

Carbonation of olivine at CO₂ supercritical conditions: Reactivity differences between synthetic and natural olivines

I. AABERG¹, K. DIDERIKSEN¹,
J.D. RODRIGUEZ-BLANCO¹, E. REGNARSSON¹,
J. OLSSON¹, H.T. JESPERSEN², K. SCHAUMBURG² AND
S.L.S. STIPP¹

¹Nano-Science Center, Dept. of Chemistry, University of Copenhagen, Denmark (iaaberg@nano.ku.dk)

²The Department of Science, Systems and Models, Roskilde University, Denmark

The carbonation of ultramafic and mafic rocks has been proposed as a carbon capture and storage (CCS) method. This method is promising because CO₂ would be captured in carbonate minerals that are stable for geological time spans. The challenge, however, is that the reactions which lead to the formation of carbonates are very slow. Learning more about it might offer the possibility of enhancing reaction kinetics.

Forsterite (Mg₂SiO₄) is an abundant mineral in mafic and ultramafic rocks. The purpose of this study was to investigate the differences in reactivity between synthetic and natural forsterite when exposed to pure deionised water and supercritical CO₂ (120 °C, 80 bars and 7 days of reaction). Solids were characterised with scanning electron microscopy (SEM), transmission electron microscopy (TEM), energy dispersive X-ray spectroscopy (EDXS), X-ray powder diffraction (XRD) and X-ray photoelectron spectroscopy (XPS) and solution composition, with atomic absorption spectroscopy (AAS).

After reaction, synthetic forsterite had transformed partly to magnesite (MgCO₃), with well defined crystals of up to 25 μm in size and to spherical particles, consisting dominantly of SiO₂.

Unreacted natural forsterite (Fo_{91.1}) had highly heterogeneous surface composition and morphology. Reaction produced very fine grained alteration products that were difficult to identify unambiguously. Thus, only a few indications of carbonate mineral formation could be observed. Our results show that natural and synthetic forsterite react very differently. After reaction, etch pits are visible on the natural samples and AAS shows Mg in solution, suggesting that the different behaviour could be caused by inhibited magnesite nucleation and growth. This implies that the complex nature of natural material should be taken into account when predicting mineral carbonation.

Dissolved and particulate iron concentrations and isotopic compositions in the South Atlantic and Southern Ocean

C. ABADIE*¹, F. LACAN¹, A. RADIC¹
AND F. POITRASSON²

¹LEGOS (CNRS/UPS/IRD/CNES), Observatoire Midi Pyrénées, F-31400, Toulouse, France

(*correspondance : cyril.abadie@legos.obs-mip.fr)

²GET (CNRS/IRD/UPS), Observatoire Midi Pyrénées, F-31400, Toulouse, France

Iron is an essential micronutrient for phytoplankton. It has been shown that in High Nutrient Low Chlorophyll areas (HNLC), Fe is a limiting factor for phytoplankton growth. Therefore, Fe has an influence on the carbon cycle. Its sources to the ocean remain a matter of debate. It has been suggested that aerosol inputs and reductive dissolution within oxygen depleted sediments were the main sources of Fe to the water column, although recent studies highlighted that the non-reductive dissolution within oxic basins is another potential source of Fe.

We obtained new results on Fe concentrations and isotopic compositions in both the particulate and dissolved phases of Fe (PFe and DFe) in seawater, in the oxic South Atlantic and Southern Ocean, off the South African coast towards Antarctica. During the Bonus GoodHope cruise in 2008, seawater samples have been taken from five stations, along a section from 36.50°S 13.12°E to 57.55°S 0.04°E. Dissolved and particulate Fe concentrations range from 0.05 to 0.72 nmol.L⁻¹ and from 0.13 to 4.65 nmol.L⁻¹, respectively. Particulate Fe and Al concentrations are correlated for three stations in the Northern part of the section suggesting lithogenic inputs of particulate iron originating from the Agulhas Current.

Iron isotopic compositions obtained so far range from -0.04‰ to 0.32‰ in δ⁵⁶Fe for PFe and from -0.71‰ to 0.27‰ for DFe. With an average isotopic composition of 0.09‰ in the Northern part of the section –close to that of the continental crust, ~-0.07‰ - the signature of the particles confirm their lithogenic origin. The lighter isotopic signatures for both DFe and PFe in the Upper Circumpolar Deep Water (UCDW) may be related to the remineralization of organic matter.

Isotopically slightly heavier DFe than PFe at the northernmost station of the transect (~500 km away from the African margin) suggests a non-reductive release of DFe from the African margin sediments. This could be a major source of Fe in oxic basins, which are much more widespread than oxygen minimum zones in the global ocean.

Rare earth elements in marine sedimentary pore fluids

APRIL N ABBOTT¹, BRIAN HALEY², JAMES MCMANUS³
AND CLARE REIMERS³

¹CEOAS, Oregon State University, USA
(aabbott@coas.oregonstate.edu)

²CEOAS, Oregon State University, USA
(bhaley@coas.oregonstate.edu)

³CEOAS, Oregon State University, USA
(mcmamus@coas.oregonstate.edu)

⁴CEOAS, Oregon State University, USA
(creimers@coas.oregonstate.edu)

The rare earth elements (REE) are powerful geochemical tracers with a number of geochemical applications. Here, we present REE concentrations from sediment pore fluids extracted from cores taken from sites along the Oregon and California margins. Our sites represent continental shelf-to-slope settings, which lie above, within, and below the oxygen minimum zone of the Northeast Pacific. These sites are characterized by varying degrees of net iron reduction; the shelf sites are generally iron-rich (where near surface, pore water Fe concentrations can exceed 100 μM), whereas slope sediments generally have less-pronounced iron reduction zones that penetrate deeper into the sediments. REE concentrations show a shallow (upper 2-10 cm) subsurface peak across all sites (up to two orders of magnitude higher than sea water), and notably these peaks do not consistently coincide with peaks in dissolved iron. Normalized patterns of fourteen REEs show distinct and large variation in the MREE enrichments and HREE to LREE ratios with core depth. These REE pore fluid enrichments highlight the potential importance of continental shelf and slope sediments as a source of REEs to the ocean's water column.

Sr-Nd isotopic study of Papandayan area, West Java: Mapping the extent of Argoland beneath Java, Indonesia

M. ABDURRACHMAN^{1*} AND M. YAMAMOTO¹

¹Bandung Institute of Technology, Bandung 40132, Indonesia
(*correspondence: mirzam@gc.itb.ac.id)

²Akita University, Akita-shi 010-8502, Japan

Southern West and East Java have been suggested by several researchers as the "home" of micro continent since Late Cretaceous [1, 2, 3], uncertainty still remains as to whether the two fragments are linked forming part of a larger micro-continent. For this reason, Sr-Nd isotopic ratios of Papandayan and adjacent Cikuray volcanoes (Papandayan area) on the volcanic front in the Triangular Volcanic Complex (TVC) were employed to gain a better of tectonic development in Java. The eruptive product of Papandayan volcano comprises medium-K series with high $^{87}\text{Sr}/^{86}\text{Sr}$ (0.705243-0.705907) and low $^{143}\text{Nd}/^{144}\text{Nd}$ (0.512504-0.512650) ratios. The Cikuray volcanic rocks are in contrast to Papandayan, belong to low-K series, with low $^{87}\text{Sr}/^{86}\text{Sr}$ (0.704172-0.704257) and high $^{143}\text{Nd}/^{144}\text{Nd}$ (0.512823-0.512858) ratios. Our study shows that the contrasting Sr-Nd isotopic ratios in Papandayan area can be explained by the mixing of clear mantle wedge (I-MORB + AOC \pm Indian Sediments) with Australian Granites as the missing "Argoland" which have separated from Western Australia in the Late Jurassic and collided to SE Sundaland in the Late Cretaceous [4]. We argue that the presence of "Argoland" beneath Southern West Java was responsible for Sr-Nd isotopic ratios diversity in Papandayan area as well as in TVC. Therefore, the suture zone should be laid between both volcanoes and Papandayan volcano probably is the only of Quaternary volcanoes which is underlain by "Argoland". If that so, the extension of East Java continental fragment can be continued to the West Java.

[1] Abdurrachman (2011) *Min Mag*, **75** (3), 401. [2] Smyth *et al* (2007) *Earth & Planetary Sci. Lett.* **258**, 269-282. [3] Clements & Hall (2007) *IPA31st*. [4] Metcalfe (2011) *Gondw. Res.* **106**, 97-122.

Multidisciplinary study on the oceanic plate: implications from the research on petitspot volcanoes

N. ABE¹ AND T. FUJIWARA²

¹IFREE, JAMSTEC, Japan (abenatsu@jamstec.go.jp)

²IFREE, JAMSTEC, Japan (toshi@jamstec.go.jp)

Petitspot is a cluster of small volcanic knolls on the oceanic lithosphere [1]. It is a kind of intraplate volcanism, similar to monogenetic volcanoes of alkaline basalts in continental plate, although there is no mantle upwelling beneath the eruption fields. Therefore, it is not related any OIB activities. The source region of the petitspot magma is expected not at very deep, but just around the boundary between the lithosphere and asthenosphere [2]. It is thought to be erupted through the small fracture on the oceanic lithosphere [1]. Petitspot volcanoes often include ultramafic xenoliths and xenocrysts that provide us many information about the chemical and physical properties of the lower oceanic lithosphere between 40 to 70 km deep without any affection of OIB [3-5]. Therefore, study on the petitspot volcanism and its ejecta is one of the most suitable research on the actual state of the oceanic plate [6, 7]. The multidisciplinary research including rock and sediment samplings, and surface and sub-seafloor geophysical surveys on the petitspot and the plain old oceanic plate around have been conducted since 2005 to reveal mechanism of the petitspot volcanism and background physics of the oceanic lithosphere and asthenosphere beneath the northwestern Pacific [6, 8-10]. However, the petitspot volcanism and its global activities are still unclear due to few rock and data samplings from the petitspot fields and the scarcity of the global detail bathymetry data.

Here we present the petrology of the ultramafic xenoliths, which shows less deformed, and the fertility and variation of the melt extraction, and the feature of the petitspot volcanism with geophysical and morphological features in the eruption fields found up to now. Then, we would like to propose the next step of the oceanic lithosphere.

[1] Hirano *et al.* (2006) *Science* **313**, 1426; [2] Machida *et al.* (2009) *GCA*, **73**, 3028; [3] Abe *et al.* (2006) *GCA*, **70**, A1; [4] Yamamoto *et al.* (2009) *Chem. Geol.*, **268**, **313**; [5] Harigane *et al.* (2011) *EPSL*, **302**, 194; [6] Abe *et al.* (2010) Proceedings Petit-Spot Workshop 2009, P.60; [7] Pilet *et al.* (2013) This Volume; [8] Fujiwara *et al.* (2007) *Grl*, **34**, L13305; [9] Baba *et al.* (2013) JPGU 2013 Abstract; [10] Hirano *et al.* (2013) *Geochemical J.*, In Press.

Time-related changes in the Si isotopic composition of Palaeo- to Mesoarchaean granitoids

K. ABRAHAM^{1,2}, S.F. FOLEY³, A. HOFMANN⁴,
D. CARDINAL¹ AND ANDRÉ L.¹

¹Section of Mineralogy–Petrography–Geochemistry,
Royal Museum for Central Africa, Leuvensesteenweg 13,
Tervuren, B 3080, Belgium

²Department of Earth Sciences, South Parks Road, Oxford
OX1 3AN, UK

³ARC Centre for Core to Crust Fluid Systems, Macquarie
University, North Ryde, 2109 NSW, Australia.

⁴Department of Geology, University of Johannesburg, South
Africa

Archaean TTG magmas are regarded to have formed by melting of amphibolite or eclogite. They are succeeded by more potassic melts in the late Archaean, suggesting that the latter melts might have formed by successive melting of the earlier TTG gneisses. Here we use Si isotopes to test this model because the light Si isotopes are expected to be enriched in the residual Mg-rich phases [1,2]. The comparison of leucosomes and melanosomes from two amphibolitic migmatitic TTG gneisses from the Archaean Iisalmi block (central Finland) confirms an isotope fractionation linked to partial melting in the range of $\Delta^{30}\text{Si}=+0.2\text{‰}$ with the restite being isotopically lighter. Si isotopes determined on four different generations of granitoid plutons from the Barberton Mountain Land (South Africa) demonstrate a gradual $\delta^{30}\text{Si}$ change from -0.17‰ at 3.55 Ga up to $+0.02\text{‰}$ at 3.1 Ga, the earliest TTGs being close to products of mantle differentiation and I-A granite types [1,3], while the younger K-rich granites are isotopically heavier, in agreement with their derivation by melting of older TTG gneisses.

[1] Savage *et al.* (2011). *Geochim. Cosmochim. Acta* **75**, 6124-6139 [2] Savage *et al.* (2013). *Earth Planet. Sci. Lett.*, **365**, 221-231. [3] Savage *et al.* (2012). *Geochim. Cosmochim. Acta* **92**, 184-202

Assessment of seasonal variations in the mineralogical and geochemical features of sulfide mine tailings

P. ACERO¹, R. PÉREZ-LÓPEZ², C. AYORA³, D. QUISPE²
AND J.M. NIETO²

¹Earth Sciences Department, Univ. Zaragoza, c/Pedro Cerbuna 12, 50009 Zaragoza, Spain.

(*correspondence: patriace@unizar.es)

²Geology Department, Univ. Huelva, Campus 'El Carmen' s/n, 21071 Huelva (Spain)

³Institute of Environmental Assessment and Water Research, IDÆA-CSIC, c/Jordi Girona 18, 08034 Barcelona (Spain)

Two sulfide mine tailings impoundments with very different proportions of pyrite from the Iberian Pyrite Belt (SW Spain) have been exposed to weathering during more than forty years under semi-arid climate conditions. Therefore, the examination of their evolution may contribute to shed light on the main processes controlling the element mobility in sulfide mine tailings with a well-developed and variable vadose zone.

For this purpose, a combination of different methodologies and techniques was applied, including the characterisation of primary and secondary mineralogy by XRD and μ -XRD, SEM-EDS and μ -XRF, study of mineral geochemistry and elemental mobility by sequential extractions and determination of pore gas profiles. The evolution of pore water hydrochemistry in vertical profiles was also examined and interpreted by geochemical and reactive transport modelling. These methodologies were applied both at field scale and in complementary laboratory column experiments.

The results of this study suggest that the main factors controlling the evolution of abandoned mine tailings under semi-arid conditions are their initial mineralogy and the degree of water saturation, which is mainly determined by the grain size and by the balance between evaporation and water infiltration. These factors determine not only the input of oxygen (and, therefore, the dissolution rate of sulfide minerals and the redox conditions) but also the type of secondary minerals precipitated, which is key for the mobilization of potentially pollutant elements. For instance, the existence of pyrite amounts larger than 80% in the vadose zone of one of the studied impoundments seems to promote not only a greater sulfide dissolution but also the existence of extremely acidic pH (below 1) that hinder the formation of secondary precipitates and give the appearance of unreacted tailing. However, the extreme low pH allows the solute load to remain in solution, increasing its pollutant potential.

Development of the U-series dating technique for the EDML ice core

S.M. ACIEGO

Department of Earth and Environmental Sciences, University of Michigan, Ann Arbor, MI 48109-1005, USA
(*correspondence: aciego@umich.edu)

Determining the absolute ages of ice within ice cores, ice sheets and glaciers remains non-trivial especially for the oldest ice (>100ka). While both insolation and Be-10 records have proven invaluable in creating ice-core timescales, neither can be used to evaluate the length of hiatuses, the extent of ice folding in ice cores, or the age of ice at the bottom sections of ice cores. U-series recoil from mineral aerosols (dust) into the ice matrix is one possible technique for determining the absolute age of ice, independent of any other parameters [1].

The well-dated upper section of the EPICA Dronning Maud Land (EDML) ice core (down to 150 ka at 2415.7 m) provides excellent constraints to verify uranium ages in a high accumulation site in the Atlantic sector of East Antarctica. In the lower 300 m the ice core climate records are disturbed due to tilting and folding of the ice. And, due to the uncertainties in flow models, it is impossible to determine if the discontinuity is resolvable (i.e., some climate record is accessible), or if the ice is too incoherent. Here, we show initial results verifying the U-series technique on samples of known age, which will allow us to apply the technique to disturbed ice in the future.

U-series recoil ages of ice samples are calculated using an age equation that includes an ejection factor, the fraction of daughter products implanted into the ice relative to the total number produced, based on the surface to volume ratio of the dust grains. This parameter is measured by specific surface area determination (BET) using a magnetically levitated balance designed at ETH [1] and manufactured by Rubotherm GmbH for the University of Michigan. Standard measurements of BAM PM103 indicate that we have achieved S_{BET} precision of better than 0.5%, equivalent precision to that of the original prototype.

Results from the well-dated section of the ice core, including surface area of dust, radiogenic and radioactive isotopic compositions of the soluble seasalt component and ^{238}U parent concentrations in the soluble component and mineral dust are applied to the U-series age equation.

[1] Aciego et al (2011) Quaternary Science Reviews **30**, 2389–2397.

Highly siderophile element geochemistry of upper mantle xenoliths from NE Bavaria

L. ACKERMAN^{1,2}, YU. KOCHERGINA^{2,3}, P. ŠPAČEK⁴
AND T. MAGNA²

¹Inst. Geology, Academy of Sciences CR, Rozvojova 269, CZ-16500 Prague, Czech Republic; (ackerman@gli.cas.cz)

²Czech Geological Survey, Klarov 3, CZ-11821 Prague, Czech Republic

³Faculty of Science, Charles University, Albertov 6, CZ-12843 Prague, Czech Republic

⁴Inst. Geophysics, Academy of Sciences CR, Bocni II, CZ-14134 Prague, Czech Republic

Concentrations of highly siderophile elements (HSE) in upper mantle xenoliths reflect variable degrees of partial melting and melt/fluid metasomatism by the agents of variable compositions (e.g., basaltic, alkaline, carbonatitic). During melt percolation, HSE can be strongly fractionated between each other depending on sulphur saturation of the infiltrating melt and melt/rock ratios; this can also affect ¹⁸⁷Os/¹⁸⁸Os.

Osmium isotope compositions coupled with HSE abundances are presented for a suite of spinel lherzolite/harzburgitic xenoliths from NE Bavaria, Bohemian Massif, that underwent variable degrees of partial melting (~4–18%) and subsequent pervasive metasomatism by alkaline–carbonatitic melts with a significant contribution of recycled crustal material.

The samples have highly variable Re–Os concentrations (9–123 ppt and 0.1–3.5 ppb, respectively) and display subchondritic to superchondritic ¹⁸⁷Os/¹⁸⁸Os (0.11348–0.13304). Primitive upper mantle-normalized patterns exhibit convex-upward shapes with significant I-PGE fractionation. Palladium contents are very low (0.09–2.07 ppb) whereas Pt contents vary greatly (0.16–6.4 ppb). Depletion ages (T_{RD}) for the whole suite scatter between 0.3 and 2.0 Ga suggesting variable perturbation of Re–Os system during metasomatism. However, the 2.0 Ga age obtained for the sample with the most depleted character appears to represent the age of the lithospheric mantle from the studied area.

While low Pd and Re contents can be explained by varying degrees of partial melting, the low I-PGE contents imply that they were removed during melt percolation of sulphur-undersaturated melt causing sulphide breakdown and I-PGE removal. On the other hand, subchondritic ¹⁸⁷Os/¹⁸⁸Os ratios in majority of samples suggest that metasomatism has only a collateral effect on Os isotopic compositions which, therefore, may provide reliable depletion ages even in pervasively metasomatized mantle.

Crystal/melt partitioning of volatiles during near-solidus melting of peridotite

JOHN ADAM¹, MICHAEL TURNER¹, ERIC HAURI²
AND SIMON TURNER¹

¹GEMOC, Department of Earth & Planetary Sciences, Macquarie University, NSW, 2109, Australia

²Carnegie Institution of Washington, 5424 Broad Branch Road, Washington, D.C. 20005, USA

Concentrations of H₂O, F, Cl, C and S in experimentally produced peridotite phases (including clinopyroxene, orthopyroxene, olivine, garnet, amphibole, mica) and co-existing melts were analysed by secondary ion mass spectrometry (SIMS). The experiments were conducted at 1025–1190 °C and 1.0–3.0 GPa on hydrous nepheline basanite mixes. Mineral/melt partition coefficients calculated from the data indicate that there is a negative correlation between partition coefficients for H₂O and absolute H₂O concentrations in melts. Because of this, the relative compatibilities of H₂O and other (non-volatile) incompatible elements (e.g. La and Ce) also depend on H₂O concentrations in melts. This may explain some of the variability in H₂O/LREE found in undegassed MORB and OIB glasses. Cl appears to be less compatible than H₂O during peridotite melting, whereas F is more compatible. Neither C nor S is significantly retained in silicate minerals during peridotite melting but may be held in residual graphite and sulphides. Thus they may be relatively compatible during mantle fractionation. The experimental data have implications for the history of volatile recycling within the mantle and thus also for the development of MORB and OIB magmatism.

Characterizing the mechanisms of soil organic matter stabilization as organo mineral complexes

NADIA K. ADAM

¹Department of Geology & Geophysics, University of Wyoming, Laramie, WY 82071, USA; Biomineral Systems LLC, South Bend, IN, 46615, USA (*Nadia.K.Adam@gmail.com)

Terrestrial soils constitute the principal pool of terrestrial carbon with 2300 Peta g organic carbon in the top 3 m of which 50-75% exists as < 2 μm sized organo-mineral complexes [1]. It is therefore critical to uncover mechanisms of SOC stabilization in organo-mineral complexes. Because C K- NEXAFS (Near edge x-ray absorption fine structure) spectroscopy has shown that SOC is composed of individual biopolymers of plant and microbial origin such as lignin, polysaccharides and lipids [2], our goal was to characterize the mechanism of sorption of organic biomolecules on a dominant, and well-characterized Fe-oxide mineral, hematite.

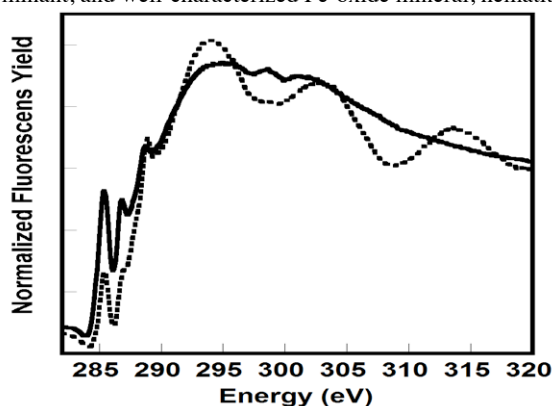
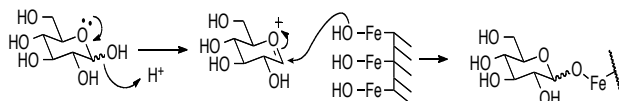


Figure 1: C K-XANES spectra of dextrose (black) and dextrose sorbed on hematite (grey) obtained in electron yield mode at Synchrotron Light Source, Wisconsin.

The C K-XANES spectrum of dextrose sorbed on hematite show marked differences compared to the spectrum for free dextrose. These changes could be attributed to C-O-Fe bonding through hydroxyl groups on hematite as shown below. This bonding upon sorption is hypothesized to shield organo-mineral complexes from enzymatic mineralization.



[1] Christensen (2000) *Eur. J. Soil Sci.* **52**, 345-353. [2] Lehmann *et al.*, (2008) *Nat. Geosci.* **1**, 238-242.

Combining life cycle (LCA) and risk (RA) assessments of TiO₂ nanomaterials: Use of a Bayesian network

VERONIQUE ADAM¹, GAETANA QUARANTA²
AND STEPHANIE LOYLAUX-LAWNICZAK³

¹LHyGeS – 1 rue Blessig – 67084 Strasbourg Cedex (veronique.adam@etu.unistra.fr)

²LHyGeS – 1 rue Blessig – 67084 Strasbourg Cedex (quaranta@unistra.fr)

³LHyGeS – 1 rue Blessig – 67084 Strasbourg Cedex (s.lawniczak@unistra.fr)

Nanomaterials are more and more present in consumer products, and are released into environmental compartments at every stage of their life cycle. Consequently, risks associated with nanoparticles need to be characterized, even if they still include a lot of uncertainties. We will focus in this communication on the production of TiO₂ nanoparticles and their insertion in cements. An assessment tool combining lifecycle and risk assessments would allow stakeholders to make decisions based on absolute results that could be compared from one life cycle to another (e.g. comparison of the sulfate process with the chloride process for the manufacturing of TiO₂ nanoparticles). Furthermore, a wider range of impact/risk categories (e.g. terrestrial ecotoxicity, aquatic ecotoxicity, or impact on human health) would be assessed, giving a comprehensive view of the system under study.

Bayesian networks are used in the risk assessment of contaminants, especially regarding ecotoxicity [1,2]. Major advantages of these networks are that they can provide satisfying results even under high uncertainty, and that they can be readily updated as new information becomes available. Given the little knowledge acquired at present regarding environmental impacts of nanomaterials, both these points make Bayesian networks very useful for their risk assessment.

The objective of this communication is to present a Bayesian network as a tool for the combined risk and lifecycle assessment of TiO₂ nanomaterials. A new methodology for a combined risk and lifecycle assessment could be presented, including a primary modeling structure and a new score combining the results of life cycle assessment and risk assessment.

[1] Borsuk, Stow & Reckhow (2004), *Ecological Modelling* **173**, 219-239. [2] Money, Reckhow & Wiesner (2012), *Science of the Total Environment* **426**, 436-445.

^{238}U - ^{230}Th and ^{235}U - ^{231}Pa disequilibria from the island of Fogo, Cape Verde

KATHERINE ADENA^{1*}, TIM ELLIOTT¹
AND RICARDO RAMALHO¹²

¹Bristol Isotope Group, School of Earth Sciences, University of Bristol (katherine.adena@bristol.ac.uk, tim.elliott@bristol.ac.uk)

²Lamont-Doherty Earth Observatory, Columbia University

The Cape Verdes Archipelago sits on one of the largest bathymetric swells in the ocean, rising 2.2km above the abyssal plain in the tropical North Atlantic. The rise is located near the point of rotation of African plate, such that the islands have experienced very little lateral movement in relation to the underlying plume over their ~20Ma lifespan. This makes Cape Verde an excellent location to examine plume dynamics under an ocean island, without the complication of lateral plate movement. There are ten islands arranged in a horseshoe, open to the west. The northern and southern islands display distinct isotopic signatures, despite their close proximity to one another. A suite of samples historical samples has been collected from the island of Fogo in the southern island chain. Samples have been collected from the 1995, 1951, 1852, 1847, 1816, 1785, 1769 and 1680-1725 eruptions, all located within the caldera. These samples have been analysed for Pb isotopes show little significant variation $^{206}\text{Pb}/^{204}\text{Pb} = 18.93$ - 19.24 , $^{207}\text{Pb}/^{204}\text{Pb} = 15.55$ - 15.63 and $^{208}\text{Pb}/^{204}\text{Pb} = 38.81$ - 39.04 . On the contrary the samples show a notable range in ($^{230}\text{Th}/^{238}\text{U}$) disequilibrium (1.091-1.226). The variation in ($^{230}\text{Th}/^{238}\text{U}$) is not clearly related to crustal contamination and we are exploring the influence of melting rate.

Coupled ^{238}U - ^{230}Th and ^{235}U - ^{231}Pa disequilibrium measurements from young mafic lavas are strongly dependent on the melting rate of their mantle source. Pyroxenite and egolite lithologies have much higher melt productivities than peridotite and this is reflected in ^{230}Th and ^{231}Pa excesses. We will attempt to explore the range in ($^{230}\text{Th}/^{238}\text{U}$) by coupling these measurements with analyses of ($^{231}\text{Pa}/^{235}\text{U}$) to get a more detailed picture of the melting process and to see if this variability can potentially be related to changes in the modal mineralogy of the source. Initial data shows large excesses for ($^{231}\text{Pa}/^{235}\text{U}$). We will present a fuller data set and its interpretations for the melting processes occurring beneath the Cape Verde Islands.

N isotope geochemistry during low grade metamorphism of coal and coal-related rocks: Case study of the anthracite field of Pennsylvania

MAGALI ADER^{1*}, JEAN-PAUL BOUDOU²
AND ERIC DANIELS³

¹Institut de Physique du Globe de Paris (*correspondence: ader@ipgp.fr)

²LAC, CNRS, UPR3321, University of Paris South, 91405 Orsay cedex, France (jpb.cnrs@free.fr)

³ChevronTexaco Energy Research & Technology Company, Richmond, California, USA (ericdaniels@chevron.com)

The evolution of the nitrogen speciation and isotopic composition in sedimentary rocks undergoing burial diagenesis and very low grade metamorphism has been seldom investigated so far. Yet it is a key issue in the reconstruction of the past nitrogen biogeochemical cycle, in the estimation of nitrogen input fluxes in subduction zones and in the understanding of molecular nitrogen genesis in the crust. Here we intend to partly fill this gap by studying the nitrogen partitioning and isotope fractionation between organic matter and minerals in coals and carbonaceous shales of the anthracite field of Pennsylvania. In this work, $\delta^{15}\text{N}$ results have been obtained on fixed-ammonium in the mineral phase of samples for which previous results on the kerogen $\delta^{15}\text{N}$ were available [1,2]. Taken together these results show that in organic and ammonium-rich samples, ammonium $\delta^{15}\text{N}$ values are more positive than the source organic nitrogen. Since, during the maturation process, nitrogen is liberated from the organic matter without isotopic fractionation [1,2], it comes that part of the generated nitrogen must have been lost with a lower $\delta^{15}\text{N}$ than its source organic matter. This nitrogen may have been lost in the form of molecular nitrogen which can then migrate and accumulate in reservoir structures. In contrast, in organic and ammonium-poor samples, ammonium $\delta^{15}\text{N}$ values are similar to those of the organic matter, suggesting that the generated nitrogen has been quantitatively fixed as ammonium in the mineral phase. In these samples, the efficiency of nitrogen retention as fixed-ammonium in the rock seems to be controlled by the ratio of generated nitrogen over the amount of host minerals for ammonium. The possibility that nitrogen was lost at this stage therefore needs to be carefully considered in studies aiming at reconstructing the past nitrogen biogeochemical cycle from bulk sedimentary rocks $\delta^{15}\text{N}$.

[1] Ader *et al* (1998) *org. geochem.* **29**, 315-323. [2] Boudou *et al* (2008) *GCA* **72**, 1199-1221.

Fluid evolution recorded by alteration minerals along the P2 reverse fault and associated with the McArthur River U-deposit

E. E. ADLAKHA^{*1}, K. HATTORI¹ AND E.G. POTTER²

¹Department of Earth Science, University of Ottawa, Ottawa, Ontario, Canada, K1N 6N5

(*correspondance: eadla028@uottawa.ca);

(keiko.hattori@uottawa.ca)

²Geological Survey of Canada, Ottawa, Ontario, Canada, K1A 0E8 (eric.potter@nrcan-nrcan.gc.ca)

The basement rocks along the P2 fault are extensively altered, particularly where they host the McArthur River Zone 2 uranium ore body. Two generations of tourmaline occur along the P2: i) early, euhedral-subhedral, coarse-grain (>0.5 mm), 1-2 cm wide veins and isolated grains of dravite (Mg-tourmaline), and ii) later fine-grain (<0.2 mm), radial magnesiofoitite (alkali-deficient dravite) forms veinlets (< 2 mm), overgrowths on earlier dravite, and grains disseminated within fine-grain illite. Fe-clinochlore, coarse-grain illite, rutile and hematite are ubiquitous along the P2 and occur as pervasive replacement minerals or veins, and post-date dravite crystallization.

To ensure minerals were free of inclusions, individual grains were first inspected with BSE-SEM at highest magnification and elemental peaks were then carefully monitored during trace element analysis (LA-ICPMS). Dravite [(□_{0.4}Na_{0.6})(□_{0.2}Mg_{1.9}Fe_{0.5}Ca_{0.2}Ti_{0.2})(Al_{5.9}Fe_{0.1})(Si_{5.7}Al_{0.3}O₁₈)(BO₃)₃(OH_{3.8}F_{0.2})] contains 1.24 (± 0.09, 1σ) wt% TiO₂, 89 – 280 ppm Zn, 51 - 630 ppm Cr, 190 - 1500 ppm V, and atomic F/Cl ratios range 98 – 11000. Magnesiofoitite [(□_{0.7}K_{0.1}Na_{0.2})(□_{0.4}Fe_{0.1}Mg_{2.0}Al_{0.5})Al₆(Al_{0.1}Si_{5.9}O₁₈)(BO₃)₃(F_{0.02}O_{H_{3.98}})] contains 65 – 260 ppm V, 2.9 - 110 ppm Cr, 0.2 – 3.7 ppm U, and 0.2 – 34 ppm Th, and ranges 3.2 - 80 atomic F/Cl. Dravite and magnesiofoitite contain low Li (< 12 ppm) and high Ni (1 – 28, 13 – 250 ppm, respectively); however, they also show contrasting trace element behaviours: dravite is enriched in LREE relative to HREE ([Ce]_N/[Ce]_N^{*}) > 1, and has a positive Eu anomaly, whereas, magnesiofoitite is enriched in HREE relative to LREE ([Ce]_N/[Ce]_N^{*}) < 1, and has a negative Eu anomaly. Chlorite [(Fe_{1.9}Mg_{2.6}Al_{1.4})(Si_{2.7}Al_{1.3}O₁₀)(OH)₈] contains significant Li (40 - 669 ppm), and Mn (803 – 4083 ppm); illite [(K_{0.9})(Al_{1.8}Mg_{0.1}Fe_{0.1})(Si_{3.2}Al_{0.8}O₁₀)(OH)₂] contains significant B (17 – 250 ppm), Li (<4.9 – 144 ppm), Ti (36 – 14500 ppm), Rb (343 - 692 ppm), U (<0.01 – 0.6 ppm), Sn (1.2 – 148 ppm), and Ba (78 – 1670 ppm); and both minerals show atomic F/Cl ratios > 10. High F/Cl, U, Th and B, and a negative Eu anomaly in alteration phases suggests a contribution of pegmatite to the fluid.

The non-trivial limitation of methanogenesis in the deep sediment of Lake Kinneret (Israel)

M. ADLER^{1*}, W. ECKERT², Z. RONEN³ AND O. SIVAN¹

¹Dep. Of geologiacl and Environmental Sciences, Ben-Gurion University of the Negev, Israel (*correspondence: sela@post.bgu.c.il, oritsi@bgu.ac.il)

²Israel Oceanogrphic and Limnological Research, Yigal Allon Kinneret Limnological Laboratory (werner@ocean.org.co.il)

³Zuckerberg institute for water research, the J. Blaustein institutes for desert research, Ben-Gurion University of the Negev, Sde-Boqer campus (zeevrone@bgu.ac.il)

The goal of this study was to investigate the non-trivial ending of methanogenesis in the deep sediments of Lake Kinneret, where substrate is still available. *in situ* profiles showed that in the deep sediment acetate and dissolved organic carbon concentrations increase. Incubation experiments showed acetate accumulation in the non-treated samples with time in the deep sediment, indicating that this substrate is not used, and that acetogenesis rather methanogenesis dominate the deeper sediments. Addition of substrates (acetate; dimethyl sulfide (DMS); H₂/CO₂ 4:1 atmosphere) did not significantly enhance methanogenesis in the deep sediments within the first 3 weeks. After 100 days of incubation with DMS methane concentration increased in all depths and in the deep sediment there was a change in the colour from brown to black as a result of iron sulfide mineral precipitation. The results indicate that methanogenesis is limited in the deep sediment of Lake Kinneret and that acetate or other electron donors are not limiting factors. The results give indication for the mechanism of methanogenesis inhibition.

www.minersoc.org

DOI:10.1180/minmag.2013.077.5.1

Geochemistry of ancient estuarine deposits on the example of pokurskaya suit sediments (West Siberia)

AFONIN I.V., TATYANIN G.M. AND TISHIN P.A.

Tomsk State University, heaven05@list.ru Tomsk, Russia

An object of study is the fragment of the pokurskaya suit (upper cenomanian) situated in the axial part of the West Siberian sediment pool (J₁-Pg) in the zone of changing sea facies to land ones. Geochemical regime of accumulating the sediments (precipitation) of the local estuarine basin was studied. Within the cut studied, there are four rock complexes fixing two transgressive cycles. First of them consolidates the beds (пласты) PK2 and PK1-2, and second one consolidates beds PK1 and K (turonian). At the same time PK1, PK2, PK1-2 fix (set) estuarine facies, whereas K sets shelf ones. The pattern of distribution of Na₂O+K₂O/Al₂O₃, Mn/U, Sr/Ba, Ce/Ce*, Ti/Zr, Fe/Mn let us mark out eight geochemical cycles within the estuarine cut. Maximum values are (Na₂O+K₂O)/Al₂O₃, Sr/Ba, Mn/U that indicates high activity of P₂O₅ and sets local peaks of the upwelling.

Lateral geochemical variability of sediments demonstrates their facial conditions. Thus, sediments of the main channel are characterized by high ratios of Mn/U (over 200), Ce/Ce* (1,2-1,45), Ti/Zr (0,04-0,86), and low content of Sr/Ba (0,23-0,13).

Sediments of the rising tide-low tide zone of the mouth differs from the channel zone by lower contents of Ce/Ce* (1,05-1,10), Mn/U (90-120), and higher content of Sr/Ba (up to 0,30).

The rocks formed in "bor" lagoons are diagnosed using parameter values, which show increasing of Sr/Ba (0,26-0,43), relative stability Ce/Ce* (0,99-1,02), and abrupt change of Fe/Mn (38-84).

Variety of coefficients Sr/Ba (0,28-0,32), Fe/Mn (44,9-35,1), and dispersion Ti/Zr (0,01-0,04) determine facial conditions of the coastal-sea zone.

This study was funded by the Russian Ministry of Education and Science (projects 5.3143.2011, 14.B37.21.0686, 14.B37.21.1257).

Multi-observable thermochemical tomography: A new framework in integrated studies of the lithosphere

JUAN C. AFONSO¹, JAVIER FULLEA², JAMES CONNOLLY³,
NICHOLAS RAWLINSON⁴, YINGJIE YANG¹
AND ALAN G. JONES⁵

¹CCFS-GEMOC, Macquarie University, Sydney, Australia

²IGEO, Universidad Complutense de Madrid, 28040, Spain

³Inst. Geochem. Petrol., ETH Zurich, Switzerland

⁴RSES, Australian National University, Canberra, Australia

⁵Dublin Institute for Advanced Studies (DIAS), Ireland

Current knowledge of the present-day thermochemical structure of the lithosphere and upper mantle essentially derives from four independent sources: i) gravity field and thermal modelling, ii) modelling of --different-- seismic data, iii) magnetotelluric studies, and iv) thermobarometric and geochemical data from exhumed mantle samples. Unfortunately, significant discrepancies and/or inconsistencies in predictions between these sources are still the rule rather than the exception, which leads to a lack of confidence in our knowledge of important features of the lithosphere and upper mantle. Moreover, thorough analyses of uncertainties and sensitivities within and between these methods are often neglected, which further exacerbates the problem.

In this talk, I will present a new thermodynamically-constrained multi-observable probabilistic inversion method, particularly designed for high-resolution (regional) studies of the present-day thermochemical structure of the lithosphere and upper mantle. The key aspects of the method are: (a) it exploits the increasing amount and quality of geophysical datasets; (b) it combines multiple geophysical observables with different sensitivities to deep/shallow, thermal/compositional anomalies into a single thermodynamic-geophysical framework; (c) it uses a general probabilistic (Bayesian) formulation to appraise the data; (d) no initial model is needed; (e) a priori compositional information relies on robust statistical analyses of a large database of natural mantle samples; and (f) it provides a natural platform to estimate realistic uncertainties. Assembling this "large" problem required a collaborative effort between thermodynamicists, mineral physicists, geophysicists and geochemists, and marks the first step towards real multi-observable thermochemical tomography studies of the Earth (as opposed to traditional seismic tomography). I will present results for both synthetic and real case studies, which serve to highlight the advantages and limitations of this approach.

Paleoarchean felsic magmatism: A melt inclusion study of 3.45 Ga volcanic rocks from the Barberton Greenstone Belt

A. AGANGI¹, A. HOFMANN² AND V. KAMENETSKY³

¹Department of Geology, University of Johannesburg,
Auckland Park 2006, South Africa. (aagangi@uj.ac.za)

²Department of Geology, University of Johannesburg,
Auckland Park 2006, South Africa. (ahofmann@uj.ac.za)

³Centre of Excellence in Ore Deposits, University of
Tasmania, Hobart, Tasmania 7001, Australia.
(dima.kamenetsky@utas.edu.au)

Archean felsic magmatism spatially and temporally associated with the Barberton Greenstone Belt (BGB) of Southern Africa can be broadly subdivided in an early (≥ 3.2 Ga), Na-rich series that formed the tonalite-trondhjemite-granodiorite (TTG) series, and a generally later (~ 3.1 Ga), K-rich series akin to modern granites [1].

Felsic volcanic rocks in the BGB are less abundant than their intrusive counterparts, and are mostly strongly deformed. The 3.45 Ga old Buck Ridge Volcanic Complex (BRVC; [2]) contains the least deformed felsic volcanic rocks in the BGB. However, widespread alteration (silicification, K-metasomatism) of these rocks involved strong mobilisation of major and some trace elements [3].

Quartz-hosted melt inclusions have been used to obtain information on the unaltered melt composition. Whole-rock compositions of the least altered samples bear strong resemblance with coeval TTG intrusions, and can be modeled as a mixture of modal phenocrysts (Na-plagioclase, quartz, Fe-Ti oxide, apatite) and melt as indicated by melt inclusion analyses, thus suggesting a cogenetic relationship between the BRVC and TTG intrusions. This is also confirmed by whole-rock concentrations of fluid-immobile trace elements. Further, melt inclusions have moderate Cl contents (≤ 0.7 wt.%), low F and low S (≤ 0.12 and < 0.02 wt.%, respectively). The moderate Cl and low F/Cl suggest a sea water contribution to the melting protolith [4]. These characteristics are interpreted as due to melting of source rocks that have undergone sea floor metamorphism, although in an Archean context this does not have immediate tectonic implications.

[1] Moyen, 2011. *Lithos* **123**, 31-36. [2] de Vries *et al.*, 2006. *Prec. Res.* **149**, 77-98. [3] Hofmann and Harris, 2008. *Chem. Geol.* **257**, 221-239 [4] Pyle and Mather, 2009. *Chem. Geol.* **263**, 110-121.

Magmatic and hydrothermal history of felsic rocks within oceanic core complex (MAR, 13°31'-13°35' N)

O.A. AGEEVA*, A.N. PERTSEV AND O.M. ZHILICHEVA

IGEM RAS, Staromonetny per., 35, Moscow, 119017 Russia
(*correspondence: ageeva@igem.ru)

Felsic plutonics and dykes – oceanic plagiogranites (OPG) – spatially associate with inactive hydrothermal fields and are regarded as the products of gabbro/dolerite hydrous melting within the oceanic core complex at 13°31'-13°35' N, Mid-Atlantic Ridge. We used cathodoluminescence (CL) and SIMS analytics to reveal mineralogical and geochemical features, and distinguish main stages of the OPG formation.

The OPG lithology includes: metadolerite - amphibolite veined by hornblende plagiogranite; coarse-grained gabbro with biotite-bearing plagiogranite veins; massive hornblende and amphibole-free OPG. The CL image (Fig. 1) demonstrates relationships between mineral assemblages, corresponding to three successive stages: mafic igneous (Pl_1 , Cpx_1), felsitic igneous (Qtz , Bt , Pl_2 , Cpx_2 , Zrn) and hydrothermal (Qtz , Pl_3 , $Chl \pm Cpx_3$).

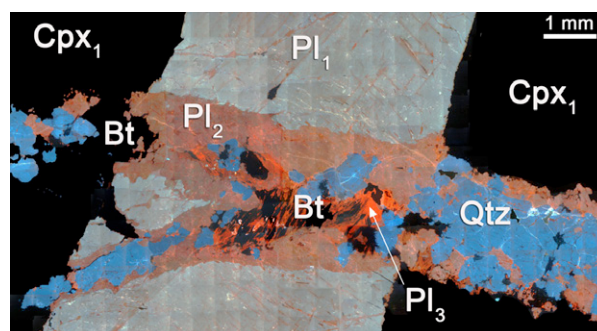


Figure 1: The OPG-vein in gabbro (CL image).

The trace-element data allow distinguishing: (1) mafic (gabbroic) fractionation; (2) felsic (OPG) fractionation; and (3) hydrothermal processing. Pl_1 (An65-60) and Cpx_1 show core-to-rim REE enrichment being appreciably depleted as compared to Pl_2 and Cpx_2 respectively. Felsic stage associates with subsequent REE enrichment of Pl_2 (An47-27) and Cpx_2 . The hydrothermal stage exhibits Pl_3 (An17-5) and Cpx_3 that are significantly depleted in REE.

Modelling the impact of C4 Biofuel Crops (*Miscanthus* spp) on soil carbon storage in different climates

F. A. AGOSTINI^{1*}, N. RONCUCCI² AND G. M. RICHTER¹

¹Rothamsted Research Harpenden, Herts AL5 2JQ UK

(*correspondence: francesco.agostini@rothamsted.ac.uk)

²Scuola St. Anna Università di Pisa (N.Roncucci@sss.up.it)

Background and Methods

The simulation of soil organic carbon (SOC) dynamics under biofuel crops, in addition to their fossil fuel offset, is critical for the evaluation of carbon (C) sequestration [1]. We tailored the RothC model [2] to simulate C3- and C4-SOC stock changes under *Miscanthus*. The expanded model (RothC_M) is designed to be coupled to a crop model, using residue inputs to the soil from the respective plant parts. The model used data from a 14-year *Miscanthus* trial at Rothamsted (UK) to calibrate turnover rates of C in litter, rhizomes and roots and the decomposability of their residues. Parameters were evaluated on a 10-year trial at Pisa (Italy).

Results and Discussion

Combining residues when applying inverse modelling (A) underestimates inputs (Tab. 1), while the estimate based on yield (B) matches RothC_M for *M. x giganteus*, but not for *M. sinensis*, possibly due to overestimating belowground inputs.

Method	A		B	C
	Low	High		
Genotypes				
Gig-1 (Italy)	3.50	6.12	8.20	8.01
Gig-1 (UK)	3.55	6.40	6.09	6.38
Sin-11	1.60	3.13	5.97	3.24

Table 1 Estimated C inputs (t ha⁻¹ yr⁻¹) to SOC by inverse modelling using RothC 26.3 [2] with default values of residue decomposability (A), based on yield [3] (B), and RothC_M (C)

Calibrated RothC_M simulates accurately SOC changes in the UK. However, in Italy the calibrated model needed further adjustment of rhizome, root and root exudate turnover to simulate observed SOC. Observations and modelling of C3 and C4 SOC indicate a C sequestration of approximately 1.8 and 3 tC ha⁻¹ yr⁻¹ in the UK and Italy, respectively.

Further simulation will test the hypothesis of a delay in rhizome turnover using new observations, and discuss the sensitivity of the model to parameter changes.

[1] Lemus and Lal (2005) *Critical Reviews in Plant Sciences*, **24**, 1-21. [2] Coleman *et al* (1997) *Geoderma*, **81**, 29-44. [3] Hillier *et al* (2009) *Global Change Biology Bioenergy*, **1**:267-281.

Synergistic Arsenic and Pb incorporation into synthetic jarosite

J. AGUILAR-CARRILLO*, M. VILLALOBOS AND F.M. ROMERO

Geochemistry Department, Geology Institute, UNAM, 04510 México D.F., Mexico

(*correspondence: jaguilarc@geologia.unam.mx)

Jarosite can incorporate many ionic substitutions into its general structure $KFe_3(SO_4)_2(OH)_6$ [1], making it especially suitable for trapping unwanted, potentially toxic species in the environment. This mineral has been shown to incorporate arsenic in acidic environments (e.g. acid mine drainage), as well as in metallurgical processes where its precipitation is used for the long-term disposal of arsenical waste [2,3]. Anionic substitutions in jarosite have been reported to affect in turn its cationic substitutions [4]. However, the effect on its cationic retention capacity is not yet well understood. The goal of this work was to investigate the influence of As(V) incorporation into the jarosite mineral structure on its Pb(II) retention capacity.

K-jarosite and arsenojarosites [$KFe_3(SO_4)_{2-z}(AsO_4)_z(OH)_6$] were synthesized, for which the arsenate substitution ranged from 16 to 80 mol% (of As+S), and Pb(II) retention experiments were performed equilibrating these at pH 2.

The Pb(II) retention capacity was increasingly enhanced by the presence of As(V) in the jarosite structure, reaching values of up to almost one order of magnitude higher Pb(II) retention for the highest As-jarosite investigated as compared to the As-free jarosite. This suggests a generalized synergistic effect of cationic heavy metal retention with arsenate incorporation.

The specific mechanisms of Pb(II) retention in this synergistic process will be presented for the different systems investigated, as well as their influence on the jarosite structure. Also, the effect of different modes of incorporation of both species during the jarosite synthesis will be shown.

The results of this work have important environmental implications: through the synergistic process encountered, remediation enhancement of cationic pollutants is possible in a concomitant fashion with arsenate attenuation in acidic mining and metallurgical environments.

[1] Dutrizac & Kaiman (1976) *Can. Mineral* **14**, 151-158. [2] Savage *et al* (2005) *Chem. Geol* **215**, 473-498. [3] Slowey *et al* (2007) *Appl. Geochem* **22**, 1884-1898. [4] Kendall *et al* (2013) *GCA* DOI: 10.1016/j.gca.2013.02.019

Isotopic signatures in a tropical transitional estuarine/marine ecosystem influenced by the largest agricultural and aquaculture activities in Mexico

AGUIÑIGA-GARCÍA S., G. RODRÍGUEZ-FIGUEROA, A. SÁNCHEZ-GONZÁLEZ AND F.J. ROMO-RÍOS

Centro Interdisciplinario de Ciencias Marinas, Instituto Politécnico Nacional, Avenida de IPN s/n, Col. Playa Palo de Santa Rita, Apto Postal 592, La Paz, Baja California Sur 23096, Mexico

Assess the anthropogenic pressures on coastal ecosystems are of primary concern. This project is focused in San Ignacio-Navachiste-Macapule, Sinaloa, Mexico, a transitional ecosystem influenced by the largest agricultural and aquaculture activities. Nitrogen and carbon stable isotopes have been evaluated in sediments to estimate spatial variability and its correlations with inputs of carbon and nitrogen derived from natural and anthropogenic sources. The d-15N values ranged from 6 to 10.6‰ from marine-estuarine gradient. Sedimentary organic matter positive d-15N values were influenced by a mixture of aquaculture (sediment pond d-15N = 8.53‰), sewage (12‰) and agriculture drainage (3‰). These land-marine areas were associated with fine grain size, high content of the macronutrient (15 µM NO₃) and negative d-13C values (-25.4‰) as a result of mangrove (-27.3‰), aquaculture (-16.8‰) and positive C4 terrestrial plants (-14.6‰). In contrast, lowest d-15N values were correlated with coarse grain size, 5 µM NO₃ and positive (-19 ‰) d-13C values, of marine environment. The estuarine/marine pattern has an anthropogenic component that be traced in the spatial scale.

The origin of myrmekite in the Boroujerd granitoids, Sanandaj-Sirjan Zone

VAHID AHADNEJAD

Geology Department, Payame Noor University, Tehran 19395-4697, I. R. Iran. (v.ahadnejad@gmail.com)

The Boroujerd Plutonic Complex (BPC) is one of the major Jurassic plutonic complexes in the Sanandaj-Sirjan Zone (SSZ). The BPC consists of a suite of calc-alkaline dioritic to granitic rocks. The abundance of myrmekitic texture is a major petrographic characteristic in the BPC that implies an emplacement into a high-strain shear zone. This is confirmed by mylonitic microstructures in the studied rocks [1]. The abundance of calcic plagioclase rather than its sodic type and absence of K-feldspar imply a Ca-metasomatism as a major geochemical factor for myrmekites. Locally, there is some K-metasomatism signs such as K-feldspar overgrowth on plagioclase [2], remnant plagioclase islands in microcline crystals, and paths of microcline in plagioclase.

[1] Rasouli, J., Ahadnejad, V., Esmaeily, D. 2012. A preliminary study of the anisotropy of magnetic susceptibility (AMS) of Boroujerd granitoids, Sanandaj-Sirjan Zone, West Iran. *Natural Science*, **4**, 91-105. [2] Collins, L.G., 1997. Myrmekite formed by Ca-metasomatism: ISSN 1526-5757, Electronic Internet Publication, No. 4. <http://www.csun.edu/~vcgeo005/revised4.htm>

Regional deep water anoxic conditions during the Hirnantian extinction event

ANNE-SOFIE C. AHM¹* CHRISTIAN J. BJERRUM¹
AND EMMA U. HAMMARLUND

¹Nordic Center for Earth Evolution and Department of Geoscience and Natural Resource Management, University of Copenhagen, DK-1350 Copenhagen K, Denmark (*correspondence: annes.ahm@geo.ku.dk)

²Nordic Center for Earth Evolution (NordCEE) and Institute of Biology, University of Southern Denmark, DK-5230 Odense C, Denmark

The Late Ordovician Hirnantian glaciation (~444 Ma) coincided with a marine carbon cycle perturbation, and one of the largest mass extinction events in the Phanerozoic. However, the underlying causes leading up to the extinction event are not fully understood. It has been suggested that a Hirnantian expansion of anoxic conditions, driven by the glacio-eustatic sea-level fall, acted together with the reduction of habitats as the major kill mechanism [1]. To further resolve the end-Ordovician water column chemistry, a multi-proxy geochemical approach was applied to a new drill core and surface material from a deep-water section in central Nevada. Here, enrichments in U and Mo suggest euxinic conditions at the onset of the Hirnantian. Furthermore, ratios of highly reactive iron over total iron (Fe_{HR}/Fe_T) increases from the Katian to values of ~0.5 in the Hirnantian stage, indicating an anoxic water column. We argue that the onset of the Hirnantian can be linked to an euxinic event and that these observations are evidence of expanding anoxia during the first stages of the marine regression which has been lacking documentation at shallower-water sections.

[1] Hammarlund *et al.* (2012) *Earth Planet. Sci. Lett.* **331-332**, 128-139.

Petrography and diagenesis of Pab sandstone, implications for hydrocarbon exploration in southern Pakistan

SAJJAD AHMAD

Department of Geology, University of Peshawar, Khyber Pukhtunkhwa, Pakistan, 25000
(dr.s_ahmed@upesh.edu.pk)

In this study the petrography, diagenetic fabric and hydrocarbon reservoir rock characterization of the Cretaceous Pab sandstone is carried out. Mostly the rock type is arkosic arenite but feldspathic Greywacke is also seen. The dominance of mono-crystalline quartz, alkali feldspar and heavy minerals (Tourmaline, Zircon, and Garnet) point to a provenance source dominated by acidic igneous rocks. Presence of the Quartz overgrowth with mostly concavo-convex boundaries along with the presence of some point and sutured contacts is the major modification caused by the increased geothermal gradient and pressure in the middle to final phase of diagenesis. The synthesis of petrographic, diagenetic and plug porosity permeability data confirms a good hydrocarbon prospect of the unit in the region.

The Microbe-Mineral Interactions In The Acidic Podzol Soil

ENGY AHMED* AND SARA HOLMSTRÖM

Department of Geological Sciences, Stockholm University,
Stockholm, Sweden (engy.ahmed@geo.su.se)

Iron is a key component of the chemical architecture of the biosphere. Due to the low bioavailability of iron in the environment, microorganisms have developed specific uptake strategies, like siderophores, which are operationally defined as low-molecular-mass biogenic Fe(III)-binding compounds, that can increase iron's bioavailability by promoting the dissolution of iron-bearing minerals. In the present study, we aimed to investigate the composition of hydroxamate siderophores in the soil horizons of the acidic podzol, and study how they are affected by the presence of specific mineral types and microbial communities.

Three different minerals (apatite, biotite and oligoclase) were inserted in the soil horizons (O (organic), E (eluvial), B (upper illuvial), and C (mineral)). After two years, soil samples were collected from both the bulk soil (next to the minerals) and from the soil attached to the mineral surfaces. The concentration of ten different fungal tri-hydroxamates and five bacterial ones were determined by high-performance liquid chromatography coupled to electrospray ionization mass spectrometry (HPLC-ESI-MS). In addition, total microbial composition and diversity were studied.

Our field experiment succeeded in describing the relationship between the presence of siderophores, soil horizon and mineral type, in addition to understanding the interaction between mineral type and soil microbial composition. A wide range of fungal and bacterial hydroxamates were detected throughout the soil profile. On the other hand, the presence of the minerals completely altered the diversity of siderophores. In addition, each mineral had a unique interaction with hydroxamates in the different soil horizons. There were also a good relationship between the microbial diversity and the siderophore distribution.

Keywords: Podzol soil, Siderophores, Weathering

Hydraulic properties and fresh water prospect of the Ganges River Basin, Bangladesh

NUR AHMED

Hydrogeologist, Institute of Water Modeling, Dhaka-1206
(nurgeo3@gmail.com)

Bangladesh is a lower riparian country in the floodplains of three major rivers- the Ganges (Padma), the Bhramaputra and the Meghna and their tributaries and distributaries which forms the largest delta in the world. Ganges River Basin in Bangladesh has been strongly influenced by tectonics, manifested as delta switching and subsidence and shows fluvio/deltaic plains depositional environments. Groundwater development was started in the early sixties and extended rapidly during the late 1976. Presently, 80% of our national water demand fulfill by groundwater. The lean season flow of the Ganges has decreased since the commissioning of the Farakka Barrage in India during 1975. Climatic change is accelerating the siltation and subsequent dry season, and also limitation of the surface water that's why total water demands stressed on the groundwater. Ganges River basin areas of Bangladesh have started facing water problems, including the drying up of wells during peak irrigation period and lowering of water table and chemical(As,Fe,Cl,Mn,Mg²⁺) problem. The study area shows arsenic contamination in shallow groundwater aquifers which makes the water unfit not only for human consumption but also for agriculture and environment. In some places deep aquifers show saline water. Between these two aquifers fresh water aquifer is found which the main water source of the area. This paper is mainly concerned with the delineation, extension, recharge and discharge areas of the fresh water aquifer and calibrates hydraulic properties of the aquifer. It also throws light on scope of development of the fresh water aquifer without arsenic contamination or saline water intrusion.

Key words: Ganges river Basin, groundwater, water quality.

Petrology and origin of Yozgat Intrusive Complex, Central Anatolia, Turkey

M.A. AKÇE^{1*2} AND Y.K. KADIOĞLU³⁴

¹Bozok University Dept. of Geological Eng., 66100 Yozgat, Turkey (*correspondence: mavni.akce@bozok.edu.tr)

²Bozok University Science and Technology Application & Research Center, Yozgat, Turkey

³Ankara University Dept. of Geological Eng., Ankara, Turkey

⁴Ankara University Earth Sciences Application & Research Center, Ankara, Turkey

Yozgat Intrusive Complex (YIC) is located in the north part of the Central Anatolian Crystalline Complex (CACC). YIC represents the biggest intrusive body of the CACC and clarifies magmatism evolved during the late Cretaceous and Paleocene. YIC is mainly composed of granitic, gabbroic, monzonitic and syenitic rocks forming a complex of different sources and compositions in Central Anatolia. The composition of granitic rocks of YIC is in the range from alkali feldspar granite to the tonalite. The monzonitic rocks are in composition of monzonite and quartz monzonite. The syenitic rocks are in composition of syenite, foid syenite and foid monzosyenite. The gabbroic rocks of YIC are mostly exposed at the top of the hills and have a sharp contact with the felsic intrusive body.

Whole rock geochemistry reveals that granitic, gabbroic and monzonitic rocks are subalkaline whereas syenitic rocks are alkaline in nature. Granitic and monzonitic rocks have a calc-alkaline and gabbroic rocks have a tholeiitic character. Granitic rocks are peraluminous and metaluminous, and monzonitic and syenitic rocks are metaluminous in character. Tectonic discrimination diagrams suggest that the most granitic rocks of YIC are syn-collisional granite whereas monzonitic and syenitic rocks are post-collisional granite. The ORG-normalized elemental patterns of all the felsic intrusive rock units show similar patterns which are characterized by enrichment in large ion lithophile (LIL) with respect to high field strength (HFS) elements. Chondrite-normalized rare earth elemental patterns of granitic, monzonitic and syenitic rocks reveal almost a slight trend. Light rare earth elements (LREE) show enrichment compared to heavy rare earth elements (HREE). These elemental patterns show that the magma is mostly influenced by the crust. All these geological, petrological and geochronological data indicate the progressive evolution of the YIC magmatism respectively from calc-alkaline granites through shoshonitic monzonites to alkaline foid syenite compositions caused by crustal thinning.

Diversity of melts migration process within the uppermost mantle along a mid-ocean ridge: An example from the northern Oman ophiolite

N. AKIZAWA¹, S. ARAI¹, A. TAMURA¹ AND K. OZAWA²

¹Department of Earth Sciences, Kanazawa Univ., Kakumamachi, Kanazawa, Ishikawa, 920-1192, JAPAN

²Department of Earth and Planetary Science, Tokyo Univ., Hongou7-3-1, Bunkyo-ku, Tokyo, 113-0033, JAPAN

Dunite bands and veins in the ophiolitic mantle peridotite are interpreted as fossil melt conduits within the suboceanic mantle. In particular, concordant dunite bands are possibly important as the melt conduits through which parental melts of MORB (mid-ocean ridge basalts) were transported to shallower mantle beneath the ridge axis. However, no detailed petrological data of concordant dunite bands and surrounding peridotites have been published. We conducted sampling of concordant dunite bands and its aureole from various "stratigraphic levels" in the mantle section of an estimated ancient-segment center and its end in the northern Oman ophiolite. They are thick and high in frequency at segment center, but are thin and low at segment end. Dunite bands are almost pyroxene-free, and their orthopyroxenes, if any, are vermicular in shape.

Mineral chemistry shows systematic variations in the wall peridotites toward the dunite bands. In ambient residual peridotites, rare earth element (REE) patterns of clinopyroxene incline from light-REE (LREE) to heavy-REE (HREE) monotonously. The REE pattern of clinopyroxene in dunites and surrounding peridotites show various shapes, depending on the position, the segment center to end: U-shaped at the segment center, and gentle slope from HREE to LREE at the segment end.

We conducted calculation for REE enrichment of clinopyroxenes in dunites by using 1-D steady state modeling, which duplicates simple fractional melting process and influx melting process. The results indicate that melt volume was less to form dunite bands of segment center, whereas was high at segment end. This contrast dues to difference of dunite band distribution between segment center and end; degree of melt/peridotite interaction was high at segment center to form dunite bands, but not at segment end.

Trace element distribution in an extremely basic environment in mine tailings

L. ALAKANGAS AND L. JINMEI

Luleå University of Technology, 97187 Luleå, Sweden

Element distribution in a 10 years old low-sulphide and high-carbonate tailings profile covered with a 50cm thick fly ash layer have been investigated. The dissolution of fly ash created an extremely basic environment (pH >11) in the underlying tailings. This resulted in a depletion zone where weathering of Ca-, Fe-, Mg- and Mn-silicates was extensive. Only quartz and K-, Na-, Ca-feldspars covered with CaCO₃ remained. The depletion zone was 47cm thick, which indicates a very high weathering rate due to the presence of hydrated hydroxyl ions. Chromium and Ni were accumulated in the depletion zone, while Cd and Cu showed a relatively unchanged content. These elements were added from the ash layer. Chromium and Ni were not identified by scanning electron microscope, but found in the residual phase by sequential extraction, indicating insoluble phases. Elements such as Fe, Pb and S were depleted in the upper part of the tailings, but accumulated together with Cd and Cu, 20cm below the depletion zone, where the pH decreased to circum-neutral. Detailed determination of secondary phases present in the accumulation zone is in progress and the result will be presented. The ash layer was hardened due to pozzolanic properties which reduced the oxygen diffusion which was confirmed by oxygen analysis. Alkaline materials are often used in remediation of contaminated areas, but should be carefully used to avoid leaching of metals. Accumulated elements can be remobilized by changes in the chemical environment when for example the weathering front moves downward and/or the lime content is exhausted.

Development of *in situ* measurements of REE in deep groundwater using Diffusive Gradient in Thin Film

L. ALAKANGAS^{1*}, M. ÅSTRÖM², F. MATHURIN²,
M. FAARINEN³ AND B. WALLIN⁴

¹SKB, Äspö HRL, SE-572 29 Oskarshamn, Sweden

(*correspondence: linda.alakangas@skb.se)

²School of Natural Sciences, Linnaeus Univ., SE-391 82 Kalmar, Sweden

³ALS Scandinavia, SE-977 75 Luleå, Sweden

⁴Geokema AB, SE-181 46 Lidingö, Sweden

The Äspö Hard Rock Laboratory (HRL), SE Sweden, is an underground facility where the Swedish concept for storage of nuclear fuel waste is tested under natural repository conditions [1]. This laboratory also offers an environment for researchers interested in conducting experiments as well as testing equipment *in situ* at the deep granitoid subsurface.

An ongoing activity at the Äspö HRL is monitoring of hydrogeochemistry where several borehole are characterized and sampled every year since two decades. The program includes the rare earth elements (REE), which generally however occur in concentrations below detection limit with the utilizes conventional sampling and analytical techniques.

In order to develop a monitoring-technique with which the REEs can be detected above the detection limit, a principle with passive samplers, DGT (Diffusive Gradient in Thin-Film) [2], has been tested. The DGT technique makes it possible to determine labile trace elements, such as REE, by allowing the metals in solution to accumulating to binding agents over a defined period of time.

To obtain as little disturbance as possible and maintain the pressure and the reduced state in the bedrock fractures a special designed container was constructed. The container can hold three DGT's and are constructed in stainless steel to maintain a high pressure of 50 bar and the inside is made of PEEK polymer material to minimize the risk of contamination.

The sampling was performed in three boreholes at depths of -144 m, -280 m and -450 m at three different locations in the Äspö HRL tunnel. Different deployment times were tested (1-4 weeks) and the results are compared with spot sample measurements (<0.45 µm). Overall, the technique works well and the results show that DGT can be used to monitor low-levels of REE (and other trace metals) in reduced groundwater in deep-lying bedrock fractures.

[1] SKB (2012) Annual Report 2011. SKB TR-12-03 [2] Zhang *et al* (1995) *Anal. Chem.* **67**, 3391-3400

Contrasting volatile contents in the lunar mantle and anorthosites

EMMANUELLE ALBALAT¹, PETER LUFFI², CIN-TY LEE²,
AND FRANCIS ALBARÈDE^{1,2},

¹Ecole Normale Supérieure de Lyon, 69007 Lyon, France,
(emmanuelle.albalat@ens-lyon.fr)

²Department of Earth Science, Rice University, Houston TX
77005, USA

The enrichment of lunar basalts in heavy Zn isotopes has been used to support large-scale evaporation of lunar volatiles in the aftermath of the Moon-forming event [1]. A remarkable property of Zn is that the Zn/Fe ratio does not significantly fractionate during magmatic processes [2], which reflects the very similar ionic radii of the two elements. We measured trace and major elements by LA-ICP-MS in individual mineral grains and basaltic fragments from 17 lunar samples, among which high-Ti and low-Ti basalts, pyroclastics, the Mg-suite, ferroan anorthosites (FAN), breccias and soils. Among the volatile elements, some of them are siderophile (Ge, $T_{50} = 883$ K), some other lithophile (Zn, $T_{50} = 726$ K) or chalcophile (Cu, $T_{50} = 1037$ K)[3]. Here we show that the Zn/Fe ratios in the source of mare basalts is about two orders of magnitude less than in the terrestrial mantle, which demonstrates that the interior of the Moon is very depleted in volatiles. On the other hand, the Zn/Fe ratios of FAN plagioclase are 1-2 orders of magnitude higher than in lunar basalts. Mineral and melt data indicate that plagioclase preferentially incorporates Zn and Cu relative to Fe by more than an order of magnitude. The nearly constant Ge/Si ratios observed for all samples argue against variable Zn/Fe fractionation upon core segregation. A first possibility is that the higher contents of volatile elements in anorthosites relative to the source of mare basalts reflects the preferential uptake of these elements from the magma ocean by crystallizing anorthite. Alternatively FAN may have been derived from a magma ocean distinctly enriched in volatile elements relative to the deep lunar mantle. The non-chondritic Th/U ratio of FAN inferred from their Pb isotopes [4] is representative of their parent melts and suggests that the latter interpretation should probably be preferred.

[1] Paniello R *et al* (2012) *GCA* **42**, 1075-1090. [2] Le Roux V. *et al et al* (2010) *GCA* **74**, 2779-2796. [3] Lodders (2003) *Astrophys. J.* **591**, 1220-1247. [4] Premo *et al* (1999) *Internatinal Geology Review* **41:2**, 95-128.

The URGE project in Italy: The Acerra–Pomigliano-Marigliano conurbation

S. ALBANESE*¹, A. LIMA¹; C. REZZA¹, G. FERULLO¹,
B. DE VIVO¹, W. CHEN² AND S. QI².

¹Università degli Studi di Napoli Federico II - Napoli, Italy.
(* correspondence: stefano.albanese@unina.it)

²School of Environmental Studies, China University of
Geosciences, Wuhan, China

The URGE project has as the main objective the production of the geochemical maps of 12 european urban areas using a shared sampling and analytical procedures.

In the framework of the URGE (Urban Geochemistry) project, aiming at the production of the geochemical maps of 12 european urban areas, the north-eastern sector of the Napoli metropolitan area (Italy), namely the Acerra-Pomigliano-Marigliano area has undergone a geochemical characterization based on 145 soil samples collected over an area of 90 sqkm.

This area has been selected on the basis of previous regional studies [1, 2, 3] and because of both the presence of an historical industrial settlement on it (mainly devoted to plastic materials and synthetic fibres production) and of an incinerator which came into operation in March 2009.

The main objective of the study was to define the local geochemical baselines both for 53 elements (among which the toxic ones) and for some organic compounds, including PAHs and OCPs. Furthermore, the study aimed at supporting epidemiological researches and at establishing a record of the actual environmental conditions to evaluate the future impact of the incinerator on both the territory and the public health.

Preliminary results showed that 1) the most urbanized areas of the conurbation are characterized by concentrations of Pb, Zn and V exceeding the trigger limits established by the Italian Environmental law (D.Lgs. 152/2006); 2) agricultural soils, in the surroundings of the urbanized areas, are enriched in Cu, Co, Cd, Be and Ni, 3) in the incinerator area Se, Hg, Cu, Cd and Sb baselines are generally higher than in the rest of the territory.

Furthermore, the PAHs distribution pattern and their diagnostic ratios suggested that the agricultural waste burning in the rural sector of the study area could be a relevant source of pollution.

[1] Albanese *et al* (2007) *JGE* **93**, 21-34. [2] Cicchella *et al* (2008) *GEEA* **8** (1), 19-29. [3] De Vivo *et al* (2006) *Aracne* Editrice, Roma. 324 pp.

Improved dust representation in the Community Atmosphere Model

S. ALBANI^{1,2*}, N. M. MAHOWALD¹, A. T. PERRY¹,
R. A. SCANZA¹, C. S. ZENDER³, N. G. HEAVENS⁴,
V. MAGGI², J. F. KOK¹ AND B. L. OTTO-BLIESNER⁵

¹Department of Earth and Atmospheric Sciences, Cornell University, Ithaca NY, USA

(*correspondence: s.albani@cornell.edu)

²Department of Environmental Sciences, University of Milano-Bicocca, Milano, Italy

³Department of Earth System Science, University of California, Irvine, Irvine CA, USA

⁴Department of Atmospheric and Planetary Sciences, Hampton University, Hampton VA, USA

⁵National Center for Atmospheric Research, Boulder CO, USA

Aerosol-climate interactions constitute one of the major sources of uncertainty in assessing anthropogenic and glacial radiative forcing. We recently focussed on improving the representation of mineral dust in the Community Atmosphere Model and assessing the impacts of the improvements in terms of direct effects on the radiative balance of the atmosphere and climate impacts.

We simulated the dust cycle while using different parameterization sets for dust emission, size distribution, and optical properties. Comparing the results of these simulations with observations of concentration, deposition, and aerosol optical depth allow us to refine the representation of the dust cycle and its climate impacts. Our findings indicate that the magnitude of the dust cycle is sensitive to the observational datasets and size distribution. In addition, the direct radiative forcing of dust is strongly sensitive to the optical properties and size distribution.

Our results from simulations applying the refined parameterization set indicate a net top of atmosphere direct dust radiative forcing of -0.22 ± 0.12 W/m² for present day and -0.33 ± 0.18 W/m² at the Last Glacial Maximum. These estimates are smaller than previous model simulations due to changes in size distribution, modeled spatial distribution and optical parameters.

We analyze the climate impacts in response to the direct radiative forcing deriving from the refined dust parameterizations.

Isotopes of disease

FRANCIS ALBARÈDE

Ecole Normale Supérieure de Lyon, 69007 Lyon, France
(albarede@ens-lyon.fr)

Transition metals are essential components of hundreds of proteins in the human body. They achieve a large spectrum of critical biological functions, such as oxygen transport (Fe), electron shuttling (Cu), structural control and protein degradation (Zn). Their binding to a variety of amino acids is controlled by bond energy, e.g., 'hard' histidine vs 'soft' cysteine, by their structural environment, and by the redox and pH conditions of biological fluids. The different cellular stores of metal are in constant flux and are regulated by gene expression which reacts to a complex pattern of physiological signals. Metal isotope compositions in organs and body fluids provide an enormous source of untapped information relevant to normal and pathological conditions. Spectacular patterns of isotope fractionation are observed in some organs such as the liver and the kidney, and in blood components as well. To a large extent, these patterns reflect the binding of metals with different amino acids, variable redox states and electronegativity. Ab initio calculations indicate that heavy isotopes tend to bind to O-rich ligands (hydroxide, carbonate, phosphate), whereas light isotopes are positively fractionated by S-bonds. Formation of blood cells (erythropoiesis) takes place with very large and coupled Cu-Fe isotope fractionation, the disruption of which clearly signal pathological, and in general, abnormal conditions. The recent years have seen the emphasis being laid on genetic diseases, such as Fe in hemochromatosis and Cu in Wilson disease, and neurodegenerative pathologies such as the Alzheimer disease for Zn. Now that preliminary ground work on metal isotopic variability in the human body is being laid, the opportunity of using some isotopes as biomarkers has never been stronger. Particularly promising are the isotopes of Cu, the concentrations of which are known to vary in multiple forms of cancer, and of Zn, which is making a forceful entry as a biomarker of prostate cancer in the wake of PSA discredit. The enormous challenge of using isotopes to quantitatively assess the parameters of metal homeostasis at the cellular level in relation with gene expression and regulation will clearly engage the upcoming generation of isotope geochemists, biochemists, and health scientists.

www.minersoc.org

DOI:10.1180/minmag.2013.077.5.1

A mass fractionation law for high-transmission MC-ICP-MS

FRANCIS ALBARÈDE, PHILIPPE TELOUK
AND EMMANUELLE ALBALAT¹

¹Ecole Normale Supérieure de Lyon, 69007 Lyon, France,
(albarede@ens-lyon.fr)

Russell *et al*'s [1] exponential law provides the standard form used for the correction of the mass bias on isotopic ratios measured by mass spectrometry and more specifically since 1992 for MC-ICP-MS. It is nevertheless expected to fail as soon as the ion/atom efficiency exceeds the percent level and preliminary observations on new-generation MC-ICP-MS confirms this prediction. At 100% transmission, the mass bias must be unity. The physics of mass fractionation in the torch involves collisions with abundant neutral argon atoms, the formation of a shock wave in the interface, and the presence of a boundary layer in the nozzle, and is therefore particularly complicated. At low transmission, the ratio between two isotopes 1 and 2 is affected by a factor $(M_1/M_2)^\beta$, where M is the atomic mass. The mass fractionation factor β remains essentially constant and equal to ~ 2 across the mass range, which suggests that the velocity of radial expansion is proportional to mass [2], but this law has not received a universally accepted physical justification.

At high transmission, the exponential law breaks down. What is the relationship between mass fractionation and transmission? A simple conservation principle applied to the fraction lost suggests an example of a transmission-compliant mass fractionation law:

$$R_{\text{meas}} = R_{\text{true}} \times \frac{(M_1/M_2)^\beta}{(1 - n/n_0) + (n/n_0)(M_1/M_2)^\beta}$$

in which n/n_0 is the transmission. At the limit, the exponential law is obtained when $n/n_0 \rightarrow 0$, while the mass bias disappears when $n/n_0 \rightarrow 1$. Other forms involving different functional relationships are also possible and need to be tested. The instrument transmission for a particular element is an essential parameter of mass fractionation laws and should therefore be recorded with the best possible precision. We will present data on the isotope compositions of various elements across the mass range that will allow the present model to be tested.

[1] Russell WA *et al* (1978) *GCA* **42**, 1075-1090 [2] Maréchal *et al* (1999) *Chem. Geol.* **156**, 251-273.

The Y-3 tephra: New insights

P. G. ALBERT^{1,2*}, M. HARDIMAN³, J. KELLER⁴,
E.L. TOMLINSON⁵, U.C. MÜLLER⁶, V.C. SMITH²
AND M. MENZIES¹

¹Earth Sciences, Royal Holloway University of London, UK

²RLAHA, University Oxford, UK

(paul.albert@rlaha.ox.ac.uk)

³Geography, Royal Holloway University of London, UK

⁴Albert-Ludwigs-University Freiburg, Germany

⁵Geology, Trinity College Dublin, Ireland.

⁶Institute of Geosciences, Frankfurt, Germany

The 'Y-3' tephra is a crucial stratigraphic marker within the central Mediterranean region, reported occurrences within palaeoenvironmental archives occur at or close to the Marine Isotope Stage 3/2 transition, which in turn is linked to the onset of Heinrich Stadial 3 (HS3) [1]. Consequently this tephra offers enormous potential to assess potential leads and lags between Mediterranean archives. Until now the type locality Ionian Sea Y-3 tephra has remained poorly characterised. Consequently, numerous other distal tephras occurring in broadly similar stratigraphic positions and displaying a similar trachyte composition have been correlated to the Y-3 tephra without the appropriate geochemical validation.

Here we present the first grain-specific major, minor (EPMA) and trace element (LA-ICP-MS) characterisation of the Y-3 tephra recorded in its type locality of the Ionian Sea (M25/4-12). The High-K phono-trachyte geochemistry of the Ionian Sea Y-3 supports a provenance from within the Campi Flegrei caldera consistent with previous interpretations. Geochemical glass data reveals problems with a correlation between the Ionian Sea Y-3 and the proposed proximal equivalent, the VRa Tufi Biancastri unit. As a result the VRa age must not be imported to the Ionian Sea Y-3 tephra.

Using the new diagnostic major, minor and trace element chemistry of the type locality Y-3 tephra we are able to assess and establish precise distal-distal tephra correlations. Robust identification of the Y-3 in the Tenaghi Philippon (Greece) sedimentary archive both offers an opportunity to determine a precise age for this distal marker and assess its stratigraphic position in the context of a high resolution palaeoenvironmental archive. A Bayesian-based ¹⁴C age model provides an age of 29, 350-30, 160 cal yrs BP for the Y-3 tephra. The Y-3 tephra resides within the latter part of a period of reduced total tree pollen percentages, which is related to drier stadial conditions. The independent age of the Y-3 tephra and its environmental context suggests that this marker tephra post dates the onset of both HS3 in the Mediterranean region and GS-5 in the INTIMATE event stratigraphy [2].

[1] Zanchetta *et al*, (2008) *JVGR* **177**, 145-154; [2] Blockley *et al*, (2012), *Quat. Sci. Revs.* **36**, 2-10.

Biogeochemistry of manmade lake nearby industrial city, Riyadh, Saudi Arabia

IBRAHIM MASHHOUR AND MAJED ALBOKARI*

Atomic Energy Research Institute (AERI), King Abdulaziz City for Science and Technology (KACST), P. O. Box 6086, Riyadh 11442, Saudi Arabia.
(mbokari@kacst.edu.sa)

Extremophiles are microbes that have the ability to maintain a life cycle in severe environments such as those characterized by high salt (halophiles) and high temperature (hyperthermophiles). A manmade lake (pond) nearby the second industrial city at the south of Riyadh, Saudi Arabia with estimated area of 25 square kilometer and 20 meter depth, which was created accidentally, is characterized as extreme environments whereas TDS reaches around 7700 ppm and the temperature of surrounded area hits 60 °C in summer and goes down -2 °C in winter. The lake has been fed by all type of wastewater ranges from treated wastewater generated from facilities of the industrial city, draining system of rainfall and portable sewage tanks. A discharge channel (stream) somehow connected to the lake from facilities of industrial city via underneath the highway was built recently. This work aimed to measure physico-chemical properties, selected heavy metals (Cr, Mn, Fe, Co, Ni, Cu, Zn, As, Cd, Pd) and presenting bacteria along the stream and the lake itself in order to propose a hypothesis regarding biogeochemistry behaviour of indigenous microorganisms.

Practically, nitrates, carbonates and sulfates clearly decreased by 41.5%, 28.5%, 14.0%, respectively, from stream part to lake itself. Similarly, level of Cr, Mn, Fe, Co, Zn, Cd and Pd decreased as sampling have been collected along stream to lake. On the other hand, concentrations of Ni and As increased by 46% and 27 %, respectively while Cu didn't show any significant change. On the bacterial level, microbiological conventional methods produced 62 isolate (38 isolated from lake's samples and 24 isolated from stream's samples) and identified using state-of-art RiboPrinter microbial characterization system, which is based on pattern of DNA bands. *Aeromonas hydrophila* species represented 10% of total isolates from lake's samples while *Klebsiella pneumonia* species found to be 50% of isolates from stream's samples. In such an open complex ecosystem, many variables are accounted to have certain behavior like chemistry of elements and geological structure of the area. Moreover, shifts in bacterial species profiles and changes in physico-chemical between stream and lake can be linked to each other and lead to isolate novel species.

Analysis of fluid inclusions with fs-LA-ICP-MS

M. ALBRECHT*¹, I.T. DERREY¹, I. HORN¹, S. SCHUTH¹, F. MELCHER² AND S. WEYER¹

¹Leibniz Universität Hannover, Institut für Mineralogie, GER
²Federal Institute for Geosciences & Natural Resources, GER
(*correspondence: m.albrecht@mineralogie.uni-hannover.de)

Hydrothermal Cu deposits are one of the most significant type of ore deposits for many metals (e.g. Cu, Zn, W, Mo, Au). Fluids are responsible for the transport and the enrichment of those metals [1]. To learn about the conditions that led to metal enrichment in fluids, we want to investigate the composition of fluid inclusions from ore deposits *in situ* by femtosecond laser ablation inductively coupled plasma mass spectrometry (fs-LA-ICP-MS; using an ElementXR@MS).

For this purpose a new analytical setup is developed by combining a heating freezing stage with our deep UV ($\lambda = 196\text{nm}$) fs-LA-ICP-MS system. By freezing the fluids, we are aiming to expand the signal length of the ablated fluid inclusion and with that to minimize analytical uncertainties compared to previously applied nanosecond LA-ICP-MS techniques [2].

Preliminary test measurements of a frozen standard solution relative to the NIST610 glass, resulted in an analytical uncertainty of 10% (1σ) for the analyses of e.g. Cu, Zn, Pb, Ag and other trace elements. We also tested our method by the analyses of natural high saline (>20wt% NaCl_{eq}) fluid inclusions in hydrothermal quartz veins from Cornwall, UK and with synthetic fluid inclusions in quartz of different salinities. First results indicate that inclusions of a size between 10 μm to 30 μm and in a depth up to ~50 μm can be analysed with a success rate of > 60%. ²³Na is used for internal standardization. For several isotopes, including ⁴⁴Ca, ⁶⁶Zn, ⁹⁵Mo, ⁸⁵Rb, ¹³³Cs and ²⁰⁸Pb we achieved signals significantly above the detection limit (3σ of background) for a duration of 20 to 40 seconds.

In future investigations, we want to apply this technique to analyse natural fluid inclusions from different ore deposits and synthetic fluid inclusions from HP/HT experiments.

[1] Heinrich *et al* (2003), *Geochim Cosmochim Acta* **67**, 3473-3496. [2] Pettke *et al* (2012), *Ore Geology Reviews* **44**, 10-38.

High pressure fluid evolution derived from veins in UHP eclogites (Dabieshan, China)

N. ALBRECHT^{1*}, G. WÖRNER¹, Y. XIAO²
AND A.M. VAN DEN KERKHOFF¹

¹Geoscience Center Göttingen, 37077 Göttingen, Germany

(*correspondence: nalbrec@gwdg.de)

²School of Earth and Space Sciences, Hefei 230026, China

Fluids linked to deep burial form and evolve under (ultra-) high pressure (UHP) conditions and are characterized by enhanced element solubilities [1], resulting in transport and fractionation of both fluid-mobile and nominally immobile elements [2]. Reconstructing UHP fluid evolution is thus essential for a better understanding of element mobility and redistribution among Earth's reservoirs.

Representing fossil pathways of fluid flow, we sampled mineral veins in UHP eclogites from the Triassic Dabieshan continental collision zone. Three vein generations are distinguished based on mineralogy and field evidence: (1st) early UHP near-peak qtz + rt veins, (2nd) HP post-peak phg + ep/czo + brs + ap + qtz + rt ± ky ± omp ± pg ± zo veins and (3rd) late HP retrograde ab + phg + ep/czo + qtz veins.

Petrography, microthermometry and Raman analyses reveal pure high density N₂ inclusions (0.56 g/cm³) in eclogitic quartz and three assemblages of aqueous inclusions in vein and eclogitic qtz: (i) primarily trapped CaCl₂ + NaCl ± MgCl₂ brines (30–35 wt% NaCl_{eq}), (ii) primary to pseudosecondary CaCl₂ + NaCl solutions (17–27 wt% NaCl_{eq}), (iii) secondary NaCl-bearing fluids (0–12 wt% NaCl_{eq}). Homogenization temperatures among the aqueous groups are bimodally distributed, clustering at 200 and 400°C. High salinities clearly correlate with high T_H and low salinities with low T_H. Zoning in vein epidote minerals from LREE- and LILE-rich allanitic cores to slightly resorbed, depleted clinzoisite and overgrowths of trace element-poor epidote mirrors the solute depletion trend indicated by fluid inclusions.

The results reflect an evolution from highly saline, trace element-rich brines near the metamorphic peak towards low salinity, trace element-poor solutions along the retrograde path. The earliest fluids are interpreted to originate from prograde dehydration and their initially high solute content is 'consumed' by precipitation of vein minerals and likely by late dilution with meteoric waters. The nitrogen is suspected to be progradly inherited from metasedimentary lithologies in which the sampled eclogite bodies are embedded.

[1] Kessel *et al* (2005) *Nature* **437**, 724-727. [2] Xiao *et al* (2006) *GCA* **70**, 4770-4782.

Primary magmas, fractionation modelling and mantle sources of Etnean lavas

G. ALESCI¹, P.P. GIACOMONI¹, M. COLTORTI¹
AND C. FERLITO²

¹Univ. of Ferrara, Italy (giuseppe.alesci@unife.it)

²Univ. of Catania, Italy (cferlito@unict.it)

A backward mass balance fractionation was used to reconstruct the primary composition of Etnean magmas and get some inferences on the petrological composition of their mantle sources. The entire evolution of Etna magmatism, from Tholeiitic period to Recent Mongibello, were taken into consideration. fO₂ activity was estimated using [1] and Fe³⁺/Fe²⁺ ratio were calculated according to [2] equation. The least differentiated products for each alkaline period were identified and about 15 to 20% of a solid assemblage made up of olivine (87 to 100%) was added to re-equilibrate the basalts with mantle olivine (Fo₈₇). If clinopyroxene is added to equilibrate the lavas with mantle olivine a much higher percentage (>40%) of solid fractionation is needed. A further subtraction of 20-25% of a solid assemblage constituted by ol (6-18%), cpx (26-55%) and plag (25-48%) is needed to get to the most differentiated erupted lavas. Taking into account the volume of the erupted magmas this modeling can be used to evaluate the quantity of material intruded below the volcano edifice. Calculated major element compositions of the primary magma is well comparable with those obtained by melt inclusions study [3] and references therein, while trace element patterns fit well with those reported in the literature. These compositions are also similar to those found in the Iblean Plateau [4] apart from a slight enrichment in Rb, Th and U and a depletion in Ti, Hf, Y and Yb, indicating the presence of discrete percentages of volatile-bearing phases, that is amphibole and phlogopite, in the Etnean mantle sources.

[1] France *et al* (2010) *J. Volcanol. Geotherm. Res.* **189**, 340-346. [2] Kress and Carmichael (1988) *Am. Mineral.* **73**, 1267-1274. [3] Collins *et al* (2009) *Geology* **37**, 571-574. [4] Beccaluva *et al* (1998) *J. Petrology* **39**, 1547-1576.

Speciation of uranium products formed during *in situ* biostimulation of the Old Rifle, CO aquifer

D. S. ALESSI¹, N. JANOT², J. S. LEZAMA-PACHECO², E. I. SUVOROVA¹, J. M. CERRATO³, D. E. GIAMMAR³, P. M. FOX⁴, K. H. WILLIAMS⁴, P. E. LONG⁴, K. M. HANDLEY⁵, K. W. WRIGHTON⁵, C. S. MILLER⁶, L. YANG⁴, R. BERNIER-LATMANI¹ AND J. R. BARGAR²

¹Environmental Microbiology Laboratory, Ecole

Polytechnique Fédérale de Lausanne, Switzerland

²Chemistry and Catalysis Division, Stanford Synchrotron Radiation Lightsource, SLAC National Accelerator Laboratory, Menlo Park, CA, USA

³Department of Energy, Environmental, and Chemical Engineering, Washington University, St Louis, MO, USA

⁴Earth Sciences Division, Lawrence Berkeley National Laboratory, Berkeley, CA, USA

⁵Department of Earth & Planetary Sciences, University of California, Berkeley, CA, USA

⁶Department of Integrative Biology, University of Colorado, Denver, CO, USA

Uranium bioremediation strategies focus on the addition of a reduced carbon source to stimulate the growth of indigenous microbial communities in subsurface sediments. This growth leads to conditions that promote the reduction of soluble U(VI) species in groundwater to relatively insoluble and immobile U(IV) species. Field studies to date focus on U(IV) products formed in deep sulfate reducing conditions, which have been identified as uraninite (UO_{2+x}), monomeric or mononuclear U(IV) species that lack crystal structure and are associated with biomass or iron-bearing minerals, and phosphate coordination polymers to which U(IV) is bound. However a systematic molecular-to-pore scale characterization of changes in U(IV) product speciation and stability as bioremediation proceeds is not extant.

In this study, we deployed sediment reactors into a groundwater well at the Old Rifle, CO aquifer during biostimulation with acetate. Sediments were harvested as the aquifer progressed through metal- and sulfate-reducing regimes, and were characterized by spectroscopic, microscopic, wet chemical, and microbiological techniques. U(IV) product local structure and reactivity exhibits little apparent change despite large changes in redox state, accumulated uranium in the sediments, and microbial community structure. This result suggests that similar U(VI) reduction mechanisms may be operating throughout the biostimulation campaign.

The link between the origin of organic matter and GEMS in extraterrestrial materials

CONEL M. O'D. ALEXANDER^{1*}, LARRY R. NITTLER¹ AND RHONDA M. STROUD².

¹DTM, 5241 Broad Branch Rd., NW, Washington DC 20015, USA (*correspondence: alexander@dtm.ciw.edu).

²Naval Research Laboratory, 4555 Overlook Av., NW, Washington DC 20375, USA.

There appears to be a genetic relationship between chondrite matrices, interplanetary dust particles (IDPs) and cometary material. All are dominated by fine-grained, crystalline silicates (predominantly olivine and pyroxene) with similar ranges of properties, along with amorphous silicates or GEMS (glass with embedded metal and sulfide) and organic matter. They also contain circumstellar grains (stardust), many of which are GEMS-like.

There have been longstanding debates about whether GEMS and the organic matter are interstellar or solar in origin, although these are rarely linked. Interstellar silicates are almost entirely amorphous. Therefore, the crystalline material must be products of high temperatures in the nebula. In primitive materials, crystalline silicates into which Na, Al, Ca, etc. could have gone are rare, and they are presumably in GEMS that formed along with the crystalline material. Organic matter is abundant in the ISM, but would have been destroyed during formation of the crystalline silicates. If all GEMS are also high-T nebular products, then almost no ISM dust can have survived and the organic matter in chondrites, IDPs and comets must also be solar in origin. Hence, it is of paramount importance to determine whether or not most GEMS are solar or interstellar [1].

The fraction of ISM silicate grains that are circumstellar is estimated to be ~0.3% [2]. Therefore, the stardust in chondrites/comets should have been accompanied >100 times as many ISM grains. 1-6% of GEMS are stardust [3], which suggests that the remaining GEMS must be interstellar. Yet the crystalline silicates require that a significant fraction of GEMS are solar. We will use meteoritic and IDP data to try to resolve the conflicting estimates of the abundances of solar and interstellar GEMS. This will provide important constraints on the production and processing of dust in the ISM, and on the origin of organic matter in primitive extraterrestrial materials.

[1] Alexander *et al* (2007) *Protostars&Planets V*, p 801-814.

[2] Zhukovska *et al* *A&A* **479**, 453-480. [3] Keller & Messenger (2011) *GCA* **75**, 5336-5365.

High-Cr minerals from the Matoush uranium deposit in the Otish Basin, Quebec, Canada

P. ALEXANDRE¹, R. PETERSON¹, K. KYSER¹,
D. LAYTON-MATTHEWS¹ AND B. JOY¹

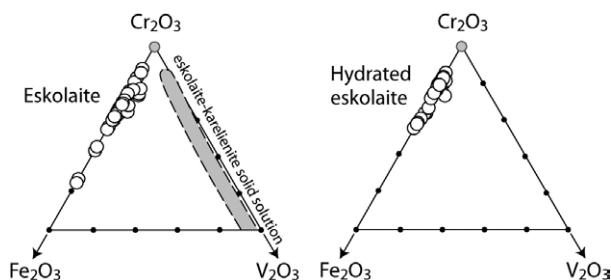
¹Queen's University, Department of Geological Sciences,
Kingston, ON, K7L 3N6, Canada
(alexandre@geol.queensu.ca, peterson@geol.queensu.ca,
kyser@geol.queensu.ca, lmatthews@geol.queensu.ca)

High-Cr paragenesis is observed at the enigmatic Matoush uranium deposit, Otish Basin (Quebec, Canada), which is associated with the bimodal and very narrow (<2 m) Matoush dike intruding the sandstones of the Indicator Formation. In addition to uraninite, both silicate (Cr-dravite and Cr-muscovite) and oxide (eskolaite) high-Cr minerals are present in large amounts. While high-Cr dravite and high-Cr muscovite have been described previously, eskolaite, Cr₂O₃, has not been studied extensively.

The highest Cr contents observed in the Matoush silicates, obtained by electron microprobe, are comparable with those documented in the literature, with Cr₂O₃ of up to ca. 22 wt% in Cr-muscovite (or chromphyllite) and ca. 37 wt% in Cr-dravite.

Complete solid solutions between hematite (Fe₂O₃), eskolaite, and karelianite (V₂O₃) are theoretically possible, but only the complete Cr-V substitution has been documented. In contrast, the Matoush eskolaite contains significant amounts of Fe, with up to 37% wt% Fe₂O₃ substitution, and minimal V (typically under 0.5 wt% V₂O₃).

A hydrated Fe-Cr oxide with the hematite structure is also observed to be closely associated with eskolaite at Matoush. This phase has the same Cr-Fe-V ratio as eskolaite, but with ca. 14 wt% H₂O. Synthetic hematite with significant OH is known to occur and exhibits increased c axis length with increased OH substitution. Rietveld analysis of the X-ray powder diffraction data of the Matoush material is best fit using a model that includes anhydrous eskolaite and a second hydrated crystalline Fe-Cr oxide with the hematite structure and a larger c axis dimension.



Measurement of $\delta^{34}\text{S}$ and $\delta^{33}\text{S}$ values in wild animal hair samples by MC-ICP-MS

Y. ALFAYFI^{1*}, M. WIESER¹, C. DUBESKY²
AND M. MUSIANI³

¹Department of Physics and Astronomy, University of
Calgary, Canada
(*presenting author, email: yalfayfi@ucalgary.ca)

²Department of Research and Graduate Education, Faculty of
Veterinary Medicine, University of Calgary, Canada.

³Faculty of Environmental Design, University of Calgary,
Canada.

Sulfur isotopic compositions vary widely in nature, which give much scope to trace sources and processes of sulfur components in biological systems. The investigation of the diets of wild animals using the sulfur isotopic composition of hair has been demonstrated to be a powerful tool in ecological investigations [1]. The challenge is to measure these differences in sulfur isotope abundances accurately from small amounts of sample. The use of multiple collector inductively coupled plasma mass spectrometry enables reliable determination of the isotopic composition of ³²S, ³³S, and ³⁴S from microgram quantities of S [2, 3, 4]. This requires that the sulfur is separated from the sample matrix and possible spectral interferences are resolved by the mass spectrometer. Sample digestion using microwave techniques or on-line combustion of the sample to SO₂ using an elemental analyzer ensures that sulfur is prepared in a form suitable for analysis. The high mass resolving power of the Thermo Scientific Neptune ensures that isotopes of sulfur are resolved from polyatomic ions, in particular isotopologues of oxygen. We developed a method to measure accurately and precisely $n(^{34}\text{S})/n(^{32}\text{S})$ and $n(^{33}\text{S})/n(^{32}\text{S})$ free from spectral interferences that might affect the results, which was demonstrated by plotting $\delta^{34}\text{S}$ and $\delta^{33}\text{S}$ values on a three-isotope plot. The analytical methods for the MC-ICP-MS were applied to study the diet of wolf and caribou in Canada revealing subtle variations in sulfur isotopic composition in the hair samples from these animals. Initial data show that these results can be used to assist in the identification of the principal sources of food in wild animal populations.

[1] Zazzo *et al* (2011), *Rapid Commun. Mass Spectrom.* **25**, 2371–2378. [2] Das *et al* (2012), *J. Anal. At. Spectrom.* **27**, 2088–2093. [3] Craddock *et al* (2008), *Chemical Geology.* **253**, 102–113. [4] Amrani, *et al* (2009), *Anal. Chem.* **81**, 90287–9034

Distribution of Ta and Nb between silicate and aluminofluoride (salt) melts

Y.O. ALFERYEVA*, T.I. SHCHEKINA
AND E.N. GRAMENITSKIY

Lomonosov Moscow State University, Russia, Moscow,
GSP-1, Geological dep, Petrology 119991
(*correspondence: YanaAlf@ya.ru)

Experiments in the model system Si-Al-Na-Li-H-F-O at $T=800^{\circ}\text{C}$ and $p=1\text{kbar}$ show possibility of equilibrium crystallization of fluorine minerals (cryolite, topaz, villiomite) or the origin of immiscible aluminofluoride melt (brine) in case of high fluorine concentration in the system. The area of coexistence of two immiscible silica and salt melts extends for both nepheline- and quartz-normative compositions of silica melts.

In case of two melts coexistence tantalum and niobium are distributed into the silicate melt. By virtue of the different values of partition coefficients the ratios of tantalum to niobium in residual aluminosilicate melt increase.

The experimentally determined phase relations are in general agreement with compositions of topaz and/or cryolite bearing granites from different regions.

In natural systems, in the final stages of crystallization high amounts of incompatible elements can lead to the separation of salt melt. Brine appears to be an effective concentrator of significant ore elements such as REE, Y, Sc, U, Th, Mo, W etc. [1]. Occurrence of salt melt can also lead to increasing of Ta/Nb ratio in the most evolved varieties of rare metal granites observed in numerous massifs [2].

[1] Gramenitskii & Shchekina (2001) *Geochem.Int.* **43**, 39-52.

[2] Syritso *et al.* (2001) *Petrology* **9/3**, 268-289

Modelling single phase bimolecular reactive transport directly on pore-scale images

ZAKI ALHASHMI*, BRANKO BIJELJIC
AND MARTIN J. BLUNT

Department of Earth Science and Engineering, Imperial
College London, London SW7 2AZ, United Kingdom
(*correspondence: zaki.al-nahari09@imperial.ac.uk)

Geochemical reaction rates estimated in geological porous media are found to be significantly lower than those measured in the laboratory. Traditional advection dispersion reaction equations (ADRE) frequently cannot accurately describe reactive transport in heterogeneous porous media. Therefore, there is still a lack of understanding of the integration between coupled transport and geochemical reactions at multiple scales. We simulate the transport of fluid reactants (A and B) directly on *mm* sized images obtained using micro-CT scanning with a resolution of a few microns. We use a streamline-based particle tracking method for simulating flow and transport. For reaction to occur, both reactants must be within a diffusion distance of each other in a time step. We assign a probability of reaction (P_r), which is a function of the reaction rate constant (k_r) and the diffusion length. Firstly we validate our model for reaction only against analytical solutions of the bimolecular reaction ($A + B \rightarrow C$). Then we couple reaction and transport to perform simulation on the micro-CT images. We find that heterogeneity of the pore structure plays a significant role in altering the average reaction rates. The heterogeneous pore structure prevents contact between reacting species, thus decreasing the reaction rate. We validate the model through predicting the experiments by Gramling *et al* [1].

[1] Gramling *et al* (2002) *Environmental Science & Technology* **36**, 2508-2514

Triple O-Isotope analyses of pallasite olivine revisited: A cautionary tale

ARSHAD ALI¹, NEIL R. BANERJEE¹, IFFAT JABEEN¹,
KIM TAIT², BRENDT HYDE² AND IAN NICKLIN²

¹Western University, London, ON, Canada; aali287@uwo.ca

²Royal Ontario Museum, Toronto, ON M5S 2C6, Canada

Pallasites belong to the stony-iron meteorite group consisting of almost equal amounts of olivine and metal. Precise O-isotope compositions of olivine from 10 main group pallasites are determined using an improved laser fluorination IRMS method [1]. Our data from all pallasites are consistently more enriched than previous studies [2, 3]. However, the $\Delta^{17}\text{O}$ values are in agreement with [3]. Ziegler & Young [4] obtained similarly enriched $\delta^{17}\text{O}$ and $\delta^{18}\text{O}$ values for pallasites and unpublished data from the Carnegie Institution (CIW) in [4] also agrees with our data. To explain the observed discrepancy in delta values for same pallasites, we partially lased Brahin's single olivine grain in 5 steps at increasing degree of laser power. Our hypothesis is the discrepancy in delta values might be due to incomplete reaction of olivine, one of the most resistant minerals to fluorination. The $\delta^{18}\text{O}$ values are observed to increase $\sim 1.8\text{‰}$ from the 1st (least complete) to 5th (most complete) reaction step and the triple O-isotope plot of these data fall on a half-slope line. Our data demonstrate that partial or incomplete reaction causes mass-dependent fractionation and results in lighter $\delta^{17}\text{O}$ and $\delta^{18}\text{O}$ values. Our experiment explains the discrepancy of data between reaction of olivine in conventional Ni-tubes [2] and laser reactions with BrF_5 (this study). Inconsistencies in reaction progress may also help explain differences observed in laser fluorination methods at different labs worldwide [e.g., 3,4]. Our study highlights the importance of considering factors that might affect reaction progress such as: 1) the effect of fluoride residues covering unreacted sample; 2) the sample holder dimple profile (i.e., V-shaped; this study); and 3) the effect of melting the sample before fluorination as adopted by [3]. In our study we utilized a sample size optimized in order to limit the effect of buildup of fluoride residues. We also make use of continuous and blast laser modes to uncover the unreacted sample during the final stages of the reaction. Our specially designed sample holder dimples have a V-shaped profile that concentrate the material in the center to more effectively lase the sample. We are now applying these improvements to a wide variety of pallasites and other meteorites to decipher their origin.

[1] Ali *et al* (2013) *44th LPSC*, #2873. [2] Clayton & Mayeda (1996) *GCA* **60**, 1999-2017. [3] Greenwood *et al* (2006) *Science* **313**, 1763-1765. [4] Ziegler & Young (2011) *42nd LPSC*, #2414.

Origin of the orthopyroxene fibrous in the ultrarefractory lithospheric domains beneath easternmost Canary Islands

MOHAMED M ALI ABU EL-RUS

Geology Department, Assiut University, Assiut 71516, Egypt
aliabuelrus@yahoo.com

The mantle xenoliths from easternmost Canary Islands, exhibit a complex evolutionary history comprising events of depletion, serpentinization, dehydration and enrichment. Each of these events left imprints on both texture and chemistry of the xenoliths. The imprints of depletion event(s) are shown in the complete disappearance of the clinopyroxene porphyroclasts and the ultra-refractory nature of the xenoliths compared to the abyssal peridotites sampled along mid-ocean ridges and oceanic fracture zones. Compositionally, the study xenoliths resemble the recycled oceanic mantle peridotites (OII-u) sampled by worldwide ocean island volcanism. The development of porous clusters of fibrous orthopyroxene at the expense of primary olivine and orthopyroxene characterizes the event of hydrothermal alteration forming serpentine minerals which were later dehydrated into fibrous orthopyroxene. The signature of serpentinization is also shown in the wide variations of several highly incompatible element ratios that might remain constant over variable degrees of melting (e.g. Rb/Ba, U/Th); the poor correlations between several LILE with HFSE and the decoupling between Sr and Nd isotope ratios. During the Canary Islands magmatism, the peridotite xenoliths have been subjected to interaction with silicic carbonatite melt which is shown in the development of clinopyroxene rims and neoblasts at the expense of olivine and orthopyroxene minerals and the enrichment in strongly LREE relative to HREE. The petrographic observations, however, indicate that dehydration of serpentine minerals and formation of anhydrous fibrous domains has occurred long time before the activity of Canarian plume. We therefore favour a model in which serpentinization of the mantle xenoliths might occur when they, like other OII-u peridotites, were parts of a mantle wedge in an old subduction zone fluxed by large volume of aqueous fluids released from downgoing oceanic crust. Dehydration of the xenoliths might occur during their residence for a while in the hot convecting asthenospheric mantle and before their accretion to the present oceanic lithospheric mantle and interaction with Canarian intraplate magmatism.

Apatite exsolution as an indicator of Udachnaya grospydite UHP history

T.A. ALIFIROVA^{1*} AND L.N. POKHILENKO¹

¹V.S. Sobolev Institute of Geology and Mineralogy SB RAS,
Novosibirsk, 630090, Russia
(*correspondence: taa@igm.nsc.ru)

Earth's mantle interiors characterizing by their heterogeneous composition contain a small fraction of rare rock types. Grospydite xenoliths well studied in kimberlites of Daldyn-Alakit region (Yakutia, Russia) [1, 2] are of special interest among the representatives of unusual rocks composing mantle. We represent new data on mineralogy and evolution of grospydite xenolith LUV134/10 from Udachnaya kimberlite pipe (Yakutia).

Kyanite and Grt-1 are poikiloblastically included into the Cpx-1. Grt-2 + polycrystalline Qtz compose large (up to 8 mm) symplectites. Cpx-1 is nearly all replaced by tiny Cpx-2 + Pl symplectites and preserved in relics and inclusions in kyanite and garnet. Kyanite usually contains quartz inclusions, some of them may indicate their high-pressure origin [3]. Minerals contain evident exsolution textures. Grt-1 comprise numerous rutile and apatite needles. Kyanite is with rutile lamellae. Cpx matrix has Rt + Ilm rods, and Cpx-1 relics contain tiny apatite precipitates (confirmed by Raman).

Grossular garnet usually has 3.02-3.04 Si apfu and Na₂O up to 0.15 wt %. Cpx-1 is omphacite with significant admixtures of Ca-Ts and Ca-Es components (7 and 4 mol. % respectively). The presence of majoritic component in preserved garnet suggests its stability at pressures > 6 GPa, but reconstructions of original garnet composition presumably will raise the bar. Apatite precipitation in Cpx-1 allows us to declare original pyroxenes could have had about 200-400 ppm P. Considering experimental data [4], precursor pyroxene is believed to be stable at pressures no less than 6 GPa. Thus, the further findings of apatite lamellae in pyroxenes may serve as reliable indicator of ultra-high pressure stage in rock history.

With respect to mineralogical data we suppose the rock to be subjected to successive decompression and cooling within mantle reservoir.

The study was supported by RFBR grant No. 12-05-31411, and Grant of President of Russia MD-1260.2013.5.

[1] Sobolev *et al* (1968) *J Petrol* **9**, 253-280. [2] Spetsius (2004) *Lithos* **77**, 525-538. [3] Korsakov *et al* (2009) *Eur J Mineral* **21**, 1313-1323. [4] Konzett *et al* (2012) *Contrib Mineral Petrol* **163**, 277-296.

Grain size and REE patterns as tools to identify coastal depositional environments in Moreton Bay (southeast Queensland, Australia)

F. AL-KAABI^{1*} AND M.GASPARON^{1,2}

¹School of Earth Sciences, The University of Queensland,
Brisbane, QLD, 4072, AUSTRALIA
(*f.alkaabi@uq.edu.au)

²National Centre for Groundwater Research and Training,
AUSTRALIA

Statistical grain size analysis of Holocene sediments across Moreton Bay revealed three different depositional environments: fluvial, aeolian and marine-tidal. The distribution of rare earth elements (REE) and yttrium was analyzed in each type of deposit to assess their suitability as a geochemical indicator of depositional environments.

Fluvial deposits are characterized by almost flat REE patterns and a positive Eu anomaly. In contrast, aeolian deposits are enriched in heavy REEs (HREE) relative to light REEs (LREE), and show a negative Eu anomaly. Fluvial deposits are enriched in REEs compared with aeolian deposits. Tidal deposits along small embayments are enriched in LREE relative to HREE, but show variable Eu anomalies. Relative to Ho, Y shows a strong negative anomaly in some of the fluvial sediments, but only a slight negative anomaly in tidal sediments. In contrast, Y/Ho > 1 values characterize aeolian sediments. The presence and abundance of organic matter within the deposits does not seem to have any influence on REE abundances and patterns.

In general, total REE concentrations mimic Th distribution across all depositional environments, and the extent of LREE/HREE fractionation correlates with Nd/Fe ratio [1]. The distribution of europium anomalies (Eu/Eu*) [2] is consistent with variations in Hf, Nb and Zr distributions.

This study confirms that REEs are a powerful geochemical indicator of depositional environments even in a complex and dynamic setting such as a tidal estuary.

[1] H. Elderfield, R. Upstill-Goddard and E.R. Sholkovitz *Geochim. Cosmochim. Acta* **54**, 971-991 (1990) [2] S.O. Tweed, T. Weaver, I. Cartwright and B. Schaefer *Chem. Geol.* **234**, 291-307 (2006)

Holocene dust record in a NW European peat bog: A multiproxy approach

MOHAMMED ALLAN*¹, GAËL LE ROUX^{2,3}, SOPHIE VERHEYDEN⁴, NADINE MATTIELLI⁵, JÉRÉMIE BEGHIN⁶, NATALIA PIOTROWSKA⁷ AND NATHALIE FAGEL¹

¹ AGEs, Département de Géologie, Université de Liège, Allée du 6 Août, B18 Sart Tilman B-4000, Liège, Belgium, (mallan@doct.ulg.ac.be; nathaliefagel@ulg.ac.be)

² Université de Toulouse ; INP, UPS; EcoLab (Laboratoire Ecologie Fonctionnelle et Environnement) ; ENSAT, Avenue de l'Agrobiopole, 31326 Castanet Tolosan, France,

³ CNRS; EcoLab; 31326 Castanet Tolosan, France, (gael.leroux@ensat.fr)

⁴ Royal Belgian Institute of Natural Sciences, Jenner straat 13, B-1000 Brussels, Belgium (Sophie.verheyden@naturalsciences.be)

⁵ Université Libre de Bruxelles, Avenue FD. Roosevelt 50, B-1050 Bruxelles, Belgium (nmattiel@ulb.ac.be)

⁶ Palaeobiogeology-Palaeobotany-Palaeopalynology, Department of Geology, University of Liege, Belgium

⁷ Department of Radioisotopes, GADAM Centre of Excellence, Institute of Physics, Silesian University of Technology, Gliwice, Poland (natalia.piotrowska@polsl.pl)

Dust deposition in southern Belgium is estimated from the geochemical signature of an ombrotrophic bog. The analyses of Rare Earth Elements (REE) and lithogenic element concentrations as well as Nd isotopes were performed by HR-ICP-MS and MC-ICP-MS respectively, in a ~ 6 m peat section representing 5300 years, from 30 BC to 5300 BC dated by the ¹⁴C method. REE concentration variations in peat samples were used as a dust proxy and the Nd isotopes to trace the sources. Peat humification and testate amoebae were used to evaluate hydroclimatic conditions. The range of dust deposition varied from 0.03 to 4 g m⁻² yr⁻¹. The highest dust fluxes were observed from 800 to 600 BC, and from 3200 to 2800 BC and correspond to cold periods. The εNd values show large variability, between -5 and -13, identifying three major sources of dust: local soils, distal volcanic and desert particles. By comparing our results with the dust recorded in other peat bogs and ice cores from different latitudes, we evidence that the Misten peat is a valid archive for dust deposition.

CO₂ emissions from arc volcanism: sources, rates and uncertainties

P. ALLARD

IPGP-Sorbonne Cité, UMR7154 CNRS, 75005 Paris, France (pallard@ipgp.fr)

Arc volcanism is one key geological manifestation of chemical exchanges between the Earth's mantle and surface reservoirs through plate subduction processes. Global quantification of the deep carbon cycle, in particular, requires improved knowledge of the CO₂ output from arc volcanoes, of respective carbon contributions from subducted slabs, mantle degassing and arc crusts, and hence of the proportion of total subducted carbon recycled back into deeper mantle. Here I present an updated review of these different aspects and their uncertainties.

Chemical and isotopic data for high-temperature (450-1040°C) volcanic gases from various subduction zones worldwide, combined with melt inclusion data, provide the most pristine information on magmatic arc volatiles. High CO₂/³He ratios in these gases compared to MOR fluids evidence systematic addition of crustal-derived carbon whose origin (subducted sediments, altered oceanic slab, or arc crust) can be discriminated from the δ¹³C vs CO₂/³He relationship and other geochemical tracers. In most cases, slab-derived carbon is the prevalent (70-95%) component of CO₂ emitted by arc volcanoes, except at a few documented volcanoes in continental arcs (e.g. Italy) where magma-carbonate crustal interaction is a significant to important source.

Published estimates of the global CO₂ output from arc volcanism, assessed from different proxies (fluxes of S, ³He, ²¹⁰Po or/and magma supply rates), vary within an order of magnitude and, over time, tend to increase with increasing data for volcanic plume emissions but also crater lakes, hydrothermal systems and soil degassing. When compared to global budgets for subducted carbon, the current figures suggest a carbon recycling efficiency of between ~50 and 100% through arc volcanism, with obviously contrasted implications for the deep carbon cycle. Hence, measuring CO₂ fluxes and δ¹³C vs CO₂/³He at much more numerous arc volcanoes worldwide is badly needed in order to better constrain this important aspect. This is one key objective of the international DECADE project sponsored by the Deep Carbon Observatory (DCO).

www.minersoc.org

DOI:10.1180/minmag.2013.077.5.1

Mount Etna: Storyboard of an exceptional basaltic volcano

P. ALLARD

IPGP-Sorbonne Cité, UMR7154 CNRS, 75005 Paris, France
(pallard@ipgp.fr)

Mount Etna, in Sicily, has fascinated observers since the Antiquity and, over the past decades, has gradually become one the most intensively studied/monitored volcanoes on Earth. Several features contribute to make it one exceptional basaltic volcano-laboratory: its peculiar tectonic setting and magma geochemistry (intraplate-type alkali basaltic magmatism in the context of African-European continental plate collision), its persistent activity and wide spectrum of eruptive styles (from lava effusions, lava fountains, Strombolian to Plinian explosions), its huge gas emissions (among the strongest ones worldwide), and its quite easy access (favourable to maintenance of dense monitoring networks and field testing of new technologies). These different aspects have long attracted scientists from various disciplines but also promoted increasingly pluri-disciplinary sounding of the deep roots of the volcano and its behaviour. Moreover, the continuous survey of Etna, under the responsibility of INGV, responds to the need of forecasting its eruptions and mitigating the risks to which its densely populated surroundings are exposed.

In this keynote talk, I'll provide a review of the progresses in our present-day understanding of how Mount Etna works, based on available geophysical, geochemical, petrologic and modelling information. I'll outline how multi-disciplinary investigations of major eruptive events in the past 15 years has greatly improved this understanding and the eruption forecasting capability. Finally, I'll attempt to show how the lessons learnt on Mount Etna, as well as the methodologies used on this volcano, can have broad applications to numerous other volcanoes worldwide.

Nonlinear chlorinated solvent sorption and its impact on remediation in surficial sedimentary aquifers

R.M. ALLEN-KING^{1*}, Z.W. MUNGER¹, D. CARLONE¹,
I. KALINOVICH¹, J.A. SALVADÓ¹, A.J. RABIDEAU²,
L.S. MATOTT², A. SINGH² AND D. LAMBERT²

^{1*}correspondance: richelle@buffalo.edu

²Dept. of Geology, University at Buffalo, SUNY

³Dept. of Civil, Structural, and Environmental Engineering,
University at Buffalo, SUNY

Contaminants stored in aquifer regions accessible only by diffusion produce 'tailing' in response to remediation wherein a rapid initial mass and/or concentration reduction is followed by sustained release at a low rate (or concentration). Our project combines laboratory experiments to parameterizing nonlinear sorption and intragranular diffusion with field scale simulations to explore the importance of contaminant sorption on tailing in surficial sedimentary aquifers.

The project examines chlorinated solvent behavior using trichloroethene (TCE) as our probe compound. The samples selected for study are kerogen-containing marine sedimentary rocks representative of the source rocks for surficial glacial aquifers in our region (southern Ontario, Canada and New York, USA). The equilibrium sorption isotherms collected spanned nearly five orders of magnitude in aqueous concentration. All samples showed nonlinear behavior with Freundlich isotherm slopes less than unity. Of the 11 candidate models common in the literature fit to the isotherm data, the dual-mode Polanyi-partition was the only model ranked as plausible for all of the samples via the corrected Akaike Information Criterion. We find that the best fit parameter sets for the three samples taken from a stratigraphic sequence in Ontario are consistent (within a factor of three) when the partitioning and sorption capacity parameters are normalized by the fraction organic carbon content. This finding is consistent with prior reports that document greater isotherm nonlinearity for more condensed carbonaceous matter.

Ongoing experiments are documenting TCE uptake and release rates to granular samples that are modeled as intragranular diffusion retarded by nonlinear sorption. Projection to plume scale transport and remediation through simulation shows that the influence of nonlinear sorption and/or pore diffusion is variable and sensitive to the combination of aquifer material (sorption characteristics and particle size) and plume history (age).

A record of carbonyl sulfide from Antarctic ice over the last 1000 years

SAMUEL J. ALLIN¹, WILLIAM T. STURGES¹, JOHANNES LAUBE¹, DAVID ETHERIDGE², MAURO RUBINO², CATHY TRUDINGER², MARK CURRAN³, ANDREW SMITH⁴ AND ROBERT MULVANEY⁵

¹School of Environmental Sciences, University of East Anglia, UK

²CSIRO Marine and Atmospheric Research, Australia

³Australian Antarctic Division and Antarctic Climate & Ecosystems Cooperative Research Centre, Australia

⁴Institute for Environmental Research, Australian Nuclear Science and Technology Organisation, Australia

⁵British Antarctic Survey, National Environment Research Council, Cambridge, UK

Carbonyl sulfide (COS) is a trace gas, present in the troposphere, and also in the stratosphere, where it contributes to the stratospheric sulfate aerosol layer. It has both natural and anthropogenic sources. Natural processes include uptake by plants, while oceans, wetlands, volcanism and biomass burning all contribute to natural COS emissions.

We have measured COS in Antarctic ice cores from Dronning Maud Land, drilled in 1998, the DE08 core drilled at Law Dome in 1987, and the DSS0506 core drilled in 2006. Ice samples with COS gas ages between about 1050 AD and the early 20th century have been examined. A large volume ice crusher at the CSIRO Marine and Atmospheric Research laboratory was used to extract air from bubbles occluded in the ice cores. These air samples were analysed for CO₂, CH₄, CO and ¹³CO₂ at CSIRO, and then for COS and several halocarbons at the University of East Anglia on a high sensitivity gas chromatograph/tri-sector mass spectrometer system.

Initial results indicate that good sample integrity can be achieved. Measurements from the DML samples indicate low and uniform abundances across the last few hundred years, and at concentrations significantly below those in the modern-day atmosphere. Measurements in more recent ice from DE08 show the start of increasing concentrations in the early 1900s, confirming earlier evidence that the global atmospheric abundance of COS has increased as a result of industrial activity during the 20th century.

Enhanced subsidence and sediment dynamics in Galveston Bay- Implications for geochemical processes and fate and transport of contaminants

M.E. ALMUKAIMI¹* AND T.M. DELLAPENNA¹

¹Texas A and M University at Galveston., Galveston, TX 77554, USA (*correspondence: malmukaimi@tamu.edu; dellapet@tamug.edu)

Galveston Bay is the second largest estuary in the Gulf of Mexico. The bay's watershed and shoreline contains one of the largest concentrations of petroleum and chemical industries in the world, with the greatest concentration within the lower 15 km of the San Jacinto River/Houston Ship Channel (SJR/HSC) [1]. Extensive groundwater withdrawal to support these industries and an expanding population has resulted elevated subsidence, with the highest subsidence in lower SJR/HSC, of over 3 m (3 cm yr⁻¹) and has decreased seaward throughout the bay to 0.6 cm yr⁻¹ near Galveston Island [2]. Mercury (Hg) contamination is well documented throughout the bay sediments [1, 3]. Sediment vibra-cores were collected throughout the bay systems. ²¹⁰Pb and ¹³⁷Cs geochronologies from these cores were used to determine sedimentation rates and correlated to Hg profiles to estimate input histories. The results shows sedimentation rates of 4 cm yr⁻¹ in areas with subsidence of comparable rates, indicating that sedimentation kept pace with subsidence. Moreover, Hg core profiles correlated with radioisotope geochronologies and show significant input of Hg beginning around 1940, with a peak around 1971, and a dramatic drop off in concentration afterwards, demonstrating it to be a valuable geochronology tool. In addition, Hg concentrations were found to be dramatically higher proximal to the SJR/HSC and progressively decreasing seaward and to distal parts of the bay.

[1] Santschi *et al* (2001) *Mar Env Res* **52**, 51-97. [2] Coplin & Galloway (1999) *U.S Geo Sur Cir* **1182**, 35-48. [3] Morse *et al* (1993) *Mar Env Res* **36**, 1-37.

Deep geothermal reservoir analysis in the Upper Rhine Graben using a geochemical and isotopic multi-tracer method - first results

S. AL NAJEM^{1*}, F. FREUNDT², M. ISENBECK-SCHRÖTER¹, AND W. AESCHBACH-HERTIG²

¹Institute of Earth Sciences, Heidelberg University, INF 236, 69120 Heidelberg, Germany (*correspondence: Sami.AINajem@geow.uni-heidelberg.de)

²Institute of Environmental Physics, Heidelberg University, INF 229, 69210 Heidelberg, Germany

It is state of the art in geothermal exploration to use various geophysical methods (eg. 3D-seismic), which are rather expensive. This work presents the first results of a new characterization of a hydrogeochemical reservoir in the Upper Rhine Graben with a combination of methods from hydrogeochemistry and isotope hydrology in near surface groundwater. For this purpose natural geochemical tracers as well as rare earth elements, ³He/⁴He ratios, and radiogenic isotopes (Sr, Nd, Pb) are investigated in the northern Upper Rhine Graben, close to Groß-Gerau, Germany.

Geochemical analysis show three different types of fluids and various mixtures. CaHCO₃-dominated waters represent quaternary aquifer conditions whereas MgSO₄-dominated waters have a tertiary origin. Higher saline NaCl-dominated waters show an impact of mantle fluids revealed by ³He/⁴He isotope analysis [1]. The ratio is highest where the main fault of the northern Upper Rhine Graben crosses the Rhine river. This suggests that the fault is hydraulically active and connects deep fluids with the shallow aquifer.

Further investigations of rare earth element patterns as well as radiogenic isotopes (Sr, Nd and Pb) identify the origin, the ascent as well as the retention time of the deep fluids more precisely [2]. Water-rock interactions and mixtures of different fluids in the reservoir and during the ascent are estimated and simulated using geochemical and hydraulic models. Thus, the geometry of the aquifer, the temperature and the quantity of the ascending deep fluid in the reservoir is estimated.

The region was chosen to test the multi-tracer method due to its well-studied geology and the marked saltwater anomaly. The aim is to identify the most useful tracers of deep geothermal fluid circulation, which consecutively can be applied to other regions with less prior information.

[1] Kenned & van Soest (2007) *Science* **318**, 1433-1436. [2] Loges *et al* (2012) *Applied Geochemistry* **27**, 1153-1169.

Se(IV) uptake by Äspö diorite: Micro-scale distribution

URSULA ALONSO¹, TIZIANA MISSANA¹, ALESSANDRO PATELLI², DANIELE CECCATO³, MIGUEL GARCÍA-GUTIÉRREZ¹ AND VALENTINO RIGATO³

¹CIEMAT, Avda. Complutense 40, 28040 Madrid, Spain

²CIVEN, Via delle Industrie 9, 30175 Marghera, Italy

³INFN-LNL Viale dell' Università 2, 35020 Legnaro-Padova, Italy

Selenium is one of the radionuclides with major contribution to the total radiation dose in nuclear waste geological repositories. The performance assessment of a repository demands sound retention data sets with minimised uncertainties, for all the material composing the natural and engineered barriers. The high heterogeneity of crystalline rock necessarily contributes to the high uncertainties on sorption parameters. Furthermore, Se is a redox sensitive element, with a complex geochemical speciation, for which to maintain controlled redox conditions during the whole experiment is particularly relevant.

In this study, Se(IV) sorption onto diorite samples from the Äspö underground research laboratory was studied by micro-Particle Induced X-ray Emission (μ PIXE). Äspö diorite samples were extracted, handled and transported under anoxic conditions. Sorption experiments were carried out in Äspö groundwater (pH 7.9 and EC = 13.36 mS/cm), both under oxic and anoxic conditions, for comparison.

Selenite distribution on Äspö diorite surface was heterogeneous both under oxic and anoxic conditions, being higher its retention under anoxic conditions. The main retentive minerals were identified and surface distribution coefficients (K_a) were determined on main diorite minerals. Sorption values ranged from zero, on quartz or K-feldspars, to higher values in Fe-bearing minerals ($K_a \sim 7 \cdot 10^{-5}$ m) under anoxic conditions.

Average surface distribution coefficients could be determined accounting for the mineral occurrence (%) of diorite samples and the obtained values were compared to the bulk distribution coefficients (K_d) determined on same samples by batch experiments (Se- K_d (oxic) ~ 2 mL/g and Se- K_d (anoxic) ~ 8 mL/g).

Acknowledgments: This study has received funding from EU Seventh Framework Programme (FP7/2007-2011) under the grant agreements N° 269658 (CROCK, Crystalline Rock Retention processes and N° 2620109 (ENSAR, European Nuclear Science and Applications Research).

Reactivity of acid gases in gas-brine-mineral systems

T. ALPERMANN¹* AND C. OSTERTAG-HENNING¹

¹Federal Institute for Geosciences and Natural Resources,
Stilleweg 2, 30655 Hannover, Germany
(*correspondence: Theodor.Alpermann@bgr.de)

Acid gases like CO₂ and H₂S may constitute a substantial fraction of the raw natural gas in sour gas fields, large gas fields in e.g. Kazakhstan and China exhibit H₂S contents of more than 10 %. Because of its toxicity, H₂S requires a proper waste management which is usually assured by a *Claus*-type sulfur plant producing elemental sulfur from H₂S. However, selling problems of produced sulfur on the world market and costly procedures due to governmental allowance of low SO₂ emissions by sulfur plants provoke economic challenges for sour gas production. The ever increasing global production of sour gas thus raised the question of other disposal options than *Claus* plants for H₂S and acid gas mixtures.

The geologic storage of acid gases in deep strata is one alternative disposal option with potentially economic advantages. Therefore, the injection of CO₂/H₂S mixtures of diverse composition has been practiced in Canada since 1989 [1]. Surface monitoring of the injection sites did not reveal any leakage, yet, but possibly occurring subsurface processes related to acid gas injection have been scarcely investigated.

To gain insight into potential geochemical reactions within the injection horizon, experiments were conducted which investigate the interaction of acid gases, brines and different types of minerals under the anticipated storage conditions. The experiments were carried out in sealed gold capsules which were first loaded with a mineral and brine followed by the application of CO₂ or CO₂/H₂S by a specifically manufactured gas-loading device [2]. After the treatment of the reaction matrices at 120°C and 120 bar, the obtained product mixtures were analyzed by means of headspace GC-TCD/FID/SCD for CO₂, hydrocarbon and sulfur gases. In addition, the fluids and solids have been analysed by ICP-OES and a variety of microscopic methods.

The results of the experiments will contribute to a more detailed understanding of geochemical processes connected to the geologic storage of acid gases that may affect the integrity of the reservoir rock and the cap rock.

[1] Bachu & William (2004) *Geol. Soc. Special Publ.* **233**, 225-234. [2] Boettcher *et al* (1989) *American Mineralogist* **74**, 1383-1384.

Geochemical Exploration for Platinum-Group Elements in Mafic/Ultramafic Complexes from the Arabian Shield

AL-SALEH AND AHMAD MUHAMMAD

Geology and geophysics Department, King Saud University,
Riyadh, Saudi Arabia

The Arabian Shield, which occupies most of the western half of the Arabian Peninsula, has been the target of extensive exploration activities for the past four decades. So far no platinum occurrences have been documented, and the relatively high PGE values reported for certain areas are associated with uneconomic chromite and Cu-Ni deposits. This project was launched as a reconnaissance program intended for the assessment of the PGE potential of some of the more promising mafic/ultramafic complexes in the Arabian Shield, with more detailed follow-up work to be undertaken at a later stage if significant anomalies were identified. Alaskan-type complexes are considered highly prospective for PGE, and a number of these were selected for preliminary soil surveys and lithogeochemistry. No anomalous values for Pt, Pd or their pathfinders were detected from the heavy mineral concentrates, and any associated Cu mineralization correlates poorly with the compatible elements thus indicating a hydrothermal origin. The very high Cu/Pd ratios from rock samples devoid of copper mineralization suggests that separation of a sulphide liquid had occurred and that PGE were largely scavenged from the magma reservoir prior to emplacement. If true, this would render these Complexes unlikely hosts for PGE mineralization. An unexpected result was the extremely low concentrations of PGE in the stream sediments of layered complexes in comparison with those from massive, gabbroic sub-volcanic plutons; on average, a sub-volcanic intrusion would have a soil content of Pt ranging from 0.5 to 3 ppb, whereas sediments derived from layered complexes would typically return values of no more than 0.1 ppb for both Pt and Pd. However, the Wadi Kamal layered complex is an exception since it contains well-known horizons of Ni-Cu mineralization overlain by conspicuous gossans; the PGE values from soil and rock samples obtained so far were highly erratic and the overall PGE potential of this complex awaits further work in the next stage of the project. An interesting discovery was made at the pyroxenite body of Wadi Amarah where well-developed soil anomalies (60-75 ppb combined Pt & Pd) are encountered at the outer contacts of this intrusion; follow-up work is planned to locate the source of these anomalies.

Numerical simulation of fluid–rock interaction upon CO₂ injection into a carbonate-hosted saline aquifer

PETER ALT-EPPING¹ AND LARRY W. DIAMOND²

Rock–Water Interaction, Institute of Geological Sciences,
University of Bern, Switzerland

(*correspondence: alt-epping@geo.unibe.ch)

We run reactive transport simulations to understand the transient chemical processes that occur in a carbonate-dominated aquifer during and after the injection of CO₂. The model, its design and its initial and bounding physico-chemical conditions, are patterned after the Upper Muschelkalk-Gipskeuper aquifer-seal pair in the Molasse Basin in Northern Switzerland. Porosity and permeability measurements on samples from the Muschelkalk indicate a strong correlation. Both the porosity and permeability distribution reflect natural heterogeneity related to the sedimentary, diagenetic and tectonic history of the aquifer. The heterogeneous permeability structure of the aquifer controls the dynamics and the shape of the CO₂ plume and thus affects the efficiency of residual and solubility trapping. The dissolution of CO₂ into the brine entails a lowering of the *pH* and hence the dissolution of the primary carbonate mineralogy. Because the brine remains at local equilibrium with the carbonates, the dynamics of the CO₂ plume and the CO₂-enriched brine is reflected by the mineral alteration pattern. Although the drop in *pH* is associated with carbonate dissolution, the *pH* recovers in certain regions of the aquifer faster than in others, thus leading to a complex pattern of carbonate dissolution and reprecipitation. This evolving pattern of carbonate dissolution/reprecipitation implies that chemical constituents that are initially incorporated in or that coexist with primary carbonate minerals may be released into the fluid, then later removed from the fluid by reprecipitation when conditions have changed.

Mass balance calculations suggest that CO₂ injection into a carbonate rock releases additional CO₂ due to mineral dissolution. Thus trapping of CO₂ in a carbonate aquifer requires that the seal remains tight over long periods of time. The increase in reservoir pressure during injection, the dynamics of the CO₂ plume and the perturbation of chemical conditions in the reservoir will initiate mass transfer across the aquifer-seal interface and initiate chemical reactions on either side of the interface. We explore the extent of species mobilization and transfer across the reservoir/seal interface, identify the type of reactions that occur as well as their implications for the tightness of the caprock.

Organic facies variation from well data on the bituminous Miocene units, Northwestern Anatolia (Sevinç/Ağapınar-Eskişehir), Turkey

MEHMET ALTUNSOY^{1*}, İLKER ŞENGÜLER², NESLIHAN ÜNAL¹, SELİN HÖKEREK¹ AND ORHAN ÖZÇELİK¹

¹Department of Geological Engineering, Akdeniz University,
07058 Antalya, Turkey (*correspondence:

altunsoy@akdeniz.edu.tr); (oozcelik@akdeniz.edu.tr;
nunal@akdeniz.edu.tr; selinhokerek@akdeniz.edu.tr)

²General Directorate of Mineral Research and Exploration,
06800 Ankara, Turkey (ilkersenguler@gmail.com)

In the region, the Miocene units consist of conglomerate, sandstone, claystone, coal, marl, siltstone, bituminous shale and limestone. Some 60 samples of bituminous units from the Miocene succession were collected from ES-07 well, in the north-western part of Turkey (Sevinç/Ağapınar-Eskişehir). 24 core samples were screened for total organic carbon (TOC) content. Selected samples were then analyzed by Rock-Eval pyrolysis. Visual kerogen analysis and vitrinite reflectance measurements were also undertaken. Detailed data from bituminous Miocene sediments made it possible to construct an organic facies framework using different zonations. Organic facies type B, C, CD and D were identified in the investigated units. Alteration colors of organic materials are yellow and dark yellow. Spore colors of these samples are yellow and dark yellow (SCI:2-3.5). Organic facies B is related to bituminous shale lithofacies. This facies is characterized by average values of HI around 509 (equivalent to type II Kerogene), TOC around 7.77%, and an average of S2 of 40.81 mg HC/g of rock. This facies is laminated and well bedded, and usually contains a higher percentage of terrestrial residual organic matter. Organic facies C is related to marl, coaly marl and coal lithofacies. This facies is composed of organic matter with average values HI around 153 (equivalent to Type II/III Kerogene), TOC around 28.05 and S2 between 3.97 and 83.77 mg HC/g sample. Organic facies C is the “gas-prone” facies. The organic matter is dominated by terrestrial debris in various stages of oxidization. Most coals are organic facies C. The organic facies CD is related to the coaly marl, marl and shale lithofacies. This facies is characterized by average values of HI around 73 (equivalent to Type III Kerogene), TOC around 13.10%, and an average of S2 of 13.97 mg HC/g of rock. An organic facies D, associated with marl, sandy marl, coaly marl and limestone lithofacies, displays values of HI around 163 (equivalent to Type III Kerogene) and TOC around 2.94%. S2 varies between 0.01 and 5.53 mg HC/g of rock.

Source and sinks of iodine in the hyperarid Atacama Desert of northern Chile

F. ALVAREZ^{1*}, A. PEREZ^{1,2}, G.T. SNYDER³, G. VARGAS^{1,2}, Y. MURAMATSU⁴ AND M. REICH^{1,2}

¹Department of Geology, University of Chile, Santiago, Chile
(*correspondence: fernanda.alvarez.a@gmail.com)

²Andean Geothermal Center of Excellence (CEGA)

³Department of Earth Science, Rice University, Houston, TX, USA ⁴Chemical Department, Gakushuin University, Tokyo, Japan

Iodine is a strongly biophilic element, and its global distribution is dominated by marine sediments. In continental settings, the occurrence of iodine minerals is restricted to hyper-arid environments. The Earth's largest iodine crustal anomaly is hosted in the Atacama Desert where the occurrence of iodine minerals is constrained to the nitrate-iodine deposits located along the eastern side of the Coastal Cordillera, and the supergene zones of copper deposits in the Central Depression and Precordillera.

The iodine occurrence, source and mechanism(s) of enrichment in this region have been scarcely studied. In this work, we present iodine concentrations and isotopic ratios (¹²⁹I/I) of the nitrate deposits, supergene copper ores, marine sedimentary rocks, geothermal fluids, groundwater and meteoric water of the Atacama Desert.

Iodine is highly enriched in the nitrate deposits, with a mean concentration of ~700 ppm. These anomalous values are followed by soil samples above supergene copper deposits, and Mesozoic shales and limestones averaging ~50 ppm. Regarding the aqueous reservoirs the highest concentrations were measured in groundwater below nitrate deposits (3.5-10 ppm) and in geothermal fluids (1-3 ppm). In nitrate ores, the calculated ¹²⁹I/I ratios range from ~300 to ~400x10⁻¹⁵. Supergene iodine minerals in copper deposits present values between 200 and 550x10⁻¹⁵ and ratios obtained from marine rocks vary from 300 to 400x10⁻¹⁵. Isotopic ratios of groundwater below nitrate deposits is ~200x10⁻¹⁵.

Results show a strong iodine enrichment in Atacama reservoirs compared to average crustal values. Three essential processes are required to reach such concentrations: (1) the presence of an enriched iodine source, (2) the removal of iodine by fluids from the source to the surficial reservoirs, and (3) the accumulation and preservation of iodine in these reservoirs. Isotopic ratios in nitrates and supergene iodine minerals are in agreement with previously reported ¹²⁹I/I ratios in crustal fluids derived from organic material (200-400x10⁻¹⁵). Mesozoic shales are the most probable source for iodine because of the similar ¹²⁹I/I ratios with rock reservoirs, high organic content and regional occurrence.

Origin of felsic microgranular enclaves from Salto Pluton, SE, Brazil

ADRIANA ALVES, VALDECIR DE ASSIS JANASI AND GIOVANA PEREIRA

Instituto de Geociências, Universidade de São Paulo

The 590 Ma Salto Granite Pluton, part of the post-orogenic Itu Rapakivi Province (590-580 Ma), SE Brazil, is mainly composed of coarse-grained hornblende-biotite red granite. This main unit was invaded by a body of zoned rapakivi granite which varies from a porphyritic facies dominated by fine-grained matrix (porphyry granite) to a cumulate granite in the eastern deeper portions. Abundant felsic microgranular enclaves (fme) with ellipsoidal shape and dimensions up to 4 m occur within both the red granite and the rapakivi granite, and are interpreted as products of a recharge event of the chamber by a hotter comparatively more mafic magma.

The fme are modally and chemically similar to their host granites. However, they show a slightly more primitive character with SiO₂ contents of ~ 70% against 72-75% observed for the granites and higher Fe, Mg, Ti and Ca contents. These evidences suggest that the enclaves might represent thoroughly hybridized liquids similar to those that gave origin to the porphyry granites. The hypothesis is also supported by the fact that enclaves increase in number and size towards the porphyry unit.

Xenocrysts in textural disequilibrium show LREE patterns different from those observed for the whole rock samples. In general, there is a significant superiority in La/Sm_N ratios and liquids calculated to be in equilibrium with such xenocrysts represent more mafic magmas, depleted in such elements.

A similar scenario is suggested for Ba and Sr contents of liquids. It is noteworthy that analyzed crystals from the porphyry unit also show indicatives of a pre-crystallization story in more mafic liquids. However, the modeled liquids show normalized profiles that are parallel to those of their whole rocks, suggesting that the granite magma was the significantly superior in volume compared to the more mafic endmember.

A MELTS model was designed for the investigation of the origin of the abundant rapakivi texture observed in xenocrysts within the fme. The predicted amount of LREE expected to be found in plagioclase rims are considerably superior to the observed values, suggesting that the rapakivi texture was probably developed in the more mafic magma, therefore in a stage previous to the thorough hybridization of the mafic and the felsic endmembers.

Arsenic dissolution from Japanese paddy soil by a dissimilatory arsenate-reducing bacterium *Geobacter* sp. OR-1

S. AMACHI^{1*}, D. T. DONG¹ AND N. YAMAGUCHI²

¹Chiba Univ., 648 Matsudo, Matsudo-shi, Chiba 271-8510, Japan (*correspondence: amachi@faculty.chiba-u.jp)

²National Institute for Agro-Environmental Sciences, 3-1-3, Kan-nondai, Tsukuba, Ibaraki 305-8505, Japan (nyamag@affrc.go.jp)

Dissimilatory As(V) (arsenate)-reducing bacteria may play an important role in arsenic release from anoxic sediments in the form of As(III) (arsenite). Although respiratory arsenate reductase genes (*arrA*) closely related with *Geobacter* species have been frequently detected in arsenic-rich sediments, it is still unclear whether they directly participate in arsenic release, mainly due to lack of pure cultures capable of arsenate reduction. In this study, we isolated a novel dissimilatory arsenate-reducing bacterium, strain OR-1, from Japanese paddy soil, and found that it was phylogenetically closely related with *Geobacter pelophilus*. OR-1 also utilized soluble Fe(III), ferrihydrite, nitrate, and fumarate as electron acceptors. OR-1 catalyzed dissolution of arsenic from arsenate-adsorbed ferrihydrite, while *Geobacter metallireducens* GS-15 did not. Furthermore, inoculation of washed cells of OR-1 into sterilized paddy soil successfully restored arsenic release. Arsenic K-edge X-ray absorption near-edge structure (XANES) analysis revealed that strain OR-1 reduced arsenate directly on the soil solid phase. Analysis of putative ArrA sequences from paddy soils suggested that *Geobacter*-related bacteria, including those closely related to OR-1, play an important role in arsenic release from paddy soils. Our results provide direct evidence for arsenic dissolution by *Geobacter* species, and support the hypothesis that *Geobacter* species play a significant role in reduction and mobilization of arsenic in flooded soils and anoxic sediments.

The lost city hydrothermal field: A geochemical analog for Nili Fossae, Mars

ELENA S. AMADOR^{1*}, JOSHUA L. BANDFIELD¹, DEBORAH S. KELLEY² AND WILLIAM J. BRAZELTON²

¹Earth and Space Sciences Dept., University of Washington (*correspondence: esamador@uw.edu)

²School of Oceanography, University of Washington

Nili Fossae, Mars contains a mineralogical suite similar to that found at the Lost City Hydrothermal Field (LC) off the mid-Atlantic ridge. The LC is a zone of active serpentinization where the interaction of seawater with the underlying mafic and ultramafic bedrock drives geochemical reactions producing serpentine, brucite, magnetite, and the release of high pH fluids enriched in H₂ and CH₄ [1]. Dense microbial communities subsequently use the abiotically produced H₂ and CH₄ as an energy source to drive metabolisms such as methanogenesis [e.g. 1].

We have acquired fifteen variably altered gabbros, serpentinites, talc-rich fault rocks and carbonates from the LC and characterized their mineralogical variability and spectroscopic characteristics in the thermal infrared and visible/near-infrared (VNIR). These results have been placed into geochemical and astrobiological context with respect to the mineralogically similar units found in Nili Fossae, Mars.

The mineralogy of LC rock samples were determined by measuring their thermal emission spectra. VNIR reflectance measurements were made to determine the spectral characteristics of mineral phases present in order to compare with similar data collected for Mars.

Data from the CRISM VNIR imaging spectrometer orbiting Mars has shown the presence of serpentine, Mg-carbonates, talc and/or saponite within an olivine-rich basaltic unit in Nili Fossae [2-5]. The comparison of VNIR spectral characteristics of the LC samples to the surfaces found in Nili Fossae has shown that the two field sites have similar mineralogical suites.

Mineralogy provides an indication of the geochemical conditions present during the time of mineral formation, and prior studies at LC have shown that the geochemical conditions associated with serpentinization-associated reactions are amenable to the growth of microbial communities. Given that the mineralogy at Nili Fossae, Mars is similar to that at LC, it is possible that similar geochemical conditions, and therefore energy sources for microbial metabolisms, may have been present in Nili Fossae early in Mars' history.

[1] Kelley *et al* (2001) *Nature*, **42**, 145-149. [2] Ehlmann *et al* (2010) *GRL*, **37**, L06201. [3] Brown *et al* (2010) *EPSL*, **297**, 1-2, 174-182. [4] Viviano *et al* (2012) *LPSC XXXIII*, Abs. 2682. [5] Hamilton & Christensen (2005) *Geology*, **94**, 433-436.

He and Ar diffusivity in basaltic glasses and melts

JULIEN AMALBERTI^{1*}, PETE BURNARD¹
AND DIDIER LAPORTE²

¹CRPG-CNRS, Vandoeuvre-lès-nancy, France,
(amalbert@crpg.cnrs-nancy.fr)

²MV, Clermont Ferrand, France

Recent models of the relative and absolute noble gases abundance in oceanic basalts have proposed that degassing has occurred out of equilibrium [1-2]. In order to constrain the lack of noble gas diffusion data at magmatic conditions, we measured He and Ar diffusivities in silicate liquids and glasses by inducing diffusion profiles at high temperatures (up to 1550°C), and using classical vacuo stepped heating experiment.

We observe (Fig 1) that He and Ar diffusivities converge at high temperature, as do the Ar isotope diffusivities, such that their diffusivities are equal at $T > 750$ C, consistent with diffusion compensation.

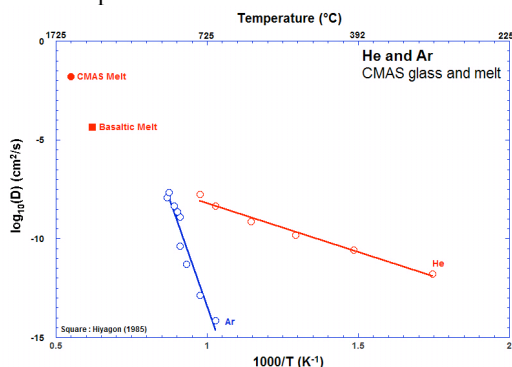


Figure 1: Blue: Ar in glass; Red: He in glass (line) and liquids (circle and square).

Our data suggest that even if disequilibrium degassing occurs during magmatic volatile loss (as suggested from other tracers [3]), this will not significantly fractionate relative noble gas abundances due to similar He and Ar diffusivities at magmatic conditions.

[1] Aubaud, C. Pineau, F., Jambon, A. Javoy, M., (2004) *Planet. Sci. Lett.* **222**, 391–406. [2] Gonnermann, H.M. and S. Mukhopahdyay, (2009). *Nature*, **459**: 560 - 564. [3] Blank J., Delaney J., Des Marais D., (1993) *GCA*. v.**57**, 875–887.

Studies of Air Quality Index of industrial area of Jamshedpur, East India

BALRAM AMBADE

Department of Chemistry, National Institute of Technology,
Jamshedpur-831014, Jharkhand, India;
(bambade.chem@nitjsr.ac.in)

Air pollution is a major environmental concern in many cities around the world. The major causes of air pollution include rapid industrialization/urbanization and increased none environmentally friendly energy production. The purpose of this paper to highlight the ambient air samples were collected between Jan 2000 to June 2011 in the urban-industrial area of Jamshedpur city, by the high volume sampler, quality of air were monitored. The particulate matter (PM₁₀ & PM_{2.5}), Sulphur dioxide (SO₂), Nitrogen oxide (NO_x), Ozone (O₃), Suspended particulate matters (SPM) and Mercury (Hg) which give a fair idea of pollution load carried by the air. The monitoring data were collected from two sites randomly selected in Jamshedpur city. The Air Quality Index (AQI) of PM₁₀ & PM_{2.5} concentration was found to be moderate, alike results are found in gases like SO₂, NO_x and O₃ concentrations were discussed.

Keywords: Urban-industrial area, High volume sampler, Ambient air, Air Quality Index

Performance of Pb Multi Ion Counting array in Triton Plus TIMS

YURI AMELIN AND MAGDALENA HUYSKENS

Research School of Earth Sciences, Australian National University,
(yuri.amelin@anu.edu.au, magda.huyskens@anu.edu.au)

In analysis of picogram quantities of Pb using a single ion counting multiplier, as commonly used in U-Pb dating, precision is limited by the number of Pb atoms of each isotope registered by the multiplier during an analysis. Using an array of ion counters offers substantial increase in the total counts for each isotope and hence potentially better precision.

Here we report performance of an array of five ion counting multipliers: three regular SEMs and two compact discrete-dynode multipliers (CDDs), spaced for simultaneous measurement of Pb isotopes (**Table 1**, below), which is the configuration of the ANU Triton Plus.

Step	L5 (Plus block)				L4	Dispersion quadrupole (Volts)
	IC4 CDD	IC3 SEM	IC2 SEM	IC1 SEM	IC5 CDD	
1	205	206	207	208	(209)	-2
2	204	205	206	207	208	0
3	(203)	204	205	206	207	+7
4	202	(203)	204	205	206	+9
5	201	202	(203)	204	205	+16

Cross-calibration by sequential measurements of a single stable ion beam, followed by data acquisition in static mode, relies on the stability of relative yields of the multipliers. In our system, the ratios of multiplier yields drift by 0.05-0.1% per hour (after initial 2-hour settling). This method is thus applicable only to measurements requiring 0.05-0.1% uncertainty, and is impractical if higher precision is required.

An alternative way of using the multiplier array is to treat each channel as an individual detector, and pool the measured isotopic ratios. This approach does not depend on the multiplier yield stability, and can potentially produce precise and accurate results. However, it requires changing the dispersion quadrupole settings between the mass steps (Table 1) to keep the peaks aligned, and to circumvent the effects of imperfect peak flats that are common for CDDs. Our tests have shown that setting the dispersion quadrupole to $\pm 10V$ changes the signal SEM yields by 0.1-0.3%, and to $\pm 20V$ by up to 1.2%. No similar effect is observed for Faraday cups.

Our tests indicate that the Pb Multi Ion Counting array in its present form is adequate for measurements at 0.05-0.1% level of precision and accuracy. Achieving a precision level of 0.01-0.02% as required by modern U-Pb geochronology would require either radical improvement in the multiplier yield stability, or a more thorough understanding of the interplay between the zoom optics and the multipliers.

Vulnerability and resilience of soil organic matter to environmental change

WULF AMELUNG^{1,2}, MICHAEL HERBST²,
ALEXANDRA SANDHAGE-HOFMANN¹, NELE MEYER¹
AND HARRY VEREECKEN²

¹Institute of Crop Science and Resource Conservation, Soil Science and Soil Ecology, University of Bonn, Nussallee 13, 53115 Bonn

²Agrosphere Institute (IBG-3), Forschungszentrum Jülich GmbH, 54225 Jülich

Soil organic carbon is one of the largest carbon pools on Earth. Huge amounts of soil C were lost, when soil was converted to cropland in the 18th and 19th Century. However, there is evidence that since the 1950, there is again an increase in carbon storage in the terrestrial biota, with still unclear relations to the contents of soil organic matter (SOM). Yet, different mechanisms contribute to losses and re-accrual of SOM after disturbance.

We will present and discuss some recent knowledge, compiled with own research, on the differential response of SOM to changes in climate, land use and soil attributes across different temporal and spatial scales. We surmise short-term heterotrophic respiration processes to provide a first indication on the vulnerability of soils to environmental change, with different sensitivity of SOM stocks against, e.g., climate induced changes in soil temperature, water content and soil properties. In the medium-term, these processes are increasingly linked to changes in soil structure and material translocations, whereas in the long-term decoupling processes to other element cycles and between surface soil and subsoil appear to contribute to an impaired resilience of soils and their organic matter to environmental change. The degree at which these processes re-couple to climate, management and socio-economy turn future projections into a challenging task. The examples will focus on agricultural systems from temperate and subtropical climates.

High-grade sperrylite zone reveals primitive source in the Sudbury impact structure

DOREEN E. AMES¹, JACOB J. HANLEY², GYÖRGYI TUBA¹
AND SIMON JACKSON¹

¹Geological Survey of Canada, Ottawa (dames@nrcan.gc.ca)

²Saint Mary's University (jacob.hanley@smu.ca)

Earth's largest impact craters had transient craters that penetrated 30-40 km depth and collapsed to form ~200 km impact craters with perturbations of the Moho [1]. The Sudbury impact structure is the eroded remnant of a larger 150-200 km multi-ring crater and uniquely revealing at present-day surface the crustal impact structures in the crater floor below the igneous complex [2].

The Paleoproterozoic Broken Hammer Cu-Ni-PGE deposit, is hosted by impact-induced pseudotachylitic breccias in the crater floor within Neoproterozoic gneiss and granites. A high-grade PGE-only zone is composed of major coarse epidote-quartz, minor chlorite-sperrylite-merenskyite, with sperrylite crystals up to 4 mm, and trace michenerite. Isolated sperrylite grains in epidote or quartz contain inclusions of gold, petzite, galena and alessite, whereas complex intergrowths of Pd-, Bi- and Ag-tellurides are associated with specular hematite and cassiterite, suggesting high fO₂ conditions. *in situ* trace element analyses of euhedral epidote and chlorite precipitated along growth zones in hydrothermal quartz reveal increasing Mg, Zn, Fe and Ni towards the rims. Late-stage Cpy-millerite penetrates the core of extensional epidote-quartz-sperrylite veins.

Early formed epidote that hosts coarse sperrylite analyzed by TIMS yielded a narrow range of low age corrected ⁸⁶Sr/⁸⁶Sr ratios from 0.705948 to 0.706457 with a primitive non-radiogenic source supporting a mantle origin [3,4]. This implies that initial impact destabilized the crust-mantle boundary resulting in rapid fluid-gas release and transport of precious metals from the mantle along deep-seated faults to the footwall environment of the SIC.

In situ LA-MC-ICP-MS Sr isotope analysis of epidote and calcite in early syn-PGE ore, later Ni-Cu and Cu-PGE vein ores and post-mineralization phases will be used to trace the evolution of fluids in the Sudbury crater.

[1] Christenson *et al* (2009), *EPSL*, 284, 249-257. [2] Ames *et al* (2008), *Econ. Geol.* **103**, 1057-1077. [3] Kerr and Hanley (2011) *Min. Mag.* **75**, 1174. [4] Hanley and Ames (2012) *PACROFI-XI*, **11**, 39-40.

Trace elements in olivine characterize the mantle source of subduction-related potassic magmas

E. AMMANNATI*^{1,2}, S. F. FOLEY^{2,3}, R. AVANZINELLI¹,
D.E. JACOB^{2,3} AND S. CONTICELLI¹

¹Dipartimento di Scienze della Terra, Università di Firenze, Italy (* correspondence: edoammo@gmail.com)

²Institut für Geowissenschaften, Johannes Gutenberg-Universität Mainz, Germany.

³CCFS, Dept. Earth and Planetary Sciences, Macquarie University, North Ryde, NSW 2109, Australia.

Trace elements in olivine have recently been shown to provide useful means to investigate the upper mantle, allowing identification of olivine-free (pyroxenitic) reservoirs in the source of OIBs [1]. But few studies are available of magmatic rocks at destructive plate margins [2]. Here we present the first comprehensive set of major and trace element analyses on olivine from subduction-related Plio-Quaternary magmatism of the Italian Peninsula.

16 rock samples covering the full compositional range from calc-alkaline to ultrapotassic occurring within the Italian magmatic region were selected for their primitive character (Mg# = 60-80) and the presence of olivine at the liquidus. 200 olivine crystals were analyzed for major and trace elements (Ca, Mn, Ni) using EPMA, and more than 100 have been analyzed for trace elements using LA ICP-MS.

Olivine phenocryst cores show a large compositional variability among the different magmatic suites. Olivine from the Lucanian region has the highest Na and Al, whereas most elements have lower concentrations compared to the other Italian regions and fall within typical mantle values. The olivine crystals from the lamproite-like samples (Tuscan Region) bear evidence of an olivine-depleted, pyroxenite-bearing source resulting from Si- and K-rich metasomatism of previously depleted mantle: the olivine crystals are remarkably enriched in Ni (up to 5,000 ppm) with high Cr and low Mn and Ca contents. Olivines from plagioclite rocks of the Roman Region show trace element contents that differ from those of the lamproite-shoshonite suite (extremely low Ni, low Cr and elevated Mn and Ca). This could be explained by a metasomatic reaction in the presence of excess Ca. Li enrichment (up to tens of ppm) in olivine from the Tuscan and the Roman Province indicate the recycling of crustal material into the mantle wedge as a primary cause of the metasomatism [2].

[1] Sobolev *et al* (2005) *Nature* **434**, 590-597. [2] Prelević *et al* (2013) *Earth & Planet. Sci. Lett.* **362**, 187-197.

Mineral transformations and bacterial diversity in As-rich waste dumps

F. Y. AMOAKO^{1*}, J. MAJZLAN¹ AND E. KOTHE²

¹Friedrich-Schiller-University, Institute of Earth Science, Jena, Germany

(*correspondence: Felix-Yebo.Amoako@uni-jena.de)
(Juraj.Majzlan@uni-jena.de)

²Friedrich-Schiller-University, Institute of Microbiology-
Microbial Phytopathology, Jena, Germany
(Erika.Kothe@uni-jena.de)

Weathering and mineral transformation of sulphidic waste generate Fe-rich secondary phases which retain metals and metalloids in metastable, nano-crystalline, or amorphous phases. Since fate and chemical stability of the pollutants are important factors for their impact on the environment, this research address microbial impact on highly weathered waste materials from the Medieval dumps in the Kaňk deposit, Kutná Hora (Czech Republic), Rotgülden-Salzbürger Land (Austria) and a historical mine from Chyžné (Slovakia).

The olive-green and yellow powdery secondary mineral phases were identified using mineralogical methods, such as, powder X-ray diffraction and electron microscopy, and confirm the presence of kaňkite ($\text{FeAsO}_4 \cdot 3.5\text{H}_2\text{O}$), (para)scorodite ($\text{FeAsO}_4 \cdot 2\text{H}_2\text{O}$) bukovskýite [$\text{Fe}_2(\text{AsO}_4)(\text{SO}_4)(\text{OH}) \cdot 9\text{H}_2\text{O}$], and zýkaite [$\text{Fe}_4(\text{AsO}_4)_3(\text{SO}_4)(\text{OH}) \cdot 15\text{H}_2\text{O}$]. These minerals form in a clay-rich matrix which acts as a seal for the weathering eluate solution.

The bacterial diversity was assessed by cultivation to study the role of microorganisms in the weathering processes and their influence on the mineral transformation, thereby leading to the release of the pollutants. So far 25 bacterial and 9 fungal isolates were obtained from the deposits which show low colony forming units and hence low microbiological prevalence. The bacteria are mainly coccoid strains with slow growth rates on arsenate containing media; two aerobic, nine anaerobic, ten facultative-anaerobic and the rest are neutral. Nineteen bacterial strains are gram positive and six strains are gram negative. Eighteen bacterial strains are siderophore producers and the rest are neutral. Nineteen bacterial strains are resistant to 5-, 10- and 20 mM arsenate concentrations, with 5 strains resistant to 1 M arsenate. The fungi are high spore producing isolates, and will be categorised as ascomycetes, basidiomycetes, yeasts or zygomycetes.

Establishing a biomarker from trace element incorporation patterns in abiotic and biotic magnetite

M. AMOR^{1,2*}, V. BUSIGNY¹, A. GÉLABERT¹,
G. ONA-NGUEMA², M. THARAUD¹, E. ALPHANDÉRY^{2,3},
M. DURAND-DUBIEF³, I. CHEBBI³ AND F. GUYOT¹

¹ Institut de Physique du Globe de Paris, Sorbonne Paris cité,
Univ Paris Diderot, UMR 7154 CNRS, 1 rue Jussieu,
75005 Paris, France (*correspondence: amor@ipgp.fr)

² Institut de Minéralogie et de Physique des Milieux
Condensés, UMR 7590 CNRS, 4 place Jussieu, 75005
Paris, France

³ Nanobactérie, Hôpital Cochin-Paris Biotech Santé, 24 rue
Méchain, 75014 Paris

Magnetite (nominally $\text{Fe}^{3+}_2\text{Fe}^{2+}\text{O}_4$) is a widespread iron oxide found at the Earth surface. It precipitates through either abiotic or biotic processes (magnetotactic bacteria, dissimilatory iron-reducing bacteria, iron-oxidizing bacteria). Magnetite provides part of the magnetic signal in various sediments such as carbonate platforms, paleosols and Banded Iron Formations. Identification of biotic magnetite in ancient sediments remains a key point to trace life evolution over geological times. Although magnetic properties allow identification of recent magnetotactic bacteria fossils, crystallographic characteristics do not appear to be suitable for unambiguous biotic magnetite identification. In this study, we propose to focus on geochemical tools to better understand the origin of fossilized magnetite. Trace elements incorporation in magnetite has been widely studied for enhancing magnetic properties but has never been explored as a potential biomarker. In the present work, we show results of both abiotic and biotic magnetite nanoparticles which were synthesized in presence of multi-elements in the precipitation media. Nanoparticles were then washed to remove adsorbed elements on magnetite surface. Magnetite were characterized using Transmission Electron Microscopy and X-Ray Diffraction. Elements incorporation was quantified with Inductively Coupled Plasma-Atomic Emission Spectroscopy and Inductively Coupled Plasma-Mass Spectrometry. Partition coefficients between solutions and magnetites were finally estimated for each element. Elemental incorporation patterns in abiotic magnetite was quantified and compared with magnetite precipitated by bacteria in order to establish criteria for biomagnetite identification. Elements of the first transition metals series show partition coefficients between mineral and fluid (normalized to Fe) close to 1 in abiotic magnetite but appear more concentrated in biotic magnetite.

Eocene pCO₂ reconstructions using boron isotopes in “glassy” planktonic foraminifera

E. ANAGNOSTOU^{1*}, E.H. JOHN², K.M. EDGAR²,
P.N. PEARSON², C.H. LEAR², R.D. PANCOST³
AND G.L. FOSTER¹

¹Ocean and Earth Science, National Oceanography Centre
Southampton, UK

(*correspondence: e.anagnostou@noc.soton.ac.uk)

²School of Earth and Ocean Sciences, Cardiff University, UK.

³School of Chemistry, University of Bristol, UK.

The Cenozoic climate transition marks the most recent climatic shift in Earth's history from a greenhouse to an icehouse world (~53-33 Ma). This interval is characterized by a gradual deep-sea [1] and high-latitude [2] cooling of ~10°C and only moderate cooling of the tropics [2], culminating in Antarctic glaciation at the Eocene/Oligocene transition (EOT).

Although a decline in the CO₂ content of the atmosphere (pCO₂) has been suggested as the trigger for final transition into the ice house [3], currently available early Eocene pCO₂ records are rather variable and appear only weakly correlated with climate variations for this interval. For this reason, using multicollector ICPMS, we generated a new record of boron isotopes (δ¹¹B) in planktonic foraminifera, a proven proxy of seawater pH [e.g. 4]. We utilised multi-species depth profiles from very well preserved “glassy” planktonic foraminifera recovered by the Tanzanian Drilling Project from five time slices spanning 53-37 Ma. We discuss our new reconstructions of seawater pH and derived pCO₂ concentrations, in view of estimates of seawater δ¹¹B composition and alkalinity.

[1] Zachos *et al* (2001) *Science* **292**. [2] Bijl *et al* (2009) *Nature* **461**. [3] Pearson *et al* (2009) *Nature* **461**. [4] Sanyal *et al* (1996) *Paleoceanography* **11**.

A common origin for terrestrial and lunar indigeneous water

M. ANAND^{1,2*}, R. TARTÈSE¹, J.J. BARNES^{1,2},
I.A. FRANCHI¹ AND N. A. STARKEY¹

¹Planetary and Space Sciences, The Open University, Walton
Hall, Milton Keynes, MK7 6AA, UK (*correspondence:
Mahesh.Anand@open.ac.uk)

²Department of Earth Sciences, The Natural History Museum,
Cromwell Road, London, SW7 5BD, UK

Variable but significant amounts of “water” have been measured in samples derived from the lunar interior [1-7], challenging the long-standing paradigm of a bone-dry Moon. Based on elevated D/H ratios measured in mare basalt apatites (> 500 ‰), lunar “water” has been inferred to be of cometary origin [3]. In contrast, it has been argued that CI-chondrites (δD ~ 100 ‰) are also a viable source for lunar H, and that the elevated apatite δD values reflect intense H₂ degassing during magma ascent and emplacement [8].

New OH and D/H analyses in apatites from Apollo basalts and basaltic meteorites, carried out at The Open University using the NanoSIMS 50L, confirm that apatite in Apollo mare basalts have elevated δD values > 400 ‰ and a wide range of OH contents (300-7300 ppm). Apatites in meteorites MIL 05035 and LAP 04841 expand our range for mare basalt δD values down to ~ 200 ‰. These δD variations are consistent with ~ 85 to 99 % degassing of H₂, starting from a CI chondrite-type δD value of 100 ‰. In the ~ 4.3 Ga basaltic lunar meteorite Kalahari 009, 8 out of 9 analyses define an average δD value of -15 ± 47 ‰ for corresponding OH contents of 500 to ~ 4000 ppm. We interpret this D/H ratio as that of an undegassed basalt, directly reflecting the H isotope composition of the lunar mantle. This is in good agreement with recent analyses carried out in melt inclusions in Apollo 17 orange glasses [9]. As this D/H ratio is similar to that of the bulk Earth [10], these new data suggest that terrestrial and lunar hydrogen share a common origin.

[1] Barnes *et al* (2013) *Chem. Geol.* **337-338**, 48-55. [2] Boyce *et al* (2010) *Nature* **466**, 466-469. [3] Greenwood *et al* (2011) *Nature Geosci.* **4**, 79-82. [4] Hauri *et al* (2011) *Science* **333**, 213-215. [5] Hui *et al* (2013) *Nature Geosci.* **6**, 177-180. [6] McCubbin *et al* (2010a) *PNAS* **27**, 11223-11228. [7] Saal *et al* (2008) *Nature* **454**, 192-196. [8] Tartèse & Anand (2013) *EPSL* **361**, 480-486. [9] Füre *et al* (2013) *LPS XLIV*, Abstract #2108. [10] Lécuyer *et al* (1998) *Chem. Geol.* **145**, 249-261.

Petrology And Geochemistry Of Pyroxene Granulite Of Somvarpet, South Western Dharwar Craton, Karnataka, India

*ANANTHA MURTHY K S¹, JAYARAM G N¹,
LINGADEVARU M² AND GOVINDARAJU¹

¹Dept. of Applied Geology, Kuvempu University,
Jnanasahyadri, Shankaraghatta - 577 451, Karnataka
²Dept. of Geology, School of Earth Sciences, Central
University of Karnataka, Gulbarga-585 106, Karnataka
(Ks.Amurthy@Yahoo.Com)

The Somvarpet area forms a part of high grade granulite terrain in the Western Dharwar Craton. The area mainly consists of peninsular gneiss, Charnokites, pyroxene granulites and mafic enclaves. The Pyroxene granulite, which forms one of the major lithological unit, occurs as large parallel bands with in the peninsular gneiss and exhibit metamorphic textures (Granoblastic and porphyroblastic textures), which are often superimposed on relict mafic igneous textures (ophitic, sub-ophitic and intergrowth textures). Mineralogically, the rock essentially contains Ortho and Clino Pyroxenes, and Plagioclase. Quartz, Garnet and Hornblende occur as accessory minerals, whereas, Ilmanite, Rutile, Apatite, Spene and Iron oxides are the minor minerals.

Geochemically, the Pyroxene granulites show tholeiitic affinity with iron enrichment, which is a characteristic feature of Archean tholeiites. Variation in trace element concentrations, particularly, Rb, Th, U and Pb, would indicate their instability during metamorphism. To understand the tectonic setting of pyroxene granulites, the analysis were plotted on various known discriminate diagram, the plots fall well within the basaltic and Island arc tholeiitic fields. The average concentration of Rb (6.60ppm) of pyroxene granulite of Somavarpet is very low compared to the Archean tholeiites (12ppm), probably, due to the loss of Rb during granulite facies metamorphism and it is substantiated by the plot of K Vs Rb, where, the pyroxene granulites follow depleted granulite trend. The Pyroxene granulites of the area exhibit slightly fractionated REE patterns, mainly due to, LREE enrichment rather than the HREE depletion.

Redox-sensitive metals and their isotopes: The Holland legacy of early ocean exploration

ARIEL D. ANBAR^{1,2*} AND TIMOTHY W. LYONS³

¹School of Earth & Space Exploration, Arizona State
University, Arizona, USA
²Department of Chemistry & Biochemistry, Arizona State
University, Arizona, USA
³Department of Earth Sciences, University of California -
Riverside, California, USA

“How lucky I am to have something that makes saying
goodbye so hard.” – A. A. Milne

In 1984 [1], Dick Holland noted the striking correlation between the abundances of Mo and U on the one hand, and organic carbon on the other, in Devonian black shales. He speculated that the slope of this correlation should scale with the abundances of these elements in ancient oceans, which in turn should scale with environmental redox conditions. These few paragraphs gave rise to a new theme in deep time paleoredox research – trace metals as paleoredox proxies – much of it centered on the question that dominated Dick's interest in his later years: how and when did the Precambrian atmosphere and oceans become rich in O₂?

Over the following ~30 years, and particularly in the last decade, analytical advances turned this speculative vision into a rich and mature field. The development of ICP-MS paved the way for the assembly of large datasets of Mo and U abundances in sedimentary rocks through time. The coupling of multiple detector arrays to ICP-MS instruments opened the door to exploration of variations in the isotope abundances of these and other redox-sensitive elements, revealing a new and unexpected dimension of paleoenvironmental information.

We will assess the future of this field in light of insights it has yielded. For example, there is now broad confirmation of a Paleoproterozoic "Great Oxidation Event" (GOE), but also evidence of a complex fabric of mild but detectable, possibly variable, "whiffs" of environmental oxygenation preceding this event. Further, it is now documented that widespread oxygen deficiency persisted in the oceans in the wake of the GOE, but the extent of ocean euxinia was apparently of limited extent. And new ideas and insights have emerged about the effects of changes in the abundances of bioessential metals, especially Mo, on ecosystem evolution.

[1] H. D. Holland (1984). *The Chemical Evolution of the Atmosphere and Oceans*. Princeton University Press, 598 pp.

Asian monsoon circulation strength inferred from multicentury tree-ring stable isotope chronologies from southeast Asia

K.J. ANCHUKAITIS^{1*}, M.H. GAGEN², D. MARTIN-BENITO³, B.M. BUCKLEY³, C. UMMENHOFER¹
AND ALLEGRA N. LEGRANDE⁴

¹Woods Hole Oceanographic Institution, Woods Hole, MA 02540 USA (* correspondence: kja@whoi.edu)

²Department of Geography, Swansea University, Swansea, UK

³Lamont-Doherty Earth Observatory of Columbia University, Palisades, NY 10964 USA

⁴NASA Goddard Institute for Space Studies, New York, NY 10025 USA

The large-scale dynamic circulation of the Asian monsoon over the last several centuries can be inferred from the oxygen isotope ratios of the annual rings of long-lived tropical conifer species from southeast Asia. Here, we present replicated, multicentury stable isotope series from *Fokienia hodginsii* growing in the Bidoup Nui Ba National Park site in the southern highlands of Vietnam. This isotope chronology is significantly negatively correlated with summer monsoon surface wind speeds over the Bay of Bengal and the adjacent region, indicating that stronger (weaker) onshore winds are associated with lower (higher) oxygen isotope values. Ring width and isotopes show particular coherence at multidecadal time scales, and together allow past precipitation amount and circulation strength to be disentangled. Estimates of the strength of past monsoon circulation provide data for validating general circulation model simulations of the response of the Asian monsoon to changes in radiative forcing and an independent estimate against which to evaluate long-term changes in the Asian monsoon as reflected in other terrestrial and marine proxies as well as forced last millennium general circulation model simulations.

Duration of prograde metamorphism in the inverted Barrovian sequence, Sikkim Himalaya, India

ROBERT ANCZKIEWICZ^{1*}, SUMIT CHAKRABORTY²,
SOMNATH DASGUPTA³ AND DILIP K MUKHOPADHYAY⁴

¹Polish Academy of Sciences, Kraków, Poland,
(ndanczki@cyf-kr.edu.pl)

²Ruhr Universität, Bochum, Germany

³Indian Institute of Science Education & Research-Kolkata, India

⁴Indian Institute of Technology Roorkee, Roorkee, India

The Lesser Himalaya in Sikkim expose a uniquely well preserved Barrovian metasedimentary sequence that displays little tectonic disturbance and is inverted in terms of both pressure and temperature. The sequence seems to be continuous from chlorite-biotite grade until muscovite dehydration reaction with well developed all intermediate zones inbetween.

We determined timing and duration of Barrovian metamorphism by Lu-Hf garnet dating of all individual Barrow zones from garnet isograd up to muscovite out reaction. Garnet is well preserved and shows broad cores with sigmoidal inclusion trails pointing to synkinematic crystallization, which occasionally are surrounded by narrow, inclusions poor rims. Bulk and single crystal dating resulted in highly precise ages showing progressively older dates with increasing metamorphic grade and higher structural level. The youngest, garnet zone rocks yielded 10.6±0.2 Ma age that is followed by 12.8±0.3 and 13.7±0.2 Ma ages obtained for staurolite and kyanite grades, respectively. Sillimanite zone garnets gave 14.6±0.2 Ma age. Structurally highest rocks, arguably marking the top of the sequence, yielded 16.8±0.1 Ma. All ages are interpreted as reflecting garnet growth on a prograde path, which is indicated by Rayleigh style Lu distribution.

High precision of bulk garnet ages was verified relatively to the duration of single crystal growth by chemically controlled high resolution single garnet dating. Five zones dated from the synkinematically grown core yielded precise analyses, which do not show any resolvable time difference and together define a 13.7±0.2 Ma isochron age. Two fractions from narrow, postkinematically grown rim define a 9.9±3.8 Ma date. Much lower precision of the rim is inevitable consequence of Rayleigh style Lu distribution. These data point to a very fast synkinematic core crystallization, which was followed by a slower phase of rim formation. The data show that age precision is not only analytical but closely resembles the real pace of metamorphic crystallization within the Lesser Himalaya. Lu-Hf dating constraints duration of Barrovian metamorphism from garnet to sillimanite zone as 4.0±0.3 Ma, which compares well with earlier estimates of Baxter *et al* (2002) who determined the duration of metamorphism as 2.8±3.7 Ma. for classical (not inverted), Barrovian sequence in Scotland.

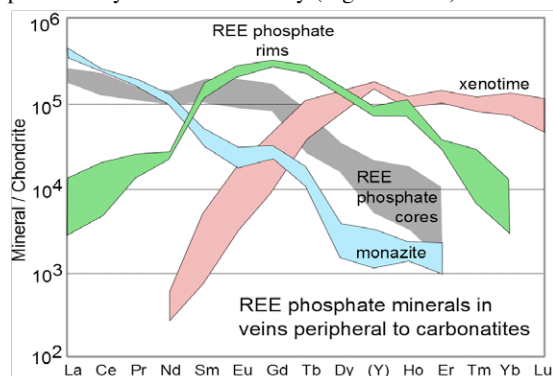
REE fractionation at the Bear Lodge REE+Au deposit, USA: Evidence from mineral chemistry

A.K. ANDERSEN^{1*}, P.B. LARSON¹ AND M.C. ROWE²

¹School of the Environment, Washington State University,
Pullman, USA (*correspondence: akandersen@wsu.edu)

²School of Environment, Univ. of Auckland, Auckland, NZ

The Bear Lodge alkaline intrusive complex hosts one of North America's largest REE deposits. Carbonatites in the central Bear Lodge have REE patterns similar to other carbonatites worldwide, with concentrations decreasing slightly from La to Lu, typical for partial melts from the mantle. Recent exploration reveals zones of HREE- and HFSE-enrichment, much of it hosted by hydrothermal veins peripheral to the LREE-enriched carbonatites. A district-wide zonation from LREE to HREE is reflected by mineralogy. The central carbonatites host REEs in the fluorocarbonate minerals, bastnäsite, synchysite, and parisite, and the carbonate minerals ancylite and carboxenite. Monazite, xenotime, and hydrated REE-phosphates of the rhabdophane group are common in the peripheral veins. New electron microprobe data show typical REE patterns for monazite and xenotime. Hydrated REE phosphates show a zonation similar to that observed district-wide (LREE to HREE), with rims particularly enriched in Eu-Dy (Figure below).



Recent experimental studies show HREEF²⁺ complexes are less strongly associated than LREEF²⁺ complexes at hydrothermal temperatures (>150°C), suggesting the fluids cooled below 150°C or that a different ligand, such as phosphate or chloride was involved. REE-phosphates (monazite) are known to be highly insoluble, suggesting phosphorous was important during precipitation, but not necessarily during transport. Potential external sources of phosphorous include Paleozoic sedimentary units containing abundant phosphatic microfossils or detrital apatite.

Uranium isotopes in anoxic sediments

M.B. ANDERSEN^{1,2*}, D. VANCE^{1,2}, R. HERDSMAN¹,
S. LITTLE^{1,2}, A. MATTHEWS³, T. LYONS⁴
AND S. ROMANIELLO⁵

¹School of Earth Sciences, University of Bristol, UK

²IGP, ERDW-ETHZ, 8092 Zurich, Switzerland

³Institute of Earth Sciences, University of Jerusalem, Israel

⁴Department of Earth Sciences, University of California, USA

⁵School of Earth & Space Explorator, Arizona State
University, USA

Elemental and isotopic proxies in marine archives are important tools for reconstructing the chemical evolution of the ocean through time. One sought-after parameter is past ocean redox, for which the Mo isotope tool is relatively mature [e.g., 1]. Uranium's redox sensitive behaviour has also served as a useful indicator for redox conditions in marine sediments [2]. Recent improvements in our ability to measure the ²³⁸U/²³⁵U ratio has also highlighted the potential for significant redox-induced isotopic variability at the Earth's surface [3,4]. However, the ground-truthing of any such tracer requires knowledge of the singularity of the signal, potential diagenetic overprinting and local vs. global processes, all of which have to be addressed.

To advance our understanding of ²³⁸U/²³⁵U in marine archives, and its response to ocean chemistry, we have measured U isotopes in anoxic marine sediments from modern euxinic settings (Black Sea and the Cariaco Basin) and in organic-rich Mediterranean sediments (sapropels) formed during the last glacial cycle. The sediments from euxinic settings are characterised by high U enrichment factors and all show ²³⁸U/²³⁵U moderately heavier than seawater (~0.4 ‰), consistent with published Black Sea data [4]. In contrast, U incorporation into the Holocene Mediterranean sapropel (S1), likely formed under anoxic but non-euxinic conditions, shows lower U enrichment but significantly heavier ²³⁸U/²³⁵U signatures (~1 ‰) compared to the euxinic sediments.

The ²³⁸U/²³⁵U signatures suggests different U incorporation into the two types of anoxic sediments likely linked to the specific mechanism of U reduction or the ocean setting. This observation suggest that the ²³⁸U/²³⁵U in marine archives can potentially fingerprint anoxic versus euxinic water conditions and may provide a paleo-redox proxy to be used in tandem with, for instance, Mo isotopes.

[1] Arnold *et al* (2004) *Science*, **304**, 87-90. [2] Barnes & Cochran (1990), *EPSL*, **97**, 94-101. [3] Stirling *et al* (2007), *EPSL*, **264**, 208-225. [4] Weyer *et al* (2008), *GCA*, **72**, 345-359.

Mantle jets and mantle plumes

DON L. ANDERSON

Seismological Laboratory, Caltech (dla@gps@caltech.edu)

Because of internal heating and effects of viscosity and pressure mantle flow is characterized by large sluggish upwellings. Jets and plumes have been introduced into mantle dynamics and geochemistry because of the perceived need for narrow hot and rapid upwellings to fuel Hawaii and other intraplate volcanoes. These imply a fluid strongly heated from below, no internal heating, non-Stokes law behaviour, flow controlled by external forces and an important role for inertia and momentum. Jets and plumes, as defined in fluid dynamics, and as used in geodynamic and geochemical modeling, are precluded by the equations of fluid dynamics and solid-state physics. The underlying homogeneity, isotropy, adiabatic and thin plate assumptions are ruled out by seismology.

Like Morgan plume hypothesis, the McKenzie-Bickle geotherm and mantle jet hypotheses and whole mantle convection scenarios violate fluid dynamic and lattice dynamic scaling relations and the 2nd law of thermodynamics, and do not satisfy well-constrained unsmoothed seismic models that allow for anisotropy. Physics, and geochemical modelling, show that the outer 200 km of the mantle is an appropriate source for intraplate magmas, including their diversity, volumes, compositions and temperatures. The thermal overshoot of boundary layer convection and the subadiabaticity of the deep geotherm explain the relative temperatures of Hawaiian and midocean ridge magmas. Anisotropy shows that the ridge source is in the transition zone.

Top-down processes, driven by secular cooling, fertilize and cool the mantle and create shear boundary layers that are responsible for shear-driven upwellings and intraplate volcanoes. The upper boundary layer of the mantle is a metasomatised, sheared melange that has all the attributes required to explain volcanoes such as Hawaii and the largest igneous provinces.

ca. 1750 Ma arc-related metamorphism in the southern Arunta Complex, central Australia?

J. R. ANDERSON^{1*}, D. E. KELSEY¹, M. HAND¹
AND W. J. COLLINS²

¹Centre for Tectonics, Resources and eXploration (TRaX),
University of Adelaide, S.A., 5005 (*correspondence:
jade.anderson@adelaide.edu.au)

²University of Newcastle, N.S.W. 2308

The Arunta Complex, central Australia, is a ~200,000 km² poly-metamorphic complex, with a cryptic record of tectonism from the Paleoproterozoic to the Paleozoic. The Arunta Complex records evidence for ~200 Myr of orogenic activity between ca. 1800–1600 Ma, but with the exception of minor magmatism interpreted to have arc-related petrogenesis [1], evidence for subduction-related magmatism and high pressure metamorphism is limited.

This study uses calculated pressure-temperature phase diagrams and *LA-ICP-MS* U–Pb monazite geochronology to investigate a series of granulite facies supracrustal and magmatic rocks from the southern Arunta Complex.

High-grade, regional metamorphism occurred at ca. 1760–1740 Ma. This timeline has previously been interpreted as an igneous event, including magmatism with subduction-related geochemical signatures in the south-eastern Arunta region (Calcalkaline–Trondhjemite Suite). However, recent evidence has highlighted that metamorphism also occurred during this time in the eastern Arunta Complex [2]. If the ca. 1750 Ma magmatism is arc-related, it is possible that we have characterised the thermal structure of the arc (medium pressure, apparent thermal gradient of ~25–35 °C/km).

The characterisation of the physical conditions of the crust in the southern Arunta Complex at ca. 1760–1740 Ma may provide supporting evidence from a metamorphic standpoint for an active margin in the southern proto-North Australian Craton. If so, the ca. 1760–1740 Ma regional metamorphism is an important constraint for deciphering the Proterozoic tectonic evolution of the Arunta Complex and North Australian Craton.

[1] Zhao & McCulloch (1995) *Precambrian Research* **71** 265–299. [2] Whelan *et al* (2011) *Annual Geoscience Exploration Seminar (AGES)*, Record of Abstracts **Record 2011-003**, 40–42.

Constraining rates of trace element supply and removal using long-lived thorium isotopes

ROBERT F. ANDERSON^{1*}, CHRISTOPHER T. HAYES¹,
MARTIN Q. FLEISHER¹, LAURA F. ROBINSON², KUO-
FANG HUANG², HAI CHENG^{3,4}, LIJUAN SHA^{3,4}, R.
LAWRENCE EDWARDS⁴, YANBIN LU⁴
AND S. BRADLEY MORAN⁵

¹Lamont-Doherty Earth Observatory of Columbia University,
Palisades, NY, boba@ldeo.columbia.edu
(* presenting author)

²Woods Hole Oceanographic Institution, Woods Hole, MA +
University of Bristol, Bristol, United Kingdom,
Laura.Robinson@bristol.ac.uk

³Institute of Global Environmental Change,
Xi'an Jiaotong University, Xi'an, China,
cheng021@umn.edu

⁴University of Minnesota, Minneapolis, MN,
edwar001@umn.edu

⁵University of Rhode Island, Narragansett, RI,
moran@gso.uri.edu

Radioactive disequilibria within naturally occurring U- and Th-decay series have been exploited to constrain the rates of a variety of processes in the ocean. Here we will illustrate the use of ²³⁰Th and ²³²Th to investigate certain processes that supply and remove trace elements, including:

1) Boundary Scavenging - the enhanced removal of trace elements by scavenging to particles in biologically productive ocean margin regions. Contrasting results from the North Pacific and North Atlantic Oceans reveal some expected findings and some surprises.

2) Bottom Scavenging - the enhanced scavenging of dissolved ²³⁰Th by resuspended particles in benthic nepheloid layers. New evidence from the US GEOTRACES program will require reinterpretation of features in certain historical ²³⁰Th profiles that were previously attributed to Atlantic overturning circulation. The rapid scavenging in benthic nepheloid layers that is evident in dissolved ²³⁰Th profiles may apply to other particle-reactive trace elements as well.

3) Supply of trace elements by mineral aerosols (dust) - a new method employing ²³⁰Th and ²³²Th has gained a great deal of attention recently. We will examine evidence that raises questions about certain assumptions inherent in this approach including, most importantly, the assumption that ²³⁰Th and ²³²Th occur in the same chemical form and, therefore, have equivalent chemical residence times in the upper water column.

Adsorption of natural organic matter at the water/gibbsite interface

K. ANDERSSON^{1*}, J. P. L. KENNEY¹, P. PERSSON¹
AND T. KARLSSON¹

¹Departemnt of Chemistry, Umeå University, 901 87 Umeå,
Sweden

(*Correspondence: kristoffer.andersson@chem.umu.se)

Aluminum (Al) is one of the earth's most abundant elements and constitutes about 8% of the earth's crust. It exists mainly as silicates, oxides and hydroxides, combined with other elements or in complexes with natural organic matter (NOM). Speciation is a key factor for understanding the environmental impact of Al. It is therefore important to determine the chemical forms of Al that predominate in different natural media and under varying geochemical conditions. Adsorption of NOM to Al-based mineral surfaces is an important process that can alter the speciation of Al by influencing the rate and extent of dissolution of the mineral and thereby the overall solubility of Al. In this work, aquatic NOM from the Suwannee river (IHSS) has been studied in the presence and absence of an Al mineral surface (Gibbsite), using both *in situ* FT-IR spectroscopic measurements coupled with potentiometric titrations, and wet-chemical methods. These experiments were conducted as a function of time, pH, and concentration in order to follow the adsorption of NOM and the possible dissolution of the mineral surface.

Previous studies have indicated that fulvic and humic acids primarily adsorb to the surface of bohemite in an outer-sphere fashion with only minor formation of inner-sphere complexes [1, 2]. Our preliminary results indicate a significant shift in the asymmetric stretch of the carboxylate group in NOM at pH 3.5-5.5, possibly pointing towards a high amount of inner-sphere complexes at the gibbsite surface. Formation of inner-sphere complexes at the surface could promote a ligand-induced dissolution of the minerals. These indications are further supported by batch experiments where a dissolution of the gibbsite mineral are observed. Thus, complexation with NOM could potentially be one of the most important factors, other than pH, for controlling the solubility of Al in environmental systems.

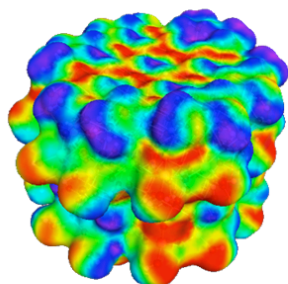
[1] Yoon *et al*(2005) *Langmuir* **21**, 5002-5012. [2] Yoon *et al*(2004) *Langmuir* **20**, 5655-5658.

Predicting the protonation behavior of the kaolinite surface

M.P. ANDERSSON AND S.L.S. STIPP

Nano-Science Center, Department of Chemistry, University of Copenhagen, Denmark,
(ma@nano.ku.dk, stipp@nano.ku.dk)

Clay minerals, known for their ion exchange capacity, have an impact on environmental issues such as uptake of contaminants from ground water and retention of oil in reservoirs. Kaolinite is believed to play an important role in enhancing oil recovery by low salinity water flooding, where decreasing Ca^{2+} and Mg^{2+} concentrations in the injected solution increases the amount of oil that can be generated from sandstone reservoirs. The ability of kaolinite to act as an ion exchanger depends on its atomic surface structure, pH and in particular, on its protonation state. This is especially true for metal ions, which compete with protons for bonding sites on surface oxygens.



COSMO surface of the kaolinite cluster model

We have used the implicit solvent model, COSMO-RS, to predict the pK_a values of kaolinite surfaces, using a molecular cluster consisting of 512 atoms, to represent a kaolinite surface. Using a cluster allows us to determine basal plane and edge protonation properties using the same model. We found that the pK_a values could be classified

according to surface composition. Al-OH_2 groups had a median pK_a value of 5.5 and were generally more acidic than SiOH groups with a median pK_a value of 10.6. The standard deviation was 2 to 3 pH units for most surface sites. Using our calculated pK_a values, we were able to estimate the point of zero charge (PZC) for kaolinite for the various surface sites, which has been difficult or impossible, using experimental approaches. The kaolinite edge has a PZC of 3.7 and the AlOH basal plane a PZC of 7.7. This has the consequence that the PZC for kaolinite samples ranges between 4 and 6 and is geometry dependent... Higher values are found for flat particles where the basal plane behavior dominates over edge effects. Our results help explain why the PZC of kaolinite can differ significantly depending on the nature of the kaolinite samples (i.e. the surface to edge ratio, the diameter of particles) used in experiments.

Phase transition in aluminous silica at lowermost mantle P-T conditions

D. ANDRAULT¹, R.G. TRØNNES², Z. KONÔPKOVÁ³,
W. MORGENROTH⁴ AND H.-P. LIERMANN³

¹LMV-UBP-CNRS-IRD, Clermont-Ferrand, France

²Natural History Museum, University of Oslo, Norway

³DESY, Hamburg, Germany

⁴Department of Crystallography, Frankfurt, Germany

Using Al-bearing SiO_2 glasses with 4 and 6 wt% Al_2O_3 as starting materials, we investigated the phase transition from the CaCl_2 -structured to the $\alpha\text{-PbO}_2$ -structured phase (seifertite) at pressures and temperatures corresponding to the lowermost mantle. The experiments were conducted with synchrotron-based *in situ* X-ray diffraction in the laser-heated diamond anvil cell. The transition from the CaCl_2 -structured phase to seifertite occurs between 113 and 119 GPa at 2500 K. Comparison with previous results shows a decrease of the transition pressure with increasing Al-content. A tentative phase diagram reports the minerals compositions as a function of pressure in the $\text{SiO}_2\text{-Al}_2\text{O}_3$ system. This diagram includes a binary loop compatible with an Al partition coefficient between CaCl_2 -form and seifertite between 0.55(5) and 1.

Based on the X-ray pattern refinement, our samples show a very small 0.3(2) % volume decrease across the transition. Still, the transition could very well be associated with a more significant change in density if the Al substitution mechanisms are different in CaCl_2 -form and seifertite. The most likely situation is that Al-substitution occurs via O-vacancies in the CaCl_2 -form and via extra interstitial Al in seifertite. That would result in a ~1.5-2.0 % density increase at the transition pressure for silica containing 5 wt% Al_2O_3 . This value is of the same order of magnitude than the estimated difference in density between peridotitic mantle and basaltic lithologies in the lowermost mantle.

www.minersoc.org

DOI:10.1180/minmag.2013.077.5.1

Can Saharan dust explain extensive clay deposits in the Amazon Basin? radiogenic isotopes as tracers of transatlantic transport

M.O. ANDREAE^{1*}, W. ABOUCHAMI¹, K. NÄTHE¹,
A. KUMAR¹, S.J.G. GALER¹, K.P. JOCHUM¹,
E. WILLIAMS², A.M.C. HORBE³, J. W.C. ROSA⁴
AND V.H. GARRISON⁵

¹Biogeochemistry Department, Max Planck Institute for Chemistry, Mainz, Germany (*m.andreae@mpic.de)

²Massachusetts Institute of Technology, Cambridge, MA

³Departamento de Geociências, Universidade Federal do Amazonas, Manaus, AM, Brasil

⁴Instituto de Geociências - Universidade de Brasília, Brasília, Brazil

⁵U.S. Geological Survey, St. Petersburg, Florida, USA

Previous studies have shown that Saharan dust transport across the Atlantic acts as an important source of mineral nutrients to the Amazon rainforest. The Belterra Clay, which outcrops extensively across the Amazon Basin, has been proposed to result from dry deposition of African dusts. We have investigated this hypothesis by measuring the radiogenic isotopic composition (Sr, Nd and Pb) of a suite of samples from the Belterra Clay, African source regions, dusts deposits from various locations along the air mass transport, and some Caribbean islands to characterize dust in the source and receptor regions.

Our results identify distinct isotopic signatures in the Belterra Clay samples and the African sources. The Belterra Clay displays radiogenic Sr and Pb isotope ratios associated with low ϵ_{Nd} values. In contrast, Bodélé samples and dusts deposits show lower Pb isotope ratios, variable $^{87}Sr/^{86}Sr$, and relatively homogeneous Nd isotopic compositions, albeit more radiogenic than those of the Belterra Clay.

Our data show unambiguously that the Belterra Clay is not derived from African dust deposition, but results from weathering and erosion under humid tropical conditions. That Saharan dust contributes to the fertilization in the Amazon Basin cannot be ruled out, however, since the African dust isotopic signature is expected to be entirely overprinted by local weathering sources. In contrast, radiogenic isotope data obtained on aerosol filters collected in the US Virgin Islands and Tobago are similar to those of aerosols from Mali, demonstrating that the African dust isotope signal is detectable and transported as far as Central and South America. We conclude that radiogenic isotope systems are powerful tracers of provenance and can be used to fingerprint dust sources and atmospheric transport patterns.

Hymenoptera pollinator effect on environment

O. ANJOS^{1,3}, O. GONÇALVES¹ AND L. NUNES¹

¹IPCB/ESA – Instituto Politécnico de Castelo Branco, Castelo Branco, Portugal.
(ofelia@ipcb.pt)

²Centro de Estudos Florestais, Instituto Superior de Agronomia, UTL, Lisboa, Portugal

There are several studies reporting the evidence that pollinators are declining as a result of local and global environmental degradation. Operation Pollinator is an international biodiversity program, supported by Syngenta, to boost the number of pollinating insects on commercial farms. It works by creating specific habitats, tailored to local conditions and native insects.

The aim of this work is to increase the ecological suitability of pollinator populations through improved food availability for pollinator employing strategies for surrounding landscape.

Two cherry orchards, located in Fundão, Portugal, were studied: one was installed a patch meadow with flowery prairie with the purpose of increasing pollinator's number; other with poor native biodiversity. It was identified the main groups of insects visiting the cherry blossoms and the surrounding flora, during the flowering cherry trees.

This review was conducted through observation and analysis of pollen in pollinator's nests, artificially placed in the orchards in order to evaluate the visiting flowers.

There was a greater number of pollinating insects in the orchard with higher biodiversity and it was found that insects visited other flora along with the cherry blossoms. The Hymenoptera identified belong to genus: *Andrena*; *Apis*; *Eucera*; *Tropinota*; *Anthophora*; *Osmia*; *Xylocopa*. The orchard where haven't been installed the patch meadow, shows a lower number of visiting insects as well as lower species variability. The increasing of pollinators protects the environment and increases the fruit production and quality. The findings of the sweeter fruit, with the increased number and diversity of insects leads to the conclusion that the environment benefits from the increase in pollinators with more balanced environment, it's a winning environment for everyone.

The conservation of pollinator habitat can also enrich overall biodiversity and the ecosystem services, protect soil and water quality.

Keywords: pollinators hymenoptera; biodiversity; pollen.
Acknowledge: To Syngenta by the financial support of the project.

Application of geochemistry in shale gas exploration: A case study from Cambay Basin, Gujarat, India

ANNAPURNA BORUAH*, M. A. RASHEED,
SYED ZAHEER HASAN, P.H.RAO, AND B. KUMAR

Petroleum Research Wing, Gujarat Energy Research and Management Institute, Gandhinagar, Gujarat, India.
(*Correspondence: Annapurna_1910@yahoo.in)

Shale gas is an unconventional hydrocarbon resource as the shale acts both as a source and reservoir for the gas. Gas can be stored in the shale either in the pore spaces or as adsorbed gas on to the organic matter. Characterization and evaluation of the source potential of a rock is made by using parameters like (1) Total Organic Carbon (2) Rock-Eval Pyrolysis (3) Elemental analysis of C, H, N, O and S (4) Vitrinite Reflectance (5) Visual Kerogen Analysis (6) Extract SARA Analysis (7) Gas Chromatograph of extracted bitumen (8) Pyrolysis Gas-Chromatography (9) Gas Chromatograph-Mass Spectrometry of extracted bitumen and (10) Isotope composition of carbon and hydrogen. For commercial shale gas exploration TOC content of the shale should be more than 2%, mature to post mature zone i.e. oil window to gas window ($R_o > 0.7\%$, $T_{max} > 445^\circ\text{C}$). The kerogen in the shale must be gas prone. At higher temperature zone gas can be generated by insitu cracking of oil. In this study, total 15 shale samples were collected from Broach and Jambusar areas of Cambay Basin, Gujarat, India. The analytical findings reveal that the Shales are found rich in organic matter (1- 5%), maturity (0.7- 1.2VRo), kerogen type II, III marine, hydrogen index <100, thickness is more than 500m and area extent is more than 53000square km. The organic richness attains the oil window at the depth of 2000m and below this depth gas window starts. Finally the laboratory findings highlight the positive prospects for shale gas exploration and exploitation in Cambay Basin.

Keywords: Shale Gas, Geochemical, Exploration.

Quantification of the magma fluxes feeding the growth of a shallow magma reservoir (Soufrière Hills, Montserrat)

C. ANNEN*¹, M. PAULATTO², R.S.J SPARKS¹,
T.A. MINSHULL³ AND E. KIDDLE¹

¹Department of Earth Sciences, University of Bristol, Wills Memorial Building, Queen's Road, BS8 1RJ, Bristol, UK
(*correspondence: catherine.annen@bristol.ac.uk)

²Department of Earth Sciences, University of Oxford, South Parks Road, Oxford OX1 3AN, UK

³Ocean and Earth Science, National Oceanography Centre Southampton, University of Southampton, European Way, Southampton SO14 3ZH, UK

Shallow andesite intrusions in arcs participate to the formation of new continental crust. The SEA-CALIPSO experiment revealed a low-seismic-velocity volume beneath Soufrière Hills (Montserrat) extending vertically from 4 to at least 7.5 km depth and attributed to the presence of melt [1]. By simulating the growth of a magma body by accretion of andesitic intrusions we calculated spatial distributions of temperature and melt fraction and the corresponding seismic wave velocities, which were smoothed to be comparable with tomography results.

The size and intensity of the synthetic velocity anomaly are controlled by the diameter of intrusions, the rate at which they are emplaced, i.e. the total duration of the intrusive episode, and the intruded magma initial heat content (including latent heat). We were able to reproduce the tomographically determined velocity anomaly with a relatively wide range of intrusion diameters (4 to 10 km) and magmatic episode durations (6,000 to 150,000 yrs), but, because of a trade off between these two parameters, the corresponding magma fluxes are restricted to $0.7 - 5 \times 10^{-3} \text{ km}^3/\text{yr}$.

The velocity anomaly can be reproduced with a chamber containing high melt-fraction magma or with a mush of crystals and melts. The range of magma ages in the modelled magma chambers is much wider than the crystal residence time of the erupted andesite [2]. This suggests that eruptions tap small pockets of recently assembled magma and that the velocity anomaly might be mostly due to a non-eruptible mush.

[1] Paulatto, Annen, Henstock, Kiddle, Minshull, Sparks, & Voight (2012), *Geochemistry Geophysics Geosystems* **13**. [2] Zellmer, Sparks, Hawkesworth & Wiedenbeck (2003) *J. Petrol.* **44**, 1413-1431.

Allergic and Respiratory Health effects of combustion aerosols

ISABELLA ANNESI-MAESANO¹ AND YOUSSEF HASSANI²

¹EPAR Department, UMR-S 707 INSERM and UPMC Paris VI, Medical School Saint-Antoine 75012 Paris (isabella.annesi-maesano@inserm.fr)

²EPAR Department, UMR-S 707 INSERM and UPMC Paris VI, Medical School Saint-Antoine 75012 Paris (youssef.hassani@gmail.com)

Health effects of combustion aerosols from 3 different aerosols will be dealt with, namely: 1) traffic-related aerosols, 2) indoor combustion aerosol and 3) wildfire aerosol.

1) Traffic-related PM was assessed in the French 6C Study at specific addresses *in situ* (PM_{2.5}) and through a dispersion model (PM₁₀) and related to allergic and respiratory health of children living close to the addresses. After adjustment for confounders and NO₂ as a potential modifier, in the 5338 school children of the survey the odds of suffering from EIB and flexural dermatitis at the period of the survey, past year atopic asthma and SPT positivity to indoor allergens were significantly increased in residential settings with PM_{2.5} concentrations exceeding 10 microg/m³ (WHO air quality limit values). For the 4,907 children who had resided at their current address for the past 3 yrs, asthma (exercise induced, past year and lifetime) was significantly positively associated with PM₁₀. In the same children, PM₁₀ were significantly positively associated with eczema (lifetime and past year), lifetime allergic rhinitis and sensitisation to pollens. Among the 2,213 children residing at their current address since birth, the associations persisted for lifetime asthma (1.4 (1.0-2.0)) and for sensitisation to pollens (1.2 (1.0-1.9)).

2) After adjusting for confounders, an increased prevalence of past year asthma was found in the classrooms with high levels of PM_{2.5} (OR 1.21; 95% CI 1.05 to 1.39), compared with others. The relationship was observed mostly for allergic asthma. A significant positive correlation was found between EIA and the levels of PM_{2.5} in the same week.

3) Wildfire combustion aerosols emissions between 2006 and 2010 have been modeled for Europe and will be related to health outcomes.

Determination of REE in carbonaceous geological samples by inductively coupled plasma mass spectrometry

YU.V. ANOSHKINA

Tomsk State University 36 avenue Lenina, Tomsk, 634050, Russia (julianoshkina@gmail.com)

The results of laboratory research on the optimization of sample preparation of carbonaceous rocks are presented. Research were carry out using reference materials of black shales SLG-1, SChS-1, metamorphic shale SSL-1 (Russia), cody shale SCo-1, green river shale SGR-1b, coal CLB-1(USA).

In order to explain the dependence between amount of carbonaceous substances in geological samples and degree of extraction of rare earth elements (REE) precipitates were analyzed after each steps of acid digestion using scanning electron microscope TESCAN Vega LMU with energy-dispersive spectrometer Oxford Instruments INCA Energy 350. The research of element-structural changes in precipitates at each steps of acid digestion was monitored by atomic emission spectrometry Grand and FT-IR stectrometry «Nicolet 6700». The necessity of removal of carbonaceous substances was shown. For determining the temperature range of pre-firing carbonaceous substances was used Simultaneous Thermal Analysis by STA 409 PC Luxx. Following conditions: 800 °C during 8 hours in ceramic crucibles into muffle furnace were chosen as optimal for pre-firing. Using the oxidative addition (LiNO₃) at the stage of pre-firing was suggested as alternative conditions. This step allows to reduce the temperature down to 550 °C and time to 2 hours.

Optimal conditions for the acid decomposition of carbonaceous rocks with subsequent determination of trace elements by ICP-MS were found. The scheme includes pre-firing with LiNO₃, open beaker heating with HF, microwave-digestion program with mixture of HF and HNO₃, open beaker procedure of consecutive evaporation with HCl and HNO₃ sequentially. In was added at a concentration of 10 µg L⁻¹ to act as internal standard for correction of matrix effect, signal drift and instrumental instability. Geological reference materials USGS BCR-2, BHVO-2 was analyzed for quality control. All measurements were performed on an Agilent 7500 cx (Agilent Technologies Inc., USA). The results are consistent with published data.

This study was funded by the Russian Ministry of Education and Science (projects 5.3143.2011, 14.B37.21.0686, 14.B37.21.1257).

Phosphorus retention in sediments of a eutrophied lake: Role of organic phosphorus

N. ANSEMS^{*1}, D.W. O'CONNELL², J. WIKLUND², T. BEHRENS¹ AND P. VAN CAPPELLEN²

¹Utrecht University, Faculty of Geosciences, Budapestlaan 4,3584 CD Utrecht, Netherlands.

(*correspondence: nienke.ansems@un-igrac.org)

²University of Waterloo, Ecohydrology Research Group, 200 University Avenue West, Waterloo, ON N2L 3G1, Canada

Phosphorus (P) cycling in aquatic sediments has traditionally been described from an abiotic viewpoint: following Mortimer's classical model, phosphate release from sediments is controlled largely by the oxidation-reduction cycle of iron (Fe). However, biotic processes and organic P (org-P) phases could play an important, if not more important, role. To analyze the fate of P, sediment cores were collected in the oxygenated epilimnion and the anoxic hypolimnion from Lake 227 of the Experimental Lake Areas (ELA) in Ontario, Canada. This experimental lake has been artificially fertilized with P since 1969. Lake 227 is a unique lake, as it has undergone a rapid transition from oligotrophic to eutrophic conditions. ²¹⁰Pb dating and chemical extractions were complemented by ³¹P NMR spectroscopy to elucidate sediment P speciation.

The sediment cores contain an historical record of in what extent and in what form P is retained while sediments were subjected to different prevailing conditions. A comparison is made between oxic and anoxic conditions under oligotrophic and eutrophic conditions. The results show that under eutrophic conditions, org-P plus humic-metal-phosphate complexes represent the major pool of reactive sediment P in Lake 227. The formation of the humic complexes is one of the mechanisms accounting for the high retention of P in the sediments since artificial fertilization started. The role of redox dependent Fe-bound P seems to be of secondary importance. Our work highlights the power of whole-lake manipulation to gain a mechanistic understanding of the role of sediment processes in phosphorus cycling.

Oxyanion adsorption on schwertmannite and iron precipitates from acid mine drainage

J. ANTELO^{1*}, S. FIOL², D. GONDAR², R. LOPEZ² AND F. ARCE²

¹Dept. Soil Science and Agricultural Chemistry. University of Santiago de Compostela. 15782 Santiago de Compostela. Spain (*correspondence: juan.antelo@usc.es)

²Dept. Physical Chemistry. University of Santiago de Compostela. 15782 Santiago de Compostela. Spain

The formation of acid mine drainage implies the weathering and oxidation of the iron sulphide minerals present in mining areas and the formation of large amounts of secondary iron precipitates. The presence of these secondary iron precipitates can be considered of great importance, since they are naturally occurring scavengers for the arsenate and other anionic species found in these highly polluted aquatic systems and their presence controls the mobility and availability of the contaminants[1]. Due to the abundance of arsenate species in AMD environments and the high retention capacity of schwertmannite at acidic pH, many studies have focused on the retention of As(V) or As(III). However, the number of adsorption studies carried out with other oxyanions of environmental interest, such as chromate or molybdate, is limited

The adsorption of different oxyanions has been studied on synthetic schwertmannite and on natural iron precipitates obtained from AMD waters. The adsorption of arsenate, phosphate, chromate and molybdate was examined in relation to pH, and anion exchange between these oxyanions and the sulphate ions present in the crystalline structure of the schwertmannite or the iron precipitates was also analysed. The affinity sequence for the different oxyanions is similar in both the synthetic and natural samples: $\text{AsO}_4 \approx \text{PO}_4 > \text{MoO}_4 > \text{CrO}_4$.

Evidence of anion exchange reactions in schwertmannite was obtained, since sulphate ions are released from the iron minerals following oxyanion adsorption. The oxyanion adsorption process for these secondary iron minerals is controlled by two mechanisms: surface complexation with iron hydroxyl groups and anion exchange with the sulphate groups present in the crystalline structure.

[1] Burton, Bush, Traina, Johnston, Watling, Hocking, Sullivan & Parker (2009), *Environ. Sci. Technol* **43**, 9202-9207.

Sulfate-oxygen isotope insight into anaerobic methane oxidation in estuarine sediments

GILAD ANTLE^{1*}, ALEXANDRA V. TURCHYN¹,
ALICIA DAVIES¹, MICHAL ADLER², VICTORIA RENNIE¹,
BARAK HERUT³ AND ORIT SIVAN²

¹ Department of Earth Sciences, University of Cambridge,
Cambridge CB2 3EQ, UK. (ga307@cam.ac.uk)

² Department of Geological and Environmental Sciences, Ben
Gurion University, Beer Sheva 84105, Israel.

³ Israel Oceanographic and Limnological Research, National
Institute of Oceanography, Haifa 31080, Israel.

Methane production is driven mostly by microbially mediated methanogenesis. In marine sediments, this naturally produced methane is almost entirely consumed by anaerobic methane oxidation (AOM) coupled to bacterial sulfate reduction (BSR). This coupling between AOM and BSR remains enigmatic. We use the sulfur and oxygen isotope composition of aqueous sulfate ($\delta^{18}\text{O}_{\text{SO}_4}$ and $\delta^{34}\text{S}_{\text{SO}_4}$ respectively) consumed through AOM to further our understanding of this critical microbially-mediated process. We focus on highly stratified estuaries in the coastal area of Israel (the Yarkon and the Qishon). At these sites, sulfate is rapidly consumed and methane concentrations subsequently increase suggesting a coupling between sulfate and methane consumption.

Although the pore fluid geochemistry (e.g. sulfate and dissolved inorganic carbon concentration profiles) are similar at the studied sites, the isotope geochemistry (e.g. the $\delta^{34}\text{S}_{\text{SO}_4}$, $\delta^{18}\text{O}_{\text{SO}_4}$, and $\delta^{13}\text{C}_{\text{DIC}}$ in the pore fluid and the $\delta^{34}\text{S}$ of the sedimentary pyrite) is fundamentally different among the sites. Because the sulfur and oxygen isotopes in pore fluid sulfate are indicative of the relative intracellular fluxes of sulfur intermediates during BSR, we conclude that the isotope geochemistry require that the mechanism of BSR differs among the studied sites and in different sulfate-methane transition zones. We use a model for the various intracellular steps during BSR to explore what may cause these differences. We conclude that the geochemical interpretation of these sites may underrepresent the processes occurring in the subsurface as suggested by the isotope data. This suggests that recycling of sulfur intermediates may be fundamentally different in BSR coupled to AOM than when coupled to standard organic matter oxidation.

Groundwater contamination potential - vulnerability assessment

I.M.H.R. ANTUNES¹, M.T.D. ALBUQUERQUE¹
AND S.F. OLIVEIRA¹

¹Polytechnic Institute of Castelo Branco, Portugal,
(imantunes@ipcb.pt;teresal@ipcb.pt;
sandrinfidalgo@ipcb.pt)

Águeda watershed is a sub-catchement of the Douro river (northern Portugal) and it is distributed on both Spanish and Portuguese territories. The main core of this work is the achievement of a methodological tool able to be used for vulnerability assessment in transboundary watersheds.

Groundwaters' vulnerability mapping was carried out by two different methodological approaches: DRASTIC and DRASTIC Pesticide [1].

DRASTIC is a numerical index derived from ratings and weights assigned to seven parameters – Deep to water, net Recharge, Aquifer media, Soil media, Topography, Impact of the vadose zone and hydraulic Conductivity. The obtained values raises between 23 (not vulnerable) to 230 (highly vulnerable). Drastic Pesticide uses the same parameters with the reassignment of attributes' weights to stress the importance of agricultural activities.

DRASTIC's map for Águeda watershed shows three spatially distributed vulnerability classes: low (102 - 119), moderate (120 - 139) and moderate to high (140 - 154). The low vulnerable zones occupy almost 78% of the all area while the moderate vulnerable zones correspond to 21% of the remaining area. The moderate to high vulnerable zones represents less than 1% of the total area and it is localized in the central part of the Águeda watershed overlapping the tertiary sedimentary aquifer and the mostly populated area.

DRASTIC Pesticide map shows four spatially distributed vulnerability classes: low (120 - 139), low to moderate (140 - 159), moderate to high (160 - 179) and high (180 - 195). The high proportion increases considerably in the central zone of the Águeda watershed representing more than 20% of the land parceling.

Although similar hydrogeological intrinsic characteristics are observed in the central watershed's area obvious differences can be stressed when anthropogenic activities are taken into consideration. Feasibility studies and the development of specific monitoring activities must be addressed in future work.

[1] Aller L, Bennet T, Lehr JH, Petty RJ, Hackett G. 1987. DRASTIC: a standardized system for evaluating ground water pollution potential using hydrogeologic settings. EPA/600/2-87/035, U.S. Environmental Protection Agency, Ada, Oklahoma, 641 pp.

Selective Cs sorption in biotite on granite

Y. AOI¹, K. FUKUSHI¹, T. MORISHITA¹ AND A. KAMEI²

¹Kanazawa University, Kanazawa, Japan,

²Shimane University, Shimane, Japan

(aoi9856@stu.kanazawa-u.ac.jp presenting author)

The radiocesium released from the Fukushima Daiichi nuclear power plant is retained at the surface soils around the power plant (Tanaka *et al* 2012). Abukuma granite distributes in the most of the affected areas. Therefore, the contaminated soil minerals has been originated from Abukuma granite (e.g. Kamei *et al* 2003). Mica and/or vermiculite are thought to be the one of the candidate for the host phases of radiocesium. It is reported these hardly desorped radiocesium (Qin *et al* 2012). The purpose of the present study is to elucidate of Cs sorption mechanism of biotite in Abukuma granite.

The thin section made from Abukuma granite was soaked in the solution containing 10 μ M Cs⁺ in 0.01 M NaCl solution at pH 4, 5 and 6 for 24 hours. The thin sections after the reaction with Cs were analyzed by means of electron probe micro analyzer (EPMA).

Abukuma granite was composed of quartz, plagioclase, feldspar, amphibole, biotite and chlorite. Chlorite is alteration products from biotite. Among these minerals, Cs distribution was observed only in biotite.

According to the quantitative analysis by EPMA, biotite contains Cs up to 6.7 wt%. Biotite accumulated Cs several tens of thousands times than that of Cs in solution. The Cs concentration in biotite was negatively correlated with K concentration in biotite. These observations suggested that Cs selectively sorbs on biotite in granite and the sorption mechanism is considered to be the cation exchange reaction in the inter layer of biotite.

[1] H. Qin, Y. Yokoyama, Q. Fan, H. Iwataki, K. Tanaka, A. Sakaguchi, Y. Kanai, J. Zhu, Y. Onoda and Y. Takahashi, *Geochemical Journal*, Vol. **46**, pp. 297 to 302, 2012 [2] K. Tanaka, A. Sakaguchi, Y. Kanai, H. Tsuruta, A. Shinohara, and Y. Takahashi, *J. Radioanal. Nucl. Chem.*, in press. A. Kamei, T. Takagi, K. Kubo, *Geol. Surv. Japan*, vol. **54**, p.395 – 409, 10 figs., 2 appendix tables.

Geology, lithostratigraphy and geochemistry of the oldest Eoarchean BIFs, Northern Labrador

S. AOKI^{1*}, M. SHIMOJO¹, S. SAKATA², S. YAMAMOTO¹, A. ISHIKAWA¹, T. HIRATA² AND T. KOMIYA¹

¹Earth Science and Astronomy, the University of Tokyo, Tokyo, 153-8902, Japan *shogo@ea.c.u-tokyo.ac.jp

²Laboratory for Planetary Sciences, Kyoto University, Japan

Banded Iron Formation (BIF) is chemical sediment, which is a key of deciphering chemical evolution of seawater throughout the Precambrian. However, there are found only few pre-3.6 Ga BIF: the 3.71-3.83 Ga Isua supracrustal belt and Akilia Island, >3.75 Ga Nuvvuagittuq supracrustal belt and the Nulliak supracrustal belt, respectively. Recently, reassessment of zircon U-Pb dating suggested that the Nulliak supracrustal belts were formed >3.9 Ga [1]. This work presents the geology and geochemistry of the oldest BIF in the earth, in the Nulliak supracrustal belts, Labrador.

Geology and lithostratigraphy shows that there are two types of BIFs in the area: thin BIF layers associated with mafic rocks and BIF layers interlayered with carbonate rocks, respectively. The former is typical Algoma-type BIF, common in the Eoarchean supracrustal belts. The latter is also thin and sporadically distributed in the area, similar to the Superior-type BIF but its lithostratigraphy is similar to the Algoma-type BIF, uncommon in the Eoarchean BIF. Mineral assemblages of the BIFs are similar each other, and comprises magnetite + quartz + actinolite + cummingtonite, which are typical of amphibolite facies assemblages for BIFs.

PAAS-normalized rare earth elements plus yttrium distribution diagrams (REY_{SN}) of the BIFs exhibit positive La_{SN} + Y_{SN} anomalies, super-chondritic Y/Ho values and LREE, MREE depletion relative to HREE. The geochemical characteristics are shared with modern seawater. In addition, the REY patterns lack negative Ce anomaly whereas display large positive Eu anomaly, suggesting reduced and hydrothermal fluid-influenced seawater. On the other hand, their high abundances of Al₂O₃ and HFSE contents suggest that detritus input was common in the sedimentary environments of the Nulliak supracrustals. In addition, their high abundances of Ni and Zn contents (>50 ppm) indicate that the >3.9 Ga seawater was enriched in the transitional metals due to high hydrothermal activities or alteration of (ultra)mafic crusts, analogous to the Archaean BIFs [2].

[1] Shimojo *et al.*, (2013), *Mineral. Mag.*, this volume. [2] Konhauser *et al.*, (2009), *Nature* **458**, 750-753.

Microbial activity below the Iheya North deep sea vent constrained by quadruple sulfur isotopes

SHINNOSUKE AOYAMA^{1*}, MANABU NISHIZAWA²,
KEN TAKAI² AND YUICHIRO UENO^{1,2,3}

¹Department of Earth and Planetary Sciences, Tokyo Institute of Technology

(*correspondence: aoyama.s.ab@m.titech.ac.jp)

²Precambrian Ecosystem Laboratory, Japan Agency for Marine-Earth Science and Technology (JAMSTEC)

³Earth-Life Science Institute, Tokyo Institute of Technology

Sulfate reduction is the predominant microbial metabolisms in the seafloor environment. The sulfate reduction is generally slow due to the limitation of substrates under the stationary seafloor. On the other hand, hydrothermal system may host active microbial sulfate reduction possibly due to the water circulation. In 2009, a drill ship "CHIKYU" drilled Iheya North hydrothermal system in the Okinawa Trough. For evaluating the sulfate reducing activity, we analysed sulfur isotopes (³²S/³³S/³⁴S/³⁶S) of pore water sulfate and mineralized sulfide extracted from the core samples. The observed ³⁴S-enrichment and decreased sulfate concentration in the upper and intermediate section suggest sulfate reduction took place below the seafloor. On the basis of our model calculation, apparent isotope effect ³⁴ε is estimated to be -21‰ and the occurrence of sulfate reduction is only in the upper part of the seafloor hydrothermal system, that is the recharge zone of seawater. The observed fractionation together with the slight Δ³³S enrichment all indicate that the sulfate reduction is not thermochemical process but microbial process with high reaction rate. Also, roughly ~50% of mineralized sulfide is estimated to have been deposited from microbial reduction below the seafloor. The rapid seawater circulation in the Iheya North hydrothermal system may be critical to support active microbial sulfate reduction below the seafloor.

A database for calculating geochemical reactions of CO₂ and gas mixtures at high (P, T, salinity)

C.A.J. APPELO^{1*} AND D.L. PARKHURST²

¹Hydrochemical Consultant, Amsterdam NL

(*correspondence: appt@hydrochemistry.eu)

²US Geol Survey, Denver, Co, USA, dlpark@usgs.gov

For calculating gas properties at high pressure an equation of state for gases [1] was programmed in PHREEQC, version 3 [2]. The solubility can be calculated from the fugacity coefficient of the gas and its aqueous molar volume, with accurate results in solutions of various salinities up to 1000 atm and 200°C.

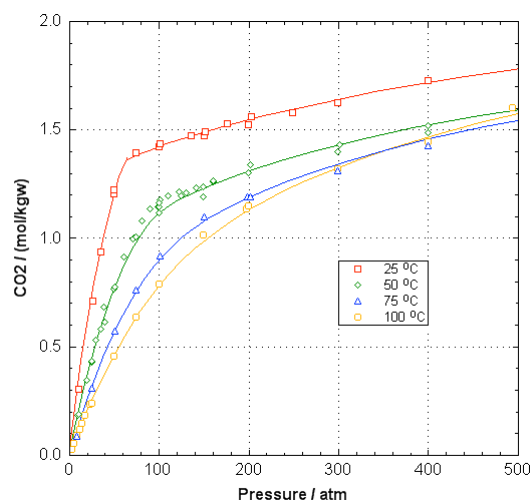


Figure 1. Solubility of CO₂ in pure water as a function of pressure, 25-100°C. Data from literature, lines from PHREEQC.

For modeling gas solubilities and mineral scales at high *P-T* and saline conditions, Pitzer.dat was adapted [3, 4].

[1] Peng and Robinson (1976) *Ind. Eng. Chem. Fund.* **15**, 59-64. [2] http://wwwbr.cr.usgs.gov/projects/GW-C_coupled/phreeqc/index.html [3] Pabalan and Pitzer (1987) *GCA* **51**, 2429-2443. [4] Holmes and Mesmer (1986) *JSC* **15**, 495-517.

Carbonate mineralisation in the supergiant Olympic Dam deposit

O.B. APUKHTINA^{1*}, V.S. KAMENETSKY¹ AND K. EHRIG²

¹CODES, UTAS, Hobart, Tasmania 7001, Australia

(*correspondence: olgaa@utas.edu.au)

²BHP-Billiton, GPO Box 1777, Adelaide, SA 5001, Australia

The supergiant polymetallic Olympic Dam (OD) deposit is characteristically enriched in carbonate minerals. The relationships between carbonates and other minerals (hematite, magnetite, pyrite, Fe-Cu sulfides, uranium minerals), as well as the source of carbon remain unresolved.

OD is a breccia complex within the Mesoproterozoic granite that was intruded by ultramafic and mafic dykes. The ore minerals are associated with gangue minerals such as barite, fluorite, quartz, apatite and carbonates. Carbonate minerals occur in the association with the sulfides (particularly chalcopyrite) and gangue minerals.

Carbonates in the deposit increase in concentration towards the edges and at depth. REE-fluorocarbonates (e.g. bastnäsite-(Ce), synchysite-(Ce)) postdate the most common Ca-Mg-Fe-Mn carbonate minerals (siderite, calcite, dolomite-ankerite ss).

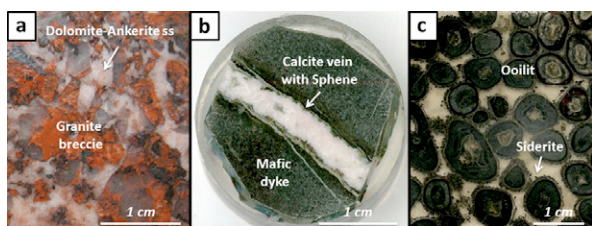


Figure 1: Some examples of carbonate textures.

In most cases carbonates appear as veins in different lithologies (mafic dykes, granite, mineralised breccia, figs. 1a,b) and rarely as oolitic rocks (fig. 1c). In addition, many carbonates occur in brecciated rock both as clasts and breccia cement (fig. 1a), providing evidence for numerous faulting and breccia-forming events. Various textures of carbonate-bearing rocks imply carbonate deposition in several stages.

The relative age of different carbonate generations based on dating of associated minerals (apatite, titanite, rutile, monazite) and $\delta^{13}\text{C}$ and $\delta^{18}\text{O}$ isotope signatures will be presented at the conference.

Reconstruction of redox conditions during deposition of Jordan oil shale using inorganic geochemical records

S. AQLEH^{1*}, S. VAN DEN BOORN², O. PODLAHA²,
C. MÄRZ¹, T. WAGNER¹, S. W. POULTON³
AND S. KOLONIC⁴

¹Newcastle University, School of Civil Engineering and Geosciences, UK (Correspondance: s.aqleh@ncl.ac.uk)

²Shell Global Solution, Rijswijk, The Netherlands

³University of Leeds, School of Earth and Environment, UK

⁴Jordan Oil Shale Company B.V., Amman, Jordam;
New adress: SPDC of Nigeria Ltd., Nigeria

With the global rise in petroleum demand the pressure on finding conventional hydrocarbon resources has increased substantially and has led to a shift in focus from conventional to unconventional resources. The situation is particularly precarious for Jordan as it imports ~97% of its current energy needs, which underlines the importance of finding alternative energy resources within Jordan and explains the increased focus on the huge reserves of oil shale in the country which exceed 65 billion tons [1]. Oil shales are characterized as thermally immature packages of fine-grained organic-rich sediments that require artificial heating to generate hydrocarbons [2].

Here we present an inorganic geochemical study of thick sections of oil shale from two neighbouring core-holes in Central Jordan. Bulk geochemical records (total sulphur, total carbon and total organic carbon) along with inorganic geochemical proxies (Fe sequential extraction and trace metals) are used to reconstruct the paleodepositional environment of the oil shale, with special emphasis on understanding the mechanisms behind high-frequency and high-amplitude variations in TOC content that characterize these deposits. The proxy records show that TOC and S_{total} vary in phase but exhibit high amplitude variability, while carbonates contribute the largest fraction to the sediments. Trace metal and Fe speciation data indicate that the depositional environment fluctuated between anoxic and euxinic conditions. The strongest enrichment in redox sensitive trace metals (e.g. Mo and V) and TOC occur in euxinic sediments. The subtle fluctuations in oxygen deficiency at the reducing end of the redox scale are believed to exert an important control on organic matter enrichment and quality.

[1] Alali, J. (2006). International Conference on Oils Shale: "Recent Trends in Oil Shale", Amman, Jordan. Paper no. Rtos-A1. [2] Dyni, J. R. (2003). *Oil Shale*. **20**, 193–252.

Diagenetic mobilisation of Fe and Mn in hydrothermal sediments

ALFRED AQUILINA¹, WILLIAM B. HOMOKY¹,
LAURA E. HEPBURN¹, SETH G. JOHN², TIMOTHY M.
CONWAY², TIMOTHY LYONS³ AND RACHEL A. MILLS^{1*}

¹Ocean and Earth Science, National Oceanography Centre
Southampton, University of Southampton, SO14 3ZH, UK
(*correspondence: rachel.mills@soton.ac.uk,
alfred.aquilina@soton.ac.uk, w.homoky@soton.ac.uk,
laura.hepburn@soton.ac.uk).

²Department of Earth and Ocean Sciences, University of South
Carolina, Columbia, SC29208, USA (sjohn@geol.sc.edu,
tconway@geol.sc.edu).

³Department of Earth Sciences, University of California,
Riverside, 900 University Ave. Riverside, CA 92521,
USA (timothy.lyons@ucr.edu).

The Bransfield Strait is a tectonically-active marginal basin between the Antarctic Peninsula and the South Shetland Islands. We present data linking diagenetic metal cycles to hydrothermal activity on *Hook Ridge*, a submarine volcanic edifice in the Central Basin. Water column E_h -anomalies, visual observation of fluid flow at the seafloor, and pore-fluid chemistry confirm hydrothermal activity on *Hook Ridge* [1]. Concentration-depth profiles of NO_3^- , Mn^{2+} and Fe^{2+} indicate early stage, suboxic diagenetic reactions. However, compared to a nearby reference site, the sediment surface at *Hook Ridge* is enriched in solid phase Fe (reactive oxides and carbonates) and Mn, and underlain by elevated pore-fluid Fe and Mn content (Fig. 1).

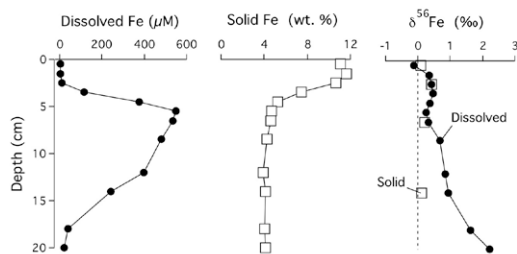


Figure 1. Down-core concentration and isotope composition of Fe in sediments and pore-fluids from *Hook Ridge*.

The isotope composition of dissolved pore-fluid Fe maxima ($\delta^{56}\text{Fe}_{\text{dissolved}} = +0.29 \pm 0.05 \text{‰}$) is similar to the solid phase isotope composition ($\delta^{56}\text{Fe}_{\text{solid}} = +0.21 \pm 0.15 \text{‰}$; Fig. 1), and distinct from light values that typify reductive Fe dissolution. Deeper dissolved Fe isotope compositions are consistent with Fe-sulfide reactions. Hydrothermal sediments are routinely overlooked as a significant source of metals to seawater, but *Hook Ridge* sediments indicate vigorous diagenetic mobilisation and enrichment of Fe and Mn with potential to impact Fe-limited primary production in the Southern Ocean.

[1] Aquilina *et al* (2013), PLoS One, 8(1) e54686

Distribution, correlation and health risk assessment of heavy metal contamination in surface soils around an industrial area, Hyderabad, India

A. KESHAV KRISHNA¹ AND K. RAMA MOHAN²

¹CSIR-NGRI, Habsiguda, Uppal, Hyderabad-500 007, INDIA
(* correspondence: keshav_krishna@ngri.res.in)

²CSIR-NGRI, Habsiguda, Uppal, Hyderabad-500 007, INDIA
(kmgri@rediffmail.com)

Due to rapid industrialisation and urbanisation there has been much concern over the soil contamination with heavy metals. One such example is soils of Kazipalli (Hyderabad), India which has become a serious environmental problem. This region hosts several industrial activities which are the main source for hazardous waste which include pharmaceuticals, drugs, metal, packing, machinery and chemicals. Soil samples from fifty seven (57) sampling sites were collected from this industrial zone and were analyzed for heavy metals (HM) like As, Cr, Cu, Ni, Pb and Zn. Concentrations ranged from 4.4-796.3 mg/kg for As, 9.7-598.6 mg/kg for Cr, 7.9-183.5 mg/kg for Cu, 10.2-129.6 mg/kg for Ni, 25.3-1830 mg/kg for Pb and 23.8-879 mg/kg for Zn.

Application of factor and cluster analysis indicates that heavy metal contamination in soils originates from industrial activities which are of anthropogenic origin. Pearson's correlation analysis showed that there exists close correlations among As-Pb, Cr-Ni, Cu-Zn. Contamination of soils in the study area were further classified for geoaccumulation index (I_{geo}), enrichment factor (EF), contamination factor (CF) and contamination degree (C_{deg}). The values of pollution index (PI) and integrated pollution index (IPI) indicated that metal pollution levels were in order of $\text{As} > \text{Pb} > \text{Cu} > \text{Cr} > \text{Zn} > \text{Ni}$. Potential ecological risk indices (PERI, RI) showed the area suffered with high As contamination, followed by Cr, Cu, Pb, Ni, and Zn. The health risk assessment based on average daily doses (ADD) of individual elements were calculated using exposure parameters and reference doses from integrated databases of USEPA. Further, the average levels of chronic and carcinogenic risk based on hazard quotient (HQ) and hazard index (HI) are presented in the form of stock plots and tables. These results are important for the development of proper management strategies to decrease point and non-point source of pollution by different remediation methods.

Ancient fragments in the subcontinental lithospheric mantle beneath the Carpathian-Pannonian Region

LÁSZLÓ ELŐD ARADI^{1*}, CSABA SZABÓ¹, JOSE MARIA GONZALEZ-JIMENEZ², WILLIAM GRIFFIN², SUZANNE Y. O'REILLY² AND KEIKO HATTORI³

¹Lithosphere Fluid Research Lab, Eötvös University, Hungary

²CCFS/GEMOC, Dept. of Earth and Planetary Sciences, Macquarie University, NSW 2109, Australia

³Department of Earth Sciences, University of Ottawa, Canada

*correspondance: aradi.laszloelod@gmail.com,

http://lrg.elte.hu

The Carpathian-Pannonian region (CPR) was formed by lithospheric extension accompanied by mantle flow and upwelling in the Neogene. Plio-Pleistocene alkali basalts brought fragments of the lithospheric mantle at five places in the CPR: Styrian Basin (Austria, Slovenia), Little Hungarian Plain, Bakony-Balaton-Highland (Hungary), Nógrád-Gömör (Hungary, Slovakia) and Perșani Mountains (Romania).

Several sulfide-bearing lherzolite xenoliths from the CPR were chosen to determine their PGE-distribution and Re-depletion ages (T_{RD}). Both whole-rock and *in situ* analyses show fractionated PGE patterns, which are controlled by partial melting of the upper mantle indicated by the correlation between Al_2O_3 and IPGE/PPGE. This is also supported by the major- and trace- element contents of the rock-forming minerals. *in situ* PGE analyses on sulfide grains show high and variable abundances of Os, Ir, Ru and Rh, with decreasing abundance from Rh to Au and a strong negative Pt anomaly. The total concentrations of PGEs range between 4 and 796 ppm.

The Re-depletion model ages range from near-zero to 1.6 Ga. Most of the T_{RD} ages are older than the oldest (Paleozoic) crustal rocks of the CPR. The main peaks at 0.6-0.8 Ga could be related to the breakup of Rodinia. The remainder of the model ages scatter between 0.95 and 1.35 Ga, which are probably related to the amalgamation of Rodinia. Outliers as old as 1.6 Ga (from Nógrád-Gömör) suggest that the subcontinental lithospheric mantle beneath the region may contain ancient domains dating from the assembly and breakup of the Columbia supercontinent, but these have been overprinted by numerous metasomatic events.

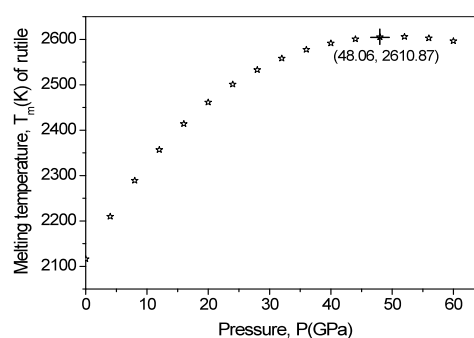
This research was funded by the Hungarian Science Foundation (OTKA, 78425 to Cs. Szabó).

Melting of Rutile under Pressure

S. ARAFIN, R. N. SINGH, YOUSUF AL-SAIDI AND A.K. GEORGE

Physics Department, College of Science, Sultan Qaboos University, Box:36, Al-Khouth 123, Oman

Rutile is one of the polymorphs of TiO_2 . Out of the total mass of the Earth's crust, amount of rutile found in nature ranges from 0.5% at the upper crust to 0.8% at the bottom crust [1]. It is used in photovoltaic devices, integrated wave guides, gas and humidity sensors, and solar cells. Research on rutile is important to earth scientists because a complete understanding of the composition and thermal state of the Earth's interior depends on information about the elastic properties of this mineral at high pressure and temperature [2].



Information on pressure dependence of the melting temperature of rutile is scanty. Fritz [3] has measured the pressure dependences of the six elastic constants of single-crystalline rutile (TiO_2) by using ultrasonic techniques and a pressure range of 0–2 GPa. We present here pressure dependence of the melting temperature and thermophysical properties such as enthalpy, viscosity and diffusivity of rutile using a semi-empirical approach based on Lindemann's law. The pressure range used in the present study is 0–60 GPa. Our preliminary results show that the melting maximum of rutile is 2610 K and it occurs at 48 GPa.

- [1] Rudnick, R.L. and Fountain, D.M., 1995, *Rev. Geophys.*, **33**(3), 267-309 [2] Isaak, D.G., Carnes, J.D., Anderson, O.L., Cynn, H. and Hake, E., 1998, *Phys Chem Minerals*, **26**, 31-43. [3] Fritz I.J., 1974, *J. Phys. Chem. Solids*, **35**, 817-826.

Secular change of the chromite concentration process from the Archean to Phanerozoic

S. ARAI^{1*} AND A.H. AHMED^{2,3}

¹Kanazawa Univ., Kanazawa 920-1192, Japan

(*Correspondence: ultrasa@staff.kanazawa-u.ac.jp)

²Geology Dept., Helwan Univ., Cairo, Egypt

³Fac. Earth Sci., King Abdulaziz Univ., Jeddah, Saudi Arabia
(ahmh2jp@yahoo.com)

We examine the secular change of properties of podiform chromitites and their host peridotites to understand the evolution of the upper mantle through Earth's history. Podiform chromitites are very rare in the Archean ophiolites. They got gradually abundant in ophiolites from the early Proterozoic to the Phanerozoic. The size of chromitite pods is mostly small (1 to 20 m x 0.5 to 3 m) in the Precambrian ophiolites, while remarkably larger (up to hundreds meters x several tens of meters) in the Phanerozoic ophiolites. The Archean chromitites show a very restricted and highly refractory composition of chromian spinel: Cr# [Cr/(Cr + Al)] from 0.74 to 0.93 and TiO₂ content less than 0.3 wt%. The Cr# of spinel in the host harzburgite is also high, around 0.7. In the late Proterozoic ophiolites, podiform chromitites are much more abundant than in the Archean and early Proterozoic ones. Al-rich chromitite varieties started to appear in the late Proterozoic ophiolites, although the majority are Cr-rich.

Podiform chromitites are very common and large in size in the Tethyan ophiolites of the late Paleozoic to Mesozoic age. Their host mantle peridotites have a wide range of spinel composition with an intermediate Cr#, around 0.5, serving as the most common host for large podiform chromitites in the Phanerozoic ophiolites. With a few exceptions all known Phanerozoic ophiolites have less refractory peridotites and chromitites than the Precambrian ophiolites. Diversity in chromian spinel chemistry and PGE contents in podiform chromitites become more distinct in the Phanerozoic ophiolites.

If the tectonic setting of ophiolite formation has been kept the same, the distribution of Cr within the mantle to crust has been changed possibly with time. Larger amounts of Cr were possibly transported to the crust by high-degree partial melts and concentrated as the stratiform chromitite in the Precambrian, and, in contrast, have been stored as the podiform chromitite within the mantle as podi in younger times in the Earth's history.

Archean regional metamorphism of the 3.8-3.7 Ga Isua Greenstone Belt, SW Greenland: Geothermal gradient of the Archean subduction zone and implication for global carbon cycle

T. ARAI^{1*}, S. OMORI², T. KOMIYA³
AND S. MARUYAMA^{4,1}

¹Department of Earth and Planetary Sciences, Tokyo Institute of Technology, Tokyo 152-8551, Japan

(*correspondence: arai.t.am@m.titech.ac.jp)

²The Open University of Japan, Chiba 261-8586, Japan

³University of Tokyo, Tokyo 153-8902, Japan

⁴Earth-Life Science Institute, Tokyo Institute of Technology, Tokyo 152-8551, Japan

The 3.7-3.8 Ga Isua Supracrustal Belt (ISB), southwest Greenland, constitutes the oldest accretionary complex on Earth [1]. Detailed microscopic and microprobe analyses of metabasites in the area revealed that the western ISB underwent regional metamorphism from lower to upper amphibole facies, which record subduction-related progressive metamorphism [1]. Analysis of isochemical phase diagram of the metabasites quantitatively estimated the Archean geothermal gradient along the subducting plates as an intermediate P/T-type metamorphic series. In addition, the correlation of the modal abundance of carbonate minerals in the MORB-related metabasites with its metamorphic grade suggests that the carbonate minerals were formed prior to its subduction at the convergent boundary. Subduction of carbonated oceanic crusts is considered as one of the main mechanism to reduce the atmospheric CO₂ [2]. Previous works reported that the less metamorphosed 3.1 Ga Archean MORB in Pilbara Craton, Western Australia, contain 30 vol% of carbonate minerals on average, due to the hydrothermal carbonation reaction with the CO₂-rich Archean seawater at the mid-ocean ridge [2], whereas 3.8Ga Archean MORB in the study area rarely contain carbonate minerals. Comparison of the Archean geothermal gradient and stability fields of carbonate minerals of the metabasite suggests that most of carbonate minerals in the oceanic crusts could not have been stably transported into the mantle under the geothermal gradient. The line of evidence indicates that most of the carbonate minerals trapped in the oceanic crusts could have returned to the surface at the subduction zone at least in the Archean 3.8Ga even though the Archean oceanic crusts were highly carbonated.

[1] Komiya *et al* (1999) *Journal of Geology* **107**, 515-554.

[2] Shibuya *et al* (2012) *EPSL* **321-322**, 64-73.

The role of brines in metamorphism and anatexis

L.Y. ARANOVICH

Institute of Geology of Ore Deposits RAS, 119017 Moscow, Russia (lyaranov@igem.ru)

A number of observations point to a potentially wide participation of brines in high grade metamorphic processes. Those are findings of alkali and alkali earth halides as daughter crystals in fluid inclusions; appreciable amount of Cl measured in granite melt inclusions in minerals and direct observations on high temperature halides present in intergranular space in the high grade rocks [1]. Thermodynamic mixing properties of concentrated water-salt fluids at high P-T differ greatly from those of water-non-polar gas mixtures: the former are characterized by a large negative deviation from ideal solutions [2], while the latter exhibit positive deviation from ideality. This difference has two major petrologic implications: unlike water-gas fluids, the presence of brines strongly increases melting temperature of quartzofeldspathic rocks and decreases dehydration of water-bearing minerals. Operation of brines may help to resolve the “granulite paradox”: extensive dehydration without hole-sale melting. New experimental results [3] show that there is a large range of P-T space in which subsolidus deep crustal metasomatism may take place at low H₂O activity via migrating fluids. Brines may implant K₂O and silica into the mid-crust and thus condition it for anatexis. Brine-assisted anatexis differs greatly from rock melting in pure H₂O or in CO₂-H₂O fluids. Large changes in feldspar compositions in equilibrium with melts can result from small shifts in fluid compositions. Contours of constant fluid H₂O on the solidus minimum (H₂O isopleths) have strongly positive dP/dT slopes. As a consequence, rising accumulations of granitic magma may be fluid saturated and even increase their melting capacity with decreasing depth because of the great pressure dependence of H₂O activity in salt solutions. These results offer an explanation for mid-crust migmatization and granite production: rising hot brines may provoke rock melting at some threshold of decreasing depth in the range 15-20 km. Because of their enhanced capacity for metasomatism, leading to eventual melting at appropriate conditions of temperature, pressure and H₂O activity, concentrated brines should be considered as possibly important agents in crustal evolution.

- [1] Markl & Bucher (1998) *Nature* **391**, 781-783.
 [2] Aranovich & Newton (1996) *Contrib. Mineral. Petrol.* **125**, 200-212. [3] Aranovich *et al* (2013) *EPSL* (submitted).

The origin of lithium in playas in Nevada, USA: Constraints by lithium isotope ratio

D. ARAOKA^{1*}, H. KAWAHATA¹, T. TAKAGI²,
 Y. WATANABE², K. NISHIMURA³ AND Y. NISHIO⁴

¹AORI, The University of Tokyo, Japan

(*correspondence: araoka@aori.u-tokyo.ac.jp)

²National Institute of Advanced Industrial Science and Technology (AIST), Japan

³Japan Agency for Marine-Earth Science and Technology (JAMSTEC), Japan

Lithium is an industrially useful element with extremely low reduction potential whose compounds are used in many ways, especially in secondary lithium-ion batteries. Highly concentrated lithium resources are often formed in salt crusts and playas by evaporative enrichment, and lithium-rich brine in playas is a major raw material for lithium production. Moreover, lithium isotopic ratios ($\delta^7\text{Li}$) have recently been identified as a tool for investigating water-rock interactions [1, 2]. Thus, to determine the origin of lithium in playas, we conducted leaching experiments to evaluate the effect of leaching processes on $\delta^7\text{Li}$. Then we determined lithium and strontium isotopic ratios and contents and trace element contents of various lacustrine and evaporite deposit samples collected from playas in Nevada, USA. In samples from the playas, $\delta^7\text{Li}$ values were much lower than those in river water [3] and groundwater samples [1] from around the world, but they were close to those of upper continental crust [4]. On the basis of temperature dependence of lithium isotope fractionation during water-rock interactions [5], these results indicate that the highly concentrated lithium in playas was supplied mainly through high-temperature water-rock interactions associated with local hydrothermal activity and not directly by low-temperature weathering of surface materials. This study, which is the first to report lithium isotopic compositions in playas, demonstrated that $\delta^7\text{Li}$ may be a useful tracer for determining the origin of lithium and evaluating its accumulation processes in playas.

- [1] Tomascak (2004) *Rev. Mineral. Geochem.* **55**, 153-195. [2] Tang *et al* (2007) *Int. Geol. Rev.* **49**, 374-388. [3] Misra & Froelich (2012) *Science* **335**, 818-823. [4] Teng *et al* (2004) *Geochim. Cosmochim. Acta* **68**, 4167-4178. [5] Wunder *et al* (2006) *Contrib Mineralog Petrol* **238**, 277-290.

Application of CSIA for evaluating the fate of chlorinated compounds in low permeability sediments

R. ARAVENA^{1*}, B. L. PARKER², G. LIMA³, S. CHAPMAN⁴
AND D. ADAMSON⁵

¹University of Waterloo, Waterloo, Ontario, Canada

(*correspondence : roaraven@uwaterloo.ca)

^{2,4}University of Guelph, Guelph, Ontario, Canada

³University of Toronto, Toronto, Ontario, Canada

⁵GSI Environmental, Houston, Texas, USA

Clayey and silty aquitards are natural barriers that can protect aquifers at sites impacted by DNAPL contamination, with the degree of protection depending on geologic, hydrogeologic and geochemical characteristics. The most effective aquitards are those in which contaminant transport is diffusion controlled, provided the aquitard is sufficiently thick (>20 ft or so) to prevent diffusive breakthrough. If the aquitard is thin but unfractured, upward hydraulic gradients and/or chemical or biological degradation may be required to prevent diffusive breakthrough. The purpose of this presentation is to discuss the state of the art of the science relevant for evaluating processes of contaminant distribution and fate in clay aquitards with emphasis on the application of CSIA.

Two sites contaminated with chlorinated compounds were used in the investigation. A high resolution monitoring network, aquitard cores, microbiological tools and CSIA were used to evaluate the distribution and fate of the contaminants in the aquifer and the aquitards.

VOC's concentration profiles showed the highest concentration of parents and daughter products are observed near the aquitard and diffusion was controlling contaminant transport in the aquitards. Much lower concentration or no VOC's were observed in the underlying aquifer at both sites. The isotope data showed that biodegradation was also controlling the VOC's concentration in the aquitard. The microbial data is also in agreement with the isotope data. Results of the detailed investigation confirmed the aquitard at both sites has apparently good integrity, therefore no or minor impact in the underlying aquifer is expected at the study sites.

Tracing perturbations in the oxygenation of the Cenozoic ocean using Molybdenum isotopes

COREY ARCHER¹, SUNE NIELSEN², KEVIN BURTON³
AND JAMES R. HEIN⁴

¹Institute of Geochemistry and Petrology, Dept. of Earth Sciences, ETH Zurich, Switzerland
(corey.archer@erdw.ethz.ch)

²Dept. of Geology and Geophysics, Woods Hole Oceanographic Institution, MA, USA

³Department of Earth Sciences, Durham University, Science Labs, Durham, UK

⁴US Geological Survey, 400 Natural Bridges Dr., Santa Cruz, CA, USA

In recent years studies of Mo and its isotopes have come to the fore as indicators of palaeoredox conditions of the Earth's atmosphere and oceans. Particular interest has focussed on tracing the evolution of the oxygenation of the atmosphere and oceans during key periods of Earth's history such as the Great Oxidation event¹, or the resultant changes in ocean chemistry during the Proterozoic Eon². By contrast few studies have focussed on changes in oceanic redox conditions through the Cenozoic, with existing data suggesting that essentially constant, and modern like redox conditions have prevailed for the last 60-70 Myr³. This observation is perhaps surprising considering evidence for substantial changes to the ocean-atmosphere system at the start of the Cenozoic^{e.g.4}.

Here we present new Mo isotope data from a well dated Pacific Ocean ferromanganese crust, potentially unique tracers of ocean chemistry, spanning the entire Cenozoic. Our data shows a small but significant 0.3‰ ($\delta^{98/95}\text{Mo}$) positive Mo isotope anomaly from modern ferromanganese crust values starting at the beginning of the Cenozoic, and lasting for much of the Cenozoic before returning to modern values. These data therefore imply a Cenozoic ocean with a heavier Mo isotope composition than the present day. The Mo isotope anomaly is consistent with the processes inferred to have caused major changes in seawater sulphur and thallium isotopes during the Early Cenozoic^{4,5}, and indicates that marine ferromanganese precipitation and organic carbon burial rates were significantly higher and lower, respectively, in the Early Cenozoic than present day.

[1] A.D. Anbar *et al*, *Science*, 2007, **317**, 1903. [2] G.L. Arnold *et al*, *Science*, 2004, **304**, 87. [3] C. Siebert *et al*, 2003, *Earth Planet. Sci. Lett.* **211**, 159. [4] U.G Wortmann & A. Paytan, 2012, *Science* **337**, 334. [5] S.G. Nielsen *et al*, 2009, *Earth Planet. Sci. Lett.* **278**, 297

Why wind energy?

CRISTINA L. ARCHER

(carcher@udel.edu)

Wind energy has a relatively minor role in our current energy mix, but it can be one of the most important players in our future energy mix. Humans are extraordinarily effective at transferring carbon from the Earth to the atmosphere, mainly for the purpose of generating useful energy. This carbon-based energy choice has impacts on the Earth's climate, from the carbon cycle to air pollution, but also on other human factors, such as population growth and GDP. Most negative impacts can be eliminated by a green economy in which energy comes from renewable sources, such as wind. Wind will be evaluated in terms of its global potential, variability, effects on climate, and limitations. Preliminary findings also suggest that offshore wind farms can provide the additional benefit of protecting coastal communities during hurricanes.

Geochemistry and mineralogy of Philippine Nickel laterite deposits

CARLO A. ARCILLA, RUSSEL ONG, MERYL CALIBO AND
CHERRISSE FERRER

National Institute of Geological Sciences, University of the
Philippines, Quezon City, Philippines,
(caloy.arcilla@gmail.com)

Increased worldwide demand for steel has led into exploitation of nickel coming from Nickel-enriched soils weathered from ultramafic ophiolites. The Philippines is the second largest producer of nickel laterites which are mostly fed into blast furnaces in China. We have conducted extensive mineralogical and geochemical studies on these laterites comprising: 1) XRD and Rietveld refinement to identify mineralogical phases of laterites, 2) sequential extraction studies to delineate phases wherein nickel is enriched preferentially and 3) major and trace element analyses of laterite stratigraphy. We find that iron oxides and hydroxides dominate the limonite phase, not clay minerals, the latter only occurring in the lower "saprolite" phases which are dominated by serpentine-type minerals. While olivine precursors dominate the peridotite bedrock of laterites, we notice that pyroxene-rich horizons give rise to higher-grade nickel laterites. Trace element analyses also reveal surprisingly enriched concentrations of some rare-earth elements and other elements (e.g. Sc, Ti, V) that are not included in payment credits for the ores.

Subduction zones as probes of mantle composition

RICHARD ARCULUS

Research School of Earth Sciences, Australian National University, ACT 0200 (richard.arculus@anu.edu.au)

On a global basis, the genesis of the majority of primitive island arc and backarc magmas is through partial melting of ultramafic parental lithologies in the mantle wedge overlying subducted lithospheric slabs. A combination of slab-derived, fluid-fluxed melting with some decompression melting are assumed to dominate these modes of magma genesis in current convergent margin settings.

The composition of fluxing agents spans a large range, including rare earth- and high field strength element-strongly depleted low-K basalts, to highly enriched high-K basalts, plus a range of high-Mg, intermediate-Si magmas including boninites and high-Mg andesites. Abundant examples of active submarine eruptions of the latter types have been sampled in the past decade in the Tonga-Lau system. Their genesis involves fluid-fluxed partial melting of highly refractory, clinopyroxene-poor parental lithologies, probably at the high temperature end of the spectrum of backarc-arc-mantle wedge thermal regimes.

The addition of fluxing agents serves as a potent probe of the lithological heterogeneity of the mantle wedge that would not otherwise be subject to partial melting given refractory mineralogical characteristics. A spectrum of basalt-to-boninite magmas with high field strength and rare earth element abundances substantially lower than the majority of primitive mid-ocean ridge basalts, occurs widely in the intra-oceanic arcs of the western Pacific. Mixing of partial melts from refractory lithologies with those generated from more fertile protoliths also appears to be widespread in the western Pacific arc-backarc systems.

Another minor but widespread arc magma type is high-Ca-Mg “ankaramites”, possibly formed through partial melting of mantle wedge orthopyroxene-free wehrlite; this protolith likely originates as sub-Moho cumulates formed during fractional crystallisation of earlier generation hydrous arc magmas.

In contrast, alkali basalt magmas including very high-K types (some are phlogopite-phyric) hosting peridotite xenoliths, with high U/Nb typical of arcs generally, are rare magma types in the western Pacific arcs, but nevertheless indicative of the existence of highly metasomatised mantle wedge sources. The spectrum of mantle lithologies tapped during magma genesis at convergent margins is plausibly an excellent guide to the compositional variability of the upper mantle worldwide.

Aqueous contamination by oxyanions. The use of Zn-Al sulphate layered double hydroxides for waste water treatment

C. ARDAU*¹, A. DAVANTES², E. DORE¹, F. FRAU¹
AND P. LATTANZI¹

¹Department of Chemical and Geological Sciences, University of Cagliari, Via Trentino 51, 09127 Cagliari, Italy
(*correspondence : carla.ardau@tiscali.it)

²LECIME, UMR7575 CNRS-Chimie ParisTech, 75005 Paris, France

Sorption is regarded as one of the most promising technologies for the treatment of waste waters, due to its efficacy and cost-effectiveness. Layered double hydroxides (LDHs) is a class of compounds with general formula $[M^{2+}_x M^{3+}_x(OH)_2](A^n)_{x/n} \cdot mH_2O$. Possible cationic and anionic associations are widely variable (e.g. $M^{2+} = Mg, Zn, Cu$; $M^{3+} = Al, Fe$; $A^n = CO_3^{2-}, NO_3^-, SO_4^{2-}$). Thanks to their large surface area, and high anionic exchange capacity, LDHs are extensively investigated for their possible use as removers of pollutant oxyanions from waters.

LDHs form spontaneously in a wide range of environments, including mine areas. Zn-Al-sulphate LDHs were found to precipitate from surface waters interacting with mine wastes [1]. Their effectiveness in attenuation of As content in NAMD (Net Alkaline Mine Drainage), observed in natural systems, was the starting point of our investigation.

Synthetic Zn-Al-sulphate LDHs were reproduced in laboratory and tested in several batch sorption experiments, first for the uptake of As and, then, for less conventional environmental oxyanion pollutants (Mo, W and Sb).

The first results in the use of these LDHs as removers of pollutant oxyanions (up to ~90% As(V); up to ~54% Mo; W and Sb work in progress) encourage further investigations. Since the affinity for LDHs strictly depends on the combination of anion charge density and size [2], a key point for sorption efficacy is the anionic form of the investigated pollutant (e.g. $H_2AsO_4^-$, $HAsO_4^{2-}$ or AsO_4^{3-}), and of potential competitors in solution (e.g. HCO_3^- and CO_3^{2-}). For some of elements (Mo), possible polymerisation phenomena must also be considered (see also Davantès *et al.*, this issue). Therefore, the optimal pH conditions must be specifically evaluated for any oxyanion and waste water composition in order to enhance the LDHs uptake efficacy.

[1] Ardau *et al.*, (2011). *N. Jb. Miner. Abh.* **188/1**, 49–63. [2] Miyata S, (1983). *Clays Clay Miner.* **31 (4)**, 305–311.

High-pressure behavior and phase transitions of thaumasite

M. ARDIT^{1*}, G. CRUCIANI¹, M. DONDI²,
G.L. GARBARINO³ AND F. NESTOLA⁴

¹Dept. of Physics and Earth Sciences, Univ. of Ferrara, 44100, Ferrara, Italy

(*correspondence: rdtmtt@unife.it, cru@unife.it)

²ISTEC - CNR, 48018, Faenza, Italy
(michele.dondi@istec.cnr.it)

³ESRF, BP 220, 38043, Grenoble Cedex, France
(gaston.garbarino@esrf.fr)

⁴Dept. of Geosciences, Univ. of Padova, 35131, Padova, Italy
(fabrizio.nestola@unipd.it)

Thaumasite, $\text{Ca}_3\text{Si}(\text{OH})_6(\text{CO}_3)(\text{SO}_4)\cdot 12\text{H}_2\text{O}$, is a rare mineral with a hexagonal structure based on cylindrical columns of $[\text{Ca}_3\text{Si}(\text{OH})_6(\text{H}_2\text{O})_{12}]^{4+}$ running parallel to the *c* axis, among which the SO_4^{2-} and the CO_3^{2-} groups are hosted. Thaumasite is unique because i) is the only known mineral stable at ambient *P-T* conditions that possesses silicon hexa-coordinated by hydroxyls; ii) is an indicator of sulphate attack in concretes (deterioration due to thaumasite formation especially occurs at subzero *T*). The thermal behavior of thaumasite has been investigated at *LT* and *HT* [1-3], and it was found that the thaumasite structure collapsed because of a severe dehydration above 417 K [3]. At all events, reports on the *HP* response of the thaumasite structure are lacking.

In this work, the *HP* evolution of the thaumasite structure was investigated using synchrotron XRPD, up to 19.5 GPa. Although during the Rietveld refinements no symmetry changes have been observed, the unit-cell decreasing with *P* is characterized by two strong discontinuities in the 1.38–3.53 GPa and 7.40–15.02 GPa *P*-ranges, respectively. Hence, three distinct compression regimes can be defined, with the thaumasite structure that retains the same $P6_3$ space group. These isosymmetric transitions occur with an increasing of the unit-cell parameters, revealing that the thaumasite structure becomes stiffer after each discontinuity. Comparing the *LT* and *HT* data from literature [1-3] with those collected under *HP* conditions, it is interesting to underline that the variation of the axial ratio *a/c* as a function of the normalized cell volume V/V_0 describes an ideal inverse relationship [4].

[1] Jacobsen *et al* (2003) *Phys. Chem. Miner.* **30**, 321-329. [2] Gatta *et al* (2012) *Am Mineral.* **97**, 1060-1069. [3] Martucci & Cruciani (2006) *Phys. Chem. Miner.* **33**, 723-731. [4] Hazen & Finger (1984) *Comparative crystal chemistry*. Wiley, New York, pp 231.

Trace element composition in a migmatite-granite complex (NW Portugal): Protolith and melting process constraints

M. AREIAS, M. A. RIBEIRO AND A. DÓRIA

CGUP/DGAOT-FCUP, Porto, Portugal
(maria.areias@gmail.com)

In NW Portugal a migmatite massif surrounding a synorogenic granite occurs within the axial zone of the Variscan Orogen. This massif includes: metatexites (patch and stromatic) and diverse granitoid rocks including: (i) diatexites, (ii) leucocratic granites, (iii) and two-mica mesocratic granites. The patch metatexites show anastomosed foliation marked by aligned Bt between grains of Qtz + Pl ± Grt_(Alm-Prp). The Grt can be total or partially replaced by Crd + Qtz + Sil. There are coarser biotite selvage skirting fibrolytic Sil + Qtz + Pl + Crd + Bt ± Kfs clusters. The stromatic metatexites have micaceous and quartz-feldspathic bands. The former contain Bt + Sil + Crd + Grt + Qtz + Pl. The latter contain large crystals of Qtz + Pl + Kfs+Bt. The diatexites have Qtz + Pl + Kfs + Bt and schlieren with Bt + Sil + Crd ± Grt. The leucocratic granitic bodies have essentially Qtz + Pl + Kfs and Bt and/or Tml clusters. The two-mica granites have Qtz + Pl + Kfs + Bt + Apt and rare schlieren of Bt + Sil ± And ± Grt ± Zrn. In all lithologies Kfs_(Or77-90) is anhedral and replaces plagioclase.

The geochemistry study shows that all granitoid rocks are peraluminous, calc-alkaline with high K. The variation in HSFE is positively related to the content of FeO_(t) + MgO and LILE don't show any correlation. The migmatites REE chondrit-normalized patterns are very similar to each other and to NIBAS standard [1]. The leucocratic granites have a REE pattern similar to leucosome, with positive Eu anomaly and variable HREE fractionation. The diatexites show variable REE fractionation and no Eu anomaly. The mesocratic granites show a REE pattern typical of two-mica granites. The enrichment in HREE is related with (i) accessory minerals retention in the melanosome, and (ii) the presence/absence of garnet in granites and leucosomes. This variations in the composition must be related to the input of accessory minerals from the protolith and the degree of melting (Bea,1996), instead of fractional crystallization or magma mixing.

Research integrated in the activities of CGUP, with financial EU funds by FEDER/OPHP and FCT and PETROCHRON project (PTDC/CTE-GIX/112561/2009).

[1] Ugidos *et al* (2010) - *Precambrian Research*, **178**, 1-4. [2] Bea, F (1996) *J. of Petrology*, **57-5**, 521-552.

Mineral abbreviations according IUGS-SCMR recommendations.

Evolution of subglacial weathering based on multiple isotopic systems

C.A. ARENDT^{1*}, S.M. ACIEGO¹, K.W.W. SIMS²,
E.A. HETLAND¹ AND E.I. STEVENSON¹

¹EES 1100 N University Ave, Ann Arbor, MI 48109-1005
(*carliana@umich.edu)

²GG 1000 E. University Ave. Laramie, WY 82071-2000

Multiple isotope systems with distinct and specific applications provide a comprehensive overview of the evolution of subglacial hydrologic pathways, and thus weathering processes, at the Athabasca Glacier, Canada. Synthesizing traditional stable isotopic analysis of $\delta^{18}\text{O}$ and δD , traditional radiogenic analysis of $^{87}\text{Sr}/^{86}\text{Sr}$ and ϵ_{Nd} , with a non-traditional application of uranium-series isotopes, allows us to quantify seasonal subglacial evolution and the impacts on weathering processes.

We apply the hydrologic tracers $\delta^{18}\text{O}$ and δD to estimate volumes and fractions of water sources to glacial discharge originating as ice, snow, and precipitation. We coupled a $\delta^{18}\text{O}$ and δD isotope-mixing model and a Bayesian Monte Carlo estimation scheme to infer the evolving water mass contributions from these three sources. We assess the extent of these water mass interactions and melt pathways with bedrock via heavy isotopes.

The length of time that subglacial water is in contact with underlying bedrock affects hydrological pathways and the magnitude of chemical interactions. Excess ^{234}U and ^{222}Rn from alpha decay depends on this residence time via their radioactive decay. Based on our newly established techniques, we find that the residence time varies by a factor of two through the melt season and is correlated with weathering fluxes. The spatial scale of weathering processes is investigated using radiogenic Sr and Nd isotopes; the age of the bedrock exposed to subglacial weathering varies systematically. The spatial variability in weathering location is revealed by the large variation in $^{87}\text{Sr}/^{86}\text{Sr}$ and ϵ_{Nd} (0.712-0.716 and 16-35, respectively). By combining these four isotope systems, we provide a quantifiable evaluation of the meltwater evolution in a polythermal glacier.

Diagnosing petroleum fractionation processes in surface and subsurface environments using GCxGC

J. S. AREY^{1,2*}, C. M. REDDY³, R. K. NELSON³,
R. CAMILLI³, D. L. VALENTINE⁴, G. D. WARDLAW⁴,
D. NABI¹, P. DIMITRIOU-CHRISTIDIS¹ AND J. GROS¹

¹Environmental Chemistry Modeling Laboratory, Ecole Polytechnique Fédérale de Lausanne, Lausanne, Switzerland (*correspondence: samuel.arey@epfl.ch)

²Eawag, Dübendorf, Switzerland

³Woods Hole Oceanographic Institution, Woods Hole, USA

⁴University of California Santa Barbara, Santa Barbara, USA

Petroleum mixtures undergo significant compositional changes when exposed to air or water. This arises when oil is spilled on the sea surface, when deposited on the sea floor, or when extracted using enhanced recovery methods.

Using GCxGC, or Comprehensive Two-Dimensional Gas Chromatography, we can quantify thousands of individual hydrocarbon constituents in oil, including many biomarkers and structural isomers. Further, GCxGC instrument retention times convey information about the phase partitioning properties of each analyzed solute, indicating its tendency to dissolve into water, volatilize into air, or remain in oil phase. Applying GCxGC together with models of environmental behavior, we can differentiate physical fractionation and biotransformation processes acting on thousands of hydrocarbon constituents in diverse surface and subsurface environments.

In this talk, I will describe diverse examples in which GCxGC allows us to disentangle volatilization, dissolution, and biodegradation processes acting on petroleum mixtures. Case studies include: oil evaporation and dissolution on the open sea; oil weathering on contaminated coastlines; fractionation of oil deposited on the deep ocean floor; and anaerobic oil biodegradation in a subsurface reservoir. An outlook into anticipated future developments is also given.

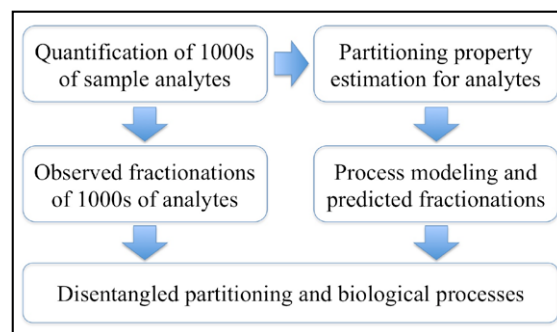


Figure 1: Elucidating fractionation processes using GCxGC.

Sorption of Pb(II) from aqueous solution by Greek attapulgite clay

A. ARGYRAKI^{1*}, P. MESSINI¹ AND V. ZOTIADIS²

¹University of Athens, Panepistimiopolis Zographou 15784 Athens Greece

(*correspondence: argyrazi@geol.uoa.gr)

²Edafomichaniki S.A., E. Papadaki 19, 14121 Athens, Greece

Attapulgite clay mined in Grevena, Greece is a readily available material with proven efficiency in the treatment of heavy metal contaminated soil [1]. Here, we present results of laboratory batch experiments aiming to compare raw and heat treated attapulgite clay for the adsorption of Pb(II) from aqueous solution.

Powdered attapulgite clay was supplied by Geohellas S.A. Samples were heat treated in muffle at temperatures of 130, 330, 500 and 800 °C for 4 hours. P-XRD analysis before and after heating at different temperature revealed that attapulgite crystal lattice gets destructed from 330 °C -a lower intensity of the main peak is observed. The comparative study of Pb adsorption efficiency of heat treated and non-treated material was performed for adsorbent dose of 2 to 15 g/L, initial Pb(II) concentration 50 mg/L, maximum shaking time 2h and pH 4. The effect of ionic strength was studied by varying the concentration of NaNO₃ from 0 to 0.5 mol/L. All experiments were carried out in a chamber set at 22 °C.

At least 90% of the metal was retained with a dose of adsorbent of 5 g/L for all tested materials while an increase in the amount of dose of adsorbent to 10 g/L reached almost 100% retention for all materials. With the exception of attapulgite clay heated at 800 °C, maximum adsorption was achieved within the first 5 minutes of reaction. A decrease in adsorption was observed as the concentration of NaNO₃ was raised probably due to competition between Na⁺ and Pb²⁺ for the adsorption sites.

Complexation and ion exchange are probably the main adsorption mechanisms at the studied pH. Heat treatment induces dehydration (zeolitic H₂O loss) at low temperatures (e.g. <150 °C) and dehydroxylation at higher temperatures (350- 510 °C), while the complete destruction of the clay occurs at temperatures over 550 °C [2]. Our data imply that significant changes in adsorption capacity of the used clay are related to alteration of nanoporosity and reduction of its specific area after calcination in temperatures > 550 °C.

[1] Zotiadis *et al* (2012) *J. Geotech. Geoenviron. Engineering* **138**, 633-637. [2] Galan and Singer (2011) *Developments in Clay Science* **3**, p.15.

Temperature determination from speleothems through fluid inclusion and clumped isotope techniques

M. M. ARIENZO^{1*}, P. K. SWART¹, S. T. MURRAY¹ AND H. B. VONHOF²

¹University of Miami, Miami FL 33149, USA

(*correspondence: marienzo@rsmas.miami.edu, pswart@rsmas.miami.edu, smurray@rsmas.miami.edu)

²Vrije Universiteit Amsterdam, Amsterdam, The Netherlands (h.b.vonhof@vu.nl)

Traditionally carbon and oxygen isotope analyses have been used to unravel the paleoclimate history of speleothems. However, the δ¹⁸O of a carbonate is dependent both on the variations in temperature and the δ¹⁸O of the water. In order to solve for the second unknown, an additional proxy is needed and such proxies include fluid inclusions, and/or clumped isotopes. Here we present results from both fluid inclusion and clumped isotope analysis on speleothems from the Bahamas.

Fluid inclusion isotope analysis is the analysis of water filled cavities in speleothems. These cavities preserve drip water at the time of formation and isotopic analysis provides information on the formation water (δ¹⁸O_w) and temperature can be calculated. Here we present a new technique utilizing cavity-ring down spectroscopy (CRDS) for δ¹⁸O and δD analysis of fluid inclusions and compare the acquired data to that measured on the Amsterdam Device, a crusher system linked with an IRMS developed at the VU University Amsterdam [1]. Our results demonstrate an average standard deviation on fluid inclusion isotopic analysis of 0.5 ‰ δ¹⁸O and 2.0 ‰ for δD, which is comparable to other IRMS fluid inclusion analytical methods [1].

In addition to fluid inclusions, clumped isotope analysis of the calcite has been conducted. Our results support an offset between the δ¹⁸O_w measured on the fluid inclusions and the δ¹⁸O_w calculated using the temperature calculated from Δ47. This is similar to the offset observed in the literature for speleothems [2]. To better elucidate the drivers of the Δ47 offset, cave monitoring has been conducted in the Bahamas, including *in situ* calcite farming. Preliminary results from the cave monitoring support an increasing Δ47 offset along a growth band for samples which are thought to precipitate in equilibrium.

[1] Vonhof *et al* (2006) *Rapid. Comm. Mass Spec.*, **20** 2553-2558. [2] Kluge, T., Affek, H. P (2012) *Quaternary Science Reviews*, **49** 82-94.

Systematic understanding of adsorption of oxyanions of Cr, Mo, and W at solid/water interfaces

D. ARIGA,¹ M. TANAKA,¹ T. KASHIWABARA²
AND Y. TAKAHASHI¹

¹Hiroshima University, (m124560@hiroshima-u.ac.jp)

²Japan Agency for Marine-Earth Science and Technology

Adsorption of trace elements on iron (oxyhydr)oxides is related to their concentrations and isotopic compositions in natural waters. Among various elements, adsorption of oxyanions of chromium (Cr), molybdenum (Mo), and tungsten (W) which are congeners have been studied here with an emphasis on chromate, because the adsorption mechanism on ferrihydrite is different between molybdate and tungstate which form outer- and inner- sphere complexes, respectively, but not evident for chromate. Therefore, fundamental understanding of the adsorption mechanisms of chromate is essential to discuss these issues. We performed (i) extended X-ray absorption fine structure (EXAFS) analysis for chromate on the three Fe (oxyhydr) oxides (i.e. ferrihydrite, goethite, and hematite), (ii) adsorption experiments of chromate on Fe (oxyhydr) oxides with different conditions of pH and ionic strength, and (iii) quantum chemical (QC) calculations to reveal difference of attachment modes (inner- or outer-sphere complexes) and surface structures such as monodentate-mononuclear, bidentate-binuclear, or bidentate-mononuclear complexes.

EXAFS analysis and adsorption experiments revealed that chromate forms almost outer-sphere complexes with slight amount of inner-sphere complexes on ferrihydrite. In contrast, most of chromate forms inner-sphere complexes on goethite and hematite. Moreover, the chromate forms mainly a bidentate-binuclear complex as inner-sphere complexes based on EXAFS analysis and QC calculations.

In addition, the QC calculation results showed that the stabilities of the hydrated species in aqueous solution and outer-sphere complex on solid surface for oxyanions may govern the determination of attachment modes of oxyanions and the distribution at the solid-water interfaces.

The experimental results of attachment mode for oxyanions will be interpreted by linear free energy relationship (LFER) using pK_{a-avg} ($= (pK_{a1} + pK_{a2})/2$) to explain the adsorption behaviors of these divalent oxyanions. We found that the LFER using the pK_{a-avg} value is essential to explain the adsorption behavior, in particular the preference of outer- and inner-sphere complexes on ferrihydrite, compared with LFER based on either pK_{a1} or pK_{a2} value.

Geological and geochemical features of the Sarıçayır (Yenice/Çanakkale) Skarn deposits

FETULLAH ARIK AND İLKUNUR AKIŞ

Selcuk University, Geological Engineering Department,
Konya, Turkey

(correspondence: fetullah42@hotmail.com)

The Sarıçayır Skarn Deposit is located around the Sarıçayır village and 70 km southwest of Çanakkale. Oligo-Miocene magmatic, metamorphic and volcanic rocks crop out in the study area. The Karakaya complex is the basement of the study area. Structural basement of the Karakaya Complex is represented by the Nilüfer unit that mostly consists of metabasic rocks. Hodul unit which is dominated by arkosic sandstones was emplaced over the Nilüfer unit. Both of the Nilüfer and Hodul units are metamorphosed to green schist facies. The units of the Karakaya complex are cut by Oligocene Karadoru granitoid and Sarıçayır alkali granites and covered unconformably by the Oligocene Çan volcanics, consist of andesitic pyroclastics and lavas.

Nilüfer and Hodul units were affected by the intrusion of Karadoru granitoid and Sarıçayır alkali granite. Contact metamorphism and skarn zones have been developed between the Karadoru granitoid and the Nilüfer and Hodul units. Contact metamorphism appears to have extended from albit-epidot hornfels to hornblend hornfels facies. Skarn zone, on the other hand, appears to have developed in the type of garnet-epidot skarn.

Skarn type mineralization was developed adjacent to Sarıçayır alkali granite contacts with the limestones belonging to Nilüfer units which are located northwest of Sarıçayır village. Also, epidote and quartz fillings are observed within fractures and faults of the Sarıçayır alkali granite [1].

Garnet, tremolite and epidote were determined in the skarn zone. Also, pyrite, chalcopyrite, sphalerite, galena, digenite and cinnabar were observed as ore minerals. Chemical data obtained from samples indicated that enrichment of the copper, lead, zinc, arsenic and iron-oxide contents. Thus Fe_2O_3 contents reach up to 57.54 % together with 60.6 ppb Au. In addition Cu, Pb, Zn, As and Ag 4656 ppm, 8101 ppm, 3700 ppm, 2500 ppm, and 8.3 ppm respectively.

[1] Arık and Akış (2011) Geological and geochemical features of Skarn Deposits Around The Sarıçayır (Yenice/Çanakkale) District, Selcuk Univ. Sci. Res. Fund. Projects, 112p,

Igneous sapphirine in Ambatomena, southern Madagascar

M. ARIMA^{1*}, K. KIMOTO¹, R. RAKOTONDRAZAFY²,
N. O. T. RAKOTONANDRASANA¹ AND
M. A. RANAIVOSON¹

¹Yokohama National University, Yokohama 240-8501, Japan
(*correspondence: arima@ed.ynu.ac.jp)

²University of Antananarivo, Antananarivo, Madagascar
(raymondrakoto@gmail.com)

Sapphirine is commonly thought to be metamorphic, and igneous sapphirine is rare [1]. We examined sapphirine-bearing intrusions of early Paleozoic age (~487 Ma) in Ambatomena, southern Madagascar [2]. The Ambatomena rocks intrude highly deformed granulite facies quartofeldspathic gneisses. The rocks consist of sapphirine, spinel, cordierite, plagioclase and orthopyroxene with subordinate amounts of ruby corundum and phlogopite. The anhedral corundum grains show melt-reaction coronas of spinel and sapphirine. The rocks contain abundant sapphirine-orthopyroxene symplectites and in some places cordierite-orthopyroxene symplectites were developed. Sapphirine grains in contact with corundum and spinel are more aluminous than the 7:9:3 composition (up to 68 wt% Al₂O₃). The sapphirine-spinel geothermometry [3] suggests equilibrium temperatures for the sapphirine-spinel paragenesis around 930~1060°C at 5 kb.

The Ambatomena assemblages represent crystallization of sapphirine and associated minerals from aluminous silica undersaturated melts at high temperatures. Petrographic features suggest the following igneous crystallization sequence; (1) crystallization of corundum from melt, (2) subsequent reaction of corundum with melt to produce spinel and sapphirine, (3) reaction of spinel with melt to form orthopyroxene and sapphirine, and (4) final crystallization of plagioclase, cordierite, and phlogopite from residual melt. This sequence is broadly comparable to the liquidus phase relations in the forsterite–diopside–anorthite–silica system reported by Liu and Presnall [4].

[1] Giovanardi *et al*, *European Journal of Mineralogy*, **25**, 17-31, 2013. [2] Giuliani *et al*, *Mineral Deposita*, **42**, 251-270, 2007. [3] Sato *et al*, *Gondwana Research*, **9**, 398-408, 2008. [4] Liu and Presnall. *Journal of Petrology*, **41**, 2-20, 2000.

Adsorption of MS2 virus to natural organic matter and model surfaces

ANTONIUS ARMANIOUS^{1*}, THÉRÈSE SIGSTAM²,
TAMAR KOHN² AND MICHAEL SANDER¹

¹Institute of Biogeochemistry and Pollutant Dynamics,
Department of Environmental Systems Science, ETH
Zurich (antonius.armanious@env.ethz.ch)

²Environmental Engineering Institute, School of Architecture,
Civil and Environmental Engineering, EPF Lausanne

Previous studies showed that viruses adsorb to natural organic matter (NOM) surfaces with varying affinities. Adsorption to NOM is an important fate process: it may affect the transport of viruses in the environment and it may enhance virus inactivation because NOM-water interfaces are reactive microenvironments. Despite its importance, virus adsorption to NOM remains poorly understood on a mechanistic level. Here, we systematically studied the adsorption of the bacteriophage MS2, a model virus, to different NOM films and to gold surfaces that were uncoated or coated with self-assembled monolayers (SAM) of alkylthiols with -CH₃, -OH, -COO⁻ and -NH₃⁺ end groups. The well-defined chemical properties of the gold and SAM allowed assessing the relative contribution of van der Waals forces, the hydrophobic effect, hydrogen bonding and electrostatic forces to MS2 adsorption. The integrities of the formed NOM and SAM films were verified by ellipsometry and contact angle measurements. MS2 adsorption was studied as a function of solution pH and ionic strength using quartz crystal microbalance with dissipation monitoring that has ng/cm² sensitivity. Negatively charged MS2 adsorbed to gold and all tested SAM surfaces except to the negatively charged carboxylate-terminated SAM surface. No virus adsorption was detected to the different NOM films at pH ≥ 5 and low ionic strength (*I* = 10 mM). Adsorption to NOM films increased with increasing ionic strength. These findings suggested that MS2-NOM electrostatic repulsion and possibly steric stabilization forces dominated over attractive interactions arising from the hydrophobic effect, hydrogen bonding, and van der Waals forces. Implications for the interactions of proteins and engineered nanoparticles with NOM will be highlighted.

Rethinking mantle geochemical heterogeneity: New insights into mantle geology

P. ARMIENTI AND D. GASPERINI

¹Dipartimento di Scienze della Terra, Università di Pisa, via S. Maria, 53, 56126 Pisa, Italy . (armienti@dst.unipi.it)

²Departament de Geoquímica, Petrologia i Prospecció Geològica, Universitat de Barcelona, Martí i Franqués s/n, 08028 Barcelona, Spain.

Classical statistical data analysis constrains the upper mantle geochemical and mineralogical complexity introducing the concept of Mantle Reservoirs. This concept is based on the underlying assumption that the mean composition of wide mantle volumes may be attained by significantly smaller representative samples. We argue that this underlying hypothesis needs to be checked and non-linear methods are able to reveal how mantle compositional heterogeneity cannot be conceived as a deviation from a mean value. Non-linear analysis methods reveal that the mutual distribution of isotope and immobile trace element of Ocean Island Basalt mantle sources mirrors the intrinsic spatial organization of the mantle revealing the systematic occurrence of strange attractors in the geochemical signals. This supports the evidence for a chaotic mantle, bridging the discrepancy between geochemical and geophysical views of mantle composition, and overcomes the impasse of the twenty years-old theories on mantle reservoirs. Our results confirm that the vertical scale of mantle heterogeneity is similar to its horizontal organization, as revealed by MORB sampled at ridge axes, and reinforces the conclusion that this structure is inherited from an ancient convection regime, probably affecting the whole mantle scale.

PTt path of rising magmas. An ascent rate meter recorded in lava volatile contents

PIETRO ARMIENTI¹ AND CRISTINA PERINELLI²

¹DST – Pisa University (armienti@dst.unipi.it)

²DST – Pisa University (c.perinelli@dst.unipi.it)

Experimental and theoretical investigations prove that the triggers of volcanic eruptions are related to the ascent rates at depth, which control the exsolution and expansion of volatile components. Volatile loss (mainly H₂O and CO₂) in turn cascade affects on a variety of parameters (crystallinity, viscosity, volume, composition) all able to strongly affect the dynamic of the ascent rate. The complex feedbacks of ascent rate and volatile content may be recorded at shallow levels by the composition of melt inclusions and at depth, by early liquidus phases which are sensible to pressure, temperature and volatile content.

Among these, pyroxene has been identified as a valid tracer of the PT path of ascent of magma providing dP/dT estimates that may be related to dZ/dt (Z=depth) through kinetic considerations on crystal growth and nucleation. The recent introduction of a clinopyroxene hygrometer now opens the possibility to relate the water content to pressure and temperature, extending at considerable depths our record of P, T, t, X_{H₂O}.

Since degassing of non ideal CO₂-H₂O mixtures is strongly non-linearly dependent on pressure, the volatile contents of lavas, as revealed by the mineralogical and melt inclusion record, can be matched by a unique PTt path that is coherent with the thermodynamic modelling of gas exsolution.

This new tool to define the PTt path of magmas is here applied to some recent eruptions of Mt Etna.

Simulating the climatic impact of Large Igneous Provinces using a mid-Miocene case-study

DAVID I. ARMSTRONG MCKAY¹, TOBY TYRRELL¹,
PAUL A. WILSON¹ AND GAVIN L. FOSTER¹

¹Ocean and Earth Science, University of Southampton
Waterfront Campus, National Oceanography Centre
Southampton, Southampton, SO14 3ZY
(correspondence: D.Armstrong-McKay@noc.soton.ac.uk)

Large Igneous Provinces (LIPs) have occurred throughout Earth's history, erupting great quantities ($>10^4$ km³) of lava in long-lived ($>10^5$ y) events that have been linked to major environmental disruptions [1]. While the largest LIP eruptions are widely considered to have had a significant impact on global climate through basalt CO₂ degassing [2–4], the impact of the more numerous smaller LIPs is disputed [5–7]. Here we test the hypothesis that LIPs had a greater impact on Earth's climate history than previously estimated because of the degassing not only of erupted basalts but also intruded, underplated and pyroxenite-enriched magma [1, 4, 8]. We use biogeochemical box models to investigate the potential impact of the Columbia River Basalts (CRB) during the mid-Miocene, as a more rigorous model-data comparison is enabled by the better palaeorecords from this relatively geologically recent event. Comparison of our simulations to palaeorecords [5, 9, 10] of mid-Miocene changes in oceanic carbonate compensation depth (CCD), $\delta^{13}\text{C}$ in benthic foraminifera and atmospheric pCO₂ suggests that an emission of ~2000–4000 Pg of carbon between ~16.2 and 15.8 Ma is required to reproduce the palaeorecords, although additional mechanisms are required to match the CCD palaeorecord beyond ~15.8 Ma. This flux is within the estimated range of potential carbon emissions when including non-extrusive sources. Our results indicate that with these additional CO₂ sources the CRB could have played a significant role in the mid-Miocene Climatic Optimum, and implies that other LIPs could have also had a greater climatic impact than currently estimated.

[1] Coffin & Eldholm (1994) *Rev. Geophys* **32**, 1–36. [2] Grard *et al* (2005). *EPSL* **234**, 207–221 [3] Paris *et al* (2012) *Clim. Past Discuss.* **8**, 2075–2110. [4] Sobolev *et al* (2011) *Nature* **477**, 312–316. [5] Foster *et al* (2012) *EPSL* **341-344**, 243–254. [6] Eldholm & Thomas (1993) *EPSL* **117**, 319–329. [7] Self *et al* (2006) *EPSL* **248**, 518–532. [8] Bryan & Ernst (2008) *Earth-Sci Rev* **86**, 175–202. [9] Pälke *et al* (2012) *Nature* **488**, 609–614. [10] Holbourn *et al* (2007) *EPSL* **261**, 534–550.

Constraining the history of the Mojavian lithosphere with Sr, Nd, Hf, and Os isotopes of peridotite xenoliths from Dish Hill, California

R.M.G. ARMYTAGE^{1*}, A.D. BRANDON¹,
A.H. PESLIER^{2,3} AND T. J. LAPEN¹

¹Earth and Atmospheric Sciences, University of Houston,
Houston, TX, 77204, USA, *armytage@uh.edu

²Jacobs Technology, JETS., Houston, TX, 77058, USA

³Astromaterials Research and Exploration Science, NASA-Johnson Space Center, Houston, TX, 77058, USA

The ¹⁸⁷Os/¹⁸⁸Os ratios in mantle xenoliths have been used to constrain continental growth histories [e.g. 1]. However, there is debate over the degree to which model Os ages reflect large-scale mantle melting linked to continental growth [2], or averaged-out end members after a multi-stage-history of partial melting, melt-rock interaction and metasomatism [3]. Combining different isotopic systematics can help constrain the nature and timing of melt extraction and secondary melt or fluid interactions in subcontinental lithospheric mantle.

A suite of 16 spinel-bearing Cr-diopside peridotite xenoliths from Dish Hill, CA, a Plio-Pleistocene cinder cone in the Mojave Desert were first characterized for major and trace elements (bulk-rock and main phases), then analysed for Os, Hf, Nd and Sr isotopes, with the lithophile isotopic analyses being obtained on cpx separates.

The ¹⁸⁷Os/¹⁸⁸Os ratios fall on two aluminachron [4] trends, with T_{PUM} at 2.12±0.08 Ga and 1.39±0.10 Ga. These two distinct trends are supported in correlations of ¹⁸⁷Os/¹⁸⁸Os versus melt depletion indices such as Cr# in spinel. This signal of two mantle melting events is not present in the Hf isotope data. The correlations between εHf and melt depletion indices are weak. There is also evidence that Hf is decoupled from Nd as the peridotites that lie off the εHf-εNd terrestrial array of [5] also display LREE enrichments. High Nb/Zr and La/Lu ratios in cpx in one of the peridotites suggest a HFSE-LREE metasomatic component.

The combined isotopic data points to the lithosphere mantle under Dish Hill being formed in two ancient mantle melting events, and overprinted by at least two metasomatic components. There is no evidence in this xenolith suite of underlying Farallon oceanic lithosphere as proposed by [6].

[1] Pearson *et al* (1995) *EPSL*, **134**, 341-357. [2] Pearson *et al* (2007) *Nature* **449**, 202-205. [3] Meisel *et al* (2001) *GCA*, **65**, 1311-1323. [4] Reisberg and Lorand (1995) *Nature* **376**, 159-162 [5] Vervoort *et al* (1999) *EPSL*, **168**, 79-99. [6] Luffi *et al* (2009), *JGR*, **114**, B03202

Downward injection of sulfide slurries: their role in the formation of Ni sulfide deposits

N.T. ARNDT¹, S.J. BARNES², J. ROBERTSTON²,
C.M. LESHNER² AND S. CRUDEN²

¹ISTerre, Univ Grenoble, CNRS UMR 5275, Grenoble, France, (arndt@ujf-grenoble.fr)

²CSIRO, 6151 Perth, Australia Steve.Barnes@csiro.au

³MERC, Laurentian Univ. Sudbury, Canada (mlesher@laurentian.ca)

Magmatic Ni-Cu sulfide deposits form when mafic-ultramafic magma interacts with rocks of the continental crust, which decreases the solubility of sulfide in the magma or adds sulfur to cause the segregation of immiscible sulfide liquid. Strongly chalcophile Ni, Cu and PGE concentrate in the sulfide and if this phase accumulates, an ore deposit is formed. Most models identify gravitative settling of dense sulfide liquid as the cause of sulfide accumulation but inspection of the textures and structures of orebodies indicates that the process is not so simple. Many ores consist of crystal mushes or breccias that are injected in pulses into the host intrusions; layers of massive sulfide commonly penetrate rocks beneath the intrusions.

These features can be explained if sulfide-rich masses of magma migrated from higher in the magmatic plumbing system. As magma ascends, the pressure drops and, particularly if the magma assimilates country rocks, it loses heat. This causes crystallization, which may be accompanied by the appearance of sulfide droplets. The density and the viscosity of the magma increases. Many ore-bearing intrusions are saucer-shaped with flat, sill-like bases and sloping margins. As magma flows up these margins, a dense and viscous sulfide-bearing mush accumulates near the lower border while crystal-free liquid ascends along the upper part. The process differentiates the magma, producing evolved decanted liquids that flows erupts as flood basalt. The magma interacts with the sulfide in the lower part of the conduit, enriching the sulfide in chalcophile metals. The mush layer periodically becomes unstable and slumps down the conduit, to be injected as pulses into the sill-like portions of the intrusions.

Effects of climate change and changes in atmospheric CO₂ levels on sources of terrestrial aerosol precursors

A. ARNETH¹, W. KNORR² AND M. WU²

¹Karlsruhe Institute of Technology, Institute for Atmospheric Environmental Research (IMK-IFU) (almut.arneth@kit.edu)

²Lund University, Dept. Physical Geography and Ecosystem Analysis (Wolfgang.knorr@nateko.lu.se; Minchao.wu@nateko.lu.se)

The terrestrial biota is a significant source of aerosols and aerosol precursors. Emissions of biogenic volatile organic compounds, for instance, are known to contribute to the growth of secondary organic aerosols and hence exert a negative radiative forcing. Wildfire, as a second example, is a large source of black carbon, with a large positive climate forcing. Hence changes in terrestrial aerosol and aerosol precursor emissions constitute a large and highly uncertain factor in the assessment of future climate-pollution interactions, especially when dealing with the question: to what extent would climate effects of pollution control be counteracted by possibly enhanced biogenic and fire emissions?

From a terrestrial sources perspective, addressing this question requires a consistent, process-based modelling framework, to take into consideration a number of direct and indirect factors that affect emissions collectively. Both fire and BVOC emissions respond rapidly and directly to short-term weather effects, like warm temperatures enhancing BVOC emissions. Fire occurrence directly responds to hot dry conditions immediately. However, over years and decades, climate trends and trends in atmospheric CO₂ concentration also play an important role. For example, wetter conditions and/or higher CO₂ levels can enhance fuel and enhance rather than reduce fires. Vegetation productivity and changing composition must be taken into consideration, both for BVOC emissions and fire regimes. Changes in vegetation composition in response to changing fire regimes can also affect BVOC emissions regionally, while direct human land use is an additional crucial component to be considered for the assessment of future aerosol precursor emissions from terrestrial ecosystems, for both BVOC and fire.

Sneaky sulfate signals: Isotope fingerprints reveal *cryptic* pathways

G.L. ARNOLD* AND B. BRUNNER

Center for Geomicrobiology, Department of Bioscience,
Aarhus University, Aarhus, Denmark (*correspondance:
gail.arnold@biology.au.dk)

The presence of sulfate in deeply buried methanic marine sediments traditionally considered to be sulfate-free (e.g. Holmkvist *et al* [1]) implies that sulfur (S) cycling is an ongoing process in the deep biosphere, reflecting catabolic pathways where S constituents act as shuttles between compounds that are being oxidized on the one side and reduced on the other side. The pivotal role of the S constituents in such processes often remains hidden or 'cryptic' because while the S compounds are continuously reduced and re-oxidized, the overall inventory of the S constituents remains constant. Exploring cryptic S cycling is of importance for two reasons. First, it provides insight into how microbial processes under energy limitation work, and if/how, specialized microorganisms share the already small amount of available energy to carry out different biochemical reactions. Second, it potentially challenges or at least transforms the paradigm that there is a sequential cascade of electron accepting processes in the environment across redox gradients, with the energetically most favorable electron acceptor consumed first and the least attractive process carried out last. In other words, dissimilatory sulfate reduction could occur in presence of Mn(IV) or Fe(III), or in the methanogenic zone.

We elucidate deep sulfate cycling in the Aarhus Bay sediments and at other sites by looking at both the S and oxygen (O) isotope composition of sulfate, which is affected by sulfate generation and consumption in combination with a numerical model. The combined S and O isotope signature of sulfate allow us to disentangle the processes responsible for sulfate production, such as oxidation of reduced organic and inorganic S and dissolution of barite from processes that consume sulfate, such as sulfate reduction.

Whereas cryptic sulfate generation is evident from the observation of sulfate in the methanic zone, where sulfate has canonically been presumed not to be present, this is not the case for the main sulfate reduction zone in marine sediments. Here, only the analysis of the combination of concentration and S and O isotope composition profiles of sulfate reveals the hidden intricacies of S cycling.

[1] Holmkvist *et al* (2011) *Geochim. Cosmochim. Acta* **75**, 3581-3599.

Functional contrasts and functional redundancy in Arctic bacterial communities in the oxic water column and anoxic sediments

C. ARNOSTI¹*, Z. CARDMAN¹, A.D. STEEN¹,
K. ZIERVOGEL¹ AND A. TESKE¹

¹UNC Chapel Hill, Dept of Marine Sciences, Chapel Hill, NC 27599, USA (*arnosti@email.unc.edu)

Investigation of enzymatic activities and bacterial community composition in the water column and sediments of an Arctic fjord of Svalbard during two summers captured the transition from a fully oxidized water column to anoxic, sulfate-reducing sediments. In 2008, water column bacterial clone libraries were dominated by members of the phylum *Verrucomicrobia* and the subphylum *Flavobacteria* (Fig. 1), known as aerobic degraders of polysaccharides. Some Svalbard phylotypes were specifically related to single cells attaching to and presumably taking up laminarin and xylan [1]. In addition to these substrates, chondroitin sulfate and fucoidan were hydrolyzed in the water column. In sediments, phylotypes of the anaerobic *Bacteroidetes* and sulfate-reducing *Deltaproteobacteria* were prominent, and a greater range of polysaccharides were hydrolyzed. Despite considerable differences in water column community composition between 2007 [2] and 2008, patterns of enzyme activities were largely constant. We therefore have evidence of functional redundancy among water column communities of differing composition, which nonetheless use the same comparatively narrow spectrum of substrates relative to their benthic counterparts.

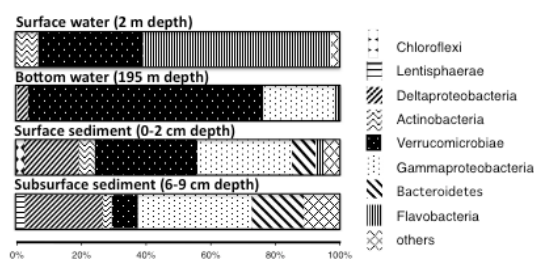


Figure 1. Bacterial 16S rRNA gene clone library composition of water column and sediment samples.

[1] Martinez-Garcia *et al* (2012). *PLoS One* 7:335314. [2] Teske *et al* (2011). *AEM* 77:2008.

Comparing properties of natural biogenic with biomass burning particles in Amazonia

PAULO ARTAXO^{1*}, LUCIANA V. RIZZO², JOEL F. BRITO¹,
HENRIQUE M. J. BARBOSA¹, ELISA T. SENA¹,
GLAUBER G. CIRINO³, ANDREA ARANA³
AND ANA M. SERRANO³

¹Instituto de Física, Universidade de São Paulo, Rua do Matão, Travessa R, 187, 05508-090, São Paulo, Brazil.

(*correspondence: artaxo@if.usp.br)

²Departamento de Ciências Exatas e da Terra, Universidade Federal de São Paulo, Rua Prof. Artur Riedel, 275, 09972-270, Diadema - São Paulo, Brazil.

³Instituto Nacional de Pesquisas da Amazonia – INPA. Av André Araújo, 2936, Manaus - AM. 69060-001, Brazil.

The Large Scale Biosphere Atmosphere Experiment in Amazonia (LBA) is a long-term (20 years) research effort aimed at the understanding of the functioning of the Amazonian ecosystem. The strong biosphere-atmosphere interaction is a key component of the ecosystem functioning. Two aerosol components are the most visible: The natural biogenic emissions of particles and VOCs, and the biomass burning emissions.

Two aerosol and trace gases monitoring stations were operated for 4 years in Manaus and Porto Velho, two very distinct sites, with different land use change. Manaus is a very clean and pristine site and Porto Velho is representative of heavy land use change in Amazonia. Aerosol composition, optical properties, size distribution, vertical profiling and optical depth were measured from 2008 to 2012. Aerosol radiative forcing was calculated over large areas. It was observed that the natural biogenic aerosol has significant absorption properties. Organic aerosol dominates the aerosol mass with 80 to 95%. Light scattering and light absorption shows an increase by factor of 10 from Manaus to Porto Velho. Very few new particle formation events were observed. Strong links between aerosols and VOC emissions were observed. Aerosol radiative forcing in Rondonia shows a high -15 watts/m² during the dry season of 2010, showing the large impacts of aerosol loading in the Amazonian ecosystem. The increase in diffuse radiation changes the forest carbon uptake by 20 to 35%, a large increase in this important ecosystem.

Compositional heterogeneity of the upper mantle beneath the Siberian craton: Reconciling thermal, seismic and gravity data

IRINA ARTEMIEVA, MATIJA HERCEG, YULIA
CHEREPANOVA AND HANS THYBO

IGN, Univ. Copenhagen, Denmark, (irina@geo.ku.dk)

We present a new regional model for the upper mantle structure below the Siberian craton. The model includes (i) thermal model of the lithosphere structure constrained by surface heat flow data, (ii) seismic velocity heterogeneity constrained by global tomography models corrected for temperature variations in the upper mantle, (iii) and a new regional model for the density structure based on the GOCE satellite gravity data. We also present a new regional seismic crustal model SibCrust, which is used to calculate crustal correction to gravity field. Thermal model and seismic tomography models are used as independent constraints on lithosphere thickness, required to convert mantle residual density anomalies to density heterogeneity. New regional upper mantle model is compared with regional and world-wide petrological data on upper mantle velocities and densities constrained by mantle-derived xenoliths. The results indicate a significant compositional heterogeneity of the lithospheric mantle of the region. Seismic velocity and density anomalies cannot be explained by variations in mg# alone. Compared to the adjacent orogenic belts and the West Siberian basin, density structure of the cratonic mantle is in a close agreement with isopycnic condition, although significant regional variations are well correlated with basement topography.

Planning cement materials for a sustainable future

G. ARTIOLI

Dipartimento di Geoscienze, Università di Padova, I-35131
Padova, Italy (gilberto.artioli@unipd.it)

Binders and cements are crucial materials in past and modern human activities. Critical issues to be addressed for a sustainable use of cements include the global generation of CO₂ during mass production of Portland clinkers, the use of recycled materials in the formulations, and the development of alternative, durable and environmentally-compatible binders. Ultimately, the proper life cycle assessment (LCA) of the mass produced cements must be considered in order to save georesources, although this is a rather challenging task [1].

The expanding use of geopolymers [2, 3] and alkali-activated binders [4] for building applications follow this trend, although further progress is urgently needed in determining the chemico-physical, mechanical, and durability properties of alternative materials. Some of the systems currently under investigation will be reviewed, with emphasis on advantages and pitfalls.

[1] Huntzinger & Eatmon (2009) *J. Cleaner Production* **17**, 668-675. [2] van Deventer *et al* (2012) *Miner. Eng.* **29**, 89-104. [3] van Deventer *et al* (2010) *Waste Biomass Valoriz.* **1**, 145-155. [4] Shi *et al* "Alkali-activated cements and concretes". Taylor & Francis, 2006.

The stochastic treatment of mineral surface reaction kinetics

R. S. ARVIDSON^{1*}, C. FISCHER¹ AND A. LÜTTGE^{1,2}

¹MARUM / Fachbereich GEO (FB5), Universität Bremen,
Klagenfurter Straße, D-28359 Bremen Germany
(*correspondence: rsa4046@uni-bremen.de)

²Rice University, Houston, TX 77005, USA

There is increasing divergence in approaches describing the geochemical kinetics of mineral surface reactions. The first approach, for which there is long-standing traditional support and a large number of observational data, assumes that the most systems are essentially deterministic, i.e., imposing a given set of initial conditions or a perturbation will always produce the same result at a later time. The well-known mathematical representation of this approach is a set of coupled ordinary differential equations: the change in a given chemical species' concentration as a function of environmental conditions, constrained by heuristically determined parameters (rate constants, overall activation energies, etc.). In contrast, the second approach, supported by more recent work [1], argues that the intrinsic variability of certain mineral-fluid systems preclude such a deterministic treatment. Although well-documented, this intrinsic variability is not well understood. At the moment, neither the presence or absence of significant variations in rate under specific conditions has a consistent explanation. Furthermore, even if deterministic outcomes could be represented by probabilistic functions (by assuming fluctuations are negligible), the deterministic approach provides no explicit defense for this assumption [2].

As an initial step, we wish to assess the amplitude of intrinsic rate variation, and thus need to examine the history of dissolving surfaces over time. We present preliminary results of (1) a large number of direct observations of a fixed area of a dissolving mineral surface at constant undersaturation over time, and (2) model simulations of a similar surface, in which contributions of surface defect density, distance to grain boundaries, and other parameters can be varied. These observations of real mineral surfaces and their virtual equivalents permit comparison of the rate's distribution over the surface and its deviation from an arbitrary mean value. This resulting statistical treatment may be a precursor to a generalized stochastic model of mineral surface reactions, and resolution of otherwise inconsistent observations of reaction rate.

[1] Fischer *et al* (2012) *Geochim. Cosmochim. Acta* **98** 177-185. [2] Gillespie, D. T. (1976) *J. Comp. Phys.* **22**, 403-434.

Spherulites in trachytic melts

F. ARZILLI^{1*}, M. VOLTOLINI², L. MANCINI¹,
M.R. CICCONE³, G. GIULI³ AND M.R. CARROLL³

¹Elettra-Sincrotrone Trieste S.C.p.A., 34149 Basovizza,
Trieste, Italy (*correspondence:
fabio.arzilli@elettra.trieste.it)

²Lawrence Berkeley National Laboratory, Cyclotron Rd,
94720 Berkeley, California, USA

³School of Science and Technology – Geology Division,
University of Camerino, Italy

Spherulites are cluster of radiating crystals that occur commonly in rhyolitic melts under highly non-equilibrium conditions [1-2]. Textural data on spherulites of alkali-feldspar and pyroxene are shown in this study. Spherulites grew in trachytic melts during cooling and decompression experiments with water-saturated conditions. The aim of this work is to better understand the growth of spherulites as a function of undercooling (ΔT), P_{H_2O} , time and superheating. Experiments were carried out using Cold Seal Pressure Vessel apparatus at pressure range of 30 ÷ 200 MPa, temperature range of 750 ÷ 850 °C and duration of 2 ÷ 16 hours.

This study presents preliminary quantitative data on spherulitic morphologies obtained both by electron microscopy (SEM) and phase-contrast synchrotron X-ray microtomography. Because experiments were performed at different experimental durations, the evolution of spherulites can be studied and furthermore the crystallographic misorientation, the changes in size and the aspect ratio can be measured.

Three kinds of spherulites occurred during our experiments: (i) spherulites characterized by widely spaced crystals arranged radially around the nucleus, in agreement with previous observations [3-4]; (ii) spherulites characterized by acicular and tiny fibers radially aggregated; (iii) spherulites characterized by the transition from a single crystal into a polycrystalline spherulite (densely branched spherulitic morphology).

The preliminary results about alkali feldspar spherulites show that their growth rate is about 10^{-7} cm/s. Spherulites were grown between 100 and 200 MPa, thus at high water contents. Moreover, low ΔT along with large superheating can enhance the nucleation and growth of spherulites. Therefore, low ΔT , large superheating and high P_f conditions can trigger the crystallization of spherulitic morphologies.

[1] Watkins J. *et al* (2008) *Contrib. Mineral. Petrol.* **157**, 163-172. [2] Grànàsy L. *et al* (2005) *Phys. Rev.* **72**, 011605. [3] Keith, H. D. and Padden F. J. (1963) *J. Appl. Phys.* **8**, 2409–2421. [4] Lofgren G. (1971) *J. Geophys. Res.* **76**, 5635-5648.

From death of a glacier to the beginning of life in soil: A case study in the Swiss Alps

J. ASCHER^{1*}, C. MAVRIS², F. FORNASIER³, M.
CECCHERINI¹, G. PIETRAMELLARA¹ AND M. EGLI²

¹Dept. of Agrifood and Environmental Science, University of
Florence, Italy (*correspondence: judith.ascher@unifi.it)

²Dept. of Geography, University of Zurich, Switzerland

³CRA-RPS Gorizia, Italy

Pedogenesis starts just after deglaciation, with microbial primary succession playing a key role in soil ecosystem development. The progressively exposed moraines of the Morteratsch Glacier (Upper Engadine, Switzerland) offer a full time sequence, from 0 to 150 yrs [1]. We assessed geological, physico-chemical and microbiological parameters (microbial biomass, microbial community structure and selected soil enzyme activities) along the age gradient of the proglacial area. We set up a *double-nested-PCR-DGGE* approach on intracellular DNA extracted from the topsoil (0-10 cm) to monitor bacterial and fungal succession along the chronosequence, capable to detect also low numbers of target sequences occurring in early stage soils.

Increasing soil age was characterized by microbial biomass increase and, as expected, by a dynamic community succession. Both parameters displayed in turn a high positive correlation with SOM content (N_{tot} and C_{tot}) and pH decrease (0 yrs: pH 8.11 – 150 yrs: pH 5.64). High correlations with enzymes, biochemical markers reflecting soil activity, were also detected. Numbers of microbial phylotypes were lowest in the youngest soils (0-4 yrs), increased in the intermediate aged soils (4-110 yrs), and decreased again and plateaued in the oldest soils (110-150 yrs).

Our findings confirm that soil microbiota undergo drastic variations both in terms of biomass and community composition according to substrate availability, with interactive adaptation to the differing stages of soil development.

[1] Mavris *et al* (2010) *Geoderma* **155**, 359-371

Melt modified mantle lithosphere beneath Dalnyayay pipe

ASHCHEPKOV I.V.¹, NTAFLS T.², SPETSIS Z.V.³
AND R.F.SALKHOV³

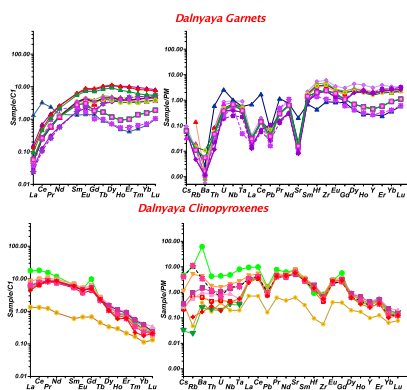
¹ IGM SD RAS, Novosibirsk, Russia, igora57@mail.ru

² University of Vienna Althanstr. 14 1090 Wien, Austria

³ Company "ALROSA", Mirny 678170 Russian

Mantle xenoliths (>100) from Dalnaya pipe (Yakutia) were studied by EPMA and LAM ICP MS. In deformed and porphyroclastic Cpx is more Fe-rich and HT and may associate with microilmenites. The splitted geotherm (33 to 45mwm-2) are traced by coarse and deformed varieties varieties respectively from 7.5 to 2GPa. Essential inflection and heating detected by PT for OPx ~3GPa referring to Ca-enriched pyroxenitic garnets two more heating intervals are found ~ 7-6 and 5GPa. Continuous branches of growth with decreasing P of Fe# for Gar and low - Fe Cpx Fe# 6 to 12# suggest that primary mantle layering beneath this pipe was smoothed by interaction with melts. The refertilization trend (Fe#9-15% rising upward in two branches refer to the joint crystallization of Ilm - low-Cr Ilm - Cpx - Gar found in intergrowth referring to protokimberlite melts evolution.

In the PFO2 diagrams garnets and Cpx show continuous reduction to the lithosphere base to 4ΔQMF, and a bit higher for Cpx. Ilm - garnet trend is rising upward between -2 -0 ΔQMF. The diamond grade is higher for the porfiric kimberlites containing higher sub Ca garnet from dunites representing melt path veins. Trace elements for olivine show lower Ni and higher Al, Ca, Ti for the deformed veins. Trace elements determined for Gar and Cpx from 13 xenoliths from the middle part of mantle section reveal very similar patterns in the incompatible part in general suggesting reactions with the protokimberlite melts.



Grant RBRF 11-05-00060

Composition and interior structure of the HED Parent Body

HELEN O. ASHCROFT*, BERNARD J. WOOD
AND JON WADE

Department of Earth Sciences, University of Oxford, South
Parks Road, Oxford OX1 3AN, UK

(*correspondence: helen.ashcroft@earth.ox.ac.uk)

Estimates for the major and trace element compositions of the Howardite-Eucrite-Diogenite (HED) parent body mantle have been derived using geochemical information from the HED meteorites [1] and the observation that refractory lithophile elements occur in chondritic relative proportions [2]. The putative mantle compositions (Table 1) were then used to investigate differentiation processes within Vesta.

	MgO	Al ₂ O ₃	SiO ₂	CaO	FeO
PM1	29.7	3.01	42.3	2.40	22.6
PM2	32.8	3.33	46.7	2.65	14.6

Table 1. Major element composition (wt%) of two putative mantle compositions (PM1 and PM2).

These estimates were combined with new information from DAWN [3] to model the interior structure of Vesta. Mantle compositions imply a mantle mineralogy of approximately 60% olivine and 40% pyroxene. We estimate crustal thickness of 10-20 km and a core mass fraction of 15% for a body with mantle composition PM1, and 20-30 km and 19% respectively for PM2. Combining this information with experimentally determined crystal-melt and melt-metal partition coefficients (e.g. [4]), the trace element distribution throughout the protoplanet was then calculated, including estimates of Ba/W for Bulk Silicate Vesta of 29-32 for PM1 and 48-67 for PM2.

Initial results from one-atmosphere and piston cylinder experiments confirm that basaltic melts can be derived from these putative mantle compositions with olivine replacing pyroxene as the 1 atm liquidus phase as increasing amounts of mantle are added to eucritic starting compositions. We are currently determining crystal-melt partitioning behaviour for a diverse range of refractory trace elements. The data will be used to further constrain the igneous history of Vesta.

[1] Sack *et al* (1991) *Geochim. Cosmochim. Acta* **55**, 1111-1120. [2] MetBase™ [3] Russell *et al* (2012) *Science* **336**, 684-686. [4] Wade *et al* (2012). *Geochim. Cosmochim. Acta* **85**, 58-74

Improved crustal *PTtD* evolution constraints using TitaniQ thermobarometry

KYLE T. ASHLEY*,¹, RICHARD D. LAW¹, DONALD W. STAHR III¹, JAY B. THOMAS², MARK J. CADDICK¹, FRANK S. SPEAR² AND LAURA E. WEBB³

¹Department of Geosciences, Virginia Tech, Blacksburg, VA 24061, USA (*correspondence: ktashley@vt.edu)

²Department of Earth and Environmental Sciences, Rensselaer Polytechnic Institute, Troy NY 12180, USA

³Department of Geology, University of Vermont, Burlington, VT 05405, USA

Applications of the Ti-in-quartz (TitaniQ) thermobarometer provide insight into the conditions, timing, mechanisms and rates of metamorphism and deformation. Our work on Vermont metapelites has documented quartz growth with respect to microstructural contexts as resulting from (a) early prograde growth; (b) quartz-producing metamorphic reactions; (c) precipitation from deforming micaceous domains; and (d) retrograde Si-charged fluid influx. In each case, the TitaniQ thermobarometer (with known pressures and activity estimates) reveals temperatures for these events, which all resulted in new quartz growth. However measurements of dynamically recrystallized quartz (notably through subgrain rotation) from Vermont and the Sutlej Valley (NW India) show that new subgrains usually exhibit [Ti] much lower than expected for the temperatures at which deformation occurred. This is an artifact of the mechanisms driving recrystallization in an attempt to minimize internal lattice strain. Defects aligned into subgrain boundaries may provide pathways for Ti to leave the crystal during formation of nearly strain-free subgrains. Increased lattice strain from Ti substitution may be reflected in the systematic increase in uncertainties of lattice refinements with single crystal X-ray diffraction measurements with increasing [Ti]. Therefore application to quartzites where only scarce weak interconnected phases are present to accommodate strain is problematic.

Ti diffusion from garnet porphyroblasts into quartz inclusions has recently been shown to be an effective technique for constraining metamorphic time scales [1]. In Vermont, this diffusion modeling suggests heating after encapsulation and cooling to 450 °C must have occurred in a short amount of time (<1.2 Myrs). Preliminary application to the Sutlej Valley suggests very similar time scales for metamorphic evolution. Coupled growth and diffusion modeling of large (ca. 4–5 mm diameter) garnets attaining low peak temperatures (<600 °C) have been unable to effectively discriminate *T-t* histories at the resolution of Ti-in-quartz diffusion modeling.

[1] Spear *et al* (2012) *Contrib Miner Petrol* **164**(6), 977–986.

Thermodynamics of melts from shock wave experiments and a simplified speciation model

P. D. ASIMOW, C. W. THOMAS AND A. S. WOLF¹

¹Division of Geological and Planetary Sciences, California Institute of Technology, Pasadena CA 91125 USA; (asimow@gps.caltech.edu)

Although the thermodynamics of melts nominally falls outside the boundaries of a “thermodynamics of minerals” session, the subjects are intertwined by melting and crystallization and by the critical planetary dynamics that arise from differences between the physical, thermochemical, and transport properties of solids and liquids.

An extensive campaign of shock wave experiments on liquid compositions in the CaO-MgO-Al₂O₃-SiO₂-FeO system now provides constraints on the equations of state (EOS) of multicomponent melts at all terrestrial mantle pressures. The results can be compared to *ab initio* and empirical molecular dynamics (MD) simulations, static experiments, and geophysical observations. Key material property conclusions that have emerged include: (1) a negative temperature dependence to the sound speed, at least for Mg₂SiO₄ melt; (2) clear composition dependence to the effective partial molar volume of the FeO component, presumably related to composition-dependent coordination or spin states; and (3) universal behavior of the Grüneisen parameter, increasing upon compression at a near-uniform rate. Earth science conclusions at this stage include: (4) an absence of cases where mid-mantle magma ocean crystallization can give rise to a neutrally buoyant solid assemblage, at least initially near the liquidus; and (5) the near impossibility of finding a bulk composition in MgO-SiO₂-FeO and an extent of partial melting consistent with phase equilibrium and geophysical constraints for partially molten ultra-low velocity zones at the core-mantle boundary.

Given the expense and limitations of current MD methods for the study of silicate liquids and the challenge of linking microscopic data (e.g. spectroscopy) to mesoscopic data (e.g. EOS) or macroscopic observations (i.e., geophysics), it is helpful to develop simplified models that capture certain key aspects of melt behavior. We have extended the hard-sphere model into a coordination-number dependent, predictive model of speciation and equation of state for silicate liquids, *CHASM*. Currently the model has been calibrated on solid structures for SiO₂, MgO, and MgO-SiO₂ binary systems. It reproduces the pressure-dependence of coordination statistics from MD and allows insight into the natural origins of phenomena (1), (2), and (3) above.

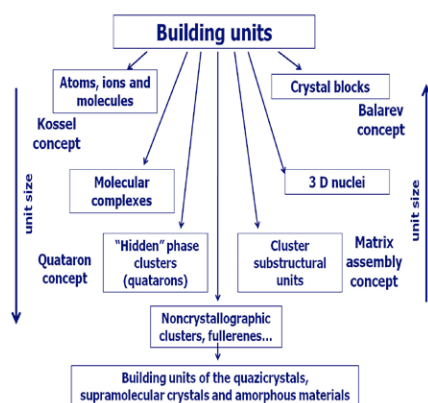
Prenucleation nanoclusters as building units in the crystal growth

A.M. ASKHABOV

Institute of Geology, Komi Science Centre, UralBranch, RAS, Syktyvkar, Russia

The problem of building units is central in the crystal growth theory. Throughout many decades there competed two conceptual ideas.

According to the first, crystals grow by joining to them of already formed in environment crystal blocks (Balarev concept). According to the second, building units are separate ions, atoms and molecules (Kossel concept).



In principle, realization of these two extreme variants does not contradict the general laws of physics and chemistry. As a matter of fact, the majority of modern theoretical models of

crystals growth are constructed on their basis. At the same time, for a long time already another idea – on building units as particles larger than separate atoms or molecules, but not being crystalline particles (3 D nuclei) – is discussed. There were suggestions about participation in growth of crystals of intermediate formations (complexes, associates, clusters etc.) of which existence testified the results of numerous experimental (not only spectroscopic) researches of crystal-forming media. However on this basis it was not possible to develop the alternative concept of crystal growth because of arising contradictions with classical theory of nucleation.

We developed a new approach to the analysis of processes of nucleation and growth of crystals which comes from the possibility of formation and existence in supersaturated media of special forms of the connected atoms – nano-size pre-nucleation clusters of “hidden” phase called quatarons [1, 2]. Quatarons owing to their properties are ideal structures as building units. Namely they are the basic growth units and not geometrically and energetically stabilized clusters or another clusters substructural units. Thus an old problem of establishing the nature and sizes of building units in the process of crystals growth is solved.

This work is supported by Programs of RAS: 12-U-5-1026, 12-T-5-1022, Scientific School 1310.2012.5, RFBR 11-05-00432a.

[1] Askhabov (2004) Proc. of the Russian Miner. Soc . CXXXIII, No.4, 108-123.[2] Askhabov & Kamashev (2012) Proc. of 34th Int. Geological Congress, Brisbane, Australia, 5-10 August. P. 2162.

Timing of Northern Hemisphere climate transitions during the last glacial period from precisely-dated speleothem data

Y. ASMEROM^{1*}, V. POLYAK¹ AND M. LACHNIET²

¹Dept. of Earth & Planetary Sciences, Univ. of New Mexico, Albuquerque, NM 87131, USA(*correspondence: (asmerom@unm.edu, polyak@unm.edu)

²Department of Geoscience, University of Nevada, Las Vegas, NV 89154, USA(matthew.lachniet@unlv.edu)

Previous $\delta^{18}\text{O}$ results of last glacial period precipitation variability in the south western United States from Fort Stanton cave, New Mexico (FS-2) [1], matched changes in Greenland temperatures [2]. We inferred changes in winter precipitation, which were related to changes in the meridional shifts in the position of the polar jet stream, reflecting changes in the polar to equator temperature gradient in the Northern Hemisphere (NH).

We report high-resolution chronology and oxygen and carbon isotope data on another Fort Stanton Cave stalagmite (FS-AH-1), taking advantage of the higher growth rate compared to FS-2 (3 $\mu\text{m}/\text{yr}$ vs 11 $\mu\text{m}/\text{yr}$), newer refinements in the half-lives of ^{234}U and ^{230}Th , a new high purity ^{233}U - ^{236}U spike and much improved efficiency from our upgraded Neptune multi-collector ICP-MS. The new chronology, between 48.4 - 11.2 kyr B.P., has 2- σ errors in the range of 100 years for most of the segments, including conservative estimate of the uncertainties in the initial $^{230}\text{Th}/^{232}\text{Th}$ ratios.

Our results show that last glacial stadial (Heinrich Events, HE) and interstadial (Dansgaard/Oeschger Events, D/O) are matched very well in timing, amplitude and duration between the FS-AH-1 and NGRIP [2] with a higher age precision than the ice core data. The lack of systematic pattern in the lead-lag relationships between the ice core and FS-AH-1 D/O and HE chronology suggests that differences are due to chronology and not climatic lags. Thus, FS-AH-1 provides a more precise chronology for the NGRIP record. One significant difference, our record, similar to some North Atlantic records, shows two HE 1 cooling excursions, occurring immediately after two IRD (ice-rafted detritus) events [3] and match temperature sensitive $\delta^{18}\text{O}$ marine core data from subtropical Atlantic [4]. The difference between the two records may reflect greater sensitivity of our record to circulation-driven NH temperature gradient variability.

[1] Asmerom *et al*, 2010, *Nature Geoscience* **3**, 114- [2] Rasmussen *et al*, 2005, *GRL*, **111**, 1- [3] Bard *et al*, 2000, *Science* **289**, 1321- [4] McManus *et al*, 2004, *Nature* **428**, 834-

www.minersoc.org

DOI:10.1180/minmag.2013.077.5.1

Petrochemical typification of the oolitic iron ores from the Bakchar deposit (Westen Siberia)

E.M. ASOCHAKOVA

Tomsk State University, Russia, ev.asochakova@gmail.com

The Bakchar deposit is confined to the Upper Cretaceous and Paleogene deposits overlapped by a rather thick Neogene-Quaternary rock body (160-200 m). The iron ores are related with several horizons: Narymskian, Kolpashevskian, Tymskian and Bakcharskian. The depth of productive strata varies from 2 to 40 m. The iron ore horizons are traced throughout the entire area of the deposit, as well as outside its borders and are separated by the barren and weakly ferruginous rocks that overlap each other often with washouts.

While researching the ore horizon of the Polinyansk site, we classified the iron ore types, which differ from each other in structural characteristics, a mineral composition of the cementing mass, as well as in the specific locations of these types in the section. There are three main types of ores in the section structure. First type includes goethite-hydrogoethite (oolite) ore, which are brownish-yellow cemented or loose sediments. The second one is glauconite-chlorite; it has a firm weakly cemented composition and greenish-grey color. The third transitional type of ores has characteristics of both goethite-hydrogoethites and glauconite-chlorite formations.

In order to verify validity of ore type classification, we processed statistically all the data of the X-ray fluorescence analysis (Na_2O , MgO , Al_2O_3 , SiO_2 , P_2O_5 , K_2O , CaO , TiO_2 , MnO , $\text{Fe}_2\text{O}_3\text{tot}$) using the software "STATISTICA".

The group clustered analysis using k-means clustering method allowed us to define one of three classes for each ore sample. The samples of ores are objects for clustering. The number of these classes was chosen according to the amount of ore types in the section described above. Clustering the samples of ore chemical compositions distinguishes clearly locations of different ore types in the ore horizon based on the change of chemical composition.

Using a factor analysis, two main factors were defined, which took more than 70 % of dispersion over. The components of the clastic part (SiO_2 , K_2O , MgO , Al_2O_3) and the ore part ($\text{Fe}_2\text{O}_3\text{tot}$, P_2O_5 and L.O.I.) influenced the variation of chemical composition of the oolite iron ores significantly.

This study was funded by the Russian Ministry of Education and Science (projects 5.3143.2011, 14.B37.21.0686, 14.B37.21.1257).

Performance and gas-flow effects of an active 2-volume sampling chamber using a 213 nm laser ablation system for inductively coupled plasma-mass spectrometry

D ASOGAN^{1*}, D. A. GREEN¹, S. SHUTTLEWORTH²
AND J. W. ROY²

¹CETAC Technologies, Omaha, NE 68144, USA

(*correspondance: dasogan@cetac.com)

²Photon Machines Inc., Bozeman, MT 59715, USA

Laser ablation-ICP-MS technology has been rapidly improving for the past decade. The sampling chamber design of any laser ablation system is vital to ensure minimal elemental fractionation (by minimizing particle condensation/agglomeration), and enhance aerosol transport to improve accuracy, precision and sensitivity.

Improvements in sampling chambers design has led to higher spatial resolution and greater precision, which subsequently improves the quality of data in applications such as (bio-)imaging and geochronology respectively.

This paper discusses for the first time the use of an active 2-volume cell, which uses multiple gas flows to effectively transport laser aerosols for high spatial resolution (fast washout) and stability using a 213 nm laser ablation system. Performance characteristics are presented that highlight its versatility to multiple application types and also the importance of choosing the right gas flows for the particular ICP-MS system in use.

Bimetasomatism in the Eclogite Facies: Evidence from the Tauern Window, Austria

DONJA ASSBICHLER^{1,2} AND ALEXANDER PROYER^{1,3}

¹Department of Earth Sciences, University of Graz, Austria

²now at: Department of Geo- and Environmental Sciences, LMU Munich, Germany, donja.assbichler@min.uni-muenchen.de

³now at: Department of Geology, University of Botswana, Private Bag UB 00704, Gaborone, Botswana; alexander.proyer@mopipi.ub.bw

Mineralogical and compositional changes of eclogite and adjacent calcareous metapelite and talc schist from the Eclogite Zone, Austria, were investigated in order to understand fluid-mediated compositional changes during subduction zone metamorphism. Whereas the eclogite in contact to the metapelite shows almost no change in volume, minor gain of Si, Ca and Na and loss of Mg, the metapelite shows a 30% volume loss, mainly as SiO₂, depletion of Ca and enrichment of K, Mg, Fe and Na – the latter two stemming from an external source. Trace element changes are less spectacular but corroborate changes in the major elements (Sr goes with Ca, Ba with K, etc.)

The eclogite in contact to the talc schist also underwent no significant change in volume, but minor enrichment in Mg and depletion in Na. The talc schist is ultrabasic in composition and of uncertain origin. It experienced more than 30% volume loss towards the contact, where Mg, Fe, Si, Na and Ti are depleted and no major element is enriched.

These changes in bulk composition are expressed in mineralogical, textural and mineral chemical changes of considerable complexity, and are not just limited to the very obvious retrograde interactions. The earliest composition changes are already manifest in the cores of garnets and demonstrate a rather continuous interaction throughout the entire metamorphic history. As the lithological boundaries are planar over distances of tens of metres at least, the volume losses are not induced by folding but rather by (pure or general) shear. Some composition changes cannot be explained by material exchange between the two lithologies (bimetasomatism) alone but must have been caused by advection parallel to the lithological boundaries. Rare garnets and epidotes with oscillatory zoning patterns near the contact indicate local abundance of fluid. The compositional changes are too systematic and complex to be explained as primary (volcano-)sedimentary layering or mixing of clays and ashes.

Characterization of CaCO₃ polymorphs grown in silica hydrogel in the presence SO₄²⁻ or CrO₄²⁻ by XAS

J.M. ASTILLEROS^{1,2*}, J. GÖTTLICHER³, N. SÁNCHEZ-PASTOR^{1,2}, R. STEININGER³ AND L. FERNÁNDEZ-DÍAZ^{1,2},

¹Department of Crystallography and Mineralogy, Complutense University, Madrid, Spain. (*correspondence: jmastill@ucm.es)

²Institute of Geoscience (CSIC, UCM), Madrid, Spain

³ANKA Synchrotron Radiation Facility, Karlsruhe Institute of Technology (KIT), Hermann-von-Helmholtz-Platz 1, D76344 Eggenstein Leopoldshafen, Germany

It has been noted that the presence of tetrahedral anions like SO₄²⁻ and CrO₄²⁻ in the medium for synthesis strongly influence CaCO₃ crystallization by promoting the formation of vaterite or vaterite/aragonite with respect to calcite. This influence has been related to either interface phenomena, such as preferential adsorption of these ions on particular sites on the surface of a specific polymorph or to changes in the relative free energy of the polymorphs due to differential incorporation of the tetrahedral anions. In order to confirm the incorporation of SO₄²⁻ and CrO₄²⁻ into the structure of the different CaCO₃ polymorphs and to study how and to what extent it may occur, crystals of calcite, aragonite and vaterite were grown in the presence of high concentrations of one of these anions using the silica gel method and were studied by X-ray absorption spectroscopy (XAS) at the Cr and S K edges in the XANES and EXAFS (only for Cr) regions. Measurements were conducted in the SUL-X beamline of the ANKA synchrotron radiation facility at the KIT (Germany). In all the experiments calcite was the most abundant polymorph in the precipitate, while vaterite and aragonite appeared as minor phase. While calcite grew as elongated single crystals, both aragonite and vaterite appeared as spherulitic aggregates. The incorporation of SO₄²⁻ and CrO₄²⁻ was confirmed in the three polymorphs, with significantly higher concentrations in calcite. In the case of calcite XAS spectra were recorded on differently oriented single crystals. Differences are very small and may point to a possible preferential orientation of the tetrahedral SO₄²⁻ anion in the structure. Finally, the comparison between spectra from the three polymorphs evidenced slight differences between those corresponding to calcite and aragonite. Differences are most marked to the spectrum of vaterite for SO₄²⁻ (Cr contents in vaterite were too low for a reliable comparison).

This work was supported by MECC-Spain under the grant CGL2010-20134-C02-01.

Coupling magnetic and molecular techniques to study microbial-mediated iron and carbon cycling

ESTELLA A. ATEKWANA^{1*}, SILVIA ROSSBACH², CAROL L. BEAVER², FARAG M. MEWAFY¹ AND LEE SLATER³

¹Oklahoma State University, Stillwater, OK, USA

(*correspondence: estella.atekwana@okstate.edu)

²Western Michigan University, Kalamazoo, MI, USA

(silvia.rossbach@wmich.edu)

³Rutgers University-Newark, New Jersey, USA

(lslater@andromeda.rutgers.edu)

Dissimilatory iron-reducing bacteria are able to reduce iron coupled to organic carbon oxidation, often producing magnetic mineral phases. Magnetic susceptibility (MS) measurements can therefore play an important role in identifying zones where microbial-mediated iron mineral transformation is occurring so that these zones can be studied by microbiological techniques. We investigated the MS and microbial community variations in a hydrocarbon-contaminated aquifer where iron-reduction and methanogenesis are occurring. Our results show two zones of elevated MS at the contaminated locations; one occurred within the zone of water table fluctuation and coincident with high concentrations of Fe(II) and organic carbon. The second was observed in the vadose zone and associated with the methane plume. Using the polymerase chain reaction technique, *Geobacter* species were found to be present in these two zones. At the background location, *Geobacter* species were limited to the upper soil layer. Therefore, *Geobacter* species could be the main drivers of magnetic mineral formation in these zones. Using molecular methods, including denaturing gradient gel electrophoresis and DNA sequencing, we observed that *Smithella* and other syntrophic species were dominant in the zone of peak magnetic susceptibility coinciding with zones of iron reduction and methanogenesis. Our results suggest that the integration of geophysical and microbiological methods will be of value for iron and carbon cycling studies.

Post depositional transformation of Ni-rich birnessite

AMY ATKINS^{1*}, CAROLINE L. PEACOCK²
AND SAMUEL SHAW³

¹School of Earth & Environment, University of Leeds, Leeds, UK. jhs5aa@leeds.ac.uk (* presenting author)

²School of Earth & Environment, University of Leeds, Leeds, UK. C.L.Peacock@leeds.ac.uk

³School of Earth, Atmospheric and Environmental Sciences, University of Manchester, Manchester, UK. Sam.Shaw@manchester.ac.uk

Birnessite is the dominant Mn oxide in marine sediments. However, under diagenesis and mild hydrothermal conditions the phyllo-manganate birnessite transforms to the tectomanganate todorokite [1-3]. Across significant areas of the seafloor birnessite is therefore a transient mineral phase. This is important because scavenging of dissolved trace metals to birnessite exerts a strong control on the concentration of these species in seawater. In particular, in the modern oceans the sorption of Ni to birnessite is the primary control on Ni oceanic concentration [4]. Ni is a bioessential element, required by primary producers and methanogenic bacteria [5]. As such understanding the sequestration of Ni to birnessite, and its fate and mobility during the transformation of birnessite to todorokite, is key to elucidating the feedbacks between Ni abundance, oceanic productivity and ultimately air-sea gas exchange. The presence of Ni in birnessite is traditionally believed to aid recrystallization to todorokite, where Ni is eventually retained in the todorokite structure, providing a potential sink for dissolved Ni [2]. Here we present the results of a novel todorokite synthesis, where we transform Ni-rich birnessite under conditions representative of marine diagenetic and mild hydrothermal settings. We have performed a time resolved study, combining XRD, BET, HR-TEM and XAS to fully characterise the transformation pathway and determine the fate and mobility of Ni during the transformation. Results facilitate our interpretation of recently collected μ -XRF and μ -XAS data, mapping Ni speciation and distribution in natural diagenetic and hydrothermal marine ferromanganese-rich sediments. We find that Ni retards the transformation of birnessite to todorokite under diagenetic and mild hydrothermal conditions, and is ultimately rejected from the neoformed todorokite during a late stage dissolution recrystallization process.

[1] Burns & Burns (1977) Mineralogy of ferromanganese deposits. In *Marine Manganese Deposits* (Elsevier, Amsterdam). [2] Bodeř *et al* (2007) *GCA* **71**, 5698. [3] Feng *et al* (2010) *GCA* **74**, 3232. [4] Peacock & Sherman (2007) *Chem. Geol.* **238**, 94. [5] Mulrooney & Hausinger (2006) *FEMS Microbiol. Rev.* **27**, 239.

Dynamics of Zn in an urban soil-plant system : Coupling isotopic and EXAFS approaches

A.M. AUCOUR¹, J.P. BEDELL², M. QUEYRON²
AND G. SARRET³

¹LGL-TPE, Université Lyon 1, CNRS, F-69622 Villeurbanne Cedex (*correspondence: aucour@univ-lyon1.fr)

²LEHNA, ENTPE, F-69518 Vaulx-en-Velin (jean-philippe.bedell@entpe.fr)

³ISTerre, Univ. Grenoble 1, CNRS, F-38041 Grenoble Cedex 9 (geraldine.sarret@ujf-grenoble.fr)

Zn isotope compositions can be an effective tool for monitoring Zn cycling in the soil-plant system. Zn isotope fractionations have been reported for model systems (humic acids, oxo-hydroxides, plant and nutrient solution) and in few natural systems. In the soil-plant system, studies combining isotopic and molecular approaches are necessary to identify abiotic and biotic processes controlling Zn isotope cycling.

This study is focused on Zn dynamics in an infiltration basin receiving urban stormwater and colonized by *Phalaris arundinacea* and *Typha latifolia*. The Zn isotope compositions were determined in the various plant organs (root, rhizome, stem, leaves), in fractions of the substrate (bulk sediments, DTPA and CaCl₂ sediment extracts, litter), in suspended and dissolved material from the water entry. The Zn speciation was also studied by EXAFS spectroscopy in the same compartments.

The EXAFS spectra were comparable in the various plant organs and indicated mainly an association of Zn with organic acids, with Zn in octahedral coordination. In contrast, the isotopic study evidenced an enrichment in light isotopes of the aerial biomass ($\delta^{66}\text{Zn}$ of -0.26‰ to -0.03‰) relative to underground biomass (-0.03 to 0.26‰) that is linked to translocation processes. Both Zn speciation and isotope composition of litter differed from that of the plant organs. The EXAFS data indicated that litter Zn was in tetrahedral coordination, corresponding to high affinity sites. The isotopic composition of litter (0.18 to 0.22‰) was enriched in heavy isotopes relative to aerial biomass and got close to that of sediment (0.14 to 0.19‰). Litter formation is thus accompanied by Zn exchange between the decomposing plant and the sediment. The Zn speciation is drastically modified from organic complexes and weakly sorbed species in entry material to phyllosilicates in the sediment. Zn in phyllosilicate is considered as a stable form. Its remobilization by the plant is however indicated by the litter-sediment exchange.

U-Pb ID-TIMS zircon ages and coupled Lu-Hf S-ICP-MS data - A tool for terrane characterisation and determination of paleogeographic affinities: An example from the Caledonides

LARS E. AUGLAND¹, ARILD ANDRESEN²
AND MARK STELTENPOHL³

¹GEOTOP, UQAM CP 8888, Succ. Centre-Ville, Montréal, Québec, Canada H3C 3P8, (augland.lars_eivind@courrier.uqam.ca)

²Department of Geosciences, University of Oslo, P. O.Box 1047 Blindern, 0316 Oslo, (arild.andresen.geo.uio.no)

³Department of Geology, 210 Petrie Hall, Auburn University, AL 36849, (steltmg@mail.auburn.edu)

Lu-Hf solution ICP-MS data from zircon fractions that have been dated by U-Pb ID-TIMS provide robust information on the sources of magmatic rocks. When combined, the complementary data sets can be used as a tool for terrane characterisation and source rock identification allowing correlation of spatially separated terranes and providing information on their provenance.

In the Scandinavian Caledonides several suspect/exotic terranes are occurring and here we report U-Pb ages and Lu-Hf isotopic data from a number of magmatic rocks, ranging from tonalites to granites, from the highest tectonostratigraphic levels in the Ofoten-Troms region (Upper and Uppermost Allochthons). Ages range from 484 Ma to 449 Ma with $\epsilon_{\text{Hf}(t)}$ varying from + 9.6 to - 6.2. The combined U-Pb and Lu-Hf data provide a new basis for terrane correlations in the area and supports previous suggestions that all of these terranes are entirely exotic with respect to Baltica. Furthermore, the Lu-Hf isotopic data indicate that the different terranes comprise different crustal segments, from ophiolitic terranes most likely formed during westward subduction east of the Laurentian continent (present day coordinates) to terranes formed on the actual Laurentian margin prior to the Caledonian continent-continent collision. The new data can thus give new constraints on crustal accretionary processes and interactions between the continents during the Caledonian orogen. S-ICP-MS Lu-Hf data from magmatic arc rocks in the North East Greenland Caledonides (Augland *et al* 2012) show a similar $\epsilon_{\text{Hf}(t)}$ range to the granitic rocks analysed in this study and we suggest that the exotic terranes with Laurentian age and Lu-Hf isotope signatures had their pre-collisional provenance in the East Greenland segment of the Laurentian margin.

Predictive Bayesian models for risk modeling of geologic carbon capture and storage leaks using natural analogues

CAITLIN AUGUSTIN¹, PETER SWART²
AND KENNETH BROAD³

¹University of Miami Abess Center for Ecosystem Science and Policy, (c.augustin@umiami.edu)

²University of Miami Rosenstiel School of Marine and Atmospheric Science, (p.swart@rsmas.miami.edu)

³University of Miami Abess Center for Ecosystem Science and Policy, (kbroad@miami.edu)

Modelling the risks of geologic carbon capture and storage (GCCS) involves many conceptual and quantitative uncertainties. In the development of subsurface carbon dioxide (CO₂) injection as a large-scale greenhouse gas solution, the ability to quantify its uncertainties and risks will play a key role. Published GCCS risk analyses have been based on failure mode and effects analysis, fault-tree analyses, and sensitivity analysis. [1] These analyses have been useful in characterizing risks, but have not yielded quantitative information on the likelihood of a leakage or spill occurring.

Leaked CO₂ is difficult to locate and quantify because monitoring techniques are not widely deployed. Moreover, the released CO₂ may be transported, sequestered or diluted based weather patterns and surrounding ecosystems. Changes in barometric pressure, temperature, and make deterministic fate models nearly impossible to deploy since even the presence of CO₂ is difficult to assess. With GCCS, it will be impractical and impossible to collect comprehensive empirical data regarding geologic reservoir leaks. There is a clear need to introduce statistical technique that integrates limited available data with stochastic modelling. Predictive Bayesian statistical techniques have been developed and demonstrated for exploiting limited information for decision support in many other applications, this paper will adapt and apply them to GCCS. [2]

Natural subsurface CO₂ deposits provide a reasonable analogue for the migration pathways and surface leakage scenarios encountered with GCCS. This paper is concentrated on the development of the conceptual predictive Bayesian model based on theory and literature review. This paper will present predictive leakage scenarios modelled on historic natural subsurface CO₂ leakage data collected from national and international databases.

[1] Goldschmidt, Wildenborg, A.,F.,B., *et al* (2005) In: Benson, S.M (Ed.) *Elsevier*, Ch. **33.**, 1293–1316 [2] Englehardt, J.D. (1995) *Journal of Environmental Engineering*, **121**, 455-464

Sulphides and Ti-Minerals in granulate xenoliths: Tracers of cratonic crust formation

SONJA AULBACH^{1,2}, BIBIANA FÖRSTER¹
AND THOMAS CHACKO²

¹Goethe-University, Fachinheit Mineralogie, Frankfurt, Germany, (s.aulbach@em.uni-frankfurt.de)

²University of Alberta, Department of Earth and Atmospheric Sciences, Edmonton AB, Canada

The trace-element composition of the common accessory minerals in granulites - sulphides (sf), rutile (rt) and ilmenite (ilm) - contains important petrogenetic information regarding the formation and evolution of the continental crust (CC) [1]. Eclogitic rt and ilm are significant hosts to many high field-strength elements (HFSE), but show contrasting partitioning and therefore fractionate geochemically diagnostic trace-element pairs, such as U-Th, Nb-Ta, Zr-Hf, W-Mo and W-Hf [2,3]. Some of the HFSE (e.g. Cr, Co, Sn, Sb, Mo, W) are chalcophile and siderophile elements (CSE), which are measurable in sulphides. A reconnaissance LAM-ICPMS study of Ti-minerals and sf in four mafic granulite xenoliths (MGX) from the Diavik kimberlites of the central Slave craton (Canada) broadly confirms experimental trace-element systematics - with interesting exceptions - and shows that sf strongly partitions Ni, Co, As and Sb, whereas W, Sn ± Mo concentrate in rt, and Cr, Zn, Ga favour ilm.

Bulk-rock CSE abundances, calculated from concentrations in MGX sf, rt and ilm weighted by modes, balance the abundances of W and Pb in CC [4], but show large excesses for Ni, Cr, Co, Sn, Mo, Sb and As. This suggests a cumulate origin for the MGX and enrichment by (seawater?) fluids. Sf- and rt- ± ilm-saturated melting of such lower CC should generate melts depleted in these elements. Since this is not observed in the upper CC [4], upper CC is probably not related to lower CC by igneous processes.

Segregation of sf-bearing cumulates in the lower CC was recently proposed to explain Cu depletion in the upper CC [5]. Sf in MGX have trace-element concentrations within the range of sf inclusions in diamonds from meta-gabbroic source rocks, which have been shown to control Cu, Se, Te, Mo, Re and PGE in the bulk rock [5]. Since only Cu and Se show complementary depletions in CC, the processes generating the crustal CSE pattern must be more complex.

[1] Stimac and Hickmott (1994) *Chem Geol* **117**, 313-330. [2] Zack *et al* (2002) *Chem Geol* **184**, 97-122. [3] Klemme *et al* (2006) *Chem Geol* **234**, 251-263. [4] Rudnick and Gao (2005) *Treatise on Geochemistry* 3, 1-64. [5] Lee *et al* 2012 *Science* **336**, 64-68. [6] Aulbach *et al* (2012) *GCA* **93**, 278-299.

Cannibalization of previous Na-rich clinopyroxenes by ascending basic magmas of the Garrotxa Volcanic Field (NE, Spain)

M. AULINAS*, G. GISBERT, D. GIMENO
AND D. GASPERINI

Dep. Geoquímica, Petrologia i Prospecció Geològica,
Universitat de Barcelona. 08028 Barcelona, Spain
(*correspondence: meritxellaulinas@ub.edu;
ggisbert@hotmail.com; domingo.gimeno@ub.edu;
gasperinidaniela@gmail.com)

The Garrotxa Volcanic Field (GVF) is a Quaternary monogenetic volcanic field belonging to the NE Spain volcanic province, recording a Neogene alkaline intraplate magmatic activity consequence of the rift-type extensional tectonics that has affected the eastern margin of Iberia since late Oligocene. The GVF is mainly characterized by alkaline basaltic rocks (basalts and basanites) both potassic and sodic in affinity. In general, mineral assemblage includes olivine and clinopyroxene phenocrysts and microphenocrysts, and a groundmass formed mainly by variable amounts of plagioclase and Fe-Ti oxides. Clinopyroxenes (cpxs) are not petrographically homogeneous and two types are distinguished: (I) Non to normal zoned phenocrysts with beige centres often surrounded by thin brown rims and (II) reversely zoned phenocrysts with green rounded cores wrapped by a beige mantle and an outer brown rim. The green cores (diopsides with Na₂O up to 1% and Al₂O₃ up to 7%) in Type II cpxs show petrographic and chemical evidences in agreement with a xenocrystic nature (e.g. sharp optical and chemical contrast between cores and mantles, rounded shape, high Fe/Mg ratios, or coexistence of type I and type II phenocrysts in a single sample). In this sense, their chemical compositions are in accordance with cpxs crystallized from a more evolved liquid than the primitive ascending basanitic magmas in which they are included. These xenocrysts seem to be petrographically and chemically related to cpxs from clinopyroxenite and gabbroic cumulates which can be found in some of the GVF samples. Therefore, we hypothesize that green cpxs were entrapped or cannibalized by the basic rising magmas. Preliminary cpx-melt calculations indicate that mantles of type II cpxs crystallized at maximum of ca. 30 km depth and consequently, cannibalization occurred at higher depths. This is consistent with the presence of green cpx-bearing mafic and ultramafic cumulates at or near the crust mantle-boundary.

Linking mantle melting and eruption rates at Stromboli volcano: A U-series perspective

R. AVANZINELLI^{1,2}, A. BRAGAGNI¹, L. FRANCALANCI¹,
H. FREYMUTH² AND T. ELLIOTT²

¹Dipartimento di Scienze della Terra, Università degli Studi di Firenze, Italy. E-mail, riccardo.avanzinelli@unifi.it
²Bristol Isotope Group, University of Bristol, UK

Over the last several hundred years, the steady-state activity of Stromboli volcano has been characterised by persistent mild explosive eruptions, ejecting black scoria bombs. Periodically, lava flows and paroxysms, ejecting also light-coloured pumices, interrupt the 'normal' activity. A degassed and highly porphyritic basaltic-shoshonitic magma (HP-magma), is erupted by the normal activity and lava flows, whereas a slightly more mafic and volatile-rich magma with low phenocryst content (LP-magma) is erupted as pumices only by the paroxysms. Whilst the former is considered as deriving from a shallow level reservoir, the latter has a deeper origin and might resemble the primitive melts generated from the mantle source.

We present new U-series disequilibria measurements on a suite of HP and LP magmas from the present-day activity of Stromboli volcano. Small but significant differences are observed in (²³⁸U/²³²Th), (²³⁰Th/²³⁸U) and (²²⁶Ra/²³⁰Th) between HP and LP magmas, testifying and further constraining the complex processes occurring in the shallow level magma chamber (e.g. crystal fractionation, mixing, recycling of material from previous activity).

On the contrary, the variation of (²³⁰Th/²³²Th) seems to be little affected by the shallow level processes and can be used to constrain the melting regimes beneath the volcano. This is particularly true for the LP magmas that should reflect the composition of the primitive magma. Indeed, the LP data show an impressive time-related constant variation of (²³⁰Th/²³²Th) during the last 15 years that is interpreted as an increase in the melting rate of the mantle source. More importantly this variation can be directly related with the increase in eruption rate that is suggested by both observation (increase of major explosive events and lava flows) and estimates based on the volcano morphology and erupted volumes. This suggests that U-series, and (²³⁰Th/²³²Th) in particular, can represent an important tool to estimate the rate of magma production and then possibly forecast the eruption rates in basaltic volcanoes such as Stromboli.

The variation in (²³⁰Th/²³²Th) is also discussed with the aim of estimating the turnover times of both the HP and LP systems.

Melt generation in the West Antarctic Rift System: The volatile legacy of Gondwana subduction?

K.B. AVIADO¹, S. RILLING², S.B. MUKASA¹,
J.G. BRYCE¹ AND J. CABATO¹

¹Department of Earth Sciences, University of New Hampshire, Durham, NH 03824, USA

²Department of Earth and Environmental Sciences, University of Michigan, Ann Arbor, MI 48105, USA

The West Antarctic Rift System (WARS) represents one of the largest extensional alkali volcanic provinces on Earth, yet the mechanisms responsible for driving rift-related magmatism remain controversial. The failure of both passive and active models of decompression melting to adequately explain the observed volume of volcanism has prompted debate about the relative roles of thermal plume-related melting and ancient subduction-related flux melting. The latter is supported by roughly 500 Ma of subduction along the paleo-Pacific margin of Gondwana prior to the breakup of this supercontinent beginning in the Jurassic, although both processes are capable of producing the broad seismic anomaly imaged beneath most of the Southern Ocean. Olivine-hosted melt inclusions from basanitic lavas provide an unambiguous means to evaluate the volatile budget of the mantle responsible for active rifting beneath the WARS. We present H₂O, C, Cl, F, and S concentrations determined by SIMS for 5 WARS lavas from Northern Victoria Land (NVL) and Marie Byrd Land (MBL). Initial results for the lavas exhibit water contents ranging from 0.5 up to 3 wt % that are positively correlated with Cl and F. Coupling between Cl and H₂O indicates metasomatic enrichment by subduction-related fluids produced during dehydration reactions; coupling between H₂O and F, which is more highly retained in subducting slabs, may be related to partial melting of slab remnants [1]. Application of source lithology filters [2] to major oxide data shows that primitive lavas (MgO wt % >7) from the Terror Rift, considered the locus of on-going tectonomagmatic activity, have transitioned from a pyroxenite source to a volatilized peridotite source over the past ~4 Ma. Integrating the volatile data with the modelled characteristics of source lithologies suggests that partial melting of lithosphere modified by subduction processes is the source of pyroxenite and volatiles in the mantle beneath the present-day rift. The earliest magmatic activity preferentially removed the most readily fusible components from the mantle, resulting in transition to a metasomatized peridotite source over time.

[1] Straub & Layne, (2003), *GCA* [2] Herzberg & Asimow, (2008), *G³* [3] Rilling *et al.*, (2009), *JGR*.

Modeling the evolution of the isotopic composition of atmospheric xenon through time

G. AVICE* AND B. MARTY

CRPG/CNRS, BP 20, 54501, Vandoeuvre-lès-Nancy, France

(*correspondence: gavice@crpg.cnrs-nancy.fr)

Even if the isotopic compositions of terrestrial H, N and Ar are clearly chondritic, atmospheric xenon is not chondritic in two ways : it is depleted relative to lighter noble gases, and it is isotopically enriched in its heavy isotopes relative to chondritic or solar components (the so-called xenon paradox). Recently, xenon trapped in Archean samples was found to be isotopically intermediate between Chondritic and Atmospheric [1], which was interpreted as resulting from prolonged loss of atmospheric xenon to space at least until the Archean eon. Such preferential loss could be related to the low ionization potential of Xe and, possibly, to the 10 fold enhanced flux of hard UV light during the first Ga of solar evolution [2].

In order to explore the geochemical consequences of this possibility, we have developed a numerical box model in which atmospheric xenon evolves through time due to degassing from the mantle with no isotopic fractionation, and escapes from the atmosphere to the outer space with enrichment in its heavy isotopes. The model is constrained by the initial conditions (cosmochemical Xe isotopic composition from the literature; Xe initial abundance equivalent to a few % carbonaceous chondrite [3]), the variation in the Xe isotope composition through time [1,4] and the present-day Xe composition of the mantle and of the atmosphere.

The combination of the two processes, permits to reproduce with accuracy (few % difference) the current isotopic composition of the Earth's atmosphere. In particular, the model explains the well known but unexplained atmospheric under-abundance of Xe isotopes from the fission of ²⁴⁴Pu (T_{1/2} = 82 Ma). When corrected for prolonged Xe loss into space, the I-Pu-Xe age of the atmosphere shifts from >100 Ma to 45±5 Ma.

[1] Pujol *et al* (2011) *EPSL* **308**, 298-306 [2] Ribas *et al* (2005) *The Astrophysical Journal* **622**, 680-694 [3] Marty (2012) *EPSL* **313-314**, 56-66 [4] Pujol *et al* (2009) *GCA* **73**, 6834-6846

Anaerobic oxidation of methane by sulfate in hypersaline groundwater at the Dead Sea aquifer

N. AVRAHAMOV^{1*}, G. ANTLER^{1,2}, Y. YECHIELI^{3,4},
I. GAVRIELI³, S. JOYE⁵ AND O. SIVAN¹

¹Department of Geological and Environmental Sciences, Ben Gurion University of the Negev, Beer-Sheva

²Department of Earth Sciences, University of Cambridge

³The Geological Survey of Israel, Jerusalem

⁴Department of Environmental Hydrology & Microbiology, Zuckerberg Institute for Water Research, Blaustein Institutes for Desert Studies, Ben Gurion University of the Negev, Sede Boqer, Israel

⁵Department of Marine Sciences, University of Georgia, Athens, GA (*correspondence: katzavn@bgu.ac.il)

Anaerobic oxidation of methane (AOM) with sulfate as an electron acceptor is not a process that is expected to occur in salt-stressed environments, since the energy yield is extremely low. Still, AOM appears to function even in hypersaline cold seeps sediments in marine environment. Here, we document geochemical evidences for AOM process in the continental hypersaline environment of the Dead Sea aquifer. We explored this process through chemical and isotope measurements of sulfate and methane in groundwater with salinity range of 40-225 Cl g·L⁻¹ along the Arugot alluvial fan next to the DS. Oxygen values of this groundwater vary from absence to very low (0 to 0.16 mg·L⁻¹). Sulfate concentrations and isotopes indicates BSR. Mass balance of carbon system parameters as well as the association between methane concentrations to the apparent net sulfate reduction show that methane serves as the main electron-donor. The calculated sulfur isotope enrichment factor might hint high reduction rates of sulfate when methane is used as a substrate.

Comparison of ²H, ¹⁸O, ³H and radionuclides migration in groundwater near the liquid waste injection site (Tomsk-7, Russia)

I.A. AVRAMENKO¹, I.V. BLAZHENNIKOVA²
AND I.V. TOKAREV³

¹(i.a.avramenko@gmail.com)

²(blazhennikova@mail.ru)

³(okarevigor@gmail.com)

Groundwater near the site injection of the liquid radioactive waste of the Siberian Chemical Combine (former Tomsk-7, Russia) was studied. There are six (from I to VI) sandy aquifers (the numbers are follow from the crystalline basement to the Earth surface) in this multilayer hydrogeological system. Radioactive solutes (including a high activity waste) are injected into the II and III aquifers on the depth of 270–350 m. Total activity of the buried waste is about 800 millions Curie. The nitrates, gamma radiation, temperature were used for monitoring of the radioactive waste distribution in aquifers for 1963-2000.

Natural water of II and III aquifers has no tritium, because their age is several thousand years according to the helium and radiocarbon dating. The tritium (³H) concentration in radioactive waste is very high, and also the stable isotopes composition (²H and ¹⁸O) of natural and man-made water is very different. These isotopes are the best tracers of water, as they form its molecule, whereas the radionuclides of waste are the reactive components, which decay with time and adsorb on the clayey part of sediments. Therefore comparison the behavior of conservative and non-conservative tracers allow to estimate of the retardation factor *in situ*. More than 200 wells have been tested for localization of the boundary between the natural water and man-made solutes. We used the ³H, ²H and ¹⁸O monitoring to improve the safety prediction of the waste disposal and also for verification and calibration of the numerical model.

Polyphase evolution of the Eastern Ghats Belt (India) - A multi mineral approach using Rb-Sr and U-Pb ages

EMELIE AXELSSON*, KLAUS MEZGER
AND IGOR M. VILLA

Institute of Geological Sciences, University of Bern,
Baltzerstrasse 3, 2012 Bern, Switzerland.
(*correspondence: axelsson@geo.unibe.ch)

The Eastern Ghats Belt (EGB) is a granulite facies metamorphic belt along the east coast of India. It is a patchwork of discrete crustal segments with distinct geological histories. It records the formation and destruction of at least two earlier supercontinents, namely Colombia (ca 2.1-1.8 Ga) and Rodinia (ca 1.0-0.9 Ga); as a part of the amalgamation of India, east Antarctica, and Australia into the SWEAT (SW United States and East Antarctica) terrane.

Four crustal domains with unique isotopic signatures and ages can be distinguished within the EGB [1]. The highest-grade metamorphism was attained during the regional metamorphism at ca 950 Ma. The subsequent evolution was proposed to be slow cooling at a rate of ca. 1-2°C/Ma [2].

To reconstruct the post-peak evolution after the 950 Ma metamorphic imprint, Rb-Sr biotite ages were determined from biotite-rich metapelitic gneisses. These ages cluster around 500 Ma for most of the Eastern Ghats belt. The analysed biotite samples have high Mg content, and the general mineral assemblage is that typical of high temperature granulites: plag + phl + sil + grt and, depending on the protolith, kfs, crn or crd. Common accessory mineral phases are: rt, zrc, spl, ap, spr.

Very young biotite ages like these are unlikely to be the result of slow cooling from the granulite facies conditions at ca 950 Ma. Instead they record a low-grade static thermal overprint of the orogenic belt. This overprint coincides with high-grade metamorphism in southern India and Sri Lanka (ca 580-550 Ma), corresponding with the Pan-African orogeny. The young ages on a regional scale extend the known area of the pan-African overprint in India significantly.

[1] Rickers, K., Mezger, K., Raith, M. (2001), *Precambrian Research*, **112**:28. [2] Mezger, K., Cosca, M.A. (1999), *Precambrian Research*, **94**:251-271

Petrological and Geochemical Constraints on the origin and evolution of the Early Campanian porphyritic rocks from the Eastern Pontide Magmatic Arc, NE-Turkey

FARUK AYDIN

Department of Geology, Karadeniz Technical Univ., 61080,
Trabzon, Turkey (faydin61@gmail.com)

Petrogenesis of the porphyritic rocks in the Eastern Pontides, NE Turkey, play a critical role in determining the nature of the continental crust and mantle dynamics during late Mesozoic subduction processes. In this study, we described, for the first time, the early Campanian (81±0.5 Ma) porphyritic rocks cutting the late Cretaceous volcanic units in the region. The porphyritic rocks were observed as small stocks (< 1km²) in the study area and they generally contain mafic magmatic enclaves (MMEs). The host porphyritic rocks comprise quartz diorite and tonalite (SiO₂= 64–70 wt%, Mg#= 0.40-0.52) and the MMEs are gabbroic diorite in composition (SiO₂= 51–57 wt%, Mg#= 0.36-0.50). The host rocks have a microgranular porphyritic texture, and they contain 15-25% phenocryst of plagioclase and amphibole with a matrix composing plagioclase ± quartz ± orthoclase ± apatite ± zircon ± Ti-magnetite. Compared to the host rocks, the MMEs are finer grained, and they contain higher proportion of ferromagnesian phases and less feldspar minerals.

Geochemically, the samples usually show a high-K calc-alkaline composition and I-type features with metaluminous character. The host porphyritic rocks and the MMEs are characterized by enrichment of LILE and depletion of HFSE with negative Nb and Ti anomalies. The chondrite-normalized REE patterns are fractionated [(La/Yb)_N = 5-17] and moderately display Eu anomalies (Eu/Eu* = 0.5-1.2). All samples have weak concave-upward REE patterns, suggesting that amphibole and garnet played a significant role in their generation during magma evolution. The host rocks and their enclaves are isotopically indistinguishable. Sr-Nd isotopic data for all of the samples display $I_{Sr} = 0.7085-0.7087$, $\epsilon_{Nd} (81 \text{ Ma}) = -6.0$ to -6.9 , with $T_{DM} = 1.38-1.63$ Ga. Pb isotopic ratios are (²⁰⁶Pb/²⁰⁴Pb) = 18.61–18.69, (²⁰⁷Pb/²⁰⁴Pb) = 15.66–15.69 and (²⁰⁸Pb/²⁰⁴Pb) = 38.78–38.90.

All geochemical results and the Ar–Ar crystallization age, combined with previous regional studies, suggest mixed-origin magma generation in a subduction setting.

**Distribution of Cu, Pb and Zn in
Astragalus pycnocephalus Fischer and
Verbascum euphraticum L. Plants on
Pb-Zn Mining Area in
Akdagmadeni, Yozgat, Turkey**

NASUH AYDIN¹, GÜLLÜ KIRAT² AND CEMAL BÖLÜCEK³

^{1,3}Balikesir University, Faculty of Engineering and Architecture. Department of Geological Engineering, BALIKESİR (nasuhaydin@hotmail.com.tr; cbolucek@balikesir.edu.tr)

²Bozok University, Faculty of Engineering and Architecture. Department of Geological Engineering, YOZGAT (gullu.kirat@bozok.edu.tr)

The study area is located in Akdagmadeni where 104 km East of Yozgat city and geologically lies within igneous and metamorphic rocks of Akdag Massive. There are several skarn type Pb, Zn deposits which formed by regional contact metamorphism.

Soil and plant samples were collected from both mineralized and unmineralized areas. The plants *Astragalus pycnocephalus* Fischer and *Verbascum euphraticum* L. were examined. Analysis were carried out by Inductively Coupled Plasma-Mass Spectrometry (ICP-MS) method.

Cu, Pb and Zn values of the soil samples were found to be in the range of (*A. pycnocephalus*) 13.1- 418.4 mg kg⁻¹; 29.87- 7839.53 mg kg⁻¹; 48.6- 10000 mg kg⁻¹ (*V. euphraticum*) 32.5- 419.4 mg kg⁻¹; 52.96- 9909.13 mg kg⁻¹; 115.1- 10000 mg kg⁻¹, respectively.

Pb and Zn values of most plant samples collected from study area were 10 times higher than the plants from unmineralized areas. Pb and Zn concentration time values were found to be in the range of 463 – 548 mg kg⁻¹; 17.4 – 23.3 mg kg⁻¹, respectively. Translocation factor changed from 0.13 to 4881. Enrichment coefficient of most plant samples were lower than 1. *A. pycnocephalus* and *V. euphraticum* can be used as hyperaccumulator plants for both Pb and Zn. However, these plants cannot be used as hyperaccumulator for Cu.

Keywords: *A. pycnocephalus*, Akdag Massive, Contact Metamorphism, Hyperaccumulator, Pb-Zn Deposit, *V. euphraticum*.

**The late Ediacaran (605-580 Ma)
anorogenic alkaline magmatism in
the Arabian–Nubian Shield:
A case study of the Serbal Ring
complex, south Sinai, Egypt**

MOKHLES K. AZER

Geology Department, National Research Centre, 12622-Dokki, Cairo, Egypt (mokhles72@yahoo.com)

The Serbal pluton is late Neoproterozoic (605-580 Ma) post-collisional A-type granites in southern Sinai, Egypt (northernmost Arabian–Nubian Shield, ANS). It is characterized by discontinuous ring-shaped outcrops that was later dislocated by a faults. The Serbal pluton intrudes late Neoproterozoic metamorphic and calc-alkaline rocks. The majority of Serbal pluton is composed of alkali feldspar granite and riebeckite granite with gradational contacts; the former represents the outer zone, while the latter represent the inner zone. The Serbal granites include wide variations of accessory minerals including zircon, apatite, titanite, Fe-Ti oxides, fluorite, allanite, pyrochlore and samarskite. The Serbal granites are highly evolved in composition (75.98-78.52 wt.% SiO₂) and display the typical geochemical characteristics of A-type granites with high SiO₂, Na₂O+K₂O, FeO*/MgO, Ga/Al, Zr, Nb, Ga and Y and low CaO, MgO, Ba, and Sr. They are rich in REE than monzogranite (country rock) and show extreme Eu-negative anomaly (Eu/Eu* = 0.01-0.23). The peralkaline to peraluminous characteristics of the Serbal granites suggested that they have been evolved through different differentiation trends which controlled by varying fluorine contents of the parent magma. The chemical characteristics indicate that the riebeckite granite shares in many features of granites with the tetrad REE effect which manifested by the very low ratios of Eu/Eu*, (La/Yb)_n, La/N, Zr/Hf and K/Rb and by the very high K/Ba. The Serbal granites exhibit an alkaline nature of within plate tectonic setting, while the monzogranite of country rocks displays calc-alkaline characteristics of island-arc tectonic settings. The Serbal pluton evolved through fractional crystallization of a parental magma derived through partial melting of juvenile crustal protolith. This crustal protolith has been extracted from a source having geochemical and isotopic data similar to those of the mantle origin. Mineral geothermometry points to the formation of the silicic magma of the Serbal granites at high temperatures, up to 650–850°C at a shallow depth of emplacement (<10 km). This magma erupted after the end of the Pan-African orogeny due to the thinning and extension of continental crust. This stage is characterized by the sudden and radical change from typical subduction-related calc-alkaline magmatism to post-tectonic alkaline (peralkaline) magmatism.

Discovery and characterization of contrasting siderophores produced by related nitrogen fixing bacteria using high resolution LC-MS

OLIVER BAAR, DAVID H. PERLMAN,
ANNE M. L. KRAEPIEL AND FRANÇOIS M. M. MOREL*

Princeton University, Princeton, NJ, USA

(*correspondence: morel@princeton.edu)

Azotobacter vinelandii (AV) and *Azotobacter chroococcum* (AC) are closely related N₂ fixing bacteria. Whereas the structures and physiological functions of siderophores produced by AV have been much studied, those of AC remain unidentified beyond a general chemical characterization. Here we have exploited the characteristic iron isotopic fingerprint to identify known and unknown siderophores and characterize them structurally using ultra-sensitive high-resolution nano-flow UPLC-MS on an LTQ-Orbitrap XL platform.

Interrogation of preliminary data for AV revealed many putative Fe-chelators with high abundances, including those previously identified and other, yet unreported compounds.

Siderophores produced by AC were unrelated to those of AV. Many AC siderophores possess aliphatic side chains of variable length with corresponding changes in hydrophobicity. Current work investigates how these chemical differences in siderophore production relate to different metal acquisition strategies and occupation of different ecological niches.

Using isotopic analysis of copper to assess copper transport and partitioning in wetland systems

I. BABCSANYI*, F. CHABAUX, V.M. GRANET
AND G. IMFELD*

Laboratory of Hydrology and Geochemistry of Strasbourg (LHyGeS), University of Strasbourg/ENGEES, CNRS, 1, rue Blessig, 67 084 Strasbourg CEDEX

(*correspondence: imfeld@unistra.fr,
izabella.babcsanyi@etu.unistra.fr)

Copper isotopes (⁶⁵Cu/⁶³Cu) are potentially powerful new geochemical proxies for transport and oxidation–reduction processes in hydromorphic soils, rivers and lake sediments. However, the integrative signal of δ⁶⁵Cu has not been used so far to investigate the transport and partitioning of copper in wetland systems with respect to both hydrological and biogeochemical conditions. Here we used copper isotopes to investigate the copper cycling in a stormwater wetland (as a ‘natural laboratory’) that regularly received copper-contaminated runoff from a 42 ha vineyard catchment (Rouffach, Alsace, France). Runoff water, suspended solids, sediments and plants were regularly collected throughout the period of copper-based fungicides application (May to July 2011) to establish the copper mass balance and study isotopic fractionations.

60 to 93% of copper in runoff was associated with suspended solids, which were efficiently retained by the wetland (93 to 96%). Copper bound to suspended solids had negative isotope signatures (−0.33 to −0.1 ± 0.1‰), whereas dissolved copper was enriched in ⁶⁵Cu (0.23 to 1.35 ± 0.06‰). Dissolved copper retention largely varied (68 to 95%) and became depleted in ⁶⁵Cu when passing through the wetland (δ⁶⁵Cu_{inlet}–δ⁶⁵Cu_{outlet}: 0.03 to 0.77 ± 0.08‰). This isotopic shift suggests that copper rapidly sorbed to organic matter or mineral phases of the wetland sediments. Under high-flow conditions, copper was less retained by the wetland and was likely mobilised from the wetland sediments. This was attested by a lower δ⁶⁵Cu value of the outflowing dissolved copper, thereby reflecting the contribution of sediment-bound copper (0.02 ± 0.1‰). Copper uptake by the vegetation (*Phragmites australis*, Cav.) was not a significant retention process in the wetland, and accounted for less than 1.5% of the total copper amount in the wetland.

We anticipate our results to be a starting point for using copper isotopes in a comprehensive approach to evaluate processes affecting copper cycling in hydro-biogeochemically dynamic systems, such as wetlands or hyporheic zones.

High-precision Nd isotope and HFSE analysis of Deccan Traps weathering profiles

MICHAEL G. BABECHUK^{1*}, MIKE WIDDOWSON²,
MICHAEL MURPHY³ AND BALZ S. KAMBER¹

¹Trinity College Dublin, Dublin, Ireland

²The Open University, Milton Keynes, United Kingdom

³University College Dublin, Dublin, Ireland

Accurately quantifying the flux of elements from landmasses during pedogenesis necessitates knowledge of the parent rock chemistry and some control on whether allochthonous materials (e.g., dust) have been added to the profile during exposure. This is important, for instance, in calculating weathering rates from U-series isotopes in young profiles or interpreting stable isotope depth signatures. The Deccan Traps provide an ideal natural laboratory for studying chemical weathering due to the thick succession of mafic flows which have been weathered to varying degrees on different time scales. In addition, the isotopic and elemental composition of the basalt parent rock contrasts significantly with most potential dust sources (e.g., Archean-Proterozoic crust of the Dravidian Shield).

Deeply weathered laterite of the Deccan Traps has experienced significant accumulation of aeolian material during its long exposure history. For example, in a full laterite profile near Bidar, an upward increase in Th concentration and accompanying decrease in the Nb/Th ratio is evident from the base to top. If Nb is assumed to be immobile during pedogenesis and least affected by dust addition, Th is enriched up to 400% relative to the parent rock in the most contaminated samples. Variations in the Nb/Th ratio are well correlated with the ¹⁴³Nd/¹⁴⁴Nd ratio, implicating the source of the contaminant as being incompatible element enriched and less radiogenic than the Deccan basalt.

Near Chhindwara, a sub-Recent weathering profile is exposed which spans across two identifiable basalt flows. The individual flows can be fingerprinted with variations in their HFSE composition, highlighting another important consideration in mass balance calculations of a weathering profile. Even more interesting, however, are the uppermost samples of the lower exposed flow with alkali element, HFSE ratios, and subtly less radiogenic Nd isotope values which again suggest contamination with an allochthonous component. This is interpreted to represent the entrainment of sediment in the lava flow top during emplacement or the accumulation of dust during post-eruption volcanic quiescence prior to the emplacement of the overlying flow.

U-Pb dating vs. Sr isotope chemostratigraphy on Neoproterozoic carbonates: Shedding light on blind dating?

M. BABINSKI¹, G.M. PAULA-SANTOS¹;
M. KUCHENBECKER², S. CAETANO-FILHO¹,
R.I.F. TRINDADE³ AND A.C. PEDROSA-SOARES²

¹Instituto de Geociências, Universidade de São Paulo, São Paulo, SP, Brazil. (babinski@usp.br)

²Instituto de Geociências, Universidade Federal de Minas Gerais, Belo Horizonte, MG, Brazil.

³Instituto de Geofísica, Universidade de São Paulo, São Paulo, SP, Brazil.

Sr isotope ratios of carbonate rocks have been extensively used for global correlations especially on Precambrian rocks due to lack of fossils and scarcity of dating targets to constrain their depositional ages. This “blind dating” procedure has been questioned before but it is still commonly used. Here we present a case study on carbonates from the basal units of the Bambuí Group (central Brazil) where Sr, C, and O chemostratigraphy was combined with U-Pb ages from detrital zircons recovered from pelitic intercalations. Our results show a strong incompatibility between ⁸⁷Sr/⁸⁶Sr ratios and the detrital zircons record.

The Bambuí Group is composed of a carbonatic-pelitic succession which overlies a glacial diamictite (Jequitáí Fm.) correlated to the Sturtian or Marinoan ice-ages. U-Pb ages from detrital zircons from the diamictite sets the maximum depositional age at 875 Ma. The cap carbonate that overlies this diamictite has δ¹³C negative values and was dated at 740 ±22 Ma, indicating a Sturtian age. Limestones and dolostones overlying the cap carbonate show δ¹³C values around 0 ‰. Upsection, carbonates are organic-rich limestones displaying highly positive δ¹³C values. All carbonates, including those overlying the diamictite, show ⁸⁷Sr/⁸⁶Sr ratios between 0.7074 to 0.7076. These ratios are compatible with depositional ages as old as 650 Ma according to the global Sr isotope evolution curves available in the literature. However, detrital zircons yielded U-Pb ages as young as 540 Ma, pointing to depositional ages close to the Precambrian-Cambrian boundary or even younger, when more radiogenic Sr isotope ratios (ca. 0.7085) are expected. This may result from a restricted sea context for the Bambuí carbonate platform; consequently their Sr isotope ratios do not correspond to that of contemporaneous oceans. Several lines of evidence suggest this is not an unusual scenario for Neoproterozoic carbonate platforms. Our work shows that worldwide correlations based only on Sr isotopes must be considered with caution.

Rocky constraints on catabolic energy supply in the seafloor

W. BACH¹, W.-A. KAHL¹, N. JÖNS¹, A. TÜRKE¹
AND O. PLÜMPER²

¹Geoscience Department, University of Bremen, Klagenfurter Str., 28359 Bremen, Germany (wbach@uni-bremen.de)

²Department of Earth Sciences, Utrecht University, Budapestlaan 4, 3584 CD Utrecht, The Netherlands

Reactions between circulating seawater and oceanic basement release reduced components, which can be used as electron donors by chemolithoautotrophs in the seafloor. High-temperature axial hydrothermal vent systems show a pronounced influence of basement composition on metabolic diversity, with ultramafic hosted systems supporting a greater range of catabolic reactions, including anaerobic ones [1].

We investigate the influence of temperature (2-110°C), rock composition (basalt vs. peridotite), and permeability on energy availability for a seafloor biosphere away from axial vents where seawater circulation through fractured basement takes place at lower temperatures.

In fresh basalt, oxidation of ferrous iron is the main energy source at low temperatures (<25°C) and under oxic conditions. Increasing extents of alteration of glassy lava will build up palagonite rims as diffusive barriers between the fractures and unaltered glass, which slow down the rates of alteration. Palagonite has little or no ferrous iron and is enriched in U and K. Unless new fractures form and allow circulating seawater to interact with fresh material, the principal source of energy will change to dihydrogen produced radiolytically by U and K. At moderate temperatures (25-60°C), recharge of oxygenated seawater is sluggish and anaerobic metabolic reactions become more important. At high temperatures (60-110°C), the metabolic energy demand has increased relative to the energy supply, making growth more difficult for microbes.

In mantle peridotite, abundantly exposed in rift mountains along slow spreading ridges and commonly strongly serpentinized, oxidation of ferrous iron is also the main energy source at T<25°C. Brucite dissolves in contact with cold seawater, increasing permeability of the rock and pH in the interacting fluid. Serpentinites are often pervasively affected by low-T reactions, indicating that new permeability develops in the course of interaction with seawater. At T>25°C, dihydrogen yields are very high throughout. While the increased energy supply and permeability will facilitate microbial growth, high pH and the dearth of CO₂ in the interstitial solutions may impede it.

[1] Amend *et al.* (2011) *GCA* **75**, 5736 - 5748.

Contaminant geochemistry and migration in three different mine sites in Finland – Comparison of anthropogenic and geogenic contamination for risk assessment

S. BACKNÄS¹* K. TURUNEN¹ A. PASANEN¹
T. KARLSSON¹ AND L. SOLISMAA¹

¹Geological Survey of Finland, P.O.Box 1237, FIN-70211 Kuopio, Finland (*Correspondence: soile.backnas@gtk.fi)

Areas with bedrock abundant in ore minerals have naturally high amount of harmful elements in soil as well as in ground and surface waters. After the beginning of the mining the anthropogenic contamination also tends to increase. Thus, it is important to estimate the effects of mining activity and water treatment methods to the geogenic background when assessing the long term effects to the surrounding environment. In this study, geochemical and anthropogenic contaminant geochemistry and transport in soil at three different mine sites in Finland: Suurikuusikko, Siilinjärvi and Luikonlahti, were characterized by using extraction methods and mineralogical studies. Water samples were analyzed for metal and metalloid concentrations, anions and physico-chemical properties. Also groundwater and geochemical modeling software were used to study the groundwater flow paths and hydrogeochemistry.

The results show that the geogenic background, the hydrogeology of the site and concentrations of harmful elements in mine wastes and waters must be considered in risk assessment of mine sites. When evaluating the risks, the concentration levels must be compared to geochemical background, but also the ratio of available, potentially mobile and total concentrations must be studied, because the mining activities tend to increase the proportion of potentially mobile and available elements. Due to residues of chemicals used in enrichment process and weathering of minerals during the process, the concentration profile of harmful elements in waters can be used to distinguish the anthropogenic and geogenic contamination. Results also indicate that fractures of crystalline bedrock are important pathways for contaminant migration to environment and should be studied using geophysical methods and groundwater flow modeling when assessing the environmental effects of mines.

Surface complexation on birnessite controls Pb distribution in highly contaminated soil and karst groundwater

C.G.D. BACON¹² AND D.M. SHERMAN^{2*}

¹School of Earth Sciences, University of Bristol, UK, BS8 1RJ
(*correspondence: dave.sherman@bristol.ac.uk)

²Golder Associates (UK) Ltd, Bourne End, UK, SL8 5AS
(cbacon@golder.com)

At the historic mineries of Priddy near Bristol, soils are heavily contaminated with up to 2000 mg/kg Pb. However, porewater concentrations of Pb are undersaturated with respect to natural common Pb minerals such as cerussite. Scanning electron microscopy and EDX analysis revealed that the Pb in Priddy soil is associated with a poorly-crystalline Mn oxide phase. The Mn oxide phase contains up to 40 wt. % Pb. Using μ -EXAFS spectroscopy, and μ -XRD, we identified the Mn oxide as birnessite, similar to the poorly crystalline microbial δ -MnO₂ described by Villalobos *et al.* [1]. However, the origin of the birnessite in Priddy soil is unclear. Using μ -EXAFS, we find that Pb is complexed on both edge and vacancy sites, as proposed by [2].

The hydrology of the mining area drains into a complex network of caves, with the resurgence at Wookey Hole. Within the caves are extensive coatings of birnessite (as identified using XRD and Raman spectroscopy). We hypothesise that this birnessite is of microbial origin as found elsewhere [3]. The soil birnessite must be reduced to release dissolved Mn(II) which is then oxidized in the dark cave system by chemolithoautotrophic bacteria. The secondary birnessite in the cave also contains up to 40 wt. % Pb. μ -EXAFS shows that Pb associated with this birnessite in both edge and vacancy surface complexes.

We hypothesise that the complexation of Pb by birnessite controls the dissolved Pb concentration in soil pore water and groundwater. To test this, we have performed a series of batch sorption edge experiments with synthetic birnessite and fit these to derive equilibrium expressions and constants for the possible surface complexation reactions. Using our surface complexation model, we are predicting the concentration of Pb in soil porewater and groundwater. However, a reactive transport model needs to account for the microbial birnessite recycling.

[1] Villalobos *et al.* (2003) *Geochim. Cosmochim. Acta.*, **67**, 2649-2662. [2] Villalobos *et al.* (2005) *Env. Sci. Tech.*, **39**, 569-576. [3] White *et al.* (2009) *J. Caves Karst Stud.*, **71**, 136-147.

U-Pb and Hf isotope characteristics of zircon from chromitites at Finero

I.YU. BADANINA¹, K.N. MALITCH^{1,2}
AND E.A. BELOUSOVA²

¹Institute of Geology and Geochemistry of the Uralian Branch of Russian Academy of Sciences, Ekaterinburg, 620075, Russia (*correspondence: dunita2009@rambler.ru)

²GEMOC ARC National Key Centre, Macquarie University, Sydney, NSW 2109, Australia (ebelouso@els.mq.edu.au)

The Finero phlogopite-peridotite represents a metasomatized residual mantle harzburgite, exposed at the base of the lower-crust section in the Ivrea Zone, Western Alps [1]. Previous studies point to one or more Late Paleozoic mantle metasomatic events in the Finero peridotite, although there is little agreement regarding the relative timing of different events or the source of the metasomatizing agents.

Studied chromitite samples derived from the dump in the prospecting trenches of Alpe Polunia and Rio Creves. Dominant zircon population is pale pink and show different shapes (subhedral, subrounded or elongated). In cathodoluminescence (CL), the main set of population is represented by complex grains, which show development of core-rim relationship (most likely recrystallized rim on a preserved core). Subordinate zircon grains are colourless, with a smoky cathodoluminescence and almost no internal pattern. Three main U-Pb age clusters have been identified. The youngest cluster, typical for subordinate zircon population and rims in complex grains from dominant population, yielded two ²⁰⁶Pb/²³⁸U ages (e.g., 208.6 ± 4.0 Ma, MSWD=2.0, n=8 and 194.9 ± 3.4 Ma, MSWD=0.45, n=3, respectively). The other clusters represent cores and rims in the composite grains, with ages 288.3 ± 7.3 Ma (MSWD=3.3, n=6) and 248.6 ± 3.3 Ma (MSWD=0.13, n=8), respectively. In Lu-Hf systematics, zircons of all age populations show a relatively narrow spread in ¹⁷⁶Hf/¹⁷⁷Hf(t) values, with majority (~90 %) falling between 0.282652 and 0.282533. An increase in ¹⁷⁶Hf/¹⁷⁷Hf(t) ratio from old to young zircon populations defines a trend, which follow CHUR evolution curve.

Our data do not concur with the assumption [2] of a single metasomatic event during chromitite formation. In contrast, a prolonged formation and multistage evolution of zircon growth is considered a feature typical of a metasomatized subcontinental mantle at Finero.

This investigation was supported by the Uralian Branch of Russian Academy of Sciences (grant 12-P-5-1020).

[1] Hartmann & Wedepohl (1993) *GCA* **57**, 1761-1782.
[2] Grieco *et al.* (2001) *J. Petrol.* **42**, 89-101.

The effect of 1,10-phenanthroline on the oxidative dissolution of iron monosulfide (FeS)

C.E. BADICA* AND P. CHIRITA

University of Craiova, Department of Chemistry, Calea Bucuresti, 1071, Craiova 200512, Romania

(*correspondence: badica.catalina@gmail.com)

The effect of 1,10-phenanthroline (a Fe²⁺ ligand) on the oxidative dissolution of synthetic iron monosulfide (FeS) was tested by using electrochemical methods. The experiments were performed in air-saturated HCl solutions with the concentration of 1,10-phenanthroline in range 0-1 mM, at pH 5 and 25°C. The corrosion current densities (i_{corr}), corrosion potentials (E_{corr}) and values of the components of equivalent circuit that fits the Electrochemical Impedance Spectroscopy (EIS) data were determined.

i_{corr} values are quasi-constant when the concentration of 1,10-phenanthroline varies between 0 and 0.5 mM. When the concentration of 10-phenanthroline exceeds the value of 0.5 mM, i_{corr} increases from 30.7 $\mu\text{A cm}^{-2}$ up to 38 $\mu\text{A cm}^{-2}$. E_{corr} increases from -393 mV up to -338 mV when the concentration of 1,10-phenanthroline increases from 0 to 0.5 mM. At higher concentrations of ligand, E_{corr} decreases down to -355 mV. The values of the components of equivalent circuit that fits EIS data were found to be in agreement with the variation of i_{corr} and E_{corr} .

Our conclusion is that the oxidative dissolution of FeS in the presence of 1,10-phenanthroline is the result of two processes with opposite effect: 1) the inhibiting adsorption of 1,10-phenanthroline on the FeS surface and 2) the promoting effect of 1,10-phenanthroline on the breakage of Fe-S bond.

This work was supported by a grant of the Romanian National Authority for Scientific Research, CNDI-UEFISCDI, project number 51/2012.

Earth's building blocks: The "Core Spyglass"

JAMES BADRO¹, JOHN BRODHOLT², JULIEN SIEBERT^{1,3} AND RICK RYERSON^{1,4}

¹Institut de Physique du Globe de Paris, France

²University College London, United Kingdom

³Université Pierre et Marie Curie, Paris

⁴Lawrence Livermore National Laboratory, USA

The details of Earth's accretion, and the nature of Earth's building blocks in particular, are still poorly understood. One way to constrain accretionary processes is to understand the major differentiation event that took place during accretion: core formation. Earth's core formed during accretion as a result of melting, phase-separation, and segregation of accretionary building blocks (meteorites, planetesimals, protoplanets). Extensive melting lead to the formation of a Magma Ocean, and the bulk compositions of the core and mantle depend on it evolution (pressure, temperature, composition) during accretion. The entire process left a compositional imprint on both reservoirs: in the silicate Earth, in terms of siderophile trace-element concentrations (a record that is observed in present-day mantle rocks); and on the core, in terms of major element composition and light elements dissolved in the metal (a record that is observed by seismology through the core density-deficit).

Constraining accretionary processes by looking at the core has been studied for almost ten years. Based on partitioning of slightly siderophile elements, the current paradigm is that Earth must have formed under very reducing conditions, followed by a complex oxidation mechanism to reach the present-day redox state. In the light of new partitioning data under extreme conditions, we will show here that Earth can form at a constant redox state (the present-day value), or even form in relatively oxidized conditions (that of carbonaceous or ordinary chondrites). This paradigm shift is strengthened by the fact that oxidizing conditions favour oxygen solubility in the core, which is a requirement both for the inner-core density jump and outer core density deficit.

Advances in instrumentation based on cavity enhanced laser absorption spectroscopy

DOUGLAS BAER, MANISH GUPTA, FENG DONG,
ELENA BERMAN, TOM OWANO
AND ROBERT PROVENCAL

Los Gatos Research, Mountain View, CA, USA

Novel instrumentation based on high-resolution laser absorption spectroscopy now allows high precision measurements of gas concentration and isotopic ratios continuously, in real time, and without preconcentration. These analyzers employ tunable lasers that operate in the near-infrared and mid-infrared spectral regions and employ an optical cavity as a measurement cell. The simple operation of these instruments allows measurements almost anywhere. The laser wavelength is continuously and repetitively scanned over selected absorption features of target isotopologues to record high-resolution absorption lineshapes at data rates of 1 Hz or faster. The integrated areas of the measured lineshapes enable determination of the respective isotope-specific concentrations directly. No longer constrained to operate in a laboratory, these analyzers offer opportunities to record measurements in remote sites in less-developed areas. This presentation will summarize recent developments at LGR in both hardware and software analysis that enable measurements of isotopic ratios in carbon dioxide ($\delta^{13}\text{C}$, $\delta^{18}\text{O}$, CO_2), methane ($\delta^{13}\text{C}$, CH_4), nitrous oxide ($\delta^{15}\text{N}\alpha$, $\delta^{15}\text{N}\beta$, $\delta^{18}\text{O}$, N_2O) and water (liquid and vapor; $\delta^2\text{H}$, $\delta^{17}\text{O}$, $\delta^{18}\text{O}$, H_2O) in ambient air and in complex gas samples. An overview of the current performance of LGR instruments and perspectives on future developments will be presented.

Ca isotope fractionation in a permafrost-dominated boreal ecosystem (Kulingdakan watershed, Central Siberia)

M.-L. BAGARD^{1*}, A.-D. SCHMITT^{1,2}, F. CHABAUX¹,
O.S. POKROVSKY³, J. VIERS³, P. STILLE¹, F. LABOLLE¹
AND A.S. PROKUSHKIN⁴

¹Université de Strasbourg-CNRS LHyGeS, 1 rue Blessig,
67084 Strasbourg Cedex, France

(*correspondence: mbagard@unistra.fr)

²Université de Franche-Comté-CNRS, 16 route de Gray,
25030 Besançon Cedex, France

³Université Paul Sabatier-CNRS, 14 Avenue Edouard Belin,
31400 Toulouse, France

⁴V.N. Sukachev Institute of Forest, Krasnoyarsk, Russia

Ca isotope compositions were measured in different compartments (stream water, soil solutions, rocks, soils and soil leachates and vegetation) of a small permafrost-dominated forested watershed in the Central Siberian Plateau. Our results show that only the processes related to vegetation activity significantly fractionate Ca isotopes within the watershed. These fractionations occur during Ca uptake by roots and along the transpiration stream within the larch trees. Biomass degradation then significantly influences the Ca isotopic compositions of soil solutions and soil leachates via the release of light Ca. Furthermore, organic and organo-mineral colloids originated from organic matter degradation are thought to affect the Ca isotopic composition of soil solutions by preferential scavenging of ^{40}Ca . This imprint of organic matter degradation on the $\delta^{44/40}\text{Ca}$ of soil solutions is much more significant for the warmer south-facing slope of the watershed than for the shallow and cold soil active layer of the north-facing slope, indicating that the available stock of biomass and the decomposition rates are critical parameters that regulate the impact of vegetation on the soil-water system. Moreover, the obtained $\delta^{44/40}\text{Ca}$ patterns contrast with those described for permafrost-free environments with a much lower $\delta^{44/40}\text{Ca}$ fractionation factor between soils and plants, suggesting particular processes related either to the presence of permafrost or to the specific features of organic matter degradation in permafrost environments. Finally, biologically induced Ca fractionation observed at the soil profile scale is not visible in stream and river waters, whose isotopic variability in the course of the year is likely controlled by the lithological heterogeneity of the sources. As such, we suggest a negligible influence of biologically related fractionation on the long-term Ca isotopic signatures of riverine fluxes carried to the ocean.

Effect of Fe(II) ions on the sorption of selenite onto chlorite

MIN HOON BAIK* AND JONG TAE JEONG

Korea Atomic Energy Research Institute, Daejeon, Republic of Korea (mhbaik@kaeri.re.kr)

It has been reported that Fe(II)-bearing minerals or Fe(II) ions can reduce oxoanionic selenite (Se(IV)O_3^{2-}) either to Se(0) or Se(-II) and then decrease the mobility of the selenite in subsurface environments [1, 2]. In this study the effect of Fe(II) ions on the sorption of selenite onto chlorite surfaces was investigated as a function of selenite concentration, Fe(II) concentration, and pH.

The sorption of Se(IV) onto chlorite surfaces followed the Langmuir isotherm regardless of the presence of Fe(II) ions. The Se(IV) sorption was enhanced at a pH > 6.5 when the Fe(II) concentration was higher than 5 ppm because of the increased sorption of Fe(II) onto chlorite surfaces. XANES (X-ray absorption near edge structure) spectra of the Se K-edge showed that most of the sorbed Se(IV) was reduced to Se(0) by Fe(II) sorbed on the chlorite surfaces, especially at pH > 9. The combined results of field emission scanning electron microscopy and X-ray diffraction also showed that elemental selenium and goethite were formed and precipitated on the chlorite surfaces during the sorption of selenite. Consequently it can be concluded that Se(IV) can be reduced to Se(0) in the presence of Fe(II) ions by the surface catalytic oxidation of Fe(II) into Fe(III) and formation of goethite at neutral and particularly alkaline conditions.

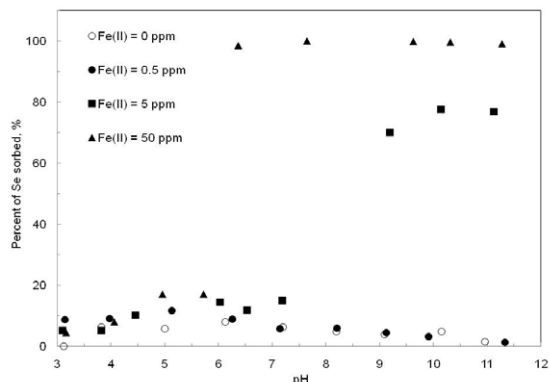


Figure 1: The sorption of Se(IV) onto chlorite surfaces as a function of pH at different concentrations of Fe(II) ions.

[1] Charlet *et al.* (2007), *Geochim. Cosmochim. Acta* **71**, 5731-5749. [2] Scheinost *et al.* (2008), *J. Contam. Hydrol.* **102**, 228-245.

Horizontal gene transfer in phylogenetically-distant taxa that induce the formation of modern wrinkle structures: Implications for the interpretation of Earth's earliest microbialites

J.V. BAILEY¹ AND B.E. FLOOD¹

¹Dept. of Earth Sci., University of Minnesota, Minneapolis, MN 55455, USA (*correspondance: baileyj@umn.edu)

Wrinkle structures in rocks dating back to the Archean are commonly interpreted to represent the stabilizing influence of cyanobacteria on sediments because the trapping and binding of sediment by these phototrophic microbes is known to produce similar features in modern tidal flat settings [1]. Our observations of modern sediments show that, like cyanobacteria, chemolithotrophic taxa within the Beggiatoaceae can produce features that are reminiscent of those found in the ancient rock record. Despite similarities in cell morphology and division patterns, the Cyanobacteria and the Beggiatoaceae are generally considered to be phylogenetically-distant clades in rRNA-based phylogenies. However, our comparisons of *Beggiatoa* and cyanobacterial genomes show that these organisms share many genes that potentially code for phenotypic traits such as chemotaxis, filament formation, and the production of extracellular polymeric substances. Some of these genes may underlie the similar biostabilizing influences these organisms impart on sediments. Our analyses further suggest that at least some of these genes may have been acquired via horizontal gene transfer. The presence of multiple biostabilizing clades in the modern, as well as the potential for extensive horizontal gene transfer over 3.5 billion years of evolution, complicates the interpretation of ancient sedimentary features using solely morphological criteria.

[1] Noffke (2007) *Gondwana Research*, **11**, 336–342.

Development of a novel TOF-SNMS to analyze sub-micron noble gas distribution

K. BAJO^{1*}, S. ITOSE², M. MATSUYA², M. ISHIHARA³,
K. UCHINO⁴, M. KUDO², I. SAKAGUCHI⁵
AND H. YURIMOTO¹⁶

¹Hokkaido Univ., Sapporo 060-0810, Japan

(*correspondance: bajo@ep.sci.hokudai.ac.jp)

²JEOL Ltd., Akishima 196-8558, Japan (sitose@jeol.co.jp,
matsuya@jeol.co.jp, kudo@jeol.co.jp)

³Osaka Univ., Toyonaka 560-0043, Japan
(ishihara@phys.sci.osaka-u.ac.jp)

⁴Kyushu Univ., Kasuga 816-8580, Japan
(uchino@ence.kyushu-u.ac.jp)

⁵NIMS, Tsukuba, Japan (sakaguchi.isao@nims.go.jp)

⁶CRIS, Hokkaido Univ., Sapporo 001-0021, Japan
(yuri@ep.sci.hokudai.ac.jp)

Overview of the instrument

Ion beam for secondary ion mass spectrometry (SIMS) down to 10 nm can reveal new perspectives for cosmochemistry and material sciences. We have developed LIMAS (Laser Ionization Mass Nanoscope [1]) that is a time-of-flight sputtered neutral mass spectrometer (TOF-SNMS) with non-resonant laser post-ionization system. LIMAS is mainly composed of Ga focused ion beam (FIB) for sputtering, femtosecond laser for post-ionization of the sputtered particles, and high mass resolution multi-turn mass spectrometer of which mass resolving power of ${}^4\text{He}^+$ ($m/z=4$) is 8,500 (FWHM) after 90 cycles.

One of our goals is to determine micro-distribution of noble gases in solids derived from solar wind (SW) irradiation. An ultra-fine ion probe and post-ionization procedure should reveal the processes of the solar-gases were implanted and the surface layer was lost by space weathering because SW implanted layer is less than 100 nm and high spatial resolution *in situ* He analysis has never been done.

The spatial resolution for ${}^4\text{He}$ was achieved ~50 nm which was evaluated by using ${}^4\text{He}$ implanted Si-wafer (dose: 2×10^{16} ions/cm²). A detection limit of the present system is about 10^{18} atoms/cm³ for ${}^4\text{He}$. The performance of LIMAS should be improved towards higher sensitivity and lower background noises because bulk concentrations of solar-He in gas-rich meteorite are 10^{16} – 10^{18} atoms/cm³ [2] for rocky material (density ~ 3 g/cm³).

[1] Ebata *et al.* (2012) *SIA*, **44**, 635–640. [2] Goswami *et al.* (1984) *SSRv*, **37**, 111–159.

The association between iron and carbon in freshwater colloids

S. BAKEN^{1*}, J.P. GUSTAFSSON²³ AND E. SMOLDERS¹

¹KU Leuven, Dept of Earth and Environmental Sciences,
Kasteelpark Arenberg 20 bus 2459, 3001 Leuven,
Belgium (*correspondence: stijn.baken@ees.kuleuven.be)

²KTH, Dept of Land and Water Resources Engineering,
Teknikringen 76, SE-100 44 Stockholm, Sweden

³SLU, Dept of Soil and Environment, Box 7014, SE-750 07
Uppsala, Sweden

Iron and carbon are important constituents of natural colloids, which intimately links the fate of these two elements in riverine systems. Iron may strongly affect the binding of trace metals by organic matter, e.g. through competition for binding sites, which highlights the importance of a correct appreciation of the Fe speciation in surface waters. However, the chemistry of Fe and C in natural colloids is complex and depend on many factors including the pH, the Fe:C ratio, and the redox speciation of Fe [1-3].

Two areas with a contrasting Fe chemistry were studied: a lowland area with widespread seepage of iron-rich groundwater, and an upland peat area. Samples of ten oxic, well-mixed streams were subjected to cascade filtration using conventional filtration (1.2 μm , 0.45 μm , 0.1 μm) and cross-flow ultrafiltration (CFF; 5 kDa). The colloidal fraction, here operationally defined as between 0.45 μm and 5 kDa, was isolated by CFF and subsequently freeze-dried. The speciation of colloidal Fe was determined by EXAFS spectroscopy at the Fe K-edge (MAX-lab, Lund, Sweden).

In the rivers draining upland peat, Fe and C were predominantly recovered in the fraction between 5 kDa and 0.1 μm . Conversely, in the rivers draining the lowland with extensive seepage of iron-rich groundwater, Fe was most abundant in the >0.1 μm fraction, whereas C was predominantly present <0.1 μm . The EXAFS data reveal that colloidal Fe speciation is different in both study areas. It exists as mononuclear Fe complexed by dissolved organic matter, as colloidal hydrous ferric oxides (likely stabilized by adsorbed organic matter), or as a mixture of these. The colloidal Fe concentrations show considerable seasonal variability. Overall, this study contributes to a better understanding of colloidal Fe speciation and of its interaction with organic C.

[1] Sjöstedt *et al.* (2013) *Geochim Cosmochim Acta* **105**, 172–186. [2] Allard *et al.* (2004) *Geochim Cosmochim Acta* **68**, 3079–3094. [3] Lyvén *et al.* (2003), *Geochim Cosmochim Acta* **67**, 3791–3802.

Asian Monsoon moisture transport 1999-2005 and its implications for palaeomonsoon reconstructions

ALEXANDER J. BAKER¹, HARALD SODEMANN²,
KATHLEEN R. JOHNSON³, JAMES U. L. BALDINI¹
AND JEROEN VAN HUNEN¹

¹Department of Earth Sciences, Durham University, Science Laboratories, South Road, Durham DH1 3LE, UK.

²Institute for Atmospheric and Climate Science, Swiss Federal Institute of Technology, CH-8092 Zurich, Switzerland.

³University of California at Irvine, 3206 Croul Hall, Irvine, CA 92697, USA.

The Asian summer monsoons affect the livelihood of the world's most populous regions. Predictions of future monsoonal variability require reliable palaeoclimate reconstructions from proxy data. Speleothem $\delta^{18}\text{O}$ records from Chinese cave sites are assumed to provide direct palaeomonsoon intensity records, but recent research suggests $\delta^{18}\text{O}$ integrates a more complex climate signal. We detected the sources modern monsoonal precipitation across China using a Lagrangian precipitation source diagnostic and reanalysis data. Our results show that monsoonal precipitation (May-August) in this region is primarily derived from the northern and western Indian Ocean; identification of this signal is consistent with recent GCM results. We also find that recycled moisture over continental Indo-China is an important contributor to west-to-east moisture transport during the monsoon season. These data highlight the importance of proxy site location and improve our ability to isolate the precipitation amount or monsoon intensity signal in palaeomonsoon reconstructions.

Trace element and ^{26}Al – ^{26}Mg constraints on silicate differentiation of the HED parent body

J. BAKER^{1*}, J. DALLAS², M. SCHILLER³, J. CREECH² AND
M. BIZZARRO³

¹School of Environment, University of Auckland, New Zealand (*correspondence: j.baker@auckland.ac.nz)

²School of Geography, Environment and Earth Sciences, Victoria University of Wellington, New Zealand

³Centre for Star and Planet Formation, Natural History Museum of Denmark, Denmark

The howardite–eucrite–diogenite meteorites are considered to originate from the asteroid Vesta. Diogenite meteorites appear to be mafic cumulates with a pyroxene-dominated mineralogy, whereas eucrites are basaltic in mineralogy and composition. However, the relationship(s) between these products of silicate differentiation of their parent asteroid(s) remain enigmatic, if indeed they originated from the same parent body as is suggested by their common three-oxygen isotope compositions.

We have conducted a detailed *in situ* major and trace element study of minerals (pyroxene and plagioclase) in a large number of diogenites and non-cumulate eucrites ($n = 44$) by LA-ICPMS. We have also analysed to ultra-high precision ($\delta^{26}\text{Mg}^* \pm 0.002\text{‰}$) the Mg isotopic composition of the same bulk meteorites by MC-ICPMS. Significant variations in $\delta^{26}\text{Mg}^*$ related to ^{26}Al decay in the first 5 Myr of the Solar System are evident amongst the suite of diogenites ($\delta^{26}\text{Mg}^* = -0.011\text{‰}$ to $+0.013\text{‰}$) and eucrites ($\delta^{26}\text{Mg}^* = +0.004\text{‰}$ to $+0.0040\text{‰}$). Despite their limited range in mineral major element compositions, mineral trace element concentrations vary widely. For example, moderately incompatible heavy rare earth element concentrations in pyroxene vary by more than two orders of magnitude (e.g., Yb = 0.02 to 3.1 ppm).

Trace elements such as Yb in pyroxene and Sr in plagioclase co-vary with bulk rock $\delta^{26}\text{Mg}^*$ values, which potentially implies rapid magmatic differentiation of a magma ocean. However, the large range of trace element abundances is difficult to reconcile with any simple co-genetic model for partial melting or crystallization of diogenites (cumulates) and eucrites (residual liquids) from a common parent body or magma ocean. Stable Mg isotopic compositions ($\delta^{25}\text{Mg}$) of eucrites appear to be distinct from those of both diogenites and terrestrial basalts, which might imply that diogenites and eucrites originated from separate parent bodies or that eucrites are the product of a formation process (i.e., residual liquids of extensive fractionation of an ultramafic magma body) that is fundamentally different to the partial melting processes that produces basaltic magmas on Earth.

Environmental fate, transport, and bioavailability of CeO₂ nanoparticles in stream mesocosms

LEANNE F. BAKER^{1*}, RYAN S. KING¹,
JASON M. UNRINE² AND COLE W. MATSON¹

¹Baylor University, One Bear Place #97266, Waco, TX, USA
76798-7266 (*correspondence: leanne_baker@baylor.edu)

²University of Kentucky, Lexington, KY, USA 40546-0091
(jason.unrine@uky.edu)

Emissions from wastewater treatment facilities (“press”-type exposures) and accidental spills (“pulse”-type exposures) are two possible entry routes of engineered nanomaterials into aquatic environments. Significant uncertainty exists regarding the processes governing transport and environmental fate of these novel materials. Outdoor, 1870L recirculating stream mesocosms were treated with either 1) a one-time addition (pulse) of acetate-coated cerium dioxide nanoparticles (CeO₂ NPs) to achieve aqueous concentration of 10 mg NPs/L or 2) a 25-day continuous exposure (press) of the same amount of CeO₂ NPs as 1), a third stream served as a control. Mesocosms were lined with unglazed ceramic tiles and stocked with fish, invertebrate, plant and microbial species. CeO₂ NPs are known to be insoluble, so total Ce concentrations measured by ICP-MS served as a proxy for CeO₂ concentrations. Results suggested rapid aggregation of CeO₂ NPs in the pulsed dose. Aqueous concentrations were between 0.24-0.37 mg/L 12-76 hours after NP addition, declining to 0.02 mg/L by cessation of the experiment on day 30. Aqueous Ce concentrations in the press-dosed stream averaged 1.2 mg/L on day 15 (12% of target) and 1.1 mg/L (11% of target dose) on day 25. Five days after completion of NP dosing in press mesocosms (day 30 of experiment), aqueous concentrations of Ce had declined to an average of 0.46 mg/L, which was still higher than any Ce concentration measured in the pulse-dosed stream. Consequently, the concentration of Ce in periphyton was lower in the press-dosed stream on day 30 (average of 9.08 μg/g of dry sample) than in the pulse-dosed stream (average of 13.11 μg/g). The press dose resulted in longer-range transport of NPs, such that periphyton concentrations of Ce in the lower reaches of the press-dosed stream were nearly double those observed for the pulse-dosed stream (6.4 μg/g vs. 3.3 μg/g, respectively), likely because of a reduced particle-particle interaction and subsequent aggregation relative to the pulse addition. These results suggest that exposure scenarios may play a significant role in determining the environmental fate, transport, and bioavailability of stable metal oxide nanomaterials.

Development of fertile magma at El Teniente, Chile: Implications for porphyry-style mineralisation

M.J. BAKER^{1*}, P.N. HOLLINGS² AND D.R. COOKE¹

¹CODES, University of Tasmania, Hobart 7001, Australia
(*correspondence: bakermj@utas.edu.au)

²Dept. of Geology, Lakehead University, Thunder Bay,
Ontario, Canada, P7B5E1

El Teniente porphyry Cu-Mo deposit is located in the Andean Cordillera in the central Chilean porphyry belt, which is host to a number of world-class late Miocene-Pliocene porphyry copper deposits. El Teniente is considered one of the world’s largest copper deposit in terms of contained metal, with a total identified resource of over 16 billion metric tonnes (Gt) at 0.554 % Cu [1] and 7.8 Gt at 0.018 % Mo [2].

A series of calc-alkaline intermediate to felsic porphyritic sills and dikes, collectively termed the Teniente Plutonic Complex, are spatially associated with magmatic-hydrothermal breccias and veins that host mineralization at El Teniente. They were emplaced between 7.1-4.9 Ma, although previous work has suggested a 7.10 ± 0.41 Ma age for a sample of the porphyry may be inherited [3,4].

Samples from the Teniente Plutonic Complex have been analysed for Rb/Sr and Sm/Nd isotopic compositions. ε_{Nd} values are consistently positive, ranging from 2.4 to 3.2, whereas ⁸⁷Sr/⁸⁶Sr_i values are between 0.70388 and 0.70421. When compared to other intrusive rocks from Central Chile [5], El Teniente rocks display broadly similar trends, implying that a geologic event led to an abrupt decrease in ε_{Nd} values ca. 5 Ma. The isotopic data reflect localized assimilation of crustal material into the mantle wedge as a result of subduction erosion adjacent to a zone of ridge subduction [5], rather than intra-crustal contamination, consistent with a subduction-erosion model [6]. The data suggest the Teniente Dacite Porphyry and associated mineralization was emplaced as several discrete intrusions over a ca. 1 million year period. This process has implications for the relationships between porphyry emplacement and Cu-Mo mineralization in central Chile.

[1] CODELCO Annual Report (2009). [2] Camus (2002) *CODES Special Pub.* **4**, 1-38. [3] Makshev *et al.* (2004) *SEG Special Pub.* **11**, 15-54. [4] Cannell *et al.* (2005) *Economic Geology* **100**, 979-1003. [5] Hollings *et al.* (2005) *Economic Geology* **100**, 887-904. [6] Stern & Skewes (1995) *Revista Geologica de Chile* **22**, 261-272.

Cl in magmas: A tool for degassing processes

H. BALCONE-BOISSARD^{1*} AND G. BOUDON²

¹ISTeP, Université Pierre et Marie Curie, Paris, France

(*correspondence : helene.balcone_boissard@upmc.fr)

²Institut de Physique du Globe de Paris, Paris, France

Volatiles are responsible of magma ascent from reservoir to surface. For differentiated melt, H₂O is the main volatile species, the behavior of which control the eruptive style. But H₂O is generally difficult to measure precisely that limits the dataset available. Halogens are interesting to study and particularly Cl that is easier to analyse in volcanic glass (residual glass and melt inclusions) by electronic microprobe at the concentrations that occurred in natural samples.

Cl is generally controlled by its partitioning into the H₂O phase that explains a wide range of behavior. Here we present different results on Cl behavior in magmas, from basic to acid composition, in order to highlight how Cl may be a useful parameter for degassing processes. In rhyolitic melt, Cl follows H₂O behaviour and provides the same information of closed- vs. open-system degassing. In alkali magmas such as phonolitic or trachytic magmas, Cl content in magmatic melt may be buffered in precised (P, T, composition) domain corresponding to magma storage at depth in equilibrium with a two-phase fluid composed of H₂O-rich vapor and a brine. At that conditions, Cl content depends on the pressure at which the magma is stored, and thus acts as a barometer. The pressure at which the magma is deduced from the solubility law corresponding to the melt composition studied. In some cases, Cl may only behaves as a pure incompatible and non-volatile element and images a stratified reservoir. Whatever the composition, effective Cl degassing potentially affecting the environment.

We illustrate these different behaviors with data on glass (melt inclusions and residual glass) from different eruptions from various contexts (Vesuvius, Etna, Azores, Lesser Antilles and Vanuatu arc).

Cyclic dolomitization of limestone at Oker (Germany)

ANDRE BALDERMANN¹, ARTUR P. DEDITIUS¹,
CHRISTIAN P. STICKLER¹, ALBRECHT LEIS²
AND MARTIN DIETZEL¹

¹Institute of Applied Geosciences, Graz University of
Technology, Rechbauerstraße 12, 8010 Graz, Austria;
(baldermann@tugraz.at)

²Institute of Water, Energy and Sustainability, Joanneum
Research, Elisabethstraße 18, 8010 Graz, Austria

Magnesium and sulfur are one of the major elements that control dolomitization in marine, low-temperature environments. However, conditions and reaction mechanisms, which are related to dolomitization are poorly understood.

We investigated partly dolomitized limestone (Oker, Langenberg, Germany) of Upper Jurassic age (~153 Ma) that was deposited in a shallow marine, sabkha environment. X-ray diffraction (XRD), δ¹⁸O and δ¹³C isotope measurements, and electron microprobe (EMP) analyses were completed on porous dolomite, sandwiched by layers of limestone.

The lower limestone layer consists of micritic calcite (-1.7 to -2.9‰ of δ¹⁸O and 1.3 to -0.7‰ of δ¹³C, VPDB), which formed under marine conditions. EMP analyses revealed low-Mg calcite (LMC) of (Ca_{0.96-0.99}Mg_{0.004-0.03}Sr_{0.001}Na_{0.01}Fe_{0.002})_{0.99-1.0}CO₃. Samples from the contacts between dolomite and limestone layers contain LMC, high-Mg calcite (HMC), and dolomite, which are associated in single grains. The dolomite core, (Ca_{0.97-1.14}Na_{0.01})_{0.97-1.14}(Mg_{0.75-0.97}Fe_{0.02}Mn_{0.01})_{0.76-0.99}[(C_{0.998-1.0}S_{0.002})O₃]₂, is ~10 μm in diameter, and is surrounded by LMC, (Ca_{0.86-0.99}Mg_{0.006-0.05}Fe_{0.004}Na_{0.002}Mn_{0.001})_{0.96-0.97}CO₃, and subsequently deposited HMC, (Ca_{0.64-0.78}Mg_{0.19-0.32}Fe_{0.004}Na_{0.003}Mn_{0.002})_{0.91-0.99}CO₃. The “pure” dolomite (2.2 to 1.7‰ of δ¹⁸O and 1.7 to -0.1‰ of δ¹³C, VPDB) comprises of 2-50 μm sized euhedral crystals of (Ca_{1.02-1.12}Na_{0.02})_{1.02-1.13}(Mg_{0.82-0.94}Fe_{0.02}Mn_{0.002})_{0.83-0.97}[(C_{0.994-1.0}S_{0.006})O₃]₂, and shows alternate growth zones of S and Fe. XRD data confirm non-stoichiometric dolomite with 51-54 mol% of CaCO₃. The degree of order in dolomite, in respect to dolomite super structure, decreases from 83% to 42% with increasing S contents from 0.02 to 0.06 S [a.p.f.u.], respectively. The upper limestone layer contains no dolomite or HMC, and displays marine conditions; i.e., micritic LMC (-1.8 to -3.4‰ of δ¹⁸O and -1.6 to -4.0‰ of δ¹³C, VPDB).

The euhedral shape and the (Fe, S)-growth zoning of the dolomite crystals, and the alternate zones of dolomite, LMC, and HMC suggest dolomitization via dissolution of primary carbonates and subsequent cyclic and abrupt changes in the chemical (Mg, Fe, and S), and isotopic composition of the interstitial solutions.

A distinct tectono-metamorphic evolution at the southern edge of Tisia Mega-Unit revealed by monazite and xenotime age dating

D. BALEN¹, P. HORVÁTH², F. FINGER³ AND P. KONEČNÝ⁴

¹Faculty of Science, University of Zagreb, Croatia

(*correspondence: drbalen@geol.pmf.hr)

²Rhodes University, Grahamstown, Republic of South Africa

³Division of Mineralogy, University of Salzburg, Austria

⁴Dionýz Štúr Institute, Bratislava, Slovak Republic

The Slavonian Mountains (Pannonian Basin, Croatia) are the area of particular significance within Tisia Mega-Unit. This large unit, with complex internal structure, encompasses three huge southward dipping Alpine nappe systems that expose characteristic lithologies of south-eastern part of Pannonian Basin basement. Complexes of the central nappe system (i.e. Bihor) outcrop along the 5.5 km long, NNW–SSE trending Kutjevačka Rijeka transect. This transect is one of the most prominent geological cross-sections that reflects a complex history of the metamorphic and igneous evolution, giving insight into crustal evolutionary processes and their relationship to deformation and metamorphism.

Our previous age dating of monazite from the representative rock complexes along Kutjevačka Rijeka transect, combined with geothermobarometric data, revealed complex structure and metamorphic history that includes a pre-Variscan (Ordovician to Silurian; 444±19 and 428±25 Ma) and a Variscan (356±23 Ma) medium-grade metamorphism [1, 2]. The primary focus of this study is on surprisingly large extent of very low- to low-grade Alpine metamorphism recorded in the parametamorphic rocks (chloritoid and chlorite schists) along the transect. The Th–U–Pb age dating on xenotime grains within the chloritoid schist gave an average age of 120±36 Ma, peak metamorphic conditions reaching 3.5–4 kbar and 340–380 °C. The age of 219±81 Ma obtained on Yb-rich xenotime (inherited?) core domain(s), implies a possible existence of older low-grade metamorphic phase(s) [3]. Two distinct penetrative low-grade metamorphic foliations recorded in the chlorite schists are accompanied by existence of two populations of small (~3.5 μm) low-Th monazites, giving an average age 99±15 Ma. Histogram of obtained ages shows two peaks at 120 and 80 Ma while age modelling recognized two peaks at 113±20 and 82±23 Ma. Those ages argue against "stratigraphic doubts" that contradict Alpine metamorphism in the area.

[1] Balen *et al.* (2006) *Miner Petrol* **87**, 143–162. [2] Horváth *et al.* (2010) *Lithos* **117**, 269–282. [3] Balen *et al.* (2013) *Int J Earth Sci*, in press.

Contribution of fungi and bacteria to the Mg biogeochemical cycle in podzolic soils

C. BALLAND-BOLOU-BI^{1*}, E. B. BOLOU-BI²,
S. J. M. HOLMSTRÖM¹ AND N. G. HOLM¹

Stockholm University, Dept. of Geological Sciences,

Stockholm, Sweden (*Clarissebolou-bi@geo.su.se)

Uppsala University, Dept. of Earth Sciences, Air, Water and

Landscape sciences, Uppsala, Sweden

Silicate mineral weathering is a key process in soil formation through leaching of essential elements (Mg, Fe, Al), which sustain plant growth and determine the chemistry of soil solutions and exchange complex. Biological role on silicate mineral weathering remain to date a scientific challenge due to the strong relation between plant growth, silicate mineral weathering and CO₂ cycle. However, some constraints, such as microflora associated to plants, are unresolved allowing to quantify biological impact on silicate mineral alteration in the soil and on major cation biogeochemical cycle. Soil microorganisms (fungi and bacteria) play a major role in the availability of nutrients in soils. They participate in weathering of primary materials through the production of low-molecular masses organic acids (LMMOAs). The objective of this study is to quantify the impact of microorganisms (bacteria and fungi) during granite bioweathering and to better understand and quantify the contribution of microflora to Mg biogeochemical cycle.

For this, we lead several experiments of geological material (granite) bioweathering to investigate the impact of fungi and bacteria on the release of Mg from granite during 42 days. The microbial communities were directly isolated in November 2011 from different horizon (O, E, B) of a podzolic soil under 3 different tree species (Scots Pines, Spruce, Birch) in Norunda (Sweden). To characterize mechanisms of dissolution, we monitored low-molecular organic molecules produced by microorganisms, microbial biomass, pH, Mg released and Mg isotope ratio variations.

Result indicates that pH decreases significantly from 6.5 to 4–5 during the first week of the experiments and then roughly stabilizes over time. In contrast, in all experiments, the fraction of released Mg is strong until 30 % at the end of the experiments. There is a positive correlation between the Mg leached from phlogopite and the carbon produced (LMMOAs and biomass) by microbial communities. Whatever the tree species, the microbial communities isolated from the upper part of the organic horizons of the soil are less efficient to weather the granite and don't produce great quantities of LMMOAs. Preliminary isotope analyses indicate that δ²⁶Mg in the leaching solutions collected at the end of the experiments are close to the initial value of the granite. Only leaching experiments performed with microbial communities isolated from the upper part of the organic horizons induce a high enrichment in the light isotope (~ -1.0‰) in the solution, suggesting a biotic effect that will be investigated.

DOI:10.1180/minmag.2013.077.5.2

www.minersoc.org

Combined Halogen (Cl, Br, I) and noble gas mantle geochemistry

C. J. BALLENTINE¹, R. BURGESS¹, H. SUMINO²,
D. HILTON³, D. GRAHAM⁴, P. VAN KEKEN⁵,
D. CHAVRIT¹, L. RUZIE¹, P.L. CLAY¹, B. JOACHIM¹,
B. WESTON¹, L.D.A. JEPSON¹ AND M. BROADLEY¹

¹U. Manchester, (chris.ballentine@manchester.ac.uk)

²U. Tokyo, (sumino@eqchem.s.u-tokyo.ac.jp)

³UCSD, (drhilton@ucsd.edu)

⁴OSU, (dgraham@coas.oregonstate.edu)

⁵U. Michigan, (keken@umich.edu)

Not yet two decades ago the community view of the mantle structure had converged on a mantle geochemically layered at 670km depth. This model has passed on, is no more, ceased to be, expired and is now history. Killed, by geophysical observation. Although the layered mantle is now an ex-model the geochemical observations used to support it remain; the formation, location and evolution of a volatile rich mantle reservoir capable of fluxing the mantle beneath mid ocean ridges with accretionary volatiles, such as ³He, still attracts significant attention.

High precision multi-collector noble gas mass spectrometry is providing us with new detail of the mantle system. MORB basalts and mantle-derived CO₂ natural gas fields show a MORB-source mantle with light and heavy noble gases, and therefore associated volatiles, that originate as a trapped component in accreting meteorites [1]. New data from Iceland nevertheless, shows that the Iceland OIB source region is incompatible with this source simply providing the noble gases now in the upper mantle [2]. An additional volatile input into the mantle is today through recycling noble gases with a seawater signature [3], while dry subduction may have operated on the Early Earth to introduce accretionary volatiles into the mantle [4].

Heavy halogens (Cl, Br, I), in combination with noble gases, are a powerful tool to understand the subduction of volatiles and highly incompatible elements in detail [5]. Due to low Br and I concentrations, new techniques only now allow us to determine: accretionary material characteristics; partitioning data; and investigate the different terrestrial reservoir halogen mass balance. We present an overview of progress in this new field and discuss how the combined halogen/noble gas data might be used to reconcile the apparent need for a volatile-rich reservoir that fluxes the shallow mantle with the new Icelandic data [2].

[1] Holland *et al.*, *Science* (2009); [2] Mukhopadhyay, *Nature* (2012) [3] Holland and Ballentine, *Nature* (2005); [4] Tolstikhin and Hofman *PEPI* (2005); [5] Sumino *et al.*, *EPSL* (2010)

Reconstructing the Rheic: Geochemical analysis of ocean lithosphere from the Variscides

A.R. BAND^{1*}, T.L. BARRY¹, A.D. SAUNDERS¹
AND J.B. MURPHY²

¹University of Leicester, Leicester, LE1 7RH.

(correspondence: arb37@le.ac.uk, tlb2@le.ac.uk & ads@le.ac.uk)

²St. Francis Xavier University, Antigonish, B2G 2W5.
(bmurphy@stfx.ca)

Although the Rheic Ocean dominates palaeo-geographic reconstructions of central Europe during the Palaeozoic, many factors regarding its general evolution & internal tectonic configuration are inadequately constrained [1]. A major component in aiding a better understanding of these factors is the accurate assessment of suture zones & associated metabasite suites within the internal Variscides. As such this study focuses on the geochemistry of the Lizard- Cornwall, Sudetes-Poland, Acatlan-Mexico & Ossa-Morena, Careon, Morais-Iberian ophiolite complexes. Sampling within these complexes focused on the least deformed mafic members in order to fully assess the geo-tectonic setting of basalt genesis. Major, trace and rare earth element data (XRF & ICP-MS) has been examined and shows general LREE depletion & a lack of significant Ta, Nb or crustal derived element anomalies for all complexes. The new geochemical data enables an accurate discrimination of the geo-tectonic setting for each complex and aids in constraining future palaeo-geographic reconstructions of the enigmatic Rheic basin. The lack of crustal contamination & origins within the upper mantle, facilitates use of some samples for a future Hf-Nd isotope study aimed at fingerprinting the Devonian upper mantle and furthering our understanding of the origin & evolution of the Dupal anomaly [2]. Additionally, we will use the isotope data to investigate models to explain the apparent depleted nature of the source of Rheic Ocean basalts [3].

[1] Kroner & Romer (2013) *Gond Res.* In press. [2] Dupre & Allegre (1984) *EPSL* **71**, 71–84. [3] Murphy *et al.* (2010) *Lithos* **123**, 165–175.

Clumped isotope thermometry in Belemnite shells from the Early Cretaceous Karai Shale Formation, Trichinopoly, India

YOGARAJ BANERJEE, PROSENJIT GHOSH*
AND RAMANANDA CHAKRABARTI

Centre for Earth Sciences, Indian Institute of Science,
Bangalore 560012, India (* pghosh@ceas.iisc.ernet.in)

Well-preserved Belemnites fossils are hosted in the upper Albian Karai Shale Formation, India, which represents an offshore high stand depositional environment (1,2). It has been argued that $\delta^{18}\text{O}$ variability in these Belemnites – growth bands reflect seasonal –paleo-temperature changes in the sea water (2). We investigate paleo-seawater temperatures by analyzing clumped isotopes (Δ_{47}) in 15 petrographically and chemically well-characterized unaltered samples of Belemnite guard shells. Sample powders were drilled from the exterior growth bands, avoiding the outermost portion. $\delta^{18}\text{O}$ and $\delta^{13}\text{C}$ were also determined. Our Δ_{47} measurements yield a temperature range of 20°C ($\Delta_{47} = 0.667 \pm 0.005$) to 42°C ($\Delta_{47} = 0.624 \pm 0.005$) using the Ghosh *et al.*, (2006) thermometry equation. The spread in Δ_{47} values together with $\delta^{13}\text{C}$ and $\delta^{18}\text{O}$ and inferred salinity values allowed characterization of the 15 samples into three suites with distinct temperature and salinity ranges. Considering the nektonic behaviour of Belemnites (3), we propose an alternative mechanism to explain the spread in our paleo-temperature data by invoking the role of thermohaline circulation during Early Cretaceous, similar to modern mid-latitude modern oceanic conditions.

[1] Sundaram *et al.* (2001) *Cret.Res* **22**, 743-762. [2] Zakharov *et al.* (2011) *Cret.Res* **32**, 623-645. [3] Mutterlose *et al.* (2010) *EPSL* **298**, 286-298.

Major and trace element geochemistry in groundwater of Patancheru Industrial Area, Andhra Pradesh, India

B. DASARAM*

CSIR-NGRI, Habsiguda AND Uppal, Hyderabad-500 007,
India (*correspondence: bdram11@gmail.com)

Patancheru Industrial Development Area is located about 40 km from Hyderabad City, A.P. This is one of the contaminated areas identified by the Central Pollution Control Board (CPCB) New Delhi. More than 200 small and large-scale industries manufacture pharmaceuticals, paints, pesticides and chemicals and metallic products in this region. All effluents drain through the area to join the main Nakkavagu stream, which merges into Manjira River, and is one of the major drinking water sources to some parts of Hyderabad and adjoining areas.

During pre- and post-monsoon seasons the ground water samples were collected from open and bore wells. The samples were analysed for major, minor and trace constituents. Several heavy and toxic trace elements were estimated by Inductively Coupled Plasma Mass Spectrometry (ICP-MS). The geochemical data obtained was utilized to assess the extent of pollution and its impact on human health. Some of the toxic and trace elements (As, Se, Pb, Cr, Cu and Mn) were found to be more than the desirable levels in drinking water (WHO guidelines). The Contour maps for these trace elements were prepared to know their spatial and temporal distribution and to identify the point source and transport of the contaminant. These studies would emphasize the need to adopt some remedial measures and combat pollution.

Geochemical characteristics and correlation of oil-source in Minfeng area for Dongying depression, Bohai Bay Basin, Eastern China

BAO DONGMEI^{1*} AND JIANG YOU LU² AND JIANG LIN¹

¹PetroChina Research Institute of Petroleum Exploration & Development, Beijing 100083, China
(bdmei@petrochina.com.cn)

²Earth Resource College, China University of Petroleum, Dongying, Shandong 257061, China

The Minfeng area is located in the northeast of Dongying Depression. The characteristics of the gas chromatography of saturated hydrocarbons and the steroid terpane biomarkers show that there are three sets of source rocks with obvious differences including the upper part of the fourth member of the Shahejie Formation (simplified as Es4s), the middle part of the third member of the Shahejie Formation (simplified as Es3z), and the lower part of the third member of the Shahejie Formation (simplified as Es3x). There are four types of oil.

Further studies focus on oil-source correlation. Based on the techniques of fingerprint identification, scatter diagram analysis and mathematical statistics, the results indicate that oils in reservoirs of the second member of the Shahejie Formation (simplified as Es2) (from 7 to 10 sand units) of Yong3 fault-block, Es2 (No.4 sand unit) of Yong51 fault-block and Yanjia area came from Es4s source rock. Oils in reservoirs of Minfeng sag came from Es3z and Es3x source rocks. Oils in reservoirs of Es2 (No.3 and No.5 sand units) of Yong3 fault-block, Yong66 fault-block, Yong12 fault-block, Yong51 fault-block are mixed by oils coming from Es4s and Es3x. Oils in reservoirs of Es2 (No.3 and No.5 sand units) of Yong2 fault-block, Yong63 fault-block came from Es3z source rock.

It is possible to infer that oils from Es4s source rock, which were mainly along the favorable sandbodies and unconformity, migrated laterally from sag to Yanjia area and eventually filled in the sandy conglomerate bodies of Es3 and Es4 because of lack of oil-source faults. Oils are diverse types because of many oil-source faults in Yong Anzhen area. It implies that traps in Yonganzhen area formed in the same period according to the distribution of the types of oils on the plane. Early generated oil accumulated in the reservoir which was near to the source rocks. With the further burial depth of the source rocks, overlying source rocks gradually entered the hydrocarbon generation period, the oil began to accumulate in traps which were further distance from the source rocks.

Direct atmospheric O₃ and O₂ signatures from the deep past and their first-order pattern

HUIMING BAO

Department of Geology and Geophysics, Louisiana State University, Baton Rouge, LA 70803
(bao@lsu.edu)

The isotope compositions of atmospheric O₃ and O₂, two of the most important molecules in the atmosphere, offer us windows to the deep history and evolution of the Earth. Sulfate is an oxyanion capable of recording direct O₃ and/or O₂ signatures from the distant past. Recently, an improved understanding of the triple oxygen isotope systematics of various sulfur oxidation processes has demonstrated that secondary atmospheric sulfate bears O₃ signature ($\Delta^{17}\text{O}$ positive), while sulfate of oxidative weathering origin bears O₂ signature ($\Delta^{17}\text{O}$ negative). The ultimate source of the ¹⁷O anomalies in O₃ and O₂ is the Chapman reaction in the stratosphere, which via stratosphere-troposphere exchange links the concentrations and triple oxygen isotope compositions of atmospheric O₂, CO₂, and O₃ to the rates of bioproductivity, weathering, and organic burial on the Earth surface.

Despite many unfilled gaps in its record, I propose here that, from existing data, a first-order temporal pattern for sulfate $\Delta^{17}\text{O}$ for the last 3.5 billion years has emerged. There are three outstanding features. (1) The Marinoan O-17 Depletion (MOSD) event at 635 Ma is a clear anomaly in which the $\Delta^{17}\text{O}$ of sulfate reached as negative as -1.64‰ . The most viable explanation for this event is a post-glacial, ultra-high pCO₂ world, which is consistent with the "snowball" Earth hypothesis. Data for other alleged "snowball" Earth periods are lacking at this time, and other secondary "depletion" events are predicted. (2) The Archean sulfate has an average $\Delta^{17}\text{O}$ value of $-0.05 \pm 0.05\text{‰}$, while the post-Archean sulfate has an average $\Delta^{17}\text{O}$ at $-0.12 \pm 0.05\text{‰}$ (MOSD data excluded), a pattern that is consistent with the lack of O₃ shield, i.e. the absence of Chapman reaction, in the Archean. However, the role of thermal alteration has yet to be examined. (3) The oldest sulfate with distinct positive $\Delta^{17}\text{O}$ values has been traced back to the Eocene (~35 Ma). However, if O₃ became essential in atmospheric oxidation of SO₂ as soon as the ³³S anomaly ceased to exist in rock records, $\Delta^{17}\text{O}$ -positive sulfate should have been produced since the Early Proterozoic Era. Bear in mind that any geological record is the net result of production and destruction. By understanding the geologic context of sulfate records, and by exploring diverse and continental deposits in particular, we shall piece together a first-order, direct geological record of atmospheric O₂, O₃, and CO₂ for the last 3.8 billion years.

U-Pb dating of hydrothermal zircon and its implications for the metallogeny of the Dongping gold deposit in North China

ZHIWEI BAO¹, WEIDONG SUN¹ AND CHUANGJIU LI²

¹ CAS Key Laboratory for Mineralogy and Metallogeny, Guangzhou Institute of Geochemistry, Chinese Academy of Sciences, Guangzhou, 510640, China

²Guangdong Nonferrous Metals Geological Exploration Institution, Guangzhou, 510080, China

The large Dongping gold deposit is located in the northern margin of the North China Craton, northwestern Hebei province, China. The ores are hosted by the Shuiquangou syenite complex and consist mainly of auriferous quartz veins and K-feldspar altered and silicified disseminated ores, both of which are characterized by low sulfide volumes, Te-rich and As-poor. U-Pb dating of zircons from the hornblende syenite on the western margin of the complex yields an age of crystallization of 400±3.5Ma. The close spatial relation of the gold mineralization with the syenite complex, and S, Si, and Pb isotope compositions of the ore-related minerals, suggest that the ore deposit might be genetically related to the syenite complex. However, almost all of the published age of ore-formation vary in range of 157~177 Ma (⁴⁰Ar-³⁹Ar ages of hydrothermal K-feldspar^[1-2]), which caused considerable controversy over the metallogeny of the Dongping gold deposit. Morphology, cathodoluminescence image and rare earth element concentrations of zircons from the first stage disseminated ore and grey auriferous quartz vein, and late stage low grade quartz vein suggest that the zircons are neocrystallized hydrothermal. The hydrothermal zircons from the disseminated ore and auriferous grey quartz vein are dated at 389±1.0Ma and 385±5.7Ma, respectively, which are close to the crystallization age of the syenite complex and might have been formed during post-magmatic hydrothermal processes. Considering the two type of ores are dominant parts of the ore deposit, we argue that the pervasive post-magmatic hydrothermal alteration is the main ore forming stage. U-Pb dating of the hydrothermal zircon from the low grade auriferous quartz vein yields an age of ~140Ma, which represents Yanshannian hydrothermal superimposition. Thus, the Dongping gold mine is a post-magmatic hydrothermal ore deposit with later stage hydrothermal overprint.

[1] Jiang & Nie (2000), *Geol Rev* **46**, 621-627. [2] Hart *et al.* (2002), *Miner Deposit* **37**, 326-351

Distribution of rare earth elements in marine Co-rich ferromanganese crusts of the South Atlantic

A.P.M.G. BARANDAS^{1,2}, M.A.I. DUARTE¹
AND J. ENZWEILER^{2,*}

¹LAMIN (Laboratório de Análises Mineralis) - Geological Survey of Brazil (CPRM) (ana.barandas@cprm.gov.br)

²University of Campinas, P.O. Box 6152, CEP13083-970, Brazil, (*correspondence:jacinta@ige.unicamp.br)

Rare earth elements (REE) are of great geological, technological, economic and strategic interest. The increasing use of REE in high-tech products and the restrictive politics of some countries for commercialization of some REE raw products resulted in search for new deposits of these elements as well as the feasibility of unexplored reserves. One of the possible sources of REE are cobalt-rich seamount ferromanganese crusts. These are unconventional ores abundant in the deep ocean. Co-rich crusts are enriched in metals such as Co, Pt, REE, Ti, Ni, Tl, Te, Zr, W, Mo and Bi. The chemical and mineralogical characterization of Co-rich crusts occurrences has been carried out in several oceans [1,2]. In the South Atlantic, they are well known in the Rio Grande Seamount [3]. Ferruginous vernadite is a common phase in Co-rich crusts and moderate amounts of carbonate-fluorapatite (CFA) are found in thick crusts, as well as low amounts of quartz and feldspar[4].

In this work, samples of cobalt-rich crusts from the Rio Grande Seamount, South Atlantic were chemically characterized. Trueness of analytical data was checked by analysis Co-rich seamount crust reference materials GSMC-1 and GSMC-3 [5]. The content of REE in the analysed samples is variable (Σ REE 320-3,100 mg/kg) and only 5-10% of these totals it is of heavy REE. Almost all samples show strong enrichment in Ce, as evidenced by PAAS normalized REE patterns. Such type of finding was previously interpreted as related to hydrogenetic Fe-Mn crusts [6]. Their formation is ascribed to the oxidative scavenging of Ce and its preferential removal from seawater by hydrous Fe-Mn oxides.

[1]Kato *et al* (2011) *Nature Geoscience* **4**, 535-539.

[2]Yingchun *et al* (2009) *Journal of Rare Earths* **27**, 169-176.

[3]Souza (2000) *Brazilian Journal of Geophysics* **18**, 455-466.

[4]Cronan (1999) Handbook of Marine Mineral Deposits, in: CRC Press. Cap. 9, p.239-279. [5] Wang *et al* (2003) *Geostandards and Geoanalytical Research* [6] Kuhn *et al*

(1998) *Earth and Planetary Science Letters* **163**, 207-220.

On regularities in accumulation and distribution of elements in living matter of natural and technogenic ecosystems

NATALIA BARANOVSKAYA

Tomsk Polytechnic University, Tomsk, 634050, Russian Federation

(*correspondence: natalya.baranovs@mail.ru)

The task of gaining information on element composition of living matter was set by V.I. Vernadskiy at the beginning of the last century. In spite of the long history of study in this problem, there is still a number of questions to be answered.

For this purpose we have revealed the regularities in accumulation and distribution of elements in living matter on the sites with various rates of natural-technogenic ecosystem transformations. The research is based on the results of up-to-date high-sensitivity analytical methods – instrumental neutron activation and inductively coupled mass-spectrometric plasma (ICP-MS).

Living matter is not homogeneous in its composition. The analysis of materials obtained by us attests the fact that in regularities of element mean content distribution in living matter the conformities of their accumulation are observed that correspond to general distribution laws for material objects: that of Mendeleev-Clark on element distribution in different masses and Oddo-Harkins rule on element interchange with even and uneven numbers. It was revealed that in the zones of geochemical abnormalities conditioned by geologic and metallogenetic features there is an increase in concentration of specific elements in composition of living organisms against the background of observing geochemical regularities. Element composition of living matter is subjected to significant transformation in the zones of technogenesis. In such zones the disruption in basic element accumulation regularities is observed. As a result it was stated that technogenic factor has an effect on organism of modern urban residents in the form of intensive accumulation of such elements as lead, gold and cadmium.

The results of research in living matter from different sites shows that the indicators of its internal changes under the influence of the environment are mostly the element relationships. The most informative is Th/U, as well as the relationship of rare-earth elements and some others.

Geochemistry of mineral springs ecosystems of Baikal region

NATALIA BARANOVSKAYA, BULAT SOKTOEV*,
LEONID RIKHVANOV AND TATIANA PERMINOVA

Tomsk Polytechnic University, Tomsk, 634050, Russian Federation

(*correspondence: bulatsoktoev@gmail.com)

The Baikal rift area is characterized by a rich variety of mineral springs. The research of microbial communities has been started quite recently, but there is a lot of information showing the important role of microbial communities of hot springs in the evolution of life in the Precambrian [1].

The complex studies in thermal springs have shown that severe environmental conditions (high temperature, alkaline pH and high sulfide content) contribute to the development of specific microbial communities, having significant biodiversity and high intensity of biogeochemical processes, comparable to the microbial communities of neutral thermal spring. The main feature of these communities is the formation of microbial mats, often in collaboration with travertines [1].

The objective of our study is to identify geochemical features of different springs in the Baikal rift area. Thus, the mat samples were taken in several springs of the Baikal region in the summer of 2012. The chemical composition was determined by multi-element neutron activation analysis (Department of Geoecology and Geochemistry of Tomsk Polytechnic University, Russia).

The data shows that the mats of different mineral springs are characterized by absolutely different content of elements. Thus, mats of the tonic spring are characterized by the largest content of Na, the mats of methane spring – that of Ca. The mats of some springs are characterized by higher content of some elements. For instance, the mats of cold Arangatuy stream have higher content of Ba, Ce, Nd, Th, Tb, Yb, Ta, Sm. We should bear in mind the higher accumulation of the mats in the stream of U (177 mg/kg).

All this suggests that the mats help to assess biogeochemical role of microorganisms in ecosystems, shows an important role of microbial communities in hot springs in the evolution of life on the Earth, as well as taking an active part in the formation of travertine.

[1] Namsaraev *et al.* (2011) *Academic Publishing House "Geo"*. 302 p.

Petrological constraints on formation of the martian crust

D. BARATOUX^{*1}, M. MONNEREAU¹, M.J. TOPLIS¹,
K. KURITA², H. SAMUEL¹, R. F. GARCIA¹
AND M. WIECZOREK³

¹Institut de Recherche en Astrophysique et Planétologie,
CNRS & Université Paul Sabatier, Toulouse III, 14. Av.
Edouard Belin, 31 400 Toulouse.

(*correspondance: david.baratoux@irap.omp.eu)

²Earthquake Research Institute, University of Tokyo, 1-1-1
Yayoi, Bunkyo-ku, Tokyo, Japan

³CNRS, Institut de Physique du Globe de Paris, 5, rue Thomas
Mann. Université Paris Diderot, 75205 Paris Cedex 13,
France.

The 4 Ga-record of Martian volcanic activity has been characterized over the last decade by various remote sensing instruments, including gamma ray spectroscopy and visible/near-infrared spectroscopy. Based on these data, the martian crust is viewed as a basalt-dominated world with limited crustal differentiation. This relatively simple situation (when compared to the Earth) may be responsible for observed trends in surface chemistry and mineralogy with age, such as an increase with time of the abundance of high-calcium pyroxene relative to that of low-calcium pyroxene. Indeed, petrogenetic modeling suggests that these trends can be explained in terms of variable degrees of partial melting of a martian mantle of constant composition [3,4], providing a quantitative estimate of the average cooling rate of the martian interior. On the other hand, further work is needed to reconcile this model with the existence of distinct geochemical mantle reservoirs inferred from the analysis of the SNC meteorites. The idea that the martian mantle has been cooling for at least the last 4 Ga, as constrained from data spanning the entire Noachian-Hesperian-Amazonian periods, has several petrological, geochemical and geophysical implications. For example, mineralogical transitions observed around 3.7 Ga may be related to minor changes in mantle temperature. Furthermore, even the oldest exposed surface rocks could be an expression of this ancient volcanism rather than being associated with a mantle overturn following the crystallization of a magma ocean. In light of these results, we also argue that the density of the martian crust should be revised to higher values, in agreement with [5]. A lower density contrast with the mantle implies a thicker crust for which a basalt-eclogite transition would appear to be very likely (at least in some regions), providing a motivation to explore mechanisms of crustal recycling and implications for the fate of heat-producing elements.

[1] Baratoux, D., *et al.* (2011). *Nature*, **472**, 7343, 338-341.

[2] Baratoux, D., *et al.* (2013) *JGR-Planets*, **118**; 1-6. [3] Grott, M. and Wieczorek, M. (2012), *Icarus*, **221**, 43-52.

Hydrogeochemical and isotopic characterization of the Saturnia thermal aquifer

A. BARBAGLI^{1*}, F. BROGNA¹, E. GUASTALDI¹, G. LIALI¹,
C. REZZA² AND M. TROTTA¹

¹CGT Center for GeoTechnologies, University of Siena, Via
Vetri Vecchi, 34 - 52027 S. Giovanni Valdarno, Italy.

(*correspondence: barbagli.alessio@gmail.com)

²Corso Italia n 16,80011, Acerra, Naples Italy.
(carmelarezza@yahoo.it)

The thermal area of Saturnia was discovered and visited for several centuries before the Roman Empire and is still one of the most visited thermal springs in the world. It is located in central Tuscany between the Monte Amiata and the Tuscan volcanic area to the south. Herein, we study the thermal aquifer by chemical and isotopic analyses.

At first time, chemical-physical analyses have been used to a preliminary choose between all the sampled waters. Later, some elements and compounds (Na, Ca, Mg, K, Cl, SO_4^{2-} , NO_3^- , total alkalinity, Li, Sr, B, F, SiO_2 , CO_2 , Sb, As, Se, Fe, Mn, Hg e Pb) have been analyzed ad used to classified the previously chosen samples. In particular, Lithium (according to [1]), Boron and Strontium shows that the main important host of the studied thermal water is the calcareous geological formation of "Calcare Cavernoso"; high values of Selenium, according to [2, 3], also shows the influence of volcanic fluids in the thermal anomalies of the Saturnia thermal area.

Finally, some isotopes have been analyzed (^2H ; ^3H , ^3He , ^4He , ^{13}C , ^{18}O , ^{86}Sr , ^{87}Sr) to obtain others important information. The isotopes in the water molecule show that the recharge area of the thermal aquifer is located some km towards north regarding to the Saturnia spring, and his residence time is greater than 30 years. The $^{87}\text{Sr}/^{86}\text{Sr}$ ratio, measured in the Saturnia thermal water, allowed distinguish the aquifer (according to [4]) from the other host of the near thermal aquifer of Mt. Amiata, sampled in Bagni San Filippo. The isolation from the surface infiltration during the underground flow of the thermal water of Saturnia has been checked by the values of $\delta^{13}\text{C}$. And by the analysis of $^3\text{He}/^4\text{He}$, sampled in a larger area, the influences of the mantle in the Saturnia thermal area has been excluded, in according to [5].

[1] Brondi *et al* (1973), *Geothermics* **2**, 142-153. [2] Aiuppa *et al* (2005), *Chemical Geology* **216**, 289-311. [3] Floor *et al* (2012), *Applied Geochemistry* **27**, 517-531. [4] Cortecchi *et al* (1994), *Mineralogia et Petrographica acta* **37**, 63-80. [5] Hooker *et al* (1985), *Geochimica et Cosmochimica Acta* **49**, 2505-2513.

Probing the interactions between iron oxides and sediment organic matter using X-ray absorption spectroscopy

ANDREW BARBER^{1*}, KARINE LALONDE¹
AND YVES GÉLINAS¹

¹GEOTOP and Concordia University, 7141 Sherbrooke West,
Montreal, Quebec, H4B 1R6

(*correspondence andrew.jack.barber@gmail.com;
k_lalonde@hotmail.com; yves.gelinas@concordia.ca)

Sediments and sedimentary rocks make up the largest sink for organic carbon on the planet while approximately 20% of the organic carbon found within marine sediments is bound to reducible iron oxide species [1]. Here we use Scanning Transmission X-ray Microscopy (STXM) as well as X-ray Absorption Near Edge Spectroscopy (XANES) in order to probe the local environment of iron oxide-bound organic matter within a variety of marine surface sediments and water column suspended particles. STXM data was collected on beamline 10ID-1 (SM) at the Canadian Light Source, where we analyzed regions with iron co-localized organic carbon, and then obtained spatially relevant NEXAFS images and spectra for these regions at both the carbon K-edge and iron L_{2,3} edge. From these we are able to determine the speciation of both carbon and iron with a spatial resolution of 40 nm. We see important contributions from aromatic and carboxyl functionalities independent of the presence of iron but see an increase in the relative proportion of aliphatic functionalities in the presence of iron-organic mineral phases.

XANES spectra at the iron K-edge were collected at beamline X26a at the Brookhaven National Synchrotron Light Source and were used to probe the effect bound organic matter has on the X-ray absorption spectra of iron. A shift towards lower energies was seen at the iron edge for synthetic iron oxides precipitated in the presence of organic matter, demonstrating that we can distinguish between iron oxide-bound organic matter and pure iron oxide minerals. XANES spectra were also collected on a variety of surface sediment samples; using linear combination fitting and well-defined end-members, we were able to determine the proportion of sediment iron which is bound to organic matter based on the effect of organic matter on the synthetic iron co-precipitates.

[1] Lalonde, Mucci, Ouellet, Gélina (2012), *Nature* **483**, 198-200

The role of iron in the diagenesis of organic carbon and nitrogen in sediments: A long-term incubation experiment

ANDREW BARBER,¹ KARINE LALONDE,¹
ALFONSO MUCCI² AND YVES GÉLINAS^{1*}

¹Concordia University, Montreal, Quebec, Canada

(*correspondence: Yves.Gelinas@concordia.ca)

²McGill University, Montreal, Quebec, Canada

The burial and preservation of organic matter (OM) in marine sediments is tightly coupled to the diagenetic cycles of iron and manganese. These strong iron-OC complexes, formed within the oxic layer of the sediment, are transferred to the deeper anoxic sediment layers through sedimentation, physical reworking and bioturbation; and are metastable over geological timescales [1]. Using a long-term (400-day) incubation, we examined the effect of iron on the early diagenetic transformations of OM in marine sediments. The fate of fresh, algal-derived DOM was monitored by tracking its stable carbon isotopic signature ($\delta^{13}\text{C}$). We demonstrate the incorporation of the ^{13}C -depleted tracer into the sediment through sorption (adsorption and co-precipitation with iron oxides). In the presence of iron oxides, we observed increased transfer of the dissolved algal material to the solid phase, revealing the role of iron in shuttling OM from sediment porewaters to sediment particles. Furthermore, we show that the presence of iron has a differential effect on OC and organic nitrogen (ON), with preferential preservation of OC and accelerated degradation of ON in the presence of reactive iron oxide surfaces. Hence, we propose that redox-sensitive metals may play a crucial role in regulating the global redox balance through increased carbon preservation as well as controlling the concentration of reactive nitrogen species in the open ocean.

[1] Hease *et al.* (1997) *Geochim. et Cosmochim. Acta* **61**, 63-72.

U behaviour under acid mine drainage conditions: Preliminary results from an experimental approach in Río Tinto area (Spain)

L. BARBERO¹, M. KETTERER², M. BASKARAN³,
A. HIERRO⁴, J.P. BOLÍVAR⁴ AND M. CASAS-RUIZ¹

¹Universidad de Cádiz, Spain, (luis.barbero@uca.es)

²Northern Arizona University, USA

³Wayne State University, USA

⁴Universidad de Huelva, Spain

Preliminary results show that dissolved U and Th concentrations in water samples collected from río Tinto area is 2-3 orders of magnitude higher than that in the environmental base-levels in undisturbed areas with $^{234}\text{U}/^{238}\text{U}$ activity ratios (UAR) much higher than 1, thus indicating a strong disequilibrium. Taking into account that under low pH conditions, congruent dissolution rates are high, this disequilibrium is surprising. Different waste pile rocks that include bedrock Fe-oxi-hydroxides, gossans and country rocks have been used for conducting a set of leaching experiments. Results indicate that: 1) Distilled water leaching, although creating an acidic media very rapidly, do not generate leachates with UAR higher than 1.8 in most cases UAR being close to unity; 2) Leaching with different mixtures of acetic acid and ammonium oxalate lead to very high UAR ratios in leachates from Fe-bearing ochre bedrock sediments; 3) Sulphuric acid leaching experiments also generate leachates with high UAR ratios in Fe-rich materials, this not being dependent on acid concentration; and 4) Sulfuric acid leaching after annealing of Fe-oxi-hydroxides at 800°C during several hours results in leachates with UAR close to unity. All these results indicate that not only the leachant but also the extent (?) of radiation damage in Fe-oxi-hydroxides play an important role in the origin of U isotope disequilibrium under acidic conditions.

Melting of an hybrid source below the Danakil Region

E. BARBIERI¹, A. CIPRIANI^{1,2}, D. BRUNELLI^{1,3}
AND E. PAGANELLI¹

¹Dipartimento di Scienze Chimiche e Geologiche, Università degli Studi di Modena e Reggio Emilia, 41100 Modena, Italy

²Lamont-Doherty Earth Observatory of Columbia University, 10964 Palisades, NY, USA

³Istituto di Scienze Marine, Geologia Marina, CNR, Via Gobetti 101, 40129 Bologna, Italy

The Danakil region is a modern example of rifting located atop a mantle plume. Along the rift system, a large number of shield volcanoes erupted large volumes of tholeiitic magmas with a wide compositional range, generally enriched in incompatible and trace elements, reflecting the source heterogeneity and the variability of melting processes that contributed to their generation. The Danakil lavas represent the combined product of continental rifting and ascending mantle plume processes.

Major and trace elements were analyzed in modern lavas sampled from the Erta Ale Chain and the Asal region and compared to literature data. Although highly enriched in trace elements, our lavas are significantly different when compared to the Oligocene main lava suites generated in the earliest stages of mantle plume activity. Based on La/Sm, Rb/Sr and Zr/Nb ratios and REE abundances they are intermediate between the high-Ti primitive lavas and the low-Ti tholeiitic basalts erupted 30 Ma ago due to the arrival of the plume-head. Trace elements abundances and geochemical modelling indicate that our lavas derive from a "hybrid" source characterized by a great complexity, possibly a metasomatized sublithospheric-mantle component that includes hydrous phases and melting at depths lower than those that generated the Oligocene lavas.

The wide compositional range of the Afar lavas suggests that those modern lavas erupted along the rift are not simply the product of melting of a deep mantle plume but derive from a composite source resulting from the interaction between the plume tail and the surrounding sublithospheric mantle previously metasomatized by the plume activity. As a consequence, this very complex and heterogeneous source undergoes extremely variable melting processes as testified by the characteristic chemistry of each volcanic complex.

Further geochemical and isotopic investigations will help to better constrain the signature and contribution of each of the reservoirs and to what extent the mantle is metasomatized by hydrous phases below the Afar region.

Geochemical analysis of the pigments and affinity of the Jurassic calcareous algae *Solenopora jurassica*

HOLLY E. BARDEN¹ PHILIP WITHERS² JULIA BEHNSEN²
UWE BERGMANN³ PHILLIP L. MANNING^{1,4}
ROY A. WOGELIUS¹ AND BART E. VAN DONGEN¹

¹Williamson Research Centre for Molecular Environmental Science, School of Earth Atmospheric and Environmental Sciences, University of Manchester, Williamson building, Oxford Rd, M13 9PL
(holly.barden@postgrad.manchester.ac.uk)

²Manchester X ray Imaging Facility, The School of Materials, The University of Manchester, Oxford Road, Manchester, M13 9PL

³SLAC, National Accelerator Laboratory, Linac Coherent Light Source, Menlo Park, CA 94025, USA

⁴Department of Earth and Environmental Sciences, University of Pennsylvania, Philadelphia, PA 19104, USA

The enigmatic fossil calcareous algae *Solenopora jurassica* is known for its distinctive pink and white banding. Though widely accepted as an algae, there has been some debate over its taxonomic affinity, as well as the derivation of its visible banding pattern which thought to be seasonal. Despite these hypotheses little geochemical work has been carried out to test them. This study represents the first in depth geochemical analysis of this fossil in order to study its affinity and the possible seasonal origin of its banding pattern. Seasonal growth is shown by differences in calcite density, and increased Mg/Ca molar ratios and chlorine levels indicate higher temperatures during the time that white bands were deposited when compared to the pink bands. Pyrolysis gas chromatography mass spectrometry and infrared spectroscopy show the presence of tetramethyl pyrrole, protein moieties and carboxylic acid groups, indicative of the red algal pigment phycoerythrin. This supports the identification of *S. jurassica* as an algae, given that the pigment is only known to occur in cyanobacteria and algae. There is no evidence that the fossil is bacterial and no other taxonomically indicative biomarkers were identified.

Serpentinites as catalysts for vapor conversion of methane in the Earth crust

VICTOR BARELKO¹, OLEG SAFONOV², NATALIA BYKOVA¹, VICTOR DOROKHOV¹ AND LEONID BYKOV¹

¹Institute of Problems of Chemical Physics, Russian Academy of Science, Chernogolovka, Russia (barelko@icp.ac.ru)

²Institute of Experimental Mineralogy, Russian Academy of Science, Chernogolovka, Russia (oleg@iem.ac.ru)

Serpentinites of the oceanic lithosphere are an active source of reduced gases, such as H₂, CH₄, as well as an abiogenic source of complex hydrocarbons. Appearance of H₂ is related to the serpentinization of ultrabasic rocks of the oceanic floor. However, production of H₂ in the CH₄ and H₂O-bearing fluids is possible according to the catalytical reaction known as «vapor conversion of methane», since serpentinite composition and structure can serve as close analogy of the artificial catalysts. We performed an experimental study of the reaction of the methane conversion by vapor using massive lizardite-antigorite serpentinite, which in addition to serpentine contains chromite, magnetite and few chlorite. The sample has not crushed to the fraction 0.5-0.71 mm before experiment. The volume ratio H₂O/CH₄ in the reaction zone was 8-10/1, filtration rate through the rock 1 cm-thick layer was 0.5-0.6 cm/s, while the time of the contact of the vapor-methane mixture with serpentinite was 1.5-2 s. During interaction with the vapor-methane mixture, serpentinite was partially dehydrated with presumable formation of olivine and silica-rich aqueous solution. Chromatography shows that the conversion of CH₄ to H₂ increases with temperature and reaches 14 % at 825°C. The conversion of CH₄ to CO and CO₂ at 825°C is 3 % for both components. Along with H₂, CO and CO₂ the reaction products include ethanol and methanol, which do not form on standard catalysts. The present experimental results support the conclusion on the high catalytical effectiveness of serpentinite: at short time of contacts of the vapor-methane flux with this rock resulted in relatively high degree of conversion. Experiments inspire testing of the catalytical properties of other crustal rocks.

Spatially resolved fully simultaneous determination of large numbers of isotope concentrations and isotope ratios by LA-MH-ICP-MS

D. ARDELT, W. BARGER*, M. REIJNEN AND O. PRIMM

SPECTRO Analytical Instruments GmbH, Boschstr. 10,
47533 Kleve, Germany
(*correspondence: willi.barger@ametech.com)

Laser Ablation-ICP-MS has developed into a powerful tool for the determination of elements, element ratios and isotope ratios in solid samples. The analysis of more and more elements with high spatial resolution and from ever smaller sample sizes is a challenge for this technology.

The development of a fully simultaneous ICP-MS brings several advantages for resolving this challenge: 'all' elements and isotopes can be determined in the same analytical run without sacrificing analysis time for any isotope. The simultaneous measurement also allows elimination of correlated noise, like flicker noise from the plasma or noise generated by the ablation process itself.

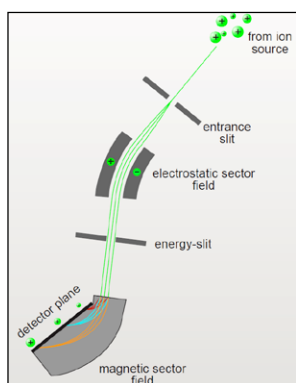


Figure 1: Mattauch-Herzog MS with Solid State Detector.

A double focussing sector field mass spectrometer in Mattauch-Herzog (MH) geometry (Figure 1) was combined with a 4800-channel, large CMOS based semiconductor direct ion detector, placed in the focal plane of the magnet. Each of the channels operates fully simultaneously, using two different amplifications, covering the mass range from ~5 to 240 amu.

The use of this new technology with laser ablation, for simultaneous chemical imaging of large numbers of isotopes, and analytical results for relevant samples, will be presented, with special emphasis on the expected advantages of the fully simultaneous detection.

Microstructures and compositions of melt inclusions from Jubrique (S Spain): Implications for anatexis

AMEL BARICH¹, ANTONIO ACOSTA-VIGIL¹,
CARLOS J. GARRIDO¹, BERNARDO CESARE²
AND OMAR BARTOLI²

¹Instituto Andaluz de Ciencias de la Tierra, CSIC, Univ.
Granada, Spain
(amelbarich@iact.ugr-csic.es)

²Dipartimento di Geoscienze, Univ. Padova, Italy
(bernardo.cesare@unipd.it)

Melt inclusions (MI) are small droplets of silicate liquid trapped by minerals growing either with or from the melt [1]. Most MI in anatectic terranes appear partially or totally crystallized due to slow cooling at depth, and have been named "nanogranites" [2]. MI represent a new and powerful method to study anatexis, because they can give information about melt compositions at the source region of crustal granites, including concentrations of H₂O [3].

There are very few studies of nanogranites, and only one has reported the presence of MI along a prograde metamorphic sequence from metatexites to diatexites [4]. We present a new occurrence of nanogranites along the prograde metamorphic sequence of Jubrique, located on top of the Ronda peridotites (S Spain). Jubrique represents a complete though strongly thinned (≤ 5 km) section of upper to middle-lower continental crust, ranging from carbonates and low-grade phyllites at the top to felsic Grt-bearing metatexites and granulites at the bottom and in contact with the peridotites.

MI show partially irregular to well faceted negative crystal shapes and occur in cores and rims of Grt porphyroblasts. They show a variable size, from ~5-10 μm to several tens of μm in diameter; some of them reach up to ~200-300 μm . Because of the large size, nanogranites at Jubrique have the potential to be remelted and analyzed by EMP but also by LA-ICP-MS. Nanogranites are composed of rare glass, daughter phases Qtz, Pl, Kfs, Bt and Ms, and solid inclusions of Ky and less frequently Gr, Hc, Rt, Ilm, Zrn, and Mnz. Ky was the main solid phase that favored the trapping of MI by poisoning crystal surfaces during Grt growth.

Previous studies concluded that anatexis in the granulites occurred in the Sil field during decompression and thinning. The presence of Ky+Rt within MI, and their occurrence in the high-P cores of Grt, indicate that partial melting in granulites and migmatites initiated at high P conditions, and that most Grt in these rocks crystallized in the presence of melt.

[1] Cesare *et al.* (2011) *J. Virt. Expl.*, **40**, paper 2. [2] Cesare *et al.* (2009) *Geology*, **37**, 627-630. [3] Bartoli *et al.* (2013) *Geology*, **41**, 115-118. Bartoli (2012) Ph.D. Thesis, Univ. of Parma, Italy.

Study of Zsolnay building ceramics in aspect of deterioration by environmental factors

ÁGNES BARICZA^{1*}, BERNADETT BAJNÓCZI²,
MÁRIA TÓTH² AND CSABA SZABÓ¹

¹Lithosphere Fluid Research Lab, Institute of Geography and Earth Sciences, Eötvös University, H-1117, Budapest Pázmány Péter sétány 1/c, Hungary

²Institute for Geological and Geochemical Research, Research Centre for Astronomy and Earth Sciences, Hungarian Academy of Science, H-1112 Budapest, Budaörsi u. 45, Hungary

(*correspondance: baricza.agnes@gmail.com)

The Zsolnay products are the one of the most famous Hungarian ceramics. The glazed building ceramics produced by the Zsolnay Factory were often applied to decorate the buildings, mainly around the turn of the 19th-20th century and since their outplacements the ceramics have suffered numerous environmental and human influences. Our purpose is to observe the alterations by environmental factors considering that these ceramics have never been studied in this aspect before. The studied objects were used on two buildings in Budapest. We have examined the major characteristics of the glaze and the ceramic body on two buildings in Budapest, the depositions on the surface of the glazed and the unglazed sides of some selected ceramics. Several types of Zsolnay ceramics were used as building materials on these buildings. We distinguished different kinds of damage, black deposition layer and alterations. Natural and artificial particles (e.g. carbonaceous and Fe-rich), spherules and a characteristic gypsum layer frequently cover the studied objects. Traces of biological activity (hyphaes) were also found and connected to these organic residues calcium-oxalate (weddelite) was identified. On some samples the glaze has started to weather and the lead leached from the thin surface layer of glaze by rainfall and, if this phenomenon continues for a long period, it will result in the deterioration of the whole glaze.

Trends in urban biogeochemistry at the Anthropocene

S. BARLES*

Université Paris 1 Panthéon-Sorbonne, 191 rue Saint-Jacques, 75005, Paris, France

(*correspondence: sabine.barles@univ-paris1.fr)

As socio-natural sites [1], cities *create* a specific biogeochemistry [2], mainly because they attract huge amounts of materials concentrated in very small areas. This *urban metabolism* is the result of two intertwined phenomena: the natural processes on one hand, the technical ones on the other. Its study calls for an interdisciplinary approach as illustrated in [3]. In order to better characterise urban metabolism, we chose Paris urban area as a case study. By crossing historical methods and material/substance flow analysis, we were able to describe long term trends and changes. These results, together with other ones for other cities, allow to give a general insight into urban key issues in terms of biogeochemistry.

The very characteristic of cities is the externalisation of a great (and up to now growing) part of their metabolism. Cities were borne from a specialisation that made possible for some people to not produce their food and then to develop other activities in specific places – cities. This externalisation peaks with industrial revolution(s) with, for instance the partial externalisation of water cycle, the one of urban by-products transformation, etc. The shift of cities from sink (up to the end of the 19th century) to source of emission to air and water for substances like N or P is another characteristic of cities metabolism. This is due to changes in waste management and to the devalorisation of urban fertilisers (especially human manure) that occurred at the beginning of the 20th century together with the increase in fossil fuel consumption (for N).

As a result, urban metabolism goes far beyond the urban limits and cities can be considered as one of the main drivers of biogeochemical cycles, considering both their direct and indirect impacts on them. Today, one of the great challenges faced by urban managers and biogeochemists is the improvement of urban metabolism (its *re-internalisation*?), its transformation from a constraint to an asset – for the provision of nutrients, the reduction of urban heat island, etc.

[1] Winiwarter & Schmid (2008) In: Knopf (ed.) *Umweltverhalten in Geschichte und Gegenwart*. Tübingen: Narr. [2] Kaye *et al.* (2006) *Trends Ecol. Evol.* **21**, 192-199. [3] Svirejeva-Hopkins & Reis (eds.) (2011) In: Sutton *et al.* *The European Nitrogen Assessment*. Cambridge Univ. Press.

Investigating instrumental mass bias in MC-ICP-MS using isotope ratio plasma profiles

J. BARLING¹, N. S. BELSHAW¹ AND A. N. HALLIDAY¹

¹ Department of Earth Sciences, University of Oxford, South Parks Road, OX1 3AN, UK (jiej@earth.ox.ac.uk)

In multi-collector inductively-coupled-plasma mass spectrometry (MC-ICP-MS) heavy/light isotope ratios are fractionated to high values relative to the true value. Accurate and precise correction of this instrumental mass bias is a prerequisite for accurate MC-ICP-MS isotope ratio data. However, understanding of this phenomenon is limited.

As a step towards gaining insight into the processes involved in generating instrumental mass bias we have measured the variation of heavy/light isotope ratios as sampling depth in the plasma is varied. These axial plasma profiles were measured at ~250 μm intervals over a sampling depth of ~3.5 mm. Each experiment consisted of 6 profiles sampled over the same sampling depth range but tuned at different sampling depths.

Pb and Mg were chosen as the analytes. These elements though very different in mass have similar first and second ionisation potentials, therefore any differences in heavy/light isotope ratios variation with sampling depth should be mass dependent. All profiles were curvilinear. For Pb the heavy/light isotope ratio (²⁰⁸Pb/²⁰⁶Pb) increased with decreasing sampling depth, whereas for Mg (²⁶Mg/²⁴Mg) it decreased. ²⁰⁸Pb/²⁰⁶Pb values on individual profiles varied by 0.56 – 0.70% of the average value measured on the profile and the magnitude of variation increased as the tuned sampling depth decreased. Variation in ²⁶Mg/²⁴Mg was much greater, 1.1 – 1.3% of the average value measured on each profile and increased dramatically to 7.1% for the profile tuned at the shallowest sampling depth. If only ratios measured at the tuned sampling depth on each profile are considered, the trends are reversed e.g. ²⁰⁸Pb/²⁰⁶Pb generally decreases with decreasing sampling depth.

These apparent variations in instrumental mass bias with sampling depth in the plasma result from a combination of processes occurring during transport of the analyte through the plasma (e.g. radial mass dependent dispersion of ions and atoms and ionisation potential effects) and additional mass dependent effects produced during sampling and transport through the interface. The contrast in apparent mass bias response between Mg and Pb allows us to speculate on the relative significance of plasma versus interface processes in producing the instrumental mass bias.

Subduction channel or fossil rifted margin? Serpentinite geochemistry of the Punta Rosa Unit, Western Alps

JAIME D. BARNES¹, MARCO BELTRANDO²,
CIN-TY A. LEE³, STACI LOEWY¹ AND EMILY CHIN³

¹Department of Geological Sciences, University of Texas, Austin, Texas, USA 78712, (jdbarnes@jsg.utexas.edu)

²Dipartimento di Scienze della Terra, Università di Torino, Via Valperga Caluso 35, 10125 Torino, Italy

³Department of Earth Science, MS-126, Rice University, Houston, Texas 77005, USA

The Punta Rosa unit (PR), now stacked in the Valaisan domain (Western Alps) preserves evidence of Mesozoic mantle exhumation at the seafloor, despite having undergone pervasive Alpine deformation/metamorphism. Serpentinites are overlain by slivers of continental basement or meta-sedimentary breccia and have been interpreted as an ocean-continent transition (OCT) based on structural data [1]. However, similar lithological associations throughout Alpine-type orogens are often interpreted as subduction-related “tectonic mélanges” [e.g., 2]. Here we present the first geochemical study of PR serpentinites to further test the interpretation of their tectonic setting.

Stable isotope and major and trace element compositions of PR serpentinites with varying distances from the contact with meta-sedimentary material were determined. δ³⁷Cl, δ¹⁸O, and δD values range from +1.1 to +2.7‰, +7.0 to +8.5‰, and -50 to -73‰, respectively. δ³⁷Cl values are some of the highest reported for serpentinites and increase towards the contact with the metasediments, indicating interaction with metasediments/altered oceanic crust during Alpine subduction/exhumation. O and H isotope data are consistent with low-T interaction with seawater (with partial resetting of H by meteoric fluids) or slab-derived fluids. Bulk serpentinite samples have high REE concentrations, compared to typical mid-ocean ridge serpentinites, with nearly flat to slightly convex up REE patterns (La_N/Sm_N = 0.38 – 0.62; La_N/Yb_N = 0.20 – 0.47; Sm_N/Yb_N = 0.41 – 0.89). These high REE concentrations are similar to those observed in OCTs (Iberia Abyssal Plain; Newfoundland) [3] and the Malenco and Platta peridotites (Switzerland), which are the type localities for preserved OCTs [4]. Serpentinite geochemistry supports stratigraphic and structural evidence for an abyssal origin of the PR serpentinites, providing a powerful tool to determine tectonic setting in poorly exposed/highly deformed metamorphic units.

- [1] Beltrando *et al.* (2012) *Tectonophysics* **579**, 17-36. [2] Gerya *et al.* (2002) *Tectonics* **21**, doi:10.1029/2002TC001406. [3] Kodolányi *et al.* (2012) *J Petrology* **53**, 235-270. [4] Müntener *et al.* (2010) *J Petrology* **51**, 255-294.

Archean andesites as products of plume/crust interaction?

STEPHEN J. BARNES¹, CARISSA ISAAC²
AND MARCO L. FIORENTINI²

¹CSIRO, Perth, Western Australia, (steve.barnes@csiro.au)

²University of Western Australia, Perth, WA,
(20685898@student.uwa.edu.au)

A key line of evidence for Archean plate tectonics rests on the presence of andesites, the signature rock type of modern subduction zones. This study considers the petrogenesis of andesites from the 2.7 Ga East Yilgarn Craton (EYC) in Western Australia, a richly mineral-endowed terrane that has been a prime focus of debate between proponents of a uniformitarian, plate-tectonic driven interpretation, and advocates of an alternative plume-driven model. While EYC andesites have incompatible trace element characteristics similar to those of modern island arc andesites, they have unusually high Ni, Cr and MgO contents. This suggests the possibility that they contain a substantial mantle plume component. To test this hypothesis, we consider the major and trace element compositions of these rocks in relation to the entire assemblage of EYC volcanic rocks with ages between 2690 and 2710 Ma, including komatiites, plume-derived basalts and dominantly dacitic felsic rocks. The dacite component occurs as part of a bimodal association with simultaneously erupted komatiites, has characteristic TTG-like trace element chemistry, and chondritic to slightly depleted Nd and Hf isotopic characteristics. This component is interpreted as the partial melting product of underplated juvenile or near-juvenile mantle-derived mafic material. Numerical modelling of fractionation of plume-related tholeiitic basalts coupled with contamination by the TTG-like dacite component provides a good fit to all of the essential major and trace element characteristics of the EYC andesites, and is also consistent with the chondritic to slightly depleted Nd and Hf isotopic characteristics of the andesites [1]. Thus, a rock type previously taken as a key line of evidence for plate tectonic processes can be explained just as well by an alternative plume-driven mechanism, consistent with the overwhelmingly plume-derived character of basalts and komatiites across the entire craton [2]. This explains a paradox, noted in a number of Archean volcanic rock sequences, that apparently subduction-related rocks are interleaved with voluminous basaltic magmatism derived from 1000 km-scale plume-head arrival events. The problem is moot if Archean andesites are products of plume, not subduction zone, magmatism.

[1] Barley ME *et al.*, (2003) AMIRA Project 624 final report.

[2] Barnes SJ *et al.*, (2012), *Aust J Earth Sci* **59**, 707-735.

Isotopic tracing of ancient metal production using geological and mining archaeological research – Gaul mining from Limousin and Morvan (France). A case study

S. BARON*¹, B. CAUUEY¹ AND C.G. TAMAS²

¹TRACES-CNRS, 5, allées A. Machado, 31058 Toulouse Cedex 09, France.

(*correspondence: sbaron@univ-tlse2.fr)

²University Babes-Bolyai, 1, M. Kogalniceanu str., 400084 Cluj-Napoca, Romania

The isotopic tracing from mines/ore bodies to archaeological materials (slags, metals, objects) constitutes a powerful tool in metal provenance studies. The progress of high resolution mass spectrometers (MC-ICP-MS) during the last decade currently facilitates accurate analyses of traditional and non-traditional isotopes, allowing thus precise and consequently more accurate interpretation [1]. Nevertheless, these high precision isotope analyses on ores are often carried out in an elusive way ignoring the geological approach as well as the mining archaeology background. The currently used lead isotope ores database is not completely relevant for the tracing of the ancient metals for several reasons: i) the isotopic composition of the analysed ores is usually not linked with their mineral paragenesis, and ii) the analysed ores are not those really exploited by the ancient miners. Furthermore, the ancient *chaîne opératoire* from ores to metal(s)/objects is not systematically considered [2].

Through an example of metal production in Gaul (France) during Protohistoric times, we demonstrate the importance of establishing a geochemical tracing based on geological and chronological/archaeological samples.

Our aim is to characterize the mining activity and the metal production at regional scale (Limousin and Morvan) and in a second stage to acquire the isotopic and trace element signature of the exploited ores and the produced metals (Au, Ag and Sn). This approach based on geological, mining archaeological and geochemical studies will refine the tracing of the metals at least for Limousin (5th to 1st centuries BC) and Morvan (2nd to 1st centuries BC) and will allow to obtain isotopic data bases needed for relevant metal provenance studies.

Acknowledgments: Research carried out in the frame of ANR MINEMET project (France).

[1] Rehkämper *et al.* (2004). *Handbook of Stable Isotope Analytical Techniques*, Elsevier Science Ltd Eds, 1258pp. [2] Baron *et al.* (in press), *Archaeometry*.

Silica and germanium cycling in a coastal shelf environment: Insights from northern Gulf of Mexico

JOTAUTAS J. BARONAS^{1*}, DOUGLAS E. HAMMOND²,
WILLIAM M. BERELSON³, JAMES MCMANUS⁴
AND SILKE SEVERMANN⁵

¹Department of Earth Sciences, University of Southern California, 3651 Trousdale Pkwy, Los Angeles, CA 90089, USA (correspondence: baronas@usc.edu)

²College of Earth, Ocean, and Atmospheric Sciences, Oregon State University, 104 CEOAS Admin Bldg, Corvallis, OR 97331-5503, USA

³Institute of Marine & Coastal Science, Rutgers University, 71 Dudley Road, New Brunswick, NJ 08901-8521, USA

The Ge/Si ratio recorded in sedimentary opal covaries with glacial-interglacial cycles as far back as the Mid-Miocene [1], demonstrating its potential as a proxy for Si cycling. However, there are multiple mechanisms potentially influencing the Ge/Si recorded. These include the intensity of terrestrial rock weathering, variations in the size of the diagenetic Ge sink, and biological fractionation by marine silicifiers.

We have measured Ge and Si concentrations in the water column and sediment pore waters in the Gulf of Mexico (GOM). Results indicate extensive fractionation, enriching the shelf surface water Ge/Si to 2.3 (all Ge/Si ratios are in $\mu\text{mol/mol}$), significantly higher than the main Si source - the Mississippi River (Ge/Si = 1.5). Preliminary box model calculations predict a fractionation factor of $R_{\text{biogenic silica}}/R_{\text{water}} = 0.5-0.6$, where R is Ge/Si ratio. GOM deep water (500-2100 m Ge/Si = 0.82-0.86) is also enriched relative to the published global ocean values (Ge/Si = 0.70-0.76). Porewater observations in coastal sediments (Ge/Si = 0.3-0.7) and modelling suggest that 10-30% of Ge is diagenetically sequestered into an unidentified (possibly iron-rich) authigenic precipitate.

[1] Shemesh *et al.* (1989) *Paleoceanography*, **4**(3), 221–234.

Ferrian chromite formation in podiform chromitites from south-central Chile

F. BARRA^{1,2*}, F. GERVILLA³ AND M. REICH^{1,2}

¹Dept. of Geology, University of Chile, Santiago, Chile
(*correspondence: fbarrapantoja@ing.uchile.cl)

²Andean Geothermal Center of Excellence (CEGA),
University of Chile, Santiago, Chile

³Dept. of Mineralogy and Petrology, University of Granada,
Granada, Spain

The metamorphic basement of the Coastal Cordillera in south-central Chile comprises two units with contrasting characteristics. The Eastern series is characterized by high T/low P conditions, whereas the Western Series represent high P/low T metamorphic conditions [1]. These units have been interpreted as an accretionary prism, where the Eastern series formed by frontal accretion and the Western series was produced by basal accretion [2]. The Western series comprises mainly metapsammopelitic rocks, metabasites and minor serpentized ultramafic rocks. The serpentinite bodies are scattered within the Western series and show variable degrees of serpentization. Although most of these serpentinites have accessory chromian spinels, only in one locality podiform chromitites have been found. Here we present the chemical composition of these chromitites determined using electron microprobe analysis (EMPA) in order to provide some insights on the formation of ferritchromite as an alteration product of chromite.

Chromitites are highly brecciated with a matrix completely altered to Cr-rich chlorite. Chromite spinel grain cores are high-Al in content, whereas ferrian chromite (i.e., ferritchromite) is Fe⁺³ rich and usually formed along cracks and margins. The observed pattern of alteration is similar to that described for other locations [3] with volume reduction associated with dissolution of chromite and formation of porous chromite. Unaltered chromite cores show Cr# [Cr/(Cr + Al) atomic ratio] = 0.65–0.70, Mg# [Mg/(Mg + Fe⁺²) atomic ratio] = 0.50–0.70, and Fe⁺³/(Fe⁺³ + Fe⁺²) < 0.15. The chemical composition of chromites evolved towards higher #Cr (0.75–0.95), lower #Mg (0.40–0.10), and higher #Fe (0.20–0.40). The observed trend is consistent with a reaction of chromite with olivine to produce chlorite. The alteration process is concomitant with mass loss and development of a porous texture in chromite.

[1] Aguirre *et al.* (1972) *Kristalinikum* **9**, 7–19. [2] Willner *et al.* (2005) *J Petrology* **46**, 1835–1858. [3] Gervilla *et al.* (2012) *Contrib Mineral Petrol* **164**, 643–657.

Reconstructing past hydrology from annual cycles in trace elements in a Moroccan Stalagmite

J.J. BARROTT*, C.C. DAY AND G.M. HENDERSON

Department of Earth Sciences, University of Oxford, UK
(*correspondance: julia.barrott@earth.ox.ac.uk)

We present annually resolved trace element and stable isotope data from a laminated Mid-Holocene north Moroccan stalagmite. All reported analyses were performed on the same 200- μm micro-milled calcite samples, yielding an entirely inter-comparable dataset. In addition to $\delta^{18}\text{O}$, $\delta^{13}\text{C}$, Mg, Sr, Ba, U and P, we present the first measurements of Cd in speleothem carbonate. Recent cave-analogue experiments [1] demonstrate that Cd/Ca is highly sensitive to variation in the amount of calcite precipitated from solution, with high Cd/Ca particularly indicative of low degrees of prior calcite precipitation. We employ a multi-proxy approach, using Cd alongside other trace elements and stable isotopes to reconstruct changes in hydrology at this site.

With the exception of $\delta^{18}\text{O}$, highly distinct annual cycles occur in all reported proxies and correspond closely to changes in laminae colour. The observed annual cycle in Cd/Ca implies that % calcite precipitated is a major driver of annual trace element cycles in this sample. The agreement between the trace elements, laminae colour and $\delta^{13}\text{C}$ agrees well with that expected in calcite precipitated in a site where rainfall is highly seasonal. Weaker correlations with $\delta^{18}\text{O}$ reflect the more integrated nature of the information recorded by oxygen isotopes, indicating that some regional signal is being captured.

Despite differences in seasonal cave ventilation these observations show remarkable agreement with annual trace element cycles from a modern speleothem at St Michael's Cave, Gibraltar [2], which lies 27 km northwest of our site. Such a parallel between sites gives confidence that trace element geochemistry can potentially be used for robust regional palaeoclimate reconstruction, and perhaps also for the careful extrapolation of monitoring studies between sites.

[1] Day & Henderson, *Geochimica et Cosmochimica Acta*, in review. [2] Matthey, Lowry, Duffet, Fisher, Hodge, & Frisia (2008), *Earth and Planetary Science Letters* **269**, 80-95.

Ancient recycled nitrogen isotope signatures in Siberian xenoliths

P. H. BARRY^{1*}, D. R. HILTON² AND L. A. TAYLOR¹

¹Planetary Geosciences Institute, Dept. of Earth and Planetary Sciences, University of Tennessee, Knoxville, TN 37996
(*Correspondence: peter.barry@utk.edu)

²Scripps Institution of Oceanography, La Jolla, CA 92093

Siberian xenoliths display compelling evidence for a recycled crustal origin. In order to assess if nitrogen is also recycled in ancient subducted-oceanic crust we have measured N-isotopes ($\delta^{15}\text{N}$) and elemental (N_2/Ar) ratios for a suite of peridotitic and eclogitic xenoliths (n=10) from two petrologically-distinct kimberlite pipes (i.e., Udachnaya and Obnazhennaya). Additionally, all samples have been well-characterized, mineralogically, petrographically, and for major and trace element chemistry.

Crustally-derived xenoliths (Gt, Cpx and Ol) of Siberia are believed to originally be derived from subducted oceanic crust which has since amalgamated to form the Siberian craton. The occurrence of non-mantle-like oxygen isotope signatures in Siberian xenoliths suggests that these lithologies are artifacts of partially-melted subducted ocean crust [1, 2]. Subsequently, this material was transported to Earth's surface via kimberlitic volcanism. The age of Siberian xenoliths have been constrained to be within 2.7 - 3.1 Ga using Re-Os and Sm-Nd isotope dating techniques [3]. $\text{Mg}\#_{\text{Gt}}$ ranges from 86 - 96, suggesting relatively primitive magmas. Major and trace element chemistry indicates that these samples have been subjected to varying degrees of metasomatism. Due to the antiquity of these particular xenoliths, they represent prime targets for N-isotopes, which have been previously suggested to show a secular variation throughout Earth history [4].

N-isotopes ($\delta^{15}\text{N}$) of Siberian xenoliths range from -0.7 to -10.8 ‰ and are consistent with both upper mantle (MORB = -5 ± 2 ‰) and recycled contributions (modern sediments = $+6 \pm 2$ ‰). N_2/Ar values range from 32 to 178, spanning both atmospheric (84) and typical mantle values (84-164). Cpx mineral separates retained the most nitrogen gas. Notably, all Obnazhennaya samples display N-isotope values above the MORB range, indicating a larger contribution from a recycled component vs. Udachnaya samples, which span the MORB range. These results suggest xenoliths of different kimberlite pipes sample isotopically-distinct parts of the mantle, and may preserve varying mantle/crustal contributions throughout Earth history.

[1] MacGregor and Manton, (1986). [2] Taylor and Anand, (2004). [3] Pearson *et al.*, (1995). [4] Marty and Dauphas, (2003).

Tracking Indian-type mantle at its western limit during the closure of Neo-Tethys and opening of the Indian Ocean

T.L. BARRY^{1*}, J.H. DAVIES² AND I.L. MILLAR³

¹Dept. of Geology, University of Leicester, Leicester, UK
(correspondence: tlb2@le.ac.uk)

²School of Earth & Ocean Sci., Cardiff University, Cardiff, UK (daviesjh2@cf.ac.uk)

³NERC Isotope Geosciences Lab., Keyworth, Notts, UK.
(i.l.millar@bgs.ac.uk)

Since the work of Mahoney *et al.* [1] on old west Indian Ocean and east Tethyan MORBs, we have known that Indian-type (DUPAL) mantle resided beneath at least parts of Neo-Tethys at the time of opening of the Indian Ocean. Furthermore, work on a ~350 Ma ophiolite from China [2] demonstrates that Indian-type mantle must have contributed, in some places, to MORB genesis during the formation of Paleo-Tethys. Together, this evidence suggests that Indian-type mantle has at least to some extent remained within the shallowmost asthenosphere during multiple Wilson cycles, over 100's millions of years.

In the western Pacific the margins of the Indian-type mantle have been recognised and, in places, mapped adjacent to Pacific-type mantle [e.g. 3-5]. Detailed work along this boundary has shown that very little mixing has taken place, but what happened to the Indian-type mantle at its western limit during the diachronous closure of Neo-Tethys?

Using robust Hf-Nd isotopes on an extensive suite of MORB rocks from Neo-Tethyan ophiolites, extending from the Himalayas, through the Mediterranean and Europe, to earliest central Atlantic and proto Caribbean ocean crust, we assess where Indian-type mantle occurred beneath Neo-Tethys. Inferences from these results are then linked to 3D numerical spherical geodynamic models (run using mantle circulation code TERRA) and used to investigate models of how this isotopically distinct Indian-type mantle may have been preserved in the upper mantle during successive events of ocean closure and re-opening, with little apparent tendency to mix laterally.

[1] Mahoney *et al.*, (1998) *J. Pet* **39**, 1285-1306. [2] Xu & Castillo (2004) *Tectonophysics* **393**, 9-27. [3] Pearce *et al.*, (1999) *J. Pet* **40**, 1579-1611. [4] Kempton *et al.*, (2002) *Geochem Geophys Geosyst* **3(12)**, 1074. [5] Nebel *et al.*, (2007) *EPSL* **254**, 377-392.

Water contents of natural anatectic melts: constraints from NanoSIMS analysis of remelted nanogranites and glassy inclusions

OMAR BARTOLI¹, BERNARDO CESARE¹, ANTONIO ACOSTA-VIGIL², LAURENT REMUSAT³ AND STEFANO POLI⁴

¹ Dipartimento di Geoscienze, Univ. Padova, Italy; email: omar.bartoli@unipd.it; bernardo.cesare@unipd.it

² Instituto Andaluz de Ciencias de la Tierra, CSIC, Univ. Granada, Spain; email: aacosta@ugr.es

³ Muséum National d'Histoire Naturelle, Paris, France; email: remusat@mnhn.fr

⁴ Dipartimento di Scienze della Terra, Univ. Milano, Italy; email: stefano.poli@unimi.it

Formation, extraction and ascent of hydrous anatectic melts to upper crustal levels represent the most important mechanisms for the reworking of the Earth's continental crust [1, 2]. In this scenario, the water content of melts is of prime importance in the formation and evolution of the continental crust and so far the experimental approach has been largely applied for obtaining constraints on the water content of anatectic melts.

The study of melt inclusions hosted in peritectic phases of partially melted rocks represents a recent, small-scale powerful approach to a better understanding of melting in the continental crust [e.g. 3-5]. Successful experimental rehomogenization of the inclusions to a glass allows the direct analysis of the natural anatectic melts produced in the source region of crustal magmas [5]. This approach provides the precise melt composition for the specific anatectic rock under study.

We report the results of NanoSIMS analyses on melt inclusions hosted in peritectic garnet of partially melted metasedimentary rocks. Data are discussed in order to i) combine information from classical petrology and melt inclusions, ii) compare them with previous estimations from experiments and thermodynamic calculations and iii) deal with new questions, such as the water content heterogeneities of natural anatectic melts in the source region.

[1] Brown *et al.* (2011) *Elements*, **7**, 261-266. [2] Sawyer *et al.* (2011) *Elements*, **7**, 229-234. [3] Cesare *et al.* (2009) *Geology*, **37**, 627-630; [4] Acosta-Vigil *et al.* (2012) *J. Pet.*, **53**, 1319-1356. [5] Bartoli *et al.* (2013) *Geology*, **41**, 115-118.

Fate and impacts of nano-CeO₂ in an activated sludge bioreactor

L. BARTON¹, M. AUFFAN², A. MAISON²,
C. SANTAELLA³, L. OLIVI⁴, N. ROCHE⁵, J. Y. BOTTERO²
AND M. WIESNER¹

¹Duke University, Durham, NC: leb40@duke.edu,
wiesner@duke.edu

²CEREGE, France: auffan@cerege.fr, maison@cerege.fr,
bottero@cerege.fr

³LEMIRE, CEA Cadarache, France:
catherine.santaella@cea.fr

⁴ELETTRA Sincrotron, Italy: luca.olivi@elettra.trieste.it

⁵University Aix-Marseille, France: nicolas.roche@univ-amu.fr

Widespread use of Engineered Nanomaterials (ENMs) in a myriad of consumer products and technologies has led to release of ENMs to the environment. A likely first route of environmental exposure of ENMs is through the waste stream. Within wastewater treatment plants (WWTPs) ENMs undergo transport and transformation processes different from traditional organic contaminants. Understanding ENM-specific fate and transport is thus a critical void in current nanomaterial research.

In this study, we tracked the mobility and transformations of a common ENM, CeO₂, to determine release concentrations and the nature of the ENMs released from WWTPs in solid and effluent. An aerobic bioreactor seeded with sampled activated sludge was dosed with pristine and citrate coated CeO₂ chronically at environmentally relevant concentrations for a six week period. Two samples of CeO₂ were employed to observe the impact of surface chemistry on fate. During the lifetime of the reactor, affinity of the ENM for the solid versus liquid phase was measured and it was observed that > 90% of the added CeO₂ associated with the solid phase regardless of the surface coating. In addition, Ce speciation was monitored with XANES to explore the CeO₂ transformations. It was found that after 5 weeks in the reactor environment, strong reduction of the Ce(IV) in the ENM to Ce(III) occurred. Reduced Ce(III) was only measured in association with the solid phase indicating the key role of the microbial communities in promoting this reduction. In addition, it was seen that the citrate coating altered the kinetics of this reduction by preventing it until consumption of the coating by the bacteria. Determination of the interaction with the biomass and nature of the Ce(III) complexes is ongoing. Studies such as these can help inform the modeling community attempting to predict exposure and risk of ENMs released to the environment.

New interpretation of kinematics and morphogenesis of block structures of the Black Sea-central transcaucasian terrane

LEVAN BASHELEISHVILI

¹Javakishvili Tbilisi State University A. Djanelidze geology
institute, Georgia,
levanbash@yahoo.com

Modern structure of the Black Sea-Central Transcaucasian Terrane is mainly conditioned both by meridional and latitudinal fault systems. They encompass different depth of the Earth's crust crystalline basement. They as a whole make a mosaic-block pattern. The analysis of lithofacies and thicknesses of sedimentary cover sometimes establishes their autonomous and inverse nature of development as well as differentiated kinematics. The research data enables to make the following conclusions: The Caucasian molasse depression (within the territory of Georgia) is divided into eastern and western subsiding zones by the Dzirula (crystalline basement) salient; they are also divided by faults into separate restricted blocks. Westwards and eastwards of the central uplift zone, along the faults is outlined a gradual "stepwise" submergence and tilting of blocks of the crystalline substrate. In the modern literature the analogous structures are known as the so called "tilt" blocks and kinematically they are related to tensile strains.

Thus, in contemporary structure of the pre-Alpine crystalline basement of the South Caucasian molassics depression (along the latitudinal profile) is marked the existence of tension structure mainly in condition of stepped-inclined blocks, which subsequently turn into the so-called listric faults. The appearance of this one is bound up, on the one hand, with uplift of the mantle masses in some parts of the region and on the other hand, with advance of the Arabian plate to the north and connected with them lateral squeezing out of masses both to the west and the east especially at the late-orogenic (collision) stage of development.

Effects of heating on the leaching of U-Th series radionuclides in a suite of natural minerals

BASKARAN, M¹ AND GARVER, E¹

¹Department of Geology, Wayne State University, Detroit, MI-48202, USA; Baskaran@wayne.edu

The differences in the extent of leaching (with 0.1 N HNO₃ for ~25 days) and recoil of U-Th series radionuclides [U (²³⁴U), Th (^{230,234}Th), Ra (^{224,226,228}Ra), Pb (^{210,212}Pb), ²¹⁰Po, ²²⁸Ac and ²²²Rn] from a suite of natural minerals (zircon, monazite, thorite and cerite) were assessed at room temperature and after heating these minerals at 200°C and 600°C. Our results indicate the following: i) The concentrations of U-Th series radionuclides in the leachate depend on the amount of the accumulated radiation dose in the minerals; ii) The amount of radionuclides leached from annealed (200°C or 600°C) minerals is lower by 3 orders of magnitude compared to unannealed minerals; and iii) The differences in the daughter/parent ratios of a number of pairs in the ²³⁸U and ²³²Th series (²¹⁰Po/²¹⁰Pb, ²²⁸Ac/²²⁸Ra, ²³⁴Th/²³⁸U, ²¹²Pb/²²⁴Ra, ²²⁴Ra/²²⁸Th and ²²²Rn/²²⁶Ra) between the heated and unheated minerals range over several orders of magnitude.

This study provides insight on the location of ²³⁸U and ²³²Th and possibly their daughter products in mineral grains (in particular, if they are located in grain boundaries), the effects of track density on the leaching of U-Th series radionuclides from mineral grains, the effects of the internal radiation damage on the escape of radon and the leaching of other non-gaseous daughter products in the U-Th series. This study has implications on the assessment of the performance of nuclear wasteforms in groundwater environment. This study has also bearing on the mobility of U-Th series radionuclides in rocks/minerals that are in contact with erupting magma.

We will present possible mechanisms for the differences in the extent of leaching of radionuclides between the heated and unheated minerals in our presentation.

Internal Lu-Hf isotope systematics of the quenched angrite D'Orbigny and two plutonic angrites

R. BAST^{1*}, E. E. SCHERER¹, K. MEZGER², M. FISCHER-GÖDDE³ AND P. SPRUNG³

¹Institut für Mineralogie, Westfälische Wilhelms-Universität Münster, D-48149 Münster, Germany (*correspondence: Rebecca.Bast@uni-muenster.de)

²Institut für Geologie, Universität Bern, CH-3012, Switzerland

³Institut für Planetologie, Westfälische Wilhelms-Universität Münster, D-48149 Münster, Germany

The long-lived radioactive decay of ¹⁷⁶Lu to ¹⁷⁶Hf chronometrically provides a precise and disturbance-resistant chronometer for dating early Solar System processes. However, some meteorites (e.g., the quenched angrite Sah 99555 [1]) show excess ¹⁷⁶Hf [1-3], resulting in Lu-Hf dates significantly older than the Solar System. One possible explanation for this is that irradiation in the early Solar System produced the short-lived isomer ^{176m}Lu (t_{1/2} = 3.7 hr) and thus accelerated the ¹⁷⁶Lu-decay [4-5].

In contrast to the results of Sanborn *et al.* [6], we found excess ¹⁷⁶Hf in the quenched angrite D'Orbigny and the plutonic angrite NWA 4801. Our internal Lu-Hf isochrons yield dates of 4760 ± 64 Ma for D'Orbigny (8 fractions) and 4635 ± 19 Ma for NWA 4801 (10 fractions). The initial ¹⁷⁶Hf/¹⁷⁷Hf values are 0.279736 (37) and 0.279788 (89), respectively, which are in the same range as the CHUR values of [7-8] back-calculated to 4567 Ma, and 3-6 ε-units higher than the initial Hf isotope composition of the Solar System suggested by Bizzarro *et al.* [1].

Our new data do not preclude irradiation on the angrite parent body as a possible cause for the old apparent ages. However, not all Lu-Hf dates are too old: our 8-point Lu-Hf isochron for the plutonic angrite NWA 4590 yields 4580 ± 46 Ma, which is in agreement with the Pb-Pb age reported by [9-10]. Its initial ¹⁷⁶Hf/¹⁷⁷Hf value of 0.279794 (16) agrees with the CHUR values of [7-8] back-calculated to 4567 Ma.

[1] Bizzarro *et al.* (2012) *G³* **13**, 10.1029/2011GC004003. [2] Blichert-Toft *et al.* (2002) *EPSL* **202**, 167-181. [3] Bast *et al.* (2012) *LPSC* **43**, abstr. 2542. [4] Thrane *et al.* (2010) *Astrophys J* **717**, 861-867. [5] Albarède *et al.* (2006) *GCA* **70**, 1261-1270. [6] Sanborn *et al.* (2012) *LPSC* **43**, abstr. 2039. [7] Blichert-Toft & Albarède (1997) *EPSL* **148**, 243-258. [8] Bouvier *et al.* (2008) *EPSL* **273**, 48-57. [9] Amelin & Irving (2007) *LPI Contrib* **1374**, 20-21. [10] Amelin *et al.* (2011) *LPSC* **42**, abstr. 2542.

Zeolites and mafic phyllosilicates in Livingston Island, Antarctica

J. BASTIAS¹, F. FUENTES², L. AGUIRRE¹, F. HERVÉ^{1,2},
F. FERNANDOY² AND A. DEMANT³

¹Departamento de Geología, Universidad de Chile, Plaza Ercilla 803 8370450, Chile (joaquinbastias@ug.uchile.cl)

²Escuela de Ciencias de la Tierra, Facultad de Ingeniería, Universidad Andres Bello, Abate Molina 140 8370116, Chile (ffuentes@unab.cl)

³Laboratoire de Pétrologie Magmatique, Université Aix Marseille III, 13397 Marseille Cedex 20, France

The present work is a report on the geochemistry and petrology of the very low-grade alteration minerals developed in the volcanic successions from Punta Hannah (PH) and Shirreff Cape (SC), Livingston Island, Antarctica.

The outcrops consist of andesitic-basaltic rocks from volcanic successions assigned to the Upper Cretaceous [1]. These rocks are one of the most extensive volcanic exposures in the South Shetland Islands.

The alteration minerals occur in amygdules, veins, veinlets, groundmass, or patches. This replacement of the phenocrysts can be partial, affecting the crystal edges and fractures or total. Primary plagioclases have been strongly altered to albite, zeolites and calcite, and clinopyroxenes to mafic phyllosilicates and celadonite.

Petrographic, XRD and EMP analyses show the occurrence of the zeolites: laumontite, stilbite, faujasite and heulandite in PH, and natrolite and analcime in SC. Mafic phyllosilicates correspond to interstratifications between chlorite and trioctahedral smectite. Chlorite layer percentages range between 57% and 84%, and display diabantine compositions [2]. Equilibrium temperatures of mafic phyllosilicates from PH, calculated using two geothermometers [3, 4], range between 160 and 190°C for those with chlorite layer percentages above 75%. This range is in agreement with temperature estimates for zeolites of 150–230°C. Zeolites from SC suggest temperatures below 150°C.

The characteristics of these rock successions indicate a Ca-Na remobilization in the light of albitization and the widespread occurrence of Ca-rich zeolites. Hydrothermalism and burial processes would account for the genesis of the secondary minerals.

Project Anillo CONICYT ACT 105 financed the research.

[1]Leppe *et al.* (2007) *UGSG Srt Rsrch Pprs* 1407. [2] Hey (1954) *MinMag* **30**, 272-292. [3] Cathelineau (1988) *Cly Min* **26**, 471-485. [4] Jowett *et al.* (1991) *SEG Jnt Annl Mtng* **16**, A62.

FreeGs thermodynamic database project: implementation, lessons, and future?

E. N. BASTRAKOV^{1*}, L. A. I. WYBORN¹, T. P. MERNAGH¹
AND A. CHALNEV²

¹Geoscience Australia, Canberra, ACT 2601, Australia

(*correspondence: Evgeniy.Bastrakov@ga.gov.au)

²DIISR, Canberra, ACT 2601, Australia

Increasing demand in reactive-transport modelling for the purposes of CO₂ sequestration, use of geothermal energy, and nuclear waste disposal requires ready access to standardised thermodynamic data. These must be adopted for multiple formats for ever increasing number of modelling applications.

FreeGs [1, 2] is a web-enabled database developed at Geoscience Australia by the Predictive mineral discovery Cooperative Research Centre (2001-2007). It was intended as a unified Australian hub of thermodynamic data for geochemical modelling for economic geologists. The database was complemented by integrated software to calculate thermodynamic properties of species and chemical reactions at elevated temperatures and pressures. The end users had put a critical emphasis on the following decisive features:

- High end-user usability in an interactive mode
- Transparency of the compiled data
- Extensibility (data formats & incorporated models)
- Options for remote access and maintenance

In the interactive mode, FreeGs readily facilitates (1) comparison of TD data compiled from different sources, (2) their model presentation via alternative algorithms (equations of state), and, (3) output of data in alternative formats (e.g., $\Delta g(T,P)$ vs $\log K_r(T,P)$).

Despite these features and a friendly web GUI, practical usage of the database system by the scientific community was rather limited. As we see it, the development of a human interface and integration with calculation algorithms were over-emphasised at the expense of the implementation of the data delivery web service. That hindered efficient access to data by external parties and created avoidable development and maintenance overheads.

The future of a similar database will lie in the realm of a database located on a cloud server with (1) HTML access ("find and read") for simple and infrequent interactions, and (2) web service for the delivery of plain standardised data that can be further processed by users applications as needed.

[1] Bastrakov *et al.* (2005) *GCA* **69**, A845. [2] Voigt *et al.* (2007) *Pure and Applied Chemistry* **79**, 883-894.

A new strategy for identifying shales with high gas retention using noble gas, nitrogen and carbon

S. BASU^{1*}, A. P. JONES¹ AND A.B. VERCHOVSKY²

¹Dept Earth Sciences, University College London, Gower S., London WC1E 6BT, UK (*correspondence: sudeshnabg@yahoo.com, adrian.jones@ucl.ac.uk)

²PSSRI, Open University, Milton Keynes, MK7 6AA, UK (a.verchovsky@open.ac.uk)

Noble gases have been used to distinguish between hydrocarbon maturities, and evaluate the fracture network in a shale [1]. Carbon and nitrogen isotopic ratios, and noble gases, have the potential to identify the origin of shale gas. A combined study using all three simultaneously can strengthen previous applications, and have the potential of further utilizations. But such studies on shale gas cuttings are non-existent.

The preferential adsorption of Xe and Kr is higher for kerogen than shales [2]. So, distinct fractionation pattern should set apart organic-rich shales. In conjunction with carbon and nitrogen isotopes, C/N and N/Ar ratios, they can provide useful insights on the type of sedimentary organic matter. A combination of stepwise combustion and vacuum crushing can be used to decouple the free and bound gases.

Acknowledgement: We thank the BG Group for a Research Grant 2013-17

[1] Hunt, Darah & Poreda (2012), *AAPG Bulletin* **96**, 1785-1811. [2] Prinzhofer (2013), *Noble Gases in Oil and Gas Accumulations* In: The Noble Gases as Geochemical Tracers Burnard P. (ed.) 225-248.

A new analytical protocol for high precision EPMA of olivine

V.G.BATANOVA^{1,2} AND A.V.SOBOLEV^{1,2}

¹ISTerre, University J. Fourier, Grenoble, France, valentina.batanova@ujf-grenoble.fr

²Vernadsky Institute of Geochemistry RAS, Moscow, Russia

Composition of olivine provides critical information on the composition and origin of primary mantle derived melts and their sources. Especially informative are minor and trace elements Ni, Mn, Ca, Al, Cr, Co, Ti, Zn, P, Na [1, 2], which being in the concentration range over 10 ppm are assessable by EPMA.

Long counting times (up to 300 sec) on WDS at high beam current (300 nA) reported in [1] yield precision of individual analysis around 30 ppm (2 standard errors) for Ni, Mn, Ca, Al, Cr and 300 ppm for Fo content of olivine. Here we report 2-3 fold improvement of EPMA precision for larger range of trace elements in olivine (Ni, Mn, Ca, Al, Cr, Co, Ti, Zn, P, Na).

The analytical protocol built up on brand new JEOL JXA 8230 EPMA in ISTerre, UJF, Grenoble, France. Facility has tungsten source gun, is equipped by five WDS and one SDD EDS and placed in the environment with controlled temperature (22±0.3 degrees C) and humidity (50±3%).

The analytical conditions are the following: acceleration voltage 25kV, 900 nA beam current, WDS recording for trace elements (Ni, Mn, Ca, Al, Cr, Co, Ti, Zn, P, Na) and EDS recording for Si, Mg, Fe, total counting time 12 minutes, ZAF correction. Instrumental drift during analytical sessions is monitored by repeated measurements of olivine standards. For trace elements this protocol yields detection limits from 3 to 10 ppm and average precision of individual analysis of 10 ppm (2 standard errors). For Fo of olivine precision is 300 ppm (2 standard errors).

Comparison of EPMA and LA ICP-MS data for the large range of olivine compositions suggests that accuracy of EPMA is similar to precision noted above. For elements with concentration over 100 ppm the obtained EPMA precision and accuracy are better than these of LA ICP-MS. For the concentration of elements between 50-100 ppm both methods show similar precision and accuracy; and for concentration between 10-50 ppm LA ICP-MS yields better precision and accuracy. Spatial resolution of EPMA, however, is significantly better: 3-5 micrometres compared to 30-50 for LA ICP-MS. This makes our new EPMA protocol of great advantage for measurement of zoned or small olivine grains.

[1] Sobolev *et al.*, 2007. *Science* **316** (5823), p.412-417. [2] De Hoog *et al.*, 2010. *Chemical Geology* **270**, p. 196-2015

Delineation of groundwater zones using weighted overlay analysis of hydrochemical and multiple isotopic data, Ulaanbaatar, Mongolia

BATSAIKHAN BAYARTUNGALAG¹, SEONG-TAEK YUN^{1*},
KYOUNG-HO KIM¹, BERNHARD MAYER²
AND SANG-TAE KIM³

¹Korea University, Department of Earth and Environmental Sciences, Seoul, South Korea
(*correspondence: styun@korea.ac.kr)

²University of Calgary, Geoscience, Canada

³McMaster University, School of Geography and Earth Sciences, Hamilton, Canada

The water demand in Ulaanbaatar (UB), the capital of Mongolia, is quickly increasing due to significant population growth. Municipal water supply in UB depends solely on groundwater withdrawn from alluvial aquifer that is developed along and near the Tuul River. To overall understand the status of groundwater in UB, we performed a hydrochemical and environmental isotopic survey. Concentrations of cations and anions, $\delta^{13}\text{C}$ of dissolved inorganic carbon, $\delta^{15}\text{N}$ and $\delta^{18}\text{O}$ of nitrate, and $\delta^{34}\text{S}$ and $\delta^{18}\text{O}$ of sulphate were analysed. Three major hydrochemical types of groundwater occur in UB: 1) Ca-HCO₃ type, 2) Ca(-Mg)-HCO₃ type, and 3) Ca(-Na)-Cl(-NO₃) type. Types 1 and 2 mainly occur in forest and grassland areas at outskirts of UB and represent the natural water chemistry without anthropogenic contamination. Type 3 occurs predominantly in urbanized areas and is characterized by increased concentrations of TDS, Cl+NO₃ (and NO₂)+SO₄ due to significant contamination. The $\delta^{15}\text{N}$ and $\delta^{18}\text{O}$ values of nitrate in type 3 groundwater indicate the main source of contamination from latrines (manure) and sewage. To delineate several groundwater zones under contamination risks, we conducted digital image processing techniques of remote sensing and GIS. Then, multi thematic maps on lithology, slope, land-use, lineament, drainage, soil and rainfall were integrated in a raster based GIS (i.e., weighted overlay analysis) to identify the weighted factors of groundwater contamination and to classify and map the groundwater zones as very poor, poor, good, and very good in relation to contamination susceptibility. The results of this study will be helpful for planning schemes for sustainable groundwater management in UB.

Raman spectroscopy and powder diffraction study of synthetic Coffinite (USiO₄) at high pressures

J. D. BAUER¹, S. LABS², S. WEISS³, L. BAYARJARGAL¹,
H. CURTIUS², W. MORGENROTH¹, D. BOSBACH²,
C. HENNIG³ AND B. WINKLER¹

¹Goethe-Universität Frankfurt am Main, Inst. f. Geowissenschaften, 60438 Frankfurt am Main, Germany
(*correspondence: J.Bauer@kristall.uni-frankfurt.de)

²Forschungszentrum Jülich GmbH, Inst. f. Energie- und Klimaforschung – Nukleare Entsorgung (IEK-6), 52425 Jülich, Germany

³Helmholtz-Zentrum Dresden Rossendorf, Inst. f. Ressourcenökologie, 01314 Dresden-Rossendorf, Germany

Coffinite, USiO₄, can form under reducing conditions from UO₂ in contact with silica-rich waters (Langmuir's criterion) [1]. Spent nuclear fuel (SNF) consists to > 90% of UO₂, therefore the safety assessment for a final repository in deep geological formation will benefit greatly if coffinite is taken into account as a potential secondary phase. While high pressures are not of specific relevance for a final repository for SNF, its structural behaviour at high pressures is of general interest to understand the phase stabilities and to benchmark model calculations. The high pressure behaviour of coffinite has been studied before on natural and synthetic samples [2,3]. A pressure-induced irreversible phase transformation from the zircon- to the scheelite-type structure was found at about 15 GPa using an alcohol-water mixture as a pressure medium [3].

Here, synthetic coffinite was studied under high pressure conditions in the diamond anvil cell with neon as quasi-hydrostatic pressure medium up to pressures of 35 GPa. The samples are free of impurities of UO₂, as characterized by XRD and HRTEM. Powder diffraction experiments with synchrotron radiation indicate a pressure-induced phase transformation at 18-20 GPa. In contrast to the earlier high pressure study [3], this transformation is reversible on pressure release and no UO₂ is formed during the process. A detailed data analysis is currently in progress.

Raman spectra were obtained up to a pressure of 18 GPa. Further measurements at higher pressures are on-going.

Financial support from the German Federal Ministry of Education and Research (BMBF) under grants 02NUK019C and 02NUK019E is gratefully acknowledged.

[1] Langmuir (1978), *Geochim. Cosmochim. Acta* **42**, 547-569

[2] Liu (1982), *Earth Plan. Sci. Lett.* **57**, 110-116 [3] Zhang *et al.* (2009), *Am. Min.* **94**, 916-920

Oxygen and hydrogen stable isotopes in Alpine waters and fine-grained soils near Saas Fee, Switzerland

KERSTIN K. BAUER^{1*}, THIERRY ADATTE¹
AND TORSTEN W. VENNEMANN¹

¹Institut des sciences de la Terre, Géopolis, Université de
Lausanne, CH-1015 Lausanne, Switzerland
(*correspondence: kbauer@unil.ch)

Samples of soil and surface water were collected along a transect of 30 km with 1600 m of difference in altitude in the valleys of Saas Fee and Visp in the Swiss Alps. Mineralogical, chemical, and isotopic (O and H) compositions were measured to study the water-rock interactions, clay mineral formation, and the influence of altitude on the isotopic composition of soils during weathering of the parent rock, in order to draw conclusions for the usability of hydrous minerals derived from alpine soils for paleoelevation studies.

Waters have a range of $\delta^{18}\text{O}$ and δD values typical of those for precipitation and glacial melt water, decreasing with altitude of the catchments. The major dissolved ions characterize the composition of the substrate lithologies by elevated contents of Ca, sulphate, K, and Mg ions. This is also the case for the mineralogical composition of the soils that corresponds to the occurrence of ophiolitic material in higher elevations and granitic gneisses and schists in lower regions. While phyllosilicates from early-stage weathering and transformation of illite and chlorite to interstratified minerals (vermiculite, illite-vermiculite, chlorite-vermiculite and illite-smectite) are present, their abundance is relatively low. The isotopic composition of the fine earth fraction and the $< 2 \mu\text{m}$ clay component in the soil was in average identical, and corresponds to the range of values of the host rock material. This suggests that the present climate and this environment do not allow for the neoformation of larger quantities of clay minerals in contact with ambient water.

Pore scale visualization of chemical gradients at biogeochemical interfaces using micromodels and Raman microspectroscopy

T. BAUMANN*, C. METZ, N. P. IVLEVA
AND R. NIESSNER

Institute of Hydrochemistry, Technische Universität München,
81377 München, Germany
(*correspondence: tbaumann@tum.de)

Biogeochemical interfaces (BGI) are controlling the fate of organic chemicals at the interface between the terrestrial and the aquatic environment. BGI are highly dynamic in the spatial and temporal domain. One of the key features of BGI is their limited temporal and spatial accessibility which is hard to imitate in conventional laboratory test designs.

Processes at BGI can be visualized and quantified using microfluidic structures mimicking the pore topology of the soil, so called micromodels. In combination with Raman microspectroscopy chemical information can be retrieved from a micromodel experiment with a spatial resolution on the order of $1 \mu\text{m}^2$ and a temporal resolution in the s-range. To increase the sensitivity, silver nanoparticles have been added to the water phase flowing through the micromodel to make use of the amplifying surface-enhanced Raman effect. Currently chemical gradients of moderately lipophilic substances have been acquired with a limit of detection of 10^{-8} mol/L. Challenges to overcome include the interactions between silver nanoparticles and target analytes which might alter the mass transfer rates, and the settling of nanoparticles in the channel.

As high resolution acquisition comes with a limited field-of-view (FoV) and, e.g., the growth of a biofilm outside of the FoV alters the flow pattern, the flow velocity has to be monitored using fluorescent latex beads and single particle tracking. For a fast measurement of well-defined variables, like the pH-value or the oxygen concentration, thin film polymers with encapsulated sensor dyes are chosen.

When looking at microbial growth in porous media, not only the development of a biofilm changes the flow paths and the accessibility to the microbes, but also the development of locally confined gas bubbles, as with *P. denitrificans*. Here, the growth rate is correlated with bacterial activity and the results indicate different bacterial densities in pore bodies and pore throats.

Diverse hydrothermal venting at the Jan Mayen vent fields, AMOR

T. BAUMBERGER^{1*}, M.D. LILLEY², R.B. PEDERSEN¹, I.H. THORSETH¹ AND A. STENSLAND¹

¹Centre for Geobiology, University of Bergen, 5007 Bergen, Norway

(*correspondence: tamara.baumberger@geo.uib.no)

²School of Oceanography, University of Washington, Seattle, WA 98195, USA (lilley@u.washington.edu)

The basalt-hosted Jan Mayen vent fields (JMVF) are located at 71° N on the southern end of the ultra-slow spreading Mohns Ridge (AMOR). Over the past few years, scientific cruises have repeatedly visited and extensively sampled these vent fields. Researchers have identified several types of hydrothermal venting and have noted significant differences in hydrothermal fluid compositions within relatively short distances. The types of venting range from focused high-temperature fluid venting from numerous chimney structures, to low-temperature diffuse fluid flow areas. In addition free gas bubbles were observed being released from the seafloor. The chemical composition of the high-temperature endmember vent fluids is primarily characterized by high concentrations of carbon dioxide together with low hydrogen and methane concentrations. Fluids from the diffuse flow areas are characterized by an increased concentration of methane, which is strongly reflected in the hydrothermal plume observed above these diffuse systems. High concentrations of dissolved methane together with low concentrations of dissolved hydrogen were measured in the water column close to the seafloor for the diffuse flow hydrothermal plume, while high hydrogen/low methane concentrations were found in the high-rising non-buoyant plume. The main constituent of the gas bubbles, however, was carbon dioxide. In addition, at 560 m water depth along the flank of a high-temperature venting chimney, formations of gas hydrate were observed. A few tens of meters away, a ridge segment with several small chimneys with a flame-like discharge was observed, suggesting subcritical phase separation through boiling at relatively low pressures. Here we present a study on the diverse geochemical fluid and gas characteristics of the Jan Mayen hydrothermal systems located on the ultra-slow spreading Arctic Mid-Ocean Ridge and compare the results with the fluid composition of other mid-ocean ridge hydrothermal systems.

The SwissSIMS ion probe facility

L. BAUMGARTNER¹ AND A.-S. BOUVIER¹

¹ISTE, University of Lausanne, Lausanne, Switzerland, (lukas.baumgartner@unil.ch)

A new ion probe laboratory, housing a CAMECA IMS 1280-HR has been established at the University of Lausanne, Switzerland in the Institute of Earth Sciences. The SIMS facility was obtained through funding from the Swiss National Science foundation, the universities of Bern, Geneva, Lausanne, and the ETHZ. It is organized as a Swiss National Facility, with a scientific steering committee. The instrument was installed in the second half of 2012, and it passed specification late 2012. The NanoSIMS facility of the EPFL under the direction of Dr. Anders Meibom is housed in the same building. The combination of facilities offers the users a unique opportunity for *in situ* surface analysis.

We will focus on basic and applied research in all domains of earth science. The IMS 1280-HR is equipped with high-intensity cesium and oxygen primary ion sources, 5 interchangeable electron-multiplier spectrometers (EMS) or Faraday cup and 2 fixed Faraday cups for multi-collection and one electron multiplier and two Faraday cups for mono-collection. The magnetic sector is stabilized with a Hall probe to improve reproducibility of isotopic ratios; transmission is optimized for IMS sensitivity.

So far we have tested and adapted existing methods on using NIST or MPI-DING standards and we improved existing method for *Cl* isotope measurements [1]. We are currently developing and establishing various carbonate standards for *O* and *C* isotopes, in house quartz standards for *O* and *Si* isotopes, as well as standards for oxygen isotopic composition for olivine, titanite, biotite for *O* isotopes. We are now ready to start the first scientific projects.

[1] Bouvier & Baumgartner, Session 201, Golschmidt 2013

Geochemical mapping in urban area of an old mercury mining town (Idrija, Slovenia)

Š. BAVEC¹, M. GOSAR^{1*}, H. BIESTER² AND H. GRČMAN³

¹ Geological survey of Slovenia, Dimičeva ulica 14, SI-1000 Ljubljana, Slovenia (spela.bavec@geo-zs.si, correspondence: mateja.gosar@geo-zs.si)

² Technical University Braunschweig, 38106 Braunschweig, Germany (h.biester@tu-bs.de)

³ Agronomy Department, Centre for Soil and Environmental Science, Biotechnical Faculty, University of Ljubljana, Jamnikarjeva 101, 1000 Ljubljana, Slovenia (helena.grcman@bf.uni-lj.si)

Detailed soil geochemical survey tackles the urban area of Idrija, which is the oldest mining town in Slovenia with about 7000 population. Strong legacy of 500 years of mercury mining and ore processing in Idrija have resulted in widespread contamination. Environmental impacts on a regional scale caused by atmospheric emissions from the Idrija ore roasting plant were established in investigations of mercury spatial distribution in soil on regional scale [1, 2].

This study is part of the URGE project (Urban Geochemistry) and brings into focus urban area of Idrija town. Soil was systematically sampled (45 sampling sites) in 4 km² of Idrija urban area. Two soil horizons (0-10 cm and 10-20 cm) were sampled in order to distinguish between different metal sources. Samples were prepared and analysed according to URGE project. A sampling model grid was developed for collection of 9 soil samples per km². Due to higher population density, the density of samples was increased in the town centre. Contents of potential harmful elements were determined using aqua regia digestion. As expected, Hg contents were extremely elevated and ranged from 8 to 1210 mg/kg with a median of 60 mg/kg for upper soil horizon and from 7 to 1550 mg/kg with a median of 50 mg/kg for lower soil horizon. Spatial distribution analysis shows that higher contents appear along river banks, where ore residues were dumped in the past and in the part of the studied area, where soils overly rocks containing mercury ore. Other potential harmful elements didn't show critical elevations according to legislation. so the study was further directed into analysis of mercury species and their water-soluble and bio-accessible portions using different extraction methods.

[1] Gosar & Šajn (2001) *Geologija* **44**, 137-159. [2] Gosar *et al.* (2006) *Sci Total Environ* **369**, 150-162.

The Chronology of Dehydration

ETHAN F. BAXTER¹, BESIM DRAGOVIC^{1,2}
AND MARK J. CADDICK²

¹Department of Earth and Environment, Boston University, 685 Commonwealth Ave, Boston MA, 02215 USA

²Department of Geosciences, Virginia Tech, 5060 Derring Hall, Blacksburg, Virginia 24061 USA

The global geologic water cycle including the hydration and dehydration of the lithosphere during tectonic and metamorphic processes plays a first order role in shaping our planet. In subduction zones, dehydration is responsible for mantle melting, arc magmatism, seismic triggering, slab densification, and more. It is challenging to constrain the rate and timing of paleo-dehydration unless a passive mineral marker of the dehydration process can be identified and dated in the dehydrated rock residue. We use thermodynamic modeling to show that the growth of garnet may be used as a proxy for dehydration in diverse bulk rock compositions and tectonic contexts. Generally, as garnet grows in a subducting rock, fluid is produced due to metamorphic dehydration of hydrous precursor phases including chlorite, lawsonite, epidote, and amphibole. We quantify the proportional relationship between garnet and water production in common lithologies along three representative subduction geotherms [1]. Over the garnet growth interval ~400 to 700 °C (and corresponding depths for each geotherm) the average production ratio for altered MORB compositions is 0.52 (wt % water per vol % garnet) in cooler geotherms (Honshu and Nicaragua) and 0.27 in hotter (Cascadia) geotherms, with predictably lower ratios if the input basalt previously experienced less hydrous alteration. Over the same interval the water production ratios are approximately 50 % lower for pelitic sediment (0.24 and 0.13, respectively). Garnets can also be dated at high precision (<±1 Myr) with the Sm-Nd (or Lu-Hf) system, thus constraining the timing of dehydration by proxy. With large single crystals (>5mm diameter), concentric growth zoned garnets may be microsampled and dated from core-to-rim, thus constraining the duration of dehydration. When coupled with thermodynamic analysis, a complete P-T-H₂O chronology can be extracted. Example P-T-H₂O chronologies from Sifnos, Greece reveal rapid, focused dehydration around 46 Ma spanning just hundreds of thousands of years [2].

[1] Baxter & Caddick 2013, *Geology*, in press, doi:10.1130/G34004.1 [2] Dragovic *et al.* 2012, *Chemical Geology*, v. **314-317**, p. 9-22.

Precise U-Pb (ID-TIMS) and SHRIMP ages on single zircon for Achaean TTG rocks on Baltic Shield

BAYANOVA T., MITROFANOV F., MOROZOVA L., NITKINA E., SEROV P., FEDOTOV D. AND LARIONOV A.

bayanova@geoksc.apatity.ru felix@geoksc.apatity.ru
 morozova@geoksc.apatity.ru nitkina@geoksc.apatity.ru
 serov@geoksc.apatity.ru fedotov@geoksc.apatity.ru
 larionov@mail.wplus.net

Voche-Lambina polygon lies on the boundary between Belomorian mobile block and Central –Kola domain (Morozova *et al.*, 2011). New neorhaean U-Pb data on single zircon from TTG of international polygon named of the Voche-Lambina yielded 3158.2 ± 8.2 , which are situated on Central-Kola block in the Baltic Shield. Zircon are characterized by low concentration U and Pb, low U/Th ratio with 0.2. REE diagrams of grey gneisses reflect high fractionation $La/Yb > 30$, enriched by light REE and depleted by heavy $Yb < 0.6$ ppm. Model Sm-Ng ages on the rocks have protolith from with the ages 3.4 to 3.2 Ga, positive ϵNd from +1.29 to +3.3, ISr equals 0.702. Precise age of amphibolites metamorphism has been dated on single zircon with 2704.3 ± 5.9 Ma. In the frame of the Central-Kola domain there is an Ingosersky TTG complex. Firstly U-Pb dating on single zircon from Bt-gneisses reflects 3149 ± 49 Ma. Metamorphic alterations were in 2725.2 ± 2.5 Ma and connected with origin of Amf-Bt gneisses and 2733.6 ± 6.6 with Bt-Amf gneisses. (Nitkina *et al.*, 2012). Achaean gneisses in Monchegorsk ore region were firstly dated in the Central-Kola domain and near Murmansk. Single zircon from gneisses in Monchegorsk region which are the basement for Paleoproterozoic PGE layered intrusions with U-Pb ages on zircon and baddeleyite from 2.4 to 2.5 Ga (Bayanova *et al.*, 2009) has 3.16 Ga and single zircon with 2776 ± 3 Ma is considered as amphibolites metamorphism. New U-Pb (ID-TIMS) data on single zircon from high alimunia gneisses near Murmansk in the Central-Kola domain gave 3.17 Ga, core from these zircon population has the age 3695 ± 5 Ma by SHRIMP. Time of amphibolites metamorphism was dated with 2753 ± 3 Ma. Therefore based on the new data on single zircon from TTG and gneisses from Central-Kola domain leads to the long history of continental crust origin in the Baltic Shield from 3.16 to 3.7 Ga.

We thank to D. Wasserburg for 205 Pb artificial spike, J. Ludden for 91500 and Temora standards, F. Corfu, V. Todt and U. Poller for assistance in the establishing of the U-Pb method for single zircon and baddeleyite grains. The study is contributed and supported by IGCP 599 and Department of Earth Sciences RAS, program 4.

Improvements of the coherent and precise ice core dating tool Datice: new data and parameterization

L. BAZIN^{1*}, A. LANDAIS¹, G. DURAND², C. RITZ²,
 M. MONTAGNAT², B. LEMIEUX-DUDON³
 AND D. RAYNAUD²

¹LSCE, CEA-CNRS-UVSQ, 91191 Gif sur Yvette, France
 (*correspondence: lucie.bazin@lscce.ipsl.fr)

²LGGE, CNRS-UJF, St Martin d'Herès, France

³LJK, Grenoble, France

Recently, we published the new ice core reference chronology AICC2012 common for 5 ice cores (EDC, EDML, Vostok, TALDICE and NorthGRIP) back to 800 ka (thousand of years before 1950) [1, 2]. To construct this optimized chronology we used the “Datice” Bayesian tool [3], using a background chronology and data constraints (absolute and orbital age markers, stratigraphic links between the ice cores) for both the ice and gas phases.

One of the limitations of AICC2012 was the lack of a good characterization of variance associated with the thinning background scenario respecting the deformation history. We thus propose a new definition of this variance using numerous data of microstructure and fabric for the EDC ice core [4].

A second limitation of AICC2012 was the lack of orbital constraints on the long EDC ice core. We present a new high-resolution record of $\delta^{18}O_{atm}$ and $\delta O_2/N_2$ between 100-800 ka obtained on EDC ice of high quality exempt of gas loss. Together with the complete record of air content [5], another orbital dating tool, we provide an important step for improving the reference ice core chronology for Antarctic ice cores.

[1] Veres *et al.* (2012) *CPD* **8**, 6011-6049. [2] Bazin *et al.* (2012) *CPD* **8**, 5963-6009. [3] Lemieux-Dudon *et al.* (2010) *QSR* **29**, 8-20. [4] Durand *et al.* (2007) *CP* **3**, 155-167. [5] Raynaud *et al.*, in prep.

High- to low- pressure features of compound xenoliths: implications from Fe-Ti-Ca metasomatism and glass formation

BAZIOTIS, I.^{1,4}, ASIMOW, P.D.², NTAFLIOS, T.³, KORONEOS, A.¹ AND POLI, G.⁴

¹Department of Mineralogy, Petrology and Economic Geology, Aristotle University of Thessaloniki, 54124, Thessaloniki, Greece, baziotis@metal.ntua.gr

²California Institute of Technology, Division of Geological and Planetary Sciences, Pasadena, California, USA

³Department of Lithospheric Research, University of Vienna, 1090, Vienna, Austria

⁴Department of Earth Sciences, University of Perugia, 06100, Perugia, Italy

Mantle xenoliths preserve invaluable information on chemical and thermal events in the earth's mantle and on the ages and rates of such events. The presence of Fe-Ti oxides such as ilmenite or armalcolite in areas affected by mantle metasomatism, for example, could constrain the oxidation state of the metasomatic event and provide information about the metasomatic agent(s). Here we focus on lherzolite- and clinopyroxenite- rich xenoliths from Cima Dome (California) and Chino Valley (Arizona), their unusual mineral assemblages, and their formation.

Fe-Ti minerals identified in the selected xenoliths include armalcolite and ilmenite. In the Chino Valley clinopyroxenite, Nb-rich and Nb-free rutile both occur, either included in or included by ilmenite. Moreover, ilmenite is initially replaced by Fe-oxide + kassite (a rare hydrous Ca-Ti oxide). Both ilmenite and rutile are rimmed by titanite. These successions imply a change from Fe-Ti to Ca-rich silicate metasomatic agents percolating through the host rock. In the amphibole-bearing lherzolite from Cima Dome, Ti-rich pargasite is surrounded by glass-1, spinel, plagioclase, clinopyroxene, olivine and armalcolite. The latter is entrained within the glass pocket and has a skeletal crystal shape suggesting rapid growth at high pressures ~1.0 GPa and low oxygen fugacity at mantle depths. The presence of glass-1 is associated with rapid melting and breakdown of pargasite to Ol+Cpx+Spl+Gl-1 en route to the surface. Glass-2 is observed along grain boundaries of pyroxenes and olivine, however is Si-enriched and depleted in Ca, Mg, Al, Ti compared to glass-1. Both samples suggest extended multi-stage histories involving partial melting to form primary minerals, a period of metasomatic alteration, and a short timescale of decompression upon eruption.

Storage of Initially Organic Nitrogen in Silicate Minerals and Volcanic Glasses

G. E. BEBOUT^{1*}, K. E. LAZZERI¹, A. P. PALYA¹, L. D. ANDERSON-SMITH¹, M. R. M. IZAWA², N. R. BANERJEE² AND C. A. GEIGER³

¹Department of Earth and Environmental Sciences, Lehigh University, Bethlehem, PA, USA. *geb0@lehigh.edu

²Department of Earth Sciences, University of Western Ontario, London, Canada.

³Material Sciences, Universität Salzburg, Salzburg, Austria.

We are investigating pathways by which initially organic N can be incorporated and stored in silicate minerals and glasses, focusing on phases other than the clays and micas, the latter known to house N as NH₄⁺. Despite its volatility, N is surprisingly compatible in various silicates, largely as NH₄⁺, but also as molecular N₂ in microporous phases (e.g., beryl, cordierite, zeolites, melanophlogite). These species can provide a record of ancient organic processes.

Along relatively warm prograde P-T paths, a significant fraction of the organic, mica-bound N in metasedimentary rocks can be lost at lower grades, due to partitioning into H₂O-rich fluids generated by breakdown of layer silicates such as chlorite. This N loss could affect the degree to which ancient (e.g., Archean) low-grade suites can be used to extract paleo-environmental information. However, at higher grades, the remaining N is retained to a surprising degree, even in rocks that experience partial melting, in phases such as K-feldspar and cordierite. Thus uptake and long-term storage of atmospheric/organic N in early-formed continental crust is possible (Goldblatt *et al.*, 2006). $\Delta^{15}\text{N}$ values for coexisting cyclosilicates (N₂) and micas (NH₄⁺) in some pegmatites and metasedimentary rocks indicate preservation of N isotope fractionations like those predicted by theoretical studies.

Incorporation of N with organic $\delta^{15}\text{N}$ in seafloor basalts can result in a seafloor N budget rivaling that in overlying sediments, strongly influencing the N subduction budget (Li *et al.*, 2007). Our work on palagonitized volcanic glasses on the modern seafloor and in Mesozoic basalts, some of the glasses bearing microbial ichnofossils, demonstrates this uptake and that analyses of such glasses could be useful in the search for signs of ancient life on Mars. Low-grade metabasalts in the Abitibi Complex (2.7 Ga) contain small amounts of N, now in mica, with organic $\delta^{15}\text{N}$ that could reflect Archean seafloor incorporation of sedimentary/organic N, likely via a pore fluid. Melanophlogite, a silica clathrate found in low-T hydrothermal settings, contains up to 1700 ppm of N₂ also with organic $\delta^{15}\text{N}$. Our ongoing work considers the extent to which such phases can store N without isotopic change for geologically significant time periods.

Thermal conductivity of (Mg,Fe)O from ambient to deep mantle conditions

M.M. BECK^{1,2}, V. HAIGIS³, F.R. SCHILLING²
AND S. JAHN^{1*}

¹GFZ German Research Centre for Geosciences,
Telegrafenberg, 14473 Potsdam, Germany
(*correspondence: jahn@gfz-potsdam.de)

²Institute of Applied Geosciences, Karlsruhe Institute of
Technology, Kaiserstr. 12, 76131 Karlsruhe, Germany

³UMR 8640, Département de Chimie, ENS, 24 rue Lhomond,
75231 Paris Cedex 05, France

The thermal conductivity κ is one important physical property that controls the structure and the dynamics of the Earth's mantle [1,2]. Furthermore, κ influences the heat flux at the core-mantle-boundary and thus the generation of the Earth's magnetic field [3]. In spite of its significance, this parameter is insufficiently constrained due to the great technical challenges to measure thermal transport properties at pressure and temperature conditions relevant for the lower mantle. Here, we use an alternative approach and predict the thermal conductivity of model (Mg,Fe)O by equilibrium molecular dynamics simulations. We first investigate the effect of isotope disorder on κ in pure MgO with natural isotopic composition by randomly distributing the three most abundant Mg isotopes in the simulation cell. At ambient conditions we find that earlier simulations of Haigis *et al.* [5], which used an average isotope mass for all Mg ions, overestimate the thermal conductivity by about 32%. This overestimation is comparable to the predicted 46% from phonon lifetime calculations [4]. With rising temperature, the influence of isotope disorder on κ decreases and becomes almost insignificant at deep mantle conditions. Next, we analyse how the substitution of 10% or 20% of Mg by Fe masses affects κ . Due to the larger mass difference between Fe and Mg ions compared to that between Mg isotopes, the reduction is now much larger at ambient conditions and still relevant at pressures and temperatures of the lower mantle. Combining our new results with those of Manthilake *et al.* for (Mg,Fe)SiO₃ perovskite [6], an aggregate mantle of 20% (Mg_{0.80}Fe_{0.20})O and 80% (Mg_{0.97}Fe_{0.03})SiO₃ perovskite has a thermal conductivity of 10±2 W/(m K) at 3000 K and 138 GPa.

[1] Dubuffet & Yuen (2000) *Geophys. Res. Lett.*, **27**, 17-20.
[2] Naliboff & Kellogg (2007) *PEPI* **161**, 86-102. [3] Gubbins & Sreenivasan (2007) *PEPI* **162**, 256-260. [4] Tang & Dong (2010) *PNAS* **107**, 4539-4543. [5] Haigis *et al.* (2012) *EPSL* **355**, 102-108. [6] Manthilake *et al.* (2011) *PNAS* **108**, 17901-17904.

Composition of the oceanic crust: where have all the noble metals gone?

H. BECKER^{1*} AND C. MEYER²

^{1*}Institut für Geologische Wissenschaften, Freie Universität
Berlin, Germany, hbecker@zedat.fu-berlin.de

²Institut für Geologische Wissenschaften, Freie Universität
Berlin, Germany, chmeyer@zedat.fu-berlin.de

It has been speculated that the low noble metal abundances of many evolved MORBs may reflect sulfide fractionation, either during melting, or, as a consequence of fractional crystallization in the oceanic crust [e.g., 1].

The depletion of incompatible noble metals and Re in lherzolitic fractional melting residues from the depleted mantle [2] can be used to estimate bulk peridotite-silicate melt partition coefficients for these elements at the specific P-T- f_{O_2} - f_{S_2} conditions of melt extraction ($D_{Pd} \approx 0.7$, $D_{Au} \approx 0.12$, $D_{Re} \approx 0.08$). The data for Re are in good agreement with bulk partition coefficients calculated from experimental data at suitable upper mantle f_{O_2} . Calculated abundances of these elements in primitive melts at 5-10 % melting are 10 ppb for Pd, 10 to 6 ppb for Au, and 2 to 1 ppb for Re. This contrasts with typical abundances in MORB of 0.05-2 ppb Pd and 0.1-3 ppb Au, whereas Re shows good agreement [e.g., 1,3,4]. Because partial melting of depleted mantle lherzolite cannot explain noble metal abundances in "primitive" MORBs, fractional crystallization in the crust is commonly invoked [1,3]. New data for the PGE+Re in different lithologies of the lower oceanic crust at hole 735B (crust formed by very slow spreading at the SW Indian ridge), indicate even lower abundances of Pd, Au and Re than in many MORBs. Clearly, the main site of fractionation of the PGE must be deeper than the drilled section. Recent data from lower crust of the Wadi Tayin section of the Oman ophiolite suggests significantly higher PGE abundances in fast spreading oceanic crust [5]. However, even these higher abundances fall short of expected concentrations in the oceanic crust. We conclude from this that most of the noble metal fractionation in MORB magma likely occurs during magma transport in the uppermost mantle. Dunites and harzburgites from the mantle section of the Oman ophiolite are strongly enriched in Pt, Pd and Re, thus providing hints for such fractionation processes [6, 7].

[1] Hertogen *et al.* (1980), *GCA* **44**, 2125-2143. [2] Wang, Z. *et al.* (2013), *GCA* **108**, 21-44. [3] Rehkämper *et al.* (1999), *GCA* **63**, 3915-3934. [4] Gannoun *et al.* 2007, *EPSL* **259**, 541-556. [5] Peucker-Ehrenbrink *et al.* (2012) *Geology* doi: 10.1130/G32431.1 [6] Lorand *et al.* (2009) *Terra Nova* **21**, 35-40. [7] Hanghoj *et al.* (2010) *J. Petrol.* **51**, 201-227.

Component specific Hf-W dating of Allende and Vigarano CV3 chondrites

BECKER^{1*}, M., KRAHNER¹, K., HEZEL, D.C.¹, SCHULZ, T.² AND MÜNKER, C.¹

¹ Institut für Geologie und Mineralogie, Universität zu Köln, Germany, (*correspondence: maik.becker1@gmx.net)

² Department of Lithospheric Research, University of Vienna

The formation of chondrules, matrix and other components of chondrites is not yet fully understood. Knowing their relative formation ages and genetic relationships can provide crucial information on their formation conditions. Short lived radionuclides can provide new insights into the chronology of the formation of early solar system materials. In the past, the ²⁶Al-²⁶Mg system has been mainly used for this purpose, but recently the ¹⁸²Hf-¹⁸²W system emerged as a promising tool to date chondrule formation. Thus, components of chondrites that never underwent high temperature metamorphism, like CV3 chondrites, are well suited candidates for Hf-W investigations. Earlier studies of Allende chondrules with the Al-Mg und Pb-Pb systems indicate that they formed up to 3.2 Ma after CAI formation¹⁻⁴.

We prepared 23 Allende and 13 Vigarano separates for Hf and W isotope measurements, covering both reduced and oxidized CV chondrites. These include pure handpicked chondrule and matrix fractions as well as magnetic separates and bulk aliquots. The separates all define isochrons which indicates a contemporaneous formation of all components. The ages defined by the isochrons suggest formation of Allende and Vigarano components within 3 Ma after CAI formation. These ages are consistent with chondrule formation ages obtained from other isotopic systems.

Notably, W and Hf concentrations in chondrule and matrix fractions from Allende and Vigarano vary considerably. Chondrules from Allende exhibit high Hf/W ratios (2.5 to 3.0), whereas matrix and strong magnetic fractions exhibit low Hf/W ratios (0.5 to 0.9). Unlike in Allende, Vigarano contains chondrules with extremely low Hf/W ratios. As suggested from petrological observations, these low ratios can be attributed to the presence of metal inclusions within the reduced Vigarano chondrules.

[1] Bizzarro *et al.* (2004) *Nature* **432**, 275-278; [2] Connelly *et al.* (2008) *Astroph. Journal* **675**, L121-L124; [3] Connelly & Bizzarro (2009) *Chem. Geol.* **259**, 143-151; [4] Amelin & Krot (2007) *Meteor. & Plan. Sci.* **42**, 1321-1335.

Actinide redox processes on iron sulfides: an electrochemical, microscopic, and computational approach

UDO BECKER^{1*}, KE YUAN¹ AND DEVON RENOCK²

¹Department of Earth and Environmental Sciences, University of Michigan, Ann Arbor, MI 48109, USA, ²Department of Earth Sciences, Dartmouth College, Hanover NH, 03755 (*correspondence: ubecker@umich.edu)

Little is known about the reaction mechanism of actinyl complexes on mineral surfaces, i.e. the role of the redox potential, the nature of the reductant, the importance of minerals in terms of providing catalytic surfaces, the role of anions in solution that polarize a mineral surface to promote or inhibit electron transfer, and the activated states that may slow down the kinetics of the redox process.

In order to resolve these, electrochemical studies using a micropowder electrode technique were performed in combination with a quantum-mechanical and microscopic (AFM) approach. The electrochemical approach allows us to determine the specific redox potential of actinide reduction on a given mineral surface. For example, uranyl reduction takes place at -0.22 V on hematite, -0.17 V on magnetite, and at -0.14 V on pyrite. Further electrochemistry experiments were performed on machinawite, in order to be able to compare these with quantum-mechanical calculations on the thermodynamics, charge and spin transfer, and electrochemical potential for reduction and oxidation to occur. The calculations show that the energy gain of the co-adsorption of hydroquinone (as an analogue for microbial reduction) and uranyl is on the order of 0.5 eV (≈50 kJ/mol) as compared to the separate adsorption of uranyl and hydroquinone. Similar co-adsorption on FeS (mackinawite) reveals that Fe(II) cations in the mineral surface become high spin (Fe(II) in bulk mackinawite is low spin), thereby increasing its potential for electron transfer.

Atmospheric CO₂ starvation of trees arrests mycorrhizal-driven silicate weathering

DAVID BEERLING¹, JOE QUIRK¹, LYLA TAYLOR¹,
STEVE BANWART² AND JONATHAN LEAKE¹

¹Department of Animal and Plant Sciences, University of Sheffield, Sheffield S10 2TN, UK. Email: d.j.beerling@sheffield.ac.uk

²Kroto Research Institute, North Campus, University of Sheffield S3 7HQ, UK

Trees dominate terrestrial silicate mineral weathering by converting solar energy into chemical energy that fuels roots and their ubiquitous nutrient-mobilizing fungal symbionts. These biological activities regulate atmospheric CO₂ over geological timescales by driving calcium and magnesium fluvial ion export and marine carbonate formation. However, the important stabilizing feedbacks between CO₂ and biotic weathering anticipated by geochemical carbon cycle models remain untested. This presentation will show experimental evidence for a non-linear feedback across a Cenozoic CO₂ range from 1500ppm to 200ppm, whereby low CO₂ curtails mineral surface alteration via trenching and etch pitting by arbuscular mycorrhizal and ectomycorrhizal fungal partners of tree roots. Integrating our experimental findings into a process-based model revealed a CO₂ drop from 1500ppm to 200ppm caused the flux of calcium and magnesium weathered from silicate rocks to drop three-fold. It is proposed that 'low' CO₂ effectively acts as a 'carbon starvation' brake on tree-driven weathering. These findings have implications for the role of forests and fungi in regulating Earth's minimum atmospheric CO₂ concentration over the Cenozoic.

Ore deposits and lithosphere evolution in the early Earth

*G. C. BEGG^{1,2}, W.L. GRIFFIN¹,
SUZANNE Y. O'REILLY¹, AND J. M.A. HRONSKY^{1,3}.

¹CCFS/GEMOC, Macquarie University, Sydney, Australia

²Minerals Targeting Intl., 17 Prowse St., W. Perth, WA 6005, Australia

³Western Mining Services (Aust.) Pty Ltd, 17 Prowse Street, W. Perth, WA 6005, Australia

(*correspondence: graham.begg@bigpond.com)

Plate tectonic processes, including subduction-related magmatism, rifting and collision are critical for the formation of many types of magmatic and hydrothermal ore deposits. Given the evidence for the existence of plate tectonic processes from as early as 3.9Ga, the absence of significant mineral deposits older than about 3Ga is attributed to either of a failure to survive, or the absence of another key ore-forming environment. Subcontinental Lithospheric Mantle (SCLM), which appeared between ca 3.6-3.0 Ga, provides the solution to understanding both of these issues. Pristine SCLM, formed as a residue of high temperature plume melting, is depleted (Fe-poor), buoyant, refractory, and has very high viscosity. These traits make for a durable lithosphere, a home for mineral deposits, in contrast to the easily removed (subducted, delaminated) dense oceanic lithospheric mantle. Integration of geological, geophysical and geochemical data from the crust and mantle, indicates that Archean SCLM underlies the majority of today's continental crust. Plate tectonics (forces, fluids, magmas) has resulted in metasomatism, fracturing, melting and suturing of the SCLM. These processes, along with the impact of mantle plumes and the rise of atmospheric oxygen, have provided the metals, energy and focus for ore systems in a range of associated crustal environments.

Seismic anisotropy changes across upper mantle phase transitions

CAROLINE BEGHEIN^{1*} AND KAIQING YUAN¹

¹ Dpt. of Earth and Space Sciences, UCLA, Los Angeles, CA 90095-1567, USA (*correspondence: cbeghein@ucla.edu)

Constraining mantle flow near the mantle transition zone (MTZ) can help better understand its role in Earth's thermochemical evolution and mantle dynamics. Using a higher mode surface wave seismic dataset [1] we modeled global 3-D azimuthal anisotropy in the top 1000km of the mantle, thereby providing constraints on mantle deformation to much greater depths than in previous studies.

Our model unravels significant seismic anisotropy in the MTZ, challenging common views of mantle deformation, and reveals a striking correlation between minima in anisotropy amplitudes, changes in the fast axes of propagation, and the location of phase transitions. This relation between anisotropy changes and phase transformations suggests lattice preferred orientation of anisotropic material in the deep upper mantle.

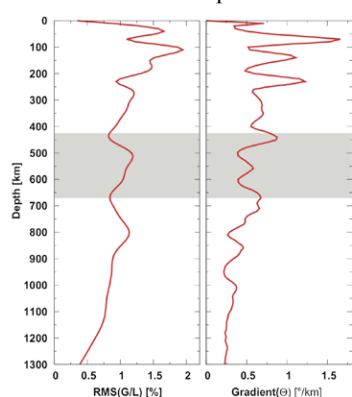


Figure 1: Root mean square anisotropy amplitude (left) and average vertical gradient of fast axis (right)

The detected global changes in the fast axes could indicate mantle flow layering, consistent with mantle geochemistry. The interpretation of our results in terms of convection style and therefore in terms of heat transport is however non-unique due to a lack of laboratory data on MTZ mantle anisotropy. Seismic anisotropy might not be a good proxy for mantle flow at these depths, in

which case whole mantle convection cannot be ruled out.

Nevertheless, our model provides unique new constraints on mantle deformation and advances toward a better understanding of Earth's convective pattern and heat transport will require stronger constraints on the effects of pressure, temperature, melting, and water content on the deformation mechanisms and slip systems of MTZ materials.

[1] Visser *et al.* (2008) *Geophys. J. Int.* **172**, 1016-1032.

Volatile distribution in the Taupo Volcanic Zone, New Zealand

FLORENCE BÉGUÉ^{1*}, DARREN GRAVLEY¹, ISABELLE CHAMBEFORT², CHAD DEERING³ AND BEN KENNEDY¹

¹University of Canterbury, Christchurch, New Zealand,

(florence.begue@pg.canterbury.ac.nz * presenting author)

²GNS Sciences, Wairakei Research Centre, Taupo, New Zealand,

³University of Wisconsin-Oshkosh, Oshkosh, USA,

The central Taupo Volcanic Zone (TVZ) is an actively rifting continental arc where more than 6000 km³ of rhyolitic magma has erupted from at least eight caldera centres over the past 1.6 Ma. The extensive magmatism in the TVZ is intimately associated with the high heat flux and active geothermal systems. These geothermal systems have previously been subdivided into two groups: 1) low-gas (i.e. CO₂), high Cl, low B and Li/Cs ratio systems suggested to have chemical affinities with basaltic (and rhyolitic) magmas, and 2) high-gas, low Cl, high B and Li/Cs ratio systems having chemical affinities with andesitic magmas.

Here we present new trace and volatile data on quartz-hosted melt inclusions from eight large, rhyolitic eruptions to examine the relationship between slab-derived fluid input and the geographic distribution of the two chemical groups observed in the present-day hydrothermal systems.

Based on trace element and volatile content, the rhyolites can also be subdivided into two distinct groups; R1 which is enriched in Li, Ba and B, and has Cl contents of ~0.2 wt%; and R2, which has lower content of these fluid-mobile elements, but higher Cl contents (0.25 to 0.35 wt%) than R1.

These differences in volatile contents are related to distinct parental magmas (i.e. two distinct sources), with “wetter” R1 having a higher slab-fluid component compared with the “drier” R2. The difference in chlorine content between R1 and R2 magmas is related to the Cl solubility, which increases with decreasing H₂O content (i.e. higher Cl content in the drier R2 melts).

A comparison between the new volatile data on the rhyolites and these present-day geothermal systems reveals that the observed differences in the fluid composition of surface springs are correlated with the distribution of the two rhyolite types. We, therefore, suggest that the variation in geothermal fluids does not necessitate a separate andesitic magma as a source, but is a continuation of different slab-derived fluid contributions producing slightly different rhyolite types. While the correlation observed here is strong, we do not rule out the influence of fluid-rock interaction as a possible contributor and this remains to be explored.

DOI:10.1180/minmag.2013.077.5.2

www.minersoc.org

Constraints on the Composition of the Lower Continental Crust from Joint Inversion of P- and S-wave Seismic Velocity Data

MARK D. BEHN^{1*}, OLIVER E. JAGOUTZ²,
DONNA J. SHILLINGTON³ AND PETER B. KELEMEN⁴

¹*WHOI, Woods Hole MA, USA, mbehn@whoi.edu

²MIT, Cambridge MA, USA, jagoutz@MIT.EDU

³LDEO, Palisades NY, USA, djs@ldeo.columbia.edu

⁴LDEO, Palisades NY, USA, peterk@ldeo.columbia.edu

Seismic velocity data constitute one of the primary constraints on the bulk composition of the lower continental crust. P-wave velocity data are frequently used to infer the composition of the deep crust and to support petrologic models for the origin of the continental crust. Unfortunately, recent work has demonstrated that a large range of compositions can be associated with the same P-wave velocity, rendering the interpretation of these crustal velocity models to be highly non-unique. Alternatively, the ratio between P- and S-wave velocity (V_p/V_s) can be directly inferred from receiver function studies (though not the absolute P- or S-wave velocity). However, V_p/V_s ratios alone also lead to highly non-unique estimates for lower crustal composition.

In order to provide more robust constraints on lower crustal compositions, we calculate elastic properties for an expansive suite of crustal compositions (anhydrous and hydrous) and invert for major element chemistry as a function of P- and S-wave velocity over a range of pressure and temperature conditions. We show that the combination of P- and S-wave data significantly improves compositional resolution, particularly when *a priori* pressure and temperature constraints can be used to determine whether the lower crust resides in the alpha- or beta-quartz stability field.

We apply this inversion technique to a range of geologic settings with high quality P-wave S-wave data (e.g., cratonic North America, the African and Indian shields, and the Aleutian arc crust—which may represent a building block for continental crust). Compositional models for each region are derived based on expected crustal geotherms, along with complementary estimates for lower crustal physical properties including density and viscosity. These data are then used to test different models for crustal evolution.

Geodynamic implications from element fluxes in the Tonga-Lau system

CHRISTOPH BEIER¹, MARCEL REGELOUS¹
AND KARSTEN M. HAASE¹

¹GeoZentrum Nordbayern, Universität Erlangen-Nürnberg,
Schlossgarten 5, D-91054 Erlangen, Germany,
christoph.beier@fau.de

It is well known that lavas from active back-arc spreading centres contain a 'subduction component' (e.g. high Pb/Ce, U/Nb), the strength of which decreases with increasing distance of the spreading axis from the volcanic arc. However, it is not well understood how the Ba-, Pb- and U-rich subduction component is transported from the subducting plate to the shallow melting zone underneath the ridge axis. Many tectonic models for subduction zones assume vertical transport of fluid or aqueous melt from the surface of the subducting slab to shallower levels beneath the back-arc spreading axis, and the decreasing subduction signal with distance from the arc is thought to result from a decreasing fluid release from the subducting slab at greater depths. To test these hypotheses, we present new data from the Tonga-Kermadec arc, a 3000 km long arc in the southwestern Pacific, along with new and published data from the Valu Fa, Central and Eastern Lau back-arc basin spreading centres. The distance between the arc and back-arc increases from less than 10 km at ~23°S to ~150 km at 19°30'S, allowing the interaction between the arc and back-arc melting regimes to be constrained. Assuming that Nb is immobile in fluids, and that Ba/Nb, Th/Nb ratios are not fractionated during melting, we map out the subduction-related enrichment of Ba and Th underneath the Tonga Arc-Lau Basin system, and show using mass-balance arguments that the simplistic model of vertically rising fluids or melts is unrealistic. We suggest that the overlap in melting zones beneath the arc and beneath the back-arc spreading centre allows horizontal flow of melt from beneath the arc towards the back-arc (i.e. in the opposite direction to the flow of solid mantle induced by plate subduction) at shallow levels in the mantle, and this best explains a subduction zone signature underneath the back-arc. Our work demonstrates for the first time that melt can be focussed from the extreme edges of the melting zone underlying an active spreading ridge to the ridge axis, over distances of up to 200 km. Our model provides an alternative explanation for $(^{238}\text{U}/^{230}\text{Th}) > 1$ in back-arc lavas, and indicates horizontal melt flow velocities of 0.4-1 m/y.

Contrasting style of Iron formations deposited before and after the GOE

BEKKER ANDREY¹

¹ Dept. of Geological Sciences, University of Manitoba,
Winnipeg, Manitoba R3T 2N2, Canada;
bekker@cc.umanitoba.ca

Iron Formations are typically interpreted to indicate anoxic deep-water conditions before the rise of atmospheric oxygen and ocean ventilation. However, deposition of iron formations continued after the Great Oxidation Event (GOE) in shallow-marine conditions above the fairweather wavebase. Their deposition on several continents at ca. 1.89 Ga has been linked to a mantle plume breakout event and indicates development of the shallow-water redoxcline in the global ocean separating deep-water, anoxic and ferruginous conditions from shallow-water oxic and well-mixed environments. Iron oxidation at the dynamic redoxcline has been linked to iron-oxidizing microbial ecosystems, oxygenic photosynthesizers, and abiotic iron oxidation. In contrast, Archean iron formations were typically deposited below the storm wavebase and lack indicators of wave or storm activity. Conspicuous absence of Archean iron formations with granular structures and Fe-coated grains might indicate lack of mechanisms for quantitative iron oxidation in Archean shallow-marine settings, suggesting that oxidizing conditions and a strong redoxcline were lacking even in highly productive shallow-marine settings. Iron isotope values of Archean and Paleoproterozoic iron formations are also consistent with non-quantitative Fe-oxidation in the Archean oceans arguing against a significant role of oxygenic photosynthesis in deposition of Archean iron formations. It seems therefore likely that anoxygenic photosynthesis in depositional settings with low sedimentation rates is responsible for deposition of Archean iron formations. The prediction from the contrasting style of deposition of iron formations before and after the GOE is that deposition of iron formations occurred at lower sedimentation rates before the rise of atmospheric oxygen. If this is the case, it has implications for scavenging capacity of iron oxyhydroxides and thus interpretation of geochemical records of iron formations.

Ge, related trace elements, and Ge isotopes in sphalerite from the Saint-Salvy deposit (France) by LA-ICP-MS and MC-ICP-MS.

BELISSONT, R.^{1,2}, BOIRON, M.-C.¹, LUISAIS, B.²,
AND CATHELINAU M.¹

¹GeoRessources, Université de Lorraine, Vandoeuvre-les-Nancy, France

²CRPG, CNRS, Vandoeuvre-les-Nancy, France
remi.belissant@univ-lorraine.fr

The recent increasing worldwide demand in germanium (Ge) encourages research for the understanding its geological cycles and the factors controlling its concentration in minerals. Ge occurs in a wide variety of geologic environments and though it averages 1.6 ppm in the Earth's crust, high Ge contents may occur in both oxide and sulphide minerals (up to 100–3000 ppm), especially sphalerite so that Zn ores represent a major source of Ge, with coal. The Ge-bearing sphalerite of the Saint-Salvy Zn-Ge-Ag-(Pb-Cd) vein-type deposit was subjected to an integrated mineralogical, geochemical and Ge isotopic study in order to understand the mechanisms and processes that conduct Ge and related minor/trace elements (e.g. Cu, In, Ga, Ag, Sb, Sn) to be enriched in sphalerite regarding source, transport, and deposition conditions.

In situ analyses of trace elements using LA-ICP-MS, coupled with optical and electron microscopy and multivariate statistics, pointed out an opposite distribution of Ge between compositional zoning types in sphalerite, with contents ranging from 15 to 2580 ppm. In *rhythmic bandings*, Ge anticorrelates with Fe, Cd, In and Sn, and averages 500 and 200 ppm within light brown and dark brown bands, respectively. In *sector zonings*, Ge is enriched and correlates with Cu, Ga, Sb, Ag and As, and averages 1100 ppm. Cu would enhance the incorporation of trace elements, being involved in many coupled substitution mechanisms, among which the most notable: $2\text{Zn}^{2+} \leftrightarrow \text{Cu}^{+} + \text{Sb}^{3+}$. In addition, the main coupled substitutions $3\text{Zn}^{2+} \leftrightarrow \text{Ge}^{4+} + 2\text{Ag}^{+}$ and $3\text{Zn}^{2+} \leftrightarrow \text{In}^{3+} + \text{Sn}^{3+}$ also occur. Trace element features of the sphalerite from Saint-Salvy compared with those of other deposits worldwide revealed to be efficient to discriminate among genetic types of ores, which may find interests in exploration guidance. Bulk Ge isotope analyses by MC-ICP-MS showed $\delta^{74}\text{Ge}_{\text{NIST3120a}}$ ranging from -1.97 to +1.01‰ ($\pm 0.25\%$ 2 σ SD) that positively correlate with Ge content and highlight large sub-surface fractionation processes during sulphide precipitation in low temperature hydrothermal open system.

Funded by LABEX RESSOURCES21 (ANR-10-LABX-21).

Photophysical studies of biologically produced macromolecules

E. BELKASEM¹, L. SWANSON¹, A. ELAYATT²
AND M.E. ROMERO-GONZÁLEZ^{2*}

¹Department of Chemistry, The University of Sheffield,
Sheffield S3 7HF, UK (chp08esb@shef.ac.uk)

²Kroto Research Institute, The University of Sheffield,
Sheffield S3 7HQ, UK (m.e.romero-gonzalez@shef.ac.uk)

The attachment of microbes to solid surfaces is controlled by the macromolecular structure of the cell wall as much as driven by functional genes that are induced to produce cell wall macromolecules. We present here a quantification of the molecular conformation and sorption forces involved in the attachment of cell wall macromolecules such as lipopolysaccharides (LPS), alginates and extracellular polymeric compounds (EPS) extracted from bacteria. Our hypothesis is that the molecule-surface interfacial forces mediate the physicochemical interactions of bacteria cell wall, and its adaptation to the host environment. Photophysics techniques were used to investigate adsorption of biopolymer onto mineral surfaces which should act as model systems for bacterial growth. Adsorption of dilute aqueous solution of macromolecules was studied as a function of pH in the presence of alumina and silica using Time resolved anisotropy studies (TRAMS), fluorescence and ICP-MS. The alumina and silica particles were used to mimic active sites existing on the surface of kaolin-like particles. It was found that LPS for example, had a high adsorption affinity for Al₂O₃ and in contrast adsorbs weakly to SiO₂ surface. Strong adsorption was observed at low pH for both minerals. The dependence of adsorption on the mineral concentration was also examined at different pH conditions: the adsorption amount was observed to increase by increasing the mineral concentration. Macromolecular folding and conformation of the LPS, alginate and EPS at the solid-solution interface was also quantified using TRAMS. The results showed a high pH and ionic strength dependence demonstrating that macromolecule adhesion is favoured and mediated by ions such as H⁺ and Ca²⁺ in solution. These findings indicate that proton bridges and van der Waal forces are responsible for interactions at the interface. A model for macromolecule adhesion at the interface including the role of ions in solution and folding was proposed. This model is representative of the behaviour of biological macromolecules at the aqueous-surface interface in natural environments. The processes described here have a direct implication on bacteria mediated mineralisation via concentration of ions from solution.

Magma, solutions and metals

AARON BELL¹, ADAM SIMON^{2*}, ELIZABETH TANIS²
AND LAURA BILENKER²

¹Institute of Meteoritics, University of New Mexico

²Earth & Environmental Sciences, University of Michigan
[*simonac@umich.edu]

Holland^[1] demonstrated experimentally that Cl-bearing magmatic-hydrothermal aqueous fluids can scavenge metals from silicate melt and transport the metals into the surrounding crustal environment where fluid-rock reactions and decompression may cause metal precipitation and form ore deposits. Specifically, the abundance of Cl in the fluid phase was demonstrated to be a master variable that controls the total mobilized quantity of metal. Holland^[1] stated: "It remains to be seen just how useful these criteria will turn out to be; the results of preliminary tests are encouraging". This was a prescient statement indeed. Over the ensuing four decades, scientists have constructed a wonderful house of experimental knowledge on the scaffolding that Holland built, and these data guide our understanding of the incredible role of aqueous fluids in magmatic-hydrothermal systems.

Our research group continues to investigate experimentally the mobility of transition row metals, high field strength, and rare earth elements in aqueous fluids ranging from those exsolved from silicate melt in shallow-level magma chambers to fluids evolved during the blueschist to eclogite transition in subduction zones. Specifically, we are investigating how the complexity of aqueous fluid, i.e., dissolved chloride salts, fluorine, albite, etc., affects element mobility.

Data for the mobility of iron in a silicate melt – aqueous fluid – magnetite – sulfide assemblage indicate that the mass transfer of iron can moderate oxygen fugacity, sulfide stability, the composition of ferromagnesian silicates, and the fractionation of stable iron isotopes. These data have important implications for using iron as a geochemical fingerprint for processes that form porphyry, high-sulfidation, iron-oxide-copper-gold (IOCG), and iron-oxide-apatite (IOA) deposits. New data for the mobility of Y (a proxy for the heavy-REE) and Nb (a proxy for all HFSE) in xenotime- and rutile-saturated aqueous fluids, respectively, indicate that these elements are orders of magnitude more soluble at the moderate temperature and high pressure conditions where fluids evolve in subduction zone environments. These new data have significant implications for element recycling during the high-pressure metamorphism that accompanies subduction, and ultimately for evolution of continental crust.

[1] Holland, H.D. (1972) *J. Economic Geology*, **67**, 281-301.

Solubility of Nickel Ferrite (NiFe₂O₄) from 100 to 200°C

ALEXANDRE BELLEFLEUR¹, MARTIN BACHET¹,
PASCALE BENEZETH² AND JACQUES SCHOTT²

¹ EDF R&D Site des Renardières, Avenue des Renardières
77818 Moret Sur Loing, (alexandre.bellefleur@edf.fr)

² GET Toulouse University, 14 Avenue Edouard Belin 31400
Toulouse (benzeth@get.obs-mip.fr)

Nickel ferrite is one of the oxides present on surfaces of the components of the primary circuit of pressurized water reactors (PWR). Its dissolution contributes to the release of nickel in the primary water, at the origin of the contamination phenomenon. A complete understanding of the behavior of nickel in the primary circuit must include solubility measurements of nickel oxides, including mixed oxides such as nickel ferrite.

The solubility of nickel ferrite was measured in a Hydrogen-Electrode Concentration Cell (HECC), which has been described in [1], at temperatures of 100°C, 150°C and 200°C and measured *in situ* pH between 4 and 5.25. The experimental solution was composed of HCl and NaCl (0.1 mol.L⁻¹). Based on previous studies ([2,3]), pure nickel ferrite was experimentally synthesized by calcination of a mixture of hematite Fe₂O₃ and bunsenite NiO in molten salts at 1000°C for 15 hours in air. The so obtained powder was fully characterized. After the experiment, the powder showed no significant XRD evidence of Ni(II) reduction. Nickel concentration was measured by atomic absorption spectroscopy and iron concentration was measured by UV spectroscopy. The protocol has been designed to enable the measurement of both dissolved Fe(II) and total iron [4].

The solution was slightly undersaturated relative to nickel oxide [1] and to both hematite and magnetite. The nickel/iron ratio indicated a non stoichiometric dissolution. The solubility measurements were compared with equilibrium calculations using the MULTEQ database. The solubility of nickel ferrite in a reducing acidic solution is reasonably well described by the available thermodynamic data.

[1] Palmer *et al.* (2011) *J. Solution Chem.* **40**, 680-702.

[2] Hayashi *et al.* (1980) *J. Materials Sci.* **15**, 1491-1497.

[3] Ziemniak *et al.* (2007) *J. Physics and Chem. of Solids.* **68**, 10-21. [4] Bénézech *et al.* (2009) *Chem. Geol.* **265**, 3-12

Alternative nitrogenases in terrestrial ecosystems?

JEAN-PHILIPPE BELLENGER, YAN XU, XINNING ZHANG,
AND ANNE KRAEPIEL¹²³⁴

¹Chemistry department, Sherbrooke University, Sherbrooke,
Quebec, J1K2R1, Canada

²Department of Molecular and Cellular Physiology, School of
Medecine, Stanford University, Stanford, CA 94305, USA

³Gesoscience department, Guyot Hall, Princeton University,
Princeton, NJ 08544, USA

⁴Chemistry department, Princeton University, Princeton, NJ
08544, USA

Recent studies have shown that molybdenum (Mo), which is used in the Mo-nitrogenase, can limit N₂ fixation in temperate and tropical ecosystems. This suggests that alternative nitrogenases, which use V or Fe in place of Mo, may contribute to N₂ fixation. The acetylene reduction assay (ARA) is commonly used to estimate N₂ fixation rates but requires the use of an adequate conversion ratio (R ratio = acetylene reduction/N₂ fixation). The theoretical value for R is 3-4, but measured values in the field range from less than 1 to more than 10. In this study, we show that even in pure cultures, the R ratio is variable and dependent on the culture growth phase. Nonetheless, low R values (below 2) can be consistently attributed to N₂ fixation by alternative nitrogenases. Interestingly, an analysis of the literature shows that low R ratios are measured almost exclusively in soils, and are not found in the surface oceans (where Mo is abundant, and alternative nitrogenases are unlikely to be important) or in plant symbioses (which do not possess the genes for the alternative nitrogenases). The low R ratios may thus be indicative of alternative nitrogenases in soils. In a series of microcosm experiments with temperate soils from New Jersey, we were able to confirm that alternative nitrogenase genes were present, and expressed, even though N₂ fixation did not appear to be Mo-limited. The R ratios were low at the beginning of the incubations, suggesting that alternative nitrogenases contribute to the bulk to N₂ fixation in these samples. The R ratios also tended to increase over time, possibly reflecting depletion of the fixed carbon pool, or increased contribution from the Mo-nitrogenase. The possibility that alternative nitrogenases may contribute to N₂ fixation in systems that are not Mo limited is intriguing and deserves further investigation.

Development of the La-Ce systematics : application to arc magmas

N. BELLOT¹, M. BOYET¹, C. PIN¹, C. CHAUVEL²,
R. DOUCELANCE¹ AND D. AUCLAIR¹

¹Laboratoire Magmas et Volcans, Université Blaise Pascal, CNRS UMR 6524, 5 rue Kessler, 63038 Clermont-Ferrand, France

correspondance : n.belloc@opgc.univ-bpclermont.fr

²ISTERRE, Maison des Géosciences, CNRS, 1381 rue de la piscine 38400 Saint Martin d'Hères, France.

In the 1980's, the ¹³⁸La-¹³⁸Ce systematics ($T_{1/2} = 302$ Ga) has been developed [1,2]. Since La/Ce fractionation is strong in some superegene conditions (due to the occurrence of Ce⁴⁺), this isotope system is able to offer new information on the material involved in the genesis of magma in subduction zones. Here, we present Ce isotope data measured on Martinique lavas that have been thoroughly characterized in a previous study [3].

The Ce purification involves 3 steps: 1) REE isolation in HCl medium on cationic resin; 2) La-Ce-Pr-Nd separation using 2MLA acid; 3) purification of the Ce fraction using LnSpec resin. The Ce isotopic compositions were measured as the oxide species by TIMS, (Triton). In order to increase the signal size of the two minor isotopes (¹³⁶Ce and ¹³⁸Ce), ¹⁴⁰Ce was not measured. The oxygen isotope composition is determined *in situ* following the method developed by [4]. ¹³⁸Ce/¹⁴²Ce ratios are normalized to ¹³⁶Ce/¹⁴²Ce=0.01688. ¹³⁸Ce/¹³⁶Ce ratio measured in the AMES standard is equal to 1.33745±4 (n=10, or ¹³⁸Ce/¹⁴²Ce=0.0225761±7) in agreement with previous measurements [4]. The ¹³⁸Ce/¹⁴²Ce ratios measured on the standard basalts BHVO-2 and BCR-2 are 0.0225662±15 (n=13) and 0.0225684±13 (n=3), respectively. The ¹³⁸Ce/¹⁴²Ce ratios of the Martinique lavas define a large range (0.0225660 – 0.0225706) showing that the Ce isotopic system can be a powerful tool to trace heterogeneities in the source of arc lavas.

The Ce isotopic tracer applied to 30 Martinique lavas shows a clear correlation with Nd, Sr and Pb isotopes suggesting a varying contribution from sedimentary material. Complementary data on sediments located in front of the arc should provide further constraints on the mixing relationships between sedimentary components and the mantle wedge underlying the Lesser Antilles arc.

[1] Tanaka *et al.*, 1982, Nature **300**; [2] Dickin, 1987, Nature **325**; [3] Labanich *et al.*, 2010, EPSL **298**; [4] Willbold, 2007, JAAS **22**.

Rb and Sr adsorption at the Quartz(101) – water interface

F. BELLUCCI^{1*}, S.S. LEE¹, Z. ZHANG¹, P. FENTER¹
AND D.J. WESOLOWSKI²

¹Argonne National Laboratory, Argonne, IL, 60439, USA

²Oak Ridge National Laboratory, Oak Ridge, TN, 37831, USA

Quartz is an abundant and ubiquitous rock-forming mineral in Earth's continental crust, and influences the chemistry of numerous aqueous systems [1]. The sorptive property of quartz changes the mobility of ions in water while its dissolution process controls long-term silica cycling through the earth system. Batch experiments [2, 3] showed that the dissolution rate of quartz at near-neutral pH increases substantially in the presence of cations while the degree of enhancement depends on the choice of cation. However, the detailed understanding on the mechanism remains unclear mainly because of the lack of atomic-scale information on the processes to explain the complexity of the interface chemistry. Molecular-scale investigation of the quartz surface-cation interaction is the first step in understanding this cation-induced mechanism. Here, we report on Rb⁺ and Sr²⁺ cation adsorption at the quartz(101)-water interface observed in 10mM salt solutions at pH 10 using x-ray reflectivity (XR) and resonant anomalous XR measurements.

The best fit models of the experimental data suggest that Rb⁺ adsorbs at an average height of 2.7 Å above the surface (defined as the average position of the two terminal oxygens), which may be a mixture of inner- and outer-sphere species. Adsorbed Sr²⁺ is prevalently located at 4.6 Å above the surface, suggesting the formation of an outer sphere complex. The occupancies of these complexes with respect to the unit cell area (UC) are 0.19 Rb⁺/UC, and 0.07 Sr²⁺/UC. The smaller coverage of Sr²⁺ compared to that of Rb⁺ is likely due to the difference in cation valency. The charge of the quartz(101) surface calculated based on the coverages at pH 10 is approximately 0.14 to 0.21 e⁻/UC or ~1 e⁻ for 5 to 7 UC.

[1] Schulz, M.S. and A.F. White, *Geochim. Cosmochim. Acta*, 1999, **63** (3-4): p.337. [2] Dove, P.M. and D.A. Crerar, *Geochim. Cosmochim. Acta*, 1990, **54** (4): p.955. [3] Dove, P.M., *Geochim. Cosmochim. Acta*, 1999, **63** (22): p.3715.

Pyroxenites from mantle section of Voykar Ophiolite (Polar Urals) – pathways for melt and fluid migration

I.A.BELOUSOV^{1,2}, V.G.BATANOVA^{2,3}, A.V.SOBOLEV^{2,3}
AND G.N.SAVELIEVA⁴

¹CODES, Hobart, Australia, ivan.belousov@utas.edu.au

²Vernadsky Institute of Geochemistry RAS, Moscow, Russia

³ISTerre, University J. Fourier, Grenoble 1, France

⁴Geological Institute RAS, Moscow, Russia

Late stages of formation of rocks from mantle section of Voykar Ophiolite were shown to take place in SSZ environment [1,2]. Dunite bodies and pyroxenite veins mark different stages of melt migration [2]. Best evidence for SSZ environment is preserved in mineral compositions from pyroxenite veins – high #Cr of spinel and LILE enrichments in Cpx and high-Al amphibole. Pyroxenite compositions display variability which is a function of their modal compositions, morphological features and spatial location.

Minerals from orthopyroxenites usually have high mineral #Mg, are most depleted in incompatible elements, show low Al in pyroxenes and spinel ($\#Cr^{Sp} > 0.6$). Other group of pyroxenites with high mineral #Mg is represented by thin (cm-scale) clinopyroxenites and websterites and complex dunite-pyroxenite veins. Their major element compositions were equilibrated with adjacent harzburgites. Minerals from thicker websterites and clinopyroxenites have lower #Mg and subparallel boninite-like trace element patterns of Cpx [1]. Cpx compositions across harzburgite-pyroxenite contacts show depletion in HREE (opposite to harzburgite-dunite contacts) and Zr and enrichment in LREE and Sr. High-Al amphibole from websterites display trace element patterns with different LREE/HREE and MREE/HREE ratios, which could reflect their formation from melt to fluid-like agent.

Therefore, Voykar mantle section pyroxenite veins represent pathways for melts variously depleted in incompatible elements or in some cases fluids with boninite-like trace element patterns and elevated silica contents. Those melts were produced by melting of hybridized mantle source formed as a result of transformation of mantle olivine to orthopyroxene under the influence of slab-derived fluids/melts [2]. Different areas of massif could be arranged in order of increasing HREE contents in Cpx from dominated type of pyroxenite which could reflect relative depth or degree of melt fractionation.

[1] Belousov *et al.*, 2009. Dokl Earth Sci, **429** (1), p.1394-1398. [2] Batanova *et al.*, 2011. JP, **52** (12), p.2483-2521.

New insights into the history of an ophiolite from zircons

E.A. BELOUSOVA^{1*}, J. M. GONZÁLEZ-JIMÉNEZ¹, I.T. GRAHAM², W.L. GRIFFIN¹ AND SUZANNE Y. O'REILLY¹

¹GEMOC/CCFS, Macquarie University, Sydney, Australia
(elena.belousova@mq.edu.au)

²School of Biological, Earth and Environmental Sciences,
University of NSW, Sydney, Australia

The Coolac Serpentinite Belt is part of the Tumut ophiolitic complex in the Lachlan Fold Belt, southeastern Australia. The 63 km belt contains a high proportion of massive (unfoliated) ultramafic rocks that have undergone only lower greenschist-facies metamorphism [1]. New U-Pb, Hf- and O-isotope and trace-element data have been obtained for zircons from the rocks of the belt. These include zircons separated from two (high-Al and high-Cr) massive chromitites and rodingites and grains recovered from gullies draining mainly weakly serpentinised massive porphyroclastic harzburgite. The Belt is either faulted against, or intruded by, the S-type Young Granodiorite. Zircons from the Young Granodiorite collected at the contact with the serpentinite belt were also studied to refine the tectonic relation and timing of the granitic magmatism.

The U-Pb age obtained on the zircons from the serpentinite belt display a wide range of ages, from Silurian to Paleo-Proterozoic, with the main age population clustering around 430 Ma. This main peak coincides within the analytical error with the age obtained for the Young Granodiorite (427.6 ± 3.2 Ma) and inherited zircon ages for plagiogranites from the Belt [1]. The ages for the inherited zircon populations in the granodiorite correlate well with the older zircon populations from the Coolac ultramafic rocks.

Most of the Coolac zircons have negative ϵ_{Hf} and heavy (>6) $\delta^{18}O$ indicative of a crustal origin. Combined with U-Pb age information, this implies that the zircons in the peridotites are xenocrystic. One possibility is that zircons derived from subducted sediments were incorporated into the ophiolitic rocks (as in the Luobusa (Tibet) ophiolite [2]). However, the similarity of the Coolac ophiolite-derived zircons with those from the Young Granodiorite may indicate that they were introduced into the Coolac peridotitic complex during the granitoid magmatism and thus may carry no information on the origin of the Tumut ophiolitic rocks. In the latter case, the Coolac rocks should be older than the granitic magmatism of the 420–390 Ma age of the Lachlan Fold Belt.

[1] Graham *et al.* (1996) *Geology* **24**, 1111-1114. [2] Yamamoto *et al.* (2013) *Island Arc* **22**, 89-103.

Monomeric and polymeric silica sorption on calcite

D.A. BELOVA^{1*}, O.N. KARASEVA², L.Z. LAKSHTANOV^{1,2}
AND S.L.S. STIPP¹

¹Nano-Science Center, Department of Chemistry, University of Copenhagen, Copenhagen, Denmark (db@nano.ku.dk)

²Institute of Experimental Mineralogy RAS, Chernogolovka, Russia (olga@iem.ac.ru)

Literature data about sorption of dissolved silica by calcite is fairly sparse and contradictive. Klein and Walter [1] investigated silica uptake at pH 6-8.3 and reported adsorption to be strongly pH dependant, with a maximum at pH 6. On the other hand, in flotation studies where sodium silicate was used as a depressant to suppress the flotation tendency of calcite, the experiments were mostly performed at pH > 8 and silica adsorption by calcite was reported to reach maximum at pH 9 to 10 [2, 3, 4]. In addition, the role of silica polymer adsorption in suppressing calcite flotation is unclear. Some authors [2] did not find any relationship with polymeric silica while others [3, 4] reported polymer adsorption to be responsible for suppression. Our study aimed to clarify the pH dependence of silica uptake by calcite and the importance of silica polymers in the process.

We investigated sorption of dissolved silica on calcite at 25 °C in calcite equilibrated solutions with pH ranging from 6 to 11, with varying initial silica concentration (≤ 2 mM) and surface area to liquid ratio (≤ 480 m²/L). The experimental conditions were designed such that polymeric silica introduced with the concentrated stock solution is stable at pH > 9 but unstable at lower pH.

Silica uptake was observed to increase with pH. At pH 11, almost 50% of the dissolved silica was removed from the solution, while no silica sorption was found at pH 6.1. The presence of stable silica polymers at pH > 9, is at least partly responsible for this pH dependence. At pH 8.3, we observed a significant, but temporary uptake of silica. It was released again to solution after several hours. This is consistent with silica being dominantly adsorbed as polymeric species and desorbed in response to depolymerisation.

[1] Klein and Walter (1995) *Chem. Geology* **125**, 29-43 [2] Marinaki and Shergold (1985) *Int. J. Miner. Process.* **14**, 177-193. [3] Hanumantha Rao *et al.* (1989a) *Colloids Surf.* **34**, 227-239. [4] Hanumantha Rao *et al.* (1989b) *Int. J. Miner. Process* **26**, 123-140.

Melt evolution from the mantle wedge to the crust: insights from South Kamchatka and West Bismarck arc xenoliths

A. BÉNARD^{1*}, S.R.B. MCALPINE¹, O. NEBEL¹,
P.M.E. TOLLAN², R.J. ARCULUS¹ AND D.A. IONOV³

¹Research School of Earth Sciences, Australian National University, ACT Australia 0200

²Department of Earth Sciences, Durham University, Durham, UK

³PRES-Lyon & UMR6524-CNRS, Saint-Etienne, France
(*correspondence: antoine.benard@anu.edu.au)

Rare xenoliths carried by recent andesites or arc tholeiites are the only direct witnesses of active sub-arc processes. We present a detailed study on such xenoliths from Avacha volcano in southern Kamchatka (Russia) and Ritter volcano, West Bismarck Arc (Papua New-Guinea Region). Avacha is located on a 'mature' subduction zone (~120 km Pacific slab depth, ~40 km crustal thickness). Harzburgites cut by websteritic veins, as well as massive olivine- and hornblende-clinopyroxenites and hornblendites occur in Avacha andesitic deposits (≤ 7000 yrs. BP). Based on the compositions of minerals, melt inclusions and interstitial glass, we infer that the websteritic veins formed from high-Ca boninites (HCB). Unlike a previous study [1], this inference is consistent with recent reports of complementary low-Ca boninites (LCB) in these rocks [2]. Similar datasets show that clinopyroxenites and hornblendites crystallized respectively at Moho and mid-crustal depth, producing residual liquids similar to Avacha andesites. Modelling suggests that these 'cumulate' rocks can form from an ascending HCB melt, modified by fractionation and melt-rock reactions in the lithospheric sub-arc mantle.

Ritter is part of an active and complex subduction zone (~120 km depth for the Solomon Sea Plate slab and ~20 km crustal thickness). Harzburgites, pyroxenites and dunites are found in picritic arc tholeiites (≤ 125 yrs. BP) from Ritter. We show with the same toolbox, that pyroxenites and dunites are former primitive sub-arc melt channels. Evidence for LCB percolation in veins through these samples supports the current generation of boninitic mantle melts, like for Avacha.

In line with literature datasets on exhumed arc sections, we propose that boninites are common primary mantle wedge liquids in various types of subduction zones. Supported by our dataset on harzburgites, this puts direct constraints on mantle wedge melting beneath arcs. The possible HCB-andesite liquid line of evolution leads us to re-examine melt ascent and element flux models for subduction zones.

[1] Ishimaru & Arai (2011), *CMP*. [2] Bénard & Ionov (2012), *G3*.

Non-traditional stable isotopes and surface complexation models for ion binding to humic substances (NICA-Donnan) and oxide mineral surfaces (CD-MUSIC)

M.F. BENEDETTI¹

¹Université Paris Diderot – Sorbonne Paris Cité – IPGP – UMR CNRS 7154, Paris France ; benedetti@ipgp.fr

Non-traditional stable isotopes (i.e. Zn, Fe, Ni and Cu) are increasingly used for environmental studies [1]. Considering the wide range of possible sorbents (Mn or Al oxides, phyllosilicates, carbonates, biologic surfaces...), the importance of the reactions at the sorbent/water interface for these numerous studies emphasized the importance of modelling approaches that are needed to quantify the isotopic fractionation of these elements caused by their sorption at mineral/water, organic moieties/water interfaces.

The present work will show how the use of EXAFS spectroscopy and CD MUSIC and NICA Donnan modelling can help to better understand the changes in isotopic ratio. Zn isotopic fractionation upon sorption onto Hydrated Ferric Oxide (HFO) and goethite will be discussed to assess the influence of reactions at the Fe-(hydr)oxide/water interface on the isotopic distribution of Zn [1]. The Zinc isotopic fractionation during interaction onto natural organic matter will be discussed. The Donnan Membrane device was successfully adapted for isotopic measurements and used to separate Zn bound to the PHA from free Zn²⁺ ions in solution and allowed the measurement of isotopic ratios of free Zn²⁺. The NICA-Donnan model, is used to simulate the corresponding isotopic fractionation and the composition of free Zn in the Seine river, France and allows a better understanding of Zn isotope fractionation mechanisms associated with organic matter binding [2].

[1] D.M. Borrok, R.B. Wanty, W. Ian Ridley, P.J. Lamothe, B.A. Kimball, P.L. Verplanck, *et al.*, *Applied Geochemistry*, **24** (2009) 1270–1277. [2] F. Juillot, C. Marechal, M. Ponthieu, S. Cacaly, G. Morin, M. Benedetti, *et al.*, *Geochimica Et Cosmochimica Acta*, **72** (2008) 4886–4900 [3] D. Jouvin, P. Louvat, F. Juillot, C.N. Maréchal, M.F. Benedetti, Zinc Isotopic Fractionation: Why Organic Matters, *Environ. Sci. Technol.* **43** (2009) 5747–5754.

In-situ IR spectroscopic study of forsterite carbonation in wet-scCO₂

P. BENEZETH¹, J. CHEN², O. QAFOKU², H.T. SCHAEF², C.J. THOMPSON², C. PEARCE², A.R. FELMY², ALAIN BONNEVILLE², K.M. ROSSO² AND J.S. LORING^{2*}

¹Géosciences Environnement Toulouse (GET)-CNRS, 14 Avenue Edouard Belin, 31400 Toulouse, France (benezeth@get.obs-mip.fr)

²Pacific Northwest National Laboratory (PNNL), Richland, WA 99352 (*correspondence: john.loring@pnnl.gov)

Capturing and storing CO₂ in basaltic formations is one of the most promising options for reducing the effects of energy production from fossil fuel on the Earth. These geologic reservoirs have high reactive potential for CO₂-mineral trapping due to an abundance of divalent-cation containing silicates, such as forsterite (Mg₂SiO₄). Recent studies [1-4] have shown that carbonation of these silicates is more effective in wet scCO₂ conditions, encountered near a CO₂ injection well, than in dry and/or CO₂-saturated aqueous fluids. More interestingly, formation of magnesite under supercritical fluid conditions has been reported in some of these previous studies at temperatures as low as 35°C [3], in spite of its known sluggish formation under aqueous scenarios.

In this study, we used high pressure IR spectroscopy to investigate the carbonation of nanometer-sized forsterite at 35 and 50°C by systematically titrating water that subsequently dissolves in scCO₂ at 90 bar. The results show that at low total dissolved water concentrations, only highly structured adsorbed water and bicarbonate are detected at the forsterite surface. However, as the water concentration increases up to a critical value, but below H₂O-saturated scCO₂, a more liquid-like water film is detected on the forsterite particles, the bicarbonate concentration decreases and magnesite precipitates, as shown in our *in situ* IR spectra, as well as from *ex-situ* XRD, TGA and SEM analyses.

The results of these studies provide important insights into metal silicate carbonation mechanisms in low water scCO₂ environments. They reinforced the concept of a water threshold for carbonation to occur, which has also been demonstrated for steel corrosion in the presence of wet scCO₂ [5]. These results will also constrain thermodynamic models and molecular dynamic simulations used to predict mineral trapping extent in basaltic host rocks.

[1] Kwak *et al.* (2011) *Int. JGGC.*, **5**, 1081-1092. [2] Loring *et al.* (2011) *ES&T*, **45**, 6204-6210. [3] Felmy *et al.* (2012) *GCA*, **91**, 271-282. [4] Schaefer *et al.* (2013), *ES&T*, **47**, 174-181. [5] McGrail *et al.* (2009) *Energ. Proc.*, **1**, 3415-3419.

Mantle Potential Temperature Trend for the Central Atlantic Magmatic Province

ALAN BENIMOFF AND JOHN H. PUFFER J

¹Dept. of Engineering Science and Physics, College of Staten
Island/CUNY, Staten Island, NY 10314

²Dept. of Earth and Environmental Sciences, Rutgers
University, Newark, NJ 07102,

Recently published high precision geochronology by Blackburn *et al.* [1] dates each of eight basaltic magmatic events intruded and extruded during the Central Atlantic Magmatic Province (CAMP) over a 0.6 Ma time span. Each of the four major CAMP magma compositions including High titanium quartz normative, High Iron quartz normative, Low titanium quartz normative, and Olivine normative are represented. Geochemical data from a variety of sources are available for each of the eight basaltic units and being applied to PRIMELT2 software developed by Herzberg and Asimow [2] that will enable the determination of mantle potential temperatures. These data will enable us to calculate temperature trends that will have a direct bearing on the petrogenesis of CAMP magmatism. Preliminary data yield mantle potential temperatures for the mean High titanium quartz normative and Olivine normative primary compositions determined by Salters *et al.* [3] of 1394°C and 1449°C respectively. These temperatures are lower than the > 1500°C melting range generally applied to the mantle plume model but are consistent with decompression melting of a subduction enriched subduction metasomatised sub-continental lithospheric mantle source (SCLM). The temperature trend that we establish will allow us to further evaluate the application of mantle plume and SCLM source models to CAMP.

[1] Blackburn *et al.* (2013) *Scienceexpress*, 21 March 2013 / Page 1/ 10.1126/science.1234204. [2] Herzberg, C. and Asimow, P.D., (2008) *Geochem. Geophys. Geosyst.*, **9**, Q09001, doi:10.1029/2008GC002057. [3] Salters *et al.* (2003) *Geophys. Monogr. Ser.*, **136** 163-177, AGU, doi:10.1029/136GM09

Planets, Minerals and Life's Origin

STEVEN A. BENNER^{1,2}

¹Foundation for Applied Molecular Evolution, PO Box 13174,
Gainesville FL 32604

²The Westheimer Institute for Science and Technology, 720
SW 2nd Ave., Gainesville FL 32601

Four paradoxes stand astride any effort to understand how life originated on Earth:

(a) The Tar Paradox. Organic molecules, given energy and left to themselves, devolve into complex mixtures, "asphalts" better suited for paving roads than supporting Darwinian evolution. Any scenario for origins requires a way to allow organic material to escape this devolution into a Darwinian existence, where replication with imperfections, where the imperfections are themselves heritable, allows natural selection to avoid a tarry fate.

(b) The Water Paradox: Water is commonly believed to be essential for life. So are biopolymers, like RNA, DNA, and proteins. However, the biopolymers that we know find water corrosive. Any scenario for origins must manage the apparent need of life for a substance (water) this is inherently toxic to life.

(c) The Single Biopolymer Paradox. Even if we can make biopolymers prebioically, it is hard to imagine making two or three (DNA, RNA, proteins) at the same time. At the same time, genetics versus catalysis place different demands on the behavior of a single biopolymer intended to support life. Catalytic biopolymers should fold, for example, while genetic biopolymers should not fold. Catalytic biopolymers should contain many building blocks; genetic biopolymers should contain few.

(d) The Probability Paradox. Some biopolymers, like RNA, strike a reasonable compromise between the needs of genetics and the needs of catalysis. However, emerging data suggests that RNA is more likely to deliver catalytic power that destroys RNA than catalytic power that makes RNA.

This talk will review experimental data that makes suggestions about early planetary environments and mineralogy that might avoid, mitigate, and possibly resolve certain of these paradoxes. Key are the presence of minerals, including borates and molybdates, that interact with organic species that are intermediates between atmospheric carbon dioxide and dinitrogen and RNA. Productive interaction requires as well a subaerial environment having only intermittent interaction with water. Recent data suggests that such environments might even be found today on Mars.

An integrated isotopic-geologic view of early continental crust formation from the oldest rock record

VICKIE C. BENNETT^{1*} AND ALLEN P. NUTMAN²

¹*Research School of Earth Sciences, The Australian National University, Canberra, Australia;

vickie.bennett@au.edu.au

²GeoQuest Research Centre, School of Earth and Environmental Sciences, University of Wollongong; allen.nutman@gmail.com

A cornerstone of Earth sciences for many years was the assumed complementary of mantle and crustal chemical evolution, with extraction and recycling of continental crust through time thought to be the main processes controlling the composition of the upper mantle. This view has been brought into question following discoveries of extinct nuclide signatures in Archean rocks (e.g. ¹⁴²Nd, ¹⁸²W) requiring early differentiation and/or a non-chondritic Earth. Linked to this are questions of which isotopic and geochemical monitors of continental crust formation processes and continental mass are most reliable.

Here we present an integrated geochemical and geologic examination of Archean continent formation with an emphasis on the patterns of ¹⁷⁶Hf and ¹⁴³Nd isotopic variations. Focus is on the largest extent of early crust located within the 3000 km² Eoarchean Itsaq Gneiss Complex of SW Greenland. This complex preserves evidence of several temporally and spatially distinct episodes of juvenile crust formation between ~3.89 Ga and 3.66 Ga, which are dominated by TTG rocks. In each event, TTG suites were emplaced into slightly older gabbros, basalts and andesites, which have geochemical signatures consistent with fluid-fluxing of upper mantle sources. The TTG suites are characterized by magmatic zircon with initial εHf of ~0 and positive whole rock initial εNd of +4 to +2. The most likely geodynamic settings for generation of this early crust were convergent plate boundary environments analogous with, but not identical to, modern island arcs. The pattern of near constant εHf values in primitive granitoids for >300 m.y. argues against derivation of these magmas by repeated sampling of a mafic crustal source, from reworking of older crustal material, or from a mantle source previously experiencing large amounts of Hadean crustal extraction. Starting at 3.66 Ga, granitic rocks first begin to show Hf isotopic evidence for reworking of older crust. Varying ¹⁴³Nd isotopic compositions of Eoarchean rocks likely reflect early Sm/Nd fractionation unrelated to crustal extraction. We propose that the shift to correlated ¹⁷⁶Hf-¹⁴³Nd isotopic temporal trends, as typify Phanerozoic style arc accretion processes, began as early as ~3.5 Ga.

Geochemistry and Carbon Management

SALLY M. BENSON

Energy Resource Engineering Department, Stanford University, Stanford, California

Without a doubt, meeting human energy needs while dramatically reducing greenhouse gas emissions is one of the grand challenges of our time. Geochemistry plays a critical role in assessing both the impacts of changing the chemical composition of the atmosphere due to emission of greenhouse gases and designing solutions. Over the coming decades, a radical transformation of our energy system is needed to reduce global greenhouse gas emissions by over 80%. Solutions for achieving needed emission reductions include improving energy efficiency, shifting to renewable energy resources for producing electricity, reducing emissions from fossil fuel by capturing and storing CO₂, switching from coal to natural gas for power generation, and sustaining use of nuclear power. In this paper, the critical role that geochemistry plays in developing and evaluating solutions is highlighted. Examples from carbon dioxide capture and storage, nuclear waste disposal, shale gas development, and providing the critical materials for renewable energy and storage systems are provided. Over the coming decades, Earth's resources will be taxed in new and unforeseen ways. The discipline of geochemistry will play a crucial role in anticipating and responding to these challenges.

Intracellular calcification by cyanobacteria: a significant controlled biomineralization process

KARIM BENZERARA*¹, FÉRIEL SKOURI-PANET¹,
MARIE RAGON¹, NITHAVONG CAM^{1,3}, JINHUA LI¹,
CELINE FERARD¹, JEAN-FRANÇOIS LAMBERT³,
THOMAS GEORGELIN³, MAGUY JABER³,
DAVID MOREIRA² AND PURIFICACION LOPEZ-GARCIA²

¹IMPMC - ERC Calcyan, CNRS & UPMC, 75005 Paris, France, *correspondence: karim.benzerara@upmc.fr

²Ecologie, Systématique et Evolution, UMR 8079 CNRS & Université Paris-Sud, France

³Laboratoire de Réactivité de Surface, UPMC & CNRS, Ivry-sur-Seine, France.

Cyanobacteria had a pivotal role on several global geochemical cycles throughout Earth's history in particular, by biomineralizing CaCO₃. Calcification by cyanobacteria has so far been considered exclusively as an induced extracellular biomineralization process. However, we recently discovered deep-branching cyanobacteria that form intracellular amorphous Ca-Mg-Sr-Ba carbonates [1]. The existence of such intracellularly calcifying cyanobacteria may modify significantly our view on the past and modern role of cyanobacteria in the formation of carbonate deposits and the degree of control they achieve on this geochemically important process. However, several questions remain open: is this biomineralization process widespread phylogenetically or restricted to one single species? Does it occur under specific or diverse environmental conditions? To what extent do phases formed intracellularly by these cyanobacteria differ from abiotically-formed carbonates?

We will address these questions using diverse approaches including high spatial and spectral resolution spectromicroscopies and molecular biology.

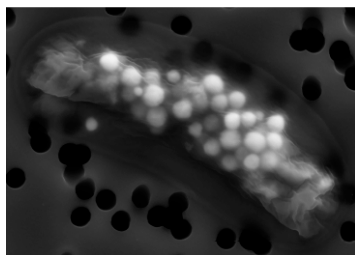


Figure 1: SEM image of *Candidatus Gloeomargarita lithophora*.

[1] Couradeau, Benzerara, Gérard, Moreira, Bernard, Brown Jr., López-García (2012), *Science* **336**, 459-462.

Polysulfides as intermediates in the bacterial metabolism of stored sulfur

J.S. BERG*, J. MILUCKA, A. SCHWEDT,
A.-C. KREUTZMANN AND M.M.M. KUYPERS

Max Planck Institute for Marine Microbiology, 28359
Bremen, Germany

(*correspondence: jberg@mpi-bremen.de)

Zero-valent sulfur is a key intermediate in the microbial oxidation of sulfide to sulfate. Many sulfide-oxidizing bacteria therefore produce and store large amounts of sulfur intra- or extracellularly. It is still not well understood how the stored sulfur is metabolized as the most stable form of S⁰ under standard biological conditions – orthorhombic α -sulfur – can most likely not be utilized by bacterial enzymes.

In this study, the speciation of sulfur in single cells of living bacteria was investigated by Raman spectroscopy. Four different strains of *Beggiatoa* were used to compare the chemical nature of sulfur under various ecological and physiological conditions. Results showed that in microaerobic cultures at circumneutral pH, stored intracellular sulfur consisted of S₈ rings and inorganic polysulfides (S_n²⁻). Linear sulfur chains were detected during both the oxidation and reduction of stored sulfur suggesting that S_n²⁻ species comprise a pool of activated sulfur utilized by bacteria. The formation of S_n²⁻ results from the cleavage of sulfur rings, either biologically by membrane-bound thiol groups and glutathione or chemically by the strong nucleophile HS⁻. It is likely that *Beggiatoa* in the environment utilize both of these mechanisms to generate S_n²⁻ intermediates as they migrate vertically between oxic and sulfidic sediment zones.

With Raman spectroscopy it was possible to further track the fate of sulfur during its oxidation to sulfate. Unexpectedly high concentrations (up to ~2 M) of internal sulfate were detected in *Beggiatoa* sp. Although the reason for the intracellular accumulation of sulfate remains unknown we could show for the first time that *Beggiatoa* contain sulfate in concentrations 100-1,000-fold higher than that of the external environment.

Non-classical nucleation of minerals and the multiple roles of additives

JOHN K. BERG*, MATTHIAS KELLERMEIER, ASHIT RAO, HELMUT CÖLFEN AND DENIS GEBAUER

Physical Chemistry, University of Konstanz, D-78457 Konstanz, Germany, [*correspondence: john.berg@uni-konstanz.de, denis.gebauer@uni-konstanz.de]

Recent reports have demonstrated the existence of stable clusters of calcium carbonate (CaCO₃) prior to nucleation through various experimental methods and also computer simulations [1, 2, 3, 4]. In contrast to classical notions, it appears cluster aggregation, not the assembly of their constituent ions, plays the significant role in nucleation of amorphous calcium carbonate (ACC), which later transforms into crystalline polymorphs.

This multi-stage process can be influenced by additives in several ways, which is of particular interest for biomineralization, as various additives, *e.g.* proteins, polysaccharides, and inorganic salts, are present throughout the nucleation processes. Though many systems have been investigated [5, 6, 7], the exact roles of additives are yet unknown, especially when it comes to mechanistic insights.

In the current contribution, we summarize the concept of non-classical nucleation of CaCO₃ by means of pre-nucleation clusters and recent advancements, including other mineral systems. Moreover, through potentiometric titration assays in the presence of additives, we exemplify the role of additives from simple salts to complex proteins on the early stages of precipitation, *e.g.* pre-nucleation cluster stability, time of nucleation, solubilities of the subsequently-formed phases, and on further phase transformations to the various crystalline polymorphs. Beyond insight into the fundamentals of biomineralization, understanding of the effect of additives on crystallization is also crucial in the creation of biomimetic materials and the formulation of novel anti-scalant methods of industrial importance.

[1] Gebauer, *et al.* (2008), *Science* **322**, 1819-1822. [2] Gebauer & Cölfen (2011), *Nano Today* **6**, 564-584. [3] Demichelis *et al.* (2011), *Nat. Commun.* **2**, 590. [4] Pouget *et al.* (2009), *Science* **323**, 1455-1458. [5] Gebauer *et al.* (2009) *Adv. Mater.* **21**, 435-439. [6] Gebauer *et al.* (2011) *Phys. Chem. Chem. Phys.* **13**, 16811-16820. [7] Picker *et al.* (2012) *Z. Kristallogr.* **227**, 744-757.

3D visualisation of core formation in deforming planetesimals

M. BERG*¹, I.B.BUTLER¹, S.REDFERN², Y.LEGODEC³ AND G.D. BROMILEY^{1,4}

¹School of Geosciences, Grant Institute, University of Edinburgh, Edinburgh, UK maddy.berg@ed.ac.uk*

²Dept. Earth Sciences, University of Cambridge, UK

³Inst. de minéralogie et de physique condensés, Université Pierre et Marie Curie, Paris, France

⁴Centre for Science at Extreme Conditions, University of Edinburgh, Edinburgh, UK

Deformation may significantly enhance permeability of small fractions of metallic melt in a solid silicate [1]. This is an important factor in constraining processes of core formation, as a permeable network in solid silicate could have led to segregation of a core and mantle much earlier than previously thought, importantly long before the onset of a molten silicate 'Magma Ocean'. Few experiments examine effects of low strain-rate deformation at realistic conditions of core formation in small planetary bodies. In addition, 3D melt geometry and permeability is usually inferred indirectly from 2D textural analysis of polished sample slices.

We have conducted experiments on a synthetic solid olivine – liquid FeS system at extreme P-T conditions using the rotational Paris-Edinburgh Cell (roPEC), and have analysed 3D melt geometry of quenched samples have using micro- and nano-tomographic imaging techniques. Deformation at strain rates as low as 10⁻⁶ s⁻¹ aids grain boundary wetting and the formation of melt veins that appear to locally 'drain' certain areas of the sample. Results support theories of complex, multi-stage core formation in which pre-differentiated planetary bodies collided to form the Earth. These proto-cores may have sunk directly to the Earth's centre without re-equilibration with the Earth's mantle, which has major implications for the inferred geochemical composition of the lower mantle [2].

[1] Rushmer, Petford, Humayun, & Campbell (2005) *Earth and Planetary Science Letters* **239**, 185-202. [2] Rudge, Kleine & Bourbon *Nature Geosci* **3**, 439-443 (2010)

Voluminous outburst of silicic low $\delta^{18}\text{O}$ magma in NE-Iceland inferred from zircon $\delta^{18}\text{O}$ and U-Pb geochronology

BERG S. E.^{1,2*}, TROLL, V. R.², RIISHUUS, M. S.¹, BURCHARDT, S.², DEEGAN, F. M.^{2,3} AND HARRIS, C.⁴

¹ Nordic Volcanological Center, Reykjavik, Iceland (*sylvia@hi.is)

²Dept. of Earth Science, CEMPEG, Uppsala University, Sweden

³Laboratory for Isotope Geology, Swedish Museum of Natural History, SE-104 05 Stockholm, Sweden

⁴Dept. of Geological Sciences, University of Cape Town, Rondebosch, South Africa

The Borgarfjörður Eystrí area in NE-Iceland represents the second-most voluminous outcrop of silicic eruptive rocks in Iceland and is a superb locality to unravel bimodal volcanism (c.f. “Bunsen-Daly” compositional gap), which has struck petrologists as abnormal for this tectonic setting for decades. Several explanations have been proposed; closed system fractional crystallisation, partial melting of hydrothermally altered crust, or partial melting of an underlying fragment of old continental or oceanic crust. To contribute to a solution to this issue we focus on zircon to unravel the origin, timing and evolution of voluminous evolved rhyolites in the Neogene silicic volcano complexes in the greater Borgarfjörður Eystrí area. We report zircon U-Pb geochronology and $\delta^{18}\text{O}$ values measured by SIMS, and on whole rock $\delta^{18}\text{O}$ values of felsic and intermediate units from Dyrfjöll and Breiðavík central volcanoes. With this new dataset we are able to decipher timing, primary magmatic processes, as well as contamination and/or post emplacement alteration. Zircon U-Pb ages of key units reveal prolonged silicic activity represented by several rhyolite flows as the systems were gradually building up (from 13.42 ± 0.15 to 12.79 ± 0.15 Ma), followed by explosive caldera forming volcanism in the Breiðavík and Dyrfjöll centres (12.44 ± 0.27 and 12.40 ± 0.19 Ma). The lifetime of these volcanic centres ended abruptly with eruption of a dacite flow at 12.26 ± 0.33 Ma and younger basaltic volcanism. Zircon $\delta^{18}\text{O}$ values range from 1.1 to 4.7 ‰ (n = 179), corresponding to $\delta^{18}\text{O}_{(\text{magma})}$ values of 3.3 to 6.0 ‰. These data imply significant contamination by hydrothermally altered crust. Whole rock $\delta^{18}\text{O}$ values ranging from 2.9 to 18.5, confirm contamination by hydrothermally altered material but also indicate the influence of low-temperature alteration in some samples. We propose a relatively short, though violent, eruptive episode of the Borgarfjörður Eystrí volcanoes, with voluminous and explosive outbursts of felsic volcanics from a low $\delta^{18}\text{O}$ magma source, likely spanning 1 M.yrs. in total duration.

Pyroxenites and the construction of oceanic arc roots

J. BERGER¹, R. CABY² AND J-P. BURG¹

¹Geological Institute, ETH Zurich, 8092 Zurich, Switzerland (julien.berger@erdw.ethz.ch)

²Géosciences Montpellier, Université de Montpellier II, 34095 Montpellier, France

Pyroxenites are a major component of arc roots. They bear important information on the igneous and metamorphic evolution of arcs. In the Jijal and Sapat complexes of the Cretaceous Kohistan oceanic arc (Himalaya, Pakistan), pyroxenites formed by reactive flow of basalts within residual mantle peridotites [1,2]. In the Talkeetna Jurassic arc (Alaska), pyroxenites are high-pressure fractionation products of primitive hydrous basalts [3].

The Neoproterozoic Amalaoulaou oceanic arc root (Gourma belt, West Africa) exposes dykes of spinel and garnet pyroxenites cutting across interlayered garnet granulites and plagioclase pyroxenites [4]. Spinel pyroxenites were crystallized at about 1.0 GPa. Isobaric cooling down to 850-900 °C induced the formation of garnet around spinel. In the vicinity of the pyroxenite dykes, lower crustal gabbros were partially molten leading to the formation of garnet granulites and garnet-clinopyroxene-rutile residues.

Spinel pyroxenites were fractionated from a primitive hydrous basalt (Mg# ~ 60-70). Calculated equilibrium liquids are similar to melt-like hornblende gabbros forming the middle to lower crust of the Amalaoulaou arc. One peculiar orthopyroxene-rich spinel pyroxenite found as a xenolith within the garnet granulites shows high Mg# and Cr content but high incompatible elements contents (LREE, Zr, Nb). It is interpreted as a product of melt-peridotite reaction before the intrusion of the garnet granulite precursor.

The strong planar-linear, high-temperature fabric of spinel pyroxenites in dykes is oblique to layering and metamorphic foliation of garnet granulites. These dykes are representing magma paths where the primitive mantle-derived basalt differentiated en-route by segregation of pyroxene and spinel. The Kohistan and Amalaoulaou complexes do not display a thick sequence of cumulate pyroxenites. Instead, scattered cumulate pyroxenites resulted from fractionation and/or melt-rock reaction in dykes or channels.

[1] Garrido *et al.* (2007) *Geology* **35**, 683-86. [2] Bouilhol *et al.* (2009) *Lithos* **107**, 17-37 [3] Greene *et al.* (2006) *J. Pet.* **47**, 1051-93. [4] Berger *et al.* (2011) *Contrib. Min. Pet.* **162**, 773-96.

Fluoride in groundwaters of regolith and bedrock (0-900 meters depth) in a granitoidic setting, SE Sweden

T. BERGER^{1*}, F. MATHURIN¹, H. DRAKE¹
AND M. ÅSTRÖM¹

¹School of Natural Sciences, Linnaeus University, 39233 SE-Kalmar
(*correspondence: tobias.berger@lnu.se)

Parts of Scandinavia show elevated fluoride in groundwaters which can be linked to the igneous host bedrocks of the Baltic Shield [1]. We investigated fluoride in groundwaters down to 900 meters depth in a small area located in southeastern Sweden. Just north and south of the study area intrusions of fluorine-rich (average 0.43 wt%) 1.45 Ga old granites are situated [2, 3]. Fluoride in private excavated wells are approximately five times higher here compared to Sweden in general [4]. Groundwaters in regolith (boreholes with plastic-casings; 0.3 mm slot screens) and fractures in the bedrock (boreholes with packed-off sections) were monitored for several years and were evaluated with respect to fluoride hydrogeochemistry. In addition, fluorine content in the host rock minerals have been investigated using wavelength dispersive spectrometry.

Fluoride in the regolith groundwaters ranged from below level of detection (LOD, <0.2 mg/L) to 5.1 mg/L (median 1.4 mg/L) and were overall stable over time. In the bedrock groundwaters, concentrations ranged from below LOD to 7.4 mg/L (median 2.7 mg/L). The area closest to the Göttemar granite showed the highest fluoride concentrations in both water types, which suggests presence of F-rich secondary mineral coatings on fracture walls (fluorite is overrepresented here) and F-rich glacial deposits originating from the intrusion of the Göttemar granite as major sources.

This granite and associated greisen contain higher amounts of F-rich fluorite and apatite, than surrounding rocks and in addition, biotite, muscovite and apatite are much more F-rich. Further on, the fluoride concentrations in the bedrock groundwaters increased closer to the surface in waters classified as of meteoric origin [5]. This pattern may indicate a downward transport of fluoride from the regolith into the bedrock fracture system.

[1] Lahermo & Backman (2000) Rep. of Inv. **149**, GTK. [2] Berger *et al.* (2012) Aq. Geochem **18**, 77-94. [3] Kresten & Chyssler (1976) GFF **98**, 155 – 161. [4] Tröjbom & Söderbäck (2006) SKB rep. **R-06-18**, 149. [5] Mathurin *et al.* (2012) Environ. Sci. Technol. **46**(23), 12779-12786.

Carbonate clumped isotope thermometry in the subsurface

KRISTIN D. BERGMANN^{*1}, SAID AL-BALUSHI², J
OHAN P. GROTZINGER¹ AND JOHN M. EILER¹

¹California Institute of Technology, 1200 E California Blvd
Pasadena, CA 91125

(*correspondence: bergmann@caltech.edu)

²Petroleum Development Oman, Muscat, Sultanate of Oman

The carbonate clumped isotope thermometer potentially can be used to reconstruct the temperature and $\delta^{18}\text{O}$ of the ocean in the distant past. However, there is considerable uncertainty regarding how the thermodynamically controlled, temperature dependent abundance of carbonate groups containing both ^{13}C and ^{18}O , is affected during burial. There is evidence that both recrystallization and solid state diffusion within the crystal lattice are important processes. There is likely a time-depth dependence to these processes, though the details of these dependencies are currently poorly constrained. This study explores how the burial and exhumation history modifies the primary distribution of isotopes in host carbonates from the subsurface and surface of Oman. The study includes rocks of Eocene to Neoproterozoic age that sit at current burial depths of 360 m to 5850 m. Additionally, we analyzed exhumed carbonates from the same formations, estimated to have been buried from 1-2 km up to 8-10 km.

Results from this work suggest two dominant modes of diagenesis: 1) Texturally well preserved carbonates measured from the subsurface yield seawater compositions similar to today of around 0‰ with Phanerozoic samples yielding temperatures <40°C and Neoproterozoic samples yielding temperatures <60°C. 2) Highly recrystallized carbonates affected by low-water-to-rock diagenesis sit close to the current geothermal gradient. Samples exhumed from depths >8km yield higher temperatures (120-150°C) and very enriched fluid compositions (~8‰) and also indicate low water-to-rock diagenesis.

From shale oil to shale gas: mineralogical and geochemical evolution of Barnett Shales

S. BERNARD¹, R. WIRTH², A. SCHREIBER²,
H-M. SCHULZ² AND B. HORSFIELD²

¹LMCM, UMR 7202, MNHN and CNRS, Paris, France
(sbernard@mnhn.fr)

²GFZ German Research Centre for Geosciences,
Telegrafenberg 14473 Potsdam, Germany. (wirth@gfz-
potsdam.de, schreiber@gfz-potsdam.de, schulzhm@gfz-
potsdam.de, horsf@gfz-potsdam.de)

Tight oil is a rapidly growing unconventional energy resource that is increasingly viewed as an abundant global commodity. An issue is that tight oil reservoirs are highly heterogeneous. As a result, fluid production assignments and mixing, drainage zone definition and reservoir performance remain poorly constrained. Here, we report the characterization of samples from the organic-rich Mississippian Barnett shale gas system (Fort Worth Basin, Texas, USA) at varying stages of thermal maturation. Using a combination of compositional organic geochemistry and spectromicroscopy techniques, including transmission electron microscopy (TEM) and scanning transmission X-ray microscopy (STXM - 5.3.2.2. ALS STXM Polymer beamline [1] - 10ID-1 CLS SM beamline [2]), we document the mineralogical and geochemical evolution of the investigated samples and evidence the net increase in sample geochemical heterogeneity with increasing maturity [3]. We distinguish kerogen from bitumen in samples of oil window maturity from the estimation of aromaticity and polarity using STXM-based XANES spectroscopy. The formation of nanoporous pyrobitumen has been inferred for samples of gas window maturity, likely resulting from the formation of gaseous hydrocarbons by secondary cracking of precursor bitumens. By providing *in situ* insights into the origin and fate of organic fluids as a response to the thermal evolution of the macromolecular structure of kerogen, the present contribution constitutes an important step towards better constraining reservoiring within unconventional systems.

[1] Kilcoyne *et al.* (2003), *J. Synchrotron radiat* **10**, 125-136,
[2] Kaznatcheev *et al.* (2007), *Nucl. Instr. Meth. Phys. Res. A* **582**, 96-99, [3] Bernard *et al.* (2012), *Int. J. Coal Geol.* **103**, 3-11.

Flux particle size and composition effects on the evolution of sanitary-ware vitreous body

A. BERNASCONI^{1*}, N. MARINONI¹, V. DIELLA², A.
PAVESE^{1,2}, F. FRANCESCONI³ AND K. YOUNG⁴

¹Earth Science Department, University of Milan, via Botticelli
23, Milano, Italy

²National Research Council, IDPA, Section of Milan, via
Botticelli 23, Milano, Italy

³Ideal Standard International, Ceramic Process Technology,
via Cavassico Inferiore 160, Trichiana (BL), Italy

⁴Sibelco, Group Central Laboratory, Moneystone Quarry,
Whiston, Stoke on Trent ST10, 2DZ, United Kingdom

A combination of three industrial flux compositions (sodium feldspar > 67 wt.%, potassium feldspar > 69 wt.% and a 1:1 mix of them) and two particle size distributions (d₅₀ ≈ 45 and 75 μm) have been used to prepare sanitary-ware slips (flux amount about 25 wt.%). Samples have been fired up to 1200 °C, and then characterized in terms of water absorption, density, X-ray diffraction (at ambient and HT conditions) and micro-structure occurrence by Scanning Electron Microscopy.

Despite of the small differences in the samples, some trends have been observed. Water absorption and interconnected porosity (obtained by density measurements) are minimized if sodium feldspar is used, suggesting a better densification, in agreement with [1]. The same effect is achieved by decreasing the flux particle size, which leads to a higher reactivity of the starting slip, in keeping with [2]. The application of RIR-Rietveld method [3] to powder diffraction patterns shows that also differences in phase composition are present: in particular, the highest glass content has been observed if the smallest flux particle size is used, in combination with a sodium bearing feldspar. Moreover, observations from HT-powder diffraction experiments (thermal range 900-1100°C) do not yield significant differences in the feldspar thermal decomposition as a function of flux composition and particle size.

[1] Das & Dana (2003) *Termochimica Acta*, **406**, 199-206. [2] Alves, Melchiades & Boschi (2012) *Journal of European Ceramic Society*, **32**, 2095-2102. [3] Gualtieri (2000) *Journal of Applied Crystallography*, **33**, 267-278.

Microbial extracellular polymeric substances modulate the product of uranium biomineralization

R. BERNIER-LATMANI¹, P.P. SHAO¹, L.R. COMOLLI²,
M. STYLO¹, D.S. ALESSI¹ AND J.R. BARGAR³

¹École Polytechnique Fédérale de Lausanne, CH-1015
Lausanne, Switzerland

(* correspondence: rizlan.bernier-latmani@epfl.ch)

²Lawrence Berkeley National Laboratory, Berkeley, CA
94720, USA

³Stanford Synchrotron Radiation Lightsource, SLAC National
Accelerator Laboratory, Menlo Park, CA 94025, USA

Microbial biomineralization influences the cycling and sequestration of a variety of metals and metalloids in the environment. Uranium biomineralization by *Shewanella oneidensis* MR-1 was shown to produce two distinct U(IV) products under different chemical conditions. Here, we report that the uranium product is modulated by the formation of extracellular polymeric substances (EPS), a biological response that improves cellular resistance to U toxicity. When imaged by cryo-electron microscopy and analyzed by X-ray absorption spectroscopy, the two uranium products have distinct morphologies and atomic environments. This difference is shown to be due to the presence or absence of EPS using a spectro-microscopy method –scanning transmission X-ray microscopy (STXM)– that can differentiate amongst carbon biomolecules and localize U. When EPS is present, U is largely associated with it instead of the cell surface. Furthermore, we show that when the suspected U reductases are removed by mutation, EPS production and cellular viability decrease. Hence, the structure of the product of uranium biomineralization is intricately linked to the formation of EPS. We posit that a single U(IV) product is favored in the subsurface due to the prevalence of biofilms and because EPS are major component of those structures.

Hydromagnesite reactivity in aqueous solutions

U.-N. BERNINGER^{1,2,*}, V. MAVROMATIS¹,
G. JORDAN², J. SCHOTT¹ AND E.H. OELKERS¹

¹GET, CNRS, UMR 5563, Toulouse, France

(* corresponding author, berninger@get.obs-mip.fr)

²Dept. f. Geo- u. Umweltwiss., LMU, München, Germany

Hydromagnesite ($\text{Mg}_5(\text{CO}_3)_4(\text{OH})_2 \cdot 4\text{H}_2\text{O}$) is the most common hydrous Mg-carbonate occurring at Earth's surface environments. It usually forms as a secondary phase in alkaline and Mg-rich natural waters where magnesite (MgCO_3) formation is inhibited by the strong hydration of aqueous Mg [1]. Formation of hydromagnesite is commonly mediated by microbiological activity [2], so that its dissolution and growth may be closely coupled to promoting primary productivity in aquatic environments.

A critical factor defining the role of minerals in natural processes is the link between their dissolution and precipitation rates. In accord with transition state theory, precipitation rates should be readily calculated from corresponding dissolution rates using simple functions of chemical affinity. This possibility has proven to be challenging to validate due to the difficulty in measuring the precipitation rates of most minerals in the laboratory. The relative ease to which hydromagnesite precipitates at ambient conditions makes it ideally suited to assess the link between dissolution and precipitation rates.

Hydromagnesite dissolution and precipitation rates have been measured in closed-system reactors from far to near to equilibrium conditions in $\text{NaHCO}_3/\text{Na}_2\text{CO}_3$ bearing aqueous solutions at pH from 8.5 to 11.2 and temperatures from 25 to 75 °C. Resulting rates (r) have been modeled using:

$$r = k(1 - \Omega^\sigma)^n$$

where k is the surface area normalized rate constant, Ω the saturation degree of hydromagnesite, σ the Temkin's coefficient [3] ($\sigma = 0.2$), and n the reaction order ($n = 1$). Preliminary data interpretation suggests that the rate constants describing dissolution are from one to two orders of magnitude faster than those describing precipitation. For example, at 25 °C and pH 8.5 dissolution and precipitation rate constants were determined to be 3.0×10^{-9} and 5.4×10^{-11} mol/m²/s, respectively. Such differences could be attributable to the changing density of reactive sites on the mineral surface as a function of fluid saturation state.

[1] Lippmann, F. (1973) *Sedimentary Carbonates* Springer (New York). [2] Shirokova *et al.* (2013) *Aquat. Geochem.* **19**, 1-24. [3] Temkin, M. (1963) The kinetics of stationary reactions. *Dokl. Akad. Nauk SSSR*, **152**, 782–785.

Recovering and refurbishing of the SILNUC code, a tool to mitigate and prevent amorphous silica scaling

FERNANDO L. BERRO JIMÉNEZ¹, GIORGIO VIRGILI¹,
ILARIA MINARDI¹ AND LUIGI MARINI²

¹West Systems, www.westsystems.com

(f.berro@westsystems.com; g.virgili@westsystems.com;
i.minardi@westsystems.com)

²Consultant in Applied Geochemistry, I-55049, Viareggio
(LU), Italy (luigimarini@appliedgeochemistry.it)

Modelling the fate of silica in geothermal brines is of utmost importance to prevent and mitigate amorphous silica scaling both in surface installations and in the geothermal reservoir upon reinjection of spent fluids.

In principle, these theoretical predictions can be done using the software code SILNUC which was written by Weres and coworkers over thirty years ago. In practice, as far as we know, only the listing of this software is presently available in their report [1]. Thus, we decided to try to recover and refurbish this code.

SILNUC models the homogeneous nucleation and growth of colloidal particles of amorphous silica. It comprises three major algorithms.

The first one is the molecular deposition or particle growth algorithm. The Runge-Kutta approach is used to compute the particle radii and the dissolved silica concentration, both as a function of time. The second one is the nucleation algorithm, which simulates the generation of classes of colloidal particles. The third one specifies the temperature, pH, and fraction of water lost through steam separation as functions of time. Review of the recent literature is also planned during refurbishing of the SILNUC code.

[1] Weres O., Yee A., Tsao L. (1980) *Kinetics of silica polymerization*. Report LBL-7033, Lawrence Berkeley Laboratory, University of California.

The oxidation states of cerium and europium in silicate melts as a function of oxygen fugacity, composition and temperature

A.J. BERRY^{1,2,3*}, A.D. BURNHAM¹, H.R. HALSE^{1,3,4},
G. CIBIN⁴ AND J.F.W. MOSSELMANS⁴

¹Department of Earth Science and Engineering, Imperial
College London, South Kensington, SW7 2AZ, UK

²Research School of Earth Sciences, Australian National
University, Canberra, ACT, 2601, Australia

(*correspondence: Andrew.Berry@anu.edu.au)

³Department of Earth Sciences, Natural History Museum,
London, SW7 5BD, UK

⁴Diamond Light Source Ltd, Didcot, OX11 0DE, UK

Ce and Eu are the only rare earth elements (REE) to occur in oxidation states other than REE³⁺ under terrestrial magmatic conditions. The stability of Ce⁴⁺ and Eu²⁺ results in anomalous, chondrite normalised, abundances of these elements relative to the other REE due to the effect of oxidation state on trace element partitioning [1]. The link between oxidation state and oxygen fugacity (fO_2) means that fO_2 may be determined if Ce⁴⁺/Ce³⁺ or Eu²⁺/Eu³⁺ can be evaluated directly or inferred from the magnitude of an anomaly.

Ce and Eu L_{III}-edge XANES spectra were used to determine Ce⁴⁺/Ce³⁺ and Eu²⁺/Eu³⁺ in melts *in situ* [2], and quenched to glasses, as a function of fO_2 (from -14 to +6 log units relative to the quartz-fayalite-magnetite, QFM, buffer), composition (MORB plus ten Fe-free systems), temperature (1200-1500 °C) and pressure (1 atm and 1 GPa). Ce⁴⁺/Ce³⁺ and Eu²⁺/Eu³⁺ vary systematically with the thermodynamically predicted dependence on fO_2 . For both elements higher oxidation states are favoured by less polymerised compositions (large values of optical basicity and NBO/T) and lower temperatures. Pressure appears to have a negligible effect. A general expression for Eu²⁺/Eu³⁺ in geological melts has been derived. An fO_2 window, beginning near QFM, exists where both Ce⁴⁺ and Eu²⁺ are stable. Coexisting Ce and Eu anomalies in minerals such as zircon are thus not necessarily related to plagioclase fractionation. In Fe-bearing compositions, neither Ce⁴⁺/Ce³⁺ nor Eu²⁺/Eu³⁺ are preserved on quenching from a melt to a glass due to electron exchange reactions between Ce⁴⁺ and Fe²⁺ and Eu²⁺ and Fe³⁺. This limits oxybarometry to estimates of Ce⁴⁺/Ce³⁺ and Eu²⁺/Eu³⁺ determined from partitioning derived anomalies.

[1] Burnham & Berry (2012) *GCA* **95**, 196-212. [2] Berry *et al.* (2003) *J. Synch. Rad.* **10**, 332-336.

Experimental investigation of K incorporation into tourmaline at high temperature and pressure

ELEANOR J. BERRYMAN^{1*}, BERND WUNDER²
AND GERHARD FRANZ¹

¹Technische Universität Berlin, Ackerstr. 75, 13355 Berlin, Germany

(*correspondence: eleanor.berryman@mailbox.tu-berlin.de)

²GFZ German Research Centre for Geosciences, Telegrafenberg, 14473 Potsdam, Germany

Tourmaline's extensive stability in pressure-temperature space and ability to incorporate a multitude of elements in its structure have motivated investigation into its potential as a recorder of its formation conditions, especially in terms of temperature and composition [1]. However, the discovery of microdiamond-bearing K-dominant dravitic tourmaline, with up to 0.576 apfu K (2.76 wt.% K₂O), in the Kokchetav Massif, Kazakhstan, [2] has increased interest in the relationship between formation pressure and tourmaline's composition, particularly with respect to the incorporation of K. Indeed, a comparison of tourmaline's composition with its inclusion mineralogy has revealed a correlation between K incorporation and increasing pressure [3]. However, whether or not the presence of microdiamond inclusions is sufficient evidence for high pressure formation of K-dominant tourmaline has been questioned [4].

A series of piston-cylinder and hydrothermal synthesis experiments was conducted to begin addressing the absence of experimental data on K-bearing tourmaline and to investigate the effect of pressure and fluid composition on the Na/K ratio of hydrothermal dravitic tourmaline (NaMg₃Al₆Si₆O₁₈(BO₃)₃(OH)₃OH). Approximate unit cell dimensions were determined by Rietveld refinement of X-ray diffraction patterns and chemical formulae were calculated from electron microprobe analyses. To date, the highest pressure and temperature conditions investigated (40 kbar, 700°C) have yielded dravitic tourmaline with up to 0.7 apfu K when exposed to a pure KCl fluid. This is the first time Na-absent "potassium dravite" has been synthesized experimentally.

[1] van Hinsberg *et al.* (2011) *The Canadian Mineralogist* **49**, 1-16. [2] Shimizu & Ogasawara (2005) *ÖMG* **150**, 141. [3] Shimizu & Ogasawara (2013) *Journal of Asian Earth Sciences* **63**, 39-55. [4] Marschall *et al.* (2009) *Journal of the Geological Society, London* **166**, 811-823.

Deconstructing the dissimilatory sulfate reduction pathway: Isotope fractionation of a mutant unable to grow on sulfate

EMMA BERTRAN¹, WILLAM D. LEAVITT²,
ANDRÉ PELLERIN¹, GRANT M. ZANE³, JUDY D. WALL³,
DAVID T. JOHNSTON² AND BOSWELL A. WING¹⁴

¹Department of Earth and Planetary Sciences and GEOTOP, McGill University;
emma.bertran@mail.mcgill.ca

²Department of Earth and Planetary Sciences, Harvard University

³Department of Biochemistry, University of Missouri

⁴Department of Environmental Sciences, Weizman Institute of Science

Dissimilatory sulfate reduction plays a significant role in shaping the sulfur isotope composition of sedimentary sulfides, which are, in turn, a record of Earth's surface redox history. The fractionation produced by this microbial metabolism is controlled by the flux of sulfur through the respiratory reaction network and the isotopic effect associated with each reaction. Although the net isotope fractionations of this metabolism have been well studied, unravelling the isotopic influence of each component of its pathway is still a challenge. The sulfite to sulfide reduction step is a particularly complicated one. Its full biochemistry is not fully understood and the associated isotope effect is inferred from fractionations associated with the entire metabolic pathway. Here, we investigated a mutant strain of *Desulfovibrio vulgaris* Hildenborough in batch and continuous culture to address these issues. This deletion mutant is missing its QmoABC complex, a principal enzyme in the reduction of adenosine phosphosulfate (APS) to sulfite. Thus, this strain is incapable of using sulfate as a terminal electron acceptor. By hindering APS reduction, this mutation also eliminates sulfite disproportionation. In all experiments, lactate and sulfite consumption are concomitant with sulfide and thiosulfate production. Rates of thiosulfate production were one order of magnitude larger in batch than continuous culture experiments. Results from batch culture show a δ³⁴S between sulfite and sulfide of ≈ -9 ‰. The two components of the thiosulfate pool (sulfonate and sulfane moieties) present a large ³⁴S/³²S fractionation, with sulfonate more ³⁴S enriched than sulfane by 30 ‰. However, the net fractionation between thiosulfate and sulfite is ≈ +1 ‰. This is inconsistent with isotopic observations of abiotic thiosulfate formation. Steady-state models are presented to understand the mechanism of fractionation during sulfite reduction and incorporate this step into the overall metabolism of sulfate reduction.

***In-Situ* Monitoring Of Water-Rock Interaction By Micro FT-IR- An Example Of Calcium Silicate Hydrate Formation-**

HIROKI BESSHO^{1*}, SATORU NAKASHIMA¹,
MAI HAMAMOTO¹, NAOKI NISHIYAMA¹,
RYOTA TONOUE¹, YUSUKE KIRINO¹,
TADASHI YOKOYAMA¹ AND HIROSHI SASAMOTO²

¹Department of Earth and Space Science, Graduate School of Science, Osaka University, Toyonaka 560-0043, Japan
(*Corresponding author: hbessho@ess.sci.osaka-u.ac.jp)

²Japan Atomic Energy Agency. Tokai 319-1194, Japan

In the geological disposal of high level radioactive wastes, cementitious grout materials are planned to be used and Calcium Silicate Hydrates (C-S-Hs) are supposed to be formed by water-rock interactions. The current study presents a new methodology of monitoring the C-S-H formation *in situ* by micro Fourier transform infrared (FT-IR) spectroscopy.

An *in situ* hydrothermal cell was constructed from titanium alloy with a diamond window to allow the transmission of an IR beam (Fig.1). In this study, thin sections of quartz were placed in the cell, with the remaining space filled with saturated Ca(OH)₂ solution. The *in situ* hydrothermal cell was then sealed and heated at 140 °C at a pressure of 3 MPa. IR spectra were collected every 5 minutes for 24 hours using an IR microspectrometer.

Fig.1

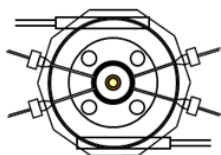


Fig.2

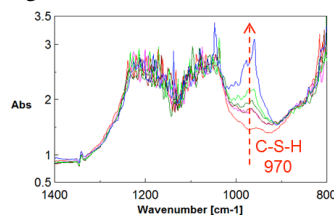


Fig.1 The schematic figure of the *in situ* hydrothermal cell
Fig.2 Infrared spectral changes with time for 5 hours at 140 °C. The absorption band around 970 cm⁻¹ (C-S-H) increased with time.

An IR absorption band around 970 cm⁻¹ due to stretching vibration of Si-OH increased with time indicating the increasing formation of C-S-H (Fig.2). The temporal changes with 5 minute intervals of the peak heights in the first 240 minutes can be used to determine apparent formation rate constants of the C-S-H. Based on these experimentally determined kinetic parameters, mechanisms and rates of the C-S-H formation processes can be discussed.

Water in Na montmorillonite - A neutron scattering study

M. BESTEL^{14*}, F. JURANYI¹, T. GIMMI²⁴,
M. A. GLAUS², L. R. VAN LOON², M. ZAMPONI³
AND L. W. DIAMOND⁴

¹Laboratory for Neutron Scattering, Paul Scherrer Institut, 5232 Villigen PSI, Switzerland

(*correspondance: martina.bestel@psi.ch)

²Laboratory for Waste Management, Paul Scherrer Institut, 5232 Villigen PSI, Switzerland

³Forschungszentrum Jülich, Centre for Neutron Science at FRM II, 85747 Garching, Germany

⁴Institute of Geological Sciences, University of Bern, 3012 Bern, Switzerland

Swelling clays, like Na montmorillonite, are important sealing materials for radioactive waste repositories. The negative charge of crystalline layers is compensated by cations surrounded by water in interlayers. At low hydration, all water is located in interlayers in up to 2 molecular water layers; at higher hydration, interparticle pores between clay particles also contain water.

To model and understand transport properties, e.g. water diffusion, it is important to know the water distribution at different hydrations and densities. Relative fractions of water in the two pore environments were measured directly and for the first time using Fixed Window scans on a neutron backscattering spectrometer. The decisive parameter was found to be the water content (total water / dry clay). In the range from 0 to 0.7 g/g the obtained water amount in the interparticle pores increases monotonically, but not linearly from 0 to 64%. These results were compared with values obtained based on surface area measurements.

They were also used to derive local diffusion coefficients from quasielastic neutron scattering. In the literature local diffusion coefficients can be found only for low hydrations (1 or 2 water layer) because of the difficulties in interpretation of the spectra when more than one water population exists. Here, from our combination of methods (quasielastic neutron scattering and fixed window scans) we can present local diffusion coefficients for up to 4 water layer in the interlayers.

Carbon flow from volcanic CO₂ into soil microbial communities of a wetland mofette

F. BEULIG^{*1}, D. M. AKOB², B. VIEHWEGER³,
M. ELVERT³, V. HEUER³, K.-U. HINRICHS³
AND K. KÜSEL¹

¹ Friedrich Schiller University Jena, 07743 Jena, Germany

(*Correspondence: felix.beulig@uni-jena.de)

² U.S. Geological Survey, 430 Reston, Virginia

³ University of Bremen, 28359 Bremen, Germany

We investigated mofettes, i.e., cold Volcanic CO₂ exhausts, in a wetland area in the NW Czech Republic. Here, continuous emanations of CO₂ lead to lower pH and anoxic conditions. Recent findings suggest that such alteration might cause a shift of the microbial community towards anaerobic and acidophilic organisms.

In this study we i) analyzed differences in the active archaeal and bacterial community structure in different depths of a mofette compared to the surrounding wetland soil by 16S rRNA pyrosequencing and ii) used DNA- and lipid-based ¹³C-CO₂ Stable Isotope Probing (SIP) to identify microbial communities which can incorporate the emanating CO₂.

16S rRNA pyrosequencing revealed that the overall active bacterial community composition was similar for the mofette and reference soil in all sampled depths. However, in the mofette soil *Acidobacteria* showed a higher relative contribution (55% to 70%) compared to the wetland reference (17% to 22%) primarily consisting of sequences closely related to *Cand. Koribacter* sp. and isolate „Ellin 624“ of Subdivision 1. The active archaeal community of the mofette soil was dominated by methanogens in all depths which were not represented in the wetland reference soil.

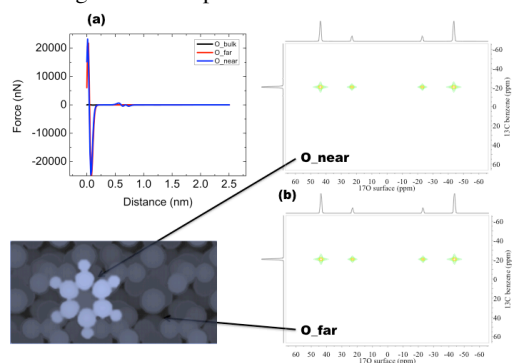
Analysis of incorporation of ¹³C-labeled CO₂ into PLFAs and ether-lipid derived hydrocarbons in the mofette soil showed continuous enrichment over 28 days in almost all bacterial and archaeal biomarkers. Archaeal CO₂ utilization was restricted to the first 10 cm of the soil, while a depth-independent labeling pattern was found for bacterial biomarkers. Archaeal 16S rRNA and formyl tetrahydrofolate synthetase (*fts*) gene labeling analysis of the first 10 cm suggested that ¹³CO₂ was potentially utilized chemolithoautotrophically by two novel groups of acetogens and methanogens, with the latter primarily being affiliated with the family *Methanoregulaceae*. On the other hand, bacterial 16S rRNA gene labeling analysis indicated a non-obligate autotrophic utilization of ¹³CO₂ by bacterial families of the *Anaerolineaceae*, unclassified *Bacteroidetes* and *Syntrophaceae*.

Characterization of hydrocarbon and functionalized silica nanoparticle adsorption on mineral surfaces through advanced First Principles techniques

ROCHELE C.A. BEVILAQUA¹, V. A. RIGO¹
AND CAETANO R. MIRANDA^{1*}

¹ Universidade Federal do ABC – UFABC - Santo André-SP – Brazil – caetano.miranda@ufabc.edu.br

Atomistic simulations have come to play an increasingly important role in advancing understanding of the fundamental properties related to the hydrocarbon and nanoparticles interaction with mineral surfaces. In this work, we will present an integrated methodology based on First Principles methods to characterize the surface properties (structural, energetic and electronic) and the adsorption of hydrocarbons and functionalized (hydroxylated, sulphonic acid and pegylated) SiO₂ nanoparticles within mineral surfaces (Carbonate and Silicates). The simulations were based on the Density Functional Theory (DFT) with solid state Nuclear Magnetic Resonance calculations (1) and simulation of noncontact Atomic Force Microscopy (nc-AFM) (2) including van der Waals corrections (3). It was possible to assign the peaks in the NMR spectra for all structures studied and determine the force distance models based on simulated AFM. Our results show a chemical shift differentiation for atoms located on different sites (bulk and surface) for calcite and silicate systems as well as the differences on force versus distance curves. Interestingly, the presence of hydrocarbon molecules also modifies the chemical shift of adsorbed the Ca and Si sites with respect to the pristine and isolated surfaces. Calculated AFM forces allow us the differentiation between the different chemical sites and a clear understanding of the adsorption processes. Within the combining theoretical AFM and NMR simulations with DFT with van de Waals, it should be possible to elucidate the coordination environment of chemical species in many important complex materials in the context of geochemical phenomena.



AFM forces(a) and (b) 2D ¹⁷O-¹³C spectra for benzene adsorbed on CaCO₃ surface

- [1] Pickard, C. J. and Mauri, F. PRB **63**, 245101 (2001). [2] T.-L.Chan *et al.*, PRL **102**, 176101 (2009). [3] V. A. Rigo, C. O. Metin, Q. P. Nguyen, and C. R. Miranda, J. Phys. Chem. C, **116**, 24538 (2012).

Strata-specific bacterial diversity in aquifers of the Thuringian Basin/Germany

A. BEYER^{1,2*}, K. BUROW¹, E. KOTHE¹
AND G. BÜCHEL²

¹Institute of Microbiology – Microbial Communication,
Friedrich Schiller Univ., Jena, D 07743, Germany
(*correspondence: andrea.beyer@uni-jena.de,

²Institute of Applied Geology, Friedrich Schiller Univ., Jena,
D 07743, Germany

The INFLUINS (Integrated fluid dynamics in sedimentary basins) project investigates coupled dynamics of near surface and deep flow patterns of fluids, transported materials and component substances in the Thuringian Basin. The extensive basin landscape is located in eastern Germany and belongs to the Triassic period of Bunter sandstone (Buntsandstein), shell limestone (Muschelkalk) and Keuper, which crop out at the surface. Older sediments and Permian (Zechstein) can be found at the edges of the basin.

With microbial investigations, we are analyzing the bacterial diversity of groundwater at different locations to see whether there are special patterns in bacterial distributions originating from the different rock strata. Furthermore, we are interested in the bacterial diversity of drilling cores and salt formations from the same locations. This will facilitate understanding fluid movement in the Thuringian Basin. We determined bacterial community from water samples out of nine natural springs and sixteen groundwater wells by cultivation and subsequent morphological, physiological and molecular identification.

First results show that the largest proportions were found to be members of Bacilli and γ - proteobacteria, including the genera *Pseudomonas*, *Marinomonas*, *Bacillus*, *Marinobacter* and *Pseudoalteromonas*.

Next steps will be a comparison of cultivation-dependent and cultivation-independent methods to gain further information on bacterial strains which were uncultivable or suppressed by other bacteria strains.

Experimental Calibration of a Garnet-Clinopyroxene Geobarometer for Mantle Eclogites

BEYER, C^{1*} AND FROST, DJ¹

¹Bayerisches Geoinstitut, University of Bayreuth, 95440
Bayreuth, Germany
(*christopher.beyer@uni-bayreuth.de)

We present a geobarometer applicable to eclogitic mantle xenoliths based on the exchange reaction involving the incorporation of Al in 4-fold coordination present as Ca-Tschermak in omphacitic clinopyroxene coexisting with garnet solid solutions. The barometer is calibrated with piston cylinder and multi-anvil experiments between pressures of 3 to 7 GPa and temperatures from 1200 to 1542 °C. Starting materials are synthetic mixtures of varying basalt compositions (hydrous N-MORB), yielding a homogeneous biminerally garnet-clinopyroxene phase assemblage. We expand our own data set by implementing additional experimental studies conducted in eclogitic systems granting the applicability to a wider range of eclogitic compositions. All experiments are buffered in terms of Al with garnet as the Al-bearing phase. Our calibration reproduces the experimental pressures with 0.4 GPa within the 95% confidence interval. The barometer was then tested with natural eclogites from various mantle xenolith locations covering a wide P-T-X regime. The herein presented barometer opens up the possibility to determine pressures of formation for biminerally eclogite xenoliths without requiring additional accessory phases. With this barometer we provide an additional tool to investigate the P-T state of upper mantle heterogeneities.

Organic carbon export in Taiwan: insights from marine sediments

OLIVIER BEYSSAC¹, VALIER GALY²
AND CHIH-CHIEH SU³

¹ CNRS, IMPMC Paris, France.

Olivier.Beyssac@impmc.upmc.fr

² Woods Hole, USA. vgaly@whoi.edu

³ National Taiwan University, Taiwan.

Terrestrial organic C (OC) delivered to the ocean by rivers is a mix of recent OC and fossil OC derived from erosion of rocks. Burial of fossil OC in marine sediments is a simple recycling of reduced carbon and has no effect on atmospheric CO₂ and O₂ levels. Conversely, its oxidation consumes atmospheric O₂ and returns CO₂ to the atmosphere. In large-scale erosion systems (Himalaya), only graphite resists to oxidation during river transport and/or transient storage in floodplains. In contrast, disordered fossil OC observed in mountainous bedrocks and mountain rivers disappear during transport in large rivers, and are not observed in marine sediments [1]. In addition, such large scale systems may act like a CO₂ pump as a huge amount of modern OC is delivered and buried in the Bengal Fan marine sediments [2].

Here, we investigate the isotopic composition (¹⁴C, ¹³C), organic geochemistry and structure (Raman spectroscopy) of OC in recent turbidite deposits all around Taiwan. We show that the bulk OC is primarily composed by terrestrial modern and fossil OC, but also includes marine OC. We discuss the geochemistry of OC in marine sediments with respect to the modern and fossil OC sources on the Taiwan island. We quantify the respective contributions of these three end-members to the total OC, and discuss the sediments provenance based on the structure and geochemistry of fossil OC. Comparison of the OC in marine sediments with data existing for Taiwanese rivers [3] allows for discussing the carbon budget of erosion. In particular, unlike large-scale systems, fossil OC is massively transferred to marine sediments during erosion in Taiwan. Globally, such small-scale systems with very active erosion and short transfer to the ocean may act as an important sink for OC in the long-term carbon cycle.

[1] Galy V. *et al.* (2007) *Nature* **450**, 407-410. [2] Galy V. (2008) *Science* **322** 943-945. [3] Hilton R.G. *et al.* (2010) *GCA* **74** 3164-3181.

Assimilation of sediments embedded in the oceanic arc crust: myth or reality?

R. BEZARD^{1,2*}, J.P. DAVIDSON¹, S. TURNER²,
C.G. MACPHERSON¹, J.M. LINDSAY³ AND A.J. BOYCE⁴

¹Durham University, UK.

²CCFS/GEMOC, Macquarie University, AUS.

³School of Environment, The University of Auckland, NZ.

⁴ Scottish Universities Environment Research Center, UK.

*rachel.bezard@mq.edu.au

Volcanic products from oceanic arcs afford a unique opportunity to study the subduction factory. Although most of these products are not primitive, the impact of assimilation of the arc crust is often ignored with the consequence that trace element and isotopic compositions are commonly attributed only to varying contributions from different source components. This jeopardises the integrity of recycling mass balance calculations. Here we use Sr and O isotope mineral data from a suite of volcanic rocks from the Lesser Antilles arc to show that assimilation can be significant in oceanic arc basement. Analysis of ⁸⁷Sr/⁸⁶Sr in single plagioclase phenocrysts from the Soufrière Volcanic Complex (St Lucia) reveal isotopic heterogeneity within and among hand samples ranging from 0.7083 to 0.7094. δ¹⁸O measurements show extreme variation beyond the mantle range: up to +10.9‰ for plagioclase, +11.8‰ for quartz, +9.8‰ for amphibole and +9.5‰ for pyroxene. Such ⁸⁷Sr/⁸⁶Sr isotope disequilibrium and extreme δ¹⁸O values strongly argue for assimilation of material located within the arc crust. A positive correlation between mineral δ¹⁸O and the whole rock radiogenic isotopes shows that assimilation seems to be responsible for the isotopic heterogeneity observed in St Lucia but also in the whole Lesser Antilles since St Lucia covers almost the whole-arc range of isotopic composition. This highlights the need for detailed mineral-scale investigation of oceanic arcs suites to quantify differentiation that could lead to misinterpretation of source composition and subduction processes.

Constraining the Thermal History of an Ultra-hot Orogen from Metamorphic Reaction History and Garnet-Orthopyroxene Diffusion Modelling Studies

S.K.BHOWMIK^{1*} AND S. CHAKRABORTY²

¹Department of Geology & Geophysics, Indian Institute of Technology, Kharagpur 721 302, India

(*correspondence: santanu@gg.iitkgp.ernet.in)

²Institut fuer Geologie, Mineralogie und Geophysik Ruhr-Universitaet Bochum, D-44780, Germany (Sumit.Chakraborty@rub.de)

The southern margin of the Central Indian Tectonic Zone experienced a history of metamorphism at different sets of conditions during the Proterozoic. A primary, high temperature assemblage of aluminous orthopyroxene ($X_{Mg} = 0.585$) + calcic plagioclase (An_{49-52}) + magnesian ilmenite ($X_{MgTiO_3} = 0.06-0.07$) experienced three recrystallization events (M_1 with a T_{Max} of ~ 1000 °C at 9.5 kbar and M_2 at 900°C, 6.7 kbar and M_3 at 770°C, 7.5 kbar) to produce two generations of garnet, orthopyroxene and biotite. We have integrated observations on metamorphic reaction textures, mineral compositional zonation, calculated pseudosections, available geochronological data, and diffusion modelling of compositional profiles in garnet and orthopyroxene to constrain the timescale of thermal evolution for this complex sequence. We find that at least a three stage thermal history is necessary to account for all observations consistently. Cooling rates on the order of 10^3 °C/ my indicate that high temperatures of M_{1-3} metamorphism were sustained for tens of million years, providing evidence of a long lasting (i.e. > 60 my) regional metamorphic event.

The origins of detrital clays on the East China Sea shelf

L. BI¹, S. Y. YANG^{1*}, C. LI¹, Q. WANG¹ AND J.T. LIU²

¹State Key Lab. of Marine Geology, Tongji Uni., Shanghai 200092, China

(*correspondence: syyang@tongji.edu.cn)

²Institute of Marine Geology and Chemistry, National Sun Yat-sen University, Kaohsiung, Taiwan 80424

There are two kinds of sediment source-to-sink (S2S) systems on the East China Sea shelf. One is “large river/delta – wide shelf – huge input – slower sediment transfer – strong anthropogenic impact” represented by the Changjiang (Yangtze) River; another is “mountainous river – narrow shelf – huge input – rapid sediment transfer – extreme climate event” represented by the rivers in Taiwan Island. To study the contributions of these two S2S systems to clayey sediments accumulated on the shelf, a total of 66 clay samples were selected from the shelf, the Changjiang and mountainous rivers entering the East China Sea. A multivariate analysis technique (EOF) was used to process elemental geochemical data.

The covariance between elements explained by the first two eigenmodes is about 76%. The first mode can explain about 62% of the data variability, in which elements are divided into two groups according to the sign of their eigenvectors. One group is dominated by Ca, Fe, Mg, Mn, P, Co and another by Al, Si, K, Na, Ti and REE. We interpret Mode 1 to be different clay mineral assemblages in the source areas. The second mode can explain about 14% of the data variability. One group consists of K, Na, Rb and LREE while the other elements belong to another group. Mode 2 probably indicates the proportion of non-clay minerals in the clay sediments. Based on the corresponding eigenweights of each sample, the spatial distribution patterns of the clays were revealed. The clay from the Changjiang River was primarily transported southeastward and formed an inner shelf mud belt that mixes with the Taiwan-derived clays in northern Taiwan Strait. Some clay from the Changjiang River may disperse eastward and mix with the clay sourced from the old Yellow River delta in the southwestern Yellow Sea. The oceanic circulation in the East China Sea predominately controls the dispersal and deposition of detrital clays on the shelf.

Acknowledgements: This work was supported by NSFC research fund (Grant No: 41076018, 41225020).

Enhanced stability and inhibited dissolution of uraninite by nanoparticulate iron sulfide under oxic conditions

YUQIANG BI AND KIM HAYES*

University of Michigan, Ann Arbor, Michigan 48109, USA
(*correspondence: ford@umich.edu)

Redox transition of uranium from dissolved U(VI) species to insoluble U(IV) precipitates can result in successful sequestration of uranium in contaminated soils and sediments. Recent studies have shown that naturally-occurring mackinawite (FeS) can provide an electron source for U(VI) reduction and retard uraninite reoxidation upon oxygen intrusion [1]. However, few studies have provided mechanistic and kinetic information on the interactions of uraninite with FeS solid under oxic conditions. The present study investigated the mechanism(s) and reaction kinetics of inhibited U(IV) reoxidation and transport by nanoparticulate FeS. The oxidative dissolution of uraninite by dissolved oxygen (DO) in FeS-bearing groundwater were conducted using batch and flow-through reactors as a function of pH, FeS content, DO and calcium concentrations, to assess the impact of critical geochemical factors on UO₂ dissolution kinetics. The results indicated that the dissolution rate of UO₂ decreased by an order of magnitude when FeS was present relative to control. The rate decreased rapidly with decreasing DO levels and increasing FeS content. In the presence of Ca²⁺, the rate was even lowered owing to the formation of Ca-containing passivation layer on uraninite surfaces. Until the depletion of FeS, DO concentration remained at significantly low levels, suggesting FeS was an effective oxygen scavenger. During the inhibition period, dissolved Fe(II), Fe(III) hydroxides, and elemental sulfur were produced from FeS oxidation. In contrast, uraninite remained as U(IV) solid as verified by X-ray absorption spectroscopy (XAS) and X-ray photoelectron spectroscopy (XPS). Although dissolved Fe(II) was not shown to reduce U(VI) under oxic conditions, residue FeS particles was responsible for inhibiting UO₂ dissolution by reducing soluble U(VI). This study suggests that naturally-occurring FeS may serve as an oxygen scavenger and a U(VI) reductant for effective uranium sequestration. These findings have direct implications for our understanding of uranium redox transition and long-term stability in the subsurface.

[1] Bargar *et al.* (2013), *PNAS*

The Mesozoic dolomites of the Levant margin - evaluating dolomitization style and mechanism from configuration and stable isotope geochemistry

O.M. BIALIK^{1*}, I. HALEVY¹ AND J.A. HIGGINS²

¹Weizmann Institute of Science, Rehovot 76100, Israel
or.bialik@weizmann.ac.il (*correspondence)
²Princeton University, Princeton, NJ 08544, USA.

The record of the Levantine margin provides a unique window into dolomitization through the Mesozoic [1] and dolomitization in general. Ample carbonate sediments have accumulated through the Triassic, Jurassic and Cretaceous in this region, maintained at relatively shallow burial depth [2], and currently exposed at the surface. We examined the depositional configuration, and the geochemical and stable isotope compositions across several limestone-dolostone transitions, with the intention of inferring the paleoenvironmental trends leading to these transitions and the style of dolomitization in these rocks.

Sequences were selected based on the presence of repeated interchanges between limestone and dolostone, in settings where the occurrence of the dolomite is likely to be derived from early diagenetic processes and interaction with marine or evaporated marine water. Three different settings were targeted: *i*) sub-tidal, open marine, evaporite-free (Cretaceous), *ii*) intertidal, open marine, evaporite-free (Jurassic), and *iii*) restricted lagoon, in association with sulphate evaporites (Triassic). In each case, a cross-section was sampled at a spatial resolution of about 50 cm to evaluate lithological changes and variability in stable isotope ratios. Following the identification of transitions of interest, these were sampled at a spatial resolution of 1-3 cm.

Mineralogy and Ca to Mg ratios in the carbonates were determined by X-ray diffractometry, and the isotopic ratios of carbon and oxygen ($\delta^{13}\text{C}$ and $\delta^{18}\text{O}$) were measured by mass spectrometry. Sedimentary textures were investigated in hand samples and in some cases by petrographic microscopy. The results of these analyses will be presented and their implications for mechanisms of dolomite genesis discussed. Future work will include analysis of Ca and Mg isotope ratios in the samples to further illuminate dolomitization mechanisms.

[1] Sass & Katz (1982) *American J. Sci.* **282**. 1184-1213. [2] Gvirtzman (2003) *Isr. J. Earth Sci.* **53**. 47-61.

Links between diel vertical migrations and ocean oxygen

D. BIANCHI, E.D. GALBRAITH, K.A.S. MISLAN,
C. STOCK, J.L. SARMIENTO AND D. CAROZZA

Diel vertical migration of zooplankton and micronekton - the largest migration on Earth, is a major but poorly quantified component of the ocean's biological pump. The impact of this migration on oceanic oxygen has received relatively little attention, partly due to the lack of a predictive framework. By using a global synthesis of acoustic data we show that diel vertical migrations are characterized by coherent large-scale patterns, which are strongly correlated with the distribution of subsurface oxygen. Open ocean oxygen minima, when present, emerge as potential refuges for vertical migrators. Including a representation of the respiratory needs of migrating populations in a three-dimensional ocean model suggests that, by focusing respiration in poorly-ventilated regions of the upper ocean, diel vertical migrations intensify oxygen depletion at the upper margin of oxygen minimum zones. This coupling between migrating animals and marine oxygen may have important implications for fisheries and oxygen minimum zone chemistry in a changing ocean.

The river Po: geochemical fluxes and related insights on weathering processes and erosion rates

BIANCHINI G.¹, MARCHINA C.^{1*}, KNOELLER K.²
AND PENNISI M.³

¹ Dip. Fisica e Scienze della Terra, Università di Ferrara, Italy
(corrispondece: *mrcchr@unife.it)

² Dep. Catchment Hydrology, Helmholtz Centre for
Environmental Research – UFZ, Halle, Germany

³Istituto di Geoscienze e Georisorse, CNR, Pisa, Italy

The Alps and the Apennines both convey water and sediments to the Po river that is the most important fluvial system of the Italian Peninsula, characterized by a length of 650 Km, an hydrological basin of 74000 km² and an average discharge of 47 Km³/yr. Major and trace elements, stable isotope composition of water and radiogenic strontium isotopes were used to characterize the sources and fluxes of solutes. Compared with the local meteoric isotopic signature, stable isotopes ($\delta^{18}\text{O}$ between -10.8 and -9.2; δD between -70.0 and -65.4) reveal that most of the recharge occurs in the north-western part of the basin, i.e. conveyed mainly from the highlands. Although subordinate, carbonatic lithologies are preferentially involved in the weathering processes inducing the typical Ca-HCO₃ hydrochemical facies and a specific strontium isotopic signature ($^{87}\text{Sr}/^{86}\text{Sr}$ 0.7090-0.7092) that is intermediate between that of Mesozoic carbonates (0.707-0.708) and felsic igneous and metamorphic rocks (> 0.701). The data also provide insights on the erosion and denudation rates of the orogens bordering the basin. The observed TDS (average and median of 39 measurements are 268 and 292 mg/l, respectively) suggest that a solute flux in the order of $13 \cdot 10^6$ t/yr is transferred from the Po River toward the Adriatic Sea. A total erosion of $68 \cdot 10^6$ t/yr is estimated within the Po River drainage basin, assuming that solute represent a fraction (of ca 20%) of the weathering products. This estimation conforms to other recent investigations [1].

[1] Hinderer *et al*, 2013. *Earth Science Review* **118**, 11-44.

CO₂ Dissolution rates during CO₂ injection: a consequence and measure of reservoir heterogeneities

M.J. BICKLE^{1*}, K. DANIELS¹, J. NEUFELD¹,
N. KAMPMAN¹, A. GALY¹, H.J. CHAPMAN¹, Z. ZHOU², B.
DUBACQ¹, M. WIGLEY¹, O. WARR²
AND C.J. BALLENTINE²

¹ Dept. Earth Sciences, University of Cambridge, Downing
St., Cambridge CB2 3EQ, UK (correspondence:
mb72@esc.cam.ac.uk)

² School of Earth, Atmosphere and Environmental Sciences,
University of Manchester, M13 9PL, UK

CO₂ dissolution during and after injection into geological storage sites is potentially an important mechanism for stabilising and securing the storage but may lead to enhanced fluid-mineral reactions with both positive and negative consequences for the security of storage. Important questions are how does reservoir heterogeneity influence CO₂ dissolution rates and does the tendency of the low-viscosity CO₂ to finger during injection increase dissolution rates? Here we evaluate the rates of possible CO₂ dissolution in an injection setting by simple pseudo-1D flow modelling with diffusion in the orthogonal direction and compare this with numerical modelling of flow and diffusion in 2D. The results show that the magnitude of CO₂ dissolved is strongly controlled by the rapid flow of brines determined by reservoir heterogeneities. The consequences for fluid-mineral reactions are that these may be strongly localised and this could have important implications for feedbacks between flow and permeability changes in reservoirs.

The results are tested against an injection experiment which utilised CO₂ injection for enhanced oil recovery (EOR) in which we monitored sampled fluid chemistries for 6 months after initiation of CO₂ injection into a five-spot pattern. Interpreting the results required 1) identifying the various water masses present in the reservoir as a consequence of a long history of water injection and then 2) modelling changes in fluid chemistry in terms of CO₂ injection and fluid mineral reactions. The results show a surprisingly rapid increase of dissolved CO₂ in the extracted brines and that this rise was accompanied by initial rapid dissolution of carbonate minerals but longer term dissolution of silicate minerals. The rates of carbonate dissolution are sufficient to cause small increases in formation porosities but these would cause significant increases in the permeability of sandstones which exhibit power law permeability-porosity relations with an exponent of ~9.

Fluid geochemistry of the deep CO₂-rich Caprese Reservoir (Northern Apennines, Italy)

G. BIOCCHI¹, F. TASSI^{1,2}, M. BONINI²,
F. CAPECCHIACCI², G. RUGGIERI², G. CHIODINI³,
A. BUCCIANTI¹ AND O. VASELLI^{1,2}

¹Dipartimento di Scienze della Terra, Università di Firenze via
La Pira 4, 50121 Firenze, Italy (*correspondence:
gabriele.biocchi@unifi.it)

²Istituto di Geoscienze e Georisorse, Consiglio Nazionale delle
Ricerche, sezione di Firenze via La Pira 4, 50121 Firenze,
Italy

³Istituto Nazionale di Geofisica e Vulcanologia, Sezione di
Napoli, OV, via Diocleziano 328, 80124 Napoli, Italy

The chemical and isotopic composition of (i) CO₂-rich fluids exploited from Caprese Reservoir (CR) by the ~5,000 m deep Pieve Santo Stefano 1 (PSS1) borehole located in the Upper Tiber Basin (Northern Apennines, Italy) and (ii) natural gas discharges located in the surrounding of the Mt. Fungai ophiolitic-bearing complex (Ligurian Units), are presented and discussed.

The CR fluids are hosted in fractured dolostones layers of Burano Fm. [1] and consist of CO₂-, N₂-rich gas phase and saline (~82 g/L) NaCl brine. The δ¹³C-CO₂ and δ¹⁵N-N₂ values are interpreted as produced by mixing of deep fluids originated by mantle degassing and thermometamorphic processes involving Mesozoic limestones. Water isotopes and ³H values indicate that the CR brine is recharged by a long (>50 yr) hydrologic circuit fed by meteoric precipitations.

The naturally discharging gases from the study area are fed by CR, likely due to the fact that the steep Arbia Val Marecchia Line transverse tectonic elements provide preferential paths for these deep-seated fluids, favoring their uprising up to the surface gas vents [2]. The interaction of the ascending CR gas with ophiolite-bearing Ligurian Units and Cervarola-Falterona Unit produces secondary H₂, H₂S and light hydrocarbons in Mt. Fungai gases.

[1] Trippetta *et al.* (2013) *Int. J. Greenh. Gas Con.* **12**, 72-83.

[2] Bonini (2009) *J. Struct. Geol.* **31**, 44-54.

Precise U–Pb zircon CA-ID-TIMS ages and Sr isotopes for the Plana pluton, Srednogie, Bulgaria

BIDZHOVA, L.^{1*}, NEDIALKOV, R.¹, OVTCHAROVA, M.²
AND VON QUADT, A.³

¹ Sofia University “St. Kliment Ohridski”, Sofia, Bulgaria
(*correspondence: lora.bidzhova@colostate.edu)

² University of Geneva (maria.ovtcharova@unige.ch)

³ IGP, ETH, Zurich (albrecht.vonquadt@erdw.ethz.ch)

We report new, high precision CA-ID-TIMS U–Pb single zircon ages for the Plana pluton, a part of the ABTS belt in SE Europe. The pluton is located at the Central Srednogie - Rhodopes border, ~60km SE of Sofia. *in situ* differentiation of high potassium calc alkaline magmas produced gradually varying rock compositions [1]. We analyzed a granite from the central parts of the pluton (A); and a monzogabbro-diorite from the periphery of the pluton (B).

The three youngest grains in (A) overlap and yield a weighted mean ²⁰⁶Pb/²³⁸U age of 77.87±0.07 Ma (2σ, MSWD=1.01), our best estimate for the crystallization age of the granite. Two zircons, interpreted as antecrysts, are concordant at ~78 Ma. The remaining two grains, interpreted as xenocrysts, are concordant at ~440 Ma. In (B), two of five grains are concordant at ~440 Ma; the remaining three zircons are discordant and older. Ages of ~440 Ma, are also reported for inherited zircons in other Upper Cretaceous intrusives and Variscan granitoids from Central and Eastern Srednogie [2, 3, 4]. The presence of inherited zircons provides direct evidence for wall-rock assimilation.

Comparison of our data with published U–Pb ages [3, 5] suggests that the Plana pluton crystallized in the late stages of Upper Cretaceous magmatism in Srednogie. Initial Sr isotopes of seven studied rocks are between 0.7043 and 0.7050, within the range of the least radiogenic Upper Cretaceous rocks in the Srednogie region. Studies from Central Srednogie show a trend toward younger and more mantle-influenced magmatism from north to south [5]. Our high precision 77.87 Ma age, and the mantle-dominated Sr isotope signature of the rocks, correlate the Plana pluton with the magmatic activity of southern Central Srednogie.

We thank Momchil Dyulgerov and Svetoslav Georgiev for analytical help, and Judy Hannah and Holly Stein for support

[1] Bidzhova *et al.*, 2007, *Advances in Reg. Geol.*; [2] Carrigan *et al.*, 2005, *Lithos*; [3] Georgiev *et al.*, 2012, *Lithos*; [4] Peytcheva & von Quadt, 2004, 5th *Mediterran. Symp. Greece*; [5] von Quadt *et al.*, 2005, *Ore Geol.Rev.*

Colloidal properties of biomineralized nanoselenium: implications for bioremediation, resource recovery and environmental transport

BIELSER, J.M.¹, EVANGELOU, M.W.H.²,
WINKEL L.H.E.^{3,4} AND LENZ, M.^{1,5}

¹ Institute for Ecopreneurship, University of Applied Sciences and Arts Northwestern Switzerland (FHNW),
Gründenstrasse 40, CH-4132 Muttenz,

² Institute of Terrestrial Ecosystems, ETH Zürich, CH-8092 Zurich

³ Institute of Biogeochemistry and Pollutant Dynamics,
Department of Environmental Sciences, ETH Zurich, CH-8092 Zurich

⁴ Swiss Federal Institute of Aquatic Science and Technology (Eawag), Überlandstrasse 133, Postfach 611, CH-8600 Dübendorf

⁵ Sub-Department of Environmental Technology, Wageningen University, NL-6700 EV Wageningen

Microbial selenium (Se) bioremediation is based on conversion of water soluble, toxic Se oxyanions to water insoluble, biogenic pure elemental Se of particle sizes in the nanometer range (bioNSe). The colloidal stability of the bioNSe suspensions hamper a straightforward removal and recovery by gravitational settling. BioNSe that is not removed from suspension may leave bioremediation reactors with the effluent and is subject to transport and re-oxidation to the original toxic oxyanions. For the first time, colloidal stability fields of pure bioNSe were determined by electrophoretic mobility (ζ-potential) measurements¹ and column settling experiments (ICP-MS). It was demonstrated that circumneutral pH, commonly applied in bioremediation, prevents settling of bioNSe, since the particles are strongly negatively charged. Counter cations and protons were used to screen efficiently this intrinsic negative charge. In this manner, settling could be significantly accelerated (up to 86.2 ± 3.5% within 0.5 h) at cation concentrations that would only increase overall treatment costs to minor extents. The ζ-potential measurements showed furthermore, that significantly dissimilar transport behaviour is to be expected in different natural waters (salt, dissolved organic matter rich), which can result in accumulation of Se in certain environments, if bioNSe leaves bioremediation reactors.

[1] Buchs, B.; Evangelou, M. W. H.; Winkel, L. H. E.; Lenz, M. *Environ. Sci. Technol.* 2013, **47**, 2401–2407.

Opening the foraminiferal proxy black box a bit further

JELLE BIJMA*¹, ANIEKE BROMBACHER²,
ANTJE FUNCKE¹, ELLA HOWES¹, KARINA KACZMAREK¹,
NINA KEUL³, GERALD LANGER⁴, GERNOT NEHRKE¹,
LENNART DE NOOIJER⁵, MARKUS RAITZSCH¹
AND GERT-JAN REICHART⁵.

¹Alfred Wegener Institute for Polar and Marine Research,
Bremerhaven, Germany (jelle.bijma@awi.de;
antje.funcke@awi.de; ella.howes@awi.de;
Karina.Kaczmarek@awi.de; gernot.nehrke@awi.de;
markus.raitzsch@awi.de)

²Department of Earth Sciences, Utrecht university, The
Netherlands (j.f.a.brombacher@students.uu.nl)

³Geoscience, LDEO, Palisades, NY, USA;
(nkeul@ldeo.columbia.edu)

⁴Dept. of Earth Sciences, Cambridge University, UK;
(gl345@cam.ac.uk)

⁵Marine Geology, Royal NIOZ, Texel, The Netherlands;
(Lennart.de.Nooijer@nioz.nl; Gert-Jan.Reichart@nioz.nl)
(*correspondence: jelle.bijma@awi.de)

Even though our geochemical proxy toolbox is ever increasing and our analytical techniques are getting more sophisticated, our fidelity at reading past ocean climate information has only slightly improved. This is mainly due to the fact that most relationships are still empirical and controlled by more than just the target parameter. The outstanding challenge is to open the black box and develop a mechanistic understanding of proxy incorporation and preservation. We have carried out a whole suite of laboratory experiments to better understand the calcification processes and the pathways of Mg, Sr, Ba, U and B using confocal laser microscopy, TEM, AFM and simultaneous analyses of B/Ca and $\delta^{11}\text{B}$ using femtosecond laser ablation and MC-ICP-MS. Together, the results show a high degree of biological control during calcification and proxy incorporation. We have used the benthic foraminifers *Ammonia aomoriensis*, *Amphistegina lessonii*, *Heterostegina depressa* and the planktonic foraminifer *Orbulina universa*. Lessons learned and a tentative model will be presented.

Experimental constraints on Fe isotope fractionation in fluid-melt-oxide-sulfide assemblages

LAURA BILENKER*¹, ADAM SIMON¹,
CRAIG C. LUNDSTROM², NORBERT GAJOS²
AND ZOLTAN ZAJACZ³

¹University of Michigan, Ann Arbor, MI, USA
(*bilenker@umich.edu)

²University of Illinois, Urbana-Champaign, IL, USA

³Institute of Geochemistry and Petrology, ETH Zürich

We report the first experimental data that quantify directly the effect of a fluid phase on stable iron isotope fractionation at magmatic conditions. Our investigation was stimulated by the hypothesis that degassing causes the heavy iron isotope signature measured in degassed rhyolites [1,2], but published experimental studies of iron isotope fractionation lacked a fluid phase.

We used a rhyolite melt, NaCl-bearing aqueous fluid, and magnetite or pyrrhotite. Charges were run at 400, 600, or 800°C, 150 MPa for mineral–fluid, and 800°C and 100 MPa for mineral–melt–fluid; f_{O_2} was buffered at ~NNO. Isotopic compositions of starting and quenched phases were obtained by MC-ICP-MS. Time-series runs and the three-isotope method were used to assess equilibrium

Our data indicate that rhyolite melt at 800°C is isotopically lighter than co-existing fluid ($\Delta_{\text{melt-fluid}} \sim -0.20\text{‰} \pm 0.07$ 1SD). Magnetite behaves as predicted ($\Delta_{\text{fluid-magnetite}} \sim +0.75\text{‰} \pm 0.07$ 1SD at 800°C), becoming isotopically heavier relative to both fluid and melt. An andesite-fluid experiment (FMQ+0.5, 1000°C, 150 MPa) yielded an isotopically lighter melt relative to the starting glass, consistent with the coexisting fluid being isotopically heavier than andesite melt. These data suggest that fluid exsolution from silica-rich melts is not the cause for the increased $^{56}\text{Fe}/^{54}\text{Fe}$ ratio in degassed rhyolites. Interestingly, magmatic and hydrothermal magnetite show distinct iron isotope signatures, suggesting that the iron isotope values of minerals deposited by these processes may serve as geochemical fingerprints of the source reservoir for iron. Additional data from sulfide runs support the observation that individual minerals can fractionate iron differently and that pyrrhotite preferentially incorporates ^{54}Fe into its structure ($\Delta_{\text{melt-pyrrhotite}} \sim -0.75\text{‰} \pm 0.01$ SD at 800°C).

These data corroborate the hypotheses that both fluid exsolution and crystal fractionation could influence the isotopic composition of a melt, but perhaps not as predicted. Owing to the importance of melt degassing as a critical process for the formation of ore deposits, our data may also help resolve debates regarding the origin of deposits that may have formed by either magmatic or hydrothermal processes.

[1] Potraissou and Freyrier (2005) Chem. Geol., **222**, 132-147, [2] Heimann *et al.* (2008) GCA, **72**, 4379-4396

Magmas going through Icelandic crustal filter

ILYA N. BINDEMAN¹, ANDREY GURENKO²,
OLEG MELNIK³ AND ALEXANDER SOBOLEV⁴

¹Dept. of Geological Sciences, University of Oregon, Eugene, USA;

(bindeman@uoregon.edu)

²CRPG/CNRS, BP 20, 54501 Vandoeuvre-lès-Nancy, France

³Univ J. Fourier, Grenoble, France

⁴Univ J. Fourier, Grenoble, France

Eruption of large-volume basalts in large igneous provinces and hotspots occurs throughout areas of preexisting thick crust and crust overloaded by early eruptions from the same plume. Iceland represents a good testing ground for estimating the amounts of upper crustal contamination of mantle-derived magma in long-lived propagating rifts - magmatic pipelines going through the isotopically fingerprinted low- $\delta^{18}\text{O}$ thick crust affected by rain and glacial meltwaters. We report analyses of individual primitive olivines across Iceland and demonstrate that the Icelandic plume is not severely depleted in ^{18}O neither contains higher than mantle values (5.2-4.6‰ for $\text{Ol} > \text{Fo}_{86}$). We observe a positive correlation of Fo and $\delta^{18}\text{O}(\text{olivine})$ down to Fo_{75} suggesting that crustal differentiation and assimilation is responsible for low- $\delta^{18}\text{O}$ evolved olivines and host basalts. We report new data and interpretation of oxygen isotope diversity in olivines from large volume rift basaltic eruptions and investigate in detail olivine-basalt oxygen isotopic equilibria. Up to 3‰ variations of Fo_{75} to Fo_{86} olivines suggest rapid transformation of mantle-derived magmas in the magma plumbing systems. Low- $\delta^{18}\text{O}$ values of large volume basalts (e.g. Laki, Veidivotn), with $\text{MgO} < 5\text{wt}\%$, require that tens of percent of a low- $\delta^{18}\text{O}$ mafic component was added to normal- $\delta^{18}\text{O}$ mantle derived basalt. Only limited $\delta^{18}\text{O}$ whole rock heterogeneity is present in large volume basalts suggesting effective mixing and homogenization prior to eruption. Diffusive reequilibration of disequilibrium olivines and plagioclase require hundreds of years, and their longest residence is in the semi-frozen cumulates underneath volcanoes. Rapid transport along a bifurcating network of dikes and sills inside of the hyaloclastitic upper crust provide a viable mechanism for crystal entrainment and basalt mixing by forced convection. We provide a simple numerical model of this process. We further discuss the effect of flowing basalt in upper crustal lithologies leading to crustal melting and generation of low- $\delta^{18}\text{O}$ silicic melts with heterogeneous crystal cargos.

Rhyolites-Hard to Produce, Easy to Recycle: Isotopic diversity in zircons as petrogenetic tool

I. BINDEMAN¹, A. SIMAKIN², D. DREW¹ AND D. COLON¹

¹ Dept Geological Sciences, University of Oregon, Eugene, OR, 97403, USA;

(bindeman@uoregon.edu)

²Inst Physics of the Earth, RAS, Moscow, Russia

Rapid pace of discovery of oxygen isotope diversity in zircons and other minerals in large volume ignimbrites worldwide suggests that this phenomenon characterize many silicic units studied so far by *in situ* methods. We report new results from calderas in the Snake River Plain: Picabo, early Bruneau, in addition to previously reported Yellowstone and Heise), Kamchatka, and rhyolites from rifts of Iceland (Askja, Hekla, Torfajokull). As low- $\delta^{18}\text{O}$ oxygen values fingerprint petrogenesis to the upper crust, these observations lead to a model of silicic magma by "double-recycling" of zircon-saturated, silicic to intermediate rocks. Initial melts are produced slowly in diverse batches and the isotopic signature of zircons record their immediate environment of growth. Next, magma batches with diverse zircons merge into larger-volume magma bodies, which mix crystals together and erupt quickly. Concave-up crystal size distributions of zircons and quartz in studied voluminous ignimbrites can be explained by just two episodes of reprecipitation.

Following the melting simulation of [1] we use visco-plastic rheology for surrounding rocks to explain the formation of magma batches generated side by side and merging them together. We observe: 1) Fast convective melting with low heat dissipation. 2) Efficient mixing on large (kilometers) horizontal scales, due to the vigorous flow field induced by compositional convective melting of silicic predecessors by superheated rhyolites. Chaotic, meter-scale vortexes of altering directions cause disintegration of the liquid parcels to diminishing size. The marker method allows us to track particle mixing (i.e., how zircons with diverse isotopic values brought together). 3) Mechanical interaction of the closely-spaced sills in hot visco-plastic upper crust with low yield stress (<100 MPas) leads to mechanical failure (both brittle and plastic) of separating screens leading to the coalescence of sills into a single body. We suggest that analogous processes of rapid two-stage segregation may characterize granitic batholith, and large supervolcanic magma bodies formed by remelting.

[1] Simakin A., Bindeman I., 2012, EPSL, 337-338, 224.

Space-Time Kriging of Precipitation Reconstructed at 12-km Grid Intervals from Tree-Ring Records

FRANCO BIONDI¹²³

¹DendroLab, University of Nevada, Reno, USA;
franco.biondi@gmail.com

²CIRES, University of Colorado at Boulder, USA;
Franco.Biondi@Colorado.EDU

³Graduate Program of Hydrologic Sciences, University of Nevada, Reno, USA; fbiondi@unr.edu

Understanding and preparing for future hydroclimatic variability greatly benefits from long (i.e., multi-century) records at seasonal to annual time steps that have been gridded at km-scale spatial intervals over a geographic region. Kriging is a geostatistical technique commonly used for optimal interpolation of environmental data, and space-time geostatistical models can improve kriging estimates when long temporal sequences of observations exist at relatively few points on the landscape. Here I present how a network of 22 tree-ring chronologies from single-leaf pinyon (*Pinus monophylla*) in the central Great Basin of North America was used to extend hydroclimatic records both temporally and spatially. First, the Line of Organic Correlation (LOC) method was used to reconstruct October-May total precipitation anomalies at each tree-ring site, as these ecotonal environments at the lower forest border are typically moisture limited. Individual site reconstructions were then combined using a hierarchical model of spatio-temporal kriging that produced annual anomaly maps on a 12x12 km grid during the period in common among all chronologies (1650-1976). Hydro-climatic episodes were numerically identified and modeled using their duration, magnitude, and peak. Spatial patterns were more variable during wet years than during dry years, and the evolution of drought episodes over space and time could be visualized and quantified. The most remarkable episode in the entire reconstruction was the early 1900s 'pluvial', followed by the late 1800s drought. The 1930s 'Dust Bowl' drought was among the top ten hydroclimatic episodes in the past few centuries. These results directly address the needs of water and natural resource managers with respect to planning for 'worst case' scenarios of drought duration and magnitude at the watershed level.

The absolute Cr isotopic ratios of the components of carbonaceous chondrites

J.L. BIRCK* AND C. GÖPEL

IPGP, 75238 Paris, France

(*correspondance: birck@ipgp.fr), (gopel@ipgp.fr)

Non linear isotopic anomalies are common for Cr in carbonaceous chondrites at the mineral scale where percent level variations are common for ⁵⁴Cr [1,2]. When these anomalies are small relative to the dispersion of mass discrimination during TIMS measurements, the identity of the anomalous isotope(s) is not unambiguous. For the stepwise dissolution fraction of C1 and C2 carbonaceous chondrites former experiments designate ⁵⁴Cr as the major varying isotope and ⁵³Cr as varying only according to ⁵³Mn decay. Nevertheless below about 10 ε variations some effects can still be present on the two normalizing isotopes ⁵²Cr and ⁵⁰Cr. As evaporation and condensation in the forming solar system is a credible possibility, significant fractionation can also be present between the components that constitute carbonaceous chondrites. We address this issue in this presentation.

In Orgueil, Tagish Lake, Tafassasset and Paris, dissolution fractions in which non-mass-dependent ⁵⁴Cr effects can spread up to close to 2% [1-3] were investigated. A Neptune MC-ICPMS was used in the medium resolution mode (M/ΔM~5000) to avoid interferences from Ar compounds in the Cr mass range. ⁵³Cr/⁵²Cr ratios are measured within a 0.05 δ (permil deviation relative to NIST 979). Radiogenic contributions on ⁵³Cr can be subtracted using the TIMS data obtained on the same Cr fractions.

⁵³Cr/⁵²Cr ratios in fractions from stepwise dissolution in C1 and C2 chondrites [1-3] are identical to their respective whole rocks within 0.1 δ. This implies that despite large differences in ⁵⁴Cr the other three isotope: ⁵⁰Cr, ⁵²Cr and ⁵³Cr are initially in identical proportions in all the mineral fractions investigated with the present procedure. At present, carbonaceous chondrites seem to contain only two primordial Cr isotopic components: one with normal ⁵⁰Cr, ⁵²Cr, ⁵³Cr and a deficit in ⁵⁴Cr, and a second one which consists of pure ⁵⁴Cr. Data on new, recently found carbonaceous chondrites will also be presented [4].

[1] Rotaru M. *et al.* 1192. *Nature* **358** 465-470. [2] Trinquier *et al.* (2007) *Astrophys. J.* **655**, 1179-1185. [3] Petitat M. *et al.* 2011. *Astrophysical Journal* **736** 23-30. [4] Göpel *et al* (2013) *MinMag* this volume.

Protracted cooling from Neoproterozoic metamorphic events in the NW Highlands, Scotland investigated using garnet Lu-Hf and Sm-Nd geochronology

A. BIRD^{1,2}, M. F. THIRLWALL² AND R. STRACHAN³

¹Department of Geography, Royal Holloway, Egham, Surrey, TW20 0EX, anna.bird@rhul.ac.uk

²Department of Earth Sciences, Royal Holloway, Egham, Surrey, TW20 0EX, m.thirlwall@es.rhul.ac.uk

³School of Earth & Environmental Sciences, Burnaby Road, Portsmouth, PO1 3QL, rob.strachan@port.ac.uk

The Moine Supergroup of the Northern Highland Terrane in Scotland records several orogenic events. The earliest of these is the Knoydartian (830–740 Ma). All previously published evidence for this event comes from West Inverness-shire. Lu-Hf and Sm-Nd garnet geochronology records much more widespread Neoproterozoic metamorphism, with evidence from Shetland to Mull. This data also shows that the Morar Group has been affected by the Renlandian event of the Valhalla Orogen. It also demonstrates that the younger limit of Morar Group deposition is older than previously thought (>950 Ma).

All of the samples all record a systematic difference between the Lu-Hf and Sm-Nd ages, the Sm-Nd ages being 10–20% younger than the Lu-Hf ones. Garnet cores and rims have been dated using Lu-Hf and Sm-Nd and the difference between the cores and rims is the same for both isotopic systems. This suggests that the difference between Sm-Nd and Lu-Hf is due to the difference in closure temperatures. One exception gives Lu-Hf and Sm-Nd ages which are within error and could suggest that this sample records garnet growth in both isotopic systems or relates to very fast cooling.

Iron Oxidation and Reverse Electron Flow In a Photoferrotroph

BIRD, LINA¹, NITSCHKE, WOLFGANG²
AND NEWMAN, DIANNE^{*1}

¹California Institute of Technology, Pasadena, Ca, USA
(linabird@caltech.edu)

(* correspondence: dkn@caltech.edu)

³CNRS Marseilles, France (nitschke@imm.cnrs.fr)

Biological iron oxidation is of interest to geobiologists as an oxygen independent mechanism of ferric iron production. *Rhodospseudomonas palustris* TIE-1 is a versatile purple phototroph with the ability to grow using ferrous iron (Fe(II)) as the sole electron donor. Previous studies showed that the *pio* operon, encoding an outer membrane porin, a decaheme cytochrome, and a high potential iron protein (HiPIP), are vital to Fe(II) oxidation. This work further explores the iron oxidation pathway through *in vitro* characterization of the HiPIP and *in vivo* visualization of photosynthetic electron transport with flash induced absorbance spectrometry. *In vitro* studies showed that the HiPIP can donate electrons to the reaction center at a rate much slower than that found in energy generation. Our *in vivo* studies, however, show that antimycin (a *bc₁* complex inhibitor) blocks reduction of the quinone pool by Fe(II), indicating that electrons may reduce the quinone pool of the cell through the *bc₁* complex instead of through the reaction center as previously thought. We have also found that the quinone pool of *R. palustris* TIE-1 is reduced by Fe(II) over short time scales even in mutants lacking the *pio* genes, although the precise rates of this reaction were not determined. These results indicate that the mechanisms of iron oxidation are more complex than originally thought, and that the path electrons take from Fe(II) to carbon reduction is similar to the pathway found in acidophilic Fe(II) oxidation.

Crystallization kinetics of apatite nanocrystals from amorphous calcium phosphate in water by *in situ* synchrotron powder diffraction

H. BIRKEDAL^{1*}, H. LEEMREIZE¹ AND C. J. S. IBSEN¹

¹INANO & Department of Chemistry, Aarhus University, Aarhus 8000, Denmark
(*correspondence: hbirkedal@chem.au.dk)

Crystallization of minerals from amorphous precursor phases is emerging as a major pathway for crystallization in several systems but remains poorly understood. Here we use *in situ* X-ray diffraction to study the crystallization kinetics of nanocrystalline apatite from amorphous calcium phosphate in water. We find a striking dependence of crystallization behavior on whether K⁺ or Na⁺ is used as counter ion.

In situ X-ray diffraction experiments were performed with ~10 s time resolution [1, 2, 3]. The data were analyzed by Rietveld refinement procedures determining the nanocrystal size, the amount of crystalline material present, the lattice constants, and the background [1, 2]. The amorphous precursor phase was clearly observed in the first time points [2] and was gradually replaced by the nanocrystal diffraction pattern of the forming apatite phase.

The crystals were found to be formed as almost spherical crystallites that soon after formation started growing preferentially in the *c*-axis direction of the hexagonal apatite crystals giving needle-shaped nanocrystals. This rapid anisotropic growth was followed by an Ostwald ripening stage, with slower crystallite size growth rates. During this stage, growth was preferentially perpendicular to the *c*-axis slightly lowering the shape anisotropy.

Using K⁺ instead of Na⁺ as counter ion resulted in drastic changes in growth kinetics. Sodium allows the incorporation of dissolved carbonate into the forming apatite while potassium does not. This difference led to more rapid crystallization for sodium as a counter ion and resulted in crystallites with different sizes and size anisotropies.

The present work provides detailed insights into how anisotropic crystal morphologies develop and shows that seemingly innocent changes in environment, such as choice of counter ions may have profound impacts on crystallization behavior.

[1] Ibsen & Birkedal (2010) *Nanoscale* **2**, 2478-2486. [2] Ibsen & Birkedal (2012) *J. Appl. Cryst.* **45**, 976-981. [3] Jensen *et al.* (2010) *Chem. Mater.* **22**, 6044-6055.

Origin of porphyries related to Cu-Mo mineralization, California-Vetas district, Colombia

THOMAS BISSIG^{*1}, LUIS C. MANTILLA²
AND CRAIG J.R. HART¹

¹Mineral Deposit Research Unit, University of BC, Vancouver, Canada.

(*correspondence: tbissig@eos.ubc.ca)

²Universidad Industrial de Santander, Bucaramanga, Colombia.

Porphyry Mo- Cu mineralization in the California-Vetas district, Eastern Cordillera, Colombia is coeval with 10.9 - 8.4 Ma granodiorite porphyry stocks and overprinted by epithermal Au-Ag mineralization. Mineralization is hosted by Grenvillian-aged paragneisses (Bucaramanga Gneiss) and Late Triassic to Early Jurassic peraluminous granites with > 70% SiO₂ and metaluminous diorites with SiO₂ 54.9 - 60.4 wt%. Late Miocene rocks are weakly peraluminous granodiorite porphyries with SiO₂ 61- 67%, sharing some characteristics with adakite-like rocks widely associated with porphyry mineralization elsewhere in the Andes. Although Miocene rocks do not have low Y (<15 ppm) or depleted HREE, they have high Ba (930-1500 ppm), high Ba/La (28 to 50), high Sr (850 to 1100 ppm), high Sr/Y (50-78) only minor Eu anomalies and depleted MREE compared to the Mesozoic granites (400-700 ppm Ba; Ba/La 14-25; 80-150 ppm Sr; Sr/Y 2.5-14), and diorites (900 -1200 ppm Ba; Ba/La 20-32; 610-750 ppm Sr; Sr/Y 22-25). Their initial ⁸⁷Sr/⁸⁶Sr ratios of 0.7052-0.7066 are significantly less radiogenic than those of the Mesozoic diorites (0.70712-0.7072), granites (0.7094-0.710) and the paragneiss (0.7144-0.7332, @ 199 Ma). Miocene granodiorite porphyries represent water-rich subduction related melts. Their initial ⁸⁷Sr/⁸⁶Sr is less radiogenic than Neogene Caribbean sediments, precluding a sedimentary source for the high Sr and Ba. Instead, a fluid source from serpentinized lithospheric mantle, fluxing the overlying subducted oceanic crust and mantle wedge is suggested. The geochemical signal may have been enhanced by the overlapping subducting Nazca and proto-Caribbean slabs at depth.

Estimating the role of competing ions on the arsenic mobilization processes in the aquifers of Bengal basin by surface complexation modeling

A. BISWAS^{12*}, J.P. GUSTAFSSON¹³, H. NEIDHARDT⁴,
D. HALDER¹², A.K. KUNDU², D. CHATTERJEE²,
Z. BERNER⁴ AND P. BHATTACHARYA²

¹KTH Royal Institute of Technology, SE-100 44 Stockholm, Sweden

(*correspondence: ashis@kth.se)

²University of Kalyani, 741235 Kalyani, West Bengal, India

³Swedish University of Agricultural Sciences, SE-750 07 Uppsala, Sweden

⁴Karlsruhe Institute of Technology, D-76131 Karlsruhe, Germany

This study investigates the relative roles of the different competing ions on the arsenic (As) mobilization in the sedimentary aquifers of Bengal basin by surface complexation modeling of the temporal variability of As in shallow (<50 m) groundwater. Two sets of piezometers (2 × 5 = 10), installed at the two sites with relatively contrasting dissolved As concentration in groundwater, were monitored bi-weekly for As and other hydrogeochemical parameters over a period of 20 months. The estimation of the standard deviation (SD) for As(III) reflects strong temporal variation (SD ≥ 10 µg/L) in all the piezometers of two sites over the monitoring period. Particularly, the variation is more prominent in the shallowest part of the aquifer, where the site specific cyclic trends are evident. While, As(V) shows significant temporal variation in the piezometers of high As site only and no specific trend is reflected in the variation.

Two different surface complexation models (SCMs), developed for ferrihydrite and goethite have been explored to account for the observed temporal variation in As(III) and As(V) concentrations. The SCM for ferrihydrite has provided the better estimation for both As(III) and As(V) variations. Among the different competing ions, PO₄³⁻ appears as the major competitor of As(III) and As(V) adsorption onto ferrihydrite and the competition ability decreases in the order PO₄³⁻ >> Fe(II) > H₄SiO₄ = HCO₃⁻. It is further revealed that a small decrease in pH significantly increases the concentration of As(III) and decreases the As(V) concentration and vice versa. The present study suggests that the reductive dissolution of Fe oxyhydroxides alone cannot explain the observed high As concentration in groundwater of the sedimentary aquifers. Perhaps, the reductive dissolution of Fe oxyhydroxides followed by competitive sorption reactions with the aquifer sediment is the processes conducive for As enrichment in the groundwater of Bengal basin.

Neoproterozoic late to post-collisional, quartz-bearing ultrapotassic syenites from southernmost Brazil

MARIA DE FATIMA BITENCOURT^{1*}, LAURO VALENTIM STOLL NARDI¹, GIUSEPPE BETINO DE TONI¹ AND LUANA MOREIRA FLORISBAL²

¹ Instituto de Geociências, Universidade Federal do Rio Grande do Sul, Av. Bento Gonçalves, 9500, Porto Alegre 91500-000 RS, Brazil. fatimab@ufrgs.br; lauro.nardi@ufrgs.br; gdetoni@ufrgs.br

² Instituto de Geociências, Universidade de São Paulo, Rua do Lago, 562, São Paulo, 05508-080, SP, Brazil. geoluana@yahoo.com.br

Continental collision is registered in southernmost Brazil at ca. 650 Ma by tectonic interleaving of paragneisses and orthogneisses of different ages under granulite facies metamorphic conditions. Megacrystic and fine-grained syenites are intrusive subparallel to the main gneissic banding and have locally undergone subsolidus deformation at around 700 °C. The syenites contain slightly perthitic K-feldspar and variable proportions of pyroxene, amphibole and red biotite, with small amounts of plagioclase and quartz. Their crystallization age is 642 ± 10 Ma (U-Pb zircon LA-MC-ICP-MS), determined in least deformed variety. Their main geochemical features (SiO₂ 58-62 wt%) are high HFSE, REE, Rb, Sr, and Ba contents, as well as K₂O/Na₂O ratios (4-10), typical of ultrapotassic rocks. The trace-element patterns suggest that they are derived from OIB-type sources. Their initial ⁸⁷Sr/⁸⁶Sr ratios vary from 0.719 to 0.729, and ¹⁴³Nd/¹⁴⁴Nd ratios from 0.5116 to 0.5118. Similar values for both isotope ratios have been reported for post-collisional ultrapotassic magmatism in southwest Tibet. Melting of phlogopitic, Rb-enriched mantle sources may account for the extremely high Sr_(i) values found in the studied syenites. The ultrapotassic character, trace-element and isotope patterns are consistent with sources previously affected by subduction, and are therefore compatible with structural data indicative of post-collisional setting.

The Lu-Hf BSE parameters and the early Earth zircon record

M. BIZZARRO¹ AND J.N. CONNELLY¹

¹Centre for Star and Planet Formation, University of Copenhagen, Copenhagen K, 1350 Denmark

The long-lived ¹⁷⁶Lu-to-¹⁷⁶Hf decay system is a powerful tool to understand ancient chemical fractionation events associated with planetary differentiation. Intrinsic to application of such isotopic tracers to study the early Earth is knowledge of chondritic reference values for the Lu-Hf system (bulk silicate Earth, BSE) and the precise value of the decay constant for the parent ¹⁷⁶Lu isotope. Using a BSE estimate based on chondrite meteorites [1], detrital Hadean zircons (>3.8 Gyr) from the Jack Hills metasedimentary belt record extremely enriched Hf-isotope signals suggesting early extraction of a continental crust (>4.5 Gyr) but fail to identify a prevalent complementary depleted mantle reservoir. However, this conclusion assumes that the present-day Hf-isotope composition of bulk chondrite meteorites can be used to estimate the composition of BSE. Recent internal ¹⁷⁶Lu-¹⁷⁶Hf systematics of the pristine 4564.58±0.14 Myr SAH99555 angrite [2] define a Lu-Hf age that is ~300 Myr older than the age of the solar system [3]. This confirms the existence of an energetic process yielding excess ¹⁷⁶Hf in affected early formed solar system objects through the production of the ¹⁷⁶Lu isomer (t_{1/2}=3.9 hours). This conclusion is now supported by new ¹⁷⁶Lu-¹⁷⁶Hf data of eucrite meteorites [4]. This implies that chondrite meteorites contain excess ¹⁷⁶Hf (~5ε-unit) and their present-day composition may not be used to infer the Lu-Hf parameters of BSE. Using a revised BSE estimate based on the SAH99555 isochron, we note that Earth's oldest zircons preserve a record of coexisting enriched and depleted hafnium reservoirs as early as 4.3 Gyr in Earth's history, with little evidence for the existence of continental crust prior to 4.4 Gyr. This contrasting interpretation of the early zircon record requires reassessing the validity of using chondrites to define the Lu-Hf BSE parameters. To better understand the extent of ¹⁷⁶Hf excesses in meteorites and the solar system's initial ¹⁷⁶Hf/¹⁷⁷Hf value, we initiated a ¹⁷⁶Lu-¹⁷⁶Hf study of additional quenched angrites via the internal isochron approach, including D'Orbigny, NWA 1670 and NWA 7203. Our new U-corrected Pb-Pb dates for these meteorites indicate coeval formation of NWA 7203, SAH99555 and D'Orbigny. NWA 1670 crystallized ~1 Myr earlier and, thus, is the oldest known angrite.

[1] Bouvier *et al.* (2008) *EPSL* **273**, 48 [2] Connelly *et al.* (2008) *GCA* **72**, 4813 [3] Bizzarro *et al.* (2012) *G-cubed* **13**, Q03002 [4] Righter *et al.* *LPSC* **44**, 2745

Sulfur isotopic evidence for sources of volatiles in Siberian Traps magmas

BENJAMIN A. BLACK^{1*}, ERIK H. HAURI²,
STEPHANIE M. BROWN¹ AND LINDA T. ELKINS-TANTON²

¹MIT EAPS, Cambridge, MA USA, bablack@mit.edu
(* presenting author)

²Carnegie Institution of Washington, Washington, DC, USA

We present new measurements of δ³⁴S in melt inclusions from the Siberian Traps. The Siberian Traps flood basalts transferred a large mass of volatiles from the Earth's mantle and crust to the atmosphere [1]. The eruption of the large igneous province temporally overlapped with the end-Permian mass extinction, and also generated ore deposits of major economic importance. Constraints on the sources of Siberian Traps sulfur and other volatiles are critical for determining the overall volatile budget, the role of assimilation of crustal materials, and genesis of Noril'sk massive sulfide deposits. Sulfur isotopic ratios vary among mantle and crustal materials, with characteristic mantle δ³⁴S values around 0±2 ‰ with respect to Vienna Cañon Diablo Troilite (VCDT), and crustal δ³⁴S values between -50 ‰ and +40 ‰. In conjunction with previously published whole rock measurements from Noril'sk [2], our sulfur isotopic data suggest that crustal assimilation was widespread and heterogeneous—though not universal—during the emplacement of the Siberian Traps. Evidence for open-system degassing implies that episodes of explosive volcanism may have been phreatomagmatic. Carbon concentrations constrain minimum entrapment depths of melt inclusions to shallow crustal depths. Magmas likely interacted with sedimentary materials depleted in ³⁴S such as shale or coal, in addition to evaporites enriched in ³⁴S. These crustal materials may have increased the total volatile budget of the large igneous province, thereby contributing to Permian-Triassic environmental deterioration.

[1] Black *et al.* (2012) *EPSL* **317-318**: 363-373. [2] Ripley *et al.* (2003) *GCA* **67**: 2805-2817.

Chlorite dissolution experiments under CO₂ saturated conditions

JAY R. BLACK^{1,2} AND RALF R. HAESE^{1,3}

¹Cooperative Research Centre for Greenhouse Gas Technologies, CO2CRC

²Geoscience Australia, GPO Box 378, Canberra, ACT 2601, Australia (jay.black@ga.gov)

³The University of Melbourne, VIC 3010, Australia (ralf.haese@unimelb.edu.au)

The injection and long-term storage of supercritical CO₂ (scCO₂) into geological reservoirs is seen as an important option to mitigate rising levels of atmospheric CO₂. Predicting what changes take place to geochemical and petrophysical properties of a reservoir once CO₂ has been injected requires an understanding of how mineral dissolution and precipitation proceed. The dissolution of CO₂ in groundwaters in contact with an scCO₂ plume leads to a decrease in the pH of pore fluids, driving the system far from equilibrium and accelerating the dissolution of minerals in the reservoir. Experiments exposing a siltstone to CO₂ saturated fluids have shown that the dissolution of carbonates and clays, including chlorite, lead to increased porosity and permeability in a sample of a siltstone caprock [1].

The dissolution kinetics of chlorite have been extensively studied [2], but not under CO₂ saturated conditions. Here we present the results of batch reactor experiments on a clinoclone chlorite (CCa-2, The Clay Minerals Society); testing the potential effects of pH, chloride and bicarbonate concentration, temperature and pressure (pCO₂) on the dissolution rate of the mineral. The dissolution rates observed are of a comparable magnitude (c. -12 log mol m⁻² sec⁻¹ at 50°C) to previous studies, but the proton promoted dissolution normally observed is not as prominent. The results suggest that dissolved bicarbonate affects the dissolution mechanism and new rate laws are presented accounting for the effect of [HCO₃⁻]. An apparent activation energy for the dissolution process of 19 kJ mol⁻¹ is calculated assuming a simple empirical rate law with an Arrhenius form. This result is much lower than the activation energy of 88 kJ mol⁻¹ previously reported under acidic conditions [3], and often used in geochemical models under all pH regimes. However, it is consistent with the results of a recent study using flow-through techniques [4].

[1] Armitage *et al.* (2013) *Nature Geosci.* **6**, 79-80. [2] Lowson *et al.* (2007) *Geochim. Cosmochim. Acta*, **71**, 1431-1447. [3] Ross, G.J. (1967) *Can. J. Chem.* **45**, 3031-3034. [4] Smith *et al.* (in press) *Chem Geo.*

U-Pb thermochronology and the thermal history of planetary crusts

TERRENCE BLACKBURN¹

¹Carnegie Institution for Science

U-Pb accessory phase thermochronology (minerals: apatite, titanite and rutile) allows estimates of cooling rates of rocks as they pass through moderate temperatures (400-800 °C). Despite a growing number of datasets employing these techniques, these data--like all thermochronologic data-- are highly non-unique and can often be interpreted as the result of any number of geologic scenarios. This problem of non-uniqueness can largely be resolved by exploiting the U-Pb system's dual decay scheme, where two parent isotopes, ²³⁸U and ²³⁵U, decay to daughter isotopes ²⁰⁶Pb and ²⁰⁷Pb respectively. The difference in decay rates between parent isotopes imposes a time-variant parent and instantaneous daughter isotopic composition for any point in Earth's history. This new thermochronologic methodology works to capture this isotopic evolution using the variation in the time of Pb retention between both: 1) samples of different crustal depths, where variations in the timescale of cooling result from the thermal gradient within a conductively cooling crust, and; 2) crystals of different size, where volume diffusion behavior, in particular for slowly cooled systems, result in larger crystals retaining lead at higher temperatures and over a longer and older timescales in comparison to smaller crystals, which retain lead at lower temperatures and at younger times. The differences in U/Pb and ²⁰⁷Pb/²⁰⁶Pb among samples from different depths, and within each sample—between grains of different size — can be used to reconstruct the long-term thermal histories within planetary crusts. By moving beyond assigning nominal closure temperatures to dated minerals one can avoid the cooling rate uncertainties that propagate from experimental diffusion kinetics. The sensitivity to cooling rate lies in the topology of U-Pb data and has been demonstrated using forward modelling to be highly insensitive to diffusion kinetics. I'll work to demonstrate how this methodology can be employed to reconstruct the thermal histories of: 1) the continental lithosphere through reconstruction of thermal histories of lower crustal xenoliths, and; 2) the chondrite parent bodies, through reconstruction of chondrite meteorite thermal histories. In each example, I'll focus on interpreting thermochronologic data with the aid of thermal models in order to elucidate the relative roles of heat conduction, production and advection (erosion/burial) and in doing so provide constraints on the timing and processes controlling continent stabilization and the assembly of planetesimals.

The reactivity of microbially-reduced goethite: assessing the potential of a naturally-occurring waste material for mine drainage remediation

N. BLACKWELL^{1*}, W. T. PERKINS¹, A. EDWARDS²,
D. B. JOHNSON³, K. B. HALLBERG³, G. W. GRIFFITH²,
J. M. BEARCOCK⁴ AND B. PALUMBO-ROE⁴

¹Institute of Geography and Earth Sciences, Aberystwyth University, UK (*correspondence: nlb09@aber.ac.uk)

²Institute of Biological, Environmental and Rural Sciences, Aberystwyth University, UK

³School of Biological Sciences, Bangor University, UK

⁴British Geological Survey, Keyworth, UK

Naturally occurring iron (Fe) oxides are ubiquitous in nature, particularly at abandoned mine sites where extraction processes have resulted in the oxidation of Fe-bearing sulphide minerals. Goethite, an Fe(III) oxide, is stable over a wide range of Eh and pH conditions and is present at several coal mine drainage treatment systems in the South Wales Coalfield, UK.

Microbial investigations at the Ynysarwed mine in the Coalfield revealed the presence of bacteria closely related to known Fe(III)-reducing species within the goethite deposit. Microcosm experiments designed to investigate the activity of these naturally-occurring bacteria were prepared using sodium acetate as the electron donor and the naturally occurring goethite as the electron acceptor.

After 100 days the solid phase Fe(II) content was determined and the results show an increase from ~1.5% Fe(II) in the starting material to ~9% in the microbially-reduced material. No increase in Fe(II) was observed in the kill or live controls. Dilute acid extractions (0.1M HCl) of the material, designed to solubilise Fe(II) weakly bound to the goethite crystal surface, recovered 97-99% of the total Fe(II).

The ability of Fe(II) bound to the surface of goethite to reduce potentially harmful elements has been shown in several studies. The reactivity of microbially-reduced natural goethite and its ability to remove problematic elements, such as zinc (Zn), from natural mine waters through addition of the slurried reduced material (5g L⁻¹ dry weight) was investigated. The results show a 5-fold increase in Zn removal from a circum-neutral mine water when compared to natural goethite. These data show the potential of naturally-occurring mine waste for the remediation of contaminated mine waters.

The Fate of Small Active Margin River POC in the Marine Environment

NEAL BLAIR^{1*}, CATHERINE GINNANE²,
LAUREL CHILDRESS¹ AND LONNIE LEITHOLD³

¹Earth & Planetary Sciences, Northwestern University, Evanston, IL 60208, USA (*correspondence n-blair@northwestern.edu)

²GNS, PO Box 30-368, Lower Hutt 5040 New Zealand, (c.ginnane@gns.cri.nz)

³Marine, Earth & Atmospheric Sciences, North Carolina State University, Raleigh, NC 27695-8208, USA (leithold@ncsu.edu)

Small active margin rivers export a mixture of particulate organic carbon (POC) pools derived from contemporary primary production, aged soils and uplifted sedimentary rocks. These pools are expected to exhibit a wide range of reactivities in the marine environment because of their vastly different ages and diagenetic histories. The stable carbon and radiocarbon isotopic compositions of sedimentary POC and pore water dissolved inorganic carbon (DIC) from the Waiapu River shelf, New Zealand were measured to determine the fate of the exported riverine POC. The Waiapu River exports material that is dominated by fossil C derived from the rapidly eroding Cretaceous to Paleocene mudstones (riverine POC $F_{\text{mod}} \sim 0.3$). Shelf sediments incorporate both riverine and marine POC as indicated by an enrichment in ¹³C and accumulation of ¹⁴C-rich material ($F_{\text{mod}} \sim 1$).

Porewater DIC carbon isotope compositions are controlled primarily by the addition of remineralized organic carbon to a seawater background. In the case of the Waiapu shelf, DIC $\delta^{13}\text{C}$ values indicate preferential oxidation of terrestrial OC nearshore (~60 meters water depth) with a transition to more marine C-supported remineralization further offshore (80-130 m water depth). In all cases, the remineralized C is modern in age, thus no appreciable oxidation of fossil C or aged soil C is evident.

Oxidation of the modern terrestrial OC is far from complete based on POC isotopic data from both the Waiapu and the adjacent Waipaoa system. The terrestrial OC is well preserved in areas of fine-grained sediment accumulation as a result of rapid and episodic deposition. On balance, we argue that small active margin river continental margins have the potential to be efficient carbon sinks regardless of POC age.

Expanding potential source area studies of dust in East Antarctica by integrating trace element chemistry and radiogenic isotopes

M. BLAKOWSKI^{1*}, S. ACIEGO¹, B. DELMONTE²
AND C. BARONI³

¹University of Michigan, Ann Arbor, MI, USA

(*correspondance: mollybla@umich.edu)

²University of Milan-Bicocca, Milan, Italy

³University of Pisa, Pisa, Italy

By studying dust records preserved in Antarctic ice cores, we can evaluate variability in dust source areas over geologic timescales. For instance, it has been determined that during the Last Glacial Maximum (LGM), South America was the dominant dust source for the entire East Antarctic Plateau [1,2], whereas ice core analyses from the Talos Dome reveal that the fraction of large particles deposited during the Holocene was significantly greater than during the LGM, indicating contribution from proximal, Antarctic sources. These findings differ from cores drilled further inland on the East Antarctic Ice Sheet (EAIS), such as the Dome C core [1,3,4].

Here we provide new results of trace Rare Earth Element (REE) chemistry and Sr-Nd, Hf signatures of <5 μ m diameter and bulk samples from 19 potential source areas (PSAs) in northern and southern Victoria Land (NVL and SVL), including from the ice-free McMurdo Dry Valleys (MDV). Because records from the Talos Dome currently suggest that ice-free areas such as the MDV may be important sources for local, wind-driven dust transport on the EAIS after the LGM, we expect to observe similar trends when comparing our PSA samples from SVL to Holocene dust profiles from the Taylor Dome core, and likewise from NVL to Holocene profiles in the Talos core. ⁸⁷Sr/⁸⁶Sr and ϵ_{Nd} compositions from our PSAs are similar to existing PSA records from Antarctica.

At present, Sr and Nd isotopic systems are commonly used to identify dust provenance in Antarctic ice cores [1], however, such studies have yet to be complimented with Hf signatures and REE chemistry. Thus, forthcoming results from this study may be especially useful for distinguishing dust flux evolution during the last deglaciation.

[1] Delmonte *et al.* (2010) *Journal of Quaternary Science* **25**, 1327-1337. [2] Gaeiro *et al.* (2007) *Chemical Geology* **238**, 107-120. [3] Delmonte *et al.* (2002) *Annals of Glaciology* **35**, 306-312. [4] Kohfeld and Tegen (2007) *Treatise on Geochemistry*, 1-26.

Modelling the migration of mercury in a column experiment: biotic against abiotic mechanisms

P. BLANC^{1*}, A. BURNOL¹, J. HARRIS-HELLAL¹
AND V. LAPERCHE¹

¹BRGM, BP36009, 45060, Orléans, France

(*correspondance : p.blanc@brgm.fr)

Apart from the behavior of mercury in terrestrial surface aquatic environment, few data are still available concerning its migration in subsurface and deep aquifers. A column experiment had been design in order to reproduce the Hg methylation by sulphate and iron reducing bacteria. Based on the experimental results, a modelling exercise had been carried out to enlighten the chain of reactions responsible for methylmercury formation in such an environment.

The numerical modelling is realised by using the Phreeqc-2 code [1] and the Thermodem database [2]. The hydrodynamics of the column is first parameterized by modeling a tracer test, allowing to realistically adjust a double porosity model. Then, the inorganic part of the model inputs include the solid substrates used (silicic sand + iron hydroxydes previously spiked with a mercury nitrate solution) and the inflowing solution. In the latter cases, this includes the chemical perturbations induced by three successive bacterial inoculation events. The organic part of the model strats from the inoculum preparation and takes into account the nature of the bacterial load (sulphate and iron reducing) and the addition of an organic substrate (Na-Lactate).

For the parameters pH, Eh, [S]_T, [Fe]_T and [Hg]_T, a satisfactory agreement is found by considering only the inorganic part of the chemical system. The total dissolved mercury concentration is slightly improved by adding a non electrostatic Hg surface complexation model. Methyl mercury is also produced. However, its amount in the analysed samples is shown to depend strongly on the presence of potential methyl donors in the inflowing solution.

[1] Parkhurst and Appelo (1999) USGS WRIR 99-4259, [2] Blanc *et al.* (2012) *Appl. Geochem.* **27**, 2107-2116.

Computational science in nuclear waste management: *ab initio* investigation of f-elements bearing Monazite.

A.BLANCA-ROMERO*¹, G. BERIDZE¹
AND P. M. KOWALSKI¹

¹ Forschungszentrum Juelich GmbH, Institute of Energy and Climate Research - IEK-6: Nuclear Waste Management, D-52425 Juelich, Germany
(*correspondence: a.blanca.romero@fz-juelich.de, p.kowalski@fz-juelich.de)

A safe disposal of nuclear waste is of great importance not only for the nuclear engineering but also for the general safety of society. One of the challenges in nuclear waste storage is to find suitable materials that are able to immobilize minor actinides such as Np, Am and Cm. The monazite-type orthophosphates are known to be able to incorporate actinides into their structure and preserve their crystalline character. Because of its resistance to radiation damage and chemical durability monazite is a promising host matrix [1]. In our institute we perform systematic experimental and computational studies of monazite ceramics that aim into in-depth understanding of the properties of these materials and their behavior upon incorporation of actinides. In our research we extensively use first-principles calculations to complement the experimental effort. Combination of both approaches allows us to learn how to reliably compute “tricky” 4f and 5f materials using modern methods of computational quantum chemistry.

In this contribution we present a systematic first-principles studies of the structural, thermodynamic, electronic and vibrational properties of Monazite-type LnPO₄ ceramics (where Ln=La, Ce, Pr, Nd, Sm, Eu, Gd, Tb, Dy). The calculations were performed using Density Functional Theory (DFT) with different variations of the generalized gradient approximation as well as with the DFT+U approach to correct for the strong on-site Coulomb repulsion. We calculated the structural parameters, vibrational frequencies, and the enthalpies of formation as well as the excess enthalpies of solid solutions of these compounds. Our results are confronted with a variety of experimental data (structural data [2,3], solid formation and solution enthalpies [3,4], IR and Raman spectroscopies [3,5]) and previous DFT calculations [3]. We will show that such a comparison allows for a proper assessment of the computational methods, and a better constraint of Hubbard U parameter for DFT+U method.

[1] H. Schlenz, J. Heuser, A. Neumann *et al.* (2013) in press
[2] H. Schlenz and J. Heuser (2013) in press [3] J. R. Rustad (2012) *American Mineralogist* **97**, 791 [4] K. Popa, R. Konings, and T. Geisler (2007) *J. Chem. Thermodynamics* **39**, 236 [5] K. Ruschel *et al.* (2012) *Miner. Petrol* **105**, 41.

First-principles investigation of equilibrium iron isotope fractionation in oxide and sulfide minerals

MARC BLANCHARD^{1*}, CARLOS PINILLA¹, FRANCK POITRASSON², MERLIN MÉHEUT², MICHELE LAZZERI¹, FRANCESCO MAURI¹ AND ÉTIENNE BALAN¹

¹IMPMC, Université Pierre et Marie Curie, CNRS, IRD, 4 place Jussieu, 75252 Paris Cedex 05, France
(*correspondence: marc.blanchard@impmc.upmc.fr)
²GET, CNRS-Université de Toulouse, IRD, 14-16 avenue Edouard Belin, 31400 Toulouse, France

The equilibrium isotope fractionation factor between two phases, which is a key parameter for the interpretation of isotopic variations among natural samples, can be determined from their reduced partition function ratios, also called β -factors. In most cases, β -factors cannot be measured directly but they can be calculated from vibrational properties following various approaches. For solids with Mössbauer-sensitive elements like Fe, the β -factor can be determined either from Mössbauer spectroscopy by measuring the temperature dependence of the isomer shift [1], or from nuclear resonant inelastic X-ray scattering spectra (NRIXS) by measuring the partial density of states of the resonant atom or by using the moments of the raw NRIXS spectrum [2,3]. An alternative approach consists in determining the theoretical vibrational density of states of the solid using first-principles calculations [4].

In this presentation, the Fe β -factors of oxide and sulfide minerals (mainly hematite, goethite and pyrite) computed using first-principles methods based on density functional theory with or without the addition of a Hubbard U correction (DFT and DFT+ U) will be compared with the available Mössbauer- and NRIXS-derived data. While all three methods must give consistent results, discrepancies are observed in some cases. The possible sources of discrepancy will be discussed.

[1] Polyakov (1997) *GCA* **61**, 4213-4217. [2] Polyakov *et al.* (2005) *GCA* **69**, 5531-5536. [3] Dauphas *et al.* (2012) *GCA* **94**, 254-275. [4] Blanchard *et al.* (2009) *GCA* **73**, 6565-6578.

Cosmogenic ^3He and ^{10}Be production rates at high elevation (> 3800 m)

P.-H. BLARD¹, R. BRAUCHER², D. BOURLES²
AND J. LAVE¹

¹CRPG, UMR 7358 CNRS-Université de Lorraine,

Vandoeuvre-lès-Nancy, France, blard@crpg.cnrs-nancy.fr

²Aix-Marseille Université, CNRS-IRD UM 34 CEREGE,

Aix-en-Provence, France

Recent cross-calibrations of cosmogenic ^3He in pyroxene and ^{10}Be in quartz [1] showed that, at low elevation (< 2000 m), the $^3\text{He}/^{10}\text{Be}$ production ratio was probably ~40% higher than the value of ~23 initially defined in the 90's. This recent update is consistent with the last independent determinations of the sea level high latitude production rates of ^{10}Be and ^3He , that are about 4 and 125 $\text{at}\cdot\text{g}^{-1}\cdot\text{yr}^{-1}$, respectively [e.g. 2, 3]. However, major questions remain about these production rates at high elevation, notably because the elevation dependence of the $^3\text{He}/^{10}\text{Be}$ production ratio is controversial [4]. It is thus crucial to produce new high precision cross-calibration data at high elevation.

Here we report new precise measurements of ^3He in pyroxenes and ^{10}Be in quartz, from dacitic moraines located at 4820 m in the Southern Altiplano (22°S, Tropical Andes). The obtained $^3\text{He}/^{10}\text{Be}$ production ratio is 33.3 ± 0.9 (1σ). This value is statistically undistinguishable from the production ratio measured at 1333 m [1], which reveals that the $^3\text{He}/^{10}\text{Be}$ production ratio in pyroxene and quartz is almost invariant with elevation. When combined with the absolute ^3He production rate locally calibrated in the Central Altiplano, at 3800 m, from a 15.3 ± 0.5 ka old surface, these new data permit to define the absolute production rate of cosmogenic ^{10}Be at high elevation. After scaling to sea level and high latitude, this calibration yields a sea level high latitude P_{10} ranging from 3.7 ± 0.2 to 4.1 ± 0.2 $\text{at}\cdot\text{g}^{-1}\cdot\text{yr}^{-1}$, depending on the used scaling scheme.

This new refinement of the cosmogenic dating tool will significantly improve both the accuracy and the precision of paleoglaciologists chronologies in the Tropical Andes.

[1] Amidon *et al.* (2009) *Earth Planet. Sci. Lett.* **280**, 194-204.

[2] Putnam *et al.* (2010) *Quat. Geochron.* **5**, 392-409.

[3] Blard *et al.* (2006) *Earth Planet. Sci. Lett.* **247**, 222-234.

[4] Gayer *et al.* (2004) *Earth Planet. Sci. Lett.* **229**, 91-104.

Calcium isotopes in evaporites constrain sulfate- vs calcite-rich seawater chemistry

C.L. BLÄTTLER* AND J.M. HIGGINS

Department of Geosciences, Princeton University, Guyot Hall,
Princeton, NJ 08544, U.S.A.

(*correspondence: blattler@princeton.edu)

The calcium-isotope behavior of evaporite formations is proposed as a new method for constraining the composition of ancient seawater. Evaporite cycles that reach the halite facies are expected to record a different range of calcium-isotope values depending on the initial major-element chemistry of seawater. In the modern ocean, where sulfate is far in excess of calcium (28 mmol/kg SO_4^{2-} compared to 10 mmol/kg Ca^{2+}), approximately 90% of the initial calcium is removed as carbonate or sulfate minerals by the time halite saturation is attained. In contrast, an excess of calcium relative to sulfate, as suggested for intervals such as the Cretaceous and the Silurian [1], leads to significant depletion of sulfate, but a much smaller proportion of calcium removed at the point of halite saturation. Isotopic fractionations associated with the precipitation of carbonates, gypsum, and anhydrite lead to Rayleigh distillation of calcium within an evaporite basin, where precipitates from more concentrated brines become enriched in the heavy isotopes of calcium, dependent on the total amount of calcium removed. The range in calcium-isotope ratios obtained by sampling different stages of the carbonate-sulfate evaporite facies is therefore diagnostic of initial sulfate- or calcium-rich seawater.

In beaker evaporation experiments, the $\delta^{44/42}\text{Ca}$ value of modern sulfate-rich seawater becomes enriched by 1.2‰ from its initial composition to the beginning of halite precipitation, whereas the $\delta^{44/42}\text{Ca}$ of a calcium-rich and sulfate-poor solution evolves by <0.2‰. The $\delta^{44/42}\text{Ca}$ values of accompanying precipitates demonstrate the same characteristics, but are offset from the fluid by 0.5–0.7‰. Analyses of geological evaporites from various Phanerozoic periods show how this behavior translates to natural samples as well. This new method provides an independent test for variations in the major-element chemistry of paleoseawater.

[1] Lowenstein *et al.* (2001), *Science* **294**, 1086–1088.

The study of the ferriferous mineral water in Kareliya by isotopic and chemical tracers.

BLAZHENNIKOVA I.V.¹, AVRAMENKO I.A.²
AND TOKAREV I.V.³

¹ blazhennikova@mail.ru

² i.a.avramenko@gmail.com

³ tokarevigor@gmail.com

From 1979 to 2012 the ferriferous mineral water in Karelia (northwest of Russia) was studied by monitoring the isotope and chemical tracers.

In 1979-1980 stable isotopes (²H, ¹⁸O) had fractionated composition (on the plot $\delta^2\text{H}$ vs. $\delta^{18}\text{O}$ the points shifted right from the meteoric line), which was caused by cryogenic metamorphism at partial freezing of water in the last glacial period. The composition of stable isotopes has strongly changed for the last 25 years (the points fit on the global meteoric line now). Other isotope tracers ($\delta^{13}\text{C}$, ³He, ⁴He, ²⁰Ne, ²³⁴U/²³⁸U, ³H) also have changed and become closer to the recharge water. So the isotope data show that the water of the studied area in 1979-1980 was formed by mixing "old" and "young" components. But now we observe the rapid penetration of the atmospheric precipitation and gradually disappearance of the "old" component.

Though the seasonal variations are detected, the average chemical composition of the mineral water (major components and microelements) has not changed for the last decades in contrast to the isotope tracers. Probably the relative constancy of the chemical composition indicates that iron accumulation in the water is due to melanterite (Fe[SO₄] \cdot 7H₂O) dissolution. Melanterite has formed from pyrite during the last glaciations and filled cracks and pores. The reserves of this mineral are not known and because of the rapid changes in the isotopic characteristics we can talk about the over-exploitation of the mineral water deposit. Data suggests the need for strict sanitary control of water quality.

Selenium distribution linked to monsoon climate in the Chinese Loess Plateau

TIM BLAZINA¹*YOUBIN SUN² MICHAEL BERG¹
LENNY H.E. WINKEL^{1,3}

¹ Eawag: Swiss Federal Institute of Aquatic Science and Technology, 8600 Duebendorf, Switzerland
(*correspondence: tim.blazina@eawag.ch)
michael.berg@eawag.ch, lenny.winkel@eawag.ch

² Institute of Earth Environment, Chinese Academy of Sciences, 710075 Xi'an, China, sunyb@ieecas.cn

³ Swiss Federal Institute of Technology (ETH) Zurich, 8092 Zurich, Switzerland, lwinkel@ethz.ch

Selenium (Se) is a vital trace element for human health with a narrow range between deficiency and toxicity. Diets deficient in Se have been linked with various diseases, while those with an excess can lead to toxicity. Predicting where Se deficiency/toxicity occurs is challenging due to the heterogeneous terrestrial distribution of Se and limited knowledge on what controls this heterogeneity. It has been proposed that the largest natural flux of Se to the terrestrial environment is via wet deposition from the atmosphere.

Our research uses the loess-paleosol and red clay deposits on the Chinese Loess Plateau (CLP), the largest area of windblown sediments on Earth and one of the best available records of climate change, to elucidate how atmospheric deposition of Se relates to its terrestrial distribution. We present a 6.8Ma record of variation in the Se concentration in the Lingtai section from Central CLP. In interglacial climatic periods from 2.31-1.56Ma and 1.6-1.3Ma, we find very strong positive correlations ($R^2=0.97$ and 0.85 respectively) between Se concentration and summer monsoon index, a proxy for effective precipitation. In later interglacial periods from 1.26-0.83Ma and 0.78-0.16Ma, the strong positive correlation with precipitation is absent or there is a negative correlation ($R^2=0.21$ and 0.50 , respectively) and we find dust input plays a greater role. As both precipitation and dust inputs are determined by the strength of the East Asian Monsoon, we are able to show that Se deposition in the CLP (at the Lingtai section), is directly related to past changes in the monsoon climate system.

Methanotrophic bacteria drive seasonal anoxia and the formation of a benthic nepheloid layer in a deep alpine lake

J. BLEES¹, H. NIEMANN¹, C. B. WENK¹, J. ZOPFI¹, M. VERONESI², C. J. SCHUBERT³ AND M.F. LEHMANN¹

¹Department of Environmental Sciences, University of Basel, Basel Switzerland; moritz.lehmann@unibas.ch

²Institute of Earth Sciences, University of Applied Sciences of Southern Switzerland, Canobbio-Lugano, Switzerland

³Swiss Federal Institute of Aquatic Science and Technology (EAWAG), Kastanienbaum, Switzerland

We investigated the composition and formation mechanisms of a seasonal benthic nepheloid layer (BNL), a layer of high suspended particle concentration, in the monomictic southern basin of Lake Lugano. During stratified water column conditions, lasting from early summer until winter mixing in January/February, the BNL developed from the sediment-water interface and expanded 20–30 m into the water column, in tandem with the rising redox transition zone. Methanotroph-derived fatty acids ($C_{16:1\omega5-8}$), with $\delta^{13}C$ values as low as -90‰, dominated the fatty acid pool within the BNL. Based on C-isotope data, we calculated that up to 98% of the lipid carbon is methane-derived, suggesting that the BNL is primarily composed of aerobic methane oxidising bacteria. The lipid composition indicates that the methanotrophic community in the BNL in Lake Lugano is dominated by Type I methanotrophic bacteria. Total cell numbers ranged between 0.9 and 3.6×10^6 cells mL⁻¹ during full development of the BNL. In incubation experiments we determined CH₄ turnover rate coefficients that translate into potential CH₄ oxidation rates as high as $20 \mu\text{M d}^{-1}$. The corresponding cell-specific rates were up to 49×10^{-5} pmol cell⁻¹ h⁻¹, which is reasonable for Type I methanotrophic bacteria. CH₄ oxidation in the BNL was limited by the diffusive supply of O₂ from the upper hypolimnion, implying that CH₄ oxidation is the primary driver of the seasonal expansion of the anoxic bottom water volume, and explaining the vertical migration of the BNL in response to its own O₂ consumption. Our study demonstrates that methanotrophic activity at the interface between oxic and anoxic water masses can drive the formation of a BNL. Such a layer of high bacterial density and high CH₄ oxidation potential may thus function as an efficient CH₄ barrier, preventing CH₄ transport into surface waters, and eventually evasion to the atmosphere.

Niobium Mineralization in a Magnetite-Rich Carbonatite, Elk Creek, Nebraska (USA)

¹M. BLESSINGTON, ¹R. KETTLER, ²P. VERPLANCK AND ³G.L. FARMER

¹Department of Earth and Atmospheric Sciences, University of Nebraska, Lincoln, NE, 68588-0340, USA

²U.S. Geological Survey, Central Mineral Resources Science Center, Box 25046, Denver Federal Center, MS-973, Denver, CO 80225-0046, USA

³Department of Geological Sciences, University of Colorado, Boulder CO 80309-0399, USA

The Elk Creek carbonatite is a roughly circular 7km*7km intrusive carbonatite-alkaline syenite complex located in Southeast Nebraska. The complex is overlain by younger marine sediments and quaternary glacial till – No surface exposure exists, but drill cores collected by Molycorp in the 1970s-80s have been made available to the public for research. The carbonatite comprises several geochemically distinct intrusive phases with notable anomalous enrichment in rare earth elements and niobium. These phases include a dolomite-magnetite carbonatite (“magnetite beforite”) phase which consists of two lobes, each approximately 0.1 square kilometer in size and extending downward to the maximum extent of drilling (900 meters). This dolomite-magnetite carbonatite is typically an aphanitic microbreccia including accessory apatite, biotite, and pyrite. Hematite dusting on mineral surfaces is pervasive, and veining is widespread. Fragments of dolomite-magnetite carbonatite are also present in a spatially-associated breccia along with fragments of apatite-dolomite carbonatite.

XRF analysis of a powdered bulk sample of the dolomite-magnetite carbonatite yields data that indicate that the dolomite-magnetite carbonatite differs from other carbonatite phases in that it has much higher Ti, Th, and W compared to the other intrusive phases. It also differs from the other intrusive phases in that Fe > Mg and it is depleted in light REE relative to the other rocks. The magnetite carbonate also contains micron-scale (0.01-0.10mm diameter) accessory niobium pyrochlore, disseminated in dolomite and biotite, in economically-significant concentrations (10,000ppm or higher Nb in bulk sample). The prevalence of pyrochlore across the entire complex is directly related to the presence of this dolomite-magnetite carbonatite.

Tuning the Torch for Lead Isotopes: The Battle in Lugdunum

JANNE BLICHERT-TOFT¹

¹ENS Lyon, 69007 Lyon, France (jblicher@ens-lyon.fr)

To celebrate Francis Albarède's pioneering work in developing high-precision, high-throughput Pb isotope analysis by Tl doping and sample-standard bracketing MC-ICP-MS [1], I here review some selected contributions by the Lyon group to cosmochemistry, geochronology, Mars, mantle geochemistry, and archeometry using this technique. The superior precision of MC-ICP-MS compared to unspiked Pb TIMS work led us to revisit several classic but crucial questions involving Pb isotopes. We determined the age of the Solar System from Pb-Pb measurements of refractory inclusions in meteorites [2], a result only now confirmed by independent means despite tumultuous revisions of U isotope compositions and major improvements in analytical precision and blanks since our early work. We further re-determined the initial Pb isotope composition of the Solar System and the solar nebula Th/U [3] and found Pb isotope evidence that some asteroids accreted and differentiated within only one million year of the formation of the Solar System [4], thereby placing constraints on nebular evolution. Our Pb-Pb ages of SNCs [5], the shergottites in particular, are important because they finally bring the ages of Martian meteorites (4.1 Ga) into agreement with cratering chronology and satellite observations for Mars, as well as with extinct radioactivities, but are controversial because ages inferred from other chronometers are far younger (160 Ma). The high throughput of MC-ICP-MS further changed the geochemical approach to understanding mantle heterogeneities in volcanic time series, such as in Hawaii [6], and the exploring of length and time scales of isotopic heterogeneities along the world's mid-ocean ridges and, hence, the deep Earth, allowing for full-fledged spectra amenable to physical and statistical modeling to be obtained [7, 8]. A spectacular new result is the evidence of Pb-Hf isotopic 'toggles' along the SEIR, and their random distribution, indicating that the local mantle has lost all memory of its mixing history [9]. Another key result was the Pb-Hf correlation in Hawaiian lavas showing that entrainment of the upper mantle by plumes is minimal [10]. We currently apply Pb isotopes to tracking Pb ore provenance in ancient Rome in order to shed new light on the heavy metal record of local economic activity, urban development, and warfare.

[1] White *et al.* (2000) [2] Bouvier *et al.* (2007) [3] Blichert-Toft *et al.* (2010a) [4] Blichert-Toft *et al.* (2010b) [5] Bouvier *et al.* (2009) [6] Blichert-Toft & Albarède (2009) [7] Agraniér *et al.* (2005) [8] Meyzen *et al.* (2007) [9] Hanan *et al.* (submitted) [10] Blichert-Toft *et al.* (1999).

Impact of long-term nitrogen deposition on the fate of nitrogen in peatlands

CHRISTIAN BLODAU^{1,2} KATARZYNA ZAJAC²
AND YUANQIAO WU¹

¹University of Münster, christian.blodau@uni-muenster.de

²University of Bayreuth, katatzyna.zajac@uni-bayreuth.de

Large areas of northern peatlands in Europe and North America have been affected by elevated long-term nitrogen deposition at levels of 0.5 – 2 g N m⁻² yr⁻¹, and in extreme cases up to 5 g N m⁻² yr⁻¹. The consequences of this deposition for the fate of nitrogen, especially the allocation of the element between vegetation and peat and the mobility in dissolved form, and for the carbon cycle are only poorly known to date. We investigated this issue using ecosystem modelling based on a long-term fertilized site and experimentally with mesocosms from five different European peatlands that have been exposed to range of 0.2 to 5 g N m⁻² yr⁻¹. The mesocosms were placed in a greenhouse under controlled light and water table conditions for a period of 160 days after an initial equilibration period. We added a ¹⁵N-NO₃ tracer with irrigation water to determine how the allocation of nitrogen in these peatlands differed and also investigated the carbon exchange and productivity of the sites under these conditions. The results show that the Sphagnum moss layer was not severely impaired at any site and that even under severely N polluted conditions nitrogen was still taken up by the moss layer. The effectivity of the moss filter for the element declined, however, and some breakthrough occurred, whereas nitrogen in the pristine sites seemed to be indirectly transferred into peat by the root system of vascular plants. Overall more nitrogen was taken up by vascular plants in the more polluted sites. Elevated nitrogen deposition lead to raised ammonium and DON concentrations even at lower deposition levels but strongly elevated nitrate concentrations only occurred at the most polluted site. Substantial differences in carbon cycling between sites did not occur in the mesocosm experiments. The ecosystem modelling exercise using the new model PEATBOG showed that the most important impacts of nitrogen deposition are to be expected are through indirect changes in the ecosystem structure, which was altered from moss to shub and then grass dominated in the simulated system. The replacement of plant functional types lead to a higher rate of nitrogen processing in the system and higher productivity and carbon uptake. Also in the simulations the peatland remained a sink of nitrogen with only moderately raised nitrogen export.

Characterization of metabolically active microorganisms in an hydrothermal active field in the Okinawa Trough (IODP Exp. 331)

MACRO BLÖTHE*, ANJA BREUKER
AND AXEL SCHIPPERS

Federal Institute for Geosciences and Natural Resources
(BGR), Stilleweg 2, D-30655 Hannover, Germany
(marco.bloethe@bgr.de; anja.breuker@online.de;
axel.schippers@bgr.de)

The BGR project, as part of the post-cruise research of IODP Expedition 331, Deep Hot Biosphere, shall test the hypothesis that the quantitative microbial community composition and the cultivable microorganisms in hydrothermally influenced deeply-buried marine sediments are significantly different from those in cold and temperate deeply-buried marine sediments. The previously successfully applied molecular techniques real-time PCR (qPCR) and catalyzed reporter deposition - fluorescence *in situ* hybridisation (CARD - FISH) shall be used as well as cultivation and stable isotope-probing to proof the existence of a deep hot biosphere, to describe it and to isolate novel microorganisms. The domains *Archaea*, *Bacteria* and *Eukarya* as well as the JS1 candidate group, *Chloroflexi*, *Geobacteraceae*, *Crenarchaeota* and the functional genes *dsrA*, *mcrA*, *aprA*, and Rubisco (*cbbL*) have been quantified via qPCR. All genes have been detected in different copy numbers. The overall order of abundance is *Archaea* > *Bacteria* > *Eukarya*. Directly after IODP Expedition 331 in October 2010, culture media were inoculated with IODP samples at different temperatures and the enrichment cultures are maintained since then. Growth is continuously checked about every three months and in case of growth, colonies are picked and transferred to fresh media. Several aerobic and anaerobic enrichments have been obtained so far. To explore microbial activity in the original samples microcalorimetric measurements showed a considerable activity at 90°C which was partly attributed to microbial activity. The microcalorimetric measurements revealed activity of thermophilic microorganisms in the IODP Exp. 331 samples.

Sulfur and iron speciation in warm deep sediments affected by dry deposition of iron

B. BLONDER¹* AND A. KAMYSHNY, JR.¹

¹Department of Geological and Environmental Sciences, The Faculty of Natural Sciences, Ben-Gurion University of the Negev, P.O. Box 653, Beer Sheva 84105, Israel,
(*correspondence: blonderbarak@gmail.com,
alexey93@gmail.com)

The Gulf of Aqaba is a unique natural laboratory for a research of the impact of atmospheric dry deposition on biogeochemistry of marine sediments. Atmospheric iron deposition is 3.65 mmol m⁻² year⁻¹ [1], and total iron content of sediment at 700 m depth is 2.0 – 5.7 mmol kg⁻¹ wet sediment. We sampled sediment at four locations with various overlying water depths.

At water depths 300 – 700 m the depth of oxygen penetration into warm upper sediment (c.a. 21°C) is 8-14 mm. In anoxic sediments, combination of moderate TOC content (0.1-0.6%) with high sulfate concentration (32 mM) fuels organoclastic bacterial sulfate reduction. Concentrations of Fe(II) in the pore-waters are as high as 78 μM, and concentrations of dissolved Mn are as high as 76 μM. Combination of low hydrogen sulfide concentration in pore-waters (≤0.37 μM), low concentrations of soluble sulfide oxidation intermediates ([S₂O₃²⁻] ≤ 0.55 μM, [SO₃²⁻] ≤ 0.14 μM) and low sedimentary S⁰ content (≤0.37 mmol kg⁻¹ wet sediment) indicate that transformation of hydrogen sulfide to pyrite is fast enough to prevent sulfide oxidation by Fe(III) phases. Pyrite is the main sulfur pool in the sediment solid phase, and its content is up to 10.6 mmol kg⁻¹, with a maximum at 15 – 25 cm bsf.

At the shallow sediments (21 m water depths) penetration depth of oxygen is only 1 mm, and hydrogen sulfide concentration in pore-waters is as high as 12 μM. Dissolved iron and manganese concentrations below 5 cm bsf are lower than in the deeper sediments <1 μM and <0.5 μM, respectively. Concentrations of sulfide oxidation intermediates in pore waters ([S₂O₃²⁻] < 4.05 μM, [SO₃²⁻] < 3.64 μM) as well as in the solid phase [S⁰] = 0.07-1.37 μmol kg⁻¹ wet sediment are higher than at deeper locations.

The sediment of the Gulf of Aqaba presents an interesting example of transition of pore-water composition with depth from sulfidic (H₂S-rich) to ferruginous (Fe(II)-rich).

[1] Chase *et al.* (2006) *Global Biogeochem Cy* **20**, GB3017.

Mass independent isotope fractionation of mercury: Why it is such a useful tool in biogeochemistry and ecology

J. D. BLUM¹

¹Dept of Earth and Environmental Sciences, University of Michigan, Ann Arbor, MI 48109
(jdblum@umich.edu)

Mercury is a globally distributed and highly toxic heavy metal with both natural and anthropogenic sources. Its mobility, toxicity and bio-accumulative properties change dramatically as it is transformed through microbial, photochemical and dark abiotic reactions in the environment. Multiple biogeochemical transformations of mercury determine its movement and bioavailability, and knowledge of these processes can aid in developing strategies for minimizing human and wildlife exposure to its most toxic forms. The seven stable isotopes of mercury fractionate in the environment due to an unusually wide range of physical processes. Mass-dependent fractionation (MDF) occurs during most biotic and abiotic reactions that have been investigated. Mass-independent fractionation (MIF) of mercury can be caused by the magnetic isotope effect, the nuclear volume effect and by UV self-shielding. Each fractionation mechanism imparts a diagnostic pattern of isotopic variation and thus mercury isotope ratios can be used to unravel complex biogeochemical pathways for mercury. Large-magnitude MIF of odd isotopes is uniquely produced by photochemical reactions, which are important because they can degrade mercury from the toxic methylated form to a volatile gas. In addition to isotopic fingerprinting of sources, MIF and MDF in natural samples have been calibrated against experimental determinations of fractionation factors to identify reactions in natural systems and estimate their reaction progress. Because MIF is unaffected by biotic processes it preserves a memory of biogeochemistry before entry into the base of foodwebs.

Seawater Trace Metals in acidified condition: an accumulation study in the blue mussel *Mytilus galloprovincialis* off Vulcano Island submarine vents (Italy)

BOATTA F.^{1*}; D'ALESSANDRO W.²; GAGLIANO A.L.¹;
FEDERICO C.²; CALABRESE S.¹; LIOTTA M.^{2,3};
MILAZZO M.¹ AND PARELLO F.¹

¹DiSTeM University of Palermo, via Archirafi, 36, 90123 Palermo, Italy (*fulvioboatta@gmail.com)

²INGV, Palermo, via U. La Malfa 153, 90146 Palermo, Italy

³DiSTABiF; Seconda Università degli Studi di Napoli, 43, 81100 Caserta, Italy

Ocean acidification is linked to the increasing concentration of atmospheric anthropogenic carbon dioxide, and this process might have negative ecological and economic effect worldwide.

Areas with naturally high levels of CO₂ can help us to achieve a better understanding of this issue. Submarine vents in the Levante Bay of Vulcano Island (Italy) are CO₂-dominated resulting in seawater acidification, and producing a stable pH gradient (from 8.2 down to 5.5) across the bay [1]. We now know that ocean acidification is tightly linked to the mobility and bio-availability of heavy metals.

In that area a transect covering the pH conditions which will be found up to the end of this century has been individuated and a Blue Mussels transplant experiment was done along this gradient in order to estimate the trace metal accumulation capability related to the seawater acidification.

Major and Trace elements were analyzed both in seawater and in the mussels' tissue.

At the end of the experiment, the animals showed an increase of concentration for some elements such as Fe and V with respect to blanks.

The present study provides preliminary data on a particular aspect related to the ocean acidification problem.

[1] Boatta *et al.* (2013) Marine Pollution Bulletin, in press.
DOI: 10.1016/j.marpolbul.2013.01.029

MgSO₄ phases: hydration, spectroscopy and S isotope partitioning

EMA BOBOCIOIU AND RAZVAN CARACAS

Laboratoire de Geologie de Lyon (LGLTPE) CNRS UMR 5276, Ecole Normale Supérieure de Lyon Université Claude-Bernard Lyon 1, 46, allée d'Italie, 69364 Lyon cedex 07, France

We study the relative stability of several magnesium sulfate minerals using first-principles calculations based on the density functional theory in the ABINIT implementation. These phases might be present on the surface of Mars or on a variety of smaller icy bodies from the outer solar system. Our calculations show that, if involved in the water cycle of Mars, the magnesium sulfates must be already present as hydrated phases: the anhydrous phases are easily absorbing water and, in turn, the complete dehydration of these phases requires large temperature, unattainable on Mars. We equally compute the Raman and infrared spectra of several phases to offer reference spectra for *in situ* spectroscopic identification. Apart from the appearance of the water bands, the hydration also changes the position of several lower-frequency bands. Using the spectroscopic calculations we determine the influence of hydration on the S isotope partitioning. We show that it is highly dependent on the temperature. For temperatures specific to the surface of Mars, hydration of the anhydrous phase leads to an enrichment in the S³⁴. The effect on the already hydrated phase is opposite: further hydration enriches lighter isotopes.

Partitioning of trace elements between Na-bearing majoritic garnet and melt at 8.5 GPa and 1500–1900°C

A.V. BOBROV^{1*}, YU.A. LITVIN², A.V. KUZUYURA², A.M. DYMSHITS³ AND T. JEFFRIES⁴

¹Geological Faculty, Moscow State University, Moscow, Russia (*correspondence: archi@geol.msu.ru)

²Institute of Experimental Mineralogy, Chernogolovka, Russia

³Sobolev Institute of Geology and Mineralogy, Novosibirsk, Russia

⁴National History Museum, London, UK

The new experimental data on trace element partitioning between Na-bearing majoritic garnet and melt at 8.5 GPa and 1500–1900°C applicable to partial melting of Na-rich eclogite is presented. The Na-bearing garnet is a liquidus phase of the system at 1850–1650°C being accompanied by enstatite-rich pyroxene at lower temperatures. With the temperature decrease, Na concentration in garnet increases up to >1 wt % Na₂O due to progressive incorporation of Na majorite (Na₂MgSi₅O₁₂). Most of the studied trace elements are incompatible, except for Er, Tm, Yb (in some runs), Lu, and Sc (in all runs), which partition into garnet. The main feature of the trace-element partitioning in our experiments is the different behaviour of the LREE (La, Ce, Pr) in comparison with MREE and HREE (Nd, Sm, Eu, Gd, Tb, Dy, Y, Ho, Er, Tm, Yb, and Lu). Significant increase of D values for LREE with increase of Na₂O concentration in garnet is observed. As predicted from lattice strain, partitioning coefficients for REEs entering the X site of garnet exhibit a near-parabolic dependence on ionic radius. Other elements including the LILE (Rb, Sr, Ba), Sc, as well as Zn, Ta, and Pb have a clear affinity for aluminosilicate melt. The results of the study are applied to the formation of inclusions of Na-bearing majoritic garnets in diamonds and equilibrium melts, which are significantly enriched in LREEs being very similar to kimberlitic and OIB melts.

This study was supported by the Russian Foundation for Basic Research (project no. 12-05-00426).

Nitrifying potential in *Beggiatoa* mats from marine mangroves

AUDREY BOC^{1*}, OLIVIER GROS¹, ANNIET M. LAVERMAN² AND MATHIEU SEBILO³

¹ Equipe Biologie de la Mangrove, UMR 7138, Laboratoire de Biologie Marine, Université des Antilles et de la Guyane, 97159 Pointe-à-Pitre, Guadeloupe, France aboc@univ-ag.fr (*presenting author)

² Sysiphe, UMR 7619 UPMC/CNRS, Université Pierre et Marie Curie, 75252 Paris Cedex 05

³ Bioemco, Equipe Géochimie organique et minérale de l'environnement, UMR 7618 UPMC, Université Pierre et Marie Curie, 75252 Paris Cedex 05

Marine mangroves are intertidal marine ecosystems found in tropical and sub-tropical areas. A development of white bacterial mat can be found in Guadeloupian marine mangroves. This mat consists of a layer of micro-organisms deposited above the anoxic sediment consisting of eukaryotes (e.g. diatoms, nematodes) and prokaryotes (e.g. filamentous cyanobacteria, filamentous sulfur-oxidizing bacteria, archae). Most of the filamentous bacteria found in the mat belong to the genus *Beggiatoa*. These bacteria contain genes encoding both for sulfur oxidation (production of sulfate) and ammonium oxidation (production of nitrate).

The aim of this study was to determine the potential for nitrification in these *Beggiatoa* mats. Potential nitrification rates were carried out with the *Beggiatoa* mat collected in a marine mangrove. The *Beggiatoa* mat or filaments were amended with sea water containing different NH_4^+ concentrations and incubated under oxic conditions. The increase in nitrate concentration was measured after 15 hours of incubations. Potential nitrification rates showed a large variation ranging from 0.2 to 2200 μg nitrate $\text{N L}^{-1} \text{h}^{-1}$. Our study showed the potential for nitrification in *Beggiatoa* filaments, implying an important link between the N and S cycles, by sulfur oxidizing bacteria, in these mangrove systems.

Examination of Magma Degassing Paths Based on Melt Inclusions

R. J. BODNAR¹, R. ESPOSITO², E. GAZEL¹, L. MOORE¹, M. STEELE-MACINNIS¹ AND P. WALLACE³

¹Dept. of Geosciences, Virginia Tech, Blacksburg, VA 24061 USA. rjb@vt.edu; egazel@vt.edu; moorelr@vt.edu; mjmaci@vt.edu

²DISTAR, Università degli Studi di Napoli Federico II, Napoli, 80134, Italy. rosario.esposito3@unina.it

³Dept. of Geological Sciences, University of Oregon, Eugene, OR 97403 USA. pwallace@uoregon.edu

In a landmark paper, Newman *et al.* [1] suggested that the CO_2 and H_2O contents of volcanic glasses could be used to understand magma degassing processes. This approach was immediately adopted by Anderson *et al.* [2] and applied to melt inclusions (MI) in quartz phenocrysts from the Bishop Tuff to investigate the pre-eruptive volatile contents and pressures in the magma chamber during phenocryst growth and MI entrapment. In the nearly three decades since these pioneering studies, numerous MI studies have been conducted to determine magma degassing paths using this method.

The scientific basis for using $\text{CO}_2/\text{H}_2\text{O}$ systematics in MI is robust and supported by experimental data, but several unstated assumptions are required for the results to accurately define a magma degassing path. First, the trapped melt must have been at volatile saturation. Additionally, the melt (glass) that is analyzed must represent the melt that was originally trapped and must be free of any post-entrapment modifications (or it must be possible to reverse these processes before analysis or account for these changes by other means). Thus, post-entrapment crystallization on the walls of the MI, diffusional loss of H_2O from the MI and exsolution of a vapor bubble after MI entrapment are all processes that will affect the $\text{CO}_2/\text{H}_2\text{O}$ systematics of the MI.

Examination of data from a variety of sources suggests that in many cases there is clear evidence for post-entrapment modifications (primarily shrinkage bubble formation) that have not been corrected for during analysis or data interpretation. Moreover, recent studies have shown that these modifications can produce "false degassing paths" that cannot be distinguished from true degassing paths. It is also critical that MI be studied within a paragenetic context in order to constrain relative times of MI formation, and that other indicators of crystallization progress and/or depth of formation be monitored along with the $\text{CO}_2/\text{H}_2\text{O}$ systematics to confirm that the volatile data record a degassing history.

[1] Newman *et al.* (1988) *J. Volcanol. Geotherm. Res.* **35**, 75-96. [2] Anderson *et al.* (1989) *Geology* **17**, 221-225.

Cordierite nucleation and growth rates in the Torres del Paine contact aureole

¹ ROBERT BODNER, ² LUKAS BAUMGARTNER
AND C. THOMAS FOSTER

1 University of Lausanne, Switzerland, Institute of Earth Sciences [robert.bodner@unil.ch]

2 University of Lausanne, Switzerland, Institute of Earth Sciences [lukas.baumgartner@unil.ch]

3 University of Iowa, USA, Department of Geoscience [tom-foster@uiowa.edu]

The Torres del Paine (~ 12.59 Ma) intrusion consists of three granite and four mafic batches, which formed within 160 ± 11 ka (Michel *et al.* 2008, Leuthold *et al.* 2012). It intruded into fine grained pelites, sandstones, and conglomerates of the Cerro Toro and Punta Barrosa formations at a depth of 2-3 km. Its contact aureole is characterized by the occurrence of porphyroblastic cordierites (crd). The crd forming reactions are the chlorite break-down reaction (ca. 480°C) and the phengite break-down reaction (530-550°C), which is accompanied by a modal decrease in biotite and the appearance of k-feldspar

We present differences of crystal size distributions (CSDs) in a 400m long sample profile from the igneous contact to the outer part of the aureole. Samples close to the contact have the smallest crystals (radius < 0.06mm), while samples at 400m from the intrusion contain the largest crystals (radius < 0.09 mm). The maximum population density decreases from 11.5mm^{-4} close to the intrusion to 9.5mm^{-4} at distances between 200 and 400m from the intrusion. T-t paths close to the intrusion are characterized by rapid heating (e.g. to 610 °C at 40 m), while the temperature increases much slower to the cordierite-in reaction temperature in the outer aureole. The observation on crd textures were fit with with a numerical nucleation-crystallization model. We assumed diffusion controlled mineral growth and we tested different nucleation laws (e.g. Ridley and Thompson 1986, Carlson *et al.* 1995). The large differences in the temperature-time paths for samples of similar chemistry allowed us to fit nucleation and growth parameters by matching calculated and observed textures.

The resulting parameters indicate rapid completion of reaction before the thermal peak in the inner parts of the contact aureole, and continued reaction after the thermal peak in the outermost contact aureole. In the innermost part of the aureole the overstepping is several tens of degrees (50-150 °C), depending on the nucleation model and the choice of parameters. Calculations with these parameters further show a narrow transition zone (~ 5m width) of full reaction to no reaction between the prograde contact aureole and the unreacted host rock, indicating a relatively sharp isograd for sampling purposes.

Interpretation of Calcium Isotope Variations in Marine Fossil Records

BÖHM, F. AND EISENHAUER, A.

Geomar, Helmholtz Centre for Ocean Research Kiel, Kiel, Germany; fboehm@geomar.de; aeisenhauer@geomar.de

Many studies indicate the existence of calcium isotope excursions and trends in sequences of fossil marine carbonates (e.g. [1, 2]). However, interpretation of these calcium isotope variations is still controversial [3]. Several studies explain calcium isotope excursions as indicators of an imbalance between the major calcium fluxes in the oceans, riverine input and output by carbonate sediments (e.g. [2, 4]). These studies tend to neglect the direct coupling between calcium and carbonate ion fluxes in both weathering and carbonate precipitation. As a consequence the neglect may lead to very unlikely scenarios for the corresponding ocean carbon cycle. Here we present a simple numerical model to calculate mass balances for both marine calcium and carbonate ion concentrations in response to changes in the weathering and carbonate sediment fluxes. The model results clearly show that neither weathering nor carbonate sedimentation may explain observed calcium isotope variations unless extreme scenarios for the inorganic carbon cycle are assumed. Hence alternative explanations other than weathering and carbonate sedimentation are necessary to explain the calcium isotope excursions observed in the Phanerozoic record.

Yet for interpretation of the marine Ca isotope record it has not been taken into account that precipitation rate has a significant influence on calcium isotopes in calcium carbonate minerals [5, 6, 7]. Nielsen *et al.* [8] recently suggested that the influence of the $\text{Ca}^{2+}:\text{CO}_3^{2-}$ ratio on precipitation rate has a significant impact on calcium isotope fractionation. Variations of the marine $\text{Ca}^{2+}:\text{CO}_3^{2-}$ ratio by up to one order of magnitude may have occurred in the Phanerozoic oceans and may explain at least some of the observed calcium isotope trends.

[1] Farkas *et al.* (2007) *Geochim. Cosmochim. Acta*, **71**, 5117-5134; [2] Blättler *et al.* (2011) *Earth Planet. Sci. Lett.*, **309**, 77-88; [3] Fantle (2010) *Amer. J. Sci.*, **310**, 194-230; [4] De La Rocha and DePaolo (2000) *Science*, **289**, 1176-1178; [5] Lemarchand *et al.* (2004) *Geochim. Cosmochim. Acta*, **68**, 4665-4678; [6] Gussone *et al.* (2005) *Geochim. Cosmochim. Acta*, **69**, 4485-4494; [7] Tang *et al.* (2008) *Geochim. Cosmochim. Acta*, **72**, 3733-3745; [8] Nielsen *et al.*, (2012) *Geochim. Cosmochim. Acta*, **86**, 166-181;

Weathering processes and supergene formation of uranium bearing minerals at U-mines in the Saint-Sylvestre Area (French Massif Central)

FLORA BOEKHOUT^{1*}, MARTINE GÉRARD¹,
VANNAPHA PHROMMAVANH², MICHAEL DESCOSTES²
AND GEORGES CALAS¹

¹Institut de Minéralogie et de Physique des Milieux
Condensés, Université P&M Curie, IRD, France,
martine.gerard@impmc.upmc.fr, calas@impmc.upmc.fr

²AREVA, BG Mines, R&D, Paris la Défense, France
vannapha.phrommavanh@areva.com,
michael.descostes@areva.com

(*presenting author)

In France, uranium mines were exploited between 1945 and 2001 leading to the production of 76,000t of U but also 200 Mt of waste rocks. We present the supergene evolution of waste rock piles generated during mining operations at the Vieilles Sagnes site (Fanay) located in the Saint-Sylvestre leucogranite complex (northwestern Limousin, French Massif Central). This two-mica granite was emplaced at 324 ± 4 Ma and hosts an important U-ore mineralization deposited at 270-280 Ma, due to sustained hydrothermal circulation.

At the Vieilles Sagnes site mining operations between 1957 and 1965 generated waste rock piles of dominantly granitic rocks that have been exposed to supergene processes since the mining time. The U content of the blocks in the waste rock pile is 10-120 ppm, while in the ore body it is around 1000-3000 ppm.

To assess their supergene evolution and the neo-formation of uranium bearing phases two trenches were excavated through the waste rock pile, enabling the sampling of both superficial blocks and samples from the interior of the pile. Granitic blocks, proto-soils and alteration products that form the matrix of the waste rock pile, as well as paleo-soils underlying the rock pile were sampled.

The micromorphology, mineralogy and geochemistry of the samples representative of the different horizons of the profile investigated were examined by optical microscopy, and SEM observations, XRD and ICPMS whole rock analyses, respectively.

The degree of weathering of the granitic blocks is evidenced by the occurrence of chlorite and kaolinite alteromorphs after biotite and smectite and kaolinite after feldspar. The liberation of Fe gives rise to the local formation of Fe-phosphates and sulphates. Magmatic and hydrothermal U-bearing minerals release U as alteration and arenisation of the granites take place. So far no coffinite or uraninite from the initial mineralization have been observed.

Preliminary results suggest that the migration of uranium and formation of uranyl phosphates is at least partly associated with the supergene formation of Fe-phosphates. U-sorption onto clay minerals also seems to play an important role in decreasing U-mobility during meteoritic weathering.

Non-mass-dependent oxygen isotope enrichments in O₃ and CO₂: New insights from experiments, observations, and modeling

K.A. BOERING^{1*}

¹ Departments of Chemistry and of Earth and Planetary
Science, University of California, Berkeley, Berkeley,
California, 94720-1460 USA
(boering@berkeley.edu)

Results from recent laboratory experiments, atmospheric observations, and photochemical kinetics modeling provide new insights into the anomalous ¹⁷O and ¹⁸O enrichments in ozone and their transfer to carbon dioxide. In particular, new observations of the triple oxygen isotope composition of stratospheric CO₂ reveal surprisingly large anomalous enrichments that vary with latitude, altitude, and season. The triple isotope slopes were $1.95 \pm 0.05(1\sigma)$ in the middle stratosphere and 2.22 ± 0.07 in the Arctic vortex versus 1.71 ± 0.03 from previous observations and a factor of 4 times larger than the mass-dependent value of 0.52. Kinetics modeling of laboratory measurements of CO₂-ozone isotope exchange demonstrates that non-mass-dependent isotope effects in ozone formation alone quantitatively account for the ¹⁷O anomaly of CO₂ in the laboratory, resolving long-standing discrepancies between models and laboratory measurements. Model sensitivities then provide a framework for understanding ¹⁷O in stratospheric CO₂ and the larger three isotope slopes observed there than in laboratory experiments and, thus, a firmer foundation for the many biogeochemical and paleoclimate applications of ¹⁷O anomalies in tropospheric CO₂, O₂, minerals sulfates, and fossil bones and teeth, all of which derive from isotope exchange between ozone and stratospheric CO₂. Finally, measurements of the pressure and bath gas dependence of the ¹⁷O and ¹⁸O enrichments in ozone in bulk photochemistry experiments in the laboratory [1] provide new insight into and constraints on the physical chemical origin of the dynamically-driven symmetry isotope effects in ozone formation.

[1] Feilberg, Wiegel, & Boering (2013), *Chem. Phys. Lett.* **556**, 1-8.

Algal mats of the North Pole: How sea ice melt can cause anoxic spots on the Arctic deep-sea floor

ANTJE BOETIUS,
FRANK WENZHÖFER^{1,2,3} AND THE SCIENTIFIC TEAM OF
RV POLARSTERN ARK 27-3

¹Alfred Wegener Institute Helmholtz Center for Polar and
Marine Research, D-27515 Bremerhaven

²Max Planck Institute for Marine Microbiology, D-28359
Bremen

³MARUM Center for Marine Environmental Sciences,
University of Bremen, D-28359 Bremen

The centric diatom *Melosira arctica* forms kelp-like accumulations under the Arctic sea ice, in the form of meter-long filaments, anchoring in troughs and depressions under ice floes. These mat-forming algae are extremely sensitive to warming and melting of the ice, leading to their rapid sedimentation. The research icebreaker POLARSTERN visited the ice-covered eastern-central basins between 82° to 89°N and 30° to 130°E in summer 2012 in the framework of the expedition ICEARC. By September, the Arctic sea ice had declined to a record minimum of 3.6 million square kilometers. Consequently, we observed the massive sedimentation of sub-ice algal biomass of up to 150 g C per m² (median: 9 g C per m²) to the deep-sea floor of the Arctic basins. Patches of algal mats of 1-50 cm in diameter covered up to 10% of the seafloor at 3300-4500m water depth. *in situ* and *ex situ* microprofiling of diffusive oxygen fluxes into sediments covered by algal aggregates showed elevated rates of 5-6 O₂ mmol m⁻² d⁻¹, compared to <0.4 mmol m⁻² d⁻¹ in the surrounding sediments. Apparently only sediment bacteria, and large mobile megafauna were able to profit of the ice-algae deposition event. In cores covered by *Melosira* strands, oxygen penetration in the sediment was reduced to a few mm as compared to the surrounding sediment, where oxygen penetrated >50 cm deep. From the *in situ* oxygen profiles we conclude that the sinking *Melosira* strands had contributed >85% of total carbon flux to the deep-sea floor in 2012, but that such massive algal falls were previously rare. Our observations support the hypothesis that the thinning ice cover enhances under-ice productivity and export. If this phenomenon repeats seasonally, substantial changes in the biogeochemistry and biodiversity of the ice-covered Arctic basins are expected.



Figure 1: Sea cucumbers feeding on freshly deposited algal mats at 4500 m water depth

Aqueous Li⁺ speciation and ancient climate monitoring

STUART BOGATKO¹, PHILIPPE CLAEYS²,
FRANK DE PROFT¹ AND PAUL GEERLINGS¹

¹Free University of Brussels, General Chemistry, Pleinlaan 2,
1050, Brussels, Belgium. Email: sbogatko@vub.ac.be

²Free University of Brussels, Earth System Science, Pleinlaan
2, 1050 Brussels, Belgium

Lithium is recognized as a valuable trace metal in the area of ancient climate monitoring. This arises from the isotopic composition of Li in seawater being strongly influenced by continental weathering, one of the major sources of Li in seawater, and the incorporation of aqueous Li⁺ into calcium carbonate shells. By systematically analyzing the isotopic composition of Lithium in ancient calcium carbonate it is possible to reconstruct a record of Li isotope fractionation (IF) in seawater over the past 68 Ma. Due to the close association of Li IF with ancient weathering, this record is able to provide critical information concerning the ancient earth climate.

Previous studies base their paleo-reconstructions on the close correspondence between modern values of Li isotope ratios in calcium carbonates and seawater. Implicit is the assumption that Li IF is not sensitive to environmental conditions such as Temperature and pH. This assumption is not supported from a molecular structure point of view; there is little information concerning the identity and molecular structure of aqueous Li⁺ species and it is not clear to what extent ligand coordination effects may play in the incorporation of Li⁺ into calcium carbonate.

We have carried out a theoretical (Density Functional theory) study of aqueous Li⁺ speciation including effects of ligand coordination, temperature and solution pH. We have calculated the isotope exchange equilibrium constant associated with the Li Acid/Base equilibrium and can constrain it to positive values. The consequences of this species dependent IF are then studied using a model for Li-Carbonate coordination. We define an effective IF to model temperature and pH induced changes in Li IF in Li-Carbonates. We predict that under normal oceanic conditions Li IF is not sensitive to pH but may be significantly influenced by temperature.

Based on our results we revisit the basic assumption that Li IF is not sensitive to environmental conditions such as Temperature and pH. Namely, our observation of significant species dependent Li IF strongly suggests that the mechanism through which Li is incorporated into calcium carbonate is not sensitive to the Li speciation.

Geochemical spectra as an integral characteristic of the concentration and dispersion of elements in soils, peats and natural waters

L.G. BOGATYREV¹, E.Y. POGOZHEV²,
E.A. POGOZHEVA¹ AND I.I. ANTONOVA¹

¹ Department of Soil Science, Moscow State University, Russia

(*correspondence: pogozhevaea@mail.ru)

²“Geoforum”, Vernadsky avenue, 51, Moscow, Russia

Geochemical spectra are the useful tool for comparison of elements concentration or dispersion in the different components of the biosphere. In this work elements distribution patterns were studied in soil samples from Yakutia, West Siberia and European Russia. Geochemical spectra were also obtained for particle-size fractions and ortsteins isolated from some soils of taiga zone, as well as for natural waters.

Geochemical spectra depend largely on soil mineralogical composition. Investigation of the elemental composition of sand, silt and clay fractions showed clear divergence of their geochemical spectra. Geochemical spectra of iron-manganese nodules from different horizons of sod-podzolic soils were quite similar. This suggests that they were formed in single geochemical space from similar soil formation products and in presence of similar soil solutions. This supposition also seems to be true for mineral horizons of alluvial soils and underlying peats. Probably, geochemical spectra of elements for soils are inherited from the parent rock and represent some sort of the “genetic code” [1]. Preservation of this code is determined by the lifetime of the soil. soil geochemical spectra provides stable functioning of terrestrial ecosystems.

This work was supported by RFBR grant No 13-0500542.

[1] Bogatyrev et al. (2003) *Eurasian Soil Sci.* **36** 501-510.

Zircon from Mesoarchean enderbites of Volgo-Uralia: U-Pb age, REE, Hf- and O-isotope compositions

S.V. BOGDANOVA^{1*}, E.A. BELOUSOVA², B. DE WAELE³
AND A.V. POSTNIKOV⁴

¹Department of Geology, Lund Univ., SE-22362, Sweden

(*correspondence: Svetlana.Bogdanova@geol.lu.se)

²GEMOC ARC National Key Centre, Macquarie Univ. Sydney, NSW 2109 Australia (elena.belousova@mq.edu.au)

³SRK Consulting, Level 1, 10 Richardson Street, West Perth WA 6005 (bdewaele@srk.com.au)

⁴Gubkin State University of Oil and Gas, Moscow, Russia (apostnikov@mtu-net.ru)

As shown by numerous drillings, Archean charnockitic rocks are common in most of the lower crust in southern Volgo-Uralia, which is one of the major crustal megablocks of the East European Craton [1]. They are mainly enderbites that form large bodies (e.g. the Kolyvan intrusion, this study). Zircon from the enderbites contains relics of inherited cores with magmatic oscillatory zoning. These are surrounded by CL black-and-bright alternating bands of curved metamorphic rims. The crystallization age of the cores is between 3140±7 Ma (SHRIMP) and 3127±46 Ma (LA-ICPMS), while the outmost CL-bright rims are ca. 1945 Ma. The ages in-between are interpreted as a result of different degrees of Pb-loss caused by the high grade metamorphism. The ingressive recrystallization of primary magmatic zircon correlates with depletion in REE, which is observed consistently in each studied core-rim pair. No differences in O-isotope composition are detected between the cores and rims; the δO¹⁸ values vary from ca. 5 to 6.5. The Hf-isotope compositions of magmatic cores (-3 to -9 εHf) and metamorphic rims (-14 to -28 εHf), and their similar crustal model ages from 3.42 to 3.86 Ga, imply Eo- to Paleoproterozoic crustal sources for the charnockitic magmas and very little, if any, juvenile additions during the metamorphic event at ca. 1945 Ma. The dated Kolyvan enderbites belong to calc-alkaline, meta- to peraluminous, mainly ferroan series, also indicating substantial participation of crust in charnockitic melt sources relevant to a continental arc setting at 3.1 Ga. We reported similar results on rocks from the Bakaly block to the northeast of the Kolyvan region [1] confirming widespread Early Archean crust in Volgo-Uralia.

[1] Bogdanova *et al.*, 2010, *Am.J.Sc.* **110**, 1345-1383.

Element accumulation in peat of the Vidrino highmoor

A.A. BOGUSH^{1*}, V.A. BOBROV¹, G.A. LEONOVA¹,
G.N. ANOSHIN¹, S.K. KRIVONOGOV¹,
L.M. KONDRATYEVA², YU.I. PREIS³
AND A.E. MALTSEV¹

¹Institute of geology and mineralogy SB RAS, Koptyug Pr. 3, Novosibirsk 630090, Russia (*coresspondence: annakhol@gmail.com)

²Institute of aquatic and ecological problems of Far-East Branch RAS, St. Kim Yu Chen 65, Khabarovsk 680000, Russia (kondrlm@rambler.ru)

³Institute of Monitoring of Climatic and Ecological Systems SB RAS, Academichesky ave. 10/3, Tomsk 634055, Russia (preisyui@rambler.ru)

Almost 90 years ago, V.I. Vernadsky [1] created the holistic doctrine of the Biosphere where he demonstrated the primacy of life as a geological force. Concentrative function of living matter plays a significant role in biomineralization, which is the process when living organisms assemble structures from naturally occurring inorganic compounds [2].

The purpose of this work was to investigate biomineral formation in peat and show an important role of living matter in element accumulation. The objects were peat of the Vidrino highmoor (south-east of the Baikal region, Russia).

The high concentrations of Zn and Cu (500-600 g/t) were determined in peat of the Vidrino highmoor in the layers of early Holocene (360-440 cm) which were formed in period 11-8.5BP. It was shown that authigenic sulfides of Zn and Cu with micron dimension (0.5-3 µm) were formed in the plant cells of sphagnum. Also particles of native silver (5-7 µm) were found out in the peat of the Vidrino highmoor and which were accumulated in cell membrane of sphagnum. The mechanism of silver micro-particles formation in the cell membrane of sphagnum was proposed in this work.

The obtained results show a considerable role of biogenic mineral formation in the investigated peat that is a very important result in discussion about genesis of ore formation in which the preference is given to physical and chemical processes and often the role of living matter is not considered. This research was supported by the RFBR grant 11-05-12038-ofi-m-2011 and grand OPTEC.

[1] Vernadsky (1926) *The Biosphere*. Leningrad. [2] Leadbeater and Barker (1995) *Biomineralization and scale production in the Chrysophyta* // In: *Chrysophyte algae*. Sandren, Smol, Kristiansen, eds., Cambridge, UK: Cambridge University Press.

A tool for exploring the impact of crustal contamination: The Magma Chamber Simulator

WA BOHRSON¹, FJ SPERA², MS GHIORSO³
AND J. CREAMER²

¹ Geological Sciences, Central Washington University, Ellensburg, WA 98926, USA
(*correspondence:bohrson@geology.cwu.edu)

² Earth Science, University of California, Santa Barbara, CA 93106, USA

³ OFM Research - West, 7336 24th Ave NE, Seattle, WA 98115, USA

The Magma Chamber Simulator is a new computational tool that quantifies the impact of simultaneous recharge, assimilation and crystallization on melt±solids±fluid in a magma-recharge magma-wallrock composite system. Enthalpy from magma cooling/crystallization and recharge heats wallrock (WR). When the fraction of anatectic melt attains or exceeds a critical percolation limit of ~0.05-0.15, assimilation begins. Magma cooling/crystallization, addition of recharge magma and anatectic melt, and WR heating continue until magma and WR reach thermal equilibrium. For each simulation step, thermodynamic and material balance assessment provides major/trace element and isotopic compositions, masses and temperatures of all phases in each part of the composite system. Initialization includes bulk composition, temperature and pressure of all subsystems, as well as relevant solid/melt and solid/fluid partition coefficients. Simulation of high alumina basalt intruding dioritic to granitic WR at 500-550°C and 0.1 GPa yields a large volume of dacitic melt at equilibrium temperatures of 950-975°C. Assimilation enhances pyroxene crystallization but suppresses plagioclase; this and addition of anatectic melt yield a melt body up to 5x larger than that generated by FC alone. Selected trace element and isotopic results for magma show that, at the equilibrium temperature, Sr isotopes are >0.708, with only 2% of Sr contributed by crust. Nd isotopes are <0.5126, with ≤11% of Nd from crust. In contrast, the total mass of anatectic melt assimilated is ~40%, highlighting the critical difference between mass of element and total mass of assimilated melt. Trace element results also illustrate that variations in mass of element and mass of magma melt can yield dilutions of incompatible element concentrations in contaminated magma, providing an explanation for systems that have "decoupled" trace element and isotopic signatures. Because the MCS predicts detailed phase abundance, mass and compositional information, exploration of a wide range of open-system problems in igneous petrology is possible.

Mineral Surface Hydroxyl Group Identity and Reactivity

JEAN-FRANÇOIS BOILY

¹Department of Chemistry, Umeå University, Sweden
(jean-francois.boily@chem.umu.se)

Mineral surfaces are reactive transformation centres and sinks for gases, solutes and solvents. These surfaces are populated by (hydr)oxo functional groups that can undergo protonation, ligand exchange, and form extensive networks of hydrogen bonds (Figure 1). Knowledge of the types, distributions and orientations of these groups is consequently essential understanding molecular-scale processes taking place at mineral surfaces.

This work is focused on the properties of hydroxo groups on important crystallographic planes of synthetic nano-sized (α , β , γ)-FeOOH particles exposed to vacuum, water vapor and carbon dioxide. Vibration spectroscopic signatures of isolate and hydrogen bonded hydroxo groups on these minerals will be presented alongside predictions from molecular dynamics simulations. This body of work forms the basis for a molecular-scale understanding of reactions taking place at surfaces of geochemically relevant mineral particles.

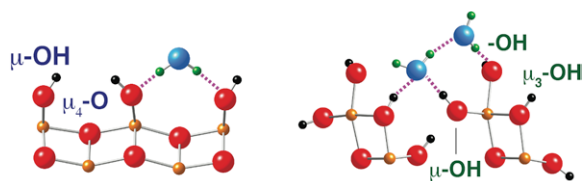


Figure 1. Schematic representation of dominant configurations of gaseous water molecules (blue) adsorbed on the (010) (left) and the (001) (right) planes of γ -FeOOH.

[1] Song X., Boily J.-F (2013) *Chem. Phys. Lett.*, **560**, 1-9. [2] Song X., Boily J.-F (2012) *Phys. Chem. Chem. Phys.* **14**, 2579-2586. [3] Boily J.-F (2012) *J. Phys. Chem. C* **116**, 4714-4724.

Reaction chain modeling of denitrification reactions during a push-pull test

A. BOISSON^{1,2}, P. DE ANNA^{1,3}, O. BOUR¹,
T. LE BORGNE¹, T. LABASQUE¹ AND L. AQUILINA¹

¹Géosciences Rennes-OSUR, UMR CNRS 6118, University of Rennes 1, France

(correspondence : Olivier.Bour@univ-rennes1.fr)

²Now at : BRGM, D3E/NRE, Indo-French Centre for Groundwater Research, Hyderabad, India
(a.boisson@brgm.fr)

³Now at : Massachusetts Institute of Technology, Cambridge, MA, USA (pdeanna@mit.edu)

Field quantitative estimation of reaction kinetics is required to predict biogeochemical reactions in aquifers. We extended the analytical solution developed by Haggerty *et al.* [1] to model an entire 1st order reaction chain and estimate the kinetic parameters for each reaction step. We then evaluated the ability of this solution to model experimental results from a push pull test in a fractured crystalline aquifer (Ploemeur, Brittany). Nitrates were used as the reactive tracer, since denitrification is a sequential reduction of nitrates to nitrogen gas occurring in a chain reaction ($\text{NO}_3^- \rightarrow \text{NO}_2^- \rightarrow \text{NO} \rightarrow \text{N}_2\text{O} \rightarrow \text{N}_2$) under anaerobic conditions. The kinetics of nitrate consumption and by-products formation (NO_2^- and N_2O) during autotrophic denitrification were quantified by using a reactive tracer (NO_3^-) and a non-reactive tracer (Br^-). Comparison of the Br^- and NO_3^- breakthrough curves showed that 10 % of the injected NO_3^- molar mass was transformed during the 12 hour experiment. Similar results, but with slower kinetics, were obtained from laboratory experiments in reactors. The good agreement between the model and the field data shows that the complete denitrification process can be efficiently modeled as a sequence of first order reactions. The variability of biogeochemical reactivity in the field will be also discussed.

[1] Haggerty *et al.* (1998), *Ground Water* **36** (2), 314–324.

Copper contamination of lake sediments in the vicinity of Konin (Poland)

IZABELA BOJAKOWSKA*, STANISŁAW WOŁKOWICZ
AND JOANNA KRASUSKA

PGI-NRI, 4 Rakowiecka, 00-975 Warsaw, Poland
(izabela.bojakowska@pgi.gov.pl)

Copper is an element essential to the life of many organisms. However, excessive concentrations of copper can be toxic. Due to the harmful effects of copper to aquatic organisms, its *PEC* level in sediments has been fixed at 149 mg kg⁻¹.

Sediment samples were collected from the 5-cm thick surface layer of the profundal zone of 14 lakes located in the near Konin (central Poland). Determinations of the concentrations of Al, Ag, As, Ba, Ca, Cd, Co, Cr, Cu, Fe, Mg, Mn, Ni, P, Pb, S, Sr, Ti, V and Zn were determined by ICP-AES methods from solutions obtained after digestion in aqua regia. The Hg concentration determinations were made using TMA method and the organic carbon content (TOC) was determined by coulometric titration method.

The concentrations of the some trace elements varied over a wide ranges of content: for Cu - 9-674 mg/kg, Ba 57-409 mg/kg, Hg - 0.058-0.366 mg/kg, Ni - 5-25 mg/kg, Pb - 16-53 mg/kg, Sr - 53-758 mg/kg and Zn - 30-184 mg/kg. It has been found that the sediments of five lakes (Gosławskie, Licheńskie, Pałnowskie, Ślesieńskie, and Wąsosko-Mikorzyńskie), whose waters are included in the power plant cooling system, are characterized by much higher contents of Cu, Ba, Hg, Mn, Sr and Zn, as compared to the other lakes. The average concentrations of Cu, Ni, Pb, Hg and Zn in the sediments of the latter lakes are comparable with the concentrations of these elements in sediments of lakes from other regions. The sediments of lakes included in the Konin-Pałnów power plant cooling system are conspicuous by a very high concentration of Cu (avg. - 415 mg/kg), which is 35-times higher than its average concentration in lake sediments (7 mg/kg). The average content of Ba in the sediments of these lakes is three times higher; of Ni, Hg and Zn - twice higher.

The studies of the Konin region lakes sediments have shown that they contain high Cu concentrations that may cause harmful effects on aquatic organisms. However, it is necessary to perform further tests to determine the copper content in fish tissues due to the fact that these lakes are used for recreational and angling purposes on a large scale.

A comparison of Pitzer databases for nuclear waste disposal modelling

FRANK BOK^{1*}, ANKE RICHTER¹
AND VINZENZ BRENDLER¹

¹Helmholtz-Zentrum Dresden-Rossendorf e.V., Dresden, Germany, (*correspondence: F.Bok@hzdr.de)

For the modelling of different chemical aspects of a nuclear waste repository in salt rock, the Pitzer formalism is necessary. Therefore, a comprehensive database with the relevant species reaction constants and associated ion-ion interaction parameters including temperature-dependencies is required. A number of different tailored Pitzer databases are available [1]. To judge their capabilities and limitations we performed comparative calculations for well-defined chemical systems (binary or ternary solubility diagrams). To avoid possible deviations due to different speciation codes all databases were transformed into the format specific for Geochemist's Workbench [2]. Additionally, model results are compared to experimental values from the literature.

Most results for the Oceanic Salt Systems (Na⁺, K⁺, Ca²⁺, Mg²⁺ / Cl⁻, SO₄²⁻ - H₂O) at 25 °C show a good agreement between experiment and model. At higher temperatures, sparse temperature-dependent data causes strong differences in the results.

For the radionuclides (e.g. Nd, Np), the solubility of their amorphous hydroxides in high salinar solutions was calculated as a function of pH. Missing anionic hydroxo-complex species or less reliable data produce inadequate predictions of the increasing solubility of mineral phases (e.g. fresh amorphous Nd(OH)₃ or NpO₂(OH) in the strongly alkaline medium. This demonstrates the importance of complete chemical speciation data.

Caesium was chosen as example for a fission product. Only minor differences can be found in the calculated solubility diagrams and the occasional absence of solubility data for Cs phases is not significant for real-world scenarios due to the high solubility of these phases in comparison to other salts.

The revealed discrepancies illustrate the need for further database work. Joint benchmark activities could help to identify missing or weak data, enhance the quality of all databases and consequently increase the confidence in modelling results.

[1] <http://www.thereda.de> [2] Bethke, C.M. (2008), "Geochemical and Biogeochemical Reaction Modeling" 2nd Ed., Cambridge University Press, 123-134 (see also: <http://www.gwb.com>).

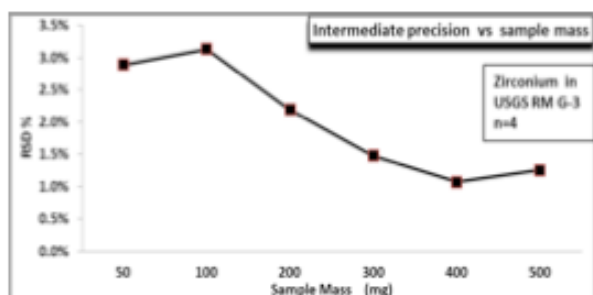
The determination of homogeneity of geological reference material

SYED N. H. BOKHARI AND THOMAS MEISEL

¹ General and Analytical Chemistry, Montanuniversität, 8700 Leoben, Austria (*correspondence: syed-nadeem-hussain.bokhari@unileoben.ac.at)

Reference materials (RM) support measurements in geological research due to the degree of homogeneity, traceability and confidence interval of their property values. Homogeneity testing is essential in certification of reference materials, as it should demonstrate the validity of the certified values and their uncertainties. Ingamells sampling theory [1] has been applied to test homogeneity of IAG Candidate RM trachyandesite (MTA), rhyolite (MRH), RM CGL MGL-AND andesite and uncertified USGS Granite (G-3). The sample digestion for test portions 50 mg to 500 mg was performed following the protocol [2] by sodium peroxide sintering and measurements with ICP-MS.

It is proposed that at least 300 mg is the minimum test portion size for trachyandesite (MTA) and Granite G-3 and 100 mg test portion for Rhyolite (MRH) and MGL-AND andesite to assure acceptable precision less than 2%. Complete digestion of all the analytes including mineral zircon is possible with sample/Na₂O₂ ratio 1:6.



In establishing reference values for reference materials, the contribution of detectable heterogeneity to the overall uncertainty of individual reference values has been quantified. The method has been developed to recover all analytes in particular zircon for 50 mg test portion size but it is suggested that 50 mg test portion is not representative for the particular rock types. It is also recommended to use ICP-MS as a tool of analysis as WD-XRF cannot determine homogeneity in specified test portion due to lower detection limits.

[1] Ingamells & Switzer (1973) *Talanta* **20**, 547-568.

[2] Meisel *et al. Geostand. Newsl.* **26**, 53-61.

Isotopic Studies of Rapid Carbonate Precipitates

J. R. BOLES^{1*}, S. OMELON² AND G. GARVEN³

¹University of California Santa Barbara, CA, 93106, USA

(*correspondence: boles@geol.ucsb.edu)

²University of Ottawa, Ottawa, ON, K1N 6N5, Canada

³Tufts University, Medford, MA, 02155, USA

In geologic systems, where crystallization is *rapid*, the carbonate isotopic systems may be out of equilibrium. Our studies of well scales in hydrocarbon production tubing and tunnel speleothems indicate carbonate to be out of equilibrium when growth rates exceed mm/year. Calcite scales resulting from CO₂ degassing results in covariance in ¹³C and ¹⁸O of the precipitate where the limited CO₂ degasses from a thin fluid film. Vaterite occurrences have extremely light isotopic values (>10 per mil) relative to calcite scales in the same reservoir.

Recent experiments to sequester CO₂ from coal combustion involve *extremely rapid* CaCO₃ precipitation, and oxygen values 10 to 20 per mil lighter than expected for equilibrium. These observations suggest that during extremely rapid crystallization rates the low mass light isotopes are preferentially incorporated into the carbonate, as observed by McCrae [1]. Light isotopes may reach the reaction site, and may form CaCO₃ species in solution more rapidly, once crystallization rates exceed some threshold rate. We are currently conducting experiments to determine the relation between crystallization rate, carbonate poly morph type, and stable isotopic composition, by CaCO₃ precipitation by CO_{2(g)} addition at different CO₂ partial pressures in calcium chloride solutions at neutral pH.

[1] McCrae, J.M. (1950) *J. Chem. Phys.* **18**, 849-857.

Water storage in the Earth's mantle

N. BOLFAN-CASANOVA¹ AND ANAIS FÉROT

¹Laboratoire Magmas et Volcans, CNRS, Université Blaise-Pascal, OPGC, Clermont-Ferrand France,
* correspondance : N.Bolfan@opgc.univ-bcpclermont.fr

Experiments were performed under water-saturated conditions in the MFSH and MFASH systems as a function of pressure and temperature from 2.5 to 13.5 GPa covering the whole depth range of the upper mantle. Water contents were analysed by Fourier transform infrared spectroscopy [1] and water values reported here use the new extinction coefficient for olivine [2]. The incorporation of Al enhances water incorporation in olivine and pyroxene, but only at pressures of 2.5 and 5 GPa. The partitioning of water between pyroxene and olivine is very high (4.4) at 2.5 GPa and below 1250°C, but decreases to an average value of 1.2+/-0.4 for higher pressures and temperatures. At 13.5 GPa and 1400°C, the water content of olivine is 1100±200 ppm wt H₂O. We conclude that the water storage capacity of the upper mantle just above the 410 km discontinuity can be anchored to ~900 ppm wt H₂O. If we interpret that the Low Velocity Layer observed near 350 km is due to mantle melting, we can constrain the water content of the mantle at that depth to be ~650±150 ppm wt H₂O. This new value is twice higher than previous estimates for the mantle source of Mid Oceanic Ridge Basalts but within the range of OIB sources.

[1] Férot A. and Bolfan-Casanova N.(2012), *EPSL* **349-350**:218-230. [2] Withers *et al.* (2012) *Chem. Geol.* **334**, 92-98.

Gujba age formation revisited : a possible use as time anchor

J. BOLLARD¹, J.N. CONNELLY¹ AND M. BIZZARRO¹

¹Centre for Star and Planet Formation, University of Copenhagen, Øster Voldgade 5-7, Copenhagen K, 1350 Denmark

The meteorite Gujba is a primitive CBa carbonaceous chondrite (Bencubbin-type) that differs markedly from common chondrites. It displays a high metal abundance (metal/silicate ~1.7-3), a depletion in volatile elements, a quasi absence of CAIs and matrix, and large silicate chondrules (up to one cm) [1]. Metal and silicates are proposed to have both formed by condensation in a high temperature environment, as completely molten droplets and both exhibit quench textures. These features suggest a formation from a vapour-melt plume produced by a giant impact between planetary embryos after dust in the protoplanetary disk had largely dissipated [2]. This supposed formation in a single event followed by a rapid cooling predicts that all chronometric systems closed at the same time such that Gujba is an ideal candidate to anchor the short-lived chronometers onto an absolute timescale.

We have undertaken a project to date individual Gujba chondrules, using the precise assumption-free U-corrected Pb-Pb dating method [4,5] to first confirm the single-event formation model and refine its absolute age.

Five cm-sized chondrules from a single slab of Gujba have been extracted and characterized by SEM. Three of them have been processed by a stepwise dissolution method [4]. Using a ²⁰²Pb-²⁰⁵Pb double spike, we analyzed the Pb isotopic composition by thermal ionization mass spectrometry to obtain well-constrained internal isochrons on single chondrules. For now, ages were calculated using the ²³⁸U/²³⁵U ratio of 137.786±0.013 that was determined by [5] for inner solar system materials except CAIs.

Three chondrules have been dated with ages that range from 4562.61±0.28 to 4562.32±0.48 Myr, with a weighted average of 4562.52±0.44Myr. This is ca 1 Myr older than previously published absolute Pb-Pb age [2], when it is adjusted for a U isotopic composition of 137.786. If the adjusted-age from [2] is correct, this discrepancy could suggest different populations of chondrules within Gujba, which, in turn, requires a new formation model.

[1] Rubin A.E. (2003) *GCA*, **67**, 3283 [2] Krot A.N. *et al.* (2005) *Nature*, **436**, 989 [3] Yamashita K. *et al.* (2010) *APJ*, **723**, 20 [4] Connelly J.N. & Bizzarro M. (2009) *Chem. Geol.*, **259**, 143 [5] Connelly *et al.* (2012) *Science*, **358**, 651.

Isotopic composition of water vapour in strong convective updrafts

M. BOLOT^{1*}, E.J. MOYER² AND B. LEGRAS¹

¹Laboratoire de Météorologie Dynamique, CNRS/ENS, UMR 8539, Paris, France (*correspondance: bolot@lmd.ens.fr)

²Department of the Geophysical Sciences, University of Chicago, Chicago, USA

The isotopic composition of water is a tracer of interest for understanding convective processes, and the last decade has seen a surge of modelling and observational studies in that field. Yet, the physics of convective clouds governing the transformation of water across its different phases is potentially very complex and the exact dependence of isotopic compositions upon it is not well known nor has been extensively documented since the pioneering work of Jouzel *et al.* [1]. Important processes to consider include kinetic effects that arise from super-/subsaturated conditions due to liquid-ice disequilibrium in mixed phase zones and to lengthy phase adjustment over ice; isotopic re-equilibration between vapour and a variable reservoir of cloud liquid water; and different routes to cloud glaciation (freezing vs. the Wegener-Bergeron-Findeisen process). Using a simplified adiabatic model, we clarify the role of those processes in altering the isotopic composition of water vapour in strong convective updrafts.

We find that the deuterium-excess, which is the conventionally used metric of the joint distribution of deuterium and oxygen 18, is highly sensitive to cloud physics at low temperatures (< -30°C), with a complicated structure of variability resulting from multiple factors. We propose new metrics that relate deuterium and oxygen 18 isotopic ratios at cloud base and cloud top and that are better related to the structure of evolution of those isotopic ratios [2]. We show that, in a statistical sense, those metrics are respectively informative on the level of supersaturation reached by the cloud upon the completion of glaciation (which removes the control of saturation by liquid water); and on the temperature at which cloud glaciation is effective. The retrieved information can serve as a probe of the physics of deep convective clouds.

[1] Jouzel, Merlivat & Roth (1975), *J. Geophys. Res.* **80** (36), 5015-5030. [2] Bolot, Legras & Moyer (2012), *Atmos. Chem. Phys. Discuss.* **12**, 22451-22533.

Early Eocene Climatic Optimum: numerical modelling of the impact of the Neo-tethys closure.

BRAHIMSAMBA BOMOU^{123*}, GUILHEM HOAREAU⁴,
YANNICK DONNADIEU³, GUILLAUME LE HIR²
AND DIDIER MARQUER¹

¹UMR-CNRS 6249 Chrono-environnement, Univ. de Franche-Comté, 16 route de Gray, 25030 Besançon Cedex, France (*correspondence: bomou@ipgp.fr)

²Institut de Physique du globe de Paris, 4 place Jussieu 75005 Paris, France

³LSCE/UVSQ/IPSL CEA Saclay, Orme des Merisiers, F-91191 Gif-sur-Yvette, France

⁴Environmental Hydrogeochemistry, Dept. Geosciences, Univ. of Pau, BP 1155, 64013 Pau Cedex, France

The Early Eocene Climate Optimum (EECO, 53-50 Ma) was the warmest interval of Cenozoic time. This warm climatic interval was induced by a high atmospheric $p\text{CO}_2$. Several mechanisms have been proposed to explain this climatic anomaly (e.g. LIP of North Atlantic). However one of them seems to be the most convincing in term of carbon fluxes degassing: the Neotethys closure, resulting in large amounts of pelagic carbonates recycled as CO_2 in arc volcanoes during the subduction process. Hoareau *et al.* (submitted) [1] have modelled the volume of subducted sediments and the related amount of CO_2 and CH_4 emitted at active arc volcanoes along the northern Tethys margin. The volume of hemipelagic carbonates and the Indian continental margin carbonate sediments subducted, can produced a maximum of 3.7×10^{18} mol CO_2 /Ma during the EECO, corresponding to a maximum of 85% of the modern CO_2 outgassing rate. A numerical modelling has been performed to test the impact of these carbon fluxes on the climate using a model of biogeochemical cycles of carbon (COMBINE) coupled with a general circulation model (FOAM). Different parameters, as the size of Greater India continental margin and the timing of the continental subduction, have been tested in order to reconstruct the potential scenarii which could occurred during this interval.

[1] Hoareau G., Carry N., Marquer D., van Hinsbergen D.J.J., Vrielynck B. & Walter-Simonnet A. (submitted) *Did Neotethys subduction rates contribute to the Early Eocene Climatic Optimum?* Submitted to EPSL.

Highly variable ^{15}N -enrichments in Solar System reflect different routes of interstellar N isotopic fractionation

BONAL L.*, HILY-BLANT P., FAURE A. AND QUIRICO E.¹

¹IPAG, Institut de Planétologie et d'Astrophysique de Grenoble, UJF-Grenoble 1 / CNRS-INSU, France, [lydie.bonal@obs.ujf-grenoble.fr]

Large nitrogen (N) isotopic variations are observed in our Solar System ($^{14}\text{N}/^{15}\text{N} \sim 50$ to 450), with most of the objects being ^{15}N -enriched compared to the presolar nebula (PSN, $^{14}\text{N}/^{15}\text{N} = 442$) [1]. We suggest that these variations originate from distinct sampled N interstellar reservoirs. Indeed, N-bearing molecules detected towards dark clouds may be divided into two groups, whether they carry the amine (-NH) or nitrile (-CN) chemical function. Our recent observations towards interstellar dense clouds, together with a review of data from the literature, suggest these two reservoirs are characterized by distinct isotopic ratios [2]. Compared to the PSN, (i) nitrile carriers (e.g., HCN) might be systematically enriched in ^{15}N ($^{14}\text{N}/^{15}\text{N} = 100$ -320) and (ii) amine carriers (e.g., NH_3) are characterized by comparable isotopic ratios ($^{14}\text{N}/^{15}\text{N} \sim 400$). Gas-phase chemical networks suggest that nitriles derive from N while amines are formed via N^+ , product of the dissociative ionization of N_2 . The $^{14}\text{N}/^{15}\text{N}$ exchange reactions are therefore different for nitriles and amines, most likely with different timescales and efficiency [2], explaining the differential fractionation of these two reservoirs.

The proposed scenario [2] appears to explain several observations on Solar System objects. In particular, the absence of significant ^{15}N -enrichments in interstellar clouds, as previously assumed, is no longer a valid argument to reject an interstellar origin of organic precursors in primitive cosmomaterials.

[1] Marty *et al* (2010) *GCA* **74**, 340 [2] Hily-Blant *et al.* (2013) *Icarus* **223**, 582.

A bimodal crystallite size distribution for mackinawite (FeS)

BONE, S.E.¹ SPOSITO, G.¹
AND BARGAR, J.R.²

¹University of California, Berkeley, CA

²Stanford Synchrotron Radiation Lightsource, Menlo Park, CA

The nanomineral mackinawite (tetragonal FeS, space group P4/nmm), ubiquitous in sulfidic sediments, impacts the cycling of metals and metalloids through sorption and reduction reactions. The crystallite size, hence the specific surface area, of FeS precipitated from supersaturated solutions is poorly described; variations in crystallite size may arise from differences in mineral synthesis conditions and from differences in measurement techniques used to estimate crystallite size. Transmission electron microscopy (TEM) images and X-ray diffraction (XRD) patterns have been used to study FeS crystallite size. However, XRD is sensitive to the largest crystallites and identification of small crystallites in TEM images can be difficult when the crystallites are embedded in a matrix of aggregated particles.

In this research, we employ a combination TEM, XRD, and Fe K-edge extended X-ray absorption fine structure (EXAFS) spectroscopy to estimate the size of FeS crystallites formed under varying conditions of pH, ionic strength and reaction time. X-ray absorption spectroscopy is sensitive to the smallest crystallites, providing an estimate of size that is complementary to TEM and XRD. Furthermore, we calculate crystallite size distributions that are able to reconcile the XRD-, TEM-, and EXAFS spectroscopy-derived estimates of size. We suggest that the crystallite size may be bimodal, with a larger number of crystallites less than 2 nm in size than has previously been estimated using TEM and XRD. The presence of numerous small (< 2 nm) crystallites will have large ramifications for the properties of FeS, including its solubility and the rate and mechanism of particle growth. Lastly, the crystallite size distribution can be used to inform studies of particle reactivity by constraining the reactive surface area and the number of surface sites.

Demixing instability in dense molten MgSiO₃

STANIMIR A. BONEV^{1,2} AND BRIAN BOATES¹

¹Department of Physics, Dalhousie University, Halifax, Nova Scotia, Canada B3H 3J5

²Lawrence Livermore National Laboratory, Livermore, California, 94550, USA

The phase diagrams of MgSiO₃ and MgO are studied from first-principles theory for pressures and temperatures up to 600 GPa and 20,000 K. We present evidence for a vast pressure-temperature regime where molten MgSiO₃ decomposes into liquid SiO₂ and solid MgO. The demixing transition is driven by the crystallization of MgO - the reaction only occurs below the high-pressure MgO melting curve. The predicted transition pressure at 10,000 K is in close proximity to an anomaly reported in recent laser-driven shock experiments of MgSiO₃. We also present new results for the high-pressure melting curve of MgO and its B1-B2 solid phase transition, with a triple point at 327 GPa and 11,800 K. Comparison with experimental measurements and explanation of the observed phase boundaries in terms of the computed free energies will be discussed.

Clumped isotope thermometry of marbles as an indicator of the closure temperatures of calcite and dolomite with respect to solid-state reordering of C–O bonds

MAGALI BONIFACIE¹, DAMIEN CALMELS¹
AND JOHN EILER²

¹Institut de Physique du Globe de Paris, France
(bonifaci@ipgp.fr, calmels@ipgp.fr)

²California Institute of Technology, Pasadena, CA, USA

Carbonate clumped isotope thermometry is based on the temperature-dependent preference of rare isotopes ¹³C and ¹⁸O to bond with each other within lattices of carbonate minerals (as measured by Δ₄₇ of CO₂ extracted by phosphoric acid digestion). In rocks that have experienced burial and/or high temperature histories, this phenomenon may be controlled by solid-state diffusion of C and O within the mineral lattice. Here we examine this issue through clumped isotope measurements of a variety of natural marbles that differ in metamorphic environment, age, cooling rates, grain sizes, and mineralogical and chemical compositions; and compare them to heating experiments conducted at laboratory timescales.

Calcitic marbles increase in Δ₄₇ (by a range of ~ 0.05‰) with decreasing cooling rates (from ~ 100 to few °C/My), suggesting that ¹³C–¹⁸O reordering during cooling is controlled by solid state diffusion. Also, dolomite marbles are systematically lower in Δ₄₇ (by at least 0.06‰) than calcitic marbles, all other factors being the same. This does not appear to reflect differences between calcite and dolomite in the temperature dependence of clumping or the fractionation on acid digestion; rather, it appears that the blocking temperature with respect to solid-state ¹³C–¹⁸O reordering is significantly higher in dolomite (~300°C) than in calcite (~150–200°C), due to currently unknown chemical and/or structural controls.

These data are relevant for the use of clumped isotope thermometry to study deeply buried sedimentary carbonates and carbonate bearing diagenetic, metamorphic and igneous rocks. Perhaps most importantly, this work suggests that authigenic or early diagenetic dolomite may provide a means of recovering clumped isotope surface temperature records from even deeply buried sedimentary sections and sub-greenschist facies metamorphic rocks.

Underestimation of the authigenic fraction of Cu and Ni in organic-rich sediments and particles

P. BÖNING^{12*}, H. FRÖLLJE¹² AND H.-J. BRUMSACK¹

¹ICBM, University of Oldenburg, 26129 Oldenburg, Germany

(*correspondence: p.boening@icbm.de)

²Max-Planck Research Group for Marine Isotope Geochemistry, 26129 Oldenburg, Germany

Organic-rich sediments from marine environments typically show authigenic enrichments in Ni and Cu. However, the exact determination of the authigenic metal level is difficult given the considerable level of the lithogenic metal background. The authigenic metal level can be estimated according to $M_{\text{auth}} = M_{\text{total}} - (M/\text{Al}_{\text{background}} \cdot \text{Al}_{\text{total}})$ while M = metal of interest and Al = aluminum. Alternatively, a metal enrichment factor (EF) is calculated according to $\text{EF} = M/\text{Al}_{\text{total}} / M/\text{Al}_{\text{background}}$. Both techniques rely on the appropriate use of the M/Al ratio of the lithogenic background. For the latter, the M/Al ratio of average shale or crust is widely applied as lithogenic background in marine geochemistry. Here, we show that the authigenic level of Cu and Ni in sediments and particles (upwelling areas of Peru, North and South Chile, Gulf of California, Norwegian Kyllaren fjord and German Wadden Sea) is significantly underestimated when using the M/Al ratio of average shale or crust as lithogenic background. The correlation between Cu/Al and Ni/Al with organic carbon in the samples indicates the apparent M/Al ratio of the background, which is 2-4 times lower than the M/Al ratio of shale or crust. A prerequisite for our technique is high linearity and high quality of correlation ($r^2 \geq 0.8$) otherwise the lithogenic background cannot be exactly determined. The resulting higher authigenic level of Cu and Ni underlines their use as productivity indicators in modern and paleo records while the enrichment of Cu and Ni shifts from moderate to high if it is assessed via EFs.

The stable chromium isotopic composition of Lunar basalts

P. BONNAND^{12*}, I.J. PARKINSON¹³ AND M. ANAND⁴⁵

¹Department of Environment, Earth and Ecosystem, The Open University, Milton Keynes, UK.

²Department of Earth Sciences, University of Oxford, Oxford, UK (*correspondence: pierre.bonnand@earth.ox.ac.uk).

³Bristol Isotope Group, School of Earth Sciences, University of Bristol, UK.

⁴Department of Physical Sciences, The Open University, UK.

⁵Department of Earth Sciences, The Natural History Museum, UK.

Planetary formation has been widely studied using major-element constituents of planetary mantles [e.g. 1]. The Moon's formation is a highly debated topic and it has been proposed that the Moon is the result of a Mars-sized impactor which collided with the proto-Earth [2]. Non-traditional stable isotopes have been used to try to understand the formation of the Moon and its differentiation [e.g. 3].

Chromium isotopes are fractionated during core formation and differences in Cr isotopic composition between meteorites and the Earth's mantle suggest that light Cr isotopes have been preferentially partitioned into the metal fraction [4]. Lunar samples are characterised by a lack of nucleosynthetic anomalies for Cr isotopes [5].

In the absence of samples from the Moon's interior and in order to better constrain the lunar mantle composition and understand its formation we report stable chromium isotopic composition for a suite of low-Ti and high-Ti mare basalts. We find resolvable Cr isotopic variations within the lunar sample suite but no clear differences between low-Ti and high-Ti basalts. There is no correlation between $\delta^{53}\text{Cr}$ and $\delta^{18}\text{O}$. However, Cr isotopes seem to be correlated with $\text{Mg}\#$ and TiO_2 content which suggest that Cr isotopes are fractionated during magmatic differentiation on the Moon. The more primitive samples have Cr isotopic composition similar to the Earth's mantle.

These results suggest that the terrestrial and lunar mantles have similar stable Cr isotopic composition. This implies that processes responsible for the difference in isotopic composition between the Earth's mantle and chondritic material occurred before the formation of the Moon.

- [1] Dauphas *et al.* 2009, *EPSL*, **288**, 5855-5863. [2] Cameron 1997, *V. Icarus*, **126**, 126-137. [3] Liu *et al.*, 2010, *GCA*, **74**, 6249-6262. [4] Moynier *et al.* 2011, *Science*, **331**, 1417-1420. [5] Qin *et al.* 2010, *GCA*, **74**, 1122-1145.

Fungi-mineral interface : hotspot of weathering in soils

S. BONNEVILLE^{1*}, A. BRAY², A. SCHMALENBERGER³,
D.J. MORGAN², A. BROWN⁴, S. BANWART⁵
AND L. G. BENNING²

¹U.R. Biogéochimie et Modélisation du Système Terre –
Université Libre de Bruxelles, BE
(*steeve.bonneville@ulb.ac.be)

²School of Earth and Environment – University of Leeds, UK

³Department of Life Sciences – University of Limerick, IE

⁴Institute for Materials Research – University of Leeds, UK

⁵Kroto Research Institute – University of Sheffield, UK

Throughout geological times, tectonic forces have continuously exposed rocks to the slow but inexorable actions of weathering at the Earth's surface. This geological process forms soils upon which the entire terrestrial biosphere depends. Weathering of primary rocks also has a key-role in the carbon cycle as the alteration of Mg- and Ca- silicates coupled to the deposition in sediments of Mg- and Ca-carbonates results in a net flux of CO₂ from the atmosphere to the lithosphere. Over geological timescales, this transfer controls atmospheric CO₂ levels and hence the climate. Initially conceptualized in terms of abiotic dissolution reactions alone, there is now growing evidence that plants and their root-symbiotic partners, mycorrhiza, are key to the weathering because of their impressive capacity to interact physically and chemically with minerals.

In soils, mycorrhiza grow preferentially around, and on the surface of nutrient-rich minerals, making such contact zones potential hot-spot of mineral alteration. Here, we present a compilation of results and observations from alteration experiments in which ectomycorrhiza (*Paxillus involutus*) were grown symbiotically with a pine tree (*Pinus sylvestris*) in presence of freshly-cleaved biotite under humid, yet undersaturated, conditions typical of soils. Using FIB (Focussed Ion Beam), cross-sections of fungi-biotite interfaces were sampled along single, surface-bound hypha and analysed for (i) their contents in Si, O, Fe, Al, Mg and K at a nanometer-resolution (by STEM-EDS) and for (ii) the speciation of redox-sensitive elements (by STXM) [1]. In parallel to the biotite characterization, the chemical conditions in the near-environments of hypha and their biochemical composition were analyzed by molecular probes coupled to confocal microscopy and synchrotron-based μ -FTIR. This dataset shed light into mechanisms and also allowed for a first estimation of chemical alteration rates at the interface between fungi and rock-forming minerals [2].

[1] Bonneville Et Al. (2009) *Geology*, **37**, 615–618

[2] Bonneville Et Al. (2011) *GCA*, **75**, 6988-7005

XAS and isotopic approaches to identify Zn and Cu sources in the Seine River watershed

C.A. BONNOT^{1*}, A. GELABERT¹, G. MORIN², P. LOUVAT¹
AND M.F. BENEDETTI¹

¹ Université Paris Diderot, Sorbonne Paris Cité, Institut de
Physique du Globe de Paris, UMR 7154 CNRS, F-75013
Paris, France, (* correspondence: bonnot@ipgp.fr)

² UPMC, UMR CNRS 7590, IMPMC, Paris, France

In order to preserve the global freshwater resource, new directives on water policy have been established imposing a good ecosystem status for 2015. For the Seine-Normandie basin, it includes the metals sources determination in order to identify the metal amount resulting from the geochemical background, and the metal amount arising from industrialisation. The combination of isotopic and XAS approaches should allow to identify the different sources, and to understand the different processes controlling the Zn and Cu cycling. Variations on the $\delta^{66}\text{Zn}$ and $\delta^{65}\text{Cu}$ can provide information relative to the main sources of metals. XAS spectra study (through the knowledge of Zn and Cu speciation) is needed to understand the processes acting on the rivers (isotopic fractionation induced by biogeochemical processes [1,2,3] versus water mixing) and determine the bioavailability of Zn and Cu. As a potential Zn source, the sediment dynamics in the river have been investigated. To do so, sediment traps representative of river bottom sediments have been analysed using XAS at the Zn K-edge. In these samples, poorly crystallized Zn sulfides constitute the Zn major species, and could explain the presence of ZnS in suspended particulate material in the river water column. In addition, two “geographic” sampling campaigns have been performed to estimate the impacts of the different environmental conditions on the Zn/Cu signal, and to help locating the potential metal sources in the system. These two campaigns highlight a general seasonal effect linked to the discharge, in addition to punctual concentration anomalies.

[1] Gélabert *et al.* (2006) *GCA* **70**, 839-857. [2] Jouvin *et al.* (2009) *ES&T* **43**, 5747-5754. [3] Juillot *et al.* (2008) *GCA* **72**, 4886-4900

Paroxysmal degassing at Mt. Etna in 2011-12

E. BONNY^{1,2}, C. MANDON^{1,2}, S.A. CARN², A.J. PRATA³,
M. COLTELLI⁴ AND F. DONNADIEU¹

¹Observatoire de Physique du Globe (OPGC), Laboratoire
Magmas et Volcans, Université Blaise Pascal, 63038
Clermont-Ferrand, France (ebonny@mtu.edu)

²Dept. of Geological and Mining Engineering and Sciences,
Michigan Technological University, Houghton, MI 49931,
USA (scarn@mtu.edu)

³Norwegian Institute for Air Research, Kjeller, Norway

⁴INGV-CT, 95123 Catania, Sicily, Italy

Between January 2011 and April 2012, Mt. Etna produced a series of 25 paroxysmal lava fountaining events, representing a significant change in its eruptive style. Understanding the causes and impacts of this activity is crucial for improved hazard assessment at Etna, and for refinement of models of the volcano's magma plumbing system. Sulfur dioxide (SO₂) emissions associated with most of these paroxysms were measured by the ultraviolet (UV) Ozone Monitoring Instrument (OMI) on NASA's Aura satellite and the Atmospheric Infrared Sounder (AIRS) sensor on the Aqua satellite. The ground-based OPGC VOLDORAD 2B L-band Doppler radar system, operated in cooperation with INGV-CT, also detected the associated ash plumes, providing accurate constraints on the timing and duration of the lava fountains. We present a comprehensive analysis of the OMI and AIRS SO₂ data for the Etna paroxysms in 2011-12. Back trajectory analysis of the observed SO₂ clouds using the HYSPLIT trajectory model indicates that SO₂ emissions generally coincided with the peak lava fountain intensity detected by VOLDORAD. By combining the UV OMI and IR AIRS SO₂ measurements we constrain the SO₂ loss rate in the Etna SO₂ clouds, many of which were tracked for several days after emission. Using SO₂ loadings corrected for the time of emission, we observe a correlation between SO₂ production and inter-paroxysm repose time. Comparison of the erupted magma mass estimated from the radar data and the SO₂ loadings also indicates a vast excess of gas in the emissions. Of the two models typically invoked for explosive basaltic eruptions (the rise speed dependent (RSD) and collapsing foam (CF) models [1]) we propose that our dataset supports the CF mechanism as the predominant driver for paroxysms at Etna in 2011-12. Satellite data indicate low or undetectable ash content in the drifting eruption clouds, suggesting efficient separation of ash and gas in the eruption column, with implications for aviation hazards.

[1] Parfitt (2004) *J. Volcanol. Geotherm. Res.* **134**, 77-107.

Dissolved gases and radioactivity in spring waters of southeast Brazil

D. M. BONOTTO

Instituto de Geociências e Ciências Exatas, UNESP,
Rio Claro, Brasil (dbonotto@rc.unesp.br)

Twenty two spring water samples from spas located at São Paulo and Minas Gerais states, southeast Brazil, have been sampled and analyzed for temperature (T), conductivity (C), pH, redox potential Eh, dissolved gases O₂, CO₂, H₂S and radionuclides ²²⁸Ra, ²²⁰Rn and ²²²Rn. The samples provided from different geological contexts, i.e. Paraná sedimentary basin, Poços de Caldas alkaline massif and high grade metamorphic suites. The RAD7 portable detector (DurrIDGE Co.) has been used for ²²⁰Rn and ²²²Rn analyses, as well traditional potentiometric/colorimetric methods and radiochemical steps followed by gamma ray spectrometry through NaI(Tl) scintillation detector.

The following data range has been found: T=21.7-28.4 °C; C=0.04-4.73 mS.cm⁻¹; pH=5.56-9.38; Eh=-115-122 mV; O₂=1.3-9.0 mg.L⁻¹; CO₂<1.0-800 mg.L⁻¹; H₂S=<1.0 - 3064 µg.L⁻¹; ²²⁸Ra=<5.4-123.2 mBq.L⁻¹; ²²⁰Rn=<0.1-23.4 pCi.L⁻¹; ²²²Rn=0.6-2020 pCi.L⁻¹. Such great variability of values reflects the different lithologies, mineralogy of the rock matrices, discharge and climatic conditions, among others factors.

According to the Brazilian Code for Mineral Waters (BCMw) established by Register 7841 published on 8/8/1945, in terms of T values, the springs analyzed are cold (<25°C) and hypothermal (25-33°C). Several significant correlations were found involving the parameters analyzed, for instance: Eh and pH (r=-0.58), H₂S and C (r=0.64), T and ²²²Rn (r=-0.61), T and ²²⁰Rn (r=-0.42), ²²²Rn and ²²⁰Rn (r=0.59). Neither O₂ nor CO₂ and H₂S exhibited significant correlation with T, as expected, however, this scenario may modify if an expanded database including values for mesothermal, isothermal and hyperthermal waters is taken into account. According to the BCMw, in terms of radiological aspects, the springs analyzed can not be considered thoriferous as the ²²⁰Rn activity concentration is lower than 26.9 Bq.L⁻¹. One spring may be classified as weakly radioactive, as exhibited ²²²Rn activity concentration between 67.2 and 134.5 Bq.L⁻¹. Most of the ²²⁸Ra activity concentration data were below the detection limit, whereas one spring exhibited a value exceeding the guideline value of 0.1 Bq.L⁻¹ established by the Brazilian Health Ministry Register 2914 published on 12/12/2011. Therefore, the acquired data are relevant for the appropriate management and use of the studied spring waters.

Complexation of Sr in aqueous solutions equilibrated with silicate melts: Implications for fluid-melt partitioning

M. BORCHERT^{1*}, M. WILKE², C. SCHMIDT²,
K. KVASHNINA³ AND S. JAHN²

¹ Deutsches Elektronen-Synchrotron, Hamburg, Germany (* correspondence: manuela.borchert@desy.de)

² Helmholtz Zentrum Potsdam GFZ GeoForschungsZentrum, Potsdam, Germany

³ European Synchrotron Radiation Facility, Grenoble, France

Fluid-melt partitioning of Sr, Ba, La, and Y strongly depends on fluid and melt composition [1-2]. That is, partition coefficients of these elements increase with i) salinity of the fluid and ii) increasing alumina saturation index (ASI: $Al/(Na+K)$ in moles) of the silicate melt (Fig.1).

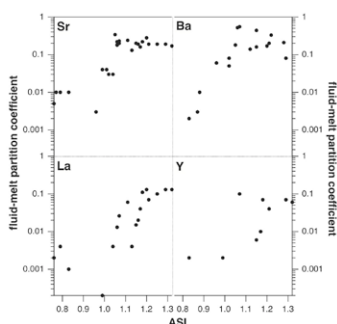


Fig. 1. Fluid-melt partition coefficients of Sr, Ba, La and Y as function of melt composition at 750°C, 200 MPa, and using a chloridic fluid.

On one hand, the distinct affinity for chloridic fluids points to a preferential complexation of these elements with chlorine. On the other hand, the strong dependence on melt composition suggests that a different release of melt components into the aqueous fluid in peralkaline systems changes the speciation in the aqueous fluid. Up to now, the exact nature of the complexation in the fluid is not clear.

Here, we present experimental and theoretical data on the complexation of Sr in three fluid-melt systems. X-ray absorption spectroscopy was applied to probe the local environment around Sr in silicate-bearing fluids, i.e., peralkaline or peraluminous melts completely dissolved in the aqueous fluid, and in various model systems, e.g., crystalline compounds, silicate glasses, and aqueous solutions. In order to decode the complexation of Sr in model systems and silicate-bearing fluids, theoretical spectra are calculated either using model structures, by testing several small cluster geometries or based on snapshots of trajectories produced with MD simulation to account for atom movements in aqueous solutions. Experimental data clearly show differences in the local environment around Sr in studied silicate-bearing fluids. Theoretical spectra point to a predominant formation of i) SrO_6 cluster in chlorine-free peralkaline fluids, ii) distorted SrO_6 clusters in chloridic-peralkaline fluids, and iii) complexes that very likely incorporate Cl in chloridic-peraluminous fluids.

[1] Borchert *et al.* (2010a), *GCA* **74**, 1057-1076. [2] Borchert *et al.* (2010b), *Chem. Geol.* **276**, 225-240.

Formation of arsenic bearing apatite from calcite. Chemistry and microstructures

STACEY BORG^{1,2*}, WEIHUA LIU¹, MARK PEARCE¹, JAMES CLEVERLEY¹ AND COLIN MACRAE³

¹ CSIRO Earth Science and Resource Engineering, Australia (*correspondence: stacey.borg@csiro.au)

² CODES ARC Centre of Excellence in Ore Deposits, University of Tasmania, Hobart, Australia

³ CSIRO Process Science and Engineering, Australia

Apatite, a calcium phosphate mineral, can form naturally as solid solutions with between 0-100% of the phosphate anions substituted with compatible molecules in the crystal lattice [1]. Arsenate, $As^V O_4^{3-}$ is one such molecule, and there are many examples in nature of high As bearing apatite [2].

In order to track the chemistry of ancient fluids that formed the observed composition variation in apatite and related mineral deposits, a series of hydrothermal synthesis experiments were performed, aiming to establish a relationship between apatite composition and fluid chemistry. Utilising a general method from a previous study [3], we have generated a range of synthesised apatite samples starting from calcite, primarily by reaction with phosphate (PO_4^{3-}), substituting with similar molecules (e.g. AsO_4^{3-} , SO_4^{2-}). Chemical analysis of thus formed apatite-like compounds show differing level of incorporation depending on the molecule being substituted, while SEM and CL mapping of grains show very interesting and complex textures and element distribution patterns. Two stage experiments, where one solution composition is reacted with pure calcite, then a different solution is reacted with the product, show that phosphate is an important driver for As-bearing apatite growth, and that arsenic incorporated into the apatite structure is not readily remobilised. This level of understanding is important when considering natural apatite samples as indicators to track ore fluids.

[1] Pan and Fleet (2002) *Rev. Mineralogy* **48**, 13-49. [2] Mailloux *et al.* (2009) *Appl. Environ. Microbiol* **75**, **8**, 2558-2565. [3] Kasioptas *et al.* (2011) *Geochimica et Cosmochimica Acta* **75**, **12**, 3486-3500.

Meter-scale chemical interaction between pyroxenite-derived melts and mantle peridotites in the Northern Apennine ophiolites (Italy)

G. BORGHINI^{1,2,3}, E. RAMPONE¹, A. ZANETTI⁴, C. CLASS²,
A. CIPRIANI^{2,5}, A.W. HOFMANN^{2,5},
S.L. GOLDSTEIN² AND M. GODARD⁶

¹DISTAV, Università di Genova, 16132 Genova,

Italy (correspondence: giulio.borghini@unige.it)

²LDEO, Columbia University, Palisades NY 10964, USA

³Dip. Scienze Terra, via Botticelli 23, 20133 Milano, Italy

⁴CNR-IGG, Sez Pavia, via Ferrata 1, I-27100 Pavia, Italy

⁵DSCG, Università di Modena e Reggio Emilia, Italy

⁶MPI für Chemie, P.O. Box 3060, 55020 Mainz, Germany

⁷UMR CNRS, Université Montpellier 2, Montpellier, France

Mantle peridotites from the Northern Apennine ophiolites are characterized by the occurrence of cm-thick pyroxenite layers originated by rather deep segregation of MORB-type melts. Our recent work documents that during the pyroxenite emplacement portions of the country peridotite have been significantly modified in their modal, chemical and isotopic compositions by reaction with melts percolating from pyroxenite veins [1]. Here we report the results of detailed bulk and mineral major and trace element profiles carried out through pyroxenite-peridotite boundaries to investigate the physico-chemical parameters governing the melt-rock reaction process. Relative to the peridotites far (> 2 m) from the pyroxenite veins, wall-rock peridotites show i) modal orthopyroxene enrichment at the expense of olivine, ii) higher Al, Ca, Si contents and slightly lower Mg# iii) Al-richer spinel and lower-Mg# pyroxenes. Moreover, clinopyroxenes in the wall-rock peridotites have LREE-depleted patterns and initial $\epsilon\text{Nd}(430 \text{ Ma}) = +4.7\text{--}+7.6$, pointing to a reaction with an enriched tholeiitic silica-saturated melt. Along the pyroxenite-peridotite traverses, clinopyroxenes record a trace element gradient: at the pyroxenite-peridotite contact they have the lowest MREE-HREE abundances, with lower Sm/Nd ratios than the distal pyroxenite-free peridotites. The overall REE abundances progressively increase away from the pyroxenite-peridotite boundary up to about 20 cm as a result of percolative reactive flow at decreasing melt mass. Beyond 20 cm from the contact, the HREE content decreases with distance from the pyroxenite, while the LREEs remain at nearly constant level, pointing to a more efficient chemical buffering of the host peridotite on the HREE composition of the percolating melt through ion exchange chromatographic-type processes.

[1] Borghini *et al.* (2013), *Geology*, in review.

How do organic molecules affect interactions of water with environmental sorbents?

M. BORISOVER

Institute of Soil, Water and Environmental Sciences, ARO,
The Volcani Center, Bet Dagan, Israel;
correspondence: vwmichel@volcani.agri.gov.il

Water is the integral component of environmental phases and interfaces (e.g., in soils and sediments) and affects their structure and reactivity. Sorption interactions of water with environmental phases can be probed by their response to sorption of organic molecules. Such a test examines a sorbent hydration in a local microenvironment specific for a given probe. However, the direct measurement of the response of water-sorbent interactions to the presence of organic molecules at environmentally relevant conditions is difficult, due to typically low organic sorbate concentrations. Therefore, the use of the model-free thermodynamic approach [1] is proposed which allows determining the effect of organic compounds on sorbent-water interactions from the equilibrium sorption isotherms of organic molecules measured at varying water activities. The analysis included the data on (1) organic vapor sorption on such important soil components as minerals (i.e., quartz, clays, metal oxides) and organic matter (OM), and (2) the liquid phase sorption on the model soil OM. The amount of water *expelled* from a sorbent or *co-sorbed*, per an organic molecule sorbed, was obtained for different extents of sorbent hydrations. The water-expelling effect of organic molecules on minerals was analyzed by using Linear Free Energy Relationship (LFER). The LFER analysis suggested (i) the significance of organic sorbate polarizability associated with n - and π - electrons in driving water into the sorbent phase and (ii) the control of water driving-out effect by molecular size, H-bond acidity and basicity of sorbates. As distinct from minerals, water interactions with strongly hydrated OM phases (i.e., at water activities approaching one) become enhanced upon sorption of multiple organic sorbates containing oxygen, nitrogen or sulfur atoms. This OM hydration enhancement may involve several water molecules per a sorbed organic molecule and seems to be cooperative, which may need to be incorporated into models of organic compound sorption by soils and sediments. Importantly, this effect of the OM hydration enhancement suggests that a pre-hydration of OM does not necessarily create the OM configuration appropriate for further accommodation of other molecules.

[1] Borisover (2012) *Adsorption*, DOI 10.1007/s10450-012-9446-7).

⁵⁷Fe Mössbauer spectroscopy of pantelleritic melts

N. BOROVKOV¹*, K.-U. HESS¹, K. T. FEHR¹, C. CIMARELLI¹, D. B. DINGWELL¹ AND A. GÜNTHER¹.

¹Department of Earth and Environmental Science, Ludwig Maximilians Universität, Theresienstr. 41/III, 80333 Munich, Germany (*correspondence: nikita.borovkov@min.uni-muenchen.de)

Fe species in the melt can include 4-Fe²⁺, 5-Fe²⁺, 4-Fe³⁺, and 5-Fe³⁺. The relative proportions between these species can vary according to bulk glass composition and oxygen fugacity conditions. RedOx state and coordination of Fe can considerably affect important physical properties (density and viscosity) of magma, even where bulk composition and Fe content are constant. A set of silicate glasses with pantelleritic composition have been synthesized at different oxygen fugacity conditions (from air down to IW buffer) and then were analyzed by ⁵⁷Fe Moessbauer spectroscopy (MB). The spectra were taken at 298K in transmission mode and fitted by applying an extended Voigt-based lineshape according to [1]. The MB spectra of all samples display three lines which can be described to two different doublets. One doublet with an isomer shift (IS) of ca. 0.9 mm/s relative alpha-iron and a quadrupole splitting (QS) of ca. 2 mm/s can be attributed to ferrous iron. The second doublet with IS of ca. 0.3 mm/s relative alpha-iron and QS of ca. 0.9 mm/s can be attributed to ferric iron. The later values are close to that of ferric iron on tetrahedral site in ferrobaltic glasses [2]. With increasing oxidation the QS of ferric iron increases slightly from 0.85 mm/s (0.3 Fe³⁺/Fetotal) to 0.95 mm/s (0.8 Fe³⁺/Fetotal) where a decrease of QS for ferric iron as a function of oxidation was observed. The IS of 0.9 mm/s for ferrous iron remains constant up to an oxidation state of about 0.6 Fe³⁺/Fetotal and with increasing oxidation a rapid decrease to IS of 0.6 mm/s at 0.8 Fe³⁺/Fetotal occurs. At the oxidation state of 0.6 Fe³⁺/Fetotal the constant QS of 2.0 mm/s for ferrous iron increases up to 2.45 mm/s at 0.8 Fe³⁺/Fetotal in contrast to ferrobaltic glasses, where a QS of 2.0 mm/s remains constant over the whole oxidation state [2]. Meanwhile, for tektites and alumino-silicate glasses [3, 4] the doublet with IS of 0.9 mm/s and 0.6 mm/s was attributed to ferrous iron on a five-fold and four-fold coordinated sites, respectively.

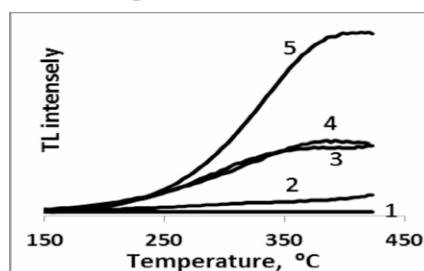
[1] Lagarec and Rancourt (1997) *Nucl. Instr. And Meth. B* **129**, 266-280. [2] Botcharnikov *et al.* (2005) *Geochim. Cosmochim. Acta* **69**, 5071-5085. [3] Rossano *et al.* (1999) *Phys Chem Minerals* **26**, 530-538. [4] Rossano *et al.* (2008) *Phys Chem Minerals* **35**, 77-93.

Luminescence of products of hypergenesis ore deposits

N.N. BOROZNOVSKAYA, L.A. ZYRYANOVA, T.S. NEBERA AND A.V. PAVLOVSKAYA

Tomsk State University, Tomsk, Russia
(boroznovskaya@mail.ru)

Luminescence analysis (L) can be successfully used in mineralogical studies of hypergene products. We studied the spectra of roentgenoluminescence (RL), and the thermoluminescence (TL) of minerals the oxidized zone Rubtsovsk deposit (Russia, Ore Altai). Found that the species composition of the loose mono and polymineral formations consisting of basic sulphate Cu, Pb, Al, and clay minerals can be determined from the characteristic spectra of RL and TL schedules. L studied minerals associated with defects in silicon-aluminum-oxygen tetrahedra, the excited states of oxygen and the presence of other native defects. Monoclinic dickite is diagnosed by the intense RL at $\lambda = 350-360$ nm, and very different from the triclinic kaolinite, which is characterized by weak luminescence in a wide wavelength range (285-300 and 340-350 nm). RL of kaolinite varies depending on the degree of crystallization and structural regularity. Halloysite is allocated by short-wave radiation with a peak in the spectral range 290-310 nm. In contrast to clay minerals alunite and osarizavaite spectra RL very low in intensity. Quantitative ratios of clay minerals and sulfates in their common units can be determined from the graphs of TL ignition minerals up to 450 °C.



Studied the L of hypogene and hypergene barite. RL spectra of barite formed in the oxidation zone differ from those of RL hypogene barite primary sulfide ore intense radiation in the wavelength range of 350-400 nm due to the excitation of oxygen. Thus, the study of products of hypergene luminescence methods allow: 1) to determine the degree of crystallinity of the mineral aggregates and order of the crystal lattice of minerals; 2) to use the luminescence for diagnostic purposes; 3) to solve individual genetic issues.

This study was funded by the Russian Ministry of Education and Science (projects 5.3143.2011, 14.B37.21.0686, 14.B37.21.1257).

Anthropogenic fractionation of zinc isotopes

DAVID M. BORROK^{1*} AND ANITA THAPALIA²

¹School of Geosciences, University of Louisiana at Lafayette, Lafayette, LA 70504

(*correspondence: dborrok@louisiana.edu)

²Department of Geological Sciences, University of Texas at El Paso (athapalia@miners.utep.edu)

Zinc (Zn) is used in many industrial processes, including the galvanization of steel and the vulcanization of rubber. Due to its relatively low volatilization temperature, Zn is emitted to the atmosphere in greater quantities than any other trace metal worldwide. The fractionation of stable Zn isotopes during anthropogenic processing provides a potential opportunity to understand and evaluate the sources, transport, and accumulation of pollutant Zn in the environment.

Here we present the results from a series of investigations of Zn isotopes in anthropogenic systems, including a new investigation of lake sediment cores from seven urban lakes and one reference lake in the USA. The time-resolved records of sediment (and Zn) accumulation suggest that, on average, the $\delta^{66}\text{Zn}$ (measured relative to JMC 3-0749L) of Zn from sediments deposited during intense urbanization is $0.09 \pm 0.07\text{‰}$ ($n = 12$), while the average isotopic signal for sediments deposited prior to urbanization (and in the non-urban reference lake) is $0.33 \pm 0.07\text{‰}$ ($n = 23$). The anthropogenic isotope signal for Zn fits well with previous investigations of Zn processing related to combustion, which may suggest that automobile emissions and waste burning are important contributors to urban Zn pollution. The natural background isotopic signal of Zn for lake sediments is similar to that reported for many igneous rocks. This may suggest that processes like weathering, transport, and biological uptake do not appreciably change the isotopic signature of the natural lake sediments.

This lake sediment study, as well as previous investigations of Zn-contaminated sediments, water, and atmospheric particles confirm that Zn isotopes can be useful to help distinguish between natural and anthropogenic Zn sources. However, because of the small amounts of fractionation and overlapping isotopic signatures, Zn isotope investigations are most successful when they are combined with other chemical and/or isotopic measurements.

Antigorite dissolution rates as a function of pH at 25 and 80 °C

O. BOSCH, J. DECLERCQ, V. MAVROMATIS AND E. H. OELKERS

¹GET, Université Paul Sabatier-CNRS/UMR 5563, Toulouse, France (*corresponding author bosch@get.obs-mip.fr)

Antigorite ($\text{Mg}_3\text{Si}_2\text{O}_5(\text{OH})_4$) is a common serpentine mineral that could provide the divalent metal cations required for mineral carbonation as part of carbon storage efforts. Such carbonation could occur via the dissolution of acidic CO_2 saturated H_2O . Antigorite dissolution into this fluid would both release aqueous Mg and neutralize the fluid promoting carbonate precipitation [c.f. 1].

In an attempt to better quantify this carbonation process antigorite dissolution rates have been measured as a function of pH from 2 to 10 temperatures of 25 and 80°C in closed system reactors. Rates were calculated from measured aqueous Mg and Si concentrations

$$r = (dC/dt)v/S$$

where r is the dissolution rate, dC/dt is the time derivative of Mg or Si concentration, v is the fluid volume in the reactor and S is the surface area.

Magnesium is released preferentially at the beginning of most of the experiments compared to silica suggesting the importance of Mg for proton exchange reactions in the antigorite dissolution mechanism. Also similar to the behavior of other Mg-silicate minerals including talc and tremolite [2], antigorite dissolution rates decrease systematically with increasing pH over the whole pH range considered in this study; antigorite dissolution rates at pH 2 are ~1.5 orders of magnitude faster than corresponding rates at pH 10. The addition of ~0.1 mol/kg citrate to the aqueous fluid appears to increase constant pH rates by less than an order of magnitude suggesting that the addition of organic ligands would be an inefficient method to accelerate the carbonation of Mg silicate minerals.

[1] Oelkers *et al.* (2008) *Elements* **4**, 333-337. [2] Saldi *et al.* (2007) *GCA* **71**, 3446-3457.

Insights on the protracted evolution of the deep crust of the Arabo-Nubian Shield.

BOSCH DELPHINE*

¹* Géosciences Montpellier, Montpellier France.
(delphine.bosch@gm.univ-montp2.fr)

The Arabian-Nubian Shield (ANS) represents a mosaic of more than 15 Neoproterozoic juvenile island-arc terranes (850-600 Ma) formed in the Mozambique ocean realm. In spite of amalgamation events that subsequently led to accretion of the ANS, most exposed terranes are characterized by low- to moderate metamorphic overprint, greenschist-facies rocks being prevalent in the shield. It is thus difficult to examine how and when the lower crust of the ANS formed since it is mostly inaccessible. In this study, we analysed 3 gneisses from Zabargad Island (Egypt) corresponding to lower crustal units exposed at surface level during the Oligo-Miocene thinning of the ANS lithosphere related to the Red Sea rifting. Zircons from a felsic granulite have both low and high Th/U ratios (0.3 and 0.07), but yield undistinguishable ages of 652 ± 10 Ma, which we interpret as dating the age of the protolith and its conversion to granulite. Some zircons however yield low Th/U ratios and a significantly younger age of 597 ± 4 Ma, reflecting a second metamorphic event, possibly related to collision between island arc terranes of the ANS and the Saharan craton on the West. Monazites from a granulitic gneiss yield a much younger age of 497 ± 2 Ma which may reflect far-field stress associated to the latest stages of amalgamation of eastern Gondwana. Lastly, zircons extracted from a granulitic gneiss sampled at the contact with the Northern peridotite massif yield an age of 25.1 ± 0.4 Ma related to contact metamorphism during juxtaposition of the hot peridotite and lower crustal units. Gneisses from Zabargad island constitute a unique window to look at the polymetamorphic evolution of high-grade lower crustal units of the ANS.

Micro-fracturing induced by radioactivity of minerals: consequences on the permeability of rocks.

V. BOSCHERO^{1,2}, A.M. SEYDOUX-GUILLAUME¹, M. MARCOUX², C. NOIRIEL¹ AND L. ORGOGOZO¹

¹ GET, UMR5563 CNRS-UPS-IRD, Université de Toulouse, 14 av E. Belin, 31400 Toulouse, France

² IMFT, UMR5502 CNRS-INPT-UPS, 2 Allée du Professeur Camille Soula, 31400 Toulouse, France

Some rocks may contain radioactive (U-Th) minerals ranging from micrometric to millimetric sizes. These minerals are submitted to intense self-irradiation (α -decay of U and Th chains) that can lead to amorphization and also modify their environment by irradiating the host minerals. Amorphization induces volume increase, leading to the formation of cracks which eventually connected into a network through the rock. This fracturing allows fluid circulation, and promotes alteration of source minerals and dispersion of elements (e.g. Pb and U). These observations highlight the importance of understanding the impact of radiation damage on radioactive transport by fluids passing through such fractured rocks. The aim of this study is, through the characterization of natural samples, to explore the consequences of such fracturing on the ability of rocks to transfer radioactive elements within fluid phases. The study was made up of imaging, laboratory measurements and numerical modelling.

First, the permeability of natural rocks with high-level of radioactivity, was measured. Such low permeability needs the use of specific gaz-permeameter. In agreement with the Klinkenberg effect, permeability of the samples can be obtained.

In a second step, these results were compared with those from numerical modelling. For that, the geometry of a micro-fracture network was used after SEM image processing. The model simulates both the flow in the fractures and the reactive transport associated with the dissolution of the radioactive minerals and helped us to evaluate the flow and the transport heterogeneity in a natural sample, induced by this local fracturation surrounding radioactive minerals.

For a better understanding of this process, the use of X-ray CT-scan is necessary to develop a 3D model.

Carbonation of serpentinite mine tailing: the example of Montecastelli mine (Tuscany, Italy)

BOSCHI C.¹, DINI A.¹, BEDINI F.¹, BANESCHI I.¹,
NATALI C.¹ AND DALLAI L.

¹Istituto di Geoscienze e Georisorse, CNR (Pisa, Italy);
c.boschi@igg.cnr.it

Carbonation of serpentinite or asbestos mine tailing is a passive, weathering-related process that take advantage of the thermodynamically driven natural transformation of ultramafic rocks into carbonate and thus it is cost and energy effective. The enhancement of this natural weathering is a challenge including multiple advantages: CO₂ capture, and remediation of asbestos tailing. Here, we present an example of natural carbonation of a small mine dump at Montecatelli (Tuscany, Italy).

At Montecatelli (Tuscany, Italy), a pluri-kilometric body of serpentinite, embedded in shales, has been deeply eroded by the Pavone River providing good exposures and sections. The central portion of the serpentinite body host a small copper ore deposit that was intermittently exploited during the XIX century, and was definitively closed in 1869. Bornite, chalcocite, chalcocite and pyrite veinlets and nodules, in a chlorite-serpentinite-brucite-amphibole soapy gangue, characterize narrow deformation zones crosscutting the serpentinites. Most of the low-grade Cu-ore extracted in the past was not reliable for industrial processing and directly dumped in front of the entrances of the mine, forming by the time a small mining dump. Mining activity stopped 60 years ago.

Intense natural carbonation produced crust of hydrated Mg-carbonates (hydromagnesite, nesquehonite, manasseite, pyroaurite, brugnatellite) coating the serpentinite clasts of the mining dump and the serpentinite walls of the mine tunnels.

The Montecatelli carbonated serpentinite mine tailings represent an example of rapid atmospheric CO₂ uptake. Their study improved our knowledge of the carbonation processes. Future quantification of the amount of carbon sequestered in geologic samples from Montecatelli would give an estimate for the sequestration capacity of ultramafic mine tailings in general and will provide a framework for the development of standard protocol for enhanced mineral sequestration at mine sites.

The Behavior of Beryllium in Soils and Aquatic Environments

VANESSA BOSCHI^{1*} AND JANE K. WILLENBRING¹

¹University of Pennsylvania, 240 South 33rd Street
Philadelphia, PA 19104; *vaboschi@sas.upenn.edu

Beryllium is an important metal utilized in a diverse range of applications. Aside from its numerous industrial uses, it is as a central tool used in the field of geochronology and geomorphology. Recent work indicates ⁹Be leached from mineral lattices during weathering processes moves through a landscape adsorbed to soil particles and in solution. As such, the flux of ⁹Be from rivers is indicative of the weathering extent of soils within the catchment. Another isotope, cosmogenic ¹⁰Be, is formed in the atmosphere and is precipitated onto the Earth's surface, adsorbing onto surface sediments. The concentration of ¹⁰Be in soils and sediments scales with the residence time of sediments in a landscape. Although these applications are dissimilar, they require an understanding of the behavior of beryllium in soils and aquatic environments. A better understanding of the mobility of beryllium will help constrain its use for such geologic techniques.

In order to evaluate the interactions of beryllium with soil and aquatic related materials, we selected model organic compounds and minerals to perform distribution coefficient experiments. Model organic compounds such as graphite, cellulose, an amine compound and phenolic acid in addition to dissolved organic matter samples were selected on the basis of their chemical composition and potential ability to adsorb beryllium. Clay-sized fractions of montmorillonite, illite, kaolinite and hectorite were also selected. The retention of beryllium onto each of these compounds was evaluated over a pH range and various equilibration times to determine which conditions allowed for the greatest retention of beryllium. Preliminary results conclude that mineral compounds more efficiently adsorb beryllium relative to the selected model organic compounds. Retention of beryllium increases with increasing pH from 2 to 6. We also examined the effect of pH on the speciation and colloidal nature of beryllium. For beryllium concentrations typical of natural soil solutions, we find that the colloidal behavior of beryllium may play a significant role in its mobility within soils.

Determination and quantification of fatty acids in speleothems and cave drip water using HPLC-ESI-IT/MS

J. M. BOSLE^{1*}, D. SCHOLZ² AND T. HOFFMANN³

¹Institute of Inorganic and Analytical Chemistry, Johannes Gutenberg-University Mainz, Germany;

(*correspondece: bosle@uni-mainz.de)

²Institute for Geoscience, Johannes Gutenberg-University Mainz, Germany;

(scholzd@uni-mainz.de)

³Institute of Inorganic and Analytical Chemistry, Johannes Gutenberg-University Mainz, Germany

(hoffmannt@uni-mainz.de)

Cave drip water, speleothems and the proxies preserved within them have significant potential to record palaeoenvironmental changes in the regional vegetation [1]. The most common proxies measured in stalagmites are inorganic proxies, in particular oxygen isotopes [2]. More recently the importance of organic matter analyses in this field is examined. This study focuses on the research of lipid biomarkers. The lipids contained in stalagmites originate from the overlying soil and different plants, bacteria and fungi. Therefore different compositions of lipids may provide records of environmental changes [3].

In the following the development of a new method for the extraction of fatty acids (FA) from stalagmites and cave drip water and their measurement by HPLC-ESI-IT/MS (high performance liquid chromatography coupled to electrospray ion trap mass spectrometry) is presented. Five different FAs with chain lengths from C12 to C20 were applied as analytical standards. A mixture of these was used to optimize the separation by HPLC. The FAs were measured in negative polarity, so a time consuming derivatization of the analytes was not necessary. To simulate the extraction of the FAs several spiking experiments were performed. Solid phase extraction and liquid liquid extraction were used for the extraction procedure. Both methods were optimized and good reproducibilities with deviations below 10% were achieved. Quantitative analyses were accomplished and the limits of detection determined. As a proof of principle, first applications to the actual samples were successfully fulfilled. To testify the role of the FAs as palaeoclimate proxies further experiments will be performed.

[1] Blyth *et al.*, (2008) *Quaternary Sci Rev* **27**, 905-921.

[2] Fairchild *et al.*, (2006) *Earth-Sci Rev* **75**, 105-153.

[3] Blyth *et al.*, (2006) *Org Geochem* **37**, 882-890.

Sub-micrometer scale chemical mapping of complex monazites: the contribution of the NanoSIMS.

V. BOSSE^{1*}, A. DIDIER¹, J.L. PAQUETTE¹, S. MOSTEFAOUI² AND J.L. DEVIDAL¹

¹ Clermont Université, Université Blaise Pascal, Laboratoire Magmas et Volcans, BP 10448, 63000 Clermont-Ferrand, France. (*V.Bosse@opgc.univ-bpclermont.fr)

² Laboratoire de Minéralogie et Cosmochimie du Muséum, UMR 7202, CNRS INSU, Muséum National d'Histoire Naturelle, 57 Rue Cuvier, 75231 Paris Cedex 05, France

Monazite [(Ce,La,Nd,Th)PO₄] is a very robust geochronometer which can record and preserve U-Th-Pb ages in various geological environments. For around ten years, monazite has also been increasingly studied because it is a key tracer for geological processes, especially fluid/rock interactions. Monazite grains often display variable chemical compositions at the grain scale and complex chemical zoning, sometimes correlated to age domains, reflecting the changes in physical and chemical parameters of the host rock. The development of *in situ* techniques (EMPA, LA-ICPMS, SHRIMP) enables the combined study of chemical and isotopic characteristics in the monazite at the scale of few μm . However, many recent studies show that: (1) it is not always possible to correlate age and chemical domains at these scales, (2) monazite often display very complex chemical zoning at infra μm scale and (3) TEM analyses show strong perturbations of the crystal lattice between 10 and 200 nm. In order to better understand the ages recorded by monazite it is necessary to obtain chemical informations at nm scale. In this context, the NanoSIMS appears to be the best suited tool.

We present here chemical elements (⁸⁹Y, ¹³⁹La, ²⁰⁸Pb, ²³²Th and ²³⁸U) NanoSIMS images and analyses obtained in monazites studied in thin section or separates. ⁸⁹Y, ¹³⁹La, ²⁰⁸Pb, ²³²Th and ²³⁸U ion images were obtained in monazite areas previously studied with EMPA and dated with LA-ICPMS. The NanoSIMS maps allow to characterise isotopically and chemically distinct domains that were not distinguishable on WDS X-ray maps. ²⁰⁸Pb/²³²Th maps derived from NanoSIMS images offer the possibility to correlate different age domains with the measured ²⁰⁸Pb/²³²Th ages obtained at larger scale (few μm) by LA-ICPMS.

These results are very promising for compositional and isotopic mapping with a highest spatial resolution in the monazite geochronometer.

Simulation of physical and chemical processes of polluted air masses during the Aegean-Game airborne campaign using WRF-Chem model

E. BOSSIOLI^{1*}, M. TOMBROU¹, J. KALOGIROS², J. ALLAN³, A. BACAK³, S. BEZENTAKOS⁴, G. BISKOS^{4,5}, H. COE³, G. KOUVARAKIS⁶ AND N. MIHALOPOULOS⁶

¹Department of Physics, Univ. of Athens, 15784 Athens, Greece

(*correspondance:ebossiol@phys.uoa.gr, mtombrou@phys.uoa.gr)

²Nat. Observatory of Athens, 15236 Athens, Greece (jkalog@noa.gr)

³The School of Earth, Atmospheric and Environmental Sciences, Univ. of Manchester, M13 9PL, UK (hugh.coe@manchester.ac.uk, james.allan@manchester.ac.uk, asan.bacak@manchester.ac.uk)

⁴Univ. of the Aegean, Mytilene 81100, Greece (bezantakos@env.aegean.gr)

⁵Fac. of Applied Sciences, Delft Univ. of Technology, Delft 2628BL, The Netherlands (biskos@aegean.gr, g.biskos@tudelft.nl)

⁶Department of Chemistry, Univ. of Crete, Heraklion 71003, Greece (mihalo@chemistry.uoc.gr, kouvarak@chemistry.uoc.gr)

The chemical and dynamic processes as well as the atmospheric composition, in the Planetary Boundary Layer (PBL) over the Aegean Sea, are investigated during an 'Etesian' event (29/8-9/9/2011) based on modeling results and a combination of airborne and ground observations. During this period atmospheric parameters, concentrations of gaseous species and size-resolved aerosol chemical composition have been measured using instrumentation flown on the UK's BAe-146-301 Atmospheric Research Aircraft operated through FAAM [1,2]. The simulations were performed by the on-line meteorological and chemical transport WRF-Chem model. Anthropogenic and on-line calculated natural (biogenic, sea-salt) emissions have been considered. Fire emissions generated by the FMI Fire Assimilation System [3] have been also included. The horizontal and vertical distribution of gaseous and aerosol species is interpreted in relation to the evolution of the PBL, and is shown that the model captures the geographical and temporal variations observed.

[1] Tombrou *et al.* (2013) *Advances in Meteorology, Climatology and Atmospheric Physics* 1239-1244. [2] Bezentakos *et al.* (2013) *ACPD* **13**, 5805-5841. [3] Sofiev *et al.* (2009) *ACP* **9**, 6833-6847.

Polyoxometalates and Their Effect on Tungsten Speciation and Transport

BENJAMIN BOSTICK^{1*} AND JING SUN¹²

¹Lamont-Doherty Earth Observatory, Palisades, U.S.A., bostick@ldeo.columbia.edu

²Columbia University, New York, U.S.A, AND Lamont-Doherty Earth Observatory, Palisades, U.S.A., jingsun@ldeo.columbia.edu

Tungsten (W) is a toxic element with complex aqueous speciation. Tungstate, W(VI), is the dominant oxidation state of tungsten in soils, forms a variety of insoluble tungstate minerals, and often adsorbs strongly to iron oxides. This W(VI) often is significantly more readily transported than expected based on the available thermodynamic data. We have examined the role of metastable and heteropolyatomic polytungstates in enhancing the solubility of tungsten in natural systems. We have measured W concentrations following reaction with model soil minerals, and natural soils, over a variety of solution compositions and reaction periods in which a variety of polytungstate species may form in solution. In particular, we examined the effect of initial W(VI) concentration and speciation, pH, and the presence of silicate and phosphate on W(VI) sorption. The speciation and structure of adsorbed W(VI) on ferrihydrite also were examined using synchrotron-based X-ray absorption spectroscopy (XAS). Adsorption isotherms and envelopes show a complex relationship between pH and W(VI) adsorption, with more W(VI) retained at circumneutral pH. Adsorption was less extensive in solutions containing more polymeric species, suggesting that these species do not adsorb to ferrihydrite surface as strongly as does the tungstate anion. Polyoxometalate (POM) clusters form in the presence of phosphate, or persist as metastable complexes for sufficient duration to considerably enhance the solubility and transport of tungsten in natural environments. XAS confirmed that tungstate usually represents the bulk of adsorbed W(VI), but polytungstates also appear to be adsorbed to the mineral surface, particularly in systems in which W(VI) was most soluble. Equilibrium adsorption onto ferrihydrite was not achieved and takes more than one month; this unusually slow adsorption is due to the slow decomposition of weakly-adsorbing polyatomic anions to monomeric tungstate anions. The kinetic stability of metastable polytungstates thus may further enhance W solubility in natural waters and its migration in natural environments.

Relating U-Th-Pb ages of accessory minerals to metamorphism: A case study from the Barrovian sequence of the Central Alps, Switzerland

KATE BOSTON^{1*}, DANIELA RUBATTO¹,
JÖRG HERMANN¹, YURI AMELIN¹ AND MARTIN ENGI²

¹Research School of Earth Sciences, the Australian National University, Building 142 Mills Rd Acton ACT Australia.
(Correspondence: Katherine.Boston@anu.edu.au)

²Institute of Geological Sciences, University of Bern,
Baltzerstrasse 1 + 3 CH3012 Bern Switzerland.

Accessory minerals allanite, monazite and rutile from amphibolite facies rocks across the Barrovian sequence of the Central Alps (Switzerland) were investigated for composition and U-Th-Pb ages. The growth ages of these minerals record stages of prograde and peak metamorphism.

Allanite formed during the prograde path at 26-33 Ma. It occurs aligned along an early foliation that is overprinted by later generations of mica. In some cases, the foliation along which allanite is aligned is only preserved in garnet. Rutile from one metapelite in the central region also records a ~33 Ma age. Zr-in-rutile thermometry yields a temperature of 550±20°C, which is lower than the 620°C peak temperature deduced from the main mineral assemblage [1], indicating that rutile crystallised under prograde conditions. We interpret this early age as the time when the rocks reached peak pressure conditions.

The timing of peak temperature conditions is recorded in monazite, rutile and, in one sample, allanite rims. Monazite yields an age of 22 Ma and grew at the expense of allanite and after the first stage of garnet growth. In monazite-bearing samples, allanite is preserved as inclusions in garnet, whereas monazite is part of the matrix. Zr-in-rutile thermometry suggests that 23 Ma rutile in a calcschist records the timing of peak temperature conditions. 20 Ma allanite rims in one metapelite crystallised on older (27 Ma) cores, and are also interpreted to reflect the timing of peak to retrograde conditions.

Through multi-mineral geochronology a prograde metamorphic history, spanning some 10 Ma, can be reconstructed: from prograde greenschist facies to peak amphibolite facies conditions. The observation that 33 Ma prograde rutile is preserved despite the later temperature peak at 22 Ma suggests a closure temperature of Pb in rutile in excess of 620°C.

[1] Todd & Engi (1997) *J. metamorphic Geol.* **15**, 513-530

A multi-isotope (H, O, C, S, B, Mg, Ca, Ba) approach to study diagenesis in Black Sea-type sediments

M.E. BÖTTCHER^{1*}, L. LAPHAM^{2,11}, N. GUSSONE³,
U. STRUCK⁴, D. BUHL⁵, A. IMMENHAUSER⁵,
K. MÖLLER⁶, C. PRETET⁷, T.N. NÄGLER⁶, O. DELLWIG¹,
B. SCHNETGER⁸, H. HUCKRIEDE⁹, S. HALAS¹⁰
AND E. SAMANKASSOU⁷

¹Leibniz IOW, D-18119 Warnemünde, FRG

(correspondance:michael.boettcher@io-warnemuende.de)

²CfG, Aarhus University, Denmark

³Mineralogy, Münster University, FRG

⁴Museum für Naturkunde, Berlin, FRG

⁵Sediment & Isotope Geology, Bochum Univ., FRG

⁶Isotope Geology, University of Bern, Switzerland

⁷Geol. & Paleont., Univ. of Geneva, Switzerland

⁸ICBM, Univ. of Oldenburg, FRG

⁹Thüringer Landesanst. Umwelt & Geol., Jena, FRG

¹⁰Institute of Physics, UMCS, Lublin, Poland

¹¹current: University of Maryland, Salomons, USA

Like The Black Sea, The Baltic Sea Has Switched Between Fresh Water And Brackish Water Modes. The Changes In Paleo-Environmental Conditions Caused Downcore Gradients In The Concentrations Of Dissolved Species In The Pore-Waters With Consequences For Microbial Activity And Physicochemical Water-Solid Interactions Associated With Multiple Stable Isotope Fractionation Processes. Here, We Introduce A New Combined Multi-Isotope And Trace Element Approach To Investigate Diagenesis In These Non-Steady State Systems.

In a Gotland Basin core, it is found that concentrations of conservative elements and the pore water H-2 and 18-O contents decrease with depth due to diffusion from brackish waters into underlying fresh waters. A downward increase and decrease of Ca and Mg concentrations, respectively, is associated with decreasing Ca-44 and Mg-26 isotope values. B-11 isotope values decrease in the limnic part. An increase in Ba concentrations with depth is associated with a slight increase in Ba-137/134 isotope values. Microbial activities lead to an increase in DIC, but a decrease in SO4 concentrations and in C-13 contents of DIC with depth. Desorption of Ba from glacial sediments due to downward diffusing ions is responsible for the formation of sedimentary barites. S-34 and O-18 isotope values of barites suggest that these were formed in glacial sediments from pore waters strongly depleted in O-18. Impacts of diagenetic processes on multi-isotope signals in pore waters and authigenic phases are discussed. Mixing between brackish and fresh waters, solid-liquid interactions, and transport reactions explain most of the observed isotope variations along the vertical pore water profile.

High Velocity Collisions Recorded in Asteroidal Meteorites: New Ways to Constrain Planet Formation

W.F. BOTTKE^{1,2} AND S. MARCHI^{1,2}

¹ Southwest Research Institute, Boulder, CO, USA

² Center for Lunar Origin and Evolution, NLSI

It was recently shown that ⁴⁰Ar–³⁹Ar ages in meteorites reflect unusually high impact velocities exceeding 10 km/s [1]. Compared with typical impact velocities for main-belt asteroids of about 5 km/s, these collisions produce 100–1,000 times more highly-heated material by volume. It was proposed that the ⁴⁰Ar–³⁹Ar ages between 3.4 and 4.1 Gyr ago from Vesta, the H-chondrite parent body and the Moon record impacts from numerous main-belt asteroids that were driven onto high velocity and highly eccentric orbits by the effects of the late migration of the giant planets. The timing of these asteroidal and lunar impact signatures help define the so-called Late Heavy Bombardment.

An intriguing implication of this work concerns the ⁴⁰Ar–³⁹Ar events seen between ~4.4–4.53 Gyr ago among many stony meteorite groups. Although some of those ages may reflect cooling through the blocking temperature after igneous crystallization, others are unambiguously related to early impact events on primordial asteroids during the planet formation era [e.g., 2]. More recent impacts in the main asteroid belt ejected this material off the parent body, allowing it to reach Earth through dynamical processes. We postulate that these early high-velocity impacts likely came from leftover planetesimals residing in the terrestrial planet region, many of which had highly eccentric and inclined orbits. If true, these ~4.5 Gyr ago events constrain the nature and decay rate of this putative population, as well as early planet formation processes. Using numerical simulations, we will explore the implications of these results in our talk. We will also probe how these same methods and data allow us to glean insights into the timing of the giant impact that formed the Moon.

[1] Marchi, Bottke *et al.* (2013) *Nature Geosci.*, **6**, 303-307.

[2] Bogard, D. D. (2011) *Chem. Erde Geochem.* **71**, 207-226.

Hypersaline volatiles in a palladium-enriched mafic pegmatoid from the 2.48 Ga East Bull Lake intrusion, Sudbury District, Ontario, Canada

BRANDON BOUCHER¹, JACOB HANLEY¹
AND RICHARD JAMES²

¹Saint Mary's University, Halifax, NS, Canada. B3H 3C3

(boucher.brandon.m@gmail.com;

jake.hanley@gmail.com)

²MERC, Laurentian University, Sudbury, ON, Canada

(rjames@laurentian.ca)

The East Bull Lake intrusion (EBLI) is a Paleoproterozoic mafic-ultramafic (low-Ti, high-Al tholeiitic) intrusion located roughly 90 km west of Sudbury, ON. The intrusion itself consists primarily of massive- and layered leucogabbro and leucogabbronorite and is interpreted to be the product of crystallization of partial melts from sublithospheric depleted mantle, a remnant of a ~2.48 Ga large igneous/metallogenic province. The heavily contaminated lower zones of the intrusion host disseminated-blebby PGE-Cu-Ni sulfide mineralization (up to ~10s ppm PGE locally in massive sulfide pods).

Microthermometry was conducted on fluid inclusion assemblages containing late-stage magmatic-hydrothermal fluids in interstitial quartz from a mineralized pegmatitic leucogabbro from the central portion of the intrusion. The FIAs contain three-phase liquid-rich inclusions with halite daughter phases. Final homogenization occurred by halite dissolution at temperatures significantly higher than vapour bubble disappearance. Using a method for calculating minimum trapping pressures at the T of homogenization [1,2], FIAs not influenced by post-entrapment modification show minimum trapping pressures from 1.6-3.0 kbars, with final homogenization temperatures ranging from 291° to 367°C (bulk salinities of 38-44 wt% NaCl equiv.) For comparison, Ti-in-quartz thermometry for fluid inclusion-rich domains in the quartz indicate crystallization from 650-750°C. The data suggest that if the inclusions are primary then actual trapping pressures are significantly higher than the minimum values estimated above, constraining the depth of emplacement of the mineralized intrusion to at least 18km.

The study provides first constraints on the nature of late-stage magmatic-derived fluids associated with the EBLI and provides a means for comparison to other mineralized intrusions that show involvement of magmatic fluids in the redistribution of chalcophile/highly siderophile ore metals.

[1] Lecumberri-Sanchez *et al.* (2012) *Geochim et Cosmochim acta* **92**, 14-22. [2] Becker *et al.* (2008) *Econ. Geol.* **103**, 539-554

Deep crustal melting revealed by Pb isotopes and seismology in the western US

R.A. BOUCHET¹, J. BLICHERT-TOFT^{1,2}, A. LEVANDER²,
M.R. REID³ AND F. ALBAREDE^{1,2}

¹Ecole Normale Supérieure de Lyon, 69007 Lyon, France
(romain.bouchet@ens-lyon.fr)

²Rice University, Houston, Texas 77005, USA

³Northern Arizona University, Flagstaff, Arizona 86011, USA

In comparison to the uniform coverage of the western US (WUS) provided by the USArray, the NAVDAT database shows many poorly sampled regions. We therefore measured the Pb isotope compositions of crustal xenoliths from numerous volcanic and plutonic rocks across the Colorado Plateau (CP), and also sampled felsic plutonic rocks outcropping east of it, where data for the crust have been particularly scarce. When possible, we separated low-U/Pb K-feldspars to obtain the Pb isotope composition of the host magmas. We combined our new data with literature Pb isotope data from ores and felsic plutonic rocks, all of which we cast into the geologically informative variables of Pb model ages, U/Pb, and Th/U using a two-stage model. These parameters were then imaged on isotopic maps of the WUS using grid-cell averaging. Comparing the isotopic maps to seismic maps of tomographic anomalies [1] and Moho and LAB depths determined from receiver functions [2] leads to the following observations: (1) Pb model ages match geological ages only where the continental mantle is cold and the Moho is deep. Elsewhere, Pb model ages have been reset. (2) While U/Pb does not vary systematically with other geochemical or seismic data, Th/U, as inferred from measured ²⁰⁸Pb/²⁰⁶Pb systematics, is high in the Snake River plain, in Northern Utah, along the Uinta Mountains, along the western rim of the CP, along the Rio Grande Rift, and in the Laramide uplifts in Colorado, all places where Vp/Vs is high, and represent regions of either crustal thinning or basement exposure. We suggest two scenarios: (1) The Th/U systematics, which are not visibly controlled by heat flow, attest to thinning of the local continental crust above hot mantle. Lateral removal of the upper and middle crust, by extensional faulting or channel flow, allowed the uplift of deep high-Th/U crustal rocks and their melting. (2) Exhumation of basement rocks by either deep-seated Laramide style thrust faults or as metamorphic core complexes provides access to deeper levels of the crust, providing the observed high Th/U values.

[1] Schmandt and Humphreys, *EPSL*, 2010 [2] Levander and Miller, *G-Cubed*, 2012.

Large river floodplains: weathering without erosion?

J. BOUCHEZ¹, M. LUPKER², J. GAILLARDET³,
C. FRANCE-LANORD⁴, P. LOUVAT³ AND L. MAURICE⁵

¹GFZ - Helmholtz Centre Potsdam, Potsdam, Germany

²ETH, Zürich, Switzerland

³IPGP – CNRS, Paris, France

⁴CRPG – CNRS, Vandoeuvre-les-Nancy, France

⁵GET – IRD, Toulouse, France

On their journey to the ocean, large river sediments undergo a series of sedimentation, temporary storage and reworking episodes in active floodplains, in which time is available for sediments to mature chemically. Weathering affecting material eroded from tectonically active mountain belts in these flat, non-erosive areas is a potential mode of coupling between erosion and weathering fluxes at the continental scale.

We quantified the chemical fluxes associated with weathering of sediments in the floodplains of the Amazon and Ganga river systems [1,2]. To this end, river sediments were sampled upstream and downstream four river reaches across these basins. Sampling along depth-profiles grants access to the whole grain size and chemical composition range of river sediment. Weathering intensities of major elements (i.e. losses of Na, K, Mg and Ca) associated with chemical weathering in floodplains were examined as a function of grain size and integrated over the entire grain size range. Finally, we computed weathering fluxes, using a steady-state mass balance model at the scale of the river reach.

Across the four river reaches (Marañon, Beni, Madeira, and Ganga rivers), two consistent features emerge: (1) significant carbonate dissolution and subsequent Ca and Mg release to the dissolved load; (2) retention of K and Mg in the silicate phase of the sediment. These observations are in agreement with what is predicted from mineral kinetics. In this respect, sediment transport time across the river reach is a controlling factor on the floodplain weathering flux. However, across the studied river reaches, the variable extent of Na and Ca release by plagioclase dissolution points at an additional control on the intensity, namely the potential exhaustion of weatherable minerals before the sedimentary material enters the floodplain (be it in modern soils of the erosive area, or during ancient weathering episodes).

Altogether, our results show that floodplains constitute the predominant locus of weathering in the Gangetic system but not in the Amazon Basin. However, CO₂ consumption fluxes associated with silicate weathering in floodplains in these two river basin floodplains is on the order of magnitude as those resulting from weathering in their erosive areas.

[1] Bouchez *et al.*, 2012, *Chem. Geol.* **332-333**: 166-184 [2] Lupker *et al.*, 2012, *Geochim. Cosmochim. Acta* **84**: 410-432

Biogeochemical responses to gamma irradiation treatment of Alberta oil sands fluid fine tailings

RYAN BOUDENS^{1*}, THOMAS REID¹, JAN CIBOROWSKI¹
AND CHRIS WEISENER¹

¹Great Lakes Institute for Environmental Research, University of Windsor, Windsor, Canada
(*boudens@uwindsor.ca, weisener@uwindsor.ca)

Exploitation of the oil sands in Alberta has created large volumes of waste materials termed fluid fine tailings (FFT). These materials are stored in large settling basins to allow adequate separation of the oil sands process water and the FFT. The separated water in these holding areas are used either for future processing or it is allowed to settle before reclamation into functional wetlands and end pit lakes. A major concern is the presence of Naphthenic Acids (NA); these are a toxic, recalcitrant group of carboxylic acids naturally released from bitumen during the extraction process. An unexplored treatment option to promote or speed the degradation process and reduce *in situ* effects of NA's is gamma irradiation. In this study we examined the development of chemical REDOX gradients; and kinetic responses of indigenous microbes inoculated into irradiated FFT material using laboratory microcosms.

The systems will be set up using representative young and aged FFT material in both oxic and anoxic environments. Temporal changes to porewater and headspace water geochemistry was tracked along with *in situ* microsensor profiles and microbial community succession patterns. These results will have implications in development of a model framework to optimize treatment based on biogeochemical responses to waste type.

Closed system vs. open system degassing: a combined textural and geochemical approach

G. BOUDON^{1*} AND H. BALCONE-BOISSARD²

¹Institut de Physique du Globe de Paris, Sorbone Paris Cité Paris, France (*correspondence : boudon@ipgp.fr)

²ISTeP, Université Pierre et Marie Curie, Paris, France

Eruptive styles of volcanoes span a wide range of dynamic, from effusive to explosive. They depend on the magma composition, the volume of ejected magma and the magma ascent conditions in the conduit, from the reservoir to the surface. Magmas with the same composition and pre-eruptive conditions can generate different eruptive styles (eg. multistyles eruptions) evidencing the dominant effect of the ascent conditions of magmas. Understanding the behavior of the volatile phase in relation with the rheology of the magma (viscosity) during magma ascent is one of the main stake.

A detailed study of the textural characteristics (vesicularity, microcrystallinity) of the products of explosive eruptions associated to their composition and volatile content (pre-eruptive and residual) allow to better define the relations between the magma behavior in the upper part of the conduit and the eruptive style. In low-viscous basic magmas, pre-eruptive volatile content is low (2-3 wt%) and bubbles move independantly in the melt, with a higher ascent velocity. Their coalescence forms large bubbles that blow up at the surface: the explosivity is low (strombolian eruptions). On the contrary, in high-viscous differentiated magmas, the pre-eruptive volatile content is high (up to 5-7 wt%) and bubbles display generally the same ascent velocity. The magma reaches the surface with a large proportion of bubbles (up to 75vol%) as an unstable foam, the fragmentation of which generates a high explosivity (plinian to vulcanian eruptions). In some cases, with similar magma composition and volatile content, part of the volatiles may escape through permeable conduit walls generating a bubble flattening and melt microcrystallisation, which in turn increase the magma viscosity, decreasing its ascent rate. At the vent, this magma is partly degassed with a very low explosivity potential (dome-forming eruptions), excepting some particular cases. All intermediate eruptive style exist between high and low explosivity, depending of the behavior of the magma during its ascent in the conduit.

We'll discuss all these cases including the extremes and inusual cases as basaltic plinian eruptions or explosive dome-forming through several examples taken in recent eruptions.

Thermodynamics of Lower Mantle Minerals

M.A. BOUHIFD¹, D. ANDRAULT¹
AND N. BOLFAN-CASANOVA¹

¹Laboratoire Magmas et Volcans, CNRS UMR 6524,
Université Blaise Pascal, Clermont-Ferrand, France

There is a general consensus that the Earth's lower mantle is mostly composed of (Mg,Fe)SiO₃ perovskite (Mg-Pv) and (Mg,Fe)O ferropericlasite (Fp). Knowledge of the chemical and physical properties of these minerals is, therefore, essential for understanding the structure and dynamics of the lower mantle.

In this work, we performed a new compression study of Mg-perovskite (MgSiO₃) and periclasite (MgO) phases synthesized at variable conditions of the Earth's lower mantle by using pure Mg₂SiO₄ as a starting material. In our experiments a Double-sided Laser-Heated Diamond Anvil Cell at the ESRF – ID27 (Grenoble) was used up to 100 GPa and 3000 K. The equation of state (EOS) at various conditions of *P* and *T* for Mg-Pv and Fp were obtained by integrating the available experimental data into a single P-V-T EOS to constrain the elastic parameters (bulk modulus, densities, etc ...) under conditions of the Earth's lower mantle, which provides a basis for evaluating the compositional models of the Earth's lower mantle.

In this study, we will also combine our new results and the existing data in the literature to discuss and compare the combined effects of Fe and/or Al on the EOS of both phases and the chemical constraints that we can obtain from such comparisons. Finally, we will discuss our results on the light of the most recent studies on the melting curves of the lowermost Earth's mantle and the stabilization of the ultra-low velocity zones associated with partial melting at the core-mantle boundary [*e.g.* 1-3].

[1] Andrault *et al.* (2012) *Nature* **487**, 354-357. [2] Andrault *et al.* (2011) *EPSL* **304**, 251-259. [3] Fiquet *et al.* (2010) *Science* **329**, 1516-1518.

C and O isotope compositions of the Matongo carbonatite (Burundi) : new insights into alteration and REE mineralization processes

P. BOULVAIS*¹, S. DECREE², C. COBERT¹, G. MIDENDE³,
L. TACK², V. GARDIEN⁴ AND D. DEMAIFFE⁵

¹ Géosciences Rennes – UMR 6118 - Université de Rennes 1
(France)

(*correspondence : philippe.boulvais@univ-rennes1.fr)

² Royal Museum for Central Africa, Tervuren (Belgium)

³ Université de Bujumbura (Burundi)

⁴ LGL-TPE, UMR CNRS 5276 Université Lyon 1/ENS-Lyon
(France)

⁵ Université Libre de Bruxelles (Belgium)

The Matongo carbonatite intrusion is part of the Neoproterozoic Upper Ruvubu alkaline plutonic complex (URAPC), located in Burundi along the western branch of the East African Rift. This alkaline complex, which also comprises feldspathoidal syenites, diorites, quartz-bearing syenites and granites, emplaced around 750 Ma [1].

Most of the oxygen and carbon isotope compositions obtained on the several carbonatitic facies are typical of carbonatites: the δ¹⁸O values are between 7.2 and 8.5‰ (vs. SMOW), the δ¹³C values are between -4.7 and -5.4‰ (vs. PDB). These values correspond to the magmatic signature of the intrusion. Some samples show a significant increase in the δ¹⁸O value, between 11 and 20‰, with an extreme value of 21.6‰. Rare Earth Element fractionation is visible in the most isotopically altered samples, which points to mobilization of these elements. The site of re-deposition of the leached elements may well be found in distal hydrothermal veins, which contain albite, calcite, apatite and REE-fluorocarbonates. The Matongo carbonatite thus appears as a complete metallogenic hydrothermal system where both the source and sinks of REE are identified.

[1] Tack *et al.* (1996), In *Petrology and geochemistry of magmatic suites of rocks in the continental and oceanic crusts*. A volume dedicated to J. Michot (Demaiffe, ed.), ULB-MRAC, Brussels, **219-226**, 91-114.

Hadean crustal relics and evidence for lifetime of early crust

B. BOURDON^{1*}, A.S.G. ROTH², M. GUITREAU^{1,3},
J. BLICHERT-TOFT¹ AND S.J. MOJZSIS^{1,4,5},

¹ENS Lyon, CNRS and UCBL, Lyon, France

²ETH, Zürich, Switzerland

³University of New Hampshire, Durham, NH, USA

⁴University of Colorado, Boulder, CO, USA

⁵Hungarian Academy of Sciences, Budapest, Hungary

* Correspondence: bernard.bourdon@ens-lyon.fr

The Nuvvuagittuq supracrustal belt (Québec) and the Acasta gneiss complex (NWT), Canada represent some of the oldest crustal remnants on Earth and are thus outstanding archives for inferring the early history of the continental crust. There are, however, controversies about how existing data should be interpreted in terms of geochronology and time scales. In this study, Sm-Nd isotope data, combined with U-Pb dating and Lu-Hf isotope data, were examined.

We analyzed thirteen samples, previously dated by U-Pb, zircon and Lu-Hf geochronology from the Acasta gneiss complex for high-precision ^{146,147}Sm-^{142,143}Nd-systematics. The ¹⁴⁷Sm-¹⁴³Nd data yield an alignment corresponding to an age of 3371 Ma age. Ten out of the thirteen samples show negative ¹⁴²Nd anomalies with an average deficit of -9.6±5 ppm.

We show that, unlike previous claims, the ¹⁴⁶Sm-¹⁴²Nd systematics are susceptible to resetting. Furthermore, when combined with the corresponding ¹⁴⁷Sm-¹⁴³Nd and ¹⁷⁶Lu-¹⁷⁶Hf data for the same samples, these data provide a fairly accurate picture of the evolution of Nuvvuagittuq and Acasta rocks. To examine quantitatively the effect of thermal resetting, we designed a new model whereby isotopes undergo exchange in a closed system at whole rock lengthscale. The Nuvvuagittuq mafic rocks were only partially reset, implying that direct dating of these rocks is not possible. In contrast, the degree of resetting was more extreme in Acasta, which yields rather constant ¹⁴²Nd anomalies, while the ¹⁴⁷Sm-¹⁴³Nd system records a younger age of ~3400 Ma. In both cases, the existence of negative ¹⁴²Nd anomalies can be attributed to Hadean crustal extraction between 4500 and 4300 Ma. The lifetime of this crust was investigated using time-dependent box models, including recycling into the mantle, and is shown to persist over 0.5-1 Gyr. In addition, the existence of positive ¹⁴²Nd anomalies in younger rocks was found to depend strongly on this parameter, and on the mantle stirring time.

Diffusive heavy metal fluxes in bottom river sediments

ALAIN C.M. BOURG^{1*} AND CHRISTOPHE MOUVET²

¹EA4592 Georessources and Environment, Dept Geosciences,
Univ. of Pau, BP 1155, 64013 Pau Cedex, France

(*correspondence: alain.bourg@univ-pau.fr)

²BRGM, BP 6009, 45060 Orléans Cedex 2, France

Suspended particles are scavengers of contaminants in streams. When they become deposited on the river bed they can act as efficient traps. Early diagenetic processes in bottom sediments are known to induce diffusive fluxes towards the overlying water in lakes and seas for some elements and downwards for others [*e.g.*, 1, 2].

We applied to a river one of the methodologies commonly used for non turbulent water bodies, i.e., porewater *peepers*. The Lot River (in SW France) was selected because of its history of long-term metallic contamination and the consequent concern about the possible re-entering in the river dissolved flux of previously trapped heavy metals. The benthic pore water samplers (with a 10 mm vertical resolution) were installed manually by a SCUBA diver at a depth of ca. 2 m in a slow channel of the river.

The interstitial water redox potential, pH, dissolved sulfate and phosphate all decrease with depth, contrary to Fe and Mn which increase with depth. All of this is coherent with diagenesis.

For Cd and Zn we observe a peak in dissolved concentration 1 to 3 cm below the sediment-water interface, this implies a double flux, one towards the river and the other towards the sediments. This last component is in favor of removal of Cd and Zn from the river flux to the ocean, but in turns it might cause some concern for groundwater supply in local well fields in alluvial aquifers. These observations are explained in terms of geochemical processes.

[1] Gaillard *et al.* (1986) *Mar. Chem* **18**, 233-247. [2] Gaillard *et al.* (1987) *Chem Geol* **63**, 73-74.

Particulate matter in São Paulo City: comparison between industrial and urban area

BOUROTTE C.^{1*}, FORNARO A.², FORTI M.C.³,
CAVICCHIOLI A.¹ AND MIRANDA R.¹

¹EACH-University of São Paulo, Rua Arlindo Bétio, 1000, CEP 03828000 São Paulo-SP, Brazil (*correspondence: chrisbourotte@usp.br.)

²IAG-University of São Paulo, Rua do Matão, 1226, CEP 05508-090, São Paulo-SP, Brazil

³INPE, Centro de Ciência do Sistema Terrestre CCST, C.P.515 - CEP 12245-970, São José dos Campos-SP, Brazil

Airborne particulate matter in urban atmosphere is derived from natural and anthropic sources. The chemical composition of coarse and fine particles is critical when considering their hazardous effect. This particulate matter study is part of a greatest research project that investigates the relationship between aerosols, road dusts and surface soils.

The sampling sites are located in two region (eastern and western zones) of the São Paulo City, in the two Campi of the University of São Paulo that present distinct characteristics i.e. industrial and commercial/residential backgrounds. The eastern area (EACH) is located in the floodplain of the Tietê River, near several industries, a highway and the international airport. The western area (Butantã) is located in a commercial and residential area and submitted to intense vehicular traffic.

The particulate matter (PM_{2.5} and PM_{2.5-10}) was continuously collected during day and night periods, simultaneously in the two areas. Sampling was initiated on August 22th, 2012 and finalized on December 7th, 2012 in the eastern area and from July, 7th to September 9th, 2012 in the western area. This period includes winter and the beginning of summer (raining season). Black Carbon and multi-elemental composition were quantified in the fine fraction by reflectometry and FRX, respectively.

The results show that particulate matter concentrations during winter, in the eastern area were 23.70 ±13.05 µg m⁻³ in the fine fraction and 42.73 ±37.71 in the coarse one. Concentrations in the western area were 21.09 ±14.00 µg m⁻³ in the fine fraction and 16.19 ±8.17 µg m⁻³ in the coarse one. During summer, concentrations were lower and similar between the two fractions. Concentrations were 20.05 ±7.72 µg m⁻³ and 21.75 ±13.93 µg m⁻³ in the fine and coarse fraction, respectively, in the eastern area. In the western area, concentrations were 17.25 ±8.36 µg m⁻³ and 17.09 ±8.12 µg m⁻³, in fine and coarse fraction, respectively. During winter, higher concentrations in the coarse mode in the industrial area may be due to higher soil resuspension since the vegetation area is reduced comparing with the western one. Chemical analysis are still being done but preliminary results showed that for the industrial area, black carbon contributed to 18.2% of the fine particulate matter mass. The elements with higher concentrations were S, Si, Fe, K, Al, Na, Zn, Pb and Cd.

New method for precise Cl isotopes measurement by SIMS

A.-S. BOUVIER¹ AND L. BAUMGARTNER¹

¹ISTE, University of Lausanne, Lausanne, Switzerland

Chlorine is an important volatile element. Its two stable isotopes are used to track the global halogen cycle and to determine fluid sources. Chlorine isotopes are fractionated by fluid/rock interaction, degassing, diffusion and mineralogical transformation. However, the range of Cl isotopes on Earth may be relatively limited [e.g., 1], requiring precise measurements of δ³⁷Cl. Usually Cl isotopes are measured by TIMS or IRMS, and only a few measurements have been performed so far by ion probe. Previous SIMS studies reported a reproducibility of 0.8 to 1.5‰ (2 Standard Deviation (SD)) for glasses with > 200 ppm Cl [e.g., 1, 2]. We develop a new SIMS method to improve the precision of δ³⁷Cl measurements. Analyses were done on a CAMECA IMS 1280-HR, using a cesium source. One analysis consists of two minutes presputtering using a 25µm raster to clean the surface, followed by 7 minutes of analysis using a ~10µm rastered beam. ³⁷Cl and ³⁵Cl were simultaneously measured on electron multipliers in multicollection mode.

Results show internal precisions as good as <0.2‰ (2SE) and reproducibility (spot to spot) of 0.6 to 0.8‰ (2SD) for standard glass with Cl content down to 100 ppm. For standard glasses with Cl content < 100 ppm (down to 5 ppm), the reproducibility reaches 1.5‰ (2SD).

With this precision reached it is now possible to investigate *in situ* δ³⁷Cl variations at small scale, even in minerals with low Cl content, using the appropriate standard material.

1. Straub and Layne, (2007), AGU Fall Meeting 2007, abstract #V41B-0610.
2. John *et al.* (2010), Earth and Planetary Science Letters, **298**, p. 175-182.

Lu-Hf and Sm-Nd systematics of the first solids in the Solar System

A. BOUVIER¹ AND M. BOYET²

¹University of Minnesota, Minneapolis, MN, USA.
(abouvier@umn.edu)

²Laboratoire Magmas et Volcans, Clermont-Ferrand, France.
(m.boyet@opgc.univ-bpclermont.fr)

Hafnium-176 excesses are found in bulk chondrite and eucrite isochrons, and in some (not all) eucrite [1] and angrite mineral isochrons [2,3]. It was proposed that cosmic rays accelerated by supernova(e) shocks in the early Solar System could produce a higher decay rate of a ¹⁷⁶Lu isomer within the irradiated planetary materials [2]. This hypothesis complicates the direct determination of the initial Lu-Hf isotopic composition of the Solar System and by extent that of the terrestrial planets [4]. The interpretation of the earliest terrestrial Lu-Hf isotopic records relies on knowing these initial conditions [5].

Such external irradiation sources should affect any objects already formed and exposed in the protoplanetary disk. We thus investigated the stable and radiogenic Lu-Hf and Sm-Nd compositions of CAIs, the first solids formed in the Solar System. The selected five CAIs were formed after injection of ²⁶Al into the protoplanetary disk [6]. The ¹⁴⁴Sm/¹⁵²Sm ratios have the largest variations with p-process deficits typically at ~250ppm. Deficits in ¹⁴⁹Sm (<100ppm) are correlated to excesses in ¹⁵⁰Sm within the same CAI suggesting small neutron capture effects. All stable Nd isotope ratios have deficits smaller than 50ppm. The bulk CAIs have no resolvable Hf isotopic variations for ¹⁷⁴Hf, small positive anomalies (<20 ppm) for ¹⁷⁸Hf and ¹⁸⁰Hf which demonstrate minimal corrections (<40ppm) for ¹⁷⁶Hf/¹⁷⁷Hf ratios. The bulk and mineral ¹⁴⁷Sm-¹⁴³Nd and ¹⁷⁶Lu-¹⁷⁶Hf isochron ages for three melted CAIs together are 4519 ±140 Ma (MSWD =0.77, ¹⁴³Nd/¹⁴⁴Nd_i = 0.50675 ±20) and 4560 ±190 Ma (MSWD =59, ¹⁷⁶Hf/¹⁷⁷Hf_i = 0.27985 ±15) respectively. We thus interpret the anomalous Lu-Hf isochron slopes [1,2] as the consequence of secondary parent body processes. Our direct determination of the initial ¹⁷⁶Hf/¹⁷⁷Hf of the Solar System is consistent with, but less precise than, those obtained from present CHUR values and from updated bulk chondrite isochrons [7].

[1]. Righter et al. (2013), 44th LPSC, A#2745. [2]. Thrane et al. (2010), ApJ **717**, 861-867. [3]. Sanborn et al. (2012), 43rd LPSC, A#2039. [4]. Bizzarro et al. (2012), *Geochem. Geophys. Geosyst.* **13**, Q03002. [5]. Harrison (2009), *Annu. Rev. Earth Planet. Sci.* **37**, 479-505. [6]. Krot et al. (2012), *MAPS* **47**, 1948-1979. [7]. Bouvier et al. (2008), *EPSL* **273**, 48-57.

Ion concentration at the kaolinite – water interface

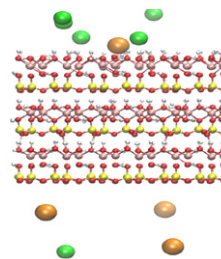
N. BOVET*, T. BAUR, T. CLAUSEN, M. OLSSON,
B. LORENZ AND S.L.S. STIPP

Nano-Science Center, Department of Chemistry, University of Copenhagen, Denmark (*bovet@nano.ku.dk)

Kaolinite is a clay present in soils, sediments and rocks, including sandstones and carbonates, as well as shales and mudstones. Its high surface area and large cation exchange capacity make it reactive in natural environments. For example, it plays an important role in uptake of contaminants in the environment and in tertiary oil recovery.

To observe the surface chemical composition of kaolinite, as it is during contact with solution, we used X-ray photoelectron spectroscopy (XPS) with the fast freezing technique. This allows the mineral - fluid interface to be preserved and investigated, even under ultrahigh vacuum which is necessary for XPS, because the ion distribution is “frozen in” as it was in the original liquid phase.

Solutions investigated were NaCl, CaCl₂ and Ca(C₂H₅COOH)₂ at pH 5.5, in their reaction with pure kaolinite (KGa1-b). The results show that the relative ion concentration is different at the surface than in the bulk, consistent with electrical double layer (EDL) theory. We also observed that the ratio of Ca and Cl ions is not constant with distance out from the interface. For low CaCl₂ concentrations (< 6 mM), the Ca:Cl ratio is higher at the interface, whereas at higher Ca concentration, more negative counter ions, i.e. Cl, are present to balance charge. Results from molecular dynamics (MD) simulations (figure) and atomic force microscopy (AFM) experiments complement the XPS results with structural information to build a full picture of interface interaction.



MD simulation snapshot of Ca (orange) and Cl (green) adsorbed on kaolinite during exposure to solution. Water is present but we have made it invisible.

The co-evolution of Fe-,Ti-oxides and other microbially induced mineral precipitates during the diagenesis of sandy sediments

D.M. BOWER¹, D.R. HUMMER², A. KYONO³,
A. STEELE¹ AND J. ARMSTRONG¹

¹Geophysical Laboratory, Carnegie Institution of
Washington, Washington, D.C., 20015,
(dbower@ciw.edu,asteel@ciw.edu,jarmstrong@ciw.edu)

²Department of Earth and Space Sciences, UCLA, Los
Angeles, CA, 90095, (dhummer@ess.ucla.edu)

³Division of Earth Evolution Sciences, University of Tsukuba,
Tsukuba, Ibaraki 305-8572, Japan,
(kyono@geol.tsukuba.ac.jp)

Ilmenite (FeTiO₃) and related Fe-,Ti-oxides are ubiquitous components of modern beach sands and are often associated with “fossil” microstructures in ancient sedimentary rocks [1,2]. The mineral composition of the ancient sedimentary rocks we see today, however, differs from what was originally formed in the sediments billions of years ago. This change in composition is usually attributed to long, complicated histories and atmospheric influences, while the contribution of microbes is not typically considered. Here the goal is to understand the co-evolutionary path of microbes and minerals in sandy, shallow sub-aquatic environments under early diagenetic conditions. Laboratory experiments were done to document the precipitation of minerals on cyanobacterial cellular material as well as the phase changes in natural ilmenites to determine if microbes passively influence mineral phase pathways. The precipitates, ilmenite grains, and fossilized cells were analyzed using scanning electron microscopy (SEM), x-ray diffraction (XRD), and micro Raman spectroscopy. The results show that microbial fossilization occurs and a variety of mineral phases precipitate under early diagenetic conditions (T<70°C) in wet, sandy environments. The minerals that form in the presence of microbes differ in crystal habit and chemical composition from those without microbes. This study aids in understanding the microbial role in diagenesis and helps redefine geochemical biosignatures that can be used for the detection of ancient microbial life in sedimentary rocks on Earth as well as for future planetary life exploration missions.

[1] Morad & Aldahan (1982) *Journal of Sedimentary Petrology*, **52**, 1295-1305. [2] Bower (2011) *Journal of Raman Spectroscopy*, **42** (8), 1626-1633.

Using Genomics to Reveal the Secrets Underlying the Ecological Success of Marine Diatoms

CHRIS BOWLER¹

¹ Head of Environmental and Evolutionary Genomics Section,
Institut de Biologie de l'Ecole Normale Supérieure, Paris,
France. cbowler@biologie.ens.fr

Diatoms are thought to be the most successful group of eukaryotic phytoplankton in the modern ocean. Recently completed whole genome sequences from two species, *Thalassiosira pseudonana* and *Phaeodactylum tricornutum*, have revealed a wealth of information about the evolutionary origins and metabolic adaptations that may have led to their ecological success. A major finding is that they have acquired genes both from their endosymbiotic ancestors and by horizontal gene transfer from marine bacteria. This unique melting pot of genes encodes novel capacities for metabolic management, for example allowing the integration of a urea cycle into a photosynthetic cell. Our studies focus on *P. tricornutum* and exploit the availability of techniques for reverse genetics, digital gene expression profiling, genome and epigenome maps, ecotypes with differential capacities to adapt to different conditions, and distinct morphotypes that can be induced to change shape in response to ecologically relevant stimuli. Using these resources we explore both the physiological functions of diatom gene products and the evolutionary mechanisms that have led to diatom success in contemporary oceans.

A next objective is to explore the functional roles of diatom biodiversity in the world's oceans. With biology becoming quantitative, systems level studies can now be performed at spatial scales ranging from molecules to ecosystems. Biological data generated consistently across scales can be integrated with physico-chemical contextual data for a truly holistic approach. While the marine planktonic ecosystems that diatoms inhabit comprise the base of the ocean food web, and are crucial in the regulation of Earth's biogeochemical cycles and climate, their organization, evolution and dynamics remain poorly understood. The *Tara* Oceans expedition was launched in September 2009 for a 3-year study of the global ocean ecosystem aboard the schooner *Tara*. A unique sampling programme encompassing optical and genomic methods to describe viruses, bacteria, archaea, protists and metazoans in their physico-chemical environment has been implemented. The project aims to generate systematic, open access datasets usable for probing the morphological and molecular makeup, diversity, evolution, ecology and global impacts of plankton on the Earth system, as well as to explore and exploit their biotechnological potential.

Global distribution of sulfate reduction rates in marine sediments

M. W. BOWLES^{1*}, J. M. MOGOLLÓN², S. KASTEN²,
M. ZABEL¹ AND K.-U. HINRICH¹

¹ MARUM Center for Marine Environmental Sciences,
University of Bremen, Bremen, Germany

(*correspondence: bowlesmw@uni-bremen.de)

² Alfred-Wegener-Institut für Polar- und Meeresforschung,
Bremerhaven, Germany

Sulfate is the dominant terminal electron acceptor in marine sediments. Sulfate reduction proceeds under anoxic conditions and is supported by a variety of electron donors (e.g. hydrogen, acetate, methane, propane, and butane), most of which are supplied by the decomposition of sedimentary organic matter. Consequently, a combination of primary productivity and water column depth is often thought to control sulfate reduction throughout most of the ocean's seafloor [1, 2]. However, global models of sulfate reduction do not resolve the many different physical and ecological parameters that are encountered on a global scale, and that ultimately play a major role in driving local and regional sulfate reduction rates. We sought to better determine sulfate reduction rates on a global scale, irrespective of region or location by 1) including sulfate profiles from diverse settings and 2) compiling multiple geochemical parameters that are relevant to sulfate reduction and can help discern the magnitude of sulfate reduction rates. All available sulfate concentration profiles from DSDP/ODP/IODP (to Exp. 312) and additionally those in the database Pangaea (www.pangaea.de) were compiled reaching a total >600 non-repetitive concentration profiles. Basic metadata describing the cores was included, such as water depth and distance to shore. Water column data such as minimum percent O₂ saturation, bottom water O₂, NO₃⁻, PO₄³⁻, and concentrations of surface water chlorophyll a and POC [3, 4] were included as additional variables that describe the biogeochemical setting of the cores. All compiled data and concentration profiles were applied to a training algorithm to estimate global sulfate reduction rates. The result was the most precise depiction of global sulfate reduction rates at the highest resolution to date. Our model serves as a platform for the examination of biogeochemical processes on the global scale and lets us predict energetic constraints for microbial metabolism in the subseafloor.

[1] Canfield (1991) *AJOS* **291**, 177-188. [2] Middelburg *et al.* (1997) *DSR* **44**, 327-344. [3] Levitus & Boyer (1994) *NOAA Atlas NESDIS* [4] *NASA*, Aqua-MODIS

Geometry of carbon and oxygen isotope exchange fronts in the Alta aureole, Utah: Records of hydrodynamic dispersion and scale-dependent permeability during infiltration-driven metamorphism

J. R. BOWMAN*

Dept. of Geology and Geophysics, Univ. of Utah, Salt Lake City, UT 84112 USA (*corr: john.bowman@utah.edu)

A carbon (C) isotope exchange front, periclase reaction front and an oxygen (O) isotope exchange front are developed with increasing distance from the igneous contact in dolomitic marbles of the south Alta aureole, Utah in response to infiltration-driven metamorphism of the marbles. Their relative distances from the igneous contact, approx. 100, 200 and 380 m, respectively, are consistent with down-temperature infiltration of water-rich fluid [X(CO₂) <0.1 to 0.15] that was equilibrated isotopically with the adjacent Alta stock. At the aureole scale both the C and O isotope exchange fronts exhibit significant dispersion: there is significant variation in both δ¹⁸O and δ¹³C values at any given position for ≥50 to 100m to either side of the geometric centers of both fronts. Applications of one-dimensional models of advection-dispersion to these aureole-scale dispersed fronts yield a minimum dispersion coefficient of 2E-8 m²/sec. However at outcrop and bedding scale, steep, coherent gradients in both δ¹⁸O and δ¹³C exist at or near bedding boundaries between marble layers of contrasting lithology and isotopic compositions; modeling of these profiles requires much lower diffusion/dispersion coefficients in the range of 7E-12 to 1E-14 m²/sec.

The variable characteristics of the exchange fronts can be explained by scale-dependent heterogeneity and anisotropy in permeability of the marbles. Both C and O exchange fronts are characterized by significant dispersion at the aureole scale because of significant bed-to-bed variations in permeability, which are reflected by significant bed-to-bed variations in δ¹⁸O and δ¹³C values. These bedding-controlled variations in permeability lead to significant permeability anisotropy, with permeability parallel to bedding >> permeability normal to bedding. In contrast, permeability within individual beds appears to be relatively homogeneous, as suggested by relatively consistent mineral modes and homogeneous δ¹⁸O and δ¹³C values within individual beds, and by steep, highly coherent δ¹⁸O and δ¹³C gradients preserved at or near bedding boundaries.

Petrologic and Metasomatic Controls on H and Cl Abundances and Isotopes in Lunar Rocks

JEREMY W. BOYCE^{1,2}, ALLAN H. TREIMAN³, JOHN M. EILER², CHI MA², YUNBIN GUAN², JAMES P. GREENWOOD⁴, JULIANE GROSS⁵ AND EDWARD M. STOLPER²

¹Dept. of Earth & Space Sciences, UCLA
(jwboyce@alum.mit.edu)

²Division of Geological and Planetary Sciences, Caltech

³Lunar and Planetary Institute, Houston TX

⁴Dept. of Earth & Environmental Sci, Wesleyan University

⁵Dept. of E & P S, American Museum of Natural History

Abundances and isotopic compositions of H and Cl have been measured in apatites from twelve lunar samples, permitting systematic comparison of relationships between these properties and other petrologic and geochemical characteristics. High $d^{37}\text{Cl}$ values are found in relatively H-rich apatites, apparently falsifying the hypothesis that elevated $\delta^{37}\text{Cl}$ arises only from single-stage degassing of anhydrous magmas. Nevertheless, high $\delta^{37}\text{Cl}$ is preferentially associated with relatively low H apatites and so seems to be a property of relatively degassed reservoir(s). The most H-rich apatites tend to have 'low' $\delta^{37}\text{Cl}$, $< +25\text{‰}$. Higher $d^{37}\text{Cl}$ values ($> +25\text{‰}$) are seen only in highlands rocks and breccias, and the highest value is in a rock that may be from an impact melt/breccia sheet. Among the eight mare basalts analyzed by us and others, δD of apatite shows no correlation with H abundance or $\delta^{37}\text{Cl}$. δD is, however negatively correlated with pyroxene homogeneity [(minimum Mg#)/(maximum Mg#)]; basalts that experienced protracted thermal histories (igneous, impact, or metamorphic) have low δD . Finally, it is common to observe both significant heterogeneity in abundance and isotopic composition of H and Cl within apatites from a single sample, or even individual crystals, indicating a lack of equilibrium.

These results can be interpreted in terms of planet-scale evolution; for example, the high $d^{37}\text{Cl}$ of highlands rocks could be inherited from a partially degassed (H-poor) magma ocean. However, it is also possible that elevated $d^{37}\text{Cl}$ in some samples arose through devolatilization during impact metamorphism and/or metasomatism of the crust. Variations in δD could represent mixing of a high δD ($> +500\text{‰}$) component in pristine igneous rocks (either because this is a signature of their mantle sources or because of magmatic degassing) with a low- δD component like solar wind implanted into regolith. If so, much of the volatile element geochemistry of lunar rocks may reflect crustal and near-surface processes.

Hot spring environments as accessible portals into the metabolic underpinnings of the deep hot biosphere

ERIC S. BOYD¹, ERIC A. ALSOP², EVERETT L. SHOCK³ AND JASON A. RAYMOND⁴

¹Department of Chemistry and Biochemistry, Montana State University, Bozeman, MT, USA, eboyd@montana.edu

²School of Earth and Space Exploration, Arizona State University, Tempe, AZ, USA, ealsop@asu.edu

³Department of Chemistry and Biochemistry, Arizona State University, Tempe, AZ, USA, eshock@asu.edu

⁴School of Earth and Space Exploration, Arizona State University, Tempe, AZ, USA, jraymond@asu.edu

The Earth's crust contains an extensive and diverse deep biosphere that is sustained by chemical energy under dark and oligotrophic conditions. Much remains unknown and in need of discovery in these ecosystems due to their deep and hard-to-reach nature. Herein, it is proposed that much information directly relevant to the deep, hot, biosphere of continental subsurface systems is directly accessible in the form of sediments and near-subsurface investigation in the globally relevant hot springs of Yellowstone National Park (YNP), Wyoming, USA. We investigated the composition of ~30 community metagenomes in YNP using a suite of bioinformatic and ecological modeling tools. The results suggest that the metabolic composition of microbial mat communities can be accurately predicted based on the physical and chemical attributes of the environment. Of particular significance is the strict temperature-dependent demarcation noted between the metabolic composition of chemotrophic communities and phototrophic communities as well as the pH-dependent demarcation in the metabolic composition of chemotrophic communities. . Additional results from modeling and *in situ* activity-based studies will be presented that reveal the environmental constraints that shape the distribution of metabolic processes in these accessible portals to the deep hot biosphere.

Seasonal variation in biological methane production in a subglacial ecosystem

ERIC S. BOYD¹, TRINITY L. HAMILTON²,
TERRA SPOTTS³, JOHN E. DORE⁴, PETER CANOVAS⁵,
JEFF HAVIG⁶, JOHN W. PETERS⁷, EVERETT L. SHOCK⁸
AND MARK SKIDMORE

¹Department of Chemistry and Biochemistry, Montana State University, Bozeman, MT, USA, eboyd@montana.edu

²Department of Geosciences, Pennsylvania State University, College Park, PA, USA, trinitylh@gmail.com

³Department of Earth Sciences, Montana State University, Bozeman, MT, USA, scheerterra@gmail.com

⁴Department of Land Resources and Environmental Sciences, Montana State University, Bozeman, MT, USA, jdore@montana.edu

⁵Department of Chemistry and Biochemistry, Arizona State University, Tempe, AZ, USA, peter.canovas@asu.edu

⁶Department of Geosciences, Pennsylvania State University, College Park, PA, USA, jeffhavig@gmail.com

⁷Department of Chemistry and Biochemistry, Montana State University, Bozeman, MT, USA, john.peters@chemistry.montana.edu

⁸Department of Chemistry and Biochemistry, Arizona State University, Tempe, AZ, USA, everett.shock@asu.edu

⁹Department of Earth Sciences, Montana State University, Bozeman, MT, USA, skidmore@montana.edu

Reports of seasonal plumes of methane emanating from the near sub-surface of Mars have fueled speculation that they may be the result of biological activity. The biological production of methane is catalyzed by a unique group of anaerobic archaea, the methanogens. Common to all methanogens is a unique metabolic pathway that enables methane production from a limited number of substrates such as H₂ + CO₂, formate, CO, methanol, methylamines, and acetate. Methanogens live close to the thermodynamic limit of life, a problem exacerbated at extremes of cold temperature. Here, we present genetic, physiological, geochemical, and thermodynamic data in support of the presence of a unique and active assemblage of methanogens in the near freezing (~0-1°C) and oligotrophic subglacial environment of Robertson Glacier, Alberta, Canada. Dominant methanogens present in the RG sediments may constitute a new order that bridges the physiologically distinct *Methanomicrobiales* and *Methanosarcinales* lineages. Methane flux measurements (2011) indicate seasonal variation in the release of methane from this permanently cold extraterrestrial analog environment.

What are the ¹⁴⁶Sm-¹⁴²Nd reference parameters for the Earth?

M. BOYET¹, A. BOUVIER², A. GANNOUN¹
AND R.W. CARLSON³

¹Laboratoire Magmas et Volcans, Université Blaise Pascal, CNRS UMR 6524, 5 rue Kessler, 63038 Clermont-Ferrand, France. boyet@opgc.univ-bpclermont.fr

²Department of Earth Sciences, University of Minnesota, 310 Pillsbury Drive SE Minneapolis, MN 55455-0231, USA.

³Carnegie Institution of Washington, Dept. of Terrestrial Magnetism, Washington DC 20015, USA.

Since the first publication of high precision ¹⁴²Nd/¹⁴⁴Nd ratios in chondrites [1], different early Earth differentiation models have been proposed. The excess in ¹⁴²Nd measured in terrestrial samples relative to the average chondrite value requires that all terrestrial rocks sampled by volcanism over the Earth's history come from a geochemical reservoir characterized by a super-chondritic Sm/Nd ratio. Some authors proposed that the complementary enriched reservoir has been lost during the Earth's accretion [2,3] whereas others suggested that a hidden reservoir may have been preserved in the deep Earth [1,4]. The measurement of stable Sm and Nd isotope ratios in chondrites has created additional confusion in the interpretation of ¹⁴²Nd deviation. Different groups of chondrites clearly have different ¹⁴²Nd signatures and variations in stable Sm and Nd isotopes were found [5-7], all of which likely reflect different mixtures of r-, s-, and p-process nucleosynthetic products.

We will present a summary of the data available on Sm-Nd systematics of chondrites as well as new data obtained on enstatite chondrites (whole rocks and leaching experiments), achondrites and CAIs from CV3 chondrites. On the basis of these results, carbonaceous chondrites must be considered as a minor constituent of the Earth. Enstatite chondrites overlaps with the terrestrial ¹⁴²Nd/¹⁴⁴Nd ratio. CAIs Sm/Nd-¹⁴²Nd/¹⁴⁴Nd isochrons pass through the terrestrial value.

Considering the level of precision now achieved on Sm-Nd isotope measurements and looking at the results obtained on stable Sm and Nd isotopes our opinion is that the Earth-chondrite difference in ¹⁴²Nd suggests that silicate part of Earth experienced a very early differentiation event. However these models will be discussed considering these new results.

[1] Boyet & Carlson 2005, *Science* **309**; [2] O'Neill & Palme 2008, *Phil. Trans. R. Soc. A* **306**; [3] Caro *et al.* 2008, *Nature* **452**; [4] Andreasen *et al.* 2008, *EPSL* **266**; [5] Andreasen & Sharma 2006, *Science* **314**; [6] Carlson *et al.* 2007, *Science* **316**; [7] Gannoun *et al.* 2011, *PNAS* **108**.

A bioturbation-induced decrease in atmospheric oxygen across the Precambrian-Cambrian boundary

R.A. BOYLE¹, T.W. DAHL^{1,2}, A.W. DALE³,
G. SHIELDS-ZHOU⁴, M. ZHU⁵, M.D. BRASIER⁶,
D.E. CANFIELD⁷ AND T.M. LENTON¹

¹Earth System Science Group, College of Life and Environmental Sciences, University of Exeter, UK

²Natural History Museum of Denmark, University of Copenhagen, Denmark.

³Geomar Helmholtz Centre for Ocean Research, Kiel, Germany.

⁴Department of Earth Sciences, University College London, UK.

⁵Nanjing Institute of Geology and Palaeontology, Chinese Academy of Sciences, Nanjing, China.

⁶Department of Earth Sciences, University of Oxford, UK.

⁷Institute of Biology and Nordic Centre for Earth Evolution, University of Southern Denmark.

Bioturbation is the reworking of sediments by animal motility, and its emergence across the Precambrian-Cambrian boundary occurred against the backdrop of major changes in the biogeochemical cycles of oxygen, phosphorus and organic carbon. Bioturbation substantially increases sedimentary phosphate content, limiting the phosphate available for primary production and thus reducing the marine organic carbon burial flux, which is the source of atmospheric oxygen over geological timescales. We use simple modelling to show how an increase in marine organic phosphate burial associated with the onset of bioturbation caused a net decrease in atmospheric oxygen across the Precambrian-Cambrian boundary. The resulting deoxygenation of the ocean restricted the spread of oxygen-demanding bioturbating animals, and established negative feedback loops that stabilised atmospheric oxygen at a lower level. Although more data are needed to quantitatively constrain model parameters, our results are supported by evidence for a resurgence of anoxic and sometimes euxinic conditions in the early Paleozoic.

[1] McIlroy, D. & Logan, G. (1999). *Palaeogeography* **14**. 58-72.
[2] Och, L. & Shields-Zhou, G.A. (2012). *Earth Science Reviews* **110**. 26-57. [3] Papineau, D. (2010). *Astrobiology* **10** (2). 165-181. [4] Maloof, A.C., Porter, S.M., Moore, J.L., Dudas, F.L., Bowring, S.A. Higgins, J.A., Fike, D.A. & Eddy, M.P. (2012). *GSA Bulletin* **122**. 1731-1774. [5] Ingall, E.D., Bustin, R.M. & Van Capellen, P. (1993). *Geochim. Cosmochim. Acta* **57**. 303-316. [6] Redfield, A.C. (1958). *Am. Sci.* **46**. 205-221. [7] Betts, J.N. & Holland, H.D. (1991). *Paleogeog. Palaeoclimatol. Palaeoecol.* **97**. 5-18. [8] Catling, D.C., Glein, C.R. Zahnle, K.J. & McKay, C.P. (2005). *Astrobiology* **5** (3). 415-437. [9] Schroder, S. & Grotzinger, J.P. (2013). *J. Geol. Soc. Lond* **164**. 175-187.

The rate of iron compounds precipitation from AMD waters in the Łęknica region (the Muskau Arch, western Poland)

P. BOŻECKI AND G. RZĘPA

AGH - University of Science and Technology, Faculty of Geology, Geophysics and Environmental Protection, Department of Mineralogy, Petrography and Geochemistry, Krakow, Poland (pbozecki@agh.edu.pl)

The Muskau Arch is a large horseshoe-shaped glaciotectonic belt formed mainly during the Mid Polish Glaciation. Lignite deposits containing pyrite were excavated there till the end of the 70-ties of the 20th century. Abandoned excavations are recently filled with water forming large so called "anthropogenic lake district" (with about 110 reservoirs). Oxidation of sulphide leads to the generation of abundant quantities of sulphuric acid. Therefore many of these lakes, especially at the Łęknica area, are of acidotrophic type characterized by low and very low pH values (usually < 4.0). This is associated with the formation of numerous ochreous precipitates as a consequence of iron oxidation and hydrolysis.

The aim of this study is to assess the precipitation rate of iron compounds from acid mine drainage waters. Experiment was conducted in over one year period, from July 2009 to September 2010, in eleven locations. For this purpose, unglazed ceramic plates (dimensions: 10x10 cm) were, after removing possible traces of iron, placed on the bottom of selected lakes. The plates were collected monthly and the amount of precipitated iron compounds was evaluated by the determination of Fe leachable in hydrochloric acid. Mineralogical analyses of the precipitates using X-ray diffractometry and SEM-EDS were carried out as well.

The amount of precipitated iron compounds turned out to be very variable, ranging from ca. 50 [mg Fe*cm⁻²] per month to nearly 13 000 [mg Fe*cm⁻²] per month. The average value for all monitored locations was approximately 1100 [mg Fe*cm⁻²] per month.

X-ray diffractometry indicate that the only mineral phase formed was schwertmannite – poorly crystalline iron oxyhydroxysulfate. Images obtained with use of scanning electron microscope reveal the presence of numerous bacteria structures, confirming that the precipitation of schwertmannite was microbially-mediated.

This work was supported by AGH-UST (Faculty of Geology, Geophysics and Environmental Protection statutory grant).

Coupled LA U-Pb chronology of detrital zircon and rutile: A powerful provenance tracer

L. BRACCIALI^{1,2*}, R.R. PARRISH^{1,3},
M.S.A. HORSTWOOD¹ AND Y. NAJMAN²

¹NERC Isotope Geosciences Laboratory, British Geological Survey, Keyworth, UK

(*correspondence: laur@bgs.ac.uk)

²Lancaster Environment Centre, Lancaster University, UK

³Department of Geology, University of Leicester, UK

The development of improved precision dating methods, increased diversity of methods and proliferation of high spatial resolution approaches in recent years has made a dramatic impact to Earth Science research. However, focusing on the right method/procedure to address different geological problems is essential to solve problems and maximise the impact of research. Dating techniques are widely applied to provenance studies in order to discriminate between potential source areas, to track the evolution of river drainage basins, to assess sediment budgets and erosion patterns across orogens and to infer feedback relationships between erosion, tectonics and climate. These methods involve high throughput analysis, and it is not uncommon to lose sight of the complexity of zircon and other grains in relation to the problem being addressed.

We have developed a new approach to LA-ICP-MS U-Pb dating of rutile and characterised two new reference materials [1]. We have also refined an approach to LA ICP-MS U-Pb dating of detrital zircons that uses CL imaging to identify and date all zircon components with a focus on very thin (<5 μm) rims that record the latest growth events that otherwise would be missed due to their <5 μm width on a polished surface.

U-Pb dates on zircon and rutile records medium- to high-temperature igneous and metamorphic crystallisation events and cooling through ~500 °C, respectively. The U-Pb analysis of detrital zircon and rutile from the same sample allows tracking of multiple crystallisation and tectono-thermal events of the source areas over a broad range of temperatures in a much more definitive and revealing manner than zircon alone. This is key to provenance studies where the detritus is sourced from areas with complex polyphase metamorphic histories such as collisional orogens. We have applied our method to Himalayan-derived sediments in the Eastern Himalaya to unravel Neogene tectonic-erosion relationships, and have found rutile and zircon rim ages as young as 1 and 5 Ma, respectively, inferring derivation from the Namche Barwa eastern syntaxis area.

[1] Bracciali et al. (2013) *Chemical Geology*

Insight on formation and evolution of cratonic mantle: Re-Os dating of single sulfides from Somerset mantle xenoliths (Rae Craton, Canada)

A. BRAGAGNI^{1*}, A. LUGUET¹, D. G. PEARSON²,
R.O.C. FONSECA¹ AND B. A. KJARSGAARD³

¹ Steinmann Institute, Universitaet Bonn, Germany

(*correspondence: bragagni@uni-bonn.de)

² Department of Earth and Atmospheric Sciences, University of Alberta, Edmonton, Canada

³ Geological Survey of Canada, Ottawa, Canada

Cratonic mantle xenoliths provide an unique opportunity to study the formation and evolution of the Archean lithosphere. However, widespread metasomatic processes that cause profound textural and geochemical changes, make it difficult to determine the original melting age. Mantle xenoliths from Somerset Island (North Rae Craton) are characterized by a large range of whole-rock Re-depletion ages (T_{RD}) ranging between 1.3 and 2.8 Ga [1]. Moreover, the oldest samples have low Pd/Ir ratio inherited from the original melting process, whereas younger samples are characterized by variable enrichments in Pd, Pt and Re suggesting extensive metasomatic overprint [1].

To better constrain the age distribution in the mantle root of the Rae Craton and to evaluate whether cratonic lithosphere formation may be older than recorded by the whole-rocks, we performed a Re-Os isotopic study on sulfides from four mantle peridotite xenoliths showing variable HSE (highly siderophile elements) signature (Pd/Ir=0.03-0.6). Sulfides (down to $\varnothing < 10 \mu\text{m}$) were micro-sampled from thick sections, with Os extracted via μ -distillation and analyzed by N-TIMS.

Sulfides from the peridotite with the most HSE residual signature yield T_{RD} ages of 2.7-2.8 Ga, in agreement with its whole rock T_{RD} age. Sulfide T_{RD} ages from metasomatised xenoliths vary from 2.8 Ga to future ages, with the 2.8 Ga age significantly older than the whole rock T_{RD} ages (even T_{MA}). The 2.7-2.8 Ga age, recorded in sulfides from three xenoliths out of four, overlaps with widespread magmatism in the Rae Craton [2] suggesting possibly a synchronous event of crustal and lithospheric mantle formation. Our results show that xenoliths with residual HSE signatures are likely to preserve the original melting age while the more metasomatic xenoliths have been rejuvenated by extensive addition of 'younger' sulfides.

[1] Irvine *et al.* (2003) *Lithos* **71**, 461-488. [2] Hartlaub *et al.* (2004) *Precambrian Research* **131**, 345-372.

Ocean drilling: MORB geochemistry in the third (and fourth) dimension

BRANDL, P.A.¹, REGELOUS, M.¹, BEIER, C.¹
AND HAASE, K.M.¹

¹GeoZentrum Nordbayern, FAU Erlangen-Nürnberg,
Schlossgarten 5, 91054 Erlangen, Germany

Most of our knowledge on the composition and formation of the oceanic igneous crust derives from lava samples collected from active ridge axes by dredging or submersible. However, lavas erupted at the ridge axis eventually make up the lowermost part of the extrusive section. If these differ in composition from those emplaced off-axis, then compilations of axial mid-ocean ridge basalt (MORB) may not yield an accurate estimate of the composition of the bulk crust.

Lavas drilled from the oceanic crust provide another way to estimate the composition of the bulk crust. In addition, they record changes in MORB chemistry over both long and short timescales. We have shown previously [1] that mantle temperatures recorded in the major element composition of ancient drilled MORB vary systematically over long timescales (10^6 - 10^8 a) in rifted ocean basins due to continental insulation effects. The chemical stratigraphy of lavas from individual drillsites could be used to investigate chemical changes over 10^3 - 10^5 a timescales, which may result from variations in fractionation, magma replenishment rates or source and melting effects.

We carried out major element analysis of 340 fresh glasses (>110 also for trace elements) from 30 different DSDP and ODP sites in the Atlantic and Pacific. First results indicate that lavas from single drill sites are remarkably uniform in their chemical composition when compared to the chemical variation present at the corresponding segment of the active ridge axis. We find systematic chemical variations with depth, sigmoidally shaped in the slow-spread crust of site 417D (Atlantic) and irregularly-shaped in the drillcore of site 1256D, drilled into superfast-spreading crust. This may indicate major differences in the residence time of magma in crustal magma chambers as well as in the magma replenishment rate, e.g. size and time intervals of rising magma batches. The oscillation between magmatic differentiation and magma recharge may be responsible for some of the globally observed trace element patterns in MORB as recently suggested by [2] but based on predominantly dredged samples.

[1] Brandl et al. (2013), *Nature Geoscience*, doi: 10.1038/ngeo1758. [2] O'Neill, H.St.C and Jenner, F.E. (2013), *Nature*, doi: 10.1038/nature11678.

Testing models for continental growth and melt-rock interaction from ¹⁸⁶Os-¹⁸⁷Os isotopes in southwest usa mantle xenoliths

A. D. BRANDON*

Department of Earth and Atmospheric Sciences, University of Houston, Houston, TX 77204, USA
(*correspondance: abrandon@uh.edu)

Melting in the convecting mantle results in lower density residual peridotite that may stabilize as subcontinental lithospheric mantle (SCLM), results in juvenile crust production, and is likely a primary mechanism to grow continents over Earth history. Peridotite and pyroxenite xenoliths provide a compositional record of formation and subsequent modification of the SCLM.

Xenolith samples 3 classic locales in the Southwestern United States - Dish Hill (California), Kilbourne Hole (New Mexico), and Vulcan's Throne (Arizona), span an 860 kilometer-wide region within two crustal provinces, the 2.0-2.3 Ga Mojavia, and the 1.7-2.0 Ga Yavapai-Mazatzal provinces. Preliminary ¹⁸⁷Os/¹⁸⁸Os data for spinel-bearing peridotites show positive correlations with melt depletion indicators such as Al₂O₃. Applying the aluminachron age concept gives ¹⁸⁷Re-¹⁸⁷Os model ages ranging from 2.0 to 2.3 Ga, broadly consistent with the ages of the overlying continental crustal provinces. If so, these data support models where continental growth is directly linked to stabilization of its underlying SCLM via partial melting in the convecting mantle. It also indicates that large off-craton continental regions may grow in rapid pulses through large-scale mantle melting events. A potentially viable alternative is that the aluminachrons record melt-rock interaction subsequent to earlier partial melting. If so, then these data instead only provide minimum model ages of partial melting via the lowest ¹⁸⁷Os/¹⁸⁸Os ratio measured in each suite and thus may be unrelated to the initial stages of juvenile crust production leading to continental growth, and alternatively represent later continental magmatic processes.

To further evaluate the timing and mechanisms of SCLM stabilization and evolution and their potential link to continental growth, Os isotope data for pyroxenites from these locales will be presented to constrain compositional signatures imparted to the peridotites via melt addition or melt-rock interaction. Further, the first high-precision ¹⁸⁶Os-¹⁸⁷Os measurements of continental peridotite xenoliths will be obtained to monitor Pt-Re-Os fractionation events. Coupled ¹⁸⁶Os-¹⁸⁷Os fingerprints partial melting versus melt-rock interaction to the Os budgets of each of these xenolith suites.

Solid solution formation and uptake of Radium in the presence of barite

F. BRANDT^{1*}, M. KLINKENBERG¹, V.L. VINOGRAD^{1,2},
K. ROZOV¹ AND D. BOSBACH¹

¹Institute of Energy and Climate Research (IEK-6),
Forschungszentrum Jülich, Germany; f.brandt@fz-
juelich.de (*presenting author), m.klinkenberg@fz-
juelich.de, k.rozov@fz-juelich.de, d.bosbach@fz-
juelich.de

²Institute of Geosciences, Goethe University, Frankfurt
(Germany); v.vinograd@kristall.uni-frankfurt.de

The phase relations in the BaSO₄-RaSO₄-H₂O system may determine the solubility of radium in natural waters due to the formation of a solid solution. In the near-field of nuclear waste repositories for spent fuel, radium may enter a system in which barite is in equilibrium with the aqueous solution. Thermodynamically, a Ra_xBa_{1-x}SO₄ solid solution is expected to form as solubility controlling phase rather than RaSO₄. However, due to a lack of reliable data, the solid solution system RaSO₄-BaSO₄-H₂O is currently not considered in long term safety assessments for nuclear waste repositories. The solubility product of the pure RaSO₄ endmember is poorly constrained between pK_{RaSO₄} = 10.26 to 10.41 by only very few experimental data [1,2]. Published interaction parameters W_{BaRa} of the RaSO₄-BaSO₄-H₂O system varies widely in different studies [3, 4] between 0.9 and 3.9 - 6.5 kJ/mol.

In this study we have combined experimental data, atomistic calculations and thermodynamic modeling to study in detail how a radium containing solution will equilibrate with solid BaSO₄ under repository relevant conditions. Batch sorption experiments at close to equilibrium conditions indicate the formation of a Ra_xBa_{1-x}SO₄ solid. Our first principles calculations based on the single defect method [5] indicate a value of $W_{BaRa} = 2.5 \pm 1.0$ kJ/mol, implying a non-ideal solid solution. Thermodynamic assessment calculations indicate that the final experimental Ra(aq) concentration at room temperature and 90 °C can be matched with $W_{BaRa} \approx 1.5$ kJ/mol and pK_{RaSO₄} \approx 10.41.

[1] Lind, S. C., *et al* (1918). *J Am Chem Soc* **40**, 465-472. [2] Paige, C. R. *et al.*(1998). *Geochim. Cosmochim. Acta* **62**, 15-23. [3] Zhu, C., 2004. *Geochim. Cosmochim. Acta* **68**, 3327-3337. [4] Curti, E., *et al.* (2010). *Geochim. Cosmochim. Acta* **74**, 3553-3570. [5] Sluiter & Kawazoe (2002) *Europhys Lett.* **57**, 526-532.

The co-ordination of Boron in foraminiferal calcite

OSCAR BRANSON*¹, SIMON REDFERN¹,
KARINA KACZMAREK², TOLEK TYLISZCZAK³
AND HENRY ELDERFIELD¹

¹Department of Earth Sciences, University of Cambridge,
Downing St, Cambridge CB2 3EQ, UK.

(*correspondence: ob266@esc.cam.ac.uk)

²Alfred Wegener Institute, Am Handelshafen 12, D-27570
Bremerhaven, Germany. (Karina.Kaczmarek@awi.de)

³ALS Beamline 11.0.2, One Cyclotron Road, MS 6R2100
Berkeley, CA 94720, USA. (Ttyliszczak@lbl.gov)

The analysis of boron in foraminiferal calcite is a burgeoning palaeo-proxy for past ocean-acidification events [1]. This is particularly relevant to today's 'carbonated ocean' [2]. However, considerable uncertainty surrounds the mechanisms of boron incorporation into the shell. Foraminiferal calcite is known to be highly chemically heterogeneous [3], and understanding how boron fits into this complex structure is central to our understanding of, and confidence in, this important proxy.

We have applied synchrotron NEXAFS spectroscopy to examine the distribution and coordination of boron in foraminifera at the nm length scale.

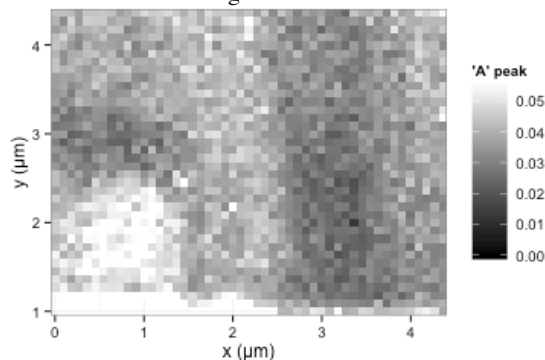


Figure 1: A Scanning Transmission X-ray Microscope (STXM) image of a section of foraminifera test at the trigonal B edge, showing variations in the concentration of B [4].

STXM results reveal clear homogeneity in boron concentration, which appears to be uniformly hosted in a trigonal coordination in the calcite crystal lattice (BO₃ groups). Analysis of boron coordination is ongoing.

[1] Spivack, et.al. (2002) *Nature* **363**, 1-3 [2] Elderfield (2002) *Science* **296**, 1618-1621 [3] Erez (2003) *Rev. Min. Geochem.* **54**, 115-149. [4] Fleet & Muthupari (2000) *Am. Min.* **85**, 1009-1021.

The establishment of the steady-state activity at Stromboli volcano (Italy): evidence from diffusion and mixing processes revealed at mineral scale

ELEONORA BRASCHI¹, CHIARA M. PETRONE²,
LORELLA FRANCALANCI^{1,3} AND SIMONE TOMMASINI³

¹CNR-IGG, Sezione Firenze, Via G. LaPira, 4, Firenze, Italy

²The Natural History Museum, Dept Earth Sciences,
Cromwell Road, SW7 5BD London, UK

³Università degli Studi di Firenze, Dipartimento di Scienze
della Terra, Via G. La Pira, 4, Firenze, Italy

The present-day activity of Stromboli is characterized by strombolian explosions ejecting black scoriaceous lapilli and ash. This persistent activity is interrupted by effusive eruptions and more energetic explosions (paroxysms) also emitting a small volume of light pumices. The entire system is in a persistent steady-state activity whose driving forces are still not completely understood. Investigating the evolution of the plumbing system toward the present-day condition is thus crucial to better constrain and understand the onset and development of the present-day activity.

We studied in detail two selected samples representative of the transitional eruptive period from the more explosive phase forming the Pizzo Sopra la Fossa tuff cone (ca. 2 ka) to the present-day activity: (i) an older spatter-lava sample (shoshonite) from the Post-Pizzo fountain-fed fallout activity; (ii) a large and flattened, black scoriaceous spatter (shoshonitic basalt) probably ejected during one of the early paroxysms of the present-day activity. Both samples have similar paragenesis with phenocrysts of olivine, clinopyroxene, plagioclase. We recognize several types of clinopyroxene textures with different recurrence among the two samples. In detail, multiple banded clinopyroxene with evident resorption features, characterizes the older sample, recording several pulsatory intrusions of new mafic magmas into the system and pointing to the establishment of the steady-state condition. Contrarily, single diffused band and/or patchy cores are found in the present-day sample. We applied the diffusion chronometry to suitable clinopyroxene crystal zones to estimate the timing of these refilling events in the shallow magma reservoir from the Post-Pizzo period onward pointing to a progressive transition toward the present-day steady-state conditions.

A $\delta^{13}\text{C}$ record from marine carbonates deposited below diamictites between ca. 2430 and 2440 Ma

A.T. BRASIER^{1*}, A.P. MARTIN², V.A. MELEZHNIK^{3,4},
A.R. PRAVE⁵, D.J. CONDON² AND A.E. FALLICK⁶

¹FALW, Vrije Universiteit Amsterdam, De Boelelaan 1085,
1081HV Amsterdam, The Netherlands

(*correspondence: a.t.brasier@vu.nl)

²NIGL, BGS, Keyworth, UK

³Geological Survey of Norway, Postboks 6315, Sluppen, NO-
7491, Trondheim, Norway

⁴Bergen Univ., Postboks 7803, NO-5020 Bergen, Norway

⁵Dept of Earth and Env. Sciences, Univ. of St Andrews, St
Andrews, KY16 9AL, Scotland, UK

⁶SUERC, East Kilbride, Scotland, G75 0QF

Palaeoproterozoic Polisarka Sedimentary Formation diamictites underlain by marine carbonates and overlain by volcanic ash sediments were recovered from International Continental Scientific Drilling Program Fennoscandian Arctic Russia - Drilling Early Earth Project (ICDP FAR-DEEP) Hole 3A (Kola Peninsula, NW Russia). The tuff yielded 2434 Ma dated zircons, constraining deposition of the diamictites and underlying carbonates to within an interval ca. 2430 to 2440 Ma. The carbonate rocks originally included aragonitic limestones deposited mostly in a deep-water setting. They record two inorganic carbon $\delta^{13}\text{C}$ excursions, from values of ca. 0‰ to minima of ca. -5.4‰ as the diamictite is approached. Mg/Ca ratios correlate strongly with $\delta^{13}\text{C}$ in the sections containing the excursions. Combined with petrographic observations, this correlation reflects secondary alteration of the first excursion, and resedimented dolostone clasts in the second excursion. It is tempting to speculate that these dolostone clasts were deposited in penecontemporaneous shallow-marine waters as the global glaciation began. Their low $\delta^{13}\text{C}$ values might reflect input of oxidised atmospheric methane to the ocean surface (and therefore the cause of the glaciation), while the majority of the ICDP FAR-DEEP Hole 3A carbonates record deeper-marine inorganic carbon $\delta^{13}\text{C}$.

Dolomite formation within microbial mats from the Dohat Faishakh sabkha, Qatar

MARISA BRAUCHLI¹, TOMASO R. R. BONTOGNALI^{2*},
JUDITH A. MCKENZIE², CHRISTIAN J. STROHMENGER³,
JEREMY JAMESON³, FADHIL SADOONI⁴
AND CRISO GONO VASCONCELOS²

¹Institute of Evolutionary Biology and Environmental Studies,
University of Zürich, Switzerland

²ETH Zürich, Geologisches Institut, Zürich, Switzerland
(*correspondence: tomaso.bontognali@erdw.ethz.ch)

³ExxonMobil Research Qatar, Doha, Qatar

⁴Environmental Studies Center, Qatar University, Doha, Qatar

The hypersaline coastal sabkha of Dohat Faishakh (Qatar) was one of the first settings recognized as a rare modern geological environment where dolomite formation occurs (Illing *et al.*, 1965). Although the origin of dolomite remains one of the most debated subjects in sedimentary geology, microbial mediation has been recently proposed as a possible solution for this controversy. Until now, the relationship between microbial activity and dolomite precipitation in the Dohat Faishakh sabkha has not been evaluated. The limited previous studies of the Dohat Faishakh sabkha considered dolomite formation to be the result of a penecontemporaneous replacement of authigenic aragonite. However, no conclusive evidence confirms this hypothesis. To evaluate whether a “microbial factor” is important in this classic evaporitic environment, we collected core samples along a transect from the lower intertidal to the supratidal zone of the sabkha. A preliminary investigation of the sampled sediments revealed a close association between buried microbial mats and dolomite. The exopolymeric substances constituting the microbial mats are recognized as an important component for dolomite nucleation. We, therefore, hypothesize that the main factor controlling the occurrence of dolomite within the sediments of the Dohat Faishakh sabkha is the presence of an organic matrix (i.e., the buried microbial mats) and not a replacement process transforming primary aragonite into dolomite. Aragonite and dolomite likely precipitate nearly simultaneously from highly evaporated marine waters. The presence/absence of an organic matrix determines whether the carbonate minerals will have a dolomitic vs. an aragonitic composition. Applying a geomicrobiological approach to study mineral formation beneath the Dohat Faishakh sabkha will provide new insights into evaporite mineral associations in the rock record, as well as into extraterrestrial environments, as evidenced by recent observations of evaporitic sediments on Mars.

[1] Illing *et al.*, 1965, SEPM Spec. Publication **13**, p. 89-111.

A new aqueous phase protocol for the mechanism generator GECKO-A used for the CAPRAM mechanism extension

P. BRÄUER¹, C. MOUCHEL-VALLON², A. TILGNER¹,
R. WOLKE¹, B. AUMONT² AND H. HERRMANN^{1*}

¹Leibniz Institute for Tropospheric Research (TROPOS),
Permoserstr. 15, D-04318 Leipzig, Germany.

(*correspondence: herrmann@tropos.de)

²LISA, UMR CNRS 7583, Universités Paris Est Créteil et
Paris Diderot, 61 Av. du Général de Gaulle, 94010 Créteil
cedex, France.

The ubiquitous abundance of organic compounds in natural and anthropogenically influenced eco-systems has put these compounds into the focus of environmental research. To investigate the chemistry of organic compounds in the tropospheric multiphase system, explicit modelling can provide a useful tool.

However, the oxidation of large organic molecules (typically $C_{>5}$) involves a huge number of intermediate compounds produced during the oxidation process. Furthermore, most of the needed experimental thermodynamic and kinetic data are unavailable in the literature. Therefore, the creation of explicit mechanisms relies on automated self-generating mechanism construction as achieved with GECKO-A (Generator for Explicit Chemistry and Kinetics of Organics in the Atmosphere) for the gas phase.

As the chemistry in deliquescent particles and cloud droplets can be important for the oxidation process, a protocol has been developed to describe the degradation of aliphatic organic compounds in the aqueous phase. This aqueous phase protocol has been implemented into GECKO-A and was used to advance the aqueous phase mechanism CAPRAM 3.0n (Chemical Aqueous Phase Radical Mechanism). The latest CAPRAM version was extended by about 3500 reactions, where, besides the addition of new subsystems, branching ratios were introduced in the mechanism.

Box model studies were performed with a non-permanent cloud scenario to reveal more insights into the degradation and formation of organic compounds in deliquescent particles and cloud droplets as well as the feedback on gas phase concentrations. Detailed time-resolved investigations of the chemical fluxes assisted the investigations of concentration-time profiles. Comparisons with previous model studies and experimental data from field and laboratory investigations were used to validate the mechanism generator and show significant improvements in the generated model results.

Rhenium-Osmium Isotope Geochronology of the Neoproterozoic Fifteenmile Group, Coal Creek Inlier, Yukon, Canada

STEVEN A. BRAUN*¹, ALAN BRANDON¹, FRANCIS A. MACDONALD², DAVID VAN ACKEN³ AND ROBERT A. CREASER³

¹Department of Earth and Atmospheric Sciences, University of Houston, Houston, TX 77204, (Correspondance: *steven.braun@exxonmobil.com)

²Department of Earth & Planetary Science, Harvard University, 20 Oxford St. Cambridge MA, 02138

³1-26 Earth Sciences Building, University of Alberta, Edmonton, Alberta, Canada, T6G 2E3

New ¹⁸⁷Re-¹⁸⁷Os isotope data on organic rich mudrocks from the Neoproterozoic Fifteenmile Group, Coal Creek Inlier, Yukon, Canada provide direct age control for biomineralizing scale microfossils [1] and the termination of the Bitter Springs isotopic stage in northwest Canada. The uppermost Reefal Assemblage of the Fifteenmile Group has a preliminary ¹⁸⁷Re-¹⁸⁷Os isochron age of 752 ±44 Ma (2σ; Model-3; MSWD 4.2; ¹⁸⁷Os/¹⁸⁸Os_i 0.42 ±0.22). The obtained age is identical within error to ¹⁸⁷Re-¹⁸⁷Os ages from the correlated Wynniatt Formation, Victoria Island, Canada [2]. This result is also in good agreement with known U-Pb TIMS zircon analysis which brackets the sampled portion of the Upper Fifteenmile Group between 811.0 and 717.4 Ma [3]. If the ~750 Ma age model is correct, the Bitter Springs isotopic stage could be younger or extend longer than previously thought (~800 Ma). A younger age for the Bitter Springs Stage may also impact global paleogeographical reconstructions based on anomalous global paleomagnetic records from the Bitter Springs stage [4]. These measurements also represent an important benchmark for the ¹⁸⁷Os/¹⁸⁸Os_i composition of Neoproterozoic seawater. The ¹⁸⁷Os/¹⁸⁸Os_i record is an emerging seawater proxy which has the ability to trace rapid climatic perturbations [5]. This proxy record can provide independent confirmation of climatic fluctuations observed in important Neoproterozoic ⁸⁷Sr/⁸⁶Sr, δ¹³C reference sections [6]. Further ¹⁸⁷Re-¹⁸⁷Os work on samples from the Fifteenmile Group is ongoing.

[1] Cohen *et al.* (2011) *Geology* **39**, 539-542. [2] van Acken *et al.* (2012) *MinMag*, Abstract #272. [3] Macdonald *et al.* (2010) *Science* **327**, 1241-1243. [4] Swanson-Hysell *et al.* (2012) *Am. J. Sci.* **312**, 817-884. [5] Turgeon & Creaser (2008) *Nature* **454**, 323-326. [6] Halverson & Shields-Zhou (2011) *Geol. Soc., Lon. Mem.* **36**, 51-66.

How bugs get their food: Linking mineral surface chemistry to nutrient availability

A.W. BRAY^{1,2*}, E.H. OELKERS², S. BONNEVILLE^{1,3} AND L.G. BENNING¹

¹Cohen Geochemistry, School of Earth and Environment, University of Leeds, LS2 9JT, United Kingdom (*correspondence: a.bray@see.leeds.ac.uk)

²Géochimie et Biogéochimie Experimentale, GET CNRS, UMR 5563, 14 av. Edouard Belin, 31400 Toulouse, France

³Faculté des Sciences, Département des Sciences de la Terre et de l'Environnement, Université Libre de Bruxelles, 50 av. F.D. Roosevelt, 1050 Brussels, Belgium

The bio-acquisition of mineral-bound key nutrients by microorganisms is currently of great interest because of our desire to understand soil nutrient cycling. It has been shown that fungi seek out nutrient sources through expansive mycorrhizal networks, acting as biosensors for 'tasty snacks'. The mechanism by which fungi extract nutrients from minerals is by combining bio-mechanical forcing of the structure [1] with subsequent chemical alteration [2]. Usually, release of nutrients from minerals is discussed in terms of bulk chemical content. Here, we present data showing the importance of the surface composition of biotite, a key terrestrial source of primary nutrients (in particular potassium), to influence nutrient availability. This gives us new insights into the mechanisms by which microorganisms weather minerals, aiding in soil formation.

A suite of batch potentiometric and electrokinetic titrations (pH 1-12 and 25 °C), were carried out to determine the surface chemistry and reactivity of biotite by quantifying protons consumed and metals released. Potassium was found to be preferentially removed from the biotite surface down to an average depth of ~ 20 nm at all pH values. A slight pH dependency of this removal and the proton consumption profile suggest a significant portion of K was removed from the structure immediately upon contact between the biotite surface and the fluid. The existence of such a K depleted surface suggests that microorganisms are required to physically break the mineral structure to access nutrients from newly created surfaces. Our data set underpins the need for an initial bio-mechanical forcing of the mineral surface prior to its chemical alteration, leading to increased weathering.

[1] Bonneville *et al.* (2009) *Geology* **37**, 615-618. [2] Bonneville *et al.* (2011) *GeoChim. Cosmochim. Ac.* **75**, 6988-7005.

Biogeography of serpentinite-hosted ecosystems

WILLIAM J. BRAZELTON^{1,4*}, DAWN A. CARDACE²,
GRETCHEN L. FRUH-GREEN³, SUSAN Q. LANG³, MARVIN
D. LILLEY⁴, PENNY L. MORRILL⁵, KATRINA I. TWING¹
AND MATTHEW O. SCHRENK¹

¹East Carolina University, Greenville, NC, USA.

(*correspondence: wbrazelton@gmail.com)

²University of Rhode Island, Providence, RI, USA

³ETH-Zurich, Switzerland

⁴University of Washington, Seattle, WA, USA

⁵Memorial Univ. of Newfoundland, St. John's, NL, Canada

Ultramafic rocks in the Earth's mantle represent a tremendous reservoir of carbon and reducing power. Upon tectonic uplift and exposure to fluid flow, serpentinization of these materials generates copious energy, sustains abiogenic synthesis of organic molecules, and releases hydrogen gas (H₂). To date, however, the "serpentinite microbiome" is poorly constrained: almost nothing is known about the microbial diversity endemic to rocks actively undergoing serpentinization.

We have obtained metagenomic and 16S rRNA tag sequence datasets from fluids and rocks collected in serpentinizing ophiolites in California, Canada, and Italy. The samples include wells which directly access subsurface aquifers, rocks obtained from drill cores into serpentinites, and natural, high-pH serpentinite springs that are presumably representative of deeper environments within the ophiolite complex. Our results point to potentially H₂-utilizing Betaproteobacteria thriving in shallow, oxic-anoxic transition zones and anaerobic Clostridia thriving in anoxic, deep subsurface habitats. Similar bacterial taxa and genes encoding hydrogenase enzymes were also observed in seafloor Lost City hydrothermal chimneys, indicating that we are beginning to identify a core serpentinite microbial community that spans marine and continental settings.

These data represent a unique opportunity to examine biogeographic patterns among a specialized set of organisms and genes and to explore their evolution during the uplift and obduction of mantle rocks onto continents over geological time scales. We are currently testing for correlations between these metagenomic data and the geochemical conditions and the geological histories of the host rocks with an ultimate goal of inferring an integrated metagenomic-biogeochemical natural history of the serpentinite habitats.

Characterization of natural gem diamonds and UV light sources using fluorescence spectroscopy

C.M. BREEDING* AND Y. LUO

Gemological Institute of America (GIA), Carlsbad, CA, USA

(*correspondence: christopher.breeding@gia.edu)

Gemologists have used fluorescence reactions to long wave ultraviolet light for identification of gemstones for decades. Simple visible observations of fluorescence color, intensity, pattern, and duration have proven invaluable for separating natural diamonds and other gemstones from synthetic or treated equivalents. Fluorescence viewing and imaging, however, can only provide a limited amount of information about the lattice defects that produce the luminescence. Spectroscopy provides details about the nature of the fluorescence, the combinations of defects that produce the observed colors, and the effects of different excitation sources. Spectra collected from natural gem diamonds show blue fluorescence from N3 defects (415 nm), green from H3 (503.2 nm) and H4 (496 nm), orange/red from N-V centers (575, 637 nm), and yellow from a combination of several defects associated with a visible absorption band at 480 nm. Using variable excitation, three dimensional maps (excitation, emission, fluorescence) of the luminescence spectra from each defect reveal complexities that cannot be discerned visually. In addition to this fundamental fluorescence information, spectroscopy also allows characterization of the excitation light source output and evaluation of how it affects the fluorescence produced from a diamond. A wide range of UV light sources are currently used in the gem and mineral industry with large differences in output intensity and wavelength. Small variations in bulb/LED and filter materials can significantly impact the visual fluorescence, leading to inconsistent results. The use of fluorescence spectroscopy provides additional detail that is not available from visual observation to help to identify subtle differences produced by variable light sources as well as many of today's modern gemstone treatments.

Hydrochemical patterns in a structurally controlled geothermal system

M. BREHME¹, C. HAASE², S. REGENSPURG¹, I. MOECK¹, F. DEON¹, B. WIEGAND³, Y. KAMAH⁴, G. ZIMMERMANN¹ AND M. SAUTER³

¹Helmholtz Centre Potsdam - GFZ German Research Centre for Geosciences, International Centre for Geothermal Research, Telegrafenberg, 14473 Potsdam, Germany

²Institute for Geosciences, Kiel University, Ludewig-Meyn-Strasse 10, 24118 Kiel, Germany

³University of Göttingen, Applied Geology, Goldschmidtstr. 3, 37077 Göttingen, Germany

⁴Pertamina Geothermal Energy, Jl.M.H. Thamrin No.9, Jakarta 10340, Indonesia

In this study, we investigate a magmatic structurally controlled geothermal reservoir in North Sulawesi-Indonesia focusing on structural geology and hydrochemistry. A combination of a thermal-hydraulic model with hydrochemical modelling is the goal of this study. The running geothermal system is located above a subduction zone surrounded by a complex network of faults and repetitive volcanic eruptions.

Analyses of the samples collected from wells, hot springs, rivers and lakes show typically two types of water. Acid high saline waters were found in the northern reservoir area (pH: 2.7-3.2, electrical conductivity: 4620-9700 $\mu\text{S}/\text{cm}$). A similar water type rises above this reservoir through several hot springs (pH: 1.8-2.7) and a lake (pH: 2.5) located above the reservoir. A second type of reservoir water was observed in the South where wells show a pH range of 4.2 to 6.5 and conductivities from 400 to 1729 $\mu\text{S}/\text{cm}$. Neutral hot springs occur in the surrounding area with pH values ranging of 5.8 to 7.0. While the northern and southern reservoirs are only 2km away from each other we observe strong difference between the water types. This is assumed to be due to laterally low permeability in the fault network. All the data analysed in this study converges to a consistent hydrotectonic model, which shows different reservoir compartments controlled by complex fault systems.

In addition to the conceptual model a hydrochemical model was set up in PHREEQC and suggests scaling from both water types such as Fe- and Si-bearing minerals. In this context, a cycle including hot water production, surface mixing and several reinjection scenarios was simulated. Modelled precipitations will eventually be compared with XRD-analyses of cores, precipitation-, alteration- and rock-samples in order to calibrate the hydrochemical model.

$\delta^{97/95}\text{Mo}$ in molybdenites from the Azegour skarn (Morocco)

BREILLAT NOEMIE^{1,2}, GUERROT CATHERINE¹, NEGREL PHILIPPE¹ AND MARCOUX ERIC²

¹BRGM, ISTO, UMR 7327, BP 36009, 45060 Orléans, France (n.breillat@brgm.fr)

²Univ d'Orléans, ISTO, UMR 7327, 45071 Orléans, France

Molybdenum (Mo) isotopes are frequently used to investigate ocean and lake (paleo-)redox conditions. In the frame of mineral resources, only few studies have been performed regarding Mo-Re-Os isotopes. The aim of this study is to understand the source, processes and mobility of metals concentrations using Mo isotopes on molybdenites in different ore deposits. The present study focuses on the Azegour skarn (Morocco). Located in the High-Atlas, the Azegour site is one of the rare Mo-W-Cu exploited skarns (three historic mines). It is formed by a granitic intrusion (271±3Ma) in cambrian volcano-sedimentary serie composed by schists, volcanic complex (andesites, pyroclastites) and carbonate formations (calcareous and dolomites). The skarn takes place in the carbonate formations where pyroxenites and grenatites occurred. The grenatites being the Mo-bearing minerals in the form of molybdenites.

Molybdenites sampling has been performed in the main mine (Azegour) and in the Tizgui mine (1km north of the Azegour mine). The Mo isotopic composition has been determined on molybdenites using a MC-ICP-MS Neptune after aquaregia dissolution and adjustment to $[\text{Mo}] = 1\mu\text{g}\cdot\text{g}^{-1}$. The $\delta^{97/95}\text{Mo}$ ratios have been normalized to NBS3134 and a reproducibility of 0.07‰ (2 σ) is reached.

Presently, we have analysed 12 molybdenites from Azegour and 2 from Tizgui and 14 others are in progress. Regarding the first 14 samples, the $\delta^{97/95}\text{Mo}_{\text{NBS}}$ ratios vary between -0.40 and 0.32‰ for Azegour and between 0.08 and 0.30‰ for Tizgui. It is worth noting that variations can occur either at the whole site (difference of about 0.72‰) but also at the cm scale in the same sample (here the largest observed difference is up to 0.40‰).

Regarding the Azegour skarn, there is no direct relationship for explaining the Mo fractionation in molybdenites between the facies or the two sites of sampling. Different processes will be discussed to explain the observed variability (redox conditions prevailing during the molybdenites deposits, late metamorphism phase...). Further investigations using Pb and S isotopic compositions will help deciphering the oxidation state and the origin of molybdenites regarding the possible different fluids.

Experimental constraints on HSE fractionation during basalt genesis

JAMES M BREANAN

Earth Sciences, University of Toronto,
(brenan@es.utoronto.ca)

Terrestrial basalts are characterised by CI-normalised depletions in the highly siderophile elements (HSE), as well as moderate to large interelement fractionation within the group; the IPGE (Os, Ir, Ru) are relatively depleted compared to the PPGE (Rh, Pt, Pd), Au and Re. The overall low abundance of the HSE in basalts is attributed to core formation, whereas the origin of the fractionation within the HSE group has been less certain. Experiments and empirical observations indicate that Ir, Ru and Rh are compatible in olivine, as is Ru in ferric-iron-poor chromian spinel, and both phases strongly reject Pt, Pd, Re and Au. It is expected, but unproven, that cpx and opx will exhibit broadly similar partitioning behaviour as olivine. This sense of fractionation is correct for terrestrial basalts, but the magnitude of partition coefficients is too low to account for the overall depletion levels.

Residual sulfide, either as liquid or crystalline MSS, has a significant impact on basalt HSE levels, owing to large sulfide-silicate partition coefficients. Crystalline MSS can be stable with silicate melt if the silicate liquidus is suppressed by water. Based on known MSS-sulfide melt partitioning, MSS-silicate melt partitioning can impose a strong inter-HSE fractionation, whose sense and magnitude is similar to terrestrial basalts. With the exception of Au, however, direct measurements of MSS-silicate melt partitioning of the HSE have not been done. If melting occurs at higher temperatures, MSS is replaced by sulfide liquid. Experiments show that Re and Au are significantly less compatible than PGE in sulfide liquid at moderately oxidised conditions, accounting for the relative enrichment of Re and Au in terrestrial basalts. It is not clear, however, if sulfide liquid can impose IPGE/PPGE fractionation on silicate melt, as partition coefficients for these elements are currently too imprecise.

Recent measurements indicate sulfide-silicate partition coefficients for the PGE are on the order of 10^6 or larger. Since the mass fraction of sulfide liquid decreases during melting, this implies that the PGE content of residual sulfide could reach 1000s of ppm, leading to saturation in the less soluble PGE, such as Os, likely alloyed with Ir and Ru. The HSE content of terrestrial basalts might therefore be controlled by a combination of metal solubility and sulfide-silicate partitioning. Detailed modelling of this behaviour is considered by Mungall [this session].

Evidence for supernova injection into the solar nebula and the decoupling of *r*-process nucleosynthesis

G.A. BRENNECKA¹, L.E. BORG¹ AND M. WADHWA²

¹Lawrence Livermore National Laboratory, Livermore, CA, USA 94550 (brennecka2@llnl.gov)

²School of Earth and Space Exploration, Arizona State University, AZ, USA 85287

Variations in the non-radiogenic isotope abundances of meteoritic materials have long been interpreted as nucleosynthetic signatures resulting from the input of distinct materials produced from *p*-, *s*-, and *r*-processes [e.g., 1-8]. Previous studies of the Solar System's first solids, calcium-aluminum-rich inclusions (CAIs), have demonstrated that isotopic compositions of various elements differ from terrestrial compositions and may be modeled using addition or subtraction of different nucleosynthetic components [6-8]. However, these studies did not determine the isotopic compositions of multiple elements spanning a large mass range in the same CAIs. We present for the first time an integrated study of Sr, Mo, Ba, Nd, and Sm isotope compositions determined on multiple coarse- and fine-grained CAIs from the Allende CV3 chondrite.

The data demonstrate that the isotopic compositions of these elements in CAIs are uniform and yet distinct from the average Solar System, necessitating that CAIs were formed in a homogenous and isotopically distinct reservoir. Taken in whole, the observed mass-independent anomalies cannot be explained by: (1) presence of presolar components, (2) simple addition/subtraction of *r*-process nuclides, (3) incomplete digestion of the sample, (4) nuclear field shift fractionation, or (5) neutron capture. Relative to terrestrial standards, CAIs contain positive *r*-process anomalies in isotopes $A < 140$ and negative *r*-process anomalies in isotopes $A > 140$. Previous work has suggested that multiple supernova sources are required to account for the proportions of short-lived isotopes in the early Solar System [9]. The fundamental difference in the isotopic character of CAIs around mass 140 is consistent with [9] and necessitates (1) the existence of multiple sources for *r*-process nucleosynthesis, and (2) the injection of supernova material into a reservoir untapped by CAIs.

[1] Hidaka *et al.* *EPSL* **214**, 455 (2003) [2] Andreasen & Sharma *Science* **314**, 806 (2006) [3] Carlson *et al.* *Science* **316**, 1125 (2007) [4] Andreasen & Sharma *ApJ* **655**, 874 (2007) [5] Qin *et al.* *GCA* **75**, 7806 (2011) [6] Burkhardt *et al.* *EPSL* **312**, 390 (2011) [7] Moynier *et al.* *ApJ* **758**, 45 (2012) [8] Schönbachler *et al.* *EPSL* **216**, 467 (2003) [9] Qian *et al.* *ApJ* **494**, 285 (1998).

Noble gases as physiological tracers for gas dynamics in human blood

M.S. BRENNWALD¹, C. LUNDBY², Y. TOMONAGA¹
AND R. KIPFER^{1,3}

¹Eawag, Dep. Water Resources and Drinking Water, Swiss Federal Institute of Aquatic Science and Technology, Switzerland

²Center for Integrative Human Physiology (ZIHP), Institute of Physiology, University of Zurich

³Institute for Geochemistry and Petrology, Swiss Federal Institute of Technology Zurich, Switzerland

The exchange of the inert noble gases (He, Ne, Ar, Kr, Xe) between gas and liquids is controlled solely by the gas-exchange kinetics in the gas/liquid interface, and by the solubility equilibrium (Henry's Law). Noble gases are therefore excellent tracers for the physical processes involved in gas/fluid exchange, and they have widely been applied as environmental tracers in aquatic systems. Here, we present our first attempts in using noble gases to trace physiological processes in the human body, such as the gas exchange in the lung or the gas distribution within the human organism.

Blood samples were taken from an atecubital vein. Samples were transferred into copper tubes (sample containers) without exposure to air or any other gas phase, and copper tubes were sealed. After coagulation of the blood, the samples were centrifuged to separate the liquid blood plasma from the blood cells. Blood samples were then analysed by vacuum extraction and mass spectrometric quantification of the dissolved gases using the standard methods used for water and sediment samples.

While breathing ambient air, noble gas concentrations in blood plasma were very similar to those in air saturated water. However, the ³He/⁴He ratio was 10% higher in blood than in air-saturated water, which is possibly due to the difference in diffusivities of ³He and ⁴He isotopes in the air/blood interface of the lung. Also, the heavier noble gases were found to be enriched in the blood-cell fraction relative to the blood plasma.

Breathing air enriched with noble gases resulted in an increase of the noble gas concentrations in the blood, and a new steady state was attained within a few minutes. All noble gas concentrations increased with the same kinetics. This suggests that gas exchange is not limited by diffusion through the air/blood interface in the lung, and that solubility equilibrium is attained in the lung. In contrast to O₂, which is bound to hemoglobin, the steady-state noble gas concentrations were considerably lower than expected, which points to a secondary partitioning or loss of noble gases within the body.

Recent advances of noble gas geochemistry in aquatic systems

M.S. BRENNWALD^{1,2}, C. MADEN³, N. VOGEL¹,
Y. TOMONAGA¹ AND R. KIPFER^{1,3}

¹Eawag, Dep. of Water Resources and Drinking Water, Swiss Federal Institute of Aquatic Science and Technology, Switzerland

²Dep. of Environmental Systems Science, Swiss Federal Institute Technology, Switzerland

³Institute for Geochemistry and Petrology, Swiss Federal Institute of Technology Zurich, Switzerland

Noble gases and bio-geochemically conservative transient trace gases (SF₆, CFCs) in aquatic systems have commonly been used to determine water residence times and to reconstruct past environmental and climatic conditions.

Recent conceptual and experimental developments have considerably extended the applicability of noble gas and transient gas analysis in aquatic systems. The mechanistic understanding of the formation of excess air (EA), a surplus of dissolved atmospheric gases commonly observed in groundwater, now allows robust interpretation of EA as a proxy for the hydraulic conditions during groundwater recharge, e.g., in areas that were covered by ice sheets during the LGM. Recent experimental breakthroughs now allow noble gas analysis in sediment pore fluids and in fluid inclusions of speleothems to reconstruct environmental condition from minutes amounts of water. Furthermore, the coupling of vacuum systems commonly used for noble gas analysis with and gas chromatographic methods allow combined analysis of noble gases and other gases (e.g., SF₆, CFCs, O₂, N₂) from a single water sample. This facilitates reliable EA correction for SF₆ and CFCs improving ground water dating. Finally, portable membrane-inlet mass spectrometers enable continuous and real-time analysis of noble gases and other dissolved gases directly in the field, allowing, for instance, quantification of O₂ turnover rates on small time scales.

In presenting these recent achievements, we intend to stimulate a broader discussion to define future applications of noble gases in conventional and unconventional aquatic systems.

How isotopic hydrogeochemical tools can help policy makers to target priority area for drinking water preservation?

A. BRENOT^{1*}, L. GOURCY², E. PETELET-GIRAUD²
AND PH. NEGREL²,

¹BRGM Rhône-Alpes, 151, boulevard Stalingrad 69626 –
Villeurbanne Cedex – France (*correspondence :
a.brenot@brgm.fr)

²BRGM, 3, avenue Claude-Guillemain BP 36009 45060 –
Orléans Cedex 2 – France (l.gourcy@brgm.fr ;
e.petelet@brgm.fr ; p.negrel@brgm.fr)

The main objective of the Water Framework Directive (2000/60/EC) is to prevent further deterioration, protect and enhance the status of aquatic ecosystems in Europe. In details, WFD enforces member states to identify the hydrosystems that should be protected for present or future use as drinking water. In this context, water policy makers of the Rhône-Méditerranée-Corse district (south-eastern part of France, covering 1/5 of the French territory) plan to list and delimit all the areas related to groundwater that present outstanding interests regarding quality and quantity for drinking use.

Our study is focused on two groundwater bodies located on the Rhône-Méditerranée-Corse district that have been identified as being of primary importance and/or at risk by the policy makers. These groundwater bodies (Isere alluvial aquifer and molasse aquifer) are used for drinking water supply for the large cities of Lyon, Grenoble and Albertville, to a lesser extent. Objectives were to characterize and better understand the origin of water and dissolved elements of these aquifers in order to identify the areas of major interest and protect them in priority. For that purpose, combined geochemical analysis of major and trace elements, and isotopes ($\delta^{18}\text{O}$ and $\delta^2\text{H}$ of water, ^3H , $\delta^{34}\text{S}_{\text{SO}_4}$ and $\delta^{18}\text{O}_{\text{SO}_4}$ of sulfates, $^{87}\text{Sr}/^{86}\text{Sr}$) have been successfully applied. This approach, in addition to geological and hydrogeological information, allow to identify groundwater units in each aquifer that i) present an uniqueness functioning and recharge and ii) permit low cost production for drinking purpose (water treatments reduced). For instance, the Isere alluvial aquifer presents high concentrations up to $3\mu\text{g/L}$ in As and Sb due to weathering of local rocks in the Alpes mountains. Hydrogeochemical knowledge, and especially isotopic tools, allow to target the groundwater units whose recharge area are less controlled by high As and Sb contents.

Lithium isotopic composition of the Tonga-Kermadec arc and its constraints on subduction recycling

RAUL BRENS JR.*¹, XIAO-MING LIU^{2,3},
ROBERTA RUDNICK³, SIMON TURNER¹
AND TRACY RUSHMER¹

¹Department of Earth & Planetary Sciences, Macquarie
University, Sydney, NSW 2109, Australia
(*correspondence: Raul.Brens@mq.edu.au)

²Geophysical Laboratory, Carnegie Institute for Science,
Washington, DC 20015, USA

³Department of Geology, University of Maryland, College
Park, Maryland 20782, USA

Understanding elemental transfer within subduction zones is integral to quantifying crust-mantle exchange and recycling. Lithium is water-soluble and potentially a useful tracer of subduction zone processes. We have analyzed the lithium concentrations and isotopic compositions of a suite of lavas from the Tonga-Kermadec island arc, as well as a depth profile through forearc marine sediments from ODP hole 204, and lavas from the Fonualei back-arc spreading center in order to trace how lithium isotopes manoeuvre through an intra-oceanic subduction zone.

The $\delta^7\text{Li}$ of the entire suite of sediments and lavas vary from 0.3 to 14.4. The depth profile, along with published data from another nearby core sample (DSDP 595/596), shows a systematic increase in $\delta^7\text{Li}$ (1.2 to 14.4) with depth. This is in relation with the sediment type; lithium isotopic signatures for pelagic sediments are often lighter because of fractionation from weathering, while volcanogenic sediments can be lighter or heavier as a direct result of their alteration effects.^[1] The $\delta^7\text{Li}$ of hole 204 pelagic sediments overlap that of the mantle, but range to lower values (1.2 to 5.2), while the $\delta^7\text{Li}$ of volcanogenic sediments are higher than the mantle (7.2 to 14.4). Thus, the Li isotope variation in the subducting sediments greatly exceeds that observed in the lavas. The fact that $\delta^7\text{Li}$ in some arc lavas (0.3 – 7.6) falls outside the range of MORB requires enrichments by fluid transfer of lithium from the sediments (which is reinforced with published B/Be data). Lavas from the back-arc spreading center ($\delta^7\text{Li} = 3.0 - 5.0$) show no variation from the widely accepted lithium isotopic signature range of the MORB (1.5 – 5.5), suggesting that there is little Li transfer from the slab in the back-arc.

[1] Chan, L.-H., Leeman, W.P., Plank, T., (2006). Lithium isotopic composition of marine sediments, *Geochem. Geophys. Geosyst.*, **7**, 6.

Electron flow in bacterial multi-heme cytochromes

M. BREUER¹, D.M.A. SMITH², J. BLUMBERGER¹
AND K.M. ROSSO^{2*}

¹University College London, London, UK

²Pacific Northwest National Laboratory, Richland, WA, USA

(*correspondence: kevin.rosso@pnl.gov)

Understanding mechanisms and kinetics of electron transfer processes in environmental systems is an important frontier for molecular theory and computation. This presentation addresses elementary aspects of predicting electron transfer rates, demonstrates the essentiality of computational molecular simulation relative to lacking experimental probes, and establishes a new methodological state-of-the-art for this purpose, using bacterial multi-heme electron transfer proteins as the case study.

Electron transport to extracellular solid metal oxides by metal-reducing bacteria is a fundamental biogeochemical process optimized by evolution to catalytic perfection. To shed light into why and how individual electron transfer steps in associated multi-heme cytochromes are combined into overall molecular function, we carried out extensive computer simulations of the recently crystallized decaheme cytochrome MtrF. We report redox potentials of individual hemes, reorganization energies and electronic coupling matrix elements for heme-to-heme electron transfer in MtrF explicitly solvated in water. The free energy profile for electron flow along various evident heme 'wire' pathways was computed using thermodynamic integration and classical molecular dynamics, and could be related to differences in the charged amino acids local to specific hemes. Reorganization free energies yield a range consistent with theoretical expectations for partially solvent exposed cofactors, and reveal an activation energy range surmountable for electron flow. Quantum mechanical calculations of electronic coupling matrix elements show a clear correlation between couplings and endergonic steps of through-protein electron transfer, suggesting that the protein evolved to harbor low-potential hemes for thermodynamic range without slowing down electron flow.

Because the individual hemes are not easily distinguished spectroscopically in such proteins, none of these insights are experimentally accessible. The theory and simulation campaign on this system is thus not only enabling a fundamental advance in understanding bacterial electron transfer protein function and key design elements, but it also provides a window into the broader biogeochemical context by the evident selection pressure underlying its purpose.

Storage of Hadean oceanic crust in the Kaapvaal subcratonic mantle

G.P. BREY^{1*}, Q. SHU^{1,2}, A. GERDES¹ AND H.E. HOEFER¹

¹Institut für Geowissenschaften, Goethe-Universität,
Altenhöferallee 1, D-60438 Frankfurt, Germany
(*brey@em.uni-frankfurt.de)

²China University of Geosciences (Beijing), Xueyuan Road
29, Haidian, Beijing, China. 100083;

Eclogites from the subcratonic lithosphere appear to be ancient and Re-Os isotope data from eclogite xenoliths from Newlands on the Kaapvaal craton suggest that some may date back to the Hadean [1]. If mantle eclogites are products of subduction of oceanic crust [2], their ages place strong constraints on the beginning of plate tectonics. The calculated bulk rock compositions of a subset of biminerally and of kyanite and corundum bearing eclogite xenoliths from the Bellsbank diamond mine (about 30 km north of Newlands) have similar flat middle to heavy REE patterns. Their range and that of their calculated major element compositions lies within the range of modern day mid ocean ridge basalts and gabbroic rocks. The kyanite- or corundum-bearing eclogites (3 samples) display positive Eu anomalies and show depletion in the more incompatible trace elements except for an enrichment in U and Th. In accord with earlier work we interpret them as former plagioclase rich cumulates which were possibly slightly modified by dehydration during subduction and during metamorphism. We interpret the biminerally eclogites with overall higher abundances of the more incompatible trace elements (2 samples; no Eu anomaly) as clinopyroxene-rich cumulates. Based on the chemical similarities we regard these eclogites as a cogenetic suite.

The Lu-Hf two-point isochrones from these samples with temperatures of last equilibration above 920 °C give kimberlite eruption age (= 120 Ma for Bellsbank), i.e. garnet and clinopyroxene were in continuous isotopic exchange in the mantle until the time of eruption. The reconstructed bulk rock Lu-Hf isotopic compositions of four of the five samples plot along a line in an isochron diagram which yields 4.12 ± 0.27 Ga (MSWD = 0.04) with $\epsilon_{\text{Hf}_i} \sim 0$. The reality of an Hadean age is supported by the extremely high $\epsilon_{\text{Hf}_i(120\text{Ma})}$ values up to 1004 and 1006 respectively for coexisting cpx and garnet. Further support comes from garnet model ages between 3.13-3.5 Ga. These are minimum possible ages. Values of $\delta^{18}\text{O}$ lower than the mantle (2.5‰ to 4.8‰ in garnets) are consistent with low temperature sea floor alteration as their cause. This supports the existence of oceans 4.1 Ga ago. The eclogites and their MORB-like compositions imply modern day potential mantle temperatures, at least locally, and subduction underneath microcontinents in the Hadean.

[1] Menzies *et al.*, Lithos (2003); [2] Jacob, Lithos (2004)

Zeolites as ion exchanger in harsh ultra-alkaline conditions

E. BREYNAERT*, L. VAN TENDELOO, E. GOBECHIYA, W. WANGERMEZ, B. DE BLOCHOUSE, J.A. MARTENS, C.E.A. KIRSCHHOCK AND A. MAES

KULeuven - Center for Surface Chemistry and Catalysis.
Kasteelpark Arenberg 23. B-3001 Heverlee. Belgium.
(*correspondence: eric.breynaert@biw.kuleuven.be)

Cement based waste disposal is among the more important options to provide safe storage of non-recyclable often highly toxic waste.[1] Despite all engineering efforts, potentially contaminated ultra-alkaline concrete derived pore waters (pH 12 – 14) will always remain associated with cement based waste disposal. To avoid contamination of the environment due to slow leaching of the metals from these waste forms, engineered barriers are built around the waste disposal sites in order to provide containment. Such engineered barriers, needed to increase the safety level of the waste disposal sites, always incorporate a sorption sink capable of reducing the concentration levels of the toxic metals below specified safety limits.

Zeolites typically crystallize in alkaline, Na/Si/Al rich aqueous conditions and exhibit cation exchange properties.[2, 3] Therefore this family of crystalline porous materials has a significant potential as sorption sink in engineered barriers optimized to function in ultra-alkaline concrete derived pore waters

Cs⁺ sorption was evaluated as function of Cs⁺ concentration (10⁻¹¹ up to 10⁻⁵ mole L⁻¹) and time (up to 180 days). The sorption results obtained in ultra-alkaline concrete pore water were compared with data obtained in electrolyte solutions at pH 8 containing identical Na⁺, K⁺ and Ca²⁺ concentrations.

The isotherms demonstrated an unexpected increased Cs⁺ sorption in pH 13 solutions as compared to pH 8 solutions with similar cation content. Sorption results in ultra-alkaline concrete pore water as function of time indicate chabasite and clinoptilolite as two zeolite frameworks stable in these conditions. This confirms results obtained in zeolite formation/transformation studies that indicated a strong stabilizing effect of the alkali cations on specific zeolite frameworks. Binary sorption isotherms confirmed that the selectivity series and calculated selectivity coefficients expected for chabasite and clinoptilolite at trace concentrations (<10⁻⁴ M Cs⁺) are also valid in ultra-alkaline aqueous conditions.

[1] Cote & Bridle (1987) *WM&R* **5**, 55–66. [2] Grutzeck *et al.* (2004) *Cem. Concr. Res.* **34**, 949–55. [3] Barrer (1985) *Surf. Sci. Catal.* **24**, 1–26.

Determination of sources and flowpaths of nitrate in a karstic watershed

C. BRIAND^{1*}, M. SEBILO², V. PLAGNES¹, P. LOUVAT³ AND T. CHESNOT⁴

¹ UPMC Univ Paris 06, UMR Sisyphe, 75252 Paris Cedex 05, France (*correspondence : cyrielle.briand@upmc.fr)

² UPMC Univ Paris 06, UMR Bioemco, 75252 Paris Cedex 05, France

³ Institut de Physique du Globe de Paris, Université Paris-Diderot, UMR CNRS 7154, 75238 Paris cedex, France

⁴ Eurofins Expertises Environnementales, Site St Jacques II, 54521 Maxeville, France

The Marseillon spring is a strategic resource for the drinking water supply of the Aquitaine region (SW of France). Fed by deep Cretaceous limestone aquifer and local infiltration (favored by karstic limestone outcrop), it is threatened by increasing nitrate concentrations (from 10 to 25 mg/L in 20 years).

Measurement of $\delta^{15}\text{N-NO}_3^-$ and $\delta^{18}\text{O-NO}_3^-$ coupled with $\delta^{11}\text{B}$ allows a good discrimination between the multiple potential sources of nitrate in the area [1]. Additional microbiological markers (bacteriophages, bacteroidales) can offer better precision over the origin of fecal contamination [2].

This work presents a dynamic approach based on these natural isotopic and microbiological tracers measured over samples of Marseillon's groundwater and local surface waters collected from October 2010 to January 2013. Their evolutions within each compartment allow a better understanding of nitrate origin and flow paths in the studied watershed.

[1] Bronders *et al.* (2012), *Environ. Forensics* **13**, 32-38. [2] Briand *et al.* *Environ. Chem* (in press).

Modifications of Cu isotopic ratios in coastal sediments in relation to the increased use of copper based antifouling paints

N. BRIANT^{1*}, R. FREYDIER¹, F. ELBAZ-POULICHET¹,
C. BANCON-MONTIGNY¹ AND S. DELPOUX¹

¹Laboratoire HydroSciences UMR 5569, CNRS, Universités
Montpellier I & II, IRD, Place Eugène Bataillon, CC
MSE, 34095 Montpellier cedex 5, France
(*correspondence : nicolas.briant@univ-montp2.fr)

Cu is released in water by weathering processes and human activities. It is widely applied on vines and used as a biocide in antifouling paints. This study aimed to assess the potential of Cu stable isotopes to identify Cu sources in coastal sediments.

For this study, sediment cores were collected from three sites in the marina of Port Camargue on the French Mediterranean coast. This marina, the largest in Europe, was built around forty years ago and has never been dredged. Sediment samples (<63 μ m fraction), antifouling paints were analyzed for copper concentration and Cu isotope ratios. Isotopic measurements were performed using a Neptune Multi Collector ICP-MS after a double separation on anionic resin.

Copper concentrations in antifouling paints (7 different brands) ranged from 6 % w/w to 36 % w/w. Their $\delta^{65}\text{Cu}$ values varies from 0.55 to 0.97‰. Close to the boat maintenance area, Cu concentrations in sediment cores exhibited an increase from the bottom to surface with a maximum value of 1961 $\mu\text{g}\cdot\text{g}^{-1}$ at 7 centimeters depth. In parallel $\delta^{65}\text{Cu}$ values increased from 0.08‰ at the bottom of the core up to 0.52‰ around 5 cm depth (Figure 1). This evolution toward $\delta^{65}\text{Cu}$ values similar to those observed in antifouling paints in surface sediments, indicates that copper isotopes are good tracers of copper contamination by antifouling paints in a coastal marina.

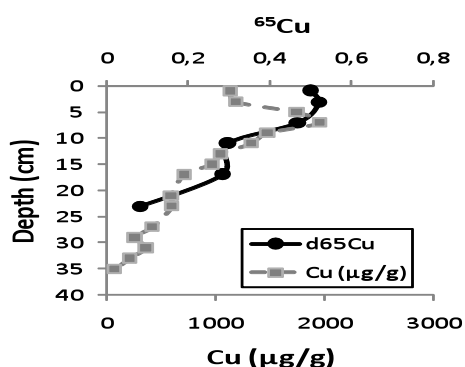


Figure 1: Depth profile of $\delta^{65}\text{Cu}$ and copper concentration in sediments from Port Camargue Marina.

Understanding the marine biogeochemical cycle of Pb in the equatorial Atlantic

L.J. BRIDGESTOCK^{1*}, M. PAUL¹, T. VAN DE FLIERDT¹, M.
REHKÄMPER^{1,2}, E. ACHTERBERG³ AND M. LOHAN⁴

¹Imperial College London, London, SW7 2AZ, UK

(*correspondence:luke.bridgestock07@imperial.ac.uk)

²Natural History Museum, London, SW7 5BD, UK

³University of Southampton, Southampton, SO14 3ZH, UK

⁴University of Plymouth, Plymouth, PL4 8AA, UK

The biogeochemical cycle of Pb has been significantly perturbed by anthropogenic activity over the past 100 years, with transient changes in the relative importance of different anthropogenic Pb sources [1]. Lead isotopes are an effective tracer of anthropogenic Pb emissions, and the short residence time of Pb in ocean surface waters (~2 years, [2]) make them a useful recorder of recent Pb sources in a particular region. Furthermore, the comparatively conservative behaviour of Pb isotopes in intermediate and deep waters enables tracing advection of pollutant Pb [3].

A newly developed method, using TIMS in conjunction with a Pb double spike, has been applied to the measurement of the Pb isotopic compositions ($^{206}\text{Pb}/^{204}\text{Pb}$, $^{207}\text{Pb}/^{206}\text{Pb}$ and $^{208}\text{Pb}/^{207}\text{Pb}$) and concentration of seawater depth profiles and surface seawater samples collected in the eastern equatorial Atlantic Ocean during the GA06 UK GEOTRACES cruise in 2011. The data are used to assess the current importance of anthropogenic versus natural Pb inputs to this region, and the advection of anthropogenic Pb into deep waters.

The Pb concentrations of surface waters (17-26 pmol/kg) are comparable to those determined in the early 1990's in the region [4], suggesting a stable Pb flux over the past 20 years. The Pb isotope composition of surface waters between 8° N and 3° S (1.163-1.169, $^{207}\text{Pb}/^{206}\text{Pb}$) are similar to those determined for Saharan dust [5]. In contrast, surface waters in the North Equatorial Current have higher $^{207}\text{Pb}/^{206}\text{Pb}$ ratios (1.173-1.174), a signature which can be attributed to advection of Pb from the west, fingerprinting eastern US emissions. A deep water maximum in Pb concentration (3000 m; 46 pmol/kg) located close to the mid Atlantic ridge is interpreted to represent hydrothermal input of Pb.

[1] Wu & Boyle (1997), *GCA*, **61**, 3279-3283. [2] Bacon *et al.* (1976), *EPSL*, **32**, 277-296. [3] Alleman *et al.* (1999), *Geophys. Res. Letters*, **26**, 1477-1480. [4] Helmers & Rutgers (1993), *Journal of Geophys. Res.*, **98**, 20,261-20,274. [5] Scheuvsens *et al.* (2013), *Earth-Science Rev.*, **116**, 170-194.

Heavy metals characteristics in the gold and iron mine soils in the upstream area of Miyun Reservoir

MERYEM BRIKI¹, XINGXING HUANG¹, PANPAN JU¹, CAI LI¹ AND HONGBING JI^{*12}

¹Department of Environmental Engineering, Civil and environmental Engineering School, University of Science and Technology Beijing, Beijing 100083, China (brimer@hotmail.fr)

²The State Key Laboratory of Environmental Geochemistry, Institute of Geochemistry, Chinese Academy of Sciences, Guiyang 550002, China (*correspondence: hongbing.ji@yahoo.com)

Metal contamination of soil from anthropogenic sources is an important global issue. Some recent studies have worked on the importance of metal contamination of soils in ecologically sensitive areas that are the source sites of drinking water. In this study, a preliminary survey of soil contamination had been carried out around the Miyun Reservoir, Beijing, China. Some results as follows: (1) the metal concentrations in the gold and iron mines soil samples exceed the background soil levels in Beijing, and the content of heavy metal in gold mine soils are higher than those of iron mine soils with Ti and Mn as an exception; the pollution of heavy metals in mine soils have reached a serious degree, and Hg is the most serious pollution element of all selected elements in gold mine soils. (2) Selected elements have been found the residual fractions is the most predominant in all gold and iron mine soil samples; the distribution of Ni in gold mine was similar to that of iron mine; Mn had the greatest acid-soluble per portion (27.95% and 23.24%, respectively) reflecting that Mn was more mobile and potentially more bioavailable in the study areas; the acid-soluble and reducible portion of Cd (20.06%, 16.45%) in gold mine was significantly higher than that of iron mine (3.70%, 1.36%), and as well as Pb. (3) the selected heavy metals in both soil samples have different degrees of enrichment; the pollution degrees of gold mine soil samples was aligned to Pb>Hg>Cd>Cr>Cu>Zn>Co>As, while Pb>Cd>Cr>Co>Cu>Zn>Hg>As for iron mine soil samples.

Zn immobilization by *Lumbricus terrestris* calcium carbonate biomineralized granules

LOREDANA BRINZA^{1*}, J. FRED W. MOSSELMANS¹, PAUL F. SCHOFIELD², ERICA DONNER⁴, ENZO LOMBI⁴ AND MARK E. HODSON³

¹ Diamond Light Source, UK, (*correspondence: Loredana.Brinza@diamond.ac.uk; Fred.Mosselmans@diamond.ac.uk)

²Natural History Museum, London, UK (p.schofield@nhm.ac.uk)

³University of York, York, UK, (mark.hodson@york.ac.uk)

⁴University of South Australia, Australia (Erica.Donner@unisa.edu.au; Enzo.Lombi@unisa.edu.au)

Many species of earthworm secrete granules of calcium carbonate. In this study we investigated the incorporation of Zn into granules produced by the earthworm *L. terrestris*, cultured in an agricultural soil (Hamble) amended with Zn and a soil from a former Zn mine (Cwmystwyth, UK).

Bulk and μ -X-ray diffraction were used to determine granule mineralogy. Both vaterite and calcite were detected.

Synchrotron μ -X-ray fluorescence (XRF) was used to determine the distribution of Zn within granules. Zn occurred in concentric zoning (Fig. 1) and as discrete hotspots. X-ray absorption spectroscopy was used to determine the Zn bonding environment within the calcium carbonate granules. The Zn exhibited several different speciations; replacing Ca in the calcite structure and as the minerals hydrozincite, $Zn_5(CO_3)_2(OH)_6$ and aurichalcite, $(Zn,Cu)_5(CO_3)_2(OH)_6$.

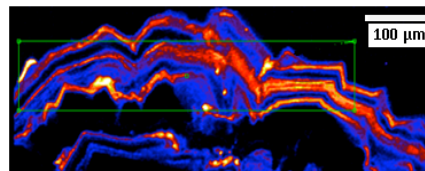


Figure 1: XRF map showing Zn distribution as concentric rims on the edge of a slice of a granule originating from Hamble soil amended with 750 ppm Zn. XRF average Zn concentration for this granule is 64 ppm and the bulk concentration from digested granules from this treatment is 164 ppm.

Zn is immobilized within biomineralized granules. Although, the degree of Zn uptake and granule production rates indicate that these biogeochemical processes have a less significant impact on Zn mobility compared to that for Sr [1] and Pb [2] at contaminated sites.

[1] Brinza et. al. (2013) *Geochim. Cosmochim Acta* DOI, 10.1016/j.gca.2013.03.011; [2] Fraser et. al. (2011) *Geochim Cosmochim Acta* **75**, 2544-2556.

High sensitivity of ammonia and nitrite oxidation rates to nanomolar oxygen concentrations

L.A. BRISTOW^{1,*}, T. DALSGAARD², L. TIANO³,
D.B. MILLS¹, O. ULLOA⁴, D.E. CANFIELD¹,
N.P. REVSBECH³ AND B. THAMDRUP¹

¹Nordic Center for Earth Evolution, Institute of Biology,
University of Southern Denmark, Odense, Denmark

²Department of Bioscience – Arctic Research Centre, Aarhus
University, Silkeborg, Denmark

³Department of Bioscience – Microbiology, Aarhus
University, Aarhus, Denmark

⁴Departamento de Oceanografía, Universidad de Concepcion,
Casilla 160-C, Concepcion, Chile

(*correspondence: lbristow@biology.sdu.dk)

To date it remains unclear as to whether ammonia and nitrite oxidation can co-occur alongside and hence supply substrates for fixed N loss via either denitrification or anammox under nanomolar oxygen (O₂) concentrations. Both culture and field based studies have been restricted to O₂ concentrations greater than 0.25 μM. With O₂ concentrations regularly observed to be less than 10 nM in the core of oxygen minimum zones (OMZ) it is essential to assess the oxygen sensitivity of these processes at these levels.

Sampling was undertaken across the oxycline in the seasonal OMZ off Concepcion, Chile to determine rates of ammonia / nitrite oxidation from short-term incubations at manipulated O₂ levels between 5 nM and 20 μM. Rates of both ammonia and nitrite oxidation were detectable to the limit of our O₂ measurements and demonstrated a strong dependence on nanomolar concentrations of O₂. Michaelis-Menten kinetics fitted to this data produced half saturation constants (K_m) of 330 and 780 nM O₂ for ammonia and nitrite oxidation respectively. These values were consistent across multiple depths sampled in this study and are shown to be applicable across OMZ systems. These K_m values must be included in future modelling studies, in order to more realistically assess the impacts of ocean deoxygenation on nitrogen cycling.

Titration curves, column experiments, and reactive transport models

S. M. BRITZ^{1,*}, U. NOSECK¹, V. BRENDLER²,
AND M. STOCKMANN²

¹GRS Braunschweig, D-38122 Braunschweig, Germany
Germany (*correspondence: susan.britz@grs.de)

²Helmholtz-Zentrum Dresden-Rossendorf, D-01314 Dresden

Surface reactions related to e.g. transport and retardation processes in groundwater systems are correlated with geochemical conditions that vary in time and space. For long-term safety analysis of radioactive waste repositories it is of great interest to better understand and to realistically assess these geochemically driven surface and transport reactions, since they might strongly impact radiation exposure.

To get an advanced insight into these processes column experiments are conducted and subsequently modeled with the geochemical speciation code PhreeqC, Version 2.18 (coupled with UCODE_2005). In order to set-up realistic reactive transport models so-called surface complexation parameters (SCP) such as surface site density, specific surface area, and protolysis constants need to be derived from titration experiments of relevant mineral phases.

Two different titration techniques are conducted for muscovite and orthoclase: continuous and batch titration. Derived results are compared offering an insight into pH-influencing reactions that contribute to surface reactions but also to cation exchange and mineral dissolution.

In column experiments different solids are applied: natural sediments from the Gorleben site, Germany and pure mineral phases (orthoclase, muscovite, quartz). Parameters such as pH, ligands, ionic strength, and cation concentrations are varied in each experiment to reflect realistic environmental conditions. Moreover, transient pH conditions are applied in selected columns.

Both types of experiments (titration, column experiments) including each geochemical variation provide data to model reactive transport processes of hazardous pollutants more realistically in groundwater-flow driven environments with PhreeqC. Calculations will be conducted and first results offered for discussion.

This project is funded by the German Federal Ministry of Economics and Technology (BMWi) under contract no. 02 E 11072A and 02 E 11072B.

Recycled volatiles beneath the Western Antarctic Rift

M.W. BROADLEY^{1*}, C.J. BALLENTINE¹, L. DALLAI²
AND R. BURGESS¹

¹SEAES, University of Manchester, M13 9PL, UK
(michael.broadley@postgrad.manchester.ac.uk)

²CNR, Institute of Earth Sciences and Resources, Pisa, Italy
(dallai@igg.cnr.it)

The Western Antarctic Rift System (WARS) represents an area of long lived extension between East and West Antarctica. The origin of this rift is poorly understood, with both an actively up-welling plume and passive rising of the asthenosphere being championed as the cause [1]. To explore the origin and evolution of the rift, a suite of 11 mantle xenoliths from Northern Victoria Land have been analysed for their halogen and noble gas isotopic signatures.

Noble gas and halogens are excellent tracers of volatiles within the mantle; providing a key source of information on the underlying mantle which is driving the rift. The fluid inclusions present within mantle xenoliths provide the best medium through which magmatic volatiles can be transported to the surface and still be able to retain a pristine magmatic signature. Noble gas and halogens contained within these fluid inclusions are released by in vacuo crushing and analysed through mass spectrometry.

Noble gas signatures extracted from the fluid inclusions show MORB like ³He/⁴He ratio of 7.4R_A whilst the ²⁰Ne/²²Ne ratios are indicative of a deeper primordial mantle source. Halogen analysis has shown the samples to be extremely enriched in iodine with I/Cl ratios ranging from a MORB like 0.09148 x 10⁻³ to highly enriched value of 54.6 x 10⁻³. These values are indicative of mixing between mantle and subduction fluid endmembers.

Halogen ratios indicate that seawater derived volatiles have been incorporated into the mantle during subduction. Volatiles were released from the slab at depth possibly by the breakdown of antigorite. This fractionated the halogens further causing an increase in the I/Cl ratio seen within the xenoliths [2]. Noble gas ratios indicate that the driving force of the rift is the convecting upper mantle, with an addition of a deeper mantle volatile source. Geochemical data, along with seismic evidence [3], suggests that slab detachment during the Cretaceous created localised convection currents which brought some primordial mantle up from depth. The rising mantle would have exerted a force on the bottom of the Antarctic Plate causing it to break apart.

[1] Rocchi *et al* (2002) *J.Geophys. Res* **107** (B9) 2195.

[2] John *et al* (2011) *EPSL* **308**, 65-76 [3] Finn *et al* (2005). *Geochem. Geophys. Geosyst.* **6** issue 1.

Phototrophs and ore formation

J. J. BROCKS^{*1}, B. J. BRUISTEN¹, A. PAGÈS²
AND K. GRICE²

¹Research School of Earth Sciences, The Australian National University, Canberra, ACT 0200, Australia.

(*correspondence: Jochen.Brocks@anu.edu.au)

²WA Organic & Isotope Geochemistry Centre, Curtin University, WA 6845, Australia.

Sediments of the 1.64 Ga Barney Creek Formation (BCF) in northern Australia host one of the largest stratiform Pb-Zn deposits in the world. An early fraction of the zinc sulfide may have formed by discharge of zinc-rich fluids from a proximal fault into sulfidic bottom waters, causing syndimentary precipitation of ZnS onto the sea floor (SEDEX model).

As the BCF contains the oldest known, thermally well-preserved molecular fossils (biomarkers) in the world, it is the ideal location to study the role of microorganisms and biogenic organic matter in this process. Solvent extracts of the sedimentary rocks yielded aromatic carotenoids produced by phototrophic sulfur bacteria, including extremely high concentrations of okenane from purple sulfur bacteria (Chromatiaceae) and chlorobactane produced by green-pigmented green sulfur bacteria (Chlorobiaceae) [1]. As okenone was exclusively known from planktonic Chromatiaceae, we envisaged a planktonic phototrophic community inhabiting a euxinic deep water system [2], consistent with a SEDEX component to ore formation. However, precursors of almost all fossil aromatic carotenoids have now also been discovered in microbial mats [3]. We present biomarkers from mat facies in the BCF and discuss whether the finely laminated sediments represent phototrophic microbial mats that thrived under a shallow, fully oxygenated water column or benthic mats that formed in a deep sulfidic basin.

[1] Brocks *et al.* (2005) *Nature* **437**, 866-870. [2] Brocks *et al.* (2008) *GCA* **72**, 1396-1414. [3] Pagès *et al.* (2012) *17th AOGC*, Sydney, 60-61. Pagès *et al.* (2013) *GCA* (submitted).

Probing the water content of the Earth's mantle: Hydrogen mobility under extreme conditions

J. BROOKE*, G. BROMILEY, K. WHALER
AND C. GRAHAM

Department of Geosciences, Grant Institute, University of
Edinburgh, UK (jennifer.brooke@ed.ac.uk) (*presenting
author)

Research over the past few decades has shown that nearly all of the nominally anhydrous minerals (NAMs) of Earth's mantle can incorporate substantial amounts of water as structurally bound hydrogen. This has important implications for understanding the geochemical and geophysical properties of Earth's interior as the presence of water influences numerous mantle properties and processes^[1,2]. Water, as hydrogen, has been invoked to reconcile differences between conductivity models and geophysical observations of the mantle, but the amount present is yet to be satisfactorily quantified – with experimental estimates differing by several orders of magnitude^[3,4]. Hydrogen-deuterium exchange experiments performed under mantle conditions are presented, that provide data on hydrogen mobility in olivine directly comparable with electrical conductivity data. These results will be used in conjunction with existing estimates of conductivity and magnetotelluric survey data in order to constrain the water content and conductivity of olivine, and thus the upper mantle.

[1] Du Frane & Tyburczy (2012), *G³*, 13, Q03004. [2] Smyth, Frost, Nestola, Holl & Bromiley (2006) *Geophysical Research Letters*, **33**, L1501. [3] Wang, Mookherjee, Xu & Careto (2006) *Nature*, **443**, 977-980. [4] Yoshino, Matsuzaki, Yamashita & Katsura (2006) *Nature*, **443**, 973-976.

Evaluating proxies for oxygen fugacity at the Mariana arc

MARYJO BROUNCE^{1,2*}, KATHERINE KELLEY¹
AND ELIZABETH COTTRELL²

¹University of Rhode Island, Graduate School of
Oceanography, Narragansett RI 02882, USA

²National Museum of Natural History, Smithsonian Institution,
Washington DC 20562, USA

Arc basalts are more oxidized than mid-ocean ridge basalts, but existing proxies for studying fO_2 present contrasting explanations for this offset. The $Fe^{3+}/\Sigma Fe$ ratio proxy indicates that the mantle wedge has higher fO_2 than mid-ocean ridge source mantle. In contrast, trace element proxies (V/Sc, Zn/Fe*, and [Cu]) suggest that the fO_2 of the upper mantle is uniform. Additionally, the $D_V^{ol/melt}$ proxy suggests that arc magmas are oxidized at the time of high-Mg olivine fractionation. We present major and trace element concentrations and $Fe^{3+}/\Sigma Fe$ ratios (μ -XANES) for melt inclusions and their olivine hosts from five Mariana arc volcanoes and Mariana Trough submarine glasses to compare the [Cu], Zn/Fe*, $D_V^{ol/melt}$, V/Sc, and $Fe^{3+}/\Sigma Fe$ ratio proxies for calculating fO_2 .

The Zn/Fe* proxy returns $Fe^{3+}/\Sigma Fe$ ratios of primary mantle melts and is sensitive to variations in Zn/Fe^*_{source} . After accounting for source composition, the Zn/Fe* proxy yields agreement with calculated primary $Fe^{3+}/\Sigma Fe$ ratios for arc and back-arc glasses. Similarly, the [Cu] of arc melt inclusions are consistent with non-modal equilibrium melting of a source between QFM+1 and QFM+2, and fractional melting between QFM and QFM +0.5 for back-arc magmas. The V/Sc proxy returns more reduced primary fO_2 s than the Fe-based proxy for all samples, however fO_2 s for arc melt inclusions calculated using $D_V^{ol/melt}$ (QFM+2.7 \pm 0.3) are systematically more oxidized than their measured $Fe^{3+}/\Sigma Fe$ ratios indicate (QFM+1.3 \pm 0.3), suggesting that there may be a significant water, pressure, or source composition effect on the partitioning behaviour of V and Sc. These results show that the Fe-, Zn/Fe*, and [Cu]-based proxies for fO_2 are in broad agreement and are consistent with an arc mantle source that is more oxidized than mid-ocean ridge source mantle.

Petrogenesis of peraluminous granites from deep crustal sources

CAITLIN BROWN^{1*}, MICHAEL BROWN¹
AND PHILIP PICCOLI¹

¹University of Maryland, College Park, USA
(*correspondence: cbrown88@umd.edu)

The study of exhumed high-grade continental crust formed at convergent plate margins reveals important details about the petrogenesis of granites and contributes to a better understanding of processes responsible for the differentiation of the continents. The Fosdick migmatite–granite complex, West Antarctica, records evidence of two melting events, during the Devonian–Carboniferous and in the Cretaceous. A Devonian–Carboniferous calc-alkaline granodiorite suite emplaced into a Lower Paleozoic metasedimentary sequence (outside the complex) and their granulite facies equivalents (inside the complex) represent the sources and make this region ideal for the study of processes and mineral behavior during polycyclic anatexis at granulite facies conditions using a combined petrologic and geochemical approach. We report 20 new LA–ICP–MS U–Pb zircon ages extending the age ranges as follows: protolith granodiorite suite 377–339 Ma; Devonian–Carboniferous anatectic granites 369–350 Ma; and, Cretaceous anatectic granites 119–96 Ma. The discovery of Devonian anatectic granites suggests that melting occurred earlier than previously thought. New geochemical data for 48 samples extends a limited dataset from earlier work. The major and trace element geochemistry of paragneisses and orthogneisses is consistent with the hypothesis that they are the high-grade equivalents of the metasedimentary sequence and granodiorite suite respectively. The metasedimentary sequence has K₂O of 2.15–4.32 wt%, Sr of 95–207 ppm and Rb of 96–216 ppm, whereas the calc-alkaline granodiorite suite has K₂O of 2.23–5.01 wt%, Sr of 90–418 ppm and Rb of 88–381 ppm. Devonian–Carboniferous granites are either high Sr (225–363 ppm) or low Sr (95–108 ppm) types with variable K₂O (2.73–6.85 wt%) and Rb (131–284 ppm). Cretaceous granites are either high Sr (207–298 ppm) or low Sr (90–167 ppm) types with variable K₂O (3.21–8.89 wt%) and Rb (80–284 ppm). Limited isotope data indicates that Devonian–Carboniferous granites were derived primarily from the granodiorite suite, whereas Cretaceous granites were derived from mixed sources (the metasedimentary rocks, the granodiorite suite, or their high-grade equivalents). Additional Sr and Nd isotope and REE data currently being collected will better constrain the sources of the granites and allow an evaluation of the role of accessory minerals such as apatite and monazite during crustal melting events.

Beneficial uses of engineered nanoparticles and the behavior of natural and engineered nanoparticles in the environment

GORDON E. BROWN, JR.^{1*}, CLEMENT LEVARD²,
CRISTINA CISMASU³, F. MARC MICHEL⁴, RUI MA⁵,
YUHENG WANG⁶, GEORGES CALAS⁶,
GUILLAUME MORIN⁶ AND GREGORY V. LOWRY⁵

¹Dept. of Geological & Environmental Sciences, Stanford University, Stanford CA 94305, USA
(*correspondence-gebjr@stanford.edu)

²CEREGE, Europôle Méditerranéen de l'Arbois, BP 80, 13545 Aix en Provence, Cedex 04, France

³Earth Sciences Division, Lawrence Berkeley National Lab, Berkeley, CA 94720, USA

⁴Dept. of Geosciences, Virginia Tech, Blacksburg, VA 24061, USA

⁵Dept. of Civil & Environmental Engineering, Carnegie Mellon University, Pittsburgh, PA 15213, USA

⁶Institut de Minéralogie et de Physique des Milieux Condensés, 4 Place Jussieu, 75252 Paris, Cedex 05, France

Engineered nanoparticles (ENPs), including Ag(0), Au(0), C-nanotubes, ZnO, TiO₂, Fe₃O₄, have many beneficial uses ranging from catalysts used for efficient production of chemicals (e.g., Au(0)) and photocatalytic degradation of organic pollutants (e.g., TiO₂) to water treatment to remove As (e.g., Fe₃O₄) and use as antibacterial agents (e.g., Ag(0) and ZnO). Here we will review some of these uses, as well as some of the transformations that ENPs undergo in different environments (e.g., sulfidation of Ag(0) and ZnO ENPs), which can significantly alter their properties (e.g., solubility) and result in lowered risk. We will also review some of the lessons learned about the behavior of ENPs from microscopic studies of engineered and natural nanoparticles, in particular the sorptive properties of Fe₃O₄ ENPs in removing As from drinking water. We will also discuss some insights about the use of nanoparticles as environmental indicators gained from ab initio thermodynamics studies of the morphologies developed by NPs under different environmental conditions.

Geochemistry and mineral exploration

GRAHAM BROWN

Anglo American, Carlton House Terrace, London, SW1Y 5AN, (graham.brown@angloamerican.com)

Mineral exploration is a multi-disciplinary team effort, in which conceptual geological thinking and traditional geological field work play leading roles. Geochemistry, when properly integrated into the process, is a key component for exploration, from initial targeting through to resource definition.

Anglo American's base metal discovery track record over the past decade (including ten significant discoveries) illustrates this point, where so-called conventional geochemical techniques played an important role in many of those discoveries.

Stream sediment geochemistry in areas of well developed topography, and soil geochemistry in areas of residual soil profiles are very effective techniques and played a role in the discoveries of the Morro Sem Boné Ni-laterite deposit, Brazil, and the Boyongan Porphyry Cu deposit, Philippines. In areas of thicker and/or transported overburden, surface geochemistry is unreliable, and Anglo American has preferred the more direct approach of drilling through the cover and sampling the base of regolith or top of bedrock (as used in the discoveries of the Gergarub Zn-Pb VMS deposit, Namibia, and the Sakatti Ni-Cu-PGE deposit, Finland). In addition to surface media geochemistry, lithochemical methods have been used in regional reconnaissance, and more locally for detecting distal effects of mineralisation, particularly around blind targets.

Fast and relatively cheap multi-element analysis by ICP-MS and computer software to aid interpretation have been the most significant technological advances over the last twenty years. More recently, portable XRF technology has enabled real-time decision-making in the field.

Anglo American actively supports geochemistry-related R&D through engagement with several key research centres globally (e.g., CODES and MDRU), and funding of PhD students. Strategic alignment of research objectives with the long term needs of industry is a key challenge, as is the gap in undergraduate teaching in applied exploration geochemistry at universities.

The fate of Archean primary crust and the transition to subduction

MICHAEL BROWN^{1*}, TIM E. JOHNSON²
AND JILL A. VANTONGEREN³

¹University of Maryland, College Park, USA
(*correspondence: mbrown@umd.edu)

²University of Mainz, Germany (tjohnson@uni-mainz.de)

³Yale University, USA (jill.vantongeren@yale.edu)

Petrological data and thermal models indicate Archean mantle potential temperatures (T_p) were up to 240°C hotter than at present, but with a similar variation (~100°C). Higher T_p generated thick MgO-rich ultramafic primary crust (PC) and highly residual lithospheric mantle (LM). Subduction and plate tectonics were unlikely. The preserved volume of PC is low suggesting that most is missing, which we address by modelling the equilibrium mineral assemblages for a range of metamorphosed (hydrated) PC compositions and complementary residues for a Moho T of 1000°C. We use calculated compositions of primary melts and complementary residues of high-MgO non-arc basalts as proxies for the secular change in composition of PC and LM. The density of LM decreases slightly with increasing T_p , whereas that of PC increases dramatically. The base of PC with MgO >21–22 wt%, produced at T_p >1600°C, was unstable at crustal thicknesses >45 km (>1.5 GPa), even when fully hydrated. Archean low-MgO eclogites and TTGs were derived from basaltic compositions and require that the PC was fractionated. Although the thermal structure of the mantle in the Hadean and Eoarchean is poorly constrained, heating from radioactive decay exceeded surface heat loss in the interval before 3.0 Ga and Archean geodynamics was probably variable, controlled by the spatial range in T_p . This regime was likely dominated by delamination/convective downwelling of PC that may have partially melted to produce basalt or refertilized the underlying mantle causing additional melting and crustal thickening. The resulting magmatic additions form plateau-like crust. Archean continental crust is dominated by TTGs. Collision of plateaux and/or plateaux overriding PC lithosphere was responsible for inducing melting to generate this TTG crust. Post 3.0 Ga tectonics was dominated by the onset of subduction, plate tectonics and a transition to the supercontinent cycle, consistent with the dominance of secular cooling since 2.5 Ga, and the rare occurrence of paired metamorphism and scarcity of eclogite in orogenic belts from the Mesoproterozoic to Paleoproterozoic. The onset of subduction may have triggered an overturn of the LM, as evidenced by T_{RD} model ages for the LM.

Multiple isotopic tracers to monitor remediation of uranium solution mining

SHAUN T. BROWN¹, JOHN N. CHRISTENSEN¹,
DONALD J. DEPAOLO¹, ANIRBAN BASU¹,
PAUL W. REIMUS², ARDYTH M. SIMMONS²
AND JEFF HEIKOOP²

¹UC Berkeley and Lawrence Berkeley National Lab
(stbrown@berkeley.edu, jnchristensen@lbl.gov,
anirbanbasu@berkeley.edu, depaolo@eps.berkeley.edu)

²Los Alamos National Lab, (preimus@lanl.gov,
asimmons@lanl.gov, jheikoop@lanl.gov)

Roll front uranium deposits form by interaction of U-bearing groundwater with reduction-oxidation gradients in the host sediments. This redox gradient in many roll-front deposits can be visually identified by hematite staining on the oxic side and green-gray sediment color on the anoxic side. A dark boundary between these two zones is concentrated in U(IV) minerals and other reduced metals such as Se and Mo. Solution mining of roll-front deposits perturbs natural redox conditions by oxidizing U (and other metals) in the main ore body for economic recovery. This perturbation coupled with an extensive monitoring well network provides a unique opportunity to assess the natural recovery of reducing conditions after the cessation of mining as a remediation strategy.

We have conducted a characterization survey of groundwater, mining fluids and complimentary ore body sediment core from the Smith Ranch mine in eastern Wyoming, USA for ⁸⁷Sr/⁸⁶Sr, $\delta^{34}\text{S}$ sulfate, $\delta^{238/235}\text{U}$ and the ²³⁴U/²³⁸U activity ratio. Sampling locations include both active and inactive mining sites. Monitoring wells surrounding the ore body have 4-22 ppb U, 68-413 ppm SO₄, ²³⁴U/²³⁸U activity ratio 2.9-5.5, $\delta^{34}\text{S}$ -16.6-10.8‰, $\delta^{238/235}\text{U}$ is between 0-2‰ for most samples.

Acid leachates of sediment core from a previously mined unit have low ²³⁴U/²³⁸U activity (0.6-1.6) compared to groundwater outside the ore zone. $\delta^{34}\text{S}$ spans nearly 52‰ (-48 to +3.8‰) and most samples have $\delta^{238/235}\text{U}$ between -2 and 0‰. The depletion of ²³⁸U in dissolved U(VI) as indicated by negative $\delta^{238/235}\text{U}$ suggests U(VI) reduction in the groundwater. There are no observed correlations between ²³⁴U/²³⁸U activity and $\delta^{238/235}\text{U}$. However the U activity ratio does correlate with depth. The low (²³⁴U/²³⁸U) in the ore zone will be a sensitive tracer for quantifying the migration of ore zone U to uncontaminated groundwater.

Iron availability controls phytoplankton ecophysiology in the South Atlantic Subtropical Convergence Zone

THOMAS J. BROWNING¹, HEATHER A. BOUMAN¹,
GIDEON M. HENDERSON¹, C. MARK MOORE², CHRISTIAN
SCHLOSSER², GLEN A. TARRAN³
AND E. MALCOLM S. WOODWARD³

¹Department of Earth Sciences, University of Oxford, South Parks Road, Oxford, UK. (thomasb@earth.ox.ac.uk)

²National Oceanography Centre Southampton, University of Southampton, European Way, Southampton, UK.

³Plymouth Marine Laboratory, Prospect Place, The Hoe, Plymouth, UK.

Measurements of phytoplankton photophysiology using Fast Repetition Rate fluorometry (FRRf) from the UK-GEOTRACES 40°S Atlantic cruise (GA10; JC068) have characterized two dominant ecophysiological regimes which are interpreted on the basis of nutrient limitation. South of the South Subtropical Convergence (SSTC) in the Antarctic Circumpolar Current (ACC) of the Eastern Atlantic Basin, waters are characterized by elevated chlorophyll concentrations, dominance by larger phytoplankton cells, and low F_v/F_m values. The reason for the low F_v/F_m values was iron (Fe) limitation, which was confirmed via 24 hour on-board Fe addition incubation experiments. Fe supply to these waters, either through artificial bottle additions or natural downstream enrichment from Gough Island in the Central Atlantic, resulted in significantly increased F_v/F_m. Satellite images suggest a broader region of enhanced chlorophyll concentrations around the SSTC of the Western Atlantic relative to the Eastern Atlantic, which is hypothesised to be a result of higher iron supply from the South American continent. To the north of the SSTC at the southern boundary of the South Atlantic Gyre, phytoplankton are characterized by high values of F_v/F_m, which coupled with the low macronutrient concentrations and increased presence of picocyanobacteria, are interpreted as conditions of Fe replete, balanced macronutrient-limited growth.

Seismic anisotropy as a constraint on composition in the lower crust

*SARAH J. BROWNLEE¹, BRADLEY R. HACKER²,
ALAN CHAPMAN³, JASON SALEEBY⁴
AND GARETH SEWARD²

¹Wayne State University, Department of Geology

(*correspondence: sarah.brownlee@wayne.edu)

²University of California, Santa Barbara, Department of Earth Sciences

³University of Arizona, Department of Geosciences

⁴California Institute of Technology, Geological and Planetary Sciences

Our current interpretation of the composition of the middle and lower crust comes mainly from seismic observations, yet it remains a challenge to link seismic observations directly to composition. This is because isotropic seismic properties are similar across a range of compositions. Taking anisotropy into account allows for further refinement of our interpretation of composition provided that anisotropy is characterized for candidate rock types. This study uses electron backscatter diffraction (EBSD) measurements of crystallographic preferred orientation of minerals to calculate seismic anisotropy in samples of the Pelona-Orocopia-Rand (POR) schist from the Mojave region of southern California. The goals of this work are to characterize the seismic anisotropy of the POR schist and its relationship to observed lower crustal anisotropy in the region, and to refine predictions of lower crustal composition based on seismic anisotropy.

Velocity anisotropy in individual samples of the POR schist ranges from ~2–11% in V_p and ~3–15% in V_s , which is consistent with results of [1] for lower crustal anisotropy in southern California. When all schist samples are averaged together, the velocity anisotropy is significantly reduced to ~6% in V_p and ~8% in V_s . The symmetry of V_s anisotropy is roughly uniaxial with a unique slow axis perpendicular to foliation for all samples. Samples with significant modal quartz or amphibole have near orthorhombic V_p symmetry with slow velocities perpendicular to foliation. Maximum V_p is ~parallel to lineation, except in samples with significant quartz displaying prism- $\langle a \rangle$ slip; for these sample V_p -max is parallel to foliation, perpendicular to lineation. Modal quartz content is inversely correlated to isotropic V_p/V_s ratios, and mica and amphibole are positively correlated with anisotropy. Relative mica/amphibole contents can be distinguished using a combination of isotropic V_p , and V_s anisotropy. Quartz content can be estimated from V_p/V_s ratios.

[1] Porter *et al.* (2011), *Lithosphere*, **3**, 201–220

Pockets of Proterozoic hydrocarbons and implications for the Archaean

B.J. BRUISTEN^{1*}, A.J.M. JARRET¹, R. SCHINTEIE^{1,2},
J. COLANGELO-LILLIS¹, L. REUNING³, R. LITTKÉ³
AND J. BROCKS¹

¹RSES, Australian National University, Canberra, ACT 0200, Australia. (*correspondence:

Benjamin.Bruisten@anu.edu.au)

²Geological and Planetary Sciences, Caltech, Pasadena, CA 91125, USA. (Richard@caltech.edu)

³LEK & Institute of Geology and Palaeontology (EMR), RWTH Aachen University, 52056 Aachen, Germany.

Precambrian biomarkers convey invaluable information about the early evolution of life, ancient ecosystems, redox conditions, climate and depositional environment and prospective petroleum systems. They are however thermally unstable, easily obliterated by contamination and thus extremely difficult to find. This is particularly true if conditions favourable for biomarker preservation had to prevail for more than 2.5 billion years – the prerequisite for finding Archaean biomarkers. Many organic geochemists abandoned this hope after original discoveries of Archaean biomarkers proved to be of younger origin [1,2] but our study of ca. 550–825 Ma old sediments from the Centralian Superbasin now shows that biomarkers can be preserved in distinctive pockets in seemingly barren areas, even if sections are metamorphosed in parts. Most Centralian sections seem empty. Yet, eventually we identified intervals with preserved biomarkers in three drill cores. A detailed investigation of 825 Ma sediments in drill core Mt Charlotte-1 revealed maturity variations that are most likely due to hydrothermal influence and in turn control the hydrocarbon preservation. Sediments might appear metamorphosed after localized, subtle alteration by hydrothermal fluids but protected intervals can still contain biomarkers. The same might be true for Archaean sediments and we might still find those protected intervals with indigenous biomarkers that allow us to glimpse the early life on earth.

[1] Rasmussen *et al.* (2008) *Nature* **455**, 1101 – 1104. [2] Brocks (2011) *GCA* **75**, 3196–3213.

Evidence for melt accumulation in the subridge melting region: A mantle residua perspective

D. BRUNELLI^{1,2}, M. SEYLER³ AND E. PAGANELLI¹

¹Dipartimento di Scienze Chimiche e Geologiche, Università di Modena e Reggio Emilia, 41100 Modena, Italy

(daniele.brunelli@unimore.it; emanuele.paganelli@unimore.it)

²Istituto di Scienze Marine, ISMAR-CNR, Via Gobetti 101, 40129 Bologna, Italy

³UFR Sciences de la Terre, CNRS FRE 3298, Géosystèmes, Université Lille 1, Bâtiment SN5, Cité Scientifique, F-59655 Villeneuve d'Ascq CEDEX, France
(monique.seyler@univ-lille1.fr)

Melt extraction from the mantle has been shown to be driven by channelization favoured by melting of source heterogeneities possibly leading to melt accumulation both on- and off-axis¹. Here we present a REE study of clinopyroxene in residual abyssal peridotites showing that melt extraction rarely follows fractional melting trends at the typical dredge haul scale (<1 km). Instead local melting trends reveal REE pattern evolution usually driven by infiltration of relatively enriched melts frequently accompanied by melt accumulation. Estimated compositions of the infiltrating melts suggest they derive by mildly enriched heterogeneities and/or grt-field melting of a DMM-like source². Observed data can be modelled by open system melting in which instantaneous melts represent the mix of influxing and locally generated melts and where the melt exceeding the critical mass porosity escapes. The out coming scenario shows a possible intermittent behaviour where melting switches from near-fractional to near-batch. In open system melting this behaviour is imaged by fluctuations of the critical porosity/degree of melting value, where the critical mass porosity is a proxy of the accumulated melt fraction.

Lower thermal settings and spreading rates could favour the retention of the compositional trends associated to fluctuations in the melting regime. Accordingly, we found that the statistical distribution of REE trends accounts for a more effective melt accumulation and enriched melt infiltration along the South West Indian Ridge with respect to the Mid Atlantic Ridge.

[1]Katz & Weatherley, 2012. *EPSL* Vol. **335-336**, Pp. 226-237. [2] Seyler *Et Al.*, 2011. *G3* Vol. **12** (9), Doi:10.1029/2011gc003585.

Lifestyles of the slow and lonely – A story told by sulfate isotopes

B. BRUNNER*

Center for Geomicrobiology, Department of Bioscience, Aarhus University, Aarhus, Denmark
(*correspondance: benjamin.brunner@biology.au.dk)

Sulfur is a bio-essential component of any living organism and is at the same time heavily used by microbes for energy yielding (dissimilatory) processes. Dissimilatory sulfate reduction (DSR) coupled to the oxidation of organic matter plays a pivotal role in the re-mineralization of organic matter in marine sediments, which is owed mostly to the high concentration of sulfate in the overlying seawater relative to other energetically more favorable electron acceptors such as oxygen or nitrate. When sulfate is depleted methane becomes the end product of organic matter degradation. At the interface between downward diffusing sulfate and upward diffusing methane (sulfate-methane transition) sulfate is consumed by sulfate reduction coupled to the anaerobic oxidation of methane (SR-AOM). In the classic view, DSR is thus confined to the main sulfate zone, a redox zone where the more favorable electron acceptors are absent.

Thanks to new findings, such as i) the discovery of sulfate generation in methanic sediments well below the main sulfate zone, the so-called “cryptic sulfur cycle” (Holmkvist *et al.* 2011 [1]), ii) the discovery that SR-AOM utilizes biochemical pathways different from DSR (Milucka *et al.* 2012 [2]) and iii) the discovery of sulfur oxidation by cable bacteria (Pfeffer *et al.* 2012 [3]) our view on sedimentary sulfur cycling has recently been dramatically changed and broadened.

Stable sulfur and oxygen isotope tracing of these newly discovered processes in the environment and in the rock record could provide us with compelling insights into these so far unrecognized biochemical sulfur transformations. However, there is a complication/caveat: we do not yet know what isotope signature we should look for.

I hypothesize that the sulfur and oxygen isotope effects of oxidative and reductive sulfur cycling mediated by microbes in the deep biosphere – organisms that live a slow and lonely life – may provide clues to what isotope signatures to expect.

[1] Holmkvist *et al.* (2011) *Geochim. Cosmochim. Acta* **75**, 3581-3599. [2] Milucka *et al.* (2012) *Nature* **491**, 541–546. [3] Pfeffer *et al.* (2012) *Nature* **491**, 218–221.

Chances and challenges in applying sulfur-oxygen isotope relationships of sulfate to studying sulfur cycling in engineered environments

B. BRUNNER*

Center for Geomicrobiology, Department of Bioscience,
Aarhus University, Aarhus, Denmark
(*correspondance: benjamin.brunner@biology.au.dk)

In recent years, our understanding of the mechanics of sulfur and oxygen isotope fractionation by sulfate reducing microorganisms has drastically improved. Based on multi-step sulfate reduction models, we are not only able to answer the question of why there is a large range of sulfur and oxygen isotope fractionations related to this process, but can also predict sulfur-oxygen isotope fractionation relationships (Brunner *et al.* 2012 [1]).

While this progress is exciting, it does not automatically provide new insight into sulfur cycling in perturbed ecosystems, such as polluted soils and aquifers, sites where sulfate reduction can be anthropogenically stimulated as a means to remove or sequester organic and inorganic contaminants.

Such systems are often highly complex because they are affected by different modes of microbial and abiotic sulfur cycling (i.e., reductive and oxidative processes), non-steady state conditions, and by mixing of waters from different sources. Additional challenges arise from the fact that monitoring of such systems is typically restricted to a few sampling points and cannot be carried out continuously.

Despite these complications, by comparing the combined sulfur and oxygen isotope signature of sulfate to the predicted sulfur-oxygen isotope relationship for sulfate reduction, it should be possible to tease out crucial information about sulfur cycling in engineered ecosystems, such as the extent to which sulfate is reduced, and the extent to which reduced sulfur is re-oxidized to sulfate.

Approaches where natural abundance sulfur and oxygen isotope signatures are combined with the outcome of stable isotope tracer experiments and evaluated by comparison to numerical models yield promising results. However, such modeling efforts can only yield meaningful conclusions when appropriate model assumptions are chosen. The evaluation and definition of these assumptions may prove to be the biggest challenge in deciphering sulfur cycling in engineered environments.

[1] Brunner *et al.* (2012) Isotopes in Environmental and Health Studies **48**, 33–54.

The stability of uraninite in anaerobic conditions: Revisiting Cigar Lake and Oklo Natural Analogues

JORDI BRUNO¹ AND KASTRIOT SPAHIU²

¹Amphos 21, Barcelona, (jordi.bruno@amphos21.com)

²SKB, Stockholm, (kastriot.spahiu@skb.se)

Recent experimental work indicates that the UO₂ matrix of the spent nuclear fuel is stable under the reducing conditions imposed by hydrogen evolution as the result of the anaerobic corrosion of the steel components.

There are a number of hypothesis concerning the mechanisms and processes that activate the hydrogen molecule on the UO₂ surface. They basically imply the catalytic effect of some of the metallic particles in the fuel, as well as the potential activation by alpha and gamma radiation.

One of the key remaining issues is to which extent the proposed mechanisms operate in the long-term of a spent fuel repository.

In this context, it is interesting to discuss to which extent the extensive information generated in previous natural analogue projects can be used to verify or falsify some of the mechanistic hypotheses. In particular, what concerns to the long-term validity of the proposed mechanisms.

Among the various natural analogue studies of uranium deposits, the Cigar Lake ore deposit in Canada and the Oklo fossible reactors in Gabon, provide some interesting observations and data under anaerobic conditions that may illustrate some of the key stabilisation processes under hydrogen conditions.

The objective of this presentation will be to discuss the findings of the Cigar Lake and Oklo natural analogue projects which may contribute to enlighten some of the open questions regarding the long-term validity of the so-called hydrogen effect in the stability of the UO₂ spent nuclear fuel matrix.

Metal isotopic distributions in mycorrhizal trees: Weathering manifestations and within-plant fractionations

J.G. BRYCE¹, E.A. HOBBIE², T.D. BULLEN³,
J. BLICHERT-TOFT⁴, J. COLPAERT⁵, C.J. HOFF¹,
M.F. MEANA-PRADO¹, P. TELOUK⁴
AND M. VADEBONCOEUR²

¹UNH Department of Earth Sciences, Durham NH, USA,
(julie.bryce@unh.edu)

²Earth Systems Research Center, UNH-EOS, Durham NH,
USA.

³USGS Water Resources Research Center, Menlo Park, CA,
USA

⁴Ecole Normale Supérieure de Lyon, Lyon, France.

⁵Hasselt University, Diepenbeek, Belgium.

Although it is well known that organisms contribute significantly to the weathering process and to the distribution of elements within continental environments, the degree to which biota actively drive weathering versus the degree to which organisms benefit from nutrients released during largely inorganic weathering processes remains unknown [1]. Furthermore, the relative influence of different organisms on key elemental cycles, such as the base cations, especially Ca and Mg, is poorly understood. To address these questions, we have carried out a series of geochemical studies on semi-hydroponically cultured trees (*Pinus sylvestris*, *Acer saccharum* and *Betula alleghaniensis*) grown with appropriate mycorrhizal symbionts (ectomycorrhizal or arbuscular) in different geologic substrates (carbonate versus granitic) and under different nutrient regimes (N-limited in high or low nutrient supply and P-limited). Plant tissues across these biogeochemical experiments were studied for elemental abundances and Pb, Ca and Mg isotopic signatures. We conclude from our approach that: (1) Pb isotopes effectively complemented elemental signatures to identify key mineral dissolution reactions (e.g., the dissolution of phosphate phases in P-limited cultures); (2) for the same geologic substrate, arbuscular fungus did not demonstrate substantive phosphate dissolution; (3) the presence of mycorrhizal fungus significantly affected the Ca and Mg elemental distributions within the plant tissues but had a more muted effect on the Ca isotopic distributions; (4) foliar and root tissues recorded distinctive isotopic compositions (e.g., differences up to 0.6‰ $\delta^{44/40}\text{Ca}$); and (5) ectomycorrhizal symbioses may drive Mg isotopic variations during weathering.

[1] Brantley *et al.*, *Geobiology*. 2011.

Nanomagnetism of iron meteorites identified by X-ray photo-emission electron microscopy

J.F.J. BRYSON¹, J. HERRERO ALBILLOS², F. KRONAST³,
G. VAN DER LAAN⁴, S.A.T. REDFERN¹
AND R.J. HARRISON¹

¹Department of Earth Sciences, University of Cambridge, UK
(correspondence: jfjb2@cam.ac.uk)

²ICMA, University of Zaragoza, Spain
(Julia.Herrero@unizar.es)

³BESSY II, HZB, Berlin, Germany
(florian.kronast@helmholtz-berlin.de)

⁴Diamond Light Source, UK,
(Gerrit.vanderlaan@diamond.ac.uk)

Paleomagnetic signals stored within meteorites are a key source of information regarding many processes in the early solar system. An increasing body of traditional macroscopic paleomagnetic evidence suggests that, while molten, the liquid cores of the meteorite's parent asteroids generated magnetic fields with comparable strength to those of present-day Earth. We have applied nanoscale magnetic techniques to show that spinodal nanostructures within meteorites are capable of providing a time-resolved record of dynamo activity of their parent asteroids - analogous to that stored in the Earth by the spreading ocean crust - across the first 100-200 Ma of the asteroid's history, a prospect that could revolutionise our understanding of asteroid development.

To investigate this magnetic nanostructure, we performed the first meteoritic high-resolution X-ray photo-emission electron microscopy experiments (on the Tazewell IIICD iron meteorite). The results display a distinct and unique magnetic pattern that is dependent on the underlying nanostructure. The spinodal region, termed the 'cloudy zone' (CZ), extends 2-10µm and is composed of tetrataenite (chemically ordered FeNi) embedded in a hitherto unobserved ordered Fe₃Ni phase. Within this region, a complex magnetic state is observed with interlocking groups of all three tetrataenite twin orientations. A clear variation in the amount of each twin with increasing lateral distance across the CZ (decreasing age of tetrataenite formation) is also present. The observed magnetisation pattern bears resemblance to anti-phase boundaries (APBs) that appear to coarsen over time. These results provide both a fundamental understanding of the CZ magnetisation as well as the magnetic state formed in the absence of a dynamo field. Chondritic meteorites can carry an analogous magnetic remanence that was influenced by a dynamo field. By comparing the results in this study to those of chondritic meteorites, we will identify both the direction and magnitude of this dynamo field over a 100 Ma period.

Experimental and theoretical study of malachite solubility in ammonia aqueous solutions

T.M. BUBLIKOVA, T.V. SETKOVA* AND V.S. BALITSKY

Institute of Experimental Mineralogy Russian Academy of Science, Acad. Osipian st, 4, Chernogolovka, Russian Federation, (*correspondence: tmb@iem.ac.ru)

Experimental and theoretical investigations of malachite solubility was carried out as a part of search of copper carbonates (malachite and azurite) crystallization conditions [1]. The solubility of $\text{CuCO}_3 \cdot \text{CuOH}_2$ was studied experimentally in 1.0, 2.0, 3.0M ammonia solutions at temperatures of 25, 50, 75°C. Moreover, thermodynamic calculations were performed for indicated ammonia concentrations and temperatures. An initial material was placed in ampoules made of thermal-resistant glass, then it was grouted of ammonia solution of necessary concentration. The ampoules were sealed and placed into thermostat. After equilibration the ampoules were unsealed, and an aliquot part of the solution was filtered and analysed for a total copper content. We used the volumetric iodometric method for estimation of the copper content and a total CO_2 content in solution was determined using AN-7529 express-analyzer.

The experimental study have shown that the equilibrium copper content increases with ammonia concentration increasing and decreases with temperature rise in ammonia solutions. Malachite is unstable in the ammonia solution at given condition it decomposes with tenorite forming, that was confirmed by the thermodynamic calculations. The results of the thermodynamic calculations and the experimental study of malachite solubility has a satisfactory fit in general (Fig.1).

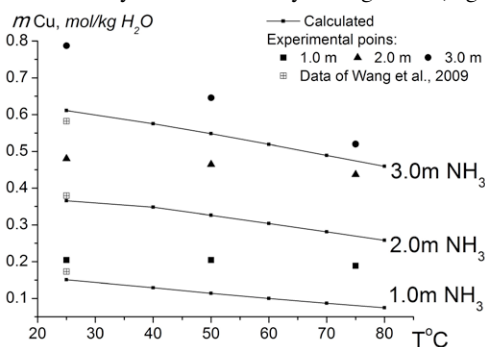


Figure 1: Calculated and experimental data of malachite solubility as functions of NH_3 concentration and temperature.

[1] Balitsky & Bublikova (1990) *Prog. Crystal Growth and Charact.* **21**, 139-161. [2] Wang *et al.* (2009) *Hydrometallurgy*, **99**, 231-237.

Geochemical processes affecting stream water at European scale investigated by differential scaling operator (perturbation) in the simplex metric

A. BUCCIANTI¹, J.J. EGOZCUE²
AND V. PAWLOWSKY-GLAHN³

¹Dep. of Earth Science, University of Florence (I)

(*correspondence: antonella.buccianti@unifi.it)

²Dep. Applied Mathematics III, UPC, Barcelona (E)

³Dep. Inf. Mat Aplicada i Estadística, Univ. of Girona (E)

Compositional data consist of vectors whose components are parts of some whole. Their statistical analysis performed in the real Euclidean sample space is not able to capture their features. Data in fact lies in a constrained space, called simplex, where to characterise the difference, or changes from one composition to another, specific operators have to be considered. In this contribution, perturbation, the group operator working in the geometry of the simplex sample space [1], is applied to analyse the differences in the chemical composition of the solutes of stream waters at European scale [2]. The analysed data are from the FOREGS (Forum of European Geological Survey) [3] database. New numerical and graphical tools are proposed to investigate the behaviour of elements or chemical species in the constrained space. In the FOREGS project, running stream waters were collected from the small, second order, drainage basins (<100 km²) at the same site as the active stream sediments. Starting from the analytical results matrix, chemical data of some selected variables, considering their geochemical affinity, were ranked by taking into account their conductivity values. Perturbation vectors from one composition to the subsequent one are calculated and results plotted in variation diagrams. The aim is to investigate the relative behaviour of the ions and chemical species, as well as the effect of weathering and dilution processes on a European scale, by considering the use of calculus operators working in the simplex geometry. The possibility to model processes at the base of the distribution of chemical elements/species (e.g., presence of trends depending on space, chemostatic behaviour, ...) is also explored.

[1] Aitchison and Ng (2005), *Statistical Modeling*, **5**, 173-185. [2] Buccianti (2011), *Zeitschrift fur Geologische Wissenschaften*, **40**(4-5), 295-305.

[3] <http://www.gtk.fi/publ/foregsatlas/>

X-ray study of high pressure induced densification of lithium disilicate glass

S. BUCHNER^{1*}, A. S. PEREIRA^{1,2}, J. C. DE LIMA³
AND N. M. BALZARETTI¹

¹LAPMA, Physics Institute, UFRGS, ZIP 91501-970, Brazil
(*correspondence: silviobuchner@gmail.com),
(naira@if.ufrgs.br)

²Escola de Engenharia, UFRGS, ZIP 91501-970, Brazil
(altair@if.ufrgs.br)

³Centro de Ciências Físicas e Matemáticas, UFSC, 88040-970, Brazil (jcardoso.delima@gmail.com),

Lithium disilicate glass ($\text{Li}_2\text{O} \cdot 2\text{SiO}_2$) is a very interesting vitreous material, because, besides several important technological applications (e.g. biomaterial to produce prostheses and implants), shows a large difference between the T_g and T_c values. This is important for the investigation of the crystallization mechanism on vitreous phases, as it allows the independent study of the nucleation and growth stages. In this work, we have investigated the effect of high-pressure processing in the induction of structural changes in the amorphous phase. This can give place to polyamorphism and/or to the generation of possible seeds for a crystalline phase nucleation. Using toroidal type high-pressure chambers, glass samples were processed at 2.5 GPa, 4 GPa, 6 GPa and 7.7 GPa at room temperature. X-ray diffraction using synchrotron radiation was used to obtain the radial distribution functions in order to follow the structural changes at different ranges. Compared to a pristine sample, the main change observed for the samples processed up to 6 GPa was associated to the distortion of the SiO_4 tetrahedra, as already observed in the literature. However, for the sample processed at 7.7 GPa, we have identified a drastic change in the RDF, which points for the production of a different amorphous phase with a local structure closer to that observed for the Li_2SiO_3 crystalline phase.

The ^{15}N and ^{18}O isotopic signature of abiotic reduction of nitrite by iron

CAROLYN BUCHWALD^{1*} COLLEEN HANSEL²
DAVE JOHNSTON³ AND SCOTT WANKEL⁴

¹266 Woods Hole Road, Woods Hole, MA 02543
(*correspondence: cbuchwald@whoi.edu)

²266 Woods Hole Road, Woods Hole, MA 02543
(chansel@whoi.edu)

³20 Oxford Street, Cambridge, MA 02138
(djohnston@eps.harvard.edu)

⁴266 Woods Hole Road, Woods Hole, MA 02543
(swankel@whoi.edu)

Evidence is mounting for the importance of interactions between reactive intermediates of multiple elemental cycles. For example, while previous studies have shown that oxidation of Fe(II) by nitrate (NO_3^-) and nitrite (NO_2^-) – a reactive intermediate of both reductive and oxidative N cycling processes – the controls on these reactions in the environment are poorly understood. Moreover, the N product of abiotic, anaerobic NO_2^- reduction by Fe(II) can include nitrous oxide, nitric oxide, ammonium or dinitrogen gas – yielding a myriad of implications for the fate of N across all types of ecosystems. Furthermore, we posit that these types of reactions may represent an important control on the dual NO_3^- and NO_2^- isotopic composition in Fe-rich, reducing environments low in organic carbon (e.g., aquifers). To date, however, the kinetic isotope effects of these processes remain uncharacterized.

Here we present the first investigation of the dual isotope systematics of abiotic NO_2^- reduction by Fe(II) under a variety of environmentally relevant pH values and reactant concentrations. In our experiments, we observe a rapid decrease in NO_2^- postively correlated with Fe(II) concentrations, followed by a second phase of slower NO_2^- reduction, possibly implying the involvement of secondary Fe(II)/Fe(III) mineral phases. Samples were collected for NO_2^- N and O stable isotope analyses in order to determine the isotope effects associated with abiotic NO_2^- reduction by Fe(II). As many studies suggest a potential for anaerobic, abiotic nitrogen transformations coupled with iron cycling, the N and O isotope effects determined here will be helpful for using dual isotopes of nitrite (and nitrate) to decipher the biogeochemical fate of N in host of important environments including soils, sediments, wastewater treatment plants and aquifers.

Evaluation of atmospheric flows of mineral substances in the south-eastern coast of Baikal Lake during the last 200 years

V.V. BUDASHKINA* AND V.A. BOBROV

Institute of geology and mineralogy SB RAS, Koptyug Pr. 3, Novosibirsk 630090, Russia (*correspondence: budash@igm.nsc.ru)

Oligotrophic bogs are capable to maintain in its peat deposits the mineral substance of atmospheric aerosol. The study of microelement composition of the stratified horizons allows us to determine the changes in chemical content of atmospheric aerosol under the influence of natural and anthropogenic factors in the historical time.

Dulihinskoe bog, located in the territory of the Baikal State Biosphere Reserve, took our attention as an object for retrospective geochemical monitoring. In the center of the bog (N 51°31', E 105°00') there were selected the top 47 cm of the 4-meter peat packs of 11000 years old [1] in the form of the monolith with square 22 * 13 cm². There was defined naturally radioactive (²¹⁰Pb, ²²⁶Ra, ²³²Th, ²³⁸U, ⁴⁰K) and anthropogenic (¹³⁷Cs, ²⁴¹Am) elements in ash samples and held AAS determination of 19 chemical elements.

²¹⁰Pb permanently come from the atmosphere and disintegrated over the time in peat horizons, whereas ¹³⁷Cs, ²⁴¹Am supply was only in 1953- 1963 years [2]. Distribution of ²¹⁰Pb and ²⁴¹Am allowed us to allocate layers, formed in the 19-20th centuries, for which we calculated the rates of accumulation of mineral matter [3] (see table).

Table1: The average annual speed of substance inflows.

The obtained values of the elements proceedings on the earth surface for the second half of the XX century are commensurate the values for the Western Siberia, subjected to anthropogenic impact. Flows of mineral substances remain rather high and in the middle ages, that we explain by the proximity of mountain systems (Khamar-Daban) [3], in contrast to the Western Siberia with its arid environments.

[1] Bezrukova et al (2000) *The problem of the environment, climate reconstruction of the Holocene and Pleistocene of Siberia* **2**, 36-47. [2] Gavshin et al (2004) Reports of the RAS **396**, 804-807. [3] Bobrov et al (2012) *Heavy metals and radionuclides in the environment* **1**, 82-90.

Evaluation of the Lu-Hf-in-lawsonite geochronometer

G. BUDDÉ* AND E.E. SCHERER

Institut für Mineralogie, Westfälische Wilhelms-Universität Münster, Corrensstraße 24, 48149 Münster, Germany (*correspondence: gerrit.budde@uni-muenster.de, escherer@uni-muenster.de)

We present an evaluation of the recently established Lu-Hf-in-lawsonite geochronometer [1, 2] including a reliable separation procedure for lawsonite. For this purpose, four blueschist-facies rocks from the island of Syros (Greece) and the Tavşanlı Zone (Turkey) were investigated, covering a wide range of different lawsonite occurrences, as well as pseudomorphs after lawsonite.

The developed mineral separation procedure involves magnetic and density separation as well as hand-picking and yields almost pure lawsonite concentrates. Lutetium and hafnium concentrations as well as Hf isotope ratios were obtained by using a selective digestion technique for mineral separates [3], a single-column separation procedure for element purification by ion exchange [4], and high-precision isotope ratio measurements by MC-ICP-MS.

Lawsonite showed elevated Lu concentrations of 0.4-1.4 ppm and very low Hf contents of <0.1 ppm. The ¹⁷⁶Lu/¹⁷⁷Hf values of 0.6-4.4 are comparable to other minerals used for Lu-Hf geochronology and allow obtaining well-defined isochrons and precise ages. However, bulk pseudomorphs after lawsonite do not preserve the Lu and Hf concentrations or Hf isotope ratios of the former lawsonite after its prograde breakdown. The obtained Lws-WR age (50.3±1.2 Ma) of the HP-LT metamorphism on Syros is in excellent agreement with previously published geochronological and geothermobarometric studies [e.g., 3]. The Lws-WR ages (87.5±1.1 Ma, 89.3±1.8 Ma) of two metabasites from the Tavşanlı Zone provide the first tight constraints on the onset of HP-LT metamorphism in this region [e.g., 5].

Due to its relatively small P-T stability range and elevated Lu/Hf values, lawsonite is well suited for Lu-Hf geochronology and has proven to be a powerful tool to date high pressure-low temperature metamorphic events. This geochronometer allows dating lawsonite growth in rocks of the lawsonite-blueschist subfacies and offers numerous prospects for investigating different subduction zone processes.

[1] Mulcahy et al. (2009), *Geology* **37**, 987-990. [2] Vitale Brovarone & Herwartz (2013), *Lithos*, in press. [3] Lagos et al. (2007), *Chem. Geol.* **243**, 16-35. [4] Münker et al. (2001), *G³* **2**, 1064. [5] Okay & Whitney (2010), *Ophioliti* **35**, 131-172.

Method for measurement of argon isotopes in helium flow for K/Ar geochronology

S.Y. BUDNITSKIY¹, A.V. IGNATIEV²
AND T.A. VELIVETSKAYA³

¹Far Eastern Geological Institute FEB RAS, Russia,
Vladivostok. (Budnitskiy_Serg@mail.ru)

²FEGI FEB RAS, Russia. (Ignatiev@fegi.ru)

³FEGI FEB RAS, Russia. (Velivetskaya@mail.ru)

We present a method for the measurement of argon isotopes in the potassium-argon (K/Ar) geochronology of the controller based on the series (conventional) mass spectrometer operating in dynamic mode. Installation for the quantitative measurement of isotopes of argon laser system has a sample preparation, based on CO₂ laser, where the isolation and purification of argon is in a continuous flow of ultra-pure helium. The system is based on the mass spectrometer MAT-253 (Thermo Scientific), equipped with the detectors Faraday m/z 36, 37, 38, 39 and 40 and use chromatographic purification system.

Instead of the traditional method of isotope dilution of 38-argon method is comparing the signals from the sample gas and gas-standard of known isotopic composition (by air) before and after the measurement of each sample. This method, using of air argon as the reference gas has an advantage over conventional method of 38-Ar isotopic dilution: there is no contamination of the sample by ⁴⁰Ar/³⁶Ar incoming from a tracer 38-argon; a quantity of argon in a dose is invariable for several years; availability of 40Ar/36Ar air ratio monitoring by reference gas.

A sample is placed in multi-charge chamber. The chamber contains 10 to 35 samples, depending on the size. To release the argon from a sample the CO₂ laser is used. The gas that was released during fusing, primary treatment is the U-shaped trap, placed in liquid nitrogen. Next argon helium flow passes through the capillary chromatography column for purification of argon from contaminants.

This method is an alternative method for measuring the argon isotopes in the static mode and can be used for analysis of radiogenic argon N * 10⁻¹² g with the same sensitivity and accuracy, the method is simpler and more reliable. Small amounts of radiogenic argon extracted from geological samples require high stability, low backgrounds, minimal content of argon in the blank experiment, and high sensitivity of the isotope ratio mass spectrometer.

The presented method has been successfully used to solve geological, geochronological and geosheological issues.

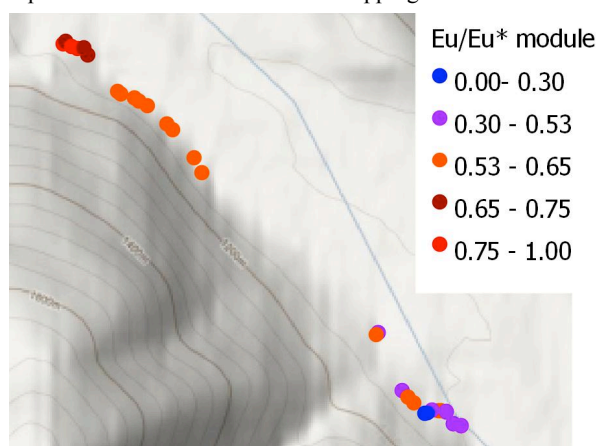
[1] Ignatiev A.V *et al.* Laser CF-MS technique Ar isotopes measurement for K/Ar geochronology // JESIUM-2008. SFIS. France, 2008. P. 58

GIS mapping of geological features of the Baikal mountain region based on integrated geochemical indicators

A. BUDYAK AND A. PARSHIN

Vinogradov Institute of Geochemistry SB RAS, Russia.
(correspondence: budyak@igc.irk.ru)

Baikal mountainous area and Kodar-Udokan structural-formational zone are perspective to search for deposits of noble and rare metals. The studies 2009-2012, the authors created a spatial database including geological and geochemical information for the various objects of the ore zone. For the analysis of this information is required to cartographically display more than 50 layers of geochemical data. Classical overlay-based GIS representation of such a large data set makes it difficult visual analysis. The authors found some mathematical and geographical distribution patterns of useful component that allowed the development of mathematical tools, providing spatial calculations of integrated geochemical indicators - "modules", which are comprehensive indicators of certain ore-forming processes. Form of their representation is suitable for GIS-mapping.



For example, the figure shows the calculation of Eu/Eu* module. Well traced the species change of rocks of different stratigraphic levels, to lying on each other. This approach provides the ability to make geological conclusions, based on visual analysis of only 5-7 data overlays. Created GIS software can serve as a navigator geochemical exploration.

Quantifying more than half the periodic table of elements in uranium ore concentrates: Results of the IAEA's interlaboratory comparison 2011-2012, and two new quality control materials

S. BÜRGER, S. BOULYGA AND M. PEŃKIN

International Atomic Energy Agency, A-1400 Vienna, Austria

The analysis of trace elements (impurities) in uranium ores and uranium ore concentrates (UOC), as well as uranium-bearing materials in general, is performed in a variety of fields, e.g., in geochemical research, for quality control in the production stream converting uranium ores to nuclear fuel, as material signatures in nuclear forensics, or in international nuclear safeguards to support the verification of States' declarations.

An interlaboratory comparison on the quantification of impurities in UOC was organized by the International Atomic Energy Agency (IAEA) during 2011-2012. The goal was to probe the analytical capabilities of the participating laboratories (i.e., the current state-of-the-practice), to determine any differences between laboratories and their potential causes, to identify chemical elements that are problematic and/or difficult to analyse with established analytical techniques, and to assess the measurement uncertainties. Six participating laboratories were tasked to quantify 69 impurity elements – more than half the periodic table – in two different UOC materials. The impurity concentrations, normalized to uranium content, covered more than six orders of magnitude. Inductively-coupled plasma mass spectrometry (ICPMS) was the main technique used by the participating laboratories.

A summary of the comparative results will be presented, highlighting the current state-of-the-practice in ICPMS analytical approaches as employed by the participants. Lessons learned, including the identification of polyatomic interferences and the challenge of estimating measurement uncertainties, will be discussed. This interlaboratory comparison yielded consensus values for the two UOC materials. They are suitable for future use as quality control materials addressing gaps in the availability of reference materials for impurity elements in uranium-bearing materials.

C, N₂, Ar, He in fluid inclusions in a garnet lherzolite from Oasis Jetty, East Antarctica

BUIKIN A. I.¹, VERCHOVSKY A. B.², SOLOVOVA I. P.³
AND KOGARKO L. N.¹

¹Vernadsky Institute of Russian Academy of Sciences, Moscow, Russia (bouikine@mail.ru)

²The Open University, Milton Keynes, UK

³IGEM RAS, Moscow, Russia

To reveal the sources and evolution of fluids during mantle metasomatism under East Antarctic we have carried out optical, thermobarogeochemical and Raman-spectroscopy investigations and studied C, N, Ar and He isotopic and elemental ratios in Px separate from Oasis Jetty garnet lherzolite by stepwise crushing method. The sample contains abundant fluid inclusions of different generations and compositions. The applied methods have revealed two major fluid activity stages. The early stage fluid inclusions are characterized by the most complex composition and high pressures (>13 kbar), some of them reach 10 μm in size. The late stage fluid inclusions (P ≥ 5-7 kbar) are all very small (2-5 μm and less); the predominance of CO₂ over all other gases is dramatically increasing in them, as well as the role of H₂O.

Our isotope-geochemical data confirm the existence of these two fluid sources. The high pressure and larger size fluid inclusions of the early stage mostly opened at the very first crushing steps are characterised by low C/N₂, C/Ar, N₂/Ar (31-34) ratios, typical for the MORB chilled glasses δ¹³C values in CO₂ (-4.7‰), heavy nitrogen (up to +2.05±0.28‰), and slightly elevated ⁴⁰Ar/³⁶Ar ratios (up to 533±10). The late stage fluid inclusions being progressively opened with increasing number of strokes are better characterized by the gases extracted at the very last crushing steps. They have 2-3 orders of magnitude higher C/N₂ and C/Ar ratios, close to the atmospheric N₂/Ar (86) and ⁴⁰Ar/³⁶Ar ratios (down to 370±7), lighter δ¹³C values in CO₂ (down to -6.8 ‰), and nitrogen (-2.28±0.26 ‰). The elemental and isotope ratios (N₂/⁴⁰Ar, ⁴⁰Ar/³⁶Ar, ⁴He/⁴⁰Ar*, δ¹⁵N) correlate to each other, reflecting mixing between early and late stage fluids. The latter is the result of a mixture between MORB-type mantle and atmospheric components. The early stage fluids could be the result of more complex mantle-crustal components mixture with high proportion of atmosphere derived argon. Typical for intra-plate mantle xenoliths element fractionation due to fluid-melt partitioning is observed in low ⁴He/⁴⁰Ar* ratios (0.1-0.7, compared to the mantle production ratio of 1.5-2). Some isotope fractionation (for N₂ and C) also could not be excluded.

Radiometric ^{81}Kr dating reveals 120,000 year old ice at Taylor Glacier, Antarctica

C. BUIZERT^{1*}, D. BAGGENSTOS², W. JIANG³,
R. PURTSCHERT⁴, V.V. PETRENKO⁵, E. J. BROOK¹,
Z.-T. LU³, P. MÜLLER³ AND J. P. SEVERINGHAUS²

¹CEOAS, Oregon State Univ., Corvallis OR 97331, USA

(*correspondence: buizertc@science.oregonstate.edu)

²SIO, University of California, San Diego, CA 92093, USA

³Argonne National Laboratory, Argonne, IL 60439, USA

⁴University of Bern, CH-3012 Bern, Switzerland

⁵University of Rochester, Rochester NY 14627, USA

Ancient ice can not only be obtained from deep ice cores, but also at ice sheet margins and blue ice areas (BIAs) where it outcrops due to local ice dynamics and surface ablation [1]. Determining an accurate chronology for BIA records is more challenging than for regular ice cores. Here we report the first successful ^{81}Kr radiometric dating of ancient BIA ice. ^{81}Kr ($t_{1/2} = 229$ ka) is produced cosmogenically in the upper atmosphere, and the modern ^{81}Kr -Kr ratio is used as the reference. Krypton is not reactive and is well mixed in the atmosphere. In principle ^{81}Kr dating can be used to date ice in the 50ka to 1Ma age range; it is widely applicable as all glacial ice contains trapped air; it does not require a continuous or undisturbed ice stratigraphy; and it does not suffer from *in situ* cosmogenic production in the ice (as is the case for ^{14}C). The large sample size requirement (> 40 kg) has precluded its use in ice core science to date.

Air was extracted on site from four 250 kg polar ice samples obtained from 5-15m below the surface of Taylor Glacier, McMurdo Dry Valleys, Antarctica. Krypton was separated from the air and dated using Atom Trap Trace Analysis [2]. The ^{81}Kr radiometric ages agree with independent stratigraphic dating techniques within 6ka. ^{85}Kr analysis shows that the samples are free of modern air contamination, validating our sampling strategy and experimental methods. We show that ice from the Eemian interglacial (130-120ka BP) can be found in abundance near the surface of Taylor Glacier. Our study paves the way for reliable radiometric dating of ancient ice in BIAs and margin sites, greatly enhancing their scientific value as archives of old ice and meteorites. As sample size requirements continue to decrease, ice core ^{81}Kr dating might be a future possibility.

[1] Bintanja (1999) Rev. Geophys. **37** 337-359. [2] Jiang *et al.* (2012) Geochim. Cosmochim. Ac. **91** 1-6.

Geochemical types of tantalum and niobium mineralization from the rare metal-bearing granites and pegmatites of the Western Mongolia

O.V. BUKHAROVA* AND A.A. BAEVA

Tomsk State University, Tomsk, Russia (getina@ggf.tsu.ru)

Tantalum-niobates are typical representatives of the rare metal mineralization in Middle Paleozoic and Early Mesozoic pegmatites and amazonite granites of the Western Mongolia (the Mongol Altay, the Charchirinsk upland region). They are seen in association with beryl in pegmatites, and characterized by heterogeneous composition of minerals, which is displayed in variability of Ta/Nb ratio from 0,3 to 3,0 from the grain core to boundaries. Tantalum-niobates in granites have microscopic sizes (2,5-150 μm) and are present as poikilitic inclusions in rock-forming minerals of protolithionite-microcline-albite paragenesis, more rarely in accessory fluorite and magnetite. At the same time, tantalum niobite grains are chemically homogeneous, but differ from each other by various Ta/Nb (0,03-0,4) and Ti/Nb (0,02-9,8) ratio, as well as significant content of LREE (20 wt.%), Sn (up to 4 wt.%). Ilmenorutile (Ta+Nb from 3-12 to 23-27 wt. %), columbite-(Mn), columbite-(Fe), tantalite-betafite, betafite, and polycrase were defined in the rocks studied. These elements show acid-base conditions for mineral-forming environment. Changing alkalinity during pegmatite crystallization is noted within some zonal minerals as transforming of columbite into ilmenorutile (Ta/Nb-1,3; Ti/Nb-3,1), and tantalite-betafite (Ta/Nb 2,5 до 3,0; Ti/Nb-0,5). Iron content coefficient (FeO/MnO) varies significantly (non-manganese up to 8,6), at the same time late non-manganese varieties are often enriched in REE, U, or Y. Despite the similar patterns of chemical evolution defined for granitoid melts, the differences in U, Pb, Y, F, W, Sn, LREE, Th contents observed in tantalum-niobates of pegmatite and amazonite granites indicate heterogeneous crust magma sources and their intrusion under different paleogeodynamic conditions.

This study was funded by the Russian Ministry of Education and Science (projects 5.3143.2011, 14.B37.21.0686, 14.B37.21.1257)

A “non-CHONS” stable isotope view on weathering and hydrology

T.D. BULLEN

U.S. Geological Survey, Menlo Park, CA 94025, USA
(correspondence: tdbullen@usgs.gov)

The past 15 years have witnessed a remarkable expansion in our knowledge of “non-CHONS” stable isotope systems (that is, stable isotope systems other than Carbon, Hydrogen, Oxygen, Nitrogen or Sulfur). The metals and metalloids studied thus far having demonstrated isotopic variability span the periodic table, vary from major to trace element abundances in natural materials and have a broad range of geochemical affinities and behaviors. Highly precise stable isotope measurements for these elements are currently obtainable using multi-collector ICPMS, TIMS and SIMS instruments, potentially allowing efforts at cross-platform validation of data accuracy. In surveying the rapidly building literature on the topic, it is becoming increasingly clear that we have spent as much effort determining why the “non-CHONS” stable isotope systems behave as they do in our laboratory and field-based experiments (e.g. the focus on distinguishing equilibrium from kinetic isotope effects, biotic from inorganic controls, natural from anthropogenic signals) as we have in using the isotopes to tell us unique information about the systems we are studying. Now that we have gained a broad understanding of isotope fractionation mechanisms and their implications for natural isotope distribution patterns for at least some of the non-CHONS stable isotope systems, the time is ripe to concentrate on demonstrating and promoting the utility of these systems for understanding Earth processes such as physical and chemical weathering and their intricate linkage to hydrology. In the broad realm of weathering and hydrology research, the greatest attention has been directed to the Li, B, Mg, Ca, Fe and Si stable isotope systems and each seems to have found one or more particular testable niches (e.g., Li isotopes to distinguish silicate from carbonate weathering, Ca isotopes to discern biotic influences on global flux calculations, Fe isotopes as a (paleo)redox proxy and potential biosignature). More recently, additional redox proxies such as U, Tl and Cr stable isotopes and tracers of biological processing such as Sr and Ba stable isotopes have been explored. This presentation will highlight some new directions for linked weathering/hydrology research in which the non-CHONS stable isotope systems can play a key role, as well as some of the challenges remaining as we move these stable isotope systems from “non-traditional” to the mainstream.

The societal impact of urban and environmental geochemistry: Pathways to success

T.D. BULLEN

U.S. Geological Survey, Menlo Park, CA 94025, USA
(correspondence: tdbullen@usgs.gov)

Taken together, the fields of urban and environmental geochemistry represent a relatively new, broad and important branch of geochemical research. Given the obvious, that urban and environmental geochemistry focuses on where people live, it could be expected that ever-expanding scientific endeavors in this field would have considerable impact on policy, regulatory decision making and public perception of the importance of sound science. There are many examples of “success stories”, where sound science and persuasive communication has resulted in changes in the way we do business as a society (e.g. implementing limits on stack emissions in response to the effects of acid rain, regulating sulfate loading in the Everglades to limit methylation of mercury, encouraging green space in urban areas to lessen impacts of hydrologic rerouting). On the other hand, the ongoing debate over the validity of climate change science as a driver of policy implementation reveals that scientists are not always the best communicators when forced to defend their science to non-scientists. Because science is complicated and has a language all its own that can be difficult for non-scientists to grasp, it is important that research results having policy implications be carefully communicated to the people charged with making and implementing policy. In this regard, the scientific logic and approach must be beyond question and implemented without bias toward a particular position or outcome. However, possible outcomes should be anticipated and potential solutions considered. Results need to be communicated at an understandable level, keeping the message on target but as simple as possible. And scientists need to stand their ground, letting the science speak for itself. Perhaps most importantly, we need to make sure that policy experts are invited to participate in our scientific conferences and workshops and to make presentations outlining their needs and perspectives, thus allowing the conversation to begin early in the process of developing regulatory policy. This presentation will showcase a collection of success stories in which urban and environmental geochemical research has influenced policy at the local, national and international level, and will attempt to identify the underlying pathways to that success.

The structure and emplacement of the Rocche Rosse obsidian lava flow, Lipari, Aeolian Islands, Italy

L. BULLOCK*, R. GERTISSER AND B. O'DRISCOLL

School of Physical and Geographical Sciences, Keele University, Keele, Staffordshire, ST5 5BG, UK

(*correspondence: l.a.bullock@keele.ac.uk)

Satellite image analysis and field-based, structural mapping of the Rocche Rosse obsidian lava flow, Lipari (Aeolian Islands, Italy) provide important constraints on silicic lava flow emplacement and deformation.

High resolution satellite imagery of the flow surface identifies large scale structures, such as two well-developed flow lobes, pronounced lineaments which are prevalent along the extent of the flow, and prominent crescent-shaped ridges (ogives), typically 20-80 m in length, spaced 10-15 m apart and parallel to flow-frontal margins. Structural features measured include a pervasive foliation (flow banding), small-scale folding and flow ramps. Small-scale folding is superimposed on larger scale folding (parasitic folds), and recumbent folding is also apparent. In general, data on the ground match with structures inferred from the satellite image. Foliation and lineation orientation patterns vary across the flow, generally showing a flow parallel and flow perpendicular arrangement. A prevailing stretching lineation follows the large-scale lineament features, and surface folding is traceable along the surface ridges identified by the satellite image.

It is proposed that the structural features outlined formed over a progressive series of flow emplacement and deformation, from initial extrusion, constrictional and compressional forces, polyphase folding, brittle deformation and devitrification in the solid state. Variations in structural trends relate to areas of complex and progressive deformation. The Rocche Rosse lava flow is emplaced endogenously as a continuous, composite lava flow, with two flow lobes (formed as the advancing flow divided).

We show that while structures associated with obsidian lava flows are remarkably complex, they are inherently related and form sequentially during continuous effusion, preserve evidence for progressive deformation, and can be used to decipher mechanisms of obsidian flow emplacement, in unprecedented detail.

Setschenow constants for prediction of salting-out of petroleum hydrocarbons in brines

A.S. BURANT^{1,2}, G.V. LOWRY^{1,2}
AND A.K. KARAMALIDIS^{1,2}

¹National Energy Technology Laboratory-Regional University Alliance (NETL-RUA), Pittsburgh, PA 15236 USA

²Department of Civil and Environmental Engineering, Carnegie Mellon University, Pittsburgh, PA 15213 USA
(Correspondance to akaramal@andrew.cmu.edu)

Large scale implementation of carbon capture, utilization, and storage (CCUS), as well as the management of produced water associated with energy production activities (including extraction of natural gas from shale plays) requires a better understanding of the interaction of petroleum hydrocarbons with highly concentrated brines. It is not well known how very high levels of electrolytes influence the solubility of hydrocarbons. The objective of this study is to determine if existing salting-out parameters, called Setschenow constants, are applicable to predict the decrease in aqueous solubility of petroleum hydrocarbons, including polycyclic aromatics hydrocarbons (PAHs), phenols, and thiophenes, due to high levels of electrolytes in concentrated oilfield brines.

We measured the solubility of important organic compounds found in oilfield brines, such as naphthalene. Electrolytes studied include NaCl and CaCl₂, which are the most common salts found in oilfield brines (*1*). The organic compounds in the brines were extracted with a 100 µm polydimethylsiloxane (PDMS) fiber using solid phase microextraction (SPME) and analyzed by an Agilent 6890 gas chromatograph coupled with a flame ionization detector (GC-FID).

We hypothesize that existing Setschenow constants measured at lower ionic strengths (e.g. up to seawater) will also predict the salting-out effect at very high ionic strengths expected in brines (5M) for a range of compound classes of interest. These results are expected to have implications for enhanced oil recovery, CCUS, and any other industry that deals with produced waters. If valid, the solubility of these compounds can be readily modeled using existing Setschenow constants determined at lower ionic strengths.

[1] Kharaka, Y. K.; Hanor, J. S. 5.16 - Deep Fluids in the Continents: I. Sedimentary Basins. In *Treatise on Geochemistry*; Holland, E.-C. H. D.; Turekian, K. K., Eds.; Pergamon: Oxford, 2003; pp 1–48.

New sedimentary $^{231}\text{Pa}/^{230}\text{Th}$ records from the northern Brazilian margin over MIS3

P. BURCKEL^{1*}, C. WAELBROECK¹, J.-M. GHERARDI¹ AND S. PICHAT²

¹Laboratoire des Sciences du Climat et de l'Environnement, Gif sur Yvette, France (*correspondence: pburckel@lsce.ipsl.fr, Claire.Waelbroeck@lsce.ipsl.fr, Jeanne.Gherardi@lsce.ipsl.fr)

²Laboratoire de Sciences de la Terre, Ecole Normale Supérieure de Lyon, Lyon, France (spichat@ens-lyon.fr)

The region of the North Eastern Brazilian margin is of major interest in the study of the variability of the oceanic circulation because of the large part of the Atlantic Meridional Overturning Circulation passing through it. Moreover this region has been extensively studied leading to a good chronostratigraphical framework of its marine sediment cores [1, 2, 3]

In order to better understand the changes in the AMOC during Heinrich events, we chose to study two sediment cores at different water depths so that we may observe not only changes in the intensity of circulation of the water masses influencing the cores, but as well changes in the vertical extent of these water masses.

Due to the difference in particle reactivity of ^{231}Pa and ^{230}Th in the water column sedimentary $^{231}\text{Pa}/^{230}\text{Th}$ (Pa/Th) may be used to record changes in AMOC [4, 5], although particle scavenging may bias the signal in certain cases. In the case of the western equatorial Atlantic region, the sedimentary Pa/Th vertical profile measured on recent sediment is consistent with a dominant role of the AMOC, rather than particle scavenging, thereby demonstrating that Pa/Th can indeed be used to monitor changes in water mass overturning rates in that region [6].

We present new Pa/Th records from the last glacial and in particular from periods of rapid circulation changes associated with Heinrich events. Our results show that the Pa/Th ratio changed along with other proxies such as the benthic foraminifer carbon isotopic ratio.

[1] Arz (1998) *Quat. Res* **50**, 157-166. [2] Arz (1999) *EPSL* **167**, 105-117. [3] Jaeschke (2007) *Paleoceanography* **22**, PA4206. [4] Yu (1996) *Nature* **379**, 689-694. [5] McManus (2004) *Nature* **428**, 834-837 [6] Lippold (2011) *Geophys. Res. Lett* **38**, L20603.

Halogen abundances of the martian mantle

RAY BURGESS^{*1}, JULIA ANN CARTWRIGHT² AND JUSTIN FILIBERTO³

¹SEAES, University of Manchester, Oxford Rd, Manchester, M13 9PL, UK, (ray.burgess@manchester.ac.uk)

²Division of Geological and Planetary Sciences, California Institute of Technology, Pasadena, CA91125, USA.

³Geology Department, Southern Illinois University, Carbondale, IL 62901, USA

The surface of Mars is relatively halogen-rich, with a mean Cl concentration of 0.49wt% [1]. In contrast, little is known about the martian interior halogen composition, nor how it compares with the Earth's mantle, where subduction recycling of halogens occurs. Insights into the halogen composition of the martian interior can be gained from shergottite meteorites, whose parental magmas were formed by partial melting of the martian mantle. North West Africa (NWA) 6234 is an olivine phyric shergottite [2], it is unweathered [2] and relatively undegassed, having likely crystallised at depth within the martian upper crust [3]. We analysed bulk and mineral separates of NWA6234 to determine Cl, Br and I by extension of the ^{40}Ar - ^{39}Ar technique. *In-vacuo* crushing experiments released only 2-10% of total halogens indicating that the major fraction is located within solid phases (melt inclusions or phosphate minerals). Stepped heating yielded constant molar Br/Cl = 0.0040 ± 0.0004 and I/Cl = 0.000358 ± 0.000046 throughout the release, indicative of a single halogen-bearing component. With the total Cl released (59 ppm), and assuming the basalt formed by 10-20% partial melting of the source, this implies a martian mantle Cl composition that is very similar to the terrestrial MORB source (4 ppm Cl [4]) and in agreement with a recent finding based on apatite chemistry [3]. However, NWA 6234 Br (560 ppb) and I (110 ppb) concentrations indicate a mantle enrichment of between 4-8 times and 30-70 times respectively relative to MORB. Thus, the martian interior is either less degassed of its heavy halogens compared to the Earth, or it formed with higher abundances.

[1] Keller *et al.* (2007) *JGR* **111**, E03S08; [2] Filiberto *et al.* (2012) *MAPS* **47**, 1256-1257; [3] Gross *et al.* (2013) *EPSL* doi.org/10.1016/j.epsl.2013.03.16; [4] Ruzie *et al.* (2012) V31A-2762, AGU Fall Meeting.

Constraining the modern riverine sulfur isotopic budget

ANDREA BURKE¹, JESS F. ADKINS¹,
JÉRÔME GAILLARD², R. MAX HOLMES³,
JAMES W. MCCLELLAND⁴, BERNHARD PEUCKER-
EHRENBRINK⁵, LAURA F. ROBINSON⁶,
ROBERT G.M. SPENCER³ AND BRITTA M. VOSS⁵

¹California Institute of Technology, USA;
(aburke@caltech.edu)

²Institut de Physique du Globe de Paris, France

³Woods Hole Research Center, USA

⁴University of Texas at Austin, USA

⁵Woods Hole Oceanographic Institute, USA

⁶University of Bristol, UK

The sulfur cycle has an important influence on global climate, for instance through weathering and aerosols, and is intricately linked to both the carbon and oxygen cycles. However, many aspects of the modern sulfur budget are not well understood. We present new $\delta^{34}\text{S}$ and $\delta^{33}\text{S}$ measurements on aqueous sulfate from more than 50 rivers from different geographical and climatic regions. These data were measured by a new MC-ICP-MS method that requires only 5 nmol of sulfate [1], with typical isotopic uncertainties of only 0.1‰. Combined with previously published sulfur isotope data, more than 44% of the world's freshwater flux to the ocean is involved in this estimate of the global riverine sulfur isotopic budget. We find a large range in the $\delta^{34}\text{S}$ of rivers, both temporally and spatially. Riverine $\delta^{34}\text{S}$ values range from -2‰ to 14‰, and some smaller tributaries lie outside of this range. Time series data from the Fraser River show a seasonal cycle in the $\delta^{34}\text{S}$ of more than 3‰.

Combined with major anion and cation data, the sulfur isotope data allows us to tease apart the relative contributions of different processes to the modern sulfur budget, including the oxidative weathering of pyrites, the weathering of sedimentary sulfates, and anthropogenic influences. These data yield important insights into the modern sulfur cycle and the weathering of sulfur bearing minerals, and are first order terms in balancing the modern sulfur isotopic budget. The large range of sulfur isotopic ratios in modern rivers also has implications for our interpretation of the past changes in the sulfur isotopic composition of seawater. Secular changes in the lithologies exposed to weathering through time could play a major role in driving the variations in $\delta^{34}\text{S}$ in seawater over the Phanerozoic.

[1] Paris *et al.* (2013), *Chemical Geology* **345**, 50-61.

Aerosols and plant leaf surfaces

J. BURKHARDT^{1*}, M. HUNSCHE² AND S. PARIYAR¹

¹INRES-Plant nutrition group, University of Bonn, Bonn,
Germany (*correspondence: j.burkhardt@uni-bonn.de)

²INRES- Horticultural science group, University of Bonn

Aerosols are ubiquitous and have always been part of the atmospheric environment of plants, while plant surfaces are probably the major terrestrial sink of fine aerosols. The deposition of fine aerosols is strongly influenced by leaf surface micro-roughness. Given constant aerosol concentrations over evolutionary timescales, plants have possibly developed leaf surface adaptations to control particle accumulation. Depending on the respective environment, plants may benefit from the nutrient content of aerosols or use them as a humidity sensor, but deposited particles may also promote leaf pathogen growth or act as desiccants [1].

The impact of aerosol exclusion on plant water relations was investigated in greenhouses, using pine seedlings, sunflower, and bean plants. Transpiration rates were lower for plants grown in filtered air (FA) than for plants grown in ambient air (AA) [2], and further effects were observed under increased CO₂ concentrations. Humidity fluctuations within an environmental scanning electron microscope (ESEM) caused a differentiated expansion of salt particles on leaf surfaces. This was related to the position of the ions within the Hofmeister series and reflected their impact on water surface tension [3]. A similar order applied when the drought tolerance of plants was measured after spraying leaves with different types of salt solutions.

Our results show that aerosol deposition strongly contributes to the ecophysiological reactions of plants, both in natural and in polluted conditions. Strong global increases of fine dust concentrations due to anthropogenic pollution or land use change may thus have world-wide impacts on plant communities.

[1] Burkhardt (2010) *Ecol. Monographs* . **80**, 369-391. [2] Pariyar *et al.* (2013) *Env. Exp. Bot.* **88**, 43-52. [3] Burkhardt *et al.* (2012) *New Phyt.* **196**, 774-787.

The redox state of diamond-forming fluids: Constraints from Fe³⁺/Fe²⁺ of garnets

A.D. BURNHAM*, S.C. KOHN, C. POTISZIL,
M.J. WALTER, G.P. BULANOVA, A.R. THOMSON
AND C.B. SMITH

School of Earth Sciences, Wills Memorial Building, Bristol,
BS8 1RJ, UK. (*correspondence: ab12908@bristol.ac.uk)

Inclusions in diamonds afford unique glimpses of deep lithospheric and asthenospheric minerals, allowing the thermal and chemical state of the mantle to be characterised. In the host diamonds, the concentration of N, ¹⁵N/¹⁴N and ¹³C/¹²C all give information about the origin of fluids in the mantle. The speciation in these fluids is uncertain in many cases, with considerable debate as to whether CH₄ or CO₂ is the predominant component in the transport of C [1,2]. As methane and carbon dioxide (or carbonate) represent reduced and oxidised C respectively, this redox signature should also be reflected in other mantle minerals.

Redox conditions of diamond-forming regions in the mantle can be found from the Fe³⁺/Fe²⁺ ratio of garnets as determined by X-ray absorption near edge structure (XANES) spectroscopy [3]. We present Fe³⁺/Fe²⁺ data for several suites of diamonds: Argyle, Western Australia; Juina, Brazil; Diavik, Canada; Udachnaya, Russia; Murowa, Zimbabwe. For the first three sets of diamonds, both eclogitic and peridotitic garnets were analysed, allowing the two distinct diamond-forming events to be contrasted.

For suites in which olivine and orthopyroxene coexist with garnet, the *f*O₂ of the diamondiferous paragenesis was calculated following [2].

Our work aims to couple the *f*O₂ information obtained from garnets to trace element data and (for the eclogitic samples) their oxygen isotope ratios, allowing the geochemical evolution of the slab during subduction to be robustly constrained.

[1] Thomassot *et al.* (2007) *EPSL* **257**, 362-371. [2] Stagno *et al.* (2013) *Nature* **493**, 84-88. [3] Berry *et al.* (2010) *Chem. Geol.* **278**, 31-37.

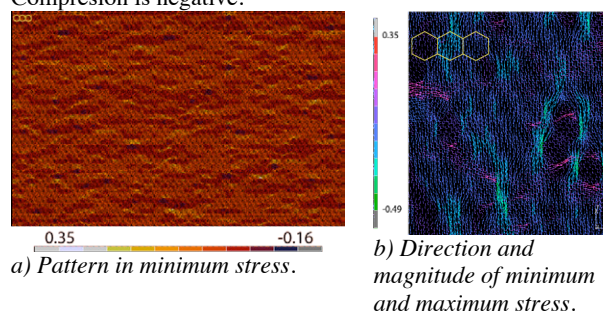
Patterning in stress: A new insight into the development of phase separation in metamorphic rocks

PAMELA C. BURNLEY

University of Nevada, Las Vegas, Department of Geoscience,
(Burnley@physics.unlv.edu)

The development of slaty cleavage, foliation and compositional banding in metamorphic rocks is understood to result from mass transport by either dissolution or diffusion under the influence of a non-hydrostatic stress field. Explanations for how compositional differentiation initiates generally rely on high shear strains to orient pre-existing features or folding of a pre-existing foliation to form a pattern of fold noses and limbs that lead to preferential dissolution. Based on 2D plane-strain finite element models, I propose a new low-strain mechanism for the formation of compositional banding based on mass transport between local regions experiencing varying levels of differential stress caused by the variations in the single crystal elastic properties of the constituent minerals in the rock. Models were constructed of 2574 hexagonal grains each containing 48 elements. Grains were assigned elastic properties appropriate for crystals of quartz, feldspar and mica in a variety of crystallographic orientations. Compression results in local variations in the differential stress that are ~30% of the total load and a pattern minimum stresses that mimics foliation. This pattern could serve as a template for mass transport of the most mobile chemical components leading to phase separation.

Figure 1: Model is shortened by 0.2% vertically. The size of grains in each view is given by the yellow hexagons. Compression is negative.



Coupling of arsenic mobility to microbial sulfate reduction in subsurface environments

EDWARD D. BURTON, SCOTT G JOHNSTON
AND DAVID ADAMS

Southern Cross GeoScience, Southern Cross University, PO
Box 157, Lismore, New South Wales, Australia;
(ed.burton@scu.edu.au)

Arsenic mobilisation is an important concern in many subsurface soil, sediment and groundwater systems. In such systems, microbial sulfate reduction often dominates anaerobic electron flow, thereby leading to the production of aqueous sulfide and the formation of iron sulfide species. However, the effects of microbial sulfate reduction on arsenic mobility in subsurface environments is poorly constrained.

This presentation describes some of our recent discoveries illustrating how arsenic mobility is coupled to subsurface sulfur biogeochemistry, especially to the production of sulfide via microbial sulfate reduction.

Our approach has been to conduct a series of integrated studies on this topic, including (i) abiotic mono-mineralogical batch experiments¹, (ii) advective-flow column experiments² and (iii) anoxic incubation experiments with complex arsenic-contaminated floodplain soil.

The results show that microbial sulfate reduction can have contradictory consequences for arsenic; either substantially retarding or greatly enhancing arsenic mobility. These vastly divergent outcomes depend on multiple factors, including hydrological flow conditions, the presence or absence of elevated porewater sulfide concentrations, aqueous arsenic concentrations and reaction time.

The fact that sulfate reduction can both retard or enhance arsenic mobility, depending on environmental conditions, represents a serious challenge for managing arsenic-contaminated systems. In particular, it implies that great caution must be exercised when aiming to exploit natural sulfur biogeochemistry as a strategy for mitigating arsenic mobility in subsurface environments.

[1] Burton *et al.*, *Environ. Sci. Technol.* (2013), **47**, 2221-2229. [2] Burton *et al.*, *Chem. Geol.* (2013), **343**, 12-24.

Unradiogenic lead in the mantle source of Mid-Ocean Ridge Basalts

KEVIN W. BURTON¹ AND IAN J. PARKINSON²

¹Durham Isotope Centre, Department of Earth Sciences,
Durham University, Durham. DH1 3LE, UK
(kevin.burton@durham.ac.uk)

²Bristol Isotope Group, School of Earth Sciences, University
of Bristol. BS8 1RJ, UK (Ian.Parkinson@bristol.ac.uk)

The isotope composition of lead (Pb) in the silicate Earth appears to be far too radiogenic for evolution from chondritic (primitive solar system) material over 4.57 billion years, the so-called 'Pb paradox'. Loss of Pb to the core, storage in the lower continental crust, or arrival in a late veneer, have all been proposed as mechanisms to account for this imbalance, but each remains problematic. Recently it has been suggested that the upper mantle itself, could serve as a complementary reservoir of unradiogenic Pb, sourced in either sulphide [1] or silicate minerals [2], but it remains unclear why such material is not sampled by oceanic basalts.

This study presents high-precision double-spike Pb isotope data for the constituent phases of Mid-Ocean Ridge Basalts (glass, plagioclase and sulphide) from a single ridge segment from the FAMOUS region (36°50'N) on the Mid-Atlantic ridge. Separated phases from individual samples show a remarkable variation in Pb isotope composition, greater than that seen for all basalts previously analysed from this ridge segment. These variations cannot be explained by assimilation of seawater altered oceanic crust or by contamination from the Azores hotspot, both of which carry a radiogenic Pb isotope signature. Rather they indicate mixing between an early extremely unradiogenic melt, from which plagioclase crystallised, sourced by mantle material showing long-term depletion of U, and a later more radiogenic melt sampled by the glass. Elemental data suggest that the mantle source of this early melt was small-degree, water-rich with a garnet-like signature. Therefore, at least, some of the Pb in the Earth's mantle that is sampled by MORB is unradiogenic and complements the radiogenic composition seen in many oceanic basalts and continental crust. It remains to be seen whether variations in ²⁰⁷Pb-²⁰⁶Pb seen in other ridge segments reflect a similar contribution from an unradiogenic source.

[1] K.W. Burton *et al.* (2012) Unradiogenic lead in Earth's upper mantle. *Nature Geoscience* **5**, 570-573. [2] J. M. Warren, S. B. Shirey (2012) Lead and osmium isotopic constraints on the oceanic mantle from single abyssal peridotite sulfides. *Earth. Planet. Sci. Letts.* **59-360**, 279-293.

Reconciling ground deformation and degassing activity at Mt. Etna

M. BURTON¹, P. ALLARD² AND G. PUGLISI³

¹IPG Paris (pallard@ipgp.fr)

²INGV PI, Via della Faggiola, 32, 56126 PISA
(burton@pi.ingv.it)

³INGV-OE, piazza Roma 2, 95125 Catania, Italy,
(*correspondence: puglisi-g@ct.ingv.it)

Etna exhibited both steady inflation and persistent degassing between 1993 and early 2001. The source volume increase associated with the inflation was deduced using a Mogi model to fit the observed deformation pattern. The mass of SO₂ released in the same period was produced by degassing magma. With knowledge of the original S concentration dissolved in the parental magma it is possible to determine a minimum mass of magma consistent with the observed gas emissions. This mass of degassed magma is more than two orders of magnitude larger than the mass of erupted magma in the same period, implying that the degassed magma was endogenously stored within the volcano. We wish to test the hypothesis that this stored degassed magma was responsible for the observed inflation of the edifice.

An initial comparison of the volume of degassed magma compared with the change in volume associated with the ground deformation reveals that the former is 4 times greater than the latter, suggesting that our hypothesis is incorrect. However, when a combination of magma compression and viscoelastic deformation of hot crustal material heated is taken into account, the deformation source volume changes can, instead, be successfully reconciled with the volume of degassed magma.

Thus, it appears we cannot exclude the hypothesis that during the observation period ground deformation at Etna was controlled by permanent storage of degassed magma in the plutonic zone 5-8 km beneath the surface. In this manner, the constant magma supply indicated by the persistent degassing of the volcano produces a quiescent accumulation of degassed magma at the roots of the volcano, slowly pressurizing and inflating the edifice.

A global volcanic CO₂ flux inventory

MICHAEL BURTON¹, GEORGINA SAWYER²
AND DOMENICO GRANIERI³

¹INGV Pisa, Italy, (burton@pi.ingv.it)

²MetOffice, UK, (georgina.sawyer@metoffice.gov.uk)

³INGV Pisa, Italy, (granieri@pi.ingv.it)

CO₂ degassing from the Earth has played a fundamental role in controlling climate through a series of feedback mechanisms including CO₂ removal through weathering in proportion to the magnitude of greenhouse warming produced by CO₂ in the atmosphere. Constraining CO₂ emission rates from volcanic sources would allow an improved understanding of the relative magnitude of natural and anthropogenic outputs today, shed light on the role of volcanic emissions in the pre-industrial climate and improve our knowledge of carbon recycling through the mantle. Notwithstanding this, the flux of CO₂ from the Earth remains poorly quantified. The uncertainty in our knowledge of this critical input into the geological carbon cycle led Berner and Lagasa (1989) to state that it is the most vexing problem facing us in understanding that cycle.

To date, CO₂ fluxes have been directly measured on approximately 23% of the world's actively degassing subaerial volcanoes. Here we present an updated assessment of the global volcanic CO₂ flux, based on these empirical observations. We use this inventory to extrapolate to an estimate of global volcanic CO₂ emissions, and to investigate rates of carbon recycling through the mantle.

Disequilibrium melting recorded in isotopic and trace element compositions of a pulsed granitoid, Mt Kinabalu, Borneo

ALEX BURTON-JOHNSON¹, COLIN G MACPHERSON¹,
ROBERT HALL² AND GEOFF M NOWELL¹

¹Department of Earth Sciences, Durham University, Durham, UK, DH3 1LE.

(alexander.burton-johnson@durham.ac.uk)

²Southeast Asia Research Group, Department of Earth Sciences, Royal Holloway university of London, UK, TW20 0EX

Geochemical heterogeneity in silicic systems - and by implication heterogeneities in the continental crust - can be derived from the melting processes or variations in their deep source regions. Mixing and assimilation during the ascent and emplacement of silicic plutons are also invoked to explain observed heterogeneities. We present a range of geochemical data collected from the zoned granite and granodiorite pluton of Mt Kinabalu in NW Borneo to provide insight into the role of such processes in development of this body and the timescales over which they occur.

The Mt Kinabalu pluton is an isolated post-orogenic intrusion. It formed following the Miocene orogenic inversion event recorded in NW Borneo that emplaced attenuated S. China crust, similar to the attenuated Mesozoic tonalitic crust of the South China Sea, beneath the region's ophiolitic basement. Post-orogenic extension and rapid related uplift (aided by the fast erosion rates of the region) led to dehydration partial melting of the tonalitic crust.

Melting resulted in the emplacement of five petrographically distinct major units at ~ 0.2Ma intervals, the first four between 7.85 and 7.22Ma (U-Pb in zircon, [1]). The oldest unit possesses significantly more radiogenic Sr and Pb and less radiogenic Nd isotope ratios than later units. This could be interpreted as evidence for isolated derivation or mixing of multiple sources, or contamination of one source. However, there is no accompanying variation in $\delta^{18}\text{O}$ or trace element ratios. More substantial trace element variation is displayed between the later units that display little isotopic contrast with one another. Instead, we interpret the isotopic data and trace element variations as the result of progressive disequilibrium melting under increasingly warmer conditions of the same region of relatively homogeneous crustal source rocks.

[1] Cottam, Hall, Sperber & Armstrong (2010), *Journal of the Geological Society* **167**, 49-60.

Transport of carbon colloid supported nano zero-valent iron

JAN BUSCH^{1*} AND SASCHA OSWALD²

¹Institute for Earth and Environmental Science, University of Potsdam, Potsdam, Germany

(*correspondence: jan.busch@uni-potsdam.de)

²Institute for Earth and Environmental Science, University of Potsdam, Potsdam, Germany (sascha.oswald@uni-potsdam.de)

Nano zero-valent iron (nZVI) is an emerging technology for *in situ* groundwater remediation. Due to its high reactivity, nZVI is able to dechlorinate organic contaminants and render them harmless. Carbo-Iron is a newly developed composite material consisting of activated carbon colloids ($d_{50} = 0.6\text{-}2.4 \mu\text{m}$) that are dotted with nZVI particles. These particles combine the sorption capacity and mobility of activated carbon colloids and the reactivity of nZVI. Results from column tests and a two dimensional laboratory aquifer test system are presented: Column tests using columns of 40 cm length were filled with porous media. A particle suspension was pumped through the system. Results show, addition of a polyanionic stabilizer such as Carboxymethylcellulose (CMC) is required to enhance mobility. Ionic strength and pH concentrations in an environmental relevant range do not interfere significantly with transport, but particle size was found to be crucial. Another experiment was performed in a two dimensional aquifer test system. The test system contains a sand filled container with an inner size of 40 x 5 x 110 cm and seven ports on each side. A constant flow of water was applied from the left to the right side through all ports and the middle port was fed with a Carbo-Iron suspension. Results show transport through the laboratory aquifer within few exchanged pore volumes, and breakthrough of ~60% of the injected concentration of Carbo-Iron at the outlet. Deposits of immobile Carbo-Iron were found to be decreasing with distance from the injection port. No gravity effects were observed. Results suggest high mobility of carbon supported nZVI under environmental relevant conditions. Carbo-Iron might be helpful to deliver nZVI into contaminated aquifers. Here 1D and 2D results support the design of a field test and application of Carbo-Iron for nZVI delivery.

Delta ^{34}S of discrete authigenic framboidal pyrite: A powerful palaeo-indicator for barrier estuary closure

*RICHARD T BUSH¹, LEIGH A SULLIVAN¹,
MICHELLE L BUSH¹ AND NICK WARD¹

¹Southern Cross GeoScience, Southern Cross University, 1
Military Rd, Lismore, NSW, 2480, Australia
(*Correspondence: richard.bush@scu.edu.au)

This study relates microscale isotopic variability of discrete authigenic framboidal pyrite to the palaeo-depositional conditions of a barrier-estuary on the east coast of Australia. Light sulfur isotope (^{32}S) is preferentially utilised in microbially mediated pyrite formation, with the extent of fractionation dependent on how 'open', or 'closed', the depositional environment is to a replenishing supply of sulfate. An open system has an unlimited supply of the preferred, light sulfate during sedimentation. In a closed system, all of the sulfate, light and heavy (i.e. ^{34}S), is eventually utilised.

Intact sediment cores were collected from the lower Richmond River floodplain. Sampling encompassed the last 6000 years of sedimentation, extending to a depth of 5m. The isotope composition of discrete pyrite framboids was determined on select layers using secondary ion mass spectrometry[1]. The striking result was an anomalous enrichment of ^{34}S in pyrite at 1.7- 2.5m depth, with $\delta^{34}\text{S}$ peaking at +50‰. (-20 to +10‰ is the normal range for estuarine sediments). The microscale isotopic variability between pyrite framboids in this layer had a broad distribution, consistent with that theoretically predicted by Seal and Wandless^[1] for a 'closed' system. This study provides the first demonstration of microscale sulfur isotope frequency distribution as a tool for identifying in the sediment record, periods of closure of barrier estuaries or other coastal embayments to marine influences.

[1]. Seal, Wandless (2006), *Reviews in Mineralogy and Geochemistry*, **61**, 633-670.

Nitrogen cycle in the late Archean ferruginous ocean

VINCENT BUSIGNY¹, OANEZ LEBEAU¹, MAGALI ADER¹,
BRYAN KRAPEZ² AND ANDREY BEKKER³

¹IPG-Paris and Univ. Paris Diderot, Sorbone Paris Cité, France
²Institute for Geoscience Research, Curtin Univ., Australia
³Dpt of Geological Sciences, Univ. of Manitoba, Canada

The Hamersley Group comprises a Late Archean sedimentary succession, which is thought to record the prelude to the atmospheric oxygenation in the early Paleoproterozoic, the so-called Great Oxidation Event (GOE) dated at around 2.4 Ga. In the present work, drill-core samples of sedimentary rocks from the upper Mount McRae Shale and Brockman Iron Formation deposited before the GOE at ~2.5 Ga were examined in order to characterize the environments and ecosystems prevailing during their deposition. We analyzed the concentration and isotopic composition of C in carbonate and organic matter, bulk N content and its isotopic composition, and major element concentrations.

The $\delta^{13}\text{C}_{\text{carb}}$ values, ranging from -10.7 to -3.2 ‰, reflect diagenetic carbonate precipitation, with markedly negative values representing Fe-rich carbonates formed via organic matter mineralization with ferric oxyhydroxides. In contrast, $\delta^{13}\text{C}_{\text{org}}$ and $\delta^{15}\text{N}$ values record primary isotope signatures derived from ancient living organisms. The near constant $\delta^{13}\text{C}_{\text{org}}$ values at -28.7 ± 0.8 ‰ are interpreted as reflecting photoautotrophs thriving on a large pool of dissolved inorganic carbon. Whole-rock N analyses show highly variable concentration, between 1.3 and 785 ppm, and $\delta^{15}\text{N}$ values range between 0.4 and 13.4 ‰. Inverse relationship between $\delta^{15}\text{N}$ and $\delta^{13}\text{C}_{\text{carb}}$ values characterize the Brockman Iron Formation. We propose that N and C biogeochemical cycles were connected via Fe redox processing in the water column and in sediments of the Late Archean ocean. Several models coupling N and Fe biogeochemical cycles are considered involving different redox states of the water column. Similar positive $\delta^{15}\text{N}$ values might record very different N biogeochemical cycles under fully anoxic, redox-stratified, and oxic conditions of the ocean. Interpretation of N isotopes in terms of N biogeochemical cycle thus requires independent constraints on the redox structure of the ocean.

Relating grain-scale weathering observations to catchment-scale critical zone morphology

H.L. BUSS^{1*}, O.W. MOORE¹, M. CHAPELA LARA¹,
M. SCHULZ² AND A.F. WHITE²

¹School of Earth Sciences, University of Bristol, Bristol BS8 1RJ, UK
(*h.buss@bristol.ac.uk, o.moore@bristol.ac.uk)

²US Geological Survey, Menlo Park, CA 95025, USA
(mschulz@usgs.gov, afwhite@usgs.gov)

It is well known that chemical weathering and porosity development in rocks are coupled. It is less understood how these coupled processes, which operate at the mineral grain-scale, impact larger-scale phenomena such as watershed fluxes and regolith and landscape development. The Bisley watershed in the Luquillo Critical Zone Observatory (Puerto Rico) is formed on meta-volcaniclastic bedrock that is blanketed by thick regolith comprised of thin soil overlying saprolite embedded with corestones. Saprolites here are highly leached; as a result, most chemical weathering fluxes are attributed to weathering at the bedrock-saprolite interface. However, corestone surfaces and fractures represent multiple “bedrock-saprolite interfaces” distributed throughout the regolith profile. Here we compare macro-scale weathering profiles (m’s thick) in saprolite to micro-scale (mm’s thick) profiles across corestone weathering rinds. Buried corestones were sampled by drilling two boreholes (27 and 37 m deep).

Weathering fronts are most dramatic in rinds on corestone fractures and surfaces. For example, ~40% of the protolith Mg is lost over ~3 mm of rind. In saprolite hand-augered to a corestone at 9.3 m, the final 20% of protolith Mg is lost over ~8 m. These fronts may reflect different weathering mechanisms as well as different weathering rates.

Pyrite crystals, which are of low abundance in these rocks and not detected by powder XRD, were identified by SEM in many of the thin sections and appear to be the first mineral to weather. In thin sections containing fracture surfaces, pyrite is associated with increased porosity and dissolving plagioclase and amphibole grains. These associations are observed even cm’s inboard of the visible weathering rinds. Although present only in trace amounts, pyrite appears to play a controlling role in secondary porosity development and weathering of the major minerals by releasing sulfate during oxidative dissolution, creating micro-environments of highly reactive, low pH fluid within the corestones. Where the bedrock contains more pyrite, corestones may split and shrink more readily, affecting mineral weathering rates and larger-scale phenomena such as the size and distribution of corestones within the regolith profile.

Organic geothermometry: Defining metamorphic grades in coal

J.P. BUSSIO¹, R.J. ROBERTS¹ AND N.J. WAGNER²

¹Department of Geology, University of Pretoria, South Africa;
(John.Bussio@up.ac.za)

²School Chemical & Metallurgical Engineering, University of Witwatersrand, Johannesburg, South Africa,
(Nicola.Wagner@wits.ac.za)

Mechanical and chemical variations created during metamorphism of organic compounds is an overlooked subject. The fundamentally structure of organic materials is analogous to that of inorganic materials such as minerals and rocks, but the organic equivalents are subject to generalities of both structure and chemistry which has left the interpretation of the metamorphic products of these materials vague and unspecific. The physicochemical nature of the coal and its macerals is currently quantified using thermogravimetric proximate analysis, which aims define the properties of coal through the quantification of moisture %, ash%, volatile% and calorific value.

A new approach was used to analyse the physicochemical character of the coal in close proximity to a dolerite intrusion on both macro and micro scales. Macro scale structural analysis has been done through the use of a Schmidt hammer to quantify *in situ* physical variation within the coal. In conjunction, conventional proximate analysis was employed to estimate the “chemical” variations within the coal. It was expected that the fundamental link between chemical properties and physical character would be displayed in the resultant analysis, but no direct link between the proximate analysis and Schmidt hammer results was observed, either as a result of inherent heterogeneity of coal or a display of the short comings of the proximate analysis method. In light of these results, a new approach was applied by using pressurized liquid extraction (PLE) combine with two dimensional gas chromatography time of flight mass spectrometry (GC*GCTOFMS) to produce detailed chromatograms of the organic constituents of the coal. The technique will allow quantification of the organic components within the coal. Due to the variable sensitivity of organic compounds to fluids, salinity, pressure and temperature, it may be possible to define not only the temperature of metamorphism but also the type *i.e.* metasomatic or contact and also the salinity of the metamorphic fluid.

Characterization of a novel multicopper oxidase that oxidizes Mn(II)

C. N. BUTTERFIELD¹, A. V. SOLDATOVA², T. G. SPIRO²
AND B. M. TEBO^{1,*}

¹ Division of Environmental and Biomolecular Systems,
Oregon Health and Science University, Beaverton, OR
97006, USA (*correspondence: tebo@ebs.ogi.edu)

² Department of Chemistry, University of Washington, Seattle,
WA 98195

Manganese (Mn) oxides are some of the most reactive mineral phases in the environment and control the distribution and bioavailability of a variety of toxic and essential elements. Mn oxide minerals are believed to be formed either directly or indirectly through the activities of microorganisms. The ability to oxidize Mn in several phylogenetically distinct groups of bacteria has been attributed to enzymatic oxidation by a multicopper oxidase (MCO), a family of proteins that utilize multicopper atoms in catalytic sites to oxidize their substrates, typically Fe(II) or phenolic compounds, in one electron reactions. Here we report the expression, purification and partial characterization of a Mn-oxidizing MCO and preliminary efforts to reconcile the one-electron chemistry of MCOs with the two-electron oxidation of Mn(II) to Mn(IV) oxide.

Many attempts have been made to purify the suspected Mn-oxidizing MCO from a variety of different bacteria, including species of *Pseudomonas*, *Leptothrix*, *Pedomicrobium* and *Bacillus*. In many species of marine *Bacillus* it is the mature spores that oxidize Mn(II). Oxidation occurs on their exosporium, the outermost layer of the spore, encrusting them with Mn(IV) oxides. Previous studies identified the *mxn* genes, including *mxnG*, a putative multicopper oxidase, as responsible for the two-electron oxidation of Mn(II). Its characterization, however, has been hampered by the difficulty in obtaining purified protein. By purifying active protein from the *mxnDEFG* expression construct, we found that the resulting enzyme is a blue (Abs max 590nm) complex containing MnxE, MnxF, and MnxG proteins. The complex oxidizes both Mn(II) to Mn(III) and Mn(III) to Mn(IV) resulting in the formation of a Mn(IV) oxide mineral. X-ray absorption spectroscopy of the Mn mineral product confirmed its similarity to Mn(IV) oxides generated by whole spores or purified exosporium. With the purification of active Mn oxidase, we will be able to unravel the mechanism of Mn oxidation and broaden our understanding of Mn oxide mineral formation and the bioinorganic capabilities of MCOs.

Inventing the Phanerozoic biological pump - and inducing Snowball Earth

N. J. BUTTERFIELD

Department of Earth Sciences, University of Cambridge,
Cambridge, UK CB2 3EQ (njb1005@cam.ac.uk)

Export production in the modern oceans is dominated by relatively large/biomineralizing eukaryotic phytoplankton, often accelerated by animal-mediated repackaging in the form of fecal pellets, appendicularian houses and carcasses. Prior to the evolution of animals, and the co-evolutionary radiation of photosynthetic eukaryotes, the biological pump would have worked in a fundamentally different fashion. The transition between these two alternate states appears to have begun in the mid-Neoproterozoic (Tonian/Cryogenian), and achieved a recognizably Phanerozoic condition in the early (but not earliest) Cambrian.

Modern aquatic ecosystems exhibit marked hysteresis between clear-water eukaryote-dominated conditions and an alternative turbid-water cyanobacterial state, typically mediated by suspension-feeding metazoans. In marine shelf environments, the particular ability of sponges to draw down turbidity-inducing DOC, and actively select for larger more export-prone phytoplankton, imparts a first-order control on the biological pump. This in turn presents the circumstances for a more general exploitation of the water column by eumetazoans, especially bilaterians, leading to multi-trophic food-webs, enhanced ventilation and complex feedback effects on nutrient cycling and export.

Biomarker evidence suggests that Proterozoic export was dominated by cyanobacteria. The first quantitatively significant occurrence of eukaryotic steranes appears shortly before the Cryogenian glaciations, along with a novel suite of eukaryotic microfossils. Although there is no direct fossil record of animals at this time, there is a case for recognizing these changes as a co-evolutionary consequence of newly introduced animal activity. Intriguingly, current molecular clock analyses place the first appearance of simple (sponge-grade) animals in this same mid-Neoproterozoic time-frame.

Changes to the mid-Neoproterozoic biological pump are likely to have induced major increases in oceanic alkalinity, leading to a draw-down of atmospheric CO₂ and potentially triggering Cryogenian glaciation [1]. As such, the pronounced evolutionary, biogeochemical and climatic perturbations of the terminal Proterozoic may all be causally linked to the evolutionary appearance of animals.

[1] Tziperman, E., *et al.* 2011. Biologically induced initiation of Neoproterozoic snowball-Earth events. *PNAS* **108**:15091-96.

Experimental study on interaction of the H₂O-NaCl fluid and model peridotite at 6 GPa

V.G. BUTVINA AND O.G. SAFONOV

¹ IEM RAS, ul. Institutskay, 4, Chernogolovka, Moscow district, 142432, Russia, (butvina@iem.ac.ru)

In order to study the effect of NaCl on the Al₂O₃, CaO, Na₂O-rich H₂O-bearing peridotite transformation at pressures above 3 GPa, we have conducted the experiments on interaction of model peridotite $For_{57}En_{17}Prp_{14}Di_{12}$ with the H₂O-NaCl fluid at 6 GPa and 1050-1450°C. Starting materials were mixtures of oxides, Mg(OH)₂ and jadeite (mg): SiO₂ (37.04); Al₂O₃ (3.66); CaO (3.62); Mg(OH)₂ (48.30); MgO (4.14), NaAlSi₃O₆ (3.24). NaCl added at 8 wt. %, that corresponds to mole fraction of $X_{NaCl} = NaCl/(NaCl+H_2O)$ in the fluid 0.05. The present experiments were performed using Pt capsules of 0.02 mm of the wall thickness.

In absence of NaCl in the fluid, the assemblage Fo+Opx+Cpx+Grt was observed in the solidus of the model peridotite, while melting began at about 1200-1300°C. Clinopyroxene shows the increase of jadeite content with increasing temperature. Addition of NaCl reduces melting temperature down to 1050-1100°C. Amount of orthopyroxene and garnet in solidus decreases, the Al content in orthopyroxene decreases, and the jadeite content of clinopyroxene increases in presence of NaCl. These relationships can be described by the following reactions:

(1) $1/4 Mg-Ts + 7/4 En + 1/2 NaCl + 1/4 H_2O = Fo + 1/2 Jd + 1/2 HCl$; (2) $1/4 Prp + 5/4 En + 1/2 NaCl + 1/4 H_2O = Fo + 1/2 Jd + 1/2 HCl$; (3) $1/4 Grs + 11/4 En + 1/2 NaCl + 1/4 H_2O = Fo + 3/4 Di + 1/2 Jd + 1/2 HCl$,

(where Mg-Ts – Mg- Tschermack molecule, MgAl₂SiO₆ in orthopyroxene, En – enstatite, Fo – forsterite, Prp – pyrope, Grs – grossular, Di – diopside, Jd – jadeite). These reactions show the destabilization of Grt-Opx association in the presence of the H₂O-NaCl fluid.

Thus, addition NaCl in the H₂O-peridotite system does not influence on phase assemblages. However, changing of mineral compositions, mostly increase of the jadeite content in clinopyroxene, results in the decrease of melting temperature. Present experiments further support our conclusion [1] that the effect of interaction of alkali chlorides with silicates in complex peridotite assemblages overpowers the effect of the reduced H₂O activity in the brine fluid [2].

[1] Safonov & Butvina (2013) Doklady, in print. [2] Chu *et al.* (2011) Contrib **162**, 565-571.

Pyroxene megacrysts in anorthosites: Revealing continental crust-forming processes at Moho depths

G.M. BYBEE^{1*}, L.D. ASHWAL¹ AND S.B. SHIREY²

¹School of Geosciences, University of the Witwatersrand, Private Bag 3, WITS, 2050, South Africa

(*correspondence: grant.bybee@wits.ac.za)

²Department of Terrestrial Magnetism, Carnegie Institute for Science, 5142 Broad Branch Road, Washington D.C. 20015, USA

The mismatch between bulk, intermediate compositions (SiO₂ > 60 %) of the continental crust and predicted basaltic compositions (SiO₂ < 50 %) of mantle-derived melts in crust-forming environments poses a major problem in models of crustal evolution and requires that a mafic component be physically separated from felsic end-members. Although information from the Moho, where some of these poorly understood crustal differentiation processes are thought to occur, is rare, giant (up to 1 m in length), high-pressure (30-40 km) pyroxene megacrysts and comagmatic Proterozoic anorthosite massifs provide insight into crust-mantle differentiation processes at these depths. Using Nd and Pb isotopes, we provide direct evidence for megacryst crystallization in isotopically homogenous magmas that ponded at the Moho (Figure 1). These megacrysts are 110-130 m.y. older than the comagmatic anorthosites that host them, indicating that the magmatic system is long-lived. In combination with EC-AFC modeling, these data also indicate that Proterozoic anorthosites are derived from melting of the depleted mantle at long-lived Andean-type margins. This evidence for ultramafic cumulate formation illustrates that fractionation of ponded magmas at the Moho is a significant mechanism in crustal differentiation and that the loss of these dense phases to the deeper mantle may represent an important component of crustal recycling.

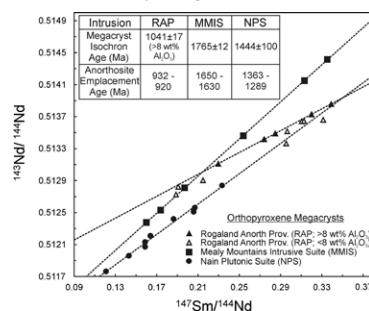


Figure 1: Isochronous high-pressure megacrysts in three Proterozoic anorthosite massifs from Canada and Norway.

Geochemistry of trace elements in gas phase of thermal springs

A.YU.BYCHKOV^{1,2}, I.YU.NIKOLAEVA¹
AND S.YU.NEKRASOV¹

¹Moscow State University, Moscow, Russia
(bychkov@geol.msu.ru)

²Vernadsky Institute of Geochemistry RAS, Moscow, Russia

The composition of the thermal waters studied well, but there are only few articles on the geochemistry of trace elements in thermal springs gas phase. Samples of the coexisting liquid and gas phases were collected in thermal springs of Kamchatka peninsula (Russia): Mutnovsky volcano, Uzon Caldera, Geyser Vally, Karymsky volcano. For the sampling of thermal springs specially designed installation was used, wells of Mutnovsky geothermal plant was studied by standard two-phase separator of steam-water mixture. More than 200 samples of coexisting gas and liquid was collected. In samples the concentration of major and trace elements and hydrogen and oxygen isotope composition were determined.

The distribution of high volatile elements, such as boron and arsenic in geothermal wells steam-water mixture was found close to experimental data. However gas phase condensates from thermal springs compared with the liquid phase are enriched with boron and arsenic. This cannot be explained by the equilibrium distribution of components by experimental data. This effect is observed only for thermal springs with superheated steam and correlates with the isotopic composition of the condensates. Perhaps distribution of the superheated steam is determined by the equilibrium at high temperatures in the depth of hydrothermal system. Boron concentration of the condensate can be used to detect the temperature of the gas phase separation and deep boiling. The calculations show good agreement with other geothermometric methods.

For nonvolatile elements, such as REE, Ga and others, distribution coefficients were calculated. Some correlations between the partition coefficients were shown. So, for LREE they are higher than for HREE. These coefficients can't be calculated from thermodynamic data, since the speciation of elements in the gas sufficiently studied. New experiments of solubility in the gas phase can explain distribution coefficients, as shown by the example of gallium. For this element the gas form Ga(OH)₃ was determined by gallium oxide solubility in vapor. This experimental data can explain the dependence of the distribution coefficient of the pH of thermal water.

This study was supported by RFBR 12-05-00957.

Subduction modification of Western North America lithosphere - Priming for destruction?

B.L. BYERLY* AND J.C. LASSITER

Jackson School of Geosciences, University of Texas at Austin,
Austin, TX, USA (* benbyerly@utexas.edu)

Destruction of continental lithospheric mantle has been recognized to be an important process that may affect the preservation of continental crust [1]. Geochemical data from mantle xenoliths indicate that the majority of the Proterozoic lithospheric mantle beneath the central Rio Grande Rift (RGR) has been convectively removed [2]. Weakening of the lithospheric mantle by addition of metasomatic fluids/melts during Laramide flat-slab subduction followed by increased mantle flow due to Farallon slab roll-back may have triggered this lithosphere destruction. If metasomatism is related to the recent deformation/destruction of the lithosphere beneath the RGR, then mantle metasomatism recorded in remnant lithospheric mantle xenoliths should also be recent.

We examined the trace element and Sr-Nd-Os-Hf isotopic composition of two suites of lithosphere-derived spinel-peridotite xenoliths from Cerro Chato (Eastern Colorado Plateau margin) and Elephant Butte (central RGR) to constrain the timing and source of mantle metasomatism. ¹⁸⁷Os/¹⁸⁸Os ranges from 0.114-0.126 and T_{RD} ages for the most depleted samples range from 1.6-2.2 Ga; similar to the age of the crust in the region [3]. Both suites of xenoliths are LREE-enriched with variable negative HFSE anomalies relative to REE. (La/Sm)_N in cpx ranges from 2-14 and is correlated with ⁸⁷Sr/⁸⁶Sr which range from 0.7031-0.7045. ε_{Nd} ranges from 4-10 and ε_{Hf} ranges from 17-304. There is no correlation between ¹⁴³Nd/¹⁴⁴Nd and Sm/Nd which suggests metasomatism is recent. This is consistent with young (< 250 Ma) Nd model ages for the xenoliths. A Hf pseudoisochron (using WR Lu/Hf due to equilibration above Lu-Hf closure temperature) yields an age of ~1.0 Ga, which is younger than the Os model ages. The young Hf age may be the result of mixing and partial resetting of Hf isotopes by metasomatism as evidenced by a correlation between 1/[Hf] and ¹⁷⁶Hf/¹⁷⁷Hf. The most radiogenic sample has a DM-model age of 1.45 Ga which is close to the age of the overlying crust. Arc-like metasomatic signatures and young Nd model ages are consistent with metasomatism being recent and related to Farallon slab subduction. This may have primed the Colorado Plateau for deformation similar to that observed in the RGR.

[1] Lee, C.T. *et al.* (2001) *Nature*, **411**, 69-73 [2] Byerly, B., Lassiter, J.C. (2012) *EPSL*, **355-356**, 82-93 [3] Wendlandt, E. *et al.*, (1993) *EPSL*, **166**, 23-43

Microbial redox cycling of surface Fe-ions in magnetite nanoparticles

JAMES M BYRNE*, NICOLE KLÜGLEIN
AND ANDREAS KAPPLER

Geomicrobiology, University of Tuebingen, Germany
(*correspondence: james.byrne@uni-tuebingen.de)

Iron is an essential element for all microbes, with different oxidation states by some even used as an electron source or as a terminal electron acceptor. The phototrophic iron-oxidizer *Rhodospseudomonas palustris* TIE-1 uses energy from light and electrons from ferrous Fe(II) for growth and respiration, whilst *Geobacter sulfurreducens* combines the oxidation of organic compounds or hydrogen with the reduction of ferric Fe(III). Iron is almost exclusively observed to be bioavailable to the bacteria as aqueous Fe(II) or in poorly crystalline Fe(III) (oxyhydr)oxides such as ferrihydrite. More crystalline iron minerals such as magnetite or siderite are not usually considered to be biologically active. Magnetite is a mixed valent iron oxide $\text{Fe}^{\text{II}}(\text{Fe}^{\text{III}})_2\text{O}_4$ which is often seen as the end member product of the microbial reduction of ferrihydrite, though very rarely as a result of microbial oxidation of Fe(II).

This study focuses on the oxidation of superparamagnetic magnetite nanoparticles (~20 nm) by strain TIE-1 and the potential mineralogical changes which result. Through *in situ* magnetic measurements and iron extraction methods, we found that the cells are capable of directly oxidizing the surface of magnetite nanoparticles and thereby decrease the overall magnetic susceptibility of the mineral. This effect occurs in the absence of any aqueous Fe(II) in the growth medium and only magnetite provided as the electron donor. Significantly, this process can be reversed through Fe(III) reduction by *G. sulfurreducens*, which in turn leads to an enhancement of the magnetic properties of the nanoparticles. Changes in magnetic properties were also detected in experiments using magnetite with varying stoichiometric ratios (i.e. $\text{Fe}^{\text{II}}/\text{Fe}^{\text{III}}$). Such effects were not observed in abiotic experiments which did not contain any bacteria.

These results demonstrate that iron ions bound at the surface of crystalline minerals such as magnetite are bioavailable for microbial respiration and can potentially be used as a source of iron in reducing or oxidizing conditions, with the potential to cycle the surface redox properties depending on the conditions present. Such modifications may provide a route towards enhancing remediation strategies that are based on the highly reactive surface of magnetite. These effects may also have implications on paleomagnetic measurements in microbially active environments.

DOI:10.1180/minmag.2013.077.5.2
www.minersoc.org

Mass independently fractionated sulfur isotopes in HIMU lavas reveal Archean crust in their mantle source

R.A. CABRAL^{1*}, M.G. JACKSON¹, E.F. ROSE-KOGA²,
K.T. KOGA², M.J. WHITEHOUSE³, M.A. ANTONELLI⁴,
J. FARQUHAR⁴, J.M.D. DAY⁵ AND E.H. HAURI⁶

¹Boston University, Boston, MA 02215

(*correspondence: racabral@bu.edu)

²Universite Blaise Pascal, Laboratoire Magmas et Volcans,
CNRS, UMR 6524, Clermont-Ferrand, France

³Swedish Museum of Natural History, Laboratory for Isotope
Geology, SE-104 05, Stockholm, Sweden

⁴University of Maryland, College Park, MD 20742

⁵Scripps Institution of Oceanography, La Jolla, CA 92093

⁶Department of Terrestrial Magnetism, Carnegie Institution of
Washington, Washington DC 20015

Ocean island basalt (OIB) lavas from Mangaia, Cook Islands (Polynesia) exhibit an extreme HIMU (high- μ , or high $^{238}\text{U}/^{204}\text{Pb}$) signature that has been attributed to melting of ancient recycled oceanic lithosphere within their mantle source. However, the residence time of subducted materials in the mantle is uncertain and model-dependent, and compelling evidence for their return to the surface in regions of mantle upwelling beneath hotspots is lacking. Here we report new SIMS data supporting our original finding of anomalous sulfur isotope signatures indicating mass-independent fractionation (MIF) in olivine-hosted sulfides from 20-million-year-old ocean island basalts from Mangaia (most extreme $\Delta^{33}\text{S}$ measurement = $-0.34 \pm 0.08\text{‰}$) [1]. Terrestrial MIF sulfur isotope signatures were generated exclusively through atmospheric photochemical reactions until about 2.45 billion years ago. Therefore, the discovery of MIF sulfur in these relatively young OIB lavas suggests that sulfur once at the Earth's surface was subducted into the mantle before 2.45 billion years ago and recycled into the mantle source of Mangaia lavas. These data provide evidence for ancient materials, with negative $\Delta^{33}\text{S}$ values, in the mantle source of Mangaia lavas. Our data also complement evidence for recycling of the sulfur content of ancient sedimentary materials to the subcontinental lithospheric mantle that has been identified in diamond-hosted sulfide inclusions. This Archean age for recycled oceanic crust also provides key constraints on the length of time that subducted crustal material can survive in the mantle, and on the timescales of mantle convection from subduction to upwelling beneath hotspots.

[1] Cabral *et al.* (2013) *Nature* doi:10.1038/nature12020

Heavy metals of the Santiago Island (Cape Verde) topsoils

CABRAL PINTO, M.M.S.^{1,2,3*}, E.A. FERREIRA SILVA¹,
SILVA, M.M.V.G.² AND J. SOUSA BRITO³

¹Geobiotec Center, University of Aveiro, Portugal

²Geociencias Center, University of Coimbra, Portugal

(*marinacp@ci.uc.pt)

³University Jean Piaget, Santiago Island, Cape Verde

In this work we present maps of Estimated Background Value (EBV) of some harmful metals (As, Cd, Co, Cr, Cu, Hg, Mn, Ni, Pb, V, Zn) in the soils of the Santiago Island and analyse their relationships with the geological cartography. We also carried out Risk assessment on the soils. The geochemical survey (sampling of 249 soil samples, sample preparation, analysis, data treatment and mapping) was conducted following the guidelines of the International Project IGCP 259. The concentration of selected elements were determined in the fraction <2mm. Each sample was digested with aqua regia and analyzed by ICP-MS. Heavy metals in Santiago Island topsoils were mostly originated from the weathering of underlying bedrocks. The EBV spatial distribution of the metals allowed us to establish relationships between the geological formations. These relationships were confirmed by the results of Principal Component Analyses (PCA). The metals with higher loadings in PC1 (Co, Cr, Ni, Cu and V) clearly show the influence of a rich lithology in siderophile elements, and metals typical of basic rocks. The high values of Geoaccumulation Indices for these elements demonstrated that the Santiago soils may have higher Co, Cr, Ni, Cu and V risks which are caused by its higher natural origin. The metals with higher loadings in PC2 (As, Hg, Cd, Zn and Pb) are also taken as a natural lithogenic factor, because the metals hot spots are mainly located at areas with soils derived from pyroclastic deposits of MV and AS Formations. However, contamination of As, Hg, Cd, Zn and Pb occurred in some areas that may have a human-influenced source.

Combustion carbonaceous particles: Evolution of their impacts

HELENE CACHIER^{1,2*} AND CATHY LIOUSSE²

¹Laboratoire des Sciences du Climat et de l'Environnement,
Gif sur Yvette (France)

²Laboratoire d'Aérodologie, Toulouse (France)
(helcachier@gmail.com)

Combustion using either fossil or vegetation fuels both emit a complex array of particles. The resulting aerosol contains primarily polymeric substances which properties substantially vary with the nature of fuels and combustion conditions. Hence, inventories firstly distinguish fossil fuel and "biomass burning" emissions, but furthermore domestic versus industrial or traditional versus modern usages. Future evolutions expected in emerging countries are likely to influence the local and regional impact of particles on atmospheric balances and population health.

Combustion particles have been traditionally described by their BC/OC content a key parameter allowing a minima assessments of their different impacts. More or less recent works, however, let suggest that carbon aerosol chemical complexity must be traced by other proxies among which the prominence of humic-like substances (HULIS) is now recognized. Interplays between HULIS contents and carbon particle radiative properties ("brown carbon"...) and water solubility ("WSOC" content) have to be investigated. In this context, aerosol partitioning into BC and OC and the lack of analytical agreement might be also revisited.

Petrologic preconditioning: A predisposition to polymetamorphism?

MARK J. CADDICK^{1*}

¹Department of Geosciences, Virginia Tech, Blacksburg, VA,
USA. email: (caddick@vt.edu)

Attainment of high or ultra-high temperatures (HT/UHT) in thickened continental crust requires significant heat input or generation, with a major thermal barrier being the latent heat requirement for melting. Melting or melt crystallization can thus buffer temperature on a local to regional scale [e.g. 1], with an additional (though far smaller) effect associated with sub-solidus dehydration reactions [2]. Incomplete retrogression of many amphibolite and granulite facies rocks implies that fluid influx during cooling is less pervasive than loss during heating [e.g. 2], so that these rocks effectively represent 'partially depleted residua'.

Subsequent heating (M_2) of previously metamorphosed (M_1) rocks requires less energy associated with melting if melt extraction during M_1 significantly reduced the rock's melt fertility. Thermodynamic calculations suggest that if a rock experienced significant melt loss at 850 °C in M_1 , the energy required to re-heat that rock to 800 °C during M_2 (calculated as the difference in specific enthalpy from 400 to 800 °C) may be > 15 % less than required without the prior metamorphism. The extent of this energy difference is a function of (i) the pre- M_1 melt fertility, (ii) the efficiency of melt and H_2O loss during M_1 and (iii) the specific $P-T$ histories involved. Furthermore, substantially different results are obtained by considering isochemical or progressively fluid + melt-depleting thermodynamic systems.

A consequence of this 'preconditioning' is that large granulite facies terranes can require substantially less energy to reach upper-amphibolite grade conditions than previously unmetamorphosed equivalents. This effectively pre-disposes them to high-grade metamorphism in later orogenic events (if they are not pervasively rehydrated in an intermediate step). Recognition of this polymetamorphism is difficult if $T_{M1} > T_{M2}$ because little M_2 mineral growth is expected, but resetting of mineral compositions and compositional zoning might be expected. 'Cryptic' polymetamorphism is thus unsurprising in many cases. Furthermore, the presence of large preconditioned bodies can strongly influence the apparent thermal evolution of orogenic belts, substantially modifying both conduction and fluid flow pathways.

[1] Stüwe (1995) *Tectonophysics* **248**, 39-51; [2] Connolly & Thompson (1989) *Contrib. Mineral. & Petrol.* **102**, 347-366.

^{224}Ra : ^{228}Th disequilibrium in coastal sediments: Implications for the transfer across the sediment-water interface

PINGHE CAI^{1*} SHIYUN PENG¹, WILLIARD S. MOORE²
XIANGMING SHI¹ GUIZHI WANG¹ AND MINHAN DAI¹

¹State Key Laboratory of Marine Environmental Science, Xiamen University, Xiamen 361005, P. R. China
*(Correspondence: (caiph@xmu.edu.cn), (shiyunpeng@stu.xmu.edu.cn), (kidsxm_0110@foxmail.com), (gzh(wang@xmu.edu.cn), (mdai@xmu.edu.cn)

²Department of Earth and Ocean Sciences, University of South Carolina, Columbia, South Carolina 29208, USA
(moore@geol.sc.edu)

We utilized $^{224}\text{Ra}/^{228}\text{Th}$ disequilibrium in the sediment to investigate the processes that regulate dissolved transfer across the sediment-water interface. Depth profiles of dissolved and surface-bound ^{224}Ra and ^{228}Th in the upper 0-20 cm sediment were measured using a delayed coincidence counter during a cruise to the Yangtze estuary from 15 to 24 August 2011. Along with ^{224}Ra and ^{228}Th , depth profiles of ^{234}Th were collected to determine the bioturbation rate in the sediment. At most study sites, a marked deficit of ^{224}Ra relative to ^{228}Th was observed in the upper 0-10 cm sediment. In contrast, ^{224}Ra was in excess with respect to ^{228}Th in the upper 0-5 cm sediment at the river mouth, possibly due to redistribution of ^{224}Ra from the mid-salinity region. By modeling the ^{224}Ra profiles in the sediment using the general diagenetic equation, we demonstrated that in most cases molecular diffusion and bioturbation together can account for only ~20-30% of the measured flux of ^{224}Ra . We concluded that other mechanisms, especially irrigation, must be invoked to explain the remnant 70% of the observed deviation of ^{224}Ra relative to ^{228}Th in the sediment. On the basis of the $^{224}\text{Ra}/^{228}\text{Th}$ disequilibrium in the sediment, we proposed an invaginated interface model to quantify the transfer rate of other dissolved species across the sediment-water interface. We have utilized the invaginated interface model to determine the benthic consumption rate of dissolved O_2 . The result reveals that O_2 consumption is an important loss term of dissolved O_2 in the Yangtze estuary and must be considered as one of the mechanisms that lead to hypoxia in this area.

The effect of zinc, nickel and cobalt on fluoride removal by low cost materials: Zeolite and calcite

QIANQIAN CAI^{1*} BRETT TURNER¹, DAICHAO SHENG¹
KRISTIAN KRABBENHOFT¹ AND SCOTT SLOAN¹

¹Centre for Geotechnical and Materials Modelling, Civil Surveying and Environmental Engineering, The University of Newcastle, University Drive, Callaghan, N.S.W., 2308, Australia
(*correspondence: Qianqian.Cai@uon.edu.au)

Spent Pot Lining (SPL) is a by-product of the electrolytic process in the smelting of aluminium. Historical disposal of SPL from the Hydro Aluminium smelter at Kurri Kurri, NSW, Australia has rendered the nearby groundwater contaminated as high as 2000 mg/L fluoride, which is far beyond the drinking water limitation of 1.5 mg/L. The excessive intake of fluoride, however, can lead to fluorosis. Since SPL leachate is in fact a complex chemical cocktail which also contains other contaminants like metal ions, it is necessary to understand how these chemicals will behave during the defluoridation process. This research aims to determine the effect of zinc, nickel, cobalt on the fluoride removal by zeolite and calcite. For this purpose, a range of "free-drift" kinetic tests have been conducted.

The tests were carried out at 20°C and a stirring rate of 200 rpm with $150\mu\text{m}$ zeolite or calcite. The initial concentration of synthetic fluoride solution was about 200 mg/L, which reflected the "average" concentration of fluoride contamination in groundwater at the Hydro Aluminium site. The fluoride solution was spiked with known amounts of either Zn, Ni or Co. Fluoride concentrations & pH were measured every 10 seconds using the respective ion-selective electrodes and spot checked by ion chromatography (IC). Selected samples were sent for ICPMS analysis for total metals.

Results show that the presence of metals can enhance the fluoride adsorption by zeolite with fluoride removal generally increasing with metal concentration. The best fluoride adsorption occurs with the addition of 100 mg/L Ni^{2+} . It exhibits an approximately 20% higher percentage adsorption than the blank (no metals). As for the calcite, the sample with Zn^{2+} exhibit the highest fluoride removal of around 90%, while the samples with the addition of Co^{2+} and Ni^{2+} are found to inhibit defluoridation compared with the blank. The kinetic study indicates that the experimental data are well fitted by the pseudo-second order kinetics model and Hill logistic model, with the latter resulting in a better fit overall.

Andesitic dyke swarms in the Araç-Boyalı foredeep basin, N Anatolia: Evidence for Eocene extension

R. EZGI CAKIROGLU^{1*} M. CEMAL GÖNCÜOĞLU¹
MICHELE MARRONI² AND LUCA PANDOLFI²

¹Department of Geological Eng., Middle East Technical University, Ankara-Turkey

(*correspondance: ezgi.cakiroglu@metu.edu.tr)

²Dipartimento di Scienze della Terra, Università di Pisa, Italy

A number of dykes and sills have been investigated in the Araç-Boyalı Flysch Basin, a foreland basin formed on the platform of the Sakarya Composite Terrane following the closure of the Intra-Pontide Ocean during the Late Cretaceous – Late Paleocene. The andesitic dyke swarms, characterized by well-developed chilled margins, flow textures and elongated vesicles, intrude the basin sediments, among which massive and pillow lavas, as well as lava and pillow breccias are also found.

Major element data plotted on SiO₂ indicates plagioclase, pyroxene and biotite fractionation, as well Fe-Ti oxides in the samples, that are andesites and andesitic basalts of calc-alkaline character. Tectono-magmatic discrimination diagrams of lavas as well as the dykes are indicative for destructive plate margin volcanism. Lava and dyke samples display similar patterns in REE and Spider diagrams. A depletion of heavy REE, enrichment of LREE is observed, as well as a marked Nb-Ta trough, characteristic of arc magmas. Based on low Mg numbers, together with low compatible trace element concentrations and low Nb/La ratios, compositions of examined samples might have been modified by assimilation processes.

Geochemical characteristics of the volcanic rocks reveal that they are products of continental arc magmatism within the Sakarya Composite Terrane above the N-ward subducting Izmir-Ankara oceanic lithosphere of Neotethys.

Similarities in major, minor and trace element geochemistry are in favour of dykes being the feeders of the Eocene lava flows within the Eocene basins that formed as a result of post-collisional extension.

Environmental mineralogy: Bridging the gap from microscopic to macroscopic

G. CALAS, G. MORIN T. ALLARD L. GALOISY,
F. JUILLOT G. ONA-NGUEMA¹ AND G.E. BROWN, JR.²

¹Institut de Minéralogie et de Physique des Milieux Condensés, Université P&M Curie, Paris, France
(georges.calas@upmc.fr)

²Dept. of Geological & Environmental Sciences, Stanford University, Stanford CA 94305, USA.

Minerals provide a large wealth of environmentally relevant information during their formation and further evolution, through their substituted trace/minor elements and structural -often radiation-induced- defects. A unified view of their behavior comes from the possibility to determine element speciation in fluids, minerals and mineral surfaces, atomic substitution processes in mineral lattices, using molecular-scale observations derived from structural, experimental and theoretical approaches.

The first focus will be on the structural evolution of nuclear glasses during aging (alteration, irradiation), showing the molecular-scale mechanisms that govern glass stability. Matrix stability relies on the synergy between glass/gel components, with a major role played by the competition for local charge compensation. Crystal chemistry considerations explain the differences observed in the leaching behavior during under-saturated and open conditions.

The second part is devoted to the mineralogical control of the distribution of heavy elements such as Zn, As, Pb or U in geochemical anomalies and sites contaminated through industrial/mining activities. Combining mineralogy and element speciation provides unique information on the behavior of heavy elements during low-T processes, showing the respective importance of low-solubility phases and sorbed species and illustrating the key mechanisms that inhibit short- and long-term contaminant dissemination. Trapping of heavy metals by Fe/Mn oxyhydroxides is an efficient natural attenuation process in acid mine drainage (AMD) waters. The dynamics of metal speciation and concentration in AMD systems provides an interesting picture of the complex interplay among source terms, geochemical conditions, hydrological fluxes, and bacterial activity

A last example will concern radiation-induced defects in minerals, used to trace short-lived uranium daughter elements. The high specific area of clays makes them sensitive to ground-level radiation doses, providing information on the past transfer of radionuclides in the geosphere, helping to model uranium-bearing fluid migration.

S burden in CFBs: A new approach

SARA CALLEGARO¹ DON R. BAKER²,
ANDREA MARZOLI¹ ANGELO DE MIN³ HERVÉ
BERTRAND⁴ TINA GERAKI⁵ CECILIA VITI⁶
AND FABRIZIO NESTOLA¹

- ¹Università di Padova, IT; (sara.callegaro@unipd.it);
(andrea.marzoli@unipd.it); (fabrizio.nestola@unipd.it)
²McGill University, Montreal, CA; (don.baker@mcgill.ca)
³Università di Trieste, IT (demin@univ.trieste.it)
⁴Univ. Ec. Norm. Sup Lyon, FR;
(herve.bertrand@ens-lyon.fr)
⁵Diamond Light Source, UK; (tina.geraki@diamond.ac.uk)
⁶Università di Siena, IT; (cecilia.viti@unisi.it)

Most Phanerozoic Large Igneous Provinces (LIPs) are associated in age with, and may have triggered, major mass extinctions. This is epitomized by the synchronicity of the Central Atlantic magmatic province (CAMP; c. 201 Ma) and the Deccan Traps (c. 66 Ma) with the end-Triassic and the end-Cretaceous biotic crises, respectively. However, LIPs not associated to mass extinctions are also recorded, as in the case of the Paranà-Etendeka (PE; c. 134 Ma). Although climatic forcing caused by huge emissions of volcanic gases such as SO₂ and CO₂ is now accepted, precise estimates of gas contents of the basalts and their gas emission masses and rates are still poorly constrained. The differences in environmental impact of these three LIPs may reflect their different gas outputs. Here we illustrate a new approach of estimating magmatic SO₂ emissions. First, the pyroxene/melt S partition coefficient was measured by micro-XRF (Diamond synchrotron, UK) and ion microprobe (WHOI, USA) on experimentally crystallized augites and basalts. S contents were then measured by in-situ micro-XRF in augite phenocrysts from representative rocks of the three considered LIPs. Selected natural clinopyroxene crystals were verified to be devoid of fluid or sulphide inclusions through Transmission electron microscopy (TEM, Siena) thus legitimating the applicability of the partition coefficient and the extrapolation of S burden in primitive magmas starting from S measured on augites. S in the pristine magmas ranges between 100 and 1500 ppm, consistently with results obtained by Self *et al.* (2008) on melt inclusions from Deccan basalts. CAMP and Deccan magmas seem systematically richer in S than PE ones, an observation that correlates well with the severity of the associated biotic crises. Thus, emissions of S (along with other volatiles) appear as important factors for assessing the global environmental changes and may play a significant role in triggering mass extinctions.

[1] Self S., Blake S., Sharma K., Widdowson M., Sephton S., 2008. *Science* **319**, 1654-1657.

Recycling of subducted crust in the source of within-plate CAMP basalts from southeastern North America

SARA CALLEGARO¹ HERVÉ BERTRAND² ANDREA
MARZOLI¹ MASSIMO CHIARADIA³ LAURIE REISBERG⁴
CHRISTINE MEYZEN¹ AND GIULIANO BELLINI¹

- ¹Università di Padova, IT; (sara.callegaro@unipd.it);
(andrea.marzoli@unipd.it); (christine.meyzen@unipd.it);
(giuliano.bellini@unipd.it)
²Univ. Ec. Norm. Sup Lyon, FR; (herve.bertrand@ens-lyon.fr)
³Université de Geneve, CH (Massimo.Chiaradia@unige.ch)
⁴CRPG-CNRS-UL Nancy, FR; (reisberg@crpg.cnrs-nancy.fr)

Basaltic dykes and sills of the Central Atlantic magmatic province (CAMP) were intruded between 202 and 195 Ma in southeastern North America (SENA) during Pangea break-up. We aim to constrain the mantle source of these magmatic bodies and their evolution path with new combined geochemical data (major and trace elements, Sr-Nd-Pb-Os isotopes). While Sr-Nd isotopic compositions for SENA rocks (⁸⁷Sr/⁸⁶Sr_{200Ma} 0.70438-0.70880 and ¹⁴³Nd/¹⁴⁴Nd_{200Ma} 0.51251-0.51204) fall within the low-Ti CAMP field, Pb-Pb isotopes (²⁰⁶Pb/²⁰⁴Pb_{200Ma} = 17.46-18.85, ²⁰⁷Pb/²⁰⁴Pb_{200Ma} = 15.54-15.65, ²⁰⁸Pb/²⁰⁴Pb_{200Ma} = 37.47-38.76) are peculiar for this area of the CAMP and span a wide range of compositions, notably extending towards low ²⁰⁶Pb/²⁰⁴Pb_{200Ma} values. Based on the generally unradiogenic Os isotopic compositions (¹⁸⁷Os/¹⁸⁸Os_{200Ma} = 0.127-0.144) and the lack of correlation between these and other geochemical markers, the role of crustal contamination in the evolution of SENA tholeiites is constrained to be less than 10%. Hence, the isotopic variation is interpreted to reside within the mantle source and a process other than crustal assimilation was responsible for conveying the observed continental trace element signature (positive anomaly in Pb and negative anomalies in Ti and Nb) to these magmas. For this process, we hypothesize shallow recycling of subducted lower and upper crustal materials within the upper mantle. Pseudo-ternary mixing models show that a maximum of 10% recycled crust is enough to explain both the SENA dyke trace element patterns and their isotopic heterogeneity. Furthermore, though a thermal contribution of a mantle plume is not completely excluded due to the relatively high mantle potential temperatures (1430°-1480° C) calculated from SENA primitive olivines, its chemical contribution was negligible (less than 5%).

Effect of mineral structure and composition on carbonate clumped isotope measurements

DAMIEN CALMELS¹, MAGALI BONIFACIE¹,
AMANDINE KATZ¹ AND JULIEN SIEBERT²

¹IPGP, Sorbonne Paris Cité, Univ Paris Disderot, UMR 7154
CNRS, F-75005 Paris, France (calmels@ipgp.fr)

²IMPMC, Université Pierre et Marie Curie, UMR CNRS 7590,
IPGP, 75005 Paris, France

Carbonate clumped isotope thermometry relies on the temperature-dependent extent of bonding of ^{13}C - ^{18}O within CO_3^{2-} ion groups in solid carbonate minerals. The measure of the abundance of $^{13}\text{C}^{18}\text{O}^{16}\text{O}_2^{2-}$ ion groups cannot be performed on the carbonate mineral itself and requires Δ_{47} measurement of CO_2 extracted by phosphoric acid digestion (i.e., the excess of ^{13}C - ^{18}O bonds in extracted CO_2 relative to a random distribution). Theoretical studies predict variations in the degree of ^{13}C - ^{18}O clumping from one carbonate to another [1] and small but analytically resolvable differences in Δ_{47} of CO_2 extracted from various types of carbonates equilibrated at a given temperature [2]. In contrast, published calibrations of carbonate clumped isotope thermometer do not show distinguishable difference among the different types of carbonate investigated (mostly biogenic and inorganic calcite, aragonite and carbonate-apatite [3]). However, some coexisting carbonate phases supposed to have grown or been re-equilibrated at the same temperature show different Δ_{47} values (e.g., Bonifacie *et al.*, same meeting).

We will present results from a series of experiments on a variety of natural and synthetic carbonate minerals. These experiments have been designed to investigate the possible effects of mineral structure and chemical composition on Δ_{47} values.

This study is relevant for key issues related to the use of Δ_{47} , and in particular in refining application of the Δ_{47} thermometry to the variety of carbonate minerals found in the geological record.

[1] Schauble *et al.* (2006), *GCA* **70**, 2510-2529. [2] Guo *et al.* (2009), *GCA* **73**, 7203-7225. [3] Eiler (2011), *QSR* **30**, 3575-3588

Carbon isotopic composition and flux variations of CO_2 emitted from the soil of Mt Etna

M. CAMARDA*, S. DE GREGORIO, R. FAVARA,
F. GRASSA AND S. GURRIERI

Istituto Nazionale di Geofisica e Vulcanologia, sezione di
Palermo, via Ugo La Malfa 153, 90146 Palermo, Italy.

(*Correspondence: m.camarda@pa.ingv.it)

Since 1987, periodic soil CO_2 flux measurements on the south-western sector and on the eastern flank of Mt Etna have been performed to monitor volcanic activity. Many studies have demonstrated that soil CO_2 flux is closely related to the magma dynamics of Mt Etna. To further confirm this relationship and better understand the influence of rising magma on soil CO_2 emission, we periodically measured the $\delta^{13}\text{C}$ values as well as the soil CO_2 flux at several points in both areas of Mt Etna. The comparison between $\delta^{13}\text{C}$ values and soil CO_2 flux revealed two groups of data with different behaviours: (i) data arranged along mixing lines between organic and depth origins of CO_2 ; (ii) data with high soil CO_2 fluxes and $\delta^{13}\text{C}$ values with organic marker. The variations in $\delta^{13}\text{C}$ in (i) are temporally well correlated with the total amount of the soil CO_2 emitted in the areas. This result strongly corroborates the primary role played by magma dynamics in the control of soil CO_2 flux in the analysed areas. In addition, the values of flux of (ii), notwithstanding the organic marker, displayed synchronised variations with the total amount of the soil CO_2 emitted in the area and hence with the $\delta^{13}\text{C}$ values of group (i). The recorded synchronism suggests that the measurements in group (ii) are also to some extent influenced by magma dynamics. It can be supposed that: increase in flux in (i) is directly derived from the release of CO_2 from ascending magma, whereas the increase in soil CO_2 flux in (ii) is mainly due to the enhancement of stress linked to magmatic intrusion.

Evaluation of potential explanations for the offsets in Δ_{47} amongst various taxa of naturally occurring modern carbonate organisms

ROSEMARIE E. CAME

¹Department of Earth Sciences, University of New Hampshire, Durham, NH 03824, USA (rosemarie.came@unh.edu)

For more than half a century, the $\delta^{18}\text{O}$ paleotemperature proxy has been applied with great success using marine carbonate fossils, yet progress has been limited because carbonate $\delta^{18}\text{O}$ is a function of both calcification temperature and the $\delta^{18}\text{O}$ of the water in which precipitation occurred, thereby requiring an assumption about past seawater $\delta^{18}\text{O}$. The recently developed carbonate “clumped isotope” paleothermometer (Δ_{47}) has the potential to circumvent this difficulty because the “clumping” of ^{13}C and ^{18}O atoms in a carbonate mineral lattice occurs independently of seawater $\delta^{18}\text{O}$ [1]. Furthermore, carbonate $\delta^{18}\text{O}$ and Δ_{47} -derived temperature are obtained simultaneously – in the same phase – allowing a calculation of seawater $\delta^{18}\text{O}$ using a single sample aliquot.

Initially, the relationship between Δ_{47} and calcification temperature was empirically derived using inorganic calcites that were grown at known temperatures [1]. Since that initial calibration study, several naturally occurring modern carbonates have been analyzed, and some yield Δ_{47} values that are consistent with the relationship derived for inorganic calcite (e.g., deep sea corals) [2], whereas others appear to be offset to values that are slightly higher (e.g. surface corals) [1] or slightly lower (e.g. otoliths) [3]. The differences observed between various taxa are not fully understood. Using both published and unpublished modern calibration data sets, several possible explanations for these offsets will be evaluated, including: “vital effects”, mineralogical offsets, and differences in the sample preparation protocols of various Δ_{47} laboratories.

[1] Ghosh *et al.* (2006) *Geochim. Cosmochim. Acta* **70**, 1439–1456. [2] Thiagarajan *et al.* (2011) *Geochim. Cosmochim. Acta* **75**, 4416–4425. [3] Ghosh *et al.* (2007) *Geochim. Cosmochim. Acta* **71**, 2736–2744.

Nickel isotopic composition of modern seawater and rivers

V. CAMERON^{1*} AND D. VANCE²

¹Bristol Isotope Group, School of Earth Sciences, University of Bristol, UK

(*correspondence: glxvc@bristol.ac.uk)

²Institute of Geochemistry and Petrology, Department of Earth Sciences, ETH Zürich, Switzerland

(derek.vance@erdw.ethz.ch)

The oceans are the most important repositories for the fallout from continental activities, such as weathering, mediating its flux of elements through a variety of processes including biogeochemical cycling. The abundances and stable isotopes of transition metals have been key tools in understanding and deciphering the totality of these processes through time and, certainly, ongoing development of isotopic systems will continue to reveal new insights into Earth processes. Here we present the first dataset for the Ni isotopic compositions of seawater and rivers.

Dissolved Ni was analysed in several major river systems, including the Amazon and Chang Jiang. In general, rivers exhibit substantial variability in both Ni concentration (2.2–35 nmol kg⁻¹) and $\delta^{60}\text{Ni}$ (0.29–1.34‰). Most of the rivers are isotopically heavy with the exception being two rivers that have isotopic compositions that overlap the lithogenic range observed for silicate rocks and sediments [1]. The variability noted in these data may be attributable to isotopic fractionation during chemical weathering or partitioning between dissolved and suspended load, both of which have been put forward to explain similar features in other isotopic systems. However, further studies will be required to resolve the detailed processes.

The range of seawater Ni concentrations was 3.1 nmol kg⁻¹ at the surface to 11.2 nmol kg⁻¹ at depth, confirming the surface to depth partitioning seen previously, and correlating with nutrient elements such as phosphate and silica. Seawater Ni isotopic data from the Atlantic and Pacific oceans produced three conspicuous outcomes: (i) relative homogeneity of all samples, with an average $\delta^{60}\text{Ni}$ of 1.44±0.15 (2σ); (ii) without exception, the Ni isotopic compositions are heavier than that of the dissolved riverine input; (iii) a missing light sink for Ni.

[1] Cameron *et al.* (2009) *PNAS* **106**, 10944–10948.

In-situ isotopic analysis of volatile fluids from subsurface carbon reservoirs

RICHARD CAMILLI¹ AND ANTHONY N. DURYEY²

¹Woods Hole Oceanographic Institution, Dept. of Applied Ocean Physics and Engineering, Deep Submergence Laboratory, MS#7, Woods Hole, MA 02543, USA.

²Monitor Instruments Company LLC., 290 E Union Rd, Cheswick, PA 15024, USA.

Technological advances are moving analytical laboratory sensors into the field. This transition eliminates sample collection and transport requirements for offsite analysis, improving spatial and temporal resolution of data, while decreasing operations costs and latency. We present a miniaturized isotope ratio mass spectrometer (IRMS) for in-situ analysis of gases and volatile hydrocarbons from subsurface carbon reservoirs.

This new instrument, which uses a compact double-focusing mass analyzer is capable of rapid spectrum scans across a 2-200AMU range for quantitative characterization of a broad range of volatile compounds including hydrocarbons and reduced gases at concentrations to less than one part-per-billion. Its multiple fixed-cup collectors enable simultaneous isotopic ratio precision to better than one per-mil. This fully self contained IRMS requires less than 20W of power and displaces a volume of approximately 10 liters.

We present an overview of the IRMS design in two differing embodiments, a TETHYS configuration for marine operation on subsea robotic vehicles, and a configuration with integrated gas chromatograph (GC) for field applications such as logging-while-drilling. Results from laboratory testing of GC-IRMS configuration indicate isotopic precision of better than $\delta 0.25\%$ analysis of mixed natural gas with total cycle times of less than five minutes. Marine operations using the TETHYS configuration for real-time analysis of dissolved water column hydrocarbons and gases indicate sensitivities better than 1 part-per-billion and isotopic precision to better than $\delta 1\%$ with measurement cycle times of seconds. This provides an efficient method for locating and classifying biogenic and thermogenic seafloor seeps from subsurface carbon reservoirs.

A rheological and textural characterization of the fall-out phase of the large volume Pozzolane Nere mafic ignimbrite (Colli Albani Volcano, Rome)

S. CAMPAGNOLA*, C. ROMANO, A. VONA AND G. GIORDANO

Geological Science Department, University of Roma Tre, L.go S.L.Murialdo, 1 00146 Rome, Italy

(*correspondence: silvia.campagnola@uniroma3.it)

The Pozzolane Nere ignimbrite (PNR) represents one of the largest explosive events in the history of the Colli Albani volcano (407 ka, Vulcano Laziale period). The PNR is tephri-phonolitic in composition and is characterized by a basal scoria fallout deposit with an east-trending axis of dispersion overlain by a low aspect ratio ignimbrite, estimated at 30km³ as bulk volume. Despite extensive studies on the deposits of the volcano, the mechanisms governing the explosive activity of these very undersaturated magmas are still poorly known. In order to improve our understanding on the origin of these high-energy eruptions (VEI 6), petrological and minero-chemical analyses of the five PNR fallout sub-layers were performed. Results from the VSD of the selected scoriae suggest an uneven distribution of nucleation events with VNDs (on the order of 10⁸-10⁹ cm⁻³) higher than those observed in literature for mafic explosive eruptions and more comparable to VNDs pertaining to explosive eruptions of evolved composition. Textural and minero-chemical investigations of the samples have been combined with their rheological characterization. Low T measurements (690°C < T < 800°C) were performed by micropenetration technique, while the high T viscosities of fully molten (1250°C < T < 1569°C) and partially crystallized specimens (1100°C < T < 1225°C) were measured at 1 bar in air with a concentric cylinder viscometer. Above the liquidus temperature, viscosity ranges from 10^{1.04} to 10^{3.64} in good agreement with the viscosity model by Giordano *et al.*^[1]. In the subliquidus region, isothermal crystallization experiments allowed to quantify the role of crystals on the rheology of PNR magmas. The increase of apparent viscosity together with the onset of strain rate- and strain-dependent behavior could play a critical role during PNR degassing history, governing the elevated explosivity of these very undersaturated magmas.

[1] Giordano et al. (2008) Earth and Planetary Science Letters 271, 123-134

Evidence against a chondritic Earth

IAN H. CAMPBELL AND HUGH ST C. O'NEILL

Research School of Earth Sciences, The Australian National University, Canberra, ACT, 0200, Australia

The $^{142}\text{Nd}/^{144}\text{Nd}$ ratio of the Earth is greater than the solar ratio as inferred from chondritic meteorites, which challenges a fundamental assumption of modern geochemistry—that the composition of the silicate Earth is 'chondritic', meaning that it has refractory element ratios identical to those found in chondrites. The popular explanation for this and other paradoxes of mantle geochemistry, is an incompatible element hidden layer deep in the mantle, which must include 40% of the mantle's heat producing elements in order to explain the Nd anomaly. This requires the mantle plumes to carry at least 40% of the mantle's heat budget, which is inconsistent with constraints on the plume heat flux that put this figure at less than 30%. Furthermore the sudden drop in the temperature of mantle plumes that occurred a ~2.5 Ga is interpreted to indicate that the D", which is commonly interpreted to be the hidden layer, did not form until that time. If the hidden layer (D") formed after the first 10 Myr of the Earth's evolution it cannot be responsible for the Earth's $^{142}\text{Nd}/^{144}\text{Nd}$ anomaly. Either the matter from which the Earth formed was not chondritic, or the Earth has lost incompatible elements rich matter by collisional erosion in the later stages of planet formation.

Mining, microbes, and models: Integrating microbial Fe(II) oxidation, hydrolysis, precipitation, and biogeochemical modeling, with application to acid mine drainage at Iron Mountain

KATE M. CAMPBELL¹, CHARLES N ALPERS²,
D. KIRK NORDSTROM¹, ALEX E. BLUM¹
AND MICHAEL B. HAY³

¹U.S. Geological Survey, Boulder, CO, USA,
(kcampbell@usgs.gov)

²U.S. Geological Survey, Sacramento, CA, USA

³ARCADIS U.S., Inc., Boulder, CO, USA

Acid mine drainage (AMD) is a major environmental concern because of high concentrations of acidity (low pH), sulfate, iron, and other elements. One important process affecting AMD chemistry is microbial Fe(II) oxidation. As Fe(II) oxidizes, a variety of Fe(III)-bearing minerals can precipitate, affecting the immobilization of elements such as Cu and Zn, as well as redox cycling of trace elements such as As and Sb. Precipitation can also cause costly management problems when it interferes with treatment efforts. An example of this problem occurred at the Iron Mountain Mine (CA, USA) where a pipeline carrying AMD to a treatment plant has developed scaling because of Fe(II) oxidation and Fe(III) precipitation inside the pipe. The scale accumulation has clogged flow and caused spillage of AMD, requiring expensive periodic cleaning of the pipeline.

Laboratory Fe(II) oxidation experiments were conducted using synthetic AMD with Fe(II)-oxidizing bacteria, and compared to experiments using natural AMD from Iron Mountain. Changes in pH, Fe(II), Fe(III), and trace elements were measured over time. The precipitates formed were characterized, and the microbial community was identified (16S rDNA). Water samples and scale collected from four locations along the pipeline also were characterized.

We developed a geochemical model to evaluate our understanding of coupled biotic and abiotic processes in AMD. Key processes included in the model are equilibrium reactions for all measured constituents, microbial Fe(II) oxidation kinetics, Fe(III) hydrolysis and polymerization, mineralogy, solubility, Fe(III) precipitation kinetics, and As(III) oxidation. This work highlights the utility of geochemical models as a means of improving quantitative descriptions of fundamental biogeochemical processes in AMD. Based on the geochemical model and laboratory experiments, we developed a potential mitigation strategy for the scaling problem that avoids costly pipeline maintenance.

www.minersoc.org

DOI: 10.1180/minmag.2013.077.5.3

Exploring the preservation of alkaline-carbonatitic extrusive rocks in relation to continent formation

L.S.CAMPBELL^{1*} A. DYER² C. WILLIAMS³
AND P.R. LYTHGOE¹

¹School of Earth, Atmospheric and Environmental Sciences, University of Manchester, Williamson Building, Oxford Road, Manchester M13 9PL. UK

(*correspondence: L.S.Campbell@manchester.ac.uk)

²Department of Chemistry, Loughborough University, Ashby Road, Loughborough, Leicestershire LE11 3TU. UK

³School of Applied Science, University of Wolverhampton, Wulfruna Street, Wolverhampton, WV1 1SB. UK

Mineral reaction paths related to continental alkaline-carbonatitic extrusive rocks are examined in the context of a “zeolitic masquerade” hypothesis [1]. The hypothesis suggests that zeolitic alteration reactions are the first steps in a gradual stabilization of these bedded successions, as the highly reactive volcanic deposits change from glasses via zeolites to authigenic feldspars, clays and SiO₂ phases. Reported reaction progressions are suggestive of trends in which Si/Al increases with time as wider, Si-saturated fluids react with earlier-formed phases in continental environments. It is not known how trace elements such as the REE and HFSE behave at each stage of reactive progression as no systematic study of these elements has been made for wide occurrences of natural zeolites. But our preliminary data indicate that the first-formed, low-Si zeolites (e.g. phillipsite), reflect the REE patterns of the original volcanic glasses. Modifications to trace element signatures of altered successions are very likely to occur as reactions progress with exposure to wider crustal fluids. Some of these modifications will be dependent on the ion-selectivity properties of different zeolite minerals in the reaction paths, but fluid controls are certainly evident. A preliminary exploration of possible examples in the geological record, of recognition and stabilization of reactive successions, is discussed.

[1] Campbell *et al* (2012) *Mineralium Deposita*, **47**, 371–382.

Sodium rich magmas parental to Catanda carbonatitic lavas (Angola): Melt inclusion evidence

M. CAMPENY^{1*} V. KAMENETSKY² J.C. MELGAREJO¹
J. MANGAS³, A. BAMBI⁴ AND J. MANUEL⁴

¹ Faculty of Geology, University of Barcelona, Catalonia

*(correspondence: mcampeny@ub.edu)

² CODES ARC, Univ. of Tasmania, Australia

³ Dept. de Física, Univ. Las Palmas de Gran Canaria, Spain

⁴ Dept. Geologia, Univ. Agostinho Neto, Luanda, Angola

Remains of highly eroded carbonatitic volcanic edifices occupy a region of 50 km² in the vicinity of the Catanda village, Kwanza Sul province, Angola. Carbonatitic lava flows and pyroclastic deposits are present in the area forming sequences of volcanic materials up to 600 metres in thickness.

We have studied the composition of the melt inclusions preserved in the primitive mineral phases of the lavas such as calcite, apatite, Na-rich cuspidine and spinel. Most inclusions are composed by calcium carbonates enriched in Na (up to 18 wt.%), K (up to 7 wt.%) and with significant S contents (Fig.1a). Alkaline chlorides such as sylvite and halite are also found among daughter phases (Fig.1b), as well as periclase, olivine, monticellite and clinopyroxene. Na-rich apatite, perovskite and pyrochlore are also found in this assemblage, arguing for important role of alkalis and fluorine.

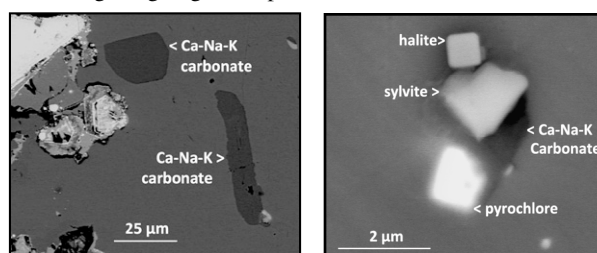


Figure 1: a) Calcium-alkaline carbonate included in calcite. b) Alkaline chlorides, carbonate and pyrochlore inside calcite.

The presence of alkalis in the melt inclusions hosted by main phenocryst mineral suggests that the parental magma compositions were Na- and K-rich. We consider that postmagmatic processes removed much of the alkaline elements from the Catanda lavas.

Gadolinium anomalies in Atibaia River water (SP, Brazil)

F. F. CAMPOS^{1*} AND J. ENZWEILER²

University of Campinas - UNICAMP, Institute of Geosciences, Campinas, SP, Brazil

^{1*}(correspondence: francisco.campos@ige.unicamp.br)

²(jacinta@ige.unicamp.br)

Stable synthetic chelates of gadolinium find wide use as contrast agents for magnetic resonance imaging (MRI). After administration to patients, the chelate is excreted in urine. Anthropogenic anomalies of Gd were measured in river water and groundwater samples by several authors, because the chelates are remarkably stable when passing wastewater treatment plants (WWTP) [1]. Despite that, even in densely populated areas small watersheds should be free of Gd anomalies in absence of discharge of raw or treated sewage.

In this work we studied three small sectors of Atibaia River, in São Paulo state, Brazil. River water was sampled, filtered through 0.22 μm syringe filters and acidified with distilled HNO_3 to $\text{pH} < 2$. Trace elements were measured by ICP-MS, without sample pre-concentration. The results of rare earth elements (REE) were normalized by the PAAS [2].

The first sector is the most pristine among the three. It is upstream, covers about 100 km of the river course and no Gd anomaly was detected in the water samples. The second sector comprises samples from Anhumas Creek, a tributary of Atibaia River, where it crosses an urban area and has two WWTPs. Gd anomalies were present even before the first WWTP, and their magnitude is comparable to anomalies described for some major German rivers [3]. Immediately after the WWTPs, Gd concentration increases reaching the same values of discharged effluents from WWTPs in Bremen (Germany) [3] and higher than those found in Berlin (Germany) [4] and in the Hérault watershed (South France) [5], but lower than in some other Berlin canals [4]. Anomalies calculated as Gd/Gd^* [3] resulted in up to fifty-fold enrichment of Gd over background concentrations. The third sampled sector is Atibaia River where it crosses an industrial and urban area, before ending at a dam. In this area, the Gd/Gd^* values were only useful to mark an anomaly at the discharge of a WWTP. The other samples showed strong influence of the industrial park, with enrichment in light REE, resulting in a poor Gd/Gd^* anthropogenic signal.

[1] Verplanck *et al* (2010) *Environ. Sci. Technol.* **44**, 3876–3882. [2] McLennan (1989) *Rev. Mineral. Geochem.* **21**, 169–200. [3] Kulaksız & Bau (2007) *Earth Planet. Sci. Lett.* **260**, 361–371. [4] Raju *et al* (2010) *J. Anal. Spectrom.* **25**, 1573–1580. [5] Rabiet *et al* (2009) *Chemosphere*, **75**, 1057–1064.

C-, Cr-, Sr-isotope stratigraphies and rare-earth elements in carbonate and BIFs of the Neoproterozoic Jucurutu Formation, Seridó Belt, NE Brazil

M. S. CAMPOS¹, A. N. SIAL¹, C. GAUCHER², R. FREI³, V. P. FERREIRA^{1*}, R. C. NASCIMENTO⁴, M. M. PIMENTEL⁵ AND N. S. PEREIRA

¹NEG-LABISE, Dept. Geology, UFPE, Recife, Brazil

* (correspondence: valderez@ufpe.br)

²Fac. Ci., Univ. de la Republica, Montevideo, Uruguay

³Inst. Geogr./Geol., Univ. of Copenhagen, Denmark

⁴Dept. Geol., FUA, Manaus, Amazonas, Brazil

⁵Inst. Geosc., UFRGS, Porto Alegre, Brazil

The Jucurutu Fm. in the Seridó Belt, NE Brazil, encompasses fine- to coarse-grained amphibolites-facies marbles, locally with cross-bedding and stromatolite structures. BIFs of three localities in this belt comprise itabirites (actinolite- or cummingtonite-itabirite) and tremolite schist iron ores and are overlain by marbles of the Jucurutu Formation. Diamictites of uncertain stratigraphic position exhibit clasts up to 0.6 m long (augen-gneisses, quartzites and bi-gneisses) and a fine-grained clay matrix.

C-isotope stratigraphic pathways for the Jucurutu Fm. show negative $\delta^{13}\text{C}$ values at the base followed upsection by positive values. At the Ferro do Bonito Mine, values as low as -12‰ are found in carbonates just above the contact with underlying BIF, followed by values $\sim -5\text{‰}$ and then by positive values ($+4$ to $+10\text{‰}$) upsection. $\delta^{13}\text{C}$ values for carbonates that overlie BIFs at Riacho Fundo and at Serra da Formiga are all positive. The difference of $\delta^{13}\text{C}$ behavior between basal carbonates at Mina do Bonito (negative) and Riacho Fundo and Serra da Formiga (positive) localities results, perhaps, from different stages of BIF deposition. $^{87}\text{Sr}/^{86}\text{Sr}$ values for Jucurutu Fm. carbonates lie ~ 0.7074 , a value commonly observed in late Cryogenian to early Ediacaran.

BIFs yield negative $\delta^{53}\text{Cr}$ values (-0.4 to -0.1‰), Ce/Ce^* from -0.4 to 0.7 (17 among 21 samples support anoxic depositional environment) and were probably formed as accumulation of Fe^{+2} in an ice-capped anoxic ocean. Their deposition was followed by post-glacial cap carbonate deposition (Ce/Ce^* from 0.4 to 0.5) in an oxic environment.

Evaluation of the influence of Radon Carried by Evapotranspiration of Equatorial Forests (northeastern of Brazil) in the Formation of Atmospheric Aerosols

T. CAMPOS^{1*}, J.J. HOELZEMANN² AND R. PETTA³

¹Federal University of Rio Grande do Norte, Brazil.

*(correspondence@thomascampos@geologia.ufrn.br)

²Federal University of Rio Grande do Norte, Brazil.
(judith.hoelzemann@inpe.br)

³Federal University of Rio Grande do Norte, Brazil.
(petta@ccet.ufrn.br)

Atmospheric aerosols cause great impact on climate, in this context and excluding the human activity, their production is closely related to the presence of ions in the atmosphere. These ionized molecules are formed both by the action of Cosmic rays from space, as the Gamma radiation from terrestrial materials, and even Alpha radiation from Radon gas, constituting an ionic groups with dimensions ≤ 1.5 nm and influencing the amount of atmospheric aerosols in a given region, mainly in areas of forests. This fact is due to the transport of radon gas into the air dissolved in groundwater by evapotranspiration of trees, since the alpha and Beta radiation from the disintegration of radon gas vented directly from soils and rocks has little power of penetration into the atmosphere [1]. This paper show our study about the ionic particulate correlation and variation with the radon emanations in an atmosphere of equatorial forest environment from the Atlantic Dune and Caatinga forests, respectively on the coastal plain and hinterland depression of the Rio Grande do Norte State.

The measurements of atmospheric ion clusters by a air ions counter (AlphaLab® system) and active-passive measurements of radon gas in the atmosphere, soil and water through emanometer (AlphaGuard®, RADELEC® systems). The Alpha and Gamma regional radiation (RAD-7® system and RS-230® spectrometers). Based on these data, we will try to prove that climate change comes from deforestation also has to do with the reduction of radon gas in the atmosphere, which acts as an inductor of formation and clumps of ions, and not only with the decrease of aerosols from the biological activity of trees and plants, which both affect the formation of clouds.

[1] E.R. Jayaratne, X. Ling, and L. Morawska (2011) *Environ. Sci. Technol.* **45**, 6350–6355.

Geochemical characteristics and tectonic significance of mafic cumulates in Kuluncak ophiolite (Malatya), SE Turkey

M. CAMUZCUOĞLU^{1*}, U. BAĞCI¹, J. KOEPKE²
AND P. E. WOLFF²

¹Mersin University, Department of Geological Engineering,
33343-Çiftlikköy-Mersin, Turkey (*correspondence:
mcamuzcuoglu@mersin.edu.tr.)

²Institute for Mineralogy, University of Hannover,
Callinstrasse 3, D-30167 Hannover, Germany

The regionally important Kuluncak (Malatya) ophiolite in the Eastern Tauride, composed of mantle tectonites, ultramafic-mafic cumulates, isotropic gabbros, a sheeted dike complex, plagiogranite, extrusives and pelagic cover sediments. The mafic cumulates of the ophiolite suite are observed in Hekimhan region, represented by olivine gabbro and gabbro, displaying mesocumulate and orthocumulate textures. The whole rock major and trace element geochemistry of the mafic cumulate rocks indicate that the primary magma generating the Kuluncak ophiolite is compositionally similar to those observed in modern island arc tectonic settings. The REE concentrations of the mafic cumulates exhibit spoon-shaped REE patterns, with La_N/Sm_N and Sm_N/Yb_N ratios ranging from 0.21 to 2.60 and from 0.68 to 1.36, respectively. The crystallization order for the cumulate rocks is olivine ($Fe_{63.7-86.9}$)±chromian spinel, clinopyroxene ($En_{41.01-55.43}$, $Fs_{4.2-14.29}$, $Wo_{35.84-48.2}$), plagioclase ($An_{73.4-93.67}$) and orthopyroxene ($En_{76.81-83.51}$, $Fs_{15.68-21.47}$, $Wo_{0.73-1.85}$). The cumulus and postcumulus minerals do not show significant zoning. The presence of anorthite-rich plagioclases ($An_{73.4-93.67}$) in the mafic cumulate rocks indicates hydrous conditions at the time of oceanic crust generation. Highly magnesian olivine ($Mg\#_{63.36-86.75}$), clinopyroxene ($Mg\#_{74.96-92.09}$), orthopyroxene ($Mg\#_{77.55-84.33}$) and their coexistency in the cumulate gabbroic rocks are indicative of suprasubduction zone environment. All the evidences suggest that the Kuluncak ophiolite were formed in a suprasubduction zone tectonic setting during the closure of the Inner Tauride in Late Cretaceous.

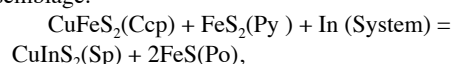
Supersolidus and subsolidus equilibria in indium-bearing magmatic-hydrothermal systems

P.A. CANDELA*, P.M. PICCOLIAND, S.M. KAYSER
AND J.R. NANCE

Laboratory for Mineral Deposits Research, Dept. of Geology,
University of Maryland, College Park, MD USA

Indium demand has increased due to its use as a capacitive sensor in touch screens. The metal is commonly a by-product of mining of VMS, granite-related, and other ores, wherein the most common host mineral is sphalerite. Murakami and Ishihara [1] report sphalerite analyses from indium deposits that range up to In/Zn ~ 0.006 by weight (0.35 wt % In). At current metal prices, the contribution of these two commodities to revenue are equal for In/Zn ~ 0.003; that is, in some cases, indium revenue can exceed zinc revenue. We suggest that deposits with significant indium require a suitable mineralogical host (e.g., zinc or tin sulfides), and higher temperatures of formation. Coupled substitution of Cu(I)+In(III) for 2Zn (defining CuInZn₂, the roquesite (rq) exchange component) accounts for indium incorporation into sphalerite.

Defining the fugacity of In (metal) in the 5 component ore system Cu-Fe-Zn-In-S, the subsolidus low-variance assemblage:



can be written in terms of chemical potentials at a given P&T. Consideration of the sulfur fugacity-dependence of the associated higher variance Po-absent, and Py-absent equilibria suggest that, for a given fugacity of In, increasing sulfur fugacity leads to increasing rq component in Sp. Incorporation of In into Po (FeS-Fe₂S₃ ss) is hypothesized to occur along the InFe(III)₁ exchange vector, and, in Cu-bearing Po, as Cu(I)In(III)Fe(II)₂.

Reconnaissance experiments have been performed to evaluate the behavior of In in the supersolidus and subsolidus realms. Cold-seal experiments were performed at 800°C and 100MPa, durations of 5-15 days, and activity of In metal = 0.05 to ~1, to evaluate the partitioning of In between Po and rhyolite melt. Results of the experiments demonstrate the affinity of In for Po (i.e. sulfides) relative to silicate melts (D~2-20). Subsolidus experiments were performed in sealed silica tubes at T = 500°C for the starting assemblage of pyrite, pyrrotite, chalcopyrite, sphalerite and indium sulfide. Results are consistent with In concentrations: Sp > Ccp ~ Po, including wt % levels of In in Sp

[1] Murakami & Ishihara (2113) *Ore Geol. Reviews* **53**, 223-243.

Sulfate was a trace constituent in the oceans of the early Earth

DONALD E. CANFIELD¹*SEAN A. CROWE^{1,2}
CARRIAYNE C. JONES^{1,2} GUILLAUME PARIS³
JESS F. ADKINS³ ALEX L. SESSIONS³
JAMES FARQUHAR⁴ AUBREY ZERKLE⁵ SANG-TAE KIM⁶
AND SULUNG NOMOSATRYO⁷

¹Nordic Center for Earth Evolution (NordCEE) and Institute of Biology, University of Southern Denmark, 5230 Odense M, Denmark *(corr: dec@biology.sdu.dk)

²Department of Microbiology and Immunology, Univ. of British Columbia, Vancouver, BC, Canada, V6T 1Z3

³Division of Geological and Planetary Sciences, Caltech, Pasadena, California, 91125, USA

⁴Department of Geology, University of Maryland, College Park, Maryland, 20742, USA

⁵Earth and Environmental Sciences, University of St. Andrews, St. Andrews, Fife, Scotland, KY16 9AJ

⁶School of Geography and Earth Sciences, McMaster University, Hamilton, ON, Canada, L8S 4K1

⁷Cibining Science Centre, Cibnong Bogor, 16911, Indonesia.

Bo Barker Jørgensen has contributed more than anyone to uncovering the secrets of the microbial sulfur cycle, and this work provides the foundation for exploring sulfur cycle evolution through time. Here, we report on the sulfur biogeochemistry of Lake Matano, South Sulawesi, Indonesia, whose low sulfate concentrations, clear waters and ferruginous conditions provide an analogue to the nature of ocean chemistry during much of the Archean Eon (≥2.5 billion years ago). We focused in on the fractionations associated with sulfate reduction in the anoxic water column of the lake, using a newly developed MC-ICP-MS technique [1] to obtain sulfate δ³⁴S values at sulfate levels as low as 1 micromolar. Within the chemocline of the lake, the δ³⁴S of sulfate varied from 7 per mil to 40 per mil, yielding fractionations of >25 per mil at sulfate concentrations down to ≤ 5 micromolar. These fractions are greater than previously observed at such low sulfate levels. The δ³⁴S of sulfides in the chemocline varied from 7 per mil to -15 per mil, and this range is comparable to the range of values observed in shales from the Paleo- and Mesoarchean Eons. We conclude that seawater sulfate concentrations through this time were probably less than 20 micromolar most likely < 5 micromolar based on independent modelling of the Archean sulfur cycle. There is an increase in the range of shale δ³⁴S values in the Neoproterozoic Eon, suggesting greater fractionations accompanying higher sulfate levels associated with mild oxygenation of the surface environment.

[1] Paris, G *et al* (2013) *Chemical Geology*, **345**, 50-61.

Geochemical signature of microbial activity during the deposition silica-stromatolite according to REE behaviour and Zr-Hf relationship

M. CANGEMI* AND P. CENSI¹

Department of Earth and Marine Sciences, University of Palermo, Via Archirafi, 36 – 90123 Palermo, Italy
*(correspondence: mariannacangemi@gmail.com)

Interactions between organic and inorganic species during the deposition of silica-stromatolites and associated microbial mats under hydrothermal conditions have been highlighted according to geochemical REE behaviour coupled to Zr-Hf fractionations.

In the studied system, dissolved SiO₂ derived from the leaching of outcropping volcanic rocks during interactions with hydrothermal fluids represents the raw material allowing to the deposition of stromatolites under the effects of severe microbial activity. At the same time microbial colonies also produce large amount of extracellular polymeric substances (EPS) that compete against bacterial surface into fractionating REE, Zr and Hf with respect to dissolved phase. Onto bacterial cell membranes (enriched in stromatolites) both specific polyphosphate binding sites and non-specific carboxyl O-donor groups occur differently partitioning HREE and MREE, depending on the REE/bacterial surfaces ratio [1]. EPS (occurring mainly in microbial mats) behave similarly to humic substances with respect to dissolved REE, due the similar nature of their surfaces where phenolic and carboxyl binding sites occur [2]. As a consequence REE, mainly Ce, are removed by EPS from dissolved phase and strongly enriched onto microbial mats. This process involves positive Ce anomalies and REE enrichments in the latter materials and consequently reduce the REE/bacterial surface ratio in forming stromatolites that preferentially bind HREE onto polyphosphate groups. During these processes a preferential Y and Zr with respect to Ho and Hf leads to higher Y/Ho and Zr/Hf ratios in microbial mats than in stromatolites suggesting that these ratios could represent a suitable geochemical signature of microbial activity in hydrothermal systems.

[1] Takahashi *et al.* (2005). *Chem Geol* **219**, 53–67. [2] Pourret *et al.* (2008). *Chem Geol* **251**, 120–127.

Controls of microbial nitrate/ nitrite respiration in polar marine sediments and implications for global climate change.

A. CANION¹ AND J.E. KOSTKA²

¹Florida State University, Tallahassee, FL, USA
²Georgia Institute of Technology, Atlanta, GA, USA

An estimated 50 to 70% of the global removal of marine N occurs in sediments, and N removal from continental shelves comprises approximately half of the total sediment contribution. Despite the importance of nitrate/ nitrite respiration to the marine nitrogen cycle, surprisingly few studies have addressed the significance of temperature as a physical control of nitrate respiration. We have been studying the mechanisms and controls of N removal in permanently cold sediments collected in the fjords of Svalbard, Norway, for the past five years. As for other biogeochemical processes, rates of denitrification and anammox in cold (1-2 °C) Arctic sediments approach those measured in temperate marine sediments. Denitrifying bacteria were isolated and shown to follow a psychrotolerant to psychrophilic growth response. Both denitrification and anammox exhibited temperature response characteristics consistent with a predominately psychrophilic community, but microbes with the anammox pathway appeared to be more adapted to permanently-cold sediments. Long term (weeks) warming experiments indicated that increases in temperature of 5 to 10 °C above *in situ* temperatures had little effect on the temperature response of denitrification and anammox, but increases of 25 °C shifted denitrification towards a predominately mesophilic community and eliminated anammox activity. When compared to previous temperature response data for other respiration processes in permanently cold sediments, it is apparent that there is considerable variability in *Topt* and activation energy, *Ea*, which may be driven by substrate availability. These results suggest that the effects of low temperature are modulated by other environmental factors to control rates of N removal in these Arctic coastal sediments.

Most recently, we have investigated the temperature regulation of microbial communities that mediate nitrogen removal in nearshore sediments over a 50° latitudinal gradient at subtropical (Gulf of Mexico), temperate (Wadden Sea), and Arctic (Svalbard) sites. The apparent activation energy of denitrification was two-fold higher in subtropical versus temperate and arctic sediments, indicating a mesophile-dominated community. Results reveal adaptation of N₂-producing microbial communities to *in situ* temperatures.

B, Pb, Sr isotopic imprint of crustal and mantle rocks from the slab-mantle interface: The Cima di Gagnone example (Central Alps)

E. CANNAO¹* S. AGOSTINI² M. SCAMBELLURI^{1,2}
AND S. TONARINI²

¹DISTAV, Università di Genova, Corso Europa 26, 16132 Genova, Italy *(correspondence: enrico.canna@unige.it)
²IGG-CNR, Via G. Moruzzi, 1, 56124 Pisa, Italy

In subduction zones, the slab-mantle interface represents a key setting for tectonic mixing of slab- and mantle-derived materials and for fluid-mediated mass transfer from the slab to the overlying mantle. Element exchange between different lithologies and element release to fluids in this environment can be traced by B, Pb, Sr isotopic systems. Here we focus on the Cima di Gagnone case-study, where pelitic schists and gneisses enclose peridotite lenses, like in a top-slab mélange [1]. The ultramafic rocks, hosting eclogitized and rodingitized MORB mafic rocks, derive from serpentinized oceanic peridotites that underwent subduction dehydration [1,2]. Serpentinization also occurred during prograde exchange with fluids derived from the host rocks, once the oceanic serpentinized peridotites were accreted to the mélange [3]. Potential precursors for Gagnone, e.g. Alpine HP serpentinized peridotites from Erro-Tobbio (ET), display high B (20 ppm), $\delta^{11}\text{B}$ (13-20‰), B/Nb > 140 [4] and scarce enrichments in radiogenic Pb, Sr. At Cima di Gagnone $^{87}\text{Sr}/^{86}\text{Sr}$ and $^{206}\text{Pb}/^{204}\text{Pb}$ ratios of ultramafites (0.7055-0.7109 and 17.7030-18.4939, respectively) indicate exchange with the host rocks ($^{87}\text{Sr}/^{86}\text{Sr}$ up to 0.7208; $^{206}\text{Pb}/^{204}\text{Pb}$ up to 18.9846). Negative $\delta^{11}\text{B}$ of ultramafic rocks (-1 to -10 ‰) point to a mixed effect of (1) dehydration of serpentinized precursors, leading to heavy ^{11}B loss into fluids and to light B isotopic compositions of residual rocks, combined with (2) exchange with fluids from the host crustal rocks. Several ultramafic samples with relatively low Pb and Sr isotopic ratios, like in the ET, and with low B/Nb (<45) and $\delta^{11}\text{B}$ (-9 ‰), may represent the dehydration products of serpentinized peridotites less affected by crustal exchange. These data document the rock and fluid compositions attained in a top-slab mélange and point to release to fluids of $\delta^{11}\text{B}$, radiogenic Sr and Pb, which may strongly affect mantle wedge metasomatism and arc magmatism.

[1] Trommsdorff (1990) *Mem. Soc. Geol. It.* **45**, 39-49. [2] Evans *et al.* (1979) *American Mineralogist* **64**, 15-31. [3] Scambelluri *et al.* (submitted). [4] Scambelluri and Tonarini (2012) *Geology* **40**, n.10, 907-910.

Source of magmas that generated eruptive products at Mt. Somma-Vesuvius and Campi Flegrei based on melt inclusions data

CLAUDIA CANNATELLI¹* ROSARIO ESPOSITO¹
ANNAMARIA LIMA¹ BENEDETTO DE VIVO¹
AND ROBERT J. BODNAR²

¹DISTAR, Università degli Studi di Napoli Federico II, Via Mezzocannone 8, Napoli, 80134, Italy (*Correspondence: claudia.cannatelli@unina.it), (rosario.esposito3@unina.it), (anlima@unina.it), (bdevivo@unina.it)

²Department of Geosciences, Virginia Tech, 4044 Derring Hall, Blacksburg VA, 24061 USA

Mt. Vesuvius and Campi Flegrei volcanic systems are located in the Campanian Volcanic District, and are considered among the most hazardous volcanic areas in the world. They lie in the proximity of the densely populated area that comprises the city of Naples, with more than 3 million people at immediate risk if an eruption occurs. The goal of this study is to understand the origin of magmas that have generated the eruptive products of these volcanic systems, by studying the major and trace element systematics of melt inclusions trapped in phenocrysts.

Melt inclusions were selected based on host rock age and provenance, i.e. all of the eruptive products of Vesuvius (from 25ky to 1944AD), Campi Flegrei (18-0.5ky) and Campanian Ignimbrite (from 250ky to 39ky) have been investigated. Incompatible elements (Zr, Th, Hf, etc) show an inverse variation with MgO, in particular Th/Hf ratios show a constant trend, indicating a genetic link between the magmas over time. More evolved melt inclusions in Vesuvius pre-1631 products (first, second and part of the third cycle) show compositions that overlap with those of the most evolved melt inclusions in Campanian Ignimbrites. Less evolved magma compositions of Campi Flegrei (Solchiaro, Fondo Riccio and Minopoli 1) overlap with compositions of magma trapped in less evolved Campanian Ignimbrite-hosted melt inclusions and Vesuvius 1906-hosted melt inclusions eruptive products.

Similarities in the trace element systematics for the melt inclusions in Vesuvius, Campi Flegrei and Campanian Ignimbrites phenocrysts lead to the conclusion that these magmas likely originated from the same deep source.

Comparison of PFLOTRAN and TOUGHREACT numerical codes for reactive transport modelling of CO₂ storage in saline aquifers

B. CANTUCCI¹* P. ORSINI² AND F. QUATTROCCHI¹

¹Istituto Nazionale di Geofisica e Vulcanologia, Via di Vigna Murata 605, 00143 Rome, Italy

(*correspondence: barbara.cantucci@ingv.it)

²BLOSint Ltd, University of Nottingham Innovation Park, Triumph road, NG7 2TU (paolo.orsini@blosint.com)

CO₂ geological storage in deep saline aquifers needs specific requirements in terms of safe storage and enduring containment of injected gas.

In order to understand the behaviour of CO₂ and predict the effect of geochemical reactions on trapping mechanisms and porosity/permeability variations, numerical models are an important tool.

Due to the large time and length scales involved, realistic numerical solutions, including thermal, hydrogeological and geochemical effects, are computationally demanding and the use of parallel software is necessary.

In this work a large scale model of an Italian reservoir, potentially suitable for CO₂ storage, is used as case study to compare two reactive transport codes, TOUGHREACT [1] and PFLOTRAN [2]. Pflotran is an open-source, 3D reservoir simulator, for sub-surface multiphase, multicomponent reactive flows with parallel capabilities.

The simulation model consists of an offshore structure with an area of more than 100 km² and a vertical development of 3 km, hosting a thick carbonatic reservoir. Two simulations were performed at different scales, considering advective and diffusive transport of the considered species at non-isothermal conditions and mineral reactions kinetically controlled. The feedback between flow and geochemical reactions, implemented in PFLOTRAN, has been customised in order to comply with the model implemented in TOUGHREACT.

At the time of writing the Authors are finalising the comparison between PFLOTRAN and TOUGHREACT solutions. However, from the preliminary results, some divergences found are likely to be due to the different EOS used to compute the dissolution of supercritical CO₂ in brine. Grid sensitivity analysis and boundary condition effects are also being investigated as part of the software comparison.

[1] Xu *et al.* (2006) *Computer & Geosciences* **32**, 145–165.

[2] Hammond *et al.* (2012) *Groundwater Reactive Transport Models* **5**, 142–160.

Research on particles carried by ascending gas flow of earthquake ruptures

JIANJIN CAO^{1,2*}, SONGYING LUO¹, PEIXIN LAI¹, ZHENGYANG WANG¹, YIPENG LIAO¹ AND JIE YI¹

¹Department of Earth Science, Sun Yat-sen University, Guangzhou, China

² Guangdong Key Laboratory of Geological Process and Mineral Resources Exploration, Guangzhou, China

* correspondence: (eescjj@mail.sysu.edu.cn)

Last century, Kristiansson and Malmqvist put forward that element contents of material carried by the the naturally occurring ascending gas flow from earth interior were analyzed and the data can be used in exploration of metal deposits. [1] Many researchers studied the application effect in metal deposits of the method. [2] We proposed and studied that the concealed metal deposits were detected using the type, size, shape, structure, chemical composition of the particles carried by the ascending gas flow. [3]-[5] In the last few years, It's the first time that we proposed that release of a large amount of particles in gases from Earth's interior were caused by earthquake and the characteristics of the particles can be used in earthquake prediction.

We studied that the type, size, shape, structure, chemical composition of particles as well as gathering characteristic among the particles, which were carried by the ascending gas of ruptures generated by the “5.12” great wenchuan earthquake, using the individual particle analysis technology of a transmission electron microscopy. Similarities and differences in the particle characteristics of ascending gas between the ruptures generated by the “5.12” great wenchuan earthquake and the fault without earthquake occurrence were compared. Abnormal particles, which are rich in metals such as Pb, Hg, Cu, Os, were found in the ascending gas of ruptures generated by the “5.12” great wenchuan earthquake.

The particles offered the new data that derives from the depth for study on causes of earthquake. This research provided a new method for earthquake prediction. It can enrich theory of nanogeoscience.

The authors acknowledge the support of the National Natural Science Foundations of China (Grant Nos. 41072263, and 41030425) and the National High-Tech Research and Development Program of China (Grant No. 2008AA06Z101).

[1] Kristiansson *et al.* (1982) *Geophysics*, **47**, 1444–1452.

[2] Wang *et al.* (1999) *Journal of Geochemical Exploration* **66**, 85–97. [3] Cao *et al.* (2009) *Journal of Geochemical Exploration* **101**, 247–253. [4] Cao *et al.* (2010) *Science China Earth Sciences* **53**, 1647–1654. [5] Cao. (2011) *Geochemical Journal* **45**, e9 ~e13.

Abiogenic Fischer-Tropsch synthesis of methane at the Baogutu reduced porphyry Cu deposit, western Junggar, NW-China

MINGJIAN CAO^{1,2*} KEZHANG QIN^{2*} GUANGMING LI²
NOREEN J. EVANS³ AND LUYING JIN^{1,2}

¹Key Laboratory of Mineral Resources, Institute of Geology and Geophysics, Chinese Academy of Sciences, P.O. Box 9825, Beijing 100029, China
(*caomingjian@mail.iggcas.ac.cn)

²University of Chinese Academy of Sciences, Beijing 100049, China (*kzq@mail.iggcas.ac.cn)

³John de Laeter Center for isotope Research, Dept. Applied Geology, Curtin University, Perth WA 6845

Methane is widely developed in hydrothermal fluids from reduced porphyry copper deposits (RPCDs; proposed by Rowins, 2000), but its origin remains enigmatic. The occurrence of methane in fluids at the Late Carboniferous Baogutu RPCD in western Junggar, Xinjiang, NW-China (our unpublished data; Shen *et al.*, 2010), presents an excellent opportunity to address this problem. A systematic study including fluid inclusion microthermometry and Laser-Raman, hydrothermal mineral H-O isotope analyses was conducted to constrain the origin of CH₄ and CH₄-rich fluids.

The wide range of δD values (-86.7 ± 11.2 ‰, $n = 21$) and $\delta^{18}O$ ($+3.8 \pm 1.4$ ‰, $n = 21$) for water within quartz most likely results from water-rock interaction with water/rock ratios (wt% in O) ranging from 0.25~3 and 0.2~1 for a closed system and open system, respectively, but not from mixing with meteoric water. Detailed Laser-Raman analyses indicate CO₂ in apatite included in granodiorite porphyry phenocrystic biotite records the early stage magmatic stages, whereas later hydrothermal fluids containing CH₄ with trace CO₂ are found in inclusions in vein quartz.

We propose that the magmatic CO₂ was reduced to CH₄ by Fischer-Tropsch type (FTT) reactions in the presence of H₂, which was probably generated during the early Ca-Na hydrothermal alteration with hydration of hornblende + clinopyroxene to actinolite + magnetite + sphene + albite. Therefore, the methane of fluids at the Baogutu RPCD was not produced via thermogenesis or bacteriogenesis but instead formed during late hydrothermal alteration by FTT reactions.

[1] Rowins S. M. (2000) *Geology* **28**, 491–494. [2] Shen *et al.* (2010a) *Chem. Geol.* **275**, 78–98.

Molecular geochemistry as indicators of seal integrity and relevance to shale oil exploration

TINGTING CAO, MAOWEN LI, JIANG QIGUI
AND ZHIMING LI

Sinopec Exploration and Production Research Institute

Recent development in unconventional shale petroleum production in North America has led to significant changes in the global energy outlook. Production of shale oil from organic rich source rocks has brought complex geochemical, geological and engineering challenges which are distinct from those related to conventional systems. This study compares the marine petroleum systems in the Devonian-Mississippian Bakken Formation of the Williston basin in North America and the lacustrine petroleum systems in the Eocene-Oligocene Shahejie Formation in the Zhanhua Depression of Bohai Bay Basin, China, to identify key geological controls for viable shale oil plays. In particular, we pay attention to the role of seal integrity in the retention of petroleum fluids within the mature source rock systems. In the Williston basin there are two opposing schools of thought that infer either the Bakken Formation or the Lodgepole Formation as the primary source rock for the Madison-reservoired oils in the Canadian Williston Basin. While there is geochemical evidence for significant mixing of Bakken and Lodgepole oils in the Madison reservoirs, multivariate statistical analysis of a large geochemical data set indicating that oil mixing appears to be geographically dependent and restricted by a northeast-southwest-striking zone, where fracture or fault systems are inferred to have provided high permeability zones allowing Bakken-derived oil to migrate upward across the Lodgepole Formation. The areas without significant fault or fracture systems favour either lateral oil migration along porous beds in the middle Bakken reservoirs or oil retention within the Bakken source rocks leading to overpressure zones. In the Zhanhua Depression, in contrast, molecular geochemical data suggest two contrasting hydrocarbon migration scenarios: dominant short-distance lateral migration in over-pressured central sag areas, and vertical migration along fault and fractures to the shallow reservoirs in the Guantao Formation. As oil production from the shale dominated intervals in the Zhanhua Depression show clear relationship between the production locations to the proximity of regional fault systems, delineating the relationship holds the key in the target selection of shale oil exploration.

A potential steel passivating layer: fe-saponite and chlorite growth on steel in high P,T engineered barrier experiments

F.A.CAPORUSCIO^{1*} AND M.C.CHESHIRE²

¹EES-14, LANL, Los Alamos, NM, 87545 USA

(*correspondence:floriec@lanl.gov)

²EES-14, LANL, Los Alamos, NM, 87545

Experimental work for the US Used Fuel Disposition campaign has started to characterize the stability and alteration of a bentonite-based Engineered Barrier Systems (EBS) with different waste container materials in brine at higher heat loads and pressures.

Experiments were run at ~150 bar 300° C for 6 weeks. Unprocessed bentonite from Colony, Wyoming was used as the clay buffer. Redox conditions were buffered at magnetite-iron oxygen fugacity. A K-Na-Ca-Cl-based brine replicated deep groundwater compositions. The experimental mixtures were brine-clay-various steels with a liquid/clay ratio of ~9. Reaction mineralogy and aqueous geochemistry of each experiment was evaluated.

No smectite illitization was observed in these reactions. It would appear that illitization was retarded due to a limitation of K⁺ in the closed-system. However, notable clay mineral reactions occurred at the steel surfaces. Authigenic chlorite and Fe-saponite grew with their basal planes perpendicular to the steel plate, forming a 10 – 100 µm thick ‘corrosion’ layer. The steel plates act as a substrate for chlorite/Fe-saponite growth. XRD and microprobe analyses of the silicate mantling on the low-carbon steel indicates the phase is a Fe saponite with a composition of (Na_{0.09},Ca_{0.03}) (Fe_{2.20}Mg_{0.12}Al_{0.86}) (Al_{0.58}Si_{3.42})O₁₀(OH)₂. Stainless steel (304) is mantled by a chlorite/Fe saponite mixture. This phyllosilicate mix is high in Fe (33.99 wt% FeO), Cr (1.35 wt % Cr₂O₃) and Ni (1.34 wt % NiO).

Mineral growth on the waste containers was influenced by the container, clay buffer, and fluid compositions, in addition to pressure and temperature conditions Results show that the waste container may act as a substrate for chlorite /saponite growth in response to corrosion and the chlorite /saponite can act as a passivating agent.

Biotite and phlogopite dissolution: Topographic observation by VSI

C. CAPPELLI^{1*}, J. CAMA² F.J. HUERTAS¹, C. FISCHER³ AND A. LÜTTGE³

¹Instituto Andaluz de Ciencias de la Tierra (IACT), CSIC-UGR, Avenida Fuentenueva s/n., 18002 Granada, Spain (*correspondence: chiaracappelli@ugr.es)

²Institute of Environmental Assessment and Water Research (IDAEA), CSIC, Jordi Girona 18-26, 08034 Barcelona, Catalonia, Spain

³University of Bremen – Department 5 Geosciences, Bibliothekstraße 1, 28359 Bremen, Germany

The dissolution kinetics of two micas (biotite and phlogopite) was investigated by vertical scanning interferometry (VSI). Topographical data at the basal surface during dissolution at pH 1 and 2 (25 -100 °C) of nitric and oxalic acid solutions were used to determine the micas’ dissolution mechanisms.

Single biotite and phlogopite fragments of approximately 100 mm² were reacted in 250 mL of acidic solution up to 44 days. The cleavage surfaces were examined by VSI before and after the reaction.

On the one hand, the biotite dissolution in nitric acid was dominated by step-edge retreat together with a phenomenon of layer peeling at the step edges [1]. At longer reaction times dissolution channels developed, leaving mineral islands. In the presence of oxalic acid, biotite step-edge retreat was also observed. In addition, formation of rounded etch pits of different size and density, depending on the experimental conditions, took place by covering the surface rather uniformly. Moreover, some peculiar dissolution microstructures were found at the mineral-solution interface.

On the other hand, VSI images of phlogopite surface showed step-edge retreat and formation of triangular crystallographically controlled etch pits [2,3] of different size, being non-homogeneously distributed over the basal surface. In the presence of oxalic acid, the phlogopite dissolution features were similar to those observed in nitric acid, but higher etch pit density and etch pit alignment were observed.

Hence, as the mechanisms that control the dissolution of the different mica minerals depend on the presence/absence of oxalic acid, it is necessary to study the effects of the compositional factor and the presence of inorganic ligands on the dissolution kinetics of micas.

[1] Turpaul and Trotignon (1994) GCA **58**, 2761-2775 [2] Rufe and Hocella (1999) Science **285**, 874-876 [3] Stübner, Jonckheere and Ratschbacher (2008) GCA **72**, 3184-3199

Fe-Si system: a potential major component of the Earth's core

RAZVAN CARACAS¹, MATTHIEU VERSTRAETE²,
REBECCA FISCHER³ AND ANDREW CAMPBELL³

- 1) Laboratoire de Geologie de Lyon (LGLTPE) CNRS UMR 5276, Ecole Normale Supérieure de Lyon, France; (razvan.caracas@ens-lyon.fr)
- 2) University of Liege, Institut de Physique, Bat. B5, Liege, Belgium
- 3) Department of the Geophysical Sciences, University of Chicago, 5734 E Ellis Ave, Chicago, IL 60637, USA

We investigate the phase diagram of the Fe-Si system, the solubility limits of Si into hcp Fe, and the effect of Si on the thermal and electrical conductivities of iron. For this we perform first-principles calculations based on the density-functional theory and the density-functional perturbation theory.

First we build a series of hcp supercells; we replace some of the Fe atoms with Si in various amounts and configurations. In this way we mimic the dissolution of silicon into hcp and take into account a realistic solid solution. Silicon slightly increases the specific volume of iron, but the differences levels out at high pressures. We show that the density and seismic profiles of the core can be easily matched by Fe-Si alloys with small amounts of Si. Further phonon analysis suggests that stoichiometric Fe₃Si is dynamically unstable at high pressure. This results in decomposition into Si-bearing hcp Fe and Fe-bearing B2 FeSi. Then we follow the evolution of the Fe-FeSi immiscibility gap as a function of pressure.

Finally we compute the electrical and thermal conductivities of Si-bearing hcp iron at inner core conditions. We obtain that a relatively small amount of Si decreases the conductivity of iron, but then this quickly reaches saturation.

Based on these considerations we conclude that Si can be a major light element of the Earth's core.

Mantle-derived fluids in Central Mediterranean: Geochemical and geophysical constrains on sources of fluids and migration

CARACAUSI A¹, F. GRASSA¹, V. PENNINO², A. RIZZO¹,
AND A. SULLI²

- ¹Istituto Nazionale Geofisica e Vulcanologia, via Ugo La Malfa 153, 90146, Palermo, Italy. (a.caracausi@pa.ingv.it)
- ²University of Palermo, via Archirafi 36, 90123, Palermo, Italy. (atilio.sulli@unipa.it)

The geodynamics of the central Mediterranean is characterized by the interaction between the European plate and the African's. In this setting Sicily is a sector of the Apennine-Maghrebide accretionary prism, which is located between two areas affected by extensional tectonics (Sicily Channel to the south and the Thyrrenian back arc basin to the north).

Significant mantle-derived helium ($0.4 < R/Ra < 2.8$; $R = {}^3\text{He}/{}^4\text{He}$ in the sample, Ra in atmosphere) is found in the CH₄ and N₂-CO₂ rich fluids released in central western Sicily, a region without evidence of recent magmatism. CH₄-dominated gases are released from mud volcanoes localized in an area of both low heat flow and seismicity. On the contrary CO₂ is mainly associated to the thermal groundwater circulating mainly in Mesozoic limestone over an area characterized by high seismicity and heat flow anomaly. Total carbon dissolved in thermal water is a mixture of mantle-derived and crustal inorganic CO₂, while CH₄-dominated fluids show a mixing between a ³He rich and CH₄-poor term and a CH₄-rich and ³He-poor one typical of crustal reservoir of gases. The computed mantle derived He, much higher than stable continental areas, indicates that the transfer of fluids is controlled by tectonic mechanism through the crust. Finally, recent geophysical investigations discovered the occurrence of active lithospheric faults that could control the transfer of mantle derived fluids from the sources to the crust and throughout this towards the surface.

Magma dynamics at Mount Etna (Italy) inferred from geochemistry of gas emissions

CARACAUSI A., MARTELLI M., PAONITA A.
AND RIZZO A.*

Istituto Nazionale di Geofisica e Vulcanologia – Sezione di
Palermo, Via Ugo La Malfa 153, 90146 Palermo, Italy
(*correspondence: a.rizzo@pa.ingv.it)

Since 2007 we have performed a geochemical monitoring of some fumaroles located in the rim of Voragine crater at Mount Etna. The acquired data have been integrated with those from peripheral gas emissions, monitored since 1996. As a first step, the gas mixtures have been quantitatively corrected for post-magmatic processes such as interaction with shallow aquifers. Then, the systematics of He-Ar-CO₂ allowed us to assess the degassing path of the emitted gases and the absolute pressures at which are released. As a result, peripheral gases are fed by volatiles exsolved from magma batches residing in a range of pressure comprised between 200 and 400 MPa, while summit fumaroles get also gases from lower pressures (~130 MPa). These pressures well agree with geophysical and petrological investigations that recognize ponding zone of magma at 5-12 km b.s.l. and at 2-3 km b.s.l.

In addition to pure magma degassing processes, also mixing of the volatiles exsolved at different pressures occurs and influences the chemical and isotope variations, especially of crater fumaroles. Indeed, temporal monitoring of $\delta^{13}\text{C}_{\text{CO}_2}$ and He/Ar ratio showed that variable proportions of mixing as well as variable degassing pressure strongly depend on magma dynamics at depth. In particular, a progressively deep component seems to prevail during pre-eruptive phases reflecting magma recharge at depth, while the pure degassing component pertains to shallow volatile component prevailing during post-eruption periods.

Finally, long-term monitoring of $^3\text{He}/^4\text{He}$ ratios from both peripheral and crater gases has allowed us to systematically recognize phases of increase of the isotope ratios, occurred months before the onset of eruptive activity at all the sampled emissions. Considering what above stated, these phases would be related to refill of the plumbing system by ^3He -rich magmas, being thus very primitive and rising directly from the mantle. Recently, this behavior has been also recorded before 2011-2012 and 2013 volcanic activities, which have been characterized by frequent episodes of fire fountains and lava flows from the New South East Crater (NSEC). We point out that the last phase of magma recharge at depth is still ongoing suggesting that the new eruptive period, started in early 2013, could be further fed in the following months.

μ -XRD, μ -XRF, and μ -XANES synchrotron analyses of heterogeneous mine-waste materials related to AMD processes

C. CARBONE¹, G. GIULI,² S. CONSANI² P. MARESCOTTI²
AND G. LUCCHETTI²

¹DISTAV, Corso Europa 26, Univeristy of Genova, Italy
²Scuola di Scienze e Tecnologie, Sezione di Geologia
University of Camerino, Italy

In this work, we studied the mineralogical and chemical variations of some representative mine-waste samples from the Fe-Cu sulphide Libiola Mine, by means of combined synchrotron-based μ -XRD, μ -XRF, and μ -XANES analyses performed at ESRF beamlines (Grenoble). Mine waste is acid generating (Marescotti *et al.*, 2010) and is characterized by a high amount of completely to partially altered sulphide-rich mineralizations. Other than acid generation, the major environmental problem is the mobilization of potential toxic elements (PTEs) that can be concentrated in waters and soils. We studied three different Fe-oxides and -oxyhydroxides rich samples representative of a) stratified crust formed by the ageing of soft precipitates formed from acid mine waters discharged at mine adits, b) partially altered massive pyrite-rich mineralizations which contain the transition from unaltered to completely altered sulphide-mineralizations (Carbone *et al.*, 2012), and c) partially altered stockwork pyrite-rich mineralizations.

In this study, we demonstrated that the combined use of micro-synchrotron-based techniques (performed at ID18f and ID21 beamlines) can be successfully applied to monitor the alteration processes that occur between sulphides and their oxidation products. In particular, the combined use of μ -XRD and μ -XRF highlighted a different behaviour of some ecotoxic elements, such as Zn and As, during the evolution of the alteration process. A quantitative analysis of the sulphide/sulphate ratio was performed using the μ -XANES S k-edge spectra, while the Fe k-edge spectra were used in order to obtain the distribution of Fe³⁺ between primary and secondary phases.

[1] Marescotti, P., Azzali, E., Servida, D., Carbone, C., De Capitani, L., Grieco, G., Lucchetti, G., 2010. *Environmental Earth Sciences* **61**, 187-199. [2] Carbone, C., Marescotti, P., Lucchetti, G., Martinelli, A., Basso, R., Cauzid, J., 2012. *Journal of Geochemical Exploration* **114**, 109-117.

The summit activity at Mt. Etna from 1995 to 2001: A multidisciplinary approach to investigate the long-term processes of the magmatic plumbing system

D. CARBONE¹, R.A. CORSARO², F. GUGLIELMINO³
AND G. PUGLISI^{4*}

¹INGV-OE, piazza Roma 2, 95125 Catania, Italy,
(carbone@ct.ingv.it)

²INGV-OE, (corsaro@ct.ingv.it)

³INGV-OE, (guglielmino@ct.ingv.it)

⁴INGV-OE, (*correspondence: puglisi-g@ct.ingv.it)

The integration of volcanologic observations, petrologic data, microgravity and ground deformation acquired at Etna from 1995 to 2001, provided the opportunity to investigate the long-term dynamics of Mt. Etna during a period when the activity was restricted to the summit craters.

Temporal patterns of major and trace elements indicate that the variability of bulk rocks composition is due to fractional crystallization and mixing between residing and new intruding magmas. Microgravity data show that from late-1996 to mid-1999 and from late-2000 to mid-2001, strong gravity decrease occurred, centered on the upper southeastern sector of the volcano. The gravity decreases coincide with an increase in the rate of the seismic strain release. Ground deformation show, from 1994 to the onset of the 2001 eruption, an almost continuous expansion of the volcano mainly due to magma accumulation into the western sector of the volcano. Therefore, the anti-correlation between gravity and seismicity in the eastern flank is not strictly connected to movements of magma and/or change of its chemical and physical properties. Conversely, these data suggest an increase of micro-fracturing along the NNW–SSE structural trend, implying a local density (gravity) decrease coupled with an increase in the release of seismic energy.

From 1996 to 1999 the inferred increase in the rate of fracturing and acceleration of deformation in the volcano eastern flank led to the ascent of conspicuous magma volumes that promoted the reactivation of the South-East and Voragine summit craters, with sustained an intense explosive and effusive activity until the end of 1999. The increase of rate of fracturing from late-2000 to mid-2001 enhanced the formation of a preferential path for magma ascent to the surface and the onset of the July 2001 flank eruption.

Control of magma recharge and buoyancy on the frequency and magnitude of volcanic eruptions

LUCA CARICCHI¹ CATHERINE ANNEN²
AND JON BLUNDY²

¹Section of Earth and Environmental Sciences, University of Geneva, Rue des Maraîchers 13, CH-1205 Geneva, CH

²Department of Earth Sciences, University of Bristol, Wills Memorial Building, Queen's Road, BS8 1RJ, Bristol, UK

The frequency at which volcanic eruptions occur is inversely proportional to the volume of magma released in a single event. The basic requirements for a volcanic eruption to occur are that enough heat is supplied to the crust to assemble a body of eruptible magma and that overpressure is sufficient for the magma to reach the surface without solidifying. Starting from these basic principles we used thermo-mechanical calculations and Monte Carlo simulations to quantify the relative contribution of magma fluxes and the physical properties of the crust on likelihood and volume of volcanic eruptions. The calculations were performed considering the periodic input of magma in pulses of different size and shape injected at various frequencies. The average rate of magma supplied to the upper crust over hundreds of thousands of years appears to control the volume of magma that can potentially be released during a single eruption, whereas the time interval between short-lived pulses of magmatism, affects the total duration of magma injection preceding an eruption. Our calculations reconcile the relationship between erupted volume and upper crustal magma residence times, and replicate the correlation between erupted volumes and caldera dimensions. Our modelling shows that relatively small and frequent eruptions are triggered by magma injection while buoyancy is important to trigger large eruptions. These calculations permit to identify the physical processes controlling the relationship between frequency and magnitude of volcanic eruptions and increase our capability of determining the temporal evolution of volcanic activity in different volcanic systems.

Systems biology studies on the stress response of perchlorate, chlorate oxidative and nitrosative stress in *Desulfovibrio alaskensis* G20

HANS K. CARLSON^{1,2*} MARK R. MULLAN^{1,2},
ADAM M. DEUTSCHBAUER² MORGAN N. PRICE²,
ADAM A. ARKIN^{1,3} AND JOHN D. COATES^{1,2,3*}

¹Energy Biosciences Institute, University of California, Berkeley, Berkeley, CA (*correspondance: jdcoates@berkeley.edu, carlsonh@berkeley.edu)

²Department of Plant and Microbial Biology, University of California, Berkeley, Berkeley, CA

³Lawrence Berkeley National Laboratory, Berkeley, CA

The chloroxyanions, perchlorate and chlorate, are potent inhibitors of sulfate-reducing bacteria, and as such are promising as treatments for biosouring in oil reservoirs. To understand the mechanism of inhibition, tagged transposon pools of the model sulfate-reducer, *Desulfovibrio alaskensis* G20 were stressed with the intermediates of respiratory perchlorate reduction: perchlorate, chlorate and oxygen.

The G20 mutant fitness profiles for (per)chlorate stress compared with other stressors such as nitrate, nitrite, nitric oxide and the reactive oxygen species hydrogen peroxide and hypochlorous acid reveal both overlapping and unique targets and mechanisms of resistance. Physiological, biochemical and transcriptomic studies were used to further define the cellular response to (per)chlorate. Taken together our results suggest that (per)chlorate toxicity appears to be a combination of oxidative stress alongside competitive inhibition of transport systems and enzymes involved in sulfate reduction. This work provides a starting point for developing new treatments to inhibit sulfate reduction in engineered ecosystems, including possible synergistic interactions between stressors.

Making Earth

RICHARD W. CARLSON

Carnegie Institution of Washington, Washington, DC, 20015
USA: (rcarlson@ciw.edu)

Our understanding of the steps involved in Earth formation have been transformed by huge improvements in the isotopic measurement techniques employed in geo/cosmochemistry. Modern techniques can: provide chronological precisions of well less than a million years on events happening over 4.5 billion years ago; allow the application of a wide variety of extinct radionuclides as chronometers and tracers that are sensitive to different key processes in planet formation and differentiation; and resolve isotopic variability in the Solar nebula that can provide clues to its structure and the origin of the building blocks of the terrestrial planets. The identification of an increasing number of stable isotope variations between meteorites and Earth has reopened the question of whether meteorites can be used to accurately infer the composition of the bulk-Earth. This basic compositional datum likely will have to come from direct measurement of Earth composition, for example the determination of bulk-Earth U and Th abundances via geoneutrinos. Improved chronological precision now allows clear resolution of many key steps involved in planet formation. Earth gained its characteristic depletion in volatile elements compared to chondritic meteorites within a few million years of Solar system formation. Ages for other events, however, must be interpreted in the context of a prolonged interval for Earth formation. For example, core formation on Earth is dated at 4.47-4.53 Ga, but this age range likely just reflects a mean age for a sequence of core forming events that occurred with each impact between a large planetesimal and the growing Earth. The last major impact into the growing Earth, likely the one responsible for Moon formation, appears to have occurred relatively late in Solar system history. The oldest reliably dated lunar crustal rocks give ages between 4.36 and 4.41 Ga, which overlap the I-Xe age of Earth's atmosphere, the U-Pb model age of Earth's mantle, the Sm-Nd and Lu-Hf model ages of the lunar mantle, and the oldest ages for zircons from western Australia and mafic metamorphic rocks from northern Quebec. Some Archean rocks derive from sources created in this early differentiation event, but mantle convection appears to have mixed away much of the evidence for this event in Earth's interior by 2.7 Ga. By ~4.4 Ga, Earth's surface and shallow interior had cooled to the point where liquid water was present on the surface and cycles of basaltic magmatism followed by hydration and remelting of the basalt to produce the felsic rocks typical of continental crust already had begun.

Preserving Fertile MORB Mantle in the Continental Lithosphere

RICHARD W. CARLSON¹ AND DMITRI A. IONOV²

¹Carnegie Institution of Washington, Washington, DC, 20015
USA: (rcarlson@ciw.edu)

²PRES-Lyon & UMR6524-CNRS, 42023 Saint Etienne,
France: dmitri.ionov@univ-st-etienne.fr

The shallow mantle beneath the Tariat region of central Mongolia is composed predominantly of fertile peridotite [1]. Of over 110 peridotite xenoliths recently collected from four localities in the Tariat region, over 90% are lherzolites. The remainder include subequal amounts of harzburgite and veined pyroxenite-peridotites. The median Mg#, Al₂O₃, and CaO contents of the Tariat collection are 89.4, 3.87 and 3.23, respectively. Modeling major element compositions indicate that most samples experienced 0-6% partial melt removal at 1 GPa [2]. Clinopyroxenes, on average, are moderately LREE depleted (average chondrite normalized La/Sm = 0.45). Most whole rocks show small, if any, depletions in Re and Pd compared to other HSE. ¹⁸⁷Os/¹⁸⁸Os for samples with more than 3.2% Al₂O₃ range only from 0.126 to 0.131. Samples with Al₂O₃ ranging from 3.1 to 1% Al₂O₃ define a correlation with ¹⁸⁷Os/¹⁸⁸Os suggesting an “alumichron” age of ~2 Ga. The most refractory samples, however, show no correlation with Os isotopic composition, with ¹⁸⁷Os/¹⁸⁸Os from 0.114 to 0.128; they also are commonly enriched in iron and LREE. In contrast to the indicators of fertility in most samples, new Sr, Nd and Hf isotopic data for acid-leached clinopyroxene separates from fertile lherzolites plot within the range of modern MORB with ⁸⁷Sr/⁸⁶Sr from 0.7021 to 0.7026 and εNd from +7.7 to +9.8, overlapping earlier results [3] and εHf from +13.3 to +18.5. One metasomatized harzburgite gives ⁸⁷Sr/⁸⁶Sr (0.7045) and εNd (+1.5), within the range seen for Cenozoic Mongolian basaltic volcanism [4], but retains a high εHf of +11.5, which suggests recent overprinting of Sr and Nd, but less so Hf, by melts similar to the regionally widespread basalts. The crustal section in this part of the Central Asia Orogenic Belt consists of various terranes mainly accreted in the Paleozoic [5]. The composition of the mantle lithosphere beneath at least the Tariat region suggests that a significant slice of fertile MORB mantle was accreted with the overlying crust, perhaps allowing an unusually clear look at a section of convecting asthenosphere less altered than typical of exposed abyssal peridotites.

[1] Ionov, D.A., *CMP* **154**, p455, 2007. [2] Ionov and Hofmann, *EPSL* **261**, p620, 2007. [3] Stosch *et al.*, *GCA* **50**, p2601, 1986. [4] Barry *et al.*, *J. Petrol.* **44**, p55, 2003. [5] Kroner *et al.*, *GSA Memoirs* **200**, p181, 2007.

Nitrogen in bivalve shell & soft tissues: Implications for N sequestration and cycling in coastal waters

RUTH H. CARMICHAEL*¹² D. JOE DALRYMPLE¹²
P. BIANCANI¹², C. KOVACS¹, W. WALTON³
AND E. DARROW¹²

¹Dauphin Island Sea Lab, Dauphin Island, AL 36528,
(*correspondence: rcarmichael@disl.org)

²University of South Alabama, Mobile, AL 36688

³Auburn University Shellfish Laboratory, Dauphin Island, AL 36528

There is growing interest in the role of bivalve shellfish in biofiltration, particularly with regard to N sequestration and removal from coastal waters. We quantified N assimilation into tissues of several bivalve species, linking N to anthropogenic sources for management, and defining timescales of N sequestration or removal that may affect ecosystem functions (particularly biogeochemical cycling). These data are important as urbanization and other human activities increasingly alter food supply and habitat for bivalves and we recognize historical global loss of commercial bivalves, due to combined habitat loss and over harvest. We found that N assimilated into bivalves largely depended on food quantity and quality, which determined growth (rate of N assimilation) and %N content in both soft tissues and shell. N assimilation rates & %N are at least affected by species-specific physiology, feeding habits, ontogeny and genetics, and cannot be generalized due to site-specific variation in food supply and environmental attributes. Similarly, biodeposition that allows N sequestration via burial or biogeochemical processes depended on food quantity and quality as well as environmental variation. Stable isotope analysis was used to successfully link biological responses to anthropogenic N sources across temporal and spatial scales, even when effects on growth or survival were not measurable. More data are needed to define timescales of sequestration, particularly in older reefs and for deposited shell. Ultimately these data can be combined from different regions to estimate global losses of N sequestration capacity through time due to bivalve depletion and predict capacity of sequestration or removal through restoration and farming activities. Interestingly, external N loading appears to have a positive influence on N removal capacity of bivalves by increasing growth rates and N storage in tissues, but external N loaded is greater than enhanced N sequestration and removal capacity in most cases, particularly in areas with increasingly limited available habitat.

^{40}K - ^{40}Ca constraints on the source of dissolved Calcium in Himalayan rivers

G. CARO¹ AND C. FRANCE-LANORD¹

¹CRPG-CNRS, Université de Lorraine, 15, rue Notre Dame des Pauvres, Vandoeuvre-les-Nancy. (caro@crpg.cnrs-nancy.fr;) cfl@crpg.cnrs-nancy.fr

This study investigates the potential of the ^{40}K - ^{40}Ca system for quantifying the contribution of silicate and carbonate lithologies to the Ca dissolved load of major Himalayan rivers. The ^{40}K - ^{40}Ca decay scheme has geochemical properties similar to the ^{87}Rb - ^{87}Sr system but its application as a tracer has been hampered by the analytical precision required to measure small variations on the large ^{40}Ca isotope (96.9%). This difficulty can now be overcome using the Finnigan Triton TIMS, which allows measurement of the $^{40}\text{Ca}/^{44}\text{Ca}$ ratio with external precision of 0.3-0.5 ϵ -unit [1]. Previous work showed that dissolved loads from the Ganga (in Patna) and Brahmaputra (in Guwahati) carry radiogenic ^{40}Ca excesses of $+1.4\pm 0.3$ and $+0.9\pm 0.3$ ϵ -units, respectively [1]. Since the ^{40}Ca composition of seawater remained constant and indistinguishable from the mantle value ($\epsilon^{40}\text{Ca}=0$) for the past 3.5 Ga [1], radiogenic Calcium must originate from the weathering of felsic rocks, or, alternatively, from metamorphosed carbonates having experienced isotopic exchange with surrounding silicates, as previously documented for ^{87}Sr . In order to test these hypotheses, we performed high-precision ^{40}Ca analyses in bedload carbonates from rivers draining the major Himalayan rock units, and in whole-rock dolostones with highly radiogenic $^{87}\text{Sr}/^{86}\text{Sr}$ from the Lesser Himalaya. Our results show that whole-rock and bedload carbonates are characterized by an $\epsilon^{40}\text{Ca}=0$ despite having highly variable $^{87}\text{Sr}/^{86}\text{Sr}$ ratios (0.71-0.86). A small excess (<1 ϵ -unit) was found in one dolomitic sample with $^{87}\text{Sr}/^{86}\text{Sr}\approx 0.86$ but given its extreme $^{87}\text{Sr}/^{86}\text{Sr}$ signature, this marginal lithology is bound to have a negligible influence on the Himalayan riverine ^{40}Ca budget. Overall, it appears that the major carbonate units of the Himalaya were not significantly affected by metamorphic redistribution of ^{40}Ca . These preliminary results suggest that radiogenic signatures measured in the Ganga and Brahmaputra are derived from the weathering of silicate lithologies, and highlight the potential of the ^{40}K - ^{40}Ca scheme as a tracer of silicate weathering in the Himalayan system.

[1] Caro *et al.* (2010) *EPSL* **296**, 124-132

Detoxification of milk contaminated by aflatoxin M1 using clay minerals and effects on milk quality

A. CARRARO¹, A. DE GIACOMO², M.L. GIANNOSSI, L. MEDICI³, L. PALAZZO², V. QUARANTA², V. SUMMA³ AND F. TATEO¹

¹ Institute of Geosciences and Earth Resources, National Research Council (CNR), c/o Department of Geosciences, University of Padova, 35131 Padova, Italy (tateo@igg.cnr.it)

² Istituto Zooprofilattico Sperimentale della Puglia e della Basilicata, Foggia, Italy

³ Institute of Methodologies for Environmental Analysis, National Research Council (CNR), Tito Scalo (PZ), Italy

Mycotoxins are widespread toxic substances produced by moulds in human and animal foodstuffs. Some of them, such as aflatoxin B1 (AFB1), are very toxic even in small amounts. The modern approach to the problem (and the link with public health) started in the 60s. After decades of studies, it appears that variations in nutritional habits and climatic conditions during the human history have emphasized epidemics and acute mycotoxin toxicity [1]. A main problem is the presence of AFM1 in milk and dairy products. The maximum amount in the European Union is 50ng/L (25ng/L for lactants). AFM1 is resistant to thermal and chemical treatments, so mineral sorbents are highly advisable. Clay minerals are suitable, but only a few data are available, as most studies deal with AFB1 which is absent in milk. To test the role of clay minerals in detoxifying milk, some bentonites and a kaolin were selected for the experimental work. The clay was added to milk and left to settle. Kaolin was less effective than bentonites, but was still able to detoxify contaminated milk, even using a little amount of kaolin (2.4% of the milk suspension). Among bentonites (beidellite-montmorillonite, ferruginous and saponite types), a saponite clay showed the highest sorbent capacity, in agreement with general theoretical consideration about its higher cell surface (available for AFM1) and less surface hydrophobicity. Fat, protein and lactose are slightly affected by clay treatments of milk; protein adsorption increases with the bentonite-milk ratio.

The climatic changes observed and predictably point to a wider diffusion of mycotoxins and health effects [1], and push toward the search for safe, cheap and accessible food treatments.

[1] Piva *et al.*, 2006. Accademia dei Georgofili, Quaderni **2005-III**, 1-18.

Arsenic anomalies in shallow groundwater and sediments (Venetian Plain, Italy)

A.CARRARO¹, P.FABBRI², A.GIARETTA¹, L.PERUZZO¹, F.TATEO¹ AND F.TELLINI¹

¹Institute of Geosciences and Earth Resources, National Research Council (CNR), c/o Department of Geosciences, University of Padova, Padova, Italy (peruzzo@igg.cnr.it)

²Department of Geosciences, University of Padova, Italy

A pilot area within the Venetian Plain was selected to assess the arsenic contamination of groundwater and sediments. The area represents a typical residential, industrial and agricultural organization of most western countries, and is also devoid of hydrothermal, volcanic or anthropogenic source of arsenic. The unconfined aquifer reservoir varies from a predominantly gravel composition in the north to a sandy and silt-clay composition further south, including peat layers. The hydrochemical features of groundwater are rather homogeneous, featuring low mineral content and a Ca-bicarbonate signature. In contrast, the redox state is highly variable: oxidizing conditions are predominant in the northern and coarse parts of the aquifer, whereas reducing potentials prevail in the southern and silt-clay parts. Several well waters contain arsenic in excess of drinkable limits (10 ppb), and most of these wells are located in the southern area. A large portion of the studied area has a high probability of containing nonpotable water (up to 150 ppb As). Remarkably, arsenic “hot spots” (As >300 ppb, up to 431 ppb) were identified at the transition from gravel to silt-clay sediments. Some private wells are used for farm activities and domestic purpose, especially where the public pipe network is absent. The analyses of sediments point out that the expected covariance of As and Fe (observed in many young sedimentary aquifers) is absent, whereas a regular increase of arsenic content and organic matter is detectable throughout all lithologies (sand, silt, clay and peats). The highest concentration of arsenic in peats is about 300 ppm, whereas the average in organic-poor sediments is 11 ppm (n = 10, std.dev. = 8.4, organic matter < 1%). The organic sediments in the area are a candidate source of arsenic in groundwater and this feature represents a prospecting tool in search of safe water. Another effective help in this task is the downhole decrease of arsenic in groundwater [1]: below 200m the average arsenic content in the area is 8 ppb.

[1] BGS & DPHE (2001) British geologic survey report WC/00/19, vols 1–4, BGS, Keyworth

Tracing Lead sources and chronologies in sediments and coral cores in Kuwait

CARRASCO, G.^{1*} BOYLE, E.A.¹ ZHAO, N.^{1,2}, NURHATI, I.³, GEVAO, B.⁴ AND AL-GHADBAN, A.N.⁴

¹Earth, Atmospheric and Planetary Sciences Department, Massachusetts Institute of Technology, Cambridge MA, USA (* presenting author).

²Woods Hole Oceanographic Institution, Woods Hole MA, USA.

³Singapore-MIT Alliance for Research and Technology, Singapore,

⁴Kuwait Institute for Scientific Research, Kuwait City, Kuwait,

The objective of this study was to reconstruct detailed input chronologies of Pb and other trace metals in the Kuwaiti marine environment, influenced by the Shatt-al-Arab River’s load (SaAR), using seawater, and sediment and coral cores. Pb concentrations were determined by plasma mass spectrometry using resin preconcentration and isotope dilution (ID) for seawater, a “Graney leach” extraction and ID on sediments, and cleaning, dissolution and ID on corals. Pb isotopic distributions in seawater, sediments and corals were determined using multicollector magnetic sector plasma mass spectrometry after anion exchange purification of Pb.

Seawater Pb concentrations are high in the northern stations, including Kuwait Bay (KB). They show combined anthropogenic and riverine sources, while waters at a coral reef near Qaruh Island (QI) show high Pb.

Comparing the Pb concentration and isotopic fractionation in two sediment cores near KB and near the SaAR outflow with a coral core near QI helped us discern trends, potential sources, and some events for the past ~60 years in the region. The coral core shows more pointed events and trends, which resemble more the data from the anthropogenic-influenced station near KB than that from the lower-Pb concentration SaAR station. The QI coral core and the KB sediment core data suggest a decreasing trend in the Pb concentrations after 1990, possibly linked to Pb phase out in the Kuwait area, which agrees with the increasing Pb206/Pb207 ratios. The change of lead isotopic signal in the coral lags the change of lead concentration signal by 3-4 years.

Pb data from two more cores and surface sediments upstream the SaAR are currently being analyzed, and will be added to the current interpretation, as well as data for other metals (Cd, Cu, Ag, U) from the sediment and coral cores.

Mineralogy, Geochemistry and Metals content in tailings, sediments and soils next to some metallic ore deposits in east central Mexico

ALEJANDRO CARRILLO-CHAVEZ^{1*}, NORMA CRUZ²,
ERIK SALAS², CAROLINA MUÑOZ¹, ALICIA AUDIFRED³
AND GILLES LEVRESSE¹

¹Centro de Geociencias-UNAM, Juriquilla, Queretaro, 76230, Mexico, (ambiente@geociencias.unam.mx) (*presenting author), (caromt@geociencias.unam.mx), (glevresse@geociencias.unam.mx)

²Posgrado Ciencias de la Tierra UNAM, Juriquilla, Queretaro, 76230, Mexico, (normalcruz@geociencias.unam.mx), (esalasm@geociencias.unam.mx)

³Faq. Química, Univ. Autónoma de Queretaro, Queretaro, 76200, Mexico, (audifred@uaq.mx)

Several metal sulfides ore deposits (epithermal veins and skarn type deposits) occur in the central east portion of Mexico (Sierra Madre). Historically, some of these deposits have been exploited since the 1500's and 1600's. Currently, there are millions of tons of mine waste material with high content of potentially toxic metals. The ore material contains stibnite, cinabar, realgar, chalcopyrite, galena, sphalerite, and minerals with Ag, Au and As. The mine waste material contains considerable amounts of Cd, Cr, Co, Cu, Ni, Pb, Hg, As, and Sb, posing a treat to the local population.

Some of the mine tailings consist of abundant metal oxides and metal sulfides. Redox reactions locally produce pH around 2 in leachates, and high metal content. Secondary mineralogy includes malachite, goethite, ferrihydrite, jarosite group minerals and gypsum, among others. The geochemical activity is controlled by the seasonal rains (from June to September), along with high evaporation rates. These factors produce acid mine drainage, metal leaching, redox and dissolution-precipitation reactions. Most important, high amounts of heavy metals and As are incorporated and transported in sediments, soil and surface water. As and metal content in tailings is up to 7 gr/Kg of As, 1 gr/Kg of Cu, 5 gr/Kg of Zn and 3 gr/Kg of Pb. River sediments concentrations are: As = 2.5 gr/kg, Cu = 0.146 g/Kg, Zn = 1 g/Kg, and Pb = 0.117 g/Kg. For agricultural soils (small patches of land along river terraces) As and metals concentrations are: As = 0.117 g/kg, Cu = 0.022 g/kg, Zn = 0.087 g/kg, and Pb = 0.037 g/kg. For surface water (seasonal mountain creeks) the As and metals concentrations are: As = 0.05 mg/l; Cu = 0.01 mg/l; Pb <0.017 mg/l, and Zn = 0.01 mg/l. The ultimate goal is to understand the geochemical controls of As and heavy metals in this environment. This work is financed by UNAM-PAPIIT Grant IN 112311.

Crystallization kinetics in hydrous magmas subject to decompression

C. AGOSTINI¹, F. ARZILLI^{1,2}, P. LANDI³
AND M.R. CARROLL¹

¹School of Science and Technology – Geology Division, University of Camerino, Via Gentile III da Varano, I-62032 Camerino, Italy (correspondence: michael.carroll@unicam.it)

²SYRMEP Group, Elettra-Sincrotrone Trieste S.C.p.A., SS 14, Km 163, 5 in Area Science Park, 34012 Basovizza, Trieste, Italy

³Istituto Nazionale di Geofisica e Vulcanologia, Sezione di Pisa, via della Faggiola 32, 56126 Pisa, Italy

Recent experimental work on crystallization kinetics in water-saturated magmas from Stromboli (Shoshonitic basalt) and Campi Flegrei (Trachyt-Phonolitic) provide insights into how magma decompression can significantly affect crystal abundances and thus melt physical properties during magma movement within the crust of the Earth.

Water-saturated samples of a primitive Stromboli basalt were subjected to isothermal (1075°C) decompression from 100 MPa to final pressures of 75 to 5 MP and samples were allowed to crystallize at the final pressure for times of 0.5 to 16 hr. Measured crystal growth rates show a strong dependence on time, varying from $\sim 10^{-6}$ cm/s in the shortest experiments to $\sim 10^{-8}$ cm/s in the longest experiments. The experimental results, combined with observations on natural samples, suggest timescales of hrs to several weeks for crystallization of small Plag crystals (<200 microns, not showing resorption textures) in Stromboli scoria. Observed variation of Plag composition with P(H₂O) suggest depths less than ~400 m for the upper part of the Stromboli feeding system.

Experiments on a trachytic composition from the Campi Flegrei (Naples) area studied the effects of decompression and cooling on alkali feldspar (Afs) crystallization. Afs is the main phase present in this trachyte and its abundance can strongly vary with small changes in pressure, temperature and water content in the melt, implying appreciable variations in magma physical properties and eruptive behavior. Results obtained show large variations with ΔT , time, and melt water content. In general, at small ΔT growth dominates crystallization, whereas at large ΔT nucleation dominates. Time also is important variable during crystallization, because long experiment durations involve more nucleation events. This is an important aspect to better understand magma evolution in the magma chamber and in the conduit, and consequent effects on magma rheology.

Geochemical and geomechanical influences on the permeability of wellbore cement fractures exposed to CO₂-rich brine

SUSAN CARROLL¹, STUART WALSH¹, HARRIS MASON¹,
AND WYATT DU FRANE¹

¹ Lawrence Livermore National Laboratory, Livermore, CA
94551 USA; (carrroll6@llnl.gov); (walsh24@llnl.gov);
(mason42@llnl.gov); (dufrane2@llnl.gov)

The objective of this work was to quantify the relationships between chemical alteration, deformation, and permeability at the wellbore/caprock interface important to long-term geologic carbon storage through experiment and modeling. The core flood experiments span variable pCO₂, flow rate, and cement – caprock fracture apertures at 60°C and 24.8 MPa. We used x-ray computed micro tomography to spatially resolve the fracture surface and the extent of alteration, three dimensional digital image correlation to spatially resolve plastic deformation resulting from chemical alteration, and time dependent solution chemistry and pressure to track coupled evolution of chemical alteration and mechanical deformation. Coupled processes between chemical alteration and material compressibility were largely responsible for decrease in permeability despite measured porosity increase at the cement/caprock interface. CO₂-rich brines alter wellbore cement into distinct portlandite depleted, carbonate, and aluminum-bearing amorphous silicate layers and change the compressibility of cement at the wellbore/caprock interface. Dissolution of portlandite from the cement resulted in plastic deformation of the surface contacts restricting flow paths and lowering the overall permeability. Chemical alteration of the cement was controlled by ion diffusion through cement and its alteration layers, as well as calcite equilibrium at the carbonate/amorphous silicate boundary and analcime equilibrium at cement/caprock interface.

Uncertainties in global CCN and cloud drops: which aerosol processes are important?

K.S. CARSLAW^{1*}, L.A. LEE¹, K.J. PRINGLE¹,
C.L. REDDINGTON¹ AND G.W. MANN¹

¹School of Earth and Environment, University of Leeds, Leeds
LS2 9JT, UK (*correspondence: k.s.carslaw@leeds.ac.uk)

Aerosol-cloud interaction has remained the largest uncertainty in the radiative forcing of climate through all IPCC assessments. Despite this persistent problem, very little research has been done to tackle the problem of uncertainty reduction directly. Here, we use new uncertainty analysis techniques to identify the leading causes of uncertainty in global CCN and cloud drop number (CDN) concentrations. The primary aims are to quantify a statistically robust “error bar” for these modelled quantities, to identify which parameters contribute most to uncertainty in different locations, and to ultimately direct research efforts towards model processes that have the greatest bearing on the uncertainty. By using Bayesian emulators we can perform a Monte Carlo statistical sampling of a complex global aerosol model across the entire space of dozens of parameters simultaneously – effectively performing many thousands of simulations for the cost of a few hundred. This approach then enables the model data to be analysed using variance decomposition so that a fraction of the uncertainty can be attributed to each parameter. We rank the importance of the parameters for CCN, CDN and first indirect forcing between 1750 and 2000. From among 28 parameters, the fraction of uncertainty caused by aerosol processes is approximately equal to that caused by emissions, but with very different spatial patterns. The parameters that are important for uncertainty in CCN and CDN are very different to those that are important for forcing, which is dominated by emissions that affect CCN under pre-industrial conditions. Finally, we introduce the Global Aerosol Synthesis and Science Project (GASSP), a community effort to reduce uncertainty in global CCN using extensive *in situ* measurements and model sensitivity and uncertainty fields.

Organics in the mix: how important are they for the uncertainty in global aerosol-climate effects?

K.S. CARSLAW^{1*}, L.A. LEE¹, C.E. SCOTT¹,
K.J. PRINGLE¹, C.L. REDDINGTON¹, G.W. MANN¹,
D.V. SPRACKLEN¹, F. RICCOBONO²,
U. BALTENSPERGER²
AND J. KIRKBY³ AND THE CERN CLOUD TEAM

¹School of Earth and Environment, University of Leeds, Leeds LS2 9JT, UK (*correspondence: k.s.carlaw@leeds.ac.uk)

²Paul Scherrer Institute, 5232 Villigen, Switzerland.

³CERN, CH-1211, Geneva, Switzerland.

Secondary organic aerosol (SOA) is one of the most challenging problems to solve in global aerosol-climate science, but how does it rank alongside other uncertainties in global models? Here, we perform a comprehensive uncertainty analysis of a global model to try to put SOA uncertainty in context. We quantify the uncertainty in modelled concentrations of CCN on a global scale due to 28 parameters related to aerosol and precursor gas emissions, aerosol processes and model structures. The unique approach, using emulation and variance analysis, enables the CCN variance in every grid box of the model to be decomposed into contributions from each parameter, including parameter interactions. The global production of biogenic SOA was perturbed between 5 and 360 Tg a⁻¹, and anthropogenic SOA between 3 and 160 Tg a⁻¹. The anthropogenic SOA uncertainty is ranked 7th out of 28 and accounts for about 5% of the global mean CCN uncertainty, somewhat higher than for anthropogenic SO₂ (although the latter emissions are assumed to be known to within ±50%, much better than for SOA). Biogenic SOA is only about half as important. Given the large assumed SOA uncertainty, these results suggest a rather low importance of SOA production to global CCN uncertainty. These results are based on the assumption that secondary organics do not contribute to nucleation, only to particle growth. However, the latest measurements suggest biogenic secondary organics need to be included in the nucleation rate expression. When such a mechanism is used in the model, we obtain better agreement with the seasonal cycle of particle concentration measurements and a much greater contribution of SOA uncertainty to the overall uncertainty in CCN. The sensitivity of CCN to SOA therefore depends on the extent to which organics control nucleation.

Changes in amino acid nitrogen isotopic composition patterns during phytoplankton degradation

D.CARSTENS^{12*}, C.J. SCHUBERT², A. DEEK³
AND M.F. LEHMANN¹

¹University of Basel, Institute of Environmental Geosciences, Bernoullistr. 30, 4056 Basel, Switzerland (*correspondence: doerte.carstens@eawag.ch)

²Swiss Federal Institute for Aquatic Science and Technology (Eawag), 6047 Kastanienbaum, Switzerland

³Trinationales Umweltzentrum, 79576 Weil am Rhein, Germany

The isotopic composition of organic nitrogen (N) in marine, estuarine and lacustrine sediments is often used to reconstruct paleoenvironmental conditions. Bacteria-mediated degradation and sedimentary diagenesis can modify the isotopic composition of the organic matter (OM). In order to study the biogeochemical mechanisms behind N isotope shifts in bulk organic N during early diagenesis, and to verify the robustness of algal amino acid (AA) δ¹⁵N patterns during partial degradation, as well as the integrity of amino acid-based degradation indicators, we conducted incubation experiments, in which we simulated the decay of algal OM (*Fragilaria crotonensis*) under controlled oxic and anoxic conditions. During progressing decomposition, we monitored the concentration and N isotopic composition of bulk OM and of particulate amino acids (AAs).

Particulate N concentrations decreased during the 300 day experimental period from 4 mg L⁻¹ to 1 mg L⁻¹ in the oxic and to 2 mg L⁻¹ in the anoxic set-up. In both experimental settings, the δ¹⁵N values of the particulate N increased during simulated degradation. The δ¹⁵N shift was more pronounced in the oxic (3.5‰) than in the anoxic (1.9‰) incubation. The total particulate AA concentrations decreased by 55% in the anoxic and by 46% in the oxic environment. Bacterial buildup, most pronounced in the initial degradation phase and under oxic conditions, was indicated by an increase in the concentration of D-glutamic acid (D-Glx), which is unique to bacteria. After two days of incubation, most AAs were enriched in ¹⁵N relative to the fresh bulk diatom biomass, independent of the redox conditions. In the course of the experiments, however, both the AA composition and N isotopic composition showed trends that were distinctive for oxic versus anoxic degradation. Overall, our findings show that bacterial degradation and biosynthesis during early sedimentary diagenesis overprint initial diatom δ¹⁵N-AA patterns and contribute to the alteration of bulk N isotope signatures.

Evidences for a persistent link between Greenland climate and northeastern Pacific Oxygen Minimum Zone on millennial timescales under interglacial conditions

OLIVIER CARTAPANIS^{1*} KAZUYO TACHIKAWA¹
OSCAR E. ROMERO² AND EDOUARD BARD¹

¹Aix-Marseille Université, CNRS, IRD, Collège de France, CEREGE UM34, 13545 Aix en Provence, France (* present adress at McGill University, Montreal H3A 2A7, Canada, correspondence: olivier.cartapanis@mcgill.ca)

²Instituto Andaluz de Cs. de la Tierra (CISC-UGR), Ave. de las Palmeras 4, 18100 Armilla-Granada, Spain

The intensity and/or extension of the northeastern Pacific Oxygen Minimum Zone (OMZ) varied in phase with the high northern latitude climate on millennial timescale during the last glacial period, indicating the presence of atmospheric and oceanic teleconnection under glacial conditions. While millennial-scale variability during the last interglacial is well known from Greenland and northern Atlantic records, a possible relationship with the NE Pacific OMZ has not been yet demonstrated. Here, we present a new geochemical dataset for core MD02-2508 (23°27.91'N, 111°35.74'W, 606 m water depth), retrieved from the northern limit of the modern OMZ, spanning the last 120 ka. High-resolution XRF scanning measurements deliver information on terrigenous fraction, marine organic matter, biogenic opal and carbonates, alongside with biological productivity and redox sensitive trace element content (Mo, Ni, Cd). The geochemical proxies (opal content based on Si/Ti, Cd/Al and Ni/Al) show that high productivity occurred during the last interglacial. Highly-resolved opal reconstruction shows strong millennial-scale variability matching all Dansgaard-Oeschger interstadials throughout the last interglacial, while Mo/Al indicates reduced oxygenation during these events. Extremely high opal content during warm interstadials corresponds to high diatom productivity. Despite the different climatic and oceanic settings between glacial and interglacial periods, NE Pacific OMZ rapid variability seems to be tightly coupled to high northern latitude climate, mainly via atmospheric processes.

Anorthosite deposits: Fragments of early Mars

J. CARTER¹ AND F. POULET²

¹European Southern Observatory, Vitacura, Santiago, Chile (jcarter@eso.org)

²Institut d'Astrophysique Spatiale, Université Paris-Sud, 91405 Orsay cedex, France (francois.poulet@ias.u-psud.fr)

We here report the detection of near-infrared spectral signatures indicative of the presence of a new rock type on Mars of anorthosite composition. On Mars, there are several reasons to explain why such rocks would not have been formed during its primordial differentiation (wetter mantle, sequestration of aluminum at depth in dense majorite and garnet phases and shallower pressure of plagioclase stability) (Elkins-Tanton *et al.*, JGR, 2005)

We will then discuss the setting properties of these intriguing deposits. The few occurrences of anorthosite in comparison to the large number of other minerals (including mafic and altered ones) suggest that the formation process of anorthositic rocks was likely rare on Mars and mainly restricted to early Mars. Their detection at several locations on Mars provides new constraints into magmatic (plutonic) evolution during early Mars.

Exploring a 60-year record of Mn deposition by comparing atmospheric dispersion models to soil chemistry profiles in Ohio (USA)

M.R. CARTER^{1*} AND S.L. BRANTLEY¹

¹Geosciences Dept., The Pennsylvania State Univ., University Park, PA 16802 (*mcarter@psu.edu)

Atmospheric deposition of metals emitted by anthropogenic activities has been a significant source of metal loading into soils worldwide. A ferromanganese refinery, located in Marietta, OH, is currently the largest US emission source of manganese (Mn) into the atmosphere. Particulate emissions during production are up to 35% manganese oxide (MnO) by weight and predominantly range in diameter from 0.05 to 0.4 μm , making them both highly mobile and respirable. In order to assess the role of soils in Marietta as sinks for atmospherically-derived Mn, a series of soil cores were collected at a range of distances (1-45 km) from the refinery. The results show that enrichment of soil-surface Mn is 10 times that of the parent material and decreases in surface concentration as a function of increasing distance from the refinery. Total mass of Mn added to soils per unit land area integrated over the soil depth was calculated to be 75 mg Mn cm^{-2} near the refinery. In contrast, a net loss of Mn was found in soil profiles at a distance of 45 km from the facility. Enrichment of chromium (Cr) by more than a factor of 3 was also found in surface soils near the refinery, consistent with the production of ferrochromium at the Marietta plant. Mn deposition rates were also estimated with an atmospheric dispersion model (SCIPUFF) using recent meteorological data and emission rates for the refinery. When scaled appropriately, this model-derived deposition can reproduce the soil-derived value as long as deposition rates in previous decades were more than 3 orders of magnitude greater than today's rates. This model-soil discrepancy may be due to enforcement of air quality standards, such as the Clean Air Act. We are furthermore exploring other possible explanations for the discrepancy. These results suggest that coupling soil measurements with atmospheric dispersion modelling could help identify locations where deposition rates have changed dramatically.

Nb/Ta decoupling under low $f\text{O}_2$

C. CARTIER¹, T. HAMMOUDA¹, M.A. BOUHIFD¹,
M. BOYET¹ AND J.L. DEVIDAL¹

¹Laboratoire Magmas et Volcans, UBP, CNRS UMR 6524, 5 rue Kessler, 63038 Clermont-Ferrand, France.

Correspondence: (c.cartier@opgc.univ-bpclermont.fr)

The high field strength elements Nb and Ta are thought to behave like geochemical twins since they have similar ionic radii and the same valence (5+) and thus should not be fractionated during magmatic processes. As both elements are refractory, the bulk Earth is thought to have a chondritic Nb/Ta ratio ($=19.9\pm 0.6$, [1]). However, and in contrast to Mars and other asteroids, lunar and terrestrial rocks all display a subchondritic ratio (Nb/Ta= 14 ± 0.3 and 17.0 ± 0.8 respectively, [1]). One way to explain this paradox is to invoke the incorporation of Nb by the core during a high pressure segregation ($>25\text{GPa}$) and moderately reducing $f\text{O}_2$ (IW-1.5), because in these conditions Ta is lithophile whereas Nb is moderately siderophile [2].

Here we present new metal/silicate melt trace element partition coefficients obtained on enstatite chondrite material at 5 GPa and under variable oxygen fugacities (IW to IW-8). Experiments have been conducted in the multianvil apparatus between 1580 and 1850°C, using doped material. Trace elements were analyzed using laser ablation ICP-MS on metal and silicate liquid phases.

Our results show that below about IW-4 and at 5GPa, both Nb and Ta are siderophile. When plotted as a function of oxygen fugacity, metal/silicate partition coefficients display slopes that depend on the valence state of the element in the silicate liquid. Our results show that under extremely reducing conditions ($< \text{IW-4}$) Nb is changing from Nb^{5+} to Nb^{2+} and Ta is changing from Ta^{5+} to Ta^{3+} in the silicate melt. This valence contrast generates a fractionation of the Nb/Ta ratio in the silicate, that consequently presents Nb-depleted Nb/Ta ratios.

These results suggest that Nb and Ta can be extracted by metal/silicate separation at low pressure (5GPa) and fractionated in the silicate if the segregation occurs at low oxygen fugacity ($< \text{IW-2}$). Since proto-Earth probably created from differentiated small bodies before undergoing high pressure events, these new results should then be considered in the Earth's accretion models.

[1] Münker *et al.* (2003), *Science* **301**, 84-87. [2] Wade and Wood (2001), *Nature* **409**, 75-78.

Re-investigating the nitrogen budget in the upper continental crust

PIERRE CARTIGNY¹, VINCENT BUSIGNY¹
AND ROBERTA RUDNICK²

¹Laboratoire de Géochimie des Isotopes Stables, IPG-Paris, France, (cartigny@ipgp.fr), (busigny@ipgp.fr)

²Department of Geology, University of Maryland, USA, (rudnick@umd.edu)

Nitrogen in sediments primarily results from its original sequestration from the atmosphere by biological activity (as opposed e.g. to abiotic processes). After its cycling in ocean, burial, diagenesis, magmatism and/or metamorphism, some nitrogen will ultimately enter the continental crust where it can be stored over geological periods of time. Its amount and isotope composition remain however little constrained.

Upper continental crust N-budget has been estimated by various authors between 40 and 80 ppm NH₄ but all these studies rely on a same data compilation of Wlowska (1972). A value of ~80 ppm NH₄, means that a about 1/5 of atmospheric nitrogen is presently stored in the upper continental crust.

To better address this issue, we have initiated a re-investigation of the nitrogen content and isotope composition of the upper continental crust. Representative loesses and shales previously studied for major and trace elements (although Rb is commonly lacking) were thus considered.

Results illustrate substantial variations in N-contents from ~100 to ~1000 ppm NH₄, yet with little variability in δ¹⁵N-values (5.8 ± 1.2 ‰ vs. AIR, 1σ). The latter suggest that N-isotopes are little affected during processes related to shale formation *sensu lato*. Contrasting with present day sediments and metasediments showing a strong positive correlation between N-contents with potassium and other large ion-lithophile elements, shales display inversely correlated relation with K-, Cs, or Nb/Cs contents.

Instead nitrogen contents show a striking positive correlation with the Chemical Index of Alteration (r² = 0.8), and therefore display positive relationship with e.g. Li-contents, SiO₂/Al₂O₃ and inverse relationship with K/U, etc...

Considering upper continental crust K/U-ratios leads to re-evaluate the budget of nitrogen in this reservoir by a factor from 2.5 to 5, suggesting that large amounts of nitrogen (up to 50%) of early atmosphere is presently stored in the upper continental crust.

[1] Wlowska (1992) Nitrogen. In Handbook of Geochemistry (Wedepohl, Ed.) Springer.

Evidence of sulfur degassing in komatiite-hosted Ni-PGE ores

STEFANO CARUSO¹, MARILENA MORONI¹,
CARISSA ISAAC², MARCO L. FIORENTINI²,
STEPHEN J. BARNES³, BOSWELL WING^{4,5}
AND JOHN CLIFF²

¹Earth Sci. Dept, University of Milano, Italy (stefano.caruso88@gmail.com); (marilena.moroni@unimi.it)

²CET/CCFS, The University of Western Australia, Perth, Australia (marco.fiorentini@uwa.edu.au); (john.cliff@uwa.edu.au)

³CSIRO Earth Science and Research Engineering, Perth, WA (steve.barnes@csiro.au)

⁴EPS and GEOTOP, McGill University, Montreal, Quebec, Canada (boswell.wing@mcgill.ca)

⁵ESER, Weizmann Institute of Science, Rehovot, Israel

The Wannaway komatiite-hosted Ni-PGE sulfide deposit is located in the Archean Ni-rich Kambalda Domain, Yilgarn Craton, Western Australia. This typical Type 1 orebody occurs at the base of a komatiite flow overlying sulfide-rich black shales and metabasalts and is characterized by a pyrrhotite-pentlandite assemblage with minor chalcopyrite and PGE-bearing Ni-Co sulfosalts. Detailed petrographic and mineralogical studies of a drillcore across the mineralized sequence were the basis for ion probe multiple S isotope analyses on pyrrhotite and pentlandite in basal massive to matrix/disseminated ore facies, and in black shales. Plots of δ³⁴S vs. Δ³³S can separate the effects of mass-dependent fractionation (δ³⁴S variability without Δ³³S variability) from mass-independent fractionation (Δ³³S variability). Non-zero values of Δ³³S fingerprint crustal S reservoirs in the Archean, characterized by intense photochemical reactions between S-bearing gases and unshielded solar UV rays [1]. In the δ³⁴S-Δ³³S diagram, both komatiite-hosted ore and black shale samples plot at positive non-zero values of Δ³³S, compatible with sulfur saturation of magma via assimilation of S-rich sediments. However, ore and black shales show different δ³⁴S-Δ³³S patterns. Black shales possess remarkable dispersion in Δ³³S, in contrast to the flat Δ³³S arrays for both ore-related pyrrhotite and pentlandite, which are in textural, chemical and isotopic equilibrium. Ore data for both phases display shifts in δ³⁴S values related to stratigraphy and sulfide mineralogy, and testify to progressive lowering of δ³⁴S signatures from basal massive ore upwards. Such a trend may correlate with intense isotopically heavy SO₂ outgassing of the lava [2], as proposed for similar isotopic imprints observed in other komatiite-hosted ores [3].

[1] Jamieson *et al.* (2006), *Econ. Geol.*, **101**, 1055-1061. [2] Marini *et al.* (2011), *Rev. Min. Geoch.*, **73**, 423-492. [3] Isaac *et al.* (2012), I.G.C., Brisbane, 5-10th August 2012.

Some examples of applications of X-ray Circular Magnetic Dichroism in Earth Sciences

C. CARVALLO*¹, Y. GUYODO¹, P. SAINCTAVIT¹,
M.-A. ARRIO¹, R. L. PENN², G. ONA-NGUEMA¹
G. MORIN¹ AND F. LAGROIX³

¹Institut de Minéralogie et de Physique des Milieux Condensés, Université Pierre et Marie Curie, 4 place Jussieu, 75005 Paris, France (*correspondence : carvallo@impmc.upmc.fr)

²Institute on the Environment, University of Minnesota, 207 Pleasant Street St, Minneapolis, MN 55455, USA (rleepenn@umn.edu)

³Institut de Physique du Globe de Paris, 75238 Paris Cedex05, France (lagroix@ipgp.fr)

XMCD is an element-, site-, and symmetry-selective technique and allows determination of the site occupancies in iron oxides and oxyhydroxides and the magnetization associated with these ions. A number of unresolved questions related to the distribution of ions on magnetic networks in magnetic minerals of interest in Earth Sciences can be tackled with XMCD. We show three examples of such studies carried out at IMPMC. XMCD spectra of a well characterized synthetic sample of 6-line ferrihydrite, at both K and L_{2,3} energy edges of iron, demonstrate unambiguously the presence of tetrahedrally coordinated Fe(III) in the mineral structure, which was a highly debated question. In a different study, N-type self-reversal magnetization in titanomaghemite from a sample of submarine basalt was identified as a reversal of the tetrahedral and octahedral magnetic subnetworks, because the XMCD spectrum at Fe K-edge of the N-type titanomaghemite at 20 K is a mirror image of the spectrum at 300 K. Finally, XMCD experiments carried out to compare the Fe²⁺/Fe³⁺ ratio in nanomagnetite chemically produced from lepidocrocite and nanomagnetite biogenically produced by the Fe-reducing bacterium *Shewanella putrefaciens* show that the biogenic nanomagnetite contained a higher amount of Fe²⁺ than the abiogenic nanomagnetite.

The first comprehensive dataset of ²³⁶U in the North Atlantic ocean

N.CASACUBERTA^{1,3} M.CHRISTL¹ J.LACHNER¹
M.R.VAN-DER-LOEFF² P.MASQUE³ AND H.-A.SYNAL¹

¹Laboratory of Ion Beam Physics, HPK G26, Schafmattstrasse 20, ETH-Zurich, CH-8093 Zurich, Switzerland.

²AWI-Geochemistry, Alfred Wegener Institut für Polar- und Meeresforschung, am Handelshafen 12, 27570, Bremerhaven, Germany.

³Institut de Ciència i Tecnologia Ambientals, Universitat Autònoma de Barcelona, 08193, Bellaterra, Spain..

Developments in accelerator mass spectrometry (AMS) allow determining very low levels of ²³⁶U/²³⁸U in Ocean waters. As a result, ²³⁶U is emerging as a new anthropogenic tracer and its potential in oceanography is currently being explored [1,2]. In this study the first comprehensive dataset of ²³⁶U/²³⁸U in the North Atlantic Ocean is presented. ²³⁶U was determined in 90 seawater samples (3 L each), collected during the GEOTRACES cruise GA02 in 2010 along the Northwest Atlantic Ocean. The cruise track was designed to follow the path of the North Atlantic Deep Water (NADW) from its formation region to the relatively deep parts of the western Atlantic Ocean basins. The sources of ²³⁶U in the North Atlantic are (i) global fallout and (ii) releases of the European reprocessing plants in La Hague and Sellafield. The results show a broad variation of ²³⁶U/²³⁸U ratios, from (44±15)×10⁻¹² in the deep western equatorial Atlantic Ocean to (1477±91)×10⁻¹² in the overflow waters passing Denmark Strait, all ratios being significantly above the theoretical pre-anthropogenic level of ocean water. This evidences that the whole transect (from 64°N to 2°N) in the North Atlantic Ocean is dominated by anthropogenic ²³⁶U. The calculated inventories of ²³⁶U increase by a factor of five from the southernmost station to the North indicating that besides the fallout derived ²³⁶U the water column in the North Atlantic is already significantly influenced by releases from the European reprocessing plants. Seawater samples from the Arctic Ocean and the South Atlantic Ocean are currently processed, to get a more comprehensive picture of this isotope in the Atlantic Ocean.

[1] Sakaguchi *et al.* (2012). Earth and Planetary Science Letters **333-334**, 165-170. [2] Christl *et al.* (2012). Geochimica and Cosmochimica Acta **77**, 98-107.

Residence time analysis of active volcanic systems: Rb-Sr isotope study of Ischia and Pantelleria

M. CASALINI^{1*}, R. AVANZINELLI¹
AND S. TOMMASINI¹

¹Dipartimento di Scienze della Terra, Università di Firenze, Italy (*correspondence: martina.casalini@unifi.it)

Numerous active and potentially high-risk volcanoes do occur in the Italian peninsula and therefore understanding their dynamics is crucial for volcanic hazard assessment. Here we present a study on the active volcanic systems of Ischia and Pantelleria, representing two high-silica volcanoes emplaced in subduction related and within-plate geodynamic settings, respectively.

Ischia is characterised by a continuous transition from trachy-basalt to phonolite. The geochemical and radiogenic isotope data of its volcanic products demonstrate a two-steps evolutive process: the first step, controlled by fractional crystallization plus crustal assimilation (AFC), drives magma composition from trachy-basalt to moderately differentiated trachyte; the second step, controlled only by fractional crystallisation (FC), drives the magma composition to the more differentiated products (phonolite) determining very low Sr (a few ppm) and high Rb (>500 ppm) contents due to extreme plagioclase and K-feldspar fractionation.

Pantelleria island displays a bimodal magmatism made up by alkali-basalt and differentiated products, which evolve from trachyte to peralkaline rhyolite (i.e. Pantellerite) through FC processes. Pantelleritic rocks also show extremely low Sr and high Rb contents.

The active volcanic systems of Ischia and Pantelleria, despite belonging to different geodynamic settings, are characterized by the occurrence of strongly differentiated products with anomalously high Sr isotope compositions that cannot be justified by the assimilation of crustal material.

This characteristic could be explained by ⁸⁷Sr in-growth in long-lived magma chambers, due to the high Rb/Sr of the most evolved rocks. To explore this hypothesis we carefully screened and selected a number of evolved samples: from these we separated the rock-forming minerals (sanidine and clinopyroxene) and groundmass/glass in order to determine Rb and Sr content by isotope dilution, along with Sr isotope composition. The extremely low diffusion coefficients of Sr in feldspar and clinopyroxene makes them suitable candidates to estimate the timing of crystallisation and, by inference, the magma residence time. The calculated crystallization times for the two islands are here compared and discussed in terms of the chemical and physical characteristics of the magmas.

Crystals modulate non-explosive gas transfer at Stromboli volcano, Italy

K. CASHMAN¹, A. RUST¹, I. BELIEN²,
J. OPPENHEIMER¹ AND A. SOLDATI¹

¹School of Earth Sciences, University of Bristol, UK
(gkvc@bristol.ac.uk)

²Exxon Mobil Upstream Research, Houston, TX

Stromboli is best known for its eponymous frequent and mildly explosive eruptions. Most of Stromboli's gas loss (~90%), however, occurs by non-explosive mechanisms, either passively or via periodic small gas bursts known as "puffing". Passive degassing probably occurs across the entire magma surface beneath the crater terrace; puffing, in contrast, is focused into one or a few central vents that are stable over the short term but migrate with time. What, then, controls the spatial and temporal patterns of non-explosive gas loss? One clue comes from volcanic clasts ejected during normal Strombolian activity, which show that the near-surface magma has ~50% crystals. To explore the effect of crystals on gas migration, we have run experiments using 50:50 mixtures of golden syrup and rice (an anisotropic particle that is neutrally buoyant and approximates plagioclase in shape) fluxed by air; this allows us to investigate the effect of varying gas flux through static 'magma' columns. A first order observation is that, at steady state, the amount of gas retained within the column (the gas holdup) increases with increasing gas flux from below. Gas holdup is achieved by trapping small bubbles within the particle-melt suspension. Importantly, these small bubbles are created by interaction of the gas with the suspension by bubble splitting either around particles or by expansion after passage between two particles into a particle-poor space. At the same time, larger parcels of gas migrate through the suspension by creating transient fractures. The pressure increase required to fracture the suspension causes quasi-periodic gas release to the surface; the fracture is transient because of healing by viscous flow. These observations suggest physical mechanisms to explain both passive degassing and puffing. Passive degassing is best explained by the slow rise of individual bubbles through the crystal-melt suspension, with bubble size modulated by the size and spacing of crystals. Puffing activity is more analogous to quasi-periodic fracturing and gas release; healing of fracture paths explains the migration of puffing vents around the central crater terrace. The location of puffing in the center of the crater terrace further suggests focusing of the steady gas supply from depth at the center of the elongated shallow magma storage region.

Late-Variscan fayalite-bearing granites in Sardinia: The lower crust connection

L. CASINI¹*, A. PUCCINI¹, S. CUCCURU¹, G. OGGIANO¹
AND G. SECCHI¹

¹ University of Sassari, Department of Science of Nature and Environmental Resources, Via Piandanna, 4 - 07100 Sassari, Italy

The Variscan [340 – 260 Ma, 1] Corsica-Sardinia Batholith (C-SB) emplaced discordantly across the orogenic structure, from the roots zone to the Gondwana foreland. Despite the scarcity (< 5%) of mafic rocks, most pre-300 Ma plutons are peraluminous biotite granites derived from dehydration melting of pre-Variscan granitoids and subordinate metasediments [2]. Lower crustal granulites observed in the deeply exhumed section of the chain [3] are thought to have developed in consequence of extensive melt extraction. The post-300 Ma granites in south Sardinia [4], instead, display the following crustal characters: ϵNd from -6 to -12, δO^{18} between 7 and 12‰, and Sr_i (₂₉₀) between 0.703 and 0.715. The rare but systematic occurrence of fayalite or pyroxene as Fe-buffering phase indicates that these A-type melts derived by partial melting of anhydrous, poorly evolved crustal material under high-T (> 900°C), low $f\text{H}_2\text{O}$ and $f\text{O}^2$ conditions [5].

Nd_{DM} model ages of post-300 Ma granites in south Sardinia are in the range 1600 - 1700 Ma, about 1 Ga older than those calculated in Corsica [6]. This implies a older lithosphere, probably accreted at the northern margin of Gondwana (S Sardinia) in early Paleozoic. The observation that this part of the chain never reached a significant crustal thickness during the Variscan event (i.e., > 40 km) support the hypothesis that granulites formed before the Carboniferous.

[1] Paquette *et al.* (2003) *Chem. Geol.* **198**, 1–20. [2] Casini *et al.* (2012) *Tectonophysics* **544**, 31–49. [3] Gaggero *et al.* (2012). *MinMag*, this volume. [4] Dack (2009) PhD Thesis, Boise State University. [5] Huang *et al.* (2011) *Geology* **39**, 903–906. [6] Cocherie *et al.* (1994) *Chem. Geol.* **115**, 173–211.

A new hypothesis for the origin of HIMU and FOZO mantle end-members

PATERO R. CASTILLO

Scripps Institution of Oceanography, Univ. of California, San Diego, La Jolla, CA 92093-0212 USA
(pcastillo@ucsd.edu)

It is widely accepted that the bulk of intraplate magmas, best represented by ocean island basalts (OIB), originate from crustal materials that had previously been subducted into the mantle. It has also been proposed that after ~b.y. of residence, such subducted materials form a number of mantle source reservoirs, represented by end-members with extreme Sr-Nd-Pb isotopic compositions^[1]. The first subducted material to be recognized was mid-ocean ridge basalt (MORB)^[2], and this was later fine-tuned as having a long time integrated (~b.y.) high U/Pb ratio (HIMU) and producing OIB with the most radiogenic Pb isotopic ratios ($^{206}\text{Pb}/^{204}\text{Pb} > \sim 19.0$)^[1,3]. However, it is becoming more evident that the compositional connection between subducted MORB and HIMU basalts is problematic^[1,4]. As an alternative hypothesis, I propose that recycled Archaean calcium carbonate (CaCO_3) is the main source of the distinct Pb-Sr isotopic and major-trace element compositions of the “classical” HIMU and Proterozoic and younger carbonate for the “younger” HIMU or FOZO end-member. This hypothesis is consistent with some of the available observations, experimental results and inferences from these data. For example, the $^{87}\text{Sr}/^{86}\text{Sr}$ and K contents of carbonates are low in the Archaean, but started to increase in the Proterozoic^[5]. CaCO_3 subduction into the deep silicate Earth may also provide important clues to the seismic velocity structure and convection in the mantle. However, the carbonate recycling hypothesis is based primarily on qualitative data and the few existing analyses of Archaean carbonates, which are expected to have very high U/Pb if precipitated out of seawater in equilibrium, do not have original Archaean seawater U/Pb ratios^[6]. Future quantitative testing of the hypothesis can be done when analytical data for unmodified Precambrian carbonates become available.

[1] White, W. (2010), *Ann. Rev. Earth & Planet. Sci.* **38**, 133–160. [2] Hofmann A. & White, W. (1982), *Earth Planet Sci Lett* **57**, 421–436. [3] Kogiso, T., Tatsumi, Y., Shimoda, G. & Barseczus, H. (1997), *J Geop Res* **102**, 8085–8103. [4] Stracke, A., Hofmann, A. & Hart, S. (2005), *G³* **6**, Q05007. [5] Veizer, J. & Mackenzie, F. (2003), *Treatise in Geochemistry* **7**, 369–407. [6] Kamber, B., Bolhar, R. & Webb, G. (2004), *Precambrian Research* **132**, 379–399.

C-isotope evidence for $p\text{CO}_2$ and volcanic forcing during the early Aptian OAE 1a – The Cau section (SE Spain)

J.M. CASTRO^{1*}, G.A. DE GEA¹, R.D. PANCOST
M.L. QUIJANO³ AND B. DAVID A. NAAFS²

¹Dept. Geología, CEATierra, Univ. Jaén, E-23071. SPAIN
(*correspondence: jmcastro@ujaen.es)

²School of Chemistry, Univ. Bristol, BS8 1TS, UK

³Dept. Química Inorgánica y Orgánica, CEATierra, Univ. Jaén, E-23071. SPAIN

The Early Aptian Oceanic Anoxic Event (OAE1a) represents a major perturbation in the global carbon cycle and is linked to environmental, biotic and sedimentary changes. The isotopic signature of OAEs consists of a positive $\delta^{13}\text{C}$ excursion, interpreted as the result of massive deposition of organic matter and subsequent ^{12}C drawdown.

Most investigations consider that high atmospheric CO_2 concentrations related to volcanic outgassing [1] played a main role during OAE1a, but only few studies estimate $p\text{CO}_2$ during this time interval [2]. Here we test the use of the offset between the $\delta^{13}\text{C}_{\text{carb}}$ and $\delta^{13}\text{C}_{\text{org}}$ as a qualitative proxy for $p\text{CO}_2$ ($\Delta^{13}\text{C}$, [3]), which has been proved useful for the OAE2 [4].

We explore the temporal variations in $p\text{CO}_2$ from an expanded section of the OAE1a (Cau section, Spain). The high resolution study combining C-isotope stratigraphy and biostratigraphy, has led to a precise correlation with other well known sections from the Tehuacan domain.

Our results suggest that $p\text{CO}_2$ increased during the prelude of OAE1a. Intriguingly, it maintained stable high concentrations during most of the positive isotope excursion, despite a putative OM burial event, then dropped in a relatively short time at the end of OAE 1a. This episode of high $p\text{CO}_2$ was punctuated by several short-lived cooling episodes [5], but high temperatures were rapidly recovered. This is consistent with a maintained volcanic forcing, demonstrated by Os isotope data [1, 6]. This study has proven the value of the $\Delta^{13}\text{C}$ as a $p\text{CO}_2$ proxy, and confirmed the link between volcanic outgassing and organic matter deposition in balancing the global climate change during OAE1a.

[1] Tejada *et al.* (2009) *Geology* **37**, 855-858. [2] Heimhofer *et al.* (2004) *EPSL* **223**, 303-318. [3] Kump and Arthur (1999) *Chem. Geol.* **161**, 181-198. [4] Jarvis *et al.* (2011) *Paleocenanography* **26**, PA3201; [5] Dumitrescu *et al.* (2006) *Geology* **34**, 833-836. [6] Bottini *et al.* (2012) *Geology* **40**, 583-586.

Advances in Our Understanding of the Noble Gas Thermometer in Groundwater - New Applications

M.C. CASTRO*, C.M. HALL, R.B. WARRIER
AND K.C. LOHMANN

University of Michigan, Ann Arbor, Michigan 48105, USA
(*correspondence: mcastro@umich.edu)

Noble gases are conservative tracers and their concentrations in recharge areas of groundwater systems are a function of temperature, pressure, and excess air. Consequently, noble gas temperatures (NGTs) are regarded as robust indicators of past climate. Until recently, however, limited attention had been placed on processes taking place in the unsaturated zone and at the water table/soil air interface capable of impacting NGTs. In recent years, we highlighted the potential impact of O_2 depletion without corresponding CO_2 build-up in the unsaturated zone on noble gas partial pressures, leading to a bias to low NGTs. A recent study in Michigan showed, however, that recharge conditions can be significantly modified by large precipitation events such as Hurricane Ike and bring O_2 depleted soil air back to standard conditions.

Atmospheric noble gases were also measured in high-altitude springs in the Galapagos Islands. These revealed the presence of a unknown pattern with atmospheric He excesses and Ne, Kr, and Xe depletion together with relative Ar enrichment. A rainwater noble gas study was subsequently carried out in Michigan and revealed the presence of two patterns both with He excesses. The first one, associated with low pressure systems, presence of fog and light rainfall, displays a pattern remarkably similar to that previously identified in the Galapagos Islands. The second one, associated with the passage of frontal systems, displays a mass-dependent depletion pattern with respect to surface conditions. Precipitation is characterized by thunderstorms, heavy rainfall, and high cloud ceiling heights. This rainwater study suggests that noble gases dissolved in rainwater and in shallow aquifer systems where infiltration is rapid can be used to trace weather patterns.

Trace element and contaminant fate during Fe(II)-catalyzed iron oxide surface transformations

J. G. CATALANO^{1*}, K. G. BECKER¹, A. J. FRIERDICH^{1,2},
M. A. G. HINKLE¹, Y. LUO^{1,3} AND B. OTEMUYIWA¹

¹Earth & Planetary Sciences, Washington Univ., St. Louis,
MO 63130 USA (*correspondence: catalano@wustl.edu)

²Dept. of Geosciences, Univ. of Wisconsin, Madison, WI
53706 USA

³Gemological Institute of America, Carlsbad, CA 92008 USA

The biogeochemical cycling of iron involves primarily the alternation of iron between oxidized and reduced forms. Recent work has shown that when microorganisms initiate such cycling a cascade of secondary abiotic processes occur through reaction of aqueous Fe(II) and solid Fe(II) oxide minerals. These reactions involve oxidative Fe(II) adsorption, electron transfer into or through the mineral solid, and atom exchange between dissolved Fe(II) and solid Fe(III) [1-3]. This results in mineral recrystallization that proceeds through a surface growth and dissolution mechanism [4]. The resulting dynamic surface transformations may affect the fate of iron oxide-associated trace elements and contaminants.

We have investigated the effect of dissolved Fe(II) on the repartitioning of elements adsorbed on or incorporated in goethite and hematite. Adsorbed As(V), which is structurally incompatible with iron oxides, is unaffected by the presence of Fe(II). In contrast, adsorbed Ni(II) and Zn(II) incorporate into iron oxide mineral structures in the presence of Fe(II). Fe(II) also induces the release of incorporated Ni and Zn back into solution; this is inhibited when insoluble elements co-substitute into goethite or hematite. Redox-active substituting elements, such as Cu(II), Co(III), and Mn(III/IV), undergo coupled reduction and repartitioning upon introduction of aqueous Fe(II). Preliminary stable isotope measurements show that Zn repartitioning during Fe(II)-catalyzed iron oxide recrystallization produces a fractionation distinct from that produced by Zn adsorption and that differs between goethite and hematite. These studies show that the effect of Fe(II) on the fate of trace elements and contaminants is dependent on the compatibility of these elements with the iron oxide structure. The observed element repartitioning demonstrates new pathways for contaminant entrapment and micronutrient release and suggests that iron oxides may not be reliable recorders of trace elements in the rock record.

[1] William & Scherer (2004) *ES&T* **38**, 4782. [2] Yanina & Rosso (2008) *Science* **320**, 218. [3] Handler *et al.* (2009) *ES&T* **43**, 1102. [4] Catalano *et al.* (2010) *GCA* **74**, 1498.

Hydrothermal alteration of the products of transformation of cement-asbestos

M. CATALANO¹, A. BLOISE¹, N. E. BELLUSO²,
C. B. CANNATA¹, E. BARRESE¹, R. DEROSA¹
AND A. F. GUALTIERI³

¹University of Calabria, Arcavacata di Rende (CS), Italy

²University of Torino and IGG-CNR, Torino, Italy

³University of Modena e Reggio Emilia, Modena, Italy

In some European countries the transformation products of cement-asbestos (CATP) can be recycled to produce stoneware tile mixtures, bricks, and concrete incorporated into mortars or to provide both refractoriness and reinforcement to other materials (e.g., road beds) [1]. Not recycled CATP materials must be moved in controlled landfill. An interesting study deals with the fate of the CATP placed in the landfill where solutions could percolate. Can the growth of fibers, perhaps asbestos, occur over a long period of time? The present work studies the experimental conditions involved in the transformation of the CATP and the resulting products. For two sets of reactions, two different deeply characterized CATP mixtures (KC2S; KA) were used. KC2S contained ferrite, periclase, ternesite Ca(OH)₂, merwinite, wollastonite, yeelimite; KA contained akermanite, amorphous, merwinite, bredigite, wollastonite, quartz, calcite, magnetite. The CATP, after addition of H₂O as reactant, was hydrothermally altered in the following range conditions: temperature from 300 to 360 °C; pressure between 15 and 200 MPa; time from 168 to 504 h. Samples have been characterized in detail through XRPD, SEM-EDS and TEM-AEM. Some altered samples showed a large amount of Ca-inosilicate fibrous phases as hillebrandite, foshagite. Other products (i.e. Ca-garnet, brucite, monticellite) were also detected together with low amount of starting material relicts.

[1] Gualtieri, Giacobbe, Sardisco, Saraceno, Lassinantti Gualtieri, Lusvardi & Cavenati Zanatto, (2011) *Waste Manag.* **31**, 91–100.

Component geochronology of the ca. 3920 Ma Acasta Gneiss

N.L. CATES^{1*}, S.J. MOJZSIS¹²³, G. CARO⁴,
M. D. HOPKINS¹, D. TRAIL⁵, O. ABRAMOV¹⁶
M. GUITREAU²⁷ J. BLICHERT-TOFT² AND W. BLEEKER⁸

¹University of Colorado, Boulder, CO, USA

²ENS & UCBL1, Lyon, France

³Hungarian Academy of Sciences, Budapest, Hungary

⁴CNRS, Vandoeuvre-les-Nancy, France

⁵Rensselaer Polytechnic Institute, Troy, NY, USA

⁶USGS, Flagstaff, AZ, USA

⁷University of New Hampshire, Durham, NH, USA

⁸Geological Survey of Canada, Ottawa, Canada

* (cates@colorado.edu)

The oldest compiled U-Pb zircon ages for the Acasta Gneiss Complex (AGC) in the Northwest Territories of Canada span about 4050-3850 Ma; yet older ca. 4200 Ma xenocrystic U-Pb zircon ages have also been reported for this terrane. The AGC comprises gneissic exposures across several large basement domes, but only a small portion (~5x5 km) of one such dome has been documented in the detail required to investigate a complex history. To better understand this history, ion microprobe ^{235,238}U-^{207,206}Pb zircon geochronology was combined with whole-rock (WR) and zircon rare earth element compositions ([REE]_{zirc}), Ti-in-zircon thermometry (Ti^{inh}) and ¹⁴⁷Sm-¹⁴³Nd geochronology for a subdivided ~60 cm² slab of Acasta banded gneiss comprising five separate lithologic components. Results were compared to other variably deformed AGC granitoid- and plagioclase-hornblende gneisses. Micro-sampling shows that different gneissic components host distinctive [Th/U]_{zirc} vs. Ti^{inh} and [REE]_{zirc}, correlative with zircon age populations and WR compositions, but not with ¹⁴⁷Sm-¹⁴³Nd isotope systematics. Lattice-strain theory used to model D_{WR}^{zircon} [REE] reconciles the U-Pb zircon geochronology only for the ca. 3920 Ma age component, which also preserves strong positive Euanomalies. Modeling shows that the magmas which gave rise to the indigenous ca. 3920 Ma component formed at ~IW (iron-wüstite) to <FMQ (fayalite-magnetite-quartz) oxygen fugacities. Emplacement of the AGC was contemporaneous with the Late Heavy Bombardment (LHB Later superimposed Eoarchean events (3850-3720 Ma) are reminiscent of formation times for the Nuvvuagittuq Supracrustal Belt in northern Québec, and the Manfred Complex in Western Australia. Equilibration of the ¹⁴⁷Sm-¹⁴³Nd whole-rock chronometer occurred at the scale of individual components over the course of one or more of these later events.

Fe-serpentines to Fe-chlorites experimental synthesis: An iron metal- shale interaction between 60 and 300°C

M. CATHELINÉAU¹, R. MOSSER-RUCK¹, I. PIGNATELLI¹,
M.C. CAUMON AND L. TRUCHE¹

¹GeoRessources, CNRS, Université de Lorraine, 54500, Vandoeuvre-les-Nancy, France

Interactions between a shale and iron metal have been studied experimentally at 90, 150 and 300°C, as well as at decreasing temperature from 90 to 50°C. These experiments simulate the mineralogical and chemical reaction of clays in contact with steel in high level nuclear waste repository, at the highest temperature to test the potential kinetic effects due to the rather short duration of the experiments with respect to the waste disposal time scale, and the experiments at decreasing temperatures to simulate the effects of the progressive cooling in the waste site due to decline of the radioactive heat (ANDRA research programme). The starting products are : a shale from the Callovo-Oxfordian series from the Paris basin (Quartz, illite and I/S rich in illite, calcite), a fluid which composition is close to the interstitial fluids of the geological formations, and iron metal added as plates or powder. The effects of the liquid on rock ratio (L/R), iron/ clay ratio (I/C) have been tested. The following mineral assemblages have been found as run products:

- di- sm > Fe-serpentine, so-called berthierine-like or greenalite for high iron/clay ratio or Fe rich di Sm + Fe rich tri-Sm for low iron/clay ratios (near neutral pH) at 90°C
- di-octahedral smectite (di-sm) > saponite at 150°C > trioctahedral Fe-chlorite + feldspar + zeolite (300°C).

New experiments at decreasing temperatures have produced other Fe-serpentines within the 60-80°C range such as cronstedtite. Thus, at each temperature, illite and I/S are unstable, and replaced by Fe-rich silicates at low temperature and Fe-Al silicates above 150°C. Within the range 60 -90°C, quartz is almost entirely dissolved as illite and I/S up to the total consumption of iron. Iron silicates are in competition with iron carbonates (siderite) and iron oxide (magnetite). Iron silicates are predominant near neutral pH when pCO₂ is not too high, and magnetite is found in most run samples but in low amounts, and iron/clay ratio >1. A thermodynamical modelling of the main mineralogical changes has been undertaken to interpret experimental data.

A framework for understanding the first and second rises of O₂

DAVID C. CATLING¹

¹Dept. Earth and Space Sciences/ Astrobiology Program,
Univ. of Washington, Box 351310, Seattle WA, USA

Oxygenation of the atmosphere and oceans was determined by key source and sink fluxes of O₂. In terms of reductants, key fluxes are: (1) the escape of hydrogen to space F_E, (2) the 'net' flux of O₂ associated with the burial of organic carbon and sulfide derived from sulfate, F_B, (3) the flux to the atmosphere of aerial volcanic and metamorphic gases F_{VM}, (4) the continental oxidative weathering flux F_W, which depends on atmospheric pO₂, (5) reductants associated with seafloor volcanism F_{OV}, and (6) seafloor weathering F_{OW}. The last two fluxes connect seafloor redox to the surface environment. The seafloor weathering flux depends on pO₂ through downward mixing of O₂ and marine sulfate.

I propose a model where the relative magnitude of these fluxes determine three redox stages of Earth history with different mean states: I. anoxic (before 2.4 Ga), II. oxic (Proterozoic) and III. highly oxic (after late Neoproterozoic).

In state I, an anoxic atmosphere is relatively rich in hydrogen-bearing species, by definition, and so F_E is non-negligible. Thus, F_B < F_{VM} and F_E ≈ F_{VM} + F_{OV}. Since F_E is (to first order) proportional to the concentration of atmospheric CH₄, a model solution gives 100s to 1000s of ppmv CH₄ for reasonable F_{VM} + F_{OV}. The transition from I to II is reached when F_B exceeds F_{VM}. These two fluxes are small compared to gross biogenic gas fluxes, but the redox state of the atmosphere is set by small differences between large fluxes. In state II, enough O₂ allows continental weathering, and F_W is non-negligible. F_E (though persistent for probable mid-Proterozoic CH₄ levels) is small compared to other fluxes. A balance is F_B ≈ F_{VM} + F_{OV} + F_{OW} + F_W. Seafloor volcanic and weathering fluxes buffer O₂ in the deep ocean to low levels. F_W depends on O₂ and a model solution in state II gives O₂ mixing ratios of 0.2-2% absolute. In state III, seafloor buffering is exhausted and the dominant balance is F_B ≈ F_{VM} + F_{OV} + F_W ≈ F_W, allowing Phanerozoic O₂ levels of 10-30%.

Driving state I to II are hydrogen escape [1] and possible geologic evolution affecting volcanic fluxes [2, 3]. The possible drivers of state II-III include hydrogen escape and sulfide burial and subduction [4].

[1] Catling D. C. *et al.* (2001) *Science* **293**, 839. [2] Kump L. R., Barley M. E. (2007) *Nature* **448**, 1033. [3] Holland H. D. (2009) *Geochim. Cosmochim. Acta* **73**, 5241. [4] Catling D. C. *et al.* (2002) *Astrobiology* **2**, 569.

Archaeological practices validating mineralogical and geochemical analyses in metal provenance studies. The gold mines from central Gaul (France) case study

B. CAUET*¹, C.G. TAMAS², S. BARON¹ AND J. MILOT¹

¹ TRACES-CNRS, 5, allées A. Machado, 31058 Toulouse Cedex 09, France. (*corresponding author: cauet@univ-tlse2.fr)

² University Babes-Bolyai, 1, M. Kogalniceanu str., 400084 Cluj-Napoca, Romania

A quality protocol regarding the selection of materials used and/or formed during the chaîne opératoire from the ore of an Ancient mine to the produced metal is proposed. This protocol, based on many archaeological findings during the 90ies is applied here for Limousin (France) Au province exploited during Gaul times.

The Gaul mining in Fouilloux deposit (3rd to end of 1st c. BC) was focused on a quartz vein with native gold, electrum and sulfides (arsenopyrite, stibnite etc.) with a N60 strike and a dip of 62° to the NW. The exploitation started in an open pit with several benches going down to a depth of 20 m and afterwards continued in underground closely following the ore body on another 10 m depth. The underground stope follows the dip of the ore body and has 2 to 2.5 m width. Pillars have been preserved within the ore body by the Gaul miners for safety reasons. The pillars are high grade (around 90 g/t Au) and represent a certified archaeological ore occurrence which is used for metal tracing.

Ore treatment workshops were discovered nearby with remnants of the Ancient metallurgy (e.g. archaeological roasted ore) and remainders of the produced gold. A low open furnace for the gold metallurgy and a touchstone preserving golden traces was discovered in Fouilloux, as well as crucibles in Cros Gallet-Nord gold mine situated nearby. These artifacts allowed reconstitution of the various operations of the chaîne opératoire of gold production from La Tène in Limousin and will be used for metal tracing.

Archaeo-Metallurgical experimental operations using gold ore from a third Gaul mine, Laurieras allowed us to produce materials which will be also analyzed, i.e. raw ore, grilled ore, slags, and gold brought out directly from the crucible.

Mineralogical and geochemical analyses are ongoing on the materials obtained through experimental works on Au ore from Laurieras. The results obtained on experimental products will be compared with the results on archaeological materials discovered in Fouilloux and Cros Gallet-North Gaul mines.

Acknowledgments: Research carried out in the frame of ANR MINEMET project (2012-2015).

Source apportionment of organic matter by isotope analysis, AMS PMF and HNMR techniques

D. CEBURNIS¹* J. OVADNEVAITE¹, A. GARBARAS², S. SZIDAT³ M. RINALDI⁴, S. DECESARI⁴, K.E. YTTRI⁵, V. REMEIKIS², M.C. FACCHINI⁴ AND C.D. O'DOWD¹

¹School of Physics and Centre for Climate and Air Pollution Studies, Ryan Institute, National University of Ireland Galway, Galway, Ireland

(*correspondence: darius.ceburnis@nuigalway.ie)

²Center for Physical Sciences and Technology, Institute of Physics, Vilnius, Lithuania

³Department of Chemistry and Biochemistry & Oeschger Centre for Climate Change Research, University of Berne, Berne, Switzerland

⁴Institute of Atmospheric Sciences and Climate, National Research Council, Bologna, Italy

⁵Norwegian Institute for Air Research, Kjeller, Norway

Particulate carbonaceous matter (PCM) is a significant contributor to ambient particulate matter originating from intervening sources which contribution is difficult to resolve due to chemical complexity of PCM and often internal mixture of aerosol particles.

Carbon isotope analysis of stable and radioactive carbon offers a method for quantitative source apportionment of three principal sources of PCM due to their unique isotopic signatures: i.e. marine, continental (non-fossil) and fossil fuel sources [1] while additional specific tracers will allow splitting into more specific sources or primary and secondary sources [2]. AMS PMF analysis allows splitting into PCM property specific sources based on degree of oxygenation and fragmentation markers of OM. HNMR factor analysis is based on common chemical structures – aromatic, aliphatic, mono, di-acids – arising from typical sources.

All three methods were applied to resolve PCM sources over the Northeast Atlantic ocean during common sampling periods demonstrating their convergence on sources and suggesting a more reliable albeit complex approach to source apportionment.

This work was supported by the HEA-PRTLI4, EC IPs EUCAARI, GEOMON, EMEP, EPA-Ireland, ESA (SToSE: OSSA), EC ACTRIS.

[1] Ceburnis *et al.* (2011) *Atmos Chem. Phys.* **11**, 8593–8606.

[2] Yttri *et al.* (2011) *Atmos Chem. Phys.* **11**, 9375–9394.

An absorption method for porewater characterization in low-permeability sedimentary rocks

MAGDA CELEJEWSKI* AND TOM AL

University of New Brunswick, Earth Sciences

(*correspondence: m.celejewski@unb.ca
tal@unb.ca)

Determination of porewater geochemistry in low-permeability rocks is challenging due to small fluid volumes and the difficulty of extracting representative samples. Several porewater extraction techniques are available, but the ability of each to provide representative samples is suspect. The objectives of this study are to develop a method of extracting a representative sample of *in situ* porewater from low-permeability rocks using absorption into a cellulosic membrane, and to quantify porewater solute concentrations.

The feasibility of porewater extraction using absorption into cellulosic membranes has been demonstrated in trials with shale drill cores. Solute mass is measured with ICP-MS and water-content is measured with near infrared (NIR) spectrometry which together provide a measure of solute concentrations.

Interactions between the membrane and porewater solutes were investigated by assessing preferential adsorption of solutes to the membrane and the reversibility of solute leaching. The NIR spectrometer was calibrated to account for the influence of dissolved salt mass on the vibrational energies of H-O bonds in water. The method was tested by adding a known mass of synthetic porewater to membranes, and comparing the known solute concentrations to those determined from the leachable solute mass and the measured water-content.

Experimental results indicate that preferential adsorption of porewater solutes (Na, Cl, Mg, Ca, K, Sr, and Br) to the cellulosic membrane is statistically insignificant and that solutes are reversibly leachable. The relative error for NIR water-content based on the 95% confidence limits ranges from 2 to 7%. The relative difference in solute concentration between the known values and those calculated from solute-mass and water-content data range from 0 to 17%. The greatest relative differences occur when the measured water-content is very low and near the NIR detection limit.

Work to date has demonstrated that porewater can be extracted from low-permeability rock samples, and porewater solute concentration determinations are possible.

Calculated P-T paths for the blueschist-facies metapelites from the Ile de Groix (France)

STEPHEN CENTRELLA^{1,2*} MICHEL BALLEVRE², P
 AVEL PITRA² AND PHILIPPE YAMATO²

¹ Inst. für Mineralogie, University of Münster, Corrensstrasse
 24, 48149, Münster, Germany (*correspondence:
 s_cent01@uni-muenster.de)

² Géosciences Rennes, UMR 6118, Université de Rennes 1,
 35042 Rennes, France

For a long time, the “Ile de Groix” has been the subject of many studies because it shows blueschist-facies rocks of Palaeozoic ages which are quite uncommon along the Variscan belt. Despite all these studies, there are still uncertainties on (i) whether peak P-T conditions vary or not across the island and (ii) how variations in the amount and causes of retrogression could control the apparent spatial zonation of the metamorphism. In order to check the different potential hypotheses, a detailed study of four samples of garnet-bearing metapelites has been performed.

In all samples, garnet preserves a growth zoning (core to rim bell-shaped decrease of Mn, increasing XMg), which, associated with the inclusions and the matrix minerals, allow to define the successive mineral parageneses. Calculated pseudosections using Thermocalc allow to define the prograde part of the P-T path, culminating in the eastern part at 22.5 kbar and 525°C. Decompression is nearly isothermal until the equilibrium between garnet and matrix was reached at 16.5 kbar and 515°C. A different P-T path is deduced for the western part of the island, where garnet growth zoning displays a more complex pattern, with bell-shaped Mn in the cores, but Mn-rich overgrowths observed in some samples. These patterns cannot result from differences in bulk-rock chemistry, but evidence differences in P-T paths.

Pressure-induced phase transitions in coesite

ANA ČERNOK^{1*}, TIZIANA BOFFA BALLARAN¹,
 RAZVAN CARACAS², NOBUYOSHI MIYAJIMA¹,
 ELENA BYKOVA¹, VITALI PRAKAPENKA³,
 HANNS-PETER LIERMANN⁴ AND LEONID DUBROVINSKY¹

¹Bayerisches Geoinstitut, Universität Bayreuth,
 Universitätsstrasse 30, D-95440 Bayreuth, Germany
 (Ana.Cernok@uni-bayreuth.de *presenting author)

²Centre National de la Recherche Scientifique Laboratoire de
 Géologie de Lyon (LGLTPE) UMR 5276 Ecole Normale
 Supérieure de Lyon 46, allée d'Italie, 69364 Lyon, France

³Center for Advanced Radiation Sources, The University of
 Chicago, Argonne National Laboratory, Building 434A,
 9700 South Cass Ave, Argonne, IL 60439, USA

⁴Photon Sciences, Deutsches Elektronen-Synchrotron (DESY),
 Notkestraße 85, 22607 Hamburg, Germany

High-pressure behavior of coesite was studied using diamond-anvil cells with neon as the pressure transmitting medium and applying *in situ* Raman spectroscopy and single crystal X-ray diffraction up to pressures of ~55 GPa. The experimental observations were complemented with theoretical computations of the Raman spectra under similar pressure conditions. We find that coesite undergoes two phase transitions and does not become amorphous at least up to ~ 52 GPa. The first phase transition (coesite I to coesite II) occurs at ~ 23 GPa and the second transition (coesite II to coesite III) occurs at ~ 35 GPa.

The *ab initio* calculations give an insight into the initiation mechanism of the first phase transition. Based on the instability of phonon modes we imply that the phase transition is displacive in nature and related to shearing of the four-membered rings of SiO₄ tetrahedra upon compression. The transition to the lowest-symmetry phase, coesite III, is possibly a first order phase transition which leads to a very distinct structure. It was previously widely accepted that coesite undergoes pressure-induced amorphization at significantly lower pressures (30 GPa) and none of the metastable high-pressure polymorphs has been reported. We are currently analyzing crystallographic data of the high-pressure metastable polymorphs coesite II and coesite III.

Origin and burial of organic carbon depending upon the environmental setting in the southwestern East/Japan Sea

H.J. CHA^{1*} AND M.S. CHOI²

¹Chungnam National University/Research Institute of Marine Sciences, , Daejeon, Republic Of Korea
(*correspondence: hcha80@chol.com)

²Chungnam National University/Department of Oceanography/Graduate School of Analytical Science and Technology, Daejeon, Republic Of Korea,
(mschoi@cnu.ac.kr)

Box core sediment samples were collected from the southwestern part of the East/Japan Sea and analyzed for sediment chemical composition, organic carbon, C/N and C/P ratios and C and N isotopes ratios together with pore water dissolved species. The southwestern East/Japan Sea, consists of continental shelf, continental slope and deep ocean basin. Sediments of the southwestern East/Japan Sea, especially over the Ulleung Basin, are characterized in high organic carbon concentrations (0.3 to 4.1%) and very high organic carbon burial flux (2.7 - 11.5 gC. m⁻². yr⁻¹) considering that the sea is a hemipelagic sedimentary setting and there is no large river entering into the sea.

From C/N and C/P ratios and C and N isotopes of the sediments, sediments of the southwestern East/Japan Sea are thought mostly of marine origin except those over the Korean coasts and some volcanic islands. where C/N, C/P ratios and C and N isotopes show more or less terrestrial input.

After deposited, organic carbon is decomposed by both aerobic and anaerobic processes (reduction of Fe/Mn-oxides and/or sulfate depending upon the environmental setting). Even though the sediments of the southwestern East/Japan experience oxidation of organic carbon by sulfate reduction, burial fluxes of organic carbon is still very high in the sediment(2.7 - 11.5 gC. m⁻². yr⁻¹) compared to other areas with similar water depth.

The recovering of weathering propagation rates from the analysis of ²³⁸U-²³⁴U-²³⁰Th-²²⁶Ra nuclides in regoliths

FRANÇOIS CHABAUX, ERIC PELT,
RAPHAEL DI CHIARA-ROUPERT, SOPHIE RIHS
AND PETER STILLE

The potential of U-series nuclides for investigating weathering processes has been recognized since the 1960s. It results from the dual property of the nuclides to be fractionated during water-rock interactions and to have radioactive periods of the same order of magnitude as the time constants of many weathering processes. The recent progression in this field of research is clearly related to the analytical developments made over the last decades in measuring the ²³⁸U series nuclides with intermediate half-lives (i.e., ²³⁴U-²³⁰Th-²²⁶Ra). The majority of studies made in this field of research has been based up to now on the analysis of ²³⁸U - ²³⁴U - ²³⁰Th nuclides and the use of the three activity ratios (²³⁴U/²³⁸U) - (²³⁰Th/²³⁴U) - (²³⁰Th/²³²Th). They provided important theoretical elements for the determination of regolith production rates in weathering profiles (e.g., Dequincey *et al.*, 2002; Chabaux *et al.*, 2003; 2013 ; Pelt *et al.*, 2007 ; Dosseto *et al.*, 2008; Ma *et al.*, 2010).

Here we propose to present the principle of the approach developed for recovering the regolith propagation rates from the analysis of U-series nuclides in a series of samples collected along the main weathering direction of the system. We will especially show how a simple modeling of U-series nuclides, based on mathematical formalism assuming a continuous gain and loss of the different U-series nuclides within a weathering profile, allows ones to recover such propagation rates. We will also highlight that the use of the ²³⁸U-²³⁴U-²³⁰Th nuclides together with the ²²⁶Ra nuclide allows for a better determination of the regolith production rate than together with the ²³²Th nuclide. Based on the results obtained by this approach it is suggested that the weathering and erosion processes in humid tropical or equatorial contexts are close to steady state, which would be not the case in area affected by important quaternary climatic variations (dry tropical or temperate context) or for soil systems significantly modified by human activity.

[1] Chabaux *et al.* 2003. *Comptes Rendus Geosciences* **335**, 1219-1231. [2] Chabaux *et al.* (2013). *GCA*, **100**, 73-95 [3] Dequincey *et al.* 2002. *Geochimica et Cosmochimica Acta* **66**, 1197-1210. [4] Dosseto, A., Turner, S.P., Chappell, J., 2008. *Earth and Planetary Science Letters* **274**, 359-371. [5] Ma, L., Chabaux, F., Pelt, E., Blaes, E., Jin, L., Brantley, S.L., 2010. *Earth and Planetary Science Letters* **297**, 211-225. [6] Pelt, E., Chabaux, F., Innocent, C., Navarre-Sitchler, A.K., Sak, P.B., Brantley, S.L., 2008. *Earth and Planetary Science Letters* **276**, 98-105.

Making the planet Mercury: Constraining Mercury's core formation and composition through laboratory experiments

NANCY L. CHABOT¹* E. ALEX WOLLACK²,
RACHEL L. KLIMA¹ AND MICHELLE E. MINITTI¹

¹Johns Hopkins University Applied Physics Laboratory,
Laurel, MD, 20723, USA (*correspondence:
Nancy.Chabot@jhuapl.edu)

²Princeton University, Princeton, NJ, 08540, USA

In 2011, MESSENGER became the first spacecraft ever to orbit Mercury and since then has returned a wealth of new data that is revolutionizing our understanding of the Solar System's innermost planet. Elemental composition information [1-3] has revealed that Mercury's surface is Fe-poor, but not Fe-free, and also S-rich. Gravity information [4] has led to new models proposed for Mercury's internal structure, notably with a large S- and Si-bearing metallic core with a top layer of solid FeS. Thus, the overall picture of Mercury is of a terrestrial planet very different from Earth, Venus, and Mars. As such, Mercury provides important constraints on planet formation in the inner Solar System.

In this work, we present results from an experimental study to understand the conditions and compositions involved during core formation on Mercury. Specifically, we use the Fe and S contents measured on Mercury's surface to constrain the amount of S and Si in Mercury's core. In total, 19 metal-silicate experiments were conducted at 1 atm and 1500°C, with varying amounts of S and Si in the metallic phases. We find that none of the experiments are able to match both the wt% levels of Fe and S measured on Mercury's surface, indicating a more complex history for the measured silicate compositions or that the Fe is meteoritic. To produce 2-4 wt% S in the silicate, as measured on Mercury's surface, our experimental results indicate core compositions with >3 wt% Si and a range of S and Si combinations. Nearly all of the determined S and Si core combinations yield bulk planetary Fe/Si and/or S/Si ratios that do not overlap with common chondrites, suggesting that Mercury formed from unique starting materials or is the remnant of a once larger body.

[1] Nittler *et al.* (2011) *Science* **333**, 1847-1850. [2] Weider *et al.* (2012) *JGR* **117**, E00L05, 10.1029/2012JE004153. [3] Evans *et al.* (2012) *JGR* **117**, E00L07, 10.1029/2012JE004178. [4] Smith *et al.* (2012) *Science* **336**, 214-217. [Acknowledgements] NASA grant NNX12AH88G; Student Research Participation Program at APL administered by the Oak Ridge Institute for Science and Education.

Biostimulation of silica and sulfur on crude oil biodegradation

SITI KHODIJAH CHAERUN^{1,2} AND XIAO-LEI WU^{1*}

¹ Department of Energy and Resources Engineering, College of Engineering, Peking University, Beijing, China
(#Presenting author: (skchaerun@gmail.com);
*(Correspondence: xiaolei_wu@pku.edu.cn)

² Laboratory of Environmental Biogeosciences and Mining Biotechnology, Division of Genetics and Molecular Biotechnology, Institut Teknologi Bandung, Indonesia

Clays have been used for stimulating oil spill bioremediation to prevent the eutrophication of the marine sites, showing that SiO₂ in the form of clays facilitates bacterial usage of hydrocarbon [1]. Likewise, sulfur (S), a component of crude oil, is reported to be a stimulator for oil biodegradation. Hence, in the current work, biostimulation of silica (Si) and S was employed for enhancing biosurfactant production by a novel species of *Pseudoclavibacter* sp. and *Dietzia* sp. DQ12-45-1b using the D-Daqing crude oil as sole carbon source for bioremediation purposes. Silica (in liquid form) enhanced bacterial growth and biosurfactant production for both strains. Interestingly, Si was capable of being stimulatory for an inactive cell of *Pseudoclavibacter* sp., thus shortening its lag phase. High S concentration did not inhibit or stimulate bacterial growth and biosurfactant production of both strains. Thus, dissolved Si derived from the Earth's crust is not inhibitory and even environmentally and economically beneficial for biosurfactant-producing bacteria. It can thus be concluded that the Si in liquid form could be considered to be a more eco-friendly and economical material source for the improvements in reliability, cost efficiency and speed of oil bioremediation.

This work was supported by a grant from National Natural Science Foundation of China (31070107, 31225001) to XLW.

[1] Chaerun & Tazaki (2005) *Clays Miner* **40**, 481-491.

K-feldspar geochronology: Not just ³⁹Ar

A.N. CHAFE¹, J.M. HANCHAR¹ AND I.M. VILLA^{2,3}

¹Memorial University of Newfoundland, St. John's, Canada;
(a.chafe@mun.ca)

²Universität Bern, Switzerland; (igor@geo.unibe.ch)

³CUDAM, Università di Milano Bicocca, Italy

Bell-shaped Pb diffusion profiles are not found in U-Pb mineral chronometers; instead, patchy intra-grain age variations match heterochemical recrystallization [1]. Fluids most efficiently control micro-chemistry, micro-textures and the isotope record [2-5]. Is K-Ar different from U-Pb?

Some authors [6] propose that K-feldspar (Kfs) loses Ar in nature and the laboratory by the same mechanism, volume diffusion out of discrete "domains", so that a lab experiment can be inverted to yield a thermal history; they assume that ambient temperature alone uniquely controls Kfs ages.

We re-sampled and re-investigated the archetypal Kfs MH-10 [6]. We duplicated age spectra and Arrhenius trajectories of [6]; this is where agreement ends. The self-similarity of Arrhenian non-linearities demonstrates that "small domains", which were argued to be mathematically justified [6] even if physically untenable [7], are untenable mathematically as well. We characterized the sample by cathodoluminescence and electron microprobe, discovering at least 5 fluid-produced, heterochemical, diachronic mineral generations. This confirms [8]. Each diachronic Kfs generation has a different Ca/Cl/K signature. This confirms [9]. MH-10 records a geohydrologic history of fluid interactions; its laboratory staircase spectrum is an effect of degassing a mixture of unrelated Kfs generations. This forbids reconstructing its "thermal history". In the own words of [6], the insight gained from MH-10 must be extrapolated to all existing Kfs samples. Thus, no Kfs must be used as a "thermochronometer" unless it were to be proven to be unaffected by patchy recrystallization and to have an isochemical Ca/Cl/K signature. What Kfs is suitable for instead is a detailed reconstruction of the hydrochronology of a rock.

[1] Williams et al, *Ann Rev EPS* **35** (2007) 137 [2] Cole et al, *GCA* **47** (1983) 1681 [3] Lasaga, *Miner Mag* **50** (1986) 359 [4] Putnis, in: Harlov & Austrheim, *Metasomatism and the Chemical Transformation of Rock*, Springer (2013) [5] Villa & Williams, in: Harlov & Austrheim, *Metasomatism and the Chemical Transformation of Rock*, Springer (2013) [6] Lovera et al, *Contrib Mineral Petrol* **113** (1993) 381 [7] Villa, *GCA* **61** (1997) **689** [8] Villa & Hanchar, *GCA* **101** (2013) 24 [9] Villa, *Geol Soc London Spec Pub* **378** (2013)

Coupling HTO tracer experiments and tomography imaging to monitor the effects of celestite porosity clogging on diffusion properties in porous media

A. CHAGNEAU^{1,2,3}, F. CLARET³, B. MADÉ⁴, M. WOLF⁵,
F. ENZMANN⁵ AND T. SCHÄFER^{1,2}

¹ KIT-INE, P.O. Box 3640, 76021 Karlsruhe, Germany.

(aurelie.chagneau@kit.edu) t(horsten.schaefer@kit.edu)

²Freie Universität Berlin, Berlin, Germany.

³Brgm, 3 avenue Claude Guillemin, BP 36009, Orléans cedex
2, France. (f.claret@brgm.fr)

⁴andRA, 7 rue Jean Monnet, 92298 Chatenay-Malabry Cedex.

⁵Johannes Gutenberg-Universität Mainz, Mainz, Germany.

The focus of the present study is to characterize the effects of porosity clogging on the effective diffusivity of porous materials under geochemical perturbation. A systematic experimental approach was used, and coupled to pore network and reactive transport modeling.

The experiments were performed in diffusion cells composed of a column filled with synthetic silica spheres (SiLi beads) or purified sea sand and two reservoirs, containing a SrCl₂ and a Na₂SO₄ solutions. Prior to the mineral precipitation experiments the transport properties were characterized by means of conservative radiotracer (HTO) tests and revealed D_e values of (4.79 ± 0.24) × 10⁻¹⁰ m² s⁻¹ and (4.20 ± 0.21) × 10⁻¹⁰ m² s⁻¹ for SiLi beads and sea sand, respectively. The precipitation of celestite (SrSO₄) in the porosity and the subsequent evolution of the diffusivity were monitored by HTO and computed tomography (CT).

The CT resolution varied from 11 to 15 μm. The data were implemented into a pore network model (GEODICT) in order to estimate porosity and diffusivity of the materials, but also to monitor the precipitation processes in a non destructive way. The model was calibrated on a diffusion cell filled with SiLi beads of 400-600 μm particle size. The segmented CT porosity of 0.365 was comparable to 0.361 ± 0.047 for HTO radiotracer tests, giving confidence in the approach used. In addition, the porosity was cross-checked by mercury intrusion porosimetry measurements, which gave values of 0.389 and 0.413, in good agreement with the two precedent ones. In addition to the pore network modeling, a reactive transport model was developed to reproduce the data using Archie's law, in order to extend its applicability to very small effective porosities.

Rare-earth deposits in igneous rocks: A mineralogist's perspective

ANTON R. CHAKHMOURADIAN¹, ANATOLY N. ZAITSEV²
AND EKATERINA P. REGUIR¹

¹Department of Geological Sciences, University of Manitoba,
Winnipeg, Manitoba, Canada (correspondence:
chakhmou@cc.umanitoba.ca)

²Department of Mineralogy, St. Petersburg State University,
St. Petersburg, Russia

Globally, some 70% of advanced rare-earth exploration projects have focused their efforts on mineral deposits associated with igneous rocks (or their weathering products). Three groups of igneous deposits have attracted the most attention: (1) carbonatites; (2) peralkaline silica-undersaturated rocks; and (3) peralkaline anorogenic granites. The first two groups accounted for ~50% of the global production of rare earth elements (REE) prior to 1995. Deposits associated with carbonatites show the lowest levels of Y and heavy REE in their budget ($Y/Nd \leq 0.3$) among the three groups, but are least depleted in Eu ($Eu/Eu^* = 0.7-1.1$); these characteristics are in marked contrast to those of rare-earth ores in anorogenic granites ($Y/Nd \geq 0.8$; $Eu/Eu^* \leq 0.3$). Postorogenic carbonatites associated with saturated alkali syenites have shown the greatest promise as a primary REE source (fluorocarbonates, monazite). Extreme enrichment of carbonatitic magmas in light REE cannot be explained satisfactorily with simple melting models. The presence of REE phases in their mantle source, low degree of contamination by crustal material, and fortuitous interplay between aF^- and $a(PO_4)^{3-}$ appear to be prerequisite to the formation of a commercially viable deposit. In anorogenic carbonatites, appreciable REE mineralization commonly develops through breakdown of apatite, calcite and other primary low-grade REE hosts during their hydrothermal reworking (fluorocarbonates, ancylite, monazite) or lateritic weathering (monazite and other secondary phosphates). A variety of minerals forming large-tonnage deposits in peralkaline undersaturated rocks have been proposed as the ultimate solution to looming critical-metal shortages; however, only loparite has been extracted and processed industrially to date. It remains to be seen if any of the other REE-bearing minerals (e.g., eudialyte) are amenable to profitable metal recovery. These minerals crystallize from extremely evolved melts derived by protracted fractional crystallization of aegirine, feldspars and nepheline (\pm sodalite) from basanitic magma in anorogenic extensional settings.

Timescales of metamorphism: A Hierarchical distribution

SUMIT CHAKRABORTY¹

¹Institut fuer Geologie Mineralogie und Geophysik, Ruhr-
University Bochum, Germany
(Sumit.Chakraborty@rub.de)

Several tools now provide us information on the timescales of metamorphism: geodynamic modelling, spatially resolved isotopic dating, and diffusion modelling of compositional zoning are some of these. Using the different tools on the same set of rocks reveals processes that occur on a hierarchy of timescales. Geodynamic modelling as well as isotopic dating indicate that orogenies can last over hundreds of millions of years, spatially resolved isotopic dating and direct geological evidence indicates that individual metamorphic rocks go through their pressure-temperature cycles on timescales of a few million years, and individual reactions (e.g. melting) occur within a few hundred thousand years. Combination of the various tools can provide more detailed insights into thermal histories; these can be verified using thermomechanical modeling with realistic boundary conditions. For example, isotopic dating using systems with different closure temperatures provides absolute points along the T-t path of a rock and diffusion modelling helps to determine how these "dots" are connected. Diffusion modelling is now able to resolve non-linear cooling histories and it is found that cooling rates can vary (i.e. increase as well as decrease) significantly during cooling from peak temperatures, and the use of a single, average cooling rate to characterize metamorphic rocks is misleading. Moreover, cooling at high temperatures is not always associated with exhumation and other processes that may act as a thermal sink need to be considered. Finally, we find that regional metamorphic P-T cycles can be very short (e.g. ~ 3 m.y.) or relatively long (~ 20 m.y.), depending on the tectonic setting. Examples from the Himalaya and a UHT metamorphic sequence in the Central Indian Tectonic Zone will be used to elucidate these situations.

Neoproterozoic island arc magmatism and gold mineralization: Examples from eastern Dharwar craton, India

MANIKYAMBA, C*, ADRIJA CHATTERJEE LINGAMURTY, E. RAJANIKANTA SINGH, M.

National Geophysical Research Institute (Council of Scientific and Industrial Research) Uppal Road, Hyderabad 500 606
 *(corresponding author email: cmaningri@gmail.com)
 (adrija.geo@gmail.com; (elmgeology@gmail.com); (rajanimumut@gmail.com)

Four linear arcuate greenstone belts dominate in the eastern Dharwar craton having variable proportions of gold mineralization along which Hutti is the only working mine at present. The Sandur greenstone terrane; the Ramagiri-Penakacherla-Hungund; Hutti-Jonnagiri-Kadiri-Kolar and Narayanpet-Gadwal-Velligallu linear, composite greenstone terranes of eastern Dharwar craton are evidenced with gold mineralization in different lithounits. The plume magmatism in the western sector has resulted in concentration of iron, manganese and other base metals deposits whereas the arc magmatism in the eastern sector contributed for the concentration of gold at some places. Subduction-accretion has been recognized as a predominant process in the growth of continental crust and its mineralization in eastern Dharwar craton. Most of the greenstone belts in eastern Dharwar craton have a complete spectrum or a few litho units that represent intraoceanic island arc process. Sandur belt has komatiite-tholeiite sequences along with calc-alkaline volcanic rocks representing plume-arc accretionary process. Komatiites, oceanic island basalts, arc basalts, Nb-enriched basalts and adakites are present along the Ramagiri-Penakacherla-Hungund belt representing the dominance of island arc process where Penakacherla belt has abundant gold mineralization. Arc-back-arc basalts with adakites were reported at Hutti; high-Mg basalts along with arc basalts are preserved at Jonnagiri; arc basalts along with Nb-enriched basalts, adakites, Mg-andesites, dacites and rhyolites occur in Kadiri belt and Kolar has ultramafic rocks that reflect on mantle plume magmatism. In Narayanpet-Gadwal and Velligallu belts boninites are present at Velligallu and Gadwal which are associated with Nb-enriched basalts, arc basalts, Mg-andesites and adakites. The identification of the rocks deposited at Neoproterozoic convergent margins provide significant constraints on the island arc magmatism, plume-arc accretionary process and concentration of gold in few greenstone belts of eastern Dharwar craton.

Evolution of basaltic melt during mantle refertilisation at shallow depths of spreading ridges, through experimental studies of liquid compositions in equilibrium with plagioclase + spinel lherzolite at low pressures (0.75 and 0.5 GPa)

F. CHALOT-PRAT¹, T.J. FALLOON², D.H. GREEN³ AND W.O. HIBBERSON⁴

¹CRPG/CNRS, Université de Lorraine, BP20, 54501 Vandoeuvre Les Nancy, France (*correspondence: chalot@crpg.cnrs-nancy.fr)

²School of Earth Sciences - IMAS, PB79, Hobart, Tasmania 7001, Australia (Trevor.Falloon@utas.edu.au)

³School of Earth Sciences - CODES, University of Tasmania, PB79, Hobart, Tasmania 7001, Australia (David.H.Green@utas.edu.au)

⁴RSES, the Australian National University, Canberra, ACT0200, Australia

The presence of plag+sp lherzolites among ocean floor samples and in some ophiolite complexes invites speculation on their origin and relationships to processes of magmatism and mantle refertilisation beneath mid-ocean ridges. We have determined experimentally, in the (Cr+Na+Fe+Ca+Mg+Al+Si) system, the compositions of liquids and 5 co-existing minerals in the six phase assemblage [Liq+Ol+Opx+Cpx+Plag+Sp] at 0.5 and 0.75 GPa [1,2]. As compositions of mineral phases are pressure dependent, our results may be used to quantify the P-T and compositional evolutionary paths of both liquids and residues during mantle refertilisation at shallow depths. The major variations in liquid compositions are related to plagioclase composition. Liquid compositions, silica-oversaturated for $An_{plag} \geq 40$ but critically silica-undersaturated for $An_{plag} \leq 25$, are unlike natural MORB glasses, providing no support for MORB genesis by extraction of near-solidus melts from plag-lherzolite at low pressure. Comparisons with natural mineral compositions of plag+sp-refertilised lherzolites from the literature infer that the refertilisation process by reactive porous flow of magma within the oceanic lithospheric mantle took place at depths of up to 30 km ($0.75 \text{ GPa} \leq P \leq 1 \text{ GPa}$) beneath the sea floor.

[1]Chalot-Prat, Falloon, Green, Hibberson (2010), *Journal of Petrology* **51**, 2349-2376; [2]Chalot-Prat, Falloon, Green, Hibberson (accepted) *Lithos*

IBA quartz chemistry to track phase separation in intrusive rock

I. CHAMBEFORT¹, W.J. TROMPETTER² AND F. BEGUE³

¹GNS Science, Wairakei Research Centre, NZ,
(i.chambefort@gns.cri.nz)

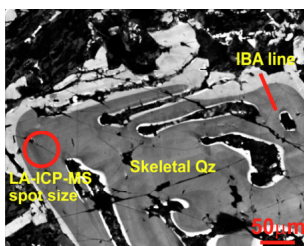
²GNS Science, National Isotope Centre, NZ,

³Univ. of Canterbury, NZ,

Undercooling and fast crystallisation textures such as myrmekites, granophyric and dendritic and skeletal growths have often been associated with subsolidus crystallisation due to H₂O loss. The exsolution of the fluid phase initiates the nucleation of quartz, K-feldspar and plagioclase by quenching at the binary eutectic.

A combined study of cathodoluminescence imaging and detailed chemistry was applied to tonalitic intrusive rock from the Ngatamariki Geothermal Field, New Zealand. The intrusions underwent phase separation at an estimated depth of 1.6 km and produced a large phyllic alteration halo in the country rocks. The working hypothesis is that the last stage of the magmatic mineralogy has recorded the exsolution stage in their chemistry. Quartz phenocrysts in the tonalite are up to 8 mm in diameter and embayed. Also present are small (<2 mm) skeletal quartz grains cocrystallising with a myrmekitic / granophyric groundmass.

Cathodoluminescence on quartz, LA-ICP-MS and Ion Beam Analysis (IBA) were done on rounded and skeletal quartz phenocrysts to track variations in Ti, Al, F, Li and B from core to rim in the different CL zones. The outer rims of the skeletal quartz and groundmass quartz are brighter in CL than the large phenocrysts, suggesting enrichment in Ti and other trace elements (figure). A 15 µm proton beam was raster scanned over the sample to produce elemental maps. Ti and Al were detected via X-rays; F via γ-rays, B and Li via (p,α) nuclear reactions. The IBA techniques give spatial precision to the micron scale and ppm LODs allowing detailed chemistry to track the volatile loss.



Acknowledgements: We thank Mighty River Power for the use of the rock sample. The project is funded by GNS Science CSA geothermal and ion beam innovations research programs, and the Royal Society of New Zealand Marsden Fund GNS1203 to IC.

Combined diffusion studies in sanidine, quartz and orthopyroxene: Timescales of magma mixing in the Bishop Tuff

K.J. CHAMBERLAIN^{1*}, D.J. MORGAN²
AND C.J.N WILSON¹

¹SGEES, Victoria University of Wellington, PO Box 600
Wellington, 6012, New Zealand (*correspondence:
katy.chamberlain@vuw.ac.nz; colin.wilson@vuw.ac.nz)

²SEES, University of Leeds, Leeds, LS2 9JT, UK
(d.j.morgan@leeds.ac.uk)

The ~0.76 Ma Bishop Tuff (eastern California) is an archetypal product of a compositionally stratified magma chamber. A key issue regarding the evolution of the melt-dominant magma body that has arisen from recent studies involves understanding the nature and timing of late-stage mixing with a compositionally contrasting melt. This melt is reflected, for example, in the CL-bright rims on quartz and Sr- and Ba-rich rims on sanidine reported in ignimbrite samples erupted from vents along the northern caldera rim [1, 2, 3].

We use ternary feldspar thermometry combined with 1D diffusion models to calculate timescales for diffusion of key elements in three crystal phases of the Bishop Tuff. We show that Sr in sanidine, Fe-Mg in orthopyroxene and Ti in quartz all indicate mixing timescales of <150 yrs, in contrast to the ~2000 yr timescale from Ba in sanidine. The anomalously long timescales obtained from Ba diffusion in sanidine have implications for the application of this chronometer to low-T (~800 °C) rhyolitic systems. The short timescales modelled indicate that the “contaminant” magma causing the growth of these rims was a relatively transient feature in the ~ 70 kyr history of the melt-dominant magma chamber [4].

[1] Anderson *et al.* (2000) *J. Pet.* **41** 449-473. [2] Peppard *et al.* (2001) *Am. Min.* **86** 1034-1052. [3] Wark *et al.* (2007) *Geology* **35** 235-238. [4] Chamberlain *et al.* (2013) *manuscript in prep.*

Melts in a single lava flow from a multiply subduction-modified mantle column below Central Italy

S. CHANEVA¹, I. NIKOGOSIAN¹, M.J. VAN BERGEN¹
P.R.D. MASON¹ AND MARTIN WHITEHOUSE²

¹Department of Earth Sciences, Utrecht University, the Netherlands (simonachaneva@gmail.com)

²Swedish Museum of Natural History, Box 50007, SE104 05 Stockholm, Sweden

Latera stratovolcano, situated in the northernmost part of the Roman Magmatic Province (Central Italy), represents a late activity stage of Quaternary volcanism in the Vulcini complex. Lava compositions range between leucite-bearing ultrapotassic (HKS) and shoshonitic (SHO). We determined major-element, trace-element and Pb-isotope compositions of homogenized melt inclusions (MI) trapped in Fo-rich olivines (Fo₉₁-Fo₈₇) that were separated from samples of a voluminous lava flow with SHO affinity (Selva Del Lamone flow, SDL) and a HKS lava. Two populations of magmatic olivine, MI and spinel have been distinguished in the SDL lava, based on morphologies and compositions of host olivines and inclusions. A wide range in CaO contents of Fo-rich olivine points to crystallization from compositionally different primary melts. We infer that the SHO lava comprises two distinct mantle-derived alkali-rich melts: (1) "normal" SHO type, compositionally closest to the host rock; and (2) "low-CaO" high-Na₂O melt with lamproitic affinity. The MI from the SDL lava show an extreme Pb-isotopic diversity: ²⁰⁶/₂₀₄Pb = 18-19.2, ²⁰⁷/₂₀₄Pb = 14.6-16, ²⁰⁸/₂₀₄Pb = 36.5-40.5, each group being characterized by its own signature. The composition of the host lava appears to be a mixture of (at least) three isotopically distinct end-members. The MI form arrays between MORB-source-like mantle and various crustal/sedimentary end-members, including both upper and lower continental crust. Former Alpine and Adriatic subduction systems may have affected mantle sources of the SHO magma, whereas the HKS source was influenced by the Adriatic system, similar to the rest of the Roman Magmatic Province. A relatively recent thermal event, possibly promoted by detachment of the Adriatic slab, must have been responsible for the simultaneous melting of heterogeneous domains in the mantle column below the volcano that reflect superimposed imprints from multiple subduction systems.

Abnormal K-feldspars from the Lower Cambrian Hetang Formation in the Lower Yangtze Area: Implications for hydrothermal activities

CHAO CHANG¹, WENXUAN HU^{1,2} AND XIAOLIN WANG^{1,2}

¹School of Earth Sciences and Engineering, Nanjing University, Nanjing, 210093, P.R. China

²Institute of Energy Sciences, Nanjing University, Nanjing, 210093, P.R. China

The Lower Cambrian black rock series are widely distributed throughout the Yangtze Platform in South China. At the lowermost part of the strata, there is a thin sulfide ore horizon rich in Cu, Mo, Co, Ni, PGE, Se, As, Hg, Sb, Ag, and Au. Based on geochemical characterization on certain segment of the strata, some researchers tried to figure out the formation mechanism of the horizon. However, no agreement on this question has been obtained yet, and the main argument is whether or not hydrothermal activities have played an important role in the formation process.

In this study, systematic analyses were carried out on the lithology and mineralogy of samples throughout the whole strata. Unexpectedly, abundant K-feldspars with abnormal composition were found. In terms of the electron probe microanalyses (EPMA), it is found that the K-feldspars can be subdivided into two types: Ba-rich K-feldspars and Ba-poor K-feldspars. The Ba-rich K-feldspar is characterized by high BaO content ranging from 1.34 % to 9.08 %; the K₂O and SiO₂ concentrations range from 7.24 % to 10.50 % and from 59.37 % to 69.70 %, respectively. The Ba-rich K-feldspar is found in veins, or occurs as thin rims of the Ba-poor K-feldspars in the matrix. The Ba-poor K-feldspar is depleted in BaO content ranging from 0.06 % to 1.08 %; the K₂O and SiO₂ content range from 5.22 % to 15.47 % and from 63.07 % to 73.13 %, respectively. The Ba-poor K-feldspar mostly occurs as anhedral grains in the matrix.

Furthermore, it is revealed that the plots of BaO and SiO₂ concentrations of the Ba-rich K-feldspar show a linear correlation, which is similar to those of hyalophane (or celsian). However, the K₂O-BaO relation is totally irregular. In addition, it is also observed that the K₂O-SiO₂ relation is basically linear, which shows that the K-feldspar could form in a continuous sequence from low K₂O content to high K₂O content; the endpoint could represent normal K-feldspars.

In conclusion, it is suggested that the K-feldspars were immature in composition and might precipitate from rapid cooling of hydrothermal fluids. We are searching for further evidence to support this new formation mechanism for abnormal K-feldspar.

Multiple controls on the geochemistry of early Cenozoic volcanism in Victoria, Australia

T-J. CHANG, J. HERGT, G. HOLDGATE,
M. WALLACE AND D. PHILLIPS

School of Earth Sciences, The University of Melbourne,
Parkville, Victoria, Australia, 3010

Early Cenozoic volcanism in Victoria (resulting in the so-called 'Older Volcanics' province) has received little attention compared to younger volcanic provinces in Australia. Magmatism occurred intermittently between ~20 to 40Ma and new trace element and isotope data for a number of subprovinces reveal wide geochemical variations both locally and regionally.

These rocks are dominated by alkali basalts and basanites, and all samples are reasonably fresh with typical mineral assemblages including olivine, clinopyroxene, and plagioclase, with or without nepheline. Mantle xenoliths have been observed in 4 samples. The MgO and SiO₂ contents range between 3.2-11.1wt% and 41.1-52.1 wt% respectively and the wide range in magnesium numbers (39-69) indicate that the magmas vary from primitive (perhaps even primary) to evolved in composition. Although trace element compositions broadly resemble those of modern OIB; in detail, mantle-normalised patterns show distinct differences between subprovinces. The transitions between subprovinces coincide with large-scale faults, that separate different structural zones in Victoria, indicating possible structural control over the magma chemistry. Ce/Pb and Nb/U ratios range between 11.4-33.3 and 23.8-60.9 respectively, with lower values reflecting the effects of crustal assimilation. Initial ⁸⁷Sr/⁸⁶Sr (0.70285-0.70507) and ¹⁴³Nd/¹⁴⁴Nd (0.512659-0.513021) ratios are corrected using new ⁴⁰Ar/³⁹Ar or ⁴⁰K/³⁹Ar ages. Isotopic compositions of the younger basalts (20-30Ma) form a distinct trend along the mantle array whereas the older basalts (~40Ma) scatter around Bulk Silicate Earth. Together, these new observations reveal that the earliest period of volcanism in the Older Volcanics province tapped a relatively homogeneous mantle source, and that magmas migrated to the surface without significant assimilation of continental crust. In contrast, the younger magmas interacted with and assimilated crustal material, modifying their compositions prior to eruption. The extent to which the mantle source rocks for this younger group may also have varied is under investigation. In addition, the role of the large-scale structures in channelling magmas to the surface, and/or influencing their ability to interact with crust, is an important component of this study.

Characteristic Elements of Products of Designations of Origin selected from Yangchun in Guangdong Province, China

CHANG XIANG-YANG, LIU HUI, FU SHAN-MING,
CHEN NAN, LI DONG-MEI AND ZHAO XIAO-FENG

School of Environmental Science & Engineering, Guangzhou
University, Guangzhou 510006, China

Kaempferia Galanga L. which is the product of designations of origin was selected from Shuangjiao town, Yangchun, Guangdong Province, China. The plants and soil profile samples were collected and the element content, element speciation, and lead isotope ratio were determined. Through the multivariate statistical analysis to ascertain the characteristic elements and multi-element group, and provide evidence for establishing the elements- isotope fingerprints of product identification system, the following conclusions:

A group of chemical elements in the plant could indicate the special effect from the special environment where the plants grown, with a closely relationship to the plants growth, those elements are called characteristic elements. According to the results of the analysis of weight, the characteristic elements of Kaempferia Galanga L. were Mn, Zn, Mg, Sr, Cu, Ni and Fe.

The factor analysis and cluster analysis were used for the purpose of the group of elements. The result of factor analysis showed that Cu, Co, Ni, Pb, Sr were the common element group in Kaempferia Galanga L. and soil. The cluster analysis showed that Co, Cr, Cu, Mg, Sr, Zn were the common element group in Kaempferia Galanga L. and soil. The results of the two methods can corroborated each other.

According to the results of the cluster analysis, Co/Ni, V/Co, Mg/Mn, Mn/Sr, Ni/Fe, Zn/Mn, Zn/Sr, V/Cr and V/Cu nine elements ratios was selected, and the change trend of consistent of elements ratios in the Kaempferia Galanga L. with corresponding soil profiles. The elements ratios could be identified as an important tracer tool.

The correlation analysis between elements speciation of soil and Kaempferia Galanga L. showed that effective state of element in soil had a significant relationship with the element content in Kaempferia Galanga L. The level of effective state of element of Fe, Mg, Mn, Pb and Zn in the research area was higher, but the level of Sr, Ti, V was lower.

Lead isotope ratios showed that the sources of lead in the soil profile and Kaempferia Galanga L. were very stable, lead isotope ratios of Kaempferia Galanga L. were very close to the distribution characteristics of soil region. ²⁰⁶Pb/²⁰⁸Pb-²⁰⁶Pb/²⁰⁷Pb showed significant correlation further proves the product with soil were homology. Lead isotope could be used as the criterion of fingerprint identification of products of designations of origin.

The Project was supported by National Natural Science Foundation of China (Grant Nos. 40772201, 41073003).

Geochemical characteristics and petrogenesis of Cenozoic igneous rocks in the Georgian Caucasus

YU-HAN CHANG^{1*}, SUN-LIN CHUNG¹,
AVTO OKROSTSVARIDZE² AND ZURAB JAVAKHISHVILI²

¹ Department of Geosciences, National Taiwan University, Taipei, Taiwan (*correspondence: r01224107@ntu.edu.tw)

² Institute of Earth Sciences, Ilia State University, Tbilisi, Georgia

Cenozoic magmatism in the Caucasus-Iran-Anatolia (CIA) region can simply be divided into two main stages that pre- and post-date, respectively, the onset of the Arabia-Eurasia collision. The pre-collisional stage has been generally related to the Neotethyan subduction. The post-collisional stage has been ascribed to rollback and then breakoff of the subducted slab or other geodynamic processes such as delamination of thickened lithosphere. In Georgia, located ~500 km north of the Zagros suture zone, the pre-collisional rocks, with SiO₂ ranging from ~45-64 wt.%, are more heterogeneous in certain incompatible elements such as potassium and LREE than the post-collisional rocks, despite the latter show a wider range of SiO₂ (45-72 wt.%). Thus, in contrast to the post-collisional rocks that plot in the median- to high-K calc-alkaline suite, the pre-collisional rocks are dominantly of intermediate compositions (SiO₂ ≈ 60 wt.%) and vary from low- to high-K calc-alkaline to shoshonitic in nature. However, rocks from both stages are characterized by the “arc signature” including enrichment in LILE (e.g., Rb, Ba) and depletion in HFSE (e.g., Ti, Nb, Ta). While isotopic determination is still in progress, Sr-Nd isotope data obtained so far from post-collisional rocks indicate that they have an isotopically uniform mantle source similar to other post-collisional magmas in the CIA region. We are also working on precise dating of the pre-collisional rocks. The result, together with geochemical and isotopic constraints, will hopefully help us better understand the petrogenesis that we suspect to have affiliated with a back-arc system.

Understanding controls on Ca isotopes in human blood and urine

M.B. CHANNON^{1*}, G.W. GORDON¹,
Q. SHOLLENBERGER¹, J.L.L. MORGAN², J.L. SKULAN³,
S.M. SMITH² AND A.D. ANBAR¹

¹Arizona State Univ., Tempe, AZ 85287

(#correspondence: mchannon@asu.edu)

²NASA Johnson Space Center, Houston, TX 77058

³Geology Museum, Univ. of Wisconsin, Madison, WI 53706

Calcium isotopes fractionate during bone formation, favoring light Ca isotopes. During bone resorption, Ca isotopes are released into the blood and soft tissue with little or no discrimination. This fractionation process may be a powerful biomarker for diseases that effect the skeletal system such as osteoporosis, multiple myeloma, and cancers that metastasize to bone. However, in order to translate this biomarker to a clinical setting, we must understand all the factors contributing to the Ca isotopic composition of blood and soft tissue in the body.

It was previously shown that Ca isotopic composition of urine reflects changes in bone mineral balance correlated to bone loss during bed rest [1-2]. The most recent study [2] involved 12 patients on bed rest for 30 days with a controlled diet. Both urine and blood were collected from participants throughout the study, as well as meal and beverage samples for isotopic analysis. This study showed that the Ca isotopic composition of urine becomes lighter as bed rest progresses, in correlation with bone resorption. Here we present new data of blood, meals, and additional urine analyses from this study.

We find variable Ca isotope ratios among meals that tend towards heavier values for breakfasts, lighter values for dinners, and intermediate values for lunches. We also find a large range within and between beverages. We investigate whether the compositional differences in meals is reflected in urine isotope ratios over a 24 hour period by measuring each urine void from the same participants for one full day of the study.

We also find that blood has a systematically lighter isotopic composition than urine. We explore the possibility of a renal fractionation [3] involving Ca-binding proteins that might explain the difference between the Ca isotope ratios of blood and urine. Nevertheless, blood tracks the same trend as urine during the progression of bed rest, and therefore the compositional difference between blood and urine does not obscure the signal of bone resorption.

[1] Skulan *et al.* (2007) *Clinical Chem.* **53**, 1155-1158. [2] Morgan *et al.* (2012) *PNAS.* **109**, 9989-9994. [3] Heuser and Eisenhauer (2010) *Bone.* **46**, 889-896.

Elastic wave velocities of polycrystalline $\text{Mg}_3\text{Al}_2\text{Si}_3\text{O}_{12}$ -pyrope garnet to 24 GPa and 1300K

J. CHANTEL¹, G. MANTHILAKE^{1,2}, D. FROST³,
C. BEYER³, Z. JING⁴ AND Y. WANG⁴

¹ Université Blaise Pascal, Laboratoire Magmas et Volcans, Clermont-Ferrand, France

² CNRS, UMR 6524, LMV, Clermont-Ferrand, France

³ Bayerisches Geoinstitut, University Bayreuth, Germany

⁴ University of Chicago, Chicago, IL, USA

The most accurate method to investigate the mineralogy and chemistry of the mantle at depths greater than 150 km is through the analysis of compressional (P) and shear (S), seismic waves and comparison with the same velocities calculated for expected mineral assemblages. Regional variations in seismic wave velocities could originate from either chemical or thermal heterogeneities and experimental measurements of wave velocities of candidate phases at high pressures and temperatures are required to differentiate between these causes. In the transition zone, rocks formed from subducted basaltic crust are rich in garnet and its mineral proportion and chemistry differs from typical ultramafic mineral phases, which are dominated by olivine polymorphs wadsleyite and ringwoodite. Although the sound velocities of olivine polymorphs at relevant pressures have been well documented, those of garnet have not been investigated in its stability field.

We have successfully measured the acoustic wave velocities for synthetic polycrystalline pyrope garnet ($\text{Mg}_3\text{Al}_2\text{Si}_3\text{O}_{12}$) were to 24 GPa and temperatures up to 1300K by ultrasonic interferometry combined with energy-dispersive synchrotron X-ray diffraction in a 1000-ton press and a T-25 multi-anvil module (13ID-D, APS). Specimen lengths at high pressures (P) and temperatures (T) are directly measured by X-ray radiography methods, while elastic wave travel times and X-ray diffraction data were collected. Two dimensional (P - T) linear fittings of the present data yields the following parameters: $K_{S0} = 168.5$ (2) GPa, $\delta K_S / \delta P = 4.49$ (2), $\delta K_S / \delta T = -19.9$ MPa/K, $G_0 = 88.5$ GPa, $\delta G / \delta P = 1.59$ (1) and $\delta G / \delta T = -8.9$ MPa/K which is consistent with earlier results at lower pressures except for a significantly lower G_0 and $\delta G / \delta T$. Compressional (V_p) and shear (V_s) wave velocities as well as the adiabatic bulk (K_S) and shear (G) moduli exhibit monotonic increase with increasing pressure and decrease with increasing temperature, respectively. The observed linear pressure and temperature dependence in both V_p and V_s is in contrast to the non-linear behavior of V_p and V_s for majorite garnet with the pyrolite composition, in particular for V_s .

Stability of polycyclic aromatic hydrocarbons at upper mantle conditions

A.D. CHANY SHEV^{1,2*}, K.D. LITASOV^{1,2}, A. SHATSKIY^{1,2}, Y. FURUKAWA³ AND E. OHTANI³

¹Sobolev Institute of Geology and Mineralogy, Novosibirsk, 630090, Russia

(*correspondence: chanyshhev_90@mail.ru)

²Novosibirsk State University, Novosibirsk, 630090, Russia

³Tohoku University, Sendai, 980-8578, Japan

The origin of deep-seated hydrocarbons was widely discussed in relation to the study of C-O-H fluid. The estimation of $f\text{O}_2$ conditions in the deep mantle indicate that it can be in equilibrium with reduced fluids and $f\text{O}_2$ in mantle rocks can be fluctuated near that for the iron-wustite buffer at the depth below 300 km [1]. The calculations of fluid compositions at these conditions in the C-O-H system indicate the dominant CH_4 - H_2O mixture, with subordinate H_2 , and heavier hydrocarbons [1]. However, some theoretical calculations predict that heavy hydrocarbons, such as alkanes, alkenes, polycyclic aromatic hydrocarbons (PAH), can become stable in the mantle fluids at 300-600 km and deeper [2].

Here we determined stability and chemical reactivity of PAHs at upper mantle pressures. PAHs were selected according to abundance in natural samples [3] and meteorites. The starting materials were from naphthalene to coronene. The decomposition parameters were detected by *in situ* X-ray diffraction and laboratory multi-anvil experiments. In the pressure range of 6-9 GPa selected PAHs become unstable at temperatures of 873-1023 K. After experiments we analyzed products using matrix-assisted laser desorption/ionization method (MALDI). As a result, the formation of polymers of starting materials at 7 GPa and 773-873 K was determined. The polymers have atomic masses up to 5000 Da.

The P-T parameters for the PAHs stability field do not correspond to the upper mantle conditions; indicating that PAHs in diamonds and other mantle minerals [3] would have secondary origin. Indeed, data for PAHs stability is important for near-surface geodynamics of small and large planetary bodies as PAHs are widely observed in the Universe [4]. The work is supported by RFBR No 12-05-00841.

[1] Frost & McCammon (2008) *Annu. Rev. Earth Planet. Sci.* **36**, 389-420. [2] Zubkov (2001) *Geochemistry* **39**, 131-154. [3] Kulakova *et al.* (1982) *Doklady Earth Sciences* **267**, 1458-1461. [4] Ehrenfreund & Cami (2010) *Cold Spring Harb Perspect Biol.* **2**, doi: 10.1101/cshperspect.a002097.

The variation of Sr isotopes ($^{87}\text{Sr}/^{86}\text{Sr}$ and $\delta^{88/86}\text{Sr}$) in river waters after Typhoon Morakot at a small catchment, southwestern Taiwan

H. C. CHAO^{1,2}, C. F. YOU^{1*}, H. C. LIU¹
AND C. H. CHUNG¹

¹Department of Earth Sciences, National Cheng Kung University, Tainan, Taiwan, R.O.C. (*correspondence: cfy20@mail.ncku.edu.tw)

²Present Address: Department of Geography, National Changhua University of Education, Changhua, Taiwan, R.O.C. (ekman60@gmail.com)

Radiogenic Sr isotope ($^{87}\text{Sr}/^{86}\text{Sr}$) is a robust tool for provenance identification in hydrology, affected mainly by chemical weathering and climatic changes. Owing to technical improved MC-ICP-MS, stable Sr isotopes ($^{88}\text{Sr}/^{86}\text{Sr}$) in natural materials have become available recently. In this study, weekly river waters, bed loads and suspend particles were collected through dry and wet season from a small drainage catchment (161 km²), Hou-ku River in southwestern Taiwan, to study effects of intense rainfall event (2000 mm/3 days, Typhoon Morakot). Dissolved major/trace elements, hydrogen, oxygen, and strontium isotopes ($^{87}\text{Sr}/^{86}\text{Sr}$ and $\delta^{88}\text{Sr}$) in river waters were measured to investigate changes on chemical and isotopic characteristics after the typhoon events. For a better constrain on the end member compositions, carbonate phases were chemically removed before acid digestion. Radiogenic and stable Sr isotopes in carbonate and residual phases were measured precisely. Dissolved major elements indicates that the watershed was predominated by silicate weathering, but trended toward carbonate weathering after the rainfall. This event causes all elemental concentrations to drop; however, respective element/chloride ratios were increased 2 to 10 folds. High dissolved $^{87}\text{Sr}/^{86}\text{Sr}$ was evident in dry season, but low ratio after the rainfall event. Both carbonate and residual phases show higher radiogenic Sr isotopes in the suspend particles (0.70987 – 0.71043 and 0.72591 – 0.72729, respectively) than the bed loads (0.70954 – 0.71013 and 0.72047 – 0.72134, respectively). Stable Sr isotopes show no significant variation ($\delta^{88}\text{Sr} = 0.24 - 0.31 \text{ ‰}$) after the event. However, all solids show lower $\delta^{88}\text{Sr}$ (0.05 – 0.17 ‰) than the river waters, preferential leached of heavier Sr. In summary, the extreme rainfall event did not alter Sr isotopes ($^{87}\text{Sr}/^{86}\text{Sr}$ and $\delta^{88}\text{Sr}$) in river waters; contain higher stable isotopes than the associated sediments.

Mg isotopes: Insights into weathering in a tropical volcanoclastic regolith

M. CHAPELA LARA^{1*}, H.L. BUSS¹,
P.A.E. POGGE VON STRANDMANN²,
C. DESSERT³ AND J. GAILLARDET³

¹School of Earth Sciences, Univ. of Bristol, Bristol BS8 1RJ, UK (*correspondence: M.ChapelaLara@bristol.ac.uk, h.buss@bristol.ac.uk)

²Dept. of Earth Sciences, Univ. of Oxford, Oxford OX1 3AN, UK (philipvs@earth.ox.ac.uk)

³Institut de Physique du Globe de Paris, 75252 Paris Cedex 05 France (dessert@ipgp.fr, gaillard@ipgp.fr)

Mg is an important constituent of silicates and a major nutrient and its stable isotopes have been shown to fractionate during geochemical and biological reactions. Mg isotope ratios therefore hold promise as a useful tracer of (bio)geochemical processes in the critical zone. We present preliminary results on the Mg isotopic composition of porewater and stream water (baseflow and stormflow), along with elemental data from depth profiles (1.0 - 9.3 m) in bulk regolith and exchangeable cations taken at 4 sites along a topo-sequence in a well-constrained catchment over volcanoclastic bedrock at the Luquillo Critical Zone Observatory, Puerto Rico.

Mg and K concentrations corrected for rain input and evapotranspiration indicate weathering contributions to pore water solutes. Pore water concentrations are relatively invariant with time below 0.5 m depth (2.0 m depth in the deepest profile). Above these depths, Mg concentrations vary in space and time, with all profiles showing overall higher concentrations in the surface layers, suggestive of biological influence. In contrast, $\delta^{26}\text{Mg}$ values in the deepest profile show a clear trend towards heavier $\delta^{26}\text{Mg}$ with increasing depth (-0.83‰ to -0.18‰) suggesting mixing between atmospheric Mg at the surface and a dissolving, isotopically heavier phase at depth. An excursion towards heavier $\delta^{26}\text{Mg}$ at the soil-saprolite interface (-0.7‰, ~1m depth) indicates a change in controlling processes. A similar heavy excursion is present at the same depth in 3 of the 4 profiles.

Stream water at baseflow is isotopically heavier than the pore waters and becomes progressively lighter with increasing stage. These results may indicate that watershed export of Mg is dominated by deep-weathering processes during baseflow with contributions from rain and shallow soils during storms.

First Finding of Picrobasaltic Melts on Iturup Island, Kurile Island Arc

I. CHAPLYGIN, I. SOLOVOVA AND M. YUDOVSKAYA

Institute of Geology of Ore Deposits (IGEM RAS), 109117
Moscow, Russia (maiya@igem.ru)

Basaltic magmatism occurs extensively in the Kurile island arc, but more magnesian magmas (picrobasalts) were not previously reported. The subvolcanic picrobasaltic massif of Ksenolitnaya Cove, Iturup Island, contains xenoliths of olivine with rare clinopyroxene crystals. Primary melt inclusions were found in olivine from both the xenoliths and their host rock. The inclusions are surrounded by decrepitation haloes. Melting of daughter phases in the melt inclusions was observed at 1170–1225°C. The inclusions in the xenoliths and rock have similar compositions with low SiO₂ (up to 45 wt %) and high MgO (up to 12 wt %), CaO (up to 17.5 wt %), H₂O (≥1 wt %), F (up to 0.3 wt %) and P₂O₅ (up to 0.4 wt %). A comparison of the whole-rock compositions of basic volcanics from the Kurile island arc and the obtained data for melt inclusions suggests that extremely primitive mantle melts with very high CaO contents were trapped in the inclusions. The similarity of major- and trace-element characteristics and temperatures of olivine-hosted melt inclusions from the picrobasalts and xenoliths suggests a cumulate origin of the latter during the crystallization of a primary mantle melt in a magma chamber.

This study was supported by the Russian Foundation for Basic Research and the Russian Program for the Support of Leading Scientific Schools.

Strontium isotopes map fluid flow in a natural CO₂ Reservoir, Green River, Utah, USA

HAZEL CHAPMAN^{1*}, NIKO KAMPMAN¹, MIKE BICKLE¹,
ANDREAS BUSCH² AND JAMES P EVANS³

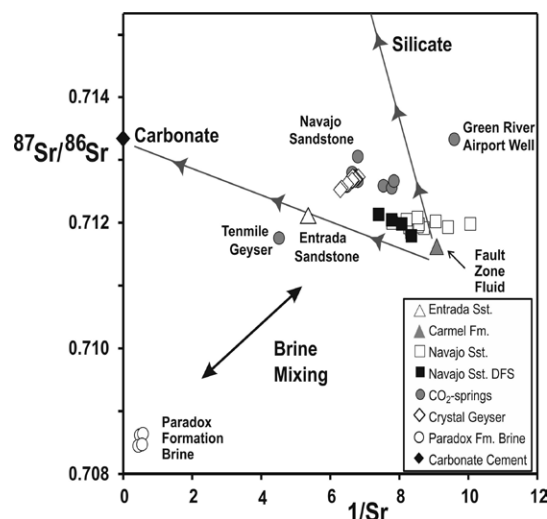
¹ Department of Earth Sciences, University of Cambridge,
Downing Street, Cambridge CB2 3EQ, UK
(*correspondence: hjc1000@cam.ac.uk)

² Shell Global Solutions International, Kessler Park 1, 2288
GS Rijswijk, The Netherlands

³ Department of Geology, Utah State University, 4505 Old
Main Hill Logan, UT 84322-4505

Strontium isotopes offer a powerful constraint in the study of subsurface fluids and are used here to map fluid transport in a natural CO₂ reservoir adjacent to a cold water CO₂-geyser and a CO₂-leaking extensional fault at Little Grand Wash, at Green River in Utah.

The strontium isotopic ratios with associated chemical data in this sequence of porous sandstone layers with intervening caprocks are used to constrain the CO₂-charged fluid sources, fluid-fluid mixing and mineral reactions caused by CO₂ migration within the fault damage zone. Carbonate and silicate fractions have been analysed in Wingate, Kayenta, Navajo and Entrada sandstones, gypsum rich layers, the low permeable Carmel caprocks and shale bands within the Entrada Sandstone. The mixing trends from deep brine, sandstone reservoirs and shale-rich cap-rock are well illustrated by 1/Sr versus ⁸⁷Sr/⁸⁶Sr ratios. The mineralogical changes enhance the sealing properties of cap-rocks for underground storage.



Molybdenum speciation and distribution in ancient euxinic shales by μ XRF and μ XANES spectroscopy

ANTHONY CHAPPAZ^{1*}, JEFFREY P. FITTS²
AND TAIS W. DAHL³

¹Institute for Great Lakes Research – Dep. of Earth and Atmospheric Sciences, Central Michigan University, Mount Pleasant, MI 48859, USA

²Department of Civil & Environmental Engineering, Princeton University, Princeton, NJ 08544, USA

³Natural History Museum of Denmark, University of Copenhagen, DK1350 Copenhagen, Denmark.

Molybdenum is a redox sensitive metal used to investigate oxygen content in ancient oceans from sedimentary records. Specifically, Mo enrichment, Mo/TOC ratio and ⁹⁸Mo-isotopic signature in black shales are determined to characterize euxinic deposition, seawater Mo concentration, and global ocean oxygenation, respectively. However, these approaches are based on bulk rock analyses without a comprehensive understanding of chemical burial pathway(s). Here, we bridge this gap using μ -XRF and μ -XANES to investigate Mo speciation and distribution in drill core samples from the ~500 Ma Alum shale formation.

The Mo distribution in our shale samples demonstrates a homogenous enrichment (~100 ppm) relative to average upper crust (~1 ppm), superimposed by enrichments in 0.1 mm thick lenses within certain sedimentary lamina. The μ -XRF elemental maps show a consistent correlation of Mo and Fe abundance and that Mo-rich lenses are particularly poor in Rb (e.g. clay minerals) and Br (e.g. organic matter). However, the apparent decoupling between Mo and organic matter in the lenses is tentative and needs further validation. The Mo speciation was determined using μ XANES spectra and compared to bulk XANES analyses of modern euxinic sediments where two types of Mo compounds were identified: Mo(IV)-S and Mo(VI)-O [1]. In our samples the Mo-rich lenses host both species, while the matrix contains only the Mo(IV)-S compound.

The Mo-Fe association is consistent with our previous study showing that both Mo species display an Fe atom in the second or third shell. Further, the reduced Mo(IV)-S compounds appear to be pristine precipitates from Cambrian seawater, whereas post-depositional oxidation cannot be ruled out for the oxidized Mo(VI)-O species. Conclusively, the pristine Mo(IV)-S in the matrix may serve as better targets for paleoredox investigations relative to bulk rock analysis.

[1] Dahl *et al.* (2013) *GCA* **103** 213-231, [2] Helz *et al.* (1996) *GCA* **60** 3631-3662

Trace-gas measurements in firn and ice cores using CRDS instruments

J. CHAPPELLAZ^{1*}

¹LGGE/CNRS, BP 96, 38402 St Martin d'Hères, France

(*correspondence : jerome@lgge.obs.ujf-grenoble.fr)

Ice cores and polar firn air provide a unique means to reconstruct polar temperature as well as atmospheric composition changes. They notably help to understand the feedbacks at work between natural climate variability and biogeochemical cycles controlling the atmospheric composition.

The iconic curves of greenhouse gas (CO₂, CH₄, N₂O) concentration changes over the last 800,000 years have been produced through painstaking discrete measurements over years of laboratory work. Stable isotopic ratios of the three greenhouse gases (used to better understand the causes of greenhouse gas concentration changes) are also investigated through discrete measurements. They typically require a full day work in the laboratory for acquiring one or two data points, and they are still far from reaching the time span and resolution of mixing ratio measurements.

Since four years, the availability of Cavity Ring-Down Spectroscopy (CRDS) instruments with enough sensitivity and precision for ice core applications, has largely changed the way firn air and ice core samples are handled. I will show and discuss the results recently obtained on firn air measured in the field and on different ice cores, the latter combining a continuous-flow analysis (CFA) extraction technique and a CRDS instrument, using either WS-CRDS (Picarro) or OF-CEAS (SARA) technology. Clear advantages of these new analytical settings are : speed of measurements, instrumental precision, saving of raw material, compatibility with field work, resolution of fine features along the core. But as with any new technique, there are drawbacks. Notably the difficulty to obtain accurate measurements with the coupled CFA-CRDS setup (calibration with discrete measurements is still needed), and the smoothing and possible drift of the CFA system.

I will also provide a short review on our current developments at the interface between laser physics and ice core / paleoclimate applications. This concerns the OF-CEAS measurements of trace-gas isotopic ratios, as well as an embedded OF-CEAS spectrometer for real-time *in situ* measurements of water isotopes and greenhouse gases inside an ice sheet.

Thermodynamic study of monoclinic pyrrhotite in equilibrium with pyrite by solid-state galvanic cell technique

DMITRIY A. CHAREEV*¹ AND EVGENIY G. OSADCHII¹

¹ Institute of Experimental Mineralogy, Russian Academy of Sciences, Chernogolovka, Moscow District, 142432 Russia (*correspondence: chareev@iem.ac.ru)

The reaction $7\text{FeS}_2(\text{cr}) + 12\text{Ag}(\text{cr}) = 8\text{Fe}_{0.875}\text{S}(\text{cr}) + 6\text{Ag}_2\text{S}(\text{cr})$ was studied by measuring the temperature dependence of the electromotive force (EMF) of the all-solid-state galvanic cell with common gas space:



The measurements were carried out in the flow of argon at atmospheric pressure, and AgI was used as a solid electrolyte. As a result of the measurements of EMF as a function of temperature the nonlinear trend was obtained which characterize the equilibrium monoclinic pyrrhotite + pyrite (mpo+py). For these measurements, the lower temperature limit (490 K) corresponds to the equilibrium pyrite+metallic silver (EMF=0); and the upper temperature limit of linear part (565 K) is determined by the temperature of monoclinic pyrrhotite decomposition. From linear low temperature experimental results of this study and literature data for Ag_2S , the temperature dependence of the gaseous sulfur activity was determined in pyrite+monoclinic pyrrhotite (mpo+py) equilibrium:

$$\log f_{\text{S}_2}(\text{mpo+py}) = 14.08 - 14406 \cdot T^{-1}, \\ (490 < T/\text{K} < 565).$$

Radium Isotopes as Tracers of Boundary Exchange Processes Along the US GEOTRACES North Atlantic Zonal Transect

M.A. CHARETTE¹, P.J. MORRIS¹², W.J. JENKINS¹, P.B. HENDERSON¹ AND W.S. MOORE²

¹Department of Marine Chemistry and Geochemistry, Woods Hole Oceanographic Institution, Woods Hole, MA 02543 USA

²Present address: School of Earth Sciences, University of Bristol, Bristol, BS8 1RJ, UK

³Department of Earth and Ocean Sciences, University of South Carolina, Columbia, SC 29208 USA

Radium isotopes are produced in sediments via the decay of thorium isotopes and are generally soluble in seawater. As such, the radium quartet (^{224}Ra , ^{223}Ra , ^{228}Ra , ^{226}Ra) has been used as tracers of ocean boundary inputs and mixing processes. We measured radium isotopes on the US GEOTRACES North Atlantic cruises in 2010 and 2011, which crossed a number of key ocean boundary features including the Mediterranean outflow, the Mauritanian upwelling and oxygen minimum zones (OMZ) along western Africa, a hydrothermal plume over the mid-Atlantic Ridge (MAR), and the broad continental margin of the northeastern US. Radium isotope features at these locations will be discussed in the context of their potential to quantify fluxes of trace elements and isotopes (TEIs) from common sources. Notable observations include: (1) evidence of substantial sediment-water interaction in the benthic boundary layer along the OMZ, (2) decoupling between ^{223}Ra and the other Ra isotopes over the MAR, and (3) significant continental inputs (e.g. submarine groundwater discharge) in the western Atlantic. Finally, we present results from an upper ocean 2-D mixing model based on our ^{228}Ra data along the OMZ, which can form the basis for interpreting the dissolved and particulate iron cycle in this region.

Compositional variability of ultramafic lavas on Mercury: Implications for surface mineralogy and mantle sources

B. CHARLIER^{1,2}, O. NAMUR² AND T.L. GROVE¹

¹EAPS, Massachusetts Institute of Technology, Cambridge, MA 02139, USA

²Institut für Mineralogie, Universität Hannover, Callinstrasse 3, 30167 Hannover, Germany

Measurements of major element ratios obtained by the MESSENGER spacecraft using x-ray fluorescence spectra are used to calculate absolute element abundances of lavas at the surface of Mercury. We discuss calculation methods and assumptions that take into account the distribution of major elements between silicate, metal, and sulfide components and the potential occurrence of sulfide minerals under reduced conditions. Available compositional data for the northern volcanic plains and for intercrater plains and heavily cratered terrain display significant variations although they share common silica- and magnesium-rich characteristics (basaltic komatiites to komatiites). The inferred mineralogy at Mercury's surface should be dominated by orthopyroxene, plagioclase, minor olivine if any, clinopyroxene (augite), and tridymite. Two compositional groups are distinguished based on mineral components, particularly by the presence or absence of clinopyroxene. Melting experiments at one atmosphere demonstrate that these compositional groups cannot be simply related to each other by any fractional crystallization process, suggesting differentiated source compositions and implying multi-stage differentiation and remelting processes for Mercury. Magma ocean crystallization followed by adiabatic decompression of mantle layers during cumulate overturn and/or convection would have produced adequate conditions to explain surface compositions. Thus, the surface of Mercury is not an unmodified quenched crust of primordial bulk planetary composition. Ultramafic lavas from Mercury have high liquidus temperatures (1450-1350 °C) and very low viscosities, in accordance with the eruption style characterized by flooding of pre-existing impact craters by lava and absence of central volcanoes.

New tricks with old tracers: Sr stable isotope variations in an evolved volcanic system investigated using an ⁸⁴Sr-⁸⁷Sr double spike

B.L.A. CHARLIER^{*1}, I.J. PARKINSON² AND C.J.N. WILSON^{3,1}

Dept. Phys. Sci., The Open University, Milton Keynes, UK.

(*correspondence: bruce.charlier@open.ac.uk)

²School of Earth Sciences, University of Bristol, UK.

(ian.parkinson@bristol.ac.uk)

³SGEES, Victoria University of Wellington, New Zealand

(colin.wilson@vuw.ac.nz)

Strontium is a refractory lithophile element with four stable isotopes, ⁸⁴Sr, ⁸⁶Sr, ⁸⁷Sr and ⁸⁸Sr. However, ⁸⁷Sr is also produced by the long-lived radioactive decay of ⁸⁷Rb, and this parent-daughter isotope system has long been a key pillar of geochronology and geochemical tracing. Conventional Sr isotopic measurements made using TIMS or MC-ICP-MS are corrected for instrumental mass fractionation assuming a value for the ⁸⁸Sr/⁸⁶Sr ratio of 8.375209. This internal normalisation permits the measurement of ⁸⁷Sr/⁸⁶Sr ratios to a very high precision. However, normalisation to a fixed ⁸⁸Sr/⁸⁶Sr ratio using a mass-dependent fractionation law assumes that the stable isotope ratio is uniform in natural samples and erases the possible signature of any mass-dependent natural variation in the ⁸⁸Sr/⁸⁶Sr and ⁸⁴Sr/⁸⁶Sr ratios. In this study, we present high-precision Sr stable and radiogenic isotope data (determined using a double spike and TIMS) along with trace element data for a suite of samples from a single evolved volcanic system (Huckleberry Ridge Tuff, Yellowstone). Strontium stable isotope values vary by up to ~0.5 ‰ and correlate well with Ba and Eu/Eu* variations in whole rocks and glass separates. Our data suggest that crystallisation of sanidine (± plagioclase) and/or mixing of melts that have experienced such fractionation is the main driver for the stable isotope variations. Sr-isotopic studies on volcanic rocks require re-evaluation.

Paleo-denudation rates at the Plio-pleistocene transition from *in situ*-produced cosmogenic ^{10}Be : Method and new results from the Tianshan and the Himalayas

J. CHARREAU¹, N. PUCHOL¹, P.-H. BLARD¹, R. PIK¹, R. BRAUCHER², L. LEANNI², D. BOURLES², J. LAVE¹ AND O. BEYSSAC³

¹CRPG-CNRS, BP 20, 54501, Vandoeuvre les Nancy, FRANCE (charreau@crpg.cnrs-nancy.fr)

²Aix-Marseille Université, CNRS-IRD UM 34 CEREGE, Aix-en-Provence, France, (bourles@cerege.fr)

³IMPMC, cc115, 75005 Paris, FRANCE (olivier.beyssac@impmc.upmc.fr)

Denudation that controls the mass transfer from the uplifting highlands to the lowlands basin and links climate and tectonics is a key factor governing the evolution of the Earth's surface. Quantitative records of past denudation rates are therefore critical, especially at the Plio-pleistocene transition, when the onset of Quaternary glaciations may have enhanced worldwide denudation rates.

To independently reconstruct denudation rates from sedimentary archives, we applied an innovative approach based on the analyses of *in situ*-produced cosmogenic ^{10}Be in ancient sediments. A pioneer study carried out in the Northern Tianshan (Central Asia) has shown a possible transient, from 4 to 2 Ma, increase in denudation rate in the drainage basin [1]. Continuing this work, we present here new cosmogenic paleo-denudation records from four different locations: three from both sides of the Tianshan range and one from the Surai section, in the Siwaliks (the southern piedmont of the Himalayas). While all these records have displayed local, and sometimes significant, variations of denudation rates since ~10 Ma, they do not show synchronous increase in denudation at the Plio-Pleistocene transition. These results challenge the paradigm of a worldwide increase in denudation rates that would be induced by the Quaternary climate variability.

Thanks to independent constraints: paleoelevation from oxygen and carbon isotopic records of paleosol carbonates, source tracking using new Raman spectra of graphite particles in the Surai section, the inherent uncertainties of the method were reduced. However, a critical step is now to understand how the material is transferred to the basin and what are the main factors that control the distribution of current denudation.

[1] Charreau *et al.*, *EPSL*, 2011

Deglacial trends in the oxygen content of intermediate waters in the southwest Pacific

ZANNA CHASE*¹, ASHLEY TOWNSEND², HELEN BOSTOCK³ AND HELEN NEIL³

¹Institute for Marine and Antarctic Studies, University of Tasmania, 7000, Australia (*correspondence: Zanna.Chase@utas.edu.au)

²Central Science Laboratory, University of Tasmania, 7000, Australia (Ashley.Townsend@utas.edu.au)

³National Institute of Water and Atmospheric Research, Wellington 6421, New Zealand (Helen.Bostock@niwa.co.nz; Helen.Neil@niwa.co.nz)

Intermediate waters of the Southern Ocean – Antarctic Intermediate Water (AAIW) and Subantarctic Mode Water (SAMW) – ventilate a large portion of the intermediate depths of the ocean. They are important in the uptake of carbon dioxide from the atmosphere and they transport nutrients and oxygen to the low latitude thermocline. These processes are sensitive to climate change. Indeed, observations between 1970 and 1990 show that Southern Ocean intermediate waters have experienced the largest decrease in oxygen of any ocean region, driven by a decrease in the exchange of water between the surface and the interior [1].

Here we use redox sensitive trace metals to examine the response of intermediate water oxygenation to the most recent deglacial warming. Excess Re, U and Mn records from cores bathed by Antarctic Intermediate Water on the Campbell Plateau (700 – 1200 m), southeast of New Zealand, suggest an increase in bottom water oxygen during the deglaciation. This trend is consistent with a rapid increase in benthic foraminiferal $\delta^{13}\text{C}$ at the start of the deglaciation at intermediate depth in the northern Tasman Sea, suggesting a ventilation event [2]. In contrast, redox-sensitive metals from the Chile margin, near the present-day locus of maximum AAIW production, indicate a decrease in intermediate water oxygenation upon deglaciation, a trend that has been interpreted to reflect a deglacial decrease in AAIW ventilation [3]. This presentation will examine intermediate water records from both sides of the Pacific in an effort to untangle the influences of biological productivity, ventilation and circulation.

[1] Helm *et al.* (2011), *Geophys. Res. Lett.* **38**, doi:10.1029/2011GL049513. [2] Bostock *et al.* (2004), *Paleoceanography* **19** doi:10.1029/2004PA001047. [3] Muratli *et al.* (2010). *Nature Geoscience* **3**, 23–26.

Contrasted iron-speciation in obsidians and tektites: A spectroscopic study

CHASSÉ, M.^{1*}, GALOISY, L.¹, LELONG, G.¹
AND CALAS, G.¹

¹Institut de Minéralogie et de Physique des Milieux Condensés (IMPMC), UPMC; 4, Place Jussieu, 75252 Paris Cedex 05, France.

(*correspondence : mathieu.chasse@impmc.upmc.fr)

Iron has long been known to play an important role in determining the properties of natural magmatic liquids. The determination of the sites occupied by ferrous and ferric cations in volcanic glasses may provide information on the physico-chemical conditions prevailing at the magmatic stage as well as on the cooling conditions of the magma. We discuss Fe speciation in calc-alkaline rhyolitic glasses (obsidians) and tektites, using optical absorption spectroscopy (OAS) and electron paramagnetic resonance (EPR). In obsidian, OAS reveals a major contribution of Fe²⁺ in a regular octahedral site, an unusual environment in synthetic glasses and tektites where this cation is mostly 4- and 5-coordinated [1], [2].

The presence of Fe-oxide nano-clusters, suspected since a long time from previous EPR studies [3], is confirmed by variable-temperature OAS in all obsidians investigated. By contrast, tektites do not show such contribution. Specific absorption bands, assigned to Fe-Fe and Fe-Ti intervalence charge transfers (IVCT), are characterized by a spectacular intensity dependence as a function of temperature over 1000 K (1000K-10K). This thermally-activated behavior shows an activation energy similar to that observed for IVCT in various minerals. The evidence of specific Fe²⁺ sites and of IVCT processes, indicate the presence of Fe-oxide clusters. These clusters, showing a local re-arrangement around Fe, are related to the cooling history of the glass, as they are not found in the medium range structure of synthetic glasses [4]. The existence of these clusters and their nature seem to be related to the conditions of formation of the investigated obsidians and they may clarify the information brought by these glasses about its magmatic history.

[1] S. Rossano *et al.* (1999) *Phys. Chem. Minerals*, **26**(6) : 530–538. [2] L. Galois *et al.* (2001) *Chem. Geol.*, **174**(1-3) : 307–319. [3] G. Calas & J. Petiau (1983) *Bull. Minéral.*, **106**(1-2) : 33–55. [4] C. Weigel *et al.* (2008) *Phys. Rev. B*, **78**(6) : 064202.

Thermodynamics and Kinetics of Fe(II)-Fe(III) Electron Transfer Across Interfaces

S. CHATMAN¹, P. ZARZYCKI², S. KERISIT¹,
V. ALEXANDROV¹, C.I. PEARCE¹ AND K.M. ROSSO^{1*}

¹Pacific Northwest National Laboratory, Richland WA, USA
(*correspondence: kevin.rosso@pnl.gov)

²Polish Academy of Sciences, Warsaw, Poland

Fe(II)-Fe(III) electron transfer is a key exchange in the biogeochemical cycle of iron. For most environmentally relevant conditions this exchange involves interaction between soluble ferrous iron and solid-phase iron (oxyhydr)oxides, with possible involvement of electrical conduction through the solid-state. This presentation addresses global thermodynamic limits and molecular-scale controls on the kinetics of this exchange from selected observations and simulations of Fe(II) interaction with hematite, goethite, and magnetite.

Single crystal single surface potentiometry and amperometry on hematite were used to examine the pH-dependence of surface electrical potential, the kinetics of protonation/deprotonation, and current flow from one crystallographic face to another, examining the effect of aqueous Fe(II) addition. The data reveal a pH-dependent energy band model with the iron redox couple in solution that is compatible with the magnitude and direction of face-to-face Fe(II)/Fe(III) current flow through the semiconductor bulk. Despite structural distinctions, in a similar fashion Fe(II) interaction with Fe_{3-x}Ti_xO₄ nanoparticles at various amounts of pre-oxidation shows a reversible topotactic Fe(II) uptake and release consistent with surface deprotonation and protonation, respectively. Synchrotron Fe L-edge x-ray absorption and magnetic circular dichroism spectroscopies are used to map Fe site occupancy and valence before and after pre-oxidation and Fe(II) recharge. Molecular simulations of Fe(II) adsorption and subsequent interfacial electron transfer with Fe(III) at hematite and goethite surfaces reveal the importance of surface net charge, the protonation state of bridging ligands, and proton coupled electron transfer to facilitate the electron exchange into the solid. Aspects covered will include thermodynamic energy requirements for bulk crystal conduction, including heat dissipation in the solid, and possible free energy sources sustaining bulk currents, Fe(II) adsorption energies and the kinetics of electron injection, and the structural dependence of Fe(II)-Fe(III) electron exchange through the crystal lattice, towards a new, more comprehensive mechanistic model for these systems.

Geochemical signatures of volcanic rocks from Kadiri greenstone belt, Dharwar craton, India: Implications on gold mineralisation

ADRIJA, CHATTERJEE^{1*}, LINGAMURTY, E¹,
RAJANIKANTA SINGH, M¹ AND MANIKYAMBA, C¹.

¹[National Geophysical Research Institute (Council of Scientific and Industrial Research)

Uppal Road, Hyderabad 500 606,

(adrija.geo@gmail.com, elmgeology@gmail.com)

(rajanikumtum@gmail.com), (cmaningri@gmail.com)

The Neoproterozoic Hutti-Jonnagiri-Kadiri-Kolar composite greenstone terrane is the largest (~500km) unique belt with abundant gold mineralisation which is being mined at Hutti. Kadiri greenstone belt is situated in the south central part of this largest arcuate belt, consisting of a variety of island arc volcanic rocks such as arc basalts, Nb-enriched basalts, adakites, dacites and rhyolites resembling with Phanerozoic intraoceanic island arc volcanic rocks. In this linear belt, north of Kadiri, plume-arc accretionary processes have been established at Jonnagiri belt.

Arc basalts of Kadiri have moderate SiO₂ and MgO with slightly enriched LREE and flat HREE. Nb-enriched basalts resemble with arc basalts with high Nb content (7-10 ppm). Adakites of Kadiri have elevated Al₂O₃ (12-16 wt%), low Yb (0.77-1.25 ppm) with high (La/Yb)_N (14.6-33.9 ppm), Zr/Sm (14-50) and low Nb/Ta (5.4-16.9) with positive Eu anomalies.

The enrichment of gold at the northern (Hutti) and southern end (Kolar) of this composite greenstone terrane with the occurrence of intraoceanic island arc rocks at Kadiri belt reflect on the island arc processes which appear to have deposited gold at Hutti and Kolar due to suitable structure and lithological conduits at these places. These plume-arc interaction also explains the crustal growth due to subduction accretion in the eastern Dharwar craton.

Nd-Hf isotopic composition of the upper continental crust

C. CHAUVEL¹, M. GARÇON¹, S. BUREAU¹, S. GALLET²
AND B.M. JAHN³

¹ISTerre, Grenoble, France; (catherine.chauvel@ujf-grenoble.fr)

²Geoazur, Nice, France

³Institute of Earth Sciences, Taiwan

Knowledge of the average composition of the upper continental crust is crucial to establish not only how it formed but also when. While well constrained averages have been suggested for its major+trace element composition (e.g., Taylor and McLennan, 1985; Rudnick and Gao, 2003), no value exists for its Nd and Hf isotopic compositions even though radiogenic isotopic systems provide valuable information on its average model age.

Here we present Nd and Hf isotopic data determined on a large number of loess deposits from several continents. We demonstrate that these deposits have very uniform Nd and Hf isotopic compositions and that these data can be used to establish an average Nd-Hf isotopic composition for the upper continental crust: $\epsilon_{Nd} = -10.3 \pm 1.2$ and $\epsilon_{Hf} = -13.2 \pm 2$. This average falls on the Terrestrial Array as defined by Vervoort *et al.* (1999, 2011) demonstrating that the two parent-daughter ratios are not decoupled during crust formation. Trace element data acquired on the same set of samples allow us to calculate an average ¹⁴⁷Sm/¹⁴⁴Nd ratio for the upper continental crust: 0.1193±0.0026, a value slightly higher than previous estimates. We estimate the average Nd extraction age of upper continental crust from the depleted mantle at $T_{DM}(Nd) = 1.82 \pm 0.07$ Ga. This model age is entirely consistent with previous suggestions made for example by Goldstein *et al.* in 1984.

Assuming that the Hf model age of the upper continental crust cannot be younger than its Nd model age, we can suggest a value for the very poorly known ¹⁷⁶Lu/¹⁷⁷Hf ratio of the upper crust. Our estimate is ¹⁷⁶Lu/¹⁷⁷Hf = 0.0125±0.0005, a value significantly lower than commonly used values (0.0150 - 0.0159; Griffin *et al.* 2002, Goodge & Vervoort 2006, Hawkesworth *et al.* 2010) but higher than the Rudnick & Gao estimate (0.0083). Using our preferred value, the average Hf upper crust differentiation age is about 300 Ma younger than when using a ratio of 0.0159. The impact of our new ¹⁷⁶Lu/¹⁷⁷Hf ratio on crustal model ages of zircon populations is not simple to evaluate in detail but the Hf model ages calculated with this new Lu/Hf ratio could be younger by up to 500 Ma.

The halogen cycle in subduction zones: Insight from back-arc basin basalts

D. CHAVRIT^{1*}, L. RUZIE¹, R. BURGESS¹, D.R. HILTON²,
H. SUMINO³, J. SINTON⁴ AND C.J. BALLENTINE¹

¹S.E.A.E.S., University of Manchester, Manchester, UK

(*presenting author, deborah.chavrit@manchester.ac.uk)

²Scripps Institution of Oceanography, La Jolla, USA

³GCRC, University of Tokyo, Tokyo 113-0033, Japan

⁴University of Hawaii, Honolulu, USA

The extent to which the subduction process preserves the volatile elements signature of the downgoing slab and the mechanisms by which these elements are transferred into the mantle wedge are not well understood. Halogens (Cl, Br, I) are good candidates to trace these processes, due to their incompatibility and their relatively high concentrations in seawater and marine sediments. A technique developed at the University of Manchester [1] allows the high precision measurements of these elements on neutron-irradiated samples using noble gas mass spectrometry.

To better constrain the cycle of halogens in subduction zones, we analyzed the halogens in 15 volcanic glasses (BABB) from three back-arc basins which are known to contain slab-derived components *viz* Manus basin, Lau basin and Mariana trough.

The three back-arc basins have relatively constant Br/Cl weight ratios ($4.0 \pm 0.4 \times 10^{-3}$) which are 2x higher than the mid-ocean ridge basalts (MORB) value [2]. The I/Cl weight ratios (0.9 to 7.1×10^{-5}) range from values close to seawater to MORB values. These results suggest that the halogen composition of the BABB mantle source is affected by a slab-derived component. However, the I/Cl ratios positively correlate with Ba/Nb ratios that are between 5-33 (weight), which reflect the extent of the slab contribution. Thus, it indicates the presence of an unknown end member with a MORB-like Ba/Nb ratio and with low I/Cl and high Br/Cl ratios. It is notable that the halogen ratios of this component are similar to that of the fluid phases trapped in altered oceanic crust [3]. Another component with higher Ba/Nb, higher I/Cl and lower Br/Cl ratios, is consistent with the presence of a sedimentary-derived component. The possible origins of the signature of the halogen BABB mantle source will be discussed by comparing with the different components characterizing the subducted oceanic crust.

[1] Johnson *et al.* (2000), *GCA* **64**, 717-732; [2] Ruzié *et al.* (2012), V31A-2762 AGU Fall Meeting; [3] Chavrit *et al.* (2012), *Mineral. Mag.* **76** (6), 1566.

A new approach for LA-ICP-MS using a high sensitive mass spectrometer

R. CHEMNITZER^{1*} AND M. HAMESTER¹

¹Bruker Daltonik GmbH, Fahrenheitstr. 4, 28359 Bremen, Germany

(*correspondence: Rene.Chemnitzer@bruker.com),
(Meike.Hamester@bdal.de)

The geochemical characterization of samples includes the elemental distribution but also the isotopic composition for a broad range of elements. Laserablation coupled to an ICP-MS has become an indispensable method. New instrumental developments allow resolutions to single-digit μm spots and new ablation cells show improved transport characteristics.

With a high sensitive ICP-MS (Bruker auroraElite) these developments lead to a tremendous increase in information. The work presents results from a LA-ICP-MS setup that provides the highest sensitivity currently available and shows results of the quantitative and isotope ratio analysis of zircon samples and other minerals.

Different parameters were investigated:

Laser

- Spot size (Laser)
- Energy density

ICP-MS

- Sample introduction / plasma
- 3-D ion focusing
- Scan speed

The results verify that the considerable higher sensitivity leads to new alternative approaches in LA-ICP-MS, that will be discussed in detail.

Si isotope systematics of acidic alteration of fresh Kilauean basalts

S. M. CHEMTOB^{1,2*}, G. R. ROSSMAN², E. D. YOUNG³,
K. ZIEGLER⁴, J. M. EILER² AND J. A. HUROWITZ⁵

¹Washington University, St. Louis, MO

(*correspondence: chemtob@levee.wustl.edu)

²California Institute of Technology, Pasadena, CA; ³UCLA, Los Angeles, CA; ⁴U. New Mexico, Inst. of Meteoritics, Albuquerque, NM; ⁵Jet Propulsion Lab, Caltech.

Silicon isotopes are fractionated by low-temperature aqueous processes, making them potentially useful as a weathering proxy. Previous authors have reported that secondary minerals like clays and opal are lower in ³⁰Si/²⁸Si than the dissolved reservoirs from which they precipitated [1-2]. Young basalts from Kilauea, on the big island of Hawai'i, frequently feature opaque amorphous silica coatings, 2-80 μm thick, that form *in situ*, apparently by acidic surface leaching [3]. Here we show that, in contrast to secondary minerals in other settings, these coatings have higher δ³⁰Si than their basaltic substrate (which is presumed to be the source of Si in the surficial solutions from which the coatings precipitate).

Silica coated basalt samples were collected from 1974 and 1998 flows along Kilauea's East and Southwest Rift Zones. We removed the coating material by scraping and then dissolved it in dilute HF and HNO₃ [4]. The resulting solutions were purified by ion-exchange chromatography and analyzed by MC-ICP-MS. Basalt glasses had δ³⁰Si = -0.10 to -0.24‰; silica coatings had δ³⁰Si = +0.92 to 1.36‰. These isotopic compositions are difficult to reconcile with previously reported fractionation factors (i.e. Δ³⁰Si_{solid-aqueous} < 0‰). We hypothesize that the atypical direction of fractionation is a result of unusual aqueous Si speciation (e.g. fluoride, chloride and/or sulfate complexation).

Batch experiments in which fresh glassy basalt gravel was reacted in HCl or HF (0.1 or 1 M) at 60° C replicated Hawaiian amorphous silica layer morphology. The fluids preferentially mobilized Al, Mg, Fe, Na, and Ca, leaving behind amorphous silica residues up to 100 μm thick. In HCl-bearing experiments, reacted fluids were ³⁰Si-enriched (up to δ³⁰Si = 2.29‰). HF-bearing experiments produced ²⁸Si-enriched fluids, suggesting preferential incorporation of ³⁰Si into precipitated silica or volatilization of ³⁰Si. These results indicate that fluid chemistry influences the direction and magnitude of Si isotope fractionation during weathering.

[1] Georg *et al.* (2007), *EPSL* **261**, 476-490. [2] Milligan *et al.* (2004) *Limnol. Oceanogr.* **49**, 322-329. [3] Chemtob *et al.* (2010), *JGR* **115**, 2009JE003473. [4] Ziegler *et al.* (2010) *EPSL* **295**, 487-496.

First Tritium-Helium Dating Results of Groundwater in Central Taiwan

AI-TI CHEN¹ TSANYAO FRANK YANG¹
TSUNG-KWEI LIU¹ YUJI SANO² NAOTO TAKAHATA²
KUAN-YU CHEN³ AND YUNSHUEN WANG⁴

¹ Department of Geosciences, National Taiwan University, Taipei, Taiwan, R.O.C.

² Department of Chemical Oceanography, Atmosphere and Ocean Research Institute, The University of Tokyo, Tokyo 164-8639, Japan

³ Industrial Technology Research Institute, Taipei, Taiwan, R.O.C.

⁴ Central Geological Survey, MOEA, Taipei, Taiwan, R.O.C.

We applied Tritium-Helium (T-He) dating method (Clarke *et al.*, 1976), for the first time, to obtain the ages of groundwater from central part of Taiwan as a case study. The groundwater wells are located on the recharge area of Jhoshui river basin and Beigang River. Three groundwater samples have been collected from different monitoring wells, which are artificial and all around 100 meters deep, and the altitude of them are less than 402 meters. Samples sent to University of Utah and University of Tokyo for further T-He dating analysis. We could obtain total helium-3 concentrations in groundwater samples, although they might contain different signatures other than radiogenic source from tritium decay. In order to obtain the radiogenic helium-3 concentration, we needed to eliminate helium-3 concentrations of air-saturated water and terrigenous source in spite of air contamination. In this study, we can successfully separate the radiogenic source of helium-3 from terrigenous (crustal) source, assuming no air contamination for the studied samples. After helium-3 corrections, we can obtain the age results ca. 7-25 years, which are consistent with each other from the analysis results of two independent labs. The result suggests that the T-He dating technique could be a good method for determining the age of young groundwater in Taiwan.

Origin of highly differentiated granites from South China: Implications for W-Sn deposits

B. CHEN*, X.H. MA AND Z.Q. WANG

School of Earth and Space Sciences, Peking University,
Beijing 100871, China,
(binchen@pku.edu.cn) (*presenting author)

Voluminous composite granite plutons occur in South China, accompanied by large-scale W-Sn deposits. Each composite pluton is composed of major phase granites and highly evolved late-stage granites. Traditionally, the late-stage granites are thought to be residual melts from the former via fractionation, and ore-forming materials and fluids are from granite magma itself. We propose a different model for the origin of highly evolved granites and related W-Sn mineralization, based on studies on the Qianlishan composite plutons that are composed of major phase coarse-grained biotite granites (163 Ma) and late-stage fine-grained granites (153 Ma). The major phase granites show features of normal granites, with LREE enrichment and medium negative Eu anomalies in the chondrite-normalized REE patterns. The late-stage granites are highly evolved, with non-CHARAC trace element features (very high K/Ba, and low K/Rb and Zr/Hf), and show HREE enrichment, huge negative Eu anomalies and typical “tetrad effect” in the REE patterns. We suggest that the late-stage granites were unlikely derivatives from the major phase granites via fractionation, but rather, derived from melting of the Proterozoic lower crust in a new tectono-thermal event, triggered by underplating of basaltic magma. Small amounts of basalts were involved in the source, as suggested by the higher $\epsilon_{Nd}(t)$ values of the late-stage granites (-5.6 to -7) than the major phase granites ($\epsilon_{Nd}(t) = -8$). The late-stage granites show common occurrence of ilmenite, euhedral quartz enclosed in feldspar, and interstitial fluorite, suggesting a low fO_2 , water-deficient and fluorine-rich feature for them. Addition of fluorine would significantly lower the solidus temperature and viscosity of magma, and thus prolong the process of magma evolution and facilitate fractional crystallization. Prolonged magma process would (1) enhance the interaction between granitic melt and meteoric water from country rocks, causing the formation of “tetrad effect” of REE patterns and non-CHARAC trace element features of the late-stage granites, and (2) heat and drive the circulation of meteoric water that subsequently, together with fluorine, extract ore-forming materials from country rocks through complexation, forming skarn-type W-Sn deposits in Ca-rich country rocks. So, the W-Sn deposits were genetically linked with the highly evolved granites.

Synthesis, toxicity and reactivity of several types of NZVI

JIawei CHEN

State Key Laboratory of Geological Process and Mineral Resources, China University of Geosciences, Beijing 100083, China.
Email(chenjiawei@cugb.edu.cn)

An emerging technology for the treatment of contaminated land and water is the use of nano-scale zero-valent iron (here after NZVI), which can rapidly dechlorinate chlorinated organics or immobilize heavy metals in contaminated groundwater [1-5]. The field demonstrations of applying nano-Fe⁰ technology for source remediation are promising.

Here, we report synthetic methods, surface property modification, mobility, toxicity and reactivity of several types of NZVI. These materials include commercial NZVI, fresh-made NZVI, NZVI supported on clay minerals, NZVI coated by CMC. It showed different bactericidal activity of these NZVI to *Escherichia coli*. The reactivity of these materials was also compared for Cr(VI) reduction and TCE degradation. Besides batch experiments and column test, in-situ remediation in a big sand-box was performed for iron and NZVI.

We paid more attention to the effects of pH, natural organic matter and ageing time on the reaction systems. During the process of water-pollutant-NZVI interaction, the different performance of several types of NZVI inferred that particle surface property is very crucial to NZVI application. Cost-efficient and long-term useful NZVI should be addressed more in the future.

This study was supported by Fundamental Research Funds for the Central Universities (2010ZD14, 2012123), China Geological Survey (1212011120288) and National Program of Control and Treatment of Water Pollution (2009ZX07424-002).

[1] Zhang, WX. (2003) *Journal of Nanoparticle Research* **5** (3-4): 323-332. [2] Lowry GV. (2005) *Environmental Science & Technology* **39** (5): 1338-1345. [3] Kanel, SR. (2006) *Environmental Science & Technology* **40** (6): 2045-2050. [4] Zhao DY. (2007) *Water Research* **41** (10): 2101-2108. [5] Chen JW. (2011) *Water Research* **45** (5): 1995-2001

Petrogenesis and geochronology of the Xilushan granitic complex in the Bengbu Uplift: Constraint on the timing of the Yanshan Movement

JIE CHEN XIANG WANG* AND XIAOJUN WANG

State Key Laboratory for Mineral Deposit Research, Nanjing University, Nanjing 210093, China
(* correspondence: xwang@nju.edu.cn)

The Xilushan granitic complex in the Bengbu Uplift, southeastern margin of the North China Block (NCB), consists of a gneissic monzogranite and a porphyritic granodiorite.

The gneissic monzogranite shows fracturing, deformation and anatectic textures, indicating it has suffered post-crystallization migmatization. It contains mainly two zircon phases: igneous zircon (IZ) and metamorphic zircon (MZ). IZ shows strong CL brightness and clear oscillatory zoning, and its contents of Hf, U, Th and REE are comparatively low. It yields a weighted mean age of 223.6 ± 2.9 Ma, representing the intrusion age of the gneissic monzogranite. MZ shows extremely weak CL brightness, weak to absent oscillatory zoning, and its contents of Hf, U, Th and REE are high and variable. It yields a weighted mean age of 156.1 ± 2 Ma, and this age is interpreted as representing the climax of compressional orogenesis of the Yanshan Movement.

The porphyritic granodiorite has low abundances of HREE and Y, high contents of Sr and resulting high Sr/Y ratios, reflecting that the magma derived from partial melting of the base of the thickened lower crust. It plots in the field of post-orogenic granite in the Rb vs. (Y+Yb) discrimination diagram. The zircon from this rock is generally of magmatic origin, showing strong CL brightness, fine-scale oscillatory zoning and developed sector zoning, and relatively low contents of Hf, U, Th and REE. It has a weighted mean age of 133.6 ± 1.3 Ma, considered to be the onset time of the post-orogenic calc-alkaline magmatism of the Yanshan Movement.

According to the two ages of metamorphic and magmatic events revealed by the Xilushan complex and the previous studies on the tectonics in the NCB, the Yanshanian movement in the NCB can be divided into three successively evolutionary periods: (1) Compressional orogenesis period (180-156 Ma); (2) Stress transformation period (156-135 Ma); (3) Extensional collapse period (135-125 Ma).

Iron isotopes in the suspended load of the Seine River (France): natural versus anthropogenic sources

JIUBIN CHEN^{1,2}, VINCENT BUSIGNY²,
JÉRÔME GAILLARDET² AND PASCALE LOUVAT²

¹ State Key Laboratory of Environmental Geochemistry, Institute of Geochemistry, CAS, Guiyang 550002, China.
² Institut de Physique du Globe de Paris, Sorbonne Paris Cité, Univ. UMR 7154 CNRS, 75238 Paris, France

The determination of fluxes and isotope compositions of Fe transported to the ocean is essential for understanding global surface Fe cycle. Fe isotope composition in anthropogenically-impacted rivers is poorly constrained up to now. We present the first Fe isotope data in suspended particulate matter (SPM) of the Seine River (France). Iron concentrations and isotope compositions (also major and trace elements) were measured for two sample sets: a geographic transect along the river to estuary, and a temporal series collected in Paris. While Fe concentration in SPM clearly increases downstream, Fe isotope composition shows a very slight decrease ($\delta^{56}\text{Fe}$ from 0.10 to -0.07%). Calculation of Fe enrichment factor relative to Al points to the anthropogenic input ($\sim 17\%$ higher than the natural background). Correlations between Fe concentration and isotopic compositions with those of Zn (from a previous study) confirm that Fe is mainly derived from a mixing of natural and anthropogenic sources. The natural sources are dominantly composed of clay materials, with minor carbonates and heavy minerals. Sulfides and organic matter may be the main anthropogenic Fe phases, and dominate during low-water and high-water stages, respectively.

Our data have two major implications. Firstly, although Fe flux from continents to ocean is significantly increased after anthropogenic input, polluted rivers bring a Fe isotope signature essentially indistinguishable from the natural detrital Fe flux. Secondly, the markedly positive $\delta^{56}\text{Fe}$ values measured in the Pacific Ocean (up to 0.6%), which contrast with the mostly negative (or 0%) $\delta^{56}\text{Fe}$ values in Fe sources to the ocean (hydrothermalism, rivers, marine benthic Fe flux, atmospheric particles), are unlikely to be produced by anthropogenic Fe input, supporting the explanation of Fe isotope fractionation related to phytoplankton assimilation processes.

Seawater derived sulfur contributions to the Archean VMS deposits: Multi-sulfur isotope evidences from the Neo-Archean Jaguar Deposits, Western Australia

M. CHEN^{1,2}, I. CAMPBELL^{2*}, Y. XUE², W. TIAN¹
AND T.R. IRELAND²

1. SESS, Peking Univ., Beijing, China (mmchen@pku.edu.cn)
2. RSES, Australian National Univ., Canberra, ACT 0200, Australia (*correspondence: ian.campbell@anu.edu.au)

The contributions of seawater sulfate to Archean VMS deposits remain equivocal; do they resemble modern seawater in the role of contributing sulfur to modern black smokers? Additionally, in magnitude, how much sulfur seawater can contribute to form an Archean VMS deposit?

Seawater sulfate plays a key role in modern black smoker systems. Estimations based on MDF $\delta^{34}\text{S}$ of sulfur isotope are typically ranging from 10% to 40%, or even up to 80% [1, 2]. While for Archean VMS deposits, which have been widely believed to be the analogous of modern black smokers, the seawater contributions have been under-estimated. One case study in the Kidd Creek shows a small contribution of seawater sulfate down to ~3%, and this value therefore implies a very low seawater sulfur concentration [3]. For further investigation, we report *in situ* SHRIMP SI multi-sulfur isotopic analyses (^{32}S ^{33}S ^{34}S) of pyrites from Jaguar VMS deposits in the Yilgan Craton, Western Australia. Taking MIF $\Delta^{33}\text{S}$ features of ore sulfides as the mixing of magmatic sulfur and reduced seawater sulfate, we estimate the quantity of seawater contribution to the sulfur budget of Jaguar VMS deposits. The estimated result is 16%-21%, much higher than 3% in Kidd Creek case. Samples from other reported Archean VMS deposits, including Dresser formation, Agnew-Wiluna belt and Alexo greenstone belt, are also quantitatively assessed. The assessment reveals that the magnitude of seawater sulfate contribution to Archean VMS deposits can be as much as that of modern sea-floor hydrothermal systems, while the case of Kidd Creek cannot represent a global-scale event for understanding the seawater derived sulfur contributions to Archean VMS deposits.

- [1] Ono et al (2007) *Geochim Cosmochim Acta* **71**, 1170-1182.
[2] Peters et al (2010) *Chem Geol* **269**, 180-196. [3] Jamieson et al (2013) *Nat Geosci* **6**, 61-64.

From diagenesis to metagenesis, geochemical changes of the late Paleozoic shale and mudstone, periphery of Songliao basin

SHUWANG CHEN^{1*}

¹ Shenyang Center of Geological Survey, CGS, China
(presenting author: sycswgeology@163.com)

With wide spread area of dark shale and mudstone occurred in the peripheral area of Songliao basin, NE China, the late Paleozoic terrane with abundant organic material has been considered as important target strata to evaluate regional potential of shale gas resources. How about the maturity of this shale and mudstone and what is the main factor to control it is more debatable. The contact metamorphism about the strata associated with the Mesozoic igneous activity is in the focus of this study, funded by China Geological Survey.

The shale and mudstone samples of outcrop and drill from different distance to the belt of contact metamorphism were collected. The intrusive and volcanic samples related to the Mesozoic activity were also collected. Analysis about the shale and mudstone are mainly of R_o , illite crystallinity, TOC and the content of absorbent gas. Analysis about the related Mesozoic igneous bodies includes the mineral manometer and the fluid inclusions.

All evidence indicates that contact metamorphism is an important factor to control the maturity of the shale and mudstone. Statistics of the analysis data of R_o and illite crystallinity indicates that the maturity ranges from diagenesis to metagenesis. The mineral manometer combined with homogenization temperature of fluid inclusions shows that some Mesozoic intrusive bodies characterized as hot sources have high crystallization temperature and great emplacement depth, while the others characterized as warm point have low crystallization temperature and low emplacement depth. The contact belt related to the hot intrusive bodies always presents as large scale and high metamorphism degree, while the belt related to cool intrusive bodies presents as small scale and low degree. The contact belt presents as small scale and low metamorphism degree associated with the Mesozoic volcanic eruption. The late Paleozoic shale and mudstone away from hot intrusive bodies and covered with Mesozoic volcanic rocks always possess catagenesis to diagenesis of maturity and have high TOC and high content of absorbent gas.

Late Quaternary Nd-Hf isotope evolution of the Weddell Sea and the abyssal Southern Ocean

TIAN-YU CHEN¹, MARTIN FRANK¹, RAINER GERSONDE²
AND ANNE OSBORNE¹

¹ GEOMAR Helmholtz Centre for Ocean Research Kiel,
Germany

² Alfred Wegener Institute for Polar and Marine Research,
Bremerhaven, Germany.

The Southern Ocean deep circulation has played a critical role in regulating the atmospheric CO₂ concentration over glacial-interglacial time scales. While Nd and Hf isotopes have been demonstrated to be effective tracers of water mass circulation and continental weathering inputs to the deep ocean, relatively little is known about glacial-interglacial Hf isotopic evolution in Southern Ocean or the Nd isotope evolution of waters fully bathed in Antarctic bottom water. We present Nd-Hf isotope time series from the Weddell Sea margin (PS1388-3, water depth 2526 m) and abyssal Southern Ocean (PS2082-1, water depth 4610 m, abyssal Agulhas Basin) over the last 250 kyr in order to better understand the deep circulation and weathering inputs.

Nd isotope signatures of sediment leachates of PS2082-1 are consistent with previously published records from the neighboring Cape Basin revealing less radiogenic signatures in interglacials and more radiogenic signatures in glacial. However, ϵ_{Nd} values of the last glacial maximum (LGM) in the Agulhas Basin are systematically more radiogenic by about $\sim 0.7 \epsilon_{Nd}$ units than the Cape Basin records, which may imply a higher Pacific contribution. In contrast, Hf isotope signatures of the same leachates show an opposite evolution trend compared with Nd isotopes (i.e., less radiogenic in glacial), implying the Hf isotopes may be controlled by high southern latitude weathering regime changes. All PS2082 leachate data of Nd-Hf isotopes are within the seawater data range constrained by surface scrapings of Fe-Mn nodules and modern seawater from the Southern Ocean, supporting a seawater origin for the leachate Nd and Hf isotope signatures.

Surprisingly, Nd isotope compositions of PS1388-3 leachates have nearly invariant signatures (ϵ_{Nd} : ~ -12.0) over glacial-interglacial times and are much less radiogenic than the abyssal Southern Ocean, while the Hf isotopes show radiogenic peaks ($\epsilon_{Hf} > +8.0$) after deglaciations. The results indicate that these signatures have been controlled by Antarctic weathering inputs, while dissolution of fresh surfaces of minerals with high Lu/Hf after deglaciations may explain the radiogenic Hf peaks.

Pb isotope evidence from the Oka carbonatite complex for a distinct mantle reservoir

WEI CHEN^{1*} AND ANTONIO SIMONETTI¹

¹ Department of Civil & Environmental Engineering & Earth Sciences, 156 Fitzpatrick Hall, University of Notre Dame, Notre Dame IN, 46556 USA

(*correspondence: wchen2@nd.edu; simonetti.3@nd.edu)

Pb isotope data from young (<200 Ma-old) carbonatite complexes plot well within the fields defined by present-day mid-ocean ridge basalts (MORBs) and oceanic island basalts (OIBs). Thus, one interpretation is that carbonatites are derived from similar mantle components (i.e., HIMU, EMI, EMII, DMM) sampled by modern oceanic basalts. Here, we report new in-situ Pb isotopic data for calcite, nepheline, and melilite from various rocks types associated with the Oka carbonatite complex (Québec, Canada). Linear trends observed in Pb vs. Pb isotope diagrams (e.g., Fig. 1) reflect open-system behavior involving mixing of at least two distinct mantle reservoirs. However, the unradiogenic ²⁰⁷Pb/²⁰⁴Pb and ²⁰⁸Pb/²⁰⁴Pb ratios for given ²⁰⁶Pb/²⁰⁴Pb values (e.g., Fig. 1) for Oka and associated alkaline rocks from the Monteregean Igneous Province (MIP) are distinct, and point to the involvement of an unidentified (depleted) mantle reservoir. This unradiogenic ²⁰⁷Pb/²⁰⁴Pb isotopic composition may be attributed to U/Pb fractionation early in Earth's history. Moreover, in-situ Sr and Nd isotope compositions for apatite from Oka overlap those for basalts derived from "FOZO", which suggests derivation from a deep mantle source.

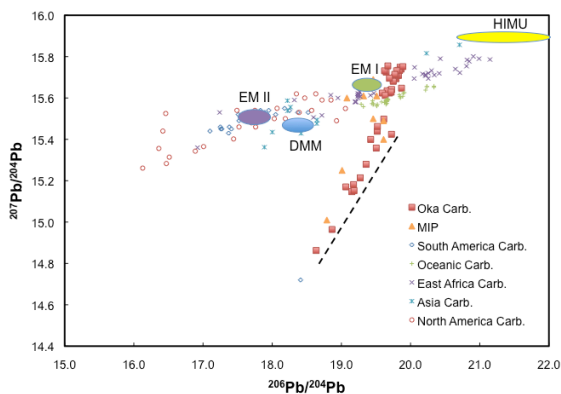


Figure 1 Pb isotope ratios for Oka and MIP intrusions.

Ultrasensitive portable multiple laser continuous-wave cavity-ringdown spectrometer for CH₄ isotope analysis

Y. CHEN¹, K.K. LEHMANN², P. MAHAFFY³, V. HOLMES³
P. MOREY³ AND T. C. ONSTOTT¹

¹ Princeton University, Dept. Of Geosciences, Princeton, NJ 08544, USA

² University of Virginia, Dept. of Chemistry, Charlottesville, VA, 22904, USA

³ NASA's Goddard Space Flight Center, Greenbelt, MD 20771, USA

A portable NIR CW-CRD spectrometer was developed for stable isotope analyses of atmospheric CH₄ on Earth and Mars. The system consists of three DFB Laser diodes, two of which are tuned to the absorption peaks of ¹²CH₄ and ¹³CH₄ and the third of which is used to measure the baseline. A MEMS optical switch rapidly alternates the lasers feeding the cavity to measure absorbance of these two isotopic molecules of CH₄. This measurement scheme avoids the high uncertainty data usually measured when the wavelength being tuned at waist of absorption line shape and overcomes partially the long-term drifting of the traditional CRDS system, thus fulfilling the high precision requirement for isotope analysis of trace gas methane. The detection limit of this system is to 1.4x10⁻¹² cm⁻¹ with integration time of 5 minutes. For ambient air on Earth which contains 1.8ppm CH₄, under 100 torr pressure, the ¹³CH₄ absorbance is 1.8x10⁻⁹cm⁻¹, thus the equivalent precision of the δ¹³C will be less than one per mil for CH₄ in the atmospheric concentration.

Keyword, CW-CRDS, Isotopic ratio, Methane, greenhouse gas

The structural analysis of Dunhua basin, China

S.Y.CHENG¹ AND Y.J. LI²

¹School of Earth Sciences and Resources, Chang'an University, Xi'an,710054,Shaanxi Province, China (chengsanyou@126.com)

²Shaanxi Provincial Research Academy of Environmental Science, Xi'an,710061,Shaanxi Province, China (hkyliyingjie@126.com)

By means of two dimensional structure-stratigraphy interpretation of several seismic profiles and magnetic and gravity data, the paper analyzed the structural features and forming mechanism of Dunhua basin.

The results show that Dunhua basin perform as the two east-west trend fault depressions, the uplift between the fault depressions and the controlling normal faults were intersected with Dunmi fracture in an acute angle, and the Dunmi main fracture also formed a deep fault depression. Consequently the northern fault depression and southern fault depression that are the two east-west trend fault depressions, are all typical dextral strike-slip and extension basins in which major strike-slip fault is the Dunmi fracture.

The seismic data shows that the Dunmi deep fault depression developed a large number normal faults that obliquely with the Dunmi fracture within the Lower Cretaceous stratum. Dextral strike-slip faulting began in Early Cretaceous, and the fault depressions were happened again in Paleogene. According to interpretation of the gravity and magnetic section, Dunhua basin was transformed by thrust fault between Cretaceous and Neogene, and the main thrust direction pointed to the north. The thrusting may be associated with tectonic inversion after the late Cretaceous in the northeast area, China, which resulted in sinistral transpression along the Dunmi fracture.

This work was financially supported by the National Natural Science Foundation of China (41073027) and the Special Fund for Basic Scientific Research of Central Colleges, Chang'an University (CHD2012JC 073).

Living in soil pores: physical and nutritional constraints for microbial decomposers of soil organic matter

CHENU C.¹, NUNAN N.¹, JUAREZ S.¹, MOYANO F.¹,
RUAMPS L.¹, OTTEN W.², SCHMIDT S.², GARNIER P.³
AND MONGA O.⁴

¹ AgroParisTech, CNRS, UMR Bioemco, 78850 Thiverval Grignon, France (chenu@grignon.inra.fr)

² Symbios, Univ Abertay, Dundee, UK

³ INRA UMR EGC, 78850 Thiverval Grignon, France

⁴ IRD UMMISCO, Cameroun.

Soil microorganisms live in a complex 3-D framework which can cause a variety of micro-environments to develop that are more or less suitable for microbial growth, activity and survival. In particular, the soil pore system controls the accessibility of substrates and oxygen to microorganisms and the local moisture conditions. Experiments, in which the location of microorganisms and substrates and the soil structure were manipulated, showed how the heterotrophic soil respiration depended on the size of pores and on their connectivity. In turn we show how microorganisms may change substrate diffusivity at the scale of their habitat, by exuding EPS. In all, characteristics of the habitat seem to have more impact on heterotrophic respiration than microbial community structure. We present innovative models explicitly representing soil structure and how microhabitats control the activity of microorganisms and hence the fluxes of C in soil.

Geophysical evidences for eclogites beneath the West Siberian basin

YULIA CHEREPANOVA^{1*} AND IRINA M. ARTEMIEVA¹

¹Oester Voldgade 10, DK-1350, Copenhagen, Denmark,
(*correspondence: yc@geo.ku.dk)

The West Siberian basin is the world's largest intracontinental sedimentary basin. Its basement is formed through a number of collisional and accretional events during late Proterozoic-Paleozoic. The amalgamation, completed in the late Permian, was followed by a large-scale rifting and eruption of flood basalts in the Permian-early Triassic (ca 250 Ma). Active subsidence of the basin started in late Triassic with the main event only in Jurassic [1].

The West Siberian basin lacks surface topography, whereas the reliefs of the Moho and the top of the basement have amplitudes of ca. 20 km and 15 km, respectively [2]. The near-zero free air gravity over the basin indicates that it is in the isostatic equilibrium.

Assuming no effect of dynamic topography on basin subsidence, we examine the relative contributions of the crust and the lithospheric mantle to maintaining the surface topography. Lithosphere buoyancy is controlled by thicknesses and densities of the crust and the lithospheric mantle, composition, metamorphic state, and temperature. Crustal thickness and density are constrained by our new regional crustal model SibCrust, which is based on all existing seismic data [2]. Lithosphere thickness and temperature are constrained by the thermal model TC1 [3]. Our modelling shows large high-density anomaly (3.5 – 3.65 g/cm³) in the upper mantle below the axial part of the basin along the major rift. This result is supported by the seismic velocity variation in the mantle along four ultra-deep reflection/refraction PNE profiles and by stretching factor. We propose that high density body in the mantle is caused by eclogitization and its presence can explain a substantial part of the subsidence of the West Siberian Basin.

[1] Vyssotski *et al.* (2005), *Marine and petr. geol.* **23**, 93-126;
[2] Cherepanova *et al.*, *Tectonophysics*, in press; [3] Artemieva and Mooney (2001), *J. Geophys. Res.*, v.**106**, 16387-16414.

$^{238}\text{U}/^{235}\text{U}$ variations in high- and low-temperature uranium deposits

I.V. CHERNYSHEV*, V.N. GOLUBE,
A.V. CHUGAEV AND A.N. BARANOVA

IGEM of Russ. Acad. of Sciences, Moscow 119017,
Staromonetny per., 35 (cher@igem.ru)

$^{238}\text{U}/^{235}\text{U}$ ratio was analysed by high-precision MC-ICP-MS method using ^{233}U - ^{236}U double spike. Double spike was prepared from monoisotopes ^{233}U and ^{236}U and calibrated relative to CRM-112A standard in which $^{238}\text{U}/^{235}\text{U}$ value was accepted as 137.844 ± 24 according to [1]. Long-term reproducibility ($\pm 2\text{SD}$) of $^{238}\text{U}/^{235}\text{U}$ results estimated for three reference samples (total 87 analyses) is better than 0.07‰.

High-T U-deposits from some regions previously dated by U-Pb method were involved in this study. 1) Transbaikalia, Russia: the Streltsovsky, Otyabrsky and Antei deposits in volcanogenic Streltsovsky ore field (Mz); the Khadatkanda skarn deposit (Pz). 2) Erzgebirge, Germany: the Schlemma-Alberoda granite-related deposit (Pz). 3) Tyan-Shan, Uzbekistan: the Chauli volcanogenic deposit (Pz). 4) Athabaska Basin, Canada: the Shea Creek and McArthur “unconformity” deposits (Prz). 5) Cage district, Canada: uraninite ore showing (Prz).

$^{238}\text{U}/^{235}\text{U}$ ratio was measured in pitchblende (more rarely in uraninite and coffinite) local microsamples of 10-50 μg weight separated directly from polished sections. $^{238}\text{U}/^{235}\text{U}$ values for listed deposits (total 44 analysed samples) yield 137.710-137.828 interval (i.e. 0.86‰) which only in part coincides with range for zircons 137.772-137.908 [2]. At the same time the individual deposits display 0.12-0.70‰ variations. Owing to analyses of local microsamples the distinctions of $^{238}\text{U}/^{235}\text{U}$ ratio up to 0.45‰ were documented for different pitchblende spherulites growth zones as well as for U-mineral phases formed during different periods of mineralization.

Ore samples from low-T U-deposits of “sandstone” (or “paleo-valley”) type Dybryn and Khiagda (Vitim region, Russia) demonstrated wider range of $^{238}\text{U}/^{235}\text{U}$ values 137.738-137.881 (i.e. 1.0‰) which is statistically “heavier” as compared with high-T U-deposits. This data are in agreement with results obtained for 40 concentrates of “sandstone” type ores from USA, Canada and some other regions [3].

Financial support by RFBR (grant N12-05-01060-a)

[1] Condon *et al.* (2010) *Geochim. Cosmochim. Acta* **74**, 7127-7143. [2] Hiess *et al.* (2012) *Science* **335**, 1610-1614. [3] Brennecka *et al.* (2010) *Earth Planet. Sci. Lett.* **291**, 228-233.

Near-infrared measurements of water speciation in hydrous $\text{Na}_2\text{Si}_2\text{O}_5$ melt using HDAC

NADEZDA CHERTKOVA^{1*}

¹Institute for Study of the Earth’s Interior, Okayama University, Misasa, Japan

(*correspondence: nadezda@misasa.okayama-u.ac.jp)

In situ study of water speciation in silicate melts is important for the construction of water solubility models and prediction of physical properties of hydrous melts at high temperature and high pressure. Water speciation in $\text{Na}_2\text{Si}_2\text{O}_5$ melt (anhydrous NBO/T = 1, structural analogue of basaltic melt) was examined by FTIR spectroscopy in an externally heated diamond anvil cell (HDAC) [1]. Hydrous $\text{Na}_2\text{Si}_2\text{O}_5$ glass, containing up to 5.9 wt% water, was used as starting material without any additional pressure medium. Experimental pressure was monitored with the pressure- and temperature-dependent Raman shift of ^{13}C diamond [2].

At temperatures above 650 °C and at pressures above 1.6 GPa only a homogeneous melt phase was observed (Fig. 1a). Near-infrared spectra of this phase contain absorption peaks corresponding to molecular H_2O (at $\sim 5200\text{ cm}^{-1}$) and structurally bound OH groups (at $\sim 4500\text{ cm}^{-1}$). Assuming a constant ratio of molar absorptivities for these bands and knowing the total water content in the melt, concentrations of water species are estimated to be 2.0 wt% as molecular H_2O and 3.9 wt% as OH groups at 800 °C and 2 GPa.

Comparison of the OH/ H_2O ratio in the quenched glasses at ambient conditions and in the melts at high temperature shows significant increase of OH species concentration with temperature. At this point, it is difficult to evaluate the effect of pressure on water speciation.

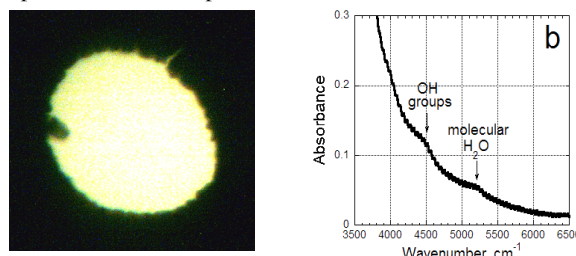


Fig. 1: (a) Sample chamber of HDAC with hydrous $\text{Na}_2\text{Si}_2\text{O}_5$ melt (5.9 wt% water) and ^{13}C diamond pressure marker.

(b) Near-infrared absorption spectrum of the melt at 800 °C.

[1] Bassett *et al.* (1993) *Rev. Sci. Instr.* **64**, 2340-2345. [2] Mysen & Yamashita (2010) *Geoch. Cos. Acta* **74**, 4577-4588.

Chemical composition of Changjiang river sediments: Climate or lithology control?

B. CHETELAT¹, C-Q. LIU¹, Q. WANG¹ AND G. ZHANG¹

¹SKLEG, Institute of Geochemistry, CAS, 46 Guanshui Road, 550002 Guiyang, PR of China

We present major and trace elements data in particulate suspended matter (SPM) collected in the Changjiang main channel and its main tributaries. Suspended sediments are derived from a mafic source related to the Emeishan Large Igneous Province (ELIP) in the Upper Reach and from a more felsic source in the Middle/Lower Reaches. The difference in chemical composition between the two sources has a strong influence on the apparent weathering intensity. Although the apparent loss of soluble elements follows a climatic gradient from the Upper Reach to the Lower Reach, the co-variation of weathering indices with different proxies for igneous differentiation suggests that a lithologic control can not be ruled out. By taking into account the variability in chemical composition of the parent rocks, we show that river suspended sediments from the upper reach may have not experienced less intense chemical weathering than those transported by rivers from the Lower/Middle Reaches characterized by higher runoff and surface temperature. We argue that the relationships observed for different indices of weathering with climate might be an artifact and are partly driven by the change in chemical composition of the sediments parent-rocks.

U-Pb LA-ICPMS dating of common Pb-bearing accessory minerals using VizualAge / Iolite

D.M. CHEW^{1*}, J.A. PETRUS² AND B.S. KAMBER¹

¹Dept. of Geology, Trinity College Dublin, Dublin 2, Ireland (*correspondence: chewd@tcd.ie, kamberbs@tcd.ie)

²Department of Earth Sciences, Laurentian University, Sudbury, Canada (japetrus@gmail.com)

Precise and accurate U–Pb LA-ICPMS dating of many U-bearing accessory minerals (e.g. apatite, titanite and rutile) is often compromised by common Pb. We present here a general approach to common Pb correction in U–Pb LA-ICP-MS dating using a modified version of the VizualAge [1] U-Pb data reduction package for Iolite [2].

The approach was tested on apatite and titanite age standards (for which there are independent constraints on the U-Pb crystallization age) using a Thermo Scientific iCAP-Qc (Q-ICP-MS) coupled to a Photon Machines Analyte Excite 193 nm ArF Excimer laser. A 50 μm spot was used in all experiments. The Durango (31.44 ± 0.18 Ma) and McClure Mountain (523.51 ± 1.47 Ma) apatite standards yielded U-Pb TW concordia intercept ages of 31.97 ± 0.59 Ma (MSWD = 1.09) and 524.5 ± 3.7 Ma (MSWD = 0.72) respectively. The Fish Canyon Tuff (28.201 ± 0.046 Ma) and Khan (522.2 ± 2.2 Ma) titanite standards yielded U-Pb TW concordia intercept ages of 28.78 ± 0.41 Ma (MSWD = 1.4) and 520.9 ± 3.9 Ma (MSWD = 4.2) respectively, demonstrating the suitability of the common Pb correction approach.

The modified version of VizualAge / Iolite first applies a common Pb correction (using either the ²⁰⁴Pb or ²⁰⁷Pb methods) to the user-selected *age standard* integrations and fits session-wide “model” U–Th–Pb fractionation curves to the time-resolved U-Pb standard data. VizualAge / Iolite then applies this downhole fractionation model to the unknowns and sample-standard bracketing (using a user-specified interpolation method) is used to calculate final isotopic ratios and ages. In addition to live concordia diagrams which allow for visualising of data while adjusting integration intervals [1], the modified version of VizualAge incorporates a ²⁰⁷Pb-corrected age channel calculated for a user-specified initial ²⁰⁷Pb/²⁰⁶Pb ratio. All other conventional common Pb correction methods (e.g. the ²⁰⁴Pb method or intercept ages calculated from linear arrays on a concordia or isochron) can be performed offline.

[1] Petrus & Kamber (2012), *Geostandards and Geoanalytical Research*, 36, 247–270. [2] Paton *et al.* (2011), *Journal of Analytical Atomic Spectrometry*, 26, 2508–2518.

Holocene Marine Reservoir Correction (ΔR) Variability in the Eastern Bay of Bengal

H.-W. CHIANG^{1*}, Y. WANG², J. BRUCE H. SHYU³
C.-C. WANG³, LIN THU AUNG⁴, PHYO MAUNG MAUNG⁵
OO THAN⁵, SOE THURA TUN⁴ AND C.-C. SHEN³

¹Earth Observatory of Singapore, Nanyang Technological University, Singapore (*correspondence: hwchiang@ntu.edu.tw)

²Division of Geological and Planetary Sciences, California Institute of Technology, Pasadena, USA

³Department of Geosciences, National Taiwan University, Taipei, Taiwan, R.O.C.

⁴Myanmar Earthquake Committee, Myanmar Engineering Society, Myanmar

⁵Department of Meteorology and Hydrology, Myanmar

We present the regional marine reservoir corrections (ΔR) for the northeastern Bay of Bengal spanning two time periods, the past 300 years and the mid-Holocene. ΔR values were calculated using paired measurements of MC-ICPMS U-Th dating and AMS ¹⁴C dating on 6 pristine fossil corals from Ramree and Cheduba Islands, western Myanmar.

The results show an average ΔR of 126±43 yr (1 σ , n=3) for 175-278 years before AD 1950, which is significantly higher than the published modern values of 7±35 yr and 29±74 yr from the Andaman Islands [1] and the southeastern Bay of Bengal [2] separately. This ~100yr difference indicates that applying global marine reservoir age directly to younger-than-1000-years coral terraces might introduce errors to the calibrated ages. Our ΔR however is consistent with the mean of 158±68 yr from the western Indian Ocean [2]. It thus suggests the ¹⁴C-depleted deep Indian Ocean water can influence as far east as the western coast of Myanmar; although large amount of fresh water from the Ganges River is believed to greatly reduce the vertical mixture. Less variation in the past 300 yrs inferred no major change in large-scale circulation. In contrast, ΔR dramatically fluctuated during 8.0-6.9 ka BP, from as high as 553±34 yr down to -35±32 yr.

This interval coincided with the period of strong Asian summer monsoon in mid-Holocene. Thus we believe the fluctuated ΔR values are resulted from (1) the stronger upwelling induced by strong monsoon wind and (2) the enhanced ocean-atmosphere gas exchange due to heavy rainfall and surface runoff.

[1] Dutta *et al.* (2001) *Radiocarbon* **43**, 483-488. [2] Southon *et al.* (2002) *Radiocarbon* **44**, 167-180.

Isotopic signature of naturally Cr(VI) contaminated spring waters from Western Tuscany (Italy)

L. CHIARANTINI^{1*}, S. AGOSTINI¹, I. BANESCHI¹,
M. GUIDI¹, C. NATALI¹, S. TONARINI¹ AND R. FREI²

¹CNR-Istituto di Geoscienze e Georisorse, Pisa, Italy

(*correspondence: laura.chiarantini@igg.cnr.it)

²Institute of Geography and Geology, University of Copenhagen (robertf@geo.ku.dk)

Weathering of serpentinites produces soils and sediments with high Cr concentrations. High Cr (VI) contents (up to 50 $\mu\text{g/l}$) have also been found in some spring waters spilling out from serpentinite bodies that outcrop in Western Tuscany. A section of a multidisciplinary research program (RESPIRA) is aimed to enhance the understanding of serpentinite rocks weathering processes in order to assess the mobility and bioavailability of Cr. Petrographic and mineral-chemical analyses of both rocks and soil samples highlight the occurrence of minerals able to release Cr (III) containing significant Cr amounts, such as chlorites (Cr_2O_3 up to 8 wt%). The absence of Mn-oxides, permitting to rapid oxidise Cr(III), implies that local presence of Cr (VI) in waters have to be ascribed to other processes.

Sr-Pb isotopes of serpentinites suggest an interaction with recent, low-T, waters, whereas most soils display larger Sr-Pb isotopic ranges indicating a significant contribution of both elements from crustal sedimentary rocks. All spring waters display Mg-HCO₃ chemical composition and a Sr-Pb isotopic signature fitting within the serpentinites and soils range.

Cr isotopes are generally used to investigate Cr(VI) reduction occurred in contaminated ground waters, during biotic and abiotic processes, which produces a strong positive fractionation of residual unreduced Cr(VI) as well as a powerful tool for to reconstruct the redox state of ancient sea water. Nevertheless, little is know about fractionation effects accompanying Cr (III) oxidation although little positive fractionation has been experimentally demonstrated. The spring waters preliminary investigated for Cr isotopes are strongly positively fractionated ($\delta^{53}\text{Cr}$ values between +1 and +3‰) as observed in other naturally Cr (VI) contaminated ground waters [1]. The observed strong positive fractionation can be the result of both Cr oxidation and partial back reduction of soluble Cr (VI). Further investigations on serpentinite spring waters can contribute to better understand Cr isotopes behaviour during natural Cr redox reactions.

[1] Izbicki *et al.* (2008) *Appl. Geochem* **23**, 1325-1352.

U-Pb geochronology and source constraints for late S-type Variscan magmatism related to Sn-W metallogeny: The Logrosán granite pluton (Central Iberian Zone)

E. CHICHARRO^{1*}, C. VILLASECA²,
P. VALVERDE-VAQUERO³, E. BELOUSOVA⁴
AND J.A. LÓPEZ-GARCÍA¹

- ¹ Department of Crystallography and Mineralogy, Complutense University of Madrid (*correspondence: evachicharro@ucm.es, jangel@ucm.es)
² Department of Petrology and Geochemistry, Complutense University of Madrid (granito@ucm.es)
³ Spanish Geological and Mining Institute (IGME) (p.valverde@igme.es)
⁴ Dpt. Earth and Planetary Sciences, GEMOC, Macquarie University. (ebelouso@els.mq.edu.au)

S-type tin-bearing granites intruded along the Central Iberian Zone (CIZ) during syn- and late-kinematic stages of the Variscan orogeny. The Logrosán cupola belongs to the Central Extremadura Batholith (CEB) which crops out within the epizonal domains of the CIZ. This granitic body intruded the Neoproterozoic Schist-Greywacke Complex (SGC). The Logrosán cupola is a felsic, perphosphoric, and strongly peraluminous (ASI=1.2-2) tin-granite (Sn=11-67 ppm). The most evolved facies are well-exposed in the topographic heights at the centre of the granitic cupola. Major and trace element geochemistry (e.g. CaO, Rb, Sr) shows no fractional crystallization trends suggesting the input of felsic batches derived from a deeper magma reservoir. Besides, the Sr-Nd and Hf isotopic signatures indicate that the Logrosán granite was derived by partial melting of heterogeneous crustal sources (initial ⁸⁷Sr/⁸⁶Sr ratios from 0.7134 to 0.7311; εNd between -4.3 and -4.0 and εHf(t) from 2.0 to -4.6 for Variscan zircons). An age for the granite emplacement of ca. 308 Ma (U-Pb Zrn & Mnz CA-ID-TIMS) indicates that the granite is coeval with other related plutons in the region. U-Pb LA-ICP-MS dating has identified a predominant group of Neoproterozoic inherited zircon with juvenile Hf-isotope composition (εHf up to +14.6; LA-MC-ICPMS data) similar to that of zircons from the SGC. This evidence suggests that the Logrosán granite was partially derived from melting a metasedimentary protolith similar to the Neoproterozoic SGC.

Microaerophilic biological methane cycling 2.6-2.1 billion years ago

ERNEST CHI FRU^{1,2*}, EMMA HAMMARLUND^{2,3},
LAURISS NGOMBI-PEMBA⁴, EMMA ARVESTÅL^{1,2},
STEFAN BENGTSO^{1,2} ABDERRAZZAK EL ALBANI⁴
PER ANDERSSON¹ AND MAGNUS MÖRTH⁵

- ¹ Swedish Museum of Natural History, Department of Palaeobiology.
² Nordic Center for Earth Evolution (NordCEE), Box 50007, SE-105 05 Stockholm, Sweden.
³ Southern University of Denmark, Institute of Biology, Campusvej 55, Dk-5230 Odense M, Denmark.
⁴ Institut de Chimie des Milieux et Matériaux de Poitiers (IC2MP) UMR 7285 CNRS - Université de Poitiers 4, rue Michel Brunet (Bât B27) 86022 Poitiers cedex.
⁵ Baltic Nest Institute Sweden and Department of Geological Sciences, Stockholm University, SE-106 91 Stockholm, Sweden.

We present a new and undescribed biogeochemical mechanism explaining the demise of the Archaean methane greenhouse atmosphere in the palaeoproterozoic using Cu, Fe, C_{org} stable isotope systematics and microbial culture experiments. Based on Cu-Fe chemistry, we infer that oceanic Cu levels, hundreds to thousands of scales above that of modern oceans, orchestrated the transition into a previously unknown Cu-resistant microbial ecosystem after the rise of atmospheric oxygen. The associated Neoproterozoic emergence of Cu-dependent microaerophilic methanotrophy, ~2.8-2.5 Ga, provided a resilient biological filter against continuous catastrophic methane input into the Palaeoatmosphere, between ~2.6-2.1 Ga. Methane oxidation by this process peaked at ~50% increase by ~2.1 Ga, relative to the Neoproterozoic. We propose that microaerophilic Cu-dependent methane oxidation was the second most important process for primary productivity after H₂-driven methanogenesis during the Palaeoproterozoic. It facilitated the accumulation of extremely low d¹³C_{org} isotopic excursions and was intensely active from the start to the end of the Huronian glaciation, facilitating biospheric oxidation.

¹⁵N-Enrichment of amino acids for studying trophic structure and energy flow in food webs

YOSHITO CHIKARAISHI¹ NANAOKO O. OGAWA²MASASHI TSUCHIYA³ AND NAOHIKO OHKOUCHI⁴

Institute of Biogeosciences, Japan Agency for Marine-Earth Science and Technology, Yokosuka, JAPAN,

¹(ychikaraishi@jamstec.go.jp), ²(nanaogawa@jamstec.go.jp), ³(tsuchiyam@jamstec.go.jp), ⁴(nohkouchi@jamstec.go.jp),

To better understand the trophic linkages and energy flow in complex networks of ecosystems, we recently have employed compound-specific stable isotope analysis (CSIA) of amino acids as a relatively new tool. In particular, the CSIA has been used to estimate trophic position (TP) among animal species, using a following equation:

$$TP = [(\delta^{15}N_{Glu} - \delta^{15}N_{Phe} + \beta)/TEF] + 1$$

where β represents the isotopic difference between glutamic acid and phenylalanine in aquatic algae (-3.4‰), and C3 ($+8.4\text{‰}$) and C4 higher plants (-0.4‰), and TEF represents trophic enrichment factor ($7.6\text{‰} = \Delta\delta^{15}N_{Glu} - \Delta\delta^{15}N_{Phe}$) at each shift of trophic level (Chikaraishi *et al.*, 2010). By using this CSIA, the estimation error on the TP has been suggested to be 0.12 unit as 1σ for aquatic (Chikaraishi *et al.*, 2009) and 0.17 for terrestrial environments (Chikaraishi *et al.*, 2011). Thus the CSIA of amino acids potentially reduces the uncertainty on the TP estimates compared to the traditional bulk isotope method by approximately 1/10 or more.

However, the validity of such estimates is dependent on the consistency of both β and TEF values. In the presentation, we will discuss whether the β value is universal among different producers and also whether the TEF value scales with trophic level, based on the experimental results for a number of organisms in our study and previously published literatures.

[1]Chikaraishi *et al.*, 2009. *Limnol. Oceanogr.: Meth.* **7**, 740-750. [2] Chikaraishi *et al.*, 2010. In: Ohkouchi *et al.* (Eds.), *Earth, Life, and Isotopes*, Kyoto University Press, pp. 37-51. [4] Chikaraishi *et al.*, 2011. *Ecol. Res.* **26**, 835-844.

CO₂ and advective heat fluxes in central Apennine, Italy

CHIODINI G.¹, CARDELLINI C.², CALIRO S.¹, FRONDINI F.² AND CHIARABBA C.³

¹INGV, sezione di Napoli, giovanni.chiodini@ov.ingv.it

²Università di Perugia, (carlo.cardellini@unipg.it)

³INGV, CNT-Roma, (claudio.chiarabba@ingv.it)

Carbon dioxide Earth degassing process affecting the Apennine belt was quantified on the base of the carbon mass balance of the regional aquifers. The deeply derived CO₂ resulted in $\sim 2\text{-}2.5 \times 10^{11}$ mol/a that represents $\sim 10\%$ of the estimated present-day total CO₂ discharge from the sub aerial volcanoes of the Earth. The groundwaters enriched in CO₂ systematically display a slight temperature anomaly, which becomes significant when the differences between the water temperatures at the springs and the temperature of corresponding recharging meteoric waters are compared. These temperature differences, together with the hydrogeologic parameters of the different aquifers, have been used to compute the total amount of heat by geothermal warming which results of $\sim 2.1 \times 10^9$ J/s. This geothermal warming implies heat fluxes higher than 300 mW/m² in a large sector of the Apennines, i.e. values in average higher than those affecting the famous geothermal provinces of Tuscany and Latium. This finding is in some way surprising because so far the central Apennines is though to be a cold area. This high heat and CO₂ flux opens a new vision of the Apennines belt and requires the existence, at depth, of a thermal and fluid source such as a large magmatic intrusion. Recent tomographic images of the area confirm the presence of such intrusion visible as a broad negative velocity of seismic waves. This study reveals how the investigations based on large groundwaters systems are important for a more reliable estimation of both deep CO₂ and heat fluxes in orogenes.

Entropy and reactive solute transport in porous media

G. CHIOGNA ^{*1}, D. L. HOCHSTETLER ², A. BELLIN ³,
P. K. KITANIDIS ² AND M. ROLLE ^{1,2}

¹ Center for Applied Geoscience, University of Tübingen,
Sigwartstr. 10, 72076 Tübingen, Germany

(correspondence: gabriele.chiogna@ifg.uni-tuebingen.de)

² Department of Civil and Environmental Engineering,
Stanford University, 473 Via Ortega, CA 94305, Stanford,
USA

³ Dipartimento di Ingegneria Civile ed Ambientale, Università
di Trento, via Mesiano 77, 38123 Trento, Italy

Mixing processes significantly affect reactive solute transport in porous media. Contaminant degradation in environmental aquatic systems can be limited either by the availability of one or more reactants, brought into contact by physical mixing, or by the kinetics of the (bio)chemical transformations. Appropriate metrics are needed to accurately quantify the interplay between mixing and reactive processes. The exponential of the Shannon entropy of the concentration probability distribution has been proposed and applied to quantify the dilution of conservative solutes either in a given volume (dilution index) or in a given water flux (flux-related dilution index). We propose using entropy-based metrics of mixing to reactive transport in porous media. Adopting a flux-related framework, we show that the degree of uniformity of the solute mass flux distribution for a reactive species and its rate of change are informative measures of physical and (bio)chemical processes and their complex interaction (Figure 1).

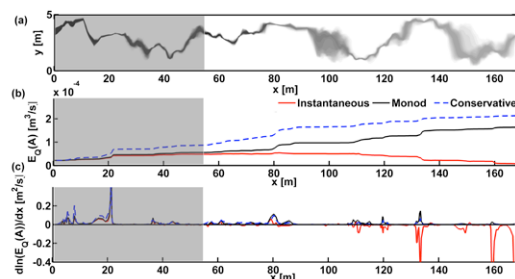


Figure 1: Steady-state conservative plume (a). Flux-related dilution index of compound A for the conservative and two reactive cases (b) and the spatial derivative of its natural logarithm (c) in a heterogeneous domain considering: instantaneous kinetics (red line), double Monod kinetics (black line) and conservative transport (blue dashed line).

Electrochemical investigation of iron monosulfide oxidation by hydrogen peroxide

P. CHIRITA ^{1*} AND C.A. CONSTANTIN ¹
AND M.L. SCHLEGEL ²

¹University of Craiova, Department of Chemistry, Calea
Bucuresti 107I, Craiova Romania (*correspondence:
paulxchirita@gmail.com)

²CEA, DEN/DANS/DPC/SEARS//Laboratory for the
Engineering of Surfaces and Lasers, F-91191 Gif-sur-
Yvette, France (michel.schlegel@cea.fr)

Aqueous oxidation of synthetic iron monosulfide (FeS) by H_2O_2 in HCl solutions was investigated by electrochemical techniques. Corrosion current densities (i_{corr}) and corrosion potentials (E_{corr}) were measured as a function of $[\text{H}_2\text{O}_2]$ (0.001 to 0.1 M) and pH (2 to 11) at temperatures from 30 to 45°C. Experiments were carried out in a conventional three electrode cell assembly with a Pt counter electrode and saturated calomel reference electrode.

It was found that, i_{corr} decreases (E_{corr} increases) from 0.27 mA cm^{-2} (-364 mV) down to 0.019 mA cm^{-2} (up to -57 mV) when pH increases from 2 to 5 (7). Thereafter they remain roughly constant up to pH 11. $[\text{H}_2\text{O}_2]$ and temperature have a more complex effect on FeS oxidative dissolution. At pH 2.5 and 45°C, i_{corr} increases from 0.16 mA cm^{-2} ($[\text{H}_2\text{O}_2]=0.001$ M) up to 0.35 mA cm^{-2} ($[\text{H}_2\text{O}_2]=0.002$ M), and then it decreases down to 0.2 mA cm^{-2} ($[\text{H}_2\text{O}_2]=0.1$ M). In similar conditions, E_{corr} increases when $[\text{H}_2\text{O}_2]$ increases. At $[\text{H}_2\text{O}_2]=0.005$ M and pH 2.5, E_{corr} increases (i_{corr} decreases) from -348 mV (0.19 mA cm^{-2}) up to -304 mV (down to 0.16 mA cm^{-2}) when temperature increases from 30°C to 40°C (35°C). Thereafter E_{corr} decreases (i_{corr} increases) to -372 mV (0.24 mA cm^{-2}).

The experimental results indicate that at low pH H_2O_2 is an effective oxidant of FeS. The complex effect of $[\text{H}_2\text{O}_2]$ and temperature on mineral aqueous oxidation is likely the result of the several reactions. Among these reactions we note: FeS oxidation; $[\text{H}_2\text{O}_2]$ decomposition and formed O_2 adsorption on mineral surface.

The authors greatly appreciate support from IFA-CEA Program (Project C1-04).

SHRIMP U-Pb detrital zircon ages for metasedimentary rocks from the Seosan Group at western margin of the Gyeonggi Massif, Korea, and their tectonic implications

DEUNG-LYONG CHO¹

¹Geological Research Division, Korea Institute of Geosciences and Mineral Resources, Daejeon, 305-350, Republic of Korea (dlcho@kigam.re.kr)

The Gyeonggi Massif (GM) located at the central part of Korean Peninsula is one of the major tectonic units where Precambrian basement rocks are widely exposed. Recent studies reveal that Precambrian rocks in the GM are mostly consist of Paleoproterozoic (1.89-1.82 Ga) para- and orthogneiss, and small bodies of Neoproterozoic (0.90-0.75 Ga) TTG and alkali pluton. Mesoproterozoic sedimentary succession and igneous activities in the GM, however, have not been well defined yet.

In this study, sensitive high-resolution microprobe (SHRIMP) U-Pb age dating is carried out for detrital zircons from metasedimentary rocks of the Seosan Group (SG) which unconformably overlies the ~1.87 Ga basement rocks at western margin of the GM. Samples are mica-schist (SS3) and quartzite (SS6) from the Soguri Formation, and biotite gneiss (Btgn) from Ibugri Formation of the SG. In cathodoluminescence image, most of the zircons show oscillatory zoning patterns, and rarely present core-rim structure. Zircon ages from the SS3, SS6 and Btgn have ranges of 3.15-1.86 Ga, 2.84-1.78 Ga and 3.02-1.82 Ga, respectively. In age spectra, they have distinct peaks at ~1.87 Ga and ~2.54 Ga, and minor peaks exist between these ages. Only a few of the ages are older than 2.75 Ga.

The youngest detrital zircon ages in this study constraint sedimentation of the SG after ~1.8 Ga, and the age spectra are very similar to those reported from Meso- to Neoproterozoic sedimentary succession in the North China Craton [1], that is Changcheng, Jixian and Qingbaikou Groups in ascending order, which deposited after the Lüliang movement at ~1.8 Ga. On these bases, it can be concluded that (1) protolith of metasedimentary rocks of the SG derived from North China Craton; (2) western margin of the GM is correlated with North China Craton.

[1] Wan *et al.*, (2011) *Gondwana Research* **20**, 219-242.

Determination of ²³⁸U, isotope Uranium(²³⁴U/²³⁸U), ²²²Rn and gross alpha in the ground water of the Goesan area in Korea

S.Y. CHO¹ WK. YOON¹ B.W. CHO¹, Y.Y. YOON¹
K.Y. LEE¹ Y.C. KIM¹ AND M.H. KOO²

¹KIGAM, Daejeon 305-350, Korea (sycho@kigam.re.kr),
²Kongju National University

Ground waters generally contains various amount of radio-activity. Measurement of natural occurring radionuclides in groundwater is important for environmental and public health studies.

The measurement of the activity concentrations of ²³⁸U, isotopic Uranium(²³⁴U/²³⁸U), gross alpha and ²²²Rn in sample of ground water is very important in the general study of radionuclide migration that is the source of the radio-nuclides dissolved in the water. Liquid scintillation counting (LSC) is an effective technique for the determination of radionuclide and measurement of radio activity in water samples using LSC which is one of the most common screening techniques applied in ground water.

The activity concentrations of the ²³⁸U, isotopic Uranium (²³⁴U/²³⁸U), gross alpha and ²²²Rn are reported for 55 natural water samples collected from public wells in the sample area. This method is dependent on sample preparation procedures and the setup of measurement conditions, which are typically individual to each of counting laboratories. The aim of this project was to get an overview of the distribution of natural radionuclide activity concentration levels in the ground water sampled from the area. The study area is located in Goesan (36° 35' N, 127° 37' E), Korea. The ²²²Rn could be extracted easily from the water sample(10mL) using a 10 ml commercial organic scintillant. Gross alpha activity was measured in the water sample using LSC method. The sample preparation in this methods was based on the evaporation of relatively small sample(200ml) and measurement in the LS spectrometer with alpha/beta discrimination feature. Determination of ²³⁸U concentration using individual coupled plus mass spectrometry(ICP-MS) and partial sample are solvent extraction method which was utilized to measure isotopic Uranium(²³⁴U/²³⁸U) content in the ground water. The ²³⁸U, isotopic Uranium(²³⁴U/²³⁸U), gross alpha and ²²²Rn, major ion concentrations and physico-chemical parameters were also measured.

The results revealed that the concentrations of Gross alpha, ²²²Rn and ²³⁸U ranged from 0 to 174.9(pCi/L), from < 94 to 29,300(pCi/L), from < 0.1 to 293(ppb), respectively. The isotopic Uranium(²³⁴U/²³⁸U) activity ratio varied between 0.39-1.75.

Development of an *in situ* K-Ar dating technique using LIBS-QMS combination

Y. CHO¹*Y. N. MIURA² AND S. SUGITA³

¹Dept. Earth & Planetary Science, University of Tokyo, Kashiwa, Chiba, 277-8561 Japan

(*correspondence: cho@astrobio.k.u-tokyo.ac.jp)

²Earthquake Research Institute, Univ. Tokyo 113-0033 Japan

³Dept. Cmplx. Sci. & Engr., Univ. Tokyo, Chiba 277-8561, Japan

The age of a rock is one of the most critical parameters for understanding the nature of the sample. Age determination of some key samples not only reveals the history of the specific rocks but also enables us to determine the age of planetary surfaces. In fact, absolute age determination of the planetary surfaces relies on the correlation between crater number density and the ages obtained by Apollo and Luna missions (chronology function) [1]. However, the chronology curve has a 0.5-1 Gyr of uncertainty due to the lack of returned samples. Determining the shape of the chronology function is important not only for determining accurate age, but also for understanding the temporal variation of the impact flux to the Earth-Moon system. In-situ age measurements and/or sample-return mission(s) are crucial to resolving this problem.

We have been developing an in-situ dating method using K-Ar system for future planetary landing missions on the Moon or Mars. In our method, K and Ar in a sample are extracted by the laser ablation and measured with laser-induced breakdown spectroscopy (LIBS) and a quadrupole mass spectrometer (QMS) as well as an optical microscope to measure the volume of laser ablation pits [2, 3].

Using our instrument we obtained the model ages of three previously measured samples with known K concentrations and ages: 2.1±0.3 Ga for a hornblende (K₂O=1.12 wt%, 1.75 Ga), 1.8±0.2 Ga for a biotite (K₂O=8.44 wt%, 1.79 Ga), and 2.0±0.3 Ga for a plagioclase (K₂O=1.42 wt%, 1.77 Ga). Since the three samples have similar ages and different K concentrations, we should be able to construct a “virtual” isochron by plotting the concentrations of K and radiogenic ⁴⁰Ar. The slope of the isochron simulated with our experimental data yields 1.78 Ga of age. This value is in good agreement with known values of 1.79 Ga.

[1] Stöfler & Ryder (2001) *Space Sci. Rev.*, **96**, 9-54. [2] Cho *et al.* (2011) *PERC Planet. Geology Field Symposium* Abstract #30. [3] Cho *et al.* (2013) *LPSC. XXXIV*, Abstract #1505.

Functionalized Carbon Nanotube for Forward Osmosis Membrane: Fabrication and Desalination Application

HYEON-GYU CHOI¹ MOON SON¹ HOSIK PARK¹
AND HEECHUL CHOI^{1*}

¹School of Environmental Science and Engineering, Gwangju Institute of Science and Technology, 1 Oryong-dong, Buk-gu, Gwangju, Republic of Korea (hgstyle@gist.ac.kr, moons@gist.ac.kr, phosik@gist.ac.kr)

(*correspondence: hcchoi@gist.ac.kr)

Forward osmosis (FO) has huge potential to replace with reverse osmosis due to the fact that it operates with osmotic pressure difference and low fouling tendency [1]. In this study, we synthesized the functionalized carbon nanotube blended polymeric membrane and evaluated performance for desalination application. Firstly multi-walled carbon nanotubes (MWCNTs) were functionalized by acid treatment [2]. By blending the MWCNTs, cellulose acetate based composite membrane was synthesized using phase inversion [3]. To characterize the MWCNTs and the membrane, SEM, TEM, FT-IR, and contact angle measurement were utilized. Lab-scale forward osmosis system was operated to evaluate membrane performance for desalination application.

It was confirmed that the functionalized MWCNTs has carboxylic group by acid treatment [3]. The hydrophilic group increase the hydrophilicity of the membrane resulting in enhanced water permeated flux. After 6 hours operation of lab-scale FO system, 47% of water permeated flux increased by 1% CNT blended. Salt ion rejection was not hindered by the presence of CNT (99% when 0% CNT and 97% when 1% CNT blended respectively), marginal reduction in salt rejection was caused by thinner membrane thickness due to increased viscosity of the polymer solution by CNT blending [4],[5]. Even small amount of MWCNTs was blended (i.e., 1 wt%), water permeated flux dramatically increased whereas the salt ion rejection of the membrane was not decreased much compared to bare cellulose acetate membrane. This study showed the capability of MWCNTs to increase forward osmosis membrane performances for desalination application.

[1] Cath *et al.* (2006) *J. Membr. Sci.* **281**, 70-87. [2] Liu *et al.* (1998) *Science* **280**, 1253-1256. [3] Celik *et al.* (2011) *Water Res.* **45**, 274-282. [4] Han and Nam. (2002) *J. Membr. Sci.* **202**, 55-61. [5] Amirilargani *et al.* (2010) *J. Polym. Res.* **17**, 363-377.

Pb isotope ratios in stream sediment around two abandoned mines originating from one ore deposits

J-W. CHOI^{1*}, K. LEE¹ AND E-J. YOO W-S. LEE¹
AND J-S. HAN¹

¹National Institute of Environmental Research, Incheon, Korea
(*correspondence: cjl111@korea.kr.)
(panthallasa@korea.kr, ejyoo@korea.kr.)
(boystone@korea.kr.) (nierhan@korea.kr)

Recently Pb isotope ratios have been successfully used for tracing sources and transports of pollutants from mine sites [2]. In addition, Pb isotope ratio data allowed to estimate relative contributions when there are more than two sources for Pb [3]. We measured Pb isotope ratios of stream sediment and soils around two abandoned mines, DJ and ID mine, originating from one ore deposits. Potential sources existed such as agricultural land, farm house and artificial pool near DJ mine, while no additional sources were found around ID mine. Pb isotope ratios determined in this study provided identification of the sources for Pb in the sediment and assessment of the contributions from those sources to neighboring areas.

The sediment samples collected in the main stream from each mine were commonly characterized by: 1) relatively high concentrations, 2) general decrease in concentrations depending on proximity to mine, 3) constant isotope ratios, and 4) distinguished isotopic compositions from those of tributary stream and downstream areas. This suggests that the Pb in the main stream sediment was affected by Pb pollutants from mines in both sites. The inverted Pb concentrations versus ²⁰⁸Pb/²⁰⁶Pb and/or ²⁰⁷Pb/²⁰⁶Pb ratios plots showed linear correlation between main stream sediment, tributary sediment and downstream sediment. According to binary mixing equation, the relative contributions of Pb from DJ and ID mines to corresponding downstream area were 35~36 % and 37~42 %, respectively. The relative contributions of each source to downstream area calculated by IsoSource program were 35~67 % for main stream, 17~65 % for tributary stream, 0~3 % for agricultural soil, 0~14 % for farm house and less than 1 % for artificial pool.

[1] Fernández-Caliani *et al.* (2009) *Water Air Soil Pollut.* 200, 211-226. [2] Ettl *et al.* (2006) *Environ. Pollut.* 142, 409-417. [3] Hansmann and Köppel (2000) *Chemical Geology* 171, 123-144.

Stable Pb and Cd isotopes in the riverwaters and soils near the Zn-refinery, Korea

MANSIK CHOI^{1*}, JONGKYU PARK¹, DONGJUN CHANG¹
SOJEONG PARK¹ AND JONGUO CHOI²

¹Chungnam National University, Daejeon, Korea
(aska4332@naver.com.) (fightgood@naver.com.)
(zzung1009@nate.com)

²National Institute of Environmental Research, Incheon, Korea. (cjl111@korea.kr)
*(correspondence: mschoi@cnu.ac.kr)

In order to estimate the contribution of refinery borne metals in riverwaters and soils near Zn-refinery and to differentiate them from mining borne metals [1,2], this study collected riverwaters and soils with distance from the refinery to the artificial lake far away 50km. Waste and discharged water, ore and sludge were also collected and analyzed for concentrations of Cu, Zn, Cd and Pb, and isotopes of Cd and Pb using MC ICP/MS.

High concentrations of Cu, Cd, and Pb in riverwaters and soils were observed even in far distance and were correlated with Zn. Based on Pb isotopes, the contribution of refinery borne Pb was identified only in riverwaters and soils within 5 km, which showed the Pb isotopes from imported ores, while samples far away 5 km showed the Pb isotopes from local ores [3] nearby the refinery. $\epsilon^{114/110}\text{Cd}$, isotopic ratio normalized to NIST 3108, showed negative values in soils and positive in riverwaters which indicated the fractionation from ore through the evaporation during refinery. Although the definite decision of the mixing between refinery borne metals and background was not easy, it was evident that refinery borne Cd contributed substantially to samples within 5 km. Size sorting in soils and mixing of enriched heavy isotopes from carbonate deposits with refinery borne metals in riverwaters were responsible for the distribution of $\epsilon^{114/110}\text{Cd}$.

This study was supported by Grant 2012M3A2A1050969 of the National Research Foundation of Korea under the Ministry of Education, Science, Technology, Korea.

[1] Wombacher *et al.*, (2004). *GCA*, 68(10): 2349-2357. [2] Gao *et al.* (2008). *ACA*, 612: 114-120. [3] Jeong *et al.* (2012). *JAES*, 61: 116-127

Mineralogical and microtextural properties of soils by erosion during the rainy season in the Andong area, southeastern part of Korea

CHOO CHANG-OH¹, JEONG GYO-CHEOL^{2*}
AND NAM KOUNG-HOON³

¹Andong National University, Andong, Korea
(mineralogy@hanmail.net)

²Andong National University, Andong, Korea
(*correspondence: jeong@andong.ac.kr)

³Andong National University, Andong, Korea
(namsoil@naver.com)

Along with geochemical information on weathering properties, properties of mineralogy and microtexture of soils are helpful to better understand the causes and patterns of soil erosion and landslide[1]. A total of annual soil loss in the Andong area, the southeastern part of the republic of Korea, amounts to one million tons due to heavy rainfall. We analyzed soils on natural slopes using XRD and SEM.

The most common minerals in soil on natural slopes are quartz, feldspars, illite, kaolinite, vermiculite, and iron oxides. Based on XRD data, the content of quartz in sandstone areas varies from 53.3 to 80.2 wt% while it ranges from 13.6 to 23.2 wt% in gneiss areas. According to SEM observation, fine particles comprising soil vary in size and shape with different geology. They are generally subrounded or elongated with rough surfaces, moderately compacted with some voids. Quartz and feldspars in soils are relatively coarser and frequently densely coated with illite with submicron in size and amorphous iron oxides. Most feldspars show rough surface with dissolution cavities or etch pits. In the same site, the content of quartz and feldspars increases with increasing the rate of soil erosion. The differences in mineralogy and soil texture are attributed to different slope angles and lithology, together with erosion rates. The mineralogical and microtextural properties of soil on natural slopes are important for determining soil erosion by rainfall because fine particles such as clays have great specific surface area and expandability.

[1] Jeong *et al.* (2011) *Nat Hazards* **59**, 347-365.

Anomalous isotope fractionation of sulfur (AIF-S) during thermochemical sulfate reduction by solid organic matter

A.P. CHORNEY¹ Y. WATANABE¹ AND H. OHMOTO¹

¹NASA Astrobiology Institute and Department of
Geosciences, University Park, USA, (apc5060@psu.edu);
(yxw129@psu.edu); (hqo@psu.edu)

Watanabe *et al.* [1] found distinct AIF-S signatures in the products of Na₂SO₄ reduction by glycine at 150-200°C: $\Delta^{33}\text{S}$ values up to +0.92 ‰ for H₂S and up to +2.06‰ for Cr-reducible S. Here we report the results of new series of experiments using various mixtures of alanine, glycine, Na₂SO₄, and H₂SO₄ at 200-300°C.

We have found that the $\Delta^{34}\text{S}$ ($= \delta^{34}\text{S}_{\text{prod}} - \delta^{34}\text{S}_{\text{mit,SO}_4}$) and $\Delta^{33}\text{S}$ ($= \delta^{33}\text{S} - 0.515 \delta^{34}\text{S}$) values greatly vary depending on the starting materials, presence of various reaction products (H₂S, S⁰, Cr-reducible S, HCl-soluble S, and organic S), temperature, pH, and reaction time. For example, mixtures of the two amino acids and Na₂SO₄ generated H₂S with much larger ranges in $\Delta^{34}\text{S}$ (-10.6 to +15.5 ‰) and $\Delta^{33}\text{S}$ (+0.5 to +2.3 ‰) and more consistent $\Delta^{36}\text{S}$ fractionation (+.4 to +1.4‰) compared to the experiments using a single type of amino acid and/or H₂SO₄. Under some experimental conditions we also observe changes from positive to negative $\Delta^{33}\text{S}$ fractionation (+.21 to -.22) in H₂S with time when reduction rates were high. In the experiments where large fractions of the initial SO₄²⁻ were reduced, the residual SO₄²⁻ possessed $\Delta^{34}\text{S} = -.27$ to 7.85‰ and $\Delta^{33}\text{S} = -.15$ to .01‰. These data suggest the AIF-S signatures resulting from TSR are dependent on the degree of polymerization/dehydration of the organic matter, which affect its surface characteristics.

Our experimental data on sulfides and sulfates are similar to those in more than 60 percent of the AIF-S signatures in pre-2.4 Ga sedimentary rocks. If we consider the additional isotope effects due to Rayleigh distillation and recycling, our data can explain all the data reported on natural rocks.

Our experimental data, therefore, provide strong supportive evidence for the hypothesis that most (if not all) AIF-S signatures in geologic materials were created during thermochemical sulfate reduction, rather than by atmospheric UV reactions of volcanic SO₂. This suggestion is also supported by the fact that large Archean AIF-S signatures are typically found in kerogen rich pyritic black shales and the recent discoveries of large AIF-S in post-2.2 Ga materials that have undergone high-temperature reactions between organic matter and sulfate.

[1] Watanabe *et al.* (2009) *Science* 324, 370-373

Critical Zone Evolution by Jerks

J. CHOROVER¹, P. BROOKS², A. HARPOLD², M. LITVAK³
J. MCINTOSH², J. PELLETIER⁴, J. PERDRIAL¹, P. TROCH²
AND C. RASMUSSEN¹

¹Department of Soil, Water and Environmental Science,
University of Arizona, Tucson, AZ, 85721, USA

²Department of Hydrology and Water Resources, University
of Arizona, Tucson, AZ, 85721, USA

³Department of Biology, University of New Mexico,
Albuquerque, NM, 87131

⁴Department of Geosciences, University of Arizona, Tucson,
AZ, 85721, USA

One challenge of Critical Zone (CZ) science is the effective prediction of internal structure formation (vegetation, soil, bedrock fractures) over geomorphic time scales. Another involves forecasting how evolved structure at any geologic time shapes CZ dynamic response (water, solute, gas, sediment) to contemporaneous pulses (“jerks”) such as precipitation inputs to semi-arid systems or catastrophic wildfire. Dissipative products of reactions among oxidants, reduced carbon, water, and silicates include gases, solutes and sediments. The stoichiometry and speciation of efflux is dynamic and convolves upgradient processes. Models are needed to convolve how these coupled physical, biological and chemical processes respond to climate (e.g., EEMT) to enable better prediction of such CZ parameters as watershed chemical denudation rate, soil depth distribution, water transit time, and stream solute flux. An improved understanding of the mechanistic underpinnings of such predictions, however, and why they succeed or fail, requires direct observation of parallel data streams generated in situ, such as those produced by the Critical Zone Observatories (CZOs). Data from the Jemez-Catalina (JRB-SCM) CZO indicate that climatic forcing that varies significantly between years drives corresponding differences in dissipative element flux, speciation, and stoichiometry. The bimodal annual precipitation regime of AZ and NM implies that formation of observed porous geomedia structure, solid phase (bio)geochemical composition, fluid flowpaths, etc., occurs disproportionately during brief episodes of water and carbon throughflux and/or disturbance, and our measurements support this hypothesis. Sub-catchment locations with elevated reaction rates appear to control overall system behavior, and the type of precipitation input is key; snowmelt pulses contribute to CZ weathering at depth, whereas flashy summer monsoon rains during peak biological activity generate hydrochemical discharges enriched in organic ligand-metal complexes and nanoparticles from near surface flow paths.

Role of Black Carbon for Radioactive Iodine Sorption

SUNGWOOK CHOUNG¹, MINKYUNG KIM¹, MIN-GYU KIM²
AND WOYONG UM^{1,3}

¹77 Chungam-lo, Nam-gu, Pohang, 790-784 Republic of
Korea, (schoung@postech.ac.kr)

²77 Chungam-lo, Nam-gu, Pohang 790-784 Republic of
Korea,

³Energy and Environment Directory, Pacific Northwestern
National Laboratory, 902 Bartelle Blvd., P7-54, Richland,
WA99354, USA

Natural organic matter (NOM) plays an important role in determining the fate and transport of iodine species such as iodide (I⁻) and iodate (IO₃⁻) in groundwater system. Although NOM exists as diverse forms in environments, prior iodine studies have mainly focused on sorption processes of iodide and iodate to humic materials. This study was firstly conducted to determine the iodide and iodate sorption potential for a particulate NOM (i.e., black carbon [BC]). A laboratory-produced BC and commercial humic acid were used for batch sorption experiments to compare their iodine sorption properties. The BC exhibited >100 times greater sorption capability for iodide than iodate, while iodide sorption was negligible for the humic acid. The sorption properties of both adsorbents strongly depend on the initial iodine aqueous concentrations. After sorption of iodide to the BC, X-ray Absorption Fine Structure (XAFS) spectroscopy results indicated that the iodide was converted to electrophilic species and chemically interacted with carbon atoms of polycyclic aromatic hydrocarbons present in the BC (Figure 1). The computed distribution coefficients (i.e., K_d values) suggest that the BC materials retard significantly the transport of iodide in environmental systems containing even a small amount of BC.

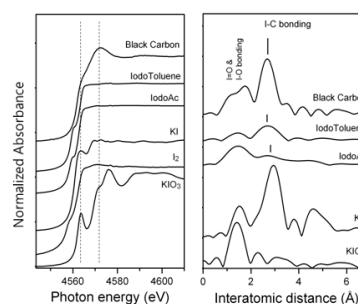


Figure 1. XAFS results.

Niche partitioning in early Eocene mammalian faunas: New insights into a C3 ecosystem from tooth morphology, microwear, and stable isotopes

HILARY CHRISTENSEN¹

¹The Carnegie Institution of Washington, Geophysical Lab,
5251 Broad Branch Rd NW, Washington, DC 20036
(hchristensen@ciw.edu)

The stable isotopic composition of biological tissues can provide information about an animal's diet, and as preserved in crystalline tooth enamel can persist unaltered for millions of years. This makes stable isotope techniques very important tools in the study of life history and ecology in extinct animals. In such cases, however, the sources of isotopic variability are often difficult to pinpoint. The present study introduces a novel method for the evaluation of dietary signal in mammalian stable isotope ecology by combining stable isotope analysis with these independent dietary indicators. Phosphate $\delta^{18}\text{O}$ and carbonate $\delta^{18}\text{O}$ and $\delta^{13}\text{C}$ values from the tooth enamel of an early Eocene mammalian fauna exhibit a wide range of values, especially for an ecosystem composed entirely of C3 plants. Comparison with microwear and morphological results show that the ^{18}O variability in these animals stems from differential reliance on ^{18}O -enriched leaf water as a proportion of water intake (high-fiber herbivores= more leaf water, frugivores= more meteoric water), while the ^{13}C variability likely stems from feeding on plants growing in different microhabitats. The dietary information available from microwear and morphology allows the sources of stable isotopic variability to be addressed, providing a powerful tool to the interpretation of isotopic values in both fossil and living systems.

Unravelling sources of ground-level ozone in the intermountain western U.S. through Pb isotopes

JOHN N. CHRISTENSEN¹ PETER WEISS-PENZIAs²,
SHAUN T. BROWN¹ CHARLES MCDADE³ DAN JAFFE⁴
AND MAE GUSTIN⁵

¹Lawrence Berkeley Natl. Lab., (jchristensen@lbl.gov)

²Univ. of California, Santa Cruz CA, (pweiss@ucsc.edu)

³Crocker Nuclear Lab., Univ. of California, Davis CA

⁴Univ. of Washington, Bothell WA, djaffe@u.washington.edu

⁵Univ. of Nevada, Reno NV, (mgustin@cabnr.unr.edu)

The Western United States (US) is subject to pollution transported across the Pacific from Asia. One component of aerosol pollution is lead (Pb), an element that can be readily traced back to sources using isotopic fingerprints. Over the past decade China has emitted $\sim 7 \times 10^9$ g/yr of Pb to the atmosphere with the principal source being coal combustion. The isotopic composition of aerosol Pb from China is distinct from sources in the Western US. In [1] it was shown, using data from Northern California, that the amount of Pb sourced in Asia/China (termed Trans-Pac Pb, ng/m³) could be determined from the aerosol Pb isotopic composition. Here we explore the combined use of Pb isotopes and back-trajectory analyses to constrain the sources of ozone and its precursors to remote areas of the intermountain Western US. The EPA is considering lowering the ozone standard from 75 ppbv (MDA8= Maximum Daily 8-hour Average) to 60-70 ppbv. This will result in remote areas of the intermountain west being out of compliance, despite a lack of significant local sources. Sources suggested as culprits for ozone exceedance events in the remote west include long-range transport from Asia, regional transport from the Los Angeles/Las Vegas area, exchange/intrusion of stratospheric air to the surface, and wildfires. We used a combination of Pb isotope fingerprinting and back-trajectory analyses to distinguish sources of ozone to Great Basin National Park located in eastern Nevada. We found that during discrete Chinese Pb events (>1.1 ng/m³) trans-Pacific transported ozone was 4 ± 5 ppbv above 15 year averages for those dates. In contrast, dates characterized by regional transport from the Los Angeles and Las Vegas areas were 19 ± 3 ppbv above the long-term averages, and those characterized by high-altitude transport were 21 ± 5 ppbv above. The latter is indicative of long range free troposphere transport, most of these samples had modest concentrations of Trans-Pac Pb (ave. 0.43 ng/m³). Our data constrain the average background concentration of Asian sourced Pb in air to 0.3 ± 0.2 ng/m³ in the western US.

[1] Ewing *et al.* (2010) *ES&T* **44**, 8911-8916

www.minersoc.org

DOI: 10.1180/minmag.2013.077.5.3

Speciation of phosphorus in soils peripheral to meltwater ponds in Victoria Land, Antarctica

HANNAH CHRISTENSON, JENNY WEBSTER-BROWN
AND IAN HAWES¹

¹Waterways Centre for Freshwater Management and Gateway Antarctica, University of Canterbury, Christchurch, New Zealand (*correspondence: hannah.christenson@pg.canterbury.ac.nz), (jenny.webster-brown@canterbury.ac.nz), (ian.hawes@canterbury.ac.nz)

Meltwater ponds are the most common habitat for terrestrial biota on continental Antarctica. The productivity of benthic cyanobacteria (the dominant biomass) is considered to be limited by phosphorus (P) availability in inland areas, but sources of P and factors limiting its bioavailability are poorly understood. Consequently it is difficult to predict how productivity will be affected by climate change-induced increases in pond size and volume. As part of a larger research programme to determine the P biogeochemical cycle for meltwater ponds, this study has explored P concentration and speciation in the soils near the ponds to identify additional potential sources of P to the pond water during periods of increased temperature and meltwater volume.

Over three years (2011 – 2013), soils were collected (together with sediments, waters and biological material) from 15 ponds from 3 areas of the Dry Valleys, and from 7 ponds in the McMurdo Ice Shelf /Ross Island region in Victoria Land, representing inland and coastal meltwater environments respectively. Concentrations of P were up to an order of magnitude higher in the soils of coastal ponds (mean = 2.2 g/kg), compared to inland pond soils (mean = 0.32 g/kg). P speciation, determined using standard sequential extraction methods indicated that <3% of the P in the soils was in a form that might be readily released during flooding or during the seasonal anoxia that develops in meltwater ponds. However, up to 10% was in a form that could be released under alkaline conditions (pH>10), as can occur during period of intense photosynthesis during summer months in the ponds.

The remaining P (70 to 99%) is refractory and less likely to be readily dissolved during soil flooding, though weathering of apatite and/or dissolution of refractory oxide phases may release P in the longer term, particularly from the relatively P-enriched coastal soils. In coastal ponds on the McMurdo Ice Shelf, pond sediments had <25% of the readily exchangeable P concentration in adjacent soils, and <80% total P, confirming immediate *and* longer term release of soil P into pond water.

Green rust sulphate - making space for interlayer cations

B.C. CHRISTIANSEN¹, A. KATZ^{1,2}, N. BOVET¹,
H.O. SØRENSEN¹, M.P. ANDERSSON¹, S. NEDEL¹ C.
FRANSEN³ K. DIDERIKSEN¹ AND S.L.S. STIPP¹

¹ Nano-Science Center, Department of Chemistry, University of Copenhagen, Denmark; (bochr@nano.ku.dk)

² Present address: Institut franco-allemand de recherches de Saint-Louis – ISL, Saint-Louis Cedex, France

³ Department of Physics, Technical University of Denmark, Denmark

Green rusts (GR) are layered double hydroxides with brucite like Fe(II),Fe(III) hydroxide layers. The surplus charge from Fe(III) is balanced by incorporation of anions and in some cases also cations. GR can reduce a range of redox sensitive compounds, e.g. nitrate, chromate and chlorinated solvents. GR forms readily in the laboratory at ambient temperatures, neutral pH and slightly reducing conditions, can be stable under groundwater conditions, making it a good candidate for contaminant remediation

Although GR has been the subject of numerous studies, several structural aspects are poorly understood. Interlayer ions for example, define the interlayer spacing, which in turn impacts interlayer accessibility for redox sensitive compounds and thereby the reactivity of GR. We have investigated interlayer incorporation of a range of monovalent cations (Na⁺, K⁺, Rb⁺ and Cs⁺) in GR_{SO4}. Synchrotron X-ray diffraction demonstrated that the interlayer spacing correlates with radius of the cations, showing that they intercalate.

X-ray photoelectron spectroscopy showed that interlayer incorporation differs greatly among cations and is correlated with the stability constant for the X⁺-SO₄⁻ ion pairs. Infrared spectroscopy showed that sulfate symmetry was affected differently by the incorporated cations. If interlayer spacing limits anion or cation availability for reaction, our results indicate that the identity of the incorporated monovalent cation would also affect reaction rates.

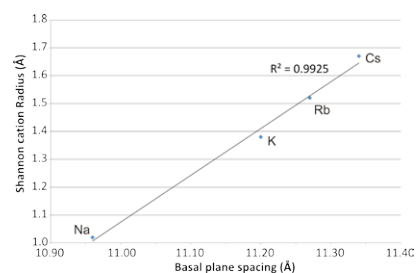


Figure 1. Correlation between GR_{SO4} basal plane spacing and ionic radius of cations in solution during formation.

Airborne *in situ* measurements of HDO/H₂¹⁶O confirm strong influence of convection on isotopic composition of upper tropospheric humidity

EMANUEL CHRISTNER*¹ CHRISTOPH DYROFF¹,
SHAHROKH SANATI¹ AND ANDREAS ZAHN¹

¹KIT – Karlsruhe Institute of Technology, Institute for Meteorology and Climate Research, Karlsruhe, Germany
(*correspondence: emanuel.christner@kit.edu)

Atmospheric water is an enormously crucial trace species. It is responsible for ~75% of the natural greenhouse effect [1] and carries huge amounts of latent heat. The isotopic composition of atmospheric water vapor is an elegant tracer for a better understanding and quantification of the extremely complex and variable hydrological cycle in Earth's atmosphere, which in turn is a prerequisite to improve climate modeling and predictions.

In this context, water-isotopologues (here the isotope ratio HDO/H₂¹⁶O) can be used to study the atmospheric transport of water, as H₂¹⁶O and HDO are fractionated during several transport-related processes (evaporation, cloud condensation, rainout, re-evaporation, formation of ice).

During more than 20 long-distance flights across or close to the equator, HDO/H₂¹⁶O of convectively lofted air was measured *in situ* in the upper troposphere (UT). These measurements confirm the large impact of tropical strong convection on the isotopic composition of atmospheric water. In comparison to a Rayleigh model we find on average an enhancement of δD by more than 100 ‰ above three continents (Africa, South America, East Asia, Fig. 1). A meridional profile illustrates the transport of convectively lofted air to higher latitudes by Hadley circulation.

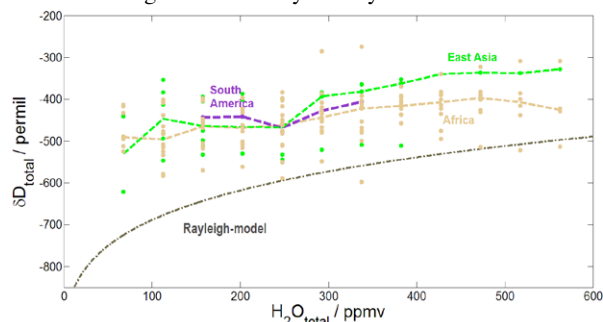


Figure 1: Enhanced tropical δD shows impact of convection on isotopic composition of humidity in the UT. Black line: Rayleigh model.

[1] Schmidt *et al.* (2010), *JGR*, **115**, D20106.

An integrated approach to build surface complexation models for chromate on iron oxides

MARIA CHRYSOCHOOU^{1*} NADINE KABENGI² MICHAEL MACHESKY³ CHAD JOHNSTON¹ AND JAMES KUBICKI⁴

¹University of Connecticut, Storrs, CT 06268, USA

(correspondence*: maria.chrysochoou@uconn.edu)

²Georgia State University, Atlanta, GA 30303, USA

³Illinois State Water Survey, Champaign, IL 61820, USA

⁴Pennsylvania State University, University Park, PA 16802, USA

This study presents Surface Complexation Models (SCMs) for chromate (CrO₄²⁻) adsorption on ferrihydrite and hematite that were formulated and calibrated using complementary techniques to investigate the mechanisms and energetics of adsorption. Specifically, Attenuated Total Reflection – Fourier Transform Infrared (ATR-FTIR) and Extended X-ray Absorption Fine Structure (EXAFS) spectroscopies were applied to investigate the surface species formed under different pH, surface loading and ionic strength conditions; Flow Adsorption Calorimetry (FAC) analyses determined the enthalpies of adsorption and provide additional evidence for surface speciation; Density Functional Theory (DFT) calculations provided bond lengths, vibration frequencies and comparative enthalpy values. SCMs were formulated using the CD-MUSIC framework and calibrated taking both proton adsorption data and observed surface species distributions into account.

The results indicate that ferrihydrite and hematite present similar behavior in terms of the type of species formed, with some differences in the relative distribution and adsorption energetics that can be traced back to the mineral structure and properties. Monodentate complexes are dominant on both minerals at low chromate loadings and pH>5, while bidentate complexes are favored at acidic pH and high surface loading. No protonation of the surface complexes was observed under any conditions. More total heat of adsorption was observed on the ferrihydrite surface compared to the hematite.

The conditions at which bidentate complexes take over are dependent on ionic strength and on the presence of carbonate, as indicated by the ATR analyses and the SCMs, respectively. The calibration of the model also indicated that the distribution of the two species as a function of pH is very sensitive to the log K values. Overall, an improved fit to adsorption edges was obtained for both minerals compared to previously published models.

Magma components of the Gangdese batholith, southern Tibet: Decoded by zircon Hf and O isotopes

M.-F. CHU^{1*} S.-L. CHUNG² X.-H. LI³ H.-Y. LEE²
AND S.Y. O'REILLY^{4,5}

¹Institute of Oceanography, National Taiwan University, Taipei 106, Taiwan

(*correspondence: meifei@ntu.edu.tw)

²Department of Geosciences, National Taiwan University, Taipei 106, Taiwan

(sunlin@ntu.edu.tw, haoyanglee@ntu.edu.tw)

³Institute of Geology and Geophysics, Chinese Academy of Sciences, Beijing, China (lixh@gig.ac.cn)

⁴Australian Research Council Centre of Excellence for Core to Crust Fluid Systems and GEMOC, Department of Earth and Planetary Sciences, Macquarie University, North Ryde, NSW 2109, Australia (sue.oreilly@mq.edu.au)

The Gangdese batholith, southern Tibet is the largest of the Transhimalayan batholiths produced by the Neo-Tethyan subduction. Zircon U-Pb age data show that the emplacement of the Gangdese batholith occurred during ca. 200 and 40 Ma, and can be divided to the Jurassic, Cretaceous and Paleogene stages. Zircon Hf isotope data indicate that, in addition to the juvenile mantle signature observed in both of Mesozoic stages, the Paleogene Gangdese is characterized by significant Hf isotopic shift suggesting the involvement of old continental crust in the magma source, which we interpret as a result of Himalayan sediment subduction related to the advancing India. Here we report new zircon O isotope data measured by Cameca 1280 that, combined with published zircon Hf isotope data, identify four magma source components of the Gangdese batholith. These are (1) a depleted mantle [$\epsilon_{\text{Hf}}(\text{T}) \approx +20$; $\delta^{18}\text{O} \approx +4.6$], representing the depleted mantle wedge of the Gangdese arc magma system; (2) an enriched mantle [$\epsilon_{\text{Hf}}(\text{T}) \approx +8$, yielding crustal model age of ~ 600 Ma; $\delta^{18}\text{O} \approx +5.5$], resulting from subduction zone enrichment; (3) an old continental crust [$\epsilon_{\text{Hf}}(\text{T}) < -5$; $\delta^{18}\text{O}$: up to $+8.5$], only in the Paleogene stage owing to the sediment subduction; and (4) a new component revealed in the Cretaceous and Paleogene stages that has high Hf and O isotope ratios [$\epsilon_{\text{Hf}}(\text{T}) \approx +13$, yielding crustal model age of ~ 350 Ma; $\delta^{18}\text{O}$: up to $+7.5$]. The fourth component, marked particularly with its high O isotope ratio, is interpreted to be derived from hydrothermally altered Neo-Tethyan oceanic crust and/or subducted arc-derived sediments.

Dynamic carbon cycle in the Ediacaran Yangtze Basin

XUELEI CHU^{1*}

¹Institute of Geology and Geophysics, Chinese Academy of Sciences, Beijing 100029, China

(*correspondence: xlchu@mail.iggcas.ac.cn)

Extraordinarily large fluctuation in the Neoproterozoic carbon isotope records implies strong perturbations of global carbon cycle. Rothman *et al.* [1] proposed a two-box dynamic model with intertwined pools of inorganic carbon (IC) and dissolved organic carbon (DOC) to explain the unusual carbon isotope excursions and their link to the early animal evolution. Decoupled carbon isotopes of sedimentary carbonate and organic carbon from the fossil-rich Doushantuo Formation (635–551 Ma) in the Yangtze area of South China may be explained by this dynamic model.

The Doushantuo Formation in the Yangtze area is divided into four lithostratigraphic members up section. Member I of ~ 6 m cap dolostone was the fast deposition in a nonsteady-state carbon cycle during the aftermath of Marinoan glaciation, which explains the irregular track of ϵ (isotope fractionation between carbonate and organic carbon) vs. $\delta^{13}\text{C}_{\text{carb}}$ plot. At member II of ~ 70 m with alternated organic-rich shale and dolostone, stable $\delta^{13}\text{C}_{\text{org}}$ values and $\delta^{13}\text{C}_{\text{carb}}$ fluctuations over 10‰ suggest a large DOC reservoir in the depth of the Yangtze basin during the earlier Ediacaran [2]. Bristow & Kennedy [3] and Jiang *et al.* [4] disagreed a large DOC reservoir on global scale. However, a large DOC pool is enough to influence the overlying IC reservoir in basin in a redox-stratified ocean [5]. The intercept of $\delta^{13}\text{C}_{\text{carb}}$ axis (-30.5%) suggests that most DOC should be derived from the degradation of photoautotrophs. After the oscillation of sea-level at member III of ~ 70 m dolostone with imbedded chert and alternating limestone-dolostone, stable $\delta^{13}\text{C}_{\text{org}}$ values and variable $\delta^{13}\text{C}_{\text{carb}}$ values ($\sim 5\%$) occurred in overlying 10–20-m-thick black shale (member IV) suggesting a still existing DOC reservoir in the deep water. Furthermore, an intercept of -40% indicates a large amount of DOC should be mostly derived from the degradation of heterotrophic organisms.

[1] Rothman *et al.* (2003) *PNAS* **100**, 8124–8129. [2] McFadden *et al.* (2008) *PNAS* **105**, 3197–3202. [3] Bristow & Kennedy (2008) *Geology* **36**, 863–866. [4] Jiang *et al.* (2010) *EPSL* **299**, 159–168. [5] Li *et al.* (2010) *Science* **328**, 80–83.

A comprehensive separation procedure for precise determination of Re, Ir, Ru, Pt and Pd in geological samples

Z.-Y. CHU^{1*}, R. J. WALKER², J.-H. GUO¹, Y. YAN¹,
Y.-H. YANG¹ AND Y.-B. ZHANG¹

¹Institute of Geology and Geophysics, Chinese Academy of Sciences, Beijing, China, (*correspondence: zhychu@mail.igcas.ac.cn)

²Department of Geology, University of Maryland, College Park, MD 20742, USA

It is difficult to precisely determine Re, Ir, Ru, Pt and Pd in geological samples due to the low abundance of these elements. Moreover, the potential polyatomic interferences on Ru, ZrO interferences on Pd, and HfO interferences on Ir and Pt, make precise determination of these elements more challenging. In this study, we have developed a comprehensive method for separation of Re, Ir, Ru, Pt and Pd in geological samples based on anion exchange method, in order to realize reliable isotope dilution (ID) analyses of these elements.

The Re, Ir, Ru, Pt and Pd are firstly group-separated in Re-Ru, Ir-Pt and Pd by using 2 mL Biorad AG 1 X 8 (100-200 mesh) anion exchange columns. Subsequently, the Re-Ru is further purified using 0.25 mL Biorad AG1 X 8 (100-200 mesh) anion exchange columns. The Ru can also be further purified via a microdistillation method by using 50 μ L of CrO₃-H₂SO₄ solution as an oxidant. The Ir-Pt and Pd are further purified using Eichrom-LN columns to completely remove potential HfO and ZrO interferences, respectively.

After this comprehensive separation procedure, the Re, Ru, Ir, Pt and Pd can be precisely measured by ID-MC-ICP-MS. The Ru further purified by microdistillation method can also be measured by ID-NTIMS method.

Finally, the USGS reference materials BHVO-2, BCR-2, BIR-1a and DNC-1 are measured and the analytical results of Re, Ir, Ru, Pt and Pd are in good agreement with the published values.

Thermodynamic potentials of Au-Hg binary solid solution

K.V. CHUDNENKO^{1*} AND G.A. PAL'YANOVA²

¹Vinogradov Institute of Geochemistry, SB RAS, Irkutsk, Russia (*correspondence: chud@igc.irk.ru)

²Sobolev IGM, SB RAS, Novosibirsk, Russia

Standard thermodynamic functions ($\Delta_f G^0$, S^0) of Au_{1-x}Hg_x (0 \leq x_{Hg} \leq 0.2) solid solution have been calculated using the formalism of Redlich-Kister method [1]:

$$G^{ex} = x_1 x_2 ({}^0L + {}^1L(x_1 - x_2)) \quad (1)$$

Parameters of equation (1) were obtained by regression analysis of the data [2]:

$${}^0L \text{ (J/mol)} = 1500 + 4.05T$$

$${}^1L \text{ (J/mol)} = -7499.99 + 2.15T.$$

The excess entropy of solid solution was evaluated from equation [3]:

$$S^{ex} = - \left(\frac{\partial G^{ex}}{\partial T} \right)_P$$

Excess thermodynamic functions were used to calculate the standard thermodynamic properties of Hg solid solution in (Au) with mercury content 1-20 at. % (Table 1).

Solid solutions	$\Delta_f G^0$, J/mol	S^0 , J/(mol·K)
Au0.99Hg0.01	-179	48.177
Au0.98Hg0.02	-319	48.752
Au0.96Hg0.04	-555	49.79
Au0.94Hg0.06	-750	50.745
Au0.92Hg0.08	-916	51.648
Au0.9Hg0.1	-1056	52.513
Au0.88Hg0.12	-1174	53.348
Au0.86Hg0.14	-1272	54.159
Au0.84Hg0.16	-1353	54.949
Au0.82Hg0.18	-1417	55.721
Au0.8Hg0.2	-1466	56.477

Table 1: Standard thermodynamic properties of Au-Hg solid solution

The obtained data can be used in different software packages for developing physicochemical models in natural and technological processes with participation of gold and mercury.

The work was supported by 12 and 48 Integration projects grants of SB RAS.

[1] Hillert (2008) Phase equilibria, phase diagrams and phase transformations, Cambridge. [2] Okamoto & Massalski (1989) *Bulletin of Alloy Phase Diagrams* **10**, 50-58. [3] Anderson (2005) Thermodynamics of natural systems, Cambridge.

A contribution from radiogenic isotope study to metal source and timing of gold orogenic deposits: A case of Nezhdaninsky deposit, Yakutia, Russia

A.V. CHUGAEV* I.V. CHERNYSHEV,
N.S. BORTNIKOV AND G.N. GAMYANIN

IGEM of Russian Acad.Sci., 35 Staromonetny, Moscow
Russia (chug@igem.ru)

The relation of orogenic gold deposits to a magmatic activity is still yet controversial. The U-Pb and Rb-Sr (rock forming minerals) isotope ratio of the intrusive rocks associated with the Nezhdaninsky world class gold deposit (NGD) (Au>470 t) hosted by the Permian carbonaceous-clastic sequence was studied [1]. The lamprophyre dikes has the concordant U-Pb zircon age of 121 ± 1 Ma, (ID-TIMS) and the isochron Rb-Sr age of 121.0 ± 2.8 Ma and are temporally close to the auriferous veins aged at 119.0 ± 4 and 132 ± 12 Ma. The Kurum granodiorites and the Gel'dy stock quartz diorite aged at 94 ± 1 Ma and 92.6 ± 0.8 Ma, respectively, postdate the NGD and were not parts of this mineral system.

A study of 62 galena samples from NGD and several ore occurrences and K-feldspar from intrusive rocks using high-precision ($\pm 0.02\%$) MC-ICP-MS method with $^{205}\text{Tl}/^{203}\text{Tl}$ normalization [2] showed that the predominant lead component at the NGD was derived from the Permian sedimentary host rocks. The subordinate lead was derived from Early Cretaceous magmatic rocks.

Thus, the NGD rocks formed within a time span of 25-28 Ma. This timing corresponds to two epochs of magmatic activity at the South Verkhoyansk Fold belt. The age of the NGD gold mineralization is not younger than 120 Ma [3]. The Nd-Sr-Pb isotope data on the igneous rocks and auriferous mineralization of the NGD [1, 2] suggest the Early and Late Cretaceous magma sources were formed in the Precambrian crust dated at ~ 1.8 Ga.

These data suggest the relation of the NGD to the lamprophyre and Early Cretaceous deep-seated crustal magmas and an involvement into the hydrothermal system of metals from underlying Permian clastic host rocks.

[1] Chernyshev *et al.* (2012) *Geology of Ore Deposits* **54**, N 6, 411-433. [2] Chernyshev *et al.* (2011) *Geology of Ore Deposits* **53**, N 5, 353-373. [3] Chugaev *et al.* (2010) *Doklady Earth Sciences* **434**, 1337-1342.

Surface area characterization of suspended sediment in glacial meltwater using "nano-BET"

P.M. CHUTCHARAVAN^{1*} AND S.M. ACIEGO²

¹Department of Earth and Environmental Sciences, University of Michigan, Ann Arbor, MI 48109, USA

(*correspondence: petermch@umich.edu)

²Department of Earth and Environmental Sciences, University of Michigan, Ann Arbor, MI 48109, USA

(aciego@umich.edu)

Suspended load is the greatest source of fluvial sediment flux to the ocean, on the order of 15-20 gigatons of material per year [1] and should have significant implications for global element cycling. However, the degree of element flux to the ocean is not solely dependent on the amount of material transported; the reactivity of the sediment grains must also be considered. Reactivity of sediment is primarily determined by two factors: mineralogical composition and grain surface area. Since surface area is directly related to reactivity (i.e. more surface area means more sites for a reaction to potentially occur), it is a good overall estimate of element availability for a given sample.

Our study attempts to characterize the reactive surface area of suspended sediments in glacial meltwater. The hydrology of subglacial environments, consists of a complex "plumbing" system of channels that governs the flow of water under a glacier and the overall dissolved elemental flux. However, the surface area of the suspended load from glacial meltwater, and the relationship to subglacial geology and regional climate, remains uncharacterized due to the difficulty of measurements. Surface areas calculated by mineral shape and size underestimate reactive surface area by several orders of magnitude and conventional gas adsorption techniques require at least one gram of sample, often unattainable in the field.

Recent developments [2] have made it possible to measure the BET surface areas of milligram size samples with nano-scale precision. Using this new method, suspended sediment samples from two alpine glacier sites in Canada and Alaska were collected and analyzed. Results will demonstrate how the reactive surface area of suspended glacial sediments changes over the melt season and help provide better constraints for element availability in glacial meltwater.

[1] Jones *et al.* (and references therein) (2012) *Geochim. Cosmochim. Acta* **77**, 108-120. [2] Aciego *et al.* (2011) *Quaternary Sci. Rev.* **30**, 2389-2397.

The influence of frost weathering on the release of readily available ions from granite surfaces

THOMAS CHWALEK^A NATASCHA TORRES^A,
GERHARD FURRER^B HELMUT BRANDL, BEAT MÜLLER^A
AND PETER C. HAUSER^D

^ASwiss Federal Institute for Environmental Science and Technology (EAWAG), CH-6047 Kastanienbaum, Switzerland

^BInstitute of Biogeochemistry and Pollution Dynamics, ETH Zurich, CH-8092 Zurich, Switzerland

^CInstitute of Evolutionary Biology and Environmental Studies, University of Zurich, CH-8057 Zurich, Switzerland

^DDepartment of Chemistry, University of Basel, CH-4004 Basel, Switzerland

Hundreds of research studies concerning frost weathering of minerals were conducted during the last century. Regardless of a long history of inquiries, the quantitative insights of frost weathering products are still elusive. Frost weathering is mainly attributed to the increase of surface area without any chemical changes. This study represents the first attempt to evaluate readily available ions released by frost weathering with the use of capillary electrophoresis (CE) and a capacitively coupled contactless conductivity detection (C⁴D) detector. An new easy-to-handle sampling technique called "Drop-on-Stone" (DoS) was used to sample rock surface areas. Aare Granite samples undergoing different amounts of freeze-thaw cycles were analyzed for a continuous increase of cations and anions. Particular attention was given to the first weathering steps. Complementary SEM pictures of the sampled areas were taken during the weathering experiments. The results illustrate the initial release of ions during the first few freeze-thaw cycles. This indicates that frost weathering is able to raise surface concentrations of readily soluble cations and anions. These ions serve as the primary nutrient source for organisms and are essential for initial soil formation in arctic and high altitude areas.

Geochemical atlas of Italian soils

D. CICCHELLA^{1*} S. ALBANESE², E. DINELLI³,
L. GIACCIO², A. LIMA², P. VALERA⁴ AND B. DE VIVO²

¹Dipartimento di Scienze e Tecnologie, Università degli Studi del Sannio. Via dei Mulini 59/A, 82100 Benevento, Italy (* correspondence: cidom@unisannio.it)

²Dipartimento di Scienze della Terra, Università di Napoli Federico II. Via Mezzocannone 8, 80134 Napoli, Italy (bdevivo@unina.it)

³Dipartimento di Scienze della Terra e Geologico Ambientali, Università di Bologna. Piazza di Porta San Donato 1, 40126 Bologna, Italy (enrico.dinelli@unibo.it)

⁴Dipartimento di Geoingegneria e Tecnologie Ambientali, Università di Cagliari. Piazza d'Armi, 09123, Italy.

The geochemical Italian Atlas was carried out as part of GEMAS project whose objective was to characterize soils of rural areas of the whole Europe. Soil samples were collected at an average sampling density of 1 site per 2500 km². Two different sample types were collected: (1) 121 agricultural soils on regularly ploughed land to a depth of 20 cm and (2) 121 grazing land soils (land under permanent grass cover) to a depth of 10 cm. All soil samples were air dried, sieved to <2 mm, homogenised and finally split into 10 sub-samples. Both sample types (Ap and Gr) were analysed at the BGR in Berlin for a suite of 41 elements by WD-XRFS. The same samples were also analysed after AR and MMI extractions by a combination of ICP-AES and ICP-MS for 53 elements. In addition, other parameters were determined: pH, TOC, total carbon and total sulphur, LOI, CEC, Sr-isotopes, Pb-isotopes, MIR-spectra. By means of a GIS software, georeferenced data of the Italian territory were used to produce the geochemical maps of all the analysed elements for both agricultural and grazing land soils. Specifically, for each element and sampling media a map reporting interpolated data and graduated dots was produced; univariate statistics and graphs were also associated to each map. The Atlas also contain: 5 maps for regional variability of factor scores of elemental associations resulting from R-mode factor analysis and 15 land use maps for some selected elements (As, Be, Cd, Co, Cr, Cu, Hg, Ni, Pb, Sb, Se, Sn, Tl, V, Zn) following the intervention criteria established by Italian Law (D.L. 152/06).

Behaviour of mineral phases during combustion of coal waste dumps – experimental study

JUSTYNA CIESIELCZUK¹

¹University of Silesia, Będzińska 60, 41-200 Sosnowiec, Poland; (justyna.ciesielczuk@us.edu.pl)

Coal waste dumps can be affected by self-heating and self-combustion processes and became an environmental problem. These processes are widely investigated, but as every coal waste dump is unique and the factors which influence and modify the processes are so numerous, it is hard to predict the behaviour of deposited wastes in any individual case. The aim of the experiment was to reduce the number of influencing factors by heating, in an oven, samples of known mineral composition under known conditions. Samples were heated at 960°C under oxidizing conditions for 74 hours in a pipe furnace (PRC 65M, Czyłok). One sample (20W) comprised 53% coal, 24% kaolinite, 21% illite/muscovite and 3% quartz. A second sample (20B) contained 11% coal, 29% kaolinite, 22% illite/muscovite, 28% quartz, 2% feldspars and 1% siderite. Each sample was mixed 1:1 with siderite (containing 76% of the mineral siderite) and pyrite (containing 79% of the mineral pyrite).

After the experiment, sample 20W was more intensely cracked than 20B, less compact but homogeneous. The presence of siderite or pyrite made 20W more compact while burning, limiting oxygen access. Besides layers of varying hematite- and magnesioferrite contents were formed.

After heating, 20B contained half of the quartz originally present and 20W one third. There was also less quartz in samples mixed with pyrite than with siderite.

Twice as much mullite was produced in sample 20W than in 20B, although both primary samples contained similar amounts of clay minerals. Additionally, euhedral mullite needles formed only in 20W.

A small amount of diopside was produced in 20B samples mixed with pyrite or siderite. Much more diopside was produced in 20W with pyrite or siderite. There was no diopside in the original 20B and 20W samples.

The presence of coal matter accelerates changes in coexisting mineral phases. As it burns during the first stage of fire, coal matter provides moisture and the space for newly-formed mineral phases.

Preliminary data on the trace elements concentration in Moldova Nouă porphyry copper deposit (Romania)

CIOACĂ MIHAELA ELENA¹ MUNTEANU MARIAN¹ QI LIANG², COSTIN GELU³ AND COSTEA CONSTANTIN¹

¹Geological Institute of Romania, Bucharest, Romania.

(*mihaela.cioaca@igr.ro);

²Institute of Geochemistry, Chinese Academy of Sciences, Guiyang China;

³Rhodes University, Grahamstown, South Africa

Moldova Nouă porphyry Cu ore deposit is associated with the Suvorov quartz dioritic intrusion from Banat Mts (Romania). The copper mineralization essentially consists of chalcopyrite, pyrite ± magnetite, molybdenite, bornite and enargite as impregnations in intensely sericitized rocks. Trace elements (Au, Ag, Mo, Re, Te, In, Ge, PGE) from bulk rock samples in the porphyry type mineralization were analyzed using ICP-MS method. The results indicate mean values of 0.35 ppm Au, 0.29 ppm Ag, 52 ppm Mo, 0.26 ppm Re, 36.23 ppm Te, 0.11 ppm In, 1.43 ppm Ge, 4.18 ppm Se, 2.32 ppm Bi and ppm As 175. PGE shows very low values (~2 ppb in total). EMPA analyses show notable concentrations of Au in enargite, tennantite and pyrite (100-1300 ppm), Ag in covellite, enargite, tennantite, chalcopyrite (100-1300 ppm) and galena (1600-3000 ppm), Se in tennantite and enargite (300-2200 ppm), galena (800-4000 ppm) and in covellite, chalcopyrite and sphalerite (20-400 ppm), Bi in all sulfides (700-1000 ppm). Ge and In have been detected in some samples of chalcopyrite, galena and sphalerite.

U-bearing hematite: A tool for dating Iron Oxide Copper Gold systems?

C.L. CIOBANU^{1*}, B.P. WADE², N.J. COOK¹, D. GILES¹,
A. SCHMIDT-MUMM¹ AND J. CLEVERLEY³

- ¹ Deep Exploration Technologies Cooperative Research Centre, The University of Adelaide, Adelaide, SA 5005, Australia (*correspondence: cristiana.ciobanu@adelaide.edu.au, nigel.cook@adelaide.edu.au, david.giles@adelaide.edu.au, asmumm@gmail.com)
² Adelaide Microscopy, The University of Adelaide, Adelaide, SA 5005, Australia (benjamin.wade@adelaide.edu.au)
³ CSIRO Earth Science & Resource Engineering, 6102 WA, Australia (james.cleverley@csiro.au)

Hematite, the most abundant mineral in Iron Oxide Copper Gold (IOCG) deposits in the Gawler Craton of South Australia, may incorporate significant amounts of U, W, Mo and radiogenic Pb. These elements are concentrated in hematite grains which display either oscillatory and/or sectorial compositional zoning, or are porous. The presence of U and Pb raises the potential for novel geochronology applications aimed at constraining the timing of mineralization.

Meaningful preliminary age data were obtained for U-bearing hematite by LA-ICP-MS techniques on zoned grains. In the absence of suitable, matrix-matched standards, GJ-1 zircon was used as the primary standard. ²⁰⁷Pb/²⁰⁶Pb ages obtained on the zoned hematite (1590±7, 1583±3 Ma; Fig. 1) are statistically indistinguishable from ages for emplacement of the Gawler Range Volcanics and associated Hiltaba Intrusive Suite, and consistent with a major ore-forming event in the region at ~1.59 Ga.

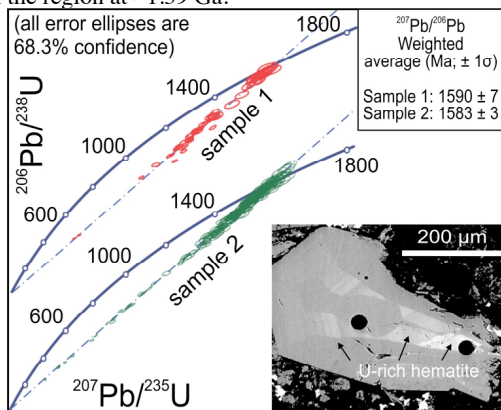


Fig. 1 U/Pb Concordia plots for dated U-hematite. All lower intercepts are at zero. BSE image shows typical zoning in dated grains.

Provided that matrix-associated mass fractionation can be constrained, and suitable standards are fabricated, the ability to date an abundant refractory mineral like hematite could represent a valuable tool for dating IOCG deposits and, potentially, other iron-bearing ores.

Subseafloor biosphere of the Canterbury basin

M.C. CIOBANU¹ G. BURGAUD², A. DUFRESNE³,
A. BREUKER⁴ V. REDOU², S. BEN MAAMAR¹,
F. GABOYER¹ O. VANDENABEELE-TRAMBOUZE¹
J.S. LIPP⁵, A. SCHIPPERS⁴ P. VANDENKOORNHUYSE³,
G. BARBIER² M. JEBBAR¹ A., GODFROY¹
AND K. ALAIN^{1*}

- ¹LM2E, UMR 6197 CNRS-UBO-Ifremer, IUEM, Plouzané, France (*correspondence: Karine.Alain@univ-brest.fr)
²LUBEM, EA3882 UBO-UEB, ESIA, Plouzané, France
³ECOBIO, UMR 6553 Univ Rennes I-CNRS, Rennes, France
⁴BGR, Hannover, Germany
⁵MARUM, University of Bremen, Bremen, Germany

The subseafloor microbiota is diverse and complex, hosting metabolically active communities down to depths of more than 1000 meters below the seafloor (mbsf), as revealed by molecular and metagenomic studies. It harbors representatives from the three domains of life, i.e., numerous endemic and/or as yet uncultured *Archaea* and *Bacteria*, in addition to bacterial endospores, protists and fungi belonging to *Eukarya*. Although background molecular data on bacterial and archaeal lineages inhabiting subsurface sediment above 1000 mbsf exists, most deep-subsurface microorganisms detected so far were refractory to cultivation. Deeply buried microorganisms form an almost untapped diversity, as sub-sea-floor prokaryotic culturability in most studies is less than 0.1% of all microscopically detected cells. So far, active prokaryotes have been discovered down to 1626 mbsf, and microeukaryotes down to 113 mbsf, but the lower limit of the deep subsurface biosphere remains elusive.

Here we report on the microbial prokaryotic and eukaryotic communities of a core of nearly 2 km collected in the Canterbury basin during IODP Expedition 317. A very stringent high-throughput 454-pyrosequencing approach targeting the 16S/18S rRNA genes for *Bacteria*, *Archaea* and *Eukarya*, along with real-time PCR analysis (genetic markers and functional genes), cell counts and cultures, were performed to assess microbial abundance, diversity and activity at different depths. Our results suggest that a diversity of microorganisms exists down to 1922 mbsf in the seafloor of the Canterbury basin and that this diversity is to a certain extent alive.

The opening phase of the 2010 summit eruption of Eyjafjallajökull volcano, Iceland: Contributions from morpho-textural and geochemical characterization of tephra

RAFFAELLO CIONI¹ MARCO PISTOLESI²,
LORELLA FRANCALANCI³ ANTONELLA BERTAGNINI⁴
CLAUDIA D'ORIANO⁴ AND ELEONORA BRASCHI⁵

¹Dip. di Scienze Chimiche e Geologiche, Cagliari, Italy;
(rcioni@unica.it)

²Dip. Scienze della Terra, Università di Pisa, Italy

³Dip. Scienze della Terra, Università di Firenze, Italy

⁴Istituto Nazionale di Geofisica e Vulcanologia, Pisa, Italy

⁵CNR-IGG, Firenze, Italy

The 2010 summit eruption of Eyjafjallajökull volcano (Iceland) started on 14 April when the eruption melted its way through the ice-filled summit caldera. We focus on the opening phase of the event (first 15-17 hours), which represents a unique opportunity to investigate triggering mechanisms and pre-eruptive dynamics.

Tephra samples were collected from the pristine fallout deposits ~4.5 km east from the crater. On the whole, the juvenile components along the eruptive sequence show a large morphological and textural variability. The peculiarity of the products of the opening phase is the presence of abundant (40 vol.%) blocky, dense, obsidian-like, microlite-poor clasts. These features suggest important quenching effects of the first body intruded at the base of the ice cover immediately before the eruption onset. Major and trace element analyses on groundmass glass of this phase highlight the occurrence of clasts with a larger compositional variability than those of the products from the following phases. Similarly, ⁸⁷Sr/⁸⁶Sr ratios determined by microdrilling on single ash clasts revealed the presence of groundmass glass with large isotopic variability, ranging from the typical values recorded in Icelandic magma, up to much higher values (⁸⁷Sr/⁸⁶Sr = 0.70668), never found in Icelandic volcanics. Conversely, plagioclase crystals from the same phase of activity have low ⁸⁷Sr/⁸⁶Sr values. These compositional and isotopic data suggest that the very first erupted magma assimilated hydrothermally altered volcanic/epiclastic rocks with high Sr isotopic ratio, possibly in the immediately pre-eruptive phase. The results confirm the importance of studying the products of the opening phases of explosive eruptions in order to get a complete understanding of pre-eruptive conditions.

Zircon U-Pb ages and δ¹⁸O in a 'contaminated' lower crustal metagabbro (Serre Massif, Calabria)

R. CIRRINCIONE¹, P. FIANNACCA^{1*} AND I.S. WILLIAMS²

¹Department of Biological, Geological and Environmental Sciences, University of Catania

(*correspondence: pfianna@unict.it)

²Research School of Earth Sciences, Australian National University

Previous dating of granulitic metagabbros from the base of a near-complete cross-section of Variscan continental crust exposed in southern Calabria has provided reliable ages of ~300-290 Ma for the late Variscan metamorphism, but less convincing ages of ~593-564 Ma for the original mafic magmatism [1,2,3]. Zircon extracted from a basal metagabbro to determine the age and nature of deep crustal magmatism has two main forms: moderately luminescent, weakly zoned overgrowths or whole grains with no core, and cores surrounded by an overgrowth. 53 SHRIMP U-Pb dates have a wide range from ~3.2 Ga to ~270 Ma. 35 cores are older than ~330 Ma, with weak clusters at 720±40, 620±35 and 560±25 Ma. The largest cluster, at 455±9 Ma (6 cores), is the youngest possibly pre-metamorphic group. Overgrowths and coreless grains (Th/U <0.3) all have dates ≤330 Ma, giving ~313 Ma as the maximum age for the youngest thermal event that produced zircon growth or recrystallization. All this zircon has high δ¹⁸O (9.3–10.6‰), indicating crystallization in the presence of sediment related fluids. Several cores in the 330-500 Ma range have the same features. Older cores have lower δ¹⁸O (6.1-9.2‰), but only three are <7.5‰. There is no preserved evidence for any zircon in the metagabbro being primary zircon crystallized from a mantle-derived magma. Instead, the oxygen isotopes have a strong sediment signature, consistent with the large amount of detrital zircon in the rock. Either the metagabbro is dominantly of metasedimentary origin, or prolonged granulitic evolution of a sediment-'contaminated' mafic magma in the deep crust has largely modified the zircon δ¹⁸O and some U-Pb dates, making it hard to determine the gabbro emplacement age. If the 455±9 Ma zircon is detrital, however, the gabbro magmatism must be younger. These inferences now need to be tested using trace element and isotopic analyses of zircon and other minerals from the metagabbro and associated rocks.

[1] Schenk & Todt (1989) *Terra Abstracts* **1**, 350. [2] Micheletti *et al.* (2008) *Lithos* **104**, 1-11. [3] Fornelli *et al.* (2011) *Mineral. Petrol* **103**, 101-122.

Eoarchean crust in the Dniestr-Bug region, Ukrainian Shield – Pb-Hf-O isotope constraints

S. CLAESSON^{1*}, L. SHUMLYANSKY^{1,2}, E. BIBIKOVA³, K. BILLSTRÖM¹, M. WHITEHOUSE¹ AND T. ANDERSEN⁴

¹ Swedish Museum of Natural History, Stockholm, Sweden

(*correspondence: stefan.claesson@nrm.se)

² Institute of Geochemistry, Mineralogy and Ore Formation, Kyiv, Ukraine

³ Vernadsky Institute of Geochemistry & Analytical Chemistry RAS, Moscow, Russia

⁴ Dept of Geosciences, University of Oslo, Norway

In the Ukrainian shield, enderbites of the Dniestr-Bug Series contain zircons as old as c. 3.75 Ga with initial Hf isotope ratios indicating their derivation from mildly depleted sources. Most Dniestr-Bug rocks are strongly tectonized and metamorphosed. We present here new U-Pb, Hf and O isotope results for zircon separated from enderbite, a supracrustal garnet-mica schist, and an assumedly clastic quartz-rich rock enclosed in enderbite.

Zircon from all these rocks yields variably discordant U-Pb ages up to c. 3.75 Ga. Hf isotope compositions for the oldest zircons indicate these crystallized from magmas with chondritic to slightly depleted isotope signatures at c. 3.75 Ga. The majority of zircons with younger U-Pb ages also appear to be ultimately derived from similar crustal sources. This supports that there was an important period of formation of continental crust at c. 3.75 Ga

$\delta^{18}\text{O}(\text{Zrc})$ for two enderbites range from mantle values to slightly more evolved compositions. $\delta^{18}\text{O}(\text{Zrc})$ up to 7.2‰ for the garnet-mica schist indicates this includes materials which in parts are derived from more evolved sources. $\delta^{18}\text{O}(\text{Zrc})$ for the quartz-rich rock stands out, with a few analyses as low as 7‰ or less, but the majority in the range 8-10‰. Few Archaean zircon crystals with such high $\delta^{18}\text{O}(\text{Zrc})$ values have been reported previously.

If the quartz-rich rock originally is a clastic sediment and the zircon has preserved its magmatic $\delta^{18}\text{O}$ signature, most of the source rocks had evolved O isotopic compositions. Secondary alteration of O in clastic zircon may also be a possibility. Alternatively, the quartz-rich rock may be heavily metasomatized enderbite and the O isotope composition of the zircons altered in a process which at the same time not has erased the original Hf isotope signature.

Clues to atmospheric evolution in Earth's ancient sediments

M.W. CLAIRE¹

¹Department of Earth and Environmental Sciences, University of St Andrews, St Andrews, Fife, KY16 9AL, Scotland, UK (m.claire@uea.ac.uk)

Sulfur isotopes are fractionated in a mass-anomalous fashion when SO_2 gas is subjected to ultraviolet light. Amazingly, the subtle fractionations (MIF-S) resulting from this process are preserved in sedimentary rocks of Archean age, but are absent in younger rocks. The MIF-S data provides direct constraints on the composition of the ancient atmosphere, and have been described as the “smoking gun” for an anoxic Archean atmosphere. In the thirteen years since their initial discovery (Farquhar *et al.* 2000), the database of Archean MIF-S has grown to include detailed temporal (and stratigraphic-level) changes in both sign and magnitude of $\Delta^{33}\text{S}$ and $\Delta^{36}\text{S}$, although our theoretical understanding hasn't advanced much beyond the notion of a 1ppm threshold concentration of atmospheric oxygen (Pavlov and Kasting, 2002). I will summarize my recent numerical modeling efforts made in conjunction with new geochemical data (Zerkle *et al.*, 2012 ; Kurzweil *et al.*, 2013 ; Claire *et al.*, 2013), which reveal how MIF-S might constrain atmospheric methane levels, the presence of an organic haze, the widespread radiation of oxygenic photosynthesis, and changes in the redox-state of the atmosphere/hydrosphere/ geosphere prior to the Great Oxidation Event.

Farquhar *et al.* 2000 *Science* ; Pavlov and Kasting, 2002 *Astrobiology* ; Zerkle *et al.* 2012 *Nature Geoscience* ; Kurzweil *et al.* 2013 *EPSL* ; Claire *et al.* 2013 (in prep)

Chemical homologue speciation in natural systems: A key to understand the anthropogenic RN fate

F. CLARET¹ C. LEROUGE S. GRANGEON¹ T. SATO²
T. SCHÄFER³ E. GIFFAUT⁴ AND C. TOURNASSAT¹

¹BRGM, 3 avenue C. Guillemin, BP 36009, 45060 Orléans Cedex 2-France

²Laboratory of Environmental Geology, Hokkaido University
Kita 13 Nishi 8, Sapporo 060-8628, Japan

³Institute for Nuclear Waste Disposal (INE), KIT Campus Nord, D-76021 Karlsruhe, Germany

⁴RA, 1 rue Jean-monnet, Châtenay-Malabry 92298, France

Anthropogenic radionuclides (RN) are generated by a wide range of industrial, medical and military activities. In a context of storage in deep geological formations or after their release in terrestrial environments by accidents, it is of paramount importance to quantify their mobility, which is partly ruled by their interaction with the solid surfaces. Usually, experiments are conducted using radiotracers at various scale from laboratory to the field in order to measure retention and retardation parameters. Although this kind of experiment is fundamental to tackle this issue, understanding the natural speciation of stable isotopes as chemical homologues to RN brings useful additional information. In particular, it sheds light on RN isotopic exchange and “irreversible” trapping mechanisms. This approach has already been used successfully to gain a better comprehension of iodine fate in the far-field of geological disposals (Claret *et al.*, 2010), which was debated in the literature, due to conflicting experimental results (from no retardation to significant retardation, depending on the study). By careful quantification of iodine reservoirs in the Callovian-Oxfordian clay rock, it was possible to provide new insights into this aspect of the iodine problem. The relevance of such approach for Sr (Lerouge *et al.*, 2010), Se and Ni, three elements with contrasted chemical behaviours and of interest for radwaste storage will be discussed based on new experimental results.

Claret, F., *et al.*, 2010. Natural iodine in a clay formation: Implications for iodine fate in geological disposals. *GCA* 74, 16-29.

Lerouge, C., *et al.* 2010. Strontium distribution and origins in a natural clayey formation (Callovian-Oxfordian, Paris Basin, France): A new sequential extraction procedure. *GCA* 74, 2926-2942.

Interfacial chemistry viewed through the lens of network analysis

A. E. CLARK*¹ A. OZKANLAR² AND M. KELLEY³

Department of Chemistry, Washington State University
(¹a uclark@wsu.edu)

² (abdullah.ozkanlar@wsu.edu)

³ (m.kelly@wsu.edu)

In prior work we have utilized a combination of density functional theory, classical molecular dynamics, and time-resolved laser-induced fluorescence to probe the surface sorption of trivalent lanthanides to various silicate minerals.[1-3] Those studies illustrated the utility and predictive capability of DFT and MD to obtain accurate bulk observable properties and average molecular scale speciation. However, interrogation of interfacial dynamics and time-dependent correlations between surface organization and reactivity have proven more difficult to quantify. Toward this end, we have recently demonstrated that the hydrogen bond network of water has many similarities to the complex and distributed networks found in computer science, and is thus amenable to new types of network information analyses that include degree distributions, network neighborhoods, and geodesic pathways.[4 – 7] Structural motifs can be elucidated within the network. The distribution of defect states and their evolution in time, in addition to a network entropy of the fluid can be also determined. Finally, hydrogen bond dynamics at the molecular and intermediate length scales (1-100's of Å) are readily quantified. In this work we re-analyze our prior MD studies of trivalent sorption to quartz through the lens of modern network analysis methods, deriving new insight into the role that interfacial organization and hydrogen bond dynamics has upon interfacial reactivity.

[1] Wander & Clark (2008), *Journal of Physical Chemistry C* 112, 8233-8241. [2] Kuta, Wander, Wang, Jian, Wall & Clark (2011), *Journal of Physical Chemistry C* 115, 21120-21127. [3] Kuta, Wang, Wisuri, Wander, Wall & Clark (2013), *Geochimica Cosmochimica Acta* 136, 204104. [4] Mooney, Corrales & Clark (2012), *Journal of Computational Chemistry* 33, 853-860. [5] Mooney, Corrales & Clark (2012), *Journal of Physical Chemistry B* 116, 4263. [6] Hudelson, Mooney & Clark (2012), *Journal of Mathematical Chemistry* 50, 2342. [7] Ozkanlar & Clark (2013), *Journal of Physical Chemistry B*, submitted.

Garnet, zircon and monazite as monitors of high-temperature metamorphic events: How useful are they?

CHRIS CLARK^{1*}

¹Applied Geology, Curtin University, Perth, WA, Australia
(*correspondence: c.clark@curtin.edu.au)

Value adding to the temporal information retrieved from the analysis of geochronometers, such as zircon and monazite, through the collection of rare-earth (REE) and trace element datasets and attempts to integrate their growth with thermodynamic datasets is a field that is rapidly evolving. This information when coupled with REE analyses of silicate minerals such as garnet, orthopyroxene and feldspar allows inferences to be made about the rates of heating, cooling and exhumation as well as the timing of partial melting experienced by rocks during orogenic cycles. Advances in analytical capabilities (e.g. laser split streaming) now allow large datasets to be collected across entire terranes enabling age-mapping of orogens to be undertaken. However, in high-temperature metapelites that seem to have all the right ingredients for these processes to be constrained (e.g. they contain garnet, zircon, monazite and rutile, they've melted and experienced temperatures in excess of 900 °C) variations in the REE partitioning between zircon and garnet varies over the length-scale of a single thin section. This presentation seeks to highlight some complexities in the application of these undoubtedly useful techniques to high-temperature metamorphic rocks from a number of terranes and hopefully provide some useful comments on developing more efficient strategies to characterise the P - T - t evolution of high-grade terranes.

Combustion aerosol over marine stratus: Long range transport, subsidence and aerosol-cloud interactions over the South East Pacific

A. CLARKE^{1*} S. FREITAG¹, J. SNIDER² J. KAZIL^{3,4},
G. FEINGOLD⁴ R. BLOT¹ T. CAMPOS⁵
AND V. BREKHOVSKIKH¹

¹University of Hawaii, Honolulu, HI, USA

(*correspondence: tclarke@soest.hawaii.edu)

²University of Wyoming, Laramie, WY, USA

³CIRES, University of Colorado, Boulder, CO, USA

⁴NOAA, Earth System Res. Lab., Boulder, CO, USA

⁵NCAR, Boulder, CO, USA

The worlds largest stratus deck over the South East Pacific (SEP) was a study target for the VOCALS (<http://www.eol.ucar.edu/projects/vocals/>) experiment in October 2008. Aerosol-cloud interactions were one major goal of the 14 flights of the NCAR C-130 aircraft reported here. Each flight covered about a 1000 km range with multiple profiles and legs below, in and above the Sc deck.

Strong aerosol sources along the coast of Chile were expected and found to influence cloud condensation nuclei (CCN) in coastal clouds. However; "rivers" of elevated CO, black carbon (BC) associated with combustion aerosol effective as CCN at <0.3%S were also common in subsiding FT. These often lay above the extensive Sc deck for over 1000km offshore and included aerosol from sources over the western Pacific as well as South America. When present above cloud, this combustion aerosol increased available CCN and decreased effective radius compared to clouds in "clean" MBL air advected from the South Pacific. Observed aerosol entrainment appeared linked to turbulence localized near cloud that significantly exceeded mean estimated entrainment rates. Surface derived sea-spray aerosol ($D_p > 40\text{nm}$) only accounted for about 20% of MBL CCN.

Pockets of Open Cell (POC) convection were consistently found in air with CO values lower than adjacent cloudy regions and similar to values over the remote South Pacific. As CO is not depleted by clouds or precipitation this suggests POC's are favored to form in clean SP air not impacted by entrained combustion aerosol. Preliminary LES model results indicate that such entrainment may help buffer MBL clouds against depletion of CCN by drizzle. The latter would delay transition of closed cell to open cell convection, potentially leading to increased lifetimes of Sc clouds. One case of entrainment of a strong "river" of pollution appears to have led to a transition from POC's back to a cloudy MBL.

Late Cretaceous sub-tropical Pacific Ocean clumped-isotope palaeothermometry

L.J. CLARKE¹* I. MILLÁN² AND S.M. BERNASCONI²

¹Division of Chemistry and Environmental Science, School of Science and the Environment, Manchester Metropolitan University, Manchester, M1 5GD, U.K. (*correspondence: l.clarke@mmu.ac.uk)

²Geologisches Institut, ETH, 8092 Zurich, Switzerland. (isabel.millan@erdw.ethz.ch), (stefano.bernasconi@erdw.ethz.ch)

Carbonate clumped-isotope palaeothermometry data are presented for the <38 micron coccolithophore-bearing fraction of Late Cretaceous (Campanian to Maastrichtian) sediments recovered from Shatsky Rise Ocean Drilling Program Site 1210, presently situated in the northwest Pacific Ocean. The predominantly coccolithophore composition of the sediments enables reconstruction of photic zone surface-ocean palaeotemperatures. Site 1210 occupied a sub-tropical palaeolatitude in the Pacific Ocean during the Late Cretaceous that resulted in relatively high sedimentation rates for an open-marine setting. Site 1210 Late Cretaceous sediments comprise nannofossil ooze that has not undergone sufficient sub-seafloor diagenesis to cause lithification and conversion into chalk or limestone, making these sediment cores ideally suited for novel application of clumped-isotope palaeothermometry. Clumped-isotope data were generated using the ETH automated mass spectrometry method of Schmid and Bernasconi [1].

The novel clumped-isotope dataset is discussed in terms of a number of critical palaeoceanographic objectives and interpretations: 1) determination of absolute Late Cretaceous sub-tropical Pacific Ocean palaeotemperatures and associated reconstruction of latitudinal palaeotemperature gradients, both via comparison to other published palaeotemperature data; 2) assessment of whether an orbital-forcing control on the sub-tropical surface ocean is evident within the clumped-isotope palaeotemperature record; and 3) use of clumped-isotope palaeotemperatures in combination with conventional $\delta^{18}\text{O}$ values in order to deconvolute a temporal seawater oxygen-isotope composition record, specifically to test the hypothesised occurrence of cryosphere development, and associated glacioeustatic sea-level change, proximal to the Campanian to Maastrichtian stage boundary.

[1] Schmid & Bernasconi (2010) *RCMS* **24**, 1955-1963.

Ocean redox dynamics during the end-Permian extinction and Early Triassic recovery

MATTHEW O. CLARKSON¹ SIMON W. POULTON²,
RACHEL A. WOOD¹ AND SYLVAIN RICHOUZ³

¹School of GeoSc., Univ. of Edinburgh, EH3 9JW, UK (*correspondence: M.O.Clarkson@ed.ac.uk)

²School of Earth & Env., Univ. of Leeds. LS2 9JT, UK

³Austrian Ac. Of Sc., c/o Univ. Graz, 26 8010, Austria

The Permian Triassic mass extinction is widely regarded as the most severe of the Phanerozoic extinctions. The event was associated with major carbon cycle disruption, not only at the Permian Triassic Boundary (PTB) but also for the entire Early Triassic. These disturbances are recorded in the $\delta^{13}\text{C}$ record of both carbonate and organic carbon, which show a series of positive and negative carbon isotope excursions (CIEs) throughout the Early Triassic. These fluctuations are also linked to minor extinctions in the Early Triassic and a delay in total species recovery until the Middle Triassic. One leading hypothesis invoked to explain these changes is oceanic anoxia, which provides a kill mechanism that is also potentially linked to observed changes in the carbon isotope record. Multiple anoxic events have indeed been identified in various sections around the world. However the link between the globally recorded CIEs and the development of anoxia is not clear, with no consistent relationship emerging.

Here we present a new record of anoxia from the Arabian platform using Fe-S-C systematics. This mixed sequence of continental margin carbonates and clastics records a shelf to basin transect for the PTB and Early Triassic, which demonstrates the distinct CIEs mentioned above. The use of Fe-speciation in tandem with carbon isotopes places the local record of anoxia in a global context, thus helping elucidate the timing, development and stability of anoxia.

Initial data show sustained anoxic, non-sulphidic (ferruginous) conditions across the PTB for both slope and basin settings. Subsequently anoxia appears restricted to the positive CIEs. Here, non-sulphidic conditions were again dominant, which is in contrast to a growing body of evidence indicating euxinic conditions for the PTB. S-isotope systematics provide further insight into controls on the observed environmental conditions at this time. Together, our approach provides a detailed examination of ocean redox variability during this interval of extreme environmental disturbance, thus enabling a greater understanding of C-cycle feedbacks and biological consequences.

Halogen (Cl, Br and I) inventory of the primitive meteorites

P.L. CLAY R. BURGESS H. BUSEMANN L. RUZIĆ.
B. JOACHIM AND C.J. BALLENTINE

The University of Manchester, SEAES, Oxford Rd.,
Manchester, UK, M13 9PL

The halogens (Cl, Br and I) are sensitive tracers of planetary processing (e.g., melting, differentiation, crust formation, etc.) due to their low abundance and incompatible nature. In order to further our understanding of the halogens response to these crucial aspects of planetary formation, extending our baseline knowledge of their concentration and distribution in the materials that accreted to form the planets (and planetesimals) is essential. The relative scarcity of halogen measurements, particularly Br and I, in the literature attests to the ultra low abundance of these elements in the primitive meteorites and thus their lack of suitability for measurement by traditional ion- and micro-probe techniques.

A systematic study of the halogens in the primitive meteorites (carbonaceous, ordinary and enstatite chondrites) was undertaken to extend the existing halogen database. Chlorine, Br and I were extracted from IR laser stepped-heating of 0.25 to 3.3 mg of neutron-irradiated samples and measured by noble gas mass spectrometry using the noble gas proxy isotopes $^{38}\text{Ar}_{\text{Cl}}/\text{Cl}$, $^{80}\text{Kr}_{\text{Br}}/\text{Br}$ and $^{128}\text{Xe}_{\text{I}}/\text{I}$. The results of carbonaceous (CV), ordinary (H, L and LL) and enstatite chondrites (EH and EL) are given here. The ordinary chondrites have variable halogen concentrations (5–600 ppm Cl, 1–1650 ppb Br and 2–390 ppb I) and very low molar I/Cl ($\sim 10^{-6}$) and Br/Cl ($\sim 10^{-4}$) ratios, comparable to those measured in some terrestrial hydrothermal fluids [1]. The EH chondrites are overall the most consistently enriched in halogens (65–330 ppm Cl, 610–2290 ppb Br and 140–180 ppb I) and show near constant I concentration, regardless of petrologic type. The EL6 Daniel's Kuil is depleted in halogens (25 ppm Cl, 60 ppb Br and 9 ppb I), which could be due to loss during metamorphism on the EL parent body. Two of three Antarctic meteorite analyses (MIL 07139; EH3) show an extreme enrichment in halogens (e.g., 6700 ppb Br); this is likely a surface phenomenon related to terrestrial weathering [2] and are therefore not included in the above ranges. Forthcoming results from CI, CM and CR chondrites, as well as extension to other petrologic types for the above groups, will further elucidate the distribution of halogens in the most primitive solar system materials.

[1] Böhlke & Irwin (1992) *EPSL*, 110: 51–66. [2] Langenauer & Krahenbuh (1993) *Meteoritics*, 28: 98–104.

Li and Sr constraints on biogeochemical processes in a tropical andesitic watershed

CLERGUE C.^{1,2*}, DESSERT C.^{1,2}, BUSS H.³, DELLINGER M.¹, CRISPI O.², ROUSTEAU A.⁴, GAILLARDET J.¹
AND BENEDETTI M.F.²

¹Institut de Physique du Globe de Paris, UMR 7154,
Université Paris Diderot

(*correspondence:clergue@ipgp.fr)

²Observatoire de volcanologie et de sismologie de
Guadeloupe et Observatoire de l'érosion aux Antilles,
Institut de Physique du Globe de Paris

³School of Earth Sciences, Univ. of Bristol, Bristol BS8 1RJ,
UK

⁴Laboratoire de biologie et physiologie végétale, Université
Antilles Guyane

In this study, we analysed Sr and Li concentrations and isotopic compositions in the surface reservoirs (soils, rocks, plants, stream and rain waters) of a small forested andesitic watershed located in the tropical rain forest of Guadeloupe. Sr is used to identify the sources contributing to soil genesis and Li is good tool to describe weathering dynamic.

Our results show that the $^{87}\text{Sr}/^{86}\text{Sr}$ ratio of unweathered andesite is 0.704. Previous studies have shown that deposition of Saharan dusts with signature around 0.717 occurs in the Caribbean. Most of soil samples Sr isotopes ratios (between 0.7086 and 0.7155) are intermediate between rainfall (0.710) and Saharan dust endmembers. That reveals the significant contribution of atmospheric deposition to soil composition and confirms previous study done in Puerto Rico (Pett-Ridge *et al.*, 2009).

The $\delta^7\text{Li}$ signature of unweathered andesite and Montserrat dusts is around 4.5‰. Because of its origin, Saharan dust signature can be estimated around 1‰. In the soil, $\delta^7\text{Li}$ signature decreases from 3.0‰ to -10.5‰ between 0 and 1250 cm. Many studies have shown that during chemical weathering Li isotopes are fractionated as ^6Li is preferentially retained in solid secondary phases whereas dissolved fraction are enriched in ^7Li . Here the decrease of $\delta^7\text{Li}$ reflects the increase of weathering intensity with depth.

In this tropical Caribbean context, with very thick and cation poor soil, Saharan minerals have strong impact on soil genesis. Because of thick saprolite layer, vegetation is isolated from primary minerals and those atmospheric inputs might constitute a significant nutrient supply for vegetation growth.

$^{16}\text{O}^1\text{H}$ signal as an indication of metamict O-contamination in zircon

J. CLIFF^{1*}, R.T. PIDGEON² AND A.A. NEMCHIN²

¹Centre for Microscopy, Characterisation and Analysis, University of Western Australia, Perth Western Australia (*correspondence: john.cliff@uwa.edu.au)

²Department of Applied Geology, Curtin Univ., Perth Western Australia

Although zircons are generally considered to be refractory with respect to oxygen isotope signatures, metamiction can make the mineral susceptible to O-isotope exchange. A variety of means are available to indicate metamict conditions, i.e. electron microscopy, common Pb contamination, Raman spectroscopy, α -damage etc., however, these methods may be inconvenient or may in some cases lead to the erroneous conclusion that the zircon is pristine. We introduce here a SIMS based technique that can provide evidence of metamiction and at the same time perform $\delta^{18}\text{O}$ analyses—namely the analysis of the $^{16}\text{O}^1\text{H}$ signal. The technique is particularly well suited to multicollector instruments and can be utilized with little to no decrease in $\delta^{18}\text{O}$ precision. In a pilot study using the technique, we found that elevated $^{16}\text{O}^1\text{H}/^{16}\text{O}$ relative to a highly crystalline standard (CZ3; $^{16}\text{O}^1\text{H}/^{16}\text{O} = 0.00136 \pm 0.00006$; mean ± 1 SD) was correlated with apparent radiation damage and we interpret an increase in this signal to indicate excess H_2O in the mineral. Although $\delta^{18}\text{O}$ in these amorphous regions varied from -7‰ to $+8.5\text{‰}$ (VSMOW; Fig. 1), regions with $^{16}\text{O}^1\text{H}/^{16}\text{O}$ values less than 6 SD above the CZ3 mean value were all interpretable as mantle $\delta^{18}\text{O}$ values. We found that the magnitude of the $^{16}\text{O}^1\text{H}/^{16}\text{O}$ on pristine zircons is dependant upon chamber vacuum and sample degassing and it is unclear if the zircon signal is detectable above background. However, at a given vacuum, four different standards gave statistically indistinguishable $^{16}\text{O}^1\text{H}/^{16}\text{O}$ values.

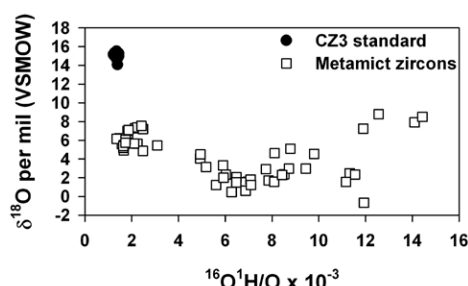


Fig 1. Comparison of $\delta^{18}\text{O}$ and $^{16}\text{O}^1\text{H}/\text{O}$ in the CZ3 standard and metamict zircons.

Doubly ^{13}C -substituted ethane

MATTHIEU D. CLOG^{1*} JOHN M. EILER¹ JARBAS V. P. GUZZO² ERICA T. MORAES² AND IGOR V.A. SOUZA²

¹Caltech, Pasadena, CA, USA (clog@caltech.edu, eiler@gps.caltech.edu)

²Petrobras R&D Center, Cempes

Most natural gas reservoirs contain significant amounts of ethane (C_2H_6). Here we examine the geochemistry of multiple ^{13}C substitutions in this molecule. Several processes can plausibly influence the abundances of $^{13}\text{C}_2\text{H}_6$ in natural gases: inheritance from larger biomolecules in source rocks; kinetic fractionations associated with thermal degradation or organic matter; isotope exchange reactions at thermodynamic equilibrium; and/or mixing of gases with different bulk isotopic composition. There is little basis for a priori predictions as to which of these processes will dominate in nature. We present the mass spectrometric techniques for measurement of $^{13}\text{C}_2\text{H}_6$ at natural abundances, using a high-resolution gas source isotope ratio mass spectrometer (the Thermo 253 Ultra), and explore the chemistry of this species through experiments and initial results on conventional thermogenic natural gases.

The high resolutions of the Ultra (up to 27,000, $M/\Delta M$) allow clean separation of obvious interferences (e.g., O_2 or CH_3OH at $m/z=32$). Most critically, we are able to discriminate the doubly-substituted isotopologues $^{13}\text{C}_2\text{H}_6$ from $^{13}\text{C}^{12}\text{CDH}_5$ at $m/z=32$. However, we find it is fastest and most precise if we analyse the sum of both singly-substituted isotopologues at $m/z=31$, $^{13}\text{C}^{12}\text{CH}_6$ and $^{12}\text{C}_2\text{H}_5\text{D}$, and then calculate $\delta^{13}\text{C}$ based on a conventional measurement of δD . We report abundances of $^{13}\text{C}_2\text{H}_6$ as an enrichment relative to a stochastic reference frame: $\Delta^{13}\text{C}_2\text{H}_6 = 1000 * ((^{13}\text{C}_2\text{H}_6/\text{C}_2\text{H}_6) / (^{13}\text{C}_2\text{H}_6/\text{C}_2\text{H}_6)_{\text{stochastic}} - 1)$.

Measurements of the $^{13}\text{C}_2\text{H}_6/^{12}\text{C}_2\text{H}_6$ ratio are limited by counting statistics down to ± 0.15 per mil (1 s.e.). The corresponding precision in $\Delta^{13}\text{C}_2\text{H}_6$ is ± 0.2 per mil (1 s.e.), when one includes the small additional uncertainties in the 31/30 ratio and conventional δD measurements. Replicate extractions of natural samples are reproducible to better than $\pm 0.5\text{‰}$. Analyses of synthetic gas mixtures confirm that fragmentation/ recombination reactions in the ion source are not a major factor. Preliminary work on ethane from thermogenic gases showed a total range in $\Delta^{13}\text{C}_2\text{H}_6$ of 4 ‰. The expected range in $\Delta^{13}\text{C}_2\text{H}_6$ due to thermodynamic equilibrium alone at typical temperatures of natural gas generation and storage is only $\sim 0.2\text{--}0.3\text{‰}$. Thus, our results suggest that proportions of $^{13}\text{C}_2\text{H}_6$ in natural gases are largely controlled by inheritance from organic precursors and/or kinetic isotope effects associated with gas generation. This is an expected result because isotopic exchange of the C-C bond in ethane is likely slow under geological conditions.

Tephra interference during amorphous silica determination - A false environmental signal?

WIM CLYMANS^{1*}, NATHALIE VAN DER PUTTEN¹,
STEFAN WASTEGÅRD², SVANTE BJÖRCK¹
AND DANIEL J. CONLEY¹

¹Department of Geology, Lund University, Sweden
(*correspondence: wim.clymans@geol.lu.se)

²Department of Physical Geography and Quaternary Geology,
Stockholm University, Sweden

Amorphous silica (ASi) is a widely applied environmental proxy that had ecological and hydrological interpretations. Volcanic eruptions can eject large amounts of igneous material to the atmosphere. The ash-outfall covers the landscape with continuous ash-deposits called tephra. The rapid weathering of tephra results in the formation of short-range ordered minerals (e.g. allophane, imogolite). The dissolution properties of short-range ordered minerals are believed to be similar to those of ASi. Soil and palaeo-environmental scientists have ignored its contribution during measurement. Nevertheless, evaluation of its exact contribution to ASi measurements or examining its dissolution behavior is lacking. We tested if tephra ASi contributes to ASi measurements during alkaline extraction, and how it interferes with sediment and lake records from the southern hemisphere.

We selected 25 well-known tephra covering a representative range of chemical composition, age, spatial provenance and sample type. A well-studied peat core from Kerguelen was used to verify its interactions with other ecological and hydrological proxies. Samples were analyzed for total ASi using the long-term sequential Na₂CO₃ (0.1M) and continuous NaOH (0.5M) method, as such obtaining detailed dissolution curves.

Amorphous Si content extracted from tephra ranged between 0.19 and 2.92 SiO₂ wt%. The extracted amount was independent of age and weakly related to its chemical composition. Detailed dissolution curves provided a distinct signature for pure tephra compared to other ASi fractions.

Palaeo-environmental studies using elevated ASi levels (> 10 SiO₂ wt%) to indicate environmental changes, encounter limited interference problems. However, our study does not exclude that increased diatom productivity could be caused by tephra weathering rather than a change in environmental conditions.

Metal behaviour during differentiation of subducted-related lavas (Hunter Ridge, SW Pacific)

GISELA COBENAS^{*1}, LEONID DANYUSHEVSKY¹
AND TREVOR FALLOON¹

¹¹CODES,ARC, Centre of Excellence in Ore Deposits, University of Tasmania, Hobart, Australia, gcobenas@utas.edu.au (* presenting author) (l.dan@utas.edu.au) (trevor.falloon@utas.edu.au)

The behaviour of key ore-forming metals during magmatic differentiation of typical island-arc lava suites from the Hunter Ridge (i.e. calc-alkaline and adakites) have been investigated using geochemistry of minerals and glass, petrographic observations, and quantitative geochemical modelling. The Hunter Ridge extends from the southern termination of the Vanuatu Trench to the Koro sea near Fiji. Calc-alkaline rocks record a protracted history of magma evolution from the very earliest stages of fractionation (i.e. before volatile loss) to eruption on the sea floor.

Metal partitioning behaviour in the principal magma components was examined (i.e. for olivine, clinopyroxene, plagioclase, magnetite, and melt). Mineral/melt partition coefficients (Ds) for Cu, Zn, V, Pb, Co and Sc were calculated directly from LA-ICP-MS analyses for phenocryst-groundmass/glass equilibrium pairs. For comparison purposes, modelling was also conducted using D values obtained from literature (where available). This approach allows us to examine, in detail, how magma ascent, crystallisation and degassing can lead either to the enrichment or depletion of ore-forming metals.

Our results provide evidence that i) Cu partitions into a H₂O-rich fluid at crustal levels as soon as volatile saturation occurs, ii) arc magmas are likely to exsolve a magmatic hydrothermal fluid before they are able to segregate an immiscible sulphide liquid, due to their higher oxidation states and volatile contents. Thus, a critical step in forming magmatic/hydrothermal ore deposits is concentrating and removing metals (i.e. Cu) from a magma before saturation of an immiscible sulphide liquid occurs. As Cu is incompatible in any of the early crystallizing silicates and oxides, its concentration in the melt will progressively increase and it will be available to partition into an aqueous fluid phase. Zn and V are strongly controlled by magnetite fractionation. Co and Sc partition into olivine and clinopyroxene from the early stages of fractionation, and magnetite once it enters the liquidus. Pb behaves incompatibly and is concentrated in the melt during magmatic differentiation.

Phosphorus availability in agricultural soils of Wallonia (Belgium) – A modeling approach

FLORIAN COBERT¹ OLIVIER POURRET²,
MALORIE RENNESON¹ AND GILLES COLINET¹

¹Université de Liège, Gembloux Agro-Bio Tech. Unité Systèmes Sol-Eau, 2 passage des déportés. B-5030 Gembloux Belgique, (florian.cobert@ulg.ac.be) ; (gilles.colinet@ulg.ac.be) ; (malorie.renneson@ulg.ac.be)

²HydrISI Institut Polytechnique LaSalle Beauvais, 19 rue Pierre Waguet, F-60026 Beauvais Cedex, France, (olivier.pourret@lasalle-beauvais.fr)

A better understanding of Phosphorus (P) behaviour in soil is needed to adapt the ordinary practices of P fertilization to the requirement of reducing agricultural impact on the environment (eutrophication of surface water) without impairing crop yields.

The aim of this study was to identify the chemical parameters that actually govern the modelling of available P in agricultural soils of Wallonia with the PHREEQC geochemical model [1]. In a first step, the chemical parameters necessary in input data to have an optimal modeling of P available in Wallonia soils were defined. During this input data calibration, our results show that it is necessary to use soil pH_{water} rather than soil pH_{KCl} and $[\text{Al}]_{\text{ox}}$ (oxalate-extractable Al) rather than $[\text{Al}]_{\text{total}}$. For other parameters, this study shows that using total content is suitable enough. In a second step, sensitivity tests were performed to quantitatively evaluate the impact of input data variations on mean P available modelled. Results of these sensitivity tests show that only pH_{water} and $[\text{Mg}]_{\text{total}}$ variations significantly influence the modelling results (i.e. mean P available in agricultural soils of Wallonia). Indeed, mean P available modelled increases by a factor 3 when the soil pH_{water} is raised from 7.3 to 8.0. The modelled values decrease of 9% and 16%, respectively, when $[\text{Mg}]_{\text{total}}$ increases of 20 and 40%, at soil $\text{pH}_{\text{water}} = 8.2$. However, results show that mean available P is not sensitive neither to soil pH_{water} nor to $[\text{Mg}]_{\text{total}}$ variations, when soil $\text{pH} \leq 7.3$.

This study has shown the high potential of PHREEQC modelling to predict available P and to estimate chemical parameters that govern P availability in Wallonia soils. As these input data parameters and PHREEQC model are calibrated, we will further try to predict the impact of various agricultural systems on the fate of P in soils.

[1] Parkhurst, D.L., Appelo, C.A.J., 1999. User's guide to PHREEQC (Version 2)

The structure of Mg-stabilised amorphous calcium carbonate

G. COBOURNE¹, G. MOUNTJOY^{1*}, A.C. HANNON², J.D. RODRIGUEZ-BLANCO³, L.G. BENNING³

¹School of Physical Sciences, University of Kent, Ingram Building, Canterbury, CT2 7NH, UK

²ISIS Neutron and Muon Source, Rutherford Appleton Laboratory, Harwell OX11 0QX, UK

³School of Earth and Environment, University of Leeds, Leeds LS2 9JT, UK

(gc262@kent.ac.uk, correspondence*:

g.mountjoy@kent.ac.uk, alex.hannon@stfc.ac.uk,

jblanco@nano.ku.dk, L.G.Benning@leeds.ac.uk)

Amorphous calcium carbonate (ACC) is thought to play a key role in biomineralisation processes in sea organisms. Very few structural studies have been performed on ACC, mainly due to its instability and tendency to crystallise into calcite. Magnesium-stabilised ACC has been prepared [1,2] with Mg:Ca ratio of 0.05:1, and has enabled neutron and x-ray diffraction measurements. The Empirical Potential Structure Refinement (EPSR) method has been used to make a model of Magnesium-stabilised ACC having good agreement with the experimental diffraction data. The model has well-defined CO_3 and H_2O molecules with an average calcium coordination of 7. The distribution of calcium in the model is homogeneous with a uniformly distributed Ca-rich network and no evidence of Ca-poor channels [3].

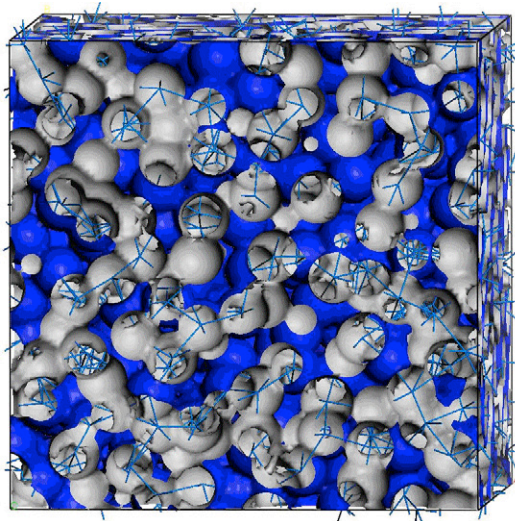


Figure 1: EPSR model of Mg-stabilised ACC with sticks showing the Ca-rich network (i.e. Ca–O–Ca)

[1] Jiang *et al.* (2010) *Nanoscale* **2**, 2358-2361. [2] Rodriguez-Blanco, Shaw & Benning (2008) *Mineral. Magazine* **72**, 283.

[3] Goodwin *et al.* (2010) *Chem. Mater.* **22**, 3197-3205.

The silicon isotopic composition ($\delta^{30}\text{Si}$) of water masses in the Atlantic

COFFINEAU N^{1*}, DE LA ROCHA C. L.¹, SCHLOSSER C.² AND WOLF-GLADROW D.A.³

¹UMR6539, LEMAR, IUEM, Université de Bretagne Occidentale, Technopôle Brest-Iroise, Place Nicolas Copernic, 29280 Plouzané, France
(christina.delarocha@unib-brest.fr)

²National Oceanography Center, Southampton, UK
(C.Schlosser@noc.soton.ac.uk)

³Alfred Wegener Institute for Marine & Polar Research, Bremerhaven, Germany
Dieter.Wolf-Gladrow@awi.de
*(correspondence: nathalie.coffineau@univ-brest.fr)

Use of silicon isotopes ($\delta^{30}\text{Si}$) as a paleoceanographic proxy requires sound knowledge of the distribution and behaviour of silicon isotopes throughout the ocean. Over the past few years considerable efforts have been made to map the silicon isotope composition ($\delta^{30}\text{Si}$) of silicic acid (dissolved silicon, DSi) and biogenic silica (BSi) throughout the ocean.

We present here new data for the $\delta^{30}\text{Si}$ of DSi of water masses in the South Atlantic and eastern North Atlantic. These data include transects from the Drake Passage to the Weddell Gyre, through the Antarctic Circumpolar Current, and through the oxygen minimum zone in the tropical eastern North Atlantic. Seven surface to deep profiles (~4000m) span the southern section of the study from the Drake Passage across the Weddell Sea and then up along the prime meridian. These samples were taken as part of the GEOTRACES Zero & Drake campaign. An additional 5 CTD profiles were taken during a tracer release experiment (MSM10/1) from Ponta Delgada in the Azores to Mindelo, Cape Verde.

These profiles add to a growing dataset from which we are building a comprehensive picture of the distribution of Si isotopes in major Atlantic water masses. This exploration of the evolution of the $\delta^{30}\text{Si}$ of water masses such as Antarctic Bottom Water, North Atlantic Deep Water, and North Atlantic Intermediate Water, enables the identification and to some extent quantification of the biogeochemical and mixing processes controlling the isotopic composition of the water masses observed at our stations.

A statistical approach to the Nd isotopes distribution in the oceans

ANTOINE COGEZ¹, CLAUDE ALLÈGRE¹,
LAURE MEYNADIER¹ AND ÉRIC LEWIN²

¹Équipe de Géochimie et Cosmochimie, Institut de Physique du Globe de Paris – Sorbonne Paris Cité, UMR 7154, Université Paris Diderot

²Équipe de Géochimie 4D, Institut des Sciences de la Terre, Université Joseph Fourier, Grenoble

The reliability of neodymium (Nd) isotopes (ϵ_{Nd} notation) to trace past ocean circulation and continental erosion builds upon our understanding of the present Nd budget in the oceans. Ocean circulation models have been used for the past decade to test the ability of different processes to explain the present Nd isotopic compositions and concentrations of the oceans. The increasing amount of ϵ_{Nd} data in seawater now allows a first statistical approach: we used Lacan *et al.* (2012) seawater data compilation, completed with sediment core tops and ferromanganese nodule and crusts data. We used different statistical methods, all contributing with relevant and each other coherent informations for the understanding of the present ocean Nd behaviour.

First, the ϵ_{Nd} variogram shows a mean correlation distance of 3500 km for the global ocean, which gives the space scale of the mixing dynamics for this element. This distance is then used to build an interpolated map of the Nd isotopic composition, using least squares method. It reveals global and regional features linked to some of the main continental sources and ocean circulation patterns.

Second, we studied the shape of ϵ_{Nd} distributions: their interpretation is based on the central limit theorem which implies that mixing processes produce gaussian distributions. After a weighting of the ϵ_{Nd} distributions by data uncertainties (analytical, sample type) and data densities in each ocean area, we compare it to the Laplace-Gauss distribution. We find that the global distribution is clearly asymmetric and multimodal, reflecting the autonomous behaviour of the different oceans and the importance of the Nd inputs in each ocean. Moreover separate ocean distributions suggest rather a better mixing inside each ocean, with distribution tails for the area of Nd inputs. Finally the Antarctic clearly reflects a mixing between the different oceans and constitutes a barrier for a direct mixing of the different oceans with one another.

Third, a box model solved with global inversion techniques let us draw some conclusions about the residence and mixing times in the different oceans and their distributions (confirming the previous remarks), the input and internal processes, and the current limitations about the interpretation of the Nd budget in the oceans.

^{186}Os mantle evidence of Hadean crust formation

JUDITH A. COGGON^{1*} AMBRE LUGUET¹,
GEOFFREY M. NOWELL² AND PETER W. U. APPEL³

¹Steinmann Institut, Universität Bonn, Poppelsdorfer Schloss, 53115 Bonn, Germany (*correspondence: jude@uni-bonn.de)

²Department of Earth Sciences, University of Durham, South Road, Durham DH1 3LE, UK.

³Geological Survey of Denmark and Greenland, Øster Voldgade 10, DK-1350 Copenhagen K, Denmark.

Crust-mantle differentiation events are recorded by the radiogenic signatures within crustal rocks and minerals and in their mantle counterparts. While the crustal record has been extensively studied and exhibits a peaked distribution of ages up to 4.38 Ga (detrital zircons) [1], corresponding statistical peaks of the mantle record only extend back to 3.3 Ga [2]. The oldest recorded mantle melting ages were measured in a single sulphide inclusion (3.9 Ga) within a xenocrystic olivine from the Lac de Gras kimberlite (Slave Craton) [3], and in two detrital, Os-rich platinum group minerals (PGM) (4.1 and 3.9 Ga) from the Witwatersrand sedimentary basin [4]. However, Eoarchean-Hadean Re-Os sulphide model ages have not revealed any statistically significant peaks.

The ^{190}Pt - ^{186}Os isotope system is demonstrably less sensitive to crustal contamination and alteration than the Re-Os isotope system. We measured whole-rock $^{186}\text{Os}/^{188}\text{Os}$ and highly siderophile element (HSE) (Os, Ir, Pt and Re) compositions of Earth's oldest known chromitites, from the >3.811 Ga Ujaragssuit nunât intrusion, Southwest Greenland to provide the first ever mantle evidence of Hadean crust-mantle differentiation. Pt-Os model ages fall into two distinct groups, reflecting the dominance of either primary or secondary PGM (e.g. alloys) in each sample aliquot. Primary PGM preserve Hadean Pt-Os ages that cluster around 4.1 Ga, with individual ages as old as 4.36 Ga. These Hadean mantle depletion ages from Greenland are consistent with the oldest zircon ages from Australia (~4.0-4.38 Ga), suggesting that global crust-mantle differentiation events occurred on Earth within the first 300 million years after accretion. These findings suggest the existence of an Os-rich mantle, similar to that observed today, by 4.1 Ga. Our study therefore supports occurrence of the "late veneer bombardement" at least 0.2 billion years earlier than previously proposed.

[1] Wilde, Valley, Peck & Graham (2001) *Nature* 409, 175-178. [2] Pearson, Parman & Nowell (2007) *Nature* 449, 202-205. [3] Aulbach *et al.* (2004) *Chem. Geol.* 208, 61-88. [4] Malitch & Merkle (2004) *Can. Mineral.* 42, 631-650.

Geochemical Windows on Coral Calcification: Cellular Mechanisms and Impacts of Climate Change

ANNE L. COHEN^{1*} THOMAS DECARLO¹,
GLENN A. GAETANI¹ AND MICHAEL HOLCOMB²

¹Woods Hole Oceanographic Institution, Woods Hole MA 02543 USA; (*acohen@whoi.edu)

²University of Western Australia, Crawley, WA 6009 Australia

Coral reefs exist because rates of calcium carbonate (CaCO_3) production by coral reef calcifying organisms exceed rates of CaCO_3 dissolution and export. Tropical reef-building corals are critical components of the reef CaCO_3 budget, producing aragonite crystals a hundred times faster than abiotic precipitation could occur under ambient seawater conditions. The ability of corals to maintain such high rates of CaCO_3 production under ocean warming and acidification is therefore critically important for the future of coral reefs worldwide. This presentation focuses on the application of geochemical and petrographic tools to uncover the fundamental mechanisms of coral calcification. Such tools provide unprecedented opportunity to probe an inaccessible, nano-sized space beneath the coral animal, revealing the origins and composition of the calcifying fluid and the ability of corals to manipulate fluid composition to induce crystal nucleation and growth on a tightly controlled diurnal schedule. Compositional and structural features of abiotic crystals grown in controlled aragonite precipitation experiments provide the crucial framework for interpreting compositional variability in coral skeletons. Application of this framework to populations of wild corals growing across natural gradients of temperature and ocean acidification is allowing us to assess the potential for corals to manipulate the composition of the internal fluid and maintain elevated rates of calcification under global climate change.

The Potassium-Argon Laser Experiment (KArLE) for *in situ* geochronology

B. A. COHEN^{1*} J. S. MILLER^{1,2} AND Z.-H. LI^{1,3}

¹NASA Marshall Space Flight Center, Huntsville AL 35812 (Barbara.A.Cohen@nasa.gov); ²Qualis Corporation, Jacobs ESSA Group; ³University of Alabama Huntsville.

Absolute dating is essential in establishing planetary geologic history, including crystallization, magmatic evolution, and alteration. Radiometric geochronology has only been accomplishable in terrestrial laboratories on returned samples and meteorites, but there is more to be gained by geochronology than money for missions to return samples. We are addressing this challenge by developing the Potassium (K)–Argon Laser Experiment (KArLE) for *in situ* dating [1,2]. KArLE ablates a rock sample, determines the K in the plasma state using laser-induced breakdown spectroscopy (LIBS), measures the liberated Ar using quadrupole mass spectrometry (QMS), and relates the two by optically measuring the volume of the ablated pit. We have constructed a full breadboard of the KArLE concept using commercial off-the-shelf parts with flight-equivalent performance [3,4] to verify measurement capabilities and operations.

We conducted end-to-end measurements on the Fish Canyon Tuff, a well-characterized Ar dating standard. Our preliminary results yield a K concentration of 8–10 wt% and ⁴⁰Ar yield of 5×10¹⁵ mol for 500-μm diameter pits (200 laser shots). An isochron constructed with these measurements gives an age of 20.6 Ma, within 25% of the accepted age of 28 Ma, and readily identifies a trapped terrestrial air component. The largest sources of uncertainty are related to procedural blanks, data analysis routines, and calibration curves, all of which we are currently improving.

In addition to achieving an *in situ* age measurement, each KArLE component conducts analyses common to planetary surface missions (e.g. elemental composition, volatile analysis, microimaging). The dual-use components make KArLE an attractive way to integrate geochronology into a payload capability. The components' flight heritage suggests that the experiment will fit on landers and rovers to Mars, the Moon, asteroids, or any rocky surface. Upcoming flight opportunities for KArLE include Curiosity 2020, Discovery, and New Frontiers missions.

[1] Swindle, T. D., *et al.* (2003) *LPSC* **34**, #1488. [2] Cohen, B. A., *et al.* (2012) *Int. Workshop on Instrumentation for Planetary Missions*, #1018. [3] Wiens R.C. *et al.* (2012) *Space Sci. Rev.* **170**, 167–227. [4] Mahaffy *et al.* (2012) *Space Sci. Rev.* **170**, 401–478.

Dynamical Mean Field Theory and Insulator to Metal Transitions in FeO and other Iron-bearing Minerals

R.E. COHEN¹ AND K. HAULE²

¹Geophysical Laboratory, Carnegie Institution of Washington, Washington, D.C. 20015 USA (rcohen@carnegiescience.edu)

²Dept. of Physics, Rutgers University, Piscataway, NJ, USA (haule@physics.rutgers.edu)

Experiments and theory show that FeO metallizes at high temperatures (~2000K) and pressures (~80 GPa) [1]. Here we use DFT+Dynamical Mean Field Theory (DMFT) with continuous time quantum Monte Carlo (CTQMC) to study the origin of the metallization. We find with increasing pressure in paramagnetic FeO in a cubic lattice a high-spin low-spin transition, with a wide transition region between characterized by intermediate occupancies of the t_{2g} and e_g states between. We find that at 300K cubic FeO remains insulating to a factor of two compression (over 600 GPa), except for a small region of high spin metal. However, at high temperatures (e.g. 2000K) a metallic state is found under compression. The metallization occurs from thermal fluctuations among different multiplets representing high- and low-spin states. We are now studying the AFM ground state, the Néel transition, and (Mg,Fe)O solid solutions. The behaviour of other transitions metal oxides such as MnO will also be presented and compared with the behaviour of FeO. This work is supported by NSF.

[1] Ohta, K., Cohen, R. E., Hirose, K., Haule, K., Shimizu, K. & Ohishi, Y. Experimental and Theoretical Evidence for Pressure-Induced Metallization in FeO with Rocksalt-Type Structure. *Phys. Rev. Lett.* **108**, 026403 (2012).

Mineralogical, geochemical characteristics and mass changes in the alteration zone at the Elmaalan (Trabzon) VMS mineralization in NE Turkey

L. COL^{1*} AND N. TUYSUZ²

¹Dept. of Geol. Eng., Gümüşhane Univ., 29100-Gümüşhane, Turkey (*correspondence: colleyla@gmail.com)

²Dept. of Geol. Eng., Karadeniz Tech. Univ., 61080-Trabzon, Turkey (ntuysuz@ktu.edu.tr)

Elmaalan (Trabzon) volcanogenic massive sulfide (VMS) mineralization lies primarily within the immediate footwall of mineralized Upper Cretaceous dacitic pyroclastics, and overlain by barren dacite and pyroclastics at hanging wall in the northern zone of the Eastern Pontide Orogenic Belt in Northeastern Turkey. Main ore minerals are pyrite, chalcopyrite, sphalerite, galena, fahlers, bornite and in less amount chalcocite and covellite together with digenite; quartz, barite, carbonates and clay minerals, sericite and gypsum are exist as gangue.

The footwall dacitic pyroclastics exposed to extreme hydrothermal alterations. The observed alterations of silicification, sericitization, Ca/Mg-rich carbonation, Fe/Mg-rich chloritization and smectization with minor scale hematization and limonitization extend outward from ore zone. The hydrothermal alteration is divided into five zones for mass change calculation toward the ore zone. The mass change calculations of these zones show that, carbonation has 13% mass loss, sericitization-carbonation (Mg)-chloritization 9% mass gain, sericitization 21% mass loss, sericitization-silicification 29% mass gain and silicification 62% mass gain. According to these results, both mass gain and mass loss occurred in footwall dacitic pyroclastics during the hydrothermal alteration. The mass change results indicate that the rate of Si, Fe, and K elements increases, whereas that of Ca, Na and Al decreases toward the ore zone.

The $\delta^{18}\text{O}$ values of solutions equilibrated with quartz, illite and chlorite vary between $-0,3\text{‰}$ and $+5,7\text{‰}$ and that of with illite/simectit and simectit are in between $+24,6\text{‰}$ and $+26,5\text{‰}$. Illite/simectit and simectit values are supposed to form low temperature and surface conditions, but quartz, illite and chlorite values may indicate that fluids become effective on mineralization and hydrothermal alteration are magmatic in origin and affected with dilution of surficial water.

Acknowledgements: This study was supported by Karadeniz Technical University Research Fund (2010.112.005.1).

Trace-element fingerprints of chromites link ultramafic massifs of the Bulgarian Rhodopes

*V. COLAS^{1,2}, J.M. GONZÁLEZ-JIMÉNEZ², I. FANLO¹, W.L. GRIFFIN², F. GERVILLA³, S.Y. O'REILLY², N.J. PEARSON² AND T. KERESTEDJIAN⁴

¹ Dept. Earth Sciences, University of Zaragoza, Spain (*correspondence: volas@unizar.es; fanlo@unizar.es)

² ARC Centre of Excellence of CCFS, and GEMOC, Sydney, Australia (jose.gonzalez@mq.edu.au; griffin@mq.edu.au); (sue.oreilly@mq.edu.au; npearson@mq.edu.au)

³ Dept. Mineralogy and Petrology, University of Granada, Spain.(gervilla@ugr.es)

⁴ Geological Institute, Bulgarian Academy of Sciences, Sofia, Bulgaria. (thomas@geology.bas.bg)

The ultramafic massifs of Yakovitsa and Dobromiritsi contain chromitites hosted in dunitic-harzurgitites are affected by amphibolite/greenschist-facies metamorphism. These massifs are interpreted as portions of a meta-ophiolitic mantle, now widespread within the crustal units of the Central and Eastern parts of the Rhodope Crystalline Massif (SE Bulgaria). Although their age is still unknown, it is very likely that the massifs were thrust over Paleozoic (570 Ma [2]) paragneisses with flysch characteristics during the Jurassic (>170-160 Ma [1]).

We report LA-ICP-MS analysis of unaltered chromite cores in chromitites from these massifs. Minor- and trace-element (Ga, Ti, Ni, Zn, Co, Mn, V, Sc) patterns of these cores from Yakovitsa and Dobromiritsi are similar to other well-characterised Cr-rich chromites in chromitite bodies hosted in the mantle sections of ophiolites. This supports (1) the ophiolitic origin of these ultramafic bodies, (2) a genetic link between the Yakovitsa and the Dobromiritsi massifs. The trace elements of the chromites strongly indicate that the chromitites crystallised from melts that originated in an arc setting. The similarity of the nature of their parental melts suggest that these massifs probably correspond to two fragments of the same portion of oceanic lithosphere developed in a back-arc setting. We plan to investigate Hf-isotope data on zircon and Os-isotope data from platinum-group minerals in the chromitites of both massifs to provide additional tests of this hypothesis.

[1] Bauer, C., *et al.* (2007). *Lithos* **150**, 207-228; [2] Carrigan, C., *et al.* (2003). *J. Czech. Geol. Soc.* **48**, 32-33

Rare earth elements as indicators of hydrothermal processes within the East Scotia subduction system

C.S. COLE^{1*} R.H. JAMES² D.P. CONNELLY²
AND E.C. HATHORNE³

¹Ocean and Earth Science, University of Southampton,
Southampton, SO14 3ZH, UK (*correspondence:
catherine.cole@noc.soton.ac.uk)

²National Oceanography Centre, University of Southampton
Waterfront Campus, Southampton, SO14 3ZH, UK

³GEOMAR, Helmholtz Centre for Ocean Research, Kiel,
Germany

The East Scotia subduction zone, located in the Atlantic sector of the Southern Ocean, hosts a number of hydrothermal sites in both back-arc and island-arc settings. High temperature (> 353 °C) 'black smoker' vents have been sampled at three locations along segments E2 and E9 of the East Scotia back-arc spreading ridge, as well as 'white smoker' (< 212 °C) and diffuse (< 40 °C) hydrothermal fluids from within the caldera of the Kemp submarine volcano. The composition of the endmember fluids (Mg = 0 mM) is markedly different, with pH ranging from 0.8 to 3.4, [Cl⁻] from 88 to 536 mM, [H₂S] from 6.7 – 200 mM, [F⁻] from 35 to 1000 μM and [Li] from 18 to 606 μM. All of the vent sites are basalt-hosted, providing an ideal opportunity for investigating the geochemical controls on rare earth element (REE) behaviour.

Hydrothermal fluids from E2 and E9 have total REE concentrations ranging from 7 – 127 nmol/kg, and chondrite-normalised fractionation patterns are either light REE-enriched ($La_{CN}/Yb_{CN} = 12.9 - 30.0$) with a positive europium anomaly ($Eu_{CN}/Eu_{CN}^* = 3.51 - 59.4$), or mid REE-enriched ($La_{CN}/Nd_{CN} = 0.61$) with a negative Eu anomaly ($Eu_{CN}/Eu_{CN}^* = 0.59$). By contrast, fluids from the Kemp Caldera have almost unfractionated REE patterns ($La_{CN}/Yb_{CN} = 0.8 - 2.2$; $Eu_{CN}/Eu_{CN}^* = 1.0 - 2.2$).

We will demonstrate that the REE geochemistry of fluids from the back-arc spreading ridge is variably influenced by ion exchange with host minerals, phase separation, competitive complexation with ligands, and anhydrite deposition, whereas fluids from the Kemp submarine volcano are also affected by the injection of magmatic volatiles which enhances the solubility of all the REEs. We will also show that the REE patterns of anhydrite deposits from Kemp differ from those of the present-day fluids, potentially providing critical information about the nature of hydrothermal activity in the past, where access to hydrothermal fluids is precluded.

Plutons are texturally modified primary igneous liquids, not cumulates

DREW S. COLEMAN^{1*} RYAN E. FRAZER¹,
RYAN D. MILLS² ALLEN F. GLAZNER¹
AND JOHN M. BARTLEY³

¹ Department of Geological Sciences, University of North Carolina, Chapel Hill, NC 27599-3315, *
(correspondence dcoleman@unc.edu); (frazer@live.unc.edu;
afg@unc.edu)

² ARES Directorate, NASA-JSC, Houston, TX 77058,
(ryan.d.mills@nasa.gov)

³ Department of Geology and Geophysics, University of Utah,
Salt Lake City, (john.bartley@utah.edu)

Existing data support a model in which chemical patterns of both shallow plutonic rocks and volcanic rocks mainly reflect melt generation in the deep crust with minimal differentiation in the upper crust. Field and petrologic features of shallow plutonic rocks reflect incremental assembly of evolving lower crustal melts, overprinted by significant textural modification. Homogeneous granodiorites reflect slow accumulation of compositionally uniform magmas that were likely feeding chemically similar, small (10¹ km³) eruptions. Zoned intrusions reflect evolution of melt composition fed from the lower crust on time scales of 10⁵ to 10⁷a, with limited upper crustal differentiation. If so, plutonic rocks are as rich a source of information about chemical evolution of the crust as volcanic rocks, and plutonic rocks provide a more complete record than volcanic rocks because they are better preserved through geologic time.

In contrast to small eruptions, magmatism related to large ignimbrites (>500 km³) may be scarcely represented in the plutonic rock record. The abnormally high magma flux necessary to generate an ignimbrite results in effective evacuation of the source. Comparable volumes of plutonic rocks that preserve such high fluxes remain unrecognized. In the Southern Rocky Mountain volcanic field, two examples are identified where the only intrusive rocks temporally equivalent to ignimbrites are dikes and ring dikes of roughly the same composition as the ignimbrite. We take this to indicate that the magmas were transported efficiently from deep sources to the surface without protracted storage in the upper crust.

Altogether, the data support a model for plutonic/volcanic rock connections in which both dominantly reflect melt generation processes with minimal overprinting by shallow crustal processes. Hypothetical links between plutonic and volcanic rocks that rely on significant shallow differentiation fail field, geophysical, geochemical and geochronological tests and should be reexamined.

Impact of curiosity-driven research on oil production through *Problem awareness*

MAX COLEMAN

NASA Jet Propulsion Laboratory, Caltech, Pasadena, CA
91109 USA (max.coleman@jpl.nasa.gov)

Much effort is applied to the process of *Technology Transfer*, whereby research is commercialised, but it appears that much less attention is given to its counterpoint and possible precursor, *Problem Transfer*. This paper describes one example of how curiosity driven research, performed in the ambience of problem awareness, by chance, had considerable impact on oil production technology. Although it happened by chance it points to the need for greater dissemination of possibly soluble problems.

A major, but relatively little known, problem of the oil industry is the cost of coproducing water with oil, including that injected into the reservoir to increase oil production. A second and also expensive problem is precipitation of mineral "scale" in the well and near-wellbore region, reducing production flow. For example, in offshore wells sulfate present in injected seawater reacts with barium in the formation water precipitating barium sulfate. The problem is ameliorated by addition to the injected water of just the right amount of a relatively expensive scale inhibitor compound.

While setting up a new stable isotope laboratory in an oil company lab and seeking materials to test, a set of water samples was analysed. This produced two surprises. Isotopic analyses of samples from a well in which chemical compositions indicated presence of injected seawater (sulfate) allowed that contribution to be quantified from a cross plot of H and O isotopes. However, the isotopes (which characterise the whole water) showed that the seawater amount had been under-estimated by a factor of two! Excitingly, those wells with no seawater contribution formed a never previously seen anti-correlation of H and O isotopes, which proved to be mixtures of underlying aquifer brine and residual water in the oil zone, with very different chemical compositions. This was significant because estimates of oil reserves involved use of the resistivity of oil zone water, until then believed to be the same as that of the underlying aquifer. Subsequently, we developed a method to analyse oil zone water by extracting it from produced, "dry" oil. The Ph.D. student involved in developing the method formed an SME to undertake this service commercially as soon as he got his degree.

Thus, curiosity-driven research, serendipity and problem awareness delivered great economic impact and indicates the need for a better managed process of *Problem transfer*.

Calibration of Raman spectroscopy to determine water contents in lunar silicate glasses

A. COLIN^{*1}, GR. DAVIES¹ J.H. HOOIJSCHUUR¹
A.R.L. NICHOLS² N. RAI¹ AND W. VAN WESTRENNEN¹

¹ VU University Amsterdam - the Netherlands
(correspondence : a.colin@vu.nl)

² IFREE, JAMSTEC, Yokosuka - Japan

Recent lunar sample analyses and remote sensing data suggest that the Moon is probably not as dry as initially thought (e.g. [1-2]). The presence or absence of water in the Moon's interior has potentially dramatic consequences for the chemical and physical properties of lunar rocks and melts during lunar evolution. It is thus critical that techniques that are able to determine the water content of lunar soils directly on the lunar surface are developed for use during future lunar lander missions. In addition, in order to establish how water influences lunar melt properties, we need to be able to measure accurately the water content of lunar melts/glasses in experiments.

Raman spectroscopy can be used to quantify reliably the water content of both silicate glasses and minerals. Raman analyses are quick, non destructive and do not require any sample preparation, contrary to more classical techniques like FTIR, SIMS or Karl-Fischer titration. Thus we are calibrating the Raman technique to quantitatively measure water content in lunar glasses. Using a piston cylinder apparatus we synthesised a range of lunar glass compositions (as identified by Apollo missions), doped with different amounts of water (0-6wt%). We confirmed that the water content is homogeneous in our standards by imaging the water content by Fourier Transform Infrared spectroscopy, and determined the absolute water content by Karl Fischer titration. We analysed the samples by Raman and found that the ratio between the water peak area at high frequency and the silicate network peak areas at low frequency, calculated according to [3] is proportional to the water content. Above 0.4wt% water the accuracy is comparable with FTIR.

We are also determining the Raman detection limits for water, using a miniaturised Raman instrument previously designed for the ExoMars mission (e.g. [4]). We are testing this instrument in an in-house vacuum chamber to simulate the extremely low pressure conditions on the lunar surface.

[1] Saal, A. E. *et al.* (2008) *Nature* 454, 192-194. [2] Pieters *et al.* (2009) *Science* 326, 568-572. [3] Le Losq *et al.* (2012) *American Mineralogist* 97, 779-790. [4] Laan E.C. *et al.* (2009) *Proceedings of SPIE* 7441, 744114.

Eclogitized serpentinites from the Rhodope Massif: Exploring the fate of serpentinites in the deep mantle

DAVID COLLINGS¹* J IVAN SAVOV¹, NIKOLAY BONEV²
AND KATHRYN ECCLES³

¹School of Earth & Environment, Univ. Leeds, LS2 9JT
(*ee09dac@leeds.ac.uk)

²Univ. of Sofia, Dept. of Geology & Paleontology, Sofia

³Department of Earth and Environment, Boston University

We report eclogitic mineral assemblages from the Avren serpentinite body on the Bulgarian-Greek border in the E. Rhodope Massif (RM). We have mapped and sampled extensively this 4x1 km body, and discovered thin bands of garnet-CPX bearing assemblages throughout the entire body. The serpentinites have variably melt-depleted protoliths and hydration history as is revealed by their wide ranges in bulk rock MgO (ave. ~31 wt%), CaO (ave. ~ 5 wt%) and Al₂O₃ (ave. ~ 7 wt%). Texturally, enstatite-diopside-Cr-spinel symplectites are common and in agreement with proposed exposures to deep mantle wedge conditions (T ~650°C and P up to 15kbar; [1]). Depending on the T and P, there are several important dehydration reaction paths recorded in the serpentinites: 1) Srp → Ant → Ol + OPX + Sp + Grt → Hbl; 2) Srp → Ant → Tc + Chl → Tr/Act → Hbl. Importantly, in association with the garnets we have discovered vesuvianite, which has been shown to be an important H₂O carrier in dewatering serpentinites in subduction zones [2]. Bulk rock trace element variations are in the range of typical mantle wedge serpentinites with Li = 0.5 ppm; Cr = 1115 ppm; Ni = 1355 ppm and [Nd/Yb]_N ~ 1. LA-ICP-MS results indicate garnets with [Nd/Yb]_N ~ 0.05 and [La/Sm]_N ~ 0.07. The EPMA data indicates that the garnets are Py₅₉Gross₁₂Alm₂₃ and the CPX are diopsides with Wo₄₆En₄₆Fs₃. The recrystallized olivines have high Mg# (~ 89). Based on Sm-Nd dating of garnets from the eclogite bands we report that the serpentinites were exposed to HP/UHP conditions during a Late Jurassic- Early Cretaceous subduction event. This timing is in agreement with metamorphic ages (U-Pb zircon rims) from adjacent parts of the RM [3,4]. Finding remnants of deeply subducted serpentinites on the surface may be rare [2, 4], but understanding their composition may shed light on the elemental fluxes associated with dewatering slabs under arc volcanic fronts. Such rocks may hold the answer for the anomalous (Vp/Vs) layers characteristic for many Western Pacific arcs (IBM, Japan, Aleutians, Kuriles)[6].

[1] Kozhokharova, 1996; [2] Halama *et al.*, 2013, *EJM*. [3] Liati, 2005, *CMP*; [4] Burg, 2011, *JVE*; [5] Debret *et al.*, 2013, *JMG*; [6] Abers, 2000, *EPSL*.

Record of Subduction Zone Carbon Cycling in HP/UHP Rocks, W. Alps

COLLINS, N.¹* BEBOUT, G.¹ COOK-KOLLARS J.¹
AND KUMP, L.²

¹Department of Earth and Environmental Sciences, Lehigh University, Bethlehem, PA, USA. *(nac211@lehigh.edu)

²Department of Geosciences, Pennsylvania State University, University Park, PA, USA.

Studies of volatiles in HP/UHP metamorphic suites can inform models of cycling among surface and deep-Earth reservoirs, including those focusing on C fluxes contributing to atmospheric CO₂ concentrations. Depending on the magnitude of the poorly constrained C flux in ultramafic rocks, on a global basis, sediments and altered oceanic crust (AOC) together deliver 70-95% of the C currently entering subduction zones (Bebout, 1995; Jarrard, 2003; Dasgupta and Hirschmann, 2010). We are investigating extents of retention and metamorphic release of C in deeply subducted AOC and carbonate-rich sediment represented by HP/UHP metapelite and metasedimentary rocks in the Italian Alps. Study of metapelite devolatilization in this suite (Bebout *et al.*, 2013, *Chem. Geol.*) provides a geochemical framework for study of C behavior along prograde P-T paths similar to those experienced in most modern subduction zones. Our results for sediments and AOC indicate impressive retention of oxidized and reduced C to depths approaching those beneath arc volcanic fronts. In metasedimentary rocks, extensive isotopic exchange between the oxidized and reduced C reservoirs results in varying shifts toward mantle values. Much of the carbonate in metabasalts has δ¹³C overlapping with that for carbonate in AOC, with some HP/UHP metamorphic veins showing greater influence of organic C signatures from metasedimentary rocks.

Carbon retained through forearcs is available for return in volcanic arcs (perhaps via partial melting) or for entrainment into the deeper mantle. On a global basis, imbalance between subducted C input and C return flux by magmatism (excluding ultramafic inputs, ~40±20% of subducted C return via arcs and ~80±20% by all magmatism; Bebout, 2013, *Treat. Geochem.*) indicates net modern C return to the mantle, perhaps a reversal of Archean net outgassing (despite more rapid subduction). Modern C subduction flux is largely influenced by carbonate-rich sediment sections entering only a few margins, and future C cycling will be affected by the duration of C subduction pulses in these regions and any new subduction in carbonate-rich ocean basins. Global C cycle models predict that a relatively small change in the subduction/volcanic C flux could significantly affect atmospheric CO₂ levels and thus global climate.

Theoretical calculations on the thermodynamics and kinetics of U(VI) homogeneous reduction by Fe(II)

RICHARD N COLLINS¹ AND KEVIN M ROSSO²

¹School of Civil and Environmental Engineering, The Univ. of New South Wales, Sydney, NSW 2052, Australia
(*correspondence: richard.collins@unsw.edu.au)

²Chemical and Materials Sciences Division, Pacific Northwest National Laboratory, Richland, WA 99354, USA
(kevin.rosso@pnl.gov)

As uranium in the (VI) oxidation state is orders of magnitude more soluble than (IV), there is intense interest in promoting the (bio)reduction of uranium in remediation settings. Fe(II) is an environmentally ubiquitous reductant, however, inconsistencies have been experimentally reported on the thermodynamics and kinetics of U(VI) homogeneous reduction by Fe(II) [1,2].

Here, as a foundation for understanding its heterogeneous reduction behavior, we report on theoretical calculations of the thermodynamics and kinetics of the one electron reduction of monomeric U(VI) (hydrolysis) species by $\text{Fe}(\text{H}_2\text{O})_6^{2+}$ in homogeneous solution. NWChem [3] was used to optimise the structures of the U and Fe monomers as well as inner- and outer-sphere complexes, pre- and post- electron transfer, by spin-unrestricted Kohn-Sham Density Functional Theory (DFT) and using the COSMO continuum solvation model. In addition to structure and free energy prediction, explicit calculation of the electronic coupling interaction was also performed, to estimate the electron transfer kinetics as defined by Marcus theory.

Calculations indicated that electron transfer via either an inner- or outer-sphere mechanism was only thermodynamically favourable for the second hydrolysis species $\text{UO}_2(\text{OH})_2(\text{H}_2\text{O})_4^0$. However, in both cases, electron transfer proceeded via a coupled electron-proton transfer mechanism – an immediate indication that electron transfer would be inhibitive slow. These results suggest that the homogeneous reduction of U(VI) by Fe(II) is either thermodynamically unfavourable or kinetically limited at environmentally relevant U and Fe concentrations at pH values < 7.

[1] Liger *et al.* (1999) *Geochim. Cosmochim. Acta* **63**, 2939-2955. [2] Du *et al.* (2011) *Environ. Sci. Technol.* **45**, 4718-4725. [3] Valiev *et al.* (2010) *Comput. Phys. Commun.* **181**, 1477.

A generic approach to geochemical multi-surface modelling of the leaching of contaminated materials

ROB N.J. COMANS¹ J.J. DIJKSTRA²
AND A. VAN ZOMEREN²

¹ Department of Soil Quality, Wageningen University, The Netherlands, (rob.comans@wur.nl)

² Energy research Centre of the Netherlands (ECN), Petten, The Netherlands

Geochemical modelling is increasingly being used in both scientific research and environmental risk assessment of contaminated materials. In this presentation an overview will be given of the development of a generic multi-surface geochemical modelling approach, to describe the speciation and solid/liquid partitioning (leaching) of major and trace elements in both soils and waste materials. The approach is based on the premise that the major reactive organic and mineral surfaces that are being considered, play a generic and determining role in the speciation and leaching of elements in these different materials.

The geochemical modelling approach is based on individual adsorption models for which generic binding parameters have been published for a wide range of elements. It currently includes reactions for aqueous speciation and mineral solubility, combined with sorption to organic matter (NICA-Donnan model), Fe/Al-(hydr)oxides (Generalized Two-Layer Model) and clay (Donnan model). As such, the model is fully based on published generic thermodynamic parameters for these different types of processes and used without any parameter fitting. Methods for the estimation of essential modelling parameters such as the potentially available/reactive fraction of elements of interest, and the type and amounts of reactive mineral and organic surfaces will be discussed. The performance of this modelling approach has been tested for a range of different elements and contaminated materials, particularly by comparing measurements and model predictions of the solid/liquid partitioning of elements over a wide pH range.

Examples will be presented of different model applications, illustrating similarities and differences in controlling processes and element speciation. These applications suggest very similar properties and contributions of the considered reactive mineral and organic surfaces in the speciation and leaching of elements among very different waste and soil materials. Finally, an outlook will be given on current work and ambitions to further develop and improve this modelling approach.

The baric behaviour of Bloedite at low and high T : A contribution to the study of icy satellites

P. COMODI¹* A. V. STAGNO² A. ZUCCHINI¹ Y. FEI²
AND V. PRAKAPENKA³

¹Earth Sciences Department, University of Perugia, Italy

(*correspondence: comodip@unipg.it)

²Geophysical Laboratory, Carnegie Institution of Washington, US

³Argonne National Laboratory, University of Chicago, US

Bloedite [$\text{Na}_2\text{Mg}(\text{SO}_4)_2 \cdot 4\text{H}_2\text{O}$], $P2_1/a$ space group, is a common constituent in evaporitic sedimentary environments and it has been suggested to be stable on icy satellites (Europa, Ganymede). The knowledge of the release of water from its structure as a function of pressure and temperature is of great interest to planetary scientists since it can be used to explain the presence of a deep ocean under the icy crust, and to understand the cryovolcanism phenomena observed from Voyager data. However, to date, there are no available data to predict possible structural modifications of bloedite (*i.e.* dehydration conditions) as a function of pressure, particularly at low temperature.

We performed *in situ* synchrotron X-ray powder diffraction experiments on natural bloedite at pressures up to 10 GPa and temperatures from ~ 100 K to ~ 570 K using diamond anvil cell technique at GSECARS, Advanced Photon Source (Argonne, USA).

The resulting negative linear thermal expansion coefficients from ambient pressure and low- T experiments are: $\alpha_c = 4.4(4) \cdot 10^{-5} \text{ K}^{-1}$, $\alpha_b = 1.4(3) \cdot 10^{-5} \text{ K}^{-1}$, $\alpha_a = 0.7(2) \cdot 10^{-5} \text{ K}^{-1}$, and $\alpha_v = 5.8(7) \cdot 10^{-5} \text{ K}^{-1}$. From high- T runs, the calculated thermal expansion coefficients are: $\alpha_c = 3.7(1) \cdot 10^{-5} \text{ K}^{-1}$, $\alpha_b = 2.5(3) \cdot 10^{-5} \text{ K}^{-1}$, $\alpha_a = 2.5(3) \cdot 10^{-5} \text{ K}^{-1}$, and $\alpha_v = 8.3(6) \cdot 10^{-5} \text{ K}^{-1}$. Non-linear thermal expansion coefficients for a and V parameters and linear for b and c were measured at 10 GPa up to 570 K. Both compression and expansion behaviours of bloedite are strongly anisotropic with a parameter more deformed with respect to b and c , in good agreement with Comodi *et al.* 2013 [1] where a strongly anisotropic compressibility was observed under HP at room temperature.

Thermogravimetric analyses were also performed at ambient pressure showing three endotherms at 410 K, 500 K and 1000 K, with weight losses of approximately 11%, 11% and 43% related to partial dehydration, full dehydration and sulphate decomposition, respectively. However, no evidence of dehydration were observed up to 570 K and 10 GPa.

Measurements of the lattice parameters of bloedite at the experimental conditions would suggest that pressure can stabilize the water molecules in the bloedite structure with implications for the extent of a thick icy crust.

[1] Comodi *et al.* (2013) Submitted to *Am. Mineral.*

K- and La- doped smectite under high pressure and temperature conditions: Implication on mantle metasomatism

ROMMULO V. CONCEIÇÃO¹*

LARISSA C. CARNIEL¹, VICENTE STEFANI²,
FLAVIA SCHENATO³, FREDERICO ALABARSE⁴,
NAIRA M. BALZARETTI² AND ANA M. XAVIER⁴

¹Instituto de Geociências, Univ. Federal do Rio Grande do Sul (UFRGS), Porto Alegre, Brazil. (*correspondence: rommulo.conceicao@ufrgs.br)

²Programa de Pós-Graduação em Ciências dos Materiais, UFRGS, Porto Alegre, Brazil.

³Comissão Nacional de Energia Nuclear (CNEN), Rio de Janeiro, Brazil.

⁴Synchrotron Soleil, L'Orme les Merisiers, Saint Aubin – BP48, 91192 Gif sur Yvette, France.

The lithospheric mantle is depleted in incompatible elements and basically anhydrous or nearly anhydrous. This region can be rehydrated and re-enriched in these elements through subduction processes that brings, among others, pelagic material. In subduction zones, smectite is one of the most important minerals that could bring together water and trace elements into the mantle. In order to test the influence of smectite in the mantle metasomatism, we are developing phase diagrams under high pressure and temperature (HPHT) in K- and La-doped smectite. Our results show that La-smectite is stable under pressures of 2.5GPa, 4.0 and 7.7GPa at temperatures up to 250°C, $\sim 300^\circ\text{C}$ and 350°C, respectively, above which they transform into a muscovite-like structure, being irreversible in such conditions. K-smectite, however, is stable at temperatures around 250°C, independently of any pressure. Above this temperature, it transforms into a I/S structure previously to changing into a muscovite structure at $\sim 450^\circ$, 350° and $\sim 300^\circ\text{C}$, under 2.5, 4.0 and 7.7GPa, respectively. These results show that pressure does not affect the stability of K-smectite, which remain stable up to 250°C under pressures up to 7.7GPa. On the other hand, higher pressures enlarge smoothly the La-smectite stability field in a very limited extension. Transformation of La-smectite into muscovite occurs directly, but K-smectite transformation occurs via I/S structure. When our results are compared to water/ice stability, we observe that La-smectite/muscovite transformation is in perfect agreement with ice/water transformation. Once ice became water, La-smectite became muscovite. However, K-smectite does not have such straightforward influence on ice/water transformation due to the existence of the I/S stability field.

Experimental melting of phlogopite-peridotite at 1 GPa – Implications for potassic magmatism

P. CONDAMINE^{1*}, E. MEDARD¹, D. LAPORTE¹
AND F. NAURET¹

¹Clermont Université, UPB/CNRS/IRD, Laboratoire Magmas et Volcans, 5 rue Kessler, 63038 Clermont-Ferrand, France (*correspondence : p.condamine@opgc.univ-bpclermont.fr)

Phlogopite has been recognized as a common phase in the subcontinental lithosphere, where it forms by percolation of ascending deeper fluids/melts. This hydrous phase is also assumed to be present in subduction zones as a result of mantle wedge metasomatism following slab dehydration. As a water repository, phlogopite could thus play a key role during partial melting in such settings and imprints peculiar trace element signatures in magmas. However, the stability of phlogopite in a natural mantle composition, as well as its fluid-absent melting reactions have never been determined.

We conducted piston-cylinder experiments at 1 GPa to determine the stability of phlogopite in both lherzolite and harzburgite under water-undersaturated conditions. Accounting for the effect of F in natural peridotites, we show that phlogopite and melt coexist over 150°C above the solidus (1015°C) at moderate degrees of melting (up to 11.5 %). The melting reactions have been quantified and appear continuous and incongruent – e.g. for lherzolite:

$$1.00 \text{ phl} + 0.95 \text{ cpx} + 0.89 \text{ opx} + 0.1 \text{ sp} = 0.93 \text{ ol} + 1.98 \text{ melt}$$

Low-degree melts are silica-saturated (from trachyte to basaltic andesite with increasing degrees of melting). Their K₂O content is buffered by the presence of phlogopite, depending on the source fertility, from ~4 wt% in lherzolite to ~7 wt% in harzburgite. We also determined the trace element partition coefficients between phlogopite and such hydrous, silica-rich melts.

Our data show that magmas with less than 4 wt% K₂O cannot be in equilibrium with residual mantle phlogopite. Conversely, magmas containing more than 7 wt% K₂O cannot come from a phlogopite-peridotite source. Potassic post-collisional lavas (e.g., from Tibet) exhibit a wide range of silica contents (60 – 45 wt% for Mg# > 0.65), with constant K₂O values (~4 wt% for southern Tibet). Such major element trends are in agreement with a phlogopite-bearing mantle source in post-collisional settings, an argument also supported by trace element partitioning models.

EARLYTIME: An initiative to evaluate and improve U-Pb and Pb-Pb dating of meteorites

J.N. CONNELLY^{1*}, Y. AMELIN², T. BLACKBURN³
AND D. CONDON⁴

¹Centre for Star and Planet Formation, University of Copenhagen, Copenhagen, Denmark;

²Research School of Earth Sciences, Australian National University, Canberra ACT, Australia;

³Carnegie Institution for Science, USA,

⁴NIGL, Keyworth, England.

Understanding the formation of the Solar System in detail requires an accurate chronological framework for meteorites with precision and accuracy of at least several 100,000 years. Only the absolute Pb-Pb chronometer, with supporting U-Pb data and uranium isotopic composition, provides assumption-free dates with this resolution. However, constructing a timeline for the first ca. 10 Myr of the Solar System using this method requires comparing dates derived from diverse materials from different laboratories and analytical methods, instrumentation and data reduction schemes.

We propose a cooperative, community-based initiative that would start with a systematic evaluation of the compatibility of U-Pb and Pb-Pb data generated by different laboratories and then seek means to improve and standardize methods to the extent possible. An important first step will be the production, distribution and analyses of synthetic standard Pb solutions mixed to replicate a typical 4.56 Ga Pb-Pb data array to test the compatibility of different mass spectrometry approaches and data reduction schemes. This will be coupled with isotopic analyses of a synthetic U solution to be used in the “age” calculation. The results of this phase will be presented as a blind test of the consistency of results from participating laboratories.

The initiative will further prioritize: 1) developing software that would standardize data reduction and presentation, 2) exploring and establishing means to reduce Pb blanks in the sample handling, dissolution and chemical separation of meteoritic materials, 3) obtaining and distributing suitable natural material(s) that will test the full analytical procedures of participating laboratories, 4) working with the well-established EARTHTIME community to evaluate the feasibility of making more ²⁰²Pb and ²⁰⁵Pb such that a Pb double spike would be widely available to the community for meteoritic work, and 4) building a consensus on the variation or consistency of the U isotopic ratio(s) of inner Solar System materials. Information about the initiative, that we propose be called “EARLYTIME”, will be made accessible via a dedicated website.

Isotope tracking of microbial sulfate reduction in oil reservoirs

MARK E. CONRAD¹, CHRISTOPHER G. HUBBARD¹,
ANNA ENGELBREKTSON² AND JOHN COATES^{1,2}

¹ Earth Sciences Division, Lawrence Berkeley National
Laboratory, Berkeley, CA, USA; (msconrad@lbl.gov)

² Department of Plant and Microbial Biology, UC Berkeley,
Berkeley, CA, USA

Seawater injection as a secondary oil recovery technique is considered to stimulate microbial sulfate reduction in oil reservoirs, leading to reservoir souring. Souring leads to major issues with oil production and refining. Several techniques to remediate souring have been tried, with the most common being addition of nitrate to the injected seawater. Tools are needed to monitor the onset of souring and track the efficiency of treatment options. Microbial sulfate reduction is known to impart large, characteristic shifts in the sulfur and oxygen isotope compositions of the residual sulfate and byproducts of the process that can be distinguished from other processes that may be occurring in the reservoir including precipitation of sulfate and/or sulfide minerals, dilution or sorption onto reservoir materials. In this contribution, we present preliminary experimental results designed to explore the use and sensitivity of isotopic signatures of sulfate and sulfide to monitor reservoir souring.

Two sets of column experiments to simulate reservoir souring and treatment with nitrate have been conducted. In the first set, seawater with and without nitrate was introduced to columns. Appearance of sulfide in the effluent from the untreated columns was observed after 5 days, but measurable shifts in the $\delta^{34}\text{S}$ of the effluent sulfate were observed after only 2 days, indicating that sulfate reduction had already begun. In the nitrate columns, sulfide in the effluent was not observed until 3 weeks after the experiment began, but a shift in the $\delta^{34}\text{S}$ of the sulfate was observed after only 1 week. In the second set of experiments, the columns were allowed to go sour before nitrate was added. Effluent sulfate dropped to less than 5% of the influent concentrations. The $\delta^{34}\text{S}$ of the residual sulfate was $\sim 60\%$ higher and the $\delta^{18}\text{O}$ was $\sim 15\%$ higher. After nitrate addition, sulfide disappeared and both the $\delta^{34}\text{S}$ and $\delta^{18}\text{O}$ values of the effluent sulfate returned to baseline after ~ 10 days. With time, the $\delta^{34}\text{S}$ of the sulfate dropped to 2% less than the influent values indicating re-oxidation of sulfide precipitates in the columns. These results indicate that isotopic monitoring of microbial sulfate reduction is highly sensitive, potentially providing early indicators of reservoir souring processes. Future work will include isotopic monitoring samples from oil reservoirs and incorporation of isotopic effects into reservoir reactive transport models.

Evaluation of precipitation isotope variability across the tropical Pacific in SWING2 simulations and observations

JESSICA L. CONROY^{1,2*} KIM M. COBB²
AND DAVID NOONE²

¹Department of Geology, University of Illinois Urbana-Champaign, IL, USA

(*correspondence: jconroy8@mail.gatech.edu)

²School of Earth and Atmospheric Sciences, Georgia Institute of Technology, Atlanta, GA, USA

³Department of Atmospheric and Oceanic Sciences, and Cooperative Institute for Research in Environmental Sciences, University of Colorado, Boulder, CO, USA

Isotope-equipped global climate models (GCMs) enable simulations of the stable isotopic composition of precipitation, but isotope simulations from different models may vary because of differences in hydrologic and isotopic fractionation schemes. However, different isotope model simulations are rarely considered together, allowing assessment of the distribution of simulated precipitation isotope variability relative to observations. Here we present an evaluation of tropical Pacific precipitation isotope variability in GCMs participating in the second Stable Water Isotope Intercomparison Group (SWING2) experiment and in observations. The tropical Pacific is an important target for such model-data comparisons, as it plays a key role in shaping global hydroclimate variability, and is home to many water isotope-based proxies of paleoclimatic change. We present examples highlighting variability in the strength of the isotopic 'amount effect' across the tropical Pacific. The models that best capture mean annual precipitation in the tropical Pacific are not the models that best simulate the mean annual stable isotopic composition of precipitation, suggesting precipitation amount is not the only influence on precipitation isotope variability in the tropical Pacific. The strength of the relationship between precipitation and precipitation $\delta^{18}\text{O}$ values varies between the western, central, and eastern equatorial Pacific. In the western equatorial Pacific, there is more variability among simulations, but precipitation $\delta^{18}\text{O}$ values have a stronger relationship with basin-wide precipitation relative to local precipitation. In the central and eastern equatorial Pacific, precipitation $\delta^{18}\text{O}$ values are strongly correlated with regional precipitation across most simulations. In many simulations of the eastern tropical Pacific, precipitation has a more spatially expansive relationship with basin-wide precipitation compared to precipitation $\delta^{18}\text{O}$ values.

Cold marine Patagonia waters and stable isotopes and trace elements from Quaternary mollusk shells

I. CONSOLONI^{1*}, G. ZANCHETTA¹, I. BANESCHI²,
L. DALLAI², M. D'ORAZIO², M. GUIDI²
AND M. TIEPOLO³

¹Dipartimento di Scienze della Terra, Università di Pisa, Via S.Maria 53, 56126, Pisa, Italy (*correspondance: consoloni@dst.unipi.it)

²I.G.G., C.N.R., Via Moruzzi 1, 56124, Pisa, Italy

³I.G.G., C.N.R., Via Ferrata 1, 27100, Pavia, Italy

Most of the Atlantic coast of Patagonia is dominated by the cold Falkland (Malvinas) current, whereas further north the upper level coastal circulation is characterised by the interaction with the saltier and warmer Brazil current.

The front of these currents changes seasonally and its position has probably been changed over a longer period of time.

Stable isotopes (¹³C/¹²C and ¹⁸O/¹⁶O ratios) and trace elements (Ba/Ca, Sr/Ca, Mg/Ca) have been used on mollusk shells preserved in fossil beach ridges for tracing past changes in the position of these two currents.

In particular, oxygen isotopic composition of *Mytilus edulis* collected from a Holocene beach ridge dated at ca. 6300 yr BP along the Bahia Camarones coast (Chubut Province, Argentina) is consistently different from the modern specimens and from Mytilidae samples collected from younger Holocene beach ridges and shell middens. On the contrary, the carbon isotopic values remain fairly homogeneous throughout the Holocene up to the present.

The changes in the oxygen isotopic composition of the shallow marine mollusk shells are consistent with changes in water temperature/salinity possibly related to fluctuations in the relative position between the Brazilian and Falkland currents, with a stronger influence of the warm and saltier Brazil current along the study area during the middle Holocene.

This is substantially confirmed by Mg/Ca ratio indicating an increase of the sea surface temperature during the middle Holocene in the Bahia Camarones area. It also found support on mollusk palaeontological data.

The effect of some new organic inhibitors on the oxidative dissolution of iron monosulfide (FeS)

C.A. CONSTANTIN^{1*}, P. CHIRITA¹, C.E. BADICA,
L.M. BIRSA², E. MATEI³, I. BALTOG³
AND M.L. SCHLEGEL⁴

¹ University of Craiova, Department of Chemistry, Calea Bucuresti 1071, Craiova Romania

(*correspondence: cristina_a_constantin@yahoo.com)

²Al. I. Cuza" University of Iasi, Department of Chemistry, 11 Carol I Blv. , Iasi 700506, Romania (lbirsa@uaic.ro)

³ National Institute of Materials Physics, Lab. Optical Processes in Nanostructured Materials, P.O. Box MG-7, Bucharest, R077125, Romania (ibaltog@infim.ro)

⁴CEA, DEN/DANS/DPC/SEARS//Laboratory for the Engineering of Surfaces and Lasers, F-91191 Gif-sur-Yvette, France (michel.schlegel@cea.fr)

The effect of some new organic inhibitors on the oxidative dissolution of synthetic FeS at 25 °C in air-saturated HCl solutions (pH 1.3) was investigated by polarization and Electrochemical Impedance Spectroscopy (EIS) methods. The studied organic inhibitors were: 4-(5-bromo-2-hydroxyphenyl)-5-methyl-2-(morpholin-4-yl)-1,3-thiazol (Pr01); 4-(2-hydroxyphenyl)-2-(morpholin-4-yl)-1,3-thiazol (Pr02) and 1-(5-bromo-2-hydroxyphenyl)-1-oxaethan-2-yl-*N,N*-diethylthiocarbamate (Pr03). The used concentration of the inhibitors was 1 mM. The inhibition efficiency (IE) was computed by the following formula:

$$IE = (1 - i_{\text{corr}} / i_{\text{corr}}^0) \cdot 100$$

where i_{corr} and i_{corr}^0 are the corrosion current densities in the presence and absence of the inhibitor, respectively.

The best IE was observed for Pr01 (54 %). The other inhibition efficiencies were: 13% (Pr02) and 31% (Pr03). The interaction between FeS and the inhibitor with the best IE was analyzed by Raman spectroscopy, and the surface of reacted FeS was inspected under Scanning Electron Microscope (SEM).

This work was supported by a grant of the Romanian National Authority for Scientific Research, CNDI-UEFISCDI, project number 51/2012.

The role of carbon dioxide from recycled sediments in the genesis of ultrapotassic magmas from lithospheric mantle

S. CONTICELLI, R. AVANZINELLI AND E. AMMANNATI

Dipartimento Scienze Terra, Università di Firenze, Italy

The central-western Mediterranean is one of the most important areas on Earth for studying subduction-related potassic and ultrapotassic magmatism derived from partial melting of lithospheric supra subduction mantle. In the circum-Tyrrhenian area leucite-free (i.e., lamproite) and leucite-bearing (i.e., kamafugite, leucitite, and plagioleucitite) ultrapotassic rocks occur in association with shoshonites and high-K calc-alkaline volcanic rocks. Four different magmatic associations are then recognised. Eastward and then south-eastward migration of magmatism with time occurred following rollback of the subducting plate. Leucite-free silica-rich lamproite are restricted to the early stages of magmatism, associated with shoshonites and high-K calc-alkaline volcanic rocks. Present day volcanic activity is restricted to the Neapolitan district where ultrapotassic rocks with contrasting geochemical and isotopic characteristics occur. Ultrapotassic rocks are strongly enriched in incompatible trace elements with variable fractionation of Ta, Nb, and Ti with respect to Th and Large Ion Lithophile Elements. Mafic ultrapotassic rocks are also variably enriched in radiogenic Sr and Pb and unradiogenic Nd. The main geochemical and isotopic signatures result from sediment recycling within the upper mantle via subduction. Selected trace element ratios suggest that high temperatures are required to generate sediment-derived melts. Recycling of carbonated pelites play an important role in the Roman province controlling the genesis of leucite-bearing magmas.

Large volumes of a metasomatic component are predicted to be accommodated within a vein network in the sub-continental lithospheric mantle. Partial melting of the pure vein mineralogy is likely to generate ultrapotassic magmas of either lamproitic or kamafugitic nature. Over time, increased interaction between the metasomatic vein lithology and the surrounding mantle dilutes the alkaline component producing shoshonites and high-K calc-alkaline rocks. The addition of a further subduction-related component shortly before magma generation is required to explain the isotopic composition of rocks from the Neapolitan district. In the last phases of circum-Tyrrhenian evolution, a within-plate component appears within south-eastern Italy. This component is evident at Vulture volcano, in the Lucanian Magmatic province (SE Italy) and at Ustica Island (SW Tyrrhenian Sea).

Sources of Fe to the North Atlantic: Insights from Fe isotopes

TIM M. CONWAY¹* AND SETH G. JOHN¹

¹Dept. Earth and Ocean Sciences, University of South Carolina, USA

*Presenting author (correspondence: tconway@geol.sc.edu)

Iron (Fe) is an important micronutrient in marine biogeochemical cycles, with dissolved Fe concentrations significantly influencing both nitrogen fixation and photosynthesis by phytoplankton throughout the surface ocean. Constraints on the marine iron cycle are therefore key to our understanding of the global carbon cycle. Dissolved Fe isotope measurements ($\delta^{56}\text{Fe}$) are a new parameter which provide a unique opportunity to discriminate between the various sources, sinks and processes controlling Fe distribution within the oceans, in a way that is not possible with measurements of Fe concentration alone.

Utilising a new method for the simultaneous extraction of dissolved Fe, Zn and Cd from seawater, followed by analysis by double-spike plasma mass spectrometry, we present the first basin-scale study of $\delta^{56}\text{Fe}$. Multiple high-resolution depth profiles from the GEOTRACES A03 North Atlantic Zonal Transect (Lisbon to Woods Hole, via Cape Verde) allow us to isotopically fingerprint different sources of Fe and assess the relative contribution of each to the dissolved Fe pool in the North Atlantic.

Close to the Mauritanian margin, where a pronounced oxygen minimum is present at depth, light $\delta^{56}\text{Fe}$ values (~ 0 to -0.5 ‰) provide evidence for a small but significant contribution of light reduced sedimentary Fe to the dissolved Fe pool, mixed with heavy Fe ($+0.5$ to $+0.7$ ‰) released from dissolving aerosols under the Saharan dust plume. Relatively homogenous heavy $\delta^{56}\text{Fe}$ values ($+0.3$ to $+0.5$ ‰) throughout the water column in the deep western basin suggests that dissolution of aerosol Fe is the dominant source of dissolved Fe to the North Atlantic ocean. The homogeneity of $\delta^{56}\text{Fe}$ values lends support to the idea that ligand-controlled exchange between the dissolved and particulate pools is important in controlling both dissolved Fe concentration and $\delta^{56}\text{Fe}$ in the North Atlantic.

We also present the first direct measurements of dissolved $\delta^{56}\text{Fe}$ in a buoyant hydrothermal plume, where values from the TAG Mid-Atlantic Ridge site (-1.3 ‰) indicate that hydrothermal vents are a source of isotopically light Fe to the oceans.

Does the redox cascade apply to permeable sediments?

PERRAN L.M. COOK^{1*}, VICTOR EVRARD¹,
MICHAEL BOURKE¹ AND RONNIE N. GLUD²

¹Water Studies Group, School of Chemistry, Monash University, Melbourne, Australia
(*perran.cook@monash.edu)

²Nordic Center for Earth Evolution, University of Southern Denmark, Odense, Denmark.

The redox cascade is a well-established paradigm that allows us to describe the sequential use of electron acceptors by microbial communities to oxidise organic matter. Sediment redox environments can be highly variable ranging from aerobic to anaerobic and back to aerobic on the timescale of minutes. The redox environment in permeable sediments is likely to be particularly variable, driven by sediment movement (re-suspension) and varying currents which can oscillate redox conditions on the timescale of minutes, hours and days. There have been no studies on the latent capacity of microbial communities or their short-term (hours–days) shifts in metabolism as the redox environment changes.

Understanding this dynamic is particularly important because it has implications for key redox reactions of global importance such as denitrification. In this talk we present the results of flow through reactor experiments on the ability of microbial communities to mineralize carbon and use electron acceptors other than oxygen over time scales of hours to days. Of key interest, our results have shown that microbial communities are able to rapidly switch to denitrification on times scales < 1 h, however this pathway can only account for a small fraction of the electron sink required for the observed rates of carbon mineralisation, pointing to the importance of the simultaneous use of other electron acceptors.

The role of natural organic matter in membrane perturbation: A model biomembrane system approach

R.L. COOK^{1*} AND L.M. OJWANG¹

¹Department of Chemistry, Louisiana State University, Baton Rouge, LA, 70803, USA

(*correspondence: rlcook@lsu.edu)

Natural organic matter (NOM) is an important component of earth's ecosystems. It is known to play a major role in biogeochemical (including redox) processes and pollutant bioavailability (and subsequent toxicity), to name just two. There are conflicting reports in regards to the ability of NOM to either lower or raise the bioavailability of pollutants. To understand these conflicting findings a mechanistic understanding is needed in terms of how NOM interacts with biomembranes. In order to make the system as simple as possible, only passive processes will be studied using of phospholipid vesicles. Our initial studies focused on the effects of pH, NOM concentration, and temperature on the ability of different humic acids to perturb the model biomembrane systems by utilizing fluorescence leakage experiments. Subsequently, wide-line ³¹P NMR was employed to investigate how the model biomembrane was being perturbed [1]. From these studies a two-step adsorption/absorption mechanism was proposed by which NOM induced biomembrane perturbation. This proposed mechanism was then further tested by kinetic studies which, in addition to supporting the proposed adsorption/absorption mechanism, also indicated two distinct components of the absorption step. Finally, the chemical components within the humic acids responsible for the perturbation of the model biomembrane system were investigated with the aid of chemically modified humic acids.

[1] Elayan *et al.* (2008) *Environ. Sci. Technol.* **42**, 1531-1536.

Computer Modeling of Pb Apatites and their Potential for Reducing Pb Levels in Drinking Water

DAVID J COOKE AND JEREMEY HOPWOOD¹

¹Department of Chemical and Biological Sciences, University of Huddersfield, UK email: (d.j.cooke@hud.ac.uk)

Due to its resistance to corrosion and maliability lead was the material of choice for water pipes from ancient times until the 20th century and many domoestic water supplies are still reliant on legacy lead piping. Over time lead will leach from the pipes into the water supply and if left unchecked can cause Pb levels in drinking water to become dangerously high. Consequently water companies the world over are investigating methods for reducing the levels of Pb present in a safe and economic way that can be applied even when pipes are inaccessible.

One solution being explored is to promote the crystallisation of lead phosphat minerals in the water pipes by adding additional phosphates to the water supply. Here we report on a combined modelling and experimenteral study exploring the Pb-apatite system.

The computer models are based on the atomistic potentials previously fitted by de Leeuw and co workers [1] to study a range of apatite minerals, which we have extended to incorporate the Pb²⁺ ion and were fitted so they reproduce the structure of Pb₃(PO₄)₃F and Pb₅(PO₄)₃Cl as well as PbCO₃, PbCl₂, PbF₂ and Pb(OH)₂ to within 1% of the experimentally determined parameters.

Initially we considered the effect on the unit cell of varying the Pb:Ca ratio and compared this to structure of crystals grown in the lab and found excellent agreement between the experimental and simulated lattice parameters, thus giving us confidence to use the computer model as a predictive tool and probe how the Pb an Ca will arrange in the structure as a function of Pb content.

Our current work is focused in two main areas. Firstly we are considering the surface properties of the minerlas and whether segregatiuon of Ca or Pb is preferable. Secondly we are probing the mineral water interacebyconsidering the competative adsorption of lead and calcium on calcium and lead rich chloro and fluoro apatitie surfaces.

[1] Rabone and de Leeuw J Comput Chem 27: 253 2006

Magmatic-hydrothermal sutures and clusters of giant porphyry Cu-(Au-Mo) deposits

DAVID R COOKE AND JOSE PIQUER¹

¹CODES, the Australian Research Council's Centre for Excellence in Ore Deposits; d.cooke@utas.edu.au

Porphyry deposits are the world's major sources of Cu, Mo and Re, and important sources of Au and Ag. They typically form in compressional orogens, either during or after subduction. The transition from extensional tectonism and widespread calc-alkaline volcanism, to a compressional tectonic regime causes inversion of the extensional structural architecture, crustal thickening and shutdown of volcanism, promoting the growth of mid- to upper-crustal intermediate-to felsic magma chambers at major structural intersections. Fractional crystallisation within the magma chamber, possibly coupled with mafic magma underplating, thermal destabilisation and volatile addition, leads to eruptions of hydrous melts and mineralising fluids from the roof of the pluton, producing elongate 'spires' of porphyry that intrude to paleodepths are surrounded and overprinted by of 1-3 km and magmatic-hydrothermal alteration and mineralisation.

Both geochemical and structural processes are fundamental to the formation of clusters of giant porphyry deposits. Several of the world's largest deposit clusters, in terms of contained metal, were localised on major suture zones that developed due to the interaction of arc-parallel and arc-oblique fault systems in the overriding plate. The Eocene—Oligocene Chuquicamata cluster of deposits in northern Chile (Chuquicamata, Radomiro Tomic, Mina Sur, Ministro Hales, Opache and the Toki cluster) was localised along a 25 km corridor controlled by the NNE-trending Mesabi fault and equivalent structures, at its intersection with the Calama-Olacapato-El Toro NW lineament. The district contains over 93 Mt of fine Cu. In the case of the world's largest porphyry Cu-Mo district, Rio Blanco-Los Bronces (> 200 Mt of fine Cu), at least seven porphyry deposits formed during the late Miocene-early Pliocene along a 12 km long, NNW-trending suture zone, with mineralised centres localised at the intersections between the major NNW-trending structures and cross-cutting NE-trending fault systems. The Paleozoic Oyu Tolgoi district in Mongolia contains at least 1749 t Au and 45.5 Mt Cu in a cluster of eight porphyry Cu-Au deposits aligned along a NNE-trending, 26 km long structural corridor. In each of these examples, conditions that promote repeated magmatic-hydrothermal activity in major upper-crustal sutures were essential for the formation of giant porphyry deposit clusters.

Thermal histories from crystal records

KARI M. COOPER^{1*} AND ADAM J.R. KENT²

¹Department of Geology, University of California Davis,
Davis, CA 95616, USA

(*correspondence: kmcooper@ucdavis.edu)

²College of Earth, Ocean and Atmospheric Sciences, Oregon
State University, Corvallis, OR 97330, USA

Many volcanic eruptions, including some of the largest ever, involve crystals stored in magma reservoirs within the crust for significant periods (10's to 100's ka) prior to eruption. Knowledge of the conditions of magma storage are critical for efforts to understand the processes that lead to initiation of eruptions and eruption dynamics, but these remain surprisingly poorly known [e.g., 1,2]. Eruption of homogeneous crystal-rich magma is often argued to reflect the mobilization of magma stored at near solidus conditions, but in other cases these are considered to reflect storage of magma at significantly higher temperatures for extended periods prior to eruption [3,4]. What has been heretofore lacking in this debate is clear observational evidence linking the thermal (and therefore physical) conditions within a magma reservoir to time scales of storage - i.e., thermal histories. We present a novel method for constraining pre-eruptive thermal histories of magmas by combining estimates of crystal residence time based on U-series systematics, textural information, and trace-element zoning in crystals.

At Mt Hood, Oregon, andesitic magmas are formed by mixing of silicic and mafic endmembers, with CSDs showing two populations of plagioclase [5]. The large (silicic-derived) population has cores >21 ka with rims that crystallized near eruption, yet preserve disequilibrium concentrations of Sr. By combining the ²³⁸U-²³⁰Th-²²⁶Ra crystal age data with diffusion calculations and with crystal growth times based on CSDs, we show that only a small fraction of the total storage duration (<<5%) has been spent at temperatures above the critical crystal fraction of 40-50%, where the magma body is easily mobilized. Partial data sets for other volcanoes suggest that similar conditions of magma storage are widespread, which predicts that largely-liquid bodies that could be imaged geophysically will be ephemeral features.

[1] Druitt, T. *et al.* (2012) *Nature* 482, 77-80. [2] Burgisser, A., and Bergantz, G.W. (2011), *Nature* 471, 212-215. [3] Bachmann, O. *et al.* (2007), *JVGR* 167, 1-23. [4] Annen, C. (2008) *JGR*, B07209, doi:10.1029/2007JB005049 [5] Kent, A. *et al.* (2010) *Nature Geosci.* 3, 631-636.

Analytical chemistry, natural organic matter and climate change: Linking chemical signatures and microbial communities that affect carbon cycling in northern peatlands

W. T. COOPER¹, M.M. TFAILY¹, J.P. CHANTON¹,
J.E. KOSTKA², X. LIN² P. CHANTON²,
J.M. STEINWEG³ AND C.W. SCHADT³.

¹ Florida State University, Tallahassee, FL, USA

²Georgia Institute of Technology, Atlanta, GA, USA

³Oak Ridge National Laboratory, Oak Ridge, TN, USA

Global peatlands sequester half as much carbon as that contained in the atmosphere. However, the response of these large carbon reservoirs to global warming remains uncertain. In this presentation the results of experiments designed to identify the reactive and refractory dissolved organic matter (DOM) pools from peatlands in the Marcell Experimental Forest, northern Minnesota, will be described, along with accompanying differences in microbial communities. These experiments included advanced analytical techniques¹ (ultrahigh resolution (UHR) mass spectrometry, PARAFAC-modeled 3-D excitation-emission matrix [EEM] fluorescence spectroscopy) and a combination of next generation sequencing and metagenomics.² Surface peat (0-10 cm) was characterized by high DOC concentrations and relatively low aromaticity. In more decomposed layers at 30-50 cm depth, UHR mass spectra identified distinctly different reactive and refractory DOM pools, as well as the appearance of lipid-like compounds of apparent microbial origin. PARAFAC-modeled EEM revealed fluorescent components (products and reactants) that were consistent with microbial processing. Below 75 cm, results indicate slower degradation of organic matter under anaerobic conditions and stable enzymatic activity. Microbial community structure corresponded strongly to the vertical stratification of dissolved organic matter (DOM) quantity and composition. Atmospheric pressure photoionization was used to selectively observe mass spectra of dissolved organic nitrogen (DON), and changes in DON were correlated to nitrogen-specific enzymatic activity in the solid phase peat. These results have important implications for predicting the fate of carbon storage in peatlands, since warming may lead to an increase in deposition of more labile DOM and enhanced phenol oxidase activity, the net effect being a release of a significant store of soil carbon to the atmosphere.

[1] Tfaily, M.M., *et al.* *Geochimica et Cosmochimica Acta*, **2013**, <http://dx.doi.org/10.1016/j.gca.2013.03.002>. ² Lin, X., *et al.* *Appl. Environ. Microbiol.* **78**, 7023-7031, **2012**.

The potential of platinum stable isotopes of Fe-Mn nodules and crusts as a paleoceanographic tracer

L. CORCORAN^{1*}, M.R. HANDLER¹, J. BAKER²,
T. SEWARD¹, J. CREECH¹ AND V. BENNETT³

¹ School of Geography, Environment and Earth Sciences,
Victoria University of Wellington, New Zealand
(*correspondence: Loretta.Corcoran@vuw.ac.nz)

² School of Environment, University of Auckland, Private Bag
92019, Auckland, New Zealand

³ Research School of Earth Sciences, Australian National
University, Canberra, ACT 0200, Australia

Fe-Mn nodules and crusts are slow-growing chemical sediments that form by direct precipitation from seawater, resulting in a record of changing seawater chemistry. In the modern oxic marine environment these sediments are also the primary sink for platinum: 80 times enrichment over pelagic sediments and up to 1300 times over UCC concentrations^[1,2], resulting in concentrations that make them amenable to Pt stable isotopic analysis.

Platinum is a non-bio-essential siderophile transition metal with six naturally occurring isotopes (¹⁹⁰Pt, ¹⁹²Pt, ¹⁹⁴Pt, ¹⁹⁵Pt, ¹⁹⁶Pt, ¹⁹⁸Pt) with a range of oxidation states (Pt⁰, Pt²⁺, Pt⁴⁺). The dominant oxidation state of platinum in seawater is thought to be Pt²⁺, with Pt⁴⁺ also present to an unknown degree^[1,3]. Variations in ocean redox state, together with changes in source fluxes to the oceans, may lead to small variations (< ±1‰) in the stable isotopic composition of marine platinum. We will present the first investigation into the Pt stable isotopic composition of marine Fe-Mn (hydroxy)oxide sediments, to investigate its potential as a paleoceanographic tracer.

A method has been established using MC-ICPMS to precisely measure Pt isotopic compositions using a ¹⁹⁶Pt-¹⁹⁸Pt double spike to correct for instrumental mass bias^[4]. Pt is separated from the Fe-Mn oxyhydroxide component of the sediments by means of anion exchange chemistry, with ≥ 80% yields and ≥ 85% purity, as determined for three natural nodule standards and a Pt standard. Preliminary results from bulk nodules from different ocean basins are indistinguishable within uncertainties but have a measurable isotopic offset from the IRMM standard and three other Pt metal standards^[4] and the suggestion of offsets from other terrestrial reservoirs.

[1] Goldberg *et al.* (1986) *App. Geochem.*, **1**, 227-232. [2] Hein, J. R. *et al.* (1997) *Manganese Mineralization: Geochemistry and Mineralogy of Terrestrial and Marine Deposits*, **119**, 123-138. [3] Jacinto & Van Den Berg (1989) *Nature*, **338**, 332-334. [4] Creech, J. *et al.* (2013) *J Anal Atom Spectrom.*, in press.

Mafic lavas constrain the chemical variability of the Society plume

C. CORDIER^{1*}, C. CHAUVEL¹ AND M. GUILLET¹

¹ ISTERre, Université Joseph Fourier, Grenoble, France.
(*correspondence: carole.cordier@ujf-grenoble.fr)

Geochemical investigation of ocean island lavas has shown that in some archipelagoes, lavas are organized in distinct chemical and geographic trends, attributed to sampling by mantle plumes of distinct chemical reservoirs located deep in the mantle [e.g., 1-2].

Here, we present new trace element and Sr-Nd-Hf-Pb isotopic compositions of 40 mafic alkaline shield-building lavas (MgO>8 wt.%) from the main islands of the Society Archipelago (French Polynesia): Mehetia (<1 Myr), Moorea (ca 1.5 Myr), Raiatea and Huahine (ca 2.5 Myr), Bora Bora (ca 3.5 Myr) and Maupiti (ca 4.5 Myr). Isotopic compositions of the mafic lavas cover the entire range known for the Society lavas (⁸⁷Sr/⁸⁶Sr = 0.703894 to 0.706053; ¹⁴³Nd/¹⁴⁴Nd = 0.512613 to 0.512898; ¹⁷⁶Hf/¹⁷⁷Hf = 0.282849 to 0.283042; ²⁰⁶Pb/²⁰⁴Pb = 18.77 to 19.55).

Recently, Payne *et al.* [3] distinguished two groups of islands along the Society chain using the relationship between published Ba/Nb and ¹⁴³Nd/¹⁴⁴Nd data. Our new data do not support this interpretation and show a continuum of compositions rather than two distinct groups. For instance, Maupiti and Huahine, assigned to different groups, not only have similar geochemical signature but also the data points for both islands are spread over the two groups. The geochemical structure of the Society plume is thus complex and the model of two parallel trends reflecting its location with respect to the DUPAL anomaly [3] needs revision.

Our dataset shows that FeO, TiO₂ and CaO decrease and SiO₂ and K₂O increase with ⁸⁷Sr/⁸⁶Sr. These correlations do not result from shallow-level processes but from changing melting depths and lithologies within the plume conduit. They also cover the entire range of major element compositions of ocean island mafic lavas [4] (e.g. SiO₂ = 42-48 wt.%, K₂O/TiO₂ = 0.1-0.7 and CaO/Al₂O₃ = 0.7-1.1). Thus, using average archipelago compositions to discuss mantle end-member lithologies leads to underestimate the internal plume variability. In the Society chain, low ⁸⁷Sr/⁸⁶Sr melts derive from deeper melting and/or from silica-poor sources (e.g., CO₂-bearing peridotite or eclogite) while high ⁸⁷Sr/⁸⁶Sr melts derive from shallower melting and/or from sources richer in SiO₂ (e.g., volatile-free peridotite).

[1] Huang *et al.* (2011), *Nat. Geosci.* **4**, 874-878. [2] Chauvel *et al.* (2012), *G3* **13** Q07005. [3] Payne *et al.* (2013), *Geology* **41**, 19-22. [4] Jackson & Dasgupta (2008), *EPSL* **276**, 175-186.

Deformation mechanisms of olivine compressed at 300 MPa and 800-1100°C

PATRICK CORDIER¹, SYLVIE DEMOUCHEY²,
ALEXANDRE MUSSI¹ AND ANDREA TOMMASI²

¹ Université Lille 1 & CNRS, UMR 8207 Unité Matériaux et Transformations, 59555 Villeneuve d'Ascq, France

² Université de Montpellier 2 & CNRS, UMR 5342 Geosciences Montpellier, 34095 Montpellier, France

Rheology of mantle rocks at lithospheric temperatures remains poorly constrained, since most experimental studies on creep mechanisms of olivine single crystals ((MgFe)₂SiO₄, *Pbnn*) and polycrystalline olivine aggregates were performed at high-temperatures ($T \gg 1200^\circ\text{C}$). In this study, we have performed deformation experiments on oriented single crystals of San Carlos olivine and polycrystalline olivine aggregate at temperatures relevant of the uppermost mantle (ranging from 800 to 1090°C) in tri-axial compression. The experiments were carried out at a confining pressure of 300 MPa in a high-resolution gas-medium mechanical testing apparatus at various constant strain rates (from $7 \times 10^{-6} \text{ s}^{-1}$ to $1 \times 10^{-4} \text{ s}^{-1}$). Mechanical tests yield differential stresses ranging from 88 to 1076 MPa. All samples were deformed at constant displacement rate and for finite strains ranging from 4 to 23 %, to provide insight into possible effects of hardening, softening or stick-and-slip. The single crystals were compressed along several crystallographic directions to test the possibility of activating different slip systems (*e.g.* [100](001), [001](100), [001](010) and [100](010)). We will present the characterization of the dislocation microstructures performed in the TEM. In particular, we present some slip plane characterizations for [001] dislocations based on electron tomography.

The disposal of spent nuclear fuel: The effect of high energy surface sites on dissolution rate

C. L. CORKHILL*, D. J. BAILEY, S. THORNBER,
M. C. STENNETT AND N. C. HYATT

Immobilisation Science Laboratory, Department of Materials Science and Engineering, University of Sheffield, Sheffield, UK. (*correspondence: c.corkhill@sheffield.ac.uk)

High energy surface sites, including grain boundaries, step edges and naturally occurring surface defects are expected to play a role in the dissolution of mineral surfaces. Spent Nuclear Fuel (SNF), composed primarily of ceramic UO₂, has grain boundaries and oxygen vacancy defects as a result of high temperature annealing within a nuclear reactor. In the safety case for the geological disposal of nuclear waste, the release of radioactivity from the repository is controlled by the dissolution of the SNF in groundwater, therefore the dissolution characteristics arising from surface features must be determined.

In this study, we demonstrate the effect of high energy surface sites on the dissolution rate of CeO₂, a SNF analogue, which approximates as closely as possible the characteristics of fuel-grade UO₂. Due to the highly refractory nature of CeO₂, dissolution was conducted at 90 °C and pH 2 (nitric acid). CeO₂ was powdered to several different size fractions and subject to dissolution. It was found that large size fractions exhibited a greater dissolution rate than small size fractions ($0.81 \times 10^{-4} \text{ g m}^{-2} \text{ d}^{-1}$ for 75 – 150 μm compared to $0.45 \times 10^{-4} \text{ g m}^{-2} \text{ d}^{-1}$ for 25 – 50 μm). Annealing the powders at high temperature removed some of the high energy surface sites and resulted in a less rapid dissolution rate ($0.21 \times 10^{-4} \text{ g m}^{-2} \text{ d}^{-1}$ for 25 – 50 μm). Monolith samples of CeO₂ were subject to dissolution and analysed periodically by AFM and ICP-MS. Initially, grain boundary dissolution was rapid (460 nm increase in grain boundary depth over 7 days), concurrent with a rapid dissolution rate (0.57 ppm d⁻¹). The dissolution rate decreased (0.15 ppm d⁻¹) when there was no longer any change in the grain boundary depth. CeO₂ powders were annealed under reducing conditions (H₂/N₂), forming non-stoichiometric CeO_{1.93}, concurrent with the formation of oxygen vacancy defects. The dissolution rate of these powders was three orders of magnitude greater than for CeO₂ powders. These results demonstrate that high energy surface sites are important in controlling the dissolution rate of SNF and provide quantitative information to reduce uncertainty in the safety case for SNF disposal.

Si isotope and Ge/Si ratios record successive cycles of dissolution/precipitation of pedogenic clay minerals

J-T. CORNELIS^{1,2*}, D. WEIS¹, J. BARLING¹,
L. LAVKULICH³ AND B. DELVAUX²

¹Department of Earth, Ocean and Atmospheric Sciences (PCIGR), University of British Columbia, 2207 Main Mall, Vancouver BC, V6T 1Z4, Canada

²Earth and Life Institute, Université catholique de Louvain, Croix du Sud 2, 1348 Louvain-la-Neuve, Belgium
(*correspondence : jean-thomas.cornelis@uclouvain.be)

³Soil Science, University of British Columbia, 127-2357 Main Mall, Vancouver BC, V6T 1Z4, Canada

Pedogenic clay minerals provide the most significant and reactive surface area in soils and as such largely govern biogeochemical processes at the interface between lithosphere and biosphere. Deciphering the mechanisms governing clay formation is therefore of the utmost importance to understand how soils will evolve and how they control the Earth's biogeochemical cycles. Pedogenetic transformations governing the dynamic of clay minerals in soils are however still not fully understood.

Compared to the original geochemical signature of clay-size minerals in the deepsoil Bw horizon of a Podzol ($\delta^{30}\text{Si} = -0.49 \pm 0.01\text{‰}$; $\text{Ge/Si} = 3.8 \pm 0.17 \mu\text{mol/mol}$), we document increasing enrichment of ^{28}Si and Ge in clay-size minerals produced during podzolization by the mobilization, transport and precipitation of carbon, metals and silicon. Partial dissolution of clay minerals previously enriched in ^{28}Si isotope and Ge in the eluvial E horizon ($\delta^{30}\text{Si} = -0.57 \pm 0.05\text{‰}$; $\text{Ge/Si} = 8.59 \pm 0.22 \mu\text{mol/mol}$) is the only process that could account for the occurrence of even lighter Si and greater enrichment of Ge in aluminosilicates in the illuvial Bh/Bs horizon ($\delta^{30}\text{Si} = -1.14 \pm 0.15\text{‰}$; $\text{Ge/Si} = 10.1 \pm 0.32 \mu\text{mol/mol}$).

This study provides consistent evidence for previously unrecognized cycles of (partial) dissolution and precipitation of pedogenic clay minerals during podzolization, leading to tertiary and quaternary silicate neof ormation. This challenges the concept that pedogenic clay minerals would be the stable end soil-product in equilibrium with soil-forming factors and suggests that they are reactive over time depending on soil physico-chemical conditions. Si isotope and Ge/Si ratios record a "mineral memory" of the soil-forming processes, and as such provide a powerful tool for the understanding of biogeochemical processes governing soil formation.

Geologic evolution of the Cerro Quema Au-Cu deposit, Azuero Peninsula (Panama)

I. CORRAL¹, M. CORBELLA¹, À. CANALS², A. GRIERA¹,
D. GÓMEZ-GRAS¹, D. NAVARRO-CIURANA¹
AND E. CARDELLACH¹

¹Departament de Geologia, Universitat Autònoma de Barcelona, 08193 Barcelona. Spain

(*Corresponding author: Isaac.Corral@uab.cat)

²Facultat de Geologia, Universitat de Barcelona, 08028 Barcelona. Spain

Central America hosts a variety of metallic mineral resources including Au, Cu, Ag, Pb, Zn, Ni, Co, Sb, W, and Al, spanning a broad range of deposit types. In Panama, Au and Cu are the most economically important metals, and they are mainly related to epithermal and porphyry copper systems.

Cerro Quema is a high sulfidation epithermal deposit located in the Azuero Peninsula (SW Panama), it is constituted by several mineralized bodies named from W to E: La Pava, Cerro Quemita and Cerro Quema. Estimated Au resources are 7.23 Mt with an average gold grade of 1.10 g/T. Cerro Quema is located in the fore-arc basin of the Panamanian Cretaceous volcanic arc. It is related to an E-W trending regional fault system, and is hosted by the dacite dome complex of the Río Quema Formation (Campanian to Maastrichtian in age).

Hydrothermal alteration consists of an inner zone of nearly pure quartz (vuggy silica alteration), with local quartz-alunite and pyrophyllite alteration (advanced argillic alteration), enclosed by a kaolinite, illite and illite/smectite-bearing zone (argillic alteration), grading to an external halo of propylitic alteration.

Gold occurs as disseminated submicroscopic grains and "invisible gold" within the pyrite lattice. Copper is associated to Cu-bearing phases such as chalcopyrite, enargite, tennantite, covellite and chalcocite.

Cerro Quema was formed by fluids derived from the emplacement of an underlying porphyry copper intrusion emplaced along E-W trending regional faults located in the Cretaceous fore-arc basin, during Paleogene times. The proposed geologic model suggests that high sulfidation epithermal deposits are not exclusive of volcanic edifices or volcanic domes related to subduction zones. This deposits can also occur in fore-arc basins, associated with acidic intrusions located between the volcanic arc front and the subduction trench. This should be taken into account for exploration in geologically similar terranes.

A two-component mantle below Mt Etna volcano: Evidences from noble gas and trace element geochemistry of primitive products

A. CORREALE^{1*}, A. PAONITA¹, M. MARTELLI¹,
A. RIZZO¹, S.G. ROTOLO^{1,2}, R.A. CORSARO³
AND V. DI RENZO⁴

¹Istituto Nazionale di Geofisica e Vulcanologia, Sezione di Palermo, Via Ugo la Malfa 153, 90146, Palermo, Italy
(*correspondence: a.correale@pa.ingv.it)

²University of Palermo, Via Archirafi 36, 90123 Palermo, Italy
(silvio.rotolo@unipa.it)

³Istituto Nazionale di Geofisica e Vulcanologia, Sezione di Catania, Piazza Roma 2, 95123 Catania, Italy
(corsaro@ct.ingv.it)

⁴Second University of Napoli, Via Roma 29, 81031, Aversa (CE), Italy (valeria.direnzo@ov.ingv.it)

A geochemical study comprehensive of major elements, trace elements and Sr-Nd isotopes in the bulk rock, coupled to noble gases analyses from fluid inclusions retained in minerals, was performed. The studied samples (basalts, trachybasalts and basanites) represent some among the most primitive products of Etnan history. The variable composition measured in trace elements (i.e. Zr/Nb=2.81–4.98, Ce/Yb=35.02–66.90, La/Yb=15.36–35.52, Th/Y=0.17–0.43) was modeled as due to varying degrees of melting of a common mantle source. We numerically simulated the process by MELTS code to calculate a melting percentage for each product and we accordingly estimated the pristine trace-elements content of their mantle source. This latter resulted to be common to all of the investigated samples and evidenced a close affinity between Etnan and Hyblean mantle. The observed coupling between trace elements and noble gases allowed us to better define the Etnan mantle, which resulted compatible with a peridotitic matrix veined by 10% of clinopyroxenites. The geochemistry of the Sr-Nd-He isotopes ($^{87}\text{Sr}/^{86}\text{Sr}=0.703321\text{--}0.703910$, $^{143}\text{Nd}/^{144}\text{Nd}=0.512836\text{--}0.512913$ and $^3\text{He}/^4\text{He}=6.7\text{--}7.6$ Ra) confirmed the relation existing between Etnan and Hyblean mantle and evidenced that mantle contamination by crustal-like fluids occurred at a variable extent in our products. The $^{87}\text{Sr}/^{86}\text{Sr}$ ratio appears correlated to the estimated degree of melting for each product, therefore the metasomatic fluids probably refertilized some portions of the mantle and promoted partial melting. In contrast, the observed decoupling between $^3\text{He}/^4\text{He}$ and $^{87}\text{Sr}/^{86}\text{Sr}$ ratios could be related to shallower processes, as magma aging or a contribution of shallow fluids, able to decrease the primitive $^3\text{He}/^4\text{He}$ of some samples.

Modeling water-gas-rock interactions using CHESS/HYTEC

JÉRÔME CORVISIER¹

¹Centre de Géosciences, MINES ParisTech, Fontainebleau FRANCE (jerome.corvisier@mines-paristech.fr)

Numerous applications of reactive-transport codes within the field of Geosciences require handling water-gas-rock interactions. Some strong but convenient assumptions could be made to simplify the problem: infinite gas source, dissolved gases, perfect gas approximation... Nevertheless, in many cases, such approaches lead to significant errors and the gaseous phase has to be more accurately represented in models.

Specific gas modules incorporating classical cubic equations of state (Redlich-Kwong, Peng-Robinson...) and their appropriate analytic solver have been developed [1,2] and implemented in the geochemical code CHESS [3] and the coupled reactive-transport code HYTEC [4].

These improvements allow the modeling of complex water-salt-gas-rock systems in various conditions. CHESS can, for example, be used to study the geochemical impact of impurities captured and possibly co-injected along with CO₂ for its geological storage. As an illustration, the code is able to reproduce the measured solubility and co-solubility of gases including gas mixtures such as CO₂-N₂ mixtures.

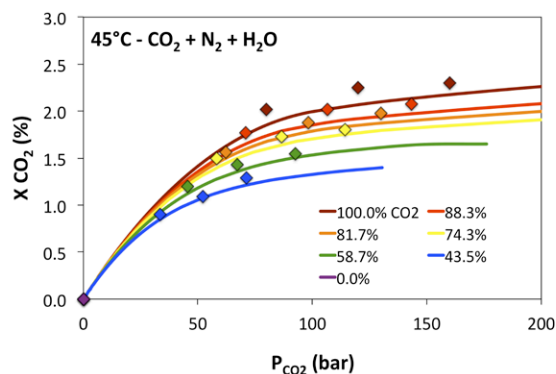


Figure Aqueous CO₂ molar fraction vs. pressure for CO₂-N₂-H₂O system (symbols correspond to measurements [5] and solid lines to CHESS simulations).

[1] Corvisier *et al.* (2012) *Geofluids VII Rueil-Malmaison (France)*, 67-70. [2] Corvisier *et al.* (2013) *Energy Procedia*, in press. [3] van der Lee (2009) *Technical report, MINES ParisTech RT-20093103-JVDL*. [4] van der Lee *et al.* (2003) *Comput. Geosci.* **29**, 265-275. [5] Liu *et al.* (2012) *J. Chem. Eng. Data* **57**, 1928-1932.

$^{87}\text{Sr}/^{86}\text{Sr}$ in gypsic soils of hyperarid settings as an altitude proxy: Results for northern Chile (19-24°S) and paleoaltimetry applications

N. C. COSENTINO* AND T. E. JORDAN

Earth and Atmospheric Sciences, Cornell Univ., Ithaca, NY 14853, USA (*correspondence: njc58@cornell.edu)

Quantification of uplift of a continental surface relative to sea level is challenging. We have developed a new altimeter proxy based on the $^{87}\text{Sr}/^{86}\text{Sr}$ ratio of incipient soils in hyperarid settings like those present in the Atacama Desert. The proposed altimeter is based on the first order topographic control on the extent of coastal fog [1]. Atmospheric advection brings offshore-generated stratocumulus clouds to the continent, generating fog that on geologically recent timescales (10^3 - 10^4 yrs) has averaged base and top altitudes of 300 and 1150 m.a.s.l., respectively. In the hyperarid desert, calcium sulfate accumulates on the surface, progressively forming saline soil [2]. Samples of Atacama's incipient soils reveal $^{87}\text{Sr}/^{86}\text{Sr}$ values clustering in two altitudinal domains (Figure 1); seawater $^{87}\text{Sr}/^{86}\text{Sr}$ (0.70916) is distinctively higher than the ratio for Atacama's incipient soils outside of the fog zone (0.70733).

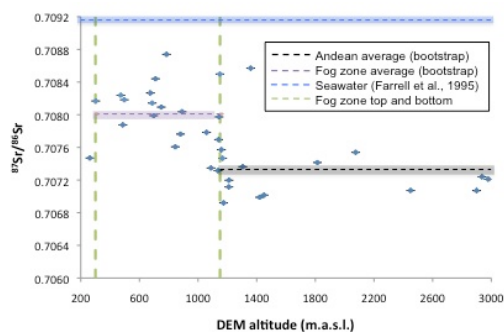


Figure 1: Northern Chile (19-24°S) modern accumulations of salts' $^{87}\text{Sr}/^{86}\text{Sr}$ and altitude of formation. Translucent color boxes represent the uncertainty in each domain's $^{87}\text{Sr}/^{86}\text{Sr}$ mean ratio. Samples from [2] and this study (N = 36).

We are investigating the use of this relationship to deduce late Miocene-Pliocene topographic history of the Nazca/South America forearc. Based on results of dated paleosols in the study area we reach a preliminary interpretation: ≥ 400 m local uplift has occurred since 5 Ma.

[1] Cereceda *et al.* (2002) *Atm. Research* **64**, 261-271. [2] Rech *et al.* (2003) *G&C Acta* **67**, 576-586.

The origin of geochemical anomalies in top soils of Eastern-Central Peloritani Mountains (Sicily, Italy)

COSENZA A.^{1*}, AYUSO R. A.², FOLEY N.², ALBANESE S.¹, LIMA A.¹, MESSINA A.³ AND DE VIVO B.¹

¹DISTAR, Università di Napoli Federico II, Via Mezzocannone 8, 80134 Napoli, Italy

(*correspondence: antonio.cosenza@unina.it)

²U.S.G.S., National Center, Mail Stop 954, Reston, VA 20192, US (rayuso@usgs.gov)

³Dipartimento di Fisica e Scienze della Terra, Università di Messina, Salita Sperone 31, 98165 Messina (antonia.messina@tiscali.it)

The Peloritani Mountains extend across the Southern Sector of the Calabria-Peloritani Arc, in NE Sicily. The arc consists of a stack of nine continental crust tectonic units *Aspromonte, Mela, Piraino, Mandanici, Ali, Fondachelli, San Marco d'Alunzio, Longi-Taormina Capo Sant'Andrea*, including Pan-African and Variscan crystalline basements and remnants of Meso-Cenozoic sedimentary covers.

In this study, we focused on 122 top soils samples collected over an area of 300 km², from the Ali to the Bafia villages (Eastern-Central Peloritani Mts.). The concentrations of 53 elements Mo, Cu, Pb, Zn, Ag, Ni, Co, Mn, Fe, As, U, Au, Th, Sr, Cd, Sb, Bi, V, Ca, P, La, Cr, Mg, Ba, Ti, B, Al, Na, K, W, Sc, Tl, S, Hg, Se, Te, Ga, Cs, Ge, Hf, Nb, Rb, Sn, Ta, Zr, Y, Ce, In, Re, Be, Li, Pd and Pt including potentially harmful metals, have been determined by ICP-MS after Aqua Regia acidification. Geochemical data have been georeferenced and interpolated geochemical maps show distribution patterns of 15 elements for which the Italian environmental law (D. Lgs 152/2006) establishes trigger limits based on geogenic values that differ for land use.

Regarding both residential and industrial/commercial land use, Pb, As and Cd concentrations in these soils often exceed the corresponding trigger limits as established by Italian law. To discriminate between anthropogenic and geogenic origin of Pb, we determined Pb isotopic compositions ($^{206}\text{Pb}/^{207}\text{Pb}$ and $^{208}\text{Pb}/^{207}\text{Pb}$) of galena hand-picked from bedrock and of soils (leach and residues) collected in the studied area. The Pb isotopic compositions of the samples indicate that the origin of most contamination is likely geogenic. This interpretation is consistent with widespread occurrence of small sulphide deposits in the area.

The presence of different heavy metal anomalies in top soils represents an interesting new finding, which could be useful for mineral exploration follow up survey, at least for commodity like Au and Ag.

Bacterial formation of Fe-phosphates in the water column of meromictic ferruginous Lake Pavin (Massif Central, France)

JULIE COSMIDIS^{1,2}, KARIM BENZERARA¹, GUILLAUME MORIN¹, VINCENT BUSIGNY², DIDIER JEZEQUEL², OANEZ LEBEAU², VINCENT NOËL¹, GABRIELLE DUBLET¹ AND GUILLAUME OTHMANE¹

¹ Institut de Minéralogie et de Physique des Milieux Condensés – Université Pierre et Marie Curie

² Institut de Physique du Globe de Paris – Sorbonne Paris Cité – Université Paris Diderot

Lac Pavin (Massif Central, France) is a deep (~92 m) stratified crater lake with anoxic and ferruginous conditions developing in the water column below ~60 m depth. Previous geochemical studies have shown that dissolved Fe(II) and phosphate (PO₄) are present at high concentrations in the anoxic monimolimnion (resp. ~1200 μM and 300 μM) and predicted the formation of vivianite (Fe(II)₃(PO₄)₂•8(H₂O)) in this layer [1,2]. We performed a detailed characterization of the mineralogy of the settling particles in the water column, and determined the potential role of anaerobic bacterial communities in Fe and P cycling in the lake. Bulk x-ray diffraction and x-ray absorption spectroscopy analyses were used to characterize the mineralogical composition and Fe redox state of Fe-bearing particles collected at different depths in the water column and sediments deposited at the bottom of the lake. In the oxygenated layer of the lake, Fe is hosted by phyllosilicates and Fe-(oxyhydr)oxides (FeOOH). Amorphous Fe-phosphates form close to the redoxcline, whereas vivianite becomes dominant in the monimolimnion. FeOOH are preserved throughout the water column and undergo reductive dissolution at the surface of the sediments, where vivianite becomes the main Fe-bearing phase. These results were confirmed by electron and scanning transmission x-ray microscopies, which showed heterogeneities in the composition and Fe redox state of the particles at the submicrometer-scale. Fe-phosphates were moreover observed to encrust microbial bodies. Based on comparisons with laboratory experiments [3], we propose that the precipitation of Fe-phosphates results from the activity of Fe-oxidizing bacteria. Polyphosphate-accumulating microorganisms could also participate in the formation of Fe-phosphates by concentrating PO₄ in the monimolimnion.

[1] Michard *et al.* (1994), *Chem. Geol.* 115, 103-115. [2] Viollier *et al.* (1997), *Chem. Geol.* 142, 225-241. [3] Miot *et al.* (2009), *Geochim. Cosmochim. Acta* 73, 696-711.

Mass specific magnetic susceptibility as a proxy to differentiate soils within the humid subtropical region

C. S. DA COSTA^{1*}

¹Universidade Estadual de Maringá. Dep. Agronomia. Av. Colombo 5790. Maringá-PR. Brazil 87020-190.

(*correspondence: aacosta@uem.br)

Magnetism (χ_{LF}) In Soils

Mass specific magnetic susceptibility (χ_{LF}) data were used to differentiate soils within the humid subtropical region of Brazil. Soils with different degree of weathering and formed under different edaphoclimatic conditions had very different magnetic behavior.

Data collected in the fine earth and clay size fraction of soils from a 200.000 Km² area of Paraná State-Brazil shows χ_{LF} values ranging from zero to more than 10.000 10⁻⁸ m³ kg⁻¹. Coarse grained multidomain magnetites were present in the sand and silt fractions of the soils while maghemite was detected in the clay size fraction. Higher magnetite contents were found in soils developed from basalts in Latosols/Oxisols. The χ_{LF} values observed for the the soils with poor drainage conditions were low (< 100 x 10⁻⁸ m³ kg⁻¹) but not all magnetite from the coarser fractions were reduced and dissolved. In the clay size fraction quantification of the iron oxides [1] shows that maghemite is the iron oxide responsible for the χ_{LF} values and detailed X-rays diffraction data that soil maghemites have extended degree of Fe for Al isomorphous substitution that decreases with increasing soil pH and less intense weathering conditions (lower average rainfall and temperature) [2]. Important bioavailable metals such as Cu, Mn, Zn and Co presented strong correlation with the χ_{LF} values specially with the magnetite content..

[1] Costa, A.C.S. *et al.* (1999) *Clays Clay Miner.*, **47**:466-473. [2] Silva, A.R. *et al.* (2010). *R. Bras. Ci. Solo*, **34**:329-337.

Bromine in basaltic volcanic systems: Experimental study on fluid/melt partitioning coefficient

MICHELA COSTA^{1*}, ALESSANDRO AIUPPA^{1,2},
GIADA IACONO MARZIANO³ AND ANTONIO PAONITA².

¹ [Dipartimento delle Scienze della Terra e del Mare – DiSTeM –
Palermo (*correspondance: michela.costa@unipa.it)]

² [Istituto Nazionale di Geofisica e Vulcanologia – INGV, sezione di
Palermo]

³ [Institut des Sciences de la Terre d'Orléans – ISTO (FR)]

Volcanic halogens play a central role not only in magmatic systems processes but also in atmospheric chemistry, since they have been shown to participate in reactions implicated in tropospheric O₃ destruction [1, 2]. Unfortunately, our current state of knowledge concerning Br behaviour in magmatic systems is still rather poor so a quantitative model of the mechanisms controlling volcanic Br degassing is currently impossible. A fundamental step is understanding Br fluid/melt partitioning coefficient ($D_{Br}^{f/m}$), which has not been investigated yet in basaltic melts. Our work has been mainly aimed to experimentally investigating the distribution of Br between a basaltic melt (Mt. Etna, Italy) and a coexisting fluid phase containing H₂O and known concentrations of Br. Experiments were carried out at ISTO-CNRS of Orléans using rapid-quench autoclaves (T~1200°C; pressure range 500-1000 bar; ~ NNO buffer). Major element in final glasses were measured by EMPA whereas bromine measurements were performed by LA-ICP-MS. In our experiments, Br was found to strongly partition into the fluid phase. This is in agreement with what Bureau *et al.* (2003) reported for an albitic composition and it means that volcanic Br contribution to the atmosphere may be significant. Since no experimental data on $D_{Br}^{f/m}$ in basaltic melts have ever been obtained so far, our study contributes to fill the lack of knowledge concerning Br. In fact, coupling together our experimental results with gas data of Mt. Etna volcanic plume and with information from melt-inclusion, our work can constrain the true Br contents dissolved in Etnean magmas and thus hopefully open the way to constraints Br behaviour during volcanic degassing paths.

[1] Aiuppa A., 2009. Degassing of halogens from basaltic volcanism: insight from volcanic gas observations. *Chemical Geology* 263 (2009) 99-109. [2] Bobrowski N., Honninger G., Galle B., Platt U., 2003. Detection of bromine monoxide in a volcanic plume. *Nature*, vol. 423. [3] Bureau H., Mètrich N., 2002. *Geochimica et Cosmochimica Acta* Vol.67 No. 9, pp 1689-1697, 2003

Frontiers in Laser Ablation U-Th/Pb Petrochronology

JOHN M COTTLE^{1*}

¹ Department of Earth Science, University of California Santa
Barbara, CA 93106-9630, USA, cottle@geol.ucsb.edu (*
presenting author)

Since the first Laser Ablation ICP-MS U-Th/Pb dates were published ~20 years ago, the field has expanded significantly, becoming a key technique for rapidly measuring spatially resolved in-situ isotopic dates. LA-ICP-MS geochronology is now integral to a broad range of studies - from determining sedimentary provenance to quantifying the timing and duration of tectonic processes. Drawing on examples from ongoing research projects at UCSB and elsewhere, this presentation will highlight recent advances and potential future directions *in situ* U-Th/Pb accessory phase geochronology. Specifically, I will focus on four key avenues of progress: 1) improvements in laser and mass spectrometry instrumentation that increase both the precision with which measurements can be made and the spatial resolution at which dates can be measured; 2) development and application of novel data acquisition and reduction methods to interrogate data and produce the best quality dates possible; 3) concomitant analysis of trace elements (Ti, Y, Zr, REE etc.) and/or other isotope systems (e.g. Sm/Nd, Lu/Hf, Li) of petrologic importance along with U-Th/Pb isotopic analysis in order to integrate dates with structural, pressure-temperature, phase relationships and geochemical data and; 4) development of campaign-style geochronology methods to elucidate the spatial and temporal scale of geologic processes at scales ranging from single crystals to entire orogens.

Redox heterogeneity in MORB as a function of mantle source

E. COTTRELL^{1,*} AND K. A. KELLEY²

¹NMNH, Smithsonian Inst., Washington, DC 20560, USA

(*correspondence: cottrell@si.edu)

²GSO, Univ. of Rhode Island, Narragansett, RI 02882 USA

Mantle oxygen fugacity (fO_2) has a first-order effect on the geochemical evolution of Earth's mantle and is predicted to influence several geophysical observables [1], yet systematic variations in mantle oxidation state at mid-ocean ridges have not previously been reported. We use XANES spectroscopy to provide $Fe^{3+}/\Sigma Fe$ ratios of submarine mantle-derived basalts from mid-ocean ridges (MORB) as a proxy for fO_2 [2]. $Fe^{3+}/\Sigma Fe$ ratios of MORB, far from plumes, decrease with indices of mantle enrichment such as $^{87/86}Sr$ and $^{208/204}Pb$ ($n=22$). In primitive glasses ($MgO > 8.5wt.%, n=19$), $Fe^{3+}/\Sigma Fe$ ratios decrease strongly with increasing trace element enrichment, such as the Ba/La ratio. The strong inverse relationship between upper mantle fO_2 and enrichment recorded by MORB glasses globally contrasts with the positive relationship hinted at by abyssal peridotite oxybarometry, and with the prediction of a positive correlation born of the expectation that Fe^{3+} can be treated as more incompatible than Fe^{2+} during mantle melting.

These data unequivocally link upper mantle oxidation state to mantle source enrichment. Further, because the data require ancient fractionation of radiogenic parent-daughter pairs, the factors that lead to variation in mantle oxidation state must be preserved on plate tectonic time scales.

Reduced lavas share isotopic and trace element signatures with low-degree carbonatitic and/or kimberlitic melts of peridotite. These include EM-1 isotopic flavor, Hf depletion relative to Nd, and strong enrichment of highly incompatible elements. Because upper mantle carbon may act to simultaneously reduce iron [3] and generate melts that share geochemical traits with our reduced samples, we propose that variations in mantle carbon lead to magmas that are reduced and enriched. Estimates of mantle carbon concentration from Siqueiros and 'popping rock' support this interpretation, though other processes that might link enrichment to reduction, such as ancient subduction of reducing sediments or mobilization of reduced fluids at depth, cannot be ruled out.

[1] Dasgupta, R. *et al.*, 2013, *Nature* 493, 211-215, doi:10.1038/nature11731. [2] Cottrell, E. and Kelley, K., 2011, *Earth Planet. Sci. Lett.* 305, 270-282, doi: 10.1016/j.epsl.2011.03.014 [3] Stagno, V. *et al.*, 2013, *Nature* 493, 84-88, doi:10.1038/nature11679

Volcanic degassing of the Gunbarrel large igneous province and its environmental repercussions

GRANT COX¹, GALEN HALVERSON², MATT HURTGEN³,
ANDRE POIRIER⁴, LUCIE THEOU- HUBERT⁵
AND BOSWELL WING⁶

¹ (grant.cox@mail.mcgill.ca)

² (galen.halverson@mail.mcgill.ca)

³ (matt@earth.northwestern.edu)

⁴ (poirier.andre@uqam.ca)

⁵ (lucie.hubert-theou@mail.mcgill.ca)

⁶ (boswell.wing@mail.mcgill.ca)

It has long been known that large volcanic eruptions have the capacity to influence the global environment (McCormick *et al.*, 1995; Payne *et al.*, 2008; Self *et al.*, 2008). Five principal mechanisms exist through which volcanic activity can perturb the environment: 1) cooling due to loading of atmospheric sulfate (McCormick *et al.*, 1995); 2) warming due to loading of atmospheric CO_2 ; 3) ocean acidification through elevated levels of oceanic CO_2 (Fraile-Nuez *et al.*, 2012; Hall-Spencer *et al.*, 2008); 4) ocean anoxia caused by an enhanced weathering flux of reduced volcanic material to the oceans (Sinton and Duncan, 1997); 5) ocean anoxia caused by an increased delivery of bio-limiting nutrients to the oceans (Frogner *et al.* 2001, Sinton & Duncan 1997).

Due to their size and duration, Large Igneous Provinces (LIP) have often been implicated in global environmental catastrophes, such as mass extinctions (e.g., Wignall, 2005; Wignall, 2001). However, this simple relationship between eruptive size and environmental impact is complicated by the fact that unlike typical volcanic eruptions, which occur over short time intervals (i.e. days), the eruption of LIP occurs over a few million years.

The compilation of marine carbonate isotope ratios ($d^{13}C$) for the Neoproterozoic suggests a major perturbation to the global carbon cycle at ~780 Ma, coinciding with the eruption of the Gunbarrel LIP. We have used $d^{34}S$ and [S] from volcanic rocks associated with this LIP along with trace element geochemistry of coeval marine carbonates to assess what impact, if any, the Gunbarrel LIP may have had on the surface environment during the Neoproterozoic.

Nucleogenic neon-21 production rates for geochronology

STEPHEN E. COX^{1*}, KENNETH A. FARLEY¹
AND DANIELE J. CHERNIAK²

¹Division of Geological and Planetary Sciences, California Institute of Technology, Pasadena, CA 91125
(correspondence: scox@caltech.edu)

²Department of Earth & Environmental Sciences, Rensselaer Polytechnic Institute, Troy, NY 12180

The (U-Th)/Ne chronometer is a potentially powerful technique for dating minerals that contain U and/or Th and oxygen and/or fluorine. For example, zircon, hematite, and apatite have sufficiently high nucleogenic neon fractions that ²¹Ne chronometry is practical. Because neon is produced via α particle capture by oxygen and fluorine, dating accuracy depends on reaction cross sections and the calculated α stopping power in the material being studied. Despite being derived from the same cross section data, published ²¹Ne production rates vary by tens of percent [1,2]. To reduce this uncertainty we implanted α particles in two materials with very different stopping powers, quartz and barium tungstate, to measure the production rate of ²¹Ne from α particles in the ²³⁸U, ²³⁵U, and ²³²Th decay series.

We find production rates that agree with predicted rates following the production model in [1], with uncertainties of 2-5%. Uncertainties are ~4% for ²¹Ne/⁴He ratios extrapolated to other minerals and are <2% for ²¹Ne concentrations measured by isotope dilution, so (U-Th)/Ne age uncertainties will be <5% when nucleogenic fractions are high.

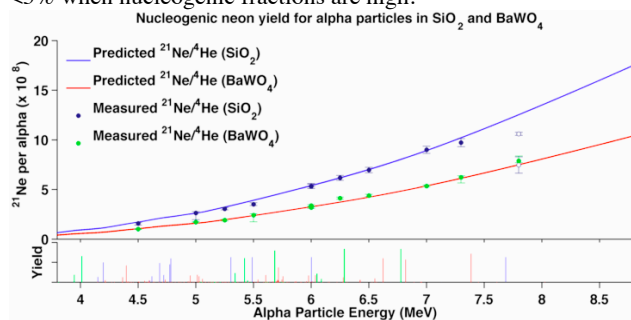


Figure 1: Ratios of nucleogenic neon to implanted helium in samples of quartz and barium tungstate compared to predicted yield following the approach of [1]. Open symbols showed evidence for helium beam contamination during implantation and are low for that reason. The lower plot shows alpha yields of the ²³⁸U (blue), ²³⁵U (red), and ²³²Th (green) decay chains.

[1] Gautheron, Tassan-Got, & Farley (2006), *EPSL* **243**, 520-535. [2] Leya & Wieler (1999), *JGR* **104**, 15,439-15,450.

Which age is the true age? Unravelling within-flow ⁴⁰Ar/³⁹Ar age variations in Faroe Islands basalt lavas

E.L. CRAMER^{1*}, S.C. SHERLOCK¹, A.M. HALTON¹,
S. BLAKE¹, T.L. BARRY², S.P. KELLEY¹
AND D.W. JOLLEY³

¹Dept. of Environment, Earth and Ecosystems, The Open University, Walton Hall, Milton Keynes, MK7 6AA. UK.
(*correspondence: Elizabeth.Cramer@open.ac.uk)

²Dept. of Geology, University of Leicester, University Road, Leicester, LE1 7RH. UK.

³Geology and Petroleum Geology, School of Geosciences, University of Aberdeen, Meston Building, Aberdeen, AB24 3UE. UK.

Previous dating of basaltic igneous rocks from the Faroe Islands by radiometric techniques (Ar/Ar and K/Ar) has proved problematic [1].

The Ar/Ar technique assumes that the rapid cooling rates of lavas is sufficient to close the argon system uniformly, preventing any loss or gain of argon from the lava during cooling. Therefore, an Ar/Ar age for a basalt should be independent of where in the lava a sample is collected. However, in practise, within-flow age variations of more than 10% have been found.

Forty-eight samples were collected from vertical transects through five basalt lavas from the Faroe Islands and radiometric ages were obtained by Ar/Ar step-heating analysis of whole-rock basalt, taking care to pick only visually fresh material and avoiding any signs of alteration (e.g. vesicle fills).

Surface exposure samples from two lavas yield average plateau-ages of ~46 Ma and ~51 Ma respectively (with individual samples ranging from 35 Ma to 55 Ma). Drill core samples from three lavas yield average ages of between ~56 Ma and ~57 Ma. The spread of ages for lavas analysed using drill core is considerably less than that for the surface exposure samples, suggesting that the highly variable Ar/Ar ages may reflect the effects of surface weathering.

We have performed a suite of geochemical analyses on all these samples which will ultimately allow evaluation of these post-emplacement alteration effects on the Ar/Ar system.

While we use a case study from the Faroe Islands Basalt Group, our results are important for accurately interpreting Ar/Ar ages from any basaltic system.

[1] Passey & Jolley (2009), *Earth & Environmental Science Transactions of the Royal Society of Edinburgh*, **99**, 127-158.

Characterisation of depleted uranium munitions residues by synchrotron X-ray microanalysis

D.E. CREAN^{1,2}, F.R. LIVENS², M.C. STENNETT¹,
D. GROLIMUND³, C.N. BORCA³ AND N.C. HYATT^{1*}

¹Department of Materials Science and Engineering, University of Sheffield, UK

(*correspondence: n.c.hyatt@sheffield.ac.uk)

²School of Chemistry, University of Manchester, UK

³Swiss Light Source, Paul Scherrer Institute, Villigen, Switzerland

The testing and use of depleted uranium (DU) munitions has resulted in the contamination of a number of sites worldwide. Interaction of DU munitions with armoured targets on impact produces particulate residues mainly composed of uranium oxides [1]. Although these residues are well characterised on formation, there is uncertainty surrounding their long term fate in the environment.

Using a complementary suite of synchrotron X-ray microanalyses, we have characterised a set of ~30 yr. environmentally aged DU particles recovered from soils at MOD Eskmeals, UK. Two areas of the site were sampled, an surface soil and a disposal pit for contaminated timbers.

Particles in surface soils had a distinctive spherical morphology and were composed of uranium oxides, U₃O₇ and U₃O₈. X-ray diffraction (μ -XRD) and X-ray absorption spectroscopy (μ -XAS) mapping were used to resolve distribution of these phases and corresponding U oxidation states, revealing distinct domains of each oxide. These data are consistent with DU particles as formed, and indicate that, at this site, primary morphology and U speciation are persistent in the environment.

In contrast, U in disposal pit soils was speciated mainly as U(VI) phosphate hydrate phases such as meta-ankoleite (K(UO₂)(PO₄)·3H₂O). A combination of X-ray fluorescence (μ -XRF), μ -XRD and μ -XANES mapping was used to resolve domains of U₃O₇, likely residual primary particles, surrounded by a widespread distribution of U(VI) phosphate hydrates, suggestive of a substantial alteration layer.

This study indicates that the environmental stability of DU munitions residues is highly variable and sensitive to deposition environments. Additionally, the utility of high spatial resolution synchrotron X-ray microprobe techniques to resolve micron-scale heterogeneity in U chemistry in complex environmental samples was demonstrated.

[1] Handley-Siduh, *et. al* (2010), *Sci. Total Environ.* **408**(23) 5690-700.

Platinum Stable Isotope Tracing of Earth's Accretion and Differentiation

JOHN B. CREECH^{1*}, JOEL A. BAKER²,
MONICA R. HANDLER¹, MARTIN SCHILLER³
AND MARTIN BIZZARRO³

¹School of Geography, Environment and Earth Sciences, Victoria University of Wellington, PO Box 600, Wellington 6140, New Zealand.

(*correspondence: john.creech@vuw.ac.nz)

²School of Environment, The University of Auckland, Private Bag 92019, Auckland, New Zealand

³Centre for Star and Planet Formation, Natural History Museum of Denmark, University of Copenhagen, DK-1350 Copenhagen, Denmark

The platinum group elements (PGEs; Ru, Rh, Pd, Os, Ir, Pt) are highly siderophile and strongly sequestered into metallic cores during planetary differentiation. However, PGE abundances in Earth's mantle are higher than predicted from low-pressure metal-silicate partitioning experiments. These relative excesses are reconciled in models by considering either late addition of chondritic material or very different physical conditions during core formation. The Pt stable isotope system represents a novel tool for investigating this problem.

Using recently developed methods for highly precise measurement of Pt stable isotopes by double-spike MC-ICPMS [1] and chemical separation of Pt from geological materials [2], we have characterised the Pt stable isotopic compositions of iron meteorites (as a proxy for Earth's core) and chondrites (as a proxy for the undifferentiated Earth as well as proposed late veneer material) and compare these with data for samples of Earth's mantle. Pt is concentrated in iron meteorites (ca. 3–40 ppm; [3]) compared with undifferentiated meteorites (ca. 0.7–5.0 ppm; [4]), and core formation is thus expected to produce a fractionation in Pt stable isotope ratios, particularly if changes in redox state are involved (Pt²⁺ versus Pt⁰). The composition of such materials are expected to be isotopically distinct from undifferentiated meteorites. By identifying these isotopic fingerprints in Earth's mantle, it should thus be possible to constrain the potential sources or processes responsible for the PGE distribution in Earth's mantle.

[1] Creech *et al.* (2013). *Journal of Analytical Atomic Spectrometry* (In press). [2] Creech *et al.* (in prep). [3] D'Orazio and Folco (2003). *Geostandards and Geoanalytical Research* **27**, 215-225. [4] Tagle and Berlin (2008). *Meteoritics & Planetary Science* **43**, 541-559.

Microbial Metabolism in Serpentine Fluids

M. CRESPO-MEDINA^{1*}, W. J. BRAZELTON¹, K. I. TWING¹,
M. D. KUBO², T. M. HOEHLER³
AND M. O. SCHRENK¹

¹East Carolina University, Greenville, NC, U.S.A

(*correspondence to: mcrespomolina@gmail.com)

²SETI Institute, Mountain View, CA, U.S.A

³NASA Ames Research Center, Moffett Field, CA, U.S.A

Serpentinization is the process in which ultramafic rocks, characteristic of the upper mantle, react with water liberating mantle carbon and reducing power to potentially support chemosynthetic microbial communities. These communities may be important mediators of carbon and energy exchange between the deep Earth and the surface biosphere. Our work focuses on the Coast Range Ophiolite Microbial Observatory (CROMO) in Northern California where subsurface fluids are accessible through a series of wells. Preliminary analyses indicate that the highly basic fluids (pH 9-12) have low microbial diversity, but there is limited knowledge about the metabolic capabilities of these communities. Metagenomic data from similar serpentine environments [1] have identified Betaproteobacteria belonging to the order Burkholderiales and Gram-positive bacteria from the phylum Clostridiales, as key components of the serpentine microbiome.

In an effort to better characterize the microbial community, metabolism, and geochemistry at CROMO, fluids from two representative wells (N08B and CSWold) were sampled during a recent field campaign. The wells selected can be differentiated in that N08B had cell counts ranging from 10^5 - 10^6 cells mL⁻¹ of fluid, and abundance of the Betaproteobacterium *Hydrogenophaga*. In contrast, fluids from CSWold have lower cell counts ($\sim 10^3$ cells mL⁻¹) and an abundance of *Dethiobacter*, a taxon within the phylum *Clostridiales*. Geochemical characterization of the fluids includes measurements of dissolved gases (H₂, CO, CH₄), dissolved inorganic and organic carbon, volatile fatty acids, and nutrients. Microcosm experiments were conducted with the purpose of monitoring carbon fixation and metabolism of small organic compounds, such as acetate, while tracing changes in fluid chemistry and microbial community composition. These experiments are expected to provide insight into the biogeochemical dynamics of the serpentine subsurface at CROMO and represent a first step for developing RNA based Stable Isotope Probing (RNA-SIP) experiments to trace microbial activity at this site.

[1] Brazelton *et al.* (2012) *Frontiers in Microbiology* 2:268

Experimentally quantifying metabasalt dissolution kinetics at 25°C and pH 2-12

T. CRITELLI^{1,4*}, G. D. SALDI², D. DAVAL³,
C. APOLLARO¹, E. H. OELKERS⁴, J. SCHOTT⁴,
R. DE ROSA¹, K. G. KNAUSS² AND L. MARINI⁵

¹DiBEST, University of Calabria, I-87036 Arcavacata di Rende (CS), Italy

(*correspondence: teresa.critelli@unical.it, apollaro@unical.it, derosa@unical.it)

²ESD, LBNL, Berkeley, USA

(gdsaldi@lbl.gov, kgknauss@lbl.gov)

³LHyGeS, Université de Strasbourg- CNRS UMR 7517, Strasbourg, France (ddaval@unistra.fr)

⁴GET, Université Paul Sabatier-CNRS/UMR 5563, Toulouse, France (jacques.schott@get.obs-mip.fr), (eric.oelkers@get.obs-mip.fr)

⁵Consultant in Applied Geochemistry, I-55049, Viareggio (LU), Italy (luigimarini@appliedgeochemistry.it)

Despite the large number of studies reporting individual minerals dissolution rates, less is known about the dissolution rates of whole rocks. This lack of data motivated this study of the dissolution kinetics of a metabasalt from the Mt. Reventino area (Southern Italy). Experiments were performed on crushed and sieved metabasalt at 25°C using mixed-flow reactors. The interpretation of our experiments takes account of the contributions of the dissolution of each distinct mineral to model the chemical evolution of the aqueous phase. Individual mineral surface areas were estimated by distributing the total crushed rock BET surface area among the different minerals present in the metabasalt (chlorite, amphibole, epidote, albite, and phengite) as a function of their modal abundances. Then, by adopting the literature dissolution rate of epidote [1], the temporal evolution of cation concentrations were used to retrieve the dissolution rates of the other minerals. Dissolution rates for chlorite, amphibole, albite, and phengite retrieved from the pH 2 experiments are within an order of magnitude from each other. This observation contrasts with corresponding rates reported in the literature and suggests that mineral dissolution rates are affected by presence of other minerals in multi-phase rocks.

[1] Marini (2007) In *Thermodynamics, Kinetics and Reaction Path Modeling*, 470.

Carbonates of the 2.0 Ga Zaonega Formation: REE and Sr isotopic indications of their origin

A. E. CRNE^{1*}, A. LEPLAND¹, B.S. KAMBER²,
V.A. MELEZHNIK¹, A.R. PRAVE³, A.E. FALICK⁴,
A.T. BRASIER⁵ AND D.J. CONDON⁶

¹Geological Survey of Norway, Trondheim, Norway
(*correspondence: alenka.crne@ngu.no)

²Department of Geology, Trinity College Dublin, Ireland

³University of St. Andrews, St. Andrews, UK,

⁴SUERC, East Kilbride, UK

⁵Faculty of Earth and Life Sciences, Vrije Universiteit
Amsterdam, Netherlands

⁶NERC Isotope Geoscience Laboratory, BGS, Keyworth, UK

The Paleoproterozoic Zaonega Formation, Onega Basin, Russian Karelia represents a deep-water, mixed siliciclastic-carbonate depositional system in a magmatically active basin. It is characterized by rocks extremely enriched in organic matter. FAR-DEEP drillholes intersecting Zaonega Formation hold lithological evidence for one of the earliest generations and spilling of oil/asphalt onto the sea floor, with part of the hydrocarbons being generated due to syn-sedimentary magmatic activity. Geochronologic maximum-minimum constraints of 2.09 ± 0.07 and 1.98 ± 0.02 Ga for the Zaonega Formation indicate its deposition partially overlapped with and/or post-dated the 2.22-2.06 Ga Lomagundi-Jatuli positive carbon isotope interval.

High $\delta^{13}\text{C}_{\text{carb}}$ (up to +10 ‰) suggest that the Zaonega Formation records the end of the Lomagundi-Jatuli Event. However, synsedimentary magmatic activity, and petroleum generation together with extensive post-depositional alteration of carbonates, poses challenges in using these carbonates for interpretations of global environmental changes.

We report new data to assist with interpreting the conditions under which the carbonates precipitated. Carefully characterized carbonate samples were analyzed for REE and Sr isotopes. High $^{87}\text{Sr}/^{86}\text{Sr}$ ratios suggest alteration by post-depositional fluids. Variable REE profiles and changes in magnitude of the Eu anomaly imply that most carbonates were considerably influenced by hydrothermal fluids, but carbonates with sea-water geochemical characteristics are also present. *in situ* REE data show that this complexity is visible both in possibly primary and clearly later carbonate phases and that hydrothermal fluids were important during some carbonate precipitation and during later burial. Contribution from organic diagenesis remains to be evaluated. Whole rock data from these rocks should be therefore viewed cautiously with respect to assessing the Paleoproterozoic carbon cycle.

Reactive Oxygen Species (O_2 , O_2^- and H_2O_2) control Manganese redox cycling in the euphotic zone: role of reactive intermediates

P. L. CROOT¹, M.I. HELLER² AND K. WUTTIG³

¹Earth and Ocean Sciences, School of Natural Sciences,
National University of Ireland, Galway (NUI Galway),
Galway, Ireland (peter.croot@nuigalway.ie)

²University of Southern California (USC), Los Angeles,
California, USA (miheller@usc.edu)

³GEOMAR, Helmholtz Centre for Ocean Research Kiel, Kiel,
Germany (kwuttig@geomar.de)

Manganese (Mn) is an essential element for oceanic phytoplankton as it plays a critical role in photosynthesis, through its unique redox chemistry, as the active site in photosystem II and in enzymes that act as defences against reactive oxygen species (ROS), most notably for protection against superoxide (O_2^-), through the action of superoxide dismutase (SOD), and against hydrogen peroxide (H_2O_2) via peroxidases and catalases. The distribution and redox speciation of Mn in the ocean is also strongly controlled by reactions with ROS. Here we examine the connections between ROS and dissolved Mn species in the upper ocean using a combination of field data from the Tropical Pacific and Atlantic, with laboratory data under controlled conditions. We find that reactions with Mn are a significant pathway for the dismutation of O_2^- in the Tropical Atlantic in surface waters where Mn concentrations are elevated due to Saharan dust input. Modelling of our data suggest it is unlikely that significant concentrations of Mn(III) are produced in the euphotic zone, as in the absence of evidence for the existence of strong Mn(III) ligands in seawater, Mn(II) reacts with O_2^- to form the short lived transient manganese superoxide, MnO_2^+ , which may react rapidly with other redox species in a similar manner to O_2^- . Experiments with the strong Mn(III) chelator, desferrioxamine B (DFB), in seawater indicated that Mn(III) species are unlikely to form significant concentrations via oxidation of the the pre-cursor Mn(II) complex, as this species is only a minor species under natural ambient conditions due to the high side reaction of DFB with Ca.

Oxygenic photosynthesis 3 billion years ago

SEAN A. CROWE^{1,2}, LASSE N. DØSSING^{3,1},
NIC J. BEUKES⁴, MICHAEL BAU⁵,
STEPHANUS J. KRUGER⁴, ROBERT FREI³
AND DONALD E. CANFIELD¹

¹Nordic Center for Earth Evolution (NordCEE) and Inst. of Biol., U. of Southern Denmark, Odense, Denmark (correspondence*: sacrowe@mail.ubc.ca)

²Depts. of Microbiology & Immunology and Earth, Ocean, & Atmos. Sci, Univ. of British Columbia, Vancouver, BC, Canada

³Dept. of Geosci. and Natural Resource Management, Univ. of Copenhagen, Copenhagen, Denmark

⁴Dept. of Geology, Univ. Johannesburg, Johannesburg, South Africa

⁵Dept. of Earth and Space Sci., Jacobs Univ., Bremen, Germany

Prior to the evolution of oxygenic photosynthesis, life on Earth was dominantly anaerobic with an estimated activity level of 1000 times less than today[1]. With the evolution of biological oxygen producers, oxygen became available to fuel aerobic metabolisms, increasing the abundance and activity of the biosphere and changing the dominant modes of metabolism. The first long-term oxygenation of the atmosphere took place around 2.3 billion years ago (Ga) during the Great Oxidation Event (GOE)[2] and oxygenic photosynthesis must have evolved by this time. Geochemical proxies, however, suggest transient atmospheric oxygenation dating back to 2.6-2.7 Ga[3,4,5], while molecular clocks indicate the possible evolution of oxygenic phototrophs as early as the Mesoproterozoic[6].

We examined the distribution of Cr isotopes and redox-sensitive metals in the approximately 3 billion year old Nsuze paleosol and in the near-contemporaneous Ijzermyn iron formation from the Pongola Supergroup, South Africa. These measurements reveal atmospheric oxygen concentrations of some 10⁻⁴ of present day levels. This mid-Archean oxygenation of Earth's atmosphere implies that oxygenic photosynthesis evolved at least 3 billion years ago, more than 600 million years before the GOE. Despite possible fluctuations in oxygen levels, oxygenic phototrophs have likely fueled Earth's aerobic biosphere since at least 3.0 Ga.

[1] Des Marais, D. J. (2000) *Science* **289**, 1703-1705; [2] Guo, Q. J. *et al.* (2009) *Geology* **37**, 399-402; [3] Wille, M. *et al.* (2007) *Geochim. Cosmochim. Acta* **71**, 2417-2435; [4] Anbar *et al.* (2007) *Science*, **317**, 1903-1906; [5] Frei, R. *et al.* (2009) *Nature* **461**, 250-U125; [6] Schirmer, B. *et al.* (2013) *PNAS*, EE, 1-6.

Geochemical changes in wet dune slacks: natural or anthropic driven?

A. CRUCES^{1*}, S. MOREIRA¹, M.C. FREITAS¹, M. LEIRA¹,
M.R. CARVALHO¹, C. ANDRADE¹, T. FERREIRA¹,
L. CANCELA DA FONSECA² AND M.C.R. SILVA¹

¹Universidade de Lisboa, Fac. Ciências, Departamento de Geologia, Centro de Geologia. 1749-016 Lisboa, Portugal (*correspondence: a.cruces@fc.ul.pt)

²Universidade de Lisboa, Centro de Oceanografia. 1749-016 Lisboa, Portugal

Lagoa da Sancha (LS) and Poço do Barbaroza de Baixo (BB), located in the Portuguese SW coast, are smaller than 0.4km² wet dune slacks including shallow (<1m) open-water bodies, which occasionally dry out in summer. Both environments are part of a Natural Reserve since 2000. BB is a blind depression, whereas LS collects inputs from a 35km² watershed. Bottom sediments are CaCO₃-free organic muds, LS materials being peculiar in comparison to BB due to hyperacidity, lower organic and higher heavy metals contents.

Field surveys conducted since 2002 show that BB is an oligohaline to freshwater (0.2 -3.8‰) and slightly acidic to slightly alkaline (pH 5.9-7.6) environment, with DO of 3-7mg/l and low values of Eh (environments near reducing conditions: -110 to +150mV). The water chemistry shows that BB has medium to high mineralization (0.060 meq/l).

In the late 1980's, LS shared similar environmental parameters: salinity (2.5-5‰, exceptionally up to 12‰ due to overwash or evaporation), dissolved oxygen (3-12mg/l) and pH (6.0-8.0). It hosted diverse macrobenthos, ictyo and avifaunas. However, surveys performed after 2001, show a drastic change in this system, with almost complete elimination of those organisms. Although LS waters remain mainly subsaturated to saturated (DO 2.8-9.5mg/l), all the other parameters are substantially different. The LS hydrosome became strongly oxidant (Eh:+315 to +546mV), acidic (pH: 2.7 to 3.8), the salinity dropping to 0-4.3‰. Also, it shows lower mineralization (0.026 meq/l), but the heavy metals content is up to 3 orders of magnitude higher than in BB (17mg/l Fe, 1.8mg/l Mn, 3.4ug/l Cu, 57ug/l Co, 83ug/l Ni, 18ug/l Cu). Such values resemble the composition of waters associated with acid mine drainage or metalliferous leaching.

Until present the extreme changes at LS have been interpreted as related to sulphide oxidation, a meteorological-driven hardly reversible consequence of prolonged bottom exposure during dry years. However, the recent discovery of an illegal industrial waste disposal proximal to LS opens a new hypothesis for that dramatic change related to anthropic contamination conveyed through groundwater circulation.

Harvesting, storage and saving of energy using microporous minerals

G. CRUCIANI^{1*}

¹Dept. of Physics and Earth Sciences, Univ. of Ferrara, 44100, Ferrara, Italy (*correspondence: cru@unife.it)

Given that up to 40% of energy demand in Europe (up to 80% in North America) is used in buildings, the R&D of sustainable technologies for heating and cooling of residential buildings is a key priority in many countries. Among the most promising technological solutions are the heat pumps, in particular those using adsorption (Adsorption Heat Pumps, AHP). The typical working cycle of these machines, encompassing three temperature levels, utilizes a low temperature heat source (e.g. solar or geothermal) to evaporate the working fluid (e.g. water) or activate (i.e. dehydrate) the adsorbing material. In the triggered thermodynamic cycle, heat is released to the environment at an intermediate temperature by the (exothermic) adsorption process by the fluid condensation, while the heat is taken from the environment at the highest T level during the endothermic desorption process.

Zeolites and related microporous minerals are among the most suited adsorbing materials both due to their efficiency and sustainability. The exothermic enthalpy of hydration, thermodynamically stabilizing the otherwise metastable anhydrous zeolite structure [1], explains the endothermic nature of the dehydration phenomenon in these minerals. Therefore, the H₂O desorption from zeolite at low T (e.g. T = 130-150°C from evacuated solar collectors) can be exploited to store heat which can be released to the environment during the next vapour adsorption. The thermal stability of several zeolite topologies [2] makes the ad/desorption cycle fully reversible. In AHPs and Solar Coolers, one evaporator and one condenser are connected to zeolite tanks which can be dehydrated at low T by solar or geothermal heat. Double tanks, cyclically operated in antiphase, allow to make use of both the release to (heating) and the subtraction from (cooling) the environment of the adsorption and condensation heat. Use of natural zeolites for solar cooling has been reported since 80-ties in USA for the chabazite from Bowie, and for chabazite and clinoptilolite in Italy [3].

Solar Heat Storage (SHS) systems can be designed by coupling the physisorption on zeolites to the chemisorption related to transformation between different hydration state(s) in crystalline phase(s) higher energy density (e.g. sulphates).

[1] Navrotsky *et al.* (2009) *Chemical Reviews*, **109**, 3887. [2] Cruciani (2006) *J Phys Chem Solids*, **67**, 1973. [3] Tchernev (2001) *MSA Rev. Miner. Geochem*, **45**, 589.

Sulfide Sites in the Arctic Ocean: Jan Mayen and Loki's Castle

M.I.F.S. CRUZ^{1,2*}, A.F.A. MARQUES¹,
A.S.C.A. DIAS^{1,3}, R.B. PEDERSEN³, J.M.R.S. RELVAS¹
AND F.J.A.S. BARRIGA¹

¹ Creminer FCUL LARSyS, Department of Geology, University of Lisbon, Portugal, (*correspondence: micruz@fc.ul.pt)

² Centre for Geobiology, Department of Earth Science, University of Bergen, Norway

³ University of St Joseph, Macau, China

There is a growing consensus on the need of exploiting the resources of the ocean floors. High latitude oceans, and ocean floors, are not easy to study, for obvious reasons, but the recent discoveries of hydrothermal vents in the Arctic Ocean opened new ground for exploration for metal resources. Jan Mayen and Loki's Castle on the Mohns Ridge are two known sites of interest [1].

The Jan Mayen hydrothermal field was discovered in 2005 at ≈71°N; it is located at water depths ranging from 550 to 700 m and the measured temperatures reached 270°C. It is composed of two separate vent fields, set 5 km apart, named Trollveggen and Soria Moria, respectively. Host rocks tend to be alkaline basalts [2].

The Loki's Castle hydrothermal field was discovered in 2008 at ≈73.30°N, at a water depth of 2400m and with a maximum recorded temperature of 317°C. Host rocks are mainly MORB, although some ultramafic rocks are exposed nearby [3].

At both sites, ROV collected samples of chimney fragments and their surrounding deposits revealed pyrite, chalcopyrite and sphalerite as the main sulfides present. Jan Mayen's whole rock analyses for the chimney fragments depict maximum metal contents for Fe of 6.5wt%, for Zn 39.9wt% and for Cu 1wt%; while Loki's Castle samples contain a maximum of 31wt% Fe, 5.4wt% Zn and 2.4% Cu.

The dominant sulfide phase at Jan Mayen is sphalerite followed by pyrite, while at Loki's Castle pyrrhotite and pyrite predominate. Predominant non-sulfide phases at Jan Mayen are barite and silica, while Loki's non-sulfide phases are composed mainly of talc/serpentine and anhydrite.

	Fe (wt%)		Zn (wt%)		Cu (wt%)	
	Max	Avg	Max	Avg	Max	Avg
Jan Mayen	6.5	4.9	39.9	18.2	1.1	0.4
Loki's Castle	31	9.9	5.4	0.1	2.4	0.6

Samples from both these hydrothermal systems are currently being studied in order to understand their genesis, and better constrain their metal content and possible economic interest.

[1] Pedersen *et al.* (2010), AGU Monogr. Ser., vol. **188**, 67 – 89. [2] Pedersen *et al.* (2005). AGU Fall Meeting, abstr. #OS21 C-01. [3] Pedersen *et al.* (2010) *Nat Commun*, **1**(8): 126.

This work has been funded by FCT through PEST-OE/PEst-OE/EEI/LA0009/2011

Geodynamic kinetics: Metamorphic reaction rates in subduction zones

ALICIA M. CRUZ-URIBE¹ AND MAUREEN D. FEINEMAN¹

¹The Pennsylvania State University, University Park, PA
16803 (amc472@psu.edu, mdf12@psu.edu)

Existing models of fluid release due to dehydration reactions in the subducting slab are based on the assumption that reactions approach equilibrium on timescales comparable to the rate of subduction. Yet there are no field-based measurements of the rates of prograde reactions in subducting slabs, making it difficult to assess the applicability of equilibrium thermodynamics in petrologic models of fluid release. The best constrained field-based metamorphic reaction rates are from regional metamorphic settings and describe a relatively robust relationship between temperature (T) and reaction rate (R_{net}):

$$\log R_{net} = 0.0077T - 12.1$$

Here we assess the applicability of regional reaction rates to fluid-producing reactions that occur during prograde metamorphism of subducting slabs.

We estimate the degree of reaction completion within a dynamic subduction setting by integrating the temperature dependence of regional reaction rates with a thermal model of a cold subduction zone (North Honshu) [1], assuming a subduction rate of 39 mm/yr. Our models show that regional reaction rates are considerably slower than subduction rates at temperatures below $\sim 600^\circ\text{C}$, such that subduction would significantly outpace the progress of metamorphic reactions in the slab. In order to create the assemblages exhumed in subduction channels (e.g., blueschist, eclogite), either (1) grain sizes must be very small; for instance, on the order of $100\ \mu\text{m}$ or less, or (2) the kinetic environment of the subducting slab is fundamentally different than in other regional metamorphic settings. We propose that the dynamic nature of subduction zones (high dT/dt) results in conditions that are far from equilibrium (large ΔG_{rxn}), driving faster reaction rates in these systems. The dramatic increase in dT/dt at $\sim 80\ \text{km}$ slab depth due to slab-mantle coupling would then drive dehydration reactions in a race to “catch up” to the thermal state of the slab, the result of which would be a pulse of fluid released at around this depth. Thus even continuous reactions could run to completion over a relatively short depth interval, explaining the pulse-like fluid release inferred from some arc magmas and exhumed subduction terranes.

[1] Syracuse *et al.* (2010) *Phys Ear Planet Int* **183**, 73–90.

Interrelation between tuffs and organic rich source rock in Chang7 Formation, Triassic, Ordos Basin, Central China

CUI JINGWEI^{1*}, ZHU RUKAI^{1,2}, WU SONTAO^{1,2}
AND BAI BIN^{1,2}

¹Research institute of petroleum exploration and development, PetroChina, Beijing, China

²State key laboratory of enhanced oil recovery, Beijing, China
(*corresponding author: jingwei.cui@126.com)

Organic rich source rocks development modes and controlling factors were summarized. Modes is including black sea molde, the upwelling molde, and hydrotherm molde. The controlling factors are primary production, anoxic enviroment, and sedimentation rate. Interrelation between organic rich sedimentation rate and tuff in the Ordos basin was reported rarely and tuff may erupted by the active of Qinling mountain orogeny and Sublacustrine hydrothermal activity. We used organic geochemistry and inorganic trace mentals to analyzed the source rock and tuff of T₃y, Ordos basin, central China after core fine description.

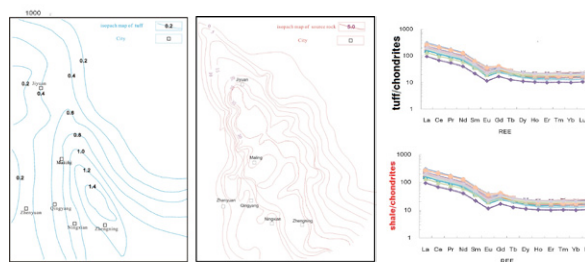


Fig.1 Comparisons of the distibution and REE of Tuffs and source rocks

Interrelation of tuffs and high quality source rocks determinted by the following evidences,

- 1) The tuffs were interbed the Chang7 high quality source rock and have the same distribution in the Ordos Basin, especially in the Chang7³ oil subformation.
- 2) Tuffs and the source rocks have the same Rare earth element (REE) distribution, which indicate the same source. Tuff contribute nutrient elements (P, Fe and N) for organic rich shale developemnt.
- 3) Paleo-depth and paleo-salinity analyses indicated the water is fresh and the maximum water depth are below 120m. Organic rich shale development mode is tuff simulation the mass plankton growth, which lead to high TOC.

$\delta^{13}\text{C}$ record of black carbon in Daihai Lake sediments, northern China: An indicator of terrestrial environmental changes

LINLIN CUI¹ AND XU WANG¹ AND JULE XIAO¹
AND ZHONGLI DING¹

¹Key Laboratory of Cenozoic Geology and Environment, Institute of Geology and Geophysics, Chinese Academy of Sciences, P.O. Box 9825, Beijing, 100029, China; (cuilinlin@mail.iggcas.ac.cn)

We measured the carbon isotope ratio of black carbon (BC) from the Daihai Lake sediment core (DH99a) in northern China to examine the effectiveness and sensitivity of the $\delta^{13}\text{C}$ values of BC ($\delta^{13}\text{C}_{\text{BC}}$) as a potential indicator of terrestrial environmental changes. We first performed a statistical study on the available data regarding carbon isotope fractionation (CIF) during the conversion of C3 and C4 vegetation to BC and observed that the mean CIF for BC produced from C3 plants is -0.3‰, whereas that for BC from C4 plants is -1.7‰. The $\delta^{13}\text{C}_{\text{BC}}$ record in the DH99a sediment core spanning the last ca 10,000 years displayed large variations from -23.7‰ to -29.2‰, which suggests that C3 plants dominantly occupied the Daihai Lake region during the Holocene. The most negative $\delta^{13}\text{C}_{\text{BC}}$ peaks coincided with high values of tree percentages and grain sizes, which occurred under relatively wetter climatic conditions during the middle Holocene (ca 6500-3200 cal. yr BP) and an interval between 1700 and 1350 cal. yr BP. In contrast, the least negative $\delta^{13}\text{C}_{\text{BC}}$ values corresponded to low values of tree percentages and grain sizes during relatively drier phases of the early and late Holocene. The generally negative correlation of the $\delta^{13}\text{C}_{\text{BC}}$ values with the tree percentages and grain sizes was thought to reflect a negative correlation of the $\delta^{13}\text{C}_{\text{BC}}$ values with the monsoon precipitation. We then developed a computational model to reconstruct the changes in annual precipitation over the Daihai Lake region. The inferred annual precipitation was highly variable, ranging from 170 mm lower to 310 mm higher than present during the middle Holocene, whereas the annual precipitation was generally ~70 mm lower than that at present during the early and late Holocene. The general features of the inferred precipitation changes are generally consistent with those reconstructed using pollen data of the same sediment core. Meanwhile, the $\delta^{13}\text{C}_{\text{BC}}$ values tend to register some extreme variations of monsoon precipitation, which were not reflected in the pollen assemblages. We conclude that the $\delta^{13}\text{C}_{\text{BC}}$ values in the Daihai Lake sediments may serve as a sensitive and reliable proxy for monitoring monsoon precipitation.

Dissolved iron and the co-limitation of phytoplankton growth in the Beaufort Sea, Arctic Ocean

J.T. CULLEN^{1*}, J. ZHOU^{1,2}, R.L. TAYLOR³
D.M. SEMENIUK³ AND M.T. MALDONADO³

¹ University of Victoria, School of Earth and Ocean Sciences, P.O. Box 3055 STN CSC, Victoria, British Columbia, Canada V8W 3P6 (* correspondence: jcullen@uvic.ca)

² Hangzhou Dianzi University, Department of Environmental Science and Engineering, Hangzhou 310018, P.R.China

³ Department of Earth, Ocean and Atmospheric Sciences, University of British Columbia, Room 2020, Earth Sciences Building, 2207 Main Mall, Vancouver, British Columbia, V6T 1Z4, Canada (mmaldonado@eos.ubc.ca)

Here we report six vertical profiles of dissolved Fe concentrations [DFe] and results of a shipboard grow-out experiment to investigate the potential for nitrate (NO_3^-), light, and Fe co-limitation of phytoplankton in the Beaufort Sea in late summer. A range of [DFe] from 0.11 to 2.04 nM is observed, with the maximum values occurring in subsurface waters near continental shelf sediments. Clear surface maxima in [DFe] exist at stations with freshwater input from melting sea ice.

Nitrate additions to incubation bottles enhanced phytoplankton growth, demonstrating that the late summer community was N limited. In the treatments with additions of NO_3^- but not Fe, biomass doubled with increasing light, indicating light limitation. In NO_3^- enriched treatments, co-limitation of primary production by Fe and light was observed at light levels $\leq 10\%$ surface irradiance, which corresponded to depths ≥ 33 m. These results suggest that, in addition to NO_3^- and light, Fe may control primary productivity in the Beaufort Sea, and seasonal changes in light, NO_3^- , and Fe availability may differentially control Arctic phytoplankton growth.

The effect of the inclusion of online aerosol-cloud feedbacks on solar radiation feedback

CURCI GABRIELE^{1,*} AND PAOLO TUCCELLA¹

¹Department of Physical and Chemical Sciences, CETEMPS, University of L'Aquila, Via Vetoio, 67100 L'Aquila, Italy (* correspondence: gabriele.curci@aquila.infn.it)

The intricate feedbacks between aerosol and clouds are currently regarded as the single major uncertainty in future climate projections and are believed to have a significant role also on weather prediction. Aerosol-clouds interactions are explicitly simulated only in three-dimensional models that solve both meteorological and chemical processes at the same time (online models). One such model is WRF/Chem. Recent developments, carried out in collaboration with NOAA, include the implementation of cloud feedbacks with the up-to-date module for the organic fraction, based on the Volatility Basis Set (VBS) approach. We test the skills of this state-of-science model for short term (few days ahead) forecast of solar radiation at the European scale. Results are evaluated against ground based observations of the downward shortwave radiation from the Baseline Surface Radiation Network (BSRN), cloud cover information from the International Satellite Cloud Climatology Project (ISCCP), and satellite data. We highlight the importance of including the representation of interactions among meteorology, radiation and chemistry for a better solar energy forecast.

Atmospheric methane concentration at the ClimaDat network sites

R. CURCOLL¹, J.-A. MORGUÍ^{1,2,*}, A. ÀGUEDA¹, O. BATET¹, C. GROSSI¹, M. NOFUENTES¹, P. OCCHIPINTI¹, R. ARIAS¹, A. MARTÍNEZ¹ AND X. RODO^{1,3}

¹Institut Català de Ciències del Clima (IC3), Dr. Trueta 203, 08005 Barcelona, Spain (roger.curcoll@ic3.cat, *(correspondence: josep-anton.morgui@ic3.cat, (alba.agueda@ic3.cat, (oscar.batet@ic3.cat, claudia.grossi@ic3.cat, (manel.nofuentes@ic3.cat, paola.occhipinti@ic3.cat, (rosa.arias@ic3.cat, ariadna.martinez@ic3.cat, (xavier.rodó@ic3.cat)

²Departament d'Ecologia, Universitat de Barcelona, Diagonal 645, 08028, Barcelona, Spain

³Institució catalana de Recerca i Estudis Avançats, Barcelona, Catalunya, Spain

Atmospheric concentrations of methane were obtained in continuous analyses by a Cavity Ring-Down Spectrometer (CRDS) [1] at six sites belonging to the ClimaDat network in Spain. ClimaDat measures the natural variability of the atmospheric gases related to processes that integrate changes, and that are influenced by the uncoupling and the displacement associated to climate change. Temporal and spatial heterogeneity are addressed and the source of air masses is inferred by Lagrangian backtrajectory models [2]. Synoptic meteorological situations acts a modulating drive of the pattern of the variability at the different sites, as shown in Figure 1 for the GIC3 site. A comparison of 2013 NRT series is presented.

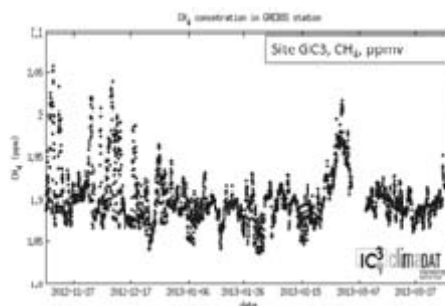


Figure 1: Time series of mean hourly values of CH₄ with a disrupted pattern of concentration cycles.

[1] Crosson (2008) *Applied Physics B* **92**, 403-408. [2] Font *et al.* (2011) *Atm. Chem. Phys.*, **11** : 1659-1670.

P-T modelling and geochronology of the Barberton Granite Greenstone Belt, South Africa: Rates of tectonic processes in the Archaean

CUTTS, K.A.^{1*}, STEVENS G.¹, HOFFMANN J.E.²,
BUICK, I.S.¹, FREI, D.¹ AND MÜNKER, C.²

¹Centre for Crustal Petrology, Department of Earth Sciences,
Stellenbosch University, Private Bag X1, Matieland 7602,
South Africa, *(correspondence: cuttsk@sun.ac.za;)

²Universität zu Köln, Institut für Geologie und Mineralogie,
Zülpicher Str. 49b, 50674 Köln, Germany

The Barberton Granite Greenstone Belt (BGGB) of South Africa is an exceptionally well preserved Meso-Paleoarchean metamorphic supracrustal belt, within which metamorphic studies have considerable potential to advance our understanding of tectonic processes in the Archaean crust. In this study, metamorphic P-T analysis has been combined with garnet Lu-Hf and monazite U-Pb geochronology, to directly date the amphibolite facies metamorphism within the Stolzburg terrane of the BGGB and constrain the P-T path. A garnet-biotite-chlorite bearing sample yields a Lu-Hf garnet age of 3233 ± 17 Ma and a garnet-staurolite-kyanite bearing sample produces a U-Pb monazite age of 3191 ± 9 Ma. Phase diagrams and garnet compositional modeling indicate a clockwise P-T evolution reaching peak P-T conditions of 8.5 kbar and 640 °C. The duration of metamorphism is estimated to be 50 to 20 Ma based on differences in age between U-Pb and Lu-Hf systems and durations needed to fit models of diffusionally modified garnet chemical zoning. Based on similar shaped clockwise P-T paths over the entire Stolzburg terrane it is probable that the metamorphism occurred in response to crustal thickening due to an accretionary tectonic process.

The difference in the ages obtained from the Lu-Hf and U-Pb systems constrains the rate of burial to 0.5-2.5 mm/yr, while the time required for garnet diffusion provides estimates on rates of exhumation (0.25-0.5 mm/yr). These estimates are consistent with burial via crustal thickening in modern orogens, however the exhumation rates are an order of magnitude slower than what is expected for exhumation of continental crust in the modern plate tectonic regime (cm-mm/yr). Plausibly, higher volumes of mafic and ultramafic rocks in the meso-Archaean proto-continental crust reduce the buoyancy of the lower crust compared to modern orogens leading to slower rebound. Against this scenario of slower exhumation, the high-pressure amphibolite facies conditions documented imply a relatively cool Meso-Archaean continental crust.

www.minersoc.org
DOI: 10.1180/minmag.2013.077.5.3

An *in situ* trace element study of peridotites from the Gakkel Ridge

M.E. D'ERRICO, J.M. WARREN¹ AND M. GODARD²

¹Stanford University, 450 Serra Mall, Stanford, CA 93405
(mderrico@stanford.edu); (warrenj@stanford.edu)

²Université Montpellier II, Montpellier, France
mgodard@univ-montp2.fr

Abyssal peridotites from the Gakkel Ridge provide constraints on the roles of ridge segmentation, on-axis cooling, and pre-existing heterogeneity on melt generation at ultraslow spreading rates. At a rate of 6-15 mm/yr, the Gakkel Ridge has a very thin crust and no major transform faults along its entire length. A thick lithospheric lid due to on-axis conductive cooling is predicted to limit the degree of melting. However, we present geochemical data that demonstrates significant compositional depletion in peridotites.

Peridotites in this study span the boundary between the Western Volcanic Zone and the Sparsely Magmatic Zone. We report *in situ* laser ablation ICP-MS trace element data for Cpx, Opx and olivine from a total of 14 samples. Based on lithology and rare earth element (REE) patterns, the harzburgite and lherzolite samples have each been divided into two groups. Group I harzburgites and lherzolites display typical REE patterns, with depletions in light REE relative to heavy REE. A single harzburgite in group II has a spoon-shaped pattern with enriched light REE, yet another sample within the same dredge has a typical REE pattern. Group II lherzolites have the highest degrees of depletion of any samples in this study. The small length-scale of compositional variability combined with thin oceanic crust suggests that pre-existing heterogeneity accounts for some of the depletion observed in peridotite compositions. The Gakkel peridotites thus provide evidence for a mantle that is the consequence of both inherited depletion and recent melting.

Mysteries of subseafloor sedimentary life

STEVEN D'HONDT^{1*}

¹Graduate School of Oceanography, University of Rhode Island, Narragansett Bay Campus, Narragansett, RI 02882, USA (dhondt@mail.uri.edu)

In recent years, multiple research groups have tremendously advanced understanding of subseafloor sedimentary life. Microbes in subseafloor sediment are now known to be abundant, diverse and characterized by extraordinarily low mean rates of activity.

Some discoveries challenge our sense of what is possible. For example, per-cell energy fluxes are far below the rates believed necessary for reproduction. What mechanisms might allow cells to reproduce at such low rates? Or do many of them live for millions of years without reproducing?

Bulk population studies show that a very large fraction of these cells is active. However, we know essentially nothing about cell-to-cell variation in respiration, biomass turnover or reproduction. Furthermore, we do not clearly understand how organic-fueled respiration can persist for tens of myrs at very slow rates.

Subseafloor community structure is largely unexplored. We have very limited understanding of the ways in which subseafloor microbes compete and almost no understanding of how they cooperate. Roles of viruses, eukaryotes, resting stages and bacterial spores in subseafloor ecosystems are largely unknown.

The proximate causes and ultimate consequences of natural selection in subseafloor communities remain unknown. For the most part, we do not yet know the genetic potential of subseafloor microbes, the extent to which their potential is expressed, or the conditions under which they are expressed. The actual limits to subseafloor life are not yet known.

Advancing understanding of these issues will yield fundamental insight into the nature of life.

Characteristics of olivine and diopside crystals in magma erupted at Stromboli during the 2003, 2007 and 2009 paroxysms: implications for magma ascent dynamics

C. D'ORIANO^{1*}, M. PISTOLESI², A. BERTAGNINI¹,
R. CIONI^{1,3}, M. POMPILIO¹ AND N. MÉTRICH⁴

¹Istituto Nazionale di Geofisica e Vulcanologia, sezione di Pisa, Italy (*correspondence: dorian@pi.ingv.it)

²Dip.to di Scienze della Terra, Università di Pisa, Italy

³Dip.to di Scienze della Terra, Università di Cagliari, Italy

⁴Institut de Physique du Globe de Paris, Paris, France

We present the results of morphological and compositional study on crystals associated with three paroxysmal explosions occurred at Stromboli in 2003, 2007 and 2009. Although with variable volume of emitted products, all the eruptions involved a deep-seated, volatile-rich, low-porphyricity magma (LP) ejected as pumice. Pumices are almost aphyric, highly vesicular and include portions of a shallow-derived, crystal-rich, moderately vesicular scoria (high porphyricity, HP magma type). We extracted about 1000 crystals (olivine and diopside) in the size interval between 1 and 0.125 mm. Three types of crystals are characterized by complex textures and compositions related to variable degrees of interaction between the LP and HP melts. The fourth type consists of transparent, light coloured crystals (light green for pyroxene), euhedral or sub-euhedral with some skeletal edges. They contain in some cases melt inclusions and are characterized by an homogeneous composition, and in some cases by a more evolved rims. Only this type of crystals is in equilibrium with the LP magma. The variable abundances of the different crystal types in the studied samples suggest the occurrence of different pre-eruption dynamics associated with the paroxysms at Stromboli. Real CSD was performed on olivine and diopside crystals in equilibrium with the LP magma. Results show that, during the 2003 event, crystallization occurred in a single step, while two different events of nucleation can be identified in the 2007 eruption. Equilibrium crystals are very rare in the 2009 paroxysm (the smallest of the three events considered) and they mainly occur as fine grained crystals (0.250-0.125 mm).

Results of this study are discussed in terms of crystallization – degassing processes, timing and modalities of magma ascent during paroxysms at Stromboli and possible relationships with signals recorded by the monitoring network.

Thermodynamics of almandine-spessartine garnet solid solutions

EDGAR DACHS, CHARLES A. GEIGER, ARTUR BENISEK
AND MICHAEL GRODZICKI

Material Science and Physics, Universität Salzburg,
Hellbrunnerstrasse 34, A-5020 Salzburg, Austria

The heat-capacity, C_p , behavior of a series of well characterized natural and synthetic almandine (Alm)-spessartine (Sps) garnets $[(\text{Fe}_x\text{Mn}_{1-x})\text{Al}_2\text{Si}_3\text{O}_{12}]$, was measured between 3 and 300 K using relaxation calorimetry and between 282 and 764 K using DSC methods.

All garnets show a λ -type anomaly at low temperatures resulting from a paramagnetic-antiferromagnetic phase transition. The temperature of the magnetic transition for Alm-rich garnets lies between those of end-member Alm at 9.2 K and Sps at 6.2 K, but is shifted to lower values between 3.5 and 4.5 K for garnets with $X_{\text{Sps}} > 0.5$. The low-temperature C_p data yield calorimetric entropies at 298 K (S_{298}), from which the excess entropy of mixing (ΔS_{ex}) of the join was calculated. By applying the phonon dispersion model of Komada and Westrum (1997), the lattice heat capacity was calculated for each solid-solution member. This allowed a decomposition of S_{298} into its vibrational (S_{vib}) and magnetic (S_{mag}) contributions.

The C_p data show that $\Delta S_{\text{ex}} \approx 0$ at 298 K for the Alm-Sps binary and thus the entropic interaction parameter $W_S \approx 0$. An analysis of published Fe-Mn exchange experiments between garnet and ilmenite giving W_G , together with this W_S term, allows W_H to be calculated. The resulting value is in satisfactory agreement with that calculated from phonon line broadening in infrared spectra of Als-Sps garnets using the autocorrelation method. ΔH_{ex} is asymmetric with a maximum in Sps-rich compositions. ΔG_{ex} is also asymmetric with a maximum of ~ 0.7 kJ/mol at $X_{\text{Sps}} \sim 0.60$ for temperatures between 500 °C and 1000 °C.

Our new subregular activity model for Alm-Sps garnets yields temperatures for Mn-rich metamorphic assemblages that agree with those from Fe-Mg biotite-garnet thermometry.

U isotopes disentangle atmosphere-ocean oxygenation dynamics

TAIS W. DAHL¹, JAMES N. CONNELLY¹,
BENJAMIN C. GILL², DONALD E. CANFIELD³
AND MARTIN BIZZARRO¹

¹Natural History Museum of Denmark, University of
Copenhagen, DK1350 Copenhagen, Denmark.

²Dept. of Geosciences at Virginia Tech, Blacksburg, VA
24061, USA.

³Nordic Center for Earth Evolution, Institute of Biology, Univ.
of Southern Denmark, DK5230 Odense, Denmark.

Anoxic marine zones were common in early Paleozoic oceans (542–400 Ma) [1–4], and they profoundly influenced atmospheric pO₂ via feedbacks associated with marine phosphorous recycling, global primary productivity and marine organic carbon burial [5–6]. Uranium (U) isotopes in carbonate rocks track the extent of ocean anoxia, and carbon (C) and sulphur (S) isotopes track the burial of organic carbon and pyrite sulphur and thus the sources of oxygen to the atmosphere. When used in combination, these proxies allow one to study the dynamics between ocean anoxia and oxygen liberation to the atmosphere over million-year time scales.

Here, we report high-precision uranium isotopic data in marine carbonates deposited during the Late Cambrian 'SPICE' event. Results document a well-defined -1.7 negative ε²³⁸U excursion that occurs at the onset of positive carbon and sulphur isotope excursions, consistent with expanded marine sinks of reduced C, S and U as expected during the expansion of marine anoxia. However, the ε²³⁸U excursion peaks before the δ¹³C and δ³⁴S excursions, marking a period of continued O₂ release from the marine C and S cycles after the oceanic anoxic event. Simple biogeochemical ocean modeling reveals that the different behaviors of the various isotope systems occurred because organic carbon and pyrite were buried with negligible U at high deposition rates in shallower oxygenated settings.

This second stage of the SPICE event suggests high weathering rates and P delivery from the continents to overcome the limited P-recycling from smaller anoxic marine zones. Intriguingly, this marine nutrient boost, perhaps induced by a tectonic-driven sea level drop, comes before the diversification of phytoplankton and the development of more extended trophic chains marking the beginnings of the Great Ordovician Biodiversification Episode.

[1] Gill *et al.*, (2011) *Nature*, **469** 80–83, [2] Dahl *et al.*, (2010) *PNAS*, **107**(42) 17911–15, [3] Berner & Raiswell (1983), *GCA*, **47** 855–862, [4] Berry & Wilde (1978), *Am. J. Sci.*, **278**, 257–275. [5] Van Capellen & Ingall (1996) *Science* **271**, 493–496. [6] Lenton & Watson (2000) *GBC* **14**, 249–268. [7] Servais *et al.* (2008) *Lethaia* **41**, 99–109.

Micro-X-ray-diffraction investigations of an altered cement-clay interface

R. DÄHN^{1*}, P. SCHAUB¹, D. POPOV², P. PATTISON³,
A. JENNI⁴, U. MÄDER⁴ AND E. WIELAND¹

¹Paul Scherrer Institut, 5232 Villigen, Switzerland

(*correspondence: rainer.daehn@psi.ch)

²Carnegie Institution of Washington, Argonne 60439, USA

³EPFL, 1015 Lausanne, Switzerland

⁴University of Bern, 3012 Bern, Switzerland

Cement-based materials and argillaceous rocks play an important role in multi-barrier concepts developed worldwide for the safe disposal of radioactive wastes in deep geological repositories. An approximately 180 million year old marine clay-rich sediment (Opalinus Clay) was identified and selected as the first-priority host-rock for the disposal of high-level radioactive waste in Switzerland. Both materials, i.e. Opalinus Clay and cement used for construction of the repository, are heterogeneous mineral assemblages with discrete nano- to micro-scale particles. Hardened cement paste (HCP) consists of mainly calcium (aluminium) silicate hydrates, portlandite, calcium aluminates, and some minor phases such as calcite and hydrotalcite, in hyper-alkaline environment (pH > 11), while Opalinus Clay (OPA) is a mineral assemblage consisting mainly of illite, illite-smectite mixed layers, kaolinite, quartz and calcite in near neutral conditions. Micro-scale information on the chemical reactions and the secondary phases formed in the disturbed zone at the HCP/OPA interface with its large chemical gradients is almost completely lacking.

In this study synchrotron-based micro-X-ray-diffraction (microXRD) was employed to characterise the complex heterogeneous phase assemblages at the HCP/OPA interface. MicroXRD with a beam size focussed down to a few micrometres makes it possible to perform a variety of novel diffraction experiments on fine-structured materials with a high spatial resolution. For example, micro-diffraction experiments allow probing of heterogeneously composed materials, which show chemical and structural alteration zones on a micrometre scale. The investigated samples were obtained from a long-term Cement/OPA-Interaction experiment ("CI-project") in the Mont Terri Rock Laboratory (St-Ursanne, Switzerland). The alteration zone was found to extend over a few hundred micrometres into the concrete material. First microXRD data of the HCP/OPA interface will be presented here.

Geochemical assessment in environmental assessment of human settlements

DEYI DAI^{1*}, YINGXUE RAO²
AND SHENGGAO CHENG¹

¹School of Environmental Studies, China University of Geosciences, Wuhan, PRC

(*correspondence author: xintata@yahoo.com.cn)

²College of Public Administration, South-Central University for Nationalities, Wuhan PRC.

Introduction and Methods

Environmental assessment of human settlements (EAHS) has two types in different levels, one is strategic environmental assessment (SEA), another is environmental impact assessment of project (EIA). From Geochemical perspective, EAHS reveal the relationship between human health and environmental characteristics or changes [1]. It uses geochemical principle and method to evaluate the environmental quality of human settlements, and also to predict the environmental change (figure 1).

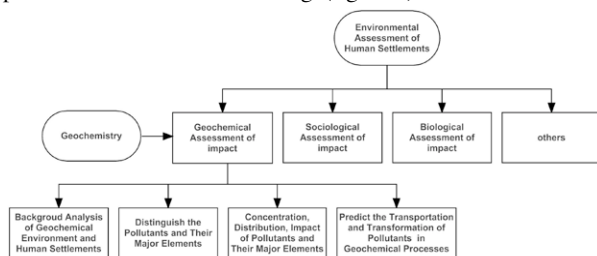


Figure 1: Relationship between EAHS and geochemistry.

The focus of assessment is to confirm the geochemical factors in environment. It is based on comprehensive analysis of environmental characteristics and human settlements' characteristics. Then, relative indexes would be selected for EAHS. Assessment is established on evaluation of the selected indexes. Finally, it proposes protective measures of environmental engineering, and conclusions of EAHS would be made.

Geochemical analysis is an important basis for EAHS. Environmental impact formed by the interaction between geochemical environment and human settlement. Strategic environmental assessment (SEA) of human settlements proposes more promptly support in policy and technology for environmental protection.

[1] Yuguo *et al.* (2006) *Journal of Earth Sciences and Environment* **28**: 81-86.

Redox-sensitive controls on the Proterozoic nitrogen cycle

STUART DAINES^{1*}, TIMOTHY M. LENTON¹

¹University of Exeter, UK,

(*correspondence: s.daines@exeter.ac.uk)

Primary production in the Proterozoic ocean is thought to have been strongly nutrient limited, with a range of hypotheses focusing on lack of phosphorus, nitrogen and/or trace metals. It has been argued that phosphorus lost its controlling role as ultimate limiting nutrient, and that all nitrogen could have been drained from the ocean by denitrification in the transition from anoxic to oxic conditions [1], resulting in a feedback maintaining low atmospheric oxygen, and ecological constraints on eukaryote diversification. However, high rates of nitrogen fixation in contemporary anoxic basins and during Phanerozoic OAEs suggest enhanced nitrogen fixation can compensate [2].

Here we use a spatially structured biogeochemical model, GENIE, to examine the role of the nitrogen cycle in controlling ecosystem productivity and ocean redox state. The physiological cost of nitrogen fixation is considerably reduced in low oxygen environments [3], hence nitrogen fixation can maintain production in a mixed anoxic/oxic regime at a level set by P as the ultimate limiting nutrient. Extensive denitrification is predicted, with small NO_3^- and NH_4^+ reservoirs and a short N residence time ~ 300 – 500 yr.

Spatial redox structure influences the expression of isotope fractionation, hence scenarios could potentially be constrained by N isotope data [4].

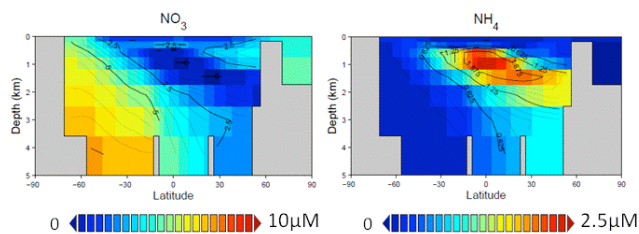


Figure 1: Meridional sections for $[\text{NO}_3^-]$ and $[\text{NH}_4^+]$ in mixed oxic/anoxic regime.

[1] Fennel *et al.* (2005) *Am. J. Sci.* **305**, 526–545. [2] Kuypers *et al.* (2004) *Geology* **32**, 853. [3] Großkopf & Laroche (2012) *Front. Microbio.* **3**, 236. [4] Beaumont & Robert (1999) *Precamb. Res.* **96**, 63–82.

Making natural materials clean – and model samples dirty.

K. N. DALBY*, N. BOVET, M.P. ANDERSSON, K. JUHL
AND S.L.S. STIPP

Nano-Science Center, Department of Chemistry, University of
Copenhagen, Denmark
(*kdalby@nano.ku.dk)

To improve interpretation of experimental geochemical data, simulations are used. However, theoretical approaches require a certain number of assumptions; otherwise computational requirements become astronomical. Thus, molecular models usually use flat or minimally stepped, pure, “clean” surfaces, e.g., no carbon contamination of the sort that comes from the environment, called “adventitious carbon” (AC). AC is extremely difficult to remove and ubiquitous on all mineral surfaces exposed to air or water.

However, surface analysis with X-ray photoelectron spectroscopy (XPS) and atomic force microscopy (AFM) clearly demonstrate that such a layer modifies the reactivity of quartz (SiO₂) surfaces. New density functional theory (DFT) modelling of carbon containing compounds on calcite surfaces also supports previous XPS results - that AC can change the affinity of the surface for organic molecule attachment, even simple alcohols..

We have developed a fast and easy method for producing “clean” surfaces analogous to those used in modelling (Figure 1) which does not change surface structure. Combined with the development of organic self assembled (SAM) monolayers, for use in deriving experimental data of a model “dirty” system that can be explored theoretically, we can begin to bridge the gap between experiments and models.

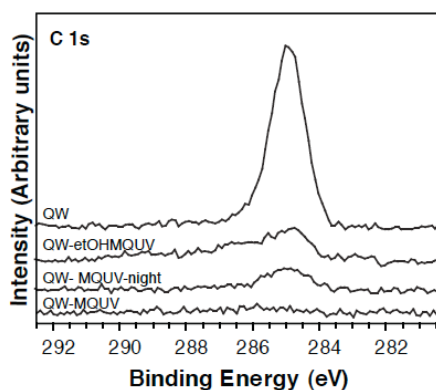


Figure 1: XPS C 1s spectra from quartz wafers (QW) treated (with ethanol (etOH), MilliQ water (MQ) and UV ozone (UV)) to remove the adventitious carbon peak at 285.0 eV.

The Carnian Pluvial Event negative CIE at Cave del Predil (early Late Triassic, Italy): a new link to Wrangellia volcanism

J. DAL CORSO^{1*}, G. ROGHI², M. RIGO^{1,2}, P. GIANOLLA³,
M. CAGGIATI³, G. GATTOLIN¹, R.J. NEWTON⁴, H.C.
JENKYN⁵ AND N. PRETO¹

¹Dipartimento di Geoscienze, Università degli Studi di
Padova, via Gradenigo 6, 35131, Padova, Italy
(*correspondence: jacopo.dalcorso@unipd.it).

²Istituto di Geoscienze e Georisorse, CNR, via Gradenigo 6,
35131, Padova, Italy.

³Dipartimento di Fisica e Scienze della Terra, Università di
Ferrara, via Saragat 1, 44100, Ferrara, Italy.

⁴School of Earth and Environments, University of Leeds,
Woodhouse Lane, LS2 1JT, Leeds, UK.

⁵Department of Earth Sciences, University of Oxford, South
Parks Road, OX1 3AN, Oxford, UK.

A ~4‰ negative C-isotope excursion (CIE) in higher plant *n*-alkanes has recently been discovered coincident with the onset of the Carnian Pluvial Event (CPE) [1], during which a major climatic and biotic turnover occurred [2]. This C-cycle disturbance has been linked to the eruption of the Wrangellia oceanic plateau (western North America), a Large Igneous Province (LIP) that is thought to have extruded up to 1 million cubic kilometres of basalts during the early Late Triassic [3].

C-isotope analyses of bulk organic matter from stratigraphic sections in the Cave del Predil area (Julian Alps, north eastern Italy) reveals an early Carnian ~6‰ negative CIE corresponding to the onset of the CPE [4]. The negative CIE occurs just below the level recording the first major terrigenous input and change in vegetation type to a hygrophytic flora that can be correlated with the existing stable C-isotope curve from the Dolomites [1].

Our new data show that the major negative CIE at the onset of the CPE can be correlated at least regionally and likely represents a global signal. This C-cycle perturbation could have been caused, directly or indirectly, by the release of large amounts of CO₂ during the coeval eruption of the Wrangellia LIP that led to the Carnian climatic, environmental and biological changes.

[1] Dal Corso *et al.* (2012), *Geology* 40, 79–82. [2] Simms and Ruffell (1989), *Geology* 17, 265–268. [3] Greene *et al.* (2010), *Geosphere* 6, 47–73. [4] Roghi *et al.* (2010), *Palaeogeogr. Palaeoclimatol. Palaeoecol.* 290, 89–106.

Clumped isotopes and concretions: The Prairie Canyon member of the Mancos Shale, Colorado

A. DALE^{1*}, C. M. JOHN¹, P. MOZLEY², P. C. SMALLEY³
AND A. H. MUGGERIDGE¹

¹Royal School of Mines, Imperial College London, UK, SW7
2BP (*correspondence: annabel.dale07@imperial.ac.uk)

²Department of Earth and Environmental Science, New
Mexico Tech, Socorro, New Mexico 87801, USA

³BP, Chertsey Road, Sunbury-on-Thames, Middlesex TW16
7BP, UK

Carbonate concretions and septarian fracture fills have been key in developing our understanding of early burial processes in siliciclastic rocks [1]. Often, septarian fractures and concretion matrix cements have unusually light $\delta^{18}\text{O}$ values. A common explanation for near-shore marine concretions is that they precipitated at the sediment-water interface in aquifers of mixed meteoric-marine water [2][3]. Alternatively, the light $\delta^{18}\text{O}$ could be due to precipitation at higher temperatures during burial. It is often difficult to distinguish between the two hypotheses, which has hindered previous interpretations of the mechanisms of concretion formation and the timing of diagenetic processes.

Here, we apply the novel carbonate 'clumped' isotope palaeothermometer [4] to Fe-dolomite/ankerite concretions and calcite septarian fracture fills from the Upper Cretaceous Prairie Canyon Member. The derived temperature is independent of the bulk isotopic composition, so the parent fluid can be back-calculated. Our results show that the fracture fill precipitated between 107-117°C, corresponding to depths of up to ~3 km. The parent fluid has a $\delta^{18}\text{O}$ value of 0.5 ± 0.13 (VSMOW), consistent with slightly ^{18}O -enriched Cretaceous seawater. Interpretation of the concretion matrix is complicated by mixed phases of cements and by the non-linear mixing of clumped isotopes, which can lead to an uncertain temperature. However, even accounting for this, a temperature trend from cooler cores ($34^\circ\text{C} \pm 8$) to hotter edges ($53^\circ\text{C} \pm 1$) is observed. Therefore, the light $\delta^{18}\text{O}$ values, at least in the Prairie Canyon, are caused by higher temperatures during burial and not meteoric mixing.

We would like to acknowledge a BP-EPSCRC Case Studentship for funding this project.

[1] Irwin *et al.* (1977), *Nature* **269**, 209-213 [2] Balsamo *et al.* (2012), *J. Geol. Soc.* **169**, 613-626 [3] Coniglio *et al.* (2000), *J. Sed. Res.* **70**, 700-714 [4] Ghosh *et al.* (2006), *Geochim. Cosmochim. Acta.* **70**, 1439-1456

Rapid core formation and an early 'vener' on Earth: Highly siderophile elements in pre- lunar mantle domains

CHRISTOPHER W. DALE¹ KEVIN W. BURTON¹,
ABDELMOUHCINE GANNOUN², IAN J. PARKINSON³,
HELEN M. WILLIAMS¹ AND STEPHEN MOORBATH⁴

¹Dept. Earth Sciences, Durham University, DH1 3LE, UK;
(christopher.dale@durham.ac.uk)

²Lab. Magmas et Volcans, UBP, Clermont Ferrand, France

³CEPSAR, Open University, Milton Keynes, MK7 6AA, UK

⁴Dept. Earth Sciences, University of Oxford, OX1 3PR, UK

Highly siderophile elements (HSEs) are strongly sequestered into metallic planetary cores, leaving silicate mantles almost devoid of HSEs. Late accretion of primitive meteoritic material, after core formation had ceased, partially replenished HSEs in planetary mantles and occurred within a few million years of solar system formation on most parent bodies (1), but probably later on Earth, after a final episode of core formation associated with the giant Moon-forming impact (50-150 million years later (2)).

Ancient isolated domains in Earth's mantle, which formed prior to the giant impact, have recently been recognised by anomalies in the short-lived ^{182}Hf - ^{182}W isotope system. These domains - such as the source of 3.8 billion-year-old Isua basalts (3) - might represent mantle that largely escaped late accretion. Here we show, however, that the Isua source mantle had HSE abundances at ~60% of the present-day mantle, inconsistent with a pre-late accretion model.

Such early-formed domains require preservation through the Moon-forming giant impact and isolation thereafter, precluding subsequent addition of HSE by mixing with material accreted later. Thus, their HSE contents were set by early 'pre-lunar' late accretion, while the Hf-W system was still extant. This early HSE replenishment requires that core formation was rapid and ceased early, and therefore, on the basis of W isotope evidence, implies a high degree of equilibration of metal with mantle silicate during accretionary impact events. The retention of such early HSE-enriched mantle also implies incomplete giant impact-related melting of Earth's mantle. Conversely, the HSE budget of the Moon was reset during its formation, thereby partially accounting for the disparity in HSE content and apparent late accretion rates between the Earth and Moon.

(1) C.W. Dale *et al.* (2012), *Science*, **336**, 72. [2] M. Touboul *et al.* (2007), *Nature* **450**, 1206 [3] M. Willbold *et al.* (2011), *Nature* **477**, 195.

Organics in the Mix during SAPUSS

M. DALL'OSTO¹, X. QUEROL¹ AND THE SAPUSS TEAM²

¹IDAEA-CSIC, c/Jordi Girona 18-26, Barcelona, Spain
(manuel.dalosto@gmail.com)

²see reference below [1]

In this work we illustrate the results of the organic aerosols measurements taken during the SAPUSS experiment (Solving Aerosol Problems By Using Synergistic Strategies) in Barcelona (Spain) during autumn 2010 [1]. Two supersites were chosen: Urban background (UB) and Road site (RS) on which

Simultaneous measurements with High Resolution Aerosol Mass Spectrometry (HR-ToF-AMS) were taken; Positive Matrix Factorization (PMF) was applied revealing five different organic aerosol factors.

Simultaneous single particle mixing state measurements with Aerosol Time Of Flight Mass Spectrometry (ATOFMS) were classified by ART-2a algorithm, resulting in eighteen specific particle types internally mixed with a number of organic and inorganic species.

Simultaneous aerosol filter measurements at 12 hours resolution were taken, and concentrations of thirtysix neutral and polar organic compounds were obtained by GC-MS; subsequently classified by MCR-ALS apportioning six OA components (two were of primary anthropogenic OA origin, three of secondary OA origin while a sixth one was not clearly defined).

This presentation aims at summarising key SAPUSS findings on organic aerosol source apportionment, on the role of organics in new-particle formation and on the interactions of organics and inorganics components.

[1] Dall'Osto *et al.*, 2012. *Atmos. Chem. Phys. Discuss.*, **12**, 18741-18815, 2012

Activity of cable bacteria and electro-physical properties of gradient systems studied with a novel microsensor for electric potential

LARS RIIS DAMGAARD*, NILS RISGAARD-PETERSEN
AND LARS PETER NIELSEN

Institute for Biosciences, Aarhus University, Ny Munkegade
114-116, DK-8000 Aarhus C, Denmark.

(*correspondence: lrd@biology.au.dk)

Activity in sediments and biofilm are thought to be confined to steep chemical gradients and cascades of coupled co-localized redox processes. Recently, however, filamentous bacteria of the family Desulfobulbaceae were found to transfer electrons over centimeter distances to couple spatially separated oxidation and reduction processes (1, 2). For this new exciting research area we have developed a novel microscale sensor for measuring electric potential at micrometer and microvolt scales. Microprofiles of electric potential in marine sediment dominated by such 'cable bacteria' allowed identification of involved electron donors and acceptors as well as the localization and quantification of the bio-electrical currents. Electrical conductivity – and in turn diffusivity – of sediment and other soft substrates could also be measured with the aid of the electric potential microsensor, and possibly it can help elucidate the nature of conductivity in microbial nanowires and cable bacteria.

[1] Nielsen, L. P., N. Risgaard-Petersen, H. Fossing, P. B. Christensen, and M. Sayama (2010), Electric currents couple spatially separated biogeochemical processes in marine sediment, *Nature*, **463** (7284), 1071-1074. [2] Pfeffer, C., *et al.* (2012), Filamentous bacteria transport electrons over centimetre distances, *Nature*, **491** (7423), 218-221.

Dissolved iron behavior in the estuarine waters; Irt and Esk River, west Cumbria, UK

EHSAN DANESHVAR¹

¹Tyn e Coed, Llandudno, LL30 1SA,
(ehsan.daneshvar@cgg.com)²

The aqueous geochemistry of the Ravenglass estuary and its feeding rivers (Irt and Esk) has been studied to assess if, where and when aqueous iron is lost from the river water and accumulates as part of the sediment in the estuary. The River Irt contains twice as much dissolved iron as the River Esk but all iron concentrations are much lower in the estuary samples than in the feeding rivers. Aqueous iron undergoes large-scale accumulation in the Ravenglass estuary. Iron concentrations are lowest at high tide at all sampling sites on the Ravenglass estuary. Iron concentrations are highest at low tide for the Irt arm of the estuary but are highest on the falling tide between high and low tide. Iron in estuary samples decrease rapidly as salinity increases with low iron in all estuary samples once salinity exceeds 5,000 mg/lit. Iron also decrease as pH increases. The loss of iron is presumably due to flocculation of colloidal iron oxides, hydroxides and iron-organic complexes. Fluvial aqueous iron does not behave conservatively on mixing with seawater; most iron is lost from the water column at an early stage of river water mixing with estuary water. The site of primary iron-loss from the water occurs towards the heads of estuaries but this site will move as a function of time within the tide cycle.

Geochemistry and significance of Carboniferous-Permian volcanic rocks in the western of Inner Mongolia, China

BEN DANG^{1,2*}, HONG ZHAO^{1,2}, LU-JUN LIN¹,
QIAN-QIAN GAO¹ AND MING LIU¹

¹College of Earth Sciences and Resources, Chang'an University, Xi'an 710054, China;

²Key Laboratory of Western China's Mineral Resources and Geological Engineering, Xi'an 710054, China
(*correspondence: dangben@126.com)

The western region of Inner Mongolia located in the south rim of Central Asian Orogenic Belt[1], which belong to the key component of Tianshan-Xing'An Orogenic system. Carboniferous-Permian volcanic rocks are widespread in the area. However, at present, the study of petrogenesis and tectonic setting are weak relatively. Based on the regional geological survey, combined with the analysis of petrology and petrogeochemistry characteristics of Carboniferous-Permian volcanic rocks, the genesis of the rocks and tectonic setting have been discussed. It provides petrogeochemistry proofs for clarifying the properties of Carboniferous-Permian basin and palaeo-tectonic setting. The volcanic rocks in the area are intermediate-acidic volcanic rocks mainly and a small amount of basic volcanic rocks. The geochemistry characteristics of the basic volcanic rocks (Basalts, basaltic-andesite) show as follows. Most of the sample of the basic volcanic rocks belong to sub-alkaline series, a little are alkaline series. Mg# ranges from 0.29 to 0.86. The high field strength elements Nb, Ta and Ti are strong depletion. Light rare earth element (LREE) is mild richer than heavy rare earth element (HREE). (La/Yb)_N ranges from 1.68 to 10.1. Eu anomalies is not obvious ($\delta\text{Eu}=0.64\sim 1.08$). REE distribution patterns are slightly right-inclined. Nb/U is generally low 1.35~9.78. Ti/V ranges from 20 to 100 (centralized in 50). $\epsilon\text{Nd}(t)$ is higher(+1.10~+6.35). Geochemistry comprehensive analysis indicate that Carboniferous-Permian volcanic rocks in the area show not only the signature of within plate setting as a whole, but also that of subduction zone. Synthesizing the regional geological characteristic and the research achievement in the neighbouring area, we conclude that the Carboniferous-Permian magmatic activity in study area generated in within-plate rift valley setting, and probably related to mantle plume affair, with variable degrees of contamination of crust during magma ascending.

[1] Dobrestsov *et al.*(1995) *International Geology Review*, 37,335–360.

Non-adiabatic calculations of ultraviolet absorption cross section of Sulfur Monoxide; Isotopic effects on the photodissociation reaction

SEBASTIAN O. DANIELACHE¹, TOMOYA SUZUKI¹
AND SHINKOH NANBU¹

¹Faculty of Science & Technology, Sophia University, Japan
(sebastian.d@sophia.ac.jp)

Understanding the mechanism of the sulfur isotopic fractionation of SO₂ in a reduced atmosphere and under high fluxes of UV light has become a key feature in explaining the mechanisms that produced the large sulfur mass independent fractionation (S-MIF) signal deposited in the geological record [1,2]. However, all modeling studies conducted for the Archean atmosphere assume that the life time of the intermediate product after the photodissociation of SO₂ (SO) is short lived and no further photochemistry can produce additional isotopic enrichment or depletion. We set out to test this hypothesis by theoretically calculating the ultraviolet absorption cross sections of the main and substituted sulfur monoxide isotopologues. The theoretical framework for this work includes a newly developed R-Matrix expansion. The calculated absorption cross section of ³²S ¹⁶O were compared with reported experimental spectra, calculations and experiments are in good agreement although there is some concern with certainty of the experimental data. Our calculations show that according to the energy of the photon flux the involved excited states can produce a fast photodissociation or a long lived SO* photoexcited fragment. In order to test these new results the obtained spectra were introduced in an improved sulfur isotope photochemical Archean model [3]. The improvement to our model includes the addition of hydrocarbon chemistry, chemical formation and deposition of organic sulfur haze.

[1] Danielache *et al.*. (2008) *J Geophys Res* **113**, D17314. [2] Farquhar *et al.*. (2001) *J Geophys Res* **106**, D32829. [3] Ueno *et al.*. (2009) *PNAS* **106**, 14784-14789.

Modelling the propagation and dissolution of CO₂ into reservoir brines: implications for CO₂ sequestration.

KATHERINE DANIELS¹, MIKE BICKLE¹, PEDRO WATERTON², DUNCAN HEWITT³, JEROME NEUFELD^{1,3,4},
NIKO KAMPMAN¹, ALEXANDRA MASKELL¹
AND HAZEL CHAPMAN¹

¹Department of Earth Sciences, University of Cambridge,
Downing Street, Cambridge CB2 3EQ, U.K.

²Department of Earth & Atmospheric Sciences, University of
Alberta, Edmonton, Alberta, Canada, T6G 2E3

³Institute of Theoretical Geophysics, Department of Applied
Mathematics and Theoretical Physics, Centre for
Mathematical Sciences, Wilberforce Road, Cambridge,
CB3 0WA, U.K.

⁴B.P. Institute for Multiphase Flow, Bullard Laboratories,
Madingley Road, Cambridge, CB3 0EZ, U.K.

The Earth's climate is changing and the release of carbon dioxide (CO₂) and other greenhouse gases into the atmosphere is recognised as the principal cause. Long-term and secure geological storage of CO₂ through Carbon Capture and Storage (CCS) within reservoirs is seen as a solution; however, knowledge of the trapping mechanisms, in conjunction with understanding the effect of injected CO₂ on the reservoir formations themselves, is fundamental to assessing the viability of long-term storage. Developing a greater understanding of the flow of CO₂ through a porous medium and the associated reactions between the host rock formation and the fluid is therefore of great importance to understanding whether a CO₂ storage site is likely to fail.

Dissolution of CO₂ into ambient brine is a prospective stable trapping mechanism. This study examines the enhanced rates of dissolution found during injection into a layered, heterogeneous formation using analogue experiments and numerical models. The analogue experiments, designed to approximate an Enhanced Oil Recovery (EOR) setting, show that during fluid propagation, pore-scale viscous fingers grow and retreat providing an increased surface area between the flow and the ambient reservoir fluid, which is likely to enhance the dissolution of CO₂ in reservoir brines. The numerical simulations provide a useful comparison with the analogue experiments and give constraints on the timescale and magnitude of CO₂ dissolution and the consequent fluid-mineral reactions in a heterogeneous reservoir. The study addresses whether carbonate or silicate mineral dissolution can provide the CO₂ with a leakage pathway through corroded caprocks and fault seals, or assist pathway sealing.

Influence of organic molecules on aggregation of TiO₂ nanoparticles

KARIN DANIELSSON*, JULIÁN GALLEGO-URREA,
MARTIN HASSELLÖV AND CAROLINE M. JONSSON

University of Gothenburg, Department of Chemistry and
Molecular Biology, Gothenburg, Sweden
(karin.danielsson@chem.gu.se) (* presenting author)
(julian.gallego@chem.gu.se), (martin.hasselov@chem.gu.se),
(caroline.jonsson@chem.gu.se)

Nanotechnology is a rapidly growing industry, which leads to an increased amount of synthetic nanoparticles released into the environment. However, the fate and behavior of synthetic nanoparticles in the environment are not well-known. Titanium dioxide (TiO₂), a naturally occurring mineral, is one of the most used metal oxide nanoparticles due to its special properties. Nanoparticles generally have higher reactivity than larger particles of the same material. As the particle size is decreased to the nanometer size range (1-100nm), the surface chemistry changes and this might influence the surface charging and aggregation behavior. Further, nanoparticles can interact with natural organic material (NOM), such as humic and fulvic acids, which is present in most natural waters. Adsorption of NOM affects the surface speciation and net charge of the nanoparticles and is therefore of great importance for their colloidal stability. This might alter the mobility of nanoparticles in surface waters and in soils, thus determining their bioavailability and toxicity.

The focus of the present study was to investigate the aggregation behavior of synthetic nanoparticles in aqueous solution as a function of time and pH in the presence of organic molecules. Synthesized and well-characterized TiO₂ (anatase) nanoparticles were used as test nanoparticles and selected phenolic carboxylic compounds were used as model substances to mimic the interactions of nanoparticles with NOM. The aggregation and surface charging of the particles were studied by simultaneously monitoring the changes in particle size and zeta potential during the reactions. Results show that the concentration of organic molecules, and the type and number of functional groups affect the aggregation behavior of TiO₂ nanoparticles in aqueous solution.

Testing accuracy of combined zircon (²³⁸U/²³⁰Th) and (U-Th)/He dating against radiocarbon dating

M. DANIŠÍK^{1,2*}, P. SHANE³, A.K. SCHMITT⁴, A. HOGG⁵,
G.M. SANTOS⁶, N.J. EVANS², S. STORM³, K. FIFIELD⁷,
J. LINDSAY³ AND B. ALLOWAY⁸

¹The University of Waikato, Hamilton, New Zealand,
(m.danisik@waikato.ac.nz) (* presenting author)

²John de Laeter Centre for Isotope Research, Curtin
University, Perth, Australia

³University of Auckland, Auckland, New Zealand

⁴University of California Los Angeles, Los Angeles, USA

⁵Radiocarbon Laboratory, University of Waikato, Hamilton,
New Zealand

⁶University of California, Irvine, USA

⁷Australian National University, Canberra, Australia

⁸Victoria University, Wellington, New Zealand

Combined ²³⁸U/²³⁰Th disequilibrium and (U-Th)/He dating of zircon [1] is a novel approach for dating young (<350 ka) volcanic eruptions. This method has been successfully applied in various settings [2,3], however its accuracy has not been rigorously tested and validated by independent methods.

In this study we apply the combined ²³⁸U/²³⁰Th disequilibrium and (U-Th)/He zircon dating to the deposits of the coeval Rotoiti (ROR) and Earthquake Flat (EQF) eruptions in the Taupo Volcanic Zone, New Zealand, to investigate consistency of the method. In addition, wood sampled below and above the Rotoiti tephra is dated by high-precision radiocarbon method to provide independent constraints on the accuracy of the zircon eruption ages.

The two independent methods revealed concordant ages, which are also in accord with the stratigraphic position of the samples. Based on these results we assign new ages of ~45 ka to the ROT and EQF eruptions, which is by ~16 kyr younger than the currently accepted age, which has implications for paleoclimatic reconstructions and hazards assessment. This study proves the combined ²³⁸U/²³⁰Th disequilibrium and (U-Th)/He dating of zircon reliable at late Quaternary time scale and also demonstrates reliability of the radiocarbon dating method at higher end of its sensitivity at ~50 ka.

[1] Schmitt *et al.*. (2006) *J. Volcanol. Geoth. Res.* 158 (3-4), 281-295. [2] Schmitt *et al.*. (2010) *Earth Planet. Sci. Lett.* 295 (1-2), 91-103. [3] Schmitt *et al.*. (2011) *Contrib. Mineral. Petrol.* 162 (6), 1215-1231.

Measuring denudation rates with the ^{10}Be (meteoric)/ ^9Be isotope ratio in catchments with different lithologies

N. DANNHAUS^{1*}, F. VON BLANCKENBURG¹,
H. WITTMANN¹, P. KRAM² AND M. CHRISTL³

¹ GFZ German Research Centre for Geosciences, Potsdam, Germany (*correspondance: nadine.dannhaus@gfz-potsdam.de)

² Czech Geological Survey, Prague, Czech Republic (pavel.kram@geology.cz)

³ ETH, Zurich, Switzerland (mchristl@phys.ethz.ch)

Unlike *in situ*-produced cosmogenic nuclides, determining denudation rates with the new ^{10}Be (meteoric)/ ^9Be ratio does not depend on the presence of quartz. In the Critical Zone cosmogenic ^{10}Be and its stable counterpart ^9Be mix to a characteristic rate that is dependent on the denudation rate, the fraction of ^9Be released from primary minerals, and the ^9Be concentration of the parent bedrock [1]. This rate can be determined either on the reactive phase (adsorbed onto or precipitated in secondary minerals) of sediment or on the dissolved phase in stream water. The reactive beryllium can be separated by a sequential extraction method described in [2]. Dissolved cosmogenic ^{10}Be is concentrated from a water sample by co-precipitation with iron(III)-hydroxide.

We applied this new method to three small catchments in the Slavkov Forest, Czech Republic. Each catchment is underlain by different bedrock, namely granite, amphibolite, and serpentinite. These diverse lithologies are ideal to investigate the potential of the $^{10}\text{Be}/^9\text{Be}$ isotope system under various geochemical conditions (e.g. different acid-base chemistry of stream and soil water). Resulting $^{10}\text{Be}/^9\text{Be}$ ratios in the reactive and dissolved phase differ only within a factor of two for each catchment, indicating almost complete equilibration of the isotopes. We used these $^{10}\text{Be}/^9\text{Be}$ ratios to calculate denudation rates that turned out to be highest for the ultramafic and lowest for the granitic catchment.

One advantage of this new approach is that it can be applied to any lithology, provided that the bedrock ^9Be concentration is known. The second novelty of this system is that a denudation rate can be determined from a $^{10}\text{Be}/^9\text{Be}$ ratio measured in the dissolved fraction of stream water.

[1] von Blanckenburg *et al.* (2012) *EPSL* **351-352**, 295-305.

[2] Wittmann *et al.* (2012) *Chem. Geol.* **318-319**, 126-138.

Influence of geological setting on geochemical baselines of heavy/trace elements in soils of Medak district, Andhra Pradesh, India

SUJATHA DANTU

CSIR - National Geophysical Research Institute, Hyderabad, India – 500 007
(sujathadantu@rediffmail.com)

A collection of 878 soil samples (557-topsoil 0-25 cm depth interval, 321-subsoil 70-95 cm depth interval) were taken from 557 sites (representing a density of 1 site/17 km²) derived from the major rock types in the Medak district of Andhra Pradesh, India. The concentration of 29 elements (major: Si, Al, Fe, Mn, Mg, Ca, Na, K, Ti, P and trace: As, Ba, Cd, Co, Cr, Cu, F, Mo, Ni, Pb, Rb, Se, Sr, Th, U, V, Y, Zn, Zr) was determined on the < 2 mm soil fraction by X-ray fluorescence spectrometry. The sampling sites were not directly influenced by any external pollution. The geochemical baseline values for each element in soils developed on different litho-units are presented. The median concentrations of Ni, Pb, Rb, Sr, Y, Zn, Zr, Si, Al, Fe, Mn, Mg, Ca, Na, Ti and P were measured to be significantly lower while the median concentrations of Ba, Cd, Co, Cr, Cu, F, Mo, Se, Th, U and K were found to be higher than the world median soil values. The distribution patterns of element concentrations are primarily influenced by the lithology. By contrast, the concentrations of Co, Cu, Fe, Mn, Ti, V and Zn are high in soils developed on basaltic terrain while the soils developed on granitic and gneissic terrain exhibited high elemental concentrations of K, Pb, Rb, Si, Th and Y. High concentration of radioactive elements in soils in certain pockets of the study area appear to characterize the igneous rocks formed over considerable periods of time and also by subsequent addition of Th derived from the erosion of the neotectonically uplifted rocks [1]. Enrichment of the elements in the soils developed on different rock variants reflected the elevated levels in the parent material and or fixation (adsorption) in soils by weathering processes. Further elemental concentrations are also related to the size of soil particles therefore, the loss or gain in clay, silt and sand size fractions of soil by wind or hydrological transport may cause differences in element enrichment at regional or local scale. It is therefore, evident that most of the differences in geochemical values of elements are controlled by the bed rock. These results indicate that regional geology is an important determinant of soil geochemical baselines for soil pollution assessment.

[1] Sujatha Dantu (2010) *Environ Monit Assess*, 170: 1-4, 681-701.

LA-ICPMS imaging of micro-inclusions and high compositional gradients in minerals

L.V. DANYUSHEVSKY^{1*}, S.J.M. MEFFRE¹
AND S.E. GILBERT¹

¹CODES CoE, University of Tasmania, Private Bag 79,
Hobart, Tasmania, 7001, Australia (*correspondence:
l.dan@utas.edu.au), (Sebastien.Meffre@utas.edu.au),
(sgilbert@utas.edu.au)

Imaging of trace element distribution in a range of geological materials using quadrupole LA-ICPMS is an actively expanding area of geochemical micro-analysis. Determining compositions of diagenetic and hydrothermal sulphide minerals using in-situ analytical techniques presents a significant challenge due to common high compositional gradients (several orders of magnitude over several microns) and wide-spread occurrence of micro-inclusions. Accurate imaging of trace and minor element distribution in such minerals offers significant advantages for genetic interpretations [1], complementing conventional spot analyses. Simultaneously resolving high concentration gradients for a wide range of elements with LA-ICPMS requires fast-response, small-volume ablation cells; minimal mixing within the laser-ICP interface; and short dwell and total sweep times on the ICPMS. The technique developed uses a set of parallel lines with spacing equaling the laser beam size, thus covering the entire sample surface. Pre-ablation of each line is essential for removing surface deposition from previous ablations. Regular measurements of the background and calibration standards are required for controlling memory effects and instrumental drift in sensitivities. Use of square rather than round beam shape is preferred, although not critical for this application. The beam size is determined by size and composition of bands and micro-inclusions of interest. Lines are ablated at 10 Hz and a constant speed covering the size of the beam in 1 sec, resulting in each position on the surface being ablated 10 times. Total sweep times are 0.2-0.3 seconds resulting in 3 to 5 sweeps being recorded each second. The effective pixel size along the lines is dependent on instrumentation design and can be minimised by advanced image processing, to be ~ 1.3-1.5 times the beam sizes. Accurate imaging of gentle compositional gradients (<10 times), especially over short distances (up to several beam diameters) requires a different approach with signal smoothing and slower rastering. Challenges of image quantification will be discussed.

[1] Large *et al.* (2009) *Econ. Geology* **104** 635-668.

Reactivity of U(VI) with H₂, CH₄ and C under hydrothermal conditions

M. DARGENT¹, L. TRUCHE¹ AND J. DUBESSY¹

¹GéoRessources, Université de Lorraine, 54500 Vandoeuvre-lès-Nancy, France (*correspondence:
maxime.dargent@univ-lorraine.fr)

Giant Unconformity-type U deposits are characterized by massive uraninite often associated with graphite. It has been demonstrated that U was first transported by acidic brines under the form of uranyl chloride complex and further reduced locally into uraninite [1]. However, the reaction mechanism and kinetics of U(VI) reduction into immobile U(IV) remain poorly understood [2]. The objective of our experimental investigations is to measure uranyl chloride reduction rate as a function of the nature of the reducing agent and under hydrothermal conditions relevant for unconformity-type deposits.

We demonstrate that U(VI) reduction occurs readily at temperature above 100°C whatever the reducing agent considered. 10 µm octahedral uraninite crystals precipitated. The initial activation stage probably corresponds to the first uraninite crystals nucleation. Reaction rate measurements allow us to rank the efficiency of electron donors: H₂ > CH₄ > C, and to evaluate the respective activation energies. Furthermore the reaction rate also depends on chlorinity. This suggests that the reaction mechanism is partly controlled by the speciation of uranyl in chloride solutions. This point is highlighted by a Raman spectroscopic study [3].

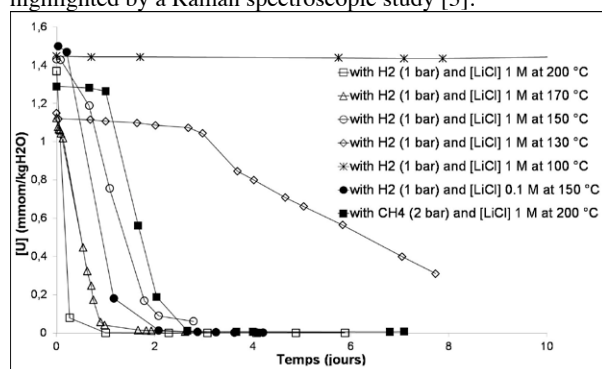


Figure 1: U(VI) concentration (mmol/kgH₂O) vs time (day) for different chlorinity, reductants and temperatures.

[1] Richard *et al.* (2011) *Nature Geosciences* **5**, 142-146. [2] Yeo & Potter (2010) *Summary of Investigations 2010* **2**, 13p. [3] Dargent *et al.* (2013) *Eur. J. Mineral.* (in press)

The shocking state of baddeleyite in basaltic shergottite NWA 5298

J.R. DARLING^{1*}, D. E. MOSER², I. BARKER², K.T. TAIT³,
K. CHAMBERLAIN⁴ AND A.K. SCHMITT⁵

¹University of Portsmouth, UK (*darling@port.ac.uk)

²Univ. of Western Ontario, London, Ontario, CAN

³Royal Ontario Museum, Toronto, Ontario, CAN

⁴University of Wyoming, Laramie, Wyoming, USA

⁵UCLA, Los Angeles, USA

Meteorites from Mars offer unique insights into the age and evolution of the planet's crust. In order to fully understand this precious archive, it is critical to separate the effects of shock metamorphism that occurs during ejection from endogenic crustal processes.

Here we show that in the case of the highly shocked shergottite NWA 5298, this evolution can be resolved by combining electron beam microstructural techniques (CL, EBSD) with in-situ U-Pb SIMS analyses. We focus upon the effects of shock metamorphism on the U-Pb systematics of baddeleyite (ZrO₂) – a micron-scale phase common to many shergottites. Unlike zircon, the relationship of shock heating and deformation with retention of radiogenic Pb is poorly known.

Baddeleyite grains from a single polished thin section show a wide array of deformation microstructures. These include fracturing, varying degrees of amorphization and granulation, plastic deformation, and recrystallization due to post-shock fluids: reflecting local variations in shock pressures and waste heat. SIMS U-Pb isotope analyses of these grains reveal variable degrees of age resetting, broadly correlated with microstructure and preservation of primary igneous CL zonation. Of the 19 analysed grains, four of the oldest six U-Pb dates are from grains which exhibit oscillatory growth banding. Degree of Pb loss (as much as 80%) is also broadly correlated with degree of growth of post-shock zircon reaction rims. The zircon reaction rims are linked to release of Si-rich fluids during quenching of shock melt pockets during transit to space. These findings, contrary to the results of shock loading experiments [1], indicate that baddeleyite U-Pb ages can be reset under certain shock metamorphic pathways. The U-Pb data are thus useful for determining both the primary age of the meteorite assemblage and bracketing the time of its Earthward launch.

[1] Niihara *et al.*, (2012) EPSL, 341-344, 195-210

Interstellar and interplanetary solids in the laboratory

E. DARTOIS^{1,2*}

¹CNRS-INSU, Institut d'Astrophysique Spatiale, UMR 8617,
91405 Orsay, France (*correspondence:
emmanuel.dartois@ias.u-psud.fr)

²Université Paris Sud, Institut d'Astrophysique Spatiale, UMR
8617, bât 121, 91405 Orsay, France

The interstellar medium is a physico-chemical laboratory where extremes conditions are encountered, and whose environmental parameters (e.g. density, reactant nature, radiations, temperature, time scales) define the composition of matter.

Whereas cosmochemists can spectroscopically examine collected extraterrestrial material in the laboratory [e.g. 1,2,3,4,5,6], astrochemists must rely on remote observations to monitor and analyze the physico-chemical composition of interstellar solids [e.g. 7,8,9,10,11].

The observations give essentially access to the molecular functionality of these solids, rarely elemental composition constraints and isotopic fractionation only in the gas phase. Astrochemists bring additional information from the study of analogs produced in the laboratory, placed in simulated space environments.

In this presentation I will briefly touch some observations of the diffuse interstellar medium (DISM) and molecular clouds (MC), setting constraints on the composition of organic solids and large molecules in the cycling of matter in the Galaxy and try to draw some commonalities and differences between materials found in the Solar System and Interstellar dust.

[1] Orthous-Daunay *et al.* (2013) *Icarus* 223, 534–543. [2] Dartois *et al.* (2013) 224, 243–252. [3] Brunetto *et al.* (2011) *Icarus* 212, 896–910. [4] Kebukawa *et al.* (2011) *Geochim. Cosmochim. Acta* 75, 3530–3541. [5] Sandford *et al.* (2006) *Science* 314, 1720–1724. [6] Flynn *et al.* (2003) *Geochim. Cosmochim. Acta* 67, 4791–4806. [7] Spoon *et al.* (2007) *The Astrophysical Journal* 654, L49-L52 [8] Dartois & Muñoz Caro (2007) *Astronomy and Astrophysics* 476, 1235-1242 [9] Van Dienenhoven *et al.* (2004) *The Astrophysical Journal* 611, 928-939. [10] Chiar *et al.* (2002) *The Astrophysical Journal* 570, 198-209. [11] Pendleton *et al.* (1994) *The Astrophysical Journal* 437, 683-696.

Tracing whole-Earth carbon from the Hadean to present

RAJDEEP DASGUPTA¹

¹Dept of Earth Science, Rice University, Houston, TX, USA

In response to the evolving thermal vigor and fugacity of oxygen and other volatiles, the behavior and fate of carbon and its partitioning between various layers of Earth - atmosphere, silicate Earth, and metallic core - varied through geologic time [1].

During the first few tens of millions of years of the Hadean Eon, carbon that participated in the core-forming, deep magma ocean, partitioned strongly into the metallic core. The Moon on the other hand, having a much shallower magma ocean likely held on to a large fraction of its bulk carbon. With almost all carbon of the chondritic building blocks being lost to space, restricted to nascent atmosphere, or sunk to the core, the silicate liquid mantle soon after core segregation was probably carbon-poor. Processes such as late bombardment of volatile-rich material, entrapped C-bearing metallic liquid in lower mantle solids, and ingassing from a C-rich atmosphere had opportunities to replenish mantle carbon by the end of the Hadean Eon. The crustal recycling zone temperature also likely was hotter until ~1.5 Ga; such slab thermal structure along with inconsistent subduction cycle might have hindered deep ingassing of surficial carbon. Massive release of CO₂ at the Archean and Paleoproterozoic volcanic arcs thus might have supplied the necessary dose of greenhouse gas in the atmosphere to offset the dimmer early Sun, sustaining liquid water on Earth's surface.

The P-T paths of subducting slabs of the Phanerozoic support transporting crustal carbonates past arc-magmatic depths, setting up systematic deep transfer of surficial carbon to the interior. Magmatic release of CO₂ balances the subduction input of carbonates and organic carbon. The proximal carrier-magma delivering mantle carbon to the exosphere depends chiefly on the thickness of the thermal boundary layer and mantle potential temperature - most strongly carbonated magma being the key agent beneath cratons, mildly carbonated magma for mature oceanic lithosphere, and basalts with trace amount of dissolved carbon beneath mid-oceanic ridges.

This talk will trace the origin of mantle carbon in the Earth-Moon system from the time of accretion, core formation, and magma ocean crystallization and will attempt developing a framework of carbon ingassing and outgassing fluxes in different time periods of whole Earth evolution.

[1] Dasgupta (2013), *RiMG* 75, 183-229.

Deep subduction of carbon and sulfur constrained by laboratory experiments

RAJDEEP DASGUPTA^{1*}, MEGAN DUNCAN¹, SÉBASTIEN JÉGO¹ AND KYUSEI TSUNO¹

¹Dept of Earth Science, Rice University, Houston, TX, USA
(*correspondence: Rajdeep.Dasgupta@rice.edu)

The fate of volatile elements such as carbon and sulfur during subduction is critical because of their influence in a number of key aspects of planetary differentiation including partial melting, atmospheric chemistry and habitability, mobility and enrichment of ore forming metals, and redox evolution of the planetary interior. Yet, the efficiency of carbon and sulfur via subduction of crust is unresolved. Here we use phase equilibria experiments on carbonate-, sulfide-, and sulfate-bearing crust and sediments, plus experimental data and models of CO₂ and sulfur solubility in hydrous siliceous melt as a function of fO_2 to constrain the recycling efficiency of carbon and sulfur.

Carbon: Carbonate minerals are stable along P-T paths of most downgoing slabs and generation of carbonatitic melt is only possible for hot subductions and/or from deeply (>200 km) subducted sediments. In the absence of carbonate melting, transfer of carbon to sub-arc mantle is limited by solubility of CO₂ in rhyolitic melts. Experiments and thermodynamic modeling suggests that wt.% level CO₂ may be dissolved in rhyolitic melts generated by hydrous-fluid-fluxed melting of crust and sediments, with solubility diminishing with decreasing fO_2 in the presence of graphite. However, the extent of graphite and carbonate breakdown remains limited by the extent of hydrous melting, with the latter being controlled chiefly by bulk water content.

Sulfur: Sulfur content of downgoing crust is estimated to be lower than that of carbon, but sulfur content of pyrrhotite-saturated, slab melts is only ~100 ppm [1]. For anhydrite-saturated crust ($fO_2 > FMQ+3$), slab melts contain 1000s of ppm S, yet elimination of sulfate from slab requires large extent of slab melting and extensive flushing by hydrous fluids. With subducting slab being largely dehydrated approaching sub-arc depths, stability of sulfur-bearing phases in ocean crust is likely at all fO_2 . Further, sulfur addition to wedge mantle is most efficient via fluid addition (rather than melt) and fluids even at reduced conditions may be sufficiently rich in sulfur to elevate mantle wedge abundance.

Constraints on relative efficiency of deep subduction of carbon and sulfur will be presented and likely carrier of carbon versus sulfur to the arc source will be evaluated.

[1] Jégo & Dasgupta (2013), *GCA* 110, 106-134.

Reduction of Cu(II) adsorbed to bacterial cells: A role for Fe(II)?

CHRISTOPHER J. DAUGHNEY^{1*}, PETER J. SWEDLUND²,
MAGALI MOREAU-FOURNIER³, SARAH L. HARMER⁴,
BERNT JOHANNESSEN⁵, RACHEL FRANZBLAU⁶
AND CHRISTOPHER G. WEISNER⁶

¹GNS Science, Lower Hutt, New Zealand (*correspondence:
c.daughney@gns.cri.nz)

²University of Auckland, Auckland, New Zealand,
(p.swedlund@auckland.ac.nz)

³GNS Science, Wairakei, New Zealand (m.moreau-
fournier@gns.cri.nz)

⁴Flinders University, Bedford Park, Australia,
(sarah.harmer@flinders.edu.au)

⁵Australian Synchrotron, Clayton, Australia,
(bernt.johannessen@synchrotron.org.au)

⁶University of Windsor, Windsor, Canada
(franzbl@uwindsor.ca, weisener@uwindsor.ca)

Laboratory experiments were performed to track the fate of dissolved Cu(II) and Fe at a fixed pH of 5.2 during the gradual, incremental oxidation of dissolved Fe(II) and precipitation of iron oxide in the presence of *Anoxybacillus flavithermus* cells. X-ray absorption spectra of wet pastes were collected at the Cu K-edge and the Fe K-edge at the Australian Synchrotron and at the Australian National Beamline Facility in Japan. The samples consisted of 3 ppm Cu(II) that had been allowed to equilibrate with the bacteria alone, abiotic iron oxide without bacteria, or the bacteria-iron oxide composites. Standards included aqueous solutions of Cu(II) perchlorate, Cu(II) formate and Cu(II) nitrile(tris)methylphosphonic acid, and powdered Cu₂O. Fe standards included aqueous solutions of Fe(II), Fe(II) citrate and Fe(II) phosphate, and powdered lepidocrocite and ferrihydrite. The EXAFS data for the bacteria-iron oxide composites showed that under the experimental conditions Cu in the solid phase was associated predominantly with carboxyl structures on the bacterial cell walls, not with bacterial phosphoryl structures or with binding sites on the iron oxide. These results are consistent with previous studies. The XANES data indicated that the solid phase Cu existed partially as Cu(I), with a ratio of Cu(I) to Cu(II) that was proportional to the concentration of solid phase Fe(II). Tests revealed that beam damage was negligible under the conditions employed. Hence, the occurrence of Cu(I) was not an artefact, and so we hypothesise that reduction to Cu(I) was facilitated by oxidation of Fe(II) that was co-adsorbed to the bacterial cells. This type of reaction that has direct relevance to natural environments, where bacteria and Fe(II) often coexist, and may play an important role in the transport of many different types of redox-sensitive contaminants. The immobilization of metal cations in bacteria-bearing settings should not be examined independently of progressive oxidation, hydrolysis and precipitation of iron.

MC-ICPMS and NRIXS: A Stereo View of Iron Isotopic Fractionation in Silicic Magmas

N. DAUPHAS¹, M. ROSKOSZ², M. TELUS³, M.Y. HU⁴, E.E. ALP⁴, F. MOYNIER⁵, C.K. SIO¹, F.L.H. TISSOT¹, F.Z. TENG⁶, D. NEUVILLE⁷, P.I. NABELEK⁸, P. CRADDOCK⁹,
L.A. GROAT¹⁰ AND J. ZHAO⁴

¹Origins Laboratory, The University of Chicago

²Université de Lille 1, France

³University of Hawaii at Manoa

⁴Argonne National Laboratory

⁵Washington University in St. Louis

⁶Dept. of Earth & Space Sciences, University of Washington

⁷Institut de Physique du Globe de Paris

⁸University of Missouri

⁹Schlumberger-Doll Research Center

¹⁰University of British Columbia

Silicic rocks show trends of increasing $\delta^{56}\text{Fe}$ values with increasing SiO₂ content [*e.g.*, 1-3]. These trends have been ascribed to Soret effect, fluid exsolution, and magmatic differentiation. To understand the cause of Fe isotopic variations in silicic magmas, we measured the Mg, Fe, Zn, and U isotopic compositions of a range of migmatites, granites, and pegmatites with well-characterized petrologic and geochemical contexts [3]. No clear positive correlation is found between the isotopic compositions of Mg, U and Fe, which rules out the process of Soret diffusion. Zinc can easily be mobilized by aqueous fluids as chloride complexes. Pegmatites and some granitic rocks with high $\delta^{56}\text{Fe}$ values also have high $\delta^{66}\text{Zn}$ values. However, some granites with high $\delta^{56}\text{Fe}$ values have unfractionated $\delta^{66}\text{Zn}$ values and were presumably poor in fluids (A-type granitoids). For these samples, iron isotopic fractionation during magma differentiation is the most likely interpretation. We used the technique of Nuclear Resonant Inelastic X-ray Spectroscopy at the Advanced Photon Source to measure the mean force constant of Fe in basalt, andesite, dacite, and rhyolite glasses. We find a sudden increase in the force constant of Fe²⁺ from dacite to rhyolite. The β -factors derived from these force constants [4,5] were used in a model of magma differentiation using Rhyolite-MELTS. The correlation between $\delta^{56}\text{Fe}$ and SiO₂ is well explained by magmatic differentiation.

- [1] Poitrasson & Freyrier (2005) *Chem. Geol.* 222, 132-147.
[2] Heimann *et al.* (2008) *Geochim. Cosmochim. Acta* 72, 4379-4396. [3] Telus *et al.* (2012) *Geochim. Cosmochim. Acta* 97, 247-265. [4] Dauphas *et al.* (2012) *GCA* 94, 254-275. [5] Hu *et al.* (2013) *Phys. Rev. B* 87, 064301.

Linking nm-scale characterizations of altered silicate surface to macroscopic dissolution rate laws: New insights based on diopside

DAMIEN DAVAL^{1,2}, ROLAND HELLMANN³, GIUSEPPE D. SALDI², RICHARD WIRTH⁴ AND KEVIN G. KNAUSS²

¹LHyGeS, Université de Strasbourg – CNRS, Strasbourg, France; (*correspondance: ddaval@unistra.fr)

²ESD, LBNL, Berkeley, USA; kgknauss@lbl.gov, gdsaldi@lbl.gov

³ISTerre, Université Grenoble 1 – CNRS, Grenoble, France; roland.hellmann@obs.ujf-grenoble.fr

⁴GFZ, German Research Centre for Geoscienceserre, Potsdam, Germany; wirth@gfz-potsdam.de

The interfacial zone between a bulk fluid and a mineral surface is where all exchange of matter and energy occurs during chemical weathering. However, our knowledge is still limited with respect to understanding where and how the rate-determining dissolution reactions take place. A complicating factor is the commonplace formation of amorphous Si-rich surface layers (ASSL), which may hinder contact between the fluid and the mineral surface. Previous studies showed that the protective ability of ASSL critically depended on properties inherited from the parent silicate mineral, which remain yet to be unraveled.

To address the role of ASSL, we investigated the dissolution of a common silicate (diopside), and related the bulk dissolution rate (determined in classical flow-through experiments) with the nanoscale dissolution rate and surface chemistry of its individual prevalent faces (by combining vertical scanning interferometry (VSI) measurements of the topography of reacted cleavages and transmission electron microscopy (TEM) characterizations of the ASSL). While ASSL were evidenced on all of the investigated faces, only those formed on (110) and (1-10) were passivating, thereby controlling the reactivity of the underlying faces. The (110) and (1-10) faces intersect the highest density of Mg-O-Si and Fe-O-Si bonds, and this specificity may explain the passivating behavior of the corresponding ASSL. Moreover, we evidenced an inverse relation between aqueous silica concentration and the bulk dissolution rate of crushed diopside grains, which suggest that the (110) and (1-10) faces are predominant in a powder. By considering ASSL as a separate phase that can control silicate dissolution rates, extrapolated laboratory-based rates at conditions relevant to the field can be lowered by up to several orders of magnitude, thereby decreasing the large gap between laboratory and natural rates. This has important implications for more accurately modeling chemical weathering reactions.

In situ real time infrared spectroscopy study of (poly)molybdate ions sorption into layered double hydroxides

A. DAVANTES¹, C. ARDAU², G. LEFEVRE^{1,*}

¹LECIME, UMR7575 CNRS-Chimie ParisTech, 75005 Paris, France (*correspondence : gregory-lefevre@enscp.fr)

²Department of Chemical and Geological Sciences, University of Cagliari, Via Trentino 51, 09127 Cagliari, Italy

Due to the high anion-exchange capacities (2-3 meq/g) and their relatively low cost, layered double hydroxides (LDHs), also known as anionic clays or hydroxalclite-like compounds (described with the general formula $[M^{2+}_x M^{3+}_x (OH)_2] (A^n)_{x/n} \cdot mH_2O$) have been studied for application in wastewater treatment by intercalated oxyanions [1,2].

The aim of this study was to investigate the sorption mechanism of molybdate anion and to obtain the speciation of molybdate inside the LDH structure after sorption in a Zn/Al sulphate-carbonate LDH.

To the best of our knowledge, it is the first time that sorption of molybdate anion into layered double hydroxides is studied by attenuated total reflection (ATR) FTIR spectroscopy [3]. *in situ* analysis of the sorption processes into the LDHs interlayer (exchanged of (poly)molybdate ions with sulfate or carbonate ions) allowed us to identify the high affinity of LDH towards $Mo_7O_{24}^{6-}$, which sorbs even though it is a minor species in comparison with other protonated heptamolybdate ions.

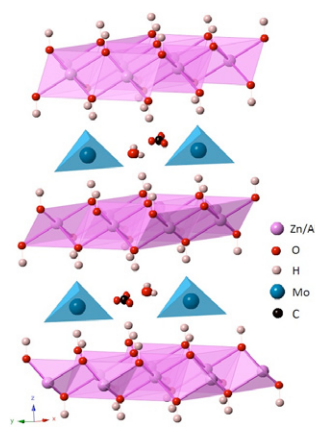


Figure 1: Structure of a layered double hydroxide, with interlayer molybdate and carbonate anions.

[1] Goh *et al.* (2008) *Water. Res.* **42**, 1343–1368. [2] C. Ardau *et al.*, (2012) *Applied Clay Sci.* **65**, 128-133. [3] G. Lefèvre. (2004) *Adv. Colloid Interface Sci.* **107**, 109-123.

Radon activity around active faults in a geothermal environment

JONATHAN DAVIDSON^{*1}, DARREN GRAVLEY¹,
ANDY NICOL² AND JERRY FAIRLEY³

¹University of Canterbury, 22 Kirkwood ave, Ilam,
Christchurch, New Zealand

(*correspondence : jrj davidson@gmail.com)

²GNS Sciences, Lower Hutt

³University of Idaho, Moscow, ID

Variation in radon gas concentration has been associated with faults and faulting processes at several locations globally. The Central Taupo Volcanic Zone (TVZ) is an active volcanic rift which hosts more than 20 geothermal fields. The geothermal activity is only occasionally associated with fault traces visible at surface, however it is possible that many active faults have been buried by recent volcanic deposits (blind faults). In order to detect these faults and their prospectivity for geothermal energy, soil gas Radon surveys have been proposed over areas potentially hosting blind faults.

We surveyed soil gas around the Rehi fault and the Paeroa fault, both substantial faults (i.e. slip rates 0.5-1.5 mm/yr) in the TVZ, with the purpose of showing the relationship between soil gas Radon activity and active faults. We used an electrostatic precipitation Radon detector (Durrige RAD7) to measure Radon activity of two Radon Isotopes (²²⁰Rn and ²²²Rn) in soil gas sampled at 1m depth. We also collected several soil samples at the location and depth of the gas measurements, for further testing of Radon emanation potential in a laboratory setting.

Our data show a clear relationship between faults and Radon activity at several locations. However, the isotope activity ratios and the laboratory testing show that this activity variation is in most cases due to shallow and local soil processes, not faulting processes. This leads us to conclude that in the TVZ measuring Radon activity in soil gas may not be a reliable technique for detecting faults in the sub-surface.

Exceptionally high Radon activity for ²²⁰Rn and ²²²Rn isotopes was however recorded in steam vents around the Waikite geothermal spring, a boiling bicarbonate spring which flows at ~60 l/s at the base of the Paeroa fault scarp. Preliminary data support the idea that the Radon isotopic ratio can be used to determine the travel time and flow path of steam from the source to the detector. These Radon isotopes constrain the flow model for the Waikite geothermal spring and could be used in environmental and hydrological studies of other bicarbonate geothermal springs.

Characterization of Baddeleyite Oxygen Isotopes and Microstructure

JOSHUA H.F.L. DAVIES^{*1}, RICHARD A. STERN¹,
LARRY M. HEAMAN¹, DESMOND E. MOSER²
AND ERIN L. WALTON³

¹University of Alberta, Edmonton, Alberta, Canada

*(jdavies1@ualberta.ca)

²University of Western Ontario, London, Ontario, Canada

³Grant McEwan University, Edmonton, Alberta, Canada

The oxygen isotopic composition of Precambrian mafic and alkaline rocks is often difficult to determine by conventional methods due to overprinting by hydrothermal alteration or metamorphism. Baddeleyite (ZrO₂) is a uranium-bearing accessory phase in these rocks, and due to improved extraction and *in situ* techniques is increasingly targeted for U-Pb geochronology. We have investigated the δ¹⁸O composition of baddeleyite from various settings to assess its suitability for recording primary δ¹⁸O values, potentially creating a valuable tool for tracing magma petrogenesis through time.

SIMS oxygen isotope analyses of potential mineral standards (baddeleyite megacrysts from Phalaborwa and Mogok) have uncovered various analytical complexities relating to matrix and orientation effects between baddeleyite and the incoming ion beam.

Here we present oxygen isotope data from metamict and thermally annealed baddeleyite. We have characterised the degree of metamictization using Raman spectroscopy, cathodoluminescence imaging and EBSD analysis. With the crystallographic information, we show how crystal orientation and degree of metamictization affect the instrumental mass fractionation during SIMS analysis, and how these effects can potentially be mitigated.

Interaction between CO₂-rich brine and marly shale under supercritical CO₂ conditions

G. DÁVILA¹, L. LUQUOT¹, J. M. SOLER¹ AND J. CAMA^{1*}

¹Institute of Environmental Assessment and Water Research (IDAEA-CSIC), Jordi Girona 18-26, Barcelona 08034, Catalonia, Spain
(*correspondence: jordi.cama@idaea.csic.es)

Geological CO₂ sequestration at a pilot-plant scale is going to be performed at Hontomin (Spain). The reservoir rocks are mainly fractured limestones and the caprock is made up of marly shales, with an average composition (wt%) of 56% calcite, 21% quartz, 17% illite, 3% clinocllore and albite and trace amounts of pyrite, gypsum and anhydrite. An experimental study was performed to (1) evaluate mineral dissolution/precipitation processes as a sulfate- and CO₂-rich brine circulates through an open fracture and (2) to quantify the effects these processes may exert on fracture permeability.

Percolation experiments under CO₂ supercritical conditions ($p_{\text{total}} = 15 \text{ MPa}$, $p_{\text{CO}_2} = 8 \text{ MPa}$, $T = 60^\circ\text{C}$) were performed using two synthetic CO₂-rich brines (sulfate-free and sulfate-rich) that circulated at constant flow rates (0.2, 1 and 60 mL/h) through artificially fractured shale cores (7.5 mm in diameter and 18 mm in length).

The pH of the injected solution was acidic (~3). In the case of the sulfate-free solution the interaction mainly promoted the dissolution of calcite. Permeabilities remained almost constant. At flow rates 0.2 and 1 mL/h, fracture permeability ($k_{\text{initial}} \sim 1 \times 10^{-12} \text{ m}^2$) decreased slightly ($k_{\text{final}}/k_{\text{initial}} = 0.8$). Under the highest flow rate (60 mL/h), permeability ($k_{\text{initial}} = 17 \times 10^{-12} \text{ m}^2$) increased slightly ($k_{\text{final}}/k_{\text{initial}} = 1.2$). In the experiments with sulfate-rich solution (synthetic Hontomin groundwater), calcite dissolution and gypsum/anhydrite precipitation were the dominant processes. At the lower flow rates (0.2-1 mL/h), the fracture permeabilities ($k_{\text{initial}} 1-20 \times 10^{-12} \text{ m}^2$) decreased remarkably ($k_{\text{final}}/k_{\text{initial}} \leq 0.03$), as expected from the precipitation of sulfates. However, at the highest flow rate (60 mL/h) the permeability ($k_{\text{initial}} = 22 \times 10^{-12} \text{ m}^2$) increased significantly ($k_{\text{final}}/k_{\text{initial}} = 4$), showing a dominant dissolution effect under those fast-flow conditions.

The Chicago Instrument for Laser Ionization: progress and promise

A. M. DAVIS^{1,2,3*}, T. STEPHAN^{1,2}, M. J. PELLIN^{1,2,3,4},
D. ROST^{1,2}, M. R. SAVINA^{1,4}, R. TRAPPITSCH^{1,2}
AND N. LIU^{1,2}

¹Chicago Center for Cosmochemistry

²Dept. of Geophysical Sciences, Univ. of Chicago, Chicago, IL 60637 (*correspondence: a-davis@uchicago.edu)

³Enrico Fermi Inst., Univ. of Chicago, Chicago, IL 60637

⁴Materials Science Div., Argonne National Laboratory, Argonne, IL 60439

Current state-of-the-art secondary ion mass spectrometers (SIMS) have reached lateral resolution of 50–100 nm and useful yields of a few percent or less. CHILI (the CHicago Instrument for Laser Ionization), a resonance ionization mass spectrometry (RIMS) nanobeam instrument, is designed for isotopic and chemical analysis at the few-nm scale with a useful yield of ~40%. CHILI is equipped with a COBRA-FIB high resolution liquid metal ion gun for sputtering samples and an e-CLIPSE Plus field emission electron gun for imaging samples, both at the few-nm scale. Both Orsay Physics guns are installed and tested. A built-in optical microscope is installed and demonstrates a diffraction-limited resolution of <1 μm. It will be used for overview imaging and for laser ablation (with a Photonics Inc. 351 nm Nd:YLF laser) of larger samples. A piezoelectric stage capable of reproducible nm-scale motions and equipped with a sample holder that will accept a wide variety of sample mounts is operational. The flight tube for the time-of-flight mass spectrometer is mounted vertically above the sample chamber, under vacuum and leak-free. Resonance ionization will be done with six Ti:sapphire tunable solid state lasers of our own design pumped with three Photonics 527 nm 40W Nd:YLF lasers, which will allow isotopic analysis of two to three elements simultaneously. The pump and tunable lasers have been shown to meet specifications, but are awaiting completion of a beam combiner to introduce all tuned laser beams on a single line through the sample chamber.

CHILI will have broad applications in geochemistry and cosmochemistry. Its strengths will be in isotopic and chemical analysis at lateral resolutions and concentrations beyond the current state-of-the-art. Among the applications currently planned are isotopic analyses of material returned to Earth by spacecraft: Stardust–cometary and contemporary interstellar dust; Genesis–solar wind; Hayabusa–asteroidal material. Also well-suited to CHILI's capabilities are presolar grains, which inform us about stellar nucleosynthesis, and refractory inclusions and chondrules, useful for early solar system chronology.

Episodic growth of vein calcite in a stable continental setting: potential application of U-Pb dating by LA-ICPMS and ID-TIMS methods

D. W. DAVIS¹, A. PARMENTER² AND A. CRUDEN³

¹Dept. of Earth Sciences, University of Toronto, 22 Russell St. Toronto. ON Canada M5S 3B1, (correspondance: dond@es.utoronto.ca)

²Nuclear Waste Management Organization, 22 St. Clair Avenue East. Toronto. ON. Canada M4T 2S3

³School of Geosciences, Monash University, Building 28. Clayton, Australia 3800

The application and utility of LA-ICPMS and ID-TIMS for U-Pb isotopic dating of secondary fracture calcite infilling has been explored. These complementary methods were applied to test a hypothesis regarding the timing of emplacement of joints and calcite-filled veins within the Devonian Lucas Formation on the eastern flank of the Michigan Basin, in southern Ontario, Canada.

Outcrop fracture cross-cutting relationships, vein morphology consistent with generation under high pore fluid pressure, and knowledge of a basin-scale concentric fracture pattern were interpreted to suggest that prominent NNW-striking and broadly ENE-striking fracture populations were emplaced contemporaneously during the Paleozoic Era.

Initial trials determined that calcite-filled vein samples collected from shallow core (< 35 m depth) and shoreline outcrops had high U (1-10 ppm) concentrations and sufficient radiogenic Pb to permit successful dating by laser ablation. LA-ICPMS analyses of the calcite infilling (n = 141) defined two age clusters in all veins regardless of their orientation, one with a relatively small number of analyses at around 56 Ma and a broader peak around 100 Ma. These results were independently confirmed by ID-TIMS with single-grain analyses at 51±2 Ma and over the range 85±2 Ma to 109±4 Ma.

Agreement between the two methods suggests that the LA-ICPMS ages are reliable. The results indicate that new crystal growth occurred episodically during the Late Cretaceous and early Paleogene, although the age of fracturing may have been older. The LA-ICPMS method appears to be suitable for yielding meaningful U-Pb isotopic ages and represents a useful geochronologic tool for interpreting the timing of vein emplacement.

Berea Sandstone permeability pre and post reaction with supercritical CO₂ in 1% NaCl brine

G.K.W. DAWSON^{1*}, D. BIDDLE², C. KHAN², X. JIANG², S.D. GOLDING¹ AND V. RUDOLPH²

¹School of Earth Sciences, University of Queensland, Brisbane, Australia (*correspondence: g.dawson@uq.edu.au)

²School of Chemical Engineering, University of Queensland, Brisbane, Australia (v.rudolph@uq.edu.au)

The injectivity of CO₂ into saline formations greatly depends upon the properties and behaviour of geological materials close to injection points. We have constructed custom built geochemical reactors and permeability apparatus to investigate the behaviour of geological materials in response to CO₂ sequestration. Samples being tested include drill core material from a future Australian CO₂ sequestration reservoir-seal set [1, 2] and well-characterised materials such as Berea Sandstone to validate our procedures. Two different sized cubic sister sample sets of Berea Sandstone cut aligned to bedding laminations were obtained for initial experiments.

The permeability of as-received samples of Berea Sandstone was found to be compromised by surface deposits of mineral fines thought to be the product of sample cutting and milling. Permeability in the bedding plane for as-received samples was also less than the orthogonal to bedding orientation. In contrast, the permeability of samples gently cleaned using a sonic bath was significantly higher, and gave the expected result of bedding plane permeability being greater than the perpendicular to bedding orientation.

The brine permeability of sonic bath cleaned Berea Sandstone increased 14% (from 240 to 275 mD) following reaction with supercritical CO₂ immersed in 1% NaCl for 360 hours at 50 °C and 10 MPa. Geochemical analysis of the dissolved ions in the experiment water indicated significant mobilisation of cations, especially calcium, magnesium, iron, manganese, potassium, and silicon, thought to be the product of carbonate and reactive silicate dissolution and clay cation exchange. SEM-EDS analysis of unreacted samples detected partially pore-filling ankerite and also vermiculite-smectite alteration of phlogopite flakes. Dissolution of reactive minerals observed, especially ankerite, is one possible reason for the measured permeability increase [3].

[1] Farquhar *et al.* (2013) *MinMag*, this volume. [2] Pearce *et al.* (2013) *MinMag*, this volume. [3] Moore *et al.* (2004) *Geophys. Res. Lett.* 31, L17610.

Hydrogen isotope fraction in lipids of syntrophically associated sulfate-reducing bacteria

K.S. DAWSON^{1*}, A.L. SESSIONS¹ AND V.J. ORPHAN¹

¹Division of Earth and Planetary Science, California Institute of Technology, Pasadena, CA 91125, USA

(*correspondence: kdawson@caltech.edu)

The microbially mediated anaerobic oxidation of methane (AOM) is carried out by methanotrophic archaea (ANME) in syntrophic association with sulfate-reducing bacteria (SRB). This energetically limited metabolism is made thermodynamically feasible by the exchange of hydrogen, electrons, fixed nitrogen and potentially other unknown chemical species between the archaeal and bacterial partners. Understanding the metabolic interplay between the ANME and SRB in consortia is made difficult by the lack of cultured representatives. However, methanogenic archaea, closely related to their AOM counterparts, and SRB also form syntrophic consortia in both the environment and in laboratory grown co-cultures.

Zhang *et al.* [1] demonstrated that the central metabolic pathway is reflected in the hydrogen isotopic fractionation between bacterial fatty acids and growth water. Here we examine the metabolic role of the sulfate reducing bacterial partner through hydrogen isotopic fractionation of bacterial fatty acids from both cocultures of *Desulfococcus multivorans* and *Methanosarcina acetivorans* and sediment cores associated with a variety of active methane seep settings in Hydrate Ridge (offshore Oregon, USA).

[1] Zhang, X, Gillespie, A.L., Sessions, A.L. (2009) *PNAS*, **106**:31, 12580-12586.

Stalagmite trace-element reconstruction of terrestrial hydrology: Results from cave-analogue studies

DAY, C.C.¹ AND HENDERSON, G.M.¹

¹Department of Earth Sciences, University of Oxford, UK, (chrisd@earth.ox.ac.uk)

We report trace-element data from a series of carbonate growth experiments in cave-analogue conditions with the goal of better understanding environmental controls on trace-element incorporation in stalagmites. The experimental setup closely mimics natural processes (e.g. precipitation driven by CO_2 -degassing, low ionic strength solution, thin solution film) but with a tight control on growth conditions (temperature, pCO_2 , drip rate, calcite saturation index and the composition of the initial solution). Calcite is dissolved in deionized water in a 20,000 ppmV pCO_2 environment, with trace-elements (Li, Na, Mg, Co, Sr, Cd, Ba, U) at appropriate concentrations to mimic natural cave drip-waters. This solution is dripped onto glass plates (coated with seed-calcite) for controlled stalagmite growth [1].

Over a wide range of temperatures (7, 15, 25, 35°C), drip rates (2, 6 and 10 drips per minute) and solution calcite saturation indices ($SI_{\text{calcite}} = 0.1, 0.2, 0.3, 0.4, 0.5, 0.6$ at 15°C), $D(\text{Sr})$ was shown to be statistically invariant. $D(\text{Mg})$ has a relationship with temperature defined by $D(\text{Mg}) = 0.01e^{0.02[40.006]T}$, but temperature is not expected to be the dominant control on Mg/Ca in cave calcite due to the larger impact of calcite precipitation on Mg/Ca. Over short timescales, in conditions where temperature is well buffered in most caves, the fraction of calcium remaining in solution (f) is likely to be the dominant control on Mg/Ca and other trace-element ratios. Cd/Ca is shown to be highly-sensitive to variation in the amount of calcite precipitated from solution, with high $Cd/Ca_{\text{stalagmite}}$ particularly indicative of a low amount of prior calcite precipitation (PCP). Overall, the varied response of trace-elements to temperature and to hydrological factors (e.g. PCP and drip rate) ensure that their combined use, together with other proxies, is well suited for reconstructing terrestrial hydrological conditions.

[1] Day, C.C., & Henderson, G.M. 2011. Oxygen isotopes in calcite grown under cave-analogue conditions. *Geochimica et Cosmochimica Acta*, **75**, 3956–3972.

Timing and nature of late accretion

JAMES M.D. DAY¹

¹Scripps Institution of Oceanography, La Jolla, CA 92093-0244, USA (jmdday@ucsd.edu)

There is overwhelming evidence for varying amounts of late accretion additions of the highly siderophile elements (HSE: Re, Os, Ir, Ru, Rh, Pt, Pd, Au) after core formation to fully differentiated inner Solar System planetary bodies. HSE abundances in rocky mantles of planets point to the cessation of core formation and continued accretion of broadly chondritic materials as a key process during the final stages of planet formation. Here I consider the fundamental relationships between late accretion additions, their timing, and potential correlations of HSE abundances with mantle oxidation state and volatile contents. On Earth, there is direct access to upper mantle materials, albeit these sample sets may not be completely unbiased. There is also the possibility that some diogenites represent lower crustal or mantle samples from their parent body. Because of a lack of definitive mantle samples from most fully differentiated bodies, establishing estimated HSE abundances of mantles occurs through derivative melts. A means for estimating mantle HSE abundances is to utilise the compatible behaviour of the HSE and MgO. Using this method, it is possible to estimate mantle HSE abundances for Earth, the Moon and Mars at $\sim 0.009 \pm 0.003$, $\sim 0.0002 \pm 0.0001$, $\sim 0.007 \pm 0.004$ (2σ), respectively. Using these mantle estimates, apparent correlation between HSE abundances and fO_2 in planetary bodies breaks down.

It has been shown that the petrology of diogenites are consistent with HSE being set within these meteorites during crystallization, within ~ 2 -3 Ma of Solar System initial (SSI). The timing of post-core formation accretion to diogenites contrasts with timing constraints from Mars, within the first 100 Ma of SSI, and with the Moon within the first ~ 150 Ma as defined by crystallization ages of the oldest ferroan anorthosites. Constraints on post-core formation accretion for Earth are less well constrained, but must have been set prior to 4 Ga. These results suggest that, in some manner, parent body size exerts influence on post-core formation late accretion. Simplistically, smaller-sized bodies melt, differentiate and cool faster than larger-sized bodies, in part because of more limited accretion of increasingly massive impactors. Thus HSE abundances in rocky planets reflect the timing of cessation of core formation, as well as the degree to which planetary mantles are able to convect and homogenise the HSE. As planetary mantles become more convectively sluggish, additions of HSE will lead to increasing mantle heterogeneity.

Highly siderophile element constraints on intraplate magmatism

JAMES M.D. DAY¹

¹Scripps Institution of Oceanography, La Jolla, CA 92093-0244, USA (jmdday@ucsd.edu)

Ocean island basalts (OIB) and continental flood basalts (CFB) represent volcanic rocks that are unassociated with conventional plate tectonic boundary magmatic processes and that may require anomalous thermo-chemical and/or tectonic conditions to induce small- to large-scale melting of their mantle sources. Studies of the highly siderophile element (HSE) geochemistry of these and other forms of intraplate magmas have the potential to provide answers to questions regarding mantle sources and potential core-mantle interactions, if the effects of assimilation, fractional crystallization and melting processes can be elucidated.

HSE (Os, Ir, Ru, Pt, Pd, Re) abundance and $^{187}\text{Os}/^{188}\text{Os}$ data for OIB and CFB illustrate the importance of sulphides during both mantle partial melting and modification of primary melts during transit through the lithosphere. The interplay of partial melting and lithological/mineralogical heterogeneity of the mantle source are also important, with lower degrees of partial melting resulting in sampling of more fusible materials (e.g., grain-boundary sulphides [1]). This relationship suggests that intraplate magmas derived from large degrees of partial melting will provide a broader mantle sampling than those derived from lower degrees of partial melting. Alkalic HIMU (high $^{238}\text{U}/^{206}\text{Pb}$) OIB with high-Os abundances (>50 ppt) that have elevated $^{187}\text{Os}/^{188}\text{Os}$ (ratios up to 0.175), and hence long-term (>1 to 2 Ga) Re/Os fractionations, have $^{186}\text{Os}/^{188}\text{Os}$ within the range of abyssal peridotite compositions. Likewise, enriched mantle (EM) OIB that have $^{187}\text{Os}/^{188}\text{Os}$ that dominantly reflect contributions from peridotite with only minor contributions from recycled sediment or continental crust and/or lithospheric mantle materials lack evidence for long-term Pt/Os fractionations. In contrast, some Hawaiian picrites have $^{186}\text{Os}/^{188}\text{Os}$ ratios consistent with a mantle source with high time-integrated Pt/Os with respect to average upper mantle composition [2]. Evidence for long-term Pt/Os fractionations retained in higher-degree tholeiites may implicate radiogenic outer core contributions, or sampling of isolated mantle source reservoirs that have evolved with supra-chondritic Pt/Os over >2 to 3 Ga time-scales.

[1] Harvey, J. *et al.* (2011) *Geochim. Cosmochim. Acta*, **75**, 5574-5596; [2] Ireland, T.J. *et al.* (2011) *Geochim. Cosmochim. Acta*, **75**, 4456-4475.

Unconventional shale gas

A. M. DAYAL, SNIGDHARANI MISHRA
AND DEVLEENA MANI

CSIR-National Geophysical Research Institute
Uppal Road, Hyderabad -700007, India
(dayalisotope@rediffmail.com)

Shale gas is natural gas produced from carbonaceous shale formations that typically function as both the reservoir and source rocks for the natural gas. Carbonaceous shales are organic-rich shale formations that were previously regarded only as source rocks and seals.

Shales are deposited as muds in low-energy environments such as tidal flats and deep water basins. During the deposition of these very fine-grained sediments, there can also be accumulation of organic matter in the form of algae, plant, and animal derived organic debris. Natural gas is stored in shale in three forms: free gas in rock pores, free gas in natural fractures, and adsorbed gas on organic matter and mineral surfaces.

For gas-shale production in 1998, light sand fracturing (water fracture treatment) was introduced and has been successful in many areas. Micro-seismic fracture mapping has also been successfully used to improve the evaluation of hydraulic fracturing in horizontal wells. The unconventional gas reservoir will produce less gas for the longer period of time compared to the high permeability reservoir. It is estimated that we have 16,000 Tcf gas as shale gas. This data indicates that there is enough opportunity to explore unconventional energy as future source of energy.

Anomalous kinetics of reactive Fronts in porous media

PIETRO DE ANNA, TANGUY LE BORGNE, MARCO DENTZ
AND ALEXANDRE TARTAKOVSKY

¹MIT, Cambridge (MA)

²University of Rennes 1 (FR)

³CSIC, Barcellona (SP)

⁴PNNL (WA)

The dynamics of reactive transport phenomena in porous media derive from the interaction of microscopic mass transfer and reaction processes. The understanding of observed reaction behavior requires the quantification of these microscale processes and their impact on the large scale reaction and transport behavior. Here we study the mixing limited (fast) reaction $A + B \rightarrow C$ at the pore-scale, and its effective behavior on the mesoscale, as a paradigmatic case that allow us to provide a connection between local mixing properties and global reaction kinetics.

Interpreting Molybdenum isotopes as a proxy for the spatial distribution and intensity of ocean de-oxygenation events in an Earth System Model

ROS DEATH^{1*}, ANDY RIDGWELL¹, SANDRA ARNDT¹,
FANNY MONTEIRO¹, DAVE SHERMAN²
AND DEREK VANCE³

¹School of Geographical Sciences, University of Bristol,
University Road, Bristol, BS8 1SS (*correspondence:
ros.death@bristol.ac.uk)

²School of Earth Sciences, University of Bristol, Queens Rd,
Bristol, BS8 1RJ

³Institute of Geochemistry and Petrology, ETH Zurich, Main
Building, Sälimstrasse 101, 8092 Zurich, Switzerland.

Molybdenum (Mo), and its isotopes, are used as a proxy for global ocean redox states. This proxy has already been applied to investigate the degree of euxinia in the Proterozoic ocean [1] and the spatial extent of de-oxygenation during the Mesozoic [2]. However, at intermediate oxygen states the interpretation of $\delta^{98/95}\text{Mo}$ is difficult because of the complex non-linear system controlling the spatial and temporal pattern of Mo sequestration into the sediments. We aim to investigate this complexity in the Earth System Model GENIE. The model will be enabled with a relatively complete description of redox-dependent dynamics of marine iron and sulphur cycling and so providing us with a powerful tool to describe the water column dynamics of Mo (plus its sources and sinks). In particular the model will allow us to examine the role of iron-sulphide minerals in the scavenging of Mo, which is a key process in its removal from the global oceans.

Here we present preliminary results of the evaluation of the model for the present-day ocean and an outline for its application to past climatic states where ocean euxinia is present, taking OAE2 as a test study.

[1] Arnold, G.L. *et al.* (2004) *Science* 304, 87-89 [2] Pearce, C.R. *et al.* (2008) *Geology* 36, 231-234

Interactions of dissolved CO₂ with Cadmium Isotopes in the Southern Ocean

H. DE BAAR^{1,2*}, S. VAN HEUVEN², R. MIDDAG³,
I. NEVEN¹, M. KLUNDER¹, J. VAN OOIJEN¹, Z. XUE⁴,
W. ABOUCHAMI⁵, M. REHKAMPER⁴ AND S.J. GALER⁵

¹Royal Netherlands Institute for Sea Research, P.O. Box 59,
1790 AB

Den Burg, The Netherlands, *(correspondence:
Hein.de.Baar@nioz.nl)

²University of Groningen, Groningen, The Netherlands

³University of Otago, Dunedin, Otago, New Zealand

⁴Imperial College London, London SW7 2AZ, UK

⁵Max Planck Institute for Chemistry, Mainz, Germany

Cadmium has a biochemical function in the carbonic anhydrase (CA) class of enzymes for CO₂ metabolism in photosynthesis by algae [1,2]. This occurs either by substitution for Zn in the common Zn-CA, or as a genuine Cd-CA as found in certain marine diatoms [2]. The CA enzyme class is pivotal for conversion of bicarbonate [HCO₃⁻] to CO₂. This CA also appears responsible for high Cd/P uptake ratio by plankton at low ambient aqueous CO₂ [1]. The uptake of Cd has been related to ambient Cd, Zn, Mn and Fe [3, 4]. Also the Mn/P uptake ratio of plankton has been shown to be dependent [5] on ambient dissolved Fe [6] in the Southern Ocean.

Here we report the first ever observations of strong correlations in ocean surface waters of dissolved aqueous CO₂ with dissolved Cd and with the stable isotope ratio ¹¹⁴Cd/¹¹⁰Cd [7,8]. This is observed along the 0°W meridian in both the Antarctic Circumpolar Current and the Weddell Gyre, as well as in the Weddell Sea proper and also in Drake Passage. This uniform trend in several surface water masses hints at a uniform biochemical mechanism. The relationships in the Southern Ocean between the relative uptake of aqueous [CO₂] versus [HCO₃⁻] by algae [9] and the biological Cd isotope fractionation [7,8] will be discussed. Parallel trends of apparent Cd/PO₄ uptake ratio and interactions with Mn, Zn and Fe will be presented. Conceivable implications for paleoceanography will be mentioned.

[1] Cullen and Sherrell (2005) *Limnol. Oceanogr.*, 50: 1193.

[2] Xu *et al.* (2008) *Nature*, 452: 56. [3] Sunda and Huntsman (2000) *Limnol. Oceanogr.*, 45:1501. [4] Cullen (2006) *Limnol. Oceanogr.*, 51: 1369. [5] Middag *et al.* (2013) *Limnol. Oceanogr.*, 58: 287. [6] Klunder *et al.* (2011) *Deep-Sea Res. II*, 58: 2678. [7] Abouchami *et al.* (2011) *Earth Planet. Sci. Lett.* 305: 83. [8] Xue *et al.* (2013) *subm. Earth Planet. Sci. Lett.* [9] Neven *et al.* (2011) *Deep-Sea Res. II*, 58: 2636.

Measuring mineral dissolution kinetics using an automated flow-through module

B. DE BAERE*, K.U. MAYER AND R. FRANCOIS

Department of Earth, Ocean and Atmospheric Sciences,
University of British Columbia, Vancouver BC, Canada
V6T 1Z4 (*correspondence: bdebaere@eos.ubc.ca)

We have developed a purpose-built flow-through dissolution sample introduction module. Until now, this experimental set-up has been used to carry out sequential leaching [1]. The application we present here is the quantification of mineral dissolution rate constants.

As a proof of concept study, we measured the dissolution kinetics of the mineral calcite. Individual calcite fragments from Chihuahua, Mexico were gradually dissolved using a leaching sequence covering pH 2-6 (using time-dependent proportions of DIW and HNO₃). The effluent was sent to an Agilent 7700 ICP-MS and analysed for ^{43,44}Ca.

In parallel, we developed a simple geochemical reactive transport model in PHREEQC based on the forward rate equations as published by Plummer *et al.* [2]. Surface area was estimated from the geometric surface area of the fragment. In order to optimize the forward model dissolution rate constants to best reflect the experimental data, PEST software (model-independent parameter estimation) was used to run a reverse model in a weighted least squares sense.

We are able to generate optimized dissolution rate constants ($k_1 = 1.18 \times 10^{-6}$ and $k_3 = 8.73 \times 10^{-11}$ moles cm⁻² sec⁻¹, correlation coefficient between optimized model and experimental data $R^2 = 0.998$) which are within an order of magnitude or less of previously published studies [3, 4].

The key benefits of this newly developed technique include (1) time efficiency – in this study a typical leaching sequence lasted ~ 100 minutes; (2) extensive data coverage (here, n = 2000) which is of particular value to optimize the fit between model and data; and (3) automation – the entire leaching sequence is fully programmed. This approach has thus the potential to rapidly generate a large database of dissolution rate constants for a wide range of minerals.

[1] Haley and Klinkhammer (2002) *Chem. Geol.* **185**, 51-69.
[2] Plummer *et al.* (1978) *Am. J. Sci.* **278**, 179-216 [3] Chou *et al.* (1989) *Chem. Geol.* **78**, 269-282 [4] Busenberg and Plummer (1986) In: F.A. Mumpton (Ed.), *Studies in Diagenesis*. USGS Bulletin **1578**: 139-168.

Can diffusion cause discrepant Lu-Hf isochrons in meteorites?

V. DEBAILLE*¹, Q.-Z. YIN² AND Y. AMELIN³

¹Lab. G-Time, Université Libre de Bruxelles, Belgium
(*correspondance: vinciane.debaille@ulb.ac.be)

²Dept. of Geology, University of California in Davis, USA
(qyin@acdavis.edu)

³Research School of Earth Sciences, Australian National University, Australia (yuri.amelin@anu.edu.au)

The ¹⁷⁶Lu-¹⁷⁶Hf isotopic system, widely used for dating cosmochemical and geological processes, still suffers from two uncertainties. First, Lu-Hf isochrons for some early Solar System materials have excess slope of unknown nature. Second, unlike the well constrained Sm/Nd value to within 2% for chondritic uniform reservoir (CHUR), the Lu/Hf ratios in chondrites vary up to 18% [1], hence questioning the CHUR value for Lu/Hf. Even the 3% dispersion of Lu/Hf ratios [2] among the chondrites of low metamorphic grade, is greater than the dispersion of Sm/Nd among all studied chondrites. In order to better understand the Lu-Hf systematic of chondrites, we analyzed mineral fractions from the Richardton H5 chondrite to construct an internal Lu-Hf isochron, and set up a model to evaluate the role of diffusion in perturbing the Lu-Hf system.

The isochron yields an age of 4647±210 millions years (Ma) (MSWD= 9.4). Low precision is caused by relatively small spread the ¹⁷⁶Lu/¹⁷⁷Hf ratios from 0.02 to 0.05. Combining this study with the phosphate fractions measured in [3] yields a slope of 0.08855±0.00072, translating to a ¹⁷⁶Lu decay constant of 1.862±0.016 x 10⁻¹¹ year⁻¹, in agreement with the terrestrial value of 1.867±0.008 x 10⁻¹¹ year⁻¹ [4]. Richardton phosphates show an extreme variation of the ¹⁷⁶Lu/¹⁷⁷Hf ratios from 0.8 to 143 [3], identifying phosphates as a major host of Lu. This is critical as apatite has substantially higher diffusion rates of REE [5] than most silicate minerals that comprise meteorites.

The model shows that preferential diffusion of Lu compared to Hf from apatite to other minerals can produce apparent older isochron, and that among parameters that influence the rate of diffusion, the temperature seems the main factor influencing the disturbance. This suggests, similarly to [2], that only type 3 chondrites with lowest metamorphic grade should be used to determine the Lu decay constant and the CHUR values.

[1] Patchett *et al.* (2004), *EPSL*, 222 29- 41. [2] Bouvier *et al.* (2008), *EPSL*, 273, 48-57. [3] Amelin (2005), *Science*, 310, 839-841. [4] Söderlund *et al.* (2004), *EPSL*, 219, 311-324. [5] Cherniak (2000), *GCA*, 64, 3871-3885.

Iron oxidation state in serpentinite during subduction: implications on the nature of the released fluids at depth

DEBRET B.^{1*}, ANDREANI M.², MUNOZ M.³, BOLFAN N.¹, CARLUT J.⁴, NICOLLET C.¹ AND SCHWARTZ S.³

¹LMV, Université Blaise Pascal, Clermont-Ferrand, France
(*correspondence: B.Debret@opgc.univ-bpclermont.fr)

²Laboratoire de Géologie de Lyon, ENS- Université Lyon 1, France (muriel.andreani@univ-lyon1.fr)

³ISTerre, Université Grenoble 1, France (manuel.munoz@ujf-grenoble.fr)

Serpentinites may be present in more than 40% of the oceanic lithosphere that formed at slow to ultra-slow spreading centers. Serpentine could thus be one of the most abundant hydrated minerals recycled into the mantle in subduction zones. Prograde metamorphism in subducted serpentinites is characterized by the destabilization of lizardite into antigorite, and then into secondary olivine. The nature of the released fluid (e.g. H₂O vs H₂) during those phase transitions is controlled by redox reactions and can be inferred from Fe oxidation state of serpentinite. We used whole rock analyses, magnetic measurements, SEM observations and μ XANES to establish the evolution of Fe_{total} and magnetite content in serpentinite as well as Fe speciation in serpentinite minerals from the ridge to the subduction setting.

At the mid-ocean ridge, during the alteration of peridotite into serpentinite, the iron is mostly redistributed between magnetite and oceanic serpentinite (usually lizardite). The Fe³⁺/Fe_{total} ratio in lizardite and the modal magnetite progressively increase with the local serpentinization degree to reach 0.8 and 7 wt% respectively in fully serpentinized peridotites.

During subduction, the Fe_{total} of serpentinite remains constant (=7-10 wt%, depending on the primary mode of the peridotite) while the magnetite mode decreases from greenschist to eclogite facies to reach less than 2% under the eclogite facies. Also, the Fe³⁺/Fe_{total} ratio in serpentinite progressively decreases down to 0.2 during the transition from lizardite to antigorite.

Our results show that, in the first 70 km of subduction, the transition from lizardite to antigorite is accompanied by a global reduction of Fe in serpentinite and in serpentine. This redox reaction allows the oxidation of reduced oceanic phases such as sulfurs, and the formation of oxidized fluid. At greater depths, the beginning of antigorite dehydration leads to an increase of Fe³⁺/Fe_{total} in the remaining antigorite implying the formation of reduced fluids (e.g. H₂, CH₄).

The National Geochemical Survey of Australia (NGSA) project

PATRICE DE CARITAT¹

¹Geoscience Australia, GPO Box 378, Canberra ACT 2601, Australia

The National Geochemical Survey of Australia (NGSA) project (www.ga.gov.au/ngsa), part of Geoscience Australia's Onshore Energy Security Program 2006-2011, was carried out in collaboration with all state and territory geological surveys. It delivered Australia's first national geochemical atlas, the underpinning geochemical database, and a series of reports and papers.

Catchment outlet sediments (mostly similar to floodplain sediments) were sampled in 1186 catchments covering ~6.2 million km² or ~81% of the country (on average one sample per 5200 km²). Samples were collected at two depths (0-10 cm and ~60-80 cm), each sieved to two grain size fractions (<2 mm and <75 μ m) and analysed for total, aqua regia, and Mobile Metal Ion[®] element contents; other analyses (pH, electrical conductivity, grain size distribution, spectroscopy, etc.) were also performed.

Results to date have been used to: (1) investigate first-order controls on the geochemical makeup of Australian regolith in comparison to Europe; (2) compile preliminary, multi-continental, empirical 'Global Soil' reference values; (3) produce continental-scale soil pH maps; (4) map Fe oxide mineralogy and soil colour; (5) investigate the level and distribution of bioavailable elements in Australia; (6) determine element associations by multivariate statistical methods and compare resulting patterns to independent geoscience datasets; (7) model the distribution of soil carbonate using multiple environmental covariates; (8) assess the potential of the dataset for mineral prospectivity analysis (e.g., for base metals, U, Au and REEs); (9) select salt lakes to be investigated for their potential to host potash, Li and B resources; (10) ground truth, infill and 'correct' airborne radiometric concentration data for K, U and Th; and (11) shed light on the phenomenon of disequilibrium in the radioactive decay chain of U by comparing actual to estimated U concentrations at the continental scale.

The NGSA project was Australia's first national-scale geochemical survey, requiring certain strategic decisions to be taken about sampling medium, density, etc. The resulting atlas and dataset have proven useful and applicable to many end-uses, but limitations and challenges exist as in every geochemical survey.

© Commonwealth of Australia (Geoscience Australia)

Atmospheric aerosol nucleation in the Po Valley during the PEGASOS-SUPERSITO experiment

S. DECESARI¹, A. MARINONI¹, G. P. GOBBI¹, A. HAMED², A. LAAKSONEN², H. E. MANNINEN³, V. POLUZZI⁴ AND M.C. FACCHINI¹

¹Institute of Atmospheric Sciences and Climate, National Research Council of Italy, Bologna, I-40129, Italy
(*correspondence: s.decesari@isac.cnr.it)

²Department of Applied Physics, University of Eastern Finland, Kuopio, FI-70211, Finland

³Division of Atmospheric Sciences, Department of Physics, University of Helsinki, Helsinki, FI-00014, Finland

⁴Centro Tematico Regionale Aree Urbane, Arpa Emilia-Romagna, Bologna, I-40138, Italy

Aerosol nucleation, or new particle formation (NPF), is a very common phenomenon in the atmosphere, exerting an important feedback on the climate system by sustaining cloud condensation nuclei (CCN) concentrations in areas relatively far from pollution sources. In forest areas, NPF was put in relation to biogenic VOC photochemistry, while the mechanisms triggering nucleation in more anthropized environments are more elusive. North Italy is exemplificative of such an environment, with forested mountain ridges and urban and rural areas extending over the low lands (the Po Valley). During the PEGASOS-SUPERSITO field campaign in June-July 2012, the frequency of NPF in the rural Po Valley was very high (87% of the days) compared to the Apennine mountain ridge (35%). At the low-elevation rural site, nucleation started in the first two hours following sunrise, before the mixing layer development, in an atmospheric layer characterized by reduced ozone concentrations, high NO_x, relatively high anthropogenic VOC levels (200 ppt of toluene), ppt-level of isoprene, and moderate SO₂ concentrations (1 ppb). Clearly, the pool of possible precursors for nucleating particles in the Po Valley was dominated by anthropogenic species. Finally, the combination of the observations carried out at the ground stations with simultaneous measurements performed with mobile platforms provided evidence of the fact that NPF in the Po Valley was not driven by emissions from point pollution sources (such as power plants) but occurred in the background air over vast sectors of the valley. Continuing developing experimental and modelling tools to understand the subtle mechanisms underlying new particle formation will greatly improve our ability to assess the impacts of such pervasive aerosol source at the global and regional scales.

KINETIC14 : A PHREEQC compatible mineral kinetic database

J. DECLERCQ^{1*} AND E.H. OELKERS²

¹ Geosciences Environnement Toulouse (GET), 14 av. Edouard Belin, 31400 Toulouse, France
(*correspondence: declercq@get.obs-mip.fr)

² Geosciences Environnement Toulouse (GET), 14 av. Edouard Belin, 31400 Toulouse, France
(oelkers@get.obs-mip.fr)

Developped within the CarbFix project [1], KINETIC14 is an add on to PHREEQC [2], allowing calculation of the temporal evolution of mineral-fluid reactions during natural geochemical and industrial processes, and laboratory experiments.

Building upon previous efforts [3,4] this KINETIC14 has been built from a detailed synthesis of dissolution and precipitation rate data available in the literature. When coupled with PHREEQC, KINETIC14 provides the dissolution rates for 98 minerals as a function of temperature, fluid phase composition, and the chemical affinity of the fluid phase with respect to the mineral phase of interest. Mineral-fluid interfacial surface areas required for modelling the evolution of the fluid phase with these rates can be calculated using a variety of geometric models or from user input.

The rate equations chosen to fit available data within KINETIC14 are based on transition state theory and dissolution mechanisms that take explicit account of reactions occurring on mineral surfaces, including metal for proton exchange reactions, multi oxide minerals and proton adsorption/desorption for simple oxides. Despite the substantial scatter that is pervasive in dissolution rate data reported in the litterature, the majority of fitted rates are within 0.8 log units of their experimentally measured counterparts.

Mineral precipitation rates are generated directly from the corresponding dissolution rate equations; the validity of this approach will need to be assessed with future research.

Upon final validation, KINETIC14 will be made publicly available.

[1]Matter *et al.* (2011) *Ener. Proc.* **4** [2]Parkhurst and Appelo (1999) *USGS* [3] Marini (2007) *Dev. Geochem.* **11** [4] Palandri and Kharaka (2004) *U.S.G.S., Open File Report*

Origin of heterogenite (CoOOH) as illustrated by rare earth element fractionation

SOPHIE DECREÉE¹ AND OLIVIER POURRET²

¹Royal Museum for Central Africa, Tervuren, Belgium
(sophie.decree@africamuseum.be)

²HydriSE, LaSalle Beauvais, Beauvais, France
(olivier.pourret@lasalle-beauvais.fr)

The Katanga Copperbelt (DR Congo) hosts around half of the world's known reserve of mineable cobalt. Heterogenite (CoOOH) is the most abundant oxidized cobalt mineral in this belt. It was ultimately derived from the oxidation of carrolite (CuCo₂S₄), during a Pliocene weathering event. The latter led to heterogenite concentration in the near-surface, as "cobalt cap" [1]. However, the detailed processes leading to the formation of heterogenite are not yet well constrained. Here, these processes are investigated through the study of REE distribution, which is an underexplored but powerful tool to understand the formation of oxyhydroxides [2]. Indeed, since these elements behave as a coherent group, REE fractionation can be used as tracer of processes. In this way, studied heterogenite REE patterns display two major types: (i) the first type is Middle REE enriched, with negative cerium anomaly and relatively low REE content; (ii) the second one is Light REE enriched, without cerium anomaly and with higher REE content.

Weathering processes leading to heterogenite mineralisation mainly consist of water-rock equilibrium. At high Co activity, heterogenite precipitates at near-neutral pH as well as manganese oxide (i.e., pyrolusite). REE are mainly fractionated in between these two solid phases: heterogenite REE patterns are clearly the opposite ones of manganese oxides. As cobalt activity decreases, heterogenite stability field shifts to alkaline pH. In these conditions, REE speciation is mainly driven by carbonate complexation, resulting in the formation of the heterogenite type with a LREE enriched REE pattern.

Both REE signatures are consistent with the formation of heterogenite in a two-step *per descensum* model, in which this mineral (i) forms as residual deposits - similar to laterite - in association with Mn oxide, in the immediate near-surface environment, and (ii) is deposited from a carbonate-bearing fluid, due country rock dissolution, in deeper part of the oxidation profile.

[1] Decrée *et al.* (2010), *Mineralium Deposita* 45, 621-629.

[2] Pourret & Davranche (2013), *Journal of Colloid and Interface Science* 395, 18-23.

Crustal versus source processes on the Northeast volcanic rift zone of Tenerife, Canary Islands

DEEGAN, F.M.^{1,2*}, TROLL, V.R.², BARKER, A.K.², HARRIS, C.³, CHADWICK, J.P.⁴, CARRACEDO, J.C.⁵ AND DELCAMP, A.⁶

¹Dept. Geosciences, Swedish Museum of Natural History, Stockholm, Sweden. Frances.Deegan@nrm.se

²Dept. Earth Sciences (CEMPEG), Uppsala University, Sweden.

³Dept. Geological Sciences, University of Cape Town, South Africa.

⁴Science Gallery, Trinity College Dublin, Ireland.

⁵Dept. de Física, Universidad de Las Palmas de Gran Canaria, Spain.

⁶Dept. Geography, Vrije Universiteit Brussels, Belgium.

The Miocene-Pliocene Northeast Rift Zone (NERZ) on Tenerife is a well exposed example of a major ocean island volcanic rift. We present elemental and O-Sr-Nd-Pb isotope data for dykes of the NERZ with the aim of unravelling the petrological evolution of the rift and ultimately defining the mantle source contributions.

Fractional crystallisation is found to be the principal control on major and trace element variability in the dykes. Differing degrees of low temperature alteration and assimilation of hydrothermally altered island edifice and/or sediments elevated the primary $\delta^{18}\text{O}$ and the Sr isotope composition of many of the dykes, but had little to no discernible effect on Pb isotopes. Minor degrees of sediment contamination, however, may be reflected in the Pb isotope composition of a few samples that plot to slightly higher $^{207}\text{Pb}/^{204}\text{Pb}$ values.

Once the data are screened for alteration and shallow level contamination, the underlying isotope variations of the NERZ reflect a mixture essentially of Depleted Mid-Ocean Ridge-type Mantle (DMM) and young High- μ (HIMU, where $\mu = ^{238}\text{U}/^{204}\text{Pb}$)-type mantle components. Furthermore, the Pb isotope data of the NERZ rocks ($^{206}\text{Pb}/^{204}\text{Pb}$ and $^{207}\text{Pb}/^{204}\text{Pb}$ range from 19.591-19.838 and 15.603-15.635, respectively) support a model of initiation and growth of the rift from the Central Shield volcano (Roque del Conde), consistent with latest geochronology results [1]. The similar isotope signature of the NERZ to both the Miocene Central Shield volcano and the Pliocene Las Cañadas central edifice suggests that the central part of Tenerife Island was derived from a mantle source of semi-constant composition through the Miocene to the Pliocene. This can be explained by the presence of a discrete "blob" of HIMU material, ≤ 100 km in vertical extent, occupying the melting zone beneath central Tenerife throughout this period. The most recent central magmatism on Tenerife appears to reflect greater entrainment of DMM material, perhaps due to waning of the blob with time.

[1] Carracedo *et al.* (2011) *Bull. Geol. Soc. America*, **123**, 562-584.

Genetic classification based on AFM

¹DEEVSALAR, R., ¹GHOORBANI, M.R., ¹GHADERI, M
AND ²AHMADIAN, J

(Deevsalar@gmail.com), (ghorbani@modares.ac.ir),
(mghaderi@modares.ac.ir); Department of Geology,
Tarbiat Modares University, Tehran 14115-175, IRAN;
Payam Noor University, P.B: 19395-3697 Tehran, IRAN
(Jamshidahmadian@yahoo.com)

Genetic relationship between different groups of rocks in an association of basic to intermediate rocks from a cogenetic suite (Malayer-Boroujerd Plutonic Complex, western Iran), including basic dykes, mafic bodies and intermediate rocks plotted on AFM diagram makes such trends on the diagram that can be easily distinguished and therefore a conjunction point with one of the three lines on AFM triangle by best fitted trend line is expected. Olivine fractionation can be properly projected on FM line of the AFM diagram. Any point on the FM line has an MgO/FeO ratio that can be calculated using the values of these oxides in the plotted samples and equations of best fitted line for them on two variable diagrams MgO-(K₂O-Na₂O), FeO-(K₂O-Na₂O) and FeO-MgO. MgO/FeO is converted to Mg# and indicates the olivine composition. With different degrees of fractionation of this mineral from mafic parent magma, new compositions on previous trend can be calculated and their position on this line can be correlated with the plotted samples.

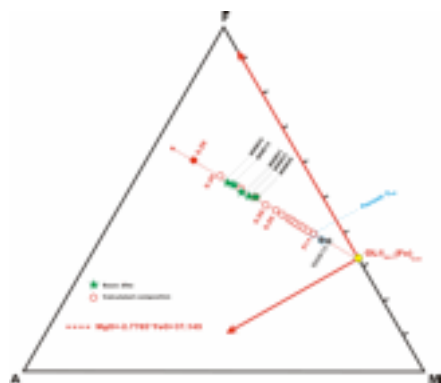


Figure 1. Differentiation trend for the basic dikes.

Mineral fractionation vector on Harker diagrams shows that olivine along with plagioclase fractionation plays an important role in generation of these samples (MBPC). Therefore, AFM diagram has properly exaggerated the role of olivine and can be used as an indicator of parental classification and investigation on petrogenesis and intra-group genetic relationships of samples on Harker diagrams

Isotopic composition of Sulfur in enstatite meteorites

C.DEFOUILLOY¹, F. MOYNIER², E. PRINGLE²,
J.-A. BARRAT³ AND P. CARTIGNY¹

¹Institut de Physique de Globe de Paris, 1 rue Jussieu, 75238
Paris, France (correspondence: defouilloy@ipgp.fr)
²Washington University in St Louis, One Brookings Drive, St
Louis, MO 63130, USA. (moynier@levee.wustl.edu)
³Université de Brest, Iace Nicolas Copernic, 29280 Plouzane
cedex, France. (barrat@univ-brest.fr)

Enstatite meteorites are the most reduced meteorites. They comprised two groups: the Enstatite Chondrites, considered to be primitive meteorites and subdivided into EH and EL (respectively, Fe-rich, and Fe-poor), and the Enstatite Achondrites (or Aubrites), which are differentiated meteorites. Several elements (O, Cr, Xe, Mo, Ni, but not Si) show similar compositions between Enstatites and Earth, suggesting a possible Enstatite origin for the Earth [1]. Yet, the genetic relationship between Enstatite groups remain unclear, some authors proposing a single Enstatite Chondrite parent body, while others have shown discrepancies between Enstatite groups and argued they could not be related.

Sulfur is a volatile element which could help apprehend the mechanisms underwent by the Enstatite parent body or parent bodies. We therefore initiated an extended database of high-precision S isotopic compositions (³³S/³²S, ³⁴S/³²S, ³⁶S/³²S) in Enstatite meteorites. Preliminary results show that sulfide content may vary from one group to another, from nearly 0 up to 3 wt% in Aubrites and EL6 and 3 to 5 wt% in EH3). Seventeen Enstatite meteorites have been studied so far. 11 of them contained enough Sulfur to be measured (5 EH3, 5 EL6 and one Aubrite). Sulfur isotopic composition is measured on a Mat 253 Mass Spectrometer, with a precision of 0.01 per mil for ³²S, ³³S and ³⁴S and 0.1 per mil for ³⁶S. No clear distinction appear in isotopic composition between the 3 groups studied (EH3, EL6 and Aubrite). The average $\delta^{34}\text{S}$ is of -0.40 ± 0.26 (1 σ), which is lower than chondritic values, but also slightly lower than the previously reported $\delta^{34}\text{S}$ for Enstatites [2]. $\Delta^{33}\text{S}$ (-0.026 ± 0.005) is very homogeneous and within error of the CDT value. $\Delta^{36}\text{S}$ shows a greater variability (-0.012 ± 0.144), with several positive values measured in EH3 and the Aubrite. A larger number of samples will allow us to determine the extend of spallation processes and the slight differences with other chondrites [3].

[1] Javoy *et al.* (2010) *Earth Planet. Sci. Lett.*, **293**, 259-268.
[2] Gao and Thiemens (1993) *Geochim. Cosmochim. Acta*, **57**, 3171-3176. [3] Hulston and Thode (1965) *J. Geophys. Research*, **70**, no. 14, 3475-3484.

Redundant data in geochemical calculations: Helpful or not?

F. DE GASPARI^{1,2*}, M.W. SAALTINK¹
AND J. CARRERA²

¹ GHS, Department of Geotechnical Engineering and Geosciences, Universitat Politècnica de Catalunya, UPC-BarcelonaTech, Barcelona, Spain

(*correspondence: francesca.de.gaspari@upc.edu, maarten.saaltink@upc.edu)

² GHS, Institute of Environmental Assessment and Water Research (IDAEA), CSIC, Barcelona, Spain (jesus.carrera.ramirez@gmail.com)

Geochemical speciation problems require the solution of non-linear systems by means of numerical methods that can be computationally demanding and sometimes can even fail to reach convergence. The performances of those numerical methods have been therefore studied in the last decades in order to increase their robustness and to find the most suitable ones for different types of systems and constraints [1, 2].

Often the amount of information available about a geochemical system can be redundant, that is, exceed the requested minimum so that a least square fitting may be necessary [3]. In those cases, models can account for data uncertainty. The effect of error in data has been studied for specific problems such as solubility equilibrium or mixing fraction calculations [4, 5].

However, little attention has been paid to the contribution that redundant data might have in the characterization of geochemical systems and in particular which types of systems are most likely to take advantage of additional data.

We present an algorithm able to handle redundant uncertain constraints and the systems that have been analyzed in order to understand the importance of considering different types of extra data in equilibrium calculations.

[1] Brassard & Bodurtha (2000) *Comp. & Geo.* **26**, 277-291.

[2] Carayrou *et al.*, (2002) *Environm. and En. Eng.* **48**(4),

894-904. [3] Albarede & Provost (1977) *Comp. & Geo.* **3**,

309-326. [4] Cabaniss (1999) *App. Geochem.* **14**, 255-262. [5]

Parkhurst (1997) *WRR* **33**(8), 1957-1970.

Continuous soil CO₂ flux measurements in a fumarole field of Mt Etna

S. DE GREGORIO*, M. CAMARDA, S. CAPPUZZO
AND S. GURRIERI

Istituto Nazionale di Geofisica e Vulcanologia, sezione di Palermo, via Ugo La Malfa 153, 90146 Palermo, Italy

(*Correspondence: s.degregorio@pa.ingv.it)

We present data from seven months of continuous measurements in the summit area of the Mt Etna volcano. The monitoring began in September 2012 and continued without any maintenance until the present (April 2013). The monitoring site is placed at “Belvedere” on the southeastern flank of the volcano, about 1.5 km away from the New Southeast Crater (NSEC) at altitude of about 2700 m a.s.l. This site is characterized by a low-temperature fumarole field. Performing soil CO₂ flux measurements in such a hostile environment, particularly during the winter, is extremely challenging, and we took advantage of an innovative device named CADEMASO [1]. This device determines soil CO₂ flux by measuring the pressure transient in a closed polymeric tube inserted into the soil. The station recorded hourly soil CO₂ flux and soil temperature. The data set revealed two distinct periods with different characteristics. During the first period, which lasted until the second decade of November, the soil temperature was almost constant around 80°C with small fluctuations, whereas the soil CO₂ flux displayed wide oscillations. During the second period, the soil temperature values displayed sharply and long lasting increments, as high as the measurement limit (225°C). As regards the soil CO₂ flux, an overall decrement of the values was observed and several clearly defined peaks were recorded. The beginning of the last period coincides with the first signs of a new reactivation of the activity of the NCSE, after a period of rest of about seven months.

[1] De Gregorio *et al.*, (2013) *Chem. Geol.* **341**, 102–109

Heavy boron isotopes in secondary olivine from the HP Voltri Massif: implications for the boron cycle in subduction zones

J.C.M. DE HOOG^{1*} AND K. HATTORI²

¹Grant Institute, School of Geosciences, Edinburgh, United Kingdom EH9 3JW (*correspondence: ceesjan.dehoog@ed.ac.uk)

²Dept. of Earth Sciences, University of Ottawa, Ottawa, Canada (khattori@uottawa.ca)

The Erro-Tobbio peridotite (Voltri Massif, Ligurian Alps, Italy) contains high-pressure rocks that have been subducted to peak conditions close to the upper stability limit of serpentine (650°C at 25 kbar; [1]). Secondary olivine occurs in partially dehydrated serpentinites in association with Ti-clinohumite (Ti-Chu). It has high Mg# (Fo86-87), MnO (0.3-0.4 wt%) and NiO (0.2-0.3 wt%) and contains magnetite inclusions attesting to its secondary origin. Olivine has variable but very high H₂O (up to 0.7 wt%) which correlates with high TiO₂ (up to 0.85 wt%) and F contents (5-51 ppm). FTIR spectroscopy indicates a high proportion of Ti-Chu-like defects in the olivine as the cause of high H₂O, F and TiO₂. Olivine also has very high B (8-20 ppm) and Li (3-70 ppm) contents, but these are not correlated with H₂O contents. Antigorite from the same sample has lower B (8-10 ppm) and Li (0.1 ppm) contents than olivine while F contents are comparable (15-47 ppm).

In-situ boron isotope analysis (Cameca 1270 SIMS) shows that olivine is enriched in heavy B ($\delta^{11}\text{B}_{\text{SRM951}} = +17$ to $+23\%$). No difference exists between Ti-rich and Ti-poor olivine. These high values are nearly identical to those of whole-rock high-pressure serpentinites from the same area ($\delta^{11}\text{B} = +17$ to $+24\%$; [2]). This indicates that little B isotope fractionation occurs during subduction dehydration of serpentine. Moreover, the high B and F contents of secondary olivine imply that these elements remain in the rock during serpentine dehydration. Hence, subduction of ultramafic rocks may introduce significant B isotope anomalies and fluorine into the deeper mantle.

[1] Scambelluri *et al.* (1995) *Geology* **23**, 459-462. [2] Scambelluri and Tonarini (2012) *Geology* **40**, 907-910.

Evaluation of the corrosion behaviour of potential plutonium wasteforms under conditions relevant for geological disposal

G. DEISSMANN^{1,2*}, F. BRANDT¹, S. NEUMEIER¹, G. MODOLO¹ AND D. BOSBACH¹

¹Forschungszentrum Jülich GmbH, Institute of Energy and Climate Research IEK-6: Nuclear Waste Management and Reactor Safety, 52425 Jülich, Germany (*correspondence: g.deissmann@fz-juelich.de)

²Brenk Systemplanung GmbH, 52080 Aachen, Germany

One important component of a safety case for a geological disposal facility for radioactive waste is to demonstrate an understanding of the corrosion behaviour of and the consequent radionuclide release from the disposed wastes. Plutonium is generated during the operation of nuclear reactors from uranium present in the nuclear fuels through capture of neutrons and can be recovered during reprocessing. Although the current preferred policy on the long-term management of separated civil plutonium in the UK is reuse as MOX fuel, at least a part of the UK plutonium inventory is likely to be designated for geological disposal. However, experimental data on the durability of plutonium wasteforms under repository conditions is rather limited to date and a detailed understanding of relevant processes that govern long-term radionuclide releases from the wasteforms on a molecular level is still missing [1].

On behalf of the NDA RWMD, we performed a review on the performance of plutonium wasteforms under conditions relevant for geological disposal in the UK. This work included the elicitation of corrosion rate data for the potential wasteforms, based on available experimental data and analogue evidence from other nuclear wasteforms, such as HLW-glasses and spent nuclear fuels. Generic candidate plutonium wasteform types addressed in this study comprised nuclear waste glasses (i.e. borosilicate glasses and phosphate glasses), ceramic wasteforms, and low-specification "storage" MOX. Due to the character of the current UK disposal programme, which is in a generic stage where no preferred disposal concept or type of host rock has yet been selected, a range of possible environmental conditions in the repository near-field were considered. The elicited ranges and distributions of the corrosion rates for the various wasteforms can be used in Post-Closure Safety Assessment models to calculate performance measures such as mean annual individual risks related to plutonium disposal with time.

[1] Deissmann *et al.* (2012) *MinMag*, **76**, 2911-2918.

Insights into the uranium speciation in the mill tailings of the COMINAK mine at Akouta, Niger

A. DEJEANT^{1,2,*}, L. GALOISY¹, G. CALAS¹, V. PHROMMAVANH³ AND M. DESCOSTES³

¹Institut de Minéralogie et de Physique des Milieux

Condensés, Université Pierre et Marie Curie, Paris, France (dejeant@impmc.upmc.fr) (*presenting author),

²Université Paris-Diderot, Paris, France

³AREVA, BG Mines, R&D, Paris la Défense

The world's largest uranium underground mine, at Akouta (Niger), has been mined for more than 40 years. About 14 million tons of mill tailings were accumulated on site. The ore beneficiation process, based on an oxidative dissolution in sulfuric acid, reaches an extraction efficiency of up to 92-96% with some U remaining in the tailings. This study aims to assess the U mobility and trapping mechanisms in mill tailings for reprocessing/rehabilitating.

The Akouta U deposit (Guezouman) occurs in continental lower Carboniferous sandstone, containing quartz and feldspar with detrital clays and organic matter. Micro-phases of pitchblende are associated with coffinite and minor U-Ti and U-Mo oxides, with an average U concentration of 4000 ppm associated with trace metals (e.g. V, Zr, Mo).

U concentration measured along a vertical profile within the 30m high tailings pile shows that U is reconcentrated at three levels: at the base, at 14.5m and in the gypsum-rich surface crust, referred to as *gypcrete*. U speciation has been investigated by scanning electron microscopy (SEM) and synchrotron-based X-ray Absorption Spectroscopy (XAS). All tailings samples contain U^{IV} and U^{VI} with an increase in U-oxidation state at shallower depth in the pile. Fresh tailings collected right out of the mill, before storage, are the most reduced. The presence in fresh tailings of ore-inherited U^{VI}-phases, identified by SEM, is in agreement with XAS analyses, showing that they mainly contain non-uranyl species. Older stored tailings where U reconcentrates contain micron-sized secondary U^{VI}-phases (uranyl sulfates and phosphates). This illustrates the importance of post-storage U-transport and trapping. The post-disposal dissolution of residual pitchblende/coffinite is a source of mobile U. However, further precipitation of secondary U-phases and efficient U sorption on Fe oxides and clays limit the extent of U migration within the tailings.

Mediterranean Sapropel S1: Synchronous basin-wide Preservation versus Productivity Signals

GERT J. DE LANGE^{*1}, C. SLOMP¹, C. CORSELLI², ELISABETTA ERBA³, J. THOMSON⁴ AND A. REITZ⁵

¹Geosciences-Utrecht, NL; gdelange@geo.uu.nl

²University bicocca Milano, IT

³Università degli Studi di Milano, IT

⁴Southampton, UK

⁵Geomar-Kiel, DE

Formation of the most-recent eastern Mediterranean S1 sapropel occurred from ~ 11 - 5 kyr 14C ago. The timing of deposition of all such distinct, organic-rich units (sapropels), is precession-related and associated with humid climate conditions. The last of such 'humid periods', simultaneous with a sustained circum-Mediterranean wet period including a vegetated Sahara. The end of this period coincides with a high manganese-oxide peak in all 30 studied cores and concurs with an abrupt re-ventilation event at 5.7 kyr for the deep-water.

We demonstrate that the most recent sapropel (S1) formed synchronously between 9.8 and 5.7 14C ky BP at all water depths greater than a few hundred metres. As a consequence of increased fresh water (monsoon) input, surface waters had a reduced salinity and concomitantly the deep (> 1.8 km) eastern Mediterranean Sea was devoid of oxygen during 4,000 years of S1 formation (De Lange et al., 2008). This has resulted in a differential basin-wide preservation of S1 determined by water depth, as a result of different ventilation/climate-related redox conditions above and below 1.8 km. Climate-induced stratification of the ocean may thus contribute to enhanced preservation of organic matter, i.e. formation of sapropels (and potentially black shales).

De Lange G.J., Thomson J., Reitz A., Slomp C.P., Principato M.S., Erba E., and Corselli C. (2008) Synchronous basin-wide formation and redox-controlled preservation of a Mediterranean sapropel. *Nature Geo* 1, 606-610.

Temporal change from young HIMU to EM1 source along the Pitcairn-Gambier chain

H. DELAVAUT¹, C. CHAUVEL²

¹ (helene.delavault@ujf-grenoble.fr)

² (catherine.chauvel@ujf-grenoble.fr)

Plume volcanism is one of the most puzzling features of present-day activities of the earth. The origin of this type of volcanism is matter of debate but it is generally agreed that its source is hot material containing some potentially recycled material. Most studies concentrate on strong plumes (Hawaii, Réunion) but weaker plumes such as Polynesia or St Helena can provided complementary information.

Here we present geochemical data on samples coming from the Pitcairn-Gambier alignment in Polynesia. This chain consists of Mururoa (11.9-10.7 Ma), Fangataufa (11.5-9.6 Ma), Gambier (7.1-5.3 Ma) and Pitcairn Islands (0.95 Ma) as well as the Pitcairn seamounts (0.45 Ma). We report trace elements and Pb isotopic data on basaltic samples with MgO>7% and we use these data to constrain the source of magmas and its evolution through time.

The most striking feature is the presence of Nb (and Ta) positive anomalies (defined as Nb/Nb* with Nb*=(Th+La)/2) in most lavas. In addition, the size of this Nb anomaly decreases with time: it equals 1.6-1.7 in Mururoa, Fangataufa and Gambier lavas; the value decreases to 1.2 in the younger Pitcairn Island and it is absent in the most recent lavas of Pitcairn seamounts. Because the size of the Nb anomaly is not correlated to MgO, its presence cannot be associated with fractionation of a mineral phase. We believe that it is a source feature because it correlates with Pb isotopic compositions that also decrease with time: ²⁰⁶Pb/²⁰⁴Pb is about 19.57 in Mururoa, 19.04 in Gambier, 18.31 in Pitcairn Island and finally only 17.71 in the Pitcairn seamounts.

To our knowledge, the only islands where positive Nb anomalies were observed are Tubuai and Mangaia, two HIMU Islands with ²⁰⁶Pb/²⁰⁴Pb>21 but in both islands, the size of the Nb anomaly never exceeds 1.5. The similarities between the trace element and isotopic characteristics of typical HIMU islands and the old islands in the Pitcairn chain suggest that they share a common origin but the lower Pb isotopic ratios observed in Mururoa, Fangataufa & Gambier suggest a more recent enrichment of U and Th relative to Pb. Finally, both trace element and isotopic changes through time along the Pitcairn-Gambier chain suggest that the source that melted to produce the lavas, started with “young HIMU” characteristics and evolved with time to a clear EM1 type in the most recent volcanic products.

DFT studies of the interaction of water with (Fe,Ni)-sulfide surfaces and clusters

NORA H. DE LEEUW,* ALBERTO ROLDAN, SAIMA HAIDER, DAVID SANTOS CARBALLAL AND UMBERTO TERRANOVA

Department of Chemistry, University College London, London WC1H 0AJ, UK. (n.h.deleeuw@ucl.ac.uk)

Reactive iron sulfide compounds that are formed at hydrothermal vents are implicated as catalysts in Origin of Life theories, which suggestion is lent credence by their widespread presence as redox centres in contemporary enzymes – thereby also suggesting their potential as benign modern-day catalysts for CO₂ conversion. These applications highlight the need for a thorough understanding of the properties of these minerals and especially their surface reactivity as well as nucleation and growth from solution.

We have used Density Functional Theory calculations (GGA+U [1]) to investigate the interaction of water with the spinel-structured greigite Fe₃S₄ and violarite FeNi₂S₄ minerals, and compared them with the oxide analogue magnetite Fe₃O₄. We have studied water adsorption at the (001) and (111) surfaces, where the metal ions are in different oxidation states. Using the Nudged-Elastic-Band and Dimer methods we have calculated the energy barriers to the dissociation of water at the surfaces, and the role of co-adsorbed water, through a number of pathways, where the presence of nickel in the surfaces notably affects the surface reactivity towards water, which also influences the co-adsorption and activation of CO₂ at the surfaces.

We also present preliminary findings on *ab initio* molecular dynamics simulations of the nucleation of (FeS)_n clusters from aqueous solution. Iron sulfides are widespread in the environment, but although the formation of the principal geologically stable iron sulfide, pyrite (FeS₂), via meta-stable Fe-S precursors, is reasonably well understood, still little is known about the reactions that control the nucleation and growth of the precursor Fe-S compounds that are crucial in the pyrite pathway, e.g. mackinawite and greigite. Field and laboratory data have shown the existence of small aqueous species (FeS_{aq}), whose role in the formation mechanism of the first condensed FeS mackinawite phase is crucial [2]. However, despite these studies, the stoichiometry and size of FeS_{aq} are still unknown. Our simulations predict hydration shells and stability constants and compare with experiment, where available.

[1] Devey *et al.* (2009) Phys. Rev. B, 79, 195126. [2] Rickard and Luther III (2007) Chem. Rev., 107, 514.

Modelling trace metal partitioning into calcium carbonate from solution

NORA H. DE LEEUW,^{1,2*} SERGIO RUIZ-HERNANDEZ,¹
AND RICARDO GRAU-CRESPO¹

¹ Department of Chemistry, University College London,
London WC1H 0AJ, UK. (n.h.deleeuw@ucl.ac.uk)

² Department of Earth Sciences, Utrecht University, Utrecht,
The Netherlands

Calcium carbonates are well known to contain significant concentrations of trace metals; Manganese for example is incorporated into calcite via dissolution-recrystallization processes, where the maximum solubility of Mn is controlled by its reaction with calcite and the mixing thermodynamics of the (Mn,Ca)CO₃ solid solutions.

Sr and Mg found in coral fossils are used as proxies for the reconstruction of past climates, based on correlations found between the Sr/Ca or Mg/Ca ratios and the sea surface temperature (SST) during biomineralization. Magnesium is always present in corals but with typical Mg/Ca ratios well below the ratio of in seawater. The variation found for the Mg/Ca ratio with SST is about four times that of the Sr/Ca ratio, thus promising higher resolution in climate change reconstructions. However, although it was initially thought that the Mg in corals occupies lattice positions in aragonite, recent experimental data seem to suggest otherwise.

We have used a combination of molecular dynamics simulations and grand-canonical statistical mechanics to investigate the mixing thermodynamics of Ca, Mn, Sr and Mg in carbonate solid solutions. Our results show a small degree of Ca/Mn ordering in calcite-structured minerals, in agreement with recent experiment, whereas most aragonite-structured Ca/Sr solid solutions are metastable with respect to separation into a Ca-rich and Sr-rich phase. However, the concentration of Sr in coral aragonites lies in the miscibility region of the phase diagram and formation of separated Sr-rich phases in coral aragonites is therefore thermo-dynamically unfavourable.

We have also calculated the equilibrium partitioning of Mg between aqueous solution and the bulk and surfaces of aragonite, including the effect of the different Mg and Ca chemical potentials. Results show that the total Mg content in the aragonite particles was found to be highly surface-dependent but too small to account for the measured Mg/Ca ratios in corals. It is therefore likely that most Mg in corals is either highly metastable in the aragonite lattice or located outside the aragonite phase of the coral skeleton, which has clear implications for its use as a proxy in paleothermometry.

Mesoarchean Tectonic Evolution of the Carajás Domain, Carajás Province, PA, Brazil.

M.A.S. DELINARDO*¹, L.V.S. MONTEIRO², R.P. XAVIER¹, C.P.N. MORETO¹, G.H.C. MELO¹, R.C. BENEDETTI¹ AND D.F.M. SOUSA¹

¹Geoscience Institute, Univ. of Campinas., SP 13083-870
(correspondence: *marcodelinarado@gmail.com)

²Univ. of São Paulo, São Paulo, SP 05508-080

The Carajás Province represents an Archean block located in the southeastern part of Amazon Craton, in the north of Brazil. The province is subdivided into two domains (1) Carajás at north and (2) Rio Maria at south.

The Carajás Domain is composed of Mesoarchean basement represented by ortho- and migmatitic rocks and tonalitic to granodioritic composition and several intrusive and tectonically imbricated calc-alkaline granites [1][2][3][4][5]. The Mesoarchean evolution of the Carajás Domain occurred between 3.0 and 2.83 Ga [5]. Tonalitic to granodioritic crust with high La/Yb was formed between 3.0 and 2.92 Ga. It was followed by events of high-grade metamorphism, migmatization and emplacement of calc-alkaline I-type tonalites, monzogranites, and granites with volcanic arc signature between 2.87 and 2.83 Ga [2][3][4]. The basement is covered by ca. 2.76-2.73 Ga metavolcano-sedimentary units of the Carajás Basin and crosscut by 2.74 Ga granites and gabbro-norites and 1.88 Ga A-type granites [5][6].

The geochemical and geochronological data suggest that the development of a subduction zone related to an arc setting may be responsible for formation of the most ancient rocks of the Carajás Domain. The youngest Mesoarchean rocks may have formed in an event of crustal reworking associated with the final subduction stage, as indicated by metamorphic, structural and geochemical evidences.

The relationship of these events with the juxtaposition of the two tectonic domains of the Carajás Province is still uncertain. However, Neoproterozoic magmatic and tectonic events have been recorded only in the Carajás Domain.

[1] Araújo *et al.* (1988) *proc of 7^o Congres Latin Amer Geo*, 324-338. [2] Machado *et al.* (1991) *Precambrian Research* **49**, 329-354. [3] Moreto *et al.* (2011) *Miner. Deposita* **46**, 789-811. [4] Feio *et al.* (2013) *Precambrian Research* **227**, 157-185. [5] DOCEGEO (1988) *proc. of 35^o Congres Bras Geol*, 11-54. [6] Dall'Agnol & Oliveira (2007) *Lithos*. **93**, 215-233.

Location of cation impurities in NGRIP deep ice revealed by cryo-cell UV-laser-ablation ICPMS

DAMIANO DELLA LUNGA¹, WOLFGANG MÜLLER¹, SUNE OLANDER RASMUSSEN² AND ANDERS SVENSSON²

¹ Dept. of Earth Sciences, Royal Holloway University of London, Egham TW20 0EX, United Kingdom

(*correspondence: damiano.dellalunga.2011@live.rhul.ac.uk)

² Centre for Ice and Climate - Niels Bohr Institute, University of Copenhagen, Juliane Maries Vej 30, 2100 Copenhagen Ø, Denmark.

The nature and location of cations impurities in ice cores provide useful insights about paleoclimate. Proxies for sea ice extension, dust atmospheric supply and the identification of annual layers are based on seasonal variabilities of soluble and not soluble impurities in ice. Furthermore, impurities play an important role in ice grain growth, which generally increases with depth, but is interrupted by many periods where the grain size sharply decreases, in correspondence of glacial-interglacial transitions [1]. The distribution of different impurities, led by this phenomenon, has never been directly observed in experiments on ice [2].

Using a recently developed methodology unique at Royal Holloway University of London [3], *in situ* chemical analysis of ice with unprecedented spatial (and thus time) resolution is achievable using cryo-cell UV-laser ablation inductively-coupled-plasma mass spectrometry (UV-LA-ICPMS). A volume of NorthGRIP ice (50x11x11 mm, HxWxD) have been analysed by using a series of 2D grids of laser spots at a resolution >300 µm over the surface of the volume. The sample surface (depth ~ 2717 m) has been smooth and cleaned using a metal free ZrO₂ blade mounted on a custom-built teflon vice used to remove ~2mm of ice to avoid contamination. A small liquid nitrogen reservoir covered by a teflon worksurface has been embedded in the proximity of the cryo cell, for keeping samples below -20 °C during loading procedures. N₂ is constantly blown on samples via a custom-made hood fitted with a vent, preventing contamination and refrosting from air.

Major elements indicative of sea salt contribution (Na, Mg) and dust concentration (Al, Ca, Fe, K) were measured simultaneously. Results proves the reliability of the technique in identify where impurities preferentially lies and which type of impurity they are (soluble or insoluble).

[1] Durand *et al.*, (2006). JGR-Earth Surface, 111(F1), F01015.

[2] Ohno *et al.*, (2005). EPSL, 232(1-2), 171-178. [3] Müller

et al., (2011). JAAS, 26(12), 2391-2395.

Lithium isotopic composition of the dissolved load in the Amazon River basin

M. DELLINGER^{1*}, J. GAILLARDET¹, J. BOUCHEZ², D. CALMELS³, P. LOUVAT¹, C. GORGE¹ AND L. MAURICE⁴

¹IPGP – Géochimie et Cosmochimie, 75238 Paris, France

(*correspondence: dellinger@ipgp.fr)

²GFZ (German Centre for Geosciences), 14473 Potsdam, Germany

³IPGP – Géochimie des isotopes stables, 75238 Paris, France

⁴LMTG-IRD, 14 avenue Edouard Belin, 31400 Toulouse, France

Silicate weathering reactions constitute a major aspect of the Earth's engine as they consume atmospheric CO₂ and influence the composition of the ocean and continental crust over long time scales. The investigation of past climatic variations requires geochemical proxies of silicate weathering. Lithium isotopes are a promising new geochemical proxy for silicate weathering and have notably been used recently to demonstrate the change of weathering regime during the Cenozoic based on the marine record [1]. However, the parameters controlling the extent of Li isotope fractionation during continental weathering and the associated fractionation factor are still poorly known. Here, we report the Li isotope composition of river-borne material in the largest Earth's River system, the Amazon River basin to characterize Li isotope fractionation at continental scale.

The Li isotopic composition of the dissolved load ($\delta^7\text{Li}$) is highly fractionated toward heavy values (up to 31‰) compared to river bed sand (-1.39 to +3.85‰) and suspended sediments (-6.80 to -0.50‰). The dissolved Li concentrations are the highest in the headwater of the Beni River that drains shale rocks (0.3 to 2 µmol.L⁻¹) and the lowest in the rivers draining the shield areas (< 0.1 µmol.L⁻¹). In the Madeira basin, the $\delta^7\text{Li}$ of the dissolved load increases from the Andes to the floodplain and displays a global inverse relationship with the Li/Na ratio. The fraction of Li incorporated into secondary weathering products during the contemporary weathering cycle is the dominant control of the dissolved Li isotope composition and is related to the geomorphic regime. This work has important implications for the determination of weathering mass budget based on Li isotope and about the importance of secondary product formation.

[1] Misra and Froelich (2012) *Science*, **335**(6070), 818-823

Uptake of SO₂, HCl and O₃ on volcanic ash

P. DELMELLE^{1*} AND M. ROSSI²

¹ Earth & Life Institute, Université catholique de Louvain, Louvain-la-Neuve, Belgium (*correspondence: pierre.delmelle@uclouvain.be),

² Laboratorium für Atmosphärenchemie, Paul Scherrer Institut, Villeggen, Switzerland (michel.rossi@psi.ch)

Mineral dust linked to soils from arid and semi-arid regions represents a significant fraction of the tropospheric aerosol mass. Many studies suggest that surface reactions involving mineral dust aerosol influence tropospheric chemistry. A largely neglected source of airborne mineral dust is silicate ash produced during explosive volcanic eruptions. The flux of ash into the atmosphere is not well constrained but may be >20 % of the annual mineral soil dust load. However, a single major eruption can inject a mass of fine (100 μm) ash with a total solid surface area on par with that emitted annually to the atmosphere by Saharan desert dust storms. In contrast to mineral dust, surface reactions of trace atmospheric gases on ash have not been studied. As a consequence, we have a limited understanding of the effects of volcanic activity on the chemical composition of the atmosphere.

The heterogeneous reactions of SO₂, HCl and O₃ on representative volcanic ash samples were investigated at room temperatures using a Knudsen cell. Volcanic ash varies in composition and mineralogy depending on source magma conditions. It is expected that natural ash samples will have different reactivities. Our results indicate that the uptake coefficients of SO₂, HCl and O₃ on volcanic ash compare with the values reported for mineral dust. No evidence was found for a significant compositional effect, and measurements performed with synthetic materials suggest that it is the glassy component which primarily drives the ash surface reactivity. Additional experiments are being performed and the new dataset will be integrated to provide a mechanistic description of the heterogeneous reaction of SO₂, HCl and O₃ on volcanic ash.

An inverse modelling approach for assessing CO₂-exposure experiments on Ketzin sandstone

M. DE LUCIA*, S. FISCHER, A. LIEBSCHER AND M. KÜHN

GFZ German Research Centre for Geosciences, Telegrafenberg, 14473 Potsdam, Germany (*delucia@gfz-potsdam.de)

For 24 months, reservoir sandstone samples from the Stuttgart Formation at the Ketzin pilot CO₂ storage site in Germany were exposed to synthetic brine and pure CO₂ at 55 bar and 40 °C [1]. Only minor mineralogical changes were directly observed after the experiments, making it difficult to discriminate natural variability of the samples from CO₂-induced alterations. During the progress of the experiments fluid samples were taken from the autoclaves in order to track the reactivity of the rock samples as reflected by changes in brine composition. Even these results show high variability and at times qualitatively opposite concentration trends for some dissolved species.

In order to assess the significance and plausibility of the analytical results and to reproduce the experiments numerically we developed and applied a computational two-step inverse modeling approach. Firstly, an extensive set (several thousands) of equilibrium simulations was generated representing all possible combinations from a predetermined pool of minerals supposed to represent all phases in the sandstone samples. These simulations were ranked based on their matching the average brine analysis. Highest ranked simulations were then re-run including kinetics of mineral reactions, with rate laws taken from literature [2]. Secondly, a more fine-grained iterative calibration of selected kinetic models, including a quantitative assessment of reactive surfaces, was built up in conformity to likelihoods estimated from the ensemble of generated simulations. Major uncertainties in the Ketzin sandstone experiments concern reactions involving Fe²⁺, K⁺ and Al³⁺; the other measured brine data were well matched.

This inverse modeling approach is computationally intensive (the simulations were run using a Pitzer database and generated via the R/PHREEQC interface [3]) but allows setting up models that are consistent to a set of otherwise intricate observations, where it is difficult to discriminate between measurements errors, biased thermodynamic data and erroneous parametrization of the models themselves. The outcome is a set of *possible* models and *ranges* in the parameters, which will then be considered i.e. for long-term predictions of the fate of Ketzin reservoir.

[1] Fischer *et al.* (accepted), *Envir Earth Sciences* [2] Palandri & Kharaka (2004) *USGS Open File Report* 2004-1068 [3] De Lucia & Kühn (2013), *Geoph Res Abstracts* **15**, EGU2013-9719

Seawater as the common Si source for both Archean BIF and cherts: insights from silicon isotopes

C. DELVIGNE^{1,2}, A. HOFMANN³, D. CARDINAL^{2,*}
AND L. ANDRÉ^{1,2}

¹Department of Earth Sciences and Environment, Université Libre de Bruxelles, Brussels, Belgium

²Department of Geology and Mineralogy, Royal Museum of Central Africa, Tervuren, Belgium

³Department of Geology, University of Johannesburg, South Africa

*Now at Laboratoire d'Océanographie et du Climat: Expérimentations et Approches Numériques, Université Pierre et Marie Curie, Paris, France

In an attempt to bring new insights into the identification of the silicon source(s) of Archean BIF, we compare silicon isotopic compositions of Si-rich mesobands of BIF and S-cherts ranging in age from 3.25 Ga to 2.5 Ga. We observe a progressive temporal 0.6‰ increase in $\delta^{30}\text{Si}$ signatures of Si-rich mesobands of BIF from $-1.80 \pm 0.62\%$ at 3.25 Ga to $-1.18 \pm 0.37\%$ at 2.5 Ga. Interestingly, this trend is parallel to the increasing $\delta^{30}\text{Si}$ trend recorded in cherts [1, 2, 3]. The common gradual change in the Si isotopic composition through time suggests that both Si-deposits had a main common Si-conveyor: the seawater. However, the comparison of both trends also reveals a systematic 1.5‰ difference between the two parallel trends where the BIF trend is the light one. We suggest here that such systematic 1.5‰ difference is most likely related to the respective genetic process that gave rise to both types of Si-rich deposits: a high to low-temperature geothermal seawater circulation for cherts [4] and a Si adsorption onto Fe-oxyhydroxides for BIF in which Si-rich mesobands are of diagenetic origin [5].

[1] Robert and Chaussidon (2006) *Nature* **443**, 969-972.

[2] Van den Boorn *et al.* (2007) *Geology* **35**, 939-942.

[3] Van den Boorn *et al.* (2010) *Geochim. Cosmochim. Acta* **74**, 1077-1103. [4] Abraham *et al.* (2011) *Earth Planet. Sci. Lett.* **301**, 222-230. [5] Delvigne *et al.* (2012) *Earth Planet. Sci. Lett.* **355-356**, 109-118.

Earthworms produce highly stable amorphous calcium carbonate

BEATRICE DEMARCHI¹, LIANE G BENNING², ANDY BROWN³, JOHN HARDING⁴, COLIN L FREEMAN⁴, KIRSTY PENKMAN¹ AND MARK E HODSON⁵

¹BioArCh, Department of Chemistry, University of York, UK (beatrice@palaeo.eu, kirsty.penkman@york.ac.uk)

²School of Earth and Environment, University of Leeds, UK (l.g.benning@leeds.ac.uk)

³Institute for Materials Research, University of Leeds, UK (a.p.brown@leeds.ac.uk)

⁴Dept Materials Science and Engineering, University of Sheffield, UK (j.harding@sheffield.ac.uk) (c.l.freeman@sheffield.ac.uk)

⁵Environment Department, University of York, UK (mark.hodson@york.ac.uk)

Many species of earthworm secrete granules of calcium carbonate. The earthworms *Lumbricus terrestris* and *L. rubellus* are the main granule producers in European soils. The granules begin as micron-scale spherulites of amorphous calcium carbonate within the earthworm's calciferous glands. These spherulites agglomerate and crystallise prior to secretion of granules up to 2 mm in diameter into the digestive tract and, ultimately, into the soil. The secreted granules are predominantly calcite but may contain aragonite, vaterite and amorphous calcium carbonate [1, 2, 3].

Granules subsampled from granule sets recovered from a range of chemically distinct soils and stored dry for over two years since their production contained between 2 and 14 % amorphous calcium carbonate and had elevated relative concentrations of glutamic acid / glutamine (Glx). After a further two year period amorphous calcium carbonate concentrations measured on further subsamples of these granule sets lay in the range 0 – 13 %; the relative amino acid composition of the granules was investigated by reverse-phase HPLC. No significant relationship was found between granule elemental composition and amorphous calcium carbonate content nor between the amorphous calcium carbonate contents determined after two and four years.

We ascribe the lack of relationships to the compositional heterogeneity of the granules and are currently performing spatially explicit analysis of the granules using Fourier transform infrared spectroscopy, electron microprobe analysis and electron backscattered diffraction. Controls on amorphous calcium carbonate stability will be discussed.

[1] Lee *et al.* (2007) *Geology* **36** 943-946. [2] Fraser *et al.* (2011) *Geochimica et Cosmochimica Acta* **75** 2544-2556. [3] Brinza *et al.* doi: 10.1016/j.gca.2013.03.011

A novel method of stable H and O isotope analyses of inclusion-hosted waters based on laser spectroscopy

DEMÉNY, A.¹ AND CZUPPON, GY.¹

¹Institute for Geological and Geochemical Research, RCAES, Hungarian Academy of Sciences, Budapest, Budaörsi út 45., (demeny@geochem.hu), (czuppon@geochem.hu)

Laser spectroscopy is a relatively recently developed technique that can be effectively used for coupled H and O isotope analyses of water samples. Since the aim of the present study was to extract water from fluid inclusions, a vacuum-based liquid water isotope analyser was chosen (Los Gatos Research, LWIA-24d). Inclusion-bearing samples were vacuum-crushed in stainless steel tubes and the released water was cryogenically transferred to the spectroscope's inlet using a vacuum line. When the fluid contained CO₂ (e.g. on the base of microthermometric analyses), the water was purified by releasing CO₂ at -80 °C. Memory and amount effects, as well as isotope shifts related to the isotope range measured were determined by introducing standard waters injected into glass capillaries. Amount effects for both H and O isotope compositions were quantified by multiple analyses of a calcite vein. On the base of a set of samples (calcite, quartz and fluorite veins, as well as speleothems), whose H isotope compositions had been measured by IRMS it can be stated that the precision of H isotope analyses achieves or even exceeds that of the IRMS analyses with a significant reduction in analysis time and cost. The determination of O isotope compositions raises more problems. It is demonstrated that the δ¹⁸O values are prone to alteration during the water release depending on extraction temperature and duration. Although the measured values may not be equal to the real compositions, internal variations can have a meaning, e.g., in paleohydrological studies.

The study was supported by the Hungarian Research Fund and the Hungarian State (project No. CK 80661).

Episodic fluid flow in a subduction zone

C. DE MEYER^{1*}, L.P. BAUMGARTNER¹, D. RUBATTO² AND A.-S. BOUVIER¹

¹ISTE, University of Lausanne, Switzerland

(*correspondence: caroline.demeyer@unil.ch)

²Research School of Earth Sciences, Australian National University, Canberra, Australia

The Zermatt-Saas Zone in the Western Alps contains the remnants of the Jurassic Piemonte-Ligurian ocean subducted to eclogite facies metamorphic conditions during the Eocene. The garnets have complex zonation documenting multiple resorption and growth periods. In-situ SHRIMP analyses of oxygen isotopes measured along profiles across the central sections of the garnets show multiple steps in δ¹⁸O values with variations of up to 5 ‰. The core of the garnet has δ¹⁸O values of 14-15 ‰. A sharp decrease to 9-10 ‰ is followed by a gradual increase to 14-15 ‰. The oxygen isotope variations in the garnets correlate with sharp jumps in grossular content. The decrease of the δ¹⁸O value during garnet growth indicates infiltration of an isotopic lighter fluid. Fluid infiltration drives the metamorphic decarbonation reactions, promoting garnet growth. The ultramafic and mafic rocks, which are intercalated with, or underlying the calcschists are the likely source of the fluids. Preliminary δ¹³C in-situ SIMS analyses of graphite inclusions suggest variable fluid sources during garnet growth. The multiple growth intervals suggest multiple pulses of fluid infiltration. While zones of adjacent garnet grains can be correlated, individual garnets have different size zones. This points towards localized fluid pathways on sub-centimeter scale. Mineral zoning in subducted carbonate-bearing rocks do not only register changing pressure and temperature conditions, but also changes in fluid composition due to circulation of fluids between ultramafic, mafic and meta-sedimentary units of the subducting slab.

The multiple structures of vaterite

RAFFAELLA DEMICHELIS^{1*}, PAOLO RAITERI¹
AND JULIAN D. GALE¹

Nanochemistry Research Institute, Department of Chemistry,
Curtin University, Perth WA, Australia.

(*presenting author - raffaella.demichele@curtin.edu.au)

(p.raiteri@curtin.edu.au, j.gale@curtin.edu.au)

Vaterite (CaCO₃) is a metastable polymorph that plays a fundamental role in the nucleation and crystal growth of calcium carbonate under biogenic conditions. In particular, the nucleation of vaterite is often observed from amorphous calcium carbonate precursors, with biomolecules acting as structural stabilizers [1,2].

Because of the role of vaterite in biomineralization, the nature of its disordered structure has been object of intense debate for several decades, leading to a multitude of different structural models [3,4,5]. Through first principles calculations, a link between the most recent models proposed in the literature has been established [6]. This new model, consisting of multiple structures, is in agreement with all of the current experimental evidence. The disorder of vaterite is here interpreted in terms of different orientations of the carbonate anions, different stacking sequences of the carbonate layers, and possible chiral forms. Hence, vaterite should be considered as a combination of different forms exhibiting similar average properties, rather than a single “disordered” structure. Furthermore, chirality represents a new and important direction for future investigation that may influence which of the possible vaterite structures is obtained.

More generally, a wide variety of structures exhibiting minor structural and energetic differences might exist in nature, as a result of nucleation in different environments and at different conditions, which might promote the formation of a particular stacking sequence or chirality.

[1] Hasse *et al.* (2000) *Chem.–Eur. J.*, **6**, 3679.

[2] Cartwright *et al.* (2012) *Angew. Chem. Int. Ed.*, **51**, 11960

[3] Mugnaioli *et al.* (2012) *Angew. Chem. Int. Ed.*, **51**, 7041

[4] Wang & Becker (2009) *Am. Mineral.*, **94**, 380

[5] Demichelis *et al.* (2012) *CrystEngComm*, **14**, 44

[6] Demichelis *et al.* (2013) *submitted* on February 22nd

Comparison of trace metal bioaccumulation potential in the three different ocean's zones

L.L. DEMINA

Shirshov Institute of Oceanology, 117997, Nakhimovsky pr,
36, Moscow, Russia.

l_demina@mail.ru)

An estimation of the trace metal' accumulation potential (TMAP) of the biological communities based on the integrated median average content of metals and average biomass of the dominated organisms was proposed [Demina, 2011]. A comparison of the TMAP in the three geochemically different zones such as: 1. coastal and estuarine areas (plankton, macroalgae and mollusks) 2. euphotic layer of the ocean (phytoplankton), and 3. deep-sea hydrothermal vent fields (bottom fauna), is made in this work (table). These areas are known to be a highly productive ones, where the biogeochemical processes are very intensive. Average biomass of In the hydrothermal biotopes the *Bathymodiolus spp.* bivalve mollusks demonstrate the largest biomass (whole bodies) – up to 60 kg·m⁻² [1].

Metal	1	2	3
Mn	470	6.3	894
Fe	9128	105	63060
Co	19.4	0.54	258
Ni	78.5	1	1092
Cu	102	6.3	4272
Zn	656	24.7	17100
As	7.8	5.7	2142
Cd	7.1	0.3	142
Pb	87	4.19	1013

Table: Trace metal bioaccumulation potential in the biomasses of the dominant communities (mg·m⁻² of the biotope).

From the comparison it follows that benthic fauna of hydrothermal fields (column 3) is characterized by the highest value of bioaccumulation potential of nine metals, which exceeds from tens to thousands times that in the estuaries (column 1) and euphotic zone of the open ocean (column 2). Thus, the hydrothermal fauna may be considered as a newly discovered local biological filter of the ocean.

[1] Demina (2011) *Dokl. Earth. Sci.* **439**, 981–986. [2] Demina *et al.* (2013) *J. Mar. Sys.*, in press, <http://dx.doi.org/10.1016/j.jmarsys.2012.09.005>

Geochronological and geochemical constraints on the construction of the Lluta pluton, Tacna (Peru)

SOPHIE DEMOUY¹ MATHIEU BENOIT¹
MICHEL DE SAINT-BLANQUAT¹
AND JEAN-LOUIS PAQUETTE²

¹GET - 14 av. Edouard Belin, F-31400 Toulouse

²LMV - 5 rue Kessler, F-63038 Clermont-Ferrand

Looking at the active margin scale, subduction-related magmatism leads to the emplacement of voluminous intrusive rocks into the crust, forming large plutonic belts parallel to the trench. Due to long-term magmatic activity in single region, these plutonic belts become highly complex in terms of structural features, emplacement history, and geochemical signatures.

Along the Western margin of South America, subduction has been ongoing since ~570 Ma. In this study, we present the emplacement history of the Lluta pluton, located at the southeastern end of the Peruvian Coastal Batholith, in the Tacna area. This pluton can be considered as an archetype of the Cretaceous to Paleocene magmatic arc activity and gives insight to the emplacement mechanisms of composite batholiths.

To unravel the emplacement history of the Lluta pluton, we performed major and trace element whole rock analyses on 21 samples, Sr and Nd isotopic measurements on 8 samples, and laser-ablation inductively coupled mass spectrometry (LA-ICPMS) U-Pb analysis on 5 samples.

The Lluta pluton intruded sedimentary Jurassic strata, after which the whole crustal sequence was tilted about 28° towards the west. The pluton has since been exhumed exposing more than 70 km² at the surface, and providing a cross section through the different levels of the pluton. The lithologies vary from gabbro to granite.

The gabbroic intrusion, located at the base of the pluton yields an age of 72.4 ± 0.5 Ma, whereas the various dioritic to granitic intrusions at lower crustal levels yield younger ages between 62.8 ± 0.4 and 62.0 ± 0.4 Ma. The entire dataset however displays a strong geochemical arc signature, that fits within the range of plutonic arc signatures in southern Peru. Initial Sr isotope ratios range is 0.70445-0.70575 and initial Nd isotope ratio range is 0.51248-0.51260.

Integration of the entire dataset illustrates the discontinuous construction of a single pluton in a subduction context. Isotopic signatures suggest either a varying amount of crustal contamination or magma mixing processes for the different lithological units, and show that the parental magmas are slightly more juvenile than those of the northern Coastal Batholith section of Arequipa.

Effects of carbonate assimilation on magma from Sumbing volcano, central Java, Indonesia and implications for Merapi

SCOTT DEMPSEY¹, COLIN G MACPHERSON¹,
ROBERT HALL² AND JON DAVIDSON¹

¹Department of Earth Sciences, Durham University, Durham, UK, DH3 1LE. (scottdempsey@chemostrat.com)

²Southeast Asia Research Group, Department of Earth Sciences, Royal Holloway University of London, UK, TW20 0EX

Sumbing volcano is situated at the southern end of a NNW-SSE trending chain of volcanoes in central Java that lies ~ 50 km east of a parallel chain, which includes Merapi. Sumbing has received little attention partly due to its dormancy since 1730. New petrological and mineralogical data along with whole rock major and trace element and Sr-Nd-Hf-Pb isotopic analyses were conducted for 20 volcanic rocks collected from Sumbing in 2009.

There are two petrographic and chemical magma groups. *Pyroclastic deposits* are predominantly fragments in lahars at the base of the volcano and contain ubiquitously higher percentages of Ca-bearing mineral phases such as clinopyroxene and highly altered plagioclase feldspar. The latter display a large range in anorthite (An) content. In contrast, a group of *lavas* show much less evidence for mineral-melt disequilibrium, are orthopyroxene (enstatite) rich and display more restricted plagioclase compositions.

The pyroclastic deposits are more silica undersaturated than the lavas and contain higher concentrations of CaO, Ba, Sr and have elevated ⁸⁷Sr/⁸⁷Sr, all of which overlap fields for Merapi. Correlations between degrees of silica saturation, Sr/Nb and ⁸⁷Sr/⁸⁶Sr suggest that these magmas become progressively enriched in Ca, Sr and ⁸⁷Sr/⁸⁶Sr with increasing silica undersaturation i.e. more contaminated rocks have lower SiO₂. In contrast, the lavas display little variation in these properties, beyond what would be expected from closed system differentiation. We interpret the two groups as originating from similar parental magma but displaying the effects of having experienced (pyroclastic) or escaped (lava) interaction with carbonate in the arc crust.

The lavas at Sumbing suggest that all magma erupted from Merapi has interacted with crustal carbonate. Therefore, Sumbing lavas provide the best estimate of parental melt characteristics of the arc front in central Java.

Geochemistry of Betul Mafic Layered Intrusion, Central India: Implications on Proterozoic Mantle Evolution and Ni-Cu-PGE Metallogeny

SUBBA RAO DENDULURI VENKATA, MANAVALAN SATYANARAYANAN AND DRONA SRINIVASA SARMA

CSIR-National Geophysical Research Institute, Uppal Road, Hyderabad 500007. Mail: (dvsubarao3s@rediffmail.com)

Precambrian crust of Central India is divided into northern Bundelkhand craton and southern Bastar craton separated by Central Indian Tectonic Zone (CITZ). The Betul Layered Complex (BLC) emplaced into the Mesoproterozoic Betul supracrustal belt (1.5-0.85 Ga) occur in CITZ. In this study we present the geochemical characteristics of the mafic-ultramafic rocks with particular relevance to the nature of contemporaneous sub-continental lithospheric mantle and Ni-Cu-PGE mineralization. BLC is characterized by metamorphosed ultramafic-mafic rocks emplaced into Betul belt consisting of bimodal volcanics and metasediments hosting VMS ores formed under a continental arc setting. The BLC exhibits primary mantle mineralogy (ol, opx, cpx, amp, phl) with secondary metamorphic mineral assemblages. The BLC rocks are subalkaline tholeiites and record Fe enrichment and fractionation trends. High concentrations of Cr, Ni and Cu indicate the presence of accessory chromite and Ni-Cu sulphides. Compositional heterogeneity is noticed with enrichments of LILE and Pb, and depletion of Nb, Zr-Hf suggesting mantle wedge of these rocks has been metasomatically enriched with the fluids derived from subducting slab. SEM-EDS study on gabbros from BLC has revealed that they contain unusual native gold, Ni-Cu, Ni-Co, Fe-Cu sulphide and Fe-Ti-Si phase with platinum group mineral inclusions and are genetically related to the magmatic hydrothermal fluids. PGE geochemistry is characterized by a high total PGE content of 1.2-1.5 ppm and have fractionated patterns (PPGE>IPGE; high Pd/Ir = 11 to 147) resembling the interstitial variety of mantle sulphide type and also fractionated PGE patterns of basalt (Mondal, 2011). It is considered that the Mesoproterozoic period witnessed extensive ultramafic-mafic magmatism with orthomagmatic ores and existence of a long lived metasomatically enriched mantle source, VMS ores and convergent margin tectonic settings. The geochemical characteristics of the BLC rocks corroborates the above proposition.

Mondal SK (2011). *Jour. Geol. Soc. India*, 7: 295-302.

Assessing the dissolution of marine sediment with ^{230}Th , and the impact of dissolution on sedimentary $^{231}\text{Pa}/^{230}\text{Th}$

FEIFEI DENG^{1*}, GIDEON M. HENDERSON¹, ALEX L. THOMAS¹, WILLIAM B. HOMOKY² AND RACHEL A. MILLS²

¹Department of Earth Sciences, University of Oxford, Oxford, (*feifei.deng@earth.ox.ac.uk)

²Ocean and Earth Sciences, National Oceanography Center, Southampton, University of Southampton, SO14 3ZH, United Kingdom (w.homoky@sotom.ac.uk)

Dissolution of marine sediment at the seafloor takes place in all ocean basins and is an important process controlling the release of chemicals from sediment back into seawater, and in setting the composition of marine particulates buried in sediment. Assessing the rate and extent of this dissolution is therefore critical for understanding of internal cycling of many chemical species in the ocean. In this study, we test the use of ^{230}Th , whose flux to the seafloor is assumed constant and well known, to assess sediment dissolution.

Sediment samples were collected during UK-GEOTRACES Cruise GA10E (D357) from the slope of the Cape Basin in the SE Atlantic. Intact core-top sediments and three short cores were selected for this study from a range of water depths. Samples of shallow-margin and deep-sea sediments are bathed in different water masses and vary in particle flux and compositions. Our results show that ^{230}Th concentrations increase from low core-top values to a depth of ~3cm and are constant below this depth. These observations can be best explained as a result of sediment dissolution in the upper centimetres of the sediment core. Core-top ^{230}Th measurements thus provide a tool to quantify the rate of sediment dissolution at the seafloor and assess the magnitude of this process in various ocean settings. Dissolution rates derived from ^{230}Th measurements have been used on these cores to assess the burial of organic biomarkers, and the fluxes of metals from upper centimetres of sediment back to overlying water column.

Measurements of ^{231}Pa on the same sediment aliquots were also conducted to assess the impact of the observed sediment dissolution on $^{231}\text{Pa}/^{230}\text{Th}$ ratios (a proxy for past rates of ocean circulation, and particle flux). Results show that, despite the large dissolution indicated by ^{230}Th profiles, $^{231}\text{Pa}/^{230}\text{Th}$ ratios appear to be almost unaffected, indicating the robustness of sedimentary archives as records of the $^{231}\text{Pa}/^{230}\text{Th}$ as a paleoceanographic proxy.

Rethinking primary organic aerosol emission inventories with a focus on wood combustion in Europe

H. A. C. DENIER VAN DER GON^{1*}, A. J. H. VISSCHEDIJK¹, R. BERGSTRÖM², D. SIMPSON³, J. GENBERG⁴, C. FOUNTOUKIS⁵ AND S. N. PANDIS⁵

¹TNO, PO Box 80015, 3508 TA, Utrecht, the Netherlands
(*correspondence: hugo.deniervandergon@tno.nl)

²Swedish Meteorological and Hydrological Institute, 601 76 Norrköping, Sweden

³EMEP MSC-W, Norwegian Meteorological Institute, Oslo, Norway

⁴Division of Nuclear Physics, Department of Physics, Lund University, Lund, Sweden

⁵Institute of Chemical Engineering Sciences, Foundation for Research and Technology Hellas (FORTH), Patras, Greece

In Europe, residential wood combustion (RWC) is the largest source of organic aerosol (OA). Recently OA modelling has significantly improved since the introduction of the Volatility Base Set approach [1]. However, these new insights had no impact on the primary particulate matter (PM) emission inventories in Europe. To quantify the importance of RWC our “traditional” OA inventory derived from reported PM emissions was used as input for 2 CTMs, PMCAMx and the EMEP model, revealing major underestimations of OA in winter time, especially for regions dominated by RWC. A new RWC emission inventory was constructed that also accounted for condensable particles, increasing RWC emissions with a factor of 2-3 but with substantial inter-country variation.

The new emission grid served as input for the CTMs and a significant improvement between measured and predicted black carbon (BC) [2] and organic carbon (OC) was found, further supported by levoglucosan campaign measurements. The results suggests that primary aerosol (PM) inventories need to be revised to include the semi-volatile OA that is formed almost instantaneously due to cooling of the flue gas or exhaust. A further analysis indicated that this is, based on the measurement protocol, not appropriate for European road transport emissions but industrial OA emissions may also be underestimated. We will also show that the choice of emission inventory influences the assessment of the effectiveness of reducing BC emissions from RWC as a mitigation strategy for decelerating global warming.

[1] Robinson *et al.*, Science, 315, 1259-1262, 2007. [2] Genberg *et al.*, ACPD, 13, 9051-9105, 2013

Petrology and Raman Characterization of Leucitites within the Ultrapotassic Rocks: Afyon, NW Turkey

K. DENİZ¹, Y. K. KADIOĞLU^{1,2}, T. KORALAY³, B. GULLU⁴, M. A. AKCE⁵ AND C. O. KILIÇ¹

¹Ankara Uni. Faculty of Eng. Dept. of Geological Eng., Ankara, Turkey and (kdeniz@eng.ankara.edu.tr)

²Ankara Uni. Earth Sciences Application & Research Center

³Pamukkale Uni. Dept. of Geological Eng., Denizli, Turkey

⁴Aksaray Uni. Dept. of Geological Eng., Aksaray, Turkey

⁵Bozok Uni. Dept. of Geological Eng., Yozgat, Turkey

NW Anatolia was exposed to alkaline volcanic activity during Miocene to Quaternary. These alkaline volcanic rocks show potassic and ultrapotassic character. Alkaline volcanic activity can be differentiated into five main groups as a leucitites, leucite phonolite, phonolitic tephrite, thrachyandesite and alkaline basalts. The first stage volcanic activity is represented by leucitites which have hypocrystalline texture and composed of leucite, melilite, augite, diopside, analcime, hematite and magnetite. Leucite phonolites and phonolitic tephrites have porphyritic texture and respectively leucite, sanidine, augite, nepheline, opaque minerals comprise the main mineral compositions. Thrachyandesites represent the third stage of volcanism and have hyloplitic porphyritic texture with augite, plagioclase, sanidine, nepheline and phlogopite. The last stage of volcanism contains alkaline basalts which show flow texture. The main mineral composition consist of augite, phlogopite, plagioclase and opaque minerals. Leucite gives a strong Raman shift in 500-530 cm⁻¹. Analcime gives a strong Raman shift in 389-484-673 cm⁻¹ and 1113 cm⁻¹. Augite type pyroxene group gives Raman shift in 324-357-390 cm⁻¹, 506 cm⁻¹, 666 cm⁻¹, 835 cm⁻¹ and 1010-1046 cm⁻¹. Diopside gives different Raman shift from augite in 963 cm⁻¹. Opaque minerals are hematite and minor magnetite in composition. Hematite gives Raman shift in 395-487-599-1293 cm⁻¹. Magnetite gives Raman shift in 649 cm⁻¹. Sanidine gives a strong Raman shift in 470-520 cm⁻¹. Whole rock geochemical data reveal that alkaline volcanic rocks are ultrapotassic and metaluminous in compositions. The ultrapotassic rocks both show enrichment in LILE and LREE with respect to HFSE and HREE. The Ba, Rb and Sr contents are enriched relative to mantle component. *The data obtained from petrological studies suggest that Afyon ultrapotassic volcanic rocks derived from lithospheric mantle source and were affected by subduction zone metasomatism during late stage of Cenozoic extensional magmatism in Western Anatolia.*

Chemical Continuous Time Random Walks

MARCO DENTZ

(marco.dentz@csic.es)

The Gillespie algorithm models chemical reactions as random walks in particle number space. The reaction lag times are exponentially distributed based on the assumption that the system is well mixed. We propose a generalization of this method and introduce non-exponential reaction lag time distributions, which may reflect the impact of incomplete mixing on the chemical reactions. From such a chemical continuous time random walk, we derive a generalized chemical Master equation. We present test cases to study the impact of non-exponential reaction times on the overall reaction behavior.

Generation of a multi-annuli corona sequence in two-pyroxene gabbro, Fiordland, New Zealand: intrusion, rapid post-magmatic cooling and transformation of gabbro to high-*P* granulite

DE PAOLI, M. C.¹, FITZHERBERT, J. A.²
AND CLARKE, G.³

¹ ETH Zürich, Institute of Geochemistry and Petrology, Zurich 8092, Switzerland.

² Geological Survey of NSW, Maitland, NSW 2320, Australia.

³ School of Geosciences, University of Sydney, Sydney, NSW, 2006, Australia.

Arc-related gabbroic intrusives of the Pembroke Valley, New Zealand preserve an unusual and unique sequence of coronas developed between igneous Fe-Mg silicates, Fe-Ti oxides and matrix plagioclase. The igneous assemblage does not contain garnet, constraining the depth of gabbro intrusion to less than *c.* 35 km at temperatures above 1000°C. Two distinct stages of corona crystallisation (*C*₁ and *C*₂) at lower-crustal levels have been identified. *C*₁ coronas involve symplectic intergrowths of Ca-amphibole-kyanite-clinopyroxene-K-feldspar-plagioclase-clinozoisite-quartz ± orthopyroxene, and formed during incipient hydration at the boundary between the two-pyroxene- and garnet granulite-facies at *c.* 25-35 km depth and temperatures of ≈ 800°C. Both igneous and *C*₁ corona mineral assemblages are crosscut by a series of ramifying anorthositic veins. Adjacent and parallel to these veins, igneous and *C*₁ corona minerals are pseudomorphed by garnet-clinopyroxene-rutile-bearing *C*₂ coronas within the selvage zones to the central vein. *C*₂ coronas formed via dehydration and recrystallisation of igneous and *C*₁ mineral assemblages in the garnet granulite-facies at pressures of ≈ 1.1 GPa (*c.* 30-35 km depth) and temperatures of ≈ 750°C. The sequence of corona annuli development at Pembroke represents the post-magmatic recrystallisation of gabbroic lithologies at constant or slightly increasing pressure and declining temperature. U-Pb isotopic ages of magmatic and recrystallised zircons indicate that the timing of intrusive and garnet granulite forming events were separated by as little as 11-17 Myr. This implies that the process of cooling (isobaric or up pressure) to produce high-pressure granulites is not just restricted to decreasing heat flow in old continental root zones, but may also occur in a transient setting during relatively rapid (11-17 Ma) isobaric cooling of young mafic under-plate in an intracontinental arc setting.

www.minersoc.org

DOI: 10.1180/minmag.2013.077.5.4

Geochemical characteristics of volcanites, as a reflection of subduction decay (Northern flank of Bureja-Jziamusy superterrains)

INNA DERBEKO

Institute of Geology and Nature Management FEB RAS,
Blagoveshchensk, Russia, (derbeko@mail.ru)

The magmatic activity was widely shown in the end of Mesozoic on the territory of the Northern flank of Bureja-Jziamusy superterrains. The three complexes of andesite formations were formed during 120-105, 111-105 Ma. The volcanites of the complexes have got some geochemical differences. The rocks enriched with Sr (up to 1029 ppm) were formed at the first stage, with the depletion of Nb (4-10), Ta (0.49-0.80), Rb (20.4-43.5), Th (1.70-4.97), Y (8-29), Ti (3100-3300). The lowering of the content of Sr (230-910 ppm), but growth of Rb and Th occurred at the second stage. The quantity of the rest of the elements is the same as in the first complex. The content of Sr (190-642 ppm) reduces, but the amount of Zr (129 - 412), Hf (3 - 13), Nb (7 - 39) in ppm is heightened in the volcanites of the third complex. Geochemical characteristics of the third complexes rocks are displaced to the same characteristics of the intra plate formations. All the rocks of the researched complexes relate to the calc - alkali series and low and high potassic groups. The rocks are characterized with oversubductional type of microelements distribution. The diagram of Sc/Ni - La/Yb [2] confirms that the rocks are oversubductional. But the content of the complexes is different. Some of the authors unite the lowering of the Sr concentration and growth of Ce, Th with the decay of the subduction. The fact is observed in the rocks of the researched complexes in the direction from the volcanites of the first to the volcanites of the third complex.

[1] McKenzie, Chappel (1972) *Contr. Miner. Petrol.* **35**. P. 50-63. [2] Rollinson (1995) *Using Geochemical Data: Evaluation, Presentation, Interpretat.* London. 352 p.

Differences in shale weathering on ridgetops and slopes along a latitudinal climosequence

A. L. DERE¹, T. S. WHITE¹, L. E. LEIDEL¹
AND S. L. BRANTLEY¹

¹Penn State University, 315 Hosler Building, University Park, PA, USA (*corresponding author: ald271@psu.edu) (tsw113@psu.edu); (le15098@psu.edu); (sxb7@psu.edu)

Regolith, the mantle of physically, chemically, and biologically altered material overlying parent material, covers much of Earth's continents but the rates and mechanisms of regolith formation are not well known. In an effort to quantify the influence of climate on shale weathering rates, a transect of study sites has been established on Silurian shales along a climatic gradient in the Northern Hemisphere as part of the Susquehanna Shale Hills Critical Zone Observatory, PA, USA. The climate gradient is bounded by a cold/wet end member in Wales and a warm/wet end member in Puerto Rico; in between, temperature and rainfall increase to the south through New York, Pennsylvania, Virginia, Tennessee and Alabama. Soil depth and geochemistry were measured both on ridgetop positions (where water flow is largely vertical through the soil profile) and on slope positions (where water moves both vertically and laterally downslope). The depth of ridgetop soils increases from north to south along the climate gradient, with shallow soils (~ 30 cm) in Wales and Pennsylvania and increasingly deep soils to the south (394 cm in Tennessee). Similarly, the extent of chemical depletion in ridgetop surface soils increases from <20% elemental depletion in the north to 100% depletion of some elements in the south. Soil depths on slopes, however, do not vary much along the transect and range from 52-86 cm across the Appalachian sites. In these slope soils the extent of weathering is similar across the Appalachian study sites; Mg, K and Al, for example, are ~40% depleted at the soil surface at all of the study sites. One working hypothesis based on limited quantitative assessments of regolith age in the Appalachians suggests that ridgetop and slope soils may be more or less the same age. In this model, the increasing ridgetop soil thickness along the transect is a function of warmer and wetter climate to the south. In slope positions, however, where downslope water flow leads to decreased fluid residence time, thinner and less weathered soils are observed. Alternately, southern soils are much older than northern soils due to impacts of the Last Glacial Maximum and similar erosion rates across the study region have left an eroded mantle of uniform thickness on top of bedrock slopes.

Petrochemical characterization of the basalts and rhyolites erupted along the central axis of the Main Ethiopian rift

ROSANNA DE ROSA^{1*}, CARMELO FERLITO², EUGENIO NICOTRA^{1,2} AND PAOLA DONATO¹,

¹Università della Calabria, Via P. Bucci 15/B, 87036

Arcavacata di Rende (CS), Italy. (derosa@unical.it)

²Università di Catania, Corso Italia 57, 95129 Catania, Italy

In continental domain rift zones are the sites of the most extensive magma production. The opening of continental rifts and their consequent oceanization are accompanied by the intrusion and emission of magmas. The relationship between the timing and style of the rift opening and the type of magma associated is still not fully understood. The Main Ethiopian Rift (MER) represents one of the most active continental rifts in which the volcanic activity has produced basaltic flows from fissural eruptions and rhyolitic central volcanoes. In order to characterize the products cropping out within the northern and central branches of the MER, we have carried out an extensive sampling of lava flows, monogenetic scoria cones and obsidianaceous central edifices (Fantale, Kone, Boseti). On the collected samples major and trace elements analysis and mineralogical and petrographic observations have been performed. Preliminary data confirm a close relationship between geochemical composition and the morphology of the volcanic edifices and structures. In particular, central edifices present a rather homogeneous rhyolitic compositions, whereas recent fissural activity is dominated by basaltic lava fields. These two distinct types of products occur along en-echelon tectonic segments, located within the central portion of each branch of the rift. Branches are joined by transitional areas, in which monogenetic scoria cones with the most primitive compositions crop out. The chemical data have been used to model the features of the magma sources and the processes affecting magmas during their ascent towards the surface.

Metal mobility in hydrothermal fluids: experimental investigations

I. T. DERREY*, R. E. BOTCHARNIKOV, M. ALBRECHT, I. HORN, S. WEYER AND F. HOLTZ

Institut für Mineralogie, Leibniz Universität Hannover, GER (*correspondence: i.derrey@mineralogie.uni-hannover.de)

Hydrothermal fluids are crucial in the formation of ore deposits, as they are the main transport medium leading to the selective concentration of elements in the Earth's crust and, among others, metals of economic interest. Fluid inclusions in minerals do not just enable us to probe natural fluids from depth, but also provide an opportunity to investigate fluids in high P/T experiments [1]. With the development of LA-ICP-MS techniques it has become possible to analyze major, minor and trace element concentrations in fluid inclusions [2].

Thus, synthetic fluid inclusion studies are an ideal tool to study metal transport and partitioning in hydrothermal fluids and to provide key data necessary for the quantification of transport properties. Partly due to difficulties in producing decent sized synthetic fluid inclusions at low temperatures, previous studies were mostly focused on conditions above. By combining the two current methods of host mineral pretreatment (thermal cracking [1] and HF etching [3]), we are able to synthesize fluid inclusions in quartz with a size in excess of 20 μm at T down to at least 400 °C. This gives us the opportunity to study the conditions and processes responsible for the mobility of metals at low temperatures. Experiments are conducted in cold seal pressure vessels at T=400-600 °C and P up to 200 MPa with the aim to unravel the transport and partitioning of metals occurring in porphyry copper deposits.

We have been implementing a new technique to analyze fluid inclusions by LA-ICP-MS, which is based the combination of a femtosecond laser with a heating-freezing cell and a sectorfield ICP-MS. During the ablation with a fs-laser the inclusion remains frozen until entirely evaporated, resulting in a considerably longer signal analysis time. This allows reducing the analytical error on the analyzed element concentrations.

Results for Au and Mo solubility in fluids of varying composition obtained at different P and T will be presented. Preliminary data indicate that solubilities of Mo are higher than expected if extrapolated from high T data of [4].

[1] Sterner & Bodnar (1984), *GCA* 48, 2659-2668. [2] Günther *et al.* (1998), *J Anal Atom Spectrom* 13, 263-270. [3] Li & Audetat (2009), *Am Mineral* 94, 367-371. [4] Zhang, Audetat & Dolejs (2012), *GCA* 77, 175-185.

Resolving inconsistent sedimentary carbon mass balances: Implications for ancient C and S cycles

L. A. DERRY¹

¹Dept. of Earth & Atmospheric Sciences, Cornell University, Ithaca NY USA (derry@cornell.edu)

Inventory and isotope mass balance estimates of the organic carbon/ Σ carbon ratio (X_{org}) of the upper crust (dominated by sediments) appear to differ systematically. Inventory-based estimates yield $X_{org} \approx 0.10$ to 0.17, while $\delta^{13}C$ mass balance estimates are 0.19 to 0.34. The $\delta^{13}C$ mass balance approach typically assumes a steady state form $\delta_{in} = f_{org}^{bur} \delta_{org} + f_{carb}^{bur} \delta_{carb}$, where f_{org}^{bur} is the burial fraction of organic carbon. Over long times the time integrated value of f_{org}^{bur} should approach the value of X_{org} , and δ_m should approach the mean $\delta^{13}C$ value of the upper crust. If the inventory-based estimates of X_{org} are approximately correct, the isotope mass balance approach as conventionally applied cannot be. Two modifications to the $\delta^{13}C$ mass balance can reconcile the discrepancy. First, increasing data indicates that even in the modern environment with $pO_2 = 0.21$, the oxidation of old carbon is incomplete [1]. Second, a substantial fraction of carbon is returned to the ocean-atmosphere system as isotopically depleted CH_4 [2]. At low pO_2 though to be characteristic of the Precambrian, the oxidative weathering efficiency of kerogen was lower, implying a larger fraction of C recycling via methanogenesis. In that case the revised steady state isotopic mass balance implies both lower absolute and fractional burial rates of sedimentary organic carbon than for Phanerozoic conditions. The generation and oxidation of CH_4 was a dominant term in the organic carbon mass balance at low pO_2 . Model results show that large CH_4 fluxes result in low steady state marine SO_4 levels via AOM, consistent with inferences from $\delta^{34}S$ studies of Proterozoic sediments [3].

[1] Blair & Aller (2012) *Ann Rev Mar Sci* **4**, 401-423. [2] Etiope *et al.* (2011) *Planet. Space Sci.* **59**, 182-195. [3] Li *et al.* (2010) *Science* **328**:80-83.

Pb-Zn-Cd-Hg multi isotopic characterization of the Loire River Basin, France

A.M. DESAULTY¹, R. MILLOT¹, D. WIDORY^{1,2},
C. GUERROT¹, C. INNOCENT¹, X. BOURRAIN³,
G. BARTOV⁴ AND T.M. JOHNSON⁴

¹BRGM, Laboratory Division, Orléans, France
(*correspondance : am.desaulty@brgm.fr)

²UQAM/GEOTOP, Earth Atm. Sci. Dept., Montréal, Canada

³Agence de l'Eau Loire Bretagne, Orléans, France

⁴University of Illinois, Department of Geology, Urbana, USA

The Loire River in Central France is approximately 1010 km long and drains an area of 117 800 km². Upstream, the Loire river flows following a south to north direction from the Massif Central down to the city of Orléans, 650 km from its source. The Loire River is one of the main European riverine inputs to the Atlantic Ocean. Over time, its basin has been exposed to numerous sources of anthropogenic metal pollutions, such as metal mining, food industry, agriculture and domestic inputs. The Loire River basin is thus an excellent study site to develop new isotope systematics for tracking anthropogenic sources of metal pollutions.

We have chosen to analyze the isotope composition of cadmium (Cd), zinc (Zn), mercury (Hg) and lead (Pb). These heavy metals have been chosen for their toxicity, even at low levels, to humans. The main goal of this study is to characterize 1) the sources and behavior of these heavy metals in the aquatic environment, and 2) their spatial distribution using a multi-isotope approach. Sources responsible for the release of Pb-Zn-Cd-Hg in the Loire basin were sampled and analysed for their concentrations and corresponding isotope compositions. We also analyzed river waters and suspended solids samples, known to play an important role in the transport of heavy metals through river systems. Biota samples (mussels, oysters), as natural accumulators of metal pollutants, were also analyzed.

All trace elements were analysed in the BRGM laboratories using a Q-ICPMS. Pb-Zn-Cd isotope compositions were measured using a Neptune MC-ICPMS at the BRGM. Hg isotope compositions were measured at the U. of Illinois using a Nu Plasma MC-ICPMS. To analyse Zn and Cd, we carried out a two-steps analytical development: 1) a chromatographic separation, followed by 2) analysis on the MC-ICPMS.

The results showed that, on their own, each of these isotope systematics reveals important information about the geogenic or anthropogenic origin of these metals. Considered together, they are however providing a more integrated understanding of the overall budgets of these pollutants at the scale of the Loire River Basin.

Swelling induced by alpha decay in monazite and zirconolite ceramics: a XRD and TEM comparative study.

X. DESCHANELS¹, A.M. SEYDOUX-GUILLAUME*², V. MAGNIN³, A. MESBAH¹, M. TRIBET⁴, S. PEUGET⁴

¹ ICSM, UMR 5257, BP 17171, 30207 Bagnols-Sur-Cèze, France.

² GET, CNRS-UPS-IRD, Université De Toulouse, 14 Av E. Belin, 31400 Toulouse, France.

³ Isterre, UMR5275 CNRS, Université Joseph Fourier, 38041 Grenoble, France.

⁴ CEA/DTCD/LMPA Centre De Marcoule, BP 17171, 30207 Bagnols-Sur-Cèze, France.

Zirconolite and monazite are potential ceramics for the containment of actinides (Np, Cm, Am, Pu) produced by reprocessing spent fuel. Alpha decay is the main disintegration mode for actinide elements. This phenomena induces structural changes on the ceramics (amorphisation, swelling...). In order to study these effects two parallel approaches based on external irradiations and short-lived actinides doping (²³⁸Pu) were used. On one hand, plutonium oxide was incorporated into the monazite and the zirconolite structure. On the other hand, external irradiations with Au ions were used to simulate energy deposits corresponding to the recoil nucleus.

For both irradiations, zirconolite samples become amorphous at room temperature for a critical dose close to 0.3 dpa and the magnitude of the swelling at saturation is similar (about 6%). Ballistic processes are predominant in the damaging of this structure. On the contrary the swelling and the amorphisation of monazite sample depend on the nature of the irradiation. Ion irradiated samples present a saturation swelling close to 7% and are metamict for a critical dose close to 0.3 dpa while the swelling measured on ²³⁸Pu doped samples is only 2% and they remain crystalline up to $7.5 \times 10^{18} \alpha/g$, i.e. 0.7 dpa. The different behavior observed between doped and externally irradiated monazite samples can be interpreted in terms of annealing effects induced by ionizing radiation. The ratio electronic-to-nuclear stopping seems to be a key parameter for the damage recombinaison in monazite. Evidence of alpha annealing is observed on the monazite structure.

Timescales of partial melting and UHP exhumation, Papua New Guinea

DESORMEAU, J.W.¹, GORDON, S.M.¹, LITTLE, T.A.², BOWRING, S.A.³

¹Dept. of Geological Sciences, University of Nevada, Reno, NV, USA; (jd112657@umconnect.umn.edu)

²Dept. of Geography, Environmental and Earth Sciences, Victoria University, Wellington, New Zealand

³EAPS, MIT, Cambridge, MA, USA

To understand how crustal rocks are subducted to mantle depths and subsequently exhumed, it is crucial to determine the relative timing and relationship of the host migmatites to the UHP-HP eclogites. The Pliocene UHP terrane of southeastern Papua New Guinea (PNG), exposes large areas of migmatitic gneiss within domal structures found throughout the D'Entrecasteaux Islands, including Goodenough, Fergusson, and Normanby Islands. These gneisses reveal abundant evidence for partial melting during exhumation. Zircons analyzed using U-Pb chemical abrasion thermal ionization mass spectrometry (CA-TIMS) geochronology from eclogite suggest UHP metamorphism began at ca. 5 Ma, and Ar-Ar thermochronology indicates exhumation of the rocks to the surface by ca. 2 Ma. To evaluate the role of partial melting in the exhumation of this UHP terrane, U-Pb CA-TIMS geochronology was applied to zircons separated from multiple leucosomes and dikes across the three islands. Previous U-Pb results from the UHP locality and other parts of the western Fergusson Island dome reveal melt-present deformation in the form of foliation-parallel leucosomes with crenulated margins that formed from ca. 3.5–3.0 Ma and weakly-deformed cross-cutting dikes at ca. 2.4 Ma. In comparison, zircons from a similarly deformed foliation-parallel leucosome within Goodenough dome to the west reveal melt crystallization from ca. 4.7–2.7 Ma. The youngest igneous rocks are felsic non-deformed intrusions which contain zircons as young as ca. 1.8 Ma. Finally, in the south, Normanby dome records the development of the host orthogneiss by ca. 5.9 Ma and emplacement of deformed granodiorite sills by ca. 4.1 Ma. Zircons from non-deformed granodioritic and andesitic dikes yield similar crystallization ages to Goodenough Island, with zircons as young as 1.8 Ma. The emplacement of the gneiss domes within the upper crust occurred by ca. 1.9–1.8 Ma, based on the late dikes, and is similar across the entire PNG UHP-HP terrane. The results indicate that exhumation of the PNG UHP-HP terrane was aided by multiple stages of partial melting that increased the overall buoyancy of the subducted crustal material.

Silicon stable isotope constraints on the pathways of thermocline nutrient replenishment

G. F. DE SOUZA*, R. D. SLATER AND J. L. SARMIENTO

Program in Atmospheric and Oceanic Sciences, Princeton University, Princeton, New Jersey, USA

(*correspondence: gfds@princeton.edu)

The continued action of the ocean's biological carbon pump, driven by photosynthetic productivity at its sunlit surface, is contingent upon the supply of nutrients from the nutrient-rich abyss to the permanent thermocline. Increasingly compelling evidence implicates the Southern Ocean in this replenishment of thermocline nutrients, via the wind-driven upwelling of deep waters and the subduction of Subantarctic Mode Water (SAMW) to the base of the permanent thermocline [1].

The recent modelling study of Palter *et al.* [2] estimated that SAMW supports between 33% and 75% of photosynthetic productivity at low latitudes, a range that hinges upon uncertainties in the pathways of the meridional overturning circulation (MOC). A novel opportunity to reduce this uncertainty is presented by the oceanic distribution of the stable isotope composition of silicic acid in seawater, $\delta^{30}\text{Si}$. It has been argued by de Souza *et al.* [3,4] that the oceanic $\delta^{30}\text{Si}$ distribution, and particularly the meridional gradient in Atlantic deep water $\delta^{30}\text{Si}$ values, provides strong support for a dominant Southern Ocean supply of silicic acid to the thermocline. Here, we combine these novel data constraints with a suite of ocean general circulation models in order to provide improved quantitative estimates of the importance of the SAMW contribution to the thermocline nutrient inventory.

Model variants that upwell a greater proportion of deep water within the Southern Ocean produce a more pronounced Atlantic deep water $\delta^{30}\text{Si}$ gradient, a result that provides further support for the importance of nutrients supplied by the Southern Ocean in maintaining low-latitude productivity. More broadly, these results pertain to the role of the Southern Ocean in the closure of the MOC, and ultimately to the driving mechanisms thereof [5].

[1] Sarmiento *et al.* (2004) *Nature* **427**, 56-60. [2] Palter *et al.* (2010) *Biogeosci.* **7**, 3549-2568. [3] de Souza *et al.* (2012) *Glob. Biogeochem. Cyc.* **26**, GB2035, doi: 10.1029/2011GB004141. [4] de Souza *et al.* (2012) *Biogeosci.* **9**, 4119-4213. [5] Kuhlbrodt *et al.* (2007) *Rev. Geophys.* **45**, RG2001, doi: 10.1029/2004RG000166.

Dynamic of organic carbon in small volcanic mountainous tropical watersheds (Guadeloupe, FWI)

C. DESSERT^{1,2}, E. LLORET³, M.F. BENEDETTI¹, E. LAJEUNESSE^{1,2}, O. CRISPI² AND J. GAILLARDET¹

¹ Institut de Physique du Globe de Paris (IPGP), Université Paris-Diderot, Paris, France (dessert@ipgp.fr)

² Observatoire Volcanologique et Sismologique de Guadeloupe (OVSG), Observatoire de l'Erosion aux Antilles (ObsErA), IPGP, Guadeloupe (FWI)

³ Department of Renewable Resources, University of Alberta, Canada (lloret@ualberta.ca)

In the tropical zone, small mountainous watersheds are affected by intense meteorological events. If the increase of the frequency and/or intensity of these extreme meteorological events (storms, cyclones) is confirmed [1, 2], it could lead to an increase of the export of dissolved and suspended material derived from soils.

We studied the geochemistry of three small watersheds around the Basse-Terre volcanic Island (FWI) during a four years period, by measuring dissolved organic carbon (DOC) and particulate organic carbon (POC) concentrations [3]. The mean annual yields range between 1.9-8.6 tC km⁻² yr⁻¹ and 8.1-25.5 tC km⁻² yr⁻¹ for DOC and POC, respectively. Floods and extreme floods account for 43% of the yearly water flux and represent 55% of the annual DOC flux, and more than 85% of the annual POC flux. These results show that organic carbon fluxes are largely underestimated if high temporal resolution sampling is not performed.

The important carbon export in Guadeloupe is induced by high intensity of precipitation leading to high runoff, high slopes, and high organic matter contents in Andosols and ferralitic soils. Even if the surface of volcanic and mountainous tropical islands is low compared to continental area, organic carbon yields in this specific context are so important that this surface can represent a significant proportion of the global annual carbon export. This total export is estimated to 2.4 ± 0.6 MtC yr⁻¹ for DOC and at 5.9 ± 2.4 MtC yr⁻¹ for POC. In addition, the quality of terrestrial organic matter (POC/DOC and C/N ; slightly degraded) arriving to the ocean is different from the one of large tropical river origin.

Our results show that tropical volcanic islands are significant pools of organic carbon for oceans and the effect on global carbon budget is still a matter of debate.

[1] Emmanuel (2005) *Nature*, **436**. [2] Trenberth (2005) *Science* **308**. [3] Lloret *et al.* (2011) *Chem. Geol.*, **280**.

CO₂ injection into submarine, CH₄-hydrate bearing sediments: geochemical implications of a hydrate conversion technology

C. DEUSNER, E. KOSSEL, N. BIGALKE,
M.G. GHARASOO, AND M. HAECKEL

GEOMAR Helmholtz Centre for Ocean Research Kiel,
Wisshofstr.1-3, D-24148, Kiel, Germany

With the aim of emission neutral energy production, combined CH₄-hydrate exploitation from and CO₂ storage in marine gas hydrate reservoirs is investigated. Little is known about the geochemistry of hydrates and their host sediments before, during and after production. Results from the recent *Ignik Sikumi* gas hydrate field trial have indicated that the injection of a CO₂-rich fluid into the hydrate reservoir produces mixed hydrates in a slow conversion process. This and the awareness of potential effects of natural and technically induced heterogeneity drives the ambition to understand hydrate conversion on the pore scale.

Our recent studies suggest that the injection of heated, supercritical CO₂ is beneficial for both CH₄ production and CO₂ retention at different hydrate reservoir temperatures ranging from 2 °C to 10 °C [1]. Yet, our findings can only be explained by the induction of a variety of spatial and temporal processes which result in substantial bulk heterogeneity, characterized by formation of mixed CO₂-CH₄-hydrates, hold-up of hydrate-derived CH₄ gas in pore spaces, permeability changes and temperature dependent CO₂-channeling. Interestingly, while CH₄ production and CO₂ retention yields varied considerably between different experiments, water production was largely similar. Using online IR-based sensor technology and Raman spectroscopy, distinct intervals of water and gas production could be identified, which suggest, that the slow formation of CO₂- or mixed CO₂-CH₄-hydrates was responsible for increased CH₄ production yields. Additional Magnetic Resonance Imaging (MRI) experiments were performed to visualize the intrusion of liquid CO₂ into the sediment/hydrate matrix.

It is a central objective of our studies to improve available transport-reaction models and strengthen the link between pore scale and reservoir modelling, by finding empirical relations suitable for implementation in current numerical simulators.

[1] Deusner *et al.* (2012) *Energies* 5, 2112-2140

Isotopic and stoichiometric constraints on marine denitrification from a global inverse circulation model

C. DEUTSCH^{1*}, T. DEVRIES¹, P. RAFTER²
AND F.PRIMEAU³

¹Department of Atmospheric and Oceanic Sciences,
University of California, Los Angeles, CA, USA

²Department of Geosciences, Princeton University,
Princeton, New Jersey, USA

³Department of Earth System Sciences, University of
California, Irvine, USA

A major impediment to understanding long-term changes in the marine nitrogen (N) cycle is the persistent uncertainty about the rates, distribution, and sensitivity of its largest fluxes in the modern ocean. We use a global ocean circulation model to obtain the first 3-dimensional estimate of marine denitrification rates that is maximally consistent with available observations of nitrate deficits and the nitrogen isotope ratio of oceanic nitrate. We find a global rate of marine denitrification in suboxic waters and sediments of 120–240 TgN/yr, which is lower than many other recent estimates. The difference stems from the ability to represent the spatial structure of suboxic zones, where denitrification rates of 50–77 TgN/yr result in up to 50% depletion of nitrate. This depletion reduces the effect of local isotopic enrichment on the rest of the ocean, allowing the N isotope ratio of oceanic nitrate to be achieved with a sedimentary denitrification rate about 1.3–2.3 times that of suboxic zones. This balance of N losses between sediments and suboxic zones is shown to obey a simple relationship between isotope fractionation and the degree of nitrate consumption in the core of the suboxic zones. The global denitrification rates derived here suggest that the marine nitrogen budget is likely close to balanced.

Holocene peat bog records of atmospheric dust fluxes in Southern South America

F. DE VLEESCHOUWER^{1,2*}, H. VANNESTE^{1,2}, N. MATTIELLI³, A. VANDERSTRAETEN³, N. PIOTROWSKA⁴, A. CORONATO⁵ AND G. LE ROUX^{1,2}

¹Université de Toulouse, INP, UPS, EcoLab (Laboratoire Ecologie Fonctionnelle et Environnement), ENSAT, Avenue de l'Agrobiopole, 31326 Castanet Tolosan, France (*correspondence: francois.devleeschouwer@ensat.fr)

²CNRS, EcoLab, 31326 Castanet Tolosan, France (francois.devleeschouwer@ensat.fr.)

(heleen.vanneste@ensat.fr, gael.leroux@ensat.fr)

³Laboratoire G-Time, Département des Sciences de la Terre et de l'Environnement, Université Libre de Bruxelles, Belgium (nmattiel@ulb.ac.be, auvdstra@ulb.ac.be)

⁴Department of Radioisotopes, Institute of Physics, Silesian University of Technology (natalia.piotrowska@polsl.pl)

⁵CADIC-CONICET, Ushuaia, Argentina (acoronato@cadic-conicet.gob.ar)

Little attention has been given to Holocene pre-anthropogenic dust records in terrestrial environments, especially in the Southern Hemisphere. Yet they are important to 1/ better understand the different particle sources during the Holocene and 2/ to tackle the linkage between atmospheric dust loads and climate change and 3/ to better understand the impact of dust on Holocene palaeoclimate and palaeoenvironments in a critical area for ocean productivity. In the PARAD project, we explore the use of a broad range of trace elements and radiogenic isotopes (Pb, Nd) as dust proxies. By coupling these findings with biological proxies (plant macrofossils) and detailed age-depth modelling, we expect to identify and interpret new links between atmospheric dust chemistry and climate change. In this contribution, we will present the elemental and isotopic signatures of two peat records from Chilean and Argentinean Tierra del Fuego, covering the Holocene. We provide here the first high-resolution dust flux records for the Southern South American Holocene. Results will also encompass density, ash content, grain size analyses, macrofossil determination and radiocarbon age modelling. Preliminary linkage of dust fluxes with change in vegetation and climate can be seen in our results. Single dust peaks originate from volcanic events while others are to be explained by regional to long range dust transport from Southern South dust source (local soils, glaciers, fluvio-glacial plains, dry lakes and valleys and perhaps, pampa materials).

High performance reactive transport simulation of hyperalkaline plume migration in fractured rocks

L.M. DE VRIES^{1*}, J. MOLINERO¹, H. EBRAHIMI¹, U. SVENSSON² AND P. LICHTNER³

¹ Amphos 21 Consulting S.L., Passeig Garcia Faria, 49-51, E-08019, Barcelona, Spain

² Computer-aided Fluid Engineering AB, Barcelona, Frankes väg 3, S-371 65 Lyckeby, Sweden.

³ OFM Research, Guest Scientist LANL, Los Alamos, NM 87545, USA.

Integration of hydrogeology and geochemistry is crucial for several problems in Earth Sciences and Engineering. One of the challenges for such integration is the large amount of computational resources needed due to the high non-linearity of the resulting system of equations. Taking advantage of new developments of powerful numerical tools, and based on high performance parallel computing, the solution of regional-scale hydrogeochemical models has become possible. A software solution, denoted iDP, has been developed which serves as an interface between DarcyTools [1] and PFLOTRAN [2]. The project is financed by SKB, the Swedish Nuclear Fuel and Waste Management Company. iDP has been applied for the first time in the Mare Nostrum III, a new facility of the Barcelona Supercomputing Centre. A total of 25,000 processor cores during 5 days were used to solve a large-scale (100 Mcells), long-term (10,000 years) simulation of the hydrogeochemical behaviour of an hyperalkaline plume produced by the dissolution of grout used during the construction of a deep geological repository for spent nuclear fuel. The simulation integrates the complex 3D groundwater flow accounting for the Discrete Fracture Network (DFN) of the site, and the complexity of the geochemical system involved in cement grout dissolution and secondary minerals precipitation within the flowing fractures.

[1]. Svensson, U, Ferry, M. (2010) Darcy Tools version 3.4. User's Guide, SKB R-10-72 (available at www.skb.se)

[2]. Lichtner, P.C., Hammond, G.E., Bisht, G., Karra, S., Mills, R.T., and Kumar, J. (2013) PFLOTRAN User's Manual: A Massively Parallel Reactive Flow Code.

Method development and validation for B isolation from Roman glass

V. DEVULDER^{1,2*}, P. DEGRYSE¹ AND F. VANHAECKE²

¹ Katholieke Universiteit Leuven, Celestijnenlaan 200E, Heverlee, Belgium
(*correspondence: Veerle.Devulder@ees.kuleuven.be)
(Patrick.Degryse@ees.kuleuven.be)

² Ghent University, Krijgslaan 281-S12, Gent, Belgium
(Frank.Vanhaecke@ugent.be)

The provenancing of the raw materials used in Roman glass production is of great interest in archaeological sciences as the corresponding information can give more insight into the trade routes in ancient times and the glass manufacturing process. Glass is made from sand as silica source and natron as a flux. The major source of this flux is thought to be the evaporites from the Wadi Natrun region in Egypt. This assumption is mainly based on the writing of Pliny the Elder, a Roman author, and some geochemical evidence [1]. However, Pliny also mentions other sources [2]. But until now, no unambiguous evidence exists for the exploitation of other natron sources for glass production in the Roman empire. The isotopic composition of B, determined by means of multi-collector ICP-MS (MC-ICP-MS), might provide this valuable information as B is introduced into the glass with the flux and different flux sources (i.e. lakes) can have different B isotopic signatures. Therefore, a method for isolation of B from archaeological glass was developed and validated. After sample dissolution, B is isolated via a two-step separation process, based on the use of a strong cation and an anion exchange resin. Only Sb (which is used as decolorizer or opacifier) was not completely separated from B, but its presence did not exert a significant influence on the $\delta^{11}\text{B}$ determination. The sample preparation method and some first sample results will be presented.

[1] Shortland *et al.* (2006), *Journal of Archaeological Science* 33, 521-530. [2] Dotsika, E. (2009) *Journal of Geochemical Exploration* 103, 133-143

Classical vs. non-classical pathways of crystallization

J. J. DE YOREO^{1*}, D. LI¹, M. H. NIELSEN², L. M. HAMM³
AND P. M. DOVE³

¹Pacific Northwest National Laboratory, Richland, WA 99352, USA, (james.deyoreo@pnl.gov)

²Department of Materials Science and Engineering, University of California, Berkeley, 94720 USA,

³Department of Geosciences, Virginia Tech, Blacksburg VA 24061, USA (pdove@vt.edu)

Recent investigations on diverse mineral systems suggest formation begins with pre-nucleation clusters and proceeds by particle-mediated growth processes involving amorphous or disordered precursors, with the primary nanoparticles often found to be co-aligned in the final crystal. Little is known, however, about the energetics of pre-nucleation clusters, the role of mineral interfaces in altering formation pathways, or the mechanism by which co-alignment of primary particles occurs. Here we analyze the impact of pre-nucleation clusters on predictions of classical nucleation theory (CNT) and report results of novel *in situ* TEM, AFM and optical investigations of both the early stages of CaCO_3 and Ca-phosphate nucleation and post-nucleation oriented aggregation of ferrihydrite nanoparticles.

Our analyses show the classical barrier to homogeneous calcite nucleation is prohibitive even at concentrations approaching the ACC solubility limit [1]. Introducing a population of metastable clusters can dramatically reduce the barrier, but clusters stable with respect to the free ions will increase it. To explore the impact of surfaces on barriers, we examined calcite nucleation on alkane thiol SAMs and found it to be described well by CNT through a reduction in the barrier due to decreased interfacial free energy, which we found scales linearly with SAM-crystal binding free energies, as expected classically. In contrast, AFM data in the Ca-phosphate system [2] shows the amorphous precursor phase forms at supersaturations too low to be sensible within CNT.

To follow initial growth after nucleation, we investigated the interactions between ferrihydrite nanoparticles using high-resolution fluid cell TEM [3]. The particles undergo continuous rotation and interaction until they find a perfect lattice match. A sudden “jump to contact” then occurs over < 1nm, followed by lateral ion-by-ion addition at the contact point. We show that direction-specific interactions drive oriented attachment and likely result from electrostatic forces.

[1] Hu *et al.* (2012), *Faraday Disc.* **159**, 509-523.

[2] Habraken *et al.* (2013) *Nature Comm.* **4**, 1507.

[3] Li *et al.* (2005), *Science* **306**, 1014-1018.

The composition of the new continental crust through time

BRUNO DHUIME^{1,2}, CHRIS HAWKESWORTH¹
AND PETER CAWOOD¹

¹ University of St Andrews, Department of Earth & Environmental Sciences, UK (b.dhuime@bristol.ac.uk)

² University of Bristol, Department of Earth Sciences, UK

Recent models on continental growth suggest that ca. 65% of the present volume of the continental crust was present by 3 Ga, and that the rates of continental growth were significantly higher before 3 Ga than subsequently. This change has been tentatively linked to the onset of subduction-driven plate tectonics and discrete subduction zones. If correct this represents a fundamental change in the evolution of the Earth, with implications for the nature of the magmas generated, the efficiency with which crustal material is returned back into the mantle and the cooling history of the Earth.

Because of the poor preservation of rocks and minerals after billions of years of crustal evolution, a major uncertainty remains about the composition of new, juvenile continental crust in the Hadean and the Archaean and hence the conditions and the tectonic setting(s) in which it was generated. One way forward is to evaluate the composition of new continental crust from the time-integrated parent/daughter ratios of isotope systems in magmatic rocks subsequently derived from that new crust.

Crustal differentiation processes produce a large range of highly fractionated Rb/Sr ratios because of the highly incompatible character of the Rb-Sr system. As a consequence mafic crust typically has Rb/Sr at least five times lower than intermediate/felsic bulk crust. We calculated time-integrated Rb/Sr in crustal material with pre- and post-3 Ga Nd model ages. Preliminary data indicate that time-integrated Rb/Sr were, on average, much lower in the Hadean/Mesoarchaean than subsequently. This suggests that new continental crust was principally mafic over the first 1.5 Ga of Earth evolution, that a large volume of pre-3 Ga crust may have been associated with intraplate magmatism, and that ~3 Ga may indeed mark the onset of plate tectonics on Earth.

Simulation of water–rock interaction and porosity evolution in a granitoid-hosted enhanced geothermal system

L.W. DIAMOND AND P. ALT-EPPING

Rock–Water Interaction, Institute of Geological Sciences, University of Bern, Switzerland (*correspondence: diamond@geo.unibe.ch)

Numerical simulations based on plans for a deep geothermal system in Basel, Switzerland are used here to understand chemical processes that occur in an initially dry granitoid reservoir during hydraulic stimulation and long-term water circulation to extract heat. A question regarding the sustainability of such enhanced geothermal systems (EGS) is whether water–rock reactions will eventually lead to clogging of flow paths in the reservoir. A reactive transport model allows the main chemical reactions to be predicted and the resulting evolution of porosity to be tracked over the expected 30-year operational lifetime of the system.

The simulations show that injection of surface water to stimulate fracture permeability in the monzogranite reservoir at 190 °C and 5000 m depth induces strong redox reactions. Although new calcite, chlorite, hematite and other minerals precipitate near the injection well, their volumes are low and more than compensated by those of the dissolving wall-rock minerals. Thus, during stimulation, reduction of injectivity by mineral precipitation is unlikely.

During the simulated long-term operation of the system, the main reactions are the hydration and albitization of plagioclase, the alteration of hornblende to an assemblage of smectites and chlorites and of primary K-feldspar to muscovite and microcline. Within a closed-system doublet, the composition of the circulated fluid changes only slightly during its repeated passage through the reservoir, as the wall rock essentially undergoes isochemical recrystallization. Even after 30 years of circulation, the calculations show that porosity is reduced by only ~0.2%, well below the expected fracture porosity induced by stimulation. This result suggests that permeability reduction owing to water–rock interaction is unlikely to jeopardize the long-term operation of deep, granitoid-hosted EGS systems.

A peculiarity at Basel is the presence of anhydrite as fracture coatings at ~5000 m depth. Simulated exposure of the circulating fluid to anhydrite induces a stronger redox disequilibrium in the reservoir, driving dissolution of ferrous minerals and precipitation of ferric smectites, hematite and pyrite. However, even in this scenario the porosity reduction is at most 0.5%, a value which is unproblematic for sustainable fluid circulation through the reservoir.

Sulfurization of humic acids during early diagenesis in surface sediments of a tropical upwelling system

RUT DIAZ^{1*}, URSULA MENDOZA¹, MICHAEL E. BÖTTCHER², MANUEL MOREIRA¹, WILSON MACHADO¹, R. CAPILLA³ AND ANA L. ALBUQUERQUE¹

¹Projeto Ressurgência Team, Programa de Geoquímica Ambiental, Universidade Federal Fluminense, Outeiro São João Baptista s/n. - Niterói RJ 24020-150, Brazil
(*correspondence: rutdias@geoq.uff.br)

²Geochemistry & Isotope Geochemistry Group, Marine Geology Section, Leibniz Institute for Baltic Sea Research Warnemünde, D-18119 Warnemünde, Germany.

³Petrobras–Cenpes, Cidade Universitária, Ilha do Fundão, RJ 21941-915, Brazil

The early diagenesis of sulfur and the potential impact on sulfurization of humic acids (HAs) was followed in several short sediment cores from the continental shelf under the influence of a tropical upwelling system (Cabo Frio, Brazil). Besides contents and elemental stoichiometries of organic matter (OM), HAs, and the kerogen fractions, their stable isotope composition of carbon, nitrogen and sulfur was followed and compared, for instance, with the composition of sedimentary pyrite. Based on ²¹⁰Pb and ¹⁴C dating, the investigated parts of the sediments span a range up to 2 ka cal BP.

The stable carbon and nitrogen isotope compositions of OM indicate a dominant marine source with no significant contributions from anthropogenic N sources, as also found in the HA fraction. It is found, that the atomic C/N ratios of HAs increased with depth with a corresponding shift towards negative in the stable sulfur isotope ratios. The sulfur isotope ratios cover a range between -8 and +5 ‰, being significantly enriched in the lighter isotope compared to sea and pore water sulfate (about +21‰), but depleted with respect to co-existing pyrite (between -27 and -42‰). Sulfur isotope ratios do not correlate with the S/C ratios, but indicate an increasing contribution of diagenetic sulfur with depth, which is estimated based on a stable sulfur isotope mass balance approach.

Anoxygenic Cyanobacterial Mats in Middle Island Sinkhole, Lake Huron: An Analogue of the Precambrian

GREGORY J. DICK^{1,2,*}, LAUREN KINSMAN-COSTELLO¹, NATHAN D. SHELDON¹, BOPI A. BIDDANDA³, DANIEL N. MARCUS¹, ALEX A. VOORHIES¹, MICHAEL J. SNIDER³, AND TIMOTHY M. GALLAGHER¹

¹Dept. Earth and Environmental Sciences (*correspondence: gdick@umich.edu), ²Dept. of Ecology and Evolutionary Biology, University of Michigan, Ann Arbor, MI, 48109, USA, ³Annis Water Resources Institute, Grand Valley State University, Muskegon, MI, USA

Cyanobacteria are well recognized as the innovators of oxygenic photosynthesis and as critical agents of Earth's oxygenation. Although most of the evolutionary history of cyanobacteria was characterized by low-O₂ and/or redox-stratified environments, little is known about cyanobacteria that operate under these conditions or the potential signatures that they might leave in the geologic record. The Middle Island Sinkhole (MIS) in Lake Huron (USA) provides a valuable analogue of such Precambrian cyanobacterial mat systems. Groundwater rich in sulfur and low in O₂ fosters benthic cyanobacterial mats that thrive under persistent low-O₂, sulfidic conditions. Just beneath the mats is a thin calcite-rich layer of carbonate followed by organic-rich sediments with sulfate-reducing and methanogenic communities [1].

MIS mats are capable of both oxygenic and anoxygenic photosynthesis and have genes for sulfide oxidation (sulfide quinone oxidoreductase) [2]. However, genes for the biosynthesis of hopanoids, a commonly used biomarker of cyanobacteria, are absent [2]. Metatranscriptomic data points to the prevalence of viral predation, transposases, and the production of accessory pigments for light harvesting. To further evaluate potential geologic signatures of anoxygenic cyanobacterial mat systems, we are now characterizing the stable carbon and nitrogen isotope composition of the organic fraction of mats and sediments as well as mineralogy and carbon isotope content of carbonates.

[1] Nold, S. *et al.* (2010) *Appl Environ Microbiol* 76:347-351; [2] Voorhies, A. *et al.* (2012) *Geobiol* 10: 250-267.

Focused Mantle Melting

H.J.B. DICK^{1*} AND H. ZHOU²

¹Woods Hole Oceanographic Inst., Woods Hole, MA 02543

(*correspondence: hdick@whoi.edu)

²Tongji University, Shanghai China (zhouhy@tongji.edu.cn)

Na₈ and Fe₈ represent the composition of mid-ocean ridge basalt corrected for fractional crystallization back to bulk MgO of 8 wt.% (Klein and Langmuir, JGR, 1987). Decreasing Na₈ is widely accepted as reflecting increasing extents of mantle melting, while increasing Fe₈ greater depths of melting due to higher mantle potential temperature. Variations in these variables over several oceanic rises are consistent with hotter deeper melting with proximity to the associated mantle hotspots. However, this interpretation of Na₈-Fe₈ does not fit all ocean rises. Some have thin crust over the rise (Zhou and Dick, Nature, 2013) while others have high Na₈ and low Fe₈ at the peak of the rise, opposite to the prediction based on KL87. Their approach assumed a constant mantle source composition, which thus presents a problem given the variability of mantle mineralogy along ocean ridges. While the rationale for decreasing sodium with extent of melting is well understood and accepted (e.g.: Dick *et al.*, 1984), this is not the case for Fe₈. The explanation of KL87 was that melts from different depths would pool and escape the mantle, and thus record an average melting depth. This explanation however appears inconsistent with substantial mineralogic evidence in abyssal peridotites for shallow melt re-equilibration. Thus a thermodynamically consistent explanation for Fe₈ has until now not been found.

It is widely accepted that at ocean ridge melt focusing to the ridge axis occurs in the underlying mantle. We have thus undertaken modeling of focused melting beneath ocean ridges using PMELTS (Ghiorso *et al.*, G3, 2002) to see if variations in depth of melting or mantle source composition can provide a thermodynamically consistent explanation for Fe₈. This is done by successively removing solid increments while conserving melt during incremental batch equilibrium melting as an analog for the ocean ridge melting regime. This differs from modeling fractional melting, by the same technique, in that we progressively remove solid from the bulk composition rather than melt. This represents an evolving bulk composition in such a way that it explains why Fe₈ increases with increasing depth and temperature of melting, but also shows that the effect of varying mantle source composition is at least as important as the effect of temperature. Thus, by varying both temperature and mantle composition we can explain increasing Fe₈ with decreasing Na₈ over ocean rises with both thick and thin crust.

Osmium isotope records of continental weathering and volcanism spanning the Paleocene-Eocene Thermal Maximum

ALEXANDER J. DICKSON,^{1,2} ANTHONY S. COHEN,²
ANGELA L. COE,² MARC DAVIES,² EKATERINA
SHCHERBININA³ AND YURI GAVRILOV³

¹Department of Earth Sciences, University of Oxford, South Parks Road, Oxford, OX1 3AN, United Kingdom.

²Department of Environment, Earth and Ecosystems, Centre for Earth, Planetary and Space Science, The Open University, Walton Hall, Milton Keynes, MK7 6AA, United Kingdom.

³Geological Institute, Russian Academy of Sciences, Pyzhevsky 7, Moscow 119017, Russian Federation.

The Paleocene-Eocene Thermal Maximum (PETM) was one of several brief global warming events that took place superimposed on a long-term warming trend during the early Eocene. The cause of the rapid warming has been attributed to the introduction of large amounts of carbon dioxide to the atmosphere and oceans, but the trigger for initial carbon release, and the mechanisms that sequestered it back into non-exchangeable reservoirs have been debated.

New osmium (Os) isotope records spanning the PETM are presented from four sites located in the Arctic and Tethys Oceans. All sites exhibit an increase in ¹⁸⁷Os/¹⁸⁸Os ratios during the PETM compared to pre- and post-event background values. The magnitude of this increase is consistent between sites and previously published records, and indicates a ~40% increase in the flux of radiogenic Os from weathered continental rocks to the oceans during the main phase of global warming.

The new Os-isotope data also contain two lines of evidence that support the role of volcanism as a trigger for the PETM. Firstly, the Arctic-Ocean record exhibits a shift to more radiogenic ¹⁸⁷Os/¹⁸⁸Os ratios >50,000 yrs prior to the onset of the PETM (as defined by the negative carbon isotope excursion), associated with volcanic uplift of the North Atlantic Seaway and hydrographic restriction in the Arctic Basin. Secondly, the Tethys sites exhibit a rapid excursion to very low ¹⁸⁷Os/¹⁸⁸Os ratios coincident with the onset of the PETM, indicating a larger flux of unradiogenic (volcanic-derived) Os to the oceans at this time. The new data suggest that volcanic activity became pronounced close to, but preceding, the start of the PETM, and therefore could have set in motion climate-system feedbacks (such as ocean circulation changes) that eventually triggered the release of large amounts of carbon at the Paleocene/Eocene boundary.

Incorporation of a Pertechnetate analog – Perrhenate – by Sodalite in Competition with other Anions

JOHNBULL DICKSON¹, JAMES HARSH¹ AND ERIC PIERCE²

¹Washington State University, Pullman, WA, USA,
(j.dickson@wsu.edu)

²Oak Ridge National Laboratory, Oak Ridge, TN, USA

Spent nuclear fuel/waste is dubbed “one of the most hazardous substances ever created by humans” and the U.S. is credited with 104 nuclear power plants that have already generated 70,000 metric tons of radioactive waste. Currently these spent nuclear fuel/wastes are being stored in swimming-pool-like tanks, and steel/concrete tanks at reactor sites in 33 U.S. States due to lack of permanent repository (C&EN, 2012). Radionuclide contamination at nuclear sites and power plants are a worldwide hazardous waste problem. Technetium-99 (⁹⁹Tc), a long-lived radionuclide at select DOE waste sites, presents a major concern due to its long half-life (211,000 y) and high mobility in oxidized subsurface environments. ⁹⁹Tc contamination has been found in the sediments beneath the Washington State Hanford Site Tank Farms after leakage of caustic, Al-rich, and high ionic strength high-level waste (HLW) solutions. Due to these releases, ⁹⁹Tc inventory (5.31x10³ Ci) is predicted to leach into the ground water table at concentrations in excess of the MCL of 53 µg L⁻¹. Interestingly, nearly 50 years after the release of the contaminant into the environment, most of the ⁹⁹Tc persists in the deep subsurface sediment. We hypothesize that the formation of feldspathoid-type minerals within native Hanford sediment is sequestering ⁹⁹Tc. Previous studies demonstrated ⁹⁰Sr and ¹³⁷Cs incorporation into feldspathoid minerals, such as sodalite, that formed as a result of contact between Hanford primary silicate minerals and HLW solutions [1, 2]. To elucidate the role of competing anions on TcO₄⁻ incorporation, we used ReO₄⁻ as an analog to synthesize various anionic sodalites. The pure and mixed anion-bearing sodalites were characterized by XRD, XRF, electron microprobe, and wet digestion. ReO₄⁻ concentrations in the resulting sodalite samples ranged from 13 mmol kg⁻¹ in the mixed-anionic sodalites to 760 mmol kg⁻¹ in the pure ReO₄⁻ sodalite. Prolonged aging appeared to increase crystallinity; however, enclathration of ReO₄⁻ into the sodalite framework with time was inconsistent. Using the 211 x-ray diffraction peak of sodalite, the unit cell parameter linearly increased with increasing anionic radius. These data imply that ⁹⁹Tc found in Hanford tank waste stream loaded with smaller competing anions (NO₃⁻, NO₂⁻, Cl⁻, SO₄²⁻, etc.) is unlikely to be sequestered into sodalite. As sodalite group mineral can deform to host guest anions of varying ionic sizes, detailed information on the structural refinements for these various mixed anion-bearing sodalites will shed light on the tilting/deformation of sodalite framework structure. Our future work will be directed at elucidating these structural changes and conditions under which Tc incorporation might be favored.

[1] Chorover, *et al.* 2008, GCA 72, 2024-2047. [2] Deng Y., *et al.* 2006, Applied Geochemistry, 21, 1392-1409.

Formation and transformation of nanocrystalline iron carbonate precursors

K. DIDERIKSEN¹, C. FRANDSEN², N. BOVET¹, A.F. WALLACE³, T. ARBOUR⁴, J. DEYOREO⁵, S.L.S. STIPP¹ AND J. F. BANFIELD⁴

¹Nano-Science Center, Dept. of Chemistry, University of Copenhagen, Denmark (knud@nano.ku.dk)

²Dept. of Physics, Technical University of Denmark

³Earth Sciences Division, Lawrence Berkeley National Laboratory, USA

⁴Dept. of Earth & Planetary Science, University Of California, Berkeley, USA

⁵Molecular Foundry, Lawrence Berkeley National Laboratory, USA

Fe(II)-carbonates, such as siderite, form in environments where O₂ is scarce, e.g. during marine sediment diagenesis, corrosion and possibly CO₂ sequestration but little is known about its formation pathways. Precipitates from carbonate solutions containing 0.1 M Fe(II) with varying pH produced broad peaks in X-ray diffraction and contained Fe and CO₃ when probed with X-ray photoelectron spectroscopy.

In pair distribution function (PDF) analysis, peaks are limited to interatomic distances below 1.5 nm. The peaks are well defined compared to those for amorphous calcium carbonate and differ in position from those for known iron carbonates and hydroxides, indicating that a previously unidentified nanocrystalline iron carbonate had formed. Also, Mössbauer spectra differ from that expected for known iron carbonates and suggest a less symmetric structure. Replica exchange molecular dynamics simulations of Fe-carbonate clusters yield PDF peak positions that agree well with those from experiments. PDF measurements of samples aging in solution coupled with refinement with the software PDFgui show that the material transforms to siderite within hours and that the transformation rate depends on pH (Fig. 1).

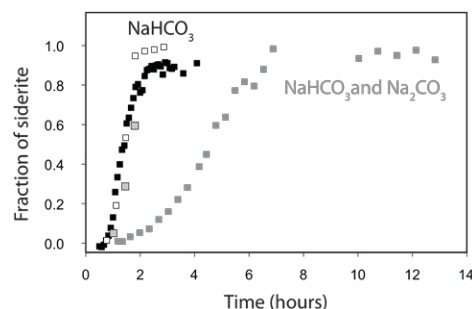


Figure 1: Fraction of siderite as a function of time from PDF

NanoSIMS mapping combined to *in situ* trace element analyses and U-Th-Pb dating in monazite: a chemical record of three successive events.

A. DIDIER^{1*}, V. BOSSE¹, S. MOSTEFAOUT², J. BOULOTON¹, J.L. DEVIDAL¹ AND J.L. PAQUETTE¹

¹ Clermont Université, Université Blaise Pascal, Laboratoire Magmas et Volcans, BP 10448, 63000 Clermont-Ferrand, France.

(*Correspondence : a.didier@opgc.univ-bpclermont.fr)

² Laboratoire de Minéralogie et Cosmochimie du Muséum, UMR 7202, CNRS INSU, Muséum National d'Histoire Naturelle, 57 Rue Cuvier, 75231 Paris Cedex 05, France

Monazite is an accessory mineral used for U-Th-Pb dating usually displaying complex chemical and isotopic zoning reflecting physical and chemical changes in the host rock. Chemical variations in the monazite were described at nm-scale while isotopic variations are known at few μm scale. In order to better understand the ages recorded by monazite it is necessary to obtain informations at smaller scale. In this context, the NanoSIMS appears to be the best suited tool. We present ⁸⁹Y, ¹³⁹La, ²⁰⁸Pb, ²³²Th and ²³⁸U, mapping on monazite from metapelitic xenoliths enclosed in andesitic lava (Slovakia). The xenolith/lava interaction is characterized by the growth of a plagioclase-bearing corona surrounding the xenolith and the overgrowth of magmatic garnet on partially resorbed metamorphic garnet. NanoSIMS images and LA-ICP-MS trace elements measurements evidenced variations of the HREE, Y and Eu contents in monazite correlated to breakdown and/or growth of garnet and plagioclase. Three domains have been distinguished: a first one corresponding to the core of the monazite grains is inherited from the metapelite protolith (308 ± 9 Ma) and characterized by low Y, HREE content and low Eu negative anomaly. A second domain crystallized during the growth of the plagioclase magmatic corona (high negative Eu*) and the resorption of the metamorphic garnet (low HREE and Y contents). A third domain crystallized with the presence of the plagioclase corona (high negative Eu*) and during the crystallization of the magmatic garnet (low Y, HREE contents) is dated at 13 ± 5 Ma, i.e. the age of the andesitic lava. Owing to its small size, the second domain was not accurately dated. ²⁰⁸Pb/²³²Th map performed with NanoSIMS demonstrates that it has the same isotopic ratio and corresponding age than the third domain. Thus monazite is able to track and date all mineralogic reactions occurring in the metapelites during the thermo-metamorphism resulting from xenolith/lava contact.

Detection of a dissolved alpha emitter by electro-precipitation

A. DIENER¹, C. WILHELM¹ AND U. HOEPPENER-KRAMAR¹

¹ Karlsruher Institut für Technologie, Sicherheitsmanagement Analytische Labore, 76344 Eggenstein-Leopoldshafen (correspondence: alexander.diener@kit.edu)

The drinking water distribution system is vulnerable to radioactive contaminations which could arise by nuclear accidents or by terrorist's attack. In this regard, alpha emitters (e.g. Po-210, U-235, Np-237, Pu-239, Am-241) could be brought into reservoirs or water treatment plants. The task of our research is the development of an *in situ* measurement system which bases upon electro-precipitation of the dissolved alphas on artificial surfaces.

Therefore, we wanted to figure out which elements in drinking water disturb our measurements. It consists of the sensor (diamond doped Si-waver), NaNO₃ as electrolyte and Am-241 as radioactive tracer. Published median or maximum concentrations for European drinking water were the basis for the synthesis of typical or highly concentrated drinking water for main (HCO₃, Ca, SO₄, Cl, Na, K, Mg, NO₃) and minor elements (Sr, F, Ba, PO₄, Zn, B, Br, Cu, I, Fe, Li, Al).

The results (Fig.1) show that the chemical yield is highest (~25%), if there is only the radioactive tracer next to the electrolyte present in solution. The median concentrations of the main and minor elements disturb only slightly while high concentrations of Ca, Mg, F, Ba, PO₄ let the yield decrease significantly, with a loss of up to 50%.

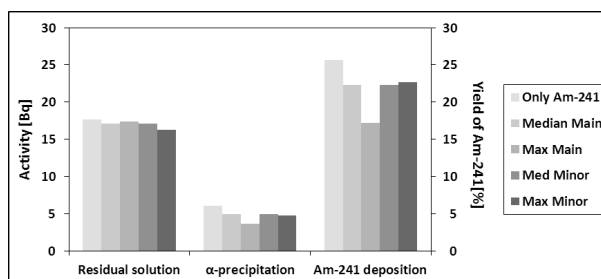


Fig.1: Comparison of the average amount of precipitated Am-241 (initial 21 Bq activity).

Towards *in situ* determination of sulfur speciation in fluids at high P-T at controlled redox conditions

M. DIETRICH^{1*}, H. BEHRENS¹, C. SCHMIDT²
AND M. WILKE²

¹Institut für Mineralogie, Leibniz Universität Hannover, Callinstr. 3, 30167 Hannover, Germany (*correspondence: m.dietrich@mineralogie.uni-hannover.de), (h.behrens@mineralogie.uni-hannover.de)

²Chemie und Physik der Geomaterialien, Sektion 3.3, Helmholtz-Zentrum Potsdam, Deutsches Geoforschungszentrum, Telegrafenberg, D 324, D-14473 Potsdam, Germany (christian.schmidt@gfz-potsdam.de), (max.wilke@gfz-potsdam.de)

Sulfur-bearing fluids play an important role in the degassing of magmas and in the formation of certain types of ore deposits. Since high temperature fluids are often not quenchable, central issue in this study is to investigate sulfur speciation in such fluids *in situ* at high pressure and temperature using Raman spectroscopy. Therefore a new sapphire-based cell is developed which allows abrupt or continuous changes of pressure at constant temperature, operating at pressures up to 200 MPa and temperatures up to 800°C. The concept is based on a flexible gold bag which separates the pressure medium from the fluid inside the cell to avoid any reaction between the sample fluid and steel components. Oxygen fugacity (f_{O_2}) is a key parameter determining the stability of sulfur species in the fluid. In the experiments the redox conditions are either pre-adjusted by the loaded fluid components or controlled by adding a specially designed open buffer capsule filled with Fe/FeO, Co/CoO, Ni/NiO or other redox pairs. Corundum powder on top of the buffer material acts as a getter for transition metal ions. Thus, penetration of these ions to the volume probed by Raman spectroscopy is avoided. First tests with the Fe/FeO buffer demonstrate the efficiency of the buffer assembly. Raman spectra recorded on the post-experimental solution show mainly HS⁻ besides a small amount of sulfate. EDX (energy dispersive X-ray spectroscopy) analyses of the buffer after the experiment indicate formation of Fe-spinel in the reaction zone of the capsule but FeO and metallic iron was also found. These observations give evidence that the buffer assembly has high potential to control redox conditions in the spectroscopic cell.

Ambient aerosol measurements and particle characterization at highly frequented motorways in Germany

DIETZE V, BAUM A, KAMINSKI U, SURKUS B, STILLE P,
WENZEL M AND GIERÉ R

¹Deutscher Wetterdienst (DWD), Referat Lufthygiene, Zentrum für Medizin-Meteorologische Forschung, 79104 Freiburg, Germany (volker.dietze@dwd.de)

²Bundesanstalt für Straßenwesen (BASt), Referat V3 – Umweltschutz, 51427 Bergisch Gladbach, Germany

³Laboratoire d'Hydrologie et de Géochimie de Strasbourg, Université de Strasbourg, UMR 7517 CNRS, 67084 Strasbourg, France

⁴Institut für Geo- und Umweltwissenschaften, Albert-Ludwigs-Universität, 79104 Freiburg, Germany

Based on projected future climate scenarios (e.g. heat waves with droughts) in combination with the assumption of no additional reduction in particle emissions, the Intergovernmental Panel on Climate Change (IPCC) predicts a general decrease in air quality in the future. A recent study estimates that in central Europe, the contribution of non-exhaust particulate matter (e.g. brake dust, tire wear, as well as suspension and re-suspension from the road surface) to total traffic emissions will increase to 80 – 90% by the end of this decade [1].

With the competence of BASt and DWD, and in cooperation with the Universities Strasbourg and Freiburg, a long-term monitoring program for coarse and fine particulate matter [2] was started in early 2013. To validate in a first approach the above-mentioned prediction [1], intense field measuring campaigns during different meteorological conditions are being carried out. The aim of this study is to determine size and optical density of individual particles (d_p ; 2.5 - 10 μm) by using computer-controlled single-particle optical microscopy. For selected samples, the chemical composition as well as geometric and morphological characteristics of individual particulates will be analyzed by manual, semi-automated, and fully computer-aided Scanning Electron Microscopy (SEM) combined with energy-dispersive X-ray (EDX) spectroscopy (Genesis, EDAX). Particles will be classified according to their chemical composition and assigned to, e.g., various mineral classes, which provide source information.

[1] Rexeis, M., Hausberger, S. (2009): Atmospheric Environment 43, 4689–4698;

[2] Kaminski, U., Fricker, M., Dietze, V. (2013): Meteorologische Zeitschrift 22, (in press).

Evidence from *n*-alkanes for ancient organic matter sources in Lake Superior

NADIA DILDAR^{1*} AND FRED J LONGSTAFFE^{1*}

¹Department of Earth Sciences, The University of Western Ontario, London, Ontario, N6A 5B7, Canada

(*correspondence: ndildar@uwo.ca, flongsta@uwo.ca)

Stable carbon isotopic compositions and abundances of individual *n*-alkanes have been analyzed for sediment cores from the Ile-Parisienne, Duluth and Caribou sub-basins of Lake Superior to investigate the source(s) of organic matter since 11,000 cal yr BP. In Lake Superior, the individual abundances of C₂₁ to C₃₁ *n*-alkanes are very much higher than obtained for C₁₇ or C₁₉ *n*-alkanes. The relative contributions of terrestrial versus aquatic organic matter have been estimated using the following ratio of *n*-alkane abundances: [C₂₅ to C₃₁]/[C₁₇ to C₂₃]. This ratio is highest in the glacial (≥ 8800 cal yr BP) sediments, and then decreases upwards in the postglacial (< 8800 cal yr BP) sediments. This trend suggests a progressive decrease in the relative abundance of terrestrial higher plants versus macrophytes in the post-glacial lake sediments. The carbon isotopic compositions of the C₂₅ – C₃₁ *n*-alkanes are more or less constant (–32 to –29 ‰) in each core over the entire sampling interval. These results suggest similar sources for these compounds throughout glacial and post-glacial times. However, the C₂₁ and C₂₃ (macrophytic) *n*-alkanes exhibit a pronounced shift in carbon isotopic composition from –29 to –37 ‰ over a ~800-1100 year period beginning at the boundary between glacial and post-glacial sedimentation. The much lower carbon isotopic macrophyte signature suggests quite different conditions for formation of the C₂₁ and C₂₃ *n*-alkanes found in the post-glacial sediments. This shift was likely a response to the massive alteration of the climate system, and associated aquatic and catchment ecosystem reorganization – including plant species changes – that occurred during this time.

Pleistocene weathering and climate evolution in southern Italy: data from intermontane basins

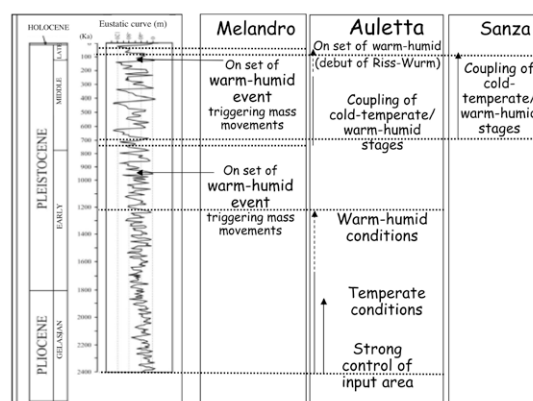
PAOLA DI LEO^{1*}, SALVATORE IVO GIANO², DARIO GIOIA², IOLANDA PULICE¹ AND MARCELLO SCHIATTARELLA²

¹ CNR-IMAA, Tito scalo (PZ), Italy (*correspondence: pdileo@imaa.cnr.it)

² Dipartimento di Scienze, Basilicata University, Potenza, Italy (marcello.schiattarella@unibas.it)

³ CNR-IBAM, Tito scalo (PZ), Italy (dario.gioia@ibam.cnr.it)

In order to reconstruct the Pleistocene climate- and morpho-evolution of southern Italy, a multidisciplinary approach has been adopted and a multiproxy dataset implemented using geomorphological, mineralogical and geochemical information collected from three intermontane basins of the southern Apennines axial zone (Melandro, Auletta, and Sanza basins, Basilicata and Campania regions). To get this goal, a quantitative evaluation of eroded rock volumes were estimated by comparing uplift and erosion rates using both geological and geomorphological markers such as paleosols, weathering horizons, erosional surfaces, and paleolandslides. Besides, the calculated erosion rates were set in the evolving paleoclimate scenarios defined by means of proxies based on mineralogy (specifically clay minerals distribution) of soils, paleosols, weathering horizons developed onto differently aged erosion/depositional surfaces, and of continental sediments from key areas of southern Apennines, and on geochemical distribution of major, trace, and rare earth elements, and of stable isotopes. Since erosion rates from the three basins investigated are quite similar in a mid- long-term time interval (~1 Ma),



mineralogical and geochemical data may be used as suitable and comparable proxies to decipher the evolution of paleoclimate conditions. Coupling of cold-temperate/warm-humid climate stages seems to be the recurrent condition responsible for the genesis and evolution of ancient landscapes of the orogenic belt – including regional-scale erosional paleosurfaces – as well as a control factor in triggering mass movements.

GEMAS results at a regional scale: the Alps

E. DINELLI^{1*}, V. LANCIANESE¹, S. ALBANESE², M. BIRKE³, B. DE VIVO², M. GOSAR⁴, E. HASLIGER⁵, P. HAYOZ⁶, H. REITNER⁷, I. SALPETEUR⁸
AND GEMAS PROJECT TEAM

¹I.G.R.G, Università di Bologna, via S.Alberto 163, 48123

Ravenna (*correspondence: enrico.dinelli@unibo.it)

²Dipartimento di Scienze della Terra, Università di Napoli 'Federico II', Napoli, Italy

³Federal Institute for Geosciences and Natural Resources (BGR), Hannover, Germany

⁴Geological Survey of Slovenia Ljubljana, Slovenia

⁵Austrian Institute of Technology (AIT)

⁶Federal Office of Topography, Swiss Geological Survey;

⁷Geological Survey of Austria (GBA)

⁸BRGM, Mineral Resources Division

The GEMAS project involved the sampling and analysis of agricultural and grazing land soil over Europe at a sample density of 1 sample per 2500 Km². Among the complete database we selected the samples collected in the alpine mountain range partially exceeding the border of the Alpine convention and considering important geographic boundaries as the Rhone river to the West, the Danube river to the North and the Po River course to the South as major boundaries for sample selection.

We worked either on the total chemical content derived from XRF analysis and on the Aqua Regia data set for a total of 132 sites of grazing land soils and 119 sites for agricultural soil.

The analysis of the data set indicate minor differences between the two soil types. There is a clear control of bedrock geology, even if sample density is too low for the complex geology of the alpine mountain range. There are numerous several point anomalies for single elements associated either to known important mining areas or minor mineralizations or to various kinds of anthropogenic contributions. There are few sites with multi element anomaly in South Tyrol (Ag, Cd, Pb, Zn) located close to a well known mining area, and Slovenia. There are also extensive anomalies covering large area as displayed for example by As that between Switzerland and Italy displays a strong anomaly, important even on a continental scale [1], and recognized also in other matrices such as bottled mineral waters [2]. Also uranium shows a large anomalous area between in the central Alps between Austria and South Tyrol, related to mineralization.

[1] Tarvainen *et al.* (2013) *Applied Geochemistry* **28**, 2-10.

[2] Birke & Reimann (2010) *Geochemistry of european bottled water*, Borntraeger

Anthropogenic sulfate in the atmosphere decrease the carbon uptake by karst in rural area of SW, China

HU DING¹, CONGQIANG LIU^{2*}, YUNCHAO LANG³
AND TAO ZE LIU

State Key Laboratory of Environmental Geochemistry,
Institute of Geochemistry, CAS, China

¹ (dinghu@vip.skleg.cn)

² (liucongqiang@vip.skleg.cn)

³ (lanyc822@163.com)

³ (liutaoze81@163.com)

Sulfuric acid as a weathering agent has been recognized recently as not only enhancing weathering but also lowering CO₂ consumption rates. However, the impact of sulfuric deposition on carbonate weathering is still poorly explored, with most studies mainly focussed on large rivers that generally integrate over a number of processes and often average the situation from various backgrounds. In this study, we investigated the chemical compositions of rainwater and stream water of a karstic rural catchment located in Huanjiang County, Guagxi Province, SW of China to understand the impact of the atmospheric anthropogenic sulfate on carbon uptake by karst at rural area. The results showed that the sum of concentrations of Ca²⁺ and Mg²⁺ ([Ca²⁺+ Mg²⁺]) of stream water were in excess with respect to HCO₃⁻ ([HCO₃⁻]), with a mean [Ca²⁺+ Mg²⁺]/[HCO₃⁻] ratio of 1.1. Sulfate acid accounted for the excess of Mg²⁺ and Ca²⁺ relative to HCO₃⁻. The involvement of sulfuric acid in carbonate weathering caused about 6.5% increase of weathering rates, and meanwhile 14.8% decrease of the CO₂ consumption rates, of which the involvement of atmospheric anthropogenic sulfate accounted for about 9.6%. The data available at present indicate that even in the rural karst region of southwest China, the involvement of anthropogenic sulfate can largely decrease the carbon uptake rate by carbonate weathering.

This work was supported by the National Natural Science Foundation of China (Grant No. 41203090, 41073099 and 41003008).

The Chemical and Isotopic Characters of Suspended Particulate Materials in the Yangtze River and Their Environmental Implications

T. P. DING^{1,2,*}, J. F. GAO^{1,2}, G. Y. SHI³, F. CHEN³,
C. Y. WANG AND X. R. LUO

¹MLR Key Laboratory of Metallogeny and Mineral Assessment, IMR, CAGS, Beijing 100037, China.

*Correspondence: tding@cags.ac.cn

²MLR Key Laboratory of Isotope Geology, CAGS, Beijing 100037, China.

³Hydrological Bureau, CJW, Wuhan 430010, China

The mineral, chemical and isotopic compositions of the Suspended particulate materials (SPM) in the Yangtze River were determined systematically on the samples collected in the period of 2003 ~ 2007.

Large spacial and temporal variations of SPM contents are observed in the Yangtze River, reflecting the changes of flow speed, runoff and SPM supply. Significant SPM sedimentation in the Three Gorge Reservoir leads to increase of embankment washout in downstream section and reduction of sedimentation in the Dongting Lake, Poyang Lake and the estuary. The difference on mineral compositions indicates that the chemical weathering activity in the Yangtze area is more intensive than in the Yellow River area.

The SiO₂ and Na₂O contents in SPM of the Yangtze are higher than those of the Yellow River, reflecting the difference on weathering conditions. The (CaO + MgO)/SiO₂ ratio in the Yangtze SPM decreases downstream, reflecting also the change of weathering conditions.

The Co, Ni, Cu, Zn, Pb and Cd contents in the Yangtze River SPM are higher than the average values of the upper crust rocks. The contents of Cu, Zn, Pb and Cd in the Yangtze River SPM are several times higher than in the bed sediments, probably reflecting increase of mining activities in recent years. The REE distribution pattern of Yangtze River SPM is similar to that of upper crust, indicating that the source rocks in the Yangtze basin have chemical compositions similar to upper crust.

The δ³⁰Si variation range (-1.1‰ to 0.3‰) of the Yangtze SPM is similar to that of shale and lower than that of granite rocks, reflecting the silicon isotope fractionation in weathering process. The decrease trend of δ³⁰Si from upper reaches to middle and lower reaches may be interpreted by the increase of clay minerals downstream.

*This work was supported by the Ministry of Science and Technology (2004DIB3J081) and the Ministry of Land and Resources (Item No.20010209).

Sub-continental Nb/Ta and Zr/Hf amphibolites: implications on subduction metamorphism

XING DING^{1*} AND WEIDONG SUN²

¹State Key Laboratory of Isotope Geochemistry, Chinese Academy of Sciences, Guangzhou, P. R. China, (xding@gig.ac.cn) (* presenting author)

²Key Laboratory of Mineralogy and Metallogeny, Chinese Academy of Sciences, Guangzhou, P. R. China, (weidongsun@gig.ac.cn)

Mobilities and fractionations of high field strength elements (HFSEs), especially Nb and Ta within subducting slab, are important for deciphering the formation of the continental crust (CC)[1-4]. Here we report mineral and geochemical studies on epidote garnet amphibolite facies metagabbro located near the margin of an eclogite zone in the Tongbai-Dabie orogenic belt, central China. The samples were hydrated during prograde metamorphism of the Triassic plate subduction.

Major minerals such as amphibole, garnet, rutile and ilmenite and bulk rocks of the garnet amphibolite show overall lower Nb/Ta and Zr/Hf than the continental crust (sub-continental), suggesting major Nb/Ta and Zr/Hf fractionations during gabbro to amphibolite transformation. Nb/Ta in bulk rocks varies from 9.4 to 15.5, with the average of 11.3 while Zr/Hf changes from 30.7 to 36.3, with the average of 33.8. Notably, Nb/Ta in rutile varies from 11.5 to 24.2, with the average of 15.3 whereas Zr/Hf ranges from 12.7 to 51.7, averaging 23.8. LA-ICPMS *in situ* trace element analyses of rutile and amphibole grains display remarkable chemical zonations. In general, the cores of rutile are usually small with much higher Nb, Ta concentrations and lower Nb/Ta ratios compared to the thick rims. Such HFSE fractionations may be explained by diverse external fluid activities: the gabbro first absorbed low Nb/Ta fluids that were released during blueschist to amphibolite transformation in deeper portions of the subducting slab, followed by acquiring external fluids with elevated Nb/Ta released during amphibolite to eclogite transformation. Fluids with various Nb/Ta signatures can be transferred to cold regions within a subducting plate and also to the mantle wedge through fluid-rock reaction.

[1] Ding *et al.* (2013) *J. Geol.* **121**, doi: 10.1086/669978.

[2] Xiao *et al.* (2006) *Geochim. Cosmochim. Acta* **70**, 4770-4782. [3] Liang *et al.* (2009) *Chem. Geol.* **268**, 27-40. [4] Ding *et al.* (2009) *Int. Geol. Rev.* **51**, 473-501.

Petrological and textural constraints on explosive activity of the last 2ka of Turrialba volcano (Costa Rica)

A. DI PIAZZA^{1*}, C. ROMANO¹, G. DE ASTIS², A. VONA¹
AND G.J. SOTO³

¹Dip. di Scienze, Univ. Roma Tre, Italy

(andrea.dipiazza@uniroma3.it) (*presenting author)

²Istituto Nazionale di Geofisica e Vulcanologia Roma-1, Italy

³Instituto Costarricense Electricidad, San José, Costa Rica

We present here a throughout investigation of the last 2ka volcanic activity of the Turrialba volcano (Costa Rica), which shows signs of potential reawakening since 2006. In particular we choose two magmatic end members: a basaltic and an andesitic eruption. Mineral assemblage is composed by abundant plagioclase (An₃₀ – An₇₂), clino- and orthopyroxenes, and olivine crystals (Fo₆₉ – Fo₈₀). We studied the stratigraphy of proximal, intermediate and distal outcrops of the two eruptions. We calculated the parameters describing the vesicles spatial arrangement of our samples (i.e. the size, shape and number), as it records the conditions of ascent and degassing which determined the different explosivity of these eruptions. The andesitic samples were classified in two classes, differing in density and porosity: pumices (0.6 – 1.2 g/cm³; porosity 79-61%) and scoriae-like clasts (1.5 - 1.7 g/cm³; porosity 54-32%). Samples show maximum dimension of vesicles between 0.6 and 0.3 mm. The Vesicle Number Density is in the range 2.28–6.60 x 10⁸ cm⁻³, values comparable to those related to Plinian eruptions (e.g. Vesuvius 79 A.D.: 10⁸ - 10⁹ cm⁻³). The basaltic magma feeding the last observed eruption at Turrialba, generates highly porphyritic scoriae and bombs, with a final stage made of breadcrust bombs. Vesicle dimensions range between 0.30 – 2.37 mm. VND values range between 9.74 x 10⁵ cm⁻³ and 3.9 x 10⁶ cm⁻³ (values similar to Stromboli volcano or Hawaiian volcanoes activity). We can classify the 1864-66 A.D. activity as a powerful Strombolian eruption. This study highlights a wide spectrum of degassing processes which occurred at Turrialba volcano in the last 2ka, providing new insights into the eruptive behavior of this volcano.

Short crystal history in the recent magmatic system of Santorini volcano, Greece: inferences from micro-Sr isotope data

SARA DI SALVO¹, LORELLA FRANCALANCI¹,
TIM H. DRUITT² AND ELEONORA BRASCHI³

¹ Dipartimento di Scienze della Terra, Università degli Studi di Firenze, via la Pira, 4, Firenze, Italy.

² Clermont Université, Université Blaise Pascal, Laboratoire Magmas et Volcans, Clermont-Ferrand, France.

³ CNR-IGG, Sezione di Firenze, via La Pira, 4, Firenze, Italy.

Magma mineral phases retain the history of changing physical and chemical conditions during their growth due to the frequent occurring of mineral/liquid elemental and isotopic disequilibria. In many volcanic systems, indeed, bulk rock compositions often represent a mechanical mixture of various phases with possible different origin. Accordingly, analyses of ⁸⁷Sr/⁸⁶Sr on core-rim traverses of minerals give us the chance to understand the dynamics and timescales of magmatic processes during the ascent of magma to the surface. Micro-Sr isotope analyses, by microdrilling, have been used, therefore, for better understanding the volcanic system of the last 3.6 ka of Santorini history, from the huge explosive event of the Minoan eruption to the successive Kameni activity. The latter originated the Palea- and Nea-Kameni islets, inside the Minoan caldera, through nine mainly effusive subaerial events, from A.D. 46-47 to 1950. The erupted products are dacitic lavas including basaltic to andesitic enclaves, with Sr isotopes increasing with time in both enclaves and host lavas.

We focussed our micro-analytical study on the plagioclase crystals of the rhyodacitic pumices from the Minoan eruption and of the oldest and youngest post-caldera dacitic lavas. Different types of plagioclase have been identified based on textures and zoning patterns. Anorthite content overall varies between 35-90% in both systems. Contrarily to many other volcanic systems, ⁸⁷Sr/⁸⁶Sr values of plagioclase do not largely change within the single eruptive event and generally reflect the respective whole-rock values, except for some xenocrysts in Kameni lavas coming from the mafic enclaves. The different crystal types of the Minoan pumices have similar ⁸⁷Sr/⁸⁶Sr values, which are higher than those of the Kameni plagioclases. Our data suggest that the Kameni plagioclases record a short history, indicating small resident time and possible crystallization during the magma ascent, whereas the Minoan crystals do not testify any relationships with both the coeval mafic magmas and the later Kameni system.

Succession of soil microbial communities and enzyme activities in artificial soils

FRANZISKA DITTERICH¹, CHRISTIAN POLL¹, GEERTJE J. PRONK^{2,3}, KATJA HEISTER², INGRID KÖGEL-KNABNER^{2,3} AND ELLEN KANDELER¹

¹Institute of Soil Science and Land Evaluation, Soil Biology Section, University of Hohenheim, Emil-Wolff-Str. 27, D-70593 Stuttgart

²Technische Universität München, Lehrstuhl für Bodenkunde, Emil-Ramann-Straße 2, 85354 Freising

³Institute for Advanced Study, Technische Universität München, Lichtenbergstrasse 2a, D-85748 Garching

Microorganisms colonize selectively minerals and organo-mineral complexes. Less well known is whether the complexity of mineral composition of soils might determine microbial communities. The use of artificial soils that differ only in their mineral composition, but not in their organic composition, offers a unique possibility to study these microorganisms-mineral-interactions in soils. For the current study, a series of artificial soils of eight different compositions was designed from simple 2 component systems to more complex 3 to 4 component systems. The components used were the clay minerals illite and montmorillonite, ferrihydrite and boehmite as representation of iron and aluminum oxides, and charcoal. The formation of artificial soils was initiated by incubating these materials with sterilized manure as organic C source and a microbial community extracted from a natural arable soil for up to 18 months at 20°C in the dark. We quantified the enzyme diversity and the abundance of eight groups of bacteria at the phylum or class levels by using qPCR to characterize the function and structure of the microbial community of the original artificial soils. Simple 2 component systems using either illite or montmorillonite as clay component as well as treatments including charcoal showed a trend for lower abundance of soil microorganisms and lower enzyme activities. We detected a microbial succession of the soil microbial community from a dominance of *r* strategist (e.g. β -proteobacteria) during the first six months of the incubation towards systems with a higher dominance of *K* strategist (e.g. acidobacteria). The succession of enzyme activities gave clear evidence that nutrient limitations developed over time. Multivariate analysis of phospholipid fatty acid patterns revealed that nutrient limitation might also change the specificity of microbial colonization of different artificial soils towards more similar microbial population in all treatments at the end of the incubation.

Analysis of minerals in biofilms Using atomic force microscopy and raman spectroscopy.

MARIA DITTRICH^{1*}, THOMAS SCHMID² AND YONG ZHU¹

¹University of Toronto Scarborough, 1265 Military Trail, Toronto, ON, Canada, M1C 1A4 (*correspondence: mdittrich@utsc.utoronto.ca)

²Department of Chemistry and Applied Biosciences, ETH, Zurich, Wolfgang-Pauli-Str. 10, HCI D323, 8093 Zurich, Switzerland, (schmid@org.chem.ethz.ch)

Although biofilms play a significant role in geochemical cycling, the detailed structure and composition of biofilms is not known. Minerals within biofilms may be crucial for the transport of contaminants as surface reaction sites, e.g. for adsorption. A better understanding of these processes at the molecular scale will generate the basis for predictions at larger scales. An additional benefit of this approach will be an improved insight into the consequences that these processes have concerning the fate of inorganic pollutants in natural environments.

In order to obtain a better understanding of the structure of biofilms, spatially resolved chemical information is needed. Therefore, biofilms from different origins, e.g. grown in hot springs, and the precipitates from biofilms at the iron-rich spring, Bonifazius-spring (Scuola, Switzerland) were examined by atomic force microscopy (AFM) and Raman spectroscopy.

AFM images of the Fe-precipitates showed that the precipitates size can be from tens of nanometers to tens of micrometers, and their shapes of the precipitate varied from spherical, leaf-shape to irregular polygon. Raman spectra indicate that the spectral features of the precipitate are different, but are originated mainly from Goethite structure (FeOOH).

The AFM images resolved cell and extracellular polymeric substances (EPS) structures in the case of cyanobacterial biofilm. With the distinct Raman spectra, differentiation between EPS and cell material was possible. The Raman spectra at the supposed cell regions showed beta-carotene bands, whereas the other regions did not show any bands or much weaker beta-carotene bands. The obtained Raman map composed of specific marker bands was in good agreement with the different topological features of the AFM image, thus combining topographical and chemical information.

Geochemistry surveying of Kooh Kaftari metamorphism area (Iran - Shahrood)

DIVAN.Y¹., HASSNNEZHAD.A.A² AND ZAHIRI.R³

- 1.M. S. C. Economic geology, Department of Geology, Damqhan university., [Iran]
- 2.Assistant PROF. Economic geology, Department of Geology, Damqhan university[Iran]
- 3Assistant PROF. Mineralogist, Department of Geology, Damqhan university.,[Iran]

Metamorphism area of KoohKaftari in central part of Iran Located in 342000 to 348000 east and 3966000 to 3950000 north. This areas metamorphism was regional metamorphism with green schist facies or higher[1]. This study aimed to understand the economically major and minor elements in the region and their potential economic power. 15 prepared samples were sending to Labwest laboratory in Australia to analysis the samples by ICP-MS and ICP-OES for 61 main elements. All of the geochemical sample results mentioned as a group and the average were compared by the Continental Crust Clarke and upper Continental Crust Clarke to find the enrichment ratio of the area. Finally, elements such as Cr, Ba had positive enrichment and elements such as U, Zr had depleted, which indicate a lack of proper mineralization's of U, Zr in metamorphic rocks of there. Results of this comparison are presented in Table 1.

Elements	kooh kaftare	Continental crust		Upper continental crust	
		Clarke	EF	Clarke	EF
Fe%	3.74	5.63	0.66	3.52	1.06
Ca%	3.63	4.15	0.87	2.57	1.1
Ba	781.28	425	1.84	628	1.24
Cr	110.14	100	1.10	92	1.20
Zr	8.67	165	0.05	193	0.04
U	1.37	2.7	0.51	2.7	0.51

Table 1 - Comparison of mean values of metamorphic rocks of the continental crust and continental crust with average pigeon mountain upper.

[1] Huber, H. and Stocklin, J. (1956). Geological Report on the Torud- Moaleman area. N. I. O.C

Analysis of the turquoise color alteration based on the FTIR studies

DIVAN.Y¹., ZAHIRI.R² AND HASSNNEZHAD.A.A³

- 1.M. S. C. Economic geology, Department of Geology, Damqhan university., [Iran] (Yassind6@gmail.com)
- 2.Assistant PROF. Mineralogist, Department of Geology, Damqhan university.,[Iran] (zahiri@du.ac.ir)
- 3.Assistant PROF. Economic geology, Department of Geology, Damqhan university[Iran] (a.hassannezhad@du.ac.ir)

The Neyshabour turquoise ore of the NE Iran is at 36°, 28' latitude and 58°, 20' longitude. The XRF results (table 1), are obtained of the blue and green turquoise samples. Concerning to that the turquoise by the Fe increase and Al decrease has color alteration from the blue (B) to the green (G) rang, in this study we analyzed this variation by infrared spectrometry FTIR method and the results has shown at figure 1

Element	B	G	Element	B	G
Al ₂ O ₃	34.48	31.64	TiO ₂	0.04	0.07
Fe ₂ O ₃	1.57	6.68	SO ₂	0.60	0.66
CuO	9.61	9.27	Sb ₂ O ₃	0.60	0
P ₂ O ₅	30.04	28.22	L.O.I	21.11	19.66

Table 1: XRF The results

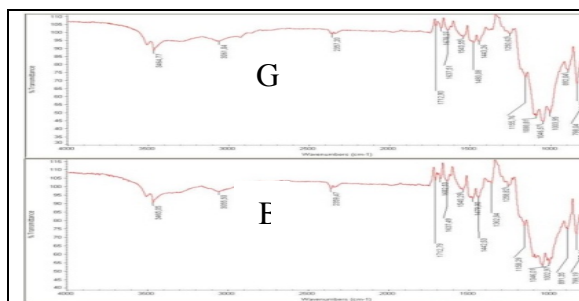


Figure 1: FTIR graphs

[1] Ray L. Frost ., B. Jagannadha Reddy., The molecular structure of the phosphate mineral turquoise Raman spectroscopic study., Journal of Molecular Structure 788 (2006) 224–231

Computational studies of hydrolysis reactions of CO₂ and actinides

DAVID A. DIXON,* K. SAHAN THANTHIRIWATTE, JOSHUA MOON, JESSICA DUKE AND VIRGIL E. JACKSON

Department of Chemistry, The University of Alabama, Shelby Hall, Box 870336, Tuscaloosa AL 35487-0336.

*(correspondence: dadixon@bama.ua.edu)

Advances in theory, algorithms, software, and computer architectures have made it possible to begin to calculate reliably the thermodynamics for geochemical processes in solution. The sequestration of CO₂ in geological formations can be used to mitigate global warming. A substantial amount of fundamental chemistry knowledge is still needed to ensure that the CO₂ does not have additional environmental impacts and that it remains in the subsurface. The supercritical CO₂ that is pumped into the ground will interact with H₂O and with various minerals. The properties and reactions of H₂O-CO₂ nanoclusters have been calculated at high levels of electronic structure theory and will be discussed. Issues with the electronic structure methods will be described. A surprising result is that CO₂ clusters can impact the hydrogen bonding in small H₂O clusters, which may impact reactivity. The important role of Lewis acid-base interactions in determining the structure of the clusters will be discussed. The hydrolysis of CO₂ in the presence of geochemically relevant metal ions in aqueous solution will be discussed. The metal cations can reduce the reaction barriers in part by changing the thermodynamics of the relevant reactions. The reactions of UO₂²⁺ with phosphates is of importance for extraction processes and for environmental remediation. The difficulties in predicting reliable properties for such systems will be discussed, especially for the solvation energetics. An important result is the critical role of CN 5 in the equatorial plane for these compounds. We find that there is both monodentate and bidentate binding depending on the nature of the PO₄H_x^{y-} and the number of water molecules in the first solvation shell. These studies have been performed at the density functional theory and correlated molecular orbital theory levels with a self consistent reaction field to model the continuum solvent.

This work is supported by the U.S. DOE Office of Sciences (BES).

Geochemical evidence for multiple gold mineralisation events in the Witwatersrand Basin

ROGER D. DIXON¹

¹Department of Geology, University of Pretoria, Pretoria, South Africa (roger.dixon@up.ac.za)

There are currently a number of competing hypotheses for the origin of the gold in the conglomeratic reefs in the Witwatersrand Basin, from hydrothermal to alluvial and variations between the two extremes. Though it has long been theorised that the gold deposits of the Witwatersrand Basin are at least partially hydrothermal in origin, there has been insufficient trace element analysis of gold and associated minerals from around the basin to evaluate this hypothesis, mainly due to inadequacies of routine analytical techniques.

A basin-wide study looking at the composition of gold produced in the different gold fields in the Witwatersrand Basin, and the composition of individual gold grains from different reefs, has been conducted utilising ICP-OES and LA-ICP-MS, and shows that the gold produced in each goldfield is compositionally distinct and that sediment source area is the main factor in determining the trace element distribution.

Results of the analysis of large gold grains from the Vaal Reef and gold associated with carbon derived from microbial mats in the Carbon Leader Reef, reveals the presence of at least three distinct types of gold.

The first type consists of alluvial gold which has been transported from source area and deposited in the calm conditions of the braided stream depositional environment.

The second type consists of very fine particles of colloidal gold precipitated from suspension during deposition of the sediments. At the same time that the gold was being precipitated from suspension, other elements in colloidal suspension were also being precipitated, such as uranium, thorium, silver, aluminium and iron.

Subsequent to deposition, one or more hydrothermal events remobilised much of the colloidal gold and this was redeposited as a third type of gold with distinct elemental and isotopic trace element signatures. Where carbon was present this redeposition took place almost in-situ, and where carbon was absent gold was redeposited from solution at some distance, in higher reefs and associated with cross-cutting quartz veins.

A combined isotopic and XAS study of Cr incorporation into marine carbonates: Towards verifying Cr isotopes as a palaeoredox proxy

S.K. DIXON^{*1}, C.L. PEACOCK², I.J. PARKINSON³,
M. A. FEHR¹ AND R.H. JAMES⁴

¹Department of Environment, Earth and Ecosystems, The Open University, Milton Keynes, UK.

(S.K.Dixon@open.ac.uk) (* presenting author)

²School of Earth and Environment, University of Leeds, Leeds, UK. (C.L.Peacock@Leeds.ac.uk)

³School of Earth Sciences, University of Bristol, Bristol, UK.

⁴Marine Geosciences, National Oceanography Centre, Southampton, UK.

Recent studies of Cr stable isotope fractionation in experimental and natural systems indicate that Cr isotopes can be used to track past changes in ocean oxygenation [1-3]. A record of dissolved oxygen concentration in seawater is crucial for understanding past climate changes, and for predicting future climate scenarios.

Marine carbonates are enriched in Cr by a factor of 10⁴ relative to seawater and have shown potential as a suitable archive phase; they are thought to record the Cr isotopic composition of seawater, however, this assumption needs to be verified. It has been demonstrated for other elemental systems e.g. Mg and B, that isotope fractionation can occur during elemental sequestration, thus we set out to determine the molecular mechanism of Cr incorporation into marine carbonates and to quantify any isotope fractionation that occurs during Cr uptake.

Synthetic calcite and aragonite were prepared in the presence of Cr, following the method of Bots *et al.*, 2011 [4]. Precipitates and initial solutions were analysed for Cr isotope composition by MC-ICP-MS. In tandem, selected subsets of the Cr-enriched precipitates were subject to synchrotron X-ray absorption spectroscopy, to determine the oxidation state and local coordination environment of Cr, and thus the molecular mechanism of Cr uptake in marine carbonates.

This work demonstrates how a mechanistic understanding of trace element uptake can improve interpretation of empirically determined isotope fractionation factors and provide a theoretical underpinning for a novel and developing palaeo-redox proxy.

[1] Ellis *et al.*, (2002), *Science* **295**, 2060-2062. [2] Bonnard *et al.*, (2011), *J. Anal. At. Spectrom* **26**, 528-535. [3] Frei *et al.* (2011), *Earth and Planet. Sci. Lett.* **312**, 114-125. [4] Bots *et al.*, (2011), *Geology* **39**, 331-334.

Hydrochemical and isotopic study of CO₂ rich groundwater in the Gyeongsang sedimentary basin, South Korea

HYUN-KWON DO¹, SEONG-TAEK YUN^{1*}, KYOUNG-HO KIM¹ AND BERNHARD MAYER²

¹Korea University, Department of Earth and Environmental Sciences, Seoul, South Korea

(styun@korea.ac.kr) (* correspondence)

²University of Calgary, Geoscience, Canada

As a natural analogue study of geologic carbon storage in deep aquifers hosted in clastic sedimentary formations, we investigated CO₂ rich groundwater in the Gyeongsang sedimentary basin, southeastern of South Korea. Data of hydrochemistry and multi isotopes ($\delta^{18}\text{O}$ - δD of water, $\delta^{13}\text{C}$ of dissolved carbonate, $\delta^{34}\text{S}$ of dissolved sulfate), together with ¹⁴C dates, were collected from 16 naturally seeping CO₂ rich groundwater. The CO₂ rich groundwaters are mainly of Ca-(Mg)-HCO₃ type (average pH = 6.1) and are very high in total dissolved solids (TDS) (up to 3393 mg/L) and alkalinity (up to 2512 mg/L). The concentrations of Ca²⁺, Cl⁻ and SO₄²⁻ are also high with the positive correlations with TDS. Thus, it is suggested that CO₂ rich groundwater was evolved through strong water-rock interactions. The results of ¹⁴C dating support a long residence time of inorganic carbon (35,720 to 44,780 BP). The $\delta^{18}\text{O}$ (-9.2 ± 0.6‰) and δD (-63.0 ± 4.4‰) data indicate that CO₂ rich waters were derived from local meteoric water. The $\delta^{13}\text{C}$ values of dissolved carbonates (-9.2 to -1.5‰) indicate the origin of dissolved carbon from mantle-derived CO₂. Careful examination of hydrochemical and isotopic data also indicates that mixing process occurred between uprising CO₂ and shallow groundwater during fluid ascending.

Archaean TTG discriminant criteria applied to Phanerozoic granitoids – significance from a study case in the Getic basement, South Carpathians

ANCA DOBRESCU

Geological Institute of Romania, Bucharest 32, Romania;
(ancadobrescu2003@yahoo.com)

A comparison to Archaean TTGs was made on two Ordovician granitoids [1] from Buchin (BG) of I-type and Slatina-Timis (STG) of I-S-type from the Getic basement (NE Semenic Mts.) - South Carpathians, because of peculiar trace elements behavior. Diagnosed as trondhjemites-tonalites-granodiorites-granites, the samples fit geochemically to Archaean TTGs [2] except higher K_2O contents (1.48-3.91%) and slightly lower $(La/Yb)_N$ (10.56-39.93). Low Y (4-12 ppm), mid-high Sr (554-965 ppm) and Sr/Y (48-175), small to no Eu anomalies, (-) Nb-Ti anomalies, low Nb/Ta and HREE ($Yb < 1.3$ ppm) signify variable clinopyroxene, Ti-phase, amphibole, garnet, +/- scarce plagioclase in the residue [2, 3, 4]. The rocks overlap Archaean-Ptz TTG composition [5] close to the amphibolites batch melting products on Nb-Ta-Zr/Sm diagram; alternatively [6] the rocks plot close to the eclogite melting field. The TTG signature tempted us to plot the samples on the discriminant diagrams for Archaean TTGs [7]. The diagrams on immobile elements (Y, Yb, La, Ce, even Sr, SiO_2) plot BGs systematically in the high pressure (HP-TTG) group and STGs in the medium pressure (MP-TTG) group. The diagrams using LILE (K, Eu) plot BGs in the K-group and STGs in the low pressure (LP-TTG) and K-group of enriched sources. MgO , FeO , SiO_2 used as indicators for T^0 /degree of melting plot the BGs in and around LP-TTG and K-group. In the BG-STG case as Phanerozoic granitoids, the conclusion on immobile elements behavior refers to pure melts related to source/P-depth conditions, while the rest of elements relate the end-rocks to the subsequent evolution during ascent and emplacement. The HP-MP coupled with moderate T^0 are consistent with early stages of continental collision - proper setting for an origin related either to partial melting of heterogeneous old continental crust eclogitized at its lower part because of wet conditions induced by a former subduction, or to partial melting triggered at the continental crust/oceanic crust/mantle tectonic contact during collision (setting described in [8, 9]).

[1] Dobrescu *et al.* (2010) *Proc. XIX, CCBGA Spec.* 99, 225-232. [2] Drummond & Defant (1990) *J. Geophys. Res.* 95, 21503-21521. [3] Rollinson & Martin (2005) *Lithos* 79, ix-xii. [4] Martin *et al.* (2005) *Lithos* 79, 1-24. [5] Foley *et al.* (2002) *Nature* 417, 637-640. [6] Rapp *et al.* (2003) *Nature* 425, 605-609. [7] Moyen (2011) *Lithos* 123, 21-36. [8] Conovici (1999) *PhD th.* [9] Săbău (1999) *PhD th.*

Asymmetric plate tectonics and asymmetric mantle convection

CARLO DOGLIONI¹

¹Sapienza University, Roma, Italy
(carlo.dogliani@uniroma1.it)

Subduction zones have hinges which move toward or away with respect to the upper plate. Assuming null the velocity of the upper plate, the velocity of the subduction is given by $V_S = V_H - V_L$, where V_H is the velocity of the subduction hinge, and V_L is the velocity of the lower plate. In case of subduction hinge diverging relative to the upper plate, the subduction results faster than the convergence rate, whereas in case of subduction hinge converging relative to the upper plate, the subduction is slower than the convergence. The dip of slabs, topography, type of rocks, foredeep subsidence rates, metamorphic P-T path, plus a number of other parameters characterize the two end-members of related orogens (Doglioni *et al.* 2007, ESR). This antithetic behaviour appears as geographically tuned, i.e., west versus east or northeast. Moving along the tectonic equator described in Crespi *et al.* (2007, GJI) and Cuffaro and Doglioni (2007, GSA SpPu), slabs having the hinge diverging relative to the upper plate occur dominantly along W-directed subduction zones. This implies a 3-5 times faster subduction recycling of the lithosphere along those margins with respect to the opposed E- or NE-directed subduction zones. Moreover, delamination and thicker asthenospheric mantle wedge occur along W-directed subduction zones. A thicker lithosphere with faster shear waves and few hundreds meters deeper oceanic bathymetry characterizes the western limb of rift zones (Panza *et al.* 2010, *Geology*), suggesting a global asymmetry of plate tectonics, and consequently of the primary mantle convection. This setting reconciles with the westward drift of the lithosphere. However, only a shallow source (LLAMA, Anderson, 2011, JP) of the hotspot reference frame matches the global tectonic asymmetry as the one described, where the net rotation of the lithosphere relative to the mantle amounts to more than 1°Ma. An astronomical input is required in order to satisfy this geodynamic configuration (Riguzzi *et al.* 2010, *Tectonophysics*).

Tracing the origin and evolution of the parental magmas of the Grey Porri Tuffs, island of Salina, Italy.

DOHERTY, A.L.^{1*}, BODNAR, R.J.², CANNATELLI, C.³, ESPOSITO, R.³, DE VIVO, B.³ AND MESSINA, A.³

¹ University of Messina, Messina, Italy (*correspondence: doherty.angelal@gmail.com)

² Virginia Tech, Blacksburg, VA, USA

³ University of Naples (Federico II), Naples, Italy

The interbedded scoria-pumice-ash tuffs of Monte dei Porri, known as the Grey Porri Tuffs (GPT), appear to be the result of the mixing of two or more compositionally-different magmas. A more evolved trachyandesite-trachydacite magma, represented by melt inclusions (MI) trapped in feldspar of the pumice, was intruded by a basaltic magma, represented by MI in olivine of the same unit.

H₂O/CO₂ modelling indicates that MI in the feldspars of the pumice units were entrapped at ~0.6 kb. Magma-wall interaction had begun, evidenced by slight positive Zr anomalies and also low volatile element abundances (primarily: 1.7-2.8 wt % H₂O and 1019-1749 ppm S) which may indicate shallow system degassing. Feldspars of the pumice unit also show strong zonation and more sodic compositions than the scoria, which range from An₅₈₋₈₁.

The MI in olivine of the pumice units, interpreted to represent the mafic magma, were entrapped at higher pressures, ~1.7 kb, based on H₂O/CO₂ modelling. The olivine hosts had Fo-contents of Fo₇₉₋₈₃. The intrusion introduced a large amount of volatile components into the system; it contained 4.1-5.1 wt % H₂O, 3227-4032 ppm S, 187-492 ppm CO₂ and 3149-3855 ppm Cl. The subsequent eruption entrained the feldspar and clinopyroxene from the evolved melt, and the olivine from the mafic intrusion, and deposited the pumice units, which have an andesitic bulk composition.

Subsequent evolution in the mixed remnants of the magma produced a melt with a composition that is intermediate between the previous two. MI in the calcic feldspar (An₈₄₋₉₃), olivine (Fo₇₁₋₈₂) and clinopyroxene (augite and diopside) show overlapping major and trace element compositions, suggesting they may have had similar evolutionary histories. MI compositions and volatile element abundances approach those of the pumice units (the olivine-hosted MI contain 2.4-3.8 wt % H₂O, 169-570 ppm CO₂, 1495-3587 ppm S and 3165-3705 ppm Cl), suggesting that there may have been continual input from below, with the bulk rock compositions of the erupted GPT scoria units having a low-silica basaltic-andesite composition, more mafic than the majority of the MI from the same units.

Acid rock drainage in Antarctica – importance for global iron cycling in the Southern Ocean

DOLD, B.¹, GONZALEZ-TORIL, E.², AGUILERA, A.², LOPEZ-PAMO, E.³, CISTERNAS, M.E.¹ AND AMILS, R.²

¹ Instituto de Geología Económica Aplicada (GEA), Universidad de Concepción, Concepción, Chile.

(Bernhard.Dold@gmail.com), (mcistern@udec.cl)

² Centro de Astrobiología (INTA-CSIC), Madrid, Spain.

(etoril@cbm.uam.es), (aaguilera@cbm.uam.es),

(ramils@cbm.uam.es)

³ Instituto Geológico y Minero de España (IGME), Madrid, Spain. (e.lopez@igme.es)

We describe biogeochemical processes that lead to the generation of acid rock drainage (ARD) and rock weathering on the Antarctic landmass and describe why they are important sources of iron into the Antarctic Ocean. During three expeditions, 2009 – 2011, we examined three sites on the South Shetland Islands in Antarctica. Two of them displayed intensive sulfide mineralization and generated acidic (pH 3.2 – 4.5), iron-rich drainage waters (up to 1.78 mM Fe), which infiltrated as groundwater (as Fe²⁺) and as superficial runoff (as Fe³⁺) into the sea, latter with the formation of schwertmannite in the sea ice. The formation of ARD in the Antarctic was catalyzed by acid mine drainage microorganisms found in cold climates, including *Acidithiobacillus ferrivorans* and “*Thiobacillus plumbophilus*”. The dissolved iron (DFe) flux from rock weathering (non-mineralized control site) was calculated to be 0.45 x 10⁹ g DFe yr⁻¹ for the nowadays 5468 km of ice-free Antarctic rock coastline what is in the order of magnitude of glacial or aeolian input to the Southern Ocean. Additionally, the two ARD sites alone liberate 0.026 and 0.057 x 10⁹ g DFe yr⁻¹ as point sources to the sea. The ARD point sources are between 1000 and 2300 times more efficient than non mineralized rock weathering for iron liberation. The increased iron input correlates with increased phytoplankton production close to the source. This might even be enhanced in the future by a global warming scenario, when more of the Antarctic coastline will be ice-free, and could be a process counterbalancing global warming.

Tracking high-pH reaction fronts in MX-80 bentonite using infiltration techniques and 4D CT

F. DOLDER^{1*}, U. MÄDER¹ AND A. JENNI¹

¹RWI, University of Bern, Geological Sciences, Bern 3012, Switzerland

(*correspondence: florian.dolder@geo.unibe.ch, urs.maeder@geo.unibe.ch, andreas.jenni@geo.unibe.ch)

Geological storage of radioactive waste foresees bentonite as backfill material enclosing spent fuel drums. Concrete is proposed as building material for tunnel reinforcement or as backfill. The emplacement of high-pH cementitious material next to clay generates a chemical gradient in pore water chemistry that drives diffusive transport. Laboratory studies and reactive transport modeling predict significant mineral alteration near interfaces [1].

We aim to characterize and quantify the cement/bentonite skin effects spatially and temporally, focusing on the advective-diffusive transport domain resolved at intermediate spatial scales. Equipment made of carbon fiber and plastics holds a cylindrical sample under confining pressure and imposes a constant hydraulic gradient to drive a small advective flux. Compacted and saturated MX-80 bentonite and sand/bentonite mixtures are used. Infiltration of high-pH pore-fluids into the bentonite plug alters the mineral assemblage over time. The related change in phase densities, porosity and local bulk density is tracked by CT scans during ongoing infiltration. The resulting micrographs describe the electron density distribution in 3D and as a function of time. Electron densities are transformed into material densities using reference materials and are calculated on the basis of the data of the NIST [2]. After 1-2 years the experiment is stopped and the samples subjected to post-mortem analysis.

In a first experiment running for >6 months, MX-80 bentonite ($\rho_{wet}=1.875 \text{ g/cm}^3$) is used as starting material, and a synthetic cement pore fluid of pH 13.4. The reaction front is tracked in the CT and appears as precipitations in the thin filter separating bentonite and infiltration fluid, and as an evolving zone of higher density in the bentonite next to it. Simultaneously, hydraulic conductivity is decreasing by 58% over 6 months.

[1] Fernández R, Mäder U K, Rodríguez, M, Vigil de la Villa R and Cuevas J (2009) *European Journal of Mineralogy* 21, 725-735. [2] Phillips, D. H. and J. J. Lannutti (1997) *NDT & E International* 30(6), 339-350.

Estimating fluid fluxes from equilibrium properties and transport theory: pitfalls and solutions

DAVID DOLEJŠ¹

¹Institute of Petrology and Structural Geology, Charles University, 128 43 Praha 2, Czech Republic

(correspondence: david.dolejs@natur.cuni.cz)

Aqueous fluids are efficient mass transport agents and reactive fluid flow occurs in diverse settings including compaction of porous sediments, thermal perturbations in oceanic crust, prograde metamorphic reactions in continental orogens and subduction zones, or during plutonic and volcanic degassing. We will address several issues pertaining to accuracy and extrapolability of thermodynamic data, magnitude of reaction progress in temperature and pressure gradients, and separation of equilibrium vs. disequilibrium effects, i.e., closed- vs. open-system fluid-mineral interaction. Standard reaction enthalpies and volumes directly provide gradients in mole amounts of reaction progress or mineral precipitated, n , per unit temperature or pressure. Evaluation of mineral solubilities reveals that $\partial n/dP$ are significant and critically moderate $\partial n/dT$ for fluid reactions along geotherms vs. at constant pressure. Highly charged species are responsible for retrograde solubility effects during isobaric (lateral) flow, but along geotherms ($7\text{-}20 \text{ }^\circ\text{C km}^{-1}$) the $\partial n/dT$ are monotonous and nearly identical for a variety of rock-forming phases. Estimation of integrated fluid fluxes is frequently biased towards two limiting approaches: (i) local equilibrium with host rocks, with reaction progress driven by pressure and temperature gradients only, or (ii) disequilibrium fluid-rock interaction at constant or variable temperature and pressure. We extend conventional transport theory to include the disequilibrium effects and demonstrate that these two approaches yield the lower and upper limits of the flux, respectively, that may differ by several orders of magnitude. A model application to hydrolytic alteration of peraluminous granites reveals time-integrated fluid fluxes from 10^2 to $10^6 \text{ m}^3 \text{ m}^{-2}$, which covers the plausible range observed globally. If the magnitude of disequilibrium is constrained by modal proportions or volume conservation, the fluid fluxes become bracketed and smaller, $10^{2-3} \text{ m}_f^3 \text{ m}_r^{-2}$. We conclude that vein-producing fluid fluxes may be several orders of magnitude lower than previously indicated for fracture- or shear zone-related flow, and low fluxes support alternating periods of episodic flow and stagnant fluid-rock interaction. Such discontinuous flow mechanism is more consistent with cycles of transient permeability enhancement and subsequent chemical or mechanical sealing.

Sr-Nd-Hf-Pb isotope mapping of Tien Shan in Uzbekistan

A. DOLGPOLOVA^{1*}, R. SELTMANN¹, R. ARMSTRONG¹,
E. BELOUSOVA², R. PANKHURST³, D. KONOPELKO⁴
AND R. KONEEV⁵

¹NHM, Department of Earth Sciences, CERCAMS, London SW7 5BD, UK (*correspondence: allad@nhm.ac.uk)

²Macquarie University, GEMOC, NSW, 2109 AUSTRALIA (elena.belousova@mq.edu.au)

³BGS, Keyworth, Nottingham NG12 5GG, UK (rjpankhurst@gmail.com)

⁴St. Petersburg State University, Geological Faculty, St. Petersburg 199034, RUSSIA (konopelko@inbox.ru)

⁵NUUZ, Department of Geology, Tashkent, UZBEKISTAN (ri.koneev@gmail.com)

Sr-Nd-Hf-Pb isotope mapping combined with U-Pb zircon SHRIMP ages and Re-Os sulphide geochronology of granitoids from profiles across terrane boundaries in Uzbekistan reveal distinct reservoir types (cratonic vs turbiditic), corresponding to diverse nature and origin of granitic magmatism and its hosted ore-forming processes. Three main tectonic domains are recognized: Middle Tien Shan, Southern Tien Shan and Karakum microcontinent.

Sr-Nd isotopes (whole-rock) of all domains show a wide range of ϵNdt (-5 to +7) and ($^{87}\text{Sr}/^{86}\text{Sr}$)t predominantly between 0.704 and 0.707, indicating involvement of both mantle-derived material (e.g., subduction of oceanic crust) and older crustal sources (Mesoproterozoic model ages).

The large range of **Hf-isotope** compositions found in zircons of granites from Kurama, Middle Tien Shan, ($\epsilon\text{Hf} \sim -6$ to +5) suggest recycling of older heterogeneous crustal protolith(s). In the Southern Tien Shan involvement of subducted oceanic crust is exemplified by juvenile ϵHf values of up to +14 (Sultan-Uvais) and +16 (Teksquduk-Kyzylkum). However, Permo-Carboniferous granitoids crossing all terrane boundaries exhibit predominantly crustal signatures indicating Neoproterozoic protoliths.

Pb isotopes (whole-rock) exhibit a present-day range of $^{206}\text{Pb}/^{204}\text{Pb}$ 18.229-20.718, $^{207}\text{Pb}/^{204}\text{Pb}$ 15.607-15.823 and $^{208}\text{Pb}/^{204}\text{Pb}$ 38.077-39.827. These are in full agreement with Sr-Nd-Hf isotopes indicating the dominance of a crustal component as well as crust-mantle mixing processes.

The granitoid samples from Middle Tien Shan, Southern Tien Shan and Karakum microcontinent show a variation of crustal to mixed signatures with a significant contribution of older components. *This is a contribution to IGCP-592 sponsored by IUGS-UNESCO.*

Competitive adsorption/desorption of arsenate and phosphate at the ferric hydroxide-water interface

RONA J. DONAHOE^{1*} AND GHANASHYAM NEUPANE²

¹Dept. of Geological Sciences, University of Alabama, Tuscaloosa, AL 35487-0338; rdonahoe@ua.edu

²University of Idaho - Idaho Falls, 1176 Science Center Dr., Suite 306, Idaho Falls, ID 83402; gneupane@uidaho.edu

The kinetics of $\text{As}_{(\text{V})}$ and PO_4 adsorption/desorption on ferric hydroxide were investigated at pH 4 and pH 8 in 0.1 M NaCl. Individually, these oxyanions showed similar adsorption on the substrate and greater adsorption at pH 4 than at pH 8. In competitive adsorption experiments, greater adsorption of $\text{As}_{(\text{V})}$ compared to PO_4 was observed at both pH conditions. Sequential loading of $\text{As}_{(\text{V})}$ followed by PO_4 , and vice versa, was aimed at studying the co-oxyanion induced desorption kinetics of $\text{As}_{(\text{V})}$ and PO_4 (Fig. 1). The kinetic data were successfully fit by pseudo-second order, Elovich, and power-function equations.

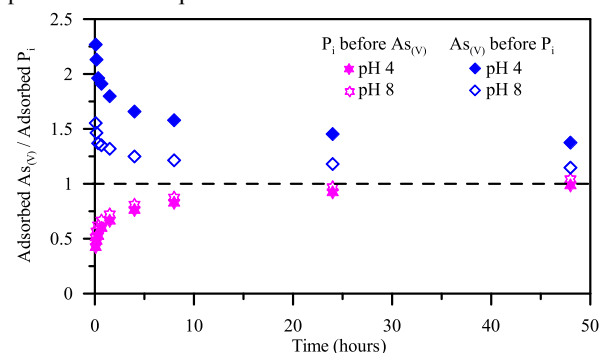


Fig. 1. Molar ratio plots for sequential loading of co-oxyanion after pre-equilibration of $\text{As}_{(\text{V})}$ or PO_4 (P_i) on ferric hydroxide at pH 4 and 8.

Selected samples were used for the As K-edge EXAFS spectroscopy to understand the changes in adsorption mechanisms of $\text{As}_{(\text{V})}$ with time in the presence/absence of PO_4 . EXAFS analysis indicated the presence mononuclear (^2E) and binuclear (^2C) bidentate $\text{As}_{(\text{V})}$ surface complexes. Fe coordination numbers (CN) increased with increasing time and decreased with addition of PO_4 into the system. Relatively, the higher proportion of CN associated with ^2E , compared to ^2C , was decreased after the addition of PO_4 . The competitive desorption study indicates that the excessive input of PO_4 due to the overuse of fertilizers could mobilize $\text{As}_{(\text{V})}$ from contaminated geomedias through competitive desorption.

Outcrops of X-5 and X-6 tephra markers along the Southern Tyrrhenian coast of Italy

P. DONATO^{1*}, P. ALBERT^{2,4}, M. CROCITTI³, R. DE ROSA¹,
AND M. MENZIES⁴

¹Università della Calabria, Via P. Bucci 15/B, 87036 Rende (CS), Italy. (donatop@unical.it)

²RLAHA, University of Oxford, UK.

³ Università di Bari, Via Orabona 4, 70125 Bari (BA), Italy

⁴Earth Sciences, RHUL, UK

Volcaniclastic layers interbedded in the sedimentary sequences of Marine Isotope Stage (MIS) 5 have been the subject of many tephrostratigraphic studies over the past decades. In particular, two important markers, named the X-5 (105 ± 2 ka) and X-6 (107-108 ka) tephras were recognised in many Mediterranean marine and lacustrine sequences. First identified within Ionian Sea marine cores [1] these marker tephras have since been recognised in Tyrrhenian Sea cores [2] and terrestrially at Lago Grande di Monticchio [3,4].

In a recent paper [5] the two tephras were identified in the lacustrine sequence of Sulmona basin and along the Cilento coastline. Here we present new petrographic and microanalytical data on volcaniclastic deposits outcropping in the Cilento area. Trace element concentration determined on single glass shards by LA-ICP-MS unequivocally confirms these volcaniclastic levels as the X-5/TM-25 and X-6/TM-27 markers tephras. Moreover, additional investigations of a volcaniclastic level outcropping in Valle del Crati (northern Calabria), near the village of Tarsia, allows a correlation of this level with the X-6 marker tephra. The associated age of the X-6 (107-108ka) is in contrast with the previous thermoluminescence age of this level (42-25 ka [6]).

Volcaniclastic deposits with similar characteristics to those along the Cilento coastline have also been recognised along the Lucania and Calabria Tyrrhenian coast. The mineralogical assemblage (alkali feldspar + diopsidic to salitic clinopyroxene + plagioclase + feldspathoids \pm biotite and amphibole) and the trachytic composition of the glasses strongly suggest a correlation of these layer with the X-5 and X-6 tephras. Further trace element analysis is required to reinforce links to the Cilento levels.

[1] Keller *et al.* (1978), *Geol. Soc. Am. Bull.* **89**, 591-604. [2] Paterne *et al.* (2008), *J. Volcanol. Geoth. Res.* **177**, 187-196. [3] Wulf *et al.* (2004), *Quat. Int.* **122**, 7-30. [4] Wulf *et al.* (2012), *Quat. Sci. Rev.* **58**, 104-123. [5] Giaccio *et al.* (2012), *Quat. Sci. Rev.* **56**, 31-45. [6] Carobene *et al.* (2006), *Quat. Int.* **148**, 149-164.

Mg and Fe isotope constraints on the genesis of Paleoproterozoic magnesite deposits, NE China

A. DONG, X. K. ZHU, S. Z. LI, Y. WANG, Z. H. LI

Laboratory of Isotope Geology, MLR, Institute of Geology, CAGS, Beijing, 100037, PR China
(aiguo.dong@gmail.com)

As the world famous magnesite mineralization belt, the Paleoproterozoic magnesite deposits in eastern Liaoning, NE China, accounting for about 30% of the whole world reserves, have experienced multi-geo-processes (evaporation deposit, regional metamorphism etc.), and the genesis is still in debate: chemical deposition or metasomatism. In this study, Mg and Fe isotope compositions of carbonate and magnesite were determined for tracing the genesis of the magnesite deposits. The $\delta^{26}\text{Mg}$ values (*ca.* -1.5‰ to DSM3) of the magnesite are in the range of the Mg isotope composition of the carbonate, differing from the magmatic source ($\delta^{26}\text{Mg}$ values *ca.* -0.25‰) and present seawater ($\delta^{26}\text{Mg}$ values *ca.* -0.83‰). Furthermore, if consider about recent stimulation experiments that the abiotic chemical precipitation could produce a large range of Mg isotope fractionation (*ca.* -2‰ for the calcite precipitation and *ca.* -1.19‰ for the magnesite precipitation at 150°C) from aqueous to solid, the Mg isotope results are consistent with a chemical precipitation origin. This view is also supported by the fact that the $\delta^{56}\text{Fe}$ values of the deposits (range from -1.0 to -0.13‰ to IRMM, with an average value of -0.43‰) are compatible to the Fe isotope composition of the sedimentary carbonates.

Sources of arsenic in groundwater based on geological and hydrogeochemical properties of an arid/semi-arid area in Yinchuan Plain, China

YIHUI DONG, TENG MA*, CHUNYAN TIAN⁴, JUNWEN ZHANG, LIN LIU¹² AND FUCUN ZHANG⁵

¹School of Environmental Studies, China University of Geosciences, Wuhan, 430074, China
(*correspondence: mateng@cug.edu.cn)

²State Key Laboratory of Biogeology and Environmental Geology, China University of Geosciences, Wuhan, 430074, China

³Department of Environmental Engineering, Technical University of Denmark, DK-2800 Lyngby, Denmark

⁴Department of hydrogeology and Engineering Geology, Guangdong Geological Survey, Zhanjiang, 524049, China

⁵Centre of Hydrogeology and Environmental Geology Survey, China Geological Survey, Baoding, 071051, China

Yinchuan Plain is a newly discovered high-arsenic groundwater area in the Yellow River Basin, China, with an arsenic range of 9µg/L in groundwater. 81 water samples were collected for chemical analysis along the direction from western Helan Mountain to the central plains. The hydrochemical types gradually change from HCO₃, SO₄-HCO₃ types to HCO₃-Cl and Cl-HCO₃ types. High arsenic groundwater is mainly distributed in the Yellow River floodplain of eastern Helan country and subsidence center area of western Pingluo country, within the depth of 40m in phreatic water.

Arsenic was detected in rocks from Helan Mountains in varying degrees: arsenic in sedimentary rocks, which were significantly influenced by weathering, such as mudstone, sandstone and shale, was respectively 6.5mg/kg, 2.5mg/kg and 5.9mg/kg. Surface water, groundwater and wind transported arsenic in rocks to the plain. The coal-bearing strata in Helan Mountains and arsenic rocks are the main native sources of high arsenic environment in the study area. Analysis results of borehole sediments showed that high arsenic layers appeared in the depths of 18m, 41m and 92m below the surface. Limnetic facies sediments in lacustrine plain were the other essential source of groundwater arsenic. In addition, human activities have accelerated migration and enrichment of arsenic into groundwater.

A Phanerozoic CO₂ history driven by tectonics

YANNICK DONNADIEU¹, YVES GODDERIS², GUILLAUME LE HIR³, VINCENT LEFEBVRE^{1,2} AND ELISE NARDIN²

¹LSCE – CNRS, CE Saclay, Orme des Merisiers, 91191 Gif/Yvette, France – (yannick.donnadieu@lsce.ipsl.fr) (vincent.lefebvre@lsce.ipsl.fr)

²GET – CNRS, Toulouse, France – (yves.godderis@get.obs-mip.fr)

³Institut de Physique du globe de Paris, 4 place Jussieu 75005 Paris, France – (lehir@ipgp.fr)

Our understanding of the geological regulation of the carbon cycle has been deeply influenced by the contribution of Bob Berner with his well-known model GEOCARB. Here, we will present a fundamentally different carbon cycle model that explicitly accounts for the effect of the paleogeography using physically based climate simulations and using 22 continental configurations spanning the whole Phanerozoic. We will show that several key features of the Phanerozoic climate can be simply explained by the modulation of the carbon cycle by continental drift. In particular, the continental drift may have strongly impacted the runoff intensity as well as the weathering flux during the transition from the hot Early Cambrian world to the colder Ordovician world. Another fascinating example is the large atmospheric CO₂ decrease simulated during the Triassic owing to the northward drift of Pangea exposing large continental area to humid sub-tropics and boosting continental weathering. Conversely, our model fails to reproduce the climatic trend of the last 100 Ma. This is due to the highly dispersed continental configurations of the last 100 Ma that optimize the consumption of CO₂ through continental weathering. This discrepancy may be reduced if we account for a larger influence of the Earth degassing flux on the atmospheric CO₂ evolution, which could come from the increase contribution of the pelagic component on the oceanic crust on the global carbonate flux and from the many sub-marine LIPs occurring during the Late Cretaceous.

V. Lefebvre, Y. Donnadieu, Y. Godd ris *et al.*, Was the Antarctic glaciation delayed by a high degassing rate during the early Cenozoic ? , *Earth and Planetary Science Letters*, in press.

E. Nardin, Y. Godd ris, Y. Donnadieu *et al.*, Modeling the early Paleozoic long-term climatic trend, *Geological Society America Bulletin*, doi: 10.1130/B30364.1, 2011

Y. Godd ris, Y. Donnadieu, C. De Vargas *et al.*, Causal or casual link between the rise of nannoplankton calcification and the tectonically-driven massive decrease in Late Triassic atmospheric CO₂, *Earth And Planetary Science Letters*, **267**, 247-255, 2008

First preliminary map of deep CO₂ degassing in Alpine region

MARCO DONNINI^{1,2}, FRANCESCO FRONDI^{1*}, CARLO CARDELLINI¹, STEFANO CALIRO³, GIOVANNI CHIODINI³, IVAN MARCHESINI² AND FAUSTO GUZZETTI²

¹ Università degli Studi di Perugia. Dipartimento di Scienze della Terra. Perugia, Italy (*correspondence: frondini@unipg.it)

² Consiglio Nazionale delle Ricerche, Istituto di Ricerca per la Protezione Idrogeologica. Perugia, Italy

³ Istituto Nazionale di Geofisica e Vulcanologia, Osservatorio Vesuviano. Perugia, Italy

Processes of CO₂ degassing affect almost all tectonically active areas and metamorphic environments. Here we show the first preliminary map of deep-CO₂ degassing of the Alps based on more than 1000 chemical analyses of springs (both data from literature and new data). Using PHREEQC, for each point we estimated the total dissolved inorganic carbon (TDIC) and through an isotopic and mass balance approach we estimated the values of C_{carb}, carbon deriving from carbonate dissolution, and C_{inf}, the sum between atmospheric CO₂ dissolved by rainwater and biogenic CO₂. C_{deep}, carbon deriving from deep degassing, has been computed considering that [1]: $TDIC = C_{carb} + C_{inf} + C_{deep}$. C_{carb}, given by Ca+Mg-SO₄, has been estimated for springs fed by carbonate aquifers. The flux of deep CO₂ associated to each spring discharge is given by $C_{deep} \times Q/A$, (Q: flow rate, A: recharge area), or by $C_{deep} \times IE$, (IE: effective infiltration, $IE=Q/A$). IE for each basin have been estimated using a water balance model [2]. Finally we prepared the CO₂ degassing map using GSLIB [3]. The results show that CO₂ production of Alps is 3 times lower than CO₂ production in Central Italy [4], but locally (like in Engadine, Lucomagno Pass, Valtellina etc..) CO₂ fluxes are one order of magnitude higher than the baseline of geothermal regions [5]. The highest deep-CO₂ degassing areas are located along the more important alpine tectonic structures and in the basins external to the alpine chain. In these areas more detailed investigations should be performed in order to obtain a complete evaluation of the extent and distribution of the CO₂ anomalies of the Alps.

[1] Chiodini *et al.* (2000) *Journal of Geophysical Research* **105**. [2] Rossi *et al.* (2013) *XIV GRASS e GFOSS meeting*. [3] Deutsch and Journel (1988) *Oxford Univ. Press* [4] Chiodini *et al.* (2004) *Geophysical Research Letters* **31**. [5] Kerrick *et al.* (1995) *Chemical Geology* **121**.

Alpine weathering and carbon cycle

MARCO DONNINI^{1,4*}, JEAN-LUC PROBST^{2,3}, ANNE PROBST^{2,3}, FRANCESCO FRONDI¹, IVAN MARCHESINI⁴ AND FAUSTO GUZZETTI⁴

¹ Università degli Studi di Perugia. Dipartimento di Scienze della Terra. Perugia, Italy (*correspondence: marco.donnini@tiscali.it)

² University of Toulouse ; INPT, UPS ; Laboratoire Ecologie Fonctionnelle et Environnement (EcoLab), ENSAT, Castanet Tolosan, France

³ Centre National de la Recherche Scientifique (CNRS), EcoLab, ENSAT Castanet Tolosan, France

⁴ Consiglio Nazionale delle Ricerche, Istituto di Ricerca per la Protezione Idrogeologica, Perugia, Italy

On geological time-scales the fluxes from atmosphere to solid Earth depend on weathering of silicates and carbonates, biogenic precipitation and removal of CaCO₃ in the oceans and volcanic gases – seawater interactions. Here we estimate the atmospheric CO₂ uptake by weathering in the Alps, using the dissolved loads of 33 Alpine rivers sampled during dry and flood seasons. The dissolved load of streams originates from atmospheric input, pollution, evaporite dissolution, and weathering of carbonate and silicate rocks. We applied the MEGA (Major Element Geochemical Approach) geochemical code [1, 2] to the chemical compositions of the selected rivers in order to quantify the atmospheric CO₂ consumed by weathering. The steps were: (1) subtraction of the rain contribution, (2) the remaining (Na+K) comes from silicate weathering. The average molar ratio $R_{sil} = (Na+K)/(Ca+Mg)$ was estimated for each basin following well known lithological classification [2, 3], (3) lastly we estimated the (Ca+Mg) originating from carbonate weathering. Depending on time-scales we considered different equations for the quantification of the atmospheric CO₂ consumed by weathering [5]. The results show the net predominance of carbonate weathering on fixing atmospheric CO₂ and that, considering different time scales, there is about one order of magnitude of difference on the atmospheric CO₂ fixed by weathering.

[1] Amiotte-Suchet (1995) *Sci. Géol. Mém. Strasbourg* **97**. [2] Amiotte-Suchet and Probst (1996) *Sci. Géologiques Bull. Strasbourg* **49**, 101–126. [3] Meybeck (1996) *Bulletin De La Société Géologique* **39**, 3–77. [4] Meybeck (1987) *Am. J. Sci* **287**, 401–428. [5] Huh (2010) *Society of London, Special Publications* **342**.

Basalt, granite, rhyolite, and schist weathering as affected by plants and microorganisms

KATERINA DONTSOVA^{1,2*}, DRAGOS G. ZAHARESCU^{1*},
CARMEN BURGHELEA¹, JON CHOROVER², RAINA MAIER²
AND TRAVIS HUXMAN³

¹University of Arizona, Biosphere 2, Tucson, Arizona, U.S.A.
(dontsova@email.arizona.edu)(* presenting author),
(zaharescu@email.arizona.edu),
(bcarmen@email.arizona.edu)

²University of Arizona, Soil Water and Environmental
Science, (chorover@cals.arizona.edu),
(rmaier@ag.arizona.edu)

³University of California, Irvine, (thuxman@uci.edu)

In order to survive in nutrient poor environments, plants and microorganisms developed a number of strategies to accelerate weathering of the minerals in the soil and rock. This study looks at the role of plant-microbial associations in mineral weathering. Four different rocks, basalt, granite, rhyolite, and schist were used as substrate for growth of Ponderosa pine (*Pinus ponderosa*) and Buffalo grass (*Bouteloua dactyloides*) with and without mycorrhiza. There was also a bacteria-only and killed controls. Two types of mycorrhizal fungi were used, *Rhizopogon evadens*, an ectomycorrhiza-forming fungi associated with Ponderosa pine and VAM mycorrhiza-forming *Glomus intraradices* used to inoculate Buffalo grass. Plants were seeded into plastic columns containing rocks inoculated with microbial community obtained from basalt.

To detect changes in soil solution composition resulting from weathering processes, drainage solution was collected and analyzed to determine electrical conductivity, pH, quantify concentrations of organic and inorganic C, total N, anions and cations. After four month a set of columns was sacrificed and root and shoot biomass, concentrations of C, N, and lithogenic elements in plant material, as well as plant root lengths was determined.

All four rocks experienced weathering. Both electrical conductivity and pH of drainage solutions, indicator variables for weathering reactions were higher than measured in water used for irrigation. Electrical conductivity of drainage solution was also higher in planted treatments compared to control, and in pine compared to grass treatment. Concentrations of lithogenic elements in soil solution were also affected by plants, with nutrient cations depleted relative to rare earth elements in planted treatments, compared to microbial and abiotic controls. In addition, it was observed that mycorrhizal infection of the plants affected plant biomass and root length.

Rapid regolith formation over volcanic bedrock and implications for landscape evolution

ANTHONY DOSSETO¹, HEATHER L. BUSS²
AND P.O. SURESH³

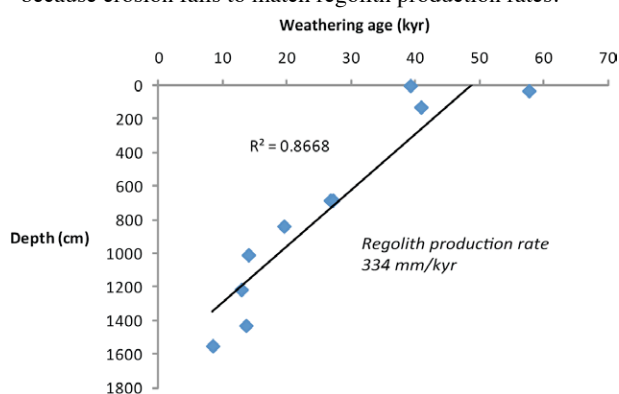
¹Wollongong Isotope Geochronology Laboratory, School of
Earth and Environmental Sciences, University of
Wollongong. E-mail: (tonyd@uow.edu.au)

²School of Earth Sciences, University of Bristol.

³Department of Environment and Geography, Macquarie
University.

The ability to quantify how fast weathering profiles develop is crucial to assessing soil resource depletion and quantifying how landscapes evolve over millennia. Uranium-series isotopes can be used to determine the age of the weathering front throughout a profile and to infer estimates of regolith production rates, because the abundance of U-series isotopes in a weathering profile is a function of chemical weathering and time. This technique is applied to a weathering profile in Puerto Rico developed over a volcanoclastic bedrock.

U-series isotope compositions are modelled, revealing that it takes 40-60 kyr to develop an 18m-thick profile. This is used to estimate an average regolith production rate of 334 ± 46 mm/kyr (Fig. 1; [1]). This value is higher by a factor of up to 30 when compared to production rates estimated for weathering profiles developed over granitic or shale lithologies. This *quantitatively* underpins the lithological control on rates of regolith production (in a neighbouring watershed but over a granitic bedrock, production rates are only ~30-40 mm/kyr). Moreover, by comparing these results to a compilation of soil erosion rates, it is clear that landscapes are controlled by the balance (or imbalance) between regolith production and erosion: soil-mantled landscapes are the result of a relative balance between production and erosion, whereas in cratonic areas, thicker weathering profiles are generated because erosion fails to match regolith production rates.



[1] Dosseto, *et al.*, 2012. Earth and Planetary Science Letters 337–338, 47–55.

Cerium isotope systematics of oceanic carbonatites

R. DOUCELANCE^{123*}, N. BELLOT¹²³, M. BOYET¹²³
AND T. HAMMOUDA¹²³

¹ Clermont Université, Université Blaise Pascal, Laboratoire Magmas et Volcans, BP 10448, F-63000 CLERMONT-FERRAND

² CNRS, UMR 6524, LMV, F-63038 CLERMONT-FERRAND

³ IRD, R 163, LMV, F-63038 CLERMONT-FERRAND

(*correspondence: doucelance@opgc.univ-bpclermont.fr)

Oceanic carbonatites have been reported only at the Cape Verde and Canary archipelagos, North Atlantic Ocean. Geochemical studies based on stable, radiogenic and noble gas isotopes have led to the general consensus that their parental magmas originate in the mantle. Two contrasted models, however, have been proposed for the origin of the carbon of their source: recycled marine carbonates via subduction [1, 2] vs. primordial carbon [3].

Marine carbonates [4] show REE patterns distinct from those assumed or measured for mantle and mantle-derived reservoirs (D⁷⁷: [5]; Lower Mantle: [6]; DMM: [7]; MORB: [8]). Notably chondrite-normalized La/Ce and Sm/Nd ratios have inverse values. Consequently old recycled carbonates are likely to display $\epsilon_{\text{Ce}} > 0$ (ϵ_{Ce} is the $^{138}\text{Ce}/^{142}\text{Ce}$ variation relative to the Bulk Earth $\times 10000$) and $\epsilon_{\text{Nd}} < 0$ ($^{143}\text{Nd}/^{144}\text{Nd}$ variation relative to the Bulk Earth $\times 10000$) with time, whereas mantle-related materials will show $\epsilon_{\text{Ce}} \leq 0$ and $\epsilon_{\text{Nd}} \geq 0$. Thus coupled Ce and Nd isotope systematics appear to be a powerful tool to decipher between the two proposed origins for the carbon of oceanic carbonatites.

We have measured Ce and Nd data on carbonatites from the Cape Verde and Canaries archipelagos, together with basaltic samples from the same locations. We have also determined ϵ_{Ce} and ϵ_{Nd} values for Tamazert carbonatites (Marocco) as it has been proposed that the Cape Verde, Canary and Tamazert carbonatites share a common source [9]. Our first measurements on oceanic samples argue in favor of recycled marine carbonates in the source of oceanic carbonatites.

[1] Hoernle *et al.* (2002) *Cont. Mineral. Petrol.* **142**, 520-542. [2] Doucelance *et al.* (2010) *GCA* **74**, 7261-7282. [3] Mata *et al.* (2010) *EPSL* **291**, 70-83. [4] Plank & Langmuir (1998) *Chem. Geol.* **145**, 325-394. [5] Tolstikhin *et al.* (2006) *Chem. Geol.* **226**, 79-99. [6] Doucelance *et al.* (2003) *GCA* **67**, 3717-3733. [7] Workman & Hart (2005) *EPSL* **231**, 53-72. [8] Hofmann (1988) *EPSL* **90**, 297-314. [9] Bouabdellah *et al.* (2010) *J. Petrol.* **51**, 1655-1686.

Dramatic seasonality of biogeochemical signatures in watersheds underlain by continuous and discontinuous permafrost

THOMAS A. DOUGLAS

U.S. Army Cold Regions Research and Engineering Laboratory; 9th Avenue, Building 4070 Fort Wainwright, Alaska 99703; 907-361-9555; (Thomas.A.Douglas@usace.army.mil)

High latitude watersheds experience two extreme seasons: 6-9 months of cold, snow covered winter and a warm, bright, summer. Between these seasons is the spring freshet, a dramatic two to three week period when up to three quarters of the yearly precipitation runs off. The summer to winter transition is far less remarkable as temperatures and light slowly decrease until winter arrives. The intense seasonality and transitions in Arctic rivers are associated with unique biogeochemical signatures, a landscape scale “view” of vegetation, soil, weathering, and water column processes.

Discerning sources or fluxes of compounds out of Arctic rivers is difficult in large rivers because they represent the combined effect of innumerable plot-scale melt water sources, each coming from different soil and vegetation types, each experiencing a slightly different melt timing and evolution, and each following its own timing. Work at Arctic sites typically means field work in remote locations with sparse ancillary data and this provides added challenges.

Spring melt is characterized by an ionic pulse of solutes, dissolved organic carbon and other nutrients (ammonium, phosphate and nitrate) leached by snow melt water from the surface organic mat of vegetation and near-surface soil. Summer and fall flows are comprised largely of shallow flow from a deepening seasonally thawed (“active”) layer. During late summer with an expanded active layer or at sites where permafrost is degrading these processes may be associated with an increasing mineral weathering signal into watersheds. The watershed biogeochemical response to precipitation in continuous and discontinuous terrains may also yield insight into subsurface permafrost geomorphological characteristics. Winter processes are the least studied or understood but overflow ice (“aufeis”) provides access to deep, old waters.

This presentation will focus on using water stable isotopes, major ion concentrations, and permafrost delineation to identify biogeochemical sources in watersheds draining continuous and discontinuous permafrost. Field sites represent permafrost terrains in Alaska from the North Slope to the Interior. Biogeochemical processes associated with scaling, meteorology, and climate warming will be discussed.

Accretion and differentiation processes in the ureilite parent body

H DOWNES^{1,2,3}, C L SMITH², F A J ABERNETHY⁴, J S HERRIN⁵ AND A J ROSS^{2,3}

¹Dept of Earth and Planetary Sciences, Birkbeck University of London, UK. E-mail: (h.downes@ucl.ac.uk)

²Natural History Museum, London UK.

³Centre for Planetary Sciences, UCL, London UK

⁴Physical Sciences, Open University, Milton Keynes UK

⁵Nanyang Technological University, Singapore.

Ureilite are carbon-rich meteorites which provide a wealth of information about early Solar System processes. The ureilite parent body (UPB) accreted from a carbon-rich precursor, but our new step-combustion $\delta^{13}\text{C}$ and $\delta^{15}\text{N}$ values for pristine ureilite samples strongly support the suggestion [1] that this precursor was not a known type of carbon-rich chondrite. A strong correlation between Fo in olivine and $\delta^{18}\text{O}$ is interpreted to result from heterogeneous accretionary mixing between two nebula-derived end-member compositions.

Heat derived from decay of short-lived radioactive isotopes caused the UPB to heat up and to differentiate into an metallic partial melt and silicate mantle. Little evidence of the metallic partial melt remains, other than frozen Fe-Ni metal droplets in some ureilites [2]. These metal droplets often contain Si, indicating extremely reducing conditions [3]. Depletion in Ge, As, Au, Pd, Ni, and enrichment in Ir, Os, Re [4], suggest that these metals may be restites from core formation.

LREE-depletion of the residual silicate mantle, together with silicate melt droplets, melt inclusions, and pyroxene-rich mantle lithologies, suggests that the UPB mantle underwent partial melting to form basaltic magmas. However, the UPB did not heat up sufficiently to reach a magma ocean stage and hence did not homogenize in terms of its mg# and $\delta^{18}\text{O}$ [5].

While it was undergoing heating and partial melting, the UPB was disrupted by a major impact. Graphite was transformed to diamond by this event [6]. Following this disruption, a single daughter rubble-pile asteroid formed by reaccretion [7]. This body is sampled by present-day ureilites, providing a fossilised example of early asteroidal accretion and differentiation processes.

[1] Warren (2011) *GCA* **75**, 6912-6926. [2] Herrin *et al.* (2007) *LPSC*, Abst 3345. [3] Smith *et al.* (2010) 73rd Ann Met Soc Meeting, Abst 5221. [4] Herrin *et al.*, (2008) 71st Ann Met Soc Meeting, Abst 5327. [5] Downes *et al.* (2008) *GCA* **72**, 4825-4844. [6] Ross *et al.* (2011) *MAPS* **46**, 835-849. [7] Herrin *et al.* (2010) *MAPS* **45**, 1789-1803.

Iron and manganese reduction and associated phosphorus release in coastal Baltic Sea sediment

KENNETH DOWNS* AND VOLKER BRÜCHERT

Department of Geological Sciences, Stockholm University, 10691 Stockholm, Sweden

*(correspondence: kenneth.downs@gmail.com)

The long-term release of phosphorus from sediments is considered the central problem for eutrophication of the Baltic Sea. In this study the sedimentary pools and long-term release rates of sediment-bound phosphorus were assessed in relation to iron and manganese reduction rates in the topmost 8 cm of coastal Baltic Sea sediment. We report porewater and solid-phase data of dissolved iron, manganese, inorganic and organic phosphorus from sediment from a near-shore station on the Eastern Swedish coast of the central Baltic with oxygenated bottom water. Rates of iron and manganese reduction were determined from porewater gradients and from anaerobic bag incubations at in-situ temperatures. Anaerobic bag incubation experiments were conducted over 33 days to quantify the changes in pool size of reactive Fe and Mn and phosphorus (ascorbic acid-extractable, citric-acid dithionite extractable, and oxalate-extractable) fractions.

The data indicate high initial rates of iron reduction in the topmost 5 cm, which decreased substantially after 18 days. Manganese reduction rates were insignificant below 1 cm depth. Rates of iron reduction were highest between 1 and 2 cm depth and decreased sixfold to 5 cm depth. Ascorbic acid extractable iron comprised about 50% of the total reactive iron in the topmost cm of sediment and decreased linearly over time. There was a pronounced lag effect of 8 days between the disappearance of reactive iron compounds and the increase in free dissolved iron and phosphorus in the topmost cm of sediment suggesting an intermediate accumulation of an iron-phosphorus complex that was not accessible to the extractions and spectrophotometric analytical methods employed here. Possibly phosphorus accumulated as an iron polyphosphate complex that was subsequently broken down under more reducing conditions. Operationally defined dissolved organic phosphorus (DOP) comprised 50% of the total dissolved phosphorus in the topmost cm of sediment. The initial rates of DOP and DIP release were equal in the topmost two centimeters, but DOP accumulation was significantly slower below 3 cm depth consistent with lower overall carbon degradation rates at depth. These data provide new quantitative constraints on the pool size and rates of phosphorus release from sediments and will improve our predictions of long-term eutrophication effects in the Baltic Sea.

Tracing episodic microbial oxidation of biogenic methane deep in fractured granite using $\delta^{13}\text{C}_{\text{calcite}}$

H. DRAKE^{1*}, C. HEIM², M. ÅSTRÖM¹
AND M. WHITEHOUSE³

¹Department of Biology & Environmental Science, Linnaeus University, 39182 Kalmar, Sweden. (*correspondence: henrik.drake@lnu.se, mats.astrom@lnu.se)

²Geoscience Centre Göttingen, Georg-August Univ., 37077 Göttingen, Germany. (cheim@gwdg.de)

³Laboratory for Isotope Geology, Swedish Museum of Natural History, 10405 Stockholm, Sweden, (martin.whitehouse@nrm.se)

Fossil and active microbial oxidation of methane (AOM) has been described from many settings worldwide, e.g. at cold seeps, and can be traced by extremely depleted $\delta^{13}\text{C}$, e.g. of authigenic carbonates (generally -65 to -45‰ [1]). We here show signs of AOM in a substantially less studied environment - deep in fractured granitoids within a shield area (Laxemar, Sweden). Here, the methane gas concentration is currently low, but nevertheless, microbial AOM is evidenced by the most $\delta^{13}\text{C}$ -depleted calcites ever reported (to our knowledge); down to -125‰ V-PDB (SIMS data). These $\delta^{13}\text{C}$ values rule out any other source than biogenic methane. The preferential depth of AOM (-350 to -650 m, cf. [2]) marks the shift from the microbial DOC consumption in the groundwater at shallower depths to methanotrophic at greater depth where DOC is depleted. Marine $\delta^{18}\text{O}_{\text{calcite}}$ values show that AOM was initiated by intrusion of SO_4^{2-} -rich marine waters causing sulphate reducing bacteria (SRB) to outcompete prevailing methanogens for H_2 , and instead methane oxidisers formed consortia with SRB, as shown by SRB-specific biomarkers trapped within the calcites (GC-MS and ToF-SIMS evidence). Low contents of dissolved carbon prevented dilution of $\delta^{13}\text{C}_{\text{calcite}}$ by other C sources than AOM, explaining why $\delta^{13}\text{C}_{\text{calcite}}$ is much lower than in other AOM-settings where $\delta^{13}\text{C}_{\text{calcite}} \gg \delta^{13}\text{C}_{\text{methane}}$ [1]. The extremely large intra-crystal $\delta^{13}\text{C}$ -variation (up to 109‰) and related $\delta^{18}\text{O}$ -variation show that AOM was episodic and e.g. succeeded by intrusion of sulphate-poor glacial water ending the AOM activity. The discovered deep AOM-zone must therefore be fossil, i.e. $\delta^{18}\text{O}$ and $\delta^{13}\text{C}$ of the calcites and modern groundwater are uncorrelated, and instead related to a pre-Holocene transgression of marine waters.

[1] Aloisi *et al.* (2002), *EPSL* **203**, 195-203

[2] Drake *et al.* (2012), *Geochim Cosmochim Acta* **84**, 217-238

O and Hf isotopic evidence in zircons for crustal recycling in caldera complexes and rifts, Picabo volcanic field, Yellowstone hotspot track

D. DREW¹, I. BINDEMAN¹, K. WATTS², A. K. SCHMITT³,
B. FU⁴ AND M. MCCURRY⁵

¹Dept. of Geological Sciences, University of Oregon, Eugene, USA (*correspondence: dld@uoregon.edu)

²U.S. Geological Survey, Menlo Park, CA, USA

³Dept. of ESS, UCLA, Los Angeles, CA, USA

⁴RSES, Australian National University, Canberra, Australia

⁵Dept. of Geosc., Idaho State University, Pocatello ID, USA

We report oxygen isotope diversity in zircons of large volume rhyolites of the Picabo volcanic field (10.4-6.6Ma) of the Snake River Plain (SRP), highlighting the generation, by shallow remelting, and rapid assembly of diverse magma batches prior to caldera forming eruptions. *In situ* measurements of ϵ_{Hf} and $\delta^{18}\text{O}$ coupled with U-Pb geochronology and whole rock Sr and Nd isotopes elucidate the processes by which large volumes of rhyolite are produced, starting with large-scale (up to ~40-60%) melting of Archean crust followed by plume driven remelting of volcanics in rift zones and caldera complexes. Similar to Heise and Yellowstone, the Picabo volcanic field produced a series of voluminous rhyolites that become progressively lower in magmatic $\delta^{18}\text{O}$ (from 7.9 to 3.3‰) and demonstrate increasing zircon $\delta^{18}\text{O}$ diversity through time (from <1‰ in early eruptions to >5‰ in late-stage). In contrast, zircon ϵ_{Hf} remains relatively homogeneous within units, with average ϵ_{Hf} ranging from -28 to -5.3 (with rare $\epsilon_{\text{Hf}}(0)=-47$ zircons reflecting pure Archean crustal melts). The temporal trend in $\delta^{18}\text{O}$ emphasizes the importance of remelting hydrothermally altered intracaldera rhyolites during caldera burial. However, the early appearance and overabundance of low $\delta^{18}\text{O}$ rhyolites suggests that hydrothermal preconditioning of the crust was facilitated by Basin and Range extension and metamorphic core complex formation. The preservation of diverse isotopic signatures in zircon, corroborates the importance of rapid batch assembly and eruption of heterogeneous melts with diverse crystal cargoes. Our interpretations highlight the mechanism by which large volume rhyolites are generated, processes applicable to producing rhyolites worldwide that are facilitated by plume driven volcanism in an extensional tectonic regime. Our newly discovered low- $\delta^{18}\text{O}$ rhyolites contribute to the growing database of greater than 10,000 km³ of low and diverse $\delta^{18}\text{O}$ rhyolites of the SRP, advancing our understanding of the 16 million year history of silicic volcanism.

Characterization of ternary surface complexes of lead chloride on hematite in dependence of temperature and salinity – experimental versus modeled data

DEJENE LEGESSE DRIBA¹, SIMONA REGENSPURG¹,
MARCO DE LUCIA² AND STEFAN PEIFFER²

¹GFZ German Research Centre for Geosciences, International Centre for Geothermal Research, Potsdam, Germany, dejene@gfz-potsdam.de,

regens@gfz-potsdam.de

²GFZ German Research Centre for Geosciences, Section 5.3, Hydrogeology, Potsdam, Germany

marco.delucia@gfz-potsdam.de

²Department of Hydrology, University of Bayreuth, Bayreuth, Germany S.Peiffer@uni-bayreuth.de

Adsorption of aqueous metal cations onto mineral surfaces can affect metal speciation and mobility in a range of geologic systems. In order to accurately model metal speciation and transport on iron-oxides, the effect of pH, temperature and ionic strength on its adsorption property and stability constants must be determined. The surface complex modeling approach CD-MUSIC (chargedistribution multi-site complexation) requires the definition of many parameters including equilibrium constants for protonation and deprotonation, metal sorption and back ground electrolyte sorption reactions etc.

However, the lack of many of those parameter particularly for Pb adsorption onto hematite surface requires the implementation of experimentally determined data.

In this study, Pb+2 adsorption experiments were performed in hematite bearing NaCl solutions as a function of pH value (3-9), ionic strength (0.5M and 5M) and temperature (25-150 °C). The required surface complex parameters (SCP) were derived through an iterative procedure of fitting the experimental data-set with simulation results by implementing the geochemical speciation code PhreeqC coupled with the non-linear optimization program UCODE_2005. Model results reveal that the simulation represents well the experimental conditions and reflects the dependency of Pb adsorption on different experimental parameters. In addition, it was found that lead-chloride ternary complex adsorption configuration provides a good fit to all Pb+2 adsorption data. Accordingly, the derived SCP data set will furnish for the development of a thermodynamically consistent surface complex database to estimate lead sorption in a geological environment of high temperatures and salinities.

The influence of flow field heterogeneity on the observed $\delta^{53}\text{Cr}$ fractionation factor during abiotic chromate reduction

J.L. DRUHAN^{1*}, K. MAHER¹, K.L. WEAVER¹
AND C.N. MCCLAIN¹

¹Department of Geological and Environmental Sciences, Stanford University, Stanford, CA, 94305

(*correspondence: jdruhan@stanford.edu)

Hydrogeochemical processes governing groundwater quantity and quality are often inferred from fluid samples that are the flux-weighted average of a heterogeneous system. The stable isotope ratios of these samples are commonly interpreted through simplified fractionation relationships that inherently assume a homogeneous chemical composition and fluid residence time. Here, we present application of an isotope-specific rate expression for chromate reduction in the CrunchFlow reactive transport code to simulate the steady state distribution of $\delta^{53}\text{Cr}$ across multiple realizations of a spatially correlated heterogeneous flow field (Figure). Our results demonstrate that a flux-weighted average value collected across the mean flow gradient yields a variable observed fractionation factor despite a fixed ratio of kinetic rate constants for the isotopologues of chromate. This variability is thus directly attributable to the physical heterogeneity of the porous media. We demonstrate that for a specified correlation function and characteristic length scale of the permeability structure, the observed fractionation factor is predictably linked to the fluid residence time distribution. These simulations serve as the basis for a series of flow-through column experiments using simplified heterogeneity to demonstrate variability in observed fractionation factors.

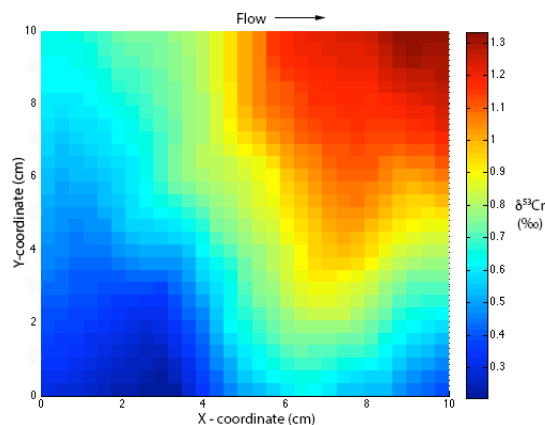


Figure: steady state $\delta^{53}\text{Cr}$ across a heterogeneous flow field

The adsorptive behaviour of Am and Tc on Fe-bearing minerals

R.DRUTEIKIENĖ*, B.LUKŠIENĖ, V.REMEIKIS,
J.ŠAPOLAITĖ AND R.GVOZDAITĖ

Center for Physical Sciences and Technology, Savanorių av.
231, LT-02300 Vilnius, Lithuania
(*correspondence: ruta@ar.fi.lt)

Understanding the migration behaviour of radioactive elements in geological environments is essential for the long-term safety assessment of nuclear waste repositories and in nuclear waste management. The potential of migration of radionuclide at contaminated sites and also from the waste repository depends on their environmental behaviour. In this work, we focus on the investigation of the behaviour of redox sensitive radionuclides in the heterogeneous system containing well-defined amounts of Fe-bearing minerals under aerobic conditions.

To evaluate sorption of Am(III), as Pu(III) analogue, by geosorbents under aerobic conditions, the batch laboratory method and laboratory column method were carried out. ²⁴³Am sorption to geosorbents from aqueous solution was determined being pH-dependent. ²⁴³Am sorption onto wustite/magnetite showed negative linear relationship within pH values (pH 2.15; pH 4.00; pH 6.95; pH 9.01), while the adsorption of ²⁴³Am ions onto hematite increased with increasing pH values (correlation coefficient R=0.83, R=0.92, R=0.90, respectively).

The tests of TcO₄⁻ sorption onto iron oxides were performed under ambient conditions. The investigation of Tc sorption onto hematite under the acidic (pH 3-5) and neutral (pH 6-7) conditions suggested that pH of solution had a very slight influence on the technetium sorption. Gradual sorption of technetium, added as TcO₄⁻, in aquatic solution onto FeO/Fe₃O₄ mineral under aerobic conditions was observed. The sorption of Tc onto wustite under the acidic (pH 3,6 and 5,6) conditions was rapid - after the first 48 hours <1 % of Tc were left in solution.

Mineral hematite at neutral or slightly alkaline pH under aerobic conditions is devoted to minerals which do not sorb Tc (VII). The presence of biogenic Fe(II) as mineral wustite/magnetite can affect the removal of Tc(VII) from the aqueous solution (pH of 8-9). Results of our experiment with Tc(VII) and wustite/magnetite varies from the general assumption stating that under oxidizing conditions TcO₄⁻ is stable and consequently mobile [1].

[1] Lieser, *et al.* (1987) *Radiochim. Acta* 42, 205-213.

This work is supported by the Research Council of Lithuania under the project No MIP-066/2013

The modern hydrogeochemistry of small pools in Corchia Cave, Italy: implications for palaeoclimate reconstruction

RUSSELL DRYSDALE¹, GIOVANNI ZANCHETTA², ILARIA BANESCHI³, ISABELLE COUCHOUD⁴, MATHEIU DAERON⁵, JOHN HELLSTROM⁶, BENCE PAUL⁶, MICHAEL GAGAN⁷, ALAN GREIG⁶, ILARIA ISOLA⁸, ELEONORA REGATTIERI², AND MASSIMO GUIDI³

¹Melbourne School of Land and Environment, The University of Melbourne, Australia; e-mail: rnd@unimelb.edu.au

²Department of Earth Sciences, University of Pisa, Italy;

³Istituto di Geoscienze e Georisorse - CNR- Pisa, Italy;

⁴EDYTEM, Universite de Savoie, Le Bourget du Lac France

⁵CNRS-LSCE, Gif-sur-Yvette, France

⁶School of Earth Sciences, The University of Melbourne, Australia

⁷Research School of Earth Sciences, ANU, Australia

⁸Istituto Nazionale di Geofisica e Vulcanologia, Pisa, Italy

Several small lakes occupy a number of levels in the Galleria delle Stalattiti of Corchia Cave, Italy. An important feature of two such lakes is the presence of actively growing, subaqueous calcite mounds. Drill cores from these mounds have been the subject of investigations for several years. ²³⁴U-²³⁸U ages from the base of these cores, combined with stable isotope data from U-Pb-dated stalagmites collected metres away, suggest that some of the mounds have been growing since ~1 Ma. To provide baseline data for interpreting the geochemical variations of these cores, we commenced a study of modern lake-water chemistry, including stable isotopes of H, C and O, trace elements and organic matter content. Besides demonstrating the exceptionally stable state of these lake systems, the combining of core-top geochemistry with source-water chemistry allows us to explore water-calcite isotope and trace element partitioning, and to evaluate the suitability of this unusual speleothem-forming environment for clumped-isotope palaeothermometry. Preliminary results will be presented in this poster.

The heat relaxation P - T - t path of HP-UHP eclogites from Chinese southwestern Tianshan: constraints from P - T pseudo-sections, Lu-Hf and Sm-Nd isochron dating

DU JINXUE, ZHANG LIFEI*, SHEN XIAOJIE
AND THOMAS BADER

Key Laboratory of Orogenic Belts and Crustal Evolution,
Ministry of Education, School of Earth and Space
Sciences, Peking University, Beijing 100871, China
(*corresponding author: Lfzhang@pku.edu.cn)

Abstract: The southwestern Tianshan orogenic belt is one of the rare preserved ultrahigh pressure metamorphic belts formed by oceanic subduction in the world. However, its P - T - t path is poor constrained. In this study, four representative eclogite samples, i.e., three paragonite-epidote eclogites (Sample 211-3, H505-26 and H76-10) and one glaucophane-phengite eclogite (Sample H711-1), are selected for combined study of Lu-Hf and Sm-Nd geochronology as well as a detailed phase equilibria modeling. Porphyroblastic garnet in these four samples shows well-preserved growth zoning with the content of pyrope increasing and that of spessartine decreasing from core to rim. Phase equilibria modeling indicates that garnet in eclogites from Chinese southwestern Tianshan grew in the lawsonite-bearing eclogite facies during heating accompanied by either compression (e.g. H505-26) or decompression (e.g. 211-3, H76-10 and H711-1). Estimated peak pressures of 24-29kbar with a coesite pseudomorphs suggest that some eclogites underwent UHP metamorphism (e.g. 211-3). Peak temperatures of 490-560°C are below the closure temperature of the Lu-Hf and Sm-Nd systems. The garnet-omphacite-whole rock Lu-Hf and Sm-Nd isochron ages, therefore, are interpreted to reflect garnet growth, i.e., HP-UHP eclogite facies metamorphism. Sample 211-3 yields a Lu-Hf isochron age of 326.9±1.3Ma which represents the first reported Lu-Hf age for UHP metamorphism in Chinese southwestern Tianshan. Another valid Lu-Hf age of 306±11Ma for Sample H76-10 and three consistent Sm-Nd isochron ages of 309±4.6Ma, 306±15Ma and 305±11Ma for Samples H505-26, H76-10 and H711-1 are obtained, reflecting high pressure eclogite facies metamorphism. Based on these new ages, a clockwise P - T - t path with heating during exhumation is obtained for HP-UHP eclogites from Chinese southwestern Tianshan, in conjunction with detailed phase equilibrium studies and previous geochronological data. This heat relaxation P - T - t path of HP-UHP eclogites indicates the slow exhumation and long journey for the heavy oceanic HP-UHP eclogite. We propose that subduction of the paleo-South Tianshan ocean began before 346Ma, blueschist-eclogite facies prograde metamorphism of subducting oceanic crust occurred at 346-333Ma, peak eclogite facies metamorphism occurred at 327-305Ma, and buoyancy-driven exhumation of subducted oceanic crust occurred at 296-226Ma.

The $\delta^{18}\text{O}$ signals of precipitation and drip water: Two hydrological years' monitoring results from eight caves in monsoon regions of China

W.H. DUAN¹, J.Y. RUAN^{2,6}, P.Z. ZHANG³, W.J. LUO⁴,
D.Z. ZHANG³, T.Y. LI⁵, L.J. TIAN¹, T. TAO¹, G.N. ZENG⁴
AND M. TAN^{1*}

¹Key laboratory of Cenozoic Geology and Environment,
IGGCAS, (*correspondence: tanming@mail.iggcas.ac.cn)
²China University of Geosciences (Wuhan), China,
³Lan Zhou University, China.
⁴State Key Laboratory of Environmental
Geochemistry, IGCAS, Guiyang 550002
⁵School of Geographical Sciences, Southwest Univ, China,
⁶Lab des Sciences du Climat et de l'Environnement, France.

To better interpret the $\delta^{18}\text{O}$ proxy of Chinese speleothems, a joint monitoring program has been carried out at eight cave sites in monsoon regions of China (fig1) since 2011. Here we outline preliminary conclusions as follows:

1. At any monitoring cave sites, precipitation $\delta^{18}\text{O}$ does not show significant amount/temperature effect at seasonal or inter-annual scale.

2. At five of six cave sites in South China, the mean annual precipitation $\delta^{18}\text{O}$ is heavier in 2012 than in 2011, which is consistent with that the short-distance source water vapor from West Pacific Ocean to China is larger in 2012 than in 2011[1]. But specially, at Xianren cave site, the $\delta^{18}\text{O}$ behaves oppositely versus other five sites, most likely because the West Pacific Ocean is a long-distance water source for this westerly farther location. While at Shihua cave and Wanxiang cave in North China, the mean annual precipitation $\delta^{18}\text{O}$ is roughly equal in the two years. Therefore, under inter-annual variation, the monitoring results from the southern caves supports the idea on the "circulation effect" of precipitation $\delta^{18}\text{O}$ [2], while, from the northern caves, they are ambiguous.

3. At most of the monitoring sites, the depleted summer precipitation $\delta^{18}\text{O}$ signals are greatly smoothed when waters filter into caves. Accordingly, vadose zone plays a significant role in modifying the $\delta^{18}\text{O}$ signals of drip waters[3].

[1] <http://www.itmm.gov.cn/grapes/jcgb>. [2] Tan (2013) Clim Dyn, doi:10.1007/s00382-013-1732-x. [3] Luo & wang (2008) Chin Sci Bull 53,3364-3370.

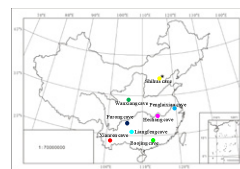


Figure1: Locations of the eight caves monitored in this study.

Trace element analysis of iron meteorites by ICP-MS

XIAOXIA DUAN^{1,2} AND MARCEL REGELOUS¹

¹ GeoZentrum Nordbayern, Universität Erlangen-Nürnberg, Schlossgarten 5, 91054 Erlangen, Germany (correspondence : duan861168@163.com)

² Institute of Geology and Geophysics, CAS, Beijing, China

Trace element measurements of iron meteorites provide important information on the processes of formation and crystallisation of asteroid cores, and forms the basis of the classification scheme whereby the number of iron meteorite parent bodies can be determined. Most existing trace element data for iron meteorites were carried out using instrumental or radiochemical neutron activation. These methods allow measurement of 10-15 trace elements in iron meteorites, but are time-consuming and expensive. Recently, attempts have been made to measure trace element concentrations in iron meteorites using inductively coupled plasma mass spectrometry [1-3]. Advantages of ICP-MS analysis include low detection limits for most elements, simple sample preparation and short analysis times. A disadvantage of quadrupole ICP-MS analysis is that molecular interferences, especially those involving Fe which makes up ~90% by weight of most iron meteorites, prevent accurate analysis of several important elements, in particular Ge.

We developed methods to remove Fe from sample solutions using ion exchange, and use a desolvating nebuliser sample introduction system to reduce other solution-based interferences. Samples are dissolved in 8M HNO₃ and loaded directly onto Eichrom TRU-spec resin. ⁵⁶Fe can be reduced by 2-3 orders of magnitude, with close to 100% recovery of most other elements, excepting Nb, Ta, Th, U, Ti, which are retained on the resin. Measurements are carried out using a Thermo X-Series2 quadrupole ICP-MS equipped with a collision cell and Aridus desolvating introduction system.

Our new method allows rapid, accurate measurement of not only the highly siderophile trace elements (including Os if solutions are not heated) and transition metals, but also many non-siderophile elements. These are not routinely measured in iron meteorites because of their very low abundance, but could nevertheless provide important new insights into the oxygen fugacity at the time of accretion and the original size of iron meteorite parent bodies.

[1] M. D'Orazio *et al.*. (2003) *Geostandards Newsletter* **27**, 215–225. [2] A. J. Campbell *et al.*. (1997) *Anal. Chem.* **71**, 939-946. [3] T. McCoy *et al.*. (2011) *Geochem. Cosmochim. Acta* **75**, 6821-6843.

Research on carbon isotopic evolution of pyrolysis methane and its dynamics

YI DUAN

Key Laboratory of Petroleum Resources Research, Institute of Geology and Geophysics, Chinese Academy of Sciences, Lanzhou, Gansu, China, duany@lzb.ac.cn.

In order to understand the genesis of coalbed methane (CBM) as a new energy, closed-system pyrolysis experiments were performed on coals with different maceral compositions and maturities and a peat representing original coal-forming material at different heating rates, and the carbon isotopic evolution of pyrolysis methane and the carbon isotopic dynamic characteristics of CBM from Qinshui Basin were studied. It was found that the carbon isotopic compositions and evolutionary history of pyrolysis methane were closely relevant to many factors, such as the properties and coalification levels of coal, initial evolution level of source rocks and heating rate and so on. The correlation between the carbon isotopic compositions of pyrolysis methane and lg(Ro) was suggested. At the same time, the carbon isotopic evolutionary history of methane from the Upper Paleozoic coal seam in Qinshui Basin and its coalbed methane genesis were determined. The results show that the CBM formed by coal with low initial evolution level and high exinite content and under conditions of high heating rate has relatively light carbon isotopic composition. The carbon isotopic compositions of pyrolysis methane from the studied samples at different heating rates were positively correlated with lg(Ro). The carbon isotopic evolution history of methane generated from the Upper Paleozoic coal in Qinshui basin was that $\delta^{13}\text{C}$ values of pyrolysis methane from Taiyuan and Shanxi Formation coals and peat in Yangcheng region have a tendency to becoming heavier with burial history, reached to the heaviest at K1 end, and then did not change. The comparative study of the carbon isotopic dynamics of pyrolysis methane showed that peat has lighter isotopic composition than coals. The carbon isotopic composition comparison of CBM from Permian system in Yangcheng region of Qinshui basin with that obtained by this experiments indicated that the carbon isotopic compositions in Yangcheng region is similar to those of CBM evolved from early Cretaceous to now, reflecting that the CBM in Yangcheng region has the feature of staged gas accumulation. Therefore, the carbon isotopic dynamics of methane is an effective method for studying CBM genesis.

Rare Earth Elements in biogenic silica of giant diatoms *Ethmodiscus rex*

A.V.DUBININ* AND E.D.BEREZHAYA

PP Shirshov Institute of Oceanology RAS, 117997 Moscow, Russia, (*correspondence: dubinin@ocean.ru)

Biogenic silica plays an important role in rare earth element cycle in the ocean. Trivalent REE distribution in ocean water is very similar to that of dissolved silica. REE content in the biogenic silica currently remains unknown. The earlier data on the REE composition [1] for diatoms *Ethmodiscus rex* from the Indian Ocean sediments were obtained without chemical pretreatment. Thus the purpose of the present work is to consider REE concentrations in the frustules of diatoms. Diatom oozes (Sta. 1537, 19°05.5'S, 24°02.9' W, depth 5000 m) were disaggregated in distilled water to remove sea salts. Fragments of diatom (size fraction >100 μm) were isolated from slurry of oozes by sieving and washing through the polyamide net.

Chemical cleaning of the diatom shells included 4 stages. 1. Dissolving in solution 0.6M $\text{NH}_2\text{OH}\times\text{HCl}$ + 1M HCl to remove coatings and micronodules. 2. Filtration through filter Millipore 0.45 μm , washing with 1M HCl and Milli-Q water. 3. Treatment with 6.3M HCl, then solution was diluted with deionized water and after heating was agitated in an ultrasonic bath. 4. Filtering is similar to stage 2. Then samples were dried to a constant weight.

REE were determined by ICP-MS in 2% HNO_3 solution with internal standards In and Re after digestion of biogenic silica in a mixture of HF and HNO_3 (ultrapure grade Fluka) in PTFE beakers. The ratio of background/signal was less than 2% for Sm, Eu, Gd and Tb, for the other REE it was less than 1%.

REE pattern in diatom shells is similar to the composition of the dissolved REE in the ocean water. The surprise is the absence of the anomalous behavior of cerium. REE content in diatom shells is lower an order of magnitude than in the carbonate lattice of foraminifera [2]. The absence of cerium anomaly may be the result of the shell formation in oxygen minimum zone in the ocean water during diatom bloom in the glacial period.

[1] Elderfield *et al.* (1981) GCA 45, 513-528. [2] Palmer (1985) EPSL 73, 285-298.

Effect of anharmonic lattice vibrations on the reaction rates in minerals

V.I. DUBINKO^{1*} AND J. F. R. ARCHILLA²

¹ NSC Kharkov Institute of Physics and Technology, Kharkov 61108, Ukraine (*correspondence: vdubinko@mail.ru)

² Seville University, E-41011, Seville, Spain (archilla@us.es)

Chemical reaction rates in minerals are shown to be accelerated by large amplitude lattice vibrations (a.k.a. intrinsic localized modes (ILM's) or discrete breathers (DB's)) that can appear in crystals with sufficient anharmonicity. As a result, Arrhenius law is violated, and the reaction rate averaged over large macroscopic volumes and times including many DB's is increased by a factor that depends on the DB statistics. The breather statistics in thermal equilibrium is considered, and the corresponding reaction rate amplification factor is derived.

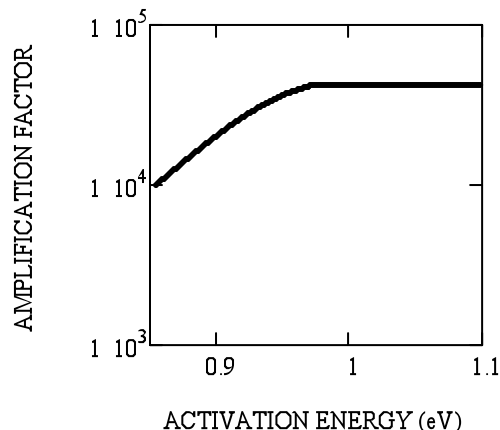


Figure 1. Amplification factor dependence on the reaction activation energy.

The model is shown to explain anomalous low-temperature reconstructive transformations in layered silicates [1] and the brittle to ductile fracture transition in α -uranium at elevated temperatures [2].

[1] J. F. R. Archilla, J. Cuevas, M. D. Alba, M. Naranjo, J. M. Trillo, J. Phys. Chem. (2006) **B110** 24112-24120. [2] M.E. Manley, Acta Materialia (2010) **58**, 2926-2935.

Fate of Ni in local reduced environments developed on lateritic Ni ores from New Caledonia

GABRIELLE DUBLET^{1,2*}, FARID JUILLLOT^{1,3}, GUILLAUME MORIN¹, EMMANUEL FRITSCH¹, JESSICA BREST¹ AND GORDON E. BROWN JR.^{2,4}

¹ Institut de Minéralogie et de Physique des Milieux Condensés (IMPMC), UMR CNRS 7590, UR IRD 206, Université Pierre et Marie Curie (UPMC), Campus Jussieu, 75252, Paris Cedex 05, France
Farid.Juillot@impmc.upmc.fr,
Guillaume.Morin@impmc.upmc.fr,
Emmanuel.Fritsch@impmc.upmc.fr,
Jessica.Brest@impmc.upmc.fr

² Department of Geological & Environmental Sciences, Stanford University, Stanford CA 94305-2115, USA
*correspondance: gdublet@stanford.edu
gordon.brown@stanford.edu

³ UFR STEP, Université Paris Diderot - IPGP, Bâtiment Lamarck, 75013 Paris, France

⁴ Stanford Synchrotron Radiation Lightsource, 2575 Sand Hill Road, Menlo Park, California, 94025, USA

In New Caledonia, the weathering of ultramafic rocks in a tropical climate produced extremely thick laterites ($\leq 80\text{m}$), particularly enriched in metals such as Ni. The main weathering pathway involved the formation of large amounts of goethite ($\alpha\text{-FeOOH}$), and X ray absorption spectroscopy (XAS) showed that the major proportion of Ni is incorporated into the structure of this Fe(III)-oxyhydroxide [1].

However, as previously reported in New Caledonia, reducing conditions can occur locally in the lateritic formations, due to the development of dolines and the accumulation of organic matter [2]. Samples from a lateritic profile characterized by X ray diffraction and ICP-AES showed the occurrence of siderite (FeCO_3) in a 4 meters thick horizon, suggesting the local reduction of Fe(III)-oxides into Fe(II)-carbonate. SEM-EDS analysis indicates significant amounts of Ni associated with siderite ($\sim 0.80\text{ wt\% NiO}$).

The speciation of Ni in this weathering context was then investigated by XAS in the solid phase, at the scale of the whole profile, and by comparison with synthetic analogues. XAS showed that Ni is mainly incorporated into the siderite structure in the reduced horizon, and is in goethite in the unreduced laterite above. This result helps understanding the trace metals behavior in altered lateritic weathering contexts, and shows the importance of local Ni trapping in reduced iron phases.

[1] Dublet *et al.* (2012) *GCA* **95**, 119–133 [2] Podwojewski and Bourdon (1996) *C.R. Acad. Sci. Paris*, **322**, series II a, 453-459

Long-time alteration of iron slags inferred from paleometallurgical heaps

M. DUBOIS AND A. GAUTHIER¹

¹LGCgE, Lille 1 University, SN5 Building, 59655 Villeneuve d'Ascq, FRANCE. Michel.dubois@univ-lille1.fr

Moulière is a large forest (area of 6800 ha) and is located on a plateau between the valleys of the Vienne and the Clain rivers (Vienne, France). Exploration by Abbé de la Croix in the nineteenth century and the work of the ONF (Office National des Forêts) have revealed the presence of numerous slag heaps. These heap associated with the iron metallurgy fall into several areas of the forest sector and outside. They are identifiable on the ground because they form mounds 0.5 to 2 m high and they are usually invaded by typical vegetation (holly - *Ruscus aculeatus* - and hawthorn). The age of these mounds is not known, but more than 10 ironworks were in operation at the time of the reformation of forests by Colbert in 1667. The establishment of the ironworks in the Forest of Moulière is related to the facility offered for logging to operate low blast furnaces. The iron ore is probably also of local origin. Whereas no significant outcrop has been actually observed, an iron-bearing sandy layer is discontinuously present in the forest underground.

A study of the mineralogical and chemical slags was carried out by optical microscopy, scanning electron microscopy (SEM) and Raman microspectroscopy in order to make a characterization, in particular for the presence of an alteration layer. Indeed, the slag storage sites offer the opportunity to study the long-term behavior of vitrified materials subjected to weathering periods of time (several centuries) well above the experimental approach.

High density slags present various dimensions from centimetric to decimetric blocks, rounded surface, sometimes within a matrix strongly the existence vacuole. They are black or red-orange. The samples exhibit a mineralogy consisting mainly of silicates (olivine (Fe_2SiO_4), quartz, feldspar) and oxides (hematite (Fe_2O_3), titanium oxide) in the periphery of the vacuoles or in forming droplets. This great disparity of mineralogical and chemical composition conditions the chemical durability of this material. Experimental studies are conducted to study the behavior of such slags.

Mantle-drip magmatism beneath the Altiplano-Puna plateau, central Andes

MIHAI N DUCEA^{1,2}

¹Universitatea Bucuresti, Facultatea de Geologie-Geofizica, Bucuresti, Romania

²University of Arizona, Department of Geosciences, Tucson, Arizona 85721, USA

Convective removal of continental lithospheric roots has been postulated to be the primary mechanism of recycling lithospheric mass into the asthenosphere under large plateaux such as the Altiplano-Puna. Convective instabilities are especially likely to develop where there is extensive intermediate arc-like magmatism in the upper plate, as the residual masses complementing these magmatic products are typically denser than the underlying mantle. Mafic volcanic rocks erupted on the central Andean Altiplano-Puna plateau during the past 25 My contain evidence of this process. Here we use equilibration temperatures, age data and geochemical constraints—primarily based on transition metals—to show that the most important source materials by mass for this mantle-derived magmatism are pyroxenites from the lower parts of the lithosphere, with only minor contributions from mantle peridotite. Pyroxenites are denser than typical upper mantle whether they are garnet bearing or not, and are therefore likely to contribute to destabilizing parts of the continental lithosphere. The pattern of melting is consistent with the process of foundering/dripping of small-scale (<50 km diameter) density anomalies in the lithosphere, where mafic volcanic fields on the plateau represent the manifestations of individual drips.

Reactivity and chemical reduction of iron oxides nanoparticles in highly alkaline medium

A. DUCHATEAU*, C. CHANEAC, J.P. JOLIVET

*anneduchateau0@gmail.com

Laboratoire de chimie de la matière condensée de Paris

Collège de France, UPMC Univ. Paris 6, CNRS, 11 Place Marcelin Berthelot 75005 Paris, France

Iron oxides play an important role in steel industry as precursors of iron. This industry is responsible for 7% of the world CO₂ rejections. Reducing the iron oxides by electrolysis in strongly alkaline medium (18 M) at 110°C is a promising way to lower the CO₂ rejections while improving steel production efficiency, that has been studied for years [1][2]. Obviously, studying the reactivity of iron oxides in this very particular medium and understanding the reduction mechanism is a key study for the process optimization. The experiments are carried out on iron oxides nanoparticles (hematite, goethite, lepidocrocite, akaganeite, magnetite) synthesized according to well known methods in order to have the most accurate comprehension of the phenomenon.

In almost all cases, the ageing of iron oxides nanoparticles in hot concentrated sodium hydroxide solution led to the formation of sodium ferrite NaFeO₂, as it was observed by Picard [2]. This phase transformation takes place according to a dissolution crystallization process whose duration is controlled by thermodynamics and depends on the starting iron oxide.

In a second step, we induced the reduction by using hydrazine as a chemical reductive agent in hot concentrated sodium hydroxide solution. At first a competition between reduction of the iron oxide and sodium ferrite precipitation is observed. Then the reduction takes place according to a two-step via solution mechanism: reduction of the starting iron oxide into magnetite, reduction of magnetite into iron.

[1]Allanore (2008) *J. Electrochem. Soc* **155**, 125-129, [2] Picard (1980) *J. Chem. Res., Synop* **8**, 252-253

Investigation of Archean mantle plume components from 2.7 Ga komatiites (Abitibi, Canada)

C. DUCHEMIN^{1*}, N. MATTIELLI¹, V. DEBAILLE¹, N. ARNDT²
AND C. CHAUVEL².

¹G-Time, Université Libre de Bruxelles, 1050 Brussels, Belgium. (*Claire.duchemin@ulb.ac.be).

²ISTerre, BP 53, 38041 Grenoble Cedex 9, France.

Komatiitic flows in Munro Township, Abitibi greenstone belt, are of two types: Al-depleted (ADK), which has low Al/Ti, and Al-undepleted (AUK) komatiites, with chondritic Al/Ti. The different geochemical types reflect source components and melting processes at 2.7 Ga.

We present new data for three thick differentiated lava flows: Fred's Flow and Pyke Hill are AUK with moderate depletion to strong REE depletion ($(Ce/Yb)_N=0.64$ and 0.34 respectively). Theo's Flow is an Al-depleted Mg-Fe rich tholeiite with HREE depletion ($(Gd/Yb)_N>1.35$) and flat LREE.

REE patterns of these flows reflect their initial geochemical signatures, and indicate differences in sources, and/or depths and degrees of partial melting probably in mantle plumes. To characterize the mantle source components, we modeled their major and trace elements. On the basis of the most primitive cumulus olivine crystals, the minimum eruption temperatures (°C) have been estimated according to calculations of [1]. Forsterite contents of olivine are 89.8% in Fred's Flow, 93.9% in the Pyke Hill flow and 84-86% in Theo's Flow and correspond to $1420\pm 43^\circ\text{C}$, $1516\pm 45^\circ\text{C}$ and $1325\pm 40^\circ\text{C}$, respectively. Parental magma compositions ($\text{CaO}/\text{Al}_2\text{O}_3\approx 1$) of Fred's Flow and Pyke Hill correspond to partial melts of a fertile mantle peridotite, whereas $\text{CaO}/\text{Al}_2\text{O}_3\approx 1.5$ of Theo's Flow suggests a higher pyroxene/garnet ratio in the source, as in pyroxene-rich peridotite [2].

External Pb-Pb isochrons have been obtained for Theo's Flow and Fred's Flow to better understand the evolution of source heterogeneities with time. The ages obtained for Theo's Flow and Fred's Flow are $2686\pm 94\text{My}$ and $2604\pm 102\text{My}$ respectively. Hf and Nd isotopes will be further investigated to propose initial isotopic signatures of the source of komatiites formed in Archean mantle plumes 2.7 Ga ago.

[1] Herzberg, C. & Asimow, P. D. (2008). *GCubed* 9, Q09001.

[2] Walter M. J. (1998). *Journal Petrol.* 39, 29-60.

Compositional gaps and melt segregation in magmatic systems: A multiphase dynamics approach

JOSEF DUFEK¹ AND OLIVIER BACHMANN²

¹School of Earth and Atmospheric Science, Georgia Institute of Technology

²Department of Earth Sciences, ETH

Compositional diversity in evolving magmatic systems is driven in large part by the multiphase dynamics of melt-crystal separation. Key to quantitative description of these systems is to accurately calculate the rate and timing of crystal-melt separation. This calculation requires accurately computing three separate, but closely linked, problems: heat transfer, phase equilibria, and multiphase dynamics, all of which can play an important role in determining the compositional and melt fraction histories of magmatic bodies. We have developed a multiphase approach to compute extraction in magmatic systems (Dufek and Bachmann, 2010) combined with an enthalpy closure from a callable library based on MELTS (Ghiorso and Sack, 1995). In this dynamics model separate phases are

We use this model to demonstrate dynamics on several different scales: We use this new model to demonstrate dynamics on several different scales: 1. Melt segregation and crystal-melt dynamics in small and moderate scale magmatic systems (using examples from Cotopaxi and the Fish Canyon Tuff), and 2. Thermal evolution on the crustal scale influenced by tectonic forcing, including shortening and extension. In all cases we explore the rate and location of fractionating phases, and the driving mechanisms for fractionation.

We have particularly applied this model to examine the production of compositional (Daly) gaps in a number of tectonic settings. Compositional gaps are common in volcanic series worldwide. The pervasive generation of compositional gaps influences the mechanical and thermal properties of the crust. We show that gaps are inherent to crystal fractionation for all compositions, as crystal-liquid separation takes place most efficiently within a crystallinity window of $\sim 50\text{--}70\text{ vol\%}$ crystals. The probability of melt extraction from a crystal residue in a cooling magma chamber is highest in this crystallinity window due to (1) enhanced melt segregation in the absence of chamber-wide convection, (2) buffering by latent heat of crystallization, and (3) diminished chamber-wall thermal gradients. This mechanical control of igneous distillation is likely to have played a dominant role in the formation of the compositionally layered Earth's crust by allowing multiple and overlapping intrusive episodes of relatively discrete or quantized composition that become more silicic upward.

Is plutonium being incorporated by magnetite under anoxic conditions?

T. DUMAS¹, D. FELLHAUER², X. GAONA²,
M. ALTMAIER² AND A.C. SCHEINOST^{1*}

¹HZDR, Inst. of Resource Ecology, 01314 Dresden, Germany
(*correspondence: scheinost@esrf.fr,
thomas.dumas@cea.fr)

²KIT-INE, 76128 Karlsruhe, Germany
(david.fellhauer@kit.edu, xavier.gaona@kit.edu,
marcus.altmaier@kit.edu)

Magnetite, which forms under anoxic conditions on the surface of corroding steel containers, is able to reduce a range of elements, including radionuclides of high relevance in the context of nuclear waste disposal, e.g. Se, Tc, U, Np, Pu [1]. Aqueous Pu(V) is rapidly reduced by nanoparticulate magnetite to Pu(III), which then forms stable, tridentate sorption complexes on the {111} faces of magnetite [2]. Trivalent lanthanides have been shown to substitute for Fe(III) in magnetite, although their ionic radii are about 1.4 times larger than that of Fe(III) (1.15-1.17 vs. 0.79 Å in six-fold coordination) [3]. To investigate if such an incorporation is also possible for Pu(III) with a similar ionic radius as the lanthanides, we conducted coprecipitation experiments with two Pu loadings of 1000 and 3500 ppm. UV-VIS spectroscopy showed an immediate reduction of Pu(V) to Pu(III) in the initial Fe(II)/Fe(III) chloride solution. After formation of the black magnetite precipitate, Pu(III) concentration in solution was below 10⁻⁹ M. X-ray Absorption Near-Edge Structure (XANES) spectroscopy confirmed the trivalent oxidation state of solid phase-associated Pu. Extended X-ray Absorption Fine-Structure (EXAFS) spectroscopy was then used to investigate the molecular structure of incorporated Pu(III) in the fresh precipitate as well as after Fe(II)-induced aging [4]. The EXAFS spectra revealed two different spectral components. The first component represents the tridentate Pu(III) sorption complex also observed during sorption experiments. The second component represents Pu(III) in a highly distorted magnetite Oh site. The proportion of the incorporated Pu(III) decreased from about 75% to 40% with Fe(II)-induced aging, while the proportion of sorbed Pu(III) increased correspondingly. Our results suggest, therefore, that Pu can be incorporated by magnetite, but will convert to sorbed species on the long time scales relevant for nuclear waste disposal.

[1] Scheinost *et al.*. (2008) *J. Contam. Hydrol.* **102**, 228-245.
[2] Kirsch *et al.*. (2011), *Environ. Sci. Technol.* **45**, 7267–7274. [3] Moon *et al.*. (2007) *Extremophiles* **11**, 859-867. [4] Boland *et al.*. (2011) *Environ. Sci. Technol.* **45**, 1327-1333.

Mineralogy and geochemistry of natural porcelanites

DELIA-GEORGETA DUMITRAS^{1*}, ADRIANA ION¹,
IOAN MILOSAN², STEFAN MARINCEA¹
AND CONSTANTIN COSTEA¹

Geological Institute of Romania, 1, Caransebes Str.,
Bucharest, Romania, RO-012271. (*correspondence:
d_deliaro@yahoo.com)
Transilvania University of Brasov, 29, Eroilor Bld., Brasov,
Romania, RO-500036. (milosan@unitbv.ro)

Natural porcelanites from Filipestii de Pădure, Romania, were analyzed from mineralogical, radiometric and geochemical point of view. These artifacts resulted from the *in situ* ignition of the relic coal in the sterile wastes issued from the mining activity, as well as from the burning of the clay formations in the couch and roof of the coal layers.

The mineralogical associations inferred by X-ray powder diffraction analyzes of 10 samples of porcelanite consist in gypsum, anhydrite, bassanite, quartz, sanidine, tridymite, mullite, cordierite, hematite, spinel, cristobalite, illite, spinel. Cell parameters for the most representative species were obtained by least squares refinement of X-ray powder data.

Anhydrite and gypsum are particularly abundant, reaching up to 45 % of the porcelanite volume. FTIR study shows in all the samples the group of bands in the 1000-1160 cm⁻¹ region materializing stretching motions of the (SO₄)²⁻ group, as well as bands characteristic to the vibrations of molecular water. SEM photos show that in some cases anhydrite postdates gypsum, pseudomorphs of anhydrite after gypsum conserving the (010) perfect cleavage of gypsum.

ICP-MS analysis pointed out the presence of a large spectrum of REE (e.g. Y, La, Ce, Pr, Nd, Sm, Eu, Gd, Tb, Dy, Ho, Er, Tm, Zb, Lu), as well as of U and Th.

The gamma-energy spectrum radiometric measurements showed the presence of the following natural radionuclides (in order of the decreasing abundance): Ra-226, U-238, K-40 and Th-232.

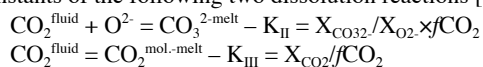
Solubility of CO₂ in rhyolitic melts as a function of depth, temperature, and oxygen fugacity – implications for carbon flux in subduction zones

MEGAN DUNCAN^{1,*} AND RAJDEEP DASGUPTA¹

¹Dept. of Earth Science, Rice University, Houston, TX, USA,
(*correspondence: Megan.S.Duncan@rice.edu)

Partial melt of subducting sediments is thought to be a critical agent in transport of trace elements and water to arc basalt source regions. Sediment melts may also carry CO₂ to arc basalt source regions, however, the carrying capacity of CO₂ in rhyolitic melts of appropriate composition and at conditions relevant for subducting slab is unknown. In particular, the solubility of CO₂ in rhyolitic sediment melt may vary significantly as a function of fO_2 , i.e. from graphite-saturated or organic carbon-bearing domains to carbonate/CO₂-saturated conditions. Yet no studies have constrained the sediment partial melt CO₂ carrying capacity under graphite saturated conditions.

We conducted experiments over 1.5 to 3.0 GPa and 1300°C on a model, natural rhyolitic melt under nominally anhydrous to hydrous conditions. CO₂ content of experimental glasses in equilibrium with CO₂-rich vapor phase was determined using FTIR spectroscopy. CO₂ was found to be dissolved both as molecular CO₂ (CO₂^{mol.-melt}) and as carbonates (CO₃^{2.-melt}). Speciation-specific CO₂ solubility data were used to constrain the pressure-dependence of equilibrium constants of the following two dissolution reactions [1] –



Further, using the thermodynamic framework given by [2], here we calculated the CO₂ content of silicate melt as a function of P, T, and fO_2 for graphite-saturated conditions, by combining the P-dependence of K_{II} and K_{III} constrained in [1] and P-T- fO_2 dependence of K_{I} of the reaction: C + O₂ = CO₂^{fluid} given by [2]. Experiments at lower temperatures are underway to constrain the T-dependence of K_{II} and K_{III} .

Using the model above, we have calculated the total CO₂ content (CO₂^{mol.-melt} + CO₃^{2.-melt}) of a sediment partial melt for a variety of subduction P-T paths [3] at fO_2 values at or below the graphite-CO₂ equilibrium. Our study suggests that ≥1 wt.% CO₂ may be dissolved in sediment partial melt at graphite saturation even at fO_2 ~FMQ-3.

[1] Duncan and Dasgupta. (in review) *GCA*; [2] Holloway *et al.*, (1992) *EJM*, 4, 105-114; [3] Syracuse *et al.*, (2010) *PEPI*, 183, 73-90.

The Caribbean plateau and OAE2: resolution of timing and trace metal release

R.A. DUNCAN^{1,2,*}, L.J. SNOW¹ AND G. SCOPELLITI³

¹CEOAS, Oregon State University, Corvallis, OR 97331 USA

(*corresp: rduncan@coas.oregonstate.edu) and

²Geology&Geophysics, King Saud University, Riyadh, KSA

³CFTA, University of Palermo, Palermo, 90123 Italy

Initial volcanism that formed a large part of the Caribbean ocean plateau coincided with ocean anoxic event 2 (OAE2), which occurred close to the Cenomanian/Turonian (C/T) boundary (~94 Ma). Increased trace metal delivery to the surface ocean during volcanic activity associated with this ocean plateau has been suggested as the cause for the depletion of seawater oxygen concentration and deposition of organic rich sediments [1]. This link is supported by isotopic excursions (Sr, Nd, Pb, Os) across the OAE2 that indicate a volcanic source. An interval of trace metal anomalies occurs in pelagic carbonate and black shale sequences of the Rock Creek Canyon section, Pueblo, Colorado at the onset of the δ¹³C global positive event [2]. The presence of these metal anomalies and isotopic profiles indicates a relationship between ocean plateau formation and ocean anoxia.

To further explore a direct connection between this ocean plateau and OAE2, we determined the distribution of major, minor and trace element abundances in marine sediments from an additional 7 globally distributed sites (Bass River, New Jersey; central Kerguelen Plateau; Baranca el Cañon, Mexico; Totumo, Venezuela; and Bottaccione, Calabianca and Novara di Sicilia, Sicily). After normalizing element concentrations to Zr, an interval of metal anomalies is present in all 8 sites. The changes in the trace metal patterns and concentrations among these sites is consistent with modeled late-Cretaceous surface circulation and a source of metals being the Caribbean plateau.

[1] Sinton&Duncan (1997) *Econ. Geol.*, **92**, 836-842. [2] Snow *et al.*, (2005) *Paleoceanog.*, **20**, PA3005.

Ion exchange and dissolution-precipitation in a zeolitic system

KRISTINA G. DUNKEL* AND ANDREW PUTNIS

Institut für Mineralogie, Westfälische Wilhelms-Universität
Münster, Corrensstraße 24, 48149 Münster, Germany
(*correspondence: kristina.dunkel@uni-muenster.de)

Zeolites are most commonly known for their ion-exchange properties. Previously, much attention has been given to the quantity of, and the necessary conditions for ion exchange. In order to better understand the underlying reaction mechanism, we investigated the reaction between a typical zeolite, scolecite ($\text{CaAl}_2\text{Si}_3\text{O}_{10}\cdot 3\text{H}_2\text{O}$), and a Na-rich fluid, with the expectation that in a solution with high Na^+ activity natrolite ($\text{Na}_2\text{Al}_2\text{Si}_3\text{O}_{10}\cdot 2\text{H}_2\text{O}$), or, with a lower probability, mesolite ($\text{Na}_2\text{Ca}_2\text{Al}_6\text{Si}_9\text{O}_{30}\cdot 8\text{H}_2\text{O}$) would form. The three minerals have very similar structures and the substitution of 2 Na^+ for Ca^{2+} and H_2O can be considered a classical cation exchange.

Against our predictions, mesolite was only observed in longer term experiments. At all reaction times, however, a reaction rim formed consisting of Na,Al-substituted tobermorite ($\text{Ca}_{4.5}\text{Si}_{5.2}\text{Al}_{1.0}\text{Na}_{1.3}\text{O}_{16}(\text{OH})_2$), a zeolite-like mineral that is of special interest because of its high selectivity for Cs.

A strong textural change from scolecite to both tobermorite and mesolite unambiguously shows that the reaction mechanism did not involve solid-state diffusion. The reaction interfaces are sharp, and the product phases form porous pseudomorphs of the original scolecite, strongly suggesting a coupled dissolution-precipitation process as the reaction mechanism. The formation of the comparatively Ca-rich tobermorite instead of the expected natrolite points to the fact that the solution at the reaction interface is not in equilibrium with the bulk solution. Similarly, it has been observed that Cs-Na exchange of the tobermorite did not start simultaneously in the whole, highly porous reaction rim, but only at the outer part.

Our results demonstrate that reaction between scolecite and a fluid with which it is out of equilibrium takes place by coupled dissolution-precipitation, both when the product phase is isostructural with the parent (as is the case for mesolite) and when it is not (as is the case for tobermorite). Moreover, there is much less fluid mobility around separate crystals in a solution than could be expected, which emphasises the importance of interfacial fluids.

Reactivity of cement and steel interfaces in geological carbon storage

S. DUPRAZ¹*, A. FABBRI² AND S. GRATALOU¹

¹ BRGM, 45060, Orléans, France (*correspondence: s.dupraz@brgm.fr)

² ENTPE, 69518, Vaulx-en-Velin, France

To some extent, carbon storage in geological environment is always submitted to leakage threats. Among the different possible scenarios, wells in contact with the storage zone are frequently regarded as the best candidates for CO_2 leakage. Wells materials, namely cement and steel, can both be corroded by the acidity of CO_2 rich fluids. Moreover, the interfaces between those materials are suggested to be the preferential pathways for fluids progressions. In order to assess this specific reactivity, a series of cement/tubing assemblies were submitted to storage conditions (150 bar of CO_2 at 65°C) during 6 weeks. Beside the assemblies interfaces, the tested parameters were the cement composition (CEM I, III and V), the cement to water ratio (0.14 to 1.24) and the salinity (0 and 20 g.l^{-1}). Carbonation of the cements and corrosion of the steel were quantified in each case as well as the resulting porosity, permeability and chemistry of the solid and liquid phases. As expected, the main conclusion of this approach demonstrate the chief role of the interfaces in the corrosion process and a surprisingly good resistance of the portland cement to such attacks.

Silicon isotope fractionation implying liquid phases at 300K: importance of configurational disorder

ROMAIN DUPUIS^{1*}, MAGALI BENOIT²
AND MERLIN MÉHEUT¹

¹GET/OMP, 14 Avenue Edouard Belin, 31400 Toulouse

(*correspondence: dupuis@get.obs-mip.fr)

²CEMES, 29 rue Jeanne Marvig 31055 Toulouse

Silicon isotope fractionation during Si precipitation in surface environments has received great interest in recent literature [1] for its potential to constrain weathering processes. *Ab initio* methods have the potential to provide independent and useful informations to understand the elementary processes responsible for such fractionations involving liquid phases [2]. In this study, we explored liquid/liquid ($\text{H}_4\text{SiO}_4/\text{H}_3\text{SiO}_4^-$) and mineral/liquid (quartz/ H_4SiO_4) fractionation of Si at equilibrium within the harmonic approximation [3]. Two 40ps trajectories of H_4SiO_4 (or H_3SiO_4^-) + 64 water molecules were simulated at 300K with the CPMD code, using BLYP functional. Then, using DFPT on configurations quenched at 0K, zone-center phonon frequencies were calculated to obtain their fractionation properties ($\ln\beta^{30/28}(\text{Liq.})$). In these systems, the effect of configurational disorder on the fractionation properties was studied in details. In parallel, $\ln\beta^{30/28}(\text{Quartz})$ have been computed to study a mineral/liquid equilibrium fractionation.

Based on a set of 10 independent configurations extracted from the trajectories, significant variations have been observed on the values of $\ln\beta^{30/28}(\text{Liq.})$. The calculated dispersion (σ) is large : **0.43‰** for H_4SiO_4 and **0.38‰** for H_3SiO_4^- . Thus, in the case of Si in solution, the configurational disorder should be taken into account for a realistic computing of fractionation properties.

The mean values of $\ln\alpha^{30/28}(\text{Quartz, H}_4\text{SiO}_4) = +2.18 \pm 0.14\text{‰}$ (SE, N=10) and $\ln\alpha^{30/28}(\text{H}_4\text{SiO}_4, \text{H}_3\text{SiO}_4^-) = +1.51 \pm 0.16\text{‰}$ (SE, N=10) at 300K have been calculated including the error due to the liquid disorder. Regarding the calculated fractionation in quartz/liquid systems, the solution is predicted to be lighter than the precipitate, inconsistently with every natural observations. Thus, the precipitation is probably a process out of equilibrium in this system. Most importantly, a significant fractionation related to a single proton exchange ($\text{H}_4\text{SiO}_4/\text{H}_3\text{SiO}_4^-$ equilibrium), is predicted.

Consequences on the explanation of silicon fractionation during precipitation will be discussed.

[1] Opfergelt, C. R. *Geoscience* 344 (2012) 723-738 [2] Kowalski et al., *GCA* 101 (2013) 285-301 [3] Rustad and Bylaska, *JACS* 129 (2007) 2222-2223

Sorption of dissolved organic matter on boom clay

D.DURCE*, C.BRUGGEMAN AND N.MAES¹

¹Belgian Nuclear Research Centre (SCK,CEN), B-2400 Mol, Belgium (*: ddurce@sckcen.be)

Dissolved organic matter (DOM) plays a significant role in a geological nuclear waste repository by enhancing or retarding the transport of radionuclides in the environment. It is thus a key aim to understand the equilibriums DOM-rock which govern the DOM mobility. DOM sorption was studied on a large variety of soils and minerals with different DOM sources [1],[2]. However, most of works was carried out after removal of the indigenous DOM, neglecting therefore some key aspects of the sorption. Boom Clay, potential host rock under study in Belgium, is a formation rich in organic matter with 1.7 wt% of TOC. The objective of this work is thus, to study the interactions of the indigenous DOM with the Boom Clay rock in undisturbed conditions. To this end, we propose to use a sequential leaching of the indigenous DOM: from a crushed solid, under a controlled pCO₂ and in a synthetic solution representative of the pore water. This method allows to quantify the fraction of soluble organic matter and the equilibrium DOM in solution/DOM sorbed.

Three different rock samples were considered with, for each, four liquid/solid ratios. No influence of the liquid/solid ratios was noticed on the amount of DOM extracted, which was estimated between 0.037 and 0.104 wt% of the total rock according to the origin of the samples. A linear behaviour in desorption was highlighted with K_ds in good agreement for all the samples. However, the dimensions of the system were observed to strongly influence the K_d values. Indeed, average K_ds of 2.7, 4.3 and 10.3 L.kg⁻¹ were measured for liquid/solid ratios of 4, 6.7 and 16.7 L.kg⁻¹ respectively. The quantification of DOM sorption is thus dependent on the studied system and the notion of K_d should be considered with care. However, the approach used here offers reference values that account for the different sorption mechanisms encountered in situ, including potential competitive effects. Behind a pure quantification of the interactions DOM-rock, our work aims at understanding the mechanisms involved and notably the influence of DOM molecular weight on sorption. Batch sorption experiments are, indeed, on-going with different size fractions of the indigenous DOM. The results and limits of the sequential leaching approach will be discussed together with the influence of molecular size on the measured K_d values.

[1] Kaiser *et al.* (2000), *Organic Geochemistry*, **31**, 711-725.

[2] Kahle *et al.* (2004), *Organic Geochemistry*, **35**, 269-276

Division by fluid incision: Biofilm patch development in porous media

W. M. DURHAM^{1,2*}, O. TRANZER^{1,3}, A. LEOMBRUNI^{1,4,5},
K. Z. COYTE⁶ AND R. STOCKER¹

¹ Department of Civil and Environmental Engineering, MIT, Cambridge, Massachusetts, USA (*correspondence: william.durham@zoo.ox.ac.uk)

² Department of Zoology, University of Oxford, Oxford, OX1 3PS, UK

³ Ecole Polytechnique, 91128 Palaiseau, France

⁴ DIIAR - SEZIONE C.I.M.I., Politecnico di Milano, 20133 Milano, Italy

⁵ Regensis Ltd, Bath BA1 5BB, UK

⁶ Centre for Mathematical Biology, Mathematical Institute, University of Oxford, OX1 3LB

Bacterial biofilms often occur in porous media, where they play pivotal roles in medicine, industry and the environment. Though flow is ubiquitous in porous media, its effects on biofilm growth have been largely ignored. Using patterned microfluidic devices that simulate soil, we find that the structure of *Escherichia coli* biofilms undergoes a self-organization mediated by the interaction of growth and flow. Intriguingly, we find that intermediate flow rates trigger the formation of striking preferential flow channels, which convey fluid around large biofilm patches (Fig. 1). At larger and smaller flow rates, biofilms form more compact patches leading to uniform flow through the matrix. A simple network model, based on the competition between biofilm growth and shear induced detachment, correctly predicts our findings. These findings may have important consequences on processes as diverse as biochemical cycling, antibiotic resistance, and water filtration.

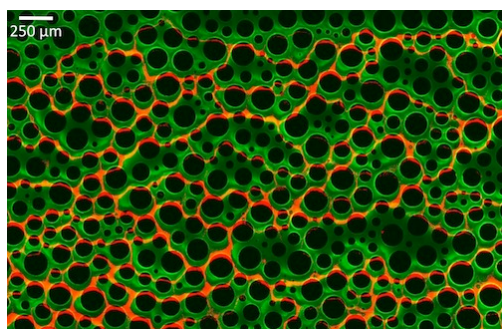


Figure 1: A microfluidic device that simulates soil colonized by *E. coli* biofilm (bacterial auto-fluorescence shown in green). Biofilm patches are intersected by channels of fluid flow (shown in red and shifted slightly downward to reveal the underlying structure), which transport nutrient unevenly through the matrix.

Assessment of the evolution of the redox conditions in a low and intermediate level nuclear waste repository (SFR1, Sweden)

LARA DURO¹, CRISTINA DOMÈNECH^{1*}, MIREIA GRIVÉ¹,
GABRIELA ROMAN-ROSS¹, JORDI BRUNO¹
AND KLAS KÄLLSTRÖM²

¹Amphos 21 Consulting S.L. Passeig de Garcia i Faria, 49-51, 1^o-1^a - E08019 Barcelona (SPAIN)

lara.duro@amphos21.com, mireia.grive@amphos21.com,
gabriela.roman@amphos21.com,
jordi.bruno@amphos21.com

²Svensk Kärnbränslehantering AB, Avd. Lågochmedelaktivt avfall, Box 250, 101 24 Stockholm Sweden.
klas.kallstrom@skb.se.

*Present address: Dept. Crist., Min., Dip. Min., Fac. Geologia, Universitat de Barcelona, c/Martí i Franquès s/n, E08028 Barcelona (Spain). cristina.domenech@ub.edu.

This study evaluates the redox conditions in 15 individual waste package types in SFR1. SFR1 contains heterogeneous wastes, with different activity levels and materials in the waste, matrices and packaging. Steel and concrete-based materials are ubiquitous in the repository. A combination of the individual models is used to assess the redox evolution of the different vaults in the repository. The results of the model indicate that O₂ is consumed through organic matter degradation and metal corrosion. The system is then kept under reducing conditions for long time periods. H₂(g) is generated due to the steel anoxic corrosion and magnetite precipitates as main corrosion product. Steel is depleted after 5,000 y to more than 60,000 y depending on the waste package type. The calculated Eh under the pH conditions imposed by the massive amounts of cements in the repository is about -0.75 V (pH 12.5) but higher redox potentials (up to -0.01 V) can be expected if the system controlling the Eh is not steel/magnetite, but Fe(III)/magnetite. If no oxic disturbances happen Eh would be kept highly reducing. In case of glacial meltwater intrusion magnetite would gradually convert into Fe(III) oxides, buffering system Eh and preventing it from oxidation for long time periods.

Greenhouse gas (CO₂, N₂O, CH₄) emissions from Llobregat (Barcelona) riverbed sediment: Effects of soil moisture and C, N, Fe substrates

T. DUTTA¹, S. RUBOL^{1,2}, S. A. VALL¹ AND J. A. TIRADO¹

¹ Hydrogeology Group, Dept Geotechnical Engineering and Geosciences, Universitat Politècnica de Catalunya-BarcelonaTech, 08034 Barcelona, Spain. Email: tanushree.dutta@upc.edu

² Dept. DICA, University of Trento, Italy Email: simonetta.rubol@upc.edu

Nutrient input to river water from adjacent agricultural and industrial areas can create soil conditions suitable for greenhouse gas emissions. In this study, we report three major greenhouse gas; CO₂, N₂O and CH₄ emissions from riverbed sediments of Llobregat River, Barcelona. In a 45 day laboratory incubation experiment, we monitored the emissions from the sediments kept at three different soil moisture conditions- 40, 60 and 80% water filled pore space with added carbon, nitrogen and iron substrates. The treatments were DI + N, DI + N + organic C, DI + N + Fe, control with DI and no DI added. Gas and soil samples were collected after 0, 1, 2, 5, 7, 10 days after the start of the experiment and then once every week. Gas samples were analyzed in a Gas Chromatograph equipped with TCD, ECD and FID detectors and soil extractants were analyzed for organic C and N. Results show that the soil had less than 1 mg per liter NH₄-N, which increased with the added C and N substrates but then decreased with time. This increased levels of C and N reflected in increased respiration, however both N₂O and CH₄ emissions remained low across all treatments in spite of the increase in C and N at all three different soil moisture conditions, which could be an indication of lack of indigenous methane-producing and denitrifying soil microbial populations.

Exploring the spatial and temporal complexity of the last interglacial sea level highstand

ANDREA DUTTON^{1*}

¹Department of Geological Sciences, University of Florida, Gainesville, FL, 32611, USA (

*correspondence: adutton@ufl.edu)

The future response of Earth's remaining ice sheets remains the most uncertain and controversial aspect of sea level-rise projections. In this context, past climate and sea-level reconstructions present a valuable opportunity to gain insight about the response of the cryosphere to warmer temperatures. Although studies of the timing, phasing, and magnitude of sea level changes on glacial-interglacial timescales have long been studied, conventional paradigms of the dynamics of this process have come under new scrutiny. In particular, studies based on chronologies and proxies derived from corals, speleothems, deep sea cores and ice cores that probe the timing of peaks in sea level as well as the length of the assumed lag between insolation and sea level response are increasingly indicating that the polar ice caps may be more sensitive than previously thought—both in the timing, frequency, and magnitude of response [e.g., 1,2].

The last interglacial period has received much attention in terms of understanding the sensitivity of ice sheets during warm climates, as much for its relevance to future climate conditions as for the accessibility of sea level indicators from this time period. New analyses of open-system U-Th age data of corals, of compilations of coral U-Th age-elevation data, and of absolute chronologies recorded by speleothems and corals are transforming our understanding of the dynamics of polar ice sheets during the last interglacial period. Of particular significance is the emerging consensus that sea level peaked somewhere around 6 to 9 meters above present [3,4], and experienced at least one if not more oscillations in sea level [5].

The state of understanding of the absolute timing, duration, and stability of the last interglacial sea level highstand will be reviewed, with particular consideration given to the unresolved complexities in the spatial and temporal signal of sea level from this time period.

Perturbation to the marine Ca isotope cycle across Oceanic Anoxic Event 2

ALICE D.C.DU VIVIER¹; ANDREW D. JACOBSON²; GREGORY LEHN²; DAVID SELBY¹ AND BRADLEY B.SAGEMAN²

¹Department of Earth Sciences, Durham University, Durham, DH1 3LE; alice.du-vivier@durham.ac.uk; david.selby@durham.ac.uk

²Department of Earth and Planetary Sciences, Northwestern University, 2145 N. Sheridan Road, Evanston, IL 60208-3130; adj@earth.northwestern.edu; greg@earth.northwestern.edu; brad@earth.northwestern.edu

Several isotope proxies (e.g., C, Mo, Nd, Os, Sr) have been used to examine the effect of OAEs on global climate and elemental cycling. Here, we evaluate the behaviour of Ca isotopes ($\delta^{44/40}\text{Ca}$) across the late Cretaceous OAE2 (Cenomanian-Turonian) in the Western Interior of North America (NA), where significant perturbations in $\delta^{44/40}\text{Ca}$ track the concomitant changes in C and Os isotope records.

We present a high-precision ($2\sigma_{\text{SD}} = \pm 0.04\text{‰}$), high-resolution (± 20 kyr) record of $\delta^{44/40}\text{Ca}$ values from the GSSP Pueblo core. A relatively large, positive excursion in $\delta^{44/40}\text{Ca}$ values occurs at the onset of OAE2. The maximum extent of variation ($\sim 0.30\text{‰}$) is ~ 8 times larger than the external reproducibility of the measurements. Several processes could explain this pattern, including mineralogical variations, changes in the fractionation factor, and perturbations to the input and output fluxes of marine Ca. We note that initial Os isotope ratios trend toward unradiogenic values during the same time interval. This trend clearly reflects the input of a mantle-like Os isotope composition, most likely derived from the emplacement of basalts of the Caribbean Large Igneous Province. Because basalts have relatively high $\delta^{44/40}\text{Ca}$ values (Huang *et al.*, 2010) compared to other marine Ca inputs, such as river runoff and submarine groundwater discharge, we infer that the Pueblo $\delta^{44/40}\text{Ca}$ record also reveals a large volcanic signature. Previous Ca isotope records for OAE2 from the UK did not record the putative basalt weathering signature (Blattler *et al.*, 2011), and were interpreted to reflect increased terrestrial weathering. The difference in Ca records from NA and the UK may reflect a combination of factors, including proximity to the LIP and an improved MC-TIMS method (Lehn *et al.*, 2013) employed in the present study. Huang *et al.*, 2010, Earth Planetary Science Letters, 292; Blattler *et al.*, 2011, Earth Planetary Science Letters, 309; Lehn *et al.*, 2013, International Journal of Mass Spectrometry (in review)

Impacts of porous structure, organic matter and mineralogy on atrazine fate in two contrasting tropical soils

C. DUWIG^{1,*}, B. PRADO², P. DELMAS³, A. GASTELUM STROZZI⁴, P. CHARRIER⁵ AND C. HIDALGO MORENO⁶

¹IRD/ LTHE UMR 5564, Grenoble, France

(*correspondence : celine.duwig@ird.fr)

²Instituto de Geología, Universidad Nacional Autónoma de México, México, DF, Mexico

³Department of Computer Science, The University of Auckland, Private Bag 92019, New Zealand

⁴CCADET, Universidad Nacional Autónoma de México, Mexico, D.F., Mexico

⁵UJF-Grenoble 1/3SR UMR 5521, Grenoble, France

⁶Colegio de Postgraduados, Texcoco, Mexico

The fate of reactive solutes in soils is the result of complex coupled processes including convective dispersive transport, sorption to organo-mineral surfaces and biochemical transformations. These processes, occurring at different space and time scales, are difficult to identify and rank by classical laboratory experiments.

Multidisciplinary studies were performed to evaluate soil characteristics impacting atrazine fate in two contrasting soil types, namely an Andosol and a Vertisol from Mexico. The 3D-macro pore networks and pore morphological parameters were calculated after imaging intact soil cores through X-ray tomography at 50 μm resolution. Reactive organo-mineral phases such as allophanes, clays, oxides and organic matter were characterized and quantified. The different processes involved in atrazine fate were studied independently and statically in closed reactors. Displacement experiments in intact cores allowed to mimic natural dynamic environmental and application conditions. A stable oxygen isotope used as water tracer permitted obtaining the convective dispersive parameters.

Water transfer in physical non equilibrium transfer was observed in the surface Vertisol and subsurface Andosol horizons and was correlated to pore shape, connectivity and size. Sorption capacity and degradation rate were compared in static and dynamic experiments. The roles of organic matter composition, clay types and pH variations were assessed. This study shows how the soil physico-chemical and microbial properties at the pore and pedon scales affect reactive solute fate at the macroscale. It also demonstrates the difficulty to decouple the different processes involved.

Ultrahigh-resolution mass spectrometry of natural organic matter from hydrothermal springs

S. DVORSKI^{1*}, M. HARIR¹, N. HERTKORN¹, N. HINMAN², M. GONSIOR³, W. COOPER⁴ AND P. SCHMITT-KOPPLIN¹

¹Helmholtz Zentrum Muenchen, German Research Center for Environmental Health, Analytical BioGeoChemistry, 85764 Neuherberg, Germany (*correspondence: sabine.dvorski@helmholtz-muenchen.de)

²Univ. of Montana, Missoula, MT 59812-1296, USA

³Center for Environmental Science, Univ. of Maryland, Solomons, MD 20688-0038, USA

⁴The Henry Samueli School of Engineering, Univ. of California, Irvine, CA 92697-2175, USA

Natural organic matter (NOM) is a highly complex mixture of organic compounds abundant and speciated in all environmental compartments (atmosphere, soils, sediments and water environments). The formation and decomposition of NOM is driven by abiotic and biotic reactions and its continual interactions with its environment. Thus the unique NOM signature reflects several key ecosystem characteristics.

Sulphur with oxidation states ranging from -2 to +6 is an essential element for any terrestrial life and an important constituent of NOM. Processes like microbial sulphate reduction, pyrite precipitation and polysulphane formation demonstrate the pivotal role of environmental sulphur chemistry for microbial life and its coupling to abiotic redox cycles. Furthermore, sulphur is crucial for environmental metal binding. The sulphur signature of NOM therefore reveals critical insights into important biogeochemical processes.

As shown recently, Fourier transform ion cyclotron resonance mass spectrometry (FTICR/MS) is a powerful tool to unravel the diverse characteristics of abiotic and biotic complexity of various NOM [1-4]. This contribution will demonstrate the capabilities of high-field FTICR mass spectra to elucidate the significant role of organic sulphur chemistry to hydrothermal springs, which feature ecosystems conditions resembling in many aspects those supposedly found in the early earth's history.

[1] Schmitt-Kopplin *et al.* (2010) *Anal Chem* **82**, 8017-8026.

[2] Gonsior *et al.* (2011) *Water Res* **45**, 2943-2953.

[3] Hertkorn *et al.* (2013) *Biogeosciences* **10**, 1583-1624.

[4] Schmitt-Kopplin *et al.* (2010) *PNAS* **107**, 2763-2768.

Chemical and Hf/W Isotopic Consequences of Lossy Accretion

CHRISTINA A. DWYER^{1*}, FRANCIS NIMMO¹
AND JOHN E. CHAMBERS²

¹Dept. Earth & Planetary Sciences, U.C. Santa Cruz, Santa Cruz, CA 95064 (*correspondence: cadwyer@ucsc.edu)

²Dept. Terrestrial Magnetism, Carnegie Institute of Washington, Washington, DC 20015

The late stages of planetary accretion involve stochastic, large collisions [1]. Many of these collisions likely resulted in hit-and-run events [2] or erosion of existing bodies' crusts [3] or mantles [4]. Here we present a preliminary investigation into the effects of lossy late-stage accretion on the bulk chemistry and isotopic characteristics of the resulting planets.

Our model is composed of two parts: (1) an N-body accretion code [5] tracks the orbital and collisional evolution of the terrestrial bodies, including hit-and-run and fragmentation events; (2) post-processing evolves the chemistry in light of radioactive decay and impact-related mixing and partial equilibration.

16 runs were performed using the MERCURY N-body code [5]; each run contained Jupiter and Saturn in their current orbits as well as ≈ 150 initial bodies. Collisional outcomes are modified from [6,7]. The masses of the core and mantle of each body are tracked throughout the simulation. All bodies are assigned an initial mantle mass fraction, y , of 0.7.

We track the Hf and W evolution of these bodies. Radioactive decay occurs between impacts. We calculate the effect of an impact by assuming an idealized model of mixing and partial equilibration [8]. The core equilibration factor is a free parameter; we use 0.4. Partition coefficients are assumed constant.

Diversity increases as final mass decreases. The range in final y changes from 0.66–0.72 for \approx Earth-mass planets to 0.41–1 for the smallest bodies in the simulation. The scatter in tungsten anomaly increases from 0.79–4.0 for \approx Earth-mass to 0.11–18 for the smallest masses. This behavior is similar to that observed.

We find there is no simple relationship between the single-stage core formation time derived from the final tungsten isotope anomaly and the actual growth history of an object.

[1] Agnor *et al.* (1999), *Icarus* 142, 219–237. [2] Asphaug *et al.* (2006), *Nature* 439, 155–160. [3] O'Neill & Palme (2008), *PhilTransRSocLondA* 366, 4205–4238. [4] Benz *et al.* (2007), *SpSciRev* 132, 189–202. [5] Chambers (2013), *Icarus*, 224, 43–56. [6] Genda *et al.* (2012), *ApJ* 744, 137. [7] Leinhardt & Stewart (2012), *ApJ* 745, 79. [8] Nimmo *et al.* (2010), *EPSL* 292, 363–370.

P–V–T equation of state of sodium majorite up to 21 GPa and 1673 K

A. M. DYMSHITS^{1*}, K. D. LITASOV¹, A. SHATSKIY¹, I.S. SHARYGIN¹, E. OHTANI², A. SUZUKI² AND K. FUNAKOSHI³

¹ Sobolev Institute of Geology and Mineralogy, Novosibirsk 630090, Russia (*a.dymshits@gmail.com)

² Tohoku University, Sendai 980-8578, Japan

³ SPring-8, Japan Synchrotron Radiation Research Institute, Kouto, Hyogo 678-5198, Japan

Garnet is one of the most abundant minerals in the upper mantle and transition zone and comprises about 40% by volume for peridotitic and up to 70% for basaltic or eclogitic lithologies [1]. With increasing pressure garnet becomes progressively enriched in Si and Na, which can be expressed as sodium majorite (Na-maj) component [2].

The *P–V–T* equation of state (EoS) for Na-maj at pressures to 21 GPa and temperatures to 1673 K was obtained by *in situ* X-ray diffraction experiments and a multi-anvil apparatus at “SPring-8” synchrotron facility. Fitting the entire *P–V–T* dataset using a high-temperature Birch–Murnaghan EoS at a fixed $K'_{0,300} = 4$ yielded $V_0 = 1474.7$ (8) Å³, $K_{0,300} = 185$ (2) GPa, $(\partial K_{0,T}/\partial T)_P = -0.028$ (4) (GPa K⁻¹) and $a = 3.17$ (14) × 10⁵ K¹, $b = 0.41$ (21) × 10⁸ K², where $a = a + bT$ is the volumetric thermal expansion coefficient. Fitting the present data to the Mie-Grüneisen-Debye EoS with Debye temperature fixed at $\theta_0 = 890$ K yielded Grüneisen parameter, $\gamma_0 = 1.31$ and 1.33 at $q = 1.0$ and 1.18, respectively.

The new data on the Na-maj were compared with previous data on majorite type garnets. The entire dataset enabled us to examine the thermoelastic properties of important mantle garnets and these data will have further applications for modelling *PT*-conditions in the transition zone of the Earth’s mantle using ultradeep mineral assemblages.

[1] Irifune & Ringwood (1987) *Earth Planet. Sci. Lett.* **86**, 365-376. [2] Gasparik (1989) *Cont. Min. Petr.* **102**, 389-405.

Laser spectroscopic *in situ* measurements of D/H in water vapor onboard a passenger aircraft

C. DYROFF^{1*}, E. CHRISTNER¹ AND S. SANATI¹

¹Karlsruhe Institute of Technology, Institute of Meteorology and Climate Research, PO Box 3640, 76021 Karlsruhe, Germany (* correspondence: christoph.dyroff@kit.edu)

Water (H₂O) is a key species in Earth’s atmosphere due to its large radiative feedback and transport of latent heat. For a better understanding, and to improve global climate models, it is vital to study the global hydrological cycle.

Isotope ratio measurements of H₂O can provide additional information to H₂O measurements alone, as they are an indicator of the transport pathways (evaporation, condensation, ice formation) of atmospheric H₂O.

We are presently deploying an *in-situ* diode-laser spectrometer [1] aboard the CARIBIC passenger aircraft [2]. On flights mostly in the northern hemisphere with occasional crossings of the tropics en route to southern Africa we have obtained the first *in-situ* meridional cross section of δD at the cruising altitude of the CARIBIC aircraft (Fig. 1). A positive gradient of ~150 ‰ from mid latitudes towards the tropics indicates an increased contribution of convective transport of near-surface H₂O vapor at 10–12 km altitude. Our findings are supported by back-trajectory calculations, and agree well with satellite-borne observations [3].

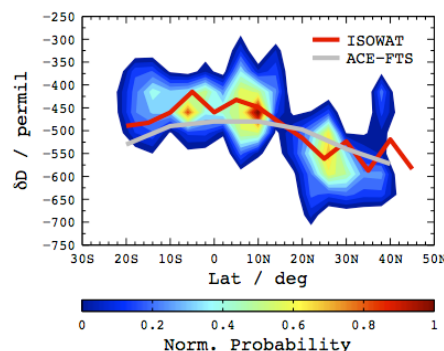


Figure 1: Meridional cross section of δD showing increased convective transport of H₂O in the tropics. Red line: mean ISOWAT. Green line: ACE-FTS annual mean.

[1] Dyroff *et al.* (2010) *Appl. Phys. B* **98**, 537-548. [2] Brenninkmeijer *et al.* (2007), *Atmos. Chem. Phys.* **7**, 4953-4976. [3] Randel *et al.* (2012) *J. Geophys. Res.* **117**, D06303.

Cosmochemical Constraints on Asteroid Accretion

EBEL DENTON S^{1,2}, MICHAEL K. EISBERG^{1,3}
AND ELLEN CRAPSTER-PREGONT^{1,2}

¹American Museum of Natural History, Central Park West at 79th St, New York, NY 10024. (*debel@amnh.org)

²Lamont-Doherty Earth Observatory of Columbia University, Palisades, New York.

³Kingsborough College, City University of New York.

Multiple lines of chemical, isotopic and textural evidence constrain how kilometer-sized bodies accreted. Km-size chondrite parent bodies were likely precursors to planetesimals and the modern planets. **First:** Chondritic meteorites (~90% of known meteorites) contain widely variant modal abundances of their primary components: Chondrules, Ca-Al-rich inclusions (CAIs), and fine-grained matrix containing insoluble organic matter (IOM) and presolar grains (PSG) including graphite and SiC [1], yet are all “chondritic” in composition [2,3]. **Second:** Chondrules, themselves highly variable in Fe/Si, combine to make rocks with bulk chondritic Fe/Si [4]. **Third:** Chondritic meteorites contain most major elements (Si, Mg, Al, Ca, Ti) and rare earth elements (REEs) in solar proportions, with the most variation in Fe, yet CAIs have highly variable REE inventories [5]. **Fourth:** Oxygen isotopes, CAI abundances, and clast sizes suggest each chondrite group formed under locally distinct conditions. Variations in Fe do not affect the present argument. That extraterrestrial materials universally tend towards chondritic major and trace element abundances is, alone, a powerful constraint on disk processes, that has been dubbed “complementarity” [2-4]. That is, the primary components (chondrules, CAIs, matrix) complement each other to produce “chondritic” bulk meteorite composition. Why is this so?

We will present major and trace element (REE) evidence that the parent bodies of chondritic meteorites accreted from local, gravitationally unstable (overdense) accumulations of material of bulk solar or dust-enriched composition [6], subjected, prior to accretion, to varying degrees of highly local heating that produced melted objects (e.g., chondrules) with varying degrees of efficiency [7].

[1] Huss GR & Lewis RS (1994) *MaPS* **29**, 811. [2] Hezel DC & Palme H (2010) *EPSL* **294**, 85-93. [3] Bland PA *et al.* (2005) *Proc. Nat. Acad. Sci.* **102**, 13755-13760. [4] Ebel DS *et al.* (2008) *MaPS* **43**, 1725-1740. [5] Boynton WV (1975) *GCA* **37**, 1119-1140. [6] Alexander C.M.O'D. *et al.* *Science* **320**, 1617-1619. [7] McNally *et al.* (2013) *LPS XLIV*, Abs. #2844.

Deformation-related chemical alteration of meta-pegmatites

TOBIAS EBERLEI^{1*}, GERLINDE HABLER¹,
RAINER ABART¹ AND BERNHARD GRASEMANN²

¹University of Vienna, Department of Lithospheric Research (*correspondence to: tobias.eberlei@univie.ac.at)

²University of Vienna, Department of Geodynamics and Sedimentology

Deformation and chemical reactions often occur contemporaneously in nature and a proper understanding of the feedback between the two is required for correctly interpreting rock microstructures and evaluating the $P-T-t-d$ evolution of rocks. Permian meta-pegmatites from the Austroalpine Matsch Unit in the Eastern Alps were deformed at conditions close to the greenschist–amphibolite facies transition during the Cretaceous [1,2], locally producing proto-, meso- and ultramylonites with finite strain gradients at the cm- to m-scale.

We focus on the relation between the Cretaceous deformation and major element re-equilibration of the major metapegmatite phases. Several white mica and feldspar generations are recognised based on combined microstructural and microchemical characteristics. A spatial relationship between specific deformation-microstructures (kink bands, micro shear zones, cracks, strain shadows) and chemical alteration is reflected by cm-sized white mica and plagioclase clasts. A fine-grained phengitic white mica generation dominates mylonitic foliation domains and compressional quadrants of clasts. Primary K-feldspar (Kfs) shows deformation-related replacement by albite, whereas secondary Kfs together with fine-grained biotite, phengitic white mica, albite and quartz precipitated in micro-fractures and extensional quadrants of large albite and muscovite clasts. Fine-grained plagioclase aggregates in the strain-shadows of albite clasts indicate deformation by dissolution-precipitation creep (DPC). The mineral compositions of fine-grained phengitic white mica co-existing with secondary Kfs, biotite, quartz and albite are consistent with $P-T$ conditions of 480 ± 30 °C and 5 ± 1 kbar.

Our results document the correlation between deformation and chemical alteration and yield quantitative PT constraints on deformation based on syntectonic phase assemblages. The study will be further extended to examine the relationship between deformation and isotopic re-setting of the Rb-Sr system in white mica.

[1] Habler, Thöni & Grasemann (2009) *Mineral. Petrol.* **97**, 149-171. [2] Froitzheim, Conti & van Dalen (1997) *Tectonophysics* **280**, 267-297.

Quantitative analysis of high resolution isotope and concentration data from a toluene-pulse experiment by reactive transport modeling

DOMINIK ECKERT^{1*}, SHIRAN QIU², MARTIN ELSNER²
AND OLAF A. CIRPKA¹

¹Center for Applied Geosciences, University of Tübingen,
Tübingen 72074, Germany
(*Dominik.Eckert@uni-tuebingen.de)

²Institute of Groundwater Ecology, Helmholtz Center
München, München 85764, Germany

A major challenge in the application of compound-specific isotope analysis (CSIA) to quantify biodegradation at contaminated field sites is the separation of microbial- and physical-induced effects on the measured isotope signal. In contrast to simple analytical tools, as the Rayleigh equation, reactive transport models can account for the complex interaction of different fractionating processes.

In this study, we analyze the high resolution toluene concentration and isotope ratio ($\delta^{13}\text{C}$) data set of a large-scale laboratory toluene pulse experiment by reactive transport modeling. We uniquely quantify degradation and sorption properties of the system, estimate the contributions of reaction-induced, sorption-induced and transverse-dispersion-induced isotope fractionation to the overall isotope signal and quantify the error introduced by neglecting individual processes (e.g. fractionation by physical processes, Michaelis-Menten degradation kinetics) in the analysis of the data. Our results show that highly resolved data of both concentration and isotope ratios are needed for unique process identification of reactive transport facilitating reliable model calibration and that the combined analysis of these highly resolved data demands reactive transport models with sufficient complexity.

Mantle control on eruption style at Kīlauea Volcano, Hawai'i

M EDMONDS¹, I SIDES¹, J MACLENNAN¹, D SWANSON²
AND B HOUGHTON³

¹Earth Sciences Department, University of Cambridge,
Downing Street, Cambridge CB2 3EQ, UK

²Hawaiian Volcano Observatory, United States Geological
Survey, Hawaii National Park, HI 96718, USA

³School of Ocean and Earth Science and Technology,
University of Hawaii at Manoa, Hawaii, USA.

Ocean island volcanoes are associated with melting of a heterogeneous mantle source. Geochemical heterogeneity might be expected to influence the way in which melts ascend and are stored and erupted, with some melts inherently more enriched in incompatible trace elements, and hence volatiles, than others. Contrasts between effusive and explosive (fountaining) behaviour in basaltic magmas has previously been explained in terms of shallow melt-gas segregation, with little geochemical control. Here we present data from a suite of melt inclusions from 25 historical eruptions of Kīlauea Volcano over the last 500 years. The deposits were emplaced via a range of eruptive styles, from effusive lava flows, fissure eruptions, high fountains and transient subplinian (gas-rich) eruptions.

The data show that more explosive styles of eruption (high fountaining and fissure eruptions) are associated statistically with more enriched melts (with higher relative proportions of Light Rare Earth Elements) with higher volatile concentrations, which ascend faster, retain their primitive nature and interact only minimally with the summit magma reservoir. Effusive styles of eruption, on the other hand, are linked statistically with more depleted melts, with lower volatile concentrations, that tend to homogenise, cool and evolve in the summit magma reservoir before eruption.

The ranges in melt volatile concentrations between the “depleted” and “enriched” end member primary melts are approximately 0.28 to 0.87 wt% water respectively and 0.17 to 0.68 wt% carbon dioxide respectively. The more volatile-rich melts are considerably more buoyant, which has a dramatic effect on their transport, storage and eruption, owing to their higher vapour content at low pressure, increasing the likelihood of explosive high fountaining styles of volcanic activity. Over time, Kīlauea’s style of eruption and magma supply rate are linked fundamentally to the geochemistry of primary melts: magma explosivity thus might be determined right at the point of separation from its mantle source region.

V.I Vernadsky: Holistic thinker and geochemical pioneer

W.M.EDMUNDS^{1*} AND A A BOGUSH²

¹School of Geography and the Environment, Oxford University, Oxford OX1 3GY, UK
(correspondence: wme@btopenworld.com)

²Institute of Geology and Mineralogy of Siberian Branch of the Russian Academy of Sciences, pr.Koptyuga 3, Novosibirsk 630090, Russia (annakhol@gmail.com)

Vladimir Ivanovich Vernadsky has only recently become recognised internationally [1,2], despite being regarded as one of the greatest names in science of the 20th century in his homeland Russia. There are several reasons for his lack of renown in the west, but mainly that his most important work “*The Biosphere*” was only fully translated into English in 1997 [1,3]. This book and the ideas it contains are now becoming regarded as one of the seminal scientific works of the last century. It defines the biosphere as a unifying, holistic concept for the earth system at a time when reductionism was the driving motivation in scientific research. Above all, for earth scientists, Vernadsky regarded life as the driving geological force. He also adopted the concept of the ‘Noosphere’ (the evolution of human thought) to emphasis man’s role as a geological agent. His publications foreshadow Gaia theory some half a century later.

This paper, coinciding with the 150th anniversary of his birth celebrates his achievements as a pioneering geochemist through his contribution in mineralogy and crystallography, geology and isotope geoscience, geochemistry and biogeochemistry, chemistry and biochemistry, pedology and hydrology, meteoritics and, the history of science and philosophy [4]. His was the first text on geochemistry [5] and also on hydrogeochemistry [2,6] published in three volumes. Vernadsky’s ideas also led to the evolution of landscape geochemistry which was promulgated by his contemporaries and students (Polynov, Fersman, Perel’man *et al.*).

[1] Margulis *et al.*(1998) In: Vernadsky *The Biosphere* Nevaumont Books, New York, 14–19. [2] Edmunds & Bogush (2012) *Appl Geochem* **27**, 1871–1886. [3] Vernadsky (1977) *The Biosphere* (Trans. Langmuir DB) Springer NewYork. [4] Vinogradov (1963) *Geokhimiya* **3** 211–214. [5] Vernadsky (1924) *La Géochimie*, Paris. [6] Shavartsev *et al.* 2006 *Geochem Int*, **44** 619–634.

Water security in low rainfall areas

W M EDMUNDS¹

¹Oxford Water, School of Geography and the Environment, Oxford University, OX1 3GY

Humans have shown a capacity over millennia to adapt to living in water scarce areas under changing climatic conditions. Today the challenges of adaptation are still water-based, but more complex due in particular to energy requirements, food security and population growth. Renewable groundwater of adequate quality is the key to water resource security in arid and semi-arid areas. Excessive and uncontrolled abstraction of mainly fossil water has already led to massive depletion of valuable reserves of groundwater in major aquifers worldwide. Access to safe drinking water supplies however remains the primary issue for most of the world’s poorest people.

Geochemistry plays a role in both the quantitative and qualitative aspects of water security. Physical parameters such as recharge estimation can best be estimated or validated using simple tools such as chloride mass balance; importantly such techniques are inexpensive and widely applicable. Residence times can be determined by a mix of radiometric and isotopic tracers as well as CFCs. Natural groundwater is widely recognised as the purest and most reliable water resource but its properties need assessment for harmful substances derived from geological sources. Above all, the needs of one quarter of the world’s population with no access to safe drinking water and one third without access to sanitation can be addressed often using basic hydrogeology coupled with simple geochemical measurement.

It is argued that rural communities may have greater opportunities for developing water security as compared with many of those in urban areas. The key lies in creating self-sufficient and productive communities based on water prioritisation. This involves *inter alia*, careful conservation and management of renewable groundwater, rainfall harvesting, underground storage - combined with education and training initiatives benefiting rural society. Policies need to be adapted and implemented to ensure that development is based on water renewability.

Synchrotron X-ray fluorescence reveals the colourful chemistry of fossils

N.P. EDWARDS^{1*}, P.L. MANNING¹, H. BARDEN¹,
W.I. SELLERS², U. BERGMANN³ AND R.A. WOGELIUS¹

¹University of Manchester, SEAES, Williamson Research
Centre for Molecular Environmental Science, Manchester,
M13 9PL, UK (correspondance:
nicholas.edwards@manchester.ac.uk)

²University of Manchester, Faculty of Life Science,
Manchester, M13 9PT

³SLAC National Accelerator Laboratory, Linac Coherent
Light Source, Menlo Park, CA, 94025, USA

Despite the widely accepted biogenic origin and composition of sedimentary organic matter, identification of endogenous chemical signals within intact fossil organisms is often met with scepticism. Fossilisation processes (both biological and geochemical) are widely believed to eradicate any original biochemical information, but many studies have identified endogenous chemistry within fossils. However, these studies have predominantly focused on biological structures composed of relatively geo-stable molecules (e.g., lignin and chitin) and have used techniques that have limitations with regards to maintaining sample integrity that preclude many fossils from analysis and provide only small scale or no spatial information. Synchrotron Rapid Scanning X-ray Fluorescence (SRS-XRF) is an advance in XRF imaging that provides decimeter scale, 2D maps of elements in ppm concentrations in large (100x100x30cm) fossils at rapid acquisition rates (~30 s/cm² at 100 micron resolution). This allows the non-destructive visualisation of chemical variation of entire fossil organisms and their enclosing matrices *in-situ*, allowing the identification of biologically and geologically derived phases. This technique has shown that certain elements correlate with, and can reveal, discrete biological structures in a range of fossil and extant organisms. Additionally, X-ray absorption spectroscopy shows that the chemical inventory of fossil tissues commonly consists of organo-metallic and organo-sulfur compounds coordinated in a manner similar to comparable extant organisms. These findings support an endogenous origin for the observed fossil chemistry and thus fossil tissues may retain useful biochemical information. For example, previously unknown remnant tooth chemistry (phosphorus) within a 50 Mya fossil reptile has been revealed, and elements (e.g., copper) associated with dark eumelanin pigmentation have been identified and mapped within feathers of an exceptionally preserved 120 Mya Chinese bird.

Coupled Fe-S-P cycling in sediments of an oligotrophic coastal basin and the role of anaerobic oxidation of methane

MATTHIAS EGGER, TOM JILBERT
AND CAROLINE P. SLOMP

Department of Earth Sciences, Utrecht University, The
Netherlands

Studies of phosphorus (P) dynamics in coastal marine sediments typically emphasize the role of coupled iron (Fe), sulfur (S) and P cycling for sedimentary P burial and release. Here, we present field results suggesting that this model may have to be extended to include interactions of reactive Fe(III) phases with methane (CH₄).

Using pore water and solid phase analyses for sediments from an oligotrophic coastal basin (Bothnian Sea) we provide evidence for the formation of Fe-bound P, possibly vivianite (Fe₃(PO₄)₂·8H₂O), below the sulfate/methane transition zone (SMTZ). Solid phase Fe and S profiles indicate that the SMTZ in these sediments has recently shifted upwards to its current position close to the sediment-water interface (< 10 cm). This upward shift is attributed to an enhanced rate of methanogenesis driven by an increased eutrophication over the past decades. Below the SMTZ, extremely high Fe²⁺ concentrations (> 2 mM) are observed, and supersaturation with respect to vivianite is reached. We suggest that the exceptionally high dissolved Fe²⁺ concentrations in this non-sulfidic zone may be explained by anaerobic oxidation of methane (AOM) coupled to the reduction of Fe-oxides. Dissimilatory iron reduction appears to be unlikely due to the presence of relatively refractory organic matter. Instead, the concurrent presence of both abundant CH₄ and reactive ferric Fe rather suggests Fe reduction coupled to AOM. The resulting release of Fe²⁺ into the pore water and subsequent formation of Fe(II)-P provides an important sink for P released during reductive dissolution of Fe-oxides within and below the SMTZ. If this P sink below the SMTZ would be absent this would likely lower the P burial capacity and enhance the diffusive P flux out of the sediment back into the overlying water column.

Thus, while AOM coupled to Fe reduction likely accounts for only a relatively small percentage of CH₄ removal, our study suggests that the impact on the sedimentary P cycle could be large.

Visualisation of detrital zircon age data relative to deposition age and identification of potential provenance regions

BRUCE EGLINGTON^{1*}, SALLY PEHRSSON²
AND DAVE EVANS³

¹University of Saskatchewan, Saskatoon, Canada;

(*correspondence: bruce.eglinton@usask.ca)

²Geological Survey of Canada, Ottawa, Canada;

(pehrsson@nrcan.gc.ca)

³Yale University, New Haven, U.S.A.; dai.evans@yale.edu

Conventional probability function diagrams are routinely used to illustrate detrital zircon age data. Where numerous samples are available from stratigraphic successions, these probability plots require a lot of space and can not capture the link between zircon age and inferred stratigraphic (depositional) age. We present an alternative view of the probability plots which emphasise the relative stratigraphic age of different samples or lithostratigraphic units while illustrating which time intervals the majority of its detrital grains come from. In effect, one views the probability curves from above with the highest frequency sections of the curves plotted in emphasised ornament and colour relative to lower probability intervals in minimised ornament and shades of grey. This methodology has been built in to the DateView and StratDB online databases and into a standalone software package (FitPDF), all available from <http://sil.usask.ca>.

Once probability distributions have been associated with lithostratigraphic units in StratDB and DateView, the online software allows users to find all samples in the DateView geochron database which match detrital age peaks. These potential provenance localities may be further refined to take into account sediment transport directions and other geological constraints, after which it is possible to generate a probability plot for the most likely provenance localities for comparison with the actual (sample) detrital age distribution.

Locality information may also be illustrated on palaeogeographic reconstructions so as to enhance the regional provenance interpretation of detrital zircon data.

This approach is illustrated using data from the Kalahari and Pilbara cratons so as to assess different models for the Vaalbara hypothesis and of collision between the Zimbabwe and Kaapvaal cratons.

Geochemistry and the spatial patterns of water management are reflected in human hair

JAMES R. EHLERINGER¹, BRETT J. TIPPLE¹,
LESLEY A. CHESSON¹ AND LUCIANO O. VALENZUELA¹

¹IsoForensics Inc., 421 Wakara Way, Salt Lake City, Utah
84108 USA (jim@isoforensics.com)

Element concentrations and isotopes of human tissues within urban regions are known to reflect human health, to provide diagnostic dietary information, and to provide region-of-origin information in a linear fashion. Here, we show the importance of isotopes of both oxygen in water and strontium within tap waters to the isotope ratios preserved within hair. We test the concept that oxygen isotopes in hair are predictable based of local drinking water values at the time that hair proteins (keratin) are initially produced within hair follicles, whereas strontium isotopes in hair reflect a progressive input from external tap waters after hair has emerged from the scalp. The contrasting inputs of oxygen and strontium isotopes to hair provide a predictable diagnostic tool that can be used in a wide array of forensics and region-of-origin studies. Since both oxygen isotope and strontium isotopes within drinking water are known to vary independently and spatially across continents in a predictable manner, the simultaneous measurement of both isotopes provides a new and powerful modern tool to reconstruct the region-of-origin of unidentified murder victims in forensic investigations.

Stable silicon isotopes in porewaters off Peru – diatom dissolution versus authigenic clay mineral formation

CLAUDIA EHLERT^{1,2*}, KRISTIN DOERING³,
KLAUS WALLMANN¹, PATRICIA GRASSE¹
AND MARTIN FRANK¹

¹GEOMAR, Helmholtz Centre for Ocean Research, Kiel,
Germany (*correspondence: cehlert@mpi-bremen.de)

²Max Planck Research Group for Marine Isotope
Geochemistry, ICBM, University of Oldenburg, Germany

³Institute of Geoscience, University of Kiel, Germany

The stable silicon isotope compositions ($\delta^{30}\text{Si}$) of dissolved silicic acid and of diatom opal have been used successfully to investigate changes in nutrient utilisation and biogeochemical cycling processes in the present and past ocean. Opal dissolution, however, might have an effect on the preserved $\delta^{30}\text{Si}$ signal of diatom opal in the sediment and therefore on the interpretation of paleo $\delta^{30}\text{Si}$ records.

To investigate the effects of dissolution processes on the preserved diatom $\delta^{30}\text{Si}$ signal we analysed the sedimentary biogenic opal content and dissolved silicic acid concentrations of the porewaters, as well as their $\delta^{30}\text{Si}$ signals in the upper 20-50 cm of three short sediment cores from different water depths within the Peruvian upwelling region. The cores show large variations in biogenic opal content ranging from 10-25% in the shallowest core to only 1-2% in the deepest one. The dissolved silicic acid concentration in all three profiles increases with sediment depth. The dissolved $\delta^{30}\text{Si}$ signature of the porewaters is unexpectedly high (+1.1‰ to +1.9‰) with the highest values occurring in the uppermost 5-10 cm of the deepest station. These $\delta^{30}\text{Si}$ signatures are significantly higher than the diatom opal (+0.6‰ to +1.0‰) and the seawater above (+1.0‰ to +1.5‰). In the shallowest profile the porewater $\delta^{30}\text{Si}$ does not show significant variations with profile depth, whereas the deepest profile is characterised by a pronounced decrease in the porewater $\delta^{30}\text{Si}$ with increasing profile depth.

Based on these results we suggest that the heavy $\delta^{30}\text{Si}$ signatures near the top of the profiles are the result of the precipitation of authigenic clay minerals with a very light Si isotope composition leaving the porewaters isotopically heavy. With increasing profile depth the effect of clay precipitation diminishes and the dissolution of diatom opal becomes dominant. So far we cannot unambiguously conclude on any significant effect of these processes on the preserved $\delta^{30}\text{Si}$ of the diatom opal itself and therefore on the interpretation of the downcore paleo records.

Early stage uptake of Se into rice (*oryza sativa japonica*) seedlings depending on medium and Se concentration

E. EICHE*, A. NOTHSTEIN AND G. KONRAD

Institute for Mineralogy and Geochemistry, KIT, 76131 Karlsruhe,
Germany (*elisabeth.eiche@kit.edu)

Selenium is a ubiquitously present trace element which is of interest because of its essentiality for human nutrition but also because of its toxicity in slightly elevated concentrations [1]. Various factors like pH-/ redox-conditions, organic matter content, microbial activity or competing ions can influence the Se cycling in the rhizosphere [1,2]. In order to investigate and quantify the influence of individual parameters on the Se uptake we carried out simple experiments in artificial and controlled systems.

The early stage uptake of Se into rice seedlings depending on the concentration was investigated in the range of 0 to 50 ppb Se using hydroponic systems. Selenium was added as Selenate (SeO_4^{2-}) to nutrient solution and to phytoagar (0, 20 ppb). The rice plants were grown in a climatic chamber and were harvested after 10 (1st harvest) and 17 days (2nd harvest), respectively.

The results show a linear increase of plant Se accumulation with increasing Se concentration in the nutrient solution. The Se enrichment was >3 times higher after the 2nd harvest compared to the 1st one. Also, 3.7 times more Se was taken up by shoots compared to roots. It is striking that already 50 ppb of Se in the nutrient solution lead to an accumulation of 10 ppm in the rice, a concentration that normally assigned to plants grown on seleniferous soils [3]. An even higher Se content of 17.1 ppm was reached (2nd harvest) if Se (20 ppb) was added to phytoagar. Generally, 6 to 8 times more Se was accumulated if the Se bearing medium was phytoagar and not the nutrient solution. This is probably due to interaction and competition of Se with other ions in the nutrient solution.

[1] Neal, R. H. 1995; in Heavy Metals in Soils, ed. Alloway, B. J. John Wiley & Sons Inc., 1995, 260-283. [2] Levander, O. & Burk, R.; in Selenium, eds. Hatfield, D. L.; Berry M. J. & Gladyshev, V. N. Springer US, 2006, pp. 399-410. [3] White *et al.*, 2004. Interactions between selenium and sulphur nutrition in *Arabidopsis thaliana*. Journal of Experimental Botany 404, 1927-1937.

Isotopic anatomies of organic molecules

JM EILER¹ AND D KRUMWIEDE²

¹Caltech, Pasadena, CA, USA (eiler@gps.caltech.edu)

²Thermo-Fisher Scientific, Bremen, Germany

Most organic molecules exist in an astonishingly large and diverse variety of isotopologues, i.e., considering all possible site-specific and multiple isotopic substitutions. These species are fractionated from one another by physical, chemical and biological processes. Thus isotopic variations of organics must involve an extraordinarily large number of independent compositional dimensions. Full analysis of even a fraction of this diversity presents a complex, challenging problem, but would potentially yield much new information about sources, conditions, reaction mechanisms and perhaps other variables.

Several emerging technologies make such measurements: chemical and/or pyrolytic preparations; IR spectroscopy, SNIF-NMR; and novel instruments and methods of mass spectrometry. Each has strengths and weaknesses, but none to date is capable of examining both site-specific and multiple-substitutions in small quantities (ng-mg) of species larger than $\sim C_3$ hydrocarbons. Most isotopic diversity of most organic compounds remains out of reach.

We describe instruments, methods and initial results of an experiment to expand this field to encompass the isotopic anatomies of organics up to ~ 300 amu, potentially bringing into play fatty acids, amino acids, isoprenoids, and similar sized compounds. The experiment uses the MAT 253 Ultra, a prototype high resolution ($M/\Delta M \sim 25,000$) multi-collector gas source mass spectrometer, and the Thermo DFS, a very high resolution (up to $\sim 80\text{-}100,000$) single collector gas source mass spec that is generally used for identification of organic compounds. We use the Ultra to precisely determine the intensity ratios of ion beams that include all isotopologues of a given compound (or its fragment ions), free from isobaric interferences by contaminant species, and then use the DFS to perform rapid scans over a narrow mass window, measuring relative proportions of isotopologues of that species at each cardinal mass. Combination of these data constrains proportions of each isotopologue at each cardinal mass. Initial experiments on butane indicate that this approach may be able to constrain $\delta^{13}C$ of ion fragments with precision of $\pm 0.1\text{-}0.2$ ‰ and δD with precision of $\pm 2\text{-}3$ ‰. We intend to combine this approach with recently invented methods for analysis of multiply substituted and position specific isotopologues of alkanes on the Ultra to create a set of techniques for characterizing proportions of a large number of isotopologues of moderate-sized organic molecules.

The impact of climate on land derived nutrient fluxes to the ocean

EYDIS SALOME EIRIKSDOTTIR¹,
SIGURDUR REYNIR GISLASON¹ AND ERIC H. OELKERS^{1,2}

¹Institute of Earth Sciences, University of Iceland, Sturlugata 7, 101 Reykjavík, Iceland, (ese@raunvis.hi.is).

²GET, CNRS/URM 5563-Université Paul Sabatier, 14 ave. Edouard Belin., 31400, Toulouse, France.

Weathering and denudation influence greatly the global elemental cycles. There are two main sources of nutrients in the oceans, recycling due to microbial degradation and influx of nutrients from terrestrial runoff [1]. Some elements are essential nutrients for photosynthesis (N, P, Si, Ca, Mg, etc) while other, such as Fe, V, and Mo catalyse biochemical transformations at key points in the carbon and nitrogen cycles. Chemical denudation is positively correlated with runoff and atmospheric temperature [2]. In this study, we demonstrate the different effects climate has on the individual elemental fluxes, derived from silicate weathering in six basaltic river catchments in NE Iceland, of which three are of glacial origin and three are non-glacial rivers.

Concentrations of suspended sediments, major dissolved elements, and some trace elements are discharge dependent while concentrations of most trace metals are discharge independent. Due to the distinct behavior of the particulate and dissolved elements, some are more sensitive to climate change than others. The climate dependence of elemental fluxes is also different between the glacial and direct-runoff rivers.

Data regression of ~ 40 years of chemical and flow was used to determine the influence of temperature and runoff on the annual fluxes of elements transported to the oceans. The fluxes of the major elements, and Sr and Mo, depended less on the climate than those of the fluxes of trace elements, including the micro-nutrients Fe and V. A change of one °C changes 1) major element, Sr and Mo fluxes, and 2) micro-nutrient fluxes by 13 – 15%, and 15 – 19%, respectively in the non-glacial rivers and by 4 – 14% and 8 – 19% in the glacial rivers. A 10% incremental runoff increase, within the runoff range of the individual river, changed the same fluxes by 7 – 9% and 10 – 15% in the non-glacial rivers and by 2 – 8% and 9 – 16% in the glacial rivers. These results show that elemental fluxes of glacial rivers are more sensitive to climate change than those of non-glacial rivers.

[1] Falkowski (2004) Vol. 8. Treatise on Geochemistry (eds. H.D. Holland and K.K. Turekian), pp. 185 – 213. [2]. Eiriksdottir *et al.* (2013), *EPSL*, **107**, 65 – 81.

Metamorphic and magmatic overprint of garnet pyroxenites from the Beni Bousera massif (Northern Morocco): Mineralogical, chemical and textural records

FATIMA EL ATRASSI^{1*}, FABRICE BRUNET²,
GILLES CHAZOT³ AND CHRISTIAN CHOPIN⁴

¹Laboratoire de G-Time, Université Libre de Bruxelles, Belgium (*Corresponding author : Fatima.El.Atrassi@ulb.ac.be)

²ISTerre, Université de Grenoble 1, CNRS, Grenoble, France

³Institut Universitaire Européen de la Mer, Brest, France

⁴Laboratoire de Géologie, Ecole normale supérieure, Paris, France

A detailed mineralogical and textural study of two garnet pyroxenites of the Beni Bousera massif, the garnet clinopyroxenite (GP) and the garnet clinopyroxenite containing graphite pseudomorphs after diamond (GGP), indicates a strong metamorphic overprint associated with the massif exhumation. In both pyroxenites, the primary assemblage [Cpx(I) + garnet +/- Opx] records temperatures in excess of 1200°C. Along the exhumation path, Cpx(I) has decomposed under sub-solidus conditions in at least two stages, which led first to pyroxene exsolution lamellae and second to garnet crystallization at the expense of the newly formed Cpx lamellae. These secondary garnets have grown in the 850-950°C temperature range. We show that these conditions are below the blocking temperature of the Mg-Fe exchange between garnet and pyroxene (ca. 1050°C) and above the blocking temperature of Mg-Fe interdiffusion in garnet. Consequently, the original composition of these secondary garnets has not been modified upon further cooling; equilibrium with the appropriate lamellar pyroxene can be used to retrieve meaningful P-T couples.

The late evolution of the Beni Bousera massif is recorded in the pyroxenites by the decomposition of primary garnet porphyroclasts into symplectite intergrowths at around 800-850°C below 10 kbar. These late conditions coincide with a major event: a temperature increase up to ca. 1050°C at most, which led to partial melting in both GP and GGP in the presence of water. The partial melting is evidenced by the presence of silicate films preserved in the graphite aggregates and the occurrence of interstitial amphibole and plagioclase.

Detailed chemical inspection of Gt-Cpx-Opx inclusions in the graphite pseudomorphs using LA-ICP-MS ablation, FEG-SEM and the electron microprobe indicates that (1) these silicates are genetically related to the same minerals in the bulk rocks and (2) they were chemically isolated from the bulk rock (included in diamond and/or graphite).

Ocean Geochemistry and Paleoproxies: Deep ocean carbonate ion through six glacial-interglacial cycles

H. ELDERFIELD

Department of Earth Sciences, University of Cambridge, CB1 1EE Cambridge UK; (he101@cam.ac.uk)

The presence of carbonate cycles in deep ocean sediments has been the subject of longstanding debate with much recent work supporting the view that changes in carbonate ion are responsible. Estimates of palaeo-carbonate ocean chemistry from boron incorporation in foraminifera provide important evidence. $[\text{CO}_3^{2-}]$ estimates also play a role in paleothermometry with debate as to the roles of ocean chemistry versus dissolution. Here we present data of behaviour of epifaunal and infaunal benthic species, factors influencing porewater $[\text{CO}_3^{2-}]$, and possibly boron coordination and emerging proxies. This is followed by evidence for elevated alkalinity in the glacial ocean with emphasis on sites within Circumpolar Deep Water.

Understanding D/H systematics of leaf wax *n*-alkanes in C₃ and C₄ plants at Stiffkey saltmarsh, Norfolk, UK

YVETTE ELEY^{1*} AND NIKOLAI PEDENTCHOUK¹

¹School of Environmental Sciences, University of East Anglia, Norwich, UK (*contact: y.eley@uea.ac.uk)

D/H ratios of *n*-alkyl lipids are becoming increasingly popular as indicators of palaeohydrological regimes. The suitability of these compounds for such applications is dependent upon the precise nature of the information they are conveying. Current interpretations of this proxy are limited by an incomplete understanding of the mechanisms responsible for the variation in *n*-alkyl lipid δD values among plant species at individual locations.

To evaluate the relative importance of environmental, physiological and biochemical factors on the D/H composition of *n*-alkyl lipids, we sampled a range of C₃ and C₄ plants at Stiffkey saltmarsh throughout 2012. The results of δD analysis of soil, xylem, and leaf waters suggest that the bulk of interspecies variation in *n*-alkane δD values (>100‰) cannot be explained by environmental and plant physiological factors. Instead, we propose that species-specific D/H fractionation during lipid biosynthesis represents a fundamental control on *n*-alkane δD values of these plants.

Our ongoing work on starch δD will allow us to identify whether variation in carbohydrate recycling may explain the range of lipid δD in key species at our site. Furthermore, we are examining whether seasonal changes in leaf wax composition, including the nature and amount of precursor compounds, affect the *n*-alkyl D/H signal. Finally, our work on chloroplast-bound phytol will allow us to investigate whether the potential existence of different NADPH pools influences the δD of compounds biosynthesized in different plant compartments. Our results indicate an integrated physical and biochemical approach is required to interpret the D/H signals contained in the sedimentary record.

Isotope anomalies of Hf and W in chondrite leachates and residues

B.-M. ELFERS^{1,2*}, S.T.M. PETERS^{1,2}, F. WOMBACHER^{1,2} AND C. MÜNKER^{1,2}

¹Institut für Geologie und Mineralogie, Universität zu Köln, 50674 Köln, Germany

(*correspondence: elfersb@uni-koeln.de)

²Steinmann-Institut, Universität Bonn, 53115 Bonn, Germany

The stepwise dissolution of primitive chondritic meteorites allows to reveal nucleosynthetic anomalies that are otherwise hidden in the bulk rock mix. Leaching experiments for Hf and W have previously been published, but in separate studies that did not include the rare p-process isotopes ¹⁷⁴Hf and ¹⁸⁰W [1, 2]. Here, we present for the first time combined Hf and W isotope data for acid leachates of several chondritic meteorites, including sufficiently precise analyses of p-process ¹⁷⁴Hf and ¹⁸⁰W for some chondrites (EET 96026 (R3), MAC 02839 (EL3) and WSG 95300 (H3.3)).

For leaching experiments, sample powders of the different meteorites were treated with 2M HCl and divided into a leachate and a residue fraction. Tungsten and Hf were separated from the same sample split using anion exchange chromatography. The W fraction was subsequently purified with TODGA resin, and Hf was further purified using Ln-Spec. Measurements were performed on a Neptune MC-ICP-MS. For the collection of the small ion beams, amplifiers with 10¹²Ω resistors were employed. Interferences from Yb, Lu and W, and Hf, Ta and Os isotopes, respectively, were sufficiently low to allow accurate interference corrections. The external reproducibilities on ¹⁷⁴Hf and ¹⁸⁰W were better than ±60 ppm and ±70 ppm, respectively, but significantly larger for small samples cuts <60 ng Hf and <150 ng W, respectively.

First data reveals that most of the Hf leachates and residues show anomalous s- and r-process patterns that are consistent with the results of [1]. First W isotope s- and r-process patterns are furthermore consistent with data reported by [2]. Neither leachates nor residues exhibit resolvable non-terrestrial ¹⁷⁴Hf, whereas both positive and negative ¹⁸⁰W signatures are resolved for almost all leachates and residues. The origin of the apparent decoupling between ¹⁸⁰W and ¹⁷⁴Hf is presently ambiguous, but possibly point towards different carrier phases for p-process Hf and W.

[1] Qin L. *et al.* (2011) *GCA*, **75**, 7806-7828. [2] Burkhardt C. *et al.* (2012) *AJL*, **753**, L6.

B and O isotopes as tracers of serpentinitization along fossil oceanic detachments, Troodos ophiolite, Cyprus

BAR ELISHA¹, YARON KATZIR¹, MEIR ABELSON²,
SAMUELE AGOSTINI³, JOHN W. VALLEY⁴
AND MICHAEL J. SPICUZZA⁴

¹Ben Gurion Univ. of the Negev, Be'er Sheva Israel,

(brelisha@gmail.com) (*presenting author)

²Geological Survey of Israel, Jerusalem, Israel;

³IGG-CNR, Pisa, Italy

⁴Univ. of Wisconsin, Madison WI 53706, USA

Serpentine lubricated detachment faults strike parallel to two segments of a paleo spreading center that are separated by the Arakapas transform in the Troodos ophiolite, Cyprus. To the north of the transform, serpentinite faulted against gabbro shows bimodal spatial distribution and covariance of B-O isotope ratios. These data indicate overprinting of fault localized, 'high temperature' oceanic serpentinitization ($\delta^{18}\text{O}=4$ to 6‰ ; $\delta^{11}\text{B}=-3$ to 3‰) by widespread late hydration at lower temperatures, forming abundant chrysotile veins ($\delta^{18}\text{O}=10$ to 12‰ ; $\delta^{11}\text{B}=7$ to 13‰). At the Limassol Forest complex, south of the transform, extensive talc-amphibole-chlorite metasomatic zones and rodingitized gabbro boudins occur within strongly foliated serpentinite shear-zones separating an ultramafic section from sheeted dykes. $\delta^{18}\text{O}$ values of serpentinite from shear-zones in the Limassol Forest have a narrow range and are invariably lower than mantle values (1 to 5.7‰ ; $n=26$), consistent with serpentinitization during seafloor spreading. $\delta^{11}\text{B}$ (Srp) values are more scattered (5 to 27‰) and weakly correlate with boron contents (2 to 60 ppm), which might be accounted for by increase in pH of water as serpentinitization progressed.

Absence of the lower crustal section above the mantle and injection of gabbroic magma followed by localized serpentinitization, metasomatism and deformation along this discontinuity are major characteristics of oceanic detachments. Isotope systematics strongly resemble those of serpentinite recovered from modern oceanic core complexes such as the Atlantis Massif. The mantle sequence of the Limassol Forest is thus suggested to have been exhumed at the footwall of an oceanic core complex. This scenario sheds light on the location of the spreading axis south of the transform and explains the highly complicated structure of the fossil ridge-transform intersection of the Limassol Forest.

Origins of anomalous ridge magmatism near Jan Mayen

L.J. ELKINS^{1*}, E.R. RIVERS¹, K.W.W. SIMS²,
J. BLICHERT-TOFT³, C. DEVEY⁴, R. CHERNOW¹,
R. DAVIS¹ AND K. MEISENHEDER¹

¹Bryn Mawr College, Bryn Mawr, PA, USA

(*correspondence: lelkins@brynmawr.edu)

²University of Wyoming, Laramie, WY, USA

(ksims7@uwyo.edu)

³Ecole Normale Supérieure de Lyon, Lyon, France

(jblicher@ens-lyon.fr)

⁴GEOMAR, Kiel, Germany (cdevey@geomar.de)

The sustained volcanism at Jan Mayen Island, located immediately south of a major fracture zone (the Jan Mayen Fracture Zone) and adjacent to two slow-spreading mid-ocean ridges (the Kolbeinsey and Mohns Ridges), has been variably ascribed to a small, isolated plume, to material siphoned northward off the larger Icelandic plume, to convection-driven edge effects along a major compositional mantle discontinuity, and to the presence of highly fusible, wet, old, garnet-bearing material derived from veins or pockets of rift-faulted or delaminated Greenland sub-continental lithospheric mantle. The compositions of volcanic rocks from both Jan Mayen Island and the immediately adjacent segments of the Mohns and Kolbeinsey Ridges likewise support the long-term presence of mantle rocks enriched in incompatible elements. While the most recent work on long-lived radiogenic isotope compositions of Jan Mayen Island magmas has supported a complex model invoking several of the above scenarios of melting, no high-resolution sampling and analysis existed for the adjacent ridge segments.

We present geochemical data for new, precisely bathymetrically located volcanic samples from the Northern Kolbeinsey and Southern Mohns segments. Preliminary geochemical and bathymetric findings suggest that both segments host long-lived, localized sources of increased magma flux associated with the most geochemically enriched melt compositions hosted by those ridge segments, which decrease in indicators of geochemical enrichment with distance from Jan Mayen Island. The surface expressions of this high magma supply include large volcanic edifices straddling the axial valleys and walls, as well as evidence for ridge axis relocations in the direction of Jan Mayen Island. This supports a sustained point source of geochemically enriched magmatic activity beneath the region, consistent with a deep-seated mantle plume.

We further provide new U-series isotopic data for all three geographic areas, which place constraints on mantle source compositions and upwelling rates beneath the region.

Dripping, thinning, melt injection, metasomatism: Geochemical consequences of small-scale convection under continents

L. T. ELKINS-TANTON^{1*}

¹DTM, Carnegie Institution for Science, Washington DC 20015 (*correspondence: ltelkins@dtm.ciw.edu)

Through a variety of physical mechanisms, the lower lithosphere is thought to be recycled into the mantle, thinning the lithosphere and creating compositional differentiation. Lithospheric thinning has been inferred from increases in crustal heat flow in specific regions, rapid regional uplift, and from the appearance of signature high-potassium magmas [e.g. 1-5]. Seismic studies also support ductile delamination in specific areas [e.g., 6].

Geochemical arguments appear to require foundering of crustal and mantle lithospheric materials to balance elemental budgets. Though continental crust and mantle are complementary reservoirs with respect to most trace elements, the continental crust is too felsic to be derived directly from the mantle [7,8]. A possible solution is the loss from the continental lithosphere through delamination of mafic residues from fractionation of mantle melts. The same process would explain the significant fractionation of thorium and lanthanum in continental crust, when they are unfractionated during the processes of subducting sediments and producing arc magmatism [9].

A spectrum of physical mechanisms have been proposed for this small-scale convection. The greatest discriminator among them appears to be rheology, that is, how ductile is the material that is sinking away? The most brittle material might sink away in the shape of a plate, while the most ductile drip off as fluids. The feasibility of these processes depends upon composition, pressure, and temperature, and all these combine to affect the surface expression and compositional ramifications, from recycling differentiated compositions back into the mantle, to producing melt that might erupt.

[1] Kay & Kay (1993) *Tectonophysics* **219**, 177-189. [2] Ducea & Saleeby (1998) *Int'l Geology Rev.* **40**, 78-93. [3] Schott & Schmeling (1998) *Tectonophysics* **296**, 225-247. [4] Lustrino (2005) *Earth Sci. Rev.* **21**. [5] Hoernle *et al.* (2006) *Earth Planet. Sci. Lett.* **248**, 335-352. [6] Jones & Phinney (1998) *J. Geophys. Res.*, **103**, 10,065 – 10,090. [7] Rudnick R.L. (1995) *Nature* **378**, 571-578. [8] Lee *et al.* (2006), *Contrib. Mineral. Petrol.* **151**, 222-242. [9] Plank (2005) *J. Petrology*.

Origin and evolution of volatiles in rocky airless bodies

L. T. ELKINS-TANTON^{1*}

¹DTM, Carnegie Institution for Science, Washington DC 20015 (*correspondence: ltelkins@dtm.ciw.edu)

Large planetesimals or asteroids, the Moon, and Mercury form a size continuum of airless bodies, but their formation histories are thought to be significantly different. While planetesimals formed from relatively lower energy accretionary impacts, they themselves continued to accrete gravitationally in more and more energetic impacts to build larger planets such as Mercury, and finally to produce the giant Moon-forming impact on the young Earth that resulted in the Moon. Despite the significant impact energy that went into producing the Moon, it was not completely dried and devolatilized during its formation [e.g., 1-3].

Part of the original evidence for a dry Moon, overturned by these recent measurements of volcanic materials, was the depleted K/U ratio compared to the Earth [4]. In contrast, Mercury shows a K content similar to the Earth and Mars, and thus may not be as depleted in volatiles as the Moon [5]. Similarly, measurements of meteorite compositions [6] indicate that neither primitive nor differentiated planetesimals were completely dried. Thus, the building blocks (planetesimals), the final planets (Mercury), and their impact debris (the Moon) all retained some fraction of their original volatile content.

In differentiated planetesimals and in the Moon and Mercury the silicate portions of the bodies were likely processed through a magma ocean stage [7]. Retention of volatiles is less likely in a planetesimal interior than it is in a planetary magma ocean. Internal heating from short-lived radiogenic aluminum 26 in small early planetesimals drives off volatiles from planetesimals above a certain size [8].

Fractional solidification in a planetary-sized magma ocean, in contrast, can retain some volatile fraction inside the planet through partitioning with solid phases and sequestration of interstitial melts. Model results for these processes will be compared with measurements from the Moon.

[1] Saal *et al.* (2008) *Nature* **454**, 193-195. [2] Boyce *et al.* (2010) *Nature* **466**, 466-470. [3] McCubbin *et al.* (2010), *PNAS* **107**, 11223-11228. [4] Tera *et al.* (1974) *EPSL* **22**, 1-21. [5] Peplowski *et al.* (2011) *Science* **333**, 1850-1852. [6] Jarosewich (1990) *MAPS* **25**, 323-337. [7] Elkins-Tanton (2011) *Ann.Rev. Earth Planet. Sci.* **40**, 113-139. [8] Young *et al.* (2003) *EPSL* **213**, 249-259.

The Global U Isotopic Cycle

TIM ELLIOTT¹, MORTEN ANDERSEN^{2*}
AND HEYE FREMUTH¹

¹Bristol Isotope Group, School of Earth Sciences, University of Bristol, Bristol, BS8 1RJ, UK (tim.elliott@bris.ac.uk)

²Institute of Geochemistry and Petrology, ETH Zürich, CH 8092 Zürich, Switzerland (*correspondence: morten.andersen@erdw.ethz.ch)

The mobility of U under oxic conditions and its enrichment in the oceanic crust has long led to speculations about the importance of these low temperature processes in the global distribution of U [e.g. 1]. Notably, the return flux of U from surface to mantle, via subduction, is potentially sufficient to perturb the mantle U abundance. This mechanism has been used as a means to explain puzzling features of mid-ocean ridge basalt (MORB) U-Th-Pb systematics [e.g. 2]. Advances in multi-collector inductively coupled plasma mass spectrometry (MC-ICPMS) allow the hitherto presumed invariant ²³⁸U/²³⁵U ratio to provide new constraints on this cycle. Recent work has shown that the U in the near surface environment can be fractionated by about 1‰ [e.g. 3,4]. Therefore, recycling of significant amounts of isotopically fractionated U from the surface to the mantle has the potential to perturb not only its U abundance but also its isotope ratio.

In order to exploit this potential we have had to tune our torch. Using a ²³³U-²³⁶U double spiking approach and by measuring intense U beams (>1nA), we have obtained precisions of ~0.02‰ on ²³⁸U/²³⁵U ratios of mantle derived samples. This provides sufficient resolution to detect the influence of recycled U in the mantle.

We have determined that the net effects of alteration and subduction leave deep recycled slab with isotopically heavy U [5]. The preferential return of this U into the upper mantle, as invoked to explain the anomalously low Th/U ratio of MORB [e.g. 2], predicts that MORB should be ~0.1‰ heavier than pristine mantle. We show that this prediction is realised in our measurements of MORB glasses relative to ocean island basalts and chondritic meteorites. Thus we provide striking, independent confirmation of the importance of recycling in shaping the U budget of the mantle courtesy of the capabilities of modern MC-ICPMS.

[1] Albarède & Michard (1986) *Chem Geol* **57** p1-15 [2] Elliott, Zindler & Bourdon (1999) *EPSL* **169** p129-145 [3] Stirling, Andersen, Potter & Halliday (2007) *EPSL* **264** p208-225 [4] Weyer *et al.* (2008) *GCA* **72** p345-359 [5] Freymuth, Andersen & Elliott this volume

Tracing changes in the biogeochemical cycling of iron during the annual subtropical spring bloom east of New Zealand

M.J. ELLWOOD^{1*}, P.W. BOYD², S. NODDER³,
D.A. HUTCHINS⁴, S.W. WILHELM⁵, A. MILNE⁶
AND M. LOHAN⁶

¹Research School of Earth Sciences, Australian National University, Canberra, Australia, (*correspondence: michael.ellwood@anu.edu.au)

²Centre for Chemical and Physical Oceanography, NIWA, University of Otago, Dunedin, New Zealand

³NIWA, Wellington, New Zealand

⁴Marine Environmental Biology, University of Southern California, Los Angeles, California, USA

⁵Department of Microbiology, The University of Tennessee, Knoxville, USA

⁶School of Geography, Earth and Environmental Sciences, University of Plymouth, UK

The turnover time of iron in the surface ocean can vary from days to weeks and months, while within cells the turnover time can be on the order of hours to days. Accordingly, the iron isotope ($\delta^{56}\text{Fe}$) composition of particulate organic matter should be sensitive to changes in the cycling of iron in the surface ocean and immediately below. Here we present data showing a dynamic change in the $\delta^{56}\text{Fe}$ composition of particulate organic matter during the development and subsequent export of phytoplankton bloom material. Our results, obtained from two FeCycle voyages in 2008 and 2012, suggest that before the onset and development of the phytoplankton bloom iron regeneration dominates the dissolved iron signal with lighter dissolved $\delta^{56}\text{Fe}$ values (-0.14‰ at 100 m to 0.07‰ at 500 m) relative to particulate iron (-0.02‰ at 60 m to 0.13‰ at 300m). In contrast, during the development and export phase of the bloom, iron scavenging and/or iron consumption by heterotrophic bacteria community appears to dominate the dissolved iron isotope signal with heavier dissolved $\delta^{56}\text{Fe}$ values (0.15‰ at 30 m to 0.16‰ at 500 m) relative to particulate $\delta^{56}\text{Fe}$ values (-0.11‰ at 30 m to -0.33‰ at 300 m). A strong relationship was also observed between particulate $\delta^{56}\text{Fe}$ and Fe/Al ratios with lighter values. The dissolved and particulate $\delta^{56}\text{Fe}$ results were modelled with Rayleigh-type functions and produced the following fractionation factors: 1.00015 prior to the onset and development of the bloom and 0.99945 during the subsequent export of the bloom material to depth. Taken together our results show that the iron isotope composition of dissolved and particulate material can be used to monitor changes in the biogeochemical cycling of iron in the marine realm.

Crystal chemistry and magnetism of Fe-serpentines based on XMCD

A. ELMALEH^{1*}, M.-A. ARRIO¹, A. JUHIN¹,
P. SAINCTAVIT¹, S.C. TARANTINO², M. ZEMA²,
A.-L. AUZENDE¹, A. SMEKHOVA^{3,4} AND A. ROGALEV³

¹IMPMC-UPMC/CNRS, Paris, France (*correspondence:

Agnes.Elmaleh@impmc.upmc.fr)

²Dep. of Earth & Environ. Sciences, University of Pavia, Italy

³ESRF, Grenoble, France

⁴now at Faculty of Physics, Moscow State University, Russia

Fe-rich layer silicates are rare on Earth, but are a major component of CM2 carbonaceous chondrites. They formed during early aqueous alteration events that affected CM2s' asteroidal or cometary parent body [1]. Bulk magnetometry (300-2 K) has proven useful for characterizing Fe-serpentines' mineralogy, close to the pole cronstedtite in CM2s [2]. Comparison with results from single crystals supports the hypothesis of a variable Fe content of serpentines along the alteration sequence of CM2s [2], similarly to terrestrial serpentinization. Site distribution and valence of iron in serpentines would directly be linked to their growth conditions (T, water-rock ratio or duration [3]). Understanding the conditions in which the reactions occurred on the parent body of CM2s thus relies on a thorough characterization of their crystal chemistry.

Here we present the results of a X-ray Magnetic Circular Dichroism study at the Fe K-edge of oriented single crystals of cronstedtite, showing a strong planar anisotropy. We measured XMCD at various angles between the *c* axis and the applied field. We will show how ligand field multiplet calculations [4] allow one to separate various contributions to the pre-edge. This would yield an estimate of the crystal chemistry of Fe in this multisite (octahedral, Oh, and tetrahedral) and multivalent (Fe^{2+,3+}) mineral, allowing for a fine characterization of this alteration mineral in meteorites. Also, XMCD suggests that the anisotropy of cronstedtite originates from the strong single ion anisotropy of Fe²⁺ in distorted Oh sites. Finally, exploring the variations of XMCD with substitutions (mostly Fe-Si) would clarify which parameters control the disruption of a long-range magnetic order in Fe-serpentines, from AF, when only Fe²⁺ is present, in Oh sites [5], to spin-glass like, in cronstedtite [2].

[1] Zolensky, Krot & Benedix (2008) *Rev. Miner. Geochem.* **68**, 429-462. [2] Elmaleh, Tarantino, Zema, Devouard & Fialin (2012) *Geochem. Geophys. Geosyst.*, **13**, Q05Z42. [3] Marcaillou, Muñoz, Vidal, Parra, & Harfouche (2011) *EPSL*, **303**, 281-290. [4] Arrio, Rossano, Brouder, Galois & Calas (2000) *Europhys. Lett.*, **51**, 454. [5] Coey, Ballet, Moukarika & Soubeyroux (1981) *Phys. Chem. Miner.* **7**, 141-148.

Estimating the Potential Evapotranspiration by using Landsat imagery

M. EL MOULAT¹, M.HAKDAOUI¹, F. T.-C. TSAI²
AND A. M. MILEWSKI³

¹Department of Geology, University Hassan II Mohammedia-Casablanca Faculty of Sciences Ben M'sik B.P 7955, Sidi Othmane, Casablanca, Morocco. (Email: m.elmoulat@gmail.com and hakdaoui@gmail.com)

²Department of Civil and Environmental Engineering, University of Louisiana State, 3418G Patrick F. Taylor Hall, Baton Rouge, LA 70803-6405. (ftsai@lsu.edu)

³Department of Geology, University of Georgia, Athens, GA 30602. (milewski@uga.edu)

Freshwater resources are becoming increasingly limited in many parts of the world, and decision makers are demanding new tools for monitoring water availability and rates of consumption. Remotely sensed data and especially Landsat imagery provides an estimate of land-surface temperature that allow mapping of evapotranspiration (ET) at the spatial scales. This work presents the utility of satellite imagery in water resource management. General modeling techniques for using land-surface temperature in mapping the surface energy balance are described, including methods developed to safeguard ET estimate. Examples are provided of how remotely sensed maps of ET derived from Landsat thermal imagery are being used operationally by water managers today: in monitoring water rights, negotiating, estimating water-use by invasive species, and in determining allocations for agriculture, urban use, and endangered species protection. To better address user requirements for high-resolution, time-continuous ET data, novel techniques have been developed to improve the spatial resolution of Landsat thermal-band imagery and temporal resolution between Landsat overpasses by fusing information from other wavebands and satellites.

Interactions between Fe(II) and arsenic species during co-sorption onto aluminum oxide and clay mineral substrates under anoxic conditions

EVERT J. ELZINGA* AND YING ZHU

Rutgers University, Department of Earth & Environmental Sciences, Newark, New Jersey, USA. (*correspondence: elzinga@andromeda.rutgers.edu)

Reductive dissolution of Fe(III)-oxides and hydroxides in suboxic and anoxic soils and sediments leads to substantial changes in aqueous geochemical conditions, including a strong increase in the aqueous concentrations of Fe(II) and trace metal(loid) species released during dissolution of Fe(III)-oxide sorbents. The fate of released Fe(II) and trace metal(loid)s is likely to be at least partially controlled by sorption reactions with mineral constituents remaining in the soil matrix, and may further be influenced by redox reactions between Fe(II) and redox-sensitive elements including As. While there have been quite a few studies addressing sorption of Fe(II), As(III) and As(V) onto common soil minerals in binary systems, very little is known about the interactions between these species in ternary systems involving co-sorption.

Here, we use a combination of batch experiments and X-ray absorption spectroscopy to study the co-sorption of Fe(II) with As(V) and As(III) onto aluminum-oxide and clay surfaces under anoxic conditions and at near-neutral pH values typical of reduced geochemical environments. We observe notable differences between the ternary and binary systems as to the extent and mechanisms of Fe(II) and As sorption. The XAS results indicate the operation of several processes, including formation of monomeric surface complexes and precipitation of Fe(II)-Al(III)-layered double hydroxides. Interactions among these processes and the significance of redox reactions in the ternary systems will be discussed.

Co-benefits of tackling poor air quality and regional climate: A focus on ecosystems

LISA EMBERSON¹, KEVIN HICKS¹ AND PATRICK BÜKER¹

¹Stockholm Environment Institute, Environment Dept. University of York, York, YO10 5DD, U.K.. (e-mail: l.emberson@york.ac.uk)

A substantial body of experimental evidence exists describing the impacts of ozone (O₃) and aerosols on important ecosystems (agro-, forest and grassland ecosystems). Much of this empirical data has been collected from co-ordinated studies conducted in North America and Europe; and more recently in Asia. Pooling these data allows the development of risk assessment methodologies which can be used to assess the benefits of emission reductions over regional to global scales. This talk describes these risk assessment methodologies focussing both on their strengths (in relation to providing estimates of a variety of ecosystem damage) as well as weaknesses and limitations (primarily associated with limited data availability for key global regions such as Asia, Africa and Latin America).

Within this context results are presented that describe benefits of emission reductions of O₃ and aerosol forming species for crop yields, forest productivity and grassland biodiversity along with benefits for near term climate. Examples of indirect benefits are also given by showing the importance of ecosystems acting as sinks for atmospheric pollution; alterations to this sink under extreme climates (e.g. heatwave type conditions) are exemplified through their influence on net atmospheric pollution concentrations and subsequent human health impacts.

Finally, the importance of considering ecosystem damage and feedbacks to the climate system within a new generation of Earth System Models, currently being developed to understand the implications of climate change, is advocated based on the evidence presented.

Characterization of the effects of grain size to mine water quality and Acid Rock Drainage (ARD) production in Kinetic Testing

R. EMBILE JR.^{1,2,3}, I.F. WALDER¹, F. MADAI²,
F. MORICZ², P. WALDER¹ AND P. RZEPKA¹

¹ Kjeoy Research and Education Center, Kjeoy 8412 Vestbygd, Norway (*correspondence: rodrigofembilejr@gmail.com)

² University of Miskolc, Miskolc H-3515 Hungary

³ Camborne School of Mines, University of Exeter

The quality of mine drainage from sulfide containing waste dumps is controlled by several factors and surface area (grain size) exposed to weathering conditions is important. However, the textural variation may control the main driving mechanisms for an acid generating or neutralizing reactions. Depending on their rates and intrinsic properties, leachate chemistry for a certain grain size can be characterized through different types of tests and analysis.

Kinetic test using humidity columns is performed on five different grain size ranges of waste rocks from the Recsk porphyry copper-skarn deposit in Hungary. Water leachate quality is analysed on a weekly basis for their pH, alkalinity, conductivity, anions, cations and dissolved metal concentrations. Results showed that finer grains produced near neutral to neutral pH and higher sulfate production rates unlike for coarser grains. This indicates that the rate of sulphide oxidation and neutralization may be only partly controlled by grain size as well as a number of interrelated factors.

Global variability of the ocean's biological pump from *in situ* measurements of the air-sea oxygen flux: A status report

STEVEN EMERSON*, SETH BUSHINSKY
AND STEPHEN RISER

School of Oceanography, University of Washington, Seattle, WA, 98195 (*correspondence: emerson@uw.edu; smbush@uw.edu; riser@uw.edu)

The ocean's biological pump is the process by which biological production exports carbon and oxygen from the ocean's euphotic zone. The geographic variability of the biological pump, along with ocean mixing and air-sea exchange, strongly influences the pCO₂ of the atmosphere and maintains the oxygen distribution below the surface ocean. We propose to determine the global variability of the biological pump by measuring the air-sea oxygen gradient using oxygen sensors on profiling floats. Oxygen mass balances at ocean time-series sites indicate the connection between net annual air-sea oxygen flux and biological carbon export and suggest a biological pump of 2 – 4 mol C m⁻² yr⁻¹ with little global open-ocean variability; however, there are only about five locations where there is sufficient data to do this calculation. Global Circulation Models and Satellite color measurements predict the biological pump varies by as much as a factor of four among the equatorial, subtropical and subarctic oceans. A better global coverage of the annual air-sea oxygen flux would provide critical calibration for the predictions based on satellite color. To accomplish this we calibrated the Aanderaa oxygen sensors in our laboratory and modified the Argo profiling instrument package so that the oxygen sensors continue recording when they surface (every five days). The oxygen sensors on our special floats are positioned well above the float body so they are in the air when the float surfaces providing a measure of the air-sea pO₂ gradient. We deployed ten of these floats in March 2013 in the Western North Pacific across the Kuroshio extension. Winkler oxygen measurements were made near the floats after deployment to calibrate them *in situ*. This abstract was written only two weeks after successfully deploying and calibrating the floats *in situ*. We will report the results of the first three months of measurements to assess how accurately it is possible to determine the air-sea oxygen flux using *in situ* oxygen measurements on Argo floats. We believe this is the next step in using oxygen mass balance to determine the global distribution of the marine biological carbon pump.

How surface heterogeneity impacts reaction rates in carbonate rocks

SIMON EMMANUEL^{1*} AND YAEL LEVENSON¹

¹The Hebrew University of Jerusalem, Jerusalem, Israel,
(simonem@cc.huji.ac.il)(* presenting author)

Due to the ubiquitous nature of calcite in natural systems, much research has focused on determining the reaction kinetics of calcite dissolution. However, the empirical rate laws derived in such studies assume that the reactivity of calcite crystals typically used in laboratory experiments is the same as the reactivity of natural carbonate surfaces that have been exposed to fluid during diagenesis. In this study, we demonstrate that the difference between polished calcite surfaces and naturally-aged calcite surfaces is significant. Atomic force microscopy (AFM) measurements show that the rate of calcite dissolution within micron-size pores of a limestone sample is much lower than the rate of dissolution in the surrounding calcite surface. In addition, we use numerical simulations to show that this difference cannot be explained using a diffusion - surface reaction model. Instead, we attribute the heterogeneous reaction rates to the high density of tiny asperities on the polished surface surrounding the pore which increase the overall reactivity of the surface. We suggest that the range of reaction rates we observe could be representative of real geological systems, helping to explain the widely reported discrepancy between laboratory and field rates. The implications for weathering, dissolution in carbonate reservoirs, and carbon sequestration are also discussed.

Tracking stable CO₂ isotopes with laser spectroscopy at Jungfrauoch

LUKAS EMMENEGGER, BÉLA TUZSONAND,
PATRICK STURM AND STEPHAN HENNE

Empa, Laboratory for Air Pollution / Environmental
Technology, CH-8600 Dübendorf, Switzerland
(lukas.emmenegger@empa.ch)

Isotope ratios of trace gases contain highly valuable information about their sources, sinks and transport processes from the local to the global scale. While isotope ratio mass spectrometry (IRMS) has been the method of choice, laser spectroscopy is rapidly gaining importance because it can deliver real-time data with unprecedented temporal resolution at moderate cost and instrument size.

We employ a quantum cascade laser absorption spectrometer (QCLAS) and perform continuous monitoring of the stable CO₂ isotopes in the free troposphere since December 2008 at the High Altitude Research Station Jungfrauoch (3580 m a.s.l.), Switzerland [1]. The instrument is based on differential absorption technique in the 4.3 μm spectral range. Being a fully cryogen-free setup, it is well suited for unattended field applications, delivering both δ¹³C and δ¹⁸O of CO₂ at atmospheric abundance with a precision of 0.02 ‰ for both δ¹³C and δ¹⁸O-CO₂ at 10 minutes integration time [2].

The high temporal resolution of the δ¹³C time series allows the detection of pollution events and the application of the Keeling plot method for source signature identification. Backward Lagrangian particle dispersion simulations are used to determine the spatial origin of these CO₂ emission sources. Furthermore, the long data series permits the analysis of yearly, seasonal and daily patterns. Footprint clustering shows significantly different wintertime δ¹³C and δ¹⁸O-CO₂ values depending on the origin and surface residence time of the air masses.

We present the development of the instrumental set-up, the improvements of the most critical parts and the resulting performance. Then, we discuss methodologies for calibration and data treatment and illustrate the advantages of measuring high time resolution isotopic signatures of CO₂ in the atmosphere with exemplary results.

[1] Tuzson, B. *et al.*, ACP, 2011, 11, 1685–1696. [2] Sturm, P. *et al.*, AMTD, 6, 423–459, 2013.

Temperature-induced phase transitions in Pb/Sr-lawsonites

M. ENDE¹, B. WUNDER², M. KOCH-MÜLLER²
AND E. LIBOWITZKY¹

¹University of Vienna, 1090 Vienna, Austria

²Helmholtz Centre Potsdam, GFZ (German Research Centre for Geoscience), 14473 Potsdam, Germany

Pb-lawsonite and itoigawaite ($\text{SrAl}_2[(\text{OH})_2\text{Si}_2\text{O}_7]\cdot\text{H}_2\text{O}$) were synthesised using either oxides [1,2], spinel phases with quartz, feldspars or glasses with stoichiometric compositions. The achieved crystal sizes reached 20 μm in maximum for the Pb-lawsonite and about 60 μm for itoigawaite.

For the syntheses a piston cylinder press at GFZ Potsdam, Germany was used. Experimental conditions were 600°C and 3-4 GPa for Pb-lawsonite and 700°C and 4 GPa for itoigawaite. Using Raman spectroscopy temperature-induced shifts of different bands were analysed. For Pb-lawsonite the most interesting one was a band at about 860 cm^{-1} , which probably arises from an AlO_6 stretching vibration [3]. It shows a minimum of two discontinuities, which could be interpreted as phase transitions at about 350 and 445 K (Fig. 1). Analyses of a band arising from a $\nu_{\text{as}} \text{SiO}_3$ stretching vibration [3] reveal a minimum of one phase transition for itoigawaite at about 225 K.

These reversible phase transitions are comparable to those of lawsonite and are mainly caused by changes of OH and H_2O groups from disordered, apparently highly symmetric positions to ordered ones at lower temperatures [4].

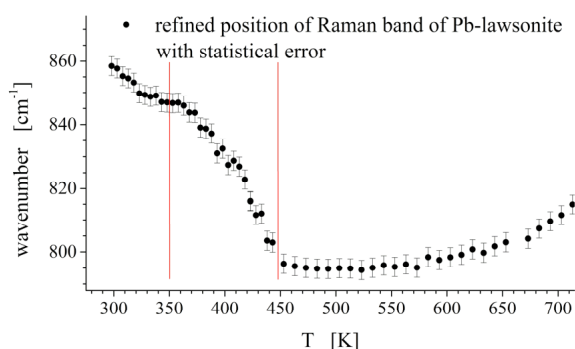


Figure 1: Raman band positions vs. temperature for Pb-lawsonite. Discontinuities probably reveal phase transitions.

[1] Dörsam *et al.* (2011) *N. Jb. Miner. Abh.* **188/2**, 99-110 [2] Liebscher *et al.* (2010) *Am. Mineral.* **95**, 724-735 [3] Le Cléac'h & Gillet (1990) *Eur. J. Mineral.* **2**, 43-53 [4] Libowitzky & Armbruster (1995) *Am. Mineral.* **80**, 1277-1285

Pressure-dependent change of ultraviolet absorption cross section of SO_2 isotopologues and S-MIF

YOSHIKI ENDO¹, SEBASTIAN O. DANIELACHE²,
YUICHIRO UENO^{1,3}, SHOHEI HATTORI⁴, MATTHEW S.
JOHNSON⁵ AND HENRIK G. KJÆRGAARD⁵

¹Earth & Planetary Sciences, Tokyo Institute of Technology, Japan (endo.y.ac@m.titech.ac.jp)

²Faculty of Science & Technology, Sophia University, Japan

³Earth-Life Science Institute (ELSI), Tokyo Institute of Technology, Japan

⁴Environmental Chemistry and Engineering, Tokyo Institute of Technology, Japan

⁵Department of Chemistry, University of Copenhagen, Denmark

Photolysis of SO_2 is known to produce anomalous sulfur isotope fractionation (S-MIF). The mechanism of the photochemical S-MIF is important for reconstructing chemistry of paleoatmosphere, though has been still poorly understood. It is important to determine isotopologue-specific UV absorption cross section accurately for estimating fractionation factor of the SO_2 photolysis. We used a dual beam monochromator in order to obtain higher accuracy cross section that is complementary to high spectral resolution Fourier transform spectrometer [1]. The results show the peak position for heavier isotopologue is red shifted relative to the lightest $^{32}\text{SO}_2$ isotopologue, though rotational structures cannot be seen due to low spectral resolution. The observed cross sections systematically changed depending on the gas pressure at certain specific wavelengths. This may suggest that S-MIF can occur when SO_2 is photolyzed even under optically thin condition and thus not by self-shielding effect in the Archean atmosphere. Also, the observed pressure dependence of cross sections may indicate S-MIF can be changed as a function of atmospheric pressure.

[1] Danieleche *et al.* (2008) *J. Geophys. Res.* **113**, 1-14.

Viruses outnumber prokaryotes in marine subsurface sediments

TIM ENGELHARDT¹, JENS KALLMEYER²,
HERIBERT CYPIONKA¹ AND BERT ENGELEN^{1*}

¹Carl-von-Ossietzky University of Oldenburg, Institute for Chemistry and Biology of the Marine Environment, Carl-von-Ossietzky Straße 9-11, D-26129 Oldenburg, Germany (*correspondance: Engelen@icbm.de, Tim.Engelhardt@icbm.de, Cypionka@icbm.de)

²Deutsches GeoForschungsZentrum GFZ, Telegrafenberg, 14473 Potsdam, Germany, Sektion 4.5 Geomicrobiology (kallm@gfz-potsdam.de)

The marine subsurface comprises nutrient-depleted and energy-limited environments, exhibiting a high microbial abundance and diversity. Sources of organic carbon in deeply buried sediments are vanishingly small and the long-term survival of indigenous microorganisms is still enigmatic. Cells are capable to live under energy-limited conditions but controlling factors for cell death in marine subsurface environments remain largely unidentified. Here, the question arises if viruses are controlling prokaryotic mortality. For this habitat, the general role of bacteriophages as a potential driver of microbial ecology was barely addressed so far [1, 2, 3]. Phages are known to contribute to carbon cycling and to control microbial communities in various marine habitats. Furthermore, they mediate horizontal gene transfer and thus, supporting the adaptation of host organisms to environmental conditions.

We found phages to be highly abundant even in deep, ancient (~14 Ma old) and the most oligotrophic subsurface sediments of the world's oceans (South Pacific Gyre). The number of viruses always exceeded that of prokaryotic cells and varied by several orders of magnitude within a comprehensive set of globally distributed subsurface sediments. Abundances of phages and cells generally decreased with sediment depth. However, an increasing virus-to-cell ratio is constituted in deeper and more oligotrophic layers, exhibiting values of up to 225 in the deep subsurface of the South Pacific Gyre. The presence of phages in enormous numbers suggests their impact on prokaryotic communities as controlling factor for cell abundance, diversity and life in the marine deep biosphere.

- [1] Engelhardt *et al.* (2011) *Environ Microbiol Rep* **3**, 459-465. [2] Engelhardt *et al.* (2013) *ISME J* **7**, 199-209. [3] Middelboe *et al.* (2011) *Aquatic Microb Ecol* **63**, 1-8.

Analysis of internal dynamics in a deep subduction channel

MARTIN ENGI¹, DANIELE REGIS^{1,2}
AND DANIEL RUBATTO³

¹Inst. of Geological Sciences, Univ. of Bern, Baltzerstrasse 3, 3012 Bern, Switzerland. (engi@geo.unibe.ch)

²Dept. of Environment, Earth & Ecosystem, The Open Univ., Milton Keynes, MK7 6AA, UK (daniele.regis@open.ac.uk)

³Research School of Earth Sciences, Australian National University, Mills Road, Canberra 0200, Australia

The spatial-temporal scales of tectonic fragmentation and mixing during the evolution of subduction channels need to be resolved. Current thinking nourished by numerical models requires critical testing against data on HP-terrains. However, deciphering natural archives of the time-integrated record of structural and metamorphic processes demands an approach that combines observations from μm - to km-spatial scales.

Our approach is shown for a case study in the Sesia Zone, a classic eclogite facies terrain in the Western Alps, Italy. The control provided by regional structural maps was extended from the meso- to the microscopic scale. Painstaking petrographic documentation was required to recognize the several generations of HP-assemblages, mineral inclusions, textural and chemical domains and to relate these in (relative) time. *in situ* dating by robust Th-U-Pb mineral chronometry was combined with thermobarometry; this allowed several stages of HP-tectonics to be discerned and metamorphic reactions to be related to the polyphase deformation. PTDT-sequences thus derived were mutually consistent for individual sample suites, but substantial differences emerged for different parts of the Sesia Zone. Their regional distribution indicates that tectonic slices (previously unrecognized) exist. Differential mobility between these lasted >20 Myr and one terrane experienced pressure cycling ($\Delta P \sim 5$ kbar). These dynamics had escaped the many previous studies and predate what has until recently been accepted as "the age" of the Sesia HP-belt, i.e. ~65 Ma.

The major challenge remains to quantify the typical mobility of fragments within this subduction channel. In the Sesia Zone fragmentation at micro- to mesoscopic scale is very common in the eclogitic micaschists; in gneissic parts mylonites are not rare. Yet estimating the total amount of strain or the magnitude of displacements between adjacent units is difficult beyond the deca- to hectometer scale of outcrops. Our ongoing regional work aims to provide better constraints on the geometry and size of mobile tectonic slices, again using the petrochronological approach described.

At this stage of our study, it is clear that (km-size) tectonic fragments were independently mobile within the subduction channel, with vertical cycling rates of 2-3 mm/a.

Challenges connected with experimental upscaling of flow and transport in porous media

A. ENGLERT*, T. VAITL, S. FRANK AND T. GOEKPINAR

Hydrogeology Department, Ruhr-University Bochum, 44801, Germany (*correspondence: andreas.englert@rub.de)

Column and sandbox experiments have a long and successful tradition in estimating flow and transport parameters of porous media. A recently developed methodology based on the combination of column and sandbox experiments might be even capable for upscaling flow and transport as follows: In a first step, a cubic Darcy cell of 0.1 m x 0.1 m x 0.1 m is used to experimentally estimate flow and transport characteristics of an unconsolidated sediment, means flow and transport is experimentally upscaled from the pore-scale to the 0.1 m- scale. In a second step, the sediment filled Darcy cell is frozen and the frozen sediment cube is extracted from the Darcy cell. In a third step, nine frozen sediment cubes are composed in a sandbox model such that a sediment body of 0.3 m x 0.3 m x 0.1 m is formed. Finally the flow and transport characteristics of the sediment body are estimated based on flow and transport experiments. Such procedure could allow for successive experimental upscaling from the pore- to the 0.1 m- to the 1 m-scale of flow and reactive transport.

First tests of the recently developed setup for experimental upscaling showed that it is feasible to form sediment cubes, extract them from the experimental apparatus and assemble them in a sandbox model. It could also be shown that the developed experimental set up is well suited to study flow and transport in single sediment cubes and sediment bodies consisting of assembled sediment cubes. Our ongoing experiments focus on improving the accuracy of the developed set up. So far, we found hydraulic conductivities (Ks) of fine gravel sediment cubes rather constant, and Ks of coarse and middle sand sediment cubes slightly changing pre- and post freezing. We also found from sandbox experiments that sediment bodies formed based on fine gravel or coarse sand sediment cubes to be rather insensitive, but sediment bodies formed based on middle sand cubes to be prone to the formation of preferential flowpath. Through procedures such like tuning of the sediment structure in sediment cubes and bodies, but also optimized drainage of sediment cubes before freezing, we are confident to enhance the developed methodology to reach an accuracy needed for proper experimental upscaling.

Cretaceous Large Igneous Provinces: the effects of submarine volcanism on calcareous nannoplankton

ELISABETTA ERBA*, CINZIA BOTTINI AND GIULIA FAUCHER

Department of Earth Sciences, Università degli Studi di Milano, 20133 Milan, Italy.
(*correspondence:elisabetta.erba@unimi.it)

During the Cretaceous the construction of Large Igneous Provinces (LIPs), forming gigantic oceanic plateaus, affected ecosystems at global scale. LIP volcanism was coeval with episodes of oxygen depletion in the oceans with consequent burial of massive amounts of organic matter known as Oceanic Anoxic Events (OAEs). Under these conditions, biota were forced to face excess CO₂ and global perturbations in the ocean-atmosphere system.

In the open ocean, coccolithophores are important carbonate rock-forming organisms, extremely sensitive to changes in physical-chemical parameters of surface waters. They are an ideal tracer for detecting the direct/indirect impacts of submarine volcanism on transient responses and evolution of calcifying biota.

We investigated calcareous nannoplankton assemblages across the early Aptian OAE1a and the latest Cenomanian OAE2, associated to the Ontong Java Plateau (OJP) and the Caribbean Plateau (CP), respectively. Massive submarine volcanism of OJP triggered a disruption in the oceanic carbonate system: excess CO₂ arguably induced ocean acidification that was detrimental to marine calcifiers, with temporary failure, but no extinctions, of rock-forming nannoconids and production of dwarf and malformed coccoliths. Similarly, during OAE2 the excess CO₂ from CP volcanism affected nannoplankton calcification inducing some coccolith dwarfism. Hydrothermal plumes during construction of both OJP and CP introduced biolimiting metals that fertilized the global ocean. However, some toxic metals might have disturbed the functioning of some intolerant coccolithophorid species.

There is a causal link between intervals of LIP submarine volcanism and changes in nannoplankton composition, abundance and biocalcification through OAE1a and OAE2. Changes in ocean chemistry, structure, and fertility during formation of oceanic plateaus might explain observed tempo and mode of nannoplankton evolution: major origination episodes might result from magmas especially enriched in biogeochemically important elements from the mantle.

Some Organic Geochemical Characteristics of Oil Shale Deposits in the Ereğli-Bor Basin, (Konya-Niğde), Central Turkey

M.S. ERDOĞAN^{1*}, S. KORKMAZ¹, G. KADINKIZ²
AND R. KARA-GÜLBAY¹

¹Karadeniz Technical University, Trabzon / Turkey

(*correspondence: mserdogan@ktu.edu.tr)

²General Directorate of MTA, Ankara / Turkey

Upper Miocene-Pliocene aged oil shale sequence, with an average thickness ranging between 72 and 160 m, has been cross-cut during the drilling studies at Ereğli-Bor basin, Central Turkey. In addition, the live oil show has also been observed in this oil shale sequence.

Paleocene-Eocene aged volcanic, volcano-clastic, clastic and carbonate rocks form the base of this basin. This basin is overlain unconformably by the Oligocene-Middle Miocene aged evaporitic rocks, carbonates and clastic rocks. The upper Miocene-Pliocene aged oil shale bearing sequence overlies this unit. The Kızılbayır formation, is overlain by the Katrandetepe formation which is composed of claystone, sandstone, siltstone, gypsum, anhydrite and oil shale. Sandstone and claystone alternations, known as Beştepeliler formation, form the upper part of the sequence. All these units are overlain unconformably by Upper Pliocene-Holocene aged clastic sediments and volcanic rocks.

According to the Pyrolysis analyses results of the selected oil shale samples, total organic carbon contents (%TOC) of the oil shale range between 1.21 and 13.98, with an average TOC value of 4.75. Hydrogen index (HI) and oxygen index (OI) values, ranging between 127-664 and 7-50 respectively, suggest that oil shales are formed by Type II kerogen. Tmax values (°C) range between 332 and 419. Considering the Tmax values, oil shales are considered to represent the immature stage, although some of them reflect the early mature stage. Pyrolysis data suggest no oil generation in the basin. The live oil show in the basin has probably formed due to the young volcanic rocks cross-cutting the oil shale which resulted oil shales to reach the thermal maturity.

Characterizing the Pb isotopic contribution of dust to seawater

A.M. ERHARDT^{1,2}, C-T. CHEIN², A.D. JACOBSON³,
C. M. MOY⁴ AND A. PAYTAN²

¹Stanford University, Stanford, CA 94305

(*correspondence: erhardt@stanford.edu)

²University of California Santa Cruz, Santa Cruz, CA 95064

³Northwestern University, Evanston, IL 60208

⁴University of Otago, Dunedin, New Zealand

Different sources of dust to the open ocean have varying effects on seawater chemistry, productivity and plankton community structure due to the release of various amounts of nutrients and trace metals. Pb isotopes in marine sediments have been used to reconstruct these dust sources (provenance). This is typically done by comparing the isotopic signature in the detrital fraction of sediments to the Pb isotope ratios of bulk dust or loess samples from dust source regions. What is missing in these studies is the isotopic composition of the seawater soluble fraction of the dust and its role in the seawater Pb isotope budget.

In this study, we characterized the Pb isotopic contribution of dust to seawater from select source regions to the Pacific Ocean through a direct simulation of dust solubility in seawater. We found that the readily leachable fraction of dust from multiple source regions to the Pacific Ocean is less radiogenic than the bulk source sample or that of the detrital fraction of sediments. Clear differences in the soluble and bulk Pb isotopic ratios of dust between the different source regions were also observed.

Knowing the true dust isotopic contribution to seawater allows for more accurate Pb mass balance calculations and clearer identification of dust sources and/or fluxes. We show preliminary results linking seawater, dust, ferromanganese, and detrital Pb isotope signatures in the Eastern Equatorial Pacific and generate a potential framework for future Pb mass balance calculations.

A comparison of shocked zircon and quartz from the Reis impact structure, Germany

TIMMONS M. ERICKSON*, STEVEN M. REDDY,
NICHOLAS E. TIMMS AND ALEXANDER A. NEMCHIN

Department of Applied Geology, Curtin University, GPO Box
U1987, Perth, WA 6945, Australia
(*timmons.erickson@gmail.com)

Shock metamorphism is well established within the zircon and quartz mineral systems. Shocked quartz has been documented in a number of impact locations on the Earth and the shock deformation mechanisms have been identified, allowing for a well constrained thermobarometer of shock conditions to be developed [1]. Zircon is an important mineral in crustal studies and also records shock metamorphism through crystallographic deformation.

Shocked zircon has been identified from a number of impact structures, however development of a thermobarometer for shock metamorphism in zircon has been limited to one empirical study [2] and work on naturally shocked zircons from the Earth [3, 4, 5] and the Moon [6]. The work of Leroux *et al.* (1999) have determined that zircon exhibits planar microstructures >20 GPa, begins to transform to reidite >40 GPa, completing conversion >60 GPa. Timms *et al.* (2012) further documented shock metamorphism of zircon and began to develop a shock deformation mechanism map. The aim of this study is to further constrain the development of shock features in zircon through the careful comparison of shocked zircon and quartz from the Reis impact structure.

We have therefore analyzed a suite of thin sections from the 14.4 Ma Reis impact structure in Germany from samples collected between 300 and 1204 m depth in the Nördlingen 1973 borehole. Previous work by Wittmann *et al.* (2006) determined shocked zircons in suevites from Reis exhibit planar microstructures, granular texture and reidite indicating samples were shocked >40 GPa, while other mineral systems indicate pressures >60 GPa. In this study shocked zircon and quartz have been analyzed petrographically and by SEM including EBSD to further resolve the correlation of shock deformation within these two mineral systems.

[1] Stöffler and Langenhorst 1994 MAPS [2] Leroux *et al.* 1999 EPSL [3] Wittmann *et al.* 2006 MAPS [4] Moser *et al.* 2011 CJES [5] Erickson *et al.* 2013 Am Min [6] Timms *et al.* 2012 MAPS

Petrology, mineral chemistry and Sr–Nd–Pb isotopic compositions of granitoids in the central Menderes metamorphic core complex: Constraints on the evolution of Aegean lithosphere slab

F. ERKÜL^{1*}, S.T. ERKÜL², E.Y. ERSOY³, İ. UYSAL⁴
AND U. KLÖTZLI⁵

¹Akdeniz Univ., Vocational School of Technical Sciences,
07058, Antalya, Turkey (*correspondance:
fuaterkul@gmail.com)

²Akdeniz Univ., Department of Geological Engineering,
Dumlupınar Bulvarı, Campus, 07058, Antalya, Turkey

³Dokuz Eylül Univ., Department of Geological Engineering,
35160, Izmir, Turkey

⁴Karadeniz Teknik Univ., Department of Geological
Engineering, Trabzon, Turkey

⁵Center for Earth Sciences, Department of Lithospheric
Research UZA II, Vienna, Austria

Salihli and Turgutlu granitoids in the central Menderes metamorphic core complex are most suitable rocks in order to understand the magma forming processes in extended terrains. They are granodiorite in composition and contain monzonitic and monzodioritic microgranular enclaves. Host rocks are geochemically similar to each other while their enclave chemistry is in contrast with low SiO₂ and high Mg# values. Mineral chemistry data confirm a chemical equilibration of distinct magma batches. Geochemical modelling suggests that these granitoids were derived from mixing of mantle and lower crustal components, which were finally modified by upper crustal contamination and fractional crystallization processes. Early-Middle Miocene syn-extensional granitoids across the Aegean region form a magmatic belt associated with roll-back of the Aegean lithosphere slab. Roll-back induced magmatism together with ductile deformation in western Turkey ceased after cooling of the Salihli granitoids at 12.2 Ma as defined in previous geochronologic work. But core-complex related magmatism was continuous in the Cycladic metamorphic core complex during Late Miocene and was followed by an active arc volcanism in the southern Aegean. Such abrupt change in the geodynamic setting of western Turkey can be explained by opening of a slab window on the Aegean lithosphere slab, which would lead to upwelling of fertile subslab asthenospheric mantle, forming transitional and finally OIB-type basalts.

Molybdenum isotopic composition of pre-GOE tidal carbonates

S. EROGLU^{1*}, R. SCHOENBERG¹, N. BEUKES²
AND M. WILLE¹

¹University of Tuebingen, Wilhelmstraße 56, 72074
Tuebingen, Germany

(*correspondence: suemeyya.eroglu@uni-tuebingen.de)

²University of Johannesburg, Auckland Park Kingsway
Campus, 2006, South Africa

The Transvaal Basin in South Africa contains one of the best preserved carbonate platforms of the Archaean. This platform was deposited between ~2.58 and 2.50 Ga [1], shortly before the 2.40-2.32 Ga great oxidation event (GOE) and is composed of alternating stromatolitic carbonates and shales. The depositional environment of the Transvaal Basin is very similar to modern tidal areas.

Variations in the isotopic abundance of the redox-sensitive transition metal molybdenum have been used in the past few years to constrain the redox conditions of Earth's atmosphere-hydrosphere system in the present and the past [2, 3]. Interestingly, carbonates and black shales from the slope of the Griqualand West Basin in South Africa, which can be well-correlated to the Transvaal Basin, shift towards heavy $\delta^{98/95}\text{Mo}$ values, which might indicate an oxygenation of the atmosphere-hydrosphere system some 100 Ma before the GOE [4, 5]. In our study we determine the Mo content and $\delta^{98/95}\text{Mo}$ composition of tidal carbonates from the platform of the Transvaal Basin, which precipitated in shallow waters and compare them to the contemporaneous deeper platform deposits of the Griqualand West Basin, in order to investigate the influence of sedimentary settings on Mo isotopic signatures. The very low Mo concentration of the carbonates generally lies around 20 ppb and most of our data cluster from +0.2 to +0.6‰ $\delta^{98/95}\text{Mo}$, but our preliminary results also reveal highly variable $\delta^{98/95}\text{Mo}$ signatures between -0.7 and +1.4‰ and indicate an influence of the depositional environment of the stromatolites on their Mo isotopic composition. This observation might be an important aspect for future interpretation of Mo isotopic compositions of chemical sediments.

[1] Sumner & Beukes (2006) *SAJG* **109**, 11-22. [2] Barling *et al.* (2001) *EPSL* **193**, 447-457. [3] Siebert *et al.* (2003) *EPSL* **211**, 723-733. [4] Voegelin *et al.* (2010) *Precambrian Res.* **182**, 70-82. [5] Wille *et al.* (2007) *GCA* **71**, 2417-2435.

Geotechnical assessment of the rock masses in Düzyurt area (Trabzon, NE Turkey)

HAKAN ERSOY¹ AND M. OĞUZ SUNNETCI²

¹Karadeniz Technical University, Department of Geological Engineering, Trabzon, Turkey, ersoy@ktu.edu.tr

²Karadeniz Technical University, Department of Geological Engineering, Trabzon, Turkey, moguzsunnetci@ktu.edu.tr

In this study, geological, hydrogeological, geotechnical properties of the rock masses in the Düzyurt Area (Trabzon, NE Turkey) were investigated. Engineering properties of geotechnical units were determined in two stages; surface and subsurface studies. Borehole applications, *in situ* testing, scan-line surveys (discontinuity direction, persistence, spacing, opening, roughness infilling material and RQD) and seismic surveys were conducted for description of geotechnical units and determination of vertical and horizontal homogeneity of these units in the site. *in situ* lugeon tests were applied for determination of bedrock permeability. During core drilling, lugeon tests were conducted and permeability of the rock masses is calculated. A total of 16 pumping tests were performed at the site in 5 boreholes. Based on the lugeon test results, permeability coefficients were calculated about 1.88×10^{-8} m/s for whole bedrock consisting of mainly limestone. According to the results, 1/2000 scaled engineering geological map was prepared. In the laboratory studies, physical and strength properties were determined on the samples collected from the boreholes and rock blocks in the geotechnical units. Rock mass strength was calculated with Hoek-Brown empirical approach using by data obtained from laboratory studies and scan-line surveys. Engineering properties of rock masses were performed with RMR system and durability of slopes in the area was investigated using kinematic analysis. GSI value for rock masses were calculated as 50. Based on the excavatability analysis of the rocks using seismic wave velocity and geotechnical properties of the rock mass, the excavatability category of rock masses is moderate-hard ripping.

A second rapid sea-level fluctuation during Termination II at Barbados

TEZER M. ESAT^{1*} AND ERDEM BEKAROĞLU²

¹Australian Nuclear Science and Technology Org., Kirrawee, Australia (*correspondence: tezer.esat@anu.edu.au)

²Ankara University, Sıhhiye 06100, Ankara, Turkey

Rapid, centennial or shorter timescale, climate variations are often superimposed over thousands of year duration orbital insolation driven climate cycles. Fast paced Heinrich events of the last glacial period are associated with ice-berg discharges and sea-level oscillations that periodically have triggered changes in the North Atlantic Ocean's thermohaline circulation. The resultant severe climate shifts have been recorded in numerous climate proxies. Such climate variability is not confined to glacial periods but extend through deglaciations and possibly into interglacial periods [1]. A definite pattern of climate change is discernible for the last six glacial terminations (T1, TII etc.) each of which appears to have gone through two major and distinct climate events. For T1 these are the Younger Dryas cold period and Heinrich event H-1 during the so-called Mystery Interval [2]. Similar features are present at T3 and T4. At T2, there is a very large >60 m sea-level oscillation called the Aladdin's Cave (AC) transition first documented at Huon Peninsula that peaks around 135.3 ka, approximately 10 m below last interglacial sea levels [3,4,5,6]. A number of marine proxy climate records of the time as well as descriptions of European lacustrine deposits of the Saalian period indicate the presence of at least two climate oscillations which would be consistent with similar climate events during T1 and TIII [2,6,7]. Along the Gordon Cummins Highway, adjacent to the West Indies University at Barbados, the road cut follows the rising sea-level during TII and there are deposits of fossil coral reefs that grew at the time in response to the rise in sea-level. Here, we have discovered a second peak in sea level at 133.5 ka, distinct from the timing of the original AC transition. The sea-level high-stand is close to the peak of the last interglacial relative sea levels at this location. However, its magnitude cannot be precisely quantified from the available data but may be as much as 90 m.

[1] Yokoyama & Esat (2011) *Oceanography* **24**, 54-69. [2] Broecker *et al.* (2010) *QSR* **29**, 1078-1081. [3] Thomas *et al.* (2009) *Science* **324**, 186-189. [4] Siddall *et al.* (2006) *Geology* **34**, 817-820. [5] Esat *et al.* (1999) *Science* **283**, 197-201. [6] Andrews *et al.* (2007) *EPSL* **259**, 457-468. [7] Risebrobakken *et al.* (2006) *EPSL* **241**, 505-516.

High frequency network sensors for integrating biogeochemical processes in the Seine River and quantifying the impact of Paris Megalopolis

N. ESCOFFIER¹, N. FLIPO², L. VILMIN²,
N. BENSOUSSAN³, A. LAVERMAN⁴, M. RAIMONET⁴
AND A. GROLEAU¹

¹Géochimie des Eaux. Univ Paris Diderot, Sorbonne Paris Cité, IGP, UMR 7154, CNRS, F-75205 Paris, France

²Centre de Géosciences. Systèmes Hydrologiques et Réservoirs. Mines ParisTech. 77305 Fontainebleau

³IPSO FACTO. 4, rue de Tilsit, F-13006 Marseille

⁴CNRS-UPMC UMR 7619 Sisyphé, Boite 125, 4 place Jussieu, 75005 Paris

The CARBOSEINE program, initiated in 2011, focuses on the urban part of the Seine river (Paris, France). It develops an integrated approach based on *in situ* sensors network in order to determine the main parameters controlling the biogeochemical carbon dynamics in the river. To do so, three on-line high frequency (every 15 min) multi-probe stations are devoted to the monitoring of the main hydrogeochemical parameters (weather, CTD, pH, phosphate, O₂, turb., chl_a) for the River downstream Paris (54 km long).

Carbon dynamics based on diel oxygen concentration variations allow the quantification of river metabolism processes over time. During algae blooms, river ecosystem shifts from heterotrophic to autotrophic on daily periods according to Net Ecosystem Production calculations. Combining Gross Primary Production and chlorophyll biomass leads to quantify the productivity of the autotrophic component, which can heavily differ from one bloom to another. Phosphate *in situ* measurements (4h freq.) demonstrates nutrient depletion without reaching the limitation level. They document the diffusive sources coming from watershed alteration, that allow algae growth upstream Paris. Moreover, these P measurements highlight the human impact variability. Comparison between probes located upstream and downstream the largest European Waste Water Treatment Plant allows to calculate the mass budget resulting from Paris megalopolis activity.

As a generic result, this high frequency observation approach constitutes a powerful tool for understanding and managing aquatic biogeochemistry in anthropic ecosystem. A challenge consists in developing an accurate data treatment strategy to segregate natural variations from human impact, with respect to different observation time scales. Finally, the generated dataset, allows to develop new modelling techniques to better define the processes representation in river numerical models.

Using textural data and fractal analysis to infer crystallization of dacites from Qorveh (W-Iran)

A. ESKANDARY^{1*}, R. DE ROSA², S. AMINI¹
AND H. MIRAJ¹

¹University of Kharazmi, Mofatteh Street, Tehran, Iran
(*correspondence: amir.eskandary157@gmail.com)

²University of Calabria, via P. Bucci I-87036 Arcavacata di Rende (CS), Italy (rosanna.derosa@unical.it)

Polybaric crystallization in a volcano feeding system generally produces concave-up trends in diagrams of crystal size distribution (CSD) of the related emitted products, a feature testified both in natural and experimental studies [1,2]. In the present work, CSD technique has been applied to plagioclase crystals in plio-Quaternary dacitic lavas of Qorveh volcano (Western Iran).

Crystal size distributions of more than 9000 plagioclases of the six collected samples were plotted in natural logarithmic scale (L_n) as the number of crystals per unit length and per unit volume ($n(L)$; mm^{-4}) vs. crystal lengths (L ; mm). According to textural and CSD data, three distinct populations of crystals were identified: 1) phenocrysts ($L > 0.6$) with coarse sieve texture and complex zoning patterns; 2) micro-phenocrysts ($0.2 < L < 0.6$) and 3) microlites ($L < 0.2$). Furthermore, CSDs show a fractal behavior, with fractal dimension ranging 2.44-2.75. In addition, based on the box counting method, also distribution patterns of plagioclase crystals present fractal dimensions.

Our study suggests a strong control on size and spatial distribution of plagioclase crystals by complex processes of crystallization related to decompression and degassing, different rates of ascent velocity and depth of crystals nucleation and growth.

[1] Armienti *et al.* (1994) *Contrib. Mineral. Petrol* **115**, 402–414. [2] Brugger, C, R. Hammer, J.E (2010) *EPSL* **300**, 246–254

Temporal evolution of subduction signatures in a continental back-arc

VENERA R. ESPANON^{1,2*}, ANTHONY DOSSETO^{1,2}
AND ALLAN R. CHIVAS²

¹Wollongong Isotope Geochronology Laboratory,

²GeoQuEST, School of Earth and Environmental Sciences,
University of Wollongong, NSW (2522), Australia
*(vre981@uowmail.edu.au)

The Andino-Cuyana Basaltic Province (ACBP) constitutes part of the Quaternary continental back arc in southern Mendoza, Argentina. This basaltic province is divided into the Llancanelo Volcanic Field (LLVF) to the north and the Payunia Volcanic Field (PVF) to the south. The younger basalts are from the PVF and they range from <10 ka to approximately 50 ka [1], while the flows from LLVF are older Pleistocene basalts [1] lacking any Holocene volcanism. The ACBP presents a range of basaltic flows providing an appropriate setting to investigate changes in back-arc geochemistry during the late Quaternary.

In this setting, this study aims (i) to quantify the relative influence of the Andean arc and subducting slab in the back-arc, and thus (ii) to identify types and timescales of processes controlling back-arc volcanism in the ACBP. For this purpose, we present a suite of geochemical data (major and trace elemental analyses, REE, ⁸⁷Sr/⁸⁶Sr, ²²⁶Ra/²³⁰Th, ²³⁸U/²³⁰Th) from the two volcanic fields and relate them to existing data from Andean arc basalts.

Our results show that basalts from the LLVF and the PVF have intraplate and arc related signatures with enrichment in LILE, HFSE and REE compared with basalts from the Andean arc. The older basalts from the LLVF and PVF have stronger arc signatures. In the PVF we observed a decrease in arc signatures from approximately 100 ka to 10 ka with a strong enrichment in LILE, HFSE and REE in the young basalts which could be related to metasomatised mantle or continental lithospheric mantle.

[1] Ramos & Folguera (2010), *Journal of Volcanology and Geothermal Research* **201**, 53-64.

Ascent of magmas associated with the Solchiaro eruption Procida Island (Italy) based on melt inclusions and glasses

ROSARIO ESPOSITO^{1*}, MATTHEW STEELE-MACINNIS²,
CLAUDIA CANNATELLI¹, ANNAMARIA LIMA¹,
BENEDETTO DE VIVO¹ AND ROBERT J. BODNAR²

¹DISTAR, Università degli Studi di Napoli Federico II, Via Mezzocannone 8, Napoli, 80134, Italy (*Correspondence: rosario.esposito3@unina.it, claudia.cannatelli@unina.it, anlma@unina.it, bdevivo@unina.it)

²Department of Geosciences, Virginia Tech, 4044 Derring Hall, Blacksburg VA, 24061 USA (rjb@vt.edu, mjmaci@vt.edu)

The Solchiaro eruption on the island of Procida is one of the few trachybasaltic eruptions in the Phlegrean Volcanic District (PVD), Italy.

The goal of this study is to provide information on the magma dynamic associated with the Solchiaro eruption based on hourglass inclusions (HI), glass embayments (GE) and melt inclusions. HI are portions of melt ± vapour connected to the outside of phenocrysts through a narrow neck, and GE are portions of melt ± vapour delimited by an indentation in a phenocryst. We have characterized the major, minor and trace elements and volatile compositions of several HI and GE glasses. The HI and GE are associated with olivines of samples from the Solchiaro eruption, representing different stratigraphic heights.

The results show a good negative correlations between the maximum contents of dissolved H₂O, CO₂ and S of HI and GE and the eruptive time (stratigraphic heights). Reversely, minimum contents of Cl and F of HI and GE show positive correlation with the eruptive time.

The H₂O and CO₂ contents of some of the early-erupted HI are the same as those of early-erupted MI [1, 2] suggesting that residence times of early-erupted olivine were short enough to preserve the original dissolved volatile contents of HI. Alternatively, some HI were quenched to a glass from a great depth (up to 8 km) under equilibrium conditions. We develop a quantitative model to understand the duration of decompression for the Solchiaro eruption based on shape and size of both the HI and the contained bubble(s) as was previously done for the Bishop Tuff [3].

[1] Esposito *et al.* (2011) *J. Petrol.* **52**, 2431-2460. [2] Mormone *et al.* (2011) *Chem. Geol.* **287**, 66-80 [3] Anderson (1991) *Am. Mineral.* **76**, 530-547.

Attachment of aspartic acid at the brucite [Mg(OH)₂]-water interface

C. F. ESTRADA^{1,2*}, D.A. SVERJENSKY^{1,2}
AND R.M. HAZEN²

¹Johns Hopkins University, Baltimore, MD 21218, USA
(*correspondence: cestrada@jhu.edu, sver@jhu.edu)

²Geophysical Laboratory, Carnegie Institution of Washington, Washington, DC 20015, USA (rhazen@ciw.edu)

The interaction of organic molecules at the mineral/water interface could play a key role in the emergence of more complex organic species in origins of life scenarios. In one such scenario, hydrothermal vents, particularly serpentine-hosted hydrothermal vents, may possibly act as a suitable environment for this process to occur. We conducted a batch adsorption study between a stable mineral product of serpentinization, brucite (Mg(OH)₂), and the amino acid aspartic acid at 25°C. We studied the adsorption of 2-500 μM aspartate onto a pure synthetic brucite at a single pH value of ~10.4 and a solid to ligand concentration of 10 g·L⁻¹ under conditions where the brucite was in thermodynamic equilibrium with the aqueous solution. The point of zero charge (pH_{ZPC}) of brucite is approximately 11.0 [1], thus resulting in weak electrostatic attraction between the weakly-positive brucite surface and the negative aspartate. We obtained an isotherm, in which the concentration of aspartate adsorbed onto brucite reached a maximum of about 0.1 μmol/m², after increasing linearly with the concentration of aspartate in solution ([Asp]_{aq}) from 2-100 μM and leveling off at 250-500 μM. We used an extended triple-layer surface complexation model (ETLM) to acquire a preliminary fit to the isotherm. The data and the ETLM suggest that the surface site density is restricted to a very low value. Model predictions also suggest that the extent of aspartate adsorption onto brucite will decrease with increasing background electrolyte concentration. In comparison with our previous batch adsorption study of aspartate onto rutile (TiO₂) [2], we conclude that aspartate adsorbs to a lesser extent onto brucite than rutile. This is the first study in which we have obtained an adsorption isotherm for a non-oxide, rock-forming mineral and an amino acid. We expect the adsorption data collected for this system at surface conditions to provide a necessary analog for future adsorption experiments at hydrothermal conditions with implications for the emergence of complex biomolecules on Early Earth environments.

[1] Pokrovsky & Schott (2004), *Geochim Cosmochim Acta* **68**, 31-45. [2] Jonsson *et al.* (2010), *Geochim Cosmochim Acta* **74**, 2356-2367.

Bacterial populations (first record) at two shallow submarine hydrothermal vents off west Mexico

A. ESTRADAS-ROMERO¹, S. DÁVILA-RAMOS²,
R.M. PROL-LEDESMA^{1*} AND K. JUÁREZ-LÓPEZ²

¹Instituto de Geofísica, Universidad Nacional Autónoma de México, Ciudad Universitaria, Delegación Coyoacán, 04510 México D.F., México
(a_estradas@hotmail.com,*correspondence: prol@unam.mx)

²Instituto de Biotecnología, Universidad Nacional Autónoma de México, Cuernavaca, Morelos. C. P. 62210, México
(sdavilar@ibt.unam.mx, katy@ibt.unam.mx)

Thermophilic and metal oxidizing bacteria were identified in shallow hydrothermal vents on the western Mexican coast. The role of these bacteria in biomineralization processes observed in the vents is explained, and the effect of the vents on biodiversity of prokaryotes is discussed. Research was done at two shallow hydrothermal vent sites: Bahía Concepción in the Baja California Peninsula and Punta Mita, in the central Pacific coast. The study focuses on the biogeochemical processes related to the different species of bacteria present in the studied sites, which are involved in the anaerobic oxidation of methane (AOM), seawater sulfate reduction and metal oxidation. Vent water shows different composition in both sites; moreover, different pH and redox conditions control bacteria diversity. The composition of the discharged water ranged from nearly sea water to lower salinity fluids with a pH about 6, and the gas phase in the hydrothermal fluids was mainly CO₂ at the Baja California site, and N₂ and CH₄ at Punta Mita. The detected bacterial lineages represented typical deep vent species.

Physical and chemical characteristics of the geothermal manifestations play a major role in the biodiversity of bacteria in shallow hydrothermal vents. In the case of the submarine vents in Bahía Concepción and Punta de Mita, the redox conditions determine the presence/absence of distinct species of bacteria: gamma, delta and epsilon bacteria as well as bacterioidetes in the oxidizing conditions of Bahía Concepción; and thermotogae, aquificae and planctomycetes in Punta de Mita. On the other hand, there are some species that are ubiquitous in shallow vents, as the halophilic and chloroflexae bacteria.

Tracing antropogenic Hg emissions in an urban area in Northeastern France

N. ESTRADE¹, C. CLOQUET¹, D. AMOUROUX²,
E. TESSIER², O.F.X. DONARD² AND J. CARIGNAN¹

¹CRPG, UMR 7358, CNRS-Université de Lorraine, France
²IPREM/LCABIE, UMR 5254, CNRS-Université de Pau et des Pays de l'Adour, France

(*correspondence: nestrade@crpg.cnrs-nancy.fr)

Mercury (Hg) isotopes are giving new insights into the study of the Hg biogeochemical cycle through large mass dependent and mass independent fractionations (MDF and MIF). A few studies have evaluated the ability to trace atmospheric Hg using both direct atmospheric measurements [1] and indirect bio-accumulators such as lichens [2,3]. Species-specific isotopic compositions of atmospheric Hg display large ranges in both MDF and MIF, and their distinct signatures suggest the occurrence of isotopic fractionation during species conversion [4]. The isotopic compositions of atmospheric depositions potentially recorded in bio-accumulators can be altered through various fractionation processes [3], leading to ambiguous interpretation of Hg isotopic composition to track down atmospheric sources. As regards anthropogenic emissions, different species-specific compositions have been suggested [5] but direct field measurements have not yet been performed.

We report species-specific Hg isotope compositions inside and at the stack of a waste incinerator located in an urban area in northeastern France. Gaseous mercury concentrations and isotope compositions were measured simultaneously in the vicinity of the waste combustor. The main results from the exhaust indicate that oxidized Hg species are slightly enriched in heavier isotopes compared to Hg⁰ species and initial Hg (waste). Diurnal variations recorded for Hg concentrations in the atmosphere are not compatible with the incinerator emissions. In contrast to incinerator emissions, isotopic compositions measured over several days of sampling display significant light isotope enrichment and indicate a little contribution of incinerator to surrounding atmosphere. Further interpretation and comparison with previously published urban topsoil and lichen compositions from the same urban area, provide us relevant informations to trace Hg anthropogenic emissions on such local scale.

[1] Sherman *et al.* (2010) *Env. Sc. Technol.*, **46**, 382-390; [2] Estrade *et al.* (2010) *Env. Sc. Technol.*, **44**, 6062-6067; [3] Blum *et al.* (2012) *Dev. Env. Sc.*, **11**, 373-390; [4] Rolison *et al.* (2013) *Chem. Geol.*, **336**, 37-49; [5] Sun *et al.* (2013) *Chem. Geol.*, **336**, 103-111

Nickel isotope fractionation in the soil to hyper-accumulating plant system

N. ESTRADE^{1*}, C. CLOQUET¹, T. DENG²,
G. ECHEVARRIA², T. STERCKEMAN² AND J.L. MOREL²

¹CRPG, UMR 7358, CNRS-Université de Lorraine, Nancy, France (*correspondence: nestrade@crpg.cnrs-nancy.fr)

²LSE, UMR 1120, INRA-Université de Lorraine, Nancy, France

Nickel stable isotopes are a promising non-traditional stable isotope system for understanding the Ni biogeochemical cycle, especially in contaminated or highly enriched environmental compartments such as ultramafic contexts. Ni hyperaccumulating plant species (e.g. *Alyssum murale*) growing in ultramafic soils can concentrate up to several weight percent in leaves and may be used in phytoremediation or phytomining. In addition to its insensitivity to redox-processes, nickel homeostasis in hyperaccumulating plants is poorly understood. In this work, we used Ni stable isotopes to document the isotopic fractionation range during accumulation processes from soil to Ni-hyperaccumulating plant species in a field investigation.

Sampling was carried out in Albania at four different sites and included the collection of several hyperaccumulating plant species as well as tolerant ones. Using two-step chemistry to isolate Ni and the double-spiking technique to correct for instrumental mass fractionation, we recorded Ni concentrations and Ni isotope compositions along the continuum of ultramafic rock, soil (different horizons), litter, roots, stems, leaves and flowers. In typical Ni-rich soil, root and litter concentrations ranged between 1-3 g kg⁻¹ dry matter. Nickel accumulation increased to 3-6 g kg⁻¹ in stems and reached up to 20 g kg⁻¹ in leaves. In contrast, tolerant species present Ni concentrations in leaves within the 0.1 g kg⁻¹ range.

Preliminary results in hyper-accumulator plant samples did not reveal large extent of isotope fractionation between roots and leaves (0.2‰). Further investigation is ongoing to confirm these results and evaluate the entire soils plants variations.

Dusts from metal smelters in Africa: Mineralogy, leaching and contaminant bioaccessibility

V. ETTLER^{1*}, M. VITKOVA^{1,2}, M. MIHALJEVIC¹
AND B. KRIBEK³

¹Institute of Geochemistry, Mineralogy and Mineral Resources, Faculty of Science, Charles University in Prague, Albertov 6, 128 43 Prague 2, Czech Republic (*correspondence: ettler@natur.cuni.cz, mihal@natur.cuni.cz)

²Department of Environmental Geosciences, Faculty of Environmental Sciences, Czech University of Life Sciences Prague, Kamycka 129, 165 21 Prague 6 – Suchbátka, Czech Republic

³Czech Geological Survey, Geologická 6, 152 00 Prague 5, Czech Republic

Dry climate and strong winds are believed to be responsible for dispersal of contaminated dust particles in areas affected by mining, mineral processing and smelting [1]. We evaluated the solid speciation, leachability and potential bioaccessibility of metals (Co, Cu, Pb, Zn) and As in fly ashes and slag dusts originating from the metal mining and smelting areas of Zambia (the Copperbelt Province) and Namibia (the Tsumeb area). Dusts were highly enriched in inorganic contaminants (up to 273 g Cu/kg, 8.9 g Co/kg, 39 g Pb/kg, 21 g Zn/kg and 437 g As/kg). Based on XRD, SEM, EPMA and HRTEM investigations, major contaminant-bearing phases were cuprospinel (CuFe₂O₄), chalcantite (CuSO₄·5H₂O), delafossite (CuFeO₂), arsenolite (As₂O₃) and minor galena (PbS), anglesite (PbSO₄), sphalerite (ZnS) and elemental Cu [2, 3]. The pH-static leaching tests indicated that contaminants were released from the fly ash mostly at low pH [2, 3], corresponding to conditions found in laterite soils from this area. We also adopted *in vitro* methods based on simulated gastric fluid (SGF) and simulated lung fluid (SLF). The maximum bioaccessibilities in SLF were relatively low (Co 16%, Cu 2%, Zn 1.2%, As 2.9%), whereas values higher than 20% were obtained for SGF (Co 80%, Cu 50%, Zn 77%, As 83%). The obtained data indicate that a severe health risk related to smelter dust ingestion/inhalation should be taken into account in these areas. This study was supported by the Czech Science Foundation (projects no. 13-17501S and P210/12/1413) and IGCP project no. 594.

[1] Ettler *et al.* (2012) *J. Geochem. Explor.* **113**, 68-75. [2] Vítková *et al.* (2011) *Appl. Geochem.* **26**, S263-S266. [3] Vítková *et al.* (2013) *Appl. Geochem.* **29**, 117-125.

Aerosol impact on the stratiform cloud and light precipitation in mid-Korean peninsula

SEUNG-HEE EUN AND BYUNG-GON KIM*

¹Department of Atmospheric Environmental Sciences, Gangneung-Wonju National University, Jibyun, Gangneung, Korea (bgk@gwnu.ac.kr)

Many observational and numerical studies have indicated that land cover and aerosol effect modify cloud property, precipitation, and further weather pattern over and downwind of urban region. Because these effects have occurred in the urban region together, it is important to understand each effect over and downwind of urban region. Eun *et al.* (2011) showed increasing trend of precipitation amount and frequency downwind of Seoul Metropolitan Area (SMA) from 1972 to 2007, for particularly light precipitation (less than 1 mm per day) and westerly condition only. It implies the possible influences of land cover change and aerosol on the precipitation in the downwind region of SMA. Based on observed results, we selected golden case (10 February 2009) to investigate the impact of aerosol on light precipitation using the Weather Research & Forecasting (WRFV3.2) model. The sensitivity run sets up 1,000 #/cm³ for the initial number concentration of cloud condensation nuclei (CCN) at SMA, but the background uses 100 #/cm³.

The results show that mean horizontal wind from surface to 850 hPa have easterly wind and approximately 5~6 m/s. Cloud thickness is about 500 m, and locates within 2 km. Also the results of cloud properties indicates that the enhanced CCN at SMA is associated with smaller effective radius (r_e ; μm) and more cloud droplet number concentration (N_c ; #/cm³) over and downwind of urban region than control run. Especially after 3-hour, change of r_e and N_c was distributed much more widely downwind of urban region. On the other hand, precipitation amount appears to widely increase in the downstream region of SMA. In the near future, further sensitivity tests need to be conducted for combined effect of land cover and aerosol effect on the light precipitation.

This research was supported by Basic Science Research Program through the National Research Foundation of Korea (NRF) funded by the Ministry of Education, Science and Technology (20120007572).

Reconciling seawater Mg/Ca reconstruction with foraminifera geochemistry

DAVID EVANS^{1*}, WOLFGANG MÜLLER¹, JONATHAN EREZ², SHAI ORON³ AND WILLEM RENEMA⁴

¹Dept. of Earth Sciences, Royal Holloway Univ. of London, UK

²Earth Science Inst., The Hebrew Univ. of Jerusalem, Israel

³Interuniversity Institute for Marine Sciences, Eilat, Israel

⁴Naturalis Biodiversity Center, Leiden, The Netherlands

* (correspondence: david.evans.2007@rhul.ac.uk)

Virtually all Paleogene seawater Mg/Ca ($\text{Mg}/\text{Ca}_{\text{sw}}$) proxy data suggests values 2-4 times lower than the present day. Despite this, the majority of studies utilising foraminifera Mg/Ca ($\text{Mg}/\text{Ca}_{\text{test}}$) as a palaeothermometer during this period have argued for ratios around twice as high as the proxy evidence suggests. This is because the use of lower $\text{Mg}/\text{Ca}_{\text{sw}}$ values resulted in unrealistically high palaeotemperature estimates. It has now been shown that this inconsistency is the result of an incorrectly assumed linear relationship between $\text{Mg}/\text{Ca}_{\text{sw}}$ and $\text{Mg}/\text{Ca}_{\text{test}}$, as detailed in Evans & Müller [2012].

In order to empirically show that this theory is applicable to foraminifera, we have produced the first combined Mg/Ca-temperature and $\text{Mg}/\text{Ca}_{\text{sw}}$ - $\text{Mg}/\text{Ca}_{\text{test}}$ calibrations for the same species, derived from both cultured and field-sampled *Operculina ammonoides*, a shallow-dwelling large benthic foraminifera. We apply these calibrations to Eocene samples from Java and the southern UK; *O. ammonoides* is the closest living relative of the abundant Paleogene *Nummulites*. We utilise laser-ablation ICPMS as a highly spatially resolved analytical technique capable of identifying newly precipitated calcite in cultured material (via a [Ba] spike), and less well-preserved areas of fossil calcite through the simultaneous analysis of proxy and diagenesis-identifying trace elements.

The consistency between our field and culture Mg/Ca-temperature calibration suggests secondary controls on Mg incorporation are less problematic for large benthic foraminifera in comparison to planktic species. Our $\text{Mg}/\text{Ca}_{\text{test}}$ - $\text{Mg}/\text{Ca}_{\text{sw}}$ calibration confirms the power relationship described by studies based on other foraminifera.

By placing reasonable constraints on palaeotemperature, our calibrations enable us to demonstrate for the first time that foraminifera-derived data imply $\text{Mg}/\text{Ca}_{\text{sw}}$ in excellent agreement with other proxy evidence.

[1] Evans & Müller, 2012, *Paleoceanography*, **27**, PA4205.

Sources of sulfur and sulfur preservation in subducted rocks: An *in situ* sulfur isotope study

K.A. EVANS*¹ A.G. TOMKINS² AND J. CLIFF³

¹Applied Geology, Curtin University, GPO Box U1987, Perth, WA 6845, Australia. (*correspondence: k.evans@curtin.edu.au)

²School of Geosciences, Monash University, Melbourne, VIC3800, Australia

³Centre for Microscopy Characterisation and Analysis, University of Western Australia, WA6009, Australia

A number of lines of evidence suggest that the sub-arc mantle is 1-2 log units more oxidised than mantle elsewhere, though this conclusion is controversial, and the processes that may contribute to sub-arc mantle oxidation are poorly understood. Sulfur has been proposed as a vector for transfer of redox budget from subducting slab to sub-arc mantle. Sulfate may be present in altered ocean crust in significant quantities, and the transfer of 8 electrons as S(+6) in sulfate is transformed to S(-2) in sulfides means that the addition of sulfate to sub-arc mantle could significantly alter mantle redox budget and oxygen fugacity on geologically reasonable timescales. However, little is known of the relative stability or solubility of sulfur-bearing phases under subduction conditions so this possibility is hard to evaluate.

Sulfur isotopes provide one way to investigate sources of sulfur, and the processes that affect sulfur content during subduction. $\delta^{34}\text{S}$ of seawater-derived sulfate is around 20‰ while $\delta^{34}\text{S}$ of magma-derived sulfides is around 0‰. Calculated fractionation of sulfur isotopes at subduction temperatures for all but the most extreme open system conditions suggest that this difference between sources should be recognisable even after significant devolatilisation. *in situ* sulfur isotope measurements of pyrite associated with high pressure mineral parageneses in high pressure mafic rocks from the Eastern Alps and from New Caledonia were performed. The New Caledonia samples contain pyrite with $\delta^{34}\text{S}$ in excess of 5‰, while samples from Pfulwe pass in the Eastern Alps contain pyrite with $\delta^{34}\text{S}$ up to 15‰. These elevated $\delta^{34}\text{S}$ values suggest that sulfur ultimately derived from seawater is preserved in these rocks to depths greater than 60km.

In situ RESOchron helium dating: Progress, pitfalls and prospects

¹NOREEN EVANS¹, BRENT MCINNES¹, BRAD McDONALD², PIETER VERMEESCH³, MIKE SHELLEY⁴ AND ESTEPHANY MARILLO SIALER

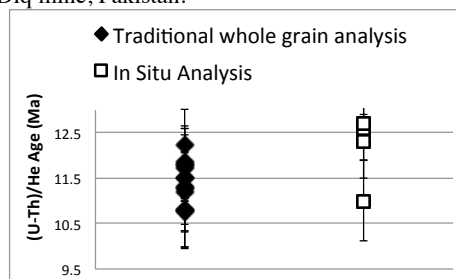
¹AuScope GeoHistory Facility, John de Laeter Centre for Isotope Research, Curtin University, Australia, (noreen.evans@curtin.edu.au);

²Department of Earth Sciences, University College London, UK;

³Laurin Technic Pty Ltd., Canberra, ACT;

⁴School of Earth Sciences, University of Melbourne, Australia

Recent advances in *in situ* double dating¹⁻³ prompted us to develop the *RESOchron*, a purpose-built laser ablation U-Th-Pb-He system (see McInnes *et al.*, this meeting). Polished zircon grains, mounted in indium, were loaded into an UHV cell where helium was extracted via 193 nm laser ablation for 30 seconds using a 33-75 μm beam at 7Hz. U and Th were subsequently analysed in an adjacent pit using traditional ELAICP-MS methods. Pit volumes were measured on a Zeiss LSM700 confocal laser microscope and (U-Th)/He ages calculated using published methods^{1,3}. The mean zircon helium age from the *in-situ* ablation experiment fell within 10% of helium ages obtained using traditional single crystal methods for an 11.4 ± 0.5 Ma subvolcanic stock from the Reko Diq mine, Pakistan.



Improvements in analytical precision require refinement of sample preparation for UHV conditions. Indium, despite being inert under high vacuum conditions, is non-ideal for zircon mounting because its high surface reflectance makes navigating around the mount and focusing the laser difficult. Due to its extreme softness, grains cannot be polished *in situ* and even slight contact can damage the surface and cause grains to shift position. Zonation of U and Th also impacts the accuracy of results, as does the accuracy of pit volume measurements as suggested previously [1-3]. Other mounting media are being explored (eg. FEP teflon) and optimization of laser protocols is underway.

[1] Boyce J.W. *et al.*, 2006, *GCA* **70**, 3031–3039; [2] Boyce J.W. *et al.*, 2009 *G-cubed* 10. doi:10.1029/2009GC002497; van Soest M.C. *et al.*, 2012, AGU Fall Meeting Abstracts, pp. B2161+. [3] Vermeesch, P. *et al.*, 2012, *GCA* **79**, 140-147.

Subseafloor microbial community in the Benguela upwelling area characterized by lipid biomarkers and intracellular DNA

T.W. EVANS^{1*}, L. WÖRMER¹, M.-A. LEVER², R. ZHU¹, L. LAGOSTINA², B. B. JØRGENSEN² AND K.-U. HINRICHS¹

¹MARUM, University of Bremen, 28359 Bremen, Germany
(*correspondence: tevans@marum.de)

²Center for Geomicrobiology, University of Aarhus, 8000 Aarhus C, Denmark

The subsurface biosphere in marine sediments is one of the least understood ecosystems on our planet. Currently, it is even subject to debate which domain of microbial life, Bacteria or Archaea, is dominant. So far, studies based on intact polar membrane lipids (IPLs) have indicated dominance of lipids associated with Archaea [1], while most DNA-based studies have suggested a higher proportion of Bacteria [2]. These contradictory results are thought to result from analytical and/or systematic biases of both techniques. In the case of IPLs, the associated organic matrix may hinder proper HPLC-MS detection due to ion suppression. In addition, both IPLs and DNA analysis may be affected by a potential pool of fossil compounds [3, 4]. To overcome these problems and achieve a more realistic view of the microbial subseafloor biosphere, novel methods were applied to samples of a transect across the Namibian Continental Margin.

We employed a new protocol for separating intracellular DNA (iDNA) from the remaining extracellular DNA-pool. For IPLs, a new method was developed and applied, based on solid phase extraction (SPE) of lipids with a phosphatic head group, resulting in strongly improved detection.

The analysis of iDNA and IPLs showed a distinct change of the microbial community. iDNA- and IPL-data were in good agreement. SPE clean-up of IPLs resulted in the detection of phospholipids that could be attributed to sulfate reducing bacteria. Previously it was not possible to detect any phospholipids in subsurface samples of upwelling areas [5]. Both iDNA and IPL analysis showed a dominance of Archaea in organic-rich sediments below the upwelling cell, while further offshore the sediments were dominated by Bacteria. Further interpretation of these trends and the downcore profile of iDNA and IPL distribution is ongoing.

[1] Lipp *et al.* (2008), *Nature* **454**, 991-994. [2] Inagaki *et al.* (2006), *PNAS* **103**, 2815-2820. [3] Xie *et al.* (2013), *PNAS* **110**, 6010-6014. [4] Dell'Anno and Danovaro (2005), *Science* **309**, 2179 [5] Lipp and Hinrichs (2009), *GCA* **73**, 6816-6833.

Revealing the 'blind spot': A simple physical model for the temporal evolution of silicate mineral weathering

JAIVIME A. EVARISTO* AND JANE K. WILLENBRING

Department of Earth and Environmental Science, University of Pennsylvania, Philadelphia, PA 19104, USA
(*correspondence: evaristo@sas.upenn.edu)

Closing the gap in the orders-of-magnitude difference between field and laboratory weathering rates has been considered essential to effectively modeling silicate mineral reactivity from centennial and millennial to geologic timescales[1]. However, what if finding the rates in the mid-range (i.e. $10^{1.5}$ - $10^{3.5}$ yr) between far-from-equilibrium conditions in laboratory experiments and near-equilibrium conditions in the field is just as useful as what we now know about the two time-dependent rate extremes? We test this hypothesis by comparing the effects of two models ("gap" or "blind spot" and "filled") of weathering rate constants k to a mineral dissolution model driven only by the physics of reaction-diffusion dynamics. The explicit neglect of intrinsic factors, like chemical composition and mineralogical structure, in this simple model is an attempt not only to put an emphasis on the frequency and, in effect, duration of time with which a mineral surface interacts with pore fluids; but also to test if the reported agreement in phenomenological effective rates $K(t)$ between numerical and analytical solutions in comparable decay systems [2] also hold true for silicate weathering rates. Preliminary findings from our model simulations indicate that (1) there is no marked difference in effective silicate weathering rates $K(t)$ (yr^{-1}) between the two models of rate constants ($4.86 \times 10^{-2} \text{ t}^{-1}$ and $4.88 \times 10^{-2} \text{ t}^{-1}$ for "filled" and "gap" distributions, respectively), suggesting that the apparent "blind spot" within the centennial to millennial range may not preclude our ability to predict mineral dissolution at these timescales; (2) the subsequent weathering beyond $t \sim k^{-1}$ exhibits a fall in rates of up to ~ 3 orders of magnitude since the effective cessation of logarithmic decay, possibly reflecting the onset of a progressively refractory stage due to finite-size effects; and (3) a simple reaction-diffusion model may be able to predict the temporal evolution of silicate weathering as an integral of both field- and lab-derived rate constants, putatively identified by a lognormal distribution and therefore the kinetic heterogeneity associated with mineral dissolution.

[1] White and Brantley (2003), *Chem. Geol.* **202**, 479.
[2] Rothman and Forney (2007), *Science* **316**, 1325.

The uplift history of the western Andes, north Chile, constrained by cosmogenic ^3He in alluvial boulders.

LAURA EVENSTAR¹, FINLAY M. STUART²
AND ADRIAN J. HARTLEY²

¹Dept. of Geology and Petroleum Geology, University of Aberdeen, Aberdeen, AB24 3UE, UK

²Isotope Geoscience Unit, Scottish Universities Environmental Research Center, East Kilbride, Glasgow, G75 0QF, UK

*Now at School of Earth Science, University of Bristol, Wills Memorial Building, Queens Road, Bristol, BS8 1RJ

Accurate timing of uplift of the Andes is essential for understanding continental tectonics processes. Current models vary from gradual uplift of the Andes from the Late Eocene due to crustal shortening/thickening [1] to rapid uplift in the Late Miocene due to large-scale mantle delamination [2]. Existing paleoelevation proxies are afflicted by either large uncertainties or reliance on assumptions about past climate-elevation histories [1]. The production rate of *in situ* cosmogenic isotopes is strongly dependent on elevation and thus has potential to constrain surface uplift histories.

The arid climate in the Atacama Desert, Northern Chile has prevailed since at least 25 Ma [3] leading to low erosion rates and high cosmogenic nuclide concentrations within alluvial boulders overlying the Pacific Planation Surface (PPS). The PPS in the Aroma Quebrada formed at < 13.9 Ma. Alluvial boulders which lie on the PPS, have high concentrations of cosmogenic ^3He that suggest deposition soon after surface formation [4]. The concentration of cosmogenic ^3He in the boulders are compared to those calculated for Early Miocene and Late Miocene uplift histories. The high concentration of cosmogenic ^3He in five boulders cannot be generated by Late Miocene uplift of the Andes (irrespective of scaling factor-production rate). The data require early uplift of the paleosurface prior to 8 Ma. This rules out rapid uplift of the Andes due to mantle delamination in the Late Miocene instead supporting progressive shortening and thickening of continental crust initiating in the Early Miocene or earlier.

[1] Barnes and Ehler (2009) *Earth-Science reviews* **97**, 105-132. [2] Garzzone *et al.* (2008b) *Science* **320**, 1304-1307. [3] Dunai *et al.* (2005) *Geology* **33**, 321-324. [4] Evenstar *et al.* (2009) *Geology* **37**, 27-30.

Nuclear materials under extreme conditions

RODNEY C. EWING*

University of Michigan, Ann Arbor, MI 48109 USA

(*correspondence: rodewing@umich.edu)

During the past forty years, the materials science of nuclear waste forms has focused mainly on the stability and long-term behavior of nuclear waste glasses and the UO_2 in used nuclear fuel. However, during this time, substantial quantities of Pu, now more than 2,000 metric tonnes, have been produced. Some 200 metric tonnes of Pu have been separated along with much lesser amounts of “minor” actinides (Np, Am and Cm). The *nuclear solution* is to prepare a mixed-oxide (MOX) fuel of Pu and U or an inert matrix fuel (IMF) to fission transuranium elements in a reactor. The *geologic solution* is to develop very durable materials for disposal in a geologic repository or a very deep borehold. However, radiation damage in the reactor or self-radiation damage due to the alpha-decay of actinides is a concern, as radiation-induced transformations of the atomic structure decrease the chemical durability.

A variety of materials, with mineral analogues, including oxides, silicates and phosphates, have been investigated because they have a high capacity to incorporate actinides, are chemically durable, and in some cases, are resistant to radiation damage. There has been substantial interest in isometric pyrochlore, $\text{A}_2\text{B}_2\text{O}_7$ (A = rare earths, actinides; B = Ti, Zr, Sn, Hf), for the immobilization of transuranium elements. Four radiation-induced transformations may occur: i) periodic-aperiodic, ii) order-disorder, iii) crystalline-to-crystalline, and iv) chemical decomposition. Certain pyrochlore compositions (B = Zr, Hf) remain crystalline to very high doses of alpha-recoil damage, which is mainly caused by ballistic interactions with the alpha-recoil nucleus.

Most recently, the radiation response of pyrochlore has been investigated using relativistic heavy ions for which high energy deposition occurs by electronic excitation. Energetic ions deposit exceptional amounts of kinetic energy (GeV) within an exceedingly short time (less than a femtosecond) into nano-scale volumes. Energy deposition is up to tens of eV/atom, forming damage tracks, very similar to fission tracks in zircon and apatite. These irradiations have been done at high pressures (>50 Gpa) and temperatures (up to 500 °C) within a diamond anvil cell (DAC). The combined use of advanced *in situ* (synchrotron X-ray diffraction and Raman spectroscopy) and *ex situ* (transmission electron microscopy) characterization techniques has shown that normal phase relations are changed by the radiation and that most materials can be amorphized.

The effect of nuclear radiation on the structure of zircon

RODNEY C. EWING*

University of Michigan, Ann Arbor, MI 48109 USA
(correspondence: rodewing@umich.edu)

In 1955, Heinrich Holland and David Gottfried published a remarkable paper in *Acta Crystallographica* on radiation damage accumulation in a suite of natural zircons from Sri Lanka [1]. The purpose of their study was to investigate the possibility of using radiation damage accumulation as a method of age determination. This was one of the first quantitative studies of damage accumulation and annealing in a complex ceramic and provided a solid basis for extrapolating radiation damage effects in actinide-bearing nuclear waste forms over geologic periods [2,3]. The paper is not only remarkable for the data, measurements of unit cell parameters and optical properties, as a function of increasing dose, but also because the interpretation of the data was in the context of a damage ingrowth model that quantifies the accumulation of amorphous domains, the accumulation of isolated defects, the formation of new crystalline structures and the change in crystallite size. The authors also recognized the possibility of alpha-particles enhancing the effects of damage accumulation and annealing caused by the alpha-recoil atom.

Subsequent studies of radiation effects have utilized P-doping experiments [4] and ion beam irradiations (MeV to GeV energies) [5,6]. Most recently, high-energy irradiations have been completed at high pressures using a diamond anvil cell [7]. These studies have provided a fundamental understanding of the radiation damage processes that has supported the use of zircon as an optic wave guide [8], the development of nuclear waste forms for excess weapons plutonium [9] and fission track dating and thermochronology [10, 11]. For all of these applications, the early work by Holland and Gottfried remains the fundamental foundation.

[1] Holland & Gottfried (1955) *Acta. Cryst.* **8**, 291-300. [2] Murakami *et al.* (1991) *Amer. Mineral.* **76**, 1510-1532. [3] Weber *et al.* (1994) *J Mater. Res.* **9**, 688-698. [4] Exarhos (1984) *Nucl. Instr. Method Phys. Res.* **B1**, 538-541. [5] Wang & Ewing (1992) *Nucl. Instr. Method Phys. Res.* **B59**, 395-400. [6] Bursill and Braunschhausen (1990) *Phil Mag.* **A62**, 395-420. [7] Glasmacher *et al.* (2006) *Phys. Rev. Lett.* **96** 195701-195705. [8] Babsail *et al.* (1991) *Nucl. Instr. Method Phys Res.* **B59**, 1219-1222. [9] Ewing *et al.* (1995) *J. Mater. Res.* **10**, 243-246. [10] Lang *et al.* (2008) *EPSL* **274**, 355-358. [11] Li *et al.* (2011) *EPSL* **302**, 227-235; Li *et al.* (2012) *EPSL* **321**, 121-127.

Formation and geochemistry of rutile from garnet gabbros of the Jijal Complex, Kohistan island arc

T.A. EWING* AND O. MÜNTENER

Institut de Sciences de la Terre, UNIL, CH-1015 Lausanne, Switzerland (*correspondence: tanya.ewing@unil.ch; othmar.muntener@unil.ch)

The Kohistan paleo-island arc preserves a ~50 km-thick section of Jurassic–Cretaceous arc crust renowned as one of the best exposures of an exhumed island arc. The lowermost Jijal Complex comprises an ultramafic and a mafic section. The latter is dominated by garnet gabbros, the origin of which is controversial. Formation of garnet in these rocks has been ascribed to dehydration melting of hornblende-bearing precursors [e.g. 1], prograde metamorphic reactions [e.g. 2] or fractional crystallisation at high pressures followed by isobaric cooling [3, 4].

Rutile (TiO₂) is an accessory phase in garnet-hornblende pyroxenites, garnet gabbros, paragonite gabbros and epidote-bearing pegmatites. In some samples garnet cores preserve ulvöspinel inclusions while garnet rims host rutile, suggesting formation of rutile at the expense of ulvöspinel. In paragonite gabbros rutile is associated with epidote–quartz intergrowths and may have formed as a result of the breakdown of clinopyroxene and garnet to form epidote and amphibole. Both reactions are consistent with isobaric cooling.

Garnet gabbros, paragonite gabbros and epidote-bearing pegmatites give Zr-in-rutile temperatures of 650–700°C. A few analysed rutiles are in contact with quartz and have indistinguishable Zr from other rutiles. These lithologies are largely zircon-free and Zr-in-rutile thus gives minimum temperatures. The Zr-in-rutile temperatures are lower than ~800–1000°C Fe–Mg temperatures for the same lithologies, and it is unlikely that this difference can be explained entirely by the lack of equilibrium with zircon. Zr content within individual grains displays little variation, arguing against diffusive re-equilibration, but it remains to rule out complete recrystallisation. Rutile from the Jijal Complex samples has Zr/Hf distinct from that of rutile from lower continental crustal metapelites, pointing to different controls on these geochemical tracers in rutile from different settings.

[1] Garrido *et al.* (2006) *J. Petrology* **47**, 1873–1914. [2] Yamamoto & Yoshino (1998) *Lithos* **43**, 219–234. [3] Ringuette *et al.* (1999) *Geology* **27**, 139–142. [4] Jagoutz *et al.* (2011) *EPSL* **303**, 25–36.

The complex dynamics of collisional orogens unveiled by numerical modeling

MANUELE FACCENDA¹, TARAS GERVA²
AND SUMIT CHAKRABORTY³

¹Dipartimento di Geoscienze, Università di Padova
(manuele.faccenda@gmail.com)

²Institute of Geophysics, ETH Zürich
(taras.gerya@erdw.ethz.ch)

³Sumit Chakraborty, Institut fuer Geologie, Mineralogie und
Geophysik, Ruhr-Universitaet Bochum;
(Sumit.Chakraborty@rub.de)

We performed numerical modelling of continental collision following oceanic subduction, and analyze metamorphic processes and the thermo-tectonic evolution of the resulting orogens as a function of key parameters such as crustal strength and radiogenic heating, fluid migration and convergence rate. The common and more important features we found for all models are crustal thickening, formation of mid-crustal partially molten levels extruding laterally, exhumation of medium to high grade metamorphic rocks with clockwise P-T-t paths and a style of post-collisional orogens that ranges from symmetric (stiff lower crust), two-sided collision zone to classical asymmetric orogen (weak lower crust). Crustal radiogenic heating favor the formation of partial melting in the mid-crust and exhumation at the surface of an inverted metamorphic sequence. Fluids affect mainly the plate boundary, reducing the viscosity of the lubricated plate interface leading to one-sided, asymmetric subduction zones. If wetting of the plate interface is very efficient, plate decoupling occurs followed by retreat and delamination of the subducting continental plate.

The results are in good agreement with geological, metamorphic, geochemical and geophysical observations from natural mountain belts (e.g. Himalaya, Western Alps, Apennines) and previous numerical studies of similar geodynamical settings.

The role of oceanic sediments in the metasomatism of subpatagonian lithospheric mantle beneath Cerro del Fraile (Argentina)

FACCINI B.¹, BONADIMAN C.¹, COLTORTI M.¹,
GRÉGOIRE M.² AND SIENA F.¹.

¹Department of Earth Sciences, Ferrara University, Ferrara,
Italy

²DTP, CNRS-UMR 5562 Observatoire Midi-Pyrénées,
Toulouse, France

A detailed petrological study of mafic and ultramafic xenoliths from the Cerro del Fraile (CF, Southern Patagonia, Argentina) was developed in order to decipher the nature of the metasomatising agents which infiltrate the mantle wedge above the Antarctic subducting Plate, as well as the role of material dragged down in the subduction zone and recycled within the South patagonian sub-arc mantle.

CF mantle xenoliths comprise peridotites, cumulitic pyroxenites and composite samples. On the basis of HREE and major element mineral melting models, the peridotites record a partial melting degree variable between 10 and 25%. They also experienced a contemporaneous or subsequent refertilisation event, caused by the percolation of SiO₂-Al₂O₃-rich slab-derived metasomatic agents. The similarity between cpx and opx of the pyroxenites and those in the pyroxenitic part of the composite samples suggests that the cumulitic process occurred within the mantle. The reaction of the variously depleted mantle with the incoming melt took place under reduction conditions ($\Delta\log fO_2$ (QFM) -1.21 to -0.34), unusual for mantle wedge settings.

Calculated melts in equilibrium with the most enriched opx and cpx in peridotites and with the pyroxenes of the cumulites have LREE, Zr (Hf), Th and U contents higher than those of AVZ natural adakites. This result speaks in favour of the melting of oceanic sediments, which are composed of a remarkable amount of manganese nodules and micronodules and, possibly, organic matter, in agreement with the estimated low oxygen fugacity conditions. The amount of sediments involved in the genesis of the infiltrating melts is larger than that previously proposed for the genesis of the erupted Patagonian adakites [1]. At mantle conditions the percolation of SiO₂-rich magmas is allowed by their high Al₂O₃ and water content and is favoured by the molar volume reduction due to the growth of opx at the expenses of olivine.

[1]. Stern, C. R. & Kilian, R. (1996). *Contribution to Mineralogy and Petrology* 123, 263-281.

Mesocosms experiments with zeolite-amended marsh soils to reduce nitrogen leaching

FACCINI B.¹, COLOMBANI N.¹, DI GIUSEPPE D.¹,
MASTROCICCO M.¹ AND COLTORTI M.¹

Physics and Earth Sciences Dep., University of Ferrara,
(barbara.faccini@unife.it)

To prevent diffuse nitrogen (N) contamination from agricultural activities the Water Framework Directive institutes a series of good practices for a sustainable agriculture in vulnerable areas. Notwithstanding, N leaching is still a major issue at the European and global scale. To increase N retention capacity of lowland soils, natural zeolites were used in an experimental field near the town of Codigoro, in the eastern part of Ferrara province (Italy), pertaining to the Po delta reclaimed marsh soils, actually 3 m below sea level. To test their effectiveness a tridimensional model 100 x 50 cm in size (divided in two sections of 50 x 50 cm each) was built. Tank was completely filled with soil composed by 8±1% of sand, 49±2% of silt, 42±2.5% of clay and 8±1.5% of organic matter, with a bulk dry density of 1.15±0.05 g/cm³. In the uppermost 20 cm of one mesocosm, the equivalent of 7 Kg/ha of natural NH₄⁺-charged zeolite was mixed with the soil, whereas the second mesocosm was fertilized with the equivalent of 270 kg/ha of urea. The filling has been done manually, compacting successive layers of about 2 cm each. During this procedure, 5TE Decagon probes were inserted every 8 cm to monitor water content, temperature and bulk soil conductivity. Suction cups were also inserted at the same depths to monitor soil water composition. The two mesocosms were irrigated with a micronizer for 2 months at an average rate of 4 mm/d. The irrigation water was taken from the irrigation channel close to the experimental field. The regular irrigation created a percolation front slowly moving downward. At the end of the experiment, duplicate core samples were excavated and analyzed for mineral N (NO₃⁻, NO₂⁻ and NH₄⁺) and for Cl⁻ and Br⁻ used as tracers. Soil water samples were also obtained by suction cups.

The mass balance of N within the two mesocosms highlighted that the natural zeolites acted as a strong buffer in N leaching, with most of the mineral N retained in the soil as adsorbed NH₄⁺. On the contrary, the mesocosm supplied with urea exhibited the greatest NO₃⁻ concentrations in both soil solutions and cores.

Aqueous carbonate speciation in equilibrium with Aragonite under subduction zones conditions

SEBASTIEN FACQ¹ ISABELLE DANIEL^{*1}
AND DIMITRI A. SVERJENSKY²

¹Laboratoire de Géologie de Lyon :Terre, Planètes,
Environnement, Université Claude Bernard Lyon 1, ENS
de Lyon, CNRS, UMR 5276, 2 rue Raphaël Dubois,
69622 Villeurbanne, France.

(*Isabelle.Daniel@univ-lyon1.fr)

²Dept. Earth & Planetary Sciences, Johns Hopkins University,
3400 N. Charles St., Baltimore, MD 21218, USA &
Geophysical Laboratory, Carnegie Institution of
Washington, 5251 Broad Branch Road NW, Washington,
D.C. 20015, USA.

In the course of subduction, carbonate minerals in the oceanic crust may survive dehydration and partial melting of the subducting slab [1-3] and transfer carbon from the surface into the deep mantle. However, the investigation of the solubility of carbonate minerals and aqueous speciation of carbon under the ranges of temperature and pressure relevant to subduction zones in the upper mantle remains largely unexplored experimentally and theoretically [4]. Here, we report a combined experimental and theoretical study of the equilibrium of CaCO₃ minerals with pure water and NaCl aqueous solutions in a larger *PT* range. The carbonate-bicarbonate speciation in the aqueous phase was first studied by *in-situ* Raman spectroscopy in a diamond anvil cell. Experimental solubilities of aragonite and relative amounts of the dissolved C-species were obtained and used to constrain a theoretical thermodynamic model of the fluid speciation and solubility in equilibrium with aragonite. In pure water at 300–400°C, the experimental and theoretical results indicate that CO₂ is a minor species in fluids in equilibrium with aragonite at *P* > 10 kbar. Instead, the CaHCO₃⁺ species becomes important until *P* > 50 kbar, where carbonate ion and CaCO₃⁰ become the dominant C-species. At higher temperatures, the theoretical model indicates that CO₂ again becomes a major species in fluids in equilibrium with aragonite depending on the pressure. The presence of sodium chloride in the fluid expands the pressure domain where the speciation of carbonate is highly variable.

[1] Yaxley & Green, (1994) *EPSL*. **128**, 313-325. [2] Molina & Poli, (2000) *EPSL*. **176**, 295-310. [3] Kerrick & Connolly, (2001) *EPSL*. **189**, 19-29. [4] Martinez *et al*, (1994) *Chem.Geol.* **207**, 47-58.

Tholeiitic vs. Calc-Alkaline Igneous Trends on the Moon: Lunar Meteorite Northwest Africa 773 vs. Apollo 15 Quartz Monzodiorite

T.J. FAGAN, Y. WAKABAYASHI, A. SUGINOHARA
AND D. KASHIMA¹

¹Waseda University, Tokyo, Japan (fagan@waseda.jp)

Terrestrial igneous rocks exhibit a wide variety of compositions, but many can be linked together as stages of magmatic evolution along chemical trends. Two of the main trends are the tholeiitic (or FeO-enrichment or Fenner) trend and the calc-alkaline (or SiO₂-enrichment or Bowen) trend. Lunar igneous rocks also show a wide range of compositions, even if only basalts are considered. Linking lunar rocks together along magmatic trends has proven difficult though, in part due to impact disruption of the surface wreaking havoc on igneous field relations.

However, impact processing can work in our favor by assembling breccias of magmatically related clasts. We use textures, pyroxene compositions ($Fe\# = Fe/(Fe+Mg) \times 100$ and $Ti\# = Ti/(Ti+Cr) \times 100$) and zoning relationships to argue that this is precisely what has happened during the formation of lunar meteorite Northwest Africa 773 (NWA 773). Clasts of olivine cumulate (OC) are characterized by pyroxene with low $Fe\#$ (20-30) and variable $Ti\#$ (10-75). Pyroxene $Ti\#$ correlates with proximity to intercumulate pockets with K,Ba-feldspar and Ca-phosphates. This increasing $Ti\#$ -trend is interpreted as a product of fractional crystallization where the $Fe\#$ was buffered by abundant surrounding mafic silicates.

Pyroxenes from other types of clasts in the breccia show a trend of $Ti\#$ and $Fe\#$ both increasing to nearly 100. Clasts with the highest $Fe\#$ and $Ti\#$ include fayalite+hedenbergite+silica symplectites and K,Ba-feldspar+fayalite+silica ± hedenbergite FeO-alkali-rich clasts. These are interpreted as the alkali-poor and alkali-rich products of silicate liquid immiscibility (SLI) after the liquid evolved to ferroan compositions. Igneous (crystallized from liquid) silica occurs only in the FeO-alkali clasts, suggesting that SiO₂-enrichment occurred only after extreme FeO-enrichment, comparable to the terrestrial tholeiitic trend.

Igneous silica also occurs in Apollo 15 quartz monzodiorite (QMD), but coexists with pyroxene having moderate $Fe\#$ (60-70), more akin to the calc-alkaline trend. Whole-rock compositions of QMD fall on a mixing line between immiscible liquids produced during experiments on a KREEP basalt composition [1], suggesting a role of SLI during formation of QMD.

[1] Rutherford et al (1976) Proc. LSC 7, p. 1723-1740.

Late quaternary sedimentary provenances in the Central Arctic Ocean inferred by Nd and Pb isotopes of fine detrital fraction

N. FAGEL*¹, C. NOT², J. GUEIBE³, N. MATTIELLI³
AND E. BAZHENOVA⁴

¹AGEs, Argiles, Géochimie et Environnement sédimentaires, Université de Liège, Belgique;

(*correspondence: nathalie.fagel@ulg.ac.be)

²GEOTOP, UQAM, Montréal, Canada;

(christelle.not@aori.u-tokyo.ac.jp)

³G-Time, Université libre de Bruxelles, Belgique ;

(nmattiel@ulb.ac.be)

⁴AWI, Bremerhaven, Germany;

EvgeniaBazhenova@gmail.com

Nd and Pb isotope signatures of sediments from Central Arctic were analysed to trace detrital particle provenance. Changes in relative contribution of different source-areas were used to reconstruct paleoceanographical changes over the last 250 kyr. Temporal changes in Nd and Pb isotopic composition confirm that sediment supply is controlled by the glacial/interglacial-deglacial variability. Pb mixing calculations suggest a major contribution from Mackenzie and Lena river areas. All interglacial-deglacial samples show isotopic values shifted towards the signature of Mackenzie end-member. Such source is consistent with their carbonate-rich lithology, detrital carbonates being mainly originated from this area and the Canadian channels. Nd mixing signature reports contribution from a third volcanic source; A compilation of trace element content of regional geological sources suggests that the most probable candidate is the Okhotsh-Chutoka province (Eastern border of Siberian platform). Our geochemical data confirm that the sediment provenances in Central Arctic remain close to the Present conditions during the earlier interglacials. Glacial stage 4 and 6 are characterised by the lowest supplies from the American margin, suggesting reduced particle supplies coming from the Beaufort Gyre to the Mendeleev Ridge.

Carbon allocation to ectomycorrhizal fungi and bacteria colonising granite

FAHAD Z, MAHMOOD S AND FINLAY RD

Department of Forest Mycology and Plant Pathology, Uppsala BioCenter, Swedish Univ. Agricultural Sciences, Uppsala, SE-75000, Sweden (*correspondence: zaenab.fahad@slu.se)

Ectomycorrhizal fungi have been postulated to mobilize essential plant nutrients directly from minerals through organic acid exudation. [1].

Laboratory microcosms were used to study mycorrhizal mycelial colonisation of granite substrate, release of organic acids, mobilisation of mineral elements and their uptake by *Pinus sylvestris* seedlings under two levels of N deposition. The effects of the mycelium were assessed by comparison with control treatments in which the mycelium was physically disrupted. Patterns of carbon allocation to different microbial taxa colonising the granite were assessed using stable isotope probing.

Colonisation of granite substrate by ectomycorrhizal mycelium resulted in significant production of organic acids after 12 weeks in comparison with uncolonised granite controls. After 24 weeks lower concentrations of a wider spectrum of organic acids were found in the treatment with intact mycelia. Significantly greater concentrations of Fe and Mn were found in the soil solution in mycelium-colonised compartments than those not colonized by mycelium, but no statistically significant effects were found on concentrations of other elements, or on plant biomass.

[1] Finlay RD et al., (2009). *Fungal Biology Reviews* **23**: 101-106.

Energy crop production on mining and smelting impacted arable land - A non-phytoremediation approach

W. FAHLBUSCH*, B. SAUER AND H. RUPPERT

Geosciences Center & Interdisciplinary Center for Sustainable Development, University of Goettingen, Goldschmidtstr. 1, D- 37077 Göttingen, Germany (*correspondence: wfahlbu@gwdg.de)

Up to 10% of the arable land in Germany is potentially contaminated by heavy metals [1]. These areas comprise flood plains of rivers, industrialized areas and also soils in the vicinity of smelter facilities e.g. in the Harz Mountains in Germany, where sulfidic polymetallic ores were mined and processed for at least 2000 years. This mining impacted land faces contamination with several elements (As, Cd, Cu, Pb, Sb, Tl, Zn). Conventional remediation techniques like excavation of the soil are often not economic. The removal of the toxic elements with hyperaccumulating plants (phytoremediation) is also not satisfying because of their commonly low yield. It would take thousands of years to reach acceptable low contamination levels.

Instead of phytoremediation we recommend to produce high yield crops with low uptake of heavy metals to leave the pollutants in the soil. The plants can be used in biogas facilities. To identify crops with a low metal uptake we measured plant and soil concentrations and the mobile/exchangeable fraction of heavy metals in a variety of polluted soils. An unpolluted soil was used as a reference. Soil material adhering to crops was mathematically corrected using titanium in the soil as a reference element [1].

These low contaminated crops can be used for biogas generation in fermentation facilities without impairing the gas output. Furthermore, the residues of the biogas production can be returned as organic fertilizer to the fields where the plants were harvested. All important nutrients are recycled back to the fields (except nitrogen) and the maximum permissible values for heavy metal in farm fertilisers can be abided. Energy crops with a low uptake of cadmium are for instance the maize cultivar Padrino, the rye cultivar Vitallo and the barley cultivar Christelle. In contrast, amaranth, sunflower and the energy beet Kyros should not be cultivated on contaminated soils for bioenergy production due to their high cadmium uptake [1].

[1] Sauer et al (2013) *Bioenergy Production as an Option for Polluted Soils – A Non-phytoremediation Approach*. In Ruppert et al (Eds.): *Sustainable Bioenergy Production - An Integrated Approach*. Chapter 14, Springer, Dordrecht, (in print).

Continuous carbon monoxide measurements along the NEEM-2011-S1 ice core: *In situ*-production and potential for atmospheric reconstruction

X. FAIN^{1*}, J. CHAPPELLAZ¹, R. H. RHODES², C. STOWASSER³, T. BLUNIER³, J. R. MCCONNELL⁴, E. J. BROOK², M. LEGRAND¹, T. DEBOIS⁵ AND D. ROMANINI⁵

¹UJF - Grenoble 1 / CNRS, LGGE-UMR 5183, Grenoble, F-38041, France (*correspondence : fain@lgge.obs.ujf-grenoble.fr)

²College of Earth, Ocean and Atmospheric Sciences, Oregon State University, Corvallis OR, USA

³Center for Ice and Climate, Niels Bohr Institute, University of Copenhagen, Copenhagen, Denmark

⁴Division of Hydrologic Sciences, Desert Research Institute, Reno NV, USA

⁵UJF - Grenoble 1 / CNRS, LIPhy-UMR 5588, Grenoble, F-38041, France

We present results of a 4-week laboratory-based campaign to measure CO mixing ratios in the North Greenland Eemian (NEEM) S1 ice core (410 m long) using an OF-CEAS spectrometer (Optical Feedback-Cavity Enhanced Absorption Spectrometry) coupled to a continuous melter system. This analytical setup generates highly precise (0.3 ppbv 1 sigma) and stable measurements of CO mixing ratios. The NEEM-2011-S1 CO record spans 1800 yr and exhibits highly variable concentrations at the scale of annual layers, ranging from 75 to 1327 ppbv. Although the most recent section of this record (i.e., since 1700 AD) agrees with existing discrete CO measurements from the Eurocore ice core and the deep NEEM firn, it is difficult to interpret in terms of atmospheric CO variation due to high frequency, high amplitudes spikes features. 68% of the elevated CO spikes are observed in ice layers enriched with pyrogenic aerosols. Such aerosols, originating from boreal biomass burning emissions, contain organic compounds, which can be oxidized or photodissociated to produce CO in-situ. We suggest that elevated CO concentration features could present a new integrative proxy for past biomass burning history. However, the NEEM-2011-S1 record also reveals an increase in baseline CO level prior to 1700 AD (129 m depth), with the mixing ratio remaining high even for ice layers depleted in dissolved organic carbon (DOC). Overall, the processes driving in-situ production of CO within the NEEM ice are complex and may involve multiple chemical, or biological, pathways.

High sulfur isotopic fractionations in a low-sulfate environment

MARIANELA FALLAS DOTTI* AND DONALD E. CANFIELD

Nordic Center for Earth Evolution (NordCEE) and Institute of Biology, University of Southern Denmark, 5230 Odense M, Denmark (*corr: nela@biology.sdu.dk)

Meromictic Lake Cadagno in Switzerland is an euxinic environment which draws scientific attention because it can be used as a proxy of early oceans. Two sites in the lake have been chosen to study the sedimentary isotopic geochemistry of sulfur. Site 1 is located in the oxic part of the lake with low sulfate concentrations (~0.5 mM). Site 2 is euxinic and it has higher sulfate concentrations than site 1 (~2mM). We explored isotopic fractionation between sulfate and sulfides and evaluated the role that disproportionation could play in these two types of environment. Canfield *et al* 2010[1] have already reported very high fractionations during sulfate reduction in the water column at site 2. However, they did not attribute these results to disproportionation. We show here higher fractionations in the sediments of site 1 than in those of site 2. The low sulfate concentrations at site 1 make it unrealistic to attribute these high fractionations to sulfate reduction alone. Thus, disproportionation seems to influence the distribution of the $\delta^{34}\text{S}$ signals in this site.

[1] Canfield *et al*, 2010. *Geology* **38**, 415-418.

New constraints on the pre-eruptive storage conditions of the Campanian Ignimbrite (Campi Flegrei, IT)

¹SARA FANARA, ¹ROMAN BOTCHARNIKOV, ²DANILO M. PALLADINO, ¹ANIKA HUSEN, ²GABRIELE MACCHI CECCARANI, ²SIMONE RIGHI AND ¹HARALD BEHRENS

¹Institute for Mineralogy, Leibniz University of Hannover, Callinstr. 3, Hannover, D-30167, Germany

²Department of Earth Science, La Sapienza University of Rome, P.le Aldo Moro 5, 00185, Rome, Italy

Solubility and phase equilibria experiments were performed on a synthetic trachyte representing the least evolved composition of the Campanian Ignimbrite (CI) eruption. H₂O and CO₂ solubilities were investigated at 1100°C and at pressure from 100 to 500 MPa for approx. 24h in an Internally Heated Pressure Vessel (IHPV). Phase equilibria experiments were performed at 100, 200 and 300 MPa and at temperature between 850°C and 1050°C in the Cold Seal Pressure Vessel (CSPV) and the IHPV under relatively oxidizing conditions (log fO₂=QFM+3.3 for IHPV; log fO₂=QFM+1 for CSPV). Run products were analysed by electron microprobe, spectroscopic techniques, Karl-Fischer titration and Carbon-Sulfur analyser.

For comparison natural samples from the juvenile parts of the CI were collected around the city of Naples and on the island of Procida. The collected products were analysed with the same techniques used for the experimental ones.

It was found that the solubility of water ($X_{\text{H}_2\text{O}}=1$) increases with pressure from 4.2 wt% at 100 MPa to 10.80 wt% at 500 MPa. The solubility of CO₂ (nominal $X_{\text{H}_2\text{O}}=0$) increases with pressure as well from 350 ppm at 100 MPa to 2700 ppm at 500 MPa. Comparing our experimental data with previous studies on the melt inclusions of the CI, a pressure between 100 and 200 MPa was evaluated for the melt prior to the CI eruption, indicating a magmatic storage region located between 2 and 6 km depth.

Comparing the paragenesis of the natural samples with those from the phase equilibria experiments, a temperature between 830°C and 880°C was estimated in the pressure range of 100-200 MPa for the magma prior to the CI eruption. Harker diagrams of experimental and natural samples were used to reconstruct the evolution of the CI melt. It is suggested that the crystal fractionation via differentiation plays a major role during the evolution of the magma prior to the CI eruption.

Variations in δD of fatty acids of Piezophilic Bacterium *Moritella japonica* DSK1 reflect biosynthetic pathways

JIASONG FANG¹ AND LI ZHANG²

¹Department of Natural Sciences, Hawaii Pacific University, Kaneohe, HI 96744, USA

²State Key Laboratory of Geological Processes and Mineral Resources, China University of Geosciences, Wuhan 430074, China

It is believed that bacterial metabolic pathways, not lipid biosynthesis, exert primary control on the variability of δD of lipids. In this study, we examined the δD of fatty acids in piezophilic bacterium *Moritella japonica* DSK1 that was grown in defined seawater medium with composite glucose as substrate at 30 megapascal. Fatty acids of DSK1 showed vastly varied δD , ranging from +44.4 to -171‰. Short-chain fatty acids (SCFA) had positive δD (average +3‰), whereas long-chain-polyunsaturated fatty acid (LC-PUFA) DHA (*cis*-4,7,10,13,16,19-docosahexaenoic acid) exhibited much depleted δD (-171‰). We show that the significant difference in δD between SCFA and LC-PUFA is a result of bacterial utilization of two distinct biosynthetic pathways that co-exist in the piezophilic bacterium. There was a wide range of hydrogen isotope fractionations between FA and growth water and between FA and substrate, but a nearly constant offset and a perfect correlation between the two fractionation factors, suggesting that the pools of hydrogens in the bacterium were metabolically linked and biosynthetically coordinated in biosynthesis of fatty acids. Thus, bacterial lipid biosynthetic pathways exert dominant, yet well-synchronized control on δD of fatty acids. Given the pressure-dependent carbon and hydrogen isotope fractionations observed in piezophilic bacterium *M. japonica* DSK1, we suggest that δD of fatty acids, together with their $\delta^{13}\text{C}$, can be used as a dual biogeochemical tracer to determine the source, diagenesis, and vertical transport of organic matter in the oceanic environments.

Geochemical evidence for volcanic activity prior to and enhanced terrestrial weathering during the Paleocene Eocene thermal maximum

MATTHEW S. FANTLE¹, REBECCA WIECZOREK¹,
LEE R. KUMP¹ AND GREGORY RAVIZZA²

¹Dept. of Geosciences, The Pennsylvania State University,
University Park, PA

²Dept. of Geology & Geophysics, SOEST, University of
Hawaii, Manoa, HI

The current study presents geochemical measurements from a gray shale sequence from the Central Basin in Spitsbergen, Svalbard Archipelago (Core BH 9/05) that samples the Paleocene Eocene thermal maximum (PETM) at extremely high resolution. The data, including Re and Os concentrations, ¹⁸⁷Os/¹⁸⁸Os, and major element geochemistry over ~60 meters of shale representing ~220 ka, suggest that a significant volcanic episode occurred just prior to or coincident with the onset of the PETM. The precise correlation between the timing of the PETM and the volcanic episode is possible due to previously published, high resolution δ¹³C organic carbon data measured in the same core. The presence of a significant volcanic component is indicated primarily by a large drop in ¹⁸⁷Os/¹⁸⁸Os (Δ¹⁸⁷Os/¹⁸⁸Os ~ -0.23) and confirmed by elemental mixing calculations. The geochemistry of the inferred ash component, which persists in the sedimentary record for ~8 ka, is distinct and consistent with the geochemistry of contemporaneous ashes in Denmark. Based on the substantial size of the ¹⁸⁷Os/¹⁸⁸Os decrease, the volcanic event must have involved widespread ash deposition in the local catchment and subsequent, rapid weathering of the ash that shifted the ¹⁸⁷Os/¹⁸⁸Os of the basin water column to <0.5. Temporally, the volcanic event coincides with (or predates by a few ka) the onset of the PETM, suggesting northwest European shelf volcanism as the trigger for the PETM.

As the planet warmed, dissolved and detrital indicators of weathering indicate a relatively short-lived <10 ka pulse of more weathered material to the basin. The pulse shifted authigenic ¹⁸⁷Os/¹⁸⁸Os to more radiogenic values and deposited clastic materials with higher Chemical Index of Alteration and lower Na/Ti, suggesting more intense chemical weathering prior to the peak carbon isotope excursion. The pulse is consistent with open ocean observations of changing ¹⁸⁷Os/¹⁸⁸Os. In addition, anoxia appears to have initiated close to the onset of the PETM, persisting for ~50 ka and ending abruptly during the recovery stage.

The inheritance of source Hf isotopic diversity in S-type granites

F. FARINA^{1*}, G. STEVENS¹, A GERDES² AND D FREI¹

¹Stellenbosch University, PB X1, Matieland 7602, South
Africa (*correspondence: fannak@gmail.com).

²Institut Für Geowissenschaften, Senckenberganlage 28, D-
60054 Frankfurt Am Main, Germany.

S-type granites typically record substantial Hf isotopic diversity within their magmatic zircon population. The 538 Ma old Peninsula pluton (South Africa) typifies this behavior exhibiting a zircon ε_{Hf(538)} range of 8ε units. In the smallest rock samples investigated (<0.5 dm³) and within individual thin sections, an ε_{Hf(538)} range is recorded that is almost as large as that recorded within the whole sample set. At all scales, the ε_{Hf} variability in the magmatic zircon fraction matches well that portrayed by the time evolved inherited zircon population, suggesting that the ε_{Hf} heterogeneity of magmatic zircon is inherited from the source [1]. However, the Hf dispersion exhibited by the inherited zircons is greater (12 ε_{Hf} units) than that shown by magmatic zircons indicating a minor degree of Hf isotope homogenization in the time interval between dissolution of detrital zircon and the growth of the magmatic fraction. Moreover, the ε_{Hf(t)} frequency of occurrence in the two populations is not identical, with a greater proportion of magmatic zircons having higher ¹⁷⁶Hf/¹⁷⁷Hf. This is interpreted to result from the relatively minor contribution of ¹⁷⁶Hf from Lu-bearing phases that did not re-equilibrate with zircon during metamorphism and partial melting. These phases have higher Lu/Hf ratios than zircon and thus their break down provides a more juvenile signature to the melt, mimicking the effect of mixing with a mantle-derived magma.

The occurrence of magmatic zircons with diverse ε_{Hf} at the sub-cm scale reflects the existence of micro domains within the melt whose Hf isotopic composition is controlled by the in-situ availability and composition of detrital zircons as well as by the ratio between detrital zircons and other Hf-bearing phases dissolved into the melt. Hf isotopic equilibration between micro domains was poor, due to the very low Hf diffusivity and short residence time of the melt in the source. Moreover, Hf homogenization is not achieved during far-field melt transport suggesting that the magma emplaces prior to any significant dissolution of inherited zircon.

[1] Villaros *et al* (2012) *Contrib Mineral Petr* **163**, 243-257.

Magnesium isotope composition of globally distributed modern brachiopods: Implications for paleo-seawater $\delta^{26}\text{Mg}$ reconstructions

JURAJ FARKAŠ^{1*}, UWE BRAND², ADAM TOMAŠOVÝCH³, KAREM AZMY⁴, JAN FIETZKE⁵ AND ANTON EISENHAUER⁵

¹Czech Geological Survey, Prague, Czech Republic, (juraj.farkas@geology.cz) (* presenting author)

²Dept. Earth Sci., Brock University, St. Catharines, Canada

³Geol. Institute, Slovak Acad. of Sci., Bratislava, Slovakia

⁴Dept. Earth Sci., Memorial University, St. John's, Canada

⁵GEOMAR | Helmholtz Centre for Ocean Research, Kiel, Germany

Magnesium isotope composition ($\delta^{26}\text{Mg}$) of marine carbonates can potentially be used as a tracer for constraining past changes in the oceanic Mg cycle. Shells of articulated brachiopods composed of diagenetically resistant calcite [1] have proven to be particularly valuable archives of isotope composition and certain physicochemical properties of past ocean water [2]. Here we present $\delta^{26}\text{Mg}$ (DSM3) and $\delta^{18}\text{O}$ (PDB) variations, and trace element (Sr/Ca, Mg/Ca) contents analysed in six different species of modern brachiopods (*T. transversa*, *T. sanguinea*, *T. septentrionalis*, *T. congregata*, *L. uva*, *M. pisum*). The sampling locations of the above species cover a global scale, thus representing major water bodies, including: North Pacific (Palau, San Juan Island), South Pacific (Doubtful Sound), North Atlantic (Bay of Fundy, Bonne Bay), and Southern Ocean (Antarctica, South Africa). Accordingly, the mean habitat temperatures (HT) of the studied shallow-water brachiopods cover a wide range from cold ($\sim 3^\circ\text{C}$, Signy Island, Antarctica), through intermediate (~ 8 to 15°C , Friday Harbour, Doubtful Sound) to warm tropical settings ($\sim 29^\circ\text{C}$, Koror, Palau). Our results indicate that samples, which plot on the 'Global Brachiopod Mg-Line' (defined by a shell MgCO_3 content relative to its HT [3]), show also a coupling between their $\delta^{26}\text{Mg}$ and $\delta^{18}\text{O}$ values ($R^2 = 0.93$; $p < 0.05$). Importantly, the overall temperature sensitivity of $\delta^{26}\text{Mg}$ in brachiopod calcite is weak ($\sim 0.01\%$ per 1°C), implying that it may be a suitable archive for paleo-seawater $\delta^{26}\text{Mg}$. Brachiopods that fall either below or above the *Global Mg-Line* yielded systematically lighter $\delta^{26}\text{Mg}$, and also elevated Sr/Ca ratios, suggesting that these were influenced by processes, such as anomalous precipitation rates (changing growth patterns) or environmental stressors.

[1] Brand and Veizer (1980) *J. Sed. Petrol.* **50**, 1219-1236. [2] Veizer *et al* (1999) *Chem. Geol.* **161**, 58-88. [3] Brand *et al* (submitted) *Chem. Geol.*

Is Late Cenozoic, post-subduction volcanism in the Sierra Nevada (California) a consequence of lithospheric downwelling?

G. LANG FARMER^{1*}

¹Department of Geological Sciences and CIRES, University of Colorado, Boulder, CO 80309 (*correspondence: farmer@colorado.edu)

Physical disaggregation of continental mantle lithosphere can trigger melting either in downgoing lithospheric material, upwelling sublithospheric mantle, or in newly exposed shallow lithosphere. A record of such disaggregation should therefore be decipherable from space-time-compositional patterns in any resulting volcanism. In practice, however, such an assessment is complex, as illustrated by Late Cenozoic volcanism with the Sierra Nevada of eastern California (U.S.). Here, geologic and geophysical observations are consistent with the Late Cenozoic, downward removal of continental margin arc lithosphere subsequent to the development of a slabless window beneath the region. In the southern Sierra Nevada, Late Cenozoic volcanism is entirely post-subduction (< 16 Ma), but only a distinctive, short-lived episode of mafic, ultrapotassic volcanism, low $\epsilon_{\text{Nd}}(\text{T})$ (~ -6 to -9) at 3.5 Ma can be convincingly linked to lithospheric removal. This link relies on chemical and isotopic data from lithospheric xenoliths entrained in older, Miocene volcanic rocks found in the same region [1]. The xenolith data suggest that only spinel peridotites embedded in shallowmost portions of Miocene mantle lithosphere had sufficiently low $\epsilon_{\text{Nd}}(\text{T})$ (~ -6 to -9) to have spawned the Pliocene volcanism. As a result, physical removal of the mantle lithosphere and exposure of this originally shallow lithosphere to supersolidus conditions is a plausible trigger mechanism for the 3.5 Ma volcanic event. In contrast, no equivalent, low $\epsilon_{\text{Nd}}(\text{T})$, ultrapotassic volcanism exists in the northern Sierra Nevada. A transition does occur in volcanic rock compositions at ~ 3 Ma, from continental arc volcanism to high HFSE and high LREE trachybasaltic andesites. Rather than being a result of lithospheric removal, this transition likely corresponds to the opening of a slab window beneath the northern Sierra Nevada and subsequent conductive heating of intact mantle lithosphere. These data illustrate that there are multiple trigger mechanisms for post-subduction magmatism along continental margins, not all of which require lithospheric downwelling or delamination.

[1] Ducea and Saleeby (1998), *Earth Planet. Sci. Letters* **156**, 101-116.

Application of multiple S-isotope studies to understanding early Earth environments and biology

JAMES FARQUHAR^{1*}, JOHN CLIFF²
AND AUBREY ZERKLE³

¹Department of Geology and ESSIC, University of Maryland, College Park, USA. (*corr: jfarquha@umd.edu)

²Centre for Microscopy and Microanalysis, University of Western Australia, Perth, WA 6009, Australia

³DEES, Univ. of St. Andrews, St. Andrews. KY16 9AL, UK.

The use of multiple sulfur isotopes to study biological signatures on the early earth has been a relatively recent development in geochemistry. This approach relies on the information about sulfur cycling that comes from determinations of $\delta^{34}\text{S}$, $\Delta^{33}\text{S}$, and $\Delta^{36}\text{S}$. During sulfate reduction, variations in $\delta^{34}\text{S}$ values arise because less energy is required to break sulfate bonds involving ^{32}S than to break bonds involving ^{34}S . Variations for $\Delta^{33}\text{S}$ and $\Delta^{36}\text{S}$ arise because of mixing and unmixing that occurs during metabolic processing by organisms such as dissimilatory sulfate reducers. On an early Earth, variations for $\Delta^{33}\text{S}$ and $\Delta^{36}\text{S}$ also were produced by mass independent processes. A key feature of measurements that include $\delta^{34}\text{S}$, $\Delta^{33}\text{S}$, and $\Delta^{36}\text{S}$ is the prospect of disentangling mass dependent biological processing from mass dependent and mass independent abiological processing.

Several approaches have been developed in the past few years to tackle the issue of biological signatures in the sulfur isotope record. These include the use of paired sulfate – sulfide evaluated using sulfur cycle models; the use of microanalytical data provided by SIMS and nanoSIMS measurements; the experimental study of isotope effects produced by pure and mixed cultures of Bacteria and Archaea; and novel approaches that tie variations in isotopic compositions to specific depositional settings.

Work to date has provided evidence for sulfate reducers in the Paleoproterozoic, and it is not inconceivable that evidence from more ancient rocks will be forthcoming in the future. Recent work has also suggested that sulfate reducers played an important role in the Neoproterozoic, and may have expressed large fractionations that were masked by the processes associated with pyrite formation. Evidence for sulfur metabolisms in addition to sulfate reduction have been proposed in the early Archean and Neoproterozoic. Work to understand, and disentangle, the role and importance of different types of sulfur metabolizing microbes on the early earth represents an important challenge that faces scientists today.

Experimental investigation of CO₂-water-rock interactions under simulated fresh-water aquifer conditions

S.M. FARQUHAR^{1*}, G.K.W. DAWSON¹, J.K. PEARCE^{1,2},
AND S.D. GOLDING¹

¹School of Earth Sciences, University of Queensland, QLD 4072, Australia (*correspondence: susan.farquhar@uqconnect.edu.au)

²Cooperative Research Center for Greenhouse Gas Technologies, Canberra, Australia

The geochemical effects of supercritical CO₂ (sc-CO₂) injection on a targeted fresh-water storage site [1] located in the Surat Basin, Queensland, Australia, were investigated using experimental reactions at simulated basin conditions. Samples from a potential reservoir, Precipice Sandstone, and from two overlying formations, Evergreen Formation and Hutton Sandstone, were mineralogically and petrographically characterised prior to submersion in purified water and exposure to sc-CO₂ at 12 MPa and 60 °C conditions for 16 days.

Fluids were sampled periodically and analysed for major and trace elements to deduce CO₂-water-rock interactions. These data were related to changes to pre-experiment sample mineralogy and texture, as observed using scanning electron microscopy with energy-dispersive spectrometry (SEM-EDS).

Incremental fluid concentrations show an initial increase in most major (e.g., Fe, Ca, Mn, Mg, Si) and trace (e.g., Sr, Ba, Zn) elements over time, indicating dissolution of minerals during reaction. Increasing dissolved Ca, Mn and Sr (\pm Mg, Fe) are partly attributed to the dissolution of carbonate minerals, with higher concentrations observed in carbonate-rich samples; extensive carbonate dissolution in calcite-cemented samples is also observed in SEM-EDS.

Relative concentrations of analytes for incremental samples from the Precipice Sandstone experiments are generally considerably lower than those from the overlying Evergreen Formation and Hutton Sandstone, excluding Al and Si, reflecting the relatively clean mineralogy of the Precipice Sandstone. Small decreases in concentrations of several major elements (e.g., Fe, Ca, Mn, Al, Na) within the Evergreen Formation and Hutton Sandstone effluents towards the end of the experiments suggest the onset of mineral precipitation, which is supported by equilibrium modelling of geochemical reactions using the Geochemist's Workbench.

[1] Farquhar, Dawson, Esterle & Golding (2013), *Australian Journal of Earth Sciences* **60**, 91–110.

Geochemical investigations of fjord sediments reveal Zr, Ni and Ca as NAO proxies in central Norway

JOHAN C. FAUST^{1,2*}, JOCHEN KNIES¹, KARL FABIAN¹,
ALBA N. RODRIGUEZ³, MICHAEL BLASCHEK⁴,
GESA MILZER⁵ AND JACQUES GIRAudeau⁵

¹Geological Survey of Norway, 7491 Trondheim, Norway,
(*correspondence: Johan.Faust@ngu.no)

²University of Tromsø, Department of Geology, 9011 Tromsø,
Norway

³Plymouth University, Plymouth, UK

⁴VU Amsterdam, Climate Change and Landscape Dynamics,
Amsterdam, Netherlands

⁵EPOC, University of Bordeaux - CNRS, Talence, France,

Sediments accumulating in fjords offer an excellent opportunity for studying land-ocean interactions and can provide high-resolution records of local responses to short-term variability in the Earth's climate. In order to increase the understanding of these records we previously investigated the inorganic/organic geochemistry of sixty surface sediment samples from the Trondheimsfjord in central Norway. By comparing our results with analyses of terrigenous sediments and bedrocks from the Trondheimsfjord drainage area we identified Zr/Al, Ni/Al and CaCO₃ as potential proxies for terrestrial input/river discharge.

Instrumental data reveal that the climate in central Norway is mainly driven by the North Atlantic current and the North Atlantic Oscillation (NAO). The aim of this study is to evaluate the applicability of Zr, Ni and Ca as proxies for changes in temperature, precipitation and NAO by comparing geochemical records with instrumental and modelling data of the last sixty years and apply these findings to Holocene sequences. For this purpose we analysed two multicores and three gravity cores from the Trondheimsfjord for their elemental composition, total organic carbon (C_{org}), nitrogen (N_{org}) and organic carbon stable isotopes (δ¹³C_{org}), grain size distribution and biomarkers. First results show that the instrumental and geochemical records coincide, confirming that Trondheimsfjord sediments provide an excellent geochemical record reflecting the intensity of river discharge and the impact of the NAO. Moreover, we found a continuous climate/weathering signal for at least the last 3000 years. Ongoing statistical verification of the connection between instrumental and sediment records will help to provide a high resolution record of Holocene climate variability in the Trondheimsfjord region.

Distribution of heavy metals and arsenic in soils of an abandoned lead mine (Central Portugal)

PAULO J.C. FAVAS^{1,4*}, JOÃO PRATAS^{2,4},
ROHAN D'SOUZA³, MAYANK VARUN³
AND MANOJ S. PAUL³

¹Department of Geology, University of Trás-os-Montes e Alto
Douro, 5001-801 Vila Real, Portugal; *
(correspondence: pjcf@utad.pt)

²Department of Earth Sciences, University of Coimbra, 3001-
401 Coimbra, Portugal

³Department of Botany, St. John's College, Agra 282 002,
India

⁴IMAR-CMA Marine and Environmental Research Centre,
University of Coimbra

The present study aims to assess contamination and distribution of heavy metals in soil around an abandoned Pb mine in Central Portugal (Barbadalhos mine also known as the Zorro mine). This mine was exploited for Pb by underground mining from 1887 till the 1940s. The mineralogy consists mainly of argentiferous galena and sphalerite (and chalcopyrite and arsenopyrite in small amounts). Samples were collected from two line transects. Line transect 1 is perpendicular to the mineralized veins. Line transect 2 is in nearby nonmineralized zone. Soil samples were collected at 20 m intervals along the line transects. Atomic absorption spectrophotometry was used after acid digestion to determine Fe, Mn, Cu, Zn, Pb, Ni, Co, Cr and Ag concentrations in the soils. To determine As content, a hydride generation system (HGS) linked to an atomic absorption device was used. Metal concentrations in soil ranged from (in mg/kg): 98-9330 (Pb), 110-517 (Zn), 7.1-50 (Co), 69-123 (Cr), 31-193 (Cu), 33400-98500 (Fe), 7.7-51 (Ni), 0.95-13 (Ag), 2.8-208 (As), and 71-2220 (Mn) along LT1; and 24-93 (Pb), 30-162 (Zn), 3.7-34 (Co), 61-196 (Cr), 21-46 (Cu), 24100-59400 (Fe), 17-87 (Ni), 0.71-1.9 (Ag), 4.3-12 (As), and 44-1800 (Mn) along LT2. Mean Pb and As concentrations were nearly 9 and 2 times the threshold for industrial soils suggested by Canadian Environmental Quality Guidelines. One way ANOVA indicated a statistically significant difference in mean content of Pb, Zn, Cu ($P < 0.001$) and Ag, As, Co, Fe and Mn ($P < 0.05$) in soil samples from the two transects. Similar distribution of Cr and Ni along the two transects indicates a non-localized distribution of the metals not limited to the mineralized veins of the region. This was confirmed by one way ANOVA where no significant difference ($P < 0.05$) was observed in mean Cr and Ni content of the soil samples.

Ion imaging of biogenic and abiogenic mineral surfaces

*MOSTAFA FAYEK¹

¹Dept. Geol. Sci., Univ. Manitoba, Winnipeg MB R3T 2N2

*(fayek@cc.umanitoba.ca)

Secondary Ion Mass Spectrometry (SIMS) is ideally suited for studies of elemental and isotopic gradients and the localization of isotopically labelled molecules. The Nano-scale SIMS (NanoSIMS) is the only technique available that can measure isotopic distributions with both high sensitivity (ppm) and high spatial resolution (i.e., 50-1000 nanometres), produce single cell images, and analyse a cell in three dimensions [1, 2]. The following two studies combine the unique capabilities of the NanoSIMS with advanced transmission electron microscopy (TEM) techniques to provide compositional and structural details of biogenic and abiogenic mineral surfaces at the nanoscale [3, 4].

Bio-precipitated minerals are typically at the nanometer scale, hydrous, and beam sensitive. We combined the nano-scale ion imaging capabilities of the NanoSIMS and advanced high-resolution (HR) TEM techniques to characterize the surfaces of *Geobacter sulfurreducens* and the bio-precipitated uranium phases, revealing the association between nutrient uptake and uranium mineral precipitation. Bio-sequestration of uranium is enhanced by addition of nutrients, and uranium is precipitated on the surface of the bacteria as nano-size crystals of uraninite (UO₂). Our results show that the biofilm shielded the UO₂ from re-oxidation and that bacteria can immobilize uranium for extended periods, even under relatively oxidizing subsurface conditions [3].

Nanoscale isotope and chemical images of grains of Amelia albite that were reacted with 2 m ¹⁸O-enriched solution of KCl show a correspondence between O-isotope exchange and K-Na exchange. The boundary between the core albite and the K-feldspar replacement is sharp and decorated with numerous pores. The distribution of Na and K, determined by electron probe microanalysis, is uniform within the core and rim and has an abrupt discontinuity at the interface. The NanoSIMS shows that the interface is also sharp in the distribution of ¹⁸O and ¹⁶O. The combined electron probe and NanoSIMS analyses indicate that both cation and isotopic exchange occurred during solution and re-precipitation of the feldspar.

Nano-scale ion imaging combined with HRTEM is a powerful technique for imaging mineral surfaces and interfaces, and tracking the uptake of radionuclides.

[1] Chandra, Smith & Morrison (2000) *Anal. Chem.* **72**, 104-114. [2] Tachikawa *et al* (2013) *GCA* 100, 11-23. [3] Fayek *et al* (2005) *Can. Min.* **43**, 1631-1641. [4] Labotka *et al* (2004) *Am. Min.* **89**, 1822-1825.

Gold associated with Neoproterozoic alkaline intrusion, Lac Bachelor, Abitibi, Canada

N. FAYOL^{1*}, M. JÉBRAK¹ AND L.B. HARRIS²

¹UQAM, Montréal, QC, H3C 3P8, Canada (*correspondence: noemiefayol@gmail.com)

²INRS-ETE, Québec, QC, G1K 9A9, Canada

Recent alkaline intrusion-related gold deposits have been recognized worldwide (e.g. Cripple Creek, Ladolam). Similar Neoproterozoic deposits are now recognized in the Canadian Superior Province but their metallogeny is still misunderstood; the Lac Bachelor gold deposit is a key example. It is located within the Desmaraisville basin, a "Timiskaming-type" basin in the Abitibi Greenstone Belt where it is hosted by a volcano-sedimentary assemblage, mafic and felsic intrusions, and associated with regional NE-SW oblique-slip faults.

Gold mineralization is located on the margin of the O'Brien stock, a polyphase alkaline quartz-syenite body which intrudes andesite and tuff. It displays porphyritic and equigranular textures. Injections of aplitic dykes occurred in late events. The O'Brien stock is mainly composed of Na- and K-feldspars, quartz, and mafic minerals. Purple fluorite is present, both disseminated in the syenite and in quartz-fluorite-pyrite veins that appears as comagmatic.

The Lac Bachelor gold deposit is characterized by several mineralized zones among which the Main zone (ZP) and the B zone (ZB) are the most economically important. A porphyry-style mineralization is present at the stock margin with quartz, quartz-magnetite, quartz-fluorite, and pyrite stockwork. Subhorizontal quartz-fluorite veins extend into the host rocks proximal to the stock. The Main and B zones are mainly localized in tuffs at the edges of the pluton and follow pre-existing discontinuities. Gold occurs in association with disseminated pyrite, magnetite, haematite, and rare chalcopyrite and pyrrhotite. In the ZP and lesser in the ZB, the magnetite is oxidized into haematite. Gold is present in highly altered (haematite-carbonate) zones associated with disseminated pyrite. The ZB is less haematized than the ZP, which is consistent with the timing: structural relations between these zones suggest that the ZB was formed first and the ZP occurred after.

The hydrothermal event is clearly related to the intrusion of the O'Brien syenite. However, fluids appear to have followed pre-existing discontinuities that focused mineralization. Results illustrate the complementary roles of magmatic and structural controls during the mineralization processes.

Hydrologic variability in coastal southwest USA

SARAH J FEAKINS*¹, MATTHEW E. KIRBY²,
MONG SIN WU¹ AND LINDA HEUSSER³

¹University of Southern California, Los Angeles, CA 90089, USA (*correspondence: feakins@usc.edu)

²California State University, Fullerton, Department of Geological Sciences, Fullerton, CA 92834 USA

³Lamont Doherty Earth Observatory, Columbia University, NY 10964, USA.

Understanding hydroclimate variability is a pressing need in the world's drylands, yet it is here that climate projections differ in the sign and magnitude of change in precipitation [1]. Within the southwest USA a different precipitation regime influences the California coast (winter only) and the interior (bimodal winter and summer). Here, we present multi-proxy reconstructions of the hydroclimate of the coastal zone. Sediments from Zaca Lake capture a sub-decadal history of wet-dry oscillations spanning 3ka whereas Lake Elsinore records climatic transitions from 33ka to Holocene.

Hydrogen isotopes in plant leaf waxes provide a record of the changing hydrological regime. Over the last 3ka, δD values of the C₂₈ *n*-alkanoic acid are highly variable across -175‰ to -125‰ in Zaca Lake. Grain size records multi-decadal variations in runoff and charcoal reveals the variable history of fire. At Lake Elsinore, a longer term shift from δD values of -190‰ at 19ka, to -120‰ at 9ka, is attributed to a shift from North Pacific to sub-tropical Pacific moisture sources, paralleling the radiative forcing trend out of the last glacial. Similarly, grain size records a long-term decrease in runoff and pollen record a transition from *Pinus* to *Quercus* indicating warming and drying. Southwest climate differs during the Younger Dryas; wet conditions found inland are linked to AMOC forcing [2]; here we show the coast remains dry.

[1] Solomon *et al.*, (2009) PNAS, **106**, 1704-1709. [2] Clark *et al.*, (2012) PNAS, **109**, E1134-1142.

Diamond dissolution in COH fluids

Y. FEDORTCHOUK

Dalhousie University, Halifax, B3H4R2, Canada
(correspondence: yana@dal.ca)

Morphology of surface features on natural kimberlite-borne diamonds indicates their interaction with fluid and greatly depends on the composition of this diamond-destructing fluid. H₂O:CO₂ ratio in the fluid dictates the degree of rounding, intensity of the pit development on {111} face, orientation and morphology of trigonal pits, and presence of other less common etch features (e.g. circular pits, hexagons). A number of different mechanisms have been proposed to explain the diversity of diamond resorption features. Application of experimental findings to natural diamonds demonstrated a relationship between diamond morphology and behavior of volatiles in kimberlite magma. However, absence of a model that relates diamond micro-morphology to the characteristics of the reacting fluid precludes more quantitative characterization of kimberlite volatile system using diamond micro-morphology. Toward this end, we conducted atomic force microscopy (AFM) study of diamond crystals from dissolution experiments with H₂O and CO₂-fluid and from natural kimberlites.

Diamond octahedra were etched in H₂O or CO₂ fluid at 1 GPa and temperature (T) = 1150-1350°C. AFM data collected in tapping and contact mode demonstrated that outside of few large etch pits (up to 2 μm depth) the roughness of the diamond surface is less than 400 nm in H₂O fluid and increases with T. In CO₂ fluid the roughness is between 600nm and 2 μm and is independent on T. Trigonal etch pits in H₂O fluid have constant diameter independent on the depth but increasing with T. In CO₂ runs trigonal pits show continuous sizes and positive correlation between the diameter and the depth. In H₂O fluid trigons are mostly flat-bottomed, whereas in CO₂ fluid they develop round bottom at higher T and more pointy-bottom at lower T. The general resorption morphology and presence of hexagonal pits in CO₂-bearing runs could be a result of the different dissolution rate in [111], [100], and [110] direction in fluids with various H₂O:CO₂ ratio. However, the more regular layer-by-layer resorption in H₂O fluid and irregular deeper material removal in CO₂ fluid may also indicate different mechanism of interaction of surface complexes formed in CO₂- and H₂O-dominated media and different rate of removal of 3- and 2-bonded atoms from diamond surface by these complexes. We conducted AFM measurements of trigonal pits on 22 micro-diamonds from four Canadian kimberlite pipes, which different geology indicates different behavior of volatiles. We use this data to examine magmatic fluid and the relative crystallization T.

Transport in active margins: Comparison of results from I^{129} and Be^{10} studies

UDO FEHN¹

¹Dept. Earth&Environmental Sciences, U. Rochester,
Rochester, NY, 14627 (udo.fehn@rochester.edu)

Active margins are the location of large-scale movement of elements and compounds between crust and mantle, including the potential for transport of marine sediments into subduction zones with subsequent release of elements from volcanoes. Two cosmogenic isotope systems have been applied for the investigation of this question: ^{10}Be (e.g. Morris *et al.*, 2002) and ^{129}I (e.g. Fehn, 2012). Although both of these isotopes have similar production modes, they differ considerably in half-lives (1.5 Ma for ^{10}Be ; 15.7 Ma for ^{129}I) and geochemical characteristics. Because Be is readily incorporated into mineral phases, ^{10}Be concentrations were determined in solid samples. Results demonstrate that in many cases marine sediments have been carried to the mobilization zone under the main arc, but that less than half of Be is transported back to the surface.

Because iodine is predominantly found in aquatic fluids, investigations were carried out on samples collected from crater lakes, fumaroles and geothermal sites at active volcanic centers. $^{129}I/I$ ratios in the fluids decrease with increasing slab age, an observation consistent with transport of iodine within marine sediments to the location of re-mobilization under the main volcanic arcs. Sediment-derived iodine was found in all study sites around the Pacific Rim, including some where ^{10}Be was absent. The observed $^{129}I/I$ ratios reflect values integrated over the full thickness of the marine sediments transported into the subduction trenches, suggesting that iodine is quantitatively released into the volcanic fluids.

Results from ^{10}Be and ^{129}I studies demonstrate transport of marine sediments into subduction zones and the subsequent integration into or release from active volcanoes. Elements such as Be are predominantly taken up by rock forming minerals and only a fraction of it reappears in surface deposits. The presence of iodine derived from marine sediments demonstrates that volatile elements are also transported to the mobilization zone, but that most of those elements are released back to the surface, preventing transport into the mantle.

[1] Morris J.D. *et al.*, *Rev. Min. Geochem.* **50**, 207, 2002 [2] Fehn U. *Ann. Rev. Earth Planet. Sci.*, **40**, 45, 2012

Tellurium stable isotope variations in chondrites

M.A. FEHR^{1*}, S.J. HAMMOND¹ AND I.J. PARKINSON^{1,2}

¹Department of Environment, Earth and Ecosystems, Centre for Earth, Planetary, Space & Astronomical Research (CEPSAR), The Open University, Walton Hall, Milton Keynes, MK7 6AA, UK (*correspondence: manuela.fehr@open.ac.uk)

²Bristol Isotope Group, School of Earth Sciences, University of Bristol, Wills Memorial Building, BS8 1RJ, UK

Different carbonaceous chondrite groups exhibit distinct stable isotope signatures for several elements including Cr, Cu and Zn reflecting mixing of two isotopically distinct reservoirs in the early solar nebula [1-2]. Furthermore, moderately and highly volatile elements such as Ag, Zn and Cd display relatively large stable isotope variations in unequilibrated ordinary chondrites that are indicative of evaporation/condensation processes due to parent body metamorphism [2-4]. Similar variations are expected also for other moderately and highly volatile elements as e.g. tellurium (Te). Previous studies revealed that Te was homogeneously distributed and well mixed in the early solar system resulting in no resolvable nucleosynthetic or radiogenic Te isotope variations in bulk meteorites [5,6]. The methods used in these studies were not specifically developed or optimized to yield precise and accurate Te stable isotope data, although the data hint at the presence of Te stable isotope variations in unequilibrated ordinary chondrites [6].

Improved methods to derive high precision and accurate Te stable isotope data were developed in this study. Tellurium isotope data are measured using a Neptune MC-ICPMS, whereas mass bias is corrected using a double spike technique. The reproducibility (2SD) of standards consuming 10 ng Te is 0.02 ‰/amu or better, whereas 2 separately processed powders of Allende reproduce to 0.03 ‰/amu. This is an improvement in precision of over 20 times compared to previous analyses that employed standard sample bracketing [6]. Initial data reveals resolvable Te stable isotope variations between different chondrite samples and an overall variability of about 1 ‰/amu. This study will obtain high precision Te stable isotope data for a comprehensive suite of ordinary, carbonaceous and enstatite chondrites.

[1] Moynier *et al.* (2011) *Science* **331**, 1417-1420. [2] Luck *et al.* (2005) *GCA*, **69**, 5351-5363. [3] Schönbachler *et al.* (2008) *GCA* **72**, 5330-5341. [4] Wombacher *et al.* (2008) *GCA* **72**, 646-667. [5] Fehr *et al.* (2004) *Int. J. Mass Spectrom.* **69**, 5099-5112. [6] Fehr *et al.* (2005) *GCA* **69**, 5099-5112.

Deep sediment melts contribute to Southwest Japan adakitic magmas

MAUREEN FEINEMAN¹, TAKUYA MORIGUTI², TETSUYA YOKOYAMA³ AND EIZO NAKAMURA²

¹The Pennsylvania State University, University Park, PA, USA

²Institute for Study of the Earth's Interior, Okayama University, Misasa, Japan

³Tokyo Institute of Technology, Tokyo, Japan

The Quaternary Southwest Japan Arc is a product of subduction of the hot, young Philippine Sea Plate beneath the Eurasian Continental Plate. The magmas erupted from the Southwest Japan Arc belong to a category of magmas commonly referred to as “adakites”. These magmas show trace element evidence for interaction with garnet at depth, and may be associated with partial melting of subducted altered oceanic crust. Also found throughout the southern Sea of Japan and scattered across Southwestern Japan, Korea, and China are alkali basalts with little apparent connection to the subduction zone. We have determined major element, trace element, and Sr, Nd, Pb, and U-Th isotopic compositions for a bimodal suite of lavas erupted at the Daisen volcanic field in the Southwest Japan Arc. These magmas consist of mildly alkaline basalts and a calcalkaline intermediate suite, separated by a ~10 wt. % silica gap. Our data suggest that the basalts are not parental to the intermediate magmas, and contain a small contribution of EM1-like mantle common in Sea of Japan alkali basalts but not apparent in the Daisen intermediate magmas. The intermediate magmas show trace element and isotopic evidence for interaction with garnet, but unlike other adakitic magmas, they show strong trace element and isotopic evidence for incorporation of significant (~25%) partial melt of subducted sediment. Recent studies [1] suggest that the ~350m sediment blanket subducted beneath Southwest Japan (Nankai) may become detached from the slab at temperatures between 650-675°C. The implications of sediment detachment are two-fold: 1) the removal of the insulating sedimentary cover would enable rapid heating of the basaltic slab surface, encouraging slab melting, and 2) the detached sediments may be relaminated at the base of the arc crust [2], where they could contribute partial melts to the slab-derived magma prior to eruption. The uncharacteristically high Al₂O₃ (17-18%) and low MgO (~2%) contents of the Daisen adakites are consistent with assimilation of significant sediment partial melts derived from depths >30km at the base of the arc crust.

[1] Behn *et al.*, *Nature Geosci.* 4 (2011) 641-646. [2] Hacker *et al.*, *Earth Planet. Sci. Lett.* 307 (2011) 501-516

Low-dimensional models of complex aerosol-cloud interactions

GRAHAM FEINGOLD^{1,*} AND ILAN KOREN²

¹NOAA Earth System Research Laboratory, Boulder, Colorado, USA (*correspondence: graham.feingold@noaa.gov)

²Weizmann Institute of Science, Rehovot, Israel, (ilan.koren@weizmann.ac.il)

The radiative forcing associated with aerosol-cloud interactions persists to be one of the largest unknowns of the climate system. To address this problem, both the aerosol and cloud communities have focused on process-level understanding of smaller components of the aerosol-cloud system. While this approach has yielded major advances in the understanding of both aerosol and cloud physics, we have been less successful at addressing the effects of aerosol perturbations on cloud systems, in which constant adjustments (feedbacks) can occur. The problem is exacerbated by the complexity of the adjustments, and the fact that they occur at a large range of spatiotemporal scales. Currently no climate model is able to address the full range of relevant scales and the processes are difficult to constrain with observations.

In this overview we will look at the aerosol-cloud system as a dynamical, self-adjusting entity and attempt to address the question of the resilience of the system to aerosol perturbation. To do so we will use a combination of observations, detailed process-modeling, and low-dimensional models that capture the essence of the system [1]. We will give examples of cloud systems that are relatively robust to aerosol perturbations, and contrast this with cases where the aerosol has locally strong effects, often through leveraging of mesoscale organization. We will highlight the important role that the aerosol plays in sustaining clouds in the very clean marine boundary layer. Finally, we will consider the possibility that aerosol-cloud interactions might be amenable to parameterization in terms of their system-wide behaviour. This may present a fruitful alternative to the current bottom-up approach to parameterization.

[1] Koren & Feingold (2011), The aerosol-cloud-precipitation system as a predator-prey problem. *Proc. Nat. Acad. Sci.*, 10.1073/pnas.1101777108.

Gasanalysis at a geothermal facility: On-line monitoring above ground and measurements in the borehole

ELVIRA FELDBUSCH^{1*}, THOMAS WIERSBERG¹,
MARTIN ZIMMER¹, HENNING FRANKE¹
AND SIMONA REGENSPURG¹

¹Helmholtz Centre Potsdam, **GFZ German Research Centre
for Geosciences, Potsdam, Germany.**

elkin@gfzpotsdam.de (* presenting author)

The formation fluid from Permian (Rotliegend) vulcanite and sandstone layers of the geothermal in-situ laboratory in Groß Schönebeck (North German Basin) contains a high volume of dissolved gases (volume ratio of liquid : gas is about 1:1 and increases up to 1 : 1.6 at reservoir conditions). It's mainly composed of nitrogen (N₂; 84-90 vol-%) and methane (CH₄; 10-16 vol-%) with minor concentrations of CO₂, H₂, He, Ethane, Kr, Propane, *n*-Buthane and *i*-Buthane. The fluid is degassed above ground and the gas composition was monitored on-line at the degasser during several circulation tests at the facility. The measurements indicated relatively constant values of gas composition over the whole production time.

Additionally, several deep fluid samples have been collected in the production well at various depths (1700m, 2200m, 4200m) to analyze changes in liquid : gas ratio and in chemical composition of formation gas in dependence of the fluid depth. The collected results show, that the beginning of degassing takes place at about 2200 m depth.

However, some samples at 4200 m appear to be above gas saturation (calculated for a gas mixture with 85 % N₂ and 15 % CH₄ in 5 M NaCl). Thus the presence of free gas in the reservoir seems likely. The impact of free gas on plant operation is still under investigation.

Noble gas constraints on reduced deep subsurface fluids

J. FELLOWES* AND C.J. BALLENTINE

SEAES, University of Manchester, M13 9PL, UK

(*correspondence: jonathan.fellowes@manchester.ac.uk)

The noble gases are conservative tracers of fluid interactions over geological time scales. By applying high precision stable isotope noble gas multi-collector mass spectrometry to deep subsurface free fracture fluids and fluid inclusions, it is possible to discern the origin (e.g. atmospheric, crustal or mantle), age and interactions of these fluids. Two distinct end-member fluids have been found in the deep Precambrian continental subsurface: (i) palaeometeoric water that falls along the global meteoric water line (GMWL) and contains atmospheric noble gas signatures and (ii) highly saline hydrothermal fluids that lie above the GMWL and contain abiogenic hydrocarbons, significant radiogenic noble gas input and fluid components billions of years old [1].

Previous noble gas studies have highlighted disparities between the neon component of free fracture fluids and fluid inclusions [2] and have used high precision heavy noble gas analysis to study free fracture fluids [3].

For this study, gas, water and rock samples have been collected from exploratory boreholes in deep mines within the Precambrian Witwatersrand basin, South Africa and Abitibi greenstone belt, Canada. By combining noble gas mass spectrometry with traditional stable isotope techniques, we aim to fully characterize these samples to relate the free fracture fluid phase with fluids trapped within hydrocarbon-rich quartz-hosted inclusions to provide constraints on the rate of abiogenic gas formation, the extent of the free fracture fluid networks and the degree of communication between deep abiogenic reduced carbon sources and the biosphere.

Here we report on our progress in the development of a sample handling and processing system that will enable us to analyze hydrocarbon-rich free fracture fluids and fluid inclusions using high precision multi-collector noble gas mass spectrometry, a key advance in the application of noble gases to crustal fluid systems.

[1] Onstott *et al* (2006) *Geomicrobiol. J.* **23**(6), 369-4143 [2] Lippmann-Pipke *et al.* (2011) *Chem. Geol.* **283**, 287-296 [3] Holland *et al* (2013) *Nature* In Press

First-principles investigations of equilibrium calcium isotope fractionation between clinopyroxene and orthopyroxene

C.-Q. FENG¹, T. QIN¹, S.-C. HUANG², Z.-Q. WU¹
AND F. HUANG¹

¹School of Earth and Space Sciences, University of Science and Technology of China, Hefei, Anhui 230026, China (fcq007@mail.ustc.edu.cn, tian91@mail.ustc.edu.cn, wuzq10@ustc.edu.cn, fhuang@ustc.edu.cn)

²Department of Earth and Planet Sciences, Harvard University, 20 Oxford St., Cambridge, MA 02138, USA (huang17@fas.harvard.edu)

Equilibrium calcium isotope fractionations between clinopyroxene and orthopyroxene, the two major Ca-bearing minerals in the upper mantle, are calculated with density functional perturbation theory (DFPT). The results suggest that orthopyroxene has higher ⁴⁴Ca/⁴⁰Ca ratios than clinopyroxene due to smaller coordination numbers (CN) of Ca in orthopyroxene than that in clinopyroxene (6 vs. 8). We further find that Ca concentration of orthopyroxene significantly influences $\Delta^{44/40}\text{Ca}_{\text{opx-cpx}}$ especially when Ca/Mg in orthopyroxene is below 1:15. Our results successfully explain the observations of variable Ca isotopic fractionation between coexisting orthopyroxene and clinopyroxene from Kilbourne Hole and San Carlos mantle peridotites, i.e., $\Delta^{44/40}\text{Ca}_{\text{opx-cpx}}$ increasing from 0.36‰ to 0.75‰ with $[\text{CaO}]_{\text{opx}}$ decreasing from 1.03wt.% to 0.75wt.% (Huang *et al.*, 2010). This reveals that crystalline environment such as the average Ca-O bond length parameter may be controlled by Ca content in orthopyroxene when Ca is a minor element. Our calculations also suggest that, although $\delta^{44}\text{Ca}$ of orthopyroxene may increase dramatically with decreasing CaO content, the average Ca isotope composition of the upper mantle is relatively constant because $[\text{CaO}]_{\text{opx}}$ is much higher than $[\text{CaO}]_{\text{cpx}}$. Furthermore, if Ca content and Ca isotope compositions of clinopyroxene and orthopyroxene are known, Ca isotopic fractionation between clinopyroxene and orthopyroxene can be used as a potential two-pyroxene Ca isotope thermometry.

[1] Huang S. *et al.* (2010), *EPSL* **292**: 337-344.

Evaluating the sulfur cycles in the early Cambrian ocean: An example from the Yanjiahe Formation, Yangtze Gorges area, South China

LIAN-JUN FENG¹

¹ Institute of Geology and Geophysics, Chinese Academy of Sciences, Beijing 100029, China, (feng.lian.jun@gmail.com)

The Yanjiahe Formation represents the earliest beginning of the Cambrian period in the Yangtze Gorges area, South China. In this study, we first report the sulfur isotope compositions of chromium-reducible sulfur ($\delta^{34}\text{S}_{\text{CRS}}$) and carbonate-associated sulfate ($\delta^{34}\text{S}_{\text{CAS}}$) from the Yanjiahe Formation. The difference between $\delta^{34}\text{S}_{\text{CAS}}$ and $\delta^{34}\text{S}_{\text{CRS}}$ from the Yanjiahe Formation is similar to that from the other basins worldwide (less than 30 per mil), reinforcing low marine sulfate concentrations across the Ediacaran-Cambrian boundary and into the Cambrian [1].

The Yanjiahe Formation has large-magnitude $\delta^{34}\text{S}_{\text{CRS}}$ ratios, ranging from 3.3 to 26.1 per mil, similar to the other basins worldwide. However, the sulfur isotope record in pyrite from the upper part (organic-rich limestone) shows more positive ratios than that from the lower part (organic-lean dolomite), probably reflecting local influences.

[1] Loyd, S.J., *et al Earth and Planetary Science Letters*, 2012. **339**: p. 79-94.

Observations of atmospheric Hg species and depositions in remote areas of China

XINBIN FENG¹, XUEWU FU¹ AND HUI ZHANG^{1,2}

¹State Key Laboratory of Environmental Geochemistry, Institute of Geochemistry, Chinese Academy of Sciences, Guiyang 550002, China

²University of Chinese Academy of Sciences, Beijing 100049, China

From September 2007, we conducted continuous measurements of speciated atmospheric mercury (Hg) and atmospheric mercury depositions at five remote sites in China. Four of these sites were involved in the Global Mercury Observation System (GMOS) as ground-based stations. These stations were located in the northwest, southwest, northeast, and east part of China, respectively, which represent the regional atmospheric Hg budgets in different areas of China. Standard Operating Procedures (SOPs) and QA/QC protocols were implemented at all the sampling sites. Data quality of atmospheric TGM concentration was controlled via periodic internal recalibration with a 25 h interval, and the emission rate of internal permeation source was calibrated every 4 months.

Our measurement data showed that the mean total gaseous mercury (TGM) concentrations were in the range of 1.60 – 2.88 ng m⁻³, with relatively higher levels observed at sites in Eastern China and Southwestern China and lower levels at sites in Northeastern and Northwestern China. Generally, TGM concentrations at most remote sites of China were higher than those reported from background sites in North America and Europe, and this is corresponding very well with the Chinese great anthropogenic Hg emissions. However, at a remote site in Northeastern China, the mean value of TGM concentrations is somewhat lower than the values of 1.7 ng m⁻³ observed in Europe and North America. Gaseous oxidized mercury (GOM) and particulate bounded mercury (PBM) were in the ranges of 3.2 – 7.4 pg m⁻³ and 19.4 – 43.5 pg m⁻³, respectively. The preliminary result on precipitation showed mean precipitation THg concentrations were in the range of 2.7 – 18.0 ng L⁻¹.

These continuous observations also helps to gain a better insight to the effects of long-range atmospheric mercury transport on TGM variations in ambient air. We showed that Northwestern India was an important source region of Northeastern Qinghai-Tibetan Plateau, indicating this area might also have relatively higher anthropogenic Hg emissions.

Sulfur runs through it: A celebration of Bo Barker Jørgensen's science and a multi-faceted element

T. G. FERDELMAN¹

¹Max Planck Institute for Marine Microbiology, Bremen, Germany; (tferdelm@mpi-bremen.de)

Behind almost every environmentally important redox transformation there lurks a sulfur transformation of some type or another. Through patient observation and elegant experimentation Bo Barker Jørgensen has over the years continuously grappled with this ubiquitous, yet slippery, element. A series of seminal papers in the late seventies set the tone for decades of research in sulfur biogeochemistry, isotope geochemistry and microbial ecology. Employing the highly sensitive radio-label technique, Bo's observation that microbial sulfate reduction is a major process in a wide variety of marine sediments [1], and one that can be tracked into deeply buried sediments (the "deep biosphere"), has provided an important fundament for our understanding of the links between in the carbon, sulfur and oxygen cycles.

Bo's exploration of biotic and abiotic sulfur transformations via sulfur oxidation state intermediates has proved equally influential. Today's research on the microbial ecology in stratified water basins owe a significant debt to the methodological approaches and concepts laid out in a paper written together with G. Kuenen and Y. Cohen, where they examined the microbial cycling of sulfur intermediates in Solar Lake [2]. Delving further into the world of sulfur intermediates and microbial ecology revealed the importance of microbial sulfur disproportionation in sediments, and the fascinating links between the giant sulfur bacteria and other element cycles, e.g. oxygen, nitrogen and phosphorus.

These strands culminate in recent studies where Bo has shown that an active sulfur cycle, complete with sulfate reduction, oxidation and disproportionation pathways, functions in the deep methane-bearing zone of marine sediments [3]. This research continues to inspire research on the paradoxical and cryptic roles of sulfur intermediates, e.g. elemental sulfur and polysulfides [4, 5] in highly reducing sulfidic environments. Sulfur, it seems, is the element that greases the redox cycles in marine environments.

[1] Jørgensen (1992) *Nature* **296**, 643-645. [2] Jørgensen *et al* (1979) *Limnol. Oceanogr.* **24**, 799-822. [3] Holmkvist *et al* (2011) *Geochim. Cosmochim. Acta* **75**, 3581-3599. [4] Milucka *et al* (2012) *Nature* **491**, 541-546. [5] Lichtschlag *et al* (2013) *Geochim. Cosmochim. Acta* **105**, 130-145.

Waste Characterisation of a Uranium Conversion Facility

T. FERNANDES^{1,3}, L. DURO¹, T. SCHÄFER², P. MASQUÉ³,
A. DELOS⁴, J.S. FLINOIS⁵ AND G. VIDEAU⁵

¹Amphos 21, Barcelona, Spain

²Karlsruhe Institute of Technology (KIT) – Institute for Nuclear Waste Disposal (INE), Karlsruhe, Germany

³Departament de Física & Institut de Ciència i Tecnologia Ambientals. Universitat Autònoma de Barcelona, Bellaterra. Spain

⁴Arcadis, Villeurbanne, France

⁵AREVA, France

At the front end of the nuclear-fuel cycle, the process of conversion of uranium ore concentrate into uranium tetrafluoride generates a waste stream. Understanding the geochemistry of this waste is fundamental for risk assessment of the final disposal.

Here we present the work carried out to characterise uranium in the decanted waste of a uranium conversion facility.

The industrial site of interest is the first step in the treatment of uranium mining concentrate. The process waste, resulting from the conversion of yellowcake into uranium tetrafluoride (UF₄) has been managed in settling basins, which were built on the tailings of a former sulphur mine. The waste contains a variety of chemicals (nitrates, carbonates, fluorides and sulphates) and radioactive elements, of which uranium contributes with 30% of the total alpha activity. The porewaters are characterised by high ionic strength, of up to 2M.

The work comprised static (batch-type) and dynamic (column) experiments of disturbed and undisturbed material obtained from the site to investigate the release of uranium. The chemical form of the uranium was also studied. Thermodynamical modelling was carried out in parallel to the laboratory work.

Static and dynamic experiments show that the release of uranium from the waste is kinetically controlled. Source term characterisation suggests U is present in different degrees of crystallinity. Although the solubility-limiting mineral phase has not been identified, it is likely to be either a U-Si phase or a phase similar to meta-schoepite. An important pH buffer effect from calcite in the waste was observed.

Calibration of the Siderite CO₂ ‘Clumped’ Isotope Paleothermometer

ALVARO FERNANDEZ¹, JIANWU TANG²
AND BRAD ROSENHEIM³

¹Department of Earth & Environmental Sciences, Tulane University, New Orleans, Louisiana 70118-5698, U.S.A., (afernan4@tulane.edu)

²Department of Earth & Environmental Sciences, Tulane University, New Orleans, Louisiana 70118-5698, U.S.A., (jtang@tulane.edu)

³Department of Earth & Environmental Sciences, Tulane University, New Orleans, Louisiana 70118-5698, U.S.A., (brosenhe@tulane.edu)

Siderite (FeCO₃) is commonly found in lake sediments, paleosol profiles and modern soils. Its presence in the geologic record has been shown to provide a useful archive of paleoclimate variables in environments that are generally exclusive of calcite (e.g. Sheldon and Tabor 2009). Clumped isotope measurements can be used to exploit the paleoclimatic potential of this archive; however, the applicability of this method is held back by the lack of clumped isotope calibrations of mineralogies other than calcite and aragonite. Here we present an inorganic calibration of siderites grown in the laboratory between 22-50° C. Synthetic siderites were precipitated by slow titration (0.15 ml/min) of a sodium bicarbonate solution with an anoxic iron (II) chloride solution followed by active degassing of CO₂ with N₂. We also report measurements of natural siderites collected from Holocene aged sediments of the Mississippi River Delta. We find no difference in the Δ₄₇ vs. temperature relationship between synthetic calcites (also measured in our laboratory) and siderites. Our results suggest that the model of Guo *et al* [1] may not accurately predict the difference in acid fractionations between the different carbonate minerals, and instead imply that a single clumped isotope calibration is appropriate for samples of different mineralogies.

[1] Guo *et al*, (2006) *GCA* **73**, 7203-7225

Priming effect and isotope ^{13}C dynamics at natural abundance during the biodegradation of lignin in a soil environment

I. FERNANDEZ*

Departamento de Bioquímica del Suelo, Instituto de Investigaciones Agrobiológicas de Galicia, IIAG-CSIC, Santiago de Compostela, Spain. *correspondence: (ifernandez@iiag.csic.es)

For the progress of isotope-based studies of decaying debris in soil profiles, factors that affect isotope ^{13}C dynamics of plant-derived biopolymers during decomposition need to be analysed. Many applied biogeochemical investigations are paying attention to isotope-ratio mass spectrometry, although for obtaining advanced accuracy when using these techniques, particularly for soil organic matter (SOM) studies at natural abundance levels, the appraisal of possible isotopic fractionation occurring during different stages of plant decomposition is essential. New insights into possible fractionation processes occurring during decomposition of a highly resistant plant component such as lignin (which remains during the last stages of vegetal decomposition) would have some important implications for assessing long-term SOM quality. Despite the direct implications for multitude of research lines, C isotopic dynamics during biological transformations of major structural biopolymers remains mostly unexplored and knowledge of the factors affecting the ^{13}C SOM fingerprint are scarce. Thus, this research evaluates the isotopic ^{13}C discrimination during the biodegradation of lignin to obtain more reliable estimates of the contribution of this highly resistant plant component to SOM buildup, as well as the influence of soil environment that may further exacerbate microbial discriminatory actions. Changes in ^{13}C composition during aerobic decomposition of the following substrates: a) hydrolytic lignin, b) soil, and c) soil+lignin mixture, were monitored over a 10 months incubation period. The results indicate that SOM decomposed faster than pure lignin. Also, soil+lignin mixture showed a synergic degradative behaviour with a greater mineralization rate than adding together soil and lignin individual rates, suggesting that priming effects can be produced during in-soil biodegradation of lignin. Isotopic fingerprint of the CO_2 released from lignin during biodegradation showed a lower ^{13}C concentration than the initial substrate and consequently, with ongoing decomposition, the solid residue became progressively ^{13}C -enriched.

Lithosphere-asthenosphere interactions (Middle-Atlas (Morocco): Geochemical highlights

L. FERNANDEZ¹, D. BOSCH¹, H. ELMESSBAHI², J.L. BODINIER¹, J.M. DAUTRIA¹ AND P. VERDOUX³

¹ Géosciences Montpellier, Montpellier France.

(laure.fernandez@gm.univ-montp2.fr)

² Université Moulay Ismail, Meknès, Maroc.

³ Université de Nîmes ,30035 Nîmes Cedex 1

The Neogene-Quaternary Middle Atlas province is the largest and youngest volcanic field of Morocco, bringing up a large variety of mantle xenoliths. The eighteen xenoliths are mainly lherzolites, but also include harzburgite, wherlite and pyroxenite. A major, trace elements & Sr-Nd-Pb-Hf isotopes study was conducted on CPX and host-rocks (WR) coupled petrographic constraints. Lherzolites show flat REE patterns with variable enrichment in LREE ie. various degrees of metasomatism. Harzburgites present a significant MREE enrichment. Sr isotopes of both WR and CPX show low ratios and define a limited range of variation ($0.7023 < ^{87}\text{Sr}/^{86}\text{Sr} < 0.7035$). Reported on the Nd-Sr diagram, they define a field extending between the DMM and HIMU compositions. Pb isotopic ratios are high and range, for $^{208}\text{Pb}/^{204}\text{Pb}$, between 38.87 and 40.54, for $^{207}\text{Pb}/^{204}\text{Pb}$ from 15.59 to 15.64, and for $^{206}\text{Pb}/^{204}\text{Pb}$ from 19.08 to 20.29. Two Sm/Nd internal isochrons have been calculated for two different volcanic sites and yield Pan-African and Alpine indicative ages. Together, these constraints allow us to propose that Middle-Atlas mantle experienced several lithosphere asthenosphere interaction processes. Such an HIMU signature is common in the European subcontinental mantle sampled by Cenozoic volcanism. At last, this study demonstrates that even in geodynamical complex zones experiencing various thinning episodes, preserved old lithospheric mantle can be present in continental lithosphere.

Thermal ageing of sepiolite/ polyamide66 nanocomposites

C. FERNÁNDEZ-BARRANCO¹, A. YEBRA-RODRÍGUEZ^{1*},
M. D. LA RUBIA-GARCÍA², A. B. RODRÍGUEZ-NAVARRO
AND J. JIMÉNEZ-MILLÁN¹

¹Department of Geology and CEACTierra, Associated Unit IACT (CSIC-UGR), Faculty of Experimental Sciences, University of Jaén, Campus Las Lagunillas s/n, 23071 Jaén, Spain (cfernand@ujaen.es; *correspondence: ayebra@ujaen.es; jmillan@ujaen.es)

²Department of Chemical, Environmental and Materials Engineering, EPS, University of Jaén, Campus Las Lagunillas s/n, 23071 Jaén, Spain (mdrubia@ujaen.es)

³Department of Mineralogy and Petrology, Faculty of Sciences, Campus Fuentenueva s/n, 18071 Granada, Spain (anava@ugr.es)

Clay/polymer nanocomposites are hybrid materials in which the nanoclay is exfoliated in the polymer matrix providing remarkable physical properties suitable for sophisticated industrial applications [1, 2]. The enhancement of the technical properties has been related to the crystallographic arrangement between the clay minerals and the polymer matrix [3]. Nanocomposites have been used commercially since Toyota first auto parts in the late 1980s. However, further effort has to be done to understand the long-term thermal stability of these materials. The aim of this work is to study the influence of the temperature on the stability (and thus the technical properties) of injection molded sepiolite/polyamide66 nanocomposites. For that purpose pure polyamide66 (PA66-S-0 samples) and sepiolite/polyamide66 nanocomposites with 5 wt.% clay loading (PA66-S-5 samples) were manufactured and injected (BABYPLAST 6/10, CRONOPLAST) to simulate industrial processing. Thermal ageing was carried out at 110 °C and 150 °C during 7, 14, 21, 28 and 35 days. Thermogravimetric analyses (TG Mettler Toledo TS 0801R0) were carried out to determine the thermal stability of the materials. Crystallinity index (W_c) was calculated with the help of Differential Scanning Calorimetry (DSC 822e, Mettler Toledo). Infrared spectra (FT-IR Bruker Tensor 27) was used to obtain the carbonyl index. The results indicate that the mass loss is not affected by the ageing. However, in PA-S-5 samples W_c decreases with the ageing and carbonyl index is higher than in pure polyamide66, thus indicating further degradation.

[1] Kojima *et al* (1993) *Mater Res* **8**, 1185-1189. [2] Wang *et al* (2004) *Appl Clay Sci* **25**, 49-55. [3] Yebra-Rodríguez *et al* (2009) *Mater Lett* **63**, 1159-1161.

Pressure-induced polyamorphism in Amorphous Calcium Carbonate: Insights into biomineral polymorph selection mechanisms

A. FERNANDEZ-MARTINEZ^{1,2,*}, B. KALKAN³,
S. M. CLARK^{3,4} AND G. A. WAYCHUNAS²

¹ISTerre, CNRS & Univ. Grenoble I, Grenoble, France.

²Earth Sciences Division, LBNL, Berkeley, USA.

³Advanced Light Source, LBNL, Berkeley, USA.

⁴Department of Earth and Planetary Sciences, Macquarie University, NSW, Australia.

* (Alex.Fernandez-Martinez@ujf-grenoble.fr)

Amorphous calcium carbonate (ACC, $\text{CaCO}_3 \cdot \text{H}_2\text{O}$) is commonly found in the earliest stages of biomineral development and as one of the metastable phases formed during the inorganic precipitation of calcium carbonate crystalline polymorphs. Recently, the existence of different amorphous polymorphs of ACC—proto-vaterite and proto-calcite—that act as precursors of the crystalline polymorphs has been suggested [1]. It has also been shown that the presence of Mg^{2+} in ACC induces an aragonite-like local order around the Ca^{2+} ions [2]. Here we show using high-pressure high-energy x-ray diffraction experiments combined with reverse Monte-Carlo modeling that ACC undergoes a reversible structural transition at ~ 9.8 GPa adopting an aragonite-like local order when its molar volume is decreased. This has been confirmed by high-pressure Raman experiments that show a discontinuous behavior of the carbonate stretching and in-plane bending modes at ~ 10 GPa. This finding could be suggesting that cationic substitutions of Ca^{2+} by smaller ions, such as Mg^{2+} , control ACC polyamorphism by reducing the molar volume of the amorphous phase. The fact that the structure is hydrated and that no signs of dehydration are found throughout the compression suggests that water is a key element in the reversibility of the transition. To our knowledge, this is the first reversible amorphous-amorphous phase transition found for an amorphous ionic system. High-pressure x-ray absorption experiments have also been performed to study the evolution of the density under pressure, allowing the first determination of the bulk modulus ($K' = 27.2 \pm 1.4$ GPa) and the density of ACC (2.18 g/cm^3).

[1] Lam, Charnock, Lennie & Meldrum. (2007) *Cryst. Eng. Comm.* **9**, 1226-1236. [2] Gebauer, Gunawidjaja, Ko *et al* (2010) *Angew. Chem. Int. Ed.* **49**, 1-4.

Microstructures and geochemistry in the subcontinental lithospheric mantle of NE Spain

M. FERNÁNDEZ-ROIG¹, G. GALÁN^{1*}, V. OLIVERAS¹, C. PIN², M. GRÉGOIRE³ AND J-L. DEVIDAL²

¹Departament de Geologia, Universitat Autònoma de Barcelona, Edifici C (sur), 08193 Bellaterra, Barcelona, Spain (*correspondence: merce.fernandez@uab.cat)

²Département de Géologie, CNRS & Université Blaise Pascal, 5 rue Kessler, F-63038 Clermont-Ferrand Cedex, France

³Université Toulouse III- Paul Sabatier, Laboratoire GET-UPS-CNRS-IRD, 14 avenue Eduard Belin, 31400 Toulouse, France

Mantle xenoliths in alkaline basaltic rocks of Neogene-Quaternary age from NE Spain are mainly anhydrous spinel lherzolites and harzburgites. New samples from different volcanoes indicate that lherzolites are more abundant than harzburgites and that they show frequent porphyroclastic and equigranular microstructures, along with protogranular varieties. Since deformation could enhance basaltic melt percolation favouring refertilization of harzburgites, the relationships between microstructures and chemistry of lherzolites are evaluated using major and trace element compositions of whole rocks and minerals.

Lherzolites show very fertile to more refractory compositions grading to harzburgites. The most fertile lherzolites are porphyroclastic, while the least fertile ones show protogranular microstructures. Based on their variable REE patterns, three main types of lherzolite clinopyroxene are distinguished: (1) highly LREE depleted ($La/Yb_N < 0.1$), (2) slightly LREE depleted ($La/Yb_N = 0.6-0.9$) and (3) LREE enriched ($La/Yb_N = 10.5-29$). These patterns are not related to any specific microstructure, although the most LREE enriched clinopyroxenes are from porphyroclastic lherzolites. Clinopyroxene from harzburgites is always enriched in LREE and MREE ($La/Yb_N = 5.6-23$, $Nd/Yb_N = 5.2-18$).

These data indicate that there is no clear relationship between deformation and lherzolite compositions. Some lherzolites could have been formed by percolation of relatively depleted basaltic melts through harzburgites, but both peridotites were affected by a subsequent alkaline metasomatic component. The most depleted lherzolites would have escaped both refertilization process and the later alkaline metasomatism.

Quantum-mechanical calculations on uranium (co)adsorption and reduction on iron and aluminum (oxyhydr)oxides

S. FERNANDO* AND U. BECKER

Earth and Environmental Sciences, University of Michigan, 2534 CC Little, Ann Arbor, MI 48109, USA (*correspondence: sfernan@umich.edu)

Minerals have been shown to promote redox reactions; *i.e.* nanoparticulate hematite catalyzes the reduction of U(VI) by Fe(II), which is otherwise kinetically inhibited in the absence of the mineral.¹ These surface-mediated redox processes are not well-understood though. The proximity effect may explain this phenomenon: a semiconducting mineral can act as a medium for electrons to be transported from one adsorbate to another one, both being spatially separated by a few Å.² To investigate the influence of semiconducting properties of iron minerals, coadsorption and reduction processes on these are compared to insulating aluminum isostructures. Aluminum (oxyhydr)oxides isostructures can be structural analogs for iron (oxyhydr)oxides while their different electronic properties enable observations of whether electron transfer is more prevalent in semiconducting than in insulating minerals.

The coadsorption of a uranyl complex and a reductant (*e.g.*, Fe(II) or H₂S) onto iron and aluminum (oxyhydr)oxide clusters was studied using quantum mechanical density functional theory (DFT) calculations. These simulations allow for visualization of electron density of states (DOS) and molecular orbitals (MOs) that are involved in electron transfer. Analyses of DOS and MOs for the (co)adsorption of uranyl on a goethite cluster (α -FeOOH, *Pnma*) show Fe *d*-orbitals overlap with U *f*-orbitals. Visualization of the MOs shows the participation of the iron atoms in the coadsorption of uranyl provide a continuous pathway where electrons from the reductant can be transferred through the goethite to the uranyl complex. Conversely, with the aluminum isostructure diasporite (α -AlOOH, *Pnma*), Al *p*-orbitals and U *f*-orbitals do not overlap, consistent with diasporite's insulating behavior.

Hirshfeld, Bader, and Mulliken analyses provide static charge and spin distributions; U(VI) atoms were shown to acquire spin density (<0.1 au) upon (co)adsorption to iron substrates. To better understand the influence of mineral substrates, the electron transfer rate is being quantified using Marcus Theory, showing if pronounced differences in the rate exist for semiconducting and insulating minerals.

[1] Liger *et al* (1999) *GCA* **63**, 2939-2955. [2] Becker *et al* (2001) *GCA* **65**, 2641-2649.

The browning phenomenon of medieval stained glass windows

J. FERRAND^{*1}, S. ROSSANO¹, C. LOISEL², N. TRCERA³,
F. FARGES⁴, E. VAN HULLEBUSCH¹, F. BOUSTA²
AND I. PALLOT-FROSSARD²

¹ Université Paris-Est, Laboratoire Géomatériaux et Environnement (EA 4508), UPEMLV, 77454 Marne-la-Vallée, France (*correspondence : ferrand@univ-mlv.fr)

²LRMH, 29 rue de Paris 77420 Champs sur Marne, France

³Synchrotron SOLEIL, l'Orme des Merisiers BP48 91192 Gif-sur-Yvette CEDEX, France

⁴LMCM, Musée National d'Histoire Naturelle, 61 rue Buffon 75005 Paris, France

In some ancient stained glass windows, the presence of manganese, coupled with the alteration by water and microorganisms [1], can induce a browning and, consequently, a loss of transparency in stained glass windows. Among the diverse alteration observed on stained glass windows, the browning phenomenon is still poorly documented and its occurrence among stained glass is not completely known.

Small pieces of ancient stained glass windows presenting brown zones at their surface have been collected mostly from French workshops. Samples have been characterized using optical microscopy, Scanning Electron Microscopy coupled with Energy Dispersive System (SEM-EDS) and microprobe analysis. In order to get insight into Mn environment in altered zones, chemical maps and X-ray Absorption Near Edge Structure (XANES) experiments have been performed at the Mn K-edge on the LUCIA beamline (Soleil synchrotron) [2] using a Si(311) double crystal monochromator and fluorescence detection mode. XANES spectra of reference compounds of inorganic and biogenic origin containing Mn under various oxidation states (II, III and IV) have been collected in order to be compared to the spectra of altered zones.

Chemical maps recorded on historical samples show that the Mn-rich alteration phases develop in Ca- and K-depleted zones. The XANES spectra of the alteration zones show significant differences with the Mn K-edge of fresh glass ensuring that a modification of the Mn environment and oxidation state occurred.

[1] G. Oriol *et al.*, (2007), *L'actualité Chimique* 312-313, 34-39. [2] A. M. Flank *et al.*, (2006), *Nuclear Instruments and Methods in Physics Research* 246, 269-274.

The Pedregal granitoid: a peculiar diatexitic rock (?) in a granite-migmatite complex

FERREIRA, J.A.¹, MARTINS, H.C.B.¹, RIBEIRO, M.A.¹,
AND FERREIRA, P.¹

¹Centro Geologia, Faculdade de Ciências, Univ. Porto R. Campo Alegre, 4160-007 Porto, Portugal (*correspondence hbrites@fc.up.pt)

The Pedregal granitoid, exposed of an area with of ca 3 km², is located in the Central Iberian Zone, northern Portugal and belongs to a synorogenic variscan granite-migmatite complex sub-concordant with the regional structures. It has an elongated shape with NW-SE trending sub-concordant with country rocks, and is a fine-grained biotite-rich granitoid with abundant small biotitic nodules (1 to 2 cm) which exhibit a internal foliation, and also metasedimentary xenoliths. The country rocks are represented by a metapelitic sequence of Edicarian age, the "Complexo Xisto-Grauváquico" (CXG).

The Pedregal granitoid is an homogeneous rock, without metamorphic differentiation, and has a isogranular texture without preferred orientation. Besides, the intergranular boundaries are consistent with a metamorphic texture marked by textural reequilibrium in solid state. Accordingly, this rock has peculiar structural/textural features, point out to a diatexitic character. The mineralogical composition of this granitoid is quartz + biotite + plagioclase + k-feldspar + zircon + apatite + titanite ± rutile, and secondary muscovite.

It is noteworthy the presence of pegmatites veins both in the granite and in the host rocks which are concordant with the main foliation of the CXG (NW-SE to NNW-SSE).

Geochemically is a peraluminous granitoid, with low SiO₂ (65 to 69 wt%) and very high Zr (390 to 435 ppm) contents. The Pedregal granitoid REE patterns show LREE enrichment much higher than the associated synorogenic granites and pegmatites (fig. 1).

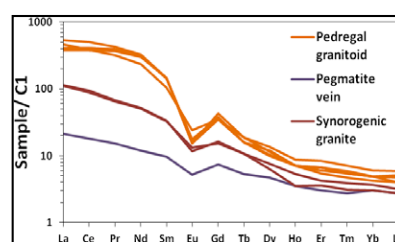


Figure 1 – REE normalized patterns.

This work has been supported by POCI 2010 (FCT-Portugal, COMPETE/FEDER).

Sequential extraction of arsenic in sediments of Paracatu, MG, Brazil

M. M. FERREIRA^{1*}, S. R. PATCHINEELAM¹,
Z. C. CASTILHOS² AND W. CALMANO³

- ¹ Environmental Geochemistry Department, Fluminense Federal University, Niteroi, RJ, Brazil (*correspondence: marcosferreira@id.uff.br)
² Center for Mineral Technology, Federal University of Rio de Janeiro, Rio de Janeiro, RJ, Brazil
³ University of Technology of Hamburg-Harburg, Hamburg, HH, Germany

Mining activity is responsible for the release of arsenic (As) for the environment, compromising the quality of soils, sediments and surface water [1]. However, the mobility and the bioavailability of As in the environment is influenced by the solid phase which it is associated. In this sense, the study evaluated samples river sediments next a great pit mining area, in the region of Paracatu city, Minas Gerais, SE Brazil, by sequential extraction method [2].

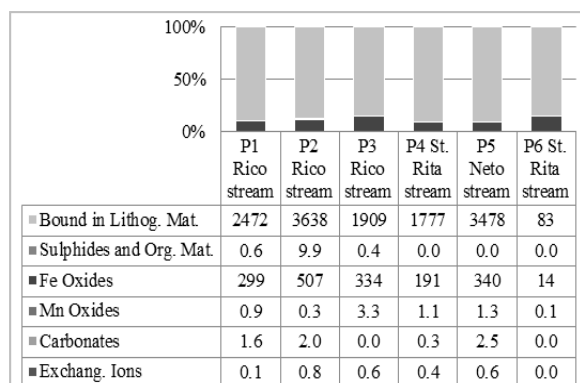


Figure 1: Arsenic speciation obtained by sequential extraction method (mg.kg⁻¹ dry weight).

Total concentrations of arsenic recorded are above of the brazilian values for quality of sediments [3, 4] and indicate a high contamination. However, this preliminary evaluation indicates the presence of As is in a form less available. For a conclusive evaluation, further studies on the mobility and bioavailability of As in the study area are needed.

- [1] Bidone *et al* (2001), *An. Acad. Bras. Cienc.*, **2**, 73. [2] Salomons & Förstner (1980) *Environ. Tech. Lett.* **1**:506–518. [3] Brasil (2004). (CONAMA). *Resol. n. 344. 25 de março de 2004*. [4] CETESB (2001). *Relatório técnico*. São Paulo, 247.

Oxygen isotope exchange (dis)equilibrium at the grain-size scale in metamorphic rocks

J.M. FERRY^{1*}, K. KITAJIMA² AND J.W. VALLEY²

- ¹Department of Earth and Planetary Sciences, Johns Hopkins University, Baltimore, MD 21218, USA (*correspondence: jferry@jhu.edu)
²WiscSIMS and Department of Geoscience, University of Wisconsin, Madison, WI 53706, USA (saburo@geology.wisc.edu, valley@geology.wisc.edu)

The approach to oxygen isotope equilibrium among minerals at the grain-size scale in metamorphic rocks was surveyed by analyzing 66 minerals (10 different: Cal, Dol, Qtz, Pl, Kfs, Grt, Ky, Di, Wo, Fo) in 20 samples (13 regional, 7 contact) using the CAMECA ims-1280 ion microprobe at the University of Wisconsin. Lithologies include marble, calc-silicate hornfels, pelite, psammite, and metamorphosed marl from California and New England (USA), Scotland, and the Swiss Alps. With few exceptions, 10-40 analyses were performed of each mineral with a 10 μm spot and an average standard deviation of 0.12‰ in silicates and 0.14‰ in carbonates. Generalizations for contact metamorphic rocks are: (1) They are distinctly less well equilibrated. Of 23 minerals analyzed, just 5 are statistically uniform in δ¹⁸O; only 1 of the 5 is a silicate (Kfs). (2) The range in δ¹⁸O measured for all grains of the same mineral in a sample is up to 10.7‰ in carbonates (Dol) and 7.4‰ in silicates (Fo). (3) Individual mineral grains of carbonate and silicate can vary in δ¹⁸O by up to 10.1‰ (Dol) and 3.1‰ (Fo). Inter- and intracrystalline variability in δ¹⁸O(Fo) scale with crystal number density and hence nucleation rate and overstepping of the Fo-forming reaction. (5) Grain-scale variability in δ¹⁸O obviates meaningful determination of oxygen isotope fractionation between most mineral pairs. Generalizations for regional metamorphic rocks are: (1) They are better but not fully equilibrated. Of 43 minerals analyzed, 17 are uniform in δ¹⁸O, including Ky and most Grt. (2) The largest range in δ¹⁸O for a given mineral in a sample is 1.5‰ (Di); the range for all but 2 analyzed minerals is ≤1.0‰. (3) The largest range in δ¹⁸O of a single mineral grain is 1.5‰ (Di); the range for all other analyzed single grains is <1.0‰. (4) Despite a measured range in δ¹⁸O(Qtz) of 9.8-21.0‰ in the 13 samples, all mineral pairs in a given sample show consistent oxygen isotope fractionation with δ¹⁸O decreasing in the same order as determined by laboratory experiment: Qtz>Cal>Kfs>Pl>Di>Ky>Grt.

Adsorption and surface complexation study of nucleotides on aluminum oxide surfaces

C. FEUILLIE^{1*}, D.A. SVERJENSKY² AND R.M. HAZEN¹

¹Geophysical Laboratory, Carnegie Institution, Washington D.C. 20015

(*correspondance : cfeuille@ciw.edu) (rhazen@ciw.edu)

²Dept. of Earth and Planetary Sciences, Johns Hopkins University, Baltimore M.D. 21218 (sver@jhu.edu)

In the context of the origin of Life, mineral surfaces might be important in the formation of the earliest biopolymers, such as nucleic acids, by trapping and concentrating their elementary bricks, as well as catalysing prebiotic reactions. The interaction of nucleotides with minerals has therefore been the focus of many studies, mainly regarding clay minerals [1] but also metal oxides such as rutile [2] or alumina [3].

Here we investigate the interactions between nucleotides, 5'-GMP, 5'-CMP, 5'-AMP and 5'-UMP, and α -alumina surfaces. We carried out batch adsorption experiments over a large range of pH, ionic strength and surface loading. Alumina adsorbs very high amounts of nucleotides $> 2 \mu\text{mol}/\text{m}^2$. We also performed surface complexation modeling in order to establish the speciation of the surface species, and the stoichiometry and the thermodynamic equilibrium constants for the adsorption of nucleotides on alumina surfaces. We used the extended triple-layer model (ETLM), that takes into account the electrical work linked to the desorption of chemisorbed water molecules during the formation of inner-sphere complexes. Results point to the formation of two surface species on the surface of corundum : a monodentate inner-sphere complex, and a bidentate outer-sphere complex, both involving interactions between the negatively charged phosphate group and the positively charged surface of alumina. This is in good agreement with previous computational results [4].

[1] Ferris (2005), *Reviews in mineralogy & geochemistry* 59, 187-210. [2] Cleaves, Jonsson C.M., Jonsson C.L., Sverjensky & Hazen (2010), *Astrobiology* 10, 311-323. [3] Arora & Kamaluddin (2009), *Astrobiology* 9, 165-171. [4] Fry, Kwon, Komarneni, Kubicki & Mueller (2006), *Langmuir* 22, 9281-9286

Sources and chemistry of nitrate in snow at Summit, Greenland

D.L. FIBIGER¹ M.G. HASTINGS² J.E. DIBB AND L.G. HUEY⁴

¹Brown University, Department of Chemistry, 324 Brook St., Providence, RI 02912, USA, dorothy_fibiger@brown.edu

²Brown University, Department of Geological Sciences/Environmental Change Initiative, Providence, RI, USA, meredith_hastings@brown.edu

³University of New Hampshire, Earth System Research Center, Insitute for the Study of the Earth, Ocean and Space, Durham, NH, USA, jack.dibb@unh.edu

⁴Georgia Institute of Technology, School of Earth and Atmospheric Sciences, Atlanta, GA, USA, (greg.huey@eas.gatech.edu)

Atmospheric nitrate deposition to snow surfaces results from reactions of NO_x (NO and NO_2) with oxidants, which produce HNO_3 that is taken up on the surface of particles or incorporated into precipitation. The concentration and isotopic composition of nitrate (NO_3^-) in ice cores have been studied with the aims of reconstructing past NO_x concentrations in the atmosphere, modeling past atmospheric oxidant concentrations and exploring variability in NO_x sources.

In a campaign consisting of two springtime (May-June) field seasons at Summit, Greenland [$72^\circ 35' \text{N}$, $38^\circ 25' \text{W}$], atmospheric and surface snow measurements were made to investigate NO_x sources contributing to the snow NO_3^- . Specifically, we look to use the nitrogen ($\delta^{15}\text{N}$) and oxygen isotopic composition of nitrate ($\delta^{18}\text{O}$, $\Delta^{17}\text{O}$) to track sources, chemistry and processing of the snow nitrate.

In surface snow collected several times each day during the springtime field seasons, $\Delta^{17}\text{O}-\text{NO}_3^-$ ranges from 5-35‰, $\delta^{18}\text{O}-\text{NO}_3^-$ from 35-85‰ vs. VSMOW, and $\delta^{15}\text{N}-\text{NO}_3^-$ from -7 to 13‰ vs. air N_2 . No relationship is found between the concentration of NO_3^- in snow and the isotopic composition of NO_3^- . A striking correlation between $\Delta^{17}\text{O}$ - and $\delta^{18}\text{O}-\text{NO}_3^-$ is found throughout both field seasons, with a slope of ~ 0.5 and $r^2 > 0.9$. This relationship appears to be a direct result of atmospheric production of NO_3^- , without significant post-depositional processing. Comparison of the $\delta^{15}\text{N}$ data with $\Delta^{17}\text{O}$ and $\delta^{18}\text{O}$ suggest a three-point mixing between three NO_3^- sources with the following isotopic compositions ($\delta^{15}\text{N}$, $\Delta^{17}\text{O}$, $\delta^{18}\text{O}$ (‰)): (1) -8, 27, 74 (2) 6, 40, 100 and (3) 16, 0, 23. While the same three NO_x pools appear to be influencing the deposited nitrate in 2010 and 2011, there appears to be different relative contributions in the two different years. The $\delta^{15}\text{N}$ of NO_x sources has not been well quantified, but by combining nitrogen and oxygen isotopic data, we are able to assign tentative identities to the three sources.

Petrology of column experiments on the interaction of young cement leachate with silicate host rock in a geological disposal facility

L. FIELD¹, A.E. MILODOWSKI¹, K. BATEMAN¹, L. JONES¹, G. PURSER¹, E.B.A. MOYCE², C.A. ROCHELLE¹ AND S. SHAW²

¹*British Geological Survey, Keyworth, Nottingham, NG12 5GG, UK*

²*The University of Leeds, Leeds, LS2 9JT, UK*

The current UK concept for the disposal of low- and intermediate-level radioactive wastes involves a mined geological disposal facility (GDF) located several hundreds of metres below the surface. The waste material will be encapsulated in a cementitious matrix within steel or concrete containers, and will be placed in disposal vaults backfilled with a cement-based material. After closure, the vaults will saturate with groundwater and become part of a modified regional groundwater flow system. Groundwater will equilibrate with the cement and produce an alkaline leachate. This will migrate from the repository into the surrounding rock and produce a 'chemically disturbed zone' (CDZ) with an elevated pH. Reactions will occur between the alkaline waters and the rock, potentially causing mineral dissolution and precipitation, which will modify the local geosphere prior to possible eventual radionuclide release. These changes in the CDZ will be critical controls on radionuclide behaviour and transport, and thus on the safety and environmental impact of a GDF. Consequently, it is desirable to understand these reactions and their impacts in terms of predicting localised changes to the transport properties of the host rock (porosity, permeability) and changes in groundwater flow, together with alteration of minerals and mineral surfaces that may have an effect on radionuclide migration and retardation. This work focuses on experiments designed to simulate the evolution of the alkaline plume from the GDF, to evaluate the spatial and temporal distribution of mineral alteration within the CDZ, and to quantify its impact on porosity and permeability.

The results presented here represent a summary of the mineralogical observations from Stage 1 of the column experiments, which investigate the interaction of a K-Ca-rich Young Cement Leachate (pH 13.1) with a "model" host rock. Significant interaction is observed within the reacted columns, with physical movement of fines, dissolution of silicate minerals, and the precipitation of secondary K-Al-bearing calcium silicate hydrate phases, all of which will impact on the transport properties of the host rock.

Syringe based flow injection MC-ICP-MS: Rotal sample consumption and rapid sample standard bracketing

M. PAUL FIELD, DAN WIEDERIN AND PAUL WATSON

Elemental Scientific, 1500 North 24th Street
Omaha, NE 68110

Sample-standard bracketing is a widely used standardization technique for the determination of precise isotope ratios by MC-ICPMS. The frequency of standard bracketing needed to compensate for mass bias drift increases with required precision and decreasing mass. Many isotope systems below 100 amu necessitate the analysis of a standard after every sample. This combined with low sample flow rates (typically $\leq 100\mu\text{L}/\text{min}$) requires that a significant amount of time is wasted during uptake and wash cycles. A newly designed, syringe driven, flow injection system precisely and accurately loads exact volumes into a loop and syringe injects them at any user defined flow rate (10-1000 $\mu\text{L}/\text{min}$). The valve on the flow injection system selects from two discrete parallel flow paths for standard and samples. This allows rapid switching between sample and standard solutions with minimal dead volume between the valve and the nebulizer. During the standard analysis the sample flow path is prepared by, 1) rapidly vacuum rinsing the uptake probe and sample loop, 2) resetting the sample syringe, and 3) accurately and precisely loading the exact sample volume into the loop. Alternatively, during sample analysis the standard side of the system is preparing for standard injection by resetting the standard syringe. The resulting benefits of flow injection MC-ICPMS are; 1) rapid wash out, 2) rapid uptake, 3) rapid sample-standard bracketing, 4) syringe controlled sample volumes, and 5) syringe controlled sample flow rates. This presentation will illustrate the utility flow injection and its benefits with respect to total sample consumption, absolute detection limits and sample standard bracketing.

Isotope imaging via LA-MC-ICPMS: A $\delta^{11}\text{B}$ study in marine carbonates

J. FIETZKE^{1*}, F. RAGAZZOLA², J. HALFAR³, H. DIETZE¹,
L.C. FOSTER², T.H. HANSTEEN¹, A. EISENHAEUER¹
AND R. S. STENECK⁴

¹GEOMAR Helmholtz Center for Ocean Research Kiel,
Germany (*correspondence: jfietzke@geomar.de)

²Dept. of Earth Sciences, Univ. of Bristol, UK

³Dept. of Earth Sciences, Univ. of Toronto, Canada

⁴School of Marine Sciences, Univ. of Maine, USA

Besides accuracy and precision of isotope ratio data spatial information can be crucial to allow for interpretation of natural samples with complex structures. Tools providing this combination may open up a new field of applications in isotope geochemistry. *Laser Ablation-Multi Collector-ICPMS* offers the analytical preconditions to achieve this challenging task.

Using a recently published method we present the first $\delta^{11}\text{B}$ 2D-images in a sample of coralline red algae [1]. The *Clathromorphum nereostratum* specimen used in this study was collected alive in 2004 off the coast of Attu island (Alaska, USA). It had been growing for more than 120 years covering most of the period of anthropogenic CO_2 emission and resulting ocean acidification. Forming annual layers of high-Mg calcite it is a promising climate archive for the high latitudes. Conventional bulk techniques appear inadequate for the determination of $\delta^{11}\text{B}$ used as pH proxy when considering the annual growth rate of about $400\mu\text{m}$. Using LA-MC-ICPMS we were able to determine the long-term decline in pH ($\sim 0.08 \pm 0.01$ pH units in 100 years). Additionally, a seasonal signal (0.1 pH units) could be identified presumably originating from strong CO_2 consumption during phytoplankton blooms in spring.

Our results clearly show a heterogeneous but systematic distribution of $\delta^{11}\text{B}$ within this sample, being the result of different phases of calcite precipitation by the alga. The seasonal cycle and spatial distribution of $\delta^{11}\text{B}$ can only be evaluated using high-resolution methods like the one applied here. Bulk techniques only would have picked up the long-term pH trend, but such measurements may have been compromised by mixing sample material from distinct phases, differing in $\delta^{11}\text{B}$. Thus, we consider this a good example of the gain in information which can be obtained using high-resolution in-situ techniques in isotope analysis.

[1] Fietzke et al (2010) J. Anal. At. Spectrom. **25**, 1953-1957

Depositional controls on spatial heterogeneity in pyrite $\delta^{34}\text{S}$: comparing the modern and ancient

DAVID A. FIKE¹, JIANXIN GAO¹ AND ROBERT C. ALLER²

¹Department of Earth & Planetary Sciences, Washington
University, St. Louis, MO 63130, USA;

(dfike@levee.wustl.edu; jianxin@levee.wustl.edu)

²School of Marine & Atmospheric Sciences, Stony Brook
University, Stony Brook, NY 11794 USA;

(robert.aller@stonybrook.edu)

The sulfur cycle plays a key role in regulating Earth's surface redox balance and provides a record of environmental and ecological change over Earth history. As new data are generated, we observe that (1) select records have more stratigraphic variability than expected; and (2) mean isotopic values differ from location to location for both sulfate and sulfide. Interpreting these ancient data is a challenge, in large part because we have only a limited understanding of sulfur isotope systematics in modern depositional environments.

Here we examine variability and mean values in pyrite sulfur isotopes from both modern and ancient strata. In the modern, we analyzed $\delta^{34}\text{S}_{\text{pyr}}$ from a series of cores taken across a gradient of water depths from the Gulf of Papua deltaic complex. In cores from physically undisturbed locations, $\delta^{34}\text{S}_{\text{pyr}}$ values were depleted ($\sim 20\text{‰}$ to 0‰) in the upper sediments, becoming progressively enriched with depth (approaching $\sim +10\text{‰}$ to $+20\text{‰}$). In general, these cores were characterized by smooth profiles with little sample-to-sample scatter ($< 5\text{‰}$ to 10‰). In contrast, cores overlain by remobilized muds had very enriched $\delta^{34}\text{S}_{\text{pyr}}$ values (up to $+35\text{‰}$, often within the remobilized near-surface samples) and large scatter in the profiles (variability between adjacent samples up to 35‰). Such drastically different isotopic signatures could easily result in divergent environmental reconstructions without knowing the depositional context of these samples. The magnitude of local, microbially driven variations in S isotopes in modern sediments is sufficiently large that uneven incorporation of these signatures during deposition and lithification can explain much of the observed discordance in chemostratigraphic reconstructions of sulfur cycling over Earth history. To illustrate the impact of depositional conditions in the ancient record, we compare coeval sedimentary strata from two late Ediacaran sedimentary basins: the Nama Group of Namibia and the Ara Group of Oman, where different depositional environments yield strongly divergent $\delta^{34}\text{S}$ data. A detailed understanding of depositional context and its impacts on $\delta^{34}\text{S}$ signals is essential for robust interpretations of geochemical data.

Light absorbing products from aqueous processing of α -dicarbonyls: matrix effects and atmospheric implications

E. FINESSI^{1*}, J.F. HAMILTON¹, M.T. BAEZA-ROMERO², A.R. RICKARD³, R.M. HEALY⁴, S. PEPPE⁵, T.J. ADAMS⁶, M.J.S. DANIELS⁶, S.M. BALL⁶, I.C.A. GOODALL⁶, P.S. MONKS⁶, E. BORRÁS⁷ AND A. MUÑOZ⁷

¹Department of Chemistry, University of York, York, YO10 5DD, UK (*correspond.: emanuela.finessi@york.ac.uk)

²Escuela Ingeniería Industrial Toledo, Universidad Castilla la Mancha, Toledo 45071, Spain

³National Centre for Atmospheric Science (NCAS), University of York, York, YO10 5DD, UK

⁴Southern Ontario Centre for Atmospheric Aerosol Research, University of Toronto, Canada

⁵School of Earth and Environment, University of Leeds, Leeds, LS2 9JT, UK

⁶Department of Chemistry, University of Leicester, Leicester, LE1 7RH, UK

⁷EUPHORE Laboratories, Instituto Universitario CEAM-UMH, 46980, Valencia, Spain

Aqueous phase chemistry of glyoxal (GLY) and methylglyoxal (MGLY) in the presence of inorganic salts has been recently identified as an important source of secondary organic aerosol (SOA) and brown carbon. However, the reversibility and the magnitude of the processes involved is still a matter of debate due to the lack of detailed speciation for such dynamic and complex systems.

In this study, a series of on- and off-line mass spectrometric techniques (FTICR-ESI-MS, LC-ESI-MSⁿ, ATOFMS) have been applied together with comprehensive gas chromatography with nitrogen chemiluminescence detection (GCxGC-NCD) and bi-dimensional nuclear magnetic resonance spectroscopy (2D-NMR) to identify the major organic products formed in bulk lab solutions with an emphasis on light absorbing organonitrogen species (ONs). The change in composition of the lab solutions as a function of different parameters was investigated. Mass spectral ions were identified as tracers for SOA generated from the uptake of gas-phase GLY and MGLY onto ammonium sulphate seeds and detected in chamber experiments conducted at the European PhotoReactor (EUPHORE). A series of light absorbing ONs, detected for the first time in chamber SOA by using off-line analyses, are presented as potential tracers for GLY- and MGLY-SOA in ambient aerosols. The relative potential of GLY and MGLY to form SOA and brown carbon through aqueous chemistry will be discussed.

Dissolution kinetics of ZrO₂ based innovative waste forms

FINKELDEI, S.* , BRANDT, F., BUKAEMSKIY, A., NEUMEIER, S., MODOLO, G. AND BOSBACH, D.

Institute of Energy and Climate Research, IEK-6, Forschungszentrum Jülich, Germany; (s.finkeldei@fz-juelich.de (*presenting author), f.brandt@fz-juelich.de, a.bukaemskiy@fz-juelich.de, s.neumeier@fz-juelich.de, g.modolo@fz-juelich.de, d.bosbach@fz-juelich.de)

Plutonium and the minor actinides (MA = Np, Am, Cm) are the main contributors to the long-term radiotoxicity of spent fuel. As an alternative to the disposal in glass or the direct disposal of spent fuel ceramic waste forms are under consideration [1]. Regarding the long-term safety, zirconia based pyrochlores (A₂B₂O₇) have outstanding properties with respect to their high radiation resistance and their high durability in aqueous environments. As a consequence of radiation damage zirconia based pyrochlores undergo a phase transition to the less ordered defect fluorite structure [2]. Recent publications have demonstrated the possibility to include e.g. Cm and Pu on regular lattice sites of the pyrochlore crystal structure [3,4].

In the open literature no systematic study of the dissolution kinetics of ZrO₂ - Nd₂O₃ pyrochlores and defect fluorites is reported. The dissolution rate is an important property of potential host phases because it defines the source term for the radionuclides in the case of water intrusion into a high level nuclear waste repository.

Here, we present new experimental data regarding the influence of the chemical composition and crystal structure on the dissolution kinetics. The dissolution experiments were carried out using a dynamic setup to ensure far from thermodynamic equilibrium conditions. Moreover, the influence of temperature and pH on the dissolution rate was studied for the defect fluorite and the pyrochlore ceramics. An initial incongruent elemental release for Nd and Zr was observed. At steady state conditions and pH = 1, the dissolution rates of pyrochlore and defect fluorite are congruent and in the range of 10⁻⁵ to 10⁻⁶ g□m⁻²□d⁻¹.

Further insight into the dissolution mechanism is gained by electron microscopy investigations.

- [1] Ewing, R. C., *et al* (2009) *C. R. Geoscience* **343**, 219-229. [2] Sickafus, K.E. *et al* (2007) *Nature Mater.* **6**, 217-223. [3] Holliday, K. S., *et al* (2013) *J. Nucl. Mater.* **433**, 479-485. [4] Nästren, C., *et al* (2009) *J. Solid State Chem.* **182**, 1-7.

Understanding shale gas plays through the application of inorganic geochemistry

A.J. FINLAY¹ AND J MARTIN²

¹Origin Analytical Ltd. 1 Ravenscroft Court, Buttington Cross Enterprise Park, Welshpool, Powys, SY21 8SL. U.K.

²Chemostrat Ltd., 1 Ravenscroft Court, Buttington Cross Enterprise Park, Welshpool, Powys, SY21 8SL. U.K.

The rapid increase in interest in exploring shale units for shale oil and gas has highlighted the need to develop a thorough understanding of shale units. Not only does possessing a detailed understanding of shale stratigraphy enable accurate volume calculations to be undertaken, but knowing the mineralogical composition of shale can provide information on rock mechanics to enable greater well completion success. In addition, a comprehensive understanding of anoxia proxies can be used to identify sweet spots in the play. All of this information can be potentially provided through the use of inorganic geochemical techniques.

This paper will discuss the application of a range of analytical techniques to shale gas plays, from rapid and non-destructive analysis by hand held X-Ray fluorescence to highly precise and accurate data produced by inductively coupled plasma mass spectrometers. In addition we will show how inorganic geochemical analysis can be integrated with other techniques such as XRD and TOC analysis to enable extra information to be gained from the analysis, for example enabling rock brittleness, a key parameter for fracking, to be established. Importantly we do not rely on samples to be provided from rare drill core, but we also analyse side wall core or drill chippings.

We will utilise case studies from UK onshore Bowland shale sections and key US shale to demonstrate the wide variety of ways that the inorganic geochemical data produced can be utilised to aid in the understanding of shale gas plays.

Immobilisation of PTEs by water treatment residual: A potential amendment for contaminated land

N.C. FINLAY*, S.A. ROBERTSON AND K.L. JOHNSON

School of Engineering & Computing Sciences, Durham University, South Road, Durham, DH1 3LE, UK.

(*correspondence: n.c.finlay@durham.ac.uk)

“Water Treatment Residual” (WTR) from the drinking water treatment process is a waste product largely composed of amorphous Al or Fe (oxy)hydroxides and organic matter and is commonly disposed of by landfill. Seasonal and geographical variations in WTRs were studied over 12-months at 10 water treatment works (WTWs) in England. Total solids ranged from 15 to 30%, of which organic matter formed 35 to 70%, Fe 25 to 37% and Al 10 to 21%. pH ranged from 4 to 7. Variation between works appears more pronounced than seasonal variation within them.

Immobilization of oxyanions such as P and As from aqueous solutions to Fe- and Al-WTR has been demonstrated [1] but research into immobilization of other Potentially Toxic Elements (PTEs) is limited. Batch experiments using aqueous solutions of Cu(II), Cd(II), Pb(II) and Zn(II) investigated the adsorption behaviour of an Fe rich WTR as a function of time, solid:solution ratio, pH and initial contaminant concentration and demonstrated effective removal of metal ions from solution. The sorption capacity of the WTR demonstrates some pH dependence, but significant sorption is observed in the low pH regime: 24% Cd, 28% Cu, and 45% Zn is sorbed at pH 3.2, 3.5 and 3.5 respectively, whilst Pb immobilisation remains > 98% from pH 3 to 9, using an initial mass load of 8.0 mg/g. The WTR’s ability to function as a metal sorbent over a broad pH range may be due to the intimate intermixture of iron (oxy)hydroxides and organic matter [2]. The fractionation of sorbed PTEs within the WTR is being determined using a new sequential extraction technique: “Chemometric Identification of Substrates and Element Distribution” [3].

These results support the hypothesis that WTRs may have potential as an amendment for remediation of contaminated land.

[1] Makris *et al* (2006), *Chemosphere* 64(5), 730-741. [2] Moon and Peacock (2012), *Geochimica et Cosmochimica Acta* 92, 203-219. [3] Cave *et al* (2004), *Geochemistry: Exploration, Environment, Analysis* 4(1), 71-86.

Modelling metal cation-phosphate competitive interactions on iron oxides

S. FIOLE^{1,*}, J. ANTELO², R. LOPEZ¹, D. GONDAR¹
AND F. ARCE¹

¹Dept. Physical Chemistry. University of Santiago de Compostela. 15782 Santiago de Compostela. Spain
(*corresponding author sarah.fiol@usc.es)

²Dept. Soil Science and Agricultural Chemistry. University of Santiago de Compostela. 15782 Santiago de Compostela. Spain

The role that iron (oxyhydr)oxides play in the speciation and bioavailability of environmental importance species such as phosphate, arsenate, sulphate, metal cations of trace elements or contaminants, has been extensively studied [1]. These mineral oxides have demonstrated to effectively retain important amounts of inorganic anions and metal cations on their surface and the mechanism of the process has been successfully explained using surface complexation models. However, the modelling sometimes fails when trying to explain adsorption data for ternary systems of the type iron oxide – inorganic anion – metal cation [2]. The enhancement of metal cation retention on iron oxides by coexisting inorganic anions has been reported by several authors [1,3]. Most of them agree that it is very difficult to establish the mechanism that produces this enhancement and three possibilities have been proposed: electrostatic enhancement, surface precipitation or formation of a ternary complex [1].

The following competitive adsorption experiments have been conducted using synthetic iron oxides: goethite – PO₄ – Cu, ferrihydrite – PO₄ – Cu, hematite – PO₄ – Cu and the same experiments were performed using natural samples with high content of iron and aluminum oxides. Attempts have been made to correct the modelling predictions for binary systems so that the interaction and mutual effect of inorganic anions and metal cations are considered and taken into account.

[1] Collins C.R., Ragnarsdottir V., Sherman D. (1999), *Geochimica et Cosmochimica Acta* **63**, 2989-3002. [2] Kanematsu M., Young T.M., Fukushi K., Green P.G., Darby J.L. (2013), *Geochimica et Cosmochimica Acta* **106**, 404-428. [3] Venema P., Hiemstra T., van Riemsdijk W.H. (1997), *Journal of Colloid and Interface Science* **192**, 94-103.

Geoneutrinos and the interior of the Earth

G. FIORENTINI

Legnaro National Laboratory (LNL-INFN), Via dell'Università, 2 - 35020 Legnaro, Padova, Italy – (fiorentini@fe.infn.it)

The deepest hole that has ever been dug is about 12 km deep, a mere dent in planetary terms. Geochemists analyze samples from the Earth's crust and from the top of the mantle. Seismology can reconstruct the density profile throughout all Earth, but not its composition. In this respect, our planet is mainly unexplored.

Geo-neutrinos, antineutrinos from the progenies of U, Th, and K decays in the Earth, bring to Earth's surface information coming from the whole planet. Differently from other emissions of the planet (e.g., heat, noble gases), they are unique in that they can escape freely and instantaneously from Earth's interior.

Detection of geo-neutrinos has become practical as a consequence of two fundamental advances that occurred in the last few years: a) development of extremely low background neutrino detectors and b) progress on understanding neutrino propagation.

Geo-neutrinos look thus a promising new probe for the study of global properties of Earth, such as the amount and distribution of long lived radioactive elements in the Earth's reservoirs.

The talk is intended as an introduction to the field, explaining to geo-scientists how geo-neutrinos are detected by physicists and to physicists why geo-neutrinos are relevant to geoscience.

Evolution of hydrogeochemical problems in Merzifon (Amasya, Turkey) aquifer with GIS

ARZU FIRAT ERSOY¹ AND FATMA GÜLTEKİN¹

¹Karadeniz Technical University, Department of Geological Engineering, 61080, Trabzon (firat@ktu.edu.tr)

Groundwater level in the Merzifon (Amasya, Turkey) aquifer has been decreased in recent years because number of wells and over pumping. Some of these wells are used for irrigation and some of are used for drinking purposes. Groundwater bearing alluvium consisting of loose gravel, sand and silt in the Merzifon-Gümüşhacıköy Basin is Plio-Quaternary aged.

Hydrogeochemical studies were conducted to establish groundwater and surface water quality in the Merzifon Aquifer. Mean pH value is 7.61, EC value is 67.59 and TDS value is 376.86 of the groundwater and surface water samples according to the analyze results. The trace element results especially Mn, Cr, Zn, As, Ni and Co are very high values in surface waters in the south of aquifer that is recharge area. Nitrate values are so high and a lot of water samples have below the limits in the aquifer.

To prevent exhausting groundwater in Merzifon Aquifer, groundwater usage should be regulated, and uncontrolled groundwater use must be terminated. Groundwater must be exploited with optimum discharge rate, must not be exceeded maximum rate. Besides, pollutants should be studied which parameters cause groundwater contamination and pollutant factors should be analyzed in water springs with intermittently.

Can we learn about bacterial attachment at mineral surfaces through colloid adsorption experiments?

CORNELIUS FISCHER^{1,2*}, MARTIN KÖNNEKE¹, ROLF S. ARVIDSON¹, KAI-UWE HINRICHS¹ AND A. LÜTTGE^{1,2}

¹MARUM, Univ. Bremen, 28359 Bremen, Germany (*correspondence: cornelius.fischer@uni-bremen.de)
²Rice University, Houston, TX 77005, USA

Colloid-surface interactions are mainly governed by electrostatic and van der Waals interactions. Nevertheless, surface topography variations on the micrometer and nanometer scale are able to alter significantly the local interaction potential. The resulting variations in the interaction energy at small separation distances may change the general interaction behaviour. Particle retention has been observed for mineral surfaces that are thought to be unable to act as collectors [1], and there is still no fundamental quantitative understanding and predictability for such phenomena. A predictive capability would be particularly important in colloid-mediated transport of radioactive material and the particle retention efficiency of barrier rocks.

Bacteria may be considered as “living particles” in the size range of large mineral colloids. Bacteria are able to modify surface area and topography of mineral and rock surfaces by corrosion. The formation of etch pits by bacteria is an important example that illustrates how bacteria govern and alter quantitatively the kinetics of mineral dissolution [2] and, consequently, the surface energy potential. Here we explore the interaction potential between well-defined surface topographies and microbes. Machined silica surfaces with building blocks in the micron to submicron scale are utilized [3]. The applied pattern results in well-defined variations of the surface energy potential. We apply this variability to study the near-field behaviour of microbes at structured mineral surfaces, i.e., the first step of microbial attachment to surfaces. Analyses using vertical scanning interferometry show the variability of microbial attachment to natural surfaces and provide quantitative constraints to these initial mineral-microbe interactions. The competition in surface interaction between “living” and “dead” colloids may provide the key to understand and predict the variability in surface reaction kinetics that is observed in nature.

[1] Fischer *et al* (2012) *Amer. J. Sci.* **312**, 885-906. [2] Lüttge *et al* (2005) *Amer. J. Sci.* **305**, 766-790. [3] Darbha *et al* (2012) *Langmuir* **28** (16), 6606-6617.

Airborne measurements of atmospheric trace gases via infra-red laser absorption spectroscopy

HORST FISCHER

Max Planck Institute for Chemistry, Mainz, Germany
(horst.fischer@mpic.de)

Recent laboratory and field studies demonstrated that replacing lead-chalcogenide tuneable diode lasers by cw operated quantum cascade lasers (QCL) results in sensitivity improvements of mid-IR TDLAS systems by a factor 2 to 3. Therefore, the MPI-C three laser TRacer In-situ Tdlas for Atmospheric Research (TRISTAR) was equipped with 3 QCL emitting at 1268.98, 2158.30, and 1759.72 cm⁻¹ to measure CH₄, CO and HCHO, respectively. In October 2005 the modified TRISTAR instrument was installed on a Lear Jet 35A as part of a scientific payload to study the photochemistry over the tropical rainforest in South America during the GABRIEL campaign. A second deployment was during fall 2006 and summer 2007 as part of the HOOVER campaign to study HO_x and its precursors in the upper troposphere over Europe. Since 2012 the instrument has been successfully flown on the new HALO aircraft during the TACTS/ESMVAL and OMO-Europe missions. These missions investigated the influence of convection and stratosphere-troposphere-transport on the photochemistry of the tropopause region. The performance of the instrument during these airborne campaigns was examined for the three species and precisions for CO and CH₄ were measured in the field to be 0.5% and 0.8% respectively (2σ). The 1σ detection limit for HCHO was ~500 pptv for a 2 second average, while post-flight signal averaging over a 2 minute time interval resulted in a 150 pptv detection limit.

Phase diagrams of FeO and Fe-Si alloys

REBECCA A. FISCHER^{*1}, ANDREW J. CAMPBELL¹, DANIEL M. REAMAN¹, DION L. HEINZ¹, PRZEMYSŁAW DERA² AND VITALI B. PRAKAPENKA²

¹Department of the Geophysical Sciences, University of Chicago, 5734 S Ellis Ave, Chicago, IL 60637, USA

²Center for Advanced Radiation Sources, 9700 S Cass Ave, Building 434A, Argonne, IL 60439, USA
(correspondence: rfischer@uchicago.edu)

Earth's core is less dense than pure iron, implying the presence of one or more lighter element(s) [1] such as Si, O, or S [2]. The phase diagrams of iron alloyed with these elements at high pressures and temperatures (*P-T*) are critical input for understanding the thermodynamics of these systems. Here we present results on FeO and a suite of Fe-Si alloys.

High *P-T* conditions (up to 200 GPa) were generated using a laser-heated diamond anvil cell. In situ X-ray diffraction to determine crystal structures was performed at beamline 13-ID-D of the Advanced Photon Source, Argonne National Laboratory. Melting was determined from diffuse X-ray scattering, by laser power-temperature relationships, and by temperature-emissivity relationships.

We have determined the melting curve of FeO [3] and clarified the location and slope of the B1/B8 phase transition [4]. We also identified an insulator-metal transition [5]. The B1 metallic phase of FeO is the stable phase at conditions of Earth's lower mantle and outer core, with possible implications for the high *P-T* character of Fe-O bonds, magnetic field propagation, and lower mantle conductivity.

FeSi has the B20 structure at 1 bar, the B2 structure at high pressures, and a wide two-phase field in between [6]. Fe-9Si has the hcp structure at high *P* and low *T*, and converts to an hcp+B2 mixture and then fcc+B2 with increasing temperature [6]. Fe-16Si has the DO₃ structure at low pressures and is an hcp+B2 mixture at higher pressures [7]. We have also measured melting temperatures for each alloy. Phase diagrams in *P-X* and *T-X* space imply that the stable phase of Fe-Si alloy at inner core conditions for compositions that match the observed density deficit is an hcp+B2 mixture [6].

[1] Birch (1952), *J. Geophys. Res.* **57**, 227-286. [2] Allègre *et al* (1995), *Earth Planet. Sci. Lett.* **134**, 515-526. [3] Fischer and Campbell (2010), *Am. Mineral.* **95**, 1473-1477. [4] Fischer *et al* (2011a), *Earth Planet. Sci. Lett.* **304**, 496-502. [5] Fischer *et al* (2011b), *Geophys. Res. Lett.* **38**, L24301. [6] Fischer *et al* (in review). [7] Fischer *et al* (2012), *Earth Planet. Sci. Lett.* **357-358**, 268-276.

Effects of SO₂-NO₂ impurities in the CO₂ stream on mineral solubility

S. FISCHER^{1,2*} AND A. LIEBSCHER¹

¹GFZ German Research Centre for Geosciences, Centre for Geological Storage CGS, Telegrafenberg, 14473 Potsdam, Germany (*fischer@gfz-potsdam.de)

²Berlin Institute of Technology, Chair of Mineralogy-Petrology, Ackerstraße 76, 13355 Berlin, Germany

Two sets of laboratory fluid-mineral experiments have been performed in order to analyze the effect of SO₂-NO₂ impurities in the CO₂ stream on the chemical reactivity of (A) siderite and (B) illite. For the siderite and illite separates, baseline XRD data with Rietveld refinements revealed a composition of (A) 69.6±1.3 wt% siderite, 26.7±1.2 wt% ankerite and 3.8±0.8 wt% quartz, and (B) 73.5±1.3 wt% illite, 10.8±1.3 wt% Ca-smectite, 11.9±0.4 wt% orthoclase, and 3.9±0.2 wt% quartz, respectively. SEM-EDS analyses yield initial structural formulae of (Fe_{0.8}Mg_{0.1}Mn_{0.1})CO₃ for siderite, (Ca_{1.0}Fe_{0.9-0.1}Mg_{0.4}Mn_{0.1})(CO₃)₂ for ankerite, and K_{0.5-0.7}(Mg_{0.1-0.2}Al_{1.8-1.9})Al_{0.4-0.6}Si_{3.4-3.6}O₁₀(OH)₂ for illite. Baseline experiments were conducted using pure CO₂ and 2 M NaCl brine at 80 °C and 20 MPa. Brine to mineral weight-ratios were 20 to 1. Run durations were one week for siderite and two weeks for illite, respectively. To study the influence of impurities, repeat experiments using identical starting conditions and analogous materials but impure CO₂ are performed. Siderite is reacted with CO₂ containing 5vol% SO₂, while illite is exposed to CO₂ containing 5vol% NO₂.

Based on XRD, SEM and ICP-AES analysis the baseline experiments using pure CO₂ yield (A) stable siderite and dissolving ankerite, and (B) unaffected illite but dissolution of the Ca-smectite component. Foci of the repeat experiments are on the potential formation of sulphates, e.g., anhydrite, during the CO₂-SO₂ runs, and the incorporation of NO₂ into the illite-smectite structure during the CO₂-NO₂ runs.

DEep CARbon DEgassing: The Deep Carbon Observatory DECADE initiative

TOBIAS P. FISCHER,¹

¹Department of Earth and Planetary Sciences, University of New Mexico, Albuquerque, NM USA
(fischer@unm.edu)

The question whether the net flux of carbon is into the mantle via subduction or out of the mantle via mantle degassing is fundamental because it provides an important framework for understanding the distribution and isotope composition of C in the mantle, the occurrence of abiotically synthesized carbon species in the mantle and crust, the presence or absence of carbon in the Earth's core, the formation of carbonated peridotite as starting material for ocean crust as well as the effect of mantle carbon release to modulate global climate through time. The Deep Carbon Observatory (DCO) Reservoirs and Fluxes Directorate is centered around the flux of carbon between different Earth reservoirs (<https://dco.gl.ciw.edu/science/deep-carbon-reservoirs-and-fluxes>) to help address some of these issues.

Volcanoes are *the* main pathway of volatiles, including carbon, from the Earth's interior to the atmosphere and hydrosphere, yet the current estimates of global C flux from volcanic regions range from 65 [1, 2] to 540 [3] Mt/yr. This order of magnitude difference in estimates is the difference between massive subduction of surface C into the mantle versus a balance between mantle input and output, with all the implications stated above. The DECADE initiative within the DCO R&F Directorate is bringing together the scientific expertise of geochemists, petrologists and volcanologists to provide constraints on the global volcanic C flux by a) establishing a data-base of volcanic and hydrothermal gas compositions and fluxes linked to PetDB and the Smithsonian Global Volcanism Program, b) building a global monitoring network to continuously measure the volcanic C flux of 10-12 yet to be selected active volcanoes, c) measure the C flux of remote volcanoes, for which no or only sparse data are currently available, d) develop new field and analytical instrumentation for C measurements and flux monitoring, and e) establish formal collaborations with volcano observatories around the world to support volcanic gas measurement and monitoring activities.

The current governance structure of DECADE includes a board of directors, a program coordination committee and several committees responsible for the key areas of the initiative (data base, network, instrumentation, and field campaigns).

[1] Allard *et al*, GRL 19, 1479-1481; [2] Williams *et al* GCA 56, 1765-1770; [3] Burton *et al* RiMG 75, 323-354

Nitrogen recycling through arc volcanism

TOBIAS P. FISCHER¹, LONG LI², ZACHARY D. SHARP¹
AND DAVID R. HILTON³

¹Dept. of Earth and Planetary Science, University of New Mexico, USA (fischer@unm.edu)

²Dept. of Earth and Atmosph. Sciences, University of Alberta, Canada (long4@ualberta.ca)

³Scripps Institution of Oceanography, Univ. of California San Diego, USA (drhilton@ucsd.edu)

Subduction is the main pathway of surface N transfer into the mantle, whereas arc volcanism can short-circuit that transfer via magmatic gas release into the atmosphere. A fundamental question is the efficiency of N recycling at subduction zones. The Central American (CA) and Izu Bonin Marianas (IBM) subduction systems are relatively well characterized in terms of N input and output and are the best candidates for evaluating N mass balance in arcs.

Stable (N) and noble gas (He) isotope and abundance characteristics show that N output at CA is dominated by the slab component ($\delta^{15}\text{N} \approx +7\text{‰}$, consistent with that of subducted Cocos Plate sediments, 5.7‰ [1]). N output fluxes vary significantly along the CA arc with Costa Rica only contributing $\sim 1 \times 10^7$ mol/yr compared to $\sim 7 \times 10^8$ mol/yr from Nicaragua [2,3]. The average slab-derived N output from the entire CA arc is estimated at 2.7×10^9 mol/yr [2], significantly higher than the input sedimentary N of 9.3×10^8 mol/yr from the Cocos Plate [1]. This imbalance implies additional N must be supplied from AOC [4] and/or subduction erosion [1]. However, both potential sources remain poorly-constrained, preventing further evaluation of N recycling efficiency and excess N delivery to the deep mantle. In contrast, the sedimentary N output flux at IBM represents only 11–51% of the input, implying that up to 90% of subducted N is potentially transferred to the deep mantle [5].

The difference in recycling efficiencies is likely related to the different thermal regimes and geometries of the two subduction zones. The contribution of crustal material by subduction erosion may also play a role. More work is needed to further constrain the processes of N release from different lithologies of subducting plates and the variability of volcanic N fluxes in arcs globally.

[1] Li & Bebout (2005), *J. Geophys. Res.* 110, B11202, doi:10.1029/2004JB003276. [2] Elkins, *et al* (2006), *Geochim. Cosmochim. Acta* 70, 5215–5235. [3] Zimmer, *et al* (2004), *Geochem. Geophys. Geosyst.* 5, Q05J11, doi:10.1029/2003GC000651. [4] Li, *et al* (2007), *Geochim. Cosmochim. Acta* 71, 2344–2360. [5] Mitchell, *et al* (2010), *Geochem. Geophys. Geosyst.* 11, Q02X11, doi:10.1029/2009GC002783.

Sedimentary and genomic insights into the evolution of iron oxidation

WOODWARD W. FISCHER¹, JENA E. JOHNSON¹, JAMES HEMP¹, LAURA A. PACE², NOAH J. PLANAVSKY¹
AND SAMUEL M. WEBB³

¹California Institute of Technology (wfischer@caltech.edu)

²University of Utah

³Stanford Synchrotron Radiation Lightsource

Iron is the most abundant redox-active element on the Earth and provides a rich source of electrons that impacts all biogeochemical cycles. Detailed observations of iron formations (IF) in the geological record demonstrate that this has been broadly true for much of Earth history, though key differences in the facies, textures, geochemistry, and mineralogy define varying styles of geobiological processes and different modes of petrogenesis.

Environmental iron oxidation processes fall broadly into four categories: abiotic photochemical, abiotic and biotic reactions with O_2 , and photobiology (e.g. anoxygenic photosynthesis). Oxidation plays an important role in concentrating iron in sediments, either by forming poorly ordered hydrous oxides or ferric and mixed-valence silicate phases. To understand processes of oxidation in ancient IF requires the ability to look through complex diagenetic and metamorphic transformations common to these deposits: in particular, the tendency toward post-depositional reduction by organic matter is common. Late Archean and earliest Paleoproterozoic IF have Fe(III)/Fe(II) that vary with paleoenvironmental depth with more oxidized facies occurring in deeper water, suggesting oxidation by anoxygenic photosynthesis. Mid-Paleoproterozoic iron formations have similar overall valence states, but the depth gradient is reversed and reflects the locus of the major oxidant at that time, O_2 . An important process outlier is provided by Neoproterozoic IF, associated with ‘Snowball Earth’ glacial deposits, are composed of nearly exclusively ferric iron, and reflects simple abiotic titration of environmental O_2 .

In this talk, we’ll discuss how these geological patterns highlight changing modes of biological iron oxidation processes through time. Since iron oxidation rates vary greatly with pH, acidophilic and neutrophilic aerobic iron-oxidizing microbes have evolved separate biochemical strategies for oxidizing iron. We use phylogenomics to show that both strategies are evolutionarily derived, implying that aerobic iron oxidation is a relatively late innovation. A similar pattern emerges from the secular distribution of filamentous microfossils interpreted to reflect aerobic iron-oxidizing microbes, which appear in the fossil record after the rise of O_2 .

Origin of the late veneer inferred from Ru isotope systematics

M. FISCHER-GÖDDE¹, C. BURKHARDT² AND T. KLEINE¹

¹Institut für Planetologie, University of Münster, 48149 Münster, Germany (m.fischer-goedde@uni-muenster.de)

²Origins Laboratory, Department of Geophysical Sciences, The University of Chicago, IL 60637, USA

Elevated abundances of the highly siderophile elements (HSE) in the Earth's mantle are commonly explained by the addition of a chondritic late veneer after cessation of core formation [e.g., 1]. Identifying the source and type of the late accreted material is a particular important issue, because the late veneer may have delivered considerable amounts of volatiles to Earth. Relative HSE abundances and Os isotope compositions of mantle materials are largely similar to those of chondrites, yet establishing a direct link of the late accreted material to a particular type of meteorite has proven difficult [2]. Ruthenium is a HSE and exhibits nucleosynthetic isotope anomalies at the bulk meteorite scale [3]. This makes Ru isotopes a promising new tool for identifying the source of the late accreted material, because the Ru isotope composition of Earth's mantle can be directly compared to that of meteorites.

We have precisely measured Ru isotopic compositions for a wide range of chondrites and iron meteorites, using the Neptune Plus MC-ICPMS at the University of Münster. All investigated meteorites, except the IAB irons but including several carbonaceous and ordinary chondrites are characterized by a deficit in *s*-process Ru relative to the Earth. Consequently, none of the meteorites nor a combination thereof can be the source of the late veneer. Our new Ru data in combination with previously published Mo isotope data for the same samples [4] show that all meteorites define a Ru vs. Mo isotope correlation [5]. This Ru-Mo correlation passes through the composition of Earth's mantle, implying that the late veneer derives from the same Ru-Mo isotopic reservoir and, hence, from the same type of material as the main building blocks of the Earth. This is because Mo, a moderately siderophile element, was delivered during the main stages of accretion, whereas the HSE Ru was mainly added by the late veneer. The Mo-Ru isotope systematics, therefore, seem to rule out an exotic outer solar system source for the late veneer, but strongly suggest an origin from the same type of inner solar system material that built Earth. The late accreted material thus may simply constitute the 'exponential tail' of accretion.

[1] Kimura *et al* (1974) *GCA* 38, 683-701. [2] Walker (2009) *Chem. Erde* 69, 101-125. [3] Chen *et al* (2010) *GCA* 74, 3851-3862. [4] Burkhardt *et al* (2011) *EPSL* 312, 390-400. [5] Dauphas *et al* (2004) *EPSL* 226, 465-475.

Earth and Mars building blocks

CAROLINE FITOUSSI^{1,*} AND BERNARD BOURDON¹

¹Laboratoire de Géologie de Lyon, ENS Lyon, CNRS and Université Claude Bernard de Lyon, France
(Correspondence : caroline.fitoussi@ens-lyon.fr)

CI chondrites, which have the closest elemental composition to the solar photosphere, have often been chosen as the reference composition for the Bulk Earth [1,2]. However, from the viewpoint of isotope compositions (e.g. Cr isotopes), it is not plausible for the Bulk Earth to have a CI chondrite composition. Another approach based on isotopic similarities between Earth and enstatite chondrites proposed that these meteorites best represented the Bulk Earth [3]. However, based on silicon isotopes, it was recently shown that enstatite chondrites cannot represent more than 15% of the Earth's mass [4]. In addition, several chemical characteristics of enstatite chondrites are distinct from those of the Earth.

Reports of nucleosynthetic and non-mass dependent isotope anomalies have shown that there is a heterogeneous distribution of isotope compositions in the nebula, and these systems (e.g. O, Cr isotopes) have even become a reliable classifying tool for various meteorite groups [5,6]. We have been looking for possible building blocks of the Earth and Mars, using these isotopic signatures in meteorites.

As target values of our model, we used the Earth and Mars compositions of measured terrestrial samples and SNC (Shergottites, Nakhilites, Chassignites) martian meteorite samples, respectively.

We propose a model that accounts for (i) all isotopic compositions of the Earth and Mars; (ii) the refractory lithophile element enrichment of the Earth compared to CI chondrites, which is one specific characteristic of the composition of our planet [e.g. 7]; (iii) the volatile element budget in Mars, which has been difficult to match, as discussed in previous models of the bulk composition of Mars [8-9]. We will discuss these results with regards to implications on the scenarios for the formation of terrestrial planets.

[1] McDonough & Sun (1995) *Chem. Geol.* 120, 223 [2] Allègre *et al* (2001) *Earth & Planet. Sci.* 185, 49 [3] Javoy *et al* (2010) *Earth & Planet. Sci.* 293, 259 [4] Fitoussi & Bourdon (2012), *Science* 335, 1477 [5] Clayton (2003) *Treatise on Geochemistry* 1.06, 129 [6] Trinquier *et al* (2007) *Astrophys. J.* 655, 1179 [7] Palme & O'Neill (2003) *Treatise on Geochemistry* 2.01, 1 [8] Lodders & Fegley (1997) *Icarus* 126, 373 [9] Sanloup *et al* (1999) *PEPI* 112, 43.

Spatial Variation of Dissolution at Fracture Boundaries

J.P. FITTS^{1*}, H. DENG¹, R. TAPPERO AND C.A. PETERS¹

¹Princeton Univ., Princeton, NJ 08544, USA

(*correspondence: fitts@princeton.edu, handeng@princeton.edu, cap@princeton.edu)

²Brookhaven National Lab, Upton, NY 11973, USA

(rtappero@bnl.gov)

Prediction of fluid flow in fracture networks is critically important to the safe and efficient advance of geologic energy technologies including oil and gas extraction, geothermal energy systems and geologic CO₂ storage. Although pore-scale mineral variation can profoundly affect fracture fluid flow [1] and the mass transfer of organics, metals and salts, major knowledge gaps exist due to the lack of experimental observations of pore-scale processes at fracture boundaries. We conducted core-flooding experiments with fractured carbonate-rich caprock samples and showed that while calcite dissolution is the primary geochemical driver of alterations to fracture geometry, permeability evolves based on a complex relationship between initial fracture geometry, mineral spatial heterogeneity and variation, fluid chemistry and flow rate [2].

To investigate the underlying causes of spatial variability of dissolution and fracture geometry alteration, we developed a new flow-through cell that enables 2D x-ray imaging of mineral-specific dissolution at a fracture surface. The parallel plate design provides an idealized fracture geometry to derive the relationship between flow rate, reaction rate, and mineral spatial heterogeneity and variation. In the flow-cell, a subsample of the carbonate-rich caprock core described above was reacted with acidified brine. The extent of dissolution was spatially correlated with calcite abundance relative to less soluble dolomite and silicate minerals, which is qualitatively consistent with the core-flooding experiment. In a second set of experiments with a limestone specimen, however, the extent of dissolution was not strictly correlated with the occurrence of calcite. Instead, the pattern and extent of dissolution suggested secondary causes such as calcite morphology, the presence of argillaceous minerals and other diagenetic features. These experimental results help define the combinations of brine chemistry, caprock mineralogy and flow rates with a high probability for geochemical alterations that increase fracture permeability.

[1] Nogues, Celia & Peters (2012) CMWR 2012. <http://cmwr2012.cce.illinois.edu>; [2] Ellis, Fitts, Bromhal, McIntyre, Tappero & Peters (2013) *Env. Eng. Sci.* 10.1089/ees.2012.0337

Iron isotopes in seawater from the Southeast Pacific and North Atlantic Oceans

JESSICA N. FITZSIMMONS^{1*}, TIM M. CONWAY², SETH G. JOHN² AND EDWARD A. BOYLE³

¹MIT-WHOI Joint Program in Chemical Oceanography, Cambridge, MA 02139, USA (*correspondence: jessfittz@mit.edu)

²Department of Earth and Ocean Sciences, University of South Carolina, Columbia, SC 29208, USA; (tconway@geol.sc.edu; sjohn@geol.sc.edu)

³Department of Earth and Planetary Sciences, MIT, Cambridge, MA 02139, USA (eaboyle@mit.edu)

Iron is an essential micronutrient for marine photosynthesis and nitrogen fixation, and low dissolved iron (dFe) concentrations limit primary production in large regions of the global ocean. Thus, understanding the sources, sinks, and internal cycling of Fe is vital to constraining its impact on the oceanic carbon cycle. Fe isotope ($\delta^{56}\text{Fe}$) measurements of dFe in seawater are a new tracer for Fe provenance and are also emerging as a useful tool for investigating Fe transformations in the open ocean.

This study presents three full-depth $\delta^{56}\text{Fe}$ profiles from the Southeast Pacific Ocean (~25°S, 70-105°W) ranging from the coastal oxygen minimum zone off of Chile to the middle of the subtropical gyre near Easter Island. Upper 1000m samples demonstrated isotopically light Fe, in contrast to enriched values in the upper ocean of the North Atlantic and Southwest Pacific [1, 2]. A distal hydrothermal vent Fe signal was also detected around 2000m depth at the two offshore stations ([dFe] of 0.86 and 1.45 nmol/kg) and corresponded to an enriched $\delta^{56}\text{Fe}$ signature of +0.5‰ at both stations.

We also present $\delta^{56}\text{Fe}$ values of size fractionated dFe at two stations sampled on the U.S. GEOTRACES cruise in the North Atlantic Ocean: one near Bermuda and one near the Cape Verde Islands. Surface dFe (<0.2 μm) $\delta^{56}\text{Fe}$ values were near +0.5‰ at both stations, while the soluble Fe (<10 kDa) portion of the dFe phase was significantly enriched in excess of +1.0‰. Subsurface soluble Fe was the same or slightly depleted compared to dFe. This demonstrates that, at least in the surface ocean, soluble and colloidal Fe are cycling independently.

[1] John & Adkins (2012) *Global Biogeochem Cy*, GB2034.

[2] Radic *et al* (2011) *Earth Planet Sc Lett* **306**, 1-10.

Iron speciation in natural and industrial dust: What can we learn from individual particle analysis?

P. FLAMENT^{1*}, K. DEBOUDT¹, H. MARRIS¹
AND R. GIÉRE²

¹ULCO/LPCA, 189A Avenue Schumann, 59140, Dunkerque, France (*correspondence : pascal.flament@univ-littoral.fr)

²Institute of Earth and Environmental Sciences, Albert-Ludwigs-Universität, D-79104 Freiburg, Germany

Iron (Fe) is considered as a main biolimiting micronutrient, whose the bioavailability controls the marine productivity in HNLC zones, then the global carbon cycle. But the extent to which human activities impact the transport of bioavailable Fe to the oceans remains a fundamental question [1]. Many recent works have demonstrated that Fe-bearing aerosols may have variable aqueous solubility, then bioavailability, related to Fe chemical speciation. More particularly, the solubility of Fe-bearing particles increases significantly, with the ferrous (FeII) content of those. The Fe-speciation in dust can be studied by transmission electron microscopy (TEM) [2], coupled with electron energy loss spectroscopy (EELS) [3]. While the TEM-EELS technique has a lower energy resolution than other techniques recently used to investigate the red-ox speciation of Fe in aerosols, such as synchrotron based X-Ray spectroscopies [4], the implementation of TEM-EELS analyses is fast and inexpensive, by comparison to synchrotron techniques and provides relevant results in term of Fe speciation with the advantage of an high spatial resolution, at the particle scale.

We present here results obtained both on desert dust collected in Senegal during the AMMA campaign and on industrial dust (Fe-Mn metallurgy plant) collected in the North of France (Dunkirk harbor). In desert dust, Fe can be present as substitution Fe in the crystalline matrix of aluminosilicate, but the existence of Fe oxide nano-inclusions has also been highlighted at the particle scale, with variable oxidation states. In alloy-making emission plumes, Fe-bearing dusts are mostly emitted from the tapping area of the electric arc furnace and Fe shows an intermediate oxidation state, at the particle scale, with an average of 2.7 ± 0.2 . It appears that, in a general manner, the iron in the smallest particles is more oxidized than in the coarser ones.

[1] Mahowald *et al* (2009) *Annu Rev Mar Sci* **1**, 245-278. [2] Gieré *et al* (2006) *Environ Sci Technol* **40**, 6235-6240. [3] Deboudt *et al* (2012) *J Geophys Res-Atmos* **117**, D12307. [4] Oakes *et al* (2012) *Atmos Chem Phys* **12**, 745-756.

Deep subduction of hot young oceanic slab required by the Syros eclogites

STAMATIS FLEMETAKIS¹, EVANGELOS MOULAS²,
DIMITRIOS KOSTOPOULOS^{1*}
AND ELIAS CHATZITHEODORIDIS³

¹University of Athens, Department of Geology, Athens 157 84, Greece (*correspondence: dikostop@geol.uoa.gr)

²Geological Institute, ETH Zurich, 8092 Zurich, Switzerland

³NTUA, Mining & Metallurgical Eng., Athens 15780, Greece

The Cycladic islands of Syros and Siphnos, Aegean Sea, Greece, represent subducted IAT and BABB remnants of the Neotethyan Pindos Ocean that formed during rifting of the southern active margin of Laurussia (Pelagonia) in the mid-Triassic, in response to northward subduction of Palaeotethys. Garnet porphyroblasts ($\varnothing=1\text{mm}$) in a glaucophane-zoisite eclogite from Kini locality on Syros are compositionally zoned and display a unique prograde heating path from a high-pressure greenschist-facies core with high X_{Sps} and low Mg\# via a blueschist-facies mantle with moderate X_{Sps} and Mg\# to an eclogite-facies rim with low X_{Sps} and high Mg\# . The outermost 35 μm of the garnet rims show flat X_{Sps} with rapidly increasing outwards Mg\# . Na-Act-Chl-Ph rimmed by Gln mark the greenschist-blueschist facies transition, whereas Pg rimmed by Omp and the incoming of Rt at the expense of Ttn signify the blueschist-eclogite facies transition.

Raman barometry of quartz inclusions in the eclogitic garnet rims coupled with elastic modelling of the garnet host [1], and Zr-in-Rt and Grt-Cpx-Ph thermobarometry revealed near-UHP P-T conditions of the order of 2.6 GPa/660°C. By contrast, the greenschist-blueschist transition lies at ~ 0.75 GPa/355°C.

Our new P-T estimates match published T distributions on the slab surface calculated for a subduction velocity of 3 cm/yr, a subduction angle of 30° and an age of incoming lithosphere of ~ 20 Ma with a shear stress of 80 MPa at the slab-mantle interface [2]. The above are in excellent agreement with published isotopic work on zircons and garnets from Syros eclogites suggesting crystallisation from magmas derived from a depleted mantle at ~ 80 Ma and constraining the event of eclogitic metamorphism at ~ 55 Ma. Diffusion modelling of the garnet outermost rims suggests a brief heating pulse of only $\sim 1,000$ years at peak T.

[1] Van der Molen (1981) *Tectonophysics* **73**, 323-342. [2] Peacock (1993) *Geol. Soc. Am. Bull.* **105**, 684-694.

Experimental approach of carbonate isotopes fractionation related to kinetic effect during travertine growth

L. FLEURENT^{1,2*}, E. GIBERT-BRUNET¹
AND F. BARBECOT²

¹UMR 8148-IDES, CNRS-UPS, Université Paris Sud-XI, Orsay, France (*leonora.fleurent@u-psud.fr)

²GEOTOP, département des sciences et de l'atmosphère, Université du Québec à Montréal, Montréal, Canada

Travertine are supposed to archive environmental conditions with high temporal resolution up to seasonal, monthly or even daily when finely laminated. It's important to understand the mechanisms of precipitation and the behaviour of isotope and major/trace elements to make environmental reconstruction.

Rate of degassing of CO₂ in rich spring is considered to influence the rate of calcite precipitation and the stable isotope δ¹⁸O and δ¹³C. Then the isotopic equilibrium is rarely maintained during the deposition of travertine suggesting that the rate of CO₂ degassing may be the main controlling factor of the disequilibrium ⁽¹⁾. Combined stable isotope (¹⁸O and ¹³C) measurement on water and on freshly precipitate travertine from rich CO₂ spring under laboratory condition have been developed in order to constrain the non-equilibrium fractionation domain.

In a 80-cm sequence cored in 2008 at the Ours gaseous spring (Massif Central, France), we have observed a disequilibrium between the calculated temperature and corresponding isotopic contents recorded in the laminated travertines, with a apparent shift of 8°C compared to the measured temperature. The main question was thus to understand the precipitation processes that either reflect or not geochemical equilibrium.

In order to understand the processes occurring between rich-CO₂ water, gaz and related travertines such as kinetic of degassing and the geochemical pathways recorded in the carbonates, laboratory tests were conducted. These experimentations allow us to identify the effect on degassing on the behaviour of isotope (fractionation factor) and chemical (partitioning) records when precipitation occurs. The isotopic signatures obtained on this core ⁽²⁾ can be thus reinterpreted with a very new geochemical insight of fractionation and interaction processes.

[1] Gonfiantini et al (1968) Earth and Planetary Science Letters pp:55-58. [2] Barbecot et al (2011) Poster Goldschmidt Congress

Borosilicate glass dissolution driven by magnesium silicate precipitation

B. FLEURY^{1*}, N. GODON¹, A. AYRAL² AND S. GIN¹

¹CEA MAR/DEN/DTCD/SECM/LCLT, BP17171, 30207, Bagnols-sur-cèze, France

*correspondence : benjamin.fleury@cea.fr, nicole.godon@cea.fr, stephane.gin@cea.fr)

²IEM, Université Montpellier 2, CC 047, Place Eugène Bataillon, 34095, Montpellier Cedex 5, France (andre.ayral@iemm.univ-montp2.fr)

This study deals with the effect of Mg-silicate precipitation on borosilicate glass dissolution mechanisms and dissolution rate. It has been shown that this precipitation is related to the consumption of elements like silicon from the altered glass layers [1]. Investigations are here performed for better understanding of the kinetically limiting mechanisms.

Leaching experiments of SON68 glass, a Mg-free borosilicate glass, were carried out in initial deionized water at 50°C with a glass-surface-area-to-solution-volume ratio of 200 cm⁻¹. After 29 days of alteration magnesium was added in order to trigger the precipitation of Mg-silicate. Additional experiments were also conducted to investigate the importance of other parameters like pH or dissolved silica on the precipitation mechanisms and their consequences on the glass dissolution rate.

Mg-silicate precipitates immediately after magnesium addition. The total amount of altered glass increases with the added amount of magnesium. It is lower when silicon is added to the solution. Increase of pH above 8 strongly accelerates Mg-silicate precipitation. A time lag is observed between magnesium addition and glass alteration resumption because silicon is first provided from partial dissolution of the previously formed alteration gel. It is finally shown that nucleation process does not limit Mg-silicate precipitation.

[1] Frugier *et al* (2008) *J. Nucl. Mater.* **380**, 8-21.

Periods of magma propagation and homogenization preserved in an upper crustal pluton over 1.2 Ma

FLOESS D^{1*}, BAUMGARTNER L¹, BRACK P²,
BRODERICK C³, CHIARADIA M³, MUNTENER O¹,
PUTLITZ B¹ AND SCHALTEGGER U³

¹University of Lausanne, CH
(*david.floess@gmail.com)

²ETH Zurich, CH

³University of Geneva, CH

Large, broadly homogeneous plutons are a major component of subduction-related batholiths. The Western Adamello Tonalite (WAT) in the Italian Alps is an excellent example of a homogeneous pluton, featuring rocks with similar texture and composition over 6 kilometers (100 km²). Locally, heterogeneous zones of up to a few hundred meters wide interrupt the homogeneous tonalite. They consist of basement xenoliths, mafic enclaves, schlieren, and hornblende-rich cumulates and are parallel to the host rock contact. Forty-five igneous samples from two transects perpendicular to the host rock contact were collected and analyzed for major and trace elements, stable and radiogenic isotopes (O, Sr, Nd), and U-Pb zircon geochronology.

U-Pb high precision dating on four samples yields ages of 37.6, 37.1, 36.7 and 36.4 Ma (youngest zircon from each sample), indicating a younging towards the internal parts of the pluton. The age spread within a single sample is over 200 ka, and no overlap between the four samples exists. Thermal models predict that a single batch intrusion of the size of the WAT would cool ten times faster than the age span of 1.2 Ma recorded by the samples. This, along with structural and chemical observations suggests incremental emplacement.

Major and trace elements show a trend towards more SiO₂-rich (evolved) compositions for the younger, internal parts. In contrast, stable isotopes only vary in the first couple of meters close to the host rock contact, indicating wall rock assimilation. A step-like increase of ⁸⁷Sr/⁸⁶Sr (and decrease of ¹⁴³Nd/¹⁴⁴Nd) coincides with the observed heterogeneous zones. The change in radiogenic isotopic values occurs over a few hundred meters, whereas the flat plateaus of similar isotope composition persist over areas that are a factor ~5 wider. This suggests that new feeder conduits are rapidly established and successive pulses of magma are isolated from the surrounding host rocks. Two such cycles can be seen in the WAT. We propose that this alternation results from processes at the level of an intermediate crustal reservoir. The general geochemical evolution, in contrast, mainly reflects changes in the deeper magma system.

Precise U-Pb ID-TIMS baddeleyite and zircon ages for the Florianópolis Dyke Swarm and its correlation to Paraná-Etendeka mafic to intermediate magmatism

LUANA MOREIRA FLORISBAL¹, VALDECIR DE ASSIS
JANASI¹, MARIA DE FATIMA BITENCOURT²
AND LARRY M. HEAMAN³

¹ Instituto de Geociências, Universidade de São Paulo, Rua do Lago, 562, São Paulo, SP, 05508-080, Brazil.

(geoluana@yahoo.com.br; vajanasi@gmail.com)

² Centro de Estudos em Petrologia e Geoquímica, Instituto de Geociências, Universidade Federal do Rio Grande do Sul, Av. Bento Gonçalves, 9500, Porto Alegre 91500-000 RS, (Brazil. fatimab@ufrgs.br)

³ Department of Earth and Atmospheric Sciences, 1-26 Earth Sciences Building, University of Alberta, Edmonton, Alberta, T6G 2E3, Canada. lheaman@ualberta.ca

The coastal region of Santa Catarina, south Brazil, features abundant mafic to intermediate dykes from the Paraná-Etendeka Magmatic Province (PEMP), which compose the Florianópolis Dyke Swarm (FDS). These are hosted by Neoproterozoic granites which locally show evidence of remelting at the contacts with the mafic dykes. NE-trending, high-TiP dykes akin to the high-Sr Urubici lava-type are predominant, and are locally crosscut by thinner, NW-trending dykes similar to the low-TiP Gramado lava-type. Basalt compositions are largely predominant, but some dykes of intermediate composition occur showing evidence of magma mingling. U-Pb ID-TIMS dates obtained on baddeleyite and zircon from both mafic and intermediate dykes yield precise crystallization ages at *ca.* 134 (±0.5) Ma. These ages coincide with the best current estimates for the climax of volcanic activity in the neighbouring PEMP lava pile, as indicated by both U-Pb and ⁴⁰Ar/³⁹Ar dates. The close chemical and temporal relations with the lavas are good indicators that the dykes must correspond to feeders of the lava pile. The ~20 Ma span of ⁴⁰Ar/³⁹Ar dates (140-120 Ma) reported in the literature for the FDS may be an overestimate of the duration of dyke emplacement in the swarm, possibly reflecting both Ar loss and, in some cases, Ar excess resulting from the contamination of the magmas by K-rich melts derived from the host granites.

Cristallinity, structure and volatile content of Panum Crater's magma

P. FLOURY¹, D. R. NEUVILLE¹, C. LE LOSQ¹
AND R. MORETTI^{2,3}

¹CNRS-IPGP, Géochimie&Cosmochimie, Paris Sorbonne Cité, 1 rue Jussieu, 75005 Paris, France.

²Seconda Università degli Studi di Napoli, Dipartimento di Ingegneria Civile, Design, Edilizia e Ambiente, Aversa (CE);

³Istituto Nazionale di Geofisica e Vulcanologia, Napoli, Italy

Despite the many studies in the literature, the influence of magma physicochemical properties, particularly viscosity, on the building and dynamics of volcanic domes is not fully understood, hitherto. The link between temperature, chemical composition and crystalline content of magmas has been assessed only partially, and still represents a major issue in Earth and Material sciences. Understanding physicochemical properties of crystal-bearing melts is of prime importance for understanding the growth and evolution of volcanic domes, as well as the transition of the eruption toward other eruptive styles. Panum Crater is the most recent dome eruption at the chain of Mono Craters in the north side of Long Valley caldera (California). It is a dome composed of obsidian and pumice, which emplaced in 1350 AD inside a tuff-ring [1]. The coexistence of these products represents an ideal case to assess physicochemical properties at the atomic level of melt structure and their role in eruptive dynamics.

In this communication, we present a large range of physical and chemical properties measurements (determination of the water concentration by Raman and FTIR spectroscopy, viscosity and density measurements, as well as C and H isotopes) to have an integral vision of the matter. Our results lead us to propose a piston-like dynamic model for the eruption based on the formation of a shallow (200-300 m), degassed, magma plug overlying a relatively volatile-rich portion of the same silicic magma that rose and expanded under closed system-degassing conditions. In our model, the sudden and preliminary gas release that flashed groundwaters and created the tuff-ring [1], formed the shallow, degassed magma plug, down to a depth determined by a rheological boundary with the lowermost magma portion. The latter acted first as a thermostat, keeping the shallow, degassed, one under superheated conditions, so preventing the onset of crystallization at shallow depth. Subsequently, the rapid expansion of the volatile-rich lowermost magma, allowed the rapid evolution of the shallow magma through the glass transition when rapidly pushed out to surface, thus forming the obsidian body which surround the highly vesiculated pumices. The model can be extended to other volcanic domes of much larger size, provided a deep source.

[1] Miller, C. D., Holocene eruptions at the Inyo volcanic chain, California: Implications for possible eruptions in Long Valley caldera, *Geology*, 13, 4-17, 1985.

L2009R2: A Cluster IDP Sampling a Diversity of Formation Conditions

G. J. FLYNN¹, S. WIRICK² AND S. R. SUTTON^{2,3}

¹Physics Dept., SUNY-Plattsburgh, Plattsburgh, NY 12901

²CARS, Univ. of Chicago, Chicago, IL 60637

³Geophysical Sciences, Univ. of Chicago, Chicago IL 60637

We performed XRF, Fe- and Cr-XANES on L2009R2, a large aggregate interplanetary dust particle (IDP) that fragmented dispersing over several hundred micrometers on impact with the stratospheric collector. Most ~8 μm pixels gave Fe-XANES spectra consistent with Fe²⁺ or Fe³⁺, but the spectrum of one pixel is consistent with Fe or Fe-Ni metal with some structural disorder. Cr-XANES was performed on eleven spots where the Cr concentration was high enough to get good quality spectra. Six areas of L2009R2 are consistent with Cr³⁺ (overplotting chromite or Cr-diopside), while four areas plot between Cr²⁺ and Cr³⁺. One area overplots the Cr²⁺ spectrum of olivine from the ureilite meteorite CMS04048. This is significant because Cr has been identified in natural terrestrial materials in only the Cr³⁺ and Cr⁶⁺ valence states [1], with only rare occurrences of Cr²⁺ in extraterrestrial materials. The most reduced Fe was found in the same area as oxidized Cr and the most reduced Cr was found in an area dominated by oxidized Fe. L2009R2 has a CI-like element abundance pattern, suggesting it consists of fine-grained matrix and larger minerals that grains aggregated into this ~50 μm particle. The XANES results on L2009R2 span a wide range of oxidation states, indicating this IDP is an aggregate of grains formed in a diverse variety of environments, some oxidizing and others reducing.

[1] Eeckhout *et al.*, *Am. Min.*, **92**, 966f, 2007.

The reduction of elemental sulfur by metal-reducing bacteria under alkaline conditions

THEODORE M. FLYNN*, EDWARD J. O'LOUGHLIN
AND KENNETH M. KEMNER

Argonne National Laboratory, Biosciences Division, Lemont,
IL 60439 (*correspondence: tflynn@anl.gov)

Metal-reducing bacteria such as *Shewanella*, *Desulfuromonas*, and *Geobacter* are abundant in many terrestrial environments, where their respiration is often linked to the reduction of ferric iron (Fe^{III}). Under alkaline conditions, however, the reduction of Fe^{III} ceases to be energetically favorable and suggests that under these conditions, metal reducers must utilize alternate electron acceptors. One possible alternative is elemental sulfur (S⁰), which is produced when ferric minerals react with dissolved sulfide such as that created by microbial sulfate reduction. Using geochemical modeling, we show that unlike the reduction of ferric minerals, the reduction of S⁰ becomes more energetically favorable as pH increases. We also show experimentally that, under alkaline conditions, *Shewanella oneidensis* is capable of reducing S⁰ to sulfide, which then reacts with ferric minerals to form Fe^{II}. We suggest that in slightly alkaline environments where both sulfate and Fe^{III} are available, metal-reducing bacteria may survive primarily by respiring the S⁰ created by sulfate-reducing bacteria.

Global variation in Fe-isotopic composition of arc basalts indicate a variably oxidised and metasomatised mantle wedge source?

JOHN FODEN^{1*}, PAOLO SOSSI^{2,1}
AND GALEN HALVERSON^{3,1}

¹University of Adelaide, Geology and Geophysics,

²Research School of Earth Sciences, ANU, Canberra ACT

³McGill University, Earth and Planetary Sciences,

New Fe-isotope data on basaltic samples from the global network of subduction arcs is used to investigate whether there is systematic variation in Fe isotopic compositions resulting from varying source oxidation. This in turn may reflect variation in slab-derived water flux.

Global arc magmas have elevated Fe³⁺/ΣFe values in the range >0.1 to 0.5 (our data set has a mean of ~ 0.35), compared to MORB with values in the range 0.1-0.2. [1,2]. For lavas, our δ⁵⁷Fe data (vs. IRMM-014) span a range from -0.2 to +0.2 (± 0.04), with a mean around +0.05. This is significantly lighter than the mean for MORB and BABBs (~+0.10) [3], though the arc data sets clearly trend towards heavier values for more fractionated samples. Light δ⁵⁷Fe values in arcs may reflect that the mantle wedge in many arcs is more depleted than MORB source [4]. Our δ⁵⁷Fe values show moderate positive correlation with Fe³⁺/ΣFe.

Using the subduction thermal parameter (ϕ) [5] which is a proxy for the thermal structure of the down going slab, we find a positive correlation of δ⁵⁷Fe where ϕ/100 > 50, but for values < 50 there seems to be a negative correlation. Interestingly we find that mineral separates from some ultramafic xenolith suites have very light δ⁵⁷Fe values (CPX as low as -0.79 & Ol at -0.66) apparently reflecting metasomatism [6] and extending the negative ϕ - δ⁵⁷Fe trend.

A possible explanation is that the iron isotopic values and trends of primitive arc basalts reflect three influences; 1. source oxidation, 2. fraction of melting and 3. impact of metasomatism.

[1] C-T. Lee et al, (2010) Nature 468, 681-685; [2] Bezos & Humler (2005) Geochim. Cosmochim. Acta 69, 711-725; [3] Teng et al, (2013) Geochim. Cosmochim. Acta, 107, 12-26; [4] Weyer and Ionov (2007) EPSL; [5] Syracuse and Abers (2006) G3; [6] Poitrasson et al, (2013) CMP .

Sorption and desorption processes of U(VI) on iron (hydr)oxide phases

H. FOERSTENDORF*, K. HEIM AND N. JORDAN

Helmholtz-Zentrum Dresden-Rossendorf, Institute of Resource Ecology, 01314 Dresden, Germany
(*correspondence: foersten@hzdr.de)

In this comparative study, the surface speciation of uranium(VI) on ferrihydrite (Fh) and maghemite (Mh) were investigated by vibrational spectroscopy. The experimental setup allows the monitoring of the surface processes at the water-solid interface in real time with a time resolution in the subminute time range. The performance of the experiments under inert gas atmosphere and under ambient conditions provides further insight into the molecular events of the binary and ternary sorption systems, respectively.

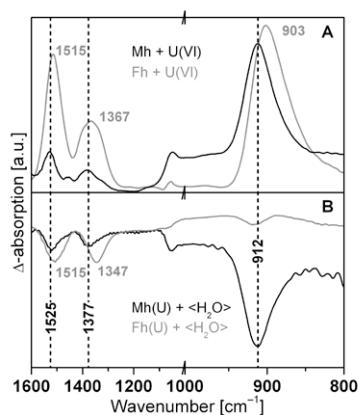


Figure 1: IR spectra of the sorption (A) and desorption (B) processes of U(VI) on ferrihydrite (Fh) and maghemite (Mh) in ambient atmosphere.

The spectra clearly demonstrate a characteristic surface speciation in dependence of the solid phase. On Fh, the formation of ternary inner sphere complexes are observed as it was derived earlier [1]. In addition, the time-resolved spectra reveal the change of the surface speciation of atmospherically derived carbonate upon U(VI) sorption [2].

From the sorption experiments on Mh, outer sphere complexation of the uranyl ion can be derived. In ambient atmosphere, contributions of carbonate ions to the U(VI) surface speciation on Mh can not be ruled out.

[1] Ulrich *et al* (2006) *Geochim. Cosmochim. Acta* **70**, 5469-5487. [2] Foerstendorf *et al* (2012) *J. Colloid Interface Sci.* **377**, 299-306.

Physical properties of CO₂-rich melts at mantle conditions: A simulation study

N. FOLLINET¹, N. SATOR¹ AND B. GUILLOT¹

¹LPTMC, Université Pierre et Marie Curie (Paris 6), Boîte courrier 121, 4 place Jussieu, 75252 Paris cedex 05, France (*correspondence: guillot@lptmc.jussieu.fr)

There are growing evidences that CO₂-rich melts play a key role in the geodynamics, chemical differentiation and degassing of the upper mantle. Experiments at HT-HP on carbonate-silicate assemblages suggest that the onset of mantle melting may start as deep as 300 km in generating carbonatitic melts at very low melt fraction [1]. The electrical conductivity anomalies measured in the asthenosphere by magnetotelluric sounding can be explained by the presence of highly conductive phases which could be CO₂-rich [2,3]. On the other hand, the composition of primary magmas at the origin of hypabyssal kimberlites has been recently reevaluated and should be transitional between carbonate and silicate melt with low SiO₂ contents [4]. Furthermore it appears that the role and abundance of the carbonatite volcanism has been underestimated [5], and recent database and world distribution map of carbonatites [6] show that a carbonatitic magmatism was abundant from the late Archean to the Phanerozoic.

However, the physical properties of carbonatites and carbonated silicate melts are poorly known. Here we present an evaluation of the physical properties of CO₂-rich melts by molecular dynamics (MD) simulation. This atomistic approach relies on the development of a realistic force field to describe the incorporation of CO₂ in a silicate melt [7] and that of a silicate component in a carbonate melt, as well. With this force field it has been possible to simulate a large composition range from carbonatites to CO₂-saturated basalts with a special emphasis on the transitional compositions (0-15wt% SiO₂). The EOS, the viscosity and the electrical conductivity of the simulated melts have been evaluated at mantle conditions. It is found that the composition has a large influence on the melt properties, a result which has important geophysical implications.

[1] Dasgupta *et al* (2013), *Nature* **493**, 211-215. [2] Gaillard *et al* (2008), *Science* **322**, 1363-1365. [3] Yoshino *et al* (2012), *Phys. Earth Planet. Inter.* **194-195**, 1-9. [4] Brooker *et al* (2011), *Bull. Volcanol.* **73**, 959-981. [5] Wooley & Bailey (2012), *Mineral. Mag.* **76**, 259-270. [6] Wooley & Kjarsgaard (2008), *Can. Mineral.* **46**, 741-752. [7] Guillot & Sator (2011), *GCA* **75**, 1829-1857.

Aerosol trace metal fractional solubility and chemical composition of marine aerosols at the CVAO

K. W. FOMBA*, K. MÜLLER AND H. HERRMANN

Leibniz-Institut für Troposphärenforschung, Permoserstr. 15, 04318 Leipzig, Germany (*correspondence: fomba@tropos.de)

The atmosphere and ocean interact in various ways that significantly affect the local and global climate. Mineral dust deposition onto the oceans plays a vital role as it provides key nutrients to the ocean biota and thereby influence the oceanic biogeochemical cycle and thus oceanic emissions. In this work we present chemical and trace metal composition of marine aerosol at the Cape Verde Atmospheric Observatory (CVAO) obtained during periods of and without Saharan dust storms.

The data were collected during intensive field campaigns and continuous measurements from January 2007 until now. During this period PM₁₀ samples were collected using a 5-stage Berner impactor for size-resolved measurements and a high volume DIGITEL DHA-80 sampler with PM₁₀-inlets.

Our observations show that about 45% of the year are dominated by remote conditions while the rest was influenced by continental and Saharan dust air masses. Continental air masses contained significant amounts of Saharan dust with trace metals and organic carbon compared to marine air masses. Dust events were observed mostly during the winter months of the year. During the events, the contribution of sea salt to the total PM₁₀ mass was found to be low. The sea salt and Saharan dust in the particle were found in the coarse mode fractions while the organics and non-sea salt components were observed mostly in the submicron fraction. Interannual and seasonal variability were observed for nearly all aerosol constituents. Strong seasonal trends were observed for ammonium and non-sea salt sulfate with peaks observed in the spring and summer, respectively.

Significant differences were observed in the trace metal composition (especially iron) between days of Saharan dust outbreaks (about 20.0 Fe, 16.4 Ca, 2.3 Ti, and 0.3 Mn $\mu\text{g}/\text{m}^3$) and days without (less than 10.0 ng/m^3). Mn was found to be the most soluble trace metal followed by Zn and Fe. Iron was mostly present in Fe (III) form with Fe (II) often found only at lower pH. Dissolution experiments at varying pH (from 5.5 to 2) showed significant increase in metal solubility at lower pH with an increase of over 3 orders of magnitude for both Fe (II) and Fe(III) and about two orders of magnitude for Cu and Mn.

The unexpected 'compatible' behavior of W during mantle melting: Implications for the W/U ratio of the lunar mantle

R.O.C. FONSECA^{1*}, G. MALLMANN², J. E. SOMMER¹, P. SPRUNG³, I. M. SPEELMANN AND A. HEUSER¹

¹ Steinmann Institute, Universität Bonn, Germany
(*correspondence: raul.fonseca@uni-bonn.de)

² Institute of Geosciences, University of São Paulo, Brasil

³ Institut für Planetologie, Universität Münster, Germany

The timing of core formation is essential for understanding the early differentiation history of the Earth and the Moon. Because Hf is lithophile and W is siderophile during metal-silicate segregation, the decay of ¹⁸²Hf to ¹⁸²W (half-life of 9 Ma) has proven to be a useful chronometer of these major planetary differentiation events. A key parameter for the interpretation of the ¹⁸²Hf/¹⁸²W chronometer is the Hf/W ratio of the primitive (i.e. undepleted) mantle. Since W is incompatible during mantle melting, its ratio relative to U and other similarly incompatible elements in basalts (e.g. Th, Ba) may be used as proxies for their mantle sources. However, the assumption that W and U are equally incompatible may be flawed for petrological systems that equilibrated over a large range of $f\text{O}_2$. Although W is typically perceived as being homovalent, evidence suggests that U is heterovalent over the range of $f\text{O}_2$ experienced in the mantle of the Earth and the Moon respectively.

Here we report partitioning data for W, U, high-field strength elements (HFSE), and Th between clinopyroxene, orthopyroxene, olivine and silicate melt. In agreement with previous studies, we show that these elements behave as homovalent elements at $f\text{O}_2$ higher than QFM. However, both W and U become more compatible at $f\text{O}_2$ lower than QFM, indicating a change in their redox state.

This result is particularly unexpected, because W is thought to be hexavalent even at very low $f\text{O}_2$. However, the much higher compatibility of W⁴⁺ as compared to W⁶⁺, means that even a small fraction of W⁴⁺ will increase the overall compatibility of W. Our results imply that under the reducing conditions in which lunar differentiation is thought to have taken place (i.e. ~IW-1), W is likely to become fractionated from U. These newly obtained partitioning data carry with them the potential implication that the W-to-U ratio of lunar basalts does not directly represent their mantle source. More high-precision measurements of W and U abundances in lunar rocks are needed to more precisely estimate the Hf/W of the Moon and thus, the age of the Moon itself.

Geophysical Evidence for Iron Mineral Transformation in a Petroleum Contaminated Aquifer

BRITTANY R. FORD^{1*}, ESTELLA A. ATEKWANA¹,
GAMAL A. AAL¹ AND ELIOT ATEKWANA¹

¹Oklahoma State University, Stillwater, OK, USA

(*correspondence: brittany.ford@okstate.edu)

Hydrocarbon-contaminated environments are excellent laboratories for understanding microbial mediated iron reduction. The excess carbon serves as an electron donor, which can stimulate microbial activity if electron acceptors, such as iron, are available. Previous studies have suggested that magnetic susceptibility (MS) measurements are a potential tool to follow microbial Fe mineral transformation. In this study, we investigated the MS and iron content variations that exist at a hydrocarbon contaminated aquifer in order to determine the major magnetic mineral present. Our results show large down hole excursions in the MS at the contaminated location coincident with peak concentrations of Fe(II) and Fe (Total), and the presence of *Geobacter* species. Variability in the down hole MS at the uncontaminated locations are not associated with peaks in Fe(II) or presence of *Geobacter* ; However, Fe(III) dominates the Fe pool. Our results also show high marked increase in the MS values in the vadose zone at the contaminated locations concomitant with higher concentrations of Fe(II) and Fe (Total). This could be evidence for the microbial reduction of Fe(III) minerals, producing magnetic mineral phases. Trace metal data will be used to determine the chemistry of the sediments and identification of the local mineralogy. With this information, we anticipate characterizing the processes that control the biogeochemical cycling of iron and carbon.

Ice age carbon dynamics of the interior Atlantic Ocean inferred from a highly resolved sedimentary depth transect

ALAN FOREMAN^{1*}, CHRISTOPHER CHARLES¹,
JAMES RAE², NIALL SLOWEY³ AND JESS ADKINS²

¹Scripps Institution of Oceanography, UCSD, La Jolla, California, USA (*Correspondance: aforeman@ucsd.edu)

²Division of Geological and Planetary Sciences, California Institute of Technology, Pasadena, California, USA.

³Department of Oceanography, Texas A&M University, College Station, Texas, USA

Many models show that the relative intensity of stratification must be a primary variable governing sequestration and release of carbon from the ocean over ice ages. The observations necessary to test these model-derived hypotheses are not yet sufficient, but sedimentary depth transects represent a promising approach for making progress. Here we present results from a suite of 24 cores spanning water depths of 1000-3700 meters, collected from the Namibian margin. This is an especially suitable location to collect vertical depth transects over ice age cycles, given that it is sensitive to the intersection of the principal water masses involved in the thermohaline circulation of the Atlantic. In aggregate, these cores allow for depth transects that have roughly 100 meter vertical resolution, and “steady state” benthic foraminiferal proxy profiles can be compiled at various points spanning the last full ice age cycle.

In this presentation, we contrast the “steady state” vertical distribution of benthic foraminiferal tracers from Marine Isotope Stages 5e, 5a, 4, and the LGM, compiled from the full suite of cores, with the transient evolution of these tracers over the last and penultimate deglaciation in a subset of the cores. The comparison between purely physical tracers (e.g. $d^{18}O$) and tracers that are sensitive to the carbon cycle (e.g. $d^{13}C$ and B/Ca) offers critical insight to the relationship between deep/mid-depth stratification and global carbon dynamics. The observation of the nonconservative behavior of mid-depth $d^{13}C$ in the South Atlantic during the so-called 'Mystery Interval,' for example, will be examined in light of the suggested carbon inputs external to the ocean-atmosphere system [1].

[1] Tessin, A.C. and D.C. Lund. (2013) *Paleoceanography* Advance online publication. doi: 10.1002/palo.20026

Lawsonite veins in eclogite as an archive of subduction zone fluids from 45-80 km depth (Sivrihisar, Turkey)

KATHERINE F. FORNASH¹, MICHAEL A. COSCA²
AND DONNA L. WHITNEY¹

¹Earth Sciences, University of Minnesota, Minneapolis USA
(forna011@umn.edu, dwhitney@umn.edu)

²USGS, Denver USA (mcosca@usgs.gov)

The lawsonite eclogite and blueschist terrane near Sivrihisar, Turkey, is a pristine archive of subduction zone fluids that were present in metabasaltic and metasedimentary rocks at depths of 45-80 km. Few rocks have returned from these depths in subduction zones without extensive overprinting of mineral assemblages and textures; Sivrihisar eclogite, however, contains unaltered lawsonite (lws) and other minerals that equilibrated at pressures of up to 2.5 GPa and 550 C. Major and trace element zoning of minerals in HP veins and host rocks, microstructures of minerals deformed at HP conditions, and the chemical and physical characteristic of lws-bearing veins record episodic mineral-fluid interaction during subduction metamorphism, likely at or near the slab interface with the overlying (serpentinized) mantle wedge. The margins of lws eclogite pods and layers contain networks of mm- to cm-scale veins containing lws + garnet (grt) + phengite (ph) (\pm paragonite). Eclogite extensively retrogressed to chlorite + epidote contains monomineralic lws veins. Lws-grt-ph veins in eclogite are rimmed by lws-grt-ph-glaucophane zones, indicating that veining occurred at least in part during decompression under lws-blueschist facies conditions. High-precision and -spatial resolution *in situ* UV laser ablation Ar/Ar dating of ph single crystals document a sequence of events, from lws eclogite metamorphism to vein formation to lws blueschist metamorphism and eclogite retrogression over the course of at least 10 million years in the Late Cretaceous.

REE distribution in granulite assemblage from lower crust of the Serre massif (Calabria-Italy)

A. FORNELLI^{1*}, A. LANGONE², F. MICHELETTI¹,
A. MUSCHITIELLO¹ AND G. PICCARRETA¹

¹Earth science and geo-environmental Dep., Bari University
Italy, (annamaria.fornelli@uniba.it)

²Institute of Geosciences and Earth Resources (CNR) - U.O.S.
of Pavia

Two samples of mafic granulites with porphyroblastic garnet were investigated for REE distribution between accessory and major mineral phases. The granulites were affected by Variscan metamorphism which began with a compressive event around 340-350 Ma and was followed by decompressional stages between 325 Ma and 280 Ma evidenced by re-setting or new growth of zircon [1, 2]. The studied samples differ for the presence/absence of amphibole and biotite. In the sample with amphibole and scarce biotite the porphyroblastic garnet is relatively rich in REE: Σ HREE=190 ppm at core and Σ HREE up to 702 ppm at rim. The garnet in the sample lacking amphibole shows decidedly higher REE abundances: Σ HREE=2463 ppm at core and Σ HREE up to 14784 ppm at rim. Both garnets show an increase of HREE in the peripheral zone due to consumption of the primary rim during corona formation and sequestration of REE in smaller volumes. The abundance and distribution of REE in the zircons from the two samples are comparable. They show REE fractionated patterns with Lu_N/Gd_N variable from 42.91 to 24.84. Even the orthopyroxenes from the two samples contain similar abundance of REE (Σ REE from 6 to 13 ppm). The difference in REE contents in garnet seems to be connected to the presence of amphibole as major mineral phase. So the empirical REE distribution coefficients (D) between zircon and garnet are controlled by REE contents of garnet in the studied rocks and caution should be placed on the use of $D_{zrn/grt}$ to infer chemical equilibrium between domains of garnet and zircon and to constrain the significance of the zircon ages.

As expected under granulite facies [3], the analysed amphibole is enriched in REE everywhere it occurs (inclusion, matrix, corona). So it appears that in the case study, the equilibrium between garnet and amphibole is indicated by the calculated DREE values which are lower than 1 from La to Dy (0.001-0.9) and higher than unity from Ho to Lu (1.5-15).

[1] Fornelli *et al* (2011) *Mineral Petrol* **103**, 101-122. [2] Fornelli *et al* (2012) *Int J Earth Sci* **101**, 1191-1207. [3] Skublov & Drugova (2003) *Can Mineral* **41**, 383-392.

The forcing of climate by CO₂ on geological timescales

GAVIN L. FOSTER^{1*} AND MIGUEL A. MARTÍNEZ-BOTÍ¹

¹Ocean and Earth Science, National Oceanography Centre
Southampton, University of Southampton, Southampton
SO14 3ZH, UK (*correspondence:
Gavin.Foster@noc.soton.ac.uk)

Understanding the role of atmospheric CO₂ in driving global climate is one of the great challenges facing Earth Scientists today. Ultimately we are driven by the pressing need to predict how hot the Earth will get in the near future. There are many ways we can achieve this increased understanding – ranging from examining the most recent historic past to basing our predictions on an understanding of the modern climate system encapsulated in numerical climate models. Increasingly the palaeo-community has been willing to contribute to the debate, since the geological record is littered with examples of warm climate states, in part associated with elevated levels of atmospheric CO₂. Whilst these provide real world examples of how the Earth System responds to CO₂ forcing, no geological period is an adequate analogue for our warm future. Furthermore, climate models suggest that a significant level of state dependency exists for climate sensitivity. Therefore examining the response of the climate system to CO₂ forcing in the Eocene, for example, does not have direct relevance due to the different continental arrangements, ice sheet configurations and vegetation. When these factors are accounted for, it has been recently shown that the available palaeo-data largely confirms the sensitivity of the Earth system to CO₂ forcing determined by climate models alone [1].

Despite this overall conformity, there are several warmer time periods in the geological record (e.g. the Pliocene) that apparently exhibit significantly elevated climate sensitivities (e.g. [1]). Importantly, these are above the range typically, but not always (e.g. [2]), achievable in climate models – clearly suggesting that the Earth can exist in states that appear to be particularly sensitive to CO₂ forcing. Such a state dependency to sensitivity has worrying implications for predictions of our warm future climate. In this contribution we use new data from a number of key periods to further probe the response of the Earth system to CO₂. This provides new insights into the possibility of “hidden” feedbacks and the likelihood of a state dependency to climate sensitivity.

[1] Rohling, E.J., *et al*, 2012. *Nature*, **491**: 683-691. [2] Stainforth, D.A. *et al*, 2005. *Nature*, **433**(7024): 403-406.

Dual explosive activity revealed by petrochemical and mineralogical data on tephra: Peculiar Roman-age eruptions of Stromboli volcano

L. FRANCALANCI^{1,2}, E. BRASCHI^{1,2}, S. DI SALVO¹,
F. LUCCHI³ AND C. M. PETRONE⁴

¹Dip. Sci. della Terra, Università degli Studi di Firenze, via La Pira 4, 50121, Firenze, Italy

²CNR, IGG, sezione di Firenze, via La Pira 4, 50121, Firenze, Italy

³Dip.Sci. della Terra e Geo-Ambientali, University of Bologna, Piazza Porta S.Donato 1, 40126, Bologna, Italy

⁴The Natural History Museum, Department of Earth Sciences, Cromwell Road, SW7 5BD London, UK

The Pizzo-Sopra-la-Fossa tuff cone of Stromboli volcano has been investigated by stratigraphic, petrographic, mineralogical, geochemical and isotopic studies. Its deposits are presently the remnant of a collapsed tuff cone formed by a thick pyroclastic sequence of bomb, lapilli and ash fallout and surge levels. The main outcrop is located above the active craters where acid fumarolic gases strongly altered the juvenile clasts. For this reason, the Pizzo-Sopra-la-Fossa sequence was poorly studied, although it represents a key point for recognising the recent evolution of Stromboli. We mainly focused our studies on Le-Croci outcrops characterized by a 6 meters thick sequence of mainly unaltered fall deposits.

Two groups of feeding magmas have been identified, a group constituted by high-K basalts to high-K basaltic-andesites (Pizzo-HKCA) and another formed by shoshonitic basalts (Pizzo-SHO). The two groups can be distinguished on the bases of petrographic, mineralogical and geochemical data. Pizzo-HKCA products have lower phenocryst contents, incompatible trace element abundances and Sr isotopic ratios, with higher ¹⁴³Nd/¹⁴⁴Nd values than Pizzo-SHO. They also show differences in mineral phase composition and zoning.

There are also clear evidences that the two magmas were erupted contemporaneously, suggesting the presence of two distinct magma reservoirs, possibly located at different depth.

Based on crucial stratigraphic correlations (S.Bartolavolas, Lower-Sequence and Post-Pizzo-series), it has been recognised that this dual explosive activity on top of Stromboli, forming the Pizzo-Sopra-la-Fossa tuff cone, occurred only 2 ka ago (during Roman-age), possibly along the activation of NE-trending eruptive fractures.

The main MORB crustal contaminant: Geochemistry of magma chamber roof experimental anatectic melts, and residues

L. FRANCE¹; J. KOEPKE²; B. ILDEFONSE³;
C.J. MACLEOD⁴; M. GODARD³ AND E. DELOULE¹

¹CRPG; UMR 7358, CNRS; Université de Lorraine;
(lyde@crpg.cnrs-nancy.fr)

²Institut fuer Mineralogie; Hannover; Germany

³GM; Université Montpellier 2; Montpellier; France

⁴School of Earth; Cardiff University; Cardiff; UK

Mid-ocean ridge basalt (MORB) is the most abundant magma type at the Earth's surface. It is widely studied to infer mantle compositions and melting processes. However, MORB liquids are also the complex end-product of a variety of intracrustal processes such as fractional crystallization, melt-rock interaction, and contamination. Deciphering the relative contribution of these processes is of first-order importance. Contamination at ocean crustal levels is likely, and may occur at magma chamber margins where fresh magmas can interact with previously hydrothermally altered rocks. Characterizing the composition of this crustal contaminant component is critical if we are to understand the relative importance of each component in the resulting MORB liquid.

In this contribution we present the results of experiments that reproduce the natural processes occurring at oceanic magma chamber roofs, by melting a representative sample of the sheeted dike complex. Anatectic melts thus produced represent the main MORB crustal contaminant. We characterize these melts for major and trace elements, showing them to be enriched in B, Zr, Hf, and depleted in Sr, Ti, V. In comparison to MORB series, we also document relative element fractionations, with enrichments of: Th relative to Ba; U relative to Nb; Nd relative to Sr; and Hf relative to Sm. We derive bulk partition coefficients for element partitioning during magma chamber roof anatexis; those are valuable tools for tracking MORB contamination.

Comparison with natural samples from the East Pacific Rise and the Oman ophiolite shows that anatectic melts can crystallize *in situ* to form oceanic plagiogranite intrusions, and that residual assemblages associated with the hydrous partial melting stage are represented by the granoblastic dikes and enclaves (also named beerbachites) commonly recognized at the root of the sheeted dike complex at present-day and fossil oceanic spreading centers.

Balancing chemical and physical erosion in the Ganga basin

CHRISTIAN FRANCE-LANORD¹, VALIER GALY²,
ANANTA GAJUREL³, JÉRÔME LAVÉ³, MAARTEN LUPKER⁴
AND GUILLAUME MORIN¹

¹CRPG-CNRS, Université de Lorraine, BP 20, Vandoeuvre-France cfl@crpg.cnrs-nancy.fr

²WHOI, Woods Hole, USA. vgal@whoi.edu

³Tribhuvan U. Kathmandu Nepal, apgajurel@gmail.com

⁴ETHZ, Zurich, Switzerland. maarten.lupker@erdw.ethz.ch

River basins at various scales undergo both physical and chemical erosion that should be balanced over long time scale. At short time scale of few years to tenth of years, it is however unlikely that steady state of erosion is verified. More likely, under variable climatic or geomorphologic conditions one term of erosion may be favoured over the other. Testing such imbalance is difficult because it requires to compare fluxes of weathering from both dissolved and particle phases.

Here we examine modern budget of erosion of three imbricated Himalayan basins: the Khudi river that is a small stream on south Himalayan flank, the Narayani drainage of central Nepal and the whole Ganga basin. Areas vary from 153 to 872000 km². This approach is based on daily sampling of suspended sediments that allow refine estimates of average composition of the dissolved and particle loads. We then compare direct weathering fluxes of Na and K deduced from dissolved load to weathering fluxes deduced from the comparison between estimated source rock and exported sediments. Uncertainties are principally linked to the net sediment flux determinations and to the knowledge of average source rock composition. For both Ganga and Narayani, the estimates tend to indicate that physical erosion and chemical erosion are close to balance within uncertainties. In contrast, the Khudi basin show clear imbalance in favour of physical erosion. This is likely due to the exceptional intensity of landslide erosion than to intensified soil erosion in this basin.

Effect of pH and temperature on zeolite precipitation rates and mechanisms from amorphous precursors

P.C.M. FRANCISCO* AND T. SATO

Laboratory of Environmental Geology, Graduate School of Engineering, Hokkaido University 060-8628 Japan
*(correspondence: pcmfrancisco@gmail.com)

The predicted precipitation of zeolites due to the dissolution of bentonite during alkaline alteration in barrier systems for the geological disposal of radioactive wastes may alter the properties of the barrier system. It is therefore important to elucidate the formation rates and mechanisms of zeolites over a wide range of conditions in order to predict their crystallization behavior in barrier conditions. Zeolite formation is typically preceded by an amorphous precursor, the transformation of which is seen as a rate-controlling step. However, the mechanism and rates of transformation remain poorly understood. This study focuses on the effect of pH and temperature on the transformation of the amorphous precursor into crystalline zeolite.

Batch zeolite synthesis experiments were carried out at pH ranging from 9.5 to 13.5 and at temperatures ranging from 25°C to 90°C by mixing NaOH, NaAlO₂ and Na₂SiO₃·9H₂O at varying proportions to achieve a fluid with the composition of 0.5 M Na, 0.24 Si and 0.03 M Al. The precipitates were extracted at different times by centrifugation and freeze drying. The supernatants were analyzed using ICP-AES for Al and Na and UV-Vis for Si. The solids were examined using XRD, FTIR, Raman spectroscopy and SEM-EDX.

Results show the rapid formation of an amorphous precursor phase, followed by slower transformation into crystalline zeolite. Crystal size distribution data suggest that the dominant transformation mechanism is dissolution and reprecipitation. Higher pH and temperature promotes rapid transformation of the amorphous precursor to zeolite. Spectroscopic data indicate lower degrees of Al substitution and lower amounts of T-OH bonds in solids formed at lower pH. These results indicate that precursor phases formed at lower pH are relatively more stable and less susceptible to dissolution. Therefore, zeolite precipitation is promoted at higher pH due to the rapid dissolution of the amorphous precursor. The results of this study show that pH controls the structure and chemistry, and therefore, the stability of the zeolite precursor phases.

Archean geodynamic: Fingerprinting sagduction vs subduction processes

CAMILLE FRANÇOIS^{1,2*}, PASCAL PHILIPPOT¹,
PATRICE REY², DANIELA RUBATTO³
AND JEAN-FRANÇOIS MOYEN⁴

¹ Institut Physique du Globe de Paris, 1 rue Jussieu, 75238 Paris, France, (*correspondance: francois@ipgp.fr)

² EarthByte Research Group, School of Geosciences, University of Sydney, NSW 2006, Sydney, Australia

³ Research School of Earth Sciences, The Australian National University, Canberra 0200, Australia

⁴ Université de Saint-Etienne, 42023 Saint-Etienne, France

The geodynamic processes responsible for the formation of Archean crust are matter of debate. Contrary to the general belief, sagduction and subduction are not incompatible processes, as both involve the deep burial and exhumation of surface and near-surface rock units. In order to better understand how to distinguish these processes, we investigated mid- to high-pressure metamorphic rocks from two key Early Archean localities: i) the East Pilbara Granite-Greenstone Terrane (EPGGT, Western Australia), considered as a reference model for sagduction [1], and ii) the Barberton Greenstone Belt (BGB, South Africa) either described in terms of subduction [2] or sagduction [3]. These two terranes display narrow belt of greenstone (ultramafic and mafic metabasalts and minor metasedimentary rocks) in association with broad TTG (tonalite-trondhjemite-granodiorite) granitoids. Estimates of the rate of heating/cooling and burial/exhumation of these granite-greenstone belts were evaluated using a combination of structural, metamorphic, and geochronological data coupled with numerical simulations.

In the EPGGT, we confirm that burial and exhumation of cold and dense greenstones is linked in time with crustal melting and granitoid dome formation. Thermobarometric, geochronological and numerical constraints indicate that metamorphism and deformation occurred within less than 10 Ma, thus implying burial and exhumation rates of some centimeters per year. The same approach applied to the BGB yielded a more complex and probably polymetamorphic history and suggest a possible different scenario. Burial/exhumation rates are possibly one order of magnitude slower and more progressive with respect to EPGGT, implying longer process.

[1] Delor *et al* (1991) *C. R. Acad. Sci. Paris* **312**, 257-263. [2] Moyen *et al* (2006) *Nature* **442**, 559-562. [3] Van Kranendonk (2011) *J. of Af. Earth Sci.* **60**, 346-352

Metakomatiites, Dynamical Modeling and the Late Veneer

E.A. FRANK^{1,*}, W.D. MAIER², R.M. CANUP³
AND S.J. MOJZSIS¹

¹University of Colorado, Dept. of Geological Sciences & Center for Lunar Origin and Evolution (CLOE), NASA Lunar Science Institute, Boulder, CO 80309-0399, USA
(*correspondence: elizabeth.frank@colorado.edu)

²UNIVERSITY OF OULU, LINNANMAA, 90014 OULU, FINLAND

³Southwest Research Institute, Planetary Science Directorate, Boulder, CO 80302, USA

During core formation, silicate mantles are stripped of their highly siderophile elements (HSEs) due to strong partitioning behavior into metal. However, the HSEs are present in mantle-derived rocks at concentrations orders of magnitude higher than expected. Analysis of komatiites shows that there is a time-dependent HSE depletion trend in late Archean and early Proterozoic samples [1]. We present data for older (>3.75 Ga) ultramafic schists to (i) show that they are metamorphosed komatiites; (ii) extend the HSE depletion trend into the Eoarchean; and (iii) evaluate models to explain this trend. One hypothesis attributes HSE enhancement to an extraterrestrial source, a late accretion event dubbed the "Late Veneer" (LV) [2]. Assuming a chondritic composition, ~1% of Earth's current mass is required to cause the observed signal. The HSEs are in chondritic relative proportions despite their dissimilar metal-silicate partition coefficients. An LV may not be exclusive to Earth: there is evidence in martian meteorites and lunar samples that these bodies may have experienced their own LVs [3,4], lending credence to an extraterrestrial explanation. Dynamical simulations have shown the presence of planetesimals at the time of the LV to be a plausible reservoir for an LV [5]. To test this possibility, simulations [cf. 6] used four different impact velocities (1.1, 1.2, 1.3, and 1.4 times Earth's v_c), three impact angles (30°, 45° and 60°), and two different impactor masses (1% and 0.1% M_e). The 1% mass assumption represents a single LV impactor, while 0.1% Earth mass impactors correlate to one of ten impactors with an equivalent total mass. The results have defined the parameter space that would have allowed large impactors to cause the HSE enhancement observed in the mantle.

[1] Maier *et al* (2009) *Nature* **460**, 620–623. [2] Chou (1978) *Proc. Lunar Planet. Sci. Conf.* IX, 219–230. [3] Day *et al* (2010) *Earth Plan. Sci. Lett.* **289**, 595–605. [4] Brandon, A.D. *et al* (2012) *Geochim. Cosmochim. Acta* **76**, 206–23. [5] Bottke *et al* (2010) *Science* **330**, 1527–1530. [6] Canup, R. (2008) *Icarus* **196**, 518–538.

Metamorphic-hydrothermal transition in the alteration of pillow and dike basalts from the Rodriguez Triple Junction

H. FRANKE¹, K. HEESCHEN¹
AND U. SCHWARZ-SCHAMPERA¹

¹Federal Institute for Geosciences and Natural Resources (BGR), D 30655 Hannover, Germany,
(Henrike.Franke@bgr.de)

Alteration processes caused by interactions between seawater and basalt are one of the main effects which modify the geochemical and mineralogical composition of the oceanic crust, alter the mineral assemblages to upper greenschist facies and may form seafloor massive sulfides at mid-ocean ridges.

A series of INDEX cruises explore the intermediate to slow spreading southern Central Indian Ridge. This area is characterized by complex structured rift valleys and isolated active volcanic edifices in the central graben. Active hydrothermal activity is associated with a small satellite volcanic ridge at the eastern rift valley wall (Kairei). Dredges and TV-grabs were used to recover fresh and altered basalt samples in the vicinity of the vent field. This study presents the effects of variable alteration processes, related to (i) high-temperature near-neutral pH seawater and isochemical metamorphic overprinting, and (ii) seawater-derived acidic hydrothermal alteration.

The tholeiitic basalts are represented by sheet flows and pillow basalts with dispersed vesicles up to cm sizes. They can be distinguished into two groups: 1) basalts with an aphyric to porphyritic texture with variable phenocrysts and 2) holocrystalline basalt sample. Both fresh basalt types display a mineral composition of major plagioclase, minor olivine, clinopyroxene, and Cr-spinel. The mineral composition of altered rock samples indicate a range from low temperature basalt seawater alteration up to upper greenschist facies-like temperatures including albite, chlorite, actinolite, epidote(?), sphene while the plagioclase is almost pristine. The seawater altered rocks contain saponite, celadonite, and palagonite within the vitrious groundmass.

Basalts at mid-ocean ridges display a variety of alteration processes which contribute to sustained element fluxes. The Rodriguez triple junction with a variety of rift-related processes is a key region to study the diverse influence of fluid flow along mid-ocean ridges.

Analysis of nanostructures consisting of the Al-pyrocatechol complex using spectroscopic ellipsometry

MARTINA FRANKE

Department of Soil Science, University of Trier, D-54296
Trier, Germany (s6mafran@uni-trier.de)

In this study, spectroscopic ellipsometry was applied by using the photon energy over the range of 1.2-5.4 eV to determine the optical properties n and k from thin films of nanostructures consisting of pure Al and the Al-pyrocatechol complex. In addition, the real and imaginary part of the dielectric function ϵ was determined. During the preparation, two types of mirrored glass were used being of different thickness of the Al film in order to examine the equality of the results. Thin films of the Al-pyrocatechol complex were synthesized by adsorption in a gas-solid phase at 50 °C in the presence of atmospheric pressure for a period of 21 days in total darkness. The modeling of the optical response from the analyzed surfaces resulted in two forms of absorption spectra which showed Al and the Al-pyrocatechol complex. In this calculation, five plots of absorption spectra were determined. At this stage, rough forms of the first spectra were transformed to a smooth form by using a smoothing-spline algorithm. The third spectra were calculated by applying a surface-excess function to eliminate the interfering optical response of Al. Concerning this matter, the second derivative of the surface-excess function was calculated and observed in the fourth absorption spectra. The fifth plot showed the reference spectra of Al. In the UV region of the metal-ligand spectrum, an absorption maximum appeared at 275 nm. Within the Vis region of the spectrum, ligand bands from the complex occurred with an absorption maximum of 525 nm. In consequence of the addition of OH auxochroms in the process of complexation, a rise of the chromophore system occurred causing an increase of the absorption intensity. Fine nanostructures of the Al-pyrocatechol complex were ascertained as a result of the spectroscopic ellipsometry.

Acknowledgement: Christoph Cobet and Norbert Esser, Institute of Solid-State Physics, Technical University of Berlin, Germany, is thanked for the glass mirrors and the spectroscopic ellipsometry.

[1] Franke M (2007) *Geochim. Cosmochim. Acta* 71 (15), Suppl. 293. [2] Franke M (2002) diploma thesis, Univer. of Trier, 187 pp. [3] Kelly M K et. al. (1993) *Surface Science* 285, p. 282-294.

Carbonatites age of the Tikshezero massive (North Karelia, Russia)

FRANTZ N.A.¹, RODIONOV N.V.² AND LOKHOV K.I.³

^{1,3} Saint -Petersburg State University, St.Petersburg, Russian Federation, (nfrantz@mail.ru),(Kirill_Lokhov@vsegei.ru)

² Centre of Isotopic Research, Russian Geological Research Institute (VSEGEI), St. Petersburg, Russian Federation, (nickolay_rodionov@vsegei.ru)

In recent years, a lot of new ages of the Tikshezero carbonatite massive were obtained. Usually for investigation zircon and baddeleyite has been used.

Baddeleyite dates converge to the age of 1.99 Ga (Rodionov *et al*, 2009; Corfu *et al*, 2011). Age of zircon from carbonatites correspond 1970±5.7 Ma (Ivanikov, Frantz, 2002) and 1959±16 Ma (Rukhlov, Bell, 2010).

It is known that baddeleyites age are reflecting age of the melt crystallization, because of their minimum sensitivity to the overprinting processes. Metamict properties of zircon from Tikshezero carbonatites do not provide correct estimation of the crystallization age.

Geochemical characteristics of zircons (Frantz *et al*, 2001, Tichomirowa *et al*, 2012) indicate their magmatic-metasomatic origin, leading to a disturbance of U-Pb isotopic system.

We obtained concordant baddeleyite U-Pb data corresponding to an age of 1997±11 Ma. (U-Th-Pb SIMS SHRIMP-II, 20 analysis of 11 baddeleyite grains were used.) Isotopic data on the subconcordant zircon-I (first generation) give exhibit 1992±13 Ma crystallization age. U-Pb data on Zircon-II (zircons overgrows on baddeleyite) and essentially discordant zircons-I can be interpreted as a discordia with parameters 2022±22 and 841±42 Ma. These data show, that zircons were not affected at the time of Svecofennian metamorphism (1764±41 Ma), which was found by isotopic data for major rock forming minerals of the Tikshezero rocks (calcite, phlogopite, amphibole), but suffered some loss of radiogenic lead at Neoproterozoic event.

Selenate sorption onto bacteria-mineral composites during the progressive addition of Fe(II)

R.E. FRANZBLAU^{1*}, C.G. WEISENER¹
AND C.J. DAUGHNEY²

¹Great Lakes Institute for Environmental Research, University of Windsor, Windsor, Canada
(correspondence: franzbl@uwindsor.ca)

²Institute of Geological and Nuclear Sciences, Lower Hutt, New Zealand

This study is focused on sorption interactions between microbes, minerals, and metals. Laboratory experiments were done to determine the fate of dissolved selenate (SeO_4^{2-}) and Fe at pH 4 during the addition and oxidation of Fe(II) and the subsequent precipitation of iron oxides in the presence of *Escherichia coli*. The experimental results suggest that selenate does not sorb to *E. coli* surfaces, in addition the presence of selenate does not affect iron oxide precipitation. In fact the presence of bacterial cells appear to influence and delay oxidation of Fe(II) and iron oxide precipitation in a mineral-bacteria composite system. In a composite system the bacterial cells also inhibit selenate adsorption onto iron oxide surfaces. Surface complexation models were used to describe the experimental data. This study is the first to show and provide a detailed understanding of metal oxyanion sorption between bacterial cells and minerals as prior studies have focused on metal cation sorption [1,2,3].

[1] Daughney (2011) *Geomicrobiology Journal* **28**, 11-22.

[2] Kulczycki (2005) *Geomicrobiology Journal* **22**, 299-310.

[3] Moon (2013) *Geochimica et cosmochimica acta* **104**, 148-164.

Retention of selenate at the water-mineral interface in the context of salt dome repositories

C. FRANZEN^{1*}, D. HERING² AND N. JORDAN¹

¹Helmholtz-Zentrum Dresden-Rossendorf, Institute of Resource Ecology, Dresden, Germany
(*:c.franzen@hzdr.de)

²University of Applied Sciences, Zittau-Görlitz, Germany

One major process controlling the mobility and bioavailability of selenium, a long-lived fission product found in nuclear waste, is the adsorption onto mineral surfaces of both the engineered and geological barrier. In this context, it is important to understand to what extent this sorption is influenced particularly by characteristic parameters as expected in deep underground repositories for high level and long-lived radioactive waste. These parameters include inter alia the presence of different background salts which are important with regard to salt domes as potential repositories.

In the present study, a combination of macroscopic sorption experiments, electrophoretic mobility and in-situ ATR FT-IR spectroscopy measurements was used to study the interaction of selenate with aged $\gamma\text{-Al}_2\text{O}_3$ in the presence of NaCl and MgCl_2 . From in-situ ATR FT-IR spectra, a change in the symmetry of the aqueous tetrahedral selenate anion can be derived evidencing the formation of a surface complex on $\gamma\text{-Al}_2\text{O}_3$. From batch experiments, we observe a dependence of selenate sorption on the ionic strength and composition of the electrolyte. Additionally, the sorption generally decreases with increasing pH. However, in the presence of 0.1 M MgCl_2 , the sorption increased again at a pH above 9.5.

The isoelectric point (pH_{IEP}) of $\gamma\text{-Al}_2\text{O}_3$ is located at pH 9.6 for low NaCl background electrolyte concentration ($I = 0.1$ M). The increase of ionic strength (up to $I = 1$ M) results in a decrease of the zeta potential for both the acidic and alkaline pH range. However, in the alkaline range the decrease of the zeta potential is more pronounced. Additionally, we observe that the pH_{IEP} is shifted to more alkaline values and finally no charge reversal is observed. In the presence 0.1 M MgCl_2 , the surface charge of $\gamma\text{-Al}_2\text{O}_3$ is positive throughout the studied pH range (3-11). Above pH 10, a sharp potential decrease occurs due to $\text{Mg}(\text{OH})_2$ precipitation. The impact of the varied parameters on the sorption of selenate in the alkaline pH range will be verified in detail.

Saprolites on- and offshore Norway: New constraints on formation processes and age

O. FREDIN^{1,2}, H. ZWINGMANN³, J. KNIES¹, R. SØRLIE⁴,
E.M. GRANDAL⁴, J.-E. LIE⁴, A. MÜLLER¹
AND C. VOGT⁵

¹Geological Survey of Norway, NO-7491 Trondheim, Norway
(*correspondence: ola.fredin@ngu.no)

²Norwegian University of Science and Technology, NO-7491,
Trondheim, Norway

²CSIRO, ESRE, Bentley, WA 6102, Australia

³Lundin Petroleum AS, NO-1366 Lysaker, Norway

⁴University of Bremen, D-28359 Bremen, Germany

The origin of landscapes in Scandinavia has been debated for more than a century and the discussion is as vigorous as ever today. In short, one school proposes that most of the geomorphology can be explained by glacial and periglacial processes, while others argue that the landscape partly is inherited from earlier etching, stripping and exhumation episodes, and has been preserved through cover of sedimentary rocks and selective glacial erosion. One key argument used by the latter proponents is the relatively widespread occurrences of saprolite in Scandinavia. Here we attempt to characterize and date these saprolites both on- and offshore Norway.

One key locality is the Utsira high, which is an offshore crystalline basement horst in the Norwegian North Sea partly overlain by Paleozoic and Mesozoic strata. The area has received significant attention recently due to large petroleum finds, specifically the Edvard Grieg (16/1-8, 2007), the Johan Sverdrup (16/2-6, 2010) and the Luno 2 (16/4-6 S 2013) discoveries done by Lundin Norway.

Significant areas of the Utsira high basement appear to be deeply weathered and saprolite is found in exploration wells. We utilize K-Ar dating of illite diagenesis and geochemical analysis of the saprolite to characterize weathering age and processes. The data suggest deep weathering of a granitic landscape during late Triassic, followed by a transgression and deposition of sedimentary strata. The K-Ar data thus agrees with the stratigraphic position of Utsira high saprolite below Jurassic sediments.

Our hypothesis is that the similar landscape and saprolite onshore Scandinavia is of similar origin and age as the offshore equivalent. Preliminary onshore data are inconclusive but more testing will be made.

Simulating Macromolecule Behaviour on Calcite Surfaces

COLIN L. FREEMAN*¹, DAVID SPARKS¹, GABRIELLA
KAKONYI^{2,3}, MARIA ROMERO-GONZALEZ^{2,3}, STEVEN
BANWART^{2,3} AND JOHN H. HARDING¹

¹ Department of Materials Science and Engineering,
University of Sheffield, Sir Robert Hadfield Building,
Mappin Street, Sheffield, S1 3JD, UK

² Department of Civil Engineering, University of Sheffield,
Sir Frederick Mappin Building, Mappin Street, Sheffield,
S1 3JD, UK

³ Kroto Research Institute, University of Sheffield, North
Campus, University of Sheffield, Broad Lane, Sheffield,
S3 7HQ, UK

Large molecular interactions with mineral surfaces remain complex to understand due to the range of conformations and multiple binding sites. Yet these molecules are vital for a large range of systems including biomineralisation, biomimetics, and cellular adhesion. Therefore it is key to understand how larger molecules behave at these interfaces.

In this presentation we explore how poly-acrylic acid (PAA) as an analogue of many biological molecules interacts with calcite surfaces. Modelling this binding with atomic scale processes is difficult due to the vast range of conformations that must be considered. We are able to model a PAA molecule of 28 monomers in a variety of conformations via the use of novel metadynamics methods and determine how the surface influences the conformation. By studying the system at a range of pHs we make comparison to experimental studies in solution and at the surface on different calcite particles. The results provide insights into how highly charged large molecules interact with these surfaces and how the structure of the molecule influences this behaviour.

The Use of Fe-Rich Compost for the Amelioration of As-Contaminated Soils

P. FREEZE*, J. HARSH, Z. SHI, R. ABI-GHANEM
AND P. OKUBARA

¹ Washington State Univ., Pullman, WA 99164-6420, USA
(*correspondence: patrick.freeze@wsu.edu;
harsh@wsu.edu; zhenqing.shi@wsu.edu;
rita_ag@wsu.edu; pokubara@wsu.edu)

Arsenic (As), a biologically harmful metal, occurs in soil as a result of lead-arsenate pesticide application, smelting, and natural occurrence. Human exposure occurs via plant uptake, dust inhalation, soil ingestion, and drinking water consumption. Heavy metal loads in urban storm-water runoff are the second most common source of lake water pollution nationwide [1]. High Fe biosolids can reduce bioavailable soil As by providing sorption sites that presumably include Fe-(hydr)oxide particles and ternary complexes with organic-FeOH functional groups [2][3] [4]. In this study, we determined (1) the adsorption, retention, and stability of As reacted with Fe-compost, (2) the model for As adsorption on iron oxides, and (3) the compost microbial community as a function of Fe content. Plating and real-time PCR showed the impact of the various iron treatments on isolated microbial species. The sustainable methods and tools utilized in this bioremediation approach to rectifying soil contamination will use organic waste, mitigate the impacts of urban development and subsequent metal loading from storm-water runoff, and ultimately improve soil quality.

[1] Jang, A., Seo, Y., & Bishop, P. L. (2005) *Environmental Pollution*, 133, 117-127. [2] Gu, B., & Schmitt, J. (1994) *Environmental Science & Technology*, 28. [3] Brown, S. L., Clausen, I., Chappell, M. A., Scheckel, K. G., Newville, M., & Hettiarachchi, G. M. (2012) *Journal of Environmental Quality*, 41, 1612-1622. [4] Mikutta, C., & Kretzschmar, R. (2011) *Environmental Science & Technology*, 45, 9550-9557.

Imogolite: An ideal mineralogical substrate for the prebiotic assembly of long polynucleotides?

JASON E. FRENCH^{1*}

¹Department of Earth and Atmospheric Sciences, University of Alberta, 1-26 ESB, Edmonton AB, Canada T6G 2E3
(*correspondence: jef@ualberta.ca)

Imogolite ($\text{HOSiO}_3\text{Al}_2(\text{OH})_3$)—a key weathering product of volcanic glass/ash—is unique among clay minerals, having the same diameter (20 Å) and long, flexible, filamentous nature as double-stranded DNA [1, 2], a nanotube structure, and a strong affinity for PO_4^{3-} adsorption, which takes place at positively charged AlOH groups on tube exteriors [2–4]. Here I propose that these chemical/morphological traits make imogolite an interesting candidate substrate for the prebiotic assembly of DNA/RNA (i.e., long polynucleotides), and that the free O⁻ of each phosphate group along the DNA/RNA backbones could represent relict detachment sites left over after the decoupling of single-stranded DNA/RNA from imogolite (Fig. 1d). New evidence to support this idea comes from the recent synthesis of imogolite/DNA hybrid hydrogels, which seem to form by interactions between AlOH groups on imogolite and phosphate groups in DNA [2]. Authigenic imogolite filaments have recently been found within microbe-sized, alpha-recoil track etch-tunnels at the glass-palagonite interface in submarine glasses (Fig. 1; [1]), and so these C- and P-rich ‘abiotic’ etch-tunnels are a fascinating new analog geological site to consider for the origin of life on Earth.

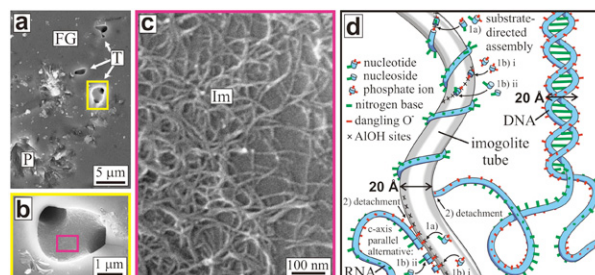


Figure 1: (a–c) SEM images of imogolite and etch-tunnels in DSDP-418A-75-3[120-123] basaltic glass. d) Hypothesis for the prebiotic assembly of DNA/RNA onto imogolite. FG – fresh glass; Im – imogolite; P – palagonite; T – etch-tunnel.

[1] French and Blake (2012) *Conference on Life Detection in Extraterrestrial Samples*, 34–35. [2] Jiravanichanun *et al* (2012) *Biomacromolecules* **13**, 276–281. [3] Gustafsson (2001) *Clays and Clay Minerals* **49**, 73–80. [4] Clark and McBride (1984) *Clays and Clay Minerals* **32**, 291–299.

Archean hydrocarbon biomarkers: Archean or not?

K.L. FRENCH^{1*}, C. HALLMANN², J.M. HOPE³, R. BUICK⁴,
J.J. BROCKS³ AND R.E. SUMMONS¹

¹MIT, Cambridge, MA, USA; *(correspondence:
klfrench@mit.edu; rsummons@mit.edu)

²MPI, Jena, Germany; challmann@bgc-jena.mpg.de

³ANU, Canberra, Australia; janetm.hope@anu.edu.au;
(jochen.brocks@anu.edu.au)

⁴UW, Seattle, WA, USA; (buick@u.washington.edu)

Understanding the origin of oxygenic photosynthesis relative to the Great Oxygenation Event (GOE) is one of the key goals in geobiology today. Archean organic biomarkers provide evidence for oxygenic photosynthesis and eukaryotes predating the GOE [e.g. 1, 2]. However, these results have been challenged and remain controversial [e.g. 3]. Resolving the controversy about the syngeneity of these compounds with their Archean host rock will clarify our understanding of the antiquity of oxygenesis and aerobiosis.

Samples were collected from three diamond drill holes in the Australian Pilbara according to unprecedented protocols during the 2012 Agouon Institute Drilling Program (AIDP). Molecular spikes, tracer experiments, negative controls, and replicate analyses of duplicate samples by multiple independent laboratories were used to constrain results.

To date, a total of seven “biomarker target” samples have been analysed from the AIDP-2 core near Ripon Hills, which intersected the Carawine and Jeerinah Formations, and the AIDP-3 core between Tom Price and Karratha, which intersected the Marra Mamba and Jeerinah Formations. Alkanes, hopanes, and steranes appear to be below detection from the interiors and exteriors of these seven samples. However, multiple samples from the Carawine Formation contain polycyclic aromatic hydrocarbons (PAHs) and diamondoids. These molecules may represent the oldest reported authigenic hydrocarbons, yet the origin of these molecules is uncertain. Replicate analyses of exact duplicate samples by additional organic geochemical laboratories will test the robustness of these current results. Interestingly, analysis of an RHDH2A drill core sample from the Carawine Formation recovered in the 1980s revealed an abundance of hydrocarbons that were absent in the new AIDP-2 Carawine Formation drill core material, suggesting contaminants were introduced during drilling, sampling, sawing, and/or storage.

[1] Brocks, Logan, Buick, & Summons (1999), *Science* 285, 1033-1036. [2] Summons, Jahnke, Hope, & Logan (1999), *Nature* 400, 554-557. [3] Rasmussen, Fletcher, Brocks, & Kilburn (2008), *Nature* 455, 1101-1104.

REE and Neodymium isotopes in sedimentary organic matter

FRESLON N.*¹, BAYON G.¹, TOUCANNE S.¹, BERMELL
S.¹, BOLLINGER C.², CHERON S.¹, ETOUBLEAU J.¹,
GERMAIN Y.¹, KRIPOUNOFF A.¹, PONZEVEVA E.¹
AND ROUGET M.L.²

¹IFREMER, F-29280 Plouzané, France

²IUEM, CNRS UMS 3113, F-29280 Plouzané, France
(*correspondence: nicolas.freslon@ifremer.fr)

Sedimentary Organic Matter (OM) collected from various depositional environments, i.e. rivers (n=25), estuaries (n=18), ocean (n=15), and cold seeps (n=12), was extracted using a mixed hydrogen peroxide/nitric acid solution, after removal of carbonate and oxy-hydroxide phases with dilute hydrochloric acid.

Our results indicate that the abundance of REE in sedimentary OM is six-to-seven orders of magnitude higher than in river water or seawater. The mean REE concentration in the H₂O₂ leachates for samples from rivers, estuaries, coastal seas and open ocean is relatively similar: ΣREE = 107 ± 89 ppm (mean ± s). In comparison, the OM fractions leached from cold seep sediments display higher concentration levels (285 ± 150 ppm). The H₂O₂ leachates for most sediments exhibit remarkably similar shale-normalized REE patterns, all characterized by a mid-REE enrichment compared to the other REE. This suggests that the distribution of REE in leached sedimentary organic phases is controlled primarily by (bio) geochemical processes (i.e. complexation), rather than by the composition of the source from which they derive (e.g. pore water, river or seawater).

The Nd isotopic compositions for OM leached from river sediments are very similar to those for the corresponding detrital fractions. In contrast, OM extracted from marine sediments display εNd values that typically range between the εNd signatures for terrestrial OM (inferred from the analysis of the detrital fractions) and marine OM (inferred from the analysis of local surface seawater). An interesting exception is the case of cold seeps OM leachates, which sometimes exhibit εNd values markedly different from both terrigenous and surface seawater signatures. This suggests that a significant organic fraction in these environments may be derived from chemosynthetic processes recycling pore water REE characterized by a distinct isotopic composition.

Overall, our results suggest that organic matter probably play an important role in the oceanic REE budget, through direct scavenging or remineralization within the water column. In addition, the use of Nd isotopes in sedimentary OM phases could offer interesting future applications in paleoenvironmental studies.

Crustal evolution and petrogenesis of silicic plutonic rocks within the Oman ophiolite – petrological and geochemical investigations

SARAH FREUND^{1*}, MARTIN ERDMANN², JÜRGEN KOEPKE², FOLKMAR HAUFF³ AND KARSTEN M. HAASE¹

¹GeoZentrum Nordbayern, Universität Erlangen-Nürnberg, Germany, (*correspondence: sarah.freund@fau.de)

²Leibniz University Hannover, Germany

³GEOMAR Helmholtz Centre Kiel, Germany

Silicic (56-79 wt. SiO₂) plutonics from mantle and crustal (plagiogranites s.l.) sections of the Oman ophiolite suggest multiple petrogenetic processes during the accretion of the Oman paleocrust at a fast-spreading ridge system, affecting major and trace elements as well as radiogenic isotopes. The mantle granites are distinctly enriched in SiO₂, K₂O, Ni and Cr but depleted in Al₂O₃, FeO, CaO and TiO₂ for a given MgO content compared to silicic crustal rocks. The mineral assemblage differs because biotite, alkali-feldspar and opaques occur in the mantle granites but are absent in comparable crustal rocks. Trace elements display high LILE, Nb, Ta and LREE contents in the silicic plutonic mantle rocks along with an increasing depletion of middle toward the HREE relative to the crustal plagiogranites. In contrast, the silicic crustal rocks are enriched in Hf, Zr and Y compared to their mantle counterparts. Furthermore, the crustal plagiogranites display a MORB-like range in Hf and Nd isotope compositions but with slightly higher ⁸⁷Sr/⁸⁶Sr, similar to their mafic host-rocks, whereas the mantle granites possess distinctly lower εHf, negative εNd values and in most cases very high Sr isotope ratios. We suggest formation of the silicic crustal intrusives by fractional crystallization and crustal partial melting processes during Oman ocean crust formation whereas the mantle granites are most likely related to subduction or obduction processes and thus must be younger.

TRACE: A multi-tracer analysis of shallow aquifers to improve geothermal potential assessment

F. FREUND^{1*}, S. AL NAJEM², W. AESCHBACH-HERTIG¹, M. ISENBECK-SCHRÖTER², B. KOBER², M. KRAML³, R. GROBE³ AND A. WENKE⁴

¹Institute of Environmental Physics, Heidelberg University, 69120 Heidelberg, Germany (*corr: ffreundt@iup.uni-heidelberg.de)

²Institute of Earth Sciences, Heidelberg University, 69120 Heidelberg, Germany

³GeoThermal Engineering GmbH, 76133 Karlsruhe, Germany

⁴Statoil ASA Nord-Norge, Molnhollet 42, 9414 Harstad, Norway

The assessment of geothermal potential for deep geothermal energy production currently relies on expensive 3D reflexion seismic methods to identify adequate fault zones and geometry of the geothermal aquifer. However, this analysis does not allow the estimation of hydraulic permeability of active faults nor provides a characterisation of the chemical properties of the deep aquifer fluid. Both factors play an important role in optimising siting of fault related geothermal wells and operation of geothermal power plants.

The TRACE project aims to combine methods from hydrogeochemistry and isotope hydrology in the analysis of shallow groundwater to develop a low cost method for deep geothermal energy exploration. The main goal is to constrain the interest area with further methods supporting geophysical exploration methods. The approach introduced in this contribution includes the measurement and evaluation of a wide range of natural isotopic and geochemical. To assess the fault permeability, the groundwater ³He/⁴He ratio will be analysed for mantle signatures pointing to deep water circulation and upward flux [1]. The hydrogeochemical analysis and transport modeling will be used to characterise the origin and flow path of the thermal water [2] and to assess its suitability for industrial scale energy production.

The Upper Rhine Graben was chosen as the project's study region, focusing on three different local areas with preexisting well and 2D/3D seismic data to allow for comparison and validation of the study results. Preliminary results from the first sampling campaign show promising data, indicating an area of increased interest where elevated helium ratios coincide with characteristic geochemical data, fault location and a previously known saltwater anomaly.

[1] Kennedy and van Soest (2007) *Science* **318**, 1433-1436 [2] He *et al* (1999) *Applied Geochemistry* **14**, 223-235

Microbial-soil organic matter linkages in response to climate warming

S.D. FREY

Department of Natural Resources & the Environment,
University of New Hampshire, Durham, NH 03824 USA
(correspondence: serita.frey@unh.edu)

Soils are the largest repository of organic carbon in the terrestrial biosphere and represent an important source of CO₂ to the atmosphere, releasing 60-75 Pg C annually through microbial decomposition of organic materials [1, 2]. Current carbon-climate models predict increased soil organic matter decomposition as global climate warms, with higher than normal soil CO₂ fluxes to the atmosphere eliciting a positive feedback to climate [3, 4]. However, results from several field studies demonstrate that while soil respiration is initially stimulated by warming, this effect often diminishes over time, with elevated soil respiration in chronically warmed soils returning to ambient levels within a few years [5, 6, 7]. Microbial decomposition of soil organic matter is responsible for as much as half or more of the CO₂ released from soils [1], and so a thorough understanding of how soil microorganisms respond to temperature is needed to accurately predict how climate warming may alter soil CO₂ fluxes [8]. This talk will synthesize data on microbial responses to climate warming, with an emphasis on microbial physiology as a driver of soil organic matter dynamics [9].

[1] Schlesinger & Andrews (2000) *Biogeochem.* **48**, 7-20. [2] Schimel (1995) *Global Change Biol.* **1**, 77-91. [3] Heimann & Reichstein (2008) *Nature* **451**, 289-292. [4] Cox *et al* (2000) *Nature* **408**, 184-187. [5] Melillo *et al* (2002) *Science* **298**, 2173-2176. [6] Oechel *et al* (2000) *Nature* **406**, 978-981. [7] Luo *et al* (2001) *Nature* **413**, 622-625. [8] Conant, *et al* (2011) *Global Change Biol.* **17**, 3392-3404. [9] Frey *et al* (2013) *Nature Climate Change* **3**, 395-398.

Mass-related U isotope fractionation during alteration of oceanic crust and release of U in subduction zones – implications for deep recycling of oceanic crust

HEYE FREYMUTH¹, MORTEN ANDERSEN²
AND TIM ELLIOTT¹

¹Bristol Isotope Group, University of Bristol, Queen's Road,
Bristol BS8 1RJ, UK (glxhf@bristol.ac.uk)

²ETH Zürich, Inst. f. Geochemie und Petrologie,
Clausiusstrasse 25, 8092 Zürich

The modification of material during seafloor alteration and subsequent processing within subduction zones is of primary importance for assessing the composition of deeply subducted material and its influence on mantle heterogeneity. It has long been known that U is added to the oceanic crust during both low and high temperature alteration of the oceanic crust, whilst some of the subducted inventory of U is returned to the surface in arc lavas. The advent of techniques to measure mass-related ²³⁸U/²³⁵U isotope fractionation with sufficient precision allows us to investigate the effect of alteration and subduction zones processes on the isotopic composition of U. This is a key step in evaluating the potential of U isotope measurements to trace deep crustal recycling. Thus we have measured the U isotopic compositions of samples from the altered, mafic, oceanic crust (AOC) at ODP site 801 as well as lavas erupted at the volcanic front of the Mariana arc. The former represents a reference site for studying the time-integrated influence of seafloor alteration and the latter constitute a well characterised sample set for which the role of slab-derived 'fluid' and sediment components can be separately recognised.

The altered oceanic crust is compositionally variable with ²³⁸U/²³⁵U similar to seawater in the top ~100 m and isotopically heavier in deeper parts. These differences are likely to be caused by oxidizing conditions in the top part of the AOC and reducing conditions in deeper parts of the AOC and isotopic fractionation occurring during the alteration of the oceanic crust. The Mariana arc lavas span a range of ~100 pm in ²³⁸U/²³⁵U and vary systematically between seawater-like compositions in samples that have been previously identified as 'fluid-rich' and heavier values similar to fresh mantle basalts in the more sediment-rich samples. These systematics indicate that either the light U in the upper mafic crust is preferentially lost to the arc lavas or that during slab dehydration of the AOC, U is fractionated to generate an isotopically light fluid and heavy residue. In either scenario the deep-subducted material is left distinctively, isotopically heavy and should be an effective tracer of deep recycled material.

Dynamics of sulfur degassing in alkaline magmas illustrated with melt and fluid inclusions

MARIA LUCE FREZZOTTI¹ AND FRANCESCA TECCE²

¹Dept. Earth and Environmental Sciences, University Milano Bicocca, Italy (maria.frezzotti@unimib.it)

²Istituto di Geologia ambientale e Geoingegneria, CNR Roma, Italy (francesca.tecce@cnr.it)

The dynamics of sulfur transfer into the magmatic fluid phase in a long-lived shallow magma reservoir has been investigated using melt and fluid inclusions in syenite xenoliths from the Sabatini K-rich volcanic complex (0.8-0.04 Ma; Roman magmatic province, Italy). Silicate melt inclusions (MI; up to 100 μm) in clinopyroxene and in sanidine have compositions in the phonotephrite-phonolite-trachyte spectrum, similar to erupted rocks. MI in sanidine argue convincingly that the pre-eruptive alkaline melt was oversaturated with respect to a sulfate-rich melt phase, and to a vapor-rich aqueous phase. Most MI show a large bubble/glass ratio and contain several pinkish-yellowish globules (1-5 μm), rich in SO_3 (6-7 wt %), SiO_2 , Al_2O_3 , alkalis, and CaO. Raman spectroscopy of globules reveals an alkali-silicate glass structure containing oxysulfur species dominantly as SO_4^{2-} , with subordinate CO_3^{2-} groups, and absence of S-S bonds. Magmatic vapor-rich brine inclusions have a microthermometric behavior consistent with the presence of up to 25 wt% sulfate in solution. Sulfur species in liquid water include an hydrated double alkali-Ca sulphate \pm anhydrite, $(\text{SO}_4)_2^{2-}$ and $(\text{HSO}_4)_2^-$ ions, and SO_2 ; CO_2 is detected in the inclusion bubble.

This case study suggests that during crystallization, sulfur supersaturation in oxidized alkaline magmas induces liquid immiscibility between silicate and sulfate melts. At these pre-eruptive stages, significant amounts of S partition as SO_2 and SO_3 (or H_2SO_4) in magmatic aqueous-rich fluids.

Isotopic constraints for sources and sinks of NO_x in the city of Berlin

M.FRIEBEL¹ AND U. WIECHERT¹

¹Freie Universität Berlin; Germany

(*correspondance: mfriebel@zedat.fu-berlin.de)

Atmospheric NO_x causes various problems in urban environments such as tropospheric ozone production and the formation of secondary aerosols. The isotopic composition of atmospheric nitrates can help to identify the sources of NO_x ($\delta^{15}\text{N}$) [e.g. 1] and to understand its reaction pathways and sinks in the atmosphere ($\delta^{18}\text{O}$) [e.g. 2].

Here, we report the results of isotopic measurements of nitrates from precipitation collected during single storm events in Berlin between March 2007 and January 2008. $\delta^{15}\text{N}_{\text{NO}_3}$ ranges from -11.6 to +2.0; mean = -4.5 (relative to AIR) and $\delta^{18}\text{O}_{\text{NO}_3}$ values range between +8.9 and +67.2; mean = +32.6 (relative to V-SMOW). The $\delta^{15}\text{N}$ values show a high variation between each rain event and can be separated into groups with values of -4.3 to +2.0 (mean = -1.2) and -11.6 to -5.1 (mean = -8.0). The $\delta^{18}\text{O}_{\text{NO}_3}$ values show a bimodal distribution with one maxima in June-July 2007 and the second in January 2008. The measured $\delta^{18}\text{O}$ values are low, especially during the spring of 2007 (+8.9 to +23.4), compared to those reported in other studies [e.g. 2].

The nature of the observed isotopic variations is complex. More positive $\delta^{15}\text{N}_{\text{NO}_3}$ values may represent NO_x originating from fossil fuel combustion (mostly fuel NO_x) and more negative $\delta^{15}\text{N}_{\text{NO}_3}$ values may be related to volatilization of nitrogen compounds from fertilized soils. This variation in the $\delta^{15}\text{N}_{\text{NO}_3}$ values could be associated with long distance transport of air masses from different source regions, since the lifetime of NO_x is approximately one day [e.g. 3] and its deposition as nitrate (residence time of 1-2 days [e.g. 3]) can be hundreds of kilometres from the nitrogen source. $\delta^{18}\text{O}_{\text{NO}_3}$ serves as a fingerprint for the reaction pathways of NO_x to nitrate. High $\delta^{18}\text{O}$ values are consistent with a high proportion of NO_x oxidised by ozone, whereas low $\delta^{18}\text{O}$ values indicate preferential oxidation by peroxy and/or OH radicals [e.g. 2]. The results show that isotope ratios of atmospheric nitrates contribute important constraints in conjunction with local concentration measurements and storm track information on the sources and fate of tropospheric NO_x and O_3 and their dynamics in the urban environment of Berlin.

[1] Hastings *et al* (2003) *JGR* **108**(D24), 4790 [2] Michalski *et al* (2011) *Hand. Env. Iso. Geoch.* 613-635 [3] Liang *et al* (1998) *JGR* **103**(D11), 13,435.

Tracing weathering and reverse weathering in floodplains using Si isotopes and Ge/Si ratios

PATRICK J. FRINGS^{1*}, ERIC STRUYF², WILLIAM GRAY³, CHRISTINA DE LA ROCHA⁴, ROGER MORMUL⁵, PABLO URRUTIA⁶, SARA EKSTRÖM⁶ AND DANIEL J. CONLEY¹

¹Department of Geology, Lund University, Sweden
(*correspondence: patrick.frings@geol.lu.se)

²Biology Department, Antwerp University, Belgium

³Department of Geography, University College London, UK

⁴Institut Universitaire Européen de la Mer, Brest, France

⁵Universidade Estadual de Maringa, Brazil

⁶Aquatic Ecology Unit, Lund University, Sweden

The role of high mountainous areas as the loci of the majority of chemical weathering (i.e. CO₂ consumption) is ambiguous due to their relatively minor surface area. Low relief areas, including floodplains, are increasingly recognised as important for river weathering flux formation, based on e.g. studies that consider longitudinal changes in water chemistry and/or suspended particulate matter composition as large rivers cross their floodplains. The integrated signals imply aging of sediment in floodplains. But in some cases, floodplains may alter weathering fluxes through chemical sedimentation, i.e. removal of elements from solution.

To directly investigate the processes occurring, we analysed material from field campaigns in two tropical floodplains – a cross-floodplain borehole survey of the upper Paraná in southern Brazil and a longitudinal survey of the terminal wetlands of the Okavango River in northern Botswana. We focus on tracing biological and weathering processes with the isotopes of Si and with Ge/Si ratios, interpreting Ge as a ‘pseudoisotope’ of Si. We analysed these, together with major and trace element concentrations, for surface water, groundwater/porewater, separated sediment fractions and aboveground vegetation.

In the Paraná, mobile elements are enriched downcore – the older sediments have accumulated e.g. K, Ca and Mg. $\delta^{30}\text{Si}$ of floodplain groundwaters is enriched by up to 1‰ relative to river water, implying in situ formation of a lighter phase. In the Okavango, observed changes in water chemistry and a $\delta^{30}\text{Si}$ decrease (~0.6‰) in dissolved Si can be interpreted as weathering of isotopically light primary and/or secondary minerals, or as intense biological recycling. Conversely, the surface water geochemistry suggests an elemental (K, Ca, Mg) sink via mineral authigenesis.

Our data suggest large floodplains are areas of both weathering and reverse weathering, adding complexity to our emerging understanding of floodplain weathering dynamics.

Mineralogical pathways involved in the formation of hydrous Mg/Ni silicate ores (New Caledonia)

EMMANUEL FRITSCH^{1*}, FARID JUILLOT^{1,2}, GABRIELLE DUBLET³, ANNE-LINE AUZENDE^{1,2}, LAURENT CANER⁴ AND DANIEL BEAUFORT⁴

¹ Institut de Minéralogie et de Physique des Milieux Condensés (IMPMC), UMR CNRS 7590, UR IRD 206, Université Pierre et Marie Curie (UPMC), 75252, Paris Cedex 05, France

*correspondance: Emmanuel.Fritsch@ird.fr, Farid.Juillot@ird.fr, (auzende@gmail.com)

² UFR STEP, Université Paris Diderot - IGP, 75013 Paris, France

³ Department of Geological & Environmental Sciences, Stanford University, Stanford CA 94305-2115, USA (gdublet@stanford.edu)

⁴ Institut de Chimie des Milieux et Matériaux de Poitiers (IC2MP), UMR 7285 CNRS, Université de Poitiers, 86022 Poitiers, France (laurent.caner@univ-poitiers.fr.) (daniel.beaufort@univ-poitiers.fr)

New Caledonia hosts one of the biggest Ni-laterite deposits in the world. Highest Ni grades are related to hydrous Mg/Ni silicate ores [1], which are best preserved at depth along serpentized faults in the saprock. Despite their importance, the mechanisms involved in the formation of the Ni silicate ores (garnierites) are still a matter of debate.

Series of fracture-controlled clay and silica infillings were investigated by optical and electron microscopy, Raman spectroscopy, X-ray diffraction and electron microprobe analyses. The first infilling stage consists of residual well-crystallized ophiolitic serpentines intimately mixed with poorly ordered serpentine-like and talc-like minerals. Talc-like minerals predominate in a second stage of infillings whereas quartz druses prevail in the ultimate infilling stage. Two crystal-chemistry pathways are attributed to the early redistribution of Ni and differentiation of white and greenish patches along the reactivated faults. In the white Ni-free deweylites, the compositional variation of clay minerals is distributed along a mixing line between Mg end-members of the serpentine-like (α -kerolite) and talc-like (β -kerolite) minerals. In the greenish patches of Ni-rich garnierites, it is distributed along a second mixing line between an Mg end-member of serpentine-like minerals and a Ni end-member of talc-like minerals (pimelite). Our results then evidence a multistage leaching of Mg and increase of the Ni and Si activities of the infilling solutions during post-obducted tectonic pulls, in agreement with a recent thermodynamic study [2].

[1] Freyssinet *et al* (2005) *Econ Geol*, 100th An Vol, 681-722.

[2] Gali *et al* (2012) *Clays Clay Miner*, **60**, 121-135.

U-Pb zircon ages from granites in the Iapetus Suture Zone in Ireland and the Isle of Man

TOBIAS FRITSCHLE¹, J. STEPHEN DALY¹, MARTIN J. WHITEHOUSE², BRIAN MCCONNELL³ AND STEPHAN BUHRE⁴

¹UCD School of Geological Sciences, Belfield, Dublin 4, Ireland (tobi.fritschle@gmx.de, stephen.daly@ucd.ie)

²Laboratory for Isotope Geology, Swedish Museum of Natural History, Stockholm, Sweden (martin.whitehouse@nrm.se)

³Geological Survey Ireland, Beggar's Bush, Dublin 4, Ireland (brian.mcconnell@gsi.ie)

⁴Institut für Geowissenschaften, Johannes Gutenberg-Universität, Mainz, Germany

Late Caledonian syn- to post-orogenic granites located in the Iapetus Suture Zone (ISZ) in Ireland and Britain have been related to A-type subduction and possible slab breakoff following the Laurentia-Avalonian collision. Lack of reliable age data (especially in Ireland) has inhibited petrogenetic investigations of these rocks. Hence, ion microprobe U-Pb analyses on zircons from Irish and Isle of Man granites have been undertaken to provide better constraints on this episode of the Caledonian orogeny.

Three stages of granitic magmatism (c. 428, 417, 397 Ma) are indicated by U-Pb dating of oscillatory-zoned magmatic zircons. The Crossdoney, Kentstown, Drogheda, Ballynamuddagh and Dhoon granites together with a rhyolite from Glenamaddy have yielded U-Pb concordia ages, interpreted as intrusion-ages, between 419.1±2.4 Ma (Ballynamuddagh) and 415.6±2.5 Ma (Dhoon) with a weighted average of 417.2±1.7 Ma (MSWD = 1.3). The Foxdale Granite and a sample from the Rockabill Granite yielded younger ages of c. 397 Ma, whereas another Rockabill sample yielded an older concordia age of 427.7±3.4 Ma.

Inherited zircons (487 to 453 Ma) occur in all three age groups, and are interpreted to have been derived from Ordovician arc magmatic rocks accreted within the ISZ. A younger group of c. 440 Ma inherited zircons occurs in the c. 417 Ma Crossdoney and Ballynamuddagh granites. These grains could be related to continued or renewed Silurian arc magmatism.

Granites in the 417 Ma age group are the most 'primitive', being metaluminous with high Mg# and low Ti, Cr, Ba and Sr concentrations, and are mineralogically I-Type, consistent with a major contribution from older arc sources. Relatively few analyses are available but granites of the 428 and 397 Ma age groups have some characteristics of S-type granites, consistent with predominantly sedimentary source rocks or contaminants.

[1] Atherton & Ghani (2002), *Lithos* 62, 65-85.

Experimental efforts to understand deep mantle melting

D.J. FROST¹, D. NOVELLA¹, R. MYHILL¹, C. LIEBSKE², AND R.G. TRØNNES³

¹Bayerisches Geoinstitut, Universität Bayreuth, 95440 Bayreuth, Germany

²Institute for Geochemistry and Petrology, ETH, Zürich, Switzerland

³Centre for Earth Evolution and Dynamics (CEED) and Natural History Museum, University of Oslo, Norway

There is evidence from seismology and from metasomatised mantle xenoliths for the presence of melting in the mantle at depths significantly greater than 50 km. At the very base of the mantle the detection of ultra low shear wave velocities may indicate melting due to the thermal boundary layer at the core mantle boundary, or may be evidence for chemical heterogeneity at the base of the mantle. On the other hand, melts that modify the roots of cratonic continental lithosphere arise from the presence of volatiles in the deep mantle. Understanding the implications and consequences of such melting requires the ability to determine the compositions and temperatures at which melting occurs under pressure.

We have performed experiments to examine simple melting relations in the systems MgO-FeO-SiO₂ and examined the effects of H₂O, CO₂ and other components on the depression of melting temperatures. The relatively simple phase relations are amenable to the thermodynamic treatment of silicate melts, which can be used to then extrapolate melting relations over much wider ranges of pressure and temperature. In addition by modelling experimental data some idea of the mechanisms by which components are incorporated in melts can be gained.

We show that melting relations of bulk silicate earth compositions at high pressure can be well described on the basis of phase relations of a simple ternary at high pressures. These results can be used to examine a partial melt origin for the existence of low shear wave velocities at the core-mantle boundary. Models for the effect of volatiles on melting relations are used to examine how melt fractions will vary throughout the upper mantle as a function of bulk volatile concentration.

The stability of carbonate melt in eclogite rocks with respect to oxygen fugacity

D.J. FROST¹, V. STAGNO², C.A. MCCAMMON¹
AND Y. FEI²

¹Bayerisches Geoinstitut, Universität Bayreuth, 95440
Bayreuth, Germany

²Geophysical Laboratory, Carnegie Institution of Washington,
Washington, DC, USA.

The redox relationship between carbon and iron species in eclogitic rocks is important for the earth's internal carbon cycle and the formation of diamond. Using a sliding Fe-Ir redox sensor the oxygen fugacity at which carbonate melts are reduced to either graphite or diamond was measured in eclogitic rock compositions. Multianvil experiments were performed between 3 and 6 GPa and temperatures between 1000–1300°C. The oxygen fugacity corresponding to the equilibrium between graphite/diamond and carbonate melt was determined. Oxygen fugacities normalized to the FMQ buffer were found to decrease with temperature, most likely as a result of dilution of the carbonate liquid with silicate as temperatures increase. In contrast to previous arguments, the carbonate melt stability field was found to extend to lower oxygen fugacity in eclogitic rocks compared to peridotite rocks.

The same set of carbonated eclogite experiments also contained monomineralic layers of clinopyroxene and garnet that allowed the ferric Fe contents of these minerals to be measured using Mössbauer spectroscopy. A relatively simple model was derived for determining the oxygen fugacity of eclogitic rocks from the compositions of garnet and clinopyroxene coupled with determinations of the garnet ferric Fe content. The model was able to reproduce the experimental data to within 0.5 log units. The equilibrium was used to estimate the oxygen fugacity of eclogitic xenoliths from the Siberian and Kaapvaal cratons. These rocks were found to record ranges of oxygen fugacity that are very similar to those recorded by peridotite xenoliths from the same localities. By assuming a typical bulk ferric Fe content of oceanic crust, we calculate that subducting eclogitic rocks would remain in the carbonate stability field until depths of at least 300 km. Ferric iron contents of cratonic eclogites appear to be lower than would be expected if they are sections of subducted oceanic crust.

Rate dependence of ⁴⁴Ca/⁴⁰Ca fractionation during inorganic aragonite precipitation from seawater

FRUCHTER, N.¹, EISENHAUER, A.¹, DIETZEL, M.², EREZ, J.³, BOEHM, F.¹, FIETZKE, J.¹ AND NIEDERMAYR, A.⁴

¹GEOMAR, Helmholtz Centre for Ocean Research Kiel, Kiel, Germany.

²Institute for Applied Geosciences, Graz University of Technology, Graz, Austria.

³The Hebrew University of Jerusalem, Jerusalem, Israel.

⁴Ruhr University of Bochum, Bochum, Germany.

In order to examine the relationship of Ca isotope fractionation and precipitation rate for inorganic aragonite formation a set of lab experiments were conducted. Therefore the CO₂ diffusion rate technique was applied (1) using natural seawater (sw). The range of precipitation rates (R = 40–4700 μmol·h⁻¹) was achieved using different initial carbonate ion concentrations (130–1080 μmol/kg sw) at temperatures of 15, 25 and 30°C.

We measured δ^{44/40}Ca of sw and the inorganic aragonite on a TIMS (TRITON, ThermoFisher) using the ⁴³Ca/⁴⁸Ca double spike method (2). In accordance with results for inorganic aragonite in diluted aqueous solutions (3) our data show that ⁴⁴Ca/⁴⁰Ca fractionation in aragonite is positively correlated to precipitation rates. Thus no significant difference in ⁴⁴Ca/⁴⁰Ca fractionation due to different salinities is observed.

The impact of precipitation rate on Ca isotope fractionation during aragonite formation is similar to observations in calcite by (4), but opposite to experimental studies and modelling results for calcite by (5) (6). Possible mechanisms for the discrepant behaviour of Ca isotope fractionation in calcite and in aragonite are discussed.

- [1] M. Dietzel *et al.*, *Chemical Geology* **203**, 139–151 (2004).
[2] A. Heuser *et al.*, *International Journal of Mass Spectrometry* **220**, 385–397 (2002). [3] N. Gussone *et al.*, *Geochimica et Cosmochimica Acta* **67**, 1375–1382 (2003). [4] D. Lemarchand and G. J. Wasserburg, *Geochimica et Cosmochimica Acta* **68**, 4665–4678 (2004). [5] J. Tang *et al.*, *Geochimica et Cosmochimica Acta* **72**, 3733–3745 (2008). [6] D. J. DePaolo, *Geochimica et Cosmochimica Acta* **75**, 1039–1056 (2011).

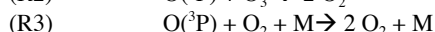
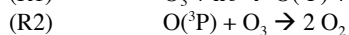
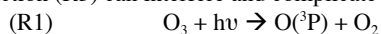
Experimental research on isotope effects in photodissociation of O₃

MARION FRÜCHTL¹, CHRISTOF JANSSEN²
AND THOMAS RÖCKMANN¹

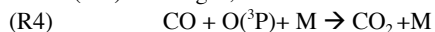
¹Institute for Marine and Atmospheric Research Utrecht,
Princetonplein 5, 3584 CC Utrecht, The Netherlands
(m.fruechtl@uu.nl, t.roeckmann@uu.nl)

²Laboratoire de Physique Moléculaire pour l'Atmosphère et
l'Astrophysique, 4 Place Jussieu, 75005 Paris, France
(christof.janssen@upmc.fr)

Ozone (O₃) has a strong influence on the radiative balance and chemical processes in the Earth's atmosphere and also exhibits a very peculiar isotopic composition. It is highly enriched in both ¹⁷O and ¹⁸O and shows a clear offset from the mass dependent fractionation line (quantified as $\Delta^{17}\text{O} = \delta^{17}\text{O} - 0.52 * \delta^{18}\text{O}$), i.e. it possesses excess ¹⁷O over what is expected based on ¹⁸O abundances. The O₃ formation reaction is the most prominent example for a reaction that leads to the formation of such mass independent isotope compositions. To what degree O₃ destruction reactions contribute to the isotopic anomaly in O₃ is still not fully understood. In particular, it has not been possible to isolate the isotope effects in the photolysis reaction (R1) from the subsequent reaction of O with O₃ (R2). In addition, the three-body recombination reaction (R3) can interfere and complicate interpretation.



Within the project INTRAMIF (Initial Training network on Mass-Independent Fractionation) we are investigating the isotope effect resulting from photodissociation of O₃. We attempt to suppress reaction (R2) and (R3) by using carbon monoxide (CO) as bathgas, which reacts with O(^3P) (R4).



In the experiments, O₃ is produced by electric discharge and exposed to different types of radiation with and without addition of CO. After reaction, the remaining O₃ is collected in a cold trap at the triple point temperature of nitrogen (63K). In order to measure the oxygen isotopes of O₃ using isotope mass spectrometry, O₃ is converted to O₂.

In this presentation we show first results of O₃ photodissociation with visible light, using CO as O(^3P) quencher.

Geochemical Modeling of Glass Alteration in Mg rich ground water

FRUGIER PIERRE¹, JOLLIVET PATRICK¹
AND GODON NICOLE¹

¹CEA Marcoule, DEN/DTCD/SECM/LCLT, BP17171 -
30207 Bagnols-sur-Cèze, (pierre.frugier@cea.fr.)
(patrick.jollivet@cea.fr),(nicole.godon@cea.fr.)

Coupling interdiffusion, through a layer passivating the glass surface, with dissolution of this layer has been the objective of a glass alteration model named GRAAL (Glass Reactivity in Allowance for the Alteration Layer) [1]. It has been implemented within the CHESS/HYTEC code. The interesting point is that GRAAL equations handle the nanometer scale interdiffusion phenomena through the passivating layer while the finite-element chemistry-transport code handles the centimeter scale transport through fluids. The model has been applied to many long term batch glass alteration experiments in Mg rich ground waters and various surface areas to solution volume ratios (S/V), following a work initiated in [1, 2]. Magnesium silicate precipitation has been proved to be a significant mechanism sustaining glass alteration. Magnesium silicate also consume hydroxide ions and its apparent solubility increases with the pH decrease. Glass alteration provides not only silica but also hydroxide ions required for magnesium silicate precipitation to go on. The strong coupling at work, visible through pH, Si and Mg variations as a function of time and glass S/V, illustrates the need for a geochemical model. Sensitivity studies on Si/Mg ratio in the magnesium silicate show that a precise knowledge of Si distribution between the depleted gel, the passivating layer, and the magnesium silicate is required for a precise prediction of pH and therefore glass alteration rate.

[1] Debure *et al* (2012) J. Nucl. Mater. 420, 347–361. [2] Jollivet *et al*. (2012) J. Nucl. Mater. 420, 508-518

Precursory Soil Radon Anomalies Related to the Major Earthquakes in Taiwan

*CHING-CHOU FU¹ TSANYAO FRANK YANG¹
TSUNG-KWEI LIU¹ CHENG-HONG CHEN¹ VIVEK WALIA²
TZU-HUA LAI³ AND CHI-YEN CHEN³

¹Department of Geosciences, National Taiwan University, Taiwan (*correspondence: d95224008@ntu.edu.tw, tyyang@ntu.edu.tw, liutk@ntu.edu.tw, chench@ntu.edu.tw)

²National Center for Research on Earthquake Engineering, NAPL, Taiwan (walia@ncree.narl.org.tw)

³Central Geological Survey, MOEA, Taiwan (hua@moeacgs.gov.tw, zychen@moeacgs.gov.tw)

Several automatic stations for soil gas monitoring were constructed on sensitive sites at the fault zone of Taiwan. Significant changes in soil-gas radon of four stations were recorded two weeks before the Jiasian earthquake (Mw = 6.4, March 4, 2010). Recurrent anomalies were observed prior to one week before precede the Wutai earthquake (Mw = 6.4, February 26, 2012) and the Nantou earthquake (Mw = 6.4, March 4, 2010) occurred at more than two stations, respectively.

The main shock occurred at 15-26 km depth, in a relatively low background seismicity area, in the middle to low crust, implying ductile beneath Central Range. Assuming that stress magnitudes are consistent with the pore-fluid pressure, a high conductivity zone at depth, which is interpreted to transfer the compressional driving force across the brittle-ductile transition, with more efficient stress interconnectivity in the high strain domain. Moreover, variations of soil gas can reflect a change in the stress-strain state of rocks, such as useful tools for earthquake surveillance.

Hence, there is obvious that the soil radon anomalies originated in stress accumulation preceding the major earthquakes. Variations of soil radon at several stations show precursory signals simultaneously that can conduce to expect the approximate location of the impending seismic event with high confidence. Continuous monitoring will allow us to better understand the relationship between soil gas variations and regional crustal stress/strain in the area.

Elemental and Os isotope variations across the K/T boundary in a marine Fe-Mn crust

YAZHOU FU^{1*}, JIANTANG PENG¹, WENJUN QU²,
RUIZHONG HU¹, XUEFA SHI³ AND JIEHUA YANG¹

¹State Key Laboratory of Ore Deposit Geochemistry, Institute of Geochemistry, Chinese Academy of Sciences, Guiyang, China (*correspondence: fuyazhoucas@gmail.com)

²National Research Center of Geoanalysis, Beijing, China

³First Institute of Oceanography, State Oceanic Administration, Qingdao, China

Marine Fe-Mn crusts grow slowly and contain distinctive laminar growth layers which have potential to document the evolution of ocean chemistry and major geologic events. The K/T boundary (KTB) is associated with the mass extinctions of terrestrial and marine organisms, most likely caused by a bolide impact or/and the Deccan volcanism. In this study, we explored the elemental and Os isotope variations in successive layers across the KTB in a marine Fe-Mn crust, MP2D06, from Line Seamount in Central Pacific Ocean.

The Fe-Mn crust has been dated using Co flux-based age model and Sr isotope stratigraphy. Then the successive layers samples from the crust spans the time interval from about 58 to 74 Ma were analysed. The element composition was determined along continuous sections of the crust using EPMA and LA-ICP-MS. The ¹⁸⁷Os/¹⁸⁸Os ratios were measured by acid digestion and ID-HR-ICP-MS.

Preliminary data show that the Ir peak does not correspond with the low Pt/Ir and Os/Ir ratios in the sections. This implies that it is difficult to decide the exact location of KTB in the Fe-Mn crust just using the concentration variation of PGE. There is a rapid decrease in ¹⁸⁷Os/¹⁸⁸Os from values 0.683 to 0.336, then followed by an increase to 0.453. The large amplitude Os isotope excursion has distinctive features to help improve the reliability of Os isotope stratigraphy in Fe-Mn crust age determinations. Mass balance estimation indicates that the ¹⁸⁷Os/¹⁸⁸Os minimum across KTB was caused by both bolide impact events and the eruption of the Deccan flood basalts.

This study was supported by NSFC (40803003, 41173020).

Experimental constraints on the magma evolution of the basanite-phonolite series from Cumbre Vieja volcano (La Palma, Canary Islands)

P. FUCHS^{1*}, R. ALMEEV¹ AND A. KLÜGEL²

¹Institute of Mineralogy, Leibniz University Hannover, Germany (*p.fuchs@mineralogie.uni-hannover.de)

²Geosciences Department, University of Bremen, Germany

Eruptive products of the recent Cumbre Vieja volcano (CV) cover a large spectrum of alkali-rich rocks ranging from basanites to phonolites. A model of the magma plumbing system is largely based on barometric studies of phenocrysts and xenoliths and includes three major intervals of magma stagnation and fractionation at mantle and crustal depths [1]. However, the relative influence of different thermodynamic parameters on phase equilibria is still unknown. We present results of an experimental study aimed for evaluating p-T- $a_{\text{H}_2\text{O}}$ - f_{O_2} conditions in the genesis of a basanite-tephrite-phonolite system. High pressure and temperature experiments (700 and 400 MPa; 1000-1175°C) in the presence of H₂O-CO₂ fluid ($X_{\text{H}_2\text{O}}$ varied between 0-1, keeping f_{O_2} between ~FMQ and FMQ+3.3) were conducted in an internally heated pressure vessel using two natural basanites with 13.7 wt.% and 9 wt.% of MgO, respectively, representing two differentiation stages in the evolution of CV magmas.

The natural phase assemblage (Ol+Cpx+Spl) was reproduced at 700 and 400 MPa, 1150-1100°C and 0.7-2.9 wt.% H₂O in the melt (H₂O^m) for the primitive basanite and at 400 MPa, 1150-1125°C and 2.2-2.7 wt.% H₂O^m for the evolved basanite. Tephritic residual melts were produced by Ol+Cpx+Spl crystallization at 400 and 700 MPa and low H₂O^m (1.4-2.9 wt.%). Phonotephritic melts were generated by Cpx+Ol+Krs+Mt crystallization at 400 MPa, 1075-1100°C and 0.7-3.1 wt.% H₂O^m. Tephriphonolitic melts were produced by Cpx+Pl+Krs-Mt+Ap crystallization at 400 MPa, 1050°C, 0.7-1.1 wt.% H₂O^m.

Our results indicate that differentiation from basanites to tephrites is possible in a pressure range of 400 to 700 MPa at least. Pl crystallization in basanites at 700 MPa is suppressed indicating that tephriphonolitic or phonolitic melts can only be generated at lower pressures or from a parent more evolved than basanite. Krs is an amphibole that can be stable even in melts with <1 wt.% H₂O^m (>0.1 $X_{\text{H}_2\text{O}}$), suggesting that CV melts are CO₂ rich and H₂O-poor even in evolved magmas. It also requires low f_{O_2} (~FMQ): higher f_{O_2} results in extensive Mt crystallization leading to qz-normative residual liquids instead of Ne-normative.

[1] Klügel *et al* (2005) *EPSL* **236**, 211-226.

Dunefield chronology in the Simpson Desert, central Australia, revealed by cosmogenic nuclide and luminescence dating

TOSHIYUKI FUJIOKA^{1*}, GERALD NANSON², STEPHEN TOOTH³, ROBERT CRADDOCK⁴, DAVID PRICE², BRENT PETERSON² AND CHARLES MIFSUD¹

¹Australian Nuclear Science and Technology Organisation, Sydney, Australia, tyf@ansto.gov.au (* presenting author), cxm@ansto.gov.au

²School of Earth and Environmental Sciences, University of Wollongong, Wollongong, Australia, (gnanson@uow.edu.au, dprice@uow.edu.au, brentp@uow.edu.au)

³Institute of Geography and Earth Sciences, University of Aberystwyth, Ceredigion, UK, (set@aber.ac.uk)

⁴Smithsonian Institution, Washington, US, craddockb@si.edu

Dune fields are among major features in arid-semiarid Australia, but our knowledge of their origin, formation mechanism and development history are incomplete. Chronology is essential for comprehensive understanding of the evolutionary history of dunefield, but conventional dating has been limited by its age range, e.g., up to ~50 ka for radiocarbon and ~300 ka for luminescence dating. In this study, we employ cosmogenic nuclide burial dating, based on ¹⁰Be and ²⁶Al measurements, to determine the dune ages within the Simpson Desert, central Australia. Total 14 sand core samples, collected from three dune ridges and associated swales, have been measured for cosmogenic ¹⁰Be and ²⁶Al. All samples show depressed ²⁶Al/¹⁰Be ratios of 2.2–4.3; with distinctive contrast to the expected ratio of 6.7 for a simple exposure sample, the measured ratios indicate the model burial ages from 0.6 to 2 Ma. Near surface samples (<5 m depth) exhibit consistent ¹⁰Be or ²⁶Al concentrations between drill holes, with a uniform burial signal of ~0.8 Ma. This observation suggests that i) sand at the site is well mixed and ii) sand particles inherit burial signals from either previous episode(s) of dune formation and/or storage in river floodplain during sediment transport. The nuclide inventory can be changed from this 'regional average' near-surface concentration only when sand particles are isolated from surface mixing (i.e., by burial under a stable sediment column within dunes). Assuming that sand now buried under dunes had nuclide concentrations similar to the current surface sand, 'inheritance corrected' burial ages can be calculated, which represent the time since the sand has been isolated from surface mixing. The corrected burial ages range 0.24–1.21 Ma. The Simpson Desert dunefield, while still active, appears to have developed over at least the last 1 Ma.

Deciphering crustal evolution from metamorphic and geochemical signatures in calc-silicate gneisses

ISIS FUKAI¹, BARBARA DUTROW^{1*}, DARRELL HENRY¹,
PAUL MUELLER² AND DAVID FOSTER²

¹Louisiana State University, Baton Rouge LA, USA

(*correspondence: dutrow@lsu.edu)

²University of Florida, Gainesville, FL, USA

Field relations, petrographic textures, whole-rock geochemistry, and thermobarometry of calc-silicate gneisses from the Sawtooth Metamorphic Complex (SMC) in central Idaho, USA, preserve details of several important stages of crustal development along the western margin of Laurentia, including: contiguous deposition of a calcareous sandstone-to-marl sequence (Fig 1), peak metamorphism to lower-granulite facies (M1; Fig. 2), followed by widespread deformation at high P-T (D1), an amphibolite-facies thermal overprint (M2), and a late-stage, heterogeneous, brittle-ductile mylonitic deformation event (D2). M2 temperature estimates of $\sim 660 \pm 40^\circ\text{C}$ from Hbl-pl thermometry are similar to conditions calculated using Ti-in-biotite (TiB) thermometry and pseudosections, suggesting these methods can be used in calc-silicates to provide useful constraints on metamorphism.

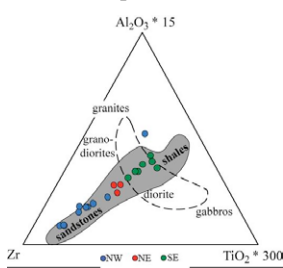


Fig. 1. Calc-silicate whole-rock geochemistry [1]

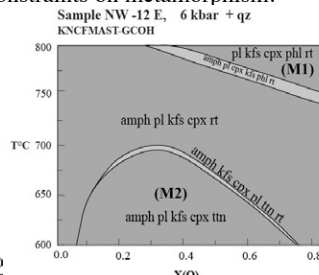


Fig. 2. Calc-silicate T-X(O) pseudosection [2]

The presence of abundant ~ 1150 - 1050 Ma Proterozoic detrital zircons in SMC quartzites and quartzofeldspathic gneisses reported in other recent work [3], coupled with protolith compositions near PAUCC, suggests calc-silicate gneisses record continuous sedimentary deposition and multiple metamorphic/deformation events that may be related to the formation/breakup of supercontinent Rodinia. As such, calc-silicates can provide valuable insight into tectonic and metamorphic events in a region.

[1] Garcia *et al* (1994) *J. of Geol.* **102**, 411-422. [2] Connolly (2005) *EPSL* **236**, 524-541. [3] Bergeron (2012) *MS Thesis*, Louisiana State University.

Changes in biological pump by ²³⁰Th-normalized flux of biogenic components in the Chilean margin sediment during the past 22kyr

M. FUKUDA^{1,2*}, N. HARADA², M. SATO¹, C. B. LANGE⁴,
H. KWAKAMI⁵, S. PANTOJA⁴, T. MATSUMOTO⁶
AND I. MOTOYAMA⁷

¹Univ. of Tsukuba, Tsukuba, Japan,

mh_(fukud@geol.tsukuba.ac.jp) (* presenting author)

²Japan Agency for Marine-Earth Science and Technology

(JAMSTEC), Yokosuka, Japan, haradan@jamstec.go.jp

⁴Univ. de Concepcion, Concepcion, Chile, clange@copas.cl

⁵JAMSTEC, Mutsu, Japan, kawakami@jamstec.go.jp

⁶Univ. of the Ryukyus, Nishihara-cho, Japan, tak@sci.u-ryukyuu.ac.jp

⁷Yamagata Univ, Japan, i-motoyama@sci.kj.yamagata-u.ac.jp

During the last glacial maximum, the atmospheric partial pressure of CO₂ ($p\text{CO}_{2\text{atm}}$) was very low, 180-190 ppm and rapidly increased to 280 ppm during the last deglaciation [1]. During glacial periods, strengthened productivity and an efficient biological pump in the North Pacific, equatorial Pacific, and Southern Oceans may have contributed to low $p\text{CO}_{2\text{atm}}$ [2]. However, there is still some controversy as to whether marine productivity was high everywhere during glacial periods. To resolve this controversy, more data are required from many regions regarding temporal changes in past export fluxes of biogenic materials. The eastern South Pacific Ocean including the Chilean marginal region, where active biological production is observed at present is target area of this study. The aim of this study is to identify changes in the ²³⁰Th-normalized export flux of biogenic components commonly used as proxies for paleoproductivity—namely total organic carbon (TOC), total nitrogen (TN) and biogenic opal (Si_{opal}) from two sediment cores collected at 36°S, off central-south Chilean covering the past 22 kyr (PC-1) and at 52°S near the mouth of Strait of Magellan, Pacific side over the past 13 kyr (PC-3). ²³⁰Th-normalized fluxes of biogenic components of sediments at 36°S and 52°S off the Chilean coast imply that the biological pump was effective during 14–8 kyr BP off central Chile, and after 5 kyr BP off central and southernmost Chile; and less effective during 22–14 kyr BP off central Chile and during 13–6 kyr BP off southernmost Patagonia [3]. That is to say, off central Chile, the weakness of the biological pump during the LGM contributed to the global rise of $p\text{CO}_{2\text{atm}}$ at that time. During 14–8 kyr BP, the increasing effectiveness of the biological pump at the PC-1 site off central Chile contributed to the global rise of $p\text{CO}_{2\text{atm}}$. At the PC-3 site, the weakening of biological pump contributed to the rise of $p\text{CO}_{2\text{atm}}$ during 13–6 kyr BP. After 6 kyr BP, the active biological pump did not contribute to the rise of $p\text{CO}_{2\text{atm}}$. In this presentation, we will also report ²³⁰Th-normalized fluxes of biogenic components at the 55°S collected from the Drake Passage sediment.

[1] Monnin (2001) *Science* **291**, 112 [2] Kohfeld (2005) *Science* **308**, 74. [3] Fukuda *Geochemical Journal* (in press)

Desorption behavior of cesium from smectite by major cations

K. FUKUSHI¹, Y. YAMASHINA¹, Y. AOI¹ AND H. SAKAI¹

¹Kanazawa University, Kanazawa, Japan,
(fukushi@staff.kanazawa-u.ac.jp (presenting author))

The radiocesium released from the Fukushima Daiichi nuclear power plant is retained at the surface soils around the power plant (Tanaka *et al* 2012GJ). The expandable clay minerals such as smectite and vermiculite are thought to be the one of the candidate for the host phases of radiocesium. The sorption behavior of cesium (Cs) on smectite has been widely studied (Cornell, 1993JRNC). On the other hand, the desorption behavior of trace Cs from smectite has not been well understood. The understanding of Cs desorption from the soil clay minerals are essential for the prediction of the migration of Cs in the surface environment. In present study, the desorption behavior of Cs from Cs bearing smectite by major cations (Na⁺, K⁺, Mg²⁺, Ca²⁺ and NH₄⁺) were systematically examined in laboratory.

The suspension of the Cs bearing smectite was prepared by reaction of 1 g/L smectite with 75 nM Cs⁺ solution in NaCl solutions at neutral pH. The desorption of Cs were examined by adding the major cations of which concentrations ranged from 10⁻³ to 10⁻¹ N to the smectite suspensions.

All cations except for K⁺ lead to the desorption of Cs from smectite when the concentrations of the added cations increased. The order of the ability for the desorption of Cs from smectite by the major cations was summarized as follow: Ca²⁺ ≈ Mg²⁺ > NH₄⁺ > Na⁺. The selectivity coefficients based on Gaines-Thomas convention relative to Na⁺ were estimated from the macroscopic desorption results. The estimated selectivity coefficients were almost consistent with previously reported values. This indicates that the exchanges of Na⁺, Mg²⁺, Ca²⁺ and NH₄⁺ to Cs⁺ in smectite are reversible reactions.

On the other hand, K⁺ plays a role for inhibition of Cs desorption from smectite. It is well documented that K⁺ lead to the shrinking of the layer space in smectite (Morodome *et al* 2009CCM). The shrinking probably makes the Cs inside the smectite layers undesorbable. Some recent studies indicated that the radiocesium in the soils affected by Fukushima Daiichi nuclear plant accident was merely leached by the high concentrations of cations (Qin *et al* 2012GJ). The effect of K in natural water is thought to be the one of the possible mechanism for the fixation of radiocesium in the soils.

Chromium solubility in chlorite and implications for subduction zone dynamics: an experimental study in the CrMASH system up to 6.5 GPa, 900°C

P. FUMAGALLI^{1*}, J. FISCHER¹, M. GEMMI²,
M. MERLINI¹ AND S. POLI¹

¹University of Milan, I-20133 Milano, Italy (*correspondence: patrizia.fumagalli@unimi.it)

²Center for Nanotechnology Innovation@NEST, Istituto Italiano di Tecnologia, Pisa, Italy

Chlorite is known to form nearly monomineralic hybrid rocks at the slab-mantle interface at subduction zones. In hydrated ultramafic systems, chlorite containing 13 wt.% of H₂O represents a good candidate for transferring water beyond the stability field of antigorite, being stable up to 4-6 GPa, 700-800°C. Although pressure-temperature stability of clinocllore has been widely investigated in the system MgO-Al₂O₃-SiO₂-H₂O, the role of Cr in modifying phase relationships is poorly assessed at the low-temperatures characteristic of subducting slabs. Despite chromium is a minor constituent of the Earth Mantle, being incorporated in almost all major mantle phases, it is expected to affect phase equilibria and to extend chlorite stability. This study mainly aims to experimentally investigate the solubility of chromium in chlorite as a function of pressure, temperature and bulk composition and evaluate its effect on phase relations.

Three different compositions with X_{Cr} = Cr/(Cr+Al) = 0.075, 0.25 and 0.5 respectively, have been investigated between 1.5-6.5 GPa, 650-900°C. Cr-chlorite only occurs in bulk with X_{Cr} = 0.15. It coexists with enstatite up to 3.5 GPa, 800-850°C, and with forsterite, pyrope and spinel at higher pressure. At P>5 GPa other hydrates occur: a Cr-bearing phase HAPY [1] is stable in assemblage with pyrope, forsterite, and spinel; Mg-sursassite coexist at 6.0 GPa, 650°C with a new Cr-bearing phase, named SAD, forsterite and spinel.

Chromium strongly partitions into spinel (X_{Cr}=0.8806), followed by orthopyroxene (X_{Cr}=0.1428), Cr-chlorite (X_{Cr}=0.0815) and garnet (X_{Cr}=0.0339).

Cr affects the stability of chlorite by shifting its breakdown reactions towards higher T and P, but Cr solubility at high P results to be reduced as compared with low P occurrence in hydrothermal environments.

[1] Gemmi *et al* (2011) *EPSL* **310**, 422-428.

Equation of state for silicate melts: Static vs. shock compression

N. FUNAMORI* AND D. WAKABAYASHI

Department of Earth and Planetary Science, University of
Tokyo, Tokyo 113-0033, Japan
(*correspondence: funamori@eps.s.u-tokyo.ac.jp)

We have recently proposed a simple and easy-to-use equation of state for silicate melts, which is applicable to a wide range of chemical composition at the pressure condition of the deep upper mantle [1]. To derive the equation of state, we assumed that silicate melts have a densified network structure (intermediate-range order) based on the knowledge from the behavior of densified SiO₂ glass under high pressure [2]. The equation of state is consistent with all the available density data of silicate melts with an SiO₂ content of about 35-55 mol% measured with large-volume presses between 8 and 22 GPa. However, the equation of state cannot explain shock-compression data. As demonstrated in Fig. 1, there are systematic differences between static- and shock-compression data. Investigation to clarify the reason of the discrepancy is now ongoing.

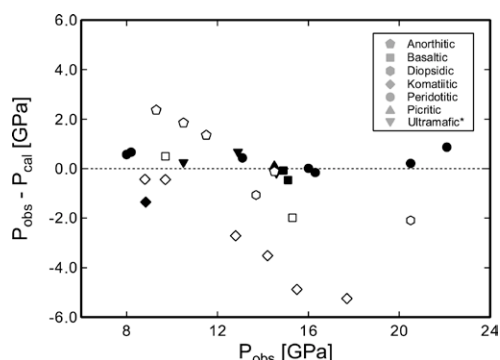


Figure 1: Deviation of experimental data from the equation of state proposed in Ref. [1] for silicate melts. Solid and open symbols represent static- and shock-compression data, respectively. (*) No specific name is given for the ultramafic data.

[1] Wakabayashi & Funamori (2013) *Phys. Chem. Minerals* **40**, 299-307. [2] Wakabayashi *et al* (2011) *Phys. Rev. B* **84**, 144103.

Element quantification in chondritic components by LA-ICP-MS

C. FUNK¹*, F. WOMBACHER¹, R. GLAUS², D. TABERSKY²,
J. KOCH² AND D. GÜNTHER²

¹Institut für Geologie und Mineralogie, Universität zu Köln,
Germany. (cfunk0@uni-koeln.de) (*presenting author)

²Laboratory of Inorg. Chemistry, ETH Zurich, Switzerland

Chondrites comprise the most primitive solar system materials available for laboratory studies. Major and trace element distribution and abundances in different chondritic components provide insights into the early evolution of inner solar system materials. Chondrites are composed of different components (e.g. chondrules, matrix, CAIs etc.) which in turn consist of heterogeneously distributed fine-grained silicates, oxides, sulfides and metals typically on the μm up to some tenth of μm scale. The different phases exhibit different laser ablation characteristics and therefore impair an accurate quantification of elemental concentrations in chondritic components. The use of femtosecond lasers that generate only minimal thermal effects during sampling, produce uniform and fine aerosols, and offer reduced matrix effects compared to nano second laser ablation can diminish this difficulty.

The small-scale chemical heterogeneity of chondritic matter makes the accurate determination of suitable internal standard elements (e.g. by electron microprobe) challenging. This problem can be circumvented if the ablation yield is calculated by the total ablated material [1]. For this purpose, all relevant major elements are analysed relative to an external standard and recalculated as oxides, sulfides, and metals. The ablation yield is then calculated from the sum of major elements. This procedure however requires a suitable external standard for major element calibration in chondrites. Compared to chondrites the commonly used NIST SRM 61x glasses have extremely low amounts of Mg, S and Fe and are therefore poorly suited for this kind of yield correction.

Considering the aforementioned problems, we purchased a nanoparticle based standard material produced by flame spray pyrolysis. This calibration material comprises major and most of the minor elements in approximately CI chondritic abundances with ablation characteristics analogous to NIST SRM 612. Quantitative analysis of the calibration material by solution nebulization ICP-MS showed good agreement with CI chondritic abundance for most elements. Measurement setup, data evaluation and applicability of the approach, composition and homogeneity of the new reference material will be presented and discussed.

[1] Liu *et al* (2008) *Chem. Geol.* **257**, 34-43.

Evidence for chondritic lunar water and nitrogen trapped in Apollo 17 volcanic glasses

E. FÜRİ^{1*}, B. MARTY¹, E. DELOULE¹ AND A. GURENKO¹

¹CRPG-CNRS, BP20, 54501 Vandoeuvre-les-Nancy, France
(*correspondence: efueri@crpg.cnrs-nancy.fr)

The notion of a largely devolatilized lunar interior has been challenged by the discovery of trace amounts of water in lunar volcanic glasses (LVGs) [1], melt inclusions [2] and apatites [3-5]. However, the caveat in the search for indigenous lunar volatiles (e.g., H₂O and N) is that any sample collected at the Moon's surface likely also contains volatiles implanted by solar wind (SW) irradiation and certain volatile element isotopes produced by spallation reactions.

Here, we first assess the proportion of solar, cosmogenic, and indigenous water (hydrogen) trapped in single Ti-rich 74002 LVGs by coupling SIMS measurements of water abundances and D/H ratios with CO₂ laser extraction-static mass spectrometry analysis of noble gases (He, Ne, Ar). Our noble gas results show that the large single Ap17 LVGs have been exposed at the lunar surface for ≤ 36 Myrs, and that they contain a negligible amount of SW-derived volatiles. Therefore, the detection of water in these primitive melts confirms the presence of a non-anhydrous mantle source within the Moon, with a chondritic isotopic signature.

Secondly, nitrogen was extracted from different 74002 grain size fractions by CO₂ laser heating. The surface-correlated N component shows a $\delta^{15}\text{N}$ value of $+4.4 \pm 7.8$ ‰ relative to air. This value likely reflects the isotope composition of N-bearing volcanic vapor that condensed onto the surface of the LVGs, and it represents a minimum estimate of the $\delta^{15}\text{N}$ signature of the melt source. Preferential loss of light isotopes from the melt, followed by condensation of isotopically light vapor [6], as well as addition of SW-derived N, may have lowered the initial $\delta^{15}\text{N}$ value. Nonetheless, the isotopic composition of indigenous nitrogen in the lunar mantle appears to be comparable to the values observed in carbonaceous chondrites (e.g., [7]).

[1] Saal *et al* (2008) *Nature* **454**, 192-196. [2] Hauri *et al* (2011) *Science* **333**, 213-215. [3] Boyce *et al* (2010) *Nature* **466**, 466-470. [4] McCubbin *et al* (2010) *PNAS* **107**, 11223-11228. [5] Greenwood *et al* (2011) *Nature Geoscience* **4**, 79-82. [6] Moynier *et al* (2006) *GCA* **70**, 6103-6117. [7] Kerridge (1985) *GCA* **49**, 1707-1714.

Effects of oxide ions on the stabilization of pentoses

YOSHIHIRO FURUKAWA^{1*}, MANA HORIUCHI¹, SAKIKO NITTA¹ AND TAKESHI KAKEGAWA¹

¹Department of Earth Science, Tohoku University, 6-3 Aza-aoba, Aramaki, Sendai, Japan (*correspondance: furukawa@m.tohoku.ac.jp)

Ribose, an aldopentose, is an essential component of RNA that has been regarded an important organic compound for the origin of life [1,2]. Thus, the formation and accumulation of ribose on the prebiotic Earth may be a requisite for the emergence of primordial RNA. However, pentoses including ribose are unstable under alkaline conditions where they typical form [3]. Formation of complexes between pentoses and several oxide ions such as borate, silicate, and molybdate, have been investigated. In particular, stabilization of pentoses by borate and silicate were demonstrated in previous studies [4,5]. However, it is still unclear which oxide ion more effectively stabilize pentoses and which pentose, among the four aldopentoses, is stabilized.

We conducted incubation experiments of each aldopentoses under several oxide ion concentrations at a fixed temperature. The experiments were conducted under an alkaline condition (pH~12) with continuous stirring. The incubation solution was sampled at a pre-determined time interval and quantitatively analyzed for residual and produced pentoses with liquid chromatography-mass spectrometry.

We confirmed the formation of pentose-borate complexes, but the pentose-silicate complexes were below the detection limit. The concentration of all residual pentoses gradually decreased with the incubation time. Both borate and silicate reduced the decrease of pentose concentration, but the stabilization effect was greater with borate. This result suggests that borate played an important role in the accumulation of pentoses on the prebiotic Earth and formation of primordial RNA.

[1] Joyce (1989) *Proc. Natl. Acad. Sci. U.S.A.* **86**, 7054-7058. [2] Bartel & Szostak (1993) *Science* **261**, 1411-1418. [3] El Khadem *et al* (1987) *Carbohydr. Res.* **169**, 13-21. [4] Ricardo *et al*, (2004) *Science* **303**, 196-196. [4] Lambert *et al*, (2010) *Science* **327**, 984-986.

Volatile content in melt inclusions of Vulcanello's explosive activity: Implications for the last 1000 years of activity at Vulcano Island (Aeolian Archipelago, Italy)

R. FUSILLO^{1*}, F. DI TRAGLIA¹, A. GIONCADA¹,
M. PISTOLESI¹, M. ROSI¹ AND P. J. WALLACE²

¹Dipartimento Scienze della Terra, Università di Pisa, Via Santa Maria 53, 56126, Pisa, Italy (*correspondence: Raffaella.Fusillo@bristol.ac.uk); present address: School of Earth Sciences, University of Bristol, Wills Memorial Building, Queen's Road, BS8 1RJ, Bristol, United Kingdom

²Department of Geological Sciences, University of Oregon, Eugene, OR 97403-1272, United States

We analysed major element and volatile (H₂O, CO₂, S, F, Cl) concentrations in olivine-hosted melt inclusions (MIs) from tephra of Vulcanello's explosive activity in order to estimate magma chamber depth. We also investigated possible petrological links with the last 1000 years of La Fossa Cone activity.

Major element compositions of MIs range from 52 to 62 wt% SiO₂, and olivine host compositions are Fo₆₅₋₇₀. Water concentrations in the MIs are variable (0.2 -1.4wt% H₂O), while CO₂ concentration is below 50 ppm for all the samples. Halogens concentration ranges from 0.1 wt% to 0.4 wt%, while S content ranges from 0.02 to 0.04 wt%.

The results showed a very shallow magma chamber (≤1 km) beneath the Vulcanello centre, as already hypothesized for la Fossa Cone [1]; major elements, S and Cl concentrations in MIs from Vulcanello's tephra are in fact comparable with those from the products of the contemporaneous activity from La Fossa Cone [2, 3].

From stratigraphic evidences [3] and MI data we hypothesize that Vulcanello and La Fossa Cone activity was fed by the same magma reservoir. We provide new data on the magmatic evolution of the last 1000 years of Vulcano's activity [4]. Our hypothesis has also implications in regard to the assessment of volcanic hazard of a resurgent volcano as La Fossa Cone.

[1] Clocchiatti *et al* (1994) *Bull. Volc.* **56**, 466-486. [2] Gioncada *et al* (1998) *Bull. Volc.* **60**, 286-306. [3] Di Traglia *et al* (2013) *Geomorphology, acc. for pub.* [4] De Astis *et al* (1997) *J. Geophys. Res.* **102**, 8021-8050

The anthropogenic contribution to carbon dioxide dissolved in seawater

F. GÄB¹* C. BALLHAUS¹ AND J. SIEMENS²

¹Steimann Institut, Universität Bonn

(*fgaeb@uni-bonn.de, ballhaus@uni-bonn.de)

²Bodenwissenschaften, Universität Bonn

(jsiemens@uni-bonn.de)

Emissions of anthropogenic CO₂ not only enhance greenhouse effects in the atmosphere and contribute toward global warming. Atmospheric CO₂ also reacts with surface ocean waters and causes ocean acidification, to an extent that marine organisms may face difficulty in sequestering CaCO₃ to build their shells. To assess how far the rate of acidification may progress in the future, reliable forecasts are needed as for the future emissions of CO₂. In addition, it must be known how much CO₂ is being exchanged across the atmosphere/seawater interface at any given pCO₂, in order to define the proportion of inorganic carbon stored in the ocean water that is anthropogenic in origin.

Exchange experiments between atmosphere and seawater are reported to quantify how much CO₂ can be exchanged between the Earth's atmosphere and ocean surface water at any given CO₂ partial pressure. The seawater came from the Aegean sea. Its total alkalinity was determined at 2698 ± 24 μmol/kg. The gases to simulate the Earth's atmosphere were commercial N₂-O₂ (4:1) gas mixtures with CO₂ ranging from < 10, 200, 280, 390, 1000, 2,000, 5,000, 20,000 and 100,000 μatm CO₂. At the present atmospheric level of CO₂ (400 μatm) about 18% of the inorganic carbon (DIC) inventory dissolved in surface seawater is due to direct exchange across the water-atmosphere interface. By far the largest proportion of the DIC in seawater, i.e. more than 80%, is derived from sources other than the atmosphere, and the concentration in seawater of this fraction is independent of short-term (human-scale) variations in pCO₂. The human contribution to the DIC of ocean surface water is defined as the carbon content that may be exchanged across the water-atmosphere interface between 280 and 400 μatm CO₂. It is quantified at ~ 115 ± 18 μmol carbon per kg seawater, or 4.5% of the total present-day DIC of surface ocean water.

That concentration is a higher than the anthropogenic contribution in mid-latitude Atlantic surface water (~ 60 μmol kg⁻¹), but (1) Aegean seawater is more alkaline than Atlantic water hence more capable of absorbing CO₂ via hydrolysis reaction; (2) the 60 μmol kg⁻¹ C dates from 1994, when the pCO₂ was only 355 μatm; and (3) any DIC derived from direct measurements of natural surface ocean waters may be a steady-state rather than an equilibrium concentration.

Secular variations in seawater chemistry controlling water-rock interaction in shallow reflux systems

T. GABELLONE* AND F. WHITAKER

School of Earth Sciences, University of Bristol, Wills

Memorial Building, Queen's Road, Bristol, BS8 1RJ, UK

(*correspondence: tatyana.gabellone@bristol.ac.uk,

fiona.whitaker@bristol.ac.uk)

Secular variations of seawater composition influence both the primary mineralogy of marine non-skeletal carbonates and also the dolomitization potential of seawater-derived fluids. Using 1D reactive transport modelling we explore the role of seawater composition in controlling early carbonate diagenesis during reflux of brines, contrasting aragonitic and calcitic seawaters based on modern and Mississippian with Mg/Ca of ~5 and ~2 respectively.

Dolomite forms from reflux of modern brines by replacement of calcite, increasing the porosity. When replacement is complete, dolomite can continue to form as primary cement ("overdolomitization") and porosity is reduced. Increasing evaporative concentration in the brine pool enhances reaction rate independent of the effect on enhanced density-driven flow. Reflux of brines formed from Mississippian seawater leads to synchronous primary dolomite cementation and replacement of calcite, with net porosity occlusion. Release of Ca²⁺ by replacement dolomitization drives gypsum precipitation from both modern and Mississippian brines of >150 ‰ salinity, particularly at higher temperatures, further occluding porosity.

Temperature is an important control on dolomitization kinetics even at relatively low temperatures, with complete replacement of calcite occurring within 130 ky at 35°C, more than twice the rate at 30°C. Fine-grained calcitic sediments characteristically have a high effective surface area and may dolomitise at rates >10 times those of coarse-grained sediments. However, this effect may be offset by the lower permeability of finer sediments which limits rates of fluid flow for a given density head drive. The effect of microbial processes appears to be critical in generating nucleation sites ("seed dolomite"), as well as altering fluid chemistry. Neither secular variations in seawater chemistry associated with changing atmospheric pCO₂, nor biological induced alkalinity variation, appear to significantly influence dolomitization.

Growth-rate induced disequilibrium of boron and divalent cations in calcite: An *in situ* approach

RINAT I. GABITOV,¹ ALEKSEY SADEKOV²
CLAIRE ROLLION-BARD³ AND BRUCE WATSON⁴

¹Mississippi State University, Mississippi State, MS, 39762, USA

²The University of Cambridge, Cambridge, CB2 3EQ, UK

³CRPG, Univ. de Lorraine, F-54500 Vandoeuvre-lès-Nancy, France

⁴Rensselaer Polytechnic Institute, Troy, NY 12180, USA

Concentrations of trace and minor elements in marine and terrestrial calcite have the potential to yield information on environmental conditions during crystallization. However, thermodynamic and kinetic effects on element partitioning in calcite are not well understood. The phenomenon of sectoral zoning (geometrically distinct distribution B, Mg, Sr, and Ba in non-equivalent vicinal faces of calcite crystals) has been reported in several studies [1-3, etc.]. The potential factors controlling element partitioning between different calcite faces and fluid include: structural difference of atomic layers at the calcite near-surface region and elements diffusion rates in those layers, difference in growth rate of crystal faces, and chemical speciation at the calcite - fluid interface [2,4,5, etc.].

We used the growth entrapment model (GEM) together with experimental data to explore B heterogeneity within single calcite crystals. The GEM describes disequilibrium fractionation of elements and isotopes between a crystal and its growth medium as a consequence of the “capture” of a chemically and isotopically anomalous near-surface region of the lattice during crystal growth [5]. We show that crystal zoning could be explained by different diffusion rates of B in the near-surface layer of the non-equivalent faces of calcite - which is not inconsistent with the extreme anisotropy of the calcite crystal structure. In addition to our B results, we will present GEM simulations for divalent cations in calcite in the context of sectoral zoning.

[1] Paquette and Reeder (1995) *Geochim. Cosmochim. Acta* 59, 735. [2] Hemming *et al* (1998) *Geochim. Cosmochim. Acta* 62, 2915. [3] Wasylenki *et al* (2005) *Geochim. Cosmochim. Acta* 69, 3017. [4] Watson (2004) *Geochim. Cosmochim. Acta* 68, 1473. [5] Gabitov and Watson (2006) *Geochem. Geophys. Geosys.* 7, Q11004, doi:10.1029/2005GC001216.

Revealing a high altitude paleoclimate record from a Southern Europe ice core

P. GABRIELLI¹, C. BARBANTE^{2,3}, L. CARTURAN⁴,
M. DAVIS¹, G. DALLA FONTANA⁴, G. DREOSI²,
R. DINALE⁵, G. DRAGÀ⁶, J. GABRIELI², N. KEHRWALD²,
V. MAIR⁷, V. MIKHALENKO⁸, K. OEGGL⁹,
U. SCHOTTERER¹⁰, R. SEPPI¹¹, A. SPOLAOR²,
B. STENNI¹², L.G. THOMPSON¹ AND D. TONIDANDEL⁷

¹The Ohio State University, USA, gabrielli.1@osu.edu

²IDPR-CNR - University Ca' Foscari of Venice, Italy

³Accademia Nazionale dei Lincei, Italy

⁴University of Padua, Italy

⁵Ufficio Idrografico – Provincia Autonoma di Bolzano, Italy

⁶Waterstones geomonitoring, Varna, Italy

⁷Ufficio Geologia, Provincia Autonoma di Bolzano, Italy

⁸Russian Academy of Sciences, Russia

⁹University of Innsbruck, Austria

¹⁰University of Bern, Switzerland

¹¹University of Pavia, Italy

¹²University of Trieste, Italy

Low latitude ice cores offer unique and detailed paleoclimate information from high elevations. However, as most of the accessible low latitude drilling sites have already been explored and as glaciers are melting worldwide, it is difficult to identify ice fields that contain novel and intact ice core records. The “Ortles Project” is an international scientific effort gathering a dozen institutes from six nations with the primary goal of obtaining a high altitude climate record from Southern Europe. Atmospheric temperatures in the entire alpine region are currently increasing at twice the rate of global temperatures and this change may be amplified at the highest elevations. Unfortunately there is a scarcity of paleoclimate information from high altitudes in the Alps to place the current rapid climate change in a paleo-perspective. To fill this gap we drilled in 2011 four ice cores on Alto dell’Ortles (3859 m, South Tyrol, Italy) the highest glacier in the eastern Alps. We have found an annually preserved climatic signal (in terms of stable isotopes, dust and major ions) embedded in the deep cold ice of this glacier. Alto dell’Ortles is the first low-accumulation alpine drilling site where both winter and summer layers can be clearly identified. From the seasonal layers in the ice core record we estimate an average accumulation rate of ~ 850 mm of water equivalent per year during the last 50 years. Preliminary annual layer counting and two absolute time markers suggest that the time period covered by the Ortles ice cores may span from several centuries to a few millennia.

Reading the melt inclusion record of pre-eruptive magmatic volatiles

GLENN A GAETANI¹*, CLAIRE BUCHOLZ¹,
ESTELLE ROSE-KOGA², NOBUMICHI SHIMIZU¹,
KEN KOGA² AND BRIAN MONTELEONE¹

¹Department of Geology and Geophysics, Woods Hole Oceanographic Institution Woods Hole, MA, 02543, USA (*correspondence: ggaetani@whoi.edu)

²Laboratoire Magmas et Volcans, Clermont Université, Université Blaise Pascal, BP 10448, 6300 Clermont-Ferrand, France

Olivine-hosted melt inclusions are one of the most important sources of information on pre-eruptive magmatic volatiles. Although the strength of the olivine largely protects inclusions from decompression and degassing during ascent and eruption, post entrapment processes can affect the concentrations of magmatic volatiles in the included melts. We investigated experimentally the potential for post-entrapment modification of H₂O, CO₂, S, F, Cl and Fe³⁺/ΣFe in olivine-hosted melt inclusions. Our results demonstrate that diffusion re-equilibrates H₂O and Fe³⁺/ΣFe in a matter of hours at magmatic temperatures. Pressure drops within the inclusions during diffusive loss of H₂O decrease the solubility of CO₂ – and to a lesser extent S – in the silicate melt. This leads to decreased concentrations in the included melt as CO₂ and S are partitioned into vapor bubbles. The concentrations of F and Cl are not affected by either diffusive loss through the host crystal or partitioning into the vapor phase.

Effects of diffusive re-equilibration were assessed by dehydrating natural inclusion-bearing olivines from Cerro Negro volcano, Nicaragua (initial H₂O = 3.8±0.3 wt%) and Mauna Loa volcano, Hawaii (initial H₂O = 0.375±0.006). Experiments were conducted using both a vertical quenching furnace and a Vernadsky heating stage. Run products were analyzed for major elements by electron microprobe and for H₂O, CO₂, S, F, Cl and D/H ratio by SIMS. Fe³⁺/ΣFe was determined by μ-XANES.

Our results demonstrate that post entrapment modification may significantly impact the concentrations of H₂O and CO₂ in included melts. The consequences of this are far less severe for olivine-hosted melt inclusions with initially low H₂O. In this case the external magma loses very little H₂O during degassing so that a H₂O fugacity gradient does not develop to drive diffusive loss. This is supported by a global compilation of melt inclusion data which show that low-H₂O melt inclusions are capable of recording entrapment pressures consistent with the upper mantle, whereas the internal pressures for melt inclusions with initially high H₂O contents never exceed crustal values.

Microorganisms in flooded underground uranium mines of East Germany

CORINNA GAGELL AND THURO ARNOLD

Institute of Resource Ecology, Helmholtz-Zentrum Dresden-Rossendorf e.V., P.O. Box 510119, D-01314 Germany, (c.gagell@hzdr.de)

After the German reunification the Wismut GmbH, formerly the 3rd largest U producer of the world, started to remediate the legacies of their U mining activities. As part of the remediation strategy the pit body was flooded to induce reductive processes. Although flooding of the mines Pöhla and Schlema-Alberoda was already finished about ten years ago, the mine water still contains elevated concentrations of toxic metals such as U, As and Ra. Thus, expensive and long-lasting monitoring and waste water treatment is required. Since microorganisms can influence the toxicity of metals directly or indirectly, one alternative approach is to use them for bioremediation. Here, the diversity of the indigenous microbial community of the mine water from Pöhla and Schlema-Alberoda is reported. *Bacteria* as well as *Archaea* were analyzed by state-of-the-art pyrosequencing of the 16S rRNA gene. Mine water samples were either filtrated or harvested from a flow cell. For the filtrated Pöhla mine water, the Pöhla flow cell, the filtrated Schlema mine water, and the Schlema flow cell 485, 697, 325 and 527 sequences, respectively, were divided into 98, 189, 188 and 89 operational taxonomical units (OTUs), respectively, belonging mainly to *Bacteria*. The bacterial sequences from the Pöhla mine were classified into *Proteobacteria*, *Verrucomicrobia*, *Bacteroidetes*, *WS3*, *Chloroflexi*, *Firmicutes*, *Acidobacteria*, *SR1*, *Actinobacteria*, *Spirochaetes* and *OD1*. For the Schlema mine *Proteobacteria*, *Acidobacteria*, *WS3*, *Bacteroidetes*, *Chloroflexi*, *SR1*, *Chlorobi*, *TM7* and *Acinobacteria* were found. The dominant bacterial phylum in all samples are the *Proteobacteria*. Higher bacterial diversities were observed in flow cells in comparison with filtrated waters. A dataset of 15786, 17872, 11404, 7780 sequences revealed 639, 643, 769 and 455 OTUs, respectively, mainly for *Archaea* of the filtrated Pöhla mine water, the Pöhla flow cell, the filtrated Schlema mine water and the Schlema flow cell, respectively. The archaeal sequences of the Pöhla as well as the Schlema mine water belong to the class of *Methanobacteria*, *Thermoprotei*, *Methanomicrobia*, *Thermoplasmata* and *Halobacteria*.

U-Pb geochronology and geochemistry of the granulite-amphibolite complex in the Asinara Island (Italy)

LAURA GAGGERO¹, GIACOMO OGGIANO²,
LEONARDO CASINI² AND MASSIMO TIEPOLO³

¹DISTAV-UNIGE Corso Europa 26, I-16132 Genoa, Italy,
gaggero@dipteris.unige.it

²Dept. Botany, Ecology, Geology - UNISS, Via Piandanna 4,
I-07100 Sassari, Italy

³IGG-CNR, Via Ferrata 1, I-27100 Pavia, Italy

In Sardinia, the Posada – Asinara mylonitic mélange zone gathers eclogitic relicts with N-MORB affinity, high-grade and medium-grade continental complexes (Carmignani *et al.*, 1992, 1994), interpreted as the southern margin of Armorica and northern margin of Gondwana, respectively. In the Asinara Island, an intermediate to high-grade granulite crust section (Oggiano and Di Pisa, 1988) attains the deepest exposed level at Punta Scorno, where a basic complex, interleaved by cm to m thick felsic layers occurs. The felsic layers were selected for U-Pb radiometric dating by ELA-ICP-MS on zircons at CNR – IGG Pavia. In the granulite-amphibolite complex, each felsic layer yielded different ranges of Concordia ages, from Neoproterozoic (672 ± 12 to 588 ± 16 Ma) until a Cambrian system closure (514 ± 22 to 506 ± 15 Ma). Early Ordovician ages spans between 491 ± 13 and 474 ± 12 Ma. Late Ordovician – Early Silurian ages fall in the 461 ± 10 to 435 ± 12 Ma interval; Devonian and Carboniferous age values also result. This points to a long-lasting, sequence of metamorphic events with episodes of partial melting, in the lower crust.

Investigation of the methanotrophic activity in the soils of a geothermal site of Pantelleria Island (Italy)

GAGLIANO A.L.¹ D'ALESSANDRO W.², QUATRINI P.³ AND PARELLO F.¹

¹University of Palermo, Dept. DiSTeM, Palermo, Italy
(*corresponding author antoninalisa.gagliano@unipa.it;
francesco.parello@unipa.it)

²Istituto Nazionale di Geofisica e Vulcanologia, sezione di Palermo, Palermo, Italy (w.dalessandro@pa.ingv.it).

³University of Palermo, Dept. STEBICEF, Palermo, Italy
(paola.quatrini@unipa.it).

Yearly, 22 Tg of CH₄ are released in to the atmosphere from several natural and anthropogenic sources [1]. The total CH₄ emission from geothermal/volcanic areas is not well defined since the balance between emission through degassing and consumption through soil microbial oxidation is poorly known.

Our purpose was to explore the methanotrophic potential and the bacterial diversity of the soils of Favara Grande, the main geothermal area of Pantelleria island, (Italy), whose emissions are in the order of 2.5 Mg/y [2]. Two of the three sites analysed, show high methane consumption (up to 950 ng/g/h), temperatures from 58 to 75 °C and pH from 5 to 6.

The total bacterial diversity analysed by PCR-TTGE of the 16rRNA gene revealed similar profiles in these two sites. The culturable methanotrophic alphaproteobacterium *Methylocystis* sp. was isolated by enrichment cultures from soil samples of the most active site. The isolated species shows a wide range of tolerates pH values from 3 to 8 and temperatures tolerance a least up to 37 °C and has a methane oxidation rate of 450 ppm/h. A larger diversity of (α - and γ -) proteobacterial and verrucomicrobial methanotrophs was detected by using a culture-independent approach based on the the amplification of the methane mono-oxygenase gene (*pmoA*).

Understanding the ecology of methanotrophy in geothermal sites will increase our knowledge of the role of soils in methane emissions to the atmosphere.

[1] Kvenvolden K.A., B.W. Rogers, 2005, Marine and Petroleum Geology 22 579-590. [2] D'Alessandro W., S. Bellomo, J. Fiebig, M. Longo, M. Martinelli, G. Pecoraino, F. Salerno, 2009, Journal of Volcanology and Geothermal Research 187 147-157.

Abiotic O₂ availability on an Early alkaline ocean through halogen-induced superoxide species

L. GAGO-DUPORT¹, S. F. BASTERO¹, C. GIL-LOZANO¹,
E.L. ADAMS¹, A. F. DAVILA² AND A .G. FAIRÉN³

¹Universidad de Vigo. 36200 Vigo. Spain.duport@uvigo.es

²SETI Institute, Mountain View, CA 94043, USA.

³Cornell University. 14853 New York, United States

Whether Early Earth oceans were acidic or alkaline and, if so what such a difference would imply in the further evolution of atmosphere and life, has been -and still is- a subject of great controversy. Because of the primitive ocean was in equilibrium with an atmosphere mainly composed of CO₂ it has been assumed the Hadean ocean was probably acidic. Alternatively, it has been suggested that reactions between sodium-rich silicates and atmospheric CO₂, leading to the formation of Na₂CO₃, may have produced an early soda ocean [1]. Both hypotheses are mainly supported by mass-balance calculations performed under the assumption of equilibrium conditions, while neglecting kinetic effects as well as simultaneous redox evolution resulting from reaction with volatiles other than CO₂.

The aim of this work is twofold: beginning with the alkaline scenario, derived from the interaction of basalt bearing minerals with water, to explore the coeval evolution of both acid-base and redox states in an ocean approaching circumneutral pH, i.e., the actual steady state. This was done through kinetically controlled geochemical calculations including transitional halogen species (ClO⁻, HClO) and iron superoxides (FeO₄⁻, Fe⁴⁺=O²⁻). Second, perform micro and nanostructural analysis through laboratory. Silica garden structures (SG), built from iron salts, were used as an instantaneous mixing device for acidic iron-rich and alkaline silica-rich regions and were used as a laboratory analogous. Resulting textures, solid phases and species forming at the acidic-alkaline interface, on both, oxic and anoxic conditions, were analyzed by UV-VIS, HREM and optical microscopy. Results of geochemical modeling show that Fe-superoxides are formed transitionally along the evolution from alkaline-oxidant conditions to neutral pH values. Significantly, the model demonstrates that, although Fe-species are not soluble in alkaline conditions -the main argument against an Early soda ocean- superoxides are. Their desestabilization near neutral pH conditions may induce precipitation of Fe⁺³ solid phases, together with O₂(g) as a byproduct and gives rise to the formation of Fe-Si composites, selforganized as layered structures.

[1] Kempe and Degens (1985) *Chem. Geol.*, **53**, 95-108.

Thermodynamics of hydration of MX80 smectite derived from hydration isotherms

H. GAILHANOU^{1*}, P. BLANC¹, A. LASSIN¹, P. VIEILLARD²
R. DENOYEL³, E. BLOCH³, B. MADÉ⁴ AND E. GIFFAUT⁴

¹BRGM, BP36009, 45060, Orléans, France

(*correspondence : h.gailhanou@brgm.fr)

²CNRS-IC2MP-UMR-7285 Hydrasa, 86022, Poitiers, France,
philippe.vieillard@univ-poitiers.fr

³LCP UMR-CNRS-6264, 13397, Marseille, France
(renaud.denoeyel@univ-provence.fr)

⁴ANDRA, 92298, Châtenay-Malabry, France
(Benoit.Made@andra.fr)

Hydration energies contribute significantly to the stability of hydrated clay minerals. However, thermodynamic data of hydration for clay minerals are still poorly known. The present study aims to improve our comprehension of the hydration processes of sodic smectite MX80, and to implement a new methodology for extracting thermodynamic data of hydration of the smectite.

A first approach consists in applying a global hydration model to extract the thermodynamic data of total adsorbed water (G, H and S) from adsorption/desorption isotherms at 25°C and 45°C. The results are in good agreement with calorimetric data at 84 and 91% RH, from [1]. As capillary water, which is present in the intergranular porosity of the clay sample, does not contribute to the thermodynamic stability of the hydrated clay mineral, a refined calculation method has been implemented to discriminate hydration water from capillary water in the total adsorbed water. The so called "hydration water" refers to interlayer water and surface recovering water of the smectite. Contrary to capillary water, the amount of hydration water depends on the nature of the smectite (nature of interlayer cations, layer charge and location of the charge). The thermodynamic properties of capillary water are calculated according to [2]. The present method allows (i) to estimate the respective amounts of hydration and capillary waters and (ii) calculate the energies of formation of the hydration water.

This work is to be extended to other hydrated clay minerals in order to refine the solid solution model from [3] and to finally provide a global predictive model for clay mineral hydration energies.

[1] Gailhanou *et al* (2012) *GCA* **89**, 279-301. [2] Lassin *et al* (2005) *GCA* **69**, 5187-5201. [3] Vieillard *et al* (2011). *GCA* **75**, 5664-5685.

Li isotopes : The ideal weathering tracer?

J. GAILLARDET¹, M. DELLINGER¹ J. BOUCHEZ²
A CALMELS C. CLERQUE¹, J.P. LOUVAT¹, C. DESSERT¹,
AND C. GORGE¹

¹IPGP – CNRS, Université Sorbonne Paris Cité, Paris, France

²GFZ - Helmholtz Centre Potsdam, Potsdam, Germany

The development of MC-ICPMS techniques has led to a considerable increase of Li isotopic data availability. Lithium has two isotopes, ⁶Li and ⁷Li which are particularly fractionated during low temperature water-rock interactions. The residence time of Li in the ocean is about 3 Myr which makes it a very good tracer of global surface geodynamics over geological time. Records of Li isotopes in the ocean are now available [1]

We have investigated the behavior of Li isotopes through the continental water cycle, by analyzing Li in large river materials, both solid and dissolved, as well as Li in smaller catchments.

Compared to other non-traditional isotopes, Li isotopes are highly discriminated during water rock interaction at the surface of the Earth, with a systematic enrichment of ⁶Li in the solid residue of weathering and a complementary ⁷Li enrichment in the dissolved load. Li is well partitioned between the solids and the dissolved phase, allowing us to measure isotopic differences between the weathering residue and the parent rocks and to establish and use mass budgets.

From our new data set, we infer that:

Li isotopes in the dissolved load are controlled by the precipitation of secondary minerals, occurring either in soils or in weathering “hot spots” in large watersheds (e.g. floodplains). Although shown in the data, the involvement of Li in the biological cycle is very weak.

Li in the river sediments traces the mixing between present-day weathering products and weathering products inherited from the geological past. Therefore, Li isotopes open the *pandora box* of the importance of geological legacy and continental recycling on chemical weathering fluxes at the global scale.

According to these conclusions, Li and its isotopes hence constitute an extremely powerful tracer of chemical weathering integrated over geological time.

[1] Misra and Froelich, 2012, *Science*. **335** (6070): 818-824

Evidence for elevated Iron flux to the Early Phanerozoic Ocean

ROBERT R. GAINES¹, RACHEL E. HAVRANEK¹,
KYLE S. METCALFE¹ AND SHANAN E. PETERS²

¹Geology Department, Pomona College, Claremont CA,
91711 USA, robert.gaines@pomona.edu

²Department of Geoscience, University of Wisconsin,
Madison, WI 53706, USA, peters@geology.wisc.edu

The Great Unconformity marks the end of a protracted episode of continental denudation that affected most of Laurentia and other continents worldwide. The processes that ultimately led to the formation of this geomorphic surface exposed crystalline basement rocks to atmospheric weathering over an area that is unprecedented in the rock record. An elevated flux of continental weathering products, immediately prior to and during the Sauk Marine Transgression, is suggested to have resulted in unique seawater chemistry during the terminal Ediacaran and Cambrian. In this study, we used whole rock geochemical data to quantify the patterns of alteration of basement rocks underlying the Great Unconformity to better constrain the chemical weathering flux to the oceans during this critical transition in the history of life. We analysed samples from seven weathering profiles developed into both felsic and mafic basement rocks at three localities in Colorado and Arizona. Our results are similar to those of Driese *et al* (2007) who also studied Cambrian weathering profiles below the Great Unconformity. Observed cation losses are similar to those found in modern weathering profiles, with the exception of Fe, which was depleted in these profiles. Thus, under Cambrian weathering conditions, Fe was preferentially leached, rather than accumulated. These results imply an elevated weathering flux of Fe³⁺ to the oceans from an exceptionally large area of exposed crystalline basement. This flux may have had several important consequences, including stimulation of primary productivity and enhanced burial efficiency of C-org, and thereby may have contributed to a rise in pO₂ during the Terminal Neoproterozoic-Early Ordovician.

Consumption-regeneration cycle of micronutrients and their isotopes in seawater

S.J.G. GALER^{1*} AND W. ABOUCHAMI^{1,2}

¹Biogeochemistry Department, Max Planck Institute for Chemistry, 55128 Mainz, Germany
(*steve.galer@mpic.de)

²Westfälische Wilhelms Universität, Institut für Mineralogie, 48149 Münster, Germany

The vertical cycling of micronutrients in seawater is well understood qualitatively, following early work by Boyle, Bruland and others. However, more quantitative models of the consumption-regeneration process are sorely needed in order to evaluate concentration profiles, and relate these to stable isotope fractionation of essential micronutrients, such as Cd, Zn, Fe and Ni, during biological utilization. Here, we have derived a mathematical formulation of micronutrient-limited cycling in the water column, where nutrients are consumed by a single phytoplankton species in the mixed layer (photic zone), and are regenerated/remineralized at depth by oxidation of sinking organic matter. This has been done within the framework of a simple 1-D advection-diffusion model of the water column, parameterized in terms of the upwelling velocity w and diapycnal mixing (eddy diffusion) coefficient κ . Simple expressions are derived for the micronutrient profiles at steady state, along with the corresponding stable isotope effects. It is shown how the depth profiles are related to those of conservative tracers (S, T) as well as AOU.

The rate of biological uptake of micronutrient in the mixed layer is assumed to follow Michaelis-Menten (Monod) kinetics. At steady state, the micronutrient consumption rate by the phytoplankton crop is balanced by the regeneration rate due to crop mortality. Interestingly, the micronutrient concentration in the mixed layer is governed by this kinetic balance and, paradoxically, not by the rate of supply of micronutrient from below. The biomass size in the mixed layer and the absolute primary production does depend on the micronutrient influx, however. This simple conceptual model suggests that there exists a self-regulating limiting micronutrient concentration for a given phytoplankton species. In reality, external factors will play a role too; these include light, which influences growth rates, and zooplankton grazing and removal from the photic zone by eddy diffusion which adversely affect mortality, as well as the mixed layer depth. Such effects, along with nutrient co-limitation and aeolian input, can easily be incorporated to yield a more realistic micronutrient cycling model.

Evaluating the role of microscopic pyrite for budgets of vital metals in Precambrian Carbonate

MEABH GALLAGHER AND BALZ S. KAMBER¹

¹Geology Department, Trinity College Dublin, Ireland
megallag@tcd.ie

The measurement of redox sensitive trace metal abundances and their stable isotope compositions is a popular tool for reconstructing the Precambrian environment. Of all Precambrian sediments, carbonates hold the best promise for reconstruction because their sedimentological origin can be inferred relative to modern analogues (e.g. microbial carbonates, abiogenic carbonates, dolomites, etc.). The redox state of ancient seawater can be reconstructed from the REE pattern in Precambrian carbonates as can be connectivity to the open ocean via Sr isotopes. It is thus tempting to apply transition metal tools to well studied Precambrian carbonates.

Here we report on trace metal distribution in previously characterised carbonates of Precambrian age. Specifically our study investigates the role of microscopic to sub-microscopic sulphides (mainly pyrite) that are often encountered in microbial carbonates. A first-order mass balance was carried out to establish how much of the metal found in the bulk rock is actually hosted in pyrite vs. carbonate. Pyrite is a dominant host of Cu but insignificant in its V and Zn content.

Apart from mass balance, a key question is whether the pyrite incorporates its metal inventory from the microbial mats, genetically older carbonates or diagenetic fluids. This was investigated with metal profiling across spheroidal pyrite of sulphate reducing bacterial origin (SRBO). For the elements V, Co, Ni, As, Mo, Pb and Bi, the profiles showed concentric zonations. In the case of V, the bell-shape profile indicates uptake from surrounding rock matrix but for Co, Ni, As, Mo, Pb and Bi, the W-shaped profiles suggest that metal was likely sourced from pore water (as was S). In this latter case, it is likely that the geochemistry of the carbonate itself reflects the marine ambient condition whereas the sulphide chemistry might reflect the diagenetic environment and erroneous conclusions could be drawn from combining the two sources of information when performing bulk rock analysis.

Finally, previous sulphur isotope studies have highlighted a variety of possible origins for the ubiquitous if minute sulphides. Our study also aimed to investigate whether one can distinguish pyrites of different origins (i.e. biogenic vs. late diagenetic forms) based on their trace metal abundances. Preliminary analysis of the dataset suggests that small grained matrix pyrite is characterised by enrichment in Mn, Co, Ni and As whereas pyrite of SRBO is depleted in these metals.

Clumped isotope thermometry of Neoproterozoic cap carbonates from northwest and southeast China

TIMOTHY M. GALLAGHER^{1*}, NATHAN D. SHELDON¹,
AND SHUHAI XIAO²

¹University of Michigan, Dept. of Earth & Environmental Sciences, Ann Arbor, MI 48109, USA
(*correspondence: tgallag@umich.edu)

²Virginia Tech, Dept. of Geosciences, Blacksburg, VA 24061, USA

Cap carbonate sequences are widely associated with Late-Neoproterozoic glacial deposits. They are of great scientific interest and have been used for stratigraphic correlation as well as for reconstructing paleoenvironmental conditions. More recently, the extent of post-sedimentary alteration of these rocks has become of great concern, calling into question whether they represent reliable environmental indicators¹.

Post Marinoan-age cap carbonates were analyzed from the Doushantuo Formation in southeast China and the Zhamoketi Formation in northwest China. Samples from two different sections of the Doushantuo Formation were analyzed to assess regional variability, while samples from the Zhamoketi Formation were included to assess variability between cratons.

To characterize the thermal history of the cap carbonates, we utilized carbonate clumped isotope thermometry. We measured the excess of mass-47 isotopologues (Δ_{47}) in order to quantify the crystallization temperature of these rocks.

Elevated temperatures (70-100°C) were found at all 3 sites. These results are lower than the maximum temperatures previously documented for the Doushantuo Formation^{1,2}, but are consistent with the temperature measurements of dolomicrite². In addition, the Δ_{47} analyses of the Zhamoketi cap carbonate record a thermal gradient, with maximum temperatures recorded at the top of the cap carbonate and declining towards the base. Temperatures also decline within a few meters above the cap carbonate. Our results better constrain the thermal diagenesis within these two formations and underscore the point that post-sedimentary thermal alteration is potentially a problem for cap carbonates on multiple cratons.

[1] Derkowski, *et al* (2013) *Geochim. Cosmochim. Acta* **107**, 279-298. [2] Bristow *et al* (2011) *Nature* **474**, 68-71.

Subduction-related to post-arc magmatism and Cu-Au-Te metallogeny in the Carpathian orogen, Romania

D.GALLHOFFER¹, A. VON QUADT¹, I. PEYTICHEVA¹²,
I. SEGHEDI³ AND C.A. HEINRICH¹

¹IGP, ETH Zurich, Switzerland (gallhofer@erdw.ethz.ch, vonquadt@erdw.ethz.ch, heinrich@erdw.ethz.ch)

²Geological Institute, BAS, 1113 Sofia
(peytcheva@erdw.ethz.ch)

³Romanian Academy, Institute of Geodynamics, Bucharest, Romania (seghedi@geodin.ro)

The Banat Region and Apuseni Mountains are the northernmost segments of the Cu-Au mineralized Apuseni-Banat-Timok-Srednogorie (ABTS)-belt in southeastern Europe. The ABTS magmatic arc formed due to northward subduction of Neotethys beneath the European continental margin during Late Cretaceous times and is associated with some of Europe's largest porphyry Cu-Au and epithermal Cu-Au deposits. Moreover, this Mesozoic subduction most likely metasomatized the Apuseni source region for a later, temporally distinct phase of magmatism. Miocene extension and consequent partial melting of the mantle source gave rise to non-arc Cu-Au-Te mineralizing calc-alkaline magmas in the South Apuseni Mountains [1].

New major and trace element whole rock data of Late Cretaceous igneous rocks show calc-alkaline to high-K calc-alkaline magma compositions and normalized trace element patterns characteristic of magmas generated in subduction zones. Samples with adakite-like signatures ($Sr/Y \geq 40$ and $Y \leq 18$) are rare. $^{87}Sr/^{86}Sr_{80Ma}$ WR ratios (0.704243 to 0.707074), $^{143}Nd/^{144}Nd_{80Ma}$ WR ratios (0.512374 to 0.512663) and initial ϵHf values of zircons point to a mantle source of the magmas that was variably contaminated by crustal components. Geochemical fingerprinting will test the possibly common source of post-subduction magmas.

In situ U-Pb CA-LA-ICP-MS dating and single-grain CA-ID-TIMS dating were conducted on zircons from igneous rocks from Banat Region and Apuseni Mts. All zircons were treated by chemical abrasion (CA) prior to dating [2]. Late Cretaceous magmatic activity in Banat Region covers a time span from 81.4 to 71.2 Ma. A distinct age zonation with younging of the magmatism from east to west is observed in the southern Banat Region.

[1] Harris *et al.* (2013) *EPSL* **366**, 122-136. [2] Mattinson (2005) *Chem Geology* **220**, 47-66.

GMS2 type station for geochemical continuous multi-parametric monitoring on Etna volcano

G. GALLI¹, F. QUATTROCCHI^{1*}, G. DI STEFANO¹,
S. GIAMMANCO², V. LONGO² AND F. PONGETTI¹

¹Istituto Nazionale di Geofisica e Vulcanologia. Sezione Sismologia e Tettonofisica. Roma. Italy (*correspondence: fedora.quattrocchi@ingv.it)

²Istituto Nazionale di Geofisica e Vulcanologia. Osservatorio Etneo. Catania. Italy (salvatore.giammanco@ct.ingv.it)

During the last twelve years three GMS2 (Geochemical Monitoring System 2) monitoring stations have been operating in three water wells on Mt. Etna: “Acqua Difesa” and “Currone” (on Etna’s south flank) and “Ilice” (on Etna’s east flank). GMS2 stations (Figure 1) every 10 minutes collect a data record composed of an array of chemical-physical parameters measured in groundwater. These data contribute to enrich our knowledge on an active volcanic system such as Mt. Etna, regarding, in particular, the chemical and physical effects of the interaction between up-rising magmatic fluids and shallow aquifers and the detection of possible pre-eruptive signals.

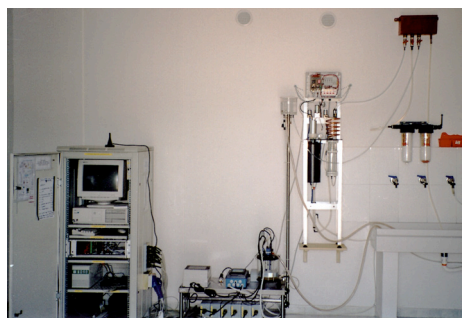


Figure 1: Field set-up of GMS2 monitoring station located at “Currone” water well (Catania, Italy)

So far, a huge quantity of data regarding temperature, conductivity, pH, redox potential, dissolved CO₂ and dissolved radon have been acquired. The peculiarity of modular GMS2 acquisition system is that it allows: 1) to operate with great simplicity during maintenance, repair and replacement of elements; 2) to gather remote data through telephone relay using mobile phone structures; 3) to control data directly from INGV Roma offices, to verify their quality and to maintain the station if necessary. GMS2 data are validated by similar, discretely acquired, geochemical data. Examples of GMS2 data are shown.

An original microscopic approach of UV-visible-near infrared spectroscopy

GALOISY L.¹, LELONG, G.¹, CALAS G.¹
AND GUILLAUMET M.¹

¹Institut de Minéralogie et de Physique des Milieux Condensés, Pierre and Marie Curie University 4, place Jussieu 75005 Paris ¹laurence.galoisy@impmc.upmc.fr

We present an original microscopic scale approach of UV-visible-near infrared spectroscopy of minerals and glasses bearing transition elements. It is based on, a microscope built with Cassegrain mirrors and coupled to a UV-visible-near infrared double beam spectrophotometer. This setting enables the collection of spectroscopic data with an adjustable spot between 120 and 20 μm, over the 250- 2600nm range. An important point is the link of the microscope to the *double beam* spectrophotometer using a spot size aperture mechanically coupled in both reference and sample beams. The angle of incidence is distributed in the range 17.8° to 32.2° with an average angle of 25.0°±0.1°.

Inside the spectrophotometer, the microscope can be associated, to a Linkam furnace to record spectroscopic data *in situ* at temperatures up to 1500°C. High pressure data can also be recorded *in situ* using a diamond anvil cell with internal pressure calibration via a laser.

Microscopic measurements at microscale and high T or P will be used to investigate the spatial evolution of element speciation in mineral and glasses.

Oldhamite CaS and potentially new mineral CaCu₂S₂ from pyrometamorphic rock of the Hatrurim formation

E. GALUSKIN¹, I. GALUSKINA¹, YE. VAPNIK², M. MURASHKO³, K. PRUSIK⁴ AND P. DZIERŻANOWSKI⁵

¹Faculty of Earth Sciences, Department of Geochemistry, Mineralogy and Petrography, University of Silesia, Będzińska 60, 41-200 Sosnowiec, Poland
(*correspondence: evgeny.galuskin@us.edu.pl)

²Department of Geological and Environmental Sciences, Ben-Gurion University of the Negev, POB 653, Beer-Sheva 84105, Israel

³Systematic Mineralogy, 44, 11th line V.O, apt. 76, Saint-Petersburg 199178, Russia

⁴Institute of Materials Science, University of Silesia, 75 Pułku Piechoty 1A, 41-500 Chorzów, Poland

⁵Institute of Geochemistry, Mineralogy and Petrology, Warsaw University, al. Żwirki i Wigury 93, 02-089 Warszawa, Poland

Oldhamite is widespread mineral of spurrite, larnite and apatite-calcite pyrometamorphic rocks of the Hatrurim formation. Pyrometamorphic rocks of the Hatrurim formation („Mottled Zone”) are located along the framing of the Dead Sea transform fault on the territory of Israel, Jordan and Palestine [1]. Oldhamite shows stable composition close to stoichiometric formula CaS. Oldhamite rarely occurs in larnite rocks enriched with copper sulphides. Larnite, brownmillerite, fluorellestadite, ye'elimite, new mineral - nabimusait (K,Ba)Ca₁₂(SiO₄)₄(SO₂)₂(O,F)₃ [2] and potentially new minerals of mayenite supergroup of the series Ca₁₂Al₁₄O₃₂F₂ - Ca₁₂Al₁₄O₃₂[F₂(H₂O)₄] [3] are the main minerals of these rocks. Periclase, vorlanite CaUO₄ and new phase Ca₃UO₆ are noted as accessory minerals. In one case oldhamite was detected as inclusion in chalcocite. Around oldhamite a phase with empirical crystal chemical formula Ca_{0.99}Cu_{2.02}S_{1.98} forms. EBSD and Raman studies showed identity of this phase to the synthetic thiocuprate CaCu₂S₂ [4].

[1] Gross, S. (1977) *Israel. Geol. Surv. Isr. Bull.*, **70**, 1-80. [2] Galuskin, E.V. *et al* (2013) *MinMag.*, **77**, 1-12. [3] Galuskin, E.V. *et al* (2012) *Abstr. Eur. Min.Conf.*, 1, EMC2012-54-2. [4] Purdy A.P. (1998) *Chem.Mater.*, **10**, 692-694.

Potential new minerals Ba₃(VO₄)₂ and hexagonal BaAl₂Si₂O₈ from rocks of the Hatrurim formation

I. GALUSKINA^{1*}, YE. VAPNIK², K. PRUSIK³, P. DZIERŻANOWSKI⁴, M. MURASHKO⁵ AND E. GALUSKIN¹

¹Univ. of Silesia, Będzińska 60, 41-200 Sosnowiec, Poland (correspondence: irina.galuskina@us.edu.pl)

²Ben-Gurion Univ. of the Negev, P.O.B. 653, Beer-Sheva 84105, Israel

³Inst. of Materials Sciences, Univ. of Silesia, 75 Pułku Piechoty 1A, 41-500 Chorzów, Poland

⁴Warsaw Univ. al. Żwirki i Wigury 93, 02-093 Warszawa, Poland

⁵Systematic Mineralogy, 44, 11th line V.O., apt.76, Saint-Petersburg 199178, Russia

Two potentially new mineral species with the end-member crystal chemical formulae Ba₃(VO₄)₂ and BaAl₂Si₂O₈ were detected in vein-like bodies of paralavas composed by coarsed-grained aggregates of rankinite, melilite, pseudowollastonite, schorlomite, fluorapatite, magnetite hosted by melilite hornfels. These rocks are confined to pyrometamorphic rocks of the Hatrurim formation in the Negev Desert, Israel [1]. Ba-minerals being in association with Ba₃(VO₄)₂ and BaAl₂Si₂O₈ are represented by the following mineral species: barioferrite BaFe₁₂O₁₉, barite BaSO₄, walstromite BaCa₂(Si₃O₉) and the next potentially new minerals of the BaCa₆[(SiO₄),(PO₄),(VO₄),(SO₄)]₄F series. The studied minerals show similar characteristics, for example EBSD patterns and Raman spectra (Fig. 1), as their well-known synthetic analogous [2, 3].

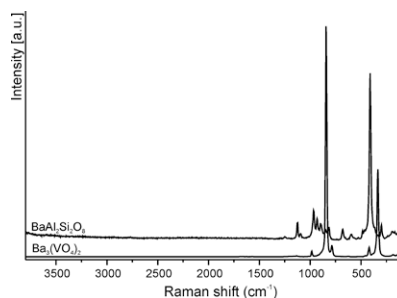


Figure 1: Raman spectra of two potentially new Ba-minerals.

[1] Gross (1977) *Geol. Survey of Israel Bul.* **70**. [2] Grzechnik & McMillan (1997) *Solid State Com.*, **8**, 569-574. [3] Kremenović *et al* (2003) *J. Phys. Chem. Solids*, **64**, 2253-2268.

Graphite formation by calcite reduction during subduction

MATTHIEU GALVEZ¹, OLIVIER BEYSSAC²,
ISABELLE MARTINEZ³ AND KARIM BENZERARA²

¹IMPMC Paris, France. Now at Geophysical Laboratory.
matthieu.galvez@gmail.com

²CNRS IMPMC Paris, France.

Olivier.Beyssac@impmc.upmc.fr

³IPG Paris, France.

The geochemistry of organic carbon in subduction zones may be strongly affected by mineral equilibria. We investigate here the geochemistry of carbon in siliceous-marbles at the direct contact with serpentinites in the Alpine lawsonite-blueschist meta-ophiolitic units of northern Corsica (France). We apply a set of spectroscopic (Raman) and isotopic methods to describe both the organic and carbonate components of the rocks across a reaction front where the equilibrium $\text{CaCO}_3 + \text{SiO}_2 + 2\text{H}_2 = \text{CaSiO}_3 + \text{C} + 2\text{H}_2\text{O}$ is evidenced.

The continuous reaction zone is composed by a centimeter thick pale nephrite layer at the contact with the serpentinites, followed by a thin wollastonite layer and a 5 to 20 cm thick dark zone composed of wollastonite, graphitic carbon, quartz but no calcite. There is a sharp (<0.5cm) transition to the overlying original metasediment composed of calcite+quartz which is significantly less rich in graphitic carbon. Raman spectroscopy shows that the graphitic carbon is better crystallized in the reaction zone compared to the non-reacted rock. Significant isotopic differences are observed apart the reaction front with $\delta^{13}\text{C}$ (graphitic carbon) and $\delta^{13}\text{C}$ (calcite) around -15‰ and 1‰ respectively in the pristine sediment far from the reaction zone, whereas $\delta^{13}\text{C}$ (graphitic carbon) is around 0‰ in the reaction zone.

We interpret the graphite in the reaction zone as formed from the destabilization and reduction of calcite under reducing conditions, possibly sustained by the underlying serpentinite body. Mass transfer calculation supports this hypothesis and shows that a complete reduction of calcite might have occurred. In addition, the temperature (430°C) of formation for this graphite is extremely low compared to any other natural process for graphite formation.

Pb isotopic composition of Himalayan Sediments

A. GALY^{1,*}, J. GATTACCECA², A.M. PIOTROWSKI^{1,3}
AND M. FRANK⁴

¹University of Cambridge, UK

(*correspondence: ajbg2@cam.ac.uk)

²BRGM, France, (julie.gatta@gmail.com)

³(amp58@cam.ac.uk)

⁴IFM-GEOMAR, Kiel, Germany (mfrank@ifm-geomar.de)

Pb- and Nd- isotopic time-series from the authigenic fraction of Central Indian Ocean sediments have been interpreted as responding to changes in the relative amount of Himalayan weathering during the Neogene [1-3]. Such interpretation relies on the lack of change in the isotopic signature of the weathering in the Himalaya. Based on detrital records from the Bengal deep-sea fan, the Nd isotopic composition of the eroded rocks remained nearly constant for the last 20My [4, 5]. However, the associated variations in the Pb-isotopes are not known, and a more precise reconstruction is hampered by the lack of information about temporal changes in the isotopic composition of dissolved Pb and Nd carried by rivers draining the Himalaya.

We present Pb- and Nd-isotope time series, from the bulk detrital and silt-sized fractions as well as the authigenic fraction of deep-sea sediment from Ocean Drilling Program Sites 717 and 718 in the Bengal fan, along with Pb- and Nd-isotopic compositions of Himalayan river bedloads. The oldest ODP samples (7-17My) have relatively uniform Pb- and Nd-isotopic compositions, characteristic of a stable input from the High Himalaya Series. The youngest samples (<1Ma) are also fairly uniform with a shift towards more radiogenic values, implying a greater contribution of the Lesser Himalaya Series. During the Pliocene (1-7Ma) the detrital fraction have more variable Pb- and Nd-isotopic composition associated with a decoupling between the bulk and silt-sized fractions. In detail, Pb-isotopic composition of the detrital is controlled by 1) the source (and correlated with ϵNd), 2) the sorting and the mineralogy as witnessed by relationship with Zr, and 3) weathering and preferential loss of radiogenic Pb. Our results suggest a strong variability in the erosion and weathering regime of the Himalaya over the Neogene with implication on the interpretation of the authigenic records in the signature of deep water of the Central Indian Ocean.

[1] Frank et O'Nions (1998) *Earth. Planet. Sc. Lett.*, **158**, 121-130 ; [2] Gourelan *et al* (2008), *Earth. Planet. Sc. Lett.*, **267**, 353-364 ; [3] Gourelan *et al* (2010) *Quaternary Sci.*, **29**, 2484-2498 ; [4] France-Lanord, Derry & Michard (1993) *Geol. Soc. Spec. Pub.*, **74**, 603-621 ; [5] Galy *et al* (2010) *Earth Planet Sc Lett*, **290**, 474-480

New views on the neogene harvesting and burial of terrestrial organic carbon

A. GALY^{1,*}, R. G. HILTON², J. SMITH¹³, R. B. SPARKES⁴
AND N. HOVIUS⁵

¹University of Cambridge, UK

(*correspondence: ajbg2@cam.ac.uk)

²University of Durham, UK, (R.G.Hilton@durham.ac.uk)

³(jcs74@cam.ac.uk)

⁴University of Manchester, UK,

(robert.sparkes@manchester.ac.uk)

⁵GFZ, Potsdam, Germany, (hovius@gfz-potsdam.de)

The temporal evolution of the $\delta^{13}\text{C}$ of marine carbonate bears contains valuable information about the global size of the organic carbon (OC) pool. C-cycle models based on the coupling of atmospheric CO_2 consumption and the fertilisation of coastal seas by continental silicate weathering enhanced by mountain building, suggest a rise in the marine OC burial rate for the entire Neogene that played a role in global cooling [1]. However, such tectonic-climate link relies primarily on the inorganic cycle, which has proven to be particularly inefficient to drawdown atmospheric CO_2 in the Himalayas [2] and only enhanced in the late Miocene as recorded in the Indian Ocean [3]. Other hypothesis linking OC burial and global cooling have been suggested, requiring changes in the biogeochemistry of the ocean [4]. Here, we show that terrigenous OC could play a role since its export from land is climatically sensitive. In Taiwan, the climatic control on the erosion and export of OC from the biosphere is moderated by the catchment geomorphology (proportion of steep hillslopes) [5]. In the Swiss Alps, we find that supply of OC from soil becomes active at a moderate threshold and runoff delivers OC to the stream with a long-term efficiency comparable to Taiwan [6]. As observed in the modern Bay of Bengal depositional system [7] or in the mid-Miocene turbidites of the Apennine (Italy), burial efficiency of terrigenous OC is particularly high. The respective role of climate and tectonic forcing and their feedbacks will be discussed with implications for the preservation of C3 biomes.

[1] Raymo (1994), *Paleoceanography*, **9**, 399-404 ; [2] Galy & France-Lanord (1999), *Chem Geol*, **159**, 31-60 ; [3] Gourelan *et al* (2008), *Earth Planet Sc Lett*, **267**, 353-364 ; [4] Vincent & Berger (1985), *Geophys Monogr Ser*, **32**, 455-468 ; [5] Hilton *et al* (2012), *Global Biogeochem Cy*, **26**, GB3014, 1-12 ; [6] Smith *et al* (2013), *Earth Planet Sc Lett*, **365**, 198-208 ; [7] Galy *et al* (2007), *Nature*, **450**, 407-410

New insights into environmental characterization of bauxite residues (red mud) from Greece

P. GAMALETOS^{15*}, A. GODELITSAS¹, A. KUZMIN²,
M. LAGOS³, S. XANTHOS⁴, T.J. MERTZIMEKIS¹,
J. GOETTLICHER⁵, R. STEININGER⁵, C. ZARKADAS⁶,
A. KOMELKOV⁶, Y. PONTIKES⁷
AND G.N. ANGELOPOULOS⁸

¹University of Athens, School of Science, 15784 Zographou, Greece (*correspondence: platon_gk@geol.uoa.gr)

²University of Latvia, Institute of Solid State Physics, Kengaraga st. 8, 1063 Riga, Latvia

³KIT, Institute for Nuclear Waste Disposal (INE), Hermann-von-Helmholtz-Platz 1, 76344 Eggenstein, Germany

⁴Aristotle University, Department of Electrical & Computer Engineering, 54124 Thessaloniki, Greece

⁵KIT, ANKA Synchrotron Radiation Facility, Hermann-von-Helmholtz-Platz 1, 76344 Eggenstein, Germany

⁶PANalytical B.V., 7600 AA Almelo, The Netherlands

⁷KU Leuven, Centre for HT Processes and Sustainable Materials Management, B-3001 Leuven, Belgium

⁸University of Patras, Department of Chemical Engineering, 26500 Rio, Greece

Bauxite metallurgical tailings (red mud from alumina production) were provided by Aluminium of Greece S.A. plant at central Greece (www.alhellas.gr) and characterized by using a combination of microscopic, analytical, and advanced spectroscopic techniques (SEM-EDS, XRF, ICP-OES/MS, HR γ -ray Spectrometry and EXAFS). Particular emphasis was given on investigating actinides, and other elements of potential environmental interest. According to XRF (performed at the PANalytical laboratories) and ICP-OES/MS measurements, the material contains Cr (2025 ppm), V (1081 ppm), Ni (933 ppm), As (164 ppm), Pb (120 ppm) and Th (111 ppm). The latter, and also minor U (15 ppm) are responsible for radioactivity (352 and 134 Bq/Kg for ²³²Th and ²³⁸U respectively) with total dose rate 285 nGy/h. Specific leaching experiments, using seawater from Greece, in conjunction with ICP-MS (performed at the INE/KIT), indicated significant release of V, which seems to be the most mobile element. Minor quantities of As and Cr may also be released in seawater. On the other hand, the release of Th, and therefore of significant radioactivity, was found to be negligible. The immobility of Th can be explained by its position in the crystal structure of Ti-oxides, as proved by the the Th L_{III} -edge EXAFS data, obtained at the ANKA Synchrotron Radiation Facility (KIT) and evaluated using the ATHENA and the EDA software packages.

Tracking down the Ediacaran isotope anomalies in a sedimentary section from Kazakhstan

ANTONIA GAMPER^{1*}, ULRICH STRUCK¹
AND GAPPAR ERGALIEV²

¹Museum für Naturkunde, Invalidenstr. 43, D-10115 Berlin,

*antonia.gamper@mfn-berlin.de

²Institute of Geological Sciences, Almaty 050010, Kazakstan

The Ediacaran-Cambrian period marks one of the most significant and vital epochs in the evolution of the Earth's ecosphere. Multicellular life, hard-shelled organisms and a bioturbating lifestyle evolved during a time of tectonic instability and fundamental biogeochemical changes in the oceans. Three major global carbonate carbon isotope excursions are assumed to be crucial for the evolution of early animal life.

Excellent preserved Ediacaran to early Cambrian strata crop out commonly in sections around the area of Zhanatas in southern Kazakhstan. However, geochemical and geochronological data from these rock sections are scarce. We determined carbonate carbon, organic carbon and nitrogen isotope data from the ~200 m thick Kyrshabakty Section including the basal late Cryogenian Aktas Tillite (Marinoan-age glacial deposit), the Ediacaran Kyrshabakty Member and the overlying lower Cambrian Chuluktau Member of Malyi Karatau Range. The section shows a high-resolution geological record of a carbonate-siliciclastic nearshore environment. Isotope data of the shallow water deposits reveal three major negative $\delta^{13}\text{C}_{\text{carb}}$ excursions. The basal Cap Carbonate overlying the Tillite shows a negative shift down to -2.4‰ which corresponds with other sections worldwide. The middle section comprises an excursion with a nadir of -9.5‰ possibly corresponding to the Shuram-Wonoka $\delta^{13}\text{C}_{\text{carb}}$ excursion (e.g. Oman, Australia). The uppermost strata are associated with a negative $\delta^{15}\text{N}$ excursion of -2.5‰ co-occurring with a pronounced negative $\delta^{13}\text{C}_{\text{carb}}$ excursion (down to -6.7‰) reflecting the global carbon isotopic trend of the Precambrian-Cambrian boundary interval (e.g. Namibia, Australia, China, Siberia). Our results suggest that the sedimentary deposits of the Kyrshabakty Member exhibit geochemical and isotopic variations of the three major profound biogeochemical fluctuations as seen in other sections worldwide. They also confirm a previously found negative $\delta^{15}\text{N}$ excursion at the Ediacaran-Cambrian transition from South China as a large to global scale anoxic event possibly accompanied by photic zone anoxia. This anoxic event may have influenced the following Cambrian Explosion of biota significantly.

Temperature dependence of water activity in organic aerosols

G. GANBAVALE*, C. MARCOLLI, A. ZUEND,
U.K. KRIEGER AND T. PETER

Institute for Atmospheric and Climate Science, ETH Zurich,
Zurich, Switzerland

(*correspondence:gouri.ganbavale@env.ethz.ch)

Atmospheric aerosols are complex mixtures of organic and inorganic compounds and influence significantly the Earth's climate. Knowledge of the composition and physical state of aerosols is essential since they play significant roles in atmospheric processes such as heterogeneous and multiphase chemistry, cloud formation, scattering and absorption of visible light and infrared radiation. At low temperatures the organic aerosol fraction is expected to be present in a liquid or glassy state since the large number of organic components depresses the temperature at which crystalline solids form [1, 2]. In the upper troposphere homogeneous ice nucleation and cirrus cloud formation take place on aerosols which grow into ice crystals by dissipating supersaturated water vapour. Homogeneous ice nucleation in supercooled aqueous solutions is independent of the nature of the solute but depends on water activity (a_w) and hence a_w of a solution is a crucial parameter for homogenous ice nucleation [3]. Activity coefficients of organic compounds in solutions may exhibit a considerable temperature dependence that has to be parameterized by models in order to achieve accurate predictions at temperatures other than room temperature.

To measure a_w over a wide composition range while focusing on low temperatures, we used different measurement techniques and instruments such as a dew point water activity meter, differential scanning calorimetry (DSC) and an electrodynamic balance (EDB). In addition we developed a setup to measure absolute vapor pressure of solutions at low temperatures. Water activity measurements were performed for aqueous organic mixtures containing the functionalities typically found in the organic aerosol fraction such as alcohol/polyol, carboxylic acids, ketones, ethers, esters, and aromatic rings. These data was used together with literature data to improve the temperature dependence of activity coefficients at low temperature in the thermodynamic group-contribution model AIOMFAC (Aerosol Inorganic-Organic Mixtures Functional groups Activity Coefficients) [4, 5].

- [1] Marcolli *et al* (2004) *J. Phys. Chem. A*, **108**, 2216 – 2224.
[2] Zobrist *et al* (2008) *Atmos. Chem. Phys.*, **8**, 5221 – 5244.
[3] Koop *et al* (2000) *Nature*, **406**, 611 – 614. [4] Zuend *et al* (2008) *Atmos. Chem. Phys.*, **8**, 4559 – 4593. [5] Zuend *et al* (2011) *Atmos. Chem. Phys.*, **11**, 9155 – 9206.

Chemical composition of the Western Arctic Ocean sediments: Recommended element abundances and potential reference material

*GAO AIGUO^{1,2} AND ZHAO DONGMEI¹

¹College of Ocean and Earth Sciences, Xianmen Univeristy, 361005, China (*correspondence: aggao@xum.edu.cn)

²State Key Laboratory of Marine Environmental Science, Xiamen University, China

The Western Arctic Ocean is the major continental margins and deep-sea system of the Earth with weathering and sedimentary characteristics similar to glacial environment. It is characterised by the broadest continental shelves, extreme environment and minimal effect of human activities so that it is much less constrained in comparison to other oceanic regions. Arctic Ocean sediments represent an outstanding archive to investigate global change and high-latitude marine geochemical processes. However, no clear understanding of their element abundances has been achieved yet. In this study, six marine sediments samples have been collected from the Western Arctic Ocean shelves and the Canada Basin, in order to provide a comprehensive representation of Arctic sediments. Samples are homogeneously mixed and analysed by ICP-MS, ICP-ES, INAA and 16 other analytical methods in 14 top geochemical institutes in China to ensure that measurements are reproducible over time and among laboratories. The abundances of 71 components (all the major and trace elements) have been determined through 3128 analyses. Owing to extensive inter-laboratory calibrations and statistical analysis, 64 of 71 elements have the highest possible standards of reliability and reproducibility and can therefore be used as recommended values for Arctic Ocean sediments, while the rest 7 components (Br, I, In, Te, C, CO₂ and H₂O⁺) are sufficiently homogeneous and stable to be used as indicative values. The results show that the elemental abundances of the Western Arctic Ocean sediments are controlled by material sources and sedimentary environments which are unique when compared with the upper continental crust or mainland and shallow-sea sediments in China. These element abundances can serve as a recommended guideline for environmental assessment, resource exploration, and global change research. Moreover, it can be used as a potential sediment standard for high-latitude/glacial geochemistry study.

Determination of the Early Palaeozoic Strata in Eastern Heilongjiang Province, NE China: Constraints from Geology and Detrital Zircon U-Pb ages

FUHONG GAO, YANG YANG, FENG WANG, AND HONG FENG

College of Earth Sciences, Jilin University, Changchun 130061, China (gaofh@jlu.edu.cn)

It has been a controversial issue whether did the Early Paleozoic strata occur in the Songnen-Zhangguangcailing Massif, NE China. This paper provides the LA-ICP-MS zircon U-Pb dating results from the Chenming Formation in the eastern Heilongjiang Province, NE China. Combined with the formation timing of the overlying strata, it is suggested that an Early Paleozoic strata is firstly determined in the NE China. Most of detrital zircons from the Chenming Formation are euhedral-subhedral in shape and display striped absorption or fine-scale oscillatory growth zoning in CL images, implying their magmatic origin. The others show dark accretionary rim formed by metamorphism. The dating results indicate that the detrital zircons from feldspathic quartz sandstone in the upper part of the Chenming Formation yield age populations of 561 Ma, 621 Ma, 683 Ma, 752 Ma, 803 Ma, 822 Ma, 851 Ma, 900 Ma, 922 Ma, 954 Ma, 1781 Ma, 1865 Ma, and 1933 Ma, suggesting that the sedimentary processes of the Chenming Formation could take place after 561 Ma.

In the study area, the Baoquan Formation occur as overlying strata over the Chenming Formation with the unconformity relationship. The detrital zircons from argillic siltstone in the lower part of the Baoquan Formation yield age populations of 425 Ma, 450 Ma, 485 Ma, 900 Ma, and 1750 Ma (Meng *et al.*, 2010) whereas the rhyolite in the upper part of the Baoquan Formation formed in 383 Ma. Taken together, we conclude that the Chenming Formation formed between 561 Ma and 425 Ma, i.e., Early Palaeozoic. Additionally, the age population of detrital zircons from the Chenming Formation reveal that the Neoproterozoic as well as Paleoproterozoic terranes could occur within the Songnen-Zhangguangcailing Massif besides the Paleozoic terranes. Combined with the distribution of geological terranes around the study area, we consider that the provenance of the Chenming Formation mainly come from the Paleozoic igneous rocks and minor Precambrian basement remnant around the study area. This is a firstly discovered Early Palaeozoic strata with the exact geochronological evidence in the eastern Heilongjiang Province, NE China.

This research was financially supported by the Natural Science Foundation of China (41272075) and the National Key Basic Research Program of China (Grant 2013CB429803).

Multi-stage gold mineralization at the Hollinger-McIntyre deposit: A LA-ICPMS mapping study

J-F. GAO^{1*}, S E. JACKSON¹ AND B. DUBÉ²

¹Geological Survey of Canada, Ottawa, ON, K1A 0E8, Canada (*correspondence: Jianfeng.Gao@NRCan.gc.ca)

²Geological Survey of Canada, 490 De la Couronne Street, Québec City, QC, G1K 9A9, Canada

The Hollinger-McIntyre gold deposit, Timmins, Ontario, is the second largest Archean quartz-carbonate vein system in the world, with a total gold production of ~1000 tonnes Au^[1]. The deposit consists of two mineralization types: an early-stage intrusion-related Cu-Mo-Au-Ag mineralization telescoped by a syn-deformation Au-pyrite-quartz-carbonate vein system that constitutes the bulk of the ore^[2].

We used a new LA-ICP-MS elemental imaging technique to map pyrite grains from the Au-pyrite-quartz-carbonate vein system. The elemental maps have revealed at least three paragenetic stages (Figure 1): (1) early stage, where invisible Au was enriched in As-rich pyrite; (2) lowering As associated with increasing Ni; Au, Cu and Zn were depleted in this stage; (3) native Au filling fractures in early pyrite grains or discrete grains associated with sphalerite and chalcopyrite in quartz veins; Ni and As were depleted in this stage. The early-stage pyrite at Hollinger-McIntyre is enriched in As and Au different from those of pyrite from Carlin-style deposits^[3], but similar to those from porphyry Au-Cu deposits (unpublished data). The latter would be compatible with the early intrusion-related Cu-Mo-Au-Ag stage.

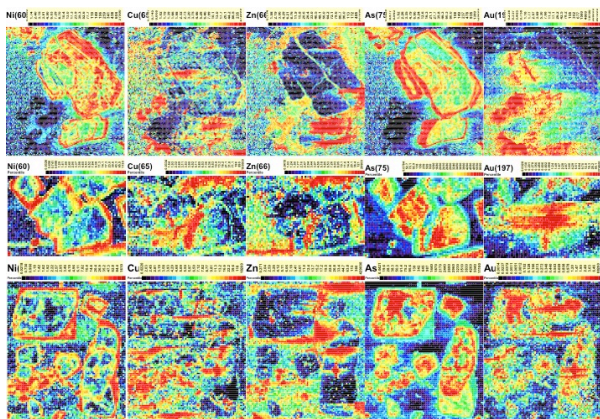


Figure 1. Mapping of selective elements for gold ore from the Hollinger-McIntyre Au deposit (Scales are in ppm).

[1] Wood *et al* (1986) Proc. Gold'86 Symposium, 56-80. [2] Burrows and Spooner (1986) Proc. Gold'86 Symposium, 23-39. [3] Large *et al*, 2009. *Econ. Geol.* **104**, 635-668.

Modeling of modern $\delta^{30}\text{Si}$ distributions in the oceans and in marine sediments

S. GAO*, D. A. WOLF-GLADROW AND C. VÖLKER

Alfred-Wegener-Institut Helmholtz-Zentrum für Polar- und Meeresforschung, Am Handelshafen 12, 27570

Bremerhaven, Germany

(*correspondence: shuang.gao@awi.de)

$\delta^{30}\text{Si}$ is used as a proxy for reconstruction of marine silicic acid utilization and Si cycling in the geological past. A better understanding of modern $\delta^{30}\text{Si}$ distribution and its control mechanism is imperative for applying this proxy with confidence.

It has been a decade since the first modeling effort on global marine $\delta^{30}\text{Si}$ distribution was accomplished [1]. There are much more field studies that have been conducted since then, which facilitates model validation and model-data comparison. In this study, we present a more sophisticated model setup compared to previous modeling studies [1, 2], aiming at representing a realistic global pattern of oceanic and sedimentary $\delta^{30}\text{Si}$ distributions and revealing possible controlling mechanisms.

Our model results suggested that surface $\delta^{30}\text{Si}$ in the North Atlantic and in the Southern Ocean (Figure 1) are largely controlled by seasonal variations of mixed layer depth and diatom primary production. The difference is up to 0.3‰ between summer and winter months, which should be considered when measuring oceanic $\delta^{30}\text{Si}$.

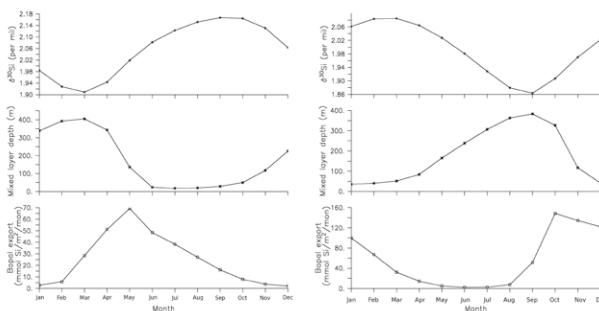


Figure 1: The seasonal variations of surface $\delta^{30}\text{Si}$ (upper 100 m), mixed layer depth and biogenic opal export in the North Atlantic (left) and in the Southern Ocean (right).

[1] Wischmeyer, De La Rocha, Maier-Reimer & Wolf-Gladrow (2003), *Global Biogeochemical Cycles* 17(3), 1083.
[2] Reynolds (2009), *Global Biogeochemical Cycles* 23.

Characteristic of Fluid Inclusion of the Xujiahe Formation in the Central Sichuan Basin, China

XIAOHUI GAO, SHIZHEN TAO AND XIA ZHAO

¹Research Institute of Petroleum Exploration & Development, Petrochina, gXH2008@petrochina.com.cn

²Research Institute of Petroleum Exploration & Development, Petrochina, tsz@petrochina.com.cn

³Research Institute of Petroleum Exploration & Development, Petrochina, zhaox601@petrochina.com.cn

The Sichuan Basin is an inner plate basin at the west of Yangzi Plate. It is a large petroliferous basin with marine carbonate deposition and terrestrial clastic deposition. Its gas bearing area can reach $18 \times 10^4 \text{ km}^2$, and the gas proven reserves, gas fields number and gas production are all the No.1 in China [1,2].

In our project we chose more than 80 samples of fluid inclusions from tight sandstone reservoirs of Xujiahe Formation in 28 wells, all of which are located in gas bearing intervals from gas fields in middle Sichuan area. The conclusions are as follows □

1. In the center of the Sichuan Basin, the maturity of source rock in the Xujiahe Formation is not high, with R_o value ranging from 0.8% to 1.2%. However, the gas reservoirs nowadays show characteristics of high gas-oil ratios and low condensate oil content ($3.8 \sim 91.9 \text{ g/m}^3$ on average). There are abundant gas hydrocarbon inclusions developed in the reservoir, with few liquid hydrocarbon inclusions, which shows that the coal measures have given priority to gas.

2. In the fluid inclusion group, the CH_4 accounts 79.62~96.42%, and C_2H_6 is about 10%, the content of C_3H_8 ranges from 3% to 5%. As to the carbon isotope of CH_4 , $\delta^{13}\text{C}_1 = -44.59 \sim -39.31\text{‰}$, $\delta^{13}\text{C}_2 = -24.82 \sim -28.05\text{‰}$, $\delta^{13}\text{C}_3 = -21.39\text{‰}$, $\delta^{13}\text{C}_4 = -22.05 \sim -20.2\text{‰}$, $\delta^{13}\text{C}_{\text{CO}_2} = -9.14 \sim -13.86\text{‰}$. The gas component and isotope in fluid inclusions coincide with the carbon isotope in the gas reservoirs today, showing that the gas hydrocarbon in the fluid inclusions can represent the residue gas in the gas reservoirs. The residue gas is mainly formed and preserved in the late stage.

3. The He and Ar associated with natural gas are positively related in content. $^{40}\text{Ar}/^{36}\text{Ar}$ and $^3\text{He}/^4\text{He}$ also has a positive correlation. He and Ar isotopic composition analysis shows that, R/Ra ratio is less than 0.5, the majority of 0.1 or less, reflecting the crust was stable then, no deep large faults or deep-source gas mix, the natural gas was mainly from the shallow crust.

[1] Dai Jinxing (1997) *et al* Formation conditions and distribution laws of giant gas fields in China: 184-198. [2] Dai Jinxing (2007) *et al*, *Natural Gas Geoscience*, **18**(4): 473-484

Li isotopes in zircon: Effects of Li substitution and kinetic fractionation

*YU-YA GAO^{1,2}, XIAN-HUA LI¹, WILLIAM L. GRIFFIN²
SUZANNE Y. O'REILLY² AND NORMAN J. PEARSON²

¹State Key Laboratory of Lithospheric Evolution, Institute of Geology and Geophysics, China Academy of Sciences, China (*correspondence: yuya.gao@mq.edu.au)

²ARC Centre of Excellence for Core to Crust Fluid Systems and GEMOC National Key Centre, Dept of Earth and Planetary Sciences, Macquarie University, Australia

In situ SIMS (Secondary Ion Mass Spectrometry) analysis of Li isotopes in zircon shows potential for studying the origin of crustal magmas. However, it is controversial whether $\delta^7\text{Li}$ in zircon reflects the magmatic sources of the zircon, or was modified by later processes. To understand Li behaviour in magmatic systems, $\delta^7\text{Li}$ and Li abundance have been investigated in whole-rock samples and zircon crystals of several standards (Temora, Plesovice, Qinghu) as well as two A-type granites from Suzhou (aluminous A-type granite) and Taohuadao (peralkaline A-type granite), east China. The measured $\delta^7\text{Li}$ values range from -12 to -1‰ for Temora, and -4 to -1‰ for Qinghu; in both cases $\delta^7\text{Li}$ is weakly correlated with ppm Li, indicating a relatively slow rate of Li diffusion. However, Plesovice ($\delta^7\text{Li} = -4 \sim +3\text{‰}$) and M257 (*in situ* zircon Li isotope standard, $\delta^7\text{Li} = 2.1 \pm 1\text{‰}$) show no sign of diffusion. This suggests that the Li diffusion rate might be controlled by the trace-element composition of zircon. Large variations in Li abundance (up to 10 ppm) and $\delta^7\text{Li}$ values (26‰) have been measured in zircons from per-alkaline and more aluminous A-type granites samples. The Li abundance in zircon from the Suzhou pluton is 10x to 100x higher than in the Taohuadao pluton. The measured $\delta^7\text{Li}$ values from Taohuadao range from -21 to 2‰ and are positively correlated with ppm Li, while the $\delta^7\text{Li}$ values of Suzhou range from -7 to +7‰ and correlate negatively with Li content. In contrast, the whole-rock lithium concentrations and isotope ratios show a more narrow range (+2 to 5‰). The possible explanation for the large variations in Li and $\delta^7\text{Li}$ values in zircon is that the diffusion of Li is controlled by different substitution mechanisms that involve other trace elements, resulting in kinetic fractionation of the Li isotopes. However, Li abundances in zircon could be a petrogenetic tracer to identify different sources of A-type granites.

First occurrence of dumortierite in Croatia: A potential evidence of tetrahedral Ti substitution for Si

V. GARAŠIĆ^{1*}, B. LUGOVIĆ¹, M. SEKUŠAK¹,
H.-P. MEYER², M. VRKLJAN¹ AND R. SCHUSTER³

¹University of Zagreb, Faculty of MGPE, Croatia
(correspondence: vesnica.garasic@rgn.hr)

²University of Heidelberg, Germany

³Geologische Bundesanstalt, Vienna, Austria

Dumortierite ($\text{Al}_6(\text{BO}_3)_2\text{Si}_3\text{O}_{13}(\text{O},\text{OH})_2$) occurs in a pegmatite vein cutting S-type granite in the Late Cretaceous magmatic-metamorphic complex of Mt. Moslavačka gora, in the SW part of the Pannonian Basin, Croatia. The granitoid pluton intruded Abukuma type series of metamorphic rocks associated with migmatites. Dumortierite-bearing vein, up to 6 cm thick, consists of coarse-grained quartz, orthoclase, microcline and albite, less abundant muscovite, biotite, pinkish andalusite and blue-coloured dumortierite. The microscopic studies identified two types of dumortierite crystals: Dum I and Dum II. The Dum I crystals are subhedral prismatic up to 16 mm in size, strongly pleochroic ranging from colourless to azure blue. The Dum II type represents bundles of parallel fibrous or acicular crystals, up to 1.4 mm long, strongly pleochroic from colourless to red violet. The Dum I crystals have lower contents of Mg (0.033-0.055 pfu) and Ti (0.001-0.011 pfu) than Dum II crystals (0.047-0.087 pfu and 0.043-0.064 pfu, respectively) whilst differences in Fe abundance (0.038-0.072 pfu vs. 0.037-0.057 pfu) and Al/Si ratios (2.35-2.47 vs. 2.27-2.49) are not significant. A Si deficiency (< of 3.0 pfu) is found in 95% of EPMA spot analysis of the dumortierite. The Si tetrahedral deficiency has been conventionally balanced by Al. A moderate correlation between 3-Si and Al ($r = 0.606$), and between 3-Si and Ti ($r = 0.609$) exists in the analysed dumortierites. Strong correlation between 3-Si and Al+Ti ($r = 0.968$) suggests that Ti in dumortierite replaces not only Al in octahedra as generally accepted, but also may substitute Si in tetrahedra.

Temperature driven stable carbon isotope ratio in marine aerosols

A. GARBARAS^{1*}, D. CEBURNIS², A. MASALAITĖ¹,
W. MAENHAUT³, J. OVADNEVAITE², C.D. O'DOWD²
AND V. REMEIKIS¹

¹Center for Physical Sciences and Technology, Vilnius, Lithuania (*correspondance: garbaras@ar.fi.lt or darius.ceburnis@nuigalway.ie)

²School of Physics and Center for Climate and Air Pollution Studies, Ryan Institute, National University of Ireland, Galway, Ireland

³Institute for Nuclear Sciences, Ghent Univ., Ghent, Belgium

Stable carbon isotope ratio mass spectrometry is evolving as a powerful tool in aerosol source apportionment studies due to unique capability of discriminating among various carbon sources [1, 2].

Stable carbon isotopic analysis was performed on the aerosol particles that were collected from 3 December 2006 until 4 March 2007 in Amsterdam Island (37.81°S, 77.5733°E), which is an atmospheric research station located in the southern Indian Ocean far from continents. The aerosol particles were sampled in fine and coarse modes. The $\delta^{13}\text{C}$ values in the fine mode ranged from -27.5 ‰ to -20.4 ‰, and in the coarse mode from -28.2 ‰ to -22.6 ‰. The concentrations of organic and inorganic species were measured in the both size fractions as reported by Claeys *et al* [3].

The measured $\delta^{13}\text{C}$ values, salts and organic carbon concentrations in the fine and coarse size fractions were combined with the isobaric air mass back trajectories, the corresponding chlorophyll concentrations and the sea surface temperature (SST). Correlation between organic carbon isotopic ratio of atmospheric aerosol and the sea surface temperature was found, corroborating significant differences in biogenic processes in the Southern Ocean.

[1] Ceburnis *et al* (2011), *ACP* **11**, 8593-8606. [2] Miyazaki *et al* (2011), *ACP* **11**, 3037-3049. [3] Claeys *et al* (2010) *J. Aerosol Sci.* **41**, 13-22.

***Clumped* isotope thermometry on ultramafic-hosted magnesium carbonates**

PABLO GARCÍA DEL REAL^{1*}, TOBIAS KLUGE²,
CÉDRIC M. JOHN², NATALIE C. JOHNSON³,
KATE MAHER¹, DENNIS K. BIRD¹
AND GORDON E. BROWN, JR¹³

¹Department of Geological & Environmental Sciences,
Stanford University, Stanford, CA 94305-2115, USA.
gdelreal@stanford.edu (*presenting author)

²Department of Earth Science and Engineering, and Qatar
Carbonate and Carbon Storage Research Center, Imperial
College London, UK.

³Department of Chemical Engineering, Stauffer III, Stanford
University, Stanford CA 94305

Magnesite (MgCO₃) and other magnesium carbonates hosted in serpentinized peridotite rocks record the final fate of CO₂-rich fluids in shallow crustal environments and provide constraints on low-temperature carbon capture and storage in ultramafic rocks. Here we determine *clumped* temperatures of mineralization for magnesium carbonates from a variety of natural ultramafic environments, and we couple our results with a laboratory-based calibration of synthetic magnesite. Our samples include: (a) massive (10's of meters thick and >100's of meters in length and depth) homogeneous, cryptocrystalline magnesite veins from the Red Mountain Magnesite Mine in the Del Puerto ophiolite of the California Coast Ranges (T = 21.5±4°C, n=7, with a maximum temperature of 31°C); (b) surficial nesquehonite (MgCO₃·3H₂O), hydromagnesite (Mg₅(CO₃)₄(OH)₂·4H₂O), dypingite (Mg₅(CO₃)₄(OH)₂·5H₂O) and artinite (Mg₂(CO₃)(OH)₂·3H₂O) from the peridotite-serpentinite belt of the California Coast Ranges (T = 21±4°C, n=6); (c) additional ultramafic-hosted magnesite deposits (Turkey, Austria, Iran) analogous to Red Mountain (T= 30.5±5°C, n=3), and (d) magnesite produced from carbonation of olivine at 60°C, 100 bars pCO₂, 0.5M NaCl, and variable (20:1 and 50:1) water-rock ratios (T=52±6°C, n=2). We use our results to constrain the δ¹⁸O composition and origin of the mineralizing fluids of the magnesite deposits at Red Mountain. Nearly identical *clumped* isotope signatures among worldwide magnesite deposits suggest that a similar set of geological processes were associated with carbonation in crustal ultramafic rocks.

Characterization of complex Fe-Mn phosphates by LA-ICP-MS methods

S. GARCÍA DE MADINABEITIA¹, E. RODA-ROBLES²,
A. PESQUERA², M.E. SÁNCHEZ²
AND J.I. GIL IBARGUCHI²

¹SGIker-Geochronology, UPV/EHU, Spain (*correspondence:
sonia.gdm@ehu.es)

²Dpt. Mineralogy-Petrology, UPV/EHU, Spain
(encar.roda@ehu.es)

Ca-phosphates in any of their variants (apatite, merrillite, etc.) are the subject of increasing interest in petrogenesis and mineralogenesis studies of igneous and metamorphic rocks from different geological settings. Their trace element characterization has been sought for and is usually done using LA-ICP-MS methods. Less abundant Fe-Mn phosphates and fluorophosphates are potential indicators of deposits of economic interest but have been so far less investigated for their trace element composition. In an attempt to improve the current knowledge on the latter type, we have analyzed complex phosphates of the triplite-zwieselite (Mn²⁺,Fe²⁺,Mg,Ca)₂(PO₄)(F,OH), triphylite-lithiophilite Li(Fe²⁺,Mn²⁺)PO₄ and graftonite-beusite (Ca, Fe²⁺, Mn²⁺)₃(PO₄)₂ series. For each series we have attempted to analyze phosphates covering the widest possible Fe-Mn compositional range. To set up the procedure we first analyzed igneous and metamorphic apatites including the classic specimens from Cerro Mercado (Durango, Mexico), initially on mineral separates and then on thick petrographic preparations. The procedure was subsequently optimized for the analysis of the Fe-Mn phosphates also in thick section. This involved the use of XSeries 2 and UP213 instruments, a SuperCell device, He as transport gas, enhanced vacuum and NIST glasses and Durango apatite for calibration and quality control purposes. Although the absence of specific CRMs implies some limitations, the method set up allows to obtain reliable results for most trace elements in the ppm range and reveals marked differences for the studied series of primary Fe-Mn phosphates, with significant variations also related to the different geological settings. Members of the triphylite-lithiophilite series present extremely low contents in all the analyzed elements, except for Zn (570-8990 ppm). In contrast, members of the triplite-zwieselite series are enriched in Nb (78-537 ppm) and Zn (437-4093 ppm), with variable contents in HREE (0-124 ppm), Ta (4-176 ppm), Y (0-280 ppm), Zr (6-233 ppm), and U (7-50 ppm). Finally, members of the graftonite-beusite series are the richest in REE, with ΣHREE up to 300 ppm and of ΣLREE up to 345 ppm. Other trace elements, such as Zn (1508-4238 ppm), Sr (3-91 ppm) and Y (0-509 ppm) occur also in significant amounts.

Modelling of Cs adsorption in natural mixed clays and the effects of ion competition

M. GARCÍA-GUTIÉRREZ¹, TIZIANA MISSANA¹,
ANA BENEDICTO¹, CARLOS AYORA²
AND KATRIEN DE-POURCQ²

¹CIEMAT, Avenida Complutense, 40, 28040 Madrid (Spain)

²IDAEA-CSIC, Jordi Girona, 18-26, 08034 Barcelona (Spain)

Cesium-137 (half-life, ~30 years) is an important fission product from the irradiation of uranium-based fuels and it has been released in the past to soils and waters as a result of nuclear accidents or weapon testing. Radiocesium is particularly relevant from an environmental point of view because it always exists as the monovalent cation Cs⁺, which presents very high solubility.

Cesium migration in the environment is mainly controlled by sorption onto mineral surfaces; in particular, it is rather strongly adsorbed onto clays by ionic exchange. Thus, with the objective of designing a geochemical reactive barrier to treat Cs-137 pollution in a salt marsh zone, several natural clayrocks were analysed as possible sorbent. The composition of the rocks was variable and within the clayey fraction the mayor clay minerals were illite, smectite and kaolinite.

The high salinity of natural waters presents in the zone obliged the understanding and quantification of the the effects of competitive ions, which may hinder cesium adsorption. Furthermore the water chemical composition variability leads to significant differences in distribution coefficients (K_d).

The semi-empiric approach in the analysis of experimental data, above all when sorption is non-linear (as in the case of Cs) is unsatisfactory.

Thus, the development of sorption models, validated by experimental data, obtained under conditions representative of the site is needed. A multisite cation exchange model, considering both the solid (mixed clays) and water composition was used to successfully explain cesium sorption in the analysed natural clayrocks and the effects of highly competitive ions present in the aqueous phase, in particular K⁺, NH₄⁺ and Na⁺.

Removing the “heavy mineral effect” to obtain a new Pb isotopic value for the upper continental crust

M. GARÇON^{1*}, C. CHAUVEL¹, C. FRANCE-LANORD²,
M. LIMONTA³ AND E. GARZANTI³

¹ISTerre, Université de Grenoble, France

²CRPG-CNRS, Vandoeuvre-lès-Nancy, France

³Laboratorio di Petrografia del Sedimentario, Università di

Milano-Bicocca, Italy (*correspondence:

marion.garcon@ujf-grenoble.fr)

Knowing the average Pb isotopic composition of the continental crust is crucial to constrain the evolution of the Earth since its formation. Current estimates are rare. Some come from Earth evolution models but most are based on data acquired from river or oceanic sediments. The latter assume that sediments are representative of their continental sources but bias can be introduced if sedimentary mineral sorting is ignored. Several authors already demonstrated that Hf isotopes are fractionated by the so-called “zircon effect”, i.e. preferential concentration of unradiogenic Hf-rich zircons in coarse sediments which produces finer sediments with much more radiogenic Hf isotopes than their continental source. Because heavy minerals have sometime extremely radiogenic Pb isotopes, we evaluate the impact of the “heavy mineral effect” on Pb isotopes of sediments.

Here, we report Pb isotopic compositions of Himalayan river sediments as well as those of several grain-size fractions and pure mineral separates. We demonstrate that Pb isotopes of both bedloads and suspended loads are biased towards more radiogenic values than their source rocks due to a “heavy mineral effect” caused by mineral sorting during fluvial transport on continents. The sparse zircons, monazites and allanites present in all samples (< 1 wt%), including suspended loads, generate a Pb isotopic variability ($37.85 < {}^{208}\text{Pb}/{}^{204}\text{Pb} < 43.16$; $15.62 < {}^{207}\text{Pb}/{}^{204}\text{Pb} < 16.18$; $17.83 < {}^{206}\text{Pb}/{}^{204}\text{Pb} < 22.58$) as large as that observed in the Earth’s mantle. Our new data suggest that mineralogical effects must be corrected for sediment Pb isotopes to be used as provenance and anthropogenic tracers. After correction of the mineralogical effect, we propose an average value for the composition of the upper Himalayan crust and a new Pb isotopic value for the Earth’s upper continental crust i.e. ${}^{208}\text{Pb}/{}^{204}\text{Pb} = 39.16$; ${}^{207}\text{Pb}/{}^{204}\text{Pb} = 15.73$; ${}^{206}\text{Pb}/{}^{204}\text{Pb} = 18.95$.

Geochemical investigations of saltwater intrusion into the coastal carbonate aquifer of Mallorca, Spain

C.GARING*, L. LUQUOT AND P. GOUZE

Géosciences Montpellier, UMR 5243 CNRS/INSU, CC60,
Université de Montpellier 2, Pl. E. Bataillon, 34095
Montpellier cedex 5, France
(*correspondence : charlotte.garing@gm.univ-montp2.fr)

Coastal aquifers often display seawater intrusion resulting in the formation of a salty water wedge progressing inland. Complex geochemical processes are likely to occur in the freshwater – seawater mixing zone of carbonate aquifers where the water becomes in disequilibrium with the rock forming carbonates [1]. The induced diagenetic activity, such as calcite dissolution and/or dolomitization [2,3,4,5], may result in significant hydrodynamic changes [6,7].

This study investigates the mass transfers in a current mixing zone located in the South-East part of Mallorca Island (Spain). Investigations were conducted in two boreholes, separated by 5 m, where repeated electrical conductivity logs of the formation and of the saturating fluid, as well as regular pore-water sampling and permanent downhole multi-parameters monitoring of the water were performed over a period of 9 years.

In the mixing zone, the significant acidification, the calcite saturation index profile and the calcium concentration profile cannot be explained by conservative mixing nor by dissolution-precipitation reactions only. Conversely, the analysis of organic carbon content and of the distinctly different time-resolved pH profiles measured in the two boreholes suggests the development of perennial biomass that enhances the calcite dissolution. Moreover, the presence of biomass seems to be correlated with the permeability and vertical connectivity at meter-scale. We speculate that the mechanism could be self-activated because the microbiological activity induces calcite dissolution and tends to increase porosity and permeability that favors biomass development.

[1] Wigley & Plummer (1976), *Geochimica et Cosmochimica Acta* **40**, 989-995. [2] Hanshaw & Back (1980), *Geology* **8**, 222-224. [3] Smart, Dawans & Whitacker (1988), *Nature* **335**, 811-813. [4] Baceta, Wright & Pujalte (2001), *Sedimentary Geology* **139**, 205-216. [5] Pulido-Leboeuf (2004), *Applied Geochemistry* **19**, 1517-1527. [6] Sandford & Konikow (1989), *Water Resources Research* **25** (4), 665-667. [7] Romanov & Dreybrodt (2006), *Journal of Hydrology* **329**, 661-673.

Proton behavior at water/silica interfaces: Reactions and proton transport

STEPHEN H. GAROFALINI* AND GLENN K. LOCKWOOD

Interfacial Molecular Science Laboratory, Department of
Materials Science and Engineering, Rutgers University
(*correspondence:shg@rutgers.edu)

A robust dissociative water potential has been used in molecular dynamics simulations to study water adsorption and reactions on silica surfaces, dissolution, and proton transport. This potential matches many structural and dynamic properties of bulk water and, when transferred to nanoconfined situations, shows the high thermal expansion of nanoconfined water. The simulations of water/silica interfaces show the appropriate dissociative chemisorption and silanol (SiOH) formation consistent with experimental data, enhanced H_3O^+ ion formation during surface reactions, and the location of weakly binding highly acidic proton adsorption sites on the silica surface, with results similar to ab-initio molecular dynamics simulations of small systems. The simulations also showed increased proton transport that is consistent with electrochemical studies that showed increased proton conductivity in mesoporous silica exposed to moisture.

In order to evaluate the proton transfer mechanisms seen at the water/silica interface, we studied proton transport in bulk water, where previous data exist. Without changing parameters used in our previous simulations mentioned above, the simulation results show proton transport in bulk water involving Eigen and Zundel complexes consistent with ab-initio calculations and H_3O^+ ion lifetimes consistent with experimental data and ab-initio calculations. H_3O^+ ion lifetimes in both the femtosecond regime and the picosecond regime are observed. The first is indicative of proton rattling between the H_3O^+ ion and an adjacent water molecule while the second is indicative of the timescale for proton transport.

The activation barriers for proton transfer between the H_3O^+ ion and an adjacent water molecule in bulk water observed in the simulations are similar to the ab-initio calculations and also show the decreasing barrier height with decreasing O-O spacing between the interacting molecules.

Genesis of quartz-rich geodes from peculiar aqueous fluids in a Cu-Zn-Pb skarn (Temperino mine, Italy) and relations with ore bodies

P.S. GAROFALO¹ AND T. PETTKE²

¹Univ. of Bologna, Dept. of Earth and Environ. Sciences

²Univ. of Bern, Institute of Geological Sciences

The Temperino deposit is an historical Cu-Zn-Pb skarn located in the the Tuscan magmatic province of Italy. It consists mainly of massive lenses of sulfide bodies, enclosed within white marble, from which chalcopyrite, sphalerite, and galena were exploited in the past ^{1,2}. These bodies occur close to trachyandesite and rhyolite porphyry dikes and within NNW-SSE trending, en-echelon and discontinuous ilvaite and hedenbergite skarn masses.

A peculiar characteristics of this deposit is the presence of quartz-rich geodes within the ilvaite and hedenbergite skarns. The geodes occur close to the sulfide lenses, have variable volumes (range: from 10-20 cm³ to 2-3 m³), and are enclosed within the massive ilvaite and hedenbergite skarns. They represent the end of the main mineralizing event at Temperino. In addition to large euhedral quartz crystals (up to 15 cm in length), geodes contain ilvaite, calcite, epidote, and small proportions of ore minerals.

We determined the physical-chemical properties of the geode fluid combining microthermometry, Raman spectrometry, EMPA, CL imaging, and LA-ICP-MS of fluid inclusions entrapped at several stages of euhedral quartz growth. The crystals show alternations of 100 µm- to 1 mm-thick bands variably enriched in Al, Na, Li, Rb, Sr, Sb, Ba, Mn, B, Cs, and Zn, so they are chemically zoned. This zoning was accounted for in the determination of inclusion compositions. Fluid inclusions host two- (L, V) to five phase (L, V, and 3 solids) aqueous fluids. Despite this, their estimated bulk salinity is unexpectedly low (0.4-2.9 wt% NaCl eq.) and does not change systematically within the crystals. The *T*_h(total) of all fluids is consistently in the 220-260 °C range and homogenization occurs mainly by bubble disappearance. The main inclusion components are (in order of relative abundance) Na, K, B, Sr, Sb, Ba, Mn, Rb, Cs, Zn, Pb, and Cu, *i.e.*, the same that make the quartz zoning.

[1] Vezzoni (2008) in Department of Earth Sciences 175 (MSc Thesis. University of Pisa, Italy). [2] Corsini *et al* (1980) *Economic Geology* **75**, 83-96.

Molybdenum in ancient glacial tillites of different ages and its bearing on atmospheric oxygenation

R. GASCHNIG¹, R. RUDNICK¹ AND W. McDONOUGH¹

¹Department of Geology, University of Maryland, College Park, MD 20742 (gaschnig@umd.edu; rudnick@umd.edu; mcdonoug@umd.edu)

Molybdenum is an important redox indicator because of its ability to exist in either insoluble +4 or soluble +6 states. The abundance and isotopic composition of Mo in black shales have been used to make inferences about global atmospheric oxygenation. While an unambiguous and dramatic rise in oxygen occurred during the ~2.3 Ga Great Oxygenation Event (GOE), Mo systematics in shales suggest that the oceans and possibly the atmosphere contained “whiffs” of oxygen as early as 2.7 Ga, implying that oxidative weathering of the continents (and Mo loss) began before the GOE. Proxies for the average composition of the upper continental crust (UCC) should reflect this loss. V.M.Goldschmidt suggested that continental glacial till deposits could be such a proxy, and thus we have studied the chemical compositions of Paleozoic to Paleoproterozoic glacial tillites.

Ancient tillites from around the world show systematic changes in Mo abundances with time, regardless of location. Mo abundances for all Paleoproterozoic (2.4-2.2 Ga) samples are comparable to the upper crustal estimate (1.1 ppm) whereas post-Paleoproterozoic samples show depletions in Mo of up to an order in magnitude. This depletion in Mo is especially apparent when compared to elements with similar compatibility in igneous environments (*i.e.*, LREE) and when all samples are corrected for quartz and carbonate dilution when normalized to Y or Al. Relatively undepleted Mo contents in Paleoproterozoic tillites implies insufficient oxygen in the atmosphere at that time to preferentially mobilize Mo during glacial erosion, or for the UCC to have developed an intrinsic oxidative weathering chemical signature. Both hypotheses place limits on the presence of any Neoproterozoic whiffs of oxygen in the atmosphere. A test of these hypotheses is available in the Mo contents of Quaternary tills derived from exclusively Archean crustal terranes, as an absence of depletion in Mo would be inconsistent with both hypotheses.

Natural hazards and scientific advice: Interactions among scientists, decision makers and the public

PAOLO GASPARINI

Università di Napoli Federico II (paolo.gasparini@na.infn.it)

The death toll of natural hazards has been dramatically increasing for a few decades. This is mainly a consequence of the increase of population density and of the vulnerability of many hazard prone areas. False and missed alarms have been harshly questioned by the population and sometimes by governmental authorities. An extreme case is the first level conviction of seven Italian scientists for the information given to the public before the Mw6.3 earthquake hitting the city of L'Aquila (Italy) and surrounding municipalities on April 6, 2009. Similar and greater disasters occurred after 2009 due to natural hazards, such as the Tohoku exceptionally violent earthquake and tsunami hitting Japan in 2011, the Christchurch earthquake sequence in New Zealand, the large floods covering central and south eastern Europe in 2006 and 2013, the floods triggered by Hurricane Irina in NE USA in 2012 etc. The reactions of public and legal authorities have been different, not reaching the extremes of L'Aquila sentence. The reactions of people and authorities to scientific information appears to be strongly conditioned by the level of risk-awareness and memory of past events. However, all the reactions of public and administrators have a common background: the lack of consciousness that we live in a probabilistic world where all scientific assessments concerning natural hazards and risks have a probabilistic character and a related uncertainty. This concept is missing in the legislation of many countries. The court of L'Aquila sentence had immediate negative consequences, at least in Italy, triggering a strongly defensive attitude in all the actors of crisis management during a natural event, hindering the implementation of innovative methodologies, such as those of early warning, that can save many lives but have inherently significant levels of false and missed alarms. Future scenarios of science - decision making people interactions must consider seriously the pros and cons of the rapidly growing role of social networks in immediate pre or during crisis information. The complexity of future communication scenarios can be approached by a widespread and transparent use of a probabilistic approach in risk governance, an advanced prevent formation of people and administrators, and the establishment of operational risk reduction guidelines. Finally a reformulation, where necessary, of the legislation on the management of risks should clarify duties and responsibilities and introduce the concept that false and missed alarms may be significant in any risk management method.

Mantle source heterogeneity beneath the Garrotxa Volcanic Field (NE Spain)

D. GASPERINI*¹, G. GISBERT¹, D. GIMENO¹,
M.AULINAS¹, P. MACERA² AND D. BOSCH³

¹Dep. Geoquímica, Petrologia i Prospecció Geològica, Universitat de Barcelona. 08028 Barcelona, Spain (*correspondence: gasperinidaniela@gmail.com; ggisbert@hotmail.com; domingo.gimeno@ub.edu; meritxellaulinas@ub.edu)

²Dip. Scienze della Terra, Università di Pisa. 56126 Pisa, Italia (macera@dst.unipi.it)

³Earth Science Department, Geosciences Montpellier (CNRS). 34095 Montpellier, France (bosch@gm.univ-montp2.fr)

The Neogene volcanism in NE Spain, which is related to the rift-type extensional tectonics affecting the eastern margin of Iberia since late Oligocene, is well represented in the basalts and basanites from the Garrotxa Volcanic Field (GVF). Geochemistry of the GVF magmas is comparable to that of the Cenozoic Eastern Atlantic and Euro-Mediterranean eruptive centers related to the European Asthenospheric Reservoir (EAR). The EAR is thought to have originated by the mixing between plume-like material (carrying a HIMU signature) and the shallower depleted mantle (DMM). The GVF mantle source and the EAR share comparable trace element distribution, enrichment levels and characteristic ranges of trace element ratios (e.g., Ba/La, K/La, Zr/Nb). However, isotope data from the GVF magmas call for the presence of a compositionally heterogeneous mantle source, which is considered to be the result of the mixing between two end-members. While a first end-member presents relatively high ¹⁴³Nd/¹⁴⁴Nd and ²⁰⁶Pb/²⁰⁴Pb values and shows geochemical features close to average EAR, the second end-member is characterized by relatively lower ¹⁴³Nd/¹⁴⁴Nd and ²⁰⁶Pb/²⁰⁴Pb and slightly higher ⁸⁷Sr/⁸⁶Sr ratios that are recurrent in EMI-type magmas. To constrain the isotope features of the GVF magmas, their Sr, Nd and ²⁰⁶Pb/²⁰⁴Pb isotopic compositions together with those of worldwide OIB, anorogenic European rocks, and lithospheric and crustal samples from the Pyrenean and Iberian domains were projected into a tetrahedron with the four classical mantle end-members (DMM, EMI, EMII, HIMU) as vertices. The three-dimensional perspective indicates that the GVF mantle source isotope characteristics are consistent with a heterogeneous lithosphere, variously metasomatized by both the EAR and EMI components, and strongly related to the local tectonic structure, e.g., crustal thinning.

www.minersoc.org

DOI:10.1180/minmag.2013.077.5.7

Calculation of the mixing ratio of wastewater effluents leakage to a pristine water source: The Israeli Experience

G. GASSER^{1,2}, I. PANKRATOV², H. GLAZMAN³,
G. RESHEF², S. ELHANANY² AND O. LEV^{*1}

¹Hebrew University of Jerusalem, Israel
(ovadia@mail.huji.ac.il)

²Israel Water Authority, Bet Dagan, Israel

³ Israel Nature and Park Authority, Israel

A methodology to estimate of the average percentage of wastewater effluents in an otherwise pristine water site was developed and applied in several vulnerable sites in Israel using mono or multiple effluent indicators. The model takes into account the levels and the uncertainty margins in the evaluation of each of the indicators in the site, in the potential effluent sources and in the uncontaminated surrounding.

Several detailed demonstrative studies exemplify the use of this model by the Israel Water Authority. In these studies we used chloride, acesulfame and carbamazepine as wastewater effluent indicators.

a The Northern Galilee springs: This research concentrated on six nearby perched springs draining upper cretaceous carbonate aquifers with Karst morphology which are influenced to an unknown extent by agricultural communities that still use septic tanks. In this site fecal contamination was found in the past, but since then the two major sources of pollution in the area were collected and diverted to a mechanical biological wastewater treatment systems.

b The Shafdan soil-aquifer treatment site. Leakage from the soil – aquifer treatment system of the Dan municipality (treating some 130 Mm³ per annum) to the coastal plain aquifer was quantified.

c The contamination of the perched Judea Mountains springs which serve for irrigation and recreation by septic wastes was explored.

In all cases we found good correspondence between the dilution predictions by the two organic tracers, whereas the chloride predictions differed somewhat and exhibited higher level of uncertainty.

Chemical influence on recoil damage annealing and impact on (U-Th)/He age in apatite

C. GAUTHERON^{1*}, R. PINNA-JAMME¹, R. KETCHAM²,
J. BARBARAND¹, L. TASSAN-GOT³, A. CARTER⁴
AND M. PAGEL¹

¹UMR IDES, UPS, France (* cecile.gautheron@u-psud.fr,
rosella.pinna@u-psud.fr, jocelyn.barbarand@u-psud.fr,
maurice.pagel@u-psud.fr)

²Jackson School of Geosciences, Austin, USA,
ketcham@jsg.utexas.edu

³IPN, UPS, France, tassango@ipno.in2p3.fr

⁴IEPS, UCL-Bbk, London, UK; a.carter@ucl.ac.uk

Apatite (U-Th)/He (AHe) age is a function of the production/ejection and diffusion of He particles in a grain of determined size and for a particular time-temperature path. Recent studies have demonstrated that He diffusion is sensitive to the amount of α -recoil damage [1-2]. As a result, new models accounting for α -recoil damage creation and annealing were created to characterize the diffusion behaviour of He in apatite, which are currently utilized in forward and inverse tools for reconstruction of T-t paths [3]. However, although these models are based on the annealing scheme used for apatite fission tracks (AFT), the effect of grain chemistry on annealing rates, shown to be critical for AFT, has not been investigated in the context of He diffusion. For this purpose, we studied the grain chemistry measured by microprobe (EMPA), laser and solution ICPMS on independent AFT dated and He degassed grains. We investigated the behaviour of sedimentary samples from Hercynian origin that shows a wide range in AFT single grain ages due to variable apatite composition (measured by Dpar, EMPA or ICPMS). Our aim was to test if apatite chemistry has an influence on the annealing rate of α -recoil damage. Dispersion of the single grain ages is large for both AFT and AHe datasets although AHe ages are systematically younger (AFT: ~14-208 Ma; N=117; AHe: ~4-76 Ma and one grain at 120 Ma; N=36). Using the thermal history reconstruction from the AFT data, we show that the poor correlation observed between AHe age and eU content can be simply explained by adjusting the annealing law parameter. For slowly exhumed samples we demonstrate that apatite grain chemistry can more easily explain some of the AHe grain age variation. This study reveals that grain chemistry can significantly influence He diffusion, and we conclude that to fully access the thermal history information in AHe ages, the potential for variation in damage annealing kinetics needs to be considered.

[1] Shuster, D. *et al* (2006). *EPSL*. **249**. 148-161. [2] Gautheron, C. *et al* (2009). *Chem. Geol.* **266**. 166-179. [3] Ketcham, R.A., *et al* (2005). *Rev. Min Geochem.* **58**. 273-310.

Interactions between glassy materials and metallophyte plants: Application to the remediation of polluted soils

A. GAUTHIER AND M. DUBOIS¹

¹LGCgE, Lille1 University, SN5 Building, 59655 Villeneuve d'Ascq-France. Arnaud.gauthier@univ-lille1.fr

The contamination of soils by heavy metals has become a really important problem, especially in some highly industrialized areas such as north of France. One of the ways of treatment is the remediation using metallophyte plants able to trap pollutants from soils. The aim of this work was to follow the evolution of a plot of polluted land in the presence of metallophyte plants (*Arabidopsis halleri*) and of a phosphated amendment. This amendment consist of a glassy matrix (Ca-Si-P) in order to increase the phosphorus concentration into the soil. Moreover the alteration of this glass produces the development of crystallized secondary phases (hydroxyapatite) which can trap heavy metals.

The contents in metals observed in plants after culture are about 2 % for cadmium and of 4 % for lead. Moreover, the contents in metals contained in the superior parts are much more important than those determined in the absence of amendment (5 and 8 % respectively for Cd and Pb). Samplings of ground were besides realized and prepared in order to observe root / soils contacts by ESEM. To try to understand the impact of this amendment on the behaviour of metals contained in the sediment, elementary mappings were made on these polished sections. These observations tend to prove that the zinc seems diffuse and integrated within the root. In the case of a stake in culture in the absence of amendment, we observe a gradient of rather weak concentration with only the presence of a zone more concentrated in periphery. In the presence of amendment, the cartography brings to light a more important concentration, with a gradual increase towards the heart of the root. A very clear border rich in lead is set up in external border, whereas this element is absent in the heart of the root. Besides, the lead distribution on the edge of the root seems to be correlated to the type of substratum of culture. So in the presence of amendment this border appears more continuous and thicker.

This study has permitted to show a great capacity of *A. halleri* to mobilize specifically zinc from solid phases of soil.

Metasomatism in the Dora Maira whiteschists investigated by SHRIMP oxygen isotopes and U-Pb geochronology

LAURE GAUTHIEZ-PUTALLAZ*, DANIELA RUBATTO, AND JOERG HERMANN

Research School of Earth Sciences, Australian National University, Canberra, ACT 0200, Australia
(*correspondence: laure.gauthiez-putallaz@anu.edu.au)

The coesite and pyrope-bearing ultra-high pressure (UHP) metamorphic whiteschists from the Dora Maira unit, Western Alps underwent pervasive metasomatism. However, the timing and setting of the metasomatism are still disputed. We analysed U-Pb and oxygen isotopes in zircon and monazite with the SHRIMP ion-microprobe, and trace-elements by Laser-Ablation ICP-MS in the major REE-bearing phases, in order to better constrain the timing of the fluid influx and its relationship to UHP metamorphism.

Zircons cores with oscillatory-zoning are dated at ~265 Ma and have a $\delta^{18}\text{O}$ of ~ 9-10 ‰. They are interpreted as magmatic relics recording the age and oxygen signature of the granitic protolith, before metasomatism. Zircon rims and the monazite grains yield an Alpine age (35-34 Ma) and a significantly lower $\delta^{18}\text{O}$ of ~ 6-7‰. For a prograde to peak metamorphic temperature of ~700-730°C, the $\delta^{18}\text{O}$ of Alpine zircon and monazites indicate equilibrium with the major metamorphic phases [1]. The core-rim $\delta^{18}\text{O}$ offset in zircon is interpreted as a shift in bulk-rock $\delta^{18}\text{O}$ corresponding to the metasomatic event that altered the granitic protolith. The zircon rims are composed of up to 4 concentric domains, different in CL emission but identical in oxygen composition and age: $\delta^{18}\text{O}$ ~6‰ and ~34 Ma. The trace-element patterns of these rims show variations from HREE-rich to HREE-depleted, which mirror the compositional variation in the garnet. This indicates zircon growth before and during progressive garnet growth. A similar record is present in monazite. According to previous petrological studies [2], garnet growth started at 25 to 30 kbar and 650°C and continued until the metamorphic peak at 45 kbar.

Thus, the granitic protolith underwent metasomatism at pressures lower than 25 kbar before the onset of garnet crystallisation, either during seafloor alteration or early prograde subduction. Prograde (25 kbar) to peak (45 kbar) metamorphism occurred over a short time-interval of 1-2 Ma corresponding to minimum burial rates of 3 to 4 cm/y.

[1] Sharp *et al* (1993), *Contrib Min Petrol* **114**, 1-12; [2] Hermann (2003), *Lithos* **70**, 163-182

Peridotite- derived sulfides in pyroxenites from the Lanzo and the Lherz ultramafic massifs?

T. GAWRONSKI^{1*}, H. BECKER² AND M. HUMAYUN³

¹Institut für Geologische Wissenschaften, Freie Universität Berlin, Germany, gawronsk@zedat.fu-berlin.de

²Institut für Geologische Wissenschaften, Freie Universität Berlin, Germany, hbecker@zedat.fu-berlin.de

³Dept. of Earth, Ocean and Atmospheric Science and National High Magnetic Field Laboratory, Florida State University, USA, humayun@magnet.fsu.edu

In the upper mantle, the abundances of highly siderophile elements (HSE: Os, Ir, Ru, Rh, Pt, Pd, Au, Re) are mainly controlled by Fe-Ni-Cu-bearing sulfides and platinum group element alloys. In order to assess the role of melt migration on the HSE distribution in mantle rocks and to constrain the HSE composition of secondary sulfide melt in mantle rocks, *in situ* LA-ICP-MS and whole rock HSE analyses on pyroxenite samples from the Lanzo (northern Italy) and the Lherz (southern France) peridotite massifs have been obtained.

More than 95% of the analysed sulfides from pyroxenites of both peridotite bodies show a pentlanditic composition with some showing subsolidus inclusions of chalcopyrite. Websterites and Al-rich clinopyroxenites display no systematic differences in HSE compositions of sulfides. Sulfides from both locales are variably depleted in Pt and Au, whereas the bulk rocks are not, indicating the additional presence of Pt-rich alloy phases and presumably native Au. Sulfides from Lanzo pyroxenites show Os, Ir and Ru abundances at 1-10 x CI chondrites, and variable Pd/Ir_(CI) of 1-7. Compared to Lanzo, sulfides (and whole rocks) from Lherz pyroxenites are more enriched in Os, Ir and Ru, with Pd/Ir_(CI) of 0.5-5. The variations of Pd/Ir in sulfides from the same thin section mostly reflect large variations of Ir abundances (in contrast to grain boundary sulfides in lherzolites, which tend to have variable Pd abundances). The presence of sulfides with suprachondritic Pd/Ir (or Pd/Os) and Re/Os in the same section as sulfides that show chondritic to subchondritic ratios of these elements is indicative of small-scale disequilibrium during magmatic processes. The compositional range of sulfides in some pyroxenites is most easily explained if sulfide melt with chondritic to subchondritic Pd/Ir and Re/Os from peridotite became mobilized during infiltration of sulfur saturated basaltic melt containing sulfide melt with high Pd/Ir and Re/Os.

Cosmogenic Nuclides, River Geochemistry, and Landforms Reconstruction methods to estimate erosion rates in Reunion Island

E. GAYER¹, P. LOUVAT¹, L. MICHON^{1,2}, C. ETZOL¹ AND M. KURZ³

¹Institut de Physique du Globe de Paris, Sorbonne Paris Cité', Univ Paris Diderot, UMR 7154 CNRS, Paris, France

²Université de la Réunion, La Réunion, France

³WHOI, Woods Hole, MA, USA

Understanding mechanisms that modify landscapes is essential for risk assessment in tropical islands. Because measurements of erosion rates are critical for understanding landform evolution, the use of cosmogenic isotopes in river sediments or the use of river load geochemistry, both to estimate average erosion rates of drainage areas have grown rapidly in recent years.

In this study we aim to estimate erosion rates of highly eroded drainage areas of the Réunion Island and we compare 3 methods of measurement : i) from cosmogenic ³He concentrations [³He_c], ii) from river geochemistry and iii) from landforms reconstruction.

The first drainage area under investigation is Cilaos Cirque, located on the south flank of the Piton des Neiges Volcano (PdN). Helium concentrations and isotopic ratios have been measured in olivine rich sands from the Grand Bras River. [³He_c] have been calculated using: (i) the ³He/⁴He ratio measured by crushing and (ii) the ³He and ⁴He concentrations measured by melting the resulting powder. Dissolved and suspended loads in Grand Bras River have also been analysed for their major and trace elements contents in order to characterise both chemical and mechanical erosion products. Finally, digital elevation model derivatives and K-Ar geochronological data have been used to reconstruct the PdN morphology and calculate the volume of material eroded over the past 70Ka. Initial results indicate average erosion rates of 1.02±0.40 and 0.47±0.16 mm/yr for the cosmogenic and river geochemistry methods respectively, while erosion rates from PdN morphology reconstruction range from 4 to 12 mm/yr. Cosmogenic and river geochemistry results show a reasonable agreement but their discrepancy with the landform reconstruction results suggests 2 questions: are the cosmogenic and river geochemistry methods suitable to quantify fast erosion rates (>>1mm/yr)? does the cosmogenic isotopes method actually provide short-term erosion estimation in fast erosion environment? Further measurements along the Grand Bras River and over other drainage areas will allow to answer these questions.

Sr and Nd isotopes of modern cold seep carbonates from the northern South China Sea

L. GE^{1*}, J.S. CHEN¹, S.Y. JIANG² AND F.T. YANG²,

¹Institute of Isotope Hydrology, School of Earth Sciences and Engineering, Hohai University, Nanjing 210098, PR China (*correspondence: gelu211@163.com)

²State Key Laboratory for Mineral Deposits Research, Department of Earth Sciences, Nanjing University, Nanjing 210093, PR China

Methane-derived carbonate precipitation, a well-known phenomenon at hydrocarbon seeps on active and passive continental margins worldwide, forms as a result of microbial oxidation of methane and bacterial sulphate reduction. Seep carbonates are generally well preserved in the sedimentary and geological records, and hence can supply information about fluid compositions, fluid sources, and fluid migration pathways over geologic time. In cold seep related studies, it is important to identify the origin of methane-rich fluids. The determination is generally inferred from stable isotopes and rare earth elements. In addition, isotopic tracers have been used for investigating the origin of fluids in continental margin sediments (Sr, Li, B and I isotopes, e.g.).

In this study, we report the Sr and Nd isotopic compositions on a series of modern cold seep carbonate chimneys from the northern South China Sea. ⁸⁷Sr/⁸⁶Sr ratios of cold seep carbonates vary from 0.709171 to 0.709269, which are indistinguishable from modern seawater (mean 0.709175), reflecting a shallow marine Sr source.

ϵ_{Nd} values of cold seep carbonates are between -8.60 and -5.38, which lie within the range of modern sea water and sediments in the northern South China Sea. The Nd isotopic characteristics imply a mixed Nd source from two end members, but different proportions of mixture.

We conclude that the Sr and Nd isotopes can be used to identify the origin of fluids at cold seep sites.

This research is funded by the National Science Foundation of China (Grant No. 41203021) and the Jiangsu Postdoctoral Sustentation Fund, China (Grant No. 1201061C) and the State Key Laboratory for Mineral Deposits Research Fund of China (Grant No. 17-1112-2).

Microbial iron reduction in marine intertidal sediments

JEANINE S. GEELHOED^{1*}, HALINA E. TEGETMEYER^{1,2}
AND MARC STROUS^{1,2}

¹Max Planck Institute for Marine Microbiology, Bremen, Germany (*correspondence: jgeelhoe@mpi-bremen.de)

²Center for Biotechnology, Bielefeld University, Germany

Oxidized iron compounds may be important electron acceptors for anaerobic respiration, in particular in marine intertidal sediments. Tidal cycles generate changes in the position of the chemocline and may drive rapid cycling of iron between oxidized and reduced iron species. The possible mechanisms for iron(III) reduction include microbial iron reduction by respiratory microorganisms, use of iron(III) as electron sink by fermentative microorganisms and the indirect reduction of iron with sulfide that is generated by sulfate-reducing microorganisms. Using geochemical and omics methods we aim to identify the microorganisms responsible for iron(III) reduction and the pathways involved.

We have incubated the microbial community from the surface layer of a marine intertidal flat using medium that contains both iron, as sparingly soluble iron(III) hydroxide, and sulfate as electron acceptors in anaerobic continuous culture with different electron donors. Batch incubations with the enriched microbial community using labelled sulfate were carried out to evaluate the importance of the production of sulfide by sulfate-reducing bacteria for the indirect reduction of iron(III).

The development of the enriched microbial community was analyzed using automated rRNA intergenic spacer analysis (ARISA), and the metagenome of this enriched community was sequenced. Sequences denoting 16S rRNA genes and universal single copy genes were used to analyse the microbial community composition. The metagenome, together with metatranscriptomic and/or metaproteomic analyses, also gives insight into substrate utilization and the pathways involved in the reduction of iron and sulfate. Based on our data, a model for carbon, sulfate and iron(III) utilization in this system is presented.

The role of the Mid-Atlantic Ridge for chemical fluxes in the Atlantic: Clues from Ra and Ac isotopes

WALTER GEIBERT¹, YU-TE HSIEH^{2,3}
AND GIDEON M. HENDERSON²

¹School of GeoSciences, University of Edinburgh, Grant Institute, The King's Buildings, West Mains Road, Edinburgh EH9 3JW; walter.geibert@ed.ac.uk

²Department of Earth Sciences, South Parks Road, Oxford, OX1 3AN, England

³now at Dept. of Earth, Atmospheric and Planetary Sciences, MIT, 45 Carleton Street, E25-623, Cambridge, MA 02142, USA,

We present data on the distribution of short-lived radium isotopes ²²³Ra and ²²⁴Ra, as proxies for their parent isotopes ²²⁷Ac and ²²⁸Th, from the deep South Atlantic (GEOTRACES cruises GA10E and GA10W), together with ²²⁸Ra and ²²⁶Ra data from the same samples. Samples were collected in-situ using submersible autonomous pumping systems (SAPS) equipped with two MnO₂-coated acrylic fibers in series. We use a new evaluation method to determine Ra adsorption efficiencies of this sampling technique with a Ra delayed coincidence counter (RaDeCC), avoiding the determination of the efficiency based on the decrease of Ra from the 1st to the 2nd absorber (1-B/A). Instead, we have individual efficiencies for each absorber. Efficiencies of the new sampling method are on average 30% (±8%) for two absorbers combined, with an average sample volume of 381 L.

Elevated ²²⁷Ac values at ~3000m across the Atlantic basin, with a maximum at the mid-Atlantic Ridge (MAR), suggest a potential effect of the MAR on the distribution of chemical species in various ways: As a source for elements that can be modeled as analogues of ²²⁷Ac; as a barrier between ocean basins; and by enhancing isopycnal mixing with long-distance effects.

Hematite/Water Interfaces Probed by Second Harmonic Generation

FRANZ M. GEIGER¹

¹Department of Chemistry, Northwestern University, 2145 Sheridan Road, Evanston, IL, 60208, USA
geigerf@chem.northwestern.edu

The Fe(III)/Fe(II) redox couple is a fundamental transformation pathway for iron oxides, however, the study of iron oxide surfaces in aqueous solution by powerful spectroscopic techniques has been limited due to "strong absorber problem". Here, we overcome this issue using atomic layer deposition (ALD) of thin films of polycrystalline α -Fe₂O₃ which were analyzed using the Eisenthal $\chi^{(3)}$ technique, a variant of second harmonic generation (SHG) that reports on interfacial potentials. The point of zero charge was found to be 5.5 ± 0.3 . The interaction of aqueous Fe(II) at pH 4 and in 1 mM NaCl with ALD-prepared hematite was found to be fully reversible and to lead to about 4 times more ferrous iron ions adsorbed per square centimeter than on fused-silica surfaces under the same conditions. The data are consistent with a recently proposed conceptual model for net Fe(II) uptake or release that is underlain by a dynamic equilibrium between Fe(II) adsorbed onto hematite, electron transfer into favorable surface sites with attendant Fe(III) deposition, and electron conduction to favorable remote sites that release and replenish aqueous Fe(II). Additional work carried out under flow conditions at pH 4 with 10 mM NaCl resulted in partially irreversible adsorption of Cr(III), the extent of which was found to depend on Cr(III) concentration, as confirmed by X-ray photoelectron spectroscopy. The interaction of Cr(III) with hematite was compared with the adsorption of Cr(III) to the silica/water interface, which is the substrate for the ALD-prepared hematite films, and found to be fully reversible under the same experimental conditions. The observed binding constant for Cr(III) interacting with the silica surface was found to be $4.0(6) \times 10^3 \text{ M}^{-1}$, which corresponds to an adsorption free energy of $-30.5(4) \text{ kJ/mol}$ when referenced to 55.5 M water. Cr(III) surface coverages were calculated to be $1.0 \times 10^{12} \text{ ions/cm}^2$ assuming a +3 charge for chromium. The observed binding constant for Cr(III) interacting reversibly with the hematite surface was calculated to be $2(2) \times 10^4 \text{ M}^{-1}$ (adsorption free energy of $-35(2) \text{ kJ/mol}$). Maximum metal ion surface coverages 8.3×10^{11} reversibly bound ions per cm², again assuming a +3 charge of chromium. The data also allows us to estimate that about 6.7×10^{12} Cr(III) ions are irreversibly bound per cm² hematite at saturation coverage. The results of this investigation are discussed in the context of surface passivation in permeable reactive barriers.

Silicon isotope variation in the Buck Reef Chert (Barberton Greenstone Belt) records early Archean basin evolution

S. GEILERT^{1*}, M.J. VAN BERGEN¹ AND P.Z. VROON²

¹Utrecht University, 3584 CD Utrecht, Netherlands
(*correspondance: s.geilert@uu.nl;
m.j.vanbergen@uu.nl)

²VU University Amsterdam, 1081 HV Amsterdam,
Netherlands (p.z.vroon@vu.nl)

Silicon isotopic signatures of chemical sediments receive growing attention, given their applicability in the search for properties of ancient seawater and the understanding of the environment in which the first life evolved. An important target is the reconstruction of secular changes in surface temperature of the Precambrian Earth, however, interpretations are problematic since controls of the isotopic signals are potentially manifold. Here we report the existence of significant silicon isotope variability in, chemically precipitated chert layers covering a continuous stratigraphic section across the ~3.42 Ga Buck Reef Chert (BRC) in the Barberton Greenstone Belt (South Africa). The $\delta^{30}\text{Si}$ values range from +0.36‰ for shallow-marine sediments in the lower part of the section to -1.25‰ for deeper water deposits in the upper part. A total shift of 1.6‰ thus accompanied chert formation in a single Archean basin in the course of deepening. Cherts at the base of the section represent silicified felsic volcanoclastic sediments and have exclusively positive $\delta^{30}\text{Si}$ values between +0.14 and +0.68‰.

Rare earth elements and yttrium patterns confirm the marine origin of the cherts and support the presumed basin evolution, from coastal shallow waters to a deep basin, well-below storm base. From the combined evidence we infer that the $\delta^{30}\text{Si}$ variations in the BRC reflect changes in the predominant origin of the silica, with terrigenous input supplying positive $\delta^{30}\text{Si}$ to shallow waters and seafloor hydrothermal sources negative $\delta^{30}\text{Si}$ to deeper levels. Our findings demonstrate the viability of silicon isotopes of cherts for reconstructing the evolution of ancient marine basins.

Complexation of oxyanions by diatom cells

A. GELABERT^{1*}, O.S. POKROVSKY², J. SCHOTT²
AND A. FEURTET-MAZEL³

¹Univ. Paris Diderot, Sorbonne-Paris-Cité, Inst. de Physique
du Globe de Paris, UMR CNRS 7154, Paris, France

²Lab. Géoscience Environnement Toulouse (GET), UMR
CNRS 5563, Toulouse, France

³LEESA, UMR CNRS 5805, Univ. Bordeaux 1, France

Diatoms are unicellular algae located at the base of short, energy-efficient food webs. Since they are widespread and exhibit strong amphoteric properties, they are expected to constitute important environmental sorbants for potential or known toxic trace elements such as Cr(VI), Mo(VI) and W(VI). However, most of the studies devoted to these oxyanions underline the lack of information regarding their mobility or their speciation in natural systems. Particularly, their interaction with microorganisms is poorly documented despite the potential control they can exert on trace elements cycling. The main goal of this study is thus to provide a surface complexation model able to describe the sorption of chromate, molybdate and tungstate ions onto diatom surfaces.

Four diatom species (*Navicula minima*, *Achnantheidium minutissimum*, *Skeletonema costatum*, *Thalassiosira weissflogii*) representative of freshwater, estuarine and marine systems were investigated. Cr(VI), Mo(VI) and W(VI) sorption isotherms as a function of pH and oxyanion concentration were collected. Experimental data were modelled assuming a constant capacitance to account for the coulombic interactions in the EDL. Both molybdate and tungstate exhibit a maximum in sorption at acidic pH, with a sorption edge between pH 4.5 and 6.5 depending on the cell/oxyanion ratio. Sorption onto the cell surface differs for these two elements with a stronger complexation constant for tungstate (logK=12.2 for *Thalassiosira weissflogii*) compared to molybdate (logK=10.5). Interestingly, freshwater species display generally a higher affinity for molybdate compared to the marine and estuarine diatoms. Chromate behaves differently, with a sorption edge around pH 7.5, but also with a strong desorption occurring at low pH (around pH 3). No reduction from Cr(VI) to Cr(III) was necessary to model chromate sorption isotherms. For the three oxyanions, the experimental data were best fitted considering monodentate mononuclear complexes with the positively charged amino groups present in the diatom cell wall structure. Because of the rigorous thermodynamic approach used in this study, this work constitutes an important step for the understanding of oxyanions cycling in natural systems.

Pre-Seismic Hydro-Chemical Anomalies in Water of Well Liaogu-1 in Shandong Province, China

JIE GENG

Earthquake Administration of Shandong Province, 5 Weiqi Road, Jinan 250021, China

Since its formal operation in 1981, the Well Liaogu-1 has showed good capability to reflect earthquakes with $M_s \geq 5.0$ within certain range around even the pre-seismic abnormal changes of hydro-chemical constituents are quite different for each earthquake. Based on fault dislocation theory and rock mechanics experiments with the data collected more than 30 years, some major results were summarized.

1, the well Liaogu-1 at a special tectonic position with good hydrogeological and borehole conditions is reliable for continuous observation, and a wealth of valuable actual observation data are obtained. Abnormal changes of hydro-chemical constituents reflected well to earthquakes $M_s \geq 5.0$ in a range of 500km around the well.

2, The synchronous abnormal changes of multiple hydro-chemical constituents in the well before the Heze $M_s 5.9$ earthquake(1983) were caused by the intensifying activity of the Liaokao fault from random to ordered fracturing, indicating local increase of tensile stress and corresponding pressure reduction around the borehole. The appearance of a complete set of medium-term, short-term and imminent anomalies is a reflection of the preparation process of the source stress field.

3, some single hydrochemical parameter displayed obvious abnormal change before the earthquakes of Datong $M_s 5.8$ (1991), Ningjin $M_s 5.8$ (1981), South Yellow Sea $M_s 5.3$ (1992) and Cangshan $M_s 5.2$ (1995), reflecting the intensification of regional tectonic stress field and the response of the tectonic sensitive area where the well Liaogu-1 located in.

4, various field-source seismic precursor characteristics of multiple constituents are of certain prediction significance. The appearance of source precursors means that earthquake with $M_s \geq 5.0$ may occur in the near future at some tectonic position on the same active fault. The appearance of field precursors means that the activity of regional stress field is intensifying and earthquake with $M_s 5.0$ may occur in a couple of weeks or months on some other active fault zone. Therefore, to distinguish field precursor and source precursor is greatly important for earthquake forecast and prediction.

Lower continental crust residue in Mesozoic EM1-type basalts from the North China craton

XIAN-LEI GENG, YONG-SHENG LIU* AND SHAN GAO

Faculty of Earth Sciences, China University of Geosciences, Wuhan, 430074, China

(*correspondence: yshliu@hotmail.com)

The origin of Enriched Mantle 1 (EM1) end-member has been in great controversy. In order to investigate the role of the lower continental crust (LCC) in generation of EM1 basalts, the Early Cretaceous (~125 Ma) Yixian and Sihetun basalts ($MgO > 10\%$) from the North China craton were collected, and their major, trace element and Sr-Nd-Pb isotopic compositions were measured. These basalts show low $\epsilon_{Nd}(t)$ (-1.48 to -11.8), low initial $^{206}Pb/^{204}Pb$ ratios (<17.306), and slightly high initial $^{87}Sr/^{86}Sr$ ratios (0.70622 to 0.70679), pointing to an origin of EM1. Enrichment of K, Pb and Sr, and depletion of Nb and Ta are also shown in these basalts. These features can not be explained by recycling of subducted oceanic crust with sediments which was usually regarded as the origin of EM1 OIBs, because dehydration will lead to depletion of K, Pb and Sr and enrichment of Nb, Ta in subducted residue that was shown in global EM1 OIBs. We suggested that involvement of ancient LCC components in the mantle source could be responsible for the generation of the above isotopic and trace element signatures.

High Mg# values (>72), low CaO/Al_2O_3 ratios (<0.65) and high Fe/Mn ratios (56-70) with low CaO (<8.5 wt%) and FeO^T (<9 wt%) contents suggest that these basalts could have been derived from a pyroxenite source produced by hybrid interaction between peridotite and Si-rich melts from subducted MORBs or foundered eclogitic LCC. MORBs have much higher $^{143}Nd/^{144}Nd$ and lower $^{87}Sr/^{86}Sr$ ratios compared to these basalts. Thus, subducted MORBs could not have been the source of the hybridizing melts. Instead, the source of the melts were most likely to be foundered eclogites that originated from ancient lower continental crust of the NCC.

Collectively, recycling of the foundered lower continental crust during the peak (~130Ma) of the lithospheric thinning of the North China craton could have played a significant role in production of the Mesozoic intraplate EM1 magmatism. Such lower continental crust components may be also present for some OIBs, especially those with continent-like trace element compositions (e.g. Aphanasey Nikitin Rise) [1, 2].

[1] Borisova *et al* (2001) *J Petrol* **42**, 277-319. [2] Mahoney *et al* (1996) *Geology* **24**, 615-618.

Constraining the nature of the western Azores mantle source using Pb-Hf-Os isotope systematics

F.S. GENSKE*^{1,2,3}, C. BEIER³, S.P. TURNER²,
A. STRACKE¹ AND K.M. HAASE³

¹Institut für Mineralogie, Westfälische Wilhelms-Universität Münster, Corrensstrasse 24, 48149 Münster, Germany, felix.genske@uni-muenster.de

²Dept. of Earth and Planetary Sciences, Macquarie University, Sydney NSW 2109, Australia

³GeoZentrum Nordbayern, Universität Erlangen-Nürnberg, Schloßgarten 5, D-91054 Erlangen, Germany

Basalts from the Azores islands in the central North-Atlantic provide an opportunity to investigate the composition of the deeper mantle brought to the surface by the Azores plume. Here, we present Hf, Pb and Os isotopes in geochemically well-characterised primitive lavas from the Azores islands. New data are presented from the islands Flores and Corvo, which are situated west of the Mid-Atlantic ridge (MAR), in addition to several submarine lavas from the far west of the Azores plateau.

The location of Flores and Corvo furthest from the inferred Azores plume is geodynamically not well understood. Radiogenic isotopes allow constraining the source composition of the Flores and Corvo lavas and allow comparison with the islands east of the MAR. Their ¹⁷⁶Hf/¹⁷⁷Hf and ²⁰⁶Pb/²⁰⁴Pb isotope ratios range from 0.282957 to 0.283069 and from 19.5166 to 19.7799, respectively, whilst ¹⁸⁷Os/¹⁸⁸Os isotope ratios range to subchondritic ratios, from 0.13970 to 0.12485. We show that, at Corvo and Flores to the west of the MAR, an enriched mantle component is present that is similar to enriched mantle underneath the eastern islands. Yet, the highly enriched, EMII-type component found on São Miguel is absent in the western lavas.

However, simple mixing of a common Azores plume component with the local depleted mantle fails to fully explain the observed isotope-trace element relationships. Differences in Nb/Zr and Ta/Hf between islands east and west of the MAR indicate the presence of an additional mantle component that is largely absent in the east, or, that unusual conditions during partial melting prevail. The latter may promote pronounced fractionation of Zr and Hf from Nb and Ta, respectively. Interestingly, a similar enrichment of Nb-Ta over Zr-Hf has been observed in MORB from the MAR to the south of the Azores plateau [1], suggesting that this signature of the high field strength elements may be a feature of the regional north Atlantic mantle or that conditions during partial melting in ridge and plume-related settings can produce these unusual trace element signatures.

[1] Gale *et al* (2011), *Geochem Geophys Geosyst.* **12** (6).

A new insight of the role of the fluids below Victoria Land (Harrow Peaks, Antarctica)

GENTILI S.¹, COMODI P.¹, BONADIMAN C.²,
COLTORTI M.² BIAGIONI C.³ AND ZUCCHINI A.¹

¹Earth Sciences Dept., University of Perugia, (Italy)

²Earth Sciences Dept., University of Ferrara, (Italy)

³Earth Sciences Dept., University of Pisa, (Italy)

This contribution presents a mineralogical and petrological study of a new mantle xenoliths population NE of Harrow Peaks (HP, 74 02.785S 164 47.466E, q. 335m). Xenoliths are entrained in Cenozoic alkaline dykes and necks intruding consolidated tuffaceous sediments. They are mainly amphibole-bearing spinel harzburgites and lherzolites similar to those found at Baker Rocks [1]. The xenoliths range from protogranular to porphyroclastic and granoblastic in texture with a medium to coarse grain size. Mg [MgO/(MgO+FeO) mol%] of primary olivine and orthopyroxene range from 86.6 to 89.5 and from 87.8 to 90.5 respectively. The high Ni contents of olivine (NiO 0.31-0.46 wt%) associated with low mg values of a few harzburgites and lherzolites would suggest Fe enrichment in this mantle domain. Metasomatic textures are widespread with amphibole and phlogopite as newly formed hydrous (metasomatic) minerals. The former occurred both disseminated and in veins whereas phlogopite is found only as tiny disseminated crystals.

X-ray powder diffraction quantitative analyses by Rietveld method were performed to determine modal composition, including amorphous phases. Moreover a detailed crystal-chemical study was developed on amphibole by means of single crystal X-ray diffraction and in-situ major and trace element (including volatiles) analyses. Among the peridotite phases amphibole is the main volatile acceptor and its study contributes to decipher the role of water circulation during metasomatic process and its effects in controlling the mantle redox conditions. Amphiboles are paragonite in composition, with partial vacancy in A site and M4 site disordered with presence of Ca, Na and Fe²⁺. Relatively low concentration of Ti (Ti ≤0.35 a.f.u.), as well as structural data of M1 site, testify that amphibole was crystallized in a low aH₂O environment [2]. Taking into account that amphiboles is equilibrated with the anhydrous parageneses (at least for Fe/Mg and Ti), aH₂O will be constrained by the degree of amphiboles dehydrogenation, as well as by the water content in coexisting nominally anhydrous phases (olivines and pyroxenes).

[1] Coltorti *et al* (2004), *Lithos* **75**, 115-139; [2] Bonadiman *et al* (2013) CMP submitted.

Photochemistry of airborne dust produces nucleation events in the troposphere

Y. DUPART¹, S.M. KING¹, B. NEKAT², A. NOWAK²
A. WIEDENSOHLER², H. HERRMANN², G. DAVID³,
B. THOMAS³, A. MIFFRE³, P. RAIROUX³, B. D'ANNA¹,
AND C. GEORGE^{1,*}

¹Université Lyon 1, CNRS, UMR5256, IRCELYON,
Villeurbanne, F-69626, France

²TROPOS - Leibniz-Institute for Tropospheric Research,
Permoserstr. 15, D-04318 Leipzig, Germany

³LASIM, Université Lyon 1, CNRS UMR 5579,
Villeurbanne, France

Dust particles acts as a sink for many gases, such as sulfur dioxide. It is well known that SO₂ reacts on dust particle surfaces leading to the production of SO₄⁻.

It is known that light-driven reactions on dust particles containing TiO₂ or Fe(III) oxides produce OH radicals from water. These radicals can convert SO₂ adsorbed onto the particles into H₂SO₄, which stays on the particles.

Here, we show that OH radicals may leave the dust particles and go on to initiate gas-phase chemistry with gaseous SO₂.

To simulate such conditions, we shone light into a flow tube containing low concentrations of dust, along with water vapor and SO₂, and monitored the particle concentrations inside the tube.

Low dust concentrations are necessary for new particle nucleation; high dust concentrations would provide enough surface area for sulfuric acid to adsorb onto the dust, instead of nucleating aerosol. These findings are supported by recent field observations near Beijing and Lyon.

Adsorption of D-Ribose and inorganic phosphate on clay minerals – molecular stabilization and phosphate condensation

THOMAS GEORGELIN¹, MAGUY JABER¹
AND JEAN-FRANCOIS LAMBERT¹

¹Université Pierre et Marie Curie – UPMC Paris VI,
Laboratoire de Réactivité de Surface, CNRS, UMR
CNRS 7609, 4 place Jussieu, 75252 Paris Cedex 05,
France

Nucleotides and more broadly DNA and RNA play a fundamental role in anabolic metabolism and are considered as "high-energy" compounds. For this reason, their prebiotic formation pose a particular problem since their synthesis is thermodynamically uphill in aqueous solution and therefore forbidden. This is a significant question in the frame of the "RNA world" models, which explain later stages of evolution, but require the previous synthesis of nucleotides and thus phosphorylations. The possible role of mineral surfaces in prebiotic processes has been considered at least since the work of Bernal (1951). This idea has been tested for several prebiotic reactions, especially the condensation of peptide bonds from monomeric amino acids, but also for phosphorylations and phosphate polymerization. Even if such reactions on mineral surfaces have a significant potential for the formation of high-energy compounds, there is little consensus as to the fundamental mechanisms that are involved. In this context, the aim of our work is to enlighten the mechanism of adsorption of nucleobases, D-Ribose, nucleosides and inorganic phosphate on different mineral surfaces, mainly clays such as montmorillonite, saponite, hectorite, Laponite (R) and also on high-surface non-porous amorphous silica. The first results obtained by XRD, TGA, ³¹P and ²⁹Si NMR show that inorganic phosphate ions deposited on these surfaces condense to polyphosphates at considerably lower temperatures than in bulk KH₂PO₄. By co-adsorption of phosphate and a nucleoside, e.g. adenosine, it appears that some surfaces promote the phosphorylation of nucleosides in the same range of temperature. In separate experiments, D-ribose adsorption and stabilization were studied since the lack of stability of ribose is another problem for RNA world scenarii. Our results show a strong stabilisation of ribose by clays and amorphous silica. A similar stabilization has been previously observed with borate minerals, whose presence in prebiotic earth environment is however open to doubt. Thus, our study shows the first example of ribose stabilization by prebiotic minerals. Phosphorylation of the sugar was also observed.

Date them all: Re-Os ages for Upper Jurassic-Lower Cretaceous shales, ammonite zones and chrons

S.V. GEORGIEV¹, G. XU¹, H.J. STEIN^{1,2}, J.L. HANNAH^{1,2},
AND H.M. WEISS³

¹AIRIE Program, Colorado State University, USA

georgiev@colostate.edu (* presenting author)

²CEED Centre of Excellence, University of Oslo, Norway

³SINTEF Petroleum Research, 7465 Trondheim, Norway

Numerical ages of Upper Jurassic and Lower Cretaceous stages are derived mostly from correlation of magneto-stratigraphic patterns of Sub-Boreal and Tethyan ammonite zones to the M-sequence marine magnetic anomalies, coupled with constraints from cycle stratigraphy [1]. The ages for Late Jurassic polarity chrons, however, are ultimately based on a model for gradually increasing Pacific spreading rates from ~170 Ma to ~125 Ma that has only a few age constraints [1]. This sequence of correlations with little radiometric age control is further complicated by the extreme faunal provincialism during the late Jurassic.

Here we present Re-Os ages for organic-rich shale from the Upper Jurassic-Lower Cretaceous Hekkingen Formation in the Norwegian Arctic. Three intervals with detailed Boreal biostratigraphy yield isochrons with precision better than 1%, including the ¹⁸⁷Re decay constant uncertainty. In the Nordkapp Basin, the base of the section in the *A. serratum* Zone (correlated with the Tethyan *P. bifurcatus* Zone, chron M29r) yields a late Oxfordian age of 157.8 Ma. In the Troms III locality to the SW, an interval in the *A. Subkitchini* Zone (correlated with the Tethyan *S. Platynota* Zone, chron M25) yields a Kimmeridgian age of 154.7 Ma. The top of the section at Troms III is no older than the Sub-Boreal *H. kochi* Zone (correlated with the Tethyan *S. boissieri* Zone, chron M16). Combined with the top of the Nordkapp Basin section, these samples yield a Valanginian age of 137.8 Ma. In addition, shales from the *A. eudoxus* or *A. autissiodorensis* Zones (Tethyan *H. beckeri* or *H. hybonotum* Zones, chron M23 or M22A) yield a less precise Tithonian (?) age of 150.3 Ma. Published Late Jurassic Re-Os ages [4,5] are critically evaluated and integrated with our new ages to refine the time scale for Upper Jurassic-Lower Cretaceous stages.

Funding: CHRONOS project (Lundin Norway AS, Eni Norge AS, and Det Norske ASA) and NRC Petromaks project 180015/S30.

[1] Gradstein *et al* (2012) *GTS 2012*; [2] Wierzbowski and Smelror (1993) *Acta Geol. Pol.* **43**, 229-249; [3] Smelror *et al* (2001) *NPF Spec. Publ.* **10**, 211-232; [4] Selby (2007) *Norw. J Geol.* **87**: 291-299; [5] Cohen *et al* (1999) *EPSL* **167**, 159-173.

Micromorphology investigations by imaging alteration, supergene and anthropogenic processes in regoliths

MARTINE GÉRARD^{1*}, LUCA TROMBINO²,
FLORA BOEKHOUT¹, AISHA KANZARI¹,
JEAN CLAUDE PARISOT³ AND GEORGES STOOPS⁴

¹IMPMC., Université P&M Curie, IRD, France,

martine.gerard@impmc.upmc.fr,

flora.boekhout@impmc.upmc.fr,

aisha.kanzari@impmc.upmc.fr (*presenting author)

²Università degli Studi di Milano, Italy,

luca.trombino@unimi.it

³IRD, CEREGE, Aix en Provence, France, parisot@cerege.fr

⁴Ghent University, Belgium, georges.stoops@ugent.be

Micromorphological investigations on undisturbed samples by microscopic and ultramicroscopic techniques allow us to interpret the processes behind the formation of regoliths, sediments and anthropogenic deposits. Keywords are fabric, groundmass composition, microstructures and pedo/biofeatures.

The composition of the micromass represents a record of the processes of alteration leading to regolith formation. The groundmass consists of fine (micromass) to coarse constituents organised with a specific spatial distribution and varying types of preservation history. Investigating the groundmass thus provides clues on the paleoenvironmental conditions, the different genetic processes behind rock and soil formation (supergene, low T hydrothermal, anthropogenic) and their impact on ecosystems or paleoenvironment.

Improvements in electron microscope imaging technology now permits us to make detailed micromorphological observations up to the nanoscale (previously limited to microscale) : another domain of observations is open in the micromass to the micromorphologists. Optimisation of the microgeochemical mapping technique is another powerful tool to gain insight in chemical migration fronts. Limits concerning homogenisation of the fabric and disappearance of rock fabric may be bypassed. However, if this new detailed information is not linked to petrographic macroscopic evidence and field observations, the analyses may remain ambiguous.

Different petrographic and electronic images of the mineral paragenesis in the micromass associated to their microgeochemical characteristics will be discussed. Examples will be given of the climatic record of different paleosoils, the impact of previous hydrothermal alteration on saprolites, the evolution of the weathering process, and neo-formation of minerals related to weathering and protosoil formation in mining waste rock piles.

He diffusion on apatite viewed by microbeam ERDA and RBS experiments

C. GERIN^{1*}, E. OLIVIERO², C. BACHELET²,
L. TASSAN-GOT³ AND C. GAUTHERON^{1*}

¹UMR IDES – CNRS-UPS, Orsay, France

(*correspondance: cecile.gautheron@u-psud.fr)

²CSNSM-CNRS/UPS (oliviero@csnsm.in2p3.fr,
bachelet@csnsm.in2p3.fr)

³IPN/CNRS-UPS, Orsay, France (tassango@ipno.in2p3.fr)

The perfect knowledge of the helium diffusion behavior in minerals is a key issue to interpreted thermochronological (U-Th)/He ages. Indeed, He age is the interplay between alpha particle accumulation produced during radioactive decay in a crystal and its diffusional loss by thermally activated diffusion. In apatite, recoil damage accumulation during α -decay is function of their production via the effective U content and their annealing [1,2,3], which depends on the temperature and grain chemistry.

The recoil damaging has been recognized has as playing an important role in helium diffusion but its annealing rate combined with the grain chemistry need to be explored. For this purpose, dedicated experiments are conducted by using microbeam ERDA (Elastic Recoil detection analysis) coupled to RBS (Rutherford Backscattering (Spectroscopy) analysis on macro apatite crystals of different compositions. He atoms have been implanted ion polished crystal at 15 keV, (mean projected range of 120 nm) deep and fluences of 10^{17} to 10^{16} He/cm²beam intensity., and the He front is plumbed with in the ERDA experiments using a 15°-15° angle after implantation and different annealing temperature heating steps. RBS and ERDA experiments are conducted on the same grain to characterize the possible effect of natural damage, induced irradiation damages and amorphization for the irradiation higher fluencedose.

ERDA and RBS analyses have been validated for apatite by Ouchani *et al* [4], giving us the possibility to extend diffusion studies toward low temperatures which are hardly attained in experiments based on in-vacuum release. In addition, the irradiation effect on the crystal surface is investigated by AFM to characterize possible high damage zones and possible amorphization. Preliminary ERDA results confirm the influence of damage and the grain chemistry on He diffusion.

[1] Gautheron et al (2009) *Chem. Geol.* **266**, 166-170.

[2] Shuster & Farley (2009) *Geochim. Cosmochim. Acta* **73**,

183-196. [3] Gautheron et al (2013) *Basin Research*,

10.1111/bre.12012. [4] Ouchani et al (1998) *Applied*

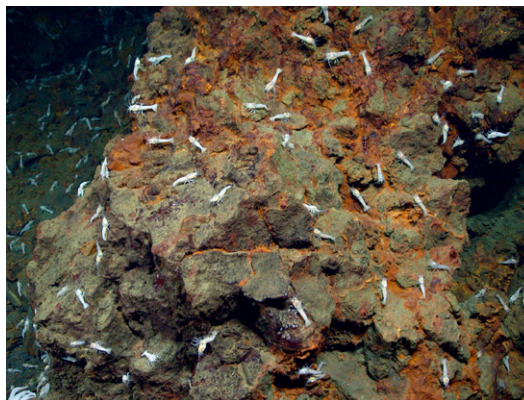
Geochemistry Geochem **13** (6), 707-714.

Hydrothermal exploration of mid-ocean ridges: Where might the largest sulfide deposits occur?

CHRISTOPHER R GERMAN¹

¹Woods Hole Oceanographic Institution, MA 02543, USA
(cgerman@whoi.edu)

Hydrothermal activity occurs along all mid-ocean ridges, and in all ocean basins. In this paper I will review what is currently known about worldwide distributions of active venting and how that knowledge has evolved since the first discovery of submarine hydrothermal activity in the late 1970s. I will pay particular attention to the case of slow spreading ridges and discuss the extent to which the incidence of high-temperature venting along such ridges might appear anomalously high when compared to the available magmatic heat budget and whether this may be attributable to a difference in the partitioning of hydrothermal heat fluxes between focussed and diffuse flow, at fast- and slow-spreading ridges. Developing this theme, I will discuss the importance of tectonically-hosted hydrothermal fields on slow spreading ridges as locales at which high-temperature fluid flow and associated polymetallic sulfide deposition can be sustained over thousand year time-scales – significantly longer than the perceived decadal lifetimes of vent-sites along fast-spreading ridges. Finally, I will close with a consideration of ultra-slow spreading ridges where venting is also now known to be widespread but where very few active vent-sites have yet been tracked to source. Surprisingly, on these ultra-slow spreading ridges, our preliminary evidence reveals that even neovolcanically hosted hydrothermal fields can apparently be sustained at any one site over sufficiently long time-scales that large polymetallic sulfide deposits can become established.



Coupled cycling of Fe and C_{org} in submarine hydrothermal systems: an ocean biogeochemistry perspective.

CHRISTOPHER R. GERMAN¹, LOUIS LEGENDRE^{2,3},
SYLVIA G. SANDER⁴, NADINE LE BRIS^{5,6}
AND SCOR WORKING GROUP¹³⁵

¹Woods Hole Oceanographic Institution, Woods Hole, USA
(cgerman@whoi.edu)

²Université Pierre et Marie Curie 6, Laboratoire
d'Océanographie de Villefranche, France (legendre@obs-
vlfr.fr)

³CNRS, Laboratoire d'Océanographie de Villefranche, France
(legendre@obs-vlfr.fr)

⁴University of Otago, Dunedin, New Zealand
(sylvia.sander@otago.ac.nz)

⁵Université Pierre et Marie Curie Paris 6, Observatoire
Océanologique de Banyuls sur Mer, France (lebris@obs-
banyuls.fr)

⁶CNRS, Observatoire Océanologique de Banyuls sur Mer,
France (lebris@obs-banyuls.fr)

Submarine hydrothermal venting was first discovered in the late 1970s. For decades the potential impact that vent-fluxes could have on global ocean budgets was restricted to consideration of processes in hydrothermal plumes in which the majority of chemical species are incorporated into polymetallic sulfide and/or oxyhydroxide particles close to the ridge-crest and sink to the underlying seafloor. This restricted view of the role that hydrothermal systems might play in global-ocean budgets has been challenged, more recently, by the recognition that there might also be a significant flux of *dissolved* Fe from hydrothermal systems to the oceans that is facilitated through organic complexation. In this paper we review field-based and modeling results, including investigations that we have carried out under the auspices of SCOR-InterRidge Working Group 135, that reveal potential relationships between C_{org} and Fe in hydrothermal plumes, and indicate that hydrothermal systems may play significant roles in both the global biogeochemical Fe cycle and the global ocean carbon cycle.

Vulnerability of soil carbon release with increasing temperature in tropical montane forests

F. GERSCHLAUER*, K. BUTTERBACH-BAHL
AND R. KIESE

Karlsruhe Institute of Technology, IMK-IFU, 82467

Garmisch-Partenkirchen, Germany (*correspondence:
friederike.gerschlaue@kit.edu, klaus.butterbach-
bahl@kit.edu, ralf.kiese@kit.edu)

Changes in terrestrial ecosystems due to shifts in climate occur in many dimensions, and include changes in the biogeochemical cycle of carbon (C) amongst others. Tropical montane ecosystems and their supportive ecosystem processes are particularly vulnerable to global warming [1, 2]. Soils from tropical forests are known to have significant effects on the global carbon cycling and climate [3] but data of these feedbacks are still scarce, for Africa in particular.

In a long term incubation experiment we investigated how increasing temperature affects soil carbon release of four different montane forest ecosystems. The Lower montane, *Ocotea*, *Podocarpus* and *Erica* forests are located along an altitudinal gradient at Mt. Kilimanjaro, Tanzania, between 1900 and 3800 m a.s.l. Soils (0-10cm and 10-30cm) of the respective sites were incubated at 15 and 25°C and 60% water holding capacity over a year's period.

Preliminary results demonstrate that at all sites at both temperatures soil from 0-10cm released more CO₂ than from 10-30cm, with exception of the *Erica* forest where 0-10 and 10-30cm had equal production rates of CO₂ at 15°C. At the first weeks of incubation soils of all sites have been very active and magnitude of cumulative CO₂ release was highest in *Ocotea* and *Erica*, medium in the Lower montane and lowest at the *Podocarpus* forest. Comparing the release of soil carbon at temperatures approx. 10°C higher than site specific mean annual temperature revealed the same order. This indicates that the *Ocotea* and *Erica* forest are of higher risk in loosing soil carbon due to increasing temperatures with climate change.

[1] Laurence *et al* (2011) *Biol. Cons.* **144**, 548-557. [2] IPCC (2007). [3] Malhi (2010) *Curr Opin in Environ Sus* **2**, 237-244.

Age and matter sources of ophiolites of the Kuznetsk Alatau, SW Siberia: New Sm-Nd isotope data

I.F. GERTNER^{1*}, T.B. BAYANOVA², T.S. KRASNOVA¹,
N.A. DUGAROVA¹, V.V. VRUBLEVSKII¹
AND G.R. SAYADYAN³

¹Tomsk State University, Russia (*labspm@ggf.tsu.ru)

²Cola Science center of RAS, Apatity, Russia

³Far East Geological Institute of RAS, Vladivostok, Russia

Ophiolites of the Kuznetsky Alatau Ridge are an ancient suture zone formed as a result of the collision of few arc island terrains on the active margin of Siberian continent during the Late Cambrian time (~500 Ma). One of typical ophiolite fragments of this region is the association of ultrabasic and basic rocks of the Barkhatnaya, Zayachiya, Severnaya, and Zelenaya mountain apexes. It is an arc-like structure, where ultrabasites are in the rims and basites are in the core. According to regional geological conclusions, the temporal range of ophiolite forming is from Early Cambrian to Late Riphean time. Our new data of Sm and Nd isotopes for the whole rocks of mantle hyperbasites and ultramafic-mafic rocks are close to the most ancient time of these rocks.

The Sm-Nd isochron based on the four whole rock samples of harzburgite, chromitite and dunite (from the Barkhatnaya apex) has a slope corresponding to the age 950±59 Ma at MSWD = 0.968 and $\epsilon_{\text{Nd}}(T) = +9.5$. The 7-point regression line based on the whole rocks magmatic peridotites and gabbroids of toleitic series is demonstrated the closed temporal interval. Its slope corresponds to the age 937±50 Ma at MSWD = 0.966 and $\epsilon_{\text{Nd}}(T) = +7.8$. The restitic ultrabasites of the Barkhatnaya apex correspond to the characteristics of the strongly depleted backarc basin -type mantle substrate whereas magmatic rocks of internal part are similar to MOR-type crust. Rocks of dike-type complex from the Barkhatnaya apex have a more young age of formation and metamorphism. The slope of Sm-Nd isochron based on the two whole rock samples and two mineral separates of diabasites corresponds to the age 679±34 Ma at MSWD = 1.86 and $\epsilon_{\text{Nd}}(T) = +8.2$. Harzburgites of the Severnaya and Zelenaya apexes are characterized a wide diapason of Nd-isotope ratios that show a contamination of mantle substrate by crust fluid matter during the recrystallization of these obduction in upper crust. According to the rate of syntectonic recrystallization of rocks the range of $\epsilon_{\text{Nd}}(T)$ parameters are changed from +7.96 to -6.51.

This study was funded by the Russian Ministry of Education and Science (projects 5.3143.2011, 14.B37.21.1257).

On the origins of Platinum-Group Minerals in ophiolitic chromitites

*F. GERVILLA¹, W.L. GRIFFIN²,
J.M. GONZÁLEZ-JIMÉNEZ², J.A. PROENZA³,
SUZANNE.Y. O'REILLY² AND N. J. PEARSON²

¹Dpt. Mineralogy & Petrology (UGR-IACT), Granada, Spain
(*correspondence: gervilla@ugr.es)

²GEMOC ARC National Key Centre, Sydney, Australia.
bill.griffin@mq.edu.au; jose.gonzalez@mq.edu.au;
sue.oreilly@mq.edu.au; norman.pearson@mq.edu.au

³Dpt. Crystallography, Mineralogy & Mineral Deposits (UB),
Barcelona, Spain (japroenza@ub.edu)

Platinum-Group Minerals (PGM) commonly occur as solid inclusions in chromitites hosted in the mantle section or the mantle-crust transition of ophiolite complexes. The most widely accepted idea is that PGMs now encased in larger chromite crystals precipitated from melts and were later mechanically trapped by growing chromite. This hypothesis, traditionally accepted by many authors, has been sustained until now on the basis of morphological features of the PGMs in the chromitites. This approach does not provide a satisfactory explanation for the PGMs beyond determining *empirically* the T - fS_2 conditions for their crystallisation from the melts that also precipitated the host chromitite. The key question of how the PGMs form and why they are found in the chromitite remains unresolved.

A major breakthrough in our understanding of the relationships between the chromitites and their enclosed PGM has come in the last few years, through new experimental data and the *in situ* analysis of Os isotopes by laser-ablation ICPMS analysis [1] Integration of these advances, a re-interpretation of the microstructures and the Os-isotope analyses of individual PGMs suggest several different origins for the PGMs in chromitites: (1) most suites of PGMs mainly record crystallisation during mixing of multiple batches of isotopically distinct melts, followed by physical entrapment in chromite; (2) some PGMs in chromitites may have been scavenged from wall-rock peridotites during migration of the parental melts of the chromitites through the mantle; (3) other platinum-group minerals may have precipitated from metasomatic fluid and/or melts that infiltrated existing chromitites. All of these processes may be required to explain the presence in the chromitites of micrometric PGMs with distinct Os-isotope compositions.

[1] González-Jiménez *et al* (2012). *Chemical Geology* **291**, 224-235.

Establishing the Magnesium isotope ($\delta^{26}\text{Mg}$) signature of early and late diagenetic dolomite types

A. GESKE^{1*}, R. GOLDSTEIN², D.K. RICHTER¹, D. BUHL¹, T. KLUGE³, C.M. JOHN³ AND A. IMMENHAUSER¹

¹Ruhr-University Bochum, Institute for Geology, Mineralogy and Geophysics, Universitätsstraße 150, 44801 Bochum, Germany (*correspondence: anna.geske@rub.de)

²University of Kansas, Department of Geology, 1450 Jayhawk Blvd., Lawrence, KS 66045, USA

³Imperial College London, ESE Department, Prince Consort Road, SW7 2BP London, United Kingdom

The Magnesium isotopic composition has been established as a paleo-climate/paleo-weathering proxy in marine and terrestrial carbonate precipitation environments. Precipitation kinetics of dolomites and dolomite precipitation models, which relate to their diagenetic environments and the commonly complex fluid chemistry, are under debate. Any independent geochemical evidence, such as specific dolomite $\delta^{26}\text{Mg}$ signatures characterizing specific dolomite formation realms, has the potential to add a valuable additional interpretation tool. This study represents a considerable advance in dolomite Mg isotope research and reviews data from previous research studies. In addition, we took advantage of well-established isotope systems in order to establish a detailed diagenetic history of each sample investigated. Proxies included oxygen ($\delta^{18}\text{O}$), carbon ($\delta^{13}\text{C}$) and strontium ($^{87}\text{Sr}/^{86}\text{Sr}$) isotopes as well as main and trace element abundances. Our data indicate that there is no unambiguous Mg isotopic pattern that characterizes specific dolomite types. At present, it seems obvious, that magnesium isotope values of different dolomite types are controlled by a complex array of factors. Burial dolomites display the widest isotope range observed. Obviously, in the burial domain, the temperature of the precipitating fluid is of interest. Therefore, we applied clumped isotope thermometry (Δ_{47}) to burial dolomites displaying end-member Mg isotope values. Our preliminary data set reveals a fair correlation between burial fluid temperature and dolomite Mg isotope signature. As the clumped isotope closure temperature for dolomite is not established yet, this could represent an interesting contrast to recent work [1] documenting that earliest diagenetic sabkha dolomites homogenized under burial temperatures of up to 450°C. The tentative working hypothesis is that the temperature of the precipitating burial fluid affects, amongst other factors, dolomite $\delta^{26}\text{Mg}$ signatures.

[1] Geske *et al* (2012) *Chem. Geol.* **332-333**: 45-64.

Natural $\text{BaCa}_6[(\text{SiO}_4)(\text{PO}_4)](\text{PO}_4)_2\text{F}$ with a new modular structure type

FRANK GFELLER¹, EVGENY V.GALUSKIN², IRINA O. GALUSKINA², THOMAS ARMBRUSTER¹, YEVEGENY VAPNIK³, ROMAN WŁODYKA² AND PIOTR DZIERŻANOWSKI⁴

¹Mineralogical Crystallography, Institute of Geological Sciences, University of Bern, Freiestr. 3, CH-3012 Bern, Switzerland

²Faculty of Earth Sciences, Department of Geochemistry, Mineralogy and Petrography, University of Silesia, Będzińska 60, 41-200 Sosnowiec, Poland

³Department of Geological and Environmental Sciences, Ben-Gurion University of the Negev, P.O.B. 653, Beer-Sheva 84105, Israel

⁴Institute of Geochemistry, Mineralogy and Petrology, Warsaw University, al. Żwirki i Wigury 93, 02-089 Warszawa, Poland

⁵Systematic Mineralogy, 44, 11th line V.O. apt. 76, Saint-Petersburg 199178, Russia

$\text{BaCa}_6[(\text{SiO}_4)(\text{PO}_4)](\text{PO}_4)_2\text{F}$ (space group *R-3m* (No.166) $a = 7.09660(10)$ Å, $c = 25.7284(3)$ Å, $Z = 3$), a not yet approved new mineral, has recently been found enclosed in paralavas confined to pyrometamorphic rocks of the Hatrurim formation, Israel.

The structure of it is easiest described as a 1:1 stacking of the two modules (1) $\{\text{Ca}_6(\text{T}^{4.5+}\text{O}_4)_2\text{F}\}^{4+}$ and (2) $\{\text{Ba}(\text{T}^{5+}\text{O}_4)_2\}^{4-}$ along the *c*-axis. Module (1) consists of close packed sevenfold coordinated Ca with (SiO_4) and (PO_4) tetrahedra filling the gaps. F is surrounded by 6 Ca atoms forming almost perfect octahedra. Module (2) is characterized by (PO_4) tetrahedra connected to sixfold coordinated Ba.

The modular stacking of $\text{BaCa}_6[(\text{SiO}_4)(\text{PO}_4)](\text{PO}_4)_2\text{F}$ presents a new structure type. The only mineral with related structure we are aware of is nabimusaite $\text{K}(\text{Ca}_{12}(\text{SO}_4)_2(\text{SiO}_4)_2)\text{O}_2\text{F}$ (space group *R-3m*, $a = 7.1905(4)$, $c = 41.251(3)$ Å, $Z = 3$) [1]. The structure of its synthetic analog has been reported before and is characterized by a 2:1 stacking of modules similar to those of $\text{BaCa}_6[(\text{SiO}_4)(\text{PO}_4)](\text{PO}_4)_2\text{F}$ but with different cations [2].

[1] Galuskin, E.V. *et al* (2013) *Min. Mag.*, **77**, 1-12. [2] Fayos, J. *et al* (1985) *Acta Cryst.*, **C41**, 814-816.

^{238}U - ^{234}U - ^{230}Th - ^{226}Ra systematics in fossil scleractinian corals

BASSAM GHALEB¹, SÉBASTIEN HUOT¹
AND CLAUDE HILLAIRE-MARCEL¹

¹GEOTOP and, département de Science de la Terre et de l'Atmosphère, Université du Québec à Montréal, Succ. Centre-Ville, Montréal, QC, H3C 3P8, Canada

The ^{230}Th -U dating method is widely used to date reef and deep-sea scleractinian (aragonitic) corals. The method relies on the assumption is that the sample remained in a closed radioactive system with respect to U and Th isotopes through time. This assumption is usually tested through mineralogical examination of the sample (i.e., through the absence of any diagenetic/secondary calcite) and the comparison of its initial $^{234}\text{U}/^{238}\text{U}$ activity ratio [$(^{234}\text{U}/^{238}\text{U})_0$], with that of the global oceanic $^{234}\text{U}/^{238}\text{U}$ activity ratio [$(^{234}\text{U}/^{238}\text{U})_{\text{marine}}$]. However, Pons-Branchu *et al.* [1] have shown that this assumption can be violated when a coral experienced an early diagenetic evolution. This results in slight ^{230}Th ages offsets without significant shifts in the initial $^{234}\text{U}/^{238}\text{U}$, due to the fact that the early diagenetic and syngenetic U-phases had a nearly similar isotopic signature. More commonly, discrete redistribution of U-series isotopes occur through time. When they result in $(^{234}\text{U}/^{238}\text{U})_0$ offsets vs [$(^{234}\text{U}/^{238}\text{U})_{\text{marine}}$], age correction models have been proposed (e.g., U-trend; Thompson *et al.*)[2]. We already proposed to use ^{226}Ra to document the relative closure of radioactive system in the ~ 10-50 ka range, through a $^{226}\text{Ra}/^{230}\text{Th}$ vs $^{230}\text{Th}/^{234}\text{U}$ pseudo-concordia approach (Hillaire-Marcel *et al.*, 2006)[3]. Here we demonstrate that slight disequilibria between $^{226}\text{Ra}/^{230}\text{Th}$ are generally observed in fossil corals of all ages, notably from the last interglacial and point to some Ra-U mobility in their aragonitic skeleton at least during the last 50 ka, thus likely earlier. We will also examine the impact of such isotopic offsets on the calculated ^{230}Th -U ages and estimate the usefulness/validity of age-corrections based on linear trend intercepts with concordia curves.

[1] Pons-Branchu *et al.* 2005, doi:10.1016/j.gca.2005.06.011.
[2] Thompson *et al.* 2003, doi:10.1016/S0012-821X(03)00121-3. [3] Hillaire-Marcel *et al.* 2006, doi:10.1016/j.gca.2006.06.506.

Geochemical considerations of the gehlenitic skarns from Valea Crişenilor – Oraviţa (Romania)

C.GHINET^{1*}, ŞT.MARINCEA¹, E. BILAL²
AND A.M. IANCU¹

¹Department INI, Geological Institute of Romania, 1 Caransebeş Str., RO-012271, Bucharest, Romania
(*correspondence: cristina.ghinet@igr.ro)

²Centre SPIN, Ecole Nationale Supérieure des Mines de Saint-Etienne, 158, Cours Fauriel, F-42023 Saint-Etienne Cedex 2, France (bilal@emse.fr)

A shallow-level pluton of Late Cretaceous age, belonging to the “banatic” magmatic and metallogenetic belt, caused extensive contact metamorphism of Cretaceous limestones and marls sequences in the Oraviţa area. In Valea Crişenilor, a small elongate apophysis of this pluton mainly dioritic, with some variations toward quartz diorite and monzonite, intruded a series of calcareous deposits of Crivina Formation deposited in Reşiţa anticlinorium. The intruded formations experienced an extended contact metamorphism with local generation of high-temperature mineral species.

The observed mineral assemblages reflect a wide range of temperature and fluid-composition space. In this respect, the metamorphic peak assemblages in the calcite-saturated rocks include wollastonite, melilite, ellestadite-(OH), titanian grossular and scarce spurrite. The estimated equilibrium temperature for this mineral assemblage is about 820-870°C with a C-rich, internally buffered pore-fluid. The aperature and infiltration of the C-poor fluids, triggering the formation of retrograde mineral assemblages comprising monticellite, vesuvianite, grandite garnets, diopside, clintonite. These assemblages formed probably near 600°C. A low-temperature retrogression affected the previous mineral paragenesis producing scawtite, hydrogrossular, hibschite, xonotlite, thomsonite.

As it is expected, the intensity of the contact metamorphism decreases from the innermost to the outermost parts of the aureole. In this respect, the mineral reactions involving carbonate and silicate minerals led to the formation of various of Si-poor silicates, but rich in Al and Ti oxides, while the next skarn zone can be circumscribed to a Si-, Mg-rich and Al-poor geochemical system, marked by the formation of gehlenite, vesuvianite ± wollastonite, garnet.

The Ca-Si ratio value is close to that of Mg-Si, suggesting a weak circulation of the fluids and a thermodynamic closed system, followed by the retrograde stage, marked by a high mobility of the chemical elements into an open system.

The future of thermodynamic databases: Community driven data systems fueled by the geoinformatics revolution

M.S. GHIORSO¹

¹OFM Research, 7336 24th Ave NE, Seattle, WA 98115, USA
(*correspondence: ghiorso@ofm-research.org)

Internally consistent thermodynamic databases are critical community resources that facilitate the calculation of heterogeneous phase equilibria and thereby support geochemical, petrological, and geodynamical modeling. These “databases” are actually derived data/model systems that depend on a diverse suite of physical property measurements, calorimetric data, and experimental phase equilibrium brackets. In addition, such databases are calibrated with the adoption of various models for extrapolation of heat capacities and volumetric equations of state to elevated temperature and pressure conditions. Finally, these databases require specification of models for the mixing properties of solid, liquid, and fluid solutions, which are often rooted in physical theory and, in turn, depend on additional experimental observations. The process of “calibrating” a thermochemical database involves considerable effort and an extensive computational infrastructure. Because of these complexities, the community tends to rely on a limited number of thermochemical databases, generated by a few researchers; these databases are often out-of-date and are universally difficult to maintain. Their longevity is generally linked to that of their creators.

Geoinformatics is poised to alter the manner in which thermodynamic databases are created, maintained, tailored, and applied. By making underlying data resources universally available, and by focusing development on a generalized web-based computing infrastructure that permits a wider community of users to evaluate those data in an internally consistent and thermodynamically rigorous context, the generation of thermodynamic data/model collections can be made more transparent and spontaneous. Through automated generation of web services that standardize the linkage between thermochemical databases and the geochemical, petrological, and geodynamical models they serve, the lag time between generation and evaluation can be shortened and a broader community of users can be empowered to participate in model creation and evaluation. A prototype system that embodies this approach to thermochemical database construction will be demonstrated. Requirements for broad-based application of this geoinformatics architecture will be discussed.

Neoproterozoic granites of Sharm El-Sheikh area, Egypt: Mineralogical and geobarometric variations

MOHAMED FOUAD GHONEIM,
BOTHINA TAHA EL DOSUKY,
MOHAMED THARWAT HEIKEL, TAMER ABU-ALAM* AND
MAHMOUD SHERIF.

¹(ghoneimf@science.tanta.edu.eg)

Sharm El-Sheikh District, south Sinai, includes representative granitic outcrops. Mineral of the hosted granites are analyzed to elucidate geobarometric variation, which could prove their evolution. The amphiboles classified as calcic and alkali amphiboles. The calcic amphiboles are Ferro-edenite while the alkali amphiboles are typically riebeckite. Amphiboles varieties are of magmatic nature. Biotites encountered mostly in monzogranites and syenogranites. They classified as merxene (Mg-rich varieties). They pertain to metamorphic-metasomatic types. Biotites have calc-alkaline affinity for the syenogranites and monzogranites. Feldspars have albite and orthoclase end-members. Coexisting amphiboles and plagioclase are used to estimate the physicochemical parameters of their crystallizing parent magma. It is clarified that syenogranites underwent temperature and pressure of formation ranges of 520-730 °C; <3 kbars. The alkali feldspar granites record 450-830 °C; <4 kbars. The riebeckite-bearing granites record the lowest temperature condition among all varieties since it estimate formation at 350-650 °C; <4 kbars.

Spatial dispersion at a watershed scale of some mining-originated metals in various solid materials

S. GHORBEL^{1*}, A. COURTIN-NOMADE¹, B. POATY¹,
C. GROSBOIS² AND M. SOUBRAND¹

¹University of Limoges, GRESE, FST, 123 avenue A. Thomas, 87060 Limoges Cedex France.

(*correspondence : sonda.ghorbel@hotmail.fr,
alexandra.courtin@unilim.fr, nedvyp@yahoo.fr,
marilyne.soubrand@unilim.fr)

²University of Tours, EA 6293 GeoHydrosystemes
Continentaux, Parc de Grandmont. 37200 Tours, France
(cecile.grosbois@univ-tours.fr)

River sediments in the french Massif Central, the largest metallogenic area in France, are ones of the most mining-impacted. The study area belongs to the Loire River basin, the largest french basin. This study deals with a former Ag-Pb mining district (Miodet sub-basin, 30 km long and 100 km²) located in the upstream part of the Loire catchment. The french Massif Central was the first area for Ag-Pb production in France. Mining activities in the studied district lasted between 1873 and 1901 and generated waste materials which constitute today dumps on ~ 24,600 m². Around 6000 t of Pb and 6 t of Ag were extracted during that period. Nowadays 100,000 m³ of tailings are still exposed to atmospheric conditions, overhanging the Miodet River.

Both tailings, located upstream of the Miodet watershed, and sediments, collected all along the river, have been sampled to evaluate the spatial dispersion of various metals (especially As, Fe, Mn, Pb and Zn) at a basin scale, 100 years after the end of mining activities. In addition, the aim of this study is to evaluate the accumulation and stability of the metal host phases within the Miodet River as well as to estimate how the anthropogenic activities infer on metals dissemination. The use of complementary approaches (Fig. 1) allow determining the partitioning and the post-depositional redistribution (mobilization/sequestration) of metals and metalloids as well as to assess their mobility.



Figure 1: Diagram presenting the applied methodology.

³⁴S enrichment during chemotrophic sulfur oxidation by bacteria

WRIDDHIMAN GHOSH¹, MASRURE ALAM¹
AND ANINDA MAZUMDAR²

¹Bose Institute, Kolkata - 700054, India

²National Institute of Oceanography, Goa - 403004, India

The three distinct proteobacteria *Paracoccus pantotrophus* (*Pp*), *Tetraethiobacter kashmirensis* (*Tk*) and *Thiomicrospira crunogena* (*Tc*) unanimously rendered kinetic enrichment of ³⁴S in the end product sulfate (SO₄²⁻) (overall fractionation ranged between -4.6‰ and +5.8‰) during chemolithotrophic oxidation of thiosulfate (S₂O₃²⁻) or tetrathionate (S₄O₆²⁻). *Pp* uses the Sox multienzyme system to oxidize S₂O₃²⁻ (but not S₄O₆²⁻) to SO₄²⁻ without any intermediate formation. *Tk* oxidizes S₄O₆²⁻ directly to SO₄²⁻, but its S₂O₃²⁻ oxidation proceeds via S₄O₆²⁻ formation. *Tc*, in its turn, oxidizes S₂O₃²⁻ to SO₄²⁻ by depositing extra-cellular elemental sulfur under low pH and oxygen. Molecular biology of sulfur oxidation in the last two species is ill-defined, even though both of them possess *sox* gene homologs in their genomes. All the studied processes were found to start with +ve Δ³⁴S values, subsequent to which (owing to Rayleigh fractionation) Δ³⁴S approached zero as δ³⁴S of produced SO₄²⁻ came close to δ³⁴S of the substrate S₂O₃²⁻/S₄O₆²⁻. In *Pp* and *Tc*, as the reactions progressed, Δ³⁴S_{thiosulfate-sulfate} values became -ve owing to continued ³⁴S enrichment in SO₄²⁻. Apparent physiological disparities notwithstanding, all the three bacteria exhibited analogous ³⁴S fractionation kinetics during S₂O₃²⁻ oxidation (and also S₄O₆²⁻ oxidation in case of *Tk*), with ³⁴S enrichment rates observed during their peak sulfate-producing stages being almost identical. This indicated the potential involvement of identical S-S bond-breaking enzymes in all these processes. Concurrent proteomic analyses detected the hydrolase SoxB in the actively sulfate-producing cells of all three species. Inducible expression of *soxB* was also observed during S₄O₆²⁻ oxidation by *Tk*, which was particularly interesting because the established Sox pathway has not yet accommodated S₄O₆²⁻ as a substrate. Notably however, no other Sox protein except SoxB was detected in lithotrophically-growing *Tk* cells even after proteomic scanning of its entire peptide map. Instead, several other redox proteins were found over-expressed during S₂O₃²⁻/S₄O₆²⁻ dependent growth, thereby indicating that there is more to S₄O₆²⁻ oxidation than SoxB alone.

The effects of sulfide and sulfate ions on degradation kinetics of chlorinated organics by nanoscale zero valent iron

S. GHOSHAL* AND C. R. SAI RAJASEKAR

¹Dept. of Civil Engineering, McGill University, Montreal, QC H3A 2K6, Canada

(*correspondence: subhasis.ghoshal@mcgill.ca)

A promising technology for the clean-up of aquifers contaminated by toxic chlorinated organic compounds is the sub-surface injection of nanoparticles of zero valent iron (NZVI) into the contaminated zones to enable rapid, *in situ* destruction of chlorinated compounds to non-toxic end products via surface-mediated electron transfer and hydrogenation reactions. However, iron oxide shells form readily on the surface of the NZVI which may reduce its reactivity over time. Although several studies have examined the reactivity of NZVI to chlorination aliphatic pollutants, there is limited knowledge on the effects of natural groundwater ions on the surface chemistry and reactivity of NZVI to target pollutants. In this study we show that sulfide and sulfate ions, which are ubiquitous in groundwater environments, may significantly alter the reactivity of NZVI.

Sulfide and sulfate ions readily react with NZVI in solution to form various iron sulfide precipitates on the NZVI surface. An FeS coating NZVI enhances the ability of the NZVI to degrade chlorinated organic compounds due to the creation of a conductive outer layer that efficiently transfers electrons from the electron rich core of the zero valent iron nanoparticle. Our studies show that the reactivity of the NZVI-FeS was distinct from the reactivity of pure FeS. Rapid dechlorination of trichloroethylene (TCE) was observed particularly at lower concentrations of sulfide (~ 2 mM). The first order TCE degradation rate constant increased from 0.013 hr⁻¹ for NZVI only to 0.432 hr⁻¹ NZVI reacted with sulfide. The surface morphology and chemistry of NZVI reacted with sulfide and sulfate were studied using TEM-EDX and X-ray photoelectron spectroscopy (XPS), and these techniques confirmed the presence of FeS at the surface and provided data on the spatial distribution of FeS. Particle size measurements by nanoparticle tracking analysis showed no observable change in the average hydrodynamic diameter of bare NZVI and NZVI reacted with sulfide and sulfate. Thus increases in reactive surface area cannot be attributed to the increase in reactivity. Rather, the increased efficiency of electron transfer through a thin FeS outer layer on the NZVI enhances NZVI reactivity.

Textural and compositional zoning of plagioclase as archive of magmatic evolution: The Mt. Etna case study

P.P. GIACOMONI¹, M. COLTORTI¹, C. FERLITO²,
C. BONADIMAN¹ AND G. LANZAFAME²

¹Dept. of Physics and Earth Sci., Univ. of Ferrara

(*correspondance: pierpaolo.giacomoni@unife.it)

²Dept. of Biol. and Earth Sci., Univ. of Catania;

(cferlito@unict.it)

Textural and compositional features of plagioclase represent an useful tool to investigate magma chamber processes and changes in physical-chemical conditions of the shallow feeding system. Notwithstanding a coherent and univocal description and classification of plagioclase textural features is still lacking, as well as their link to magmatic processes. The study of more than 130 thin sections from Mt. Etna recent eruptions (2001, 2002-2003, 2004-2005 and 2006) offer a unique opportunity to fill this gap. Classification was developed taking into account different portion of the crystals, rather than simply label a single crystal. This allows to recognize different types of core (euhedral and rounded) and rims (dusty or with melt inclusion alignment) divided by oscillatory zoned overgrowth. Thermobarometric and crystal-melt equilibrium equations have been used to estimate the oxygen fugacity in magmas [1] and the amount of dissolved water content using the hygrometers of [2]. These data were introduced in the MELT's modelling to estimate the plagioclase stability field and to calculate theoretic composition at distinct water content, thus relating each crystal portion to growth or dissolution events occurring at specific P-T-fO₂ conditions and water contents. Results suggest a rather continuous plumbing system, ruling out the hypothesis of significant magma chambers in the Etnean plumbing system. Such system is persistently filled by magmas with quite similar major element composition but different dissolved H₂O, with the initial H₂O content constraining the depth at which plagioclase crystallizes. A small number of phenocrysts nucleate at 14 km whereas most plagioclase nucleates between 7 and 4 km of depth. At this depth, mixing occur between variably H₂O-enriched magmas, causing dusty textures in more albitic plagioclase. On the other hand, volatile loss due to fast ascent decompression promotes undercooling and crystal growth enhancing melt inclusions entrapment at crystal rims.

[1] France *et al.* (2010) *J. Volcanol. Geotherm. Res.* **189**, 340-346. [2] Lange *et al.* (2009) *Am. Mineral.* **94**, 494-506.

Petrological study of Cenozoic basic lavas and melt inclusions from Northern Victoria Land (Antarctica)

P.P. GIACOMONI^{1*}, M. COLTORTI¹, S. MUKASA²,
C. BONADIMAN¹, C. FERLITO³ AND B. PELOROSSO¹

¹Dep. of Physics and Earth Sci., Univ. of Ferrara

(*correspondance: pierpaolo.giacomoni@unife.it)

²Dep. of Earth Sci., Univ. of New Hampshire

(sam.mukasa@unh.edu)

³Dep. of Biol. and Earth Sci., Univ. of Catania;

(cferlito@unict.it)

This study offers a first view of the petrologic features of basic lavas and melt inclusions (MI) in olivine phenocrysts from Northern Victoria Land (Antarctica). Samples were collected during three Italian expeditions with the aim of comparing major element composition and volatile content in the lavas and their mantle sources.

Major elements and volatiles (H₂O, CO₂, S, F and Cl) were analyzed in MI, while major and trace elements were carried out on lavas from three localities, Eldridge Bluff, Shield Nunatak and Handler Ridge.

Lavas are olivine-phyric (up to 15 %vol) with minor clinopyroxene and plagioclase in a glassy to microcrystalline plagioclase-dominated groundmass; opaque minerals are mostly magnetites and subordinately ilmenites. The great majority of lavas are basanites (42.20-45.02 wt% SiO₂ with 3.36-4.21 wt% of Na₂O+K₂O) with Mg# (MgO/(MgO+FeO) mol%, Fe₂O₃=0.15FeO) ranging from 44.87 to 60.83. Lavas from Handler Ridge are the most primitive. At similar fractionation degree, however two series can be distinguished based on K₂O and trace element contents (Rb, Ba, La, Nb and Zr).

MI in olivine phenocrysts from Shield Nunatak basanites were analysed. They are comparable to the host lavas but encompass a wider range in composition (43.68 to 48.73 wt% SiO₂, with 2.81-4.55 wt% of Na₂O+K₂O) and Mg# 49.51 to 74.44). The great majority of olivine in equilibrium with MI are more forsteritic than the enclosing crystal suggesting that MI were trapped from a less evolved magma or, most probably, that Mg-Fe interdiffusion occurred between olivine and MI after entrapment.

Most of MI have H₂O content ranging from 0.70 wt% to 1.19 wt% and CO₂ from 25 ppm to 341 ppm (H₂O/CO₂~1). At comparable H₂O contents few samples show a remarkable higher CO₂ values (1322 ppm to 3905 ppm) with a H₂O/CO₂ down to 0.8.

Magma migration at Mt. Etna in 2012-2013 detected by gas emissions and plume temperature

S. GIAMMANCO¹, G.G. SALERNO¹, A. LA SPINA¹,
L. SPAMPINATO¹, T. CALTABIANO¹, P. BONFANTI¹,
F. MURÈ¹, R. MAUGERI¹ AND V. LONGO¹

¹Istituto Nazionale di Geofisica e Vulcanologia, Osservatorio Etneo, Catania, Italy (salvatore.giammanco@ct.ingv.it)

In 2012-13 gas emissions from Mt. Etna's summit craters have been continuously observed by the automated UV-scanner network surrounding the volcano, continuous radiometric measurements from a permanent station installed on the SE flank of the volcano, discrete FTIR spectrometry surveys, and soil gas emissions periodically measured in low altitude sites on the SW and E flanks of the volcano. Integration of the parameters derived from the different methodologies allowed tracking of the episodic paroxysms from the New South-East crater (NSEC) and of the sporadic explosive activity at the Bocca Nuova crater (BN). Geochemistry data suggest temporal evolution of gas emissions compatible with a solubility-dependent progressive release of gas species typical of processes of magma migration from depth to surface. In particular, we observed a new phase of degassing that started early in June 2012, two months after the closure of the 2012 paroxysmal eruptive sequence. The new degassing phase was clearly discriminated by all the monitored parameters and firstly detected by soil CO₂ increase. This was followed by increase in SO₂ flux and NSEC volcanic plume temperature in August 2012, and in HCl flux late in October 2012. Whilst soil CO₂ flux described a complete cycle that ended in November 2012, the other geochemical parameters and radiometric data continued increasing and climaxed with the renewal of the NSEC paroxysmal events early in February 2013. The decreasing pattern of the soil CO₂ flux starting from August 2012 contrasting the rising trend of the SO₂ and HCl fluxes and temperature measured at the volcanic plume suggests magma migration from depths less than 7 km to the surface. The low soil CO₂ fluxes recorded since November 2012 seem to indicate that no further magma has been supplied to the volcano shallow feeder system, and that the 2013 eruptive events have been fed by the same magma batch that has started degassing in June 2012.

Geochemistry and petrology of the Khantaishir ophiolite (Central Mongolia)

O. GIANOLA¹, M.W. SCHMIDT¹, O. JAGOUTZ²
AND S. OYUNGEREL³

¹ETH Zürich, 8092 Zürich, Switzerland

(*correspondence: omar.gianola@erdw.ethz.ch)

(max.schmidt@erdw.ethz.ch)

²MIT, Cambridge, MA 02139-4307, USA (jagoutz@mit.edu)

³Mongolian Univ. of Science and Technology, Ulaanbaatar 46, Mongolia (oyunas@must.edu.mn)

Ophiolites are slices of oceanic lithosphere incorporated into continental crust. They often allow, in complete sections, to constrain the petrological and spatial evolution of their constituent lithologies and hence to reconstruct past oceanic basins. Oceanic lithosphere forms after seafloor spreading, which may occur at mid oceanic ridges or in proximity of subduction zones. We present a preliminary petrological and geochemical investigation of the Khantaishir ophiolite, a little studied, ~400 km² sized body located in central Mongolia, in the middle of the so called Central Asian Orogenic Belt (CAOB). Aim is to understand its formation history and to reconstruct the tectonic setting where this peculiar ophiolite originated (i.e. mid oceanic ridge or subduction zone). This ophiolite shows a complete crust/mantle transition with a highly refractory mantle composed of harzburgites displaying locally dunitic channels. Towards its top, this mantle is replaced by pyroxenites in discrete zones with a reconstructed sub-horizontal orientation. The igneous crust itself is composed of gabbro, minor gabbroite (both replaced by pyroxenites in discrete zones), intermediate dykes/sills (but not sheeted dyke complexes) and pillow lavas, capped by a sedimentary cover of cherts and limestones. Major and trace elements of the crustal rocks of the Khantaishir ophiolite are compared with chemical analyses of modern ocean crust-forming localities (i.e. the East Pacific Rise, EPR, the Mariana and the Lau backarc basins). Al₂O₃, TiO₂, MnO, Co, V and Zr vs. X_{Mg} show trends similar to those observed for the Mariana and the Lau backarc basins, rather than to that displayed by the EPR. Dykes/sills and pillow lavas of the Khantaishir ophiolitic complex are generally basaltic-andesitic to andesitic in composition (average SiO₂ of ~57%). Their low TiO₂ (<1.2%) and Ti/V ratio of ~10 contrast with MOR suites, which are basaltic (average SiO₂ ~50%) with TiO₂ values >1.2% and a Ti/V ratio between 20 and 50. This evidence suggests that the igneous crustal rocks of the Khantaishir ophiolite were originated from a mantle source modified by a subduction component.

New insights into the size of atoms from electron density distributions

G.V. GIBBS^{1*}, N.L. ROSS¹ AND B.B. IVERSEN²

¹Department of Geosciences, Virginia Tech, Blacksburg, VA 24061, USA (*correspondence: ggibbs@vt.edu)

²Department of Chemistry and iNANO, Aarhus University, DK-8000, Aarhus, Denmark

V.M. Goldschmidt recognized that one of the key variables controlling trace element partitioning is the size of the trace ion relative to the size of the site in the crystal structure in which it partitions. To date, ionic radii have been used in lattice strain models to predict partitioning behavior [1]. However traditional strategies used to determine ionic radii, based on a rigid oxygen with a fixed radius, are flawed. Analysis of electron density distributions (EDD) of over 50 oxides and silicates show that the EDD of oxygen is not spherical and displays as many different bonded radii as it has bonded interactions [2]. As a result, the bonded radius of oxygen is not fixed: it decreases systematically from 1.40 Å when bonded to an electropositive atom like K to 0.65 Å when bonded to a highly electronegative atom like N. The observation that the bonded radius of oxygen depends on the polarizing impact of the bonded atoms has profound implications for trace element partitioning. Furthermore, models that incorporate bonded radii derived from EDD's may also be useful in predicting trace element partitioning in more intractable systems such as sulphides.

[1] Blundy and Wood (2003) *EPSL*, **210**, 383-397. [2] Gibbs *et al.* (2013) *J. Phys. Chem.* **117**, 1632-1640

A half million years of suborbital variability from the Cariaco Basin: A proxy for Greenland “ice core” records?

K.A. GIBSON^{1,2*} AND L.C. PETERSON¹

¹University of Miami, RSMAS, 4600 Rickenbacker Cswy, Miami, FL 33149 (lpeter@rsmas.miami.edu)

²Now at , University of South Carolina, 701 Sumter St, EWS 617, Columbia, SC 29208 (*correspondence: kgibson@geol.sc.edu)

It is becoming increasingly apparent that rapid climate change on suborbital timescales is a persistent feature of Pleistocene climate. The best-studied archives of rapid climate change are Greenland ice cores, the longest of which presently available extends back to Marine Isotope Stage (MIS) 5e. The Cariaco Basin, located in the southern Caribbean, is a location that holds the potential to extend our understanding of suborbital scale climate variability. The basin is in a region sensitive to changes in the migration of the Intertropical Convergence Zone (ITCZ), has high sedimentation rates (≥ 30 cm/kyr) and excellent preservation due to periodic deep-water anoxia. The tight linkage between proxies for productivity in Cariaco and $\delta^{18}\text{O}$ records in Greenland has been well established [1,2], suggesting the basin could serve as a proxy for conditions in Greenland prior to MIS 5e.

We present a half-million year long scanning X-Ray Fluorescence (XRF) record of sedimentary Molybdenum (Mo) from Ocean Drilling Program (ODP) Hole 1002C in the Cariaco Basin. The Mo record appears to serve as a reasonable proxy for high latitude conditions over the last ~500 kyr. Greenland ice core $\delta^{18}\text{O}$ and Cariaco Mo records can be mechanistically linked by changes in the position of the ITCZ during the last glacial period. In earlier glacial periods, Mo enrichments covary with peaks in CH_4 from Epica Dome C and depletions in planktonic $\delta^{18}\text{O}$ from Hole 1002C, giving confidence that they record interstadial-like conditions over the full ~500 kyr studied here. The distribution of millennial-scale variability during the last six glacial periods is not consistent, and coupled with evidence for millennial-scale variability during interglacial periods, suggests that ice volume is not the only control on its occurrence. Alternative mechanisms for triggering periods of millennial-scale variability include the influence of precession on high-latitude insolation and the distribution of sea ice, or the influence of precession (and semi-precessional cycles) on the insolation and hydrologic cycle of the tropics.

[1] Hughen *et al.*, (1996) *Nature*, **380**, 51-54. [2] Peterson *et al.*, (2000) *Science*, **290**, 1947-1950

Experimental investigations on halogen-rich apgaitic phase equilibria

CHRISTOPHER GIEHL*, MICHAEL MARKS
AND MARCUS NOWAK

Eberhard Karls Universität Tübingen, Germany,
(*correspondence: christopher.giehl@uni-tuebingen.de)

High concentrations of Cl and F are known to affect phase relations in magmatic rocks. In this study, we present phase equilibrium experiments investigating an iron-rich peralkaline phonolitic composition with variable Cl and F content. The starting material resembles a potential parental melt composition of the peralkaline Ilímaussaq plutonic complex/South Greenland [1].

Nominally dry experiments were performed at 100 MPa, 1000 – 650 °C and low oxygen fugacity adjusted with graphite-lined gold capsules in an internally heated argon pressure vessel and in hydrothermal rapid-quench cold seal pressure vessels. To cover the large T interval of crystallization we applied a two-step fractional crystallization strategy. The synthesized mineral phases are titanomagnetite, fayalitic olivine, clinopyroxene, alkali feldspar, nepheline and aenigmatite (\pm native iron). Increased Cl and F concentrations additionally stabilize fluorite (CaF_2), hiortdahlite ($(\text{Ca,Na})_6(\text{Zr,Ti})_2\text{Si}_4\text{O}_{14}\text{F}_4$), Cl-bearing sodalite ($\text{Na}_8\text{Al}_6\text{Si}_6\text{O}_{24}\text{Cl}_2$) and, characteristic for apgaitic rocks, eudialyte ($\text{Na}_4\text{Ca}_2(\text{Fe,Mn})\text{ZrSi}_8\text{O}_{22}(\text{Cl,OH})_2$). ZrO_2 melt concentrations necessary to stabilize hiortdahlite and eudialyte are different (0.9 and ~1.2 wt%, respectively). Thus early hiortdahlite saturation shifts eudialyte saturation to lower T .

In the Ilímaussaq rocks, magmatic clinopyroxene shows a gap between Ca-rich and Na-rich compositions, common in evolved peralkaline rocks [2]. This gap may be induced by Ca-rich hiortdahlite and fluorite at the expense of Ca-rich clinopyroxene by reason of increasing F content in the residual melt. Na-rich clinopyroxene, not influenced by Ca-F phases, may then be stabilized coexisting with a more evolved melt at lower T . Both the Cl/OH ratio in eudialyte and Fe/Mn partition coefficients between clinopyroxene and eudialyte/aenigmatite decrease systematically with T . The comparison with existing data indicates that these ratios may have the potential for geothermometers, rarely available for apgaitic phase assemblages.

[1] Marks & Markl (2003) *MinMag* **67**, 893-919. [2] Njonfang & Nono (2003) *Eur J Min* **15**, 527-542.

BIOCOMBUST Biomass, Energy, Health

GIERÉ R, MASCHOWSKI C, MERFORT I, KÖNCZÖL M, DORNHOF R, DIETZE V, KAMINSKI U, NAZARENKO I, MERSCH-SUNDERMANN V, GMINSKI R, TROUVÉ G, DIETERLEN A, KLEINPETER J, DREWNICK F, FREUTEL F AND KRUSPAN P

¹Universität Freiburg, Germany (*giere@uni-freiburg.de)

²Umweltmedizin, Universitätsklinik Freiburg, Germany

³Lufthygiene, Deutscher Wetterdienst, Freiburg, Germany

⁴Université de Haute-Alsace, Mulhouse, France

⁵ASPA, Schiltigheim, France

⁶Max-Planck-Institut für Chemie, Mainz, Germany

⁷Holcim (Schweiz) AG, Würenlingen, Switzerland

BIOCOMBUST is a large-scale international research project on health aspects of biomass combustion. Funded by the European Union through its Funds for Regional Development (INTERREG IV Upper Rhine program), it is a cross-border collaboration between several research teams with widely differing expertise, including: mineralogy; geochemistry; pharmaceutical science; environmental medicine; combustion science; aerosol science; human biometeorology; and cement manufacturing.

The research explores the impacts of particulate emissions from biomass combustion on air quality and health. To evaluate these effects, various experiments are performed, including: biomass combustion in the laboratory, district heating facilities, and power plants; chemical, mineralogical, and structural characterization of biomass, particulate emissions, and ashes; optimization of combustion conditions; determination of ash and particulate-emission properties in relation to type of biomass, firing conditions and cooling path; identifying and tracking of particulate plumes as well as collection of emitted particulates around industrial biomass-combustion facilities; determination of cytotoxic, genotoxic, and proinflammatory effects in human lung cells as a result of particulate exposure; determination of the potential of particles to generate reactive oxygen species in human lung cells; investigation of the molecular mechanisms underlying the cell responses to particulate exposure.

The expected results will provide a basis for technical and economic applications, which eventually will lead to an improvement of both environmental and living conditions. In addition, the results will give an important boost to the sustainable expansion of the biomass industry and to the potential use of the associated ashes as secondary raw materials for the cement industry.

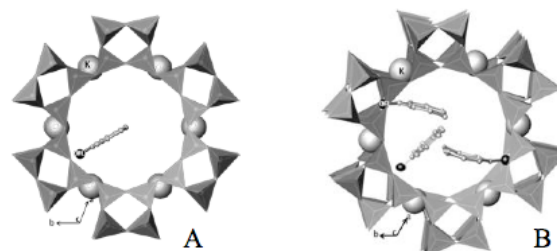
Fluorenone dye- zeolite L hybrid: a novel optical material

GIGLI L¹., ARLETTI R²., QUARTIERI S³., VEZZALINI G¹.

¹Department of chemical and Geological Sciences, University of Modena and Reggio Emilia, Italy,

²Department of Earth Sciences, University of Torino, Italy
Department of Earth Sciences- University of Messina, Italy

A major challenge facing humanity is developing renewable source of energy. Following the biological blueprint of the natural photosynthesis is possible design synthetic systems for converting light into stored energy: the so called artificial antenna systems. The encapsulation of ordered chromophore molecules into one dimensional zeolite channel systems results in host-guest compounds suitable for the development of novel optical materials such as lenses, infrared light-emitting diodes (used in telecommunications) or dye nanostructured materials for optical data storage [1]. X-ray powder diffraction study of zeolite K-L loaded with 0.5, 1, 1.5, 2 fluorenone-dye (FL) molecules per unit cell (ZL/FL hybrid) [2], was carried out to understand the functionality of these host-guest systems from the structural point of view. These data evidenced a significant change of the unit cell parameters due to the embedding of FL into the ZL 12-membered channels. The Rietveld refinements revealed that the maximum loading is 1.5 FL molecules per unit cell. A strong interaction between FL carbonyl group and two



extraframework potassium cations is proved by the short bond distances which make this composite very stable.

Fig.1 Projection along *c* axis of the ZL/FL (1 molecule) (A) and ZL/FL (1.5 molecules) composites (B) .

This work is supported by the Italian MIUR (FUTURO INRICERCA2012:ImPACTproject (RBFR12CLQD) AB

[1] St. Suárez, A. Devaux, J. Bañuelos, O. Bossart, A. Kunzmann and Gion Calzaferri Properties *Adv. Funct. Mater.* (2007), **17**, 2298–2306. [2]A. Devaux, C. Minkowski, and Gion Calzaferri *Chem. Eur. J.* 10, (2004), 2391

Properties and processing of organic aerosol in the Po valley

S. GILARDONI¹, M. RINALDI¹, M. PAGLIONE¹,
S. DECESARI¹, L. POULAIN², S. CARBONE³,
R. HILLAMO³, L. M. RUSSELL⁴, P. MASSOLI⁵,
V. POLUZZI⁶ AND M. C. FACCHINI¹

¹ISAC-CNR Bologna Italy s.gilardoni@isac.cnr.it; ²IFT Leibniz Germany; ³FMI Helsinki, Finland; ⁴SCRIPPS San Diego, CA; ⁵Aerodyne Research Billerica, MA; ⁶ARPA ER Bologna, Italy.

The chemical and microphysical properties of submicron organic aerosol (OA) strongly depend on sources and atmospheric processing.

OA properties were investigated in the framework of ARPA-ER Supersite project and Pegasos project. Observations were performed at an urban site (Bologna) and a rural location (San Pietro Capofiume) in fall 2011, summer 2012, fall 2013, and winter 2013. The suite of deployed measurement techniques included High Resolution Time of Flight Aerosol Mass Spectrometry (HR-TOF-AMS), Hydrogen Nuclear Magnetic Resonance (H-NMR), Fourier Transform Infrared Spectrometry (FTIR), together with thermo and thermo-optical analysis.

At both sites, OA represented about 50% of submicron particle mass during the colder seasons (winter and fall), and about 60% in summer. The oxygen to carbon ratio (O:C), an index of the oxidation level of OA, showed a clear seasonality with higher values in summer at the rural site. Different organic aerosol processing mechanisms characterized different areas and seasons. Photochemical processing was more relevant during summer. Fog processing was significant during fall experiments in the rural site, where frequent and prolonged fog events occurred. Van Krevelen diagram (H:C vs O:C) suggested that different processing mechanisms took place through different chemical oxidation pathways. We also present results from positive matrix factorization (PMF) analysis performed on the datasets collected at both sites.

Ultrafast Pump-Probe Studies of Geochemical Reactions

BENJAMIN GILBERT¹

¹Lawrence Berkeley National Laboratory, 1 Cyclotron Road, Berkeley, CA 94720, USA

Time-resolved spectroscopic methods provide new opportunities for understanding reaction mechanisms in all areas of the chemical sciences. In essence, ultrafast spectroscopy using the pump-probe approach can measure the rates of elementary reaction steps that occur on subnanosecond timescales, and provide chemical characterization of reaction intermediates with as much information content as conventional methods. Time-resolved versions of UV-vis, infrared, Raman, X-ray absorption and electron paramagnetic spectroscopy are now available. This presentation will give an introduction to ultrafast pump-probe studies of geochemical reactions, particularly discussing the opportunities and challenges of time-resolved X-ray absorption spectroscopy. TR-XAS is a major focus for all current and planned X-ray sources, and currently undergoing to a rapid growth in facility availability and data quality.

The pump-probe method achieves very high time resolution only when a reaction of interest can be initiated by a fast trigger pulse (the "pump"), typically a laser pulse. Thus, photochemical reactions, such as the photolysis of ferrioxalate or mineral photoreductive dissolution, are naturally suited for ultrafast studies. In addition, the photoreduction or photooxidation of organic and inorganic adsorbates at semiconductor mineral surfaces are also now being studied by ultrafast spectroscopic techniques. However, most geochemical reactions are not naturally light driven, and a major challenge is the development of strategies for reaction initiation. Photoactive dye molecules can be used to efficiently transfer electrons to iron and manganese oxide minerals, and may also permit the study of metal redox reactions in homogeneous solution.

Interpretation of spectroscopic signatures from reaction intermediates can be difficult because their nature precludes the preparation of stable reference species. Thus, simulation can play an important role in the interpretation of TR-XAS. For example, model calculations of the XAS of iron(II) sites in iron(III) oxides revealed that both valence state change and lengthening of the iron-oxygen bond length contributed to the spectral changes observed at the near-edge, confirming the polaronic nature of this reactive site.

A disordered whole-nanoparticle model for 6-line ferrihydrite

BENJAMIN GILBERT¹, J. ERBS², R. L. PENN², V. PETKOV³
AND G. A. WAYCHUNAS¹

¹Lawrence Berkeley National Laboratory, 1 Cyclotron Road, Berkeley, CA 94720, USA

²Department of Chemistry, University of Minnesota, Minneapolis, MN 55455, U.S.A

³Department of Physics, Central Michigan University, Mt. Pleasant, Michigan 48859, USA

Ferrihydrite is a probably the most widespread and environmentally important natural inorganic nanoparticle, composed of defective nanocrystals of hydrous iron(III) oxide. Recently, Michel *et al.* (2007, 2010) proposed a structural model for ferrihydrite in place of the long-accepted model by Drits *et al.* (1993). The *Drits* and *Michel* models each achieve arbitrarily good agreement with, respectively, XRD and PDF data, but not with both. Because X-ray scattering methods have a growing role in structural studies of nanoscale materials, it is essential to understand the origin of this apparent paradox. Here we present a novel structural analysis of total X-ray scattering data acquired from 6-line ferrihydrite. We generated candidate whole-nanoparticle models of ferrihydrite composed of a two-phase *Drits* model, the *Michel* model, or a *hybrid* phase based on a single-phase *Drits* model that incorporated tetrahedral Fe sites, creating a lattice in which the *Michel* model was one of many possible topologies. We implemented a reverse Monte Carlo (RMC) approach to explore alternative configurations of iron occupancies plus structural disorder, and to refine the nanoparticle structure using both the reciprocal and real-space forms of the X-ray scattering data.

Nanoparticles based upon the *hybrid* structure converged to give better agreement to the experimental total scattering data than was attained for nanoparticles based upon either the *Michel* or *Drits* models. RMC models that incorporated tetrahedrally coordinated iron sites achieved better matches to the data than RMC models with face-sharing octahedra. Long-range vacancy disorder was essential for optimum fits to the scattering data, highlighting the advantage of whole-nanoparticle models in place of unit cell models. The RMC-derived structures do not satisfy all experimental constraints, but our results suggest a route to achieving better descriptions of this, and other, defective nanomaterials.

[1] Drits, V.A., *et al.* (1993) *Clay Minerals* **28**, 185-207. [2] Michel, F.M. *et al.* (2007) *Science* **316**, 1726-1729. [3] Michel, F.M. *et al.* (2007) *Proc. Nat. Sci. Am.* **107**, 2787-2792.

Sequence of phase transitions in calcite biominerals, mapped with 20 nm resolution, and their energetics

YUT GONG¹, CE KILLIAN^{1,2}, IC OLSON¹, NP APPATHURAI³, AL AMASINO¹, MC MARTIN⁴, LJ HOLT², FH WILT² AND PUPA GILBERT^{1,5*}

¹Department of Physics, University of Wisconsin, Madison, WI 53706, USA.

²Department of Molecular and Cell Biology, University of California, Berkeley, CA 94720, USA.

³Synchrotron Radiation Center, University of Wisconsin-Madison, Stoughton, WI 53589, USA.

⁴Advanced Light Source, Lawrence Berkeley National Laboratory, Berkeley, CA 94720, USA.

⁵Department of Chemistry, University of Wisconsin, Madison, WI 53706, USA. (*correspondence: pupa@physics.wisc.edu)

We will show data from 20nm-resolution synchrotron photoelectron spectromicroscopy and microcalorimetry, demonstrating that in sea urchin biominerals the first mineral deposited is hydrated amorphous calcium carbonate (ACCH2O), which rapidly transforms into ACC, which slowly transforms into calcite [1]. The same process occurs abiotically, but it takes seconds to crystallize, whereas in the animal it takes days, hence the above phase transitions are highly bio-regulated. The energetics [2], spatial distribution of phases, and time-evolution [3] of this complex process will be presented, with particular emphasis on the role of SM50 [3], a protein that appears to stabilize ACCH2O in vitro, and may have this function in vivo [4].

[1] Y Politi *et al.* (2008) *PNAS*. [2] AV Radha *et al.* (2010) *PNAS*. [3] YUT Gong *et al.* (2012) *PNAS*. [4] CE Killian *et al.*, work in progress.

Matrix dependance for the quantification of sulphur in sulphide minerals by LA-ICP-MS

S.E. GILBERT*, L.V. DANYUSHEVSKY AND S. MEFFRE

CODES, University of Tasmania, Hobart, Tasmania, Australia, 7000 (*correspondence: sgilbert@utas.edu.au)

Matrix effects due to differences in ablation characteristics can be significant between minerals during LA-ICP-MS analyses [1, 2]. In this study we investigate the degree of matrix dependance on the quantification of sulphur between a range of sulphide minerals including pyrite, pyrrhotite, bornite, chalcopyrite, sphalerite and pentlandite.

The major element yields (sensitivity per ppm) for these sulphide minerals were compared on three laser ablation systems: a 213 nm and 193 nm Nd:YAG lasers and a 193 nm Excimer laser. Sulphur fractionation was significant for some minerals. For example, for both pyrrhotite (Fe_{1-x}S) and bornite (Cu_5FeS_4) S yields relative to Fe are consistently high on all laser systems, by up to 12 and 40 % respectively, compared to pyrite (FeS_2). In comparison no fractionation is seen between Cu and Fe [3].

These observation can in part be explained by examining the amount of melt within, and adjacent to, the laser ablation crater. The degree of melting is mineral specific and dependant on the physical properties of the mineral (ie heat capacity), as melting occurs even at low energy close to the ablation threshold. The degree of melting in each sulphide mineral was assessed with SEM imaging, by inspecting the morphology of the crater rim and deposited material adjacent to the ablation site. Very little melting occurs during pyrite ablation in contrast to pyrrhotite and bornite, which show evidence of liquid melt within and around the ablation crater.

We propose that the high yields of S relative to Fe and Cu in these minerals is due to the high volatility of S. The implications for the quantification of S in sulphide minerals, and the factors that influence the liberation of S, such as melting during ablation, are discussed.

- [1] Jackson & Gunther (2003) *JAAS*, **18**, 205-212.
 [2] Sylvester (2008) in *Laser-Ablation-ICPMS in the Earth Sciences: Current Practices and Outstanding Issues*. [3] Danyushevsky *et al* (2011) *Geochemistry: Exploration, Environment, Analysis*, **11**, 51-60.

Evolution of AFM mineral assemblages in the Jálama granitic pluton

GIL-CRESPO P.P.¹, TORRES-RUIZ J.², PESQUERA A.¹ AND RODA-ROBLES E.¹

¹Departamento de Mineralogía-Petrología, Universidad del País Vasco, PO Box 644, E-48080 Bilbao, Spain

²Departamento de Mineralogía-Petrología, Universidad de Granada, Campus Fuentenueva, E-18002 Granada, Spain

The Jálama pluton crops out in the Central Iberian Zone (Spain). It intrudes into low-grade metasedimentary rocks from the Schist-Greywacke Complex, and includes two main units: (1) the central unit, which consists of an inhomogeneous sillimanite-bearing monzogranite with hypidiomorphic seriate texture containing mainly quartz, alkali feldspar, plagioclase, muscovite and biotite. (2) the external unit, which comprises (i) a coarse-grained monzogranite with hypidiomorphic seriate to porphyritic texture including quartz, K-feldspar, plagioclase, biotite, muscovite ± tourmaline, the tourmaline being relatively abundant in places, (ii) an equigranular granite with a mineral association similar to the monzogranite, but muscovite being more abundant than biotite, and (iii) a fine- to medium-grained leucogranite containing quartz, alkali feldspar, plagioclase, muscovite and tourmaline as essential components. Based on textural relationships, mineral compositions, and AFM liquidus topologies, the sequence of AFM mineral reactions in the Jálama pluton may have evolved from $L_1 = \text{Bt} + \text{Ms} + L_2$, through $L_2 = \text{Bt} + \text{Ms} + \text{Tur} + L_3$ to $L_4 = \text{Ms} + \text{Tur}$. Biotite would react with a B-bearing melt (L_3) to produce further tourmaline during crystallization to lower temperatures, and subsequent crystallization of the residual melt (L_4) gave rise to the muscovite + tourmaline facies. The FeMg_1 exchange operator involving the crystallization of biotite and tourmaline, with an average K_D value $((\text{Mg}/\text{Fe})_{\text{tur}}/(\text{Mg}/\text{Fe})_{\text{bt}}) \sim 2.0$, covers a wide range of $\text{Fe}/(\text{Fe}+\text{Mg})$ in the AFM topology. The restricted accesibility to the three-phase Tur-Bt-Mus field of most granitic melts, nevertheless, would account for the separation of biotite + muscovite assemblages from tourmaline-bearing assemblages. The three-phase assemblage displaces toward higher $\text{Fe}/(\text{Fe}+\text{Mg})$ values with decreasing temperature based on the AFM liquidus topology. This suggests a solidus temperature for the biotite-muscovite assemblage higher than for the tourmaline-muscovite assemblage. This is consistent with the emplacement of the pluton under epizonal conditions (~200-300 MPa) at temperatures in the range of 650-800°C using the zircon saturation thermometry.

Geochemical tracing of methane from unconventional gas production

STUART M.V. GILFILLAN¹, R. STUART HASZELDINE¹,
FINLAY M. STUART² AND SUSAN WALDRON³

¹School of GeoSciences, University of Edinburgh, UK
(*correspondance: stuart.gilfillan@ed.ac.uk)

²Isotope Geosciences Unit, SUERC, East Kilbride, UK

³School of Geographical and Earth Sciences, University of Glasgow, UK.

There is significant public concern surrounding the exploitation of unconventional gas resources. Many of these concerns relate to potential methane contamination of potable water supplies in shallow aquifers. Public apprehension is predominantly linked to experiences of unconventional gas extraction in the USA where there is strong and growing public dispute around the “fracking” process. Evidence of groundwater contamination by produced gas is equivocal. Some studies have found no direct causality between fracturing and groundwater contamination. However, there is a developing group of work in the USA by individual researchers [1] and by the Environmental Protection Agency [2], which suggests that a degree of contamination of groundwater has occurred.

In such a commercially active sector, a strong suite of evidence is needed to unequivocally detect contamination and allow successful remediation litigation. Simple documentation of elevated methane content in groundwater is not sufficient to enable a legally secure diagnosis. Rival claims can be made that the methane present in the groundwater is from drilling operations which predate shale gas exploration, or that observations of hydrocarbon content, including methane gas, in shallow aquifers are due to natural processes unconnected with unconventional gas exploration. For these reasons, an extremely robust identification of methane source, or multiple methane sources, is needed. In this study we focus on providing the means to make that identification.

Using existing data, we will show how C and H isotopes, radiocarbon (¹⁴C) and noble gases (He Ne Ar Kr Xe) can be used to geochemically “fingerprint” produced gas from coal bed methane and shale gas deposits. This clear “fingerprint” can be used to distinguish any produced gas from other gas sources and provide a robust means for identifying produced methane contamination of shallow groundwaters.

[1] Osborn *et al.*, (2011) *PNAS*, Vol. **108**, No. 20, p8172-8176

[2] EPA (2011) Investigation of groundwater contamination near Pavillion, Wyoming. Environmental Protection Agency, USA.

Volcanostratigraphic controls on the occurrence of massive sulfide (VMS) deposits in the Oman Ophiolite

S. GILGEN*, L. W. DIAMOND AND I. MERCOLLI

Rock–Water Interaction, Institute of Geological Sciences,
University of Bern, Switzerland

(*correspondence: gilgen@geo.unibe.ch)

The Semail ophiolite in northern Oman is capped by up to 2 km of basaltic–andesitic lavas that host copper-dominant, Cyprus-type, volcanogenic massive sulfide (VMS) deposits. This study identifies the multiple volcanostratigraphic horizons on which the deposits are situated, based on characterization of footwall and hanging-wall lavas from 16 deposits or deposit clusters. Comparison of their field and petrographic features, compositions of igneous clinopyroxenes and whole-rock geochemical signatures permits their classification within a modified version of the established regional volcanostratigraphy.

Four extrusive units host VMS deposits: Geotimes (earliest), Lasail, Alley and Boninitic Alley (latest). The latter was known only at a few localities but the present study reveals its regional extent and significance as a host for VMS deposits. The new results show that VMS deposits sit on or near the Geotimes/Lasail and Geotimes/Alley contacts as well as entirely within the Lasail, Alley and Boninitic Alley Units. The Geotimes and Lasail Units represent Late Cretaceous, ocean spreading ridge and related off-axis volcanic environments respectively. Highest Cu grades tend to occur in deposits lying on or within the Geotimes. The Alley and Boninitic Alley Units represent younger, subduction-related volcanism prior to Coniacian–Santonian obduction of the ophiolite. Highest Au grades occur in deposits within the Boninitic Alley.

In contrast to earlier studies, the new results show that essentially every horizon that marks a hiatus in lava deposition in the Semail ophiolite, i.e. contacts between the four major eruptive units, and umbers and sedimentary chert layers within the units, has exploration potential for Cu–Au VMS deposits.

Microbial sulfur cycling in the modern Black Sea

W.P. GILHOOLY III¹, D. JOHNSTON², J. FARQUHAR³,
S. SEVERMANN⁴, M. E. BÖTTCHER⁵, B. C. GILL⁶,
A. KAMYSHNY⁷ AND T. LYONS⁸

¹Dept. of Earth Sciences, Indiana University-Purdue University Indianapolis, Indianapolis, IN, USA (wgilhoool@iupui.edu)

²Dept. of Earth and Planetary Science, Harvard University, Cambridge, MA, USA

³Dept. of Geology and Earth Systems Science, University of Maryland, College Park, MD, USA

⁴Institute of Marine & Coastal Science and Dept. of Earth & Planetary Sciences, Rutgers University, New Brunswick, NJ, USA

⁵Geochemistry & Isotope Geochemistry Group, Leibniz-Institute for Baltic Sea Research, Warnemünde, Germany

⁶Dept. of Geosciences, Virginia Tech, Blacksburg, VA, USA

⁷Dept of Geological and Environmental Sciences, Ben-Gurion University of the Negev, Beer Sheva, Isreal

⁸Dept. of Earth Sciences, University of California, Riverside, CA, USA

The evolution of Earth's oceans on geologic timescales has included episodes when basinal waters were anoxic and sulfidic (euxinic). The expansion of sulfidic bottom waters has the potential to drive significant chemical and biological changes in benthic environments. Considerable interest exists to develop tools that can be used to identify these conditions. Sulfur isotope analyses ($^{33}\text{S}/^{32}\text{S}$, $^{34}\text{S}/^{32}\text{S}$ and $^{36}/^{32}\text{S}$) in combination with other geochemical indicators show promise in studies of dynamic bottom-water conditions in low oxygen settings. Here, we present multiple sulfur isotope analyses of sulfate, dissolved sulfide, and sedimentary sulfides (AVS and pyrite) from diverse settings in the modern Black Sea to address basin-wide sulfur cycling. Within this well constrained depositional and environmental context, we describe variations in $\delta^{34}\text{S}$, $\Delta^{33}\text{S}$ and $\Delta^{36}\text{S}$ that, along with other geochemical proxies such as iron geochemistry, track the historical shoaling of sulfidic deep waters. Multiple sulfur isotope approaches are especially sensitive to oxidative and reductive pathways of microbial S metabolisms that vary in phase with changes in bottom-water redox. The processes that control the sulfur isotopic signatures are ultimately related to the interplay of rates of pyrite formation, sulfide oxidation, and diffusion of sulfide and dissolved iron in the sediments. By extrapolation, we argue that the sulfur isotope signatures may provide a tool for identifying chemocline shoaling events and ecological changes in the biologic S cycle in the geologic past.

Kinetic of H_2O_2 generation and decay during pyrite-water reactions

C. GIL LOZANO*¹, E.L. ADAMS¹, A.F. DAVILA²,
A.G. FAIREN³ AND L.G. DUPORT¹

¹Universidad de Vigo. 36200 Vigo. Spain. (corresponding author*: karolina_gil@uvigo.es)

²SETI Institute, Mountain View, CA 94043, USA.

³Cornell University. Ithaca, 14853 New York, United States

The oxidative dissolution of pyrite is driven by a complex mechanism that involves the transient formation of H_2O_2 and other reactive oxygen species [1], however, a kinetic analysis dealing with the time evolution of these species is presently lacking. In this work, we measured the real-time generation and decomposition of H_2O_2 on pyrite surfaces under different boundary conditions with amperometric biosensors. In addition, simultaneous measurement of the O_2 , Fe(II), together with Fe(III) generated as a byproduct of Fenton reaction, were done with Clark sensors, and UV-VIS spectroscopy. The observed general pathway for H_2O_2 time evolution consisted of an S-shaped stretched exponential profile, with a first stage marked by an increasing generation of H_2O_2 until a critical concentration value of peroxide was reached. From this moment on, the measured amount of H_2O_2 in solution decreased towards a nearly stationary value. Further, experiments were performed to assess the reversibility of the process and to evaluate the possible role of pyrite-generated H_2O_2 and other ROS in the long-term redox evolution in natural environments. A new kinetic model based the coupling between H_2O_2 and Fenton reaction in aqueous solution was performed to fit the experimental data. Results showed that the observed amount of peroxide at each instant can be closely related to the supply rate of Fe^{+2} resulting from pyrite dissolution, which progressively degrades H_2O_2 inducing the continuous generation of secondary ROS in solution. Thus, it can be speculated that the mineral pyrite may act as a Fenton-like reagent, able to induce long-term oxidation through the geological realm.

[1] Schoonen *et al.* (2010) *Geochim. et Cosmochim. Acta* **74** (17), 4971-4987.

Green color chemical recipes in stained glass windows of NE Spain and N Italy (XIIIth to XVth centuries)

D. GIMENO*¹, F. BAZZOCCHI¹, M. AULINAS¹,
G. GISBERT¹, M. P. RICCARDI² AND E. BASSO²

¹Dep. Geoquímica, Petrologia i Prospecció Geològica, Universitat de Barcelona. 08028 Barcelona, Spain (* presenting author) d.gimeno.torrente@gmail.com; meritxellaulinas@ub.edu; ggisbert@hotmail.com

²Dipartimento di Scienze della Terra e dell'Ambiente, Università degli Studi di Pavia, 27100 Pavia, Italia. mariapia.riccardi@unipv.it; elena.basso@unipv.it

A great number of medieval religious buildings in Europe contain stained glass windows. A number of original glass fragments (i.e. with original medieval lead framework) coming from restoration projects (Girona, Tarragona, Pedralbes Monastery at Barcelona (Spain); the Siena Cathedral, the San Petronio Basilica and the San Giacomo Maggiore church in Bologna (Italy)) have been analyzed in term of major, minor and trace elements. In contrast to the coeval glass windows of central Europe, most of the studied glass fragments are soda-glass of Mediterranean origin, whereas the imported K-glass were used only to realize some colors in the windows (in most of cases red ruby plaque glass). Concerning the technological aspects, these glass were realized starting from the colorless base glass, to which metal-transition elements were added to obtain the different colors. A first conclusion is that some elements, singularly REE associated to Nb and other trace elements characterize the source of silica, that is quartz sand or quartz cobbles. This allows to the identification of homogeneous sets of colored and colorless glass (i.e., original medieval glass) in the same windows and sites, even in the cases of subsequent widespread reposition of glass fragments over the centuries. Total content in Sr provides information on the calcium carbonate source (limestone or aragonitic shells). The different shades of the green color were obtained by using a Fe-Cu association. The study of green glass fragments by ICP-MS and laser ablation HR-ICP-MS allows to characterize different mineral salts taking into account the associated trace element metal associations. We acknowledge the technical support of the CCiT of the Universitat de Barcelona and the ICTJA-CSIC labGEOTOP, infrastructure co-funded by ERDF-EU (Ref. CSIC08-4E-001). This work has been carried out in the framework of the research group PEGEFA SGR2009 972 (Generalitat de Catalunya).

Perturbing a field diffusion experiment: First results of the DR-A test in the Mont Terri Rock Laboratory (Switzerland)

T. GIMMI^{1,2}, O.X. LEUPIN³, J.M SOLER⁴
AND L.R. VAN LOON²

¹Paul Scherrer Institute, CH-5232 Villigen, Switzerland (thomas.gimmi@psi.ch)

²Institute of Geological Sciences, University of Bern, CH-3012 Bern, Switzerland

³Nagra, CH-5430 Wettingen, Switzerland

⁴IDAEA-CSIC, E-08034 Barcelona, Spain

Clay-rich formations have repeatedly been shown to provide an appropriate environment to safely retain harmful solutes. However, a thorough understanding of diffusion of anions, cations and uncharged tracers through clay is fundamental to assess any long-term transport properties. A field diffusion experiment (DR-A) was recently started in the Mont Terri Underground Rock Laboratory (Switzerland). The aim of this experiment is to provide insights on coupled transport and sorption processes that are of central importance in clays, notably anion exclusion, competing sorption by cation exchange, anion and cation diffusion, and to test the predictive capability of transport codes.

The experimental design is based on established setups (DI-A1 and DI-A2 [1,2]) with a traced artificial pore water (APW) that should match the local geochemical conditions and which is circulated through a 1-m injection interval. The tracers included HTO, I⁻, Br⁻, Cs⁺, 85-Sr²⁺, 60-Co²⁺ and Eu³⁺. However, unlike earlier experiments, the traced APW was exchanged after 6 months by a non-matching solution (~3 times higher ionic strength, strongly increased in K content compared to the original APW) still containing the tracers. This geochemical perturbation was expected to provoke responses that can be observed in the circulated solution.

The increase of the ionic strength and the K content led to a release of Cs from the exchanger and back-diffusion into the circulated solution. So far, no clear effect on anion exclusion was observed. The data will be interpreted by several modelling groups (IDAEA-CSIC, PSI, Univ. Bern, Univ. British Columbia, Lawrence Berkeley Natl. Lab.) using codes with different representations of the coupling between ionic strength and the transport and sorption properties.

[1] Van Loon *et al.* (2004) *Radiochim. Acta* **92**, 757. [2] Wersin *et al.* (2008) *Appl. Geochem.* **23**, 678.

Understanding Long-Term Variability of Dust in Different Parts of the World

GINOUX P, MALYSHEV S AND SHEVLIKOVA E

paul.ginoux@noaa.gov

Over the last decade dust modeling has made large progress and satisfactory dust forecasting is now being provided operationally by several modeling groups. However, unsatisfactory comparison with observations, especially long-term datasets, indicates limiting factors of dust modeling. One of these factors is related to the dynamic variation of dust sources, which can be observed from satellite data. This is particularly problematic to study dust effects on climate, and feedbacks.

In this presentation, after summarizing the most prominent changes of dust concentration observed in different parts of the world, we will review several modeling approaches which were used to simulate decadal variations of dust. The recent implementation of a dust module within a dynamic land model, which is coupled with atmosphere/ocean/ice models, will be used to understand observed dust variability over the last 60 years and to evaluate the contribution of sea-surface temperature, vegetation and landuse changes to long-term variability of dust. Finally, some additional factors which may affect aeolian dust in the future will be presented.

CCN Relevant Properties of Biomass Burning Aerosol

M. GIORODANO AND AKUA ASA-AWUKU^{1*}

¹University of California, Riverside, Riverside, CA 92521, USA (correspondence akua@enr.ucr.edu)

Biomass burning contributes upto 2-3 Pg C per year to the atmosphere, of which the composition and phase are not well characterized. The oxidation of these emissions can produce additional aerosol downwind from sources that can directly and indirectly modify climate. Controlled burns were conducted at UC-Riverside's CE-CERT facility to understand the influence of aged wood smoke for aerosol cloud formation process. The emissions were diluted and injected into a 12 m³ Teflon environmental chamber. The smoke was allowed to mix in the chamber, and a suite of instrumentation measured changes in aerosol phase chemical and physical properties. The smoke is photochemically active; ultraviolet lights age the wood smoke over a 6-8 hour period and cloud condensation nuclei (CCN) properties are transient. This presentation focuses on the changes in CCN activity due to key factors that are used to quantify and predict hygroscopicity. The kappa-hygroscopicity varies significantly with photochemical age and supersaturation. A high resolution time-of-flight aerosol mass spectrometer is used to analyze aerosol chemical composition. Size distribution and CCN activity are determined with a SMPS and CCN counter.

A combined sedimentological and biomarker record across the Neoproterozoic Bitter Springs Excursion

MARTINO GIORGIONI^{1*}, AMBER JARRETT¹, MARTIN KENNEDY² AND JOCHEN BROCKS¹

¹Research School of Earth Sciences, Australian National University, Canberra, ACT 0200, Australia
(*correspondence: martino.giorgioni@anu.edu.au)

²School of Earth and Environmental Science, University of Adelaide, Adelaide SA 5005, Australia

Isotopic records from carbonate carbon of the Neoproterozoic (1000 – 542 Ma) display extremely large negative excursions, with $\delta^{13}\text{C}$ values shifting from 5‰ to 8‰ down to -4‰, -6‰, or even -12‰. The origin of such large amplitude variations is still enigmatic because they do not occur in any other geological period, except in diagenetically altered carbonate platforms [1].

In this work we focus on the Bitter Springs Excursion (BSE), which is the oldest (~800 Ma) and the least extreme in the Neoproterozoic, with $\delta^{13}\text{C}$ values shifting from 6‰ to -4‰. In respect to the other large excursions this is the only one not preceding nor followed by a large glacial event, and it is the only case in which the negative excursion is recorded both in carbonate and in organic $\delta^{13}\text{C}$ [2].

We present sedimentological and geochemical data from a new core drilled through the Bitter Springs Formation of the Amadeus Basin in Central Australia. The lower part of this unit consists of a thick succession of carbonate and evaporitic facies (Loves Creek member), whereas the upper part is dominated by red silty marlstones alternating with gray, more carbonatic facies (Jonny's Creek member). Bulk carbonate $\delta^{13}\text{C}$ is between -4‰ and -2‰ within the Loves Creek member, corresponding to the upper part of the BSE. The base of the Jonny's Creek member coincides with the end of the excursion, with $\delta^{13}\text{C}$ increasing up to 6‰. However, the $\delta^{13}\text{C}$ pattern is continuous indicating that there is no significant hiatus at the boundary between the two members.

We also present the first detailed record of indigenous [3, 4] biomarkers from within and above the BSE. Shifts in facies as well as in biomarker assemblages suggest significant ecological changes at the end of the BSE within the Amadeus Basin.

[1] Swart & Kennedy (2012) *Geology*, **40**, 87-90. [2] Swanson-Hysell *et al.* (2010) *Science*, **328**, 608-611. [3] Brocks *et al.* (2008) *Geochimica and Cosmochimica Acta*, **72**, 871-888. [4] Pawlowska *et al.* (2013) *Geology*, **41**, 103-106

Enrichment of Pb, Se, As, U and Cs in commercial cosmetic clays

K. GIOURI*, A. PAPADOPOULOS, A. BOURLIVA, E.TZAMOS, L. PAPADOPOULOU, K. NTOUANOGLOU AND A. FILIPPIDIS

Aristotle University of Thessaloniki, School of Geology, Department of Mineralogy-Petrology-Economic Geology, Thessaloniki 54124, Greece
(*correspondance:agiouri@geo.auth.gr)

Three samples, representing different commercial types of cosmetic clays (white, green and red) were analyzed for 29 trace elements (Ag, As, Ba, Be, Cd, Ce, Co, Cr, Cs, Cu, Ga, Hf, Hg, La, Mo, Ni, Pb, Rb, Sb, Sc, Se, Sr, Th, Tl, U, V, Y, Zn and Zr).

According to EC regulation [1] the presence of As, Be, Cd, Cr, Hg, Ni, P, Pb, Sb, Se, Te, Tl, Zr and their compounds is prohibited in cosmetics. However, for 16 trace elements (As, Ba, Ce, Cr, Cs, Cu, La, Ni, Pb, Rb, Sr, Th, V, Y, Zn and Zr), concentrations ranging from 10 ppm to 410 ppm have been detected in the studied clays.

Compared to the average concentration of elements in shales (average shale) [2] (Fig. 1), white clay (WC) is enriched in Pb (11.0 times), Cs (2.0 times) and U (2.0 times), green clay (GC) is enriched in As (3.3 times) and U (2.1 times), while the red clay (RC) is enriched in Se (9 times).

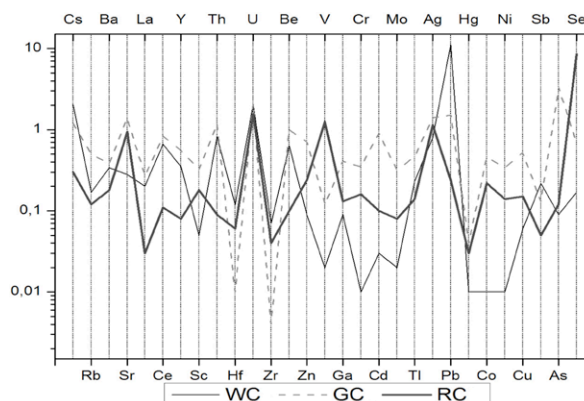


Figure 1: Average shale-normalized trace element spider diagram patterns of the studied samples; elements sorted according to their electronegativity values.

[1] E.C. Regulation 1223 (2009) *Official Journal of the European Union*, L342 (22.12.2009), 59-209. [2] Mason & Moore (1982) *Principles of Geochemistry*. Wiley, New York, 344p.

U-Pb and Hf isotopes in zircons from mantle chromitites of the Finero Peridotite (Ivrea Verbano Zone)

T. GIOVANARDI^{1,2}, A. ZANETTI^{3*}, M. MAZZUCHELLI²,
M. TIEPOLO³, F.-W. WU⁴, A. LANGONE²
AND R. VANNUCCI¹

¹Dip. Scienze della Terra e Ambiente, Univ. di Pavia, Pavia, Italy

²Dip. Sc. Chim. e Geol., Univ. di Modena e Reggio Emilia, Modena, Italy

³Istituto di Geoscienze e Georisorse, CNR, Pavia, Italy

⁴IGG, Chinese Academy of Sciences, Beijing, China

(*correspondence: zanetti@crystal.unipv.it)

The Finero Phlogopite Peridotite unit (hereafter Ph-Pd. Ivrea-Verbano Zone, IVZ: Southern Alps) is the unique worldwide example of orogenic mantle massif completely constituted by phlogopite-bearing ultramafics (mainly harzburgites, websterites and dunites) after pervasive to channelled melt migration events. A precious opportunity to provide further constraints on the petrologic and geodynamic evolution of such a mantle sequence is given by the occurrence of zircons in chromitites usually composed by Chromite+Orthopyroxene±Clinopyroxene±Amphibole.

Zircons show low CL emission and are generally homogeneous. Few grains display cores slightly darker than the rims. Zircons have up to 1420 and 800 ppm of U and Th, respectively, with Th/U ratio up to 1.6. U-Pb LA-ICP-HRMS analyses yield most concordant Lower Jurassic dates with a weighted average ²⁰⁶Pb/²³⁸U age at 187±2 Ma. A few darker cores yield Middle Triassic concordant ²⁰⁶Pb/²³⁸U ages from 242±7 Ma to 229±7 Ma. Zircons also show ¹⁷⁶Hf/¹⁷⁷Hf ratios in the range of 0.282486-0.282610, which give sub-chondritic εHf₍₁₈₈₎ (-6.0 to -1.6). The relatively high U and Th contents and the large Th/U ratios are the evidence that the chromitite zircons crystallised from a melt, which, according to the low εHf₍₁₈₈₎ values, had a marked crustal signature. This melt is analogous to that at the origin of the phlogopite harzburgites and websterites. The absence of internal zoning in zircon is interpreted as the result of homogenisation after a prolonged residence at high temperature mantle conditions. In this frame, the Lower Jurassic ages are proposed to date the cooling of the mantle sequence during exhumation for the opening of the Alpine Tethys. Conversely, the few Middle Triassic dates could represent the age of mantle metasomatism. As a whole, our data strongly support that the Finero area experienced a different geodynamic evolution with respect to the rest of IVZ.

Use of whole rock geochemistry for ignimbritic unit recognition: An example from the Sulcis area (SW Sardinia, Italy)

G. GISBERT AND D. GIMENO

Facultat de Geologia, Universitat de Barcelona, C/ Martí i Franquès s/n, 08028 Barcelona, Spain.

(ggisbertp@hotmail.com, d.gimeno.torrente@gmail.com)

In the Sulcis area (SW Sardinia, Italy) a thick Oligo-Miocene volcanic sequence formed during the drifting and rotation of Sardinia from the European continental margin to its current position. These volcanics originated by the combined effect of oceanic crust subduction under the Corsica-Sardinia microplate and increased extensional tectonics after 18 Ma. The volcanic deposits are over 600 m thick and cover an area more than 40 km in diameter which includes part of the mainland and two minor islands. This volcanic sequence consists of two differentiated halves: a lower one formed by andesitic lava domes and flows, and an upper one formed by a pile of trachytic and rhyolitic up to comenditic ignimbritic mantles, some of which cover the whole studied area. This ignimbritic sequence has been divided over the years into 18 units. The similarities between the various ignimbritic units, both macro- and microscopically in many cases, combined with the large facies variability some units may present, make the correct identification of units and correlation between zones and outcrops difficult in such a wide area, which is divided, moreover, by the sea. To solve this problem a thorough study of the ignimbritic suite was carried out involving the volcanostratigraphic revision and the whole rock geochemical characterisation of each unit. Whole rock geochemistry was analysed by means of XRF, ICP-MS and ICP-OES. A protocol was developed which allows the identification of the ignimbritic units in the Miocene Sulcis ignimbritic pile based on whole rock geochemistry. It works by projecting geochemical data of problem samples into specially-designed binary diagrams. This tool for the recognition of units using only its whole rock geochemistry has allowed us to solve many cartographic and stratigraphic doubts in the study area, proving its usefulness. From now on it can be also used by other researchers working in the area. Moreover, the methodology followed to elaborate this protocol can be applied elsewhere.

This study has been funded by the Spanish project CGL2011-28022.

Solubility and mineral storage of CO₂ in basalt

S.R. GISLASON¹, E.H. OELKERS^{1,2}, B. SIGFUSSON³,
J.M. MATTER⁴, M. STUTE⁴, E. GUNNLAUGSSON³,
I. GUNNARSSON³, E.S. ARADOTTIR³,
H. SIGURDARDOTTIR³, K. MESFIN¹, H.A. ALFREDSSON¹,
D. WOLFF-BOENISCH¹, M.T. ARNARSSON⁵
AND W.S. BROECKER⁴

¹Institute of Earth Sciences, University of Iceland, Sturlugata 7, 101 Reykjavík, Iceland, (correspondence: sigrg@hi.is)

²GET, CNRS/URM 5563-Université Paul Sabatier, 14 ave. Edouard Belin, 31400, Toulouse, France

³Reykjavík Energy, Baejarhálsi 1, 110 Reykjavík, Iceland

⁴Lamont-Doherty Earth Observatory, 61 Route 9W, Palisades, NY 10964, USA

⁵Mannvit, Grensásvegur 1, 108 Reykjavík, Iceland

The long-term security of geologic carbon storage is critical to its success and public acceptance. Much of the security risk associated with geologic carbon storage stems from its buoyancy. Gaseous and supercritical CO₂ are less dense than formation waters providing a driving force for it to escape back to the surface via fractures, or abandoned wells. This buoyancy can be eradicated by the dissolution of CO₂ into water prior to, or during its injection into the subsurface. The dissolution will further enhance mineral storage of CO₂ especially if injected into silicate rocks rich in divalent metal cations such as basalts and ultra-mafic rocks.

We have demonstrated the dissolution of CO₂ into water during its injection into a rock formation leading to its geologic solubility storage in less than 5 minutes. This process was verified via the successful injection of over 170 tons of dissolved CO₂ into porous basaltic rocks located 400-800 m below the surface at the CarbFix [1,2,3] field injection site in SW Iceland. Rock dissolution, dilution, and dispersion, caused the pH and alkalinity of the injected water to increase. Concomitantly, the concentration of most dissolved elements increased and carbonate minerals became saturated. Conservative tracers and ¹⁴C labelled CO₂ were mixed into the injected gas and water stream to monitor the subsurface transport and to assess the degree of subsurface carbonation.

[1] Gislason *et al.* (2010), *Int. J. Greenh. Gas Con.* **4**, 537 – 545. [2] Aradottir *et al.* (2012), *Int. J. Greenh. Gas Con.* **9**, 24 – 40. [3] Alfredsson *et al.* (2013), *Int. J. Greenh. Gas Con.* **12**, 399 – 418.

Dating mantle metasomatism: A new tool (U/Pb LIMA titanate) and an impostor (⁴⁰Ar/³⁹Ar phlogopite)

A. GIULIANI¹, D. PHILLIPS¹, M.K. KENDRICK¹,
R. MAAS¹, A. GREIG¹, R. ARMSTRONG², M.R. FELGATE¹
AND V.S. KAMENETSKY³

¹School of Earth Sciences, The University of Melbourne, Australia (*corresp: a.giuliani@student.unimelb.edu.au)

²Research School of Earth Sciences, Australian National University, ACT, Australia

³School of Earth Sciences, University of Tasmania, Australia

Precise dating of fluid processes in the Earth's mantle remains a major challenge for geoscientists. The U/Pb and Ar/Ar dating techniques have both been used in an attempt to constrain the timing of mantle metasomatic events; however, the Ar/Ar results have proven contentious [1]. Here we compare the ⁴⁰Ar/³⁹Ar ages obtained for large phlogopite grains from 7 mantle xenoliths from the 84 Ma Bultfontein kimberlite (Kimberley, South Africa), with U/Pb ages from metasomatic zircon and LIMA minerals coeval with phlogopite.

LIMAs are unusual titanates that occur in phlogopite-rich metasomatised peridotites [2]. LIMA minerals are enriched in incompatible elements (e.g., LILE, LREE, HFSE), with high U (250-400 ppm) and Pb (200-700 ppm) contents. U/Pb geochronology on LIMA minerals is limited by the low U/Pb ratios and high common Pb. In this study, the U, Th and Pb isotopes of LIMA minerals from three mantle xenoliths were measured by *in-situ* LA-ICP-MS. Common Pb values were determined from isotope dilution MC-ICP-MS measurements of coeval clinopyroxene grains. LIMA U/Pb ages are ~ 170-180 Ma, in agreement with a U/Pb age of 184±2 Ma obtained for a single zircon from one of the LIMA-bearing xenoliths. These results suggest a link between mantle metasomatism and Karoo magmatism in southern Africa [3].

Ar/Ar step-heating analyses of phlogopite grains were conducted using a new generation ARGUSVI multi-collector mass spectrometer. All the phlogopite samples yielded much older ⁴⁰Ar/³⁹Ar ages (up to 780 Ma) than coexisting zircon and/or LIMA minerals. We attribute these anomalously old Ar/Ar ages to the presence of excess ⁴⁰Ar in the metasomatic fluid that crystallised phlogopite [4]. We conclude that the ⁴⁰Ar/³⁹Ar phlogopite technique cannot be used to date mantle metasomatism.

[1] Phillips (2012) *Precambr Res* **208**, 49-52. [2] Haggerty (1983) *GCA* **47**, 1833-54. [3] Konzett *et al.* (1998) *EPSL* **160**, 133-145. [4] Phillips & Onstott (1988) *Geology* **16**, 542-546.

Textural evolution of a basaltic melt in function of cooling rate

¹L. GIULIANI, ¹F. CAUTI, ¹²G. IEZZI, ¹³F. VETERE,
¹²B.T. POE, ²A. CAVALLO, ²V. MISITI, ²G. VENTURA²,
S. MOLLO AND H. BEHRENS

¹Dipartimento di Ingegneria & Geologia, Università G.
d'Annunzio, Via dei vestini 30, 66100 Chieti, Italy
(*correspondance: g.iezzi@unich.it)

²Istituto Nazionale di Geofisica e Vulcanologia, Via di Vigna
Murata 605 00143 Rome, Italy

³Institute for Mineralogy, Leibniz University of Hannover,
Callinstr. 3, Hannover, D-30167, Germany

The evolution of textures has been quantified in run-products of basaltic composition solidified at 0.0167, 0.117, 1, 3, 30 and 150 °C/min from superliquidus to 800 °C. Three of these six cooling rates were run two times. At cooling rates ≤ 1 °C/min and ≥ 3 °C/min crystals are faceted and dendritic, respectively. Crystals and dendrites have been analyzed by image analysis, to obtain the proportion (area%), length and width (μm), aspect ratio, orientation of maximum axis ($^\circ$) and phase density (n/area) of objects.

As the cooling rate increases crystal and plagioclase contents monotonically decrease, whereas clinopyroxene content shows an asymmetric Gaussian-like trend; the amount of spinel is instead always < 6 area%.

The strength of the fabric (preferred orientation of crystals) is low, except for one experiment at 0.0167 and 150 °C/min due to the likely presence of a thermal gradient.

The aspect ratio of plagioclase and spinel smoothly decreases with decreasing cooling rate; conversely, the shape of clinopyroxene does not show a specific trend.

As the cooling rate increases, the abundance of tiny crystals progressively and exponentially increases. In general, the number of crystals per area, which reflects nucleation, exponentially increases as the cooling rate increases, except at 150 °C/min.

At 150 °C/min this basaltic melt is virtually glassy (< 2 area%), indicating that 150 °C/min is close to the critical cooling rate (R_c) for this melt.

Finally, run-products from three duplicated experiments show crystal content differences < 1 , 4 and 18 area% under 0.0167, 1 and 30 °C/min, respectively.

The evolution of textural parameters experimentally observed here allows us to calibrate geo-speedometers and design new glass-ceramics.

Experimental determination of chlorine isotope fractionation in Cl_2 - Cl_{aq}^- and $\text{ClOH}_{\text{aq}}-\text{Cl}_{\text{aq}}^-$

THOMAS GIUNTA*, JABRANE LABIDI HANS
AND G.M. EGGENKAMP

Laboratoire de Géochimie des Isotopes Stables, IPGP, 1 rue
Jussieu, 75238 Paris Cedex 05, France. (*correspondence:
giunta@ipgp.fr)

In nature, the most common oxidation state of chlorine is -I (Cl^-). However, in some extreme environments such as hydrothermal systems, atmosphere or Martian soils, occurrences of other oxidized form of chlorine have been recognized. *Redox* reactions are known to produce large isotopic fractionations, that have been theoretically estimated for chlorine stable isotopes at equilibrium [1].

In order to explore both the chemistry and the isotopic effects of some of these redox processes, we designed a chloride oxidation experiment. In our apparatus, liquid HCl is mixed at $\sim 20^\circ\text{C}$ with H_2O_2 , a powerful oxidant. Under a highly complex reaction pathway, this mixture ultimately leads to the formation of Cl_2 gas. The new forming gas is directly flushed out and trapped in a KOH solution, where it disproportionates into Cl^- and ClOH . In the oxidation reaction, the maximum production of Cl_2 is about 20% of the initial HCl. This experiment allows us to explore the isotope fractionation associated with three reactions: i) the oxidation of Cl_{aq}^- into Cl_2 , ii) Cl_2 degassing, iii) Cl_2 disproportionation into Cl_{aq}^- and ClOH_{aq} .

The lack of fractionation during degassing implies that $\alpha(\text{Cl}_{2\text{gas}}-\text{Cl}_{2\text{aq}}) \approx 1.000$. Assuming batch equilibrium, we can therefore determine the fractionation factors as follows:

$$10^3 \ln \alpha(\text{Cl}_{2\text{gas}}-\text{Cl}_{\text{aq}}^-) = 3.72 \pm 0.25 \text{‰ at } \sim 20^\circ\text{C}, \text{ and}$$

$$10^3 \ln \alpha(\text{ClOH}_{\text{aq}}-\text{Cl}_{\text{aq}}^-) = 3.04 \pm 0.20 \text{‰ at } \sim 20^\circ\text{C}.$$

These two values are slightly lower than the theoretically calculated values [1][2]. We will discuss the likely hypothesis to explain these discrepancies.

[1] Schauble et al., (2003) *Geochimica et cosmochimica acta*, **67** (17), 3267-3281. [2] Czarnacki et al., (2012) *Isotopes in Environmental and Health Studies*, **48** (1), 55-64.

Dating metamorphic stages in HP-terrane: Case study in the Sesia Zone (NW-Alps, Italy)

FRANCESCO GIUNTOLI, MARTIN ENGI
AND AFIFÉ EL KORH

¹Institut für Geologie, University of Bern, Baltzerstrasse 1+3,
CH-3012 Bern, Switzerland
(francesco.giuntoli@geo.unibe.ch)

The dynamics of assembly of HP-terrane is of major geotectonic significance. We report on a field-based study in the Sesia Zone, a HP-terrane formed during Alpine convergence. The three main parts of the Sesia Zone essentially derive from the rifted NW-margin of the Adriatic continent.

Micaschists showing a HP foliation (eclogite to blueschist facies) and weak (greenschist facies) retrogression were studied in detail. Assemblages comprise multiple generations of phengite, garnet, glaucophane (\pm early omphacite) and allanite, plus quartz, epidote, chlorite, and titanite rimming rutile. Microstructural and mineral-chemical data indicate that growth zones in garnet and allanite correspond to distinct HP stages. In some cases, these can be related to discrete phases of deformation (D1/D2, D3).

Garnet cores are strongly porphyroclastic, with at least two overgrowth phases. Allanite composite grains have a LREE-rich metamorphic core believed to be stable with early grt plus first generation phen (Si-rich), gln, and rutile. Allanite rims (one or more) show lower LREE and seem to be stable with second generation phen, gln and probably grt. Thermobarometry for each stage is in progress.

Preliminary Th-Pb age data for all were obtained by *in situ* LA-ICP-MS analysis: 80-74 Ma for cores and 68-62 Ma for rims (imprecise owing to small volumes). These ages compare well with the two HP stages (HP1: ~75 Ma; HP2: ~65 Ma) Regis *et al.* (2013) found in several samples of the Fondo slice of the Sesia Zone, from which pressure cycling was inferred (Rubatto *et al.* 2011). Taken together with their data, the present sample suite indicates that YoYo tectonics may have operated in one (or more?) slices, which span at least 16 km along strike of the Sesia Zone.

Field-based research continues to define the size and geometry of tectonic slices that constitute the Sesia HP terrane. Kinematic constraints quantifying the relative mobility of such fragments are sorely needed, as the scale of mixing within subduction channels is poorly known. Understanding the overall processes in subduction channels requires that results from numerical models and field data be combined.

[1] Regis *et al.* 2013 submitted to J. Petrology. [2] Rubatto *et al.* 2011, Nature Geosci., doi: 10.1038/ngeo1124.

Inferring a West Antarctica firn temperature history from a shallow ice core using a new proxy.

V. GKINIS^{1,2}, T. JONES¹, J. WHITE¹, B. VAUGHN¹,
E. STEIG³, B. MARKLE³ AND S. SCHOENEMANN³

¹Institute for Arctic and Alpine Research, University of
Colorado, Boulder, CO 80309, (v.gkinis@nbi.ku.dk)

²Center for Ice and Climate, University of Copenhagen,
Copenhagen DK 2100

³Earth and Space Sciences, University of Washington, Seattle,
WA 98195, USA, steig@uw.edu

The isotopic composition of polar ice has traditionally been used as a proxy for the temperature of the precipitation site. The validity of the method has however been challenged over the years, mainly due to apparent artifacts related to the seasonality of the precipitation, shifts in moisture source areas and others. Water isotope diffusion in firn is a process that can be used to infer past temperatures without the common problems of the traditional slope method. The method exploits the spectral information contained in the water isotopic composition time series and thus requires data sets of high resolution measured with high precision. Here we describe the method of firn water isotope diffusion and present ways to extract the firn temperature signal from high resolution $\delta^{18}\text{O}$ and δD time series. We apply this method on a 300 m shallow core from WAIS divide Antarctica (WDC2005A), sampled at a resolution of 3.3 cm and extending back to 1200 years b2k. We discuss on the findings of our temperature reconstruction and compare it to the temperature inferred with the traditional slope as well as with recent borehole temperature studies.

Metal micronutrients for anaerobic oxidation of methane

JENNIFER B. GLASS^{1*}, JOSHUA A. STEELE¹,
KATHERINE S. DAWSON¹, SHAWN E. MCGLYNN¹,
CHRISTOPHER T. REINHARD¹ AND VICTORIA J. ORPHAN¹

¹Division of Geological and Planetary Sciences, California
Institute of Technology, Pasadena, CA 91125;
(jglass@caltech.edu)(*presenting author)

Methane is produced and consumed by microbes via metabolic pathways that involve metalloenzymes [1]. Our focus is trace metal requirements for anaerobic oxidation of methane (AOM) performed by microbial consortia of sulfate-reducing bacteria (SRB) and anaerobic methanotrophic euryarcheota (ANME) in marine methane seep sediments, where porewaters are highly sulfidic (up to 25 mM HS⁻) and scavenging by sulfide mineral precipitation may reduce the availability of bioessential metals.

Using both metagenomic and metaproteomic data, we are characterizing the “metallome” of ANME/SRB consortia enriched from methane seep sediments. Iron-sulfur and heme-containing proteins are involved in reverse methanogenesis, sulfate reduction and the Wood-Ljungdahl carbon fixation pathway. Iron is likely transported by ferrous iron transporters in both symbiotic partners. Cobalt as vitamin B₁₂ is present in enzymes involved in reverse methanogenesis, carbon fixation and methionine synthesis. Genes for high-affinity cobalt uptake and vitamin B₁₂ biosynthesis are present in both symbiotic partners. Nickel as the tetrapyrrole cofactor F₄₃₀ and as Ni-Fe-S clusters is involved in reverse methanogenesis and carbon fixation, respectively. Molybdenum-iron nitrogenases [2] and molybdate (MoO₄²⁻) transporters are found in both partners, and a Mo or tungsten-containing enzyme is also involved in reverse methanogenesis.

Measurements of dissolved metal concentrations in methane seep sediment porewaters revealed that Co, Ni and Fe levels were below those required for optimal growth of cultured methanogens [1]. In contrast, dissolved Mo concentrations were generally high (~1 μM), suggesting that thiomolybdates (MoS₄²⁻) are soluble in these porewaters. The similarity in size and charge between MoS₄²⁻ and MoO₄²⁻ may allow anaerobes to transport both species through the same transporters. Results from incubation experiments using sediment with a well-characterized ANME/SRB population and low dissolved metals, designed to test if Fe, Co and Ni additions stimulate AOM activity and/or ANME/SRB growth, will also be presented.

[1] Glass and Orphan (2012) *Front. Microbiol.* **3**:61,1-20. [2] McGlynn *et al.* (2013) *Front. Microbiol.* **3**:419,1-8.

A role for liquid immiscibility in granites and granodiorites

ALLEN F. GLAZNER¹ AND JOHN M. BARTLEY²

¹Dept. of Geological Sciences, Univ. of North Carolina,
Chapel Hill, NC 27599, USA (afg@unc.edu)

²Dept. of Geology and Geophysics, Univ. of Utah, Salt Lake
City, UT 84112 (john.bartley@utah.edu)

Mafic segregations in granodioritic and granitic bodies, such as layered granodiorites (LGs) and ladder dikes (LDs), are typically interpreted to have formed by separation of mafic minerals from a more silicic magma body via processes such as gravitational settling and shear flow. In the Sierra Nevada of California and other examples, the whole-rock geochemistry and mineral chemistry of the mafic layers rule out such an interpretation and instead suggest that these layers are the heavily recrystallized products of liquid immiscibility.

LGs and LDs consist of high concentrations of biotite, hornblende, magnetite, titanite, apatite, and zircon, leading to extreme enrichments in REE, Fe, Zr, P, and Ti; Fe₂O₃^t in some LD mafic layers approaches 35 wt%, and La 1000x chondrite. LGs and LDs also have low Al and low Mg numbers (Fig. 1). These features require that the minerals in the layers were not derived from the surrounding pluton by crystal-liquid separation. Instead, they are consistent with crystallization from an Fe-rich immiscible liquid exsolved from high-silica liquid during the latter stages of crystallization. Although immiscibility is obscured in plutonic rocks owing to crystallization of the immiscible liquids, it has been proposed for several layered mafic complexes, and we suggest that it is a minor but widespread process in the late-stage evolution of granitic systems.

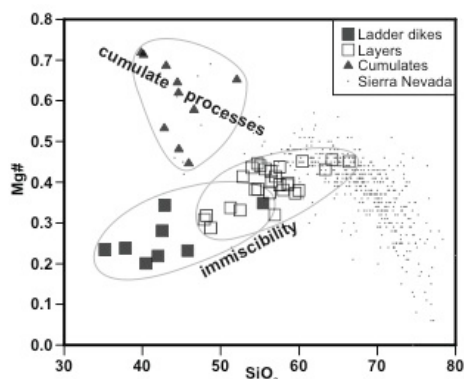


Figure 1: Mg number vs. SiO₂ for the Sierra Nevada batholith and occurrences of cumulate rocks, LDs, and LGs therein. LDs and LGs have much lower Mg numbers than cumulate rocks, consistent with immiscibility.

Heme *b* in particulate material from the Atlantic and Southern Oceans

M. GLEDHILL^{*1}, D.J. HONEY¹, M.J. RIJKENBERG^{1,2}
M.N. NIELSDOTTIR¹ AND E.P. ACHTERBERG¹

¹Ocean and Earth Science, University of Southampton,
National Oceanography Centre Southampton, UK
(martha@soton.ac.uk)

²Department of Biological Oceanography, Royal Netherlands
Institute of Sea Research, Texel, The Netherlands
(*correspondence: martha@soton.ac.uk)

Heme *b* is the iron containing prosthetic group of hemoproteins, which include *b* type cytochromes, peroxidases and catalases. We determined the heme *b* abundance in particulate material on three cruises in the Atlantic and Southern Oceans. Analysis of phytoplankton cultures indicated that we recovered approximately 18% of the total cellular iron pool in marine phytoplankton as heme *b* [1, 2]. We show that particulate heme *b* concentrations are depleted relative to particulate carbon and chlorophyll *a* in samples from the Southern Ocean and high latitude North Atlantic when compared to samples from the tropical North Atlantic Ocean. The phytoplankton communities in the Southern Ocean and high latitude North Atlantic are iron stressed during at least part of the growing season, whereas the iron supply to the tropical North Atlantic is high due to aerosol inputs. The observed lower heme *b* to carbon ratios are consistent with the patterns of iron supply and suggest a reduced capacity for photosynthetic and respiratory electron transport in high latitude phytoplankton populations. However, comparison with primary productivity determined on the same cruises showed that heme *b* use efficiency, defined as the amount of heme *b* required to fix a mole of carbon per second, was enhanced at high latitudes compared to the tropical North Atlantic. We discuss the implications of our results for phytoplankton iron requirements in the Atlantic Ocean.

[1] Gledhill (2007), *Mar. Chem.* **103**, 393. [2] Honey *et al.* (2013), *Mar. Ecol. Prog. Ser.* 243, 1.

Regional urban geochemical baseline for heavy metals and persistent organic pollutants in Dublin, Ireland (SURGE Project)

GLENNON, M.M.¹, SCANLON, R.P.^{1*}, O'CONNOR, P.J.²,
HARRIS, P.³ AND OTTESEN, R.T.⁴.

¹Geological Survey of Ireland, Beggars' Bush, Haddington
Road, Dublin 4, Ireland. (*ray.scanlon@gsi.ie).

²Independent Consultant, Dublin, Ireland.

³National University of Ireland, Maynooth, Ireland.

⁴Norges Geologiske Undersøkelse, Trondheim, Norway.

The Dublin SURGE (Soil Urban Geochemistry) Project establishes a baseline for inorganic elements and persistent organic pollutants in topsoils in Dublin, Ireland for the first time. Topsoil samples (n=1058) of 0-10 cm depth from the greater Dublin area (430 km²) were analysed for 31 inorganic elements by ICP-AES. A subset of 194 samples was analysed for polycyclic aromatic hydrocarbons (PAHs) and polychlorinated bipheyls by GC-MS and GC-ECD respectively.

Exploratory data analysis was carried out on the analytical results using bedrock, soil type and land use zones data to reveal natural and anthropogenic influences on soil geochemical concentrations. Box plots, histograms and cumulative probability curves indicate that concentrations of Pb, Cu, Zn, Hg and PAHs are strongly influenced by human activities in the docklands, the inner city and heavy industry areas of Dublin. Historical industry, domestic coal burning, reuse of contaminated soil and traffic emissions are likely sources.

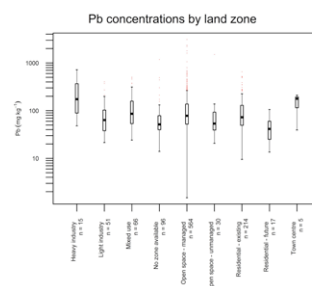


Figure 1. Box plots for Pb in topsoil showing higher median concentrations (mg/kg) in heavy industry and town centre zones.

To better understand historical anthropogenic sources of contaminants, historical industry locations were compiled and employed in a preliminary multivariate spatial analysis which demonstrates strong spatial correlations between key contaminants and certain historical industries. The project provides systematic, regional baseline data for urban soils relevant to the protection of human health, compliance with environmental legislation and urban regeneration.

Oxygen dynamics in marine sediments: From microbial to global Scale

RONNIE N GLUD^{1,2,3}

¹University of Southern Denmark

²Scottish Association of Marine Science

³University of Aarhus

Oxygen availability and dynamic are key factors regulating the biological and biogeochemical functioning of marine sediments. On microscale in has in recent years become evident that marine sediments are much more dynamic than previously anticipated. Micro scale topography, particulate sedimentation, short and long term changes in hydrodynamic are all factors that induce temporal and spatial variations in the oxygen distribution. Furthermore, macro and meio fauna activity constantly affect the distribution of microbial niches. The intense dynamic affect the microbial interactions and ecology, putting high demands on metabolic versatility and/or mobility of microbes in a constantly changing environment. Also on meso- and regional scale the awareness on the importance of spatial and temporal dynamics is increasing. The benthic seascape and its interaction with large scale hydrodynamic features lead to highly uneven deposition of organic material and thereby in large scale distribution of benthic communities and biogeochemical process rates. The presentation will – on the basis of a number of case studies, using state of the art technology – discuss and challenge our conceptual understanding on benthic O₂ dynamics and sediment functioning.

Hydrogeochemical and Isotopic Investigation around the Manisa

GÜLER GÖÇMEZ¹ AND ERKAN HAFIZOĞLU²

¹Selcuk University, Geological Engineering Department, Konya, Turkey

(correspondence: gulergoçmez@selcuk.edu.tr)

²Celal Bayar Universty Vocational High School (ehafizoğlu@hotmail.com)

Investigated area, include Manisa country, Saruhanlı district on northeast of Manisa, Karaoğlanlı district on southeast Muradiye on north and Akgedik on west. Study area contains approximately 350 km² area.

The basement of the investigation area is made up Upper Cretaceous-Paleocene aged Bornova melange which contains metasandstone, metamudstone and this units lateral and vertical transition gray coloured micritic limestones, white coloured tuff. This basement is overlaid unconformably by lower Miocene aged. Yeniköy formation including red coloured conglomerate gravelly sandstone and sandstone. This formation is overlaid conformably by Lower-Middle Miocene aged Zeytindağ formation, which contains conglomerate, sandstone, claystone, marl, shale, limestone of clay, tuff. Zeytindağ formation is overlaid unconformably by Upper Miocene aged Yamanlar volcanites that is made up andesite, dacite gravel blocks and agglomerates. Yamanlar volcanites is overlaid unconformably by Upper Miocene – Pliocene aged Aliğa formation which consist of sometimes tuff alloyed, claystone, siltstone, white - yellow coloured lacustrine limestones. All these formations are unformably is overlaid by Quaternary aged the Alluvium and slope deposits.

Investigation area, to be found in the very important structure İzmir Ankara suture zone, paleotectonic era geography of the Anatolia. According the Schoeller diagram of waters of wells in study area lines combining the anions and rations are approximately parallel. Most ions in waters Ca, Mg and HCO₃. Statics level in the drill wells is 0,26-93,5 meters. Dynamics levels 1,22-94 meters and debit is in between 15-95 lt/sn. According to physicochemical analysis of the wells in investigation area drillings which have close value run from the same area. According to isotope analysis results of the waters in this drilling. ¹⁸O values are (-6,46)-(-7,84), ²H values are (-34,95)- (-45,41) and ³H values are 0,90-3,55 . In isotopic studies, points belong to waters were nearly parallel and close to meteoric water line. So the waters have meteoric origin

Geochemistry of Fast-spreading Lower Crust: Results from IODP Expedition 345 at the Hess Deep Rift

M. GODARD¹, R. MEYER², A. SAHA³, K. M. GILLIS⁴,
J.E. SNOW⁵, A. KLAUS⁶ AND IODP EXPEDITION 345
SHIPBOARD SCIENTIFIC PARTY

¹Géosciences, CNRS-Université Montpellier 2, France;
(Marguerite.Godard@um2.fr)

²University of Bergen, Norway

³Indian Institute of Science, Bangalore, India

⁴University of Victoria, B.C., Canada

⁵University of Houston, Houston TX, USA

⁶Texas A&M University, College Station TX, USA

We report preliminary results of IODP Expedition 345 (Site U1415, Dec. 2012-Feb. 2013) to the Hess Deep Rift where propagation of the Cocos Nazca Ridge into young, fast-spreading East Pacific Rise crust exposes a dismembered, but nearly complete lower crustal section, with extensive exposures of the plutonic crust. Reasonable recovery for hard rock expeditions (15%–30%) was achieved in three holes (35–110 m below seafloor), despite water depths of more than 4500 m and challenging drilling conditions.

Olivine gabbro and troctolite are the dominant plutonic rock types at Site U1415, with minor gabbro, clinopyroxene oikocryst-bearing troctolite, clinopyroxene oikocryst-bearing gabbro, and gabbronorite. All recovered gabbroic rocks have primitive compositions except for one gabbronorite sampled in the upper rubble zone at Hole U1415E, that is similar in composition to the evolved shallow gabbros previously sampled at Hess Deep. Site U1415 olivine gabbros, gabbros and gabbronorites overlap in composition: they have high Mg# (79–87), high Ni (130–570 ppm) and low TiO₂ (0.1–0.3 wt.%). Troctolites have high Mg# (81–89), Ni (260–1500 ppm) and Cr (365–1100 ppm) and low TiO₂ (<0.1 wt.%). The main geochemical characteristics of Site U1415 gabbroic rocks are consistent with formation as a cumulate sequence from a common parental MORB melt, troctolites representing the most primitive end-member of this sequence. They overlap in composition with the most primitive of slow and fast spread crust gabbroic rocks. These primitive geochemical signatures seem however contradictory with orthopyroxene (up to 5%) in the primary mineral assemblage of the olivine gabbros. In MORB crystallization series, orthopyroxene is expected to crystallize from evolved melts. The presence of orthopyroxene in the primitive gabbroic sequence sampled at Site U1415 suggests that it was formed in a more complex magmatic system, with possible mixing with melts in equilibrium with mantle orthopyroxene.

Rates of consumption of atmospheric CO₂ through the weathering of loess during the next 100 years of climate change

YVES GODDÉRIIS¹, SUSAN L. BRANTLEY²,
LOUIS M. FRANÇOIS³, JACQUES SCHOTT¹,
DAVID POLLARD², MICHEL DÉQUÉ⁴ AND MARIE DURY³

¹Géosciences Environnement Toulouse, CNRS, France

²Earth and Environmental Systems Institute, PennState, USA

³IAG, Université de Liège, Belgium

⁴Météo-France/CNRM, CNRS/GAME, Toulouse, France

We investigate how weathering of the Mississippi Valley loess will respond over the next 100 years of climate change along a North-South transect. Using a cascade of numerical models for climate (ARPEGE), vegetation (CARAIB) and weathering (WITCH), we explore the effect of an increase in CO₂ of 315 ppmv (1950) to 700 ppmv (2100 projection). Our simulations predict that temperature increasing in the next 100 years causes the weathering rates of the silicates to increase into the future. In contrast, the weathering rate of dolomite – which consumes most of the CO₂ – decreases in both end members (South and North) of the transect due to its retrograde solubility. We thus infer slower rates of advance of the dolomite reaction front into the subsurface, and faster rates of advance of the silicate reaction front. However, additional simulations for 9 pedons located along the North-South transect show that the dolomite weathering advance rate will increase in the central part of the Mississippi Valley, owing to a maximum in the response of vertical drainage to the ongoing climate change.

The carbonate reaction front can be likened to a terrestrial lysocline because it represents a depth interval over which carbonate dissolution rates increase drastically. However, in contrast to the lower pH and shallower lysocline expected in the oceans with increasing atmospheric CO₂, we predict a deeper lysocline in future soils. In the central Mississippi Valley, soil lysocline deepening accelerates but in the South and North the deepening rate slows. This result illustrates the complex behavior of carbonate weathering facing short term global climate change. Predicting the global response of terrestrial weathering to increased atmospheric CO₂ in the future will mostly depend upon our ability to make precise assessments of which areas of the globe increase or decrease in precipitation and soil drainage.

New insights into iron mineralogy and geochemistry in Saharan dust precipitated over Greece

A. GODELITSAS^{1*}, P. NASTOS¹, T.J. MERTZIMEKIS¹,
N. CHATZIKONSTANTINOU¹, A. DOUVALIS², K. TOLI³,
J. GÖTTLICHER⁴, R. STEININGER⁴ AND R. SIMON⁴

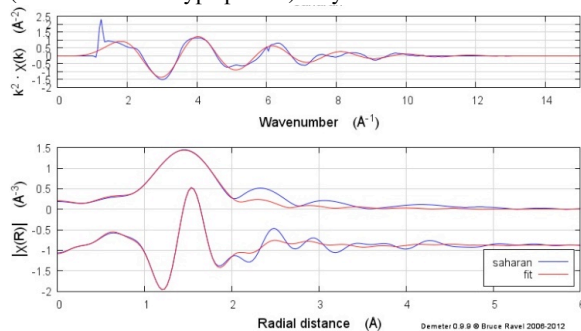
¹School of Science, University of Athens, Greece

²Dept. of Physics, University of Ioannina, Greece

³GWP Mediterranean, Athens, Greece

⁴ANKA Synchrotron Radiation Fac. KIT, Karlsruhe, Germany

The Saharan dust samples were collected on membrane filters after intense “red rain” episodes over the Greek megacity Athens. Characterization by means of bulk powder-XRD and SEM-EDS showed quartz, calcite and dolomite, as major crystalline phases and minor phyllosilicates (mostly clays). Detailed Synchrotron μ -XRF study proved that many trace elements are intercorrelated with Fe in microparticles of potential anthropogenic origin (e.g. Fe-Mn-V-Cu), as well as the presence of very hazardous elements such as Pb and As. Moreover, it was concluded that Fe also forms individual Fe-oxide and/or oxyhydroxy phases (sole Fe spots in μ -XRF maps) and besides it is frequently associated to Ca-containing phases and particularly carbonates (frequent Ca-Fe overlap in μ -XRF maps without Si or any other metal). However, Synchrotron μ -XRD study gave no clear evidence of crystalline Fe-oxides and/or -oxyhydroxides. Subsequent Mössbauer spectroscopic study showed abundant Fe^{3+} -containing constituents and minor Fe^{2+} -phases (ca. 5% paramagnetic component having Mössbauer parameters characteristic of a Fe^{2+} state). The investigation of the μ -XANES and -EXAFS (Figure below) indicated that Fe^{3+} most probably corresponds to ferrihydrite-type -XRD-“amorphous”- phases, but structural units from other Fe-oxyhydroxides, like akaganeite, and Fe^{3+} -oxyhydroxy-sulphates (schwertmannite-type phases) may also contribute.



Sequential leaching experiments, using appropriate acids and ICP-MS analyses, revealed a significant percentage of extractable Fe (and also Zn, Mn and Pb), fundamentally due to carbonate phases comprising ~60% of the material according to bulk XRD. It is herein stated that Fe in Saharan dust precipitated over eastern Mediterranean, and particularly Greece, is predominantly related to Fe^{3+} -oxyhydroxy (most probably ferrihydrite-type) phases, and to a lesser extent to Ca-(Mg)-carbonates hosting possibly the Mössbauer-detected minor Fe^{2+} component.

Direct observations of structures developed on fluorite surfaces after contact with an aqueous solution

J.R.A. GODINHO¹, C.V. PUTNIS² AND S. PIAZOLO³

¹Department of geological sciences, Stockholm University, 10691 Stockholm, Sweden; (jose.godinho@geo.su.se)

²Institut für mineralogie, University of Münster, 48149 Münster, Germany; putnisc@uni-muenster.de

³GEMOC ARC National key center, Department of earth and planetary sciences, Macquarie University, Australia; (sandra.piazolo@mq.edu.au)

In this study we used an atomic force microscope equipped with a fluid cell to observe the surface dynamics during the first minutes of contact between a solution and polished fluorite surfaces with orientations (115), (334), (104), (110) or (102). 3-D confocal profilometry was used to analyze the surface topography developed on the same surfaces for dissolution times up to 3200 hours.

The surfaces studied, with an initially high density of defects, showed fast changes during the first seconds in contact with solution. Different types of structures were observed on the surface depending on its initial orientation and the solution composition. These structures dissolved slower than the main surface persisting for at least 1620 hours of continuous dissolution. The inhibition of dissolution on the areas of the surface where the structures developed induced the growth of crystallographically controlled topography, which was linked to a variation of the surface reactivity and measured dissolution rate.

A new interpretation of traditional kinetic and thermodynamic models of dissolution applied to surfaces with high density of defects is proposed to explain the observations. It is proposed that the structures developing rapidly during the first contact with the fluid are a fluorite phase more stable than the initial surface. A new dissolution model is suggested to include the following steps: a) fast initial dissolution at defect sites; b) formation of a fluid boundary layer at the interface mineral-solution enriched in the dissolving ions; c) precipitation of a stable phase on surface defects. This model highlights the importance of considering surface defects for advancing our understanding of processes happening at the interface mineral-solution and for developing more accurate kinetic dissolution models essential in Earth and material sciences.

The pH of the Dead Sea brine: Calibrating the combination electrode measurements

R. GOLAN^{1,2}, I. GAVRIELI², B. LAZAR³ AND J. GANOR¹

¹Geological and Environmental Sciences, Ben Gurion University of the Negev, Beer Sheva, 84105, Israel

²Geological Survey of Israel, Jerusalem, 95501, Israel

³Institute of Earth Sciences, The Hebrew University of Jerusalem, 91904, Israel

While the pH is a major variable controlling the carbonate system speciation and the saturation state of carbonate minerals in aqueous systems, its measurement in hypersaline brines is not trivial. In such media, a problem with liquid junction potential may arise when employing standard pH measurements using a combination pH glass electrode.

The hypersaline Dead Sea and its predecessor, Late Pleistocene Lake Lisan, precipitated sequences of seasonal aragonite laminae during most of their geological history. The seasonality in aragonite deposition from the Ca-chloride brines was attributed to supersaturation induced by mixing of the inflowing high bicarbonate fresh runoff water in the Ca-rich lake brine [1]. This study evaluates and verifies the pH measurements in Dead Sea brine and its mixtures with deionized water using a liquid-junction-free cell [2], consisting of a pH glass electrode (Orion 81-01) and Cl⁻ ion selective electrode, ISE (Orion 9417).

The voltage of the ISEs cell is proportional to the log activities product of H⁺ and Cl⁻. A calibration curve was prepared by measuring the ISEs cell voltage per incremental addition of 32% HCl to the brine. Cl⁻ activity was calculated based on the Pitzer data base and MacInnes convention using the PHREEQc software [3]. The pH values of the unknown brines were derived from the calibration curve by measuring the cell voltage and its major ion composition.

Simultaneous pH measurements by the ISEs and a standard combination pH glass electrode (Orion 81-03, calibrated with low ionic strength buffers) were conducted for comparison. It was found that the pH difference between the measurements by the two electrode system was linearly correlated with ionic strength. Hence, by applying appropriate correction factor it is possible to use a standard combination pH electrode to measure pH of very high ionic strength solutions. The pH of the surface brine of the Dead Sea was determined to be 6.28.

[1] Barkan *et al.* (2001) *GCA* **65**, 355–368. [2] Knauss *et al.* 1990, *GCA* **54**, 1519–1523. [3] Parkhurst & Appelo (1999), *USGS WRI Rep.* 99-4259.

Syn-Variscan anorogenic volcanism in northern Gondwana: SIMS U-Pb ages and REE patterns of zircon from deep borehole in coastal Israel

T. GOLAN¹, Y. KATZIR¹ AND M.A. COBLE²

¹Ben Gurion University of the Negev, Beer Sheva 84105, Israel (tzahig@post.bgu.ac.il)

²Stanford University, SHRIMP-RG lab, CA 94305, USA

The Helez Deep 1A borehole (southern coastal Israel) penetrated a 200 m thick (5977–5767 m depth interval) felsic volcanic section, the Gevim quartz porphyry, overlying Precambrian basement rocks and overlain by Triassic shales. Previous Rb-Sr and K-Ar dating of these volcanics yielded Permian and Jurassic ages, respectively, considered as recording rifting-related magmatism in the Levant margins of the NeoTethys. We present SIMS U-Pb dating of zircons separated from rock-cuttings recovered from 4 different depths within the volcanic unit (~10 zircon grains each), which yield Early Carboniferous crystallization age for the Gevim quartz porphyry. Zircons of the two deeper samples yield calculated concordia ages of 353 ± 3 and 345 ± 2 Ma (2σ), whereas for the two shallower samples 350 ± 10 and 355 ± 15 Ma discordia intercept ages were calculated. While separated zircon is fresh and idiomorphic, feldspar and micas, the major Rb and K carriers in felsic igneous rocks, are heavily altered to clay. The Rb-Sr and K-Ar clocks were thus reset by hydrothermal alteration. This is the first discovery of Early Carboniferous volcanism in northern Africa and Arabia. It closely follows uplift and erosion of several regional 'Geanticlines' and coeval with steep crustal thermal gradients in the Levant. Zircon REE patterns measured by SIMS indicate within plate 'A-type' granite affinity. The geodynamic setting of volcanism is thus extensional rather than of Variscan compression, possibly related to rifting and detachment of Gondwanan terranes that were eventually incorporated to the Variscan orogeny.

Molybdenum drawdown during the Cretaceous OAE 2

T. GOLDBERG^{1*}, S.W. POULTON², T. WAGNER³,
AND M. REHKÄMPER¹

¹Imperial College London, London SW7 2AZ, UK,
(*t.goldberg@imperial.ac.uk)

²University of Leeds, Leeds, LS2 9JT, UK

³Newcastle University, NE1 7RU, Newcastle upon Tyne, UK

During the Cretaceous greenhouse, globally occurring events of black shale deposition were associated with widespread ocean deoxygenation. Possibly the most pronounced of these oceanic anoxic events (OAE's) was the Cenomanian-Turonian OAE2 (~94 Ma). However, although certain redox sensitive trace metals tend to be preferentially sequestered in sediments deposited under anoxic conditions, with Mo drawdown being specifically prone to euxinic settings, these elements are generally somewhat depleted in sediments deposited during OAE2. To understand the driving factors responsible for this depleted trace metal drawdown, we have studied a low latitude section from the proto-North Atlantic Ocean in high-resolution, where existing biomarker and iron-sulphur data point to a dominantly euxinic water column, with periodic transitions to ferruginous water column conditions.

We utilised a variety of redox proxies (Fe-speciation, redox sensitive trace metals and Mo isotopes), which, in combination, allows us to evaluate the detailed nature of ocean redox conditions and hence controls on trace metal drawdown. Our data suggest that very low Mo/TOC ratios at Tarfaya and elsewhere in the proto-North Atlantic may have been result of partial restriction of deep-water exchange with other ocean basins. However, the low and possibly heterogeneous $\delta^{98}\text{Mo}$ values inferred for seawater, together with low Mo/TOC ratios, point to a large decrease in the size of the oceanic Mo reservoir during OAE2 due to a major increase in Mo drawdown under euxinic conditions.

Future gas through bioconversion of stranded coals

S.D. GOLDING^{1*}, S.K. HAMILTON¹, K.A. BAUBLYS¹,
J.S. ESTERLE¹, G. TYSON¹, S. ROBBINS¹, V. RUDOLPH¹,
H. ZHENG¹, P.C. GILCREASE² AND S.L. PAPENDICK²

¹The University of Queensland, QLD 4072, Australia
(*correspondence: s.golding1@uq.edu.au)

²South Dakota School of Mines and Technology, Rapid City,
SD 57701, USA (Patrick.Gilcrease@sdsmt.edu)

The biology of methanogenesis in deep subsurface environments is not well understood, and there has been only limited work on microbial processes in coal seams despite the fact that they may support a large subsurface ecosystem potentially capable of replenishing gas depleted by coal seam gas production. To carry out field scale stimulation of microbial methane production from coal, we need to determine what makes a coal favorable for microbial methane generation, which native microorganisms are essential for the stepwise conversion of coal to methane, what fraction of coal is convertible to microbial methane and whether there are chemical or physical stimulation methods that can enhance the rates of conversion. Many of these questions are best addressed in the laboratory through enrichment experiments using coal bed formation water as the source of microbes and coal as the sole substrate [1]. However, implementation of microbially enhanced coal bed methane will necessarily involve the identification of conceptual exploration targets, which requires not only understanding of the geological history of the coal basin but also the development of ancient analogue models for microbial methane generation.

In eastern Australia, the chemical and stable isotope compositions of coal seam gases and related production waters vary systematically with depth, which reflects mixing between shallow biogenic gas and deeper thermogenic gas in higher rank uplifted coals and variations in openness of the microbial system in low rank coals. In the northern Bowen Basin, methane carbon isotope compositions become less negative with depth and highest gas production occurs at intermediate levels where the gas is of mixed origins [2]. The higher gas production is a function of saturation and permeability. Individual wells in the Surat Basin also commonly show a positively parabolic trend in gas content with depth [3], which is interpreted to reflect enhanced methanogenesis linked to hydrology. Lateral variability in gas content is less well understood and requires further research.

[1] Papendick *et al.* (2011) *Int. J. Coal Geol.* **88**, 123–134. [2] Kinnon *et al.* (2010) *Int. J. Coal Geol.* **82**, 219–231. [3] Hamilton *et al.* (2012) *Int. J. Coal Geol.* **101**, 21–35.

The $^{238}\text{U}/^{235}\text{U}$ of the Earth and the Solar System

A. GOLDMANN¹, G. BRENECKA², J. NOORDMANN¹,
S. WEYER¹ AND M. WADHWA²

¹Leibniz Universität Hannover, Institut für Mineralogie,
Callinstr. 3, 30167 Hannover, Germany
(correspondence: s.weyer@mineralogie.uni-hannover.de)

²Arizona State University, School of Earth & Space
Exploration, Tempe, AZ 85287, USA

For this study we performed high precision $^{238}\text{U}/^{235}\text{U}$ isotope analyses of 27 bulk meteorites (carbonaceous and ordinary chondrites as well as achondrites) and 12 terrestrial basalts. Additionally, we compiled high precision $^{238}\text{U}/^{235}\text{U}$ data on bulk meteorites from the recent literature in order to constrain the distribution of U isotopic heterogeneities and to determine an average $^{238}\text{U}/^{235}\text{U}$ for the solar system.

Most meteorites overlap with the U isotope composition observed for terrestrial basalts (137.78 – 137.81, [1] and this study). The most prominent exceptions are among the ordinary chondrites (Richardton H5 = 137.711 and Elenovka L5 = 137.891). Likely, different processes are responsible for the observed U isotope variations on the bulk meteorite scale, including the decay of extant ^{247}Cm [2], evaporation/condensation [3], redox processes or nucleosynthetic heterogeneities, as indicated by different relationships of $^{238}\text{U}/^{235}\text{U}$ and Nd/U for different meteorites or meteorite components.

All meteorite samples considered here (in total 45) have $^{238}\text{U}/^{235}\text{U}$ values that define a Gaussian distribution with an average value of 137.79 ± 0.03 (at 95% confidence level). The uncertainty of this value is dominated by that of the used U double spike ($\pm 0.16\%$ [4]). Notably, the average values for each of the investigated meteorite groups and that of terrestrial basalts define a narrow range between 137.787 and 137.795, which overlaps with the average value for all bulk meteorites taken together. We thus consider the average value obtained from this study ($^{238}\text{U}/^{235}\text{U} = 137.79$) to be representative for the Earth and the Solar System, consistent with earlier estimates [3, 5, 6]. We recommend using it for Pb-Pb dating if the precise $^{238}\text{U}/^{235}\text{U}$ of the sample cannot be obtained. Compared to the Pb-Pb ages based on the previously assumed $^{238}\text{U}/^{235}\text{U}$ (137.88), the new value of this study results in 0.9 Ma younger ages.

[1] Weyer *et al.* (2008) *GCA* **72**, 345-359. [2] Brennecka *et al.* (2010) *Science* **327**, 449-451. [3] Connelly *et al.* (2012) *Science* **338**, 651-655. [4] Richter *et al.* (2008) *IJMS* **269**, 145-148. [5] Brennecka and Wadhwa (2012) *PNAS* **109**, 9299-9303. [6] Hiess *et al.* (2012) *Science* **235**, 1610-1614.

In-situ determination of Fe Isotopes in Kamacite-, Taenite- and Troilite-Phases of Ordinary Chondrites

A. GOLDMANN AND S. WEYER

Leibniz Universität Hannover, Institut für Mineralogie,
Callinstr. 3, 30167 Hannover, Germany

In this study we investigated the Fe isotopic composition of metal and sulphide grains in ordinary chondrites. Recent studies [1], [2] found variations in $\delta^{56}\text{Fe}$ of up to 0.8‰ in bulk grains or grain fractions, which were manually extracted and dissolved. Here we represent the first in-situ Fe isotope analyses conducted by femtosecond laser ablation-ICP-MS. Instrumental mass bias was monitored with a Ni standard solution, which was simultaneously aspirated during laser ablation. With this method a reproducibility for replicate analyses of homogeneous standards of 0.04 to 0.06 (2 SD) for $\delta^{56}\text{Fe}$ was achieved with spot-sizes as low as 30 μm . Prior to isotope analyses metal and sulfide grains were characterized with microprobe analyses.

The analyses of over 100 metal and sulphide grains in H- and L-chondrites revealed $\delta^{56}\text{Fe}$ values with a total variation of 1.6‰, ranging from -0.8‰ to +0.8‰, relative to IRMM-014. The analyzed sulphide grains (all troilite), revealed an average $\delta^{56}\text{Fe}$ of -0.47‰. Metal grains contained 80% - 90% kamacite with an average $\delta^{56}\text{Fe}$ of 0.05‰ and 10% - 20% taenite with an average $\delta^{56}\text{Fe}$ of +0.49‰.

These first results show that the abundance of taenite in ordinary chondrites may affect the Fe isotope composition of the bulk metal and that previously observed variations in $\delta^{56}\text{Fe}$ may be the result of variations in the sampling of taenite. Larger exolutions of kamacite and taenite were generally isotopically homogeneous, i.e. did not show any diffusive exchange of Fe isotopes. The large $\Delta^{56}\text{Fe}_{\text{metal-FeS}}$ of 0.6‰ – 0.8‰ in ordinary chondrites (compared to ~0.5‰ observed for iron meteorites [3]) indicates a very low troilite-metal equilibration temperature of <300°C (calculated after [1] using data from [4] for troilite).

[1] Theis *et al.* (2008) *GCA* **72**, 4440-4456. [2] Needham *et al.* (2009) *GCA* **73**, 7399-7413. [3] Williams *et al.* (2006) *ESPL* **250**, 486-500. [4] Polyakov and Soultanov (2011) *GCA* **75**, 1957-1974.

The ICDP Dead Sea Deep Drill Core: Chronology and implications for Levant climate change

S.L. GOLDSTEIN^{1*}, A. TORFSTEIN¹, M. STEIN²
AND H. KITAGAWA³

¹Lamont-Doherty Earth Observatory, Columbia University,
Palisades, NY 10964, USA (steveg@ldeo.columbia.edu)

²Geological Survey of Israel, 95501 Jerusalem, ISR

³Nagoya University, Nagoya, JPN

The ICDP Dead Sea Deep Drilling Project recovered the longest paleoclimate record in the Middle East, including a ~450m long core in the deepest basin, and extending to MIS 7, based on the overall glacial vs interglacial lithology. Here we report the detailed chronology from ¹⁴C of organic material, stable isotopes and U-series of aragonite, changing lithology, stratigraphic correlation with subaerial deposits, XRF-scanning, and layer counting.

The Levant climate conditions are recorded in detail in the sediment layering. During wetter climate intervals varve-like alternating aragonite and detritus (aad) reflect summer and winter seasons, respectively. Less runoff means less aragonite (more mud). Gypsum layers indicate more arid climate, and halite indicates hyper-aridity.

The new chronology shows that major lithological changes coincide with the timing of MIS boundaries; for example, at MIS 2/1 there is substantial gypsum interval (during Heinrich 1) is followed by halite, and interestingly, MIS 6/5 shows a similar transition. Throughout the core, the lithological sequence in detail strongly reflects changes observed in marine and polar records. For example, full glacials (MIS 2, 4, 6) are reflected by thicker aad sequences, while strong interglacial intervals show substantial halite, gypsum, and mud, but little aad. Halite and gypsum are prominent during the warmer intervals of MIS 5 (5e,c,a), while the cooler intervals (5d,b) are characterized by mud and even aad. Short unstable intervals such as the MIS 3 D-O cycles are reflected by short sequences of aad, mud, gypsum.

The most dramatic discovery is a major desiccation event, more extreme than anything during the Holocene, now constrained to occur during MIS 5c, and indicated by an interval of rounded pebbles resembling on-shore beach deposits, overlying ~45 meters of mainly salt. The obvious question arises, why did it happen during MIS 5c rather than 5e? Possible explanations include a more intense southern monsoon during 5e that contributed runoff in the basin, or low enough P/E during both 5e and 5c. In any case, its occurrence has implications for the water-starved Middle East today, with GCM models indicating a more arid future.

Multi-element pedogeochemical prospecting in the Agrochão-Murçós area (NE Portugal)

M. ELISA P. GOMES^{12*} AND PAULO J.C. FAVAS¹³

¹Department of Geology, University of Trás-os-Montes e Alto Douro, 5001-801 Vila Real, Portugal; *correspondence: mgomes@utad.pt

²Geosciences Centre, University of Coimbra

³IMAR-CMA Marine and Environmental Research Centre, University of Coimbra

Total concentrations of chemical elements in soils of the Agrochão-Murçós area (NE Portugal) were determined in order to define potential spatial anomalies which have economic value based on a multivariate analysis and a geostatistical approach. In the area networks of quartz veins mineralized with scheelite, wolframite and rare cassiterite cut metamorphosed silurian rocks near the ceiling of small apophyses of biotite granodiorite and granite.

Soil samples were collected at 421 locations (20–30 cm depth from the surface) and were taken at intervals of 50 m within parallel sampling lines and spaced 500 m. The total concentrations were determined in each sample after being disaggregated and sieved in a 180 mesh sieve. The solutions were analysed by ICP-OES for a suite of 45 elements.

Principal component analysis and factorial kriging analysis were used to map the spatial distribution of chemical elements in soil. The analysis of the plane of the first three principal components revealed three groups of elements. A group showed a positive correlation with the first principal component and included Al, Na, Ca, Li, Ga, P, Zr, Rb, Sr, Th, U and Rare Earth Elements (REE- Y, La, Ce), while a second group of 11 elements (Fe, Sc, V, Co, Ni, Ti, Cr, Nb, Mn, Ba and Zn) showed a positive correlation with the second component. The third group included As, Cu, W and Pb. Sulfur, K and Sn are better explained isolated respectively by the axes 4, 5 and 7.

Then, the elements were analyzed separately by factorial kriging analysis. In the study area, six anomalies of W, Sn and REE were defined. Tungsten anomalies are spread across an area which coincides not only with the Rebordelo granitic massif but also to some extent with other smaller granite outcrops to the east and the surrounding metasediments. In addition there is a clear correlation with the calculated anomalies and several old Sn/W concessions in the area. The Sn distribution is such that most of the samples fall below percentile 95 and only scattered samples show small concentrations of Sn. The Sn anomaly is restricted and even this represents values of approximately 100 ppm only.

The preservation of sulfur isotope signals in low sulfate systems: How low is low?

M. GOMES^{1*} AND M.T. HURTGEN¹

¹Department of Earth and Planetary Sciences, Northwestern University, Evanston, IL, USA (*correspondence: maya@earth.northwestern.edu)

The sulfur (S) isotope difference between sulfates and sulfides preserved in sedimentary rocks ($\Delta^{34}\text{S}$) has been utilized to reconstruct ancient marine sulfate levels and oxygenation of the early Earth. Many modern lake systems have low sulfate levels (<1mM) and thus serve as useful analogs to low sulfate oceans of the early Earth. In these low sulfate systems, the preserved $\Delta^{34}\text{S}$ is typically lower than the magnitude of S isotope fractionation due to microbial S cycling (ϵ_{SR}) because $\Delta^{34}\text{S}$ is quantified as the S isotope difference between S phases (sulfate and pyrite) formed in different portions of the water column/sediment. This is a result of the reservoir effect where, at low sulfate levels, the S isotope composition of the sulfate reservoir becomes enriched in the heavy isotope of S (^{34}S) as microbial sulfate reduction occurs in anoxic portions of the water column/sediment. In turn, dissolved sulfide becomes enriched in ^{34}S with depth as it is formed from a ^{34}S -enriched sulfate reservoir. The result of this effect, which follows Rayleigh distillation theory, is that the S isotope composition of pyrite formed from ^{34}S -enriched sulfide is close to the surface water sulfate S isotope composition and $\Delta^{34}\text{S}$ is low. The reservoir effect is particularly important at low sulfate levels because the sulfate reservoir becomes enriched in ^{34}S more rapidly when the sulfate reservoir is small. However, it is not clear how low sulfate levels must be for the reservoir effect to place constraints on $\Delta^{34}\text{S}$ values. We use a combined reactive transport and Rayleigh distillation model to assess when the size of the sulfate reservoir affects $\Delta^{34}\text{S}$ values. We then compare this model to modern euxinic systems in order to better constrain how $\Delta^{34}\text{S}$ values can be used to interpret marine sulfate levels in the past.

Testing of Ce and Eu anomalies in natural zircon as a sensor of oxygen fugacity for Archean magmas

A. GONCHAROV^{1,2} AND N. KOROLEV²

¹St. Petersburg State University, Faculty of Geology, Russia (a.goncharov@spbu.ru)

²Institute of Precambrian Geology and Geochronology RAS, St. Petersburg, Russia

The recent experimental calibrations of cerium and europium partitioning between melts and zircons [1, 2] allow calculating Ce and Eu anomalies in magmatic zircons as a function of oxygen fugacity. We ran testing on current database of natural zircons from Precambrian complexes (~3500 - 2000 Ma) of the Voronezh Crystalline Massif (Eastern-European platform) to estimate redox conditions in parental magma sources.

The initial limitation was that CHUR normalized Ce and Eu anomalies in studied zircon cores show a wide variation in complex as well as in the sample, apparently due to the different origin. To separate zircon material in basic and silicic rocks produced by metamorphic or other endogenic process and identify captured or inherited zircons from ones with magmatic genesis has been used recently developed Hf-Nd isotopic systematics [3].

A study of Ce and Eu in selected zircon minerals has allowed an assessment of the redox conditions in magma source that prevailed in the upper mantle during the formation of ancient basement on Eastern-European platform. The obtained oxygen fugacity value varies from -1 to +2 ΔFMQ for most of basic complexes at temperature range: 800-1000°C and from 0 to +4 ΔFMQ at 700-900°C. Unfortunately, we did not find any correlations between ages and oxygen fugacity values in same complex, the only correlation observed is evolution of redox condition through time due to the different geodynamic settings of magma source.

[1] Trail *et al.* (2012) *Geochimica et Cosmochimica Acta* **97**, 70-87. [2] Burnham & Berry (2012) *Geochimica et Cosmochimica Acta* **95**, 196-212. [3] Lokhov *et al.* (2009) *Regional geology* (in Russian), **38**, 43-53.

Relationship between leaf C, N and soil C, N: A case study of degraded grassland in western Jilin Province

H.Y.GONG, Y.F.LI*, D.Y.WANG, S.WAN
ANDY.Y.ZHAO

College of Earth Sciences, Jilin University, Changchun
130061, China, (yfli@jlu.edu.cn* presenting author)

Carbon (C) and nitrogen (N) are crucial chemical elements to plant and soil, they play important roles in plants growth and various physiological regulation mechanism. At present it is generally believed that the loss of soil nutrients(C, N etc) is accompanied with land degradation process, and plant nutrients are the dominant source to soil C and N. Therefore, the relationship between plant leaf C, N, C/N and soil C, N, C/N has been one of the hotly-discussed issues in the ecological stoichiometry. However, the C, N stoichiometry in the leaves of *Leymus chinensis* and soil conditions from the grassland in Chang'ling county in western Jilin Province, NE China, provides insights for the above issue. Our objective is to determine how and to what extent soil organic C(SOC), total N (STN) and C/N(S-C/N) influence leaf total C(LTC), total N (LTN) and C/N(L-C/N) in the study region.

This paper reports the SOC and STN contents of 18 surface soil samples(0-20cm) and the LTC and LTN contents of 18 *Leymus chinensis* samples. The results indicate that the average content of LTC ($457.07\text{mg}\cdot\text{g}^{-1}$) is lower than the global average content ($464\text{mg}\cdot\text{g}^{-1}$), however, the LTN content($22.37\text{mg}\cdot\text{g}^{-1}$) is higher than the global average content ($20.6\text{mg}\cdot\text{g}^{-1}$), however, the C/N ratio in *Leymus chinensis* leaf (21.59) is higher than the global average value (16.0). Moreover, the contents of SOC and STN are $10.35\text{mg}\cdot\text{g}^{-1}$ and $1.11\text{mg}\cdot\text{kg}^{-1}$, respectively. The research results of Bohn *et al* indicated that the average S-C/N ratio was about 12 in the grassland of almost no land degradation, however, the S-C/N ratio of the study region is 9.44, it is lower than 12. In addition, Pearson correlations analyses done by SPSS software indicate that LTC does not exhibit evidently correlations with SOC ($r=-0.19$, $n=18$) and STN ($r=-0.16$, $n=18$). The LTN also has no significant correlation with SOC ($r=0.11$, $n=18$) and STN ($r=0.132$, $n=18$). While the LTN has a very significant negative correlation with L-C/N ratio($r=-0.918$, $n=18$). The SOC has a very significant positive correlation with STN($r=0.981$, $n=18$). Taken together, the ratio of S-C/N is considerably lower than the global average, while L-C/N ratio is higher than the global average. The variation laws of soil C, N and C/N are inconsistent with plant leaf C, N and C/N. It is suggested that plant leaf C, N and C/N can influence soil C, N and C/N, but be not necessarily leading factor.

Therefore, we conclude that high plant C, N and C/N ratio does not necessarily lead to the high regional soil C, N and C/N ratio correspondingly, they are likely caused by other factors such as soil microbial activity, the decomposition degree of plant residues, soil texture, and external environment and so on.

This work was supported by Natural Science Foundation Project of Jilin Province (201215017).

Distribution and sources of organic matter (OM) in a tropical intertidal mud bank of French Guiana

S. GONTHARET^{1*}, O. MATHIEU², J. LEVEQUE²,
M.-J. MILLOUX², S. LESOURD³, S. PHILIPPE¹,
J. CAILLAUD¹ AND A. GARDEL¹

¹LOG, INSU-CNRS UMR 8187, Université Lille Nord de France, ULCO, 32 avenue Foch, 62930 Wimereux
(*correspondence: swanne.gontharet@univ-littoral.fr, sylvie.philippe@univ-littoral.fr, jacinthe.caillaud@univ-littoral.fr, antoine.gardel@univ-littoral.fr)

²LB, CNRS-UMR 6282, Université de Bourgogne, 6 boulevard Gabriel, 21000 Dijon, France
(olivier.mathieu@u-bourgogne.fr, jean.leveque@u-bourgogne.fr, marie-jeanne.milloux@u-bourgogne.fr)

³M2C, CNRS UMR 6143, Université de Caen-Basse Normandie, 24 rue des tilleuls, 14000 Caen, France
(Sandric.Lesourd@unicaen.fr)

The 1600km-long coast of South America between the mouths of the Amazon and the Orinoco is characterized by the occurrence of Amazon-derived mud banks. These mud banks are highly unstable structures due to a combination of sedimentary processes (erosion, re-suspension, re-deposition). Depending on their elevation and tidal cycles, they can be temporally emerged, resulting to their rapid colonization and stabilization by microphytobenthos and opportunistic mangroves (i.e. *Avicennia germinans*).

Due to their rapid colonization by vegetation and their strong hydrodynamics features, mud banks represent preferential sites for accumulation and intense remineralization of organic matter (OM). The objectives of this study are (1) to characterize the distribution of sedimentary OM and (2) to identify the OM sources of sediments sampled during the 2008 Equinoctial spring tide on the landward face of the Macouria mud bank (French Guiana). Elemental and stable carbon and nitrogen isotopic compositions were measured for sediments and potential OM sources (*Avicennia germinans* leaves, microphytobenthos and suspended particulate matter (SPM)). Lower TOC and TN contents are observed, indicating either low terrestrial OM inputs and/or extensive remineralization induced by important and repeated remobilization of mud deposits. The relative contributions of mangrove plants, SPM and microphytobenthos have been estimated using the atomic TN/TOC ratio and the $\delta^{13}\text{C}$ values. OM preserved in the sediments is mostly controlled by the SPM associated with minor amounts of OM derived from mangrove plants and microphytobenthos.

Insight into the use of U- and Th-series nuclides for soil-production rates determination

A. GONTIER*¹, S. RIHS¹, E. PELT¹, M-P. TURPAULT²,
D. LEMARCHAND¹ AND F. CHABAUX¹

¹LHyGeS/CNRS, Université de Strasbourg, France -
(*correspondence: adrien.gontier@etu.unistra.fr;
rihs@unistra.fr)

²Laboratory of Biogeochemistry of Forest Ecosystems, INRA,
Champenoux, France - turpault@nancy.inra.fr

Over the last decades, the U- and Th-series isotopes were used to determine weathering rates in various environments (e.g., 1-5), but some concerns may arise about the use of these chronometers in soil profiles. The objective of this study was to address two of these concerns: the impact of a land cover change and the bedrock characteristics on these chronometers. This study was carried out in the Breuil-Chenue experimental forest site (Morvan, France) developed by INRA-BEF. In 1976, the native forest was partially clear-felled and replaced by monospecific plantations (oak, Douglas and spruce). The site is separated in two adjacent blocks which distinguished by different grain-sizes of the same granite bedrock. Three podzolic soil profiles developed on the coarse grain-size granite were sampled under the native forest, replanted oak and Douglas stands respectively and one soil profile was sampled under the native forest developed on the fine grain-size granite. Some selective extractions were performed in order to investigate the distribution of U and Th among different soil phases, including the cation exchangeable fraction, Fe-Mn amorphous oxides (ammonium-oxalate extraction) and silicate minerals.

No significant amount of U and Th was detected in the exchangeable fraction, but the oxalate-extracted phase (mainly amorphous Fe-Mn oxides and organics) holds up to 25 % of these elements, with clear pedogenic redistribution through all the profiles. In all the four different soil profiles the activity ratios of the U-series nuclides vary within a narrow range of values: from 0.94 to 0.95 for (²³⁴U/²³⁸U) and from 1.19 to 1.22 for (²³⁰Th/²³⁴U), but our results demonstrate that the podzolic pedogenic processes may significantly impact the shallowest soil layers (0-40cm), making these horizons unsuitable for U-series dating. In contrast, the deepest soil layers do not show observable vegetation-derived or grain-size effects on the U-Th series. The soil production rate can therefore be calculated from these latter.

[1] Chabaux F., *et al.* (2013). *GCA* 100, 73-95 [2] Dosseto A. *et al.* (2008) *EPSL* 274, 359-371. [3] Ma, L., *et al.*, (2010). *EPSL* 297, 211-225. [4] Pelt, E., *et al.* (2008). *EPSL* 276, 98-105. [5] Rihs *et al.*, (2011). *GCA* 75, 7707-7724.

Metal adsorption on mosses: Towards a universal adsorption model

A. G. GONZÁLEZ AND O. S. POKROVSKY

Geosciences Environment Toulouse (GET), CNRS, UMR
5563, Observatoire Midi-Pyrénées, 14 Avenue Edouard
Belin, 31400 Toulouse, France

Physico-chemical characterization was performed for four moss species (*Hypnum sp.*, *Sphagnum sp.*, *P. purum* and *B. rutabulum*) and five metals (Cu²⁺, Cd²⁺, Ni²⁺, Pb²⁺ and Zn²⁺). Chemical composition of mosses showed that all 4 mosses exhibit similar concentration of Cu and Zn. For Pb and Cd, *Sphagnum sp.* is the most enriched. The amount of metal released as a function of time for each moss allow to classify the moss species in the following order. For Cu²⁺, Ni²⁺ and Pb²⁺: *B. rutabulum* > *P. purum* > *Sphagnum sp.* ≥ *Hypnum sp.*. For Cd²⁺, *P. purum* > *B. rutabulum* > *Hypnum sp.* ≥ *Sphagnum sp.*. For Zn²⁺, this sequence is *P. purum* > *B. rutabulum* > *Sphagnum sp.* ≈ *Hypnum sp.*. During this experiment, the DOC amount measurements showed that *Sphagnum sp.* released the lower DOC concentration. The acid-base surface titration of moss species from pH 3 to 11 indicated that *Sphagnum sp.* was species with more negative excess of charge. The pH of point zero charge (pH_{PZC}) was computed as 5.01 ± 0.13, 4.64 ± 0.1, 4.96 ± 0.14 and 6.23 ± 0.25 for *Hypnum sp.*, *Sphagnum sp.*, *P. purum* and *B. rutabulum* respectively. The adsorption of metal as a function of pH showed different pattern depending on the metal and allow to classify them as following: for Cu²⁺, *P. purum* > *B. rutabulum* > *Hypnum sp.* > *Sphagnum sp.*. For Cd²⁺ and Zn²⁺, *B. rutabulum* > *Sphagnum sp.* > *P. purum* > *Hypnum sp.*. For Ni²⁺ and Pb²⁺, *B. rutabulum* > *P. purum* > *Hypnum sp.* > *Sphagnum sp.*. The metal adsorption on moss surfaces as a function of aqueous metal concentration showed a close relationship between moss species for each individual metal. The adsorption order can be expressed by following. For Cu²⁺, *P. purum* ≈ *Sphagnum sp.* ≈ *B. rutabulum* > *Hypnum sp.*. For Cd²⁺, *Sphagnum sp.* > *B. rutabulum* > *Hypnum sp.* > *P. purum*. For Ni²⁺, *Sphagnum sp.* ≈ *Hypnum sp.* ≈ *P. purum* ≈ *B. rutabulum*. For Pb²⁺, *B. rutabulum* > *Hypnum sp.* > *Sphagnum sp.* > *P. purum*. For Zn²⁺, *B. rutabulum* ≈ *Sphagnum sp.* ≈ *Hypnum sp.* > *P. purum*. Eventually, a Linear Programming Modeling was applied for experimental data in order to compute the pK_s, pK_m and pK_a.

**Simultaneous Laser Ablation
Molecular Isotopic Spectrometry
(LAMIS), Laser-Induced Breakdown
Spectroscopy (LIBS) and Laser
Ablation Inductively Coupled Plasma
Spectrometry (LA-ICP-MS) for
elemental analysis of geological
samples**

JHANIS J. GONZALEZ^{1,2}, JOSE R. CHIRINOS¹,
MEIRONG DONG¹, DAYANA OROPEZA¹, XIANGLEI MAO¹,
ALEXANDER BOLSHAKOV², JONG YOO²,
PAUL SYLVESTER³, KATE SOUDERS³,
HENRY LONGERICH³, AND RICHARD E. RUSSO^{1,2*}

¹Lawrence Berkeley National Laboratory, Berkeley, CA, USA
(Correspondence: rerusso@lbl.gov)

²Applied Spectra, Inc., Fremont, CA, USA

³Memorial University of Newfoundland, St. John's,
Newfoundland, Canada

A system that combines the capabilities and analytical benefits of LIBS, LAMIS and LA-ICP-MS was demonstrated for the analysis of samples of geological interest. The system consists of a Nd:YAG laser operated at 213 nm, for the LIBS and LAMIS measurements with a switchable spectrometer-detector system (Czerny-turner spectrograph with ICCD detection and a six channel spectrograph with CCD detection). For ICP-MS measurements a choice between a Quadrupole based system and Time-Of-Flight based system was made depending on the application. The data will show simultaneous determination of major elements such Si, Ca, Mg, C, Al, etc. with LIBS, carbon and boron isotopes determination by LAMIS, with trace composition (i.e., REE's) information from these geological samples by ICP-MS. The data are presented in the form of elemental distribution maps of major and trace elements with lateral resolution on the order of 50 μm .

**The effect of Copper in the oxidation
of Fe(II) in seawater**

MELCHOR GONZÁLEZ-DÁVILA,
J. MAGDALENA SANTANA-CASIANO,
ARIDANE G. GONZÁLEZ, NORMA PÉREZ-ALMEIDA
AND GUILLERMO SAMPERIO

Universidad de Las Palmas de Gran Canaria. Departamento de
Química. Facultad de Ciencias del Mar. 35017, Tafira.
Las Palmas de G.C. Spain. Email:
(mgonzalez@dqui.ulpgc.es)

The competition between Fe(II) and copper species has been studied in seawater at different initial Cu(II) and Cu(I) concentration (0-200nM). In addition, the effect of pH (6.2-8.5), bicarbonate concentration (2-9mM) and hydrogen peroxide concentration (0-500nM) on the Fe(II) rate constant were also studied. The Cu(II) added in solution was rapidly reduced to Cu(I), at the first 1-2 min, and it remained in solution after 40 min when Fe(II) was added. The initial copper additions increase the oxidation rate of Fe(II) under the different experimental conditions. The rate constant of Fe(II) was a second order pH dependent function at pH over 7.5 and a first order function for lower pH values. In the presence of Cu(II), a first-order pH dependence was always observed. Thus, FeOH⁺, FeCO₃ and probably FeHCO₃⁺ are involved in the process. In addition, Fe(II) oxidation rate was increased only when both carbonate and Cu(II) concentrations was over 6mM and 100nM, respectively. The effect of H₂O₂ concentrations was also function of the initial Cu(II) additions, but the oxidation rate was equally affected by H₂O₂, thus the observed effect must be only due to the presence of copper species in solution.

Evaluation of heavy metals in sediments of Chapala Lake

M. J. GONZÁLEZ GUADARRAMA^{1*},
R. E. VILLANUEVA ESTRADA²
AND R. M. PROL LEDESMA²

¹Posgrado en Ciencias del Mar y Limnología, Universidad Nacional Autónoma de México, 04510, México D. F.
(*correspondence: chuy41284@yahoo.com.mx).

²Instituto de Geofísica, Universidad Nacional Autónoma de México, 04510, México, D.F.

The Chapala Lake is the largest and most important water body in Mexico, from a geological, chemical and ecological point of view [1, 2, 3]. In this work a relationship between size grain and heavy metals is presented.

Area	Granulometry				Chemical analyzes	
	Mz (Φ)	σ (Φ)	SK	K _G	%CO ₃ ⁻²	%organic matter
Bank	6.9	2.1	0.1	1.4	4.2	1.0
Center	5.1	1.7	0.0	0.9	4.4	1.1
Lerma River	5.3	1.6	0.0	0.8	2.5	0.6

Table 1 Size grain and chemical analyzes of carbonate and organic matter in the sediments.

Area	Geoaccumulation index					
	Ba	Cr	Cu	Ni	Zn	Pb
Bank	-0.0	0.9	0.2	0.2	0.2	-0.4
Center	-1.1	0.5	0.6	0.5	0.8	-0.1
Lerma River	-1.0	0.6	0.8	0.2	1.0	-0.1

Table 2 Geoaccumulation index calculated [4] for different areas in the Chapala Lake.

According to the calculation of geoaccumulation index and the scale given by Ramos *et al* (1990), no contamination by heavy metals in surface sediments was observed. The size grain is fine; the sediment is poorly sorted, near symmetrical and leptokurtic and the mineralogical analyses show the predominance of clays. The delta of the River Lerma generates organic matter and carbonates migrate to others areas in the lake.

[1] Rosales *et al* (2000), *Environmental Geology* **39**, 378-383.
[2] Hansen *et al* (2001), Kluwer Academic/Plenum Publishers, New York. [3] Zárate del Valle *et al* (2005), *RMCGeológicas* **22**, 358-370. [4] Ramos *et al* (1990), *Lurralde* **13**, 157-164.

Neo-Archean domains in the Mediterranean and their implications

*J.M. GONZÁLEZ-JIMÉNEZ¹, C. VILLASECA²,
W.L. GRIFFIN¹, E. BELOUSOVA¹, Z. KONC³,
E. ANCOCHEA², SUZANNE Y. O'REILLY¹,
N. J. PEARSON¹, C. J. GARRIDO³ AND F. GERVILLA^{3,4}

¹CCFS Centre of Excellence and GEMOC, Macquarie University, Sydney, Australia.

(*Correspondence: jose.gonzalez@mq.edu.au

²Dpt. Mineralogía y Geoquímica and Instituto de Geociencias, Madrid, Spain

³Instituto Andaluz de Ciencias de la Tierra (CSIC-UGR), Granada, Spain

⁴Dpt. Mineralogía y Petrología (UGR), Granada, Spain

Mantle-derived rocks, including xenoliths and peridotite massifs, are widespread throughout the Mediterranean region. A synthesis of Re-depletion model ages (T_{RD}) for both whole-rock samples and *in situ*-analysed of individual sulfides from these mantle-derived rocks reveal mantle domains of different ages across the Mediterranean region.

A maximum T_{RD} age of 1.8 Ga is common to sulfides in xenoliths sampling the mantle beneath Western Europe (Calatrava Volcanic Field, Spain; Languedoc and Massif Central, France) and of whole-rock samples from Azrou (North Africa) and the Pyrenees (France). A maximum at <1.4-1.3 Ga observed in whole-rock samples from Central Europe (Bohemian and Rhenish Massifs). In contrast, Os-bearing phases in xenoliths (sulfides) and in peridotite massifs (sulfides and platinum-group minerals) from the inner Mediterranean region (Hyblean Plateau in Sicily and Kraubath Massif in Austria) all show an oldest T_{RD} peak at ~ 2.3 Ga, equivalent to the oldest whole-rock T_{MA} of 2.2 Ga for rocks of Beni Boussera in northern Morocco and the 2.4 Ga peak in sulfides from peridotites of the internal Ligurides (Italy). A peak at 2.6 Ga is defined by sulfides in mantle xenoliths from the Tallante volcanic field in southern Spain.

These data clearly identify the existence of a common Paleo-Proterozoic (~ 1.8 Ga) mantle on both sides of the Mediterranean realm, and an older (~2.2-2.6 Ga) lithospheric mantle domain within the more recent Maghrebide-Appennine-Betic front generated during the Alpine-Betic orogeny. The Mediterranean basin may contain several buoyant Archean microplates, which could have impeded the northward movement of Africa and contributed to complex tectonics in the Mediterranean basin.

Crystallization of hydroxide cobalt carbonate $\text{Co}_2\text{CO}_3(\text{OH})_2$, precursor of Co_3O_4 , at room temperature

JORGE GONZÁLEZ-LÓPEZ^{1*},
 ÁNGELES FERNÁNDEZ-GONZÁLEZ¹
 AND AMALIA JIMÉNEZ¹

¹Departament of Geology, Universidad de Oviedo (Spain)
 jgonzalez@geol.uniovi.es

The crystallization of cobalt carbonate CoCO_3 , cobalt hydroxide carbonate $\text{Co}_2\text{CO}_3(\text{OH})_2$ and its hydrated phases $\text{Co}_2\text{CO}_3(\text{OH})_2 \cdot n\text{H}_2\text{O}$ have been subject of interest in the scientific literature because they can be precursors of the so-called low-dimensional cobalt oxide-based nanomaterials. Various cobalt salts can be precursors of Co_3O_4 , but carbonates and hydroxide carbonates are the most desirable because they are readily available and because no toxic product gases are produced during their calcination. In most cases, the physical properties and applications of the oxide-based nanomaterials are in linked with specific morphologies and hence, a number of works are focused on different experimental methods to achieve these morphologies. In most of the reported experimental works the cobalt carbonate phases have been synthesized by hydrothermal methods and their transformation into cobalt oxides occurs by calcination.

At room temperature, the crystallization behaviour of Co-carbonates seems to be complex and needs to be studied in depth. Under these conditions, the precipitation of crystalline cobalt carbonates or hydroxycarbonates from soluble salt of Co^{2+} and CO_3^{2-} is prevented by the formation of Co^{2+} aqueous complexes. Therefore the obtained phases by direct precipitation in aqueous solution are amorphous. In this experimental work we have aged this amorphous phase in the remaining aqueous solution for two months. We have observed its progressive transformation into a crystalline phase with rosasite-type crystal structure $\text{Co}_2\text{CO}_3(\text{OH})_2$. The evolution of the morphology and chemical composition of the solids with aging time, have been examined by X-ray Powder diffraction, scanning electron microscopy, transmission electron microscopy an infra-red spectroscopy.

The final $\text{Co}_2\text{CO}_3(\text{OH})_2$ crystals grown by aging at room temperature show platelet morphology and are transformed into Co_3O_4 by calcination in a similar way as the crystals of this substance grown by hydrothermal methods do. Moreover, the layered crystal structure of the precursor $\text{Ca}_2\text{CO}_3(\text{OH})_2$ favors the development of lamellar morphology that, after a topotactic transformation, is approximately maintained in the cobalt oxide new phase.

Nano iron sulfides for carbon dioxide reduction

JOSIE GOODALL^{1*}, NATHAN HOLLINGSWORTH¹,
 ANNA ROFFEY¹, KATHERINE B. HOLT¹,
 GRAEME HOGARTH¹ AND JAWWAD A. DARR¹

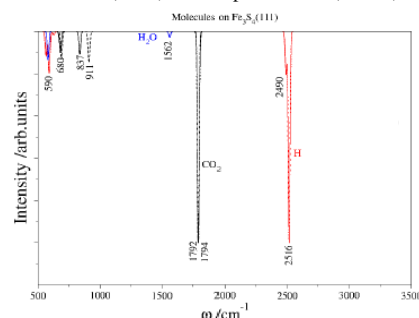
¹University College London, London, UK

*j.goodall@ucl.ac.uk

Despite the high thermodynamic stability of CO_2 , biological systems are capable of converting it into a range of organic molecules, under moderate conditions. Iron sulfide membranes formed in the warm, alkaline springs on the ocean floor are increasingly considered to be early catalysts involved the emergence of life. These anaerobic reactions are thought to have been catalyzed by small (Fe,Ni)S clusters similar to the surfaces of present day sulfide minerals.^[1]

We have synthesised iron sulfide nanomaterials using a novel methods based on continuous hydrothermal synthesis, where aqueous flows of iron and sulfide ions are brought into contact with a flow of superheated water (at 450 °C). The conditions and processes occurring during synthesis can be compared to those that might occur in hydrothermal vents.^[2,3] The electrochemical properties of these materials and their stability and activity towards CO_2 and their selectivity to products can be evaluated.

Figure 1: Simulated (solid) and experimental (dotted) IR spectra of



Greigite nanoparticles after CO_2 has been bubbled over the surface

Based on comprehensive computational investigations, a number of iron and iron-nickel sulphide nanoparticles have been designed, synthesised, tested, characterised, and evaluated for the activation and chemical modification of CO_2 at low voltages (obtainable from solar energy) and ambient conditions. Structures including greigite show evidence of interacting with CO_2 (figure 1). The electroreduction of CO_2 on iron sulfide surface has been shown to produce small organic molecules including formic acid

- [1] Russell (2005) *Economic Geology* **100**, 419-438.
 [2]Crabtree (1997) *Science* **276**, 222-222. [3]Middelkoop (2009) *Chemistry of Materials* **21**, 2430-2435

Mesoproterozoic and Paleoproterozoic igneous crust of central East Antarctica: Age and origins revealed from glacial clasts

J. W. GOODGE^{1*}, C. M. FANNING², J. D. VERVOORT³
AND C. FISHER³

¹Dept. of Geological Sciences, Univ. of Minnesota, Duluth, MN 55812 USA (correspondence: jgoodge@d.umn.edu)

²Res. School of Earth Sci., Australian Nat. Univ., Canberra, ACT 0200 Australia, (mark.fanning@anu.edu.au)

³Dept. of Earth Sciences, School of the Environment, Washington State Univ., Pullman, WA 99164, USA (vervoort@wsu.edu, chris.fisher@wsu.edu)

New SHRIMP U-Pb zircon ages from a large suite of granitoid clasts collected from glacial catchments draining central East Antarctica show that the crust in this ice-covered region was formed by a series of magmatic events at 2.00-1.90, 1.88-1.85, 1.80-1.79, 1.57, 1.48-1.43, and 1.20-1.10 Ga. The dominant granitoid populations are 1.85, 1.45 and 1.18 Ga, with some showing metamorphic overprinting at 1.18-1.15 Ga. Together, these clast ages indicate the presence in cratonic East Antarctica of a large, composite Proterozoic igneous province that reflects crustal growth across central East Gondwana. Further, they provide direct geologic support for the SWEAT reconstruction of Rodinia by correlation with Laurentia. Abundant ~1.1 Ga igneous and metamorphic clasts indicate the presence of Grenvillian orogenic belts in the interior that may reflect Rodinia assembly, and may sample crust underlying the Gamburtsev Subglacial Mountains.

In addition to U-Pb ages, we determined zircon Hf and O isotopic compositions in order to evaluate crustal history. Hf-isotope compositions were determined simultaneously with U-Pb by LA-ICP/MS in split-stream mode (LASS); O-isotope compositions were measured on SHRIMP-II in negative ion mode. Among the granitoid age populations, the following trends emerge: (1) a general pattern of increasing $\delta^{18}\text{O}$ with decreasing ϵHf , both corresponding with increasing age; (2) granitoids of ~2.0 Ga age have weakly evolved Hf compositions ($\epsilon\text{Hf} = +1$ to $+4$) and mantle $\delta^{18}\text{O}$; (3) rocks of ~1.57, ~1.79 and ~1.88-1.85 Ga age show evolved crustal compositions with $\epsilon\text{Hf} = +5$ to -8 , and $\delta^{18}\text{O} = 5.8$ - 8.3 ‰, and the ~1.88-1.79 Ga granitoids require some involvement of Archean crust; (4) rocks of 1.50-1.45 Ga age have mantle signatures with $\epsilon\text{Hf} = +5$ to $+11$; and (5) rocks of ~1.2 Ga age have crustal $\delta^{18}\text{O}$ signatures and $\epsilon\text{Hf} = +2$ to $+5$. Together, these age and isotopic data provide the first glimpse of crustal growth in central East Antarctica and suggest a varied history of relatively juvenile Proterozoic magmatism.

⁵⁴Cr isotope anomalies and Mn/Cr chronology in chondrites

C. GÖPEL^{1*}, J.-L. BIRCK¹, J. ZIPFEL², A. GALY³
AND B. ZANDA⁴

¹IPGP, 75238 Paris, France (*correspondance: gopel@ipgp.fr), (birck@ipgp.fr)

³Senckenberg Institute, 60325 Frankfurt, Germany (jzipfel@senckenberg.de)

²Dept. of Earth Sciences, University of Cambridge, UK (ajbg2@cam.ac.uk)

⁴MNHN, 75005 Paris, France (zanda@mnhn.fr)

In order for Cr to be used as a chronometer, the initial homogeneity of its isotopic composition in the solar system has to be verified. Today we have clear evidence for anomalies of ⁵⁴Cr in different meteorites whereas evidence for heterogeneity of ⁵³Mn and ⁵³Cr is less obvious [1-4].

In order to assess this problem we have performed detailed internal isotopic and mineralogical investigations of recently discovered equilibrated meteorites related to CR chondrites (Tafassasset, NWA 6901), the carbonaceous chondrite (NWA 5958) and of Acapulco. We exploit the double information provided by the Mn/Cr system: dating with ⁵³Mn/⁵³Cr and information on the nucleosynthetically distinct components witnessed by ⁵⁴Cr.

The bulk rocks of Tafassasset, NWA 6901 and NWA 5958 show positive ⁵⁴Cr values (1.333 ± 0.126 , 1.007 ± 0.188 , 0.973 ± 0.153) that are typical for carbonaceous chondrites. In contrast the Acapulco bulk rock exhibits a negative ⁵⁴Cr anomaly, similar to that observed in achondrites. The mineral phases in Tafassasset (chromite, olivine) exhibit an identical ⁵⁴Cr excess, while the ⁵⁴Cr anomaly is variable in different minerals (clinopyroxene, chromite, olivine) of Acapulco. In the ⁵⁵Mn/⁵²Cr versus $\epsilon^{53}\text{Cr}$ diagram the samples of both meteorites fall on linear trends implying variable ⁵³Mn/⁵⁵Mn ratios that are consistent with well-established chronological information [5, 6].

We will discuss the significance of such internal Mn-Cr isochrons, compare them to age information obtained from other systems and evaluate the new data in respect to the initial heterogeneity of ⁵³Cr and ⁵⁴Cr of the solar system.

[1] Trinquier *et al.* (2008) *GCA* **72**, 5146-5163. [2] Trinquier *et al.* (2007) *Astrophys. J.* **655**, 1179-1185. [3] Dauphas *et al.* (2010) *Astrophys. J.* **720**, 1577-5163. [4] Moynier *et al.* (2008) *Astrophys. J.* **671**, L181-L183. [5] Göpel *et al.* (2010) *CRAS* **342**, 53-59. [6] Renne *et al.* (2010) *EPSL* **175**, 13-26.

Experimental study of melting, texture, and phase relations of basalt (eclogite)-peridotite-fluid system at sub- and supercritical P-T

N.S. GORBACHEV*, A.N. NEKRASOV, A.V. KOSTYUK,
AND D.M. SULTANOV

Institute of Experimental Mineralogy RAS, Academica
Osipyana 4, Chernogolovka, Russia
(correspondence*: gor@iem.ac.ru)

Fluids have an effective influence on the phase relations and melting of the mantle. Depending on the P-T conditions fluid-bearing silicate systems can be in the subcritical and supercritical conditions. Melting, textures, phase relations at sub - and supercritical P-T are studied experimentally in the system basalt (eclogite)-peridotite-H₂O, H₂O+(Na, K)₂CO₃ fluid.

Experiments were carried out in piston-cylinder and anvil-with-hole apparatus by a quenching technique in the range P=2-4 GPa, T=1100-1400°C. Different texture and phase relations of quenched samples served as test that the system goes into a supercritical state. Two experimental techniques were used: Pt-Pt-peridotite ampoules at T=1350-1400°C and direct melting peridotite in Au and Au-Pd ampoules at T=1100-1200°C.

At subcritical P-T conditions quenching samples have a massive texture, due to the fact that the massive silicate glass cements solid liquidus phases. At supercritical P-T conditions observed full miscibility between melt and fluid, and in the second critical end point – between minerals, melts, and fluid. The disintegration of the experimental samples observed during quenching supercritical phase. Samples characterized by clastic-like or fragmental-like textures regardless of the composition and technique of experiments. They consist of a mixture of fritted, rolled-like relicts of Ol, Opx from peridotite, reactionary minerals, and products quenching of supercritical phase - microlites of silicate minerals and their joints needle- or dendrite-like forms, microglobules Al-Si glasses, carbonates. Separate fragments remind of “breccia”-relicts of Ol, Opx cement of reactionary Grt, Cpx. Solubility of minerals peridotite, reactionary relation between relict and neogenic reactionary minerals testify to high reactionary ability supercritical phase.

Supporting by grant RFBR № 12-05-00777a

Intra-plate tectonics and magmatism as a consequence of mantle lithosphere delamination

WERONIKA GORCZYK¹, KATHARINA VOGT²
AND BRUCE HOBBS^{1,3}

¹Center for Exploration and Targeting, University of Western
Australia,

²Swiss Federal Institute of Technology, Switzerland

³Commonwealth and Industrial Research Organization,
Australia

Most of intra-plate melting is associated with interaction of deep mantle plume with mantle lithosphere. Vast amount of mafic/felsic intra-plate intrusions are located along post-collisional lines, where for longer periods time regional tectonic conditions are more likely to be (weakly) compressional to transpressional, and more rarely extensional. Arrival of the asthenosphere-derived plume would suggest initiation of extension along the weak/post-collision zone (craton boundary). Alternatively, in compressional regime a surprisingly large range of instabilities can develop that lead to melting of the lower crust and mantle lithosphere. Unexpected structural complexity arises which is quite sensitive to the geometry and rheological properties. This has dramatic effects on melting and devolatilisation within the lithosphere and hence in the localisation of and melt emplacement. Melts extracted in these circumstances lead to emplacement of all variety of melts: mafic, intermediate and felsic, from wide range of PT conditions.

In order to investigate these intra-plate sites of deformation, melt production and crustal growth in relation to cratonic post-collisional contacts we performed a series of 2D numerical experiments by using a coupled petrological–thermomechanical numerical model. The model includes, stable mineralogy, aqueous fluid transport, partial melting, melt extraction and melt emplacement in form of extrusive volcanics and intrusive plutons.

As a case study we will present Musgrave Orogeny in Central Australia.

Hydrogeochemical characteristics in the basin area of the "Rovni" accumulation - influence of the natural radionuclides

¹V. GORDANIĆ, ¹M. VIDOVIĆ, ²V. SPASIĆ-JOKIĆ, ³D. JOVANOVIĆ AND ⁴A. SEKE

¹University of Belgrade, IHTM (gordanicv@gmail.com, mivibgd@yahoo.com)

²University of Novi Sad, Faculty of Technical Science (svesna@uns.ac.rs)

³Geological Survey of Serbia (dragan.jovanovic@gzs.gov.rs)

⁴University of Belgrade, RGF (anaseke@gmail.com)

The hydrogeochemical prospecting covered 110 km² of basin surface area of "Rovni" accumulation. Among the water flows the most significant rivers are Sušica and Jablanica, which are mostly cut in into the limestones of Mesozoic in age. The area incorporated in the eco-geochemical research is built of Palaeozoic and Mesozoic sediments, and Quaternary material. According to geological-structural characteristics of the terrain, of special significance is the presence of pyroclastic material (tuff, volcanic breccia) as well as limestones (T₂²) and bauxite ore bodies within. Average values of natural radionuclides content in bauxite are: 2.24 g/t for ²³⁸U, 14.82 g/t for ²³²Th and 0.14% for ⁴⁰K [1]. Hydrogeochemical research of radioactive elements in bauxite were conducted for all four seasons. Average uranium content for all four seasons varies within the interval 0.21-0.26 µg/l; Ra <0.05-0.09 Bq/l and Rn 0.1-4.7 Bq/l [1] Regarding the presence of Sb, Cu ore occurrences, Fe, Cu mineralization (pyritization, limonitization) in the basin area, natural radionuclide contents were determined as well as pH, Eh, Ep, microelements, gases, mineralization and anion-cation composition. Presence of natural radionuclides in water is negligible and it doesn't affect the quality of water in the future accumulation [1]. All results are presented in tables, charts and geochemical maps. Geoecological map of the basin area presents the geoecological state in the living environment before the dam construction, and it also enables making a base for evaluation of accumulation degradation during a multiyear period of exploitation.

Acknowledgement: This work has been financed by Ministry of Science and Technological Development of the Republic of Serbia (project No. OI 176018).

[1] Gordanić V. (1992) Ecological-geochemical researches of radioactive and other elements of the "Rovni" accumulation in the area of sanitary protection, fund of expert documentation of Geoinstitute, Belgrade, Serbia.

Early detection of osteolytic lesions in multiple myeloma using natural Ca isotopes

G.W. GORDON^{1*}, J.L. SKULAN¹², M. CHANNON¹, R. FONSECA³ AND A.D. ANBAR¹²

¹School of Earth and Space Exploration, Arizona State University, Tempe, AZ, 85287-1404 (*correspondance: Gwyneth.Gordon@asu.edu)

²Department of Chemistry and Biochemistry, Arizona State University, Tempe, AZ 85287-1604 (anbar@asu.edu)

³Mayo Clinic of Arizona, (fonseca.rafael@mayo.com)

Real time monitoring of bone metabolism in multiple myeloma (MM) would help clinicians detect MM onset earlier than is currently possible. A biomarker detecting incipient or asymptomatic bone destruction would help evaluate the efficacy, timing, and duration of bone-specific therapies. Naturally occurring Ca isotope ratios in serum may be such a biomarker.

Natural changes in the Ca isotope composition of blood provide quantitative information on short-term changes in net bone mineral balance (BMB), information unavailable from conventional biochemical measures of bone metabolism. Net bone gain or loss cause blood and urine to be respectively enriched or depleted in light Ca isotopes. Based on studies of bed-rest induced bone loss [1,2], a net bone mineral loss rate of about <4%/year is detectable.

Osteolytic lesions occur in >80% of MM patients and should cause negative shifts in BMB detectable by Ca isotopes. Patients with MGUS (Monoclonal Gammopathy of Undetermined Significance) progress to MM at a rate of 1-2% per year, often with the onset of osteolytic lesions. In a pilot study, Ca of blood from patients with MGUS was isotopically heavier than Ca in blood of patients with MM (n=19, p=0.01, Mann-Whitney test). This difference is consistent with osteolytic lesions in MM patients. Ca isotopes may be used in the clinic to detect bone disease early, monitor its progression, and evaluate which patients are at highest risk for rapid deterioration.

[1] Morgan *et al* (2012) *PNAS* **109**, 9989-9994. [2] Skulan *et al* (2007) *Clin Chem* **53**, 1155-1158.

Split-stream ICPMS migmatite geochemistry: significance for the rheologic evolution of the Western Gneiss Region, Norway

S.M. GORDON¹, D.L. WHITNEY², C. TEYSSIER²,
H. FOSSEN³ AND J. DESORMEAU¹

¹Geological Sciences, U of Nevada, Reno, NV, USA,
staciag@unr.edu

²Earth Sciences, U of Minnesota, Minneapolis, MN, USA

³Earth Science, U of Bergen, Bergen, Norway

Exhumed ultrahigh-pressure (UHP) terranes document the subduction of crustal material to mantle depths and its return to the Earth's surface. The Western Gneiss Region (WGR), Norway, is one of the two largest UHP terranes on Earth and consists of a UHP eclogite terrain and a HP granulite terrain that may represent overprinted eclogite; these are separated by a major strike-slip shear zone. To evaluate the geochemical and age relationships of migmatite and mafic pods in both regions, we obtained LA-ICP-MS U-Pb dates and trace-element analyses for zircon from a variety of textural types of leucosome associated with mafic pods. Five leucosomes within highly deformed migmatite in the HP granulite terrain reveal U-Pb lower-intercept ages from ca. 405 to 409 Ma and upper-intercept Proterozoic dates. The Caledonian zircons all have flat Eu anomalies and weakly steep HREE patterns, suggesting HP crystallization. Similar results were obtained from zircon rims extracted from the UHP terrain, with garnet-present \pm plagioclase-absent REE patterns and dates as old as 410–406 Ma. The new U-Pb dates suggest a similar melt crystallization history that was coeval with previously determined ages of (U)HP metamorphism of WGR eclogite. Results are consistent with the presence of partially molten crust in a large part of the WGR at HP or UHP conditions. The decreased viscosity and increased buoyancy and strain weakening induced by partial melting may have assisted rapid ascent of HP/UHP rocks from mantle to crustal depths.

Formation mechanisms of reaction zones in Mélange zones: Evidence for mechanical mixing

J.K. GORMAN^{1*}, S. PENNISTON-DORLAND¹,
R.J. WALKER¹, AND H. MARSCHALL²

¹Department of Geology, University of Maryland, College Park, MD 20742,
(*email: jgorman1@umd.edu)

²Department of Geology and Geophysics, Woods Hole Oceanographic Institution, Woods Hole, MA 02543

Three mechanisms have been proposed to operate within mélange zones to form metasomatic reaction zones between mafic rock and adjacent peridotite. These mechanisms are: 1) mass transfer by fluid flux, likely parallel to reaction zone contacts, 2) mass transfer by diffusion through an intergranular fluid perpendicular to reaction zone contacts, and 3) mechanical mixing of adjacent lithologies. This study utilizes the broad concentration ranges of highly siderophile elements (HSE) across lithologic contacts to elucidate peridotitic contributions to reaction zones. Ultimately this data can help determine the extent of mechanical mixing contribution to reaction zone formation.

Rinds from two amphibolite grade traverses from the Catalina Schist (CA) are enriched in Os, Ir, and Ru relative to the block. Initial ¹⁸⁷Os/¹⁸⁸Os ratios are distinctly lower in the rinds (0.13–0.18) compared to the blocks (0.43–2.23). Lower grade lawsonite-blueschist facies rinds have similar HSE systematics with high ¹⁸⁷Os/¹⁸⁸Os ratios (0.24–0.33) for mafic block cores and lower ratios (0.12) for the rinds. Similar to the Catalina traverses, the Stavros traverse (Syros, Greece) has very high ¹⁸⁷Os/¹⁸⁸Os ratios for the block (4.1–16.6), a low ratio for serpentinite (0.12) and an intermediate ratio for the reaction zone (0.29). ¹⁸⁷Os/¹⁸⁸Os ratios for the Lia Beach traverse (Syros, Greece) are high in the metabasalt (0.32), whereas the nearby serpentinite has the lowest ratio (0.13). The blackwall zone (thought to be formed by diffusion through an intergranular fluid) has variable ratios (0.16–0.80). Concentrations of Os in the blackwall are lower than both the core and serpentinite.

In order to produce the elemental and isotopic variations seen in the rind in the Catalina traverses and the outermost rind of the Stavros traverse, we suggest initial mechanical mixing of block and peridotite to create rind-like material on the edges of the block. The Lia Beach traverse Os data may indicate initial mechanical mixing as well as a combination of metasomatic flux parallel to the contact and diffusion across the contact. In all traverses, concentrations of other elements suggest a later-stage infiltration of fluids after peak metamorphism.

Isotopic analysis of ice core carbon dioxide inclusions by means of quantum cascade laser cavity enhanced absorption spectroscopy

PAULA GORROTXATEGI CARBAJO¹, MARINE FAVIER¹,
THIBAUT DEBOIS¹, DANIELE ROMANINI¹,
GREGORY MAISONS², MATHIEU CARRAS²,
JEROME CHAPPELLAZ³ AND ERIK KERSTEL¹

- ¹J. Fourier University of Grenoble, Laboratoire Interdisciplinaire de Physique (UMR 5588 CNRS-UJF), 38402 Grenoble, France (erik.kerstel@ujf-grenoble.fr)
²Thales Research & Technology, III-V Labs, 91767 Palaiseau, France (mathieu.carras@3-5lab.fr)
³Laboratoire de Glaciologie et Géophysique de l'Environnement (UMR 5183 CNRS-UJF), 38402 Grenoble, France (jerome@lgge.obs.ujf-grenoble.fr)

In the context of a globally warming climate it is crucial to study the climate variability in the past in order to understand which natural feedbacks can be expected on the atmospheric CO₂ concentration in a future warmer world. The composition of gas from bubbles in polar ice presents a paleo-climate archive that provides a powerful means to study the mechanisms involved in the ~40% increase in atmospheric CO₂ between glacial and interglacial climates. The source of the CO₂ released into the atmosphere during previous deglaciations can be constrained from isotopic measurements. Unfortunately, such studies have been seriously hampered by the experimental difficulty of extracting the CO₂ without contamination or fractionation, and measuring the isotope signal off-line on an isotope ratio mass spectrometer (IRMS).

Here we present an alternative method that leverages the extreme sensitivity afforded by Optical Feedback Cavity Enhanced Absorption Spectroscopy (OF-CEAS) in the Mid-Infrared. This region of the spectrum is accessed by a custom-developed Quantum Cascade Laser operating near 4.35 μm. The feedback to the laser of light that has been spectrally filtered by a high-finesse enhancement cavity has the effect of spectrally narrowing the laser emission and to auto-lock the laser frequency to one of the cavity's longitudinal modes, with clear advantages in terms of acquisition time and signal-to-noise ratio of the measurement. The line strengths in this region are about 5 orders of magnitude higher than in the more easily accessible NIR region near 1.6 μm. A small cavity volume of ~20 mL, this enables the analysis of nmol-sized samples with high precision (< 0.05‰) in a fraction of the time required by the conventional IRMS-based technique. We will show an instrument characterization and preliminary results.

Redox characterization of Fe-bearing clay minerals using electrochemical and spectroscopic techniques

CHRISTOPHER A. GORSKI^{1,2*}, LAURA E. KLÜPFEL^{2,3},
ANDREAS VOEGELIN², MICHAEL SANDER³
AND THOMAS B. HOFSTETTER^{2,3}

- ¹Pennsylvania State University, University Park, PA, USA *
(Correspondence: gorski@psu.edu)
²Eawag, Swiss Federal Institute of Aquatic Science and Technology, Dübendorf, Switzerland
³Institute of Biogeochemistry and Pollutant Dynamics (IBP), Swiss Federal Institute of Technology, ETH Zurich, Switzerland

Fe-bearing clay minerals serve as important redox buffers in natural and engineered environments, where they readily undergo electron transfer reactions with bacteria, nutrients, and contaminants. Despite much interest, modeling the extent and kinetics of these interfacial redox reactions has proven to be challenging due to the inability to describe clay mineral redox properties in terms of reduction potential (E_H) values. Such values have been difficult to obtain experimentally because of sluggish electron transfer rates and redox equilibration between clay minerals and electrodes.

Recently, we demonstrated that this challenge can be overcome using mediated electrochemical analyses, in which soluble redox mediator compounds facilitate rapid mineral-electrode electron transfer and redox equilibration [1]. In this approach, the oxidation state of the structural Fe is measured across a series of applied E_H values. In the current study, we applied this technique to four natural Fe-bearing smectites having varied structural Fe-contents, layer charges, elemental compositions, and redox histories to determine how clay mineral redox properties deviate as a function of these variables. X-ray absorption spectroscopy complimented these experiments to determine how structural molecular-scale variations influenced macroscopic redox properties.

All four smectites displayed complex redox behavior; high Fe-content smectites exhibited metastable states during redox cycling and all the smectites were redox-active over a wide range of E_H values spanning an array of redox regimes, ranging from methanogenesis to aerobic respiration. These results indicate that smectites likely play important roles in determining the fate of contaminants and biological nutrients under a variety of redox conditions.

- [1] Gorski, Aeschbacher, Soltermann, Bayens, Marques, Hofstetter, and Sander, (2012), *Environ. Sci. Technol.* **46**, 9360-9368.

Noise in Heat Flow Data

WILLIAM GOSNOLD^{1,2,3}

¹Harold Hamm School of Geology and Geological Engineering, University of North Dakota, Grand Forks, ND 58202

Temperature disturbances due to a variety of heat transport phenomena in the upper few km of the crust and the inclusion of unconventional heat flow determinations, i.e., use of bottom hole temperatures from petroleum exploration, alter the geothermal gradient and lead to inaccurate heat flow determinations. These data can be problematic in assessing the geoneutrinos flux due to radiogenic heat production because they have been included in the global heat flow database without correction. Careful analysis of heat flow data is particularly important on a local scale where inaccurate determination of surface heat flow can lead to miscalculation of radiogenic and mantle heat flow components and thus to erroneous estimation of the local background geoneutrino flux at sites where observatories could be installed. For example, high and low heat flow anomalies within a 140,000 km² area close to the Black Hills are due to gravity-driven regional groundwater flow in confined aquifers. Heat flow determined by conventional methods in Minnesota, Manitoba and Ontario has a long-period transient from ground warming after retreat of the Pleistocene ice sheet that causes under estimation of heat flow by 25 to 40 percent. We present a range of heat flow and heat production models to explore the end members of these conditions.

Nitrogen isotopic fractionation during enzymatic transamination of glutamic acid to form aspartic acid

AKIKO S. GOTO^{1*}, KASUMI MIURA²
AND YOSHITO CHIKARAISHI³

¹Institute of Science and Engineering, Kanazawa University, Kanazawa, JAPAN (akigoto@staff.kanazawa-u.ac.jp)

²Tokyo Metropolitan University, Tokyo, JAPAN

³Japan Agency for Marine-Earth Science and Technology, Yokosuka, JAPAN (ychikaraishi@jamstec.go.jp)

The trophic enrichment of ¹⁵N on amino acids from diets to consumers has recently been employed as a potential useful tool for characterizing the trophic position of organisms in ecological food webs (Popp *et al.*, 2007; Chikaraishi *et al.*, 2009). Amino acids are the basic subunit of biomass protein and major pool of nitrogen in organisms. These facts enhance our motivation to understand nitrogen flux and associated change in the isotopic composition of amino acids in animal metabolisms.

Glutamic acid generally has a significant ¹⁵N-enrichment with increase of trophic position (~8‰/each), probably due to the isotopic fractionation associated with its enzymatic deamination or transamination. To evaluate this hypothesis, we estimated the isotopic fractionation factor (α) associated with an *in vitro* enzymatic transamination of glutamic acid to oxaloacetic acid (i.e., to form aspartic acid).

The α value is estimated to be 0.9958 based on change in the observed $\delta^{15}\text{N}$ value and abundance data of glutamic acid between before and after transamination. These results are almost consistent with the α estimation in the previous study (Macko *et al.* 1986: $\alpha=0.9923$) within an analytical error. Also, the α value roughly account for that 86% of glutamic acid (which derived from diets) is deaminated and the remaining only 14% is used to configure biomass protein, when the 8‰ trophic enrichment occurs on glutamic acid from diets to consumers. These values may correspond closely to the “Ten percent law” for the transfer of energy from one trophic level to the next. Thus, we conclude that the transamination is a likely process to explain the observed trophic enrichment of ¹⁵N on amino acids.

[1] Popp *et al.* (2007) Stable isotopes as indicators of ecological change, pp. 173-190. [2] Chikaraishi *et al.* (2009) *Limnol. Oceanogr. Methods.* **7**, 740-750. [3] Macko *et al.* (1986) *Geochim. Cosmochim Acta* **50**, 2143-2146.

A study of combustion aerosols in Japan using a nonhydrostatic icosahedral atmospheric model

D. GOTO^{1*}, K. SUZUKI² AND SALSA PROJECT TEAM³

¹National Institute for Environmental Studies, Ibaraki 305-8506, Japan (*correspondence: goto.daisuke@nies.go.jp)
²JPL/CalTech, California (Kentaro.Suzuki@jpl.nasa.gov)
³Research program on Climate Change Adaptation (RECCA) / development of Seamless chemical AssimiLation System and its Application for atmospheric environmental materials (SALSA project), Japan

An aerosol-coupled global cloud-resolving model, NICAM-SPRINTARS, developed by [1] based on the aerosol module of Spectral Radiation-Transport Model for Aerosol Species (SPRINTARS; [2]) and the global cloud-resolving model of Nonhydrostatic Icosahedral Atmospheric Model (NICAM; [3,4]) is capable to simulate the aerosol processes and distributions not only in the whole globe but also over specific regions using a stretched grid system developed by [5] as a ‘seamless’ model. In the present study, we develop the seamless aerosol-transport model with the spatial resolution of about 10 km to simulate aerosols around Japan, especially the Kanto region including Megacity Tokyo.

Although in some cities near mountains the present model does not always reproduce both the meteorological and aerosol fields mainly due to large spatial resolution, around the center of Tokyo it can successfully simulate meteorological and aerosol fields such as sulfate (Figure). In the presentation, we will discuss the performance of the newly developed aerosol model.

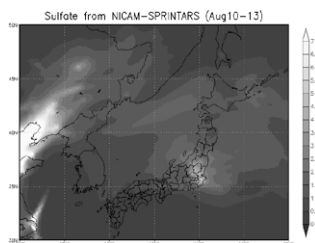


Figure 1: Simulated sulfate around Japan in unit of $\mu\text{g}/\text{m}^3$.

[1] Suzuki *et al.* (2008) *Geophys. Res. Lett.* **35**, L19817, doi:10.1029/2008GL035449. [2] Takemura *et al.* (2005) *J. Geophys. Res.* **110**, D02202, doi:10.1029/2004JD005029. [3] Tomita and Satoh (2004). *Fluid Dyn. Res.*, **131**, 1033-1050. [4] Satoh *et al.* (2008). *J. Comput. Phys.* **227**, 3486-3514. [5] Tomita (2008) *J. Meteor. Soc. Japan*, **86A**, 121-142.

Thermodynamics of solid solutions: the Margules equation and beyond

M. GOTTSCHALK*

GeoForschungsZentrum Potsdam, 14473 Potsdam, Germany, (*correspondence: gottschalk@gfz-potsdam.de)

For the thermodynamic treatment of phase equilibria the knowledge of *Gibbs free energy* G of solid solutions are essential. The thermodynamic models used for solid solutions are mostly the *regular solution*, the *Margules-*, and the *Guggenheim-equation*. The calibration of the involved parameters involves the results from phase equilibria studies. Alternatively, the lattice energy is calculated on the atomistic scale by using empirical force potentials or ab-initio calculations. Cluster expansion and applying statistical mechanics e.g. *Monte Carlo* methods are then used to evaluate G . For thermodynamic calculations parameterization of the *Gibbs free energy* rely then on the same models as for the thermodynamic approach.

The *regular solutions* and the *Margules equation* originate from fluid mixtures. A general approach can be applied to solids considering, that the molar mixing energy u depends on x_i and the occupancy x_j of neighboring adjacent or more distant sites. For *one neighbor* of the same site, u is:

$$u = \sum_{i=1}^c \sum_{j=1}^c x_i x_j u_{ij} \quad \text{with} \quad \Delta U_{ij} = 2u_{ij} - u_{ii} - u_{jj}$$

which gives us the *regular solution*:

$$u = \sum_{i=1}^c x_i u_{ii} + \frac{1}{2} \sum_{i=1}^c \sum_{j=1}^c x_i x_j \Delta U_{ij}$$

If the energy depends on *two neighboring sites*

$$u = \sum_{i=1}^c \sum_{j=1}^c \sum_{k=1}^c x_i x_j x_k u_{ijk} \quad \text{with} \quad \Delta U_{ijk} = 3u_{ijk} - u_{iii} - u_{jjj} - u_{kkk}$$

results in the *Margules equation* including a ternary term:

$$u = \sum_{i=1}^c x_i u_{iii} + \sum_{i=1}^c \sum_{j=i+1}^c x_i x_j (x_i \Delta U_{ij} + x_j \Delta U_{ji}) + 2 \sum_{i=1}^c \sum_{j=i+1}^c \sum_{k=j+1}^c x_i x_j x_k \Delta U_{ijk}$$

The above equation can also be written in the form:

$$u = \sum_{i=1}^c x_i u_{iii} + \frac{1}{3} \sum_{i=1}^c \sum_{j=1}^c \sum_{k=1}^c x_i x_j x_k \Delta U_{ijk}$$

This procedure can be extended to more complex interactions. If the energy of the site depends on the occupancy of *four* of the same site and *two* of a neighboring site:

$$U = \sum_{i=1}^{c_A} \sum_{m=1}^{c_B} x_i^A x_m^B u_{(iiii)(nm)} + \frac{1}{8} \sum_{i=1}^{c_A} \sum_{j=1}^{c_A} \sum_{k=1}^{c_A} \sum_{l=1}^{c_A} \sum_{m=1}^{c_B} \sum_{n=1}^{c_B} x_i^A x_j^A x_k^A x_l^A x_m^B x_n^B \Delta U_{(ijkl)(mn)}$$

It is important to note that these types of equations always split in a term for the *mechanical mixture* and one involving only parameters ΔU based on energy differences, which can be acquired by theoretical calculations for complex and arbitrary system.

***In situ* monitoring of reaction band formation using synchrotron radiation**

L.C. GÖTZE^{1*}, R. MILKE¹, S. SCHORR¹, R. DOHMEN² AND R. WIRTH³

¹Free University of Berlin, Institute of Geological Sciences, Berlin, Germany

(*correspondence: lutz.c.goetze@fu-berlin.de)

²Ruhr University Bochum, Institute for Geology, Mineralogy & Geophysics, Bochum, Germany

³GFZ German Research Centre for Geosciences, Potsdam, Germany

Diffusion reaction couple experiments are an essential tool in order to understand corona microstructures and underlying processes in metamorphosed and igneous natural rocks. By employing a heating attachment and synchrotron radiation we monitored the initial and transient stages of an *in situ* reaction rim formation at the nanoscale. Additionally, by miniaturising the experimental setup using thin films we could lower the temperatures and test durations that are usually applied in diffusion couple experiments.

As a model system the reaction between corundum (Al₂O₃) and periclase (MgO) that forms spinel (MgAl₂O₄) was chosen. The diffusion couples consisted of single crystal substrates of either (0001) oriented corundum with an amorphous MgO thin film on top or (111) oriented periclase which reacted with an Al₂O₃ thin film. Thin films were produced by laser ablation, and their thickness was always less than 300 nm. Experimental temperatures were varied from 700 to 1000 °C, and test durations ranged from 5 minutes to 3 hours. The texture of the *in-situ* grown spinel, i.e. the crystallographic relationship between substrate and thin film, was subsequently analysed using a four-circle diffractometer to obtain pole figures. As complementary methods to the X-ray diffraction techniques transmission electron microscopy (TEM) and atomic force microscopy (AFM) were employed.

At 700 and 800 °C no spinel formation could be observed, but the reaction layers crystallise oriented on the substrate. Spinel formation occurs at a moderate rate at 900 °C, and is rapid at 1000 °C. The time series conducted at 1000 °C points to an interface-controlled reaction regime, i.e. the thickness of spinel grows linearly with time. Microstructures within the spinel, as revealed by TEM, suggest 'counter-diffusion of the cations' as the diffusion mechanism. Diffraction spectra and pole figures show that the spinel crystallises and grows epitactically on and into the substrates.

Delayed response in sedimentary discharge from the Himalaya to the ocean at Milankovitch periods

A.T. GOURLAN^{1*}, C. VOISIN¹, C. CHAUVEL¹ AND J. BRAUN¹

¹ISTerre, Université Joseph Fourier, CNRS, BP 53, 38041 Grenoble CEDEX 9, France

(* correspondence: alexandra.gourlan@ujf-grenoble.fr)

The neodymium isotopic composition of marine sediments (ϵ_{Nd}) is often used as a proxy for past climate changes in paleoceanography studies. However, in some parts of the world ocean, the origin of ϵ_{Nd} variations in seawater over the last Glacial/Interglacial cycles remains unclear. This is particularly true in the Indian Ocean because of its connections with the Atlantic and the Pacific Ocean waters, and because of the huge Himalayan sedimentary discharge that brings low ϵ_{Nd} into the ocean. The ϵ_{Nd} variations could result of changes in the global oceanic circulation or be due to changes in the continental input controlled by continental rainfalls. Here we present a simple technique to discriminate these two interpretations at a given site, based on the correlation of $\delta^{18}O$ and ϵ_{Nd} seawater signals. We show in-phase records at site SK129-CR2 [1] (Arabian Sea) and out-of-phase records at site ODP-758 [2] (Bay of Bengal), suggesting that the two sites have recorded different phenomena through time. Arabian Site fluctuations were interpreted as changes of the thermohaline circulation and Bay of Bengal Site fluctuations as changes on the Himalayan input. As Himalayan rivers input is linked to the Earth's climate variability, we filtered the time series of $\delta^{18}O$ and ϵ_{Nd} at Site ODP 758 around the three periods related to the three main orbital parameters. We show that the time lag between $\delta^{18}O$ and ϵ_{Nd} , increases from 1000 to 2000 and then to 7000 years for the 23 ky, 41 ky, and 100 ky filtered signals. To explain the delays between temperature changes recorded by $\delta^{18}O$ and ϵ_{Nd} , two models were proposed: diffusive [3] and erosion [4] models of Himalayans. For the first time, we demonstrate that a geochemical dataset can record and thus constrain the time lag in the erosional response of an active mountain belt to climate change.

[1] Piotrowski, *et al.* (2009) *Earth Planet. Sci. Lett.* **285**, 179-189.

[2] Gourlan *et al.* (2010) *Quaternary Sci. Rev.* **29** (19-20), 2484-2498. [3] Castelltort and Van den Driessche (2003) *Sedim. Geol.*

157, 3-13. [4] Richter and Turkian (1993) *Earth Planet. Sci. Lett.* **119**, 121-131.

Relevance of model complexity for assessing contaminant leaching from a fractured degrading concrete structure

JOAN GOVAERTS, JANEZ PERKO, DIEDERIK JACQUES,
AND SURESH C. SEETHARAM¹

¹Institute for Environment, Health and Safety, Belgian
Nuclear Research Centre (SCK•CEN), Belgium,
jgovaert@sckcen.be

Cementitious materials such as concrete, used in near-surface disposal facilities for radioactive waste, play a crucial role in ensuring the waste retention capabilities within the repository. During the lifetime of the facility, the concrete is in permanent contact with infiltrating rain or soil water, which is not in the equilibrium with the cement pore water. Chemical degradation of concrete affects several properties and consequently could accelerate the leaching of contaminants from the disposal system. One important degradation process is leaching of calcium. The effect of calcium leaching encompasses loss of material's mechanical strength, change of physical properties such as porosity, permeability and change of retention capacity for contaminants.

A small-scale representation of a concrete waste container wall with a fracture going through the middle is modeled in a simplified 2D geometry. The geochemical degradation reactions are solved using iPhreeqc, which is then linked to the finite element software COMSOL Multiphysics. By taking advantage of COMSOL's unique capability of treating fracture flow and transport as an implicit 1D-boundary, the computational burden of the problem is drastically reduced.

In a stepwise manner, both the chemical and physical complexity of the model are increased. Along the way, different concrete minerals are added to the geochemical system, starting from system based solely on portlandite and ending up with a state-of-the-art description with inclusion of different C-S-H minerals. By then linking the chemical degradation to the hydraulic and diffusive properties of the concrete, several levels of complexity are again added. It is then evaluated which additions add enough safety-relevant information in order to justify the increase in computational demands. This is done by comparing Ca leaching rates and the evolution of safety relevant properties such as the total water flux through the system or the pH (which influences the mobility of contaminants). On the basis of these analyses, recommendations are made for the safety assessment modelling of large-scale disposal facilities.

Geochemical baseline mapping in India using top and bottom soil samples for environmental management

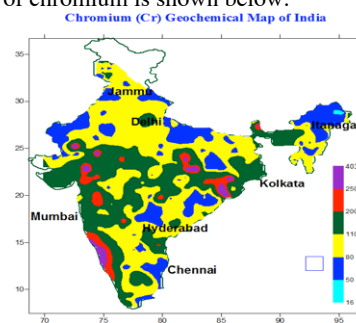
PRADIP K. GOVIL

National Geophysical Research Institute, Hyderabad, India.
(govilpk@gmail.com)

As a part of IUGS/IAGC Global Baselines Program, National Geophysical Research Institute (NGRI), Hyderabad has carried out studies leading to the preparation of geochemical maps of India for top and bottom soil for 25 elements. India is divided into 122 GRNs, out of which 118 cells of 160 x 160 sq. Km have been sampled and analysed by using X-ray fluorescence spectrometer at NGRI, Hyderabad.

Samples were collected by using the field manual (Green Book) prepared by Geological Survey of Finland. All the data is compiled and plotted by using a software SURFER to prepare the baseline maps. The data was interpreted with the underlying geology of the area. Baseline studies are useful to define the natural abundance and the spatial distribution of chemical elements in the earth's surface to which changes caused by human activities can be compared.

Geochemical maps have been interpreted and spatial correlation was found between the underlying geology and elemental abundances in the sampled media. The hot spots for the toxic metals can be seen at a glance for the whole country, which will help in taking suitable remedial measures. Mean, median, maximum, minimum and average concentrations were calculated and presented in this paper for chromium, copper, nickel, arsenic, cobalt, strontium, rubidium along with some major oxides like aluminium, iron, titanium, manganese, sulphur, calcium, magnesium, sodium, potassium and silica. Geochemical map of chromium is shown below:



Microbial uptake of phosphate during anaerobic oxidation of methane

J.S. GRAF*, J. MILUCKA, T.G. FERDELMAN
AND M.M.M. KUYPERS

Max Planck Institute for Marine Microbiology, Celsiusstrasse
1, 28359 Bremen, Germany
(*correspondence: jgraf@mpi-bremen.de)

Sulfate-coupled anaerobic oxidation of methane (AOM) in sediments is considered a major sink of methane in the ocean and plays an important role in sedimentary biogeochemical cycling of carbon and sulfur [1]. The *Deltaproteobacteria* (DSS) associated with the methanotrophic archaea (ANME) mediating AOM are capable of polysulfide disproportionation and couple the carbon and sulfur cycles during AOM [2].

Investigations using transmission electron microscopy/energy-dispersive X-ray analysis showed amorphous particles, enriched in iron and phosphorus, only present in the cytoplasm of the *Deltaproteobacteria* bacterial partner [2]. The function of these particles is yet unknown. We investigated the microbial uptake of phosphate during AOM using $^{33}\text{P}_i$ radiotracer experiments. In our studies we used highly enriched AOM cultures originating from sediments of the Mediterranean mud volcano Isis. These sediments were enriched during 9 years of continuous cultivation and consist mainly (>95%) of ANME-2 and DSS cells as determined by CARD-FISH [3].

Radiotracer incubations on our AOM cultures lasting seven days showed an accumulation of $^{33}\text{P}_i$ tracer in the biomass and a decrease of tracer in the medium in the presence methane. In controls without methane $^{33}\text{P}_i$ uptake was minimal. In methane amended samples there was a linear correlation between sulfate reduction and the disappearance of $^{33}\text{P}_i$ radiotracer in the medium. The specific activity of $^{33}\text{P}_i$ in the medium decreased (phosphate concentration remained constant) suggesting phosphorus turnover at a significant rate of ~ 3% of the sulfate reduction rate.

[1] Reeburgh, WS (2007) *Chem. Rev.* **107** (2), 486 – 513.
[2] Milucka J *et al.* (2012) *Nature* **491**, 541-546. [3] Schreiber L *et al.* (2010) *Environ. Microbiol.* **12**, 2327 - 22340

Nuclear Waste disposal: from geosciences to multigenerational safety and society

BERND GRAMBOW¹ AND SOPHIE BRETESCHE²

¹SUBATECH, UMR 6457 Ecole des Mines, Université de Nantes, IN2P3, 4 rue Alfred Kastler, 44307 Nantes

²Dept. Science Social et Gestion, Ecole des Mines de Nantes, 4 rue Alfred Kastler, 44307 Nantes

A very large quantity of highly radiotoxic nuclear waste has been accumulated worldwide in the last 30 years constituting health risks for many thousands of generations. Isolation in futur deep geological disposal facilities is considered today by national and European legislation, by governmental commissions international agencies and large parts of the scientific community as the best strategy to reduce the long term risk. Nevertheless, serious doubts remain in the public and by NGOs.

Scientific proof for the safety of long term waste isolation is provided in particular by the geosciences by detailed site characterisation, comparaisson of disposal concepts to natural analogues and by ellucidating detailed process understanding for mineral dissolution, mass transfer resistance for exemple of clays, geomechanics, hydraulics of site evolution etc.

Using examples from waste form dissolution in confined space, from the geochemistry of radionuclide migration and from water transport in clays, the paper presents how scenarios for potential radionuclide release to biosphere and potential doses to future generations can be obtained. Safety analyses generally show that doses will remain always (up to millions of years) lower than today legal limits. The validity and credibility of such analyses can be increased by qualitative lines of evidence, demonstrating the safety case.

From a societal point of view there are however a certain number of questions:

- 1) The focus on the long term risk is based on the fact that most analyses show zero risk for the first 1000 of years. However in case of reversible disposal, the repository will remain open for more than hundreds of years, with associated risks for todays generations similar to that of typical nuclear installations. Incorrect repository closure after the end of reversibility period may increase the long term risk.
- 2) The meaning of risk of very low doses to thousands of generations is chalanged the societal debate on low doses in particular after the Chernobyl desaster.
- 3) The horizon of responsibility for thousands of generations has no paralel in any human ethics

Long-term fate and transport of fission products and actinides in geosphere

BERND GRAMBOW, G. MONTAVON, A. ABDELOUAS
AND T. SUZUKI¹

¹SUBATECH, UMR 6457 Ecole des Mines, Université de Nantes, IN2P3, 4 rue Alfred Kastler, 44307 Nantes

Global natural distribution pattern of radionuclides and homologues elements between fluids and rock formations allow a certain classification of mobility with respect to charge/valence when considering the fate of radionuclides in geological formations.

Ion exchange and surface complexation allow prediction of mobility influencing environmental parameters for Se, Cs and I. Diffusion rates in compact clay are very low since the clay rock pores are so small that electrostatic repulsion limits the available space for anion diffusion and even certain of these “mobile” nuclides may show significant retardation. However, in much less compact systems like aquifers, fixation of sparingly soluble radionuclides on mobile clay particles provides additional transport vectors. In a shallow waste disposal site a complex relationships between the clay /radionuclide/solution system, influence of transportable organic matter, the colloid loads, size distribution and the hydrodynamics of the aquifer was observed.

An important issue is whether redox states or organic/inorganic speciation change along transport path.. In deep geologic conditions like those foreseen for high level nuclear waste disposal, very anoxic to reducing conditions are often attained assuring very slow migration rates of actinides, Tc(IV), Se(0) etc. but even in soils, in close vicinity to the atmosphere, microbial activity may lead to fixation of low redox states of elements like Tc.

The complex interplay between radionuclide mobility influencing factors has recently been studied for Selenium in soil type environments: competition and synergies between reactivity of different mineral surfaces (clay, quartz, calcite iron hydroxide) solution composition, microbes and their influence on bioavailability.

A factor often overlooked in assessing long term radionuclide mobility is the potential irreversible entrapment of radionuclides by slow mineral/water reactions. At solid/solution equilibrium the dynamics of dissolution and precipitation is still ongoing, allowing not only adsorption on stable surfaces but as well incorporation in the sub-surface of the mineral, protecting it from release by sorption/desorption equilibrium.

Definition of a clean energy system for decontamination of acid mine waters and recovering their metal load

J.A., GRANDE^{1*}, M.L. DE LA TORRE¹, J.M. ANDÚJAR¹,
T. VALENTE²¹ AND M. SANTISTEBÁN²

¹Centro de Investigación para la Ingeniería en Minería Sostenible (CIPIMS). Escuela Técnica Superior de Ingeniería. University of Huelva. Ctra. Palos de la Frontera s/n, 21819, Huelva, Spain,
(*correspondence: grangil@uhu.es)

²CIG-R (PEst-OE/CTE/UI0697/2011) – Centro de Investigação Geológica, Ordenamento e Valorização de Recursos, Universidade do Minho, Campus de Gualtar, 4710-057 Braga, Portugal, teresav@uct.uminho.pt

Acid mine drainage (AMD) is one of the largest hydrochemical problem resulting from anthropic activity, with consequences worldwide. For this reason is understandable the importance of innovative measures for recovering rivers affected AMD. Taken in account the substantial changes in terms of European legislation on water quality, under the framework of Directive 2000/60/EC (Water Framework Directive, WFD), the proposal of remediation measures for streams affected by AMD in the period marked by the standard has become even more relevant.

The most common techniques, applying corrective measures to mitigate the process, have high costs of installation and maintenance, or poor performance. On the other hand, the cheaper approaches often cause undesirable discharges of pollutants.

The aim of the system presented in this study is to neutralise acid mine waters and recover their metal load, using energy obtained from renewable sources. With this approach, the treated water is produced without releasing emissions into the atmosphere, without using fossil fuels and at an acceptable cost. At the same time, it allows the Cu dissolved in the waters to be separated from the rest of the metal load and sulphates. Therefore, it makes possible the metal's recovery, transforming an environmental passive into an industrial income, in an economic context in which the price of Cu reaches around 7300 US\$/ton.

Mineralogical and geochemical properties of a water dam receiving historic AMD contamination by sulfide tailings in the Riotinto Mine SW Spain

J.A. GRANDE^{1*}, T. VALENTE²¹, M.L. DE LA TORRE¹,
J.P. FERNÁNDEZ³, J. BORREGO¹,
M.A. SEQUEIRA BRAGA², P. GOMES²
AND M. SANTISTEBAN¹

¹CIPIMS - Centro de Investigación para la Ingeniería en Minería Sostenible. Escuela Técnica Superior de Ingeniería. Universidad de Huelva. Ctra. Palos de la Frontera. s/n. 21819. Palos de la Frontera. Huelva. Spain (*correspondence: grangil@uhu.es)

²CIG-R (PEst-OE/CTE/UI0697/2011) – Centro de Investigação Geológica, Ordenamento e Valorização de Recursos, Universidade do Minho, Campus de Gualtar, 4710-057 Braga, Portugal (teresav@dct.uminho.pt)

³University of Oviedo, Hydrogeophysics and NDT modeling Unit. Oviedo. Spain (pauli@uniovi.es)

The present study was performed in the Marismillas water dam, in the Iberian Pyrite Belt, SW Spain. This reservoir receives water from the Tinto River, known by its historical high levels of contamination by AMD. Additionally to soluble pollutants, sulfates and metals in the form of particulate matter have been transported for decades. Consequently, today, Marismillas is clogged by the accumulation of sulfide-rich material from the RioTinto mines.

An integrated sampling campaign was accomplished with the following objectives: i) to characterize the input waters; ii) to reveal horizons for preferential accumulation of metals, and iii) to propose a model of the clogging process.

The samples were collected in three drill cores, from the surface to the bottom. Geochemical and mineralogical analyses were performed each 10 cm.

The results indicate high average concentrations of metals and metalloids (Cu, Zn, Pb, and As > 1200 ppm). A strong accumulation of these elements (> 2000 ppm) was detected at depth 1-2 m. Geochemical trends indicate strong correlation between major elements mobilized from the source materials (sulfides and felsic host rocks). So, Fe and Al, as well as Cu and Zn are clearly associated in the sediments. Regarding mineralogy, in addition to clay minerals, the finest fraction (<2 μ m) is dominated by jarosite and goethite. Therefore, combining geochemistry and mineralogy allowed mapping the properties of dam, identifying major mineralogical hosts of environmental, but also economic relevant elements, such as REE.

A Second Lunar Magma Ocean?

MARION GRANGE* AND ALEXANDER NEMCHIN.

Curtin University, Department of Applied Geology, GPO box U1987, WA 6845, Perth, Australia.

*(correspondence: m.grange@curtin.edu.au)

The Lunar Magma Ocean (LMO) model is one of the key concepts in the current understanding of lunar evolution. It is used to explain a range of geological, mineralogical and chemical characteristics of the Moon, such as the presence of anorthositic crust, a reservoir enriched in incompatible elements and mare basalts. The LMO model suggests that the lunar crust, made up of Ferroan-Anorthosite (FAN), formed by segregation and floatation of plagioclase from the magma ocean, after ~75% of the initial liquid has crystallised as mafic cumulates. After ~95% solidification, the remaining liquid is enriched in incompatible elements (e.g. K, REE, P, U, Th, Zr...) and constitutes the KREEP reservoir. Although this reservoir has never been sampled as such, its existence is indicated by incompatible elements enrichment in some plutonic rocks, which are interpreted to be emplaced into the FAN crust. These rocks are also enriched in Mg and are referred to as Mg-suite. The presence of a KREEP component in this suite and the associated enrichment in incompatible elements also results in a widespread crystallisation of zircon in these rocks.

Very specific sequence of crystallisation predicted by the LMO model demands particular timing relationships between FAN, KREEP reservoir and Mg-suite rocks. However, absolute dating of FAN and Mg-suite samples reveals a significant overlap in ages that is inconsistent with the LMO model. In particular, the contradiction is highlighted by the recently obtained precise ages of (i) the oldest lunar zircon at 4417 ± 6 Ma [1], which must represent the youngest possible limit for the formation of KREEP reservoir and (ii) a sample of FAN at 4360 ± 3 Ma [2], which suggests the oldest limit for the lunar crust crystallisation.

The only way to resolve the controversy posed by chronological data is to accept the possibility of a second magma ocean on the Moon at ~4360 Ma, resulting from a massive impact and probably restricted to the near site of the Moon.

[1] Nemchin *et al.* (2009) *Nature Geosc.* **2**, 133-136. [2] Borg *et al.* (2011), *Nature* **477**, 70-73.

Contribution and effects of the volcanic carbon dioxide over the urban area of Naples

D. GRANIERI^{1*}, A. COSTA², G. MACEDONIO³, M. BISSON¹
AND G. CHIODINI³

¹INGV, Sezione di Pisa, Via della Faggiola 32, 56126 Pisa, Italy (*granieri@pi.ingv.it, bisson@pi.ingv.it)

²INGV, Sezione di Bologna, via Donato Creti 12, 40128 Bologna, Italy (antonio.costa@bo.ingv.it)

³INGV, Sezione di Napoli, via Diocleziano 328, 80124 Napoli, Italy (macedon@ov.ingv.it, giovanni.chiodini@ov.ingv.it)

The city of Naples is nearest to the Solfatara crater (Campi Flegrei caldera) that is a prodigious source of natural CO₂ [1]. In this study, the CO₂ plume dispersion is simulated using the DisGas code [2], under the most significant local-scale wind and hydrodynamic conditions of the atmosphere. Results showed that the western quarters of the city, as well as the inhabited area around the Solfatara, are mantled by the volcanic plume when atmospheric circulatory patterns are dominated by the common winds blowing from the sea. Under these conditions the CO₂ content in the air increases above normal values, reaching more than one thousand ppm in proximity to the Solfatara crater to a few tens of ppm several kilometres from the source (Figure 1). Simulated values satisfactory agreed with CO₂ concentrations measured by two stations inside the crater. A complete discussion of these results is presented elsewhere [3].

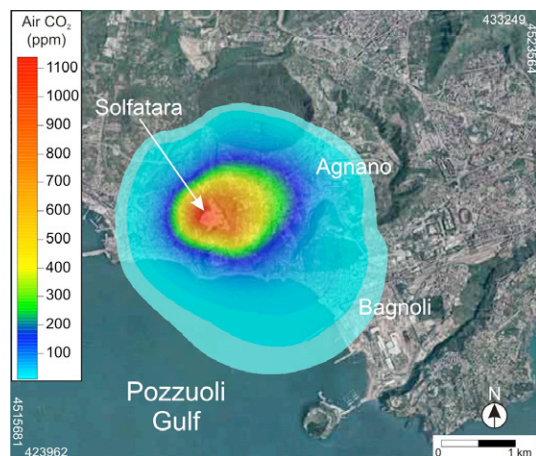


Figure 1: CO₂ plume dispersion over Naples. The concentration is expressed as values in excess of background CO₂ level.

- [1] Chiodini *et al.* (2010) *J. Geophys. Res.* **115** (B03205), 531-542. [2] Costa *et al.* (2005) *An. Geophys.* **48** (4/5), 805-815. [3] Granieri *et al.* (2013) *J. Volcanol. Geotherm. Res.* **In press.**

The kinetic effects of H₂O in metasomatic and xenolith breakdown reactions

TOM GRANT^{1,2}, RALF MILKE¹, BERND WUNDER²,
LUIZ MORALES² AND RICHARD WIRTH²

¹Campus Lankwitz, Freie Universität Berlin, Berlin 12249, Germany (tomgrant.gfz.fu@googlemail.com)

²GFZ, Helmholtz Centre Potsdam, Potsdam, Germany

The role of fluids, specifically water, in mineral replacement reactions has long been noted. Water is a vital catalyst as it lowers activation energies for reactions and increases solubilities of components for transport. The kinetic effects of fluids have been studied for solid-solid and solid-fluid reactions applicable to metamorphism but little attention has been paid to solid-melt reactions involved in metasomatism and xenolith breakdown in parent melts. We take the natural examples of olivine xenocryst breakdown in phonolite melt to form phlogopite rims and re-create these experimentally. Rim growth is parabolic with time, indicating diffusion limited reaction rates. No diffusion profiles are observed in the olivines or the melt suggesting transport via grain boundaries is rate limiting.

As the total water content is below the saturation threshold of the melt there should be no fluid phase in the system. However, addition of water to the melt significantly increases rates of reaction. This could be linked to changing transport properties of rim grain boundaries at different levels of fluid saturation. We use Dual Beam (FIB + SEM) serial sectioning to observe 3D microstructures of the rims as well as TEM to determine the presence of pores in the reaction rims. The results of this show that free fluid forms in localized regions at the micron to submicron scale and that these are not well connected. The correspondence of water content in the melt with rim growth kinetics suggests that the grain boundaries become increasingly hydrated but not completely fluid saturated. This increases the transport of components through the rims, allowing faster growth rates.

The amount of fluid present in reactions of this kind will affect the rates of xenolith breakdown which are commonly used to assess residence times and ascent rates of magmas. The kinetic and transport properties of grain boundaries during melt infiltration and reaction during metasomatism will also be strongly influenced by the levels of fluid saturation, even if the bulk melt remains water-undersaturated. Understanding the affects of fluid saturation in grain boundaries is therefore vital.

Cycling of silicic acid and nitrate in the Eastern Equatorial Pacific: Insights from stable silicon and nitrogen isotopes

PATRICIA GRASSE^{1*}, EVGENIA RYABENKO¹,
MARK A. ALTABET² AND MARTIN FRANK¹

¹GEOMAR, Helmholtz Centre for Ocean Research, Kiel, Germany

²School for Marine Science and Technology, University of Massachusetts Dartmouth

(*correspondence: pgrasse@geomar.de)

We present the first direct comparison between dissolved stable silicon ($\delta^{30}\text{Si}(\text{OH})_4$) and nitrogen ($\delta^{15}\text{NO}_3^-$) isotopes in the upwelling area off Peru to investigate the biogeochemical processes controlling nutrient cycling in one of the globally largest Oxygen Minimum Zones (OMZs). Nitrate is a generally important source of new nitrogen for phytoplankton, whereas silicic acid is a key nutrient for diatoms, which dominate the phytoplankton assemblages in upwelling areas. Silicon and nitrogen isotopes in the euphotic zone of the upwelling area are mainly controlled by biological utilization during which the lighter isotopes are preferentially incorporated into the organisms. Silicon isotopes are subject to a relatively simple cycling only influenced by utilization and subsequent dissolution of diatoms. In contrast, there are additional processes exerting control the N isotope composition of dissolved nitrate including anoxic ammonium oxidation (anammox) and/or denitrification within the OMZ. Given that the water masses feeding the coastal upwelling cells originate from the suboxic zone, the surface waters near the shelf show low $\delta^{30}\text{Si}(\text{OH})_4$ values (2‰) under strong upwelling conditions corresponding to high $\delta^{15}\text{NO}_3^-$ values (14‰). During the cruise a large mesoscale eddy was present in the study area and clearly influenced the nutrient stable isotope composition, as well as the phytoplankton community. Pronounced silicic acid limitation in the center of the eddy structure is indicated by high $\text{NO}_3^-:\text{Si}(\text{OH})_4$ ratios (~15) leading to the highest $\delta^{30}\text{Si}(\text{OH})_4$ values (3.7‰) accompanied by high $\delta^{15}\text{NO}_3^-$ values (16‰). The results show that both water mass mixing and remineralization processes influence the dissolved nitrogen and silicon isotope composition. Due to grazing of zooplankton and/or microbial remineralization a larger fraction of the nitrogen is recycled within the upper water column compared to silicic acid, which is more efficiently transferred to the deep waters. This is indicated by a smaller degree of utilization for nitrate in comparison to silicic acid in the study area. The combination of $\delta^{30}\text{Si}(\text{OH})_4$ and $\delta^{15}\text{NO}_3^-$ helps to disentangle utilization and N-loss processes and better understand paleo records and.

Determination of microbial consortia and its adaptation to environmental changes in the Neo-Archaean

NATHALIE V. GRASSINEAU¹ AND EUAN G. NISBET¹

¹Earth Sciences Department, Royal Holloway, University of London, Egham, TW20 0EX, UK

(nathalie@gl.rhul.ac.uk)

Isotopic fingerprints in Archaean sediments track metabolic processes, and are often the best evidence of biological activity. However poor and limited preservation make reconstitution of Archaean environments from rock records very challenging. Studying multiple localities around the world for one specific period helps to create a better picture of Archaean environments for this time window, but it is still a succession of snapshots, and such models can be misleading.

This work uses three cores and coexisting stromatolitic deposits from proximal but spatially different localities to reconstitute contemporary but sedimentologically varied Archaean environments. Well preserved 2.7 to 2.65 Ga sediments from the Belingwe Greenstone Belt (Zimbabwe) have been studied. The Manjeri and Cheshire Fms, laid down in a continental basin, consist of carbon- and sulphur-rich cherts and dark shales, as well as shallow-water limestones. In carbon-rich sections in cores from the Shavi and Jimmy Members, Manjeri Fm, and stromatolite surface outcrops, the overall 39‰ range for $\delta^{13}\text{C}_{\text{red}}$ and the overall 40‰ range for $\delta^{34}\text{S}$, plus $\Delta^{33}\text{S}$, molybdenum and iron isotopic information, suggest a wide spectrum of bacterial consortia, showing adaptations to environmental changes. This allows us to map out a wide sequence of microbial/sedimentary facies in coexisting microbial consortia in evolving prokaryotic communities.

Assessment of river water quality in catchments: Impact of urbanization on particle bound pollutant fluxes

PETER GRATHWOHL*¹, MARC SCHWIENTEK²,
HERMANN RÜGNER³ AND MICHAEL RODE⁴

¹Eberhard Karls University of Tübingen, Hölderlinstr. 12,
72074 Tübingen, Germany.

(*correspondence: grathwohl@uni-tuebingen.de)

²Water Earth System Science (WESS), Keplerstr. 17, 72074
Tübingen, Germany.

(marc.schwientek@uni-tuebingen.de)

³Water Earth System Science (WESS), Keplerstr. 17, 72074
Tübingen, Germany. (h.ruegner@uni-tuebingen.de)

⁴Helmholtz Centre for Environmental Research-UFZ,
Brückstr. 3a, 39114 Magdeburg, Germany.
(michael.rode@ufz.de)

Transport of many urban pollutants in rivers is coupled to transport of suspended particles, potentially dominated by storm water overflows and mobilization of legacy contamination of sediments. Concentration of these pollutants depends on the mixture of “polluted” urban and “clean” background particles. In the current study, the total concentration of polycyclic aromatic hydrocarbons (PAHs), the amount of total suspended solids (TSS) and turbidity were measured on a monthly basis in water samples from 5 catchments with contrasting land use in Southwest Germany and 3 catchments in the Bode Basin in Eastern Germany over up to 1.5 years. In addition, single flood events with large changes in turbidity were sampled at high temporal resolution. Linear correlations of turbidity and TSS were obtained over all catchments investigated. From linear regressions of turbidity vs. total PAH concentrations in water, concentrations of PAHs on suspended particles were obtained. These values comprise a robust measure of the average sediment quality in a river network and may be correlated to the degree of urbanization represented by the number of inhabitants per total flux of suspended particles. The findings are promising for other particle-bound contaminant fluxes (PCBs, phosphorus, etc.) and in terms of on-line monitoring of turbidity as a proxy for pollution.

Origin of REE patterns in AMD-impacted areas

A. GRAWUNDER^{1*}, S. MEISSNER¹, D. MERTEN¹,
S. PAŠALIĆ¹, S. KARLSSON², B. ALLARD²
AND G. BÜCHEL¹

¹Friedrich-Schiller-University, Jena, Germany

(*correspondence: anja.grawunder@uni-jena.de)

²Örebro University, Örebro, Sweden

Rare earth elements (REE; La-Lu) are a group of elements with a high potential as process indicators in the system rock/soil and water. Acid mine drainage (AMD)-impacted areas often have high concentrations of REE due to low pH. Moreover, they feature with a pronounced enrichment of middle REE (MREE) a very common phenomenon which is still under debate. Different AMD-impacted sites in Europe were investigated for REE patterns and their origins. Three of them showed the typical MREE-enrichment (Fig. 1) despite different geology (shales, volcanic rocks) and water source (lake, creek, groundwater). Based on a series of pyrite samples, it was found with H₂SO₄ - batch tests that one source for MREE enrichment is the release from pyrite under acidic conditions (Fig. 1), assuming complexation with a metastable S-species [2]. An exception was Ljusnarsberg, a former Swedish Cu mining area. For this site the REE patterns were rather enriched in light REE (LREE, Fig. 1). Saturated column experiments with heap material (pH 2.6-2.7) in combination with H₂SO₄ - batch tests of abundant minerals showed that release from a biotite group member controls the REE pattern in the open pit water to a large part (Fig. 1). Concluding, these results give a new view on REE pattern development in AMD-impacted areas.

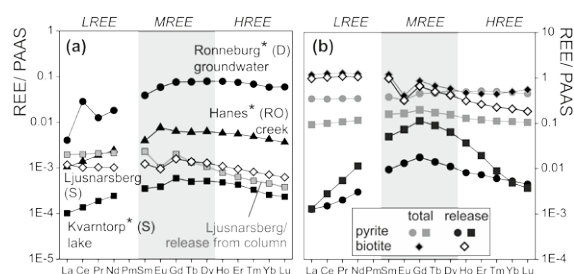


Figure 1: Examples for PAAS [1] normalised REE patterns of (a) AMD-impacted water (* from [2]) and effluent of column experiments with heap material of an AMD-impacted area; (b) total and released REE of pyrite samples [2] and biotite.

[1] McLennan (1989) *Rev. Min. Geochem.* **21**,169–200. [2] Grawunder *et al.* (subm) *Environ. Sci. Poll. Res.*

Mercury transport along the Tiber River basin (Central Italy)

J.E. GRAY^{1*}, V. RIMONDI², P. COSTAGLIOLA²,
P. LATTANZI³, O. VASELLI² AND G. PATTELLI²

¹US Geological Survey, MS 973 Federal Center, Denver, USA
(*correspondence: jgray@usgs.gov)

²Dipartimento Scienze della Terra, Università di Firenze,
50121 Firenze

³Dipartimento di Scienze Chimiche e Geologiche, Università
di Cagliari, 09127 Cagliari

The Mt. Amiata Hg district (MAMD) was an area of significant Hg mining up to the 1980s, with a total Hg production exceeding 102,000 tons. High concentrations of Hg were found in rivers, such as the Paglia River, which drains the NE part of the MAMD. In this study, stream sediment, stream water and fish were collected from the Tiber River and its tributaries to evaluate long distance Hg transport downstream from the MAMD. Along the Tiber River, samples were collected both upstream and downstream from the confluence with Paglia River to determine any adverse affects of Hg to the Tiber River.

The highest Hg concentrations in stream sediment, water and fish were found along the Paglia River, which is most proximal to Hg mines, and along the Tiber River just below the confluence with the Paglia River. Overall, Hg generally decreased with increasing distance from the MAMD, suggesting dispersion and dilution of Hg with increasing distance from mined areas. Five sediment samples exceed the probable effect concentration for Hg of 1.06 µg/g, above which harmful effects are likely to be observed in sediment-dwelling organisms. Concentrations of stream water Hg generally correlated with sediment Hg indicating that Hg is dominantly transported as particulates. The Alviano dam, located along the Tiber River, acts as a sink for Hg, where Hg contaminated sediment is deposited.

Of the fish muscle samples collected, 17% exceeded the 0.30 µg/g (wet weight, methyl-Hg) USEPA fish muscle Hg guideline recommended to protect human health. Fish with the highest Hg concentrations were collected from the Paglia River, whereas no fish collected from the Tiber River contained Hg beyond the USEPA guideline. Lower Hg concentrations in fish in the Tiber River are a result of dispersion and dilution of Hg with increasing distance from mined areas, as well as generally low methylation of Hg on the Tiber River.

Controls on the uptake of Mg, Sr and Li in benthic foraminifera *Uvigerina peregrina*

WILLIAM R. GRAY^{1*}, MARIËTTE WOLTERS^{2,3}
AND JONATHAN A. HOLMES¹

¹Department of Geography, University College London, UK;
william.gray.09@ucl.ac.uk (*corresponding author)
(j.holmes@ucl.ac.uk)

²Department of Chemistry, University College London, UK;
(m.wolthers@ucl.ac.uk)

³Department of Earth Sciences-Geochemistry, Utrecht
University, the Netherlands

The uptake of trace elements into benthic foraminiferal calcite is controlled by the temperature and carbonate ion saturation (ΔCO_3^{2-}) of the water in which calcification occurs. Trace element/Calcium ratios can potentially be used to elucidate past changes in bottom water temperature (BWT) and ΔCO_3^{2-} , providing the relationships between trace element uptake and environmental variables can be accurately constrained. Current *Uvigerina peregrina* trace element/Ca calibrations are predominantly based on the super-saturated waters of the North Atlantic. In order to constrain the effects of temperature and ΔCO_3^{2-} on trace element uptake, and assess the fidelity of trace element-temperature/ ΔCO_3^{2-} relationships in under-saturated waters we present new core top *Uvigerina peregrina* trace element/Ca data with a focus on the under-saturated waters of the North Pacific.

Core top *Uvigerina peregrina* samples were obtained from the Bering Sea, Cascadia Basin, Gulf of California and Okhotsk Sea in the North Pacific, and the Florida Straits in the North Atlantic. The core top sites were chosen to cover a wide range of bottom water temperatures (2 to 17 °C) and carbonate ion saturation states (-10 to 135 µmol kg⁻¹). Trace element/Ca ratios were analysed by quadrupole ICP-MS. Our results reveal a significant negative relationship between test size and both Li/Ca, and Sr/Ca ratios, demonstrating an ontogenetic control on trace element uptake, possibly related to changing calcification rate. Mg/Ca, Sr/Ca, and Li/Ca ratios are significantly correlated to both BWT and ΔCO_3^{2-} , however the relationship between trace element/Ca ratios and BWT/ ΔCO_3^{2-} differs in under-saturated and super-saturated waters, with Li uptake displaying a higher sensitivity to ΔCO_3^{2-} in under-saturated waters.

Magmatic and linked hydrothermal processes fractionate Mo isotopes

NICOLAS D. GREBER^{1*}, ANDREA R. VOEGELIN²,
THOMAS PETTKE¹ AND THOMAS F. NÄGLER¹

¹Institute of Geological Sciences, University of Bern,
Switzerland

(*correspondence: greber@geo.unibe.ch)

²Departement of Geosciences and Natural Resource
Management, University of Copenhagen, Denmark
(andrea.voegelin@geo.ku.dk)

Molybdenum isotope ratios in the marine sedimentary record are a valuable tool for reconstructing the evolution of atmospheric oxygen and paleo-redox conditions of the oceans. However, mass-balance models are highly dependent on the characterization of the (terrestrial) Mo sources. Recent results on the Mo isotope composition of terrestrial igneous rocks [1] and molybdenites [2] show a Mo isotope variability that is larger than previously suspected for crustal rocks and minerals. Therefore, two geochemically well-understood systems, the Kos Island Arc volcano (Greece) and the porphyry Questa Mo deposit (New Mexico, USA), were investigated systematically. The magmatic evolution of the igneous rock suite from Kos was predominantly controlled by fractional crystallization. The molybdenites from the porphyry Questa Mo deposit were produced during two distinct mineralization stages, related to two hydrothermal fluid exsolutions from an increasingly fractionated magma [3].

The magma evolution from basalt to dacite on Kos is characterized by increasing $\delta^{98}\text{Mo}$ (total $\delta^{98}\text{Mo}$ range = 0.3‰) along with increasing Mo concentrations, as expected for a highly incompatible element. The $\delta^{98}\text{Mo}$ of the molybdenites from the Questa deposit ranges from -0.48‰ to +0.40‰, with a median at -0.06‰. The median $\delta^{98}\text{Mo}$ increases from first stage (-0.17‰) to late stage molybdenites (0.21‰). Based on these results we recognize three different processes that produce systematic Mo isotope fractionation between 700 and 350°C in igneous and hydrothermal environments: (a) fractional crystallization, (b) magmatic-hydrothermal fluid exsolution and (c) molybdenite precipitation.

All these processes lead to the enrichment of heavy Mo isotopes in the more evolved magma or fluid phase. This indicates that the mean Mo isotope composition of all molybdenites ($\delta^{98}\text{Mo} \approx 0.4‰$; [2]) reflects a maximum value for Earth's upper crustal signature.

[1] Voegelin *et al.* (2012) *Geochim Cosmochim Acta*, **86**, 150–165. [2] Greber *et al.* (2011) *Geochim Cosmochim Acta*, **75**(21), 6600–6609. [3] Klemm *et al.* (2008) *Miner Deposita*, **43**, 533–552.

Multiple generations of TTG gneisses host Eoarchean supracrustals in the Innukjuak domain (Québec, Canada)

J. C. GREER¹, N. L. CATES¹, G. CARO²
AND S. J. MOJZSIS^{1,3,4*}

¹University of Colorado, Geol. Sciences, Boulder, CO, USA

²CRPG- CNRS and Université de Lorraine, Nancy, France

³Laboratoire de Géologie de Lyon, ENS & UCBL1, France

⁴MTK, Institute for Geological and Geochemical Research,
Budapest, Hungary *mojzsis@colorado.edu

The ca. 3750–3780 Ma Nuvvuagittuq supracrustal belt (NSB) in northern Québec is the best known of a dozen or so km-scale supracrustal belts (or “enclaves”) which are part of the Innukjuak domain of the northwest Superior province in Canada [1,2]. Dominantly (mafic) amphibolites and minor paragneisses in these supracrustal belts are surrounded and intruded by several generations of tonalite-trondhjemite-granodiorite (TTG) gneisses; these imparted metamorphic overprints on the enclaves beginning at ca. 3750 Ma. Previous work also documented a ca. 3650 Ma tonalitic gneiss in the core of the NSB fold belt [2; referred to here as the central tonalitic gneiss (CTG)] as well as rocks of the “Boizard suite” (Aboi), a terrane of ca. 2700 Ma granitoid gneisses that volumetrically dominate the Innukjuak domain [3]. New geochemical and U-Pb zircon geochronological data are presented for these gneisses coupled with data from a previously undated but locally significant pale granodioritic gneiss enveloping the NSB, the “Voizel suite” (Avoi; [2]).

We find that most Avoi zircons are up to ca. 3700 Ma inherited cores from multiple generations with ca. 2700 Ma igneous overgrowths. The CTG hosts mainly ca. 3650 Ma igneous cores with narrow rims. Younger zircons typically have spongy textures attributable to hydrothermal growth. Outside the NSB, Avoi rocks are the principal host for various Innukjuak domain supracrustal enclaves. Most Avoi igneous zircon cores from these localities cluster about 3550 Ma with younger metamorphic rims. Younger Avoi ages tend to be discordant. A tonalitic gneiss cross-cutting amphibolites from a supracrustal belt northeast of the NSB, and within Avoi, yielded a maximum concordant zircon age of 3653±8 Ma; it may be cogenetic with the CTG. The previously unrecognized 3550 Ma Avoi igneous event is recorded as metamorphic zircon growth within many of the NSB lithologies [4], particularly in metasedimentary units and the CTG.

[1] Cates & Mojzsis (2007) *EPSL* **255** 9–21. [2] David *et al.* (2009) *GCA* **121**, 150–163. [3] Simard *et al.* (2003) Ministère des ressources Naturelles, Québec, vol. 2002/10 [4] Cates & Mojzsis (2009) *Chem Geol* **261**, 99–114.

The oxygen isotope excess $\Delta(^{17}\text{O})$ of marine nitrous oxide

IMKE GREFE AND JAN KAISER

University of East Anglia, School of Environmental Sciences,
NR4 9TJ Norwich, UK (i.grefe@uea.ac.uk,
j.kaiser@uea.ac.uk)

The small ^{17}O isotope excess $\Delta(^{17}\text{O})$ of atmospheric nitrous oxide (N_2O) of $(0.9\pm 0.1) \text{‰}$ (vs. VSMOW) is regarded to be mainly a result of chemical in-situ production in the troposphere and the stratosphere. These mechanisms only have a negligible contribution to the global N_2O mass budget, but do significantly affect the ^{17}O excess of atmospheric N_2O because of the high ^{17}O excess of the species involved (NO_x , O_3).

However, Kaiser *et al.* (2004) suggested that the main biological N_2O sources (denitrification, nitrification) can also have an influence on the $\Delta(^{17}\text{O})$ value of atmospheric N_2O . Therefore, soils and ocean should also be considered as a source of the ^{17}O excess in atmospheric N_2O .

We present depth-resolved measurements of the ^{17}O excess in dissolved N_2O from the Atlantic Ocean, the Scotia Sea and the Weddell Sea. In the temperate, subtropical and tropical surface Atlantic Ocean, we observed $\Delta(^{17}\text{O})$ values of up to 1.5 ‰ relative to N_2O in air. Values above the tropospheric mean value of 0.9 ‰ were observed down to 300 m depth. This means that oceanic N_2O from these regions contributes to the atmospheric ^{17}O excess. In polar regions and in the deep Atlantic Ocean, the isotope excess was between 0 and 0.9 ‰. Irrespective of the oceanic net N_2O mass flux, this would lead to a net reduction of the atmospheric ^{17}O excess.

These results show that oceanic N_2O emissions need to be taken into account for tropospheric N_2O isotope budget calculations. However, further measurements in other ocean regions are needed before the net effect of oceanic N_2O on the ^{17}O excess can be established.

A 100% renewable power system in Europe – let the weather decide!

MARTIN O.W. GREINER¹, GORM ANDRESEN¹,
ROLANDO RODRIGUEZ¹, SARAH BECKER¹, ANDERS
SONDERGAARD¹, TUE JENSEN¹ AND TIMO ZEYER¹

¹Department of Engineering and Department of Mathematics,
Aarhus University, Ny Munkegaard 120, DK-8000 Aarhus,
Denmark, (greiner@imf.au.dk)

Today's overall macro energy system based on fossil and nuclear resources will transform into a future system dominantly relying on fluctuating renewable resources. At the moment it is not really clear what will be the best transitional pathway between the current and the future energy system. In this respect it makes sense to think backwards, which means in a first step to get a good functional understanding of fully renewable energy systems and then in a second step bridge from there to today's energy system. Based on state-of-the-art high-resolution meteorological and electrical load data, simple spatio-temporal modelling, time-series analysis and the physics of complex networks, fundamental properties of a fully renewable pan-European power system are determined. Amongst such characteristics are the optimal mix of wind and solar power generation, the optimal combination of storage and balancing, the optimal extension of the transmission network, as well as the optimal ramp down of fossil and nuclear power generation during the transitional phase. These results indicate that the pathways into future energy systems will be driven by an optimal systemic combination of technologies, and that economy and markets have to follow technology

A-type granites of Prydz Bay, Antarctica: Products of melting of a two-component granulite crust?

E.S. GREW^{1*}, R. MAAS², A.G. CHRISTY³, C.J. CARSON⁴,
M.G. YATES¹ AND S.D. BOGER²

¹School of Earth and Climate Sciences, Univ Maine, Orono, ME 04469, USA (correspondence: esgrew@maine.edu)

²School of Earth Sciences, Univ Melbourne, Parkville, 3010, Australia (maasr@unimelb.edu.au)

³Centre for Advanced Microscopy, Australian National University, Canberra, 0200, Australia

⁴Geoscience Australia, PO Box 378, Canberra, 2601, Australia (chris.carson@ga.gov.au)

Cambrian (519-494 Ma) A-type granites, cropping out over ~130 km along the Prydz Bay coast are structurally, texturally and mineralogically diverse. Intrusions in the SW carry hornblende, chevkinite-perrierite, allanite and titanite; those in the NE carry garnet and monazite. Fluorite is widespread; oxides include magnetite, hercynite, ilmenite and, locally, h ogbomite and hematite. The granites (SiO₂ 59.8-77.7%, ASI 0.95-1.19) are high in Fe, alkalis and K₂O/Na₂O (1.1-5.2), Ga/Al, HFSE and REE, with remarkably high Zr (322-1625 ppm), LREE (Ce 107-2101 ppm) and Th (up to 878 ppm Th; Th/U = 28-142). REE fractionation is strong (La_N/Yb_N 36-454), being more pronounced in the NE. Sr-Nd-Hf isotope ratios (⁸⁷Sr/⁸⁶Sr 0.708-0.726, ε_{Nd} -8 to -13, ε_{Hf} -4 to -14) and Nd-Hf model ages are consistent with magma sources in equivalents of the exposed Neoproterozoic ortho- and paragneisses. High ²⁰⁷Pb/²⁰⁴Pb_i (15.71-15.77) and low ²⁰⁶Pb/²⁰⁴Pb_i (17.7-18.16) indicate Pb isotope evolution in a high-μ reservoir since ~2.5 Ga, followed by a low-μ stage for several 100 Ma prior to granite formation. A ~1 Ga granulite-facies event recorded in Prydz Bay gneisses could explain the drop in U/Pb. Co-variation of REE-Y and Sr-Nd isotopes in the granites suggests at least two crustal components in the magma source. Component 1 (ε_{Nd} ~ -13, ⁸⁷Sr/⁸⁶Sr >0.72) produced melts with strong HREE fractionation and Y depletion (major residual garnet), represented by 3 of the 4 NE intrusions. Component 2 (ε_{Nd} -7 to -10, ⁸⁷Sr/⁸⁶Sr 0.708-0.714) produced melts with lower Gd_N/Yb_N (less residual garnet), represented by the SW intrusions. Both components contain the high-207/low-206 isotope signature inferred to be linked to the regional ~1 Ga granulite-facies gneisses. Since these source rocks are residual, dehydrated gneisses, it is inferred that temperatures well above the wet solidus were required for melting at ~0.5 Ga, a condition we suggest was inherited from the pre-collision thermal structure of the lithosphere in Prydz Bay.

'Kimberlitic' zircons from Paleoproterozoic Kimozero kimberlites (Karelia):

Mineralogy, geochemistry and U-Pb geochronology

J.G. GRIBAN^{12*}, A.V. SAMSONOV¹, E.B. SALNIKOVA³,
AND E.N. LEPEHINA⁴

¹IGEM RAS, Moscow, Russia,

(*correspondence: julie.griban@gmail.com)

²Lomonosov Moscow State University, Russia,

³IPGG RAS, St. Petersburg, Russia,

⁴VSEGEI RAS, St. Petersburg, Russia

The origin of xenocrystic zircons from the Paleoproterozoic Kimozero kimberlite is in discussion. The kimberlite is located in the Eastern part of the Karelian craton among the Middle Paleoproterozoic (2.1-2.0 Ga) Zaonezhskaya supracrustal sequence of the Onega trough.

Most zircons separated from the kimberlitic breccias are large (up to 1000 μm) isometric, soccer-ball shape crystals and correspond to the description of kimberlitic zircons [1]. There are two general types of inner structure of the zircons: homogenous and oscillatory zoned.

Oscillatory zoned zircons represented as cores in zircon grains. They have U-Pb isotopic age around 2.4 Ga. Their geochemical characteristics suggesting they are relicts of magmatic zircons formed from depleted, possibly, basaltic source.

The two genetic groups of homogenous zircons from Kimozero kimberlites were revealed. The zircons of Ist group are extremely depleted by all trace elements such as REE, U, Th, P, Ti, Li and have the age of 1986±4 Ma. Their geochemical characteristics are comparable with kimberlitic zircon megacrysts described for various kimberlites all over the world. Thus, the zircons are thought to be engaged from a mantle Kimozero kimberlite source. The obtained age for the Kimozero kimberlitic zircons is very close to the age of the alkaline-ultrabasic carbonatite magmatism in the North-Western part of the Karelian craton 1999 ± 5 Ma [2]. The zircons of IInd group are also depleted by U, Th, REE, but they are enriched in Hf, P, Li, Ti and have an older U-Pb age of 2406±6 Ma. Geochemical features of the zircons of IInd group are typical for lower crustal xenoliths [3]. Their crystallization was probably related with granulite metamorphism occurring 2.4-2.5 Ga ago as part of large-scale intense thermal reworking of lower crust by rising plume under the eastern part of the Baltic shield.

[1] Page *et al.* (2007) *Geochim Cosmochim Acta*. №71:3887-3903. [2] Corfu *et al.* (2011) *Central European Journal of Geosciences*. [3] Hoskin & Schaltegger (2003) *Rev. Mineral. Geochem.* 53, 27-62.

Going up or going down? Diamonds and Super-Reducing UHP assemblages in ophiolitic mantle

*W.L. GRIFFIN¹, J.S. YANG², P. ROBINSON², D. HOWELL¹, R.D. SHI^{1,3}, SUZANNE Y. O'REILLY¹ AND N.J. PEARSON¹

¹GEMOC/CCFS, Earth and Planetary Sciences, Macquarie University, NSW 2109 Australia

(*correspondence: bill.griffin@mq.edu.au)

²State Key Laboratory for Continental Tectonics and Dynamics, CAGS, Beijing 100037 China

³Inst. Tibetan Plateau Research, CAS, Beijing 100085 China

Diamonds have been reported from the mantle parts of ophiolites for ≥ 30 years, but have been widely dismissed as contaminants, because their morphology (octahedral + planar cubic faces) and isotopically light C ($\delta^{13}\text{C}$ to -27) are unlike kimberlitic diamonds. However, diamonds have now been found *in situ* in the chromitites and peridotites of many ophiolites in Tibet (Yarlung-Zangbo suture) and the Polar Urals [1]. LA-ICPMS analyses of the diamonds show LREE-enriched trace-element patterns parallel to those of kimberlitic fibrous diamonds. The patterns are distinct from those of synthetic diamonds, and the ophiolitic diamonds thus appear to be natural. However, there are also striking differences from cratonic diamonds: strong negative anomalies in Sr, Sm, Eu and Yb; extremely low Fe; high Ta and Mn-Ni-Co (present as alloy microinclusions). The diamonds are accompanied by a range of alloys, native metals, carbides and silicides; these and the low Sm-Eu imply very low $f\text{O}_2$. High-Si rutile and coesite pseudomorphs after stishovite suggest pressures ≥ 10 GPa. Finally, some peridotites yield whole-rock Re-Os T_{RD} ages back to 3.4 Ga [2]. The presence of these super-reducing ultrahigh pressure (SuR-UHP) assemblages in large ultramafic massifs raises important questions: Are the SuR-UHP rocks widespread at depth, and brought up along sutures, or are they related to the subduction process? Do the old T_{RD} ages indicate an origin as subducted SCLM, or does such ancient depleted material exist in the "convecting mantle"? How did the massifs come up rapidly enough to avoid graphitizing the diamonds? These SuR-UHP massifs carry unique information on the tectonics of collision zones, mantle convection processes, and the physical and chemical makeup of the deep mantle.

[1] Yang *et al.* (2013) *Science (subm.)*. [2] Shi *et al.* (2012) *Geol. Rev.* **58**, 649-652.

Micro-scale carbonation of single facets of Portlandite

GRAHAM GRIFFITHS¹, DAVID CHERNS², RICHARD BALL³, GEOFF ALLEN AND ADEL EL-TURKI

¹g.griffiths@bristol.ac.uk

²D.Cherns@bristol.ac.uk

³R.J.Ball@bath.ac.uk

The carbonation of portlandite to calcite is considered a key adhesive process in almost all historic mortars, right up until the beginning of the 20th century. Even in the present day, so-called "high-calcium cements", which rely on this reaction, are still widely used for cosmetic and conservation purposes. While the precursor hydroxide and the consequent carbonate have previously been extensively characterized, a subject of much current interest is the physical manifestation of the conversion between the two, i.e. by what mechanism does the reaction get from crystalline portlandite to crystalline calcite?

To study this reaction *in-situ* and at very early stages, it is necessary to generate pristine calcium hydroxide surfaces on which to perform subsequent reactions; crystalline facets of portlandite as a reactive substrate is key to isolating the reaction path of carbonation and any intermediates that may occur. To provide these facets, artificial specimens of portlandite were generated by precipitation from aqueous solution by way of a novel nitrogen-drying cell. Following exposures to pure CO_2 lasting from 1 to 48 hours, a new phase was seen growing on the portlandite surfaces, characterized using scanning electron microscopy. This was subsequently identified as highly voluminous calcium carbonate "nodules" using transmission electron microscopy, small angle electron diffraction and Raman spectroscopy. While the carbonate Raman spectra ultimately tended towards calcite, spectra taken with the first one to three hours were closer to that of an amorphous phase of calcium carbonate. In addition to its low crystallinity, this new phase was seen, using TEM, to be highly expansive; generating large volumes of carbonate with the consumption of relatively little hydroxide. This is believed to be a consequence of the sequestration of water within the rapidly formed nodules, which would then gradually stabilize to calcite with time or heating.

Simulated exposure of crude oil to sunlight and characterization using atmospheric pressure photoionization fourier transform ion cyclotron resonance mass spectrometry

MATTHEW T. GRIFFITHS¹, RAFFAELLO DA CAMPO¹, PETER B. O'CONNOR¹ AND MARK P. BARROW^{1*}

¹Department of Chemistry, University of Warwick, Coventry, CV4 7AL, United Kingdom (*correspondence: M.P.Barrow@warwick.ac.uk)

Petroleum is a vital resource and is likely to remain so for the foreseeable future, providing the primary basis of most transportation energy and being the precursor for many materials. Due to its finite availability, production of petroleum is in decline, although worldwide consumption continues to increase. Lower quality sources of crude oil have become increasingly exploited as a result. Releases of petroleum into the environment can occur, whether arising from natural seepage or from human activity, and it is known that natural processes can influence the chemical composition of these complex mixtures. The effects of solar radiation have been targeted for the following study.

A crude oil sample was divided into three allocations: one sample was exposed to ultraviolet light, the second sample was exposed to light from a SoLux lamp which mimics sunlight, and a third sample served as a control. After more than a month of exposure, the chemical compositions were determined and compared using a 12 T Fourier transform ion cyclotron resonance mass spectrometer.

Atmospheric pressure photoionization was selected as the ionization method due to its suitability for studying less polar components which may be present within crude oils, such as sulfur-containing compounds and hydrocarbons which do not incorporate any heteroatoms. The thousands of components observed were categorized according to heteroatom content, carbon number, and double bond equivalents, and profiles for each sample could be created. It was found that specific heteroatom classes more readily degraded, accompanied by an increase in oxygen-containing compound classes. The findings contribute to a better understanding of changes to the chemical composition of crude oil in the environment and possible changes in toxicity.

The behaviour of submicron inclusions during host deformation

T. A. GRIFFITHS^{1*}, G. HABLER¹, R. ABART¹ AND D. RHEDE²

¹University of Vienna, Althanstrasse 14, 1090 Vienna, Austria (*correspondence: th.griffiths@univie.ac.at)

²GFZ Potsdam, Telegrafenberg C 121, D-14473 Potsdam, Germany (rhede@gfz-potsdam.de)

Both brittle and plastic deformation strongly influence the location, rates and mechanisms of material transport in the earth's interior. Mineral reactions and diffusion can be controlled by deformation, but in turn contribute to its localisation. We investigate the mechanisms of interaction between deformation and chemical reaction in the context of re-equilibration of inclusions in a deforming host mineral.

Permian pegmatite garnets from the Koralpe, eastern Alps, contain numerous submicron sized inclusions. The pegmatitic assemblage was affected by deformation under eclogite facies conditions during the Cretaceous tectono-metamorphic event. The meta-pegmatite garnet deformed crystal-plastically at this metamorphic stage [1].

Trails of inclusions crosscutting the garnet have a coarser grain size (1-10 μm \varnothing) than inclusions outside the trails. In 10-40 μm wide zones flanking the inclusion trails the original $\leq 1 \mu\text{m}$ sized inclusions are absent, defining bleaching zones.

FEI-microprobe data showed that it is possible to form the microstructure isochemically. However, some trails were also found where inclusions have coarsened non-isochemically. In both cases no change in garnet major element composition was observed.

From their microstructural characteristics it is inferred that the trails formed at sites of healed brittle cracks. Garnet deformation has been mapped using EBSD and correlates with re-equilibration microstructures. Bleaching zones are associated with systematic very low angle lattice rotations of garnet. Additionally, lattice rotations of up to 10° occurred adjacent to already coarsened inclusions.

The new microstructural, microchemical and textural data document several different interactions between material transport, crystallization and deformation processes which contribute to the final microstructure. TEM investigations provide the opportunity to examine the types of defects present in order to help determine the mechanisms through which chemical and mechanical processes have interacted on the nanoscale.

[1] Bestmann Et Al. (2008) *J. Struct. Geol.* **30**, 777-790.

First investigations of IO, BrO, and NO₂ summer atmospheric levels at a coastal East Antarctic site using mode-locked cavity enhanced absorption spectroscopy

ROBERTO GRILLI¹, GUILLAUME MÉJEAN¹,
MICHEL LEGRAND², SUZANNE PREUNKERT²
AND DANIELE ROMANINI¹

¹Laboratoire Interdisciplinaire de Physique (LIPhy) UMR
5588, Grenoble, France.

²Laboratoire de Glaciologie et Géophysique de
l'Environnement (LGGE) UMR 5183, Grenoble, France.

The detection of highly chemical reactive halogenated species, such as BrO and IO represents a challenge for analytical techniques due to their short lifetime and very low abundance. The ability to take part to oxidative processes, such as the oxidation of dimethyl sulfide (DMS) and Mercury, increases the interest of the atmospheric community to better understand their role in the atmosphere and mainly in the Antarctica boundary layer where information from the polar ice cores, unique archive of climate proxies, can be retrieved. Detection of part per trillion (pptv, 1:10¹²) levels of BrO and IO radicals can be performed by probing rotationally structured electronic transitions in the near-UV employing mode-locked cavity-enhanced absorption spectroscopy (ML-CEAS). The technique is based on the injection of a broadband femtosecond laser into an optical resonator. The robust and transportable spectrometer provides shot-noise limited measurements for as long as 10 minutes, reaching detection limits of 0.04, 2, 10 and 200 ppt (2σ) for IO, BrO, NO₂ and H₂CO, respectively. The results of a field campaign at Dumont d'Urville Station in Antarctica during the austral summer 2011/12 highlight the differences in the oxidative capacity of the atmospheric boundary layer at coastal Antarctic sites, with the halogen chemistry being promoted to the West and the OH and NO_x chemistry on the East (Grilli *et al.*, GRL, 40, 1-6, 2013).

Inclusions in halite – evidence of mixing of evaporite xenoliths and kimberlites of Udachnaya-East pipe (Siberia)

S.N. GRISHINA

V.S. Sobolev Institute of Geology and Mineralogy, 630090
Novosibirsk, Russia
(correspondence: grishina@igm.nsc.ru)

Unknown compositional features of kimberlite magma, notably highly elevated alkalis and chlorine (up to 6 wt.%) have been declared in Udachnaya-East kimberlites [1]. These data are controversial and one question of debates is origin of chloride-carbonate segregations in unsertintinized kimberlite. It was supposed, that segregations represent pools of residual liquids and thus provide a new insights into composition of the kimberlite magma. Crustal assimilation is the alternative hypothesis and was considered theoretically [2]. We tried to use inclusion data as a new approach to clarify the origin of chloride-bearing segregations and the reasons for high chlorine content of kimberlites.

Part of chloride xenoliths in Udachnaya-East kimberlites are disaggregated and extensively altered to chloride-carbonate composition along the fractures and xenoliths boundaries. Transition from pervasive to no alteration xenoliths is correspondent to carbonate-rich and carbonate-free ones. Texture and inclusions of carbonate-free xenoliths are similar to pyrometamorphic evaporates [3]. Chloride-carbonate zones have distinctive textural features indicative of partial melting. The interaction between chlorides and kimberlites reveals by occurrence of natrocarbonatite-bearing inclusions along the fractures and boundaries both inside xenoliths and in kimberlite groundmass.

Chloride-carbonate segregations formed as a result of crystallisation of contaminated kimberlite magma in disaggregated chloride xenoliths. High chlorine content of studied kimberlites reflect syn-eruptive contamination.

[1] Kamenetsky (2012) *Lithos*, **152**, 173-186. [2] Kopylova (2013), *Earth-Science Reviews* **119** 1-16. [3] Grishina, (1992), *Eur. J. of Miner.* **4**. P. 1187-1202.

Emerald mineralization at the Anuri prospect, Nunavut, Canada

L.A. GROAT¹, A.A. BRAND¹ AND P. KLEESPIES²

¹University of British Columbia, Vancouver BC V6T 1Z4, Canada (*correspondence: groat@mail.ubc.ca)

²North Country Gold Corp., Edmonton AB T6E 5V8, Canada

Emerald has been identified in 7 intervals from 3 drill holes at the Anuri Au and Ag prospect which is located ~410 km N of Rankin Inlet in Nunavut. The prospect is within the Committee Bay Greenstone Belt, which forms part of the Rae domain of the western Churchill province. The emerald occurs in rocks of the Neoproterozoic volcano-sedimentary Prince Albert Group, primarily in an altered komatiite with a texturally and mineralogically variable matrix of biotite, actinolite, plagioclase, pyrite and occasional quartz, calcite, and accessory minerals such as apatite, titanite, rutile, chalcopyrite and molybdenite. The emerald (and colorless beryl) can occur in quartz veins, at contacts, and potentially as a hydrothermal overprint. Electron probe microanalysis shows that the dominant chromophore is Cr (with essentially no V), with a maximum content of 2.62 wt% Cr₂O₃ or 0.20 Cr *pfu*. The emerald also contains unusually high concentrations of Na (maximum 2.66 wt.% Na₂O, or 0.49 Na *pfu*), Mg (to 3.41 wt.% MgO, or 0.48 Mg *pfu*), and Fe (up to 1.99 wt.% FeO, or 0.16 Fe *pfu*). The source of the Be is likely a nearby 2718 Ma tonalite [1] which intrudes the komatiites.

[1] Skulski *et al.* (2003) Geological Survey of Canada, Current Research **C22**.

Long range transport of volcanic aerosols: The Eyjafjallajökull plume 2010

B.GROBETY^{1*}, M. MEIER¹, C. BOTTER¹, K. WEBER²,
C. FISCHER², A. VOGEL², E. GOLDENBERG³
AND R. GIÈRE³

¹Department of Geosciences, Univ. of Fribourg, Switzerland (*correspondence: bernard.grobety@unifr.ch)

²Laboratory for Environmental Measurement Techniques, University of Applied Sciences, Duesseldorf, Germany

³Institute of Geosciences, Univ. of Freiburg, Germany

The plume of the Eyjafjallajökull 2010 and its transport into European airspace gave the possibility to study how the physico-chemical properties of a volcanic aerosol are affected by long-range transport. We compared the mineralogical composition and the morphology of particles of samples of resuspended ash collected in Iceland with samples taken from an airplane, which crossed the plume over the Dutch-German border and ground samples from the town of Freiburg im Breisgau and the Vosges Mountains. A clear change in mineralogy and morphology could be observed between airborne samples taken close to the volcano and after long range transport. The ground and airborne samples taken in and over Germany are impoverished in olivine, clinopyroxene and plagioclase phenocrysts compared with Icelandic samples. The loss of these phenocrysts is a consequence of the difference in density between the volcanic glass and the mafic crystals. The aspect ratio of the particles changes also during transport. Particles with high aspect ratio (>2.5) are almost absent in the plume over Europe. Possible explanation is the higher specific surface of such particles, which will enhance the tendency of aggregation. Average physical properties (melting point, hardness) of the plume particles relevant for air traffic security after prolonged transport are thus clearly different from the one close to the emission point. When assessing the societal and environmental impact of a volcanic plume these continuous physico-chemical changes will ultimately have to be taken into account.

The role of crustal assimilation on the oxidation state of arc magmas

S.B. GROCKE^{1,2*}, E. COTTRELL¹, S.L. DE SILVA²,
B.J. ANDREWS¹ AND K.A. KELLEY³

¹Smithsonian Institution, NMNH, DC 20560, USA

(*correspondence: grockes@geo.oregonstate.edu)

²College of Earth, Ocean, and Atmospheric Sciences, Oregon State University, OR 97331, USA

³Graduate School of Oceanography, University of Rhode Island, Narragansett Bay Campus, RI 02882, USA

Oxygen fugacity (fO_2) governs magmatic evolution, phase assemblage, and gas speciation. Magmas erupted in volcanic arcs tend to be several orders of magnitude more oxidized than those at mid-ocean ridges, however the processes that lead to oxidation have not been identified. Here, we explore two mechanisms that may influence the fO_2 recorded by subduction-related volcanic rocks: 1) post- or syn-eruptive alteration, and 2) assimilation of continental crust. We use several proxies to estimate the fO_2 recorded by lavas, pumice and scoria erupted from the Central Volcanic Zone of the Andes: 1) whole rock $Fe^{3+}/\Sigma Fe$ ratios, 2) $Fe^{3+}/\Sigma Fe$ ratios in quartz- and olivine-hosted melt inclusions using micro X-ray absorption near-edge structure (XANES) spectroscopy, and 3) magnetite-ilmenite oxybarometry. Samples span a range of crustal contribution, as indicated by their radiogenic isotope compositions ($^{87}Sr/^{86}Sr = 0.705-0.712$), and cover the full suite of magma compositions erupted during the Neogene history of the arc (52 - 74 wt.% SiO_2). $Fe^{3+}/\Sigma Fe$ ratios range from 20-80% in these samples. This full range is observed for all stages of magmatic differentiation (basaltic andesites to rhyolites), all extents of crustal assimilation (30-100%), and all types of eruptive product (lavas, pumice and scoria). Comparison of the fO_2 calculated from bulk $Fe^{3+}/\Sigma Fe$ ratios (post-eruptive) versus that calculated from Fe-Ti oxides or melt inclusion $Fe^{3+}/\Sigma Fe$ ratios (pre-eruptive), enables us to quantify the effect of post- or syn-eruptive alteration. Some sample suites show excellent agreement between the three techniques employed in this study. In other cases, where pumices show evidence of alteration in hand-sample, the fO_2 recorded by bulk $Fe^{3+}/\Sigma Fe$ ratios is two orders of magnitude more oxidized than corresponding ratios from melt inclusions or oxybarometry, suggesting modification of whole rock $Fe^{3+}/\Sigma Fe$ ratios by post-eruptive processes. Our work demonstrates that care must be taken when exclusively relying on bulk techniques to determine magmatic fO_2 , as whole rock may be subjected to post-emplacement oxidation. Moreover, our results show that neither crustal assimilation nor crystal fractionation systematically oxidize bulk continental arc magmas.

Fluid-mineral interactions of CO_2/O_2 , NaCl-brines and siderite-ankerite-mixtures at geological CO_2 -storage conditions

J. GRÖGER-TRAMPE^{1*}, S. WALDMANN¹, T. NOWAK¹
AND C. OSTERTAG-HENNING¹

¹Federal Institute for Geosciences and Natural Resources

(BGR), D-30655 Hannover, Germany (*correspondence: jgroeger@uni-bremen.de)

An option considered for the geological storage of CO_2 in Germany is the injection into deep saline aquifers. The geochemical effects triggered by impurities or so called incidental associated substances in CO_2 streams are an issue for mineral trapping of CO_2 . The carbonates siderite and ankerite are possible sequestration products of mineral trapping of CO_2 or can already initially occur in the target formations.

In the presented set of experiments the effect of O_2 in the CO_2 stream on siderite-ankerite-mixtures will be investigated. These experiments are conducted in static Au-Ti-cells at 20 MPa and 353 K with CO_2 containing 4 mol% O_2 . Saline groundwater is simulated by using a 2.7 mol/kgW NaCl-brine. Solution sampling during the the experiment is performed to monitor changes in the solution composition and thus mineral dissolution and precipitation reactions. First results of a reference experiment without the addition of O_2 (to be compared with the experiment containing O_2) show the expected dissolution of the siderite-ankerite-mixture (release of Ca, Mg, Fe and Mn). During the further course of the experiment a decrease of Fe- und Mn-concentrations indicates the formation of a new mineral phase, e.g. a Mn-rich siderite. Scanning-electron-microscopy (SEM) supported this assumption by revealing Fe- and Mn-rich precipitates on the mineral surfaces which were likely formed during the experiment. This and other assumptions will be further tested by deploying isotopically labeled CO_2 in upcoming experiments.

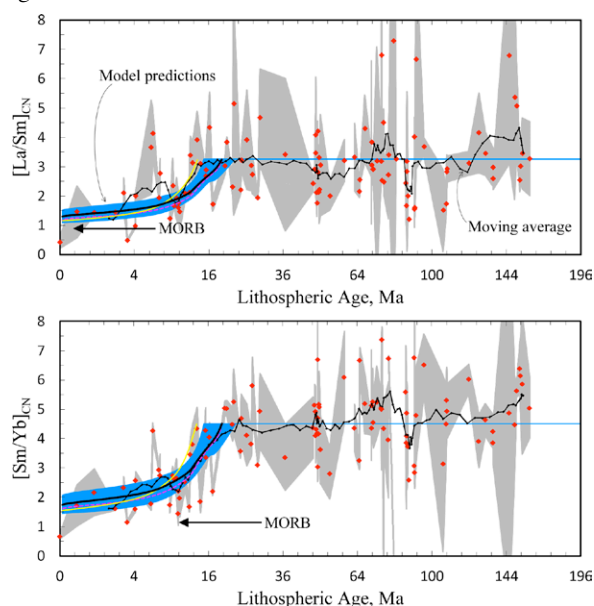
“Garnet signature” systematics and the structure of oceanic lithosphere

CHRISTOPHER J. GROSE¹ AND JUAN C. AFONSO¹

¹Department of Earth and Planetary Sciences, CCFS/GEMOC, Macquarie University, North Ryde, Sydney, NSW 2109, Australia.

Humphreys and Niu [1] showed that a geochemical database of 115 volcanic islands revealed trends in elemental systematics following the thickness of oceanic lithosphere. After performing corrections to lithospheric age estimates for volcanic islands we find that the trend with age is substantially more apparent. Specifically, we focus on La/Sm and Sm/Yb systematics, elevated values of which are thought to be a function of the presence of garnet in the melt source. The trend is not a simple function of lithospheric thickness. Values of these ratios are low for young ages (<15 Ma) and abruptly jump to a higher value which is constant over older seafloor.

To explain this structure, we combining a new thermal plate model of the oceanic lithosphere with a thermodynamic assessment of garnet stability to estimate relative values of La/Sm and Sm/Yb as a function of lithospheric age. We hypothesize that the transition to high La/Sm and Sm/Yb at ~15 Ma occurs because the LAB intersects the garnet stability field at ~50 km depth at this age. Models are in excellent agreement with observations.



[1] Humphreys and Niu (2009) *Lithos* **112**, 118-136.

Effects of nutrients on compound specific carbon fixation in phytoplankton

J. GROSSE^{1*} AND H.T.S. BOSCHKER¹

¹Royal Netherlands Institute for Sea Research, PO Box 40, Yerseke, The Netherlands. julia.grosse@nioz.nl (*presenting author)

The coastal waters of the North Sea have been affected by eutrophication over the past decades and subsequent efforts to reduce riverine nutrient loads resulted in a major shift in N:P:Si nutrient ratios. The consequent changes in the limiting resource can alter the biochemical composition of phytoplankton and translate through the food web, affecting its structure, functioning, and consequently the carrying capacity of an ecosystem.

Stable isotope tracers are widely used to estimate primary production in many ecosystems. However, beyond total carbon uptake rates limited emphasis is given to investigate into which of the major cellular compounds (amino acids, fatty acids, carbohydrates and DNA/RNA) the fixed carbon is allocated. Since all these compounds have different C:N:P requirements resource limitations should affect their biosynthesis differently.

We combine GC-c-IRMS and LC-IRMS approaches to trace stable isotope incorporation into major cellular components, such as amino acids, fatty acids and carbohydrates, and determine their concentrations and biosynthesis rates. We applied these methods to stations in the North Sea, where different nutrients are limiting.

The contributions of macromolecules to total biomass as well as their synthesis rates differ substantially between stations and the phytoplankton communities respond differently to nutrient additions by re-allocating fixed carbon to other macromolecules on short timescales (24 hours). Though still preliminary, we hope that this work will allow us to infer changes in phytoplankton stoichiometry and consequent food web changes.

Geochemistry of organic matter from Lower Ordovician Dictyonema Shale (Podlasie Depression, NE Poland)

IZABELLA GROTEK, EWA KLIMUSZKO, STANISŁAW WOLKOWICZ* AND JERZY MIECZNIK.

PGI-NRI, 4 Rakowiecka, 00-975 Warsaw, Poland
(stanislaw.wolkowicz@pgi.gov.pl)

Lower Ordovician Dictyonema Shale occur in the Podlasie Depression (NE Poland). The succession comprises from about a dozen cm to 4.0 m (2.7 m at the average) of black claystones passing gradually upwards into the brownish ones. The rocks display U-V-Mo mineralization (black shale type).

20 samples were covered by geochemical studies, including TOC, bitumen fractions, saturated hydrocarbons, aromatic hydrocarbons. Moreover, vitrinite reflectance measurements and maturity calculations were made on vitrinite-like matter.

TOC content ranges from 3,86 do 11,5% which shows shale samples also show good to very good hydrocarbon generating potential of the studied samples. This is confirmed by generation of significant amounts of hydrocarbons, ranging from 450 do 2,860 ppm. The share of hydrocarbons in bitumens ranges from 11% to 36,6%, being lower than that of asphaltenes and resins. The amounts of aromatic hydrocarbons predominate over those of the saturated ones. The coefficient of migration is low (from 0.002 to 0.013), showing that labile components are syngenetic with sediment. Analysis of n-alkanes indicated that the organic matter is here of the sapropel type. Detailed analysis of compounds of the terpane group showed low level of maturation of organic matter. This is confirmed by results of measurements of thermal maturation of authigenic organic components. Average vitrinite reflectance values range from 0,46 to 0,61% Ro, being not related to depth of burial of these rocks. The obtained data indicate low temperature diagenesis (of the order of 50-800C at the most).

Lower Ordovician Dictyonema Shale series are rich in solid organic matter and may be treated as very good parent rocks for hydrocarbon generation. At the same time they are rich in labile components. The organic matter is of marine origin and represents products of decay of algae and bacteria. Degree of its alteration is low, corresponding to early stage of oil window. Therefore, these rocks and the overlaying ones do not appear promising as a target in search for shale gas reserves.

Resolving the gap between laboratory and field rates of weathering

GRUBER, C.¹, ZHU, C.², GEORG, B.R.³ AND GANOR, J.¹

¹Department of Geological and Environmental Sciences, Ben-Gurion University of the Negev, Israel,

(*correspondence: chengrub@post.bgu.ac.il)

²Department of Geological Sciences, Indiana University, USA

³Water Quality center, Trent University, Canada

The rate of minerals' weathering is a key factor in many environmental problems such as the relationship between silicate weathering and global climate over geological timescales, the availability of inorganic nutrients in soils, geological carbon sequestration, global geochemical cycles, and the distribution of porosity and permeability in hydrocarbon reservoir rocks [1]. Weathering rates of silicate minerals observed in the lab are up to five orders of magnitude higher than those inferred from field studies. The many differences between experimental conditions in the lab and natural conditions in the field have been thoroughly discussed in previous studies, but the gap was not fully resolved.

This study is using a novel method to determine dissolution rates in a single point batch experiment by measuring the change of silicon stable isotopes ratio of a spiked solution with time. The silicon isotope ratio method is used in the present study to measure weathering rates of feldspar under ambient temperature and circum neutral pH [2]. It is for the first time that albite dissolution rate (or any silicate mineral) is described as a function of deviation from equilibrium under ambient temperature and circum neutral pH. The new experimental data confirm the extrapolation of high temperature data and numerical modeling exercise [3,4,5], and fully resolve the gap between lab measurements and field estimates. The agreement between the confirmed rate law and the field data indicates that the extensive debate on the gap reflects the so far inability to measure the dissolution rates under typical field conditions, using standard laboratory experiments.

[1] Zhu, C., *Geochim et Cosmo Acta*, 2005. **69**(6): 1435-1453.

[2] Gruber *et al.*, *Geochim et Cosmom Acta*, 2013. **104**: 261-

280. [3] Zhu *et al.*, *Geochim et Cosmo Acta*, 2010. **74**(14):

3963-3983. [4] Ganor *et al.*, *Environmental Geology*, 2007.

53(3): 599-610. [5] Zhu, C., in *Thermodynamics and kinetics*

of water-rock interaction, E.H. Oelkers and J. Schott, Editors. 2009, Mineralogical Society of America. 533-569.

Linkage between gold mineralization and hydrocarbon accumulation in the Youjiang basin, South China: Petrographic evidence

X.X. GU¹, Y.M. ZHANG¹, C.Y. WU¹, B.H. LI²,
S.Y. DONG² AND C.J. XUE¹

¹State Key Laboratory of Geological Processes and Mineral Resources, China University of Geosciences, Beijing 100083, P.R. China (bzzym@163.com)

²College of Earth Sciences, Chengdu University of Technology, China

The Carlin-type gold deposits and paleo-oil reservoirs in the Youjiang basin, South China spatially show close association, suggesting a genetic linkage between gold mineralization and hydrocarbon accumulation. Petrographic studies show that bitumen in the gold deposits is commonly present as a migrated hydrocarbon product in mineralized rocks but is absent in barren sedimentary host rocks. Bitumen dispersed in ores is closely associated and/or intergrown with ore-stage hydrothermal minerals. Bitumen occurring in hydrothermal veins and veinlets is paragenetically associated with pre-, syn-, and post-ore stage mineral assemblages. These observations suggest an intimate relationship between bitumen precipitation and gold mineralization. In the paleo-oil reservoirs, bitumen occurring with calcite is typically concentrated along pore/vein centers and along the wall of pores and fractures, indicating approximately coeval precipitation. Fluid inclusion studies show that aqueous inclusions, hydrocarbon- and CO₂-rich inclusions are dominant in the syn- and post-ore stage quartz and calcite, indicating that the ore fluid consisted of an aqueous solution and an immiscible hydrocarbon phase. In the paleo-oil reservoirs, similar types of inclusions including liquid C₂H₆, vapor CH₄, CH₄-H₂O, and aqueous inclusions occur in diagenetic pore- and fissure-filling calcite associated with bitumen. The close association of gold deposits and paleo-oil reservoirs, the paragenetic coexistence of bitumens with ore-stage minerals, and the presence of abundant hydrocarbons in the ore fluids all suggest that the gold originated, migrated and precipitated along with the hydrocarbons in an immiscible, gold- and hydrocarbon-bearing, basinal fluid system.

The research was funded by the National Natural Science Foundation of China under grants of 40930423.

Geochemical Characteristics and Tectonic Environment of Basement Granite in Weiyuan Structure, Sichuan Basin, Southwest China

GU ZHIDONG, ZHAI XIUFEN AND WANG ZECHENG

Research Institute of Petroleum Exploration and Development, PetroChina, China

(* correspondance: guzhidong@petrochina.com.cn)

Based on the deep wells drilled into the basement in Weiyuan structure, and aeromagnetic negative anomalies, the basement of Weiyuan structure in Sichuan Basin of Southwest China, is proved to be composed of granitoids.

Well core observation and thin section identification results show that syenogranite is the main rock type. The features of major elements include high Si content, high alkali value, high K₂O/Na₂O ratio, high K content but low Na content, suggesting that it belongs to high-K calc-alkaline and metaluminous - weakly peraluminous series. The LREE is rich, with HREE loss and intensely negative Eu abnormality, while the chondrite-normalized distribution shows right tilting seagull-like patterns. High field strength elements Th, U, Pb, Nd, Sm and large ion lithophile elements Cs, Rb are rich, while high field strength elements Nb, Eu, Ti, Sc and large ion lithophile elements Ba, Sr are depleted (Fig.1).

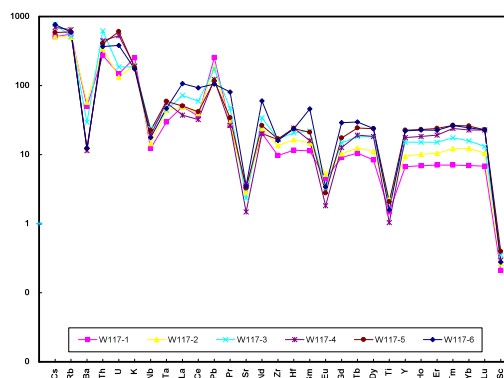


Fig.1 Spider diagram of primitive mantle normalized trace elements of basal granite in W117 well

The genetic type is A₂ granite, probably formed by highly fractional crystallization of crust molten magma mixing with a small amount of mantle magma. This type of granite is deduced to have developed from extensional rifting tectonic environment which may be related to Rodinia supercontinent break-up event in Neoproterozoic.

Total Scattering Techniques: A powerful tool to investigate size, shape and growth mechanisms of minerals at the nanoscale

A. GUAGLIARDI^{1*}, A. CERVELLINO², R. FRISON¹,
J. M. DELGADO LÓPEZ³, J. GÓMEZ-MORALES³
AND N. MASCIOCCHI⁴

¹Istituto di Cristallografia, CNR, I-22100 Como, Italy
(*correspondence: antonella.guagliardi@ic.cnr.it).

²SLS Laboratory for Synchrotron Radiation - Condensed
Matter, PSI, CH-5232 Villigen, Switzerland.

³Laboratorio de Estudios Cristalográficos, IACT (CSIC-UGR,
E-18100 Armilla, Granada, Spain.

⁴DiSAT, Università dell'Insubria, I-22100 Como, Italy.

Nanoscaled crystals (NCs) and the processes governing their nucleation and growth play a fundamental role in relevant, and diverse, fields, such as (to mention a few) geochemical cycling, mining and biomineralization. The limited coherence length of NCs, the presence of compositional and structural defects and the interaction with organic components make these systems highly complex, with a *short-range order only*. In the diffraction space, these features turn into diffuse scattering, falling between and below the Bragg peaks. The Debye equation [1] is a *Total Scattering* approach treating Bragg and diffuse scattering on an equal basis and, therefore, is able to use the *entire* information present in the experimental diffraction pattern. Conversely, conventional single-crystal and powder X-ray and neutron diffraction methods deal with Bragg intensities only. Recently, we have proposed a new, original and computationally efficient implementation of the Debye Function Analysis [2], which enabled us to *quantitatively* characterize, in terms of structure, size and shape distributions, different kinds of nanocrystalline materials [3]. Among these, citrate-controlled biomimetic apatites [4], very similar in size, shape and composition to bone apatites, have been for the first time characterized by DFA. Combining DFA and AFM, we were able to unravel the mechanism forming platy-shaped NCs from an amorphous calcium phosphate precursor. A major role of citrate in controlling the growth mechanism of the apatitic mineral clearly emerges.

[1] Debye (1915) *Ann. Phys.* **351**, 809-823. [2] Cervellino *et al.* (2010) *J. Appl. Cryst.* **43**, 1543-1547. [3] Cernuto *et al.* (2011) *Angew. Chem. Int. Ed.* **50**, 10828-10833, and references therein. [4] Delgado-López *et al.* (2012) *Acta Biomater.* **8**, 3491-3499.

High-silica rhyolites and granites: Products of the shallow crust

GUILHERME A. R. GUALDA¹ AND MARK S. GHIORSO²

¹Earth & Environmental Sciences, Vanderbilt University,
Nashville, TN 37235, USA;
(g.gualda@vanderbilt.edu)

²OFM Research - West, Seattle, WA 98115, USA;
(ghiorso@ofm-research.org)

High-silica rhyolites and granites (>75 wt. % SiO₂, anhydrous) are common features of the crust, as part of both the volcanic and plutonic records. While low crystallization pressure (<250 MPa) is typically inferred, it has been suggested that they form via polybaric evolution, with initial crystallization at relatively high pressures (> 500 MPa).

We use glass compositions derived from the EarthChem portal, selected natural examples from the literature, and rhyolite-MELTS calculations to probe the depth at which different magma compositions can form within the crust.

We demonstrate that the phase relations in the Qz-Ab-Or ternary dictate the silica content of silicic melts and cause silica content to increase with decreasing pressure. Our analysis has profound implications for the origin of silicic melts and magmas within the continental crust, specifically:

- Silicic magmas are expected to show stratification in silica contents within the crust.* Melts within the crust will show a gradient in maximum silica content; while dacites can occur over much of the crust, high-silica rhyolites are confined to the shallow levels of the crust.
- High-silica rhyolite glass can only form at low P, requiring crystallization in the shallow crust.* Polybaric evolution of magmas is confined to their possible range of occurrences. While dacites can evolve via decompression-driven crystallization over a large range of pressures (as recorded in glass inclusions), high-silica rhyolites are confined to the shallow crust (consistent with narrow range of silica contents in glass inclusions).
- The existence of high-silica pumice requires fractionation or melting at low pressure.* Whole-pumice with high-silica rhyolite composition requires melting or fractionation in the shallow crust, which precludes direct derivation of high-silica magmas from high pressures without substantial fractionation at low pressure, and shows that high-silica rhyolites and granites are intrinsic to the shallow crust.
- Low-pressure cumulates or melting residues must exist in the shallow crust.* If shallow-level fractionation is required, then crystal cumulates or partial melting residues must be present within the upper crust. The crystal cumulates necessary to form high-silica rhyolites are to be found within upper crustal granitoid plutons.

The concept of end of waste in view of developing sustainable secondary geo-materials

A.F. GUALTIERI^{1*}, A. VIANI² AND S. POLLASTRI¹

¹Dipartimento di Scienze Chimiche e Geologiche, Università di Modena e Reggio Emilia, 41121 Modena, Italy

(*correspondence: alessandro.gualtieri@unimore.it)

²Institute of Theoretical and Applied Mechanics AS, Prague and Centrum Excellence Telč, 588024 Czech Republic.

The concept of *end of waste*, adopted by the European Commission on December 2005, regards under which conditions a waste could cease to be waste and could be regarded as a non-waste material. This is a revolutionary way to think of wastes not just as refuse to be dismissed but as secondary raw material to be exploited, with an enormous social and economic impact. In this scenario, the creativity of *materials* scientists is highly stimulated and the key to success is the development of innovative and sustainable means to transform a waste into a secondary raw material of potential economic value. To this aim, stimulus comes from the so called geo-inspiring materials. This contribution presents the results of a long-term project aimed to recycle asbestos containing materials (ACMs), into secondary raw materials for various industrial applications. The high temperature product of transformation of ACM can be successfully recycled in clay bricks, rock-wool, glass-ceramics, ceramic pigments [1], geopolymers [2], concrete [3], and recently also for innovative formulations of calcium sulfoaluminate cement clinkers [4] and magnesium phosphate cements [5].

[1] Gualtieri *et al.* (2011) *Waste Man.* **31**, 91–100. [2] Gualtieri *et al.* (2012) *Constr. and Buil. Mat.* **31**, 47–51. [3] Gualtieri & Boccaletti (2011) *Constr. and Buil. Mat.* **25**, 3561–3569. [4] Viani & Gualtieri (2013) *J. Hazard. Mat.* Accepted. [5] Viani & Gualtieri (2013) *Cem. Concr. Res.* Submitted.

Mapping the natural radioactivity of Elba Island by means of geostatistical interpolation of airborne gamma-ray data

GUASTALDI E.¹, BALDONCINI M.³, BEZZON G. P.⁴, BROGGINI C.², BUSO G. P.⁴, CACIOLLI A.², CALLEGARI I.¹, COLONNA T.¹, FIORENTINI G.⁵, KAÇELI XHIXHA M.⁵, MANTOVANI F.³, MASSA G.¹, MENEGAZZO R.², MOU L.⁴, ROSSI ALVAREZ C.², STRATI V.³ AND XHIXHA G.⁴

¹CGT Center for GeoTechnologies, University of Siena, Via Vetri Vecchi, 34 - 52027 S. Giovanni Valdarno, Italy. (guastaldi@unisi.it)

²Istituto Nazionale di Fisica Nucleare (INFN), Padova Section, Via Marzolo 8 - 35131 Padova, Italy. (carlo.broggini@pd.infn.it)

³Department of Physics and Earth Sciences, University of Ferrara, Via Saragat, 1 - 44100 Ferrara, Italy. (mantovani@fe.infn.it)

⁴Istituto Nazionale di Fisica Nucleare (INFN), Legnaro National Laboratory, Via dell'Università, 2 - 35020 Legnaro, Padova, Italy. (giampaolo.buso@lnl.infn.it)

⁵Istituto Nazionale di Fisica Nucleare (INFN), Via Saragat, 1 - 44100 Ferrara, Italy (giovanni.fiorentini@fe.infn.it)

We present the maps of K, eU, and eTh radioelement abundances of Elba Island (Italy) realized by means of a geostatistical interpolation of airborne γ -ray data, performed with a module of four NaI(Tl) crystals of 16 L mounted on an autogyro. We applied the Collocated Cokriging (CCoK) multivariate estimator in a non-conventional way for interpolating the under-sampled airborne gamma-ray data using the geologic map as constraining ancillary variable. An arbitrary number has been assigned to each geological formation and used in the algorithm for estimating the radioelement abundances: the independence from the random assignment process has been tested for three distinct models. The spatial variability shows well-defined structures for the linear coregionalization models. The abundance maps indicate a distinct correlation between the geological formation and radioactivity content. High K, eU and eTh abundances were estimated in the intrusive granitic complex of Mt. Capanne and low abundances in the geological formations in the N-E sector of Elba Island. However, a clear anomaly of high K content in the Mt. Calamita promontory confirms the presence of felsic dykes and hydrothermal veins not reported in geological map of Tuscany Region at scale 1:10000. This result confirms that the internal variability of the radiometric data is not biased by the multivariate interpolation.

Dissolution rates of plagioclase feldspars at 22 °C as a function of pH and plagioclase composition

S. GUDBRANDSSON^{12*}, D. WOLFF-BOENISCH¹,
S.R. GISLASON¹ AND E. H. OELKERS¹²

¹Institute of Earth Sciences, University of Iceland, Sturlugata
7, 101 Reykjavik, Iceland
(*snorgud@hi.is), (boenisch@hi.is), (sigrg@hi.is)

²GET/CNRS, 14 Avenue Edouard Belin, 31400 Toulouse,
France (eric.oelkers@get.obs-mip.fr)

Feldspars are the most abundant mineral in the Earth's crust and thus play an integral role in the plethora of natural geochemical processes including global element cycling. Moreover, as a major reservoir of silicate mineral bound Ca, plagioclase dissolution may serve as an important source of the divalent cations required for mineral carbonation [1]. Our ability, however, to model such processes is currently confounded by inconsistencies among plagioclase rate data measured in distinct laboratories; corresponding rates reported in the literature vary by as much as 3 orders of magnitude. In addition there is a nearly complete lack of measured dissolution rates for the Ca-rich feldspars at alkali conditions. This laboratory study has been designed to overcome some of these ambiguities.

The steady state, far-from-equilibrium dissolution rates of 5 distinct plagioclases ranging in composition from albite (An_{8.9}) to anorthite (An_{88.8}) were measured in mixed flow reactors at 22±2° C and pH from 2 to 11. The dissolution rates of all plagioclases based on silica release rates show a common U-shaped behaviour as a function of pH where rates decrease with increasing pH at acid condition but increase with increasing pH at alkaline conditions. As previously observed, constant pH plagioclase dissolution rates increase with increasing anorthite content at acid conditions; measured anorthite dissolution rates are ~2.5 orders of magnitude faster than those of albite at pH~2. Perhaps more significantly plagioclase dissolution rates are independent of plagioclase composition at alkaline conditions. Preliminary interpretation and data fitting suggests that plagioclase dissolution rates are consistent with their control by the detachment of Si-rich activated complexes formed by the removal of Al from the mineral framework. Taking account of this mechanism and transition state theory yields a robust equation that describes plagioclase dissolution rates as a function of the composition of both the mineral and fluid phase over the full range of pH found in natural systems.

[1] Gudbrandsson *et al.* (2011) *Geochim. Cosmochim. Acta* **75**, 5496-5509.

Ferromanganese crusts as proxies for deep water Ni, Cu, Zn and Fe isotope variations

BLEUENN GUEGUEN^{12*}, OLIVIER ROUXEL²
AND YVES FOUQUET²

¹IFREMER, Centre de Brest, Unité Géosciences Marines,
29280 Plouzané, France (*bleuenn.gueguen@univ-
brest.fr)

²Institut Universitaire Européen de la Mer, UMR 6538,
Laboratoire Domaines Océaniques, Université de Bretagne
Occidentale, BP 80 F- 29280 Plouzané, France
(olivier.rouxel@ifremer.fr; yves.fouquet@ifremer.fr)

While ferromanganese (Fe-Mn) crusts have long been characterized by elevated concentrations of Ni, Co, and Cu arising from their very slow growth rates (1-6 mm/Ma), the sources of metals in hydrogenous seafloor deposits and their record of evolving deep sea metal fluxes remain strikingly unresolved. Temporal geochemical variations in Fe-Mn crusts were mostly investigated for paleoceanographic studies of oceanic circulation and climate variations with radiogenic isotope (Pb, Nd, Os). Since transition metals are actively involved in key biogeochemical processes, it is crucial to understand how metal oceanic sources and internal cycling responded to major oceanic perturbations in the past. As a result, unlocking the history of trace metals using transition metal isotopes is now receiving growing interest.

Here, we report high resolution Ni-Cu-Zn-Fe isotope profiles in two Fe-Mn crusts collected in the North Pacific Ocean (Apuupuu seamount, south of Hawaii). This record provide a comprehensive view of the last 6 Ma. Results show that Ni, Cu and Zn isotope variabilities are restricted with $\delta^{60/58}\text{Ni}_{\text{SRM986}} = +1.73 \pm 0.03\%$, $\delta^{65/63}\text{Cu}_{\text{SRM976}} = +0.64 \pm 0.04\%$ and $\delta^{66/64}\text{Zn}_{\text{SRM3168a}} = +2.12 \pm 0.06\%$. In contrast, $\delta^{56/54}\text{Fe}$ values range from -0.04 to -0.68‰ and differ between both crusts, albeit showing concomitant kink of Fe isotopes at ~2-2.5 Ma correlating with Pb isotope ratios. Overall, Ni, Cu, and Zn isotope records in Fe-Mn crusts are consistent with their modern oceanic values, after consideration of potential isotope fractionation during incorporation in Fe-Mn oxides, while Fe isotope record is strongly affected by local effects due to short residence time and local halmyrolitic and/or hydrothermal sources.

Investigation on neodymium isotopic fractionation occurring during HPLC separation

F. GUÉGUEN^{1*}, H. ISNARD¹, A. NONELL¹,
G. STADELMANN¹, M. AUBERT¹ AND F. CHARTIER²

¹Commissariat à l'Énergie Atomique, DEN DPC SEARS
LANIE, F-91191 Gif Sur Yvette, France,
(florence.gueguen@cea.fr)

²Commissariat à l'Énergie Atomique, DEN DPC, F-91191 Gif
Sur Yvette, France

The precise Nd isotopic composition is of major interest in nuclear (determination of nuclear fuel burn-up, ...) [1] and geosciences applications (paleoceanography, ...) [2]. Direct determination of Nd isotopic ratios in sample is hampered by isobaric interferences and chemical separation before isotopic measurements is required.

In this study, the separation of lanthanides was performed by high-performance liquid chromatography using analytical column with strong cation exchange (SCX) groups bounded to the silica surface. A gradient elution mode was used with the mobile phase containing the organic acid HMB (2-hydroxy 2-methylbutyric acid).

For this study, a *JNdi-1* standard solution was used. The Nd peak was collected in various fractions for isotope ratio measurements by MC-ICP-MS (Neptune Plus, Thermo Scientific), to evaluate Nd isotopic fractionation during elution. Raw ratios were corrected for mass bias using Nd reference values obtained by the flash evaporation method in Thermal Ionisation Mass Spectrometry [3,4].

The range of variation observed along the elution peak is about 2‰/amu, which is significant considering an external reproducibility obtained by sample standard bracketing method on the *JNdi-1* isotopic standard lower than 0.03‰ for all isotopic ratios. This trend indicates a preferential elution of heavy isotopes. This phenomenon imposes to collect the total Nd elution peak in order to determine the true isotopic ratios. The potential consequences of this behaviour on the accuracy of the measurement will be presented. This result is essential for future on-line experiments with HPLC hyphenated with MC ICPMS in order to measure accurate Nd isotopic ratios.

- [1] Bourgeois *et al.*, *J. Anal. At. Spectrom.* **26** (2011) 1660.
[2] Ilina *et al.*, *Chem. Geol.* **342** (2013) 63. [3] Dubois *et al.*, *Int. J. Mass Spectrom. Ion Process.* **120** (1992) 163. [4] Wakaki and Tanaka, *Int. J. Mass Spectrom.* **45** 323-324 (2012).

A new radiation damage based model for He diffusion in zircon

W.R. GUENTHNER^{1*}, P.W. REINERS¹, R.A. KETCHAM²,
L. NASADALA³ AND G. GIESTER³

¹University of Arizona, Tucson, Arizona 85721 USA
(*correspondence: wrg@email.arizona.edu)

²University of Texas, Austin, Texas 78712 USA

³University of Vienna, Althanstr. 14, 1090, Vienna, Austria

A key assumption in zircon and apatite (U-Th)/He dating has traditionally been that the diffusion kinetics of ⁴He in the mineral of interest are constant across a broad spectrum of chemical compositions. Increasingly, practitioners of the technique are discovering that a "one-size-fits-all" approach to these kinetics is inadequate and are developing more grain-specific diffusion models to both explain data complexities, and to better constrain time-temperature histories. Here we present diffusion measurements that show how a zircon's alpha dose, which we interpret to correlate with radiation damage, influences its He diffusivity. Results from step-heating experiments on pairs of crystallographically oriented slabs of zircon are as follows: from 1.2×10^{16} α/g to 1.4×10^{18} α/g, the frequency factor measured parallel to the c-axis decreases by ~4 orders of magnitude, causing He diffusivity to decrease (e.g. by ~3 orders of magnitude at between 140 and 220 °C). Above $\sim 2 \times 10^{18}$ α/g, activation energy decreases by a factor of two, and diffusivity increases by ~9 orders of magnitude by 8.2×10^{18} α/g. We attribute these trends to two separate, though related, mechanisms. Initially, progressive damage in-growth leads to greater tortuosity of diffusion pathways, decreasing He diffusivity. As in-growth continues, damage zones become interconnected, shrinking the effective diffusion domain size and increasing the crystal's bulk He diffusivity. We parameterize the damage-diffusivity relationship and couple it to a model describing damage annealing as a function of time and temperature (as in the RDAAM of Flowers *et al.* (2009)). This new model describes the coevolution of damage, He diffusivity, and (U-Th)/He date of a zircon.

Ferrous denitrification by biogenic hydroxycarbonate green-rust

GUERBOIS, D.^{1*}, ONA-NGUEMA, G.¹, MORIN, G.¹,
LAVERMAN, A.M.², ABDELMOULA, M.³,
MOUCHEL, JM², BARTHELEMY AND K.³, BREST, J.¹

¹IMPMC UMR 7590 UPMC-CNRS, Campus de Jussieu – 4
place Jussieu 75005 Paris
(delphine.guerbois@impmc.upmc.fr)

²Sisyphé UMR 7619 UPMC-CNRS, Campus de Jussieu – 4
place Jussieu 75005 Paris

³LCPME UMR 7564 CNRS-Université de Lorraine – 405 rue
de Vandoeuvre 54601 Villers-lès-Nancy

Nitrate is a common contaminant causing eutrophication, particularly in agricultural areas, such as in Brittany (France). In this region, natural green-rust phases (fougerite) significantly contribute to the bluish color of hydromorphic soils. These minerals are thought to form upon reduction of Fe(III)-minerals by bacterial activity under anoxic conditions [1,2]. Since synthetic green rusts phases are known to reduce NO₃⁻ to NH₄⁺ [3], potential for *in situ* denitrification involving bacterial metabolism and abiotic reduction by biogenic green-rust has been raised.

In the present study, biogenic hydroxycarbonate green-rusts, GR(CO₃), were produced in the laboratory from the reduction of either lepidocrocite or ferric oxyhydroxycarbonate [4] by *Shewanella putrefaciens* strain ATCC 12099. These biogenic Fe(II,III)-containing minerals were characterized by XRD, TEM and transmission Mössbauer spectroscopy, and their interactions with nitrite were studied. Results show that kinetics of reduction by biogenic GR(CO₃) differ from those reported for synthetic analogues [5]. In addition, XRD and EXAFS analysis of time-series samples help to elucidate the chemical mechanisms involved when green rusts get oxidized.

[1] Génin *et al.* (2001) *Appl. Geochem.* **16** 559-570

[2] Ona-Nguema *et al.* (2002) *Environ. Sci. Technol.* **36**, 16-

20. [3] Hansen *et al.* (1996) *Environ. Sci. Technol.* **30**, 2053-

2056. [4] Ruby *et al. Geochim Cosmochim Acta* (2010), **74**,

953-966 [5] Hansen (2004) *Colloque Academie des sciences*, 2004

An integrated geochemical, hydrological and hydrodynamic approach to model arsenic at a fluvial confluence

PAULA GUERRA^{1*}, CRISTIAN ESCAURIAZA¹,
CHRISTIAN GONZALEZ¹, VERONICA MORALES¹,
GONZALO PIZARRO¹ AND PABLO PASTEN¹

¹Pontificia Universidad Católica de Chile, Santiago, Chile.
(pguerra@ing.puc.cl) (* presenting author)

Fluvial confluences are natural reactors where geochemistry, hydrology and hydrodynamics can interact in complex ways to determine the fate of contaminants in a watershed. Seasonal and diurnal changes in flow, chemical composition and the non-uniform, impermanent, three dimensional field of velocities induce relevant deviations from simplified models. This is particularly relevant in watersheds receiving acid mine drainage (AMD), where confluences are primary producers of highly reactive solid phases like hydrous iron oxides (HFOs) and hydrous aluminum oxides (HAOs). We used geochemical-hydrodynamic modeling, field measurements, and laboratory experiments to study a model confluence. Our field scale model is the Azufre River (pH<2, E.C>10000µS/cm, [Fe]_{Total}~60mg/L, [Al]_{Total}~65mg/L, [As]_{Total}~2 mg/L)-Caracarani River (pH~8.6, E.C~1500µS/cm) confluence, located in the Chilean Altiplano. We performed geochemical simulations for the mixing ratio $C_{Azufre} = Q_{Azufre} / Q_{Total}$ (L/L) in a range of 0 to 0.5 and coupled them to 3D numerical simulations of flow. Heterogeneous spatial/temporal profiles of pH-induced HFOs and HAOs and a downstream buffer is achieved at pH~2.8-3.2, where As concentration is not only diluted by mixing, but also sorbed onto the assemblage of the amorphous phases (up to 30%). Experimental mixtures of natural waters in the laboratory and field measurements were consistent with our simulations. Despite the assumptions and limitations of geochemical modeling, this integrative approach allows the study of critical scenarios and highlights the importance of evaluating kinetic and equilibrium assumptions. Our study improves the knowledge on the fate of As in surface waters, vital for the design of treatment systems or monitoring programs in extreme environments such as the Altiplano.

Unraveling cryptic high-temperature polymetamorphism: An Alpine example

V.E. GUEVARA ^{*1} AND M.J. CADDICK ¹

¹Dept. of Geosciences, Virginia Tech, Blacksburg, VA 24061, USA ^{*}(correspondence: vguevara@vt.edu)

Distinguishing between mineral phases which record evidence of distinct metamorphic events in high-grade polymetamorphosed rocks is one of the most difficult tasks facing metamorphic petrologists. This is particularly challenging when attempted on rocks that have experienced partial melting in at least one of these events. Resetting of mineral equilibrium compositions during metamorphic overprinting and an evolving bulk-rock composition during partial melting or late-stage fluid fluxing mean that both conventional thermobarometry and quantitative *P-T* modeling can be ineffective or easily misinterpreted. Here, we aim to elucidate the nature of potentially polymetamorphic granulites from the Gruf Complex, Central Alps, through integration of trace element thermometry, *in-situ* geochronology, and pressure-temperature (*P-T*) pseudosection modeling of carefully chosen textural domains. The Gruf Complex contains ultrahigh temperature (UHT) granulites and remains one of the most enigmatic features within the Alpine orogenic belt. Some studies suggest that UHT conditions record peak *T* during the Eocene Alpine orogen [1], whilst others invoke UHT conditions during Permian rifting overprinted by upper amphibolite facies migmatization during Alpine orogenesis [2, 3].

Zr in rutile (rtl) and Ti in quartz (qtz) thermometry on grains in several textural domains of a single hand sample help to resolve ambiguity regarding the phases and textures that record different stages of the rock's history. Results suggest the presence of two distinct generations of biotite (bt), recording dramatically different *T*. Rtl grains within highly resorbed, high-Ti bt yield 710–780 °C. Textural association with high-*T* opx + grt ± sill assemblages suggests that they may record prograde heating leading to incomplete bt dehydration melting, and resultant formation of porphyroblastic opx with rtl inclusions that yield 810–880 °C. Rtl grains in texturally equilibrated, low-Ti bt or in matrix cordierite clearly record a later stage, low *T* recrystallization. Qtz and rtl grains in grt yield *T* of 800–850 °C, suggesting possible grt growth coeval with opx.

[1] Möller *et al.* (2012) *IGC, Abstracts* **34**, 3161. [2] Galli *et al.* (2011), *Lithos* **124**, 17–45. [3] Galli *et al.* (2012), *Contrib. to Mineralogy and Petrology*, **163**, 353–378.

Reconstruction of nutrient redox cycling in the Early Neoproterozoic

ROMAIN GUILBAUD ^{1*} AND SIMON W. POULTON ¹

¹School of Earth and Environment, University of Leeds, Leeds LS2 9JT, UK (^{*}correspondance: r.j.guilbaud@leeds.ac.uk)

A significant body of evidence suggests that the deep ocean remained anoxic until the terminal Neoproterozoic. Recent studies on mid-Proterozoic [1] and later Neoproterozoic [2,3] (<750 Ma) marine sediments indicate that water masses beneath the oxic surface ocean were dominantly ferruginous, with sulphidic conditions restricted to the continental margins. However, in contrast to the Mesoproterozoic, sulphidic continental margin conditions appear to be particularly sparse in the later Neoproterozoic, while little is known about the nature of ocean chemistry in the early Neoproterozoic. This is particularly significant since the bioavailability and the redox cycling of nutrients are prone to change dramatically when shifting from sulphidic to ferruginous conditions. Thus, the biogeochemistry of the ocean preceding the onset of the first Neoproterozoic glaciation is poorly constrained. Here, we reconstruct the evolution of coupled redox-nutrient cycling throughout a succession capturing pre- (>800 Ma) to syn-glacial sediments. Our focus is on a succession of deeper and shallower marine deposits from the Huainan region, northern China. The transect constitutes a potential archive of the biogeochemical response to linked changes in ocean redox conditions and nutrient feedbacks during the run-up to extreme climate change. Our data document the links between phosphorous cycling and ferruginous waters, under conditions characterised by low sulphate and apparent low productivity.

[1] Poulton *et al.* (2010) *Nat. Geosci.* **3**, 486–490. [2] Canfield *et al.* (2008) *Science* **32**, 949–952. [3] Johnston *et al.* (2010) *EPSL* **290**, 64–73.

Optimization of LA-ICP-MS for U-Pb dating of young zircons

M. GUILLONG^{1*}, O. BACHMANN¹ AND A. VON QUADT¹

¹ETH Zurich · Inst. for Geochemistry and Petrology,
Clausiusstrasse 25, 8092 Zürich, Switzerland
*guillong@erdw.ethz.ch

Laser ablation ICP-MS is a powerful method to determine the age of rocks by measuring U/Th/Pb isotopes. The method is fast, cheap and for many applications precise and accurate enough when using robust corrections and reference materials [1]. In this work we show the optimization of a laser ablation system equipped with a 2nd generation 2 volume constant geometry ablation cell (Resonetics: S-155LR) in combination with a high sensitivity sector field ICP-MS (Thermo: Element XR). Investigated parameters includes laser crater size, repetition rate and energy density, as well as signal length, gas flows and ICP-MS parameters with respect to, precision, accuracy, sample throughput and resolution. Results for different zircon standard reference material are shown and observations including down hole fractionation, low count rates, and the importance of integration interval settings are discussed.

The optimized instrumentation is used to determine the age of young zircons from Kos Plateau Tuff with a known eruption age of 160 ky. Due to the high sensitivity, it is possible to date these zircons using a 30 µm spot and 5Hz ablation rate with a precision similar to SHRIMP [2]. Several challenges dating zircons of this age range are addressed: Due to the low count rates on the Pb isotopes the mean of ratios is different than the ratio of the mean. For accurate dating of young zircons a U-Th disequilibrium correction is necessary, for which a precise Th/U ratio is needed, both in the individual zircons as well as in the magma. Due to the relatively fast drilling of laser ablation (~0.1 µm/pulse) we often observe inherited cores resulting in mixed signals which makes the setting of integration intervals important but can give indication about the pre-eruptive magmatic history of zircons [3].

[1] Paton *et al.* (2010) *Geochem. Geophys. Geosyst.* **11**, 1525-2027. [2] Bachmann *et al.* (2007) *Geology* **35**, 73-76. [3] Simon *et al.* (2008) *EPSL* **266**, 182-194.

On the filtering of dust by planetesimals and its consequences for the compositions of planetary systems

TRISTAN GUILLOT^{12*} AND SHIGERU IDA²

¹Université de Nice-Sophia Antipolis, Observatoire de la Côte d'Azur, CNRS, Nice, France (tristan.guillot@oca.eu)
²Tokyo Institute of Technology, Tokyo, Japan (ida@geo.titech.ac.jp)

The inner solar system, and in particular Mercury, Venus, the Earth and Mars contains very little water. Asteroids between Mars and Jupiter are known to be progressively more water-rich as they orbit further to the Sun. Yet, we know that protoplanetary disks contain vast amounts of water ice, and that the ice line (i.e. the distance at which water vaporizes) moves progressively inside of 1 AU before gas photoevaporation takes place. Ice grains could thus potentially deliver significant amounts of water there, in disagreement with the evidence in our Solar System.

We show that the inside-out formation of planetesimals can effectively filter dust and prevent icy grains from reaching the inner regions of the system. This occurs when the mass in planetesimals exceeds a threshold well below that obtained from adding the mass of solids present in the present-day Solar System. This thus explains why the inner Solar System is dry, but potentially also why other planetary systems may lead to the formation of wet, low-density planets. The potentially high solid-to-gas ratio obtained in the late phases would also help to understand the very large masses in heavy elements derived in giant planets observed by transit surveys including CoRoT and Kepler.

Magmatic evolution and intensive parameters of the Santa Maria Rhyolites, Paraná Magmatic Province, Brazil, as inferred from whole rock and mineral geochemistry

GUIMARÃES, L.F.¹, POLO, L.A.¹ AND JANASI, V.A.¹

¹University of São Paulo

The Santa Maria rhyolites correspond to a sequence of effusive glassy to hypocrySTALLINE rocks occurring as lava-domes and flows in the southern portion of the Paraná Magmatic Province, south Brazil. Detailed field work in the Soledade-Gramado Xavier region has shown that they correspond to the uppermost sequence of the low-Ti magmatism, which is characterized by a succession of pahoehoe basalt-aa basalt-dacite-rhyolite.

The rhyolite magmas have some unusual characteristics such as high magma temperatures (up to 1,000°C, as indicated by apatite saturation and two-pyroxene thermometry), high H₂O contents (2.5-3.5 wt%, estimated from the plagioclase geothermometer), and consequently lower viscosities (~104 Pa.s) compared to typical rhyolites, what could in part respond for the dominantly effusive mode of emplacement.

The rhyolites are chemically homogeneous, with 71-73 wt% SiO₂, 0.65-0.70 wt% TiO₂ and enriched in K₂O (4-5 wt%) and other incompatible elements (210–300 ppm Rb; 680–930 ppm Ba; ~350 ppm Zr and □ REE ~300 ppm) compared to the associated dacite units.

The scarce (~3-5 vol.%) 0.5-1.5 mm plagioclase phenocrysts have homogeneous cores with compositions varying from An₄₆ to An₅₄; resorption surfaces present in some crystals may be mantled by a thin, more calcic (An₅₇₋₆₀) rim. Trace-element contents determined by LA-ICPMS are also relatively homogeneous; results of inverse modeling for Ba, Sr, Rb and LREE using K_ds from literature are broadly consistent with crystallization from the host melts.

An increase in the temperature of the magmas suggested by resorption textures and inverse zoning of plagioclase may have occurred immediately prior to eruption, as a result of heating by latent heat of crystallization or, more probably, was due to injections of hotter magma, as evidenced by the occurrence of scattered dm-sized ball-shaped dacitic enclaves.

Lu-Hf isotope systematics of the ca. 3.92-3.96 Ga Acasta Gneiss Complex (NWT, Canada)

M. GUITREAU^{1,2,3*}, J. BLICHERT-TOFT¹², S.J. MOJZSIS^{1,2,4,5}, A.S.G. ROTH⁶, B. BOURDON¹², N.L. CATES⁴ AND W. BLEEKER⁷

¹Ecole Normale Supérieure de Lyon, Lyon, France

²Université Claude Bernard Lyon 1, Villeurbanne, France

³University of New Hampshire, Durham, NH, USA

⁴University of Colorado, Boulder, CO, USA

⁵Hungarian Academy of Sciences, Budapest, Hungary

⁶ETH, Zürich, Switzerland

⁷Geological Survey of Canada, Ottawa, Canada

*(Correspondence: martin.guitreau@unh.edu)

The Acasta Gneiss Complex (AGC) is a remnant Hadean (pre-3900 Ma) ancient crust composed of strongly deformed, polyphase mafic to felsic gneisses that preserve a protracted multi-stage history of magmatic emplacement, inheritance, and subsequent tectono-thermal modifications that induced generalized migmatization. The complexities observed in these ancient gneisses have been documented in previous geochronological studies of the AGC (e.g. U-Pb, ¹⁴⁷Sm-¹⁴³Nd), and are evident also in the Lu-Hf isotope systematics. Here, we report new whole-rock Lu-Hf isotope measurements which show that some AGC gneisses have been disturbed by metamorphic garnet growth and/or migmatization and mineral segregation, while others have preserved their Lu-Hf isotope systematics relatively intact. Results reveal identifiable Hadean and later (Eo- to Paleoproterozoic) magmatic events at around 3960 Ma and again at 3600 Ma, with a major metamorphic episode of the complex at ca. 3730 Ma. The oldest and least contaminated gneisses yield a mean Lu-Hf regression age of 3945 ± 91 Ma, which is in good agreement with U-Pb zircon geochronology [1]. The role of yet older crust (4000-4200 Ma) in the formation of the AGC is also evident, but this crust was not ubiquitous. Assimilation calculations show that the mantle source of the least contaminated samples in the oldest age group had Hf isotope compositions near that of the chondritic uniform reservoir (CHUR) 3960 My ago.

[1] Cates et al. (submitted)

Geochemical Characteristic of Felsic Dykes Within the Karakaya (Kaymaz) Granite Eskişehir, Turkey

B.GULLU¹, Y.K.KADIOGLU^{2,5}, O.ZOROGLU³,
T.KORALAY⁴, K.DENIZ⁵ AND C.O.KILIC⁵

¹Aksaray Uni. Dept of. Geol. Eng., Aksaray, Turkey

(*correspondance: bgullu@aksaray.edu.tr)

²Ankara Uni. Earth. Sci. App&Res. Center, Ankara

³General Directorate of Min. Res. And Exp., Ankara

⁴Pamukkale Uni. Dept. of. Geol. Eng., Denizli

⁵Ankara Uni. Dept. of Geol. Eng., Ankara

Karakaya (Kaymaz) granite is exposed to the east of Eskişehir City within the Sakarya Continent at eastern part of northwest of Anatolia. Karakaya granite has holocrystalline granular texture and mainly composed of quartz, orthoclase, oligoclase, biotite, tourmaline, \pm allanite, \pm zircon [1]. Karakaya granite covers an area of 16 km² as NW-SE trending semi elliptical shaped and cut by felsic dykes with direction of N10-35W [2].

Felsic dykes have myrmekitic and graphic textures are in composition of alkali feldspar granite and granophyr. Evolution of geochemistry of host rocks and felsic dykes indicates continuous trend between felsic dykes and their host rocks. This trend suggested the differentiation products of same magma resource for felsic dykes and host rocks.

ORG normalized elemental patterns of felsic dykes reveal enrichment with Large Ione Lithophile Elements with respect to High Field Strength Elements. Besides, chondrite normalized elemental patterns of Rare Earth Elements show prominent enrichment of Light Rare Earth Elements with respect to Heavy Rare Earth Elements.

REE characteristics of felsic dykes are calculated as $(La/Yb)_N$: 17.47–17.51, $(Eu/Eu^*)_N$: 0.63–0.77, $(La/Sm)_N$: 11.85–12.41 and $(Sm/Yb)_N$: 1.413–1.47.

High LREE/HREE values and all the field geology, petrography and geochemical data reveal that the felsic dykes are the residual melts of the mixed felsic and mafic products of mantle signature crustal source magma.

The authors wish to thank DPT (dpt-2012K120440) and Ankara University (BAP 09B4343016) for supporting Project.

[1] Gullu B.&Kadioğlu Y.K. (2010) Karakaya (Eskişehir) Granite” ISSN 1556-4800 GSA, p.43 [2] Gullu B. (2013) Phd thesis (unpublished), AU, 243 p.

Water Geochemistry of the Thermal Waters in the Eastern Black Sea Section (Ordu, Rize and Artvin), Turkey

F. GULTEKIN^{1*} E. HATIPOGLU¹
AND A. FIRAT ERSOY¹

¹Karadeniz Technical University, 61080 Trabzon,

Turkey*(correspondence: fatma@ktu.edu.tr)

(hatipoglu@ktu.edu.tr, arzu@ktu.edu.tr)

Eastern Black Sea Section is characterized by a magmatic arc developed in the Cretaceous- Tertiary. Thrust faults, strike-slip faults and normal faults are formed in the region. Accordingly, in the area strike-slip faults, trending NE-SW direction, creates lines for thermal water outlets. Sarmaşık (Fatsa-Ordu), Ayder (Çamlıhemşin- Rize), İkizdere-Rize) and Ilica (Şavşat- Artvin) thermal waters, discharging from along these faults and fractures, are located in the region.

Temperature of Sarmaşık and Ilica thermal springs, discharging from basaltic and andesitic rocks are 48°C and 38°C respectively. Thermal well waters temperature in the Ayder and İkizdere areas are 57°C and 63°C respectively. In the study area pH values are between 6.32- 8.92, EC values are between 200- 8463 μ S/cm, TDS values are between 130- 5500 mg/l. The Na-HCO₃ thermal waters of Ayder, İkizdere and Ilica are Peripheral waters. Sarmaşık thermal waters, which is classified as Na-Ca-Mg-SO₄ are Steam heated waters. While thermal waters of Ayder and İkizdere are Immature Waters, Sarmaşık and Ilica thermal waters are Partially Mature Waters. The thermal waters of Ayder and Sarmaşık are undersaturated with respect to gypsum, amorphous silica, calcite, aragonite and dolomite, but İkizdere and Ilica thermal waters are oversaturated with respect to calcite, aragonite and dolomite.

The concentration values of trace element Rb, Cs and Li vary in thermal waters of four regions. Ilica thermal waters has the highest trace element concentration. Ayder thermal water are not affected by water-rock chemistry, compared with rare elements of rock and waters. In the Sarmaşık, İkizdere and Ilica area water chemistry is similar to the rock chemistry according to rare elements content. Based on their stable isotope contents waters are meteoric in origin. Ilica and İkizdere thermal waters have a more positive values of $\delta^{18}O$ due to water-rock interaction.

Vaporization studies on laser-generated aerosols as used in LA-ICPMS

DETLEF GÜNTHER^{1*}, LUCA FLAMIGNI¹, JOACHIM KOCH¹,
OLGA BOROVINSKAYA¹, BODO HATTENDORF¹,
AND MARTIN TANNER

¹ETH Zurich, Department of Chemistry and Applied
Biosciences, Laboratory of Inorganic Chemistry

²Tofwerk AG, Uttigenstrasse 22, Thun, Switzerland

(*correspondence: guenther@inorg.chem.ethz.ch)

Non-matrix matched calibration is one of the most widely applied strategies for quantification in laser ablation-inductively coupled plasma mass spectrometry. It relies on the assumption that sensitivities obtained for the elements in standards and samples are identical in relation to the internal standards used. Based on the observation that vaporization of the elements inside the ICP was found to be significantly affected by the matrix composition, various imaging techniques were applied to study vaporization of laser-generated aerosols within the ICP for different matrices. The results obtained indicate that vaporization points of particles in the plasma are species dependent (e.g. CaO, Ca, Na₂O, Na). Therefore, the efficiency of sampling different elements is affected by their respective diffusion rates in the plasma. It will also be shown that optimization of gas flow, ICP Rf-power adjustment or optimization of the sampling position cannot overcome these matrix problems. Additionally, data acquisition at high time resolution, using an ICP-TOF-MS (Tofwerk AG, Thun, Switzerland) allows studying the signal structure in greater detail and variations in the vaporization of different elements will be discussed.

Finally, various mix gas additions to the carrier gas were tested to stimulate a more uniform vaporization process of laser-generated aerosols within the ICP and some of these results will be presented and discussed in detail.

[1] L. Flamigni *et al.* (2012), *Spectrochim. Acta B*, **76**, 70. [2] O. Borovinskaya *et al.* (2013), *J Anal Atom Spectrom*, **28**, 226.

Crust–mantle interaction of Late Jurassic Qianlishan granites in South China: Constraints from geochemistry and in-situ analyses of zircon U–Pb–Hf–O isotopes

CHUN-LI GUO^{1*}, BING YIN² AND YI-MING XU³

¹MLR Key Laboratory of Metallogeny and Mineral Assessment, Institute of Mineral Resources, Chinese Academy of Geological Sciences, Beijing, 100037, PR China

²Hu'nan Shizhuyuan Nonferrous Metals Liability Co. Ltd., Chenzhou, 423037, PR China

³Southern Hu'nan Institute of Geology and Survey, Chenzhou, 423000, PR China

The Qianlishan granitic pluton is closely related to the Shizhuyuan superlarge W–Sn–Mo–Bi polymetallic deposit. It is composed of two phases, porphyritic biotite granite and equigranular biotite granite. Representative samples from each phase were analyzed using SIMS zircon U–Pb technique, and results were 155–153 Ma and 153–152 Ma (2 σ) respectively. The granitic rocks have high SiO₂ contents (73.2–77.7 wt%) and total alkali (7.27–9.36 wt%). For example, ASI (aluminum saturation index) values of two phases are 0.91–1.01 and 1.01–1.27 respectively. K₂O/Na₂O ratios of two phases are 1.29–2.82 and 0.86–1.36 respectively. LREE/HREE ratios are 3.95–6.80 and 1.10–2.12 respectively. The second phase has more obvious Eu negative anomaly (Eu/Eu* = 0.01–0.02) than the first one (Eu/Eu* = 0.13–0.28) and the second one has more conspicuous Sr, P, Zr and Ti depletion than the first one. P₂O₅ vs SiO₂, Zr saturation thermometer, whole rock Sr–Nd and zircon $\delta^{18}\text{O}$ values proved the Qianlishan granites are belong to a high evolved I-type. Whole rock $\epsilon_{\text{Nd}}(t)$, zircon $\epsilon_{\text{Hf}}(t)$ and $\delta^{18}\text{O}$ values fall into the ranges –9.3 to –6.4, –8.0 to –1.0, and 5.24‰–7.45‰ respectively, and combined with zircon Hf two-stage model ages (T_{DM2}) of 1.45Ga–1.73Ga. Trace–element geochemistry and isotope systematics further imply that the Qianlishan granitic magmas were most probably derived by partial melting of Palaeo– to Mesoproterozoic metamorphic lower crustal rocks and there were obvious mantle materials participating in during the granite formed. Combined previous researches, it is inferred that the Qianlishan granite was produced in an extensional structural setting, which resulting in the lithosphere thinning and an influx of asthenosphere.

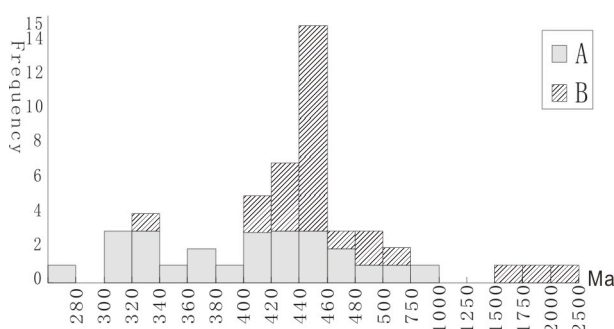
The characteristics of metamorphic basement for the Bogda late Paleozoic rift through, eastern Tianshan mountains, China

JUNFENG GUO^{1*} AND YONG LI¹

¹College of Earth Science and Land Resources, Chang'an University, Xi'an 710054, China
(*correspondence: guojunfeng540@gmail.com)

East tianshan mountains bogda rift trough located in the binding site between junggar and turpan-hami precambrian blocks, the tectonic setting is an upper paleozoic continental rift zone. Detrital zircon dating of newly discovered on the bogda orogenic north rim tectonic quartz schist shows that two sampling points apart 20 meters reflects a remarkable difference about the origin and the reformation of the metamorphic basement. The rifting from the early carboniferous, the deposition is characterized by a set of basalt and rhyolite bimodal volcanic and clastic rocks; the late carboniferous rift closed. Magmatism occurred in the tensional environment.

A sampling point on 25 zircon LA-ICP MS U-pb age analysis showed that the sample material composition, source formed in a wide range of geological time (figure 1, A sample data). B sampling point 30 zircon LA-ICP MS U-pb age analysis shows that 22 zircon of which given the relative concentration of the age of information, the weighted age of 450.3 ± 4.3 (MSWD=1.7). Batch of these zircon was short columnar or long columnar euhedral, the subhedral structure, with zircon shock rings clear, which indicate the source mass came from the magmatic, and the metamorphic protolith main diagenetic's late cambrian; sampled twice by a total of six zircon older than 540 million years, and the distribution of dating was scattered. Batch of these zircon was rounded, the weaker reflected light intensity, indicating that the metamorphic protolith old crystalline basement (fig. 1 B sample data).



Analysis of characteristics on different components of hydrocarbons in organo-clay complexes

MIN GUO¹, JINGONG CAI^{1*}, TIANZHU LEI²
AND FEI DING¹

¹State Key Laboratory of Marine Geology, Tongji University, Shanghai 200092, China

(*correspondence: jgcai@tongji.edu.cn)

²Key Laboratory of Petroleum Resources Research, Institute of Geology and Geophysics, Chinese Academy of Sciences, Lanzhou 730000, China

To investigate the characteristics of hydrocarbons with different occurrence states in clay minerals, samples of clay fraction ($<2\mu\text{m}$) were separated from argillaceous source rocks in Palaeogene of Dongying Sag in Jiyang Depression. The clay fractions were sequentially treated with Soxhlet extraction, alkaline hydrolysis, acid hydrolysis and mixed acid (10% HF and 10% HCl) processing, then the quantitative detection of GC-MS was employed to the organic components. The results show that there were great variations in the contents and the composition distribution characteristics of hydrocarbons with different treatments, a) the content of free hydrocarbons obtained by Soxhlet extraction was maximum ($603.74\mu\text{g/g}$), while the second part was the hydrocarbons obtained by mixed acid processing, and the hydrocarbons from alkaline and acid hydrolysis were the least part ($23.51\mu\text{g/g}$, $12.73\mu\text{g/g}$, respectively); b) the free hydrocarbons from Soxhlet extraction were mainly consisted of heavy components (C_{15}^+), ranged 52%~94%, 80% on average; and the hydrocarbons from alkaline and acid treatments were chiefly composed of light components ($\text{C}_1\text{-C}_{14}$), mainly ranged $\text{C}_7\text{-C}_{11}$, and the contents of light components were 73%, 77%, 65%, respectively. Through the contrastive analysis on the content of hydrocarbons in different burial depth, it can be found that the hydrocarbons were dominated with light components above 2000m, with the content more than 70%, and were dominated with heavy components below 2000m, with the content much more than 70%.

The organo-clay complexes are the main carrier of organic matter and hydrocarbons in argillaceous source rocks. It is of great significance to study the geochemical characteristics of petroleum based on different treatments in clay fractions for the migration study of petroleum and the resource evaluation of unconventional petroleum.

This work was supported by National Natural Science Foundation of China Program (Grant No. 41072089).

REE and trace element patterns across the Ediacaran-Cambrian transition, South China

QINGJUN GUO^{1*}, YINAN DENG¹, HARALD STRAUSS²,
DOROTHEE HIPPLER³, GERHARD FRANZ³
AND GUANGXU ZHU¹

¹Inst. of Geographic Sci. and Nat. Res. Research, Chinese Academy of Sciences, Beijing 100101, China
(guojq@igsnr.ac.cn)

²Westfälische Wilhelms-Universität Münster, Corrensstr. 24, 48149 Münster, Germany

³Technical University Berlin, Inst. of Applied Geosciences, Ackerstr. 76, 13355 Berlin, Germany

The Ediacaran and Cambrian interval belong to the most important periods in Earth's history. Deposits from the early Cambrian of the Yangtze Platform in South China represent a valuable source of information for the reconstruction of the evolution of marine palaeo-environments. Concentrations of REE and trace elements in kerogen as well as in bulk rocks from different depositional environments of the Yangtze platform indicate oxic conditions for shallow-water environments, and euxinic conditions in the deeper sea. The oxygenation of the water column of shallow-marine environments is manifested in two oxygenation events, one occurring in the upper Meishucunian and the second in the lower Qiongzhusian. Particularly the second oxygenation event resulted in the change of benthic redox conditions from anoxic to (sub-) oxic, which likely had an impact on the Cambrian explosion of life.

The early Cambrian Ni-Mo-PGE polymetallic ore layer, which occurs in most sections of the Yangtze Platform, shows a considerable enrichment of certain trace elements and coincides with negative $\delta^{13}\text{C}_{\text{org}}$ values. It is used as a marker for stratigraphic correlation separating the Meishucunian and the Qiongzhusian. Trace metal enrichment in associated black shales further indicates widespread euxinic conditions, although the extreme enrichment of some metals may originally come from hydrothermal plumes associated with spreading ridge volcanism. The results of this study thus provide valuable information about palaeo-environmental changes in the oceans during the Ediacaran-Cambrian transition, which may be used for the stratigraphic division of the Lower Cambrian.

Acknowledgements: The research was supported by the One Hundred Talents Program of the Chinese Academy of Sciences, the NNS Foundation of China (Nos. 40972023, 40930211, 40902003, 41173008), 973 Program (Nr. 2013CB835004) and is a contribution to the Sino-German research group FOR 736 funded by the German Science Foundation (FR 557/22-1 and HI 1553/1-2) to G. Franz and D. Hippler.

Magmatic digestion of the crust and the origin of silicic magmas in Iceland: Insights from partially melted crustal xenoliths

A.A. GURENKO^{1,2*}, I.N. BINDEMAN³
AND I.A. SIGURDSSON⁴

¹CRPG/CNRS, BP 20, 54501 Vandoeuvre-lès-Nancy, France
(*correspondence: agurenko@crpg.cnrs-nancy.fr)

²Geology & Geophysics, Woods Hole Oceanographic Institution, Woods Hole, USA

³Geological Sciences, University of Oregon, Eugene, OR 97403, USA

⁴South Iceland Nature Centre, 900 Vestmannaeyjar, Iceland

Silicic magmas play a fundamental role in the origin of the continental crust. Whether silicic magmas predominantly result from extensive fractionation of the parental basaltic melts or they originate during partial melting of the older metamorphosed oceanic crust is still a subject of debate.

We studied partially melted, glass-bearing granite to syenite xenoliths from the Tindfjallajökull Pleistocene volcanic complex, SW Iceland. EPMA and LA ICP-MS were used for analysis of major and trace elements, SIMS and single grain laser fluorination methods were applied for zircon dating and O isotope analysis of minerals and glasses. The xenoliths consist of strongly resorbed, partially melted relicts of anorthitic plagioclase and K-rich feldspar (Fsp; $\text{Ab}_{21-80}\text{An}_{1-37}\text{Or}_{1-78}$, $\delta^{18}\text{O} = 5.3\text{--}6.2\text{‰}$ given in permil relative to SMOW standard) and rounded quartz (Qz; $5.9\text{--}6.8\text{‰}$) in the mingling colorless ($5.5\text{--}6.2\text{‰}$) through pale or light brownish ($5.1\text{--}5.9\text{‰}$) to dark-brown magnetic ($4.0\text{--}5.0\text{‰}$) interstitial glass matrix. Spongy aggregates and elongated crystals of orthopyroxene ($\text{mg}\# = 62\text{--}75$, $\text{Wo}_{1-10}\text{En}_{58-77}\text{Fs}_{20-36}$) and clinopyroxene ($\text{mg}\# = 52\text{--}68$, $\text{Wo}_{34-43}\text{En}_{31-46}\text{Fs}_{16-27}$) are common. They probably have crystallized during reaction of hot mafic magmas with surrounding crustal (plagiogranitic?) rocks at $T = 800\text{--}1100^\circ\text{C}$. Magnetite ($\text{Spl}_{1-9}\text{Mag}_{58-84}\text{Usp}_{14-37}$) and rare ilmenite often form clusters with zircon and chevkinite, and together with apatite represent the accessory mineral association.

Many Icelandic lavas have systematically lower in $\delta^{18}\text{O}$ (i.e., $<5.2\text{--}5.6\text{‰}$) due to their interaction with the upper-crustal rocks altered by meteoric water, but they may contain strongly $\delta^{18}\text{O}$ -diverse olivines and zircons [1,2]. The important result of this work is that although the studied xenoliths are not low- $\delta^{18}\text{O}$, suggesting no interaction with meteoric water, they also contain low- to high- $\delta^{18}\text{O}$ ($2.2\text{--}6.3\text{‰}$) young zircons ($0.18\text{--}0.25 \pm 0.03\text{ Ma}$, 2 SD). This may suggest *in-situ* crystallization of the high- $\delta^{18}\text{O}$ zircons from the "minute" partial melts under local isotopic equilibrium. On the other hand, part of the zircon cores representing the lower end of the $\delta^{18}\text{O}$ range and being out of equilibrium with the interstitial melts could be inherited from the adjacent hydrothermally-altered crustal rocks having low $\delta^{18}\text{O}$ values.

[1] Bindeman *et al.* (2008) *GCA* **72**, 4397-4420. [2] Bindeman *et al.* (2012) *Terra Nova* **24**, 227-232.

Chromium(III) and bismuth(III) complexation to organic matter: EXAFS spectroscopy and equilibrium modelling

J.P. GUSTAFSSON^{1*}, A.G. OROMIEH¹, C. SJÖSTEDT²,
I. PERSSON¹ AND D.B. KLEJA^{1,3}

¹Swedish University of Agricultural Sciences, Uppsala, Sweden; *(correspondence: jon-petter.gustafsson@slu.se)

²Department of Chemistry, KTH Royal Institute of Technology, Stockholm, Sweden

³Swedish Geotechnical Institute, Stockholm, Sweden; Dan.Berggren.(Kleja@swedgeo.se)

The complexation of chromium(III) and bismuth(III) to mor layer material was investigated. Characterization of the products was made at MAX-Lab, Lund, Sweden, using Cr *K*-edge and Bi *L*₃-edge EXAFS spectroscopy.

The EXAFS results showed a predominance of monomeric organic complexes for chromium(III). The sorption of chromium(III) was pH-dependent. Chromium(III) complexation was found to be very slow at pH < 4, and equilibration times of three months or longer were required to reach equilibrium. For bismuth(III), complexation was quicker and found to be very strong, with more than 94 % bound at pH 1.2 also at a high bismuth(III) loading. EXAFS spectroscopy showed that the bound bismuth(III) ion is strongly distorted and interacts with a second bismuth(III) ion at ~4 Å. The complexation of bismuth(III) remained essentially unchanged even in the presence of a potent competitor such as iron(III).

The results from the spectroscopic investigation and from the quantitative solution data were used to calibrate new and improved complexation models for the Stockholm Humic (SHM) and the NICA-Donnan models. Similarities and differences in the organic complexation of the four trivalent metals chromium(III), bismuth(III), iron(III) and aluminium(III) will be discussed.

The study of Hg transformation in the Au recovery plant tailing area using thermal release technique with atomic absorption detection

M.A. GUSTAYTIS^{1*}, O.V. SHUVAEVA²,
I.N. MYAGKAYA¹ AND E.V. LAZAREVA¹.

¹Institute of Geology and Mineralogy SB RAS, Koptyug Pr. 3, Novosibirsk 630090, Russia (*goustaitis_m@mail.ru)

²Institute of Inorganic chemistry SB RAS, Acad. Lavrentiev Pr., 3, Novosibirsk, 630090, Russia

It is known that gold mining is one of the most powerful sources of mercury emission into environment. A present investigation was focuses on the Ursk tailings located in Kemerovo region (southwestern Siberia, Russia), that contains waste material produced by the cyanidation of the primary gold polymetallic ores and ores of the oxidation zone with elevated level of mercury and consisting of sand, sand-silt, silt and organic (peat mounds and buried peat).

As a result of the study it has been shown that in tailing shed wastes matereals mercury is presented as HgX₂, HgS and methylmercury at the predominance of HgCH₃⁺ and Hg²⁺, and also as impurities in pyrite and barite. Herewith in sand matter mercury is contained as oxidizing species (49-54 μg/g) and CH₃HgX (9-60 μg/g); in sand-silt - as HgX₂ (~15 μg/g), CH₃HgX (~15 μg/g) and HgS (~3 μg/g); in silt - as oxidized species (12-43 μg/g), merthylmercury (9-21 μg/g) and HgS (3-13 μg/g). In organic matter close to waste methylmercury prevails (up 25 to 2 μg/g), but in organic matter of perennially wet zone mercury exists as cinnabar and mercury selenide (Hg_{total}=2350 g/t).

It can be assumed that Hg²⁺-compounds are formed under the interaction of the shed wastes material with the components of the environment while methylmercury appears due to the presence of organic carbon in the pore solution as in the solid its concentration is negligible. As for organic carbon it may originate from the substances of peat mounds and buried peat. Mercury content in pyrite and barite doesn't generally exceed 10% of the total one.

On the base of the results of the present study and the published data as well the scheme of mercury transformation was proposed.

The study was supported by Grant 11-05-01020 from RFBR and an 2012-2013 OPTEC grant for young scientists, and was run as part of SB RAS Integration Project #94.

Relatively small degree of surface ocean acidification during the PETM in the North Atlantic

MARCUS GUTJAHR^{1,2*}, PHILIP F. SEXTON³,
PAUL N. PEARSON⁴, HEIKO PÄLIKE⁵,
RICHARD D. NORRIS⁶ AND GAVIN L. FOSTER¹

¹Ocean and Earth Science, National Oceanography Centre
Southampton, University of Southampton, UK
Gavin.Foster@noc.soton.ac.uk

²GEOMAR Helmholtz Centre for Ocean Research Kiel, Germany
mgutjahr@geomar.de (* presenting author)

³Centre for Earth, Planetary, Space & Astronomical Research, The
Open University, Milton Keynes, UK Philip.Sexton@open.ac.uk

⁴Cardiff University, School for Earth and Ocean Sciences, Cardiff,
UK PearsonP@cardiff.ac.uk

⁵Marum Centre for Marine Environmental Sciences, University of
Bremen, Germany hpaelike@marum.de

⁶Scripps Institution of Oceanography, University of California, San
Diego, La Jolla, U.S.A. rnorris@ucsd.edu

With an estimated 2,000 to 12,000 Gt of carbon released over ≤ 10 ka, the Paleocene-Eocene Thermal Maximum (PETM) is an excellent analogue for understanding the long-term effects of present-day fossil fuel carbon combustion. The carbon cycle perturbation during the PETM was initiated at ~ 56 Ma and lasted for less than 200 kyr. Temperature reconstructions indicate warming averaging $\sim 5^\circ\text{C}$. However, to date, no constraints exist for the response of surface water pH through this fossil carbon release event. If the injection of several thousand Gt of carbon occurred sufficiently rapidly relative to the mixing time of the oceans, it should have resulted in a significant drop in surface water pH that subsequently recovered to near pre-event values. The existence of such a perturbation of surface water pH can be resolved by means of the boron isotopic composition of marine carbonates.

Here the first MC-ICP-MS based boron isotope record from both mixed-layer and thermocline dwelling foraminiferal species across the PETM from DSDP Site 401 in the North Atlantic will be presented. These results are complemented by elemental records and new carbon and oxygen isotope data generated from the same samples. Although we find perturbations in our various elemental and isotopic records across the PETM-related carbon isotope excursion (CIE), the degree of ocean acidification and, hence, inferred carbon release, is surprisingly small. Carbon cycle modelling using our new boron isotope records suggests that this comparatively small degree of ocean acidification during the CIE was driven by a methanogenic source of carbon.

CO₂: Waste or resource ? The role of mineral/water interfaces

F. GUYOT

IMPMC, Université Paris Diderot, IPGP, CNRS, UPMC,
Paris, France (guyot@impmc.upmc.fr)

In the context of the anthropogenic destabilization of the carbon cycle, the CO₂ molecule is often considered as a waste to be captured and stored as far away as possible. Both nature and chemistry suggest, however, that, in some specific conditions, CO₂ can be turned into a useful resource. In this talk, I will examine how mineral/water interfaces present in several geological systems could possibly contribute to that purpose. Solid carbonates and hydrocarbonates produced by CO₂ carbonation of basic and ultrabasic minerals can sometimes be valuable materials. Their characteristics mostly depend on interfacial layers that develop at the surface of the primary minerals. Results of observations by focused ion beam coupled to transmission electron microscopy, in different contexts between 25°C and 180°C, will be given; the role of iron on their passivating properties will be shown. Abiotic hydrogen production and CO₂ reduction, a way of converting CO₂ into energetic resources, but also into strong greenhouse species, will be demonstrated at mineral/water interfaces by contrast with the fact that no such processes occur in pure aqueous phase. The actions of magnetite and of iron carbonate (siderite), will be investigated. The production yields of different organics ranging from formic acid to methanol and to methane in presence of iron-bearing mineral surfaces will be given and modeled. High resolution transmission electron microscopy of magnetite and siderite surfaces will be shown and discussed with respect to this question. Finally, recent intriguing mineral preferences concerning biological CO₂ reduction in the oceanic sub seafloor will also be examined. A tentative geomicrobiological and thermodynamic model will be proposed for understanding different routes of CO₂ reduction at those mineral/water interfaces.

The ultra-high pressure phase diagrams of SiO₂ and MgSiO₃

F. GUYOT^{1*}, A. BENUZZI-MOUNAIX², S. MAZEVET^{3,4}
AND T. TSUCHIYA⁴

¹IMPMC, Université Paris Diderot, IPGP, CNRS, UPMC, Paris, France (* correspondence : guyot@impmc.upmc.fr)

²LULI, Ecole Polytechnique, CNRS, CEA, UPMC, Palaiseau, France

³LUTH Observatoire de Paris, CNRS, UPD, Paris, France

⁴CEA-DAM-DIF, Arpajon, France

⁵Geodynamics Research Center, Ehime University, Matsuyama, Ehime, Japan

As a result of condensation sequences in protostellar nebulae and subsequent metal/silicate differentiation, planetary mantles are to first order close to an average MgSiO₃ composition. Indeed, large uncertainties exist about the Mg/Si ratios but in all cases, the question of the dissociation of MgSiO₃ or Mg₂SiO₄ into MgO and SiO₂ is crucial for understanding the mantles of terrestrial planets, the putative rocky cores of giant planets and possibly the early Earth. In this study, we have investigated the ultra high pressure phase diagram of SiO₂ using ab initio quantum calculations. We have observed an increase with pressure of the average effective Si-O coordination from 4 to 9 in both solid and liquid phases. We have calculated the melting line and extracted elementary thermodynamic parameters for the solid and liquid phases which were then used to infer dissociation pressures and temperatures of MgSiO₃. The ab initio calculated electrical conductivity of the SiO₂ liquid phase allowed us to determine the position of liquid metallic SiO₂ in the phase diagram. The thermodynamic connections between SiO₂ metallization and MgSiO₃ dissociation and the implications for rocky cores of giant planets and early terrestrial mantle will be discussed. Finally, all these results from theory will be compared with experimental results acquired at ultra high pressures in dynamical compressions, including very recent ones.

Prebiotic Simulations of Shallow Sea Hydrothermal Vents: Photochemical Reduction of CO₂ on Sphalerite

MARCELO I. GUZMAN* AND RUIXIN ZHOU

Department of Chemistry, University of Kentucky, Lexington, KY 40506, USA (marcelo.guzman@uky.edu)

A key requirement to understand the origin of life is to explain how early metabolism could have emerged. In the model of central universal metabolism [1], all carbon fixation pathways used by living organisms share at least one common intermediate [2], implying that all carbon fixation mechanisms are linked, and that a prebiotic mechanism should have used key organic compounds from present anabolic cycles. Photoelectrochemical reactions on semiconductor mineral surfaces have been proposed to play a central role in this scenario.

In this study sphalerite (ZnS) semiconductor mineral is used as a model catalyst to explore prebiotic reactions occurring in a shallow sea hydrothermal vent [3]. Sunlight free energy drives otherwise unviable reactions in the presence of ZnS mineral produced *in situ*. The material and photoelectrochemical characterization of the ZnS colloidal suspensions and comparison to commercial samples includes powder X-ray diffraction, transmission electron microscopy, energy dispersive spectroscopy, and dynamic light scattering.

Experimental results show the photoreduction of dissolved carbon dioxide (C+IV) and the coevolution of species produced from sulphide hole scavenger. The photoreduction reaction proceeds to generate formate as the main initial photoproduct. The quantum efficiency of formate production (Φ) in the ultraviolet spectrum at pH relevant to the early ocean waters ($7 < \text{pH} < 9$) follows a dependence on wavelengths described by the equation: $\Phi (\%) = 10.730 - 0.031 \times \lambda (\text{nm})$, with a coefficient of correlation $r^2 = 0.991$. The quantum efficiency does not depend on temperature between 283 and 328 K. The mechanism provides a way to capture energy from the environment while producing carbon feedstock useful in anabolism. The results of this study suggest that central metabolites could have participated in a viable enzyme-free cycle for carbon fixation in a shallow sea hydrothermal vent, where light, sulfide minerals, carbon dioxide, and other organic compounds interacted on the prebiotic Earth to generate an autonomous chemical cycle [1].

[1] Morowitz *et al.* (2000) *Proc Natl Acad Sci USA* **97**, 7704.

[2] Guzman & Martin (2010) *Chem Commun* **46**, 2265.

[3] Guzman & Martin (2008) *Int J Astrobiology* **7**, 271

Trace element partitioning between immiscible silicate and carbonate melts, based on natural melt inclusions from Kerimasi volcano, Tanzania

TIBOR GUZMICS¹ AND ZOLTÁN ZAJACZ²

¹Lithosphere Fluid Research Lab, Department of Petrology and Geochemistry, Eötvös University Budapest, Hungary

²Department of Earth Sciences, Institute of Geochemistry and Petrology, ETH Zürich, Switzerland

Although trace element partitioning between immiscible silicate and carbonate melts has been studied experimentally [1, 2], the reason for enrichment of calcicarbonatites in HFSE (=high field strength elements), REE (=rare earth elements) and Y is still controversial.

We have carried out LA-ICP-MS analyses of silicate and carbonate melt inclusions as well as rock forming minerals from two plutonic rocks (afrikandite and calcicarbonatite) from Kerimasi volcano. Melt inclusions show that immiscibility between silicate and carbonate melts occurred from a parental carbonated nephelinite magma. During liquid immiscibility Li, Na, Pb, Ca, Sr, Ba, B, REE, Y, U, V, Nb, P, Mo, W and S are partitioned into the carbonate melt whereas, Mg, Mn, Fe, Co, Ni, Cu, Zn, Al, Sc, Si, Ti, Hf, Zr and Th are partitioned into the silicate melt. Potassium, Rb, Cs, and Ta show almost no preferential partitioning. Strong distribution of sulfur (as SO_4^{2-}) and P (as PO_4^{3-}) into the carbonate melt (relative to silicate melt) could result in partitioning of Nb, Pb and all REE into the same melt. In perovskites compatibility of MREE, LREE, Ti, Zr, Nb, Ta and U increases; in magnetite that of Nb and Zn also increases during evolution of carbonate melts from afrikandite to calcicarbonatite.

We demonstrate that enrichment of calcicarbonatite rocks in LREE, Nb, Zr, Zn, Th and U is determined by both the fractionation of elements during silicate-carbonate liquid immiscibility prior to formation of these rocks and the significant changes in $D_{\text{MINERAL-CARBONATE MELT}}$ values during subsequent evolution of the physically separated carbonate melt.

- [1] Martin *et al.* (2012) *Chem. Geol.* **320-321**, 96-112.
[2] Veksler *et al.* (2012) *Geochim. Cosmochim. Acta* **79**, 20-40.

Effects of volcanic CO₂ vents on a freshwater environment, the Laacher See

S. GWOSDZ¹, I. MÖLLER¹, H. H. RICHNOW²
AND M. KRÜGER¹

¹ Federal Institute for Geosciences and Natural Resources (BGR), 30655 Hannover, Germany

² Helmholtz Centre for Environmental Research (UFZ), 04318 Leipzig, Germany

The Laacher See volcanic centre, located in the middle of the East Eifel volcanic field (Germany) discharges about 5 000 t of CO₂ per year. The CO₂ is released from multiple gas vents at the bottom of the lake. Natural CO₂ sources like Laacher See allow the determination of CO₂-induced biogeochemical alterations of ecosystems.

Therefore, biogeochemical parameters as well as microbial metabolisms, abundance and diversity were studied to assess potential effects of elevated CO₂ concentrations on that freshwater sediment ecosystem.

CO₂ seeps at the lake bottom and reference areas were localised using different hydroacoustic measurements. The flux rates and the composition of seeping gases were verified with divers and a small remotely operated vehicle (ROV). For the investigation of active metabolic pathways, cultivation experiments under aerobic and anaerobic conditions were conducted and the formation of e.g. CO₂ and CH₄ was analyzed by gas chromatography. The microbial population was characterized using quantitative real time PCR (qPCR) for 16S rRNA and functional genes, TRFLP and sequencing.

Dissolved CO₂ in bottom water as well as in sediment pore water samples had a carbon isotopic signature close to that in the gas bubbles, both confirming a magmatic origin of the gas. Analysis of water samples collected close to intensive CO₂ seeps showed a low pH and an increase of dissolved CO₂. Furthermore, geochemical and microbiological analyses of deep sediment cores from CO₂-affected and reference sites showed alterations in the carbon isotopic signature, pH, microbial activity and populations. 16S rRNA gene copy numbers of Bacteria and Archaea from CO₂ induced and reference sites varied by four orders of magnitude. Similar results could be detected for the analyzed microbial CO₂ and CH₄ turnover. Our results illustrate a CO₂ impact on the geochemistry, microbial activity and community composition caused by the increasingly anaerobic and acidic environmental conditions.

U–Pb chronology and REE geochemistry of large zircons in Estherville mesosiderite

MAKIKO K. HABA^{1*}, AKIRA YAMAGUCHI², HIROYUKI KAGI¹, KEISUKE NAGAO¹ AND HIROSHI HIDAKA³

¹Geochemical Research Center, University of Tokyo, Bunkyo-ku, Tokyo 113-0033, Japan (correspondence: kikuchi@eqchem.s.u-tokyo.ac.jp)

²Antarctic Meteorite Research Center, National Institute of Polar Research, Tachikawa, Tokyo 190-8518, Japan

³Department of Earth and Planetary Systems Science, Higashi-Hiroshima, Hiroshima 739-8526, Japan

Mesosiderites are breccias composed of almost equal proportions of silicates and Fe-Ni metal. The oxygen isotopic compositions of the silicate parts of mesosiderites and HED (howardite, eucrite, and diogenite) meteorites indicate that their parent bodies are same or located in the same region [1]. However, an origin and formation histories of mesosiderites are still enigmatic, because they have experienced complex metamorphism [2]. In this study, we report results of *in situ* analyses of large zircons found in Estherville mesosiderite.

An electron probe micro-analyser was used to identify a zircon by elemental mappings of Zr and Si and for quantitative analysis of major elements. Crystallinity and structure of zircons were evaluated by Raman spectra and cathodoluminescence (CL) images, respectively. U–Pb isotopes and rare earth elements (REE) contents were analyzed using a sensitive high resolution ion micro-probe (SHRIMP).

Two large zircons, 30 × 100 μm and 100 × 300 μm, were found. The CL images and Raman spectra indicate that the larger zircon consists of several domains. U and REE contents of the most part of the zircons are quite low compared with those in basaltic eucrites [3, 4]. However, the larger zircon has U- and REE-enriched area where U and REE contents are well consistent with those in basaltic eucrites. The ²⁰⁷Pb–²⁰⁶Pb age of the U- and REE-enriched area is 4520 ± 14 Ma (2σ, n = 3), which is younger than zircons in basaltic eucrites [3] and Vaca Muerta (mesosiderite) [5]. These results suggest that the original zircons in Estherville were similar to those in basaltic eucrites and could have recrystallized and overgrown during the metal-silicate mixing event.

[1] Clayton and Mayeda (1996) *GCA* **60**, 1999–2017. [2] Wadhwa *et al* (2003) *GCA* **67**, 5047–5069. [3] Misawa *et al* (2005) *GCA* **69**, 5847–5861. [4] Haba *et al* (2013) *LPSC* **44**, #1989. [5] Ireland and Wlotzka (1992) *EPSL* **109**, 1–10.

Oxygen transfer across the capillary fringe: Impact of transient flow conditions and coarse-material lenses

C.M. HABERER^{1*}, M. ROLLE^{1,2}, O.A. CIRPKA¹ AND P. GRATHWOHL¹

¹Department of Geosciences, University of Tübingen, Hölderlinstraße 12, 72074 Tübingen, Germany

(*correspondence: christina.haberer@uni-tuebingen.de)

²Department of Civil & Environmental Engineering, Stanford University, 473 Via Ortega, Stanford, CA 94305, USA.

We performed quasi 2-D flow-through experiments at the laboratory bench-scale to investigate the impact of transient flow conditions and a coarse-material inclusion on oxygen transfer from the unsaturated zone, across the capillary fringe (CF), to anoxic water. The experimental setup consists of a flow-through chamber with inner dimensions of 80 cm × 40 cm × 0.5 cm (Fig. 1). Glass beads with two different ranges in grain diameter were used as porous media. We applied a non-invasive optode technique to measure high-resolution vertical O₂-concentration profiles across the CF at several distances from the inlet of the flow-through chamber. In addition, the oxygen flux at the inlet and in the effluent of the flow-through chamber was monitored over time.

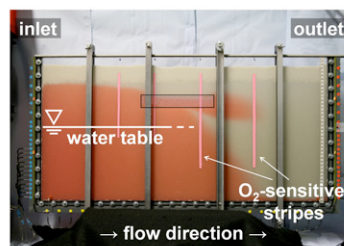


Figure 1. Experimental setup with coarse-material inclusion. The red dye (New Coccine) was used to visualize the flow field.

In homogeneous porous material, we quantified the effect of different water table dynamics, i.e., slow and fast water table fluctuations, on oxygen transfer. Enhanced O₂-supply was observed in case of slow fluctuations due to pronounced partitioning from entrapped air. In case of a fast draining water table the effect of specific yield has to be considered. The experiments performed in the heterogeneous system showed that oxygen transfer was significantly increased by the coarse-material inclusion due to flow focusing, the capillary barrier effect, and the presence of an air passage. These processes contributed to the overall enhancement of O₂-transfer through the CF to the underlying anoxic groundwater up to seven times compared to what was observed in the homogeneous experimental setup.

Influence of bacterial biomass on transport kinetics of phenanthrene

N. HACHICHO*, A. MILTNER, L.Y. WICK
AND M. KÄSTNER

UFZ - Helmholtz Centre for Environmental Research Leipzig,
Germany (*correspondence: nancy.hachicho@ufz.de)

Introduction

In soils, both pollutants and pollutant-degrading organisms are heterogeneously distributed. For an efficient site remediation by biodegradation, transport of either the pollutant or the microorganisms is necessary. Earlier studies show the effect of fungal hyphae on the transport of both chemicals and bacteria by fungal highways or pipelines [1]. In our study we investigated how the presence of bacterial biomass affects the diffusive transport of phenanthrene in aqueous solution in model systems (adapted from ref [2]) in the laboratory.

Phenanthrene Transport in Passive Dosing Systems

We studied the transport of phenanthrene from a silicone ring loaded with phenanthrene (source) to a larger clean silicone ring (sink). Both rings were placed in a vial containing 1 ml of medium with or without bacteria not able to degrade phenanthrene at different cell densities. After xy hours, source, sink and medium were analysed separately for phenanthrene.

Results and Discussion

The presence of bacterial biomass increased the medium's capacity for phenanthrene, but no difference in the phenanthrene contents in the source and the sink ring were found (Fig. 1). Further experiments with different soil bacteria with a range of surface properties and motilities will provide additional information to elucidate the role of bacterial biomass for the transport of chemicals in soil.

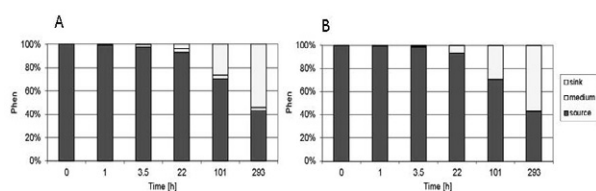


Figure 1: Phenanthrene distribution in passive dosing systems with biofilm of *Arthrobacter chlorophenicus* A6 on the surface (A) and sterile agar (B).

[1] Banitz *et al*(2012) *EnvironMicrobiolRep* 2012, 1-8. [2] Smith *et al* (2012) *Environ. Sci. Technol.* **46**, 4852–4860.

Campaign-style titanite U-Pb dating by laser-ablation ICP: Implications for crustal flow, phase transformations and titanite closure

B.R HACKER¹ A.R.C. KYLANDER-CLARK¹
T.B. ANDERSEN^{2A} AND J.M. COTTLE¹

¹Earth Science, University of California, Santa Barbara CA
93106, USA (hacker@geol.ucsb.edu)

²Geosciences, Universitetet i Oslo, P.O. Box 1047 Blindern,
0316 Oslo, Norway

U-Pb dates of titanite from >150 samples of quartzofeldspathic gneiss and leucosomes were measured across the ultrahigh-pressure (UHP) Western Gneiss Region of Norway to understand deformation and metamorphism of continental crust during subduction and exhumation. Titanite is unstable at pressures > 1.5 GPa, and, indeed, most yielded post-UHP dates. A number of titanites sampled across large areas, however, have pre-UHP U-Pb dates, indicating that the titanites survived their excursion to and return from mantle depths metastably. This has three important implications. Titanite grains can remain closed to complete Pb loss during regional metamorphism at temperatures as high as 750°C and pressures as high as 3 GPa, implying that thermally mediated volume diffusion was not the principal factor controlling resetting of the U-Pb system. Phase transformations in and deformation of quartzofeldspathic rocks can be inhibited at the same conditions.

Interpretation of extreme diagenetic settings with a new thermodynamic activity model

LAURA HAFFERT¹, MATTHIAS HAECKEL¹, VOLKER LIEBETRAU¹ AND DIRK DE BEER²

¹Helmholtz Centre for Ocean Research Kiel (GEOMAR), Germany (*correspondence: lhaffert@geomar.de, mhaeckel@geomar.de, vliebetr@geomar.de)

²Max Planck Institute for Marine Microbiology, Bremen, Germany (dbeer@mpi-bremen.de)

A thermodynamic activity model (Pitzer approach) applicable to extreme environmental pTS-conditions (up to 1000 bar, 200 °C and 6 M NaCl) coupled to an extensive mineral database has been developed. The advantage of this code is the incorporation of a comprehensive pressure correction, as well as the flexibility on the choice of input datasets, allowing fine-tuning of the model according to the relevant pTS range. This code is then integrated into our transport-reaction models, allowing for the interpretation of extreme diagenetic settings, where regular seawater models fail.

One such setting is the Mercator mud volcano in the Gulf of Cadiz, where the porewater profiles are characterised by a strong salinity gradient in the upper 1-2 mbsf created by the mixing of upward advecting hypersaline (halite and gypsum saturated) mud volcano fluids and seawater (S=35). In addition, various types of authigenic gypsum (CaSO₄·2H₂O) and anhydrite (CaSO₄) crystals, typical for evaporitic environments, were found. We show, that here the precipitation of authigenic CaSO₄ minerals is temperature driven and directly related to heat pulses that are typically occurring at mud volcanoes. The composition of the CaSO₄ mineral, in turn, is additionally controlled by the salinity gradient, raising the gypsum-anhydrite transition zone from >1 km to about 500 m sediment depth and during heat pulses (> 30 °C) even to within a few metres below the seafloor.

Another application is the geochemistry of the sediment-hosted natural CO₂ seeps in the southern Okinawa Trough. At the Swallow Chimney, located at 1380 mbsf, liquid CO₂ and CO₂ hydrates are encountered in the top decimetres below the seafloor. Here, the strong CO₂ and concomitant pH gradient induce silicate and complete carbonate dissolution downcore. However, some carbonate is reprecipitated towards the seafloor again, as suggested by the radiogenic and stable Sr isotopy. Our thermodynamic model is used to test this hypothesis and to quantify the diagenetic processes occurring in this extreme geochemical environment.

Carbon isotope gradients in the Eocene as a constraint on the biological pump, atmospheric CO₂ and the ocean's major ion composition

MATHIS P. HAIN¹, DANIEL M. SIGMAN¹, J. A. HIGGINS¹, AND GERALD H. HAUG²

¹Princeton University, (mhain@princeton.edu)

²ETH Zürich

In the modern ocean surface the δ¹³C of dissolved inorganic carbon (DIC) is high (¹³C-enriched) relative to deep waters, due to isotope fractionation during biological carbon fixation and the subsequent export of organic matter from the surface to sequester ¹³C-deplete carbon at depth, the soft-tissue component of the biological pump. In the Eocene, observations suggest that these isotope gradients were greater than today, leading to the inference that the biological pump was stronger. However, this argument ignores the much greater ocean carbon inventory under high atmospheric CO₂ levels during the Eocene, which would dilute the biologically driven δ¹³C gradients. Box model simulations indicate a number of mechanisms to resolve this discrepancy, including changes in the ocean's major ion composition and meridional temperature gradient. When using observational constraints such as temperature reconstructions, the depth of seafloor carbonate preservation, fluid inclusion data and the absence of large-scale anoxia in the Eocene ocean, we find that the δ¹³C gradients are inconsistent with atmospheric CO₂ levels greater than 1200 ppm. In these Eocene scenarios, the ocean's DIC is similar to today, but pH and buffer capacity are much lower, with implications for marine calcifying organisms.

Complete simulation of deglacial changes in atmospheric $^{14}\text{C}/\text{C}$: Implications for ocean circulation changes and CO_2 release

MATHIS P. HAIN¹, DANIEL M. SIGMAN¹
AND GERALD H. HAUG²

¹Princeton University, (mhain@princeton.edu)

²ETH Zürich

We present a new deglacial budget (production and decay) of ^{14}C , the first to correctly predict the preindustrial global activity of ^{14}C . While ^{14}C production change accounts for most of the overall decline in atmospheric $^{14}\text{C}/\text{C}$ (i.e., $\Delta^{14}\text{C}_{\text{atm}}$) since the Last Glacial Maximum, it fails to explain the rapid observed $\Delta^{14}\text{C}_{\text{atm}}$ swings during deglaciation. We use a carbon cycle model to separate the contribution of ocean CO_2 release and circulation changes to the $\Delta^{14}\text{C}_{\text{atm}}$ history, which together yield an exceptional match to available terrestrial $\Delta^{14}\text{C}_{\text{atm}}$ data, both in terms of overall deglacial $\Delta^{14}\text{C}_{\text{atm}}$ decline and millennial scale variations. The previously hypothesized but not yet identified stagnant “mystery reservoir” in the ice age ocean is not required in our simulations.

Ocean chemistry before and after the rise of atmospheric O_2

I. HALEVY¹

¹Weizmann Institute of Science, Rehovot 76100, Israel,

The tight coupling among the biogeochemical cycle of O_2 and those of the major redox-sensitive elements, such as C, Fe and S [1-3], implies that the rise in atmospheric O_2 was likely preceded, accompanied and followed by radical rearrangements in the cycles of these elements. Indeed, the rise of O_2 appears to be recorded in a variety of marine geochemical and isotopic records, especially those of Fe and S. Among others, these include traditional and mass-independent S isotope ratios [4,5], Fe isotope ratios [6], detrital O_2 -sensitive mineral grains [7], and banded iron formations [7]. Qualitative understanding of these records hinders insight into events that fundamentally reshaped Earth's surface environment. I have developed a chemically detailed, spatially resolved model of the coupled marine biogeochemical cycles of S and Fe [8], which I use here to provide quantitative constraints on ocean chemistry before and after the rise of O_2 .

Prior to the rise of O_2 , the main S reservoirs in the ocean are sulphate and thiosulphate, with concentrations up to ~60 and ~10 μM , respectively, consistent with recent constraints from mass-independent S isotopes in VMS deposits [9]. Elemental S particles (S_8), which settle rapidly, reach only sub-nanomolar concentrations, but contribute much of the S flux to the sediments. A balance between riverine and hydrothermal supply of Fe^{2+} and its oxidation in the photic zone governs water-column Fe^{2+} concentrations, which do not exceed 5 μM , unlike suggestions that mineral solubility allowed Fe^{2+} concentrations as high as ~100 μM [7]. After the rise of O_2 , sulphate becomes essentially the only marine S reservoir, and its concentration exceeds 1 mM. Sulphide concentrations in hydrothermal fluids exceed those of Fe, resulting in a decline of the hydrothermal Fe influx. Deposition of Fe (as Fe^{3+} -hydroxides) becomes limited to near-shore environments.

Among other topics, I will discuss the implications of these results to the records S isotope ratios, to metabolic S and Fe utilization, and to the observed Precambrian sedimentary record.

[1] Garrels and Lerman (1984) *Am J Sci* **284**, 989. [2] Kump and Garrels (1986) *Am J Sci* **286**, 337. [3] Hayes and Waldbauer (2006) *Phil Trans Royal Soc B* **361**, 931. [4] Farquhar *et al* (2000) *Science* **289**, 756. [5] Habicht *et al* (2002) *Science* **298**, 2372. [6] Bekker *et al* (2010) *Econ Geol* **105**, 467. [7] Holland (1984) *The Chemical Evolution of the Atmosphere and Oceans*. [8] Halevy (2013) *Proc Natl Acad Sci USA* **110**, Early Edition. [9] Jamieson *et al* (2013) *Nature Geo* **6**, 61.

Densities of dilute coenzyme M solutions to 0.80 MPa and 353.15 K

A. S. HALL¹ AND J. C. SEITZ¹ *

¹California State Univ. East Bay, Hayward, CA 94542 USA

(*correspondence: jeff.seitz@csueastbay.edu)

Sodium 2-mercaptoethanesulfonate ($C_2H_5NaO_3S_2$), also known as coenzyme M is a thiol that is essential to the process of methanogenesis [1]. Coenzyme M is a cofactor involved in methyl transfer reactions within methanogenic archaea. Given that fossil evidence of methanogenic archaea may date back to 2.8 billion years [2], methanogenesis is likely an ancient metabolic process. Determining the thermodynamic properties of coenzyme M is essential for understanding the potential for its formation and reaction properties in high P-T environments that host extremophiles and may have hosted the emergence of life.

The volumetric properties of dilute aqueous solutions of coenzyme M (0.09966 m, 0.19950 m, 0.299921 m & 0.39815 m) were obtained using an Anton Paar DMA 5000 vibrating tube densimeter. Reproducibility of density measurements was $\pm 0.00002 \text{ g}\cdot\text{cm}^{-3}$, exceeding propagated errors associated with uncertainty in the measurement of temperature, pressure, and fluid concentration.

Experimentally determined volumetric properties of coenzyme M have not been previously reported in the literature. Figure 1 shows partial molar volumes at infinite dilution (V^∞) derived from fluid density data; it is clear that V^∞ is not a sensitive function of pressure in the range examined.

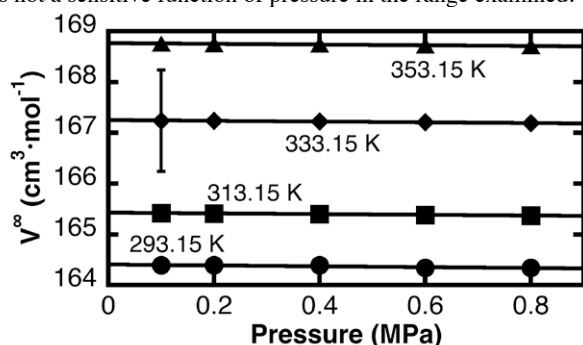


Figure 1. Experimentally determined partial molar volumes at infinite dilution of sodium 2-mercaptoethanesulfonate in aqueous solutions at 0.10-0.80 MPa and 293.15-353.15 K from this study. Lines represent simple linear regression fits to the data. The error bar represents the estimated uncertainty of $\pm 1.0 \text{ cm}^3\cdot\text{mol}^{-1}$.

[1] Balch & Wolfe (1979) *J. Bacteriol.* **137**, 256-263. [2]

Brocks *et al* (1999) *Science* **285**, 1033-1036.

Deep carbonate recycling and metasomatic enrichment of the sub-continental lithospheric mantle inferred from mantle xenoliths of the East African Rift system

S. A. HALLDÓRSSON^{1*}, D. R. HILTON¹, P. SCARSI², T. ABEBE², J. HOPP³ AND S. CHAKRABORTY⁴

¹Scripps Institution of Oceanography, UCSD, La Jolla, USA

(*correspondence: shalldor@ucsd.edu)

²IGG-CNR, Pisa, Italy

³Mineralogisches Institut, Universität Heidelberg, Germany

⁴Department of Chemistry, UCSD, La Jolla, USA

The source region of the extensive magmatism driving the East Africa Rift System (EARS) is thought to involve one or more deep-seated mantle plumes with variable interactions with overlying crust and, in particular, sub-continental lithospheric mantle (SCLM). To assess the role of SCLM in modulating the volatile systematics of plume-related material, we report new results on the He-CO₂-N₂ isotope and relative abundance of mantle xenoliths from throughout the EARS (Red Sea, Ethiopia, Kenya and Tanzania).

Our analytical approach involves crushing mafic crystals to release CO₂ and N₂ trapped in fluid inclusions. This approach was used on a suite of gas-rich xenoliths (dominantly pyroxenites, n=25). The xenoliths display a large range in He-isotopes (5.9 to 13.9R_A) but have a limited range of $\delta^{13}\text{C}$ values (-3.3 to +0.8‰), with only two xenoliths showing values lower than -2‰. $\delta^{15}\text{N}$ values range from -4.11 to +5.89‰ and CO₂/³He and CO₂/N₂ ratios vary by orders of magnitude from 0.020 to 7.0 ($\times 10^9$) and 0.42 to ~3800, respectively.

The $\delta^{13}\text{C}$ -CO₂/³He systematics of the xenoliths fall on a 2-component mixing line where the low CO₂/³He endmember is $\sim 3 \times 10^8$, significantly lower than the DMM value ($\sim 2 \times 10^9$). This low ratio is consistent with low-end estimates of DMM and the mean CO₂/³He ratio of E-chondrite [1]. Thus, our new data are consistent with enrichment of the SCLM by CO₂-rich mantle fluids with CO₂/³He ratios $\gg 3 \times 10^8$ and $\delta^{13}\text{C} \sim 0\text{‰}$ - characteristics of recycled C from subducted carbonatitic material. Such CO₂ enrichments are also associated with positive $\delta^{15}\text{N}$ values reinforcing the link between the metasomatic fluid and subduction. Notably, xenoliths with high ³He/⁴He ratios (Afar) are also associated with $\delta^{15}\text{N} > -5\text{‰}$, implying an important role for the deep-seated Afar mantle plume in supplying recycled volatiles to the SCLM. Oxygen isotope analysis (in prep) will further enable us to constrain the nature of the recycled component.

[1] Marty & Zimmerman (1999) *GCA* **63**, 3619-3633.

Volatile budgets and the late veneer

ALEX N. HALLIDAY^{1*}

¹Department of Earth Sciences, University of Oxford, Oxford, OX1 3AN, U.K. (correspondence: alexh@earth.ox.ac.uk)

The late veneer hypothesis was proposed to explain the budgets of refractory highly siderophile elements (HSEs) in the bulk silicate Earth (BSE) [1], which are too abundant to be in equilibrium with core-forming metallic liquids at low pressures. It was argued that they were added in chondritic proportions after the core formed. It has also been proposed that Earth's volatiles were added as part of this veneer after the Moon forming Giant Impact [e.g. 2]. However, a late veneer does not explain Earth's volatiles. The similarities in moderately siderophile elements [3] and identical isotopic compositions of Si [4] and W [5] in the BSE and Moon provide evidence that terrestrial core formation and accretion were limited following the Giant Impact [6]. For example, a veneer of ordinary chondrites [7] would need to be $<0.3 \pm 0.3\%$ to be consistent with W isotopes [6]. The H/C/N ratios of the BSE (including all surface budgets) are strongly non chondritic. The estimated BSE H/N is 45 whereas carbonaceous chondrites have H/N <15 [8]. If Earth's N was contributed by a CI chondritic veneer, more than 70% of the H would need to be accreted from an additional source [8] requiring that major portions of Earth's volatiles predate any putative chondritic late veneer. Earth's Ne, Ar and Kr are also too abundant to be explained with a chondritic veneer. Cometary ices do have enriched Ar relative to major volatiles [9]. This would explain Earth's heavy noble gases but with amounts that are too small to also explain the H, C and N [8]. A more likely scenario is that after incorporation of early Solar components, Earth acquired most of its volatiles during main stage accretion. This included noble gases, in roughly chondritic proportions, with some fractionation from amorphous ices. A mechanism is required that will also fractionate the BSE's H, C and N from each other, as well as deplete them relative to noble gases. Possibilities for this are losses to space and partitioning into Earth's core before and / or during the Giant Impact [8,10]. However, a volatile rich late veneer does not readily explain the data.

[1] Chou (1978) *Proc.Lun.SciConf.* **9**, 219–230. [2] Albarède (2009) *Nat.* **461**, 1227–1233. [3] Drake *et al* (1989) *GCA* **53**, 2101–2111. [4] Armytage *et al* (2012) *GCA* **77**, 504–514. [5] Touboul *et al* (2007) *Nat.* **450**, 1206–1209. [6] Halliday (2008) *Phil.Trans.R.S.L.* **A366**, 4163–4181. [7] Walker *et al* (2002) *GCA* **66**, 4187–4201. [8] Halliday (2013) *GCA* **105**, 146–171. [9] Stern *et al* (2000) *ApJ* **544**, L169–L172. [10] Hirschmann & Dasgupta (2009) *ChemGeol* **262**, 4–16.

The D/H ratio of the Deep Mantle

L. J. HALLIS^{*1,2}, G. R. HUSS^{1,2}, G. J. TAYLOR^{1,2}, K. NAGASHIMA², S.A. HALLDÓRSSON AND D.R. HITLON

¹University of Hawaii NASA Astrobiology Institute
(*Correspondance: lydh@higp.hawaii.edu)

²Hawai'i Institute of Geophysics and Planetology, University of Hawaii, 1680 East-West Road, Room 503, Honolulu, HI 96822

The ratio of deuterium (²H) to hydrogen (¹H) in the Earth's atmosphere has changed over geological time. The lighter hydrogen isotope (¹H) is preferentially lost to space via Jeans (thermal) escape, hence the atmosphere slowly becomes relatively enriched in deuterium and the ²H/¹H ratio increases. To measure the initial ²H/¹H ratio of the Earth we must sample a reservoir that has been totally isolated from surface processes.

Plate tectonics is known to drag surface water down into the upper mantle, but primitive areas of the lower mantle may be isolated from this circulation, hence uncontaminated by surface hydrogen [1,2]. Certain mantle plumes, such as those that formed the Hawaiian Islands, Iceland, and Baffin Island, appear to have tapped into primitive, un-degassed, deep mantle sources, as evidenced by helium isotope ratios in rock samples from these regions [2,3]. Therefore, ²H/¹H analyses of hydrous melt inclusions from erupted lavas at these sites could give an accurate value for the Earth's primordial water. However, oxygen isotope data suggest that some contamination from crustal material does occur in areas where the crust is thick (e.g., Iceland and Baffin Island) [4]. Therefore, comparisons between oxygen and hydrogen isotope data should be made for samples from these areas.

We are currently measuring the ²H/¹H and ¹⁸O/¹⁶O ratios in pristine olivine melt inclusions and glasses from numerous Icelandic and Baffin Island basaltic units [5,6]. A number of these units contain some of the highest ³He/⁴He ratios currently measured worldwide, indicating a primitive deep mantle origin [2,6]. Others have lower ³He/⁴He ratios. Helium isotope variations will enable us to determine whether samples with higher (more primitive) helium isotope ratios correspond to lower hydrogen isotope ratios.

[1] Williams and Hemley (2001) *Annu. Rev. Earth Planet. Sci.* **29**, 365-418. [2] Jackson *et al* (2010) *Nature* **466**, 853-856. [3] Stuart *et al* (2003) *Nature* **424**, 57-59. [4] Gurenko A. A. and Chaussidon M. (2002) *Earth. Planet. Sci. Lett.* **205**, 63-79. [5] Francis D. (1985) *Contrib Mineral Petrol* **89**, 144-154. [6] Füre *et al* (2010) *Geochim. Cosmochim. Acta* **74**, 3307-3332.

Secular trends in the global ocean revealed through trace elements in sedimentary pyrite

J.A. HALPIN^{1*}, R.R. LARGE¹, L.V. DANYUSHEVSKY¹, V.V. MASLENNIKOV², D. GREGORY¹, T.W. LYONS³ AND E. LOUNEJEVA¹

¹ARC CODES, University of Tasmania, Private Bag 126, Hobart 7001, Australia (*correspondence: jahalpin@utas.edu.au, ross.large@utas.edu.au, l.dan@utas.edu.au, ddg@utas.edu.au, Elena.Lounejeva@utas.edu.au)

²Institute of Mineralogy, Urals Branch, Russia (maslennikov@mineralogy.ru)

³University of California, Riverside, CA, USA (timothy.lyons@ucr.edu)

Sedimentary pyrite incorporates trace elements (TE) during growth at levels far beyond the host bulk rock, making it a potentially powerful proxy for seawater chemistry in the marine rock record. We have developed a novel approach to simultaneously quantify a suite of TE via LA-ICPMS in sedimentary pyrite from marine black shales, as a proxy for chemical changes in palaeo-oceans. When our sedimentary pyrite data is compared with published whole-rock data, we see similar trends. We show that the temporal TE curves for 22 elements in sedimentary pyrite can be related to secular changes on Earth over 3.5 billion years.

The Mo trend increases through time attributed to the significantly lower levels of oxygen in the atmosphere and oceans in the early Earth system [1]. The effects of the Great Oxidation Events are shown by the jumps in Mo at ~2500 Ma and 650 Ma, similar to what is seen in the bulk shale data. The broad Ni and Co trends are the opposite to Mo, attributed to cooling upper mantle temperatures and decreased eruption of komatiitic lavas from ~2700 Ma [2]. Pulses of elevated Ni and Co correspond to episodes of Large Igneous Province eruptions, particularly obvious with the Siberian Traps at the Permian-Triassic boundary. Phanerozoic trends in all TE are far more cyclical. We identify Se as being particularly redox sensitive, which allows us to explore finer-scale fluctuations through the Phanerozoic [3]. As our database expands in both scope and temporal detail, this new approach in measuring TE in sedimentary pyrite has exciting potential for chemical palaeo-ocean research.

[1] Scott *et al* (2008) *Nature* **452**, 456-459. [2] Konhauser *et al* (2009) *Nature* **458**, 750-753. [3] Large *et al* (2013) *Min. Mag.*, this volume.

The oxidation state of uranium in basaltic magmas

H.R. HALSE^{1,2,3*}, A.J. BERRY¹, P.F. SCHOFIELD², J.F.W. MOSSELMANS³, K.O. KVASHNINA⁴ AND G. CIBIN³

¹Department of Earth Science and Engineering, Imperial College London, South Kensington, SW7 2AZ, UK (*correspondence: h.halse10@imperial.ac.uk)

²Department of Earth Sciences, Natural History Museum, London, SW7 5BD, UK

³Diamond Light Source Ltd, Didcot, OX11 0DE, UK

⁴European Synchrotron Radiation Facility, Grenoble, France

Recently erupted mid-ocean ridge basalt (MORB) often exhibits disequilibria between the series of isotopes associated with the radioactive decay of U to Pb. This suggests rates of melt transport that are fast relative to the half-lives of the isotopes that are of anomalous abundance. Current U-series models are based on the assumption that U⁴⁺ is the only oxidation state of U important during the generation, transport, and differentiation of MORB magmas. However, if U⁵⁺ and/or U⁶⁺ were stable in the melt, then the chemical behaviour of U relative to Th⁴⁺ (and the other elements of the decay series) would vary significantly.

High resolution U M₄-edge X-ray absorption near edge structure (XANES) spectra were recorded for synthetic MORB and anorthite-diopside eutectic compositions glasses containing 0.5 wt % U₃O₈. Glasses were quenched from melts equilibrated at 1400 °C and a range of oxygen fugacities (*f*O₂) at one-atmosphere. The spectra were recorded in fluorescence mode at beamline ID26 of the European Synchrotron Radiation Facility, which allows U M₄-edge spectra to be acquired with an energy resolution that is not accessible at most synchrotron facilities. In addition, U L₃-edge XANES spectra were recorded for the same melt compositions *in situ* at magmatic temperatures at beamlines I18 and B18 of the Diamond Light Source.

The L₃- and M₄-edge spectra both vary systematically with *f*O₂. The M₄ spectra exhibit more complexity than the L₃ spectra and allow U⁵⁺ to be unambiguously identified as a major component in both glass compositions, and U redox ratios to be quantified. The proportions of U⁴⁺, U⁵⁺, and U⁶⁺ vary systematically in the glasses. U⁵⁺ is a significant oxidation state at the *f*O₂ conditions of MORB generation, with U⁵⁺/ΣU (where ΣU = U⁴⁺ + U⁵⁺ + U⁶⁺) varying from ~0.25 at the QFM (quartz-fayalite-magnetite) *f*O₂ buffer to ~0.1 at IW (iron-wüstite) +2.

A multi-proxy record from a late Neoproterozoic volcano-sedimentary basin, eastern Arabian Shield

GALEN P. HALVERSON¹, GRANT M. COX¹,
LUCIE HUBERT-THÉOU¹, MARK SCHMITZ²,
JAMES W. HAGADORN³, PETER JOHNSON⁴,
PIERRE SANSJOFRE¹, AND MARCUS KUNZMANN¹

¹Dept. of Earth & Planetary Sciences, McGill University, 3450 University St., Montreal QC, H3A0E8, CANADA.
(galen.halverson@mcgill.ca)

²Dept. of Geosciences, Boise State University, Boise, ID 83725, U.S.A.

³Dept. of Earth Sciences, Denver Museum of Nature and Science, 2001 Colorado Blvd., Denver, CO 80205, U.S.A

⁴6016 SW Haines St., Portland, OR 97219, U.S.A.

Small, middle to late Ediacaran intermontane basins occur in the northern and eastern Arabian shield. The Jibalah basins are a subset of these basins that are minimally deformed and concentrated along the Najd strike-slip fault system, where they likely originated as pull-apart basins during the late stages of the East African orogeny. Whereas the Jibalah basins all appear to share similar sedimentary basin evolution and are broadly the same age, the nature of the basin fill is highly variable. The 10x50 km Jifn Basin, along the northwestern extent of the Halaban-Zarghat Fault Zone, has a carbonate-rich sedimentary succession that was deposited between ~635 and 577 Ma. This succession includes a 340 m-thick shoaling upward section of mixed cherty limestone and dolostone, which overlies a basal, volcanoclastic conglomerate and in turn is overlain by a thick interval of medium- to coarse-grained arkosic sandstone. The carbonates are dominantly gravity flow deposits, transitioning upward into grainstones and heavily silicified microbial laminites—a facies that supplied many of the clasts to the deeper water gravity flow deposits. Felsic tuffs and tuffaceous siltstones, as much as 10 m-thick, occur throughout the succession. In several cases, these are directly overlain by a distinct sequence of organic-rich laminites, followed by rhythmites containing unusual, bubble-like (methane?) structures, and disrupted beds with evidence for fluid escape. We interpret the succession to record eutrophication of the water column following plinian volcanic eruptions. Here we report inorganic and organic C, O, S, and Sr isotopes, along with major and trace element abundances for the Jifn carbonates. We apply these proxies to evaluate the geochemical response in this small basin to massive input of volcanic material and to test its connection to the global ocean at a time of monumental environmental and biological change.

The ortho-para ratio of H₂O desorbed from ice: Implications for cometary coma

T. HAMA*, A. KOUCHI AND N. WATANABE

Inst. Low Temp. Sci., Hokkaido Univ., Japan
(hama@lowtem.hokudai.ac.jp)

H₂O contains two protons with nuclear spin of $I=1/2$, leading to two nuclear-spin isomers: the ortho ($I=1$, triplet, parallel nuclear spin) and the para ($I=0$, singlet, antiparallel nuclear spin) with statistical weights of 3 :1. The lowest energy level of ortho-H₂O lies about 34 K above the lowest para-level in the gas phase. Nuclear-spin temperature (T_{spin}) is defined by a given ortho-para ratio (OPR), because the OPR depends on temperature in local thermodynamic equilibrium. T_{spin} of H₂O has been observed in comet coma, and it has been derived to be ~30 K. Although the T_{spin} values have been implicated as a temperature of cold grains at molecular condensation or formation in a molecular cloud, or in the solar nebula, the correlation between T_{spin} and temperatures of ice at condensation, formation, and desorption is yet to be investigated. The present study measured the T_{spin} of H₂O that was thermally desorbed from amorphous solid water (ASW) at the desorption temperature for cometary water ices, 150 K. The ASW samples were prepared at 8 K by several procedures in an ultra-high vacuum chamber: H₂O-vapor-deposited ASW and ASW produced by photolysis of CH₄/O₂ mixed solid. The sample solids were then heated to 150 K and the thermally desorbed H₂O molecules were analyzed rovibrationally. Desorbed H₂O molecules from all ice samples were found to show T_{spin} almost at the statistical high-temperature limit, indicating that T_{spin} of gaseous H₂O molecules thermally desorbed from ice does not reflect the surface temperature at which H₂O molecules condense or form under laboratory conditions.

[1] Hama, T. *et al.*, (2011) *ApJ*, **738**, L15 (5pp).

IR spectra of thin film water sandwiched between two mineral plates

M. HAMAMOTO*, M. KATSURA AND S. NAKASHIMA

Department of Earth and Space Science, Osaka University,
Toyonaka, 560-0043, Japan (*correspondence:
mhamamoto@ess.sci.osaka-u.ac.jp)

Physicochemical behaviours of water sandwiched between minerals are important to understand water-rock interactions including rock quality degradation by water. In order to examine these properties, pure water sandwiched between two mineral plates was measured by transmission infrared (IR) microspectroscopy.

Pure water is sandwiched between two mineral plates (Fig.1) and its thickness is monitored by the absorbance at 1643.5 cm^{-1} . The measurement area ($100\times 100\text{ }\mu\text{m}^2$) is selected to be occupied totally with water. This procedure is repeated to obtain IR transmission spectra for different pure water thicknesses.

The measured spectra include effects of reflection at air/plate/water interfaces. These effects were removed and the absorption index k was calculated.

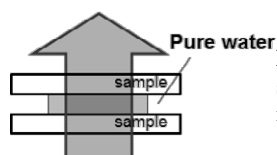


Figure 1 Pure water sandwiched between two mineral plates.

The extracted k spectra of thin film water sandwiched between two CaF_2 plates for different thicknesses from 20 nm to 1 μm were successfully obtained with high signal to noise ratio (Fig.2). These spectra match globally the k spectrum for different thicknesses within 5%. The k spectra of thin film water between different mineral plates such as Al_2O_3 and SiO_2 plates will be measured and compared.

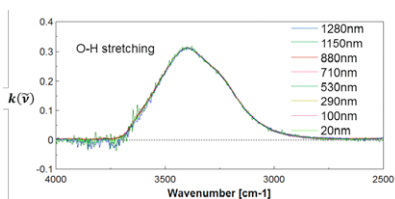


Figure 2 The absorption index k spectra of pure water with different thicknesses between two CaF_2 plates.

The sub-Arctic upper mantle, from Jan Mayen to Molloy Fracture Zone

CEDRIC HAMELIN¹ AND ROLF BIRGER PEDERSEN¹

¹Centre for Geobiology, University of Bergen, Postboks 7800,
NO-5020 Bergen, Norway.

In recent years, sub-kilometer scale studies have revealed that regional mantle heterogeneity is generally better preserved in oceanic basalts where the melt supply is low. The Mohns and Knipovich ridges in the Norwegian Greenland Sea are among the slowest spreading mid-ocean ridges (15-17mm/yr) and present extremely low melting rates. This region is therefore a favorable location to study the different scales of geochemical mantle heterogeneity.

We present new Sr, Nd, Pb and Hf isotopic data from samples collected along Mohns and Knipovich ridges, during 4 different cruises of the SUBMAR program (1999-2004). Our new dataset (≈ 90 samples) together with published data (60 samples), represent a dense sampling of the sub-Arctic upper mantle and allow us to look at regional variations as well as fine-scale, intra-segment, heterogeneity. A first order observation of geochemical variations along the ridge axis is a progressively decreasing influence of the Jan Mayen hotspot (71°N) toward the north (73°N). The rather large geochemical variations measured in samples from the northern part of Mohns ridge ($73-75^\circ\text{N}$) and along Knipovich ridge ($75-78^\circ\text{N}$), are unlikely related to hotspot-ridge interaction. The local upper mantle is influenced by the recent continental breakup and the presence of residual subcontinental lithosphere could therefore contribute to the observed geochemical variability.

Previous study of this region have documented an atypical radiogenic ϵHf values for a given ϵNd [1], which appears to be very comparable to the mantle signature discovered recently along the Mid-Atlantic Ridge near the Azores [2]. The origin of this mantle component is still a matter of debate. Our new dataset, together with published data from [1] is used to produce a detailed petrogenetic model for basalts erupted north of Jan Mayen and brings new constraints on the structure and nature of upper mantle components present in this area.

[1] Blichert-Toft, J. *et al*, 2005. *Geochem. Geophys. Geosyst.*, 6(1): Q01E19. [2] Hamelin, C. *et al*, 2013. *Chemical Geology*, 341(0): 128-139.

Laser $^{40}\text{Ar}/^{39}\text{Ar}$ dating of supervolcanoes and super gold deposits along the trace of the Miocene Yellowstone Hotspot

W. HAMES^{1*}, M. BRUESEKE² AND J. SAUNDERS¹

¹Geology, Auburn Univ., Auburn, AL 36849, USA;

²Geology, Kansas State Univ., Manhattan, KS, 66506, USA.

Early volcanism of the Yellowstone hotspot began at ca. 16.5 Ma and produced abundant and extensive bimodal volcanics in northern Nevada and adjacent portions of Idaho and Utah along with some of earth's richest gold deposits. Within eruptive centers studied, volcanism tended to occur over a ~1.5 Ma interval. Tholeiitic flood basalts in this region, that are typical of the earliest Columbia River Large Igneous Province (LIP) lavas, are typically the earliest volcanics, though they were extruded in multiple events that overlap rhyolitic magmatism. Although coarse plagioclase phenocrysts are conspicuously abundant in these basalts, they tend to be low in potassium content and have high amounts of inherited, extraneous argon, such that the most robust age dating results are for laser incremental heating of the basalt's phenocryst-free, subophitic matrix. Single crystal laser fusion ages of sanidine from the rhyolites are very precise, with some samples that yield a distribution of ages with a single mode that is consistent with analytical uncertainty. However, sanidine from rhyolites in some eruptive centers yield more complex distributions of ages that are less than ~16.5 Ma, but that range beyond analytical uncertainty and comprise multiple age modes. Single crystal incremental heating analysis of sanidines from these more complex samples tend to result in release spectra with plateau and indicate the samples are not affected by extraneous, non-atmospheric argon. We interpret that the duration of magmatism and high geothermal gradients locally promoted isotopic closure at different times, in sanidine crystals of differing size and effective diffusion dimension. Adularia is associated with gold in many of the epithermal Au-Ag deposits and ores, and is commonly of sufficient grain size to permit single crystal dating. $^{40}\text{Ar}/^{39}\text{Ar}$ fusion and plateau ages for adularia from many deposits in northern Nevada produce age distributions that are the same as the bimodal volcanics, however adularia from the Silver City district (southern Idaho) and associated Au-Ag deposits formed in one brief episode ~ 1 Ma after the earliest 16.5 Ma volcanics. In contrast with earlier models that invoke shallow crustal sources, the gold in these deposits is interpreted to have originated from a deep lithospheric or mantle source, and to have been transported by fluids to the epithermal systems as colloids.

Sensitivity boost for ICP-MS to enhance isotope ratio determinations

MEIKE HAMESTER^{1*} AND RENÉ CHEMNITZER¹

¹Bruker Daltonik GmbH, Fahrenheitstr. 4, 28359 Bremen, Germany (*correspondence: meike.hamester@bruker.com)

ICP-MS is a powerful technique for the determination of trace elements in various matrices. Beyond that ICP-MS is able to determine isotope ratios with high accuracy and precision. In principle three instrumental ICP-MS solutions exist: Quadrupole based ICP-MS, single collector magnetic sector field ICP-MS and multicollector magnetic sector field ICP-MS. General assumption is that precision and accuracy for isotope ratio measurements increases with complexity of technology used. The work will describe the achievements in isotope ratio analysis by a new quadrupole based ICP-MS (Bruker aurora Elite). Key characteristic is a very high ion transmission achieved by an optimized interface, and a unique ion optical system with low chromatic and spherical aberrations, which focuses ions into one focal point. In result sensitivities of up to 4 Mio cps / ppb can be obtained, which exceeds sensitivities of magnetic sector field ICP-MS significantly. The high sensitivity attainable allows utilization of the fast scanspeed and short integration times (0.1 msec) without the limitation due to counting statistic.

The presentation will discuss all relevant instrumental characteristics, such as:

- Abundance sensitivity
- Scan speed
- Ion detection system
- Plasma robustness

which are important to obtain highest isotope ratio precision and accuracy.

Finally results accomplished for e.g. lead and uranium isotope ratios and lead / uranium ratios will be shown.

2-Methyl hopanoid production and anoxygenic photosynthesis: A model cyanobacteria isolated from a proterozoic ocean analog

T.L. HAMILTON¹, L.M. BIRD¹, K.H. FREEMAN¹
AND J.L. MACALADY¹

¹Department of Geosciences and Penn State Astrobiology Research Center (PSARC), University Park, PA 16802 USA (*correspondence tlh42@psu.edu)

Biomarkers recovered from ancient rocks provide invaluable tools to reconstruct early Earth microbial ecosystems as well as providing clues about planetary redox evolution. Bacteriohopanepolyols (BHPs) or hopanoids are membrane lipids produced by many bacteria and are among the most abundant and extractable organic compounds in ancient sedimentary rocks. Cyanobacteria are responsible for oxygenation of the atmosphere and examining their presence in the rock record with specific biomarkers such as 2-methyl BHPs can provide key clues regarding the rise of oxygen on early Earth. However, the lack of a model cyanobacterium capable of producing 2-MeBHPs as well as observations that other bacteria also produce these lipids has hindered our understanding of these biosignatures in ancient rocks. Here we demonstrate hopanoid production and anoxygenic photosynthesis in a cyanobacterium isolated from a Proterozoic ocean analog. We isolated a cyanobacterium that produces 2-MeBHPs from a red phototrophic mat in Little Salt Spring, a karst sinkhole in Florida with low levels of both dissolved oxygen and sulfide. The hopanol content of the phototrophic mat is high and rich in 2-methyl structures which are preserved in the organic-rich bottom sediments. Furthermore, we found the cyanobacterium is capable of primary productivity by anoxygenic photosynthesis. The isolation of a cyanobacteria from an environment with a Proterozoic-ocean chemical composition that produces 2-MeBHPs and is capable of anoxygenic photosynthesis will greatly improve our understanding of the role of hopanoids in microbial physiology and ecology as well as the deposition of these biomarkers in the rock record.

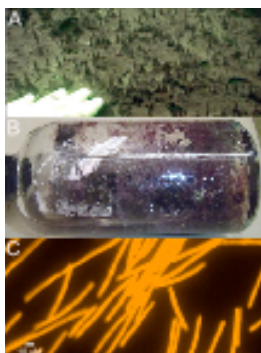


Figure 1. A. Microbial biofilm collected from Little Salt Spring at 9 m water depth at sediment-water interface, human hand for scale. B. Culture bottle incubated *in situ* in the Little Salt Spring water column after inoculation with microbial biofilm from the sediment-water interface. C. Autofluorescence of cells due to the presence of phycoerythrin.

Oxygen Minimum-Zone-like conditions from the Early Cambrian of Chengjiang, South China

E.U. HAMMARLUND^{1*}, R.R. GAINES², CHANGSHI QI³,
AND D.E. CANFIELD¹

¹Nordic Center for Earth Evolution (NordCEE) and Institute of Biology, University of Southern Denmark, 5230 Odense M, Denmark (*corr: emma@biology.sdu.dk)

²Geology Department, Pomona College, Claremont CA 91711, USA

³Yunnan Key Laboratory for Palaeobiology, Yunnan University, Kunming 650091, China

The Cambrian explosion occurred between increases in atmospheric oxygen concentration in the later Neoproterozoic Eon [1, 2] and during the Paleozoic Era [3, 4]. To further constrain chemical conditions in the Early Cambrian ocean, a multi-proxy geochemical approach was applied to two new drill cores through a portion of the Early Cambrian succession of Yunnan, South China. Our results reveal a transition in local ocean chemistry that is captured in both cores. Sulfidic conditions, which were well developed in the lower Yu'an-shan Formation (members 1-2), pass through a transitional interval into oxic conditions in the upper part of the Formation (member 4). In member 3, the interval bearing exceptionally-preserved fossils of the Chengjiang biota (~520 Ma), a prominent positive nitrogen isotope excursion occurs in both cores. This $\delta^{15}\text{N}$ excursion is noteworthy because it is indicative of extensive denitrification under oxygen-depleted conditions, and suggests that modern oxygen minimum-zone-like conditions were present. Results from Chengjiang suggest that the Cambrian radiation of the animals occurred in a relatively thin layer of shallow oxic waters that was sharply separated from toxic deep waters.

[1] Fike, *et al* 2006. *Nature* **444**, 744-747. [2] Canfield *et al*, 2007. *Science* **315**, 92-95. [3] Bergman *et al*, 2004. *Am. J. Sci.* **304**, 397-437. [4] Dahl *et al*, 2010. *PNAS* **107**, 17911-17915.

Plant establishment in sulfide ore-derived mine tailings stabilizes arsenic *in situ* despite promoting arsenopyrite oxidation

C. M. HAMMOND*, R. A. ROOT, R. M. MAIER
AND J. CHOROVER

University of Arizona, Tucson, AZ 85721, USA
(*correspondance: schowalt@email.arizona.edu)

A compost-assisted phytostabilization strategy at the Iron King Mine tailings in Arizona, USA aims to establish a self-sustaining vegetative cover as a low cost option to reduce human exposure to metal(loid) contaminants. Plant growth on contaminated land reduces dispersion of particulate matter caused by erosion, but less is known regarding the effect of phytostabilization on subsurface metal(loid) speciation and lability. Biogeochemical mechanisms controlling arsenic speciation and lability were examined in a three year 1.5 ha field trial in which dairy compost and irrigation water were added to aid plant growth. Bench-scale chemical analyses were combined with synchrotron-based X-ray spectroscopic methods applied as a function of time, depth and specific treatment. Arsenic and iron K-edge X-ray absorption near-edge structure (XANES) of untreated samples show oxidation of pyritic [FeS₂, FeAsS] minerals to ferric (oxy)hydroxide [e.g. ferrihydrite] and (oxy)hydroxide sulfates [e.g. jarosite-type minerals; XFe^(III)₃(OH)₆(SO₄)₂, where X = K⁺, H₃O⁺, Pb²⁺] in near-surface tailings, indicating an oxidation front penetrating the profile. Arsenic XANES indicate that both irrigation and compost are associated with enhancement of sulfide oxidative weathering (Figure). Importantly, an increase in As lability related to compost addition has not been observed. Sequential chemical extraction and Fe XAS results indicate that sulfide weathering may be associated with formation of an ammonium oxalate-resistant Fe mineral phase, affecting the mobility of Fe-sorbed As in the tailings.

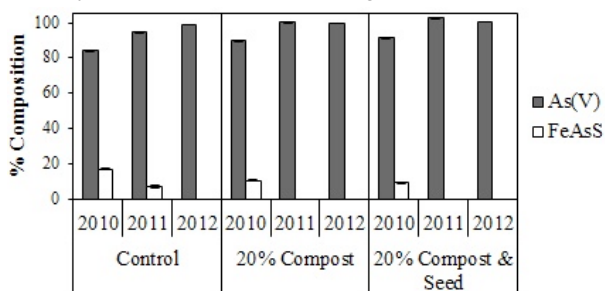


Figure 1. As K α XANES linear combination fits of amended and control field samples, fit with arsenopyrite and 2-line ferrihydrite. The binary fits, not normalized to unity, account for 99-102% of the spectral features.

Major melting on EL enstatite chondrite parent body

T. HAMMOUDA^{123*}, M. BOYET¹²³, B. MOINE²³⁴,
C. CARTIER¹²³ AND J.L. DEVIDAL¹²³

¹Université Blaise Pascal, Laboratoire Magmas et Volcans, BP 10448, F-16 63000 Clermont-Ferrand, France

(*correspondence:

t.hammoda@opgc.univ-bpclermont.fr)

²CNRS, UMR 6524, LMV, F-63038 Clermont-Ferrand, France

³IRD, R 163, LMV, F-63038 Clermont-Ferrand, France

⁴Laboratoire Magmas et Volcans, UMR CNRS 6524, Université Jean Monnet, 23 rue du Dr P. Michelon, F42023 23 SAINT-ETIENNE, CEDEX 02, FRANCE

Chondrites are amongst the most primitive objects of the solar system. Their constitutive chondrules represent either condensates, or interstellar dust that was once molten and quenched. Overall, chondrites are undifferentiated rocks that did not experience core separation associated with planetary formation. Some groups of chondrite are considered to represent building blocks at the origin of planets, including the Earth. Here we show that one group of enstatite chondrites (EL) bears evidence for large scale melting, yet showing little (if any) sign of differentiation. We have compared the two enstatite chondrite groups (EH and EL). Differences between EH and EL subtypes regarding both their bulk major element compositions as well as their mineralogy have long been recognized [1,2]. Here, we used in-situ, laser ablation inductively coupled plasma mass spectrometry (LA-ICP-MS) analyses of minerals present in both enstatite chondrite subtypes (enstatite, and the two sulfides troilite (FeS) and oldhamite (CaS)). We show that each subgroup possesses a unique signature. EH chondrite trace element patterns are compatible with condensation signature, followed by equilibration during metamorphism from type 3 to type 5. They may thus be considered as primitive. On the contrary, EL chondrite patterns are suggestive of equilibrium during large scale melting on their parent body. They may therefore evidence melting processes that would yet essentially preserve the undifferentiated nature of their parent body, except in equilibrated types (EL5-6) wherein slight melt depletion is observed. Timescales for this melting should be long enough to allow for melt / crystal equilibration, but short enough to prevent metal / silicate separation. Alternatively, melting may have occurred in a low gravity field, either a small planetary body, or a molten disk following the collision of two large objects.

[1] Keil (1968), *J. Geophys. Res.* 73, 6945-6976. [2] Wasson & Keileynen (1988), *Phil. Trans. R. Soc. Lond. A* 325, 535-544.

Noble gas isotope studies of Ningwu Ore District, Middle-Lower Yangtze River polymetallic ore belt, East China

DAN HAN¹, CHAO DUAN¹ AND YAN-HE LI¹

¹MRL Key Laboratory of Metallogeny and Mineral Assessment, Institute of Mineral Resources, Chinese Academy of Geological Sciences, Beijing, China, 100037

Different causes, such as the atmosphere, the Earth's crust, mantle and sources of abundance and of the noble gas isotopic composition is significantly different. Typical ratio of helium in the Earth's crust $^3\text{He}/^4\text{He}$ is 10^{-8} , $^3\text{He}/^4\text{He}$ value of 10^{-5} of mantle helium, difference of nearly 1000 times.

So helium argon and other noble gas isotope has become a research of crust-mantle interaction, the tracer mantle fluid mineralization and different ore-forming fluid mixed effective means and the most sensitive tracer.

In this study, the concentration and isotopic compositions of noble gases were measured in pyrite and magnetite phenocrysts of 11 iron ore from Ningwu ore district Gaocun and Dongshan, $^3\text{He} / ^4\text{He}$ ratio is $1 \text{ Ra} \sim 0.04 \text{ Ra}$, $^3\text{He} / ^4\text{He}$ ratio of air 1.4×10^{-6} . The He isotopic study shows, the environment of different $^3\text{He}/^4\text{He}$ ratio, showed there was no With the same degree of deep fluid. Typical characteristics can be seen as the mantle fluid.

Model-predicted and satellite-retrieved tropospheric NO₂ columns over East Asia

KYUNG M. HAN, CHUL H. SONG* AND SOJIN LEE

School of Environmental Science and Engineering, Gwangju Institute of Science and Technology (GIST), Gwangju, 500-712, Korea
(kmhan@gist.ac.kr; *correspondence: chsong@gist.ac.kr)

In this study, we attempted to evaluate NO_x emission fluxes over East Asia for the year of 2006, using CMAQ-predicted and OMI-retrieved tropospheric NO₂ columns. The two retrieved OMI products were taken from the Level-2 DOMINO product version 2 (using KNMI algorithm) and from the Level-2 OMNO2 product version 2.1 (using NASA algorithm). The two OMI products were well correlated (R=0.98 over Central East China). Also, averaging kernels (AKs) taken from each OMI product were applied to the CMAQ-predicted NO₂ columns (Ω_{CMAQ}) for the comparison analysis. The applied AK_{KNMI} (i.e. AK retrieved from the KNMI algorithm) to the Ω_{CMAQ} showed seasonally good correlations with the $\Omega_{\text{OMI,KNMI}}$ (R=0.75, slope=0.92). However, the Ω_{CMAQ} with the AK_{NASA} showed larger values than the $\Omega_{\text{OMI,NASA}}$ from the OMI observations despite of good correlation coefficient (R=0.75) because the AK_{NASA} are vertically even larger by factors of approximate 2 – 10 than AK_{KNMI} over Central East China (CEC). The differences between the Ω_{CMAQ} and Ω_{OMI} using the NASA algorithm were much larger than those using the KNMI algorithm during the winter episodes, whereas the differences were smaller using the NASA algorithm than those using the KNMI algorithm. In addition, this study investigated the large discrepancies between CMAQ-predicted and OMI-retrieved NO₂ columns during the winter episodes in terms of the seasonal variations of NO_x source and heterogeneous NO_x sink. First, the seasonal variation of the NO_x emissions influenced greatly in the tropospheric NO₂ columns. For example, when non-seasonal factors were applied to the CMAQ model simulation, the $\Omega_{\text{NO}_2,\text{CMAQ}}$ decreased by 38% over CEC regions during winter, compared to those from the our baseline simulation. For the latter, four parameterizations of gamma N₂O₅ were applied to the separate CMAQ model simulations during the cold seasons.

Hf isotope evidence for continental lithosphere pollution of the Asthenosphere near the Oceanographer Fracture Zone

B. HANAN^{1*}, L. DOSSO², K. SAYIT¹, S. SHIREY³
AND J. BENDER⁴

¹San Diego State University, San Diego, CA 92182-1020,

USA (*correspondence: Barry.Hanan@sdsu.edu)

²CNRS, IUEM, Ifremer, Plouzané 29280, France

³Carnegie Institution, DTM, Washington, DC 20015, USA

⁴University of North Carolina, Charlotte, NC 28223

Pb, Sr, and isotope data from a suite of basalts from ~35°, ~0-10 miles north of the Oceanographer Transform (OFZ) are interpreted as mixing between three chemically distinct mantle sources [1]. The transform offsets the ridge right-laterally by 130 km and lies within the geochemical gradient attributed to dispersion of the Azores plume and mixing with the depleted upper mantle MORB source [2]. The third mantle component's isotope and geochemical characteristics suggest that portions of the mantle in the region contain detached fragments of ancient sub-continental lithosphere. We have analyzed a subset of the the samples previously analyzed for Pb, Sr, and Nd [1] for Hf isotopes and high precision Pb isotopes.

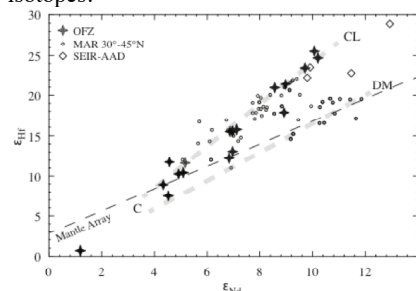


Figure 1: New Hf isotope data for the OFZ region. Also shown are published data [3-5] for the MAR and ultra-depleted MORB from

the Southeast Indian Ridge-AAD Pacific-Indian mantle boundary.

Bifurcating trends bound the data and require at least 3 mantle components. An enriched C-like (low ϵ_{Nd} and ϵ_{Hf}), common to both trends, and two depleted components, one DM like (high ϵ_{Nd} and intermediate ϵ_{Hf}), the other (very high ϵ_{Hf}) similar to ultra-depleted MORB from the AAD, where the upper mantle is contaminated by continental material entrained during Gondwana rifting. The new OFZ Hf isotope data confirm the Pb and Nd isotope results [1] indicating pollution of the upper mantle MORB source by material derived from the continental lithosphere mantle, also advocated for the Azores plume [6]. This suggests that during plume-lithosphere interaction and rifting, accompanying the early opening of the Atlantic Ocean Basin, fragments of refractory continental lithosphere mantle were incorporated into the OFZ MORB source.

[1] Shirey *et al* (1987) *Nature***325** 217-223 [2] Schilling (1975) *EPSL***25** 103-115 [3] Agranier *et al* (2005) *EPSL***238** 96-109 [4] Debaille *et al* (2006) *EPSL***241** 844-862 [5] Hamelin *et al* (2013) *ChemGeol***341** 128-139 [6] Widom *et al* (1997) *ChemGeol***140** 49-68.

Novel approaches to reconstructing sulfur cycling in methane seeps

L.G. HANCOCK^{1*}, T.W. LYONS¹, B.C. GILL²,
R.S. SHAPIRO³ AND S.M. BATES¹

¹University of California Riverside, Riverside, CA, 92521
(*correspondence: lhanc001@ucr.edu)

²Virginia Polytechnic Institute and State University,
Blacksburg, VA, 24061

³Chico State University, Chico, CA, 95929

Methane ranks among the key greenhouse gases throughout Earth history, particularly under the generally more reducing conditions of the Precambrian. The mechanisms of methane cycling have been studied extensively, but a complete understanding of its role in the chemical and organismal evolution of the ocean through time, including its closely coupled relationship to the sulfur cycle, are still largely unresolved. Modern and ancient seeps provide outstanding natural labs for studying coupled methane-sulfur cycles and their geochemical fingerprints. Many seep studies examine sulfide in pyrite, but pyrite formation in these settings is typically limited by the availability of reactive iron and thus only captures the earliest diagenetic processes. In such cases, a better way to track sulfur and its role in modulating methane production and consumption is by following the pathways of dissolved sulfate, specifically using carbonate-associated sulfate or CAS. This study focuses on modern and ancient seep sites marked by complex carbonate paragenesis and traces sulfur, carbon and oxygen isotopes to unravel ancient methane cycling, its relationship to sulfur metabolic pathways and the preservational history of proxies during early to late burial. Our initial results suggest that coupled isotopic and concentration measurements of CAS may closely track spatiotemporal variation in rates of microbial sulphate reduction as coupled to anaerobic methane oxidation. These rates in ancient settings seem highly variable spatially and temporally, as they are in modern seeps. CAS isotopic relationships also reveal the relative patterns of sulfate reduction and sulfide oxidation, thus providing an essential backdrop for interpreting thiotrophic and methanotrophic symbiosis among the seep-dwelling macrofauna.

Along-arc geochemical and isotopic variations in Javanese volcanic rocks: 'Crustal' versus 'source' contamination at the Sunda arc, Indonesia

HEATHER HANDLEY¹, JANNE BLICHERT-TOFT², SIMON TURNER¹, COLIN MACPHERSON³, RALF GERTISSER⁴

¹GEMOC, Department of Earth and Planetary Sciences, Macquarie University, Sydney, NSW 2109, Australia. (heather.handley@mq.edu.au; simon.turner@mq.edu.au)

²Laboratoire de Géologie de Lyon, Ecole Normale Supérieure de Lyon, 69007 Lyon, France. (jblicher@ens-lyon.fr)

³Department of Earth Sciences, University of Durham, Durham, UK. (colin.macpherson@durham.ac.uk)

⁴School of Physical and Geographical Sciences, Keele University, Keele, ST5 5BG, UK. (r.gertisser@keele.ac.uk)

Through detailed studies of individual magmatic systems it is possible to identify and establish the relative importance and contributions of the various potential source components and differentiation processes that modify magmatic composition, such as crustal contamination. Along-arc changes in lava geochemistry have long been recognised on Java in the Sunda arc, Indonesia, but debate still prevails over the cause of such variations and the relative importance of shallow (crustal) versus deep (subduction) contamination. We present new Pb isotope data for Javanese volcanoes, which, when combined with our recently published geochemical and radiogenic isotopic data of Javanese volcanic rocks and results from other detailed geochemical and isotopic studies, elucidate the potential changing nature of the arc crust and its control on lava chemistry. In $^{207}\text{Pb}/^{204}\text{Pb}$ - $^{206}\text{Pb}/^{204}\text{Pb}$ space the Javanese volcanic data reveal two distinct trends which can be related to either a strong control by crustal assimilation processes or source contamination by local sedimentary material on the down-going plate. Sr isotope ratios of volcanic rocks generally increase from West to Central Java, showing a wide range within individual volcanic centres and broad correlation with inferred crustal thickness, implying a strong, shallow-level control on isotopic composition. However, East Javanese volcanic rocks show significantly lower Sr and Pb isotopic ratios and extremely restricted isotopic variation at individual volcanoes. Key trace element ratios combined with radiogenic isotopic data of Javanese volcanoes reveal three distinct trends, which roughly equate with the geographical boundaries West, Central and East Java. These results provide evidence for major transitions in the crustal architecture of Java.

Oxygen fugacity in the Kaapvaal cratonic lithosphere – Evidence from Fe XANES measurements of Fe³⁺ in garnet from the Kimberley pipe

BRENDAN J. HANGER^{1*}, GREGORY M. YAXLEY¹, ANDREW J. BERRY¹, VADIM S. KAMENETSKY², DAVID PATERSON³ AND DARYL L. HOWARD³

¹Research School of Earth Sciences, The Australian National University, Canberra, ACT, 0200, Australia (*correspondence: brendan.hanger@anu.edu.au)

²ARC Centre of Excellence in Ore Deposits, University of Tasmania, Hobart TAS 7001, Australia

³Australian Synchrotron, Clayton VIC 3168, Australia

Oxygen fugacity is important in understanding the evolution of the cratonic lithosphere, but is more difficult to determine than other variables (e.g. temperature and pressure). It requires precise measurement of Fe³⁺/ΣFe in garnet in peridotite xenoliths which until recently has been practically limited to the bulk technique Mössbauer spectroscopy. However, new highly spatially resolved, *in situ* techniques such as synchrotron-based Fe K-edge XANES [1] or the microprobe-based flank method [2] are enabling precise and rapid determination of garnet Fe³⁺/ΣFe. We have combined XANES measurements with experimental calibrations of oxybarometers applicable to peridotite [3] to determine the oxygen fugacities recorded in suites of garnet peridotite xenoliths from the Kimberley kimberlite, which sampled the Kaapvaal cratonic lithosphere.

The xenoliths examined are relatively fresh. Most contain ilmenite-bearing garnet based upon the CaO-Cr₂O₃ systematics [4], although two contain harzburgitic garnet. Thermobarometry reveals a pressure range of 2.5-4.5 GPa and a temperature range of 880 – 1100 °C. Fe XANES gave garnet Fe³⁺/ΣFe values from 0.04 and 0.07. $\Delta\log f\text{O}_2^{\text{FMQ}}$ varies between -0.46 and -2.40, with most samples falling between -2.0 and -2.4 at pressures from 3.5 to 4.2 GPa. The xenoliths show a general trend of decreasing $\Delta\log f\text{O}_2^{\text{FMQ}}$ with depth, in broad agreement with previous studies [5,6].

[1] Berry *et al* (2010) *Chem. Geol.* **278**, 31-37. [2] Höfer and Brey *Am. Mineral.* **92**, 873-885. [3] Stagno *et al* (2013) *Nature* **493**, 84-88. [4] Grutter *et al* (2004) *Lithos* **77**, 841-857. [5] Woodland and Koch (2003) *EPSL* **214** 295-310. [6] Yaxley *et al* (2012) *Lithos* **140-141** 142-151.

Melt inclusions in mafic-ultramafic potassic volcanic rocks in British Columbia, Canada: A record of the transfer of PGE from mantle to crust in porphyry settings

JACOB J. HANLEY¹ AND ZOLTAN ZAJACZ²

¹Dept. Geology, Saint Mary's University, Halifax, Canada

(*correspondence: jacob.hanley@smu.ca)

²IGP, ETH Zürich, Zürich, Switzerland

Mafic-ultramafic subvolcanic intrusions composed of alkalic basalt are spatially/temporally associated with many alkalic Cu-Au deposits in the Canadian Cordillera that contain resources of platinum-group elements (PGE). In the Afton porphyry deposit, we have investigated melt inclusions preserved within leucite-clinopyroxene-olivine (>Fo₉₀)-rich basalts (18-22 wt% MgO) in order to understand their relationship to porphyry evolution/metal tenor.

Olivine-melt and melt inclusion microthermometry for primary inclusions in growth zones in clinopyroxene primocrysts constrain the liquidus T of the basalt between 1370-1520°C. However more evolved liquids, trapped as secondary inclusions in pyroxene, were likely trapped as low as ~900°C and at low pressure. Shallow depths of emplacement for the basalt sills and dykes are confirmed by pepperite textures indicating interaction of the magma bodies with wet volcanic sediments, sandstones, and mudstones. The Cr content of early melt inclusions (Cr-in-melt oxybarometry[1]), determined by laser ablation ICP-MS, and chromian spinel-olivine oxybarometry indicate that the liquids were relatively oxidized (~FMQ+1.5).

Melt inclusion analysis is essential to characterize the trace element chemistry of the basalts because the intrusions are cumulates containing non-cotectic proportions of olivine and pyroxene, and the groundmass was extensively hydrothermally altered by the adjacent porphyry stock. Early melts are most similar to high Ca-Mg, high K₂O, silica-undersaturated arc ankaramites and their differentiates, formed by partial melting of amphibole or clinopyroxene-rich cumulates in sub-arc lithospheric mantle or lower crust.

Early melt inclusions are highly enriched in PGE, containing up to ~480 ppb Pd and a high Pd/Pt ratio (~10-20), identical to that of porphyry-stage ore in the deposit. The exact mechanism by which this high Pd/Pt was inherited by the porphyry magma (i.e., fractional crystallization, mixing with/contamination by crustal rocks/melts) is being evaluated.

[1] J.Brenan (2012) personal communication

Sr isotope anomalies in meteorites: Uniform distribution of *s*- and *r*-process Sr at the planetary scale

ULRIK HANS¹, THORSTEN KLEINE², CHRISTOPH BURKHARDT¹ AND BERNARD BOURDON³

¹Institute of Geochemistry and Petrology, ETH Zurich, Switzerland (*correspondence ulrik.hans@erdw.ethz.ch)

²Institut für Planetologie, Westfälische Wilhelms-Universität Münster, Germany

³Ecole Normale Supérieure de Lyon, UCBL and CNRS, France

Planetary-scale nucleosynthetic anomalies have been identified for various refractory elements, indicating that the protoplanetary disk was not entirely mixed with respect to stellar sources or that thermal processing of solid material was uneven. In this study we re-address the presence of planetary-scale ⁸⁴Sr/⁸⁶Sr anomalies. Several bulk chondrites, eucrites, angrites as well as Ca-Al-rich inclusions (CAI) from the CV3 chondrite Allende were analyzed using the Thermo Triton TIMS at ETH Zürich in a dynamic acquisition mode. In contrast to static measurements (as used in previous studies [1]) no difference in ⁸⁴Sr/⁸⁶Sr ratios between the NBS987 standard and terrestrial rock standards was found. Furthermore, with the exception of CV and CM chondrites all bulk meteorites show within uncertainty a uniform and terrestrial ⁸⁴Sr/⁸⁶Sr. The anomaly in the CM chondrite could be due to incomplete dissolution of presolar SiC grains, while the anomalies in Allende can be attributed to the high abundance of CAI which show ⁸⁴Sr/⁸⁶Sr anomalies of up to 1.3ε, most likely due to an excess in r-process Sr. Thus, our results do not confirm the planetary-scale Sr isotope heterogeneity reported in an earlier study. Instead they indicate that overall, the Sr isotope composition of the solar nebula prior to planetary accretion was rather homogeneous, which is essential to establish the Rb-Sr chronology of volatile element depletion in the early solar system.

[1] Moynier *et al*, *Astrophys. J.* **758**:45 ,(2012)

Widespread production of extracellular superoxide by heterotrophic bacteria

C.M. HANSEL^{1*}, J.M. DIAZ², B.M. VOELKER³,
P.F. ANDEER¹ AND T. ZHANG¹

¹Marine Chemistry and Geochemistry Department, Woods Hole Oceanographic Institution, Woods Hole, MA 02543, U.S.A. (*correspondance: chansel@whoi.edu)

²Biology Department, Woods Hole Oceanographic Institution, Woods Hole, MA 02543, U.S.A.

³Department of Chemistry and Geochemistry, Colorado School of Mines, Golden, CO 80401, U.S.A.

Superoxide, a reactive oxygen species (ROS), is a powerful and versatile reactant that is toxic to living organisms and can dramatically alter the geochemical landscape through a myriad of redox reactions. (A)biotic reactions that are directly or indirectly coupled to sunlight have been the only recognized sources of environmentally relevant ROS. Phytoplankton, for instance, have previously been shown to produce ROS, yet their abundance and distribution in nature is fundamentally constrained by sunlight. Thus, although ROS production has been frequently observed in the deep ocean and at night, superoxide and other ROS are regarded as pertinent only in sunlit systems, which represent merely ~5% of the habitable environment on Earth.

Here we show that common and abundant heterotrophic bacteria are a vast unrecognized source of ROS. We analyzed extracellular superoxide production by a broad range of ecologically and phylogenetically diverse heterotrophic bacteria using a high sensitivity flow-through chemiluminescence approach. Superoxide production was detected by 27 of 30 environmentally common isolates. Rates of superoxide production normalized to the proportion of metabolically active cells varied a few orders of magnitude, between 0.02 ± 0.02 and 19.4 ± 5.2 amol cell⁻¹ hr⁻¹. Although cell-normalized rates of superoxide production by heterotrophic bacteria are lower than those measured previously for marine phytoplankton, rates normalized to cell surface area are comparable to, and in several cases greater than, those of phytoplankton. Superoxide production by a model bacterium within the ubiquitous *Roseobacter* clade involves an extracellular NADH oxidoreductase, suggesting a surprising homology with eukaryotes.

Our discovery therefore introduces the likelihood of ROS cycling in ~95% of the global habitat that is untouched by light, a paradigm shift which will certainly transform our understanding of the geochemistry, ecology, and health of a wide range of modern and ancient environments.

Venus crustal plateaus as an analog for Archean cratons and SCLM

VICKI L. HANSEN *

Dept. of Geol. Sciences, University of Minnesota, Duluth MN 55812 USA; (*correspondence: vhansen@d.umn.edu)

A hypothesis is presented suggesting that Venus' ancient crustal plateaus and their mantle roots represent analogs for Archean cratons and their underlying subcontinental lithospheric mantle (SCLM). Crustal plateaus (~1500-2500 km diameter) are quasicircular features that rise 0.5-4.0 km above Venus' lowlands, supported by low density isostatic roots, and host a distinctive structural fabric called ribbon-tessera terrain (RTT). RTT also occurs as arcuate-shaped exposures in the lowlands, widely interpreted as 'collapsed' or rootless crustal plateaus. Crustal plateaus and RTT inliers represent Venus' oldest preserved features and surfaces. RTT fabrics and their host crustal plateaus are postulated to have formed as the solidified 'scum' of huge lava ponds, formed by large bolide (>25 km diameter) impacts with ancient thin lithosphere. Bolides pierced the lithosphere, leading to massive partial melting in the upper mantle. Melt rose to form huge surface ponds, burying bolide scars; high-Mg depleted mantle melt residuum formed a robust buoyant root, leading to plateau formation, and long-term stability. The roots of lowland RTT were removed, likely due to mantle convection.

On Earth, Archean cratons comprise granite-greenstone terrains (GGTs) and associated high-Mg SCLM. Like crustal plateaus, GGTs are unique—lacking contemporary analogs—and they have been remarkably stable since formation; thus, they too record ancient geologic processes of their host.

Recent studies indicate that Late Heavy Bombardment (LHB) on Earth lasted through the Archean. Therefore, like Venus, early Earth's thin lithosphere would have been bombarded by numerous large bolides (>25 km), with a likely similar first-order response, resulting in massive partial melting of the mantle, escape of high-Mg melt to the surface (komatiites), and formation of a high-Mg residuum root, which protected the new-formed crustal features from younger planetary processes. GGTs that survived retain their roots; GGTs that lost their roots were likely accreted to stable GGTs or recycled by younger plate tectonic processes. The hypothesis suggests that Venus' crustal plateaus and Earth's GGTs both formed during LHB, when both of these young hot planets had relatively thin lithosphere, and record a unique era in the evolution of these sister planets. Large bolides punctured the thin lithospheres, which were strong enough to support the products of massive mantle partial melt; the high-Mg melt residuum roots protected these unique regions from younger planetary processes on both planets.

Numerical modeling of iron-corrosion and interaction with bentonite

C. HANSMEIER¹, G. BRACKE² AND B. REICHERT³

^{1,2}Department of Final Disposal, GRS mbH, Schwertnergasse 1, 50667 Cologne, Germany,

(¹christina.hansmeier@grs.de, ²guido.bracke@grs.de)

³Steinmann-Institute, Department Hydrogeology, Nussallee 8, 53115 Bonn, Germany, (b.reichert@uni-bonn.de)

In deep geological repositories, bentonite is preferred as a possible Engineered Barrier (EB) to isolate the High Level Waste (HLW) from the biosphere. Over time, the iron canister of the HLW corrodes under anaerobic conditions and interactions between the EB and the corrosion products of the iron canister modify the properties of the bentonite. Besides, formation water in the host rock (Opalinus clay) affects the bentonite, too.

The aim is to calculate changes in porewater chemistry, mineral dissolution and precipitation as well as its effects on permeability and porosity changes on process level to assess the long term behavior. Cation exchange and surface complexation are not considered in this model. The system is modeled as a 1D model for a timescale of 10.000 years. Due to low permeabilities of both bentonite and clay the mass transport entirely takes place by diffusion, leading to small changes of constituents only. Precipitation of corrosion products decreases the porosity of the system. For calculations the code TOUGHREACT [1] is used with PetraSim [2] as user interface. TOUGHREACT adds reactive geochemistry to the multi-phase flow code TOUGH2 [3].

[1] Xu, T., Sonnenthal, E., Spycher, N., Pruess, K.: TOUGHREACT User's Guide: A Simulation Program for Non-isothermal Multiphase reactive Geochemical Transport in Variably Saturated Geologic Media, 2006, LBNL, UC: Berkeley, California, USA. [2] Thunderhead Engineering: PetraSim 5, User Manual, 2005, Manhattan, Kansas, USA. [3] Pruess, K.: TOUGH2: A general purpose numerical simulator for multiphase fluid flow, 1990, LBNL, UC: Berkeley, California, USA.

Large geochemical variations in submarine HIMU basalts

T. HANYU^{1*}, L. DOSSO², O. ISHIZUKA³, K. TANI¹, B.B. HANAN⁴, C. ADAM⁵, S. NAKAI⁶, R. SENDA¹, Q. CHANG¹, AND Y. TATSUMI⁷

¹IFREE, Japan Agency for Marine-Earth Science and Technology, Yokosuka 237-0061, Japan

(*presenting author: hanyut@jamstec.go.jp)

²CNRS, IUEM, Ifremer, Plouzané 29280, France

³Geological Survey of Japan, AIST, Tsukuba 305-8567, Japan

⁴San Diego State University, San Diego CA 92182-1020, USA

⁵Universidade de Évora, Évora 7002-554, Portugal

⁶Earthquake Research Institute, The University of Tokyo, Tokyo 113-0032, Japan

⁷Kobe University, Kobe 657-8501, Japan

We report the geochemical compositions of submarine basalts collected by a manned submersible from Rurutu, Tubuai, and Raivavae in the Austral Islands, French Polynesia, where subaerial basalts exhibit robust HIMU isotopic signatures. The ⁴⁰Ar/³⁹Ar ages of the submarine basalts overlap with those of the subaerial basalts with the exception of one sample from Tubuai. While the major element compositions are similar between the submarine and subaerial basalts for each island, the submarine basalts exhibit much larger variations in Pb, Sr, Nd, and Hf isotopic compositions than those previously reported in subaerial basalts. The submarine basalts with less-radiogenic Pb isotopes show systematically lower abundances in highly incompatible elements than the basalts with radiogenic Pb isotopes. The overall geochemical variations are best explained by a two-component mixing between the melt derived from the HIMU reservoir on one hand and the melt from the depleted asthenospheric mantle entrained by an upwelling plume on the other. The present and compiled data demonstrate that the HIMU reservoir has uniquely low ¹⁷⁶Hf/¹⁷⁷Hf for a given ¹⁴³Nd/¹⁴⁴Nd, suggesting it being formed by subduction of an ancient slab. Moreover, the Nd/Hf ratios of the HIMU basalts, together with the curvilinear aspect of the ¹⁴³Nd/¹⁴⁴Nd–¹⁷⁶Hf/¹⁷⁷Hf mixing trend, suggest higher Nd/Hf for the HIMU reservoir than for the depleted mantle component. Such elevated Nd/Hf of the HIMU reservoir could reflect metasomatic enrichment processes of the mantle by a partial melt derived from subducted material during reservoir formation.

Impact of phenanthrene on the formation of microbial habitats in soil

J. HANZEL* AND K. U. TOTSCHKE

Chair of Hydrogeology, Institute for Geosciences, Friedrich Schiller University Jena, Burgweg 11, 07749 Jena, Germany (*correspondence: joanna.hanzel@uni-jena.de)

Recent studies reveal that there is a strong interplay between the physical soil structure and the activity of soil microorganisms [1, 2, 3]. Yet, a quantitative understanding of this feedback loop and their consequences for the soil functions remain speculative. Two-layer soil columns packed with soil material and spiked with phenanthrene in its upper layer will be used after forced-gradient transport experiment has been performed. Thin sections prepared from soil aggregates taken from different depths of the column will be analyzed to examine the impact of phenanthrene on the formation of microbial growth habitats in soil. Epifluorescent microscopy will be applied to identify growth habits of DAPI-stained cells of soil microorganisms and to determine their abundance and spatial distribution in the soil column. The microbial habitats will be examined by scanning electron microscope (SEM) and the results will be compared with the data obtained from non-spiked controls, where soil interfaces will be characterize to elucidate how the activity of phenanthrene degrading soil microorganisms alters the physicochemical soil properties. Such knowledge will contribute to a mechanistic understanding of the interactions between soil structure, habitat and microbial activity and may ultimately help to better understand soil formation and the functions of a soil.

[1] Young and Crawford (1994) *Science* **304**, 1634-1637. [2] Crawford *et al* (2012) *J R Soc Interface*, doi: 10.1097/rsif.2011.0669. [3] Hanzel and Totsche, submitted.

Alkenone record of the 19 years long time-series sediment trap samples collected at central subarctic North Pacific and Bering Sea

NAOMI HARADA^{1*}, KOZO TAKAHASHI², MIYAKO SATO¹, JONAOTARO ONODERA¹, HIROJI ONISHI³

¹Japan Agency for Marine-Earth Science and Technology (JAMSTEC), Yokosuka, Japan,

(*Correspondence: haradan@jamstec.go.jp)

²Hokusei Gakuen University, Japan

³Hokkaido University, Japan

The subarctic North Pacific including the Bering Sea is the area that efficient biological pump works [1]. According to the global compilation of sediment trap experiment [2], the subarctic North Pacific including the Bering Sea represents that biogenic opal/CaCO₃ ratios of settling particles is the highest in the world. The time-series observation of settling particles is valuable to understand the changes in the function of subarctic biological pump associated with climate changes. Thus, to understand characteristics of primary fluxes of biogenic particles, plankton assemblages and to detect the environmental variation and changes in low trophic level ecosystem associated with current climate changes, settling particulate samples were collected for 19 years by sediment trap mooring system at St. SA (49°N, 174°W, water depth 5406m) in the central subarctic North Pacific and at St. AB (53°30'N, 177°W, water depth 3788m) in the central Bering Sea from 1990 to 2010 [3]. The diatom and radiolaria having opal test were predominant components throughout the 19 years at both stations. The CaCO₃ was the secondly dominant component of settling particles [3]. The CaCO₃ was composed of calcareous nannoplanktons and micro zooplankton. *Coccolithus pelagicus* and *Eminiania huxleyi* were two major species. The relative abundance of *C. pelagicus* and *E. huxleyi* were average 55% and 42% to the total calcareous nannoplanktons [4]. Alkenone flux increased in August, September, October and November at both sites. In the presentation, more details about the alkenone flux will be shown. We will discuss the seasonal and annual changes in alkenone fluxes comparing with other components.

[1]Takahashi *et al.* (2002) *Prog. Oceanogr.* **55**, 95-112.

[2]Honjo *et al.* (2008) *Prog. Oceanogr.* **76**, 217-285.

[3]Takahashi *et al.* (2012) *Memories of the Faculty of Science, Kyushu University. Series D, Earth and planetary sciences*, **32**(4), 1-38. [4]Tsutsui *et al.* (2013) *Deep-Sea Res. II* (in press).

CO₂ degassing in a haplo-basaltic magma: An experimental approach

M. HARDIAGON¹⁻³, D. LAPORTE¹⁻³, Y. MORIZET⁴,
AND A. PROVOST¹⁻³

¹ Clermont Université, Université Blaise Pascal, Laboratoire
Magmas et Volcans, BP 10448, 63000 Clermont-Ferrand

² CNRS, UMR 6524, LMV, 63038 Clermont-Ferrand

³ IRD, R 163, LMV, 63038 Clermont-Ferrand

Correspondence: M.Hardiagon@opgc.univ-bpclermont.fr

⁴ Département de Planétologie et Géodynamique, Université
de Nantes, 2 rue de la Houssinière, 44300 Nantes, France

Basaltic magmas carry huge amounts of volatiles (CO₂, H₂O, SO₂) from their sources in the upper mantle up to the Earth surface. The dynamics and efficiency of basalt degassing are fundamental parameters for eruption dynamics, the environmental impact of volcanism, and the global cycle of volatile elements. Some models of basalt ascent and degassing are purely based on equilibrium solubility laws while others take into account disequilibrium processes such as bubble nucleation and growth (e.g. [1]). Attempts to integrate these disequilibrium processes are hampered, however, by the lack of experimental data on major variables, such as the basalt-CO₂ surface tension.

We investigated CO₂ degassing in an ascending basaltic melt by performing decompression experiments in a piston-cylinder apparatus. Series of experiments were run at a constant decompression rate and quenched at different pressures in order to characterize the kinetics of bubble nucleation and growth. The main parameters of interest are the bubble nucleation pressure P_N , the critical supersaturation pressure ΔP_N ($= P_{SAT} - P_N$, where P_{SAT} is the volatile saturation pressure), the bubble number density, the bubble size distribution and the residual CO₂ supersaturation in the melt.

A CMAS-Na basaltic glass cylinder was loaded along with silver oxalate powder (the source of CO₂) into a Pt container. The melt was first saturated with CO₂ at 2 GPa-1500°C and then decompressed at 1 MPa/s. Homogeneous bubble nucleation was observed in the experiment quenched at 1.2 GPa, but not in the ones quenched above 1.5 GPa. This yields a ΔP_N for CO₂ bubbles in basalt of 0.5 to 0.8 GPa, thus larger than the values reported in the literature (0.2 GPa [2] or 0.4-0.5 GPa [1]). Quantification of CO₂ in the decompressed quenched glasses is in progress to quantify the residual volatile supersaturation.

[1] Bottinga and Javoy (1990) *Chem. Geol.*, **81**: 225-270. [2] Lensky *et al* (2006) *Earth Planet. Sci. Lett.* **245**: 278-288.

Simulating the role of extra-cellular DNA in cellular adhesion

JOHN H. HARDING^{*1}, COLIN L. FREEMAN¹,
RACHEL WALTON², STEVEN BANWART^{2,3},
STEVE ROLFE⁴ AND MARK GEOGHEGAN⁵

¹Department of Materials Science and Engineering,
University of Sheffield, Sir Robert Hadfield Building,
Mappin Street, Sheffield, S1 3JD, UK

²Department of Civil Engineering, Univeristy of Sheffield, Sir
Frederick Mappin Building, Mappin Street, Sheffield, S1
3JD, UK

³Kroto Research Institute, University of Sheffield, North
Campus, University of Sheffield, Broad Lane, Sheffield,
S3 7HQ, UK

⁴Department of Animal and Plant Sciences, Alfred Denny
Building, University of Sheffield, Western Bank,
Sheffield, S10 2TN, UK

⁵The Department of Physics and Astronomy, Hicks Building,
Hounsfield Road, Sheffield, S3 7RH, UK

Bacteria produce a vast range of mineral deposits within the earth and are involved in the degradation of many materials. Experimental studies have demonstrated that extra-cellular DNA (eDNA) is a major component of the extra-cellular polymeric substance used to bind the bacteria to surfaces [1]. Understanding the mechanisms of eDNA attachment is necessary to understand biofilm development.

We have explored the mechanisms of attachment using molecular dynamics simulations that provide atomic-scale detail to analyse the interactions. We consider how eDNA binds at amorphous silica surfaces which provides an analogue to many geological and experimental systems. A range of different solvated cations is simulated to enable us to look at their effect on both the space-charge layer and on localised bonding. We discuss the implications of these results for bacterial attachment and the building of DNA based scaffolds on mineral surfaces comparing them with current experimental work where possible.

[1] J.S. Andrews, S.A. Rolfe, W.E. Huang, J.D. Scholes, S.A. Banwart, (2010) *Environmental Microbiology* **12**(9), 2496-2507

A record of paleoproterozoic surface ocean redox from iodine-to-calcium ratios

DALTON S. HARDISTY^{1*}, ZUNLI LU², NOAH J. PLANAVSKY³, ANDREY BEKKER⁴, XIAOLI ZHOU², TIMOTHY W. LYONS¹

¹University of California, Riverside, USA
(*correspondence: dhard003@ucr.edu)

²Syracuse University, Syracuse, USA

³California Institute of Technology, Pasadena, USA

⁴University of Manitoba, Canada

Despite geochemical inferences of surface ocean and atmospheric oxygen accumulation prior to and at the Great Oxygenation Event (GOE) at 2.4 Gyr ago, a record of oxygen accumulation in the shallow ocean has yet to be demonstrated. Iodine-to-calcium ratios (I/Ca) in carbonates have recently been revealed as a paleoredox indicator, as iodate (IO₃⁻) is restricted to oxic waters and is the exclusive iodine species associated with carbonate precipitation¹. With a similar pE to that of O₂/H₂O, the presence/absence of IO₃⁻ is a more sensitive indicator of deoxygenation than other redox-dependent elements such as manganese and nitrogen, making I/Ca ideal for evaluating *in situ* redox in the early shallow ocean. Analysis of I/Ca in a series of Archean and Proterozoic dolomites show that the initial shift in I/Ca began at the GOE with a further increase following this at the Lomagundi carbon isotope excursion (LE). A tentative threshold for surface water oxygen accumulation of > 1 μM at the GOE is inferred from the shift in I/Ca from observations at modern oxygen minimum zones². A second order control on I/Ca ratios is the total iodine reservoir size, which is largely controlled by the burial and remineralization of organic matter. The LE is widely accepted to have resulted from an intense relative increase in organic carbon burial rates. The increase in I/Ca at the LE, despite likely reduction in the total iodine reservoir size due to organic burial, suggests expanded oxygenation, potentially into deeper water settings. Increasing I/Ca from a stratigraphic section of the Mcheka Formation, representing the later stage of the LE, may reflect increasing total iodine reservoir size, as organic carbon remineralization begins to outpace burial as carbon isotopes begin to retreat from > 10 ‰ to near 6 ‰. More generally, these data highlight the potential strength of the I/Ca proxy even in Precambrian samples.

[1] Lu, Jenkyns & Rickaby (2010), *Geology* 38, 1107-1110.

[2] Rue, Smith, Cutter & Bruland (1997), *Deep-Sea Research* 44, 113-134

Dark organic matter in permanently shadowed craters on Mercury

E. R. HARJU¹, D. A. PAIGE^{1*}, M. A. SIEGLER², M. L. DELITSKY³, D. SCHRIVER⁴

¹Department of Earth and Space Sciences, University of California, Los Angeles, CA 90095, USA
(*correspondence: dap@mars.ucla.edu)

²Jet Propulsion Laboratory, Pasadena, CA 91109, USA

³California Specialty Engineering, Flintridge, CA 91012, USA

⁴Department of Physics and Astronomy, University of California, Los Angeles, CA 90095, USA.

Data from instruments aboard the MESSENGER spacecraft have confirmed that radar bright regions in permanently shadowed craters, with temperatures less than 100 K, in the north polar region of Mercury are water ice [1-3]. In areas with temperatures up to 350 K, the Mercury Laser Altimeter observed radar-dark regions which are most likely an amorphous carbon-rich organic layer with a distribution peaking around 160 K, covering and in some cases extending beyond near-surface water ice deposits [1,2].

Simple organic molecules and water are delivered to Mercury by cometary impacts. A portion of these molecules could migrate to the polar regions of Mercury and become cold-trapped in permanently shadowed craters [4,5]. The magnetic field lines of Mercury create a cusp where solar wind plasma is transferred to the planet's surface in the north polar region with a peak proton flux of 1.9 x 10⁸ cm²/s [6].

Ion radiation processes organic molecules to species with greater molecular weights and greater C/H ratios as hydrogen ions escape. This process can continue until the organics become amorphous carbonaceous material or even graphite or other forms of elemental carbon which have low albedos similar to those of the dark material observed in permanently shadowed craters. Based on estimated proton and electron fluxes to the north polar region of Mercury, 3.35 x 10²⁷ molecules/cm² of polycyclic aromatic hydrocarbons can be created from processing methane over the lifetime of the solar system. Due to the ion radiation and source of organic molecules, it is likely that the radar-dark material is highly processed carbonaceous organic material.

[1] Paige *et al* (2013) *Science* 339, 300-303. [2] Neumann *et al* (2013) *Science* 339, 296-300. [3] Lawrence *et al* (2013) *Science* 339, 292-296. [4] Zhang & Piage (2009) *GRL* 36, L16203. [5] Zhang & Paige (2010) *GRL* 37, L03203. [6] Mouawad *et al* (2011) 211, 21-36.

Sr isotope stratigraphy of carbonate fraction in oil shales

Y. HARLAVAN* AND O. GOREN

Geological Survey of Israel, 30 Malkhe Israel St., Jerusalem.

(*correspondence: y.harlavan@gsi.gov.il)

Oil shale is a term used for immature, organic-rich, fine-grained sedimentary rocks from which hydrocarbons can be produced. In Israel, these rocks are composed of four main components: carbonate, phosphate, organic matter, and detritus (mainly Al-Silicates). The studied oil shales sequence is dated by their stratigraphic position (Bio-Zone) to Campan-Maastricht.

The use of $^{87}\text{Sr}/^{86}\text{Sr}$ ratio from marine sediments is in one of two ways: to determine the Sr isotopic composition of the ocean water at deposition time, or to determine the age of the sediment based upon ocean water $^{87}\text{Sr}/^{86}\text{Sr}$ changes with time (Sr isotope stratigraphy).

In the present study we examined the potential of calcite in oil shales to reflect the $^{87}\text{Sr}/^{86}\text{Sr}$ of the ocean water at time of formation. The absence of dolomite in the studied oil shales sequence suggests that the associated calcite was not significantly altered and therefore should reflect the isotopic composition of Sr in the ocean water at time of formation. The calcite and insoluble residue fractions in oil shales from different basins in Israel, were separated using sequential extraction and their Sr isotopic composition was determined. The numerical Sr ages of the calcite was calculated [1] and results show that the numerical stratigraphic age is in good agreement with the assigned bio-stratigraphic age. Moreover, the $^{87}\text{Sr}/^{86}\text{Sr}$ ratio of the insoluble residue should reflect the source of detritus transported to these basins and may shed light on their province. The $^{87}\text{Sr}/^{86}\text{Sr}$ ratio of the insoluble residue varies and has no correlation with the Sr isotopic ratio of the calcite. This strengthens the observation that the calcite fraction in oil shales can record the $^{87}\text{Sr}/^{86}\text{Sr}$ ratio of the ocean water. Furthermore, the observed strong correlations between (1) the $^{87}\text{Sr}/^{86}\text{Sr}$ ratio and 1/Sr and (2) Sr, Ca and P concentrations in the insoluble residue, indicate a mixture of two PO_4 -minerals which are likely to be of biogenic and magmatic origin.

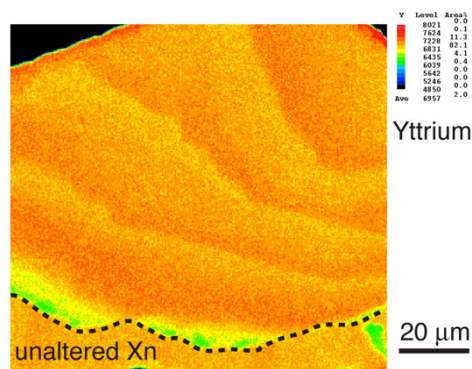
[1] McArthur, Howarth & Bailey, (2001). *Journal of Geology* **109**, 155–169. (LOWESS V5).

Experimental incorporation of U into xenotime at 900 °C, 500-1000 MPa utilizing alkali-bearing fluids

DANIEL E. HARLOV AND DIETER RHEDE

GeoForschungsZentrum, Telegrafenberg, D-14473 Potsdam, Germany (dharlov@gfz-potsdam.de)

In this study, specific areas of a natural Th-absent, low U, xenotime $[(\text{Y}+\text{HREE})\text{PO}_4]$ of uniform composition, are experimentally enriched in U + Si utilizing a NaF + H_2O fluid plus UO_2 and SiO_2 under both reducing (graphite-CO/ CO_2 buffer) and oxidizing (Mt-Hm buffer) conditions. Charge and fluid were sealed in 2 cm long, 3 mm diameter Au and Pt capsules. In the reduced experiment the Au capsule was placed in the piston-cylinder apparatus (CaF₂ assembly; graphite oven; 1000 MPa; 900 °C; 8 days). In the oxidized experiment (500 MPa; 900 °C; 4 days) the Pt capsule was packed with Hm + H_2O into a 4 cm long, 5 mm diameter Pt capsule, which was placed in the gas apparatus. BSE imaging indicates that the altered areas occur as a series of curvilinear intergrowths with sharp compositional boundaries that extend from the edge of the xenotime grain into the interior. EPMA indicates that the altered areas from both experiments are enriched in U + Si via the coupled substitution $\text{U}^{4+} + \text{Si}^{4+} = (\text{Y}+\text{HREE})^{3+} + \text{P}^{5+}$. WDS element distribution maps indicate that U + Si are concentrated close to the compositional interface between the altered and unaltered xenotime with corresponding depletion in Y+HREE. Across the altered region Y occurs as a series of concentric waves of relative enrichment and depletion with contrasting depletion and enrichment in HREE (see Y element map below).



Element movement is interpreted as a consequence of fluid-mediated coupled dissolution-precipitation in some sort of a chromatographic column effect across the altered area. Fluid-aided incorporation of U into xenotime has implications with respect to its utilization as a metamorphic geochronometer.

Phase identification of complex Cu-Fe sulfides using Time-of-Flight Secondary Ion Mass Spectrometry (ToF-SIMS)

YOGESH KALEGOWDA¹ AND SARAH L HARMER¹

¹School of Chemical and Physical Sciences, Flinders University, Bedford Park, Adelaide, South Australia 5042 (Sarah.Harmer@flinders.edu.au)

ToF-SIMS is a monolayer-sensitive surface analytical technique that has been extensively used in mineral processing to identify the elemental and molecular composition of a mineral surface. The combination of mass spectrometry and imaging makes ToF-SIMS a sensitive and capable technique for precisely identifying surface chemistry and its distribution across the surface. Traditionally, ToF-SIMS mass spectra have been used to provide the surface chemistry of an ore with little specificity to the local surface chemistry of a particular mineral phase. Some mineral specificity has been achieved by imaging particles using a major element of their composition. However, the identification of mineral phases that contain the same elements in a mixed multi-metal mineral system like chalcopyrite (CuFeS₂) and bornite (Cu₅FeS₄) presents a unique challenge for ToF-SIMS. The addition of precipitated, adsorbed, reacted and contaminant species in the outermost molecular layers produce complex mass spectra that are difficult to interpret using conventional methods.

For the effective analysis of such mineral systems, sufficient sensitivity and selectivity are required to detect significant components of the mass spectra. Furthermore the determination of surface chemistry, on a particle by particle basis, requires the selection of a particular mineral phase and statistical analysis of particles with an estimation of the variability of the value. The complex mass spectral data sets were analyzed using an adaption of principle component analysis – artificial neural networks (PCA-ANN). The analysis of ToF-SIMS data, has resulted in the successful classification of bornite, chalcopyrite, chalcocite and pyrite at different flotation stages. A method for phase identification of particles using ToF-SIMS has been used to track the surface chemistry of an individual particle throughout complex processing procedures[1].

[1] Yogesh Kalegowda and Sarah L Harmer (2012) Anal. Chem., 2012, 84 (6), 2754–2760.

Using isotopic and morphological evidence to determine biogenicity of gypsum precipitates in the Frasassi caves, Italy

KHADOUJA HAROUAKA^{1*}, MATTHEW GONZALES¹, ANTON EISENHAEUER² AND MATTHEW FANTLE¹

¹Penn State University, University Park 16802, USA

*correspondence: kuh121@psu.edu

²IFM-GEOMAR, Kiel D-24148, Germany

The process of biomineralization can leave unique fingerprints in the chemical and physical properties of a mineral, specifically in its isotopic composition and morphology. In the Frasassi cave system (Italy), gypsum forms at the cave wall-atmosphere interface as a consequence of limestone corrosion by sulphuric acid, which is produced by H₂S oxidation mediated by microbes (i.e., *Acidithiobacillus thiooxidans*). We sampled gypsum, drip water, and H₂S(g) from the Grotto Bella chamber near an active H₂S vent, and measured mineral aspect ratios, particle size, mineral and H₂S δ³⁴S_{CDT}, mineral and limestone δ⁴⁴Ca_{SRM915a}, and drip water elemental concentrations to find evidence of biomineralization. The gypsum occurs in three distinct morphologies: equant microcrystalline (<50 μm) crystals, wall crust, and needles up to 1 cm in length. The crust is characterized by small needles and aggregates of microcrystalline gypsum held together by biofilm. In Grotto Bella, smaller crystals are generally proximal to the H₂S source, whereas larger needles are found distally. The microcrystalline gypsum and needles are fractionated in δ³⁴S from the H₂S by -12 and -6‰ (2σ ≤ 1‰) respectively. The δ⁴⁴Ca of the microcrystalline and needle deposits are offset from the limestone wall by -0.04 and -0.84‰ (2σ ≤ 0.23‰) respectively. A biogenic origin of the microcrystalline gypsum may be deduced from the unusually low aspect ratios and highly negative δ³⁴S relative to the H₂S. The microcrystalline morphology may have arisen by crystal nucleation on individual cells embedded in the biofilm. The negative δ⁴⁴Ca of the needles may also suggest biogenicity, as the bacteria tend to colonize the larger gypsum needles more than the smaller morphologies.

Enhancing CO₂ sequestration in Mg-rich mine tailings

A. L. HARRISON^{1*}, I. M. POWER¹, S. A. WILSON²,
G. M. DIPPLE¹ AND K. U. MAYER¹

¹The University of British Columbia, Vancouver, V6T 1Z4, Canada (*correspondence: aharriso@eos.ubc.ca; ipower@eos.ubc.ca, gdipple@eos.ubc.ca, umayer@eos.ubc.ca)

²Monash University, Clayton, VIC 3800, Australia (sasha.wilson@monash.edu)

Mineralization of atmospheric CO₂ within carbonate minerals occurs passively in Mg-rich mine tailings via weathering of Mg-bearing primary minerals [1]. Passive carbon mineralization has been documented at the Mount Keith Nickel mine (MKM) in Western Australia [1]. Field data and reactive transport modeling indicate that passive mineralization occurs primarily via carbonation of brucite [Mg(OH)₂], and is limited by the supply of CO₂. MKM produces ~0.1-0.3 Mt brucite/yr in tailings; complete carbonation of this brucite would sequester up to 60% of mine emissions [2]. Thus, modification of tailings management practices to enhance brucite carbonation rates could provide a significant offset of emissions.

Two strategies are proposed to enhance CO₂ sequestration. First, passive carbonation could be accelerated by maximizing the exposure of brucite to atmospheric CO₂. Mineral abundance profiles from tailings of different ages at MKM and reactive transport modeling with MIN3P [1,3] were used to calculate the rate of brucite carbonation with depth below the tailings surface. It is estimated that passive sequestration would be maximized if brucite remained at the surface for twice the current duration (i.e., burial rates decreased).

A second strategy is to actively supply CO₂-rich gas streams into tailings [2]. Column experiments containing brucite were conducted to assess carbonation efficiency with injection of CO₂-rich gas into partially saturated systems akin to mine tailings. The effect of brucite grain size, water content, and reaction path length were assessed. Experimental and modeling results indicated that brucite grain size should be minimized to prevent the development of a passivating surface layer. Moreover, tailings water content should be maintained above residual saturation to optimize carbonation. The experimental rates suggest that the CO₂ sequestration potential in tailings would become limited by the brucite content rather than the reaction rate if CO₂-rich gas were supplied. These results will guide implementation of accelerated CO₂ sequestration strategies at mine sites.

[1] Bea *et al* (2012) *Vadose Zone J.* **11**. [2] Harrison *et al* (2013) *Environ. Sci. Technol.* **47**, 126-134. [3] Molins & Mayer (2007) *Water Resour. Res.* **43**, W05435.

Magnetic nanostructures in meteorites: A window on the early solar system

R. J. HARRISON^{1*}, J. BRYSON¹, N. S. CHURCH¹,
T. KASAMA², J. HERRERO ALBILLOS³

¹Department of Earth Sciences, Univ. Cambridge (*correspondence: rjh40@esc.cam.ac.uk)

²Center for Electron Nanoscopy, Technical University Denmark, Copenhagen (takeshi.kasama@cen.dtu.dk)

³ICMA, University of Zaragoza (Julia.Herrero@unizar.es)

Paleomagnetic signals recorded by meteorites are a potent source of information about processes occurring during the early solar system. This talk sets out the challenges that we face when attempting to extract meaningful magnetic information from such ancient and complex materials. To overcome these challenges we must search for the most ideal carriers of magnetic remanence (i.e. those displaying the highest magnetic stability and the highest resistance to thermochemical alteration and shock demagnetisation) – a search that leads us away from the conventional bulk paleomagnetic methods that have served us so well over the past 60 years, and towards the development of spatially resolved measurements that will take paleomagnetism to the micrometre scale and beyond.

Using a combination of state-of-the-art electron and X-ray imaging methods, we show that Fe-Ni metal carries a chemical transformation remanent magnetisation (CTRM) encoded within a spinodal decomposition nanostructure that formed continuously during slow cooling. This nanostructure is comprised of nanoscale islands of a magnetically hard phase (chemically ordered FeNi) coherently intergrown with a hitherto unobserved soft magnetic phase (chemically ordered Fe₃Ni), that developed progressively along pre-existing Ni concentration gradients. Dramatic variations in magnetic behaviour are observed across a lateral traverse of the spinodal region, which can be related to variations in the underlying nanostructure that developed during progressive cooling. Asteroid cooling models predict that spinodal nanostructures within chondritic meteorites formed during a time when the proposed asteroid core dynamo was active. We argue that microstructures forming in Fe-Ni metal from chondritic meteorites have the potential to reveal a time-resolved record of asteroid dynamo activity during the first 100-200 Ma of the asteroid's history – a record that would be the nanometre scale equivalent of the kilometre scale magnetic anomalies recorded by oceanic crust on Earth.

Reconstructing Societal Dynamics of the Ancient Maya: Insights from Nd Isotopes

E. HARRISON-BUCK¹, J. G. BRYCE², J. Blichert-Toft³

¹UNH Dept. of Anthropology, Durham NH, USA, e.harrison-buck@unh.edu

²UNH Dept. of Earth Sciences, Durham, NH 03824, USA.

³Ecole Normale Supérieure de Lyon, Lyon, France.

Ethnoarchaeological studies of cultures, such as the Maya, suggest that technical choices, such as the selection of clay and temper for pottery production, are socially informed actions that are among the strongest indicators of a group's social identity. Yet, archaeologists typically carry out stylistic analyses of artifacts (e.g. examining the painted designs on pottery), and fail to analyze the technological aspects of the material culture. Geochemical studies offer a valuable method for examining the fabric of ceramic production that can reveal changes in local pottery manufacture and exchange and can also point to significant shifts in long-distance trading activity over time. Current methods for chemical sourcing use statistical analyses to group ceramics based on elemental compositions derived from Instrumental Neutron Activation Analysis and Inductively Coupled Plasma Mass Spectrometry. Both techniques yield data that can be analyzed statistically to determine differences within and between groups in order to generally distinguish the proportion of locally made pottery from those that appear to be imports. This approach is problematic in terms of its sample preparation and study and limiting in terms of its degree of accuracy. Strontium isotopes have been commonly used in many locations in Belize watersheds, but their interpretations for sourcing local clay deposits are complicated by overprinting by carbonate-based temper. Here, we present new Nd isotope data that appear to be especially useful for isolating imported pottery and determining shared provenance for specific types of local ceramics from ancient Maya sites in the eastern Belize Watershed. The Maya pottery shows a range of up to 6 ϵ_{Nd} units, enabling the detection of specific production locales and shifting trade orientation consistent with changes in socioeconomic organization, likely resulting from new social groups entering the eastern Belize Watershed during different periods of Maya history. The Nd isotopic data, integrated with the stylistic analyses of the artifacts, clearly reveal the complexity of ancient patterns of mobility and trade, particularly at the time of the collapse at the end of the Classic period, and afford new insights into the societal dynamics of the ancient Maya.

Can mineral inclusions in metamorphic rutile help to constrain P-T conditions of formation?

EMMA HART¹, CRAIG STOREY¹ AND EMILIE BRUAND¹

¹School of Earth and Environmental Sciences, University of Portsmouth, PO1 3QL, UK. (*correspondence: emma.hart@port.ac.uk)

Peak metamorphic temperatures of rutile can already be determined using the Zr-in-rutile geothermometer [1], however little work has been carried out to develop rutile as a geobarometer.

We therefore aim to investigate the use of rutile as a single grain geothermobarometer by analysing mineral inclusions found within rutile. This work will be used in conjunction with average P-T calculations using THERMOCALC 3.3, providing a novel way of constraining conditions of rutile formation.

Rutile grains from a number of localities been characterised using EPMA. Raman spectroscopy will be used to analyse quartz inclusions in UHP rocks, e.g. Dora Maira, to determine if coesite is present.

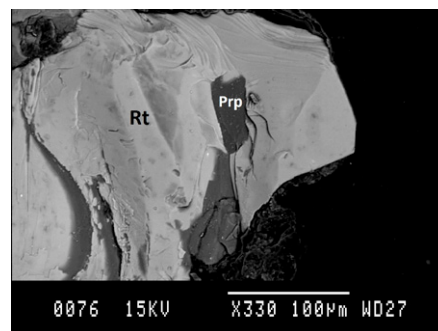


Figure 1: Back-scattered image of a rutile grain with a pyrope mineral inclusion from the Dora Maira Massif.

Preliminary EPMA data shows that inclusions in rutile comprise minerals useful for determining geothermobarometric conditions, e.g. glaucophane, omphacite and phengite. Pyrope and almandine garnet inclusions have also been discovered in UHP rocks from the Western Alps (fig. 1).

[1] Zack *et al* (2004) *Sedimentary Geology*, **171**, 37-58.

Source heterogeneities deduced from spatial and temporal geochemical patterns in continental basalts

W.K. HART^{1*} AND M.E. BRUESEKE²

¹Dept. of Geology and Env. Earth Sci., Miami Univ., Oxford, OH 45056, USA

(*correspondence: hartwk@miamioh.edu)

²Dept. of Geology, Kansas State Univ., Manhattan, KS 66506, USA (brueseke@ksu.edu)

Deciphering the mantle source(s) of basaltic magmas erupted in continental settings is challenging due to the potential geochemical and isotopic overprints imparted by continental lithosphere. In addition, both lithospheric and sublithospheric mantle reservoirs are variously implicated in continental basalt generation. As a result, intracontinental locations with extensive exposures of time-transgressive basalt flows can be extremely important for unraveling the relative contributions of these reservoirs.

In this context, we describe the spatial, temporal, chemical, and isotopic characteristics of basaltic volcanism on the Owyhee Plateau, USA. The Owyhee Plateau (OP) lies at the intersection of the Snake River Plain-Yellowstone and Oregon High Lava Plains magmatic trends; a region affected by the initial upwelling of the Yellowstone hotspot ~17 million years ago. It is the only location in the Pacific Northwest directly affected by Yellowstone-hotspot related volcanism that also contains a continuous record of basaltic volcanism over the past ~17 Ma [1]. OP basalt compositions include primitive to fractionated tholeiitic and mildly alkaline varieties with incompatible trace element and Sr, Nd, and Pb isotope ratios that are decoupled from the bulk chemistries, and that are time dependent [1,2].

The OP basalt suite reveals how mantle sources of intracontinental mafic magmas can vary as a function of time and lithospheric structure in a geographically restricted location. In this region, the heterogeneous mantle sources result from location along a distinct continental lithosphere transition, a major episode of sublithospheric mantle upwelling, and prolonged regional subduction leading to geochemical modifications of the lithosphere-asthenosphere boundary region that influence the nature of subsequent magmatism. Recent geophysical and geodynamic modeling results support these geochemical-based interpretations [3].

- [1] Shoemaker & Hart (2002) *Idaho Geol. Surv. Bull.* **30**, 313-328. [2] Hart (1985) *Geochim. Cosmochim. Acta* **49**, 131-144. [3] Long *et al* (2012) *Geochem. Geophys. Geosys.* **13**, doi: 10.1029/2012GC004189.

Melt injections and metasomatism in the continental mantle lithosphere beneath southern Africa

BEN HARTE

Centre for Science at Extreme Conditions, School of Geosciences, University of Edinburgh, King's Buildings, Edinburgh EH9 3JW, Scotland, UK. (ben.harte@ed.ac.uk)

A wide spectrum of melt-related phenomena have been identified in mantle xenoliths and xenocrysts from southern African xenoliths. At one end of this spectrum are the megacrysts of the Cr-poor megacryst suite, which appear to be direct crystallisation products from a melt body. At the other end of the spectrum are peridotite xenoliths with no megascopic signs of melt injection, but showing trace element evidence of metasomatism by melt percolation. In between these extremes are xenoliths showing apparently intrusive sheets and injected veins, as seen in the MARID suite of the Kimberley area (South Africa) and the IRPS suite of Matsoku (Lesotho). Evidence of melt intrusion, disruption and metasomatism is also shown by the polymict peridotite suite.

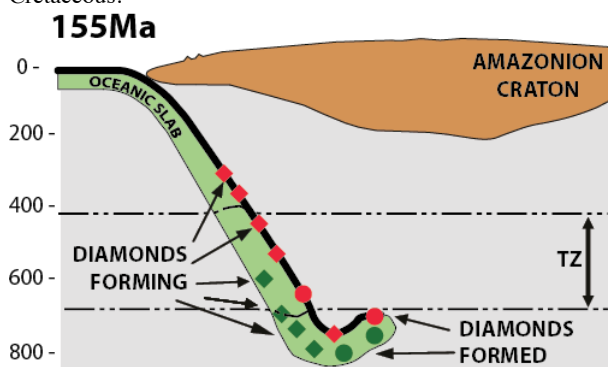
Close major-minor element compositional links exist between megacryst suite minerals, some Fe-Ti-rich high-temperature deformed xenoliths, and the metasomatised peridotite host rocks to intrusive IRPS-rich sheets. The major-minor element compositions of minerals in the Matsoku IRPS suite show close similarities to the matrix minerals of polymict peridotites. Estimates of the trace element compositions of melts percolating through Jagersfontein peridotite xenoliths evolve from compositions close to those estimated for megacryst magmas to those estimated for kimberlites. It appears that many phenomena show evidence of a lineage going back to similar Cr-poor megacryst magmas interacting over thicknesses of ca 100km with a diverse mantle lithosphere.

Subducted carbon in stagnant slabs: Evidence from 'deep' diamonds

BEN HARTE

Centre for Science at Extreme Conditions, School of
Geosciences, University of Edinburgh, King's Buildings,
Edinburgh EH9 3JW, Scotland, UK.

Evidence has been accumulating of diamonds containing mineral inclusions of unusually deep origin (250 to 800 km). In the case of 'deep' diamonds with silicate inclusions indicating basic rock protoliths, the diamonds have $\delta^{13}\text{C}$ values extending as low as -24‰ and suggestive of organic carbon. Other evidence of an initial ocean floor protoliths is shown by Eu anomalies in some inclusions. 'Deep' diamonds with inclusions indicating ultrabasic protoliths, commonly appear to have formed at depths of 500 to 750 km and have 'normal' mantle $\delta^{13}\text{C}$ values of -4 to -6‰ . However, these diamonds are also believed to be derived from subducted oceanic lithosphere in the form of hydrous meta-peridotites that have undergone dehydration reactions near the Upper/Lower Mantle boundary [1]. Time constraints from diamonds and inclusions erupted in the Juina area, Brazil, suggest the subducted lithosphere to be of early Mesozoic age, with diamond formation occurring as the oceanic lithosphere descended and formed a subducted stagnant slab near the Upper/Lower Mantle boundary (see figure). The diamonds were erupted back to the surface by kimberlites during the Cretaceous.



[1] Harte (2010), *Mineralogical Magazine* **74**, 189-215.

Colloidal metals in stalagmites: Potential for palaeohydrology

ADAM HARTLAND¹, IAN. J. FAIRCHILD², WOLFGANG
MULLER³ AND DAVID DOMINGUEZ-VILLAR⁴

¹ University of Waikato, Hamilton, New Zealand.
a.hartland@waikato.ac.nz

² University of Birmingham, Birmingham, B15 2TT, UK.

³ Royal Holloway University of London, Egham, Surrey,
TW20 0EX, UK.

⁴ Centro Nacional de Investigación sobre la Evolución
Humana, Burgos, Espana.

There is increasing recognition of the role of organic colloids and dissolved natural organic matter (NOM) in trace metal transport in karst systems. In particular, we now know that colloid-facilitated transport of trace metals responds in a coherent way to surface infiltration patterns [1] and that this may be encoded meaningfully in speleothems [2].

This study combines measurements of aqueous colloid-metal species from dripwaters, with trace metal and organic carbon data from a conjugate hyperalkaline speleothem. Thus, for the first time the capture of the inorganic and organic components of dripwaters by speleothems is studied in a quantitative way.

Our results indicate that the partitioning of NOM-transported metals into speleothems is proportional to the strength of the aqueous NOM-metal complex. In practice, this means that some metals (e.g. Cu, Zn) more closely reflect hydrological changes (readily dissociate to bind with calcite), while other elements (e.g. Co, Br) more closely encode information on NOM capture, i.e. they less readily dissociate from aqueous complexes.

We also provide evidence for kinetic effects on NOM incorporation in the speleothem and show that the ratio of certain trace metals (e.g. Cu/Ni) in stalagmites may also reflect compositional fluctuations in the NOM, consistent with high and low molecular weight trends also seen in dripwaters.

[1] Hartland *et al* (2012) *Chem. Geol.* **304-305**, 68-82. [2] Jo, K.N. *et al* (2010) *EPSL* **295**, 441-450.

Arsenic in surface sediments of a harbor sludge dumping site and a natural deposition site in the Helgoland Mud Area, North Sea

JAN F. HARTMANN¹, SABINE KASTEN², THOMAS KRENGEL¹ AND MARGOT ISENBECK-SCHRÖTER^{1*}

¹ Inst. of Earth Sciences, Heidelberg Univ., Im Neuenheimer Feld 236, 69120 Heidelberg, Germany (*corr.:

Margot.Isenbeck@geow.uni-heidelberg.de)

² Alfred Wegener Institute for Polar and Marine Research, Am Handelshafen 12, 27570 Bremerhaven, Germany

In order to analyse differences in concentration, speciation and total mobility of arsenic two different locations were studied near the Helgoland Mud Area, North Sea.

The first location is characterised by natural sedimentation, the second by deposited sediments dredged from the port of Hamburg. Porewater as well as sediment profiles were analysed with respect to arsenic compounds (As (III) and total As) and major redox species as total and reactive manganese and iron. The sediment samples were handled under inert atmosphere before and during extraction by water, phosphate, hydrochloric acid and aqua regia. Total element contents in porewater and leachable extracts of sediment fractions were analysed.

The results show a strong redox coupling of arsenic with manganese and iron. Oxidized arsenic seems to adsorb to manganese- and iron-oxyhydroxides in surface sediments. In contrast to the solid samples, the pore water data shows a release of As (III) into porewater when manganese- and iron-oxyhydroxides are reduced in the upper part of the cores. Also a remobilisation of As (V) occurs. Downward diffusing arsenic can be fixed by carbonate below the zone of manganese and iron reduction. In the anoxic parts of the sediments As (III) and As (V) are released and could be fixed at authigenic iron sulphide or arsenic sulphides formation. A sulfidic precipitation of arsenic in iron-dominated systems is limited by the occurrence of HS⁻.

Total solid-phase contents in leachable extracts of sediment fractions of the natural area show significant higher arsenic concentrations than the core of the anthropogenic dumping area. This is due to the higher fines content of the Helgoland mud area.

Higher total porewater contents of iron and arsenic in the core of the anthropogenic dumping area thus due to higher turnover rates of organic matter by iron reduction. Higher concentrations of arsenic may be due to a higher availability of iron in the dumped sediments.

Sub-arc $\delta^{11}\text{B}$: The introduction of boron isotope heterogeneity into the convecting mantle

JASON HARVEY^{1*}, CARLOS J. GARRIDO², SAMUELE AGOSTINI³, JOSÉ-ALBERTO PADRÓN-NAVARTA^{4,5}, VICENTE LÓPEZ SÁNCHEZ-VIZCAÍNO^{2,4}, IVAN P. SAVOV¹, CLAUDIO MARCHESI²

¹ School of Earth & Environment, University of Leeds, UK
feejh@leeds.ac.uk (*presenting author)

² Instituto Andaluz de Ciencias de la Tierra (IACT), CSIC-UGR, Armilla, Granada, Spain

³ Istituto di Geoscienze e Georisorse, Area di Ricerca del CNR, Pisa, Italy

⁴ Research School of Earth Sciences, The Australian National University, Canberra 0200, ACT, Australia

⁵ Géosciences, Montpellier, CNRS (France)

The Cerro del Almirez Massif in Spain preserves field evidence for the prograde transition from antigorite-serpentine (ant-serp) to chlorite-harzburgite (chl-harz) in a paleo-subducting slab. This study investigates B isotope fractionation in the sub-arc region, where fluid loss accompanies prograde metamorphism under well constrained pressure and temperature conditions (650 °C, 1.7 GPa [1]). Boron isotopes are strongly fractionated during the dehydration of ant-serp, with a sharp decrease of $\delta^{11}\text{B}$ across the ant-serp to chl-harz isograd. Ant-serp has a $\delta^{11}\text{B}$ of +22.6 ‰ (± 1.6), similar to the heaviest $\delta^{11}\text{B}$ in serpentinites recovered from the forearc region of the Mariana subduction zone [2, 3], whereas prograde lithologies preserve $\delta^{11}\text{B}$ of +3.3 ‰ (± 0.3) to $\delta^{11}\text{B}$ of -3.5 ‰ (± 0.3).

Although the rapid drop in $\delta^{11}\text{B}$ demonstrates that massive B isotope fractionation occurs at sub-arc depths, the absolute amount of boron lost during dehydration is negligible compared to B lost from the downgoing slab in the forearc at the onset of subduction (c. 85%)[4]. Lithologies on either side of the isograd contain 7-12 ppm B with only minimal loss of B accompanying dehydration. This means that any B that survives ant-serp dehydration has the potential to be transported past the sub-arc region and into the deep, convecting mantle. Prograde chlorite is not the major host of this boron - it is mostly contained in prograde olivine-hosted inclusions[5], unlikely to suffer any subsequent dehydration reactions. The delivery of B with $\delta^{11}\text{B}$ of +3.3 ‰ to $\delta^{11}\text{B}$ of -3.5 ‰ into the asthenosphere therefore provides a possible source for OIB (e.g.[6]) whose $\delta^{11}\text{B}$ is significantly lighter than primitive mantle.

- [1] Padrón-Navarta *et al* (2011) *J. Petrol.* **52**, 2047-2078.
[2] Savov *et al* (2007), *J. Geophys. Res.*, doi:10.1029/2006JB004749 [3] Pabst *et al* (2012) *Lithos* **133**, 162-179. [4] Kodolanyi and Pettke (2011) *Chem. Geol.* **284**, 351-362. [5] Scambelluri *et al* (2004) *Earth Planet. Sci. Lett.* **222**, 217-234. [6] Turner *et al* (2007) *Nature* **447**, 702-705.

Copper mineralization prevented by arc-root delamination during Alpine-Himalayan collision in Iran

MICHAEL HASCHKE¹, JAMSHID AHMADIAN², FATEMEH SARJOUGHIAN³, BEHNAM SHAFIEI⁴

¹UIT Dresden, Am Windkanal 21, 01109 Dresden, Germany

²Dept. of Geology, Payame Noor University, Tehran, Iran

³Dept. of Earth Sciences, Univ. of Kurdistan, Sanandaj, Iran

⁴Dept. of Geology, Golestan Univ., Gorgan, Iran

The formation of Cu-Au-Mo porphyry deposits in Iran is linked to continental collision, yet there are no clear temporal relations between geochemical signatures of Miocene (collisional) and Eocene (pre-collisional) intrusive arc rocks, and the presence/lack of ore mineralization. We compare geochemical scenarios from five different segments along the Urumieh-Dokhtar arc and propose a geodynamic model to explain this discrepancy. For instance, in the Natanz arc segment in central Iran, contrasting geochemical signatures of copper ore hosting Eocene and some barren undeformed Miocene diorites to granites temporally overlap with the Alpine-Himalayan collision. These changes provide key implications on the existence and lack of Cu mineralization during collisional magmatism. High Sr and low Y (and Yb) contents of Eocene arc rocks in the Natanz arc segment reflect thickened, Andean-type orogenic arc crust (~45 km), whereas barren Miocene Natanz arc rocks (21-19 Ma) indicate thin arc crust similar to collisional volcanism in Anatolia. Geochemical modeling indicates a change in the mineralogy of the melt residual, from precollisional Eocene basaltic garnet-bearing (5-30%) amphibolite to syn- or postcollisional Miocene metasomatized mantle peridotite, which can be explained by collision-induced delamination of the arc lithospheric root. Subsequent recharge of hot asthenosphere and melting of metasomatized mantle peridotite and lack of interaction with a garnet-bearing arc crustal keel explain the low Sr and high Y (and Yb) contents, the relatively enriched initial Sr isotope ratios of postcollisional Miocene Natanz rocks, and the lack of copper mineralization in postcollisional Miocene Natanz arc rocks. Arc-root delamination removes the copper- and sulfurenriched metasomatized lithospheric arc root and hydrous cumulate reservoir required to form copper ore deposits. Lack of the dense melt residues also provides an alternative explanation for the elevated, thin crustal Iranian back-arc plateau (38 km) as a result of uplift by isostatic rebound rather than uplift by anomalous shortening. Miocene arc-root delamination implies a minimum age of >21 Ma for the Alpine-Himalayan collision in central Iran.

Relationship between modern speleothem formation and surface weather in an Asian tropical cave

W. HASEGAWA^{1*}, Y. WATANABE¹, H. MATSUOKA¹, S. OHSAWA², B. BRAHMANTYO³, K. A. MARYUNANI³ AND T. TAGAMI¹

¹Earth and Planetary Science, Kyoto univ., Kyoto, Japan

(*correspondence: hasegawa-w@kueps.kyoto-u.ac.jp)

²Institute of Geothermal Science, Kyoto univ., Beppu, Japan

³Earth Sciences and Mineral Technology, Institut Teknologi Bandung, Bandung, Indonesia

For precise climate prediction, it is necessary to reconstruct high time and space resolution paleo-climate (especially past 2000 years) from paleo-climate proxies and assimilate the result to climate model. Tropical Asia, including Indonesia, is well affected by El Niño Southern Oscillation (ENSO). The ENSO does not only directly affect on precipitation in tropical Asia, but also indirectly on middle and high latitude climate through teleconnection [1]. In Indonesia, Watanabe *et al* [2] suggested inverse-correlation between $\delta^{18}\text{O}$ and $\delta^{13}\text{C}$ in speleothems and instrumental precipitation. However, relationship between modern speleothem formation and surface weather is not revealed clearly.

Thus cave monitoring program was initiated from 2011 in Petruk Cave (Central Java, Indonesia) in order to study the recording mechanism of precipitation variation into the $\delta^{18}\text{O}$ and $\delta^{13}\text{C}$ fluctuation in speleothems.

Air CO₂ concentration in Petruk Cave is fluctuated daily and seasonally until over 100 m deep site from the entrance.

It is revealed that cave air CO₂ concentration may be a significant factor that controls stable isotope value in speleothems, because temperature, humidity and drip rate in Petruk cave are nearly stable.

A scenario of precipitation recording is as follows: (1) surface rainfall cools outside air temperature; (2) cave airflow direction is inversed; (3) outside fresh air flows into the cave and air CO₂ concentration is dropped; (4) pCO₂ difference between cave air and dripwater becomes higher and calcite precipitation is promoted; (5) $\delta^{18}\text{O}$ and $\delta^{13}\text{C}$ in speleothems are decreased.

[1] Hastenrath (1991) *Climate dynamics of the tropics*. [2] Watanabe *et al* (2010) *Palaeogeography, Palaeoclimatology, Palaeoecology* **293**, 90–97.

Origin of laminations in BIF deciphered from N and Fe isotopes

K. HASHIZUME^{1*}, D.L. PINTI², B. ORBERGER³,
C. CLOQUET⁴, M. JAYANANDA⁵ AND H. SOYAMA¹

¹Dept. of Earth & Space Sci., Osaka Univ., Toyonaka 560-0043, Japan (*kohash@ess.sci.osaka-u.ac.jp)

²GEOTOP, H2X 3Y7, Montréal, Qc, Canada

³Groupe ERAMET, 75755 Paris, France

⁴CRPG-CNRS, BP 20, 54501 Nancy, France

⁵Dept. of Geology, Univ. of Delhi, Delhi 110 007, India

Elucidation of the formation process of banded iron formations (BIF) is the major purpose of this study. Not only the iron oxidation process itself, but the alternation between the quartz- and iron-rich layers may provide important clues on the emergence of the oxygen in the early atmosphere.

A >2.72 Ga old BIF from Dharwar Craton, southern India, was studied. Compositions of N, Fe and Ar isotopes, major and trace elements including REEs were analyzed among 10 qz- or Fe-oxide-rich bands from the sample. REE and trace element compositions of the samples indicate a minimal influence from the continental crust, allowing us to propose a relatively simplified view of the water column from which constituents of the BIF sample precipitated. Qz- and Fe-rich layers showed contrasting compositions of N, Fe and Ar isotopes and of REEs. A positive correlation between $\delta^{15}\text{N}$ and $\delta^{56}\text{Fe}$ values, which range from +2 to +12‰ and +0.9 to +2.2‰, respectively, is the major finding of this study. Qz-rich layers exhibit higher Eu anomalies correlated with $^{40}\text{Ar}/^{36}\text{Ar}$ ratios. This trend is explained by the contribution of a constant amount among all bands of a hydrothermal component, added to Y-rich REE and ^{36}Ar -rich Ar components, which possibly represent Archean oceanic and atmospheric air compositions, respectively, carried by Fe-bearing minerals. The lower $\delta^{56}\text{Fe}$ values observed among the Fe-rich bands could be explained either by anoxygenic photosynthetic oxidation or O_2 -mediated abiotic oxidation from an oceanic ferrous iron with a mantle origin. We explain the higher $\delta^{56}\text{Fe}$ values among the qz-rich bands by dissimilatory iron reduction (DIR) by which lighter iron isotopes are consumed faster. The qz-rich bands are N-rich, in concentrations and C/N ratios, and ^{15}N -rich, in the isotope ratio. We propose that formation of the qz-rich bands may correspond to periods when the photosynthetic biological productivity at the surface of the ocean was active. The DIR could have been enhanced during this period by supply of abundant organic matter to the iron particles. The biological activity at the ocean surface could be the switch producing the laminations in BIFs.

Net community and gross primary production in the Southern California Bight based on carbon export, dissolved O_2/Ar and triple oxygen isotopes: Exploration of how the magnitude and timing of upwelling events may influence export efficiency

W.Z. HASKELL II¹, M.G. PROKOPENKO¹,
D.E. HAMMOND¹, R.H.R. STANLEY², W.M. BERELSON¹

¹Dept. of Earth Sciences, University of Southern California, 3651 Trousdale Pkwy, Los Angeles, CA, 90089, USA
whaskell@usc.edu

²Dept. of Marine Chemistry, Woods Hole Oceanographic Institution, 266 Woods Hole Rd., Woods Hole, MA, 02543, USA

Biologically driven deviation of dissolved O_2 from equilibrium concentrations, determined from O_2/Ar ratios, has long been used as a tracer of net community production (NCP) in the oceans, as O_2 is a counterpart of carbon in photosynthesis and respiration. Over the last decade, a technique using the triple oxygen isotope composition (TOI) of dissolved O_2 has been applied in many regions of the ocean to estimate gross biological oxygen production (GOP) in the surface mixed layer. The TOI approach rests on using the deviation from mass dependent fractionation of the three oxygen isotopes (^{16}O , ^{17}O , ^{18}O) in the mixed layer to distinguish between photosynthetic *in situ* produced O_2 and atmospheric O_2 supplied through gas exchange. This “dual-tracer” approach of simultaneous measurements of Net Community and Gross Production provides estimates of NCP/GOP ratios, which reflect efficiency of carbon export. However, applications of this *in-situ* technique have been limited in productive coastal upwelling zones because the mixed layer O_2 mass balance is altered by upward advection of water from the oxygen deficient zone, which has both O_2 concentration and TOI composition out of equilibrium with the atmosphere. The Upwelling Regime In-situ Ecosystem Efficiency (Up.R.I.S.E.E.) time-series study is an ongoing effort to expand the application of the O_2 -based dual-tracer approach to the upwelling regimes. In this study, O_2/Ar and TOI measurements through the upper thermocline are combined with estimates of upwelling rates, constrained by a mass balance of ^7Be in the surface mixed layer and upwelling indices from wind stress curl. Accounting for the contribution of the deep water O_2 signal to the mixed layer O_2 and TOI inventory, we test whether the timing and/or magnitude of upwelling events affect an ecosystem's efficiency in exporting organic carbon from the surface ocean in this highly productive setting. Sediment trap deployments and budgets of DIC, DOC, and ^{234}Th are used to further constrain export estimates, and compared to NCP. Preliminary results from the first six months of a two-year study will be presented.

www.minersoc.org

DOI:10.1180/minmag.2013.077.5.8

Metals zone distribution in old ore deposits Egypt: A pathfinder for site of chief metal accumulation

MAHMOUD M. HASSAAN¹

¹mah_hassaan@hotmail.com. Faculty of Sciences, AlAzhar University-Egypt.

Geochemical zoning, is a reliable exploration criterion for revealing site of accumulation of chief ore metal. Studies established the clark of concentration CC and zoning coefficient to investigate the old exploited deposits of gold, zinc-copper, molybdenum-silver hosted by the Pan-African ophiolitic, island arc and cordilleran-extension rocks of the Nubian shield. These studies considered the general zoning sequence. Be, Ni, Co, B, Sn, U, Mo, W, As, Bi, Cu₍₁₎, Zn, Pb, Sn₍₂₎, Au, Ag, B, As₍₂₎, Cu, Sb, Hg, Te, I. The zoning sequence of Sukkari mineralization upward is Au, Sn, Mo, Zn, As, Ni, Pb, Ba favoring gold accumulation site deeper than ~ 400 m. In Abu Marwat mine the zoning sequences favored increase of gold northward as follow :Upper zone northern part Ag, Zn, Mo, Pb, Ba, Au, sn, Cu, Au and lower zone northern part Sn, Ni, Pb, Ba, Au, Zn, Cu, Mo, Ag. The recommended site of gold accumulation is meta-volcanic rocks and quartz veins bordering Wadi Abu Marwat from north and their extension under the Wadi alluvial. The study of Gattar molybdenite-silver occurrence recorded gold. The vertical zoning sequence from altitude 10 m to 953 m. is Au, Cu Pb, (Co, Ni), Ag, Zn, Sb, (Sn-W), Cr, Mo enhanced 2 mineralization phases and gold accumulation at deeper levels. In Um Zuriq mineralization at Wadi kid in Sinai, the data of a drill hole penetrated repeated sheared and altered chlorite schist and garnet biotitic andalusite schist forming two limbs of a recumbent fold placed basal mineralization zone at south western side above the top of the zone at north eastern part. The recorded sequence Cu(Zn, Pb), Au, Ag upward in the basal limb is normal and another inverted one for the upper limb. The mineralization is syngeneic to the schist. The arc-like island arc meta-volcanic rocks hosting seven As, Pb, Zn, Cu sulfides litho- structurally controlled forming a belt. In El Atshan mine variable high CC values of only Cu and Zn in all rock units favored that the volcanic magma was bearing Cu-Zn. The recorded high Pb and As contents in the talc carbonate and serpentinite enhanced its relation to dynamothermal activity during thrusting. The vertical zonal sequence is Fe, Cu, Zn (Pb-As) upward. These features were recorded at the Derhib mine. Similar deposit was recorded in Wadi Allaqi.

Late Neoproterozoic Nuqara Dokhan Volcanics, Central Eastern Desert, Egypt: Geochemistry and petrogenesis

ASRAN.M.H.HASSAN¹, NATFLOS.THEO², AMRON.T³, THARWAT.SALEM⁴, EL TAKY.M⁵

¹ Sohage Univ. Egypt.(Asran_59@yahoo.com)

² Vienna Univ.Austria (theodoros.ntaflos@univie.ac.at)

³ South Valley Univ. Egypt (t_amron@yahoo.com)

⁴ South Valley Univ.Egypt (geo_tharwat2010@yahoo.com)

⁵ South Valley Univ.Egypt (eltaky@yahoo.com)

The Neoproterozoic Nuqara Dokhan volcanics are one of the northernmost outcrops of the Arabian- Nubian Shield. The origin and tectonic setting of these rocks is highly debated. Debate concerns the tectonic setting they formed as a result of subduction (El Gabby et al, 1990) or crustal extension (Stern,1994). Nuqara dokhan volcanics comprises two main rock suites: (a) an intermediate volcanic suite, consisting of basaltic andesite, andesite and their associated pyroclastics rocks; and (b) a felsic volcanic suite composed of dacite, rhyolite and ignimbrites. The two suites display well-defined major and trace element trends and continuum in composition with wide ranges in SiO₂ (52-75.73%), CaO (9.19-0.22%), MgO(5.29-0.05%), Sr (1367-7.4ppm), Zr (688.5-172.7ppm), Cr (207-0.4 ppm), and Ni (86-0.2ppm). The Nuqara Dokhan volcanics are characterized by strong enrichment in LILE relative to HFSE and affiliated to the calc-alkaline subduction – related magmatism. Modeling results display that the evolution of these rocks was governed by fractional crystallization of plagioclase, amphiboles, pyroxene, magnetite and apatite in the intermediate varieties and plagioclase, amphibole, magnetite, apatite and zircon in the felsic varieties. The obtained mineral chemistry of these volcanics reveals: (a) Plagioclase range in composition from An₅₉ to An₅₅ in basaltic andesite and from An₄₉ to An₂₇ in andesite. (b) Alkali feldspars have sanidine composition. (c) Clinopyroxenes have augite composition. The low Al₂O₃ contents (2.055-5.588 wt %) indicate that clinopyroxene crystallized at low – pressure. (d) Amphiboles have ferro hornblende to ferro barrosite composition.

[1] El Gaby et al (1990) A.A.Balkema, Rotterdam, p.175- 184.

[2] Stern RJ (1994) Ann Rev Earth planet sci 22:319

Specific ion effects on the wettability of sandstone particle

T. HASSENKAM, J. MATHIESSEN, M.P. ANDERSSON AND S.L.S. STIPP

Nano-Science Center, Dept. of Chemistry, University of Copenhagen, Denmark (tue@nano.ku.dk)

Specific ion effects control most reactions in nature. Adhesion, between organic molecules and mineral surfaces in aqueous solution, depends not only on the behaviour of the molecule and substrate but also on the specific set of dissolved ions. The complex behaviour between ions, water and organic molecules is reflected in various versions of what is known as the Hofmeister series where ion activity depends on size, charge and electron configuration. There is a wealth of experimental data on how organic molecules interact with sandstone, from oil industry work and from environmental studies of soil, sediments and aquifers but the picture of molecular scale interactions is not clear.

By using force spectroscopy and chemical mapping with AFM (atomic force microscopy) we can observe contact behaviour with a variety of molecules on real sand grains, while solution composition is changed. By using tips functionalised to behave as pure alkane (CH₃), we have probed sand grains, and examined adhesion in NaCl solutions, with ionic strength close to that of seawater. Changing composition of the solution by adding small amounts (12 mM) of specific divalent ions (Ca²⁺, Mg²⁺), corresponding to about 2% relative to the number of Na⁺ ions, caused a dramatic adhesion increase between the alkane tips and the surface - by as much as 50%. Increased adhesion is a clear response to higher divalent ion density at the surface. However, in 0.5 M NaCl, the electrical double layer collapses to much less than the thickness of a single water molecule so the understanding of the data can only be founded in mechanisms involving ions and their behaviour specifically, at the molecular scale.

The biogeochemical ice core record: A new perspective on nitrate

MEREDITH G. HASTINGS¹, DOROTHY FIBIGER², NATHAN CHELMAN^{1,3} AND JOSEPH R. MCCONNELL³

¹Brown University, Department of Geological Sciences and Environmental Change Initiative, 324 Brook Street Box 1846, Providence, RI USA, meredith_hastings@brown.edu

²Brown University, Department of Chemistry, Providence, RI USA

³Desert Research Institute, Division of Hydrologic Science, Reno, NV USA

A major motivation in studying ice core nitrate is to reconstruct the atmospheric loading of its precursor, nitrogen oxides (NO_x). NO_x concentrations in the atmosphere play a significant role in determining tropospheric chemical composition and oxidizing capacity. Today, NO_x emissions are primarily the result of fossil fuel burning, with important contributions from biomass burning, lightning and biogenic processes in soils. The result of these emissions is deposition of nitric acid (i.e., nitrate), a component of acidic precipitation and a bioavailable nutrient. Recent studies utilizing the isotopic composition of nitrate in ice cores offer the possibility to trace the sources and chemical processes that contribute to nitrate deposition over time.

Studies of the isotopic composition of nitrate in surface snow and snowpits at Summit, Greenland reveal an atmospheric nitrate signal that is well preserved in recent snow. A seasonally resolved ice core record of the isotopic composition of nitrate, together with highly resolved (> 22 samples yr⁻¹) elemental and chemical tracers are used to investigate changes in NO_x sources and chemistry since 1760 C.E. A marked negative trend in δ¹⁵N since industrialization (pre-industrial-era average of 12.0‰ vs. air N₂ to a modern-era average of 3.6‰) parallels a nearly three-fold increase in nitrate concentration, as well as pronounced increases in tracers such as excess lead and non-sea-salt sulfur. This, along with independent estimates of oil burning and transport studies, indicate that North American oil combustion is the primary driver of the negative trend in δ¹⁵N of nitrate. The pre-industrial record of nitrate and tracers such as ammonium and black carbon ties the high, positive δ¹⁵N values to biomass burning. Overall, this record provides constraints for δ¹⁵N-NO_x source signatures, which are poorly characterized. A quantitative tracer of the pre-industrial sources and chemistry of NO_x would allow for detailing connections between the atmosphere (lightning, chemistry, transport), the biosphere (biomass burning, soils), and climate.

Rare Earth Elements in the surface Ocean under the Saharan dust belt

ED C. HATHORNE¹, MARTIN FRANK¹, MICHEL RUTGERS VAN DE LOEFF², TOBIAS ROESKE², AND JOERG RICKLI³

¹GEOMAR, Helmholtz Centre for Ocean Research Kiel, Germany (ehathorne@geomar.de)

²Alfred Wegener Institute for Polar and Marine Research (AWI), Bremerhaven, Germany

³ETH Zürich, Switzerland

The supply of trace metals to the surface ocean via dust deposition is important for primary productivity and the global biogeochemical cycle of many elements. Here we utilise the systematic variation of the chemical properties of yttrium and the rare earth elements (YREE) to investigate trace metal release from dust in the equatorial Atlantic Ocean. We present YREE data for the dissolved (<0.45 µm) and suspended particulate matter (SPM) collected from the mixed layer during Polarstern cruise ANT-XXIII/1 in Oct-Nov 2005.

Saharan dust can be traced with the Al content of the SPM revealing a broad maximum extending from 15° to 3°N. The PAAS normalised YREE patterns of the dust dominated SPM are relatively flat with a broad peak centred around Eu and Gd. This dust dominated SPM is also characterised by lower Y/Ho and Er/Nd ratios than the particulate material from outside the high Al zone.

The dissolved YREE distributions show normal seawater patterns with the relative enrichment of heavy REE over light REE. The samples with dust dominated SPM are enriched in the light and middle REE by a factor of approximately 2 compared to the other samples and a Sargasso Sea surface water. The dissolved Y/Ho and Er/Nd ratios obtained from the dust dominated SPM zone are also low compared to the samples outside the zone but display a fractionation between the SPM and the dissolved phase. This comparison indicates a consistent incongruent dissolution of the dust associated YREE which are probably mainly hosted by oxide coatings on the particles.

Hydrogeochemical assesment of Pasinler (Erzurum- Turkey) geothermal fluids

E. HATIPOGLU^{1*}, F. GULTEKIN¹ AND A. FIRAT ERSOY¹

¹Karadeniz Technical University, 61080 Trabzon, Turkey
(*correspondence:hatipoglu@ktu.edu.tr, arzu@ktu.edu.tr, fatma@ktu.edu.tr, arzu@ktu.edu.tr)

The Pasinler geothermal field is located to 37 km east of Erzurum Province. The basement of Pasinler Geothermal field consists of Upper Cretaceous ophiolitic melange, Eocene volcanic rocks, Oligocene volcanic rocks, Lower Miocene reef limestones, Upper Miocene pyroclastics, Plio-Quaternary (sandstone, marl, conglomerate) and Quaternary alluvium. The rhyolite is the reservoir for the geothermal fluid. The tuffs and marls are cap rocks of the system. The fault and related fractures around the Pasinler geothermal field provide pathways for the upward flow of geothermal fluid to the surface. The Alluvium around the Hasankale River is the most important unit as cold groundwater deposits in the study area. The thermal waters in the Pasinler geothermal fields have outlet temperatures 23 to 35°C in springs. But discharges in the wells vary between 38-52°C.

Geothermal well waters belong to the Na-Ca-Cl-HCO₃ type. The Pasinler geothermal water has discharge pH values of 6 to 7.5, electrical conductivity (EC) of 970 to 5800 µS/cm and TDS contents between 635 and 3700 mg/l. The Pasinler geothermal field is in class low enthalpy geothermal system, and its reservoir temperature was calculated as 46-169°C using silica geothermometer. The δ¹⁸O- δ²H data clearly indicate a meteoric origin for the thermal waters.

According to analyses of heavy metal contents such as Cr, Pb, Zn, Ni, Al and Cu, the Pasinler geothermal water is suitable for the Turkish Thermal Standarts, on the other hand by the amount of Fe, Mn, As, B, Br is not suitable.

Laser ablation for spatially resolved radiocarbon measurements with gas source-accelerator mass spectrometry

B. HATTENDORF¹, C. MÜNSTERER^{1,2}, R. DIETIKER¹, J. KOCH¹, L. WACKER², M. CHRISTL², H.A. SYNAL² AND D. GÜNTHER¹

¹ETH Zurich, Laboratory for Inorganic Chemistry, Wolfgang Pauli Str. 10, 8093 Zurich, Switzerland

²ETH Zurich, Laboratory of Ion Beam Physics, Schafmattstr. 20, 8093 Zurich, Switzerland

Accessing the spatial variability of ¹⁴C in solids like for example speleothems, corals or wood, traditionally required laborious and time consuming sample preparation (milling, drilling, graphitization) to allow measurements by accelerator mass spectrometry (AMS). With the availability of gas ion source AMS [1] and new sample preparation techniques and the direct measurement of gaseous carbon species (i.e. CO₂) a wider range of applications has become accessible. Laser ablation can directly produce CO₂ from carbonates at a spatial resolution of several 10 μm and is considered to complement currently available measurement strategies when high resolution radiocarbon records are of interest. In this study, a prototype laser ablation sampling unit is developed, which can be directly connected to the ion source of a gas-source AMS instrument. It comprises an ArF excimer laser (193 nm) with beam delivery optics, a specific ablation cell and sample observation system. Initial tests showed that using rectangular ablation crater of 100 μm x 700 μm can generate a sufficient CO₂ flux to allow radiocarbon measurements with the gas ion source AMS. The ablation cell was designed in order to avoid carry over effects of particulate debris from adjacent ablation spots and to ensure minimum signal dispersion at the operating conditions of the gas source AMS (i.e. 200 μL/min He as carrier gas). It consists of a volume-optimized gas expansion head with targeting and observation window and a large volume sub-unit capable of hosting sample specimen with sizes of up to 100 mm x 20 mm. The system configuration and initial results from ¹⁴C measurements will be discussed in this presentation.

[1] Ruff M. *et al*, A GAS ION SOURCE FOR RADIOCARBON MEASUREMENTS AT 200 kV, RADIOCARBON, Vol 49, Nr 2, 2007, p 307–314

SO₂ photoexcitation links polar sulfate and climate-impacting volcanism

SHOHEI HATTORI^{1*}, JOHAN A. SCHMIDT², MATTHEW S. JOHNSON², SEBASTIAN O. DANIELACHE³, AKINORI YAMADA⁴, YUICHIRO UENO^{5,6} AND NAOHIRO YOSHIDA^{1,6}

¹ Department of Environmental Chemistry and Engineering, Tokyo Institute of Technology, Japan (hattori.s.ab@m.titech.ac.jp)

² Department of Chemistry, University of Copenhagen, Denmark

³ Faculty of Science & Technology, Sophia University, Japan

⁴ Department of Earth & Planetary Science, University of Tokyo, Japan

⁵ Department of Earth & Planetary Sciences, Tokyo Institute of Technology, Japan

⁶ Earth-life Science Institute (ELSI), Tokyo Institute of Technology, Japan

Natural climate variation, such as that caused by volcanoes, is the basis for identifying anthropogenic climate change. However, knowledge of the history of volcanic activity is inadequate, particularly concerning the explosivity of specific events. Some material is deposited in ice cores, but the concentration of glacial sulfate does not distinguish between tropospheric and stratospheric eruptions. Stable sulfur isotope abundances contain additional information, and recent studies show a correlation between volcanic plumes that reach the stratosphere and mass-independent anomalies in sulfur isotopes in glacial sulfate. We describe a mechanism, photoexcitation of SO₂, that links the two, yielding a useful metric of the explosivity of historic volcanic events. A plume model was constructed including photochemistry, entrainment of background air, and sulfate deposition. Isotopologue-specific photoexcitation rates were calculated based on the UV absorption cross-sections of ³²SO₂, ³³SO₂, ³⁴SO₂, and ³⁶SO₂ from 250 to 320 nm. The model shows that UV photoexcitation is enhanced with altitude, whereas mass-independent oxidation, such as SO₂ + OH, is suppressed by *in situ* plume chemistry, allowing the production and preservation of a mass-independent sulfur isotope anomaly in the sulfate product. We are able to identify the process controlling mass-independent sulfur isotope anomalies in the modern atmosphere. This mechanism is the basis of identifying the magnitude of historic volcanic events.

Internal structure of a mid-crustal magmatic conduit: The Punta Falcone mafic pluton (Sardinia, Italy)

ANNE-CÉCILE HAUSER¹ AND FRANÇOIS BUSSY²

^{1,2}Institute of Earth Sciences, University of Lausanne, Géopolis, CH-1015 Lausanne.

(¹anne-cecile.hauser@unil.ch, ²francois.bussy@unil.ch)

The granite-hosted mid-crustal gabbroic pluton of Punta Falcone is built by many magmatic pulses with contrasting textures and composition. Gabbros can be divided into a supposedly older external zone (EZ) and a central zone (CZ) based on mineralogical, textural and geochemical arguments. CZ gabbros are more primitive in composition as indicated e.g. by higher mg-# in amphiboles. They contain relics of orthopyroxene, which are absent in the EZ gabbros. Whether the change in chemistry is due to more thorough interaction of the earlier pulses (EZ) with the host rocks during ascent/in the source region or whether it represents a change in the magma source should be resolved by radiogenic isotope compositions.

High An-contents of plagioclase as well as important amounts of amphibole in all gabbros express the high water content of the system. Phase diagrams based on water-saturated experiments allow linking the early stabilization of amphibole in the EZ gabbros (sub-euhedral grains) with cooling of the magma during ascent. The later appearance of amphibole in the CZ gabbros (poikilitic interstitial phase around euhedral plagioclase) on the other hand indicates higher temperatures for the same pressure and thus thermal maturation of the system over time. Furthermore the first pulses (EZ) crystallize as a whole with isotropic granular textures, whereas later pulses (CZ) show signs of crystal segregation and cumulate processes. They display remarkable rhythmic black and white layering at the cm-scale, which is roughly vertical and parallel to the limits of the cooling units. A second set of layers is crosscutting the main one at an angle of ca. 35°. Dark bands are defined by interstitial amphibole, which is absent in the white layers. The amount of lost liquid might reach several tens of wt%. The concentration of late crystallizing amphiboles in the dark layers indicates that liquid extraction is possibly linked to the development of the layering.

We interpret these magmatic structures as resulting from shearing of a crystallizing mush during its ascent or at its final emplacement level, with concomitant extraction of residual liquid, which escaped to higher crustal levels.

The effect of hydrothermal iron on marine dissolved organic carbon

J. A. HAWKES*¹, D. P. CONNELLY¹, A. DJURHUUS² AND E. P. ACHTERBERG¹

¹National Oceanography Centre Southampton, European Way, Southampton, UK

²University of Oxford, Department of Zoology, South Parks Road, Oxford, UK

High temperature hydrothermal vents produce particle rich plumes in particle deprived deep ocean regions. Dissolved organic carbon (DOC) may be adsorbed onto this iron rich particulate matter and as a result hydrothermal plumes may act as a sink for DOC [1]. It is estimated that the ocean's water is cycled through hydrothermal plumes on a 4000-8000 year timescale [2], making even very small DOC concentration changes in plume waters significant to the ocean budget of DOC. With an increasing variety of venting types being discovered [3,4], including environments which produce new DOC from magmatic CH₄ and CO₂ [5,6,7], a deeper understanding is required to assess the impact of hydrothermal vents on marine DOC.

We present new carbon and iron concentration data from plumes in three different hydrothermal settings: a back-arc vent site, a deep mid ocean ridge vent site and a ocean core complex hosted vent site. The plume characteristics (physical and chemical) are very different at these three sites, and samples were taken from vent fluids, diffuse areas of venting, the buoyant plumes and the dispersing (neutrally buoyant) plumes, allowing a comprehensive description of the interactions between dissolved and particulate iron and carbon in these three high-temperature vent environments. We will use the results to consider the overall impact that hydrothermal venting has on the concentration and nature of marine organic carbon globally.

[1] Bennett *et al* (2011), *Deep Sea Res. I* **58**, 922-931.

[2] Elderfield & Schultz (1996), *Annu. Rev. Earth Planet. Sci.*

24, 191-224. [3] Kelley *et al* (2005), *Science* **307**, 1428-1434.

[4] Connelly *et al* (2012), *Nat. Comm.* **3** no.620. [5] Bennett *et al*

(2011), *Geochim. Cosmochim. Acta* **75**, 5526-5539.

[6] Lang *et al* (2010), *Geochim. Cosmochim. Acta* **74**, 941-

952. [7] Lang *et al* (2006), *Geochim. Cosmochim. Acta* **70**,

3830-3042

Assessing the influence of glacial weathering on marine iron (Fe) inputs using Fe stable isotopes

S.M. HAWLEY^{1*}, H.M. WILLIAMS¹, P.A.E. POGGE VON STRANDMANN², S.R. GISLASON³ AND K.W. BURTON¹

¹Durham University, Durham DH1 3LE, UK (correspondence: s.m.hawley@durham.ac.uk, kevin.burton@durham.ac.uk, h.m.williams2@durham.ac.uk)

²University of Oxford, Oxford, OX1 2JD, UK (philipvs@earth.ox.ac.uk)

³University of Iceland, Reykjavik, 101 Reykjavik, Iceland (sigrg@raunvis.is)

Marine concentrations of bioavailable and reactive Iron can modulate the Carbon cycle and Earth's climate [1,2] Previous studies of glacial weathering [3,4] suggest that biogeochemical processes at rock-glacier interfaces promote the formation of highly bioavailable and reactive nano-particulate iron oxy-hydroxides. Consequently, because glacial weathering is a climatically dependent process the marine export of glacially derived oxy-hydroxide should strengthen the feedback loop between Fe and the climate.

Iron stable isotopes ($\delta^{57}\text{Fe}$) have potential to trace weathering Fe exports as Fe oxy-hydroxide formation has been shown to fractionate Fe stable isotopes [5]. Preliminary data from Kangerlussuaq, Greenland indicates suspended particulate and dissolved material have heavy $\delta^{57}\text{Fe}$ values (-0.20 permil) compared to the surrounding bedrock and riverine bed loads (-0.10 to 0.00 permil). This study will incorporate further Fe isotope data from glacial and non-glacial catchments in Iceland and Greenland. Both Iceland and Greenland contain glacial and non-glacial systems that drain relatively uniform rock types allowing for the effects of the different weathering regimes to be compared. Comparisons between Greenland and Iceland then allow independent assessment of the role bedrock plays in controlling Fe exports from glacial and non-glacial weathering.

[1] Martin (1990) *Paleoceanography*, **5**(1), 1-13. [2] Lalonde *et al* (2012) *Nature*, **483**, 198-200 2012. [3] Raiswell *et al* (2006) *Geochem. Cosmo. Act.* **70**, 2765-2780. [4] Wimpenny *et al* (2011) *EPSL* **290**, 427-437 [6] Severmann *et al* (2008) *Geology* **36**, 487-490.

Exhalation and inhalation of Ceria lattice Oxygen: A triple Oxygen isotope perspective

JUSTIN HAYLES¹ AND HUIMING BAO¹

¹Department of Geology and Geophysics, Louisiana State University, Baton Rouge, LA 70803 (jhayle3@lsu.edu)

Ceria (CeO_2) is a fluorite type oxide that has been studied and used extensively as an oxygen storage media in three-way catalysts, as an oxygen partial pressure regulator, as a fuel additive for the reduction of soot, and for the production of syn-gas from water and CO_2 . It is known that exposing ceria powders to low $p\text{O}_2$ and/or high temperature conditions will cause ceria to partially reduce. This partial reduction drives off oxygen from crystal lattice (exhalation) and leads to the formation of oxygen vacancies. When partially reduced ceria is exposed to high $p\text{O}_2$ environments, such as open air, the ceria powders will readily reoxidize even at room temperature. The reoxidation effectively fills the oxygen vacancies with new oxygen (inhalation). We expect that oxygen isotope fractionation is associated with both the exhalation and the inhalation processes. Understanding the isotope effect will help us explore the molecular mechanism for the dissociation, association, migration of oxygen on the surface and within the lattice of ceria.

To determine this isotope effect, we have devised an experimental procedure utilizing triple oxygen isotope labelled initial ceria powders. These powders are heated (700°C) for one hour and cooled under vacuum prior to exposure to air. By combining the results from six independent experimental sets using different initial oxygen isotope labels we have determined the kinetic isotope fractionation factors for both exhalation and inhalation using a graphical method. Our results indicate that there is a $1.6\text{‰} \pm 0.6\text{‰}$ increase in the $\delta^{18}\text{O}$ value of the remaining ceria upon heating in vacuum. When the vacuum is broken at room temperature, the heated ceria will inhale 3% to 12% oxygen from air, with a $\delta^{18}\text{O}$ of 1.6‰ ($+4.6\text{‰}$; -5.6‰). These fractionation factors are consistent with the magnitudes of kinetic fractionation associated with the dissociation and association of atomic oxygen at the surface of ceria. The issue associated with room-temperature oxygen inhalation renders ceria a poor choice of exchange medium for triple oxygen isotope analysis of CO_2 or other oxygen-bearing gases. We have discovered a similar result for yttria stabilized zirconia as well, suggesting that this behaviour may be intrinsic to the fluorite type oxides.

Contrasting tourmaline chemistry from late-Archaen orogenic gold deposits at Hutti and Hira-Buddini, eastern Dharwar craton, India: Implications for fluid source

PRANJIT HAZARIKA^{1*}, BISWAJIT MISHRA¹
AND KAMAL LOCHAN PRUSETH¹

¹Department of Geology and Geophysics, Indian Institute of Technology, Kharagpur, India-721302
(correspondence:pranjit.hazarika@gg.iitkgp.ernet.in)

Textural and chemical features of tourmaline in the proximal alteration zones of the Hutti and Hira-Buddini deposits are: (i) warping of biotite-chlorite mylonitic foliation, (ii) inclusions in pyrite, and (iii) sharp decrease of Fe at rim. These imply (i) synchronous sulfidation of the wall rocks resulting in pyrite formation and (ii) early tourmalinization and its continuation until sulfidation of wall rocks and gold mineralization.

Tourmalines from Hutti are Mg-rich ($X_{Mg}=0.63$) while the unaltered rock is Fe-rich ($X_{Mg}=0.30$). Their high Al content (> 6 apfu) implies no substitution of Al by Fe^{+3} in the Z-site. The dominant substitutions observed are $MgFe^{+2}_{-1}$, and $\square AlNa_{-1}(Fe^{+2},Mg)_{-1}$. Participation of Fe^{+2} in most substitutions suggest a low Fe^{+3}/Fe^{+2} ratio, also supported by the compositions lying on the dravite-foitite trend. These observations suggest a reducing nature for the tourmaline precipitating fluid. The Mg-rich composition of tourmaline in Fe-rich amphibolite shows insignificant chemical control of the unaltered rock on the tourmaline chemistry and suggest their formation under high fluid by rock ratio [1]. Such Mg-rich, low saline (X-site vacancy upto 0.53) and reducing nature of the fluid is suggestive of a metamorphic source [1][2].

Tourmalines from Hira-Buddini belong to dravite-schorl series with relatively low Mg ($X_{Mg}=0.53$); low X-site vacancy (≤ 0.16) and show an oxy-dravite-povandrite (O-P) trend. Dominant substitutions observed are $Fe^{+3}Al_{-1}$, $Fe^{+2}Fe^{+3}(Al_{-1}Mg_{-1})$ and minor $NaMg(\square_{-1}Al_{-1})$. Al contents of < 6 apfu is possibly due to substitution of Al in the Z-site by Fe^{+3} , as evident from the substitution types and tourmaline compositions lying on the O-P trend. Tourmalines characterized by enrichment in Fe^{+3} and Na, depleted in X-site vacancy suggest oxidizing and relatively high saline fluid, which could be either from a meta-evaporitic [3] or a late stage granitic source [4].

[1] Jiang *et al* (2002), *Chem Geol* 188, 229-247. [2] Groves and Phillips (1987), *Ore Geol Rev* 2, 287-322. [3] Cabral *et al* (2012), *Lithos* 140-141, 224-233. [4] Henry and Dutrow (2012), *Lithos* 154, 16-32.

Earth's Carbon through Deep Time

ROBERT M. HAZEN

Geophysical Laboratory, Carnegie Institution of Washington,
5251 Broad Branch Rd NW, Washington DC 20015 USA.
(rhazen@ciw.edu)

Earth's 4.567 billion year history is marked by a dramatic evolution in the chemical, physical, and biological roles of carbon [1,2]. Aspects of Earth's changing carbon cycle are revealed by a variety of investigations, including: (1) Abiotic organic synthesis, notably mineral catalyzed reactions of volcanic gases, yield essential biomolecules. Recent findings point to the critical role played by hydrogen fugacity in the synthesis and stability of these molecules [3]. (2) Small organic molecules display competitive and cooperative adsorption on mineral surfaces. We find that adsorption configurations are strongly affected by environmental conditions such as pH, ionic strength, and solute concentration [4]. (3) Experimental, theoretical, and field studies elucidate serpentinization reactions, as well as other deep interactions between C-bearing fluids and mafic and ultramafic rocks. Both volcanic and impact hydrothermal zones led to the first extensive carbonate mineral production [5]. (4) The subsurface biosphere modifies and cycles carbon. Deep microbial life often survives at metabolic rates and in concentrations far below those of near-surface communities [6]. And (5) carbon mineral evolution traces the changing diversity, distribution, and compositions (including trace and minor elements) in carbon minerals through deep time. Diamond was the first mineral in the cosmos, but many of the almost 400 known carbon minerals have appeared only recently in Earth history [7]. Collectively, these and other investigations of Earth's carbon through deep time underscore the co-evolution of the geosphere and biosphere.

[1] R.M.Hazen, A.P.Jones & J.A.Baross [Eds] (2013) Carbon in Earth. *Rev. Mineral. Geochem.* v. 75, 698 p; [2] R. Dasgupta (2013) Ingassing, storage, and outgassing of terrestrial carbon through geological time. *Rev. Mineral. Geochem.* 75, 183-229; [3] M.A.Sephton & R.M.Hazen (2013) On the origins of deep hydrocarbons. *Rev. Mineral. Geochem* 75, 449-465; [4] H.J.Cleaves *et al* (2012) Mineral-organic interfacial processes: Potential roles in the origins of life. *Chem. Soc. Rev.* 41, 5502-5525; [5] M.O.Schrenk *et al* (2013) Serpentinization, carbon and deep life. *Rev. Mineral. Geochem* 75, 575-606; [6] F.S.Colwell & S. D'Hondt (2013) Nature and extent of the deep biosphere. *Rev. Mineral. Geochem* 75, 547-574; [7] R.M.Hazen, *et al* (2013) Carbon mineral evolution. *Rev. Mineral. Geochem* 75, 79-107.

Paleomineralogy of the Hadean Eon

ROBERT M. HAZEN

Geophysical Laboratory, Carnegie Institution of Washington,
5251 Broad Branch Rd NW, Washington DC 20015 USA.
(rhazen@ciw.edu)

The Hadean Eon, encompassing Earth's first 550 million years, was a time of significant planetary evolution. Nevertheless, prebiotic Earth's near-surface environment may have held no more than approximately 420 different rock-forming or accessory mineral species that were widely distributed and/or volumetrically significant [1]. This relative Hadean mineralogical parsimony is a consequence of the limited modes of mineral paragenesis prior to 4 Ga compared to the last 3.0 billion years. Dominant Hadean Eon mineralizing processes include the evolution of a diverse suite of intrusive and extrusive igneous lithologies; hydrothermal alteration over a wide temperature range, notably serpentinization; authigenesis in marine sediments; diagenesis and low-grade metamorphism in near-surface environments; and impact-related processes, including shock mineralization, creation of marginal hydrothermal zones, and excavation of deep metamorphosed terrains. On the other hand, the Hadean Eon may have been notably lacking in mineralization generated by plate tectonic processes, such as subduction zone volcanism and associated fluid-rock interactions, which result in massive sulfide deposition; convergent boundary orogenesis and consequent extensive granitoid-rooted continental landmasses; and the selection and concentration of incompatible elements in complex pegmatites, with hundreds of accompanying minerals. The dramatic mineralogical consequences of life are reflected in the absence of Hadean biomineralization; for example, the lack of extensive carbonate deposits and the associated restricted development of skarn and cave minerals prior to 4 Ga. Most importantly, it was not until after the establishment via photosynthesis of significant near-surface redox gradients that supergene alteration, redox-controlled ore deposition, and subaerial weathering in an oxidizing environment could diversify Earth's near-surface mineralogy. These post-Hadean processes may be responsible for more than 4000 of the more than 4800 approved mineral species. Any scenario for life's origins that invokes minerals as agents of molecular synthesis, selection, protection, or organization must take into account the limited mineralogical repertoire of the time.

[1] R.M.Hazen (2013) Paleomineralogy of the Hadean Eon: A preliminary list. *American Journal of Science*, in press.

Role of bacteria on the release of cesium from illite

ALICE HAZOTTE^{1*}, THIERRY LEBEAU¹, OLIVIER PÉRON²,
TAKUMI SAITO³ AND ABDELOUAS ABDESSELAM²

¹LUNAM University, LPGN, UMR 6112, BP 92208, 44322
Nantes, France (*alice.hazotte@univ-nantes.fr;
thierry.lebeau@univ-nantes.fr)

²Subatech, UMR 6457, BP20722, 44307 Nantes, France
(abdeslam.abdelouas@subatech.in2p3.fr;
olivier.peron@subatech.in2p3.fr)

³Department of Nuclear Engineering and Management,
School of Engineering, The University of Tokyo, Japan
(takumi@flanker.n.t.u-tokyo.ac.jp)

As a result of the nuclear accident in Fukushima, various radioactive elements such as cesium were dispersed in the atmosphere before being deposited on the soil within a distance of 80km around the nuclear power plant. Cesium with half-life of 30 years and properties similar to potassium accumulates in the clays, especially illite, of the upper soil horizons.

Among soil remediation methods, phytoextraction is the most appropriate one as it can be achieved *in situ* without any change of the biophysicochemical properties of the soil. Cesium uptake by plants depends on sorption/desorption reactions to/from the soil particles and on biogeochemical processes in the rhizosphere.

This work focuses on the bacterial mechanisms involved in Cs desorption from illite by estimating the amount of Cs released by desorption and/or as the result of illite alteration. Citric acid and oxalic acid that bacteria and plants are able to produce in soils were used in this work [1-2]. Illite alteration by these same bacteria also able to form biofilms at the surface of soil particles was studied [3-4]. Eventually experimental results were compared to those obtained by modeling.

[1] Krebs, Brombacher, Borrhard, Bachofen and Brandl (1997), *FEMS Microbiology Reviews* 20, 605-617. [2] Vyas and Gulati (2009), *BMC Microbiology* 9, 174. [3] Alimova, Katz, Steiner, Rudolph, Wei, Steiner and Gottlieb (2009), *Clays and Clay Minerals* 57-2, 205-212. [4] Dong (2012), *Elements* 8, 113-118.

Multiple exsolutions in a rare clinopyroxene megacryst from the Hannuoba basalt, North China: Implications for subducted slab-related crustal thickening and recycling

DETAO HE, YONGSHENG LIU*, XIRUN TONG, KEQING ZONG, ZHAOCHU HU, SHAN GAO

Faculty of Earth Sciences, China University of Geosciences, Wuhan, 430074, China (*correspondence: yshliu@hotmail.com)

A rare large clinopyroxene megacryst (type 1) collected from the Hannuoba basalt, North China was studied. It is distinguished from the prevalent clinopyroxene megacrysts (type 2) by garnet and orthopyroxene exsolutions and by chemical and Sr-Nd isotopic compositions. The type 1 clinopyroxene megacryst has higher Cr (2100 ppm) and Mg# (83) than the type 2 clinopyroxene megacrysts as well as more evolved Sr and Nd isotopic compositions. These characteristics suggest that the type 1 clinopyroxene megacryst could have been formed by a recycled crust-related melt-peridotite reaction. The type 2 clinopyroxene megacrysts exhibit good correlations between Mg# and major and trace element compositions. Their Sr-Nd isotopic compositions cluster in the least evolved field of the Hannuoba basalt. These observations imply that the type 2 clinopyroxene megacrysts were crystallized from the host lava at high pressure.

The type 1 clinopyroxene megacryst contains abundant coherent cryptocrystalline lamellae and orthopyroxene exsolutions within it. The bulk composition of the cryptocrystalline lamellae, composed of fine plagioclase and olivine, shows typical chemical features of garnet and Sr isotopic composition similar to the clinopyroxene host. These observations indicate that the cryptocrystalline lamellae are decomposition products of garnet exsolutions in the clinopyroxene megacryst. This garnet exsolution could be caused by increasing pressure or decreasing temperature, as indicated by experimental results. Although the temperature decreases during basalt eruption, the much quicker decrease in pressure will suppress the garnet exsolution in clinopyroxene. Therefore, we suggest that the type 1 clinopyroxene megacryst could have experienced pre-Mesozoic crustal uplifting and thickening at the north margin of the North China Craton. Garnet decomposition could have taken place prior to orthopyroxene exsolution during the eruption of the host lava.

Noble gases in mantle xenoliths from the Tan-Lu fault zone, North China Craton

HUAIYU HE, FEI SU AND RIXIANG ZHU

Institute of Geology and Geophysics, Chinese Academy of Sciences, Beijing 100029, China

The Tan-Lu fault zone, which extends NNE-SSW for more than 3000km, is a major lithospheric discontinuity along the eastern Asia continent and is believed to have acted as a major channel for the ascending of asthenosphere and played an important role in the Mesozoic-Cenozoic thinning of the North China Craton (NCC) lithosphere. From North to South, there are many Cenozoic volcanic areas which are located in the Tan-Lu Fault Zone. Ultramafic xenoliths, mainly lherzolite and pyroxenite, are common in alkali basalts in these volcanic areas. Detailed petrological and geochemical studies suggest that these low Mg# peridotites (Fo 88-91) represent fragments of the newly accreted lithospheric mantle.

This study performed a comprehensive investigation of petrology, mineral chemistry and noble gases of mantle xenolith in Changle-Linqu (in the middle part of Tan-Lu Fault Zone) and Nvshan (in the south part of Tan-Lu Fault Zone) and try to trace the post destruction evolution of North China Craton (NCC) lithospheric mantle.

Olivines in wehrlites and lherzolites in Changle-Linqu and Nvshan yield $^3\text{He}/^4\text{He}$ ratio range from 6.9 to 7.6 Ra, a little bit lower than MORB value ($8\pm 1\text{Ra}$), suggest that lithospheric mantle in the Tan-Lu fault zone would thus most likely have been metasomated by melts/fluids derived from an asthenospheric reservoir or lithospheric mantle is cooling from asthenospheric. However, wehrlites and lherzolites have significant lower $^3\text{He}/^4\text{He}$ ratios, lower helium abundance and lower $^4\text{He}/^{40}\text{Ar}^*$ in Cpx than in co-exist Ol. ^4He abundance and $^3\text{He}/^4\text{He}$ ratios of Opx are lower than co-exist Ol and higher than co-exist Cpx. Our thin section study indicates there is a direct link between sieve texture/melt-pocket and low helium abundance, low $^3\text{He}/^4\text{He}$ ratios and low $^4\text{He}/^{40}\text{Ar}^*$. This may suggest that the noble gas in Cpx were lost during partial melting and there is diffusive fractionation between ^3He , ^4He , and ^{40}Ar .

Novel bionanocomposites - Chitosan Goethite Bead - for arsenic remediation

J. HE^{1,2}, F. BARDELLI¹, A. GEHIN¹ AND L. CHARLET^{1*}

¹ISTerre, Université Joseph Fourier (Grenoble), P.O. Box 53, F 38041 Grenoble, France,

(*correspondence:charlet38@gmail.com)

²School of Resource and Environmental Science, Wuhan University, Wuhan 430079, PRC

Since iron oxides/hydroxides have high sorption affinity toward both As(V) and As(III), many scientific and industrial researches focus on the application of iron oxides/hydroxides as adsorbents in water treatment. Nevertheless, most iron oxides/hydroxides are fine powders, difficult to separate from solution after the adsorption process. In this study we develop a novel method for the synthesis of chitosan-iron hydroxide composite leading to chitosan-goethite bead (CGB). Goethite nanoparticles and chitosan gel-beads were prepared simultaneously, obtaining 1mm-sized spherical bionanocomposites, consisting of homogenous distribution of the goethite nanoparticles in the chitosan phase with enhanced mechanical properties compared to pure polymer/pure mineral. The macroscopic structure of the composite determines that it can overcome the difficulty of separation procedure in water treatment, while its microscopic structure retains the superiority of nanomaterial with regard to high sorption efficiency. CGBs were characterized by Mössbauer spectroscopy to confirm the presence of goethite phase, and their morphology was investigated by FE-SEM. Batch sorption and kinetic experiments on CGB reactivity toward arsenate and arsenite were performed to quantify the sorption and diffusion-controlled kinetics of CGB with respect to As. In addition, the mechanism of arsenic uptake onto CGB was investigated by X-ray Absorption Spectroscopy (XAS), and the diffusion of As(V) and As(III) from aqueous into solid phase was monitored by micro X-ray fluorescence (μ XRF) (Fig.1) and micro X-ray Absorption Near Edge Spectroscopy (μ XANES).

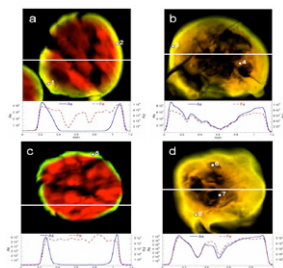


Figure 1. Color temperature distribution maps of As (green color) and Fe (red color) of As-loaded CGB samples, collected from kinetic experiments of As(V) sorption onto CGB a) at 1.5 h, b) at 120 h; As(III) sorption onto CGB c) at 1.5 h; d) at 120 h.

C4 plants expansion and the enhanced aridity from the late Miocene to Pliocene on the Chinese Loess Plateau

TONG HE, YANG CHEN, JUNFENG JI*

The MOE Key Laboratory of Surficial Geochemistry, School of Earth Sciences and Engineering, Nanjing University, Nanjing 210093, China (*Correspondence: jijunfeng@nju.edu.cn)

The Red Clay Formation, which underlies the well-known Quaternary loess sequence, extends the eolian deposits from 2.6Ma through the late Miocene making it a good archive to reconstruct Pliocene climate in North China. The carbon isotopic composition of carbonate nodules in the Red Clay Formation has been suggested as potential proxy for paleoecology. The spatial and temporal pattern of carbon isotopes will provide new evidence for the drying history from late Miocene to Pliocene.

We studied four continuous sections (Duanjiapo, Lingtai, Bajiazui and Jiaxian) of the Red Clay Formations on Chinese Loess Plateau (CLP) by stable isotope mass spectrometer. The averages of carbon isotopes were at -9.3‰ , -8.0‰ , -5.3‰ and -4.9‰ , respectively. The carbon isotopes of carbonate nodules show a northward positive gradient on CLP, suggesting an increasing trend of C4 plants abundance, which may relate with increasing aridity.

Two C4 plants expansion events were revealed from our Red Clay carbon isotope records. C4 plants greatly expanded in two intervals at $\sim 6.4\text{Ma}$ and $\sim 3.6\text{Ma}$ on CLP. The enhanced aridity may account for the two events.

Acknowledgment

This study is funded by the NSF of China (Grant No. 41021002 and 41230526).

A thermodynamic entrapment model for the quantitative description of selenite coprecipitation with calcite

F. HEBERLING^{1*}, V.L. VINOGRAD^{2,3}, R. POLLY¹

¹Karlsruhe Institute of Technology, Institute for Nuclear Waste Disposal, Karlsruhe, Germany, Frank.Heberling@kit.edu

²Forschungszentrum Jülich, Institute of Energy and Climate Research-6, Jülich, Germany

³Goethe Universität Frankfurt, Institute of Geosciences, Frankfurt, Germany

The trace element Selenium is of environmental relevance as a nutrient as well as a toxic element for animal and human life. The long lived fission product ⁷⁹Se is of special concern in the context of nuclear waste management.

A possible retention mechanism for selenite in natural environments is the structural incorporation of the trigonal pyramidal oxyanion Se(IV)O₃²⁻ into the calcite structure.

EXAFS and polarization dependent EXAFS measurements confirm, in agreement with previous results [1], the structural incorporation of selenite in calcite and the substitution of carbonate for selenite, leading to the formation of a Ca(SeO₃)_x(CO₃)_(1-x) solid solution.

Selenite incorporation, quantified in coprecipitation experiments at surface controlled steady state conditions and low supersaturation, is much higher (partition coefficient, D_{exp} = 0.015±0.012) than expected according to DFT calculations and thermodynamic considerations (D_{theo} = 2·10⁻¹⁰).

To bridge the gap between experiment and theory we present a thermodynamic entrapment model based on the assumption, that experimental observations reflect preferential incorporation of selenite into the calcite surface and subsequent entrapment upon crystal growth, while bulk DFT calculation reflect the high strain induced upon incorporation of selenite into the bulk calcite structure.

DFT calculations confirm that surface incorporation is energetically more favourable than bulk incorporation. Batch type adsorption experiments at calcite equilibrium confirm the analogy between surface adsorption (ion-exchange [2]) and coprecipitation.

The observation of growth inhibition in aragonite to calcite recrystallization experiments in the presence of selenite in solution is interpreted as experimental evidence for the energetical difference between bulk and surface incorporation of selenite in calcite.

[1] Aurelio *et al Chem. Geol.* 270, **2010**, 249-256. [2] Cheng *et al Surf. Sci.* 283, **1997**, L690-L695

Tawlah Specialized Alkaline Granite Prospect, Midyan Region, Arabian Shield, Kingdom of Saudi Arabia: Petrology. Structural Implications and REEs-RM Characterization

MOHAMED TH.S. HEIKAL¹ AND MAHER A. AMMAWY²

¹Geology Department, Faculty of Science, Tanta University, Tanta 31527, Egypt (Mohamed.heikal2010@yahoo.com)

²Geology Department, Faculty of Science, Benha University, Egypt

The Tawlah albite granites-quartz syenites is one of promising sites of REE- Ta-Nb- bearing alkaline granites in the Midyan Suite, NW Arabian Shield. The granite-syenite association is a highly leucocratic, albite-rich rocks with accessory columbite-tantalite, thorite, monazite, allanite, xenotime, zircon and cassiterite. Ages of 577± 4 Ma (Hedge, 1985) were obtained from isotopic ratios of Sr and Nd by ¹⁴³Nd/¹⁴⁴Nd and ⁸⁷Sr/⁸⁶Sr method. The precision is sufficient to indicate that the albite granite is post-orogenic with respect to Najd orogeny. The Tawlah granite is divided into albite-granite (in major) and quartz-syenite (in part). The albite granite is more highly mineralized, has higher modal albite contents and higher Nb/Ta ratios, both in whole surface rocks and in drill hole samples.

On the structural point of view, the relationship between fault system and/or shear zones reported and mineral potential provides excellent and interesting evidences of its occurrence. Bearing in mind the Najd fault zone provides interesting evidences concerning the relationship between such faults and REEs-Nb-Ta-Th mineralization. Therefore, the distribution of mineralizations are closely related to the main trends; WNW-ESE, NW-SE and ENE. On the other hand, reactivation of NW Najd fault system has been affected by Tertiary rift tectonics, leading to the development of mineralization in Tawlah alkaline granites.

On the basis of petrographic, mineralogical signature and geochemical interpretations, it is suggested that the albite granite-quartz syenite of Jabal Tawlah has a magmatic origin indicating post-orogenic overprinting of A-type granites. By analogy with other Nb-Ta-REEs -bearing granites, the sodic bulk composition of Tawlah granite can be explained by fluorine enrichment in the magma, but much of the magmatic fluorine was lost upon crystallization because the low CaO, P₂O₅ and Al₂O₃ contents of melt precluded fixation of F in crystalline phases.

In fact, the Tawlah alkaline granite prospect is considered to be a promising metallogenic site for REEs and Nb-Ta-Th, where its geologic environment, structural framework and tectonic setting are reasonable for achievement.

Why so much gold in the Archean? Some thoughts linking the Witwatersrand gold endowment to hydrothermal processes

CHRISTOPH A. HEINRICH

ETH Zurich, Department of Earth Sciences, 8092 Zürich,
Switzerland; heinrich@erdw.ethz.ch

Archean cratons constitute a tiny fraction of today's continental surface, but are disproportionately endowed by gold mineralization, amounting to more than half of the known economic resources. Through Earth's history, gold ore accumulation in veins and shear zones by metamorphic and/or deep-seated magmatic fluids broadly correlates with the rate of continental crust formation, both showing a prominent peak in the Archean at 3.2 – 2.5 Ga. The Witwatersrand basin in the Kaapvaal Craton also formed in this period, hosting some 40% of economic gold ore in fluvial conglomerate layers that also contain pyrite pebbles, uraninite grains and reduced carbon. The enrichment of these minerals within conglomerate layers occurred near the paleosurface, but the mechanism of gold deposition (clastic or early hydrothermal), the transport medium (fluvial or shallow marine water; mechanical or chemical) and the source of the gold remain debated.

Mass-balance estimations indicate that craton-scale erosion of normal crustal rocks could deliver enough gold to produce the Witwatersrand ores. However, if transport and enrichment occurred mechanically in placer deposits, this requires that particles of native gold were available in the eroding crust. The process that may have precipitated these primary gold particles may well be a critical step in the exceptional endowment of Archean crust with economic gold deposits. In today's surface environment, most of the hydrothermal flux of gold through the upper crust becomes dispersed, ending up in slightly gold-enriched black shales that are liable to recycling, but only locally contribute to later ore formation. By contrast, the acid surface environment in Archean times may have acted as a near-perfect "screen" for the precipitation of all the gold transported upward from the lower crust or the mantle by crust-forming processes. Vein deposits in greenstone belts probably trapped only a small fraction of this hydrothermal gold flux, while a far greater fraction of native gold may have been precipitated near the land surface, also above widespread granitoids. Gold particles would have been ready for further concentration by mechanical transport into conglomerate reefs, but some direct precipitation of dissolved gold by reduction on local organic material in permeable aquifers may have upgraded the ore.

Changing mantle wedge geometry and magma generation processes in the Central Andes

ROSANNE HEISTEK^{1*} AND GERHARD WÖRNER¹

¹GZG, Georg-August Universität, 37077 Göttingen, Germany
(*correspondence: rheiste@gwdg.de)

Miocene andesitic volcanoes in the Central Andes typically overly plateau-forming ignimbrites. These "early" andesites form low angle volcanic shield volcanoes succeeded by more evolved steep-sided strato-cones. These cover smaller areas and are characterized by amphibole phenocrysts. Such a transition could be either due to a change in the melting regime in the mantle wedge from decompression (hot and dry?) to flux melting (wet and lower T?) or to different magma production and effusion rates.

We studied samples that represent different ages, petrography, composition, and volcanic style in order to test differences in processes of magma generation. Based on a survey of >4000 chemical analyses (<http://andes.gzg.geo.uni-goettingen.de/>) and the distribution of SiO₂ we selected three representative sample types 1) the most mafic samples (50-55 % SiO₂), 2) the intermediate andesites representing 63 % of the data (55-60 % SiO₂) and 3) felsic samples (60-65 % SiO₂) which were identified before as important endmember magma type in the Central Andes. Using a range of geothermometers and hygrometers, we show that the most significant parameters regulating viscosity at the time of eruption remained surprisingly constant throughout Andean history (e.g. 940°C to 1020°C for 2 pyroxene thermometry). Therefore, the rate of effusion, and by implication, magma production and upper crustal stress regime rather than eruption temperature are the primary factors that influenced flow length and flow field type.

Another important parameter maybe preferential erosion of Miocene stratocones relative to distal lava fields. An increase in slab dip after a time of flat-slab subduction may increase melt production in the mantle wedge and result a change in stress regime in the upper Andean plate. Ensuing high effusion rates during the Miocene produced lava shields with stacks of long lava flows at the base of (now eroded) steeper stratovolcanoes. Erosion of the central stratocone left isolated lava fields. By contrast, lower melt production and effusion rates during the Pliocene the Quaternary reflect more diverse ascent paths and crustal magma systems with more diverse cooling, crystallization, assimilation, and mixing histories. At the same time, the depth of magma evolution changed as represented by increasing garnet signatures from Miocene to Pleistocene lavas.

Soil heterogeneity and surfactant desorption influence PAH distribution at a tar-contaminated site

KATJA HEISTER^{1*} AND ANA T. LIMA²

¹ Lehrstuhl für Bodenkunde, Technische Universität München, 85350 Freising-Weihenstephan, Germany

(*correspondence: heister@wzw.tum.de)

² Department of Earth and Environmental Sciences, University of Waterloo, Waterloo, N2L 3G1, Canada

A remediation field experiment utilising electroosmosis and a non-ionic surfactant was conducted successfully at the site of a former asphalt production plant with a long-term tar-oil contamination [1]. After 159 days, the question arose whether the scattered distribution of the polycyclic aromatic hydrocarbons (PAHs) was due to soil's heterogeneity itself or to electroosmosis efficacy [1]. In this study, we assess the heterogeneity of the soil itself by analysing various soils samples with respect to amount and type of organic matter (OM) and PAH content. No relationship between either amount of OM, amount of aromatic carbon and PAH concentrations was observed. A relationship between PAHs and tar oil (represented by aromatic carbon) was *a priori* expected. Hence, soil's heterogeneity dominated this site rather than a considerable redistribution of PAHs during the electroosmotic treatment. Batch desorption experiments were then carried out with and without 1% Tween 80 on a representative sample of intermediate OM and PAH content and a sand sample with pure tar oil. The surfactant significantly enhanced PAH desorption and inhibited microbial degradation by forming micelles that entrap PAH molecules, making them unavailable to microorganisms. The PAH aqueous phase concentrations in the batch experiments were comparable to those obtained in the field experiment. Therefore, we conclude that the surfactant seems to be inevitable for the success of the remediation. As a consequence, in order to describe the transport of desorbed PAHs, micelles should be considered instead of single PAH molecules.

[1] Lima *et al* (2012) *Electrochim. Acta* **86**, 142-147.

Noise is now signal: Capturing the relevant from the distraction

MATTHEW T. HEIZLER¹

¹New Mexico Bureau of Geology, 801 Leroy Place, Socorro, NM, 87801, (matt@nmt.edu)

It is truly an exciting time for noble gas applications, and in the particular, geochronology precision is undergoing a revolutionary increase that allows incredible insight into complex geological processes. However this improvement is not immediately allowing for new discovery in geo and thermochronology. Removing the impediment towards new discovery lies in determining the causes for age scatter that is now recorded in most geological samples. Ultra-high precision age measurements (0.1-0.2 per mil) on individual volcanic crystals typically show ~0.2% standard deviation thereby reducing the MSWD to ridiculously high values. This leads to the question "What part of the scattered distribution records the geological event of interest?" Cases can be made for the young part, the middle part and the old part. Accurate young ages can be argued for by interpreting older results to be contaminated with excess and/or inherited argon. Excluding the young part in favor of the old part implies argon loss is the cause of inaccurately young grains. Perhaps our planet operates at a high standard deviation and natural variation caused by a host of mechanisms can be averaged such that the mean value of a scattered distribution remains the preferred choice for an event such as eruption. Determining the geological uncertainty for the time of eruption of a scattered distribution has no obvious value or statistical approach. Classical crosscutting relationships or stratigraphic order will always be the ground truth measure of accuracy and proper interpretation despite the level of precision reached in 2020. In addition to volcanology studies vastly improved spatial resolution at high precision will be the norm thereby increasing the utility of *in situ* analyses. Unfortunately, in many cases argon concentration profiles occur at a spatial resolution that will continue to confound our best current instrumentation. Despite the fact that new ultra sensitive, ultra clean multicollector mass spectrometers have jumped our science surprisingly forward, another leap will be required to achieve what every thermochronologist desires – an accurate concentration profile at a geologically relevant length scale. Lastly, the seemingly straightforward task to get geochronology labs intercalibrated remains a perplexing obstacle that inhibits productivity and causes unnecessary confusion. Because calibration and operation of the new and highly stable multicollector instruments will soon become routine, we as a community can have every expectation that this nagging issue will soon be a topic of the past.

**$^{234}\text{U}/^{238}\text{U}$ in speleothems revisited:
Are there generally applicable
relationships of this proxy to past
environmental change?**

JOHN HELLSTROM

School of Earth Sciences, The University of Melbourne,
Australia

The initial activity ratio of ^{234}U to ^{238}U , ($^{234}\text{U}/^{238}\text{U}$)_i, is the ratio of ^{234}U to ^{238}U atoms at time of formation of a sample, relative to that at secular equilibrium. It is found using their measured present ratio and the known age of a sample, and is a by-product of all U-Th disequilibrium dating as well as some U-Pb dating of Quaternary samples. As such there is now an enormous body of these data in the published literature. A number of publications have addressed paleoenvironmental significance of ($^{234}\text{U}/^{238}\text{U}$)_i over the last few decades but no clear consensus has emerged, other than that this initial disequilibrium is caused by some combination of alpha recoil and selective dissolution of ^{234}U as seepage water makes its way to the cave, and that hydrological factors probably have the greatest influence. General observations are that ($^{234}\text{U}/^{238}\text{U}$)_i tends to gradually fall with time at a given location, often to values well below one in relatively old, stable settings, and that significant paleoenvironmental changes invariably lead to some form of change superimposed upon this. The nature of these latter changes remains poorly understood. They vary hugely in magnitude with ($^{234}\text{U}/^{238}\text{U}$)_i values as high as 10 and as low as 0.5 having been observed, and are sometimes highly responsive to reconstructed external environmental change and sometimes lagged by thousands of years. Here I will report progress in understanding of the hydrological significance of ($^{234}\text{U}/^{238}\text{U}$)_i in speleothems, and of its significance for paleoenvironmental reconstruction and also for dating using the U-U and U-Pb techniques

**Hidden hotspot track beneath
Eastern United States**

DON HELMBERGER, RISHENG CHU, WEI LENG AND
MICHAEL GURNIS

Seismological Laboratory, California Institute of Technology,
Pasadena, CA 91125 USA

More than two thirds of surface hotspots associated with volcanism can be explained by the interaction between a moving plate and deep-seated mantle plumes¹. Most of these hotspot tracks are observed on oceanic or thin continental lithosphere. Although there are not many traditional hotspot tracks on old continents, there are diamondiferous kimberlites indicative of deep mantle origins². This poses the question that there could be many more hotspot tracks beneath old continental regions than suggested by the record of surface volcanism. Here we show that seismic waveforms recorded by USArray from a recent Virginia earthquake reveal an unexpected linear, lower lithosphere seismic anomaly extending from Missouri to Virginia without a clear relationship to surface geology. This east-west corridor has *P* velocity reduced by 2.1% along with high attenuation and crosscuts prominent regional features suggesting a link to plate motions. We suggest that a thermal plume-like upwelling interacting with the base of the continental lithosphere can produce the requisite seismic signal. A Late Cretaceous kimberlite in Kentucky, dated 75 Ma, pins a hotspot track that bends northward beneath Virginia. Seismic data indicates that the lower lithospheric anomaly along this northeastern segment is even stronger than the east-west segment, supporting such a hypothesis.

Pre-nucleation clustering of noble metals in high-temperature magmatic liquids

H. M. HELMY^{1*}, C. BALLHAUS², R. O. C. FONSECA²,
R. WIRTH³, T. NAGEL², M. TREDOUX⁴

¹Minia University, Minia, Egypt (correspondence.
hmelmy@yahoo.com

²Steinmann Institute, University of Bonn, Bonn, Germany
(ballhaus@uni-bonn.de)

³GFZ Potsdam, Germany (wirth@gfz-potsdam.de)

⁴University of the Free State, Bloemfontein, South Africa
(mtredoux@ufs.ac.za)

The conventional view is that magmatic trace minerals nucleate and grow by assembling cationic and anionic species from the melt. Experiments reported here suggest that this view may be simplistic. We have investigated on the nanometer-scale the distribution of Pt in Fe-Cu-S sulfide matrix. When ligands like arsenic are added to the sulfide, Pt and As self-organize to Pt-As molecules, non-crystalline (Pt-As)_n clusters, PtAs₂ nanoparticles, and at very high temperature to nanometer-sized droplets of Pt-rich Fe-As melt. With the addition of As, the partitioning of Pt among sulfide phases is shifted relative to simple (As-free) systems by at least an order of magnitude. Similar to minerals crystallizing from aqueous solutions, magmatic trace minerals may grow by oriented attachment of nanoparticles and nanophases when they crystallize from magmatic solutions. This explains how noble trace elements could form discrete mineral phases in subsolidus range although their concentrations in magmatic melts do not exceed tens of ppb to few ppm. Pre-nucleation clustering should be considered when highly siderophile elements (HSE) partition coefficients determined by simple system experimentation are used to model HSE fractionations among chemically more diverse reservoirs of the Earth

[1] Tredoux *et al* (1995). *South African Journal Geol* **98**, 157–167.

Dolomite reaction rim growth under non-isostatic stress

V. HELPA^{1*}, E. RYBACKI¹, G. DRESEN¹, W. HEINRICH¹,
R. ABART², L. MORALES¹

¹GFZ Potsdam, Telegrafenberg, 14473 Potsdam, Germany
(*correspondence: helpa@gfz-potsdam.de)

²University of Vienna, Althansstrasse, 1090 Vienna, Austria

Reaction rims of dolomite (CaMg[CO₃]₂) were produced by solid-state reactions of oriented calcite (CaCO₃) and magnesite (MgCO₃) single crystals using a gas-deformation apparatus at 400 MPa confining pressure, 750 °C, and run durations ranging from 4 to 76 h. In addition, we applied a differential stress up to 40 MPa perpendicular to the contact interface.

The resulting dolomite reaction rims consist of two different textural domains. Granular dolomite grains (2.2–5 μm grain size) grew next to calcite, while elongated palisade-shaped grains (2.2–5.2 μm diameter) grew perpendicular to the magnesite interface. The thickness of the granular dolomite layer is 2.9–11.2 μm, smaller than the palisade-like layer (5.2 to 13.2 μm). Platinum markers show that the initial interface is located between granular and palisade-forming dolomite, indicating that rim growth occurred by counter diffusion of MgO and CaO.

As expected, rim thickness increased with increasing run duration. The effect of the applied load is not systematic and causes a maximum variation in rim thickness of less than 11% at fixed time.

Diffusion of MgO across the dolomite reaction rim into calcite produced newly formed magnesio-calcite grains with an average diameter of 20.7 to 34.8 μm. Grain size of magnesio-calcite grains increased with increasing distance to the dolomite boundary. The magnesio-calcite layer increased from 29.1 to 63.3 μm with time, but was also not affected by the differential stress conditions.

The experiments indicate that differential stresses up to 40 MPa do not significantly change the kinetics of reaction rim growth in the carbonate system. Possibly this is because volume diffusion is the dominant transport mechanism, which presumably is less strongly affected by deformation than grain boundary diffusion.

Picking apart paleoredox proxies: What regulates them?

GEORGE R. HELZ*¹

¹Department of Chemistry, University of Maryland, College Park, MD 20742 USA (*correspondence: helz@umd.edu)

Certain trace elements that are oxyanions (broadly defined) with long seawater mean residence times (e.g. HVO_4^{2-} , CrO_4^{2-} , AsO_4^{3-} , MoO_4^{2-} , $\text{Sb}(\text{OH})_6^-$, WO_4^{2-} , ReO_4^{2-} , and $\text{UO}_2(\text{CO}_3)_2^{2-}$) are modestly to strongly enriched relative to Earth's crust in sediments below O_2 -depleted waters. Their enrichment in sedimentary rocks is cited to support qualitative conclusions about redox conditions in ancient sedimentary basins. More nuanced, possibly quantitative conclusions require better knowledge of events that regulate conversion of these particle-inert oxyanions to particle-reactive species. Each of these elements exists in multiple oxidation states in nature, inviting the assumption that pE regulates conversions. But pE is indefinable in natural waters, so this is at best a superficial explanation. In some cases, abiotic or biotically mediated electron transfer, leading to insoluble products, is indeed a regulating mechanism (U the most studied example). In other cases (e.g. Re), evidence for an electron transfer mechanism is lacking. In sulfidic solutions, most of these oxyanions undergo $\text{O} \leftrightarrow \text{S}$ exchange. If the particle reactivity of the thioanions exceeds that of the oxyanions, then $\text{O} \leftrightarrow \text{S}$ exchange could be a deposition-regulating mechanism. Often exchanges are labile, probably abiotically and thermodynamically controlled, and thus invariant over geologic time. Important gaps remain in knowledge of what regulates deposition of these elements--for example, polysulfides' role. Recent evidence demonstrates polysulfides' importance, at least for Mo and As. Another gap concerns organic matter's role. Correlations between the above elements and TOC are well known in sediments beneath O_2 -depleted waters. Correlations might be incidental or might point to specific biotic or abiotic organic reactions that participate in trace element deposition mechanisms. Good evidence exists for organic hosting of V and Re in TOC-rich sediments, but this may arise after deposition, during early diagenesis.

Rare Earth Element distributions as tracers of micronutrient input and Nd cycling in the South Atlantic

DEBORAH J. HEMBURY*, XINYUAN ZHENG, PHILIP HOLDSHIP, PETER SCOTT, MATTHEW POINTING, AND GIDEON M. HENDERSON

Department of Earth Sciences, University of Oxford, South Parks Road, OX1 3AN, UK (*correspondence: debbie.hembury@earth.ox.ac.uk)

Concentrations of the REEs in seawater reflect their inputs and their cycling in the water column. Because the behaviour of the REE have some similarities to that of micronutrient elements (such as Fe, Zn, Cu, Cd) but are not directly biologically utilised, their distribution has potential to constrain the cycling of micronutrients. The cycling of Nd is also of particular interest because Nd isotopes are widely used as tracers of past ocean circulation. In this study, we have measured REE concentrations on filtered samples collected during the UK-GEOTRACES GA10 cruises (D357, JC068) across the South Atlantic at 40°S. CTD profiles and a full range of other chemical parameters provide a comprehensive context for these new REE measurements. REE samples were obtained for the full- water column and concentrations determined by isotope-dilution MC-ICP-MS on 250 ml samples. This samples all the major deep-water masses of the Atlantic, and a clear water-mass dependence is observed in the concentrations of heavy REEs. The light REEs show significantly less water-mass dependence, however, suggesting the importance of downward particulate transport for their cycling, with implications for the interpretation of Nd isotopes. Ce concentrations demonstrate the lack of significant input in intermediate waters, reflecting O_2 levels that are insufficiently depleted to drive Mn cycling in the sediment, but are notably high in surface waters due to additional inputs and active release from particles.

The K/Ar system for tracing fine-grained terrigenous sediments: A survey of Atlantic clay fractions

SIDNEY R. HEMMING^{1,2*}, PIERRE E. BISCAYE²,
RAHUL SAHAJPAL³, JENNIFER M. COLE^{2,4}
AND WALLACE S. BROECKER^{1,2}

¹Department of Earth & Environmental Sciences, Columbia Univ. sidney@ldeo.columbia.edu (* presenting author)

²Lamont-Doherty Earth Observatory of Columbia University

³School of Earth and Environmental Sciences, Queens College.

⁴Western Kentucky Univ., Dept. of Geography & Geology

The provenance of terrigenous sediments provides important constraints on the processes that bring them to their depositional sites in the ocean. Terrigenous sediments are formed by weathering and are delivered to the ocean by wind, water, and ice, and are redistributed within the ocean by currents. The mineralogical content and geochemical composition of sediments reflect the source rock types, weathering style and intensity, as well as sedimentary sorting evidence for sedimentary transport and delivery mechanisms. Radiogenic isotopes provide a measure of the temporal geologic history of sediments that is different depending on the geochemical characteristics of the parent and daughter isotopes. The K/Ar system in fine-grained terrigenous sediments reflects the latest stages of the geologic history of the sediments' sources. Thus the K/Ar "age" of fine-grained sediments provides a useful measure of sediment provenance, previously demonstrated by several studies (e.g., Hurley *et al.*, 1961, GSAB, 1963a, GCA, 1963b, GCA; Jantshik and Huon, 1992, *Ecolae Geol. Helv.*; Huon and Ruch, 1992, *Mar. Geol.*; Pettke *et al.*, 2000, EPSL; Hemming *et al.*, 2002, *Chem. Geol.*; vanLaningham *et al.*, 2006, JGR, 2008, QSR, 2009, EPSL; vanLaningham and Mark, 2011, GCA).

An initial survey of the <2 μm fractions of samples from the Biscaye (1965, GSAB) clay mineral study, demonstrates that in contrast to the strong latitudinally-controlled distribution of kaolinite/chlorite in Atlantic sediments, K/Ar model ages trend from oldest in the NW Atlantic to youngest in the SW Atlantic. Intermediate ages are found in the tropical belt as well as off the coast of Europe. Though the data are still sparse, the general trends are well matched to the known distribution of geologic ages of continental sources around the Atlantic basin, with extreme old ages in Canada and Greenland and extreme young ages in active tectonic settings like the southern tip of South America and the Scotia Arc.

This study will produce a map of sediment distribution that serves as a benchmark to explore ocean circulation of sediment transport questions over a variety of timescales.

The Central Indian Upper Mantle 50 MY ago: Continental crust versus oceanic crust recycling contributions within the Central Indian Basin MORB

C. HEMOND¹, H. DELAVAUULT¹, M. JANIN¹, P. DAS² AND S. IYER²

¹UMR Domaines Océaniques, Univ. Brest – CNRS, Plouzané, France. (chemond@univ-brest.fr)

²National Institute of Oceanography, Dona Paula, Goa, India

The central Indian Ocean Basin (CIOB) results from the activity of both the Central and Southeast Indian Ridges and carries also the tracks of the Rodrigues triple junction and the Reunion Hotspot 53 Ma ago.

We discuss the composition of the Indian upper mantle 50 Ma ago i.e. its level of isotope heterogeneities within a model in which the breakup of the Gondwana has introduced continental derived material in it. The potential input of Reunion hotspot derived material is also investigated.

All samples dredged in an area comprised between 72-80°E and 9-15°S. They are on axis MORB or off axis MORB seamounts and are tholeiitic in composition and slightly depleted in incompatible trace elements.

Isotopes (Sr, Nd, Hf and Pb) lead to class samples in four groups: 1) very depleted in Sr-Nd and Hf isotopes including amongst the least radiogenic Pb isotope of the Indian MORBs regarded as the depleted Indian MORB mantle 50Ma ago. 2 and 3) Similar low ²⁰⁶Pb for higher ²⁰⁸Pb and intend to have even lower ²⁰⁶Pb than the previous group but very radiogenic Sr and unradiogenic Nd or DUPAL signature. The last group has more radiogenic Pb isotopes, and slightly lower Nd for identical Sr isotopes of the DMM group. This is clearly regarded as representative of recycled oceanic crust material such as seen in Ocean Island Basalts (C, Fozo, HIMU).

Mixing models suggest three components and two stages of mixing to account for the results. The local DMM is first contaminated by African Lower Continental Crust (LCC) material such as granulites during continental breakup.

In conclusion, the very depleted local DM and the extreme DUPAL compositions support the concept of LCC contamination of the upper mantle during the Gondwana breakup as 50Ma ago, the mixing and assimilation of the LCC being less advanced than in today Indian upper mantle. This leads to more extreme resulting isotope composition than today

Evolution of photosynthesis

JAMES HEMP¹, LAURA A. PACE², JENA E. JOHNSON¹ AND
WOODWARD W. FISCHER¹

¹ California Institute of Technology (jim.hemp@gmail.com)

² University of Utah

The evolution of chlorophyll-based phototrophy was one of the most important bioenergetic innovations in the history of life on Earth, but key first-order questions about its evolution remain. Here we present genomic and biochemical data that place new constraints on the acquisition of phototrophy in different clades. There are currently six known phyla of bacteria that have chlorophototrophic members; Cyanobacteria, Proteobacteria, Chloroflexi, Chlorobi, Firmicutes, and Acidobacteria. Cyanobacteria perform oxygenic photosynthesis using H₂O as an electron donor, generating O₂ as a product. All of the other clades perform anoxygenic photosynthesis using a variety of reduced compounds as electron donors. Despite these differences, all known chlorophototrophs share only three common molecular elements; (bacterio-)chlorophyll, reaction centers, and quinol:electron acceptor oxidoreductases (complex III).

Chlorins can be classified into two types; chlorophylls and bacteriochlorophylls, with the latter only found in anoxygenic phototrophs. Recent analyses of chlorin biosynthesis pathways provide support for the evolution of chlorophyll preceding that of bacteriochlorophyll¹.

Reaction centers are proteins that convert light energy into high energy electrons. Two evolutionarily related types of reaction centers exist, RCI and RCII. Anoxygenic phototrophs contain either RCI (Firmicutes, Chlorobi, and Acidobacteria) or RCII (Chloroflexi and Proteobacteria). In oxygenic photosynthesis RCI and RCII are coupled together in series, which allows electrons to be transferred from H₂O to ferredoxin. Evolutionary analysis of reaction centers show that their distribution reflects lateral gene transfer².

Complex III proteins convert high energy electrons into a protonmotive force. There are two evolutionarily unrelated complex III's—the b₆f/bc₁ superfamily and alternative complex III (ACIII). These enzymes are part of a high potential redox module that is shared with aerobic respiration and denitrification. The distribution and evolutionary relationships of complex III and the high potential module support the inferences from chlorin biosynthesis and reaction centers and demonstrates the remarkable conclusion that most currently known anoxygenic phototrophs acquired photosynthesis after the evolution of aerobic respiration, and therefore after the evolution of oxygenic photosynthesis.

[1] Bryant and Liu (2013) *Adv. Bot. Res.*, Volume 66. [2]. Raymond, *et al* (2002) *Science* 298:1616

The zinc isotopic composition of siliceous marine sponges: Investigating nature's sediment traps

KATHARINE R. HENDRY¹² AND MORTEN B. ANDERSEN²³

¹School of Earth and Ocean Sciences, Cardiff University, Main Building, Park Place, Cardiff, CF10 3AT, UK

²Department of Earth Sciences, University of Bristol, Wills Memorial Building, Queens Road, Bristol, BS8 1RJ, UK

³ETH Zürich, Inst. f. Geochimie und Petrologie, Clausiusstrasse 25, 8092 Zürich, Switzerland

The Zinc (Zn) content and isotopic composition of marine biogenic opal has the potential to yield information about the nutrient availability, utilisation and organic matter export from surface to deep waters. Here, we report the first measurements of Zn isotope composition of deep-sea benthic sponge skeletal elements (spicules) from the Southern Ocean. Our results highlight different Zn uptake and fractionation behaviour between the two major siliceous sponge clades (hexactinellids and demosponges), which is most likely linked to sponge filter-feeding strategy and internal physiology. Hexactinellid spicule Zn isotopic compositions are not fractionated with respect to seawater, and so hold potential as proxies for past ocean Zn cycling. In contrast, demosponge spicules exhibit a wide range of Zn isotopic compositions that are related to the opal Zn concentration, most likely reflecting fractionation processes during feeding. As such, demosponge Zn isotope records may be able to shed light on past changes in photic zone organic matter formation in the ocean.

Effect of increased glacier melt on diagenetic Fe cycling in marine sediments at King George Island (Antarctica)

S. HENKEL^{1*}, S. KASTEN², H. SALA³, A.S. BUSSO³ AND M. STAUBWASSER¹

¹ Institute of Geology and Mineralogy, Uni. of Cologne, GER
*correspondence: susann.henkel@uni-koeln.de

² Alfred Wegener Institute, Bremerhaven, GER

³ Dirección Nacional del Antártico - Instituto Antártido Argentino, Buenos Aires, ARG

The glacier melt of the Western Antarctic Peninsula and its surrounding islands influences biogeochemical processes in the water column and the marine sediment by changing the flux of mineral particles and nutrients (e.g. Fe) into the ocean. Sediment and pore water samples were collected at King George Island (South Shetland Islands) to unravel how the vicinity of ice-covered and -uncovered terrestrial environment affects redox zonation and diagenetic processes in the coastal sediments. The post-depositional dissolution of Fe-minerals and the stable Fe isotope signatures of pore water and specific Fe minerals were of special interest since changing Fe supplies - as reactive particles via melting icebergs or meltwater streams or dissolved via diffusion from the sediment into the bottom water - might not only impact local biogeochemical cycles but most likely also impact productivity in the Southern Ocean.

Sediment cores of up to 45 cm length were retrieved in Potter Cove, Marian Cove, and Maxwell Bay. In vicinity to the glaciers the sediments showed an extended redox zonation. The post-oxic zone with Fe²⁺ concentrations of up to 300 μM ranged from 1 to 25 cm depth. Most probably, microbial activity in sediments close to the glaciers is sluggish due to low input of organic matter (OM). More condensed redox zones prevailed in troughs where OM from terrestrial or marine sources accumulates and in vicinity to research stations. The upward directed diffusive Fe²⁺ fluxes as inferred from pore water profiles range between 0 and $\sim 1050 \mu\text{M m}^{-2} \text{d}^{-1}$. However, the correlation to the intensity of diagenesis is not straightforward. Fe isotopes of specific minerals were used to assess the intensity of Fe cycling. With ongoing Fe-oxide dissolution, the residual Fe pool becomes enriched in ⁵⁶Fe, whereas dissolved Fe and secondary Fe-oxides become enriched in ⁵⁴Fe. Thus, easily reducible Fe oxides show lowest $\delta^{56}\text{Fe}$ values at the top of the sediment column. We suggest that the retreat of the glaciers indirectly results in higher OM fluxes to shelf areas fueling diagenetic processes/nutrient recycling.

P-T evolution of Neoproterozoic and Ordovician metamorphic rocks in the Iberian Massif, Central Portugal

S.B.A HENRIQUES^{1*}, M.L. RIBEIRO¹, A.M.R. NEIVA², G.R. DUNNING³ AND L. TAJCMANOVA⁴

¹LNEG, Dpt. of Geology, Ap.7586, Amadora, Portugal;

(*correspondence: susana.henriques@lneg.pt);

(mluisa.ribeiro@lneg.pt)

²Earth Sciences Dpt. and Geosciences Centre, University of Coimbra, Portugal (neiva@det.uc.pt)

³Earth Sciences Dpt., Memorial University, St. John's NL A1B 3X5 Canada (gdunning@mun.ca)

⁴Department of Earth Sciences, ETHZ, Clausiusstrasse 25, CH-8092, Zurich, Switzerland; (lucie.tajcmanova@erdw.ethz.ch)

The study area is located at the boundary of the Ossa Morena-Central Iberian zones in the Iberian Massif. An island arc and a continental margin setting were active during the Ediacaran period. Both events are represented in the Sardeal Complex (SC) by amphibolites and felsic orthogneisses, respectively. An Ordovician rift magmatic event is recorded, in the Mouriscas Complex (MC), by a protomylonite trondhjemite and a garnet amphibolite with a MORB signature. We present the first *P-T* diagrams based on the thermodynamic modelling, which were computed using the Perple_X. The ID-TIMS U-Pb metamorphic zircon age from the SC amphibolite is 539 ± 3 Ma. The estimated *P-T* conditions were based on the compositional isopleths for key mineral phases in the stability field (Cpx-Am-Pl-Ilm-Ttn) at 7–8 kb and 640–660° C. The ID-TIMS U-Pb metamorphic monazite age from the felsic orthogneiss is 539 ± 2 Ma. The *P-T* path indicates an evolution from 4.5 kb and 590° C in the Bt-Pl-Ms-Grt-Sil-Qtz-Rt-Ilm field towards lower pressure and temperature field Bt-Pl-Ms-Grt-Qtz-Ilm at 4.4–5 kb and 570–580° C. The ID-TIMS U-Pb igneous zircon age from MC protomylonite trondhjemite is 483 ± 1.5 Ma. The estimated *P-T* conditions were based on the compositional isopleths for key mineral phases in the stability field (Bt-St-Pl-Ms-Grt-Sil-Qtz) at 4.5–6.2 kb and 590–650° C. The ID-TIMS U-Pb igneous zircon age from the MC garnet amphibolite is 477 ± 2 Ma. The estimated *P-T* conditions were based on plagioclase and biotite isopleths in the stability field (Bt-Chl-Ep-Am-Pl-Ilm-Mag-Grt-Qtz) at 6.5 kb and 550° C. Two major geodynamic events at the amphibolite facies conditions were identified in this study. The first one, the continental arc accretion of the Ossa Morena Zone to the Iberian Autochthon passive margin (Northern margin of Gondwana) occurs at ca. 540 Ma. The second one, younger than ca. 477 Ma is probably connected to the opening of the Rheic ocean.

Parallel budgets of excess thorium and protactinium in grain-size separates of marine sediments from the North Atlantic over the past 20,000 years

LEONARD E. HENRY^{1*} AND JERRY F. MCMANUS¹

Lamont-Doherty Earth Observatory Of Columbia University,
Geochemistry Division, Palisades, Ny, 10964 Usa,

¹Lhenry@ldeo.columbia.edu (*Presenting Author)

JMcManus@ldeo.columbia.edu

Abrupt shifts in the Atlantic's circulation regime have been inferred from carbon isotopes within benthic foraminifera, geostrophic gradient shifts captured in oxygen isotopes from benthic foraminifera, changes in the burial ratio of ²³¹Pa/²³⁰Th in bulk sediment, and variations in sortable silts. Drift deposits, those regions of the ocean where the energy of currents slaken and sediment is deposited in excess of the local vertical particle flux, are often selected for ²³¹Pa/²³⁰Th and other paleoceanographic reconstructions because the sedimentation rates far in excess of the mean ocean, thus allowing for greater resolution of transient climate events than in other seafloor sediment cores. Most of the fine sediment (<20micron) that constitutes a large fraction of mass within these deposits is laterally transported. Previous work suggested the fine fraction of the sediment carries a disproportionately high concentration of excess ²³⁰Th, or ²³⁰Th_{xs}, produced by the decay of ²³⁴U in sea water and scavenged by settling particles, and extra-terrestrial helium, ³He_{ET}, two nuclides whose mass flux aids in the reconstruction of past climate events. While the results are consistent with past findings for ²³⁰Th_{xs}, we find a contrasting distribution of ²³¹Pa_{xs} that serves as a cautionary tale towards assuming that a similar size-dependence applies to all particle-reactive elements.

This study presents side-by-side size-fraction budgets of ²³⁰Th_{xs} and ²³¹Pa_{xs} over the last deglacial from core CDH19 taken from a North Atlantic drift deposit, on the Bermuda Rise. Our results suggest that ²³¹Pa_{xs} is more evenly distributed among size-fractions than is ²³⁰Th_{xs}, possibly indicating that ²³¹Pa_{xs} is less susceptible to the biasing effects of particle focusing and more sensitive to the drivers of vertical particle flux. Further, ²³⁰Th normalized fluxes of the size-fraction separates imply that the maximum changes in the ²³¹Pa_{xs}/²³⁰Th_{xs} ratio that occurs across Heinrich Event 1 are evenly distributed across all size fractions.

Element outgassing in BABB: An example from the Havre Trough

J.M. HERGT^{1*}, J.D. WOODHEAD¹, A. GREIG¹,
R.J. WYSCOCZANSKI², M.I. LEYBOURNE³, E. TODD⁴ AND
AND C. WRIGHT⁵

¹School of Earth Sciences, The University of Melbourne, VIC,
3010, Australia

(*correspondence: jhergt@unimelb.edu.au)

²NIWA, Private Bag 14901, Wellington, 6021, New Zealand

³ALS Geochemistry, North Vancouver, BC Canada V7H 0A7

⁴Alaska Science Centre, USGS, Anchorage, AK 99508-4626,
USA

⁵National Oceanography Centre, Southampton, Empress Dock,
European Way, Southampton SO14, 3ZH, UK

Trace element data have been acquired for glass rinds and corresponding whole-rock samples of back-arc basin basalts from the Havre Trough in the SW Pacific. For most elements the match in compositions between glass and whole-rock pairs is essentially identical to within analytical uncertainties. In other cases, small variations exist that can be explained by the lack of olivine (for example) phenocrysts in digests of the handpicked glass.

In contrast, volatile elements show more marked differences that we attribute to outgassing of the magmas during vesiculation and eruption. Although most researchers would agree that Cd is highly volatile, our observation is that Cd is only slightly enriched in the glass (glass averaging Cd contents only ~7% higher than rock). In contrast, the largest discrepancies between the whole rock and glass compositions are in W (enrichment factor of ~30) and Mo (enrichment factor of ~5), and these elements also show an excellent correlation with each other. Given that these two elements are broadly believed to be less volatile compared with Cd, the most reasonable conclusion might be that the glass rinds lost much of this highly volatile element prior to quenching. Similar comparisons have been made with other elements in order to assess their relative volatilities in this back-arc basin setting.

Exhumation rates from orogenic areas

FREDERIC HERMAN¹, JEAN-DANIEL CHAMPAGNAC²,
MARTEEN LUPKER² AND SEAN D. WILLET²

¹Institute of Earth Sciences, University of Lausanne,
(Frederic.Herman@unil.ch)

²Department of Earth Sciences, ETH

A critical issue in the global mass balance of sediment is assessment of the importance of the rates and links between physical erosion and chemical weathering in tectonically active, high relief regions. There are two issues in these regions. First is determining the physical erosion rates in these areas which is problematic given the high variance in measured erosion rates, low concentrations and high errors in cosmogenic ages and young thermochronometric ages. The second problem is in generalizing erosion laws calibrated to low relief areas to these high relief areas. For example, erosion laws based on linear or non-linear diffusion of hillslopes saturate at high erosion rates and high slope and have no predictive capability. We address each of these problems through a detailed analysis of a new global compilation of more than 17,000 low-temperature thermochronometric ages. Here we focus on erosion rates and topographic characteristics of the highest relief regions of the active orogenic regions of the world. We compare erosion rates to common geomorphic metrics including mean slope and relief on different scale. We find no statistically significant relationship between relief or slope and erosion rate. Our result is consistent with theory that predicts that hillslopes reach a maximum value at which there is no relationship between slope and erosion rate. Our results demonstrate the difficulty in generalizing or predicting erosion rates in high-relief areas that lack direct measurement and contrasting these values to low-uplift regions where physical processes and governing equations differ.

Experimental constraints on carbon recycling in subducted sediments and altered oceanic crust

JÖRG HERMANN¹ AND LAURE MARTIN^{1,2}

¹Research School of Earth Sciences, The Australian National University, ACT Australia. Joerg.Hermann@anu.edu.au

²Centre for Microscopy, Characterisation and Analysis, UWA, 35 Stirling Highway, Crawley WA6009 Australia.

Altered oceanic crust and sediments are the main host rocks within the subducted lithosphere to transport carbon from the Earth's surface to the mantle. Whether carbon is effectively recycled toward the atmosphere through arc magmatism located above subduction zones, or buried into the deep mantle, remains controversial.

We have conducted experiments in a carbonate-bearing metapelite and in altered oceanic crust at 2.5-4.5 GPa and 700-1000°C, i.e. under conditions relevant for subducted slabs at sub arc depth. The experiments contained 2-7 wt% H₂O, simulating interaction of the rocks with an externally derived aqueous fluid. The wet solidus in both rock types is very similar and occurs at ~700°C at 2.5 GPa and at 800-850°C at 4.5 GPa. At subsolidus conditions residual carbonates are common and they coexist with hydrous phases such as phengite, epidote and lawsonite. We have developed a new method to determine the proportion of CO₂ in the fluid, where the experimental capsules are pierced under vacuum and the gas is directly analysed with a gas chromatograph. We show that the molar proportion of CO₂ in the aqueous fluid in altered oceanic crust decreases with increasing pressure from 0.06 to 0.03 and thus 70-90% of the original carbonate are retained in the rocks. Above the solidus at pressures ≤3.5 GPa hydrous silicate melts coexists with carbonates and less than 25% of the original carbonate is dissolved in the melt. The carbonate solubility in hydrous silicate melts increases with increasing pressure. Additionally, at 4-4.5 GPa, T ≥ 850°C globules of Fe-Ca-rich carbonate-quench occur in the hydrous silicate melt in altered oceanic crust and in sediments, indicating that immiscible silicate and carbonate melts coexists. These carbonate melts contain SiO₂, Al₂O₃ and P₂O₅ and TiO₂ at a wt.% level and high amounts of U and Th. There are only accessory amounts of residual carbonate at these conditions and 90-100% of the original carbonate is removed from the protholith.

Our results suggest that fluid fluxed partial melting of altered basalts and sediments provides an efficient mechanism by which significant amounts of subducted carbon can be brought back to the atmosphere via arc magmatism on relatively short time scales of less than 10 Ma.

Mineral-fluid interactions and time-integrated fluxes in tin-bearing greisens, Krušné hory (Erzgebirge) Mts., Central Europe

MATYLDA HEŘMANSKÁ¹ AND DAVID DOLEJŠ¹

¹Institute of Petrology and Structural geology, Charles University, 128 43 Praha 2, Czech Republic

Hydrothermal fluids are major mass transport agents in the lithosphere and reactive fluid flow underlies alteration and ore-forming mechanisms in diverse settings. In contrast to our advanced knowledge of alteration mineralogy and geochemistry, little is known about the volume of fluids responsible for specific mineralization or about the nature of replacement, i.e. dissolution-precipitation reactions on the microscale. We use alteration zoning of cassiterite-bearing greisens from the Krušné hory (Erzgebirge) Mts. in Central Europe as model example to interpret the fluid-mineral reaction mechanisms and calculate the time-integrated fluid fluxes. The greisen veins and swarms are hosted by highly evolved Li-F-P-rich biotite and zinnwaldite granites with topaz and tourmaline. Magmatic plagioclase (An_{<10}) and K-feldspar (Or_{>84}Ab_{<16}) exchanged Na and K prior to greisenization. Dark micas are represented by lithian annite continuously evolving to zinnwaldite, whereas white mica corresponds to lithian Fe-bearing muscovite. Greisenization occurs in several stages: (i) breakdown of feldspars to quartz and sericite or muscovite. Silicification and muscovite formation are spatially decoupled and represent dissolution-precipitation process, which requires local transport of Al, (ii) replacement of dark mica by celadonitic muscovite under volume-conserved conditions. This reaction requires significant Al addition and Mg, Fe release, (iii) breakdown of muscovite to topaz and quartz. This is a dissolution-precipitation reaction under Al-conserved conditions but declining fugacity of HF, and (iv) hydraulic fracturing and open-space filling by quartz greisens and monomineralic veins. Thermodynamic simulation of fluid-mineral interaction during disequilibrium infiltration in a pressure-temperature gradient reveals that the formation of mica-quartz and topaz-quartz greisens requires time-integrated fluid fluxes 10² to 10³ m³ fluid per m² rock, and the corresponding fluid flow rate of 10⁻¹⁰ to 10⁻⁸ m s⁻¹. The formation of a single greisen vein with a typical volume of 10³–5·10⁴ m³ would thus require 10⁵–3·10⁷ m³ aqueous fluid that must have exsolved from an intrusion measuring 80–700 m in each dimension. This approach illustrates use of reaction stoichiometries and non-equilibrium transport theory in estimating fluid fluxes in hydrothermal ore-forming processes.

Calcification rate and carbon-isotope fractionation in coccolithophore calcite through laboratory culture experiments

M. HERMOSO^{1,*}, F. MINOLETTI², Y. CANDELIER², H. MCCLELLAND¹, G. ALOISI³ AND R.E.M. RICKABY¹

¹University of Oxford, Dept. Earth Sciences, Oxford, UK, michael.hermoso@earth.ox.ac.uk (* presenting author).

²Univ. Paris 06 and 7193, Paris, France.

³Univ. Paris 06 and 7159, Paris, France.

The physiology of marine calcifiers such as haptophytes substantially affects the fractionation of carbon isotopes into biominerals. The resultant offset from equilibrium fractionation is often referred to as the "vital effect". The geological record of climate and the composition of seawater reconstructed from sedimentary biominerals is therefore not completely faithful. The aim of this work is to examine and quantify this biologically-induced distortion of the carbon isotopic signature in coccoliths in order to develop a mechanistic understanding of the vital effect in the coccolithophores, determine species-specific fractionation factors to derive the actual composition of seawater, and eventually be able to reconstruct climates more reliably using species separation techniques for fossil coccoliths.

Calcifying strains of haptophytes were subjected to a series of perturbation experiments in the laboratory in order to determine the effect of changes in the physico-chemical composition of the ambient environment (temperature, DIC level, pH, calcium concentration and phosphate concentration) on that of the biominerals and the organic matter. For all these experiments and for all the species, the partitioning of carbon into photosynthetic versus calcification pathways seems to be the primary driver of differences in the carbon isotopic composition of coccoliths. A second-order but still important parameter to consider for interpreting carbon isotopes is the active mechanisms used by the cells to concentrate carbon (CO₂) within the chloroplast and the coccolith vesicle. Empirically revealed through pH and TDIC perturbation experiments, variations in CCM efficiency can lead to 4‰ offsets between species. Finally, frequent malformations of coccoliths are observed for specimens grown under carbon limited conditions, or when cells reach their physiological maximum division rate.

Hydrogeochemical and isotopic signatures of Carboneras-Palomares Fault Area aquifers (SE Spain)

P. HERNANDEZ-PUENTES¹, R. JIMENEZ-ESPINOSA^{1*} AND J. JIMENEZ-MILLAN¹

¹Department of Geology and CEACTierra, Associated Unit IACT (CSIC-UGR), Faculty of Experimental Science, University of Jaén, Campus Las Lagunillas s/n, 23071 Jaén, Spain (ppuentes@ujaen.es; *correspondence: respino@ujaen.es; jmillan@ujaen.es)

Groundwater from Palomares-Carboneras Active Fault Area has been studied using geochemical (major ions) and isotopic (data $\delta^{18}\text{O}$ and $\delta^2\text{H}$). The study area is located in the eastern of Betic Cordillera (SE Spain). Hydrological changes that follow major earthquakes has been investigated and found to be dependent on the style of faulting [1]. We try to establish a circulation model of groundwater and to identify the sources of fluids from aquifers and the influence of water flow on the nucleation of new earthquakes.

Chemical composition of the waters reflects different types and degrees of water-rock interaction and several geochemical families have been found:

(i) Na-Ca-Mg-SO₄-Cl and Na-Mg-Cl-SO₄ waters: extreme EC (4000-14000 $\mu\text{S}/\text{cm}$): related to Pliocene marine marls in Vera Depression and Pulpí Corridor. ii) Na-Ca-Mg-SO₄-Cl and Na-Mg-HCO₃-Cl-SO₄ waters: high EC (2000-3500 $\mu\text{S}/\text{cm}$): related to dissolution of evaporites and carbonates along deep faults. (iii) Ca-Mg-Na-HCO₃-SO₄ waters: low EC (300-1000 $\mu\text{S}/\text{cm}$): in relation to dissolution of carbonates from Sierra Cabrera, Sierra de Filabres and Sierra de Almenara.

The $\delta^{18}\text{O} / \delta^2\text{H}$ diagram indicates that the distribution of the samples define a local meteoric line less steep than the World Online rainwater. The samples are better suited to the meteoric water line of the Mediterranean, indicating that precipitation of Mediterranean origin must contribute significantly to the recharge area. However, a mixed origin, Mediterranean and Atlantic rainfalls, could be taken into account. Samples from Sierra Cabrera and Fuente Alamo springs are more isotopically depleted. While Cuatro Caños and La Zanjilla springs appear more isotopically enriched. The prevalence of more negative values of ^{18}O is associated with a greater height in recharge, regarding the two groundwater samples from the northern area.

[1] Muir-Wood and King, 1993. *J. Geophysical Research* 98-B12 (22035-22068)

Effect of trace metals and light intensity on biomarker isotopic fractionation

M.T. HERNÁNDEZ-SÁNCHEZ^{1,2*}, H. STOLL¹, A. PIOTROWSKI³, A. MILNE⁴, M. LOHAN⁴ AND R. PANCOST²

¹Geology Department, Univ. Oviedo, Oviedo, Spain. (*correspondance: maitehs@geol.uniovi.es)

²Organic Geochemistry Unit, Univ. Bristol, Bristol, UK.

³Department of Earth Sciences, Univ. Cambridge, Cambridge, UK

⁴School of Geography, Univ. Plymouth, Plymouth, UK.

Photosynthetic carbon isotope fractionation (ϵ_p) is mainly controlled by CO₂ concentrations, but also other factors such as nutrient availability, carbon uptake or cell size; thus, it can provide insights into the marine carbon cycle. Most relevant for paleoclimate and despite its high dependence on algal growth rates, alkenone ϵ_p has been invoked as a robust proxy for reconstructing ancient pCO₂ [1]. pCO₂ reconstructions rely on measured ϵ_p and a b coefficient (which integrates physiological factors affecting isotope fractionation) which is generally assumed to be constant (or corrected for cell size) over time at a given location. Previously, the wide variations in b coefficient of suspended particulate matter alkenone ϵ_p in the modern ocean was shown to correlate with seawater phosphate concentrations but in fact hypothesized to arise due to trace metal regulation of growth rate [2].

We further explore the effect of trace metal and light intensities on ϵ_p of different phytoplankton biomarkers (including alkenones) for a smaller dataset in the modern ocean. ϵ_p is positively correlated with light intensities that vary with collection depth, a trend which cannot be explained by lower growth rates at lower light but is consistent with prediction of light limitation of carbon concentrating mechanisms. ϵ_p is inversely correlated with trace metals (Co and Co+Zn), a correlation that is stronger than that bore with CO₂ concentrations. Although further research is needed, our observations suggest that trace metals and light intensity affect the b coefficient, and that variations in the b coefficient at a given site must be accounted for in calibrations to reconstruct ancient pCO₂ accurately.

[1] Pagani *et al* (2002). *Paleoceanogr.* 17, 1069. [2] Bidigare *et al* (1997). *Global Biogeochem. Cycles* 11, 279-292.

The fate of iodine-129 released from the Fukushima-Daiichi nuclear accident

MATT N. HEROD^{1*}, MARTIN SUCHY², IAN D. CLARK¹,
W.E. KIESER³ AND GWYN GRAHAM²

¹University of Ottawa, Department of Earth Sciences, Ottawa, ON, Canada, (mhero065@uottawa.ca)

²Environment Canada, Vancouver, BC, Canada

³University of Ottawa, Department of Physics, Ottawa, ON, Canada

The Fukushima-Daiichi nuclear accident (FDNA) released large amounts of fission product radionuclides into the environment in the spring and summer of 2011. Along with short lived fission products, iodine-129 (15.7 million year half-life) was also released. ¹²⁹I is recognized as a useful tracer due to its mobile geochemical behaviour. To test if ¹²⁹I released by the FDNA was reaching Canada, rain samples were collected in Vancouver from March 2011 to March 2012. Archived precipitation samples from Environment Canada's station on Saturna Island and from the National Atmospheric Deposition Program in northern Washington State were also measured to establish a pre-accident ¹²⁹I background. Groundwater from the Abbotsford-Sumas Aquifer was sampled to determine the fate of ¹²⁹I. The mean pre-accident background for ¹²⁹I in rain is 38.15×10^6 atoms/L (n=4). Immediately following the FDNA, ¹²⁹I values increased sharply to 227.2×10^6 atoms/L and quickly returned to near-background levels. However, pulses of elevated ¹²⁹I continued for several months. The ¹²⁹I in shallow (³H/³He age <1.4 yrs) [1] groundwater were unchanged through November 2012 with an average of 11.39×10^6 atoms/L (n=21). The 6-fold increase in ¹²⁹I concentrations from both Vancouver and Saturna Island are coincident, and occur directly after the initial release from the FDNA. This indicates atmospheric transport and deposition of ¹²⁹I and agrees well with the timing of elevated ¹³¹I and ¹³⁷Cs measurements in the United States [2]. The lack of groundwater response suggests that ¹²⁹I is possibly attenuated in soil, which is consistent with its geochemical behaviour.

[1] Wassenaar *et al* (2006) *Environ. Sci. Tech.***40**, 4626-4632.

[2] Wetherbee *et al* (2012) *Environ. Sci. Tech.***46**, 2574-2582

Spectroscopy and magnetic imaging at the nanoscale for the study of magnetic minerals

JULIA HERRERO-ALBILLOS^{1,2,3}

¹ARAID researcher at Centro Universitario de la Defensa. Ctra. de Huesca s/n. 50090 Zaragoza, SPAIN

²ICMA (Universidad de Zaragoza - CSIC). Facultad de Ciencias 50009 Zaragoza, SPAIN

³Julia.Herrero@unizar.es

X-ray magnetic circular dichroism (XMCD) is the preferential absorption of X-rays by a magnetic sample for left and right circular polarized light. XMCD is produced at the resonance absorption energies of the different atoms, and therefore provides element-specific magnetic information. Since its discovery in 1987 by Schütz, XMCD has been pivotal in the understanding of magnetic materials and it is nowadays routinely used in both basic and applied research in magnetism. X-rays with variable polarization at a wide range of energies are readily produced in nearly 50 synchrotron radiation facilities around the world, offering varied sample environments (temperatures, pressure, magnetic fields, etc.) and XMCD-related techniques.

One of the most exciting of those techniques is X-ray Photo-Emission Electron Microscopy (XPEEM). Using XMCD as a contrast mechanism, in combination with a spatial resolution down to 30 nm, element-specific spatially resolved magnetization maps can be obtained. Moreover, recent developments in dedicated instruments, allowing performing experiments at low temperatures (40 to 600 K), under applied magnetic fields (up to about 100 mT) and with electrical contacts, as well as time resolved experiments (in the nanosecond range) to study magnetization dynamics.

In this talk I will present the capabilities of those two techniques in the study of the fundamental properties of natural magnetic rocks and how a deep understanding of their nanostructure can shed light onto their macroscopic magnetic properties.

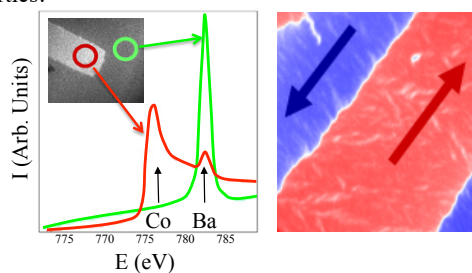


Figure 1. Capabilities of XPEEM: Chemical map and related spectra where the distribution of Co and Ba on a sample is observed (left). Magnetization map on a Fe film, with two magnetic domains (right).

Submicrometer exsolution lamellae in volcanic pyroxenes as indicators of magma residence times

J HERRIN^{1,2*}, F COSTA², Y. Y TAY¹, H LIU³
AND S PRAMANA¹

¹Facility for Analysis, Characterization, Testing, and Simulation, Nanyang Technological University, Singapore. (correspondence: jsherrin@ntu.edu.sg)

²Earth Observatory of Singapore, Nanyang Technological University, Singapore.

³School of Materials Science & Engineering, Nanyang Technological University, Singapore.

Pyroxene geothermometry is a well-established tool for the determination of thermal conditions of magmatic systems. Such applications are based largely on the presence of solvus relations within the pyroxene group that govern shifts in equilibrium composition as a function of temperature. These same solvus constraints can result in the subsolidus formation of exsolution lamellae in pyroxene. Many natural examples exist in plutonic pyroxenes. Since coarsening of these lamellae is largely a diffusion-moderated process [1], examination of their size and spacing can potentially be exploited to obtain timescales or cooling histories of magmatic systems, provided that empirical calibrations of controlling parameters (e.g. activation energies) are available. Volcanic systems present a unique challenge for this application because the pyroxene lamellae that they contain are typically nm-scale, owing to rapid cooling, and are also highly localized. Here we report the results of a chemical and crystallographic study of three suites of rhyodacitic samples. To locate, image, and analyze multiple exsolution lamellae of tens to hundreds of nm in size within clinopyroxene phenocrysts, we used a combined approach consisting of initial characterization by SEM/EPMA/EBSD, targeted FIB sampling, and detailed imaging and analysis by TEM/ATEM/SAED/EELS. Coupling these results with laboratory-calibrated models of lamellae formation and various end-member thermal cooling models of magma reservoirs [2] allows us to propose that these rhyodacites, erupted decades apart, originated from a common long-lived (several thousands of years) and relatively large (tens of km³) magma reservoir. The study of exsolution lamellae in volcanic pyroxenes should prove useful to constrain the thermal histories and sizes of magma bodies below active volcanoes, but analytical obstacles abound. One significant challenge is to obtain quantitative TEM-based chemical analysis (EDS and EELS) with sufficient precision for geothermometry.

[1] Weinbruch *et al* (2003) *GCA* **67**, 5071-5082. [2] Costa *et al* (2008) *RiMG* **69**, 545-594.

Molybdenum and uranium isotope dynamics in a Paleozoic epicontinental black shale

ACHIM D. HERRMANN¹, THOMAS ALGEO², STEPHEN ROMANIELLO³, GWYNETH W. GORDON³
AND ARIEL D. ANBAR^{3,4}

¹Coastal Studies Institute and Department of Geology and Geophysics, Louisiana State University, Louisiana, USA

²Department of Geology, University of Cincinnati, Cincinnati, Ohio, USA

³School of Earth and Space Exploration, Arizona State University, Arizona, USA

⁴Department of Chemistry & Biochemistry, Arizona State University, Arizona, USA

Reconstructing the history of global ocean anoxia during the Neoproterozoic and the Paleozoic is challenging since plate tectonic activity has destroyed the majority of the deep ocean floor from those time periods. In recent years, Mo and U isotopes have been used as a proxy to track global O₂ levels. However, these studies generally have to rely on the sedimentary record of shallow epicontinental seas. Here we present Mo and U isotope variations of a Paleozoic black shale (Hushpuckney Shale) from three different cores from across the same depositional basin to test whether global marine redox conditions can be determined reliably from a single section within an epicontinental settings.

We find that, based on Mo and U enrichment factors (EF) and nitrogen isotopes, three different intervals within the black shale can be distinguished. These intervals are characterized by strong spatial and temporal geochemical gradients that indicate that the basin experienced non uniform environmental conditions along the black shale horizon. These gradients are reflected in systematic offsets of U isotopes across the basin by up to 0.5‰. Furthermore, during the transition to the most reducing conditions (based on several geochemical proxies), the U isotopes attain their heaviest values while Mo isotopes attain their lightest values. This indicates that local redox conditions can lead to anomalous isotopic signatures as current understanding of these isotope systems suggests that both Mo and U should track each other during that transition. These results suggest that chemical gradients across an epicontinental basin can lead to local redox conditions that have a strong effect on the Mo and isotopic signatures. This spatial heterogeneity potentially challenges our ability to accurately reconstruct the accumulation of O₂ on Earth from only one section from such settings.

Natural organic matter and our current capacity to depict molecular dissimilarity in complex mixtures

N. HERTKORN*, M. HARIR, PH. SAND CHMITT-KOPPLIN

Helmholtz Zentrum München, German Research Center for Environmental Health, Research Unit Analytical Biogeochemistry, Ingolstaedter Landstrasse 1, D-85764 Neuherberg, Germany. (*correspondence: hertkorn@helmholtz-muenchen.de)

Natural organic matter (NOM) is the most abundant fraction of organic carbon on earth. NOM occurs in all terrestrial ecosystems such as soils, sediments, freshwater and marine environments, in the atmosphere and, throughout the universe, in the form of prebiotic organic matter synthesized by interstellar chemistry. NOM is an exceedingly complex mixture of organic compounds that collectively exhibits a nearly continuous distribution of properties (size-reactivity continuum).

NOM incorporates the hugely disparate characteristics of abiotic and biotic complexity. While biotic complexity derives from a plethora of evolutionary tested molecules with a rich three-dimensional structure designed to execute specific functions, abiotic molecular complexity is rather governed by "mathematical synthesis" which maximizes compositional diversity under given conditions of reaction partners, radiation and temperature. Molecular level NOM composition and structure at first depend on system characteristics and exhibit far more variance than anticipated from often rather uniform bulk parameters. Nevertheless, all NOM on earth is connected in a boundless carbon cycle.

Successful non-target molecular-level analyses of NOM attempts to characterize the entire molecular complement present in NOM by means of information-rich detection methods, like NMR spectroscopy (provides unsurpassed insight into short-range molecular order) and FTICR mass spectrometry (provides depiction of the compositional space with unsurpassed resolution).

This presentation provides an overview how modern organic structural spectroscopy can reveal key characteristics in composition and structure of various NOM. Examples will include secondary organic aerosols (SOA) as well as marine organic matter and NOM in organic chondrites.

[1] Hertkorn *et al* (2007) *Anal. Bioanal. Chem.*, **389**, 1311-1327. [2] Battin *et al* (2009) *Nature Geoscience*, **2**, 598-600. [3] Schmitt-Kopplin *et al* (2010) *Anal. Chem.*, **82**, 8017-8126. [4] Schmitt-Kopplin *et al* (2010) *PNAS*, **107**, 2763-2768. [5] Hertkorn *et al* (2013) *Biogeosciences*, **10**, 1583-1624.

Variations of $\Delta^{17}\text{O}$ in terrestrial rocks

D. HERWARTZ^{1*}, A. PACK¹ AND D.P. KRYLOV²

¹Universität Göttingen, Geowissenschaftliches Zentrum, Abteilung Isotopengeologie, Goldschmidtstraße 1, 37073 Göttingen. (*correspondence: dherwar@gwdg.de)

²Institute of Precambrian Geology and Geochronology, Russian Academy of Science, Makarova 2, 199034, St Petersburg, Russian Federation, (dkrylov@dk1899.spb.edu)

Large mass independent effects in $\Delta^{17}\text{O}$ are well known for extraterrestrial and stratospheric substances. Small variations in $\Delta^{17}\text{O}$ are expected in terrestrial rocks and minerals due to variations in the triple isotope fractionation exponent [3]. In this contribution we demonstrate that high-precision measurements of $\Delta^{17}\text{O}$ allow identification and quantification of the interaction between rocks and ancient meteoric water.

We have developed a technique to measure $\Delta^{17}\text{O}$ in silicates with a precision of 5 ppm (1 σ SD), which is an order of magnitude better than had been achieved previously. To characterize the $\Delta^{17}\text{O}$ composition of the Earth we have measured minerals from mantle xenoliths and a variety of crustal rocks and minerals. Our sample set included peculiar gneiss samples from Karelia, Russia with $\delta^{18}\text{O} = -25\text{‰}$ [2].

Silicate samples do not plot on a single terrestrial fractionation line (TFL), as frequently assumed. This is explained by differences in triple isotope fractionation exponent in high- and low-T fractionation processes as well as by interaction between reservoirs with different $\Delta^{17}\text{O}$.

Rock assemblages that have interacted with water fall on well-defined arrays in the $\Delta^{17}\text{O}$ vs. $\delta^{18}\text{O}$ space. These arrays can be utilized to reconstruct the original oxygen isotope composition of both, the samples and the hydrous fluid.

We apply our finding to reconstruct the composition of water from low- $\delta^{18}\text{O}$ rocks from Karelia (Russia) that likely interacted with glacial melt waters during a snowball Earth event.

[1] Young *et al* (2002) *GCA* **66**; [2] Krylov (2008) *Doklady Earth Sci.* **419A**.

Petrological evidence for deep lower mantle melting

CLAUDE HERZBERG

Department of Earth and Planetary Sciences, Rutgers
University, Piscataway, NJ, U.S.A.
(herzberg@rci.rutgers.edu)

Olivine phenocrysts in picrites from Baffin Island and West Greenland (BIWG) have elevated Ni contents consistent with derivation from a Ni-rich peridotite source [1]. Interaction of a silicate melt with the core may have provided the excess Ni [1]. Partial melting is consistent with experimental results on the solidus of peridotite near the core-mantle boundary [2]. Ni/Co in BIWG lavas and olivine phenocryst are also higher than those in MORB, consistent with experiments on liquid silicate/metal systems that show the effect of pressure is to make Ni more lithophile than Co [3]. But experiments at pressures near the core-mantle boundary are needed to confirm or falsify this conjecture. Also, the provenance of metal melt that supplies Ni may not be restricted to the core. Late accretion of dense metal-bearing chondritic bodies at subsonic velocities may have settled as piles on the core-mantle boundary [4].

Olivine phenocrysts in Hawaiian shield lavas have even higher Ni contents than those from BIWG [5]. Ni contents can be elevated by reaction of peridotite with either basaltic crust or partial melts of basaltic crust to make a second stage pyroxenite source. Petrological modeling indicates that the Hawaiian peridotite end-member is likely to be Ni-rich, not MORB-like, similar to BIWG. This petrological evidence supports the presence of partial melt at the base of the Hawaiian mantle plume.

Ultra low velocity zones (ULVZs) may originate by partial melting [6] and appear to be irregularly distributed at the boundaries of large low shear velocity provinces (LLSVPs) [7] which are also the proposed sites of mantle plume generation for both LIPS and ocean islands [8]. ULVZs have been located below BIWG and Hawaii [7,9], consistent with petrological inferences of partial melt.

[1] Herzberg, Asimow, Ionov, Jackson & Geist (2013), *Nature* **493**, 393-397. [2] Fiquet *et al* (2010), *Science* **329**, 1516-1518. [3] Li & Agee (1996), *Nature* **381**, 686-689. [4] Tolstikin & Hofmann (2005), *Physics Earth Planet. Inter.* **148**, 109-130. [5] Sobolev *et al* (2007), *Science* **316**, 412-417. [6] Williams & Garnero (1996), *Science* **273**, 1528-1530. [7] McNamara, Garnero & Rost (2010), *Earth Planet. Sci. Lett.* **299**, 1-9. [8] Torsvik *et al* (2006), *Geophys. J. Int.*, **167**, 1447-1460. [9] Cottaar & Romanowicz (2012), *Earth Planet. Sci. Lett.* 355-356, 213-222.

Calcium isotope fractionation in vertebrates

A. HEUSER^{1*}, A. EISENHAEUER²,
K. SCHOLZ-AHRENS³ AND J. SCHREZENMEIR

¹Steinmann-Institut, Universität Bonn, Bonn, Germany
(*correspondence: aheuser@uni-bonn.de)

²GEOMAR, Helmholtz-Zentrum für Ozeanforschung Kiel,
Germany

³Max Rubner-Institut, Bundesforschungsinstitut für Ernährung
und Lebensmittel, Kiel, Germany

Earlier investigations showed that there is considerable biological fractionation of Ca isotopes in vertebrates. Consequently it was suggested that Ca isotope fractionation may be applied as a diagnostic tool for the detection of Ca metabolic malfunctions like osteomalacia or osteoporosis. In order to further investigate Ca isotope fractionation in vertebrates, we analyzed the Ca isotopic composition ($\delta^{44/40}\text{Ca}$) of diet, feces, blood, bones and urine of Göttingen miniature pigs from an animal trial. Samples of three different groups were investigated: 1. Control group (Con), 2. Glucocorticosteroid induced osteoporosis group (GIO) and 3. Calcium and vitamin D deficiency induced osteomalacia group (-CaD).

While $\delta^{44/40}\text{Ca}_{\text{diet}}$ values are in average 0.42 ± 0.07 ‰ the observed Ca isotope variations in feces, bones, blood and urine is significantly higher. $\delta^{44/40}\text{Ca}$ values vary in total by 3.28 ‰ ranging from -0.54 ‰ (feces) up to 2.74 ‰ (urine). It is not possible to distinguish the three groups solely based on $\delta^{44/40}\text{Ca}_{\text{urine}}$, $\delta^{44/40}\text{Ca}_{\text{bone}}$ or $\delta^{44/40}\text{Ca}_{\text{blood}}$ values only. In contrast, group -CaD is clearly marked by their low $\delta^{44/40}\text{Ca}_{\text{feces}}$ values. Average $\delta^{44/40}\text{Ca}_{\text{feces}}$ of group -CaD is -0.27 ‰ while it is 0.39 ‰ and 0.28 ‰ for groups Con and GIO, respectively.

The $\delta^{44/40}\text{Ca}_{\text{feces}}$ represents the unabsorbed fraction of dietary Ca and thus can be used to identify Ca fractionation during intestinal absorption. The $\delta^{44/40}\text{Ca}_{\text{feces}}$ values of -CaD are lighter than corresponding $\delta^{44/40}\text{Ca}_{\text{diet}}$ by ~ 0.6 ‰ which indicates that Ca isotopes are fractionated during intestinal absorption. In contrast, group Con and GIO $\delta^{44/40}\text{Ca}_{\text{feces}}$ values do not indicate Ca fractionation during intestinal absorption. Observed $\delta^{44/40}\text{Ca}_{\text{feces}}$ values of group -CaD may be caused by either the addition of isotopically light Ca from intestinal fluids or fixation of light Ca isotopes in unmetabolizable compounds like Ca oxalates or Ca phytates.

Raman and IR spectroscopy of Monazite-type ceramics for the nuclear waste management

J. HEUSER^{1*}, A. BUKAEMSKIY¹, S. NEUMEIER¹,
F. BRANDT¹, H. SCHLENZ¹, N. DACHEUX², N. CLAVIER²,
A. NEUMANN³, A. HIRSCH³, D. BOSBACH¹

¹Forschungszentrum Juelich GmbH, Institute of Energy and Climate Research - IEK-6: Nuclear Waste Management, D-52425 Juelich, Germany (*correspondence: j.heuser@fz-juelich.de)

²Institut de Chimie Séparative de Marcoule, ICSM UMR 5257 – CEA / CNRS / UM2 / ENSCM, Site de Marcoule, BP 17171, F-30207 Bagnols sur Cèze Cedex, France

³RWTH Aachen University, Institute of Crystallography, D-52066 Aachen, Germany

Lanthanide monazite-type ($LnPO_4$) ceramics are promising candidate materials for the immobilisation of minor actinides resulting from reprocessing of spent fuel. Particularly with regard to the long-term safety in a deep geological repository, monazite-type ceramics present a good alternative to the widely used borosilicate glasses for the specific conditioning of actinides. In terms of their crystal structure (SG $P 2_1/n$) they offer outstanding properties concerning radiation resistance and chemical stability. Their normalised dissolution rates are several orders of magnitude lower than these of glasses [1-4]. This behaviour can also be confirmed by their natural analogues (no metamictisation occurs).

Therefore we investigated different monazite-type phases as potential waste forms for minor actinides. We prepared and characterised $SmPO_4$ - $TbPO_4$ and $SmPO_4$ - $CaTh(PO_4)_2$ solid solutions, using wet-chemical synthesis routes like precipitation at room temperature and solid state reactions (1600 °C), respectively. The presented data obtained by Raman and IR spectroscopic investigations will be discussed in conjunction with X-ray powder diffraction data as well as thermal analyses within a comparison to the available literature. An increasing distortion of the PO_4 tetrahedra should be demonstrated with increasing Th-substitution of the Ln -position. Additionally, the monazite-cheralite solid solution data will be compared to that of a Thorium containing natural monazite sample. Completely new data could be generated for the solid solutions. Results of temperature dependent Raman spectroscopic investigations on the partly metastable $(Sm,Tb)PO_4$ solid solutions will be presented, where depending on the composition one-two exothermic phase transitions are expected.

[1] Meldrum *et al* (1997) *Phys. Rev. B* **56**, 13805-13814 [2] Lumpkin (2006) *Elements* **2**, 365-372 [3] N. Dacheux *et al* (2004) *Comptes Rendus Chimie* **7**, 1141-1152 [4] Schlenz *et al* (2013) *Z. Krist.* **228**, **III**, 113-123

Searching for evidence for Mo isotope fractionation in the mantle

KATE HIBBERT^{1*}, MATTHIAS WILLBOLD^{1,2},
MORTEN ANDERSEN^{1,3} AND TIM ELLIOTT¹

¹Bristol Isotope Group, School of Earth Sciences, University of Bristol, Bristol, UK

(*correspondence: kate.hibbert@bristol.ac.uk)

²Department of Earth Science and Engineering, Imperial College London, London, UK

³Institute of Geochemistry and Petrology, ETH Zurich, Switzerland

Molybdenum is a highly siderophile element which was strongly depleted in the mantle by the process of core formation. Its mantle inventory is therefore strongly influenced by the addition of material during the late veneer when highly siderophile elements were enriched in the mantle after core formation.

Recent experimental data suggest that molybdenum isotopes are fractionated during metal-silicate equilibration, with lighter isotopes preferentially entering the silicate phase [1]. Therefore the mantle should be isotopically lighter than the chondritic material which is presumed to have accreted to form the Earth as heavy isotopes were concentrated into the core. However, the addition of the late veneer may have somewhat obscured the isotopic signature of core formation.

We describe two approaches taken to investigate the isotopic composition of the mantle relative to chondrites in an attempt to verify these experimental findings. Firstly, we measure a range of ~3.8Ga samples from Greenland which have been shown to retain an isotopic signature of the mantle prior to the addition of the late veneer [2].

Secondly, we measure the Mo isotopic composition of mid-ocean ridge basalts (MORBs) which we compare to chondrite samples in an effort to detect residual fractionation of molybdenum isotopes associated with core formation post late veneer.

MORB samples are known to carry some signature of recycling; however we suggest that they are sufficiently representative of the mantle for our purposes. Whilst scatter in both the MORB and chondrite datasets currently prevents the identification of a resolvable difference, we find a tantalising offset of 0.1 permil between the most primitive MORB sample and the least altered chondrite.

[1] Hin *et al*, AGU Fall Mtg, abs #P11A-1588 [2] Willbold *et al*, (2011) *Nature* **477**, 195-198

Isotopic evidence for an activity of the early Sun studied from the isotopic measurements of Kapoeta

HIROSHI HIDAKA¹ AND SHIGEKAZU YONEDA²

¹Department of Earth and Planetary Systems Science, Hiroshima University, Higashi-Hiroshima 739-8526, Japan (hidaka@hiroshima-u.ac.jp)

²Department of Science and Engineering, National Museum of Nature and Science, Tsukuba 305-0005, Japan

The Kapoeta meteorite (howardite) is a regolith breccia meteorite, and is known to be a highly gas-rich meteorite that experienced early irradiation by cosmic rays, however, its irradiation history is complicated and still disputed with respect to evidence of early solar irradiation. Our previous study on neutron capture history of Kapoeta suggests the existence of preirradiation materials migrating into the meteorite parent body [1]. The existence of space-weathered rims in several regolith grains in the Kapoeta meteorite is resulted from the irradiation of cosmic-ray on the regolith parent body [2]. In this study, Sr, Ba, Ce, Nd, Sm and Gd isotopic compositions of the sequential acid-leachates from the Kapoeta meteorite were determined to find systematic and correlated variations of their p-process isotopic abundances and to understand the neutron capture record due to cosmic-ray irradiation.

Significantly large isotopic excesses of ⁸⁴Sr, ¹³⁰Ba, ¹³²Ba, ¹³⁶Ce, ¹³⁸Ce and ¹⁴⁴Sm were observed particularly in the first leaching fraction (L1). Interestingly, a large isotopic shift of ¹⁵⁰Sm/¹⁴⁹Sm and ¹⁵⁸Gd/¹⁵⁷Gd due to neutron capture reactions was also found in the first fraction, corresponding to the neutron fluence of 2.6×10^{16} n cm⁻², which is more than 10 times higher than those in the other fractions. The large difference of neutron capture records of L1 from the other three suggests the existence of preirradiation materials migrating into the Kapoeta parent body.

Systematic isotopic data in this study reveal the enrichment of several p-process isotopes of the fraction L1 leached probably from a very surficial part of regolith grains of Kapoeta, suggesting the production of p-process isotopes resulted from the interaction of SCR during the regolith process of the Kapoeta parent body. The result provides isotopic evidence for an activity of the early Sun.

[1] Hidaka and Yoneda (2009) *EPSL* **285**, 173–178. [2] Noble *et al* (2011) *MAPS* **45**, 2007-2015.

Fulvic and Humic Acid interaction with Phosphate at synthetic and natural oxide surfaces

TJISSE HIEMSTRA¹, SHAMIM MIA, PIERRE-BENOÎT DUHAUT, AND BASTIAAN MOLLEMAN

¹Dept. Soil Quality, PO box 47, 6700 AA, Wageningen University, Netherlands tjisse.hiemstra@wur.nl

Fulvic acid (FA) and humic acid (HA) have a large variability in binding to metal (hydr)oxides and interact differently with oxyanions, as studied experimentally for goethite, phosphate, and a series of soil HAs that cover the large natural variation in molecular charge and size. A surface complexation approach has been developed that aims to describe the pH-dependent competitive behaviour of natural organic matter (NOM) in soil as well as model (hydr)oxide systems, using variable inner and outer-sphere complexation as well as protonation of RCOO ligands.

Modelling shows that the competition of phosphate with various HAs is linearly related to the HA charge. Expressed per unit charge, HA competes as well as FA (or even better), which is unexpected since the various humics highly differ in molecular size (~1-10 nm) suggesting variation in mean distance of approach [1]. Modelling suggests that at low loading, both FA and HAs are predominantly adsorbed in the Stern layer domain which points to a strong change of the molecular conformation of the humic acids. Our calculations suggest that the metal (hydr) oxide surfaces are efficiently covered by an ultra-thin layer of NOM. Therefore, realistic surface complexation modeling of natural systems should account for this pervasive NOM surface coverage.

From the perspective of global carbon sequestration, adsorption of NOM is also important since minerals may protect adsorbed carbon against oxidation. In soils, the reactive metal (hydr)oxide fraction consists of nanoparticles, typically representing ~3-30 m² g⁻¹ soil [2]. When covered by an ultra-thin layer of NOM, it may represent at least 0.2-2% NOM. Surface-associated NOM may be even three times higher. In our competition study, we have also included pyrogenic HA since it will be released to the environment in case of large-scale application of biochar, potentially creating Dark Earths or Terra Preta soils. Terra Preta soils are fertile, rich in carbon as well as phosphate. Our charge distribution model for NOM predicts a more than 10-fold increase in dissolved phosphate for soils rich in black carbon. This is due to the relatively high molecular charge of pyrogenic HA.

[1] Weng *et al* (2007) *J. Colloid Interf. Sci.* **314**, 107-118. [2] Hiemstra *et al* (2010) *Geochim. Cosmochim. Acta* **74**, 41-58.

Multi-stage Cl-rich fluid activity and behavior of REE-bearing minerals in a Neoproterozoic granulite terrane

FUMIKO HIGASHINO^{1*}, TETSUO KAWAKAMI¹,
M. SATISH-KUMAR², MASAHIRO ISHIKAWA³,
NORIYOSHI TSUCHIYA⁴ AND GEOFF GRANTHAM⁵

¹Department of Geology and Mineralogy, Kyoto University,
Japan (correspondance: fumitan@kueps.kyoto-u.ac.jp)

²Niigata University, Japan

³Yokohama National University, Japan

⁴Tohoku University, Japan

⁵Council for Geoscience, South Africa

Cl-rich fluid is a powerful solvent, and can coexist with CO₂-rich fluid under granulite facies conditions [1]. Despite such important roles, the scale and timing of its activity during high-grade metamorphism are still not clear. Field distribution of Cl-rich biotite, amphibole and apatite, which are evidence for the presence of Cl-rich fluid, is investigated in detail in the Sør Rondane Mountains (SRM), East Antarctica where granulites are widely exposed.

Cl-rich biotite preserved as inclusions in garnet shows linear distribution in the SRM. Among them, a pelitic gneiss from the east SRM (Balchenfjella) shows Cl-rich fluid infiltrated around near-peak metamorphism at ca. 800 °C, 0.8 GPa [2]. In this sample, monazite is present in the garnet core, whereas zircon and xenotime are included in the garnet rim. This suggests that the Cl-rich fluid infiltration that took place at the garnet core/rim boundary lead to the change of REE-bearing mineral species. This implies that Cl-rich fluid carried LREE and Th away and brought HREE, Zr and Y in. U-Pb dating of zircon included in the garnet rim gave 603±14 Ma [2], representing the timing of Cl-rich fluid infiltration. Biotite in the matrix is Cl-poor, suggesting that the retrograde metamorphism occurred in a Cl-poor environment. The rim of zircon in the matrix might represent a timing of this fluid activity (564±17 Ma), which is consistent with the zircon ages obtained from metacarbonates (ca. 545 Ma) that represent the timing of fluid activity [3, 4].

In addition, the mafic gneisses from the central SRM (Brattnipane) host cm-thick veinlets composed of garnet and Cl-rich amphibole that discordantly cut the penetrative gneissosity. In our presentation we discuss the processes associated with multi-stage Cl-rich fluid infiltration in the SRM during the peak- to retrograde stages.

[1] Newton & Manning (2010) *Geofluids* **10**, 58-72. [2] Higashino *et al* (2013) *Precam. Res.* in press. [3] Higashino *et al* (2013) *JpGU abst.* [4] Otsuji *et al* (2013) *JpGU abst.*

Magnesium isotope evidence for a link between low-temperature clays, seawater Mg/Ca, and climate

HIGGINS, J.A.^{1*} AND D.P. SCHRAG²

¹Dept. of Geosciences, Princeton University,
(jahiggin@princeton.edu)

²Dept. of Earth and Planetary Science, Harvard University,
(schrage@eps.harvard.edu)

Cooling of Earth's climate over the Cenozoic has been accompanied by large changes in the magnesium and calcium content of seawater. The processes that control these changes affect the magnesium isotopic composition of seawater, rendering it a useful tool for elucidating the processes that control seawater chemistry. We use measurements of magnesium isotopes in both pore fluids and carbonate sediments together with a numerical model of sediment diagenesis and show that the magnesium content of seawater has increased by 10-15 mmol over the last 15-25 Myr with little change in its isotopic composition. These observations are best explained by a reduction in removal of Mg from seawater in marine clays formed at low temperatures. A temperature-dependent Mg sink in marine clay directly links the major element chemistry of seawater to global climate, providing an additional explanation for the co-variation of seawater Mg/Ca and climate on ~100 million year timescales over the Phanerozoic.

Holocene records of chlorin N isotopes

MEY TAL B. HIGGINS¹, REBECCA S. ROBINSON²
AND ANN PEARSON³

¹Department of Geosciences, Princeton University;
mbhiggin@princeton.edu

²Graduate School of Oceanography, University of Rhode
Island; rebeccar@gso.uri.edu

³Department of Earth and Planetary Sciences, Harvard
University; apearson@eps.harvard.edu

Nitrogen isotope ratios measured in sedimentary chlorophyll degradation products provide a diagenetically unaltered signal of the marine nitrogen cycle during deposition. Additionally, due to taxonomic differences in fractionation associated with chlorophyll biosynthesis, these records can be used to reconstruct the cyanobacterial contribution to buried organic matter. If diazotrophic cyanobacterial contribution to biomass increases during enhanced N₂ fixation, then chlorin N isotope records may provide an additional constraint on the importance of this source of N to surface waters in the geologic past. We reconstructed low resolution records of chlorin δ¹⁵N values from the last glacial maximum to recent sediments in four oceanographically distinct settings. Samples were taken from ODP sites 1234 (Chile Margin), 1237 (Nazca Ridge, Peru), 1063 (Bermuda Rise), and core 17964 from the South China Sea. These four globally-distributed sites represent different nutrient regimes characterized by a wide range of modern P* values and potential rates of N₂ fixation. Chlorin δ¹⁵N data were compared to new or previously published bulk N data to examine for diagenetic enrichment of bulk N (causing ¹⁵N offsets to increase) or cyanobacterial contribution to export (causing ¹⁵N offsets to decrease). Preliminary data show an average δ¹⁵N offset of ~5-5.5‰ between bulk and chlorin N at all sites, suggesting predominantly algal export production irrespective of N₂ fixation regime and bulk values of δ¹⁵N.

Efficient preservation of terrestrial organic carbon offshore Taiwan: Implications for the global carbon cycle

R. G. HILTON^{1,*} AND S. J. KAO^{2,3}

¹Durham University, United Kingdom, (*correspondence:
r.g.hilton@durham.ac.uk)

²Academia Sinica, Taiwan, (sjkao@gate.sinica.edu.tw)

³Xiamen University, China.

Photosynthesis on land produces terrestrial biomass and sequesters atmospheric CO₂ within living matter. Geological sequestration of CO₂ can occur if this terrestrial organic carbon (OC) is eroded and transported to marine sediments where accumulation rates are high¹, influencing Earth's radiation energy balance. Mountain rivers draining islands of Oceania have amongst the highest erosion rates of terrestrial OC and sediment^{2,3} and it is of critical importance to understand its fate upon entering the ocean. Here we use radiocarbon (Δ¹⁴C_{org}, ‰), stable isotopes (δ¹³C_{org}, ‰) and OC content (C_{org}, %) to track terrestrial OC from Taiwan from river sediments to ocean sediment traps and box-cores collected from around the island. We account for fossil OC from sedimentary rock, while assessing the range of delivery mechanisms to the ocean by mountain rivers.

During floods at high suspended sediment concentrations, we observe efficient transfer of terrestrial OC (both fossil and non-fossil) to the deep ocean, and evidence for its longer-term preservation in marine sediments. Large amounts of terrestrial sediment are also delivered to the surface ocean by rivers, dispersing OC over a larger area³. Marine sediments sourced by this mechanism have a positive relationship between Δ¹⁴C_{org} and δ¹³C_{org}, and a negative relationship between 1/C_{org} and Δ¹⁴C_{org}. Employing end member mixing analysis and by modelling OC loss scenarios, we show that these are the product of mixing between marine OC and terrestrial OC (itself a fossil and non-fossil mixture) and that 80-100% of terrestrial OC is preserved in marine sediments, suggesting much higher burial efficiencies than previously hypothesised². Our findings allow for a conservative estimate of recent CO₂ sequestration by terrestrial OC burial across Oceania, which comprises a significant proportion of global OC burial. We thus postulate that tropical mountain islands provide a strong coupling between tectonic uplift and the carbon cycle, one that is moderated by the climatic variability that controls terrestrial OC delivery to the ocean.

[1] Galy *et al* (2007) *Nature* **450**, 407-410. [2] Hilton *et al* (2012) *Global Biogeochemical Cycles* **26**, GB3014. [3] Kao & Milliman (2008) *Journal of Geology* **116**, 431-448.

Experimental determination of the Si isotope fractionation factor between metal and silicate liquids

REMCO C. HIN¹, CAROLINE FITOUSSI^{1,2},
MAX W. SCHMIDT¹ AND BERNARD BOURDON^{1,2}

¹Institute of Geochemistry and Petrology, ETH Zurich,
Switzerland (*correspondence: remco.hin@erdw.ethz.ch)
²Ecole Normale Supérieure de Lyon and CNRS, France

The conditions of core formation on Earth are still debated and stable isotope fractionation is explored as a new tool to further constrain metal-silicate segregation conditions. It has been shown that chondrites and (ultra)mafic terrestrial silicates have different Si isotope compositions¹⁻³, although there is no consensus yet⁴. Recent experimental work has found $-1.77 \pm 0.32\%$ fractionation between liquid metal and olivine at 1800°C ⁵, which implies that Si isotope fractionation may occur during core formation in planetesimals and on Earth.

To better constrain the conditions of core formation, Si isotope fractionation between metal and silicate must be well calibrated. We therefore performed liquid metal, liquid silicate equilibration experiments at 1450°C and 1750°C at 1 GPa in a centrifuging piston cylinder at ETH Zurich. The physically segregated liquids were mechanically separated prior to dissolution by alkali fusion. After ion exchange chromatography, isotopic analyses were carried out on a Nu Instruments 1700 MC-ICPMS at ETH Zurich.

The silicate liquids had consistently heavier Si isotopes than the equilibrated metal liquids. The average fractionation factor between metal and silicate liquids ($\Delta^{30}\text{Si}_{\text{Metal-Silicate}}$) was $-1.48 \pm 0.08\%$ at 1450°C and $-1.11 \pm 0.14\%$ at 1750°C . Given a $1/T^2$ functional form, the temperature dependence of Si isotope fractionation between metal and silicate liquids can be described as $\Delta^{30}\text{Si}_{\text{Metal-Silicate}} (\%) = -4.47 (\pm 0.31) \times 10^6 / T^2$.

Our equilibrium data yield a smaller fractionation than previously deduced⁵. Calculations at 2500-3500 K for metal-silicate equilibration during core segregation on Earth imply a bulk Earth $\delta^{30}\text{Si}$ of -0.38 to -0.33 ($\pm 0.02\%$ propagated error), respectively, for a bulk silicate Earth $\delta^{30}\text{Si}$ of $-0.29 \pm 0.01\%$ and 6 wt% Si in the Earth's core. Although the calculated values fall in the range of observed chondrite Si isotope compositions, they do not match all observations for the Si isotope composition of chondrites.

[1]. Georg *et al.*, 2007. *Nature* 447, 1102-1106. [2] Fitoussi *et al.*, 2009. *EPSL* 287, 77-85. [3] Armytage *et al.*, 2010. *GCA* 75, 3662-3672. [4] Chakrabarti and Jacobsen, 2010. *GCA* 74, 6921-6933. [5] Shahar *et al.*, 2011. *GCA* 75, 7688-7697.

Combining radiogenic and stable Ca isotopes to explore sub-glacial weathering reactions

R. HINDSHAW^{1*}, B. BOURDON², J. RICKLI³ AND
J. WADHAM⁴

¹Øystein Møyilas veg 16, Trondheim, Norway
(correspondence : ruth.hindshaw@googlemail.com)

²Laboratoire de Géologie de Lyon, ENS Lyon, France

³Institute of Geochemistry and Petrology, ETH, Switzerland

⁴Bristol Glaciology Centre, University of Bristol, UK

The interpretation of weathering processes based on the stable isotopes of calcium (Ca) is complicated by the difficulty of distinguishing between source and process fractionation effects. The combination of radiogenic Ca isotopes ($\epsilon^{40}\text{Ca}$) with stable Ca isotopes ($\delta^{44/42}\text{Ca}$) would provide the ability to separate source and process fractionation effects. The aim of this study was to combine both the stable and radiogenic Ca isotope systems to investigate the sources of Ca and Ca isotope fractionation processes in glaciated environments, providing great potential to increase understanding of the behaviour of Ca during weathering.

This study is based on a one month sampling campaign to Leverett Glacier, West Greenland in July 2009. The bedrock (granite/gneiss) is of Archean age (ca 1850 Ma), theoretically old enough to have acquired radiogenic ^{40}Ca anomalies. Water samples were collected twice daily for a period of 28 days together with spot samples of water end-members (ice, supra-glacial water) and four representative rock samples from which the main Ca bearing minerals were separated.

The bulk rock samples exhibit a range in both stable ($\delta^{44/42}\text{Ca} = +0.20$ to $+0.50\%$) and radiogenic ($\epsilon^{40}\text{Ca} = -1.0$ to $+6.9$) Ca isotopic compositions. Two of the analysed mineral separates had significant radiogenic Ca anomalies: sanidine ($\epsilon^{40}\text{Ca} = +15.3$) and biotite ($\epsilon^{40}\text{Ca} = +7.7$). Radiogenic anomalies up to $\epsilon^{40}\text{Ca} = +5.3$ were detected in river water samples, coincident with an outburst event. The change in $\epsilon^{40}\text{Ca}$ measured in the river water samples during the outburst event indicates a change in the relative contribution from different mineral sources to the dissolved load of Ca. In contrast, the stable Ca isotopic composition of river water showed no discernable temporal variation and had an average $\delta^{44/42}\text{Ca}$ of $+0.60\%$, which was significantly higher than the source rocks. The combination of $\epsilon^{40}\text{Ca}$ and $\delta^{44/42}\text{Ca}$ data clearly indicates that $\delta^{44/42}\text{Ca}$ values cannot be reconciled with mixing processes and have been fractionated.

Effect of phosphate and sulfate on Fe(II)-catalyzed trace metal incorporation into and release from Fe(III) oxides

MARGARET ANNE G. HINKLE¹* JEFFREY G. CATALANO¹

¹Earth & Planetary Sci., Washington Univ., St. Louis, MO 63130 USA (*correspondence: mhinkle@eps.wustl.edu)

Trace element concentrations in natural systems are often controlled by adsorption-desorption reactions on iron oxide surfaces [1]. Biogeochemical iron cycling leads to the coexistence of aqueous Fe(II) with solid Fe(III) oxides, which undergo Fe(II)-Fe(III) interfacial electron transfer and atom exchange (ET-AE) reactions [2]. These reactions result in Fe(III) oxide recrystallization, causing the incorporation of structurally compatible adsorbates, e.g. Ni(II), into solid Fe(III) oxides as well as the release of preincorporated ions into solution [3-5]. Recent research has shown that oxoanions common to natural systems, such as phosphate, do not affect the rate or extent of Fe(II)-Fe(III) atom exchange reactions [6]. However, these species may still potentially alter trace metal incorporation and release by complexing with metals at the iron oxide surface or by changing growth and dissolution mechanisms via processes such as step pinning.

We have investigated the interaction of phosphate and sulfate with Fe(II) on goethite and hematite surfaces and the resulting impact on Ni incorporation and release. Macroscopic adsorption and ATR-FTIR studies demonstrate that oxoanions enhance Fe(II) adsorption through a direct interaction on the mineral surface. XAFS spectroscopy indicates that both phosphate and sulfate decrease Fe(II)-catalyzed Ni(II) incorporation into goethite and hematite; the effect of phosphate was more substantial. Ni(II) release from these minerals during Fe(II)-catalyzed recrystallization was also suppressed by phosphate and sulfate, with the former again producing the larger inhibitory effect. This research suggests that phosphate and sulfate affect trace element partitioning between aqueous solutions and Fe(III) oxides during Fe(II)-Fe(III) ET-AE reactions, potentially impacting contaminant fate and micronutrient bioavailability in soil and aquatic environments.

[1] Brown & Parks (2001) *Int Geol Rev* **43**, 963-1073. [2] Handler *et al* (2009) *Environ Sci Technol* **43**, 1102-1107. [3] Yanina & Rosso (2008) *Science* **320**, 218-222. [4] Frierdich & Catalano (2012) *Environ Sci Technol* **46**, 1519-1526. [5] Frierdich, Luo & Catalano (2011) *Geology* **39**, 1083-1086. [6] Latta, Bachman & Scherer (2012) *Environ Sci Technol* **46**, 10614-10623.

The future of lipids as tools to study microbes and biogeochemical processes in the deep biosphere

KAI-UWE HINRICHS¹*, JULIUS S. LIPP¹, TRAVIS B. MEADOR¹, GUNTER WEGENER^{1,2}, SITAN XIE¹

¹MARUM-Center for Marine Environmental Sciences, University of Bremen, 28359 Bremen, Germany (*Presenting author, khinrichs@uni-bremen.de)

²Max Planck Institute for Marine Microbiology, 28359 Bremen, Germany

Recent work has demonstrated that the predominant microbial intact polar lipids (IPLs) in marine sediments, i.e., glycerol-based ether lipids with a glycosidic polar headgroup, are impacted by a considerable fossil fraction derived from past microbial generations [1]. Although IPL concentration profiles provide useful quantitative constraints on slowly growing archaeal communities [1], their use as direct markers of live biomass in deeply buried sediments is compromised. Hence lipid-based investigative strategies will have to be modified in order to sustain a central role of microbial lipids in future studies of seafloor life.

Future avenues will need to focus on IPLs that have little or no fossil bias, such as phospholipids [cf. 1] or new target compounds that are diagnostic for actively growing cells as identified by culture studies. Detection of these often far less abundant compounds will require implementation of more sensitive approaches [2]. Some novel groups of orphan lipids are concentrated in the seafloor [3]; the elucidation of their biological sources and function will likely provide important clues on the deep biosphere. Novel, minimally invasive stable isotope probing assays that target microbial lipids will have a key role in quantifying microbial growth and substrate specificity [4]. This paper will review the state-of-the-art and provide new examples that illustrate future directions of lipid-based research of seafloor life.

[1] Xie *et al* (2013) *PNAS* **110**, 6010-6014. [2] Wörmer *et al* (2013) *Org. Geochem.* doi:10.1016.2013.03.004. [3] Liu *et al* (2012) *Rap. Comm. Mass Spectrom.* **26**, 2295-2302. [4] Wegener *et al* (2012) *Env. Microbiol.* **14**, 1517-1527.

Complex *in situ* cosmogenic ^{10}Be - ^{14}C data suggest Mid-Holocene climate change on the Bolivian Altiplano

K. HIPPE^{1*}, F. KOBER², S. IVY-OCHS¹, M. LUPKER³,
L. WACKER¹, M. CHRISTL¹ AND R. WIELER³

¹Laboratory of Ion Beam Physics, ETH Zürich, 8093 Zürich, Switzerland (*correspondence: hippe@phys.ethz.ch)

²Institute of Geology, ETH Zürich, 8092 Zürich, Switzerland 3
Isotope Geology and Mineral Resources, ETH Zürich,
8092 Zürich, Switzerland

³Institute of Geochemistry and Petrology, ETH Zürich, 8092
Zürich, Switzerland

In a recent study on basin-averaged denudation rates on the Bolivian eastern Altiplano, long-lived ^{10}Be and ^{26}Al have been used to provide long-term estimates on sediment production while the short-lived *in situ* ^{14}C allowed to identify interruptions of sediment exposure by episodes of sediment storage [1]. Based on comparatively low *in situ* ^{14}C concentrations sediment storage over at least the past 11- 20 ka has been suggested.

Following this approach, we have chosen to focus on one single catchment on the eastern Altiplano (~350 km²) to trace the spatial pattern of sediment deposition and quantify individual storage durations. Sediment samples were taken along the main channel and from tributaries as well as from three hilltop sites. Results from the analysis of ^{10}Be and *in situ* ^{14}C are in agreement with previous data [1] showing a high ^{10}Be content and significantly too low *in situ* ^{14}C concentrations for all but one sample, including two of the three hilltop samples. Excluding sediment storage/burial on the hilltop for obvious reasons and excluding soil mixing or slab breakoff from field observations, we propose a change in denudation rate to account for the discrepancy of ^{10}Be and *in situ* ^{14}C on the hilltop. Using a simple model of a rapid, one-step denudation increase, the two samples suggest a minimum 30-40 times increase in denudation rate about 4-6 ka ago.

Assuming that the analyzed fluvial sediments have already an inherited complex ^{10}Be - ^{14}C signal from the sediment-producing hilltop areas, the total duration of sediment storage reduces to ~1-5 ka, thus much shorter than previously assumed. Our data further show that sediment storage occurring on the floodplain does not contribute to the complex cosmogenic nuclide signal. In contrast to the channels in the upstream area, that incise a few metres in depth, the material deposited on the floodplain is apparently only rarely reworked.

[1] Hippe *et al* (2012) *Geomorphology* **179**, 59-70.

Mantle structure below the petit-spot

N. HIRANO^{1*}, J. YAMAMOTO² AND S. OKUMURA³

¹Center NE-Asian Studies, Tohoku Univ., Japan

(*correspondence: nhirano@m.tohoku.ac.jp)

²Hokkaido Univ. Museum, Hokkaido Univ., Japan

³Dept. Earth Sci., Tohoku Univ., Japan

The petit-spot volcanoes, erupted due to lithospheric bending related to the plate subduction, were found on the subducting plate off Japan and Chile trenches [1, 2]. An old and flexed lithosphere might cause brittle fractures at the upper lithosphere. Incipient melts in the asthenosphere can be squeezed upward by tectonic forces associated with plate flexure [1]. The presence of the tiny submarine volcanoes, petit-spot, is an important indicator of the stress field of the plate [3], in addition to providing information on the geochemical composition of the mantle below the petit-spot [4, 5, 6, 7].

The lavas and entrained xenolithes were newly dated and analyzed in this study. Accordingly, monogenetic petit-spot volcanoes located on the NW Pacific Plate yield ages of 1.8, 3.8, 4.2, 6.0, 6.2, 8.5, and 9.2 Ma by Ar-Ar datings, suggesting the episodic eruption of magma over a large eruption area (over 800 km of plate motion) of the concave part of the plate, but with low volumes of magma production [8]. Most of lavas have the differentiated composition of approximately 50 wt% SiO₂ and 60 of Mg number with extremely high contents of carbon dioxide. The petrography and geobarometer of peridotitic xenolithes show that they rapidly ascended through the upper lithosphere. These data implies the magma differentiated at the depth deeper than middle of lithosphere where the carbon dioxide does not exsolve in magmas.

[1] Hirano *et al* (2006) *Science* **313**, 1426-1428. [2] Hirano *et al* (2013) *Geochem. J.* **47**, in press. [3] Valentine & Hirano (2010) *Geology* **38**, 55-58. [4] Machida *et al* (2009) *Geochem. Cosmochim. Acta* **73**, 3028-3037. [5] Hirano (2011) *Geochem. J.* **45**, 157-167. [6] Yamamoto *et al* (2009) *Chemical Geol.* **268**, 313-323. [7] Machida *et al* (2013) *MinMag*, this volume. [8] Hirano *et al* (2008) *Basin Res.* **20**, 543-553.

Heavy element-stable isotope systematics for metallomics induced by the MC-ICPMS technique

TAKAFUMI HIRATA¹, SATOKI OKABAYASHI¹,
TAKESHI OHNO², KAZUMI YOSHIYA³,
TSUYOSHI KOMIYA⁴ AND SHIGENORI MARUYAMA³

¹Dept. of Earth and Planet. Sci., Kyoto Univ. Japan
(hrt1@kueps.kyoto-u.ac.jp)

²Dept. of Chem., Gakushuin Univ., Japan

³Dept. of Earth and Planet. Sci., Tokyo Inst. of Techn., Japan

⁴Dept. of Earth Sci. and Astro., Komaba, Univ. Tokyo, Japan

Continuous developments in inorganic mass spectrometry techniques, including a combination of an ICP ion source and a magnetic sector-based mass spectrometer equipped with a multiple-collector array (MC-ICPMS), have revolutionized the precision of the isotopic ratio measurements. Although the magnitude of many analytical problems is clearly exacerbated, the analytical community is actively solving problems, such as spectral interference, mass discrimination drift, high-yield chemical separation and purification processes, or reduction of the contamination of analytes, and the applications of the heavy element-stable isotope geochemistry are beginning to appear over the horizon [1, 2]. The variations in isotopic ratios of the heavy elements, such as Fe, Zn, Cu, Sr, Ce-Nd, W, or U can provide new insights into past and present geochemical and biochemical processes [2]. Among the heavy elements, mass-dependent isotopic fractionation of the bioessential metals (e.g., Ca, Fe, Zn or Cu) was extensively applied to investigate the nutritional status of elements or to evaluate the elemental metabolism for plant and animals [e.g., 1,3,4]. This is well demonstrated by the diagnosis for specific diseases through the changes in isotope ratios of the elements [5,6]. To take a full advantage of the heavy element-isotope systematics, we are currently trying to obtain *in situ* isotope ratio data of the elements using MC-ICPMS technique coupled with a femtosecond-laser ablation sample introduction technique (fLA-MC-ICPMS). Analytical advantages achieved by the fLA-MC-ICPMS technique or by the LAL-MC-ICPMS technique [7] will be presented in this presentation.

[1] Maréchal *et al* (1999) *Chem. Geol.* **156**, 359-396. [2] Tanimizu *et al* (2013) *Anal. Bioanal. Chem.*, **405**, 2771-2783. [3] Bullen and Walczyk (2009) *Elements* **5**, 381-385. [4] Moynier *et al.*, (2009) *Chem. Geol.* **267**, 125-130. [5] Walczyk, von Blanckenburg (2002) *Science* **295**, 2065-2066. [6] Aramendia *et al* (2013) *J. Anal. Atom. Spectrom.* doi: 10.1036/c3ja30349g. [7] Okabayashi *et al* (2011) *J. Anal. Atom. Spectrom.* **26**, 1393-1400.

Crystal structure in Earth's inner core

KEI HIROSE^{1*}, SHIGEHICO TATENO² A
ND HARUKA OZAWA^{1,3}

¹Earth-Life Science Institute, Tokyo Institute of Technology,
Tokyo, Japan (*Correspondence: kei@elsi.jp)

²Department of Earth and Planetary Sciences, Tokyo Institute
of Technology, Tokyo, Japan

³Institute for Research on Earth Evolution, Japan Agency for
Marine-Earth Science and Technology, Yokosuka, Japan

Composition and state of the core remain uncertain to a large extent [1], in part because static experiments performed on candidate compositions at such extreme conditions have been difficult until recently. Nevertheless, ultrahigh-pressure experimental techniques using laser-heated diamond-anvil cell (DAC) combined with synchrotron x-rays have greatly advanced in recent years. Now static experiments are being performed at the core ultrahigh pressure and temperature conditions, even beyond those at the center of the Earth [2]. Recent experimental and theoretical studies indicated that hexagonal-close-packed (hcp) structure is a stable form of iron in the Earth's inner core. Earlier calculations suggested that body-centered-cubic (bcc) Fe is stable above ~5500 K at 330 GPa [4]. However, the temperature at the inner core boundary may be as low as 5200 K, inferred from recent estimates of core-mantle boundary temperature of ~3800 K. The nature of stable crystalline phases and physical properties are strongly affected by impurity elements in the core. We have performed x-ray diffraction measurements so far up to 412 GPa and 5900 K and examined stable crystal structures of iron-compounds including Fe-10wt%Ni, FeO, Fe-9wt%Si, and Fe-S alloys under the core conditions. Considering a small density deficit, our data so far suggest that hcp is a plausible crystal structure in the inner core.

[1] Hirose *et al* (2013) *Annu. Rev. Earth Planet. Sci.*, **41**, 10.1146/annurev-earth-050212-124007. [2] Tateno *et al* (2012) AGU Fall Meet., Abstr. D112A-04.

Deep Time: How did the early Earth become our modern world?

MARC M. HIRSCHMANN

U. Minnesota, Minneapolis, MN USA (mmh@umn.edu)

One of the salient challenges in Deep Time studies is understanding how the Earth made the transition from early violent events –accretion, core formation, and impacts– to the rather normal equable conditions recorded in the Hadean Jack Hills zircons, with oceans, granitic crust derived in large part from partial melting of mature sediments, and perhaps even dynamical behavior similar to plate tectonics¹. An unresolved question is how the Earth's deep volatile cycles evolved through this time. One interpretation is that the combination of core formation, magma ocean degassing, and atmospheric loss produced an early mantle largely devoid of volatiles, which were then added chiefly in a late veneer. But if the late veneer was mixed in to the mantle only gradually over time scales of > 1 Ga², then the Hadean near surface environment would have been dominated by super-oceans, flooding protocontinents and massive supracrustal storage of C, presumably as carbonate. Similarly, the consequences of a nearly volatile-free mantle on mantle dynamics and tectonics are poorly understood. However, there is reason to believe that a significant portion of Earth's present-day volatiles were delivered to the mantle prior to the late veneer. At a minimum, the distinct noble gas compositions of the mantle and atmosphere require retention of some early (including nebular) volatiles in the mantle. But more importantly, H/C³ and N/C⁴ ratios of the bulk silicate Earth demonstrate that Earth's major volatile inventories remember the processing associated with magma ocean and core formation stages, suggesting that significant fraction of Earth's early volatiles avoided catastrophic escape or core sequestration. The mechanisms of this retention are poorly understood, but may have been critical to the early approach to dynamical and climatic stability.

[1] Hopkins *et al* (2008) *Nature* **456** 493-456. [2] Maier *et al* (2009) *Nature* **460** 620-623. [3] Hirschmann&Dasgupta (2009) *Chem. Geol.* **262** 4-16. [4] Marty (2012) *EPSL* **313** 56-66.

Chemical diffusion in the deep Earth: Is it all about grain boundaries?

MATTHEW HISCOCK¹ AND GEOFFREY D. BROMLEY¹

¹School of GeoSciences (Grant Institute) and Centre for Science at Extreme Conditions, University of Edinburgh, Edinburgh EH9 3JW, UK

Diffusion of chemical species in Earth's interior plays a controlling role in many of the large-scale processes which first formed and continue to reform the Earth through time. Traditionally, diffusivity of species has been considered to occur under subsolidus conditions mainly via lattice diffusion; i.e. the movement of species through bulk crystal structures. Recently however, researchers have started to attempt to constrain the importance of grain boundary diffusion (GBD) in the deep Earth: i.e. the mobility of species along grain boundaries. Grain boundaries provide alternative, fast pathways for mobile species which may be chemically and structurally very distinct from the bulk crystalline structure of polymineralic materials. It has recently been suggested that GBD provides a mechanism for transporting highly incompatible elements from the core into regions of lower mantle melting, and is an important component of H mobility in the upper mantle. Here we present results from an experimental study aimed at constraining the importance of GBD in 3 geochemically important but contrasting systems: H mobility in olivine, Li diffusion in olivine and Ti diffusion in quartz.

Experimental data demonstrate similar diffusivities for GBD and lattice diffusion of H under mantle conditions. When scaled to mantle grain sizes, results suggest that GBD of H is of minor importance, except at marked discontinuities in the mantle where there are abrupt changes in H solubility. In contrast, data suggest that GBD of Li is between 2 and 4 orders of magnitude faster than lattice diffusion. Differences in the behaviour of H and Li can be understood in terms of incorporation mechanisms and the contrasting nature of crystalline material vs relatively amorphous grain boundaries. Critically, these differences result in contrasting temperature dependences for GB vs lattice diffusion which imply that GBD always dominates at low temperatures. Similarly, we find that GBD of Ti in polycrystalline quartz is orders of magnitude faster than lattice diffusion, a result which has immediate implications for the applicability of the Ti in quartz geothermometer. Based on these results, we present a predictive model for determining the relative importance of GBD in the deep Earth.

Release of antimony from contaminated soil induced by redox changes

KERSTIN HOCKMANN^{1*}, SUSAN TANDY¹, MARKUS LENZ²
AND RAINER SCHULIN¹

¹Institute of Terrestrial Ecosystems, ETH Zurich, Switzerland,
(*correspondence: kerstin.hockmann@env.ethz.ch)

²University of Applied Sciences and Arts Northwestern
Switzerland (FHNW), Institute for Ecopreneurship,
MuttENZ, Switzerland

Due to its rapid growth in industrial use, soil contamination by antimony (Sb) has become a matter of increasing environmental concern. A key factor of Sb mobility in soils is its redox state, which is closely related to soil aeration and thus to the soil water regime. Under aerobic conditions, thermodynamics predicts Sb to be stable as the pentavalent $\text{Sb}(\text{OH})_6^-$, while under reducing conditions, the more toxic trivalent $\text{Sb}(\text{OH})_3$ predominates [1]. Both species strongly differ in their affinity to iron (Fe) and manganese (Mn) (hydr)oxides, which, in turn, may be reductively dissolved under reducing conditions.

Here, we investigated how the interplay of reduction, sorption and dissolution processes affects Sb mobility in saturated soil subject to alternating redox conditions induced by autochthonous bacterial communities. Columns with Sb-contaminated shooting range soil (pH 7.8) were eluted with 15 mM sodium lactate solution for ~60 pore volumes (PV), interrupted by a 24 days stop-flow phase after 30 PV. With the transition to reducing conditions, Sb(V) and Mn concentrations showed a concomitant increase, providing evidence that sorbed Sb(V) was released by reductive dissolution of Mn minerals. As reducing conditions continued, Sb was immobilized again by reduction of Sb(V) to Sb(III), since the latter binds stronger to Fe (hydr)oxides at circumneutral pH. However, as these Fe phases started to dissolve with the onset of Fe-reducing conditions, the previously bound Sb(III) was released back into the solution. Characterization of the solid phased by laser ablation inductively coupled plasma-mass spectrometry (LA ICP-MS) underpinned the important role of Mn and Fe (hydr)oxides as Sb sorbents.

Our study shows for the first time that Sb can be mobilized under reducing conditions in soil also in form of Sb(V) with the dissolution of Mn and thus provides further reason for concern that release of Sb from insufficiently drained contaminated soil may pose a significant risk to the environment.

[1] Filella, Belzile & Chen (2002), *Earth-Sci. Rev.* 57, 125 - 176.

The role of earthworm-produced CaCO_3 in the terrestrial calcium and carbon cycles

MARK E. HODSON^{1*}, EMMA A. A. VERSTEEGH² AND
STUART BLACK³

¹Environment Department, University of York, Heslington,
York YO10 5DD, UK, (mark.hodson@york.ac.uk
*presenting author)

²Department of Geography and Environmental Science,
University of Reading, Reading RG6 6DW, UK,
(e.a.versteegh@reading.ac.uk)

³Department of Archaeology, University of Reading, Reading
RG6 6AB, UK, (s.black@reading.ac.uk)

Earthworm-produced calcium carbonate granules form a considerable proportion of soil carbonate and can be preserved for up to ~2 Ma. They may play an important role in the immobilisation of metals [1,2] and can be used to reconstruct temperatures of the past [3]. The physiological function of these carbonates and their role in the terrestrial calcium and carbon cycles remain poorly understood.

Experiments were performed with *Lumbricus terrestris*, one of the two main earthworm producers of CaCO_3 granules in many temperate soils. Earthworms were kept at different temperatures (3–20 °C) and, in a separate experiment, at different atmospheric CO_2 levels (440–3800 ppm). Granule production rate was correlated with temperature ($R^2 = 0.55$, $p < 0.0005$) increasing from 0.8 to 2.7 $\text{mgCaCO}_3 \text{ earthworm}^{-1} \text{ day}^{-1}$ between 3 and 20 °C. In contrast, granule production rate only showed a non-significant increasing trend under elevated $[\text{CO}_2]$.

In the variable temperature experiment the stable carbon isotopic composition ($\delta^{13}\text{C}$ values) was measured for soils, food (manure), air, earthworm tissues, and CaCO_3 granules. $\delta^{13}\text{C}$ values show that the majority of C in the granules comes from the food offered to the earthworms. As such, $\delta^{13}\text{C}$ values of granules originating from archaeological finds could be a useful proxy for vegetation type or agricultural practice (manuring) employed by past societies. In addition it suggests that earthworms are converting carbon from a more labile organic-hosted form to a less labile mineral-hosted form.

[1] Brinza *et al* (2013) *GCA*, 10.1016/j.gca.2013.03.011; [2] Fraser *et al* (2011) *GCA* 75, 2544–2556, 10.1016/j.gca.2011.02.015; [3] Versteegh *et al* (submitted).
[3] Versteegh *et al* (2013) 10.1016/j.gca.2013.06.020

Geochronology of the Lithospheric Mantle underneath the Gibeon Kimberlite Field, Namibia

C.E. HOEFER^{1,2*}, G.P. BREY¹, T. LUCHS¹, A. GERDES¹,
H.E. HOEFER¹

¹Institut für Geowissenschaften, Goethe-Universität,
Altenhöferallee 1, D-60438 Frankfurt, Germany;

²Institut für Geochemie und Petrologie, ETH-Zürich,
Clausiusstrasse 25, CH-8092 Zürich, Switzerland
(*carolin.hoefer@erdw.ethz.ch)

Recent comparative work has shown that differences and similarities exist between the mantle underneath the Archean Kaapvaal craton and the attached Proterozoic terranes [1]. Differences are: higher average forsterite in olivines from the Kaapvaal craton, lower Al₂O₃ and CaO in their bulk rocks, Re depletion ages mostly older than 2.5 Ga and a thicker lithosphere. Similarities are: similar geothermal gradients, an overabundance of orthopyroxene in part of the mantle samples and the existence of garnets with sigmoidal REE patterns. Re depletion ages are all younger than 2.2 Ga [2].

The 70 Ma old Gibeon Kimberlite Province is located in Namibia within the mixed age Rehoboth Terrane (0.9-1.2 and 1.8-2.1 Ga). Three major localities with mantle xenoliths are known: Hanaus, Gibeon Townsland and Louwrensia. Luchs *et al* [3] distinguished for Hanaus and Gibeon Townsland two types of garnet peridotites by their REE patterns: i) peridotites with flat middle to heavy REE in their garnets and ii) a minor proportion with sinusoidal REE patterns as they are known from the Kaapvaal craton. Bulk rock isotope trace element and isotope compositions were calculated from the analysis of garnets and clinopyroxenes and their modal abundances. A Lu-Hf isochron for the peridotites with the sinusoidal REE patterns gave 1852 Ma as the age of enrichment of a previously strongly depleted mantle ($\epsilon_{\text{Hf}} = 29$). The garnet peridotites with the flat middle to heavy REE patterns yielded a Lu-Hf age of 810 Ma with $\epsilon_{\text{Hf}} = 3.3$. These ages overlap with crustal ages of the mixed age Rehoboth Terrane. We have extended our studies to samples from the Louwrensia kimberlite pipe and find a similar division as in Hanaus and Gibeon Townsland for the garnet peridotites. First results from isotope studies yield a Lu-Hf age of 1100 Ma which is within the age range of the adjoining Namaqua-Natal belt. Different mantle portions with ages reflecting different events seem to be hoisted to the Earth's surface by the Gibeon kimberlites. The grt-cpx Lu-Hf two-point isochron ages give an alignment of increasing age with decreasing temperatures between 1000 to 1200 °C. We interpret these ages as cooling ages. Since kimberlite eruption ages are obtained for some samples at 1200 °C we conclude that the closure temperature for the Lu-Hf system must lie around that temperature for peridotite systems.

[1] Bell *et al*, *Lithos*, 2003; [2] Pearson *et al*, *Chem. Geol.*, 2004; [3] Luchs *et al*, *Precambrian Research*, 2013, in press

Fe³⁺ determination in garnet: A crystal chemical test with the EPMA flank method

H.E. HOEFER^{1*}, C.E. HOEFER¹, V. MATJUSCHKIN¹,
G.M. YAXLEY² AND G.P. BREY¹

¹Institut für Geowissenschaften, Goethe-Universität,
Altenhöferallee 1, 60438 Frankfurt am Main, Germany
(*hoefer@em.uni-frankfurt.de.)

²Australian National University, Canberra, Australia

We established the „flank method“ for *in situ* determination of garnet iron oxidation state with the electron microprobe at micron-scale spatial resolution [1]. Besides the high spatial resolution, the great advantage of this method is the ability to analyse simultaneously the major element chemistry on the same spot.

The flank method has been calibrated with a large number of synthetic and natural garnets. We apply it here for the first time, to garnets with grain sizes of 10-15 µm. They were synthesized at various oxygen fugacities at high pressures. We determined Fe³⁺/ΣFe together with the major element composition.

The test for the reliability of the Fe³⁺/ΣFe determined with the flank method uses a crystal chemical approach i.e. is based on constraints from the structural formula. In garnet with general formula A²⁺₃B³⁺₂Si₃O₁₂, the number of trivalent cations on the octahedral B site is 2. A linear correlation of Fe³⁺ per formula unit and the sum of further trivalent cations plus Ti⁴⁺ must therefore exist. This is the case for the synthetic high-pressure garnets of this study (Fig. 1). The excellent correlation is independent proof of the high quality of garnet Fe³⁺ data determined using the flank method.

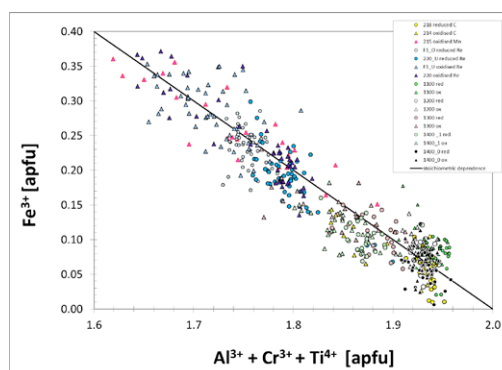


Figure 1: Fe³⁺ determined by the flank method versus the total of the remaining cations on the octahedral site.

[1] Hoefer & Brey (2007) *Am. Mineral.* **92**, 873-885.

Zircon U-Pb, Lu-Hf and REE Composition of Sorocaba and São Francisco Granites, São Paulo State, SE Brazil

TABATA HOEGER LUQUE^{1*} AND SILVIO R.F. VLACH¹

¹IGc-USP,04280-000, Brazil.*correspondence:
[tabatahl,srfvlach]@usp.br

The granitic massifs of Sorocaba (SG, 180 km²) and São Francisco (SFG, 150 km²) are located southeast of São Paulo State, southeastern Brazil. They crop out near the Paraná Basin and intrude low-grade meta-volcano-sedimentary rocks. SHRIMP U-Pb ages, Lu-Hf (LA-MC-ICP-MS) isotopic data and REE (LA-ICP-MS) abundances in zircon were considered together with WR geochemistry (XRF and ICP-MS) to understand petrogenetic processes.

The U-Pb ages for SG granodiorites are 617±4, 610±7 Ma, syeno- and monzogranites are 585±4 and 603±4 Ma. For the SFG ages are 592±3 Ma for the syeno-monzogranites and 599±4 Ma for the minor quartz-monzodiorites.

Lu-Hf isotope system from all the analyzed zircon crystals display strongly negative εHf₀ values, compatible with crustal signatures. The granodiorites εHf₀ values vary between -12.2 and -21.5. These values are slightly less evolved than those observed in the other samples; in the syeno- and monzogranites from SG, εHf₀ are between -12.8 and -33.1. Zircon crystals from quartz-monzodiorites of SFG displays εHf₀ between -30.5 and -33.5 varying in a more limited range, and the syeno-monzogranites εHf₀ varies between -32.5 and -54.4.

REE patterns are characterized by negative Eu anomalies, variable positive Ce anomalies and variable enrichment of HREE regarding to MREE. The REE concentrations were used to calculate partition coefficient data and then compared with the model from Blundy & Wood [1] considering: $r_o = \text{Zr}$ site in zircon, 0.84 Å [2]; Young's modulus for Zr was deducted from equation 15 [3]; $D_o = D_{Zr}$ and $T = \text{Zr}$ saturation temperature in WR. The best-fit curves were those of the SFG quartz-monzodiorites. Calculated partition coefficients of HREE show good correlation. Meanwhile, the LREE are slightly discrepant for the more felsic-studied rocks. Those discrepancies, joined with the other *in situ* analyses are a robust dataset that allow to analyse petrogenetic processes.

[1] Blundy, J. & Wood, B. (1994). *Letters to Nature* 372, 452–454. [2] Shannon, R. D.(1976). *Acta Crystallographica Section A* 32, 751–767. [3] Wood, B. J. & Blundy, J. D. (2003) *Treatise On Geochemistry*, 2, chap 9, 395–424

Preparation of micrometer sized soil particles for NanoSIMS analysis

C. HOESCHEN^{1*}, T. HOESCHEN², C.W. MUELLER¹,
T. RENNERT¹, J. LUGMEIER¹ AND I. KÖGEL-KNABNER^{1,3}

¹ Lehrstuhl für Bodenkunde, Technische Universität München,
85350 Freising-Weihenstephan, Germany
(*correspondence: hoeschen@wzw.tum.de)

² Max-Planck-Institut für Plasmaphysik, EURATOM
Association, 85748 Garching, Germany

³ Institute for Advanced Study, Technische Universität
München, Lichtenbergstraße 2a, 85748 Garching,
Germany

The study of biogeochemical interfaces in soils requires an adequate technique capable of revealing processes occurring at a sub-micron spatial scale.

NanoSIMS analysis provides information about elemental/isotopic distributions at such a scale. Soil architecture is revealed by imaging the spatial distribution of organic matter (e.g.: ¹²C, ¹²C¹⁴N are detected) and mineral constituents (e.g. ²⁸Si, ²⁷Al¹⁶O, ⁵⁶Fe¹⁶O).

Samples relevant in soil science obtained by density and/or particle size fractionation are usually single particles or microaggregates with sizes in the micrometer range. Organic matter potentially distributed as a thin coating (few nm) on mineral particles could be lost during the presputtering/implantation process before NanoSIMS measurement. The challenge is to prepare such primary particles as flat, well-polished samples and to investigate them in cross-section. Embedding in a carbon containing resin results in ambiguities in distinguishing between the resin and the organic matter.

We present a method for preparing polished cross sections of micrometer-sized primary soil particles. The particles were coated with a marker layer, embedded in epoxy resin and polished. In the cross section organic coatings and assemblages on the primary soil particles can be distinguished.

This method can essentially improve the quality of NanoSIMS measurements on grainy mineral samples to better characterize soil biogeochemical interfaces.

Archean mantle heterogeneities revealed by Hf-Nd isotope systematics of the 3.33 Ga Comondale komatiites

J. ELIS HOFFMANN^{1,2} AND ALLAN H. WILSON³

¹Universität zu Köln, Germany; hoffmaj1@uni-koeln.de

²Steinmann-Institut, Universität Bonn, Germany

³University of Witwatersrand, Johannesburg, South Africa

The modern Earth's mantle is strongly heterogeneous, bearing ancient depleted portions that escaped homogenization. For the Archean depleted mantle, the degree of heterogeneity is comparably unconstrained. Powerful tools to investigate the degree of depletion of the mantle at a given time are the radiogenic ¹⁷⁶Lu-¹⁷⁶Hf and ¹⁴⁷Sm-¹⁴³Nd decay systems that can be applied on mafic and ultramafic rocks that directly tapped depleted mantle sources.

Here we report the first ultra-depleted mantle reservoirs for the Palaeoarchean tapped by the extraordinary well preserved 3.33 Ga Comondale komatiites [1] from the eastern Kaapvaal Craton, South Africa. The best preserved samples yield identical Lu-Hf and Sm-Nd isochron ages of 3334 ± 27 Ma (MSWD: 0.21) and 3334 ± 13 Ma (MSWD: 0.76), respectively, also in agreement with the Re-Os regression age of 3393 ± 440 Ma [2]. Initial εHf(t) and εNd(t) values are +6.5 to +9.2 and +1.6 to +2.4, revealing a decoupling of both isotope systems during previous melt extraction in the stability field of garnet. Moreover, a contamination with older crust during ascent can be excluded. In contrast, γOs(t) values are about chondritic, hence showing also decoupling from εNd(t) and εHf(t). This can be explained by the partition behaviour of Re-Os during mantle melting under oxidized conditions, leading to no fractionation of Re from Os in the source [3]. Primitive mantle normalized trace element patterns of the Comondale lavas show strong depletion of Nb-Ta, positive Zr-Hf, Ti and Y anomalies as well as comparably enriched LREE and Th for some samples. As alteration can be excluded here, the re-enrichment process might have been related to re-enrichment processes in an arc setting. This is supported by experimental data for the Comondale suite arguing for a hydrous mantle source [4]. Overall, the Comondale komatiites are the first reported strongly radiogenic Hf isotope compositions reported from the Palaeoarchean revealing initial εHf(t) well above the average depleted mantle at 3.3 Ga.

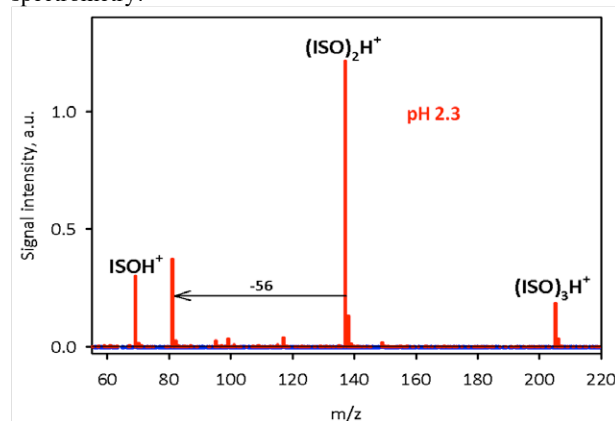
[1] Wilson and Carlson (1989) *EPSL* **96**, 89-105. [2] Wilson *et al* (2003) *Nature*, **423**, 858-861. [3] Birck and Allègre (1994) *EPSL* **124**, 139-148. [4] Barr *et al* (2009) *EPSL* **284**, 199-207.

Chemical reactions at the air-water interface in the troposphere

MICHAEL R HOFFMANN*, HIMANSHU MISHRA AND A. J. COLUSSI

Linde+Robinson Laboratory and Center for Global Environmental Science, California Institute of Technology, Pasadena, California 91125 USA
(*correspondence: mrh@caltech.edu)

An in depth investigations of chemical and physical phenomena at air-water interface are critical for understanding heterogeneous processes on cloud droplets, dew, fog, and haze aerosol. With this mind, the report that gas-phase isoprene (2-methyl buta-1,3-diene, ISO) is protonated as ISOH⁺ and oligomerized into a dimer, (ISO)₂H⁺, and a trimer, (ISO)₃H⁺, during collisions with pH < 4 aqueous microdroplets during gas-droplet collisions over 50 μs. Based on these observations, determined the probability of protonation per collision as γ ~ 10⁻⁵ corresponding to a process hindered by a 7 kcal mol⁻¹ kinetic barrier. During the λ > 305 nm photolysis of H₂O₂ in aqueous dilute ISO solutions yields C₁₀H₁₅OH species as primary products, whose formation both requires and is inhibited by O₂. A minimum of seven C₁₀H₁₅OH isomers are resolved by reverse-phase high-performance liquid chromatography and detected as MH⁺ (m/z = 153) and MH⁺-18 (m/z = 135) signals by electrospray ionization mass spectrometry.



Canonical trace element ratios and partitioning during global differentiation

A.W. HOFMANN^{1,2*}

¹LDEO, Columbia University, Palisades, NY 10964, USA

²Max Planck Institute for Chemistry, 55020 Mainz, Germany

(*correspondence: albrecht.hofmann@mpic.de)

For the past 16 years, the concept of “canonical” trace element ratios - concentration ratios that do not systematically change during global magmatic differentiation processes - has been variously questioned, declared invalid (e.g. [1]), or reaffirmed by many geochemical studies on oceanic basalts. Partitioning of such element pairs is sufficiently similar so that their ratios in melts reflect those of the source. Like isotope ratios, they are useful as tracers of mantle source composition, but they can be more diagnostic of global differentiation processes than the parent-daughter pairs of long-lived radioactive decay systems. Thus, Pb is partitioned similarly to the moderately incompatible LREE during intra-oceanic mantle melting, but it is highly incompatible (similar to U) during arc magmatism leading ultimately to formation of continental crust. Thus, although Pb isotopes do not distinguish well between continental and mantle sources, Pb/Ce ratios are sensitive discriminators. However, the basis for using Pb/Ce as a diagnostic ratio has been criticized, in part because Pb has similar ionic properties as Sr, which is strongly affected by gabbroic plagioclase fractionation, so that primary Pb/Ce ratios should be sufficiently modified to invalidate Pb/Ce as a tracer of mantle composition.

I use recent, comprehensive, high-quality data on the composition of global ocean floor basalts [2, 3, 4] to reassess canonical ratios involving Pb, Nb, Ta, K, U and other trace elements relevant to global differentiation processes. Plagioclase fractionation affects Pb/Ce ratios remarkably little, presumably due to the presence of sulfide during gabbroic fractionation. Overall, the bulk partition coefficient $D(\text{Pb})$ is between the values for Ce and Pr. $D(\text{K})$ is between Ta and La, and $D(\text{Nb})$ between Th and U. The bulk terrestrial K/U ratio is not well defined by MORB data, because K/U varies with absolute trace element enrichment [2].

[1] Sims & DePaolo (1997) *Geochim. Cosmochim. Acta* **61**, 765-784. [2] Arevalo & McDonough (2010) *Chem. Geol.* **217**, 70-85. [3] Jenner & O'Neill (2012) *Geochem. Geophys. Geosyst.* **13**, doi 10.1029/2011gc004009. [4] Gale *et al* (2013) *Geochem. Geophys. Geosyst.* **14**, doi 10.1029/2012GC004334.

CD-MUSIC to interpret drifting primary charge of ferrihydrite

A. HOFMANN¹, T. HIEMSTRA² AND J. LÜTZENKIRCHEN³

¹Géosystèmes UMR 8217, Université Lille 1, 59655

Villeneuve d'Ascq, France

²Dept. Soil Quality, Wageningen University, 6700 AA

Wageningen, The Netherlands

³INE, Karlsruher Institut für Technologie, 76344 Eggenstein-Leopoldshafen, Germany

In recent years, « environmental minerals », especially nanoparticles, have come into the focus of research because their short order structure confers them high chemical reactivity. Many of these minerals are formed in heterogeneous soil/water systems under ambient conditions. They reflect transitional, metastable phases that ultimately convert to thermodynamically stable phases, although this process can take very long periods of time. We will focus on surface complexation modeling and show how CD-MUSIC can contribute to understanding dynamic phase transformations.

When 2-line ferrihydrite is synthesized under « environmental conditions », i.e. relatively low ionic strength, no desalination and no drying steps, a material is formed which is marked by drifting of the primary charge over time and blurring of the point of zero salt effect.

Modeling these data with CD-MUSIC suggests that the affinity of electrolyte ions changes during aging of the primary material and that aggregational growth plays a role. We show that the particles' surfaces reflect the subtle changes occurring in the bulk material. Surface complexation modeling helps to decipher them, while classical spectroscopic and X-ray means hardly can.

Interaction of Eu(III) with calcite surfaces in presence of NaNO₃

S. HOFMANN^{1*} AND T. STUMPF²

¹Karlsruhe Inst. of Techn., Inst. for Nuclear Waste Disposal (KIT-INE), Eggenstein-Leopoldshafen, Germany
(*correspondence: sascha.hofmann@kit.edu)

²KIT-INE, Eggenstein-Leopoldshafen, Germany

Calcite is one of the most abundant minerals in the earth's crust, playing an important role as a geochemical barrier in nuclear waste deposits. It is known to adsorb and even incorporate many metal ions including lanthanides and actinides [1, 2]. In this study, we present the influence of NaNO₃ on the calcite surface and the uptake of Eu(III), investigated by site-selective time resolved laser fluorescence spectroscopy (TRLFS) and atomic force microscopy (AFM).

Discussion of results

TRLFS measurements with Eu(III) as a molecular probe showed that the lanthanide ion is not incorporated into the calcite crystal itself. Excitation and emission spectra (Fig. 1) differ considerably from the well-known Eu³⁺/calcite solid solution [3]. The fluorescence lifetime of this Eu³⁺/NO₃⁻/calcite species was determined to be 630 ± 50 μs, indicating the presence of only one water molecule in the first coordination shell of Eu.

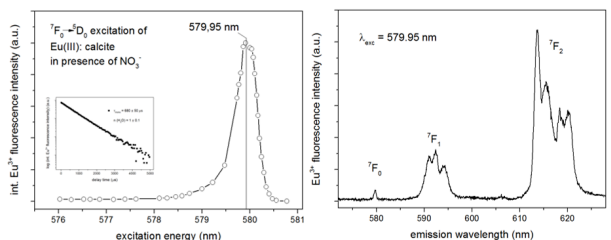


Figure 1: TRLFS excitation and emission spectra.

For further characterization of the influence of NaNO₃, calcite single crystals were equilibrated in aqueous NaNO₃ solutions (10⁻⁷ to 10⁻² M) and measured *in situ* with AFM. Images of these samples reveal critical changes of the surface morphology (roughening of the facets and rounding of step edges). An amorphous, soft layer forms rapidly on top of the calcite lattice. Europium seems to be incorporated into this layer, which is about 0.8 ± 0.1 nm thick.

[1] J. Paquette (1995), *Geochim Cosmochim. Acta*, **59**. [2] G. Aurelio (2010), *Chem. Geol.*, **270**. [3] M. Schmidt (2008), *Angew. Chem. Int. Edit.*, **47**.

Using compound-specific isotope analysis to assess biodegradation of nitroaromatic explosives in the subsurface

RETO S. WIJKER^{1,2}, JAKOV BOLOTIN^{1,2},
SHIRLEY F. NISHINO³, JIM C. SPAIN³,
AND THOMAS B. HOFSTETTER^{1,2*}

¹Eawag, Environmental Chemistry, CH-8600 Dübendorf, Switzerland, *thomas.hofstetter@eawag.ch

²Institute of Biogeochemistry and Pollutant Dynamics, ETH Zürich, CH-8092 Zürich, Switzerland

³School of Civil & Environmental Engineering, Georgia Institute of Technology, Atlanta, GA 30332, USA

Assessing the fate of nitroaromatic explosives in soils and sediments is challenging because these contaminants are present in different phases, that is bound to the organic and mineral matrix or as solid-phase residues, and transformation takes place via several competing pathways over time-scales of decades. To infer the type and extent of biotransformation of nitroaromatic compounds (NACs) from the combined evaluation of their C, N, and H isotope signatures, we have developed procedures for compound-specific analysis of 2,4,6-trinitrotoluene (TNT), dinitrotoluene isomers (2,4-DNT and 2,6-DNT), and mono-nitrotoluenes in subsurface material from a contaminated site.

Because of repeated spill events during decades of site operation as well as the perturbed subsurface at the study site, neither concentration nor δ¹³C, δ²H, or δ¹⁵N profiles provided evidence for transformation. Correlation of N vs. C and H vs. C isotope fractionation, in contrast, enabled the identification of three biodegradation routes.

Indicative trends of Δδ¹⁵N vs. Δδ¹³C and Δδ²H vs. Δδ¹³C were obtained from laboratory model systems with pure cultures for reaction pathways initiated via (i) dioxygenation, (ii) reduction, and (iii) CH₃-group oxidation. The comparison of Δδ¹⁵N vs. Δδ¹³C from field and laboratory data enabled a distinction of reductive and oxidative transformation of TNT, 2,4-DNT, and 2,6-DNT while Δδ²H vs. Δδ¹³C was used to quantify the relative shares of dioxygenation and CH₃-group oxidation. Based on the apparent kinetic isotope effects of the three biodegradation routes, our data imply that 86-89% of 2,4-DNT transformation in the field was due to dioxygenation while TNT was mostly reduced to aminonitrotoluenes and 2,6-DNT reacted via a combination of reduction and CH₃-group oxidation. Isotopic and historic site information suggest biodegradation of 2,4-DNT with half-lives of up to 9 to 17 years compared to 18 to 34 years for co-metabolic transformation of TNT and 2,6-DNT.

Multi-proxy study of shallow- and deep-water Doushantuo carbonates, Yangtze Platform, South China

S.V. HOHL¹, H. BECKER¹, S. HERZLIEB¹, Q. GUO²
AND A. GAMPER³

¹Freie Univ. Berlin, Germany, shohl@zedat.fu-berlin.de

²Institute of Geographic Sciences and Natural Resources
Research, Chinese Academy of Sciences, Beijing 100101,
China

³Museum für Naturkunde, Berlin, Germany

The wide distribution of shallow and deep-water sedimentary facies has established the Yangtze Platform in South China as a key site for the study of ocean oxidation and Ediacaran animal evolution following the Marinoan glaciation. We have studied mineralogy, textures, major and trace elements and Sr-C-O isotopic compositions of carbonates of the Doushantuo formation from shallow- (Xiaofenghe, Hubei Province) and deep-water (Yanwutan, Hunan Province) sections in order to distinguish diagenetic overprint from primary signatures and to constrain compositional variations of Ediacaran seawater in space and time. Carbonate rocks from the lower part of Yanwutan section show elevated ⁸⁷Sr/⁸⁶Sr (0.7099 to 0.7220) and high Mn/Sr. Negative correlation of ⁸⁷Sr/⁸⁶Sr with $\delta^{18}\text{O}_{\text{carb}}$ in the upper part of the section indicates meteoric fluid-rock interaction. At Xiaofenghe, ⁸⁷Sr/⁸⁶Sr in cap carbonates (D1) is near 0.713, dropping to seawater-like ratios upsection (0.7079 in D3). REE+Y patterns of deep water slope facies carbonates at Yanwutan reveal preservation of seawater signatures, cap carbonates show no Ce anomalies, but high Eu/Eu* (1.9) and enrichment in MREE, which, given the high ⁸⁷Sr/⁸⁶Sr, may reflect strong hydrothermal overprint. In contrast, the upper part of the section displays HREE enrichment, negative Ce, and variable positive Eu anomalies, indicating oxidizing conditions of deep water during this time interval. REE+Y patterns of carbonates at Xiaofenghe section are flat to variable HREE enriched, with Y/Ho_{PAS} (>2.1), indicating the presence of a seawater signature. While the cap carbonates have no Ce anomalies, D2 and D3 carbonates show strongly negative Ce anomalies, indicating precipitation from an oxidized water column. A main conclusion from the data is that deep water of the Yangtze basin was oxidized as early as the middle Doushantuo, with likely anoxic conditions before that time. Fluid-mobile elements in deepwater sections are more overprinted than in shallow water sections, presumably by hot reducing fluids of variable origin. Although fluid-mobile elements (Ba, Sr, Ca, Mg) commonly show evidence for modification by post-depositional fluid flow, REE+Y in these rocks often preserve seawater signals.

Decay constants for dating

NORMAN E. HOLDEN¹

¹National Nuclear Data Center, Brookhaven National
Laboratory, Upton, New York 11973-5000, USA

Two generations ago, the International Union of Geological Sciences (IUGS), through a sub-committee, recommended values for reporting isotopic data. A quarter century ago, the International Union of Pure and Applied Chemistry (IUPAC) recommended values for half-lives (decay constants) for a series of long-lived nuclides, many of which could be used for dating materials. The IUGS and the IUPAC recommendations differed in many cases. More than a decade ago, geochronologists began writing articles suggesting that updates should be made to the original IUGS recommendations because of the existence of more recent data on the original isotopic information that had been presented and because of the absence of any uncertainties that were associated with that data.

A few years ago, an inter-Union Task Group of members of IUGS and IUPAC was formed to make 'Recommendations for Isotopic Data in the Geosciences' and was approved by their Executive Boards. The rationale was similar, there were new data now available and the associated uncertainties need to be added to all recommended values.

The procedure for any recommendation of isotopic data would involve a re-evaluation of the measurement uncertainty budgets for each experiment, especially for the 'type-B' or non-statistical uncertainties, before combining the overall uncertainties and determining a recommended value. A number of isotopes will be discussed.

Deep fracture fluids isolated in the crust since the Precambrian

G.HOLLAND^{1,2}, B. SHERWOOD LOLLAR³, L. LI³,
G. LACRAMPE-COULOUME³, G.F. SLATER⁴
AND C.J. BALLENTINE^{1*}

¹SEAES, Manchester University, Manchester M13 9PL UK

²LEC, University, Lancaster LA1 4YQ UK

³Dept. of Earth Sciences, University of Toronto, ON, Canada M5S 3B1

⁴SGG, McMaster University, Hamilton ON Canada L8S 4K1

Water bearing macrosystems that have been isolated from the surface and preserved on geological timescales (>10Ma) are seemingly rare. Nevertheless, the unique insight they provide into the evolution of chemolithotrophic life makes these systems important areas of study. The Witwatersrand Basin in the South African Precambrian Crystalline Shield provides the case type [1,2]. Here, we have determined the noble gas concentration and isotopic composition of 6 gas samples, co-produced with water, from deep exploratory boreholes in a producing mine in the Timmins region of the Canadian Precambrian Crystalline Shield.

We show that ^{124,126,128}Xe excesses in the Timmins mine fluids can be linked to Xe isotope changes in the ancient atmosphere [3] and can be used to calculate a minimum mean residence time for this fluid of ~1.5Ga. We also resolve in all samples a clear ¹²⁹Xe signal in excess of atmospheric values. Mass fractionation and U fission can be excluded as sources of ¹²⁹Xe, and a mantle source is unlikely. We postulate ¹²⁹Xe is sourced in carbon rich metamorphic material of sedimentary origin and extracted by fluid migration processes at ~2.64Ga. Neon isotopic compositions are similar to the Witwatersrand study and are used to validate the closed system assumption for the radiogenic noble gases [1]. Closed system radiogenic noble gas residence times are 1142±64.5, 1655±789, 1498±784, 1610±825Ma for ⁴He, ²¹Ne, ⁴⁰Ar, ¹³⁶Xe respectively. Combined together, these complementary strands of evidence lend further support to the hypothesis that ancient pockets of water can survive the crustal fracturing process and remain in the crust for billions of years [4].

[1] Lippmann-Pipke *et al* (2011) *Chem. Geol.* **283**, 287-296.
[2] Lin *et al* (2006) *Science* **314**, 479-482. [3] Pujol, M. *et al*, (2011). *Earth Planet. Sci. Lett.* **308**, 298-306. [4] Holland *et al*, (2013) *Nature*, *in press*.

Influence of different organic carbon substrates on denitrification rates in riparian sediment

MELISA HOLLINGHAM^{1*}, RAOUL-MARIE COUTURE^{1,2},
FEREIDOUN REZANEZHAD¹
AND PHILIPPE VAN CAPPELLEN¹

¹University of Waterloo, Waterloo, Ontario, Canada,
(*correspondence: m.hollingham@gmail.com)

²Norwegian Institute for Water Research, Oslo, Norway

Nitrate (NO₃⁻) is an ubiquitous groundwater contaminant in agricultural and wastewater discharge areas [1]. The prediction of microbially mediated NO₃⁻ removal in subsurface environments requires an understanding of the rates at which electron donors are utilized by denitrifying microbes [2]. This study focuses specifically on the following organic carbon compounds as electron donors: glucose, acetate, adenine, cysteine and fulvic acid. Six triplicate series of flow through reactors (FTRs) containing 35cm³ of natural, organic-poor, riparian sediment were supplied for 10 weeks with solutions containing nitrate and the individual carbon compounds, along with a no-carbon added control. The organic carbon compounds were selected to yield a range of Gibbs Free Energy (ΔG) values when their oxidation is coupled to denitrification. The initial flow rate of the FTRs was 1 ml h⁻¹. Once steady NO₃⁻ concentrations were reached in the outflow, the flow rate was increased to 2 ml h⁻¹ and, subsequently, 4 ml h⁻¹. Maximum potential denitrification rates (R_{max}) measured for the different carbon substrates spanned an order of magnitude, ranging from 0 to 91nmol cm⁻³ h⁻¹. Fulvic acid did not induce denitrification, while acetate yielded the highest rate. The outflow solutions for FTRs supplied with adenine and cysteine contained ammonia and sulfate, respectively. These results are consistent with the structure of the organic components of adenine, containing an amine, and cysteine, containing a thiol group. R_{max} values for the studied carbon substrates are relatively low compared to those in the literature for similar experiments, which have values ranging from 98 to 933 nmol cm⁻³ h⁻¹ [3]. Most likely, the low rates reflect a low abundance of denitrifying organisms in the riparian sediment used.

[1] Xue *et al* (2009) *Water Research* **43** 1159-1170.
[2] Thullner *et al* (2007) *Geomicrobiol. J.* **24** 139-155.
[3] Laverman *et al* (2006) *FEMS Microbiol Ecol* **58** 179-192

Tectonic evolution of the Cerro Casale Cu-porphyry system, Chile: Implications for mineralisation

PETE HOLLINGS^{1*}, HUAYONG CHEN^{2,3}
AND DAVID R. COOKE²

¹Dept. of Geology, Lakehead University, Thunder Bay, Ontario, Canada, P7B5E1. (*correspondence: peter.hollings@lakeheadu.ca)

²CODES, ARC Centre for Excellence in Ore Deposits, Private Bag 126, Hobart, Tasmania 7001, Australia

³Guangzhou Institute of Geochemistry, Chinese Academy of Sciences, Tianhe, PO Box 1131, Guangzhou, China

The Cerro Casale porphyry Cu-Au deposit is located at the southern end of the Maricunga belt, near the northern boundary of the modern nonvolcanic, flat-slab region of the Chilean Andes (28-33°S). Oligocene andesitic volcanic rocks in the Casale district have been intruded by the Cerro Casale, Roman, Eva, Estrella and Anfiteatro dioritic to granodioritic plutons, of which the Casale diorite is the main host to mineralisation (1300 Mt @ 0.7 g/t Au and 0.35% Cu).

U-Pb dating of zircon from the mineralized granodiorite yielded an age of 13.9 ± 1.1 Ma, consistent with previous Ar-Ar ages of 13.89 - 13.91 Ma from hydrothermal biotite and alunite [1]. Weakly mineralised to barren intrusions in the district range in age from 28 to 14 Ma, with a major porphyry-high sulfidation system forming at the Caspiche prospect ~10 km to the north in the late Oligocene, implying repeated mineralising episodes in the region.

The volcanic and intrusive rocks from the Casale district are predominantly medium-K andesites and diorites. The intrusive rocks show a trend to increasing Gd/Yb_n ratios in younger samples comparable to trends in Miocene rocks related to porphyry mineralisation in Central Chile interpreted to be the result of subduction of the Juan Fernandez ridge and associated slab flattening [2]. ϵ_{Nd} values for the intrusive rocks are uniformly negative (-0.6 to -2.8), consistent with contamination by older crustal sources, and show a weak trend to less negative values with time. $^{87}Sr/^{86}Sr_i$ values range from 0.70490 to 0.70547 and increase in younger intrusions. The less negative ϵ_{Nd} in the younger intrusions in conjunction with a slight increase in Ni contents suggests a more primitive source for the mineralising magmas.

[1] Muntean, J.L., and Einaudi, M.T. (2000), *Economic Geology* 95, 1445-1472. [2] Hollings, P., Cooke, D.R., and Clark, A. (2005), *Economic Geology* 100, 887-904.

Natural Cu-Al-Fe metallic quasicrystals in the new CV3 meteorite find, Khatyrka

L. HOLLISTER*, C. ANDRONICOS², L. BINDI³,
V. DISTLER⁴, M. EDDY⁵, J. EILER⁶, Y. GUAN⁶,
A. KOSTIN⁷, V. KRYACHKO⁴, G. MACPHERSON⁸,
W. STEINHARDT⁹, M. YUDOVSKAYA⁴
AND P. STEINHARDT¹⁰

*Princeton University, Princeton, NJ 08544, USA
(correspondence: linc@Princeton.EDU);

²Purdue University, West Lafayette, IN;

³Università di Firenze, Florence, Italy;

⁴Russian Academy of Sciences, Moscow, Russia

⁵Massachusetts Institute of Technology, Cambridge, MA;

⁶Caltech, Pasadena, CA, ⁷BHP Billiton, Houston, TX;

⁸Smithsonian Institution, Washington, D.C.

⁹Harvard University, Cambridge, MA

¹⁰Dept. of Physics, Princeton University, Princeton, NJ 08544.

Khatyrka occurs as clastic grains within clay-rich layers along the banks of a small stream in the Koryak Mountains of far eastern Russia. The recovered grains share in common the presence of metallic Cu-Al-Fe alloys that include the quasicrystalline phase icosahedrite (Al₆₃Cu₂₄Fe₁₃), along with khatyrkite (CuAl₂) and cupalite (CuAl). Some of the ~ mm-sized meteorite grains clearly are CV3 (oxidized) chondrite fragments having Type IA porphyritic olivine chondrules enclosed in matrices that have the characteristic platy olivine texture, matrix olivine composition, and mineralogy of oxidized-subgroup CV3 chondrites. Other grains are fine-grained spinel-rich calcium-aluminum-rich inclusions (CAIs) with spinel oxygen isotopic compositions ($\Delta^{17}O \sim -19 - -23$ ‰) typical of such objects in CV3 chondrites. One grain is an achondritic intergrowth of Cu-Al-Fe metal alloys with forsteritic olivine ± diopside pyroxene. The latter, along with silicates from the chondritic grains, have ¹⁶O-enriched ($\Delta^{17}O \sim -4 - -8$ ‰) oxygen isotopic compositions that plot on the CCAM mixing line in the region occupied by bulk CV3 chondrites [1, 2]. Finally, some grains consist almost entirely of Cu-Al-Fe alloys. The Cu-Al-Fe metal alloys and the alloy-bearing achondrite clast are either a unique accretionary component of what otherwise is a fairly normal CV3 (oxidized) chondrite, or else formed in place via an as-yet undetermined process. Either way, the reducing conditions required to form such metallic aluminum-bearing alloys are approximately those of a hot gas of solar composition. Understanding what specific process(es) formed these alloys of two such cosmochemically-dissimilar elements as aluminum and copper remains the focus of our on-going research program.

[1] Bindi, L. *et al* (2012) PNAS, **109**: 1396-1401; [2] MacPherson, G. *et al* (2013) MAPS (submitted).

Fe(II) in early abiotic processes

NILS G. HOLM

Department of Geological Sciences, Stockholm University,
SE-106 91 Stockholm, Sweden; (nils.holm@geo.su.se)

Recently, it was suggested that Fe(II) preceded Mg(II) as an efficient co-factor in prebiotic catalysts on the early Earth [1]. Mg(II) has a special role in the folding and catalysis of biomolecules such as RNA because of its small size and ability to coordinate six oxygen atoms, including oxygens in oxyanions, in its first coordination shell [2]. In principle, Fe(II) can replace Mg(II) in this function and be even more efficient [1], but on Earth today Fe(II) is quickly oxidized to Fe(III) in the presence of molecular oxygen. However, before the Great Oxidation Event about 2.5 Ga Fe(II) would have been abundant in aqueous systems. Iron metabolism in modern organisms is controlled by small RNAs molecules (sRNA) [3]. Because of the ability of Fe(II) to coordinate oxyanions, Fe(II) minerals can catalyze the formation of pyrophosphate from activated phosphate compounds, such as acetyl phosphate, and inorganic phosphate [4]. It has also been found, that even though modern deep-sea water is oxidized, Fe(II) originating in hydrothermal fluids are stabilized because of its affinity to lipids, polysaccharides and proteins [5]. Abiotic formation of acetyl phosphate has been reported. It is, therefore, likely that Fe(II) would have been a powerful component in the formation of pre-RNA types of information molecules in early life systems.

[1] Athavale, Petrov, Hsiao, Watkins, Prickett, Gossett, Lie, Bowman, O'Neill, Bernier, Hud, Wartell, Harvey & Williams (2012), *PLoS One* 7(5). [2] Holm (2012), *Geobiology* 10, 269-279. [3] Massé, Salvail, Desnoyers & Arguin (2007), *Current Opinion in Microbiology* 10, 140-145. [4] de Zwart, Meade & Pratt (2004), *Geochimica et Cosmochimica Acta* 68, 4093-4098. [5] Toner, Fakra, Manganini, Santelli, Marcus, Moffett, Rouxel, German & Edwards (2009), *Nature Geoscience* 2, 197-201.

Compositional constraints on the mantle below part of the Andes SVZ

P.M. HOLM^{1*}, N. SØAGER¹ AND C.T. DYHR¹

¹Institute of Geosciences and Natural Resource Management,
Univ. Copenhagen, Ø. Voldgade 10, DK-1350
Copenhagen, Denmark
(*correspondence: paulmh@geo.ku.dk)

This contribution discusses along and across arc differences in Pleistocene-Recent volcanic rocks of the SVZ based on new major and trace element and Sr, Nd and Pb isotope data from the T- and N-SVZ. We limit our discussion to little evolved compositions with high Mg#. Despite their primitive character most of these arc magmas display a strong negative correlation between silica and Ba/Th. Relative HFS-depletion is not caused by residual rutile is demonstrated by La-Nb systematics. Therefore, the relative enrichment in LILEs and LREEs is a reflection of source composition and show that that continental material with e.g. low Ba/Th rather than fluid was added to a source. The pre-enrichment mantle was more depleted in the C-NVZ than in the more northern T- and N-SVZ. Furthermore, all mantle below the arc is distinctly more depleted than the back-arc mantle, and compositional variation is thus indicated both N-S and E-W. Isotopically the depleted end-member is comparable to South Atlantic MORB mantle. Two distinctly different isotopically enriched endmembers show a similar elemental crustal signature. A Pb, Sr and Nd isotopic array of the northern backarc to T-SVZ arc magmas allow the arc-backarc mantle to be identified as distinct from the upwelling enriched Río Colorado component (Søager *et al.*, in prep.). There is a general decrease in water soluble components away from the trench. This may indicate that the fluid enriched source is generated over a more shallow part of the subducting slab than the crust enriched source. We model the crustal component that is added to the source as melts of subduction eroded continental crust that reacted with the overlying mantle.

Tracing the rise of atmospheric oxygen using Cr isotopes in carbonates as a paleoredox proxy

C. HOLMDEN¹ AND A.D. BEKKER²

¹Saskatchewan Isotope Laboratory, Department of Geological Sciences, University of Saskatchewan, SK, S7N 5E2 CANADA (*correspondence: chris.holmden@usask.ca)

²Department of Geological Sciences, University of Manitoba, MB, SK R3T 2N2 CANADA (bekker@cc.umanitoba.ca)

The Great Oxidation Event (GOE) is now well-constrained in age to ca. 2.4–2.3 Ga, but questions remain whether the pathway to oxidized surface environments was gradual, oscillatory with transient oxidation events, or stepwise. Various proxies, including fractionation of Cr isotopes in iron formations (Frei *et al.*, 2009), have been used to infer, at least locally, the development of oxidizing conditions as early as 2.7 Ga. Alternatively, Konhauser *et al.* (2011) argued that Cr concentrations were low in iron formations until 2.5–2.3 Ga when acidic groundwaters formed in response to the GOE and delivered reduced Cr to shallow-water environments.

Here, we tested whether $\delta^{53}\text{Cr}$ values in shallow-water carbonates spanning the GOE might also record steps in the rise of atmospheric oxygen. Cr isotopes are fractionated by redox reactions such as those occurring during Mn-mediated Cr oxidation on the continents or Cr reduction in anoxic marine environments. In the absence of molecular oxygen, the range of Cr isotope fractionation in exogenic materials would likely be confined to the range of igneous rocks ($\delta^{53}\text{Cr} = -0.1 \pm 0.1\%$). Carbonates from 15 formations were chosen with depositional ages ranging between 2.5 Ga and 1.9 Ga. Carbonate is more abundant than iron formation in the rock record, but there are pitfalls with carbonate-hosted seawater records that must be borne in mind. These include dolomitization, local cycling effects, depositional fractionation, and detrital sediment contamination.

$\delta^{53}\text{Cr}$ data collected, thus far, show no fractionation in samples older than 2.4 Ga, a very mild amount of fractionation at ca. 2.3 Ga of $\sim 0.1\%$, and permil level fractionation at 2.15 Ga in the peak interval of the Lomagundi carbon isotope excursion. Interestingly, the fractionations are both positive and negative relative to $\delta^{53}\text{Cr}$ in igneous rocks. Although fractionated Cr may be hosted in both carbonate and lithogenic components, Cr/Al ratios support the predominantly authigenic origin of the Cr in the carbonate fraction. These data are consistent with acidic weathering at the beginning of the GOE and Mn-mediated Cr oxidation during the Lomagundi carbon isotope excursion.

The Hf-W chronology of FUN CAIs

J. C. HOLST¹, M.B. OLSEN¹, C. PATON¹,
K. NAGASHIMA², M. SCHILLER¹, D. WIELANDT¹,
K.K. LARSEN¹, J. N. CONNELLY¹, J. K. JØRGENSEN¹,
A.N. KROT^{1,2}, Å. NORDLUND¹ AND M. BIZZARRO¹

¹Centre for Star and Planet Formation, University of Copenhagen, Copenhagen, Denmark.

²Institute of Geophysics and Planetology, University of Hawaii at Manoa, HI 96822, USA

Refractory inclusions (CAIs) represent the oldest solar system solids and provide information regarding the formation of the Sun and its protoplanetary disk. CAIs contain evidence of now extinct short-lived radioisotopes synthesized in one or multiple stars and added to the protosolar molecular cloud before or during its collapse. Understanding the origin of short-lived radioisotopes is necessary to assess their validity as chronometers and constrain the birthplace of the Sun. Whereas most CAIs formed with the canonical abundance of ^{26}Al corresponding to $^{26}\text{Al}/^{27}\text{Al}$ of $\sim 5 \times 10^{-5}$, rare CAIs with fractionation and unidentified nuclear isotope effects (FUN CAIs) [1] record nucleosynthetic isotopic heterogeneity and $^{26}\text{Al}/^{27}\text{Al}$ of $< 5 \times 10^{-6}$, possibly reflecting their formation before canonical CAIs [2]. Thus, FUN CAIs may provide a time-window into the earliest solar system, but their chronology is unknown.

Using the ^{182}Hf - ^{182}W chronometer, we show that a newly discovered FUN CAI, dubbed STP-1, formed coevally with canonical CAIs [3], but with $^{26}\text{Al}/^{27}\text{Al}$ of $\sim 3 \times 10^{-6}$. Moreover, the mineralogy and the group II rare earth element (REE) pattern coupled with a ^{16}O -rich composition, suggest that the precursor material of STP-1 formed by condensation from a gas of solar composition depleted in the most refractory REEs, similar to fine-grained CAIs. The level of $^{26}\text{Al}/^{27}\text{Al}$ in STP-1 is higher than the galactic background and suggests that our Sun formed as part of a cloud that was chemically enriched by earlier generations of massive stars. The observed decoupling between ^{182}Hf and ^{26}Al requires distinct stellar origins: steady-state galactic stellar nucleosynthesis for ^{182}Hf and late-stage contamination of the protosolar molecular cloud by a massive star(s) for ^{26}Al . Admixing of fresh stellar-derived ^{26}Al to the protoplanetary disk occurred during the epoch of CAI-formation and, therefore, the ^{26}Al - ^{26}Mg systematics of CAIs cannot be used to define their formation interval. In contrast, our results support ^{182}Hf homogeneity and the chronological significance of the ^{182}Hf - ^{182}W clock.

[1] Wasserburg *et al.* (1977) *Geophys Res Lett* **4**, 299. [2] Sahijpal & Goswami (1998) *Astrophys. J.* **509**, L137-L140. [3] Burkhardt *et al.* (2012) *Astrophys. J.* **753**, L6.

Microbially-induced carbonate precipitation, Moodies Group (3.2 Ga, BGB, South Africa)

M. HOMANN^{1*}, C. HEUBECK¹, A. AIRO¹, M. TICE² AND S. NABHAN¹

¹Freie Universität Berlin, Institute of Geological Sciences, Malteserstr. 74-100, 12249 Berlin, Germany (*correspondence: martin.homann@fu-berlin.de)

²Texas A&M University, College Station, Texas 77843, USA (mtice@geos.tamu.edu)

The Archean Moodies Group, Barberton Greenstone Belt (BGB), ~3.2 Ga, represents Earth's oldest known tidally influenced siliciclastic sequence and includes well-preserved microbial mats which can be traced laterally for >15 km.

We investigated the microstructure of crinkly intertidal-facies mat morphotypes and tufted supratidal-facies mats, both preserved as abundant kerogenous laminae ~1mm thick overlying individual depositional events in medium- to coarse-grained sandstones. Mats are widely underlain by up to 40 cm long and few mm-thick monomineralic layers; microbial tufts (1-2 cm in height) show increased calcification within their interior. XRF elemental scanning of fresh slabbed and polished hand samples indicates (1) that the monomineralic layers underlying the microbial mats consist of pure carbonate (calcite, dolomite), now largely replaced by microcrystalline quartz, and that (2) Fe is enriched in the kerogenous mat remnants. SEM observations of freshly exposed kerogenous surfaces show interwoven, bundled and twisted filaments 1-3 μm in diameter, confirming mat biogenicity.

The close association of carbonate layers and microbial mats suggests that mat metabolic activity promoted their formation. An autotrophic metabolism, such as CO₂ fixation, would have increased the alkalinity of the pore fluid beneath the mat and induced carbonate precipitation. Alternatively or additionally, carbonate could have formed as a byproduct of a Fe-reducing metabolic pathway. Middle Archean photic-zone filamentous microbial mats may have, at least in its upper layers, employed a photosynthetic strategy.

Trace metal inputs from river-fed and river-starved margin sediments of the South Atlantic Ocean

WILLIAM B. HOMOKY^{1*}, RACHEL A. MILLS¹, YU-TE HSIEH^{2,3}, DEBORAH J. HEMBURY¹, E. MALCOLM S. WOODWARD⁴ AND GIDEON M. HENDERSON²

¹Ocean and Earth Science, National Oceanography Centre Southampton, University of Southampton, SO14 3ZH, UK (*Correspondence: w.homoky@soton.ac.uk, rachel.mills@soton.ac.uk, d.hembury@noc.ac.uk)

²Department of Earth Sciences, University of Oxford, South Parks Road, OX1 3AN, UK (gideonh@earth.ox.ac.uk)

³Program of Atmosphere, Ocean and Climate, Massachusetts Institute of Technology, 77 Massachusetts Avenue, Cambridge, MA 02139, USA (yuteh@mit.edu)

⁴Plymouth Marine Laboratory, Prospect Place, The Hoe, Plymouth, PL1 3DH (EMSW@pml.ac.uk)

Trace metal exchange between sediments and seawater may play an important role in providing micronutrients to the ocean. Continental margin fluxes of metals such as Fe remain poorly constrained but may be important in the global carbon cycle [1]. A selection of micronutrient trace metals have been measured in porewaters and sediments from the slopes on both sides of the South Atlantic Ocean to determine such margin fluxes to a region of high primary productivity in the surface ocean. Intact surface sediments were collected by coring activities on two UK GEOTRACES expeditions (D357 and JC068; GA10) from 12 sites between the River Plate-fed Uruguyan margin and the comparatively river-starved Cape margin of South Africa.

Macronutrient and micronutrient concentrations are principally coupled to organic carbon oxidation at all sites. Fe and Mn inputs to the South Atlantic are calculated from the relationship between porewater metal and high-resolution oxygen data. Dissolved fluxes of Fe and Mn on the Uruguyan and South African margins have notable differences in their magnitude and down-slope distribution. We show the variability of metal supply reflects (a) enhanced organic carbon respiration on the river-fed Uruguyan margin, and (b) the depleted metal substrate reservoir on the comparatively river-starved Cape margin of South Africa. This study provides new constraints on dissolved micronutrient inputs to South Atlantic deep waters which subsequently upwell in the Fe-starved Southern Ocean. It also provides information about the general role of sediments in micronutrient fluxes to seawater.

[1] Boyd and Ellwood (2010) *Nature Geoscience*, **25**(10), 675

Diffusive fractionation of lithium isotopes in polycrystalline olivine

V HOMOLOVA* AND E B WATSON

Department of Earth and Environmental Sciences, Rensselaer Polytechnic Institute, Troy, NY 12180, USA
(*correspondence: homolv@rpi.edu)

Diffusive fractionation of Li isotopes has recently been reported in silicate melts, aqueous fluids and single crystals [1, 2, 3]. Here, we present an experimental study which investigates diffusive fractionation of Li isotopes in polycrystalline olivine. The experimental procedure consists of annealing oxide powders in an iron capsule at 1.4 GPa and 1250°C for 48 hours. The annealing step produces a synthetic rock comprising olivine (Fo90) plus 15 wt% pyroxene (En92), with grains 50 - 75µm in diameter. The capsule is then sectioned, polished and juxtaposed to a spodumene powder, which acts as the Li source. The diffusion couples were held at 1.4 GPa and 700 - 1000°C for 12 - 120 hours. Li abundances and isotopic ($7\text{Li}/6\text{Li}$) profiles were analyzed using LA-ICP-MS.

Maximum lithium abundances measured near the Li source in the olivine and pyroxene reach ~550 and ~700 ppm, respectively. Li abundances decrease as a function of distance from the source to the background Li concentration of ~3 ppm. Preliminary data suggest an effective diffusivity of Li in polycrystalline olivine plus pyroxene of $\sim 5\text{E}-13\text{m}^2/\text{s}$ at the highest temperature investigated. In both olivine and pyroxene, $7\text{Li}/6\text{Li}$ ratios decrease linearly or in a concave down fashion for the entirety of the diffusion profile before abruptly jumping back up to the initial isotopic ratio of the synthetic rock. This decrease in $7\text{Li}/6\text{Li}$ along the diffusion profile is similar to previous studies investigating diffusive fractionation of Li isotopes and suggests a higher diffusivity of 6Li relative to 7Li . The shape of the isotopic profile may be replicated well with a model previously developed by [3] for Li diffusion with reaction in single crystal olivine, in which Li simultaneously diffuses via two different mechanisms. Application of the data to diffusive transport of Li in the upper mantle will be discussed. Experiments at higher temperature and utilizing alternate Li sources are underway.

[1] Richter *et al* (2003) *GCA* **67** 3905 - 3923 [2] Richter *et al* (2006) *GCA* **70** 277 - 289 [3] Dohmen *et al* (2010) *GCA* **74** 274 - 292

Abrupt variations of Indian and East Asian summer monsoons during the last deglacial stadial and interstadial

B. HONG^{1*}, Y.T. HONG¹, M. UCHIDA², Y. SHIBATA²
AND Y.X. ZHU¹

¹Institute of Geochemistry, Chinese Academy of Sciences, Guiyang 550002, China (*correspondence: hongbing@vip.skleg.cn)

²National Institute for Environmental Studies, Onogawa 16-2, Tsukuba, Ibaraki 305-0053, Japan

The recent study comparing marine and terrestrial palaeoclimate records from South Asia suggests that during the deglaciation the ISM fluctuated widely, with weaker monsoons during colder episodes, such as the Younger Dryas (YD), and stronger monsoons during warmer episodes, such as the Bølling-Allerød (BA) [1]. However, this study does not cover the palaeoclimate records from some East Asian regions influenced by the Indian Summer Monsoon (ISM), such as the Tibetan Plateau and its adjacent regions, and it does not include the activity of the East Asian Summer Monsoon (EASM). Another study on global climate evolution during the last deglaciation briefly discusses the behaviours of the ISM and EASM during the transient period and mainly focuses on the results of a few stalagmite ^{18}O records from the southern Chinese mainland [2]. To complement these studies, we present a continuous peat cellulose $\delta^{13}\text{C}$ record of ISM covering the past 15000 years. By comparing this record with a variety of other monsoon proxy records, especially with the EASM proxy records published in recent years, we attempt to clarify the abrupt variation, phase relationship, and possible forcing mechanisms of two Asian monsoons during the last deglaciation.

[1] Tiwari *et al* (2011) *J Geol Res* 1-12. [2] Clark *et al* (2012) *PNAS* 109, E1134-E1142.

Distribution, Fluxes in the water column and early diagenesis in the bottom sediments of ^{210}Po and ^{210}Pb in the sea

G.H. HONG^{1*}, H.M. LEE¹, M. BASKARAN², S.H. KIM¹,
Y.I. KIM¹ AND C.J. KIM¹

¹Korea Institute of Ocean Science and Technology, Ansan
426-744, R. Korea (correspondence: ghhong@kiost.ac)

²Wayne State University, Detroit, MI 48202,
U.S.A. (baskaran@wayne.edu)

The ^{210}Po activity, granddaughter of ^{210}Pb activity, has been widely studied to elucidate various oceanic processes, such as quantifying the scavenging and removal of particle-reactive species including organic matter. The deficit and excess of ^{210}Po with respect to its grandparent ^{210}Pb in dissolved and particulate phases in the surface ocean is well documented through the ocean. However, in deep waters below 1000 m, secular equilibrium between ^{210}Po and ^{210}Pb was observed in some areas, but a large deficiency of ^{210}Po with respect to ^{210}Pb in dissolved phase was also observed in several places in the world ocean. Recent efforts were made extensively by GEOTRACES [1, 2] to resolve the unresolved issues in determination of ^{210}Po and ^{210}Pb remaining from the earlier GEOSECS studies in late 1970s. Here we report new measurements of dissolved, particulate, and sediment porewater ^{210}Po and ^{210}Pb in a deep marginal sea in the Northwest Pacific (East Sea/Japan Sea) using the state-of-the-art measurement methods considering all relevant correction factors in the calculation of the final *in situ* their activities provided by GEOTRACES $^{210}\text{Po}/^{210}\text{Pb}$ group. The earlier discrepancy may be resolved as we can generalize the vertical distribution of dissolved ^{210}Po with respect to dissolved ^{210}Pb in the sea as the surface deficit, subsurface excess and secular equilibrium below the 500 m or 1000 m depth based on our measurements with great variation of total activities due to their variation in the sources as well as the amount of suspended particulate matter in the water column. An order of magnitude greater concentration of dissolved ^{210}Po and ^{210}Pb concentration activities were present in the interstitial waters of the bottom sediment with ^{210}Po deficit or excess with respect to ^{210}Pb in the East Sea. Detailed quantitative analysis on the distribution, chemistry, flux, and early diagenesis is presented at the meeting.

[1] Church *et al* (2012). *Limnol. Oceanog.: Methods* **10**, 776-789. [2] Baskaran *et al* (2013). in press.

Redox behavior of uranium incorporated into hematite

DERRELL HOOD¹, YI WEN¹,
LINDSAY SHULLER-NICKLES^{*1}

¹Clemson University, 342 Computer Court, Anderson, SC,
USA 29625 (*correspondence: lshulle@clemson.edu)

The development of long-term geological waste repositories is an important response to ever increasing amounts of spent nuclear fuel. One of the principle considerations at any potential storage site is the possibility for radionuclides to leach from waste forms and undergo subsurface transport. The solubility of radionuclides in the repository environment, their redox behavior, and possible incorporation into proximal mineral phases are inter-related mechanisms that synergistically affect the subsequent hydrological transport of the nuclides.

It has been shown that U(VI) can be incorporated into bulk hematite with a similar coordination environment as Fe(III) [1,2]. In this study, we analyze the incorporation of U(VI) into hematite as a possible mechanism of limiting the aqueous uranyl concentration in contaminated areas. Atomistic simulations were conducted to evaluate the incorporation mechanism (*i.e.*, substitution reaction energies and substitution geometries). The redox behavior of uranyl incorporated into bulk hematite was investigated using cyclic voltametry with a powder microelectrode. In addition, the redox behavior of uranyl incorporated into hematite is compared with that of uranyl at the hematite surface to evaluate the role of hematite as a uranyl host and as a substrate for uranyl sorption, reduction and precipitation.

The sample was preconditioned for thirty minutes at -0.25V and scanned between $\pm 0.7\text{ V}$ at a rate of 50 mV/s . Under these conditions, uranyl was observed to undergo an irreversible oxidation from U(IV) to U(VI) on the first positive voltage scan. Subsequent cycles indicate reduction and re-oxidation between U(VI) and U(V). Similar experiments examined uranyl in solution with hematite and measured comparable uranyl redox behavior. Due to the strong relation between uranium solubility and oxidation state, these initial results are significant with regards to potential aqueous uranyl immobilization.

[1] Duff (2002) *Geochimica Acta* **20**, 3533-3547 [2] Ilton (2012) *Environmental Science and Technology* **46**, 9428-9436

Os isotope constraints on crustal contamination in Auckland Volcanic Field basalts, New Zealand

J.L. HOPKINS^{1*}, A. POIRIER², M-A. MILLET³, C. TIMM⁴,
G. LEONARD⁴ AND C.J.N. WILSON¹

¹SGEES, Victoria University of Wellington, PO Box 600, Wellington, New Zealand. (*jenni.hopkins@vuw.ac.nz)

²GEOTOP, Université du Québec à Montréal, Montréal, Canada

³Origins Laboratory, Department of the Geophysical Sciences, University of Chicago, USA

⁴GNS Science, Lower Hutt, New Zealand

Basalts from the monogenetic Auckland Volcanic Field (AVF) have been inferred to derive from the partial melting and mixing of varying proportions of three distinct components from within two mantle sources: (a) ambient asthenospheric mantle consisting of mid ocean ridge-like peridotite containing HIMU-type eclogitic domains (recycled oceanic crust); and (b) a subduction metasomatised lithosphere¹. However the contribution of lithospheric (mantle and crust) contamination has not been assessed in detail. We present Re-Os isotope systematics of basalts representative of the range in the AVF geochemistry and use the differences of Os isotope systematics between crust and mantle derived lithologies to assess the extent of lithospheric contamination in these data.

Our results show there is a large range in Os concentrations (6-579ppt) and ¹⁸⁷Os/¹⁸⁸Os isotope ratios (0.123-0.547). ¹⁸⁷Os/¹⁸⁸Os vs. 1/¹⁸⁸Os diagram shows a broad positive trend (decreasing Os concentration and increasing Os isotope ratio). Samples showing only little contamination also display ¹⁸⁷Os/¹⁸⁸Os values (0.128-0.138) similar to or slightly higher than average mantle values (0.121-0.128), consistent with their derivation from partial melting of a peridotitic source containing HIMU-type eclogitic/pyroxenitic domains. The more radiogenic Os isotopic compositions (>0.15) and low Os content, entirely decoupled from tracers of the mantle sources under the AVF are suggestive of contamination of asthenospheric mantle-derived magmas by assimilation of continental crust during ascent.

[1] McGee, L.E., (2012) Melting processes in small basaltic systems: the Auckland Volcanic field, New Zealand. PhD Thesis, University of Auckland.

Ancient thermal events on 4 Vesta recorded in zircon U-Th-Pb-Ti depth profiles from a brecciated eucrite

M. D. HOPKINS^{1*}, S. J. MOJZSIS^{1,2,4}, W.F. BOTTKE^{3,4}
AND O. ABRAMOV⁵

¹ University of Colorado, Geol. Sciences, Boulder, CO USA
(*correspondence: michelle.hopkins@colorado.edu)

² Laboratoire de Géologie de Lyon, ENS & UCBL1, France

³ Southwest Research Institute, Boulder, CO, USA

⁴ Center for Lunar Origin and Evolution, NLSI

⁵ United States Geological Survey, Flagstaff, AZ, USA

Zircons in asteroidal meteorites are rare, but a modest number have been previously documented, including those in the howardite-eucrite-diogenite (HED) achondrite group. The HEDs probably originate from 4 Vesta. Sub-micrometer distributions of trace elements (Ti, U, Th) and ^{235,238}U-^{207,206}Pb ages were investigated in four zircons (>7-40 μm Ø) separated from bulk samples of Millbillillie, a brecciated eucrite. Ultra-high resolution (sub-μm) ion microprobe depth profiles reveal different age domains correlative to mineral chemistry in cores and mantles within individual zircons. These compositional differences (e.g. [Th/U]_{zrc} and Pb* isotope discordance) can be related to ancient thermal events to the crust of the parent body asteroid. Our results confirm that the crust of 4 Vesta solidified within a few million years after the formation of CAIs (4561±13 Ma), in good agreement with previous work. Subsequent zircon age re-setting occurred less than 40 Myr later (ca. 4530 Ma), which has also been seen in some ⁴⁰⁻³⁹Ar age plateaux [1]. Analytical modeling shows that for a single impactor to be responsible for this effect, it had to have been ≥10 km in diameter and at high enough velocity (>5 km s⁻¹) to account for the thermal field required to re-crystallize zircon. Model output also shows that the thermal regime from impact could have penetrated at least 10 km into Vesta's crust. Later events at ca. 4200 Ma have been recorded in an HED apatite ^{235,238}U-^{207,206}Pb age [2] and ⁴⁰⁻³⁹Ar age spectra [3]. These younger ages, as well as those coinciding with the Late Heavy Bombardment (LHB; ca. 3900 Ma) are not present in Millbillillie zircon. This is attributable to differences in mineral closure temperatures (T_c zircon >> apatite) and changes to the velocity distributions of impactors in the asteroid belt during and after the LHB.

[1] Bogard & Garrison (2003) *Meteor Planet Sci*, **38**, 669-710.

[2] Zhou *et al* (2011) *42nd LPSC*, Abs. #2575. [3] Bogard

(2011) *Chemie der Erde*, **71**, 207-226.

Early diagenetic alteration of zeolites in subseafloor sediment of the South Pacific Gyre

BRYCE HOPPIE* AND ALYSSA WITT

Department of Chemistry and Geology, Minnesota State University, Mankato, Minnesota 56001 USA
(*correspondence: bryce.hoppie@mnsu.edu)

Zeolite minerals are distributed throughout much of the subseafloor sediment of the South Pacific Gyre (SPG). Previous studies of deep-sea zeolites suggest that they form through the early diagenetic alteration of volcanic debris within the first meter of the subseafloor and subsequently undergo dissolution at burial depths exceeding 50 m. In SPG subseafloor sediment, porosities frequently exceed 80% and pore water residence times are greater than 10^5 years. Consequently, substantial opportunities exist for zeolites beneath the SPG to undergo post-depositional mineral-to-pore water interactions.

For this study, over 1,200 randomly selected zeolite crystals were isolated from clay-rich samples of SPG subseafloor sediment obtained during IODP Expedition 329. Crystals were analyzed using optical microscopy, SEM-EDS, and X-ray diffraction techniques. Strata were found to include the zeolite minerals phillipsite, $(\text{Na}, \text{K})_2(\text{Mg}, \text{Ca})\text{Al}_6\text{Si}_{10}\text{O}_{32} \cdot 12\text{H}_2\text{O}$, and harmotome, $(\text{Na}, \text{K})_2(\text{Ba}, \text{Mg}, \text{Ca})\text{Al}_5\text{Si}_{11}\text{O}_{32} \cdot 12\text{H}_2\text{O}$. The zeolites generally exhibit up to 100x increases in prismatic length within the first 4 to 15 m below the seafloor. Larger mean diameters of the phillipsite crystals correspond to elevated $[\text{K}^+]$ and $[\text{Si}^{4+}]$ whereas increased $[\text{Ba}^{2+}]$ corresponds to smaller harmotome crystals. Individual crystal volumes exhibit no consistent trend versus burial depth and do not correlate to euhedralism, a proxy for crystal dissolution; sub- and anhedral crystals are found at all depths and are particularly prevalent in the upper 10 to 25 m of the western study sites. All crystals maintain overall charge balance; however, none of the alkali or alkaline earth elements within the zeolites vary consistently with the other cations of similar electron valence or with $[\text{Al}^{4+}]$ or $[\text{Si}^{4+}]$.

These results show that SPG subseafloor zeolite minerals are not uniform or predictably variable with respect to their textural attributes or composition. Furthermore, they do not readily corroborate previous explanations of deep-sea zeolite diagenesis. Although the observed mineral characteristics could derive from local, shallow subsurface environmental disparities, they are also suggestive of cation-change and non-uniform interactions among zeolites and pore water within the SPG subseafloor environment.

A comparison of geothermometers for shallow silicic magmas

J.M. HORA^{1*}, G. WÖRNER¹, A. KRONZ¹,
AND A. K. SCHMITT²

¹GZG-Abt. Geochemie, Georg-August Universität, 37077 Göttingen, Germany (* correspondence: jhora@gwdg.de)

²Department of Earth and Space Sciences, University of California, Los Angeles, CA 90095, USA

Several geothermometers can be applied to silicic systems. Aside from 'traditional' two phase thermometers, recent calibrations involving partitioning of Si, Ti, and Zr among quartz, titanite, and zircon offer the promise of being able to extract T-t paths from zoned crystals. Recognition of P, a_{TiO_2} dependence have resulted in some controversy and revisions to these thermometers over the past few years. Difficulty in testing calibrations of these thermometers lies in having to assume values of input variables such as P and activities of components when comparing to only one or two other thermometers. Another complication is that the chemical species involved in various thermometers diffuse at different rates, and may result in comparing temperatures locked in at different times during a cooling history.

By choosing a natural system where there are more applicable thermometry equations than free variables (e.g. P, component activities), we can evaluate consistency of results among thermometers in the contexts of (a) differing diffusivities, (b) testing various calibrations of the same thermometer, and (c) a magmatic thermal history. We compared Fe-Ti oxide, amphibole, amphibole-plagioclase, two-feldspar, Zr-in-titanite, Ti-in-zircon, and Ti-in-quartz thermometers in rhyodacite dome lavas at Paríacota volcano, Chile. This also includes thermometry of U-Th-dated zircon with crystallization ages ranging from >350 ka to near-eruption (~47 ka), and oxide inclusions in titanite. This comparison indicates: (a) good agreement ($T = 740\text{--}760^\circ\text{C}$) among phases where diffusion is slow when $P = 3.5\text{ kbar}$, $a_{\text{TiO}_2} = 0.85$, $a_{\text{SiO}_2} = 1$, interpreted as conditions of crystallization, (b) progressively lower temperatures with increase in diffusivity (quartz $\approx 720^\circ\text{C}$, oxides $\approx 710^\circ\text{C}$), likely reflecting latest storage and syn-eruption temperatures, respectively; and (c) both the pressure-dependences of the Ti-in-zircon thermometer suggested by [1] and [2] agree with other thermometers, whereas the calibration of Ti-in-quartz by [3] produces the most consistent results at the low pressures and temperatures experienced by these magmas.

[1] Huang & Audetat (2012) *GCA* **84**, 75-89. [2] Ferry & Watson (2007) *CMP* **154**, 429-437. [3] Ferriss *et al* (2008) *Eur. J. Mineral.* **20**, 745-755.

Improved Pd-Ag isotopic systematics by MC-ICP-MS

M.F. HORAN*¹, R.W. CARLSON¹ AND M.SCHÖNBÄCHLER^{1,2}

¹ Carnegie Institution of Washington, Washington DC 20015

(*correspondence: mhoran@ciw.edu)

²ETH Zürich, 8092 Zürich, Switzerland

The short-lived ¹⁰⁷Pd-¹⁰⁷Ag radiogenic decay system has been used to date volatile depletion, crystallization and shock in meteorites. Palladium is siderophile with a condensation temperature (T_c) similar to Fe-metal alloy, while Ag is chalcophile with T_c several hundred degrees lower. The contrasting characteristics allow Pd-Ag data to provide chronologic information on early solar system processes complementary to that provided by other long- and short-lived systems.

Early Pd-Ag measurements by thermal ionization mass spectrometry (TIMS) yielded the first internal isochron for high Pd/Ag Group IVA iron meteorites [1]. Because Ag has only two isotopes, however, the inability to correct for instrumental mass bias limited precisions in ¹⁰⁷Ag/¹⁰⁹Ag by TIMS to 10-20 ϵ units (parts in 10,000). Over the past decade, our group refined a technique for MC-ICP-MS measurements of Ag isotopic composition by Faraday cup using added Pd to correct for mass bias [2,3]. External precision for tens of ng of Ag initially was $\pm 1.3 \epsilon$, which allowed resolution of the ¹⁰⁷Pd decay contribution to the Ag isotopic compositions in low Pd/Ag iron meteorites and pallasites. Subsequent use of wet plasma, instead of desolvation, produced more constant mass bias of Ag relative to Pd, yielding precisions of $\pm 0.5 \epsilon$, and showed Pd/Ag correlated with Ag isotope compositions in carbonaceous chondrites, but also many epsilon units of natural Ag mass fractionation effects in ordinary chondrites. [3,4]

To measure low Ag abundances (100s of pg) in volatile depleted irons, we used simultaneous collection of Ag isotopes by ion multipliers on the Nu Plasma MC-ICPMS. Mass bias was corrected by comparison with Ag standards without added Pd. Although precision was only $\pm 10 \epsilon$, a precise solar system initial ¹⁰⁷Pd/¹⁰⁸Pd of $2.8(\pm 0.3) \times 10^{-5}$ was obtained from the Group IVA iron Muonionalusta by assuming that the Pd-Ag system closed at its ²⁰⁷Pb-²⁰⁶Pb date (4565.3 ± 0.1 Ma). Pd-Ag systematics indicated the interval between volatile depletion and crystallization in the IVA parent body was short, < 0.5 Ma, suggesting that volatile depletion occurred during planetesimal breakup[5].

[1] Chen *et al*, GCA, 1990. [2] Carlson *et al*, 2001 GCA. [3] Schönbachler *et al*, Mass Spec Ion Proc., 2007 [4] Schönbachler *et al* GCA 2008. [5] Horan *et al*, EPSL 2012.

Reduction process of Cr(VI) by Fe(II) and humic acid using high-time resolution XAFS analysis

MAYUMI HORI*, KATSUMI SHOZUGAWA, AND MOTOYUKI MATSUO

Graduate School of Arts and Sciences, The University of Tokyo, Tokyo 153-8902, Japan

(*correspondence: 5953061388@mail.ecc.u-tokyo.ac.jp)

The reduction of Cr(VI) to Cr(III) starts immediately when Cr(VI) is released in the soil. However, Cr(VI) species have high mobility in subsurface soil, so the behavior of Cr (VI) released in the soil is not well understood. In this study, we clarified the detailed initial reduction process at high time resolution.

Three kinds of samples were prepared, 1) Fe(II) pellet, 2) humic acid (HA) pellet, 3) Fe(II)-HA pellet which contributed to Cr(VI) reduction in soil, and then they were spiked with Cr(VI) solution. In order to estimate the initial reduction process of Cr(VI) in samples, we continuously observed the valence of Cr and the concentration of Cr(VI) in samples after spiking Cr(VI) solution by measuring consecutively by Quick X-ray absorption fine structure (QXAFS) for several hours.

The decrease of concentration of Cr(VI) was observed for all samples just after Cr(VI) was spiked to samples. However, the reduction of Cr(VI) with Fe(II)-HA experiment showed reduction process unlike both Fe(II) and HA experiment, because of HA could also reduce Fe(III) to Fe(II). 97 % of total Cr(VI) was reduced to Cr(III) in 140 min. There were three phases of reduction processes. Firstly, there was an immediate sharp decrease of concentrations of Cr(VI), which means rapid reduction reaction. And then, the concentration of Cr(VI) gradually decreased. Thereafter, the concentration of Cr(VI) decreased sharply again, the reduction reaction was rapid. In the first phase, Cr(VI) was rapidly reduced by both Fe(II) and HA. In the second phase, Cr(VI) was mainly reduced by Fe(II). In the third phase, Cr(VI) was reduced by Fe(II), which was reduced by HA. The reduction reaction became rapid again due to increase of Fe(II). We clarified that the initial reduction process consisted of three phases, and Fe(II) and HA do different contribution to reduction of Cr(VI) in each phase.

Geochronological evidence of rapid progression of regional metamorphism in Hida Metamorphic Complex, southwest Japan

K. HORIE^{1*}, M. TAKEHARA², Y. TSUTSUMI³
AND M. CHO⁴

¹National Institute of Polar Research, Japan (*correspondence: horie.kenji@nipr.ac.jp)

²Department of Earth and Planetary Sciences, Kyushu University, Japan (3sc12025r@s.kyushu-u.ac.jp)

³National Museum of Nature and Science, Tokyo, Japan (ytsutsu@kahaku.go.jp)

⁴Seoul National University, Seoul, Korea (moonsup@snu.ac.kr)

Geochronological constraints from metamorphic rocks provide important information for understanding crustal evolution as well as metamorphic processes. The Hida Belt, situated at the northern part of southwestern Japan, consists of low P/T metamorphic rocks (Hida Metamorphic Complex) and Permo-Triassic granitoids, and is an important geological unit for discussion about crustal evolution at continental margin. In this study, zircon U–Pb geochronology was applied to the Hida gneisses and the Unazuki metamorphic rocks situated at the northeastern part of the Hida Belt to discuss the timing and the duration of regional metamorphism.

Zircon grains collected from the Hida gneisses have a dark CL response mantle and a bright CL response rim around igneous zoning core. The youngest age population of the igneous zoning core is 253 ± 5 Ma. The mantle and the rim yielded same age of 247 ± 4 Ma, suggesting a rapid progression from igneous activity to regional metamorphism. REE patterns of the rim suggest overgrowth of zircon under hydrothermal fluids.

Protoliths of the Unazuki metamorphic rocks are sedimentary and felsic volcanic rocks of late Carboniferous to early Permian age, based on the fossil evidence. U–Pb data of quartzo-feldspathic schist derived from felsic volcanics yield an eruption age of 258 ± 2 Ma, indicating that regional metamorphism occurred after 258 Ma. On the other hand, U–Pb age of a granite intruding the schist is 253 ± 1 Ma. The granite contains some xenoliths of the Unazuki schist, in which staurolite is replaced by andalusite and cordierite due to thermal flux from granitic magma. Therefore, the regional kyanite-sillimanite type metamorphism occurred between 258 and 253 Ma, suggesting a rapid metamorphic progression. Further work is needed to confirm this rapidity of crustal-thickening process.

Helium isotope map of Japan

KEIKA HORIGUCHI¹, NORITOSHI MORIKAWA¹,
MICHIKO OHWADA¹, ATSUKO NAKAMA¹
AND KOHEI KAZAHAYA¹

¹Crustal fluid Research Group, The Institute of Geology and Geoinformation, Geological Survey of Japan, AIST, Tsukuba, Ibaraki 305-8567, Japan. (keika-horiguchi @ aist.go.jp)

A helium isotope ratio ($^3\text{He}/^4\text{He}$ ratio) could be a good tracer for estimating the extent of upwelling deep fluids. This is because the helium has two origins, ^3He in terrestrial sample is considered to be a primordial isotope derived from the mantle, while ^4He is mainly from the crust. The spatial distribution of helium isotope ratios is characterized by high values of 4 to 8Ra (where Ra is the atmospheric $^3\text{He}/^4\text{He}$ ratio of 1.40×10^{-6}) along the volcanic front and in the back-arc region at northeastern Japan. In contrast forearc region shows low values less than 1Ra. This trend has simply been interpreted that helium in the back-arc region originates from the mantle and that in the fore-arc region is from the crust [e.g. 1, 2]. On the other hand, $^3\text{He}/^4\text{He}$ ratio of the southwestern Japan shows no clear and complex distribution. The complexity cause a lot of discussion for many years [e.g. 1, 3, 4, 5, 6]. However, no end to this discussion is currently in sight.

In recent 20 years, an increasing number of hot spring wells have been constructed in Japan. We collected gas and water samples from hot springs, deep wells, and mineral springs whole of Japan, and carried out the analysis of helium isotope ratio. At the same time, the helium data of previous studies are compiled.

The total number of data points is over 2000 including 1091 samples obtained in our study and 1121 samples from previous studies. We show helium isotope map of Japan.

- [1] Sano and Wakita (1985) *J. Geophys. Res.*, **90**, 8729-8741., [2] Horiguchi *et al* (2010) *Isl. Arc*, **19**, 60-70., [3] Matsumoto *et al* (2003) *Earth Planet Sc. Lett.*, **216**, 221-230., [4] Umeda *et al* (2006) *Volcanol. Geoth. Res.*, **149**, 47-61., [5] Morikawa *et al* (2008) *Geochem. J.*, **42**, 42-74., [6] Sano *et al* (2009) *Chem. Geol.*, **266**, 50-56.

Carbon isotope biosignatures: A surface-deep Earth abiotic connection

JUSKE HORITA

Department of Geosciences, Texas Tech University, Texas
79409-1053 (juske.horita@ttu.edu)

Our quest for identifying the beginning of life in terrestrial (and possibly extraterrestrial) environments has been hampered by the lack of unequivocal biosignatures in the absence of many other lines of evidence. The claim for finding early life in the ≥ 3.85 Ga Istaq Gneiss Complex at Akilia Island [1] reignited the half-century old debate on the use of low $\delta^{13}\text{C}$ values ($< -20\text{‰}$) of ancient carbonaceous materials as an isotope biosignature. It is now well demonstrated that a number of possible abiotic pathways exist near Earth-surface that lead to the synthesis of various organic and reduced carbon compounds depleted in ^{13}C due to large kinetic isotope effects [2]. Mantle carbons (graphite, diamond, dissolved carbons, carbide) with low $\delta^{13}\text{C}$ values ($< -20\text{‰}$) have previously been considered recycled sedimentary organic carbons or surface contamination. Other possible origins of these low $\delta^{13}\text{C}$ values have been suggested, including (a) possible mantle heterogeneity since the accretion from the solar nebula and the core–mantle segregation and (b) unidentified mechanisms and processes for large carbon isotopic fractionation at high temperatures and pressures.

Our recent theoretical calculations, along with some experimental studies [3], show that Si/Fe-carbide is very depleted in ^{13}C relative to other mantle compounds (diamond and calcite) even under deep-Earth conditions ($> 1000^\circ\text{C}$). Our modelling shows that redox-controlled C-cycle in the mantle between diamond and Fe-carbide can produce low $\delta^{13}\text{C}$ values ($< -20\text{‰}$) in addition to a primary mantle value ($-5 \pm 2\text{‰}$), a pattern similar to that observed from a global $\delta^{13}\text{C}$ distribution of diamond. These mantle-derived diamond and carbide with low $\delta^{13}\text{C}$ values can be brought up to near surface by mantle upwelling over geologic time. Thus, now a viable mechanism exists that can produce low $\delta^{13}\text{C}$ values of diamond and other carbonaceous materials that could have originated from the deep-Earth. Abiogenic processes that can produce carbonaceous materials with low $\delta^{13}\text{C}$ values, both near-surface and in deep-Earth, further challenge our notion of carbon isotope biosignatures for early life.

[1] Mojzsis *et al* (1996) *Nature* **384** 55-59. [2] Horita (2005) *Chemical Geology* **218**, 171-186. [3] Satish-Kumar *et al* (2011) *EPSL* **310** 340-348

Suboxic sediments as an oceanic sink of isotopically-light cadmium

T.J. HORNER^{1,2,*}, W.B. HOMOKY³, S.V. GEORGIEV⁴,
H.J. STEIN^{4,5}, J.L. HANNAH^{4,5}, R.A. MILLS³,
M. REHKÄMPER⁶ AND G.M. HENDERSON²

¹Dept. Marine Chem. Geochem., Woods Hole Oceanographic Institution, USA; *Tristan.Horner@whoi.edu

²Dept. Earth Sci., University of Oxford, UK

³Ocean and Earth Sci., National Oceanography Centre Southampton, University of Southampton, UK

⁴AIRIE Program, Colorado State University, USA

⁵CEED Centre of Excellence, University of Oslo, NO

⁶Dept. Earth Sci. Eng., Imperial College London, UK

Riverine and dust fluxes are thought to be the only two quantitatively significant sources of dissolved cadmium to the ocean. These inputs are balanced, within uncertainty, by burial of Cd into suboxic continental margin sediments [1]. Recent studies have characterized the Cd isotopic composition of the source terms [2, 3], indicating that the overall Cd isotopic composition of the inputs is isotopically lighter than average deep-ocean seawater by $\delta^{114/110}\text{Cd} \approx -0.2 \text{‰}$ [4]. The offset between seawater and the inputs implies that either the system is not in steady state, or that suboxic sediments should also be characterized by a Cd isotopic composition that is close to the input value, and therefore also fractionated toward a lighter composition than seawater.

Here, we present Cd isotopic and multi-element geochemical data for suboxic sediments that were sampled from the Cape Margin, South Africa, during the UK GEOTRACES 40 °S cruise in 2011 (D357; GA10E). Our Cd isotopic data suggest that suboxic sediments are indeed fractionated from seawater by $\delta^{114/110}\text{Cd} \approx -0.2 \text{‰}$, and represent a significant sink of isotopically light Cd in the modern oceans. Our isotopic mass balance – the first of its kind for Cd – demonstrates that the isotopic composition of suboxic sediments balances the inputs, and therefore the isotopic budget of Cd in the oceans.

We explore possible mechanisms for the immobilization of isotopically light Cd in suboxic sediments using multi-element geochemical data from both the solid phase and sediment porewaters. The temporal sensitivity of the Cd isotopic composition of deep-ocean seawater is also investigated using a simple numerical model, as well as implications for the use of Cd isotopes in paleoceanography.

[1] Morford & Emerson (1999) *GCA*, **63**(11), 1735-1750. [2] Schmitt *et al* (2009) *EPSL*, **277**(1), 262-272. [3] Lambelet *et al* (2013) *EPSL*, **361**, 64-73. [4] Ripperger *et al* (2007) *EPSL*, **261**(3), 670-684.

The LA-ICP-MS U-Th-Pb Network: Improving data standards in laser ablation geochronology

M.S.A. HORSTWOOD^{1*}, J. KOSLER², G. GEHRELS³,
S.E. JACKSON⁴, N.J. PEARSON⁵ AND P.J. SYLVESTER⁶

¹NERC Isotope Geosciences Laboratory, British Geological Survey, Nottingham NG12 5GG, UK.

(*correspondence: msah@nigl.nerc.ac.uk)

²Dept. of Earth Science & Centre for Geobiology, University of Bergen, Allegaten 41, N-5007 Bergen, Norway.
(jan.kosler@geo.uib.no)

³Dept. of Geosciences, University of Arizona, Tucson AZ 85721, USA. (ggehrels@gmail.com)

⁴Natural Resources Canada, Ottawa, ON K1A 0E8, Canada
(Simon.Jackson@NRCan-RNCan.gc.ca)

⁵Dept. of Earth and Planetary Sciences, Macquarie University NSW 2109, Australia (norman.pearson@mq.edu.au)

⁶Dept. of Earth Sciences, Memorial University, St. John's NL A1B 3X5 Canada (pjsylvester@gmail.com)

The inter-laboratory comparison (ILC) of laser ablation (LA-)ICP-MS U-Th-Pb data is currently compromised by the use of multiple and disparate 1) mass spectrometer and laser ablation platforms, 2) data processing packages and independent spreadsheets, and 3) geological factors, which in combination, result in differing results for the same materials and potentially misleading and inaccurate interpretations. Since 2006, an international network of LA-ICP-MS U-Th-Pb specialists has been addressing these issues, and measures and documentation are now in place to inform new and existing practitioners of better practice in acquiring, handling, reducing and interpreting LA-ICP-MS U-Th-Pb data. These measures include: completion and documentation of a detrital zircon-focussed ILC, a defined uncertainty propagation protocol, defined tables for publishing data and acquisition information, peer-reviewed publications [1], provision of reference material sets for long-term validation of lab performance, the running of workshops and shortcourses, recommendations with respect to the interpretation of detrital zircon data and a maintained website with resources and information (www.plasmage.org). These measures will: a) improve the standard and accuracy of published LA-ICP-MS U-Th-Pb data, b) allow better comparability of published data, c) ensure appropriate age uncertainty quantification and, ultimately, d) improve the rigour of geological interpretation. New insights into achievable ILC performance and future Network activities will be highlighted.

[1] Kosler *et al* (in review)

A global molecular ecological survey of subseafloor microbial communities

TATSUHIKO HOSHINO¹, MASAZUMI TSUTSUMI¹,
YUKI MORONO¹ AND FUMIO INAGAKI¹

¹Geomicrobiology Group, Kochi institute for Core Sample Research, Japan Agency for Marine-Earth Science and Technology (JAMSTEC), Monobe B200, Nankoku, Kochi 783-8502, Japan

Recent advances of the culture-independent molecular ecological survey such as deep sequencing enable us to provide precise and detailed views of naturally occurring microbial communities [1]. For the deep subseafloor microbial communities, an improved hot-alkaline DNA extraction method have significantly improved the cell-lysis efficiency, providing less-biased DNA pools for the subsequent molecular ecological analyses [2]. Regarding the molecular quantification, the conventional used real-time PCR assay is highly sensitive to the PCR inhibitors such as humic acids and polysaccharides in organic-rich ocean margin sediments. However, a new technique using digital PCR and microfluidic devices is free of such an inhibitory effect, providing absolute quantification of the target genes [3]. Using these newly standardized molecular ecological techniques, a new global-scale molecular survey of subseafloor microbial communities has been planned.

In this project, we have currently extracted DNA from over 200 deep-frozen samples from 15 drilling sites using a new hot-alkaline method: e.g., off Peru and eastern equatorial Pacific (ODP Leg 201), Juan de Fuca ridge flank (IODP Exp. 301), South Pacific Gyre (IODP Exp. 329), Nankai Trough (IODP Exp. 315 and 316), off Shimokita of Japan (CK0606, IODP Exp. 337), Gulf of Mexico (IODP 308), Porcupine carbonate mound (IODP Exp. 307). These environmental DNA pools provide an unprecedented opportunity to study biogeographical distribution and diversity of bacterial and archaeal 16S rRNA and some other ecologically significant functional genes with a systematic analytical scheme.

[1] Hoshino, *et al*, *Front. Microbio.*, 2, no. 231 (2011). [2] Morono, *et al*, submitted. [3] Hoshino & Inagaki, *Syst. Appl. Microbiol.*, 35, 390-395 (2012).

In situ lithium isotope measurements for spodumene using LA-MC-ICP-MS

KEJUN HOU

Key laboratory of Metallogeny and Mineral Assessment, Ministry of Land and Resources, Institute of Mineral Resources(kejunhou@126.com)

As a useful geochemical tracer, the lithium isotope system has been used to study some important geological or geochemical problems. Lithium isotope can be readily fractionated during geological processes in nature because of the large mass difference (16.7%) between its stable isotopes, ^6Li and ^7Li , whose abundances are 7.52% and 92.48%, respectively. Therefore, the application of the lithium isotopic system has important significance in the fields of cosmochemistry, continental crust weathering processes, oceanic crust thermal activity and alteration, continental plate subduction and crust-mantle material recycling, surface water geochemistry, halogenic water origin and evolution, and so on. Therefore, this technique will surely become a useful geochemical tool in the Earth sciences.(Tian *et al*, 2012)

In this study, we have developed a direct *in situ* lithium isotope analytical method for spodumene using LA-MC-ICP-MS. Our LA-MC-ICP-MS homogeneity testing results show that the four in-house spodumene standards have constant $^7\text{Li}/^6\text{Li}$ compositions. The precision of measured $\delta^7\text{Li}$ in these homogeneous spodumene is better than 1.5‰. And all of these *in situ* analytical results are in good agreement with those results measured by solution MC-ICP-MS method within error.

Stable isotopic record of a Himalayan ice core during the last millennium

S. HOU*

School of Geographic and Oceanographic Sciences, Nanjing University, Nanjing 210093, China. (*correspondence: shugui@nju.edu.cn)

A 108.8 m ice core to bedrock recovered from the East Rongbuk (ER) Glacier (28.03 N, 86.96 E, 6518 m a.s.l.) on the northeast ridge of Mt. Qomolangma (Everest) provides a high-resolution stable isotopic record of the last millennium (3044 samples). Interpretation of the Himalayan ice core δD and $\delta^{18}\text{O}$ records is multivocal. For instance, Thompson *et al* [1] suggested that the long-term $\delta^{18}\text{O}$ variability recorded in the Himalayan Dasuopu ice core was attributed to changes in local temperature, while Cai *et al* [2] suggested that precipitation, rather than temperature, was a major factor controlling $\delta^{18}\text{O}$ in precipitation on orbital time scales in the south-central Tibetan Plateau. However, the linear combination of δD and $\delta^{18}\text{O}$ (i.e., deuterium excess or $d=\delta\text{D}-8\delta^{18}\text{O}$) is a good proxy for changes in atmospheric circulation in the Himalayas [3]. A feature for the d time series of the ER ice core is the significantly positive phase during the period of middle 15th century and the significantly negative phase during the period of middle 17th century (Figure 1). Thompson *et al* (2010). *Science* 289, 1916-1919. [2] Cai *et al* (2010). *Geology*, 38(3), 243–246. [3] Pang *et al* (2012). *Climatic Research*, 53(1), 1–12. 18th century, with a reversal around middle 17th century (Figure 1). This might indicate a changeover of the atmospheric circulation regime during the 17th century. We suggest that, on the centennial time scale, the Indian Summer Monsoon weakened since the early 15th century, reaching its minimum around the middle 17th century. The time interval of the 15-17th centuries is the transition from the Medieval Climatic Optimum to the Little Ice Age, and the modification of the atmospheric processes in the Asian monsoon regime may be the reflection of global change in the climatic processes during this time interval.

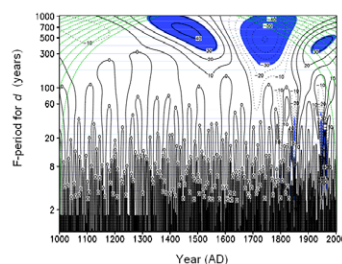


Figure 1. Result of wavelet analysis of d (solid lines stand for positive values, dotted lines for negative values, and dashed lines for the boundary effect. The shadow denotes the area passing the significant test with confidence of 95).

[1] Thompson *et al* (2010). *Science* 289, 1916-1919. [2] Cai *et al* (2010). *Geology*, 38(3), 243–246. [3] Pang *et al* (2012). *Climatic Research*, 53(1), 1–12.

The Cihai diabase in the Beishan region, NW China: Isotope geochronology, geochemistry and implications for Cornwall-style iron mineralization

TONG HOU¹ AND ZHAO-CHONG ZHANG¹

¹State Key Laboratory of Geological Processes and Mineral Resources, China University of Geosciences, Beijing, 100083, China (houtong08@gmail.com)

Diabase dykes in Cihai, Beishan region, NW China are spatially and temporally associated with 'Cornwall-type' iron deposits. U-Pb dating of zircons from a diabase dyke using laser ablation inductively coupled plasma mass spectrometry (LA-ICP-MS) yields an age of 128.5 ± 0.3 Ma. Most of the diabases show low Mg-numbers, suggesting evolved magmas. The diabase dykes show typical ophitic or sub-ophitic textures, and are dominantly composed of phenocrysts of plagioclase and clinopyroxene, with minor and varying amounts of biotite and hornblende, and minor disseminated magnetite. The diabase dykes are characterized by minor variation in SiO₂ (44.67-49.76 wt.%) and MnO (0.14-0.26 wt.%), but show a marked range of Al₂O₃ (10.66-14.21 wt.%), total Fe₂O₃ (9.52-13.88 wt.%), TiO₂ (0.66-2.82 wt.%) and relatively high MgO (4.87-9.29 wt.%) with an Mg# value [atomic Mg/(Mg+Fe²⁺)] of up to 66. The Cihai diabases possibly experienced fractional crystallization of olivine + clinopyroxene and minor crustal contamination during the differentiation process. Prominent negative Nb, Ta and Ti anomalies suggest derivation from subduction-modified mantle. Furthermore, the rocks have relatively unradiogenic Sr- and Nd-isotopic ratios. These characteristics probably reflect partial melting of a subduction component in the source mantle lithosphere through heat input from an upwelling asthenospheric mantle. Such processes probably occurred within an extensional setting during the Early Cretaceous in the Beishan area. The iron-rich fluids were derived from deep sources, and the iron ores were concentrated through a convection cell driven by temperature gradients established by the intrusion of the diabase sills. The combined processes of subduction-related enrichment in the source, shallow depth of emplacement, and the involvement of large-scale circulation of basinal brines from an evaporitic source are inferred to have contributed to the formation of the 'Cornwall-type' mineralization in Cihai.

Challenges in constraining and understanding Strombolian volcanism

BF HOUGHTON¹, J TADDEUCCI² AND M EDMONDS³,

¹School of Ocean and Earth Science and Technology, University of Hawaii at Manoa, Hawaii, USA.

²Dept. of Seismology and Tectonophysics, Istituto Nazionale di Geofisica e Vulcanologia, Roma, Italy

³Earth Sciences Department, University of Cambridge, Downing Street, Cambridge CB2 3EQ, UK

Activity at Stromboli is exceptionally well characterised on most time scales but it remains a challenge to identify what portion of that activity should be defined as "Strombolian" in the strict sense of naming the eruption style, in a fashion that is useful elsewhere. Here we look at delineating the limits of 'Strombolian style', particularly in the context of demarcation from Hawaiian fountaining eruptions.

That demarcation has generally been articulated in terms of transient versus sustained activity linked to mechanical decoupling versus partial coupling of exsolved volatiles. However, while sustained fountains are steady, they are seldom steady, and violent Strombolian events can last for minutes.

Plotting basaltic activity in viscosity-mass eruption rate space reveals some of the issues. Individual Strombolian explosions occupy the short duration, low eruption rate corner of such a plot, very clearly distinguished from high Hawaiian fountains that have durations that are 3 to 5 orders of magnitude longer and mass discharge rates that are 10 to 100 times larger. However the spectrum of activity called names such as 'low fountains', 'gas pistonning' and 'violent Strombolian' defines a grey scale between these extremes. Finally on what time scale can we define a Strombolian (or Hawaiian) 'eruption', i.e., what is the most characteristic time scale - a transient explosion of seconds duration or centuries of continual but varied activity?

Lithospheric mantle downwelling beneath the Southeast Carpathians

GREGORY A. HOUSEMAN, PIROSKA LORINCZI, YONG REN AND GRAHAM W. STUART

School of Earth and Environment, University of Leeds, Leeds, LS2 9JT (correspondance to: greg@earth.leeds.ac.uk)

The South Carpathian Project, a major seismological experiment carried out during 2009-2011 by the University of Leeds, the National Institute of Earth Physics in Bucharest, the Eötvös Loránd Geophysical Institute in Budapest, and the Seismological Survey of Serbia in Belgrade, has resulted in the most detailed tomographic images yet obtained of the upper mantle structure beneath the Pannonian – Carpathian region [1]. These images shed new light on the unique geological structure which is responsible for the damaging earthquakes that occur in the upper mantle beneath the Vrancea Zone of the South-east Carpathians. A sub-vertical high-velocity body extending down to the top of the Mantle Transition Zone is interpreted as downwelling mantle lithosphere. The main mass of fast (presumably dense) material is located directly beneath the seismic activity. The earthquakes are caused by vertical stretching at strain-rates which imply that the mantle at 200 km is moving downward at about 20 mm/yr relative to the surface.

Three-dimensional numerical experiments assuming viscous flow support the interpretation that the drip-like structure that we image may be a natural consequence of a Rayleigh-Taylor instability developing from an unstable stratification of mantle lithosphere above asthenosphere, and triggered by recent convergence of Adria and Europe. The depth distribution of seismic-moment release rate is most easily explained if this high velocity structure is produced by a Rayleigh-Taylor instability. The present high rate of tectonic activity in this region is probably short-lived on a geological scale (< 1 Myr) but is likely to increase in energy before it is abates. The circumstances of this tectonic activity support the idea that Rayleigh-Taylor instability of the mantle lithosphere requires relatively dense mantle lithosphere activated by local plate convergence.

[1] Ren, Y., Stuart, G., Houseman, G., *et al* (2002), *Earth Planet. Sci. Lett.*, 349-350, 139-152.

Newly measured enthalpies of K-Na mixing for low albite - microcline crystalline solutions

GUY L. HOVIS¹

¹Department of Geology & Environmental Geosciences, Lafayette College, Easton, PA 18042 USA

Earlier studies [1,2] on the thermodynamic mixing properties of the low albite - microcline system reported enthalpies of K-Na mixing that were nearly symmetric with regard to composition, despite a solvus [3] and Gibbs free energies of mixing [4,5] that require compositionally asymmetric relationships. To refine earlier results, new data have been collected at a particularly large number (21) of compositions across this series. Duplicate solution calorimetric experiments on each of these samples at 50 °C in 20.1 wt% HF have produced highly precise calorimetric data having an average standard deviation per sample of just 0.06% of the heats of solution. The new study, which reveals a maximum 8.7 kJ/mol enthalpy of mixing (H_{ex}) at $N_{Or} = 0.39$, demonstrates that detail in data at the sodic end of the series is crucial to definition of asymmetry in H_{ex} . The greater mixing magnitudes for this series relative to those for analbite - sanidine solutions (newly investigated via a 20-sample series) correlate well with the comparatively higher critical temperature of the low albite - microcline solvus [3] relative to that for analbite - sanidine [e.g., 6]. Entropies of K-Na mixing have been calculated by combining the new enthalpy data with Gibbs free energies of mixing derived from phase equilibrium studies [4,5]; these may be compared with entropy data based on the recent heat capacity measurements of Benisek and others [7].

[1] Waldbaum & Robie, 1971, *Z. Krist.* [2] Hovis, 1988, *J. Petrol.* [3] Bachinski & Müller, 1971, *J. Petrol.* [4] Delbove, 1975, *Amer. Mineral.* [5] Hovis, Delbove, & Roll, 1991, *Amer. Mineral.* [6] Smith & Parsons, 1974, *Mineral. Mag.* [7] personal communication.

Nitrogen isotope systematics and origins of mixed-habit diamonds

*D. HOWELL¹, R.A. STERN², W.L. GRFFIN¹,
R. SOUTHWORTH^{3,4}, S. MIKHAIL⁵, T. STACHEL²,
A.B. VERCHOVSKY⁴, A.P. JONES³,
SUZANNE Y.O'REILLY¹ AND N.J. PEARSON¹.

¹CCFS ARC Center of Excellence, and GEMOC, Macquarie University, Sydney, NSW 2109, Australia.

(* correspondence: Daniel.Howell@mq.edu.au).

²Canadian Center for Isotopic Microanalysis, University of Alberta, Edmonton, AB, T6G 2E3, Canada.

³Department of Earth Sciences, University College London, Gower Street, London, WC1E 6BT, UK.

⁴Department of Physical Sciences, The Open University, Walton Hall, Milton Keynes, MK7 6AA, UK.

⁵Geophysical Laboratory, Carnegie Institute of Washington, 5251 Broad Branch Road NW, Washington DC, 20015, USA.

Mixed-habit diamonds form when growth occurs by two different simultaneous growth mechanisms [1, 2]. The two crystal habits are smooth, flat {111} crystal faces (octahedral growth) and curved, hummocky, non-faceted surfaces with a mean orientation of {100}, but this can be inclined by up to 30° (cuboid growth). This type of growth can produce a range of centre-cross or star-shaped patterns within the diamond [3], which are the result of light-scattering defects that occur only in the cuboid sectors. When these defects are graphitized and thus opaque, the cuboid growth sectors appear much darker than the gem-quality octahedral sectors.

Analysis of this type of diamond has shown that carbon isotopes show no partitioning between growth sectors [4]. However, nitrogen contents are much higher in the octahedral sectors (enriched by up to 160% compared with that of cuboid sectors), while nickel and cobalt are partitioned into the cuboid sectors if available in the diamond-forming fluid [5]. Few nitrogen isotope data exist for these types of diamonds. One study showed no N-isotope fractionation between growth sectors [6] but the sample used in that study is not thought to be a true mixed-habit diamond.

This study compares nitrogen-isotope data obtained via SIMS and by step-wise oxidation mass spectrometry from both octahedral and cuboid growth sectors, with the goal of investigating both isotopic fractionation and the source of nitrogen in these unusually N-rich diamonds.

[1] Frank (1967) *Proc. Int. Industrial Diamond Conf.*, 119-135. [2] Lang (1974) *Proc. R. Soc. Lond.*, **A. 340**, 233-248, [3] Welbourn *et al* (1989) *J. Crystal Growth*, **94**, 229-252, [4] Howell *et al* (2013) *Am. Min.*, **98**, 66-77, [5] Howell *et al* (in press), *Chem. Geol.*, [6] Cartigny *et al* (2003), *Geochim. Cosmochim. Acta*, **67**, 1571-1576.

Sorption behavior of lithium

MANDY HOYER AND NICOLAI ALEXEJI KUMMER

TU Bergakademie Freiberg, Department of Hydrogeology,
D-09599 Freiberg, Mandy.Hoyer@student.tu-freiberg.de

Salar the Uyuni is one of the greatest sources for Li being presently assessed. It is not yet understood why one observes great Li enrichment in the delta areas of past and presently inflowing rivers. One theory is temporary sorption and subsequent desorption by clay minerals that are enriched in these inflow areas.

Li sorption on clay minerals, namely kaolinite and bentonite, and on clinoptilolite, a zeolite, was studied in batch experiments with subsequent ICP-MS analysis. Solid/solution ratio was 1:4; shaking time was 24 hours; pH was varied between 2 and 10, with focus on pH 6 and 8 as pH in the Salar is circum-neutral. Li concentration in the solutions was varied between 1.5 and 750 mM; sodium concentration between 0.01 and 5 M.

It was found that Li was sorbed by all minerals; highest sorption being achieved at lowest sodium and highest Li concentration for clinoptilolite (3890 ppm) and bentonite (3820 ppm); at 3 M Na and highest Li concentration for kaolinite (1250 ppm). Absolute Li sorption at pH 6 and 8 was similar and increased with increasing Li concentration in the initial solution at constant Na concentration. Relative Li sorption decreased due to limited exchange sites on the mineral's surface. At constant Li concentration, increasing Na caused Li sorption decreased by competition.

pH changes altered minerals' surface charge by (de)protonation, caused structural changes, or decomposition. For bentonite and clinoptilolite, pH-dependent sorption results scattered. The reason for that is not known. For kaolinite sorption was maximal at pH 2-4 which could be explained by surface complexation or incorporation in the crystal structure. Above pH 5, kaolinite probably transformed to gibbsite with effects on surface charge and on Li sorption.

This study showed that clay minerals and zeolites are effective Li sorbents and may contribute to elevated Li concentration at the freshwater inflows of Salar de Uyuni.

Thermodynamics of the C-H-O fluids: High pressure experiments on dissociation of carbonates and hydrides

R. HRUBIAK^{1*}, V. DROZD¹ AND S.K. SAXENA¹,

¹ Department of Mechanical and Materials Engineering,
Florida International University, Miami, FL 33199,
USA (*correspondence: rhub001@fiu.edu)

Understanding the chemistry of carbon in deep Earth's interior requires thermodynamic data on the multicomponent C-H-O fluid. Experimental data on such fluids at high temperature and high pressure mantle conditions is quite rare. In this study we use new experimental methods and computations to produce pressure-volume-temperature (P-V-T) equation of state (EoS) data on CO₂ and H₂ fluids to pressures of 100 GPa and very high temperatures.

The thermodynamic properties and P-V-T EoS for CO₂ and H₂ fluids are assessed by combining experimental data on equilibrium conditions for several carbonate and hydride dissociation reactions involving these fluids with P-V-T EoS' of solid phases involved in the given reactions. Experimental P-V-T data on several carbonates and hydrides used in this study was extensively collected from literature and missing P-V-T data was measured using resistively heated and laser heated diamond anvil cell and *in situ* x-ray diffraction. The P-V-T EoS' for the CO₂ and H₂ are thus self consistent with experimental phase equilibrium data and standard thermochemical data. The EoS' are also shown to be consistent with results obtained independently using molecular dynamics calculations [1].

The newly created thermodynamic database was used to calculate high pressure and temperature phase equilibrium in several binary, ternary and multicomponent systems.

The authors wish to acknowledge the support and collaboration of the Deep Carbon Observatory

[1] Belonoshko, A.B, Shi, P., Saxena, S.K. (1992) *Computer and Geosciences* **18**, 1267–1269.

Comparison of ²²⁸Ra and microstructure derived ocean mixing rates and chemical fluxes in the Cape Basin

YU-TE HSIEH^{1,2*}, WALTER GEIBERT^{3,4},
MATTHEW R. PALMER⁵, E. MALCOLM S. WOODWARD⁶,
AND GIDEON M. HENDERSON¹

¹Department of Earth Sciences, University of Oxford, UK
(*correspondence: yuteh@mit.edu; yuteh@earth.ox.ac.uk)

²Present address: Department of EAPS, Massachusetts
Institute of Technology, Cambridge, MA, USA

³School of Geosciences, University of Edinburgh, UK

⁴Scottish Association for Marine Sciences, UK

⁵National Oceanography Centre, Liverpool, UK

⁶Plymouth Marine Laboratory, UK

Diapycnal mixing from below is a critical route by which nutrients and other chemical species are introduced to the sunlit surface ocean. Instantaneous mixing rates can be assessed by shipboard measurements of velocity microstructure in the water column. Radium-228, a daughter of ²³²Th, has a half life of 5.75 years, and is mixed into the ocean interior from ocean shelves and downwards from the surface by diapycnal mixing. It therefore provides a means to assess the long-term average mixing rates in the oceans. In this study, we compare instantaneous mixing rates from velocity microstructure with long-term rates from ²²⁸Ra for waters of the Cape Basin. We use these measured mixing rates to assess the supply of nutrients to the surface ocean in this region, and the temporal variability of this supply.

Twenty five seawater samples were collected from the Cape Basin during the 2010 UK GEOTRACES cruise (GA10E) and analysed for high-precision ²²⁸Ra and ²²⁶Ra concentrations by MC-ICP-MS. We estimated vertical and horizontal ocean mixing rates from this data using 1D mixing models to derive rates of 0.9 – 2.1 cm²s⁻¹ and 3.8 × 10⁷ cm²s⁻¹ respectively. The rates of diapycnal mixing indicate sufficient nutrient supply to drive the productivity in downward organic carbon fluxes of 3.1 – 3.3 mmol C m⁻²d⁻¹ in this region – in close agreement with estimates from other proxies. The long-term averages are compared with instantaneous mixing rate and nutrient supply derived from microstructure measurements from the same cruise to assess the merits of the two approaches and variation in the mixing environment.

DFT+*U* investigations of spin crossovers in lower-mantle minerals

HAN HSU

Department of Physics, National Central University, Zhongli City, Taoyuan 32001, Taiwan (hanhsu@ncu.edu.tw)

The total electron spin of a transition-metal ion in a crystalline solid can vary with many factors, including temperature, pressure, and strain. This phenomenon, known as spin crossover, is of great technological potential, as it allows artificial control of magnetic properties of materials. Not as widely known, spin crossover may also play a significant role in geophysics. As pressure and temperature increase with depth in the Earth, iron incorporated in minerals can undergo a spin crossover. A well studied example is ferroperricite, the second most abundant mineral in the Earth's lower mantle. In this mineral, a high-spin (HS) to low-spin (LS) crossover occurs in the pressure range of 40-55 GPa, accompanied by elastic, thermodynamic, optical, and conducting anomalies.

In contrast to ferroperricite, spin crossovers in magnesium silicate (MgSiO₃) perovskite and post-perovskite, the major mineral phases in the lower mantle, have been controversial for years, due to the complicated nature of these minerals and the difficulty in probing iron spin state directly. Using density functional theory + Hubbard *U* (DFT+*U*) calculations, we investigated spin crossovers in MgSiO₃ perovskite and post-perovskite, and our results clarify the iron spin controversy in both mineral phases. We also show that Mössbauer spectroscopy, combined with first-principles calculations, can be a reliable tool to unambiguously identify iron spin state at high pressure [1-4].

[1] Hsu *et al* (2010) *Earth Planet. Sci. Lett.* **294**, 19-26. [2] Hsu *et al* (2011) *Phys. Rev. Lett.* **106**, 118501. [3] Yu *et al* (2012) *Earth Planet. Sci. Lett.* **331-332**, 1-7. [4] Hsu *et al* (2012) *Earth Planet. Sci. Lett.* **359-360**, 34-39.

Meso- to Neo-proterozoic magmatic events and their geological significance: evidences from detrital zircon U-Pb ages of the Jurassic and Cambrian sedimentary rocks in Xishan area, Beijing city, China

BO HU¹, MINGGUO ZHAI², PENG PENG² AND FU LIU²

¹Key Laboratory of Western Mineral Resources and Geological Engineering, Ministry of Education, College of Earth Science and Resources, Chang'an University, Xi'an 710054, China (hubowork@126.com)

²Institute of Geology and Geophysics, Chinese Academy of Sciences, P. O. Box 9825, Beijing 100029, China

Whether any magmatic records corresponding to the assembly and breaking up of the supercontinent Rodinia are preserved in the North China Craton (NCC) is a key issue to understand the Proterozoic tectonic evolution of the NCC and its correlation to the supercontinent Rodinia. LA-ICP-MS U-Pb dating results of detrital zircons from Jurassic and Cambrian sedimentary rocks in the Xishan area, Beijing city, central part of the NCC show that there are not only ~507 Ma cambrian age peaks, but also ~2.5 Ga, ~2.1 Ga, 1.8-1.66 Ga, ~1.56 Ga, ~1.38 Ga, ~1.14 Ga, ~912 Ma, ~814 Ma, ~740 Ma and ~630 Ma precambrian age records in Cambrian fine sandstone. Also, there are not only ~484 Ma, ~267 Ma, ~241 Ma and ~188 Ma phanerozoic age peaks, but also ~2.77 Ga, ~2.5 Ga, ~2.0 Ga, ~1.78 Ga, ~1.6 Ga, ~1.2 Ga and 848Ma precambrian age records in Jurassic silty mudstone and fine sandstone. Most of Neoproterozoic age peaks correspond to significant tectono-magmatic-thermal events previously recognized in the NCC. 1.78-1.38 Ga age peaks correspond to late Paleoproterozoic to Mesoproterozoic multi phase rifting events in the NCC. Zircon ages of 1.3-1.0 Ga and 1.0-0.6 Ga indicate that during the deposition of these sediments there have been significant contributions from 1.3-1.0 Ga and 1.0-0.6 Ga magmatic rocks in the NCC. The magmatic rocks during these periods, which were common in the South China Craton (SCC) and were explained to relate to the assembly and breaking up of the supercontinent Rodinia, were seldom reported in the NCC so far. The finding of 1.3-1.0 Ga and 1.0-0.6 Ga detrital zircons in the NCC may provide clues to understand the possible relationship of the NCC, the SCC and the supercontinent Rodinia.

This work is supported by National Nature Science Foundation of China (Grant No. 41002064) and Special Fund for Basic Scientific Research of Central Colleges, Chang'an University (Grant No. CHD2011JC163).

Altitudinal $\delta^{18}\text{O}$ gradients from Chinese stalagmites provide records of Holocene humidity variation

CHAORYONG HU¹ GIDEON M. HENDERSON² JIN LIAO¹
JIAOYANG RUAN¹ CHENGZHAN LI¹ SHUCHENG XIE¹
AND KATHLEEN JOHNSON³

¹State key laboratory of biology and environmental geology, China University of Geosciences, Wuhan, 430074 (chyhu@cug.edu.cn)

²Department of Earth Sciences, University of Oxford, South Parks Road, Oxford OX23AN, UK. (gideonh@earth.ox.ac.uk)

³Department of Earth System Science, University of California, Irvine, CA 92697.

Humidity is one of the fundamental variables controlling the energy balance of the climate, and plays a critical role in Earth's ecosystems. Its reconstruction would aid considerably in assessing the mechanisms driving past changes observed in paleoclimate records. Paleohumidity has been reconstructed qualitatively from the pollen and tree ring data, but not yet from speleothem records, due to the uncertain interpretation of speleothem geochemical proxies. Here we propose a novel proxy for paleo-humidity based on the altitudinal $\delta^{18}\text{O}$ gradient derived from two speleothems with different altitude of rainfall recharge in closely spaced caves. We then use this proxy to reconstruct a Holocene humidity record in the middle reaches of the Yangtze river. Two factors affect the altitudinal $\delta^{18}\text{O}$ gradient of precipitation, the lapse rate of temperature and relative humidity. In the case of speleothems, the cave temperature effect (negative effect) offsets the temperature induced isotopic fractionation in precipitation (positive effect), and relative humidity is likely to be the major controller of $\delta^{18}\text{O}$ gradients between speleothems with recharge from different heights. $\delta^{18}\text{O}$ in recently formed carbonate from two caves in Qingjiang valley, Hubei, China, supports this interpretation, with larger $\delta^{18}\text{O}$ gradients in periods of lower relative humidity. Based on this observation, we reconstruct Holocene relative humidity from the high resolution speleothem $\delta^{18}\text{O}$ records from Heshang and Sanbao caves. The reconstructed record indicates a slight increase in RH during the Holocene, with lowest values at 8.2 kyr BP. Independent hydrological records of Mg/Ca and $\delta^{13}\text{C}$ from the Heshang speleothem vary in a similar pattern to the altitudinal $\delta^{18}\text{O}$ gradients, which supports the reconstruction of humidity for the Holocene of this region.

Hydrochemistry and isotope evidence of groundwater evolution and recharge in Poyang Lake, South China

HU CHUNHUA^{1,2}, ZHOU PENG^{1,2}, HUANG DAN^{1,2},
LI LIYANG^{1,2} AND ZHOU WENBIN^{1,2*}

¹School of Environmental and Chemical Engineering, Nanchang University, Nanchang, 330031, China (*correspondence: ouyangyinghui@126.com)

²Key Laboratory of Lake Poyang Environment and Resource Utilization, Ministry of Education, Nanchang University, Nanchang, 330029, China

In recent decades, a systematic research of groundwater system is imperative for the increasingly prominent contradiction between supply and demand of water. In this work, environmental factors, main zwitterions, hydrogen and oxygen isotopes composition in groundwater were researched in dry season and wet season. Groundwater evolution and recharge were studied with the purposes of analyzing hydrochemical characteristics and evolution laws [1], as well as helping rebuild the geochemical evolution [2]. In addition, the recharge rates of different landscape units were estimated by hydrogen oxygen isotopes during investigation period.

The results show that: Na^+ and Ca^{2+} are the main cations of groundwater in research area, and HCO_3^- is the main anion, seasonal change has influence on spatiotemporal variation of area hydrochemistry, and its type is mainly present in $\text{HCO}_3^- - (\text{Na}^+ + \text{K}^+)$; the composition of δD and $\delta^{18}\text{O}$ has different characteristics for seasonal change, it mainly controlled by precipitation. Groundwater anions type transforms from $\text{HCO}_3^- - \text{SO}_4^{2-}$ to $\text{HCO}_3^- - \text{Cl}^-$ when the season changes from dry season to rainy season, and cation type drifting and evolving from $(\text{Na}^+ + \text{K}^+) - \text{Ca}^{2+}$ to $(\text{Na}^+ + \text{K}^+)$. The results of hydrogen and oxygen isotopic mixing ratios shows that there is significant difference on water recharging of groundwater system in different geomorphic units, and it reflects that the origin and evolution of groundwater response to geomorphology sensitively.

[1] Zhao *et al* (2007) Ecology and Environment 16, 1620-1626. [2] Hackley *et al* (2010) Geological Soc America 122, 1047-1066.

The characteristics of polycyclic aromatic hydrocarbons (PAHs) in the drainage basin of the Liao River, Northeast China

JIAN HU^{1*}, YAN-LIN ZHANG^{1,2}, BAO-JIAN LIU^{2,3}, SI-LIANG LI¹ AND JIN GUAN^{1,2,3}

¹Institute of Geochemistry, Chinese Academy of Sciences, Guiyang 550002, PR China (*correspondence: hujian@vip.skleg.cn)

²Graduate University of Chinese Academy of Sciences, Beijing 100049, China

³Guangzhou Institute of Geochemistry, Chinese Academy of Sciences, Guangzhou 510640, China

Sixteen polycyclic aromatic hydrocarbons (PAHs) in surface water and suspended particulate matter (SPM) in the drainage basin of Liao River were determined by GC/MS. The concentration and distribution characteristics, pollution levels, and sources of PAHs were discussed. The total PAHs concentration ranged from 0.41 to 76.45 $\mu\text{g}\cdot\text{g}^{-1}$ (dry weight) in SPM, and 32.57 to 108.47 $\text{ng}\cdot\text{L}^{-1}$ in surface water, respectively. The PAHs concentration in west Liao River is higher than that in east Liao River and Liao River main stream. The compositions of PAHs are predominant by low ring PAHs (two and three-ring PAHs), and the percentage of low ring PAHs in dissolved phase is higher than that in SPM. The percentage of two-ring PAHs in dissolved phase is highest with an average of 68.19%, while the percentage of three-ring PAHs in SPM is highest with an average of 66.28%, respectively. Compared with other rivers in China and the world, the PAHs concentrations in Liao River drainage basin are at a lower level, but some branches are PAHs-contaminated to some extent.

Diagnostic ratios of Ipy/(Ipy+Bpe) and Fla/Fla+Pyr were used to identify the PAHs sources, and the result suggested the main sources of PAHs would be petroleum and fossil fuel combustion-based, which are resulted from complex energy structure of Liaoning province.

This work was supported by Knowledge Innovation Program of the Chinese Academy of Sciences (Grant No. KZCX2-EW-102) and National Science and Technology Major Project of the Ministry of Science and Technology of China (Grant No. 2012ZX07503-003-001)

Mineral compositions of Lower Silurian Longmaxi Formation, Sichuan Basin, China

PEI-QING HU, JUAN SHEN AND WAN-XIANG RAO

Key Laboratory of Mineral Resources in Western China (Gansu Province) & School of Earth Sciences, Lanzhou University, Lanzhou 730000, China (hupq@lzu.edu.cn)

The Sichuan Basin is a prolific hydrocarbon region and is currently China's largest gas-producing region. In order to study the mineral properties, composition and the relationship with the organic matter characteristics in Lower Silurian Longmaxi Formation shale, 30 shales from Longmaxi Formation fresh outcrop cross sections located in Changning County in Sichuan basin were analyzed.

The analysis result shows that mineral compositions are brittle (fragment) minerals: quartz, feldspars, mica, pyrite; siliciclastic and calcite minerals: Chalcedony, calcite and dolomite; and clay minerals: Illite, chlorite and montmorillonite. These samples display significant variations in the proportions of detritus derived extrabasinal and intrabasinal sources. Quartz in particular occurs in both clay-size and silt-size fractions of both intrabasinal and extrabasinal origin and it is important that lots of dark luminescing microcrystalline (clay-size) quartz closely intergrown with clay minerals in the samples. The organic matter occurrence modes have important relationship with the mineral character. The finer fracture in the fragment minerals have huge influence to the produce and travel of the shale gas.

This study was supported by The National Basic Research Program of China (2012CB214701) and NSF of China (40873005).

Kinetic experiments of actinolite in CaCl_2 – HCl – H_2O up to 400°C

SHUMIN HU*, RONGHUA ZHANG AND XUETONG ZHANG

Laboratory of Geochemical Kinetics, MLR Key Laboratory of Metallogeny and Mineral Assessment, Institute of Mineral Resources, Chinese Academy of Geological Sciences, Baiwanzhuang Road 26, Beijing 100037, P.R.China
(*correspondence: zrhsm@cags.ac.cn)

Actinolite dissolution rates in HCl – H_2O and CaCl_2 – HCl – H_2O were measured at temperature ranging from 25 to 400°C and at 23 MPa. The dissolution experiments were performed in a flow-through reactor. The results provide new insight into the rate limiting reactions governing actinolite dissolution behavior at far from equilibrium, particularly at temperatures above 300°C . As actinolite dissolves in aqueous solutions, the relative release rates for breaking various metal–oxygen bonds in actinolite are different. Results show that Ca, Mg, Fe and Al dissolve faster than Si at temperatures of 25– 300°C , but slower at 300°C . Ca and Mg release faster than Si at temperatures of 350°C – 374°C . All of release rates vary with temperatures and pH. The release rate of Si increases with temperature from 20 to 300°C , and then decreases with continued increasing temperature from 300 to 400°C . The maximum release rate of Si is reached at 300°C . Experiments show that dissolution stoichiometry of actinolite is affected by temperature and pH. Results of actinolite dissolved in CaCl_2 – HCl – H_2O indicate that the release ratios of $m_{\text{Ca}}/m_{\text{Si}}$ and $m_{\text{Mg}}/m_{\text{Si}}$ in the effluent at 200°C are close to stoichiometric number of these element moles in one mole of actinolite and actinolite dissolution in HCl – H_2O at 100°C is close to the stoichiometric.

The reacted surfaces of actinolite are observed using EPMA, HRTEM, SEM and XPS. The surface after reacted at temperature $<300^\circ\text{C}$ is quite different from that after reacted at $\geq 300^\circ\text{C}$. At temperature $\geq 300^\circ\text{C}$, metal–hydrogen exchange reaction is weak and the release rates of Si increases. HRTEM and SEM studies indicate that a Fe (Al)-rich, Si-deficient layer is formed at surface. Experiments prove that each metal–oxygen bond within the silicate structure breaks at a distinct rate, which is affected by temperature. XPS and SEM-TEM study indicates that the surface layer after reacted at 300 – 400°C is not only amorphous, but also hydrated silicate, composed of Si–O–Si, Mi–OH, and Mi–O bonds. This project is supported by the project of k[2013]01-062-014, SinoProbe-07-02-03, SinoProbe-03-01-2A and 2010G28.

Hydrocarbon geology characteristics and exploring prospect of ultradeep layers onshore China

HU SUYUN¹, ZOU CAINENG², HOU LIANHUA³
AND ZHU RUKAI⁴

¹ Research Institute of Petroleum Exploration and Development, PetroChina, Beijing, China, husy@petrochina.com.cn

² Research Institute of Petroleum Exploration and Development, PetroChina, Beijing, China, zcn@petrochina.com.cn

³ Research Institute of Petroleum Exploration and Development, PetroChina, Beijing, China, houh@petrochina.com.cn

⁴ Research Institute of Petroleum Exploration and Development, PetroChina, Beijing, China, zrk@petrochina.com.cn

As the geology knowledge becoming deeper and the exploring technology developing, the hydrocarbon exploring prospect in deep-ultradeep layers is being recognized by the world. Chinese petroliferous basins suffered divergency in Eopaleozoic, transition between marine and continent in Neopaleozoic, and strong compression in Meso-cenozoic. The basins are mainly superimposition basins, which have upper and lower tectonic layers. Previous exploration mainly focus on upper layer, in recent years, CNPC has achieved a series of discoveries in deep-ultradeep layers of petroliferous basins onshore China through strengthening hydrocarbon geology research and discovery in deep layers, which shows great prospect of hydrocarbon exploring in deep layers. Basing on newest exploring results and research, it can be proposed that:
⊖ There are two kind of sources, normal source rock and inner source resident liquid hydrocarbon cracking, which can provide hydrocarbon, causing the deep layer resource potential may be out of our expectation. ⊖ Deep-ultradeep layers onshore China are affected by several geological factors. In the deep layers of superimposed basins, there are carbonate, volcanic and clastic reservoirs. ⊕ Large area of accumulation can happen in carbonate rocks, clastic rocks and volcanic rocks in deep-ultradeep layers. The reserve abundance is not so high but the scale can be very large. ⊕ The exploring degree in deep layer onshore China is low and the remaining resource is high, it can be predicted that the deep layers onshore will become an important replace area for the oil and gas industry of our country.

Dolomitization process and its effect on the behavior of trace elements in carbonate rocks

WENXUAN HU^{1,2}, LICHAO WANG¹
AND XIAOLIN WANG^{1,2}

¹School of Earth Sciences and Engineering, Nanjing University, Nanjing, 210093, P.R. China

²Institute of Energy Sciences, Nanjing University, Nanjing, 210093, P.R. China

The origin of dolomite has been considered to be a long-standing enigma in sedimentary geology. It has been accepted that dolomitization of limestone by solutions with high Mg²⁺/Ca²⁺ ratio is one of the most important mechanisms to produce dolomite. Therefore, understanding the geochemical behaviors of major and trace elements during dolomitization is vital towards deciphering the mysterious "dolomite problem".

An example section is selected in this study of Geshan profile of the middle Triassic age in the Lower Yangtze area, China. This outcrop develops various carbonate rocks ranging from limestone, through dolomitic limestone and calcareous dolomite, to dolomite. The carbonate series represent a gradual increase in dolomitization degree.

The geochemical signatures of these carbonate rocks are well preserved as supported by two folds of evidence: (a) most of the dolomites are micritic or fine-grained with planar-s in fabric, and (b) the Mn/Sr ratios of these samples are generally less than 1. The average Sr concentrations of limestone, dolomitic limestone, calcareous dolomite and dolomite are 1357.7 ppm, 271.2 ppm, 121.8 ppm and 99.9 ppm, respectively; whereas the average Mn concentrations are 15.37 ppm, 17.46 ppm, 27.85 ppm and 44.09 ppm, respectively. Therefore, the Sr concentration of carbonate rocks decreases with increasing dolomitization processes. However, the Mn concentration shows an opposite variation trend.

Previous studies suggest that, in the dolomite lattice, Sr mainly substitutes Ca sites. However, our observations show that the Sr concentration exhibits a non-linear decrease along with the decrease of CaO content during dolomitization. This reflects that, apart from the substitution of Ca, Sr exists in dolomite in other forms, such as in the crystal defects, or in fluid inclusions. In addition, compared with the published Sr concentration in microbial dolomite precipitated in culture experiments, our results ruled out the possibility of bacterial origin for the dolomite in this report.

Carbon and Oxygen Isotopic Compositions: How to Respond the Lacustrine Environmental Factors in Northwestern and Northeastern China

HU XIAOLAN ZHAO QI

College of Resource and Environmental Sciences, Lanzhou University, Lanzhou, 730000, China

*correspondence: huxl2011@lzu.edu.cn

The sediments, that 28 closed-lake sediments from Hoh Xil, 24 from Northeastern China, 99 surface sediments from Lake Bosten, 31 from Ulungur and 26 from Heihai were collected to determine the $\delta^{13}\text{C}$ and $\delta^{18}\text{O}$ values and discussed the impacting factors to the $\delta^{13}\text{C}$ - $\delta^{18}\text{O}$. The closure and residence time of lakes can influence the correlation between $\delta^{13}\text{C}$ and $\delta^{18}\text{O}$. Mg/Ca in the bulk sediment indicates the characteristic of residence time, Sr/Ca and Fe/Mn infer the salinity of lakes. Carbonate forming and types can influence the $\delta^{13}\text{C}$ - $\delta^{18}\text{O}$ correlation. When carbonate content is less than 30%, there is no relationship both $\delta^{13}\text{C}$ and $\delta^{18}\text{O}$, and no relationship between $\delta^{13}\text{C}$ and $\delta^{18}\text{O}$. But more than 30%, carbonate content highly co-varies to $\delta^{13}\text{C}$ and $\delta^{18}\text{O}$, and has high correlation between $\delta^{13}\text{C}$ and $\delta^{18}\text{O}$ also. Vegetation condition and primary productivity of lakes can influence the characteristic of $\delta^{13}\text{C}$ and $\delta^{18}\text{O}$, and their co-varying. Organic matter content (TOC) in the sediments is higher with more terrestrial and submerged plants filling. When organic matter comes from endogenous floating organisms and algae (C/N<6), $\delta^{13}\text{C}$ value is heavy. $\delta^{13}\text{C}$ is in -4~0‰. $\delta^{13}\text{C}$ is in the range of -4~8‰ as organic matter comes from diatom (C/N=6~8). $\delta^{13}\text{C}$ is in the range of -8~4‰ as organic matter from aquatic and terrestrial plants (C/N>8).

Rapid bulk rock decomposition by ammonium fluoride (NH₄F) in open-vessels by an elevated digestion temperature

ZHAOCHU HU^{1,*}, WEN ZHANG¹, QION NI¹,
YONGSHENG LIU¹, RICHARD M. GASCHNIG², LIAN
ZHOU¹ AND LAISHI ZHAO¹

¹State Key Laboratory of Geological Processes and Mineral Resources, China University of Geosciences, Wuhan 430074, China

²Department of Geology, University of Maryland, College Park, Maryland 20742, USA

Complete dissolution is essential to achieve accurate analytical results for geological samples. Hydrofluoric acid is the most effective mineral acid for breaking up strong Si-O bonds to form SiF₆²⁻ ions in acidic solution. In this study, decomposition technique using the neutral solid compound NH₄F in open vessel (Savillex Teflon vial) has been investigated for multi-element analysis of different types of rock reference materials. The higher boiling point (260 °C) of NH₄F allows for an elevated digestion temperature in open vessels, which enables the decomposition of refractory phases. It took 1-1.5 h for Zr to be completely recovered in GSP-2 at 250 °C, which is 12 times faster than using conventional closed-vessel acid digestion at 190 °C (high-pressure PTFE digestion bomb). Unlike in NH₄F-assisted high pressure acid digestion, our results clearly indicate that adding HNO₃ severely inhibited the digestion capabilities of NH₄F for refractory minerals such as zircon in open vessel. The most outstanding advantage of the new method is that the digestion can be performed in a conventional Savillex Teflon vial instead of using a high pressure PTEF digestion bomb. Moreover, the NH₄F–open-vessel acid digestion is not hampered by the formation of insoluble fluorides, which represent another important advantage of this new sample decomposition method. Similar to HF and HNO₃, ultra-pure NH₄F can be produced using a conventional PFA sub-boiling purification system, and it does not induce new interference species in ICP-MS analysis. It is also worth emphasized and this reagent is removed by taking the sample to dryness, which is important to keep the total dissolved solid of the final solution presented to the instrument low. The developed NH₄F–open-vessel acid digestion has been successfully applied to the digestion of a series of international geological reference materials. This simple, effective, and comparatively safe dissolution method shows a great potential for the digestion of geological samples.

Fluid inclusion study of Maoping W deposit, southern Jiangxi province

R.M. HUA AND D.Q. HU

State Key Laboratory of Mineral Deposit Research, Nanjing University, Nanjing 210093, China

The Maoping tungsten deposit is a large W-Sn-polymetallic deposit discovered recently in southern Jiangxi province. It comprises two types of ore-bodies, i.e. quartz-vein type and greisenized-granite type. The present paper studies the fluid inclusions in quartz and topaz occurring in wolframite-quartz-veins, which mainly includes microthermometry and Laser Raman analysis. Besides, the homogenization temperatures of fluid inclusions in wolframite were also determined under an infra-red microscope. Result shows that fluid inclusions in both quartz and topaz are mainly of liquid-rich two-phase aqueous solution (H₂O-NaCl), in addition of small amount CO₂-bearing three-phase aqueous solution in quartz. The homogenization temperatures from quartz show wider variation range and can be divided into two main periods, indicating two stages of ore precipitation. The CO₂-bearing three-phase inclusions have similar homogenization temperatures to the higher temperature period of above inclusions, but lower salinities and different homogenizing ways. Fluid inclusions in wolframite have highest homogenization temperatures and salinities, whereas those in topaz also show high homogenization temperatures and salinities, and narrow variation range. The characteristics of homogenization temperatures and salinities from fluid inclusions in quartz reveal the multiple-stage of ore-forming process and the complexity of fluid evolution. It is concluded from this fluid inclusion that the early-stage boiling and late-stage mixing is probably the major mechanism of formation of wolframite-quartz-vein type ore in the Maoping deposit.

Silicon isotope fractionation between the upper and lower mantle of the Earth

FANG HUANG¹, ZHONGQING WU² AND SHICHUN HUANG³

¹CAS Key Laboratory of Crust-Mantle Materials and Environments, School of Earth and Space Sciences, USTC, Hefei 230026, China (fhuang@ustc.edu.edu)

²Laboratory of Seismology and Physics of Earth's Interior, School of Earth and Space Sciences, USTC, China.

³Department of Earth and Planetary Sciences, Harvard University, 20 Oxford Street, MA 02138, United States

As the second most abundant element in rocky planets, Si exhibits limited isotopic variations among different chondrite groups [1]. The $\delta^{30}\text{Si}$ of Bulk Silicate Earth (BSE), estimated based on basalts and peridotites, is higher than chondritic value. The heavier Si of BSE is proposed to be balanced by lighter Si in the Earth's core. In detail, a range of $\delta^{30}\text{Si}_{\text{BSE}} - \delta^{30}\text{Si}_{\text{Chondrite}}$ from 0.04 to 0.20‰, has been reported [e.g., 1-3]. Kempl *et al* [4] reported Si isotopic fractionation coefficient between metal and silicate under high P-T conditions, and they concluded that “the core contains between 11 and 29 wt% Si” depending on the value of $\delta^{30}\text{Si}_{\text{BSE}} - \delta^{30}\text{Si}_{\text{Chondrite}}$. Such high Si content in the core conflicts with seismic observations.

We calculated equilibrium fractionation factors of Si isotopes at high P-T conditions using density functional theory for mantle silicate minerals. Our calculations reveal significant Si isotope fractionation among mantle minerals with different Si coordination numbers (CN), especially between Mg-perovskite (CN=6) and olivine polymorphs (CN=4). Using our *ab initio* calculation and the magma ocean crystallization model of [5], the lower mantle, dominated by perovskite, is estimated to have lower $\delta^{30}\text{Si}$ (by ~0.1‰) than the upper mantle, dominated by olivine polymorphs. If such primordial Si isotope heterogeneity between the upper and lower mantle is not completely destroyed through the Earth's history, $\delta^{30}\text{Si}$ of BSE could be lighter than that inferred based on peridotites and basalts which are derived from the shallow upper mantle. Consequently, it does not require an unrealistically high Si content in the core.

[1] Savage and Moynier (2013) EPSL. [2] Chakrabarti and Jacobsen (2010) GCA. [3] Georg *et al* (2007) Nature. [4] Kempl *et al* (2013) LPSC. [5] Walter, M.J. and R.G. Trønnes, EPSL, 2004.

The mercury in the low latitude Holocene peat profile associated with monsoon variation

JING HUANG, LIMIN ZHOU AND XIANGMIN ZHENG¹

¹Key Laboratory of Geographic Information Science, Ministry of Education, East China Normal University, Shanghai, China, 200241, correspondence author: Limin Zhou, (lmzhou@geo.ecnu.edu.cn)

Mercury is key trace metal in earth surface system. The gaseous elemental Hg takes over 90% and has a long resident time in atmosphere. Mercury in ice core has been researched for a long time. The total element Hg changes from interglacier and glacier period, although there exists the argument on the driving process. The thermal lability of mercury in peat bog could be considered as an important paleoclimate proxy. The 1.3m peat core at the Caohai Lake was collected. By the AMS dating age the core covered 3.8 ka up to 9.4 ka. The total mercury concentration with the different temperature heating pretreatment associated with the organic carbon analysis including the stable carbon isotope analysis. The results show the mercury concentration is consistent with the organic carbon variation. The clear fluctuation at 8.2 ka and 4.3 ka could be detected. The mercury concentration variation is consistent with the solar radiation change from Dongge Cave which is closed to this peat core site. Compared to the mercury in the ice core, by this result, the mercury in peat at low latitude takes the different variation pattern from the high latitude region, which implies that the deposition pattern with the climate change varies with the latitude.

Unmasking enigmatic xenolithic eclogites: Progressive metasomatism on a key Roberts Victor sample

*JIN-XIANG HUANG^{1,2}, W. L. GRIFFIN¹, Y. GREAU¹,
N. J. PEARSON¹ AND S. Y. O'REILLY¹

¹CCFS/GEMOC, Macquarie University, Sydney, Australia

(*correspondence: jinxiang.huang@mq.edu.au)

²Institute of Geology and Geophysics, China Academy of Sciences, Beijing, China

Extensive studies of xenolithic eclogites have generated two contradictory hypotheses about their origin. One regards the eclogites as deep-seated magmatic rocks, while the other regards them as basaltic components of subducted oceanic slabs. To test the hypotheses, it is essential to find out if the samples being studied actually carry primary information.

Previous work on Roberts Victor eclogites (South Africa) divided the samples into Types I and II. Type I eclogites show sequential degrees of metasomatism by melts/fluids in the carbonatitic-kimberlitic spectrum; Type II eclogites may be the protoliths of Type I.

Progressive metasomatism inferred from studies of the whole eclogite suite, has now been revealed within one sample RV07-17. Four zones (progressively 1, 2, 3, and 4) are distinguished using the compositions of garnets. From Zone 1 to Zone 4, the microstructure becomes less equilibrated; secondary minerals and fluid inclusions become abundant; pyrope content of the garnets increases gradually; cpx shows progressive enrichment in MgO. The cross-cutting pattern strongly suggests that Zone 1 represents an early stage of the metasomatism, and Zone 4 the latest stage.

The garnets of Zone 1 have flat REE patterns from Lu to Sm, but a strong depletion in the LREE. Toward Zone 4, the relative abundance of the MREE of the garnets drops significantly, giving smoother patterns. A large cpx grain in Zone 1 shows a strong depletion in the LREE, but the LREE/MREE of the cpx increases from Zone 1 to Zone 4. From Zone 1 to 4, ⁸⁷Sr/⁸⁶Sr of cpx increases along with Sr content; $\delta^{18}\text{O}$ of the garnet decreases from ~8.5 to ~6.0 ‰ as the MgO content increases.

These observations indicate that the eclogite was metasomatized by Mg-rich melts/fluids, changing through time from carbonatitic to more kimberlite-like. The metasomatism has swept away all original information on compositions, making it nearly impossible to define a protolith. To know the origin of the xenolithic eclogites, and to use them as evidence for different dynamic scenarios, the least metasomatized samples must be studied more than has been done previously.

Carbon isotopic evidence for methane release during the end-Permian mass extinction

JUNHUA HUANG¹, LIDAN LEI¹, GENMING LUO^{1,2} AND
QUNFENG ZHOU³

¹State Key Laboratory of Geological Processes and Mineral Resources, China University of Geosciences, Wuhan 430074, China

²State Key Laboratory of Biogeology and Environmental Geology, China University of Geosciences, Wuhan 430074, China

³Institute of Geophysics & Geomatics, China University of Geosciences, Wuhan 430074, China

The largest mass extinction in the Phanerozoic that occurred mainly at the end-Permian about 252 Ma ago, eliminated ~90% of marine invertebrate species and ~70% of terrestrial vertebrate species [3]. The succedent recovery of the whole marine ecosystem lasted for more than 5 Ma [2]. This mass extinction was known to be accompanied by large perturbations in the global carbon cycle. However, the cause-and-effect relationship between the mass extinction and the global carbon cycle perturbation remains unclear [1].

Here we analyzed paired carbonate and organic carbon isotopic composition at the biostratigraphically-constrained Ganxi section which was located in northern deep water basin that attached to the Yangtze carbonate platform during the P-Tr transition. The $\delta^{13}\text{C}_{\text{carb}}$ underwent two episodes of negative shifts. The first one, from ~1.5‰ to 0‰, occurred before the main mass extinction horizon. The corresponding $\delta^{13}\text{C}_{\text{org}}$ also show a negative shift from ~25‰ to ~28‰. The second shift, from ~1‰ to -1‰, occurred at the lower Triassic, which might correspond to the second episode identified at the Meishan section (Xie *et al.*, 2007). However, the corresponding $\delta^{13}\text{C}_{\text{org}}$ shows a distinct positive shift from ~28‰ to ~25‰. During the extinction interval, the $\delta^{13}\text{C}_{\text{carb}}$ increased to ~1‰, and the $\delta^{13}\text{C}_{\text{org}}$ kept relatively constant.

In addition to the two episodes of general negative shifts, it is interesting to note that there are two intervals characterized by sharp negative shifts in $\delta^{13}\text{C}_{\text{carb}}$. One of them was found to occur around the P-Tr boundary, in which the $\delta^{13}\text{C}_{\text{carb}}$ declined from +1‰ to -1.3‰ within 3-cm thick strata. On the basis of recent high-resolution dating (Shen *et al.*, 2011), this shift produces a variation rate as high as 80‰/Ma for the $\delta^{13}\text{C}_{\text{carb}}$, suggesting the occurrence of huge methane release.

Our data in Ganxi section indicate that the significant negative shifts in $\delta^{13}\text{C}_{\text{carb}}$ and $\delta^{13}\text{C}_{\text{org}}$ were not caused by the mass extinction. Episodic release of methane, combining with other events, might have occurred during the mass extinction interval, which could make a contribution to the extinction and environmental perturbation.

[1] Berner (2002) *Proc Nat Acad Sci USA* 99, 4172-4177. [2] Chen & Benton (2012) *Nature Geoscience* 5, 375-383. [3] Erwin *et al.* (2002). *Boulder Geol. Soc. Amer.* 356, 363-384. [4] Shen *et al.* (2011) *Science* 334. [4] Xie (2007). *Geology* 35, 1083-1086.

Replacement of authigenic and detrital pyrrhotites by marcasite and pyrite in cold-seep sediments offshore SW Taiwan

KO-CHUN HUANG¹ AND WEI-TEH JIANG¹

¹Department of Earth Sciences, National Cheng Kung University, Tainan, Taiwan., R.O.C.
148001016@mail.ncku.edu.tw; atwtj@mail.ncku.edu.tw

Complex formation sequences of pyrrhotite, marcasite, and pyrite in two 5-m piston cores of muddy sediments offshore southwestern Taiwan were investigated by FESEM-EDS-EBSD techniques. The cored sites were characterized by a shallow sulfate methane interface at ~2 meters below seafloor and located in a ridge area (Fengliao Ridge) with cold-seep activities.

Two intriguing types of iron-sulfide microtextures were identified for the sediments. Firstly, sub-millimeter stacks of detrital pyrrhotite crystals were largely replaced by pyrite and minor marcasite. Later formed platy crystals (lathy section) of pyrrhotite developed from the edges of such stacks and were locally replaced by marcasite and pyrite as well. The second type involved the occurrence of millimeter-sized iron-sulfide nodules. The nodules had a core made of aggregates of lathy grains consisting of a mixture of pyrite and minor marcasite, and were fringed with pyrrhotite crystals and carbonate. Regardless of the microtextural differences, the marcasite EBSD data collected within single lathy grains invariably exhibited six intensity clusters aligned parallel to the long axes of the lathy grains in the {010} pole figure and two intensity clusters oriented perpendicular to the same axes in the {100} pole figure, and displayed an orientation relationship of $\{100\}_{\text{Mrc}} \parallel \{0001\}_{\text{Po}}$, $\{010\}_{\text{Mrc}} \parallel \{1000\}_{\text{Po}}$, and $\{001\}_{\text{Mrc}} \parallel \{1\bar{2}10\}_{\text{Po}}$ whenever the pyrrhotite relicts were present. No specific orientation relationships between pyrite and pyrrhotite or marcasite were detected. All of the pyrrhotites had a Fe/S atomic ratio of ~0.87.

The formation of marcasite occurred through epitaxial replacement of detrital or diagenetic pyrrhotite and was related to the oxidation of pyrrhotite that led to chemical changes in microenvironments. Relatively reducing pore fluids with low flux of hydrogen sulfide were favorable for the authigenesis of pyrrhotite. The multiple stages of phase replacement and precipitation were suggestive of temporal variations of redox conditions and hydrogen-sulfide activities associated with fluctuations of the sulfate-methane interface in the region.

Comparative characterization of charcoals prepared from pyrolysis and hydrothermal carbonization and their water extractable organic carbon

R.X. HUANG^{1*}, W.C. HOCKADAY¹, B.L.T. LAU¹,
X.W. LU² AND D. JACK³

¹ Department of Geology, Baylor University, Waco, Texas, USA (*correspondence:rixiang_huang@baylor.edu)

² Department of Civil and Environmental Engineering, University of South Carolina, Columbia, USA

³ Department of Mechanical Engineering, Baylor University, Waco, Texas, USA

Understanding the properties and the environmental behavior of charcoals produced from biomass is important within the context of carbon sequestration and sustainable agriculture. The present study compares the physicochemical properties of different types of chars and dissolved organic carbon (DOC) derived from them, as a means of making qualitative inferences about their stability and organo-mineral interactions in soils.

Chars were synthesized by slow pyrolysis at 250 °C and 500 °C and hydrothermal carbonization (HTC) at 250 °C using wheat straw as feedstock. The charcoals were characterized by solid-state ¹³C nuclear magnetic resonance spectroscopy (NMR) and thermogravimetric analysis (TGA). A higher proportion of aromatic carbons (78%) were formed in char pyrolyzed at high temperature than low temperature pyrolysis (47%) and HTC charcoals (51%). Statistical correlations between ¹³C NMR peak areas and mass loss data from TGA demonstrated that the aromatic carbons were mostly oxidized at temperature above 350 °C, while the alkyl carbons being oxidized at temperature below 350 °C. This suggests that the formation of aromatic structures was responsible for the thermal stability of charcoal. The leaching of labile organic carbon from chars was simulated using aqueous Soxhlet extraction. Leaching released a relatively small proportion of the charcoal carbon as DOC (<3%). The HTC charcoal leached more DOC than pyrolysis charcoal, and low-temperature pyrolysis charcoal leached more DOC than high-temperature pyrolysis charcoal. Spectroscopic characterization (proton and ¹³C liquid NMR and UV-vis) of the DOC implied that they are mostly low molecular weight neutral molecules (e.g., sugars and alcohols). Batch adsorption experiments showed no significant adsorption of the DOC onto kaolinite and goethite over a wide range of pH in the presence of 10 mM NaNO₃, which suggests that adsorption potential of the DOC onto common soil minerals is low.

Effects of glycine on oligomerization of methionine under high temperature and high pressure

R. HUANG^{1*}, Y. FURUKAWA¹, AND T. KAKEGAWA¹

¹Graduate school of Science, Tohoku Univ., Japan
(*correspondence: b2sm6036@s.tohoku.ac.jp)

Abiotic polymerization of amino acids seems to be an important process for the formation of the first life. Previous studies have implied the importance of pressurized conditions for the production of longer peptides, simulating the conditions of marine sediments [1, 2, 3]. These previous studies also suggest the skepticism about the formation of peptides composed of plural amino acids, showing a variety in reactivity of amino acids. In this study, we investigated the oligomerization of methionine and glycine under the conditions of high temperature and high pressure (at 175°C, 150 MPa, and 0-96 hours).

Methionine and glycine were used for representatives of each low and high reactive amino acid, respectively. Starting materials were solid methionine or solid methionine mixed with solid glycine, water, aqueous ammonia, or ammonium hydrogen carbonate. The additives other than glycine (water, aqueous ammonia, and ammonium hydrogen carbonate) are simulated decomposition products of glycine. Each starting material was sealed into a gold capsule. Then, high temperature and pressure conditions were applied using a test-tube-type autoclave system. After these experiments, experimental products were analyzed with a high performance liquid chromatograph connected to a mass spectrometer.

The rates of methionine decomposition and methionine-peptide formation were increased with additives. These rates were especially increased in samples containing aqueous ammonia and ammonium hydrogen carbonate, suggesting that ammonia promote both the production rates of peptides and the decomposition reactions of methionine. The difference in reaction rates might have been caused by the difference in pH as suggested in a previous study [4]. Our results suggest that amino acids of lower reactivity may have been activated by amino acids of higher reactivity, and then promoting peptide formation composed of plural amino acids. Such new finding may have happened commonly in prebiotic environments.

[1] Ohara *et al* (2007), *Orig Life Evol Biosph* **37**, 215–223. [2] Otake *et al* (2011), *Astrobiology* **11**, 799–813. [3] Furukawa *et al* (2012), *Orig Life Evol Biosph* **42**, 519–531. [4] Sakata *et al* (2010), *Geochim Cosmochim Acta* **74** 6841–6851.

A newly identified microorganism affecting the N cycle: Ammonium oxidation in iron reducing soils

SHAN HUANG¹ AND PETER R. JAFFE^{1*}

¹Department of Civil and Environmental Engineering,
Princeton University, Princeton, NJ, jaffe@princeton.edu
(* presentimng author)

A novel anaerobic ammonium (NH₄⁺) oxidation process coupled with iron reduction was first noted in a forested riparian wetland in New Jersey ^(1,2). In this reaction, NH₄⁺ is oxidized using ferric iron as the electron acceptor. Either this same pathway, or a very similar one, was also reported in a biological reactor ⁽³⁾, and a tropical rainforest soil ⁽⁴⁾ and coined Feammox ⁽³⁾.

Here we focus on characterizing the microbiology responsible of the Feammox process described for our previous study site ^(1,2), through an anaerobic incubation experiment and using 16S rDNA PCR-DGGE and qPCR analysis. Production of both nitrite (NO₂⁻) and ferrous iron were measured repeatedly during incubations when soil slurries were supplied with iron oxide (ferrihydrite or goethite) and ammonium chloride. Significant changes in the microbial community were observed during the incubation, and one of the dominant microbial species (an uncultured *Acidimicrobiaceae* bacterium A6), belonging to the *Acidimicrobiaceae* family, similar to *Ferrimicrobium acidiphilum* (with 92% identity), is believed to be responsible for this Feammox pathway. This novel bacterium is considered to be autotrophic since its activity increased substantially when inorganic carbon was supplied. Through qPCR analysis using specific designed primers, *Acidimicrobiaceae* bacterium A6 was also found at a storm-water detention pond, which has similar high NH₄⁺ and iron oxide content, indicated that the Feammox pathway might be widespread in soil environments.

The Feammox process provided denitrifiers and anammox bacteria with the necessary NO₂⁻ under this anaerobic incubation, and achieved total nitrogen loss via denitrification and anammox pathways. Therefore, Feammox may be an important process in the nitrogen cycle in soil environments under oxygen limited conditions, and reveals a new linkage between these two significant biogeochemical cycles (iron and nitrogen cycle).

[1] Clement *et al* (2005) *Soil Biol. Biochem.* **37**, 2323–2328. [2] Shrestha *et al* (2009) *Soil Sci.* **174**,156–164. [3] Sawayama, J. (2006) *Biosci. Bioeng.* **101**, 70–72. [4] Yang *et al* (2011) *Nat. Geosci.* **5**, 538–541.

Sm/Nd ratio of the Earth

SHICHUN HUANG¹, STEIN B JACOBSEN¹
AND SUJOY MUKHOPADHYAY¹

¹Department of Earth and Planetary Sciences, Harvard
University (huang17@fas.harvard.edu)

The composition of Bulk Silicate Earth (BSE) provides an important “roadmap” understanding the thermal evolution, mass flow and the structure of Earth’s mantle. Although it has been known since 1960s that the BSE composition is overall not chondritic [1], it is assumed that the refractory elements in the Earth are present in chondritic proportions relative to each other [2], which is the basis of many models about the compositions of BSE and depleted mantle (DM) [e.g., 3].

The ¹⁴⁷Sm-¹⁴³Nd isotopic system has been used as a “backbone” to estimate the compositions of BSE and DM. This is because both Sm and Nd are refractory elements, and all chondrites have essentially the same Sm/Nd ratio (within ±2%) [e.g., 2, 4]. BSE is assumed to have chondritic Sm/Nd and ¹⁴³Nd/¹⁴⁴Nd ratios. However, this assumption is challenged by recent ¹⁴²Nd studies [4, 5]. Specifically, Boyet and Carlson [4] reported ~20 ppm ¹⁴²Nd/¹⁴⁴Nd difference between Earth and ordinary chondrites. Although this difference could be of nucleosynthetic origin [6, 7], it has also been attributed to either early silicate differentiation of a chondritic Earth, occurred within 30 Myrs after the Earth’s formation [4], or to a superchondritic BSE, which has a Sm/Nd ratio 6% higher than the chondritic value [5].

Here we re-examine published data, and found that:

1. There is ~50 ppm ¹⁴²Nd/¹⁴⁴Nd variation in chondrites, and it is correlated with nucleosynthetic anomalies in ¹³⁵Ba, ¹⁴⁴Sm and ¹⁴⁸Nd. Consequently, the 20 ppm ¹⁴²Nd/¹⁴⁴Nd difference between Earth and ordinary chondrites must reflect nucleosynthetic origin;
2. Possible nebular processes are unable to significantly fractionate Sm/Nd ratio; consequently, it is unlikely that the Earth accreted from a nebular reservoir with a superchondritic Sm/Nd ratio;
3. Our analyses of the ¹⁴⁷Sm-¹⁴³Nd isotopic systematics of continental crust and DM suggest that BSE, or the accessible portion of BSE under the “hidden reservoir” hypothesis, has a near-chondritic Sm/Nd ratio.

[1] Wasserburg *et al* (1964) *Science*. [2] Jacobsen and Wasserburg (1984) *Earth Planet Sci Lett*. [3] McDonough and Sun (1995) *Chem Geol*. [4] Boyet and Carlson (2005) *Science*. [5] Caro *et al* (2008) *Nature*. [6] Ranen and Jacobsen (2006) *Science*. [7] Andreassen and Sharma (2006) *Science*.

Studies on the characteristics and mechanism of a heavy haze episode in Jiangsu Province, China

X.X. HUANG, T.J. WANG* AND J.L. ZHU

School of Atmospheric Sciences, Nanjing University, Nanjing
210093, China (hxxc829@hotmail.com)

(*correspondence: tjwang@nju.edu.cn)

Autumn is one of the periods that poor air quality frequently occurs in Jiangsu [1]. In this study, the characteristics and mechanism of a regional haze episode were investigated in late October 2012 over Jiangsu. The analysis was conducted with the observational concentrations of air pollutants (PM₁₀, PM_{2.5}, and CO) in 13 cities, visibility data in 5 cities, meteorological elements (relative humidity, wind speed, air temperature, precipitation in surface, upper air soundings, and synoptic situation), fire locations from FIRMS, and trajectories from the numerical models of HYSPLIT. The northern cities suffered more heavily with the highest hourly PM₁₀, PM_{2.5}, CO, ratio of PM_{2.5} to PM₁₀ exceeding 0.50mg/m³, 0.45mg/m³, 3.5mg/m³, and 0.9, respectively. The lowest hourly visibility was below 5km in the 5 cities. Backward trajectories accompanied with fire spots exhibited that pollutants from large areas of biomass burning during the harvest season mixed with local anthropogenic emissions contributed to this event. The degradation of air quality in northern cities was mainly caused by emissions from biomass burning, while the southern cities were affected by the mixed emissions. Synoptic condition was another factor, especially calm and weak wind, and relatively high temperature before rainfall.

[1] Deng *et al* (2011) *Atmos. Res.* **101**, 681-691.

Vanadium Distribution in Environmental Samples Surrounding the Slag Dump in Panzhihua, Sichuan province, P.R.China

HUANG YI^{1,2*}, ZHANG WEI¹, NI SHIJUN^{1,2}, CHEN YING¹
AND ZHONG LICHUN

¹Department of Geochemistry, Chengdu University of Technology, Sichuan, PRC, huangyi@cdut.edu.cn (* presenting author)

²Applied Nuclear techniques in Groscience Key Laboratory of Sichuan Province, PRC

Million tons of metallurgical slag bearing abundant vanadium (V) was piled outside along Jinshajiang river, upstream of Yangtze river. Vanadium distribution in water, sediment and soil samples surrounding the slag dump was studied. The results showed that from the slag dump to the downstream of the Baguanhe river, vanadium content and the pH value gradually decreased for water samples, and also vanadium content of sediment samples gradually decreased. Soil vanadium near the slag dump is usually higher than the background value of soil in Sichuan province, and the soil with the highest value was collected from the slag dump area. It is apparent that slag piling has brought a certain degree of pollution to the surrounding environment.

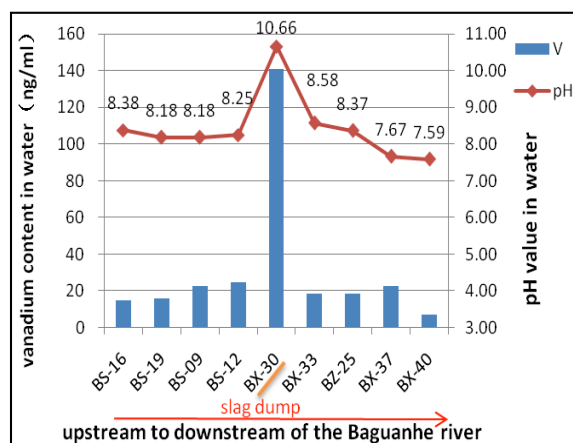


Figure 1. Vanadium concentration and pH values of water samples along the Baguanhe river

A reference Earth model for the heat producing elements and associated geoneutrino flux

Y. HUANG^{1*}, V. CHUBAKOV², F. MANTOVANI²,
R.L. RUDNICK¹ AND W.F. MCDONOUGH¹

¹University of Maryland, College Park, MD 20742, USA
(*correspondence: yu Huang@umd.edu;

rudnick@umd.edu, mcdonoug@umd.edu)

²Università degli Studi di Ferrara/ INFN, Ferrara, Italy
(chubakov@fe.infn.it, mantovani@fe.infn.it)

Geoneutrinos are electron antineutrinos emitted by beta-minus decays of naturally occurring radionuclides (e.g., heat producing element (HPEs), namely U, Th and K). The recent geoneutrino experimental results from KamLand [1] and Borexino [2] detectors reveal the usefulness of analyzing the Earth's geoneutrino flux, as it provides a constraint on the strength of the radiogenic heat power and this, in turn, provides a test of compositional models of the bulk silicate Earth (BSE). This flux is dependent on the amount and distribution of HPEs in the Earth's interior.

We have developed a geophysically-based, three-dimensional global reference model for the abundances and distributions of HPEs in the BSE [3]. The structure and composition of the outermost portion of the Earth, the crust and underlying lithospheric mantle, is detailed in the reference model, this portion of the Earth has the greatest influence on the geoneutrino fluxes. The reference model combines three existing geophysical models of the global crust and yields an average crustal thickness of 34.4 ± 4.1 km in the continents and 8.0 ± 2.7 km in the oceans, and the total mass (in 10^{22} kg) of oceanic, continental and bulk crust is 0.67 ± 0.23 , 2.06 ± 0.25 and 2.73 ± 0.48 , respectively. *In situ* seismic velocity provided by CRUST 2.0 allows estimates of the average composition of the deep continental crust by using new and updated compositional databases for amphibolite and granulite facies rocks, in combination with laboratory ultrasonic velocities measurements. An updated xenolithic peridotite database is used to represent the average composition of continental lithospheric mantle. Monte Carlo simulation is used to predict the geoneutrino flux at selected locations and to track the asymmetrical uncertainties of radiogenic heat power due to the log-normal distributions of HPE concentrations in crustal rocks.

[1] Gando *et al* (2013) arXiv: 1303.4667. [2] Bellini *et al* (2013) arXiv: 1303.2571. [3] Huang *et al* (2013) G-Cubed, doi: 10.1002/ggge.20129.

Limitations of isotopic and elemental signatures of oxygenic photosynthesis: A possible solution?

AXELLE HUBERT^{1,2*}, FRANCES WESTALL¹,
ALEXANDRE SIMIONOVICI², CLAIRE ROLLION-BARD³
AND NATHALIE GRASSINEAU⁴

¹CBM, CNRS, 45071 Orléans, France (*correspondence
axelle.hubert@cnrs-orleans.fr)

²ISTerre, Grenoble, France

³CRPG, CNRS, 54500, Vandoeuvre les Nancy, France

⁴RHU L, Egham, Surrey TW20 0EX, United Kingdom

The appearance of oxygenic photosynthetic bacteria is recognised to be one of the major processes involved in the rise of oxygen in Earth's atmosphere. This process permitted the development of more complex aerobic lifeforms. However, the timing of the appearance of oxygenic photosynthesis and that of the oxygenation of the Earth are still debated [1] and constraining the event remains a challenge.

Initially, oxygenic photosynthesis must have appeared in very localized zones [2] before having a global influence. Certain factors can influence the isotopic and elemental signatures of early oxygenic photosynthesis at the local level. These include (i) overlapping ranges of ¹³C isotopes for oxygenic photosynthetic and heterotrophic signatures, (ii) mixing of signatures in complex, multicomunity microbial mats, and (iii) diagenetic reduction of potential redox sensitive transition metals and trace elements by heterotrophs and geochemical processes caused by the predominantly (still) anaerobic environment.

We aim to disentangle the complex isotopic and elemental signatures of photosynthetic bacterial biofilms and cells in sedimentary cherts ranging from 3.5 to 1.9 Ga. We are conducting a systematic *in situ* investigation characterizing individual microbial mats so as to understand the differences between fossilized anoxygenic and oxygenic photosynthetic mats. We chose to focus on individual microbial mats as they record the composition and concentration of transition metals and trace elements, as well as C and S isotopic signatures on a very fine, local scale.

We hope to be able to understand the fine scale isotopic and elemental signatures of photosynthetic oxidation in our samples so as to contribute to the overall delineation of the record of Earth's oxygenation.

[1] Farquhar J., Zerkle A.L., & Bekker A. (2011), *Photosynthesis Research* 107, 11-36. [2] Anbar A.D., *et al* (2007), *Science* 317, 1903-1906.

A constant flux of diverse anaerobic thermophilic endospores into cold marine sediments

CASEY HUBERT,^{1*} EMMA BELL,¹ JÚLIA DE REZENDE,¹
CHINA HANSON,¹ ANA SUÁREZ-SUÁREZ,¹ IAN HEAD,¹
ALEXANDER LOY,² ALBERT MÜLLER,² CHRISTIAN
BARANYI,² TIMOTHY FERDELMAN,³ MAREN NICKEL,³
VERONA VANDIEKEN,³ CAROL ARNOSTI,⁴ VOLKER
BRÜCHERT,⁵ KAI FINSTER,⁶ KASPER KJELDSEN,⁶
AND BO BARKER JØRGENSEN⁶

¹School of Civil Engineering & Geosciences, Newcastle
University; (*casey.hubert@newcastle.ac.uk)

²Dept of Microbial Ecology, University of Vienna

³Max Planck Institute for Marine Microbiology

⁴Dept of Marine Sciences, University of North Carolina

⁵Department of Geological Sciences, Stockholm University

⁶Center for Geomicrobiology, Aarhus University

Microorganisms have been repeatedly discovered in environments that do not support their metabolic activity. In a striking example of this, experiments to determine the temperature optima for sulfate reduction in permanently cold Arctic marine sediments revealed that metabolic rates were greatest in sediment that was incubated above 50°C. This response was distinct from that associated with the local cold-adapted microbial community (that catalyzed much lower rates associated with a 20°C optimum) and is explained by the germination of endospores of diverse thermophilic *Clostridiales* that lie dormant in marine sediments but can rapidly mineralize organic matter by hydrolysis, fermentation, and sulfate reduction upon induction at 50°C. Identifying and quantifying misplaced organisms such as thermophilic endospores can reveal rates and vectors of cell dispersal that shape natural microbial diversity and biogeography. In this case, endospore germination experiments that incorporated ³⁵S sulfate radiotracer were combined with a ²¹⁰Pb sediment age model to enable the estimation of a stable supply of thermophilic bacteria into the sediment at a rate exceeding 10⁸ spores per square meter per year. Genomic comparisons indicate that the closest relatives to these and other misplaced thermophilic spores are found in warm subsurface petroleum reservoir and ocean crust ecosystems, suggesting that seabed fluid flow from deep biosphere environments may be transporting thermophiles into the cold ocean. These proposed mechanisms for the passive dispersal of microbial cells may thus connect very different provinces of the biosphere and lithosphere, and could be broadly influencing microbial community composition in the marine environment.

Coupled climate-geochemical modeling of the connections between break-up of Rodinia, weathering of continental flood basalts, snowball glaciations and the strontium cycle

LUCIE HUBERT-THÉOU¹, GRANT C. COX¹,
GUILLAUME LEHIR², YVES GODDÉRIIS³,
YANNICK DONNADIEU⁴, GALEN P. HALVERSON¹,
ANDRÉ POIRIER⁵ AND LINDSAY NELSON¹

¹ McGill University, Earth and Planetary Sciences

department, 3450 University Street, Montreal (Qc), H3A 2A7, Canada ; (lucie.hubert-theou@mail.mcgill.ca)

² IPGP, 1 rue Jussieu, 75238 Paris cedex 05 ; (lehir@ipgp.fr)

³ Geoscience Environnement Toulouse, UMR 5563, CNRS- Université Toulouse III, 14 avenue Edouard Belin, 31400 Toulouse, France ; (yves.godderis@get.obs-mip.fr)

⁴ Laboratoire des Sciences du Climat et de l'Environnement, UMR 8212, CNRS-CEA-UVSQ, Orme des Merisiers, 91191 Gif/Yvette ; (yannick.donnadieu@lscce.ipsl.fr)

⁵ Université du Québec à Montréal, GEOTOP-UQAM, CP 8888, Montréal (Qc), Canada ; (poirier.andre@uqam.ca)

Isotope records of marine seawater composition (e.g. $\delta^{13}\text{C}$, $^{87}\text{Sr}/^{86}\text{Sr}$) display significant variability at the end of the Precambrian, in particular associated with the break-up of the Rodinia supercontinent and spanning the Cryogenian snowball Earth events ca. 716 and 635 Ma. Here we explore the time interval 950–630 Ma to address the long-term evolution of the Neoproterozoic seawater chemistry and climate and to investigate perturbations to the Earth-system over this period. We apply GEOCLIM, a powerful coupled climate-geochemical model to test the effect of the breakup of the supercontinent Rodinia and the emplacement and subsequent weathering of Large Igneous Provinces (LIPs: Willouran-Gairdner, Guibei, Gunbarrel and Franklin events) on the carbon cycle. The strontium cycle and its isotopes are implemented in the model in order to assess the influence of lithologic and paleogeographic changes on the weathering of continental silicates and climate. To this end, new $^{87}\text{Sr}/^{86}\text{Sr}$ data from marine carbonates of various Neoproterozoic successions (Northwestern Canada, Eastern Greenland, Svalbard, Siberia and Saudi Arabia) were produced to build a more complete Sr isotope record spanning the Neoproterozoic and to provide initial conditions in our simulations. In addition, Sr and Nd isotopes ratios were measured on Neoproterozoic mafic rocks and Nd isotopes on fine-grained sediments to track the timing of emplacement and weathering of the major LIP relative to glaciations.

Geological history of 4-Vesta: ^{26}Al - ^{26}Mg dating on eucrites and diogenites

G. HUBLET¹, V. DEBAILLE¹, J. WIMPENNY²
AND Q-Z. YIN²

¹G-Time, Université Libre de Bruxelles, Brussels, Belgium, (ghublet@ulb.ac.be)

²Department of Geology, University of California, Davis, CA, USA

Eucrites and diogenites are achondrites belonging to a magmatic series coming from 4-Vesta. Eucrites are basaltic rocks, while diogenites are ultrabasic cumulates. We used the ^{26}Al - ^{26}Mg chronometer for precise dating of eucrites and diogenites and revealing the geological history of 4-Vesta.

Basaltic eucrite textures suggest a formation and rapid cooling on the surface in lava flows or dikes while cumulative eucrites evidence deeper and slower cooling. This study reveals that those two types of eucrites belong to two different age populations and cannot be used together for external isochrons. Ages obtained for basaltic eucrites suggest a formation of the eucrite crust during a short and ancient period of magmatic activity on 4-Vesta between 4564 to 4563 Ma. Disturbance observed for the $^{26}\text{Mg}^*/^{24}\text{Mg}$ ratio in plagioclase fraction in one basaltic eucrite (Y-792510) suggest also a metamorphism episode likely related to shock.

Results obtained for the cumulative eucrites show younger ages compared to the basaltic type. This suggests that some inner parts of Vesta were still warm until ~4560 Ma. Ghosh et al. [1] show ^{26}Al decay is probably the heating source for Vesta differentiation and basaltic eucrite magmatic activity, and may have also kept the mantle hot during a few Ma [2], explaining the slow cooling rate evidenced by the younger age of cumulative eucrites.

Finally, our incapacity to date diogenites with the ^{26}Al - ^{26}Mg chronometer suggests a younger age for them (< 4560 Ma). Diogenite are thought to be formed in intrusion within the eucrite crust during a second period of magmatic activity on 4-Vesta [3, 4], probably generated by the remelting of the magma ocean cumulates [5, 6]. This remelting cannot be related to the ^{26}Al decay because at this time, the ^{26}Al was completely extinct. A mantle overturn could be a process to explain this remelting event.

[1] Ghosh A., et al (1998) *Icarus*, 134, 187-206. [2] Zhou Q., et al (2013) *GCA*, 110, 152-175. [3] Barrat J.A., et al (2010) *GCA*, 74, 6218-6231. [4] Yamaguchi A., et al (2011) *Journal of Geophysical Research*, 116, E08009. [5] Barrat J.A. (2004) *MAPS*, 39, 1767-1779. [6] Barrat J.A., et al (2008) *MAPS*, 43, 1759-1775.

Redox controls on diagenetic incorporation of rare earth elements in fossil fish teeth

C.E. HUCK^{1*}, T.VAN DE FLIERDT¹, S.M. BOHATY², S. HAMMOND³ AND IODP EXPEDITION 318 SCIENTISTS

¹Imperial College, London SW7 2AZ UK

²Ocean and Earth Science, NOC, Univ. of Southampton, Southampton, SO14 3ZH UK

³The Open University, Walton Hall, Milton Keynes MK7 6AA UK

Fossil fish teeth and skeletal debris are considered one of the most robust archives for reconstructing Nd isotope ratios of seawater in the geological past, and have been widely used to fingerprint individual water masses and trace their distribution through time. Little systematic work, however, has been done to verify the robustness of this proxy in marginal settings and under varying bottom-water and sedimentary redox conditions.

IODP Expedition 318 recovered Paleogene drillcores from offshore of the East Antarctic margin (Site U1356; 63°18.61'S, 135°59.94'E). Strata of early Eocene age (~48 to ~49 Ma) deposited in a shelf environment during the warmest period of the Cenozoic - the Early Eocene Climatic Optimum (EECO) - show striking cyclical variations between oxidised and reduced conditions. Since Site U1356 is located proximal to the Tasman Gateway and the EECO is of particular interest for palaeoceanographic reconstructions during the early Paleogene greenhouse, we investigated the robustness of the Nd isotope signal in fish debris deposited during the early Eocene at this site.

Individual fish teeth were picked from the >125µm fraction of washed bulk sediments. Comparison between fully reductively cleaned samples and samples only cleaned with water and methanol yielded the same Nd isotopic composition, and hence the latter cleaning procedure was used for the majority of the samples. All samples were dissolved in HCl, aliquoted for major and trace element analyses, and subjected to a standard two stage ion chromatography. Neodymium isotope ratios were determined using a Nu Plasma MC-ICP-MS and major and trace element data, including rare earth element patterns, were obtained on an Agilent 7500a quadrupole ICP-MS.

Preliminary data show systematic variation in the Nd isotopic composition of fish teeth extracted from reduced and oxidised sediments. We will evaluate these findings in the context of a more comprehensive data set, including main and trace element data, and discuss the implications of varying redox conditions at the sea floor on the incorporation and preservation of seawater Nd isotopes in fossil fish teeth.

Melt-inclusion evidence for a CO₂-rich mantle beneath the western branch of the East African Rift

T.R. HUDGINS^{1*}, S.B. MUKASA² AND A.C. SIMON¹

¹Department of Earth and Environmental Sciences, University of Michigan, Ann Arbor, MI, USA

(*correspondence: hudginst@umich.edu)

²Department of Earth Sciences, University of New Hampshire, Durham, NH, USA

CO₂ in the mantle may moderate the generation of low silica magmas. Here, we present data from olivine-hosted melt inclusions that are consistent with a carbonated mantle source beneath the western branch of the East African Rift.

Twenty-four samples were collected from the Virunga province of the East African Rift. These rocks are silica-understaturated potassic lavas (kamafugites) with 38-45 wt% SiO₂ and K₂O/Na₂O>1. We quantified the abundances of major, minor, and trace elements, as well as the volatiles H₂O, CO₂, F, S, and Cl in olivine-hosted melt inclusions from five whole-rock samples. The H₂O and CO₂ concentrations range from ~0.3 to 2.5 wt% and ~30 to 9,950 ppm, respectively. The CO₂ values are consistent with molecular dynamics simulations for the solubility of CO₂ in MORB and may represent less degassed melt[1]. The melt inclusions have elevated Li concentrations (up to 117 ppm) and B/Be ratios (>10) relative to MORB (Li ~3 to 4 ppm, B/Be ~2 to 4).

Two plausible sources of the volatiles are fluids evolved during paleo-subduction, and fluid exsolved from the melting of a mantle plume. Published Nd, Hf, Sr, and Os data for rocks across the EAR western branch suggest mixing of two metasomatized mantle sources as the source of these magmas, requiring previous fluid-mantle interaction[2]. Elevated Li and B concentrations measured in arc magmas have been used as a fluid tracer to investigate the role of fluid additions to the mantle wedge. As such, volatiles subducted by the closure of the Mozambique Ocean during the Pan-African orogeny are a plausible source for the elevated CO₂ and H₂O. This scenario is consistent with evidence for long-term storage of volatiles in the mantle[3]. Other potential sources include ancient subducted slabs pooled in the lower mantle and fluids released from a partially melting mantle plume. Radiogenic and noble gas isotope studies may be required to fully distinguish the sources of the mantle metasomatism.

[1] Guillot and Sator (2011) *GCA* **75**, 1829-1857. [2] Rosenthal *et al.*, (2009) *EPSL* **284**, 236-248. [3] Pettke *et al.*, (2010) *EPSL* **296**, 267-277.

Subcontinental lithospheric mantle and mantle plume controls on crustal PGE abundance: A case study of Palaeogene magma conduits from Western Scotland, UK

H. HUGHES, I. McDONALD, A.C. KERR¹
AND A.J. BOYCE²

¹School of Earth and Ocean Science, Cardiff University, UK
CF10 3AT. (*correspondance: HughesH6@cf.ac.uk)

²Scottish Universities Environmental Research Centre, East
Kilbride, Glasgow, UK G75 0QF.

A strong correlation can be demonstrated between plume magmatism, ancient cratonic lithosphere, and the occurrence of magmatic sulphide Ni-Cu-PGE deposits [1]. Such deposits are typically located proximal to Archaean craton margins. A highly desirable combination of plume-related mafic/ultramafic igneous systems and Archaean cratons, underlain by their associated subcontinental lithospheric mantle (SCLM) keel, occur within the North Atlantic Igneous Province (NAIP). Significant mineralization has been discovered in the western portion of the NAIP (e.g. Skaergaard and Paleogene macrodykes [2,3]). Therefore, the British Palaeogene Igneous Province (BPIP) is potentially the most prospective PGE province in Western Europe.

This research focuses on the Scottish sector of the BPIP. Isolated platinum group mineral occurrences are documented on the Isles of Rum, Mull and Skye, but with limited assessment of its relationship to the province as a whole. To assess the geochemical inputs of asthenospheric (plume) vs. lithospheric 'reservoirs', a temporal and spatial evaluation of PGE abundance across the region must be adopted. This study incorporates the Paleoproterozoic Scourie dyke swarm, Caledonain lavas and small-scale intrusions, mantle xenoliths, and Palaeogene lavas and magma conduits.

Whole-rock grab samples were analysed for major and trace elements by ICP-OES and ICP-MS and NiS fire assay with ICP-MS analysis to determine PGE and Au abundances. Whole-rock PGE+Au concentrations from the 2.4 Ga Scourie Dyke swarm suggest no major removal of PGE from mantle 'reservoirs' at this time, leaving residual Archaean SCLM as 'fertile'. Permian dyke-hosted lherzolite xenoliths are in support of the shallow mantle remaining 'fertile' during this period, and may have undergone some degree of subduction-related enrichment of Au during Caledonian orogenesis. Lithogeochemical indicators (e.g. Cu/Pd ratio) highlight the occurrence of both S-saturated and -unsaturated magma batches across the BPIP, however there is no clear correlation with MgO, which may infer variable Cu/Pd of parental magmas instead. Pd/Ir suggest variable coeval SCLM contamination.

[1] Begg, G. C. *et al* 2010. *Econ. Geol.*, **105**, 1057-1070. [2] Andersen, J. C. Ø. *et al* 1998. *Econ. Geol.*, **93**, 488-509. [3] Holwell, D.A. *et al* (2012). *Mineral. Dep.*, **47**, 3-21.

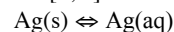
Dissolved metals in redox-state zero: A gap in thermodynamic databases

W. HUMMEL

Laboratory for Waste Management, Paul Scherrer Institut,
5232 Villigen, Switzerland (wolfgang.hummel@psi.ch)

Dissolution of metals like silver is usually considered solely as oxidative dissolution $\text{Ag(s)} \rightleftharpoons \text{Ag}^+ + \text{e}^-$.

Whereas the solubility of zero-valent mercury is well known [1], experimental data about the solubility of other metals like silver is scarce [2, 3]. The explicit equilibrium



although published and discussed in [2], is not included in any thermodynamic database. The same is true for Hg(aq).

The myth that heavy metals are "insoluble" seems to be so powerful that dissolved metal atoms do not exist in geochemical considerations. This blind spot of chemical equilibrium thermodynamics has consequences: (1) The calculated "solubility abyss" of heavy metals under reducing conditions does not exist. (2) "Unclear differences" in experimental data sets and strange model parameters are due to the ignorance of zero-valent metal species.

(1) In the field of radioactive waste disposal solubility limits of contaminants are important safety issues. In the case of metals like silver, conventional model calculations lead to a "solubility abyss" under strong reducing conditions. There, silver metal is the thermodynamically stable phase and the concentration of dissolved silver virtually drops to zero. This is an artefact due to the omission of Ag(aq).

(2) Experimental determinations of the solubility of silver sulphide, $\text{Ag}_2\text{S(s)}$, lead to large differences between data sets in acidic solutions. "The reason for this is unclear" [4]. However, these differences can be explained by considering Ag(aq) and assuming that the data sets have been measured under slightly different redox conditions. Measurements of the solubility of gold in water have been interpreted in terms of extremely strong AuOH(aq) complex formation [5]. Assuming a solubility of zero-valent gold similar to Ag(aq) the experiments can be interpreted as governed by the formation of Au(aq).

Experimental data or good estimates for Au(aq), Cu(aq), Ni(aq), Pd(aq), Pt(aq) are needed to fill the database gap.

[1] Clever *et al* (1985) *J. Phys. Chem. Ref. Data* **14**, 631-680. [2] Kozlov & Khodakovskiy (1983) *Geochem. Inter.* **20**, 118-131. [3] Dobrowolski & Oglaza (1963) *Nucleonika* **8**, 79-81. [4] Stefánsson & Seward (2003) *Geochim. Cosmochim. Acta* **67**, 1395-1413. [5] Stefánsson & Seward (2003) *Geochim. Cosmochim. Acta* **67**, 1677-1688.

Structure of carbonate-silicate melts at high P-T conditions using in situ X-ray diffuse scattering

DANIEL HUMMER¹, ABBY KAVNER²
AND CRAIG MANNING³

¹Department of Earth and Space Sciences, University of California Los Angeles, Los Angeles, CA 90095, (dhummer@ess.ucla.edu)

²Department of Earth and Space Sciences, University of California Los Angeles, Los Angeles, CA 90095, (akavner@ucla.edu)

³Department of Earth and Space Sciences, University of California Los Angeles, Los Angeles, CA 90095, (manning@ess.ucla.edu)

Carbonatites are an important class of mantle-derived magmas that may play a fundamental role in mantle metasomatism and carbon cycling. To examine compositional dependence of melt structure in the CaO-MgO-CO₂-SiO₂ system, we performed *in situ* X-ray scattering experiments in the Paris-Edinburgh press at HPCAT (Advanced Photon Source) using compositions along the CaCO₃-CaSiO₃ (Cc-Wo) and CaCO₃-Mg₂SiO₄ (Cc-Fo) joins. Both systems exhibit simple eutectic melting over a wide pressure range, with no subsolidus decarbonation reactions [1,2]. Charges were loaded using the setup of Yamada *et al* [3], and held at ~1800 °C and ~40 kbar while energy dispersive X-ray scattering spectra were recorded at each of eleven scattering angles to achieve reciprocal space coverage up to $q=32 \text{ \AA}^{-1}$.

The presence of both Cc and Wo in quenched charges confirms the retention of CO₂. Pair distribution functions (PDF) reveal local atomic structure of the liquid and, when normalized to the calcite-liquid PDF, provide a measure of silica polymerization. Results suggest that CaCO₃ forms an ionic liquid with intact CO₃²⁻ ions, in agreement with previous results [4,5]. Silicate melts show a clear signal at 1.6 Å, corresponding to Si-O in SiO₄⁴⁻ tetrahedra. Both Wo-bearing and Fo-bearing compositions also show a strong signal at 3.3 Å, corresponding to Si-Si in polymerized silica. Thus, in the presence of carbonate, even liquid orthosilicates contain silica polymers. The extent of polymerization moderately increases with carbonate content along both joins, suggesting that carbonate has a significant influence over the chemistry of molten silicates at mantle conditions.

[1] Huang & Wyllie (1974), *EPSL* 24, 305-310. [2] Huang *et al* (1980), *Am. Min.* 65, 285-301. [3] Yamada *et al* (2011), *Rev. Sci. Instr.* 82, 015103. [4] Waseda & Toguri (1977), *Metall. Trans. B* 8B, 563-568. [5] Benmore *et al* (2010), *Phys. Rev. B* 82, 224202.

Three styles of delamination found beneath the western United States

EUGENE HUMPHREYS^{1*}, BRANDON SCHMANDT² AND ALAN LEVANDER³

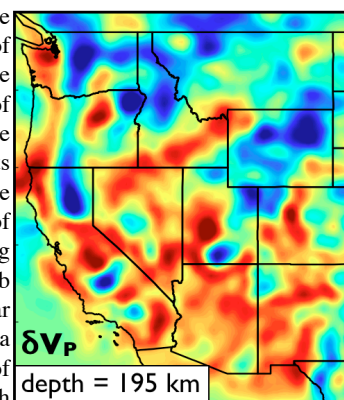
¹University of Oregon, Eugene Oregon, USA 97403
(*correspondence: genehumphreys@gmail.com)

²University of New Mexico, Albuquerque NM, USA 87131

³Rice University, Houston Texas, USA 77251

Strong seismic heterogeneity imaged across the western U.S. upper mantle implies the occurrence of segmented subduction, active upwelling associated with Yellowstone, and small-scale convection across most of the area. When put in geologic context, we

recognize three types of small-scale convective downwelling. (1) Most of the fast structures are thought to be fragments of Farallon lithosphere emplaced at the base of North America during Laramide-age flat-slab subduction. Their tabular form suggests a delamination style of detachment from North



America. Associated magmas probably involves melting of ascending asthenosphere, hydrated basal North America, and Farallon ocean crust. (2) Another type of downwelling is most reasonably explained as a delamination-style detachment of North American lithosphere. An association with volcanism suggests basalt infiltration and eclogite loading of the delaminated lithosphere, i.e., thermochemical convection. (3) A third delamination type is inferred from the young uplift of granitic batholiths that have a geochemical signature for garnet-rich restites.

Examples include delaminations related to the Columbia River Basalt eruptions (involving delamination types 1 and 3, in conjunction with arrival of the Yellowstone plume) and the ignimbrite flareup (type 1), and uplift of the southern Sierra Nevada (3 and maybe 1), Colorado Plateau margin (2) and the Transverse Ranges (1). In many cases, magmatism apparently is an integral part of delamination; it both enables mechanical detachment through the emplacement of lower crustal sills, and caused asthenosphere return flow. A general consequence of these delaminations is a remaking continent by driving mass exchange between continent and underlying mantle, and internal segregation of the continent.

Evolution of chemical and physical properties of mixed arc magmas

MADELEINE C S HUMPHREYS¹, MARIE EDMONDS²,
THOMAS CHRISTOPHER³ AND RICHARD BROOKER⁴

¹Department of Earth Sciences, University of Oxford, South Parks Road, Oxford, OX1 3AN, UK
(madeleine.humphreys@earth.ox.ac.uk)

²Department of Earth Sciences, University of Cambridge, Downing Street, Cambridge, CB2 3EQ, UK

³Montserrat Volcano Observatory, Flemmings, Montserrat, West Indies

⁴Department of Earth Sciences, University of Bristol, Wills Memorial Building, Queen's Road, Bristol, BS8 1RJ, UK

Many intermediate arc magmas arise as a result of mingling between mafic and silicic melts that may be genetically unrelated. Recharge involving mafic melts is commonly cited as the trigger for new or renewed eruptive episodes, and a mechanism for rejuvenating stalled silicic crystal mush in the mid-crust. This process has a profound effect on the chemical and physical properties of the whole volcanic system. Using geochemical microanalysis and textural observations, it is possible to identify distinct compositions of minerals and glass that reflect different elements of the volcanic system. There is abundant evidence of physical and chemical contamination of the silicic magma on the micron-scale during mingling, and entrainment of deeper plutonic material. Disequilibrium reaction textures and overgrowth rims indicate direct contact between crystals from the silicic magma and the mafic melt, including sieved plagioclase, coarse breakdown textures in hornblende and clinopyroxene overgrowth on quartz and orthopyroxene. Anomalous glass compositions overlap with the residual glass of some mafic enclaves, indicating mingling between mafic and silicic melts. Microlite/ microphenocryst compositions overlap with mafic enclave mineral compositions, suggesting incorporation of mafic crystals into the host magma.

During ascent, the mingled magma experiences volatile exsolution and decompression crystallisation. We discuss and present evidence for the chemical variations that take place in the magma during ascent through the volcanic system, including the controls on changing oxidation state due to degassing and crystallisation, and evidence for the exsolution of a dense brine. We also draw together constraints on the timescales of these processes and consider their effects on the physical properties of the evolving magma. We discuss the implications of these findings for our understanding of andesite petrogenesis and eruption triggering and style.

Clinopyroxene and its relationship to rapidly erupted, carbonate-rich magmas in Calatrava, Spain

EMMA R. HUMPHREYS-WILLIAMS*^{1,2} TERESA JEFFRIES¹
AND KEN BAILEY†²

¹Earth Sciences, Natural History Museum London, SW7 5BD
(correspondance: e.williams@nhm.ac.uk)

²Earth Sciences, University of Bristol, Bristol, BS8 1RJ

†deceased

Rapidly erupted alkaline, ultramafic magmas such as those occurring in intraplate settings offer a unique opportunity to understand lithosphere structure and rock petrogenesis. Such volcanism erupts rapidly from the mantle, entraining a dense load of xenolithic material forming up to 30% of the rock [1]. The discovery of abundant examples of carbonate-rich volcanism containing magmatic carbonate in association with ultramafic silicate glass [2], highlights the role of carbonate and carbon-rich fluids in the formation of these magmas. However, a comprehensive understanding of the petrogenesis of such magmas remains elusive and petrological observations of variably resorbed, originally euhedral crystals are just one indication of a complex magmatic history.

Clinopyroxenes from a rapidly-erupted carbonatitic tuff in Calatrava, Spain have been analysed for their major and trace element composition. Clinopyroxenes are ideal candidates for understanding melting processes as they host a significant quantity of trace elements and the partitioning behaviour is relatively well characterised. The tuff has a wide textural range of clinopyroxene which occurs alongside calcium-carbonate within fresh melilititic silicate glass. Within glassy lapilli, carbonate occurs as globules and also as a matrix between lapilli fragments.

Clinopyroxenes have Mg# 0.68-0.80 and span a wide range of major element compositions. Clinopyroxenes do not overlap with the major element composition of mantle xenolith-derived clinopyroxenes erupted in similar volcanism in Calatrava, suggesting that no clinopyroxene originates from the disaggregation of mantle xenoliths.

Melts calculated to be in equilibrium with a range of clinopyroxenes illustrate the variation of the melt composition before and up to eruption. Our data suggest that large 'xenocrystic' clinopyroxenes relate to the early stages of magma formation. Resorption of once euhedral crystals can be attributed to disequilibrium resulting from changes in composition of the melt prior to eruption.

[1] Humphreys, et. al, (2010), *Geology* **38** (10), 911-914, [2] Bailey & Kearns (2012), *Min. mag.* **76**(2), 271-284.

The influence of urbanisation on forest soils: Comparing variability and mobility of potentially toxic elements and carbon sequestration between urban regions in Scotland and Bulgaria

ANDREW HURSTHOUSE^{1*}, VANYA DOICHINOVA² AND MIGLENA ZHIYANSKI²

¹School of Science, University of the West of Scotland, Paisley, PA1 2BE, UK (*andrew.hursthouse@uws.ac.uk)

²Forest Research Institute, Bulgarian Academy of Sciences, 132 "Kliment Ohridski" Blvd., 1756 Sofia, Bulgaria (doichinova@abv.bg; zhiyanski@abv.bg)

The process of urbanization creates unique urban ecosystems and urbanized soils. Due to high pollution load and the dynamic effect of climate change in the urban environment, green infrastructure comes under increasing stress. The great potential is for urban forest areas to offer a significant contribution in mitigation of CO₂ at a small scale, but little is known about the interaction with urban soils, increasingly recognized as a sink for inputs of urban pollutants. Our study looked at a number of forest soil sites along rural-urban gradients in Glasgow, Scotland and the Sofia Region, Bulgaria.

We compared soil properties with carbon stocks, nutrient availability and potentially toxic element loads. In urban soils of Sofia carbon stocks varied between 80 - 125 tC ha⁻¹ and for Glasgow 76 - 120 tC ha⁻¹, with non-urbanized control sites: 53 - 103 tC ha⁻¹ for the Sofia region. The tree carbon stock, was higher in non-urbanized sites, because of higher tree density in these plots. The results for aboveground biomass carbon stock in urban sites varied between 34.5 - 61.7 tC.ha⁻¹ for Sofia and 45.2 - 60.8 tC.ha⁻¹ for Glasgow and in Non-Urban sites: 33.9 - 67.5 tC.ha⁻¹, and 57.3 tC.ha⁻¹ respectively.

We obtained strong correlations between mobile forms of Cu, Zn, Pb, Cd in urban soils and a number of soil parameters (pH, CEC and texture). The mobility related to soil pH (and OM for Cu) agreeing with other work in the cities. The most mobile soil fraction was found for Cd (33%). The assessment of health status of oaks tree vegetation based on indices defoliation of crown and changes in color do not correlate significantly with the bioavailable concentration of PTEs in the soils. Carbon sequestration relates strongly to management activity and the influence of PTE content is obscured.

Redox and nutrient cycling in a late Mesoproterozoic sea

K.F. HUSBAND^{1,2*}, S.W. POULTON¹, R. GUILBAUD¹, A.D. ROONEY³ AND D. SELBY⁴

¹Sch. Earth & Env., Uni. of Leeds, Leeds, LS2 9JT, UK (*correspondence: K.Husband@leeds.ac.uk)

²Sch. Civil Eng. & Geosci., Newcastle Uni., Newcastle upon Tyne, NE1 7RU, UK

³Dept. Earth & Planet. Sci., Harvard Uni., Cambridge MA 02138, USA

⁴Dept. Earth Sci., Uni. of Durham, Durham, DH1 3LE, UK

A growing body of evidence suggests that, during the so-called 'boring billion' (~1.8-0.8 Ga), the global ocean was characterised by widespread euxinia along productive continental margins, with deeper waters that remained ferruginous. In detail, however, evidence for euxinic conditions in continental margin settings is extremely scarce in the early Neoproterozoic (~1.0-0.75 Ga), with most evidence instead suggesting an expansion of ferruginous conditions. In addition, little is known about the detailed nature of ocean chemistry in the late Mesoproterozoic, prior to this apparent change in global ocean chemistry. Ocean redox conditions potentially exert a strong control on nutrient cycling, thus influencing organic carbon production and burial, and, in turn, environmental oxygen levels. However, the lack of detailed studies on late Mesoproterozoic successions means that little is known about redox-driven nutrient feedbacks at this time, and hence controls on environmental conditions towards the end of the 'boring billion' remain poorly understood.

Here, we present an integrated study of Fe-S-C systematics and P cycling in the 1.1 Ga Taoudeni Basin of Mauritania. Earlier in the succession, we find that euxinia was prevalent in mid-depth waters, with deeper waters being ferruginous. However, there is less evidence for euxinia further up the succession and instead ferruginous conditions became more widespread. Ferruginous conditions throughout the succession are commonly characterized by enhanced organic C burial, suggesting that the development of euxinic conditions was not simply driven by organic C availability. To provide further insight, we utilize P speciation and S isotope data, which together shed new light on environmental conditions during this crucial interval that marks the final stages of several hundred million years of apparent environmental stasis.

High throughput analysis of mining samples by LA-ICP-MS

ROBERT W HUTCHINSON¹ DAVID PRICE²
AND ALEX CHRIST³

¹New Wave Research (a division of ESI), 8 Avro Court, Ermine Business Park, Huntingdon, PE29 6XS, United Kingdom. (rhutchinson@esi.com)

²PerkinElmer LAS (UK) Ltd, Chalfont Road, Seer Green, Beaconsfield, Bucks HP9 2FX, UK. (david.price@perkinelmer.com).

³Bureau Veritas Australia Pty Ltd. 58 Sorbonne Cres Canning Vale Perth WA 6155. (alex.christ@au.bureauveritas.com)

Mining operations rely on fast turnaround of precise and accurate analysis of rock and soil sampled from the field. A large mine can supply up to 100,000 samples to the analytical services per month, each requiring extensive sample preparation for analysis by XRF for composition analysis and solution analysis-ICP-MS for trace elements. The latter is typically performed by sample digestion in *aqua regia*, which has cost, health and safety and disposal considerations.

Here we describe methodology and results for the trace element analysis of XRF discs by laser ablation ICP-MS. This methodology removes the solution digestion sample preparation and its associated costs and risks. Furthermore, the sample type is highly stable long-term and can be recalled for repeat analysis without the need for specialist storage.

Overall, the LA-ICP-MS methodology represents improvement in cost, manpower, throughput and risk when compared to solution ICP-MS analysis.

Indirect dating of the Guadalupian-Lopingian Boundary

M.H. HUYSKENS*, Y. AMELIN¹, R.S. NICOLL^{1,2}
AND I. METCALFE³

¹Research School of Earth Sciences, The Australian National University, 142 Mills Road, 0200 Acton, ACT, Australia. (*magda.huyskens@anu.edu.au)

²Geoscience Australia, Canberra, Australia.

³Earth Sciences, University of New England, Australia.

The Guadalupian-Lopingian Boundary (GLB) is defined by the first occurrence of the conodont species *Clarkina postbitteri postbitteri* and currently interpreted to be 259.8±0.4 Ma [1]. The Global Stratotype Section and Point (GSSP) for this boundary at Penglaitan, south China has detailed fossil and chemostratigraphy information available, but unfortunately neither magnetostratigraphy nor geochronological studies were successful at the GSSP section.

We have correlated the GSSP section to a terrestrial sequence in the southern Sydney Basin, Australia using C-isotope stratigraphy and present high-precision U-Pb geochronology for five samples covering the Wilton Formation to the Erins Vale Formation tied to C-isotopic values [2] of the drill core Bunnerong DDH 1. Based on C-isotope stratigraphy the GLB in the southern Sydney Basin is interpreted to correlate with the boundary between the Thirroul Sandstone and the Woonona Coal. Based on two bracketing U-Pb ages (256.47±0.14 Ma and 258.04±0.54 Ma, 51 m above and 65 m below the GLB respectively) the age of the GLB is interpreted to be ~ 257.5 Ma.

These new dates can be used to constrain the age of the mid-Capitanian mass extinction. This extinction was previously interpreted to coincide with the GLB, but more recent work suggests a prolonged extinction episode in the mid-Capitanian with different biota becoming extinct at different levels. There is no current consensus on placement of the mass extinction. One of the suggestions is that it occurred at the base of the *Jinogondolella granti* zone coinciding with a major sea-level regression [3]. This regression is recorded in the southern Sydney Basin by an erosive contact between the Erins Vale Formation and the Thirroul Sandstone. This regression is dated at ~ 258 Ma.

[1] Gradstein *et al* (2012) GTS 2012, pp. 1176. [2] Birgenheier *et al* (2010) *P³* **286**, 178-193. [3] Wignall *et al* (2009) *Journal of the Geological Society, London* **166**, 655-666.

Assessment of accuracy and precision for IRMS by standard material

JONG-YEON HWANG^{1*}, BO-KYONG KIM, WON-SEOK LEE,
MIN-SEOB KIM AND JIN-SEOK HAN

¹Environmental Measurement & Analysis center, NIER,
Environmental Research complex, Gyeongseo-dong, Seo-
gu, Incheon Metropolitan City, 404-708,
KOREA. (*correspondence : hjy6711@korea.kr)

The setup of optimum condition for IRMS

As a result of this study, carbon isotope composition was very precise and accurate in a narrow range as well as a wide range of sample weight. The measured $\delta^{13}\text{C}$ value that was within the certified value $\pm 2\sigma$ had the minimum carbon contents in which EMA-P1 and EMA-P2 is 102.107 μg and 116.879 μg , respectively. Although nitrogen and sulfur isotope composition was less precise and accurate than carbon, the nitrogen content (18.650 μg) and sulfur content (27.839 μg) already had been within the certified value $\pm 2\sigma$. The variation of isotope composition was also investigated by the fractionation factor $\epsilon_{\text{applied}}$ that would explain the stability for $\delta^{13}\text{C}$, $\delta^{15}\text{N}$ and $\delta^{34}\text{S}$ value. We suggest that carbon, nitrogen and sulfur isotope composition need to be determined by considering several factors; accuracy of $\delta^{13}\text{C}$ value and precision of $\delta^{13}\text{C}$ value, peak height ratio and fractionation factor $\epsilon_{\text{applied}}$.

Discussion of Results

Study on stable isotopes in contaminants is a relatively new concept with high potential of transforming a monitoring-based research paradigm into a more advanced one. In this study, a brand-new stable isotope analyzer was used and accuracy and precision were evaluated using carbon and nitrogen reference materials to establish the optimal analytical condition. And also, we can conclude that the analysis of stable isotopes in environment using a stable isotope analyzer is a promising new method for identifying the sources of contaminants.

[1] Jong-Yeon Hwang *et al* (2012) **NIER-RP2012-143**, pp.1-52. [2] Bo-Kyong Kim *et al* (2012) *J. of the Korean society for Environmental Analysis*, **15**(4), pp. 245-255. [3] Z. SHARP (2007) *Principles of Stable Isotope Geochemistry*.

Volcanic acid-sulfate analogs for early Mars

BRIAN HYNEK^{1,2*}, THOMAS MCCOLLOM¹,
KARYN ROGERS³ AND EMMA MARCUCCI^{1,2}

¹Lab. for Atmospheric and Space Physics, University of
Colorado, 3665 Discovery DR, Boulder, CO 80303 USA
²Department of Geological Sciences, University of Colorado,
399 UCB, Boulder, CO 80309 USA
³Geophysical Laboratory, Carnegie Institution of Washington,
Washington, DC 20015 USA

Owing to Mars' prolonged history of volcanism, high heat flow, and copious surface water, we assume abundant hydrothermal systems persisted for significant time periods. Life on Earth may have originated in a similar setting and assessment of putative hydrothermal systems on Mars is paramount to assessing the planet's geochemical history and astrobiological potential. To this end, we have been assessing Earth and putative Mars hydrothermal systems through fieldwork, lab experiments, geochemical modeling, and remote sensing. Fieldwork at active basaltic volcanoes in Central America and Hawaii was used to document geochemical pathways of acid-sulfate alteration and resultant mineralogy. These results were correlated with environmental parameters (T, pH, fluid:rock ratio) to define the controls on alteration pathways. We find that extremely acidic pH and high temperature fumaroles rapidly alter the parent lithology into S, amorphous Si, with occasional crusts of gypsum. Moderately acidic (pH of about 4) fumaroles lead to abundant gypsum, natroalunite, Si, and Al-smectites. Mildly acidic and cooler fumaroles produce calcite and gypsum. Correlated laboratory experiments and geochemical modeling on whole basalts and individual mineral components have further defined the controls of acid sulfate alteration over a broad range of conditions and we found that high fluid:rock and temperatures lead to rapid dissolution of primary minerals and the liberated cations lead to a range of sulfates, amorphous Si, and hematite concretions. Remote sensing data from Mars reveals discrete locales of minerals indicative of acid-sulfate alteration and some were undoubtedly hydrothermal in origin. Our terrestrial studies provide a conceptual framework for interpreting the paleoconditions of ancient martian hydrothermal systems, where we are able to use the alteration mineralogy to infer the likely conditions of formation. Further, we have characterized the microbiology within active terrestrial volcanoes. While the hottest and lowest pH sites have minimal biomass, the moderately acidic and cooler fumaroles have diverse endolithic communities of photo- and heterotrophic aerobes and anaerobes.

High rates of carbon oxidation through dissimilatory manganese reduction in sediment of Ulleung Basin in the East Sea

JUNG-HO HYUN¹, SUNG-HAN KIM¹, JIN-SOOK MOK¹,
HYE-YOUN CHO¹, VERONA VANDIEKEN²
AND BO THAMDRUP³

¹Hanyang University, Marine Sciences and Convergent
Technology, Korea; hyunjh@hanyang.ac.kr

²University of Oldenburg, Germany; verona.vandiek@uni-
oldenburg.de

³University of Southern Denmark; (bot@biology.sdu.dk).

Dissimilatory iron reduction plays an important role in the oxidation of organic carbon in continental sediments, whereas large contributions from dissimilatory manganese reduction are only known from a few locations characterized by a very high Mn content. There are very few experimental studies of these processes in deep sea sediments. As a contribution to filling this gap and obtaining a more detailed understanding of the regulation of the processes in marine sediments, we investigated experimentally the rates and relative importance of terminal electron acceptors in sediment from the slope and floor of the >2000 m deep Ulleung Basin in the East Sea. Our experiments also tested the assumptions behind the methods.

The contributions of Fe and Mn reduction were determined in anoxic incubations both indirectly by comparing total carbon oxidation rates from DIC production to the part of DIC production contributed by sulfate reduction, and directly from the accumulation of Fe(II) and Mn²⁺ over time, with corrections for reduction coupled to reoxidation of reduced sulfur species and for the adsorption of Mn²⁺. Rates obtained by the two methods agreed closely, which indicates that the stoichiometric assumptions behind the incubation approach are correct.

Dissimilatory Mn reduction accounted for ~50% of anaerobic carbon oxidation at the deep basin site, which contained more than 2.5 wt% Mn, while the process was insignificant at the slope site, which was not enriched in Mn. Here, sulfate reduction dominated with ~80% of anaerobic carbon oxidation. Both the diffusive O₂ uptake in intact cores and the depth-integrated DIC production from anoxic incubations demonstrated very high rates of carbon oxidation in these deep sediments.

Our results add the Ulleung Basin to the very small set of locations where dissimilatory Mn oxidation is important, and demonstrate that this deep basin is a hotspot of benthic mineralization, which can be related to the oceanographic characteristics of the East Sea.

Impact of Fe speciation in the aquifer sediments on ferric (hydr)oxide precipitation at the Changwon research site, Korea

S. P. HYUN*, H. S. MOON, P. YOON, K. HA
AND B.-G. CHAE

Korea Institute of Geoscience and Mineral Resources
(KIGAM), Daejeon 305-350, Korea (*Correspondence:
sphyun@kigam.re.kr)

Ferric (hydr)oxide precipitation can control the mobility of contaminants and redox conditions in an aquifer. The impact of Fe speciation on the kinetics of ferric (hydr)oxide precipitation at the sediment-groundwater interfaces was studied using the sediment samples collected from the KIGAM research site in Changwon, Korea. The research site is on unconsolidated, Quaternary floodplain deposits by the Nakdong River. Sets of sediment samples were collected at varying depths and locations within the research site. The sediment samples were wet-sieved to the sand, silt, and clay fraction, and further used for the Fe speciation characterization. Different pools of Fe present in the sediment samples were selectively extracted using ferrozine, ammonium oxalate, dithionite-citrate-bicarbonate, and hydrochloric acid. Chemical and mineralogical characterization of the sediment samples were performed using X-ray fluorescence, X-ray diffraction, and electron microscopy. Also, Fe distribution between the sediment and groundwater was modeled using the field measured groundwater chemistry data and Fe speciation results.

The results indicate alternating redox conditions along the depth of the aquifer. The alternating redox pattern suggests heterogeneities in the organic matter content and mineral composition within the aquifer, and seasonal and spatial variations in the groundwater table affected by the river water level changes. The different extraction methods resulted in independently varying or even apparently conflicting trends as functions of depth, suggesting the different quantities of Fe in the different pools. The field measured dissolved Fe(II) concentration in groundwater was up to a hundred mg/L with dissolved oxygen between 0.1 to 4 mg/L, depending on the depth and spatial location. This study suggests the potential of ferric (hydr)oxide precipitation upon the infiltration of surface water high in dissolved oxygen, to act as a sink and source of contaminants such as heavy metals and radionuclides, depending on the prevailing geochemical conditions within the aquifer. The results of this study will be used as background information in studying the kinetics of ferric (hydr)oxide precipitation.

Toward a unified method for the quantification of volatiles in magmas via FTIR

KAYLA IACOVINO^{1*}, NIAL PETERS¹
AND CLIVE OPPENHEIMER¹

¹Dept. Of Geography, University of Cambridge, Cambridge UK (*correspondance: ki247@cam.ac.uk)

Fourier Transform Infrared (FTIR) spectroscopy is a common tool used to quantify dissolved volatiles in melts. The use of this method for the analysis of melt inclusions in particular is crucial to understanding a multitude of volcanic and geochemical processes such as magma storage, crystallization, and degassing. Despite the ubiquitous nature of this technique in the literature, standard methods for the retrieval of dissolved volatile concentrations from IR spectral data are poorly defined and often rely on hand-drawn or assumed straight-line-fit background curves that introduce significant error and variation within data sets. Propogated errors from differences in “acceptable” background curves for a single IR spectrum drawn by a set of individuals (or even by a single individual at different times) can equate to variation in final retrieved volatile concentrations on the order of wt%. In an effort to reconcile this problem, we are developing a simple software package capable of retrieving dissolved volatile concentrations (i.e. H₂O, OH, CO₂, and CO₃) from FTIR spectra based on a set of standard peak fitting algorithms. By using spectroscopic first principles to define a volatile-free background spectra, peak heights, and ultimately volatile concentrations, we can eliminate variations between individual researchers that stem from the subjectivity in choosing a “good” background spectrum. In addition, the automation of this procedure by computer eliminates internal variation within data sets and expedites the process of analyzing large data sets.

Our software tool, currently in the early stages of development, will allow for the creation of volatile-free background spectra based on a curve fit to the user-input FTIR data. Subsequently, a calculation of peak heights and ultimately volatile concentrations (based on the Beer-Lambert law, given sample thickness, density, and absorption coefficient) can be performed. Our goal is to make the tool as transparent as possible in order that the user has more control over and understanding of the data transformations being performed. The program, written in Python and released under the Gnu Public License (GPLv3), is currently in alpha. We are now seeking input on the overall design, desired features, and back-end theory/computation.

REE content of phosphogypsum from Romania

AURORA MĂRUȚA IANCU^{1*}, DELIA-GEORGETA DUMITRAȘ¹, ESSAÏD BILAL², STEFAN MARINCEA¹, CRISTINA GHINET¹, CĂLIN NICOLAE¹ AND MARIA-ANGELA ANASON¹

Geological Institute of Romania, 1, Caransebes Str., Bucharest, Romania, RO-012271.
(*correspondence: aurash83@yahoo.com)

Centre SPIN, Ecole Nationale Supérieure des Mines de Saint-Etienne, 158, Cours Fauriel, F-42023 Saint-Etienne Cedex 2, France (bilal@emse.fr)

Phosphogypsum is a technogenic product remaining after the extraction of phosphoric acid from raw phosphate, mainly apatite. The original phosphate rock contains large amounts of REE, mainly replacing Ca from apatite or included in other phosphate structures. About 70% of the REE contents are stacked in the phosphogypsum obtained after sulfuric attack of the raw phosphate and much less in the case of hydrochloric attack. In Romania, the sulfuric attack through the hemidihydrate (HDH) or dihydrate (DH) procedures was extensively used to obtain phosphoric acid at Turnu Măgurele (TM), Valea Călugărească (VC), Năvodari (N) and Bacău (B).

Inductively coupled plasma - atomic emission spectrometry (ICP-AES) analyses performed on selected samples of phosphogypsum from the four deposits showed that the contents in the main REE (cerium, erbium, neodymium, thorium, ytterbium) are specific for the phosphogypsum issued from the processing of sedimentary raw phosphates. The contents are given in the table.

Occ.	Ce (ppm)	Er (ppm)	La (ppm)	Nd (ppm)	Th (ppm)	Yb (ppm)
TM	29,1 - 663,1	0,9 - 11,7	22,7 - 469,0	21,1 - 260,5	0,3 - 20,8	1,1 - 6,8
VC	30,2 - 454,2	0,8 - 7,3	35,7 - 322,5	22,3 - 188,2	0,0 - 12,8	1,6 - 5,0
N	3,9 - 165,0	1,8 - 7,7	14,5 - 135,6	3,8 - 90,6	0,8 - 6,5	1,8 - 6,1
B	19,3 - 174,8	13,1 - 18,8	36,2 - 134,2	24,5 - 104,5	1,7 - 5,2	1,9 - 6,6

Observation of geoneutrinos in Borexino

A. IANNI^{1*} AND Y. SUVOROV²

¹*correspondance: aldo.ianni@lngs.infn.it

²yury.suvorov@lngs.infn.it

Geoneutrinos are electron anti-neutrinos produced by long-lived radioactive isotopes in the earth's crust and mantle. Geoneutrinos can be detected in kton scale organic liquid scintillator detectors located in underground laboratories. The detection reaction being the inverse-beta decay which has a prompt and delayed signal. These signals are correlated in space and time. The anti-neutrino interacts with a proton from an hydrogen atom and will make a positron plus a neutron. The positron will promptly annihilate; the neutron will thermalize and be captured on hydrogen in some 250 μ s. In spite of the strong signature geoneutrino can only be detected in massive low background set-ups designed for low energy (1 MeV) neutrinos. Borexino at the Gran Sasso underground laboratory in Italy has been in operation since 2007 to search for sub-MeV solar neutrinos. The sun is a huge source of electron neutrinos. Observation of solar neutrinos provides a unique tool to study the interior of the sun. At present experimental studies of geoneutrinos are carried out with KamLAND at the Kamioka mine in Japan and with Borexino at Gran Sasso. The first attempt of a geoneutrino measurement was done in KamLAND in 2005. Only in 2010 and 2011 both Borexino and KamLAND observed at more the 4 σ C.L. a signal from geoneutrinos. The search of geoneutrinos likewise the one of solar neutrinos for the sun provides a unique tool to probe the interior of the earth. Uranium and thorium from the crust and the mantle make the geoneutrino flux on surface. The energy spectrum of the detected geoneutrinos depends on the abundance of uranium and thorium and on the different beta decays in the two radioactive chains. A spectroscopy determination of the geoneutrino signal can be done. This has been recently shown by Borexino. By means of this analysis the ultimate goal of the geoneutrino search will be the determination of the uranium and thorium content in the mantle. For this purpose a combined analysis of more than one experiment results will be necessary. In this talk we will review the present status of geoneutrino research. We elaborate on the recent results from Borexino and KamLAND. The experimental difficulties and background sources will be discussed.

Influence of osteopontin on apatite formation

C. J. S. IBSEN¹, J. OLSEN¹, D. GEBAUER², H. BIRKEDAL¹

¹iNANO & Department of Chemistry, Aarhus University, Aarhus 8000, Denmark (*correspondence: hbirkedal@chem.au.dk)

²Department of Chemistry, University of Konstanz, Konstanz 78457, Germany

The classical crystallization theories have been shown to be incomplete, particularly in the field biomineralization where non-classical crystallization pathways are widespread [1], including prenucleation clusters in solution as known in CaCO₃ and calcium phosphates [2-4]. The picture is even more complicated when additives are also considered. For calcium phosphate biomineralization in vertebrates, phosphate-rich proteins are known to be important. Herein we show how one of these, the calcium binding phosphoprotein osteopontin, drastically modifies the prenucleation behavior during calcium phosphate formation.

The formation of calcium phosphate was investigated by constant pH (8.0) titration of dilute calcium chloride into a sodium phosphate solution [2]. The calcium activity was measured *in situ* using a calcium sensitive electrode. In the osteopontin-free case, the calcium activity is lower than the added amount reflecting the formation of a bound prenucleation state [2-4]. As the supersaturation increases, an amorphous intermediate is formed which transforms into crystalline apatite upon continued titration. When introducing osteopontin an additional intermediate is observed that remains in dispersion. Both intermediates were stabilized by osteopontin in a dose dependent manner. However, osteopontin did not significantly affect the prenucleation behaviour prior to the formation of the first intermediate.

The initial amorphous phase was HPO₄²⁻-rich. As more calcium was added, the stoichiometry gradually changed towards stoichiometric amorphous calcium phosphate (ACP), with a distinct increase in the PO₄³⁻/HPO₄²⁻ ratio at the transition from intermediate 1 to 2. The final apatitic phase was also found to be calcium deficient.

For carbonates, multiple amorphous forms are known, which might influence what polymorph is formed [2]. The observed additive-stabilization of ACP could help unravel the role of additives in biomineral formation, including polymorph selection.

[1] Gower (2008) *Chem. Rev.* **108**, 4551-4627. [2] Gebauer *et al.* (2008) *Science* **322**, 1819-1822. [3] Dey *et al.* (2010) *Nat. Mater.* **9**, 1010-1014. [4] Habraken *et al.* (2013) *Nat Commun.* **4**, 1507

Titanite from the Fish Canyon Tuff: Searching for clues to pre-eruptive magma chamber processes

F. IDDON¹, G. W. MCLEOD^{1*} AND T. J. DEMPSTER²

¹Earth & Environment, University of Leeds, Leeds, LS2 9JT, UK (*correspondance: g.w.mcleod@leeds.ac.uk)

²Geographical and Earth Sciences, University of Glasgow, G12 8QQ, UK (tim.dempster@ges.gla.ac.uk)

Magma-mixing is thought to be an important mechanism for initiating large-scale pyroclastic eruptions, and as such, may play a key role in the petrogenetic history of such eruptions. However, the fragmental and often glassy nature of pyroclastic deposits, and to some extent the homogenisation associated with emplacement at the surface, may act to mask the details of plutonic level petrogenesis. The deposits rarely display visible evidence of pre-eruptive mixing, and unless there is textural or geochemical alteration of phenocrysts prior to eruption, then evidence of mixing at depth may be very sparse.

Titanite is a geochemically robust accessory mineral that has the ability to serve as a sink for trace elements; the REE and HFSE in particular. Recently, it has been shown that compositional zoning of titanite from plutonic rocks can preserve a record of the changing conditions within a magma chamber, including evidence of magma-mixing processes [1].

This study aims to assess the ability of titanite found in volcanic rocks to preserve evidence of pre-eruptive petrogenetic processes, by conducting a coupled micro-textural and geochemical analysis of titanite from the Fish Canyon Tuff, Colorado, USA. It is thought that thermal rejuvenation of the silicic magma, caused by intrusion of mafic magma at the base of the magma chamber just prior to eruption of the tuff, served as a trigger for eruption [2]. Such an input of mafic magma could induce compositional, temperature, and oxygen fugacity changes in the chamber, to which titanite could respond

Preliminary results, from this ongoing study, show titanite to have compositional zoning with cores preferentially enriched in heavy REE and rims preferentially enriched in light REE; a reflection of the changing composition of the melt. Dissolution surfaces with inclusions of ilmenite are common, and provide evidence of changing titanite/ilmenite stability; interpreted here to reflect changes in oxygen fugacity brought about by replenishment of the chamber with fresh mafic magma.

[1] McLeod *et al.* (2011) *Journal of Petrology* **52**, 55-82. [2] Bachmann & Bergantz (2003) *Geology* **31**, 789-792.

Molecular and Micro Element Remote Analysis of Leaves of the Green Plants

A. IGLAKOVA¹, A. KLIMKIN¹, V. PROKOPIEV²

¹Institute of Atmospheric Optics SB RAS, Tomsk, Russia;

²Institute of High Current Electronics SB RAS, Tomsk, Russia

Condition of the vegetative ground cover is an important determinant of environmental health. The global scale of this object requires using distant, primarily optical research techniques [1].

In particular, this may be done by measuring the fluorescence spectra and laser plasma emission during leaves surfaces ablation, which allows drawing certain conclusions about the state of photosynthetic apparatus and plant vegetation conditions [2].

This study was carried out by way of remote and laboratory tests, focused on research of fluorescence spectra in photosynthetic apparatus and plasma of green plants optical-induced breakdown under femtosecond laser radiation. Radiation wavelength of 650 ÷ 950 nm, pulse energy up to 10 mJ, length 50 ÷ 100 fs [3].

Chlorophyll fluorescence and absorption bands in the light-collecting antenna as well as the leaf reaction center with the range of 660 ÷ 800 nm were measured in the radiation spectra. The researched parameters helped to evaluate the current condition of plants photosynthetic apparatus.

Measurements of leaves micro element composition allow finding possible reasons which modify this condition.

Spectra of plasma emission from plant leaves located at 10 meter distance revealed the presence of sensitive spectral lines of atoms and ions of carbon, magnesium, iron, calcium, calcium, and copper. Lines of OH, Swan (C₂), and Cyanogen (CN) were also observed in these spectra.

[1] Ageev B.G., *et al.* // Atmospheric and Oceanic Optics. 2007. **V.20**, No.01. P. 82-86. [2] Krivonosenko A.V., *et al.* // Atmospheric and Oceanic Optics. 2012. **V.25**, No.03. P. 268-272. [3] Afonosenko A.V., *et al.* // Atmospheric and Oceanic Optics. 2012. **V.25**, No.03. P. 237-243.

Veined quartz of the Urals: Structure, mineralogy

M.A. IGUMENTSEVA¹, V.N. ANFILOGOV²

¹Miass, Chelyabinsk region, Institute of Mineralogy,
maria@mineralogy.ru

²Miass, Chelyabinsk region, Institute of Mineralogy,
anfilogov@mineralogy.ru

There are three major groups of the Ural quartz deposits: the Subpolar Urals group, the Middle Urals group and the South Urals one. The Subpolar group is represented by the typical hydrothermal veined deposits. Zhelannoe - one of the big Subpolar quartz deposit is described. It is located in monomineralic quartz sandstone. The quartz vein may be to 100 meters thick. Rutile, tourmaline, zircon and sericite are the major accessory minerals. The chief deleterious constituent in quartz is water, which is located in gas-liquid inclusions. The effective method for H₂O elimination is described. High quality quartz glass may be produced after primary quartz enriching.

The Middle Urals is represented by two giant quartz deposits: Gora Khrustal'naya and Svetlaya Rechka. Gora Khrustal'naya is represented by one quartz body which size is 380X140X160 m. The content of quartz in this body is 98.89%. Quartz deposit was formed on the big massive of quartz-diorite and granite contact. The main accessory minerals are microcline, muscovite, kaolin, hydrogoethite and pyrite. Quartz has giant crystalline structure. The specific enriching technology is described for this quartz deposit.

The South Ural group of quartz deposits is represented by quartz veins disposed in East part of the Ufaleisky gneiss-migmatite complex. Length of quartz vein area is 50 km. There are more than 3000 quartz veins on this area. Granulated quartz is prevalent for this group of deposits. Field spars, micas, rutile, sphene, ilmenite and carbonates are the main accessory minerals. Concentration of impurities in granulated quartz is as the IOTA STD. There is standard technology of quartz enriching for these deposits.

One more type of quartz deposits associated with small Naily gold deposit is vein Tolstikha. It is situated 35 km north from Miass and localized at the contact of small gabbro pluton with the large Talovskii massif of serpentized dunites, peridotites, and pyroxenites. This is a new economic quartz object. To date, the gold deposit has been mined. The vein is 1000 m along the strike, up to 50 m wide, and is traced up to 450 m deep.

Biogeochemistry of the deep mud-volcano biosphere in the Kumano forearc basin of the Nankai Trough

AKIRA IJIRI^{1,2*}, FUMIO INAGAKI^{1,2}, YUSUKE KUBO³ AND EXPEDITIONS CK09-01 AND 906 SCIENTISTS

¹Submarine Resources Research Project, Japan Agency for Marine-Earth Science and Technology (JAMSTEC), Monobe B200, Nankoku, Kochi 783-8502, Japan.
(*correspondence: ijiri@jamstec.go.jp)

²Kochi Institute for Core Sample Research, JAMSTEC, Monobe B200, Nankoku, Kochi 783-8502, Japan.

³Center for Deep Earth Exploration (CDEX), JAMSTEC, Showa-machi 3173-25, Yokohama 236-0001, Japan.

Submarine mud-volcanoes are formed by the vertical intrusion of a lower density and deformable materials from deep realm to the seabed. The mud-volcanism transports deep-sourced fluids, elements and hydrocarbons to the seafloor, of which seepages support chemosynthetic benthic life, including microbial communities that mediate anaerobic oxidation of methane with sulfate reduction. However, biogeochemical and microbiological characteristics of the deep realm of submarine mud-volcano have remained largely unknown.

In 2009 and 2012, using the deep-sea drilling vessel *Chikyu*, we drilled one of the most active submarine mud-volcanoes in the Kumano forearc basin of the Nankai Trough, off the Kii Peninsula of Japan, down to 200 meters from the summit (33°67.581N, 136°56.8085E: 1,986.7 m in water depth). Cell count and molecular analysis indicate the presence of relatively small microbial communities (less than 10⁵ cells/cm³) throughout the cored depth. Carbon isotopic compositions of bicarbonate and acetate in the pore water were found to be highly enriched in ¹³C. High concentrations of hydrogen were also observed, indicating a thermodynamically preferential condition for microbial acetogenesis via CO₂ reduction (i.e., homo-acetogenesis) rather. Radiotracer incubation experiments showed that activities of homo-acetogenesis were 2-3 orders of magnitude higher than those of homo- and acetoclastic methanogenesis.

Consequently, our accumulative biogeochemical and microbiological data indicate that the deep biosphere in the submarine mud-volcano of the Nankai Trough accretionary wedge is characterized by tectonic and sedimentological regimes, and hence different from the previously explored subseafloor biosphere in stratified sediment on the continental margins.

Exploration of the deep coalbed biosphere (IODP Expedition 337)

FUMIO INAGAKI^{1,2*}, KAI-UWE HINRICH³, YUSUKE KUBO⁴ AND IODP EXPEDITION 337 SCIENTISTS

¹Submarine Resources Research Project, Japan Agency for Marine-Earth Science and Technology (JAMSTEC), Monobe B200, Nankoku, Kochi 783-8502, Japan.

(*correspondence: inagaki@jamstec.go.jp)

²Kochi Institute for Core Sample Research, JAMSTEC, Monobe B200, Nankoku, Kochi 783-8502, Japan.

³MARUM and Department of Geosciences, University of Bremen, D-28359 Bremen, Germany.

⁴Center for Deep Earth Exploration (CDEX), JAMSTEC, Showa-machi 3173-25, Yokohama 236-0001, Japan.

Integrated Ocean Drilling Program (IODP) Expedition 337 was the first expedition dedicated to seafloor microbiology that used riser drilling technology [1]. IODP drill Site C0020 is located in a forearc basin formed by the subduction of the Pacific plate off the Shimokita Peninsula at a water depth of 1,180 m. Seismic profiles suggested the presence of deep, coal-bearing horizons at ~2 km seafloor depth. Our primary objectives during Expedition 337 were to study the relationship between the deep microbial biosphere and the seafloor coalbed and to explore the limits of life in horizons deeper than ever probed before by scientific ocean drilling. Among the questions that guided our research strategy was: Do deeply buried hydrocarbon reservoirs such as coalbeds act as geobiological reactors that sustain subsurface life by releasing nutrients and carbon substrates? To address this question and other objectives, we penetrated a 2,466 m deep sedimentary sequence with a series of coal layers at ~2 km below the seafloor. Hole C0020A is currently the deepest hole in the history of scientific ocean drilling [1].

During Expedition 337, over 1,700 microbiological and biogeochemical samples have successfully been obtained, for which rigorous contamination controls enable differentiation of contaminants from indigenous microbial communities. We conducted gas chemistry and isotopic analyses using a new mud-gas monitoring laboratory during riser-drilling operation [1], which provided the first indication of biologically mediated CO₂ reduction to methane at the 2 km-deep coalbed layers. The numbers of microbial cells are generally less than 10³ cells cm⁻³; however, increase of biomass was observed at the coal layers. Potential rates of organoclastic sulfate reduction are elevated in coalbed-bearing strata.

[1] Inagaki, Hinrichs, Kubo and Expedition 337 Scientists. *IODP Prel. Rept.*, 337 (2012).

Studies on the concentration of I-129 and I-131/I-129 ratios in soil samples collected from Fukushima Prefecture

NAOYA INAGAWA^{1*}, YASUYUKI MURAMATSU^{1*}, TAKESHI OHNO¹, CHIAKI TOYAMA¹, MUTUTO SATOU², HIROYUKI MATUZAKI³,

^{1*}Gakushuin University, Tokyo, 171-8588, Japan, naoy1121@yahoo.co.jp (presenting author),

yasuyuki.muramatsu@gakushuin.ac.jp (Correspondence),

²Fukushima Agricultural Technology Centre, Fukushima, 963-0531, Japan,

³University of Tokyo, Tokyo, 113-0032, Japan,

A large amount of I-131 was released from the Fukushima nuclear power plant accident. Radioiodine accumulates in thyroid gland and radiation risk would be enhanced. Therefore, it is necessary to obtain deposition date of I-131 in Fukushima Prefecture. Because of the short half-life of I-131 (8 days), it was below the detection limit after a few months. On the other hand, I-129 released simultaneously with I-131 still remained in soil, due to its long half-life of 1.57×10⁷ years. Therefore, I-129 can be used in the estimation of the I-131 deposition. For this purpose, it is essential to obtain I-131/I-129 ratios for calculating the amount of I-131 deposition from the I-129 analysis.

We used Fukushima soil samples in which I-131 had been measured. Iodine was separated by pyrohydrolysis and the evaporated iodine was collected in a trap solution. Stable iodine (I-127) concentrations in the trap solution were measured by ICP-MS. Solvent extraction was performed, and iodine was purified. Silver nitrate was added to precipitate AgI as a target for AMS and the I-129/I-127 ratios were measured by AMS at MALT, the University of Tokyo. For the estimation of I-129 concentrations (Bq/kg) the I-129/I-127 ratios and I-127 concentrations were used.

We obtained concentration (Bq/kg) of I-129 in soil and deposition density (Bq/m²) for more than 100 samples collected from different locations in Fukushima. It is interesting to note that a good correlation was found between the concentrations of I-131 and I-129 in soil samples. This finding suggests the possibility to estimate I-131 levels in soil at the early stage of the accident through the analysis of I-129. We obtained an average I-131/I-129 ratio as (2.1 ± 0.7) × 10⁷, although these are still uncertainties.

We also studied the concentrations of I-129 according to the soil depth. Compared to the depth profile of radiocesium, radioiodine was found to migrate faster into the deeper soil layer.

Mechanisms and kinetics of hydrogen exchange in olivine: A review from experimental and computational studies

J. INGRIN¹

¹UMR CNRS 8207, Univ. Lille 1, 59655 Villeneuve d'Ascq, France. jannick.ingrin@univ-lille1.fr

Mobility of hydrogen in mantle minerals and especially olivine has raised interest for its impact on mantle properties for many years. Nevertheless, the mechanisms and kinetics of hydrogen exchange in olivine remain largely misunderstood. We present here a review on the current knowledge of hydrogen kinetics in olivine, highlighted by recent results from experiments [1], [2] and numerical modelling [3]. In forsterite, laboratory's experiments, suggest that incorporation of hydrogen is controlled by the mobility of magnesium vacancies with a diffusion of hydrogen faster than exchange rate along direction [100] and slower in the two other directions. A common kinetics is generally observed for all OH bands, in apparent contradiction with their different origin as highlighted by numerical modelling. In olivine, diffusion of small-polarons is faster than diffusion of hydrogen. These results suggest that diffusion of polarons is anisotropic, with diffusion along [100] probably faster. Theoretical interpretations in connexion with electrical conductivity properties of olivine are discussed.

[1] Du Frane and Tyburczy (2012) *Geochem Geophys Geosyst* DOI:10.1029/2011GC003895. [2] Ingrin *et al.* (2013) *Phys Chem Mineral* DOI: 10.1007/s00269-013-0587-3. [3] Balan *et al.* (2011) *Eur J Mineral* DOI: 10.1127/0935-1221/2011/0023-2090.

The nitrogen isotope composition of volcanic fluids

S. INGUAGGIATO^{1,2}, Y. TARAN², T. FRIDRIKSSON³, S. CALIRO⁴

¹Istituto Nazionale di Vulcanologia, sezione di Palermo, Via Ugo La Malfa, 153 Palermo Italy (correspondence*: s.inguaggiato@pa.ingv.it)

²Instituto de Geofisica UNAM Coyacan Mexico D.F.04510 Mexico (taran@geofisica.unam.mx)

³Iceland GeoSurvey grensasvegur 9, 108 Reykjavik (Thrainn.Fridriksson@isor.is)

⁴Istituto Nazionale di Vulcanologia, Sezione di Napoli, via Diocleziano 328, 80124 Napoli, Italy

The main potential sources of nitrogen in volcanic and hydrothermal fluids are (i) the atmosphere; (ii) the upper mantle, including contribution from the subducting plates at the arc settings; (iii) the lower mantle at the hot spot settings; and (iv) the continental crust. The meaningful differences in $\delta^{15}\text{N}$ among the four main potential sources of nitrogen make it a useful tracer providing relevant information on the geodynamic environments in which volcanic fluids are generated.

Here we present a large and new data set of nitrogen isotope, $\text{N}_2/^{36}\text{Ar}$ and $^3\text{He}/^4\text{He}$ in fluids from more of 20 volcanic systems of different geodynamic setting including subduction zones (Mediterranean volcanoes, Mexico, Central and South America, Kamchatka); spreading zones (Socorro Island) and hotspots (Iceland, Azores, Galapagos). The goals of this work are i) to identify the relationships between the geodynamic setting and the isotopic composition of nitrogen in volcanic fluids; ii) to characterize the lower mantle (fluids with $^3\text{He}/^4\text{He}$ much higher than MORB values) in terms of $\delta^{15}\text{N}$ and iii) to understand the inhomogeneity of $\delta^{15}\text{N}$ with respect to the upper mantle.

The preliminary obtained results showed a wide range of $\delta^{15}\text{N}$ values, for estimated deep component (ASW corrected), from +7 to -16‰. The fluids related to subduction zones are characterized by values from -5‰ to +7‰, while the very light $\delta^{15}\text{N}$ (up to -16‰), were found in some gases of Iceland evidencing an important contribution from the lower mantle. We also discuss some problems related to possible effects of the nitrogen isotope fractionation ($\text{N}_2\text{-NH}_3$ system) and to the air correction procedure.

Experimental studies of catalytic properties of Iron II and III modified hydrothermal zeolites

E. IÑIGUEZ^{1*}, C. HEMMINGSSON¹ AND N.G. HOLM¹

¹(*correspondence: enrique.iniguez@geo.su.se)

Department of Geological Sciences, Stockholm University, Sweden

Zeolites are natural minerals formed by condensation of silica, alumina and some metallic hydroxides under hydrothermal systems [1], known by their porous structure and remarkable catalytic properties related to their high surface area, among others characteristics. Moreover, they present high affinity to absorb gases in their crystalline structure (i.e., H₂, N₂, CO₂), decreasing their activation energy barrier promoting recombination of between them [2]. They may occur in hydrothermal systems where constant emission of hydrogen as a product of weathering of the marine lithosphere can react with the dissolved gases in seawater [3]. Hydrothermal systems are considered present since the Hadean when the Earth's seas had formed. Therefore, the interaction of minerals could enhance the nitrogen reduction as well as its subsequent recombination into larger organics [4].

We present results of enhancement of the surface area, porosity properties, and acidity of two synthetic iron II and III zeolites and a feldspar - analcime, phillipsite, sanidine - in comparison to the native mineral. These metallic inclusions in the zeolite structure provoke an enlargement of the internal channels and cavities, as well as creating Brønsted acid sites responsible of a stronger adsorption of N₂ o CO₂.

Astrobiology, 1(2), 133–142. [1] Stonecipher (1976). *Chemical Geology*, 17, 307–318. [2] Stüeken *et al.* (2013). *Geobiology*, 11(2), 101–126. [3] Schoonen & Xu (2001). [4] Holm & Charlou (2001). *Earth and Planetary Science Letters*, 191(1-2), 1–8.

Balance of carbon in the system of geochemically linked mire landscapes

L. I. INISHEVA¹, M. A. SERGEEVA¹, N.V. JUDINA²

¹ - Tomsk State Pedagogical University, Tomsk

(*correspondence: agroecol@yandex.ru)

² Institute of chemistry of petroleum of the Siberian Branch of the Russian Academy of Science, Tomsk

According to V.I. Vernadskiy, migration of chemical elements in biosphere is carried out at direct participation of biogenic matter. The purpose of long-term researches (1996-2011 ye) was studying balance of carbon in bogs. As modeling object for researches it was accepted on territory of Vasyugan mire spurs (West Siberia).

Investigations have shown, that peat deposits of oligotrophic mires are biochemical active on all structure and the dynamic of biochemical processes is determined by hydrothermal conditions. Process of organic matter transformation in a peat deposit and formations CO₂ is determined by temperature of peatland. The greatest concentration of methane in a peat deposit is marked in damp years. As a result of this processes was confirmed with long-term dynamics of gas structure («peepers»-method), carbon balance oligotrophic mires on territory of Vasyugan mire spurs has the following kind.

Position on Landscapes mires	Receipt of carbon,	Allocation of carbon,	Deposition of carbon,
	gC/m ² *year		
Trans accumulative	267.3	97.6	169.7
Transit	235.2	66.9	168.3
Autonomy	158.0	65.2	92.8
Average	220.0	76.6	143.6

Table 1: Carbon balance of Landscapes mires.

In balance of carbon article of the charge determining carrying out of carbon with a drain of mire waters has essential value. According to our results, the average contents of carbon in mire waters, including carbon humid acids, changes from 53 up to 92,5 mg/l with limits 27,8-145 mg/l.

In a result the special kind of mire waters is formed. On the basis of the mathematical model carrying out of organic carbon by mire waters was designed 6,9 g m²/m¹. But, and in view of losses of carbon with a drain of mire waters, on oligotrophic mires deposition of carbon, and, hence, is observed peat formation process is progresses.

This study was supported by the Russian Foundation for Basic Research, project nos. 5.1161.2011.

Geochemistry of uranium and thorium in soils on the Ditrău Alkaline Massif, Eastern Carpathians, Romania

ADRIANA ION^{1,2*}

¹Geological Institute of Romania, Bucharest, RO-012271, Romania (*adi75riana@yahoo.com)

²"Al. I. Cuza" University, Iași, RO-700506, Romania

The rocks of the Ditrău Massif (syenite, nepheline syenite, hornblendite, diorite, monzonite, monzodiorite, granitoid) have naturally higher uranium and thorium contents, making the area ideal for the study of the distribution in soils of these elements. The soil types present in the investigated area, according to the Romanian Soil Taxonomic Classification are: lithosol, redzine, eutricambosol, districombosol, typical luvisol, albic luvisol, ethnic luvisol and aluviosols. Uranium and thorium were analyzed in 70 soil samples collected from an equable points net for all type of representative rocks. U and Th concentration were measured non-destructively using gamma-ray spectrometry with HPGe detector, and the uranium and thorium bearing minerals in soil samples were identified by XRD. The pH values were determined using a digital pH-meter.

U concentrations in the soil varies between 0.5 and 9.3 $\mu\text{g g}^{-1}$ (6.18-114.86 Bq/Kg) and Th concentrations from 2 to 51.3 $\mu\text{g g}^{-1}$ (8.12-208.28 Bq/Kg), whereas the Th/U ration in soil ranges from 1.87 to 19.52 $\mu\text{g g}^{-1}$. The pH varies from 3.6 to 7.3 and it controls the distribution of uranium and thorium in soil. Unlike U which is a mobile element, soluble in the U⁺⁶ state (oxidizing conditions), Th has low mobility under environmental conditions and reflects source area characteristics. XRD analysis enabled the identification of U and Th as major or trace elements in minerals like zircon, thorite, allanite, monazite, pyrochlore, aeschynite, columbite, bastnäsite. The distribution of U and Th in soils is primarily controlled by the distribution of the accessory minerals in bedrocks, and secondly by the physical and chemical stability of these minerals in the pedogenetic process. The soils developed on granitoid rocks that occur in the north-eastern and eastern parts of the massif have the highest thorium content among all types of soils. High uranium contents were determined in soil samples developed on syenite and nepheline syenite. A positive correlation between uranium and thorium occurs in almost all type of soils.

Also, the results indicate an U and Th enrichment in the clay fraction.

The origin of garnet peridotites in the Siberian cratonic mantle from chemical, modal and textural data

D.A. IONOV¹, L.S. DOUCET¹, A.V. GOLOVIN²

¹PRES-Lyon & UMR6524-CNRS, Saint Etienne, France, dmitri.ionov@univ-st-etienne.fr (*presenting author)

²Institute of Geology & Mineralogy, Novosibirsk, Russia, avg@igm.nsc.ru

Garnet peridotites, the most common rocks in cratonic mantle, are believed to be variably enriched residues of high-degree melt extraction, but the role and conditions of melting, metasomatism and deformation in their origin continue to be debated. A major problem is that peridotite xenoliths in kimberlites are usually altered during and after their transport to the surface, many are small and heterogeneous. We examine new and published [1-3] chemical, modal and textural data on several dozen large, fresh and homogeneous garnet peridotite xenoliths from the Udachnaya kimberlite in the central Siberian craton to better constrain the origin and evolution of garnet-facies cratonic mantle.

The least metasomatized garnet peridotites are similar in major oxide compositions to low-opx spl harzburgites from Udachnaya (interpreted as pristine melt extraction residues [4]) and were formed by 30–38% of polybaric fractional melting from 7–4 GPa to $\leq 1-3$ GPa. Their whole-rock (WR) Al_2O_3 and Mg#, hence melt extraction degrees, do not vary with depth. Co-variations of modal abundances, major oxides and their ratios in WR indicate that garnet is mainly a residual mineral, which survived partial melting and/or exsolved from high-T opx on cooling, whereas cpx is mainly metasomatic. Modal abundances of garnet can be estimated from WR Al_2O_3 ; rocks with $\text{Cr}\#_{\text{WR}} > \text{Cr}\#_{\text{gar}}$ contain accessory Cr-spinel.

In addition to coarse and sheared peridotites, we identify “transitional” rocks with $\leq 10\%$ neoblasts at margins of coarse olivine. Such incipient stages of deformation may have been overlooked in previous studies of altered xenoliths in the Siberian and other cratons. Regardless of deformation degrees deformed peridotites show stronger enrichments in Fe, Ti, Ca, REE than coarse peridotites, i.e. deformation is accompanied by metasomatism. Both deformed and coarse peridotites occur near the base of the lithosphere ($\geq 1300^\circ\text{C}$, 6.8 GPa). P-T estimates define a perturbed geotherm [3]; oxygen fugacity decreases with depth less than inferred previously [3, 5].

[1] Ionov *et al.* (2010) *J Petrol* **51**, 2177-2210. [2] Doucet *et al.* (2013) *CMP* **165** (6). [3] Goncharov *et al.* (2012) *EPSL* **357-358**, 99-110. [4] Doucet *et al.* (2012) *EPSL* **359-360**, 206-218. [5] Yaxley *et al.* (2012) *Lithos* **140-141**, 142-151.

Arsenic contamination in an anoxic aquifer in southwest Germany: Assessment and process studies

M. ISENBECK-SCHRÖTER*, M. MAIER, S. AL NAJEM,
N. SALM AND C. SCHOLZ

Institute of Earth Sciences, Heidelberg University, INF 236,
69120 Heidelberg, Germany (*correspondence:
Margot.Isenbeck@geow.uni-heidelberg.de)

Arsenic groundwater contamination due to the infiltration of arsenic bearing sewage has been assessed analysing groundwater and aquifer material on an abandoned industrial site in the quaternary aquifer in the Upper Rhine Rift, southwest Germany. The contamination plume is about 800 m long, 200 m wide and 20-30 m deep. Detailed studies were performed in order to investigate the redox state and the binding forms of arsenic in the water and in the aquifer material, respectively.

A cross section of four liner boreholes along the plume was drilled and analysed in detail as well as 20 direct push soundings in the center of the contamination. Groundwater was sampled using filtered groundwater wells and the direct push boreholes. The analyses lead to a detailed assessment of the contamination extension and mass. This assessment could also be used to characterize the mobility of both arsenic redox species.

The transport processes in the aquifer were studied more in detail using column experiments with contaminated material under oxic and anoxic conditions. It could be shown that surface complexation and microbial redox processes dominantly influence the arsenic mobility under anoxic conditions. The reduction of As (V) to As (III) following iron reduction seems to be the dominating process under the aquifer conditions.

Similar processes have also been observed during field studies with As (V) input into the Cape Cod Aquifer [1]. Both sites are characterized by an iron dominated redox system. They are anoxic due to contamination with sewage of organic contaminants. The sites differ in the geochemical milieu; whereas the contaminated site in the Upper Rhine Valley is a carbonate system, the Cape Cod aquifer is acidic.

We thank the RP Darmstadt, the HIM-ASG and the CDM Smith Consult GmbH for their financial and technical support.

[1] Höhn *et al.*, (2006): *J. Cont. Hydrology* **88**, 36-54

U-Pb dating of Eoarchaeon zircons using a NanoSIMS

AKIZUMI ISHIDA¹, NAOTO TAKAHATA¹, YUJI SANO¹,
JEAN DAVID², AND DANIELE L. PINTI²

¹ Atmosphere and Ocean Research Institute, the University of Tokyo (e-mail: ishiaki@aori.u-tokyo.c.jp), ² GEOTOP, Université du Québec à Montréal

Volatiles, such as hydrogen or sulphur, included in Eoarchaeon igneous rocks, have crucial information to reveal about the evolution of the early Earth. Apatite and/or glass inclusions, found in zircon crystals, are expected to preserve primitive information of such volatile elements. NanoSIMS is one of the more powerful tools for micro-scale analyses including precise *in situ* U-Pb dating of zircon.

We performed ²³⁸U-²⁰⁶Pb and ²⁰⁷Pb-²⁰⁶Pb zircon dating using a NanoSIMS 50 ion microprobe at the University of Tokyo, with the method developed by our group [1]. The targeted zircons were separated from a tonalite of the Eoarchaeon Nuvvuagittuq supracrustal belt, Superior Craton, Canada. The reported U-Pb age of this tonalite is 3661 ± 4 Ma [2]. Euhedral to subeuhedral zircon crystals were picked up. Some of them have a zoning structure. Glass or apatite inclusions, whose size were 10 to 30 micrometers in diameter, were found in the crystal.

After the correction of common lead, ²³⁸U/²⁰⁶Pb* and ²⁰⁷Pb*/²⁰⁶Pb* ratios of 20 crystals were plotted on Terra-Wasserburg Concordia diagram. They showed a Discordia suggesting recent Pb loss. The intersection of Concordia and Discordia indicates that the age of this rock is 3637 ± 19 Ma, which agrees well with previous study. Now we are trying to measure the volatile compositions of inclusions in these zircons.

[1] Takahata *et al.*, *Gondwana Res.*, 14, 587-596, 2008. [2] David *et al.*, *GSA Bulletin*, 121, 150-163, 2008.

Geo-neutrino measurements with KamLAND

K. ISHIDOSHIRO^{1*} (FOR KAMLAND COLLABORATION)

¹Research Center for Neutrino Science, Tohoku University, Sendai 980-8578, JAPAN

(*correspondence/:koji@awa.tohoku.ac.jp)

KamLAND experiment

The Kamioka Liquid-scintillator Antineutrino Detector (KamLAND) is a 1 kton liquid scintillator surrounded by 53 nuclear reactor units in JAPAN. Following the Fukushima nuclear accident in March 2011, the entire Japanese nuclear industry, which generates > 97% of the reactor neutrino flux at KamLAND, has been subjected to a protracted shutdown. The reactor-off period provides a unique opportunity to measure geo-neutrino with KamLAND.

Geo-neutrino analysis [1]

The data reported here are based on a total live-time of 2991 days, which includes the recent reactor-off period. Assuming a chondritic Th/U mass ratio, we obtain a geo-neutrino flux of $3.4^{+0.8}_{-0.8} \times 10^6 \text{ cm}^{-2}\text{s}^{-1}$ from ²³⁸U and ²³²Th at the KamLAND location. The geo-neutrino flux translates to a total radiogenic heat production of $11.2^{+7.9}_{-5.1}$ TW from ²³⁸U and ²³²Th. The flux estimation is significantly improved by the reactor-off data. The geodynamical prediction with the homogeneous hypothesis is disfavored at 89% C.L. (Fig. 1) The observed flux is in agreement with the predictions from existing BSE models (geodynamical [2], geochemical [3] and cosmochemical [4]) with in $\sim 2\sigma$.

Future prospects

The ability of discriminating between models is limited by the statistical uncertainty. KamLAND continues to measure for getting further statistics. In the future, improved measurements with higher statistics and lower background is desired. Directional geo-neutrino detection is also required to further understand the deep interior of the Earth.

[1] A. Gando *et al.*, arXiv:1303.4667. [2] D. L. Turcotte and G. Schubert, *Geodynamics, Applications of Continuum Physics to Geological Problems*, second ed. (Cambridge Univ. Press, Cambridge, 2002). [3] W. F. McDonough and S.-s. Sun, *Chem. Geol.* 120, 223 (1995). [4] M. Javoy *et al.*, *Earth and Planet. Sci. Lett.* 293, 259 (2010).

Natural analogue study on long term alteration of bentonite (1) - Geochemistry and clay mineralogy-

TOMOKO ISHII¹, HISAO SATOH², KOHEI YAMAGUCHI², JIRO ETO¹, TOSHIAKI OHE³

¹ Radioactive Waste Management Funding and Research Center, Tokyo, 104-0052 JAPAN(ishii@rwmc.or.jp)

² Mitsubishi Materials Corp., Saitama pef.,330-8508 JAPAN

³ Tokai Univ., Kanagawa pref., 259-1292 JAPAN

In order to evaluate the long-term behavior of the bentonite in geological disposal sites for TRU waste, the prediction of alkaline alteration by cement influences is very important. We conducted geochemical analyses of natural bentonite suffered from Ca-rich groundwater as a natural analogue of bentonite barrier after $\sim 100\text{kyr}$.

The drilling survey was carried out on geothermal site at a Japanese island arc basin to find similar environment to the bentonite barrier influenced by cement leachates. The hot spring water near the site has high concentration of Ca and pH. We drilled down to GL-250 m, and the tuffaceous bed was recognized in the depth of GL-240m. The sedimentary age of the bed was estimated as 8.2 - 5.6 Ma by analysis of microfossils. Post-sedimental thermal history was estimated to be 20-40 degrees by analysis of stable isotopes. According to whole-rock XRF data, this bentonite could have been altered from basalt-dacite (granite) bimodal igneous rocks. Backscattered electron imaging on the bentonite identified coexisting Na/Ca-smectite and heulandite (Fig.1).

Even in such a Ca-rich condition, Na-smectite still remains without complete conversion to Ca-smectite. Geochronology by fission track dating and ³⁶Cl/Cl suggested about 10Ma for igneous age and 2Ma for groundwater entrapment. The composition of present groundwater was estimated as the mixture of rainwater and near hot spring water from a result of principal component analysis.

It is inferred that the Na-type smectite could have coexisted with the Ca-type in the bentonite for this geologic time-scale. This natural analogue may suggest a supporting evidence of smectite stability at the repository.

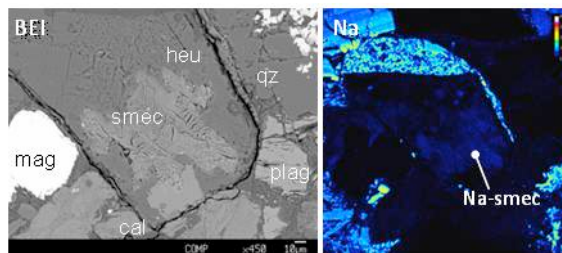


Fig.1 BEI and Na-map of the altered bentonite.

This research is a part of "Development of the technique for the evaluation of long-term performance of EBS (FY2007-2012)" under a grant from the Agency of Natural Resources and Energy, the Ministry of Economy Trade and Industry of Japan (METI).

Re-evaluation of digestion methods for accurate Re-Os isotope and highly siderophile element analyses

AKIRA ISHIKAWA^{1,2*}, RYOKO SENDA², KATSUHIKO SUZUKI² AND CHRISTOPHER W. DALE³

¹Earth Science and Astronomy, The University of Tokyo,

Tokyo 153-8902, Japan, akr@ea.c.u-tokyo.ac.jp

²IFREE, JAMSTEC, Yokosuka 237-0061, Japan

³Earth Sciences, Durham University, DH1 3LE, UK

The current database on highly siderophile elements (HSEs: Re, Au, Ir, Os, Ru, Rh, Pt and Pd) and Os isotopes in geological samples is dominated by isotope dilution methods, coupled with high-temperature sample digestion using inverse aqua regia in closed glass vessels such as Carius tubes (CT) or a high-pressure asher system (HPA). These acid digestion techniques are preferred over traditional flux fusion techniques, such as NiS fire assay, largely due to the ability to measure Re and Os on the same sample aliquot. By contrast, two major limitations - the 'nugget effect' and incomplete digestion - have often been associated with these acid digestion techniques. Recent data suggest that an additional HF step is essential to release HSEs hosted in the silicate portions of certain basaltic materials, necessitating modification of typical digesting procedures.

To address this issue, we systematically conducted analytical tests for CANMET reference material TDB-1 with varying digestion apparatus (microwave, CT, HPA), conditions (temperature, duration, sample size) and protocol (with or without HF desilicification, either before or after aqua regia attack). We found the optimum method for simultaneous determination of ¹⁸⁷Os/¹⁸⁸Os and HSE concentrations used inverse aqua regia to attack 1-2 g of powder over long durations, such as a Carius tube heated to 240°C for 72 hours, followed by an HF desilicification step after CCl₄ solvent extraction of Os. It is anticipated that extended HPA digestions will also achieve the same effect.

The method provides strong linear correlations on Os versus Ir-Ru-Pt concentration diagrams for repeat dissolutions of TDB-1, reflecting an effect of powder heterogeneity. This is further supported by a linear array on the ¹⁸⁷Re/¹⁸⁸Os and ¹⁸⁷Os/¹⁸⁸Os diagram, yielding a meaningful age of 1230 ± 47 Ma (MSWD=2.1), consistent with the Mesoproterozoic (~1265 Ma) formation of diabase TDB-1. In comparison, excellent reproducibilities for all HSEs were obtained from USGS reference material BIR-1: RSDs for 1-2 g aliquots were 7.4% Os, 4.4% Ir, 1.5% Ru, 5.2% Pt, 1.6% Pd and 0.7% Re (n=8). Thus, BIR-1 might be suitable material for narrowing the confidence intervals of HSE certified values.

Metasomatism recorded in the peridotite overlying metamorphic sole of the the Oman ophiolite: an analog of mantle-wedge events

S. ISHIMARU^{1*}, S. ARAI², AND A. TAMURA²

¹Dept. of Earth and Environ. Sci., Kumamoto Univ.,

Kumamoto 860-8555, Japan (*correspondence:

ishimaru@sci.kumamoto-u.ac.jp)

²Dept. of Earth Sci., Kanazawa Univ., Kanazawa 920-1192, Japan

Mantle peridotites have been modified to various extents at slab-mantle interface within the mantle wedge. To know the details of the event, e.g., which elements and how much amounts?, the materials from the mantle wedge are needed. Ophiolite is a place where we can investigate the slab-mantle interaction, because it has the metamorphic sole, formed at the ophiolite obduction. Its formation is interpreted as an analog of an incipient arc system transformed from the ocean floor.

The Oman ophiolite is quite famous for good exposure and preservation of the oceanic stratigraphy with widespread formation of metamorphic sole. We did systematic sampling at the southern Oman ophiolite from the sole garnet amphibolite to the peridotite up to 110 m above the amphibolite/peridotite boundary, i.e., an analog of slab-mantle boundary. The peridotite is deformed and serpentinized to various degree, and occasionally has mylonitized bands. The peridotite protolith is fertile lherzolite: the Fo content of olivine and Cr# [= Cr/ (Cr + Al) cation ratio] of chromian spinel is 90-93 and 0.11-0.35 (except for the spinels in highly serpentinized peridotite), respectively. The Al₂O₃ contents of clinopyroxenes and orthopyroxenes are high (up to 5.3 and 6.3 wt.%, respectively). Fine pyroxene grains show a low Al₂O₃ content, < 1 wt.%. The peridotites contain amphiboles irrespective of the distance from the amphibolite/peridotite boundary, and the amphiboles are not only tremolite after clinopyroxene but also hornblendes. The incompatible trace-element patterns of clinopyroxene are enriched in LREE and some LILE (Rb, Ba and Sr), and those of hornblendes show similar patterns although some show higher abundances than clinopyroxene.

The peridotites just above the metamorphic sole have been cooled as well as extensively hydrated (at least 110 m above the boundary) and enriched in fluid-mobile elements as mantle-wedge peridotites.

REE signatures of accessory minerals from Iron Oxide Copper Gold - skarn mineralization, Hillside, South Australia

R. ISMAIL*, C.L. CIOBANU, N.J. COOK, D. GILES AND A. SCHMIDT-MUMM

Deep Exploration Technologies Cooperative Research Centre, The University of Adelaide, Adelaide, SA 5005, Australia (*correspondence: roniza.ismail@adelaide.edu.au, cristiana.ciobanu@adelaide.edu.au, nigel.cook@adelaide.edu.au, david.giles@adelaide.edu.au, asmumm@gmail.com)

Hillside is an Iron Oxide Copper Gold (IOCG) mineralized system in the Gawler Craton, typified by skarn associations and genetically tied to the ~1.59 Ga Hiltaba Intrusive Suite. Incorporation of REE in skarn and accessory minerals is a valuable tool for understanding evolution of REE-enriched IOCG deposits and their footprints.

Mineralization is hosted within calcic skarns comprising prograde garnet-pyroxene-magnetite and retrograde epidote-actinolite-hematite associations. Early, high-temperature (~750 °C; Zr-in-titanite geothermometry) pyroxene skarn (I) is tied to strong albitization. Pyrite, present in the calcic skarn (II), is replaced by chalcopyrite during the late-hydrothermal (main Cu-Au ore deposition, III) stage. Titanite, apatite and allanite are abundant throughout all stages of skarn evolution from early-prograde to late-hydrothermal collapse.

REE concentrations and distributions in skarn and accessory minerals were determined by LA-ICP-MS. Whereas skarn minerals are extensively replaced in the main ore stage, accessories are still present, and their REE trends depict all stages of evolution (Fig. 1). Significantly, they record HREE-enrichment in stage III. This can be interpreted as a response to change in the fS_2 character of fluids.

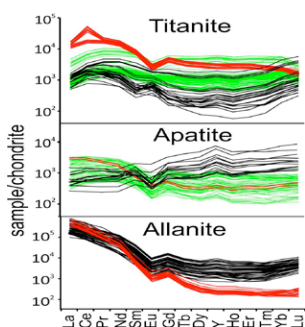


Figure 1 Chondrite-normalized REE+Y plots for accessory minerals. Red - early skarn (I); green - main calcic skarn (II); black - main sulfide deposition (III). Note progressive LREE-depletion and HREE-enrichment during evolution of the IOCG-skarn system.

The data show that REE signatures of accessory minerals from IOCG systems can help monitor development of alteration, and provide a framework for discriminating mineralized from non-mineralized systems in the region.

Mid to Late Holocene decreasing precipitation trends as reflected in $\delta^{18}O$ of speleothems from Apuan Alps (central Italy): Implications for seasonality

I. ISOLA¹, E. REGATTIERI², G. ZANCHETTA^{1,2,3}, L. ZHORNIAK², R.N. DRYSDALE⁴, J.C. HELLSTROM⁵

¹Istituto Nazionale Geofisica Vulcanologia, sez. Pisa, Italy; e-mail: isola@pi.ingv.it

²Dipartimento di Scienze della Terra, University of Pisa, Pisa, Italy

³Institute of Geosciences and Earth Resources, CNR Pisa Research area, Pisa, Italy

⁴Melbourne School of Land and Environment, The University of Melbourne, Australia

⁵School of Earth Sciences, The University of Melbourne, Australia

Changes in insolation related to Earth's orbital variations played a central role in the global-scale changes in climate of the last 11,500 cal yr. A progressive decline in summer temperature since the middle Holocene is well established from pollen and plant macrofossil data in northern and central Europe. The Mediterranean region has also become drier from the Middle Holocene to the present, with a marked precipitation seasonality that is crucial for both Mediterranean ecosystems and societies. Several records show contrasting seasonality patterns between southern and northern border regions of the central Mediterranean during Middle to Late Holocene. In this poster we present $\delta^{18}O$ stalagmite data sets from Corchia and Renella caves (Central Italy), showing long-term trends of increasing values (i.e. reduced rainfall) from Middle to late Holocene, while at secular to millennial scale they present different behavior. This difference is due to the variable recharge conditions related to changes in seasonality. These data can provide a more precise picture of the variations in the seasonality in the Mediterranean area

On the arrangement of sodium atoms around structural units and vibrational properties of a sodium borosilicate glass

S. ISPAS^{1*}, L. PEDESSEAU^{1,2} AND W. KOB¹

¹Laboratoire Charles Coulomb, CNRS UMR 5221, Univ. Montpellier 2, 34095, Montpellier, France
(*correspondence simona.ispas@um2.fr, walter.kob@um2.fr)

²Univ. Européenne de Bretagne, INSA, FOTON, UMR 6082, 35708, Rennes, France (laurent.pedesseau@insa-rennes.fr)

We have used first principles simulations in order to investigate the properties of a sodium borosilicate glass of composition $3\text{Na}_2\text{O}-\text{B}_2\text{O}_3-6\text{SiO}_2$ (NBS). This composition is similar to that of the glass wool used in our daily life. The study was carried up using first principles molecular dynamics within the density functional theory framework as implemented in the VASP code [1].

In this talk, we will present the analysis of the local environments of the three building structural units of the glass network, namely silicon atoms in 4-fold coordination, and boron atoms with 3- or 4-fold coordination. We will also discuss the local distribution of the Na atoms around the basic structural units. Indeed we have identified their preferential neighborhoods and how the nature of network former and its coordination infer on the shape of these preferential regions of Na atoms.

The vibrational properties have been equally studied, and the contributions of the various species have been identified. We have found that 3- and 4-fold coordinated boron atoms give rise to distinguished spectral features. Moreover, the partial vibrational density of the 3-fold coordinated B atoms has been found to be a weighted sum of 2 specific contributions so-called 3-fold symmetric coordinated B atoms and asymmetric coordinated B atoms.

[1] Kresse & Hafner (1993) *PRB* **47**, 558; Kresse & Furthmüller (1996) *Comp.Mater. Sci.* **6**, 15; Kresse & Furthmüller (1996) *PRB* **54**, 1116

Different diagenetic behaviors of As, Mo and Sb in Lake Biwa, Japan

TAKA AKI ITAI^{1*}, YUIKA HYOBU¹, MICHIO KUMAGAI², SHINSUKE TANABE¹

¹Center for Marine Environmental Studies (CMES), Ehime University, Bukyo-cho 2-5, Matsuyama, Ehime 790-8577, Japan (*correspondence: itai@sci.ehime-u.ac.jp)

²Sigma Research Center, Ritsumeikan University

Lake Biwa, the biggest lake in Japan, is suitable field to study diagenetic behavior of redox sensitive oxyanions, since clear diagenetic accumulation of Mn and As in surface sediment have been observed from entire lake. Redox conditions, evaluated by the depth profiles of solid phase speciation of Mn and As determined by XANES, were significantly varied depending on the sampling location within the lake. Here we show the comparison of depth profile of As, Sb, and Mo in both solid phase and porewater among various redox conditions. Of the seven stations studied, As profiles in porewater showed clear concentration peak in six. The depth of these peaks ranged from 3 to 1 cm below sediment-water interface, and arsenite was the dominant species around the areas where the peaks appeared. The peak values of As in solid phase always appeared 1-2.5 cm above the places where the peaks of porewaters were found. Predominance of arsenate in surface sediments suggested diagenetic accumulation of As, whereas As-S species becomes predominant below As peak areas in porewater. Both Mo and Sb showed cocentration peak in 5 stations. Two stations in which the peaks were not observed are in areas with most reducing conditions where no MnO_2 enrichment was observed even in the top layer (0-5 mm). In the other 5 stations, depth of the peaks in porewater were always in the following order: As>Sb>Mo. Difference in peak depth between As and other 2 elements were 0.75-1.5 cm, whereas difference between Sb and Mo were <0.75 cm. It is well known that these oxyanions have high affinity to Fe (oxy)hydroxides. However, if the dissolution of this phase predominantly controls the solid-water partitioning of these oxyanions, the porewater profile should be similar. Distinctly higher depth of As peak is likely attributed to arsenate reduction to arsenite which enhances the mobility of As. Slight differences in Mo and Sb is possibly due to high affinity of Mo to MnO_2 that reduces more easily than Fe (oxy)hydroxides. Although these relative mobility should change in more sulfidic setting like seawater, such a comparison is rather limited in freshwater system so far, thereby the finding of this study can contribute for better understanding of diagenetic behavior of these elements.

Role of acid mobilization in projected response of soluble iron supply to improvement of air quality in the future

AKINORI ITO^{1*}, LI XU² AND JOYCE E. PENNER³

¹Research Institute for Global Change, JAMSTEC, Yokohama, Kanagawa 236-0001, Japan (*correspondence: akinorii@jamstec.go.jp)

²Scripps Institution of Oceanography, University of California San Diego, La Jolla, CA 92093, USA

³University of Michigan, Ann Arbor, MI 48109-2143, USA

Acidification of dust aerosols may increase aerosol iron (Fe) solubility, which is linked to mineral properties (e.g., crystallinity, grain size and impurity content). The mixing of the mineral dust with combustion aerosols can also elevate iron solubility when aerosol loading is low. Here, we use a process-based chemical transport model [1, 2] with improved treatment of Fe in mineral dust and proton-promoted dissolution scheme to investigate the deposition of soluble iron and its response to changes in anthropogenic emissions of both primary particles and precursor gases.

Comparisons of modeled Fe dissolution curves with the measured dissolution rates show overall good agreement under acidic conditions. The improved treatment of Fe in mineral dust and the proton-promoted dissolution scheme results in reasonable predictive capability for iron solubility over the oceans in the Northern Hemisphere. Our model results suggest that iron included in aluminosilicate dust can be released in the form of ferrihydrite colloids, nanoparticles and aqueous species during the long-range transport and thus provide an important bioavailable source of iron to the oceans. As a result of considering both the atmospheric processing of mineral dust and source composition of combustion aerosols, soluble iron deposition to the subarctic North Pacific is projected to respond nonlinearly to changing emissions of fly ash and air pollutant gases (e.g., SO₂, NO₂ and NH₃). These results could have important implications for iron fertilization of phytoplankton growth, and highlight the necessity of improving the process-based quantitative understanding of the response of the chemical modification in iron-containing minerals to environmental changes.

[1] Xu, & Penner (2012) *Atmos. Chem. Phys.* **12**, 9479–9504, doi:10.5194/acp-12-9479-2012. [2] Ito (2013) *Global Biogeochem. Cycles* **27**, 1–10, doi: 10.1029/2012GB004378.

Spin transition of Fe²⁺ in ringwoodite (Mg,Fe)₂SiO₄ at high pressures

A.G. IVANOVA^{1*}, I.S. LYUBUTIN¹, JUNG-FU LIN², A.G. GAVRILIUK^{1,3}, A.A. MIRONOVICH³ AND M.YU. PRESNYAKOV^{1,4}

¹Shubnikov Institute of Crystallography, Russian Academy of Sciences, Moscow 119333, Russia (*correspondence: ani@ns.crys.ras.ru)

²Department of Geological Sciences, Jackson School of Geosciences, The University of Texas at Austin, Austin, Texas 78712-0254

³Institute for Nuclear Research, Russian Academy of Sciences, Moscow 117312, Russia

⁴0254National Scientific Center “Kurchatov Institute”, Moscow 123098, Russia

Electronic spin transitions of iron in the Earth's mantle minerals are of great interest to deep-Earth researchers because their effects on the physical and chemical properties of mantle minerals can significantly affect our understanding of the properties of the deep planet. Polycrystalline samples were synthesized in a multi-anvil apparatus using ⁵⁷Fe-enriched starting material ((Mg,Fe)O-SiO₂ mixture) at conditions of approximately 22 GPa and 2000 K. Energy dispersive x-ray elemental mapping and electron diffracton study of the sample showed that Fe predominantly presents in the ringwoodite phase γ -(Mg_{0.75}Fe_{0.25})₂SiO₄.

The electronic spin states of iron in ringwoodite were studied at high pressures up to 82 GPa using synchrotron Mössbauer spectroscopy (NFS) in a diamond anvil cell (HPCAT, Sector 16, APS, ANL). At ambient conditions, the NFS spectra reveal two non-equivalent iron species (Fe²⁺)₁ and (Fe²⁺)₂ which can be attributed to octahedral and tetrahedral sites in the cubic spinel structure of ringwoodite, respectively. High-pressure NFS spectra showed the disappearance of the hyperfine quadrupole splitting of the Fe²⁺ ions in both sites at approximately 45-70 GPa, indicating an electronic high-spin to low-spin transition. The spin transition exhibits a continuous crossover nature and is reversible at decompression.

The study was partially supported by RFBR, research projects No. 12-05-31342 and 11-02-00291. The work at the UT Austin was supported by the US National Science Foundation (EAR-0838221) and the Carnegie/DOE Alliance Center (grant DE-FG02-02ER45955). APS is supported by DOE-BES, under Contract no.DE-AC02-06CH11357.

Subseafloor basalts as fungal habitats

IVARSSON, M.^{1*} AND BENGTSON, S¹

¹Department of Paleobiology and the Nordic Center for Earth Evolution (NordCEE), Swedish Museum of Natural History, Box 50007, Stockholm, Sweden.

(*Correspondance: magnus.ivarsson@nrm.se)

The oceanic crust makes up the largest potential habitat for life on Earth, yet next to nothing is known about the abundance, diversity and ecology of its biosphere. Our understanding of the deep biosphere of subseafloor crust is, with a few exceptions, based on a fossil record. Surprisingly, a majority of the fossilized microorganisms have been interpreted or recently re-interpreted as remnants of fungi rather than prokaryotes [1-4]. Even though this might be due to a bias in fossilization the presence of fungi in these settings can not be neglected.

We have examined fossilized microorganisms in drilled basalt samples collected at the Emperor Seamounts in the Pacific Ocean. Synchrotron-radiation X-ray tomography microscopy (SRXTM) studies has revealed a complex morphology and internal structure that corresponds to characteristic fungal morphology. Chitin was detected in the fossilized hyphae, which is another strong argument in favour of a fungal interpretation. Chitin is absent in prokaryotes but a substantial constituent in fungal cell walls.

The fungal colonies consist of both hyphae and yeast-like growth states as well as resting structures and possible fruit bodies, thus, the fungi exist in vital colonies in subseafloor basalts. The fungi have also been involved in extensive weathering of secondary mineralisations. In terrestrial environments fungi are known as an important geobiological agent that promotes mineral weathering and decomposition of organic matter, and they occur in vital symbiosis with other microorganisms. It is probable to assume that fungi would play a similar role in subseafloor basalts and have great impact on the ecology and on biogeochemical cycles in such environments.

[1] Schumann *et al.* (2004) *Geomicrobiol. J.* 21, 241-246. [2] Ivarsson (2012) *Biogeosciences* 9, 3625-3635. [3] Ivarsson *et al.* (2012) *Geology* 40, 163-166. [4] Ivarsson *et al.* (2013) *Geo-Marine Letters*, DOI 10.1007/s00367-013-0321-7.

Simultaneous measurement of CCN activity and chemical composition of fine aerosols at Noto peninsula, Japan, in autumn 2012

YOKO IWAMOTO¹, KENTO KINOCHI² AND ATSUSHI MATSUKI¹

¹Institute of Nature and Environmental Technology, Kanazawa Univ., Kakuma-machi, Kanazawa 920-1192, Japan (*correspondence: iwamoto@se.kanazawa-u.ac.jp)

²Graduate School of Natural Science & Technology, Kanazawa Univ., Kakuma-machi, Kanazawa 920-1192, Japan

For the quantitative evaluations of cloud condensation nucleus (CCN) characteristics in the East Asia, CCN activity and chemical composition of atmospheric aerosols in submicrometer size range were measured at Noto Ground-based Research Observatory (NOTOGRO), located at the tip of Noto peninsula, facing the Sea of Japan, in autumn 2012.

In the atmospheric measurement, the CCN efficiency spectra, where CCN number fraction is plotted against the diameter of aerosols, were obtained at four different supersaturation (SS) conditions (0.1%, 0.2%, 0.5% and 0.8%). Hygroscopicity parameters κ [1], which depends on the chemical composition of aerosols, were estimated by the analysis of the CCN spectra. The bulk chemical composition of non-refractory submicrometer-sized aerosols was also measured by an aerosol chemical speciation monitor (ACSM).

The CCN activation diameters of ambient aerosols were clearly larger than those of pure ammonium sulfate under each SS condition. From the relationship between the estimated κ values and the CCN activation diameters, it was suggested that organics contributed to the aerosol mass especially in the size range of less than 100 nm. The contribution of organics observed in this study, based on the analysis of CCN spectra, was more apparent than those for other sites in East Asia [2, 3]. The bulk chemical composition derived by ACSM also indicated the significant mass fraction of organics in the submicrometer size range. The negative correlations between organic mass fraction and cloud droplets' diameters were observed especially under low SS conditions (<0.2%), suggesting that the initial growth rates of cloud droplets might slow by certain organics.

[1] Petters and Kreidenweis (2007) *Atmos. Chem. Phys.*, 7, 1961-1971 [2] Mochida *et al.* (2010) *J. Geophys. Res.*, 115, D21207 [3] Kuwata *et al.* (2008) *Atmos. Chem. Phys.*, 8, 2933-2948.

Clarification for Boron Sorption Mechanism in Coprecipitation with Magnesium Hydroxide

SAYAKA IZAWA¹, CHIHARU TOKORO², SHINYA SUZUKI³
AND KEIKO SASAKI⁴

¹ Waseda University, Tokyo, Japan, izasaya@ruri.waseda.jp

² Waseda University, Tokyo, Japan, tokoro@waseda.jp

³ Waseda University, Tokyo, Japan, Shinya.Suzuki55@gmail.com

⁴ Kyushu University, Kyushu, Japan, ksasakime@gmail.com

Although boron is absolutely essential in various industries, especially in glass industry, the high contaminant levels of boron in water are regulated in several countries because of its toxicity. While ion-exchange resin is commonly used to remove boron from wastewater, it is relatively expensive. In this study, boron removal by coprecipitation method using magnesium salt has been investigated. The objective of this study is to clarify how coprecipitation of boron with magnesium hydroxide occurs in order to achieve cost efficient way to treat wastewater.

We carried out three kinds of experimental studies; (i) sorption isotherm formation, (ii) XRD analysis, (iii) NMR analysis. In general, when pH is below 9.2, the predominating species is orthoboric acid, which is less adsorptive because of its low electrical activity [1]. Therefore, we carried out the coprecipitation experiments at pH 10.5 and 0.3 of ion strength. Indeed, we could achieve the best adsorption efficiency of boron to magnesium hydroxide at pH 10.5.

We found that the sorption isotherm was BET type, which suggested that the sorption mechanism of boron adsorption was changed as the initial B/Mg molar ratio increased. From XRD analysis, the crystal structure of the precipitation corresponded with magnesium hydroxide when the initial B/Mg molar ratio was less than 0.4, whereas uncertain amorphous precipitation and carbonate hydromagnesite were formed when the initial B/Mg molar ratio was larger than 0.4. Formation of the uncertain amorphous precipitation indicated that surface precipitation was formed and related to boron uptake to magnesium hydroxide when the initial B/Mg molar ratio was larger than 0.4. NMR analysis showed that boron was adsorbed onto the surface of magnesium hydroxide as three-coordinate boron. These results suggested that a part of boron was precipitated or intercalated with uncertain amorphous precipitation as three-coordinate boron during coprecipitation with magnesium hydroxide.

[1] M.M. de la Fuente García-Sotoa, E. Muñoz Camacho (2008), *Desalination*, 249, pp.626–634

Seeing through the haze: Testing the existence of a Neoproterozoic bistable organic-rich atmosphere

G. IZON^{1,2,*}, A.L. ZERKLE¹, M.W. CLAIRE¹, J. FARQUHAR³, S.W. POULTON² AND J. EIGENBRODE⁴

¹ DEES, Univ. of St. Andrews, St. Andrews. KY16 9AL, UK

(*correspondence: gareth.izon@ncl.ac.uk, aubrey.zerkle@ncl.ac.uk, m.claire@uea.ac.uk)

² School of Earth and Environ., Univ. of Leeds, Leeds. LS2 9JT, UK (s.poulton@leeds.ac.uk)

³ Dept. of Geology, University of Maryland, College Park, Maryland 20742, USA (jfarquha@essic.umd.edu)

⁴ NASA Goddard Space Flight Center, Code 699, Greenbelt, MD 20771, USA (jennifer.l.eigenbrode@nasa.gov)

The Great Oxidation Event (GOE; ~2.45–2.32 Ga) represents the onset of pervasive atmospheric oxygenation; however, ~2.7 Ga cyanobacterial microfossils and biomarkers [1] coupled with additional geochemical evidence [2], suggests a potentially earlier origin for photosynthetic O₂ accumulation. This temporal disparity implies either localised O₂ production or transient small rises ('whiffs') in atmospheric O₂ [2]. Despite the emerging data, large uncertainties surround the composition and the evolution of the Neoproterozoic atmosphere.

Analyses of sediments from the Campbellrand-Malmani platform (GKF01; ~2.65–2.5 Ga) suggest localised O₂ production, in a reducing atmosphere [3]. Importantly, within GKF01, large deviations in $\Delta^{36}\text{S}/\Delta^{33}\text{S}$ correlate with pronounced ¹³C-depletions in $\delta^{13}\text{C}_{\text{Org}}$, implying increased sedimentary incorporation of methanogenic carbon [3, 4]. Photochemical model simulations corroborate these data and predict the persistence of a bistable atmosphere poised between clear-skies and hazy conditions, implicating methane as an important component of the Neoproterozoic atmosphere.

Here, a new multiple S-isotope record from age-equivalent successions in W. Australia, combined with proxies for ocean redox and nutrient availability, will test the envisaged coupling between oceanic and atmospheric chemistry [3] whilst examining the drivers that link the two.

[1] Eigenbrode *et al.* (2009) *EPSL* **273** 323–331. [2] Anbar *et al.* (2007) *Science*. **317** 1903–1906. [3] Zerkle *et al.* (2012) *Nature Geosci.* **5** 359–363. [4] Eigenbrode *et al.* (2006) *PNAS* **103** 15759–15764.

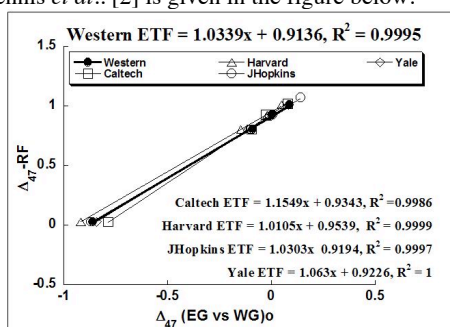
CO₂ Clumped Isotopologue Thermometry to Study Natural and Synthetic Carbonates

IFFAT JABEEN, ELIZABETH WEBB*, NEIL R. BANERJEE
AND ARSHAD ALI

Western University, London, ON, Canada N6A 5B7

ijabeen@uwo.ca, ewebb5@uwo.ca (*presenting author),
neil.banerjee@uwo.ca, aali287@uwo.ca

The distribution of rare “clumped” isotopologue species in the carbonate lattice is temperature dependent [1]. Our primary interests lie in exploiting this feature of clumped isotopologue science to explore paleoenvironments. We have established protocols to calibrate the clumped isotope thermometry of CO₂ by defining an absolute reference frame based on CO₂-H₂O equilibration experiments conducted at 10°C, 25°C, 50°C and 1000°C. A plot of experimental and theoretical equilibration intercepts has yielded an empirical transfer function (ETF) for our lab. A comparison of our ETF with Dennis *et al.* [2] is given in the figure below.



Application: Seeds from the hackberry tree (*Celtis occidentalis*) precipitate up to 70 wt. % aragonite in their endocarp. Fossil hackberry seeds have been recovered from Holocene deposits across most of N. America and have great potential as a terrestrial paleoclimate proxy. The determination of growth temperature by clumped isotopologue analysis of the seed carbonate is the first application of this emerging field to hackberries. Seed samples were obtained from 4 different locations in N. America with differing climatic conditions. Growth temperatures were calibrated using a regression developed for synthetic carbonates grown from 4 to 45°C and analysed for clumped isotopologues. This study demonstrates the potential of the isotopologue technique to terrestrial paleotemperature estimates, which can be used to estimate the δ¹⁸O values of plant waters and ancient relative humidity conditions.

[1] Ghosh *et al.* (2006) *GCA* **70**, 1439-1456. [2] Dennis *et al.* (2011) *GCA* **75**, 7117-7131.

Authigenic and exogenic mineral particles in lung tissues.

JABLONSKA M¹, JANECEK J² AND LEŚNIOK M³

¹mariola.jablonska@us.edu.pl;

²janusz.janeczek@us.edu.pl

³mlesniok@op.pl

Investigation of mineral particles by SEM and TEM in samples of lung tissues from 34 subjects who lived in the urban and industrial region of Upper Silesia, Poland, revealed the occurrence of 15 mineral species. Based on their origin inferred from chemical compositions, structural properties, and morphological features, mineral particles can be grouped into authigenic and exogenic, i.e. inhaled dust particles.

Authigenic biocalcite and Mg-biocalcite (mean-diameter <1.5 μm) are age-related ranging from 5.5 to 64.62 vol.% of mineral matter in dry lungs. They often envelop exogenic particles masking their presence. The biocarbonates formed preferably in lungs of non-smokers. The largest of all mineral particles (mean diameter > 2.5 μm) are bioapatites observed exclusively in lungs of male cigarette smokers and formed in response to pathogenic processes in lungs. Ferrihydrate and goethite are products of redox-driven reactions in lungs.

Mineral composition of exogenic particles reflects the mineral composition of atmospheric dust particles in the Upper Silesia. The inventory of abundant anthropogenic mineral particles includes: amorphous aluminosilicates, mullite, Fe-oxides, barite, trydimite, REE-phosphates metallic Fe, metal alloys, and (Zn, Fe, Pb)-sulfides. Minerals derived from natural sources and indicative of long-range transport include: micas, feldspars, pyroxenes, and amphiboles. Quartz particles are both natural and anthropogenic.

While the amount of authigenic carbonates increases with age the opposite trend is observed for aluminosilicates, silica, Fe-oxides, and metal alloys in individuals age 70 and older. The amount of barite in lungs of those individuals doubles relative to younger individuals.

Vertical differentiation of PM10 concentration and mineral composition in the first 100 m of troposphere related to meteorological conditions in the Sosnowiec urban area, S Poland

JABLONSKA M¹, JANECEK J² AND LESNIOK M³

¹mariola.jablonska@us.edu.pl

²janusz.janeczek@us.edu.pl

³mlesniok@op.pl

Airborne particulate matter (PM10) was collected in the Sosnowiec city, Upper Silesia conurbation, Poland, at 3 m and 100 m above ground level (a.g.l.) in conjunction with meteorological observations to determine the difference in both PM10 concentrations and mineral composition within the so-called free atmosphere. Samples were examined by the environmental ASEM, ATEM, and X-ray powder diffraction. Particular attention was paid to smog episodes caused by temperature inversion, and responsible for extremely high concentrations of particulate matter. We found no difference in concentrations and mineral composition of PM10 in samples collected at 3 m and 100 m a.g.l. during smog associated with almost stagnant air. The inventory of PM10 included particles originating from traffic (soot, Pb-chloride) and abundant coal combustion-related particles (soot, glassy aluminosilicates, Fe-oxides, barite, gypsum, Na- and K-chlorides) typical of low emission.

Differentiation of PM10 concentration and mineral composition was observed during inflow of air-masses associated with increased speed of wind. Mineral composition of PM10 at 3 m a.g.l. reflected local sources of anthropogenic pollution, whereas PM10 sampled at 100 m a.g.l. consisted of particles indicative of long-range transport, i.e. derived from natural sources, in addition to anthropogenic particles typical of the Upper Silesia.

Two modes of change in Southern Ocean export production over the past million years

JACCARD, S.L.¹, HAIN, M.P.², HAYES, C.T.³,
MARTINEZ-GARCIA, A.¹, ANDERSON, R.F.³,
SIGMAN, D.M.² AND HAUG, G.H.¹

¹D-ERDW, ETH Zurich, Zurich, Switzerland;
samuel.jaccard@erdw.ethz.ch

²Department of Geosciences, Princeton University, Princeton, USA

³LDEO, Columbia University, Palisades, USA

Export of organic carbon from surface waters of the Antarctic Zone of the Southern Ocean decreased during the last ice age, coinciding with declining atmospheric carbon dioxide (CO₂) concentrations, signaling reduced exchange of CO₂ between the ocean interior and the atmosphere. In contrast, in the Subantarctic Zone, export production increased into ice ages coinciding with rising dust fluxes, thus suggesting iron fertilization of Subantarctic phytoplankton.

Here, a new high-resolution productivity record from the Antarctic Zone is compiled with parallel Subantarctic data over the past million years. Together, they fit the view that the combination of these two modes of Southern Ocean change determines the temporal structure of the glacial interglacial atmospheric CO₂ record, including during the interval of "lukewarm" interglacials between 450 and 800 thousand years ago.

In addition, we present CYCLOPS model runs to separate the implied relative contribution of each parameter to the atmospheric CO₂ budget. Extending this model-based approach holds the promise to quantitatively cross-verify diverse paleoceanographic data, and to refine our mechanistic understanding of the coupling between climate, ocean biogeochemistry and atmospheric CO₂.

N and S isotope fractionation in the terminal electron acceptors during biodegradation of BTEX compounds

CHRIS JACKSON^{1*}, BERNHARD MAYER¹
AND LES STEHMEIER²

¹Department of Geoscience, University of Calgary, 2500 University Drive NW, Calgary, Alberta, Canada T2N1N4
(*correspondence: cjackson@ucalgary.ca)

²NOVA Chemicals Research Centre, 2928 16th N.E., Calgary, Alberta, Canada T2E 7K7

The biodegradation of BTEX compounds occurs under varying redox conditions [1]. Anaerobic processes are of particular interest as groundwater is often anaerobic as a result of initial mineralization of BTEX compounds [2]. Isotopic fractionation has been shown to occur for carbon and hydrogen isotopes of benzene during biodegradation [3] and other natural attenuation processes [4]. During the microbial reduction of the terminal electron acceptors (TEA) nitrate, and sulphate, significant isotope fractionation has also been demonstrated [5, 6]. The objective of this on-going project is to assess the extent of N and S isotope fractionation during BTEX biodegradation in laboratory studies and aquifers. Bioactivities of denitrifying and sulphate-reducing bacteria retrieved from a contaminated aquifer are respectively summarized in Table 1.

TEA	Carbon Source	Cells/mL
Nitrate	Benzene	9.16x10 ⁴
Nitrate	Toluene	2.05x10 ⁵
Sulphate	Benzene	1.84x10 ⁶
Sulphate	Toluene	1.12x10 ⁶

Table 1: Bioactivity measurements for benzene & toluene degrading bacterial cultures.

In laboratory studies with bacterial cultures growing on a mixed lactate/benzene carbon source, we observed biodegradation of benzene coupled with bacterial sulphate reduction evidenced by decreases of sulphate concentrations from 2500 to 216 mg/L accompanied by increases of $\delta^{34}\text{S}$ values from 0.4 to 12.7‰. Further laboratory experiments and groundwater investigations will reveal whether the coupling of isotopic tracers for BTEX and TEA compounds is a suitable approach for separating biodegradation within aquifers from other processes of natural attenuation [4] that affect both concentration and isotopic composition of BTEX compounds.

[1] Coates & Chakraborty (2004) *Appl Microbiol Biotechnol* **64**, 437-446. [2] Lovley (1997) *Indus Microbiol & Biotechnol* **18**, 75-81. [3] Mancini *et al.* (2003) *Appl & Environ Microbiol* **69**, 191-198. [4] Sin & Lee (2010) *Rapid Commun Mass Spectrom* **24**, 1636-1640. [5] Einsiedl & Mayer (2005) *Environ Sci Technol* **39**, 7118-7125. [6] Böttcher *et al.* (1990) *J Hydrol* **114**, 413-424.

Noble Gas Recycling and He-Ne-Ar Solubility in Ring Structure-Bearing Minerals

COLIN R.M. JACKSON¹, STEPHEN W. PARMAN¹,
SIMON P. KELLEY² AND REID F. COOPER¹

¹Brown University, Providence, RI, USA

²The Open University, Milton Keynes, Buckinghamshire, UK

There is increasing evidence that significant amounts of noble gases have been recycled back into the mantle. Data on the solution properties of noble gases in geologic materials remain scarce, and thus it is unclear what materials are capable of recycling noble gases and how noble gas recycling is coupled to the recycling of other volatiles.

Towards this end, we have experimentally determined He-Ne-Ar solubility in beryl and cordierite. He-Ne-Ar solubility in beryl and cordierite is very high: 7×10^{-8} , 1×10^{-7} , 2×10^{-8} in beryl, and 3×10^{-7} , 4×10^{-7} , and 4×10^{-7} in cordierite (list order: He-Ne-Ar, mol g⁻¹ bar⁻¹) which are around 10⁴ times greater than He solubility in olivine.

Experiments were conducted using an externally-heated pressure vessel (equal parts He-Ne-Ar pressure medium) and analyzed using laser-ablation, noble gas-mass spectrometry. Experiments essentially utilized a constant-source approach, where the minerals diffusively equilibrated with the imposed fugacity of noble gases present in the pressure medium. Temperatures ranged from 750-800°C, and total pressure ranged from 1.3-1.5 kbar.

Beryl and cordierite were chosen because they possess six-member tetrahedral ring structures in their lattice, and similar lattice structures are present in commonly recycled, hydrothermal minerals (e.g. amphibole, clays, serpentine). These lattice structures are large radius and commonly unoccupied (zero-charge), suggesting they are energetically favorable locations for noble gas dissolution in minerals.

Recent He and Ne solubility determinations for amphibole also indicate that noble gas solubility is correlated with the form of the unoccupied ring structures. Interestingly, the ratio of He to Ne solubility in amphibole is greater than that determined for both beryl and cordierite. Ring structure geometry differs amongst minerals, which may explain why amphibole apparently fractionates He and Ne relative to beryl and cordierite. This suggests that ring structure-bearing minerals may have diagnostic noble gas fractionations. Comparing the expected fractionations of noble gases in subducted materials to the integrated pattern of recycled noble gases in the mantle should yield insight into viable mechanisms for noble gas recycling.

Contrasting origins of an intermediate pluton and a highly silicic pluton, Never Summer Mountains, Colorado, USA

KRISTIN JACOB^{1*} AND G. LANG FARMER¹

¹University of Colorado, Boulder, Campus Box 399, Boulder, CO 80309, USA

(*correspondence: Kristin.Jacob@colorado.edu)

Field observations, whole-rock major- and trace-element geochemistry, and Sr, Nd, and Pb isotopic data were used to assess the petrogenesis of and relationship between two epizonal plutons: the intermediate Mt Richthofen stock (MRS) and the high-silica rhyolite composition Mt Cumulus stock at the ~28 Ma Never Summer igneous complex, north-central Colorado, USA. The MRS is compositionally zoned from more mafic compositions at the structurally deepest portion of the pluton (55 wt. % SiO₂, ε_{Nd}(T) -2.0, ⁸⁷Sr/⁸⁶Sr(T) 0.7049) to more felsic compositions at the structurally shallowest portion of the pluton (67 wt. % SiO₂, ε_{Nd}(T) -5.6, ⁸⁷Sr/⁸⁶Sr(T) 0.7119). Given the lack of obvious wall-rock assimilation at the level of pluton emplacement, the compositional variations in the pluton most likely reflects differences in the compositions of magmas from which the pluton was assembled. The presence of mafic enclaves in the structurally lowest portion of the pluton reveals evidence for mafic underplating. Aluminum-hornblende geobarometry of the structurally lowest rocks yields an emplacement depth of ~3 km. Taken together, we attribute the vertical zonation to mixing of two primary magmas, an early-emplaced felsic end-member with later arriving mafic magmas, which were derived from greater crustal depths and interacted in the upper crust to produce the range of intermediate compositions. In contrast, the MCS is compositionally homogeneous with 77 wt. % SiO₂, ε_{Nd}(T) -5.8, and ⁸⁷Sr/⁸⁶Sr(T) ~0.712. A close fit to a 28 Ma Sr reference isochron reveals that the MCS represent melts derived from an isotopically uniform source and could not have been derived from the adjacent isotopically heterogeneous MRS by upper-crustal differentiation. The Nd isotopic composition of the MCS is similar to that of mafic lower crustal xenoliths entrained in nearby Devonian kimberlites. Rare earth element modeling reveals a good compositional match between the MCS and calculated partial melts of the mafic, garnet-free, two-pyroxene lower crustal granulite xenoliths sampled by the kimberlites. The mafic lower crust is therefore a plausible source for the melts of MCS and early emplaced silicic material associated with the MRS.

An isotopically homogeneous inner terrestrial planet region

S. B. JACOBSEN^{1*}, M. I. PETAEV¹, S. HUANG¹
AND D. D. SASSELOV¹

¹Depts. of Earth and Planetary Sciences and Astronomy, Harvard Univ., 20 Oxford St., Cambridge, MA 02138, USA. (*email: jacobsen@neodymium.harvard.edu)

The well-established variability in isotopic compositions and water contents among various planetary materials in the inner Solar System means that bulk mixing of accreting materials, at least in some regions of the inner Solar System, was limited. We use enstatite chondrites (ECs) to explore a new model for the early evolution of the inner Solar System. In this model, the bulk of the Earth-building material originates inside the orbit of Mars (Oligarchic Growth Zone), which is isotopically homogeneous and identical to Earth and ECs. In contrast, there is a region with significant isotopic heterogeneity from Mars outwards. It is divided by the snowline (~2.7 AU) into two zones: one inside with moderate heterogeneity and another outside with much larger isotopic heterogeneity. Both zones form in a low-mass gap in the disk and therefore could never form larger planets. In this model the planets in the inner, oligarchic growth zone formed essentially dry. The Earth has received its water as a late veneer via very minor contributions from the outer regions beyond the snowline. Despite substantial isotopic variations among different chondrite groups, the isotopic compositions of the Earth's mantle are nearly identical only to ECs. Yet, there is a large chemical difference between Earth and ECs that is explained by different evolution paths from the same precursor, chemically similar to the widely accepted Earth's composition derived from mantle peridotites. This material formed in the isotopically homogeneous inner terrestrial planet region (Oligarchic Zone). The FeO-poor silicates and Ca,Mg sulfides typical of ECs resulted from a local non-nebular sulfidation of this precursor that has also changed the EC's bulk chemical composition. In this model, the identical isotopic composition of Earth and Moon is a logical outcome rather than something that has to be explained away.

Roadmaps for powering the world, U.S., and individual states for all purposes with wind, water, and sunlight

MARK Z. JACOBSON¹

¹Department of Civil and Environmental Engineering,
Stanford University, Stanford, CA 94305-4020, USA;
jacobson@stanford.edu

Global warming, air pollution, and energy insecurity are three of the most significant problems facing the world today. This talk discusses these problems and technical and economic plans to solve them by powering 100% of the world, individual countries, and states for all purposes, including electricity, transportation, industry, and heating/cooling, with wind, water, and sunlight (WWS) together with efficiency measures, within 20-40 years. New specific plans for New York and California are discussed. Relevant papers are at <http://www.stanford.edu/group/efmh/jacobson/Articles/I/susenergy2030.html>.

Impact of iron limitation on marine unicellular diazotrophic cyanobacteria

V. JACQ^{1*}, C. RIDAME¹, S. L'HELGUEN², F. KACZMAR¹
AND A. SALIOT¹

¹LOCEAN, CNRS, UPMC, 75005 Paris, France

(*correspondence: violaine.jacq@locean-ipsl.upmc.fr)

²LEMAR, CNRS,UBO, IRD, IUEM, 29280 Plouzané, France

Marine diazotrophic cyanobacteria are able to use dissolved dinitrogen (N₂) as nitrogen source for primary production. These cyanobacteria play a key role in the global carbon and nitrogen cycles as they contribute to significantly increase the oceanic N pool and thus primary production and carbon export to deep ocean. Due to the high iron (Fe) content of nitrogenase, the enzyme required for N₂ fixation, and to its low solubility in seawater, Fe is widely suspected as a key controlling factor of the activity of diazotrophic cyanobacteria. Nevertheless, the influence of Fe limitation on the recently discovered unicellular diazotrophic cyanobacteria (UCYN) is poorly understood. To address this knowledge gap, we conducted culture experiments on the UCYN *Crocospaera watsonii* WH8501 growing under a range of bioavailable Fe concentrations (from 0.017 nM to 2.53 nM). Overall, severe Fe limitation leads to significant decreases in growth rate (-60%), C, N and chlorophyll *a* contents per cell (-70%), N₂ and CO₂ fixation rates per cell (-90%) as well as in cell volume (-60%). Regarding these cellular contents and fixation rates on a volumetric basis we highlight two distinct responses of *Crocospaera watsonii* depending on the degree of Fe limitation: (i) under low Fe deprivation, cells only reduced their volume while their growth rate, cellular contents and N₂ and CO₂ fixation rates per μm³ remained maximum, and (ii) when increasing Fe deprivation, cell volume remained unchanged while growth rate, cellular contents and N₂ and CO₂ fixation rates per μm³ strongly decreased. The half saturation constant for growth with respect to bioavailable Fe of *Crocospaera watsonii* was 70% lower than that of the large diazotrophic filamentous cyanobacterium *Trichodesmium*. This indicates that UCYN are better adapted to poor Fe environments than large filamentous diazotrophs. Furthermore, the physiological response of *Crocospaera watsonii* to Fe limitation was different from that shown in a previous study on the UCYN *Cyanothece* sp, indicating potential differences in Fe requirements or Fe acquisition within the UCYN community. Conclusively, our results contribute to a better understanding of how Fe bioavailability can control the activity of UCYN and explain the biogeography of diverse N₂ fixers in ocean.

Geochemical variations in the Central Southern Volcanic Zone, Chile (38-43°S): The role of fluids in generating arc magmas

GUILLAUME JACQUES¹, KAJ HOERNLE¹², HEIDI WEHRMANN^{12*}, JAMES GILL³ AND ILYA BINDEMAN⁴

¹Collaborative Research Center (SFB574), Univ. Kiel & GEOMAR (*correspondence: gjacques@geomar.de)

²GEOMAR Helmholtz Centre for Ocean Research Kiel, Germany

³University of California, Santa Cruz, USA

⁴University of Oregon, Eugene, USA

We present new major and trace element, volatile and Sr-Nd-Pb-Hf-O isotope data from the Central Southern Volcanic Zone in Chile (CSVZ; 38-43°S). The satellitic and between stratovolcano cinder cones display different geochemical characteristics from the stratovolcanoes. The cinder cone samples have lower HREEs contents and U/Th, Pb/Ce and Ba/Nb ratios, but higher LREE, Nb and Ta abundances, and La/Yb and Nb/Yb ratios. As in the Transitional (T) SVZ (34.5-38°S), S and Cl contents are elevated in some small cinder cones of the CSVZ relative to the stratovolcanoes. They also extend to less radiogenic Pb and Sr isotopic compositions and higher $\delta^{18}\text{O}_{\text{olivine}}$ compared to the stratovolcano samples, but almost completely overlap in Nd and Hf isotopic composition. These variations are consistent with the lower-volume cinder cones forming through lower degrees of melting as a result of a lower fluid flux from the subducting slab than at the stratovolcanoes. When compared to the TSVZ ([1] Jacques *et al.*, in press), the magmas feeding the CSVZ stratovolcanoes have experienced higher fluid flux released from the subducting slab, resulting in higher degrees of melting and larger magma production.

[1] Jacques *et al.*, (in press), *GCA*

Microbial transformations of dissolved organic matter in crustal aquifer fluids at North Pond

ULRIKE JAEKEL^{*1}, JULIE MEYER², JULIE HUBER², THORSTEN DITTMAR³ AND PETER GIRGUIS¹

¹Department of Organismic and Evolutionary Biology, Harvard University, Cambridge, MA, (*correspondence: ulrikejaekel@fas.harvard.edu, pgirguis@oeb.harvard.edu)

²Marine Biological Laboratory, Woods Hole, MA, jmeyer@mbl.edu, jhuber@mbl.edu

³Max Planck Research Group for Marine Geochemistry, University of Oldenburg, Oldenburg, Germany, dtittmar@mpi-bremen.de

While recent studies have established the existence of a deep subsurface biosphere, little is known about their activity, or their influence on biogeochemical cycles. Near the Mid-Atlantic Ridge, at a site called the "North Pond", deep ocean seawater circulates through the basaltic crust, supplying the aquifer-hosted microbial community with organic matter and electron acceptors. Studies have shown that these crustal fluids contain both oxygen and nitrate, potentially enabling a variety of microbial organic matter transformations that could have implications for the composition and source of dissolved organic matter to the deep ocean. To investigate the transformation of dissolved organic matter (DOM) in crustal aquifer fluids at North Pond, we sampled fluids from CORK (Circulation Obviation Retrofit Kit) observatories. These fluids were incubated at *in situ* pressure and temperature, as well as at atmospheric pressure. Comparative analyses by Fourier Transform Ion Cyclotron Resonance Mass Spectrometry (FT-ICR-MS) generated high-resolution profiles of the molecular composition of DOM, and shed light on the transformations of DOM taking place within these fluids. Molecular analyses of the microbial community and incubations with ¹³C-labeled substrates further illustrated the potential for these microbial communities to alter the geochemical regime via their collective metabolic activity.

Meteoric ^{10}Be in soils of loessic origin- a case study of Luvisols from Northern France

M. JAGERCIKOVA¹, S. CORNU^{1*}, M. MAYOR¹,
V. GUILLOU² AND D. BOURLÈS²

¹INRA, UR1119 Géochimie des Sols et des Eaux, F-13100
Aix en Provence, France (*correspondence:
scornu@aix.inra.fr)

²Aix-Marseille Univ., CEREGE, UMR CNRS 7330, BP80,
13545 Aix-en-Provence Cedex 4, France

Meteoric ^{10}Be , due to its high affinity with soil and sediment particles, is a popular tracer in geomorphologic and environmental studies attempting to evaluate the soil production/denudation rates or soil age up to 10^7 years. However, the evolution of the ^{10}Be distribution as a function of depth is poorly known in soils, as has been shown by recent reviews [1, 2]. In this study, we have measured ^{10}Be concentrations of bulk samples and in 0-2 μm (lutum) granulometric fractions in Luvisols profiles developed on loess in Northern France. The three sites differ significantly in ^{10}Be absolute concentrations in bulk samples reflecting probably the past ^{10}Be accumulation in loess parent material. In all profiles, ^{10}Be concentrations in bulk samples show a significant correlation with the lutum content with the maximum ^{10}Be concentrations in the Bt-horizon. This result was surprising, as we expected the maximum concentration of ^{10}Be to appear at the soil surface, since ^{10}Be input occurs at the soil-atmosphere interface. Dominant adsorption of ^{10}Be to the lutum has been corroborated by measurements of ^{10}Be concentrations in lutum fraction and mass balance equation. Nevertheless, an anti-correlation has been observed between ^{10}Be concentrations in lutum and lutum content of the soils, thus outlining the dilution effect of lutum on ^{10}Be concentrations in this fraction. Contrary to the bulk samples, ^{10}Be concentrations in lutum show several maxima coinciding with the shifts in loess grain size distribution (coarse silt/fine silt), probably due to different episodes of pedogenesis occurrence. Finally, in order to quantify ^{10}Be transfers in these soils, a mass balance and numerical modelling approach of diffusion-convection equation has been used.

[1] Graly *et al.* (2010) *GCA* **74**, 6814-6829. [2] Willenbring & von Blanckenburg (2010) *ES-Reviews* **98**, 105-122.

Were ancient granitoid compositions influenced by contemporaneous atmospheric and hydrosphere oxidation states?

OLIVER JAGOUTZ

MIT, Cambridge MA, USA, jagoutz@MIT.EDU

A fundamental shift in the nature of granitoids occurs at approximately the Archean-Proterozoic boundary. Archean crust is dominated Na-rich tonalite-trondjemite-granodiorites (TTGs), whereas post-Archean granitoids are characterized by K-rich granodiorite-granite (GG). Due to the HREE depletion commonly found in TTGs indicating the presence of residual garnet, many researchers have proposed that the difference in Na/K is related to the deeper melting depth of the TTG parental liquids.

Here I present a compilation of the relevant experimental data, documenting that no correlation exists between the Na/K of derivative felsic liquids and the pressure of partial melting/fractional crystallization. Instead, the Na/K ratio of the felsic liquid best correlates with the Na/K ratio of the source. This implies that in Archean time the source material of TTG rocks must have been Na/K enriched relative to the modern. Modern granitoids are dominantly formed in a supra subduction zone environment, where a feedback loop exists between subducted materials (oceanic crust and sediments) and arc magmatism. Sea-floor weathering and the Na/K of the altered oceanic crust strongly depends on $f(\text{O}_2)$ conditions during alteration, which likely changed with earth history. During alteration under oxidized condition K_2O is fixated due to the formation of celadonite (K-Mica), whereas during anoxic condition saponite (Na-Smectite) is the stable alteration mineral. I propose that the rise of oxygen at 2600–2400 Ma triggered associated changes in $f(\text{O}_2)$ seafloor alteration conditions (Jagoutz 2012). The change in the dominant seafloor alteration mineral from reduced to oxidized causes a change in the nature of the arc magma source and provides a possible explanation for the observed transition from TTG-rocks in the Archean to the GG-granitoids in post-Archean times.

[1] Jagoutz, O. (2012) *Terra Nova*, **25**, pp 95-101

Mineral formation and evolution from a first-principles perspective

SANDRO JAHN

GFZ German Research Centre for Geosciences,
Telegrafenberg, 14473 Potsdam, Germany
(correspondence: jahn@gfz-potsdam.de)

The formation and evolution of minerals is driven by thermodynamics or, more specifically, by the tendency of a usually complex chemical system to reach the lowest energy state at the existing pressure and temperature conditions. Much of what we know about the mineralogy of the Earth's interior stems either from laboratory experiments or from natural samples that at least partly preserved the structure and chemical composition they obtained during their formation. In recent years, computational mineralogy has become a powerful complementary approach to constrain the stability of minerals and their chemistry in the wide range of conditions of the Earth's interior. First-principles simulations that are based on quantum mechanics are especially suited in this respect as they are predictive, accurate and versatile.

In this talk, I will focus on two aspects of mineral evolution: (1) the partitioning of trace elements and isotopes between minerals, melts and fluids and (2) the phase behavior of mantle minerals at high pressures and temperatures. With a number of examples from recent case studies I will illustrate how the most likely incorporation mechanisms of minor elements into minerals are obtained from the simulations and which influence the molecular structure of the fluid or melt has on the partition coefficients. I will present efficient schemes to compute Gibbs free energy differences or element exchange coefficients and conclude with explicit simulations of mineral phase transformations, which sometimes lead to the discovery of previously unknown stable or metastable crystalline phases. All calculations presented here accompany or are accompanied by experimental or analytical work and it is important to stress the new synergies that arise from such collaborations.

Reactive transport modeling of chromium isotope fractionation during Cr(VI) reduction under saturated flow conditions

JAMIESON-HANES, J.H.¹, AMOS, R.T.¹, GIBSON, B.D.¹, PTACEK, C.J.¹ AND BLOWES, D.W.¹

¹Dept. of Earth and Environmental Sciences, University of Waterloo, Waterloo, ON, Canada
(jhjamies@uwaterloo.ca, ramos@uwaterloo.ca, bgibson@uwaterloo.ca, ptacek@uwaterloo.ca, blowes@uwaterloo.ca)

Hexavalent chromium (Cr(VI)) is a very mobile groundwater contaminant most often derived from industrial processes such as tanning and electroplating, but also from naturally occurring geological sources. Reduction of Cr(VI) to the sparingly soluble Cr(III) is a common method of groundwater remediation, and is accompanied by a significant isotope fractionation. During reduction the remaining Cr(VI) pool becomes enriched in the ⁵³Cr/⁵²Cr ratio; the degree of this enrichment depends on the reductant, the mechanism of Cr removal, and is potentially influenced by transport processes [1].

Several laboratory experiments were conducted using organic carbon and zero-valent iron to treat Cr(VI) under both static and saturated flow conditions. In addition to traditional aqueous geochemical measurements, MC-ICP-MS analyses were made to determine the Cr isotope composition of the dissolved Cr(VI). Results from the analogous batch and column experiments exhibited different Cr isotope trends, suggesting that transport processes may play a role in the overall fractionation factor. The experiments were simulated using the reactive transport model MIN3P in order to further explore the influence of transport. Modeling results indicated that the interpretation of Cr isotope fractionation during reduction can be complex, particularly where multiple removal mechanisms may exist. Overall, the simulations were able to provide further insight into the isotope fractionation associated with the Cr removal processes.

[1] Jamieson-Hanes (2012) *Environ. Sci. Technol.* **46**, 6783-6789.

Structural and geochemical evidence for the origin of felsic microgranular enclaves and porphyry granite, Itu Rapakivi Batholith, SE Brazil

VALDECIR DE ASSIS JANASI¹,
GIOVANNA DOS SANTOS PEREIRA¹
AND ADRIANA ALVES¹

¹Instituto de Geociências, Universidade de São Paulo, Rua do Lago, 562, 05508-080, São Paulo, Brazil, vajanasi@usp.br (corresponding author); gsp.santos@gmail.com; adrianaalves@usp.br.

The 590 Ma Salto Granite Pluton, part of the post-orogenic Itu Rapakivi Batholith (590-580 Ma), SE Brazil, is interpreted on the basis of structural data as a westward-tilted magma chamber, whose main portion consisting of red coarse-grained hornblende-biotite granite is capped by a cupola of pink inequigranular biotite leucogranite with miarolitic cavities. This main unit was invaded by a body of zoned rapakivi granite which varies from a porphyritic facies dominated by fine-grained matrix (porphyry granite) to a cumulate granite in the eastern deeper portions. Abundant felsic microgranular enclaves (*fme*) with ellipsoidal shape and dimensions up to 4 m occur within both the red granite and the rapakivi granite, and are interpreted as products of recharge by new inputs of slightly hotter magma that broke up and froze within mushy portions of the chamber in advanced state of crystallization.

Whole-rock geochemistry helps recognize the identity of the three main magma pulses that constituted the pluton. Relative to the main body, the porphyry-rapakivi granite unit is on average slightly less felsic (0.3-0.4 wt% MgO), and has higher Ca, Ba and Sr. The *fme*, on the other hand, besides being distinctly less felsic (0.4-0.7 wt% MgO), are characterized by higher Rb and U, and lower Sr/Ba, Ba/Rb and Th/U. REE patterns ((La/Yb)_N= 14-18), (⁸⁷Sr/⁸⁶Sr)_i (0.7058-0.7074) and εNd_i (-10.0 to -10.6) do not discriminate the units, revealing the broadly cogenetic nature of all magma inputs. Very small (<3 cm) mafic microgranular enclaves (2.3-2.9 wt% MgO) had their chemical composition strongly transformed by reaction with the host granite magmas; although they are indicative that basic magmas participated in the genesis of the granites making up the pluton, these probably did not reach the exposed portions of the Salto chamber.

Financed by Fapesp, Grants 07/00635-5 and 2012/04148-0 and Ms Scholarship (2010/03300-7; to GSP)

Change in water circulation of the Bering Sea recorded by authigenic neodymium isotopes in sediments from the Bering Slope over 500 ka BP

KWANGCHUL JANG^{1*} AND YOUNGSOOK HUH¹

¹School of Earth and Environmental Sciences, Seoul National University, Seoul 151-747, Korea, wkdrhkd3@snu.ac.kr (*presenting author), yhuh@snu.ac.kr

The Bering Sea is located in the northernmost part of the Pacific Ocean, joining with the Arctic Ocean. Because of its proximity to the polar region which is sensitive to climate change, reconstructing the paleoenvironmental changes of this region is important. We analyzed the neodymium isotope ratios in Fe-Mn oxide coating of marine sediments from the Bering Slope (site U1345; water depth 1008 m) recovered during the Integrated Ocean Drilling Project (IODP) Expedition 323. The εNd value (n = 80) for the last 150 kyrs was relatively constant at an average value of -3.0 ± 0.8, which is slightly higher than the values of the Bering Strait (-4 to -6) [1]. We observed some deviations from the average εNd value. According to the tentative age model [2], trends toward unradiogenic value were observed during deglacial periods. The Yukon River whose pathway was blocked by sea ice during cold periods may have increased its input of unradiogenic material to the Bering Sea upon melting of sea ice during deglacial periods. Seasonal sea ice and brine formation may have facilitated the sinking of this unradiogenic water mass. A radiogenic εNd peak was observed in MIS 4. It may be interpreted as enhanced sinking of the Kamchatka-sourced radiogenic water as suggested by Horikawa *et al.* [2010].

[1] Dahlqvist *et al.* (2007) *Geochim. Cosmochim. Acta* 71, A196. [2] Takahashi *et al.* (2011) *Proc. IODP, 323*: Tokyo, doi:10.2204/iodp.proc.323.109.2011. [3] Horikawa *et al.* (2010) *Geology* 38, 435-438.

Fe and S redox cycling during a biostimulation episode at the Old Rifle, CO aquifer

N. JANOT^{1*}, J.S. LEZAMA-PACHECO², D.S. ALESSI³,
R. BERNIER-LATMANI³, E. SUVOROVA³, J.M. CERRATO⁴,
D.E. GIAMMAR⁴, L. YANG⁵, J.A. DAVIS⁵, P.M. FOX⁵,
K.H. WILLIAMS⁵, P.E. LONG⁵, K. HANDLEY⁶
AND J.R. BARGAR¹

¹Stanford Synchrotron Radiation Lightsource, USA,
njanot@slac.stanford.edu

²Stanford University, USA, jlezama@stanford.edu

³Ecole Polytechnique Fédérale de Lausanne, Switzerland,
rizlan.bernier-latmani@epfl.ch

⁴Washington University in St. Louis, USA,
degiammar@seas.wustl.edu

⁵Lawrence Berkeley National Laboratory, USA,
pelong@lbl.gov

⁶University of California Berkeley, USA,
kim.handley@berkeley.edu

In-situ bioremediation studies have shown that adding electron donor to groundwater stimulates the activity of metal- and sulfate-reducing bacteria, profoundly impacting the cycling and speciation of redox-sensitive elements such as iron and sulfur, and changing the redox status of contaminants such as U(VI) to insoluble U(IV) products. While numerous studies have examined the impact of bioreduction in laboratory-based studies, very few have examined Fe and S speciation changes at the molecular to pore scales *in situ* in a biostimulated aquifer. In this study, we used in-well columns to obtain direct access to sediment speciation at different time points during a bioremediation experiment at the Old Rifle site, CO, transitioning dominantly from iron-reducing to sulfate-reducing regime.

We investigated Fe and S speciation at the molecular scale using X-ray absorption spectroscopy (XAS). Chemical extractions of reduced sediments revealed the rates of Fe(II) and sulfide formation. Bulk Fe EXAFS showed a significant change of Fe redox status with ongoing bioremediation. Results provide evidence for the reduction of the entire S pool to monosulfide and elemental sulfur. The speciation of FeS grain coatings that appear under sulfate-reducing conditions was probed using electron microscopy and micro-XAS. Results showed elemental sulfur accumulating in the coatings which appear to also concentrate uranium.

REE microdistribution in laterite from Madagascar

E. JANOTS¹, F. BRUNET¹, A. BERGER², F. BERNIER¹,
M. MUNOZ¹, M. LANSON¹, N. TRCERA⁴ AND E. GNOS³

¹ISTerre, UJF-CNRS, Grenoble, France, janotse@ujf-grenoble.fr

²Institut of Earth Sciences, University of Bern, Switzerland

³Museum de Geneve, Switzerland

⁴Synchrotron SOLEIL, Gif-sur-Yvette, France

Despite of relatively low REE concentrations, laterites are attractive as REE ion-adsorption deposit because REE are sorbed on mineral surfaces (readily leached) and HREE are enriched in comparison to LREE. However, in laterites, the REE distribution is difficult to assess due to the small size of the host phases and their low REE concentrations. We present here an innovative approach to determine the microscale REE distribution by combining geochemical data (whole-rock elementary and isotopic composition) with high-resolution *in-situ* techniques including FE-SEM, EMP and synchrotron μ -XRF and μ -XAS (LUCIA beamline at SOLEIL, France). The investigated laterite developed by weathering of tonalitic rock in Madagascar. The weathering profile includes from bottom to top: fresh tonalite, saprolite, oxidized-soil layer and top-soil. Bulk-rock composition reveals REE-mobility along the profile. REE are significantly leached from the top-soil and they accumulate in the oxidized layer, which is also enriched in Mn⁴⁺ and other redox sensitive elements. In this oxidized soil, all REE concentrations are 3-4 times the bed-rock concentrations, but Ce reaches 9 times the bed-rock concentration. In all studied samples, electron images and XRF mapping indicate that the main Ce portion is hosted by REE-phosphates, which belong to the rhabdophane group in the saprolite and to the alunite-jarosite group in the oxidized-soil and top-soil. The CeIII/CeIV ratio in these minerals (determined from the Ce_LIII edge XANES) reflects that of the bulk-rock values. The highest Ce concentrations are localized in porous zones enriched in Mn-oxide of the oxidized-layer. Although cerianite and alunite-jarosite minerals appear as the main REE-hosts, Mn-oxides also contain significant REE amount. In comparison, clay-rich domains show low Ce concentrations. Our *in-situ* results confirm that phosphates are crucial REE-carriers in common laterites.

Protolith and metamorphism of Moldanubian HP granulites – a geochemical perspective

V. JANOUŠEK*, J. FRANĚK AND S. VRÁNA

Czech Geological Survey, Klárov 3, 118 21 Prague 1, Czech Rep. (*correspondence: vojtech.janousek@geology.cz)

Petrogenesis of voluminous, widespread and chemically nearly uniform felsic Moldanubian HP granulites in the Variscan orogenic root of the Bohemian Massif remains controversial. Previous studies of the best exposed Blanský les Granulite Massif (BLGM) showed that it originated by ~340 Ma HP–HT metamorphism of mid-Ordovician–Silurian [1] acid metaigneous rocks of Saxothuringian provenance [2]. Such refractory protoliths would suffer only limited chemical modification (mainly loss of U, Th, and Cs [2,3]).

Carefully selected samples from rare relict (S1) felsic–intermediate BLGM granulites help to constrain the peak mineral assemblage (Grs-rich Grt, Ky, mesoperthite) giving pressures of ~20–23 kbar (GASP barometry), higher than any previous estimates ([4] for review) and, together with geothermometric data from the same domain (~950 °C, see also [5]) support the early eclogite-facies history.

The other samples show small-scale mineral disequilibria (several mineral generations, zoning in mineral grains and various reactions related to HT decompression), contain large proportion of pre-Variscan (>400 Ma) inherited Zrn, preserve ~470 Ma Rb–Sr whole-rock errorochrons and show largely undepleted whole-rock geochemical signatures. This implies only a limited melt participation at the peak conditions [2,3].

We propose that the felsic Saxothuringian crust rich in heat-producing elements was deeply subducted [6,7] and re-laminated to the base of the Moldanubian crust. After thermal incubation, rheological weakening with a limited partial melting triggered gravitational instability and ascent of the orogenic lower crust [3,8]. The mantle contaminated by the passage of the crustal material produced characteristic K-rich magmas with crust-like Sr–Nd–Pb isotopic signatures, closely related with HP granulites in space and time [9].

Research funding: GAČR (P210-11-2358).

[1] Kröner *et al.* (2000) *CMP* **138**, 127-142. [2] Janoušek *et al.* (2004) *TRSE* **95**, 141-159. [3] Lexa O *et al.* (2011) *J Met. Geol* **29**, 79-102. [4] Franěk *et al.* (2011) *JMG* **29**, 53-78. [5] Tajčmanová *et al.* (2012) *CMP* **164**: 715-729. [6] O'Brien (2000) *Geol. Soc. London Spec. Pub.* **179**, 369-386. [7] Kotková (2011) *Geology* **39**, 667-670. [8] Maierová *et al.* (2012) *Stud. Geoph. Geod.* **56**, 595-619. [9] Janoušek & Holub (2007) *Proc. Geol. Assoc.* **118**, 75-86.

The Selva Negra: A Favourable Setting for Alkalic Au Mineralisation

NICHOLAS H. JANSEN¹, PETE HOLLINGS²
AND F. MARTINEZ-LEGORRETA³

¹CODES, ARC Centre for Excellence in Ore Deposits, Private Bag 126, Hobart, Tasmania 7001, Australia

²Geology Department, Lakehead University, 955 Oliver Road, Thunder Bay, Ontario, P7B 5E1, Canada

³SRK Consulting Mexico, Lava Street, #2, Int. 6, Cañada de La Bufa, 98619, Guadalupe, Zacatecas, Mexico

The Selva Negra volcanic rocks are located in Chiapas State, southeastern Mexico, in a complex triple junction between the North American, Caribbean, and Cocos plates. The Chiapanecan Volcanic Arc, which hosts the Selva Negra complex, activated around 3 Ma when slab flattening in central Mexico caused volcanism on the Pacific coast to change from parallel to the Middle American Trench to approximately 30° oblique to the trench. Volcanic activity was focused along northwest-oriented faults that extend from the Caribbean and North American plate boundary and likely acted as magma conduits during periods of extension.

The Selva Negra rocks occur at the northwest end of the coeval calc-alkaline arc and at the furthest point from the trench (300-330 km). They comprise widespread alkaline and LILE-enriched monzodiorite to diorite intrusions with a crystallization age of ~1.0 Ma (zircon U-Pb), trachyandesite volcanic rocks and rare basalt flows. The radiogenic isotope data suggest that the ascending magmas interacted with the thick crust (~50 km) through MASH processes. The Selva Negra rocks likely resulted from a combination of low degree partial melts of a heterogeneous mantle enriched in LILE and LREE and crustal contamination.

Alkaline magmatism is commonly associated with Au-rich deposits and several key geological parameters are favourable for their formation including rifted arc terranes, back-arc sites, extensional and post-subduction settings are [1, 2, 3]. In the case of the Selva Negra, slab flattening and the complex triple junction has refocused the magmatism 30° oblique to the trench allowing low degree partial melts and alkaline intrusions to occur at the furthest extension inland and creating a favourable setting for mineralising intrusions. Au-rich mineralisation has been intersected within the Selva Negra but remains largely underexplored.

[1] Sillitoe (2002) *Mineralium Deposita*, v. **37**, p. 788-790. [2] Richards, (1995) *Mineralogical Association of Canada, Short Course Series*, **23**, p. 367-400. [3] Hollings *et al.*, (2011) *Economic Geology*, v. **106**, p. 1257-1277.

Microbial and redox evolution in the Neoproterozoic of Australia

A. J. M. JARRETT^{1*}, S. W. POULTON², M. GIORGIONI¹,
AND J. J. BROCKS¹

¹Research School of Earth Sciences, The Australian National University, Canberra, ACT 0200. (* correspondence: amber.jarrett@anu.edu.au)

²School of Earth & Environment, University of Leeds, LS2 9JT, United Kingdom.

Availability of oxygen and a stable redox environment may have been major factors in the evolution of the Ediacaran biota [1]. Therefore, much research is focused on tracing the co-evolution of life and the redox state of marine environments through the Neoproterozoic. The Centralian Superbasin in Australia is one of the few places in the world where it is possible to study body fossils, redox conditions as well as molecular fossils in sediments ranging from the ~850 Ma Bitter Springs Formation to the Cambrian. The thick siliciclastic or evaporitic successions were deposited in a marine intracratonic basin and include evidence for two Snowball Earth events.

Here we provide first insights into the redox state of the Centralian Superbasin using Fe speciation data. In mid-shelf or deeper waters, our results document a major transition from a predominantly unstable ferruginous water column to a marine basin persistently oxygenated by at least 580 Ma. Therefore, the Centralian Superbasin became oxygenated at a time similar to other major basins worldwide [2].

We also complement the redox record with biomarker data from ~850 Ma to 570 Ma successions. We speculated that the transition from unstable redox conditions to persistently oxic conditions would also mark a transition to eukaryotic dominated ecosystems. Despite excellent organic preservation and the presence of abundant bacterial biomarkers, we did not find any evidence for a complementary increase in eukaryotic biomass. Thus, although oxygenated mid-shelf environments significantly predate the Ediacaran biota in Australia, eukaryotes such as algae and sponges did not become a dominant part of these oxic marine ecosystems for at least 20 Ma after full oxygenation [3, 4]. Therefore, the rise of eukaryotes to ecological dominance in the Neoproterozoic was not solely dependent on the availability of a stable oxygenated water column.

[1] Johnston *et al.*, (2012) *EPSL* **25-35**, 335-336. [2] Canfield *et al.* (2008) *Science* **321**, 949-952 [3] Grey (2005) *Mem. Assoc. Aust. Paleo.* **31**, 1-43. [4] Pawlowska *et al.* (2013) *Geology* **41**, 103-106.

Sealing time: Numerical simulation of water-rock interaction in volcanic systems

JASIM A.^{1*}, WHITAKER F.¹, RUST A.C.¹
AND SCOTT T.B.²

¹School of Earth Sciences, University of Bristol
(*alia.jasim@bristol.ac.uk)

²University of Bristol, Interface Analysis Centre

Clogging of porosity around active volcanos influences fluid flow paths, degassing processes and rock strength, altering the response of the volcano to deeper perturbations as well as meteoric recharge events. Water-rock interactions in systems characterised by significant gradients in temperature and pressure lead to the destabilisation of primary igneous minerals and precipitation of secondary phases. The objective of this research is to use RTM to provide a rigorous foundation for the development of a conceptual model describing the complexity of the interactions between circulating hydrothermal fluids and andesitic country rock.

Preliminary 1D simulations using TOUGHREACT permit identification of key controls, quantitative evaluation of their effects and interactions between different controls. The modelling is constrained using data from the well-studied andesitic composite Soufrière Hills Volcano (SHV) on Montserrat. Temperature is a key control on reaction kinetics and, in combination with effective reactive surface area (RSA) of component minerals, controls the evolution of mineralogy and porosity over time. Moreover we can evaluate key feedbacks between the effects of this paragenesis on permeability and the flow of fluids supplying reactants and removing alteration products. RTM simulations offer answers to questions such as; how long does the plagioclase take to disappear from the andesite? What is the rate of change of the porosity? Key challenges are better understanding of RSA and kinetics of reactions. Preliminary results allow us to start thinking about the effects of water-rock reactions in altering transport of mass and heat and implications for volcanic response and slope stability.

This work contributes to building a holistic understanding of volcanic systems within the framework of the VUELCO project (Volcanic Unrest in Europe and Latin America: phenomenology, eruption precursors, hazard forecast, and risk mitigation).

The “boring billion”: An exciting time for early eukaryotes!

E.J. JAVAUX^{1*}, J. BEGHIN¹, J-P. HOUZAY²
AND C. BLANPIED³

¹Dept Geology, Uni. of Liège, Liège, 4000, Belgium
(*correspondence: ej.javaux@ulg.ac.be)

²Fluids and Geochemistry Dpt, TOTAL, Pau, France

³Projets Nouveaux, TOTAL, Paris, France

The so-called ‘boring billion’ (~1.8-0.8 Ga) was characterized by a stratified ocean with anoxic ferruginous deep water, euxinic mid-water-column layer or wedges, and oxygenated shallow-water. These conditions are thought to have delayed eukaryotic diversification by limiting nutrient availability.

Here, we present a new, exquisitely preserved and morphologically diverse assemblage of organic-walled microfossils from the 1.1 Ga Taoudeni Basin of Mauritania. The assemblage includes diverse protists (ornamented and process-bearing acritarchs), possible multicellular xanthophyte algae, unidentified microfossils including smooth sphaeromorphs, prokaryotic filamentous sheaths and filaments, as well beautifully preserved microbial mats. Several taxa are reported for the first time in Africa.

This new microfossil assemblage, and others documented during the “boring billion”, evidence the early and worldwide diversification of eukaryotes. Stem eukaryotes appeared before or at the start of that time, had evolved a cytoskeleton, a nucleus, multicellularity, and diversified in mostly (but not only) shallow-water settings. Between 1.2 and 0.75 Ga, a major diversification of crown group eukaryotes occurred at the supergroup level, with key biological innovations such as cell differentiation, sexual reproduction, and eukaryotic photosynthesis by primary and secondary endosymbioses. Soon after the boring billion, a second diversification occurred but within supergroups, together with the evolution of eukaryotic biomineralisation and predation, and later on in the Ediacaran, tissue and organ-grade multicellularity.

Thus, the chemical state of the mid-proterozoic ocean does not entirely explain the pattern and timing of eukaryotic diversification, started well before the onset of global ocean ventilation around 0.8 Ga.

To better understand the paleobiology and paleoecology of early (stem or crown, aerobic or anaerobic) eukaryotes, we combine our morphological, microchemical and ultrastructural studies of microfossils, with high-resolution paleoenvironmental and paleoredox characterization.

The genesis of Enstatite Chondrites and the Earth.

MARC JAVOY^{1*} AND JAMES CONNOLLY²

¹Institut de Physique du Globe de Paris mja@ipgp.fr

²ETH Zurich, (james.connolly@erdw.ethz.ch)

The multielemental isotopic convergence between the Earth’s Mantle and Enstatite Chondrites (E Chondrites) likely results from a large scale high temperature isotopic equilibrium within the same isotopically homogeneous medium (« mother nebula »). High temperatures insured nearly total isotopic homogenisation, the residual differences between E chondrites and Earth being due to a temperature gradient inside the mother nebula, and/or cooling of a zone where E chondrites appear after the main accretion episode of the Earth. The mother nebula resulted from the high temperature (1550-1650K) processing of a mixture of solar gas with concentrated (150 ±20 times), dehydrated, and partially reduced CI dust, resulting in volatile (S, Na) and transitional (Si, Mg, Fe, Ni) elements’ enrichment and refractory (Al, Ca REE, actinides) elements depletion. The dust-gas proportion and the condensation temperatures are, respectively, constrained from the isotopic compositions of nitrogen and silicon. The mother nebula genesis likely took place during the Sun’s T Tauri phase. An appropriate location is the « dust chemical reactor » around 1AU, described in recent studies of T Tauri stars [1]. This also agrees with the idea that terrestrial planets accreted dominantly from a 0.7-1UA circumsolar annulus [2]. At 10⁻³ atmospheres the condensation sequence of such compositions reproduces the chemical and mineralogical composition of « primitive » EH3 Chondrites around 1150 K, and Earth’s bulk compositions at 1280-1420K, with large variations of the volatile (S, Na) contents and moderate changes of the Mg/Si ratio. The enhanced (Si +Mg)/O ratio of the dust-enriched mixture and the corresponding increase in oxygen uptake by the condensates, explain the very low oxygen fugacities observed, especially in the E chondrites’ temperature domain.

[1] Dullemond & Monnier (2010) *An Rev. Astro.Astrophys* 205-239 [2] Walsh *et al.* (2011) *Nature* **475** 206-208

Revisiting land to ocean fluxes

CATHERINE JEANDEL¹ AND ERIC H. OELKERS²

¹LEGOS (CNRS/UPS/IRD/CNES) Observatoire Midi-Pyrénées, 14 Ave Edouard Belin 31400 Toulouse France

²GET (CNRS/UPS/IRD) Observatoire Midi-Pyrénées, 14 Ave Edouard Belin 31400 Toulouse France

A large number of diverse observations reveal that substantial lithogenic material dissolution occurs at the land-ocean interface, a key area targeted by the GEOTRACES international program (www.geotraces.org).

1) The compositions and distribution of numerous elemental tracers and isotopic systems including Co, ¹⁴³Nd/ ¹⁴⁴Nd, ²³²Th/²³⁰Th, ³⁰Si/²⁸Si, ⁵⁶Fe/⁵⁴Fe in the oceans can only be accurately interpreted by taking account of a substantial input to seawater from lithogenic material from the continental shelf or margins [1].

2) Closed-system laboratory experiments show that a significant fraction of river transported material dissolves into seawater over the time scale of days to months, releasing elements and isotopes to the fluid [2].

3) A recent study demonstrated that particulate material dissolution is the dominant source of Sr to the waters the Borgarfjörður (Iceland) estuary (Jones *et al.*, in prep).

These observations suggest that from 0.5 and 10% of the mass contained in river transported particulate material is released to seawater during the first days to months following its arriving to the oceans. As the total particulate material flux to the world's oceans exceeds the corresponding dissolved load flux by as much as a factor of 30, particulate dissolution at the continental margins may be the dominant source of many of the elements present in the oceans [3].

To assess the significance of particulate dissolution on ocean chemistry, we have estimated the total global flux to seawater of a suite of elements originating from riverine transported particulate material by taking account of the average composition and mineralogy of continental and volcanic sourced particulates, together with the published dissolution rates for these minerals, measured surface areas of representative particulate materials, and mineral saturation indexes computed using PHREEQC. Results indicate that particulate material dissolution is a significant contributor to the global flux of major elements (e.g. Si, Ca, and Sr) to the oceans, and can dominate the fluxes of some critical trace elements and nutrients.

[1] Arsouze *et al.*, Biogeo., 2009; Fripiat *et al.*, Mar Chem. 2011; Radic *et al.*, EPSL, 2011; Bown *et al.*, Biogeo., 2013.

[2] Jones *et al.*, GCA, 2011; EPSL 2012; Pierce *et al.*, EPSL, 2013; Oelkers *et al.*, C.R. Geoscience, 2012. [3] Jeandel *et al.*, EOS, 2011.

Magmatic processes beneath Furnas volcano, São Miguel, Azores

A. J. JEFFERY¹, R. GERTISSER¹, B. O'DRISCOLL¹, A. PIMENTEL² AND J. M. PACHECO², S. SELF³

¹School of Physical and Geographical Sciences, Keele University, Keele, Staffordshire, ST5 5BG, UK.

(*correspondence: a.j.jeffery@keele.ac.uk)

²Centro de Vulcanologia e Avaliação de Riscos Geológicos, Universidade dos Açores, 9501-801 Ponta Delgada, Açores, Portugal

³Department of Earth and Environmental Sciences, The Open University, Milton Keynes, MK7 6AA, UK

Furnas, São Miguel, Azores is an oceanic-island caldera volcano characterised by mafic to silicic, metaluminous to peralkaline magmas, and a range of eruption styles that imply significant variation in pre- and syn-eruptive processes. Here, we investigate these processes and provide insights into the magma plumbing system of Furnas by targeting selected units within the volcano's stratigraphy. These include the products of two older caldera-forming events, namely the Povoação Ignimbrite (PI) (30,000 ¹⁴C y B.P.) and an ignimbrite interpreted to represent the second caldera-forming eruption (~12,000 ¹⁴C y B.P.), as well as the younger, sub-plinian eruptions (< ~5,000 ¹⁴C y B.P.) of the Upper Furnas Group (UFG), Furnas A-J.

The UFG spans a compositional range from metaluminous to mildly peralkaline trachyte, with agpaite indices (AI) between 0.73 and 1.13. Mineralogical assemblages of the UFG include alkali-feldspar, clinopyroxene, Ti-magnetite ± biotite, ilmenite and apatite, though phenocryst contents are typically low (< 5 vol.%). Ba and Sr concentrations are 5-115 and 2-51 ppm, respectively, whilst Nb and Zr contents are 177-303 and 1010-1498 ppm, respectively. A pronounced negative Eu anomaly (Eu/Eu* = 0.15) is present in all UFG samples. Rare cognate syenite nodules are present in Furnas J, comprising alkali-feldspar, clinopyroxene, amphibole, Fe-Ti oxides and apatite. The PI is trachytic and metaluminous (AI = 0.95-0.98), with no Eu anomaly. The mineral assemblage is similar to the UFG, but Ba and Sr contents are significantly higher (287-308 and 85-88 ppm, respectively), whilst Nb and Zr are notably lower (133-140 and 810-860 ppm, respectively) than in the UFG.

We discuss the geochemical variation of silicic magmatism at Furnas, and highlight the role of plagioclase and alkali-feldspar fractionation, alongside formation of a syenitic mush zone, in the derivation and shallow crustal evolution of Furnas magmas, as well as the temporal development of oceanic island, peralkaline magma systems.

Constraining Rates of Ocean Processes Using Tracers

W.J. JENKINS¹

¹Department of Marine Chemistry and Geochemistry, Woods Hole Oceanographic Institution, Woods Hole, MA 02543 USA

The marine environment is controlled by a complex interplay of physical, chemical, biological, and geological processes occurring over a vast array of time and space scales. Deconvoluting these processes is necessary to gain any quantitative understanding of how the ocean works and is a challenging task. Much of what we know about oceanic biogeochemical processes (and their rates) comes from the interpretation of the distributions of tracers combined with simple physical laws. Progress in measurement techniques have lead to numerous new tracer tools, including transient-, radioactive-, age-, and “steady state” tracers that have lead to remarkable insights into oceanic processes.

While we have advanced from the halcyon days of one-dimensional advection-diffusion models, we still struggle with some fundamental challenges arising from the nature of tracers and their observations. Among these are the fact that individual tracers, based on their *in situ* behavior and their boundary conditions in space and time, provide a specific, skewed measure of the ocean. Recognizing factoring in this bias is an important step forward for tracer oceanographers. Another important consideration is that the tracers’ boundary conditions and/or *in situ* behavior may not be completely defined or understood, so inclusion of these uncertainties into the confidence assigned to the results of our interpretation. Finally, we have to deal with the reality that tracer observations are usually sparse in both space and time. Although all of the above conspire to make life difficult for tracer geochemists, valuable insights can still be gained, and advances in tracer diagnostic methodologies hold considerable promise. Among the relatively new methods include Optimum Multi-Parameter Analysis (and the related Total Matrix Inversion), Transit-Time Distribution Analysis, and Age Tracer Contour Inverse Method. In this overview, I will attempt to compare these methods and tracers and point to future directions where progress may be made.

The competing roles of sulfide saturation, magma mixing and degassing during the petrogenesis of convergent margin magmas

F. JENNER^{1*}, E. H. HAURI¹, R. ARCULUS², J. A. MAVROGENES², H. ST.C. O’NEILL² AND T. H. E. WHAN²

¹Carnegie Institution of Washington, Department of Terrestrial Magnetism, Washington DC 20015-1305, U.S.A

(*correspondence: fjenner@ciw.edu)

²RSES, Australian National University, Canberra, Australia

The point at which the silicate melt becomes saturated with a sulfide phase in an evolving magmatic system depends on the initial S content and oxidation state of the parental melt. Because of their more oxidized character, evolving convergent margin magmas usually reach sulfide saturation at a more advanced stage of their evolution than mid-ocean ridge basalts (MORB). Sulfide saturation may be initiated by stabilization of magnetite: the so-called “Magnetite Crisis”, identified in the near-arc, Manus Backarc Basin submarine volcanic systems. Here we report new major and trace element data for submarine volcanic glasses from the magma-starved southern Valu Fa Ridge (SVFR), the current location of the propagating tip of backarc basin spreading of the Eastern Lau Spreading Centre in the Lau Basin, SW Pacific. The change of Cu/Se, Ag/Se and Cu/Ag with indices of evolution also indicate a Magnetite Crisis, demonstrating this process is not a localized phenomenon. In contrast, chalcophile element contents of submarine glasses from the more active Central Valu Fa Ridge (CVFR) are more scattered, which may be due to magma chamber recharge, resulting in illusion of sulfide saturation prior to the appearance of magnetite as a crystallizing phase. The systematics of chalcophile and volatile element abundances of Valu Fa Ridge samples are inconsistent with partitioning of Cu, Ag and Au into an exsolved Cl-rich brine or vapor phase during differentiation or degassing. The occurrence of volcanogenic hydrothermal sulfide deposits along the Valu Fa Ridge indicate that Cu, Ag and Au were likely leached from the host rocks during circulation of hydrothermal fluids post dating magmatic solidification, and accounting for the similarity of hydrothermal sulfide deposits in both the Manus and the Lau backarc basins.

Reactive transport in bentonite: Experiments and modelling

A. JENNI^{1*}, U. MÄDER¹ AND R. FERNÁNDEZ²

¹RWI, University of Bern, Institute of Geological Sciences,
Bern, Switzerland (*correspondence:
andreas.jenni@geo.unibe.ch, urs.maeder@geo.unibe.ch)

³Universidad Autónoma de Madrid, Departamento de
Geología y Geoquímica, Madrid, Spain
(raul.fernandez@uam.es)

Bentonite plays a key role in many engineered barrier concepts for nuclear waste repositories. Gradients in chemical composition, temperature, and water potential drive reactive transport in bentonite when acting as a barrier. Subsequent mineral reactions may influence the long-term performance of the material and are thus investigated.

The experimental approach consists of a compacted, saturated bentonite cylinder subjected to a confining pressure. In addition to chemical diffusion, an infiltration pressure leads to advective transport of an infiltrate through the cylinder [1]. As long as hydraulic conductivity (set by P_{inf} and P_{conf}) is slow compared to kinetics of phase reactions, this approach imitates a long-term diffusion-only reactive transport scenario.

Comparison of reactive transport at room temperature with an expected repository temperature of 140°C reveals that the same mechanisms operate: ion exchange in smectite, and gypsum dissolution.

Substantial differences of break-throughs and break-outs of anionic and neutral tracers, all non-reactive in this system, can be explained by anion exclusion from the smectite interlayer, where no advection is expected.

Therefore, the chosen model consists of a double porosity approach [2]: the “microporosity” domain (diffusion only), where chemistry is determined by charged smectite basal sheet surfaces and Donnan equilibrium, and the “macroporosity” (charge balanced, advective and diffusive transport). This multi-component model fits the experimental data and explains the substantial differences in tracer break-through behaviour.

[1] Dolder *et al.* (2013), this volume. [2] Galindez *et al.* (2012), Goldschmidt Conference, 884.

Origin of the Neoproterozoic zircon inheritance in the Arabian Shield

HEEJIN JEON^{1*}, MARTIN WHITEHOUSE¹
AND KHALID KADI²

¹Swedish Museum of Natural History, Stockholm, Sweden
(*correspondence: heejin.jeon@nrm.se)

²Saudi Geological Survey, Jeddah, Saudi Arabia

The Arabian Shield is the largest area of Neoproterozoic juvenile crust on Earth and consists of several oceanic island arc terranes. There is rare exposed old (pre-Neoproterozoic) crust in the shield and to date, no evidence of it at depth. However, many studies have reported pre-Neoproterozoic zircon inheritance from igneous and sedimentary rocks and even from ophiolites, whose origin is ambiguous. The cores are variously interpreted to have been inherited from the Khida (sub)terrane, the only continental terrane in the shield, attributed to the ‘contaminated’ nature of the shield by sedimentary incorporation, or to have survived subduction and transport through the mantle.

While pre-Neoproterozoic zircon core studies have been focused on determining their source(s), Neoproterozoic ones only slightly older than the host-rocks have received little attention, despite their abundance. The Neoproterozoic cores may have the same origin as the pre-Neoproterozoic ones or may be derived from another source: wall rocks, recycled materials of the juvenile arc crust, undetected older crust underneath the shield, or the mantle. In either case, new U-Pb and O isotopic data of the Neoproterozoic zircon inheritance gives insights into the evolution of the Arabian Shield

About 10 granite and sandstone samples were collected along an E-W transect across six terranes in the Arabian Shield. Zircon cores were dominantly targeted (>100 analyses) for U-Pb analysis with several rim spots in each sample for both inheritance and crystalline ages. The studied granite and sandstone were emplaced or deposited at ca. 640–610 Ma (Cryogenian–Ediacaran) and slightly older cores (mostly <800 Ma, Cryogenian) were found. The cores are clearly distinguished by discordant zoning and sometimes by different Th/U ratios from the surrounding rims. Corresponding stable O isotopic data help to determine origin of the cores in the Arabian Shield, most components of which are juvenile and newly formed. Thus, the new data of the Neoproterozoic zircon inheritance will contribute to understanding the formation processes and compositions of the terranes in the Arabian Shield.

Measurement of soil loss affected by rainfall and slopes with different rocks and slopes from Andong, Korea

JEONG GYO-CHEOL^{1*}, LEE JUN-JEONG²,
NAM KOUNG-HOON³, AND CHOO CHANG-OH⁴

¹Andong National University, Andong,

Korea (*correspondence: jeong@andong.ac.kr)

²InForworld, Seoul, Korea (jklee8103@paran.com)

³Andong National University, Andong, Korea
(namsoil@naver.com)

⁴Andong National University, Andong, Korea
(mineralogy@hanmail.net)

Since several factors such as the movement pattern of soil mass, intensity of rainfall, surface relief, soil mineralogy, or geology can affect the process of soil loss or landslide[1], it is not easy to predict them in the field. Here, we present some important factors that affect the behaviors of soil loss related to rock types, slopes, rainfall, and mineralogy. In recent years, there has been growing increase in annual rainfall in Korea and it is interesting to mention that more than 90 % of the total rainfall is recorded during the summer ranging from June to September, possibly due to climate change over the world. As a result, especially soil erosion or soil loss on natural slopes by such torrential rains became a matter of some concern on the rise. We investigated the characters of soil loss in four sites with different slope angles: two sites are gneiss, other two sites are sedimentary rocks, respectively.

Based on XRD data, constituent minerals in soils are quartz, feldspars, and clay minerals such as illite, kaolinite, and vermiculite. Soils tended to be much coarser as erosion proceeded, and especially the amount of fine particles (0.1~0.01 mm) decreased by 10 % while that of coarse particles (1.0~10 mm) increased drastically by more than 30~40 %. The rate of soil loss becomes high while the slope is steeper. As the process of soil erosion repeats, the grain sizes in soil tend to be coarser, which in turn acts as weakening the strength of the moisture holding ability in soil.

This study was supported by the GAIA Project (RE201202051), Ministry of Environment, Korea.

[1] Jeong *et al.* (2011) *Nat Hazards* **59**, 347-365

The distribution map of lead isotope compositions for galena from ore deposits in South Korea

Y.-J. JEONG¹, C.-S. CHEONG¹, H.J. CHO¹, J.Y. CHOI¹,
Y.M. AN¹, D.B. SHIN², S.J. KIM^{3A} AND J.J. HWANG³

¹Korea Basic Science Institute, Daejeon 305-333, Korea
(hero0123@kbsi.re.kr)

²Department of Geoenvironmental Sciences, Kongju National University, Kongju 314-701, Korea.

³Division of Conservation Science, National Research Institute of Cultural Heritage, Daejeon 305-380, Korea

In this study, we report the distribution map of lead isotope compositions for galena from ore deposits (n=91) in the southern part of the Korean peninsula with new and published data. The ore deposits are mostly skarn and hydrothermal-type deposits formed in close relation to the Mesozoic magmatic activities. The lead isotope compositions plot around the growth curve of the upper crust and orogene in the plumbotectonic model.

The comprehensived lead isotope data of this study indicated may be subdivided into four discrete zones that were recognized by geological consideration and statistical analysis for the ore lead composition.

Zone I geotectonically comprises the Gyeongsang basin in South Korea. Their ²⁰⁷Pb/²⁰⁴Pb ratios were characteristically low for the given ²⁰⁶Pb/²⁰⁴Pb ratios, suggesting an involvement of reservoirs with low time-integrated U/Pb and Th/U ratios such as the mantle or low crust. Zone II covers the northeastern Yeongnam massif and eastern Taebaeksan basin, lead isotopic composition of those had the most radiogenic in South Korea (²⁰⁶Pb/²⁰⁴Pb = 18.66–20.48, ²⁰⁷Pb/²⁰⁴Pb = 15.71–16.07, ²⁰⁸Pb/²⁰⁴Pb = 37.73–40.46). Zone III corresponds to the middle and southwestern parts of the Precambrian Yeongnam massif, the western part of Cambro-Ordovician Taebaeksan basin, and the Okcheon metamorphic belt. Galenas of these deposits showed the less radiogenic signature and limited variations in lead isotopic composition. The lead isotopic difference between zone II and zone III could be ascribed to the spatially-selective involvement of highly radiogenic crustal materials represented by the basement rocks (²⁰⁶Pb/²⁰⁴Pb up to 76) in the northeastern Yeongnam massif. Zone IV comprises the Gyeonggi massif of Precambrian craton in central parts of the Korean peninsula.

Such distribution map of lead isotope composition in South Korea may be useful of application for mining exploration, estimation of ancient artifacts, and environmental tracer.

Halogens in basalts of the Azores, Canaries and Tristan da Cunha

L.D.A. JEPSON^{1*}, R. BURGESS¹, V.A. FERNANDES²,
D. MURPHY³ AND C. BALLENTINE¹

¹School of Earth, Atmospheric and Environmental Sciences, University of Manchester, Oxford Road, Manchester, M13 9PL, UK (*correspondence:

lisa.abbott@postgrad.manchester.ac.uk)

²Museum für Naturkunde, Leibniz-Institut für Evolutions und Biodiversitätsforschung, Berlin, Germany

³School of Natural Resource Sciences, Queensland Institute of Technology, Brisbane, Australia

The halogens (Cl, Br, I) are moderately volatile elements that exhibit incompatible behaviour during melting, and are hydrophylic - in addition, iodine is strongly fractionated by biological processes. Although the halogens share similar geochemical properties to the noble gases, the heavy halogens in particular have been underutilized as tracers, because of the analytical difficulties related to determining their low abundances in geological materials.

Olivine and pyroxene mineral separates from basalts have been analysed from Tristan da Cunha, Canaries, and Azores ocean island groups. The halogens are assumed to be mainly sited in fluid (Canaries) and melt (Tristan, Azores) inclusions observed within the mineral phases; noble gases were liberated by a combination of crushing and stepped heating. Only bulk molar halogen ratios are quoted here.

The Tristan da Cunha basalts show Br/Cl and I/Cl ratios that extend from the range previously determined for MORB samples up to the high values characteristic of marine pore fluids, with maximum values of Br/Cl = 3.4×10^{-3} and I/Cl = 4.1×10^{-3} . This range is interpreted to represent a mixing trend between MORB and a subducted marine pore fluid or I-rich sediment signature, in the source of the Tristan da Cunha basalts.

Initial results show that the Azores basalts have a similar range in I/Cl ($9.92\text{--}253 \times 10^{-6}$) to MORB, with the Br/Cl values offset to slightly higher values ($0.62\text{--}4.22 \times 10^{-3}$). There appears to be some variation between islands, observed in the I/Cl values - with the samples from Graciosa having the highest I/Cl and Br/Cl ratios.

Crushing analyses show that the Canaries basalts have a similar range in Br/Cl ($0.456\text{--}1.07 \times 10^{-3}$) to MORB, but extend to much higher I/Cl values ($94.5\text{--}15500 \times 10^{-6}$). The data overlap with unpublished data from marine sediments. Analyses indicate the presence of a fluid component, which is not seen in the other OIBs.

Reducing uncertainty in the climatic interpretations of speleothem $\delta^{18}\text{O}$

CATHERINE N JEX^{*1,2,3}, S.J. PHIPPS^{4,5}, A. BAKER^{2,3} AND
C. BRADLEY⁶

¹Water Research Centre, School of Civil and Environmental Engineering, University of New South Wales, Sydney, New South Wales, 2052, Australia

(*correspondance: c.jex@unsw.edu.au)

²Connected Waters Initiative Research Centre, University of New South Wales, 110 King Street, Manly Vale, New South Wales, 2093, Australia

³Affiliated to the National Centre for Groundwater Research and Training (NCGRT), Australia.

⁴Climate Change Research Centre, University of New South Wales, Sydney, Australia.

⁵ARC Centre of Excellence for Climate System Science, University of New South Wales, Sydney, Australia.

⁶School of Geography, Earth and Environmental Sciences, University of Birmingham, Edgbaston, Birmingham, B15 2TT, UK.

We explore two principal areas of uncertainty associated with paleoclimate reconstructions from speleothem $\delta^{18}\text{O}$ ($\delta^{18}\text{O}_{\text{spel}}$): i. potential non-stationarity in relationships between local climate and larger-scale atmospheric circulation; and ii. routing of water through the karst aquifer. Using a $\delta^{18}\text{O}_{\text{spel}}$ record from Turkey, the CSIRO Mk3L climate system model and the KarstFOR karst hydrology model, we confirm the stationarity of relationships between cool season precipitation and regional circulation dynamics associated with the North Sea - Caspian Pattern since 1ka. Stalagmite $\delta^{18}\text{O}$ is predicted for the last 500 years, using precipitation and temperature output from the CSIRO Mk3L model and synthetic $\delta^{18}\text{O}$ of precipitation as inputs for the KarstFOR model. Interannual variability in the $\delta^{18}\text{O}_{\text{spel}}$ record is captured by KarstFOR, but we cannot reproduce the isotopically lighter conditions of the 16th to 17th Centuries. We argue that forward models of paleoclimate proxies (such as KarstFOR) embedded within isotope-enabled general circulation models are now required.

Carbon and Sr fluxes of river waters from a karstic and a granitic terrain in the Yangtze River system

HONGBING JI^{1,2} AND YONGBIN JIANG²

¹The State Key Laboratory of Environmental Geochemistry, Institute of Geochemistry, Chinese Academy of Sciences, Guiyang 550002, China

(*correspondence: hongbing.ji@yahoo.com)

²Department of Environmental Engineering, Civil and Environmental Engineering School, University of Science and Technology Beijing, Beijing 100083, China

Two typical subtropical watersheds were chosen in the Yangtze River, which have similar latitudes and climate, but distinct differences in basin lithologies. These features provide a good natural laboratory in which to investigate weathering processes, carbon and Sr fluxes in river waters. Total erosion rates, dissolved inorganic carbon flux and CO₂ uptake were 28.0 t km⁻² yr⁻¹, 2.9×10⁵ mol km⁻² yr⁻¹ and 2.3×10⁵ mol km⁻² yr⁻¹ for the granitic terrain and 70.2 t km⁻² yr⁻¹, 11.9×10⁵ mol km⁻² yr⁻¹ and 6.4×10⁵ mol km⁻² yr⁻¹ for the karstic terrain, respectively. These results indicated the karstic area plays an important role in uptake of CO₂ and DIC flux along the Yangtze River Basin. Our results revealed that the chemical erosion rate and Sr flux in the karstic terrain are twice and six times that of the granitic terrain. This indicates that the intensive carbonate weathering in the karstic area can provide much more Sr flux than that of silicate weathering in the granitic area. Our results support the conclusion the process of a non-steady state of rock cycling (e.g., the uneven distribution of dolomite through geological time) has an important meaning in elemental cycle and the global climate change (buffer effect).

Zircon U-Pb age and Hf isotope constraints on the petrogenesis of the Alpine Periadriatic intrusions

W.-Q. JI^{1*}, F.-Y. WU¹, M. TIEPOLO², A. LANGONE², AND R. BRAGA³

¹Institute of Geology and Geophysics, Chinese Academy of Sciences, Beijing 100029, China

(*correspondence: jiweiqiang@mail.iggcas.ac.cn)

²C.N.R.-I.G.G.-Pavia, 27100 Pavia, Italy

³University of Bologna, Italy

The origin of the Tertiary Periadriatic magmatism, developed along the Alpine Chain and its relationship with tectonic evolution of the Alpine Orogeny is still controversial. Integrated zircon U-Pb age and isotope study is an effective method to decipher petrogenesis of granite and crustal evolution in orogenic belt. Here we carried out zircon LA-ICPMS U-Pb and Hf isotope analyses on granitoid rocks from the major Periadriatic intrusions of the Western and Central Alps, including the plutons of Biella, Miagliano, Novate, Bergell and the Adamello batholith.

The dated granitoid rocks of different lithologies from the Biella pluton, yield identical ages of 30.5–30.1 Ma and similar $\epsilon_{\text{Hf}}(t)$ values of -5.9–1.8. The Miagliano tonalite gives an age of 32.6 ± 0.5 Ma and $\epsilon_{\text{Hf}}(t)$ value range from -5.2 to -1.3. The Novate pluton yields ages in the range of 26.5–23.5 Ma with $\epsilon_{\text{Hf}}(t)$ values vary from -8.5 to -2.5. The tonalites and the granodiorites from the Bergell plutons are dated at 32.1–30.3 Ma and 31.3–30.3 Ma, respectively. Their zircon $\epsilon_{\text{Hf}}(t)$ values vary from -5.0±0.5 to -3.2±0.3. In the Adamello batholith, the trondhjemites from Corno Alto pluton (43.2–43.0 Ma) and the tonalites from southern Re di Castello Unit (43.3–42.9 Ma) are coeval. Both units exhibit relatively high $\epsilon_{\text{Hf}}(t)$ values (5.0±0.6 – 7.7±0.3). Whereas the tonalite from Presanella pluton of north Adamello yield a young age (33.9±0.4 Ma) and low $\epsilon_{\text{Hf}}(t)$ values (-7.5±0.4).

The new data, combined with literature data, support two main stages of magma generation in the Alpine Orogen are at 43–40 Ma and 33–30 Ma. These two stages are associated with two contributions of juvenile materials during partial melting of magma source. We tentatively propose that the oldest rocks of the Periadriatic magmatism (Adamello batholith) may be related to removal of a thickened mountain root resulting from previous subduction. Partial melting at this stage was generated by the upwelling of asthenosphere, while subsequent northward magmatism of the Adamello batholith was ascribed to slab rollback. Then the ignition of the younger magmatism (33–30 Ma) along the Periadriatic Lineament is induced by slab breakoff.

Tetraether biomarker records for the last 60 kyr from a loess-paleosol sequence in the western Chinese Loess Plateau

GUODONG JIA^{1*}, ZHIGUO RAO², JIE ZHANG¹, ZHIYANG LI¹, AND FAHU CHEN^{1,2,3}

¹State Key Laboratory of Organic Geochemistry, Guangzhou Institute of Geochemistry, Chinese Academy of Sciences, Guangzhou, China (*correspondence: jiadg@gig.ac.cn)

²Key Laboratory of Western China's Environmental Systems (Ministry of Education), Lanzhou University, Lanzhou, China

In this study we present records of glycerol dialkyl glycerol tetraethers (GDGT)-derived proxies for the last 70 kyr from the Yuanbao LPS, western CLP. Temperature record reconstructed from the cyclization and methylation index of branched tetraethers (CBT-MBT) displays that the onset of deglacial warming at ~20 kyr BP precedes the strengthening of summer monsoon, which is in agreement in timing with previous CBT-MBT temperature records from the southeastern CLP. The maximal deglacial warming of ~10 °C is slightly higher than those in the southeastern CLP, perhaps due to the higher latitude and farther inland of the study site. The late Holocene temperature of ~8 °C is consistent with present mean air temperature from spring to autumn, not including winter temperature and suggesting that the growth of GDGT-producing bacteria in winter is retarded by the low temperature, and hence contributing insignificantly to its annual production. The branched/isoprenoid tetraether (BIT) Index shows higher values in the glacial loess and lower values in the Holocene paleosols, with a steady decreasing trend since the early Holocene. The decreasing trend could suggest that archaea production exceeded that of the branched GDGT producing bacteria since the early Holocene, but other possibilities, such as preferential degradation of isoprenoid GDGTs or upward increase in living archaea relative to bacteria in the paleosol profile, cannot be fully excluded. Our results thus demonstrate the need of future study on regional calibration of the CBT-MBT temperature proxy, microbial community structure in soil column and differential degradation of GDGT molecules.

A dustier world since MIS12 inferred from Sr and Nd isotopes of sediments in the western Philippine Sea

FUQING JIANG^{1*}, MARTIN FRANK², TIEGANG LI¹, TIAN-YU CHEN², YU ZHOU¹ AND ANCHUN LI¹

¹Institute of Oceanology, Chinese Academy of Sciences, Nanhai Road 7, 266071 Qingdao, P.R.China (*correspondence: fqjiang@qdio.ac.cn)

²GEOMAR Helmholtz Centre for Ocean Research Kiel, Wischhofstrasse 1-3, 24148 Kiel, Germany

Asian dust deposition in the tropical Pacific has supplied essential nutrients (e.g. Fe) to fuel bioproductivity and allows reconstruction of East Asian continental paleoclimate. Here we report a high-resolution record of dust supply to the tropical northwest Pacific over the past one million years derived from the analysis of radiogenic Sr and Nd isotopes in the marine sediments of core MD06-3050, located on Benham Rise in the western Philippine Sea.

The down-core variability of the Sr and Nd isotopic composition of the lithogenic fraction documents climatically induced changes in sediment supply from two isotopically distinct end-members: (1) Eolian dust from Asia and (2) volcanic material from the Luzon islands. The dust flux over the past one million years was closely coupled to glacial-interglacial climate cycles and showed a pronounced 100kyr periodicity. Eastern Asia has become overall dustier since MIS12 (0.47 Ma) as reflected by a marked increase of the average Asian dust flux from 0.27 to 0.45 g/(cm²-kyr). The “dustiest” conditions occurred during MIS12, MIS10 and the LGM. We suggest that this reflects increasing aridity of the Asian continent and an enhancement of the atmospheric circulation forced by changes in the eccentricity of the Earth's orbit. The higher dust flux may have amplified the internal feedbacks of the climate system and may thus serve as an explanation for the strong 100kyr glacial/interglacial cyclicity of the Late Quaternary.

Karsting mode and its features in YINGMAI-2 of North Tarim Basin, China

JIANG HUA, SUYUN HU, ZECHENG WANG
AND RUIJU WANG

PetroChina Research Institute of Petroleum Exploration & Development, Beijing 100083, China)

Distinctive heterogeneity of reservoir and its complex formation mechanism of marine carbonate rocks was focused in the fields of oil and gas exploration in China. Applying 3D seismic attributes, cores, imaging loggings and thin sections, etc, combined with fluid inclusions analysis and tectonic recovery techniques, reservoir characteristics and its formation mechanism were researched. It was concluded that it is not karst reservoir in YINGMAI-2 area, while it is reservoir controlled by faults. Reservoir space includes fracture and pore-fracture which was not or partly not filled with calcites. Furthermore, distribution of reservoir was controlled by faults. Through studying structure activities and fluid inclusion salinity, it was recognized that two types of fault-controlling karst happened, they were surface water karsting downward along faults and hydrothermal fluid upward along faults. The former was constructive for reservoir, while the latter was destructive. Based on the research, it was concluded that it was not enough to find karst crust type reservoir during oil and gas exploration, more types of reservoir should be concerned; fault-controlling karst could become prospecting fields.

Stability analysis on hydrocarbon secondary migration pathway

JIANG LIN^{123*}, BAO DONGMEI¹, HONG FENG¹²³,
HAO JIA-QING¹² AND FAN YANG⁴

¹Research Institute of Petroleum Exploration & Development, CNPC, Beijing 100083, China
jianglin01@petrochina.com.cn (*)

²State Key Laboratory of Enhanced Oil Recovery, Beijing 100083, China

³Key Laboratory of Basin Structure and Hydrocarbon Accumulation, CNPC, Beijing 100083, China

⁴School of Earth Sciences and Technology, China University of Petroleum (east China), Qingdao 26658, China

In order to accumulate in effective trap, hydrocarbon generated from source rocks has to go through a certain distance of secondary migration, therefore the process of hydrocarbon secondary migration has a great influence on hydrocarbon accumulation rate, eventually. The secondary migration process of crude oil can be divided into two types such as piston pattern and advantage pattern, the secondary migration of nature gas is an intermittent migration process composed by two basic migration ways of piston pattern and advantage pattern. The difference of secondary migration pattern leads to the differences of the migration pathway stability between crude oil and nature gas. The study used dye kerosene and nitrogen to conduct physical simulation experiment of secondary migration process respectively, discussing secondary migration pathway stability of crude oil and nature gas through way of more than once filling, and analysis its formation mechanism in view of the difference of physical characteristics of oil/gas/water and the relation of the difference between reservoir rock and oil/gas/water. The result indicates that the crude oil can change the rock wettability, and will not only alternate the free water located in the center of rock pores, but also replace the water adsorbed on the surface of porous rocks in secondary migration process. So crude oil could form a fairly stable migration pathway in the process of secondary migration, and its transport efficiency is higher. Natural gas can not change the wettability of porous rocks like crude oil does; natural gas form a relatively stable dynamic migration pathway in the process of secondary migration, the loss amount is larger while migrating.

Formation of hydroxylapatite with different morphologies and implication for biomineralization

SHU-DONG JIANG¹, QI-ZHI YAO² AND GEN-TAO ZHOU^{1*}

¹School of Earth and Space Sciences, University of Science and Technology of China, Hefei 230026, P. R. China (gtzhou@ustc.edu.cn)

²School of Chemistry and Materials Science, University of Science and Technology of China, Hefei 230026, P. R. China (qzyao@ustc.edu.cn)

Living organisms are capable of inducing and controlling the crystallization and deposition of a wide variety of minerals, but the vertebrates mainly utilize the calcium phosphates in constructing their mineral phases in both normal circumstances in bone, dentin, and tooth enamel and in pathological ectopic mineral deposits. The predominant form of the mineral in all situations is hydroxyapatite. Morphological control during mineral crystallization is one of the prominent hallmarks of biomineralization. A general consensus is that organisms can employ some of biological or organic molecules to produce crystals with special morphologies. Herein, hydroxyapatite (HAP) was synthesized in the absence of any biological or organic molecules at room temperature. The results show that different phosphate concentrations leads to the hydroxyapatite with various morphologies. However, the porous flower-like spheres are always obtained at the different concentrations of Ca^{2+} . Moreover, the initial precipitate is always an unstable amorphous calcium phosphate (ACP) at all different PO_4^{3-} concentrations used, and the generation of the HAP with various morphologies may have experienced the dissolution of the initial ACP, and then the recrystallization and self-assembly of HAP. Contrary to the common believe that crystal morphology control of biominerals is generally achieved by biological or organic molecules, our results suggest that PO_4^{3-} concentration may also play an important role in the different morphogenesis of HAP. The dependence of HAP morphology on phosphate concentration suggests that in biomineralization biological genetic and physicochemical factors can cooperatively influence the formation of HAP with unusual morphologies and hierarchical structures. As such, this provides a deep insight into biomineralization mechanism.

Engineered crumpled graphene oxide nanocomposite for environmental application

YI JIANG, WEI-NING WANG, JOHN D. FORTNER* AND PRATIM BISWAS*

Department of Energy, Environmental, and Chemical Engineering, Washington University in St. Louis, MO, 63130, United States (*Correspondence: jfortner@seas.wustl.edu; pbiswas@wustl.edu)

Graphene oxide (GO), with large specific surface area, strong hydrophilicity, and broad (chemical) functionalization possibilities, holds great promises for surface modification of engineered nanoparticles (ENPs). A one-step aerosol-based method, which utilizes evaporation-induced confinement force to crumple GO and thus effectively encapsulate ENPs, has been demonstrated to synthesize various GO-based binary and ternary nanocomposites, such as GO-magnetite (GOM), GO-TiO₂ (GOTI), and GO-TiO₂-Magnetite (GOTIM).

The as-synthesized quasi-spherical, core-shell nanostructured composites, with controllable size and functionality, have demonstrated outstanding water-stability. GOTI exhibited enhanced photocatalytic activity compared to bare TiO₂ due to increased lifetime of photo-induced holes and electrons; and reactive oxygen species, such as $\text{O}_2^{\cdot-}$, H_2O_2 , and OH^{\cdot} , have been identified by employing various radical scavenging experiments. GOM and GOTIM are ready to be magnetically recovered by one handheld magnet. Regarding nano-environment interfacial interactions, QCM-D is utilized to study deposition kinetics of GO-coated ENPs onto different model surfaces. The proposed facile aerosol-based method enables the encapsulation of nearly all pre-synthesized NPs by graphene oxide; and thus opens up many more possibilities in environmental applications, such as pollutant degradation and sensing, groundwater remediation. The potential impacts on the environment by examining the stability of the material will be examined. The compatibility with biological systems will also be discussed.

Rapid high amplitude variability in Baltic Sea hypoxia during the Holocene

TOM JILBERT¹ AND CAROLINE P. SLOMP¹

¹Department of Earth Sciences (Geochemistry), Faculty of Geosciences, Utrecht University, P.O. Box 80.021, 3508 TA Utrecht, The Netherlands.

Hypoxia (oxygen <2ml/L) is widespread in the modern Baltic Sea and has occurred intermittently throughout the Holocene. Previous studies based on the occurrence of laminated sediments have shown that during the Holocene Thermal Maximum (HTM) and Medieval Climate Anomaly (MCA), hypoxic conditions were present in the deep basins of the Baltic Sea. However, high-resolution, quantitative reconstructions of past hypoxia are lacking. Here we present sediment records of molybdenum enrichment (Mo/Al), organic carbon content (C_{org}) and the ratio of organic carbon to total phosphorus (C_{org}/P_{tot}) which facilitate the first detailed comparison between modern and past hypoxic conditions in the Baltic Sea. We show that the previously identified intervals of widespread hypoxia were in fact characterized by multiple centennial-scale hypoxic events, interrupted by periods of more oxic conditions. This rapid high amplitude variability in hypoxia intensity was likely forced by climatic oscillations – which influence the ventilation rate of the Baltic Sea – and amplified by positive feedbacks in the P cycle, which control export productivity. We show that the modern hypoxic event has a similar intensity to the most extreme past events, implying a maximum potential intensity of both hypoxia and productivity in the Baltic Sea. However, modern hypoxia intensified more rapidly than any past event, confirming the role of anthropogenic nutrient loading in forcing this coastal marine system into its current hypoxic state.

Crystallization of schwertmannite from Na-rich solutions

AMALIA JIMÉNEZ¹, ANGELES FERNÁNDEZ-GONZALEZ^{1*} AND MANUEL PRIETO¹

¹University of Oviedo, Spain, mafernan@geol.uniovi.es*

Schwertmannite is a ferric oxyhydroxysulphate ($Fe_8O_8(OH)_{5.5}(SO_4)_{1.25}$) formed in acid waters that may play a key role in the removal of toxic elements from aqueous solutions. It is generally accepted that this metastable phase is transformed into goethite and jarosite-like compounds, which infer changes in the chemical composition of aqueous solutions. Here, the objective is studying the crystallization of schwertmannite from sodium-rich solutions at ambient temperature and its stability during aging processes. For this purpose, a set of experiments was carried out by mixing $Fe_3(SO_4)_2$ (0.16M) and NaOH (0.5M) parent solutions which were kept at constant stirring (250 rpm) for specific reaction periods (1, 7, 14 and 21 days) at 25°C. Nature of the solids were characterized by X-Ray Diffraction (XRD) and Scanning Electron Microscopy (SEM). The surface of the solids was analyzed by X-ray photoelectron spectroscopy (XPS) and the binding energies of Fe2p_{3/2}, S2p, Na1s, and O1s core levels were obtained to determine the chemical state of the species. A colloidal mixture of dark brown colour is obtained at the beginning of the reaction, which changed to brown-reddish colour at the end of the period of reaction (21 days). Changes of colour in the mixture are associated with the evolution of the nature of solids as the aging process progresses. XRD reveal that the solid obtained in the early stage of experiments (1day) seems to be amorphous and evolves to a poorly crystalline phase. This phase matches with the pattern of schwertmannite which was recognized as a mineral in spite of its poor crystalline character (Bigham *et al.* 1994). Any other phases have not been identified in these diffractograms. SEM images show grains of higher size ($\approx 50 \mu m$) coexisting with grains of lower dimension ($< 5 \mu m$) in the entire aging process. All the particles displaying a shapeless morphology. The overall XPS spectra reveal the presence of sodium on the surface of schwertmannite. The binding energies obtained for Na, Fe, S and O suggest that sodium is adsorbed on the surface of the precipitates but a chemical bond is not established with iron, sulfur or oxygen. Thus, sodium has not been incorporated in the crystal structure of schwertmannite, which remains stable throughout the entire aging process at the experimental conditions used in the present work.

Bigham J.M., Carlson L. and Murad E. (1994) *Mineralogical Magazine*, **58**, 641-648.

Evidence for the microbial in situ conversion of oil to methane in the Dagang oilfield

NÚRIA JIMÉNEZ¹, MINMIN CAI^{1,2}, NONTJE STRAATEN³, BRANDON E L MORRIS¹, JUN YAO², HANS H RICHNOW¹ AND MARTIN KRÜGER³.

¹Helmholtz Centre for Environmental Research (UFZ), 04318 Leipzig, Germany

²School of Civil & Environment Engineering, University of Science and Technology Beijing, P. R. China

³Federal Institute for Geosciences and Natural Resources (BGR), 30655 Hannover, Germany

The microbial degradation of hydrocarbons in oil reservoirs affects the quality and economic value of recovered petroleum products. Recent studies suggest that anaerobic biodegradation may play a significant role in situ and the biodegradation of residual oil constituents under methanogenic conditions has been reported. Methane, like other gases, may aid in oil viscosity reduction and enhance flow characteristics through the reservoir matrix. In addition, methane may be used as a energy source.

The aim of this study was to assess the ability of indigenous microbial communities from a thermophilic oil reservoir (Dagang oilfield, China) to produce methane from crude oil under environmental conditions. The isotopic composition of reservoir fluids (H₂O, CO₂, CH₄) was analyzed, and GC-MS fingerprinting was applied to assess the oil composition in the reservoir. Microbial cell numbers were assessed by qPCR. Microcosms with ¹³C-labelled hydrocarbons were inoculated with production and injection waters to characterize these processes in vitro.

Analysis of oil samples confirmed that the majority of the oils from Dagang are highly weathered. Geochemical data from reservoir oil, water and gas are consistent with in situ biogenic methane production linked to aliphatic and aromatic hydrocarbon degradation. The bulk isotopic discrimination between methane and CO₂ was in accordance with previously reported results for methane formation during hydrocarbon degradation. Degradation experiments revealed that autochthonous microbiota is capable of producing heavy methane from ¹³C-labelled n-hexadecane or 2-methylnaphthalene. Microbial numbers in oil/water samples from production wells were abundant and the communities diverse, including methanogenic Archaea and hydrocarbon-degrading bacteria. In summary, the investigated areas of the Dagang reservoir may have significant potential for testing the viability of in situ conversion of oil to methane as an enhanced recovery method.

Occurrence of aerobic and methanogenic oil biodegradation in a water-flooded oil field

N. JIMÉNEZ^{1*}, M. CAI², Y. JUN², M. KRÜGER³ AND H.H. RICHNOW¹

¹UFZ, Permoserstraße 15, 04318 Leipzig, Germany

(*Correspondence: nuria.jimenez-garcia@ufz.de)

²University of Science and Technology Beijing - No. 30 Xueyuan Road, Haidian District, Beijing, P. R. China

³BGR, Stilleweg 2, 30655 Hannover, Germany

Water flooding is a secondary oil recovery method intending to enhance oil recovery by increasing the pressure in the oil-bearing strata. However, it can accelerate microbial oil degradation processes leading to a reduction of its quality (by changing its viscosity, sulfur content, etc.). In undisturbed subsurface oil reservoirs biodegradation is thought to be primarily anaerobic, as oxygen is practically unavailable, and methanogenesis may play a predominant role. Nevertheless, injection waters could be an oxygen source, causing alterations in the indigenous microbial communities. The conversion of oil to methane might be of interest because it does not require the supply of additional electron acceptors and methane could be recovered using the existing production infrastructure. On the other hand, aerobic oil biodegradation can involve the production of biosurfactants and other oil-releasing agents, which might favor oil production.

Oil biodegradation was investigated in a highly degraded water-flooded oil reservoir [1]. Isotopic composition of its gases was consistent with a biological origin ($\Delta\delta^{13}\text{C}$ between CH₄ and CO₂ ranging from 32 to 65‰). The reservoir contained an active microbial community, rich in syntrophic bacteria and methanogenic archaea, able to produce ¹³CH₄ and ¹³CO₂ ($\delta^{13}\text{C}$ up to 550‰) from ¹³C-labelled hydrocarbons *in vitro*. Additional laboratory experiments, using production waters, showed oil biodegradation potential not only under methanogenic but also under aerobic conditions. In both cases biodegradation patterns similar to those observed *in situ* were found: *n*-alkanes, *n*-alkyltoluenes and *n*-alkylbenzenes were removed before PAHs and biomarkers. Degradation decreased with increasing alkylation and ring number. A selective removal of some compounds like steranes or alkylated naphthalenes was observed. Further experiments will focus on studying biosurfactant production by indigenous oil degrading communities.

[1] Jiménez, Morris, Cai, Gründger, Yao, Richnow, Krüger (2012) *Organic Geochemistry* **52**, 44-54.

Geochemical studies of the weathering profile developed on the Pegmatitic terrain in Awo mining district, Southwestern Nigeria.

M.T. JIMOH^{1*}, A.T BOLARINWA² AND O. ARANSIOLA¹

¹Department of Earth Sciences, Ladoké Akintola University of Technology, Ogbomoso, Oyo State, Nigeria.

(*correspondence: jimohmustapha@yahoo.com)

²Department of Geology, University of Ibadan, Nigeria.

This study on geochemistry of the weathering profile developed on pegmatite in Awo mining district describes mobility of elements from the bedrock to the top soil. The report is targeted at obtaining the concentration of the major, trace and rare earth elements in the weathered profile revealing the degree of weathering. The pegmatite which intrudes the syenite and migmatite gneiss belongs to the NE/SW trending type.

The samples collected from the B-horizon were air dried, sieved with size of 75 mesh and analysed using X-ray Fluorescence Spectrometry (XRF) analytical technique of the digested samples at ACME Laboratory, Ontario, Canada.

The result of the major, trace and rare earth elements of the weathered soil revealed that Mg, Ca, Na and K have been extremely weathered and massively depleted. The mass percentage of these elements are Mg (-84.3%), Ca (-99.2%), Na (99.9%) and K (-96.0%). The Chemical Index of Alteration (CIA) for the soil samples 1 to 9 are 97%, 97%, 97%, 96%, 96%, 95%, 97%, 97% and 98% respectively; this shows high degree of weathering which indicate that Kaolinite is the clay mineral found in the mining site.

The analysis also shows that there is high abundance of rare metals typified by Ta (3 ppm), Nb (25.6ppm), Cs (26.3ppm), and Sn (36.7ppm), this reveals that the precambrian pegmatite of the study area rare metal bearing.

Integrated C and Cl isotope modeling of chlorinated ethenes degradation

BIAO JIN,¹ STEFAN B. HADERLEIN,¹
AND MASSIMO ROLLE^{1,2}

¹Center for Applied Geosciences, University of Tübingen, Hölderlinstr. 12, D-72074 Tübingen, Germany

²Department of Civil and Environmental Engineering, Stanford University, 473 Via Ortega, 94305 Stanford, CA, USA

We propose an integrated method to predict the evolution of carbon and chlorine isotope ratios and we apply the new approach to chlorinated aliphatic hydrocarbons dechlorination. The carbon and chlorine isotopic changes are explicitly simulated by tracking the cleavage of isotopically different C-Cl bonds of the combined carbon-chlorine isotopologues. To illustrate the proposed modeling approach we compare our method with the currently available method, in which carbon and chlorine isotopologues are treated separately. Our approach is self-consistent and provides an accurate description of dual-isotope effects regardless of the extent of the isotope fractionation and physical characteristics of the experimental system. We further applied the new approach to reproduce published experimental results on dehalogenation of chlorinated ethenes both in well-mixed systems and in situations where mass-transfer limitations control the overall rate of biodegradation. Our integrated dual isotope modeling approach is proved to be most advantageous when isotope fractionation factors of carbon and chlorine differed significantly and for systems with mass-transfer limitations, where both physical and (bio)chemical transformation processes affect the observed isotopic values.

Hydrochemical and stable isotopic assessment of water quality and its variations in rice-growing areas in East China

ZANFANG JIN, FEILI LI AND LINGXIAO CHEN

College of Biol. & Environ. Engineering, Zhejiang Univ. of Tech., Hangzhou 310032, China (jinzhanfang@zjut.edu.cn)

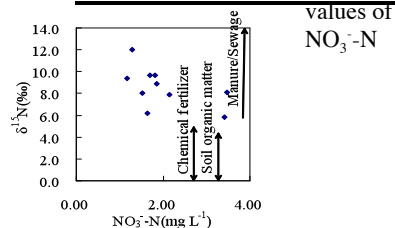
Nitrate contamination of surface-water and groundwater is a common occurrence worldwide. In drinking water, nitrate in excess of 10 mg N/L may be toxic for infants and may be responsible for increases in stomach cancer for other. The nitrogen-stable isotopic composition of nitrate has been extensively used for the identification of nitrogen sources and transformation pathways in hydrologic studies. The West Lake is a typical shallow lake located in Hangzhou city, China. East of the West Lake is on the verge of the downtown, the other three sides are surrounded by small hills. The West Lake has been in the risk of eutrophication and ecosystem degradation. Here, we have analyzed the dissolved anions in the West Lake, with the immediate goals of describing water quality and identifying the sources of nitrate in the West Lake.

All the samples were taken in the West Lake on April 4, 2012. The average pH value of water was 6.95, and all samples was weakly acidic. The average DO concentration of the surface water was 7.43 mg L⁻¹. The surface water was aerobic. The average BOD₅ and COD_{Cr} concentration of the samples was 3.0 mg L⁻¹ and 13.5 mg L⁻¹, respectively. Low BOD values and COD values reflect low burden of organic pollution in the West Lake. TP concentrations remained at a low level, was 0.075 mg L⁻¹ concentrations was low and was 0.29 mg L⁻¹. NO₃⁻-N concentration in the samples was higher than NH₄⁺-N concentrations, was 1.66mg L⁻¹. The average TN concentration was 2.48 mg L⁻¹. It was found that 75% of the surface water samples in the West Lake had higher TN concentration than the statutory limit (1.5 mg L⁻¹) for surface water (GB3838-2002). TN was the major contaminant. The δ¹⁵N_{NO3} values for the samples from the West Lake ranged from 5.8‰ to 12.0‰. It was probable that the sources of NO₃⁻-N were rainfall, manure applied to land, and agricultural fertilizer.

Table1: Water quality of the West Lake and the Environmental guideline of national quality standards for surface waters, China (GB3838-2002) (mg L⁻¹).

	Concentration/Ave.	Standard deviation	GB3838-2002/IV
DO	7.43	0.42	3.0
pH	6.95	0.04	≥ 6-9
BOD ₅	3.0	1.0	≤ 6.0
COD _{Cr}	13.5	5.1	≤ 30.0
TP	0.075	0.02	≤ 0.1
TN	2.48	0.47	≤ 1.5
NO ₃ ⁻ -N	1.66	0.29	≤ 10.0
NH ₄ ⁺ -N	0.29	0.23	≤ 1.5

Figure1: δ¹⁵N_{NO3} versus concentrations.



Halogen partitioning behavior at Earth's mantle conditions

B. JOACHIM, I. LYON, A. PAWLEY, T. HENKEL, L. RUZIE, P. CLAY, R. BURGESS AND C. J. BALLENTINE

School of Earth, Atmospheric and Environmental Sciences, University of Manchester, M139PL Manchester, United Kingdom (bastian.joachim@manchester.ac.uk)

Halogens have, because of their incompatibility, the potential to act as key tracers of volatile transport processes in the Earth's mantle. Combining Mid Ocean Ridge Basalt (MORB) [1] and Ocean Island Basalt (OIB) [2] bulk halogen concentrations with experimentally determined halogen partition coefficients (this study) allows us to investigate the halogen content and variance in different mantle reservoirs.

As starting material, we used a primitive mantle composition simplified to four components (CaO, MgO, Al₂O₃ and SiO₂), to which defined small amounts of halogens (~0.2 wt%) were added. Partition experiments were performed for 5 h at 1.0 to 2.5 GPa and 1500-1600°C.

Samples contain forsterite grains or a mixture of forsterite and orthopyroxene grains with a side length of up to 150 μm embedded in a MORB-like melt. Euhedral crystal shapes and the fact that no halogen concentration gradients are detectable within the crystals or melt indicate that experiments were performed at equilibrium conditions.

In all experiments, compatibilities of Br, Cl and F are ordered with $D_{Br}^{mineral/melt} < D_{Cl}^{mineral/melt} < D_{F}^{mineral/melt}$; e.g. $D_{Br}^{fo/melt}$ was determined to 0.128 at 1600°C ($D_{Cl}^{fo/melt} = 0.202$, $D_{F}^{fo/melt} = 0.259$; Uncertainties: ~20%). Our data combined with results of recent studies [3,4] show that fluorine and chlorine partitioning into forsterite increases by about two orders of magnitude between 1300°C and 1600°C and does not show a pressure dependence. Chlorine partitioning into orthopyroxene shows a similar temperature effect ($D_{Cl}^{opx/melt} = 0.905(81)$ at 1600°C and 2.3 GPa) but decreases significantly with increasing pressure.

By using natural bulk Cl concentrations in basalt [1,2] and assuming accumulated fractional melting [5], we are able to estimate bulk Cl concentrations of MORB (3-5 μg/g) and OIB (25-50 μg/g) source regions. Data suggest that the MORB source region is 80-95% more depleted in chlorine relative to the OIB source region.

[1] Ruzie *et al.* (2012) **V31A-2762**, AGU Fall Meeting. [2] Kendrick *et al.* (2012) *Geology* **40**, 1075-1078. [3] Beyer *et al.* (2011) *EPSL* **337-338**, 1-9. [4] Dalou *et al.* (2012) *CMP* **163**, 591-609. [5] Shaw (1970) *Geochim Cosmochim Acta* **34**, 237-243.

Advanced Antineutrino Estimation

G. R. JOCHER¹, S. USMAN, S. T. DYE
AND J. G. LEARNED

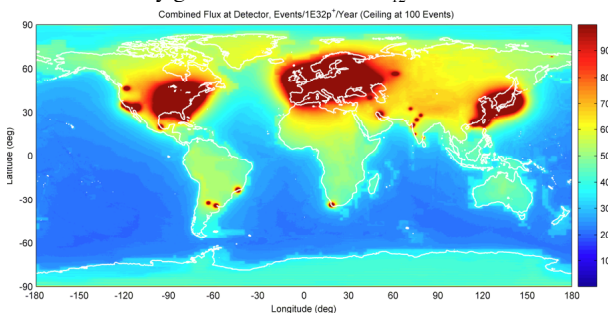
¹IAI, 15020 Conference Center Drive, Chantilly, VA, 20151
USA (correspondence: gjocher@integrity-apps.com)

Geoneutrinos are emitted via Uranium and Thorium decay within the Earth's crust and mantle, and, when observed by current antineutrino detectors can provide great insights into the inner geological workings of the Earth. Unfortunately though, these valuable geoneutrino measurements are nearly always obscured today within larger datasets populated by various types of unwanted background. Common approaches to this statistical quandary, such as trying to identify and filter out geoneutrinos from the background, are largely unsatisfactory and suboptimal. In this paper we attempt to combat this problem three ways.

First we introduce a novel mixture-distribution Bayesian estimator capable of operating in extremely low Signal to Background Ratio (SBR) environments. We show how, under real world conditions, an antineutrino signal obscured 100 times over by background (0.01 SBR) can still yield great quantities of information about a source if a moderate understanding of the obscuring background is available.

Secondly, we show how exploitation of the energy and direction vector of individual antineutrino measurements can offer far more information than that available by counts only. We show that crust-geoneutrinos can be segregated statistically from mantle-geoneutrinos in this manner.

Thirdly, we demonstrate the use of Cramer-Rao Lower Bounds for optimal detector placement. We evaluate the entire surface of the Earth and find the best spots to place a detector to study geoneutrinos and θ_{12} oscillations.



Lastly we model the entire Earth, and combine all the above methods into a large Monte Carlo simulation showing how four oceangoing antineutrino detectors, strategically placed around the world, can reduce geoneutrino flux uncertainty by 50%, and antineutrino θ_{12} oscillation uncertainty by 80% within just 1 year.

Ge/Si variations in the deep sea deduced from microanalyses of giant spicules of the sponge *Monorhaphis chuni*

K.P JOCHUM^{1*}, M.O. ANDREAE¹, J.A. SCHUESSLER²,
X.H. WANG³, B. STOLL¹, U. WEIS¹ AND W.E.G. MÜLLER³

¹Max Planck Institute for Chemistry, 55020 Mainz, Germany
(*correspondence: k.jochum@mpic.de)

²German Research Centre for Geosciences GFZ, Potsdam,
Germany

³Institute for Physiological Chemistry, Universitätsmedizin
Mainz, Germany

The exceptional longevity of the deep-sea sponge *Monorhaphis chuni* and the stability of their giant spicules provide the potential that they can be used as paleoenvironmental archives spanning the last 13 ka. To track secular variations of the geochemically similar elements Si and Ge [1] in the East and South China Sea, we used femtosecond-LA-MC-ICP-MS at GFZ and LA-ICP-MS at MPI for the high-resolution *in-situ* determination of Si isotope ratios and Ge and other trace element concentrations, respectively, in cross sections of giant spicules.

Significant variations in Si isotope ratios ($\delta^{30}\text{Si}$: from -1.9 to -3.7 ‰) and Ge concentrations (0.21-0.29 $\mu\text{g g}^{-1}$) were observed in the largest spicule collected so far (SCS-4, 2.7 m long) from a depth of 2100 m. No obvious trend in Si isotope variability could be identified in smaller and presumably younger spicules. To convert the Si isotope and Ge data into respective seawater concentrations, we used the inverse relationship of $\text{Si}(\text{OH})_4$ in seawater and $\delta^{30}\text{Si}$ in the sponge [2] as well as the linear relationship between Ge/Si in the sponge and the Ge concentration in the seawater [3]. Present-day Ge/Si is uniform and about 0.7 $\mu\text{mol mol}^{-1}$. In contrast, there are significant changes of Ge/Si in the time interval corresponding to the Younger Dryas event 11 – 13 ka BP, where Ge/Si is about 0.55 $\mu\text{mol mol}^{-1}$. A high value of 0.8 $\mu\text{mol mol}^{-1}$ was observed at the Holocene optimum around 6 ka BP. The Ge/Si pattern compares well with the results of previous studies on diatomaceous opal obtained from South Atlantic cores [4] and supports the idea of secular changes of whole ocean Ge/Si.

[1] Froelich and Andreae (1981) *Science* **213**, 205-207. [2] Hendry *et al.* (2010) *EPSL* **292**, 290-300. [3] Ellwood *et al.* (2006) *EPSL* **243**, 749-759. [4] Mortlock *et al.* (1991) *Nature* **220**, 220-223.

Kinetic isotope effect in the atmospheric reaction of the methane clumped isotopologue $^{13}\text{CH}_3\text{D}$ with OH and Cl

L. M. T. JOELSSON¹, R. FORECAST¹, S. ONO²
AND M. S. JOHNSON^{1*}

¹Copenhagen Center for Atmospheric Research, CCAR,
Department of Chemistry, University of Copenhagen,
Copenhagen, Denmark

²Department of Earth, Atmospheric and Planetary Sciences,
Massachusetts Institute of Technology, 77 Massachusetts
Avenue, Cambridge, MA 02139, USA

*Corresponding author msj@kiku.dk

Methane, as the long lived greenhouse gas with the second largest radiative forcing [1], has a significant impact on Earth's climate. Atmospheric methane abundance has undergone a critical growth from pre-industrial levels of 400-700 ppb to above 1750 ppb around year 2000, where the growth seemed to level out [1]. The recent trend, however, shows renewed growth [2]. The causes for these changes are not well known. Methane has an array of natural and anthropogenic sources. The study of clumped isotopes has proven useful for determining sources of atmospheric gases, since the formation temperature give each source contains a characteristic distribution of stable isotopes. Removal processes such as oxidation often prefer one isotopologue over another and thus shift the isotopic composition of atmospheric samples relative to the source. By characterizing the kinetic isotope effects of the sink reactions, the composition of the source can be determined.

Oxidation of methane by OH and Cl was studied experimentally in the photochemical reactor at Copenhagen Center for Atmospheric Research [5]. OH was formed from photolysis of ozone in the UV region and subsequent reaction with H₂O. Cl₂ was photolysed to obtain Cl radicals. A synthesised sample of pure $^{13}\text{CH}_3\text{D}$ was used along with natural abundance CH₄. Under the course of reaction several infrared spectra were recorded with a Bruker IFS 66v/s Fourier Transform Infrared spectrometer. The spectra were analysed using the non-linear least squares algorithm MALT [6]. The kinetic isotope effect α was obtained from the data points by linear regression as:

$$\alpha = \log\left(\frac{[^{13}\text{CH}_3\text{D}]_{t=0}/[^{13}\text{CH}_3\text{D}]_t}{[^{12}\text{CH}_4]_{t=0}/[^{12}\text{CH}_4]_t}\right)$$

We present the first results of this study.

[1] Solomon *et al.* (2007) Fourth Assessment Report of the IPCC. [2] NOAA Earth System Research Laboratory, <http://www.esrl.noaa.gov/gmd/obop/mlo/> 2013-04-12 [4] Nilsson *et al.* (2009), *Atmos. Environ.* **43** 3029–3033. [5] Griffith (1996), *Appl. Spectrosc.* **50** 59-70

Response of the biological pump to elevated ocean temperatures during the Eocene

E.H. JOHN^{*1}, P.N. PEARSON¹, B. WADE²,
H. K. COXALL³, G.L. FOSTER⁴, J. WILSON¹
AND A. RIDGWELL⁵

¹School of Earth and Ocean Sciences, Cardiff University,
CF10 3AT, johneh@cf.ac.uk (* presenting author)

²Earth Sciences, University College London, WC1E 6BT

³Department of Geological Sciences, Stockholm University,
Svante Arrhenius väg 8, SE-106 91 Stockholm, Sweden

⁴Ocean and Earth Science, National Oceanography Centre
Southampton, SO14 3ZH

⁵School of Geographical Sciences, University of Bristol, BS8
1SS.

The sensitivity of biological processes to changes in temperature is described in terms of Q₁₀, the fractional increase in metabolic rate per 10°C increase in temperature [1]. This value is greater in heterotrophs than autotrophs (e.g. [2,3]). Consequently, faster bacterial respiration rates in a warmer ocean may result in more efficient remineralisation of organic matter at shallower sinking depths with major implications for carbon and nutrient cycling. We find support for this in a series of reconstructed carbon isotope depth profiles based on well-preserved planktonic foraminifera assemblages from Tanzania and Mexico from the warm Eocene epoch. Our results suggest relatively sharp $\delta^{13}\text{C}$ gradients in the upper water column which supports hypotheses that invoke high metabolic rates in a warm Eocene ocean leading to more efficient recycling of organic matter and reduced burial rates of organic carbon [4]. We examined these ideas using a GENIE model that incorporates temperature sensitivities of primary producers and respiring bacteria, i.e. different Q₁₀ values.

[1] Arrhenius (1889) *Zeit. für Physik. Chem.* **4**, 226-248; [2] López-Urrutia *et al.* (2006) *Proc. Nat. Acad. Sci. USA.* **103**, 8739–8744; [3] Regaudie-de-Gioux & Duarte (2012) *Glob. Biogeochem. Cy.* **26**, GB1015; [4] Olivarez Lyle & Lyle (2006) *Paleoceanography* **21**, PA2007.

Quantifying nitrogen fixation in the North Atlantic using paired analyses of Cd and N stable isotopes.

S. G. JOHN¹*, T. M. CONWAY¹, K. L. CASCIOTTI²,
D. M. SIGMAN³, P. RAFTER³ AND D. MARCONI

¹Department of Earth and Ocean Sciences, University of South Carolina, Columbia, SC.

(*correspondence: sjohn@geol.sc.edu)

²Department of Environmental Earth System Science, Stanford University, Stanford, CA.

³Department of Geosciences, Princeton University, NJ.

For Cd and fixed N in the ocean, there are important similarities in the depth profiles of both dissolved concentration and stable isotopic composition ($\delta^{114}\text{Cd}$, and $\delta^{15}\text{N-NO}_3^-$). Both elements are biologically assimilated in surface waters and regenerated from sinking organic matter in the ocean interior. Preferential uptake of the lighter isotopes during biological assimilation typically leads to an increase in both $\delta^{114}\text{Cd}$ and $\delta^{15}\text{N-NO}_3^-$ in surface waters, and the isotopic signal of nutrient uptake in high latitude waters is subducted into water masses (such as Subantarctic Mode Water) that ventilate the mid-depths at low latitudes. Against this background of similar behaviour due assimilation and regeneration, differences between $\delta^{114}\text{Cd}$ and $\delta^{15}\text{N-NO}_3^-$ are expected in regions of active nitrogen fixation and denitrification, as these processes lower and raise the $\delta^{15}\text{N-NO}_3^-$, respectively, while they should not directly affect $\delta^{114}\text{Cd}$. Paired analyses of dissolved $\delta^{114}\text{Cd}$ and $\delta^{15}\text{N-NO}_3^-$ from the US GEOTRACES North Atlantic transect appear to show the expected distinction due to nitrogen fixation. Dissolved $\delta^{114}\text{Cd}$ increases from deep water into the permanent thermocline and then more sharply into the surface, due to biological assimilation, while $\delta^{15}\text{N-NO}_3^-$ decreases from deep water into the permanent thermocline, which has been interpreted as resulting from the remineralization of low $\delta^{15}\text{N}$ material from nitrogen fixation in low latitude surface waters.

Here, we use the difference between $\delta^{114}\text{Cd}$ and $\delta^{15}\text{N-NO}_3^-$ profiles in the North Atlantic to quantify the amount of low- $\delta^{15}\text{N-NO}_3^-$ 'newly fixed' nitrogen in the water column. $\delta^{114}\text{Cd}$ is used to calculate the $\delta^{15}\text{N-NO}_3^-$ profiles expected in the absence of nitrogen fixation, and the differences between this and the observed $\delta^{15}\text{N-NO}_3^-$ profiles are used to calculate the fraction and concentration of newly fixed N that has been oxidized to NO_3^- in the Atlantic interior.

Structure and fate of Zn-bearing green rust nanominerals in slightly acidic mine drainage crossing a steep redox boundary

C. A. JOHNSON¹*, G. FREYER², M. FABISCH²,
M. MURAYAMA¹, K. KÜSEL² AND M. F. HOHELLA JR¹

¹Virginia Tech, Blacksburg, VA, USA, (*correspondence: cjohns49@vt.edu, hochella@vt.edu, murayama@vt.edu)

²Friedrich Schiller University Jena, Jena, Germany, (maria.fabisch@uni-jena.de, kirsten.kuesel@uni-jena.de)

The fate and transport of inorganic contaminants in mine drainage systems are strongly dependent on pH and redox conditions. As drainage water crosses geochemical gradients, changes to the transporting particle and/or the contaminant speciation will dictate how the contaminant continues to be transported and how bioavailable it is. In order to gain insights into these processes, we examined water and sediments directly taken from a mine drainage outflow environment. Our field site is a former uranium mine near Ronneburg, Germany, where water outflow from the underground mine at pH 6 crosses a steep redox boundary. Contact with oxygen causes dramatic changes in the mineralogy of suspended particles that interact with metal(loid)s in the water and sediments. After careful sample preparation, we use analytical transmission electron microscopy to characterize the nanoscale structure and elemental composition and compare with measurements from standard bulk techniques.

The suspended particles in the anoxic mine outflow consist primarily of nanometer-thin pseudo-hexagonal Zn-bearing green rust platelets ($(\text{Fe}^{2+})_6\text{Fe}^{3+}_2(\text{OH})_{18}\cdot 4\text{H}_2\text{O}$) co-precipitated with amorphous silica. Green rusts have been found previously in groundwater systems, but are difficult to track due to rapid oxidation in aerated water. Zinc is the contaminant of second-highest concentration in the outflow. Once these particles cross the redox boundary, they undergo oxidative dissolution and rapidly co-precipitate with silica to form aggregates of spheroidal iron oxide nanoparticles. Some aggregates settle to the streambed where they get larger and grow needles, many of which are nanocrystalline goethite.

In this ongoing study, we show why knowledge of the formation, transformation, reactivity, and dissolution of nano-components are important in understanding the behavior and evolution of environmental systems.

Quantifying the isolation performance of CO₂ reservoirs: Requirements, results, and challenges

JAMES W JOHNSON¹

¹Schlumberger-Doll Research, 1 Hampshire St, MD A-139, Cambridge, MA 02139, USA, jwjohnson@slb.com

Transitioning the technical focus of CO₂ flood operations from the efficient extraction of hydrocarbons (CO₂ EOR) to the secure emplacement of CO₂ (+/- EOR) involves significant paradigm shifts for the oilfield services industry. Most important among these are new requirements to predict and monitor the fate of isolated (un-recycled) CO₂, which in turn requires baseline site (versus solely reservoir) characterization. Meeting these requirements demands the development of new modeling, monitoring, and characterization techniques. The isolation performance of engineered (and natural) CO₂ reservoirs is largely controlled by multiphase CO₂ migration, dynamic CO₂ mass partitioning among physical/chemical sinks, and reservoir/seal permeability evolution, all of which are strongly dependent upon specific integrated processes and system properties. These correlations can be quantified through reactive transport modeling, within which the operative processes of multiphase flow, geochemical mass transfer, and geomechanical deformation are explicitly integrated. In particular, important structural, compositional, and integrated-process constraints on CO₂ migration, mass partitioning dynamics, and permeability evolution can be identified, and the dependence of isolation performance (CO₂ capacity, footprint, and containment) on such migration, dynamics, and evolution can be assessed. In this paper, I will review the conceptual framework, present results obtained from applying this modeling approach to field projects, and discuss current challenges.

Manganese-oxidizing photosynthesis before the rise of cyanobacteria

JENA E. JOHNSON^{1*}, SAMUEL M. WEBB²,
KATHERINE THOMAS³, SHUHEI ONO³,
JOSEPH L. KIRSCHVINK¹ AND WOODWARD W. FISCHER¹

¹California Institute of Technology, Pasadena CA 91125
(*correspondence: jena@caltech.edu)

²Stanford Synchrotron Radiation Lightsource, Menlo Park CA 94025

³Massachusetts Institute of Technology, Cambridge MA 02139

The evolution of oxygenic photosynthesis was a singularity that fundamentally transformed our planet's core biogeochemical cycles and redox state. Here we probe the geological record for clues of the evolutionary pathway to light-driven water oxidation. One attractive hypothesis from the perspective of modern photo-assembly of the water-oxidizing complex posits a Mn(II)-oxidizing photosystem as a precursor to oxygenic photosynthesis [1,2]. We tested this hypothesis by exploring early Paleoproterozoic manganese deposits (up to 17 wt. % Mn) to test this hypothesis, captured in the 2415 ± 6 Ma Koegas Subgroup from scientific drill cores retrieved by the Agouron Drilling Project in South Africa. We utilized a novel X-ray absorption spectroscopy microprobe to make redox maps of these deposits at a 2µm scale to understand their petrogenesis and textural context. Coupled to light and electron microscopy and C isotopic measurements, we determined that all of the Mn is hosted in Mn(II) carbonate minerals produced from early diagenetic reduction of Mn-oxides with organic matter. To determine whether the Mn oxidant was molecular oxygen or a Mn-oxidizing photosystem, we examined two independent redox proxies sensitive to low levels of environmental oxygen—multiple sulfur isotopes analyzed using whole-rock IRMS and texture-specific SIMS techniques, and the presence of redox-sensitive detrital grains. Both proxies indicate O₂ was < 10^{-5.7} atm [3]. Kinetic calculations reveal that these maximal levels are several orders of magnitude too low to explain the observed Mn enrichments. The 2.415 Ga Mn deposits therefore provide strong geological evidence for an early, transitional Mn-oxidizing photosystem before the evolution of oxygenic photosynthesis.

[1] Zubay (1996) Academic Press: San Diego. [2] Allen & Martin (2007) *Nature* **445**, 610-612. [3] Pavlov & Kasting (2002) *Astrobiology* **2**, 27-41.

***In situ* immobilization of Pb using a natural Mn oxide by-product amended to contaminated soil**

K.L. JOHNSON^{1*}, C.M. MCCANN², J. TOURNEY¹, R.J. DAVENPORT², S.A. ROBERTSON¹, N.C. FINLAY¹, N.D. GREY², M. WADE² AND K. HUDSON-EDWARDS³

¹School of Engineering and Computing Sciences, Durham Univ., Durham, DH1 3LE, UK (*correspondence Karen.johnson@durham.ac.uk)

²School of Civil Engineering and Geosciences, Newcastle Univ. Newcastle, NE1 7RU, UK (clare.mccann@newcastle.ac.uk)

³Department of Earth and Planetary Sciences, Birkbeck Univ. London (k.hudson-edwards@bbk.ac.uk)

Natural Mn oxide (NMO)-coated sand byproducts from the water treatment industry were assessed as a potential remediation amendment for in situ immobilization of Pb in contaminated soils. Sorption of Pb by the NMO was found to be pH dependent in aqueous batch experiments and q_{max} was calculated. The viability of NMO amendment as a remediation strategy was determined through a 10 month outdoor lysimeter trial using naturally Pb contaminated soils mixed with 10 % by weight NMO. After 10 months available pore-water Pb did decrease but bioaccessibility data was equivocal and at odds with other literature e.g. [1],[2].

Our data, the first to explore the use of natural manganese oxides in contaminated soils suggests that it is difficult to establish a statistically significant reduction in available Pb concentrations and we suggest that this is due to the highly heterogeneous nature of Pb contamination in industrially contaminated soils. However, our electron probe X-ray mapping shows Pb immobilization on the Mn oxide coating of the sand grains, which were Pb free prior to their addition to the soils. Amendment of the Pb contaminated soil with NMO had no effect on gross microbial functioning as assessed by respiration, potential denitrification and nitrification rates. In addition, 454 pyrosequencing showed that NMO amendment did not alter soil microbial community structure or diversity. We conclude that NMO byproducts could be used as an effective soil amendment for the treatment of sites contaminated with Pb.

[1] Lee *et al.* (2011) *J. Haz. Materials* **186**, 2117-2122. [2] Beak *et al.* (2007) *EST* **42**, 779-785.

North Pacific SST variability and drought in Southwestern North America since 854 AD

K.R. JOHNSON^{1*}, S. MCCABE-GLYNN¹, C. STRONG², M. BERKELHAMMER³, A. SINHA⁴, H. CHENG⁵ AND R.L. EDWARDS⁵

¹Dept. of Earth System Science, Univ. of California, Irvine, CA 92697 (*correspondence: kathleen.johnson@uci.edu)

²University of Utah, Salt Lake City, Utah 84112

³CIRES/ATOC, University of Colorado, Boulder, CO 80309

⁴California State University, Dominguez Hills, CA 90747

⁵University of Minnesota, Minneapolis, MN 55455

Climate models predict increasing aridity in Southwestern North America (SWNA) as storm tracks intensify and shift poleward under global warming. However, precipitation in SWNA also exhibits significant natural variability, which has been linked to Pacific and Atlantic sea surface temperature (SST) regimes and the associated atmospheric circulation patterns. The North Pacific, in particular, is known to influence decadal precipitation variability in this region over the 20th century, yet little is known about its role in past droughts and pluvials. Here we present a new record of North Pacific SSTs and SWNA drought from 854 to 2007 A.D. derived from stable isotope ($\delta^{18}O$ and $\delta^{13}C$) and trace element (Mg/Ca, Sr/Ca) variations in a stalagmite (CRC-3) from Crystal Cave, located in the southern Sierra Nevada Mountains, CA (36.59°N; 118.82°W; 1,386 m). Crystal Cave drip water reflects the mean $\delta^{18}O$ of precipitation falling over the cave, which is largely controlled by moisture source region and storm track, with lower values reflecting transport from the North Pacific and higher values reflecting transport from the tropical Pacific. Storm tracks are influenced by North Pacific SST patterns and we find that CRC-3 $\delta^{18}O$ values are strongly correlated with SST anomalies in the Kuroshio Extension region in particular and we use this relationship to reconstruct KE SSTs from 854 to 2007 A.D.. A moderate correlation between $\delta^{13}C$, Mg/Ca, and Sr/Ca suggests that these proxies are linked to prior calcite precipitation, which is thought to reflect local effective precipitation. Comparison of the KE SST reconstruction with last millennium tree-ring records indicate only weak coherence between KE SST and SWNA droughts, with only some occurring during periods of warm KE SSTs, as seen in the instrumental record. $\delta^{13}C$, Mg/Ca, and Sr/Ca are, however, significantly correlated with tree ring records of drought. Through this novel multi-proxy approach, we demonstrate how records of large-scale ocean-atmosphere dynamics and local hydroclimate may be obtained from individual speleothem samples.

CO₂ photolysis produces mass independent fractionation and a ¹⁶O¹³C¹⁸O clumped isotope anomaly

MATTHEW S. JOHNSON^{1*}, JOHAN A. SCHMIDT¹,
REINHARD SCHINKE², CARL MEUSINGER¹,
ROSLYN FORECAST¹ AND JAMES R. LYONS³

¹Copenhagen Center for Atmospheric Research, CCAR,
Department of Chemistry, University of Copenhagen,
Copenhagen, Denmark

²Max-Planck-Institut für Dynamik und Selbstorganisation,
Göttingen, Germany

³Department of Earth and Space Sciences, University of
California, Los Angeles, USA

*Corresponding author msj@kiku.dk

Carbon dioxide is the main component of the atmospheres of Mars and Venus, and the early Earth. Photochemistry in these atmospheres is based on the UV photolysis of CO₂; fractionation in CO₂ photolysis impacts the isotopic composition of the photoproduct CO and O₂. For the first time, an accurate model of fractionation in CO₂ photolysis has been made, using the time-dependent methodology, yielding the temperature and isotopologue dependent CO₂ absorption cross sections: ¹⁶O¹²C¹⁶O (626), 627, 628, 636, and the clumped species 638. The calculations reproduce experimental absorption cross sections at low resolution without scaling intensity. The main results are: a) The accurate description of the temperature dependence of the CO₂ UV absorption cross section has a large impact on catalytic HOx radical concentrations in CO₂ atmospheres. b) CO₂ photolysis in the modern mesosphere has a ¹³C fractionation exceeding 300 per mil. This, together with CO₂ + O(¹D) exchange, may generate a significant CO₂ clumped isotope anomaly. c) In a CO₂ atmosphere, CO₂ photolysis produces mass independent fractionation (MIF) in the Ox reservoir. This, combined with a sink of oxygen to the surface of Mars and/or space, may impact the oxygen isotope distributions found in the Martian meteorite ALH84001 and the 'Black Beauty' meteorite NWA 7034.

Composition, formation, and role of the Si-rich surface layer during olivine dissolution

NATALIE C. JOHNSON^{1*}, KATE MAHER²,
DENNIS K. BIRD² AND GORDON E. BROWN JR¹²³

¹Department of Chemical Engineering, 381 North-South Mall,
Stauffer III, Stanford University, Stanford CA 94305
(*correspondance: nataliej@stanford.edu)

²Department of Geological and Environmental Sciences, 450 Serra
Mall, Braun Hall Building 320, Stanford University, Stanford CA
94305 (kmaher@stanford.edu, dbird@stanford.edu)

³Stanford Synchrotron Radiation Lightsource, 2575 Sand Hill Rd,
Menlo Park CA 94025 (gordon.brown@stanford.edu)

Olivine ((Mg,Fe)₂SiO₄) dissolution in the presence of water and supercritical CO₂ results in the formation of a Mg-depleted, Si-rich surface layer. The Si-rich layer may play a role in limiting olivine carbonation kinetics, but little is known about its mechanism of formation and chemical composition. This study probes the Si-rich layer by reacting olivine with a ²⁹Si-spiked CO₂-containing aqueous solution at 60°C and 100 bar, followed by analysis of the mineral products using ion microprobe depth profiling and TEM imaging of cross-sections. After 19 days of unmixed reaction, TEM imaging coupled with energy dispersive spectroscopy (EDS) revealed an amorphous Si-rich layer, 30-40 nm thick, with an average composition of MgSiO₃ [Figure 1]. The location of the Si-rich layer is visible in the image as a vertical stripe slightly lighter in color and in the plot as sharp drops in both the Mg:Si and O:Si ratios. Depth-profiling with the ion microprobe indicates that ²⁹Si penetrates >100 nm into the mineral surface. Combined TEM and SIMS results suggest that, under these conditions, the Si-rich layer forms due to a dissolution/precipitation mechanism.

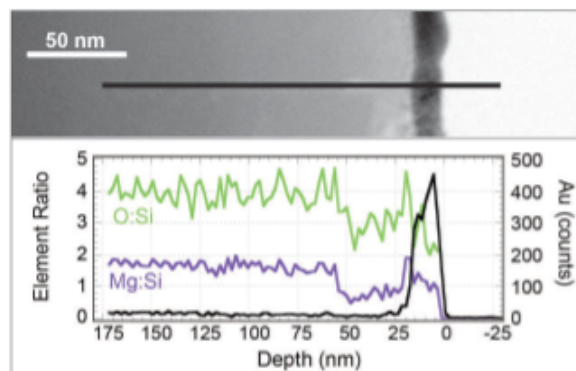


Figure 1: Scanning transmission electron microscopy image and results from an EDS line scan (location of scan marked by black line on image). Gold (black line in plot) was used to protect the mineral surface during cross section preparation.

Marine sediments as an archive of the evolution of volcanism on Montserrat

P. JOHNSON¹, E. INGLIS¹, I. MARCHANT¹, M. CASSIDY¹,
M.R. PALMER^{1*}, P.J. TALLING¹, T.M. GERON¹, S.
WATT¹ AND SHIPBOARD SCIENTISTS OF IODP LEG 340²

¹School of Ocean & Earth Science, University of
Southampton, European Way, Southampton SO14
3ZH,UK (*correspondance: pmrp@noc.soton.ac.uk)

²(http://iodp.tamu.edu/scienceops/expeditions/antilles_volcanism_landslides.html)

Island arc crust has a bulk composition that is approximately basaltic, but continental crust has a bulk andesitic composition. It has been suggested, however, that island arc crust is layered, with an upper portion that has a silicic composition similar to bulk continental crust, and a lower, mafic portion, that may be lost during transition from arc crust into continental crust. Testing of this model requires observations of clear trends in time and space that reflect the growth, evolution and differentiation of island arc crust.

Evolution of an arc centre also has geohazard implications. For example, if early activity is characterised by mafic volcanism and an absence of shallow magma storage, large-volume explosive eruptions are less likely to occur. The probability of tsunami-forming flank collapses may also increase as the crust thickens and a large, composite edifice forms. Large collapse events may also feedback into volcanic activity by releasing the confining pressure above a magma chamber, leading to the ascent of fresh, less evolved magmas, and a period of increased activity.

It is difficult, however, to test these and other models of the life cycle of an arc centre because erosion, collapses, later eruptions, etc., all obscure and destroy the subaerial record; e.g., ~75% of erupted material on Montserrat (Lesser Antilles) since 1995 has been transported to the Caribbean Sea. The best records of the evolution of arc centres are, therefore, preserved in nearby marine sediments. During IODP340 we recovered a complete sedimentary record from site U1396. This site (~30 km SW of Montserrat) comprises hemipelagic carbonate interspersed with >150 visible tephra layers extending back ~4.5 Myr (the oldest dated rocks on the island are only 2.6 Ma). We also obtained high-recovery records of collapse events from the east of the island at sites U1394 and U1395.

We present preliminary data from these IODP sites that reveal new information concerning the evolution of this arc volcanic centre.

Neoproterozoic ocean chemistry and redox evolution as inferred through sulfur isotope records

DAVID T. JOHNSTON¹

¹Dept. of Earth and Planetary Sciences, Harvard University,
20 Oxford St., Cambridge MA 02138:
johnston@eps.harvard.edu

The classic geochemical approach to reconstructing the net oxidation state of the ocean-atmosphere system is via tracking changes in the C, S and Fe cycles. Rebuilding the Neoproterozoic ocean-atmosphere and searching for the presumed second great rise in atmospheric oxygen has appropriately employed a similar approach. For example, work on the carbon cycle documents large perturbations in the marine DIC, however the interpretation of these anomalies and the links to redox budgets remain controversial. In parallel, great success has been gained through the pervasive application of Fe-based methods, which now appropriately serve as a backdrop to Neoproterozoic storylines, but record a more basal and less globally integrated signal. Parallel work on the sulfur cycle (³⁴S/³²S) carries interest, but often suffers from a lack of uniqueness in its interpretations—that is, biological and abiological processes can be hard to distinguish from one another and quantifying seawater sulfate concentrations remains elusive.

Similar to changes in global oxidation state, the role for the S cycle in Neoproterozoic ocean is not clear. A dominant electron acceptor in modern seawater, there is a thermodynamic expectation for sulfate to play a major role in anaerobic remineralization, especially given persistent anoxia in Neoproterozoic deeper water masses. However, thousands of shale analyses reveal strikingly low pyrite contents from both oxic shelves and deeper water facies, and only fleeting indications of euxinia associated with elevated organic carbon loading mark the Neoproterozoic. Viewed in parallel with pre-Sturtian sulfate evaporites and beautiful Marianoan barite crystal fans, the role of the S cycle gains added mystery. In hopes of gaining insight into the Neoproterozoic S cycle, here I present multiple sulfur isotope data from sulfides and sulfates from numerous Neoproterozoic basins. With ³³S, the opportunity exists to 1) differentiate between primary and burial diagenetic signals, 2) discern distillation from changes in biological isotope effects, and 3) uniquely track changes in classic measures of pyrite burial over long-timescales. This dataset is further viewed in light of new microbial data and modern marine sediment analyses, which together provides an independent perspective on later Proterozoic ocean-atmosphere oxygenation.

The isotopic composition and controls on modern seawater sulfate

DAVID T. JOHNSTON¹, BENJAMIN GILL²,
ANDREW MASTERTON¹, ERIN BEIRNE¹
AND WILLIAM BERELSON³,

¹Dept. of Earth and Planetary Sciences, Harvard University,

Cambridge MA 02138: johnston@eps.harvard.edu

²Dept. of Geosciences, Virginia Tech, Blacksburg, VA 24061

³Dept. of Earth Sciences, USC, Los Angeles CA 90089

The isotopic composition of seawater sulfate carries great utility for informing rates of modern biogeochemical cycling and tracking changes in oxidant budgets on geological timescales. These applications, and numerous others, lean on the analysis of modern seawater sulfate. Through decades of great work, it is broadly understood that the sulfate reservoir carries a long residence time (~ tens of millions of years), with the oxygen in sulfate turning over much more quickly (~ one million years). With this context, the modern ocean should carry a homogeneous isotopic composition. However, recent and quite provocative work suggests that oxygen minimum zones host a cryptic sulfur cycle (implicating potential effects on the isotope composition of both S and O in sulfate), while in parallel, experimental work on oxygen isotope exchange with S-bearing intermediates suggests that interpretations of ¹⁸O/¹⁶O in sulfate may also may also require updating.

To address these questions, we present ~ 200 measurements of modern seawater sulfate (³⁴S/³²S via SO₂ and ¹⁸O/¹⁶O via CO) through 10 vertical, 1-D profiles in different ocean basins with variable nutrient regimes. To complement these measurements, we targeted 4 of the profiles (BATS, SAFE and 2 profiles through oxygen minimum zones) for high precision ³³S and ³⁶S measurements generated via SF₆. With this, we first revisit decades of work on ¹⁸O and ³⁴S to place these data on a common scale (V-CDT and relative to SF₆), alleviating small but important differences in inferred compositions. The resultant isotopic composition of seawater sulfate (³⁴S/³²S, ³³S/³²S, ³⁶S/³²S, ¹⁸O/¹⁶O) allows for a series of major questions to be revisited. Of particular interest are: 1) Does the cryptic S cycle exist at a measurable scale? 2) What biogeochemical information is locked within the ¹⁸O/¹⁶O of sulfate? 3) What are the implications for the state of the marine sulfur cycle as a whole (is the modern cycle in steady-state or imbalanced)? We thank K. Casciotti, D. Capone, W. Homoky and A. Knapp for assistance in sample collection.

Iron geochemistry in redox-dynamic coastal wetlands: Consequences for trace element cycling in the environment

SCOTT G. JOHNSTON

Southern Cross GeoScience, Southern Cross University,

Lismore NSW 2480, Australia

(*correspondence: scott.johnston@scu.edu.au)

Many acidic coastal wetlands in eastern Australia contain abundant reactive iron species within their sediments due to oxidation of bioauthigenic pyrite. Redox fluctuations occur periodically within these wetlands due to changes in hydrology that are driven by natural climate variations, anthropogenic drainage and wetland remediation practices. These redox fluctuations drive complex iron geochemical cycling in the environment, influencing the bio-mineralisation, mobilisation and redistribution of iron species and co-associated trace elements. Here, we employ case-studies to explore iron redox transformations and trace element cycling within these wetlands at a variety of spatial and temporal scales. We examine the consequences for sediments, surface water and groundwater quality.

Remediation of acidic, Fe-rich wetlands via inundation with seawater can lead to mobilisation and redistribution of As and extreme enrichment of poorly crystalline Fe(III) (hydr)oxides (~40% Fe w/w) in redox-interfacial sediments. This results from a complex interplay between tidally controlled hydrology, landscape topography, sediment geochemistry and macroporosity. Highly heterogenous intertidal sediments also contain organic-rich micro-niches, where sulfate reduction occurs alongside As-bearing, pedogenic jarosite. We examine this spatial pairing of thermodynamic opposites by reacting S(-II) with As-bearing jarosite under a range of pH conditions. We quantify the corresponding iron mineral transformations and co-associated arsenic mobilisation, re-partitioning and speciation.

Anthropogenic drainage of Fe-rich acidic wetlands can also cause off-site impacts on estuarine sediments and receiving waters. Impacts include; tidally modulated discharge of low pH (~3) and metal-rich waters; elevated reactive-Fe, trace elements and REE's in downstream sediments and porewaters; drastically altered sedimentary sulfur geochemistry and; enhanced trace elements in some estuarine plant species.

We also explore how large, seasonal flood events in Fe-rich coastal wetlands can drive landscape-scale reductive mobilisation of Fe into floodplain surface waters. Anthropogenic drainage of these anoxic, C and Fe²⁺-rich waters influences the subsequent magnitude and intensity of large-scale (>40 km) riverine hypoxic events.

The Paleoproterozoic Rooiberg Group, Kaapvaal Craton, South Africa: New insights into the formation of silicic large igneous provinces (SLIPs)

OLUTOLA O. JOLAYEMI, JAMES ROBERTS
AND NILS LENHARDT

Department of Geology, University of Pretoria.

With an estimated erupted volume of 300,000 km³[2] and areal extent of ca. 200,000 km², the Paleoproterozoic (2.06 Ga) silicic volcanics of the Rooiberg Group (Kaapvaal Craton) in northern South Africa form one of the largest and oldest silicic large igneous provinces (SLIPs) known. These rocks can be sub-divided into four formations[1]: the Dullstroom, Damwal, Kwaggasnek and Schrikkloof Formations. Despite the uniqueness of these rocks and their scientific importance regarding the formation of SLIPs worldwide, the Rooiberg Group received little attention in the past. Therefore, a geochemical and petrological study was initiated to further investigate the petrogenesis of the Rooiberg Group, provide constraints on the magma forming processes and to come up with an explanation for the wide extent of its rhyolitic lava flows.

The Loskop Dam area, Mpumalanga province, ca. 120 km east of Pretoria, and one of the type localities for the Rooiberg Group, was found suitable as study area because of its good outcrop conditions and the fact that most of the formations can be found here.

The studied rocks vary from dacites to rhyolites. Comparison of major, trace and rare earth elements of the Rooiberg Group with other SLIPs around the world show remarkable similarities thus suggesting similar magma sources for the different SLIPs.

[1] Hatton, C.J. and Schweitzer, J.K. (1995), Evidence for synchronous extrusive and intrusive Bushveld magmatism. *Journal African Earth Sciences* **21**, 579-594. [2] Twist, D. and French, B.M. (1983), Voluminous acid volcanism in the Bushveld Complex: A review of the Rooiberg Felsite. *Bulletin Volcanologique* **46** (3), 225-242.

Diffusion of titanium in forsterite

M.C. JOLLANDS ^{1*}, H. ST. C. O'NEILL ¹, J. HERMANN ¹
AND C. SPANDLER ²

¹Research School of Earth Sciences, Australian National University, Canberra, ACT 0200, Australia
(*correspondence: mike.jollands@anu.edu.au)

²School of Earth and Environmental Sciences, James Cook University, Townsville, QLD 4811, Australia

Titanium diffusion in cubes of synthetic, pure forsterite has been determined as a function of chemical activity, oxygen fugacity (fO_2), crystal orientation, temperature and time at 1 atmosphere. Experimental run products were analysed using both LA-ICP-MS with a scanning rectangular beam, and EPMA in line profile mode. Experiments were conducted between 1300-1500°C, and diffusivity was shown to be positively temperature-dependent.

The experiments consistently produce non-Fickian diffusion profiles that do not fit an error function, hence diffusivity was determined from penetration distance of above-background Ti into the cubes.

In order to fix chemical activity in a three component system (SiO₂, MgO, TiO₂), the sources of Ti were four different three-phase buffers (forsterite–qandilite–periclase, forsterite–qandilite–geikielite, forsterite–geikielite–karooite, forsterite–karooite–enstatite). These were powdered and coupled to polished [001], [010] and [100] crystal faces. In all experiments, a strong positive dependence of diffusivity on silica activity was observed, with fastest diffusion in the presence of enstatite and slowest diffusion in buffers containing periclase. This result agrees with those of Ni, Co and Y diffusion in forsterite [1,2], suggesting Ti is predominantly diffusing on the M site.

Oxygen fugacity was fixed using either CO₂/CO mixtures or air, and experiments were run between $fO_2=10^{-0.7}$ and 10^{-12} . A large negative dependence of diffusivity on fO_2 is observed (slower diffusion in more oxidising conditions), possibly related to the Ti⁴⁺/Ti³⁺ transition. In addition, Ti solubility at the buffer-crystal interface increases as fO_2 decreases.

Diffusion is anisotropic; fastest along the *c* axis and slowest along the *a* axis. Contrasts between these findings and a recently presented data set in the same system [3] are currently being investigated.

[1] Zhukova et al. (2012) IGC abstract [2] Creppisson et al. (2012) EMC² abstract [3] Cherniak et al. (2012) Eos. Trans. AGU.

Geochemical mapping of $^{87}\text{Sr}/^{86}\text{Sr}$ ratios using stream sediments in Japan

Y. JOMORI^{1*}, M. MINAMI² AND A. OHTA³

¹Graduate School of Environmental Studies, Nagoya University, Chikusa, Nagoya, Japan

(*correspondence: jyomori@nendai.nagoya-u.ac.jp)

²Center for Chronological Research, Nagoya University, Japan

³Geological Survey of Japan, AIST, Japan

A series of nationwide geochemical maps of element concentrations using catchment outlet stream sediments (<180 μm) have been created by Geological Survey of Japan, AIST, in Japan [1]. The original purpose of this project was environmental assessment. Recently, the geochemical database is also applied to determinate producing area of food and tracking of human migration in archaeology. For such purposes, we have started to determine $^{87}\text{Sr}/^{86}\text{Sr}$ ratios in stream sediments of whole Japan because isotope fractionation is much smaller than concentration variation.

As a first step, we investigated appropriate grain sizes of stream sediments for the $^{87}\text{Sr}/^{86}\text{Sr}$ mapping project because it is unknown whether the fine sediments (<180 μm) are also suitable for the above purposes or not. The stream sediments were collected from two river systems. They were sieved into 6 fractions (1000–500 μm , 500–300 μm , 300–180 μm , 180–125 μm , 125–75 μm , and <75 μm), and each size fraction was measured for $^{87}\text{Sr}/^{86}\text{Sr}$ ratios by thermal ionization mass spectrometry (TIMS; VG Sector 54). The results indicate that $^{87}\text{Sr}/^{86}\text{Sr}$ ratio in <180 μm fraction shows the most representative value of bedrocks in the catchment area.

Secondly, we created the $^{87}\text{Sr}/^{86}\text{Sr}$ geochemical map using stream sediments (<180 μm) in Shikoku Island and the Kii Peninsula in Japan, to investigate the factors controlling spatial distribution of the $^{87}\text{Sr}/^{86}\text{Sr}$ ratios [2]. The $^{87}\text{Sr}/^{86}\text{Sr}$ ratios range from 0.705 to 0.719. The variation corresponds to the distributions of geological units. For example, underlying Neogene-Cretaceous accretionary complexes in the southern part of this area show the highest values (0.718–0.719), while the other regions covered by the older accretionary complexes have the lower isotope ratios. The fact suggests that detrital materials derived from the Asian continent having high $^{87}\text{Sr}/^{86}\text{Sr}$ ratio were supplied to the fore-arc basin during the Neogene and Cretaceous ages. From the results, we concluded that newly created $^{87}\text{Sr}/^{86}\text{Sr}$ maps reflect geochemical features of source rocks faithfully.

[1] Imai *et al.* (2010) Available at <http://riodb02.aist.go.jp/geochemmap/index.htm>. [2] Jomori *et al.* (in press) *Geochemical Journal*

Grain boundaries and transient porosity as fluid pathways for reaction front propagation

LAURA JONAS^{1,2}, TIMM JOHN¹, HELENE E. KING¹, THORSTEN GEISLER³ AND ANDREW PUTNIS¹

¹Institut für Mineralogie, Universität Münster, Germany

²Institut für Mineralogie, Geologie und Geophysik, Universität Bochum, Germany (Laura.Jonas@rub.de)

³Steinmann-Institut für Geologie, Mineralogie und Paläontologie, Universität Bonn, Germany

We used the pseudomorphic replacement of Carrara marble by calcium phosphates as a model system to study the influence of different fluid pathways for reaction front propagation induced by fluid-rock interaction. Grain boundaries present in the rock as well as the transient porosity structures developing throughout the replacement reaction enable the reaction front to progress further into the rock as well as to the center of each single grain until transformation is complete. Hydrothermal treatment of the marble using phosphate bearing solutions led to the formation of OH-apatite and β -TCP; the formation of the latter phase was probably promoted by ~0.6 wt.% Mg in the parent carbonate phase. Completely transformed single grains show a distinctive zoning, both in composition and texture. Whereas areas next to the grain boundary consist of nearly pure OH-apatite with a coarse porosity, areas close to the center of the single grains have a high amount of β -TCP and a very fine porous microstructure. The use of the isotope ^{18}O as a chronometer for the replacement reaction makes it possible to reconstruct the chronological development of the calcium phosphate reaction front. Raman analysis revealed that the incorporation of ^{18}O in the PO_4 tetrahedron of OH-apatite results in the development of distinct profiles in the calcium phosphate reaction front perpendicular to the grain boundaries of the marble. Through the use of the ^{18}O chronometer, it is possible to estimate and compare the time effectiveness of the different fluid pathways in this model system. The results demonstrate that the grain boundaries are an effective pathway enabling the fluid to penetrate the rock more than one order of magnitude faster compared to the newly developing channel-like porosity structures, which act as pathways towards the center of single mineral grains. Thus, after only short reaction durations, it may be possible for the fluid to progress relatively large distances along the grain boundaries without developing broad reaction fronts along the path.

Mineralogical effects on microbial diversity and accumulation in subsurface communities

AARON A. JONES* AND PHILIP C. BENNETT

The University of Texas at Austin, Austin, TX 78712, USA,
(*correspondence: aaajones@utexas.edu)

The rocks and minerals that comprise the subsurface lithology; each have properties that will potentially benefit specific microbial communities, especially those uniquely adapted to take advantage of these surfaces. We present experimental evidence that microorganisms colonize rock surfaces according to the rock's chemistry and the organism's metabolic requirements and tolerances. We investigated this phenomenon using laboratory reactors, which allowed microbial colonization of assorted surfaces by both a pure culture of the sulfur-oxidizing bacteria (SOB) *Thiothrix unzii* and a diverse mixed environmental sulfur-metabolizing microbial inoculant collected from Lower Kane Cave, WY, USA. Variations in microbial community structure on each surface were characterized and quantified by SEM, total biomass accumulation measurements, and high-throughput 16S rRNA sequencing.

We found that the combination of mineral properties such as buffering-capacity, nutrient content and aluminum content; as well as cell wall electronegativity, and competitive exclusion control biomass density and diversity of microbial communities attached to rock and mineral surfaces. Diversity analysis reveals that nearly identical communities, primarily composed of neutrophilic SOB, colonize a variety of carbonate surfaces. This resulted in aggressive dissolution of the carbonate minerals, producing a characteristic weathered surface texture. In contrast, a variety of silicate surfaces accumulate highly dissimilar communities with abundant acidophilic microorganisms colonizing only non-buffering quartz. Nutrient rich minerals consistently accumulated substantial biofilms. Nutrient poor and potentially toxic aluminosilicates accumulated very sparse, but highly diverse biofilms composed of a relatively large relative abundance of microorganisms that have been shown to have the ability to neutralize toxic aluminum. Also, Gram-positive bacteria are almost completely excluded from colonization of carbonate surfaces, but are abundant on all of the silicates.

Additionally, members of the genus *Thiothrix* (often found in mid-ocean ridge environments) show an affinity for basalt in both pure and mixed cultures, where it competitively excludes other SOB. These results suggest that adaptations to specific rocks are retained despite displacement of the organism in time and space from an ancestral rock habitat.

Is Diamond a repository of mantle helium and noble gases ?

ADRIAN P JONES¹ AND SUDESHNA BASU¹

¹Dept Earth Sciences, University College London, Gower S.,
London WC1E 6BT;
email adrian.jones@ucl.ac.uk; sudesnabg@yahoo.com

The high ³He/⁴He ratios observed in some oceanic island basalts has been explained by the presence of a primordial undegassed reservoir, a model now often considered untenable. Other geodynamic models have been suggested but need further testing [1]. Considering the very high ³He/⁴He in diamonds from pipes, and a range spanning six orders of magnitude varying with location, age and history, we propose that diamonds can be an important repository of helium and other noble gases in Earth's mantle. Residence times of billions of years are implied from preserved internal zonation. This work has evolved from combining our review of noble gas data for natural diamonds [2], with recent data and perspectives for Earth's deep carbon through time [3]. The mantle, at depths > 150 km along continental and oceanic geothermal gradients is in the diamond stability field [4]. Considering the low solubility of C and incompatibility of noble gases in mantle silicates and oxides, diamonds trapping large amounts of noble gases can crystallize within a large volume of Earth's mantle in the presence of carbonate or methane. The true amount of diamond crystallizing will be much larger than that actually erupted [5]. The noble gases can be released when diamonds graphitize or oxidize, and the mobility of a variety of small degree melts may be the rate-limiting step. It will be important to investigate the solubility of noble gases in diamond forming melt at mantle conditions.

[1] Class C and Goldstein SL (2005). *Nature* **436**, 1107.
[2] Basu S, *et al.* submitted Earth Sci Reviews 2013. [3] Hazen RM, Jones AP, Baross J (eds) *Carbon in Earth RIMG* 75, 2013. [4] Stachel T, Brey GP and Harris JW (2005) *Elements* 1, 73. [5] Shirey *et al.*, (2013) *Rev. Mineral. & Geochem.* **75**, 355.

Acknowledgement: We thank the Levrulme Trust for a Research Grant 2009-11

Entire community of microbes lacks phospholipids

JONES, C.¹, CROWE, S.A.¹, VIEHWEGER, B.², HINRICHS, K.-U.², MARESCA, J.A.³, DELONG E.⁴, NOMOSATRYO, S.⁵, FOWLE, D.A.⁶, AND CANFIELD, D.E.¹

¹NordCEE, U. Southern Denmark, Odense, Denmark

²MARUM, U. Bremen, Bremen, Germany

³Civil and Env. Eng., U. Delaware, Newark, USA

⁴Civil and Env. Eng., Mass. Inst. Tech., Cambridge, USA

⁵LIPI, Indonesian Inst. of Science, Cibinong, Indonesia

⁶Geology, U. Kansas, Lawrence, USA

Phosphorus is an essential nutrient for life, and aquatic microorganisms have strict P requirements for cellular structure, energy, function, and replication. We examined the physiological capacity of a microbial community to cope with extreme P limitation. This community lives in the surface waters of Lake Matano, an ultra-oligotrophic, stratified, ferruginous, ancient lake situated on Sulawesi Island, Indonesia. Based on dissolved nutrient concentrations in the surface waters, the elemental composition of microbial biomass, alkaline phosphatase enzyme assays, metagenomic analyses, and C-fixation assays with and without added P, we show that biomass production is P limited in the surface waters (0-100 m). The planktonic microbial community has responded to the extreme scarcity of available P through increased bulk C:P ratios (>1000), an order of magnitude higher than the Redfield ratio of 106:1. Such high C:P ratios are in part explainable by a lack of detectable phospholipids in the microbial biomass. Instead, abundant and structurally diverse betaine and glycolipids substitute for phospholipids, reducing the cellular P demand of the Lake Matano microbial community. With this observation, we show that this ability is not restricted to autotrophic organisms¹ but is universally distributed among different microbial taxa stressed by extremely low concentrations of available P. Such extreme P limitation in Lake Matano suggests that ferruginous conditions in general may lead to P limited ecosystems. This is consistent with previous work indicating P limitations on primary production during ferruginous Precambrian ocean chemistry².

[1] Van Mooy *et al.* (2009) *Nature* **458**, 69-72. [2] Bjerrum and Canfield (2002) *Nature* **417**, 159-162.

Microbial phosphate release from marine sediments: Transcriptomics and geochemistry

D.S. JONES*, B.E. FLOOD AND J.V. BAILEY

¹Dept. of Earth Sci., University of Minnesota, Minneapolis, MN 55455, USA (*correspondance: dsjones@umn.edu.)

Hydrolysis of intracellular polyphosphate (polyP) by benthic marine microorganisms is a potentially significant mechanism for phosphorus (P) flux from sediments to the water column. Additionally, polyP utilization by large sulfur (S) bacteria has been linked to phosphogenesis in episodically anoxic marine settings. Here, we combined incubations of sediment-hosted microbial communities with geochemical measurements and comparative metatranscriptomics in order to identify important polyP accumulating organisms in different marine environments and compare their activities under distinct redox conditions. We incubated sediments from two locations: (i) methane-seep sediments near Barbados that included a *Thiomargarita*-like bacterial biofilm; and (ii) sulfidic Santa Barbara Basin (SBB) sediments with no visible S oxidizing bacteria. P release from sediments of both localities was observed under anoxic conditions (Fig. 1), with and without additions of sulfide and acetate. Following incubations, sediments were immediately preserved for RNA extraction and sequencing. Metatranscriptomic analysis of the Barbados incubations revealed that, based on rRNA and *rpoB* transcripts, active microbial populations included diverse representatives of the Methanosarcinales, Bacteroidetes, and Delta-, Gamma- and Epsilonproteobacteria. However, based on identification and taxonomic classification of polyP kinase and exopolyP-ase transcripts, only certain gamma- and epsilonproteobacteria appeared to be metabolizing polyP under incubation conditions. Comparative analysis of metatranscriptomes from Barbados (where S bacteria were abundant) with metatranscriptomes from SBB (rare S bacteria) will provide insight into the identities and activities of key marine polyphosphate-metabolizing organisms, and further define their contributions to the global P cycle.

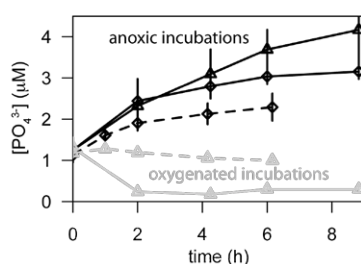


Figure 1: Dissolved phosphate changes during incubation experiments with marine sediments from Barbados (dashed lines) and the Santa Barbara Basin (solid lines).

Daily geochemical monitoring of volcanic rivers: A tool for eruption prediction?

MORGAN T. JONES^{1*}, ATHANASIOS GKRTZALIS-PAPADOPOULOUS², MARTIN R. PALMER², MATTHEW C. MOWLEM² AND SIGURÐUR R. GISLASON¹

¹Institute of Earth Sciences, Sturlugata 7, 101 Reykjavík, Iceland (* correspondence: morgan@hi.is)

²National Oceanography Centre, University of Southampton, European Way, SO14 3ZH, UK

The exsolution of volatiles and magma degassing can have a profound impact on the behaviour of volcanic systems and eruption style and frequency. Measuring volcanic degassing has traditionally focused on atmospheric emissions. However, volatiles can become dissolved in proximal water bodies en route to the surface, thus the monitoring of rivers draining active volcanoes can be integral to understanding the state of the volcano and potentially be used as a tool for predicting changes in activity or imminent eruptions. This method of monitoring is hampered by the dependence on spot-sampling due to financial and equipment constraints.

Recent advances in the design of osmotic samplers now allow for the continuous collection of water, providing a daily-averaged sample for weeks to months without the need of electricity or human supervision [1]. Deployment and testing of these osmotic samplers has been conducted in the rivers draining Mýrdalsjökull glacier and Katla volcano in southern Iceland. Preliminary results suggest that daily-averaged samples are able to track changes in volatile and metal concentrations over days to months. Results are used in conjunction with continuous monitoring of conductivity and temperature by the Icelandic Meteorological Office to highlight the differences in glacial, meteoric, volcanic and spring sources to the river chemistry from season to season. We envision that this form of sampling and monitoring can provide vital information on the behaviour and activity of volcanoes, and with further data become a potential method of eruption forecasting.

This work is funded as part of the EU collaborative project FUTUREVOLC, “a European volcanological supersite in Iceland: a monitoring system and network for the future”.

[1] Gkrtzalis-Papadopoulous *et al.* (2012) *Environ. Sci. Technol.* **46**, 7293-7300.

Effects of sediment porosity and particulate organic carbon on Fe, S and U cycling in Naturally Reduced Zones (NRZs) of a contaminated aquifer

M.E. JONES^{1*}, N. JANOT², J.R. BARGAR² AND S. FENDORF¹

¹School of Earth Science, Stanford University, Stanford, CA 94305, USA (*correspondence: mejones@stanford.edu)

²SLAC National Accelerator Laboratory, Menlo Park, CA 94025, USA

Previous studies have illustrated the importance of Naturally Reduced Zones (NRZs) within saturated sediments as a source of reduced organic compounds and hydrogen, providing electron donor for subsurface microbial respiration. NRZ's are typically characterized by low permeability and elevated concentrations of organic carbon and trace metals. However, both the formation of NRZs and their importance to the overall aquifer carbon remineralization is not fully understood.

Within NRZs the hydrolysis of particulate organic carbon (POC) and subsequent fermentation of dissolved organic carbon (DOC) to form low molecular weight dissolved organic carbon (LMW-DOC) provides electron donors necessary for the respiration of Fe, S, and in the case of the Rifle aquifer, U. Rates of POC hydrolysis and subsequent fermentation have been poorly constrained and rates in excess and deficit to the rates of subsurface anaerobic respiratory processes have been suggested.

In this study, we simulate the development of NRZ sediments in diffusion-limited aggregates to investigate the physical and chemical conditions required for NRZ formation. Effects of sediment porosity and POC loading on Fe, S, and U cycling on molecular and nanoscale are investigated with synchrotron-based Near Edge X-ray Absorption Fine Structure Spectroscopy (NEXAFS). Fourier Transform Ion Cyclotron Resonance Mass Spectrometry (FT-ICR-MS) and Fourier Transform Infrared spectroscopy (FTIR) are used to characterize the transformations in POC and DOC. Sediment aggregates are inoculated with the natural microbial biota from the Rifle aquifer and population dynamics are monitored by 16S RNA analysis.

Overall, establishment of low permeability NRZs within the aquifer stimulate microbial respiration beyond the diffusion-limited zones and can limit the transport of U through a contaminated aquifer. However, the long-term stability of NRZs and the collocated U is unknown and requires further study.

Boron cycling in the Central Andean subduction zone: Evidence for recycled components

ROSIE JONES^{1*}, LINDA KIRSTEIN¹, RICHARD HINTON¹,
SIMONE KASEMANN², TIM ELLIOTT³
AND VANESA LITVAK⁴

¹School of GeoSciences, University of Edinburgh, UK
r.e.jones-3@sms.ed.ac.uk (* presenting author)

²Department of Geosciences, University of Bremen, Germany

³Department of Earth Sciences, University of Bristol, UK

⁴Departamento de Ciencias Geológicas, Universidad de Buenos Aires, Argentina

Subduction zones, such as the active Andean margin, form large recycling systems and are the main producers of new continental crust. Some of the material which enters the subduction zone, including terrigenous and pelagic sediment and oceanic crust, is recycled to the continental crust via arc magmatism, and some re-equilibrates with the mantle. Boron has been identified as an ideal tracer for mass transfer in subduction zones, especially of recycled slab components (eg. [1, 2]). The study area is located within the Pampean flat slab segment (~27° - 33°S) of the southern Central Andes. This segment is currently volcanically inactive due to the low angle at which the Nazca plate currently subducts beneath the South American plate. This low angle has been attributed to the subduction of the Juan Fernandez Ridge, a volcanic seamount, which began intersecting the Andean continental margin during the early Miocene (~18Ma) [3]. Volcanism terminated in the region during the late Miocene (~6Ma).

A suite of Eocene – Miocene arc volcanic rocks were sampled from the southern Central Andes (28° to 32°S). Whole rock major- and trace-element data indicate variable contamination of the magmas during this interval but the source of the contamination remains enigmatic. New *in situ* analyses of boron concentrations and isotope ratios in pyroxene and zircon hosted melt inclusions were measured by SIMS, in order to identify contributions to Central Andean arc magmas from the subducting slab and sediments. This new data has been combined with high resolution, U-Pb zircon dating to provide insight into the petrogenetic evolution of magmas along the margin.

Average boron concentrations and isotope ratios obtained for the three Miocene samples are distinctly higher ($[B] = 111.7 \pm 9.0$ ppm, $\delta^{11}B = 4.47 \pm 0.86$ ‰ (2 σ)) than those obtained for the four Eocene – Oligocene samples ($[B] = 76.3 \pm 15.9$ ppm, $\delta^{11}B = -0.09 \pm 1.01$ ‰ (2 σ)). This suggests Central Andean arc magmas received a greater influence from slab derived fluids after the intersection of the Juan Fernandez Ridge and subsequent shallowing of the Nazca plate. This work demonstrates boron isotope ratios can be used in combination with high resolution U-Pb dating and major and trace element geochemistry to provide new insights into arc processes in changing geodynamic settings.

[1] Palmer (1991) *Geology*, **19**, 215 - 217. [2] Ishikawa and Nakamura (1994) *Nature*, **370**, 205 – 208. [3] Yañez *et al.* (2001) *Journal of Geophysical Research*, **106**, 6325 – 6345.

Microbially mediated phosphogenesis 2 Ga ago

LAURI JOOSU^{1*}, AIVO LEPLAND^{2,3}
AND KALLE KIRSIMÄE¹

¹University of Tartu, Tartu, Estonia. (*correspondence: lauri.joosu@ut.ee)

²Geological Survey of Norway, Trondheim, Norway.

³Tallinn University of Technology, Tallinn, Estonia.

Modern phosphogenesis is typically associated with high productivity upwelling systems where apatite (Ca-phosphate) precipitation is mediated by large sulphur bacteria [1]. They live in the upper few centimetres of sediment at oxic/anoxic interface and thrive in close association with a consortium of anaerobic methane oxidising archaea and syntrophic sulphate-reducing bacteria.

Paleoproterozoic Zaonega Formation in the Onega Basin, Karelia, Russia, is a c. 1500 m thick succession of organic-rich sedimentary rocks interlayered with mafic tuffs and lavas, containing several P-rich intervals in its upper part. Microstructure of these P-rich intervals exhibit apatitic laminae and particularly nodules up to several hundred μm in size. Individual apatite particles in P-rich lamellas and nodules occur as cylindrical apatite aggregates 0.5-4 μm in diameter and 1-8 μm in length. Cross-sections of cylindrical apatite particles reveal a thin outer rim whereas the internal parts consist of small anhedral elongated crystallites.

The sizes and shape of the nodules are similar to those of giant sulphide-oxidising bacteria known in modern and ancient settings [2, 3]. Individual apatite cylinders and aggregates have shapes and sizes similar to the methanotrophic archaea ANME-1 and ANME-2 that inhabit microbial mats in modern seep/vent areas where they operate in close associations with sulphur-oxidising microbial communities [4]. Moreover apatite in the Zaonega Formation is found in organic rich sediments exhibiting strongly negative $\delta^{13}\text{C}_{\text{org}}$ values (-37 to -34 ‰) which is interpreted to reflect the occurrence of methanotrophic biomass. We conclude that modern-style phosphogenesis, mediated by sulphide-oxidising bacteria living in consortia with methanotrophs, was established at least 2 Ga ago in response to the oxygenation of the Earth.

[1] Schulz and Schulz (2005) *Science* **307**, 416-418 [2] Bailey, Joye, Kalanetra, Flood, and Corsetti (2007) *Nature* **445**, 198-201 [3] Schulz, Brinkhoff, Ferdelman, Marine, Teske and Jorgensen (1999) *Science* **284**, 493-495 [4] Knittel, Losekann, Boetius, Kort and Amann (2005) *Applied and Environmental Microbiology* **71**, 467-479.

Rare earth element signatures of metal-rich hydrothermal ferromanganese deposit in the South-West Pacific

PIERRE JOSSO^{12,*}, EWAN PELLETER¹, OLIVIER POURRET²,
YVES FOUQUET¹, JOEL ÉTOUBLEAU¹, SANDRINE
CHERON¹, CLAIRE BOLLINGER³
AND THE SCIENTIFIC PARTIES

¹Ifremer c/Brest, Laboratoire de Géochimie et Métallogénie,
Plouzané, France (email: pierre.josso@ifremer.fr)

²HydriSE, LaSalle Beauvais, Beauvais, France

³IUEM, UMS 3113, Plouzané, France

A metal-rich hydrothermal ferromanganese deposit was discovered in the south-west Pacific during a French cruise [1]. The deposit formed at ridge axis and is hosted by pyroclastic rocks (e.g., hyaloclastite, tuffite, pumice). Mineralogical and geochemical investigation shows evidence of vertical zonation with depth. From top to bottom, we distinguished highly Ni-enriched manganese oxyhydroxides (Ni up to 4.6%) then iron oxyhydroxides ± nontronite with low metal concentrations, and barren nontronite. Here, we report rare earth element (REE) data for Fe-Mn oxyhydroxides and nontronite samples. All samples exhibit very low REE abundance (Σ REE: 12.6 – 92.7 mg/kg) and relatively low middle REE / heavy REE ratios ($Nd_n/Yb_n = 0.52 – 2.13$). This signature is characteristic of low temperature hydrothermal Fe-Si-Mn mineralization [2]. All samples have a slight negative Eu anomaly while the Ce negative anomaly is well developed ($Ce/Ce^* = 0.04 – 0.89$) and negatively correlated with Mn/Fe ratio (Mn/Fe: 0.14 – 80). This opposite correlation might implicate a strong mineralogical control of Ce content in Fe-Mn oxyhydroxides possibly related to pH [3]. This observation is to be qualified as the lack of correlation between the Σ REE and Mn/Fe ratio leads to think of the differential state of the phase's crystallinity as a control factor of the REE fractionation rather than its mineralogical nature [2].

[1] Pelletier *et al.* (2012), *Mineralogical Magazine* **76**, 2217.

[2] Bau (1999), *Geochimica et Cosmochimica Acta* **63**, 67–77.

[3] Mills *et al.* (2001), *Chemical Geology* **176**, 283–293.

Volcanoes, asteroid impacts and mass extinctions: A matter of timing

FRED JOURDAN

Western Australian Argon Isotope Facility; JdL Centre &
Dept of Applied Geology; Curtin University, GPO Box
U1987, Perth WA6845. Australia.

The history of life on Earth is punctuated by large mass extinction events, with five large ones occurring in the Phanerozoic and several smaller ones occurring between them. Isotopic and elemental chemistry shows that the extinctions are somehow linked to drastic climate changes.

The Cretaceous-Palaeogene (K-Pg) extinction event is well-documented, but controversy as to whether this was caused by an asteroid impact or the Deccan Traps has raged for many years [1,2], in particular because both events are demonstrably synchronous with the K-Pg boundary [3].

One important question is whether other significant extinction events were caused by impact, volcanism or the combination of both? To test these hypotheses, impacts and/or volcanic eruptions *must* be exactly synchronous with a mass extinction.

Quality-filtered age compilations show that whereas at least six large volcanic province – mass extinctions pairs have been recognized (including the newly added Kalkarindji – Middle Cambrian extinction pair at 510 Ma; [4]), only one asteroid – mass extinction pair has been demonstrated [5]. A possible synchronicity between extinction and impact candidates can be tested using precise geochronology. For example, our ⁴⁰Ar/³⁹Ar data on the Siljan Impact structure [6] show that the impact occur several million years before the Frasnian-Famennian boundary (~376 Ma). New data on Popigai and Chesapeake Bay [7] show that the two events are older than the mid-Eocene extinction. Some impact events (Rochechouart [8]; Araguainia [9]) have ages that make them time-compatible with a major extinction levels, but their small sizes (20–40 km) rule out any possible link.

At the face value of the current age database, large outpouring of lava is a more recurrent kill factor in the evolution of life than large impacts. Nevertheless, and largely understudied, is the potential of impact cratering events to have fostered life evolution [e.g., 10].

[1] Shulte *et al.* (2010) *Science* 327; [2] Hofmann *et al.* (2000) *EPSL* 180; [3] Renne *et al.* (2013) *Science* 339; [4] Jourdan *et al.*, submitted; [5] Jourdan *et al.*, (2012) *Elements* 8; [6] Jourdan & Reimold (2012) *MetSoc conf. abstract*; [7] Langenhorst & Jourdan, unpublished; [8] Schmieder *et al.* (2010) *MAPS* 45; [9] Tohver *et al.*, (2012) *GCA* 86; [10] Schmieder & Jourdan (2012) *GCA*, in press.

Controls on methane cycling in the Baltic Sea

B.B. JØRGENSEN^{1*}, G. REHDER²
AND BALTIC GAS TEAM³

¹Center for Geomicrobiology, Aarhus University, 8000C Aarhus, Denmark (*correspondence: bo.barker@biology.au.dk)

²Department of Marine Chemistry, Leibniz Institute for Baltic Sea Research Warnemünde, Germany (gregor.rehder@io-warnemuende.de)

³www.balticgas.net

The Baltic Sea is an ideal model to understand the environmental factors controlling methane production and methane cycling in coastal marine sediments. Salinities range from marine to nearly limnic, temperatures vary seasonally, and the stratified water column leads to widespread anoxia. During the BONUS+ project, BALTIC GAS, an international group of researchers studied sediment geophysics, free gas distribution, methane fluxes and organic carbon mineralization to determine the constraints on methanogenesis and methane emission to the water column and atmosphere.

The entire Baltic Sea region was ice-covered during the last glaciation, and modern methanogenesis primarily takes place in organic-rich sediments from the past <10,000 years. Sub-surface methane fluxes are highly dependent on the thickness of these Holocene sediments. In fact, the geographic distribution of dissolved methane and free gas can only be understood in the light of post-glacial geology as revealed by seismic-acoustic mapping combined with targeted coring and geochemical analyses. When Holocene deposits exceed a threshold thickness of 6-10 m, the methane partial pressure builds up to form gas bubbles. The underlying post-glacial clay, in contrast, may be a sink for methane.

Ebullition of free gas appears to be insignificant in the main Baltic Sea basins, yet hotspots with outgassing associated with pockmarks have been found by multibeam bathymetry, mostly in the Polish and Russian sectors. Outgassing also occurs in the most eutrophic coastal zone. Enhanced ebullition was not found associated with the low sulfate concentrations in the Bothnian Bay. Elevated methane concentrations in the bottom water are confined to the anoxic basins and methane is retained and oxidized in the chemocline of the water column. The Baltic Sea basins are thus generally robust towards methane emission to the atmosphere, although studies during extreme water level fluctuations are still lacking.

Hierarchy of two drivers of soil organic matter biodegradation: microbial habitat properties versus microbial communities

S. JUAREZ¹, N. NUNAN¹, V. POUTEAU¹, T. LERCH²
AND C. CHENU¹

¹UMR Bioemco AgroParisTech, CNRS INRA, 78850 Thiverval Grignon France (juarez@grignon.inra.fr, chen@grignon.inra.fr)

²UMR Bioemco, UPEC, Créteil France

Soil microbial communities live in a complex 3-D framework in which a range of habitats with a variety of properties exists. The importance of these habitat properties relative to the intrinsic properties of microbial communities in the regulation of soil organic matter decomposition is still unclear.

In order to uncouple effects linked to microbial habitat properties from ones linked to microbial communities, we sterilized 6 contrasted soils and performed to crossing inoculations. Each soil microbial community was extracted from its native soil by a saline solution, and inoculated in each on the six different sterilized soils. During the incubation, we measured C mineralisation as well as the microbial communities structures. Microbial habitat was the dominant determinant of SOC decomposition and of microbial community structure.

Human health risk assessment of a closed landfill based on direct gas measurements

I. JUBANY¹, E. GALLEGO², J. GIMÉNEZ^{3*}, V. MARTÍ¹³,
J.F. PERALES², F.J. ROCA AND J DE PABLO¹³

¹Fundació CTM Centre Tecnològic, Av. Bases de Manresa, 1,
08242 Manresa, Spain (irene.jubany@ctm.com.es)

²Laboratori del Centre de Medi Ambient, UPC, Avda.
Diagonal, 647, 08028 Barcelona, Spain
(eva.gallego@upc.edu, jose.francisco.perales@upc.edu,
fco.javier.roca@upc.edu)

³Chemical Engineering Department, UPC, Avda. Diagonal,
647, 08028 Barcelona, Spain (vicens.marti@upc.edu,
francisco.javier.gimenez@upc.edu,
joan.de.pablo@upc.edu.)

A human health risk assessment (HHRA) for a former landfill located at Cerdanyola del Vallès (Catalonia, Spain) was performed to evaluate the present risk of the identified receptors in the area and to the receptors of a the future urban planning. A former clay extraction activity in the area caused the existence of three 40m-deep holes which were afterwards filled with several types of industrial waste during the 80's. After landfill closing in 1995 several studies have been performed to assess the effect of the landfilled wastes to the environment. The innovative aspect of HHRA in this study was based on direct measurements of volatile organic compounds (VOC) in the urban air (immission concentrations around landfill), fluxes from the subsoil and surface emission.

Therefore, 130 VOC were identified and 70 quantified (odor, toxic and irritant compounds) in outdoor air at 4 urban sites located close to the landfill. The emission flux of the same compounds was determined in 5 points on the surface of the landfill, and soil gas composition at 5m-deep was also evaluated in the edge of the landfill. VOC were adsorbed into multi-sorbent tubes and analyzed by means of TD-GC-MS.

Several potential scenarios were defined for the HHRA: 3 for the current situation and 4 for the future situation (recreative area with surrounding buildings). USEPA methodology for HHRA was followed and toxicity values from IRIS database were used. Admissible risk was obtained in all scenarios due to low emissions. Effect of landfill on immission air measurements was calculated to be negligible.

The use of direct measurement of contaminants in air and emission fluxes allowed a more accurate HHRA with respect to the typical approach.

Enhancing the performance of GC-IRMS for small biomarker samples

DIETER JUCHELKA¹, JENS RADKE²
AND ANDREAS HILKERT^{3*}

¹Thermo Fisher Scientific, 28199 Bremen, Germany
(*correspondence: dieter.juchelka@thermofisher.com)

²Thermo Fisher Scientific, 28199 Bremen, Germany
(jens.radke@thermofisher.com)

³Thermo Fisher Scientific, 28199 Bremen, Germany
(andreas.hilkert@thermofisher.com)

The combination of Gas Chromatography with Isotope Ratio Mass Spectrometry (GC-IRMS) was introduced in 1988, opening the wide field of compound specific isotope analysis (CSIA). It combines the high purification efficiency of GC with the utmost precision of isotope ratio mass spectrometry.

Today compound specific isotope analysis of the main bioelements and their major isotopes ¹³C, ¹⁵N, ¹⁸O and ²H is a standard tool in many laboratories and is used in a wide range of applications. Consequently, this analytical tool is extending into new areas of research, in which smallest sample size at high precision is a must.

The development of more sensitive IRMS systems with optimized GC combustion and high temperature conversion interfaces is also related with modern sample introduction techniques, choice of GC columns, advanced GC technology, conversion technology and interfacing to the IRMS as well as data handling. New challenges in sample size and separation concern the improvement of sensitivity and GC resolution combined with full automation for higher sample throughput.

We will discuss in this presentation the neuralgic points in the GC-IRMS system with application examples on biomarkers and other important biomolecules linked to improvements in sample introduction techniques, GC- and reactor technology.

Partitioning of sulfur between silicate melts and volatile phases as function of fO_2 : Clues from old models for a new reference framework

PEDRO J. JUGO

Department of Earth Sciences, Laurentian University,
Sudbury, Ontario P3E 2C6, Canada (pjugo@laurentian.ca)

The partitioning of sulfur between silicate melts and coexisting volatile phases is a key parameter to understand igneous processes such as massive S degassing in explosive eruptions (e.g. Mount Pinatubo, June 1991) and the formation of porphyry deposits (which in addition to Cu, Mo, and Au, are S anomalies). It is well-established that the S content at sulfide saturation (SCSS) in a silicate melt increases exponentially with increasing fO_2 regardless of whether the system is anhydrous or the melt is in equilibrium with a hydrous phase [1, 2, 3, 4]. It is also well-established that only S^{2-} and S^{6+} species are significant in silicate melts [5], whereas S^{4+} species (in addition to S^{2-} and S^{6+}) are significant in volatile phases [6]. Thus, the stability of S^{4+} species in the volatile phase is an essential parameter controlling S partitioning. Early studies of S behaviour between volatile phases and silicate melts [7, 8] have been used extensively to describe a “sulfur solubility minimum” that has no relevance to SCSS because the experiments in those studies lacked sulfides as run products. However, those experimental studies provide useful reference models when the data are recast in a more appropriate framework (i.e. to express S partitioning between the input gas and the silicate melt). The results show that, at atmospheric pressure, a S partitioning maximum exists at fO_2 conditions that may be attributed to S^{4+} dominance in volatile phases at low pressure (and that overlap the fO_2 range corresponding to the S^{2-} to S^{6+} transition in silicate melts at high pressure). Linking the two types of data (SCSS at high P and $D_{S^{gas/melt}}$ at atmospheric P) provides a useful model to understand S mass transfer from silicate melts into volatile phases during volatile exsolution and degassing resulting from magma ascent and decompression.

[1] Jugo (2009) *Geology* **37**, 425-418. [2] Beermann *et al.* (2011) *Geochim. Cosmochim. Acta* **75**, 7612-7631. [3] Botcharnikov *et al.* (2011) *Nat. Geosci.* **4**, 112-115. [4] Zajacz *et al.* (2012) *Geochim. Cosmochim. Acta* **89**, 81-101. [5] Wilke *et al.* (2008) *Am. Min.* **93**: 235-240. [6] Symonds *et al.* (1994) *RiM.* **30**, 1-66. [7] Fincham and Richardson (1954) *Royal Soc. London Series A.* **223**, 40-62. [8] Katsura and Nagashima (1974) *Geochim. Cosmochim. Acta* **38**, 517-531.

Natural type-C olivine fabrics in garnet peridotites in North Qaidam UHP collision belt, NW China

H. JUNG^{1*}, J. LEE¹, B. KO¹, S. JUNG¹, M. PARK¹, Y. CAO¹
AND S.G. SONG²

¹School of Earth and Environmental Sciences, Seoul National University, Seoul 151-747, Republic of Korea
(*correspondence: hjung@snu.ac.kr).

²School of Earth and Space Sciences, Peking University, Beijing 100871, China.

Water is known to change the lattice-preferred orientation (LPO) of olivine, which significantly affects seismic anisotropy in the Earth's upper mantle. Research into the LPO of olivine in the deep interior of the Earth has been limited due to inadequate specimens. We report both the water-induced LPOs of olivine and the presence of large quantities of water inside olivine, enstatite, and garnet in garnet peridotites from the North Qaidam ultrahigh-pressure (UHP) collision belt in NW China. We show that the [001] axis of olivine is aligned subparallel to the lineation and that the [100] axis is strongly aligned subnormal to the foliation. This alignment is a known feature of type-C LPO of olivine formed experimentally under water-rich conditions (≥ 700 ppm H/Si) at high pressure and temperature. Enstatite possessed an LPO with the [001] axis aligned parallel to the lineation and the [100] axis aligned normal to the foliation. FTIR analysis of this specimen revealed that olivine contained concentrations of water up to 1130 ± 50 ppm H/Si in clean areas, whereas olivine, enstatite, and garnet contained considerably more water, i.e., 2600 ± 100 ppm H/Si, 5000 ± 100 ppm H/Si, and 21000 ± 200 ppm H/Si, respectively, when exsolved inclusions were visible. Confocal micro-Raman spectroscopy of these exsolved inclusions revealed that they were composed of hornblende and amphiboles. Straight dislocations were also commonly observed in olivine and are characteristic of olivine that had been experimentally deformed under hydrous conditions. These observations suggest that the type-C LPO of olivine in the North Qaidam UHP belt formed under water-rich conditions.

Geologic control of groundwater contamination in a basaltic aquifer beneath an agricultural field, South Korea

HEE-WON JUNG¹, SEONG-TAEK YUN^{1*},
KYOUNG-HO KIM¹, SANG-SIL OH²
AND KYUNG-GOO KANG³

¹Korea University, KU-KIST Green School and the
Department of Earth and Environmental Sciences, Seoul,
South Korea

styun@korea.ac.kr (* correspondence)

²Jeju Special Self-Governing Province Institute of
Environment Research, Jeju, South Korea

³Jeju Special Self-Governing Province Development
Corporation, Jeju, South Korea

Hydrochemistry data of groundwater were collected in the Gosan area, southwestern coastal part of Jeju Island, South Korea. In the western part of the study area, an impermeable clay-rich layer (Gosan Formation) locally overlies the basaltic aquifer. The Robust PCA method (ROBPCA) was used to investigate hydrochemical characteristics. The results show that principal component 1 effectively distinguishes the groundwater samples recording varying degrees of agricultural contamination. Groundwater samples whose chemistry is controlled by agricultural contamination are restricted to the eastern part of the study area, while uncontaminated water is predominantly obtained in the western part where the Gosan Formation occurs. Groundwater samples from wells near the edge of the Gosan Formation show a seasonal fluctuation of water quality (i.e., from uncontamination in a dry season to agricultural contamination in a wet season). This study suggests that groundwater below the marginal part of an impermeable layer is seasonally contaminated by a temporal extension of the pollution front during the wet season, even though the impermeable layer plays a role as a natural barrier to protect groundwater from the infiltration of surface contaminants.

PANGA: A new tool for the evaluation of noble gas data

M. JUNG^{1*} AND W. AESCHBACH-HERTIG¹

¹Institute of Environmental Physics, Heidelberg University,
69120 Heidelberg, Germany (*correspondence:
michael.jung@iup.uni-heidelberg.de)

In recent years, several new models for the description of dissolved noble gases in groundwater have been developed, because the more traditional models did not yield good results for certain data sets [1]. The oxygen depletion model was proposed in response to the observation that the classical models yielded too low temperatures for some aquifers [2]. To overcome specific problems related with unrealistically high temperature estimates of the closed-system equilibration model, a Monte Carlo-based evaluation method was developed [3].

In order to adapt and simplify the evaluation process, we created *PANGA*, a new software for the analysis of noble gas data sets. Its basic features are comparable to *Noble* [4], but it also includes more recent excess air models and provides additional features like fast Monte Carlo fitting (up to several 100,000 fits per minute) and the subsequent depiction and evaluation of the results in one- and two-dimensional histograms as well as the possibility to interactively explore the χ^2 space of noble gas fits, enabling the user to identify problems like local minima in the χ^2 surface.

Comparison tests have shown that *PANGA* is able to reproduce *Noble's* results very well. The analysis of several data sets showed that Monte Carlo results, especially parameter uncertainties, differ considerably from the original fit results in a number of cases. Therefore, it is recommended to perform Monte Carlo evaluations in all cases, especially if any kind of problematic behavior occurs, like parameters approaching physical boundaries or unrealistically high temperature estimates or uncertainties.

- [1] Sun *et al.* (2010) *Geochemistry Geophysics Geosystems* **11**
[2] Hall *et al.* (2005) *Geophysical Research Letters* **32** [3] Jung *et al.* (2013) *Chemical Geology* **339**, 291–300 [4] Peeters *et al.* (2003) *Geochimica et Cosmochimica Acta* **67**, 587–600

**Modeling the fate of the
Pharmaceuticals in an urban aquifer.
Besòs River Delta case study
(Barcelona, Spain).**

A. JURADO^{12*}, E. VAZQUEZ-SUÑE¹, J. CARRERA¹,
E. PUJADES¹², R. LOPEZ-SERNA³, M. PETROVIC⁴
AND D. BBARCELÓ^{3,4}.

¹IDAEA-CSIC (GHS, Department of Geosciences), Jordi
Girona 18-26, 08034, Barcelona, Spain.
(*annajuradoelices@gmail.com).

²GHS, UPC-Barcelona Tech, Jordi Girona 1-3, 08034,
Barcelona, Spain. (estanislaopujades@gmail.com)

³IDAEA-CSIC (Department of Environmental Chemistry) ,
Barcelona, Spain. (dbcqam@cid.csic.es)

⁴ICRA, Emili Grahit 101,17003 Girona, Spain.
(mpetrovic@icra.cat).

Pharmaceutically active compounds (PhACs) are a matter of growing concern because they might produce potentially harmful effects on ecosystems and human health. The incomplete removal of some PhACs during conventional waste water treatment represents the main source in surface and ground waters. As a result, groundwater quality can be deteriorated by the presence of PhACs. Thus, understanding their fate in the aquifer is a key environmental issue.

In this work, a multicomponent reactive transport modeling will be used to investigate the fate of the PhACs in an urban aquifer which main recharge source is the polluted River Besòs in Barcelona (Spain). River Besòs flow is heavily dependent on seasonal rainfall and it receives large amounts of effluents from waste water treatment plants. Therefore, a wide range of PhACs may be present in groundwater at similar levels or even higher than the River Besòs.

Prior inspection of the collected data suggests different behavior of the PhACs in the aquifer. As an example, ibuprofen, gemfibrozil, sulfadiazine and bezafibrate present a significant removal in when river water infiltrates the aquifer, with elimination rates ranging between 60–80%. However, other PhACs such as carbamazepine are highly persistent with elimination rates that usually below 10%. It is important to understand and quantify the different attenuation behavior of PhACs to know whether the groundwater of Besòs River Delta can be use to other purposes, such as supply ones, apart from street cleaning and water plant.

Chromium chemistry in natural waters, Iceland

HANNA KAASALAINEN^{1*}, ANDRI STEFÁNSSON¹,
INGVI GUNNARSSON² AND STEFÁN ARNÓRSSON¹

¹Institute of Earth Sciences, University of Iceland, Sturlugata
7, 101 Reykjavik, Iceland,
(*correspondence: hannakaa@hi.is)

²Present address: Reykjavik Energy, Bæjarhalsi 1, 110
Reykjavik, Iceland

Chemistry of Cr and Fe was studied in non-thermal and geothermal waters in Iceland. Chromium (Cr) is typically present at low concentrations (<1 µg/l) in natural waters, but elevated concentrations have been observed in waters with low pH values, e.g. acid mine drainage, and in association with industrial activities. Chromium occurs in two oxidation states, Cr(III) and (VI), these being characterized by different (bio)chemical behaviour and solubility. As Cr(VI) is known to be toxic but Cr(III) an essential micronutrient, it is important to determine the two oxidations states. Iron (Fe) is known to play an important role in the chemistry of Cr through adsorption on and incorporation in Fe containing minerals, and by affecting the distribution of Cr species. In natural waters, iron is present in two oxidation states (Fe(II) and (III)) and understanding its chemistry is complicated by fast oxidation kinetics, importance of colloidal forms and low solubility in the pH range of most natural waters (pH>6).

Samples were collected from non-thermal surface and spring water, surface geothermal water and geothermal well discharges, and analyzed for their major and trace element composition. Chromium and Fe speciation was determined in selected samples. The sampled waters showed wide range of composition with temperature, pH and total dissolved solids in the range of 0-184°C, 2.0-9.6, and 35-4030 mg/l, respectively. The total dissolved Fe and Cr concentrations were between <1 µg/L to 360 mg/L and <0.01 and 660 µg/L, respectively. The highest concentrations were associated with steam-heated acid-sulfate waters with the lowest pH values, whereas the concentrations in neutral to alkaline waters were low, typically <1 µg/L Cr and <100 µg/L Fe.

The main processes controlling Cr chemistry were found to depend on the water pH and rock leaching. At a low pH, Cr(III) becomes released into solution through leaching of Cr-containing minerals contained in basaltic rocks. At neutral to alkaline pH, Cr leaching from rock is limited and Cr(III) concentrations may be further reduced and controlled by solubility of Cr(III)-Fe(III) mineral phases. However, Cr(VI) mobility is enhanced associated with decreasing importance of mineral surface complexation. Indeed, Cr(VI) was frequently found to dominate over Cr(III) at pH>6 in concentrations of a few µg/L.

Deformation mechanisms in Martian Shergottites

KACZMAREK M.-A.*^{1,2}, GRANGE M.¹, REDDY S.M.¹,
AND NEMCHIN A.¹

¹Department of Applied Geology, The Institute for Geoscience
Research, Curtin University of Technology, GPO Box
U1987, Perth, WA 6845, Australia

²Now at University of Lausanne, Institute of Earth Sciences,
UNIL Mouline, Géopolis, CH-1016 Lausanne,
Switzerland
(*correspondence: mary-alix.kaczmarek@unil.ch)

Nakhla and Zagami are both clinopyroxene-rich basaltic shergottite, with some Fe-rich olivine. The microstructure, the preferred orientation of pyroxene using Electron Backscatter Diffraction (EBSD) method and the geochemistry are combined to study subsamples of both Zagami and Nakhla to decipher deformation processes that have occurred on Mars.

Nakhla displays a granular texture, essentially composed of augite, fayalite, plagioclase and magnetite. Our Zagami sample, formed by olivine, plagioclase, and whitlockite is part of the "coarse grained" portion of Normal Zagami texture [1, 2] with long prism of clinopyroxene underlying a weak preferential orientation. Complete maps of both Zagami and Nakhla samples and detailed maps of clinopyroxene single grains were obtained with EBSD. Both samples show a strong preferred orientation of clinopyroxene and CPOs display several point concentrations on <001> axes within a girdle. The relationship between the microstructure and CPOs inferred the possible activation of (100)[001] and (010)[100] slip systems. Moreover, the several point concentrations on clinopyroxene <001> axis might correspond to twinning.

Geochemical maps of clinopyroxene single grains highlight chemical zoning from augite core to pigeonite rims. Phases indexation with the EBSD is concordant with the geochemistry and highlights no variation in the slip system from cores to rims, suggesting either no variation of deformation during the evolution of the geochemical system, or a late deformation event. Inspection of clinopyroxene single grains show that Nakhla clinopyroxenes have almost no internal deformation, rather than Zagami clinopyroxenes showing complicate microtexture with possible activation of several slip systems.

Our results suggest a composite deformation related to magmatic deformation (preferred orientation and prismatic clinopyroxene) and to the shock event (single grain internal deformation and twinning).

[1] Stolper E. M. *et al.* 1979. *Geochimica Cosmochimica Acta*. **43**: 589-602. [2] McCoy T. J. *et al.* 1992. *Geochimica Cosmochimica Acta*. **56**: 3571-3582.

Bioavailability of nanoparticulate iron derived from atmospheric mineral dusts

ENIKÖ KADAR¹, JONATHAN J. POWELL³
AND ZONGBO SHI²

¹Plymouth Marine Laboratory, Prospect Place, the Hoe,
Plymouth PL1 3DH, UK email: enik@pml.ac.uk

²School of Geography, Earth and Environmental Sciences,
University of Birmingham, B15 2TT, U.K email:
z.shi@bham.ac.uk

³Biomineral Research Section, Medical Research Council -
Human Nutrition Research, Elsie Widdowson Laboratory,
Fulbourn Road, Cambridge CB1 9NL email:
Jonathan.Powell@mrc-hnr.cam.ac.uk

We have studied the composition, Fe dissolution/Fe lability, particle aggregation/size distribution, surface topology and zeta potential (i.e. colloidal stability) of Fe-rich nanoparticles (NPs) formed during simulated atmospheric processing of dust in contact with seawater under a range of environmentally realistic conditions typical in oceanic waters to shed light on putative relationships between NP structure and water parameters. These laboratory studies showed that: (i) despite the close resemblance in micromorphology, NPs formed from mineral dusts have distinct aggregation behaviour from ferrihydrite NPs; (ii) the relatively stable and monodisperse aggregates of NPs formed during simulated cloud processing of mineral dust become more polydisperse and unstable in seawater; (iii) exopolymeric substances (EPS) extracted from phytoplankton seem to "stabilise" the aggregates of dust derived NPs; iv) dissolved Fe concentration from NPs, is consistently higher in seawater in the presence of EPS and is also affected by sunlight; v) EPS-mediated Fe uptake may be responsible for enhanced bioavailability in phytoplankton.

To test the hypothesis that nanoparticulate Fe is more bioavailable than the bulk analogue we have grown marine microalgae on synthetic nano-iron substrates. Algal growth was significantly enhanced when the nanomaterials were added in equimolar concentration compared to Fe-EDTA in the optimised algal growth medium (f/2). NP addition influenced cellular fatty acid composition compared to control treatments, but this was significant only in haptophytes. The NP uptake mechanism proposed is via secretion of an extracellular matrix that binds NPs through which Fe is bioavailable via fagocytotic membrane processes and/or NP dissolution. The implications of the use of such engineered nanomaterials as Fe substrate in algal culture are discussed.

Determination the step of karst formation using GPR and Raman Spectroscopy Methods, South East Anatolia, Turkey

SELMA KADIOĞLU^{1,2} AND YUSUF KAĞAN KADIOĞLU²

¹Ankara University Faculty of Engineering Department of
Geophysical Engineering, Ankara, Turkey

²Ankara University Earth Sciences Application and Research
Center, Ankara, Turkey (kadi@ankara.edu.tr)

Ground Penetrating Radar (GPR) is used to identify the relatively shallow subsurface features at scale from centimeter up to meter. In this study dissolution of soluble rocks (Karst) including limestone and dolomitic limestone are examined using GPR and Raman spectroscopy methods around Adiyaman City in East Anatolia Turkey. Karstification led to form sinkholes, caves, and underground drainage systems. Rainwater becomes acidic as it comes in contact with carbon dioxide in the atmosphere and the soil. As it drains into fractures in the rock, the water begins to dissolve away the rock creating a network of passages. The step of the karst formation towards the inner parts of the surface of the limestone is determined using 250 and 500 Mhz GPR antenna. GPR attribute volumes is sensible and suggests that the formation of the cavities along the fracture packets exist over cavity floors elsewhere but that there is also variation in fracture intensity and in orientation over the whole system. The matrix consolidation and dissolution of the rocks are observed through the processing of the radar data. The microscopically examination and Confocal Raman spectroscopy determination studies show the degree of the dissolution is increased towards the crack and aid to form ankerite, siderite, limonite, hydrous carbonate-sulfates, vermiculite clay minerals with rare amount of albite and pyrite.

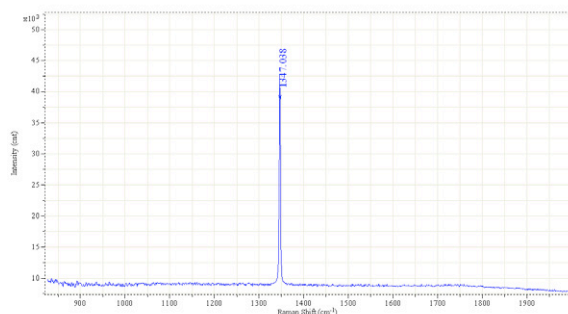
Diamond Bearing Mantle Xenoliths in Alkaline Basalts: Karacadağ Volcano, South East Anatolia, Turkey

YUSUF KAĞAN KADIOĞLU^{1,2}

¹Ankara University, Faculty of Engineering Department of Geological Engineering, Ankara, Turkey and kadi@ankara.edu.tr

²Ankara Uni. Earth Sciences Application and Research Center, Ankara, Turkey

Small Diamond crystals are determined by Raman spectroscopy within the mantle xenoliths from alkali basalts in Karacadağ Volcanic province South East Turkey. The peridotite mantle xenoliths are in the compositions of dunite and pyroxene bearing dunite and they are ranging from 1 cm up to 30 cm in size. The purpose of this contribution is to review the nature of the latest Cenozoic alkaline magmatism with respect to the geochemistry of mantle xenoliths. Diamond bearing Peridotite xenoliths in basalts of Karacadağ provide snapshots of the lithospheric mantle beneath particular regions at the time of their eruption and hence are crucial direct evidence of the nature of the mantle beneath regions. The diamond bearing peridotite mantle xenoliths suggests that these diamonds might be cogenetic with old rock provinces in the subcontinental mantle and then erupted with the latest events of the alkaline magmatism.



Raman Shift value of the diamond crystals within mantle xenoliths of Karacadağ Basalts

HSE and S-Se-Te fractionation in components of enstatite chondrites

YOGITA KADLAG¹ AND HARRY BECKER¹

¹Institut für Geologische Wissenschaften, Freie Universität Berlin, Germany. yogita@zedat.fu-berlin.de, hbecker@zedat.fu-berlin.de

Enstatite chondrites show distinct fractionations of the highly siderophile elements (HSE) that may reflect volatility control or other types of partition processes [1, 2]. To investigate the origin of the fractionation of the HSE, S, Se and Te in enstatite chondrites, we have separated the components from the unequilibrated enstatite chondrites (EH3) Sahara 97072 and Kota Kota: magnetic, slightly magnetic and nonmagnetic components in five different grain size fractions, matrix, chondrules, CAIs (Ca-Al rich inclusions) and dark inclusions. Samples were analyzed following established techniques [2, 3].

Magnetic components of both meteorites (and the chondrule fraction of Sahara 97072) are enriched in HSE, S, Se and Te compared to the bulk rocks. Au is more enriched relative to the PGE and Re in the magnetic fractions, compared to non-magnetic fractions. In contrast, S, Se and Te in the magnetic fractions are always depleted compared to the HSE. The CAI fraction and a dark inclusion from Sahara 97072 are depleted in all elements (0.3*bulk) and show a similar abundance pattern as CI chondrites. Magnetic fractions display higher Re/Os (0.08-0.19) than most non-magnetic fractions, which have Re/Os lower than Re/Os of CI chondrites.

The relative enrichments, depletions and element fractionation in the components allow some preliminary conclusions: (1) Because metal rich components display strong enrichment of Au and Pd relative to refractory HSE, but depletion of Te-Se-S (with ratios relatively close to CI), the different groups of moderately volatile elements in metal rich components are decoupled. (2) In non-magnetic silicate rich fractions, Se and S are less depleted than HSE and Te, likely reflecting low-pressure metal-silicate-sulfide partitioning [4,5].

[1] Horan, M. *et al.* (2003) *Chem. Geol.* **196**, 5-20 [2] Fischer-Gödde M. *et al.* (2010) *GCA* **74**, 356-379. [3] Wang *et al.* (2013) *GCA* **108**, 21-44. [4] Rose-Weston *et al.* (2009) *GCA* **73**, 4598-4615. [5] Mann *et al.* (2012) *GCA* **84**, 593-613.

Transformation of Silver Nanoparticles: From the Sewer to the Fly Ash

R. KAEGI¹, A. VOEGELIN¹ AND B. THALMANN¹

¹Eawag, Swiss Federal Institute of Aquatic Science and Technology, Dübendorf, Switzerland (*correspondence: ralf.kaegi@eawag.ch)

Silver-nanoparticles (Ag-NP), used in textiles and cosmetics, will eventually be discharged to the municipal sewer system. We have shown that Ag-NP are efficiently transported along the sewer channel without substantial loss to the biofilm [1]. In the wastewater treatment plant (WWTP), partially sulfidized Ag-NP attach to the wastewater biomass and are removed from the wastewater stream. In parallel, the sulfidation reaction proceeds and the Ag-NP are almost completely sulfidized when leaving the WWTP via the surplus sludge [2]. Ag₂S is very recalcitrant to oxidation as shown in a recent study where digested sludge was stockpiled for several weeks under oxic conditions [3].

In Switzerland sewage sludge is exclusively incinerated, in Germany about 50% with an increasing trend towards thermal sewage sludge disposal and on a EU level, about one third of the sewage sludge is incinerated. In order to allow for later phosphorus (P) recovery, sewage sludge has to be incinerated in monocombustion facilities. Until an economic and ecologic process for P recovery from sewage sludge ashes (SSA) has been found, the majority of the SSA are stored in separate deposits, although in Germany, a small fraction (5%) of the SSA is directly used as fertilizer.

X-ray fluorescence (XRF) analysis of fly ashes collected from monocombustion (fluid bed) facilities revealed Ag concentrations of ~10 mg/kg. X-ray absorption spectroscopy (XAS) analysis showed that Ag in the fly ash was dominantly Ag₂S. This result is in contrast to a recent study concluding that Ag₂S transforms into Ag(0) during the combustion [4], which would possibly have far reaching consequences regarding the direct application of SSA in agriculture. The differences are most likely caused by different combustion conditions between the two studies. We will further investigate the fly ash samples using electron microscopy to assess whether silver is present in the form of nanoparticles.

[1] Kaegi *et al.* (2011), *ES & T*, **49**, 3902 – 3908 [2] Kaegi *et al.* (2013), *Water Research*, doi:10.1016/j.watres.2012.11.060. [3] Lombi *et al.* (2013), *Env.Poll.* **176**, 193–197. [4] Impellitteri *et al.* (2013), *Water Research*, doi:10.1016/j.watres.2012.12.041.

Sulfur and halogen fluxes at mid-ocean ridges: Estimations based on gas compositions in MORB vesicles

T. KAGOSHIMA^{1*}, Y. SANO¹, N. TAKAHATA¹ AND B. MARTY²

¹AORI, Univ. Tokyo, Chiba, Japan
(*correspondence: kagoshima@aori.u-tokyo.ac.jp)
²CRPG, CNRS, Nancy, France

Since S and halogens (F and Cl) form various compounds on the Earth's surface, their geochemical cycles are important issues in the Earth's evolution. Though fluxes of S and halogens at MORs have been estimated using compositions of chilled margins of MORB glasses characterised as those of silicate melts derived from the upper mantle, they may be somewhat overestimated [1]. Plausible estimations based on compositions of volcanic gases released as hydrothermal fluids are necessary. We characterised gas and melt compositions retained respectively in vesicles and solids of MORB glasses and estimated MOR fluxes of S and halogens.

We analyzed MORB glasses collected at 2 sites on East Pacific Rise, 2 sites on Mid-Atlantic Ridge and 2 sites on Central Indian Ridge. After extractions of gases in vesicles by the frozen crushing method [2], concentrations of ³He were measured using a VG-5400 and those of S and halogens were measured using an ICS-2100. Concentrations of S and halogens in solids were measured using a NanoSIMS. We calculated relative molar ratios (S/³He, F/³He and Cl/³He) and estimated MOR fluxes of S and halogens calibrating against the known ³He flux (527 mol/yr [3]).

For vesicle components, global averages of S/³He, F/³He and Cl/³He are (4.2±1.6)×10⁷, (1.4±0.7)×10⁶ and (2.6±1.0)×10⁷. For bulk components, they are (0.3–1.2)×10¹⁰, (1.6–6.5)×10⁹ and (0.7–3.0)×10⁹, respectively. Using these ratios and the known ³He flux, MOR fluxes were estimated to be (2.2×10¹⁰–6.6×10¹²) mol/yr for S, (7.1×10⁸–3.4×10¹²) mol/yr for F and (1.4×10¹⁰–1.6×10¹²) mol/yr for Cl. Assuming the continuous degassing from the solid Earth, formations of atmosphere and ocean can not be achieved by the low MOR fluxes estimated based on vesicle compositions. The amount of S accumulated on the surface are calculated to be 50 times lower than its surface inventory, and halogens are calculated not to be accumulated because of dominant influxes at subduction zones. This implies a possibility that the elements were significantly degassed in the early Earth.

[1] Tajika (1998) *GRL* **25**, 3991-3994. [2] Kagoshima *et al.* (2012) *Geochem. J.* **46**, e21-e26. [3] Bianchi *et al.* (2010) *EPSL* **297**, 379-386.

Evaluating possible risks and benefits of nanopesticides application

M. KAH^{1*}, S. BEULKE², K. TIEDE² AND T. HOFMANN¹

¹Department of Environmental Geosciences, University of Vienna, Austria

(*correspondence: melanie.kah@univie.ac.at)

²Food and Environment Research Agency, York, UK

Deliberate application of nanoparticles as plant protection products within agricultural practices could result in one of the rare intentionally diffuse inputs of engineered nanoparticles into the environment. The anticipated new or enhanced activity of nanopesticides will inevitably result in both new risks and new benefits to human and environmental health. It is unclear whether the current regulatory framework is adequate for the evaluation of these new products.

A literature review [1] was carried out with the objectives (i) to explore potential applications of nanotechnology within the pesticide formulation sector, (ii) to identify possible impacts on environmental fate, and (iii) to analyse the suitability of current exposure assessment procedures to account for their novel properties within the EU regulatory context. Nanopesticides encompass a great variety of products and cannot be considered as a single category. Nanopesticides can consist of organic ingredients (e.g., active ingredient(s), polymers) and/or inorganic ingredients (e.g., metal oxides) in various forms (e.g., particles, micelles). Studies on the environmental fate of nanopesticides are scarce. Possible effects of nano-formulations on the fate of the active ingredient can be complex and reported results are often contradictory.

The current level of knowledge does not appear to allow a fair assessment of the advantages and disadvantages that will result from the use of some nanopesticides. A great deal of work will be required to successfully combine analytical techniques that can detect, characterize and quantify the active ingredient and adjuvants emanating from nano-formulations, and also to understand how their characteristics evolve with time, under realistic conditions.

A more robust risk assessments framework for nanopesticides is urgently needed. In this context, priority for research are to (i) identify the assumptions currently applied that are not valid in the case of nanopesticides, (ii) evaluate the points or situations in which differences may impact significantly on the exposure assessment outcomes, and (iii) refine or adapt current assessment protocols as required.

[1] Kah *et al.* (2013) *Crit. Rev. Environ. Sci. Technol.*
DOI:10.1080/10643389.2012.671750

Characterizing magma migration dynamics beneath Mt. Etna using combined kinetic and thermodynamic (MELTS) modelling

MAREN KAHL^{*1,2}, SUMIT CHAKRABORTY², FIDEL COSTA³ AND MASSIMO POMPILIO⁴

¹SEE, The University of Leeds, UK

(*correspondence: M.Kahl@leeds.ac.uk)

²GMG, Ruhr-University Bochum, Germany

(Sumit.Chakraborty@rub.de)

³EOS, Nanyang Technological University, Singapore

(fcosta@ntu.edu.sg)

⁴INGV - Sezione di Pisa, Italy (pompilio@pi.ingv.it)

Characterizing the routes of magma migration beneath active volcanoes is important to understand the dynamic processes in sub-surface magma plumbing systems. We present a method that combines kinetic (diffusion) and thermodynamic (MELTS) modelling of the chemical stratigraphy preserved in zoned olivine crystals to constrain the nature and dynamics of magma storage and migration beneath Mt. Etna. We used 180 olivine crystals erupted during several episodes between 1991 and 2008. The compositional and zoning record preserved in these crystals reveal five different olivine populations (i.e. Fo₇₉₋₈₃, Fo₇₅₋₇₈, Fo₇₃₋₇₅, Fo₇₀₋₇₂ and Fo₆₅₋₆₉). These can be explained as the result of multistage magma mixing and magma exchange between at least four different magmatic environments (M₀ containing olivine of Fo₇₉₋₈₃; M₁ with Fo₇₅₋₇₈, M₂ with Fo₇₀₋₇₂ and M₃ with Fo₆₅₋₆₉). Two dominant magma migration routes (M₀-M₁; M₁-M₂) have been identified in the majority of the studied eruption products and thus might represent major pathways for magma transfer. Kinetic modelling of the compositional zoning observed in the olivines reveal that most of the timescales related to the transfer of magma between the environments M₀-M₁ as well as M₁-M₂ is less than three months, though a minor population of longer timescales ranging up to 3 years was also found. Combining these results with thermodynamic modeling using the MELTS thermodynamic database [1], we aim to characterize the ambient intensive variables (e.g. P, T, fO₂) along the two most prominent magma transfer routes (i.e. M₀-M₁; M₁-M₂). Comparison of the obtained results with compositions of other mineral phases (i.e. Cpx, Plag and Ti-Mt) allows elucidating the P-T-fO₂-H₂O-time history of the magmas before eruption.

[1] Ghiorso & Sack (1995), *Contrib. Mineral. Petrol.* **119**, 197-212

Geochemical and mineralogical properties of harzburgite and dunite in Margı (NE Eskisehir) Area

ASUMAN YILMAZ AND MUSTAFA KUŞCU SÜLEYMAN

¹Aksaray Üniversitesi Mühendislik Fakültesi, Jeoloji Mühendisliği Bölümü (asuman27@hotmail.com)

²Demirel Üniversitesi, Mühendislik Fakültesi, Jeoloji Mühendisliği Bölümü

Study area which located in the Izmir-Ankara suture zone is found Tavsanlı zone peridotites. Harzburgites which is a host rock of magnesite have been subject to severe serpentinization. Dunite consists of mostly olivine, very few orthopyroxene and opaque mineral chromite. Harzburgite contains olivine, orthopyroxene, serpentine, talc, opaque mineral magnetite and chromite. Chrysotile, lizardite are common and antigorite is a small amount serpentin mineral according to the XRD. Rock has sieve / network-glass clock texture because of widespread serpentinization. REE (Rare Earth Elements) values of these rocks have positive La, Nd, Eu, Ho, Tm, Lu and negative Pr, Sm, Gd, Er, Yb anomaly by chondrites / normalized distribution and show rather depleted according to the chondrite. Can be said that mineral transformation temperature reaches amphibolite facies according to the mineral association.

Raduzhnoe – epithermal breccia-hosted deposit (Northern Caucasus, Russia)

E.N. KAIGORODOVA¹

¹Institute of Geology of Ore Deposits, Petrography, Mineralogy and Geochemistry, Russian Academy of Sciences, Staromonetny per., 35, Moscow, Russia (katmsu@mail.ru)

The **Raduzhnoe deposit** is situated in the central part of North Caucasian Mountains within Jurassic depression zone, related with extensional-transensional tectonic regime, forming horst and graben structures. Intensive tectonic and magmatic activity was associated with the closure of the Tethys Ocean and the Andean type of subduction. Block movements began in the Early Jurassic (Pliensbachian). Jurassic volcanic formations are represented by Aalenian basalt-rhyolite and Bajocian basalt-porphry-trachytic formations. Rhyolites are the most common volcanic rocks at this area. Epimagmatic hydrothermal activity related to rhyolites led to: broad development of processes of silicification of host rocks, less their kaolinization, carbonation, sulphidation, baritization, chloritization, the widespread expression of alkaline metasomatism.

The ore occurrences are confined to the PZ granite ledge and zones of intense brecciation. Composition of the breccias is quite diverse. Breccias have been changed in a varying degree during gas-hydrothermal activity. Ore minerals which have been identified at Raduzhnoe are native gold, calaverite, dyscrasite, proustite, sulfides. Au content reaches up to 215 g / t, Ag and 4000 g / t.

At the deeper levels of the breccias the pyrite content increases and galena, sphalerite and chalcopyrite appear. Polymetallic mineralization is mainly associated with hydrothermally altered basement granites and Pliensbachian sandstones. Gold and silver are being in a finely dispersed state in sulfides.

Thus, at the Raduzhnoe there are allocated two types of mineralization: gold-silver (low-sulfidation gold-silver type) and gold-silver-containing polymetallic (low-sulfidation silver-gold-base metal type) [1]. Probably gold-silver-polymetallic mineralization is earlier process and is associated with developing of the global Jurassic polymetallic belt of the North Caucasus. Gold-silver subtype of mineralization is more recent, local and related to the final (solfatar) stage of volcanism.

[1] Sillitoe R.H., Hedenquist J.W. (2003) *Soc. Econ. Geol. Spec. Publ.* **10**, 315–343.

Origin of secondary REE minerals in grusified Karkonosze granites, SW Poland

BARTŁOMIEJ KAJDAS^{1*} AND MAREK MICHALIK¹

¹Institute of Geological Science, Jagiellonian University, Kraków, Poland; (*correspondence: xszerlit@gmail.com)

Primary monazite-(Ce), which is one of the most common accessory mineral in Karkonosze granites, is absent in grusified granites from Głębock, Kowary Średnie and Miłków. In the grusified granites muscovite–thorite or cheralite–xenotime-(Y) pseudomorphs after primary monazite-(Ce) are present. Instead of monazite-(Ce) in grusified granites secondary rhabdophane-(Ce), florencite-(Ce), cerianite-(Ce), rhabdophane-(La) and rhabdophane-(Nd) are present.

Small (about 5 µm) automorphic crystals of rhabdophane-(Ce) and florencite-(Ce) occur inside sericitised plagioclases often along cleavage planes of primary feldspar. Cerianite-(Ce) occurs as thin veins or as clusters of crystals impregnating rims of the grains of grus. Rhabdophane-(La) and rhabdophane-(Nd) crystals are usually small, xenomorphic and fill large cracks inside the grains of granitic grus.

Decomposition of primary monazite-(Ce) might be the result of the activity of hydrothermal fluids [1], which could be also the main factor of the development of microcracks in granite that led to the development of grus. REE released from the decomposed monazite-(Ce) crystallized as secondary rhabdophane-(Ce) and florencite-(Ce). Chemical analysis of primary monazite-(Ce) from Karkonosze granite and secondary rhabdophane-(Ce) and florencite-(Ce) shows, that ratios of REE in primary and secondary REE phosphates are very similar.

Secondary cerianite-(Ce), rhabdophane-(La) and rhabdophane-(Nd) crystallisation could be caused by low temperature weathering, oxidizing fluids [2].

Decomposition of primary REE minerals and multistage crystallisation of secondary REE minerals in grusified granites indicates that process of grusification *sensu stricto* was preceded by activity of hydrothermal fluids, which developed microcracks in the rock and caused breakdown of primary minerals including REE phosphates. Similar observations were obtained in grusified Tatra granites [3].

[1] Berger *et al.* (2008) *Chem. Geol.* **254**, 238-248. [2] Aubert *et al.* (2001) *Geochim. Cosmochim. Acta* **6(3)**, 387-406. [3] Kajdas B & Michalik M (2011) *Min. Mag.* **75(3)**, 1135.

Addressing the nanoscale complexity of mineral-water interfaces in MD simulations: Effects of the substrate compositional disorder on the properties of surface species

ANDREY G. KALINICHEV^{1*}, NARASIMHAN L.¹
AND BRICE F. NGOUANA W.¹,

¹Laboratoire SUBATECH (UMR-6457), Ecoles des Mines de Nantes, 4 Rue Alfred Kastler, La Chantrerie, 44307, Nantes Cedex 3, France (*kalinich@subatech.in2p3.fr)

Thermodynamic, structural and transport properties of hydrated clays and clay-related materials for many geochemical, environmental, and technological applications are routinely studied by computational molecular modeling techniques. However, simulated system size limitations often impose a considerable quasi-periodicity on the distribution of the tetrahedral and octahedral site substitutions in the T-O-T clay layers. Such quasi-periodicity is then typically propagated further even if larger models are later constructed by simply multiplying the smaller ones, and the effects of this imposed structural ordering on the calculated properties of the interfaces is not obvious.

Here we report the results of molecular dynamics simulations with a new set of larger-scale muscovite and montmorillonite models which were systematically constructed to introduce as much structural disorder in the distributions of the Al/Si and Mg/Al substitutions as possible. The effects of such disorder on the local structural and dynamic properties of the interfacial and interlayer water and hydrated ions are then carefully quantified and analyzed for a number of typical monovalent and divalent cations.

The time- and space- averaged properties of the hydrated interfaces and interlayers, such as atomic density profiles, radial distribution functions, and surface diffusion coefficients, are observed to be not particularly sensitive to the specific details of the substrate disorder. However, local effects of the disordered distribution of charge-substituted sites in clay layers can be substantial and can influence the strength of the ionic and molecular adsorption at a specific surface site, the structure and dynamics of the interfacial hydrogen bonding network around it, and the molecular mechanisms of its local rearrangement.

Putting age into the equation: A new look at microbial distribution in subsurface sediments

JENS KALLMEYER¹

¹Helmholtz Centre Potsdam, GFZ German Research Centre
For Geosciences Telegrafenberg, 14473 Potsdam,
Germany, kallm@gfz-potsdam.de

At any given depth cell abundance in subsurface sediments varies by up to six orders of magnitude between sites. To a large extent this variability correlates with mean sedimentation rate and distance from land. This relationship can therefore be used to predict subsurface cell abundance.

Usually, decrease in subsurface microbial abundance at each site can be described by a logarithmic function. However, at some sites, e.g. IODP Exp. 320, Site U1334 from the equatorial Pacific Ocean, cell distribution strongly deviates from this trend and cannot be described by a simple equation.

In order to better understand why cell distribution at some sites exhibits such unusual patterns it is necessary to take a closer look at sedimentation rates and therefore sediment ages as well. The sites that were drilled by IODP Exp. 320 and 321 recovered a continuous Cenozoic record of the paleoequatorial Pacific by coring above the paleoposition of the highly productive equatorial upwelling zone at successive crustal ages on the Pacific plate. Although some of the unusual cell distribution is caused by strong geochemical gradients and diagenetic alteration fronts, the significant differences in sedimentation rates between within and outside the upwelling zone appear to be a major cause for the strong deviations in cell abundance from the expected logarithmic decline with depth.

Subsurface microbial communities have to subsist without fresh supply of organic matter, which becomes increasingly recalcitrant with increasing age. When assigning ages to cell count data from different oceanic regions, these cells vs. age correlation show less variability between sites than correlations vs. depth.

These observations suggest that subsurface microbial abundance is controlled by organic matter reactivity, which is largely controlled by sediment age. Using age instead of depth models might provide important clues about the finer details of subsurface cell abundance, especially in areas that have not fitted into previous models.

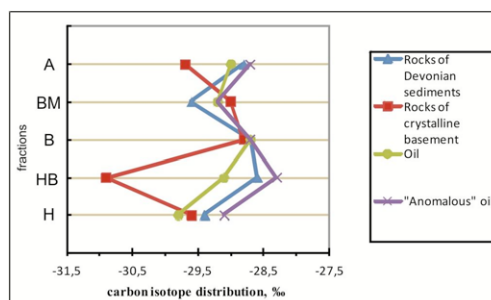
Biogenic or abiogenic hydrocarbon source of Melekes Depression

A.I.KAMALEEVA* AND E.M.GALIMOV

Vernadsky Inst. of Geochemistry and Analytical Chemistry
RAS, Kosygin 19, Moscow, 119991 Russia
(*correspondence: adelya-kamaleeva@yandex.ru)

The question of hydrocarbon origin is an important problem in Tatarstan, where some of the geologists suggest the existence of abiogenic hydrocarbon "inflow" to sedimentary oil fields. Core samples for the study of the organic matter were taken from Devonian sediments (DS), as well as from the rocks of the crystalline basement (CB). The oil was taken from the main productive complexes of seven fields within the studied areas and from the so-called "anomalous" boreholes of the Romashkinskoye supergiant field, where the inflow of deep hydrocarbons is possible. The distribution of the isotope ratios of carbon between different fractions was studied in oil and extracted bitumoids of rocks by the method [1].

In the studied oil the sufficiently common type of carbon isotope distribution by fractions was found (Figure). This type of oil consists of the sapropelic type of organic matter and mixed type, which is formed by a certain percent of humus and aquahumus materials. The "anomalous" oil completely coincides with other samples of oil. So there is no reason to assume for them any other source of hydrocarbons. Bitumoids extracted from the organic matter of DS, with a few exceptions, are of the same genetic type as the studied oil.



Bitumoids extracted from the rocks of CB carry traces of thermal and hydrothermal effects missing in the oil of sedimentary strata [2]. Therefore, they may be the product of thermal alteration of sedimentary naphthides but cannot be primary with regard to the last one. Thus, the biogenic hydrocarbon source of Melekes Depression is proved.

[1] Galimov (2006) *Organic Geochem.* **10**, 1200-1262. [2] Kamaleeva et al. (2013) *Geochemistry Int.* **1**, 13-22.

The evolving nature of terrestrial crust from the Hadean, through the Archaean, into the Proterozoic

BALZ S. KAMBER¹

¹Geology Department, Trinity College Dublin, Ireland

The ancient rock and mineral records show that Hadean crust could persist for 500-700 Ma. Notwithstanding the general longevity of evolved crust, the well-established major Precambrian time boundaries remind us that terrestrial geology did not proceed in a uniform manner. The Hadean-Archaean boundary witnessed the near-complete destruction of the Hadean crust. This crust was chemically diverse, and at least the zircon bearing magmas formed at relatively low T and had interacted with the hydrosphere. Opinions diverge as to whether these attributes imply plate tectonics. Advocates of the existence of Hadean continental lithosphere have yet to propose a plausible mechanism by which this lithosphere was destroyed. Those who appeal to internal differentiation of largely basaltic crust, aided by volcanic resurfacing, can appeal to the episodic collapse of early planetary crustal lids to explain the disappearance of Hadean crust.

Regardless of this unresolved debate, agreement exists that the entire Archaean record is dominated by greenstone-granitoid terrains. The much-improved greenstone belt geochronological database demonstrates that most of these edifices grew vertically, by repeated eruptions of new volcanic sequences on top of older ones. Although they do not represent oceanic crust, the existence of subduction and subductable oceanic lithosphere can be inferred from a variety of observations, ranging from granitoid geochemistry to diamond inclusions. It is thus proposed that the Archaean represents the era of three types of plates: continental and oceanic lithosphere as well as prominent oceanic plateaus.

The Palaeoproterozoic rock record differs in many ways. Greenstone belts have disappeared, platform sediments have become abundant and the first very high-P rocks are preserved at the Earth's surface. These phenomena reflect a change in the mechanical strength of the continents, which increased due to less internal heat production and redistribution of K, Th and U. However, the disappearance of komatiites and the unexpected lack of increase in extent of mantle depletion from 2.7 Ga to 2.0 Ga argue for mantle reorganisation. It is here proposed that a mechanical and thermal boundary layer existed in the mantle transition zone until the end of the Archaean. This led to severe depletion in the upper mantle, promoted build up of heat plumes and prevented recycling of oceanic plates into the deep mantle. Accordingly, the onset of deep recycling is dated by the ca. 2 Ga 'age' of OIB sources.

A first-order deep time reconstruction of the marine Sr/Ba ratio from microbial carbonate

BALZ S. KAMBER¹, THOMAS F. NAEGLER²,
ELIZABETH C. TURNER³, GREGORY E. WEBB⁴
AND CHLOÉ PRETET⁵

¹Geology Department, Trinity College Dublin, Ireland

²Geological Sciences, University of Bern, Switzerland

³Earth Sciences, Laurentian University, Sudbury, Canada

⁴Earth Sciences, The University of Queensland, Australia

⁵Earth Sciences, University of Geneva, Switzerland

The upper crust is enriched in Sr and Ba where they occur at a mass ratio of ca. 1.25. The dissolved river load has a Sr/Ba of ca. 1.8, whereas residual weathering profiles have a Sr/Ba of ca. 0.9, showing that Sr is more easily released. In our estuarine transects both elements behave conservatively. Once in the ocean, the fates of Ba and Sr diverge sharply. Sr has a long residence time and is homogeneously distributed whereas dissolved Ba concentration in seawater is very low and varies systematically with depth [1] (very depleted in the shallow ocean and more enriched at depth). The overall depletion and the depth structure are explained by Ba-removal as biogenic marine barite in organisms and its partial re-release at depth. Hanor [2] predicted that this type of barite formation may not have been constant through time and that marine Ba could be a proxy for sulphate concentration.

Our data from Holocene microbial carbonate faithfully record the very high but variable Sr/Ba (400-1,200) of very shallow seawater. In situ LA-ICP-MS of partly dolomitised samples clearly indicate that dolomitisation greatly increases the Ba content and our deep time reconstruction was conducted on best preserved calcite only. The reconstruction shows a very clear first-order Sr/Ba topology. The ratio remained very high (>>200) back to 555 Ma, decreased rapidly throughout the Proterozoic to 2-5 until the Great Oxygenation Event, before which it was quite constant at 10. This evolution is interpreted as a three step increase of marine sulphate levels. A second-order control on the shape of the Sr/Ba topology can be inferred from the absolute Sr and Ba concentrations in the microbial carbonate, which, for Sr, was much lower for most of the Precambrian but increased strongly after the Marinoan. This is important as it suggests a much reduced nutrient load to the Precambrian ocean with wide implications for other deep time studies (e.g. Mo in shale) that assume variable removal but constant supply of metals.

[1] Griffith and Paytan (2012) *Sedimentology* **59**, 1817-1835.

[2] Hanor (2000) *Rev. Min. & Geochem.* **40**, 193-275.

PGE-Au potential of sulphide-saturated melts from the subcontinental lithosphere

V. S. KAMENETSKY¹, R. MAAS², R.O.C. FONSECA³,
C. BALLHAUS³ AND A. HEUSER³

¹University of Tasmania, Hobart, TAS 7001, Australia;

Dima.Kamenetsky@utas.edu.au

²University of Melbourne, VIC 3010, Australia

³Universität Bonn, Bonn 53115, Germany

The origin of platinum element metal (PGE) enrichment in large magmatic nickel sulphide deposits is controversial; both primary magmatic and hydrothermal processes have been invoked. Irrespective of their exact mode of deposition, the ultimate source of such extreme enrichments of these rare metals must be PGE-enriched parental silicate melts capable of reaching sulphide saturation and efficient PGE capture in immiscible sulphide liquids. Direct observation of coexisting primary silicate and sulphide melts at the onset of silicate-sulphide liquid is impossible because of intense magmatic processing up until ore deposition. Here we report the discovery of Fe-Ni sulphide melt globules highly enriched in noble metals (Pt, Pd, Os, Ir, Au, Ag; total 150 ppm) within an unusual high-Mg andesitic glass dredged from the southern Mid Atlantic Ridge [1]. The composition of this primitive glass (8.2 wt% MgO, Mg# 67.1 mol%) indicates derivation of its parental silicate melt from a garnet pyroxenite mantle source with pronounced 'continental' isotopic (Pb, Sr, Nd, Hf, Os, O) signatures [1]. We infer that the chemical properties of this melt, notably high SiO₂ (57.3 wt%) and Ni (310 ppm) contents, promoted sulphide saturation at low pressures in a purely oceanic setting and propose that this unique example, with its likely origin in the continental lithospheric mantle, may be a useful analogue for magmatic PGE enrichment and incipient Ni-PGE- sulphide melt generation within large Ni-PGE magmatic sulphide systems.

[1] Kamenetsky, V. S. *et al. Geology* **29**, 243-246 (2001).

A two-stage scenario for the formation of the Earth's mantle and core

E. KAMINSKI^{1*} AND M. JAVOY²

¹Institut de physique du globe de Paris, 75005 Paris, France,

(*correspondence: kaminski@ipgp.fr)

²Institut de physique du globe de Paris, 75005 Paris, France,

(javoy@ipgp.fr)

Various geophysical constraints on the deep Earth point to a chemically heterogeneous mantle. Based on such constraints, Bulk Earth compositions inferred from Enstatite chondrites (E-Earth composition) predict that, whereas the Primitive Upper mantle (PUM) had a pyrolitic composition, the Primitive Lower mantle (PLoM) was enriched in Fe and Si and depleted in Mg, Ca and Al relative to PUM. We will explain how, in E-Earth formalism, this chemical heterogeneity can be related to the formation and differentiation of the Early Earth, and mantle Si and Fe variations reflect variations in the efficiency of Si and FeO dissolution in the metal phase during core formation, through the reaction $\text{SiO}_2 + 2\text{Fe}_{\text{metal}} = \text{Si}_{\text{metal}} + 2\text{FeO}$ which increases progressively the $f\text{O}_2$ of the silicate. In the simplest and most direct scenario of homogeneous accretion, we calculate by mass balance the composition and the mass fraction of the metallic extract in equilibrium with a pyrolite. The O, Si and Ni contents of this metal extract correspond to a silicate-metal equilibrium at high pressure (50±5 GPa) and high temperature (3500±500°C), in line with a giant impact scenario. The mass of pyrolite produced during that stage is significantly smaller than the mass of the Bulk Silicate Earth. Mass balance calculations then yield the composition of the proto-core and the proto-mantle prior to the giant impact. We obtain that the core of the proto-Earth was almost devoid of oxygen, hence formed under lower pressure and temperature conditions, in agreement with an early differentiation of planetesimals in the early solar system. In such a two-stage scenario of Earth's core formation, no massive silicate differentiation is required to create a pristine mantle heterogeneity. The concentration of lithophile elements in the Primitive Lower mantle, notably Ca, Al, U and Th, can then be constrained using RLE ratios in E-chondrites and in the upper mantle.

New minerals in the primary, deep-seated carbonatitic association

FELIX V. KAMINSKY¹* AND RICHARD WIRTH²

¹KM Diamond Exploration Ltd., West Vancouver, Canada

*correspondence: felixvkaminsky@aol.com

²GeoForschungsZentrum, Potsdam, Germany

In one of newly studied diamonds from the Juina area, Brazil, several new polymineral inclusions of the carbonatitic association were identified. The hosting diamond belongs, like most of the diamonds from this area, to the Deep Earth. The composite carbonate-halide-phosphate inclusion consists of magnesite, dolomite and mixed-anion phosphate micrograins along with nanograins of eitelite, halite, sylvite, phlogopite, spinel and pentlandite. The inclusion has a 'negative' shape, typical for syngenetic inclusions in diamond. The mineral assemblage comprising this inclusion belongs to the carbonate-chloride line of the primary, deep-seated carbonatitic association, which has been established among inclusions in diamond in our earlier works [1, 2]. Three new minerals for this association were identified in this inclusion: magnesite, eitelite and a mixed-anion phosphate, $\text{Na}_4\text{Mg}_3(\text{PO}_4)_2(\text{P}_2\text{O}_7)$. The presence of magnesite, within this new mineral association, provides evidence for its stability in the diamond stability field, which was earlier questioned; magnesite had been suggested to decompose with the formation of ferropicrinite and diamond. Eitelite, $\text{Na}_2\text{Mg}(\text{CO}_3)_2$, has been identified previously in alkaline-carbonatitic rocks of the Khibini Massif, Kola Peninsula, Russia [3]. The mixed-anion phosphate, $\text{Na}_4\text{Mg}_3(\text{PO}_4)_2(\text{P}_2\text{O}_7)$, has not previously been observed in the natural environment before. This mineral contains an admixture of FeO (up to 6 at.%). In other carbonatitic inclusions, Fe-phosphate $\text{Fe}_2\text{Fe}_3(\text{P}_2\text{O}_7)_4$, and aluminium fluoride AlF_3 were identified. They were found in the natural environment for the first time as well. The carbonatitic inclusions most likely originated as a high-density fluid (HDF) micro-inclusions, encapsulated in diamond during its initial growth. Such inclusions are fully miscible under mantle conditions and subsequently crystallize as polyphase mineral inclusions, during ascent of diamond to the Earth's surface.

[1] Wirth, Kaminsky, Matsyuk & Schreiber, A. (2009). *Earth Planet. Sci. Lett.* **286**, 292-303. [2] Kaminsky, Wirth, Matsyuk, Schreiber & Thomas (2009) *Mineral. Mag.* **73**, 797-816. [3] Khomyakov, Sandomirskaya & Malinovskii (1980) *Doklady* **255**, 190-192.

Sampling a natural CO₂ reservoir, Green River, Utah

NIKO KAMPMAN¹, MIKE BICKLE¹, HAZEL CHAPMAN¹, ALEX MASKELL¹, JIM EVANS² AND ANDREAS BUSCH³

¹Department of Earth Sciences, University of Cambridge, Downing Street, Cambridge CB2 3EQ (correspondence: nkam06@esc.cam.ac.uk)

²Department of Geology, Utah State University, 4505 Old Main Hill Logan, UT 84322-4505 16

³Shell Global Solutions International, Kessler Park 1, 2288 GS Rijswijk, The Netherlands

We present the initial results from a scientific drilling project to recover core and high pressure fluid samples from a natural CO₂ reservoir near Green River, Utah. We use this as an analogue to investigate fluid-flow and CO₂-fluid-mineral interactions with caprocks and fault zones likely during anthropogenic storage of carbon dioxide

Diamond drilling of drill-hole CO₂W55, adjacent to the CO₂-degassing Little Grand normal fault, recovered core from two major CO₂ reservoirs in the Entrada and Navajo Sandstones, and from the intervening Carmel Formation caprock. The well encountered CO₂-charged fluids in the basal sandstones of the Entrada Sandstone, in open fractures in the footwall damage zone of the fault penetrating the Carmel Formation, and throughout the Navajo Sandstone. Downhole wireline fluid sampling to recover high-pressure CO₂-charged fluids during drilling, and analytical methods to measure their dissolved CO₂ content and pH on-site, are presented and discussed. Measurements of CO₂ concentrations, fluid chemistry and isotope ratios from the drill-hole fluid samples are used to constrain fluid-fluid mixing, fluid-rock reactions and dynamics of CO₂ migration within the fault damage zone. Fluid-mineral reactions predicted from fluid geochemistry are compared to petrological, mineralogical, geochemical and petrophysical measurements from the reservoir and caprock core, and the implications for reservoir alteration and caprock performance are discussed.

Cyanide and thiocyanate biogeochemistry in non-polluted natural aquatic systems

A. KAMYSHNY JR.^{1*}, H. ODURO², Z. F. MANSARAY³
AND J. FARQUHAR³

¹Department of Geological and Environmental Sciences, The Faculty of Natural Sciences, Ben-Gurion University of the Negev, P.O. Box 653, Beer Sheva 84105, Israel, (*correspondence: alexey93@gmail.com)

²EAPS, Massachusetts Institute of Technology, E25-639, 77 Massachusetts Avenue, Cambridge, MA 02139-4307, USA, hoduro@mit.edu

³Department of Geology and Earth Systems Science Interdisciplinary Center, University of Maryland, College Park, MD 20742, USA, zfmansaray@gmail.com, jfarquha@glue.umd.edu

Here, we report on the accumulation of high levels of cyanide as free cyanide, complexed cyanide, iron-cyanide, and thiocyanate in sediments of the non-polluted Delaware Great Marsh (up to 230 $\mu\text{mol kg}^{-1}$). Free cyanide at concentrations which are toxic to aquatic life (up to 1.92 $\mu\text{mol L}^{-1}$) were detected in sediment pore-waters, and the concentration of total (free and complexed) cyanide in the pore waters was found to be as high as 6.94 $\mu\text{mol L}^{-1}$. The presence of hydrogen cyanide in the salt marsh sediments is attributed to processes associated with decomposition of cord grass *Spartina alterniflora* roots. The formation of iron-cyanide complexes and their adsorption onto sedimentary organic matter provide a temporary sink of cyanide, but the ultimate cyanide sink is associated with the formation of thiocyanate by reaction with sulphide oxidation products, principally polysulfides, formed by reaction with Fe(III) minerals. The formation of thiocyanate by this pathway detoxifies two poisonous compounds, polysulfides and hydrogen cyanide, in the salt marsh sediments [1]. Thiocyanate is stable under anoxic conditions, but diffuses freely through sedimentary pore waters to upper oxic sediment layers, where it may be oxidized by biologically assisted processes either to carbonyl sulfide and ammonia or to cyanate and hydrogen sulfide. Thiocyanate was also detected at concentrations up to 288 nmol L^{-1} in the water column of Lake Rogoznica (Croatia) [2] and up to 274 nmol L^{-1} in the water column of Fayetteville Green Lake (NY). Here, thiocyanate appears to be produced in the sediment and diffuse towards the chemocline, where it is consumed by abiotic or biologically enhanced oxidation.

[1] Kamyshny *et al.* (2013) *Aquat Geochem* **19**, 97-113. [2] Kamyshny *et al.* (2011) *Mar Chem* **127**, 144-154.

Petrogenesis and tectonic setting of the Nasrand granitoid pluton, southeast of Ardestan

ALI KANANIAN*, ZAHRA HAMZEHIE, FATEMEH SARJOUGHIAN AND JAMSHID AHMADIAN

Kananian@Khayam.ut.ac.ir 1 zahra.hamzei@ut.ac.ir
Fsarjoughian2@gmail.com,
jamshidahmadian@yahoo.com

The Nasrand pluton of Oligo-Miocen age, which is located in south-east of Ardestan, intruded into Eocene volcanic rocks of the Urumieh-Dokhtar magmatic belt. This pluton consists mainly of granite and granodiorite, and has been intruded by a series diabase dikes. The nasrand plutonic rocks are metaluminous, with mineralogical and geochemical characteristics of I-type calc-alkaline to high-K calc-alkaline granite. They are characterized by enrichment of LREE and LILE, depletion of HREE and HFSE, negative anomalies of Ti, Nb, P, Ba, and positive anomalies of U, K, Th, Rb, Ba, associated with high Ba/Nb ratio and interpreted to reflect emplacement of the plutonic rocks in an active continental margin. The Nasrand granitic pluton and its diabase dikes were all derived from partial melting of the lower continental crust, but it seems that the granitic rocks are slightly more fractionated than diabase dikes and may be modified by assimilation of upper crustal materials.

Keywords: Ardestan, I type granite, calc-alkaline, diabase dikes, active continental margin.

Mineralogical, petrographical and geochemical investigation of Tefenni-Burdur chromite occurrences

ALEV KAN BOSTANCI¹, DEMET KIRAN YILDIRIM¹,
MUHITTIN KARAMAN¹, ANIL SENA SERT¹
AND MURAT BUDAKOĞLU¹

¹Istanbul Technical University, Department of Geological Engineering, 34469, Istanbul, TURKEY

The lithological units consist of Late Jurassic – Early Cretaceous aged Yeşilova ophiolites, Upper Cenozoic aged Kızılcadağ ophiolitic melange, Pliocene-Quaternary aged Niyazlar Formation and Quaternary aged alluvions in the investigation area.

Yeşilova ophiolite consists of tectonites, ultramafic and mafic cumulates, isotropic gabbros, plagiogranites and basalts from bottom to top. Yeşilova ophiolite in which sheeted dike complex and pillow lavas are not seen, represents an ophiolite group with missing rock character.

In the bottom of the Yeşilova ophiolite there are tectonites, which is composed of harzburgite, dunite, serpentinized harzburgite and dunite, serpentinite and chromite masses with dunitic envelope. Tectonites are mostly serpentinized in parts where mafic dikes are dense and along tectonic lines. Tectonites are cut by many mafic dikes.

According to the metamorphic paragenesis determined in the oceanic crust rocks forming Yeşilova ophiolite, it is metamorphosed in P/T situations which does not reach the sub limit of greenschist facies.

Upper Cenozoic aged Kızılcadağ ophiolitic melange takes place tectonically on Yeşilova ophiolite. Tectonic boundary between these two units is nearly horizontal.

Role of submicron-sized particles on the ^{134,137}Cs migration in Fukushima

M. KANEKO¹, Y. NAKAMATSU¹, T. OHNUKI², K. NANBA
AND S. UTSUNOMIYA¹

¹Dept. Chemistry, Kyushu University, Fukuoka 812-8581,
Japan (utsunomiya.satoshi.998@m.kyushu-u.ac.jp)

²ASRC, Japan Atomic Energy Agency, Tokai, Japan

³Dept. Environmental Management, Fukushima University

In the vicinity of Fukushima Daiichi Nuclear Power Plant (FDNPP), ¹³⁷Cs ($T_{1/2} = 30.07$ y) and ¹³⁴Cs ($T_{1/2} = 2.062$ y) have great contribution to the radiation dose. Although the initial distribution of radionuclides derived from FDNPP accident have been reported to date, there are limited knowledge on micron- and submicron-scale distribution and migration of ^{134,137}Cs in the surface and sub-surface environments. In order to understand the fundamental mechanism of ^{134,137}Cs retention and migration in the contaminated area in Fukushima, Cs speciation in various environmental samples (soils, aerosol and groundwater) is investigated, which were collected from severely contaminated area in Fukushima.

In the soil samples, the vertical profile of ^{134,137}Cs distribution revealed that >98% of ^{134,137}Cs remained within top 5 cm. Sequential extraction of the contaminated soils revealed that most ^{134,137}Cs was strongly bound to high-affinity site of clay minerals such as illite and montmorillonite, while up to 20% of ^{134,137}Cs was present as an ion exchangeable form, suggesting that elution of ^{134,137}Cs from soil minerals would be minimal in the surface environment in Fukushima. In the size fractionation experiment, ~78% of ¹³⁷Cs was distributed in the colloid region (<1 μm) and the concentration was as high as ~3,000,000 Bq/kg. The ¹³⁷Cs radioactivity of airborne particles collected in Iitate was measured to be 12.2, 15.7, and 11.8 mBq/m³ for the size fractions of <0.4, 0.4-2.5, and >2.5 μm, respectively. ^{134,137}Cs were under the detection limit in the groundwater samples. These results clearly indicate that ^{134,137}Cs have not migrated to the groundwater system until one year after the accident, and the airborne Cs-particles were mainly derived from suspension of the fine fraction of the contaminated soils, namely Cs-bearing clay minerals.

The present study strongly suggests that the migration of ^{134,137}Cs in the surface and sub-surface environment is not governed by the adsorption-desorption cycle but by the behavior of Cs-adsorbed submicron-sized particles. Therefore, the unique physico-chemical property of Cs-bearing colloids should be taken into account for predicting the future behavior of ^{134,137}Cs in the surrounding environments in Fukushima.

Quantification of methanogenic potential in environmental samples

MASANORI KANEKO^{*1}, YOSHINORI TAKANO¹,
TAKESHI WATANABE², SUSUMU ASAKAWA²,
SEIGO SHIMA³, NANAOKO OGAWA¹
AND NAOHIKO OHKOUCHI¹

¹JAMSTEC, Yokosuka, 237-0061 Japan

(*correspondence: m_kaneko@jamstec.go.jp)

²Nagoya Univ. Nagoya, 464-8601 Japan

³Max Planck Inst. Marburg, D35043, Germany

A Ni porphyrinoid, coenzyme F430 is the prosthetic group of methyl-coenzyme M reductase, which catalyze a final step of methanogenic reactions in all methanogenic pathways including CO₂ resuction, acetate fermentation and methylotrophic pathways[1]. F430 is unstable, hence native F430 will not be persisting in sediments through a geologic time scale. Given its unique structure, functionality and lability, F430 can be a robust biomarker for a quantitative estimation of *in situ* activities of living methanogens.

Conventionally F430 was analyzed photometrically using HPLC or off-line MS [2]. Recently we have developed a high sensitive detection of F430 by a HPLC-MS/MS. This sensitivity (femto mol level) is 10⁴ to 10⁵ times higher than the conventional photometric dection and only 10² to 10⁴ methanogen cells are required for quantification of F430 in environmental samples. Our analyses indicated that concentration in paddy field ranges between 9870 and 253 fmol/g which is 1-2 orders of magnitude higher than those in marne sediments off Japan, ranging between 100 and 7 fmol/g, and 1910 fmol/g from Peru Margin (68 mbsf).

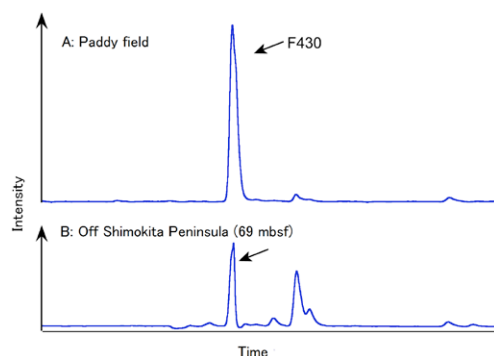


Fig. 1. HPLC-MS/MS chromatograms of derivatized F430 from a paddy field and marine sediment.

[1] Thauer (1998), *Microbiology* **144**, 2377-2406. [2] Takano, Kaneko, Kahnt, Imachi, Shima & Ohkouchi (2013), *Org. Geochem.*, in press.

Biominingalization of Strontianite (SrCO₃) by *Proteus mirabilis*

SERKU KANG¹, YUMI KIM², AND YUL ROH^{3*}

¹Chonnam National University, Gwangju, Korea,
(chodang02@naver.com)

²Chonnam National University, Gwangju, Korea,
(yumddalki@hotmail.com)

³Chonnam National University, Gwangju, Korea,
(*correspondence: rohy@jnu.ac.kr)

Microbially induced mineralization of carbonate minerals has drawn much attention in recent decades because of its practical applications such as atmospheric CO₂ fixation through mineral carbonation and solid phase capture of toxic radionuclide or metal contaminants (i.e., ⁹⁰Sr, ⁶⁰Co and Cd). The objectives of this study were to investigate the potential for microbially induced precipitation of strontianite (SrCO₃) using microorganisms enriched from rhodoliths and to identify mineralogical characteristics of the bio-precipitates.

Carbonate forming microorganism (CFM) was enriched from rhodoliths and aerobically cultured at 25°C in D-1 medium containing 30 mM Sr-acetate. The microorganisms were analyzed by 16S rRNA gene DGGE analysis to confirm microbial diversity. Mineralogical characteristics of the bio-precipitates were determined by XRD, TEM/SEM-EDS analyses.

A 16S rRNA sequence analysis showed the CFM was mainly *Proteus mirabilis* [1]. The growth of CFMs gradually increased for 16 days (OD₆₀₀ = 2.613) and then decreased until 22 days (OD₆₀₀ = 2.016) of incubation. Medium pH in the biotic group increased from acidic at first (pH = 5.3) to alkaline condition (pH = 8.6). The pH changes might induce favorable geochemical condition for Sr-carbonate precipitation. In the abiotic group, neither growth of microorganism nor changes in pH were detected.

The enriched microorganisms mediated the precipitates in D-1 medium containing 30 mM Sr-acetate. The bio-precipitates were identified strontianite (SrCO₃) by XRD analysis. SEM-EDS analyses showed that the precipitates were round in shape, and around 60 μm in size, and composed of C, O and Sr. TEM-EDS analyses showed that the Sr-carbonate minerals were irregular in shape, 60~70 nm in size, and composed of C, O, and Sr.

These results indicate that the CFM induce the precipitation of strontianite (SrCO₃) by biological processes. Therefore, CFM such as *Proteus mirabilis* may play one of important roles in Sr immobilization in Sr-contaminated water and CO₂ fixation in natural environments.

[1] Chimento et al. (2011) *Int. J. Syst. Evol. Microbiol.* **60**(1), 60-64.

Pb, Sr, Nd, Hf isotope geochemistry of South Arch lavas: Origin of the upstream side Hawaiian arch volcanism

T. KANI^{1*}, B. B. HANAN², R. KINGSLEY³
AND J.-G. SCHILLING³

¹Kumamoto University, Kumamoto 860-8555, Japan

(*correspondence: kani@sci.kumamoto-u.ac.jp)

²San Diego State University, San Diego, CA, USA

(bhanan@mail.sdsu.edu)

³GSO, University of Rhode Island, RI, USA

South Arch volcanic field is located on the crest of a broad swell surrounding the Hawaiian Islands, 200 km south of Kilauea, along the peripheral edge of the radially dispersing mantle plume stream, diverted to the NW by the migrating Pacific lithospheric plate.

Pb, Sr, Nd and Hf isotope compositions of 14 alkali basalts collected at water depths > 4 km by JAMSTEC Kaiko and Shinkai dives (K217 and S697), distinguish these magmas from shield tholeiites, rejuvenated stage, and North Arch lavas. Pb isotope compositions of South Arch lavas are more radiogenic compared to North Arch and rejuvenated lavas, but similar to Kea lavas, confirming plume compositional influence on the upstream plume periphery is stronger than downstream. In Pb-Sr-Nd multi-isotope binary plots the data clusters, with little variation, and no apparent correlation. The $^{87}\text{Sr}/^{86}\text{Sr}$ is lower and the ϵ_{Nd} higher than Hawaiian shield tholeiites indicative of a depleted source. Plots of ϵ_{Hf} against ϵ_{Nd} , $^{87}\text{Sr}/^{86}\text{Sr}$ or $^{206}\text{Pb}/^{204}\text{Pb}$ define trends oblique to the mantle array. The variation is in ϵ_{Hf} essentially at constant ϵ_{Nd} , $^{87}\text{Sr}/^{86}\text{Sr}$ or $^{206}\text{Pb}/^{204}\text{Pb}$. These relationships cannot be explained by seawater or sediment contamination, but could result from metasomatism. The results suggest that the South Arch basalt source consists of metasomatised oceanic lithosphere and plume components. The isotope characteristics of the South Arch lavas could be interpreted to represent metasomatised Pacific lithosphere, residue of a MORB-related melting event at ~100 Ma, modified by plume fluids and melts. Alternatively, the South Arch mantle source may be ancient recycled oceanic lithosphere, part of the Hawaiian plume.

Diagnosing the hydroclimate influences on soil water $\delta^{18}\text{O}$: Precipitation $\delta^{18}\text{O}$, evaporation, or moisture transport?

LISA KANNER^{1*}, NIKOLAUS BUENNING¹,
LOWELL STOTT¹, AXEL TIMMERMAN², DAVID NOONE
AND LISA SLOAN⁴

¹University of Southern California, Los Angeles, CA, USA

lkanner@usc.edu, buenning@usc.edu, stott@usc.edu

(*presenting author)

²University of Hawaii, Honolulu, HI, USA, axel@hawaii.edu

³University of Colorado, Boulder, CO, USA,

dcn@colorado.edu

⁴University of California - Santa Cruz, Santa Cruz, CA, USA,

sloan@ucsc.edu

The stable oxygen isotopic composition of soil water that is incorporated into paleoclimate proxies is often assumed to be the same as precipitation $\delta^{18}\text{O}$ in order to obtain information about past hydroclimate variations. For example, the $\delta^{18}\text{O}$ of soil water, when taken up by tree roots, is transferred to the $\delta^{18}\text{O}$ of xylem water and eventually incorporated into the tree cellulose. Thus, implicit in the use of cellulose $\delta^{18}\text{O}$ as a proxy for precipitation $\delta^{18}\text{O}$ is that evaporative influences on soil water $\delta^{18}\text{O}$ do not overprint the precipitation $\delta^{18}\text{O}$ signal.

In this study, we use an isotope-enabled land surface model (IsoLSM) to diagnose environmental influences on soil water $\delta^{18}\text{O}$ across seasonal to interannual timescales. An unperturbed control simulation from 1979-2004 reveals that in many semi-arid regions, such as the southwest United States, the $\delta^{18}\text{O}$ of xylem water is only partially related to the $\delta^{18}\text{O}$ of precipitation. At these locations, both evaporation and upward moisture fluxes in the soil water column contribute to variations in xylem water $\delta^{18}\text{O}$. For typical soil water profiles that are more depleted at depth, soil water tagging simulations reveal that in years with lower precipitation, an upward flux of deep soil moisture can lead to isotopically depleted xylem water. Consequently, this depleted cellulose $\delta^{18}\text{O}$ signal may be misinterpreted as reflecting more isotopically depleted precipitation or enhanced rainfall due to an inferred "amount effect". Thus, where these soil moisture transport processes are dominant, there is a positive correlation between xylem water $\delta^{18}\text{O}$ and relative humidity, even though a decrease in relative humidity would be expected to enrich surface water $\delta^{18}\text{O}$. Furthermore, sensitivity experiments demonstrate that for these semi-arid regions, the seasonal cycle in xylem water $\delta^{18}\text{O}$ is not driven by the isotopic composition of precipitation but instead by ground evaporation.

Crystal structures of two oxygen-deficient calcium aluminum silicate perovskites from NMR and powder X-ray diffraction

M. KANZAKI^{1*}, X. XUE¹, Y. WU² AND S. NIE²

¹Institute for Study of the Earth's Interior, Okayama Univ., Misasa, Tottori 682-0193 Japan

(*Correspondence: mkanzaki@misasa.okayama-u.ac.jp)

²School Earth and Space Sciences, Peking Univ., China

Several high-pressure phases along the $\text{Ca}_2\text{Si}_2\text{O}_6$ - $\text{Ca}_2\text{Al}_2\text{O}_5$ join have been reported to occur with oxygen-deficit perovskite structures [1], but their detailed crystal structures remained undetermined. We have successfully determined the crystal structures for two of these phases: a $\text{Ca}_2\text{AlSiO}_{5.5}$ phase synthesized at 7 GPa and 1500 °C, and a $\text{Ca}_2\text{Al}_{0.8}\text{Si}_{1.2}\text{O}_{5.6}$ phase synthesized at 11 GPa and 1500°C, both in a multi-anvil press. Here we report these results.

²⁹Si MAS NMR and ²⁷Al 3Q MAS NMR revealed one tetrahedral Si peak and one octahedral Al peak for the $\text{Ca}_2\text{AlSiO}_{5.5}$ phase, and two Si (one tetrahedral and one octahedral) peaks and one octahedral Al peak for the $\text{Ca}_2\text{Al}_{0.8}\text{Si}_{1.2}\text{O}_{5.6}$ phase.

The crystal structures were solved with an ab initio structural determination technique (using the program FOX) from synchrotron powder X-ray diffraction data (measured at BL19B2, SPring-8) using information from NMR as constraints, and were further refined using the Rietveld method (RIETAN-FP). The space groups for both phases were found to be *C2/c*. The crystal structure of the $\text{Ca}_2\text{AlSiO}_{5.5}$ phase consists of double-layers of perovskite-like AlO_6 octahedra and double-layers of SiO_4 tetrahedra, stacked alternatively in the [111] direction of cubic perovskite, forming an 8-fold superstructure. That of the $\text{Ca}_2\text{Al}_{0.8}\text{Si}_{1.2}\text{O}_{5.6}$ phase is made of triple-layers of perovskite-like AlO_6 - SiO_6 - AlO_6 octahedra and double-layers of SiO_4 tetrahedra, also stacked alternatively in the [111] direction, forming a 10-fold superstructure. The double-layers of SiO_4 in both phases are similar, having deficient oxygens at the middle with one terminal oxygen (not bonded to other Si/Al) for each SiO_4 tetrahedron. These structures are related to the merwinite ($\text{Ca}_3\text{MgSi}_2\text{O}_8$) structure, which consists of alternating single layers of MgO_6 octahedra and double-layers of SiO_4 tetrahedra. This series of oxygen-deficit perovskites provide additional insights into the local structural environments of Al- and Fe^{3+} -containing CaSiO_3 perovskite.

[1] Bläß, UW *et al.* (2007) *Phys. Chem. Mineral.*, **34**, 363-376.

Estimates of atmospheric CO₂ in the Neoproterozoic-Paleoproterozoic

YOSHIKI KANZAKI* AND TAKASHI MURAKAMI

Department of Earth and Planetary Science, the University of Tokyo, Tokyo 113-0033, Japan

(*Correspondence: kanzaki@eps.s.u-tokyo.ac.jp)

The weak luminosity of the younger Sun requires the early Earth to have more greenhouse effects than those today. The candidates for such greenhouse effect gases are CO₂ and CH₄ in the Neoproterozoic and the Paleoproterozoic. The quantification of CO₂ and CH₄ levels in the Neoproterozoic-Paleoproterozoic is a crucial issue, because the multiple glaciation events at ~2.9 Ga and ~2.4-2.2 Ga are considered to have been caused by the transitions of CO₂ and CH₄ levels.

Paleosols record vestiges of weathering by CO₂ and therefore have given estimates of atmospheric CO₂ levels. However, the CO₂ levels estimated from paleosols are less than those estimated by the climate model. Therefore, CH₄ is considered to have had a significant role as greenhouse effect gas. Because the CO₂ levels have been usually discussed indicating the contemporary CH₄ levels and vice versa, it is important to validate or assess the CO₂ levels extracted from paleosols so far. In this study, another method was developed to re-evaluate CO₂ levels from paleosols.

The new method estimates CO₂ levels operating in weathering profiles in 3 steps: (1) estimation of cation concentrations in porewater at the time of weathering from the loss amounts of cations in paleosol profiles, (2) estimation of pH in porewater at the time of weathering from likely secondary minerals in paleosols (kaolinite and smectite with no carbonates), and (3) CO₂ estimation from a charge-balance equation in porewater for dissolved CO₂ species (carbonic acid, bicarbonate ion and carbonate ion) and cations, using the estimated cation concentrations and pH. Application of the new method to modern weathering profiles has revealed that the new method reproduces modern soil CO₂ levels reasonably well, confirming the validity of the method.

Applying the new method to the Neoproterozoic-Paleoproterozoic paleosols, the CO₂ levels were calculated to be > 100 PAL at ~2.8-2.4 Ga and < 100 PAL at ~2.3-1.8 Ga. The calculated levels of CO₂ throughout the above eras were sufficient to keep the average surface temperature of the Earth more than the freezing point of water. These results indicate (i) the general decreasing trend of CO₂ throughout the Neoproterozoic-Paleoproterozoic and (ii) that it would have been more difficult to make the Earth a Snowball than previously thought.

Delineation of recharge patterns and nitrate contamination using stable isotopes of water, ^3H - ^3He , and CFCs in an agricultural basin

DUGIN KAOWN^{1*}, DONG-CHAN KOH², YOON-YEOL YOON², HEEJUNG KIM¹, JIN-YONG LEE³
AND KANG-KUN LEE¹

¹School of Earth and Environmental Sciences, Seoul National University, Seoul 151-747, Korea (*correspondence: dugin1@snu.ac.kr)

²Korea Institute of Geoscience and Mineral Resources, Groundwater Resources Group, 30 Gajeong-dong, Yuseong-gu, Daejeon 305-350, Korea (chankoh@kigam.re.kr)

³Department of Geology, Kangwon National University, Chuncheon 200-701, Korea (hydrolee@kangwon.ac.kr)

Haean basin in Yanggu (Korea) shows a bowl-shaped topography and the drainage system shows a simple dendritic pattern. Stable isotopes of groundwater, ^3H - ^3He , and chlorofluorocarbon (CFCs) combined with hydrogeochemical data were applied to delineate groundwater residence time, recharge patterns and nitrate contamination of groundwater in the agricultural basin. The study area is consisted of forests (58.0%), vegetable fields (27.6%), rice paddy fields (11.4%) and fruit fields (0.5%). Thus, most of residents in the study area practice agriculture. The concentration of $\text{NO}_3\text{-N}$ in groundwater showed 0.2 ~ 15.2 mg/L in June, 2012 and 0.4 ~ 14.8 mg/L in September, 2012. Nitrate concentrations were higher in the downgradient area than in the upgradient area due to the land use pattern and topography. The values of $\delta^{18}\text{O}$ and δD showed that groundwater is derived mainly from summer precipitation and the evidence of evaporation was observed in some wells in the paddy fields. The apparent groundwater ages using ^3H - ^3He and CFCs are ranged from 7 to 10 years in the upgradient area and from 15 to 30 years in the downgradient area. The apparent groundwater age corresponds to the different nitrate concentrations in the upgradient and downgradient area. The $\text{NO}_3\text{-N}$ concentration in recently recharged groundwater showed 3-15 mg/L while the $\text{NO}_3\text{-N}$ concentration in 30 years old groundwater showed less than 3 mg/L. The reconstructed ^3H input and initial ^3H were used to estimate groundwater mixing. A conceptual model of groundwater flow using measured apparent ^3H - ^3He and CFCs age will be developed to understand the hydrological processes of the study area.

SHRIMP U–Pb zircon dating, geochemical and petrographical characteristics of calc-alkaline Early Miocene Şapçı volcanics around Balıkesir (W Turkey)

D. KAPLAN¹, Z. ASLAN^{1*} AND B. CHEN²

¹Balıkesir Univ., Dept. Geol. Engn., Balıkesir, Turkey (*correspondence: zaslan@balikesir.edu.tr)

²Peking Univ., Dept. Geol. Engn., Beijing 100871, Peoples R China (binchen@pku.edu.cn)

Tertiary volcanic rocks are widespread in the Biga Peninsula of western Anatolian region (Turkey), and related to a collision tectonics in origin [1]. One of them, the Şapçı volcanics crop out in the northwest of Balıkesir. The volcanics consist of tuffs and lava flows in andesite and trachyandesite compositions. The rocks show microlitic, hyalo-microlitic, microlitic-porphyrific and fluidal textures. Modal minerals of the rocks are plagioclase (An_{30-49}), hornblende, biotite, Fe-Ti oxide and accessory apatite and zircon.

The SHRIMP U–Pb zircon dating from the lava yielded ages between 22.72 ± 0.19 and 22.97 ± 0.23 Ma, which are regarded as the crystallization age. The Şapçı volcanics have a composition of 60.09-66.45 % SiO_2 , 0.47-0.60 % TiO_2 , 14.64-16.38 % Al_2O_3 and 2.75-4.00 % K_2O . Petrochemically, they have high-K calc-alkaline characteristics, and exhibit similar features of volcanic arc setting. Besides, the trace element compositions are indicative of subduction-related volcanism. The volcanics have high large ion lithophile elements (LILEs) contents and low high field strength elements (HFSEs) contents compared to N-type Mid-Ocean Ridge Basalt (MORB), and have a high ratio of La/Yb, Zr/Nb. Chondrite normalized rare earth element (REE) patterns are concave upwards with $(\text{La/Lu})_{\text{CN}} = 6.72\text{--}21.84$, indicating significant fractional crystallization during the evolution of the volcanics. Furthermore, some trace element ratios indicate that the role of a subduction component and/or crustal contamination in the genesis of the Şapçı volcanics.

[1] Altunkaynak, & Genç (2008) *Lithos* **102**, 316-340.

Simulating Precambrian banded iron formation diagenesis

A. KAPPLER^{1*}, N. R. POSTH², I. KÖHLER¹,
E. SWANNER¹, C. SCHRÖDER¹, E. WELLMANN¹,
B. BINDER¹, K.O. KONHAUSER³, U. NEUMANN⁴,
C. BERTHOLD⁴, M. NOWAK⁴ AND D. PAPINEAU⁵

¹Geomicrobiology, Center for Applied Geoscience, University of Tuebingen/Tuebingen, Germany (*correspondence: andreas.kappler@uni-tuebingen.de)

²Nordic Center for Earth Evolution (NordCEE), Institute for Biology, University of Southern Denmark, Odense, Denmark

³Department of Earth and Atmospheric Sciences, University of Alberta, Edmonton, Alberta, Canada.

⁴Mineralogy & Geodynamics, Department of Geosciences, University of Tuebingen, Tuebingen, Germany

⁵Geophysical Lab, Carnegie Institution of Washington, Washington DC, USA

Sedimentary rocks as old as 3.8 billion years, such as Precambrian banded iron formations (BIFs), offer a unique archive of key past chemical and biological processes. Yet, post-depositional alterations such as diagenesis can alter these sediments and make accurate interpretation of primary processes challenging. Fe(II)-oxidizing bacteria have been proposed as key contributors to BIF deposition. One main challenge to this proposition is to understand how temperature/pressure diagenesis transforms biogenic Fe(III)(hydr)oxides formed by these bacteria.

We present diagenetic experiments of the transformation of precursor Fe(III) minerals associated with microbial biomass. Mixtures of ferrihydrite (biogenic ferric oxyhydroxide mineral proxy) and glucose (microbial biomass proxy) were incubated in gold capsules at 1.2 kbar and 170°C. Key BIF minerals are produced by electron transfer from organic carbon to Fe(III) minerals during this diagenesis. Ferrihydrite transforms to hematite, magnetite, and siderite. Silica-coated ferrihydrite mixed with glucose yields hematite and siderite. Spheroidal siderite, a structure found in IF, forms depending on the Fe(III):C ratio of primary ferrihydrite-biomass sediment. Our results thus suggest that post-depositional BIF mineralogy does not directly archive the oceanic or atmospheric conditions during their lithification. Furthermore, we argue that spherical to rhombohedral siderite structures in deep-water Fe-oxide IF can be used as a biosignature for photoferrotrophy, whereas massive siderites reflect high cyanobacterial biomass loading in highly productive shallow-waters.

The platinum group and precious metals contents of Muğla-Ortaca Area Chromites

SALIH BURAK KARABEL¹, LOKMAN GUMUS¹, DEMET KIRAN YILDIRIM¹, SERENA UZASCI SULTANYAN¹, MURAT BUDAKOĞLU¹ AND MUSTAFA KUMRAL¹

¹Istanbul Technical University, Department of Geological Engineering, 34469, Istanbul, TURKEY

The study area is located in Menteşe Region, which is called Taurus belt, Southwest of Turkey. Structural units in the area are Menderes Massive, Western Taurus Nappes, Beydağları Autochthonous and Antalya Nappes.

In general, region consists of from bottom to top allochthonous units, peridotite nappe and alluvium. Allochthonous units, include Jura aged limestone interlayered with calciturbidite. The Upper Cretaceous aged complex consist of limestone with micritic texture and marl which is formed intermediate layers.

The peridotitic unit is composed of serpentinite, serpentinized dunite, dunite and harzburgite and it is Cretaceous aged. Also Quaternary alluvium is located at the top of the peridotites.

In this study, in order to determine the geochemical and petrographic characteristics (ore and rock) major, trace and rare earth elements were analyzed around Muğla-Ortaca.

The distribution of platinum group elements for Zimparalik shows according to geochemical analyses that Pt content is between 10 ppb and 147 ppb, Pd content is between 6 ppb and 54 ppb and Ir content is between 12 ppb and 131 ppb. In addition, Au content is between 24 ppb and 135 ppb in this area.

The samples from Yemislik show that Pt content changes between 30 ppb and 138 ppb, Pd content is approximately 8 ppb, Ir content changes from 10 ppb to 100 ppb and also Au content reaches to 205 ppb.

Geophysical constraints on the water content in the lunar mantle and its implications for the origin of the Moon

SHUN-ICHIRO KARATO¹¹³

¹Yale University, Department of Geology & Geophysics, New Haven, CT, USA

Although the Moon was considered to be “dry”, recent measurements of hydrogen content in some of the lunar samples showed a substantial amount of water comparable to the water content in the Earth's asthenosphere. However, the interpretation of these observations in terms of the distribution of water in the lunar interior is difficult because the composition of these rocks reflects a complicated history involving melting and crystallization. In this study, I analyze geophysically inferred properties to obtain constraints on the distribution of water (and temperature) in the lunar interior. The electrical conductivity inferred from electromagnetic induction observations and the geodetically or geophysically inferred Q are interpreted in terms of laboratory data and the theoretical models on the influence of water (hydrogen) on these properties. Both electrical conductivity and Q are controlled by defect-related processes that are sensitive to the water (hydrogen) content and temperature but less sensitive to the major element chemistry. After a correction for the influence of the major element chemistry constrained by geophysical observations and geochemical considerations, I estimate the temperature-water content combinations that are consistent with the geophysically inferred electrical conductivity and Q . I conclude that the lunar interior is cooler than Earth (at the same depth) but the water content of the lunar mantle is similar to that of Earth's asthenosphere. A possible model is presented to explain the not-so-dry Moon where a small degree of water loss during the Moon formation is attributed to the role of liquid phases that play an important role in the Moon forming environment.

Four types of olivine from orangeites of Kostomuksha-Lentiïro area (Russia, Finland)

A.V. KARGIN, A.A. NOSOVA AND E.V. KOVALCHUK

Institute of Geology of Ore Deposits, Petrography, Mineralogy and Geochemistry of the Russian Academy of Sciences, Russia, Moscow, kargin@igem.ru

Mineral characteristics of alkaline ultramafic rocks of the Kostomuksha-Lentiïro area suggest their orangeitic rather than lamproitic nature. The orangeites are divided into three types by their macrocryst assemblages: Ol-Phl-Cpx, Ol-Phl and Phl-Carb. The Ol-Phl-Cpx orangeites of Lentiïro contain four generations of unaltered olivine that vary in composition and origin.

Olivine I is large (3-2 mm) typically rounded zoned macrocrysts. Core composition is Fo 92 with the highest content of NiO (0.33-0.37 wt. %) and the lowest CaO (0.03-0.04 wt. %). This olivine is interpreted as a xenocryst derived from depleted mantle peridotite.

Olivine IIa is represented by euhedral and subhedral phenocrysts (commonly 0.15-0.3 mm). Olivine IIa and rims of olivine I and III have the same composition - Fo 88-89 with high content of CaO (0.10-0.42 wt. %), and moderate contents of NiO (0.14-0.35 wt. %) and MnO (up to 0.07-0.21 wt. %), which is consistent with fractional crystallization trend of olivine from orangeites. This olivine crystallized from orangeitic melt at 950-960°C (content of Ca and Al [1]).

Olivine IIb is observed as microphenocryst in a groundmass (< 0.1 mm). It is Fo 86-87 with the highest content of CaO (1.19-1.40 wt. %). This olivine is the product of late-stage crystallization of evolved kimberlitic melt.

Olivine III forms medium size (commonly 1.0-1.5 mm) rounded zoned "tablet"-shaped crystals [2]. Core of olivine III is Fo 82-83 with the lower content of CaO (0.03-0.05 wt. %), NiO (0.12-0.17 wt. %) and high MnO (up to 0.40 wt. %). This generation is interpreted to represent either early stage crystallization of megacryst assemblage [3] or a product of metasomatic interaction between mantle peridotite and protokimberlitic melt [2].

[1] De Hoog J.C.M., Gall L., Cornell D.H. Trace-element geochemistry of mantle olivine and application to mantle petrogenesis and geothermobarometry // *Chem. Geol.* 2010. V. 270. P. 196-215. [2] Arndt N.T., Guitreau M., Boullier A.M., et al. Olivine and the origin of kimberlite // *J. of Petrology.* 2010. V.51. P. 573-602. [3] Moore A.E. The case for a cognate, polybaric origin for kimberlitic olivines // *Lithos.* 2012. Vol. 128-131. P. 1-10.

Calcium and magnesium isotopes reveal Earth system response in the aftermath of a Cryogenian glaciation

S.A. KASEMANN*¹, P. POGGE VON STRANDMANN²,
A.R. PRAVE³, A.E. FALICK⁴, T. ELLIOTT⁵
AND K.-H. HOFFMANN⁶

¹Department of Geosciences Univ. Bremen, 28334 Bremen, Germany (*correspondence: skasemann@marum.de)

²Dept. of Earth Sciences, University of Oxford, Oxford OX1 3AN, UK (philipvs@earth.ox.ac.uk)

³Earth Sciences, University of St Andrews, St Andrews KY16 9AL, UK (ap13@st-andrews.ac.uk)

⁴Scottish Universities Environmental Research Centre, East Kilbride G75 0QF, UK (T.Fallick@suerc.gla.ac.uk)

⁵Department of Earth Sciences, University of Bristol, Bristol BS8 1RJ, UK (tim.elliott@bristol.ac.uk)

⁶Geological Survey of Namibia, P.O. Box 2168, Windhoek, Namibia (khhoffmann@mme.gov.na)

Neoproterozoic response to, and recovery from, a postulated greenhouse state following global glaciation represents an acute test of feedbacks within the Earth system to maintain an equable environment. One explanation for the severe environmental change predicts progressive build-up of $p\text{CO}_2$ during extreme glaciation, and rapid melt back and influx of atmospheric CO_2 into the ocean [1]. A boron isotope study of post-glacial carbonates from Namibia identified a temporary ocean acidification (pH \sim 7), potentially linked to oceanic uptake of carbon dioxide [2]. $\delta^{44}\text{Ca}$ (0.4 to 1.3‰) and $\delta^{26}\text{Mg}$ (-2.1 to -1.4‰) excursions in Neoproterozoic carbonate profiles elucidate the recovery of the Earth System from such an ocean acidification event and elevated greenhouse gas concentrations in the glacial aftermath. Both isotope patterns indicate an enhanced weathering influx following the glaciation demise, and increase in global temperature and precipitation in the greenhouse aftermath. This enabled the ocean to return to normal pH after climatic amelioration. Differences in time-development of the Ca and Mg isotope patterns reflect a change from carbonate- to silicate-dominated weathering flux and suggest primary dolomite formation during “cap dolostone” sedimentation. Differences in the magnitude of both isotope patterns across the palaeocontinental margin of the Congo Craton suggest a local influence potentially overprinting and amplifying the global pattern. Thus, extreme regional signals can lead to an overestimate of the global chemical weathering flux.

[1] Hoffman *et al.* (1998) *Science* **281**, 1342–1346. [2] Kasemann *et al.* (2010) *Geology* **38**, 775–778.

Tungsten species in natural ferromanganese oxides related to its different behavior from molybdenum in oxic ocean

TERUHIKO KASHIWABARA¹ AND YOSHIO TAKAHASHI²

¹Japan Agency for Marine-Earth Science and Technology (JAMSTEC), teruhiko-kashiwa@jamstec.go.jp*

²Hiroshima University, ytakaha@hiroshima-u.ac.jp

Different concentrations of Mo and W in oxic ocean attribute to their different distributions at the seawater/ferromanganese oxide interface. Recent studies also revealed large isotopic fractionation of Mo on ferromanganese oxides, which leads to the utility of Mo isotope systems as a paleoredox proxy. In contrast to extensive attentions on Mo, chemistry of W at the solid/water interface is poorly understood. The aim of this study is to reveal the W species in natural ferromanganese oxide, which affects its different behaviors from Mo in modern oxic ocean.

Conventionally, it has been difficult to obtain high quality fluorescence XAFS spectra of trace amount of W because of interferences of intense scattering and/or fluorescence from other predominant elements, such as Fe, Mn, Ni, Cu, and Zn. Here, we applied wavelength dispersive XAFS method, where Bent Crystal Laue Analyzer was used in front of detector to selectively extract fluorescence X-rays of W [1].

We revealed that the W species are in distorted *Oh* symmetry in natural ferromanganese oxides. The host phase of W is suggested to be Mn oxides. We also found that the W forms inner-sphere complexes in hexavalent state and distorted *Oh* symmetry on both synthetic ferrihydrite and $\delta\text{-MnO}_2$. It is known that Mo forms a distorted *Oh* inner-sphere complex on Mn oxides and a *Td* outer-sphere complex on ferrihydrite, and the host phase of Mo in natural ferromanganese oxides is $\delta\text{-MnO}_2$ [2]. Therefore, the different behaviors of W and Mo at the seawater/ferromanganese oxide interface can be caused by (i) the stability of inner-sphere complexes on the Mn oxides and (ii) mode of attachment (inner- or outer-sphere) on Fe oxyhydroxides. In addition, preferential adsorption of lighter W isotopes is expected based on the molecular symmetry of the adsorbed species, implying the potential significance of the W isotope systems as paleoredox proxy similar to Mo [3].

[1] Kashiwabara *et al.* (2011) *Geochim. Cosmochim. Acta.* **75**, 5762–5784. [2] Kashiwabara *et al.* (2010) *Chem. Lett.* **39**, 870–871. [3] Kashiwabara *et al.* (2013) *Geochim. Cosmochim. Acta.* **106**, 364–378.

Future calamity of Arsenic poisoning in the groundwater of Thoubal and Bishnupur districts of Manipur (India)

A. K. CHANDRASHEKHAR^{1*}; S. H. FAROOQ²;
D. CHANDRASEKHARAM¹ AND P. THAMBIDURAI¹

¹Department of Earth Sciences, IIT Bombay, Mumbai - 400076. (*correspondance: kashyapglm27@gmail.com)

²School of Earth, Ocean and Climate Sciences, Indian Institute of Technology Bhubaneswar, Bhubaneswar-751013, (hilalfarooq@gmail.com)

Above 10 $\mu\text{g/L}$ (WHO 2001) concentration of arsenic in the drinking water lead to carcinogenic, cardiovascular disease, neurotoxicity and diabetes in the human. Arsenic poisoning in the groundwater is growing threat to a very large portion of Indian population. Along with the West Bengal, many areas of Uttar Pradesh, Jharkhand, Bihar, Chhattisgarh and Assam have been reported with higher concentrations of arsenic in the groundwater. To know the extent of arsenic poisoning in parts of Manipur a study has been carried out and 26 groundwater and samples were collected for analysis. More than 57% samples recorded arsenic > 10 $\mu\text{g/L}$ while this concentration in the surface waters samples is negligible. The highest concentration of arsenic (535 $\mu\text{g/L}$) was registered from Ngangkha Lawai Mamang Leikai area of Bishnupur district which is fifty fold of the (WHO 10 $\mu\text{g/L}$) limit for arsenic and tenfold of Indian permissible limit (50 $\mu\text{g/L}$).

In previous study the highest concentration of arsenic 200 $\mu\text{g/L}$ [2] was reported in the same area of Bishnupur district. Whereas in present study the highest concentration of arsenic is (535 $\mu\text{g/L}$) which is nearly three fold of previous study. This study shows that the arsenic concentration in groundwater is increasing with time. If situation continues, the groundwater may become highly polluted with arsenic and may become a major cause of concern to the population of this region.

In this study the presence of arsenic free water on the surface and contaminated groundwater at subsurface levels indicates the existence and functioning of arsenic release mechanism within the aquifer sediments [3].

[1] WHO 2001.[2] Jayalakshmi *et al.* (2010) *Environ Earth Sci* **62**:1183–1195 [3] Farooq *et al.*, (2012) *Applied Geochemistry*, **27**, 292-303.

Role of aggregates formed during process stabilization in a production of methane in biogas reactors

M. KASINA^{1,2*}, A. KLEYBÖCKER¹, M. MICHALIK²,
M. LIEBRICH AND H. WÜRDEMANN¹

¹Helmholtz Centre Potsdam, GFZ German Research Centre for Geosciences, 14473 Potsdam, Germany (Hilke.Wuerdemann@gfz-potsdam.de)

²Institute of Geological Science, Jagiellonian University, Kraków, Poland;

To optimise the co-digestion of sewage sludge and rape seed oil a fast increase in the organic loading rate and the addition of CaO was tested in an experimental setup. The process stability was increased by aggregate formation. These aggregates were extracted and subjected to detailed characterization using SEM-EDS, XRD, FTIR and optical microscopy. The aim of this study is to describe the aggregates in terms of their morphology and mineral composition, as well as to find the answer about the role of microorganisms in their formation. The relationship between Calcium and organics components like long-chain fatty acids (LCFA), polysaccharides and proteins and microorganisms was investigated to get a more detailed insight into biofilm formation that is known to favour syntrophic acetate oxidation and methane formation.

The aggregates differed in size (from 0.5 mm up to 0.5 cm), shape (usually rounded) and porous inner structure (different pore size) and showed a bipartite structure. In each part organic material containing calcium was the main component (LCFA-Ca).

Adsorption effects as well as precipitation of insoluble salts of LCFA and Ca formed an outer cover of aggregates and offered interfaces within the aggregate as well. The aggregate formation was stimulated by CaO addition and had a positive impact on growths of syntrophic consortia. Due to the high concentrations of short-chain organic acids phosphate accumulating bacteria (PAO) took up acids like acetate and propionate and released phosphate which precipitated with cations present in the sludge. Iron and aluminium phosphates were more common than calcium phosphates. Therefore we assume that calcium added during experiments mainly precipitated with LCFA as a strengthening material for aggregates. It was noted that precipitation of LCFA decreased their toxicity and obviously, activity of PAO and syntrophic consortia increased the pH inside the aggregates and created favourable conditions for methane production. Therefore, a stable biogas production was observed although the pH and the H₂ concentration in the liquid phase of the sludge were below optimum.

Experimental study of mineral-microbial interaction to investigate the effects of CO₂ storage

MONIKA KASINA^{1*}, DARIA MOROZOVA¹,
LINDA PELLIZZARI¹, ANDREA KASSAHUN²
AND HILKE WÜRDEMANN¹

¹Helmholtz Centre Potsdam, GFZ German Research Centre for Geosciences, 14473 Potsdam, Germany, (Hilke.Wuerdemann@gfz-potsdam.de)

²Dresden Groundwater Research Centre e.V., 01217 Dresden, Germany

The influence of biological processes on the composition of reservoir sandstones the interactions between fluids and minerals are monitored during exposure to CO₂ in long-term experiments. Samples from the core deposit were incubated with fresh reservoir fluids as inoculum for indigenous microorganisms in a N₂/CH₄/H₂-atmosphere at a temperature of 80°C and a pressure of 40 bars for half a year. Afterwards the samples were exposed to supercritical CO₂. Incubation was performed under lower temperature than in situ conditions to create more favourable growth conditions for microorganisms.

Analyses of the downhole fluids taken from a reservoir well using genetic fingerprinting methods (PCR SSCP and DGGE) revealed different DNA sequences indicating the presence of H₂-oxidising, biocorrosive thermophilic bacteria, thiosulfate-oxidising bacteria as well as some microorganisms similar to representatives from other deep environments, which have not been cultivated previously. Given a high temperature (120 – 127°C) and high salinity (up to 420 g/l) of fluids, the cells were difficult to detect because of very low numbers. The analysis of rock and fluid material from the long-term experiment after 11 and 31 months of incubation with CO₂ indicated the dissolution of major minerals and cements present in the sandstones, and secondary precipitation of new mineral phases such as quartz, albite, gypsum, halite, iron oxides and clay minerals. Changes in organic acid concentration and the release of organic components might indicate a metabolic activity of microorganisms or a mobilisation due to CO₂ exposure.

Slight indication of microbial activity like EPS formation was detected: Calcofluor white staining of carbohydrates indicates the presence of biofilms. We assume that changes observed in the samples until now were related mainly to CO₂ exposure and fluid-rock interaction. In the next steps, samples will be fed with H₂ to enhance microbial growth and molecular biological analyses will be used to characterise the changes in the biocenosis due to CO₂ and H₂ exposure.

What caused the rise of atmospheric O₂?

JAMES F. KASTING

Dept. of Geosciences, 443 Deike, Penn State University,
University Park, PA 16802 (jfk4@psu.edu)

Oxygenic photosynthesis appears to have evolved well before O₂ levels increased in the atmosphere, at around 2.4 Ga. This has led to numerous suggestions as to what may have kept O₂ suppressed and then eventually allowed it to rise. These suggestions include changes in the recycling of carbon and sulfur relative to water (or hydrogen), a switch from dominantly submarine to dominantly subaerial volcanism, gradual oxidation of the continents and a concomitant decrease in reduced metamorphic gases, a decline in deposition of banded iron-formations, a decline in nickel availability, and various proposals to increase the efficiency of photosynthesis. Several of these different mechanisms could have contributed to the rise of O₂, although not all of them are equally effective. To be considered successful, any proposed mechanism must make predictions that are consistent with the carbon isotope record in marine carbonates, which shows relatively little change with time, apart from short-lived (but occasionally spectacular) excursions. The reasons for this constancy are explored here, but are not fully resolved. In the process of making these comparisons, a self-consistent redox balance framework is developed which will hopefully prove useful to others who may work on this problem and to astronomers who may one day try to decipher spectral signatures of oxygen on Earth-like exoplanets.

Melting of FeO-SiO₂ system at high pressure and the fate of subducted banded iron formations

CHIE KATO^{1*}, RYUICHI NOMURA¹ AND KEI HIROSE^{1,2,3}

¹Department of Earth and Planetary Sciences, Tokyo Institute of Technology, Tokyo, Japan (*Correspondence: kato.c.ab@m.titech.ac.jp)

²Earth-Life Science Institute, Tokyo Institute of Technology, Tokyo, Japan

³Institute for Research on Earth Evolution, Japan Agency for Marine-Earth Science and Technology, Yokosuka, Japan

Large amount of banded iron formations (BIFs) is thought to have subducted into the deep mantle. Because of their high density, BIFs may have fallen down toward the core mantle boundary (CMB) region and might cause the ultra-low velocity zones (ULVZs) [1]. BIFs would be composed of FeO and SiO₂ in the mantle because its oxidation state is close to iron-wustite. FeO and SiO₂ form a simple binary eutectic system above 16 GPa [2]. Its eutectic temperature must be lower than the melting temperature of FeO, which is estimated to be about 3,500 K at the CMB pressure [3]. Since temperature at the CMB is most likely over 3,500 K, subducted BIFs may have melted there. In order to understand the fate of the subducted BIFs, we have conducted high-pressure melting experiments on FeO-SiO₂ binary system, using laser-heated diamond-anvil cell techniques. Results at 47 GPa demonstrate that eutectic composition is extremely FeO-rich only with < 3 wt% SiO₂. Dense FeO-rich melt should have segregated downward, while buoyant SiO₂-dominant solid residue may have recycled upward. Such FeO melt accumulating between the core and mantle could have formed Fe-rich lowermost mantle and O-rich topmost core.

[1] Dobson & Brodholt (2005) *Nature*, **434**, 731-734. [2] Kato *et al.* (1984) *J. Phys. Earth*, **32**, 97-111. [3] Boehler (1992) *EPSL*, **111**, 217-227.

Experimental studies of partial melting at the contact between limestone and pelitic gneiss

M. KATO^{1*}, Y. HIROI² AND M. ARIMA³

¹Chiba University, Chiba 263-8522, Japan (*correspondence: andkysil@gmail.com)

²Chiba University, Chiba 263-8522, Japan

³Yokohama National University, Yokohama 240-8501, Japan

Continental crust is much more diverse than oceanic crust in composition. To evaluate the significance of partial melting for interaction between such diverse lithologies during high-grade metamorphism, we performed high-pressure experiments of partial melting at the contact between limestone and pelitic gneiss, which are characteristic lithologies in Gondwana fragments such as the Highland Complex of Sri Lanka and the Lützow-Holm Complex (LHC) of East Antarctica [1].

The rock fragments of limestone from Japan were loaded in a sealed Pt capsule with powdered garnet-sillimanite gneiss from the LHC. H₂O or NaCl aqueous solution were also added to the capsule. Experiments were performed at 900 °C, 800 MPa, and 100 hours with a piston-cylinder, high-pressure apparatus at the Yokohama National University.

At the contacts between limestone and partially molten garnet-sillimanite gneiss (garnet + spinel + peraluminous liquid), different mineral assemblages are formed depending on the composition of solution as follows.

H₂O: Wollastonite, clinopyroxene, plagioclase, biotite, and subaluminous to peraluminous liquid.

NaCl aqueous solution: Clinopyroxene, plagioclase, scapolite, and metaluminous liquid.

The results show that clinopyroxene, scapolite, plagioclase, and metaluminous liquid could be formed by the melting reaction between limestone and garnet-sillimanite gneiss when NaCl aqueous solutions are involved. We attempt to discuss the origin of clinopyroxene-scapolite-bearing calc-silicate granulites that have been reported from many high-grade metamorphic terrains including Antarctica [2], Sri Lanka [3], southern India [4] based on our experimental results.

[1] Shiraishi *et al.* (1994) *Jour. Geol* **102**, 47-65. [2] Satish-Kumar *et al.* (2006) *Polar Geoscience*, **19**, 37-61. [3] Mathavan and Fernando (2001) *Lithos* **59**, 217-232. [4] Satish-Kumar and Harley (1998) *Lithos* **44**, 83-99.

Mineralization rates of organic carbon in freshwater vs marine environments and implications for carbon burial efficiencies

SERGEI KATSEV¹, SEAN A. CROWE²,
MATTHEW KISTNER¹ AND JIYING LI¹

¹Large Lakes Observatory, University of Minnesota Duluth,
(skatsev@d.umn.edu)

²NordCEE, University of South Denmark,
(sacrowe1@gmail.com)

The mineralization and burial rates of organic carbon in aquatic sediments influence the global carbon cycle and over geological time scales determine the atmospheric CO₂ and oxygen levels. As organic matter descends through the water and then sediment columns, its reactivity towards mineralization decreases. In marine environments, the decrease in organic carbon reactivity was described as a power-law function of carbon age, sometimes referred to as Middelburg power law. The relationship extends over time scales spanning eight orders of magnitude and is largely independent of temperature, exposure to oxygen, concentration of sulfate, and other factors that have been suggested to affect carbon mineralization rates. In contrast, no relationship of this kind was suggested in freshwater where conditions are typically more variable. Using a compilation of data from large lakes, we show that the reactivity of autochthonous organic carbon in fresh water decreases with time according to a similar power-law. The similarity suggests that mineralization rates of organic carbon are determined primarily by intrinsic factors rather than the characteristics of the environment. It also suggests that carbon mineralization by sulfate reduction is not fundamentally faster than by methanogenesis, with a particular implication that carbon mineralization rates in oceanic sediments 0.5Ga ago, when sulfate concentrations were low, were not particularly different from today. Our results indicate that carbon reactivity is higher in presence of oxygen, consistent with the enhanced preservation of carbon in anoxic sediments. Using the obtained relationships for oxic and anoxic mineralization rates, we calculate the theoretical burial efficiencies as a function of oxygen exposure time, which match the previously reported observational trends. In contrast to the effect of oxygen, the effect of temperature on specific (per carbon atom) carbon mineralization rates appears to be minor, suggesting that climate-related warming of lake sediments may not lead to increases in specific rates of carbon mineralization.

Highly sensitive and precise analysis of stable chlorine isotope ratio by continuous-flow isotope ratio mass spectrometry

SHINSUKE KAWAGUCCI AND UTA KONNO

Subsurface Geobiology Advanced Research Project
(SUGAR), Japan Agency for Marine-Earth Science and
Technology (JAMSTEC), 2-15 Natsushima-cho,
Yokosuka 237-0061, Japan, (kawagucci@jamstec.go.jp)

Recent advancements in continuous-flow isotope ratio mass spectrometry (CF-IRMS) enable us to determine stable isotope ratios with only subnanomolar quantities. However, the current CF-IRMS methods for stable chlorine isotope ratios ($\delta^{37}\text{Cl}$) of CH₃Cl had required more than several hundreds nano-mole CH₃Cl. We thus develop a CF-IRMS system for the $\delta^{37}\text{Cl}$ analysis that combines a sample processing procedure largely based on the highly sensitive method for the $\delta^{13}\text{C}$ analysis of CH₃Cl with the IRMS setting for the $\delta^{37}\text{Cl}$ analysis of CH₃Cl.

The newly developed system successfully reduces sample requirements (>0.6 nmol-CH₃Cl) to less than one hundredth of that required by the previous CF-IRMS systems while maintaining comparable precision in the $\delta^{37}\text{Cl}$ determination ($\pm 0.1\%$, 1σ). This system is also able to determine carbon isotope ratio for CH₃Cl with comparable precision ($\pm 0.3\%$, 1σ , >0.3 nmol-CH₃Cl) to the previous study. $\delta^{37}\text{Cl}$ -SMOC and $\delta^{13}\text{C}$ -VPDB values of CH₃Cl in commercial tank were determined to be $-6.8 \pm 0.1\%$ and $-46.9 \pm 0.3\%$, respectively.

The gas emitted from the leaves of *Myrica rubra* was collected near a harbor of Tokyo Bay (35°19.1'N, 139°39.0'E) using the vial method reported previously. On a dry weight basis, *Myrica rubra* was found to emit CH₃Cl with a flux of 3.1–3.9 ng-CH₃Cl/g-leaves/hour, whereas no CH₃Cl was detected in the empty vials. The $\delta^{37}\text{Cl}$ _{SMOC} and $\delta^{13}\text{C}$ _{VPDB} values of the leaf-emitted CH₃Cl ranged from -4.9% to -2.9% ($n=4$) and from -112.7% to -108.0% ($n=4$), respectively. The newly developed system is applicable not only to atmospheric CH₃Cl, but also to any chlorine in liquid and solid samples when appropriate treatment such as silver chloride precipitation and its methylation is combined.

Reconstruction of pH and PCO₂ by boron isotopes of unaltered ammonoids & nautiloids and the expected high alkalinity during the Cretaceous

KAWAHATA, H.¹, FUKUSHIMA, A.¹, MORIYA, K.², SUZUKI, A.³ AND ISHIKAWA, T.⁴

¹Atmosphere and Ocean Research Institute, The University of Tokyo, kawahata@aori.u-tokyo.ac.jp

²Waseda, University

³AIST, a.suzuki@aist.go.jp

⁴JAMSTEC, t-ishik@jamstec.go.jp

The reconstruction of pCO₂ during the geological time is required in order to predict the future environments. Boron isotopic ratio is an excellent proxy for pH and the relevant partial pressure of carbon dioxide in the seawater (PCO₂). By using P-TIMS method, we conducted the high precision analysis of delta 11B (+/- 0.1 per mil reproducibility) of unaltered aragonite shells of ammonoids and nautiloids mainly in the Cretaceous and in Jurassic (70-162 Ma), which were expected to be much warmer due to higher PCO₂. So far, difficulty of fresh biogenic carbonate during these periods has produced no reliable reconstruction data using foraminiferal delta 11B before Cenozoic era. Our careful assessment of secondary alteration was conducted by 1) Determination by X-ray diffraction (XRD), 2) Observation of microstructures of the nacreous layers by SEM, and 3) Measurement of trace element contents. Positive correlation between delta 11B and delta 18O (temperature) of biogenic aragonites in 80 and 86 Ma revealed that relatively deeper dwellers within the surface ocean showed lower delta 11B values, which corresponded to lower pH. It is observed in the modern vertical water column. The reconstructed maximum PCO₂ levels at late Cretaceous (80 Ma and 86 Ma) are 1,750 and 1,540 ppm, respectively. This is moderately high, coinciding with the suggestion by Breecker *et al.* (2010). Abundant deposition of biogenic carbonate during the Cretaceous requires the enhancement of alkalinity, which could be raised by 20% relative to modern value. This is indirectly supported by seawater-rock interaction in Oman ophiolite around 100Ma. Both terrestrial and ocean environments have strong buffering mechanism for pH and PCO₂ levels in moderate time scale.

Supercontinent cycle and 2nd continents

KENJI KAWAI^{1,2} HIROKI ICHIKAWA^{1,3}
SHINJI YAMAMOTO⁴ TAKU TSUCHIYA³
AND SHIGENORI MARUYAMA¹

¹Earth-Life Science Institute, Tokyo Institute of Technology (kenji@geo.titech.ac.jp)

²Department of Earth and Planetary Sciences, Tokyo Institute of Technology

³Geodynamics Research Center, Ehime University

⁴Graduate School of Arts and Sciences, The University of Tokyo

It has been thought that granitic crust, having been formed on the surface, must have survived through the Earth's evolution because of its buoyancy. Recent geological studies have suggested that a significant amount of crustal material has been lost from the surface due to delamination, continental collision, and subduction at oceanic–continental convergent margins (von Huene and Scholl 1991; Yamamoto *et al.* 2009; Ichikawa *et al.* 2013a). If so, then the subducted crustal materials are expected to be trapped in the mid-mantle due to the density difference from peridotitic materials induced by the phase transition from coesite to stishovite (Kawai *et al.* 2013). In order to study the effect of the subducted granitic materials floating around the mantle transition zone, we conducted two-dimensional numerical experiments of mantle convection incorporating a continental drift with a heat source placed around the bottom of the mantle transition zone. We found that the addition of heat source in the mantle transition zone considerably enhances the onset of upwelling plumes in the upper mantle, which further reduces the time scale of continental drift. The heat source also causes massive mechanical mixing, especially in the upper mantle. The results suggest that the heat source floating around the mantle transition zone can be a possible candidate for inducing the supercontinent cycle (Ichikawa *et al.* 2013b).

A molecular view of the reductive dehalogenase-homologous gene in subseafloor sediments

MIKIHICO KAWAI^{12*}, TAIKI FUTAGAMI¹³,
ATSUSHI TOYODA⁴, YOSHIHIRO TAKAKI²,
IKUO UCHIYAMA⁵, ASAO FUJIYAMA⁴, TAKEHIKO ITOH⁶,
FUMIO INAGAKI¹ AND HIDETO TAKAMI²

¹Kochi Institute for Core Sample Research, Japan Agency for Marine-Earth Science and Technology (JAMSTEC), Monobe B200, Nankoku, Kochi 783-8502, Japan.
(*correspondence: kawaim@jamstec.go.jp)

²Inst. Biogeosciences, JAMSTEC, Yokosuka 237-0061, Japan.

³Kyushu University, Fukuoka 812-8581, Japan.

⁴Natl. Inst. Genetics, Mishima 411-8540, Japan.

⁵Natl. Inst. Basic Biology, Okazaki 444-8585, Japan.

⁶Tokyo Inst. Technology, Tokyo 152-8550, Japan.

Recent molecular analysis of microbial communities in subseafloor sediment indicates that phylogenetically diverse bacteria utilize organohalides as the electron acceptor: e.g., diverse 16S rRNA and reductive dehalogenase-homologous (*rdhA*) genes related to the member of *Dehalococcoides* have been detected by PCR from organic-rich deep subseafloor sediments (Futagami *et al.*, 2009, 2013). Incubation experiments also demonstrated the biological degradation of organohalides (e.g., trichloroethene), indicating that organohalides support anaerobic microbial respiration in sedimentary habitats that are generally poor in bio-available electron acceptors.

To gain molecular insight into the largely unknown subseafloor reductive dehalogenation processes, we studied metagenomic pools obtained from five sediment core samples (i.e., 0.7, 5, 18, 48, 107 m in depth) at Site C9001 off the Shimokita Peninsula of Japan during the *Chikyu* Shakedown Cruise CK06-06 in 2006. From all samples examined, we detected phylogenetically remarkably diverse *rdhA*-homologous genes that affiliate to novel specific clusters, indicating that molecular characteristics of subseafloor *rdhA*-homologous genes are evolutionary and functionary more diverse than those previously expected from the modern surface biosphere (e.g., anthropogenic habitats). Consistently, the frequency of *rdhA*-homologous genes in the subseafloor metagenomic pools was found to be statistically high as compared to those in genomic sequences of over 1,800 isolated species. Interestingly, however, no or very little differences in phylogenetic distribution of *rdhA*-homologous genes were observed between five pools, suggesting that the genes are spatially evenly distributed in sediment regardless of the formation age ranging from modern to Pleistocene.

Contrasting behaviour of monazite and zircon during partial melting and fluid infiltration: An example from the Ryoke metamorphic belt, Japan

TETSUO KAWAKAMI¹

¹Department of Geology and Mineralogy, Kyoto University, Japan, t-kawakami@kueps.kyoto-u.ac.jp

Behaviour of monazite and zircon in the pelitic and psammitic migmatites are investigated in the low P/T type Ryoke metamorphic belt at the Aoyama area, Japan where regional metamorphic terrane is thermally overprinted by later granite intrusions.

Monazite grains in migmatites yield a CHIME age of 96.5 ± 1.9 Ma mainly in the core, and rims and patchy domains yield 83.5 ± 2.4 Ma. The age of ~ 97 Ma is interpreted to represent the timing of monazite growth during prograde regional metamorphism. Some monazite includes PbO-rich phases at the core/rim boundary where sharp chemical and age zonings are observed, suggesting the contribution of interface-coupled dissolution-precipitation mechanism. Patchy young domains could represent the result of fluid-related Pb loss through microcracks. Therefore, ~ 80 Ma overprint on migmatites represents the wide and combined effect of thermal input and fluid activity on the monazite grains caused by the ~ 80 Ma granite intrusions [1].

On the other hand, zircon in the same area records 90.3 ± 2.2 Ma alone except for inherited ages at the core. Between inherited core and the metamorphic rim, a thin, dark-CL annulus containing $< 2 \mu\text{m}$ melt (glass) and nano-granite inclusions is commonly developed, suggesting the presence of melt during the rim growth. In diatexites, the annulus is further truncated by the brighter-CL overgrowth, suggesting the resorption and regrowth of the zircon after peak metamorphism. This kind of zircon rim probably crystallized during the solidification of the melt in migmatites, and yields 90.3 ± 2.2 Ma. Therefore, zircon records the timing of partial melting event but not the fluid infiltration event during the ~ 80 Ma contact metamorphism [2].

Using the difference of growth timing of monazite and zircon, the duration of metamorphism higher than the amphibolite facies grade is estimated to be ca. 6 Myr [2], similar to ~ 5 Ma estimated by [3]. This duration of high-temperature metamorphism is difficult to be attained by the intrusion of a single granite sill (3 km thick), and requires additional granite intrusions [4] or alternative heat source.

[1] Kawakami & Suzuki, (2011), *Island Arc*, **20**, 439-453. [2] Kawakami *et al.*, (2013), *CMP*, **165**, 575-591. [3] Suzuki *et al.*, (1994), *EPSL*, **128**, 391-405. [4] Okudaira, (1994), *Earth Monthly*, **16**, 486-489. (in Japanese)

Synchrotron radiation X-Ray fluorescence analysis of aqueous fluids and high-Mg Andesite melt under high-temperature and high-pressure conditions

TATSUHIKO KAWAMOTO¹, KENJI MIBE²,
KEN-ICHI KUROIWA¹ AND TESTU KOGISO³

¹Institute for Geothermal Sciences, Graduate School of Science, Kyoto University, Kyoto 606-8502, Japan; kawamoto@bep.vgs.kyoto-u.ac.jp

²Earthquake Research Institute, The University of Tokyo, Tokyo 113-0032, Japan; mibe@eri.u-tokyo.ac.jp

³Graduate School of Human and Environmental Studies, Kyoto University, Kyoto 606-8501, Japan; kogiso@gaia.h.kyoto-u.ac.jp

Chemical fractionation of slab-derived supercritical fluids can play an important role in elemental transfer from subducting slab to the mantle wedge and arc magmatism [1]. Synchrotron radiation X-ray fluorescence (XRF) analysis is conducted to know elemental partition between aqueous fluids and high magnesian andesite melt with Kawai-type large-volume press at BL04B1, SPring-8, Japan. Incident X-ray is a white beam with energy ranging from 20 keV to 150 keV. During heating at a given pressure, synchrotron XRF spectra are collected from the melt and the aqueous fluid with help of X-ray radiography under HT-HP [2]. The spectra show characteristic X-ray peaks of the doped elements (Cs, Ba, Rare Earth Elements (REE)) superimposed on a continuous X-ray background. A series of experiments has been carried out to obtain partition coefficients between them at 1000-1200 °C and 0.5 - 2.2 GPa. The results suggest that (Na, K)Cl in aqueous fluids have large effects on the partition as previous studies [3]. Two slab-derived components: a melt and a fluid component are suggested to explain trace element characteristics of basalts and basaltic andesites in the Mariana arc [4]. Both components are characterized by enrichment of alkali and alkali earth elements. In addition to these, the melt component has immobile elements such as REE [4]. Such features can be explained if the fluid component is a Cl-rich aqueous fluid [3]. We suggest that slab-derived components have compositional features consistent with a Cl-rich aqueous fluid and a melt, which can be formed through a separation of a slab-derived supercritical fluid [1].

[1] Kawamoto *et al* (2012), *Proc Nat Acad Sci USA* **109**, 18695 [2] Mibe *et al* (2004) *Geochim Cosmochim Acta* **68**, 5189 [3] Keppler, (1996) *Nature* **380**, 237 [4] Pearce *et al.* (2005) *Geochem Geophys Geosys* **6**, Q07006

Difficulty of the self-replication of prebiotic RNA molecules

K. KAWAMURA^{1*}, Y. MARUOKA¹, K. HAMAHIGA¹
AND N. KONAGAYA²

¹Department of Human Environmental Studies, Hiroshima Shudo University, Hiroshima, Japan (*correspondence: kawamura@shudo-u.ac.jp)

²Department of Nutritional Sciences, Yasuda Women's University, Hiroshima, Japan

Difficulties of RNA formation

The RNA world hypothesis is supported by the discovery of ribozyme, the simulations of RNA formation under the primitive earth environments, and *in vitro* selection of a variety of functional RNA molecules. However, there are several drawbacks regarding the formation and replication of entirely prebiotic RNA molecules. First, the efficient pathway of formation of RNA monomers under the primitive earth conditions is not yet clarified. Second, the cyclization of short oligonucleotides [1], such as dinucleotides and trinucleotides, inhibits the accumulation of long RNA. This was partially solved by addition of intercalators [2]. Third, although it is true that RNA molecules preserve genetic information and enzymatic function *in vivo*, these functions are not yet elucidated for the RNA molecules formed entirely prebiotic conditions. It is known that the template-directed synthesis of oligoguanylate from activated nucleotide monomers proceeds on a polycytidylic template [3]. However, other combinations of activated nucleotide monomers on a complementary polynucleotide template proceed with very low efficiency.

Results and Discussion

We have attempted screening to enhance the efficiency of the template-directed formation of oligonucleotides. The screening was carried out in the presence of intercalator, polypeptides, metal ions, and naturally-occurring minerals. In addition, the template-directed reaction was carried out at temperature below 0 °C. Although the efficiency of the template-directed reaction was slightly enhanced in the presence of intercalator, that was generally reduced in the presence of polypeptides, metal ions, and minerals. Furthermore, the influence of very low temperatures was not also detected. These results imply the fact that the replication of RNA molecules consisting of entirely prebiotic materials would be very difficult.

[1] Kawamura & Ferris (1999) *OLEB* **29**, 563-591. [2] Horowitz *et al.* (2010) *PNAS* **107**, 5288-5293. [3] Inoue (1983) *Science* **219**, 859-862. [4] Sawai & Wada (2000) *OLEB* **30**, 503-511.

Reactive transport modelling of mineral trapping of CO₂, revised by water sampling data at Nagaoka CO₂ storage site

YUKO KAWATA*, ZIQIU XUE AND SAEKO MITO

Research Institute of Innovative Technology for the Earth (RITE), 9-2 Kizugawadai, Kizugawa-shi, Kyoto 619-0292, Japan (*correspondence: kawatayk@rite.or.jp)

Carbon dioxide capture and storage (CCS) in saline aquifer is one of the global warming countermeasure technologies. A part of injected CO₂ will be stored by reacting with formation water and reservoir rock forming minerals over many years, which is more stable for CO₂ trapping. Conducting reactive transport simulation is needed to evaluate CO₂ mineralization. However, some geochemical input data for kinetic mineral dissolution/precipitation calculation has high uncertainty. We have attempted to revise the geochemical data by matching the geochemical simulation results with sampled formation water composition, to make more realistic model for long term CO₂ behavior prediction. A series of trial runs would be needed to gain a good match, and so we used 1-D radial model for simulation-time saving. If a field-scale model is used, we have to consider lots of geological uncertainties simultaneously, which should make the study too complicated and time consuming.

Formation water was sampled twice after CO₂ injection from the observation well OB-2 at the depth of 1118m at the Nagaoka site. The concentration changes of HCO₃⁻, Ca, and Si from the first run to the second run was chosen for matching data, because only calcite is a carbonate mineral in the initial mineral composition referring to Mito *et al.* [1]. 1-D radial model was constructed with TOUGHREACT, based on the previous study. Since the reservoir pressure is already stable, CO₂ dissolved water moves mainly by the gravity effect, which can't be expressed in 1-D radial model. Instead, the diffusion coefficient was adjusted by considering HCO₃⁻ concentration. We selected reactive surface area (RSA) for varying geochemical parameter, and the initial data was based on the experimental results using reservoir rock powder. Finally, RSA value was modified to 0.015 times of the initial model, then a good matching result was obtained. This result is reasonable because the sandstone of Nagaoka site has some conglomerate, and thus should have the narrower contact area with formation water than expected. Subsequently, we performed long term CO₂ behavior simulation with this matched model.

[1] Mito, S., *et al* (2013) *Applied Geochemistry* **30**, p.33-40

Hydrogen isotope exchange between insoluble organic matter and water in chondrite parent bodies

Y. KEBUKAWA^{1,2*} AND G. D. CODY¹

¹Geophysical Laboratory, Carnegie Institution of Washington, Washington DC, 20015, USA (*ykebukawa@ciw.edu)

²Department of Natural History Sciences, Hokkaido University, Sapporo 060-0810, Japan

The high deuterium enrichment in insoluble organic matter (IOM) in chondrites has largely been attributed to small molecule chemistry prior to IOM, specifically ion-molecule reactions at low temperature interstellar medium (ISM) [1]. The hydrogen isotope (D/H) ratio of IOM tends to decrease as alteration proceeds [2]. While water in carbonaceous chondrites is more depleted in D [3]. Thus, the decrease in D/H ratio of IOM could be attributed to the hydrogen isotope exchange between D-enriched IOM precursor and D-depleted water, which could have occurred during and/or after the formation of IOM.

Cody *et al.* [4] proposed that IOM in chondrites may have formed through the polymerization of interstellar formaldehyde after the planetesimal accretion, in the presence of liquid water. Our recent study successfully enhanced production of IOM analog materials from formaldehyde in the presence of ammonia [5]. Using this formaldehyde polymer as an IOM analog we have conducted kinetic hydrogen isotope exchange experiments, starting with (1) deuterated formaldehyde polymer and normal water, and (2) normal formaldehyde polymer and deuterated water, both as a function of temperature. The three-dimensional diffusion rate control model was found to fit well the changes in the D/H ratio with time. The apparent activation energies and the frequency factors were obtained by the apparent rate constants for each temperature with the Arrhenius equation. Using these kinetic expressions, hydrogen isotope exchange profiles were estimated for time and temperature behavior, based on the assumption that the kinetic rate law is valid over all temperatures. We will discuss the δD variation observed in various chondrites, and the IOM grain size effects, based on our hydrogen isotope exchange kinetics.

[1] Robert & Epstein (1982) *GCA* **46**, 81-95. [2] Herd *et al* (2011) *Science* **332**, 1304-1307. [3] Alexander *et al* (2012) *Science* **337**, 721-723. [4] Cody *et al* (2011) *PNAS* **108**, 19171-19176. [5] Kebukawa *et al* *ApJ* under review.

Lithospheric control of plume impact: Evidence from dyke geochemistry

JAKOB K. KEIDING^{1*}, ROBERT B. TRUMBULL¹,
THOMAS M. WILL², HARTVIG E. FRIMMEL²,
MIRIAM WIEGAND³ AND ILYA V. VEKSLER¹

¹GFZ German Research Centre for Geosciences, Germany
(*correspondence: jakob@gfz-potsdam.de)

²University of Würzburg, Germany

³Karlsruhe Institute of Technology, Germany

Dyke swarms in continental flood basalt (CFB) provinces carry more information about the magmatic systems than coeval lavas since they often are less differentiated and less prone to removal by erosion. Moreover, dykes directly record the site of magma emplacement whereas eruptive vents for CFB lavas are rarely known and can be distant from the sampling site. Here we report on ~250 samples from the Early Cretaceous Henties Bay Outjo dyke swarm (HOD) in NW Namibia, which is the best exposed major dyke swarm associated with South Atlantic rifting and breakup. The goals of this research are to assess the geochemical variability of dyke magmas, to determine the composition of the mantle source and physical conditions of melting, and to understand the influence of the continental crust and lithosphere on magma composition, ascent and emplacement. And finally, we are interested in the time-space variation of these parameters.

Chemical and isotopic compositions distinguish three end-member magma groups in the HOD. In order of decreasing abundance these are: (a) crustally-contaminated tholeiites, with “spiky” trace element patterns and enriched isotope ratios ($^{87}\text{Sr}/^{86}\text{Sr}_i = 0.710\text{--}0.712$, $\epsilon\text{Nd}_i = -2$ to -7) very similar to the main series of Etendeka flood basalts, (b) MORB-like tholeiites with relative flat trace element patterns and depleted isotope ratios ($^{87}\text{Sr}/^{86}\text{Sr}_i = 0.704\text{--}0.705$, $\epsilon\text{Nd}_i = +2$ to $+6$), and (c) alkaline, trace element enriched basalts ($^{87}\text{Sr}/^{86}\text{Sr}_i = 0.7055\text{--}0.7059$, $\epsilon\text{Nd}_i = 0$ to -2). In general, dykes in the southern part of the HOD (lat. 20–23°) are more diverse and more primitive. Neither picritic nor alkaline dykes have been so far observed to the North (lat. 17–20°). Interestingly, the most primitive dykes (MgO > 6 wt.%), with the highest magmatic temperatures (1350°C) and the greatest apparent depth of melting (highest Zr/Y and Dy/Yb ratios) occur in the southern area although the proposed plume impact is farther north (Walvis Ridge). The dyke diversity may be controlled more by crustal permeability than differences in magma source.

Biogeochemical Mechanisms Underlying the Manganese Dependence of Litter Decomposition

MARCO KEILUWEIT^{12*}, PETER S. NICO³,
MARK HARMON², SUET LIU⁴, TIM FILLEY⁵,
JENNIFER PETT-RIDGE¹ AND MARKUS KLEBER²

¹Chemical Sciences Division, Lawrence Livermore National Laboratory, Livermore, CA 94550

²Crop and Soil Science, Oregon State University, Corvallis, OR 97331

³Earth Sciences Division, Lawrence Berkeley National Laboratory, Berkeley, CA 94720

⁴Advanced Light Source, Lawrence Berkeley National Laboratory, Berkeley, CA 94720

⁵Department of Earth and Atmospheric Sciences, Purdue University, West Lafayette, IN 47907

Climate change is predicted to impact the organic and inorganic composition of foliar litter, and global warming may increase soil microbial and enzymatic activity, with uncertain consequences for litter decomposition rates and pathways in soils. Recent work has identified the bioavailability of key resources (e.g. assimilable C or inorganic nutrients) as the main control of litter decomposition rates. A particularly strong correlation was established between manganese (Mn) content in needle litter and litter decomposition rates across a variety of boreal forest ecosystems, suggesting that Mn is an essential component of the decomposition pathway. There is good reason to assume that this is due to the critical role of Mn(III)-ligand complexes acting as potent oxidizers in the enzymatic breakdown of lignin. Here we related changes in Mn form and distribution to lignin transformation over the course of a 7-year litter decomposition experiment in an old growth forest ecosystem. Soft-ionization mass spectrometry, FTIR and X-ray absorption spectroscopy analyses of fresh needles, litter at different decomposition stages, and mineral soil show that the formation of oxidative Mn species is well correlated with lignin decomposition. Spatially-resolved synchrotron-FTIR and X-ray microprobe imaging revealed that microorganisms colonizing individual needles redistribute and transform reduced Mn(II) present in the vascular system of fresh needles into oxidative Mn(II/III) forms at the sites of lignin decomposition. These mechanistic insights suggest that Mn bioavailability and form are important parameters for improved model predictions of litter decomposition rates in forest soils. The response of ecosystem Mn fluxes to rising temperatures and CO₂ concentrations and, specifically, its implications for litter decomposition rates will be discussed.

Trace element systematics of pyrite from submarine hydrothermal vents

M. KEITH¹*, F. HÄCKEL¹, K.M. HAASE¹,
U. SCHWARZ-SCHAMPERA², R. KLEMD¹
AND S. PETERSEN³

¹GeoZentrum Nordbayern, Univ. Erlangen-Nuernberg,
Erlangen, 91054, Germany (*correspondence:
Manuel.Keith@gzn.uni-erlangen.de)

²Federal Institute for Geosciences and Natural Resources,
Hannover, 30655, Germany

³Geomar, Helmholtz-Zentrum fuer Ozeanforschung, Kiel,
24148, Germany

Submarine hydrothermal sulfide deposits occur at mid-ocean ridges, island arcs, and in back-arc basins. It is believed that the different wall rocks and potential magmatic volatiles [1] influence the metal budget of the hydrothermal fluid and the composition of the sulfide precipitates to variable degrees.

Pyrite is the dominating mineral in these precipitates and thus, the trace element composition of pyrite may reflect the different metal sources. However, the physicochemical composition of the fluid phase and processes such as phase separation [2] largely control the solubility and transport of metals and hence, metals enriched in the wall rock or magmas may not necessarily be concentrated in the sulfides.

Here we report on a systematic study of major and trace element concentrations on pyrites from active and inactive hydrothermal fields including the Indian and Mid-Atlantic Ridges, the Tonga-Kermadec arc, Lau back-arc, and the central Okinawa Trough. Preliminary results indicate that the pyrites show significant variations in their trace element contents irrespective of the surrounding host rocks. Pyrites from single locations have highly variable concentrations of elements like Cu, Sb, Ag, Au and Co that are most likely related to fluid evolution and changes in fluid compositions. Elements like Sb, Ag and Au have a characteristic affinity to As and Pb in pyrite, Cd correlates closely with Zn. High temperature (>240°C) As-Cu-pyrites are often enriched in Co and Au, while Ni seems to be unaffected by temperature variations. The incorporation of Co and Ni into pyrite is wall rock-independent. Bismuth appears to be enriched in pyrites from settings associated with sediments [3] and Mo may be concentrated due to seawater mixing [4].

These results indicate the complexity of trace metal contents in pyrite as a function of the physicochemical composition of the fluid phase rather than their source.

[1] de Ronde *et al.* (2011) *Miner Deposita*, **46**, 541-584. [2] Koschinsky *et al.* (2008) *Geology*, **36**, 615-618. [3] Zierenberg *et al.* (1993) *Econ Geol.*, **88**, 2069-2098. [4] Trefry *et al.* (1994) *J Geophys Res.*, **99**, 4925-4936.

Clumped isotope geochemistry of travertine carbonates in the 22-95 °C temperature range

KELE S¹*, BERNASCONI SM², KLUGE T³, JOHN CM³,
MILLÁN MI², MECKLER AN², ZIEGLER, M²,
BREITENBACH SFM², CAPEZZUOLI E⁴, ÖZKUL M⁵ AND
GÖKGÖZ A⁵, DEÁK J⁶

¹Institute for Geological and Geochemical Research, RCAES-
HAS, Budapest, Hungary (*keles@geochem.hu)

²Dept. of Earth Science, ETH Zurich, Switzerland

³Imperial College, London, Earth Sci. and Eng., London, UK

⁴Dept. of Phys., Earth and Env. Sci., Univ. of Siena, Italy

⁵Pamukkale University, Denizli, Turkey

⁶Gwis Ltd, Dunakeszi, Hungary

The formation temperature of carbonates can be estimated using both the conventional carbonate-water paleothermometry and the newly developed clumped isotope method of [1]. However, there is still a large uncertainty in the published clumped-isotope based temperature calibrations.

In this work recent travertines forming from natural springs and wells between 22 and 95 °C from Hungary, Turkey and Italy were studied for stable- and 'clumped' isotopes. Clumped isotope data showed an excellent correlation with temperature indicating equilibrium precipitation close to the spring orifice. Δ_{47} values decreased with increasing distance from the springs, which may be related to kinetic isotope fractionation due to CO₂ degassing in the different depositional sub-environments (e.g. channel, terrace-pool, cascade).

All vent travertine samples show a strong Δ_{47} -temperature relationship ($r^2 > 0.9$) defining an empirical equation with a slightly lower slope (i.e. lower temperature sensitivity) than that of Ghosh *et al.* [1]. This empirical calibration significantly extends the calibration range of the clumped isotope thermometer to temperatures of 95 °C and can be used to derive the oxygen isotope composition of travertine-depositing waters from ancient deposits to reconstruct glacial-interglacial variations in meteoric water compositions and the paleohydrological regimes of the study areas.

[1] Ghosh, P. *et al.* (2006) *Geochim. Cosmochim. Acta* **70**, 1439-1456.

Some less conventional processes in subduction zones

P.B. KELEMEN

LDEO, Columbia University, (peterk@ldeo.columbia.edu)

Emplacement of buoyant, felsic material from subduction zones into hanging wall crust may be as important as foundering of dense lithologies from the base of the crust. Building on the ideas of Hacker *et al.* (EPSL 2011), we've proposed an end-member, uniformitarian model in which continental crust forms and evolves via accumulation of buoyant, felsic material ascending from the upper crust of the subducting plate in arc-arc or arc-continent collisions (Kelemen & Behn, submitted).

More generally, fore-arc sediments can be thrust into arc crust during subduction erosion, buoyant material can be subducted to great depths and then ascend along a "subduction channel", or diapirs may rise through the hot mantle wedge beneath arcs. The latter process can efficiently recycle components from subducted sediment (greywacke, pelite, carbonate; Behn *et al.* Nature Geoscience 2011), and play a key role in global geochemical cycles. Interaction between metasedimentary diapirs and mantle peridotite may form a variety of hybrid rocks, melts and fluids.

It is more challenging to understand accumulation and transport of partial melts of subducting basalt, where these comprise a substantial geochemical component in arc lavas (e.g., W Aleutian primitive andesites). Perhaps, reaction between SiO₂-rich melt and peridotite forms an impermeable carapace of pyroxenite, beneath which melt accumulates to sufficient thickness to form diapirs (e.g., Ringwood 1975).

Diapirs may slow or stop near the crust-mantle boundary. An intriguing observation in some areas (Mt Shasta, W Aleutians) is the spatial juxtaposition of primitive magmas (Mg# ~ 0.7) with very different MgO and H₂O contents, and thus different temperatures. Perhaps hydrous, cool, primitive andesites and dacites commonly pond and equilibrate with the mantle just below the base of arc crust, while hotter primitive basalts rise rapidly through this region in cracks or porous conduits of focused flow.

Reaction-driven cracking

P.B. KELEMEN

LDEO, Columbia University, (peterk@ldeo.columbia.edu)

Hydration, carbonation, and oxidation of volatile-poor lithologies are essential to the rheology of oceanic plates, the structure of subduction zones, global geochemical cycles, and possible capture and storage of CO₂. There's plenty of energy. Mantle olivine plus H₂O or CO₂ contains 5% of the energy density (J/m³) of petroleum fuels (Kelemen and Hirth EPSL 2012). Negative feedbacks (fluid consumption fluid, falling diffusivity, increasing solid mass, decreasing solid density, crystallization in pore space, armouring of surfaces) make these processes self-limiting under many conditions. Yet, fully hydrated (serpentinite) and carbonated (listvenite) peridotites demonstrate that reaction can proceed to completion in some cases. Cracking due to stress from volume change can maintain or increase permeability and reactive surface area (MacDonald & Fyfe Tphys 1985). In systems far from equilibrium, reactions can produce kilobars of differential stress to fracture rocks, though the effect of confining pressure is uncertain. In natural samples that underwent reaction-driven cracking, the surface energy density on newly formed fractures corresponds to a strain energy density produced by kilobars of stress, consistent with thermodynamic estimates (Kelemen & Hirth EPSL 2012).

Devolatilization and melting may cause earthquakes and hydro-fracture, if fluid/melt production is rapid and permeability is low. Again, disequilibria in natural systems have energy densities ~5% of petroleum. Reaction of eclogite melt with peridotite could form an impermeable pyroxenite carapace, beneath which a column of interconnected melt grows until buoyancy leads to magma fracture. Volume change due to rapid fluid evolution from cooling melt, or from warming rocks, can cause fracture if relaxation (porous flow, viscous deformation) cannot keep pace. Shear-heating could cause rapid fluid production and fracture in localized shear zones. If fluid pressure reduces effective stress, heating will slow. With different time scales for thermal evolution and reaction progress, such instabilities could be oscillatory.

A statistical approach to the volcanic – plutonic connection

BRENNIN KELLER*, BLAIR SCHOENE,
KYLE SAMPERTON, MELANIE BARBONI,
JEFF GRONWOLD AND JON HUSSON.

Princeton University, Geosciences, Princeton, USA,
(cbkeller@princeton.edu * presenting author)

The geochemical relationship between volcanic and plutonic rocks - whether the two are geochemically identical, or if the choice between eruption and intrusion is correlated with magma chemistry - represents a major unanswered question in igneous petrology. In one endmember scenario, felsic to intermediate plutons are proposed to represent the unerupted crystal mush from which crystal-poor eruptible melts are extracted. At the other end of the spectrum, it is argued that a nearly the entire volume of magma is evacuated during large silicic eruptions, and that the probability of eruption versus intrusion is instead largely a function of magma flux.

In the first scenario, parental magmas originating at depth experience substantial fractionation during volcanic melt extraction, leading to complementary volcanic and plutonic reservoirs. In the second endmember scenario, volcanic/plutonic fractionation is negligible, but geochemical differences on average between volcanic and plutonic rocks are still possible if high- and low-flux melts have distinct geochemical characteristics that are correlated with the eruptibility of a magma.

We have compared the geochemistry of ~300,000 volcanic and plutonic rocks by Monte Carlo analysis in order to produce maximally representative average compositions that reflect the influence of meaningful physical processes. The results indicate that while volcanic and plutonic rocks in general show remarkably similar major element trends, intermediate to felsic plutonic rocks, for a given silica content, display clear enrichments in Sr and Ba and depletions in Zr, Hf, and HREEs relative to their volcanic equivalents. More subtly, intermediate volcanic rocks are found to exhibit small but distinct enrichments in FeO and depletions in K₂O relative to equivalent plutonics. These results suggest that, in the first endmember scenario above, volcanic/plutonic fractionation of plagioclase must be a key factor; while for the second scenario to hold, average water content must differ substantially between extrusive and intrusive equivalents. Further examination of trace element systematics combined with geochemical modelling allows for the discrimination between the influence of late stage crystal fractionation, versus the influence of water to suppress plagioclase relative to the ferromagnesian minerals and to delay the crystallization of most silicate minerals relative to zircon saturation.

Sulfur isotope systematics of geothermal fluids, Krafla, Iceland

N.S. KELLER¹, A. STEFÁNSSON¹, S. ONO²
AND J. GUNNARSSON ROBIN¹

¹Institute of Earth Sciences, University of Iceland, Sturlugata
7, 101 Reykjavík, Iceland (nic@hi.is)

²Department of Earth Atmospheric and Planetary Sciences,
MIT, Cambridge, MA, USA

Sulfur is among the major components in geothermal systems. It is present in various oxidation states ranging from sulfide (S^{-II}) to sulfate (S^{+VI}) and present in solid phases and fluids (water and vapor). The source of the various sulfur compounds and the processes affecting their chemistry and fluxes are complex and in many respects not fully understood. In an effort to study the complex geochemistry of sulfur in this system, we obtained new chemical and isotopic data for fluids sampled from the Krafla field, NE Iceland, an active volcanic geothermal system. High-temperature well fluids discharging water and/or steam were collected having enthalpies ranging from 852 to 2774 kJ/kg. The fluids were analyzed for various sulfur compounds including, H₂S, SO₃, S₂O₃ and S₂O₃ in the water phase and H₂S and SO₂ in the vapor phase and for sulfur isotopes including ³²S, ³³S, ³⁴S and ³⁶S on H₂S and SO₄ in the water phase and H₂S in the vapor phase. For the sulfur isotope analysis the various sulfur oxidation states were sequentially precipitated as ZnS and BaSO₄, converted to Ag₂S and analyzed by Fluorination-GC-IRMS.

The observed concentrations in the waters were SO₄ = 5.1-280 ppm, H₂S = 27.6 to 120 ppm and S₂O₃ = 0-39.1 ppm. The concentrations in the vapor were H₂S = 46-2617 mg/kg condensate. No other sulfur phases were detected. The δ³⁴S in SO₄ and H₂S in the waters were +3.4 to +13.4‰ and -1.8 to -0.2‰, respectively, and H₂S in the vapor were +0.1 to +1.3‰. The Δ³³S and Δ³⁶S follow the theoretical value for mass-dependent fractionation in all cases.

The results indicate that the δ³⁴S for H₂S in the total discharged fluid are very close to 0.0‰, suggesting magmatic origin, either through magma degassing and/or magmatic sulfide leaching. The δ³⁴S ratio between H₂S in the water and vapor is considered to reflect boiling temperatures. For SO₄, the positive isotope shift observed may be explained by H₂S oxidation to SO₄ and/or SO₄ originated from the surface either through meteoric water and/or sulfate mineral leaching and/or mixing of these two different sources.

The relationship between fO_2 and calc-alkaline affinity of arc magmas

K.A. KELLEY^{1*}, E. COTTRELL² AND M.N. BROUNCE¹

¹GSO, Univ. of Rhode Island, Narragansett, RI 20882 USA

(*correspondence: kelley@gso.uri.edu)

²NMNH, Smithsonian Inst., Washington, DC 20560, USA

Calc-alkaline differentiation, a process by which magmas become rapidly depleted in Fe early in their crystallization history, is observed exclusively in magmas in subduction zone settings and is thought to drive magmas towards the bulk composition of continental crust. Basaltic arc magmas have been proposed to achieve calc-alkaline affinity through either high magmatic H_2O , which delays the onset of plagioclase crystallization, or high magmatic fO_2 , which enhances the onset of magnetite crystallization, or both. The relative importance of H_2O , fO_2 , and magmatic bulk composition in generating calc-alkaline magma series, however, is not yet clearly resolved. Here, we present new measurements of the oxidation state of Fe (expressed as $Fe^{3+}/\Sigma Fe$ ratio) in olivine-hosted melt inclusions from basaltic arc volcanoes in the Mariana and Aleutian arcs, acquired using X-ray Absorption Near Edge Structure spectroscopy. These volcanoes span a range of calc-alkaline affinity, with THI ranging from 0.7 to 1.2 (THI = Tholeiitic Index, <1 is more calc-alkaline, >1 is more tholeiitic [1]). Measured $Fe^{3+}/\Sigma Fe$ ratios range on average from 0.23-0.28 in the Marianas, and from 0.20-0.28 in the Aleutians, which are uniformly more oxidized than more tholeiitic basaltic glasses from the Mariana trough back-arc basin (THI=1.4; $Fe^{3+}/\Sigma Fe=0.15-0.18$) or normal MORB (THI=1.6; $Fe^{3+}/\Sigma Fe=0.16\pm 0.01$). Our results show a correlation between THI and $Fe^{3+}/\Sigma Fe$ ratios at these volcanoes, such that more tholeiitic magmas contain a greater proportion of reduced Fe, and more calc-alkaline magmas a greater proportion of oxidized Fe. At the same time, the maximum dissolved H_2O contents of basaltic melt inclusions from these volcanoes also broadly correlate with THI [1], and with measured $Fe^{3+}/\Sigma Fe$ ratios, which is consistent with prior work [2], although H_2O is not the direct cause of oxidation. These findings suggest that H_2O and fO_2 may both play key roles in the development of calc-alkaline affinity in arc magmas, but their respective functions in this process may be difficult to separate in natural systems because the subducted slab delivers fluids that generate arc magmas with both elevated H_2O and fO_2 .

[1] Zimmer, M.M., Plank, T., Hauri, E.H., *et al.*, 2010, *J. Pet.* **51**, 2411-2444, doi:10.1093/petrology/egq062. [2] Kelley, K.A., Cottrell, E., 2009, *Science* **325**, 605-607, doi:10.1126/science.1174156.

Characterisation of active forest soil *Bacteria* during mineral weathering

KELLY L.C.*, UROZ S¹ AND TURPAULT M.-P.²

¹UMR1136 Interactions Arbres-Microorganismes, Centre INRA de Nancy, 54280 Champenoux, France.

²UR1138 Biogéochimie des Ecosystèmes Forestiers, Centre INRA de Nancy, 54280 Champenoux, France.

(*correspondence: laura.kelly@nancy.inra.fr)

Acidic forest soils, while nutrient-poor, are characterised by a reservoir of inorganic nutrients trapped within the minerals contained therein. Despite the significance of such reservoirs to the long-term functioning of acidic forest ecosystems, surprisingly little is known regarding the contribution of the resident bacterial communities to the weathering of soil minerals. While the influence of mineralogy on the phylogenetic composition of mineralosphere communities in soil and other terrestrial environments ^[1, 2, 3] has been demonstrated, determining the activities and contributions of individual microbial taxa to weathering processes remains an ongoing challenge. Using DNA immunocapture and high-throughput sequencing, in concert with geochemistry and traditional culture-based techniques, we investigated bacterial communities on a variety of minerals during weathering in laboratory microcosms, seeded with a forest soil-derived inoculum. Our primary objectives were i) the comparison of active and inactive bacterial community fractions and ii) to determine whether mineralogy influences the phylogenetic composition of these fractions. Such analyses brings us a step closer to understanding the composition and activities of mineralosphere bacterial communities in acidic forest soils, and the likely ecological significance of particular taxa.

[1] Uroz *et al.* (2009) *Trends Microbiol.* **17**, 378-387. [2] Kelly *et al.* (2010) *Microbial Ecol.* **60**, 740-752. [3] Lepleux *et al.* (2012) *Appl. Environ. Microbiol.* **78**, 7114-7119.

Temporal trends in the seawater osmium inventory and $^{187}\text{Os}/^{188}\text{Os}$

B. KENDALL* AND X. LU

Department of Earth and Environmental Sciences, University of Waterloo, Waterloo, Ontario, N2L 3G1, Canada
(*correspondance: bkendall@uwaterloo.ca)

Recently, several studies have used compilations of redox-sensitive metal abundances (e.g., Mo, Ni, Zn) from organic-rich sedimentary rocks (ORS) and iron formations to infer first-order temporal trends in oceanic metal inventories. These trends provide critical information about atmosphere and ocean oxygenation and associated changes in biogeochemical cycles and biological evolution. Osmium (Os) is a redox-sensitive metal that can provide information about redox conditions and crustal vs hydrothermal fluxes.

Most of the Os supplied to the modern oceans is derived from rivers (via oxidative weathering of the upper crust), with the remainder coming from cosmic dust dissolution and hydrothermal alteration of oceanic crust and peridotites. Osmium accumulates in modern oxygenated seawater (residence time of 10^4 years) but is sequestered into anoxic, organic-rich sediments. Seawater $^{187}\text{Os}/^{188}\text{Os}$ (= initial $^{187}\text{Os}/^{188}\text{Os}$ of ORS at the time of sediment deposition) also constrains the relative importance of radiogenic crustal versus unradiogenic hydrothermal (and extraterrestrial) inputs to seawater. Temporal trends in $^{187}\text{Os}/^{188}\text{Os}$ have been explored, whereas Os abundances in ORS have received less attention.

Here, we present a compilation of ^{192}Os abundances in ORS (total Os abundances are not used because of ^{187}Os contributions from ^{187}Re decay). We find that ^{192}Os abundances in pre-Ediacaran shales are low, typically <300 ppt, but still elevated above average upper crust (~10-20 ppt). The ^{192}Os enrichments and chondritic initial $^{187}\text{Os}/^{188}\text{Os}$ from Archean ORS require a oceanic Os inventory dominated by hydrothermally sourced Os. However, there is no clear change in ^{192}Os abundances across the Great Oxidation Event. This observation contrasts with a shift from chondritic seawater $^{187}\text{Os}/^{188}\text{Os}$ in the Archean to moderately radiogenic seawater $^{187}\text{Os}/^{188}\text{Os}$ in the Proterozoic, which points to an increase in the riverine flux of radiogenic Os to the oceans. To reconcile these observations, we suggest that continued widespread Proterozoic deep ocean anoxia and declining hydrothermal Os fluxes kept the oceanic Os inventory broadly similar to Archean levels. Higher ^{192}Os abundances (>300 ppt) and instances of highly radiogenic seawater $^{187}\text{Os}/^{188}\text{Os}$ in the Ediacaran Period and Phanerozoic Eon point to an increase in the riverine Os flux and oceanic Os inventory in response to late Neoproterozoic oxygenation.

Possible PGE nano structures, in magmatic systems

KENNEDY, B.^{1*}, TREDOUX, M.¹, BALLHAUS, C.², COETSEE, E.³ AND STEYL, G.⁴

¹Dept. of Geology, University of the Free State, South Africa,
(*correspondence: kennedybia@gmail.com)

²Steinmann Institute, University of Bonn, Germany

³Dept. of Physics, University of the Free State, South Africa

⁴Dept. of Chemistry, University of the Free State, South Africa

The retention of platinum-group elements (PGE) in the mantle restite is difficult to explain by conventional chalcophile models. PGE nano-structures (clusters of 10-100nm), might be the cause that magma can become enriched in PGE, during the early stages of magmatic differentiation. The study focused on the possible formation of these entities in a magmatic system. If these entities do form, to what extent might they contribute to ore forming processes in ultra mafic deposits, like the Bushveld complex.

A synthetic sulphide system was used to replicate the sulphide portion of a Cu-Ni-S ± PGE system. Sulphides are of the first ore minerals to crystallize in a magmatic environment and thus the ideal place to look for clusters. Experiments were run, using the dry powder silica charge technique. A base mixture of Cu, S and Fe, was doped with variable concentration of PGE (Pt, Pd and Ru) and As. As was chosen as stabilising chalcogene ligand. The systems were manipulated to form a mono sulphide or pyrrhotite phase (Fe_xS_x) and a melt ($\text{Fe}_x\text{Cu}_x\text{S}_x$) phase.

Nano scale PGE-ligand phases, ranging from 10-1000 nm, were measured in the synthetic samples, by high resolution SAM and TOF-SIMS. This observation indicated that the PGE may form phases, on a nano level, without sulphide saturation having been achieved. The clusters form due to the physico-chemical association of the PGE with chalcogene ligands, such as As, Fe and Cu, before formal chemical bonding, to form PGMs. A fraction of the clusters are reabsorbed into the melt, while a fraction may act as nucleation points to form nano-crystals and minerals in the incompatible sulphide, oxide or silicate phases. The clusters form during the early stages of magmatic differentiation.

Chemical behaviour may govern the secondary distribution of PGE-phases, but clustering is potentially the primary (physical) enrichment mechanism. This behaviour cannot be explained by sub-solidus immiscibility properties as has been suggested to account for the frequent presence of PGE in base metal sulphide minerals.

Spectroscopically visualising the availability of goethite-sorbed phosphate to soil microorganisms

JANICE P.L. KENNEY^{1*}, REINER GIESLER²
AND PER PERSSON¹

¹Department of Chemistry, Umeå University, Umeå, Sweden,

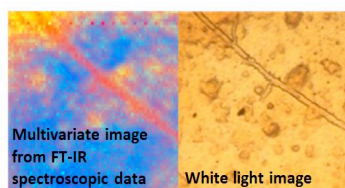
²Department of Ecology and Environmental Science, Umeå University, Umeå, Sweden (*correspondence: janice.kenney@chem.umu.se)

Phosphorus (P) is an essential nutrient, limiting biomass production in many soils. The biogeochemical cycling of P is highly influenced by soil minerals, such as goethite, which has the ability to strongly sorb soluble phosphates. However, the mechanisms by which soil microorganisms take up sorbed phosphate is still not completely understood.

In this study we investigate whether soil microorganisms can use phosphate pre-adsorbed to goethite. To test this we ran experiments under four sets of experimental conditions; with or without P (+P/-P) and with or without glucose and nitrogen (+CN/-CN). The goethite was deposited as a mineral film on BaF₂ slides, after which the soil (clay-rich oxisol from South Africa), was deposited onto the goethite films. Prior to addition to the goethite layer, half the soil was amended with glucose and ammonium sulphate (2.0 and 0.3 g per g of soil organic matter, respectively).

The experiments were monitored over 13 days using FT-IR microspectroscopy. During this time it was found that there was no significant growth of microorganisms from the soil onto the goethite mineral film in both cases where C and N were not amended to the soil (-CN). However, in both cases where C and N are amended to the soil (+CN) we see microbial growth. When there is no P added to the mineral film (+CN/-P), we see only minimal growth of yeast cells close to the soil deposition site. When there is P added to the mineral film (+CN/+P) we see significant fungal hyphae growing out onto the goethite within 6 days of incubation. The FT-IR microspectroscopy results show distinct differences in the goethite near the fungal hyphae. These results show that goethite-sorbed P is bioavailable and can greatly affect the soil microbial growth.

Blue: Phosphates
Red: Carbohydrates, proteins, lipids
Yellow: increase in polysaccharides



Submarine meteorite impact craters as potential cradles of life: Mineralogical evidence from the Onaping Formation, Sudbury

G.G. KENNY^{1*} AND B.S. KAMBER¹

¹Department of Geology, Trinity College Dublin, Dublin 2, Ireland (*correspondence: kennyg2@tcd.ie)

A difference between terrestrial versus lunar and martian impact basins is the possibility of submarine impacts. The thick melt sheet of a very large terrestrial impact acts as an effective heat source below water-filled craters and can potentially sustain prolonged phreatomagmatic activity. The Sudbury impact basin, Ontario, Canada, is the largest accessible and well-preserved example of a submarine impact. Although it is mainly known for its magmatic sulphide Ni-Cu deposits, it also hosts a number of VMS-type base metal deposits in the crater fill. Using observations from the fill, we highlight the potential importance of submarine meteorite impact craters as a location for the development of the life on the heavily bombarded early Earth.

We report the discovery of monocrystalline igneous quartz in the Onaping Fm. of the Sudbury crater fill – a complex unit composed of both the immediate fall-back of brecciated impact material and also later-formed igneous rocks. The crystallisation temperatures of the quartz grains have been calculated by applying the titanium-in-quartz thermometer to titanium contents obtained by LA-ICP-MS.

This finding provides support for continued in-crater igneous activity after the initial impact (e.g. [1]), and thus highlights the potential of submarine impact craters as sites where life might have emerged. Submarine Hadean impacts were likely common (e.g. [2]) as there is evidence for a liquid hydrosphere at this time (e.g. from abundance of halogens; [3]). From an emergence of life point of view, submarine craters are contained, confined bodies of water surrounded by highly friable rock, supporting a very high nutrient load. In addition, the hydrothermal processing of this fluid at volcanic vents was an effective factory for creating complex precursor molecules. Interestingly, the upper half of the Onaping Fm., like the overlying sedimentary Onwatin Fm., is rich in isotopically light [4] reduced carbon of possibly biogenic origin (e.g. [5]).

[1] Grieve *et al.* (2010) *MAPS* **45**, 759-782. [2] Furukawa *et al.* (2009) *Nat. Geosci.* **2**, 62-66. [3] Kramers (2003) *Precamb. Res.* **126**, 379-394. [4] Whitehead *et al.* (1990) *Chem. Geol.* **86**, 49-63. [5] Avermann (1994) *GSA Special Paper* **293**, 265-274.

Investigation of fungal decomposition of leaf lignin using synchrotron infrared microspectroscopy

J.L. KERR¹, D.S. BALDWIN², M.J. TOBIN³, L. PUSKAR³,
G. REES² AND E. SILVESTER^{1*}

¹La Trobe University, Australia (*correspondence: e.silvester@latrobe.edu.au)

²MDFRC, La Trobe University, Australia

³The Australian Synchrotron, Australia

Fungi are a major decomposer group in the aquatic carbon cycle, and are one of few groups though to be capable of breaking down woody (lignified) tissue [1]. Here we have used synchrotron Fourier transform infrared (S-FTIR) microspectroscopy to study the interface between fungal tissue and lignified leaf tissue (xylem) in two eucalypt species (River Red Gum and Snow Gum) during aquatic decomposition.

Aquatically decomposed River Red Gum leaf samples show strong depletion of lignin-bound carbohydrate immediately adjacent to the fungal tissue, spatially correlated with oxidation (de-polymerisation) of the lignin framework [2]. This observation has now been replicated with Snow Gum leaf samples (Figure 1 (a-c)) and investigated at even greater resolution using a synchrotron-coupled Focal Planar Array (FPA)-FTIR spectrometer (Figure 1(d)). S-FPA-FTIR offers sub-micron spatial resolution and can probe more subtle spatial changes in leaf chemistry at the fungal interface.

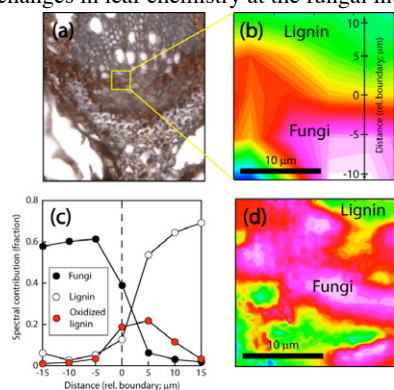


Figure 1.(a) Bright field image of Snow Gum vein; (b) S-FTIR map of fungi-xylem interface; (c) line scan across interface; (d) S-FPA-FTIR map of fungi-xylem interface.

[1] Floudas *et al.* (2012) *Science* **336**, 1715-1719. [2] Kerr *et al.* (2013) *PLOS ONE* 8(4), doi:10.1371/journal.pone.0060857

Preliminary evaluation of trace hydrocarbon speciation and abundance as an exploration tool for footwall-style sulfide ore, Sudbury Igneous Complex, Ontario, Canada

MITCHELL J. KERR^{1*} AND JACOB J. HANLEY²

¹Saint Mary's University, Halifax, NS. B3H 3C3

(*correspondence: mitchjkerr@gmail.com)

²Saint Mary's University (jacob.hanley@smu.ca)

The North Range of the Sudbury Igneous Complex (SIC) hosts footwall-style Cu-Ni-platinum group element (PGE)-rich sulfide deposits of predominantly magmatic origin but that have been influenced by multiple syn- and post-magmatic hydrothermal events. The composition of reduced carbonic phases (unsaturated and saturated hydrocarbons, C1 to C6) in fluid inclusions within the matrix of Sudbury breccia, a rock unit that is permeable to circulating volatiles and that commonly hosts footwall-style Cu-Ni-PGE deposits, has been investigated by in-line rock-crushing gas chromatography. This was done on samples from zones of breccia that are known to contain economic footwall sulfide deposits and zones barren of such deposits. Subtle but strategically significant differences have been found in the composition and abundance of bulk hydrocarbons that are released from mineralized and barren breccias when fluid inclusions are opened. These findings include: (i) statistically higher average abundances of light, saturated hydrocarbons (C1-C4) in mineralized, embayment-associated footwall packages than in breccia from barren environments (maximum difference of approx. half an order of magnitude for propane abundances; mol/g rock), and (ii) no statistically significant differences in average unsaturated hydrocarbon abundances between the two breccia environments, but differences are present when considering the spatial variations of hydrocarbons within the mineralized breccia package itself relative to massive sulfide mineralization.

Additionally, samples of breccia and quartz (from mineralized alteration assemblages) from PGE-rich environments significantly deviate from expected hydrocarbon signatures and are considerably more enriched in unsaturated hydrocarbons. It is suspected that PGE, particularly Pt, play a direct role in the catalytic dehydrogenation of saturated, into unsaturated hydrocarbon species in hydrothermal environments. These findings strongly suggest that fluid hydrocarbon signatures should be taken into consideration when exploring for Cu-Ni-PGE-rich footwall-style ore bodies as a supplemental criterion to traditional visual and geochemical approaches.

Coprecipitation: Mechanisms and quantitative models

M. KERSTEN¹

¹Gutenberg-University, Mainz 55099, Germany
(*correspondence: kersten@uni-mainz.de)

Coprecipitation is referred to as the simultaneous removal of a trace with host constituent in the aquatic environment. Solid-solution aqueous-solution (SSAS) equilibrium models have been developed to close the often huge solubility gap in the continuum between surface complexation and single-component precipitation of trace elements [1]. These models were originally developed to explain incongruent dissolution and secondary mineral formation in weathering reaction path modeling including carbonates and clay minerals [2,3]. They became of major interest, however, in long-term environmental assessment of radionuclide repositories, in particular for evaluation of near-field geochemical barrier performance. Such barrier concepts include radionuclide coprecipitation with more or less long-term stable minerals like sulfates [4], carbonates [5], and silicate hydrates [6]. More recently, the SSAS modeling concept became also of interest to manage enhanced geogenic radium leaching [7], which may occur during deep geothermal resource exploitation or hydraulic fracturing for shale gas recovery. This keynote contribution will give an overview on the most promising applications in geochemical engineering, as well as model concepts spanning from the classical Lippmann equation approach for drawing aqueous solubility diagrams of binary solid solutions [8] to the most advanced non-ideal multi-site sublattice concept [9,10].

[1] Kersten & Kulik (2005) In: Cornelis *et al.* (eds.) *Handbook of Elemental Speciation*, Vol. 2. Wiley, Chichester, pp. 651-689. [2] Glynn *et al.* (1990) *Geochim. Cosmochim. Acta* **54**, 267-282. [3] Zhu *et al.* (2010) *Geochim. Cosmochim. Acta* **74**, 3963-3983. [4] Aimoz *et al.* (2012) *Appl. Geochem.* **27**, 2117-2129. [5] Kulik *et al.* (2010) *Phys. Chem. Earth* **35**, 217-232. [6] Gaona *et al.* (2012) *Appl. Geochem.* **27**, 81-95. [7] Fernández-González *et al.* (2013) *Geochim. Cosmochim. Acta* **105**, 31-43. [8] Kersten (1996) *Environ. Sci. Technol.* **36**, 2919-2925. [9] Rozov *et al.* (2011) *Clays Clay Min.* **59**, 215-232. [10] Kulik (2011) *Cem. Concr. Res.* **41**, 477-495.

Arsenate adsorption by akaganéite

M. KERSTEN^{1*} AND N. VLASOVA²

¹Gutenberg-University, Mainz 55099, Germany
(*correspondence: kersten@uni-mainz.de)

²NAS Institute of Surface Chemistry, Kiev 03164, Ukraine

The β -type is the last among the FeOOH polymorphs for which there is yet no multi-site surface complexation (MUSIC) model, which requires information about the proton affinity of the various types of surface groups. Enigmatic behavior during acid-base titrations where protons are co-released from tunnel sites renders interpretation a challenge for akaganéite. In batch experiments, our akaganéite sample show a CIP at pH 7.7. However, the apparent surface charge is not equal to zero at this CIP but shows an offset by -0.25 C/m², obviously due to the excess tunnel site protons. We propose to monitor the chloride exchange with at least two days batch equilibration time (Fig. 1). The chloride is not significantly re-adsorbed on outer surfaces and may be used to monitor and quantify the excess tunnel HCl release. The thus corrected σ_0 vs. pH curves become sigmoidal and can be fitted to parameterize a reliable surface complexation model based on recently published site densities for singly and triply coordinated hydroxyl surface groups [1]. This provides a sound basis to set up CD-MUSIC adsorption models for arsenate and competing oxyanions. Furtheron, breakthrough curves of akaganéite based GFH fixed-bed adsorber column units can be calculated for different groundwater chemistry using a homogeneous surface diffusion model and Langmuir adsorption isotherms predicted by the surface complexation model.

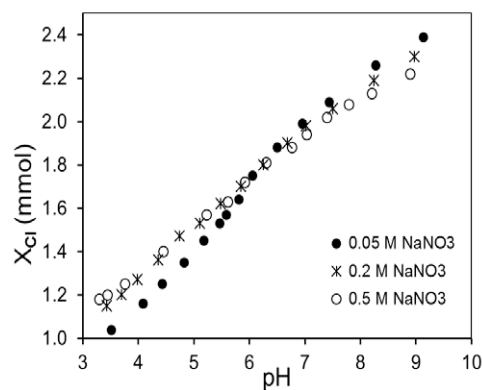


Figure 1: Tunnel chloride ion release vs. pH at different NaNO₃ electrolyte concentrations

[1] Kozin & Boily (2013) *J. Phys. Chem.* C117 (Article ASAP, DOI: 10.1021/jp3101046).

Measuring the isotope fractionation of denitrification in permeable sediments

A.J. KESSLER^{1*}, L.A. BRISTOW², M.B. CARDENAS³,
R.N. GLUD², B. THAMDRUP² AND P.L.M. COOK¹

¹Water Studies Centre and School of Chemistry, Monash Univ., Melbourne, Australia (*correspondence: adam.kessler@monash.edu)

²Nordic Centre for Earth Evolution and Institute of Biology, Univ. Southern Denmark, Odense, Denmark

³Department of Geological Sciences, Univ. Texas at Austin, Austin, Texas

Permeable sediments cover a significant proportion of the continental shelf, yet denitrification and other redox biogeochemistry in these sediments remains poorly understood. This is mostly due to the complex advective transport patterns in such sediments [1].

Despite benthic denitrification accounting for a significant oceanic nitrogen sink, no isotope effect (ϵ) associated with denitrification in permeable sediment has been published. Rather, most models assume an isotope effect of zero for this process, based on work solely in cohesive sediments [2]. However, permeable sediments could potentially impose substantial fractionation if nitrate is only partly consumed during advective transport through the sediment.

We performed flow-through column experiments to quantify the organism-scale nitrate N isotope effect (ϵ_{cell}) during benthic nitrate reduction, the first step of denitrification using sand from Kerteminde, Denmark. The value of ϵ_{cell} was $18 \pm 1\%$, consistent with ϵ_{cell} values reported in cohesive sediments [3].

In order to estimate the apparent isotope effect (ϵ_{app}) on the overlying water, a computational model was employed to simulate denitrification and associated N isotope fractionation in a rippled permeable sediment under varied conditions. Simulations indicate that ϵ_{app} varies between 2‰ and 5‰, driven by advection of partially denitrified nitrate out of the sediment.

This work has significant implications for the global marine nitrogen isotope budget, and may help to explain discrepancies between modelled and measured ocean isotope signatures [2].

[1] Boudreau *et al.* (2001) *EOS Trans. Am. Geophys. Union* **82**, 133-136. [2] Altabet *et al.* (2007) *Biogeosciences* **4**, 75-86. [3] Lehmann *et al.* (2007) *Geochim. Cosmochim. Acta*; **71**, 5384-5404.

Geochemical fingerprinting of corundum from Fiskensæset, Greenland

NYNKE KEULEN¹ AND PER KALVIG¹

¹Geological Survey of Denmark and Greenland (GEUS), Øster Voldgade 10, 1350 Copenhagen, Denmark. ntk@geus.dk, pka@geus.dk

Since the late 1960s it has been known that pink and red corundum occurs in the area near Fiskensæset (Qeqatarsuaat) in southern West-Greenland. Corundum is hosted in the Fiskensæset complex, which is part of the Archaean basement of the North Atlantic Craton. To date, c. 40 corundum localities are known in the area – a few localities yield stones of gem quality. The most promising locality, Aappaluttoq, is likely to be mined in the near future by the Canadian company True North Gems.

This study is a first attempt to find geochemical characteristics that can be used to tie the Greenlandic rubies to their area of origin. Here, we present laser ablation-ICP-MS trace element geochemistry data and oxygen isotope investigations on samples from the Fiskensæset area and other known localities in Greenland (Storø, Maniitsoq, Kapisilit, and Nattivit).

Trace element investigations of corundum grains separated from 21 hand specimen from ten localities in the Fiskensæset complex were performed on 24 different elements with LA-SF-ICP-MS at GEUS, however most of them were not detected. Our investigations of the Greenlandic corundum were concentrated on the elements Mg, Si, Ti, V, Cr, Fe, and Ga. Results are compared with data from other localities in Greenland and from internationally, well-known, ruby occurrences. Samples from Fiskensæset show a considerably higher amount of Cr (up to 14000 ppm) than found in measurements on samples from other areas in Greenland and literature data on most international samples. The Fiskensæset rubies are relatively rich in Fe and Si, but relatively poor in Ti and Ga, while V and Mg do not show very distinctive values compared to samples from other areas.

Oxygen isotope composition measurements were performed on 11 samples from Greenland at the University of Lausanne, Switzerland using an isotope ratio mass spectrometer. Samples from the Fiskensæset region yield $\delta^{18}\text{O}$ values between 1.62 and 4.20‰, which is low compared to the other areas in Greenland and world-wide.

The two methods discussed here are efficient in characterising the Fiskensæset rubies. More independent methods are necessary for a high-confidence fingerprinting.

The study of polymorphs of Wordian Amb Formation, Salt Range of Western Pakistan in relation to Geochemistry

SAJJAD KHAN¹ AND NAGHMA HAIDER²

^{1,2}Geoscience advance Research Laboratory, Geological Survey of Pakistan, Islamabad (pkpkgeo@gmail.com)

The Amb Formation of Wordian age (Martmann, 2003) was investigated for geochemistry. Twenty six samples were collected from out crop for geochemistry at Zaluch Nala of Western Salt Range of Pakistan.

The results of the collected samples displayed major oxides of K₂O, P₂O₃, Na₂O, MgO, Al₂O₃, TiO₂, Fe₂O₃, FeO, P₂O₅, SiO₂ & C (with addition of H₂O).

To find the number of polymorphs of twenty six out crop sample of thirty grams was processed one by one.

The productivity level of each sample was controlled by the comparative amount of CaO, MgO and C (both inorganic and organic).

Fifty six polymorphs species of thirty two were reported. Among these, eleven genera and nineteen species belong to trilete, six genera and nineteen species to monosaccates, twelve genera and twenty four species to bisaccates. Pollens Colpates (two species) and acolpate (one species) were also reported from the samples.

The Role of Swamps in Formation of Chemical Composition of River Waters in Western Siberia

J.A. KHARANZHEVSKAYA¹, E.S. IVANOVA^{1*},
E.S. VOISTINOVA¹ AND A.A. SINYUTKINA¹

¹Siberian Research Institute of Agriculture and Peat, Tomsk, 634050 (*ivanova_e_s@bk.ru, kharan@yandex.ru)

The landscape is characterized by the wide spread occurrence of raised oligotrophic swamps with the dominant role of the ridge-pool and ridge-lacustrine-pool systems in combination with areas of riams-oligotrophic complex piny-suffruticous-sphagnous swamps and narrow bands of transitional swamps along the periphery of watershed areas. Geographical coordinates of the area are N56°03'07" E82°22'42".

Water samples for the analysis were taken within the basin of the Klyuch River in the most typical swampy geobiocoenoses: piny-suffruticous-sphagnous with a 10-15 meter pine (point 2); piny-suffruticous-sphagnous with a scrubby pine (point 3); sedge-sphagnum (point 5).

Index	Max. allowable conc. (MAC) est. Russia	the Klyuch River	Mire		
			Point 2	Point 3	Point 5
pH	6.5–8.5	6.5	4.4	3.8	4.1
mineralization	1000	72.0	30.2	25.1	15.1
NH ₄ ⁺	1.9	3.8	6.7	6.0	3.5
COD,mgO/dm ³	15	122.2	262.4	157.7	162.2
humic acid	-	6.7	8.9	9.5	5.5
fulvic acid	-	41.1	66.6	53.1	43.3
Fe _{total}	0.3	2.5	2.9	1.8	1.3

Table: Chemical composition of swamp and river waters for 2006 – 2011 years of research, mg/dm³

The chemical composition of swamp waters of area under study is an averaged sample of the one-meter peat mire layer and represents biochemical and biological processes occurring in them. The content of water-soluble carbon in the water under study at its maximum values varies from 106.6 mgC/dm³ in point 2 to 63.4 mgC/dm³ in point 5. This index for river waters falls by 3-5 times. Due to that fact that the intensity of the peat decomposition processes in a high bog increases from the center to the periphery (from point 5 to point 2), the content of all components of the geochemical runoff increases in this direction. A high content of NH₄⁺ (5.4 mg/dm³) is observed in swamp waters: it almost three times exceeds the maximum allowable concentrations. The content of NH₄⁺ in river water is one and a half time lower – 3.8 mg/dm³. It should be also noted that the value of dichromate oxidizability in the swampy area 25 times exceeds MAC, as compared with river waters, where this index is exceeded only by 11 times. Thus, for a number of natural reasons, swamp and river waters contain high concentrations of organic and biogenic substances, the content of which in river waters is several times lower.

Isotopes of oxygen and hydrogen in natural waters from NE of Asia

N.A.KHARITONOVA, G.A.CHELNOKOV AND I.V.BRAGIN

690022, Russia, Primorsky region, Vladivostok, Prospect 100-letya 159, Far East Geological Institute Russian Academy of Science (tchenat@mail.ru)

Isotopes of oxygen and hydrogen are ideal natural tracers for describing phenomena of the water cycle so they are constituents of the water molecule. The $\delta^{18}\text{O}$ and $\delta^2\text{H}$ in waters violently rely on meteoric processes, and so infiltration into specific sediments leads to a characteristic isotopic signature which tags as the origin of groundwater as surface water-groundwater interactions. ^3H is the most attractive radioisotope for studying the principles of water circulation in nature so it is a perfect water tracer. The first particular data about the content of stable and radiogenic isotope of oxygen and hydrogen in natural water of region were presented in some studies (Chudaeva *et al.*, 1999; Kharitonova *et al.*, 2012), however simultaneous measurements $\delta^2\text{H}$, ^3H and $\delta^{18}\text{O}$ were never performed for this area.

The aims of this study are to define local meteoric waters line of Russian Far East, to identify the forming conditions of various groundwater types of area using isotopic parameters and estimate residence time of groundwater basing on tritium values.

More than 120 samples of precipitation, seawater, surface water and groundwater were collected across territory of Russian Far East during last 7 years and then analyzed for isotopic composition. Geochemical characteristics of these samples were published earlier (Chelnokov & Kharitonova, 2008).

Our data let us conclude:

1. All studied groundwater is meteoric water and shift from GMWL for some spas is the result of water-rock-gas interaction. Local meteoric water line for the southern part of Russian Far East can be determined by the equilibrium: $\delta\text{D}=7.6385\times\delta^{18}\text{O}+3.96\text{‰}$. Continental and lateral zonal distribution of stable isotopes on this territory is being observed.
2. There is the universal increasing in ^3H values in surface water from ocean to inland. Content of tritium is 20 TU in rivers of Amurskiy region, ~13 TU in rivers of Primorsky region and to ~5.5 TU in ones of Kuril Islands. Most of studied groundwater, excluding brackish waters of Rechitza outlet, have short residence time (less 50 years).

Low thermal Northern Dvina iodine water field: History of prospection and perspectives of development

I.L. KHARKHORDIN^{1*}, F.G. ATROSCHENKO¹
AND V.V. NAZIMA¹

¹Geostroyproekt Ltd., 22-th Line, 3, St. Petersburg, 199106, Russia (*correspondence: kharkhordin@rambler.ru)

²Geostroyproekt Ltd., 22-th Line, 3, St. Petersburg, 199106, Russia (fatroschenko@mail.ru)

³Geostroyproekt Ltd., 22-th Line, 3, St. Petersburg, 199106, Russia (v.v.nazima@gmail.com)

Iodine water field is located at Northern Dvina River basin, north-west of European part of Russia [1]. Uncommon features of the field are as follows.

- 1) Depth to iodine water containing aquifer is only 100-120 meters.
- 2) Iodine water field was formed at low temperature conditions (below 10 °C).
- 3) The source of iodine is organic fossils associated with marine clays (Q_{IImk}) [2]. This clays was consolidated by ice shield, iodine water was expressed into upper part of padun aquifer (V_{pd}).

At present study analysis of hydrodynamic and hydrochemical conditions of iodine water field was performed, the numerical models of groundwater flow and iodine transport were created using MODFLOW-96 [3] and MT3DMS [4] computer codes. The main issues are:

- the present day recharge through mikulinski clays is important for iodine water field existence due quaternary time, it partly compensates iodine water discharge into Northern Dvina River;
- resources of iodine water was estimated;
- limiting factor of iodine water field exploitation is fresh water upconing from low part of padun aquifer;
- strategy for iodine water field exploitation was elaborated.

[1] Malov (1980) Vodnye Resursy, No. 2, pp. 66-76 (In Russia). [2] Gurevich (1963) Izv. VUZov, Geologiya i razvedka, No. 7, pp. 123-125 (In Russia). [3] Harbauf & McDonald (1996) USGS, Open-File Report 96-495. [4] Zheng & Wang (1998) Contract Report SERDP-99, 239 p.

Provenance tracing of aerosols in the South Atlantic Ocean using Pb and Nd isotopes and select trace and rare earth elements

R. KHONDOKER^{1*}, D. WEISS, T. VAN DE FLIERDT¹,
M. REHKÄMPER¹, R. CHANCE², A. BAKER²,
S. STREKOPYTOV³, E. WILLIAMS³ AND J. NAJORKA³

¹Dept. of Earth Sciences, Imperial College London, SW7 2AZ, UK (roulin.khondoker04@imperial.ac.uk)

²University of East Anglia, Norwich, NR4 7TJ, UK

³Natural History Museum, London, SW7 5BD, UK

The atmosphere is an important pathway of delivering nutrients to ocean surface waters. These nutrients can play a vital role in marine biogeochemical processes and ultimately the global carbon cycle. However, our understanding of the atmospheric inputs and their influences on marine micronutrient cycles is limited, particularly in the South Atlantic, a region where models predict widely variable fluxes of micronutrients to the ocean from the atmosphere.

Moreover, in recent years it has become clear that atmospheric emissions from cities and human activities, such as road traffic and industrial plant emissions, can significantly impact atmospheric inputs and thus alter micronutrient fluxes to the ocean. Although air quality studies have been carried out for some cities bordering the South Atlantic Ocean, including São Paulo and Buenos Aires, the impact of emissions from such cities on marine micronutrient budgets has not been studied in detail.

Here, we present rare earth and select trace element data as well as results from Pb and Nd isotope analysis of sediments, volcanic ash, road dusts, aerosol filters and lichens from Patagonia, recent Cotopaxi, Chaitan and Puyahue volcanic eruptions, and the cities of São Paulo, Buenos Aires and Johannesburg. All sites are potential atmospheric aerosol sources for the South Atlantic Ocean. The rare earth and trace element concentration data and the isotopic results allow characterisation of the different source sites with adequate resolution to distinguish between South American and Southern African as well as anthropogenic and natural aerosol sources. This provenance information will be applied to interpret the first comprehensive geochemical data set (comprising rare earth, other trace element concentrations, and Pb, Nd isotope compositions) for aerosol filters collected in the South Atlantic Ocean at approximately 40° S during the UK GEOTRACES cruises D357 and JC068.

Mineralogy and origin of uranium deposits from central Jordan

HANI N. KHOURY

Department of Geology The University of Jordan, Amman – Jordan 11942 (khouryh@ju.edu.jo)

Secondary uranium surficial mineralization is hosted by travertine and calcrete in central Jordan [1]. The paleocirculating water in the combusted bituminous marl has oxidized the dissolved V⁴⁺ to V⁵⁺ and fixed the uranyl-ion as uranyl vanadate in strelkinite and metatyuyamunite. Carnotite was favored depending on the availability of K in solution. The uranyl vanadate minerals were precipitated from highly alkaline solutions during the dry periods after the precipitation of the thick travertine deposits.

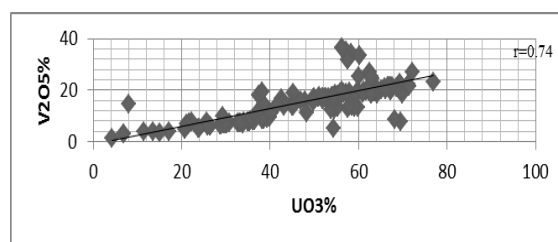


Figure 1: EDS results: UO₃ vs V₂O₅ correlation of the uranium minerals

Discussion of Results

U and V are associated in the same mineral phases as indicated in the figure above. The travertine is an evidence for discharges of hyperalkaline groundwater in the past [1]. Oxidizing alkaline circulating water oxidized dissolved V⁴⁺ to V⁵⁺, and mobilized uranium as uranyl complexes before the precipitation of uranium vanadate minerals as strelkinite and tyuyamunite and carnotite.

[1] Khoury (2012) *Environmental and Earth Science*. **65**:1909-1916.

Investigation of sediment geochemistry in areas with elevated arsenic in groundwater of Matlab, Bangladesh and Murshidabad, India

M.G. KIBRIA¹, M. HOSSAIN², P. BHATTACHARYA²,
K.M. AHMED⁶, M. VON BRÖMSEN⁵, G. JACKS²,
M.F. KIRK¹, M.S. SANKAR¹, K. TELFEYAN³, S. FORD¹,
A. NEAL⁴, T.J. HAUG³, K. JOHANNESSON³
AND S. DATTA*¹

¹Kansas State University, Manhattan, KS, USA
(sdatta@ksu.edu)

²KTH Royal Institute of Technology, Stockholm, Sweden

³Tulane University, New Orleans, LA, USA

⁴Virginia Tech, Blackburg, VA, USA

⁵Ramböll Sweden AB, Stockhome, Sweden

⁶University of Dhaka, Dhaka, Bangladesh

The assessment of the incidence of arsenic (As) and other oxyanions forming trace elements was examined in Bengal delta floodplain groundwaters from Matlab Upazila, Bangladesh and Murshidabad District, India. These field areas cover an area of about ~400km² (von Brömssen *et al.* 2008) and ~438km² (Datta *et al.* 2011) respectively. The study focuses on the sediment geochemistry and adsorption behavior of oxidised red brown and reduced grey sediments and their respective capacity to attenuate As. Sediment cores were collected at regular intervals within depth of 125m in Matlab and ~40m in Murshidabad. Detailed sequential extractions of sediments indicate relatively low amount of As released from oxidized sediments. The study describes the lithofacies, mineralogy and results of adsorption experiments on the sediments from two sites and establishes a relationship between aqueous and solid phase geochemistry along the various depths of the aquifers. DNA recovered from Matlab core samples averaged 450ng/g from course-grained samples and 800ng/g from fine-grained samples. Sequencing of the DNA is utilised to identify microbial communities and their role in the biogeochemical processes controlling the groundwater As levels. Synchrotron aided μ XANES and μ XRD studies conducted for solid state As and S speciation in the core samples at different depths indicate the occurrences of hotspots of As differently distributed in red-brown and grey sediments in both these sites. The projected outcome is to incorporate detailed sediment characteristics of the different aquifers including all possible color variations available in exploited depths within Matlab and Murshidabad respectively. Porewater from Matlab abstracted from oxidized reddish sediments, in contrast to reducing greyish sediments contain substantially lower amount of dissolved As and can be a source of safe water. This study has wider implications towards broad scale regional approach for As mitigation that incorporates the enquiry of efficiency of sediment color as a simple and easy tool for identifying safe aquifers in major As prone areas.

[1] Datta S. *et al* (2011). *Geophysical Research Letters*. **38**:2

[2] von Brömssen M. *et al* (2008). *Journal of Contaminant Hydrology* **99**:1: 137-149.

Peat and sapropel as the sources of humus for the restoration of degraded lands of the Amur region (Far East, Russia)

VARVARA KICHANOVA AND VALERY KICHANOV

Institute of Geology and Nature Management FEB RAS,
Blagoveshchensk, Russia, (barbara@mail.ru)

The natural ability of soil to produce biological products decreases each year. The problem of the land resources has become one of the largest global problems. It is connected with the growth of world population and, consequently, decrease of sown area per capita; increased area of degraded and disturbed soils. In particular, in the Amur region of degraded and disturbed lands is increasing every year. Also because of the lack of organic fertilizers, that has decreased from 63 kg/ha in 1995 to 5 kg/ha in 2011 [1]. The specific weight of fertilized area of organic fertilizers in the total sown area in 1995 was 0.5 %, in 2011 – 0.09%. Only 2% of the soils of the region (660 thousand hectares) are characterized by high soil fertility, where humus horizon reaches 20 - 40 cm sometimes 50 cm. Humus content in the upper part of the soil is from 4 up to 8%. The annual loss of humus soils of the Amur region is 0.45 tons per ha. At the same time with the loss of humus, the destruction of soil structure is mentioned, soil compaction lead to a deterioration of its physical and chemical characteristics [2]. Soil restoration is possible with the introduction of organo-mineral fertilizers produced from peat and sapropel deposits of the Amur region. The region possesses significant reserves of peat and sapropel. The total area of deposits of sapropel, in the border of the industrial depth of the deposits is 1493 ha. The total content of useful (1553 g/t) and harmful (436 g/t) elements in sapropels of Amur region in comparison with other sapropels and soils of Russia has the highest - lowest values [3]. Peat general reserves of the Amur region include 600 deposits. The total projected resources of peat, including reserves of explored fields, are 158.5 million tonnes, with 40% of the conditional humidity. Total area of the deposits is 5663.5 km² [4]. These reserves are sufficient to restore the fertility of the soils of the region.

[1] Diachenko *et al.* Amur statistical Yearbook of 2012: the Statistical collection. Blagoveschensk: Zeya. 2012. 602. [2] Pavliuk (2005) Geography of Amur region: training manual. Blagoveschensk: BGPU. 364. [3] Alekseiko *et al.* (2003) Sapropel of the Amur region: properties, production and use. Blagoveshchensk: Dalnauka. 210. [4] Vasilev *et al.* Mineral-raw material base of the Amur region at the turn of the century. (2000). Blagoveshchensk: Zeya. 168.

Ethanol Variability in Rainwater and its Impact on the Chemistry of the Troposphere

R.J. KIEBER¹, J.D. WILLEY¹, G.B. AVERY¹,
R.N. MEAD¹, F.F. GIUBBINA² AND M.L. CAMPOS²

¹University of North Carolina Wilmington, Department of Chemistry and Biochemistry, Wilmington, NC USA 28403 (*correspondence: kieberr@uncw.edu)

²Departamento de Química, Faculdade de Filosofia, Ciências e Letras de Ribeirão Preto, Universidade de São Paulo, Av Bandeirantes, 3900, 14040-901 Ribeirão Preto, SP, Brazil

We present the first detailed analysis of the occurrence and variability of ethanol in precipitation collected in coastal North Carolina (NC) USA and at the Universidade de São Paulo, Brazil. Concentrations ranged from 23 nM to 908 nM with a volume weighted average (VWA) concentration of 193 nM at the NC collection site (n=52). The VWA concentration of ethanol is more than an order of magnitude higher (2.7 µM) in Brazilian rain (n=40) relative to the NC site with the highest concentrations exceeding 10 µM. There was a great deal of variability in the abundance of ethanol between rain events at both sites driven primarily by temporal and air mass back trajectory influences.

The presence of significant quantities of ethanol in precipitation has important implications for fundamental properties of atmospheric waters including the oxidizing and acid generating capacity of the troposphere, photochemical smog formation, as well as indirect effects on solar radiative transfer and light attenuation. Also, because rainwater is an important mechanism by which CH₃CH₂OH is transported from the atmosphere to surface waters, greater wet deposition of ethanol from increasing biofuel usage could dramatically influence the biogeochemistry of receiving watersheds which typically have concentrations one to two orders of magnitude lower than rainwater.

Factors affecting fractionation of Ni and Cr in ultrabasic soils from southwestern Poland

J. KIERCZAK¹, A. PĘDZIWIATR¹, J. WAROSZEWSKI²,
AND R. TYSZKA²

¹University of Wrocław, Institute of Geological Sciences, Cybulskiego 30, 50-205 Wrocław, Poland; jakub.kierczak@ing.uni.wroc.pl, artur_pedziwiatr@op.pl

²Wrocław University of Environmental and Life Sciences, Department of Soil Sciences and Environmental Protection, CK Norwida 25/27, 50-375 Wrocław; jaroslaw.waroszewski@gmail.com, tyszkarafal@gmail.com

Weathering of ultrabasic rocks, naturally enriched in some trace elements (e.g., Ni and Cr) leads to the formation of soils having distinctive properties caused primarily by a specific chemical composition of parent rocks. The parent ultrabasic rocks commonly cause infertility of serpentine soils, which results from the low ratio of calcium to magnesium, and the high content of Ni and Cr in the parent rock and the soil.

We have analysed shallow and well drained soils (Leptosols) developed on a variety of ultrabasic rocks, from hornblende peridotite through partially serpentinized peridotite to proper serpentinite. The Ni and Cr concentrations in soils decrease upwards in analysed pedons and range from 72 to 2350 ppm for Ni and 160 to 3500 ppm for Cr. Studied ultrabasic soils have similar physicochemical characteristics (e.g., slightly acidic to neutral pH, clay content approximately 10% etc.) however mineralogical composition seems to be strongly influenced by different types of ultrabasic rocks. Soils developed on peridotites have more complex mineralogy and contain important proportions of swelling phases (smectite, vermiculite, interstratified chlorite/smectite) whereas only traces of swelling phases were detected in soil derived from serpentinite. Fractionation of Ni and Cr, estimated using the 0.05 M EDTA, aimed to determine the easily mobilizable proportions of these elements. In all studied soils proportions of Ni-EDTA extractable (5-42% of total Ni) are larger than proportions of Cr-EDTA extractable (1-7% of total Cr). The highest proportions of EDTA extractable fractions of both Ni and Cr were noted in topsoil horizons of all studied soils. Soils developed on peridotites have higher proportions of Ni-EDTA extractable than soils derived from serpentinite.

Our study shows that type of parent rock strongly influence fractionation of Ni and Cr in ultrabasic soils, however other factors (e.g., organic matter content, local climatic conditions etc.) should also be taken into account.

Residence times of ancient water in Outokumpu (Finland) revealed by noble gases

R. KIETÄVÄINEN^{1*}, L. AHONEN¹, I.T. KUKKONEN^{1,2},
S. NIEDERMANN³ AND T. WIERSBERG³

¹Geological Survey of Finland, Espoo, Finland

(* correspondence: riikka.kietavainen@gtk.fi)

²University of Helsinki, Department of Physics, Helsinki, Finland

³Deutsches GeoForschungsZentrum, Potsdam, Germany

Deep saline groundwaters in the Precambrian crystalline bedrock of Outokumpu, eastern Finland, host ecosystems that may be remarkably old. Based on water stable isotopes, these waters have been suggested to be recharged during climatic conditions up to 10°C warmer than at present, which would be indicative of residence times on the order of tens of millions of years [1].

In order to better define residence times, concentrations of radiogenic (⁴He, ⁴⁰Ar), nucleogenic (²¹Ne) and fissiogenic (¹³⁴Xe, ¹³⁶Xe) noble gas isotopes were measured in water and gas samples covering a depth range from 500 m to 2450 m in the Outokumpu Deep Drill Hole.

The observed vertical variation of geochemistry and microbiology together with hydrogeological and geophysical measurements indicate negligible fluid flow in the bedrock. Furthermore, more than 99 % of the air-corrected He is crustal in origin with an average ³He/⁴He ratio of $1.5 \cdot 10^{-8}$, and no concentration gradient indicative of diffusive flux through the crust was observed. Therefore an *in situ* accumulation model [2] using average values for porosity, density and concentrations of radioactive elements (U, Th and K) in the Outokumpu deep drill core [3] was applied to calculate residence times.

Residence times between 12 and 45 Ma are indicated by the ⁴He accumulation. Similarly, ²¹Ne and ⁴⁰Ar ages fall between 5 and 70 Ma whereas ¹³⁴Xe and ¹³⁶Xe indicate longer residence times. The results thus confirm the existence of ancient groundwaters in Outokumpu. This should be taken into account when rates of microbial metabolism, adequacy of substrates, and biological cycling of elements within the deep subsurface are considered.

[1] Kietäväinen *et al.* (2013) *Appl. Geochem.* **32**, 37-51. [2] Torgersen (1980) *J. Geochem. Explor.* **13**, 57-75. [3] Kukkonen (2011) *Geol. Surv. Finl. Spec. Pap.* **51**.

Can radioactive cesium be used as a hydrological tracer for crater lake study?

YOSHIKAZU KIKAWADA^{1*}, AYA OKAWA¹,
KO NAKAMACHI², TERUYUKI HONDA², TAKAO OI¹
AND KATSUMI HIROSE¹

¹Sophia Univ., Tokyo 102-8554, Japan.

(*correspondence: y-kikawa@sophia.ac.jp)

²Tokyo City Univ., Tokyo 158-8557, Japan.

The Fukushima Dai-ichi Nuclear Power Plant (FDNPP) accident in March 2011 resulted in serious radiological contamination in areas adjacent to the plant. Meanwhile, radioactive cesium originated from the accident was detected over a wide range of the northeastern half of Honshu, the main island of Japan. In this study, we discuss the possible use of radioactive cesium newly deposited on the ground from the FDNPP accident as a hydrological tracer for crater lake study in Japan, taking crater lakes of the Kusatsu-Shirane volcano, located about 240 km west-southwest from the FDNPP, for example. Water budget of crater lakes, especially on active volcanoes, is very complicated, because most of them are closed ones. The budget and circulation of water in active crater lakes provide very important information connected to the hydrothermal activities and subsurface structures of the volcanoes.

The Kusatsu-Shirane volcano with three crater lakes on its summit area is one of the most famous active volcanoes in Japan. Yugama, the largest and deepest one among the three is well known as an active crater lake filled with water of high salinity and strong acidity. We determined the contents of radioactive isotope of cesium, ¹³⁴Cs and ¹³⁷Cs, and the stable isotope, ¹³³Cs, and their content ratios in waters of three crater lakes of the Kusatsu-Shirane volcano collected in 2012. The obtained activity ratio of ¹³⁴Cs/¹³⁷Cs revealed that the radioactive cesium released by the accident has reached the summit area of the volcano. However, the concentration of radioactive cesium was not uniform among the three crater lake waters. This nonuniformity is most probably ascribable to the difference in the water supply and circulation system among the three. This suggests that the temporal changes in the concentration of radioactive cesium and their concentration ratios against the stable isotope can provide us useful information to clarify the water budget in the summit area of the Kusatsu-Shirane volcano. In this context, we are now investigating the temporal changes in the concentrations of ¹³⁴Cs, ¹³⁷Cs and ¹³³Cs in the crater lakes.

High-resolution imaging and quantification of Au in sulphide minerals using NanoSIMS

M.R. KILBURN^{1*} AND R. LIU¹

¹Centre for Microscopy, Characterisation and Analysis, The University of Western Australia, Crawley, 6009, Australia (*correspondence: matt.kilburn@uwa.edu.au)

With its high lateral resolution and high sensitivity, NanoSIMS is the ideal tool for mapping the distribution of trace elements within sulphide minerals. In Carlin-type deposits, Au is typically present as narrow rims along the edges or within the matrix of the sulphide grains. The low concentrations of Au in solid solution with the sulphide are notoriously difficult to detect by most in situ techniques, such as EPMA, and is thus commonly referred to as 'invisible gold'. As SIMS is very sensitive to Au, and other commonly associated trace elements such as Te and Sb, NanoSIMS provides the ability to image these elements with sub-micron resolution. At such scales it is possible to investigate the intricate relationships between the Au and associated elements to help determine the nature and evolution of the Au-bearing fluids [1]. Furthermore, through the development of ion-implanted standards, it is possible to quantify the concentration of Au directly from the NanoSIMS secondary ion images. Preliminary data also show the potential to obtain S isotope measurements from the same regions of interest.

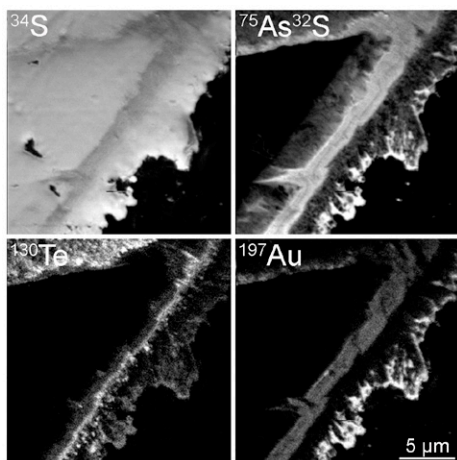


Figure 1: Secondary ion images showing the distribution of S, As, Te and Au in a pyrite grain from a Carlin-type deposit.

[1] Barker *et al.* (2009) *Econ. Geol.* **104**, 897-904.

Investigating the role of noble gases as tracers for CO₂ storage

R. KILGALLON^{1*}, S.M.V. GILFILLAN¹,
C.I. MCDERMOTT¹ AND K. EDLMANN¹

¹School of GeoSciences, The University of Edinburgh, King's Buildings, Edinburgh, EH9 3JW (*correspondence: Rachel.Kilgallon@ed.ac.uk)

The capture and long term storage of carbon dioxide (CO₂) in the subsurface is one of the most promising ways of mitigating the current level of anthropogenic CO₂ being released to the atmosphere. A major issue surrounding long term storage is the risk of failure of CO₂ containment. Developing a monitoring strategy which would allow early detection of CO₂ leakage would enable measures to be implemented to mitigate and remediate the impact of containment failure. Experiments and modelling results have shown that noble gases have the potential to act as early warning tracers for CO₂ arrival [1]. Previous studies highlight the importance of understanding the transport processes involved for calculating tracer arrival times [2].

This study uses specially constructed equipment for experiments to determine factors affecting the transport of noble gases relative to CO₂. Initial pipeline experiments using argon and CO₂ have determined the parameters required for complete mixing of the gases.

We intend to examine conservative transport processes such as the advection, dispersion and diffusion of noble gases relative to CO₂ in porous media. The existence of any non-conservative transport processes such as sorption and dissolution are also considered. These data are compared to results from core flow experiments in order to determine the relationship between CO₂ and noble gases on rock core samples. The choice of sample used for experiments are low permeability porous sandstones.

Preliminary data will establish how noble gases and CO₂ behave in porous media during migration. Upscaling of the initial results will determine how effective different noble gases could be at acting as early warning tracers in a real world storage site.

[1] Cohen *et al.* (2013) *International Journal of Greenhouse Gas Control* **14**, 18-140. [2] Carrigan *et al.* (1996) *Nature* **382**, 528 – 531.

Antimony in hydrothermal chimneys of Kolumbo shallow-submarine vent field (Santorini, Greece)

S.P. KILIAS^{1*}, A. GODELITSAS¹, P. GAMALETSOS¹²,
T.J. MERTZIMEKIS¹, P. NOMIKOU¹, J. GÖTTLICHER²,
R. STEININGER², A. ARGYRAKI¹, M. GOUSGOUNI¹
AND D. PAPANIKOLAOU¹

¹University of Athens, School of Science, 15784 Zographou, Greece (*correspondence: kilias@geol.uoa.gr)

²KIT, ANKA Synchrotron Radiation Facility, Hermann-von-Helmholtz-Platz 1, 76344 Eggenstein, Germany

Polymetallic sulfide/sulfate chimneys, collected during the NA014 expedition of the E/V *Nautilus* (2011) from the Kolumbo shallow-submarine hydrothermal field (Santorini, Greece), are exceptionally enriched in antimony (up to 2.2 wt%) [1]. SEM-EDS data show that colloform banded trace-element-rich zoned possibly biogenic Fe-sulfides show oscillatory zoning; zones "bright" in BSE are enriched in Sb (up to 11 wt%), and/or Pb, As and Si. However, preliminary SR μ -XRF elemental maps confirmed that Sb is mostly concentrated in the core relative to rim (Fig. 1).

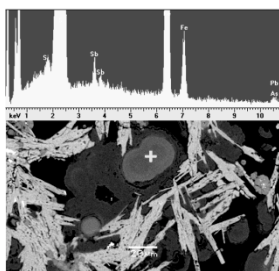


Figure 1. Colloform banded masses of amorphous trace-metal rich Fe-sulfides surrounded by barite blades

Subsequent μ -XAFS spectra, in micro-areas with accumulated Sb, have indicated a possible dominance of the relatively more toxic trivalent species (Sb^{3+}) rather than pentavalent species (Sb^{5+}) forms [2]. It is known that pyrites may accommodate Sb-ions and Sb-sulfosalt nanoparticles [3], but there are no particular studies on the nature of Sb in amorphous Fe-sulfides from recent submarine hydrothermal fields, unless stibnite is formed. Future work will include further evaluation and upgrading of the SR data in combination with microscopic investigation in nanoscale.

[1] Kilias *et al.* *Sci Rep* (2013-under review), [2] Filella *et al.* *Earth-Sci. Rev.* **80** (2007) 195, [3] Deditius *et al.*, *Ore Geol. Rev.* **42** (2011) 32

Statistical Approach and Heavy Metal Analyses of Konyaalti (Antalya, Turkey) Coast Water

S. KILIC¹, F. YALCIN² AND M.G. YALCIN^{3*}

¹Akdeniz University, Ar-Ge Lab, 07058, Antalya, Turkey, (serpilkilic@akdeniz.edu.tr)

²Akdeniz University, Department of Mathematics, 07058, Antalya, Turkey, (fusunyalcin@akdeniz.edu.tr)

³Akdeniz University, Department of Geological Engineering, 07058, Antalya, Turkey, (gurhanyalcin@akdeniz.edu.tr)

The aim of the study conducted on Konyaalti (Antalya) coast, which is one of the important coasts of Turkey, is to determine the heavy metal (Ni, As, Cr, Pb, Cd, Cu) contents in the seawater along the coastline. In this study samples were taken systematically from 35 different coastal locations. According to the EPA method 3005A (EPA 3005A, 1992), pre-treatment was applied. The fact that the seawater is rich in the elements such as Na, Ca, Cl posed a problem of contamination. Coal gas was used to prevent the contamination (e.g. $^{40}Ar+^{35}Cl-^{75}As$). DRC (Dynamic Reaction Cell) method was applied firstly with %0.1 NaCl solution as being a matrix, then by spiking As so that it is to be 20 ppb into %0.1 NaCl solution. According to the recovery data, measurements were analyzed in the ICP-MS device by using EPA method 6020A (EPA 6020A, 1997). Calibration curve (R^2) chart was drawn with the standards of 2, 5, 10, 15, 25, 50 and 100 ppb from 100 ppm VHG multi-element standard. These values were between 0.9999-0.9993 through the whole study. In the recovery process the minimum and maximum values of the 6 spikes are as follows: As (14.152 - 16.415), Pb (14.540-16.483), Ni (14.719-16.621), Cr (15.498 - 16.937), Cu (14.999-16.138), Cd (14.349-15.844). According to this, the mean percentage values of the recovery were calculated as As (%101), Pb (101), Ni (104), Cr (108), Cu (101), Cd (99). The values were determined as <2 ppb in the locations of 7, 8, 10, 13, 19, 28 and 31 for As; 3, 6-8, 10, 13, 14, 18, 19, 21, 23-27, 29-34 for Pb; 1-3, 5, 6, 8-27, 29-35 for Ni; 3, 5-8, 10, 11, 13, 18-20, 22, 24-26, 30, 31 for Cu; 2, 7, 9-16, 18, 19, 21-27, 29-35 for Cd. Maximum values were observed in the stations numbered 35 (11.19 ppb) for As; 4 (75.44 ppb) for Pb; 28 (61.3) for Ni; 5 (114.82 ppb) for Cr; 9 (65.15 ppb) for Cu; 4 (243.63 ppb) for Cd. It is thought that there is an anthropogenic effect especially in the locations numbered 4, 5 and 9.

[1] US Method EPA 3005 A, 1992, Acid Digestion of Waters for Total Recoverable or Dissolved Metals for Analysis by FLAA or ICP Spectroscopy, Revision 1, [2] US Method EPA, 6020 A, 1997, Coupled plasma mass spectrometry, Revision 1.

Petrology and geochemistry of mafic and ultramafic metamagmatic rocks emplaced within the anatectic series of the middle crust of the Variscan Pyrenees: example of the Gavarnie-Heas dome, West Pyrenees

M. A. KILZI¹, M. GREGOIRE¹, M. BENOIT¹, P. DEBAT¹,
M. ST. BLANQUAT¹ AND Y. DRIOUCH²

¹Laboratoire de Géosciences Environnement Toulouse,
Observatoire Midi Pyrénées, Université Paul-Sabatier,
CNRS, IRD, 14, Avenue Edouard Belin 31400 Toulouse
michel.gregoire@get.obs-mip.fr

²Département de Géologie, Université de Fès, Maroc

Within the anatectic formations of the middle crust of the Variscan Pyrenees occur in some massifs (Alberes, Aston, Trois Seigneurs, Lesponne...) ultramafic and mafic rocks forming polymetric or plutons mileage enclaves. The most significant example is the Héas Gavarnie Dome in the Western Pyrenees. Within this dome of metasedimentary formations affected by a common anatexis (peak conditions at around 730 °C and 4.3 kb) the mafic and ultramafic series form three massifs: the Troumouze massif in the south, mostly made of diorites; the Aguila massif consisting of diorites which contains some hornblende enclaves; the Gloriette massif, consisting of diorites and norites associated with ultramafic rocks (orthopyroxenites and hornblendites). All of these rocks are affected by variable degrees of metamorphism resulting in the development of secondary amphibole and biotite and cross cutted by a network of granitic bodies.

Petrological and geochemical studies show that these rocks mostly correspond to a basic metamagmatic series with a calc-alkaline affinity and characterized by enriched REE (432 ppm) contents, and REE fractionation processes ($(La/Yb)_N = 7.5$; $(La/Sm) = 2.5$ and $(Gd/Yb) = 1$). They have positive Eu anomalies ($Eu/Eu^* = 3.5$) and the following trace element characteristics: (1) enrichments in U; (2) Nb and Sr depletion; and (3) large positive Pb anomalies. $^{87}Sr/^{86}Sr$ isotopic ratios of mafic and ultramafic rocks range from 0.7045 to 0.7117 and ϵNd from -5.2 to -10.5. These signatures are typically crustal and show that these rocks have preserved the isotopic fingerprints of lower crustal magmatic processes

Interpretation of hydrochemistry data using Bayesian statistical approaches to delineate groundwater contamination vulnerability

HO-RIM KIM¹, KYOUNG-HO KIM¹, KYUNG-GOO KANG²,
SOO-HYUNG MOON² AND SEONG-TAEK YUN^{1*}

¹Korea University, KU-KIST Green School and the
Department of Earth and Environmental Sciences, South
Korea, styun@korea.ac.kr (* correspondence)

²Jeju Special Self-Governing Province Development
Corporation, Jeju, South Korea

Well understanding of the source(s) and landuse control of groundwater contamination is highly needed to better manage groundwater quality. In this context, we performed the interpretation of hydrochemical data of groundwater using the Bayesian statistical method in conjunction with a GIS technique to produce a spatial map showing groundwater vulnerability to contamination. In particular, we used the Weight of Evidence (WofE) method (a Bayesian probabilistic model) and relevance vector machine (RVM) regression (a Bayesian machine learning technique) that was recently developed to find out the correlations among factors influencing the occurrence of groundwater contamination. Hydrochemistry data of 46 groundwater samples from the Pyosun watershed of Jeju volcanic island, South Korea were used, because the groundwater system has been considered to be highly susceptible to surface contamination (esp., agricultural pollution) because of the short residence time in permeable basaltic aquifer.

For the combined use of WofE and RVM, hydrochemistry data were evaluated using multivariate analyses to get the initial information whether a sample is contaminated or not. The results of Principal component analysis (PCA) and Hierarchical Cluster Analysis (HCA) showed a good spatial control of hydrochemistry data in relation to the topography within the watershed. In the next step, we estimated the correlation between topography data and the results of a binary classification from multivariate analyses. The results using Bayesian statistical techniques could predict the contamination vulnerability. Thus, the integrated method developed in this study can be successfully used for evaluating the groundwater vulnerability.

Use of risk-based remediation strategy and concept of attainable clean-up level in management of groundwater contaminated sites in Korea

HUN-MI KIM^{1*}, SEONGSUN LEE¹, DUGIN KAOWN¹
AND KANG-KUN LEE¹

¹School of Earth Environmental Science, Seoul National University, Seoul 151-747, Korea (*correspondence : tweety1@snu.ac.kr), soon3311@snu.ac.kr, dugin1@snu.ac.kr, kklee@snu.ac.kr

There are recognized needs to establish a reliable and effective remediation strategy as groundwater and soil protection from DNAPL (dense non-aqueous phase liquid) contamination is one of the critical issues in Korea. Remediation performance results at DNAPL contaminated field sites have shown that achieving groundwater clean-up is very difficult due to the complexity of site characterization and contaminants (DNAPL). Therefore, a new approach is now necessary to determine the reachable clean-up level and control the groundwater contaminated sites with DNAPLs. Our research team initiated a 5-year GAIA (Geo-Advanced Innovative Action) project to intensively monitor the DNAPL contaminated site with a focus on developing clean-up options under support of Korea Ministry of Environment (KMOE). Woosan industrial complex was chosen as our field site and 16 rounds of groundwater sampling at about 90 monitoring wells were performed from 2009 to 2013. The highest concentration of trichloroethylene (TCE) which was the main pollutant in the source area of this site was 15 mg/L. According to field monitoring data and hydrogeologic condition, Risk Based Corrective Action (RBCA) program and variable remediation technologies such as soil vapor extraction, pump-and-treat, surfactant enhanced in-situ remediation, in-situ bioaugmentation and Monitoring Natural Attenuation (MNA) were performed. As a result of our field site application, we propose the following step by step- remediation strategy. The 1st step is implementation of site-specific characterization and risk-based site assessment and 2nd step is application of the chosen remediation technologies to enhance the attenuation, plume capture and mass reduction in source zone based on the 1st step result. The 3rd step is establishment of an attainable clean-up level considering the results of mass reduction when there is no further contaminant exposures and plume migration and the final step is application of the MNA until the final clean-up level of groundwater remediation is achieved.

Combined use of ED-EPMA and ATR-FTIR imaging for characterization of individual aged Asian Dust particles

HYEKYEONG KIM, HAE-JIN JUNG, HYO-JIN EOM,
XUE LI AND CHUL-UN RO

Department of Chemistry, Inha University, 253 Yonghyun-dong, Nam-gu, Incheon, 402-751, KOREA and curo@inha.ac.kr

In our previous works, it was demonstrated that the combined use of quantitative energy-dispersive electron probe X-ray microanalysis (ED-EPMA), which is also known as low-Z particle EPMA, and attenuated total reflectance FTIR (ATR-FTIR) imaging has great potential for a detailed characterization of individual aerosol particles. In this study, extensively chemically modified (aged) individual Asian Dust particles collected during an Asian Dust storm event on November 11, 2002 in Korea were characterized by the combined use of low-Z particle EPMA and ATR-FTIR imaging. Overall, 109 individual particles were classified into four particle types based on their morphology, elemental concentrations, and molecular species and/or functional groups of individual particles available from the two analytical techniques: Ca-containing (38%); NaNO₃-containing (30%); silicate (22%); and miscellaneous particles (10%). Among the 41 Ca-containing particles, 10, 8, and 14 particles contained nitrate, sulfate, and both, respectively, whereas only two particles contained unreacted CaCO₃. Airborne amorphous calcium carbonate (ACC) particles were observed in this Asian Dust sample for the first time, where their IR peaks for the insufficient symmetric environment of CO₃²⁻ ions of ACC were clearly differentiated from those of crystalline CaCO₃. This paper also reports the first inland field observation of CaCl₂ particles probably converted from CaCO₃ through the reaction with HCl(g). HCl(g) was likely released from the reaction of sea salt with NO_x/HNO₃, as all 33 particles of marine origin contained NaNO₃ (no genuine sea salt particles were encountered). Some silicate particles with minor amounts of calcium were observed to be mixed with nitrate, sulfate, and water. Among 24 silicate particles, 10 particles are mixed with water, the presence of which could facilitate atmospheric heterogeneous reactions of silicate particles including swelling minerals and non-swelling ones. Using the combined use of the two single particle analytical techniques, this work clearly shows that internal mixing states of the aged Asian Dust particles are highly complicated.

Chemical evolution of perched groundwater flowing through weathered bedrock underlying a steep forested hillslope, northern California

HYOJIN KIM^{1*}, JAMES K.B. BISHOP^{1,2}
WILLIAM E. DIETRICH¹ AND INEZ FUNG¹

¹University of California, Berkeley Dept. Earth and Planetary Science, 307 McCone Hall, Berkeley CA94709
hyojin820@berkeley.edu

²Earth Science Division, Lawrence Berkeley National Laboratory, 1 Cyclotron Road, MS 90-1116, Berkeley CA 94709, USA

At the ~4000 m² Rivendell study site on a 30° hillslope underlain by argillite along the South Fork Eel River, we have monitored the chemistry of rainfall and of groundwater that seasonally perches on dense, fresh bedrock (5 to 20 m below the surface) and flows through a weathered bedrock zone to an adjacent channel. This is a part of a collaborative study focused on coupling hydrologic, geochemical, ecological, and atmospheric processes. Water samples were collected every 1 to 3 days for five years from three wells: upslope (Well 10), mid-slope (Well 3), and downslope (Well 1).

At the beginning of the rainy season Well 10 groundwater is deep with a constant high concentration of major cations (Ca, Mg, and Na). New water arriving from seasonal storms causes water-table rise (4 to 6 m), and systematic dilution until rising water levels reach a new, significantly diluted constant value. Surprisingly, however, Si shows an opposite response and increases in concentration with rising water level. Well 3 response is generally similar. Well 1 behaves differently: its water-table is highly responsive to rainfall inputs, but its chemistry shows no significant change, except briefly during rainstorms.

Our data suggests that the deeper groundwater flow which is highly concentrated is in thermodynamic equilibrium with the argillite. Seasonal rainwater passes quickly through the soil and weathered bedrock where it rapidly uptakes major cations via cation exchange reactions and Si through amorphous silica dissolution. PCO₂ is highly elevated due to biological activity. Intensive biological activities in this layer increase the rate of mineral dissolution and thus continuously replenish exchangeable cations and the amorphous silica pool.

Ship-plume sulfur chemistry: ITCT 2K2 case study

HYUN S. KIM¹, YONG H. KIM¹ AND CHUL H. SONG^{1,*}

¹School of Environmental Science and Engineering, Gwangju Institute of Science and Technology, 1 Oryong-dong, Buk-gu, Gwangju 500-712, Republic of Korea

The ship-plume sulfur chemistry was investigated for the ITCT 2K2 (Intercontinental Transport and Chemical Transformation 2002) ship-plume experiment, using the ship-plume photochemical/dynamic model developed in this study. In order to evaluate the performance of the model, the model-predicted mixing ratios of SO₂ and H₂SO₄ were compared with those observed. From these comparisons, it was found that the model-predicted levels were in reasonable agreements with those observed ($0.56 \leq R \leq 0.71$), when the pH of sea-salt particles (pH_{ss}) was $\leq \sim 6.5$. The ship-plume equivalent lifetimes of SO₂ ($\tau_{SO_2}^{eq}$) were also estimated/investigated for this particular ship-plume case. The magnitudes of $\tau_{SO_2}^{eq}$ were found to be controlled by two main factors: (i) the mixing ratios of in-plume hydroxyl radicals (OH) and (ii) pH_{ss}. The former is governed primarily by stability conditions of the marine boundary layer (MBL), when the ship NO_x emission rate is fixed. The latter determines if the heterogeneous oxidation of dissolved SO₂ occurs via reaction with hydrogen peroxide (H₂O₂, when pH_{ss} < 6.5) or with ozone (O₃, when pH_{ss} > 6.5). According to the multiple ship-plume photochemical/dynamic model simulations, the estimated $\tau_{SO_2}^{eq}$ over the entire ship plumes ranged from 10.32 to 14.32 hrs under moderately stable (E) to stable (F) MBL conditions. These values were clearly shorter than the background SO₂ lifetime ($\tau_{SO_2}^b$) of 15.18- 23.20 hrs. In contrast, $\tau_{SO_2}^{eq}$ was estimated to be 0.33 hrs when the pH_{ss} remained at ~ 8.0 (a rather unlikely case). In addition, the SO₂ loss budget was further analyzed to estimate the influences of the two main factors on the ship-plume sulfur chemistry. The changes in the loss budget with pH_{ss} clearly showed a shift in the dominant SO₂ loss processes from heterogeneous SO₂ conversion (when pH_{ss} > 6.5) to the gas-phase oxidation of SO₂ by OH (when pH_{ss} < 6.5).

Acknowledgements. This work was financially supported by the Basic Science Research Program through the National Research Foundation of Korea (NRF) grant from the Ministry of Education, Science and Technology (MEST) (2012R1A1A2041481).

Mineralogical characterization of tremolite asbestos-containing soils

JUHYUN KIM^{1*}, JAEBONG PARK², SECKWHAN SONG³,
HOJU LIM⁴ AND YUL ROH⁵

¹Chonnam National University, Gwangju, South Korea,
fawkes3@hanmail.net

²Chonnam National University, Gwangju, South Korea,
20548pjb@chonnam.ac.kr

³Joongbu University, Chungnam, South Korea,
shsong@joongbu.ac.kr

⁴National Institute of Environmental Research, Incheon, South
Korea, limhoju@gmail.com

⁵Chonnam National University, Gwangju, South Korea,
rohy@jnu.ac.kr

Asbestos-containing soils occur mainly at ultramafic rocks and hydrothermally altered carbonate rocks in S. Korea. Remediation of asbestos-containing soils is considered a high priority by the Korean Government because these soils, if left untreated, represent a hazard to the environment and human health. The objective of this study was to show a priori physicochemical and mineralogical characterization of asbestos-contaminated soil can direct the development of remediation strategies.

Two sites (Seosan and Jaechon, S. Korea) at abandoned asbestos mines were selected for soil and mineralogical characterization. Parent rock of the two sites is hydrothermally altered carbonate rocks in S. Korea. At each site, samples were taken at soil surface. Soil preparation consisted of sieving air-dried soil through a 2-mm sieve. The sieved soils (< 2-mm) were used for soil characterization and mineralogical analysis. Following particle size fractionations, mineralogical characterization was investigated by TG-DTA, XRD, PLM, SEM and EDS analyses. Point counting was used to quantify asbestos in the whole soil and size fractionated samples.

The soil color of the both sites was dark red (Seosan site) and dark brown (Jaechon site). The soil texture of the Seosan and Jaechon sites was loam and sand, respectively. XRD analysis showed mineral assemblages of the Seosan and Jaechon site were tremolite-talc-vermiculite-quartz-diopside and tremolite-talc-vermiculite-quartz-dolomite, respectively. XRD, PLM, SEM and EDS analyses showed that the needle-shaped tremolite was observed at both soils. Size fraction between 425 μm to 2mm of the Seosan and Jaechon soils contained 1.5 % and 2 % asbestos, respectively. Therefore, the soils of the both sites were designated as asbestos-containing materials (greater than or equal to 1%) according to the criteria of the U.S. EPA. TG-DTA showed that tremolite asbestos at both soils were transformed to diopside with the temperatures about 1,100°C. These results indicated that thermal treatment of asbestos-containing soils was effective for phase transformation of the asbestos in soils.

Mineralogical and geochemical characteristics of the Korean coal ashes from the perspective of the coal and combustion types

KANGJOO KIM^{1*}, GI-YOUNG JEONG AND JAE-CHUL LEE³

¹Department of Environmental Engineering, Kunsan National
University, Jeonbuk, 573-701, Korea
(correspondence: kangjoo@kunsan.ac.kr)

²Department of Earth and Environmental Sciences, Andong
National University, Kyeongpook, 760-749, Korea

³Korea Western Power Co. Ltd., Seoul, 135-984, Korea

Fly ashes produced from 9 coal burning power plants in Korea were investigated to see the changes in mineralogical and geochemical characteristics according to the coal types and combustion methods. Our results indicate that the mineralogical and geochemical features of the fly ashes are more dependent on the combustion methods than the coals used. Five and two out of the nine investigated plants were originally constructed to burn bituminous (or subbituminous) coals and anthracite coals, respectively, by applying pulverized coal firing system. The remaining two plants burn anthracite or bituminous coals together with fine sand-sized limestone grains using the fluidized bed combustion method. According to the SEM and XRD investigation, it was revealed that spheres, mullite, and glasses were absent and sometimes illite, a clay mineral, was present in the fly ashes produced from the plants of the fluidized bed combustion method due to the low combustion temperature (800 - 850 °C). These ashes particularly contains calcite and anhydrite phases due to the co-combustion of limestone grains. The high temperature phases such as mullite and glass were observed in all the ashes of the pulverized coal firing plants. However, their contents were generally higher in the fly ashes of the pulverized anthracite coal burning plants. This is due to their higher combustion temperatures (1200 – 1500 °C) than those of the bituminous or subbituminous coal burning plants (1200 – 1300 °C). The chemical composition of the ashes also reflected the combustion methods.

Estimation of POC and Biogenic silica export fluxes using $^{234}\text{Th}/^{238}\text{U}$ disequilibrium in the Amundsen sea, Antarctic

MI SEON KIM¹ MAN SIK CHOI^{1*} AND SANG HEON LEE²

¹Chungnam National University, Daejeon, Korea
seonkim@cnu.ac.kr (*correspondence : mschoi@cnu.ac.kr)

²Pusan National University, Busan, Korea
sanglee@pusan.ac.kr

In order to understand the carbon cycle in the Amundsen Sea, the Antarctic, the export fluxes of organic carbon and biogenic silica from the euphotic zone to depth were estimated using $^{234}\text{Th}/^{238}\text{U}$ disequilibrium method. Seawaters in 14 water columns were collected during February and March 2012, and analyzed for total and dissolved ^{234}Th , and particulate organic carbon and biogenic silica.

The water column activities of total ^{234}Th showed deficiency and excess relative to those of ^{238}U . Deficiency of total ^{234}Th in the euphotic zone showed mirror images both with chlorophyll-a and fluorescence, and was consistent with the loss of nitrate, which indicated the impact of biological activity. In addition, deficiency of total ^{234}Th from deepwater was associated with the increase of total Fe/Mn concentration. Excess total ^{234}Th activity presented below the euphotic zone might be related to the active remineralization process.

The export flux of ^{234}Th estimated using the steady state model was av. $0.87 (\pm 0.25) \times 10^3 \text{dpm/m}^2/\text{day}$. The export fluxes of organic carbon and biogenic silica, which were estimated by the product of total ^{234}Th flux and ratio of $\text{POC}/^{234}\text{Th}$ ($7.08 \pm 4.27 \mu\text{M}/\text{dpm}$) and $\text{BSi}/^{234}\text{Th}$ ($0.80 \pm 0.36 \mu\text{M}/\text{dpm}$) in the sinking particles, were av. $5.85 (\pm 2.42) \text{mmol/m}^2/\text{day}$ and $0.69 \text{mmol/m}^2/\text{day}$, respectively. These fluxes were similar levels to those in the Weddell Sea during February and March 2008. Export ratios (ThE) relative to the primary production in the euphotic zone were in the range of 3~50% (av. 27.8%), which indicated less efficiency in the biological pump than the Ross sea during January and February 1997.

[1] Cochran *et al* (2000), *Deep-Sea Research II* **47**, 3451-3490. [2] Rutgers van der Loeff *et al* (2011), *Deep Sea Research Part II* **58** (25-26): 2749-2766.

Variation of As-leaching from coal ashes according to extractant pH, reaction time, and shaking methods

SEOK-HWI KIM, BYUNG-HYO KIM, KANGJOO KIM*,
BYUNG-GON JEONG AND SEUNG-HYUN CHOI

Department of Environmental Engineering, Kunsan National University, Jeonbuk, 573-701, Korea
(*correspondence: kangjoo@kunsan.ac.kr)

In this study, the leaching characteristics of arsenic (As) from the weathered coal ashes (fly ash + bottom ash mixture), which have been reclaimed in an ash pond of a power plant, and the fresh fly ashes were evaluated using various leaching experiments. The As-leaching experiments were performed considering extractant pH (5, 7, and 9), shaking methods, and extraction time as variables. Especially, the ashes were extracted repeatedly using new extractant to observe the leaching characteristics as a function of time. The As concentration in the fresh fly ash was 16.1 mg/kg. In contrast, the weathered coal ashes showed the lower concentrations 5.77-10.0 mg/kg, reflecting that a part of As already has been leached by the reaction with the pond water. The weathered ashes showed the more As leaching at lower pH, indicating that the contribution from the carbonate-bound fraction becomes greater as the pH becomes acidic. The As leaching decreases drastically as the reaction time increases. Our results also show that the As-leaching is dependent not only on the shaking speeds and stroke distances but also on the bottom areas of the reaction bottles. For example, the As-leaching was greater when the bottles with wider bottom were used even at the same shaking speed and stroke distance.

Characterization of the primary productivity using a year-long high resolution sediment trap experiment in the southwestern part of the East/Japan Sea

S.H. KIM*, G.H. HONG, Y.I. KIM, C.S. CHUNG, K.Y. CHOI AND Y.H. KIM

¹Korea Institute of Ocean Science & Technology, Ansan, R.Korea 426-744 (*correspondence: shkim@kiost.ac)

The southwestern East/Japan Sea is one of the world's most productive fishing grounds that is readily visible from the space born satellite's day-night band due to bright lights emitted from dense assemblage of fishing fleet. Traps were deployed to collect sinking particles in the depths of 1,020 m and 2,100 m at the inter-plain gap between Ulleung and Dok islands (37°25.77'N, 132°30.27'E, 2300 m) in 1999 with shorter than 10 days sampling interval. The water temperature and current at 350 m depth using RCM 7 at the site adjacent to the sediment trap mooring site were also utilized to aid our data analysis.

This high resolution temporal observations showed many important characteristics related to the productivity of the southwestern East/Japan Sea: 1) Ulleung Warm Eddy enhanced primary productivity as evidenced by a simultaneous variation in water temperature at 100 m and particulate organic carbon fluxes at 1,020 m depth.; 2) Siliceous phytoplankton species dominated spring and autumn blooms. The ratio of biogenic silica flux to particulate organic carbon flux increased during these two seasons; 3) Calcareous productivity was observed during August when surface water temperature was the highest when the ratio of calcium flux to aluminum flux peaked its maximum; 4) Small sized primary producers such as nano- or pico- plankton dominated in summer. Dissolution of sinking particulate organic carbon appeared to be great in the water column between 1,020 m and 2,100 m compare to other seasons; 5) Nitrogen fixer appeared to contribute to comparable high productivity during the apparent N-poor oligotrophic summer and the ratio of particulate organic carbon to particulate nitrogen was relatively high compared with that in other seasons.

Determination of picomolar Zn in seawater of the North and South Pacific with clean sampling methods

T. KIM^{1*}, T. GAMO¹ AND H. OBATA¹

¹Atmosphere and Ocean Research Institute, The University of Tokyo, 5-1-5 Kashiwanoha, Kashiwa-shi, Chiba 277-8564, Japan (*tjkim@aori.u-tokyo.ac.jp)

Zinc (Zn) is an essential micronutrient for bacteria and phytoplankton in the ocean. However, biogeochemical cycles of Zn have not been fully revealed yet in the ocean since determination of Zn in seawater is very difficult because of contamination problems [1]. We have established a precise determination method of picomolar level of Zn in seawater using recent clean technique. Using this method, vertical distributions of Zn were investigated.

Seawater samples were collected in the subtropical North, South Pacific and subarctic North Pacific during the R.V. Hakuho-Maru research cruises. We used Teflon-coated X-Niskin bottles, which were thoroughly cleaned with detergent, acid, and milli-Q water. Zn in seawater was determined by cathodic stripping voltammetry after UV-digestion.

We have compared three different seawater sampling methods. Teflon-coated X-Niskin samplers were 1) deployed on CTD-CMS, 2) attached to Kevlar wire and 3) attached to titanium wire. Because Zn is used as sacrificial anode in the research vessel, especially around main propellers of the Hakuho-Maru, Zn contamination was observed during Kevlar wire hydrocasts that were performed from the stern of the vessel. By minimizing the influence from the propellers, we obtained almost the same Zn concentrations within the analytical error among those three different sampling methods. In the subarctic North Pacific, surface Zn concentrations showed the decrement from west to east, indicating that high eolian dust inputs from the Asian deserts may contribute to relatively high Zn concentration in western North Pacific [2].

[1] Fitzwater *et al* (1982) *Limnology and Oceanography* **27**, 544-551 [2] Jakuba *et al* (2012) *Global Biogeochemical Cycles* **26**, GB2015.

Characterization of the white precipitates found in acid mine drainage

YEONGKYOO KIM*, CHANG-MIN LEE
AND HAE-YONG GWAK

Department of Geology, Kyungpook National University,
Daegu 702-701, Korea, ygkim@knu.ac.kr

The mobility of heavy metals released from acid mine drainage can be controlled by sorption on the iron and aluminum precipitates. There have been plenty of reports on the iron precipitates found in acid mine drainage. However, the white precipitates, mainly composed of aluminum, have not been thoroughly investigated. Previous study have reported hydrobasaluminite and gibbsite as possible phases. Recently Al_{13} -tridecamer was suggested as a possible aluminum phase in precipitates. We used chemical analysis, XRD, SEM, NMR, and sequential extraction method to characterize the white precipitates collected at three different sites.

XRD and SEM data show that most white precipitates are amorphous with small amount of gypsum. ^{27}Al MAS NMR spectra provide more detailed information on the aluminum species in precipitates, showing that there are 4- and 6-coordinated aluminums in the samples. The aluminum with 4-coordination can be assigned to Al_{13} -tridecamer, which has been known as one of the most toxic aluminum species. The calculations based on chemical and ^{27}Al MAS NMR data, show that the relative amounts of Al_{13} -tridecamer, hydrobasaluminite, gibbsite and gypsum are different for each sample. The results of sequential extraction experiment also show that each sample has different aluminum and heavy metal fractions, indicating that the toxicity caused by aluminum and heavy metals can be different for each sample. Sequential extraction results show that one sample (S-1) has higher water soluble fraction and sorbed and exchangeable fraction of aluminum than other samples. However this sample does not contain Al_{13} -tridecamer based on NMR data, indicating that careful characterization of white precipitates is needed to estimate the toxicity of aluminum of white precipitates found in acid mine drainage.

Sorption Behavior of Mercury (Hg) on Hydroxylapatite

YOUNGJAE KIM¹ AND YOUNG JAE LEE^{1*}

¹Department of Earth and Environmental Sciences, Korea University, Seoul 136-701, Korea (*Correspondence: youngjlee@korea.ac.kr)

Hydroxylapatite (HAP) has been known to be ubiquitous in various environments. Mercury (Hg) is notorious in ecosystems including humans due to its toxicity. Nevertheless, Hg interactions with HAP has been barely addressed yet. In this study, systematic batch experiments were conducted to investigate Hg sorption on HAP over a wide range of physicochemical conditions such as pH, ionic strengths, and ligands forming complexes.

Hg sorption increases with increasing pH up to pH 6.0 whereas the sorption decreases with pH at $pH \geq 7.0$. This result is in good agreement with species modeling calculation showing that $Hg(OH)_2^0$ is dominant at neutral and basic pHs. It is found that Hg sorption on HAP increases with increasing Hg concentration. At pH 5.0 and 7.0, Hg uptake by HAP steeply increases up to $[Hg]_{ini} \leq 10 \mu M$, and then gently increases at higher concentration. At pH 9.0, however, the Hg sorption on HAP shows linear slope with increasing Hg concentration.

Upon Hg sorption edges and isotherms, it is shown that the sorption is little influenced by variation of ionic strengths. This result indicates that Hg would form inner-sphere surface complexes at the HAP. In kinetics, Hg sorption on HAP reaches ~70 % of total sorbed Hg within the first 3 hr, indicating that adsorption plays a major role in controlling the initial uptake of Hg by HAP. During desorption, ~90 % of the sorbed Hg is retained by HAP suggesting that the sorbed Hg is bounded tightly to the surface and irreversible. It is also found that Hg sorption on HAP is decreased by Cl whereas Hg desorption is enhanced in the presence of Cl. These results suggest that Hg interactions with HAP are significantly influenced by various physicochemical conditions in ecosystems.

Thermal history energy balance compared with convection modeling

SCOTT D. KING*

Department of Geosciences, Virginia Tech, Blacksburg, VA 24061, USA (*correspondence: sdk@vt.edu)

Thermal history calculations are based on balancing the flux of heat into and out of the mantle with the heat generated internally due to the decay of radiogenic elements [1]. In order to reduce this balance to a tractable equation, a relationship between the surface heat flow and temperature is necessary. Often this is a relationship between the Nusselt number and Rayleigh number and variants of this relationship have been proposed based on both theory and numerical experimentation [1, 2, 3]. The power of thermal history calculations is that they can explore a large parameter space with minimal computational resources; however they provide only an average mantle temperature as a function of time.

3D spherical-shell convection calculations are becoming increasingly prevalent. These solve the conservation of mass, momentum and energy in a 3D spherical geometry; however two important aspects of thermal history modeling are infrequently employed in 3D convection calculations: a cooling core boundary condition and decreasing radiogenic heating with time. In many recent investigations the time-span of interest is such that these do not vary significantly.

This raises an interesting question: *Just how comparable are thermal history calculations and 3D spherical-shell convection calculations?* In this presentation I will compare 3D convection and thermal history calculations with the same properties. These will include temperature and pressure dependent rheology and a 'mobile lid' using the methodology outlined by *van Heck and Tackley* [4], decaying radiogenic heat sources, and a cooling core boundary condition. Even with advances in computing power, it is unlikely that solving the set of conservation equations will replace thermal history models any time soon. The goal is to assess whether given the same parameters these two formulations will produce a similar temperature history. While there are a myriad of parameters and assumptions, many of which are unknown and perhaps even unknowable (e.g., the average mantle temperature at formation), both 3D and thermal history calculations face these challenges. While the observations relevant to Earth's thermal evolution are being assessed, so to should the computational tools used to model it.

[1] Schubert, Turcotte & Olsen (2001) *Mantle Convection in the Earth and Planets*, Ch 13. [2] Gurnis (1989) *GRL* **16**, 179-182. [3] Solomatov (1995) *Phys. Fluids* **7**, 266-274. [4] van Heck & Tackley (2008) *GRL* **35**, L19312.

Distribution and migration of americium-241 in the East Pacific

NORIKAZU KINOSHITA^{1*}, MIKA NAGAOKA², TAKAHIRO SUMI³, KIYOTAKA TAKIMOTO³, AKIHIKO YOKOYAMA³ AND TAKASHI NAKANISHI³

¹Shimizu Corporation, Tokyo 135-8530, Japan.

²Japan Atomic Energy Agency, Ibaraki 319-1194, Japan.

³Kanazawa University, Ishikawa 920-1192, Japan.

(*norikazu.kinoshita@shimz.co.jp)

Anthropogenic radionuclides of plutonium-239, 240 and americium-241, that is, a decay product of ²⁴¹Pu, are present on the earth as a result of atmospheric nuclear tests carried out during the 1950s and 1960s. It is known that most of the nuclides deposited in ocean and deposition in North Pacific is higher than South Pacific due to location of the test site. Few data on ²⁴¹Am in marine environment have been reported, so far. Depth profile, residence time, applicability as a tracer of migration of the nuclide have not been well investigated yet. We have investigated on its distribution at the East Pacific by assaying large volume seawater collected in 2003.

The Am atoms were collected as hydroxides together with iron from 250 L of sea water spiked with ²⁴³Am yield tracer. The Am atoms were isolated through a solvent extraction and anion exchange procedure, followed by an assay in α -spectroemtry. The concentration of ²⁴¹Am was found low in surface water and the depths below 2000 m as well, and enhanced at the depths around 800 m. The depth profile shows a pattern similar to that of ²³⁹⁺²⁴⁰Pu [1]. Although concentration and depth of the subsurface maximum were different depends on the location, the subsurface maximum was observed in a isopycnic surface; the distribution is affected by water mass structure.

Comparing the present data on ²⁴¹Am with previous data on ²³⁹⁺²⁴⁰Pu [1], ²⁴¹Am/²³⁹⁺²⁴⁰Pu activity ratio showed constant value. Substantial differences between different locations and depths have not been observed in the profiles of ²⁴¹Am/²³⁹⁺²⁴⁰Pu ratio. The Am atoms appear to have the same residence time as those of Pu in the East Pacific.

Besides, The ²⁴¹Am inflow from North Pacific to South Pacific across the equator is observed in a depth of 500 – 1500 m along longitude of 95° W. Similar flows were observed for the Pu isotopes and the nutrients in the same area as well [1]. Our result supports a model simulation of migration in the East Pacific reported by Nakano *et al.* [2].

[1] Kinoshita *et al.* (2011) *Sci. Tot. Environ.* **409**, 1889-1899.

[2] Nakano *et al.* (2010) *J. Geophys. Res.* **15**, C06015.

Inverse modeling in a CO₂ natural analogue – long term processes in carbon dioxide storage

KIRÁLY, CS.¹, SENDULA, E.¹, SZAMOSFALVI, Á.²,
FALUS, GY.², SZABÓ, CS.¹, SZÓCS, T.²
AND FORRAY, V.¹

¹Litosphere Fluid Research Lab, Eötvös University, Hungary

²Geological and Geophysical Institute of Hungary

To guarantee the long term safety of the geologically stored CO₂, long timescale behavior of the CO₂-rock-porewater system must be well understood. The most suitable way to describe a future CCS system is study of long-term natural CO₂ accumulations and their footprint on the mineralogical and fluid compositions. One of these natural CO₂ occurrences is in the western part of Hungary, in the Little Hungarian Plane, where the studied system is composed by 38 reservoirs (26 CO₂, 10 hydrocarbon, and 2 mixed gas). The carbon dioxide is produced since 1948 for industrial purposes. The CO₂ is contained by the (late Miocene) Pannonian sedimentary sequence of a prograding delta system (mainly sandstone, siltstone and clay), in a depth of about 1400 m.

Based on the mineralogical composition of the available core samples and water chemistry data from the studied area, and using mineralogical composition of a CO₂-free brine containing sandstone from the same formation, a geochemical modeling was applied with the PHREEQC program to reproduce the observed effects and determine the major fluid-rock interactions which could have taken place in the reservoir. These interactions are believed to have a major impact on long term safety of carbon dioxide geological storage as they may strongly affect the petrophysical parameters of storage and sealing lithologies.

The work was carried out in collaboration between Eötvös University and Geological and Geophysical Institute of Hungary.

Geochemical and petrographical investigation of chromite occurrences in Burdur-Salda, Turkey

DEMET KIRAN YILDIRIM¹,
SERENA UZASCI SULTANYAN¹,
SALIH BURAK KARABEL¹, ALEV KAN BOSTANCI¹
AND MUSTAFA KUMRAL¹,

¹Istanbul Technical University, Department of Geological Engineering, 34469, Istanbul, TURKEY

Lithological units in research area from oldest to youngest are Cretaceous aged ophiolites, intrusive gabbros in ophiolites, sedimentary units mostly composed of limestones and Quaternary aged alluvials.

There are four types of chromite occurrences in the area. These are massive, nodular, disseminated and banded ores. Chromite ores which include Cr₂O₃ from 18% to 50% were bedded in podiform type. Slope directions of masses are different in northern and southern parts. It is estimated that this differences of slope depend on faulting in the region. Chromite deposits are can be seen in the outcrop, have continuities in the strike and dip directions and in the form of extensions of each other. Chromite deposits in the middle and edge parts of the ophiolitic series are small and individual appearances.

Samples from the research area were analyzed for determining the petrographical and geochemical characteristics. Samples were taken from the research region are examined according to major oxide contents to determine geochemical content ratio of this units.

The percentage of SiO₂ is between 10% an 31% and Al₂O₃ content is approximately %3-3.6. N39, which is one of five samples tested to establish Fe₂O₃ content, have the highest Fe₂O₃ content is 15,972%. It is seen that the sample is rich on account of Cr₂O₃ with the percentage of is 50,181. Moreover, the content of CaO was determined between 0,02% and 0,5% for all samples.

The Olympic Dam giant ore deposit – a fossil nuclear reactor?

MARIA KIRCHENBAUR^{1,2}, KATHY EHRIG³,
ROLAND MAAS⁴, VADIM KAMENETSKY⁵,
CHRIS BALLHAUS² AND CARSTEN MÜNKER¹

¹Institut für Geologie und Mineralogie, Universität zu Köln, Germany; ²Steinmann-Institut, Universität Bonn, Germany; Kirchenbaur@uni-bonn.de

³BHP-Billiton, Adelaide, South Australia, Australia

⁴School of Earth Sciences, University of Melbourne, Australia

⁵CODES, University of Tasmania, Hobart, Australia

The Olympic Dam (OD) supergiant Cu-U-Au-Ag deposit in the Gawler Craton of South Australia occurs within tectonic-hydrothermal breccia hosted by 1.59 Ga granite of the Gawler silicic large igneous province. With probable reserves of ~200000 t of U, OD is one of the world's largest U deposits. The high uranium content and a possible Proterozoic age of mineralization raises the possibility of Oklo-style fossil nuclear reactor activity, although a much smaller degree of burn-up, similar to that documented in many other Proterozoic and Phanerozoic U deposits, is more likely, given the low average U concentration (450 ppm) at OD. We explore this possibility using U-Sm-Nd isotope data.

High-precision U isotope data for 43 samples with U concentrations up to 10.5% were obtained by MC-ICPMS at Cologne/Bonn, employing both double spiking and standard-sample bracketing to correct for instrumental mass bias. $\delta^{238}\text{U}$ (relative to a $^{238}\text{U}/^{235}\text{U}$ of 137.856 for REIMEP 18a) ranges from -0.5‰ to +0.2‰ (average $\delta^{238}\text{U} = -0.2‰$). Only four samples yield the positive $\delta^{238}\text{U}$ expected from consumption of ^{235}U in sustained nuclear fission, well below $\delta^{238}\text{U}$ found at Oklo (up to 560‰), but consistent with the minute isotopic effects reported for other old U deposits. Depletion of ^{149}Sm by slow neutron capture, observed in many U deposits, reaches 1.5 ϵ -units and only occurs in the few samples with positive $\delta^{238}\text{U}$. Isotope ratios of Nd are indistinguishable from normal. We conclude that OD contains U with a near-natural abundance of ^{235}U , but some U-rich domains appear to have experienced a small degree of induced ^{235}U fission with associated neutron capture effects in other elements.

The vast majority of our samples (10-8000 ppm U) exhibit slightly negative $\delta^{238}\text{U}$. Consistently negative $\delta^{238}\text{U}$ (-0.3 to -0.7‰) was previously found for 'magmatic' U deposits, defined to include hydrothermal (200-400°C) deposits [1]. ^{238}U depletion in such deposits is thought to reflect natural isotope fractionation during U deposition.

[1] Bopp *et al.* (2009) *Geology* **37**, 611-614

Calibration of the Δ_{47} (clumped isotope) thermometer for biogenic and inorganic carbonate using the MIRA IRMS.

R. KIRK^{1*}, P. F. DENNIS¹, J. FARKAS² AND A. MARCA¹

¹University of East Anglia, Norwich, NR4 7TJ, UK

(*correspondence: r.kirk@uea.ac.uk)

²Czech Geological Survey, 152 00 Prague 5, Czech Republic

Using a suite of brachiopod samples collected from natural marine environments (5-22°C) and inorganic hydrothermal calcites collected from springs precipitated at up to 56°C we have determined a new calibration for the Δ_{47} isotope thermometer. This is the first reported calibration using the MIRA IRMS. All other previous determinations have been made using the Thermo-Finnegan 253 IRMS.

For all samples, 10mg of homogenised powder were reacted with ca. 2mL of 102% orthophosphoric acid for 12 hours at 25°C. CO_2 was collected by cryo-distillation after passing through sequential cold traps at -100 and -120°C to ensure complete removal of water vapour. Yields were determined barometrically before transferring the CO_2 , via a short packed column to remove any hydrocarbons, into gas tubes for mass spectrometric analysis. The MIRA mass spectrometer was operated at 8kV energy with an ionising electron current of 750 μA and $m/z = 44$ signal strengths of $4 \times 10^{-8}\text{A}$. Reported measurements are the average of 9 runs of 20 samples-reference cycles, with a 10 second integration per cycle. The measurement precision for δ^{47} approaches the shot-noise limit of ca. 0.01‰. All results are presented on the absolute reference frame outlined by Dennis *et al.* [1].

Between 5 and 56°C the Δ_{47} Vs. T relationship for both biogenic and inorganic calcite can be described by a single equation:

$$\Delta_{47} = 0.0368 (\pm 0.0037) \times 10^6 \cdot T^{-2} + 0.2345 (\pm 0.042) \\ (r^2 = 0.92)$$

The gradient of the response, within measurement error, is the same as recently reported studies [1, 2] and similar to the theoretical response [3]. There are, however, significant differences in the intercept that may result from different sample reaction conditions and procedures.

[1] Dennis *et al.* (2011) *Geochim.Cosmochim.Acta*, **75**, 7117-7131. [2] Henkes *et al.* (2013) *Geochim.Cosmochim.Acta*, **106**, 307-325. [3] Guo *et al.* (2009) *Geochim. Cosmochim. Acta*, **73**, 7203-7225.

An experimental study of the geochemical impact of CO₂ leakage in siliclastic aquifers

KIRSCH, K.¹, NAVARRE-SITCHLER, A.,² WUNSCH, A.,^{3A}
AND MCCRAY, J.E.³

¹Department of Geology and Geological Engineering,
Colorado School of Mines, kkirsch@mines.edu

²Department of Geology and Geological Engineering,
Colorado School of Mines, asitchle@mines.edu

³Department of Civil and Environmental Engineering,
Colorado School of Mines

Leakage of CO₂ from deep storage formations into an overlying potable aquifer may mobilize trace metals leading to undesirable water quality degradation. Understanding CO₂-water-rock interactions under leakage conditions is therefore an important step toward the safe implementation of geologic carbon sequestration. In this study we investigated the geochemical response of three sandstone samples from the Mesaverde Group in northwestern Colorado. Two batch dissolution experiments were conducted in which samples were reacted with water and CO₂ at partial pressures of 0.01 and 1 bar, representing natural background levels and levels expected in an aquifer impacted by a small leak of CO₂, respectively. The pH dropped sharply after CO₂ was introduced into the system, and then rebounded slightly as the minerals in the rocks dissolved. Concentrations of major (e.g., Ca, Mg, Fe) and trace (e.g., As, Ba, Cd, Pb, Sr, U) elements in the fluids increased over the 4 week duration of the experiments. These concentrations increased more in the 1 bar CO₂ experiments compared to the 0.01 bar CO₂ experiments. Throughout the experiments the concentrations of potentially toxic constituents remained below regulatory limits. Sequential extraction results suggest that carbonate minerals, although volumetrically insignificant in sandstones, are the dominant source of metals. A simple geochemical model was developed that simulates observed changes in fluid composition and supports the interpretation that carbonate minerals are an important source of metals in siliclastic aquifers impacted by CO₂ leakage.

Reaction path geochemical modelling of CO₂-SO₂-water-rock experiments

D. KIRSTE^{1,2}, J. PEARCE^{1,3}, S. GOLDING^{1,3}
AND A. FRANK^{1,2}

¹Cooperative Research Centre for Greenhouse Gas Technologies,

²Dept. of Earth Sciences, Simon Fraser University, Burnaby, BC V5A 1S6, Canada; dkirste@sfu.ca, anjaf@sfu.ca

³School of Earth Sciences, University of Queensland, Brisbane, QLD 4072, Australia; j.pearce2@uq.edu.au, s.golding1@uq.edu.au

The CO₂CRC has conducted an in depth study of the geochemical impacts of CO₂ storage with co-contaminant SO₂. In this study, laboratory experiments were conducted in static reaction vessels to investigate the chemical evolution of the CO₂-SO₂-water-rock system of core samples from 3 different geologic formations in the Surat Basin of southern Queensland, Australia. Numerical modelling of the experiments was undertaken to evaluate modelling capabilities as well as to determine which factors contribute significantly to the chemical behaviour of the system. This work reports on the geochemical modelling component of the study.

The experiments were conducted at 60°C and 120 bar with scCO₂ and scCO₂ + SO₂ in a low salinity water and 3 different rock types (see Pearce *et al.*, Goldschmidt 2013). Changes in the gas and water chemistry as well as mineralogy were determined. Static reaction path geochemical modelling using Geochemist's Workbench was conducted to simulate the experimental conditions and output of the experiments. The simulations generated provided a reasonable history match to the experiments. It was noted that the experiments and even more so the numerical models were very sensitive to redox state. In the case of the experiments it appeared that the most important contribution to redox related to aqueous phase species, particular O₂ and Fe. In the geochemical modelling, the presence of ferric iron (usually initially in the form of hematite) played a significant role in determining model outcomes. The presence of oxidised iron drove SO₂ oxidation to H₂SO₄ to take place as well as the disproportionation reaction to H₂SO₄ and H₂S leading to increased mineral dissolution and pyrite precipitation in the simulations. However, without oxidised iron the disproportionation reaction dominated leading to elemental sulphur and pyrite precipitation. The experiments and modelling clearly indicate that understanding the redox state in terms of minerals and aqueous phase of any potential sites will be critical to the geochemical behaviour.

Impacts of arc collision on small orogens: New insights from the Coastal Range detrital record of Taiwan

LINDA A. KIRSTEIN¹, ANDREW CARTER²
AND YUE-GAU CHEN³

¹School of Geosciences, University of Edinburgh, Edinburgh, EH9 3JW, UK (linda.kirstein@ed.ac.uk)

²Dept. of Earth & Planetary Sciences, Birkbeck College, London, WC1E 7HX, UK

³Dept. of Geosciences, National Taiwan University, Taipei, Taiwan, ROC

Taiwan is seen as the archetypical orogen in the development of critical wedge models of mountain building however, despite intense study the issue of how arc collision progressed along the Taiwan margin remains poorly understood. It has been suggested that punctuated collision took place (e.g. Byrne *et al.*, 2011) and therefore the classic wedge model may not be applicable. To resolve this, the detrital archive of orogenesis preserved in Coastal Range rocks of eastern Taiwan was used to reconstruct the erosional response of arc collision.

There is a distinct geographic division to the thermochronology data linked to the location of volcanic arc centres of Chimei and Chengkuangao. Detrital zircon fission-track results record grains that were exhumed from depths of 6-8 km ~6 Ma in the region between Chimei and Chengkuangao. These grains were transported and deposited into adjacent retro-foredeep basin(s) bounded by the discrete volcanic centers starting at 1.9 Myr.

South of Chengkuangao rapidly exhumed zircons are detected in sediments deposited < 1.3 Myr hence both exhumation and deposition must be fast. The pattern of exhumation and location of exhumation ages is consistent with southwards progression of arc-continent collision in a punctuated rather than sequential manner and deposition was confined to small foredeep basins.

[1] Byrne, T., Chan, Y-C., Rau, R-J., Lu, C-Y., Lee, Y-H., and Wang, Y-J., 2011, The arc-continent collision in Taiwan, *in* Brown, D., and Ryan, P.D., eds, Arc-Continent Collision: Springer Verlag, New York, p. 213-245.

Decreased export productivity at onset of Eocene hyperthermal events

SANDRA KIRTLAND TURNER^{1*}

¹Scripps Institution of Oceanography, La Jolla CA, 92093, USA *skirtlan@ucsd.edu

Hyperthermals, or abrupt global warming events, occurred frequently throughout the warm early Eocene (~56 to 47 Ma). Two lines of evidence widely used in their identification include a negative $\delta^{13}\text{C}$ excursion recorded in marine and terrestrial sources of inorganic and organic carbon and a drop in deep sea sedimentary carbonate content (wt% CaCO_3), indicative of the release of large quantities of isotopically depleted carbon to the atmosphere and oceans and subsequent dissolution of deep sea carbonates due to a shoaling carbonate compensation depth. For a number of the smaller hyperthermal events, including H2 [1], C22rH2, C22nH2, C22nH3, and C21rH1 [2], records from multiple deep sea sites show a notable offset in the timing of the $\delta^{13}\text{C}$ excursion and the wt% carbonate minimum, though carbonate content never drops below 10%, indicating deposition above the CCD throughout each event. The minima in wt% carbonate have an apparent lead of ~1 to 20 kyr compared to the minima in carbonate $\delta^{13}\text{C}$. For each event, the temporal offsets occur at multiple deep sea sites, though the magnitude of the lead varies between sites.

Experiments using the intermediate complexity Earth System model cGENIE (Grid-ENabled Integrated Earth system model) designed to reproduce these hyperthermal events show the same pattern in modeled sediment 'cores.' Hyperthermals are simulated by forcing the addition and removal of isotopically depleted carbon to the atmosphere in order to match the observed $\delta^{13}\text{C}$ excursion, with the results recorded in sediment model tracers of carbonate content and isotopes. In the model, the timing of the minimum in sedimentary wt% CaCO_2 is a function of decreased CaCO_3 export from the surface ocean occurring coincident with the addition of excess carbon to the atmosphere and oceans. In contrast, the carbonate $\delta^{13}\text{C}$ minimum records a whole ocean change in the $\delta^{13}\text{C}$ of dissolved inorganic carbon and is therefore delayed relative to the carbon addition. Both model results and observational data thus indicate an early reduction in export productivity as a consequence of small hyperthermal events.

[1] Stap, L., *et al.*, (2009), *Paleoceanography*, Vol. **24**, PA1211, 13 pp., doi:10.1029/2008PA001655. [2] Sexton, P.N., *et al.*, (2011), *Nature*, Vol. **471**, pp. 349-353, doi:10.1038/nature09826.

Geochemistry of fluids from the Eastern Carpathians and Transylvanian Basin boundary (Romania)-constraints on the origin of mineral waters and dissolved gases

BOGLÁRKA-MERCEDESZ KIS*¹ FRANCESCO ITALIANO²
CĂLIN BACIU¹ ANDREA RIZZO²
AND KRISZTINA KÁRMÁN³

¹Babeş-Bolyai University, Fântânele street 30, Cluj-Napoca, Romania (*correspondence: kisboglarka85@gmail.com)

²Istituto Nazionale di Geofisica e Vulcanologia, Via Ugo La Malfa 153, Palermo, Italy (f.italiano@pa.ingv.it)

³HAS, Institute for Geological and Geochemical Research, Budaörsi street 45, Budapest, Hungary

The Eastern Carpathians, along the Rodna-Bârgăului subvolcanic area and Călimani-Gurghiu-Harghita volcanic chain, with the Transylvanian Basin boundary, host important resources of Romanian CO₂-rich mineral waters. Results of a comprehensive study on the volatiles dissolved in artesian thermal waters discharged over a 200 km-long transect show large contents of CO₂-dominated gases.

The circulation of fluids on the study area is enhanced by tectonic fragmentations which are considered to be the main upraising path for CO₂ and mineral waters. The geochemical features of the gas phase extracted by water samples reveal amounts of CO₂ up to about 2000 cm³ STP/L_{H₂O}, and helium up to 0.02 cm³ STP/L_{H₂O}. Our investigations show that the wide range of chemical and isotopic composition can be explained in terms of contemporary occurrence of Gas-Water Interactions (GWI) affecting the circulating waters after their infiltration. Carbon (δ¹³C_{TDC} Total Dissolved Carbon, ranging from -17 to +10‰ vs PDB) and He systematics (He isotopes in the range of 0.38-0.9Ra, Ra = air-normalized ³He/⁴He ratio), coherently indicate the presence of fluids from sources located at different depths in the crust (e.g. sediments, oil reservoirs) besides minor but detectable contributions of mantle/magmatic-derived fluids.

The present work was financially supported by the RNRC, Project PN-II-ID-PCE-2011-3-0537 and by the European Social Fund and the Romanian Government through the POSDRU project "DOCTORAL STUDIES FOR EUROPEAN PERFORMANCES IN RESEARCH and INNOVATION - CUANTUMDOC" ID79407

Chalcophile element partitioning between silicate and sulphide liquids

EKATERINA S. KISEEVA¹ AND BERNARD J. WOOD¹

¹University of Oxford (*correspondence:

Kate.Kiseeva@earth.ox.co.uk, berniew@earth.ox.ac.uk)

We report the partitioning of the elements Cu, In, Tl, Pb, Ag, Zn, Cr, Co, Ni, Sb, Mn and Cd between FeS-rich sulphide liquids and anhydrous basaltic melts at high P and T. There are simple relationships between the FeO contents of the silicate melts and the sulphide-silicate partition coefficients for the individual trace elements. These relationships can be generally represented as follows:

$$\log D_{M}^{sulph / sil} \approx A + \frac{n}{2} \log[FeO]$$

where A is a constant related to the free energy of Fe-M exchange, n is a constant related to the valence of the element and [FeO] is the FeO content of the silicate melt in mole fraction or weight %. At 1.5 GPa and 1400°C, with [FeO] in weight %, we report the following values of n and A:

At 1.5 GPa and 1400°C we found, with [FeO] in weight %, the following values of A and n/2: Cu (3.33; -0.82); Pb (2.24; -1.12); Tl (1.86; -0.76); Pb (2.64; -1.09); Ag (3.47; -0.82); Zn (1.15; -0.79); Cr (1.23; -0.87); Co (2.76; -1.09); Ni (3.65; -0.84); Sb (2.56; -1.23); Cd (2.69; -0.93); Mn (0.46; -0.59).

We calculated the composition of the putative Hadean sulphide matte extracted from primitive mantle during the final stages of accretion and possibly responsible for the current "spiky" abundance pattern of chalcophile elements in silicate Earth. Starting with the current primitive mantle abundances of these elements and calculating matte composition, however, we find that it is not possible to generate an initial abundance pattern which approximates chondritic. The simple "Hadean matte" model is inadequate.

We calculated Ce/Pb and Nd/Pb ratios of basalts generated by mantle melting. Calculated Nd/Pb is essentially constant over wide ranges of partial melting and fractional crystallization with a value of ~18.6 if we assume that depleted mantle contains 65 ppb Pb. Calculated Ce/Pb varies slightly during batch partial melting from 21-29 with the canonical value of 25 being achieved at ~10% partial melting. These trends are in excellent agreement with measurements of oceanic basalt glasses. Our partitioning relationships enable calculation of the concentrations of a number of incompatible chalcophile trace elements in depleted mantle. These are as follows: 30ppm Cu, 65 ppb Pb, 7.6 ppb Ag, 12ppb In, 23 ppb Cd, 1.6 ppb Sb and 1.3 ppb Tl.

Chemical weathering and regolith development over Rajmahal basalt and Chotanagpur gneiss: A comparative study

PREMCHAND KISKU¹, JITENDRA K. PATTANAIK^{1*},
TARUN K. DALAI¹ AND S. BALAKRISHNAN²

¹Department of Earth Sciences, Indian Institute of Science Education and Research-Kolkata, Mohanpur 741252, INDIA (*correspondence: jitendra.bapi@iiserkol.ac.in)

²Department of Earth Sciences, Pondicherry University, Puducherry 605014, INDIA

Mineralogical, geochemical and field investigations were carried out on weathering profiles developed over Rajmahal basalt and Chotanagpur gneiss in eastern India to study and understand chemical weathering, elemental mobilization and development of regolith. Samples (n=38) were collected from three different locations, including fresh rock, variably weathered saprolite and soil. Variable thickness of soil cover and saprolite was observed in the study area. Fresh Rajmahal basalt consists of plagioclase phenocrysts enclosed by clinopyroxene and plagioclase groundmass, glass and opaque minerals. Chotanagpur gneiss is mainly composed of K-feldspar, plagioclase, quartz, mica and bands of mafic minerals. Weathered basalt shows red coloration along the fractures indicating precipitation of iron oxy-hydroxides.

The Chemical Index of Alteration (CIA) in the weathering profile developed over the basalt and gneiss varies from 40 to 95 and 46 to 85, respectively. High CIA values of pedoliths indicate extensive chemical weathering in the study area. Data of fresh and slightly weathered rocks plot close to the feldspar line in the A-CN-K diagram, indicating that feldspars are the most abundant minerals. Weathered samples show loss of CaO+Na₂O+K₂O, indicating extensive destruction of feldspar and clinopyroxene. XRD analysis shows progressive upward increase of clay mineral abundance in the soil profile. With respect to fresh rocks, Fe, Mn, Ti, Ni, Cr, Zr and Al are enriched, and Ca, Mg, Na, Sr and Si are depleted in the weathered basalt, whereas, in the weathered gneiss Si is enriched and Fe and Mn are depleted. For different elements, zones of leaching and accumulation vary within a profile.

Results of this study bring out the differences in the alteration and weathering of minerals in profiles developed on basaltic and gneissic rock types.

A low blank technique for the measurement of iron isotopes in seawater and results from the tropical Atlantic Ocean

J. K. KLAR^{1*}, R. H. JAMES¹, I. J. PARKINSON²,
E. P. ACHTERBERG¹ AND C. SCHLOSSER¹

¹National Oceanography Centre, University of Southampton Waterfront Campus, European Way, Southampton, SO14 3ZH, UK, (*correspondance: J.klar@noc.soton.sc.uk, r.h.james@noc.ac.uk, eric@noc.soton.ac.uk, cs2u09@noc.soton.ac.uk)

²Bristol Isotope Group, School of Earth Sciences, University of Bristol, Wills Memorial Building, BS8 1RJ, UK, (Ian.Parkinson@bristol.ac.uk)

Iron (Fe) is essential for marine photosynthesis, respiration and nitrogen uptake, but low Fe supply and low solubility under oxic conditions results in Fe-limitation of microbial communities in large parts of the world's ocean. For this reason the oceanic Fe cycle is linked to global carbon cycle. Recent studies [1, 2] have shown that analysis of the Fe isotopic composition can provide unique information about its sources, and Fe cycling within the oceans. Here we present a protocol for the accurate and precise measurement of Fe isotopes in seawater using a low blank, double-spike technique. To this end, Fe is pre-concentrated from seawater using a NTA resin, and then separated from the sample matrix by anion exchange chromatography (AG1-X8 resin). Isotope ratios are analysed by multi-collector inductively coupled plasma mass spectrometry (ThermoFisher Neptune) coupled to a sample desolvator (Aridus II or Apex-Q), and corrected for mass bias effects using a double-spike technique. Our model simulations show that the optimal spike composition is 47% ⁵⁷Fe, 53% ⁵⁸Fe, with a small amount (<0.5%) of ⁵⁴Fe, which allows precise measurements of a wide range of sample to spike mixing ratios, the optimum being ~1:1. The precision of the MC-ICPMS measurements is δ⁵⁶Fe ~0.05 ‰ (2 SD), based on replicate analyses of haematite standards.

We also present results of the preliminary analysis of Fe isotopes in seawater samples (0.2 µm filtered) collected from within the Oxygen Minimum Zone (OMZ) of the tropical Atlantic Ocean along ~12° N (GEOTRACES cruise GA06, 7 depth profiles sampled at 4 to 9 depths, ranging from surface waters to 5600 m depth). Fe concentrations ranged from 1.04 to 3.77 nM within the OMZ (located between 200 and 1000 m depth). The Fe isotope data will be used to (i) identify the sources of Fe to this region, and (ii) to identify processes of Fe cycling in oxygen minimum zones.

[1] Lacan *et al.* (2010) *Anal. Chem* **82**(17), 7103-7111. [2] John & Adkins (2010) *Mar. Chem* **119**, 65-79.

Availability of light and chemical energy determines the structure of natural sulfide oxidizing biofilms

JUDITH KLATT^{1*}, STEFFI MEYER, DIRK DE BEER¹
AND LUBOS POLERECKY¹

¹Max-Planck-Institute for Marine Microbiology, Bremen, Germany (*correspondence: jklatt@mpi-bremen.de)

In the Frasassi cave system, Italy, sulfidic streams and pools are colonized by aerobic chemolithoautotrophic biofilms. Upon emergence of this water from the caves, light becomes available and gives rise to biofilms that are additionally inhabited by highly abundant phototrophic microorganisms. The structure of these biofilms varies between two end-members, one characterized by a cyanobacterial layer on top of a distinct *Beggiatoa* layer (C/B biofilms) and the other one by an inverted structure (B/C biofilms). We used microsensors to study how this structure depends on the availability of light and chemical energy.

C/B biofilms form where the availability of oxygen, and thus of chemical energy, from the water-column is limited (<5 μM). Aerobic chemolithotrophic activity in the *Beggiatoa* layer depends entirely on the supply of oxygen from the cyanobacteria, which occurs at high incident light intensities. Therefore, light is the energy source that drives the community and the main factor that regulates the spatial organization of its dominant functional groups. In B/C biofilms, which occur at locations where oxygen in the water column is comparatively abundant (>45 μM) and continuously present, *Beggiatoa* are independent of the photosynthetic production of oxygen and outcompete the cyanobacteria in the uppermost layer of the biofilm (i.e., closest to one of the energy sources). The proliferation of cyanobacteria in these biofilms seems to be disadvantaged by the extensive interval of darkness during night and by high back scattering of light in the *Beggiatoa* layer during the day. Therefore, although the daily flux of light energy to the biofilm is much greater than the daily flux of chemical energy derived from the oxidation of sulfide with oxygen, light is only peripherally utilized. Instead, the continuity of the input of chemical energy appears to be a more important factor determining the community structure and its dominant functional traits. Our study thereby introduces a scenario, where apparent uncoupling of phototrophic and aerobic chemolithotrophic activity leads to outcompetition of photosynthetic microbes even in the presence of light showing that both microbial interactions and available thermodynamic energy must be considered to understand the biogeochemical cycling.

Spatial and temporal variation in provenance of Eastern Mediterranean sediment: Implications for Aegean volcanism

M. KLAVER*, T.T. DJULY AND P.Z. VROON

VU University Amsterdam, De Boelelaan 1085, 1081HV Amsterdam, The Netherlands (*correspondence: martijn.klaver@vu.nl)

Subducted sediment is one of the principal geochemical components of island arc magmas. Along-arc variation in subducting sediment composition is reflected in geochemical trends in the arc volcanics [e.g. 1]. The predominantly Quaternary Aegean volcanic arc is the result of northward subduction of the African plate underneath the Aegean microplate. East-west geochemical variation in Aegean arc volcanics has often been related to differences in subducted sediment composition in the Eastern Mediterranean Sea (EMS) resulting from contrasting source regions.

Recent studies [2,3,4] investigating the provenance of EMS sediment suggest mixing between Sahara dust (old, felsic) and Nile sediment (young, mafic). These studies however, lack a spatial and temporal framework as they focus exclusively on Quaternary deposits while the subducted sediment underneath the Aegean arc is Pliocene to Mesozoic in age. We present an extensive new geochemical dataset of EMS sediment samples obtained from DSDP and ODP drill cores along the Aegean arc from Quaternary to middle Miocene age.

The new dataset, in conjunction with previously published results, allows us to accurately trace the along-arc temporal variation of EMS sediment provenance. In line with previous results, we conclude that Quaternary EMS is a mix of Nile sediment, Sahara dust and autogenic carbonate or evaporite components. A clear along-arc trend in principal component can be observed, and the geochemical composition of subducting sediment is highly variable. However, in the Plio- to Miocene, the Nile component appears to be dominant in the entire EMS, leading to much less pronounced geochemical variation of subducted sediment along the Aegean arc. Hence, the assumption that east-west geochemical trends in Aegean arc volcanics are due to differences in subducted EMS sediment composition, may be unjustified.

[1] White & Dupré (1986) *JGR* **91**, 5927-5941. [2] Weldeab *et al.* (2001) *Chem. Geol.* **186**, 139-149. [3] Revel *et al.* (2010) *Quat. Sci. Rev.* **29**, 1342-1362. [4] Padoan *et al.* (2011) *GCA* **75**, 3627-3644.

Chondritic Sm/Nd in the Earth, Moon and Mars

T. KLEINE¹, C. BURKHARDT² AND P. SPRUNG¹

¹Institut für Planetologie, University of Münster, 48149 Münster, Germany (thorsten.kleine@wwu.de)

²Origins Laboratory, Department of Geophysical Sciences, The University of Chicago, IL 60637, USA

One of the most fundamental assumptions in geochemistry is that refractory lithophile elements occur in chondritic relative abundances in the bulk Earth. However, the accessible silicate Earth exhibits a ~20 ppm higher ¹⁴²Nd/¹⁴⁴Nd than most chondrites [1], and this may reflect a higher-than-chondritic Sm/Nd of the bulk Earth [2-4]. Caro *et al.* [2] argued that because the ¹⁴⁶Sm-¹⁴²Nd isochrons of the lunar and martian mantles intersect at a higher-than-chondritic ¹⁴⁷Sm/¹⁴⁴Nd and at the ¹⁴²Nd/¹⁴⁴Nd of the modern terrestrial mantle, the Earth, Moon and Mars all are characterized by a common, superchondritic bulk composition (termed 'SCHEM' [3]). Such non-chondritic compositions may result from collisional erosion of early-formed crust or may reflect assembly of the terrestrial planets from non-chondritic materials [4].

Here we re-examine the lunar and martian ¹⁴⁶Sm-¹⁴²Nd systematics and show that the lunar and shergottite isochrons intersect almost exactly at the chondritic ¹⁴⁷Sm/¹⁴⁴Nd, whereas SCHEM plots off both isochrons. This as well as evidence from the Hf-Nd isotope systematics of lunar samples [5] indicates chondritic Sm/Nd in the Earth, Moon and Mars. The ¹⁴²Nd/¹⁴⁴Nd of the lunar and shergottite isochrons at a chondritic Sm/Nd are slightly lower than albeit not clearly resolved from that of the modern terrestrial mantle, but are distinctly higher than the mean ¹⁴²Nd/¹⁴⁴Nd of ordinary and carbonaceous chondrites. We interpret these ¹⁴²Nd/¹⁴⁴Nd variations to be nucleosynthetic in origin and show them to be consistent with a heterogeneous distribution of *s*- and *p*-process Nd. Of note, the resulting nucleosynthetic anomalies in Sm and non-radiogenic Nd isotopes are small and consistent with currently available data for chondrites [*e.g.*, 6].

A nucleosynthetic origin of the ¹⁴²Nd difference between the Earth and chondrites provides further evidence that the isotopic composition of the Earth is distinctly non-chondritic [7]. However, the chemical composition of the Earth, at least for refractory lithophile elements, appears to be chondritic.

[1] Boyet & Carlson (2005) *Science* **309**, 576-581. [2] Caro *et al.* (2008) *Nature* **452**, 336-339. [3] Caro & Bourdon (2010) *GCA* **74**, 3333-3349. [4] Campbell & O'Neill (2012) *Nature* **483**, 553-558. [5] Sprung *et al.* (2013) *EPSL*, subm. [6] Carlson *et al.* (2007) *Science* **316**, 1175-1178. [7] Burkhardt *et al.* (2011) *EPSL* **312**, 390-400.

Investigation of boron, carbon, and oxygen isotope systematics in the aragonite-CO₂-H₂O system

C.D. KLEIN GEBBINCK¹, S.-T. KIM^{1*}, M. HENEHAN² AND G.L. FOSTER²

¹School of Geography and Earth Sciences, McMaster University, Hamilton, Canada (*correspondence: sangtae@mcmaster.ca)

²Ocean and Earth Sciences, University of Southampton, Southampton, UK

Calcium carbonate has been ubiquitous on the surface of the Earth. Therefore, marine and continental carbonates, such as forams and speleothems, play a critical role in paleoceanography and paleoclimatology as a key climate archive. Hence, a proper understanding of stable isotope systematics in carbonates with respect to their formational environment is important for the reconstruction of Earth's climate history.

Stable isotope systematics of boron, carbon, and oxygen in the aragonite-carbon dioxide-water system were simultaneously investigated using synthetic aragonite as a function of solution chemistry at 25 °C. A refined version of the constant addition method [1] was used to synthesize a polymorph of CaCO₃, aragonite, in aqueous solutions of various, but constant pH values and ionic strengths. The mineralogy of the carbonate was confirmed by XRD analysis and their isotopic compositions were determined by either IRMS or MC-ICPMS.

Results of our study suggest that the effect of ionic strength (~0.7 mol/kg) on the stable isotope fractionation between aragonite and water (for oxygen) as well as between aragonite and DIC (for carbon) in the aragonite-CO₂-H₂O system is negligible. In addition, boron isotope analysis of synthetic aragonite prepared from aqueous solutions of seawater-like ionic strength indicates that borate ions are preferentially incorporated into the aragonite crystal.

[1] Kim *et al.* (2007) *Geochim. Cosmochim. Acta.* **71**, 4704-4715.

Tracing old SCLM in Pan-African granitoids from Dronning Maud Land (East Antarctica) with Sr-Nd isotope signatures

I.C. KLEINHANNS^{1*}, J.JACOBS², A. K. ENGVIK³,
B.BINGEN³, N.W.ROLAND⁴, A. LÄUFER⁴
AND R.SCHOENBERG¹

¹Universität Tübingen, Wilhelmstrasse 56, D-72074

Tuebingen; *kleinhanns@ifg.uni-tuebingen.de

²Universitetet i Bergen, Allégaten 41, NO-5007 Bergen

³Norges Geologiske Undersøkelse, NO-7491 Trondheim

⁴BGR, Stilleweg 2, D-30655 Hannover

Dronning Maud Land (DML) represents the southern end of the East African Antarctic orogen that was created during the final amalgamation of Gondwana in the Neoproterozoic. The suture between parts of East and West Gondwana spans over more than 8000km from present Egypt-Arabia to present Mozambique-Antarctica. The part north of the Lurio belt (LB) is characterised by accretionary tectonics visible in the Arabian-Nubian Shield contrary to the part south that shows evidence for continent-continent collision. Within southern Mozambique and DML numerous late-tectonic granitoids are observed, which are characterised as ferroan A-type granitoids that evolved under high-T conditions. The geodynamic regime is explained by extensional tectonics within a collapsing orogen accompanied by asthenospheric upwelling through delamination of the orogenic root [1]. In this project we studied an E-W-profile along the 72°S-latitude starting from the Mühlig-Hofmann mountains (MH) (4°-7°E) via central Dronning Maud Land (cDML) (8°-14°E) and finally samples from Sør Rondane (SR) (23°-25°E). TDM (Nd) for MH and cDML samples are of Meso- to Paleoproterozoic age although the oldest (yet detected) crust in that region is of Grenville-age. We take this as evidence for the existence of an old subcontinental lithospheric mantle underneath this part of East Antarctica and its contribution to the granitoids. SR granitoids are different as they show grenville-aged TDM (Nd) and could thus have been developed by simple crustal melting. Initial Sr isotope signatures for both regions are similar and indicate homogenisation during time of emplacement. Finally, samples from the LB show large similarities with MH and cDML, but are different to SR granitoids. This allows to place certain paleogeographical constraints on Gondwana configuration.

[1] Jacobs *et al.* (2008) In: Satish-Kumar *et al.* Geol. Society, London, Spec. Pub. **308**, 69-90

Experimental study of trace element partitioning between spinel and silicate melts: Effects of oxygen fugacity and spinel composition

S KLEMME¹, CH WIJBRANS^{1,*}, C VOLLMER¹,
M MENNEKEN¹ AND J BERNDT¹

¹Institut für Mineralogie, Universität Münster, Germany,

*ineke.wijbrans@uni-muenster.de

Spinel is a common accessory mineral that occurs in a variety of rocks such as evolved basaltic magmas or chromitites in ultramafic rocks. Spinel often contain large amounts of transition metals or other redox sensitive elements, but the partitioning of these elements in these rocks is not well constrained, probably because it depends on several parameters which are difficult to disentangle: temperature, pressure, oxygen fugacity and composition of the crystals and melt.

Experiments are performed in 1 atm. gas mixing furnaces at temperatures between 1200 and 1430°C and oxygen fugacities ranging from log -12 to log -0.7. Starting materials consist of glasses in the system (Cr₂O₃-FeO)-CaO-MgO-Al₂O₃-TiO₂-SiO₂ doped with a large number of trace elements.

The experimental run products were characterized with electron microprobe for major elements and 193nm Laser Ablation ICPMS for trace elements. The experiments all contained spinels and glass, some experiments contained additional phases (olivine or plagioclase).

The Fe²⁺/Mg²⁺ ratio in spinel has little effect on trace element partitioning, but the concentration of trivalent cations such as Al, Fe and Cr appears to have an (large) effect on the partitioning of Ti, Sc and the HFSE; D values for these elements are lowest in Al rich spinels, are slightly elevated in spinels that contain chromium, and are about an order of magnitude higher in spinel high in Fe³⁺.

Our results show that partition coefficients for some elements are redox sensitive; D_{Ni}, D_{Co}, and D_{Mo} decrease slightly with increasing fO₂ and D_V decreases over four orders of magnitude. In contrast, D_{Pt} and D_{Rh} increase strongly with increasing oxygen fugacity. To investigate peculiar high Pt and Rh concentration in the some of the experimental spinels, a TEM study was performed to investigate the presence of platinum group element nuggets as inclusions in the spinel. However, preliminary TEM results show no inclusions in these spinels suggesting that the measured high D's are correct.

Research of Condensation of Supersaturated Water Vapor

A. KLIMKIN¹, A. KOZLOV², F. KRYMSKIY³, A. KURYAK¹,
S. MALYSHKIN², A. PETROV²
AND YU. PONOMAREV¹

¹Institute of Atmospheric Optics SB RAS, Tomsk, Russia,
tosha@asd.iao.ru, alex@asd.iao.ru, yupon@iao.ru;

²Institute of Chemical Kinetics and Combustion SB RAS,
Novosibirsk, Russia;

³Institute of Cosmophysical Research and Aeronomy SB RAS,
Yakutsk, Russia

Clouds in the atmosphere have a significant influence on weather conditions, and play a prominent part in the processes of energy exchange between the Sun, the surface of the Earth and the atmosphere. That is why it is important to research the mechanisms of clouds formation and the processes developing at different stages of formation. It is essential to estimate the influence of cosmic radiation, as well as other natural and anthropogenic factors on these processes.

Nucleation of droplets in the cooled water vapor requires the presence of condensation centers [1-3]. In order to observe the dynamics of droplets nucleation, the Institute of Atmospheric Optics SB RAS developed a unit on basis of the two-chambered cell with capacity exceeding 40 m³ [4] which allows creating supersaturated H₂O vapor. At that, the unit offers the possibility of controlling thermodynamic parameters under varied pressure, test gas mixture composition and influence of ionizing radiation.

The study was focused on nucleation of nanoparticles and droplets. The nucleation developed under the gradual decrease in pressure of the test gas mixture when the unit conditions were made similar to Wilson chamber, type-II. The gas mixture was also exposed to the charged particle beam under gradual pressure decrease and supersaturated H₂O vapor. To this effect the unit was equipped with the electron gun [5]. Air, binary mixtures of H₂O-CO₂ and H₂O-N₂, as well as the air with high concentration of CO₂ and N₂ were used as test mixtures.

[1] Marsh N., Svensmark H. // *Space Sci. Rev.* 2000. **V.94**, N 1–2. P. 215–230. [2] Andreas M., et al. // *Atmos. Chem. and Phys.* 2008. **V. 8**, N 16. P. 4911–4923. [3] Krimskiy G.F. // *Science and Technology in Yakutiya*. 2005. N 1(8). P. 3–6. (Russian issue). [4] Ponomarev Yu.N., Tyryshkin I.S. // *Atmospheric and Oceanic Optics Journal*. 1993. **V.6**, N 04. P. 360-368. [5] Yu. Ponomarev., et al. // *Solar-Terrestrial Physics*. 2012. **V.21**. P.58-61.

Exploring synergies of aerosol and climate mitigation strategies

Z. KLIMONT^{1*}, M. AMANN¹, S. RAO¹ AND F. DENTENER²

¹IIASA, Schlossplatz 1, 2361 Laxenburg, Austria

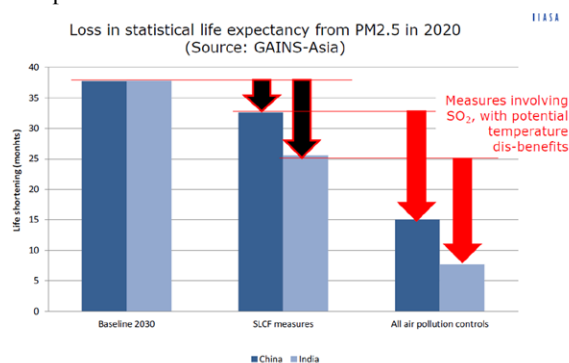
(*correspondence: klimont@iiasa.ac.at)

²JRC/IES, 21027 Ispra, Italy

Recent work has highlighted the scope for reductions of short-lived climate pollutants (SLCP) that yield significant benefits to human health and agricultural crops at the local scale while limiting temperature increase in the near-term [1, 2]. Identified measures would achieve large cuts in emissions of CH₄ and BC, but minimize further emission reductions of cooling aerosols, such as SO₂, beyond what is already implied in current legislation. Climate policies, cutting emissions of several pollutants, would also bring important health benefits [3].

While implementation of measures addressing SLCP or specific climate policies would result, beyond climate benefits, in significant air quality and ecosystem improvements, they will not be sufficient to remediate all current air quality problems and achieve sustainable air quality around the world. Additional air quality measures will need to involve further reductions of cooling aerosols, such as SO₂ emissions, which however will result in a clear climate dis-benefit, at least in the near term (Figure 1).

The presentation will review available emissions scenarios



for measures or policies that could compensate climate dis-benefits of SO₂ mitigation by co-controls of long-lived greenhouse gases.

[1] Shindell et al. (2012) *Science*, **335**, 183–189. [2] Annenberg et al. (2012) *Env. Health Persp.*, 120, 831-839. [3] Rao et al., *Global Env. Chnage* (in review).

Geochemistry of organic matter from Triassic U-bearing sandstones of Peribaltic Syneclise (N Poland)

KLIMUSZKO E., WOLKOWICZ S.* AND MIECZNIK J.B.

PGI-NRI, 4 Rakowiecka, 00-975 Warsaw, Poland
(stanislaw.wolkowicz@pgi.gov.pl)

In central parts of the Peribaltic Syneclise, Triassic rocks display sandstone type uranium mineralization. Mineralization is related to gray sandstones poor in TOC.

5 samples were covered by geochemical studies, including TOC, bitumen fractions, saturated hydrocarbons and aromatic hydrocarbons.

Small TOC values (below 0,1%) indicate poor hydrocarbon generation potential. Amounts of bitumens are small, from 70 to 170 ppm. The share of hydrocarbons in these bitumens ranges from 26,7% to 52,3%, being lower than that of the asphaltene and resin fraction. Migration coefficient of hydrocarbons is raised, ranging from 0,03 to 0,09, which suggests epigenetic origin of labile components. N-alkanes with 21 – 24 carbons in chain are most common, suggesting that the organic matter is of the sapropel type. Analyses of compounds of the terpane group showed predominance of pentacyclic compounds over the tricyclic, indicating high share of bacteria in original organic matter as well as low level of maturation. The composition changes in lower part of the studied series. In that part, tricyclic compounds predominate over the pentacyclic which indicates a higher level of maturation. Moreover, difference between contents of 17 α (H)-trisorhopane (Tm) and 18 α (H)-trisorhopane II (Ts) compounds which further supports higher level of maturation of the studied organic matter. C27 (cholestane) appears fairly common in the group of identified steranes but content of sterane C29 sterane (stigmastane) is higher which suggests some contribution of terrigenous material in organic matter. Significant share of C28 compound (ergostane) was found in lower part of the studied series which evidences presence of material of the lacustrine origin.

The Triassic rocks are poor in TOC and their hydrocarbon generation potential is very low. At the same time they yield small amounts of labile components which would be epigenetic origin. The organic matter was generally of the marine origin. In lower part of the rock series, the parent organic matter comprises material of the lacustrine type, and in the upper – organic matter of the marine type is enriched with supposedly allochthonous terrigenous material.

A microscopic and ToF-SIMS study on the Ra uptake by barite

KLINKENBERG, M^{1*}., BRANDT, F.¹, BREUER, U.²
AND BOSBACH, D.¹

¹Institute of Energy and Climate Research (IEK-6)
Forschungszentrum Jülich, Germany; m.klinkenberg@fz-juelich.de (*presenting author), f.brandt@fz-juelich.de, d.bosbach@fz-juelich.de

²ZEA-3 Analytics, Forschungszentrum Jülich, Germany;
uwe.breuer@fz-juelich.de

Long-term safety assessment studies of nuclear waste repositories for spent nuclear fuel commonly consider a scenario, in which radium released from the fuel comes into contact with an aqueous solution saturated with barium [1]. An open question is whether a Ra containing solution will equilibrate with solid BaSO₄ under repository relevant conditions due to complete recrystallization. Previous studies have indicated that uptake of Ra is not limited by pure adsorption at close to equilibrium conditions but involves a significant fraction of the bulk solid [2,3]. So far, only macroscopic data indicate that barite may fully recrystallize to radiobarite. For this microscopic (SEM) and ToF-SIMS study, samples of two different barites were prepared in batch sorption experiments to investigate the recrystallization of barite in the presence of Ra. Based on gamma spectrometry, it was observed that one barite incorporates Ra faster than the other barite.

A broad grain size distribution was determined via SEM observation for the fine grained barite. During recrystallization of the crystals, an additional effect on the grain size evolution due to the presence of Ra was detected compared to the coarsening of a blank sample due to Ostwald ripening. In contrast, the narrow grain size distribution of the coarse grained barite didn't show significant changes with time and no influence of the presence of Ra. Here, morphological changes were observed instead.

The results of ToF-SIMS indicate a homogeneous uptake of Ra into the crystals. After 443 days the integrated Ra concentration corresponds with the size of the barite particles. The Ba/Ra ratio was calculated from several ToF-SIMS measurements. The Ra/Ba intensity distribution has its maximum between 2 and 4 · 10⁻³, corresponding well with the macroscopic results from bulk solution chemistry.

- [1] Grandia, F. *et al.*: SKB Technical Report TR-08-07 2008
[2] Bosbach, D. *et al.*: SKB Technical Report TR-10-43, 2010.
[3] Curti, E. *et al.*: *Geochim. et Cosmochim. Acta*, 2010, **74**, 3553-3570.

Hybrid Multispectral Analysis (HMA): Innovative technology for continuously monitoring the biogeochemistry of urban waterways

GARY P. KLINKHAMMER¹ AND CHRIS J. RUSSO²

¹CEOAS, Ocean Admin. Bldg. 104, Oregon State University, Corvallis OR, USA 97331

²ZAPS Technologies Inc., 4314 Research Way, Corvallis OR, USA 97333

Hybrid Multispectral Analysis (HMA) uses a fiber optic spectrometer to analyze source and waste waters for multiple parameters. Hybrid refers to the HMA capability of measuring fluorescence and absorption as well as scattering to produce a rich array of optical data. No chemicals are required in HMA analysis. The optical information is then used to correct for artifacts such as turbidity and signal overlap before calculating concentrations based on laboratory calibrations performed in a clean water matrix. HMA data quality is maintained over time with automated cleaning and correction protocols. The HMA menu for source water includes TOC, nitrate, chlorophylls, turbidity, biochemical oxygen demand (BOD), total suspended solids (TSS), color, *E. coli* bacteria, fluorescent dissolved organic matter (FDOM) and other water quality parameters. Each value is displayed on a graphical web-user interface once every 2-3 minutes depending on the number of measurements in the menu. In this paper HMA data will be compared for several urban-impacted waterways including a small creek in Corvallis Oregon (Oak Creek) and a river-estuary in Sydney Australia (Parramatta River). The biogeochemistry of these urban streams will be compared to the relatively pristine, mountain-fed Santiam River in coastal Oregon. The high-resolution data from HMA allows details of important inter-parameter relationships to be examined in detail for the first time.

Abiotic reactions of nitrite during microbial Fe(II) oxidation and their influence on cell-encrustation of nitrate-reducers

NICOLE KLUEGLEIN, FABIAN ZEITVOGEL, MARTIN OBST AND ANDREAS KAPPLER*

University of Tuebingen, Centre for Applied Geoscience, Sigwartstrasse 10, 72076 Tuebingen, Germany

(nicole.klueglein@uni-tuebingen.de)

(fabian.zeitvogel@student.uni-tuebingen.de)

(martin.obst@uni-tuebingen.de)

(*correspondence: andreas.kappler@uni-tuebingen.de)

Anoxic, nitrate-reducing bacteria are widespread in soils and sediments. They use nitrate (NO_3^-) and the following intermediates (NO_2^- , NO and N_2O) as electron acceptors. In addition to heterotrophic denitrifiers, nitrate-reducers have been isolated which were suggested to couple nitrate reduction to the oxidation of Fe(II). Recently, however, it has been questioned whether the observed Fe(II) oxidation is completely enzymatic or whether it is at least partly due to an abiotic reaction between Fe(II) and the reactive N-species formed during mixotrophic growth [1,2,3]. Here we present data that demonstrates that NO_2^- is able to oxidize Fe(II) under pH-neutral and particularly under acidic conditions at high rates. Fe(II) analysis using sulfamic acid instead of HCl prevents the abiotic reaction of NO_2^- and Fe(II) during acidic extraction and yields correct Fe(II)/Fe(III) values. To evaluate the role of bacterially produced nitrite in Fe(II) oxidation, we compared two strains that were isolated as nitrate-dependent Fe(II)-oxidizers [1,2] with two heterotrophic nitrate-reducers (*Paracoccus denitrificans* ATCC 19367 & 1222) in their ability to oxidize ferrous iron and the formation of Fe(III) mineral crusts around the cells. All four tested strains oxidized Fe(II) and using SEM/TEM we observed heavy encrustation of all strains. However, the shape, crystallinity and localization of minerals inside and outside the cell varied distinctly between the strains. Applying fluorescent lectins in the CLSM, we also observed a significant production of exopolymeric substances, maybe as a protection mechanism against high Fe(II) concentrations. Our observations suggest that cell encrustation is a side effect caused by abiotic Fe(II) oxidation by nitrite during heterotrophic denitrification.

[1] Klueglein & Kappler (2013) *Geobiology* **11**, 180-190. [2] Weber *et al.* (2006) *Appl. Environ. Microbiol.* **72**, 686-694. [3] Kopf, Henny & Newman (2013) *Environ. Sci. Technol.* in press

Fluid migration along a dense, intersecting array of faults on the outer-shelf of Southern Costa Rica: Insights from 3D seismic attributes and multibeam data

JARED W KLUESNER¹, ELI SILVER¹, STEPHANIE NALE¹,
NATHAN L BANGS² AND KIRK D MCINTOSH²

¹Earth and Planetary Sci Dept, Univ California Santa Cruz,
Santa Cruz, CA, USA, (jwkluesn@ucsc.edu)

²Institute for Geophysics, Univ. of Texas, Austin, TX, USA

We use 3D seismic reflection attributes and multibeam data to map and analyze fluid-flow along a dense network of intersecting normal faults imaged on the outer shelf offshore Southern Costa Rica. Faults were imaged on the seafloor using (i) high-resolvability EM122 multibeam data, and (ii) in 3D below the seafloor using seismic reflection data, both collected during the 2011 CRISP seismic survey. Multibeam bathymetry reveals a series of high-backscatter ridges on the seafloor cut by numerous faults with roughly N-S and E-W trends. Vertical profiles within the 3D seismic volume reveal that faults have normal displacements and extend deep into the sedimentary section, some of which cut through top of the margin. Numerous indicators of fluid-migration and fluid-rich sediments, such as bright spots, dim spots, and acoustic turbidity zones, are present along fault traces imaged on vertical inlines and crosslines. Within the seismic volume we use seismic discontinuity attributes (e.g., coherency and similarity) of a dip-steered seismic volume to reveal and map fault traces in horizontal time slices. We then use a neural network of multiple seismic attributes to create a 'fault cube' and a 'chimney cube' to detect high probability zones fluid leakage along faults. Indicators of seafloor seepage, such as high-backscatter pockmarks and mounds, are imaged on the seafloor along fault traces and above seismic indicators of fluid migration. Use of seismic discontinuity attributes massively improves 3D interpretability of a very complex set of intersecting faults, and provides insight into understanding the pathways of fluids and gas within the margin of Costa Rica.

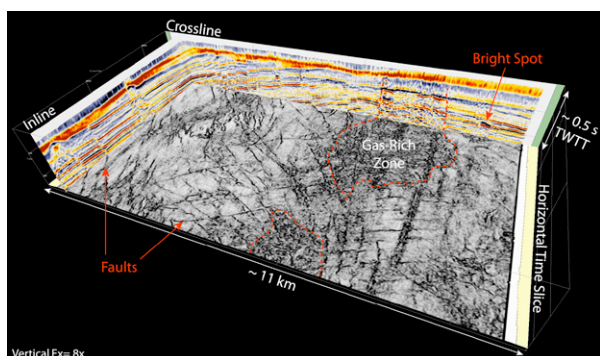


Figure 1. 3D perspective view of subset of 3D seismic data below the outer shelf of southern Costa Rica.

Constraints for the clumped isotope application in diagenetic environments involving high salt concentrations

TOBIAS KLUGE*, CÉDRIC M. JOHN
AND SIMON DAVIS

Department of Earth Science and Engineering and Qatar
Carbonate and Carbon Storage Research Centre, Imperial
College London, SW7 2BP, United Kingdom;

*correspondence: t.kluge@imperial.ac.uk

Carbonate clumped isotopes is a promising proxy for the reconstruction of mineral formation temperature and their parent fluid composition. Clumped isotopes has a wide range of potential applications, such as the reconstruction of the diagenetic history of sedimentary basins that involve fluids with a high salt concentration and elevated temperatures. As salt ion effects are known to impact bulk oxygen isotopes, here we assessed the influence of salinity on clumped isotopes in the temperature range from 20-90°C.

Samples were precipitated from a super-saturated CaCO₃ solution via N₂ bubbling. Prior to starting the carbonate precipitation the solution was equilibrated at the respective experiment temperature. Different salt ions (Na⁺, Ca²⁺, Mg²⁺) were added to the solution and compared to samples without added NaCl, MgCl or CaCl₂ to evaluate ionic effects on ¹³C-¹⁸O clumping. No effects were observed for NaCl at temperatures between 23 and 90°C and salt concentrations up to 6 molal. Preliminary results indicate that moderate concentrations of MgCl₂ (0-0.4 molal) and CaCl₂ (0-0.5 molal) have no observable influence on ¹³C-¹⁸O clumping. Furthermore, polymorphism of CaCO₃ produced no observable effect. In summary, our results indicate that carbonate clumped isotopes can be applied to carbonates precipitated from saline parent fluids without the need to correct for salt ion effects in common NaCl brines or fluids containing moderate levels of CaCl₂ and MgCl₂.

We gratefully acknowledge funding from Qatar Petroleum, Shell and the Qatar Science and Technology Park.

Petrological constraints on magma plumbing dynamics of the 2011 El Hierro eruption (Canary Islands)

A. KLÜGEL*¹, M.-A. LONGPRÉ² AND J. STIX²

¹University of Bremen, Geosciences Department, Bremen, Germany [akluegel@uni-bremen.de]

²Earth and Planetary Sciences, McGill University, Montréal, Québec, Canada [m-a.longpre@mcgill.ca]

(*correspondence: akluegel@uni-bremen.de)

A submarine eruption took place off the south coast of El Hierro, Canary Islands, from October 2011 to March 2012. The well-monitored eruption was preceded and accompanied by numerous earthquakes and ground deformation. Eruptive products sporadically rose to the ocean surface and were sampled at different stages of the eruption. We carried out a detailed geochemical and petrological study to constrain magma plumbing dynamics associated with the eruption.

All bulk lava samples are basanites with essentially identical matrix glass compositions, implying very little change in magmatic liquid composition through time. The MgO content of the bulk lava increased at the late eruptive phase due to increasing contents of ferromagnesian crystals. Final phenocryst crystallization took place at 500-710 MPa (17-24 km depth, within the upper mantle), as was determined by 73 clinopyroxene-melt pairs. This depth range for an inferred magma reservoir coincides perfectly with the depths of syn-eruptive seismicity. In contrast, the analysis of 260 CO₂-rich fluid inclusions in phenocrysts yields two pressure ranges, one at 280-440 MPa (10-16 km depth, lower crust to upper mantle) and one at 450-580 MPa (16-19 km). The shallower range corresponds well with the depths of pre-eruptive seismicity, and reflects lateral movement of magma within the lower crust over a distance of ca. 15 km before ascending to the eruptive site.

Detailed analysis of zoning patterns in olivine and clinopyroxene phenocrysts and compositions of melt inclusions reveal that at least two distinct magmas were involved in the eruption. Both magma batches were initially stored in the upper mantle, one probably at 19-25 km depth and one at 15-18 km. Diffusion modelling indicates that mixing of these magmas likely began about three months before eruption, resulting in intrusions to the lower crust and associated seismic crisis and surface deformation. Strikingly, mixing must have continued for many weeks after the onset of the eruption. The abundance of complexly zoned phenocrysts in the late eruptive products is interpreted to reflect mobilization of crystal mush and cumulates as a consequence of magma withdrawal and reservoir collapse.

Established and advanced solid-state NMR spectroscopy for a better understanding of the structure and function of natural organic matter in soils, water and sediments

HEIKE KNICKER¹, SASCHA LANGE²,
BARTH VAN ROSSUM² AND HARTMUT OSCHKINAT²

¹Instituto de Recursos Naturales y Agrobiología de Sevilla, CSIC, Adva. Reina Mercedes, 10. 4012 Sevilla, Spain

²Leibniz-Institut für Molekulare Pharmakologie FMP, Robert-Rössle-str. 10, 13125 Berlin, Germany

In geobiogeochemistry, 1-dimensional solid-state NMR spectroscopy has been proven as a powerful tool for the characterization of natural organic matter (NOM) in soils, sediments and waters. However, compared to solution NMR spectroscopy, this technique suffers from broad resonance lines and low resolution, which could be overcome by the use of 2-dimensional solid-state NMR pulse sequences. Until recently, this approach has been unfeasible as a routine tool in geochemistry, mainly because of the low NMR sensitivity of the respective samples. Alternative to the use of higher magnetic fields, considerable signal enhancements can be achieved with the new developments in the field of dynamic nuclear polarization (DNP) solid-state NMR spectroscopy. Here, the improvement is achieved by a microwave-driven transfer of polarization from a paramagnetic centre to nuclear spins. Application of DNP to magic angle spinning (MAS) spectra of biological systems (frozen solutions) showed enhancements by factors of 40 to 50 (Hall *et al.*, 1997). Applying this technique for the first time on NOM, lower but still promising enhancement factors were obtained which allowed the successful acquisition of 2D solid-state NMR spectra of such samples. In the present contribution, the possibilities and limitation of established solid-state NMR techniques in NOM research are discussed and first results obtained with solid-state DNP NMR are presented. Those first data demonstrate the great potential of the latter and that this approach opens new doors for a better understanding of biochemical processes in soils, sediments and water.

Coupling of nitrogen inputs and losses during the Permian-Triassic biotic crisis

J. KNIES*¹, S.E. GRASBY^{2,3}, B. BEAUCHAMP³
AND C.J. SCHUBERT⁴

¹Geological Survey of Norway, 7491 Trondheim, Norway
(*correspondence: jochen.knies@ngu.no)

²Geological Survey of Canada, Calgary, Alberta T2L 2A7,
Canada

³University of Calgary, Calgary, Alberta T2N 1N4, Canada

⁴Swiss Federal Institute of Aquatic Science and Technology,
EAWAG, 6407 Kastanienbaum, Switzerland

We report coupling of dinitrogen (N₂) fixation and denitrification in oxygen deficient waters in the Sverdrup Basin, Arctic Canada, during the Permian-Triassic biotic crises. Sediments deposited prior to the latest Permian extinction (LPE) event are characterized by positive δ¹⁵N values of ~9 ‰ associated with the presence of lycopane implying upwelling of denitrified waters from an expanded oxygen minimum zone (OMZ). The data show anoxic bottom water conditions were not developed in northeastern Panthalassa during the Late Permian. Promoted by dispersing coal ash from Siberian Traps volcanic, as marked by abrupt rise in C/N ratios (>20) prior to the LPE event, euxinic conditions first developed at the LPE. Nutrient-induced anoxia was likely prevalent during the Early Triassic in the aftermath of the LPE, however, the nutrient N pool was predominantly fuelled by N₂-fixing cyanobacteria.

Tellus: Regional-scale baseline geochemical mapping of soil, stream sediment and stream water for the island of Ireland

KNIGHTS, K.V¹ AND SCANLON, R.²

^{1,2}Geological Survey of Ireland, Beggars' Bush, Haddington
Road, Dublin 4, Ireland (kate.knights@gsi.ie,
ray.scanlon@gsi.ie)

Systematic geochemical surveying of the northern region of the island of Ireland, comprising Northern Ireland (NI) and the northernmost counties of the Republic of Ireland (RoI), is now complete. The Geological Survey of Ireland recently conducted regional-scale surveying of soils, stream sediments and stream waters geochemistry across the northern region of Ireland under the Tellus Border project. A survey of neighbouring Northern Ireland was completed in 2007 under the Tellus project by the Geological Survey of Northern Ireland. Multi-element analytical data for the entire region are currently being integrated to provide seamless cross-border mapped datasets. These surveys also took place alongside multiparameter low-level airborne geophysical surveys collecting magnetic field, electromagnetic and radiometric data; resulting in a high-quality and comprehensive geo-environmental database.

There are challenges in merging these data; with two ground survey designs conducted at differing densities. However the same general field collection, sample preparation and analytical methodologies have been utilised. Topsoils (c.5–20 cm) have undergone *aqua regia* ICP analyses, stream sediments (<150 μm wet-sieved fraction) by XRF and stream waters analysed by IC, ICP-MS and for DOC.

Legacy and new data have been combined and are being assessed using multivariate statistical techniques (*e.g.* factor analyses) to characterise and map factors which help to define geochemical signatures; to understand sources and processes at play. They reveal broad geogenic controls and influence of agricultural practices that overprint the rural geochemical baseline.

The region now has a rich geochemical dataset with improved detail across this geologically diverse region. Elements of interest to agricultural applications are compared to results from prior national soil surveys and the European-wide GEMAS study.

The effect of marine biological activity on aerosol generation and cold cloud formation

D. A. KNOPF^{1*}, P. A. ALPERT¹, W. KILTHAU¹,
J. RADWAY¹ AND J. Y. ALLER¹

¹School of Marine and Atmospheric Sciences, Stony Brook Univ., Stony Brook, NY, 11794-5000, USA
(*correspondence to daniel.knopf@stonybrook.edu)

Sea salt particles are a major contributor to atmospheric aerosol. Recent observations have indicated that these and other marine derived particles can be enriched in organic material (OM), particularly during periods of high primary production. This OM can impact atmospheric particulate matter loading and the ability of particles to act as cloud condensation and ice nuclei, with subsequent consequences for the global radiative budget.

Here we report the effects of marine biological activity on aerosol generation and cloud formation potential. Aerosols were produced by plunging jets and glass frits from 1000L mesocosms containing three phytoplankton species cultured in artificial seawater, exudates derived from phytoplankton, a bacterial culture, and a natural seawater microbial community. The 14-day experiments simulated bloom development as evidenced by changes in cell numbers. At each sampling time, aerosolized particles were size discriminated under dry and 80% humidified conditions, collected, and characterized. Bubble-size spectra were determined. To interpret relationships between biological activity and aerosol size distributions, we characterized concentrations of dissolved and particulate organic matter, transparent exopolymer particles, and microgels; numbers of phytoplankton and virus-like particles; and the proportion of live:dead bacteria. Aerosols were collected on substrates for single particle chemical analyses using electron and X-ray micro-spectroscopy. Water uptake and ice nucleation capabilities for temperatures as low as 200 K were determined.

As phytoplankton growth reached stationary phase, the number of particles smaller than 100 nm increased threefold. Ice active particles in a population characterized by a sea salt core with OM coating are 1.0-5.0 μm in diameter. Water uptake is observed until 220 K and 60% RH. Immersion freezing occurs between 80% and 100% RH. Deposition ice nucleation occurs below 215 K and around 70% RH. Our experiments show that biological activity can affect marine derived aerosol, with implications for cloud formation and the radiative budget.

Impact of long term wetting on hydrology and biogeochemistry of a peat bog in Ontario, Canada

KLAUS-HOLGER KNORR¹, CHRISTIAN BLODAU¹, SVEN FREI², KLAUS KASPARBAUER² AND JONAS SCHAPER²

¹Institute for Landscape Ecology, Hydrology Group, WWU Münster, Heisenbergstr. 2, 48149 Münster, Germany; kh.knorr@uni-muenster.de
²Department of Hydrology, University of Bayreuth, Universitätsstr. 30, 95447 Bayreuth, Germany

Peatlands of the northern hemisphere store vast amounts of carbon but also contribute to global methane emissions. As large areas in the boreal and temperate zones are predicted to undergo significant changes in climate and concomitant changes in hydrology, it is crucial to understand the response of peatlands to altered climatic and hydrological boundary conditions. In this study we investigated the response of peatlands to long term wetting, as especially in winter for large areas wetter conditions have been predicted. We hypothesized that long term wetting will result in changes in vegetation, concomitant changes in peat decomposability and also nutrient input from the adjacent water body.

To this end, we chose the Luther Marsh site in Ontario, Canada, that has been partly flooded since the 1950s due to the construction of a reservoir. Water management in the reservoir flooded a large part of the peatland, but also causes seasonal flooding and draining, shifting hydrological flow patterns and vegetation gradients. Hydrology was monitored by means of piezometers and pressure transducers over one growing season over a transect of 7 sites from the reservoir to the inner, pristine part of the bog. At the same sites, we obtained pore water chemistry data and dissolved gases.

Partial flooding resulted in obvious changes in vegetation, increased nutrient availability, and thus increased decomposition activity in the wet part. This was reflected more narrow CH₄ to CO₂ ratios in the pore water and higher concentrations and calculated turnover rates. Advective transport removed decomposition end products and introduced nutrient enriched reservoir water, as indicated by elevated pH and increased concentrations in Ca and Mg. DOC quality as assessed by fluorescence spectroscopy also gradually approached quality indices observed in the reservoir.

This study demonstrated that partial flooding of a peatland significantly changes vegetation and the nutritional status, resulting in a shift towards more CH₄ production and higher turnover rates.

Molecular Dynamics Study of Cement-Aqueous Solution Interfacial System: Cesium Ion Fixation

K. KOBAYASHI¹, Y. LIANG¹, I.C. BOURG²
AND T. MATSUOKA¹

¹Environment and Resource System Engineering Lab., Kyoto Univ., Kyoto 615-8540, Japan
(kobayashi.kazuya.44n@st.kyoto-u.ac.jp,
liang.yunfeng.5x@kyoto-u.ac.jp,
matsuoka.toshifumi.7x@kyoto-u.ac.jp)

²Earth Science Division, Lawrence Berkeley National Lab., Berkeley, CA 94720, USA (icbourg@lbl.gov)

Cs⁺ ion is one of radioactive species generated by nuclear electric power. It is one of the most problematic ions because of its long half-life and high mobility. Cement material is considered as a candidate for the solid fixation of Cs⁺ ions, and the engineered barrier for the geological disposal of such radioactive species. The structures of the cement is complicated, and considered as nano-crystalline aggregation phase with two distinct local structures, tobermorite and jennite, by the difference of Ca/Si ratio and the silica-chain length. The goal of this research is to detect which structural or compositional feature is essential to ionic adsorption into cement matrix.

By using molecular dynamics simulations, we have studied the aqueous solution-mineral (cement) interfacial systems for two different cement local structures (tobermorite and jennite) and two different solutions (NaCl and CsCl). It was found that Na⁺ ion could form both inner-sphere complex and outer-sphere complex, without full hydration shell and with full hydration shell at the time of adsorption, respectively. In contrast, Cs⁺ ion could only form inner-sphere complex for both mineral cases. This finding is in good correspondence with previous NMR studies [1]. Furthermore, we found that the inner-sphere complex Na⁺ is tightly binded with the deprotonated oxygen. More importantly, it was found that tobermorite presents better binding property than that of jennite. The fact that differences in cement structure and ion species may cause these differences in adsorption state and binding property will enhance our understanding on cement materials in the case of the solid fixation and the geological disposal.

[1] Viallis *et al.* (1999) *J. Phys. Chem. B* **103**, 5212-5219

Subducted halogens and noble gases in the mantle wedge peridotites

M. KOBAYASHI^{1*}, H. SUMINO¹, K. NAGAO¹,
S. ISHIMARU², S. ARAI³, M. YOSHIKAWA⁴,
T. KAWAMOTO⁵, Y. KUMAGAI⁵, T. KOBAYASHI⁶,
R. BURGESS⁷ AND C.J. BALLENTINE⁷

¹GCRC, Univ. Tokyo, Tokyo 113-0033, Japan

(*correspondence: kobayashi@eqchem.s.u-tokyo.ac.jp)

²Kumamoto Univ., Kumamoto 860-8555, Japan

³Kanazawa Univ., Kanazawa 920-1192, Japan

⁴Kyoto Univ., Beppu 874-0903, Japan

⁵Kyoto Univ., Kyoto 606-8502, Japan

⁶Kagoshima Univ., Kagoshima 890-0065, Japan

⁷SEAES, Univ. Manchester, Manchester M13 9PL, UK

Halogen and noble gas compositions are complementary tracers of H₂O (or aqueous fluids) in the mantle. Via subduction of sedimentary pore-fluids, halogens and noble gases are carried into the mantle [1, 2]. Here, we present the halogen and noble gas compositions of mantle peridotites from subduction zones (the Avacha volcano in Kamchatka, the Pinatubo volcano in Philippines, and the Horoman massif in Japan) to investigate how far the influence of subducted pore fluids extends in the mantle wedge. H₂O-rich fluid inclusions are present in the studied peridotites as previously described [3–5]. To determine noble gas and halogen compositions of the fluid inclusions and bulk peridotites, we converted halogens (Cl, Br and I) to Ar, Kr and Xe isotopes by neutron irradiation, and extracted the noble gases by *in vacuo* crushing or heating.

The Br/Cl and I/Cl values of the fluid inclusions obtained by crushing show a sedimentary pore-fluid signature with some variation between localities. The halogen ratios obtained by heating are slightly lower than crushing suggesting the presence of additional Cl in minerals such as amphibole and/or silicate glass [3] in the peridotites. Slab-derived, seawater-like noble gases are also dominant in fluid inclusions as previously reported [6, 7].

The composition of subducted halogens and noble gases in the mantle peridotites demonstrates that sedimentary pore-fluid signatures are carried beneath the island arcs through subduction and survive in the mantle wedge. Deeper subduction of pore-fluid like noble gases into the deep mantle accounts for the same signature of the convecting mantle [2].

[1] Sumino *et al.* (2010) *EPSL* **294**, 163-172. [2] Holland & Ballentine (2006) *Nature* **441**, 186-191. [3] Ishimaru *et al.* (2007) *J. Petrol.* **48**, 395-433. [4] Kumagai *et al.* (2011) *JpGU Meeting 2011*, SCG060-P07. [5] Hirai & Arai (1987) *EPSL* **85**, 311-318. [6] Hopp & Ionov (2011) *EPSL* **302**, 121-131. [7] Matsumoto *et al.* (2001) *EPSL* **185**, 35-47.

Zinc isotopes as a tool to study zinc uptake by marine phytoplankton

M. KÖBBERICH^{1*}, A. D. COX², AND D. VANCE¹

¹Institute of Geochemistry and Petrology, ETH Zurich, Switzerland

²School of Earth and Space Exploration, Arizona State University, USA

The availability of metals to marine phytoplankton has been suggested to control oceanic carbon uptake from the atmosphere and its sequestration to the deep sea. Metal variability across glacial/interglacial periods could have driven changes in the composition of atmospheric greenhouse gases [1]. Many transition metals, including zinc, are often extremely scarce in the euphotic zone and are coupled with deep enrichments, consistent with biological uptake at the surface and regeneration at depth. However, abiotic processes, such as scavenging, can also contribute to this depth cycling [2]. If the surface to depth cycling is associated with zinc isotopic fractionation, then isotopic studies should be able to elucidate the key controlling processes, both now and in the past.

Here we seek to evaluate zinc isotopes as a potential tool to track metal cycling in the oceans. Recently obtained depth profiles of dissolved zinc isotopes from the NE Pacific reveal anomalously light compositions in the shallow sub-surface immediately below the isotopically heavier euphotic zone. This dataset suggests shallow zinc recycling in the upper ocean, possibly caused by the release of biologically bound light zinc [3,4]. To our knowledge, the diatom *Thalassiosira oceanica* is thus far the only planktonic organism that has been shown to fractionate zinc isotopes during uptake [5]. We have cultured this organism, and a variety of other marine phytoplankton strains, in order to explore systematic and species-dependent changes in their isotopic fractionation. Thermodynamic reaction modelling of our experiments and natural systems elucidates zinc isotopes as a potentially powerful tool to reconstruct biological metal cycling in both modern and past oceans.

[1] Martin (1990), *Paleoceanogr.* **5**(1), 1-13. [2] Little *et al.* (in review), *Global Biogeochem. Cy.* [3] Lohan *et al.* (2002) *Deep-Sea Res. II* **49**(24-25), 5793-5808. [4] Vance *et al.* (2012), *Mineral. Mag.* **76**(6), 2486. [5] John *et al.* (2007), *Limnol. Oceanogr.* **52**(6), 2710-2714.

Noble gas signature of Tertiary alkaline basalts and xenoliths from central Europe

YU. KOCHERGINA^{1,2}, S. NIEDERMANN³, V. RAPPRICH¹
AND T. MAGNA¹

¹Czech Geological Survey, Klarov 3, CZ-11821 Prague, Czech Republic; julia.kocergina@geology.cz

²Faculty of Science, Charles University, Albertov 6, CZ-12843 Prague, Czech Republic

³GFZ Potsdam, Telegrafenberg, D-14473 Potsdam, Germany

We present preliminary He and Ar isotope data for two suites of pristine alkaline basaltic rocks associated with the Eger Rift, Bohemian Massif, in order to deconvolve the noble gas signature of the sub-continental lithospheric mantle beneath central Europe. In addition, He and Ar data were collected from xenoliths enclosed in these alkaline basalts in order to compare the noble gas isotope signature of the mantle source of the xenoliths, thought to be located at shallower depths than that inferred for alkaline volcanic rocks.

Most xenolithic and phenocrystic olivines have ³He/⁴He ratios between 4.7 and 6.6R_A, clearly more radiogenic than MORB, and rather constant despite ⁴He concentrations varying by nearly two orders of magnitude (0.1–8.9×10⁻⁸ cm³ STP/g), although the highest ⁴He concentration is associated with an elevated ³He/⁴He of 7.2R_A. The latter may suggest sampling of a convective mantle similar to MORB. Homogeneous ³He/⁴He ratios (5.5–5.7R_A; n=3) are found for olivines from the Doupovske hory volcanic complex, whereas clinopyroxene shows a slightly more radiogenic signature (4.1R_A). Collectively, He isotope data shows a remarkable homogeneity across two chemically distinct volcanic centres associated with the major Eger rift lineament, attesting to their temporally and spatially invariant lithospheric mantle source, and confirms further the observations of a homogeneous He isotope signature of the sub-continental mantle beneath central Europe [1]. ⁴⁰Ar/³⁶Ar ratios for the same samples are between 306 and 3690. Atmospheric Ar could be admixed by infiltration of air from basaltic melts; such a process of metasomatism of mantle xenoliths by basaltic melts has been reported from other localities of the Eger rift [2]. Further He and Ar isotope analyses of alkaline basaltic and basanitic rocks and xenoliths of distinct mantle layers from between 32 and 70 km in depth are in progress.

[1] Gautheron *et al.* (2005) *Chem Geol* **217**, 97-112; [2] Ackerman *et al.* (2013) *J Petrol*, under review

Trace metals in plants of Chadak gold ore field, Uzbekistan

O.KODIROV¹*, F. MARTIN² AND N. SHUKUROV¹

¹Institute of Geology and Geophysics, Academy of Sciences of Uzbekistan, 49-Olimlar, 100041, Tashkent, Uzbekistan (*correspondance: o.kodirov@gmail.com)

²University of Granada, University Campus Fuentenueva s/n 18071- Granada, Spain (fjmartin@ugr.es)

Among the set of conditions that determine the status of the biota and the environment in general, geochemical factors related to the geologic history of the area and its constituent chemical composition of rocks and soils play a major role. It is known that the chemical composition of plant communities are closely related to the concentration of some elements in soil. From this perspective, the study of the relationship between the components of geochemical environment is the main objective of our investigation.

The study area is characterized by a relatively developed mining industry, here since 1970 operates the Chadak mine and the gold-extracting factory.

Plant samples (*Artemisia absinthium* and *Phragmites australis*) were collected in the vicinity of Chadak mining area and in tailing dumps which were formed as a results of mining activity. Dry ashing was conducted in a muffle furnace at temperatures of 450 to 500°C for 3-4 hours. After the ashing the ashe dissolved in dilute HNO₃+3HCl. The final solution was analized for Cu, Zn, Pb, Mn and As with ICP-MS.

Results show that trace elements were to exceed normal concentration in plant leaves [1] and reaching (mg/kg): Cu – 37-639, Zn – 174-1798, Pb – 5-282, Mn – 361-2969, and As – 2-341, respectively.

As can be seen from the results trace elements are found in excessive or toxic concentration despite the fact, that some of these elements are essential for plants. Not always observed relationship with the soil composition as the concentration of trace metals are much higher than in soil samples. Perhaps this is due to selective ability of some plant species or such high content of trace metals related to ore deposit.

Many studies have shown that there is a correlation of trace metals in plants on the content of their mobile forms in soil solution. With this respect, future investigations on the mobile forms of trace metals are required in our studied area.

[1] Kabata-Pendias, Alina (2011) 4-th ed. *CRC Press*, 505.

Platelet degradation in diamonds. Insights from infrared microscopy and implications for the thermal evolution of cratonic mantle.

S.C. KOHN*, E. WIBBERLEY, C.B. SMITH, G.P. BULANOVA AND M.J. WALTER

School of Earth Sciences, University of Bristol, Queens Rd., Bristol, BS8 1RJ, UK (*simon.kohn@bristol.ac.uk)

Crystallographic defects in diamonds provide a wealth of information that can, in principle, be used to constrain the thermal evolution of diamond source regions. The simplest method consists of using the average N concentration and aggregation of whole diamonds of known age to obtain an estimate of residence temperature in the mantle. Detailed studies of the spatial dependence of N abundance and aggregation provide an improvement in temperature estimation and can provide constraints on multistage diamond growth events (Kohn *et al.*, in prep). However, temperature estimates can only be obtained if the diamond has been dated by an independent method and the temperature obtained is neither the maximum nor mean temperature experienced during residence in the mantle, because of the exponential temperature dependence in the kinetic equation.

In the present study we are exploring the potential of platelet degradation rate as an additional constraint on thermal histories of diamonds and their cratonic mantle hosts. The approach is to measure nitrogen abundance and aggregation in core-to-rim profiles across diamonds from Argyle (Australia) to determine apparent temperature profiles. These profiles are then compared with the degree of platelet degradation at each point. If platelet degradation occurs at a fixed rate for a given temperature, then for diamonds with a single mantle residence time there should be a clear correlation between the degree of platelet degradation and temperature. Our data show that for a single diamond such a correlation usually exists, but that for the whole data set there are wide variations in the apparent degradation rate. The diamonds with the slowest apparent rates were found to have eclogitic (E) inclusions while those with the fastest rates are peridotitic (P). For Argyle the mantle residence times are around 0.4 and 1.4 Ga for E and P respectively [1], suggesting that the degradation rate could be constant at a given T, and that the different degrees of degradation reflect the different residence times of the two parageneses.

The potential role of plastic deformation and other complicating factors in modifying the calculated temperatures and degree of platelet degradation will also be discussed.

[1] Lugué *et al.* (2009) *Lithos* **112S**, 1096-1108.

OH incorporation in quartz as a tracer of formation conditions

MARZENA A. KOHUT¹ ROLAND STALDER¹
AND JÜRGEN KONZETT¹

¹Institute of Mineralogy and Petrography, University of
Innsbruck, Austria, Marzena.Kohut@uibk.ac.at,
Roland.Stalder@uibk.ac.at, Juergen.Konzett@uibk.ac.at

Quartz as a common nominally anhydrous mineral of the Earth's crust contains traces of hydrogen as a molecular water in fluid inclusions, or as structurally incorporated hydroxyl ions. The structurally bound hydrogen commonly acts as a charge compensator, associated with point defects, such as substitution of Si⁴⁺ by Al³⁺ and/or B³⁺ with charge balance maintained by monovalent cations substitutions (H⁺, Li⁺ and Na⁺). The occurrence of hydrogen affects thermodynamic properties of minerals and influences their kinetic behavior during diffusion and phase transformations. Even small amounts of OH defects can dramatically change physical properties of minerals that are a key to understand rock-formation mechanisms within the crustal conditions.

The geochemical behavior of OH incorporation in quartz in the systems granite-tourmaline-water and granite-spodumene-water was studied in order to explain the effect of pressure and temperature on structural defect generation. Piston-cylinder experiments were carried at pressures between 5 and 25 kbar and temperatures between 800 and 1050°C. Oriented and polished quartz crystals from each run were characterized with FT-IR spectroscopy and water contents were calculated using mineral-specific and general wavelength-specific calibrations.

The OH absorption features were assigned to Al³⁺-substitution (Al-H defect, band-triplet at 3320, 3383 and 3434 cm⁻¹), B³⁺-substitution (sharp absorption band at 3597 cm⁻¹), Li⁺-substitution (weak absorption band at 3475 cm⁻¹) and hydrogarnet (4H)_{Si} defect (absorption at 3585 cm⁻¹).

In this study point defects cause various OH contents in quartz, depending on different pressures, temperatures and chemical environments. Synthesized crystals showed a negative correlation of calculated water content vs. pressure. Under lower pressures quartz incorporates more hydrogen (5 kbar: 450-750 ppm H₂O) than at higher pressures (25 kbar: 72-106 ppm H₂O). Therefore, our results imply that IR spectra of quartzes have a potential to be used as a geobarometer to indicate petrological formation conditions. Moreover, the B- and Li-specific OH absorption bands may be used to quantify the charge balancing B³⁺- and Li⁺- content that could be used as a novel and indirect analytical tool to detect traces of B and Li in quartz crystals.

Ion microprobe U-Pb dating of individual phosphate grains in Martian meteorite

M. KOIKE^{1*}, Y. OTA¹, N. TAKAHATA¹, Y. SANO¹
AND N. SUGIURA²

¹AORI, Univ. of Tokyo, Chiba, Japan, mizuho_k@aori.u-tokyo.ac.jp (*presenting author)

²School of Science, Univ. of Tokyo, Tokyo, Japan

A Martian meteorite ALH 84001 shows extremely old age of over 4 Ga and is expected as a key to the ancient history of Mars. Its crystallization age is still controversial due to the complicated impact history. While volumetrically minor, phosphates are important carriers of trace elements. Previous SIMS U-Pb dating of several merrillite and apatite grains in ALH 84001 showed ~4 Ga [1]. However, intra-grain systematics was not observed because of limited spatial resolution. In-situ analysis of a single grain will provide further information regarding cooling and reheating process. Here we measured single grain U-Pb ages using a laterally high-resolution secondary ion mass spectrometer (NanoSIMS) at Atmosphere and Ocean Research Institute, University of Tokyo.

Two polished thick sections of ALH 84001 were firstly observed by SEM-EDS. Two merrillite grains with ~100 μm in diameter were found. The sections were polished again, gold-coated and baked overnight, and then analyzed by a NanoSIMS. A 2-10 nA O⁻ primary beam was used with spot size of ~10-20 μm. An apatite from Prairie Lake circular complex, PRAP, with a known age of 1155 ± 20 Ma [2] was used as a standard of UO/UO₂-Pb/UO calibration.

For both analyzed grains, the obtained ²³⁸U-²⁰⁶Pb and ²⁰⁶Pb-²⁰⁷Pb ages show good agreement with ~4 Ga, suggesting the intra-grain U-Pb system is concordant. There is also chemical zoning of U abundance. Since diffusion rate of U in apatite is slower than Pb by ~4 orders of magnitude [3], the observed zoning was possibly made during crystal growth and preserved since then. Meanwhile, Pb may have been homogenized within a grain at crystallization (and/or later impacts), which makes single grain U-Pb dating possible. The interpretation of the ages (igneous or impact-reset) is related to the processes of crystallization and impacts. Further studies including micro scale analyses of other elements are required. This is the first report of single grain U-Pb dating of phosphates using a NanoSIMS.

[1] Terada *et al.* (2003) *Meteorit. Planet. Sci.* **38**, 1697-1703.

[2] Sano *et al.* (2006) *Geochem. J.* **40**, 597-608. [3] Cherniak (2005) *Chem. Geol.* **219**, 297-308

The effect of carbon dioxide on metal transport by geological fluids

MARIA A. KOKH^{1*}, GLEB S. POKROVSKI¹,
DAMIEN GUILLAUME¹ AND STEFANO SALVI¹

¹GET, CNRS, University of Toulouse, France
(*maria.kokh@get.obs-mip.fr)

Carbon dioxide is the second major component (after water) of most crustal fluids responsible for metal ore deposit formation. Its contents amount up to 10-20 wt% in porphyry Cu-Au-Mo fluids [1] and more than 50 wt% in metamorphic, skarn, orogenic gold, and PGE deposits [2]. In contrast to H₂O-dominated fluids, models of metal transport and deposition by high-temperature and pressure (T-P) CO₂-rich fluids are subjects to debate.

In this contribution, we combined thermodynamic modeling, based on few data available from the literature, with new solubility experiments in H₂O-CO₂-salt-sulfur systems to assess, in a systematic way, the role of CO₂ on the behavior of metals at hydrothermal conditions. Our analysis shows that the presence of CO₂ may have the following impacts on metals transport: a) the presence of CO₂ expands the field of vapor-liquid immiscibility, which causes both changes in metal solubility in the liquid phase (mostly owing to changes in pH), and a redistribution of metals between vapor and liquid; b) CO₂ decreases both water activity and the dielectric constant of the solvent, which in turn affects ion pairing and the activity coefficients of charged species; c) the formation of complexes with C-bearing ligands (CO₃²⁻, HCO₃⁻, CO, COS) may be important for some metals (e.g., Rare Earth Elements, U, Sn, Fe, Ni); and d) at high concentrations (>~50 wt%), CO₂ may also specifically solvate some non-polar complexes (e.g., AuHS(H₂S) [3]) and thus enhance their solubility.

To evaluate the contribution of these factors, we are currently investigating experimentally the solubility of major ore minerals (FeS₂, CuFeS₂, MoS₂, SnO₂, PtS, and Au) in H₂O-KCl-CO₂-H₂S supercritical fluids in the presence of acidity and redox mineral buffers, and as function of CO₂ content. Data obtained in H₂O-dominated experiments allow a revision of the available speciation models for metals in high T-P aqueous fluids. These results will provide the necessary basis for interpreting experimental runs in CO₂-rich fluids, which are in progress.

[1] Kouzmanov & Pokrovski (2012) *Society of Economic Geologists, Inc. Special Publication* **16**, 573-618. [2] Phillips & Evans (2004) *Nature* **429**, 860-863. [3] Pokrovski *et al.* (2008) *Earth & Planet. Sci. Letters* **266**, 345-362.

Using model mineral-organic matter-water interfaces as a step towards determining the fate of pollutants in the environment

P.E. KOLIC¹, B. SUBRAMANIAN¹, D.A. SPIVAK¹
AND R.L. COOK^{1*}

¹Department of Chemistry, Louisiana State University, Baton Rouge, LA 70803, USA (*correspondence: rlcook@lsu.edu)

Mineral-organic matter-water interfaces play a valuable role in our ecosystem and are a major role player in determining the bioavailability as well as the fate and transport of anthropogenic contaminants (ACs) in the environment. Anthropogenic contaminants include a vast amount of compounds that are harmful to the environment and its inhabitants. The mineral-organic matter component of the mineral-organic matter-water interface has been found to play a major role in the sorption of ACs in soils and sediments, thus decreasing their presence in other environmental compartments, such as groundwater. This mineral-organic matter component is highly complex, especially in terms of the organic matter constituent, leading to a lack of detailed chemical insight into AC sorption. In order to address this void and gain valuable information that a real soil and sediment samples cannot provide, a simpler more homogeneous mineral-organic matter model system is needed to serve as a model system. To better understand the chemical mechanism of pollutant sorption to the mineral-organic matter component, this project uses a combination of highly adjustable model synthetic mineral-organic matter sorbent systems. The model system consists of silica, a model mineral surface, functionalized with alkyl, aromatic, and O-alkyl groups to echo the natural structure of organic matter. Solid state Nuclear Magnetic Resonance (NMR) as well as a range of other techniques are used for characterization of the model synthetic mineral. Sorption and desorption batch experiment studies are performed using commonly used pesticides as model organic pollutants as an initial step towards understanding the geochemical mechanisms that occur at mineral-water interfaces.

Geochemistry of uranium in lakes of West Mongolia

KOLPAKOVA M. N.^{1,2*}

¹Tomsk Department of the Trofimuk Institute of Petroleum-Gas Geology and Geophysics, Siberian Branch of the Russian Academy of Sciences, Akademichesky ave. 4, Tomsk, 634055, Russia, marina.kolpakova@gmail.com

²National Research Tomsk Polytechnic University, Lenin ave. 30, Tomsk 634050, Russia

Natural lakes with high concentrations of uranium are widespread, for example, Van in Turkey (110 μgL^{-1}) [1], Mono in the USA, California (300 μgL^{-1}), Shar Burdiin in Eastern Mongolia (15000 μgL^{-1}) [2]. In Western Mongolia, we have also discovered lakes with concentrations of uranium as high as 3000 μgL^{-1} . In the arid climate of western Mongolia, where evaporation is by 2-3 times higher than the amount of precipitation, evaporation concentration processes contribute to the growth of salinity and content of the U. However, our investigation indicated a significant role in uranium accumulation in the waters of the upper hydrodynamic zone is provided by aquiferous rock catchment lakes. Geologically, granite massifs are widespread on the studied territory, which are known to be possessed of natural radioactivity. But the type of rock is not the main factor. The time of water-rocks interaction which determines the degree of accumulation of U in the lakes is more important. Precisely, the equilibrium-nonequilibrium state of the system water-rock determines the possibility of U concentration in the water during the whole time of its interaction with rocks: the longer interaction time, the more uranium will be concentrated in the water, of course, the other things being equal. Analysis of the lake waters equilibrium with uranium minerals shows that only a few can precipitate out of solution and only three lakes with total salinity more than 300 gL^{-1} equilibrium with the investigated minerals. Water store U by getting into the rocks of any composition and dissolving them. Uranium, in turn, forms complexes with carbonate-ions and migrate to the lakes, and precipitates in lake sediments by influence of evaporation and water-rock interaction time. In this case, the more uranium will be accumulated in the water for the entire migration path to the lake, the greater amount will be precipitated. Consequently, the lakes are a unique geochemical barrier for the migration of uranium which forms oxides, hydroxides, carbonates, phosphates, fluorides and other minerals in lakes sediment.

[1] Mehmet *et al.* (2011) *Clean-Soil, Air, Water* **39**(6), 530-536. [2] Linhoff *et al.* (2011) *Environ. Earth Sc.* **62**, 171-183.

Evaluating the efficiency of a synthetic amorphous manganese oxide for chemical stabilization of Cu in a contaminated soil

M. KOMÁREK*, L. TRAKAL, Z. MICHÁLKOVÁ
AND L. DELLA PUPPA

Czech University of Life Sciences Prague, Department of Environmental Geosciences, Kamýčká 129, 165 21, Prague 6, Czech Republic

(*correspondence: komarek@fzp.czu.cz)

Chemical stabilization techniques aim at rendering less available the metal(loid) fractions that can pose significant environmental and toxicological risks and protecting the functionality of the soil environment [1]. Recently, a synthetic amorphous manganese oxide (AMO) has been proposed as an efficient metal sorbent and stabilizing agent for contaminated soils [2]. This work aims to evaluate AMO (up to 2 wt.%) stabilization efficiency in a soil contaminated predominantly with Cu (400 mg/kg; pH 3.6) using (i) batch experiments with soil solution samplers (rhizons), (ii) small-scale columns and (iii) a novel set-up of a large-scale column experiment together with direct sampling of the soil solution and chemical extraction methods (0.01 M CaCl_2 , 0.05 M EDTA, BCR sequential extraction procedure).

The results suggest that the application of the AMO increased the soil pH and its high reactivity resulted in increased DOC concentrations originating from dissolved soil organic matter (SOM). The AMO was efficient in stabilizing Cu proved by significant decreases in Cu in soil solution, in the exchangeable fraction and CaCl_2 /EDTA extracts. When further metals (Cd, Cu, Pb, Zn) were added to the soil columns, the AMO was able to stabilize them in the subsurface layers. However, due to SOM dissolution, metals (especially Cu) bound to the organic soil phase can be released to the soil solution. This preliminary study assess the efficiency of the AMO for metal stabilization in a Cu-contaminated soil and proposes a combination of experimental set-ups evaluating the efficiency of stabilizing amendments in general.

[1] Komárek *et al.* (2013) *Environ. Pollut.* **172**, 9-22. [2] Della Puppa *et al.* (2013) *J. Colloid Interf. Sci.*, in press.

Simultaneous determination of carbon and hydrogen isotope enrichment factors of methane during microbial oxidation in a natural water environment

D. D. KOMATSU¹, U. TSUNOGAI¹, S. SATO²,
F. NAKAGAWA² AND A. TANAKA³

¹Graduate school of Environmental Studies, Nagoya University, Nagoya, 464-8601, Japan (*correspondence: ddkomatsu@nagoya-u.jp)

²Graduate school of Science, Hokkaido University, Sapporo 060-0810, Japan

³NIES, Tsukuba, 305-8506 Japan

The stable carbon and hydrogen isotope compositions ($\delta^{13}\text{C}$ and $\delta^2\text{H}$) of methane (CH_4) were analyzed using a newly developed CF-IRMS method in a hydrothermal plume in the water column of Lake Towada, Japan. The CH_4 concentration, $\delta^{13}\text{C}\text{-CH}_4$, and $\delta^2\text{H}\text{-CH}_4$ in the lake water column varied widely, ranging from 0.6 to 246.5 nM, -54.9 to $+54.2\text{‰}$ (vs VPDB), and -258 to $+762\text{‰}$ (vs VSMOW), respectively, reflecting rapid CH_4 oxidation in the water column. Rapid CH_4 oxidation was further confirmed through bottle incubation experiments of the lake water sampled below 150 m, which found an extreme increase in the values of both $\delta^{13}\text{C}\text{-CH}_4$ and $\delta^2\text{H}\text{-CH}_4$ corresponding to a decreasing CH_4 concentration, after the incubations of more than 48 hours. The isotope enrichment factors for carbon and hydrogen were determined through incubation experiments to be $-26.2 \pm 0.9\text{‰}$ and $-233 \pm 12\text{‰}$, respectively, and the rapid rate constants ranged from 0.05 to 0.67 day^{-1} . These enrichment factors were the highest values ever reported in natural environments. In addition, we found that a greater isotope fractionation occurred at larger rate constants, i.e., higher populations of CH_4 oxidizing microbes. However, we also found that the ratios between the isotope enrichment factors of hydrogen and carbon (Λ values) were always constant around 11.3 ± 0.9 , which coincides well with previous laboratory and field observations under elevated CH_4 concentration. The coincidence in the Λ value of approximately 10 between this study and previous studies indicates that the Λ value can be a robust tracer for distinguishing microbial CH_4 oxidation from the other processes such as mixing, even in environmental samples of nanomolar per liter quantities of CH_4 .

LIME Olivine and Pyroxene: Multi-Stage Thermal Histories of AOAs

M. KOMATSU^{1*}, T. FAGAN² AND T. MIKOUCHI³

¹Waseda Institute for Advanced Study, Waseda University, Tokyo 169-8050, Japan (*komatsu@aoni.waseda.jp)

²Dep. of Earth Sciences, Waseda University.

³Dep. of Earth and Planetary Science, University of Tokyo.

Low-iron, Mn-enriched (LIME) silicates are interpreted as indicators of nebular condensation conditions [1-4]. They have been identified in IDPs [1], in rare chondrules and matrices of primitive chondrites [2, 3], and in Wild 2 cometary grains [4]. LIME olivine has also been observed in amoeboid olivine aggregates (AOAs) in primitive chondrites [6, 7]. In this study, we compare the roles of nebular and asteroidal thermal processing on formation and alteration of LIME silicates in AOAs.

Most AOAs in Y-81020 (CO3.0) are compact, with closely intergrown minerals. The compact AOAs have concentric textures of anorthite \pm spinel cores, Al-diopside-rich mantles and closely-packed forsterite rims. Some AOAs appear to be more loosely-bound (fluffy). The fluffy AOAs have more irregular shapes, contain less Al-diopside and lack the well-defined concentric textures of the compact AOAs.

LIME olivines are commonly observed in AOAs in Y-81020. They typically occur (i) in the rims of compact AOAs, and (ii) as uniformly distributed grains in fluffy AOAs (see [7]). Most olivines in both types of AOAs are nearly pure forsterite (Fo_{99-100}). LIME low-Ca pyroxenes are also observed in rims of some AOAs. Their MnO concentrations are similar to those of coexisting LIME olivines.

LIME olivine and pyroxene both occur in the rims of compact AOAs in Y-81020, consistent with a model calculation that predicts Mn-enrichment with decreasing condensation temperature in the nebula [5]. AOAs in metamorphosed type 3 carbonaceous chondrites apparently lack LIME silicates [8]. We suggest that LIME silicates were originally present as primary phases in many AOAs, and then were lost during asteroidal thermal processing.

[1] Klöck W. *et al.* 1989. *Nature* **339**: 126-128. [2] Ichikawa O. and Ikeda Y. 1995. *Proc. of NIPR Symp.* 8:63-78. [3] Rubin A. 1984. *American Mineralogist* **69**:880-888. [4] Zolensky M. E. *et al.* 2006. *Science* **314**: 1735-1753. [5] Ebel D. S. *et al.* 2012. *MaPS* **47**:585-593. [6] Weisberg M. K. *et al.* 2004. *MaPS* **39**:1741-1753. [7] Sugiura N. *et al.* 2009. *MaPS* **44**:559-572. [8] Komatsu M. *et al.*, 2014. *LPSC* #1847.

Ocean sections and stoichiometry of dissolved bioactive trace metals in the North Pacific Ocean

WATARU KONAGAYA¹, LINJIE ZHENG,
TOMO HARU MINAMI AND YOSHIKI SOHRIN

Institute for chemical research, Kyoto University, Uji, Japan,
(wkonagaya@inter3.kuicr.kyoto-u.ac.jp)

Bioactive trace metals have strong influence on production and community structure of phytoplankton. In turn, such biological processes affect the distribution of bioactive trace metals. So it is clear that bioactive trace metals have interactive influence with biological processes in the ocean.

The Subarctic North Pacific Ocean is an important area sensitive to the effects from the Asian continent, where the Subpolar Gyre, consisting of the Kamchatka Current and North Pacific Current, makes the southern boundary.

We report the distribution of dissolved bioactive trace metals from the subtropic to subarctic region in the North Pacific Ocean. In this study, we used of a new automated preconcentration system and determined the concentration of nine elements.

Sea water samples were collected using clean technique in accordance with the GEOTRACES protocol. The bioactive trace metals were preconcentrated by solid extraction using NOBIAS CHELATE-PA1 chelating resin (Sohrin *et al.*, 2008) in an automated preconcentration system and determined by HR-ICP-MS.

The blank value of a procedure with the automated preconcentration system was low enough. In recovery tests, target metals were quantitatively recovered at 90-110% from seawater. The measured values of them in seawater reference material NASS-5 agreed with the certified values. We are going to report the results on ocean sections along 47°N and 165°E.

Heavy metal attenuation and mobility in the Wood Creek Sand Channel aquifer: Correlation of experimental and field study

MACOURA KONÉ^{1,3*}, K. ULRICH MAYER²
AND ANIA C. ULRICH³

¹Suncor Energy Inc., mkone@suncor.com (*presenting author),

²University of British Columbia, Earth and Ocean Sciences, umayer@eos.ubc.ca

³University of Alberta, Department of Civil & Environmental Engineering, aulrich@ualberta.ca

The storage of process affected (PA) water in tailings ponds over glacial till formations in the oil sands region in Alberta (Canada) has the potential to cause contamination of groundwater and surface water with trace metals and dissolved major ions. To predict the fate of contaminants in the aquifers underlying and adjacent to tailings impoundments, a detailed understanding of the processes controlling metal release and attenuation is required. In this study, column experiments were performed under anaerobic conditions to simulate interactions between aquifer soils and PA water. Experimental results were compared with and correlated to field observations obtained from monitoring of groundwater wells located in an oil sands facility over a time period of 6 years.

Results from the column experiments indicated that Fe, Mn, Ba, and Si were released from the sediments while other trace metals present in PA water (Zn, Cr, Ni, U, Mo, As, B, etc.) were either weakly attenuated or completely retained by the soils. A DNA extraction performed on the columns sediments identified iron and sulphate reducers suggesting that microbial reductive dissolution of Mn(IV) and Fe(III) is likely the geochemical process by which the metals were released and mobilized into the effluent solution. The groundwater monitoring results are in agreement with those from the columns. However, observed metal concentrations are much higher in the field than in the columns. Variation in the released amounts may be attributed to different materials characteristics, but are most likely due to longer residence times, and longer flow paths. Results also demonstrate that microbial reduction of Mn(IV) and Fe(III) may have important environmental implications on water quality. Potential metals of concerns include Fe, Mn, Zn, Cr and B. Concentrations of these elements measured in both the column effluent and the groundwater were above environmental standards.

These results have important applications in the prediction, protection and potential evaluation of remedial technologies for the immobilization of metals.

Evidence for mantle heterogeneity from Selenium-Tellurium systematics in peridotites

STEPHAN KÖNIG^{*1}, AMBRE LUGUET¹, JEAN-PIERRE-LORAND², D. GRAHAM PEARSON³
AND ALESSANDRO BRAGAGNI¹

¹Universität Bonn, Steinmann Institut für Mineralogie, Germany, stephan.koenig@uni-bonn.de (* presenting author),

²Laboratoire de Planétologie et Géodynamique de Nantes, University of Nantes, France,

³University of Alberta, Department of Earth and Atmospheric Sciences, Edmonton, Canada

Selenium and Tellurium belong to the group of highly siderophile elements (HSE), which may constitute key tracers for planetary processes such as formation of the Earth's core and the Late Veneer composition. Constraints on HSE systematics on the planetary scale require a solid understanding regarding the behaviour of these elements during petrogenetic processes and their abundances in the Earth's mantle. However, the upper mantle has been shown to bear significant long-term geochemical and lithological heterogeneities as a result of repeated melt depletion and re-enrichment processes. In addition to petrographic and mineralogical investigations and geochemical and isotopic studies on platinum group element systematics, these mantle heterogeneities can now be further constrained with new results obtained from Se and Te geochemistry.

Recent studies have shown systematic differences in Se/Te between fertile lherzolites and depleted harzburgites from both oceanic and continental settings. In contrast to fertile lherzolites which scatter around broadly chondritic values of ca. 9 [1,2], depleted peridotites are generally highly fractionated with up to suprachondritic Se/Te (up to 35). The increase of Se/Te correlates with decreasing Te concentrations [3]. Similar fractionations are also observed at the scale of single samples and likely result from the heterogeneous distribution of micrometer sized Te-bearing host phases in highly depleted harzburgites. The marked differences in Se-Te systematics observed between fertile lherzolites and depleted harzburgites as well as the μm -scale heterogeneity can be explained by the combined effect of i) different abundances and proportions of residual and metasomatic base metal sulfides and ii) discrete micrometric to nanometric platinum-group minerals. Together with platinum group elements, the Se-Te systematics in ophiolitic peridotites, mantle-derived peridotite xenoliths (both alkali-basalt and kimberlite-hosted) and orogenic massifs therefore provide further evidence for the mineralogical control on the heterogeneity of highly siderophile elements as well as osmium isotope signatures in the Earth's mantle.

[1] Lorand and Alard (2010) *Chem Geol* **278**, 120-130. [2] Wang *et al.* (2013) *GCA* **108**, 21-44. [3] König *et al.* (2012) *GCA* **98**, 354-366.

Depressurization-induced gas production from methane hydrate sediment formed in a giant cell

YOSHIHIRO KONNO*, YUSUKE JIN, AND JIRO NAGAO

ProTech, MHRC, National Institute of Advanced Industrial Science and Technology (AIST), Sapporo 062-8517, Japan (*correspondence: yoshihiro-konno@aist.go.jp)

We have conducted a gas production test from methane-hydrate-bearing sediment artificially formed in a giant pressure-cell to evaluate feasibility of depressurization method. Unique apparatus named High-pressure Giant Unit for Methane-hydrate Analyses (HiGUMA), which is consist of a pressure-cell with an internal volume of 1710 liter, a vertical well system, and a separator for gas and water, was used for the test.

Methane hydrate with saturation of over 60% was formed in artificial sediment made of Toyoura standard sand within the pressure-cell. Production test was performed by decreasing the pressure of vertical well from 10 MPa to 5.0 MPa. Gas production rate showed the increasing tendency during pressure reduction of the well. The gas water ratio of production fluid increased to about 150 with time. Gas from methane hydrate was successfully produced by this method.

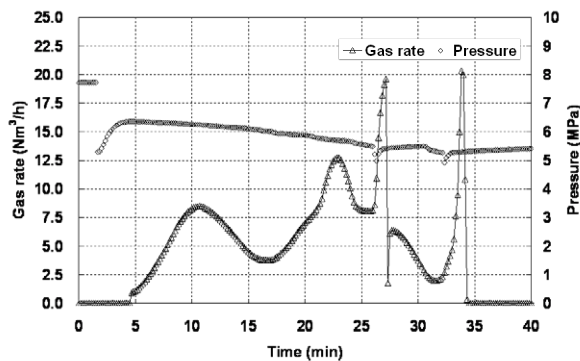


Figure 1: Time-dependent variations of gas production rate and well pressure.

Acknowledgment

This study was financially supported by the Research Consortium for Methane Hydrate Resources in Japan (MH21 Research Consortium) that carries out Japan's Methane Hydrate R&D Program conducted by the Ministry of Economy, Trade and Industry (METI).

Timing and sources of pre-collisional Neoproterozoic sedimentation along the SW margin of the Congo Craton (Kaoko Belt, NW Namibia)

J. KONOPÁSEK^{12*}, J. KOŠLER¹², J. SLÁMA¹³
AND V. JANOUŠEK²

¹Department of Earth Science and Centre for Geobiology, University of Bergen, Allégaten 41, N-5007, Bergen, Norway (*correspondence: jiri.konopasek@geo.uib.no, jan.kosler@geo.uib.no, jiri.slama@geo.uib.no)

²Czech Geological Survey, Klárov 3, 118 21, Praha 1, Czech Republic (vojtech.janousek@geology.cz)

³Institute of Geology AS CR, v.v.i., Rozvojová 269, 165 00, Praha 6, Czech Republic

Isotopic dating of detrital zircons from metasediments and of magmatic zircons from intercalated metavolcanics in the medium- to high-grade part of the Kaoko Belt in Namibia provides first robust constraints on the age of Neoproterozoic sedimentation along the southwestern margin of the Congo Craton. Zircons from metasediments directly overlying the cratonic basement suggest maximum sedimentary protolith ages of c. 1.00 and c. 1.45 Ga, and age populations comparable with protolith ages from the gneisses of the Congo/Kalahari cratons. Dating of zircons from associated metavolcanics constrains the age of the earliest preserved sediments at c. 740–730 Ma and at c. 710 Ma.

Detrital zircons from the samples collected from upper parts of the succession contain only small proportion of grains with ages similar to those from the Congo Craton. Samples show dominance of c. 1.00 Ga, c. 750 Ma and c. 650 Ma old zircon grains that can only be derived from the Punta del Este – Coastal Terrane (Dom Feliciano and Kaoko belts) that acted as an (back)arc domain at c. 650–630 Ma. Neodymium model ages for the studied metasediments provide another argument that the youngest sediments could not have been derived from the Congo Craton.

Recognition of the Punta del Este – Coastal Terrane crust as a source region for the youngest pre-collisional sediments of Kaoko Belt suggests that the c. 650–630 Ma (back)arc Punta del Este – Coastal Terrane has developed directly on top of, or very close to, the attenuated Congo Craton passive margin.

Research funding: Czech Science Foundation grant no. P210/11/1904

Geochemical zoning of the spodumene vein series of the mineral deposit Tastig Tuva, Central Asia

S. I. KONOVALENKO

Tomsk State University, Tomsk, Russia (*konov@ggf.tsu.ru)

Spatial zoning is an essential characteristic of all ore-magmatic systems. It is quite definite, if there is a logical (naturally determined) change in falling, rising, spreading trends, or in a trend from an axial deposit zone to borders of productive mineral parageneses. However, zoning is not so obvious, if scalar parameters composing a single paragenetic complex are being changed consistently along these trends. In such a case, forecast valuation of an object is often challenged. The latter refers entirely to vein series of rare metal spodumene-albite pegmatites, which are still the main industrial type of endogenous lithium deposits.

The author of the work has studied steep-grade vein series (with a pitch angle/angle of fall of 70–80°) of spodumene pegmatites from the deposit Tastig in the republic Tuva in order to define elements of such a spatial zoning. It is outcropts within the absolute altitude range (2600–2200 m), but oriented in a way, where the veins of the lying side of the series are at the maximum heights (2600–2500 m), whereas the veins of the hanging side are revealing within the height interval from 2200 to 2350 m. It was ascertained by sampling of rock-forming pegmatite feldspars, that the indicator of Rb/Ba ratio, which shows degree of a system differentiation, changes logically in accordance with the following pattern. It increases sharply from the lying side of the vein series (where it is equal 15) to its axial zone (61–73), and then decreases slightly (34) in a vein microcline of the hanging side.

The discovered pattern shows that there is rather a hidden transversal zoning within the mineral deposit, which is much more contrast in the modern erosive cut, than a poorly revealed vertical zoning. Insignificance of the last one in the type chemical features of the rock-forming potassium feldspar is probably connected with poor studying of the deep parts of the object, and that a real vertical spread of mineralization exceeds noticeably the natural cut observed (400 m).

This study was funded by the Russian Ministry of Education and Science (projects 5.3143.2011, 14.B37.21.0686, 14.B37.21.1257).

The composition of the spodumene of Asian pegmatite fields

S.I. KONOVALENKO

Tomsk State University, Tomsk, Russia (konov@ggf.tsu.ru)

The composition of the rock forming spodumene from rare metal pegmatite of the Enisei ridge, the Sangilen Plateau, the Southern Tian-Shan, the Pamir, and the Gindukush was studied using a X-ray microprobe analysis. The age of them ranges from Pre-Cambrian to Palaeogene inclusively. The spodumene demonstrates two types of bodies: classic albite-spodumene veins with profile lithium specific, and spodumene-microcline-albite complex ones (Li, Rb, Cs, Ta, Nb, Be) from zoning pegmatite fields. It is found that the main components defining a mineral composition, except of kind-forming (Li, Al, and Si), are Fe, Mn, Na, K, Ti, and partly Ca and Mg. In addition, the spodumenes of linear separate lithium vein series of albite-spodumene type are always significantly more enriched in Fe, Mn, Ti, Ca, Mg despite their age, whereas the complex-type spodumenes of spodumene-microcline-albite veins from zoning fields are constantly enriched in Na and K. The same tendency was found while sampling the spodumenes with different generations of all vein types. An early spodumene is always more contaminant than a later one, especially with Fe, Mn, and Ti. Generally, late spodumenes are less contaminant, but have more Na and K. The discovered tendency correlates with changing the color of a mineral from greenish-grey to white and pinkish-white, and with growth of excretion size (from sm to dm). Ca and Mg as contaminants are not very typical for a spodumene and always seen in minerals of lithium pegmatites from the Sangilen (Central Asia). That is probably related to localization of province veins in the carbonate suite, which is responsible for modification of initial melts that enriches these veins in Ca and Mg. Sampling demonstrates direct correlation between Al and Si. At the same time, significant Al-abundance is often seen while calculating the crystal chemical formulas. This all indicates that the isomorphic replacement of silicon by the element takes place in tetrahedrons of mineral structure.

This study was funded by the Russian Ministry of Education and Science (projects 5.3143.2011, 14.B37.21.0686, 14.B37.21.1257).

Combined accessory mineral micro-analysis: The strength of a multi-phase approach

ELLEN KOOIJMAN^{1,2}, BRADLEY HACKER²,
ANDREW KYLANDER-CLARK², LOTHAR RATSCHBACHER³
AND VLAD MINAEV⁴

¹Swedish Museum of Natural History, Stockholm, Sweden,
Ellen.Kooijman@nrm.se.

²Department of Earth Sciences, UC Santa Barbara, USA.

³Institut für Geologie, TU Freiberg, Germany.

⁴Tajik Academy of Sciences, Dushanbe, Tajikistan.

Accessory mineral micro-analysis provides a diverse and versatile toolbox for deciphering the timing and conditions of petrological processes. We explore the use of multi-mineral U-(Th)-Pb geochronology and trace-element analysis using LA-‘split-stream’-ICP-MS in a study of rare near-UHP crustal xenoliths in the Pamir (peak conditions 2.5-2.8 GPa, 1000-1100 °C, eruption ~11 Ma [1]). These direct samples of the deep crust recovered from under an active collisional orogen provide a unique opportunity to assess how orogenic roots form and evolve.

We analyzed zircon, monazite, and rutile from a variety of rocks (eclogites to grt-ky-qtz granulites) in thin section using an excimer laser coupled to a Nu Plasma HR and a Nu AttoM. This set-up provides REE-HFSE concentrations and U-Th-Pb isotope ratios—hence, petrogenetic, thermometric and age data—for small amounts of ablated analyte. Our analysis yielded 1) U-Pb ages, Ti concentrations and REE in zircon, 2) U-Pb and Th-Pb ages and REE in monazite, and 3) U-Pb ages and HFSE concentrations (incl. Zr) in rutile.

Zircon and monazite defined 6 age populations between 55-11 Ma, each typically having uncertainties of 1 Ma or better. The Ti-in-zircon and zircon U-Pb ages imply a three-stage P-T-t history, involving Barrovian metamorphism (55-20 Ma), deep burial leading to near-UHP conditions at ~12 Ma, and rapid magmatic heating shortly before the 11-Ma eruption. Monazite data complement this history. Rutile yielded ~11-Ma U-Pb dates exclusively, demonstrating the reliability of this thermochronometer.

The data show that different accessory mineral techniques are largely complementary and that their combined use is very powerful in refining and redefining geodynamic models. In addition, we demonstrate that, through ongoing development in LASS-ICP-MS technology, we are able to identify and resolve a wide range of petrological processes on a Myr time scale for Cenozoic rocks.

[1] Hacker *et al.* (2005) *J. Petrol.* **46**, 1661-1687.

Using DMT and AF4-HR-ICP-MS to characterize trace metal speciation in soil water extracts

GERWIN F. KOOPMANS, INGE C. REGELINK
AND ROB N.J. COMANS

¹Dep. of Soil Quality, Wageningen University, Wageningen,
The Netherlands
(*correspondence: Gerwin.Koopmans@wur.nl)

Diffuse contamination of soils with trace metals like Cu and Zn is an ubiquitous problem all over the world. Trace metals in 0.45 μm -filtered soil solution samples can be present in the free form or they can be associated with inorganic ligands, DOM, and inorganic colloids. Inorganic colloids like clay and Fe-(hydr)oxide nanoparticles can pass the 0.45 μm -filter, but their concentration, composition, and effect on trace metal speciation is largely unknown. For ecological risk assessment of contaminated soils, total trace metal concentrations in soil solution are often measured. However, uptake of trace metals by plants and soil organisms is not necessarily related to their total dissolved concentrations, but generally correlates best with their free concentrations. Hence, the speciation of trace metals in soil solution needs to be known to understand their bioavailability in soils. During the presentation, we will focus on the Donnan Membrane Technique (DMT) and Asymmetric Flow Field-Flow Fractionation (AF4), which can be used to measure the trace metal speciation in soil solution. The DMT allows for the measurement of free trace metal concentrations in solution [1]. Using a chemical equilibrium model in combination with the NICA-Donnan model, the complexation of trace metals with inorganic ligands and DOM can be predicted [2]. However, the role of inorganic colloids in soil solution in the binding of trace metals remains poorly understood when using this approach. An emerging analytical technique with a high potential to analyse the colloidal trace metal fraction in 0.45 soil μm -filtered solution samples is AF4. AF4 is a chromatographic-like technique for size fractionation of colloids, and allows for online multi-element detection in combination with HR-ICP-MS. We will briefly describe the analytical developments in the DMT and present examples of the application of both DMT and AF4-HR-ICP-MS to measure specific trace metal forms in soil solution extracts to demonstrate (i) the complementary character of both analytical techniques and (ii) their potential to obtain a full speciation of total dissolved trace metals.

[1] Temminghoff *et al.* (2000) *Anal. Chim. Acta* **417**, 149-157.

[2] Weng *et al.* (2002) *Environ. Sci. Technol.* **36**, 4804-4810.

Use of 10^{12} and 10^{13} Ohm resistors in TIMS analysis of Sr and Nd isotopes in sub-nanogram geological and environmental samples

J.M. KOORNNEEF¹, C. BOUMAN², J.B. SCHWIETERS²
AND G.R. DAVIES¹

¹Faculty of Earth and Life Sciences, Vrije Universiteit
Amsterdam, the Netherlands, j.m.koornneef@vu.nl

²Thermo Fisher Scientific, Bremen, Germany

Analysis of isotope ratios in small geological and environmental samples such as inclusions in diamonds or individual human hairs is ultimately limited by the detection system of the mass spectrometer. We report a technique using a TRITON Thermal Ionisation Mass-Spectrometer (TIMS) to measure sample sizes up to 10 times smaller than currently feasible. Use of current amplifiers with 10^{12} Ohm and 10^{13} Ohm resistors instead of the standard 10^{11} Ohm resistors promises a 2-3 fold and 4-5 fold improvement in signal to noise ratios, respectively. This improvement results in higher precision on analyses of small ion beams.

Internal precision and external reproducibility are both better for Sr and Nd isotope ratios collected on small samples using 10^{12} Ohm and 10^{13} compared to the standard 10^{11} Ohm resistors. At a ^{87}Sr intensity of 3 mV the internal precision (2SE) of $^{87}\text{Sr}/^{86}\text{Sr}$ is twice better for 10^{12} Ohm and 5 times better for 10^{13} Ohm resistors compared to 10^{11} Ohm resistors. The external reproducibilities (2SD) at this beam intensity are 4 and 9 times better, respectively.

We additionally tested the precision of $^{143}\text{Nd}/^{144}\text{Nd}$ measured by 10^{13} Ohm resistors in the beam intensity range usually covered by ion counting (< 3 mV or 2×10^5 cps). For a ^{143}Nd intensity of 6.25×10^4 cps (1 mV) the precision is 480 ppm (2SE) and at 2×10^3 cps (32 μV) it is 1%. At intensities higher than 2×10^4 cps the precision using the 10^{13} Ohm resistors is better than 0.2%, which is the lower limit for ion counting owing to the instability and non-linearity of ion counters. This observation indicates that the high gain amplifiers can be used instead of multi ion counting or Faraday cups equipped with the standard 10^{11} Ohm resistors in the range between 2×10^4 cps and 20 mV.

The reproducibility of $^{143}\text{Nd}/^{144}\text{Nd}$ and $^{87}\text{Sr}/^{86}\text{Sr}$ ratios for 100 pg standards using 10^{12} Ohm resistors is 176 ppm for Nd (2RSD, $n=28$) and 92 ppm for Sr (2RSD, $n=20$). Using 10^{13} Ohm resistors the reproducibility is twice better. Thus, variability in Nd and Sr isotope ratios in the 4th decimal place, e.g. $^{143}\text{Nd}/^{144}\text{Nd}$ 0.5110 – 0.5119 or $^{87}\text{Sr}/^{86}\text{Sr}$ 0.7100-0.7109, can be resolved in such small samples provided that the procedural blanks and chemical separation are optimal.

Using stable isotope tracers to elucidate the *in situ* metabolic activity of microbial populations in the cystic fibrosis lung

S. KOPF^{1,4*}, R. HUNTER², A. LARIVIERE^{2,3}, Y. HU²,
M. DIETERLE², A. SESSIONS¹, V. ORPHAN¹
AND D. NEWMAN^{1,2,4}

¹Division of Geological and Planetary Sciences and ²Division of Biology, Caltech, Pasadena, CA 91125, USA

³Children's Hospital, Los Angeles, CA 90027, USA

⁴Howard Hughes Medical Institute, Pasadena, CA 91125, USA

(*correspondence: skopf@caltech.edu)

Background

Cystic fibrosis is a genetic disorder that causes the accumulation of mucus in a variety of organs. The genetic defect allows for the colonization and chronic infection of the pulmonary system by opportunistic pathogens and ranks as the most common lethal genetic disorder in Caucasian populations. The formation of complex microbial communities and their physiological heterogeneity within the cystic fibrosis lung are suspected to contribute to rapid disease progression and antibiotic resistance. However, because of the inherent challenges of working *in situ* with human patients, very few studies of the *in situ* metabolic programs of infectious agents exist and the development of effective antimicrobial therapies is often hindered by our limited knowledge of the physiological state of microbial populations within the human host. It is currently unknown how even basic metabolic indicators, such as microbial growth rates, may correlate with disease progression.

Discussion

Here, we present a novel approach based on techniques developed in the (bio)geochemical sciences to tackle this knowledge gap. Using ²H and ¹⁵N isotope tracers, combined with GC-IRMS and nanoSIMS analytical techniques, we characterize the growth rate, community structure and metabolic state of microbes within the lungs of cystic fibrosis patients. Contrary to the traditional model of a rapidly multiplying infectious population, our results from compound specific lipid analysis of biosynthetic ²H incorporation suggest microbial activity consistent with slow growth (a physiological adaptation known to confer antibiotic resistance in the laboratory). At the same time, analyses of spatial variation in microbial activity using fluorescent *in situ* hybridization and nanoSIMS highlight metabolic heterogeneity within the microbial community. This approach provides a first glimpse at the *in situ* biosynthetic activity of pathogens involved in chronic infection of the cystic fibrosis airways and contributes to building a basis for physiologically informed laboratory experiments.

Highly dynamic cellular-level response of symbiotic coral to sudden increase in environmental nitrogen

C. KOPP¹, M. PERNICE², I. DOMART-COULON³,
C. DJEDIAT⁴, J.E. SPANGENBERG⁵, D.T.L. ALEXANDER⁶,
M. HIGNETTE⁷, T. MEZIANE⁸ AND A. MEIBOM^{9*}

¹christophe.kopp@epfl.ch

²mathieu.pernice@epfl.ch

³icoulon@mnhn.fr

⁴djediat@mnhn.fr

⁵jorge.spangenberg@unil.ch

⁶duncan.alexander@epfl.ch

⁷michel.hignette@culture.gouv.fr

⁸meziane@mnhn.fr

⁹anders.meibom@epfl.ch

Metabolic interactions with endosymbiotic photosynthetic dinoflagellates *Symbiodinium* sp. are fundamental to reef-building corals (Scleractinia) thriving in nutrient-poor tropical seas. Yet detailed understanding at the single cell-level of nutrient assimilation, translocation, and utilization within this fundamental symbiosis is lacking. Using pulse-chase ¹⁵N-labeling and quantitative ion-microprobe isotopic imaging (NanoSIMS) we visualized these dynamic processes in tissues of the symbiotic coral *Pocillopora damicornis* at the sub-cellular level. Assimilation of ammonium, nitrate, and aspartic acid resulted in rapid incorporation of nitrogen into uric acid crystals (after ~45 minutes), forming temporary N-storage sites within the dinoflagellate endosymbionts. Subsequent intracellular remobilization of this metabolite was accompanied by translocation of nitrogenous compounds to the coral host, starting at ~6 hours. Within the coral tissue, nitrogen is utilized in specific cellular compartments in all four epithelia, including mucus chambers, Golgi bodies, and vesicles in calicoblastic cells. Our study shows how nitrogen-limited symbiotic corals take advantage of sudden changes in nitrogen availability and opens new perspectives for functional studies of nutrient storage and remobilization in microbial symbioses in the changing reef environment.

Primary alkali kimberlite melt: The myth dispelled

M.G. KOPYLOVA¹, S.I. KOSTROVITSKY²
AND K.N. EGOROV³

¹University of British Columbia, Vancouver, BC V6T 1Z4,
Canada (*correspondence: mkopylov@eos.ubc.ca)

²Institute of Geochemistry SB RAS, 1a Favorskogo St.,
Irkutsk, Russian Federation, 664033

³Institute of the Earth's Crust SB RAS, 128 Lermontova St.
Irkutsk, Russian Federation, 664033

After decades of studies, the composition of the primary kimberlite melt is still poorly constrained. One of the models for the kimberlite origin suggests the melt is low in H₂O and high in alkalis, as observed in the “uniquely fresh” Udachnaya East kimberlite. Papers that proposed the alkali-rich affinity for the melt focused on geochemical evidence and did not report petrography or geology of the rocks, which are critically important for the geochemical interpretation. We present geological, petrographic and geochemical evidence that the alkali-rich affinity of the Udachnaya kimberlite and other kimberlites in Southern Yakutia relates to crustal contamination. Alkali carbonates, sodalite, gypsum, anhydrite, halite and sylvite are present in the groundmass and matrix of the Udachnaya, Mir and International'naya pipes (southern Yakutia). The kimberlites were emplaced through 2 km-thick evaporite-bearing carbonate sediments saturated with brines. In the global context, southern Yakutian kimberlites are unprecedented in the amount of the crustal carbonate and evaporite material included in the pipes. The secondary, crustal origin of Na, K, Cl and S-rich minerals is supported by the following: 1. A regional correlation between the geology and hydrogeology of the local country rocks and the kimberlite mineralogy, in particular the difference between southern and northern Yakutian kimberlites; 2. A restriction of halite or gypsum mineralization in the Mir and International'naya pipes to depths where pipes intersect country rock strata with the similar mineralogy; 3. The localization of the highest abundances of Na-K-Cl-S-bearing minerals in the Udachnaya East kimberlite at a depth interval that correlates across three magmatic phases of kimberlites and coincides with the roof of the halite-bearing country rock and an aquifer carrying anomalously Na-rich brines; 4. The presence of evaporite xenoliths and veins of halite, gypsum and carbonate cutting through the kimberlite and xenoliths; 5. The geochemical and Sr, C, O, Cl and S isotopic evidence for crustal contamination. Addition of crustal salts to kimberlite melt began prior to the volcanic fragmentation as a result of preferential melting and assimilation of evaporite xenoliths and may have continued in-situ after the pipe emplacement via reactions with external saline fluids. The hybrid, alkali-, S- and Cl-rich compositions of residual melts and fluids were trapped in secondary inclusions in olivine. Alkali-rich compositions of fluids trapped in fibrous diamonds shortly before the kimberlite emplacement cannot support the model of the alkali-rich primary kimberlite melt, as the latter is significantly more Ca-, Na-, B-, and S-rich than the K- and Ba-rich fluid inclusions.

Composition of hydrocarbon source rocks of the Hayrettin Formation (Denizli/Western Turkey): Provenance, source weathering and tectonic setting

DEMET BANU KORALAY¹

¹Pamukkale University Engineering Faculty, Department of
Geological Engineering, 20070 Denizli/TURKEY
dbkoralay@pau.edu.tr

The geochemical composition of the Oligocene hydrocarbon source rocks of the Hayrettin Formation of Denizli (Western Turkey) province were analyzed for major and selected trace elements to infer their provenance, intensity of palaeoweathering of the source rocks and tectonic setting. Total organic carbon (C_{org}, %) contents of organic matter rich rocks are between 0.21 % and 39.61 %. Plots of organic matter rich rocks on Al₂O₃ wt.% versus TiO₂ wt.% diagram and discriminant functions diagram indicate that the samples plot between the granodiorite and gabbro field, and quartzose sedimentary and mafic igneous rocks constitute the source rocks in the provenance. To constrain the climatic condition during sedimentation of organic matter rich rocks on SiO₂ wt.% versus (Al₂O₃+K₂O+Na₂O) wt.% diagram the samples plot in the field of semiarid climate. Plots of samples on bivariate discriminant function diagram reveal an active continental margin setting for the provenance. The chemical index of alteration (CIA) monitors the progressive alteration of plagioclase and potassium feldspars to clay minerals. CIA values for the Oligocene Hayrettin Formation organic matter rich samples vary from 26 to 81 with an average 70 indicating significant weathering at the source areas.

www.minersoc.org

DOI:10.1180/minmag.2013.077.5.11

Origin of High-K Ignimbrite in the Miocene Volcanism Surrounding Uşak Region (Western Turkey): Rb-Sr, Sm-Nd Isotopic Evidence

T. KORALAY¹, Y. K. KADIOĞLU²⁻³, S.Y. JIANG⁴,
K. DENİZ³ AND B. GÜLLÜ⁵

¹Pamukkale Univ., Geol.Eng. Dept., 20017 Denizli TURKEY
tkoralay@pau.edu.tr; tkoralay@gmail.com

²Ankara Univ. Earth Sci. Application&Res. Center-TURKEY

³Ankara Univ., Geol. Eng. Dept., 06100, Ankara-TURKEY

⁴Nanjing Univ., Dept. of Earth Sci., 210093, P.R.China

⁵Aksaray Univ. Dept. of Geological Eng., Aksaray

The Western Turkey is an active region formed in a complex crustal extensional regime, generating large volume of subduction and post-collisional-related magmas took place during the Middle Miocene-Quaternary time. The ignimbrite is mainly composed of plagioclase (oligoclase, andesine) + biotite + Fe-Ti oxides (magnetite, hematite) ± amphibole (brown hornblende) and has eutaxitic texture. Whole rock geochemical data reveal that ignimbrite, characterized by their trachy-andesite composition, high-K in character, show fractional crystallization primarily controlled by plagioclase, biotite, Fe-Ti oxide. The ignimbrite samples have Th/Nb (1.00-1.20), Nb/Ta (3.57-14.67), Ba/Nb (37.32-64.43), Hf/Th (0.18-0.44), K/P (16.99-34.76), Ce/P (0.06-0.10) and Th/U (1.60-4.03) incompatible element ratios and show Volcanic Arc Basalts (VAB) in character. According to spider diagrams; ignimbrite exhibits a clear enrichment in LILE and HFSE. Although it is close to Continental Crust value, there are generally slight decreases in the content of Sr, Ba, Nb, P and Ti ratios reflecting subduction related magma (Wilson, 1989). In REE diagram, it displays marked enrichment in light rare earth elements (LREE) ((La/Sm)_N = 5.03-5.97) relative to heavy rare earth elements (HREE) ((Sm/Yb)_N = 4.36-5.15). Furthermore, all samples have negative Eu anomalies ((Eu/Eu*)_N = 0.77-0.90), indicating the significant role of plagioclase in the fractional crystallization. The ignimbrite display limited range in ⁸⁷Sr/⁸⁶Sr (0.708048 to 0.708782) and ¹⁴³Nd/¹⁴⁴Nd (0.512420 to 0.512436) isotopic ratios and similar to Continental Margin Volcanics. Petrographic, geochemical and Sr-Nd isotope datas indicate that the ignimbrite evolved through fractional crystallization and crustal contamination of the parent magma were formed during the partial melting of the lower crust and mixing with the upper crust material.

Metal mobilization by iron- and sulfur-oxidizing bacteria in a multiple extreme mine tailings in the Atacama Desert, Chile [2]

H. KOREHI¹, M. BLÖTHE¹, M.A. SITNIKOVA¹, B. DOLD²,
AND A. SCHIPPERS^{1*}

¹Federal Institute for Geosciences and Natural Resources (BGR), Stilleweg 2, D-30655 Hannover, Germany (hananeh_k@hotmail.com; marco.bloethe@bgr.de; maria.alexandrovna.sitnikova@bgr.de; axel.schippers@bgr.de)

²FCFM- Universidad de Chile, Departamento de Geología, Departamento de Geología, Plaza Ercilla 803, Santiago de Chile, Chile (bernhard.dold@gmail.com)

The marine shore sulfidic mine tailings dump at the Chañaral Bay in the Atacama Desert, northern Chile, is characterized by extreme acidity, high salinity and high heavy metals concentrations. Due to pyrite oxidation, metals (especially copper) are mobilized under acidic conditions and transported towards the tailings surface and precipitate as secondary minerals [1]. Depth profiles of total cell counts in this almost organic-carbon free multiple extreme environment showed variable numbers with up to 10⁸ cells g⁻¹ dry weight for 50 samples at four sites. Real-time PCR quantification and bacterial 16S rRNA gene diversity analysis via clone libraries revealed a dominance of *Bacteria* over *Archaea* and the frequent occurrence of the acidophilic iron(II)- and sulfur-oxidizing and iron(III)-reducing genera *Acidithiobacillus*, *Alicyclobacillus* and *Sulfobacillus*. Acidophilic chemolithoautotrophic iron(II)-oxidizing bacteria were also frequently found via most-probable-number (MPN) cultivation. Halotolerant iron(II)-oxidizers in enrichment cultures were active at NaCl concentrations up to 1 M. Maximal microcalorimetrically determined pyrite oxidation rates coincided with maxima of the pyrite content, total cell counts and MPN of iron(II)-oxidizers. These findings indicate that microbial pyrite oxidation and metal mobilization preferentially occur in distinct tailings layers at high salinity. Microorganisms for biomining with seawater salt concentrations obviously exist in nature [2].

[1] B. Dold (2006). *Environ. Sci. Technol.* **40**, 752-758. [2] H. Korehi, M. Blöthe, M. A. Sitnikova, B. Dold, A. Schippers (2013). *Environ. Sci. Technol.* **47**, 2189-2196.

The biogeochemical system of chemical elements distribution in the hydrosphere

V.D. KORZH

Shirshov Institute of Oceanology, Nakhimovsky pr. 36,
Moscow 117997, Russia (E-mail: okean41@mail.ru)

The chemical elements composition of the oceanic water is a result of substance migration and transformation on river-sea and ocean-atmosphere boundaries. Stability of these processes is the main condition of the hydrosphere ecosystems stability. Detailed studies revealed three types of chemical element distribution in the ocean: 1) Conservative: concentration normalized to salinity is constant in space and time; 2) Nutrient-type: element concentration in the surface waters decreases due to the bio-consumption; and 3) Litho-generative: complex character of distribution of elements, which enter the ocean with the river runoff and interred almost entirely in sediments. The correlation between the chemical elemental compositions of the lithosphere and ocean is relatively weak ($r = 0.68$) while for river and oceanic water it is high ($r = 0.94$).

In our presentation, we shall show intensities of global migration and average concentrations in the ocean in the coordinates $\lg C_{\text{ocean}} - \lg \tau_{\text{ocean}}$, where C_{ocean} is an average element concentration and τ_{ocean} is its residence time in the ocean. In this plot elements form groups reflecting the similarity of their properties. The System indicates an existence of the relationship between three main geochemical parameters of the dissolved forms of chemical elements in the hydrosphere: 1) average concentration in the ocean, 2) average concentration in the river runoff and 3) the type of distribution in oceanic water. This allows using knowledge of two of these parameters to gain theoretical knowledge of the third. Finally, the mean concentrations of elements and patterns of their distribution in the ocean can be used to determine pre-techno-generative concentrations of elements in the river runoff [1, 2, 3].

[1] Korzh (1974), *Journal de Recherches Atmospheriques*, **8**(3-4), 653-660. [2] Korzh (2008), *J. Ecologica* **15**, 13-21. [3] Korzh (2012), *Journal of water science and its practical application* **1**, 56-62.

Accumulation mechanisms and bonding of high-tech metals in marine ferromanganese crusts

A. KOSCHINSKY^{1*}, J. HEIN², D. MOHWINKEL¹,
A. FOSTER³ AND J. BARGAR⁴

¹Jacobs University Bremen, D-28759 Bremen, Germany

(*correspondence: a.koschinsky@jacobs-university.de)

²U.S. Geological Survey, Santa Cruz, CA 95060

³U.S. Geological Survey, Menlo Park, CA 94025

⁴SLAC National Accelerator, Menlo Park, CA 94025

Marine ferromanganese crusts (Fe-Mn crusts) are abundant throughout the global ocean and provide a potential economic resource for a wide range of rare metals for high technology applications. Understanding the geochemical processes that govern the interactions of these rare metals with natural Fe-Mn oxides has far reaching implications that span the range from global-ocean geochemical balances to the development of new techniques for extractive metallurgy. In our project we used synchrotron-based XANES spectroscopy to assess oxidation states in natural samples and samples in which metals were sorbed onto synthetic and natural Fe and Mn oxides. EXAFS spectroscopy was used to resolve the local structure around the metals in these same samples. We focussed on the metals Te, Pt, Mo, Zr, and Pb.

Our results confirm that Te is largely Te(VI) in Fe-Mn crusts and predominantly bound to FeOOH by inner-sphere complexation. For most model compounds, most Te(IV) transformed into Te(VI) during sorption. These data confirm that oxidative surface adsorption is the process responsible for the extremely high enrichment of Te in crusts (up to about 200 ppm) as compared to seawater. Since Pt concentrations are too low in natural Fe-Mn crusts, we investigated Pt only on sorption samples. As for Te, the results suggest that during uptake of Pt(II) from seawater a surface oxidation to Pt(IV) on the crusts takes place, explaining the high enrichment of Pt in crusts (up to 1-3 ppm). Of the model compounds, especially Mn oxide was very effective in oxidizing Pt(II). Molybdenum (as Mo(VI)) shows a strong association with the Mn oxide phase of crusts, while in sorption and sequential leaching experiments it also strongly binds on FeOOH. Lead displays a complex distribution, especially in phosphatized crusts, where it seems to form insoluble phosphate compounds. Zirconium was found to be bound as Zr(IV) to both FeOOH and MnO₂ phases, in contrast to the expected predominant binding to FeOOH. A more detailed evaluation of the spectra is presently carried out to resolve open questions.

Petrology and geochemistry of mafic rocks in the Acasta Gneiss Complex

KEIKO KOSHIDA^{1*}, AKIRA ISHIKAWA¹, HIKARU IWAMORI² AND TSUYOSHI KOMIYA¹

¹Earth Science and Astronomy, The University of Tokyo, Tokyo 153-8902, Japan, koshida@ea.c.u-tokyo.ac.jp

²Earth & Planetary Sciences, Tokyo Institute of Technology, Tokyo 152-8550, Japan

Eoarchean crustal records are rare, so that the details of early Earth are not revealed yet. Acasta Gneiss Complex (AGC), located in the western part of the Slave Province, Canada, is one of the Early Archean terranes, and contains the oldest rocks in the world [1]. It is dominated by ca. 3.6-4.0 Ga felsic and layered gneiss suites, but minor mafic to intermediate gneiss occur as rounded to elliptical enclaves and inclusions [2]. The Acasta mafic rocks are composed of variable amounts of hornblende ± plagioclase ± quartz ± chlorite ± epidote ± biotite ± apatite ± sphene ± garnet ± clinopyroxene ± opaque ± cummingtonite, and are classified into hornblendite, garnet-bearing and garnet-free amphibolites. The garnet-free amphibolites can be further subdivided into fine- and coarse-grained amphibolites. Petrological examination and mineral composition demonstrate that all rocks underwent up to upper amphibolite facies metamorphism.

The composition of our studied samples ranges from basalt to basaltic andesite (SiO₂ = 43-57 wt%, MgO=4.1-19.1 wt%). Some systematic differences can be seen among each group in terms of major elements and chondrite-normalized REE patterns. The hornblendites have high MgO contents and show strong negative Eu anomaly, reflecting the effect of anatexis. The garnet amphibolites have high FeO contents and slightly fractionated REE patterns (La_N/Sm_N=1.2-1.8, Gd_N/Yb_N=2.0-2.2). The coarse-grained amphibolites are enriched in Al₂O₃ and LREE contents (La_N/Sm_N=1.3-5.4) with moderately fractionated MREE to HREE patterns (Gd_N/Yb_N=1.2-2.0), whereas the fine-grained amphibolites display flat REE patterns (La_N/Sm_N=0.8-1.4, Gd_N/Yb_N=1.0-1.2). MORB-normalized trace element patterns show depletion in Nb and Zr relative to Th and LREE for all studied samples. Although variable incompatible trace element patterns were possibly due to alteration during regional metamorphism, depletion in Nb and Zr contents suggest subduction zone magmatism for the mafic rock inclusions in the AGC.

[1]Bowring & Williams (1999) *Contrib. Mineral. Petrol.*, **134**, 3-16. [2]Iizuka *et al.* (2007) *Precamb. Res.* **153**, 179-208.

The heavy metals in *Halocynthia aurantium* tissues of the Japan Sea

KOSJANENKO A.A.* AND KOSJANENKO D.V.

V. I. Il'ichev Pacific Oceanological Institute, 43, Baltiyskaya Street, Vladivostok, 690041, Russia.
(E-mail: KosyanPOI@inbox.ru)*

The problem of concentration of elements of living organisms of the marine environment is of great importance. This problem was first posed VI Vernadsky [1]. Intermediate stage in the cycle of TM in the estuaries of the seas is a planktonic organisms that accumulate TM and send them to the bottom [2]. Ascidiarians (A), as bottom marine animals, are the final link in the cycle TM of the oceans and seas.

The aim was to determine the selectivity of HM accumulation various tissues ascidian *H. aurantium*. In addition, ascidians tissue use in medical applications: in recent years, mining *H. aurantium* is to produce raw materials for the production of biologically active food supplement "Haurantin" (POI FEB RAS) Overseas pharmacists from the body squirts identified cancer drugs ezteinastidin-743 and ascidin [3]. Individuals of *H. aurantium* were collected in the Kievka Bay (Sea of Japan) in 2011. For the analysis of seized samples of the following tissues: stomach, digestive gland, gonads, muscle and tunic. Analyses of the composition of animal tissues were determined by atomic absorption spectroscopy.

Tissue	Fe	Zn	Cu	Mn	Ni	Cd	Pb	Co
t	140,6	13,9	2,7	30,8	1	0,1	1	0,3
m	48,6	65,3	1,4	4,9	0,1	0	22,2	0,1
dg	898,3	29,5	7,1	24	1,3	0,2	1,4	0,8
g	41,4	202	4,3	12	0,7	0	34,1	0,4
s	344	188,4	4,2	21,1	0,9	0	344	0

Table: The concentration of heavy metals in *H. aurantium* tissues (t – tunic, m – muscle, dg – digestive glands, g – gonads, s – stomach, mcg/g.)

Thus, we can judge the selective accumulation of certain tissues purple ascidian TM in large enough quantities that can be explained by their peculiarities of life, the structure of tissues themselves and also, to a large extent, the state of their environment.

[1] Vernadsky V.I. (1965) Moscow: Nauka, 374. [2] Kasatkina A.P. *et al.* (1994) *Biologiya morya* **20**, №4, 247-251. [3] Dobryakov Y.I. *et al.* (2003) *Intern. J. on Immunorehabilitation* **5**, №2, 181.

Factors controlling elemental fractionation in laser ablation ICP-MS zircon geochronology

JAN KOSLER^{1,2*}, SIMON E. JACKSON²
AND ZHAOPING YANG²

¹Centre for Geobiology and Department of Earth Science,
University of Bergen, Allegaten 41, Bergen, N-5007,
Norway (*correspondence: jan.kosler@geo.uib.no)

²Geological Survey of Canada, Natural Resources Canada,
601 Booth St., Ottawa, Ontario, K1A 0E8, Canada
(sjackson@NRCan.gc.ca, zhayang@NRCan.gc.ca)

Fractionation of elements during laser ablation (LA) is a significant source of error in quantitative and isotope ratio analysis by ICP-MS. It has been demonstrated that phase separation and formation of particles of variable size and composition are the primary cause of laser-induced elemental fractionation [1], and that the element decoupling can be further enhanced by variable aerosol transport and processes in the ICP [2]. Interaction of laser radiation with zircon (ZrSiO₄) typically results in its thermal breakdown to ZrO₂ and SiO₂ and formation of aerosol particles with different composition, size and transport properties [3]. As a result of the preferential partitioning of U+Th and Pb into ZrO₂ and SiO₂ phases, respectively, the decomposition of zircon by transfer of laser heat can efficiently fractionate these geochronologically important trace elements, resulting in erroneous U-Th-Pb ages obtained by LA-ICP-MS dating.

Previous studies have related the laser-induced decoupling of U+Th from Pb in zircon to different element volatilisation temperatures [2], chemical composition of the zircon matrix [4] and radiation damage accumulated since the last closure for annealing in zircon [5]. Recently obtained laser ablation ICP-MS data for a suite of well characterized zircon samples with range of composition and accumulated radiation damage suggest that these factors alone cannot explain the observed variations in the rate of laser-induced elemental fractionation; they may, however, affect the kinetics of the phase separation during the thermal breakdown of zircon. Additional parameters that will be evaluated for effects on laser-induced fractionation include the composition of ambient gas during the ablation and transport properties of aerosol particles formed by laser ablation of zircon.

[1] Kuhn & Günther (2003) *Anal Chem* **75**, 747-753. [2] Guillong & Günther (2002) *JAAS* **17**, 831-837. [3] Kosler *et al.* (2005) *JAAS* **20**, 402-409. [4] Black *et al.* (2004) *Chem Geol* **205**, 115-140. [5] Allen & Campbell (2012) *Chem Geol* **332-333**, 157-165. (* Funding received from Czech Science Foundation - project number P210/12/2114).

Metagenomic insights into the response of indigenous microbial communities in beach sands to the Deepwater Horizon oil spill

J.E. KOSTKA¹, L.M. RODRIGUEZ-R.¹, W.A. OVERHOLT¹,
X. LIN¹, K. MARKS¹, K. KONSTANTINIDIS
AND M. HUETTEL²

¹Georgia Institute of Technology, Atlanta, GA, USA

²Florida State University, Tallahassee, FL, USA

Biodegradation mediated by indigenous microbial communities is the ultimate fate of the majority of hydrocarbons that enter the marine environment. A large amount of oil from the Deepwater Horizon oil spill was transported to and subsequently buried in Gulf of Mexico beaches. The objective of this research is to characterize the *in situ* response of microbial communities in parallel with the fate and chemical changes in oil hydrocarbons. Our time series database encompasses >500 sediment and water samples collected from Pensacola Beach, FL, USA, from 2010 to 2012. Illumina MiSeq and HiSeq platforms were used to obtain an average of 10000 SSU rRNA gene amplicon sequences and 35 million (100bp) paired-end reads on a subset of these samples. A bloom of bacteria was observed in parallel with oxygen consumption rates and the depletion of the majority of highly degradable oil hydrocarbons during the first 4 months after oil came ashore. SSU rRNA gene amplicon and metagenome analysis revealed an initial sharp drop in community diversity after oiling. Moreover, evidence of succession was detected across the time-series, featuring a marked increase in relative abundance of Alcanivorax spp. during the first two months (up to 40% of the community) followed by enrichment in other members of the Gammaproteobacteria (*Parvularcula*, *Hyphomonas*, *Xanthomonadales*) in subsequent months. By July 2011, community diversity had sharply rebounded, and sequences of taxa associated with oligotrophic conditions, such as the Thaumarchaeota (*Nitrosopumilus*) were detectable, whereas phylotypes associated with the oiling event were undetectable. Finally, we observed that genes for central-metabolism functions were enriched in clean samples, while genes related to peripheral metabolism (e.g. aromatics degradation, nitrogen fixation, phosphorus uptake) were enriched in oiled samples, reflecting the community response to a oil-derived carbon source and nutrient depletion. Overall, multiple lines of independent evidence from a time series describe the microbial response to hydrocarbon discharge as a succession dynamics model driven by nutrient availability and hydrocarbon chemistry.

Provenance and metamorphic conditions of very low-grade metasedimentary rocks of the Variscan accretionary prism of the Kaczawa Mts (SW Poland): Geochemical and mineralogical evidence

JOANNA KOSTYLEW¹, RYSZARD KRYZA¹
AND JAN ZALASIEWICZ²

¹Institute of Geological Sciences, University of Wrocław, ul. Cybulskiego 30, 50-205 Wrocław, Poland, e-mail: joanna.kostylew@ing.uni.wroc.pl

²Department of Geology, University of Leicester, University Road, Leicester LE1 7RH, UK

The Kaczawa Complex in the West Sudetes (SW Poland) is interpreted as a fragment of a Variscan accretionary prism. Together with neighbouring basement units, it forms a structural mosaic of the Sudetes at the NE edge of the Bohemian Massif.

Some previous studies of the Kaczawa Complex aimed at determination of the provenance and metamorphic conditions of metasedimentary rocks of the complex. These questions have become particularly important since the 1970's when some of the rocks were classified as *mélange*, rather than fragments of coherent stratigraphic successions as previously thought. Their depositional age remains controversial, though scarce conodonts suggest a Devonian - Early Carboniferous age.

We present new results of mineralogical (microprobe, XRD) and bulk-rock chemical investigations of various metasedimentary rocks from different structural units of the Kaczawa Complex.

The provenance of metasedimentary rocks of the Kaczawa Complex is assessed based on the Chemical Index of Alteration (CIA) and discrimination function analysis, using major-element and selected trace-element data (i.e. Eu/Eu*, Zr/Sc, Th/Sc, Th/U and Gd_N/Yb_N). The results point to an old continental crust as the likely main source for the sediments, with minor recycled sedimentary and trench-derived components.

Based on the white mica and chlorite chemistry, as well as on illite 'crystallinity' index, we provide further evidence that the *mélange* and some other metamudstones in the Kaczawa Complex were metamorphosed under very low-grade conditions (T < 250°C) which is in line with the accretionary prism model.

Is there an extreme pressure dependence of sulphur solubility in hydrous silicate melts?

A.V. KOSTYUK* AND N.S. GORBACHEV

Institute of Experimental Mineralogy RAS, Academica Osipyana 4, Chernogolovka, Russia
(correspondence*: nastya@iem.ac.ru, gor@iem.ac.ru)

The question of the dependence of the solubility of sulphur in hydrous silicate melts on the pressure still remains one of the most discussed and relevant. There are a lot of experimental works studying the SCSS in silicate melts, but there is no clear answer on the effect of pressure on it. We have proposed an alternative hypothesis about existence of extreme pressure dependence of sulphur solubility with a maximum at 1.5-2.0 GPa [1]. Since, the available literature data are quite extensive at P from 0.5 to 3 GPa [2-4], we decided to study experimentally peridotite-basalt-sulphide-H₂O system at P=0.1-0.5 GPa and T=1200-1300°C.

Experiments were carried out in an internal-heated pressure vessels by a quenching technique. We used Pt-peridotite ampoules filled with powder of tholeiitic basalt and FeS as starting compositions in the ratio of 3:1. The total volatile (H₂O) in system were 5 wt.%. Fugacity of sulphur and oxygen buffered by Pt-PtS and WM buffers respectively. Duration of experiments was 24 hours. Products of experiments were studied by microprobe.

There was a positive dependence of the solubility of sulphur on the pressure after experiment. The concentration of sulphur in the water-containing silicate melt at T=1200°C was 0.2±0.12wt.% at P=0.1GPa; 0.35±0.03wt.% at P=0.3GPa; 0.42±0.19wt.% at P=0.5 GPa. The sulphur concentration at T=1300°C was 0.2±0.12wt.% at P=0.1GPa; 0.27±0.06wt.% at P=0.3GPa; 0.46±0.12wt.% at P=0.5GPa. These data confirm our previous assumption about extreme pressure dependence of sulphur solubility in hydrous sulphide-bearing silicate melts. Confirmation of this theory can be very useful for a better understanding of transport of sulphide sulphur and ore elements from the deep magmatic centres to the upper levels of the Earth crust where most of known sulphide ore deposits were discovered.

Supported by grant RFBR № 12-05-31113

[1] Gorbachev N.S. *et al.* (2005) *Doklady Earth Science*, V.401, N.3, P.421-423 [2] Mavrogenes, O'Neill (1999) *Geochim. Cosmochim. Acta.* 63, 1173-1180. [3] Mysen, Popp (1980) *Amer. J. Sci.* 280, 78-92. [4] Wendlandt (1982) *Amer. Mineral.* 67, 877-885.

U-Pb, Ar-Ar isotopic dating of Kalba-Narym polychronic batholith (East Kazakhstan)

P.D. KOTLER^{12*}, A.G. VLADIMIROV^{12,3},
S.V. KHROMYKH¹², A.V. TRAVIN¹ AND O.V. NAVOZOV⁴

¹Institute of geology and mineralogy SB RAS, Novosibirsk, 630090, Russia (*: pkotler@yandex.ru)

²Novosibirsk State University, 630090, Novosibirsk, Russia

³Tomsk State University, Tomsk 634050, Russia

⁴“Topaz” geological exploration company LTD, Oskemen, 070001, Republic of Kazakhstan

Kalba-Narym granitoid batholith located on the territory of East Kazakhstan. Batholith has a polychronic structure and is composed of rocks of five intrusive complexes, which differ in composition and formation time [1].

Results of U-Pb and Ar-Ar granitoids complexes isotopic dating are: 1) kunush plagiogranite complex (U-Pb, Zrc - 306±9, 299±2 Ma); 2) kalguta association of Bt-Grt-granodiorites and Hbl-granite (Ar-Ar, Hbl (2 dates) - 286±3 Ma, Bt - 272±1 Ma); 3) Kalba granodiorite-granite complex (Ar-Ar, Bt - 5 dates from 291 to 273 Ma); 4) monastyr leucogranite complex (U-Pb, Zrc - 284±4 Ma, Ar-Ar, Bt - 6 dates from 285 to 269 Ma); 5) kainda granite complex (Ar-Ar, Bt - 5 dates from 290 to 267 Ma).

Obtained results allow us to determine the maximum duration of formation of Kalba-Narym batholith at ~ 30 million years. The formation of the main volume of granitoids occurred during a short interval - no more than 10 million years (290-280 Ma), which corresponds to most of the Ar-Ar dates. Younger Ar-Ar dates from 280 to 270 Ma can be interpreted as the result of later disbalance in K-Ar isotopic system because the north-eastern part of the batholith is adjacent to a major fault - Irtysh shear zone, within which the fixed stages of tectonic activity are 280-275 Ma and 270-265 Ma [2].

The work was supported by the Presidium of SB RAS (project № 17, 77,123), RFBR (project № 10-0500913-A), FGP “Research and scientific-pedagogical personnel of innovative Russia” (№ 2012-1.2.1-12-000-2008-8340).

[1] Navozov O.V. *et al.* (2011) *Geologiya i ohrana nedr.* **4**, 66-72. [2] Travin *et al.* (2001) *Geochemistry Int.* **12**, 1347-1351

Geochemistry of sediments from the Khai River – Nha Trang Bay estuarine system, South China Sea

S.E. KOUKINA*, N.V. LOBUS, V.I. PERESYPKIN,
G.N. BATURIN AND N.A. SHULGA

PP Shirshov Institute of Oceanology of RAS, 117997

Nakhimovsky pr. 36, Moscow, Russia

(*correspondence: skoukina@gmail.com)

The Khai River and the Nha Trang Bay form one of the major estuarine systems in the South China Sea that is inhabited by unique biota. This area now experiences a significant anthropogenic load from the local people activities and, especially, from the quickly growing tourist industry.

Trace (Cr, Ni, Cd, V, Zn, Cu, Pb, Sb, Bi, Sn, Ag, Li, Co, As, Zr, Mo, Hg), minor (Mn) and major (Al, Fe, Ti, Mg, Ca, Na, K) along with nutrients (TOC, TS, TP) and TIC were first determined in surface sediment samples from the Khai River and Nha Trang Bay along the salinity gradient.

According to the sediment quality guidelines and reference background values data on the shale, pelagic clays, average river bed sediments and rural and industrial Vietnamese soils most of the element contents that were studied were below the threshold levels, while the content of Cu, Pb, Ni and, especially Ag exceeded significantly the hazardous levels in the most of the samples from the Nha Trang Bay.

Aluminum normalization and Spearman correlation analysis revealed some specific features in distribution of elements along the salinity gradient. Thus, Ca, Ba and Sr are largely dependent on the carbonates content in sediments. Sedimentary P, Al, Fe, Mn, Ti, Na, K, Li, Co, Cs, Zn and V are most likely controlled by the accumulation of their fine grained aluminosilicate host minerals and therefore tend to increase seaward. The contents of S, As, Sn, Bi, U, Cd and Mo are slightly elevated in sediments of estuarine part of the river – sea transect. These elements may be scavenged by and/or co-precipitated with the dissolved and particulate materials of the river discharge and further deposited on the geochemical barrier within the river – sea water mixing zone.

The distribution of Ni, Cr, Zr, Cu, Pb, Sb, Hg and, especially, Ag was characterized by anomalous high concentrations in the urban area of river-sea transect. This might be due to the point anthropogenic pollution from local human activities, i.e., fishing, shipping, fueling, and waste and sewage sludge outflow. The anthropogenic and/or environmental sources of Ag in the region need special study.

Integrated geological and geophysical probing of lithospheric dynamics in a young extensional basin (Carpathian-Pannonian Region)

ISTVÁN KOVÁCS¹, GYÖRGY FALUS¹, CSABA SZABÓ², JÁNOS KISS¹, TAMÁS FANCSIK¹, ENDRE HEGEDŰS¹, ZSANETT PINTÉR², NÓRA LIPTAI² AND LEVENTE PATKÓ²

¹Geological and Geophysical Institute of Hungary, H-1143, Srefánia út 14, Budapest, Hungary

²Lithosphere Fluid Research Lab, Institute of Geography and Earth Sciences, Eötvös University, Budapest, Hungary, H-1117, Pázmány Péter sétány 1/c

Detailed analysis of numerous of mantle xenoliths from the Carpathian-Pannonian region revealed that the present lithosphere may be divided into two major sub-horizontal domains.

The shallower “layer” is characterized mostly by fine grained, equigranular to porphyroclastic xenoliths, generally displays an ‘axial [010]’ deformation pattern. Mineral constituents show high Mg#, low H₂O content in nominally anhydrous minerals (NAMs) and depleted in basaltic major elements implying that this layer may have undergone considerable depletion.

The xenoliths from the deeper “layer” show mainly coarse grained, protogranular texture with ‘A-type’ deformation pattern. Minerals usually have lower Mg# and richer in basaltic major elements. The NAMs from this “layer” show higher H₂O content than those in the shallow layer. This layering may also be seen as seismic reflections in the present lithospheric mantle 10-15 km below the MOHO, accompanied by a considerable increase in seismic velocities. Anomalous seismic anisotropy pattern showing E-W direction in contrast to the general NNW-SSE trend may be due to the fossil directions frozen in the juvenile deeper lithosphere which may be the result of an asthenospheric flow related to the Alpine collision.

Influence of long-term diagenesis on the REE content in marine reptile remains from the Middle Triassic bonebed (S Poland)

MONIKA KOWAL-LINKA^{1*}, KLAUS PETER JOCHUM² AND DAWID SURMIK³

¹A. Mickiewicz University in Poznań, Institute of Geology, Poland, (*correspondence: mokowal@amu.edu.pl)

²Max-Planck-Institut für Chemie, Mainz, Germany, (k.jochum@mpic.de)

³University of Silesia, Faculty of Earth Science, Sosnowiec, Poland (dawid@surmik.pl)

The geochemical signals recorded in fossil bones are commonly used to reconstruct conditions of sedimentary and diagenetic environments, but recent data suggest insufficient recognition of particularly the long-term impact of diagenesis on vertebrate remains. We have examined with LA-ICPMS 29 bones of marine reptiles collected from the ~247-245 Ma old (Middle Triassic) bonebed, outcropped in Żyglin (S Poland). This bonebed (a crinoidal limestone) comprises reworked vertebrate remains deposited originally in various coastal and marine settings and at different times. The two main objectives of the present study are: (1) to check whether concentrations and ratios of REE and other trace elements are useful to distinguish between relatively younger and relatively older bones in the marine bonebed, and (2) whether the early diagenetic element contents and ratios characteristic for the various depositional settings can still be deciphered.

The REE concentrations in the profiles (average Σ REE in individual profile is ~2900-3500 ppm) tend to be more or less constant. All samples are enriched in REE with regard to the PAAS. The samples/PAAS diagrams reveal “bell shaped” patterns with two peaks for Sm and Gd, a small low for Eu, and with HREE values far below the LREE values. The bones form a small cluster in the (La/Sm)_N vs. (La/Yb)_N diagram, although some samples are located distinctly outside the cluster margin. In the Ce/Ce* vs. Pr/Pr* diagram the bones reveal a slightly negative Ce_N anomaly or lack of it, and smoothly positive and negative La_N anomaly. Most of the samples display similar REE concentrations and distribution patterns, probably due to long-term diagenesis which obliterated the early diagenetic geochemical signals. Only several samples show different features.

M. Kowal-Linka is supported by the NCN grant 2011/01/B/ST10/04889, and Dawid Surmik by the NCN grant 2011/01/N/ST10/06989.

Fractionation of Si isotopes during core formation from first principles calculations

PIOTR M. KOWALSKI*¹ AND SANDRO JAHN²

¹Forschungszentrum Jülich GmbH, Institute of Energy and Climate Research - IEK-6: Nuclear Waste Management, D-52425 Jülich, Germany (*correspondence: p.kowalski@fz-juelich.de);

²GFZ German Research Centre for Geosciences, Telegrafenberg, D-14473 Potsdam, Germany.

Recently, we have developed an efficient ab initio based computational approach to predict equilibrium isotope fractionation factors between chemically and structurally complex crystalline solids, fluids and melts at high T and P [1,2]. Our method has been successfully applied to “non-traditional” stable isotopes of light elements such as B and Li, which are important geochemical tracers widely used in petrology. We have shown that we are able to correctly reproduce the experimentally observed fractionation sequences: fluid-tourmaline-mica for B and staurolite-fluid-mica-spodumene for Li isotopes with a computational uncertainty comparable to the experimental error. Moreover, with the calculations we explained the discrepancy between the results of in-situ experiments and measurements on natural samples [2].

With this well tested methodology we investigate here the Si isotope fractionation between silicate melt and liquid metal under the extreme P-T conditions of Earth's core formation (P~25 GPa, T~3000 K) that are not yet accessible to experiment [3]. The equilibrium Si isotope fractionation factors between these materials are of great interest as they are needed to understand the origin of the difference in the isotopic signatures observed between the Bulk Silicate Earth (BSE) and Chondrite meteorites [3]. It has been proposed that the observed difference reflects the fractionation of Si isotopes between silicate melt and iron-rich metal during the formation of Earth's core [4]. We will present a comparison of our predictions with the available experimental data and discuss the effect of the pressure-induced changes in the melt structure on the fractionation of Si isotopes. Our results shed new light on the origin of the excess of the heavy Si isotopes in BSE and may also help to further constrain the silicon content of the Earth's core.

[1] Kowalski, P. M. and Jahn, S. (2011) *Geochim. Cosmochim. Acta* **75**, 6112-6123. [2] Kowalski, P. M. Wunder, B. and Jahn, S. (2013) *Geochim. Cosmochim. Acta* **101**, 285-301. [3] Shahar, A. *et al.* (2011) *Geochim. Cosmochim. Acta* **75**, 7688-7697. [4] Georg, R. B. *et al.* (2007) *Nature* **447**, 1102-1106.

Characteristics of metal bearing phases in MSWI residues from Poland

P. KOWALSKI*¹ AND M. MICHALIK¹

¹Institute of Geological Sciences, Jagiellonian University ul.Oleandry 2a, 30-063 Krakow (*correspondence: p.kowalski@uj.edu.pl)

Mineralogical characteristic of MSWI (municipal solid waste incineration) residues is important, especially in time of ongoing changes in municipal waste management system in Poland. These changes leads to significant reduction of the amount of landfilled raw wastes. A way to achieve this goal is construction of nine incineration power plants with assumed slags production around two hundred thousand tons per year. The increasing slag production makes that it is essential to take a closer look into this material in terms of possible environmental pollution.

The aim of this study is mineralogical and chemical characteristics of the metal-bearing phases of the MSWI residues. Slags were collected from two the biggest incineration power plants in Poland. One of them is oriented to incineration of non-hazardous municipal waste and the other on industrial and hazardous municipal wastes.

Slags from incineration of wastes are non-consolidated, grainy materials, containing large amount of amorphous phase, mostly composed of Si-rich glass.

Metals in slags are present in several forms:

1. As large fragments which are mixed with slags grains and part of uncombusted materials (rock fragments, glass and ceramics),
2. In form of metallic inclusions in glass or minerals,
3. As a component of mineral and amorphous phases.

Metals in form of metallic inclusions are monometallic (mainly Fe, Al, Pb, Zn, Cu) or in form of alloys (Fe-Ti, Fe-Ni, Fe-Cu, Cu-Sn+Pb and Cr-Fe). Metals in minerals are concentrated mostly in form of oxides (mainly Fe and Al oxides) and in silicates, aluminosilicates and sulfates (e.g. Cu). The content of metals in glass varies in wide range. High concentration of them is connected with presence of metallic inclusions inside the glass. Content of metals in slags varies within broad range – e.g. Cu from 330 to 4900 ppm, Zn from 1500 to 4700 ppm, Pb from 50 to 6300 ppm and Cr from 300 to 600 ppm in municipal slags and from 2000 to 2500 ppm in industrial slags. These concentrations could be potentially hazardous and further studies about leaching potential and mobility of these metals are needed.

Electrolyte ion binding at iron oxyhydroxide surfaces

PHILIPP A. KOZIN*, ANDREI SHCHUKAREV
AND JEAN-FRANÇOIS BOILY

*correspondence philipp.kozin@chem.umu.se

Electrolyte ion loadings at the surfaces of synthetic goethite (α -FeOOH) and lepidocrocite (γ -FeOOH) nano-sized particles that were pre-equilibrated in aqueous solutions of 10 mM NaCl and NaClO₄ were investigated by means of cryogenic X-ray photoelectron spectroscopy (XPS) [1]. Atomic concentrations of Cl⁻ and ClO₄⁻ in acidic pH regions and of Na⁺ cations [2] in alkaline pH regions were correlated to potential determining ion (*p.d.i.*; H⁺, OH⁻) adsorption obtained by potentiometric titrations. (Fig. 1)

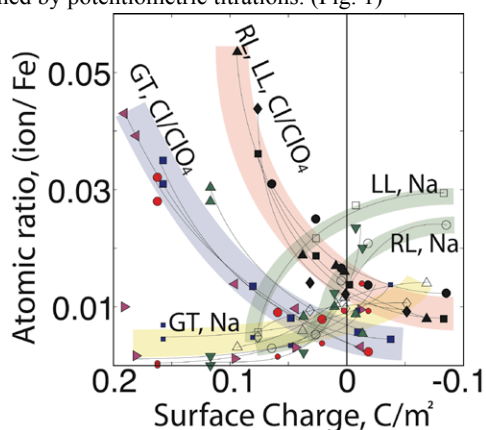


Figure 1. Ionic surface loadings as a function of surface charge developed on rod- (RL) and lath-shaped (LL) lepidocrocite, as well as in two different goethite with specific surface area of 69 (GT69) and 122 (GT122) m²/g.

The data revealed a strong dependency of *p.d.i.* and electrolyte ion adsorption on mineral particle morphology, as seen by comparison of rod- (RL) and lath-shaped (LL) lepidocrocite particles, as well as on surface roughness, as in case of samples with different surface porosity (Fig. 1). LL particles with a predominantly proton-inactive (010) surface acquired greater sodium but lower anion loadings. GT122 particles contained greater surface roughness and thereby acquired greater *p.d.i.* and anion loadings than GT69.

[1] Shchukarev (2010), *Journal of Electron Spectroscopy and Related Phenomena* **176**, 13–17. [2] Shimizu, Shchukarev, Kozin and Boily (2012), *Surface Science* **606**, 1005–1009.

Petrogenesis of mafic-ultramafic rocks from the Berit metaophiolite massif: implications for REE, PGE, base metal and Al-rich chromitite composition

¹H. KOZLU^{2A} AND V. RUDASHEVSKY

¹General Directorate of Mineral Research & Exploration, Mineralogy-Petrography, 06800 TR Çankaya/Ankara Turkey, E-mail: haticekozlu@mta.gov.tr

²CNT Labs, 1 Roentgena Str.197101, St.Petersburg, Russia

Mantle heterogeneity in terms of corundum bearing mafic rocks, as including eclogite and/or pyroxenite within peridotite is observed in Berit massif. The bulk chemical analytical results of the patterns from mafic and ultramafic rocks indicate that they relatively enriched in the REE-PGE and base metals. The refertilized and inhomogeneous mantle is capable of yielding more voluminous and compositionally diverse magma than normal. The REE and PGE distribution of high-Al chromitite patterns and mafic layers in Berit peridotite are, therefore, very important geochemical tool for determining the upper mantle heterogeneity. REE values of mafic rocks are between (La/Ce: 0.40-0.69, Ce/Yb: 1.05-16.29, La/Yb: 0.44-7.62, La/Sm: 0.88-6, La/Lu: 2.8-55) 12-165 ppm. The LREE-enrichment in peridotites are explained by interaction of the peridotites with LREE-enriched melts. The REE and PGE are generally considered to be relatively immobile during low-temperature alteration. However some elements, such as Eu, can be modified some what by hydrothermal processes. It has been determined the positive Eu anomalies in the normalised diagram for some chromitites and ultramafic mafic rock samples (dunite-pyroxenite-gabbro-diabase) from Berit metaophiolite. A relative enrichment in siderophile elements (as ppm) in the both of mafic and ultramafic rocks and in the high-Al chromitites for base metals (Ag: 0.3-0.9, Bi: 0.03-0.11, Cu: 13-2626, Ni: 134-7172, and Te: 0.1-3 ppm) is also determined. It is noteworthy that especially Pt (2.5 ppm) and Pd (4 ppm) enrichments are encountered in the high-Al chromitites.

Two chromite generations are determined in Berit: 1) primary spinel component-rich (Al₂O₃- and MgO-rich compositions); 2) developed on the boundary of grains of chromite I – chromite and II enriched by chromite and magnetite minerals (in Fe, Cr and Ti). The association of base metals (Cu, Ni, Bi, Se, Te, Au, Ag) and Ti as well as Pd and Pt itself in composition of accessory minerals has been suggested that they may be brought into chromitites by fluids in basic composition.

Migration of hydrocarbons recorded in calcite-hosted inclusions, Dead Sea area: trace elements and isotopic evidence

O.A. KOZMENKO*, E.V. SOKOL AND V.N. REUTSKY

V.S.Sobolev Institute of Geology and Mineralogy, prosp. Koptuyuga 3, Novosibirsk, 630090, Russia (*olg@igm.nsc.ru)

The mechanisms of hydrocarbon (HC) migration with water fluids, as well as the ability of container minerals such as vein calcite to preserve HC geochemical tracers, have received much recent interest [1]. Calcitic veins enclosing HC and soot carbon have been discovered in the western side of the Dead Sea rift, where basin opening induced venting of water-methane fluids [2]. All veins share similar REE spectra defined by the calcite rare earths patterns. Calcite crystallized from solutions with seawater chemistry signatures [3]. The reconstructed water generation temperatures of 55–90°C fit the regional “oil window” located at the depths 2.5–4 km. Significant negative Ce/Ce* anomaly indicates calcite growth at high oxygen fugacity. The organic matter hosted by calcite has C:N:S ratios from 30:2:15 to 15:0.1:2 (in mole fraction) and contains abundant asphaltene with trace amounts of alkanes and carbonyl groups. Measured values $\delta^{13}\text{C}_{\text{org}}$ (–26.9 to –27.2‰ PDB) and $\delta^{34}\text{S}$ (+5.5‰ CDT) are similar to those of the Dead Sea asphaltene [4]. As the obtained data imply, the calcite veins with inclusions of both oxidized and biodegraded HC and soot carbon precipitated from Ca-Na-HCO₃-Cl sediment waters that entrained crude oil drops.

[1] Rongxi *et al.* (2011) *Rus. Geol.Geoph.* **52**, 1491–1503. [2] Gvirtzman & Stanislavsky (2000) *Basin Research* **12**, 79–93. [3] Bau & Dulski (1996) *Precamb. Res.* **79**, 37–55. [4] Nissenbaum & Goldberg (1980) *Org. Geochem.* **2**, 167–180.

Gramaccioliite-(Y) – rare yttrium carrier in metamorphic rocks (Subpolar Urals, Russia)

KOZYREVA I.V.¹, AND SHVETSOVA I.V.

Institute of Geology Komi SC UB RAS, Syktyvkar 167982, Russia (¹kozyreva@geo.komisc.ru)

Gramaccioliite-(Y) is related to crichtonite group which includes the series of complex titanium and iron oxides with general formula $\text{ABC}_{18}\text{T}_2\text{O}_{38}$, where A = Sr, Pb, Ca, Na, R, REE, Ba, U; B = Mn, Y, REE, U, Zr; C = Ti, Fe³⁺, Cr и T = Fe³⁺, Mg. For the first time it was found in biotite gneisses of Piedmont province (Italy) and named in honor of Professor of Milan University Carlo Maria Gramaccioli [1]. We found gramaccioliite-(Y) on Maldynyrd Ridge (Subpolar Urals) in hematite-sericite shales. This is the first find in Russia. The mineral was found as well composed tabular crystals with trigonal habit with rhombohedral side planes, with black coloring and metal shine. In association with it we found leucoxene, rutile, anatase, apatite, cyanite, epidote, garnet, tourmaline, monazite and fuchsite, gold in important quantities. Gramaccioliite-(Y) was studied with scanning electron microscope JSM-6400 with energy spectrometer Link. The calculated empirical formulas of gramaccioliite-(Y) are as follows:

$$(\text{Pb}_{0.61}\text{Sr}_{0.27}\text{Ba}_{0.02}\text{U}_{0.02})_{0.93}(\text{Y}_{0.49}\text{Mn}_{0.37}\text{Ce}_{0.08}\text{Ca}_{0.04}\text{Nd}_{0.02}\text{La}_{0.02})_{1.01} \times (\text{Ti}_{13.53}\text{Fe}_{5.49}\text{Zn}_{0.22}\text{V}_{0.04}\text{Nb}_{0.04})_{19.33}\text{O}_{38} [1].$$

$$(\text{Pb}_{0.60}\text{Sr}_{0.39})_{0.99}(\text{Y}_{0.55}\text{Mn}_{0.42})_{0.97}(\text{Ti}_{13.32}\text{Fe}_{6.01}\text{Zn}_{0.53}\text{V}_{0.18})_{20.04}\text{O}_{38}$$

– our data.

It is noticeable that the mineral, discovered by us, differs from the one, discovered in Italy, by considerably lower quantity of impurities, and its formula is practically identical to approved one (IMA 2001–034): $(\text{Pb,Sr})(\text{Y,Mn})(\text{Ti,Fe})_{18}\text{Fe}_2\text{O}_{38}$ [1]. The formation of gramaccioliite-(Y) is conditioned by geochemical and mineralogical features of metamorphized rocks, formed on Precambrian substrate of contrasting content and modified by hypergenic processes. On the one hand the high titanium content of basites, presence of lead and zinc as galenite and sphalerite inclusions, on the other hand – rare earth and manganese anomaly, which is characteristic for rhyolites of this region – all these were favorable formation factors for complex titanium and iron oxide - gramaccioliite-(Y).

The work is completed with financial support from the Program of Basic Researches of UB RAS #12-C-5-1020 “General and local criteria of difference between high-disperse exogenous and low-temperature hydrothermal ore-forming systems”.

[1] Orlandi P. *et al.* (2004) *European Journal of Mineralogy* **16**, 171–175.

Benthic nutrient fluxes and iron-phosphorus cycling in sulfidic estuarine muds

PETER KRAAL^{1,2}, EDWARD D. BURTON¹,
RICHARD T. BUSH¹, ANDREW L. ROSE¹,
MICHAEL D. CHEETHAM¹ AND LEIGH A. SULLIVAN¹

¹Southern Cross GeoScience, Southern Cross University, PO Box 157, Lismore, New South Wales, Australia

²As per June 1, 2013: Department of Geochemistry, Utrecht University, Budapestlaan 4, 3584 CD Utrecht, The Netherlands

Estuaries are crucial geochemical filters at the land-ocean interface that have been widely impacted by human activities. We investigated sediment biogeochemistry and benthic nutrient fluxes in the shallow, eutrophic Peel-Harvey Estuary in Western Australia. Our results reveal localized deposition of organic-rich, fine-grained surface sediments characterized by high sulfate reduction rates and abundant accumulation of metastable iron (Fe) monosulfides. Core incubations showed high rates of nitrogen and phosphate release from these sulfidic surface sediments, even though they are reworked and overlain by a well-mixed, oxygenated water column. This suggests decoupling between bottom water oxygenation and sedimentary phosphorus (P) retention. Phosphate sorption experiments emphasized the stark contrast in phosphate binding capacity between the 'normal' estuarine sediments and the strongly reducing muds.

In addition, we observed rapid and extensive sulfidization of reactive Fe within centimeters of the sediment surface below the oxygenated water column, indicating that Fe speciation may not necessarily reflect bottom water oxygenation, at least under the investigated environmental conditions. These findings may be of importance to the use of Fe-based paleoredox-proxies.

Despite strongly reducing conditions, our results suggested that Fe-associated P may be an important P sink in the investigated muds. Using a combination of sequential chemical Fe and P extractions, Fe Extended X-ray Absorption Fine Structure (Fe EXAFS) and micron-scale multi-energy X-ray element mapping, we examine the nature of this Fe-P association.

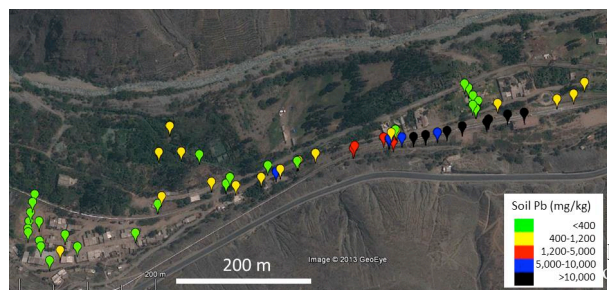
Overall, our detailed geochemical results and benthic flux measurements challenge some of the existing paradigms regarding the links between bottom water oxygenation and the cycling of essential elements such as Fe and P.

Mapping lead contamination of soil due to mining in Peru

S.X. KRAGIE¹ AND A. VAN GEEN¹

¹Lamont-Doherty Earth Observatory of Columbia University, Palisades, NY 10964, USA

An estimated 1.6 million people live within 5 km of an active mine, ore processing plant, smelter, or former mining site in Peru [1]. In a country with such a long mining history, towns have often been built on top of former mine tailings contaminated with Pb. The health consequences of allowing children to play in soil contaminated with Pb have been well documented. What is less widely known is that the distribution of Pb in soil contaminated by mining activities can be spatially highly heterogeneous. One such example along the railroad track that links the capital Lima to the main mining centers in the Andes is illustrated below.



The data show concentrations exceeding 10,000 mg/kg Pb along a 200 m section of the railroad while other sites along the rail road generally are well within the current US EPA standard of 1,200 mg/kg for residential soil where children do not play. The particularly contaminated area is a turning point for railroad cars containing ore concentrate and this has been associated with contamination of an area commonly used as a walkway. Additional examples of Pb hot-spots will be included in the poster, typically from older mining sites. Results of soil surveys around modern mining operations showing little Pb contamination will also be shown.

Handheld XRF analysers are relatively expensive and their deployment requires training. We have therefore also been testing the soils collected in Peru with a simple Pb extraction and detection protocol relying on citric acid and rhodizonate. The poster will include results from this alternative approach.

[1] van Geen *et al.* (2012) *Bull. WHO* **90**, 878–886.

U phase evolution in the bedrock around Forsmark, eastern Sweden

L. KRALL^{1*}, B. SANDSTRÖM² AND E-L. TULLBORG³

¹SKB, Stockholm University, Sweden *Lindsay.Krall@skb.se

²WSP Group, Gothenburg, Sweden

³Terralogica AB, Gråbo, Sweden

Elevated gamma emissions from some pegmatites, cataclasites, and vein fillings were found in drillcores from Forsmark, Sweden. A proposed host for nuclear waste repositories, these findings prompted interest in the geochemistry of U in the local bedrock. Coupled with existing knowledge of the site, characterization of solid-phase U has implications for the deposition, evolution, and behavior of U in this environment. A model of the low- to moderate-temperature evolution of the area was established during preceding fracture mineral studies. Four generations of fracture minerals record the relative timings and types of fluid migration and have been traced to regional events, such as orogeny and glaciation, by means of stable isotope, fluid inclusion, radiometric dating, and fracture orientation analysis [1]. This model has contributed to a working hypothesis on the stages of U alteration: 1) Palaeoproterozoic, U was introduced, likely as uraninite, by pegmatitic intrusion, 2) formation of cataclasite, U was mobilized and uraninite was altered to pitchblende then partially coffinitized, 3) Palaeozoic, U was remobilized and U-phosphate precipitated on fracture surfaces and 4) Palaeozoic or later, amorphous U-silicate formed in fractures.

Thin sections from zones of elevated gamma radiation have been analyzed using SEM-EDS. A primary (U,Pb)-oxide mineral (250 µm) confined by a rim of (Fe, Mn)-chlorite has been found in a small pegmatite. Most U phases found in pegmatites are low-Pb, probably secondary U-silicates (10-30 µm) of mutually different habit and composition (e.g. Ca, Fe, Ti, Mn, Al, and/or Ba) and are associated with minerals like chlorite, hematite, quartz, K-feldspar, and calcite. In the cataclasite, both primary (Th, U, REE)-silicates (150 µm) within pegmatite clasts and secondary U(Ca, Al)-silicates were along calcite and quartz grain boundaries. In vein fillings, disseminated grains of secondary U-silicate were found associated with laumontite, a marker within the fracture mineral generation of 1.10 – 1.03 Ga. Additionally, U-phosphates were found with pyrite, mixed layer clays, and Palaeozoic asphaltite. These findings complement the hypothesized stages of evolution and offer new U phases for integration.

[1] Sandström *et al.* (2009) *Tectonophysics* **478**, 158-174.

Drainage water chemistry reflects monolithologic Critical Zones

P. KRÁM*, J. ČUŘÍK, F. VESELOVSKÝ, O. MYŠKA, V. ŠTĚDRÁ, V. BLÁHA AND J. HRUŠKA

Czech Geological Survey, Klárov 3, 118 21 Prague 1, Czech Republic (*correspondence: pavel.kram@geology.cz)

Three small (27-55 ha) catchments covered by spruce, each underlain by geochemically contrasting rocks (LYS: granite, NAZ: amphibolite, PLB: serpentinite) were studied in the Slavkov Forest, Czech Rep [1]. Hydrochemical patterns were ascertained by concurrent stream water sampling (2001-2013) and soil water sampling by lysimeters placed at five depths in 2012-2013 (Fig. 1). Three boreholes drilled to 26-30 m probed deep critical zones. Strongly acidified LYS exhibited incomplete neutralization of acidic deposition and had chronically low drainage water pH and elevated levels of toxic Al [2]. PLB exhibited the most efficient neutralization by chemical weathering. LYS was Mg deficient with respect of spruce and ectomycorrhizal fungi, PLB was P and K deficient and NAZ was not deficient in any nutrients [1,3].

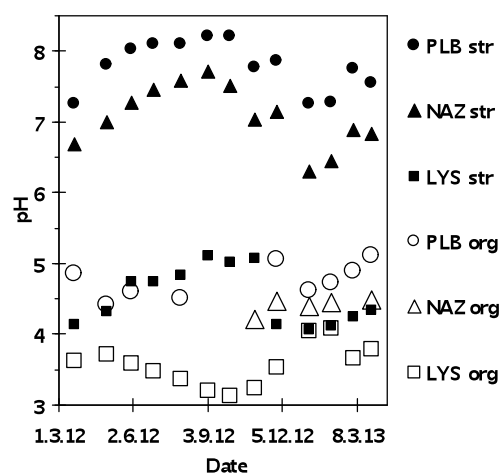


Figure 1: Temporal patterns of stream water (str) and organic horizon soil water (org) at Lysina (LYS), Na Zeleném (NAZ) and Pluhův Bor (PLB) in March 2012 - March 2013.

This study was supported by the EC (FP7 SoilTrEC 244118).

[1] Krám *et al.* (2012) *Appl. Geoch.* **27**, 1854-1863. [2] Banwart *et al.* (2012) *Compt. Rend. Geosci.* **344**, 758-772. [3] Berner (2013) *Doct. Thes.*, Lund Univ., Sweden.

Indirect evidence for the presence of secondary phosphorus in continental fine aerosol

K. KRASSOVÁN^{1*}, Z. KERTÉSZ², K. IMRE³
AND A. GELENCSE^{1,3}

¹Institute of Environmental Sciences, University of Pannonia, Veszprém 8200, Hungary (*correspondence: krassovank@uni-pannon.hu)

²Institute of Nuclear Research of the Hungarian Academy of Sciences, Laboratory of Ion Beam Applications, Debrecen 4032, Hungary (kerteszz.sofia@atomki.mta.hu)

³Air Chemistry Group of the Hungarian Academy of Sciences, Veszprém 8200, Hungary (kornelia@almos.uni-pannon.hu)

The role of the atmosphere in the biogeochemical cycle of phosphorus is generally associated with the emission of soil dust, sea-salt particles, bioaerosols and industrial aerosols. Quite independently, a reduced gaseous phosphorus compound (phosphine, PH₃) was measured over various sources such as marshes and sewage plants [1] and also in the global troposphere. Given that phosphine is a reactive gas that rapidly yields low-volatility phosphoric acid in the atmosphere [2], secondary aerosol formation can be an important sink that has never been considered in the global phosphorus cycle. In our study we present mass size-distribution measurements of phosphorus in aerosol samples collected at two locations in Hungary. The bimodal size distribution of phosphorus indicated two distinct formation mechanisms in the fine and coarse modes. As expected, the mass concentration of phosphorus was dominated by the coarse particles (aerodynamic diameter >1 μm), the contribution of fine mode phosphorus was in the range of 10–27 % (median 19 %) of the total. The contribution of biomass burning to the fine mode phosphorus was inferred from measured K concentrations and P/K ratios reported for biomass smoke [3]. It was found that biomass burning accounted for only a small fraction of fine mode phosphorus, the rest of which likely formed as secondary aerosol component from gaseous phosphine. Secondary aerosol phosphorus can be even more important in providing this essential nutrient for remote ecosystems since it is associated with fine aerosol particles which have longer residence time and thus are more prone to long-range atmospheric transport than coarse primary particles.

[1] Dévai *et al.* (1988) *Nature* **333**, 343–345. [2] Frank & Rippen (1987) *Lebensmitteltechnik* **7-8**, 409–411. [3] Echalar *et al.* (1995) *Geophysical Research Letters* **22**, 3039–3042.

Enhanced calcite dissolution in the presence of aerobic methanotrophic bacteria

KRAUSE S.¹, ALOISI G.^{1,3}, ENGEL, A.², LIEBETRAU V.¹,
AND TREUDE T.¹

¹GEOMAR Helmholtz Centre of Ocean Research, Department of Marine Biogeochemistry, Wischhofstrasse 1-3, 24148 Kiel, Germany, skrause@geomar.de, vliebetrau@geomar.de, ttreude@geomar.de

²GEOMAR Helmholtz Centre of Ocean Research Department of Biological Oceanography, Düsternbrooker Weg 20, 24105 Kiel, Germany, aengel@geomar.de

³Laboratoire d'Océanographie et du Climat : Expérimentations et Approches Numériques, UMR 7159, Université Pierre et Marie Curie, 4, Place Jussieu, 75252, Paris, France, Giovanni.Aloisi@locean-ipsl.upmc.fr

Aquatic microbial aerobic methane oxidation (MOx) causes the production of carbon dioxide, leading to decrease of liquid phase pH. Therefore, MOx activity impacts the carbonate system, potentially favouring dissolution of calcium carbonates. In addition, carbonate dissolution has recently also been attributed to microbially produced organic polymers. To date, the impact of metabolic products from MOx on carbonates has been poorly constrained. To discriminate between different mechanisms acting on carbonate stability, calcite dissolution experiments were conducted with (1) prospering cells (2) starving cells, and (3) dead cells of the methanotrophic bacterium *Methylosinus trichosporium*, as well as abiotic controls, under brackish conditions (salinity 10) near calcite saturation (saturation state (Ω) 2.22 to 1.76). Abiotic controls showed no calcite dissolution during the experiment. In contrast, dissolved calcium and total alkalinity markedly increased in experiments containing *M. trichosporium* cells, indicative for calcite dissolution. After initial system equilibration, calcite dissolution, ranging from 29.6 to 14.9 μmol l⁻¹ d⁻¹ between treatments, was observed. While concentrations of transparent exopolymer particles concentrations declined considerably over time in the presence of prospering and starving cells, concentrations increased in experiments with dead cells. Scanning electron microscopy of calcite crystals revealed surface corrosion after exposure to prospering, starving, and dead *M. trichosporium* cells. The results of this study demonstrate a strong potential impact of MOx bacteria on calcite stability, clearly facilitating calcite dissolution. In addition to CO₂ production by methanotrophically active cells and starving cells, we suggest that the release of acidic and/or calcium-chelating organic carbon compounds also facilitated enhanced calcite dissolution.

Glass ceramics and mineral materials for the immobilization of lead and cadmium from Municipal Solid Waste Incinerator ashes

KATERINA KRAUSOVA^{1*}, LAURENT GAUTRON¹, GILLES CATILLON¹ AND STEPHAN BORENSZTAJN²

¹Laboratory of Earth Materials and Environment, University Paris East – Marne la Vallée, 77454, France, (*krausovak@seznam.cz, gautron@univ-mlv.fr, gilles.catillon@univ-mlv.fr)

²Laboratory of Interfaces and Electrochemical Systems, University Pierre and Marie Curie, France (stephan.borensztajn@upmc.fr)

Waste management is one of the major global issues. Incineration is an efficient treatment since it offers both a reduction of mass and volume and a possibility of energy recovery. One of the problems of incineration is the production of bottom and fly ashes which are considered as hazardous waste with obligation of final disposal into a specific landfill.

The objective of the present study is to investigate glass ceramics and sintered ceramics as new mineral materials for a sustainable immobilization and possible recycling of these incineration wastes. Toxic elements can be incorporated into embedded crystals in a glass matrix which has a function of the second barrier, or in highly resistant crystalline structure. Based upon cations size considerations, this study is focused on Ca-rich or Ba-bearing minerals as possible hosts of lead and cadmium.

Promising results have been obtained for $\text{CaMgSi}_2\text{O}_6$ diopside-bearing glass ceramics and sintered $\text{Ba}_{1.5}\text{Mg}_{1.5}\text{Ti}_{6.5}\text{O}_{16}$ hollandite, both in terms of toxic elements incorporation and of chemical and mechanical resistance.

Stable isotope composition of anthropogenic thallium deposition

K. KREISSIG¹, M. REHKÄMPER^{1*} AND M. KERSTEN²

¹ESE, Imperial College, London SW7 2AZ, UK

(*correspondence: markrehk@imperial.ac.uk)

²Gutenberg-University, Mainz 55099, Germany

Thallium compounds are volatile at high temperature and not efficiently retained by emission control facilities of combustion sources. This study represents the first use of stable isotope ratios to apportion near-source Tl deposition to the emitter. In 1979, dust containing Tl was emitted by a cement plant near Lengerich, NW Germany. The emission event was caused by a ferric oxide additive to the powdered lime (used for the production of special cements), which contained a Tl-bearing residue of pyrite roasting. Following the emission event, sheep died and rabbits and horses were reported to loose fur and hair in the vicinity of the cement plant [1]. The cement plant owners denied responsibility for the bulk of the emissions. We determined the Tl isotope compositions ($\epsilon^{205}\text{Tl}$) of the cement dust (open symbol) and soil cores down to 100 cm depth (black symbols), and the data are in accord with a two-source mixing line (Fig. 1). Our novel isotope analysis ultimately helped the plaintiffs to settle the case by showing the causation of the pollution event, even though the emissions happened more than 30 years ago.

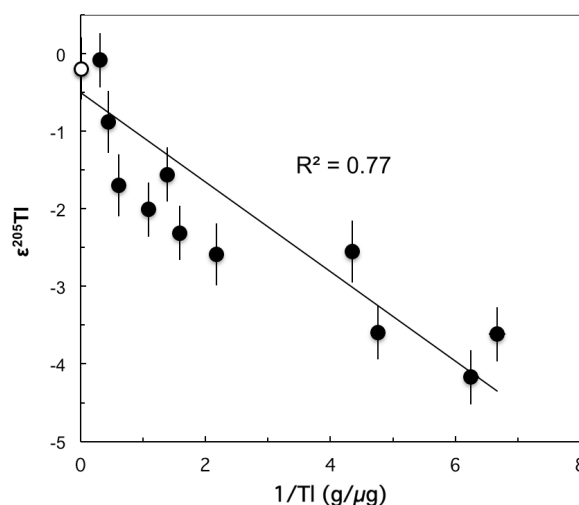


Figure 1: Tl stable isotope data vs. inverse Tl concentrations for soil samples of increasing depth from left to right.

[1] Schoer (1984) In: Hutzinger (ed.), Handbook of Environmental Chemistry, Vol. 3c. Springer, New York, 143–214.

Fractionation of Cd isotopes during evaporation and re-condensation

V. KREMSE¹, F. WOMBACHER¹, W. ERTEL-INGRISCH²,
D. B. DINGWELL² AND C. MÜNKER¹

¹Universität zu Köln, Institut für Geologie und Mineralogie,
Köln, Germany (v.kremser@uni-koeln.de)

²Ludwig-Maximilians-Universität, Department für Geo- und
Umweltwissenschaften, München, Germany

Stable isotope studies of volatile elements can provide constraints on possible scenarios of volatile element loss and redistribution [e.g. 1, 2]. Here, Cd stable isotope and volatile element fractionation during evaporation from silicate melt at about 1300 °C and during re-condensation onto Al₂O₃ condensation plates is studied experimentally, at atmospheric pressure in air and in CO-CO₂. The experiments can serve to address questions that are important for the interpretation of volatile element stable isotope data in cosmochemistry, e.g.: How much do atmospheres with variable *f*O₂ suppress (Cd) isotope fractionation? Are there conditions where volatile metal loss by evaporation can occur without measurable stable isotope fractionation? Will (kinetic) condensation result in significant stable isotope fractionation?

Our experiments show that evaporation at atmospheric pressure only yields strongly suppressed Cd isotope fractionation, with a vapor-melt fractionation factor α for ¹¹⁴Cd/¹¹⁰Cd that corresponds to -1.6‰ (air) and -0.3‰ (CO-CO₂). This compares to about -10‰ observed for evaporation into vacuum [3] and the theoretical prediction of -17.7‰ as calculated from Graham's law.

In addition, Cd also displays isotope fractionation along the temperature gradient of the Al₂O₃ condensation plates with light Cd isotopes being enriched in the condensates closest to the melt.

The observed suppressed isotope fractionation during evaporation may result from back reaction into the melt phase and more efficient Cd⁰ vapor formation at reduced conditions.

[1] Humayun & Clayton (1995) *GCA* **59**, 2131-2148.

[2] Wombacher *et al.* (2008) *GCA* **72**, 646-667.

[3] Wombacher *et al.* (2004) *GCA* **68**, 2349-2357.

A method to constrain the size of the Protosolar Nebula

KRETKE, K. A.^{1*}, LEVISON, H. F.¹, BUIE, M. W.¹
AND MORBIDELLI, A.²

¹Southwest Research Institute, Department of Space Studies,
1050 Walnut Street, Suite 400, Boulder, CO 80302, USA
*correspondence: kretke@boulder.swri.edu

²Observatoire de la Côte d'Azur, BP 4229, 06304 Nice Cedex
4, France

Observations indicate that the gaseous circumstellar disks around young stars vary significantly in size, ranging from tens to thousands of AU. Models of planet formation depend critically upon the properties of these primordial disks, yet in general it is impossible to connect an existing planetary system with an observed disk. We present a method by which we can constrain the size of our own protosolar nebula using the properties of the small body reservoirs in the solar system. In standard planet formation theory, after Jupiter and Saturn formed they scattered a significant number of remnant planetesimals into highly eccentric orbits. In this paper, we show that if there had been a massive, extended protoplanetary disk at that time, then the disk would have excited Kozai oscillations in some of the scattered objects, driving them into high-inclination (*i* >~ 50°), low-eccentricity orbits (*q* >~ 30 AU). The dissipation of the gaseous disk would strand a subset of objects in these high-inclination orbits; orbits that are stable on Gyr timescales. To date, surveys have not detected any Kuiper-belt objects with orbits consistent with this dynamical mechanism. Using these non-detections by the Deep Ecliptic Survey and the Palomar Distant Solar System Survey we are able to rule out an extended gaseous protoplanetary disk (*R_D* >~ 80 AU) in our solar system at the time of Jupiter's formation. Future deep all sky surveys such as the Large Synoptic Survey Telescope will allow us to further constrain the size of the protoplanetary disk.

Speciation and mobility of trace elements in wetland soils

RUBEN KRETZSCHMAR

Institute of Biogeochemistry and Pollutant Dynamics, ETH Zurich, Switzerland (kretzschmar@env.ethz.ch)

Wetlands including peatlands, riparian floodplains, and paddy soils play key roles in the biogeochemical cycling of carbon, sulfur, phosphorus, and many essential or potentially toxic trace elements (e.g., As, Se, Hg, Zn, Cu, Cd). Understanding the solid-phase speciation, micro-scale distribution, and mobility of trace elements in such soils is an important challenge in soil biogeochemistry. Prof. Willem van Riemsdijk and his coworkers were among the leaders in developing our current understanding of competitive sorption of cations, anions, and NOM to soil mineral surfaces. Competitive sorption of arsenate or arsenite with other anions such as phosphate or carbonate, for example, are now rather well understood and can be modelled quantitatively using the CD-MUSIC approach [1]. However, sorption and speciation changes of trace elements during reduction/oxidation cycles in soils, often coupled to iron mineral transformations and sulfur redox reactions in the presence of NOM, are still poorly understood. We therefore explored the influence of soil flooding on trace element speciation and mobility and found formation of metallic Cu(0) and metal sulfide nano-particles by suspended bacteria to be an important mechanism controlling pore water concentrations of Cu, Hg, Zn, and Pb [2]. More recently, we explored the speciation of As in different wetlands and found As(III) bound to reduced sulfur groups of NOM to be the dominant species in anoxic peat layers [3]. Subsequent model studies confirmed this newly discovered binding mechanism of As to NOM [4], which may of great importance in other NOM-rich, reducing environments. In contrast, in a mining-affected river floodplain, As was mainly present as As(V) coprecipitated with Fe(III) in poorly-crystalline mineral phases, exhibiting similarity to amorphous ferric arsenates, partly forming rims around weathering pyrite and arsenopyrite grains. The solid-phase speciation greatly influences the kinetics of microbial Fe and As reduction and release, and is therefore important for understanding As release under reducing conditions in soils [5].

[1] Stachowicz *et al.*, *J. Colloid Interf. Sci.* **320**: 400, 2008. [2] Hofacker *et al.*, *Geochim. Cosmochim. Acta* **103**: 316, 2013. [3] Langner *et al.*, *Nature Geoscience* **5**: 66, 2011. [4] Hoffmann *et al.*, *Environ. Sci. Technol.* **46**: 11788, 2012. [5] Weber *et al.*, *Environ. Sci. Technol.* **44**: 116, 2010.

Juvenile crustal growth during the Palaeoproterozoic: U-Pb-O-Hf isotopes of detrital zircon from Ghana

BÁRA D. KRISTINSDÓTTIR¹, ANDERS SCHERSTÉN¹, ANTHONY I.S. KEMP^{2,3} AND ANDREAS PETERSSON¹

¹Department of Geology, Lund University, Sölvegatan 12, SE-223 62 Lund, Sweden. anders.schersten@geol.lu.se; barakristins@gmail.com

²School of Earth and Environmental Sciences, James Cook University, Townsville, Queensland 4811, Australia. tony.kemp@uwa.edu.au

³School of Earth and Environment, the University of Western Australia, Crawley, Western Australia 6009, Australia.

The Palaeoproterozoic domains of the West African Craton (WAC) (~2.15 Ga) have been described as a fast growing segment of juvenile crust based on geochronological data and Nd-model ages. Detrital zircon from four rivers in Ghana, southeastern WAC, were analysed for U-Pb, O and Lu-Hf isotopes and a zircon population from a fifth river was analysed for U-Pb and Lu-Hf isotopes. U-Pb crystallisation ages mainly cluster between 2.24 and 2.09 Ga with a peak at ~2.14 Ga, reflecting peak magmatic activity. The zircon population from the Birim river, representing the Kibi-Winneba belt, in southeast Ghana have zircon with U-Pb ages >2.2 Ga, which is nearly absent in other rivers.

The entire zircon population has ϵ_{Hf} values ranging from 0.9 to 7.1, except four grains from the Birim river population that have negative ϵ_{Hf} . Although there are contrasts between the zircon populations from the different rivers, the data imply relatively juvenile crust without any significant reworking of ancient crustal components. ~2.2 Ga zircon from the Birim river have depleted ϵ_{Hf} , while a younger (2.15 Ga) subset of zircon requires a reworked Archaean component. Zircon from Sihili and Black Volta rivers form a loosely defined trend that suggest the reworking of mafic crust, while the others do not.

Contribution of reworked supracrustal rocks were minor during the initial growth stages as indicated by the absence of zircon with $\delta^{18}\text{O} > 6.5\text{‰}$ prior to 2.174 Ga. The proportion of grains with elevated $\delta^{18}\text{O}$ gradually increases after 2.174 Ga, suggesting increasing amounts of reworked supracrustal sedimentary components. However, these zircon grains with high $\delta^{18}\text{O}$ have depleted ϵ_{Hf} , which suggests fast reworking of young supracrustal rocks, perhaps in a maturing arc system.

Are mafic microgranular enclaves in durbachites plutonic equivalents of common minettes?

LUKÁŠ KRMÍČEK^{1*} AND ROLF L. ROMER²

¹Brno University of Technology, Faculty of Civil Engineering, Veveří 95, CZ-602 00 Brno, Czech Rep.

(*correspondence: l.krmicek@gmail.com)

²Deutsches GeoForschungsZentrum (GFZ), Telegrafenberg, D-14473 Potsdam, Germany

Durbachites are K-feldspar-phyric biotite-bearing MgO-rich rocks of syenitic composition whose formation involves the mixing of mafic high-potassium partial melts from an enriched mantle with granitic melts. Due to this process, durbachites encompass a broad compositional range and contain variable amounts of mafic microgranular enclaves (MME). The mafic members are considered to be the plutonic equivalent of common mica lamprophyres, i.e., minettes [1]. Large volumes of durbachites (e.g., the Třebíč Massif) have been emplaced in the Moldanubian Zone of the Bohemian Massif. Regionally contrasting geochemical fingerprints of mantle metasomatism and the role of mantle contribution in durbachite magmatism may be the key control on the distribution of durbachites in the Bohemian Massif. MME from the Třebíč Massif have been investigated petrologically and geochemically (including Sr-Nd-Pb isotopes) and compared with Variscan mafic dikes of the Bohemian Massif. The geochemical composition of the MME does not correspond to the composition of typical minettes from which they are noticeably shifted toward higher ⁸⁷Sr/⁸⁶Sr(i) values and more negative εNd(i) values. Moreover, the composition of MME also differs from newly recognised peralkaline lamproitic rocks cropping out around the Třebíč Massif [2]. Instead, the MME compositionally overlap with micaceous mafic dykes that could be best described as cocites [2]. Both cocites and MME show high Mg-values and are characterized – in comparison with minettes and lamproites – by a remarkable negative Eu anomaly, an extremely high positive Pb anomaly, and an unusually high Sm/La ratio. It is the particular geochemical and isotopic signature of mantle metasomatic component that is common for the durbachites and the cocite dykes and that distinguishes them from Variscan minettes of other parts of the Bohemian Massif.

Acknowledgements. This work was supported by the project FAST-S-12-1774 from BUT.

[1] Parat *et al.* (2010) *Contrib. Mineral. Petrol.* **159**, 331–347.

[2] Krmíček (2011) *PhD thesis*, Brno, 1–160.

Near-field measurements of volcanogenic sulfur: Emissions, oxidation, and neutralization

EBEN CROSS¹, SIDHANT PAI¹, ZARA L'HEUREUX¹, JAMES HUNTER¹, PHILIP CROTEAU², JOHN JAYNE², LISA WALLACE³, JENNIFER MURPHY⁴, COLETTE HEALD¹, AND JESSE KROLL¹

¹Department of Civil and Environmental Engineering, Massachusetts Institute of Technology, Cambridge MA, USA

²Center for Aerosol and Cloud Chemistry, Aerodyne Research, Inc., Billerica MA, USA

³Clean Air Branch, Hawai'i State Department of Health, Honolulu HI, USA

⁴Department of Chemistry, University of Toronto, Toronto ON, Canada

* correspondence: jhkroll@mit.edu

Volcanic activity represents a major natural source of sulfur dioxide (SO₂) to the Earth's atmosphere, and thus is an important component of the global sulfur cycle. In addition, the very high concentrations of SO₂ and particulate matter in the areas immediately surrounding volcanoes can have serious effects on human and ecological health. In order to better understand the atmospheric fate of volcanogenic emissions in the near field (in the first few hours after emission), we have carried out *in situ* studies of key sulfur species on the Big Island of Hawai'i. Measurements were made as part of MIT's Traveling Research Environmental eXperiences (TRES) program, aimed at introducing undergraduate students to environmental fieldwork. A suite of instruments for characterizing oxidized sulfur in both the gas and particle phase, including an SO₂ monitor and an Aerosol Chemical Speciation Monitor (ACSM), were deployed on a mobile ground-based platform, with sampling carried out at a range of locations on the island. To our knowledge these measurements represent the first real-time measurement of the chemical composition of volcanic aerosol. The high time resolution of the instruments, combined with the high spatial coverage of the mobile measurements, enables the characterization of the volcanic plume at different times/distances downwind of the point of emission. From these measurements we are able to track the initial lifecycle of volcanogenic sulfur, including emission, oxidation to particulate sulfuric acid, and neutralization by ammonia. Results are compared with continuous measurements taken by air quality monitoring sites on the island.

Origin of water on the chondrite asteroids: Evidence from oxygen-isotope compositions of aqueously-formed minerals

A. N. KROT^{1,2*}, P. M. DOYLE^{1,2}, K. NAGASHIMA¹, K. JOGO³, S. WAKITA³, F. J. CIESLA⁴ AND I. HUTCHEON⁵

¹HIGP, University of Hawai'i, Honolulu, HI 96822, USA.

²Hawai'i NASA Astrobiology Institute, University of Hawai'i

³Tohoku University, Sendai 980-8578, JAPAN

⁴University of Chicago, Chicago, IL 60637, USA

⁵Glenn Seaborg Institute, LLNL, Livermore, CA 94551, USA

Fayalite and magnetite in CV3.1 and CO3.1 carbonaceous chondrites (CCs) resulted from water-rock interaction on their parent asteroids at water/rock volume ratio of ~0.2 and temperatures of ~100–200°C [1,2]. The inferred ⁵³Mn/⁵⁵Mn ratios in fayalite in Asuka 881317 (CV) and MacAlpine Hills 88107 (CO-like) are $(2.77 \pm 0.48) \times 10^{-6}$ and $(2.45 \pm 0.33) \times 10^{-6}$ [3]. The ⁵³Mn-⁵³Cr ages of the CV and CO fayalite formation anchored to D'Orbigny angrite [4,5] are 3.7 (+1.1/-0.9) and 4.4 (+0.9/-0.7) Ma after CV CAIs [3] having an absolute age of 4567.3±0.16 Ma [6]. These ages are indistinguishable from the ⁵³Mn-⁵³Cr ages of calcite in CMs [7] and dolomite in CMs and CIs [7,8]. The high peak metamorphic temperatures experienced by CVs and COs of petrologic type ≥ 3.6 (≥600°C) and the old formation ages of fayalite imply a rapid accretion of their parent asteroids after chondrule formation (~2–2.5 Ma after CV CAIs) followed by a short onset of aqueous alteration. The accretion of CVs and COs predated by ~1 Ma accretion of the more extensively aqueously-altered, but less metamorphosed CMs and CIs [7,8]. Near terrestrial oxygen-isotope compositions of the CV and CO fayalite and magnetite ($\Delta^{17}\text{O} \sim -1\text{‰}$), and CM and CI carbonates and magnetite ($\Delta^{17}\text{O} \sim +2\text{‰}$ to -3‰) may indicate water in the CC parent asteroids had preferentially a local, inner Solar System origin, consistent with the inferred hydrogen-isotope composition of the CC asteroidal water [9]. The low influx of isotopically heavy (i.e., enriched in ¹⁷O, ¹⁸O, and D/H) water ices from the outer Solar System at the time of accretion of CC asteroids may be due to an early growth of Jupiter that could have prevented significant radial transport of dust and gas from outside its orbit.

[1] Krot A. N. *et al.* (1998) *MAPS* 33, 1065. [2] Zolotov M. Yu. *et al.* (2006) *MAPS* 41, 1775. [3] Doyle P. M. *et al.* (2013) *LPSC* 44, #1793. [4] Amelin Y. (2008) *GCA* 72, 221. [5] Glavin D. M. *et al.* (2004) *MAPS* 39, 693. [6] Connelly J. N. *et al.* (2012) *Science* 338, 651. [7] Fujiya W. *et al.* (2012) *Nature Commun.* 3, 1. [8] Fujiya W. *et al.* (2013) *EPSL* 362, 130. [9] Alexander C. M. O'D. *et al.* (2012) *Science* 337, 721.

Nucleosynthetic W isotope anomalies in CAI: Implications for Hf-W chronology

T.S. KRUIJER^{1,2,*}, T. KLEINE¹, C. BURKHARDT³ AND R. WIELER²

¹Institute for Planetology, University of Münster, Germany

²Institute of Geochemistry and Petrology, ETH Zürich

(*correspondence: thomas.kruijer@erdw.ethz.ch)

³Origins Laboratory, Department of the Geophysical Sciences, The University of Chicago

The application of the short-lived ¹⁸²Hf-¹⁸²W decay system to investigate the timing of early solar system processes requires knowledge of the initial Hf and W isotope compositions at the beginning of the solar system [1,2]. These can most directly be determined from Ca-Al-rich inclusions (CAI), which are the oldest yet dated objects that formed within the solar system [*e.g.*, 3,4]. However, the interpretation of W isotope data in CAI is complicated by the presence of nucleosynthetic W isotope anomalies [1], which may significantly bias the inferred initial ¹⁸²W/¹⁸⁴W of CAI [2]. The aim of this study is to explore the range of nucleosynthetic W isotope variations in CAI to better quantify the initial Hf and W isotope compositions of the solar system.

Here we report W isotope compositions for six bulk CAI (one type B, five type A) from the Allende CV3 chondrite. Tungsten isotope compositions of the CAI were measured on a Neptune Plus MC-ICPMS at the University of Münster and are reported as ϵ^{W} (*i.e.*, 0.01 % deviations from terrestrial values). The investigated CAI display large variations in $\epsilon^{183}\text{W}$, extending to much larger anomalies than previously observed [1,2] and indicating variable abundances of *s*- and *r*-process W isotopes in CAI. The CAI define a precise empirical correlation between $\epsilon^{183}\text{W}$ and initial $\epsilon^{182}\text{W}$, which allows correction of measured $\epsilon^{182}\text{W}$ for nucleosynthetic heterogeneity. The corrected $\epsilon^{182}\text{W}$ vs. ¹⁸⁰Hf/¹⁸⁴W define a bulk CAI isochron (MWS=1.5) with a precise initial ¹⁸²Hf/¹⁸⁰Hf of $\approx 1.0 \times 10^{-4}$, which when anchored to the angrite D'Orbigny [5] corresponds to an absolute age of CAI that is in good agreement with their Pb-Pb ages [3,4]. The bulk CAI isochron confirms the recently revised CAI initial of $\epsilon^{182}\text{W} \approx -3.5$ [2]. Relative to this value, magmatic iron meteorites have more radiogenic neutron capture-corrected $\epsilon^{182}\text{W}$ [6], corresponding to core formation timescales of ≈ 1 -3 Ma after CAI formation and indicating a time gap of ≈ 0.5 -1 Ma between the formation of the first solids and accretion of the oldest planetesimals.

[1] Burkhardt *et al.* (2008) *GCA* 72, 6177-6197. [2] Burkhardt *et al.* (2012) *APJ Lett.* 753, L6. [3] Amelin *et al.* (2010) *EPSL* 300, 343-350. [4] Bouvier & Wadhwa (2010) *Nat. Geosci.* 3, 637-641. [5] Kleine *et al.* (2012) *GCA* 84, 186-203. [6] Kruijer *et al.* (2013) *EPSL* 361, 162-172.

Re–Os Age and Gold Source for Mayskoe Quartz-Vein Deposit (Northern Karelia, Baltic Shield)

R.KRYMSKY¹, B.BELYATSKY², N.GOLTSIN¹, S.SERGEEV¹
AND S.BUSHMIN²

¹CIR VSEGEI, St.Petersburg, Russia,
robert_krymsky@yahoo.com

²IPGG RAS, St.petersburg, Russia, bbelyatsky@mail.ru

Mayskoe deposit located in Northern Karelia within the Svecofennian orogen near the boundary with the Belomorian–Lapland orogen is the only known gold deposit of the quartz–vein type in the Karelian–Kola region. The host Paleoproterozoic volcanogenic–sedimentary rocks metamorphosed from greenschist to amphibolite facies within the Svecofennian time. Metamorphic rocks are strongly sheared and metasomatized, where early quartz and late gold-bearing quartz veins are located. Ore association in quartz veins is represented by native gold, chalcopyrite, pyrrhotite, galena, pyrite, and sphalerite, as well as Se and Te minerals.

We investigated the Re–Os isotope system of native gold and syngenetic chalcopyrite from the eastern lode-gold quartz vein. Gold grains and chalcopyrite were manually collected from two gold-bearing milky–white quartz samples. Re and Os contents in the analyzed gold range from 1.8 to 13.8 and from 0.2 to 2.3 ppb, which is comparable with the concentrations measured in syngenetic chalcopyrite: 0.5–2.1 ppb Re and 0.1–1.0 ppb Os. According to the Os concentration, the studied samples differ significantly from hydrothermal sulfide gold deposits and are comparable with those associated with conglomerates [1]. The correlation between Re/Os and Os isotope composition for the studied samples corresponds to the age of 397 ± 15 Ma and $(^{187}\text{Os}/^{188}\text{Os})_i = 0.1469 \pm 0.0051$ ($\gamma_{\text{Os}} = +18$).

The measured Os composition of gold and chalcopyrite ($^{187}\text{Os}/^{188}\text{Os} = 0.2160\text{--}0.4376$) differs significantly from typical crustal (> 1.0) and mantle values (0.1296), and may be obtained either by mixing of Os from these sources or as a result of in situ Re decay. The age character of obtained trend is provided by the model Re–Os age of the samples: from 430 to 515 Ma, similar to the isochron one. Thus, the ore-forming fluid may have been formed in the Early Paleozoic by mixing of 75% upper mantle material and 25% Proterozoic crust and have come to quartz veins 400 m.y. ago. The primitive upper mantle ($\text{Os} = 2.5$ ppb and $^{187}\text{Os}/^{188}\text{Os} = 0.1239$), in this case, was the main source of gold. Alternatively, formation of gold-bearing mineralization was plausible realised under the influence of the Caledonian mantle plume due to remobilization of basic–ultrabasic matter (or mantle restites) of Paleoproterozoic rocks (2.0–2.2 Ga) of the Karelian–Kola region characterized by high concentrations of gold and PGEs.

[1] Kirk *et al.* (2002) *Science* **297**, 1856 – 1860.

Experimental and computational spectra and thermodynamics of biogeochemical interfaces

JAMES D. KUBICKI¹ AND NADINE KABENGI²

¹Dept. of Geosciences, The Pennsylvania State University,
University Park, PA 16802 USA (*correspondence:
jdk7@psu.edu)

²Dept. of Geosciences and Chemistry, Georgia State
University, Atlanta GA 30303

The molecular-level chemistry of biogeochemical interfaces influences dissolution of minerals, transport of bacteria and degradation of contaminants. Detailing these interactions is problematic, however, because surfaces are difficult to characterize and biological compounds can be complex. Significant advances have been made by collecting spectra (e.g., ATR-FTIR, NMR, etc.) of samples representing key biogeochemical reactions and interpreting the spectra with quantum mechanical calculations. Generally, these experimental studies are performed on simplified binary systems with one substrate and one adsorbent. Predictions of biogeochemistry in the field may be erroneous because competing reactions are not considered in the laboratory-based studies.

A missing component of these types of studies is the thermodynamics of the adsorption reactions. One can model surface complexes and the spectroscopic properties observed, but without knowledge of the thermodynamic favorability of the surface complexes, one cannot estimate their prevalence or dominance in natural systems.

This talk will focus on progress in developing methods to calculate spectroscopic properties and thermodynamics of adsorption in biogeochemical systems. The incorporation of thermodynamic data from flow-adsorption calorimetry into modeling of these adsorption reactions will also be discussed. Examples of test systems such as goethite-phosphate will be used as the basis for more complex reactions with biological compounds.

Modeling of TiO₂ nanoparticles interactions with water and ions

JAMES D. KUBICKI¹, SUNG-YUP KIM²,
ADRI C. VAN DUIN², MOIRA RIDLEY³,
MIKE MACHESKY⁴, DANIEL HUMMER⁵
AND PAUL R. KENT⁶

¹Dept. of Geosciences, The Pennsylvania State University,
University Park, PA 16802 USA (*correspondence:
jdk7@psu.edu)

²Dept. of Nuclear & Mechanical Engineering, The
Pennsylvania State University, University Park, PA 16802
USA

³Dept. of Geosciences, Texas Tech University, Lubbock, TX
USA

⁴Illinois State Water Survey, University of Illinois,
Champaign, IL 61820 USA

⁵Department of Earth and Space Sciences, University of
California, Los Angeles CA USA

⁶Center for NanoMaterials Science, Oak Ridge National
Laboratory, Oak Ridge, TN USA

Although TiO₂ is not a major rock-forming mineral, it is an important technological material, and it has been used extensively as a model for oxide-water studies. Because the surfaces of the common TiO₂ phases, rutile and anatase, have been characterized experimentally and modeled with density functional theory (DFT), they serve as good model systems for understanding the size and shape effects of nanoparticles on the oxide-water interface.

In this talk, we will present results of DFT calculations on rutile and anatase surfaces and nanoparticles interactions with H₂O. The relationship of surface site defects (i.e., corner and edge sites) to H₂O adsorption energy is investigated. DFT calculations on anatase surfaces with adsorbed ions are also presented.

These DFT calculations were then used in developing a reactive classical force field, ReaxFF, for the Ti-O-H system. The ReaxFF was used to perform molecular dynamics simulations of rutile and anatase particles in water and aqueous salt solutions. Differences in the electrical double layer around finite nanoparticles as compared with flat, infinite surfaces will be discussed.

Hybrid Pressure Coring System of D/V *Chikyu*

YUSUKE KUBO¹, YASUHIKO MIZUGUCHI²
AND FUMIO INAGAKI³

¹CDEX, JAMSTEC, 3173-25 Showa-machi, Kanazawa-ku,
Yokohama, Japan 236-0001. kuboy@jamstec.go.jp

²CDEX, JAMSTEC, 3173-25 Showa-machi, Kanazawa-ku,
Yokohama, Japan 236-0001

Submarine Resources Research Project and Kochi Institute for
Core Sample Research, JAMSTEC, Monobe B200,
Nankoku, Kochi 783-8502, Japan

Pressure coring is a technique to keep *in-situ* conditions in recovering subseafloor sediment samples, which are potentially rich in soluble or hydrated gas. Gas fractions are easily lost in regular core sampling through the pressure and temperature change during core recovery, and subsequently change the chemical components of the sample: e.g., degassing may cause critical changes and/or damages of original structures. To study original characteristics of gaseous subseafloor sediment, a New Hybrid Pressure Coring System (Hybrid PCS) was developed for the D/V *Chikyu* operation by adapting some of the existing pressure sampling technologies. Hybrid PCS is composed of three main parts: top section for the wireline tool, middle section for the accumulator and pressure controlling system, and the bottom section for the autoclave chamber. The design concept is based on that of Pressure Core Sampler used in Ocean Drilling Program, and of Pressure Temperature Core Sampler (PTCS) and Non-cooled PTCS of Japan Oil, Gas and Metals National Corporation (JOGMEC). Modifications were made on the ball valve, which operates to close the autoclave after coring. The core samples are 51 mm in diameter and up to 3.5 m in length. The system is combined with the Extended Shoe Coring System on the *Chikyu* and best suited for coring of semi-consolidated formation up to about 3400 m from the sea level. Sample autoclave is compatible with Pressure Core Analysis and Transfer System of Geotek Ltd for sub-sampling and analysis under *in-situ* pressure. The analysis includes X-ray CT scan and core logging with P-wave velocity and gamma density. Depressurization provides accurate volume of gas and its sub-sampling.

Hybrid PCS was first tested during the *Chikyu* Exp. 906 at a submarine mud-volcano in the Nankai Trough. A 0.9 m of hydrate rich material was recovered from the summit (water depth: 2000 m) and the intact hydrate structure was observed by X-ray CT scan. Hybrid PCS was also used in the following JOGMEC methane hydrate cruise, resulting in the good recovery of methane hydrate-bearing cores (approx. 69%).

Trace elements in ectomycorrhizae determined by neutron activation analysis

JAROSLAVA KUBROVÁ¹² AND JAN BOROVIČKA^{2*}

¹Institute of Geochemistry, Mineralogy and Mineral Resources, Faculty of Science, Charles University, Albertov 6, CZ-128 43 Prague 2

²Nuclear Physics Institute, v.v.i., Academy of Sciences of the Czech Republic, Řež 130, CZ-250 68 Řež near Prague
(*correspondence: borovicka@ujf.cas.cz)

In recent years, interest in the biochemical roles of macrofungi in the environment has increased rapidly. Macrofungi play important roles in biogeochemical cycling of chemical elements in the critical zone and many species are known as effective accumulators of toxic metals.

Ectomycorrhizal fungi live in symbiosis with vascular plants. In this reciprocally profitable relationship, the exchange of nutrients occurs in a mutual organ called ectomycorrhiza (pl. *ectomycorrhizae*). Ectomycorrhizae are formed on fine roots of host plants, distributed throughout the soil profile in both organic and mineral horizons, and are composed of plant biomass and fungal hyphae.

As has been repeatedly demonstrated, metal-adapted mycorrhizal fungi play as an effective biological barrier against metal toxicity in trees. Only few data have been published on concentrations of heavy metals in ectomycorrhizae: a relatively high degree of accumulation of Cd, Cu, Pb and Zn was observed from polluted sites in Norway and Poland.

In this study, we have focused on natural concentrations of trace elements in ectomycorrhizae and fine roots of *Picea abies* from pristine sites above gneissic and granitic bedrocks. Trace elements were analyzed using short-term thermal and long-term epithermal neutron activation analysis. The individual fungal species in analyzed ectomycorrhizal tips were determined by DNA sequencing (rDNA ITS molecular marker, semi-nested PCR).

According to our preliminary results, the most striking accumulation was noted in Cd. Its concentrations, however, varied in a wide range (with the highest content of 50 mg·kg⁻¹ dry weight). On the other hand, very low concentrations (mostly below 20 mg·kg⁻¹ dry weight) were found for Cu.

This research was supported by the projects 535112 (Grant Agency of Charles University in Prague) and P504/11/0484 (Czech Science Foundation).

Depth-dependent links between surface and subsurface as reflected by microbial community structures in limestone aquifers

KIRSTEN KUESEL*, MARTINA HERRMANN, ANNA RUSZNYAK, DENISE AKOB, UTE RISSE-BUHL, SEBASTIAN OPITZ AND KAI-UWE TOTSCHKE

Friedrich Schiller University Jena, Jena, Germany

*correspondence: kirsten.kuesel@uni-jena.de

One quarter of the drinking water supply for the world's population is derived from limestone aquifers, yet they are to date poorly represented in studies focussing on surface-subsurface interactions. Lithoautotrophy might be an important metabolic strategy in these oligotrophic habitats for coupling carbon cycling to the cycling of other elements, e.g. nitrogen, metals or sulphur accumulated from rock weathering. Within the framework of the AquaDiva project we started to explore the influence of surface conditions on the subsurface biosphere. We compared the diversity of microbial communities, some of their key functions, and potential links within food webs in the groundwater of a shallow, suboxic, and a deep, oxygen-rich limestone aquifer located in the Hainich region (Thuringia, Germany) below sites subjected to different land management.

Pyrosequencing of 16S ribosomal RNA revealed a clear separation of the shallow and the deep aquifer based on the structure of the active microbial communities. Results of quantitative PCR targeting *cbbl* and *cbbm* genes encoding RubisCO type I and II suggested that approximately 0.3 to 14 % of the groundwater bacterial population had the genetic potential to fix CO₂ via the Calvin Cycle. Analysis of *cbbm* and *cbbl* transcripts showed that the active CO₂-fixing bacterial communities were dominated by organisms related to *Sulfuricella denitrificans*, *Sideroxydans lithotrophicus*, *Acidithiobacillus sp.*, and *Nitrosomonas ureae* with the latter being more abundant in the deep, oxygen-rich aquifer.

Our data provide strong evidence that chemolithoautotrophy linked to metabolisms involving sulphur, iron, and nitrogen contributes to the carbon flow in a limestone aquifer. Moreover, analyses of the eukaryotic microbial communities in the groundwater revealed a diverse protist community consisting mainly of bacterial feeders such as ciliates, flagellates and amoeba but also representatives of higher trophic levels such as heliozoa and nematodes, suggesting complex food web interactions. In the light of surface-subsurface interactions, the observed geochemical and microbial patterns point to a depth-dependent impact of surface activities on the aquifer system with the shallow aquifer being more strongly affected by agricultural practices.

Origin of refractory organics in chondrites: An experimental study

M. KUGA^{1*}, B. MARTY¹ AND Y. MARROCCHI¹

¹CRPG-CNRS, Université de Lorraine, Nancy, France
(*mkuga@crpg.cnrs-nancy.fr)

Most organic matter found in chondrites occurs as insoluble organic matter (IOM). This refractory organic material has been studied through a wide range of techniques, which has provided insights in its molecular structure [1-2]. Despite these efforts, the origin, nature of precursors and synthesis of this IOM is still debated [1-3].

This study describes a Miller-Urey inspired experiment [4], designed to produce organics by condensation and polymerisation from gas molecules representative of the protosolar nebula. The experiment consists of a gas mixture (CO:N₂:noble gases = 5:0.5:0.5 + traces of H₂O) flowing at ~ 1 mbar in a quartz reactor through an electric discharge. Electrons from the plasma (average energy ~ 2 eV) initiated gas-phase chemistry by dissociating and ionizing gas molecules. At the end of the experiment, dark solids deposited on the reactor wall were recovered for ex-situ analysis by SEM, TEM, py-GC-MS, Raman and FTIR techniques. Noble gases and C, H, N content and isotopes were also measured.

TEM imaging indicates that these solids are mainly composed of amorphous carbon with small domains showing stacks of a few graphene layers. The poorly organized carbon structure was confirmed by Raman spectroscopy. Py-GC-MS, FTIR and elemental analyses indicate an aromatic material composed of small units (1-3 rings). O (carbonyl, phenol) and N (nitrile, heterocycles) functional groups were also identified. Elemental and isotopic fractionation of noble gases, similar to that observed for Q relative to Solar [4] were measured. This preliminary characterization of these synthetic organic material shares similarities with features of IOM.

Both characterization of experimental organics and the trapped noble gases suggest that ionization and dissociation of CO and N₂ in the disk, either by electrons or far-UV photons, could be a possible mechanism for formation of precursors of organics recovered in chondrites. Subsequent reaction and processing of these organic precursors during evolution of the protoplanetary disk could form the complex organic macromolecule we call IOM.

[1] L. Remusat *et al.* (2007) *CGR* **339**, 895-906, [2] S. Derenne and F. Robert (2010) *MPS* **45**, 1461-1475, [3] G. Cody *et al.* (2011) *PNAS* **108**, 19171-19176, [4] S. Miller and H. Urey (1959) *Science* **130**, 245-251. [4] R. Busemann *et al.* (2000) *MPS* **35**, 949-973

Don't forget the salty soup: Calculations for bulk marine geochemistry and radionuclide geochronology

GERHARD KUHN¹

¹Alfred-Wegener-Institut Helmholtz-Zentrum für Polar- und Meeresforschung, Am Alten Hafen 26, 27568 Bremerhaven, Germany (gerhard.kuhn@awi.de)

In reference to marine sediments I would like to add to the theme of this session: "Your data are only as good as your standards and methods!" if you remember to correct your analytical data for pore water salt.

Performing sophisticated analytics in marine geochemistry constantly aims at improving the detection limits as well as minimizing the margin of error regarding the precision and accuracy of the method. However, this holds true only if you are genuinely aware of what are you actually analyzing. The normal procedure of sample preparation for marine sediments consists of drying and grinding. Thereafter, these samples are analyzed with regards to their elementary or mineral concentrations. In the best case scenario, sampled water content data are available for calculations of physical properties, such as porosity and dry bulk density, which are both absolutely necessary for the calculation of elementary flux or geochemical budgets. In addition, based on the water content (*w*, in % of the wet weight) and a normal salinity of 3.5% (or 35 PSU), the amount of salt (*s* in mass%) in the dry sample can be determined by:

1. Calculating the mass percentage of the salty pore water (*w'*) as: $w' = w \cdot 100 / 96.5$
2. Calculate the salt as: $s = 100 \cdot (w' - w) / (100 - w)$.

This is especially important for samples with water contents above 50% (*s*=3.6%; *w*=80% *s*=14.5%), which are very common in the biogenic opal-rich, diatomaceous sediments of the Southern Ocean around Antarctica. These calculations could be improved by using known salinities, obtained through chlorine determinations, of samples or pore water directly.

Although these calculations are simple, they are often ignored, giving rise to two potential errors, sometimes greater than 14% (relative concentration). The first, greatest and often neglected mistake is a "wrong" net weight - the input is not the pure sediment but sediment + salt. For most ratios of elements, the salt content is irrelevant, but every calculation of concentrations must be corrected accordingly, also radiogenic activity calculations (e.g. ²¹⁰Pb, ²³⁰Th). Geochemists try to avoid the second error by using a salt correction when subtracting the salt related element concentrations directly from the composition analyzed.

Visualization of dynamic changes and the effects of coatings on silver nanoparticles by Surface Enhanced Raman Spectroscopy

M. KÜHN*, N.P. IVLEVA, R. NIESSNER
AND T. BAUMANN

Institute of Hydrochemistry, Technische Universität München,
81377 Munich, Germany (*correspondence:
melanie.kuehn@tum.de)

A wide variety of applications for engineered nanoparticles leads to increasing emissions into the environment. After entering the aquatic or terrestrial compartment, nanoparticles likely undergo changes caused by weathering or interactions with dissolved substances forming coatings on the particles. Hence, the surface properties will no longer be characterized by the nanoparticle itself, but rather by the properties of the coating material. Stability and transport properties particles will be altered significantly by different coating materials.

Knowledge of the development and stability of coatings is therefore crucial to predict the fate of nanoparticles in the environment. Surface enhanced Raman Spectroscopy (SERS) is a spectroscopic technique, which makes use of the signal enhancement caused by surface plasmon resonance and chemical enhancement typically found at silver nanoparticles and other nanostructured metals (e.g. Au, Cu). Thus the signal of the molecules adsorbed to the nanoparticles will be enhanced significantly and dynamic changes of the materials adsorbed to the particles can be studied. SERS is rather insensitive to dissolved molecules since the electromagnetic SERS enhancement strongly decreases with growing distance ($\sim d^{-12}$). The technique works with little sample preparation and sample volumes suitable for microfluidic experiments and environmental samples.

Citrate reduced and stabilized as well as hydroxyl-ammoniumchloride reduced silver nanoparticles were coated with humic acid, seaweed extract, and polygalacturonic acid. After adding the coating materials, the suspensions were centrifuged to remove excess coating materials. Changes of the pH-value of the solution and an exchange of the coating material were done to study the stability of the coating. Here, Raman spectroscopy gives direct access to the protonation of humic acid on the surface which immediately effects the spectrum.

The characterized nanoparticles were then brought into contact with physically and chemically heterogeneous surfaces to investigate the attachment coefficients and potential blocking. Chemical mapping using Raman microspectroscopy and SERS not only gives access to the spatial distribution of the nanoparticles but also to the chemical environment around the nanoparticles.

Water H₂¹⁸O isotope studies in the AIDA cloud simulation chamber

B. KUEHNREICH¹, J. LANDSBERG², J. HABIG⁴,
S. WAGNER¹, E. MOYER³, H. SAATHOFF⁴,
V. EBERT¹ AND E. KERSTEL²

¹PTB/TU Darmstadt, Germany (volker.ebert@ptb.de)

²University of Grenoble, France (erik.kerstel@ujf-grenoble.fr)

³University of Chicago, USA (moyer@uchicago.edu)

⁴Karlsruhe Institute of Technology, Germany
(harald.saathoff@kit.edu)

Isotopic studies can provide additional information on cloud physics, which have a significant impact on global climate. The conventional isotope-selective measurement technique, Isotope Ratio Mass Spectrometry (IRMS) is however not adapted to study dynamic processes such as cloud formation. Laser based measurement techniques offer both high precision and a fast response to follow the cloud formation process in real time. In the recent ISOCLOUD campaign at the AIDA cloud and aerosol chamber, different laser-based instruments were used to jointly obtain information about isotope ratio changes in both the water vapor and ice phases during simulated cloud formation processes. Here we report on two instruments used to quantify the H₂¹⁸O/H₂¹⁶O ratio. One of the instruments, ISO-APiCT (PTB/KIT), an open path spectrometer based on tunable diode laser absorption spectroscopy (TDLAS) measures the isotopic ratio of the vapor phase. Open-path TDLAS has been successfully applied to in-cloud studies on H₂¹⁶O [2]. The second instrument based on Optical Feedback Cavity Enhanced Absorption Spectroscopy (OF-CEAS, Grenoble/KIT) extractively samples either total water or, if connected behind a pumped counterflow virtual impactor, the ice phase only. The OF-CEAS technique has already been used in different water isotope studies, including airborne studies [3]. We show a characterization of both instruments, including their time response to sudden isotope ratio changes, as well as preliminary results obtained during ice cloud formation.

[1] Krämer M. *et al.*, *Atmos. Chem. Phys.* **9**, 3505-22 (2009).

[2] Gurlit, W. *et al.*, *Applied Optics* **44**, 91-102 (2005) [3]

Iannone R.Q. *et al.*, *J. Geophys. Res.* **115**, D10111 (2010) ;

Isot. Env. Health Stud. **45**, 303-20 (2009)

Dissolved organic matter composition across a coastal-open ocean gradient in the eastern Pacific Ocean

ELIZABETH B. KUJAWINSKI^{*1}, WINIFRED JOHNSON²
AND KRISTA LONGNECKER¹

¹Department of Marine Chemistry and Geochemistry, Woods Hole Oceanographic Institution (WHOI), Woods Hole MA 02543 [*correspondence: ekujawinski@whoi.edu, klongnecker@whoi.edu]

²MIT/WHOI Joint Program in Oceanography and Applied Ocean Sciences, Woods Hole, MA 02543 [wjohnson@whoi.edu]

Dissolved organic matter (DOM) in marine systems is an important component of the global carbon cycle whose molecular-level composition is determined by a combination of abiotic and biotic factors related to sources, sinks and transformations. Molecular-level characterization of this heterogeneous mixture has become practical only recently with the advent of ultrahigh resolution mass spectrometry (ESI FT-ICR MS). To date, systematic surveys of DOM composition in the surface and deep oceans are rare, but those conducted to date have highlighted the potential of this tool to identify new marker compounds for different biological processes. Here we examine the DOM composition along Line P in the eastern Pacific Ocean, collected during the interdisciplinary GEOMICS cruise in May 2012. We explore the shifts in DOM composition from the coast to the open ocean as well as down the depth profile at selected locations. We further explore the source of surface DOM through comparison with culture-based investigations of metabolites exuded by phytoplankton and heterotrophic bacteria. Using multivariate statistical tools, we observe significant changes in compound distributions along the primary spatial gradients of Line P, notably an increase in N:C and S:C ratios with depth. We hypothesize that microbial activity is responsible for these changes and leads to the sequestration of N and S in increasingly recalcitrant molecules. These data will provide important chemical contexts for other omics-based analyses undertaken by GEOMICS colleagues and are an integral component of an emerging systems-biology view of the ocean.

New experimental data on TiO₂ solubility in hydrous rhyolite melts: Implications for titanium-in-quartz thermobarometry

K. KULARATNE¹ AND A. AUDÉTAT^{1*}

¹Bayerisches Geoinstitut, Universität Bayreuth, 95440 Bayreuth, Germany (*correspondence: andreas.audetat@uni-bayreuth.de)

Application of the titanium-in-quartz (TitaniQ) thermobarometer to natural magmas requires estimation of the activity of TiO₂ because most natural magmas are not TiO₂-saturated. However, currently available methods to calculate TiO₂ activities in silicate melts return highly inconsistent results that commonly differ by a factor of up to two, which introduces large uncertainties in the calculated TitaniQ temperatures or pressures. In order to further constrain TiO₂ solubility in silicic melts we conducted experiments at 800-900 °C and 2 kbar in H₂O-saturated haplogranite melts with molar Al/(Na+K)-ratios ranging from 0.81 to 1.2.

Due to the slow diffusivity of Ti in silicate melts at these conditions we developed a new method to determine TiO₂ solubility. In a first step, anhydrous glasses with smooth TiO₂ concentration gradients over several millimeters were produced in an 1 atm high-temperature furnace. Pieces of these glasses were then hydrated for 3 days at 750 °C and 2 kbar at H₂O-saturated conditions in cold-seal pressure vessels, which caused crystallization of rutile in the TiO₂-rich parts of the samples. Finally, the recovered pieces were welded together with untreated ones (plus H₂O) into new Au capsules and were equilibrated at 800-900 °C and 2 kbar for 7 days, after which time the samples were rapidly quenched. In this way, forward and reverse runs could be conducted within single experiments. TiO₂ concentrations measured at the contact between rutile-bearing and rutile-free glass agree well between forward and reverse runs, suggesting that equilibrium was obtained.

An empirical best-fit model to our data predicts TiO₂ solubilities that are similar to those measured by [1], thus validating the TitaniQ model and corresponding tests on natural samples published in [2].

[1] Hayden&Watson (2007) *Earth Planet. Sci. Lett.* **258**, 561-568. [2] Huang&Audétat (2012) *Geochim. Cosmochim. Acta* **84**, 75-89.

GEMS: Gibbs energy minimization software for geochemical modeling

D. A. KULIK^{1*}, S.V. DMYTRIEVA², T. WAGNER³,
T. THOENEN¹ AND U. BERNER¹

¹Laboratory for Waste Management, Paul Scherrer Institut, 5232 Villigen, Switzerland (*dmitrii.kulik@psi.ch)

²Institute of Environmental Geochemistry, Kyiv, Ukraine

³Department of Geosciences and Geography, University of Helsinki, Finland

Geochemical modeling is relevant in ore geochemistry, CO₂/radioactive/toxic waste disposal, cosmochemistry, petrology, and hydrogeochemistry. GEMS is an advanced software tool for modeling complex systems that involve non-ideal solid solutions, fluids and aqueous solutions, mineral phases metastability, adsorption, and ion exchange. GEMS (<http://gems.web.psi.ch>) comprises the GEM-Selektor code; default thermodynamic databases; the GEMS3K kernel code [1,2] included into the GEMSFIT code [3] and available open-source for coupling into reactive transport codes.

The GEM-Selektor v.3 is the main tool for interactive geochemical thermodynamic modeling. It integrates a multi-document graphical user interface with a built-in script interpreter, a database management system, and a context-driven help browser. These features support forward- or inverse modeling tasks, plotting or exporting results, and creating GEMS3K input files. The usage is focused around a *modeling project* database that accumulates all input data and results for a given application. Any project can be shared with others, which greatly facilitates the data exchange in teams. GEMS databases equally support thermochemical and reaction-based formats of standard-state thermodynamic data. Creation of new projects is facilitated by the supplied thermodynamic databases, derived from the PSI/Nagra 12/07 [4] and the SUPCRT92 [5] datasets. Third-party databases for specific application fields are also available in GEMS format.

Current development is focused on adding the kinetics of mineral-aqueous reactions and trace element uptake; implementing sorption models using a concept of linked phase metastability; improving GEM numerical algorithms; moving to industrial NoSQL database format in connection with the general parameter-fitting code GEMSFIT. Our goal is to make GEMS the software of choice for all kinds of geochemical modelling applications.

[1] Kulik *et al.* (2013) *Comput. Geosci.* **17**, 1-24. [2] Wagner *et al.* (2012) *Can. Mineral.* **50**, 701-723. [3] Hingerl *et al.* (2013) *Comput. Chem. Eng.* (submitted). [4] Thoenen *et al.* (this conference). [5] Shock *et al.* (1997) *Geoch. Cosmoch. Acta* **61**, 907-950.

Southward transport of the Fukushima-derived radiocesium due to the subtropical mode water

Y. KUMAMOTO^{1*}, A. MURATA¹, T. KAWANO¹
AND M. AOYAMA²

¹Japan Agency for Marine-Earth Science and Technology, 2-15 Natsushima-cho, Yokosuka 237-0061, Japan (*correspondence: kumamoto@jamstec.go.jp, murataa@jamstec.go.jp, kawanot@jamstec.go.jp)

²Meteorological Research Institute, 1-1 Nagamine, Tsukuba 305-0052, Japan (maoyama@mri-jma.go.jp)

Fukushima-derived Radiocesium

The massive Tohoku earthquake and consequent giant tsunami of March 11, 2011 resulted in releases of radiocesium from the Fukushima Dai-ichi nuclear power plants. The total amount of the radiocesium derived from the direct discharge into the North Pacific Ocean was estimated to be about 4 PBq for Cs-137 [1, 2]. However, that from the atmospheric deposition contains large uncertainty mostly due to the restriction of available data in the open ocean.

Sample Collection and Radiocesium Analysis

We measured the radiocesium in seawaters from surface to 800-m depth at stations along approx.149°E line more than hundreds km away from the plants in the western North Pacific Ocean in January and February 2012. Radiocesium in the seawater was concentrated onto ammonium molybdophosphate and then measured using a gamma-spectrometry with Ge detectors.

Results and Discussion

Cs-134 was found in surface waters at all the stations from 20°N to 42°N. Activity of Cs-134 in the surface mixed layer was highest (~ 20 Bq m⁻³) in the transition area between the subarctic and subtropical regions, which was due to the direct discharge into the transition area. Below the surface mixed layer Cs-134 activity decreased sharply and was not detected in deeper layers than 400-m depth in the subarctic region and transition area. However, in the subtropical region we observed Cs-134 maxima just below the mixing layer that corresponds to about 25.3 sigma-theta, implying that the Cs-134-rich waters in the transition area have been transported southwardly to the subtropical region due to formation of the subtropical mode water.

[1] Kawamura *et al.* (2011) *J. Nucl. Sci. Technol.* **48**, 1349-1356. [2] Tsumune *et al.* (2012) *J. Environ. Radioactiv.* **111**, 100-108, doi:10.1016/j.jenvrad.2011.10.007.

Isotopic characterization of winter time aeolian dust over Cape Verde

A. KUMAR^{1*}, W. ABOUCHAMI^{1,2}, S.J.G. GALER¹,
K.W. FOMBA³ AND M.O. ANDREAE¹

¹Biogeochemistry Department, Max Planck Institute for Chemistry, Mainz, Germany (*ashwini.kumar@mpic.de)

²Westfälische Wilhelms Universität, Institut für Mineralogie, 48149 Münster, Germany

³Department of Chemistry, Leibniz Institute for Tropospheric Research, Leipzig, Germany.

Radiogenic isotope tracers are robust tools for tracking dust provenance and atmospheric transport pathways. Recent studies of African sources have shown spatial isotopic heterogeneity locally and on short time scales. High-temporal-resolution isotopic time series are thus essential for resolving seasonal changes in dust provenance. Here, we report Sr, Nd and Pb isotopic compositions of aeolian dust collected during a campaign in late winter (1-20 February 2012) on the island of São Vicente at the Cape Verde Atmospheric Observatory (16.9°N, 24.9°W).

Total suspended particulate (TSP) and PM10 (particulate matter less than 10 μ m aerodynamic diameter) were collected on acid-cleaned cellulose filters on a daily basis (~24 hrs). During the dust storm event, from 6-8 February 2012, samples were collected at shorter time intervals (every 5-8 hrs). About 1-20 cm² of filter was leached with ultrapure MilliQ water to remove sea-salt Sr and subsequently leached with 0.5 N HBr to extract the anthropogenic Pb and soluble particulate fraction. The remaining silicate fraction was fully dissolved using HF-HNO₃ acids. Isotopic measurements were obtained on all fractions by TIMS; Pb isotope ratios were corrected for instrumental mass bias using a triple spike.

The silicate fractions show consistently more radiogenic Pb and Sr compared to those of the leachates, while Nd isotopic compositions are nearly uniform in both fractions. A shift towards higher Pb isotope ratios is observed during the dust event, followed by a continual decrease. By comparison, Sr and Nd isotopes record small changes, with a noticeable excursion to low values after the dust event. Lead and Nd isotopic compositions of TSP and PM10 are similar during dusty days, in contrast to less-dusty days, suggesting that grain-size fractionation depends on dust loading. The radiogenic isotope time-series of winter dust at Cape Verde pinpoints Northwest Africa as a persistent source of dust, while an additional emission source, with more radiogenic Pb, was active during the dust storm event. These inferences are entirely consistent with analysis of air-mass back-trajectories.

The ocean's biological pump in deep time

LEE R. KUMP

Dept. of Geosciences, Penn State, University Park, PA 16802
USA lkump@psu.edu

The importance of biotic processes in the functioning of the Earth system is perhaps nowhere better demonstrated than by the vertical chemical stratification of the ocean. In the face of physical forces of homogenization, life transforms the ocean into a chemically heterogeneous environment, depleted of nutrients, and through fractionation, ¹²C in surface waters and enriched at depth. This biological pumping of nutrients to depth occurs with the sinking of organic matter and its remineralization in the deep ocean. The "health" of the ocean's biota has been inferred from reconstructed gradients in $\delta^{13}\text{C}$, with strong gradients implying a strong biological pump and loss of the gradient, e.g., during the Cretaceous-Paleogene extinction event implying collapse. However, today, the magnitude of the surface-to-deep gradient is inversely related to the rate of export of organic matter to the deep on a regional basis. Rather, it is the efficiency of the biological pump, the ability of organisms to extract nutrients from upwelling waters before those waters mix physically with waters at depth, that is reflected in the gradients, and the most efficient removal occurs in the oligotrophic gyres. The biological pump appears as a robust feature of ocean ecosystems over geologic time, as evidenced through detailed investigations of the carbon isotope gradients inferred from carbonate rocks deposited during the Paleoproterozoic, end Permian, and throughout the Cenozoic.

Heinrich Holland's big event: The Great Oxidation

LEE R. KUMP¹

¹Dept. of Geosciences, Penn State, University Park, PA 16802
USA lkump@psu.edu

Although his research delved into many problems in the geochemistry of Earth, for much of his career H.D. Holland was most passionate about what he termed "the Great Oxidation Event," i.e., the establishment of an oxygen-rich atmosphere in the early Paleoproterozoic. From the early 1960's until his passing in 2012, Holland developed and refined a deep understanding of the geological and theoretical constraints on the chemical composition and evolution of the atmosphere and ocean. This understanding, and the way that only Holland could provide simple yet deep quantification to the problem, is perhaps most elegantly displayed in his 1984 book *The Chemical Evolution of the Atmosphere and Oceans*, the manuscript of which served as my introduction to Holland's work when I was a graduate student studying under lifelong friend and scientific foil to Holland, Robert Garrels. Holland sought to answer the questions of "when did the GOE occur?", "why did it occur?", and "how high oxygen levels rose during the event and subsequently?". For Holland, the answer to "when" has been fairly well constrained by the mass-independent sulfur isotope record of the Paleoproterozoic. The answer to "how high" is rather poorly constrained by geological proxies but approximately 10% of today's level just following the GOE. But the answer of "why" continued to perplex him to the end. A diverse group of researchers has been entrained by Holland's passion for the GOE and will carry the torch forward as the timing, pathway, and mechanisms of the GOE become fully illuminated.

Organic genesis of the sulphur occurrences and their relationship with black shales in the Isparta Region, SW, Turkey

MUSTAFA KUMRAL¹ AND MURAT BUDAKOGLU¹

¹Istanbul Technical University, Department of Geological Engineering, 34469, Istanbul, TURKEY

The study area is located in the triple conjunction area of the "Isparta Angle" in the Western Taurus region of SW Turkey. Due to Neotectonic evolution of Eastern Mediterranean Region, the study area is a geologically very complicated region. The rock units are divided into two groups as either allochthonous or autochthonous. Tectono-stratigraphically, the allochthonous units are Paleozoic quartzite, black shale, limestone, arkosic sandstone, interlaminated radiolarite and autochthonous units are Triassic and Jurassic limestones, and Upper Cretaceous ophiolite. Trachyte, trachyandesite, feldspathoidal trachyandesite porphyry, tuff and pumice were formed by volcanism during the Plio-Quaternary. Recent alluvium and slope detritus cover all the rock units.

Sulphur outcrops are exposed in the Keciborlu native sulphur, Uyuzpınar volcanic gases, Daridere altered volcanic rocks, Daridere pyrite in volcanic rocks, Yakaören altered volcanic rocks, Kasımlar blackshales, Kesme road native sulphur in blackshales, İbişler village in native sulphur, Afyon volcanics, Kınık Kızıltepe altered volcanic rocks, Gölbaşı realgar, Gölbaşı gypsum and Şarkikaraagac barite occurrences. The most important sulphur deposits are found in volcanic tuff and siltstone - marl - shale interbedded unit which contains an organic matter.

Sulphur may accumulate around recent fumaroles existing and also as massive mineralization. Field studies and sulphur isotope data show that the sulphur originated from the uppercrust and probably comes from organic matter-rich Paleozoic and Triassic sedimentary rocks. The sulphur did not migrate between the Triassic and Pliocene periods. However, Plio-Quaternary volcanism was the cause of mobility of the sulphur and was followed by formation of the secondary sulphur mineralization due to post tectonic geothermal activities. $\delta^{34}\text{S}$ values of the samples coincide with other samples from different shallow marine environments. Since the isotope values of the sulphur samples are quite similar to those of organic materials, it can be concluded that the sulphur might have occurred in the same anoxic environment together with petroleum source rocks.

Seismic evidence for the α - β quartz transition beneath Taiwan from Vp/Vs tomography

H. KUO-CHEN^{1,2,3}, F. T. WU^{1,3}, D. M. JENKINS¹,
J. MECHIE⁴, S. W. ROECKER⁵, C.-Y. WANG²
AND B.-S. HUANG⁶

¹Department of Geological and Environmental Sciences, State University of New York at Binghamton, NY, USA.

²Institute of Geophysics, National Central University, Jhongli, Taiwan.

³Department of Earth Sciences, University of Southern California, Los Angeles, California, USA.

⁴Deutsches GeoForschungsZentrum – GFZ, Section “Geophysical Deep Sounding”, Telegrafenberg, 14473 Potsdam, Germany.

⁵Department of Earth and Environmental Sciences, Rensselaer Polytechnic Institute, New York, USA.

⁶Institute of Earth Sciences, Academia Sinica, Taipei, Taiwan.

Knowledge of the rock types and pressure-temperature conditions at crustal depths in an active orogeny is key to understanding the mechanism of mountain building and its associated modern deformation, erosion and earthquakes. Seismic-wave velocities by themselves generally do not have the sensitivity to discriminate one rock type from another or to decipher the P-T conditions at which they exist. But laboratory-measured ratios of velocities of P to S waves (Vp/Vs) have been shown to be effective. Results of 3-D Vp and Vp/Vs tomographic imaging based on dense seismic arrays in the highly seismic environment of Taiwan provides the first detailed Vp/Vs structures of the orogen. The sharp reduction in the observed Vp/Vs ratio in the felsic core of the mountain belts implies that the α - β quartz transition temperature is reached at a mean depth of 24 ± 3 km. The transition temperature is estimated to be 750 ± 25 °C at this depth, yielding an average thermal gradient of 30 ± 3 °C/km.

In a young orogen such as Taiwan where an extensive root system is extant and rapid deformation and uplifting are well-documented, the knowledge of the present P/T conditions and materials in the core of the orogen could help in the understanding of the dynamics of mountain building. The presence of abundant quartz in the continental crust is important in localizing deformation; while hydration weakening as one of the conditions in the feedback processes the α - β quartz transition in Taiwan may play the role. In any case, Taiwan is an excellent site where patterns of strain focusing and crustal weakening during the early stages of tectonic deformation can be explored in detail.

Isotopic and Geochemical Constraints on the Origin of Post-Collisional Mafic Tholeiites from Erkilet, Central Anatolia

BİLTAN KÜRKCÜOĞLU^{1*}, TANYA FURMAN²,
MEGAN PICKARD², ERDAL ŞEN¹, BARRY HANAN³,
PİNAR ŞEN⁴, KAAAN SAYIT³ AND TEKİN YÜRÜR¹

¹Hacettepe University, Dept. of Geological Engineering, 06800 Beytepe-Ankara, Turkey, biltan@hacettepe.edu.tr

²Pennsylvania State University, Dept. of Geosciences, University Park, PA, 16802, USA furman@psu.edu

³San Diego State University, Dept. of Geological Sciences, San Diego, CA, USA, bhanan@mail.sdsu.edu

⁴General Directorate of Mineral Research and Exploration (MTA) Balgat-Ankara, Turkey, pinar.alicisen@gmail.com

Central Anatolia is one of the most interesting region displaying extensive volcanic activity related to post-collisional extension. Besides stratovolcanoes, most monogenetic vents and smaller volcanoes (e.g., Karapınar, Develidağ, Sivas, Erkilet) are characterized by basaltic lavas that may be alkaline or tholeiitic or both. The field and geographical occurrence of Erkilet mafic lavas are generally similar to those observed in the Sivas area some 100 km to the northeast (1). These two volcanic provinces are located along an ancient suture separating the Anatolide-Tauride blocks. Erkilet basalts have incompatible trace element abundances that are enriched overall relative to primitive mantle values, but they lack the unusually high contents of large ion lithophile and light rare earth elements that typify Sivas basalts, Erciyes tholeiites, and products of the regional mantle lithosphere (2). The Erkilet basalts have low Nb-Ta contents (but not Ti, Zr, Hf) that are typical of arc lavas and suggest a contribution from a source area with rutile that remains stable during shallow melting. Their high Ba/Nb (25-36) and La/Nb (~2) values reflect these low Nb contents, and require a source region distinct from that for MORB or Sivas basalts. Low Rb/Sr (~0.01) and moderate Ba/Rb (33-36) values suggest a source with modal amphibole but not phlogopite, consistent with low Tb/Ybn values that indicate melting within the shallow mantle, i.e., above the garnet stability field. The Sr-Nd isotopic signatures of Erkilet mafic lavas are depleted relative to those of Sivas and Erciyes basalts (~0.7037, 0.5128), consistent with their smooth and OIB-like incompatible trace element abundance patterns. Their Pb isotopic values, however, plot within the range of Sivas and Erciyes basalts that are interpreted as including contributions from a mantle lithosphere affected by enrichment in fluid-mobile trace elements during an ancient subduction event (3). These isotopic signatures are consistent with trace element evidence supporting existence of an arc environment during the evolution of the source region for Erkilet basalts. Further work will explore the nature and degree of interaction between identifiable lithospheric and asthenospheric sources during extension-related melting along this ancient suture zone. [1] Kurkcuoglu 2013, submitted, [2] IGR, **43**, 508, [3] Picard, 2012, Goldschmidt, 2012, 2231.

www.minersoc.org

DOI:10.1180/minmag.2013.077.5.11

Single-crystal elastic properties of $\text{Fe}_{0.04}\text{Mg}_{0.96}\text{SiO}_3$ – perovskite at high pressure

A. KURNOSOV^{*1}, D. M. TROTS¹, T. BOFFA BALLARAN¹,
AND D.J. FROST¹

¹Bayerisches Geoinstitut, Universität Bayreuth, 95447
Bayreuth, Germany.

Perovskite structured MgSiO_3 is widely accepted to be the dominant phase in the Earth's lower mantle where it coexists with ferropericlase. An understanding of the plausible chemical variation of MgSiO_3 -perovskite (enrichment with Fe/Al) in addition to the consequent effects on density and elastic properties is important in order to understand the origin of seismic velocity anomalies in the lower mantle reported in a number of studies [1-3].

In this study two differently oriented single-crystals of magnesium silicate perovskite containing 4 mol% of the $\text{Fe}^{2+}\text{SiO}_3$ component [Mg,FeSiO_3] have been studied by means of Brillouin spectroscopy and X-ray diffraction in-situ in diamond anvil cells. Helium was used as the pressure transmitting medium and experiments were performed in the pressure range from 2 to 31 GPa. Ruby pressure markers were used to obtain similar pressure conditions in both diamond anvil cells. The Brillouin spectra were measured in symmetric platelet geometry for each crystal at different orientations in the plane of the platelet. The data at each pressure were fitted for both crystals simultaneously in order to reduce correlations of C_{ij} constants. Using the data from two crystals with different non-specific orientations we were able to obtain all 9 independent C_{ij} elastic constants for orthorhombic symmetry at 8 different pressure points. The orientation matrix and cell parameters for each crystal at every pressure point were refined using in-situ x-ray diffraction measurements. From sample densities obtained from x-ray diffraction data and simultaneous measurements of the adiabatic bulk modulus obtained from Brillouin measurements, it was possible to calculate the absolute pressure for all our experimental points. This approach allowed the elastic properties of $(\text{Mg,Fe})\text{SiO}_3$ -perovskite to be determined as a function of primary pressure, i.e. without resort to a secondary pressure standard. This consequently provides a more reliable data set to be compared with seismic data for the lower mantle.

[1] Ni *et al.* (2005), *Geophys. J. Int.* **161**, 283–294. [2] Masters *et al.* (2000), *AGU Monograph Series*, **117**, 63–87. [3] Garnero *et al.* (2005), *The Geological Society of America Special Paper*, **430**, 79–101.

Sedimentary osmium isotopic records of Mediterranean basins

JUNICHIRO KURODA^{1*}, FRANCISCO J. JIMENEZ-ESPEJO^{1,2},
TATSUO NOZAKI¹ AND KATSUHIKO SUZUKI¹

¹Japan Agency for Marine-Earth Science and Technology
(JAMSETC), Yokosuka 237-0061, Japan

(*correspondance: kurodaj@jamstec.go.jp)

²Nagoya University, Nagoya 464-8602, Japan

Mediterranean Sea has experienced an extreme event called Messinian Salinity Crisis (MSC) that represents a formation of gigantic evaporite deposits in deep basins (e.g., Ryan *et al.*, 2009). In this study we report sedimentary Os isotopic record of marine sediment cores from four Deep-Sea Drilling Project (DSDP) sites in the Mediterranean Sea (Hsü & Montadert, 1978); DSDP Site 372 in the western Mediterranean (Balearic Basin), DSDP Site 374 in the central Mediterranean (Ionian Basin), and DSDP Sites 375 and 376 in the eastern Mediterranean (Florence Rise). Osmium isotopic ratios of the pre-MSC sediments of Miocene (Burdigalian to Serravallian) in the western Mediterranean are identical to that of the coeval ocean water. In contrast, the pre-MSC sediments (Langhian to early Messinian) in the eastern Mediterranean have significantly low $^{187}\text{Os}/^{188}\text{Os}$ values than those of the Middle to Late Miocene ocean water. This suggests that Os in the eastern Mediterranean was not fully mixed with that of other seas such as western Mediterranean and North Atlantic, and that the basin isolation has already started before the MSC, probably as early as Middle Miocene. The unradiogenic Os would have been supplied to the eastern Mediterranean by selective weathering of ultramafic rocks in the surrounding ophiolite bodies, which contains high amount of non-radiogenic Os. The isotopic compositions of Os in gypsum samples from all sites are significantly lower than the end-Miocene ocean water values, suggesting isolation of all Messinian basins. Sediments from Pliocene show Os isotopic ratios more radiogenic, and close to the seawater values of Pliocene but slightly less radiogenic, indicating that Os started mixing with global seawater again. We will further discuss possible scenarios about Mediterranean hydrology during the MSC, based on the sedimentary Os isotopic records.

[1] Hsü, K.J. & Montadert, L. (1978) Initial Reports of the Deep Sea Drilling Projects 42A, Ryan, W.B.F. (2009) *Sedimentology* 56, 95-136.

Helium isotopic and concentration variations in a clinopyroxenite vein: Implications for mantle evolution

M.D. KURZ¹, V. LEROUX¹, J.M. WARREN², J. CURTICE¹,
AND S. NIELSEN¹

¹Quissett Campus, Woods Hole Oceanographic Institution,
Woods Hole, MA 02543, USA

²Geological and Environmental Sciences, Stanford University,
450 Serra Mall, Stanford CA 94305-2115, USA

In an effort to constrain the behavior of noble gases during melting and melt migration in the mantle, we have measured helium concentrations and isotopic compositions in a 10 centimeter transect through a clinopyroxenite vein in the Josephine Ophiolite (Oregon, USA). The 4 cm thick clinopyroxenite is hosted by harzburgite and was sampled with 1-2 millimeter resolution. The vein has ⁴He concentrations up to 10 times higher than the host harzburgite (5.0 to 9.0 x 10⁻⁷, as compared to 3.4 x 10⁻⁸ to 1.7 x 10⁻⁷ cc STP/gram). Because the veins are thought to form through mantle melt percolation, the enrichment confirms that helium behaves as an extremely incompatible element. There is a sharp helium concentration contrast at the vein/host interface, suggesting that the concentration variations were produced during vein emplacement, and that clinopyroxene has higher helium storage capacity. Total ³He/⁴He in the host harzburgite ranges from 6.5 to 7.1 times atmosphere (Ra), in agreement with previous measurements of the area, suggesting that mantle helium isotopic compositions are dominant (Recanati *et al.*, 2012). The bulk ³He/⁴He in the vein varies between 4.5 and 5.3Ra, significantly lower than the harzburgite, reflecting radiogenic production since vein emplacement or slab related fluxes. These data demonstrate that isotopic and concentration variations have been preserved since emplacement at ~ 157 Ma, and that mantle helium isotopic compositions are retained. The isotopic variations suggest that it may be possible to determine Th-U-He vein emplacement ages. The short length scale variations place time limits for diffusion and post-emplacement cooling below the closure temperature. This study may not be representative of the mantle, as the Josephine veins are thought to derive from a sub-arc or back-arc basin setting, and are preserved only by rapid cooling. However, these preliminary data do suggest that preferential melting of this vein type will yield lower ³He/⁴He than the host mantle, and that vein melting models therefore may not explain elevated values (unradiogenic helium) found in some oceanic basalts.

The Mo-isotopic composition of late Archean Iron Formations

F. KURZWEIL^{1*}, M. WILLE¹, R. SCHOENBERG¹
AND M. VAN KRANENDONK²

¹Department of Geoscience, University of Tuebingen,
Wilhelmstr. 56, 72074 Tuebingen, Germany,
(*correspondence: flokurzweil@hotmail.de)

²School of Biological, Earth and Environmental Sciences,
University of New South Wales, Kensington, NSW 2052,
Australia

The timing of the first appearance of free oxygen in Earth's atmosphere remains highly debated in the literature. The general view places the Great Oxidation Event (GOE) between 2.4 and 2.32 billion years ago (Ga), when oxygen concentrations rose for the first time from 10⁻⁵ to 10⁻² of the present atmospheric level. However, some redox-sensitive elements seem to indicate a pre-GOE increase in atmospheric oxygen concentrations at extremely low levels. Mo isotopes and concentrations in late Archean sediments (carbonates and black shales), for example, show $\delta^{98}\text{Mo}$ values higher than the continental crust average some 100 million years before the GOE. These positive $\delta^{98}\text{Mo}$ values are attributed to oxidation-reduction processes that per se require oxygenated oceans, in which light Mo is preferentially adsorbed onto Mn- and Fe-(oxyhydr)oxides. The subsequent increase in seawater $\delta^{98}\text{Mo}$ is thought to be preserved in black shales and carbonates. The occurrence of heavy Mo-isotope signatures in late Archean shales and carbonates infers the presence of a light Mo-reservoir in the sedimentary record. Fe-(oxyhydr)oxides are a possible candidate for such a light Mo reservoir. During early diagenesis they would form Fe-carbonates, -oxides, or -silicates and eventually iron formations (IF's). Consequently, IF's may represent the missing late Archean reservoir for isotopically light Mo.

Here, we tested this hypothesis by measuring Mo isotopes in 2.63 to 2.45 Ga old black shales and IF's of the Pilbara Craton, Australia. Both, black shales and IF's show a similar increase in $\delta^{98}\text{Mo}$ as time-equivalent shales and carbonates from the Kapvaal craton, South Africa. The youngest IF shows a highly positive $\delta^{98}\text{Mo}$ value of 1.5‰. Thus, the proposal that IF's represent the reservoir for light Mo is not confirmed by our measurements. The similarity in magnitude and trend of $\delta^{98}\text{Mo}$ through time suggests a similar removal mechanism of molybdenum from seawater by carbonates, shales and IF's. Furthermore, this observation requires the build-up of a sizeable seawater Mo-reservoir that was linked to more oxidizing conditions before the GOE.

Cathodoluminescence characterization of Norsethite



N. KUSANO¹, H. NISHIDO¹, M. MAKIO²
AND K. NINAGAWA³

¹Department of Biosphere-Geosphere Science, Okayama
University of Science, 1-1 Ridai-cho, Okayama 700-0005,
Japan (correspondence: nishido@rins.ous.ac.jp)

²Graduate School of Social and Cultural studies, Kyushu
University, 744 Motooka, Nishi-ku, Fukuoka, 819-0395
Japan

³Department of Applied Physics, Okayama University of
Science

Anhydrous double salts of MgCO_3 and BaCO_3 such as norsethite $\text{BaMg}(\text{CO}_3)_2$ have not been investigated up to date with respect to CL properties, whereas CL of dolomite structurally similar to norsethite has been extensively used to geoscience application. In this study, we have measured CL spectra of norsethite and characterize its CL emission centers.

Norsethite sample from Kremikovtsy, Bulgaria was selected for CL spectral measurements. SEM-CL analysis was conducted using an SEM combined with a grating monochromator to measure CL spectra ranging from 300 to 800 nm in 1 nm steps with a temperature controlled stage from -190 to 250 °C. All CL spectra were corrected for the total instrumental response.

Norsethite exhibits a red broad band emission in red region between 570 and 770 nm at room temperature. This emission can be assigned to Mn^{2+} as an activator by comparing with the emissions of other carbonates, but with too low concentration of Fe^{2+} as a quencher. A Gaussian curve fitting of the spectra was carried out to clarify emission components in energy units. One emission component at around 1.93 eV (641 nm) was found without the others related to defect centers. Dolomite has two emission components at 1.84 eV (673 nm) for Mn^{2+} activator in Mg site and another component at 2.15 eV (576 nm) for same activator in Ca site. This fact implies that Ba ions with large ionic size might alternate crystal field strength around Mg site in norsethite structure.

An apatite-halogen based probe for fluid-rock interaction events

CHRISTOF KUSEBAUCH¹, TIMM JOHN¹,
MARTIN WHITEHOUSE² AND ANE ENGVIK³

¹Institute for Mineralogy, Uni Muenster, Germany;
c.kusebauch@uni-muenster.de

²Swedish Museum of Natural History, Stockholm, Sweden

³Norwegian Geological Survey, Trondheim, Norway

Apatite is a typical accessory mineral in many geological settings and is stable over a wide range of pressure and temperature. Natural apatite usually occurs as a solid solution of three end members, i.e. fluor-, hydroxy- and chlorapatite and therefore reflects the F-Cl-OH activity conditions of its formation. Apatite crystallized during fluid-rock interaction can be used as a fluid probe for halogens as it reflects not only F and Cl, but Br and I concentration in the fluid. Also apatite is rather sensitive to changes in fluid composition, undergoing dissolution-precipitation reactions leading to formation of an apatite with a changed composition. This facilitates constraints on the number of fluid events and the characteristics of their potential sources.

Here, we present a halogen concentration and $\delta^{37}\text{Cl}$ study of apatite from an alteration sequence from a regional-scale metasomatic event (Bamble Sector, SE Norway). The alteration sequence comprises a complete profile from unreacted to fully altered gabbro, close to a shear zone from which a high salinity fluid pervasively altered the gabbro.

Halogens in apatite, measured in-situ by ion microprobe, show marked diversity. Whereas Br concentrations constantly decrease from the least altered (100-500 ppm) to most altered samples (10-20 ppm), F shows the opposite trend, with a constantly increasing concentration from 40-100 ppm to 2000-12000 ppm. Apatite from the most pristine samples shows low F/Cl ratios and high Br/Cl, while apatite from strongly altered samples is characterized by high F/Cl and low Br/Cl ratios. I/Cl ratios show no correlation with alteration.

Apatite from the pristine gabbro has $\delta^{37}\text{Cl}$ values $<+0.4\%$. With increasing alteration $\delta^{37}\text{Cl}$ values increase to as high as $+3.5\%$. Furthermore, there is a strong correlation between $\delta^{37}\text{Cl}$ values and F concentrations within individual apatite crystals.

The observed halogen concentrations and $\delta^{37}\text{Cl}$ values of apatite formed during the metasomatic event can be explained by a single fluid event. Characteristics of the fluid are best represented by apatite from highly altered samples (high $\delta^{37}\text{Cl}$, high F concentrations). Due to interaction with the gabbro this fluid constantly evolves to lower F concentrations and lower $\delta^{37}\text{Cl}$ values.

Ancient mobilisation of radiogenic Pb and Ti during high-grade metamorphism

M.A.KUSIAK^{1,2,3*}, M.J.WHITEHOUSE¹, S.A.WILDE²,
D.J.DUNKLEY², A.A.NEMCHIN², R.WIRTH⁴
AND K.MARQUARDT⁴

¹Swedish Museum of Natural History, Stockholm, Sweden,

²Dept. of Applied Geology, Curtin University, Perth, Australia,

³Polish Academy of Science, Inst. of Geol. Sci., Warsaw, Poland

⁴Deutsches GeoForschungsZentrum, GFZ, Potsdam, Germany

Many zircons from early Archaean gneisses in the Napier Complex of East Antarctica, are reversely discordant. High spatial resolution ion microprobe imaging reveals Y and U zonation, characteristic of magmatic zircons, together with a micro-scale patchy distribution of ²⁰⁶Pb and ²⁰⁷Pb that does not correspond to either growth zonation or crystal imperfections. Some of these patches yield ²⁰⁷Pb/²⁰⁶Pb ages >4 Ga, whereas others yield ages younger than the magmatic crystallization age. Zircons from Dallwitz Nunatak record detrital ages between 3.5 Ga and 2.5, whereas those from Gage Ridge define multiple age groups, with concordant data between 3.6 Ga and 3.3 Ga and reversely discordant data that form a distinctive ca. 3.8 Ga population. These oldest zircons are interpreted as xenocrysts, with the age of the protolith being ca. 3.3 Ga or younger. The patchy distribution of Pb is the result of mobilisation of ancient radiogenic Pb, which can lead to reverse discordance [1]; this is independent of the degree of metamictisation, oxygen isotope and REE content of the zircons. Zircons from Mount Sones which show this effect underwent high-grade metamorphism at both ~2.8 Ga and 2.5 Ga, the latter reaching temperatures of >1000°C. It is likely that one or both of these events caused re-mobilisation of Pb. However, the precise mechanism is unclear and further work is in progress in an attempt to constrain this. Importantly, Ti also exhibits a random, patchy distribution in some zircon grains. This has the potential to affect Ti-in-zircon thermometry, with implications for the accurate determination of zircon crystallization temperatures.

[1] Kusiak *et al.* (2013), *Geology* **41**, 291-294.

Quantitative 18S rDNA analysis using 3rd generation sequencing methods to determine the effects of Modified Circumpolar Deep Water, iron and siderophores on phytoplankton assemblage composition in the Ross Sea

ADAM B. KUSTKA, ASHLEY M. NEW
AND BETHAN M. JONES¹

¹Rutgers University, Newark, NJ

kustka@andromeda.rutgers.edu

We participated in the SEAFARERS cruise (along with other investigators Hatta, Kohut, Lam, Measures, Milligan and White) in the Ross Sea to test hypotheses regarding the influence of Fe supplied from Modified Circumpolar Deep Water (MCDW) and from putatively accessible and somewhat refractory forms (FeCl₃ and Fe-enterobactin) on primary production. Incubation experiments revealed widespread and chronic Fe limitation that was more pronounced in surface waters above Joides Trough than on Pennell Bank. Addition of MCDW did not stimulate growth at any station. Iron supplied as the Fe- catecholate complex enterobactin stimulated bulk chlorophyll production in a station dependent manner, which might be explained by clade-specific differences in Fe-catecholate bioavailability. We developed a quantitative approach to characterize community composition - based on amplification of the v7-v9 regions of 18S rDNA (>500 bp) and single-molecule real-time (SMRT) sequencing - which increased phylogenetic resolution compared to some previous methods. The inclusion of various xenobiotic standards immediately prior to DNA extraction and to PCR amplification allow us to evaluate absolute changes in community composition, facilitating the calculation of clade-specific growth rates under various treatments. To our knowledge, this is the first quantitative application of third generation sequencing methods in marine environments.

Impact of increasing MoO₃ loading on incorporation properties of multi-component borosilicate glass

A. KUTZER^{1*}, T. VITOVA¹, K. KVASHNINA²,
T. PRÜßMANN¹, J. ROTHE¹, E. SOBALLA¹, C. ADAM¹,
P. KADEN¹, M. A. DENECKE¹, S. WEISENBURGER¹,
G. ROTH¹ AND H. GECKEIS¹

¹Institute for Nuclear Waste Disposal (INE), KIT, 76021, Karlsruhe, Germany

(*correspondence: andrea.kutzer@kit.edu)

²European Synchrotron Radiation Facility (ESRF), 38043, Grenoble, France (kristina.kvashnina@esrf.fr)

Mo(VI)-rich residual material remaining after vitrification of high level liquid waste (HLLW) at the 'Karlsruhe Reprocessing Plant' (WAK) site can potentially be immobilized in borosilicate glass for ultimate disposal. Due to its low solubility in borosilicate glass melts, Mo(VI) tends to form molybdate-rich phases during the vitrification process. [1] These phases may crystallize during melt cooling and are able to incorporate radionuclides within their crystal structure. If water soluble alkali molybdates are formed, the release of radioactivity into the environment will be facilitated in case of water intrusion into a deep geological repository. The chemical composition of the formed phases is strongly dependent on the borosilicate glass composition used. Understanding factors favoring the formation of stable crystalline Mo(VI) phases in borosilicate glasses allows development of glass compositions capable of incorporating high Mo loadings, yet avoiding formation of soluble phases.

In this work nuclear waste simulate with varying MoO₃ concentrations vitrified in a multi-component borosilicate glass ([2]) was characterized. Powder X-ray diffraction and Raman spectroscopy studies confirm formation of crystalline CaMoO₄ and BaMoO₄ phases for MoO₃ concentrations above 4.5 wt%. Observed Mo K-edge high resolution X-ray absorption near edge structure (HR-XANES) spectral changes are correlated to different molybdate environments in the glass depending on the MoO₃ concentration. Fit analyses show that Na⁺ cations preferably compensate molybdate charge over Ba²⁺ and Ca²⁺ at low concentrations. ²⁹Si nuclear magnetic resonance (MAS NMR) spectroscopic investigations show a strong impact of the different MoO₃ loadings on the degree of silicon network polymerization of the glass. No evidence for the formation of water soluble crystalline molybdates is found, indicating that the chemical composition of the glass used is favorable for immobilization of Mo-rich nuclear waste with this specific chemical composition.

[1] Lutze and Ewing (1988), *Radioactive Wasteforms for the Future*, North Holland, Amsterdam. [2] Grünewald *et al.* (2009), *Proceedings of Global 2009*, Paris.

Correlative imaging of microbial transformations in Nature

M. M. M. KUYPERS

MPI for Marine Microbiology, Bremen, Germany
(mkuypers@mpi-bremen.de)

Correlative imaging is widely applied to obtain comprehensive information on the identity, activity and physiology of cells in eukaryotic cell biology. However, in the field of environmental microbiology this method is still little used despite its obvious potential. During the past years substantial progress was made at the MPI for Marine Microbiology (MPI-MM) to establish this method for our field. A particularly powerful approach used in our institute is the use of nano-scale Secondary Ion Mass Spectrometry (nanoSIMS) coupled to stable and radio-isotope labelling experiments to determine single-cell activity in the environment. By combining this approach with Fluorescence in situ Hybridization (FISH) we are able to link the identity of microbial cells in a complex microbial community to their in situ nutrient incorporation, which allows us to calculate cellular uptake rates and directly determine nutrient fluxes. The recent acquisitions of an Environmental Scanning Electron Microscope combined with an EDX system (ESEM/EDX) and a confocal laser Raman microscope coupled with an atomic force microscope provides further elemental, chemical-bond and structural information at a single cell level. I will present results of our correlative imaging studies of complex microbial communities in various marine environments.

Gold-sulfide jasperoids of East Kazakhstan

KUZMINA O.N.^{1,2}, DYACHKOV B.A.^{1,3},
VLADIMIROV A.G.^{2,4,5}, KIRILLOV M.V.²,
KOLPAKOV V.V.², MIZERNAYA M.A.¹
AND MAYOROVA N.P.¹

¹D. Serikbaev EKSTU, Ust-Kamenogorsk, Kazakhstan
(kik_kuzmins@mail.ru)

²Sobolev Institute of geology and mineralogy SB RAS,
Novosibirsk, Russia (vladimir@igm.nsc.ru)

³TOO "Altaiski GEI", Ust-Kamenogorsk, Kazakhstan

⁴Novosibirsk State University, Novosibirsk, Russia

⁵Tomsk State University, Tomsk, Russia

Zaisan structural zone refers to traditional auriferous region of East Kazakhstan [1]. This zone includes paleozoic ofiolites and volcanic-sedimentary sequences, those were formed as the result of oblique collision of Kazakhstan and Siberian paleocontinents [2]. Terrigen-carbonate sedimentary sequences are characterized by high contents of gold, but the ore deposits are associated with the introduction of granodiorite-plagiogranite collision magma (Kunush complex, 310-300 Ma). In result of acid magmas and carbonates interaction were formed Carlin-type gold-sulfide jasperoids [3]. This type includes the Suzdal deposit, and a number of promising gold objects (Baibura, Jhaima, etc.) [2]. In the article it is given the characteristic of Baibura ore field. Native gold from this ore field jasperoids is uniform in morphology and geochemical features. The most part of gold granules is of medium and fine dimension, preferably <0.25 mm. Gold granules are not rounded, of yellow color and interstitial, rarely crystal, morphology. Grade of gold indicates the unity of its source and the one-step process of its formation, lying in a narrow range of values 923-959‰. It was indicated the impurity of mercury in amounts up to 0.7%. Presence of mercury confirms ore field belonging to the Carlin-type gold mineralization.

[1] Narseev V.A. (2002) *Ores and Metals*, **1**, 67-70. [2] Dyachkov B.A., *et al.* (2009) *Ores and Metals*, **3**, 1-21. [3] Emsbo P., *et al.* (1999) *Geology*, **27**, 59-62. [4] Kovalev K.R., *et al.* (2012) *Geology of ore deposits*, **54**, 4, 305-328.

Rare elements of diamond-forming melt chambers formed in the mantle peridotite (estimation with use of experimental K_D at 7.0-8.5 GPa)

KUZYURA A.V.* AND LITVIN YU.A.

Institute of Experimental Mineralogy Russian Academy of Sciences, ul. Ak. Osip'yana, 4, Chernogolovka, Moscow region, (*correspondence: shushkanova@iem.ac.ru)

Based on the experimental data at 7.0-8.5 GPa [1] rare elements (RE) in the diamond-forming mantle peridotite-carbonatite and eclogite-carbonatite systems are characterized by similar partitioning coefficients (K_D^{RE}) mineral-melt. These values are also closely comparable with those for the silicate and carbonatite melts in equilibrium with mantle silicate minerals [2].

It can be assumed that a chamber of diamond-forming melts was formed within the host garnet lherzolite mantle when it was affected by a reactive "metasomatic agent" [2, 3]. It is of interest to identify those RE that came to diamond-forming melts with the mantle components, as well as those RE that were infused by the "metasomatic agent".

The contents of RE in diamond-forming carbonatite melt chambers were calculated based on the real content of RE in minerals of peridotite and eclogite parageneses in diamonds and diamond xenoliths of several kimberlite pipes [4-6] and experimental K_D^{RE} . The main contribution of RE in them is made by the mantle component. Parental melt of diamonds and inclusions in them are depleted by medium (Sm, Eu, Gd) and heavy RE (Tb, Dy, Ho, Er, Yb, Lu, Hf), in contrast to primitive peridotite [7]. They are enriched in light (Sc, Rb, Sr, Ba, La, Ce, Pr, Nd) RE and Nb, but their content by 1-2 orders of magnitude lower than in the primitive mantle peridotite. High Sr can be associated with "the metasomatic agent". Support: Grants of the President # MK-1386.2013.5, the Ministry of education and science of Russia (agreements 8317, 8378) и RFBR grant 11-05-00401, 12-05-33044, 13-05-00835.

[1] Kuzyura *et al.* (2013) *DES*. in print. [2] Litvin (2011) *H.DES RAS* **3**, NZ6066. [3] Litvin *et al.* (2012) *GeoChem. Int.* **9**, 818-847. [4] Harte & Kirkley (1997) *ChemG* **136**, 1-24. [5] Ionov (2004). *J.Pet.* **45**, 343-36. [6] Stachel & Harris (1997) *CMP* **127**, 336-352. [7] Lyubetskaya & Korenaga (2007) *JGR* **112**, B3.

Mechanisms of replacement reactions of single cerussite PbCO_3 crystals by pyromorphite, mimetite and vanadinite

MONIKA KWAŚNIAK-KOMINEK¹ AND MACIEJ MANECKI¹

¹AGH – University of Science and Technology, Krakow, Poland (kwasniak@geol.agh.edu.pl)

Formation of thermodynamically stable phases like pyromorphite $\text{Pb}_5(\text{PO}_4)_3\text{Cl}$, mimetite $\text{Pb}_5(\text{AsO}_4)_3\text{Cl}$ and vanadinite $\text{Pb}_5(\text{VO}_4)_3\text{Cl}$ are common in the environment. It is hypothesised here that lead carbonate PbCO_3 , cerussite, can be readily replaced by polycrystalline lead apatites. This process is analogous to the calcium carbonate – calcium hydroxylapatite system, where such transformation is observed. However, the mechanisms of formation of pyromorphite, mimetite and vanadinite in the presence of cerussite are unknown.

The aim of this study was to experimentally determine the mechanism of the transformation of cerussite to pyromorphite, mimetite and vanadinite and the conditions under which these phases can form. The parameters of the experiments include pH (alkalic or acidic), the presence or absence of chloride ion, and temperature (140 or 5 °C). Experiments were carried out in order to produce partially reacted crystals to provide information about structural and textural relationships between parent and product phases. Cerussite crystals were put into 2M $(\text{NH}_4)_2\text{H}_2\text{PO}_4$, 2M $(\text{NH}_4)_2\text{H}_2\text{VO}_4$ or 2M $(\text{NH}_4)_2\text{H}_2\text{AsO}_4$ to form pyromorphite, vanadinite and mimetite, respectively.

X-Ray powder diffraction was used to identify and characterize the reaction products. Microstructural relationship between parent and product phases were determined by scanning electron microscopy (SEM-EDS) and electron microprobe analysis.

In every case single cerussite crystal were replaced by polycrystalline pyromorphite, mimetite and vanadinite through dissolution of PbCO_3 followed by precipitation of lead apatite. In acidic conditions formation of shultenite PbHAsO_4 or phospho-shultenite PbHPO_4 were also observed. Products of the reaction in every case are porous, allowing fluid transport to the reaction interface. At all temperatures the product phase and its morphology are the same. Interface coupled dissolution-precipitation mechanisms are confirmed by the textural relationships.

This project is supported by Polish NCN grant No 2011/01/M/ST10/06999.

Vertical lithofacies changes of the Jeonchong tuff cone in the Miocene Eoil Basin, SE Korea: Implication of a series of eruptive and depositional processes

C.W. KWON

Geological Research Division, Korea Institute of Geosciences and Mineral Resource, SE Korea (cwkwon@kigam.re.kr)

The Miocene Eoil Basin, SE Korea, contains abundant volcanic and volcanoclastic deposits because of active volcanism during basin formation. The Jeonchon tuff cone refers to an about 25 m-thick sequence of basaltic lapilli tuff in the central part of the basin. The tuff cone is underlain by pahoehoe lavas (the Lower Eoil Basalt), lacustrine mudstone, and mouth-bar sandstone in ascending order, indicating hydrovolcanic eruption in a shallow lake. It is composed of seven sedimentary facies: massive tuff breccia (TBm), crudely stratified lapilli tuff (LTb), inverse-to-normally graded lapilli tuff (LTin), normally graded lapilli tuff (LTn), massive coarse tuff (cTm) and massive medium to fine tuff (MtM & FtM). It can be divided into five depositional units (unit I to V in ascending order) based on facies characteristics and componentry. Unit I, about 4 m thick, consists of quartz-bearing massive tuffs (MtM & FtM), suggesting contact-surface steam explosivity within mouth-bar sand. Unit II, about 1.5 m thick, consists of graded lapilli tuffs (LTin & LTn) with abundant accidental basalt clasts, suggesting bulk-interaction steam explosivity within the Lower Eoil Basalt and deposition from pyroclastic surges and ballistic fallouts of basalt clasts. Unit III consists of tuff breccia (TBm; about 3.5 m thick) and overlying stratified lapilli tuff (LTb; about 0.5 m thick), which are interpreted to have resulted from debris flows and Surtseyan fallouts associated with vent-widening explosions. Unit IV, 0.8 m-thick and composed of massive coarse tuff (cTm), suggests remobilization of pyroclasts by debris flows during volcanic quiescence. Crudely stratified lapilli tuff (LTb) of Unit V, about 15 m thick, is interpreted to have formed by sustained Surtseyan finger jets without further excavation of the substrate. The vertical lithofacies changes suggest that the Jeonchon tuff cone experienced a series of eruptive and depositional processes during growth because of the changes in depositional environments, types of the substrate (sand vs. lava), and vent geometry.

Geochemical characteristics and microbial community composition of toxic metal-rich sediments contaminated from mine tailings

MAN JAE KWON¹, BAKNOON HAM¹, YUNHO HWANG¹,
JAEYOUNG CHOI¹, MAXIM BOYANOV², KEN KEMNER²,
EDWARD O'LOUGHLIN² AND JUNG-SEOK YANG¹

¹Korea Institute of Science and Technology (KIST) –
Gangneung Institute, Gangneung 210-340 S. Korea,
mkwon@kist.re.kr

²Biosciences Division, Argonne National Laboratory, Lemont,
IL 60439 USA

The effects of extreme geochemical conditions on microbial community composition were investigated using two distinct sets of sediment samples collected near weathered mine tailings from the Songcheon Au-Ag mine, Korea. One set (SCH) was gray-colored and showed extraordinary geochemical characteristics: As (6.7-11.5%), Pb (1.5-2.1%), Zn (0.1-0.2%), and pH (3.1-3.5). The other set (SCL) was brown-colored and had As (0.3-1.2%), Pb (0.02-0.22%), and Zn (0.01-0.02%) at pH of 2.5-3.1. Terminal Restriction Fragment Length Polymorphism revealed that the bacterial communities in SCL were more diverse than those in SCH. The clones identified in SCL were closely related to acidophilic bacteria within the genus of *Acidobacterium* (18%), *Acidomicrobinae* (14%), and *Leptospirillum* (10%). Most clones in SCH were closely related to *Methylobacterium* (79%) and *Ralstonia* (19%), both of which are well-known metal-resistant bacteria. The archaeal community in SCL was relatively simple: *Thermogymnomonas* (32%) and unclassified Euryarchaeota (48%). No archaeal community was detected in SCH sediments. Although total As was extremely high, over 95% of it was in the form of scorodite (FeAsO₄·2H₂O), as confirmed by XAFS analysis. Water-soluble As was only ~208 and ~0.06 ppm in SCH and SCL, respectively, which is not known to be toxic to bacteria; As(V) as much as 1000-1300 ppm did not influence bacterial growth. Because As was present in an oxidized and stable form it is likely that other metals released from the sediment were responsible for the differences in microbial community structure (e.g., water soluble Zn was ~234 and ~6.8 ppm in SCH and SCL, respectively).

Titanite Geochronology by LA-ICPMS: Advantages and Future Objectives

ANDREW R.C. KYLANDER-CLARK, BRADLEY R. HACKER, PAUL R. RENNE AND MICHAEL A. STEARNS^{1,2,3}

¹University of California, Santa Barbara, 93106-9630

²Berkeley Geochron Center, Berkeley, CA 94709

*correspondence: kylander@geol.ucsb.edu

Titanite has been dated by U/Pb TIMS for many years, but the application of this technique has been tempered by the recognition that titanite in single samples can yield a range of dates, and moreover, titanite dating by TIMS relies on either time/cost-intensive analysis of multiple titanite fractions, or on Pb measurement of an assumed-coeval low-U/Pb phase, such as feldspar, to establish an isochron. One of the great strengths of LA-ICPMS dating is rapid throughput; by analyzing many spots with differing concentrations of common Pb, isochrons can be established from titanite analyses alone, in a fraction of the time it takes for a single TIMS analysis. Furthermore, measuring composition at the same time—in this case laser ablation split-stream ICP petrochronology (LASS)—allows one to discriminate among titanite populations.

Here, we present two examples of the strength of the LASS technique on titanite: 1) grains from the Western Gneiss Region in Norway that (re)crystallized during exhumation, and 2) those from volcanic tuffs at/near the Cretaceous–Tertiary boundary. Both cases yield dates equivalent to those produced by conventional techniques. For the Norwegian samples, younger grains contain elevated Al, Ce/Ce*, and Eu/Eu* and depleted Fe, Ta, Zr, Hf, and LREE compared to the inherited portions of the grain, exemplifying the opportunities this technique offers with respect to understanding petrologic/geochemical systematics of metamorphic/igneous processes.

Although natural standards exist with little variability in age, the incorporation of variable amounts of common Pb results in variable ²³⁸U/²⁰⁸Pb ratios, thus negating the use of that material as a primary reference material. New standards (natural or synthetic) and/or data processing methods are required to enhance the effectiveness of this technique in the future.

Novel applications of geochemistry to mineral exploration and remediation

KURT KYSER

Department of Geological Science and Geological
Engineering, Queen's University, Canada
(kyser@geol.queensu.ca)

Mineral deposits are in fact geochemical anomalies, and as such their detection and assessment of their impact on the environment should be facilitated using geochemical techniques. Although geochemistry has been used directly in the discovery of mineral deposits and more indirectly in shaping deposit models, much of the novel application of geochemistry is in formulating effective exploration and remediation strategies. Areas where recent research, application and policy intersect in the extraction of metals from the geosphere include: (1) the use of element mobility in the near surface environment to detect deposits at depth, (2) revealing element distributions in and around deposits to adequately assess the total chemical environment associated with the deposit and to refine effective and relatively benign extraction and waste disposal techniques, (3) understand the effects of both macro- and micro-environments on element mobility across the geosphere-biosphere interface to define appropriate remediation techniques associated with the extraction of diverse commodities. Research, both pure and applied, play a fundamental role in providing the techniques for these areas, but this is driven largely by what industry requires, which is driven largely by policies formulated in government agencies. Research in applied geochemistry can add value to exploration and remediation strategies provided the results are adequately conveyed to the appropriate individuals in both industry and government and there is a perceived need to develop new and novel techniques by all concerned. For example, the application of isotope tracing to elucidate the processes by which various elements move through the geosphere and into the biosphere is a novel area of research with boundless potential for exploration and remediation. This area, which is largely driven by those in research, is an evolving one wherein the historically high costs, slow turnover and general mystic are being overcome by a concerted need by all involved to better understand the processes mining has on the total environment.

www.minersoc.org
DOI:10.1180/minmag.2013.077.5.11

Non-chondritic sulfur isotope composition of the Earth's mantle: Implications on planetary differentiation

LABIDI J.¹, CARTIGNY P.¹ AND MOREIRA M.²

¹Stable isotope Laboratory, IPGP, Paris, France.

(*labidi@ipgp.fr)

²Geochemistry and Cosmochemistry Laboratory, IPGP, Paris, France

Sulfur (S) is a siderophile and moderately volatile element. Its abundance and isotope composition in accessible parts of the terrestrial mantle can therefore provide constraints on both accretion and planetary differentiation. We have investigated the ³⁴S/³²S ratio of 23 glasses dredged on the south-Atlantic ridge between 40° and 55°S. Several of the typical mantle end-members feed the source mantle of the two plumes and analyzed samples have been chosen to reflect this geochemical variability, hence offering a unique opportunity to address ³⁴S/³²S variations with respect to various mantle heterogeneities.

We show that south-Atlantic MORB display ³⁴S/³²S ratios directly correlated to ⁸⁷Sr/⁸⁶Sr and ¹⁴³Nd/¹⁴⁴Nd. These isotope trends are compatible with a binary mixing between two extreme components: The depleted mantle, having a δ³⁴S of -1.28±0.33‰, and a S-rich component with a δ³⁴S > 1.05 ± 0.10‰, that we infer to be subducted sediments (i.e. neither sub-continental lithospheric mantle nor lower continental crust) variably distributed in the sources of two local plumes. Our dataset imply that substantial amount of S survives slab devolatilization and thereby support efficient recycling of S via sediment subduction.

As the chondritic average δ³⁴S is constrained at +0.04 ± 0.31‰ [1,2], the negative value of depleted end-member consistently illustrates a non-chondritic feature. Furthermore, the amount and isotope composition of surficial S cannot balance out the depleted mantle to a chondritic value. Such distinctly non-chondritic ³⁴S/³²S ratio for the depleted mantle can only be reconciled with a core-mantle differentiation record, implying that most of the sulfur and elements of comparable volatilities have been delivered to the Earth before such planetary differentiation event.

[1] Gao *et al.*. (1993) GCA **57**, 3159-3169. [2] Gao *et al.*. (1993) GCA **57** 3171-3176.

Frequent bacteria-phage interactions in deep biosphere

JESSICA M. LABONTÉ ^{1*}, MAGGIE LAU ², ESTA VAN HEERDEN ³, THOMAS L. KIEFT ⁴, TULLIS ONSTOTT ² AND RAMUNAS STEPANAUSKAS ^{1*}

¹Bigelow Laboratory for Ocean Sciences, East Boothbay, ME

²Princeton University, Princeton, NJ

³University of the Free State, South Africa

⁴New Mexico Institute of Mining and Technology, Socorro, NM

(*correspondence: jlabonte@bigelow.org, rstepanuskas@bigelow.org)

Recent discoveries suggest that subsurface microorganisms constitute a significant fraction of the living biomass on our planet, but little is known so far about their life histories and interactions. Here, we employed single cell genomics to obtain cultivation-independent information about *in situ* bacteria-phage interactions in 0.6 to 3.8 km deep fractures in the 2.9 byr old Witwaterstrand Basin, South Africa.

Genomic sequencing of 17 single amplified genomes (SAGs) revealed viral sequences in nine SAGs, suggesting that viral infections are prevalent in these isolated communities. We recovered partial genomes of Mu-like transposable phages, retrons, and lambda-like prophages from SAGs of Firmicutes *Desulforudis* and *Thermincola*, which are known to be indigenous to deep subsurface environments. The discovered phages, while sharing some conserved genes, are highly divergent from known viruses.

Our results suggest prevalence of lysogenic host-phage systems in the studied subsurface fractures, which may be more sustainable in these extremely isolated and simple microbial communities, as compared to lytic infections. The types and genome content of the discovered phages also suggest involvement in host DNA shuffling, which may be an important mechanism for deep subsurface microbial evolution.

Core cooling and lower mantle crystallisation in the thermal evolution of the Earth

S. LABROSSE¹, J. W. HERNLUND², N. COLTICE¹

¹Lab. Géologie Lyon, ENS de Lyon, Univ. Lyon-1, CNRS, France (stephane.labrosse@ens-lyon.fr)

²Department of Earth and Planetary Science, University of California, Berkeley, California 94720, USA

Models for the thermal evolution of the Earth have traditionally assumed that the core cools at the same pace as the mantle or more slowly. The latter assumption comes from the idea that the heat flow across the core mantle boundary (CMB) is low, of order 3TW, and given by the buoyancy flux sustaining hotspot swells. The present heat imbalance of the Earth, quantified by the Urey number being lower than 0.5, and the positive feedback between mantle temperature and heat flow through temperature-dependence of the viscosity, typically lead to a thermal catastrophe less than 2 Byr ago in standard parameterised models of thermal evolution. This has pushed many authors to propose non-classical scalings of heat transfer by mantle convection.

The thermal conductivity of core material has been recently revised to values larger than 90W/m/K at the CMB and increasing with depth in the core [1]. With such values, the low CMB heat flow assumed previously would not sustain a geodynamo, even taking into account compositionnal buoyancy released upon inner core growth. A CMB heat flow larger than 10 TW is required, which can effectively solve the thermal evolution for the Earth. Indeed, when considering the CMB heat flow as a source for the mantle, its effective Urey number is in excess of 0.65, a value much easier to accommodate with standard scalings.

For the low amount of potassium usually considered as possible in the core, a large CMB heat flow implies a large cooling rate, more than 750 K in 4.5 Gyr. Dense partially molten regions at the bottom of the mantle provide the best explanations to the seismic observations of ultra low velocity zones. The large cooling of the core implies a thicker molten lowermost mantle in the past [2]. The slow fractionnal crystallisation of this basal magma ocean brings in latent heat, helping to solve the thermal evolution problem. In addition, assuming that heat producing elements partition in the melt at the pressure of the lowermost mantle, a significant fraction of the Earth budget can be stored there.

[1]Gomi, Ohta, Hirose, Labrosse, Caracas, Verstraete & Hernlund, *Phys. Earth Planet. Inter.*, Submitted. [2]Labrosse, Hernlund & Coltice, *Nature*, **450**, 866-869, 2007.

Modes of formation of the basal magma ocean

S. LABROSSE¹, J. W. HERNLUND² AND N. COLTICE¹

¹Lab. Géologie Lyon, ENS de Lyon, Univ. Lyon-1, CNRS, France (stephane.labrosse@ens-lyon.fr)

²Department of Earth and Planetary Science, University of California, Berkeley, California 94720, USA

The classical view of magma ocean crystallization is based on the assumption that the liquidus gradient is steeper than the isentropic temperature gradient, leading to crystallisation from the bottom upward. In addition, it was usually assumed that the solid thereby formed is denser than the liquid. Recent results on the phase diagram of deep mantle minerals prompt a reconsideration of these assumptions.

Some recent studies propose that crystallization of the magma ocean could start from mid-mantle and produce neutrally buoyant crystals at the same depth. This would naturally lead to a surface magma ocean and a basal magma ocean. On the other hand, some recent results [1] suggest that crystallisation should start at the bottom of the mantle and make dense solids. However, the gradual enrichment of the solid in Fe by fractional crystallization causes an unstable density increase with height and eventually overturn following a Rayleigh-Taylor instability. This would bring down highly fusible Fe-rich solid and the gravitational energy released by viscous friction would remelt it. The Fe-rich formed liquid would then be dense enough to remain at the bottom of the mantle as a basal magma ocean.

Alternatively, the formation of the core could result in a largely superheated core that would melt the mantle from below. The liquid produced could be less dense than the solid despite being enriched in iron. Its rise and subsequent freezing would be a means of rapidly transporting core superheat to the mantle as well as producing an unstably stratified solid mantle whose overturn would also create a basal magma ocean.

We explored quantitatively the outcome of these different scenarios in terms of the thickness of the basal magma ocean produced and the implied geochemical signatures, in particular regarding rare gases [2].

[1] Thomas, CW *et al.*, *J. Geophys. Res.*, **117**, B10206, 2012.

[2] Coltice, N., M. Moreira, J. Hernlund & S. Labrosse, *Earth Planet. Sci. Lett.*, **308**, 193-199, 2011.

A new database for Nd isotopes in marine environments

F. LACAN¹, K. TACHIKAWA² AND NEOSYMPA MEMBERS

¹ LEGOS (CNES/CNRS/IRD/University of Toulouse), 14 av. Edouard Belin, 31400, Toulouse, France, francois.lacan@legos.obs-mip.fr

² CEREGE, UM 34 Aix-Marseille Université-CNRS (UMR 7330), Europole de l'Arbois, BP80 13545 Aix-en-Provence, France, kazuyo@cerege.fr

Neodymium isotopic ratios in seawater have been used as a tracer of ocean circulation, continental weathering and exchange processes between dissolved and particulate phases. Over the recent years, the interest in this tracer has been growing with improvement of our knowledge on its behaviour in the modern ocean, thanks to GEOTRACES programme, and identification of archives that can preserve seawater Nd isotopic signatures. In the framework of the French INSU-LEFE project NEOSYMPA (Workshop NEODYMIUM isotopes in marine environments: SYnergy between Modern, Modelling and PAleo communities), we have updated a database for the available Nd isotopic data in the ocean, and compiled ϵ_{Nd} values for sedimentary oxyhydroxide coatings, foraminiferal tests, deep-sea corals and fish teeth/debris from the Holocene period (<10 ka). The objective of the study was to update the database of seawater-Nd isotopic ratios, to assess relationships with other more conventional water mass tracers, and to evaluate how well the marine archives could record seawater isotopic ϵ_{Nd} signatures. Based on the observed relationships between seawater Nd isotopic compositions, salinity and dissolved silica concentrations, we demonstrate that the bottom water Nd isotopic signatures in the Arctic and Nordic Seas and the Bay of Bengal are decoupled from the general trend defined between the North Atlantic and the Pacific, which suggests the importance of local dissolved-particulate interaction. Although seawater and archive samples were not systematically collected at the same sites, the general relationship observed between bottom/deepwater (> 2500 m) Nd isotopic ratios and dissolved silica concentrations allows us to evaluate the reliability of the ϵ_{Nd} values extracted from the archives. The marine archives generally show Nd isotopic ratios that agree well with estimated seawater values. We will discuss a few cases when they do not.

NEOSYMPA members: K. Tachikawa, T. Arsouze, G. Bayon, A. Bory, C. Colin, J-C. Dutay, N. Frank, J. Gherardi, A. T. Gourelan, F. Grousset, C. Hillaire-Marcel, C. Jeandel, F. Lacan, L. Meynadier, P. Montagna, E. Pucéat, M. Roy-Barman, C. Waelbroeck

Elemental patterns in agricultural and grazing land soils in Norway, Finland and Sweden – what have we learned from continental scale mapping?

A. LADENBERGER^{1*}, J. UHLBÄCK¹, M. ANDERSSON¹, C. REIMANN², T. TARVAINEN³, M. SADEGHI¹, G. MORRIS¹ AND M. EKLUND³

¹Geological Survey of Sweden, Box 670, S-751 28 Uppsala, Sweden (*correspondence: anna.ladenberger@sgu.se)

²Geological Survey of Norway, P.O. Box 6315 Sluppen, N-7491 Trondheim, Norway

³Geological Survey of Finland, P.O. Box 96, FI-02151 Espoo, Finland

The GEMAS Project (Geochemical Mapping of Agricultural and Grazing Land Soil in Europe) resulted in a large coherent data set displaying baseline levels of elements in agricultural and grazing land soil, on both a European and a regional scale. The geochemical mapping of agricultural and grazing land soil in Norway, Sweden and Finland provides an exceptional opportunity to demonstrate regional geochemical trends in arable soil. When looking at the European data set as a whole, Norway, Sweden and Finland stand out as geochemically distinct, mainly due to the old bedrock and the extent of the last glaciation, and they were thus considered valuable for a study as a separate entity.

The interpretation of the elemental maps and statistics identified several groups of factors influencing the observed trends in the geochemical patterns of Norway, Sweden and Finland, with the most important factors being bedrock geology, the presence of ore deposits, the soil type and its properties, and climate. Anthropogenic impact on soils appears to have a minor influence on the soil geochemistry of both agricultural and grazing land. In mining regions, with the natural signal from the mineralisation, it is often difficult to discriminate between the original anomaly and any anthropogenic contamination.

The results of this survey are available for a public and can be used by both local authorities and research groups.

Nucleation and growth of chrysotile nanotubes: complementary insight from macroscopic to nanoscopic measurements

R. LAFAY¹, G. MONTES-HERNANDEZ¹ AND E. JANOTS¹

¹ISTERRE, University of Grenoble I and CNRS, BP 53, 38041 Grenoble Cedex 9, France (romain.lafay@ujf-grenoble.fr)

Chrysotile is one of the most studied asbestos mineral but rare studies have focussed on the nucleation and growth processes of chrysotile because batch (or discontinuous) reactors are generally used. However, various questions still remain unanswered concerning their formation in natural systems as well as their production at laboratory and industrial scales

In the present study [1], we report new insights on the nucleation and growth processes of chrysotile nanotubes [1] by using semi-continuous experiments (i.e. sampling of reacting suspension with time). From macroscopic (N_2 sorption/desorption isotherms, X-ray diffraction, infrared spectroscopy, Thermogravimetric analyses) to microscopic (FESEM, TEM) characterization, three main reaction steps were identified for chrysotile nucleation and growth at 300°C: (1) proto-serpentine precursor formation in the first 2 hours of reaction, accompanied by brucite and residual silica gel, (2) spontaneous nucleation and growth of chrysotile between about 3 and 8h of reaction via a progressive dissolution of proto-serpentine, brucite and residual silica gel and, (3) Ostwald ripening growth of chrysotile from 8 to 30h of reaction as attested by specific surface area measurements and FESEM and TEM observations. Complementary results from batch experiments have confirmed a significant influence of temperature on kinetics of chrysotile formation. Moreover, Si/Mg ratio and molality have been experienced to better characterize the stability field of chrysotile.

[1] R. Lafay, G. Montes-Hernandez *et al.*. *Chemistry – A European Journal* (2013) DOI: 10.1002/chem.201204105

Subsurface mineral weathering in transient layers of permafrost in the Canadian High Arctic

M.J. LAFRENIÈRE¹, S. MONTROSS¹, J. HOLLOWAY¹
AND S.F. LAMOUREUX¹

¹Department of Geography, Queen's University, Kingston ON Canada, melissa.lafreniere@queensu.ca

Chemical weathering in high latitude regions has largely been dismissed as insignificant, as frozen soils limit weathering reaction rates for more than 8 months a year, and also the movement of weathered products within the soil profile. We present evidence that subsurface mineral weathering in the transient layers of permafrost soils results in the formation and subsequent ejection of authigenic clay, onto the surface.

Hundreds of active and dormant mud ejection features were witnessed and mapped during the summers of 2011 and 2012, on Melville Island, Nunavut, in the Canadian High Arctic. We measured the chemical composition of aqueous and mineral solid phases in material ejected from active features in order to determine the source of material and processes responsible for their formation.

Fluids from these mud ejections are enriched in nutrients (dissolved nitrogen and organic carbon) and trace metals. Stable isotope ratios of water extracted from the mud indicates that water is not from precipitation or surface runoff and is likely from thawed permafrost, or water stored in the transient layer over several melt seasons. Bulk mineralogy, and trace metal and major ion ratios of fluids and mineral solids indicate subsurface chemical weathering reactions are occurring at near freezing temperatures in the permafrost transient layer.

The results show that the material and solutions delivered to the ground surface are the products of extensive subsurface weathering of siliciclastic minerals to authigenic clays. These mud ejection features represent a mechanism that delivers fine grained material rich in dissolved metals and nutrients to the surface, where they are subject to mobilization and delivery to terrestrial and aquatic ecosystems.

New geochronological constraints on the Ruili Metamorphic Belt in western Yunnan, China

C.K. LAI^{1*}, KHIN ZAW¹ AND S. MEFFRE¹

¹ ARC Centre of Excellence in Ore Deposits, University of Tasmania, Hobart, Tasmania, Australia (*correspondance: chunkitl@utas.edu.au)

The Ruili Metamorphic Belt is located in westernmost Yunnan near the Chinese–Myanmar border. The belt trends NE–SW and comprises mainly augen gneiss, two-mica schist, and plagioclase amphibolite, with various generations of (meta)-granitoids. The Ruili Metamorphic Belt is located close to the Sibumasu–West Burma suture and may extend into the Mogok Metamorphic Belt in NE Myanmar, which hosts rich orogenic sediment-hosted gold and gemstone (e.g., ruby, sapphire) natural resources [1,2]. However, no regional geological correlation between these two belts has been attempted. The new U–Pb zircon age data reported here suggest a complex tectonic history for the belt, with at least four major magmatic/metamorphic phases, as follows:

1. Early Cretaceous (ca. 125–116 Ma);
2. Late Cretaceous (ca. 70–68 Ma);
3. Late Palaeocene (ca. 58 Ma);
4. Eocene (ca. 35–49 Ma).

When compared to the Mogok Metamorphic Belt in Myanmar [1–4], the Jurassic (ca. 170 Ma) and Late Oligocene–Miocene (ca. 20–25 Ma) magmatic/ metamorphic events there have not yet been found in the Ruili Metamorphic Belt, whereas Late Cretaceous metamorphism has not yet been documented in the Mogok Metamorphic Belt. Much more data will be required to clarify their heating and exhumation history and regional tectonic relations between these two belts.

[1] Barley *et al.*. (2000) *GSA abs* **59**, 18. [2] Barley *et al.*. (2003) *Tectonics* **22**, 1019. [3] Searle *et al.*. (2007) *Tectonics* **26**, TC3014. [4] Mitchell *et al.*. (2012) *JAES* **56**, 1–23.

High-Precision Mg-isotope Measurements of Peridotites and Bulk Chondrites

Y.J. LAI^{1,2*}, P.A.E. POGGE VON STRANDMANN³, T. ELLIOTT², S.S. RUSSELL⁴ AND R.A. BROOKER²

¹Isotope Geochemistry and Cosmochemistry, Inst. of Geochemistry and Petrology, ETH Zurich, Clausiusstrasse 25, 8092 Zurich, Switzerland

²Bristol Isotope Group, Dept. of Earth Sciences, Univ. of Bristol, Queens Road, Bristol, BS8 1RJ, UK

³Dept. of Earth Sciences, Univ. of Oxford, South Parks Road, Oxford, OX1 3AN, UK

⁴Dept. of Earth Sciences, Natural History Museum, Cromwell Road, London, SW7 5BD, UK

(*correspondence: yi-chen.lai@erdw.ethz.ch)

As one of the most abundant constituent elements, magnesium may have the potential of providing information on the initial composition of primordial building blocks of planetary bodies, especially the processes that fractionate isotope compositions during planetary accretion and differentiation can be studied by comparing the Mg isotope composition of the Earth and meteorites. The dominant reservoir of Mg for the bulk silicate Earth is the mantle (> 99%). This makes it possible to attain a representative samples of the bulk Earth by selecting samples that best representing the Earth's mantle. Here, we present high precision Mg isotope data (<0.03 ‰ on $\delta^{26}\text{Mg}$ based on long-term analyses of geological reference peridotite, JP-1, n=17) of tectonically emplaced peridotite massifs to avoid diffusive perturbation observed on small mantle xenoliths, which we compare with bulk chondrites, chondrules and CAIs from CV chondrites. More than 10 repeat measurements of the Mg isotope ratios on small amount of samples were obtained to reduce standard error of the determinations and gain a statistically meaningful comparison between bulk chondrites, peridotites, chondrules and CAIs. The Mg isotope data of peridotites fall within a narrow range of $\delta^{26}\text{Mg}$ values and give mean values of $-0.23 \pm 0.04\text{‰}$. However, there is a relatively large range of $\delta^{26}\text{Mg}$ values in analysed chondrules and CAIs. The Mg isotope data of carbonaceous chondrites are slightly lighter than the terrestrial peridotites. The inconsistent Mg stable isotopic composition between the Earth and carbonaceous chondrites, and hence the possibility that the Earth consists of non-carbonaceous-chondritic Mg, has important implications for Earth's bulk composition and primordial building material of the Earth.

Role of polysaccharides in calcite (re)crystallisation

L.Z. LAKSHANOV^{1,2} AND S.L.S. STIPP¹

¹Nano-Science, Department of Chemistry, University of Copenhagen, Copenhagen Ø, Denmark (ll@nano.ku.dk)
²Institute of Experimental Mineralogy RAS, Chernogolovka, Russia

Polysaccharides are often suspected for inhibiting calcite recrystallisation. Well known is the dual role of polymers in crystallisation control. They act as inhibitors when free in the solution, but when immobilized at surfaces, they can promote mineralization. This duality is shown in [1] where calcite growth, initially inhibited by alginate, resumed after alginate immobilization at the surface. Independent of supersaturation, induction time for resuming calcite growth drastically increases (Fig.1) when adsorbed concentration approaches

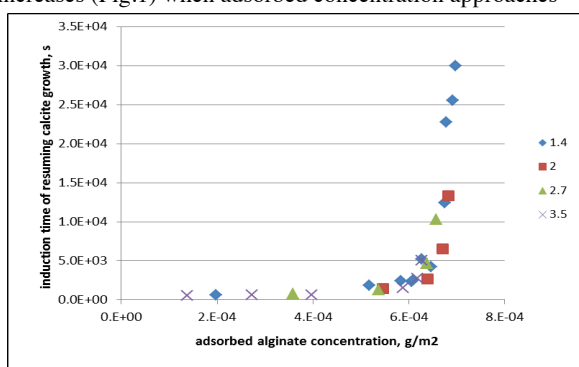


Figure 1. Induction time for calcite growth to resume after inhibition as a function of adsorbed alginate concentration for a series of solution supersaturations.

its maximum $7.5E-4 \text{ g/m}^2$. At maximal adsorption, alginate can no longer serve as a good template for calcite overgrowth. Alginate molecules spread and arrange in flat positions at the surface, where all their carboxylic groups are occupied in binding on Ca^{2+} that is part of the mineral structure, thus retarding ion transport to the surface. Under these conditions, diffusion becomes rate determining for calcite growth. Because of extremely low supersaturation, this is not the case when alginate inhibits calcite recrystallisation and the overall process proceeds in the surface kinetics range. This is the reason why the relative inhibition of calcite recrystallisation is much lower than that of calcite precipitation.

[1] Lakshatanov *et al.* (2011) *Geochim. Cosmochim. Acta*, **75**, 3945-3955.

Direct Measurements of Isotopic Fractionation Factors of Water Vapor over Ice for Temperatures below 235 K

KARA LAMB^{1*}, BEN CLOUSER¹, LASZLO SARKOZY¹,
 ERIC STUTZ¹, BENJAMIN KÜHNREICH²,
 JANEK LANDSBERG³, JAN HABIG⁴, NARUKI HIRANUMA⁴,
 STEVEN WAGNER², VOLKER EBERT⁵, ERIK KERSTEL³,
 OTTMAR MÖHLER⁴, HARALD SAATHOFF⁴
 AND ELISABETH MOYER¹

¹Department of the Geophysical Sciences, University of Chicago, Chicago, IL, USA (*correspondence: karalamb@uchicago.edu)

²Center of Smart Interfaces, Technische Universität Darmstadt, Darmstadt, Germany

³J. Fourier Laboratoire Interdisciplinaire de Physique, University of Grenoble, Grenoble, France

⁴Institute for Meteorology and Climate Research, KIT, Karlsruhe, Germany

⁵Physikalisch-Technische Bundesanstalt, Braunschweig, Germany

The use of the isotopic composition of water vapor as a tracer for convective and microphysical processes is complicated by the fact that isotopic fractionation factors have not previously been directly measured at the temperatures characteristic of much of the upper troposphere ($< 235 \text{ K}$). Instead, fractionation factor values used in models are extrapolated from measurements made at higher temperatures [1, 2]. We report on the first direct determination of the equilibrium fractionation of $\text{HDO}/\text{H}_2\text{O}$ between water vapor and ice at temperatures below 233 K, obtained during the ISOCLOUD measurement campaign at the AIDA cloud and aerosol chamber. The ISOCLOUD campaign involved a series of adiabatic expansion experiments over a range of temperatures between 190 and 233 K, during which measurements were made of water vapor and total water (vapor + ice) and their isotopic compositions. Modeling of vapor sources, sinks and ice cloud formation during the expansion experiments then allowed determination of the degree of preferential condensation of the heavier isotopologues.

[1] Merlivat, L. & G. Nief (1967) *Tellus* **19**, 122-127. [2] Ellehøj, M. (2010) Ph.D. thesis, *University of Copenhagen*

Neodymium isotopic composition and concentration in equatorial to North Atlantic seawater

M. LAMBELET¹, T. VAN DE FLIERDT¹, K. CROCKET¹,
M. REHKÄMPER¹, K. KREISSIG¹, B. COLES¹,
M.J.A. RIJKENBERG², L. GERRINGA², H.M. VAN AKEN²
AND H.J.W. DE BAAR²

¹Department of Earth Science and Engineering, Imperial College London, UK

²Royal Netherlands Institute for Sea Research (Royal NIOZ), Den Burg, Netherlands

Email: m.lambelet-salazar-serrudo09imperial.ac.uk

The Nd isotopic composition of seawater is widely used as a tracer for ocean circulation, as each individual water mass is tagged with a characteristic Nd isotope fingerprint. The reconstruction of past water mass configurations and ocean circulation are useful to understand the role of the ocean in past climate change and hence comprehend the future evolution of climate. Even though the Nd isotopic composition is often assumed to be an ideal ocean circulation tracer, our understanding of the modern cycle of Nd in the ocean is still poor. Indeed, while the continents are assumed to be the major source of Nd in the ocean, it is not yet clear how exactly water masses acquire their Nd isotopic composition.

The goal of the present study is to investigate whether Nd isotopes in seawater behave conservatively along the flow path of North Atlantic Deep Water. The samples measured to address this question were collected in 2010 on the Pelagia during the first two legs of the Dutch GEOTRACES Atlantic Ocean transect (Iceland to Brazil). Twelve seawater profiles were analysed for their Nd isotopic compositions and concentrations. Each profile comprises 10 to 12 depths, providing a better depth resolution than previous studies and covering some areas that have never been investigated for Nd isotopes or concentrations.

The new results will be discussed in the context of previously published Nd data, constraints from physical oceanography, and other proxy data collected on the same samples.

High-precision atmospheric helium isotope measurement in volcanic areas

T.F. LAN^{1*}, J.C. MABRY¹, B. MARTY¹,
P. BURNARD¹, E. FÜRI¹, J.M. DE MOOR²,
T.P. FISCHER² AND G.M. MCMURTRY³

¹CRPG-CNRS, Nancy, France

²Dept. Earth and Planetary Sciences, University of New Mexico, Albuquerque, USA

³Dept. Oceanography, University of Hawaii, Honolulu, USA
(*correspondence: tflan@crpg.cnrs-nancy.fr)

Current helium isotope analysis is sufficient to distinguish numerous geological end members, but determining the subtle isotopic variation in the air still poses a challenge to modern analytical techniques. The newly designed helium isotope measuring system, CRPG air-line, has reached the required precision to distinguish subtle differences in atmospheric helium isotopic ratios [1]. This technique marks a milestone for opening up new research directions for helium isotope study. Giving such high measuring precision, investigating geographical and temporal helium isotopic variation is within reach.

With this measuring system, we have identified that the average atmospheric helium isotopic ratios of the Big Island (Hawaii) and Afar region (Ethiopia) are 2.1-2.7 per mil higher than that in Nancy, France. Further investigation is needed to explain the cause of the difference, but comparing atmospheric helium isotopes from different tectonic settings is intriguing and may shed light on atmospheric helium dispersion patterns. Etna is an ideal place to study atmospheric helium isotopes since it has been constantly active and it offers various degassing mechanisms, such as: plumes, fumaroles, faults, and soil degassing. In June 2012, we took air samples from various sites, including the summit craters, fumaroles, Pernicana fault area, Paternò and Vallone Salato. We also took plume samples by flying through the trail on a gyroplane.

The ³He/⁴He ratio of the plume is 2.156±0.006 R_A (ratio normalized to atmospheric ratio of Nancy), while the ratio of the crater air is similar to that of Nancy. This indicates that the plume is the major helium degassing outlet of Etna, and helium seems to concentrate in the plume column rather than dispersing at the crater area. We will present the results of atmospheric helium isotope measurement of samples from Hawaii, Ethiopia and Etna; and hopefully will propose a model to elucidate the helium flux from Etna plume.

[1] Mabry, J., Marty, B., & Burnard, P. (2013), *Mineralogical Magazine*, 77(2).

Hydrothermal origin of the Paleoproterozoic xenotimes from the King Leopold Sandstone of the Kimberley Group, Kimberley, NW Australia: Implications for a ca 1.7 Ga far-field hydrothermal event

Z.W. LAN^{1*}, Z.Q. CHEN², X.H. LI¹, B. LI³
AND D. ADAMS⁴

State Key Laboratory of Lithospheric Evolution, Institute of Geology and Geophysics, Chinese Academy of Sciences, Beijing 100029, China (*correspondence: lzw1981@126.com)

²State Key Laboratory of Biogeology and Environmental Geology, China University of Geosciences (Wuhan), Wuhan 430074, China

³Centre for Exploration Targeting, ARC Centre of Excellence for Core to Crust Fluid Systems, The University of Western Australia, WA6009, Australia

⁴Centre for Microscopy, Characterisation and Analysis, The University of Western Australia, WA6009, Australia

New xenotime overgrowth ages are obtained from the Paleoproterozoic King Leopold Sandstone of the Kimberley Group, NW Australia. The concordant age of 1679 ± 13 Ma can be equated with the ca 1.7 Ga xenotime overgrowth ages within errors obtained from the Warton and Pentecost Sandstones of the same group and the ca 1.7 Ga zircon U-Pb ages from the Dingo Granite in northern Australia, and together they are consistent with the age of Capricorn orogeny. These ages are much younger than the robust SHRIMP ages (1790 ± 4 Ma) obtained from zircons from the Hart Dolerite intrusions, and thus indicate that the xenotime overgrowths recorded in the Kimberley Group are unlikely to be diagenetic in origin, but may have been resulted from a post-depositional hydrothermal event. The ca 1.7 Ga age could point to a common hydrothermal event possibly associated with the low temperature far-field Dingo Granite intrusion during Capricorn orogeny in the Paleoproterozoic Australia. The hydrothermal origin of the xenotime overgrowths is also supported by its mineral chemistry characterized by LREE depletion, MREE-HREE enrichment, higher Zr content, and lower U, Fe, and Lu contents. The differing U and Th concentrations suggest a differing chemical pore fluid would have been responsible for the formation of xenotime overgrowths from the King Leopold, Warton, and Pentecost Sandstones as the zone of xenotime precipitation was reached by siliciclastic sediments.

Regional geochemical mapping at high density sampling: Various criteria in representation of Romagna Apennines, Northern Italy

V. LANCIANESE^{1*} AND E. DINELLI¹

¹I.G.R.G., Università di Bologna, via S.Alberto 163, 48100 Ravenna (*correspondence: valerio.lancianese2@unibo.it)

Geochemical mapping is a fundamental tool in environmental monitoring and land management. For this reason, regional-, national- and global-scale geochemical mapping projects have been carried out in some countries since the late 1960s. The surveys had sample densities ranging from 1 site per 1 Km² to 1 site per 18000 Km² and each research group used different representation techniques.

In the Romagna Apennines (Northern Italy) has been conducted an high density stream sediment geochemical survey (1 sample per 5 km²): 770 samples were collected in a regional-scale area (4125 km²) and analysed for 30 elements by X-ray fluorescence spectrometry on the fraction < 180µm. In the area industrial settlements and largest towns are in the plains, agricultural areas in the hills and a wooded mountainous area is common in the upper reaches of the major streams. The area has a complex geology characterized by different geological units: Messinian gypsum, Plio-Pleistocene marls, chaotic clays with extensive outcrops of quartz-rich sandstones, carbonatic sandstones and limestones, and the extensive Serravallian-Tortonian Marnoso-arenacea Formation. In data interpretation different techniques were applied: EDA [1], IDW interpolation and Sample Catchment Basin (SCB) mapping approach [2,3]. EDA highlights very well the control of geological units and different background values using major elements. IDW interpolation point out the nature of some anomalies (Zn, Sr, V, Cr) showing the spatial distribution of geochemical data. Otherwise SCB mapping technique is useful in geochemical maps of Cu, Pb, Ba, S because identifies the effects of human activities localized along the valleys.

This study shows how in an area characterized by multiple factors, chemical elements can not be represent properly with a standardized mapping technique. Indeed, the use of different mapping techniques point out peculiarities useful for interpretation of the effect of geology or of the human impact.

[1] Bounessah & Atkin (2003) *Applied Geochemistry* **18**, 1185-1195. [2] Spadoni (2006) *Journal of Geochemical Exploration* **90**, 183-196. [3] Carranza (2010) *Geochemistry: Exploration, Environment, Analysis* **10**, 171-187.

A precise climatic sequencing of the penultimate glacial termination

A. LANDAIS^{1,*}, G. DREYFUS¹, E. CAPRON¹, J. JOUZEL¹,
V. MASSON-DELMOTTE¹, D.M. ROCHE¹, F. PRIE¹,
N. CAILLON¹, J. CHAPPELLAZ², M. LEUENBERGER³,
A. LOURANTOU², F. PARRENIN², D. RAYNAUD²
AND G. TESTE²

¹LSCE, CEA-CNRS-UVSQ, 91191 Gif sur Yvette, France
(*correspondence: amaelle.landais@lsce.ipsl.fr)

²LGGE, CNRS-UJF, St Martin d'Herès, France

³Oeschger Center, Bern, Switzerland

Based on marine and terrestrial archives, a general mechanism has been proposed for the sequence of events over terminations involving interactions between millennial and orbital scale variability and atmospheric teleconnections. In this classical view, the occurrence of an Heinrich event in the first part of the deglaciation leads to a synchronism between Northern Hemisphere cooling (Heinrich Stadial), Asian monsoon dynamics (weak monsoon interval), CO₂ rise and Antarctic warming, the end of the HS being associated with an abrupt recovery of monsoon activity and Antarctic temperature maximum. Here, we provide new high resolution gas records ($\delta^{15}\text{N}$, $\delta^{18}\text{O}_{\text{atm}}$, CO₂) over the strong Termination 2 on the EPICA Dome C ice core and show a highly detailed sequence of events over this deglaciation with no relative chronological uncertainties between the records. We show a clear decoupling between Antarctic temperature and CO₂ increases 2000 years before the end of this deglaciation. This decoupling is synchronous with a clear change in the low latitude hydrological cycle (resumption of monsoon activity), in $\delta^{13}\text{C}$ of CO₂ and probably a partial recovery of the Atlantic Meridional Overturning Circulation.

Sulfur cycling in a karstic catchment: constraints from isotopes of dissolved sulfates

Y.-C. LANG^{*}, H. DING, C.-Q. LIU AND Z.-Q. ZHAO

State Key Laboratory of Environmental Geochemistry,
Institute of Geochemistry, Chinese Academy of Sciences,
Guiyang 550002, China (*correspondence:
langyc822@163.com)

Sulfur cycling in karstic catchments in southwest China is active and has been demonstrated to be coupled with carbon cycling. Therefore, many studies have been carried out to characterize the geochemical characteristics of sulfur cycling in a karstic catchment and to understand its effects on carbon cycling. In order to understand geochemical characteristics of dissolved sulfates in diverse aquatic system of a small karstic catchment, we carried out a research on variations in sulfur isotope composition of dissolved sulfate in precipitation, streams, springs, a well, and subsurface flow in the Mulian catchment of Northern Guangxi, China. This study area with a karstic landform of typical peak clusters depression is located in 24°44' N and 108°19' E, and covers about 1.14 km². Sixty water samples were collected for sulfur isotope analysis in the catchment in summer 2007, including rainwater, well water, spring water. Other samples were collected from and the stream waters..

The average $\delta^{34}\text{S}$ value of SO₄ is -8.4‰ (n=7) in rainwater during sampling period. The one spring flowing through the clastic rocks has the highest average $\delta^{34}\text{S}_{\text{SO}_4}$ value (-5.3‰, n=9), while the other spring flowing through the carbonate rocks has the lowest average $\delta^{34}\text{S}_{\text{SO}_4}$ value (-9.1‰, n=2). There exists a positive correlation between $\delta^{34}\text{S}$ value and 1/SO₄ for sampled seven rainwaters. The data distribution of all samples can be explained in terms of three-end member mixing. The three main sources include precipitation, the sulfate in soil, and oxidation of sulfide minerals in coal seams, which indicate that the sulfur cycling might have been coupled with carbonate weathering.

Acknowledgements

This work is financially supported by National Natural Science Foundation (Grant Nos. 41073099, 41203090) and by Innovation Key Program of Chinese Academy of Sciences (Grant Nos. KZCX2-EW-102, KZCX2-YW-137).

Modeling of copper and cobalt fractionation in soils: A useful tool to predict edaphic factors influence upon Cu and Co accumulation in two metallophytes

BASTIEN LANGE^{1,2,*}, MICHEL-PIERRE FAUCON¹,
GREGORY MAHY³, PETRU JITARU¹
AND OLIVIER POURRET¹

¹HydrISE, LaSalle Beauvais, Beauvais, France

(*correspondence : bastien.lange2@lasalle-beauvais.fr)

²Laboratoire d'Ecologie végétale et Biogéochimie, Université Libre de Bruxelles, Bruxelles, Belgium

³Université de Liège, Gembloux Agro-Bio Tech, Unité Biodiversité et Paysages, Gembloux, Belgium

In Katanga (Dem. Rep of Congo), an original and unique metallophyte flora takes place on extremely copper and cobalt rich soils, deriving from Cu and Co outcrops. Among the present species, some are able to accumulate extremely high concentrations of Cu and Co in shoot, which are considered as Cu and Co hyperaccumulators. Still non-explained high variations of Cu and Co concentrations in shoot have been highlighted within this copper and cobalt flora. A good comprehension of the Cu and Co accumulation would go through a characterization of the Cu and Co speciation and bioavailability in soil. The objectives of the present study are to (i) examine variations of Cu and Co speciation in soils and Cu and Co concentrations in plants, (ii) determine which edaphic factors influence the Cu and Co accumulation in plants, and (iii) highlight the Cu and Co bioavailable fraction.

Two species have been selected as biological model: *Anisopappus chinensis* and *Crepidiorhopalon tenuis*. Plant samples and soil samples (n=146) have been collected in seven pedogeochemically contrasted sites. Concentrations of Cu and Co in plants have been measured using ICP-MS and speciation modeling (WHAM 6.0) was performed to estimate Cu and Co speciation in soils. Huge variations in the Cu and Co fractionation in soils, as well as huge variations in the Cu and Co concentration in plants have been highlighted among and within the different sites and populations. Copper is mostly bind to organic matter (OM) and Fe oxides. Oppositely, Co occurs as ionic species and has strong affinity for Mn oxides. Copper accumulation variations are mostly explained by Cu adsorbed onto Mn oxides whereas Co accumulation variations are mostly explained by Co ionic species and Co adsorbed by OM. Bioavailable Cu and Co concentrations seem to correspond not only to the Cu and Co ionic species content but also part of linked Mn oxides and OM, for Cu and Co, respectively. Eventually, this latter fraction can be mobilized and / or absorbed by plants.

Why do some andesite stratovolcanoes evolve to erupt rhyolite and/or rhyodacite and others do not?

R.A. LANGE¹, H.M. FREY² AND C.M. HALL¹

¹Department of Earth and Environmental Sciences, University of Michigan, Ann Arbor, MI, 48107, USA

(*correspondence: becky@umich.edu)

²Department of Geology, Union College, Schenectady, NY, 12308, USA

If rhyolite/rhyodacite liquid commonly forms as an interstitial melt in crystal-rich andesite/dacite magmas in sub-volcanic chambers in the upper crust, an outstanding question is why segregation and eruption of the interstitial liquid occurs in some cases but not others. An example of this variation is seen among five andesite volcanoes along the western Mexican volcanic arc, spanning >150 km of arc length; three have explosively erupted rhyodacite and/or rhyolite (Volcáns Ceboruco, Tepetitlic and San Juan) and two have not (Volcáns Sanganguey and Tequila). Hypotheses for why some andesite volcanoes erupt rhyolite/rhyodacite and others do not include: (1) the effect of mafic magma recharge, which drives the differentiating magma back to more evolved compositions and prevents the formation and extraction of interstitial rhyolitic melt; (2) segregation of interstitial melt from a crystallizing magma requires compaction and thus crystal-rich (50-70%) conditions (e.g., Dufek and Bachmann, 2010) and/or gas filter-pressing (e.g., Sisson and Grove, 1999), and the time interval in which the magma spends under these optimal conditions for melt segregation may be variable, thus limiting the ubiquity of this process; and (3) extraction of interstitial melt may be most efficient during partial melting (vs. crystallization) because of the increase in volume associated with the crystal-liquid phase change, which causes the interstitial melt to be over-pressurized (vs. under-pressurized); however, this requires an influx of hot new magma into a sub-solidus system to transfer the heat and volatiles necessary to drive partial melting of adjacent wallrock. In this study, we use a combined geochemical and ⁴⁰Ar/³⁹Ar geochronology study to test which of the three models best explains the eruptive history of Volcán Tepetitlic, an andesitic stratovolcano (~42 km³) that explosively erupted zoned crystal-poor rhyodacite-rhyolite (4-8 km³) after a 180 k.y. hiatus in volcanic activity from the central vent. The explosive eruption was synchronous with an episode of basaltic andesite volcanism (~9 km³) from three vents along the flanks Volcan Tepetitlic. Thus all three mechanisms can be tested against each other.

New insights into the evolution of the Finero Mafic Complex

A. LANGONE^{1*}, M.R. RENNA², M. TIEPOLO¹,
A. ZANETTI¹, M. MAZZUCHELLI³ AND T. GIOVANNARDI³

¹ CNR-IGG-Pavia, Pavia, Italy, langone.crystal.unipv.it

² Dip. di Fisica e Sc. della Terra, Univ. di Messina, Italy

³ Dip. Sc. Chimiche e Geologiche,
Univ. di Modena e Reggio Emilia

The Finero Complex outcrops as an antiform in the northern sector of the Ivrea-Verbanò Zone (Southern Alps). The antiform core is constituted by a mantle unit surrounded by a cumulitic sequence, i.e. the Finero Mafic Complex (FMC) [1,2]. The complex is divided in three units: a) the Layered Internal Zone (LIZ), in tectonic contact with the mantle unit; b) the Amphibole Peridotite (Amph-Pd); c) the External Gabbro. Owing to the lack of a detailed petrochemical characterisation of the FMC, we performed new major and trace element (LA-ICPMS) analyses on representative samples from the LIZ and Amph-Pd. The LIZ mainly consists of Grt-hornblendites and Hbl-gabbros, with minor anorthosites and pyroxenites. The Amph-Pd is mostly made up of Amph-bearing harburgites and dunites (Ol: Fo₈₇₋₈₂), with recrystallisation fronts along which the peridotites become modally-dominated by Amph. The Al₂O₃ content is up to 11 and 18 wt% in Cpx and Amph, respectively: it increases from the peridotites (Amph-Pd) through gabbros to the hornblendites and pyroxenites (LIZ). In the garnet-free pyroxenites and hornblendites from LIZ, Amph and Cpx have slightly LREE-depleted patterns with flat HREE (at 2 CI in Cpx) and marked positive Eu, Sr, Pb and U anomalies. Similar features are shown by the Cpx and Amph from the associated gabbros, they differ in having HREE-depleted patterns, thereby indicating chemical equilibration with garnet. Cpx and Amph from the Amph-Pd have variable LREE-enriched spoon-shaped patterns, with nearly flat HREE-pattern and positive Eu, Sr and U anomalies. The LREE gradient can be explained by interaction with percolating LREE-enriched melts, dominated by ion exchange processes. Amph-enriched peridotites, which contain the highest LREE contents are a proxy for the composition of the percolating melts. The new data suggest that the LIZ and Amph-Pd units may have crystallised from melts of cognate origin with a clear crustal component. However, the recrystallisation of the Amph-Pd cannot be explained by a closed-system evolution, pointing to significant changes in the composition of the uprising mantle melts.

[1] Rivalenti *et al.* (1984) *Tsch.Min.Petr.Mitt.* **33**, 77-99,

[2] Siena & Coltorti (1989) *N.Jb.Mineral.* **6**, 255-274

Syn to post-eruptive crystallization of phenocrysts in pahoehoe “cicirara” lavas from Mount Etna volcano (Italy)

G. LANZAFAME^{1*}, S. MOLLO², G. IEZZI³, C. FERLITO¹
AND G. VENTURA²

¹ Università di Catania, Dipartimento di Scienze Biologiche,
Geologiche e Ambientali, Corso Italia 57, I-95129

Catania, Italy. (*correspondence:
gabriele.lanzafame@gmail.com, cferlito@unict.it)

² Istituto Nazionale di Geofisica e Vulcanologia, Via di Vigna
Murata 605, I-00143 Roma, Italy (mollo@ingv.it,
guido.ventura@ingv.it)

³ Dipartimento INGEO – Ingegneria e Geologia, Università G.
d’Annunzio, Via Dei Vestini 30, I-66013 Chieti, Italy
(g.iezzi@unich.it)

At Mount Etna volcano (Italy) lavas with large plagioclase phenocrysts (PI > 40 vol.%) have been erupted during historical and pre-historical periods. If phenocrysts had crystallized inside a magma chamber or within the feeding system, viscosity would not have allowed the magma to reach the surface or at most would have produced volcanic domes. Instead, these plagioclase rich lavas, named locally as “cicirara”, present wonderful pahoehoe morphologies with ribbons ropy structures and pressure ridges, which are definitively incongruous with an intratelluric growth of the phenocrysts. We have studied the mineral compositional variations and textural features, i.e., size frequency and crystal size of the one of the most basic cicirara lava. Our findings underline that only a small amount (10–15 vol.%) of crystals equilibrated at 12 km of depth, whereas most of the phenocrysts have grown at the surface and that emplacement of low-viscosity pahoehoe lavas is therefore driven by the low degree of undercooling associated with a rapid rise to the surface of poorly degassed magmas. In these conditions the growth of the phenocrysts occur mainly after the eruption when the lava is emplaced, thus reconciling the apparent paradox of pahoehoe morphology and high PI.

Four Cycles of Oxygenation in the Phanerozoic

R.R. LARGE¹, J.A. HALPIN¹, L.V. DANYUSHEVSKY¹, V.V. MASLENNIKOV², S. BULL¹, D. GREGORY¹, T.W. LYONS³ AND E. LOUNEJEVA¹

¹University of Tasmania, Hobart, Tasmania, Australia
(*correspondence: ross.large@utas.edu.au)

²Institute of Mineralogy, Miass, Russia
(maslennikov@mineralogy.ru)

³University of California, Riverside, California, USA
(timothy.lyons@ucr.edu)

Sedimentary pyrite captures trace elements (TE) from the oceans and tracks variations in their seawater concentrations through time [1]. LA-ICPMS analysis of sedimentary pyrites, based on newly developed standards, has enabled the development of temporal ocean concentration curves for 22 TE [2].

Our results show that TE variations over the last 700 million years of ocean history have been strongly cyclical. We interpret these cycles to indicate that the Late Neoproterozoic to Phanerozoic oceans went through dramatic changes in mean oxygen content. Four major cycles are recognised: Late Cryogenian to Late Ordovician, Early Silurian to late Devonian, Early Carboniferous to Late Permian and Triassic to Quaternary. Oxygen maxima, indicated by Se, U and Mo proxies, occur at 540, 390, 310 and 0 Ma, supporting previous models [3, 4]. Oxygen minima, indicated by trace element drawdown, occur at 700, 455, 365 and 200 Ma. Extended periods of low oxygen in the oceans have led to extreme deficiency of some elements that are critical for life. The periods of extreme Se depletion coincide with the mass extinction events at end Ordovician, Late Devonian and the Triassic-Jurassic boundary, suggesting that Se-deficiency in the oceans may be a contributing cause of marine mass extinctions.

[1] Halpin *et al.* (2013) *Min. Mag.*, this volume. [2] Danyushevsky *et al.* (2013) *Min. Mag.*, this volume. [3] Berner (2006) *Am. J. Sci.* **309**, 603-606. [4] Dahl *et al.*, (2010) *PNAS* **107**, 17911-17915.

High precision isotope measurements unveil poor control of copper metabolism in Parkinson's disease

F. LARNER^{1,2*}, B. SAMPSON³, M. REHKÄMPER^{1,4}, D.J. WEISS^{1,4}, J.R. DAINY⁵, S. O'RIORDAN⁶, T.PANETTA³ AND P.G. BAIN⁷

¹Department of Earth Science & Engineering, Imperial College London, SW7 2AZ, UK

²Department of Earth Sciences, University of Oxford, OX1 3AN, UK (*correspondence: fiona.larner@earth.ox.ac.uk)

³Department of Clinical Biochemistry, Imperial College Hospitals NHS Trust, London W6 8RF, UK

⁴Department of Mineralogy, Natural History Museum, London SW7 5BD, UK

⁵Institute of Food Research, Norwich NR4 7UA, UK

⁶Department of Neurology, Imperial College Hospitals NHS Trust, London W6 8RF, UK

⁷Department of Neurosciences, Imperial College London, W6 8RF, UK

Parkinsonism is a neurodegenerative disorder, and propagates from the loss of dopaminergic cells due to oxidative stress. Disordered copper metabolism may be important in the causation of Parkinsonism, as the main Cu carrying enzyme, caeruloplasmin, is key in handling oxidative stress and is involved in the synthesis pathway of dopamine [1, 2].

The human Cu metabolism of ten Parkinsonism patients was compared to ten healthy controls with the aid of a stable ⁶⁵Cu isotope tracer. The analyses of blood serum ⁶⁵Cu/⁶³Cu ratios yielded individual isotopic profiles spanning four days. The use of multiple-collector inductively coupled plasma mass spectrometry and the associated sample preparation techniques [3] is necessary to detect the small differences in Cu metabolism between subjects with Parkinsonism and controls.

The isotopic profiles indicate that the Cu metabolism is less controlled in patients with Parkinsonism. In addition, modelling suggests that (i) 30% of the subjects affected by Parkinsonism have abnormally large Cu stores in tissues and (ii) the absorption of Cu in the gut may control subsequent Cu metabolism. This pilot investigation supports full-scale medical studies into the Cu metabolism of those with Parkinsonism [4].

[1] Vassiliev *et al.* (2005) *Brain Res. Rev.* **49**, 633-640. [2] Jenner (2003) *Ann. Neurol.* **53**, S26-36. [3] Larner *et al.* (2011) *J. Anal. Atom. Spectrom.* **26**, 1627-1632. [4] Larner *et al.* (2013) *Metallomics* **5**, 125-132.

Geochemical evolution and bioenergetic potential of shallow-sea hydrothermal fluids from Panarea Island (Italy)

DOUGLAS E. LAROWE¹, ROY E. PRICE^{1*}
AND JAN P. AMEND^{1,2}

¹Dept. of Earth Sciences, University of Southern California,
Los Angeles, CA, USA

²Dept. of Biological Sciences, University of Southern
California, Los Angeles, CA, USA

*Corresponding author: royprice@usc.edu

The shallow-sea hydrothermal fluids off Panarea Island, Italy are hot (up to 135 °C), acidic (pH 1.9-5.7), and sulfidic (up to 1 mM). Vent and pore fluids at three sites were sampled and analyzed for major and minor elements, redox-sensitive compounds, and strontium isotopes. These data were used to describe the geochemical evolution of the fluids and to evaluate the catabolic potential of 61 inorganic redox reactions for *in situ* microbial communities. Based on the geochemical data, the fluids divide into three distinct types, all depleted in Mg²⁺ and SO₄²⁻. Types 1 and 2 are much more saline than seawater, but to different degrees, whereas Type 3 fluids are seawater-like with respect to most major ions. Type 1 fluids are interpreted to be derived from a very high salinity hydrothermal reservoir fluid, while Type 2 results from the discharge of a lower salinity reservoir fluid which has perhaps undergone phase separation. Type 3 fluids may result from hydrothermal alteration of seawater in the shallow subsurface by discharging gases. Gibbs energies (ΔG_r) of redox reactions that couple potential terminal electron acceptors (O₂, NO₃⁻, Mn^{IV}, Fe^{III}, SO₄²⁻, S⁰, CO₂) with potential electron donors (H₂, NH₄⁺, Fe²⁺, Mn²⁺, H₂S, CH₄) were evaluated at *in situ* temperatures and compositions. Per mole of electron transferred, the range of ΔG_r spans from near 0 to -120 kJ (mol e⁻)⁻¹. When these Gibbs energies of reaction are normalized per kilogram of hydrothermal fluid, sulfur oxidation reactions are the most exergonic, while the oxidation of Fe²⁺, NH₄⁺, and Mn²⁺ are moderately energy yielding. The results of these calculations are consistent with available molecular microbiology (16S rRNA) data, which suggest that aerobic oxidation of H₂S may be the most common metabolism in the hydrothermal springs near Panarea.

New Sr-Nd-Pb isotopic data on Graciosa island lavas (Azores)

P. LARREA^{1,2*}, E. WIDOM², C. GALÉ¹, T. UBIDE¹,
M. LAGO² AND Z. FRANÇA³

¹Department of Earth Sciences, Universidad de Zaragoza,
Spain (*correspondence: plarrea@unizar.es)

²Department of Geology & Environmental Earth Science,
Miami University, Oxford, OH, USA

³Observatório Vulcanológico e Geotérmico dos Açores, São
Miguel, Portugal

The Graciosa island belongs to the Central Group of the Azores archipelago, to the east of the Mid-Atlantic Ridge. Three main volcanic complexes are recognized, in order of decreasing age: the Serra das Fontes Volcanic Complex (620±120 Ky [1]) composed of basaltic effusive products, the Serra Branca Volcanic Complex (350±40 Ky [1]) which presents trachytic products and the most recent Vitória-Vulcão Central Volcanic Complex formed by basaltic to trachytic terms and divided into two units: Vitória and Vulcão Central, being the latter the youngest volcanic unit [2].

A selection of nine lavas from the three volcanic complexes (basalt to trachyte compositions) have been analyzed for Sr-Nd-Pb isotopic systems. They display a small variability of ⁸⁷Sr/⁸⁶Sr (0.703356 and 0.703576) and ¹⁴³Nd/¹⁴⁴Nd (0.512883 to 0.512964) isotope ratios, and the Pb-Pb isotope ratios correlate positively (²⁰⁶Pb/²⁰⁴Pb from 19.419 to 20.096; ²⁰⁷Pb/²⁰⁴Pb from 15.588 to 15.659; ²⁰⁸Pb/²⁰⁴Pb from 39.038 to 39.520). These new Sr, Nd and Pb isotopic data suggest the involvement of two mantle components: a depleted MORB and an enriched HIMU.

The oldest samples (Serra das Fontes, Serra Branca and Vitoria Unit) of the northern half of the island have homogeneous isotopic ratios with a high influence of the MORB mantle component. In contrast, the youngest samples from the southern part of the island (Vulcão Central Unit) present more radiogenic isotopic compositions. This suggests that during the formation of Graciosa island, the composition of the mantle and/or conditions of melt generation varied with time, as recently reported in other islands from central Azores [3].

[1] Feraud *et al.* (1989) *Earth Planet. Sci. Lett.* **46**, 275-286.

[2] Gaspar (1996) PhD thesis. [3] Hildenbrand *et al.* (2012) *AGU Fall Meeting D151A-2352*.

Formation timescales of pallasite meteorites inferred from the Mg isotope composition of olivine

K.K. LARSEN*, M. SCHILLER, C. PATON
AND M. BIZZARRO

Center for Star and Planet Formation, University of
Copenhagen, Øster Voldgade 5-7, DK-1350, Copenhagen
K, Denmark (*correspondence: kirstenl@snm.ku.dk)

Early formed meteoritic materials with significantly sub-chondritic Al/Mg ratios are not influenced by in-growth of ^{26}Mg from the decay of ^{26}Al ($t_{1/2} \sim 0.73$ Myr) and thus should record deficits in the mass-independent component of ^{26}Mg ($\mu^{26}\text{Mg}^*$) inherited from the source reservoir at the time of formation. This provides a means to define their formation timescales. Moreover, potential stable isotope variability in magnesium ($\mu^{25}\text{Mg}$) can be used to track genetic relationships between early solar system reservoirs. Pallasite meteorites, consisting of large mm- to cm-sized olivine crystals (Al/Mg ~ 0) set in evolved iron-nickel metal, are ideally suited to constrain the timing of asteroidal accretion and differentiation in the early solar system. Using improved methods for high-precision Mg-isotope measurements [1], we have extended our search for deficits in pallasite meteorites [2] to diverse main group pallasites (PMGs), two pyroxene pallasites, the ungrouped Zinder and Milton pallasites and two pallasites from the Eagle Station grouplet (PESs), including 20 distinct olivine crystals from Eagle Station.

Apart from PESs, all pallasite meteorites studied here have $\mu^{25}\text{Mg}$ values that are identical to that of Earth's mantle. The PESs have $\mu^{25}\text{Mg}$ systematically lighter than PMGs and Earth's mantle; defining a weighted mean of -183 ± 23 ppm (relative to DSM-3). This composition is similar to that of the bulk Allende meteorite, supporting the view that PESs formed from a CV chondrite-like precursor [3]. Considerable variability is observed in $\mu^{26}\text{Mg}^*$, with PMGs, pyroxene pallasites and Zinder having consistently negative $\mu^{26}\text{Mg}^*$ and PESs displaying positive $\mu^{26}\text{Mg}^*$ values. Individual olivine grains from the Eagle Station pallasite have $\mu^{26}\text{Mg}^*$ values ranging from $+1.3 \pm 1.5$ ppm to $+14.8 \pm 2.0$ ppm, plausibly related to igneous evolution on the Eagle Station parent body. Such excesses may record an evolutionary history of a magmatic reservoir with super-chondritic Al/Mg ratio while ^{26}Al was still extant. Model ^{26}Al - ^{26}Mg ages constrain the differentiation of the parent bodies of PMGs, PESs, the Vermillion and Yamato8451 pyroxene pallasites as well as Zinder to <2 Myr after solar system formation.

[1] Bizzarro *et al.* (2011). *J. Anal. At. Spectrom.* **26**, 565-577.
[2] Baker *et al.* (2012). *GCA.* **77**, 415-431. [3] Shukolyukov and Lugmair (2006). *EPSL.* **250**, 200-213.

Indispensable amino acids become dispensable via bacterial symbiosis in a generalist soil detritivore

THOMAS LARSEN^{1,2*}, DIANE M. O'BRIEN³,
NILS ANDERSEN² AND MARC VENTURA⁴

¹Department of Agroecology, Aarhus University, Blichers
Allé, 8830 Tjele, Denmark.

²Leibniz-Laboratory, Christian-Albrechts-Universität zu Kiel,
24118 Kiel, Germany (*correspondence: tl@leibniz.uni-
kiel.de).

³Institute of Arctic Biology, University of Alaska Fairbanks,
Fairbanks, AK 99775-7000, USA.

⁴Biogeodynamics and Biodiversity Group, CEAB-CSIC,
17300 Blanes, Catalonia, Spain.

Detritus-feeders play a key role for stimulating microbial activity in arctic peatlands but their nutritional requirements are poorly understood. We investigated whether a dominant detritivore in arctic peatlands, the enchytraeid worm, can overcome amino acid limitations in their nutrient poor diets by supplementation from bacterial symbionts. With a new isotopic tool for identifying bacterial synthesis of indispensable amino acids (IAAs) *in situ*, we demonstrated that enchytraeids feeding on hardly digestible diets derived nearly all IAAs from symbiotic bacteria; however, it was considerably less for enchytraeids feeding on easily digestible diets. We also found evidence for substantial bacterial IAA supplementation among enchytraeids dwelling in arctic peatlands. Although symbiotic synthesis and subsidy of IAAs to hosts is well known in herbivore specialists, this study provides the first evidence for substantial symbiotic IAA supplementation among soil detritivores. Our findings suggest that digestibility and initial microbial degradation of soil litter rather than nutritional qualities such as IAA composition determine its suitability as a food resource for enchytraeids. Recent observations and climate change projections for northern high latitudes indicate wetter and warmer conditions, which would be likely to stimulate enchytraeid activity by longer seasons and increased access to older stocks of decomposing litter.

Rates of low-pH biological Fe(II) oxidation in the Appalachian Coal Basin and the Iberian Pyrite Belt

LANCE N. LARSON¹, JAVIER SANCHEZ-ESPANA²
AND WILLIAM BURGOS³

¹Department of Civil and Environmental Engineering, Penn State University, USA, ln15053@psu.edu

²Instituto Geológico y Minero de España (IGME), Ríos Rosas, 23 28003 Madrid, j.sanchez@igme.es

³Department of Civil and Environmental Engineering, Penn State University, USA, wdb3@psu.edu

Low-pH Fe(II) oxidation can be exploited for the treatment of acid mine drainage (AMD). However, natural or engineered terraced iron formations (TIFs) are underutilized for AMD treatment because of uncertainties with respect to treatment performance. To address this problem we measured the rates of Fe(II) oxidation multiple times at seven sites in the Appalachian Bituminous Coal Basin and three sites in the Iberian Pyrite Belt (IPB). Longitudinal geochemical transects were measured downstream of emergent anoxic AMD sources. Water velocities were measured at each sampling location and used to transform concentration versus distance profiles into concentration versus travel time for kinetic analysis of field data. Both zero-order rates and first-order rate constants were used to compare Fe(II) oxidation kinetics. Zero-order Fe(II) oxidation rates ranged from $8.60 - 97.0 \times 10^{-7} \text{ mol L}^{-1} \text{ s}^{-1}$ at the Appalachian sites and $13.1 - 67.9 \times 10^{-7} \text{ mol L}^{-1} \text{ s}^{-1}$ at the IPB sites. In contrast, first-order Fe(II) oxidation rate constants ranged from $0.035 - 0.810 \text{ min}^{-1}$ at the Appalachian sites and $0.003 - 0.010 \text{ min}^{-1}$ at the IPB sites. The fastest zero-order rates of Fe(II) oxidation were measured at two sites (one in Appalachia and one in IPB) where little to no oxidative precipitation of Fe(III) occurred. Laboratory-based rates of Fe(II) oxidation were measured with TIF sediments and emergent AMD collected from the seven Appalachian sites. A zero-order laboratory-based removal rate for Fe(T) was used to calculate performance criteria of $2.6 - 8.7 \text{ g Fe day}^{-1} \text{ m}^{-2}$ (GDM) for both natural and engineered TIFs. These GDM values could be used to size TIFs for AMD treatment.

Alteration and fluid flow in large continental hydrothermal systems

P.B. LARSON

School of the Environment, Washington State University,
Pullman, WA 99164-2812 USA
(correspondence: plarson@wsu.edu)

Large volumes of hydrothermally altered rocks are found in calderas and around shallow plutons in the continental crust. The alteration is the product of water/rock interaction in hydrothermal systems that are convectively driven by cooling plutons, and record mass and heat flux through the shallow crust. They often host hydrothermal mineralization. O and H isotope ratios have been used to map large hydrothermal systems at the 23 Ma Lake City caldera and the 3-4 Ma Rico hydrothermal systems, CO, in Eocene hydrothermal systems, Idaho Batholith, ID, and in the active Yellowstone system, WY, all in the USA. These studies define a general architecture for continental hydrothermal systems.

Gradual variations of O isotope ratios in the altered rocks are observed both laterally and vertically, with lower values in central hydrothermal upflow zones with higher temperatures and enhanced fluid flux, and deeper where temperatures are higher. Fluids in deeper (more than 4km) portions of the systems can include a significant magmatic component near intrusions, where they are related to the formation of porphyry deposits. Fluids in shallower portions are dominated by meteoric ground waters. Thermal profiles in the shallowest (less than about 300 meters) epithermal near-surface environments are controlled by the hydrostatic boiling curve. In all cases, fractures and other permeable zones control the most important fluid flow paths.

Argillization and acid-sulfate alteration are widespread within a kilometer or so of the paleosurface, where boiling in rising fluids can be important. Propylitization is dominant in deeper parts of the systems, and potassic and quartz-sericite-pyrite porphyry-style alteration is prevalent near some deeper intrusions. The most important mass chemical effect of propylitic alteration is hydration. Although mineral reactions are pervasive in those altered rocks, major element concentrations suggest that their flux is minimal in the propylitic environment. Ba and Sr are generally added. Leaching of nearly all components, sometimes extreme, is characteristic of shallow alteration. Diffusion models of O isotope ratio profiles in altered feldspar phenocrysts at Rico suggest a hydrothermal duration on the order of about 100,000 years, whereas the Yellowstone system has been active for at least 400,000 years, although we do not know if its activity has been continuous or intermittent.

Pre-Hallandian metamorphism in the Sveconorwegian Province – its implication on the tectonic evolution of the Baltic Shield.

S. Å. LARSON^{1*} AND E-L. TULLBORG²

¹Department of Geology, Earth Sciences Centre, Göteborg University, Box 460, SE-405 30 Göteborg, Sweden, svenake@gvc.gu.se

²Terralogica AB, Gråbo, Sweden,

It has long been debate whether the Sveconorwegian Province in SW Sweden has suffered pre-Sveconorwegian (>1.1 Ga) metamorphic imprints. However, today it is agreed upon that the pre-Sveconorwegian Hallandian (~1.45 Ga) event has influenced this province. Any older metamorphic events have not been revealed by using U-Pb geochronology on minerals hitherto.

In this study we have taken use of intrusive relations to find suitable samples in order to constrain metamorphic events. Ion-probe dating of zircon and titanite was carried out from different rock types of the Sveconorwegian Province in SW Sweden, both west and east of a N-S trending, Sveconorwegian shear zone, the Mylonite Zone. Intrusion and metamorphic ages were dated for both veined and gneissic rocks as well as for corresponding crosscutting younger rocks. In this way the formation of veins was constrained on both sides of the Mylonite Zone.

To the east in the easternmost part of the Eastern Segment formation of early veins were formed between 1.66 Ga - 1.53 Ga, and anatectic, granitoid magmas related to basic intrusions were formed at 1.53 ±0.03 Ga. To the west (Western Segment), the formation of early veins and folding is constrained between 1.61 Ga and 1.52 Ga, and formation of pegmatite related to basic intrusions to 1.54 ±0.02 Ga. Here also zircon growth indicates a Sveconorwegian thermal event in contrast to what was found in our samples from the easternmost Eastern Segment.

The findings of Pre-Hallandian (>1.45 Ga) metamorphism and magmatism across the Mylonite Zone, separating the Western and Eastern Segments of the Sveconorwegian Province in Sweden suggest that these parts of the Baltic Shield were united at least at ~1.54 Ga. Thus, it is suggested that the Mylonite Zone is a Sveconorwegian terrane boundary rather than a Sveconorwegian suture.

Modeling inverse adsorption isotope effects for CO₂ and CH₄ from experimental and field data

TOTI LARSON¹ AND JEIMIN LU²

¹Department of Geological Sciences, The University of Texas at Austin, Austin, Texas, USA.

²Bureau of Economic Geology, The University of Texas at Austin, Austin, Texas, 78713, USA.

Transport of CO₂ and CH₄ through porous media is affected by diffusion, gas-liquid partitioning, advection and adsorption processes. Adsorption, diffusion, and gas-liquid partitioning processes are affected by isotope substitution. Although considerable effort has been placed on understanding stable isotope effects associated with diffusion and gas-liquid partitioning, significantly fewer results have been measured for adsorption carbon isotope effects of CO₂ and CH₄ on geologically relevant substrates, temperatures and pressures. Early work by Bruner *et al.* (1966), Van Hook (1967) and Corcia and Liberty (1969) explored hydrogen isotope adsorption isotope effects for methane on dry and wet glass columns with limited carbon isotope results. Here we report experimentally measured carbon isotope fractionations for CO₂ on illite and quartz substrates at 298K using a 1-D column apparatus as well as preliminary field results of methane carbon isotope values from the caprock of a natural gas reservoir. Observed adsorption isotope effects are compared to diffusion effects conducted in unpacked 1-D columns. Results are modeled using an analytical solution to a coupled advection-diffusion-adsorption transport model. Measured diffusivities from diffusion experiments are in excellent agreement with binary diffusion constants calculated for ¹³CO₂-Helium and ¹²CO₂-Helium using the Fuller Equation whereby the ratio of diffusivities between ¹³CO₂ and ¹²CO₂ is 0.99909. In contrast to diffusion where ¹²CO₂ preferentially populates the front of the chromatographic peak, adsorption of CO₂ and CH₄ has the opposite effect whereby preferential adsorption of ¹²CO₂ is observed, resulting in the 'front' of the chromatographic peak becoming enriched in ¹³CO₂. Similar observations are made for methane in a shale adsorption-dominated system whereby methane furthest from the reservoir is approx. 15 permil heavier than the reservoir gas. This inverse chromatographic effect for CO₂ and CH₄ is modeled well using the Rayleigh Equation ($\alpha=1.0086$) and the transport equation (retardation factor=0.999). These results demonstrate the importance of understanding adsorption isotopic effects and potentially offers a tool to quantify surface area and/or transport distance in geological reservoirs.

Vanadium leaching from converter lime and speciation in soil: a long-term field study

M.A. LARSSON¹, M. D'AMATO², F. CUBADDA²,
A. RAGGI², I. ÖBORN¹ AND J.P. GUSTAFSSON¹

¹Department of Soil and Environment, Swedish University of Agricultural Sciences, Box 7014, 750 07 Uppsala, Sweden (*correspondence: maja.larsson@slu.se)

²Department of Food Safety and Veterinary Public Health, Istituto Superiore di Sanità, Viale regina Elena 299, Rome, 00161, Italy

Vanadium, V, is a redox-sensitive metal that is mainly used within the steel industry. Under environmental conditions, it mainly exists in oxidation states +4 and +5 [1]. Under aerobic conditions vanadium prevails as the pentavalent oxyanion vanadate, H_2VO_4^- . Vanadate is thought to be the most toxic vanadium form due to its structural similarity to phosphate [2].

In the mid-1980's, a field trial was set up in a pine forest in the south of Sweden. Granulated converter lime, containing high concentrations of vanadium, was added in different concentrations (0, 2, 7 and 10 tonne ha^{-1}). 25 years later, soil samples from the mor and from the top 20 cm of the mineral layer were taken at the site. The soils were analyzed for total and dissolved vanadium concentrations. Further, the redox form of the vanadium bound to the soils was analysed using X-ray absorption near edge structure (XANES) spectroscopy. Quantification of vanadium(IV) and vanadium(V) in the soil extracts was made with EDTA complexation followed by measurements with HPLC coupled ICP-MS [3].

The total soil vanadium concentrations generally decreased with depth, indicating some downward transport of vanadium in the profile. XANES spectra in the mor layer show similarities to reference samples of V(IV) bound to organic matter. Further down in the mineral soil, the XANES spectra suggests vanadium(V) binding to soil constituents containing aluminium. The speciation analysis of the CaCl_2 -extracts showed a higher fraction of V(IV) in samples with higher concentrations of organic matter such as in the mor samples. The extracts of the mineral soils had a larger fraction of V(V).

[1] Wanty & Goldhaber, 1992. *Geochim. Cosmochim. Acta* 56, 1471-1483. [2] Seargeant & Stinson, 1979. *Biochem. J.* 181, 247-250. [3] Aureli, Ciardullo, Pagano, Raggi & Cubadda, 2008. *J. Anal. At. Spectrom.* 23, 1009-1016.

Processed controlling recent lava fountaining activity on Mt. Etna, revealed using remote sensing measurements of volcanic gases

ALESSANDRO LA SPINA¹, GIUSEPPE SALERNO²
AND MICHAEL BURTON³

¹INGV Osservatorio Etneo, Italy, salerno@ct.ingv.it

²INGV Osservatorio Etneo, Italy, laspina@ct.ingv.it

³INGV Pisa, Italy, burton@pi.ingv.it

Open-Path Fourier Transform Infrared (OP-FTIR) spectroscopy is now an established methodology for measuring volcanic gas compositions remotely. Here we present and interpret OP-FTIR measurements collected on Mt. Etna, before, during and after a series of lava fountains which were observed between 2011 and 2013. We combine our results with quantifications of SO_2 flux, allowing the fluxes of multiple volcanic gas species to be constrained, including H_2O , CO_2 , SO_2 , HCl , and HF . These results allow an interpretative framework to be established, in which we use clearly observed geochemical precursors to the lava fountain activity to constrain the magma dynamics which produce the eruptive activity.

Thermoddem: an example of alive thermochemical database

LASSIN A.¹, BLANC P.¹, ANDRE L.¹, MARTY N.¹,
PARMENTIER M.¹, MOYARD S.², AZAROUAL M.¹,
PIANTONE P.¹, GAUCHER E.C.¹, KERVEVAN C.¹
AND TOURNASSAT C.¹

¹BRGM, 3 av. C. Guillemin, B.P. 36009, 45060 Orléans, France

²CASPEO, 3 av. C. Guillemin, 45060 Orléans, France

The basic goal of the Thermoddem thermochemical database [1] (<http://thermoddem.brgm.fr/>) is to gather standard thermodynamic data regarding chemical compounds encountered in most water-solid-gas systems, with a specific concern for environmental issues, cement phases and clay minerals. The construction of the database (since 2006) relies on a careful selection of published experimental data, constrained by a rigorous internal consistency. Data selection combines both solubility and calorimetric data in order to strengthen the coherence of the data set. A particular effort is paid to identifying the source of every data. Some examples will be presented for illustration.

A major objective of thermochemical databases (TDB) is to be integrated into coupled reactive transport modelling codes. Therefore, it is of key importance to provide database formats adapted to the most widely used calculation codes and to make them freely available on the Internet. In addition, Thermoddem includes mineralogical and geological information to help the modeller to define and to select the geochemical reactive system in agreement with the problematic to handle.

Geochemical and reactive transport modelling covers a wide range of temperature and pressure conditions, numerous reactive mechanisms (aqueous complexation, surface complexation and ionic exchanges, dissolution/precipitation or degassing reactions, kinetic processes, bacterial activity), and various contexts (dilute/saline waters, isobaric/anisobaric conditions). Models implemented in calculations codes for describing the different geochemical mechanisms evolve with time and new concepts are perpetually developed. Alive TDB have to adapt to these evolutions as for Thermoddem, which is this way developed. However one has to acknowledge that, despite the wide use of thermochemical databases, there is still a need for gathering a community that would actively contribute to help improving these tools. Furthermore a better scientific recognition could help supporting their development and maintenance.

[1] Blanc P., Lassin A., Piantone P., *et al.*. (2012) *Appl. Geochem.* 27(10), 2107-2116

How depleted is the upper mantle? Constraints from elemental-Os isotope correlations in abyssal peridotites and ocean island xenoliths

J.C. LASSITER*¹ AND B.L. BYERLY¹

¹ Jackson School of Geosciences, University of Texas at Austin, Austin, TX, USA (*lassiter1@jsg.utexas.edu)

It is generally accepted that the convecting upper mantle is depleted in incompatible trace elements as a result of prior melt extraction. However, the amount of melt depletion that has occurred and the extent to which this has effected the major element composition of the mantle is less certain. *Workman & Hart* [1] estimated the composition of MORB-source mantle utilizing both MORB and abyssal peridotite (AP) compositional trends and inferred a relatively fertile bulk composition (e.g., $\text{Al}_2\text{O}_3 > 4$ wt.%) consistent with minor long-term melt depletion of ~3-4%, assuming a primitive mantle Al_2O_3 content of ~4.4 wt.% and that the melt extracted had a roughly MORB-like composition. *Walker et al.* [2] also inferred limited long-term melt extraction (2-3%) based on Os-isotope systematics of ophiolite chromitites.

We have examined correlations between indices of peridotite fertility (Al_2O_3 , spinel Cr#) and Os-isotopes in both APs and ocean island peridotite xenoliths (OIPs) to better constrain the average $^{187}\text{Os}/^{188}\text{Os}$ of the upper mantle, the average age of melt depletion, and the extent of melt depletion required to generate the observed major element-isotope correlations. APs and OIPs have statistically indistinguishable average $^{187}\text{Os}/^{188}\text{Os}$ (0.1244 versus 0.1245), and are considerably less radiogenic on average than chromitites derived from modern ophiolites (~0.1281; [2]). Both APs and OIPs display positive global correlations between fertility indices and $^{187}\text{Os}/^{188}\text{Os}$. The Al_2O_3 - $^{187}\text{Os}/^{188}\text{Os}$ trends of both suites define aluminachron “ages” of ~1.5 Ga, similar to the average T_{Ma} ages of both populations. Combined, these trends suggest upper mantle peridotites have an average $^{187}\text{Os}/^{188}\text{Os}$ of ~0.1245 and the average age of melt depletion is ~1.5 Ga. If extraction of oceanic crust is the primary mechanism for depleting the upper mantle, then the degree of MORB melt extraction required to generate an average upper mantle Os-isotope value consistent with APs and OIPs is ~10-12%, significantly greater than previous estimates of upper mantle depletion. During mantle upwelling, the degree of melt generated from a mantle packet is a function of initial fertility. MORB therefore oversample fertile components in the mantle, which likely accounts for the apparent conflict between our estimate of average mantle peridotite fertility and that of [1].

[1] Workman & Hart (2005), *EPSL* **231**, 53-72. [2] Walker *et al.* (2002), *Geochim. Cosmochim. Acta* **66**, 329-345.

Reduction of aqueous U^{VI} by Fe^{II}: Effect of Ti^{IV} on the speciation of U^{IV}

DREW E. LATTA¹, CAROLYN I. PEARCE², KEVIN M. ROSSO¹, EDWARD J. O'LOUGHLIN¹, KENNETH M. KEMNER¹ AND MAXIM I. BOYANOV¹

¹ Biosciences Division, Argonne National Laboratory, Lemont, IL 60439 USA

² Physical Sciences Division, Pacific Northwest National Laboratory, Richland, WA 99352 USA

The solubility and mobility of uranium, a radionuclide contaminant at many sites, is highly dependent on its valence state and speciation. Transformation of aqueous U(VI) to U(IV) under the (bio-)reducing conditions found in many subsurface environments can decrease U solubility due to the precipitation of U(IV) dioxide (uraninite), a process that has been studied extensively for uranium remediation. However, recent evidence suggests that U(VI) reduction can produce complexed U(IV) species in the solid phase, such as U(IV)-phosphate precipitates or surface-adsorbed U(IV) atoms. The molecular speciation and the stability of non-uraninite U(IV) phases is poorly understood, even though this knowledge is essential in predicting uranium behavior at contaminated sites or in the design of nuclear waste repositories.

As part of understanding uranium transformations under iron reducing conditions, we examined the reduction of U(VI) by Fe(II) in the presence of Ti(IV). Ti(IV) is commonly present in natural magnetite and has been observed in the magnetic sediment fraction at the Hanford nuclear site. Titanium-doped magnetite nanoparticles of varying Ti content (Fe_{3-x}Ti_xO₄, 0 < x < 0.5) were synthesized and reacted with aqueous U(VI) in the presence and absence of bicarbonate. Analysis of the solids by U L_{III} edge x-ray absorption spectroscopy (XANES and EXAFS) indicated that Ti incorporation did not affect the ability of magnetite to reduce U(VI) to U(IV). Reactions with pure magnetite resulted in the formation of uraninite (dioxo-bridged UO₂). In contrast, reactions with Ti-doped magnetite resulted in a phase that lacked dioxo bridges between the U(IV) atoms. The latter phase was distinct from the U(IV) mineral brannerite (UTi₂O₆), suggesting that U(IV) was stabilized as a mononuclear surface complex. To understand the nature of Ti-complexed U(IV) species, U(VI) was co-precipitated with Fe(II) in the presence of carboxyl-functionalized microbeads and increasing amounts of Ti(IV). Analysis of the resulting solids indicated complete reduction of U(VI) to U(IV) and the formation of an inner-sphere U(IV)-Ti complex at Ti:U ratios as low as 1:1. The refined U(IV)-Ti distance of 3.43 Å suggests the formation of a bidentate corner-sharing complex between Ti octahedra and U(IV).

Active Carbon Cycling in Deep Subsurface Fracture Environments: Insights from RNA, Lipid and Isotopic Analyses

M. LAU^{1*}, M. LINDSAY¹, T.L. KIEFT², M. PULLIN², S. HENDRICKSON², D.N. SIMKUS³, G.F. SLATER³, B. SHERWOOD LOLLAR⁴, L. LI⁴, G. LACRAMPE-COULOUME⁴, ESTA VAN HEERDEN⁵, M. ERASMUS⁵, G. BORGONIE⁵, B. LINAGE⁵, O. KULOYO⁵, B. MAILLOUX⁶, V. HEUER⁷, K-U HINRICHS⁷, S. MAPHANGA⁸ AND T.C. ONSTOTT¹

¹Dept. of Geosciences, Princeton University, Princeton, NJ USA 08544, ²New Mexico Tech, Socorro, NM USA 87801

³SGG, McMaster University, Hamilton ON Canada L8S 4K1

⁴Dept. of Earth Sciences, University of Toronto, ON, Canada M5S 3B1

⁵University of the Free State, Bloemfontein 9300, South Africa

⁶Dept. of Environ. Sci., Barnard College, New York, NY USA 10025-6598

⁷MARUM Center for Marine Environmental Sciences, Univ. of Bremen, D-28334 Bremen, Germany

⁸Beatrix Au Mine, South Africa

This study undertook identifying 1) the metabolically active microbial communities of deep fracture water by comparison of cDNA (from RNA = active community) and DNA (total community) sequences; and 2) the C source of the active microbial community by comparing the compound specific δ¹³C and Δ¹⁴C of the PLFA and the Δ¹⁴C of the DNA with the δ¹³C and Δ¹⁴C of the CH₄, DIC, DOC and the δ¹³C of the organic acids. In this talk we will present this data for a borehole located at 1.3 kmbls. in the Beatrix Au Mine.

Comparison of the cDNA and DNA results for both Archaea and Bacteria indicates that the composition of the active community differs from that of the total DNA community. *Methanobacterium* is part of the active community, though in low abundance compared to the Bacteria. *D. audaxviator* found in both DNA and cDNA nifH results indicating that N₂ is occurring *in situ*. cDNA library also yielded pmoA gene indicating that active methanotrophy is also occurring.

The δ¹³C and δ²H of the CH₄ is consistent with methanogenesis. The Δ¹⁴C of the PLFA agrees with the Δ¹⁴C of the DNA and along with the δ¹³C of the PLFA and the Δ¹⁴C of the CH₄ indicate that the active microbial community is obtaining most of its carbon from the CH₄.

Polyelectrolyte injection increases mobility of nanoscale zero-valent iron in carbonate sand

S. LAUMANN, V. MICIĆ AND T. HOFMANN*

Department of Environmental Geosciences, University of Vienna, Vienna, Austria (*correspondence: thilo.hofmann@univie.ac.at)

The limited mobility of nanoscale zero-valent iron (nZVI) remains one major obstacle to widespread utilization of this agent for *in situ* groundwater remediation [1]. The nZVI mobility is strongly affected by aquifer heterogeneities, which include mineralogical variations [2]. In our previous study we showed that the presence of carbonates in porous aquifers significantly reduces the nZVI mobility [3]. New strategies are therefore required to improve the nZVI mobility in such porous media. This might be achieved by increasing the repulsion between nZVI and the porous media, which can be provided by the injection of anionic polyelectrolytes in the subsurface. We tested this hypothesis by studying the effects of various co-injected polyelectrolytes (natural organic matter, humic acid, carboxymethyl cellulose, and lignin sulfonate) on the mobility of polyacrylic acid coated nZVI in two model porous media; quartz and carbonate sand.

The results demonstrated that co-injection of the chosen polyelectrolytes at concentrations of 50 mg L⁻¹ does not influence the nZVI mobility in quartz sand. This can be explained by the highly negative surface charge of quartz (-40 mV), which prohibited any surface interactions with the negatively charged polyelectrolytes. Contrarily, in less negatively charged carbonate sand (-10 mV) the co-injection resulted in an increased nZVI mobility. We related this to polyelectrolyte adsorption onto the carbonate surface. Lignin sulfonate was selected to further investigate the effect of increasing polyelectrolyte concentrations (10, 25, 50, 250, and 500 mg L⁻¹) on the nZVI mobility in carbonate sand. At concentrations above 10 mg L⁻¹ an increase in nZVI mobility was observed. Furthermore, the nZVI transport distance was almost doubled when the particles were co-injected with 500 mg L⁻¹ lignin sulfonate.

Overall, the results indicated that polyelectrolyte adsorption onto the carbonate sand reduces the nZVI deposition onto aquifer grains and consequently promote its mobility, an effect which is more pronounced with higher concentrations of co-injected polyelectrolyte.

[1] O'Carroll *et al.*. (2013) *Adv. Water Resour.* 51, 104-122.

[2] Kim *et al.*. (2012) *J. Colloid Interface Sci.* 370, 1-10. [3]

Laumann *et al.*. (2013), accepted, *Environ. Pollut.*

Metal-silicate partitioning of the HSE at high pressures and temperatures in S-bearing systems

VERA LAURENZ^{1*}, DAVID C. RUBIE¹
AND DANIEL J. FROST¹

¹Bayerisches Geoinstitut, Universität Bayreuth, Universitätsstrasse 30, 95440 Bayreuth, Germany
*(correspondence: vera.laurenz@uni-bayreuth.de)

The highly siderophile elements (HSE - Os, Ir, Ru, Rh, Pt, Pd, Re, Au) are unique geochemical tracers of Earth's accretion and differentiation history. From high pressure-high temperature experimental work it is known, that the HSE were effectively scavenged from the Earth's mantle during core formation, leaving the mantle strongly depleted in HSE. After core formation was complete, a "late-veener" of highly oxidized, chondritic material then delivered a small amount of HSE back to the mantle [1]. However, the observed HSE abundances of the primitive upper mantle cannot be reproduced by any known meteorite group, questioning how the HSE abundances were established. A possible clue to this problem could lie in the effect of S on metal-silicate partitioning of the HSE: As S is known to strongly influence the partitioning behaviour of chalcophile trace elements such as Mo or Ni, it may also have played an important role for the behaviour of the HSE, especially during the late stages of accretion and core formation.

In order investigate if sulfur has an effect on the behaviour of the HSE during core formation, we studied the metal-silicate partitioning of Pt, Pd and Ru in S-bearing systems under high pressure-high temperature conditions. A molten peridotite was equilibrated with a S-bearing Fe-HSE-alloy at pressures from 6 to 18 GPa and temperatures between 2200 °C and 2400 °C in a multianvil apparatus. Sulfur concentration in the alloy varied between 5-15 wt. %. Quenched metal and silicate were analyzed by electron microprobe (major elements) while trace element concentrations were determined using LA-ICP-MS.

Results indicate that Pd and Ru, the two most chalcophile HSE, become significantly less siderophile with increasing S-content of the metal. In contrast, Pt being less chalcophile shows only a small effect. These results indicate that, besides pressure and temperature, composition also has a significant effect on the partitioning behaviour of HSE. The presence of sulfur may induce HSE fractionation during core formation and might be responsible for observed HSE abundances in the Earth's mantle.

[1] Mann U, Frost D. J., Rubie D. C., Becker H. and Audétat A. (2012) *GCA* 85, 593-316.

Denitrification rates in riparian wetlands of the Seine River are influenced by carbon quantity rather than quality

ANNIET LAVERMAN¹ CHRISTELLE ANQUETIL²
AND SYLVIE DERENNE²

¹ UMR 7619 Sisyphe, UPMC, CNRS, Paris

² UMR 7618 Bioemco, UPMC, CNRS, Paris

Benthic denitrification in riparian zones or adjacent wetlands of the Seine River could significantly improve its water quality. The goal of this study was to investigate the potential for denitrification and the factors affecting *in situ* denitrification rates with special emphasis on the role of organic matter. We measured denitrification potentials in sediments collected from four sites along the Seine River during three different seasons. Sediment characteristics (C_{org} , C:N ratio, bioavailable carbon and chlorophyll content) were determined and the sedimentary organic matter was analyzed at the molecular level (¹³C NMR and pyrolysis coupled with gas chromatography-mass spectrometry).

Denitrification rates showed large spatial and seasonal variations. They were significantly correlated with sedimentary chlorophyll concentrations, but not with biodegradable carbon, measured as the decrease in total organic carbon under oxic conditions. Algal C most likely served as a carbon source for this process. The addition of carbon, either in the form of simple organic molecules (acetate, lactate), reed or algae always increased the denitrification rates, indicating a strong carbon limitation in these sediments and a lack of discrimination against the carbon source. The latter was confirmed through examination of the molecular structure of the sedimentary organic matter from four sites. Indeed the sediments which exhibit the highest denitrification rates show the most similar organic matter chemical structures. Moreover, incubation of sediments for two months under denitrifying conditions did not induce any significant change in the chemical structure of the organic matter although the latter was contrasted from one site to another one.

Fluxes of fine particles over a semi arid pine forest: possible effects of a complex terrain

AVI LAVI¹, DELPHINE K. FARMER^{2,3}, ENRICO SEGRE⁴,
TAMAR MOISE¹, EYAL ROTENBERG¹, JOSE L. JIMENEZ²
AND YINON RUDICH^{1*}

¹ Department of Environmental Sciences, Weizmann Institute of Science, Rehovot, 76100 Israel

(avi.lavi@weizmann.ac.il, tamar.moise@weizmann.ac.il, eyal.rotenberg@weizmann.ac.il, *correspondence: yinon.rudich@weizmann.ac.il)

² Department of Chemistry and Biochemistry, University of Colorado Boulder, CIRES, Boulder, CO 80303 USA (jose.jimenez@colorado.edu)

³ Department of Chemistry, Colorado State University, Department of Chemistry Ft Collins, CO 80523 USA (delphine.farmer@colostate.edu)

⁴ Department of Physical Services, Weizmann Institute of Science, Rehovot, 76100 Israel (enrico.segre@weizmann.ac.il)

Semi-arid forests are of growing importance due to expected ecosystem transformations following climatic changes. Size-resolved flux measurements of atmospheric aerosols (0.25-0.65 μm) were conducted for the first time in such an ecosystem in the Yatir forest in southern Israel, using an optical particle counter and eddy covariance methodology. Both downward and upward fluxes were observed. Upward fluxes were not associated with a local particle source. Moreover, the flux direction correlated strongly with wind direction suggesting topographical effects. The measured effect of topography on the deposition velocity (V_d) is greater as particle size increases, as had been shown in modeling and laboratory studies [1, 2] but had not been demonstrated yet in field studies. We therefore suggest that a complex terrain and a patchy fetch affect the expected dependence of V_d on particle size and cause the observed upward particle fluxes. This hypothesis is consistent with the observed relationship between V_d and the friction velocity, the topography around the flux tower, and the observed correlation of flux direction with wind direction. The averaged V_d for 0.25-0.28 μm particles ($3.8 \pm 4.5 \text{ mm}\cdot\text{s}^{-1}$) is similar to previous particle deposition velocity measurements in mid and northern latitude coniferous forests.

[1] Belcher, *et al.* (2012), *Ann. Rev. of Fluid Mech* **44**,479-504.[2] Katul, *et al.* (2010), *Bound-Lay Meteorol* **135**,67-88.

Low Concentration Soil Exposure to ZnO Nanoparticles by Stable Isotope Labelling

A. LAYCOCK^{1,3}, M. DIEZ ORTIZ², F. LARNER¹, A. DYBOWSKA³, E. VALSAMI-JONES^{3,4}, C. SVENDSEN² AND M. REHKÄMPER^{1,3}

¹ ESE, Imperial College London, SW7 2AZ, UK

² Centre for Ecology and Hydrology, OX10 8BB, UK

³ Natural History Museum, London SW7 5BD, UK

⁴ Geography, Earth & Env Sci, U Birmingham B15 2TT, UK

The tracing of engineered nanoparticles (NPs) in the environment is hampered by analytical limitations. In particular, difficulties lie in the detection of these materials against the natural background of elements and NPs found in complex systems. To overcome these problems excessive dosing is often employed in exposures, calling into question the relevance of findings. The novel application of stable isotope labelling in conjunction with high precision isotope ratio measurements can overcome these shortcomings.

Presented here are results obtained for the exposure of the earthworm *Lumbricus rubellus* to isotopically labelled ZnO NPs in soil. To this end, ZnO NPs were synthesised using Zn enriched to 99.5% in the Zn-68 isotope relative to the natural abundance of 18.8%. The introduction of this enriched isotope into the experimental system creates distinct non-natural deviations in the diagnostic isotope ratio ⁶⁸Zn/⁶⁶Zn. Precise determination of isotope ratio changes then enables accurate detection and quantification of the isotope label in the components of the exposure system.

The study compares dietary vs. dermal uptake of ⁶⁸ZnO NPs and soluble ⁶⁸Zn from soil by *Lumbricus rubellus*. Exposures were performed simultaneously in triplicate with earthworms being sampled at 4, 8, 24, 36, 48 and 72 hours. The labelling method allows use of an environmentally relevant exposure concentration of 4 µg/g ⁶⁸Zn against a natural Zn background content of up to 1.7 mg/g. After 4 hours of dermal exposure, the enriched ⁶⁸Zn contributes about 0.02% to the total Zn concentration of an exposed earthworm but this already produces a sufficient deviation in the diagnostic ⁶⁸Zn/⁶⁶Zn ratio to be detectable when measured by high precision multiple-collector ICP-MS.

For the exposures with ⁶⁸ZnO NPs and soluble ⁶⁸Zn, our data reveal that dermal ⁶⁸Zn uptake accounted for less than 10% of the worms total uptake, with dietary ⁶⁸Zn uptake being by far the most important route. In both cases, the uptake rates determined for ⁶⁸ZnO NPs and soluble ⁶⁸Zn are identical, within error. This indicates that Zn from both nano and ionic based exposures display similar bioavailability.

Substantial changes in the salinity and paleo-hydrology of the late Quaternary Dead Sea revealed in the ICDP deep drill

B. LAZAR*¹, O. SIVAN², G. ANTLER³, Y. YECHIELI⁴, E. LEVI¹, I. GAVRIELI⁴ AND M. STEIN⁴

¹Institute of Earth Science, The Hebrew University of Jerusalem, ISRAEL 91904 (*Correspondence: boaz.lazar@mail.huji.ac.il)

² Geological and Environmental Sciences, Ben-Gurion University of the Negev, Beer-Sheva, ISRAEL 84105

³Department of Earth Sciences, University of Cambridge, Cambridge, UK

⁴Geological Survey of Israel, 30 Malkhe Israel St. Jerusalem, ISRAEL, 95501

Vertical profiles of chloride (Cl) and oxygen isotopes ($\delta^{18}\text{O}$) of Lake Lisan the late Quaternary precursor of the Dead Sea were established from analyses of pore-fluids that were extracted from cores drilled during the ICDP campaign in the deep basin of the Dead Sea at water depth of 300 m. The pore fluids data provide the first direct measurements of the composition of the Dead Sea deep brine that was evolved over the past several glacial interglacial intervals. Specifically, pore fluid profiles suggest that during the last glacial (70-14 ka BP) Cl concentrations at the bottom of the lake were not more than 2/3 of their present values and $\delta^{18}\text{O}$ reached values higher than 6.7 ‰. The low chloride values of porewaters indicate that during MIS2 the deepest part of Lake Lisan was significantly less salty than the present Dead Sea. This is compatible with the heaviest $\delta^{18}\text{O}$ values that could be produced by evaporation of the waters at the shallow southern lake margins. Continuous turbulent mixing of such an evaporated solution with the lower brine across the epi/hypolimniom interface, led the dilution of the latter and the buffering of the Sr/Ca ratios and radiocarbon reservoir ages in the epilimniom[1]. However, upon the abrupt decline of the lake to minimum levels (below 450 m bmsl)[2] e.g. at ~14-13 ka (the Bolling-Allerod period), the bottommost brine retained its highest salinity, lowest $\delta^{18}\text{O}$ and highest Sr/Ca ratios.

[1] Stein M., Lazar B., Goldstein S.L. (2013), *Radiocarbon*. Accepted. [2] Stein M., Torfstein A., Gavrieli I. Yechieli Y. (2010), *Quarter. Sci. Rev.* **29**, 567-575.

Insights into potential metabolisms of the cosmopolitan Miscellaneous Crenarchaeotal Group (MCG) from estuarine sediments using metagenomics

C. S. LAZAR^{1,2*}, B. J. BAKER³, G. J. DICK³,
K-U HINRICHS² AND A. P. TESKE¹

¹Department of Marine Sciences, University of North Carolina at Chapel Hill, Chapel Hill, NC 27599, USA
(clazar@email.unc.edu)

²Organic Geochemistry Group, MARUM Center for Marine Environmental Sciences and Department of Geosciences, University of Bremen, Bremen D-28359, Germany

³Department of Earth and Environmental Sciences, University of Michigan, Ann Arbor, MI 48178, USA

The Miscellaneous Crenarchaeotal Group (MCG) represents a frequently detected and widespread phylum-level lineage of Archaea. Their members are as yet uncultivated and hence little is known about their metabolism or their biogeochemical role in the environment. Recently, single cell genomic sequencing of one MCG cell indicated a role in protein remineralization [1]. A characteristic feature of MCG is their wide intra-specific diversity. Up to 17 subgroups of MCG based on 16S rRNA sequences have been documented [2]. In order to expand the search on potential metabolisms of the MCG, sediment cores were sampled in the White Oak River estuary (North Carolina, USA) in October 2010; these sediments have been previously shown to be strongly enriched in members of the MCG. The archaeal diversity of these sediments was screened with 16S rRNA gene libraries, accompanied by detailed geochemical analysis. Apart from one shallow sediment sample (10 cmbsf) the MCG dominated all samples, and all 17 MCG subgroups were detected. A sample at 46 cmbsf was chosen for 454 pyrosequencing using genomic DNA. Sequence read assembly yielded approximately 34,000 contigs, 15 of which contained more than 6000 bp. Many of the top contigs belonged to the MCG Archaea. Of the ten 16S rRNA archaeal sequences retrieved from the reassembled contigs, nine were affiliated with MCG and belong to six different MCG subgroups. Metagenomic characterization of archaeal community members revealed a variety of novel organic matter utilization genes including; proteases, amino acid transporters, nucleases, and lipid degradation.

[1] Lloyd *et al.*. 2013. *Nature*. **496**, 215-218. [2] Kubo *et al.*. 2012. *ISME J.* **10**, 1949-65.

A cyano-bacterial community as a possible agent of Ge accumulation in coal

E.V. LAZAREVA¹, A.V. BRYANSKAYA²,
V.V. MOROZOVA³, I.V. BABKIN³, N.V. TIKUNOVA³, O.P.
TARAN⁴, O.V. SHUVAEVA⁵ AND S.M. ZHMODIK¹

¹Institute of Geology and Mineralogy SB RAS, Pr. Koptug, 3, Novosibirsk, 630090, Russia (*lazareva@igm.nsc.ru)

²Institute of Cytology and Genetics SB RAS

³Institute of Chemical Biology and Fundamental Medicine SB RAS

⁴Boreskov Institute of Catalysis SB RAS

⁵Institute of Inorganic Chemistry SB RAS

Quasi-synchronous hydrothermal activity is critical for high Ge contents in coal [1]. The mechanism of Ge accumulation remains unknown and has been suggested to be associated mainly with sorption from thermal waters bearing 100-150 ppb Ge.

We discuss the geochemistry of a cyanobacterial community at the Uro vent in the Baikal rift and compare element abundances in its waters with those in shale [2] and brown coal [1]. The Uro community contains 350 ppm Ge (average dry-weight contents, up to 1000 ppm), which is about that in the highest-Ge coal. The Uro thermal water composition is remarkable by elevated Be, Sr, Cs, Ga, Mo, and W. Trace elements in the community have implications for the general composition of the water but not for the abundances of elements in it. Bacteria may accumulate little (Cs, Rb, Mg, Sr, K, Ca, Si, V, U, Sb) or zero (Li, Na) amounts of some elements, or be poorer in others than the water (e.g., Mo and W). The living matter of the community hyper-accumulates Ge from water with only 3.4 ppm germanium. Thus, in order to infer the water composition from buried fossils (i.e., to do inversion), one has to take into account the mobility of elements, as well as their different sorption/accumulation by bacteria. The composition of the Uro community is typically thermophilic. Syngenetic hydrothermalism may induce formation of cyanobacterial mats, along with peat generation. Therefore, accumulation by the cyanobacterial community may be the agent responsible for high Ge in coal. As our study shows, Ge contents in the hot spring water may be not very high, within a few ppm.

The work was supported by grant 11-05-00717 from RFBR and was performed as part of Integration Project SB RAS 94.

[1] Yudovich Ya.E. *Int. J. of Coal Geology*, 2003, **56**, 223–232. [2] Li *et al.*. *Geochemica et Cosmochimica Acta*, 1991, **55**, 3223-3240.

Biomorphic structure of rich ores at the Tomtor REE deposit

E.V.LAZAREVA, S.M.ZHMODIK, A.V.TOLSTOV,
B.L. SHERBOV AND N.S.KARMANOV

¹Institute of Geology and Mineralogy SB RAS, Pr. Koptug, 3,
Novosibirsk, 630090, Russia (*lazareva@igm.nsc.ru)

The Tomtor Paleozoic complex of ultramafic alkaline and carbonate rocks covers about 250 km² in northern Yakutia (Russia). It has a zoned structure with a carbonatitic core surrounded by ultramafite and foidolite and an alkaline-nepheline syenite periphery [1, 2, 3]. All rocks are weathered, the weathering profile upon P-REE carbonatite being the thickest and consisting of four layers: kaolinite-crandallite, siderite, goetite, and francolite (from top to bottom) [3]. Mineralization is the highest in redeposited and altered thinly bedded aphanitic kaolinite-crandallite ores, of slope-wash-lacustrine origin, with chemogenic phosphate [3] and Nb, Y, Sc, and REE enrichment. The richest ores are natural concentrates of Nb (up to 24%) and REE (to 39%) [1, 2, 3].

Monazite, pyrochlore, and crandallite-group minerals (goyazite, georceixite, and florencite) are main opaque phases in the rich ores. Pyrochlore occurs as euhedral cracked grains of sodic compositions, with Sr-Ba substitutions. Fine colloform aggregates of crandallite minerals make up the groundmass. Monazite exists as aggregates of 800-1200 nm long tubes, 300 nm in diameter, which perfectly correspond to pseudomorphs coating bacterial cells (monazite sheaths). Lanthanum phosphate precipitation on *Pseudomonas aeruginosa* cells was reported from experiments [4, 5].

Thus the high mineralization at Tomtor may be due to microbially mediated alteration of eluvium. Microbial fossils in the Tomtor ores were reported earlier [6] but no further study ever followed for the lack of solid proof. Prolific accumulation of monazite was possible in water of a persistent hot spring where hydrothermalism maintained a microbial community that concentrated trace elements.

The work was part of Integration Projects SB RAS #40, 94.

[1] Frolov, A.A. *et al.*. 2003. Carbonatite Deposits of Russia. NIA-Priroda, Moscow. [2] Dobretsov N.L. & Pokhilenko N.P., 2010. Russian Geology and Geophysics, 51(1), 98-111. [3] Tolstov, A.B. *et al.*, 2011. Razvedka i Okhrana Nedr, No. 6, 20-26. [4] Mullen, M. D., *et al.*. 1989. Applied and Environmental Microbiology, 55(12), 3143-3149. [5] Langley, S. & Beveridge, T. J., 1999. Applied and Environmental Microbiology, 65 (2), 489-498. [6] Zhmur, S.I. *et al.*, 1994. Doklady Earth. Sci., 336 (3), 372-375.

Understanding biogeochemical transformation and mobilization of Hg From river bank soils: South River, Virginia

O. LAZAREVA^{1*}, D.L. SPARKS¹, R. LANDIS², N.R. GROSSO², J. COLLINS³, J. A. DYER², C.J. PTACEK⁴, S. HICKS⁵ AND D. MONTGOMERY⁵

¹University of Delaware Environmental Institute, Newark, DE, USA, olazarev@udel.edu*, dlsparks@udel.edu

²DuPont, Wilmington, DE, USA,
Richard.C.Landis@usa.dupont.com,
Nancy.R.Grosso@usa.dupont.com,
James.A.Dyer@usa.dupont.com

³URS Corporation, Fort Washington, PA, USA,
joshua.collins@urs.com

⁴Department of Earth & Environmental Sciences, University of Waterloo, Waterloo, Canada, ptacek@uwaterloo.ca

⁵Stroud Water Research Center, Avondale, PA, USA,
shicks@stroudcenter.org, davemont@stroudcenter.org

Between 1929 and 1950, mercury (Hg) was extensively used by the DuPont plant in the production of rayon acetate fiber in Waynesboro, VA and released into the South River. The contamination of Hg was discovered in the 1970s and remains elevated in water, soil, sediments, and biota.

The major objective of this study is to investigate Hg dynamics within the floodplain soils at South River Mile 3.5. Our over-arching hypothesis is to test if leaching of bank soils is a significant source of dissolved or colloidal inorganic Hg (IHg). The hypotheses on Hg loading mechanism include: (1) bank soil inundation is due to horizontal flow through a highly transmissive gravel zone at the base of the bank, vertical drainage of precipitation, and upgradient groundwater flow; (2) drainage occurs mainly through gravel zone wetting an organic rich soil; (3) hydraulics facilitate the downward or upward movement of the capillary fringe affecting soil redox potential, mineral dissolution, and leaching of IHg into dissolved/colloidal phases that are either directly transported to the river or methylated within the saturated zone of the bank and subsequently released.

This investigation will demonstrate preliminary data from a number of state-of-the-art in-situ monitoring sensors, such as custom-designed redox probes, soil moisture and temperature probes, pressure transducers installed at the site; and soil and pore-water chemistry. The sensors are used to characterize geochemical gradients and how they change over time, and to enable targeted sampling at Hg loading hot spots.

***In situ* measurements of Cu isotopes in Cu sulphides**

M. LAZAROV^{1*}, I. HORN¹, S. WEYER¹
AND A. PAČEVSKI²

¹ Institute für Mineralogie, Leibniz Universität Hannover,
Callinstr. 13, 30167 Hannover, Germany
(*m.lazarov@mineralogie.uni-hannover.de)

² Faculty of Mining and Geology, University of Belgrade,
Dusina 7, 11000 Belgrade, Serbia

Previous investigations observed Cu isotope fractionation in hydrothermal or porphyry ore deposits in the order of 2‰ [1, 2]. If such Cu isotope variations occur within a single ore body or mineralisation vein, they likely point to changes of the redox conditions or salinity of hydrothermal fluids [2, 3], rather than source heterogeneities. To distinguish these processes we are developing a method of *in situ* copper isotope analyses by femtosecond LA-MC-ICP-MS.

Initial tests were conducted using in-house standards of Cu metal, brass and Cu-sulphide minerals (chalcopyrite, covellite and enargite) that are homogeneous regarding their major elements. For comparison, the copper isotope composition of these in-house standards was also analysed by solution MC-ICP-MS. In both cases in-house standards were measured relative to the Cu (NIST976) standard while Ni (NIST986) was used to monitor instrumental mass bias [3]. For replicated analyses of metal in-house standards relative to NIST976, in both laser ablation and solution modes the precision of <0.05‰ for $\delta^{65}\text{Cu}_{\text{NIST}}$ was achieved. Replicated LA-MC-ICP-MS analyses of minerals relative to NIST976 or in-house standards of the same mineral, revealed reproducibility variations for $\delta^{65}\text{Cu}$ of ~0.2‰. The laser ablation analyses of the in-house mineral standards agreed within 0.15‰ ($\delta^{65}\text{Cu}$) with those obtained by solution analyses. The larger scatter of the mineral standards (relative to metals), obtained by laser ablation, likely indicates Cu isotopic heterogeneities within the analysed minerals.

First *in situ* Cu isotope measurements of samples from the Bor hydrothermal ore deposit (East Serbia) reveals differences of ~0.35‰ in $\delta^{65}\text{Cu}$ between chalcopyrite in veins and those dispersed as small grains. These systematic variations likely imply a change in the composition of hydrothermal fluids.

[1] Zhu, X. K., O'Nions, R. K., Guo, Y., Belshaw, N. S. & Rickard, D. (2000). *Chem. Geol.* **163**, 139-149.

[2] Li, W., Jackson, S. E., Pearson, N. J. & Graham, S. (2010). *Geochim. Cosmochim. Acta* **74**, 4078-4096.

[3] Markl, G., Lahaye, Y. & Schwinn, G. (2006). *Geochim. Cosmochim. Acta* **70**, 4215-4228.

Regeneration of organophilic zeolites after sulfamethoxazole antibiotic adsorption

L. LEARDINI^{1*}, A. MARTUCCI², I. BRASCHI³,
S. BLASIOLI³, R. ARLETTI⁴ AND S. QUARTIERI¹

¹Dep. of Physics and Earth Sciences, University of Messina, Italy (*correspondence: llearnini@unime.it)

²Dep. of Physics and Earth Sciences, University of Ferrara, Italy

³Dep. of Agro-Environmental Science and Technology, University of Bologna, Italy

⁴Dep. of Mineralogical and Petrological Sciences, University of Torino, Italy

The large amount of non-biodegradable sulfonamide antibiotics used in hospitals, feedstocks and in fish farming cause their occurrence in the aquatic environment resulting in the dramatic emergence of antibiotic resistance in fish pathogens and in the transfer of these resistance determinants to bacteria in land animals and to human pathogens [1]. In Italy, it was found that sulfamethoxazole (SMX) is one of the most abundant residual drug in surface waters [2]. Recently, it has been proven that high-silica zeolites (Y, ZSM-5 and MOR) are environmentally compatible adsorbents able to effectively remove sulfamethoxazole when dissolved in aqueous matrix [3]. The effective incorporation of this pollutant inside the zeolite cavities has been demonstrated by combining diffraction and spectroscopic techniques [3].

In this work, the thermal regeneration of hydrophobic high-silica ZSM-5 and hydrophobic high-silica zeolite Y after sulfamethoxazole adsorption was investigated using *in situ* high-temperature synchrotron X-ray powder diffraction (GILDA, ESRF) to monitor the structural modifications induced by heating. The evolution of the structural features was followed both in temperature ramp (25-575°C, heating rate 10 °C/min) and in isotherm mode (120 minutes at 575 °C) by full profile Rietveld refinements.

Structure refinements demonstrate that the thermal regeneration accompanied by the full degradation of SMX is completed at about 575 °C and it does not affect the crystallinity of the sorbing materials. These results indicate that high-silica zeolite Y and high silica ZSM-5 are affordable materials for water clean-up and drug delivery.

[1] Acar *et al.* (2001) *Rev. Sci. Tech.* **20**, 797- 810. [2] Castiglioni *et al.* (2006) *Environ. Sci. Technol.* **40**, 357-363.

[3] Blasioli *et al.* (2011) *Advances in Zeolites Science and Technology*, De Frede Eds., Napoli, 49-52.

Connecting bacterial ROS cycling to the production of Mn oxides

D.R. LEARMAN^{1*}, T. ZHANG², P.F. ANDEER²
AND C.M. HANSEL²

¹Department of Earth and Atmospheric Sciences and Institute for Great Lakes Research, Central Michigan University, Mount Pleasant, MI, 48859 U.S.A. (*correspondance: deric.learman@cmich.edu)

²Marine Chemistry and Geochemistry Department, Woods Hole Oceanographic Institution, Woods Hole, MA 02543, U.S.A.

Reactive oxygen species (ROS) can drive the cycling of numerous important elements in the environment. Previously we have shown that the bacterium, *Roseobacter* sp. AzwK-3b, governs the oxidation of Mn(II) via enzymatic production of superoxide. Another ROS, hydrogen peroxide, is also important in this pathway. In fact, in reactions with only Mn(II) and abiotically generated superoxide, we find superoxide alone is not enough to produce Mn(III,IV) oxides. The scavenging of hydrogen peroxide (via the addition of catalase) is required to generate Mn oxides abiotically. Thus, *R. AzwK-3b* must produce superoxide and also scavenge hydrogen peroxide to form Mn oxides. To obtain a greater understanding of biological factors involved in this process, proteins were extracted from *R. AzwK-3b* cultures and examined for their connection to Mn(II) oxidation. Similar to the pathway identified in experiments with *R. AzwK-3b* whole cell cultures and cell-free filtrate, Mn(II) oxidation within soluble protein extracts is initiated by superoxide. Further, an in-gel Mn(II) oxidation assay revealed a protein band that could generate Mn oxides in the presence of soluble Mn(II). This Mn(II)-oxidizing protein band was excised from the gel and the peptides were identified via mass spectrometry. An animal heme peroxidase was the predominant protein found in this band. This protein is homologous to the animal heme peroxidases previously implicated as a Mn(II)-oxidizing enzyme within the *Alphaproteobacteria*, *Erythrobacter* SD-21 and *Aurantimonas manganoxydans* strain SI85-9A1. For *R. AzwK-3b*, the mechanism(s) of Mn(II) oxidation by this animal heme peroxidase is unknown, but may include scavenging of hydrogen peroxide, generation of superoxide, or production an organic ligand involved in Mn(III) complexation. Interestingly, the *Alphaproteobacteria*, *Ruegeria* sp. TM1040, is also known to generate extracellular superoxide but does not oxidize Mn(II) to Mn oxides. Interestingly, the genome of *Ru. TM1040* does not contain an animal heme peroxidase, which further suggests an important role for this protein in the formation of Mn oxides.

Enzymatic constraints on the global S cycle: the fractionation factors of Dsr

WILLIAM D. LEAVITT^{*1}, INÉS C. PEREIRA³, ALEXANDER S. BRADLEY³, WEIFU GUO⁴ AND DAVID T. JOHNSTON¹

¹Harvard University, Dept. of Earth & Planetary Science, Cambridge, MA, USA, (*wleavitt@fas.harvard.edu),

²Instituto De Tecnologia Quimica E Biologica, Oeiras, Portugal,

³Dept. of Earth and Planetary Sciences, Washington University in St. Louis, MO, USA,

⁴Dept. of Marine Chemistry and Geochemistry, Woods Hole Oceanographic Institution, MA.

Coupling quantitative geochemical models with enzyme and whole cell observations informs our interpretation of the environmental histories encoded in the geological S isotope records. Much of this preserved record is driven by the central biochemical machinery of microbial sulfate reducers (MSRs) – linking sulphate reduction to organic matter oxidation. Our present understanding of MSR sulfur isotope fractionation stem from a series of robust cellular-scale (*in vivo*) studies [c.f., 1]. Still, biogeochemical models of the S cycle lack fundamental constraints on the fractionations associated with enzymatic S transformations within the MSR pathway, rendering our best models semi-quantitative. Inspired by the early carbon isotope work on RuBisCO and the influence those studies hold on our understanding of the global carbon cycle, we extend our recent open-system *in vivo* [2] and preliminary pure-enzyme (*in vitro*) experimental work. This study is part of a broader effort to precisely calibrate the S-isotope effects associated with *in vivo* sulphate and *in vitro* sulfite reduction, each underpinned by the MSR enzyme dissimilatory sulfite reductase (Dsr).

To provide fundamental boundary conditions for the network fractionation models of MSR, we performed *in vitro* closed-bottle sulphite reduction experiments with purified DsrAB protein. From these experiments we measure the isotopic composition of all S pools: sulfane and sulfonate moieties in reduction products trithionate and thiosulfate, residual, and initial sulphite. From here we apply a modified Rayleigh model to calculate the enzyme-specific isotope fractionation factors for DsrAB (³³λ_{Dsr}, ³⁴α_{Dsr}). We repeat this procedure over a range of experimental conditions, including temperature and host species. Isotope and mass balance is conserved in all individual experimental volumes allowing us to directly calculate fractionation factors. Interestingly, the major isotope fractionation factors (³⁴α_{DsrAB}) we most often observe are significantly smaller than predicted those from equilibrium estimates, but readily fit with indirect estimates from a seminal study by Jørgensen [3].

[1] Harrison & Thode (1958), *Trans. Faraday Soc.*, **54**, 84–92.

[2] Leavitt et al. 2013. PNAS, *in press*. [3] Jørgensen (1979) *GCA* **43**, 363-374.

Nitrogen biogeochemical cycling in ferruginous Lake Pavin

OANEZ LEBEAU^{1*}, VINCENT BUSIGNY^{1*}, DIDIER JEZEQUEL¹, CARINE CHADUTEAU¹, SEAN CROWE² AND MAGALI ADER¹

¹Univ. Paris Diderot-IPGP, Sorbonne Paris Cité, UMR7154 CNRS, Paris, France *correspondence: olebeau@ipgp.fr
²Nordic Center For Earth Evolution, University of Southern Denmark, Odense, Denmark

Over geological timescales, the Earth's oceans were affected by several periods of total or partial anoxia. The timing, causes and consequences of ocean oxygenation are intimately linked to paleo- N cycling. Studies on modern analogues are essential for interpreting biogeochemical signals recorded in ancient sediments. Lake Pavin (French Massif Central) is permanently stratified with anoxic Fe-rich deep waters (from 60 to 92m depth) overlain by oxic shallow waters (from 0 to 60m depth) and can be regarded as an analogue for the ocean during periods of redox stratification with ferruginous deep waters. Such ferruginous conditions were prevalent during the Precambrian and may also have been important during Phanerozoic Ocean Anoxic Events (OAEs). In order to determine if the primary N isotope signatures are preserved or modified in this type of environment, we analyzed bulk N isotope compositions in 6 sediment cores from different depths in Lake Pavin: in the oxic zone (31.5, 26.8 and 19.5m depth), at the oxic-anoxic boundary (60m depth), at the peak of H₂S production from SO₄²⁻ reduction (65m depth) and at the bottom of the lake (90m depth). Complementary analyses of sediment traps set up at 4 different depths in the water column (25, 56, 67 and 88m depth) provide a reference frame for organic matter deposited in the sediments and allow us to test diagenetic N evolution in the water column. For the traps and cores of the anoxic layer, the N isotope composition is not significantly affected by diagenetic processes with $\delta^{15}\text{N}_{\text{tot}}$ values around -1 ‰. Such unusually low $\delta^{15}\text{N}$ values suggest a dominance of N₂-fixers in the water column, which is expected in a stratified system where nitrate is strongly depleted by denitrification at the redox boundary and N₂ is the major source of N for organisms living in the photic zone. For each core of the oxic layer, $\delta^{15}\text{N}_{\text{tot}}$ increases with depth within the sediment, from values as low as -3.3 ‰ up to +0.3 ‰. These variations are not compatible with purely oxic diagenesis but require a migration of the sediment oxycline through time, possibly due to an increase in the organic matter flux associated with eutrophication in Lake Pavin.

Stretching, Coalescence and Mixing in Porous Media

TANGUY LE BORGNE¹, MARCO DENTZ² AND EMMANUEL VILLERMAUX³

¹Geosciences Rennes, UMR 6118, Université de Rennes 1, CNRS, Rennes, France
²Spanish National Research Council (IDAEA-CSIC), Barcelona, Spain
³Institut de Recherche sur les Phénomènes Hors Equilibre, Aix-Marseille Université, 13384 Marseille Cedex 13, Francey

We study mixing in heterogeneous permeability fields, whose structural disorder varies from weak to strong. We propose a unified framework to quantify the overall concentration distribution predicting its shape and rate of deformation as it progresses towards uniformity in the medium. The concentration field is represented by a set of stretched lamellae whose rate of diffusive smoothing is locally enhanced by kinematic stretching. Overlap between the lamellae is enforced by confinement of the scalar line support within the dispersion area. Based on these elementary processes, we derive analytical expressions for the concentration distribution, resulting from the interplay between stretching, diffusion and random overlaps, holding for all field heterogeneities, residence times, and Peclet numbers. We discuss consequences for effective chemical reaction kinetics in heterogeneous media.

Rare earth elements in lake sediments in Poland

DARIUSZ LECH, IZABELA BOJAKOWSKA
AND DOROTA KARMA SZ

Polish Geological Institute – National Research Institute
(izabela.bojakowska@pgi.gov.pl)

127 sediment samples were collected from profundal zones of 87 lakes of the following lakeland areas: Greater Poland, Pomerania, Masuria and Łęczna-Włodawa. In the samples the content of REE, Sc and Y were determined by ICP-MS method, the content of Ba, Cr, Co, Cu, Pb, Zn, Ni, V, Sr, Ca, Mg, Fe, Mn, K, Na, P and S - by ICP-OES method, after aqua regia digestion, Organic carbon were also determined (TOC) by means of coulometric titration method

The REE content in analyzed sediments ranged from 4.40 to 127.44 mg/kg, the average content was 35.78 mg/kg while the geometric mean - 24.68 mg/kg. The average REE contents of individual elements were as follows: La - 6.65 mg/kg, Ce - 15.43 mg/kg, Pr - 1.74 mg/kg, Nd - 6.93 mg/kg, Eu - 0.26 mg/kg, Sm - 1.36 mg/kg Gd - 1.24 mg/kg, Tb - 0.17 mg/kg, Dy - 0.92 mg/kg, Ho - 0.17 mg/kg, Er - 0.45 mg/kg, Tm - 0.06 mg/kg, Yb - 0.35 mg/kg and Lu - 0.05 mg/kg. The concentrations of rare earth elements in studied lake sediments are comparable to the concentrations found in sedimentary rocks. REE concentrations in the sediments are most similar to their concentrations in limestone rocks; however they are lower in comparison to the REE concentrations in sandstones and clay rocks. The results showed differences in the content of REE in lake sediments in various parts of Poland. The geometric mean of REE content in the lake sediments of Pomeranian, Greater Poland and Łęczna-Włodawa Lake Districts were similar and were respectively 21.70, 20.70 and 21.50 mg/kg, while the sediments of Masuria Lake District had a higher geometric mean of REE content – 29.54 mg/kg.

The content of REE in lake sediments shows a strong correlation with the Al ($r = 0.96$), K ($r = 0.96$) and Mg ($r = 0.86$) contents, a high correlation with the Fe ($r = 0.68$), a significant correlation with the P ($r = 0.42$), S ($r = 0.40$) and organic carbon ($r = 0.38$) contents. Among the trace elements analyzed REE concentrations showed a very strong correlation with the concentration of Ni ($r = 0.92$), V ($r = 0.94$), Co ($r = 0.94$) and poor correlation with the content of Zn ($r = 0.31$), Pb ($r = 0.34$), and Cu ($r = 0.33$). REE contents in sediments also showed a negative high correlation with calcium ($r = -0.79$) and strontium content ($r = -0.53$).

Redox in silicate melts: in-situ XAS investigation of 2 redox couples

M. LECONTE¹, P. M. MARTIN², D. TESTEMALE³, C. PETITJEAN⁴ AND D. R. NEUVILLE¹

¹CNRS-IPGP, Géochimie&Cosmochimie, Paris Sorbonne Cité, 1 rue Jussieu, 75005 Paris, France.

²CEA, DEN, DEC, Cadarache F-13108 Saint-Paul-Lez-Durance, France.

³Institut Néel, Département MCMF, 38042 Grenoble, France.

⁴Institut Jean Lamour, BP 70239, 54506 Vandoeuvre, France.

The silicate melts are important materials for earth sciences, in particular for the volcanology and mass transfers and also for glass industry (glass making, ceramics and nuclear waste management). Such melts are very complex materials generally containing more than ten oxides. The presence of multivalent elements within the glass compositions can significantly affect both glass properties (rheological properties [1] for example) and technological processes. In particular in the field of nuclear waste storage where solubility, crystallization and incorporation of heavy elements are of prime importance. Consequently, the control of oxydoreduction reactions proves to be necessary for managing both vitrification processes and structural changes intervening in temperature within glasses. Magnien *et al.* [2] have shown that redox can be control at high temperature by diffusion of O₂ and O²⁻ whereas at low temperature, around the glass transition temperature by diffusion of cations according with Cook and Cooper [3]. But all these studies are made with only one redox couple, but what happens by mixing redox couple?

XANES spectroscopy is a powerful tools to investigate valence, coordination number, short and middle range order in mineral, glass and melts.

We have investigated redox of Cr and Ce silicate glass and melts at high temperature by using XANES at the Cr K-edge and Ce L3 edge. These results represent a first step to understand mixing redox couple in silicate melts and how they interact at different temperature and under different control atmosphere. These results will be present and discuss.

[1] Neuville *et al.*, (1993) *Contrib. Min. Petrol.*, 113, 571-581; [2] Magnien V, *et al.*, (2008) *Geochim. Cosmochim. Acta.*, 72, 2157-2168; [3] Cook and Cooper (1990) *J. Non-Cryst. Sol.*, 120, 207-222.

Genetic relationship between Ag-(Pb-Zn) mineralization and W-specific Mesozoic magmatism in the Nanling belt (China) based on data from the Wutong deposit

P. LECUMBERRI-SANCHEZ^{1*}, R.L. ROMER², V. LÜDERS²
AND R.J. BODNAR¹

¹4044 Derring Hall, Virginia Tech, Blacksburg, VA 24061,
USA (*correspondence: pilar@vt.edu)

²GFZ, Telegrafenberg, D-14473, Potsdam, Germany

More than 50 % of the world's total reserves of tungsten are in China, and most tungsten deposits are located in the Nanling range (Cathaysia block, southeast China). This study explores the genetic relationship between W-specific magmatic events and shallow (W)-Ag-Pb-Zn deposits in the Nanling range based on data from the Wutong deposit, Guangxi Province.

Because the temperatures obtained from mineral thermometry and homogenization temperatures of fluid inclusions are the same (~300°C), the fluid inclusion homogenization temperatures are interpreted to be approximately equal to the trapping temperatures, indicating formation at low pressures, i.e., slightly above the liquid-vapor curve. This, in turn, indicates that the deposit formed at relatively shallow levels. The C-O-Sr-Pb isotopic composition of minerals indicate that one single fluid was responsible for mineralization. The chemical composition of fluid inclusions indicates that the fluid evolved from a fractionated magma. Therefore, the Wutong deposit is likely to represent the shallow expression of a magmatic-hydrothermal system. The Sr-Pb isotopic data indicate that the magmatic fluids are associated with melting of crustal rocks of the Cathaysia block.

The age of the Wutong mineralization, obtained from h bnerite dating, is Late Yanshanian (Cretaceous). Most Ag-Pb-Zn deposits in this region are typically attributed to Late Jurassic mineralization. In contrast, Wutong is a Cretaceous system formed during the Cretaceous mineralization peak in south China. As this relatively shallow hydrothermal system is related to deeper magmatism, Cretaceous mineralization is not limited to the western limit of Cathaysia but may extend eastward at least to the Nanling range. Furthermore, regional grouping of the age of granite-related magmatism indicates that the same kind of crustal source has been melted repeatedly, possibly in different tectonic settings.

The turnover time of organic carbon in boreal riparian zones – A hydrological approach

J. L. J. LEDESMA^{1*}, T. GRABS², K. H. BISHOP^{1,2}
AND S. J. K HLER¹

¹ Department of Aquatic Sciences and Assessment, Swedish University of Agricultural Sciences (SLU), P.O. Box 7050, 750 07 Uppsala, Sweden (*correspondence: jose.ledesma@slu.se) (Kevin.Bishop@slu.se, Stephan.Kohler@slu.se)

² Department of Earth Sciences, Uppsala University, P.O. Box 256, 751 05 Uppsala, Sweden, (Kevin.Bishop@geo.uu.se, thomas.grabs@geo.uu.se)

Boreal regions are large stores of organic carbon (OC). The majority of the OC found in boreal inland waters is allochthonous, i.e. originally from terrestrial sources. Allochthonous carbon is especially dominant in headwater streams, which also show high concentration and fluxes. The link between the terrestrial and the aquatic compartments in these headwaters is dominated by organic matter-rich riparian zones (RZ). RZ have been described as near-infinite organic matter sources [1] [2] because large amounts of OC originate here and are exported to streams by lateral fluxes. But, how long can RZ sustain the high lateral OC fluxes in boreal catchments? To answer this question we estimate the turnover times of OC in 13 RZ profiles in a boreal catchment in northern Sweden by comparing pools and lateral fluxes. The lateral fluxes can be mathematically estimated using the Riparian Flow-Concentration Integration Model (RIM) approach [3] [4], in which lateral discharge and concentration profiles in the RZ are combined. Our calculations with this approach indicate that 90% of the lateral OC fluxes come from a 36 ± 18 cm (± SD) shallow soil layer accounting in all the 13 studied riparian profiles. Preliminary analyses suggest long turnover times of OC in these 'active' layers. That would imply that there is no long term supply shortage. The results from this study will have implications for the global carbon cycle in relation to human perturbations.

[1] McGlynn and McDonnell (2003) *Water Resour Res* **39**, 1090. [2] Sanderman *et al.* (2009) *Water Resour Res* **45**, W03418. [3] Bishop *et al.* (2004) *Hydrol Process*, **18**, 185-189. [4] Seibert *et al.* (2009) *Hydrol Earth Syst Sc* **13**, 2287-2297.

Archean cherts: are they reliable paleo-seawater proxies?

MORGANE LEDEVIN^{1*}, NICK ARNDT¹
AND ALEXANDRE SIMONOVICI¹

¹ISTERRE, BP53, 38041 Grenoble Cedex 9, France

(*correspondence: morgane.ledevin@ujf-grenoble.fr)

Archean cherts represent some of the oldest sedimentary rocks on Earth. It is commonly thought that they could be useful paleo-environment indicators, assuming that the silica phase retained the composition of the fluid from which it precipitated. In this study, we conducted geochemical and isotope analyses of three types of cherts (seawater-derived precipitates, fracture-filling cherts and silicified sediments) from the Barberton greenstone belt (3.5-3.2Gy), South Africa, in order to test their reliability for paleo-environment studies.

We show that Archean cherts are a mixture of (1) a silica phase that has extremely low concentrations of trace elements and contributes only SiO₂ to the bulk composition, and (2) another phase that dominates the trace element composition and varies from site to site. We calculated that 3-4% of phyllosilicate, 20% of carbonaceous matter and only 2% of carbonate is enough to control the chert chemistry and mask the silica composition. Carbonate-rich cherts could be of interest because this phase has long been known to retain oceanic fluid chemistry.

Because the silica phase is easily contaminated, the use of cherts for paleo-environment reconstructions is seriously limited and requires high purity precipitates. Massive white chert layers at Buck Reef have SiO₂ close to 100wt% and extremely low concentrations in all the trace elements. We argue that these chemical features are the sole reliable criteria available for now to recognize a pure precipitate, i.e. one that lacks continental contributions, but that they are not sufficient to rule out a possible hydrothermal contribution. Otherwise, only systematic field and petrographic studies can help to distinguish the various chert types, as their composition does not depend on the formation process.

The high purity white cherts from Buck Reef display strong LREE depletions, positive La anomalies and superchondritic Y/Ho ratios that resemble modern seawater. However, these commonly used proxies for the recognition of seawater-derived precipitates fail to distinguish the origin of the silica, these characteristics being similar to those found in hydrothermal, metamorphic and pegmatitic quartz. An unusual feature is the strong positive Sm-anomalies of these samples which have never been observed in any other terrestrial rock.

Prediction of Effects of Acetogens on Hot Spring Biogeochemistry

BRADY D. LEE¹, JOHN E. ASTON¹, MICHELLE H. LEE²
AND WILLIAM A. APEL¹

¹Idaho National Lab, P.O. Box 1625, Idaho Falls, ID 83415,
Brady.Lee@inl.gov

²Pacific Northwest National Lab, P.O. Box 999, MSIN K3-62,
Richland, WA 99352 USA, Hope.Lee@pnnl.gov

Acetogens are a broad category of obligately anaerobic bacteria that are found in a variety of ecosystems and are able to use diverse electron donors and acceptors. Activity of acetogens has been studied in many terrestrial environments, but the activity of acetogens in hot spring environments is not well understood. For this reason, acetogens in hot spring have a wider impact on hot spring geochemical cycles and microbial populations, beyond just acetogenic activity. One method to predict the impacts of versatile metabolisms on the flow of energy and material through microbial systems is metabolic stoichiometric modeling, which extracts systemic information from molecular-level network structure and conservation relationships, depending on electron donors and acceptors in the growth environment. To test this hypothesis, an initial model has been constructed from the annotated genome of the well-studied acetogen, *Moorella thermoacetica*, and the output data have been sorted against various cellular strategies, including maximal efficiency of biomass yield per substrate, and substrate consumption in the presence of high exogenous concentrations of produced metabolites. Output from such models has successfully predicted substrate concentrations that yield elevated ethanol production, as opposed to acetate, when *M. thermoacetica* was grown on CO₂ and H₂. This research has shown the utility of metabolic modeling in predicting electron donor and acceptor use and production of organic acids and alcohol in the *M. thermoacetica*. These types of models will help to predict the effects of acetogenic activity on the overall biogeochemistry in hot spring environments.

Carbon isotope and lipid biomarker stratigraphy from organic-rich strata through the Neoproterozoic Shuram excursion in South Oman

C. LEE¹, D. A. FIKE², G. D. LOVE¹, A. L. SESSIONS³, J. P. GROTZINGER³, R. E. SUMMONS⁴
AND W. W. FISCHER³

¹University of California, Riverside (clee093@ucr.edu)

²Washington University St Louis

³California Institute of Technology (wfischer@caltech.edu)

⁴Massachusetts Institute of Technology

The regulation of oxygen levels in Earth's atmosphere and oceans is inextricably linked to the carbon cycle. Carbon isotope ratios of carbonate and sedimentary organic matter provide first order insights into the operation of the carbon cycle in the geologic past. During the Ediacaran period, the ~580 Ma 'Shuram Excursion' (SE) records a dramatic, systematic shift in $\delta^{13}\text{C}_{\text{carbonate}}$ values to as low as *ca.* -12‰, lasting potentially millions to tens of millions of years in duration and constitutes the largest carbon isotope excursion known in the record [1]. The extremely negative carbon isotope values in carbonate challenges our understanding of the ancient carbon cycle and is difficult to rationalise *via* uniform carbon cycle principles. Several hypotheses have been developed to explain this behaviour, all of which make different predictions for the abundance, structure, and isotopic composition of organic carbon through the excursion [1,2,3,4].

For a direct test of these ideas, we report paired organic and inorganic stable carbon isotope ratios in addition to detailed lipid biomarker stratigraphic records from a subsurface well drilled on the eastern flank of the South Oman Salt Basin, Sultanate of Oman. This well captures thermally immature and organic-rich Nafun Group strata traversing the SE, yielding variable but primary biomarker characteristics typical of Neoproterozoic rocks from this region [5].

Despite the high organic matter contents, the carbon isotopic compositions of carbonates do not covary with those of organic phases. Furthermore, lipid biomarker data reveal that organic matter composition and source inputs varied stratigraphically, reflecting biological community shifts in non-migrated, syngenetic organic matter deposited during this interval. Together these observations imply that carbonate-organic isotopic decoupling during the SE is not a result of mixing of fossil or exogenous carbon sources (either DOC, detrital, or migrated) with syngenetic organic matter.

[1] Fike *et al.*, (2006) [2] Johnston *et al.*, (2012) [3] Schrag *et al.*, 2013 [4] Rothman *et al.*, (2003); [5] Love *et al.*, (2009)

Mineralogical characterization of chrysotile-containing soils

CHAEHYANG LEE¹, JAEBOONG PARK², SEKWHAN SONG³,
HOJU LIM⁴ AND YUL ROH^{5*}

¹Chonnam National University, Gwangju, Korea,
(chwish@nate.com)

²Chonnam National University, Gwangju, Korea,
(20548pjb@chonnam.ac.kr)

³Joongbu University, Chungnam, Korea,
(shsong@joongbu.ac.kr)

⁴National Institute of Environmental Research, Incheon,
Korea, (limhoju@gmail.com)

⁵Chonnam National University, Gwangju, Korea,
(*correspondence: rohy@jnu.ac.kr)

Asbestos-containing soils occur mainly at ultramafic rocks and hydrothermally altered carbonate rocks in S. Korea. Remediation of asbestos-containing soils is considered a high priority by the Korean Government because these soils, if left untreated, represent a hazard to the environment and human health. The objective of this study was to show physicochemical and mineralogical characterization of asbestos-contaminated soil can direct the development of remediation strategies.

Two sites (Hongseong and Gapyeong, S. Korea) at abandoned asbestos mines were selected for soil and mineralogical characterization. At each site, samples were taken at soil surface. Soil preparation consisted of sieving air-dried soil through a 2-mm sieve. The sieved soils (< 2-mm) were used for soil characterization and mineralogical analysis. Following particle size fractionations, mineralogical characterization was investigated by TG-DTA, XRD, PLM, SEM and EDS analyses. Point counting was used to quantify asbestos in the whole soil and size fractionated samples.

The soil color of the both sites was grey. The soil texture of the Hongseong and Gapyeong soils was loamy sand and sand, respectively. XRD, PLM, SEM and EDS analyses showed that the fibrous chrysotile was observed at both soils, and both fibrous chrysotile and the needle or straight-shaped tremolite asbestos existed in Gapyeong soils. Hongseong soils contained 4.8% asbestos in sand fraction and 2.5% asbestos in silt fraction. And Gapyeong soils contained 6.6% asbestos in sand fraction and 1.7% asbestos in silt fraction. Therefore, the soils of the both sites were designated as asbestos-containing materials (greater than or equal to 1%) according to the criteria of the U.S. EPA. TG-DTA showed that chrysotile and tremolite asbestos in soil at both sites were transformed to forsterite and diopside with the temperatures about 810°C and 1060°C, respectively. These results indicated that thermal treatment of asbestos-containing soils was effective for phase transformation of the asbestos in soils.

A case study for soil erosion in the Han river buffer zone, South Chuncheon, Korea

DAL-HEUI LEE¹, SUNG LAE CHUNG², WOO YOUNG CHOI³ AND SEUNG HEON CHAE⁴

¹[215 Anyang Megavalley, Gwanyang-dong 799, Dongan-gu, Anyang-si, Gyunggi-do, Korea, dalheui@yonsei.ac.kr
^{2,3,4}[215 Anyang Megavalley, Gwanyang-dong 799, Dongan-gu, Anyang-si, Gyunggi-do, Korea, sj9171@chol.com]

The objective of this study is to report the relative importance of soil management on organic content of the sediment in relation to soil erosion. The rainfall simulation experiments were carried out under different rainfall kinetic energies and geotechnical conditions. The three soil sampling sites were located on the adjacent farms of the riparian buffer zone of the Han River, Korea. Rainfall simulations were carried out within three months after soil sampling. Lechler full cone nozzles (type 460.648.30.cc) based on measurements using a Distromet Joss-Waldvogel Disdrometer. Tap water with an electric conductivity of 105 $\mu\text{S cm}^{-1}$ was used for each test. The implications of the results will aid the development of models aimed at predicting organic content due to soil erosion. The test results showed that geotechnical conditions and rainfall conditions, such as the ground slope, the compaction ratio, rainfall intensity and duration of rainfall are main factors for soil erosion. However, soil texture was determined to be the most important soil variable influencing soil erosion. Apparently, the severity of soil erosion did not exclusively determine the amount of nutrients lost in runoff from agricultural land.

Metal stable isotopes in Lake Baikal sediments

DER-CHUEN LEE^{1,*}, HSIN-TING LIU²
AND SHUN-CHUN YANG³

¹Institute of Earth Sciences, Academia Sinica, Taipei, Taiwan, ROC, dclee@earth.sinica.edu.tw (* presenting author)
²Dept. of Earth Sciences, Nat. Normal Univ., Taipei, Taiwan, ROC, 49444039@ntnu.edu.tw
³Dept. of Geological Sciences, Nat. Taiwan Univ., Taipei, Taiwan, ROC, d98224001@ntu.edu.tw

Metal stable isotopes of Fe, Zn, Mo, and Cd, have been analyzed for the authigenic portion of a gravity core from Lake Baikal, Russia, in order to study the sources and sinks for these trace metals in the Lake Baikal, the largest fresh water lake in the world, and as potential proxies for the past climate changes in the region [1]. A ~ 3 meters gravity core (GC-99; 52°05'23"N, 105°15'24"E) sampled near the bore hole of BDP-99 in Lake Baikal is used in this study. The core was sampled per cm continuously, and one sample was analyzed for every 10 cm throughout the entire core in this study. A series of leaching procedures were used to remove the carbonates, and to collect the authigenic fractions for study. Double spike technique is used for all four metal stable isotopic measurements.

In general, significant variations are observed yet no correlation is found among these four metal stable isotopes and their respective elemental concentrations. Direct ¹⁴C-dating is currently undertaken, however, using the sedimentation rate of a nearby sediment core, the 3 m GC-99 seems to have recorded the past ~ 23 ka of sedimentation history of Lake Baikal, with a shift of sedimentation rate at ~ 100 cm that has marked the YD event at ~ 12 ka. The same depth also marked the significant shift of $\delta^{97}\text{Mo}/^{94}\text{Mo}$ from -0.5 ‰ in the deeper depth to ~ -2.2 ‰ in the upper 100 cm. Similar shifts from relatively constant at -0.7 ‰ in the deeper depth to more variable, 0 to -1.5 ‰, in the upper 100 cm is also observed for $\delta^{56}\text{Fe}/^{54}\text{Fe}$. Less pronounced but nonetheless similar shifts also observed for Cd and Zn isotopes. While the variations of Cd, Zn, and Fe (to some degrees) isotopes are mostly likely reflect the biological activities, booming of diatoms, the isotopic variations of Mo and Fe (to a lesser degree) can only be explained by the changing of the redox states, towards more oxic from YD event to the present, in Lake Baikal, if the sedimentation rate is indeed correct. Nevertheless, this study marks the first time the metal stable isotopes can be used to study the connections between the local climate events and Lake Baikal using the sediment records. More data, in particular, the chronology and detailed chemical and mineralogical compositions of the sediment cores are needed in order to better constrain the relationship between the Lake Baikal and regional climate changes in the past.

[1] Kuzmin M.I. and Yarmolyuk V.V. (2006) *Geol. Geophys.* **47**, 5-23.

Geochemical processes of soil and groundwater contamination by Cr(VI) from natural sources

GIEHYEON LEE*, SEONYI NAMGUNG AND YEONJIN LEE

Department of Earth System Sciences, Yonsei University,
Seoul, Korea (*correspondence: ghlee@yonsei.ac.kr)

Soil and groundwater contamination with hexavalent chromium (Cr(VI)) is of serious concern especially in industrialized areas over the world as Cr(VI) is the 2nd most common inorganic contaminant. Reduction of Cr(VI) to Cr(III) followed by its precipitation as or directly to Cr(OH)₃(s) is generally the best strategy for Cr(VI) removal because this process substantially alleviates both the toxicity and mobility of Cr. Thereby, processes and mechanisms for Cr(VI) reduction by various reductants have been extensively investigated. Besides the anthropogenic contamination, natural Cr(VI) contamination of soil and groundwater without any anthropogenic source has been reported over the world. Since Cr commonly exists as a trace constituent of various rock forming minerals in the oxidation state of +III, the oxidation processes of Cr(III) would likely be responsible for the natural Cr(VI) contamination processes. We have investigated the potential reaction pathways of Cr(III) oxidation to elucidate the geochemical processes of natural Cr(VI) contamination.

In this study, we examined the oxidation of Cr(OH)₃(s) by birnessite. These two solid phases are those of the most common solid phases of Cr and Mn, respectively, under the near surface environmental conditions. Cr(OH)₃(s) oxidation was examined with solid suspensions containing Cr(OH)₃(s) and/or birnessite (1.0 g/L of each solid) fixed at pH 7–9 with buffers. Sparingly soluble Cr(OH)₃(s) was readily oxidized by birnessite and released substantial amounts of dissolved Cr(VI) in the mixed suspensions. The apparent rate and extent of Cr(OH)₃(s) oxidation increased with increasing pH. The oxidation was catalyzed by reaction intermediate during the early stage of reaction (ca. 10 h) at all pHs. At pH 7 the production of Cr(VI) reached plateau in about 10 d but was continued for 33 d at higher pHs until the experiments were ceased. In addition, the processes of Cr(OH)₃(s) oxidation by birnessite were substantially accelerated in the suspensions open to the atmosphere compared to those purged with N₂. The geochemical processes inhibiting or accelerating Cr(OH)₃(s) oxidation under the experimental conditions will be discussed.

Age and geochemical constraints on the genesis of Late Cenozoic volcanic rocks in central Myanmar

HAO-YANG LEE^{1*}, SUN-LIN CHUNG¹, HSIAO-MING YANG¹, CHIU-HUNG CHU¹, CHING-HUA LO¹
AND A.H.G. MITCHELL²

¹Department of Geosciences, National Taiwan University,
Taipei, Taiwan

(*correspondence: haoyanglee@ntu.edu.tw)

²Consulting Geologist, 20, Dale Close, Oxford OX1 1TU, UK

The central Myanmar basin in which Late Cenozoic volcanism occurred is marked by the existence of the dextral Sagaing fault linking the eastern Himalayan Syntaxis in the north and the Andaman Sea in the south. Here new and comprehensive age results of the volcanic rocks from volcanoes of Mt. Popa, Monywa and Singu are reported. They display two distinct stages of eruptions, including a mid-Miocene stage from ca. 14 to 13 Ma and a Quaternary stage <1 Ma, with a pronounced >10-m.y. magmatic gap in between. While calc-alkaline rocks showing arc-like lava features are abundant, an apparent change in magma composition is observed between these two stages. The mid-Miocene rocks are dominated by intermediate compositions (SiO₂ = 53–61 wt.%) and typical of high-K calc-alkaline nature. They exhibit similar Nd isotope ratios ($\epsilon_{Nd} = +2.6$ to $+1.4$), suggesting a juvenile mantle origin possibly related to the subduction of the Indian oceanic slab beneath Asia. The Quaternary rocks, however, are mainly basaltic compositions but show heterogeneities. There are (1) high-Al basalts with high-K calc-alkaline geochemistry: $\epsilon_{Nd} = +3.1$ to $+2.1$, (2) absarokites: Al₂O₃ = 13–15 wt.%; MgO = 10–12 wt.%; $\epsilon_{Nd} \approx +3.5$, and (3) intra-plate alkali basalts: K₂O = 2.6–3.5 wt.%; $\epsilon_{Nd} = +1.6$ to $+0.9$. We interpret the long magmatic gap as a consequence of transition of the Indian oceanic slab from oblique convergence/subduction to strike-slip movement. It took place in the mid-Miocene, when the dextral motion of the Sagaing fault system initiated and opening of the Andaman Sea began. All these processes were related to the India-Asia collision that caused plate reorganization and eventually “rollback” of the Indian oceanic slab in this region since 1 Ma. Thus the Quaternary volcanism renewed owing to rise of the geotherm resulted from upwelling asthenosphere and small-degree melting of different domains of pre-Miocene subduction-related enriched mantle beneath central Myanmar.

Temporal variation of compositions of volcanic gas and hot springs in the Tatun Volcano Group, Taiwan

HSIAO-FEN LEE^{1*}, TSANYAO FRANK YANG²,
HSIN-YI WEN² AND CHENG-HORNG LIN¹

¹ Institute of Earth Sciences, Academia Sinica, Taipei, Taiwan.

(*correspondence: hf_lee@earth.sinica.edu.tw,
lin@earth.sinica.edu.tw)

² Department of Geosciences, National Taiwan University,
No. 1, Sec. 4, Roosevelt Road, Taipei 10617, Taiwan.
(tyyang@ntu.edu.tw, d99224009@ntu.edu.tw)

The Tatun Volcano Group (TVG), where the geothermal and seismic activities are still very strong, is located in the northern Taiwan. In the past decade, gas samples have been collected monthly to analyze the compositions and isotopic ratios. The results show a similar composition as those of low-temperature fumaroles in other parts of the world. H₂O is the major species of these gas samples, and CO₂ is the dominant component after de-watering[1]. The high ³He/⁴He ratios (4.7~6.7 R_A) [2,3] indicate a mantle-derived degassing source in origin. The carbon isotopic values of CO₂ also exhibit a magmatic source. Since August 2004, progressive increases of HCl concentration and SO₂/H₂S ratio have been observed at Da-you-keng, the most active hydrothermal area in TVG. These variations are accompanied by rising temperature of fumaroles. From 2006 to 2009, increases of S_{total}/CO₂ ratio have been observed in many fumaroles simultaneously. The H-O isotopic values of condensed water of fumaroles from Da-you-keng and Hsiao-you-keng fall in the range away from the meteoric water line, indicating a magmatic water source. Meanwhile, the rest of data from other fumaroles are similar with previous published data of hot springs[4], which are clearly derived from meteoric water in origin.

To surveillance the potential magmatic activity of TVG, an observatory is established in October 2011. We have been collecting/analyzing the volcanic gas samples regularly, as well as the water samples from two hot springs weekly. Compare with the previous data, no significant variations of the geochemical compositions have been found in the past year until now.

[1] Lee *et al.*. (2008) *JVGR*, 178, 624-635. [2] Yang *et al.*. (1999) *Nuovo Cimento Della Societa Italiana Di Fisica C*, 22(3-4), 281-286. [3] Ohba *et al.*. (2010) *Appl. Geochem.*, 25, 513-523. [4] Shieh *et al.*. (1983) *Geol. Soc. China Mem.*, 5,127-140.

Asian monsoon hydrometeorology from TES and SCIAMACHY water vapor isotope measurements and the LMDZ simulations: implications for speleothem climate record interpretation

JUNG-EUN LEE^{1*}, CAMILLE RISI², INEZ FUNG³
AND JOHN WORDEN⁴

¹Jet Propulsion Laboratory, Pasadena, CA, US:
jungelee.kim@gmail.com

²LMD/IPSL, CNRS, Paris, France:
Camille.Risi@lmd.jussieu.fr

³Department of Earth and Planetary Science, University of California, Berkeley, CA, US: ifung@berkeley.edu

⁴Jet Propulsion Laboratory, Pasadena, CA, US:
john.r.worden@jpl.nasa.gov

Observations show that heavy oxygen isotope composition in precipitation ($\delta^{18}\text{O}_p$) increases from coastal southeastern (SE) China to interior northwestern (NW) China during the wet season, contradicting expectations from simple Rayleigh distillation theory. Here we employ stable isotopes of precipitation and vapor from satellite measurements and climate model simulations to characterize the moisture processes that control Asian monsoon precipitation and relate these processes to speleothem paleoclimate records. We find that $\delta^{18}\text{O}_p$ is low over SE China as a result of local and upstream condensation and that $\delta^{18}\text{O}_p$ is high over NW China because of evaporative enrichment of ¹⁸O as raindrops fall through dry air. We show that $\delta^{18}\text{O}_p$ at cave sites over southern China is weakly correlated with upstream precipitation in the core of the Indian monsoon region rather than local precipitation, but it is well-correlated with the $\delta^{18}\text{O}_p$ over large areas of southern and central China, consistent with coherent speleothem $\delta^{18}\text{O}_p$ variations over different parts of China. Previous studies have documented high correlations between speleothem $\delta^{18}\text{O}_p$ and millennial timescale climate forcings, and we suggest that the high correlation between insolation and speleothem $\delta^{18}\text{O}_p$ in southern China reflect the variations of hydrologic processes over Indian monsoon region on millennial and orbital timescales. The $\delta^{18}\text{O}_p$ in the drier part (north of ~30°N) of China, on the other hand, has consistently negative correlations with local precipitation and may capture local hydrologic processes related to changes in the extent of the Hadley circulation.

Treatment of fluoride containing acid wastewater using red mud

JUNG-HWA LEE, JAE GON KIM*, CHUL-MIN CHON
AND IN-HYUN NAM

Korea Institute of Geoscience and Mineral Resources,
Daejeon 305-350 Korea (ljh@kigam.re.kr,
jgkim@kigam.re.kr*, femini@kigam.re.kr,
nih@kigam.re.kr)

Capacity of red mud for the fluoride(F) removal and acid neutralization for the wastewater from a semiconductor manufactory was investigated using a batch experiment. The red mud was characterized for the chemical and mineralogical compositions using XRF and XRD, respectively. The pH was determined with 1red mud and 10distilled water after 24 hrs reaction. The point of zero charge(PZC) was determined with a potentiometric method. Red mud and wastewater was mixed at 0 – 25% of red mud. The suspension was reacted and the pH and F concentration of the solution were determined.

The red mud contained 34.3% of Fe₂O₃, 25.8% of Al₂O₃, 9.96% of SiO₂, 7.08% of Na₂O, 6.07% of TiO₂, and 5.07% of CaO. Hematite, boehmite, zeolite, quartz, anatase and calcite were identified as major minerals of red mud. The pH and PZC of red mud was pH 12.4 and pH 9.2, respectively.

The pH sharply increased and the F concentration decreased for initial 2 hrs of the reaction and then showed a steady state for all red mud content. The pH increased from 1.7 to 8.8 with increasing the red mud content. The F concentration decreased from 2,600 to 31 mg L⁻¹ with increasing to 7.5% of red mud. The F concentration of the solution was not significantly changed with increasing red mud content at > 7.5%.

The alkalinity of red mud neutralized the acidic wastewater. The F removal rate was increased with increasing content of iron oxides as major solid phases for the F adsorption at < 7.5% of red mud(pH 7.1). No significant change of F removal rate with increasing red mud content at > 7.5% might be due to the increased surface charge of iron oxide along with increased solution pH. The capacity of neutralization and F removal of red mud indicated that red mud can be utilized as a treatment agent for F containing acidic wastewater.

Hydrogeochemical characterization of urban groundwater in Seoul (South Korea) using Self-Organizing-Map technique

KYUNG-JIN LEE, KYOUNG-HO KIM
AND SEONG-TAEK YUN*

Korea University, Department of Earth and Environmental Sciences and KU-KIST Green School, Seoul, South Korea
styun@korea.ac.kr (* correspondence)

Degradation of urban groundwater quality is serious in some metropolitan cities such as Seoul, South Korea. In Seoul, depression of groundwater levels by over-pumping is considered as a major cause of groundwater contamination. In this study, we investigated spatial variations of groundwater level (i.e., drawdown) and hydrochemistry in Seoul. Field measurements and water sampling were made in 2003 and 2004 for this study. The average and maximum groundwater depths were 13.3 m and 73.3 m, respectively. The average and maximum concentrations of Cl, NO₃, and SO₄ as the potential indicators of anthropogenic contamination were high (45.5 and 189.8 mg/L, 24.8 and 528.1 mg/L, and 40.1 and 128.1 mg/L, respectively). Based on the Hierarchical Cluster Analysis (HCA) and Self Organizing Map (SOM) technique, four main clusters of groundwater samples were derived. Cluster 1 has the lowest concentrations of most solutes and represents the non-polluted groundwater; Cluster 2 contains relatively low concentrations of most solutes except NO₃; Cluster 3 and Cluster 4 are highly enriched in solutes (esp., Ca, Mg, Cl, SO₄) because of anthropogenic contamination. Cluster 3 has the high NO₃ but low HCO₃ concentrations, while Cluster 4 is opposite. The relationship between groundwater quality and groundwater depth was further evaluated by SOM. However, there is a weak correlation between spatial distributions of classified groups and groundwater depth data because of high heterogeneity of urban groundwater. On the other hand, the use of geo-SOM method showed a rather spatially classified water chemistry.

Evaluation of prokaryotes and community dynamics in Alvord Desert Hot Springs

M. HOPE LEE AND TIMOTHY MAGNUSON^{1,2,3}

¹Pacific Northwest National Laboratory, 902 Battelle Blvd, Richland, WA 99352; hope.lee@pnl.gov

²Idaho State University, 921 S. 8th Street, Pocatello, ID 83209; magntimo@isu.edu

The Alvord Desert, located in southeastern Oregon, is composed of springs which are near neutral and/or basic, and are driven by tectonic dilation of range-front faults. The thermal springs within the Alvord Desert discharge sodium-bicarbonate-chloride type water and maintain high concentrations of sulfate and chloride. Microbiological enrichments have resulted in the culturing of several organisms with biogeochemical significance including sulfate-reducing bacteria, and YeAs-1, a novel arsenic-reducing Archaea. Strain AlSe is a novel selenium-reducing thermophilic bacterium that is only 96% similar to *Carboxydocella thermoautotrophica*; AlSe has the ability to utilize organic carbon. A strain of *Thermus* spp., OPOC, was isolated, and can oxidize As(III) and reduce As(V), as well as respire on Fe(III). Zymography and proteomics confirms the expression of both arsenite oxidase (Aio) and respiratory arsenate reductase (Arr), as well as large-mass c-type cytochromes that may serve as electron transport components for Fe(III) respiration. Aerobic prokaryotes, including multiple species of *Anoxybacillus*, methanogen and methanotroph organisms have also been isolated. Together these efforts show that this ecosystem maintains a broad diversity of uncultivated microorganisms and metabolic pathways. It is expected that with continued mining of organisms, there is potential for discovering novel metabolisms that have significant implications for next-generation technologies, including carbon sequestration, biofuels, and the development of bioconversion processes yet to be conceived.

Age, geochemistry and Sr-Nd-Pb isotopes of alkaline lavas from Northern Victoria Land and Ross Sea Region, Antarctica

MI JUNG LEE*¹, JONG IK LEE¹, TAEHOON KIM¹
AND JOOHAN LEE¹

¹Division of Polar Earth System Sciences, Korea Polar Research Institute (KOPRI), Incheon 406-840, Korea, mjlee@kopri.re.kr, jilee@kopri.re.kr, tkim@kopri.re.kr, jooohan@kopri.re.kr

We present new K/Ar ages, geochemical and isotope results (Sr, Nd, Pb) on submarine basalts dredged from Victoria Land Basin of the Ross Sea, Antarctica. Subaerial samples were also collected from two areas near Mt. Melbourn in Northern Victoria Land for comparison. The volcanic rocks studied are alkaline ranging from basanite to trachybasalt. Chemically, they show the OIB-like patterns of trace element distribution and are characterized by a prominent depletion in K and Pb relative to other highly incompatible elements when normalized to primitive mantle. K/Ar ages of basalts from group A in Mt. Melbourn area range from 0.16 to 0.33 Ma and those of group B are from 1.25 to 1.34 Ma. The K/Ar determination result for submarine lavas also shows similar ranges of eruption ages from 0.46 to 0.57 Ma. In spite of their distinctly different ages of group A and B subaerial samples from Mt. Melbourn area, they show similar geochemical and isotopic features indicating common mantle sources and magma processes being shared in their magma generation. The Sr, Nd and Pb isotopic compositions of the group A and B basalts from Mt. Melbourn area display a range of values for ⁸⁷Sr/⁸⁶Sr (0.70306 to 0.70398), ¹⁴³Nd/¹⁴⁴Nd (0.51284 to 0.51293) and ²⁰⁶Pb/²⁰⁴Pb (18.498-19.667). They show a considerably higher range of ²⁰⁶Pb/²⁰⁴Pb contrast to limited compositional variations of ⁸⁷Sr/⁸⁶Sr and ¹⁴³Nd/¹⁴⁴Nd. Submarine lavas dredged from Victoria Land Basins (VLB) show slightly higher ratios of ²⁰⁶Pb/²⁰⁴Pb (18.935-19.852) and less radiogenic ⁸⁷Sr/⁸⁶Sr (0.70299-0.70340) and ¹⁴³Nd/¹⁴⁴Nd (0.51290-0.51297) isotope compositions compared to group A and B Mt. Melbourn basalts. The (La/Yb)_N in submarine lavas ([La/Yb]_N = 15.4 – 19.9) are slightly higher than those in group A and B volcanics ([La/Yb]_N = 9.8– 15.7), suggesting lower degrees of partial melting in submarine lavas. The stronger HIMU signature (higher ²⁰⁶Pb/²⁰⁴Pb and less radiogenic ⁸⁷Sr/⁸⁶Sr and ¹⁴³Nd/¹⁴⁴Nd ratios) in submarine lavas appears to be related with smaller degrees of partial melting of them, suggesting preferential sampling of the HIMU component in small degrees of melts in the Cenozoic NVL magmatism.

Cooperative and competitive adsorption of amino acids with Ca^{2+} on rutile

NAMHEY LEE¹, DIMITRI A. SVERJENSKY^{2,3}
AND ROBERT M. HAZEN³

¹ Earth Science Division, Lawrence Berkeley National Laboratory, Berkeley, CA, USA, nlee@lbl.gov

²Department of Earth and Planetary Sciences, Johns Hopkins University, Baltimore, MD, USA

³Geophysical Laboratory, Carnegie Institution of Washington 5251 Broad Branch Rd., NW, Washington D.C., USA

Amino acids are highly soluble in water and do not spontaneously organize themselves. For these molecules, it has been recognized that mineral surfaces may potentially have played an important role in their selection, organization and concentration in the prebiotic era. Here, we investigated the adsorption of the oppositely charged amino acids glutamate and lysine with and without the addition of Ca^{2+} . Without Ca^{2+} , glutamate shows maximum adsorption at a pH of ~4 and lysine shows maximum adsorption at a pH of ~9.4. In comparison, with Ca^{2+} present, glutamate showed maximum adsorption at both pH ~4 and ~10, whereas lysine showed no adsorption at all. These dramatic effects can be described as cooperative adsorption between glutamate and Ca^{2+} and competitive adsorption between lysine and Ca^{2+} . Surface complexation model calculations indicate a purely electrostatic origin of these effects. Adsorption of Ca^{2+} at high pH makes the rutile surface more positive, attracting glutamate and repelling lysine. The cooperative or competitive effects show that biomolecules can participate in complex adsorption behaviour. A fundamental understanding of amino acids speciation and coordination chemistry to oxide mineral surfaces may provide valuable insight into biomaterial and bimolecular interactions and the fate of organic acids in natural environments, as well as the possible role of mineral surfaces in the chemical evolution of biomolecules in the origin of life.

Biogeochemical control on the dissolution/precipitation of fine suspended solids from mine drainage

SANGHOON LEE¹, MINAH OH², JAIYOUNG LEE²
AND DUCKMIN KIM³

¹ Department of Environmental Engineering, Division of Biotechnology, The Catholic University of Korea (slee@catholic.ac.kr)

²Department of Environmental Engineering, University of Seoul

³Mine Reclamation and Technology Center, Mine Reclamation Corporation

Mine drainage discharges fine suspended solids (SS), as well as trace metals. Although many abandoned mining sites adapt sand filter beds to treat the SS, improved system is still in demand, as often long-term operation clogs either the sand media or the porous filter installed underneath of the bed, dramatically degrading treating capacities. The first approach was to find better filtering mediums. Fly ash, mine tailing aggregates, metal scraps and the mixed medium were compared with the current sand bed filters in the laboratory, using the mine drainage from the field. Batch and column test of 7 days revealed sand media still outperformed to other candidates. Mixing with anthracite or activated carbon on the sand filter also improved the treatability, extending to some heavy metals, as well.

Possible bioleaching of the suspended solids was also investigated to ameliorate the system by manipulation the dissolution/precipitation processes associated with the solids in the filter media. The redox transformation and biogeochemical interactions of heavy metals in the solids were examined using facultative anaerobic bacterium *Shewanella* sp. (HN-41) in batch mode and with small scale columns. This is a preliminary study carried out to determine if such process is instrumental in preventing the coagulation of solid precipitates on the sand media and the porous media. In addition, bioleaching of the metals from the suspended solids is also considered. The organism HN-41 was not influenced by pH ranging from acidic to neutral and was able to metabolize all the metal elements from the suspended solids, with high contents of metals.

[1] Healy, M.G., Rodgers, M., and Mulqueen, J., (2007), *Environmental Management*, **83**, 409-415.

Evaluating the fate of chlorinated ethene (TCE) around the near-stream zone

SEONG-SUN LEE^{1*}, HUN-MI KIM¹, DUGIN KAOWN¹
AND KANG-KUN LEE¹

¹School of Earth Environmental Science, Seoul National University, Seoul 151-747, Korea
(*correspondence : soon3311@snu.ac.kr),
tweety1@snu.ac.kr, dugin1@snu.ac.kr, kkleee@snu.ac.kr

The fate of chlorinated ethens in a near stream zone was evaluated using concentration of each component, hydrogeochemical data, microbial data and carbon isotope data. Temporal and spatial monitoring investigation show that a trichloroethylene (TCE) plume was originated from a small source zone in an industrial complex and is discharging to a stream. Groundwater geochemical data around the stream showed a region of depleted dissolved oxygen. Mass discharge of contaminants computed across transect lines showed that TCE mass discharge decreases along the groundwater flow path, whereas *cis*-DCE and VC mass discharge increases across the transect line located near the stream. TCE molar fraction is high ranging from 83 to 90% of total VOCs at a well located near the source zone. However, in the region downgradient of the source zone, molar fractions of *cis*-DCE and VC increase indicating biodegradation of TCE. The degree of chlorinated ethene transformation varies spatially due to local conditions. Reductive dechlorination likely dominated in the anaerobic region of the aquifer where TCE level was observed to decrease with simultaneous increase in *cis*-1,2-dichloroethene (*cis*-DCE) and vinyl chloride (VC). Groundwater along the transect nearest to the stream has concentrations of *cis*-DCE and VC decreased below detection limits, presumably due to anaerobic biotransformation processes at the near-stream zone. The increase in ferrous iron and manganese and decrease in TCE around the stream zone also are related with the biotransformation. Microbial community around the near-stream zone was analyzed to identify organisms which are responsible for the biodegradation. Carbon isotope ($\delta^{13}\text{C}$ of TCE, *cis*-DCE and VC) data were used to estimate the origin of contaminants source and the evidence of biodegradation around the near-stream zone. TCE isotope values (from -19.21‰ to -17.78‰) around the near-stream zone are more enriched in $\delta^{13}\text{C}$ than the $\delta^{13}\text{C}$ around the source zone (-24.45‰). These isotope results also showed the evidence of biodegradation around the stream zone. Those data and analyses indicate the contaminant plume around the stream zone have been naturally attenuated by active anaerobic biotransformation processes.

Late Ordovician volcanic rocks in South Korea: Speculation on the cause of Paleozoic regional unconformity in Sino-Korean craton

SEUNG RYEOL LEE^{1*}, DEUNG-LYONG CHO¹,
JOONBEOM PARK² AND HEEJAE KOH¹

¹Korea Institute of Geoscience and Mineral Resources, Daejeon 305-350, Korea (*correspondence: leesr@kigam.re.kr)

²US Army Corps of Engineers Far East District, Seoul 100-195, Korea

One of the distinct geologic features that distinguishing Sino-Korean block (SKB) from other east Asian blocks (e.g., South China block (SCB), Tarim block etc.) is a regional unconformity between Upper Ordovician and Middle-Upper Carboniferous on the SKB [1, 2]. The Korean Paleozoic, as a part of Sino-Korean sedimentary system, are mostly distributed in two relatively large sedimentary basins, the Taebaeksan and Pyeongnam basins, and consist of lower and upper Paleozoic strata with a great unconformity between them. The unconformity period is conventionally thought to be of non-deposition, but the cause of the unconformity is still ambiguous.

The Oknyobong Formation (OFm), consisting of volcanoclastics, tuffs, basalt and rhyolite, overlies Cambro-Ordovician strata in Taebaeksan basin [3]. It was considered to be Late Jurassic-Early Cretaceous stratum, based on incorrect age data [3]. In this study we reported SHRIMP U-Pb zircon ages and geochemical data for the volcanic rocks from the OFm. SHRIMP U-Pb zircon ages of 452.5 ± 3.2 (2 σ) Ma and 445.0 ± 3.7 (2 σ) Ma were obtained from two felsic volcanics, indicating that the OFm is of Upper Ordovician in age. Petrological and geochemical features suggest that the OFm extruded at the within-plate tectonic environment.

The Upper Ordovician within-plate volcanic activity, confirmed by the OFm, is coeval well with the Ordovician (~470 Ma) kimberlite volcanism in SKB, suggestive of regional lithospheric uplift at that time [4]. Therefore epeirogenic uplift from mantle plumes (or hotspot epeirogeny) is suggested as a possible cause of the regional development of middle Paleozoic unconformity in SKB.

[1] Kim *et al.* (1999) *GondwanaRes* **2**, 577-578. [2] Wan & Zeng (2002) *JAES* **20**, 881-888. [3] Chang *et al.* (2003) *JAES* **21**, 937-948. [4] Yang *et al.* (2009) *ChemGeol* **264**, 24-42.

Hindcast study of aerosol optical depth using retrieval of geostationary satellite over East Asia

S. LEE¹, C. H. SONG¹, M. E. PARK¹, R. S. PARK¹, J. LEE²
AND J. KIM³

¹School of Environmental Science and Engineering, Gwangju Institute of Science and Technology (GIST), Gwangju, 500-712, Korea (noitul5@gist.ac.kr, *correspondence to chsong@gist.ac.kr)

²Aerosol and Cloud Group, NASA JPL, Pasadena, and JIFRESSE, UCLA, L.A., CA, USA

³Institute of Earth, Astronomy, and Atmosphere, Brain Korea 21 Program, Department of Atmospheric Sciences, Yonsei University, Seoul, Republic of Korea

Compared with the aerosol optical depth (AOD) retrievals from polar orbiting satellites, the AOD retrievals from geostationary satellites have a high temporal and spatial resolution. Because the number of AOD retrievals from geostationary satellites is increased, a better initial condition can be prepared for better aerosol forecast or hindcast. We carried out a hindcast study of AOD over East Asia to test the effects of the initial conditions prepared the AOD data from a geostationary satellite. The retrievals from the Geostationary Ocean Color Imager (GOCI) on board the Communication, Ocean, and Meteorological Satellite (COMS) were used in this study, and the retrieved AOD data were assimilated with the AOD values simulated by the Community Multiscale Air Quality Model (CMAQ). We assimilated the two data via an optimal interpolation (OI) technique, and the OI parameters of observation and modeling errors were calculated to minimize the variance of differences between assimilated and AERONET AODs. The AERONET AODs were selected within the period of Distributed Regional Aerosol Gridded Observation Networks DRAGON in Asia (DRAGON-ASIA) campaign, and were also used for comparison with the results of hindcast studies. The 6-hour hindcast result in selected days using the GOCI retrievals showed improved AOD distributions, compared with the AOD data from DRAGON-ASIA AERONET sites. Also, using GOCI and TERRA MODIS AOD retrievals, spatial coverage of satellite retrieval can be increased. 12-hour hindcast was also carried out using the combined GOCI-MODIS data sets.

Multi-component silicate glasses and melts under compression

SUNG KEUN LEE¹

¹School of Earth and Environmental Sciences, Seoul, 151742, Korea, sungklee@snu.ac.kr

Probing the pressure-induced structural changes and the extent of disorder in multi-component aluminosilicate glasses and melts at high pressure relevant to earth's interior remains challenge in mineral physics and high temperature geochemistry. Most of the previous studies focused on the pressure-induced bonding transition in rather simple model melts (e.g., from single-component, to ternary). Recent advances in element-specific experimental probe of local structures including non-resonant synchrotron inelastic x-ray scattering (IXS) and solid-state NMR unveil previously unknown structural details of the structural changes in the diverse multi-component silicate glasses under static and dynamic compression. This progress allows us to establish a systematic relationship between pressure, temperature, composition, and melt (and glass) structures. Here, we present an overview of the recent progress and insights by IXS and NMR into electronic structures of multi-component silicate glasses at high pressure. IXS study using shock compressed basaltic glasses allowed us to constrain topology-driven densification upon dynamic compression. Contrary to an expected complexity in densification for multi-component silicate glasses, high-resolution O-17 NMR spectra for quaternary Ca-Mg- and Ca-Na aluminosilicate glasses quenched from melts at high pressure demonstrate that the pressure-induced changes in melt structures show a simple densification trend where all the experimental non-bridging oxygen (NBO) fractions at high pressure converge into a single decaying function, regardless of composition. Additionally, detailed Al-27 NMR studies of aluminosilicate glasses showed that the fraction of ^{5,6}Al at a given pressure vary nonlinearly with variations of NBO/T. ^{5,6}Al fraction increases with decreasing degree of melt polymerization from NBO/T=0 to partially depolymerized melts. Then it gradually decreases with further increase in NBO/T. A new scheme of pressure-induced structural transitions in silicate melts involving ¹⁴Al-O-¹⁴Al also includes the formation of ¹⁴Al-O-¹⁵Al. We finally show how these new structural information can be utilized to help elucidate connections between the microscopic signatures of anomalous and non-linear changes in the macroscopic properties of the corresponding liquids as well as natural magmatic processes in the Earth's interior.

Variations of soil C and N along a South-North Transect in East Central Asia: Implications for climate change

XINQING LEE, LIKE ZHANG, DAIKUAN HUANG, LU HU,
JIANZHONG CHENG, BING WANG, BIN FANG,
FANG YANG AND TSERENPIL SHURKHUUA

State Key Laboratory of Environmental Geochemistry,
Institute of Geochemistry, Chinese Academy of Sciences,
46 Guanshui Road, Guiyang 550002, Guizhou, China.
Email: lee@mail.gyig.ac.cn

The feedback of soil organic matter to global warming is important for modeling future climate change. No consensus, however, has been reached on this issue partly because the temperature sensitivity of soil organic carbon (SOC) is affected by a variety of factors such as water availability and the associated change in soil N contents. To elucidate the links between the C stock and environmental factors, we assessed the spatial variation of C and N content in the topsoil, and the concomitant changes of temperature, water availability and alkalinity in a mega-transect in East Central Asia, which is characterized by large environmental changes.

Totally 210 sites were sampled at 6 replicates using a corer along the transect. Soil C and N content and soil alkalinity change dramatically in the transect. SOC and soil organic nitrogen (SON) increases with water availability while decreases with temperature, both are associated so closely with each other that their molar ratio, C/N, is generally invariant about 12 except in the agro-pastoral transitional zone in north China. Soil pH increases with temperature and decreases with water availability. $\text{NH}_4^+\text{-N}$, which is the primary inorganic N in the soil, basically varies with SON, indicating its provenance, but is also subject to modification by soil alkalinity. $\text{NO}_3^-\text{-N}$, though derived primarily from nitrification of $\text{NH}_4^+\text{-N}$, does not follow its precursor because of precipitation leaching and re-deposition.

Statistic analyses indicate that SOC and SON contents in East Central Asia should have been influenced negatively by recent warming, which, albeit occurring primarily in the winter half year, strengthens the evaporation and enlarges the difference of wet and dry seasons, and thus reducing soil annual water availability while increasing soil alkalinity. The accelerated decomposition of SOC stock, in association with the increased soil alkalinity, enhances transformation of SON to NH_4^+ . The increased N mineralization, however, may not necessarily promote net primary production because of the decreased water availability and increased soil NH_3 volatilization.

Pressure-induced insertion of xenon into a small-pore zeolite natrolite

DONGHOON SEOUNG,¹ YONGMOON LEE,¹ HYUNCHAE
CYNN,² WILLIAM EVANS,² THOMAS VOGT,³
CHI-CHANG KAO AND YONGJAE LEE,^{1,*}

¹Department of Earth System Sciences, Yonsei University,
Seoul, Korea [yongjaelee@yonsei.ac.kr]

²Condensed Matter and Materials Division, Lawrence
Livermore National Laboratory, Livermore, USA

³NanoCenter & Department of Chemistry and Biochemistry,
University of South Carolina, Columbia, South Carolina,
USA

⁴SLAC National Accelerator Laboratory, Menlo Park,
California, USA

We report here a novel mechanism of xenon incorporation into a zeolite at moderate upper mantle PT conditions. When silver-exchanged natrolite, $\text{Ag}_{16}\text{Al}_{16}\text{Si}_{24}\text{O}_{48} \cdot 16\text{H}_2\text{O}$, a small pore auxetic zeolite is compressed under xenon medium to ca. 1.7 GPa and heated to ca. 250 degrees Celsius, significant amount of xenon is incorporated into the natrolite channel via desorption of water molecules and charge disproportionation of silver cations, resulting in ca. $\text{Ar}_8\text{Al}_{16}\text{Si}_{24}\text{O}_{80} \cdot 8\text{Xe}$. This material is recovered to ambient conditions with ca. 4% larger unit cell compared to the starting material. This process has been monitored by in situ high-pressure synchrotron XRD, and the presence of xenon and the formation of charge-disproportionated silver metal nano particles have been confirmed by XRF chemical analysis and TEM imaging from the recovered sample. Xenon incorporation under moderate pressure into Auxetic framework silicate such as natrolite is an important and overlooked confinement mechanism of heavy noble gases in geochemical environment.

Attenuated total reflection-infrared spectroscopy: a tool of choice for investigation of the sorption of oxyanions

G. LEFEVRE¹

¹LECIME, UMR7575 CNRS-Chimie ParisTech, 75005 Paris, France (*correspondence : gregory-lefevre@enscp.fr)

Attenuated Total Reflection-Infrared spectroscopy (ATR-IR) is a fast-expanding spectral techniques to *in situ* studies of the solid/solution interfaces. Several optical materials can be used as ATR crystal, but the range of probed frequency is always limited above around 700 cm⁻¹). The observation of sorbed heavy metals is therefore not possible since absorption bands of surface complexes would take place below this limit, contrary to most of oxyanions due to their polyatomic structure [1]. The first studies showed the adsorption of model ions (sulfate, carbonate) onto metal oxides, then several pollutants have been investigated (AsO₄³⁻, SeO₄²⁻,...), along with other mechanisms, as ion exchange, have been followed.

Examples amongst our recent results are presented, as the study of sorption of molybdate and tungstate ions onto hematite. Thus, the use of ATR-IR to characterize surface complexes with tungstate ions is presented for the first time to the best of our knowledge. From the comparison of spectra of solution species as monomeric and polymeric geometries, the inner-sphere behaviour of tungstate has been deduced. A first try with perhenate ions has been performed, confirming the formation of outer-sphere complexes.

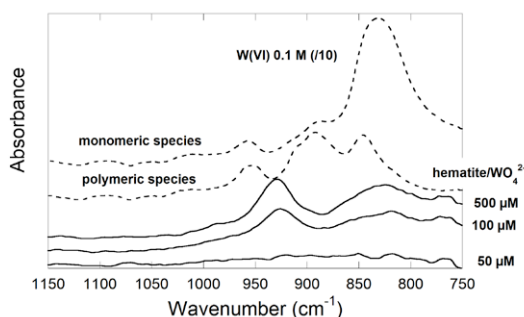


Figure 1. Spectra of tungstate solutions and adsorbed tungstate ions at pH 8.4.

[1] Lefèvre (2004) Adv. Colloid Interface Sci. **109**, 107-123.

Stable soil carbon decomposition is more sensitive to temperature. Evidence from long term bare fallow experiments

LEFEVRE R.¹, BARRÉ P.², BARDOUX G.¹, CHRISTENSEN B.T.³, GIRARDIN C.¹, HOUOT S.⁴, KÄTERRER T.⁵, MOYANO F.¹, VAN OORT F.⁶ AND CHENU C.¹

¹UPMC, CNRS, INRA AgroParisTech, Bioemco, Grignon, France

²CNRS, Laboratoire de Géologie, Paris France

³Univ of Aarhus, Tjele, Denmark

⁴INRA, EGC, Grignon, France

⁵SLU, Uppsala, Sweden

⁶INRA, Pessac, Versailles, France

The impact of climate change on the stability of soil organic carbon (SOC) remains a major source of uncertainty in predicting future changes in atmospheric CO₂ levels. One unsettled question is whether the mineralization response to temperature is the same for labile and stable SOC pools. Long-term (>25 years) bare fallow experiments (LTBF) in which the soil is kept free of any vegetation, represent a unique research platform to examine this issue as with increasing duration of the treatment, the proportion of stable SOC relative to total SOC increases.

We used soils from LTBF experiments situated at Askov (Denmark), Grignon (France), Versailles (France) and Ultuna (Sweden). We used archived soils sampled at the start of the experiments and after 25, 50, 80 and 52 years of bare fallow, respectively, when the soils had become enriched in stable SOC. Samples were incubated at 4, 12, 30 and 35 °C and evolved CO₂ was monitored. We calculated the activation energy of SOC after the same amount of respired C at the different temperatures. The activation energy was always higher for samples more concentrated in stable C, implying a higher temperature sensitivity of stable C compared to more labile C. Hence, assuming the same temperature sensitivity for different soil carbon pools in simulation models appears inappropriate.

Temporal evolution of the oxygen depletion in the bottom water of the Lower St. Lawrence Estuary: from 1930 to 2100

STELLY LEFORT^{1*}, ISABELLE DADOU², DENIS GILBERT³,
LAURENT BOPP¹, ALFONSO MUCCI⁴, YVES GRATTON⁵
AND LAURE RESPLANDY¹

¹Laboratoire des Sciences du Climat et de l'Environnement (CNRS/CEA/UVSQ), Orme des Merisiers, Point Courrier 132, Bât. 712, 91191 Gif-sur-Yvette Cedex, France

²Laboratoire d'Etudes en Géophysique et Océanographie Spatiales (UMR5566/CNRS/UPS), 14 Avenue Edouard Belin, 31400 Toulouse Cedex, France.

³Institut Maurice Lamontagne, Pêche et Océans Canada, P.O. Box 1000, Mont-Joli, QC, G5H 3Z4, Canada.

⁴GEOTOP et Department of Earth & Planetary Sciences, Université McGill, 3450 University Street, Montréal, QC, H3A 2A7, Canada.

⁵Institut National de la Recherche Scientifique, Eau Terre & Environnement (INRS-ETE), 490 rue de la Couronne, Québec, QC, G1K 9A9, Canada.

Historical records reveal that the dissolved oxygen concentration has progressively decreased in the bottom water of the Lower St. Lawrence Estuary (LSLE) during the last century and reached the severe hypoxic threshold in the 1980s where it has hovered ever since. We recently demonstrated that the physics of the system, both benthic and pelagic respirations, as well as the modification of chemical properties of the water mass entering the Laurentian Channel (originating from the North Atlantic Ocean), are the main causes of the oxygen depletion in the LSLE. Climate models forecast a strong deoxygenation of the subsurface water in the North Atlantic Ocean over the next century, that may further decrease the oxygen supply into the Laurentian Channel. We used four climate scenarios (rcp2.6, rcp4.5, rcp6.0 and rcp8.5, labeled according to the additional radiative forcing level in 2100 with atmospheric CO₂ concentrations reaching 421, 538, 670 and 936 ppm respectively) to estimate the oxygen concentration in the North Atlantic Ocean and at the entrance of the Laurentian Channel. By applying these estimated oxygen concentrations at the boundary condition of a bidimensional model validated for the 2002-2011 period, we forecast the evolution of hypoxia in the LSLE. We also estimate the contribution of the physics of the system, respirations and chemical properties of the source water to the oxygen depletion.

Coupled cycling of Fe and C_{org} in submarine hydrothermal systems: Modeling approach.

LOUIS LEGENDRE^{1,2}, CHRISTOPHER R GERMAN³
AND SYLVIA G. SANDER⁴

¹Université Pierre et Marie Curie Paris 6, Laboratoire d'Océanographie de Villefranche, France (legendre@obs-vlfr.fr)

²CNRS, Laboratoire d'Océanographie de Villefranche, France (legendre@obs-vlfr.fr)

³Woods Hole Oceanographic Institution, MA 02543, USA (cgerman@whoi.edu)

⁴University of Otago, Dunedin, New Zealand (sylvia.sander@otago.ac.nz)

We investigated the fate of dissolved Fe released from hydrothermal systems to the overlying ocean using an approach that combined modelling and field values. We based our work on a consensus conceptual model developed by members of SCOR-InterRidge Working Group 135. This model was both complex enough to capture the main processes of dissolved Fe release from hydrothermal systems and chemical transformation in the hydrothermal plume, and simple enough to be parameterized with existing field data. It included the following flows: Fe, water and heat in the high-temperature vent fluids, in the fluids diffusing around the vent, and in the entrained seawater; Fe precipitated in sulfides near the vent, and in particles onto the sea bottom away from the vent; and Fe dissolving into deep-sea waters. Through trials and errors, we transformed the conceptual model into equations, which were parameterized with field data. We used the resulting set of equations (model) to explore various scenarios of Fe emissions and transformations. The modelling exercises suggested that hydrothermal systems may play significant roles in the global biogeochemical Fe cycle.

Alteration of amorphous Fe-silicate in meteorites

C. LE GUILLOU¹, R. DOHMEN¹, T. MÜLLER¹, C. VOLLMER², D. ROGALLA³ AND H. W. BECKER³

¹Ruhr-Universität Bochum, Inst. für Geologie, Mineralogie and Geophysik., 44780, Bochum, Germany

²Universität Münster, Inst. für Mineralogie, 48149 Münster.

³RUBION facility, Ruhr-Universität Bochum, Germany.

Serpentine is ubiquitous in carbonaceous chondrites and likely the result of a hydrothermal reaction of amorphous precursors (at <100°C) as indicated by replacement textures in fine-grained matrices. To constrain the temperature and timescales of aqueous alteration, we study the mechanisms and kinetics of Fe-rich amorphous silicate serpentinization. Our approach is a combination of a novel experimental setup and multiple analytical techniques. A thin (~1 μm) layer of amorphous "FeMgSiO₄" is deposited on a substrate using a pulsed laser deposition system (laser ablation / deposition from the plasma). The film is reacted in deionized water (60°C to 190°C, 2h to 2 weeks, water to rock ratios of about 300). The geometry is ideal to follow the evolution of the reaction front by FIB/TEM, Rutherford Back Scattering (major elements composition) and Nuclear Reaction Analysis (water content) with nm scale depth resolution.

Our results reveal a systematic sequence of hydrated amorphous layers from the surface towards the pristine material: (1) silicon oxide (<50 nm); (2) a fibrous and porous layer with a composition close to Mg-serpentine; (3) thin (< 20 nm) Fe-oxide; (4) a compact layer with a composition close to Fe-serpentine. Depth profiles reveal that all layers are hydrated (10-15 wt. %). Layer boundaries are sharp. The formation sequence likely results from kinetically-controlled, interfacial dissolution-precipitation front, as previously described in glass alteration experiments. The Fe/Mg fractionation between layers may be due to the higher solubility of Mg, first leached and later precipitated after fluid had reached saturation.

Our findings of amorphous and hydrated Fe-rich silicates with a stoichiometry close to serpentine are to some degree comparable to observations made in chondrites. It may point towards shorter hydrothermal episodes as initially thought in chondrites.

Effect of coarse marine aerosols on stratocumulus clouds

Y. LHEHN¹, I. KOREN^{1*}, O. ALTARATZ¹ AND A. KOSTINSKI²

¹Dept. of Environmental Sciences, Weizmann Institute, Rehovot 76100, Israel (*correspondence: ilan.koren@weizmann.ac.il, yoav.lehahn@weizmann.ac.il, orit.altaratz@weizmann.ac.il)

²Department of Physics, Michigan Technological University, 1400 Townsend Drive, Houghton, MI 49931-1200, USA (alex_kostinski@mtu.edu)

In contrast to fine anthropogenic aerosols (radii ~< 0.5 μm), large aerosol particles are thought to enhance cloud droplet growth, promote precipitation formation and reduce cloud albedo. While shown in models, the impact of coarse aerosols on marine stratocumulus clouds lacks observational evidence. Combining satellite data from AMSR-E and MODIS, we link the amount of wind induced coarse marine aerosols (CMA), with droplet size of marine stratocumulus clouds over the southeastern Pacific.

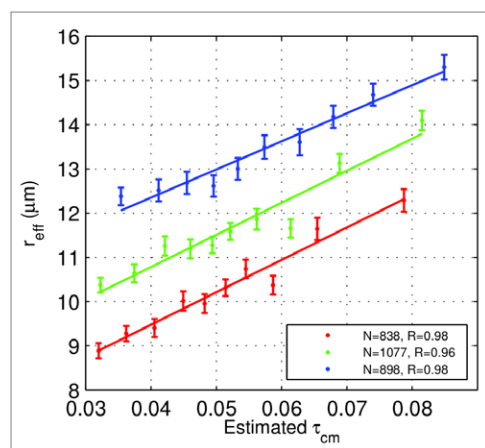


Figure 1. r_{eff} vs. τ_{cm} in a southeastern Pacific marine stratocumulus cloud field. Data are plotted for different ranges of LWP (25-50, 50-75 and 75-100 gr/m², red, green and blue, respectively).

For constrained meteorological conditions, approximately 1/2 of the change in droplet effective radius (r_{eff}) is attributed to increase in CMA optical depth (τ_{cm}), as surface winds intensify. Accordingly, a twofold increase in τ_{cm} is associated with a 1.4 μm ± 0.11 increase in r_{eff} . Our results suggest that any attempt to quantify the impact of anthropogenic and biogenic marine aerosols on marine boundary layer clouds, should take into account the opposing effect of wind induced coarse marine particles.

Ore deposits related to felsic magmatism through time

B. LEHMANN

Mineral Resources, Technical University of Clausthal,
D-38678 Clausthal-Zellerfeld, Germany

Shallow magmatic-hydrothermal ore systems, such as copper porphyries, molybdenum porphyries and tin-tungsten ore systems, as well as their epithermal superstructures, form at high level in orogenic belts (≤ 4 km) and have the same age distribution as their low-grade or non-metamorphic host environment, i.e. ≥ 90 % of their resources are of Phanerozoic age [1]. This is different from orogenic (mesothermal) gold deposits which form at deeper levels in metamorphic terrain (in a continuum of 2-20 km), with only about 50 % of gold resources of Phanerozoic age [2]. Rare-metal pegmatites (Ta-Sn-Li) form mostly in medium-grade metamorphic terrain (staurolite-kyanite stable), with spodumen present (≥ 12 km depth). Such relatively deep tectonometamorphic basement terrains are much less sensitive to erosional dispersion than the shallow orogenic domains and their ore deposits (and Ta resources) are dominantly of Precambrian age.

However, it is striking that major tantalum resources in western Australia (Greenbushes district, Yilgarn craton; Wodgina district, Pilbara craton) are all of Archean age, with about 2.8 Ga for the Wodgina and 2.5 Ga for the Greenbushes rare-metal pegmatite, respectively. The substantial rare metal enrichment in these pegmatites requires about 1000 times larger cogenetic peraluminous granite systems and an environment favorable for extreme reaction progress of magmatic fractionation processes, i.e. a reasonably thick continental crust. Further back in time, the giant Mesoarchean Witwatersrand gold-uranium placer province can be traced back to an Early Archean source domain of granitic affinity [3], underlining the presence of felsic magmatism with efficient metal enrichment already at ~ 3.1 Ga, although this domain has not survived tectonic diffusion.

The direct evidence of evolved felsic magmatism and related Ta ore formation in the Archean, and the indirect evidence for granite magmatism and large-scale hydrothermal Au-U ore formation in the Early Archean point to significant volumes of continental crust for that time. This is in accord with models of crustal evolution which suggest higher rates of crust generation in the Archean than in later times [4].

[1] Veizer *et al.* (1989) *Am. J. Sci.* **289**, 484-523. [2] Goldfarb *et al.* (2005) *Econ. Geol.* 100th Anniv. Vol., 407-450. [3] Depiné *et al.* (2013) *Miner Deposita* **48**, in press. [4] Hawkesworth & Kemp (2006) *Nature* **443**, 811-817.

Hydrocarbon Generation and Accumulation in the Unconventional Petroleum System of the Silurian Shale, Lublin Basin, Poland

ERIC LEHNE^{1*}, OLIVER SCHENK², KENNETH PETERS³
AND ARTUR STANKIEWICZ⁴

^{1*}Schlumberger DBR Edmonton, ELehne@slb.com

²Schlumberger, SIS Aachen, OSchenk@slb.com

³Schlumberger, SIS Mill Valley, KPeters2@slb.com

⁴Schlumberger, RSA Paris, AStankiewicz@slb.com

As natural gas demand increases worldwide, exploration for gas is increasingly focused on unconventional reservoirs, such as shale gas formations. The economic value of shale gas plays is determined by reservoir and completion quality. Reservoir quality parameters include porosity, permeability, clay content, cementation factors, the diagenetic history and other factors that affect the storage and deliverability of fluids contained in the pores of those rocks. Organic geochemistry input parameters for reservoir quality assessment take account of the fluid types in shale gas plays, their compositional characteristics, and the evolutionary generation history of hydrocarbons in such systems.

We constructed a numerical model for the petroleum system of the Silurian Shale to integrate parameters that influence generation and migration/accumulation of hydrocarbons in the Lublin Basin. The Silurian strata in Poland are at present the target of intensive shale gas exploration, due to relatively high total organic carbon content (TOC), and good hydraulic fracturing and production potential based on its silica content. The Silurian Shale is a marine (Type II) source rock with hydrogen index (HI) below 600 mg/g and TOC up to 12%. Vitrinite macerals from vascular land plants are absent in these shales. Thus, the visible reflectance equivalent (VRE) based on analyses of bitumen was used to calibrate the heat-flow. The reflectance data suggest that the Silurian shale is within the gas generation window in the study area.

Cyberinfrastructure Vision for Geochemistry, Petrology, and Volcanology

K. LEHNERT¹ AND L. HSU¹

¹Lamont-Doherty Earth Observatory, Palisades, NY, USA

Grand challenges in geochemistry and petrology, such as understanding the composition of and extent of fluxes between Earth's major reservoirs (core, mantle, crust, biosphere and hydrosphere), or the relationship between geologic processes and societal issues such as natural hazards and resources, require access and integration of large amounts of data and their seamless integration into dynamic models. Progress in scientific research will be greatly accelerated with a cyberinfrastructure that is guided by a community-endorsed vision. Recently, the geochemistry and petrology community has been charged with identifying key scientific and technical challenges, and next steps toward realizing the vision.

Scientific challenges are substantial in high impact, global scale research that currently is impeded by the dearth of accessible, integrated data, especially between terrestrial and marine data resources, thermodynamic models, experiments, and analytical data; lack of consistent coverage of geochemical sample specimens from geologic terrains of interest; lack of widespread sample curation and online sample catalogs; and lack of basic knowledge and communication within and outside the community.

The scientific challenges are augmented by technical challenges related to the discoverability, interoperability, and standardization of the geochemical, petrological, kinematic, and thermodynamic data currently in existence.

Steps have been proposed to reach the goal of science-supporting cyberinfrastructure in geochemistry: Data and metadata should be captured at the point of acquisition in a way that they can seamlessly be managed throughout their life cycle, including upload to repositories. Systems should be in place to promote spatial contextualization of analysis through sample registration, imagery, and links between samples (hand samples, thin sections, splits, etc.) and analytical data. Historical data should be properly brought into the integrated system. The community, especially early career scientists, must work together to produce the cultural shift to social networking, virtual collaboration, and sharing of data and knowledge.

With broad community participation and feedback, an integrated infrastructure can lead more comprehensive, well-informed, and high impact scientific advances.

Anthropogenic impact on forest soil - Pollution with PAH, PCB and OCP in Germany

P. LEHNIK-HABRINK^{1*}, B. AICHNER¹, B. BUSSIAN², S. HEIN¹ AND CH. PIECHOTTA¹

¹ Federal Institute for Materials Research and Testing, D-12489 Berlin, Germany (*correspondence: petra.lehnik-habrink@bam.de)

² Federal Environmental Agency, D-06844 Dessau, Germany

While organic pollutants have been extensively studied in urban and agricultural areas, data from forested regions are relatively rare.

Within the framework of a forest soil inventory in Germany polycyclic aromatic hydrocarbons (PAH), polychlorinated biphenyls (PCB) and organochlorine pesticides (OCP) were analyzed in 1500 soil samples taken from 3 soil horizons at 447 sites. An analytical protocol was developed and validated for the simultaneous extraction and measurement of all analytes in humic rich soil at trace level range [1]. In line with the monitoring campaign a comprehensive quality assurance concept was implemented to guarantee constant analytical measurement conditions for two years.

At most sampling sites pollutant concentrations gradually decrease with depth. Only few spots showed highest concentrations in the upper mineral soil. In the O-horizon the sum concentrations of 16 PAHs range from 104 to 14.000 $\mu\text{g}/\text{kg}$, of 6 PCBs from <1 to 106 $\mu\text{g}/\text{kg}$ and the sum of DDT and metabolites range from <1 to ca. 4.000 $\mu\text{g}/\text{kg}$.

The observed concentration of PAH, PCB and OCP reflect an ubiquitous background contamination at most sites. Relatively high concentrations of PAH and PCB are related to industrial areas and peak concentrations only of PAH are associated with open cast mining of brown coal areas. The spatial distribution of the contents of DDT and metabolites in German forest soils can clearly be attributed to historic application.

[1] Lehnik-Habrink *et al.* (2010), J Soils Sediments 10, 1487-1498

Retention and mobility of heavy metals in the carbonate-rich sulfide tailings in Dachang mine (Guangxi, China)

LIANGQI LEI¹, CIAN SONG¹ AND LIYAN YANG²

¹Earth Science Faculty, Guilin University of Technology, China; e-mail: leilq@glut.edu.cn; songcian@glut.edu.cn;
²Law school, Guangxi Normal University, China; e-mail: yangliyan891139@hotmail.com

The tailings in Bali impoundment of Dachang tin-polymetallic sulfide mine, which is located at Guangxi Zhuang Autonomous Region of P. R. China, are rich in carbonate (CaCO_3 30.2 wt%; $\text{CaMg}(\text{CO}_3)_2$ 4.4 wt%) and sulfide (Total-S 15.7 wt%). By observing and sampling successively on a plumb profile of the tailings pile and using the modified BCR (European Community Bureau of Reference) procedure for element extraction, and the secondary mineralogy and the element geochemistry etc, we have gained following conclusions: (1) Most of pyrrhotite, galena, calcite and sericite, while part of sphalerite, arsenopyrite and pyrite, were consumed in the tailings by oxidation. Sulfide oxidation resulted in generating acid mine drainage, as well as releasing heavy metals (such as Zn, As, Cd, Pb). Zinc and As were moved out from the tailings more easily and larger in quantity than Cd and Pb. (2) A hardpan with greater thickness, cemented by secondary gypsum and lepidocrocite, was formed on the tailings surface due to long-term oxidation. The hardpan could be concentrated with heavy metals which released from the original tailings through oxidation. Zinc and As appeared as active acid extractable speciation in the hardpan were prone to remigration and released in large amounts, implying that both may be key factors of heavy metals pollution in Dachang mine district. And Pb and Cd may cause less impact for the mine environment due to their lower contents as acid extractable speciation in the hardpan. However, the condition of the tailings stacking would be changed if the tailings were restored by coverage (resulted in reducing environment) or phytoremediation (resulted in development of organic matter). In these cases, heavy metals (As, Pb, Zn and Cd), which appeared as Fe-Mn oxide bound speciation and sulfide/organic bound speciation in the tailings, may be removed and produce the environmental effect.

Consequently, the carbonate-rich sulfide tailings may be similar to many other types of sulfide tailings in retention and mobility of heavy metals. It means the carbonate-rich sulfide tailings may also have the potential of releasing heavy metals.

The early Paleozoic magmatic arc of the Central Tianshan, NW China

RUXIONG LEI¹ AND CHANGZHI WU²

¹ Key Laboratory of Western China's Mineral Resources and Geological Engineering Ministry of Education, College of Earth Sciences and Resource, Chang'an University, Xi'an 710054, China, email: ruxionglei@chd.edu.cn
² State Key Laboratory for Mineral Deposit Research, School of Earth Sciences and engineering, Nanjing University, Nanjing 210093, China

Located in the Xinjiang province, NW China, the Central Tianshan zone is an important component of the Central Asian Orogenic Belt (CAOB) and crucial linkage between the Siberian, Kazakhstan, Turpan-Hami and Tarim blocks, and played a key role in the crustal evolution and collisional tectonics of the CAOB. We studied a series of the early Paleozoic igneous rock of the Central Tianshan in an attempt to understand the magmatism and tectonic setting of the early Paleozoic Central Tianshan. LA-ICP-MS zircon U-Pb dating yields 424.9 ± 5.8 Ma for the Xingxingxia granodiorite, 445.3 ± 4.6 Ma for the ore-bearing granite of Tianhudong Fe-Mo ore deposit, 466.7 ± 4.2 Ma and 452.0 ± 2.8 Ma for the meta-volcanic rocks hosting the Tianhu iron deposit in the Central Tianshan. Geochemical analyses show these rocks are generally enriched in large ion lithophile elements (LILE) such as Rb, Ba, Sr and LREE, but depleted in typical high field strength elements (HFSE) such as Nb, Ta, Ti, Y and HREE, consistent with the geochemical characteristics of typical arc igneous rock, indicating these rocks have genetic relations to volcanic arc and have been formed in a magmatic arc environment. This is also demonstrated by a number of early Paleozoic granites with ages mainly between 470 and 420 Ma which have been defined by high-precision zircon U-Pb chronology recently in Central Tianshan, such as the Hongliuhe pluton (441.4 ± 1.6 Ma), the north Xiaoyanchi monzodiorite (427 ± 8 Ma), the East Tianhu gneissose granite (466.54 ± 9.8 Ma), the mylonitized Tianger granite (441.6 ± 3.8 Ma), and the Gangou granite (428 ± 10 Ma). The geochemical and isotope features of all these granites also show calc-alkaline arc affinity. Combined with the regional geological characteristics and all the available data, it is suggested that the Central Tianshan was a magmatic arc during the early Paleozoic. The mechanism of the early Paleozoic Central Tianshan arc can be ascribed to the southern subduction of the ancient Tianshan ocean located between the Tuha block and Tarim block.

This work is supported by the NSFC(41272098) and the China Geological Survey (1212011140056).

Mineralization Characteristics And Enrichment Regularity Of Alteration-Type Gold Deposit In Eastern Qinling,China

WANSHAN LEI^{1,2*} AND YAJIAN LIU³

¹College of Earth Science and Land Resources,Chang'an University,Xi'an 710054,China

(*correspondence:lei.wanshan@gmail.com)

²Key Laboratory of Western China's Mineral Resources and Geological Engineering,Ministry of Education,Xi'an 710054,China

³Department of mineral exploration,Henan Huatai Zijin Mining Industry Co., Ltd,LuoYang, 471700,China

Luyuangou gold deposit is located in the north slope of the xionger mountains, eastern Qinling, China, which belongs to the western Henan broken-dermatofibrosarcoma area, southern margin of North China platform. According to the type of mineralization, the characteristics of mineral assemblages and the interpenetration relation between different mineral, the mineralization can be divided into three stages: Quartz-pyrite stage(I): gangue minerals was the milky white massive quartz, metal mineral was the pyrite, which

The main stage of gold mineralization. In this stage, the quartz mostly smoke gray, cut through the early quartz veins. Metal sulfide was disseminated and cloddy, which composed of pyrite, galena, sphalerite, chalcopyrite. Native gold mainly concentrated in the vein quartz, metal sulfides. Fine-grained dust-like characteristics of this stage pyrite. Carbonate stage(III): The last phase of mineralization. The combination of vein quartz, calcite and fluorite mineral appears. Poor mineralization. The existing gold body occur in the capacity seam fault invariably. The gold body assumes layered, stratiform and lenticular outputs. The boundary of ore body relies on chemical analysis to be delineated.

The BSE and EDS were used to study the Regularity of gold mineralization. The histogram shows three peak interval, 0-10%, 40-50% and 60-100%, which shows there are at least three types of Au migration and aggregation. Further investigation of ore-forming elements shows, the content of Au in gold-silver ore can be high; gold telluride ore Au content is generally not more than 40%; This shows that the combination between elements and substances allocation mechanism affects the occurrence of mineralization and ore-forming efficiency. Also shows that the multi-mode, multi-stage mineralization superimposed is the main characteristic in Alteration-Type Gold Deposit In Eastern Qinling, China.

This research is financially supported by the special Fund Basic Scientific Research of Central Colleges and the Special Fund of Basic Research Support Program of Chang'an University (Grant No. CHD2009JC159).

Do pyrolytic biomarker fragments retain some diagnosticity?

ARNE LEIDER¹ AND CHRISTIAN HALLMANN^{1,2}

¹ Max-Planck-Institute for Biogeochemistry, 07745 Jena, Germany, (aleider@bgc-jena.mpg.de, challmann@bgc-jena.mpg.de)

² MARUM, University of Bremen, 28334 Bremen, Germany

The detection of early life signatures based on lipid biomarkers in the sedimentary record is frequently hindered by an intense thermal history of the sediments, which causes cracking of parent biomarker molecules [e.g., 1]. Specific degradation products of hopanes and steranes might however still carry diagnostic value for the reconstruction of past biota when found in mature oils and sediment extracts. Laboratory studies investigating the thermal stability of kerogens and authentic biomarker standards during pyrolysis revealed some characteristic alteration products [e.g. 2, 3] but it is not known if these compounds are unique to their precursors.

We here investigate this question with heating experiments using biomarker standards (steranes and hopanes) under different time and temperature conditions as well as in the presence of a carbonaceous catalyst. Preliminary results show that e.g. 5 α -cholestane undergoes conversion to a series of benzenes, naphthalenes, biphenyls and diphenylmethanes at 350°C in the presence of activated carbon but diamondoid hydrocarbons, which are used to evaluate the thermal maturity in crude oils and condensates [e.g. 4], were not generated. Comparison of larger biomarker fragments to cracking products of spiked oils will reveal how unique they are. Such data might extend molecular geobiological approaches to basins that were hitherto precluded by their thermal maturity.

[1] Hill *et al.* (2003) *Org. Geochem.* **34** 1651–1672. [2] Abbott *et al.* (1995) *Geochim. Cosmochim. Acta* **59**, 2259–2264. [3] Seifert (1978) *Geochim. Cosmochim. Acta* **42**, 473–484. [4] Chen *et al.* (1996) *Org. Geochem.* **25**, 179–190.

Origin of brines associated with the Bou Azzer silver deposit, Anti-Atlas, Morocco: A LA-ICPMS study of individual fluid inclusions

M. LEISEN^{1,2*}, M-C. BOIRON¹, S. ESSARAJ³
AND J. DUBESSY¹

¹GeoRessources, Université de Lorraine, Vandoeuvre les Nancy, France

²present address : Andean Geothermal Center of Excellence (CEGA), Universidad de Chile, Santiago, Chile (*mleisen@ing.uchile.cl)

³Faculté des Sciences et Techniques, Département de Géologie, BP 549, Marrakech, Morocco

Determination of major and trace element concentrations including metals in fluids associated with ore deposits is essential to evaluate contrasting genetic models. Such information can be obtained by LA-ICPMS analysis of individual fluid inclusions as they represent remnants of the hydrothermal fluids responsible of ore deposition. Previous studies have determined Br and Cl concentrations in high-salinity fluid inclusions using standard multi-element solutions loaded in silica glass capillaries [1] or by using scapolite solid standards [2, 3, 4]. In this work, all metal concentrations have been calibrated using NIST 610 glass. Concentration of all elements in the fluid inclusions have been calculated as described by Leisen *et al.* (2012) [5].

Fluid inclusions associated with silver mineralisation in the Bou Azzer deposit (Anti-Atlas, Morocco) are Na-K-Ca chloride brines (Na: 30,000-60,000 ppm, K: 11,000-27,000 ppm, and Ca: 12,000-85,000 ppm). Ag content ranges from tens to hundreds of ppm. Cl/Br molar ratios range from 300 to 1,000. The Cl/Br ratios determined here are in good agreement with previously published data obtained by crush-leaching techniques [6]. The chemical characteristics of the fluid inclusions indicate that the fluids originated from evaporates that later migrated through basement rocks during a major extensional episode. These geochemical signatures do not support an epithermal model as previously suggested by Levresse *et al.* (2004) [7].

Funding: CNRS-INSU-CESSUR and French National Research Agency through the national program LABEX "Ressources 21"

[1] Stoffel *et al.* (2004) *Am. J. Sci.* **304**, 533-557 [2] Hammerli *et al.* (2013) *Chem.Geol.* **337-338**, 75-87 [3] Seo *et al.* (2011) *Chem.Geol.* **284**, 35-44 [4] Leisen *et al.* (2012) *Chem.Geol.* **330-331**, 197-206 [5] Leisen *et al.* (2012) *Geochim Cosmochim Acta*, **90**, 110-125 [6] Essaraj *et al.* (2005) *J. Afr. Ear. Sci.* **41**, 25-39 [7] Levresse *et al.* (2004) *Chem.Geol.* **207**, 59-79

Boron behavior during silicate weathering: clues from bulk mineral and intracrystalline investigations

D. LEMARCHAND^{1*}, A. VOINOT^{1,2}, P. FLORIAN³, D. NEUVILLE⁴ AND M-P. TURPAULT²

¹LHyGeS/CNRS, Univ. Strasbourg, France

(*correspondence: lemarcha@unistra.fr)

²BEF, INRA Champenoux, France

³CEMHTI/CNRS, Orléans, France

⁴IPGP/CNRS, Paris, France

How to model the behavior of a trace element in the mineral structure? What can trace elements actually tell us about the weathering conditions and history of their host mineral? In the present study, we have analyzed a series of common silicate minerals (biotite, muscovite, albite, K-feldspar) handpicked in different soil horizons developed on a granite bedrock (Morvan, France). The chemical and mineralogical weathering gradient shown by those minerals is compared with their respective B and $\delta^{11}\text{B}$ signatures. Our results evidence an excess B solubility compared to major elements in both micas, whereas it shows a relative accumulation in albite. Beside, major elements and B show parallel evolutions in K-feldspar, which is diagnostic of a stoichiometric mineral dissolution.

In order to investigate whether these distinct B behaviors are related to the B atomic environment in those minerals, we have performed solid-state ^{11}B NMR (SSNMR) analyses in similar silicate minerals. As far as we know, these SSNMR analyses are the first ones performed on such low B silicate samples (10-100 ppm). The SSNMR spectra in a B-rich plagioclase (labradorite) clearly shows a well-organized environment for B atoms but they are found in both trigonal and tetrahedral coordination whereas the mineral structure only presents tetrahedral sites. The presence of trigonal B implies the disruption of one of the tetrahedral-O bond, which should necessarily change the energy state of the B local environment. The SSNMR spectra of pristine albite and muscovite clearly demonstrate that B in those minerals is also present in both the trigonal and tetrahedral coordination, but not in well-organized environments, typically not in substitution of Si or Al in the crystal structure but rather located in crystal defects (i.e. in those crystal positions expected to be the most reactive ones).

These new observations may allow the determination of distinct B energy states in crystallographic sites and study of the differential B mobility may help characterizing processes of non-stoichiometric mineral dissolution.

The copper deposit of Gaoua, Burkina Faso: A Paleoproterozoic porphyry deposit

E. LE MIGNOT^{1,2*}, L. SIEBENALLER³, D. BEZIAT⁴, S.
SALVI⁴, A.-S. ANDRE-MAYER¹, L. REISBERG²
AND G. VELASQUEZ⁴

¹ GéoRessources, Université de Lorraine, BP239, 54506
Vandoeuvre-lès-Nancy, France

(*correspondence: elodie.le-mignot@univ-lorraine.fr)

² CRPG/CNRS, 54501 Vandoeuvre-lès-Nancy, France

³ IRD GET, 31400 Toulouse, France

⁴ GET, Université Paul Sabatier, 31400 Toulouse, France

The copper occurrence of Gaoua is located in the Boromo-Goren greenstone belt, southern Burkina Faso. In this deposit, copper mineralization is predominantly present in the form of chalcopyrite and is hosted in Paleoproterozoic volcanic and plutonic rocks of andesitic to dioritic composition.

Geochemical analyses of the host diorite and andesite suggest an island arc setting for the formation of these rocks. Brecciation is widespread, accompanied by abundant chalcopyrite ± anhydrite in the matrix, as are quartz ± carbonate veins, which commonly form stockwerk-like networks. Microthermometric analyses of fluid inclusions indicate high temperature (>400°C) and high salinity fluids (>30% wt% eq. NaCl), related to hydrothermal fluid circulation contemporaneous to diorite intrusion and andesitic volcanism. The above data suggest that the copper mineralization formed in a porphyry-type context.

Pyrites and molybdenites associated with the porphyry mineralization were dated by the Re-Os method. The resulting isochron yields an age of 2170 ± 40 Ma, corresponding to a pre-Eburnean magmatic accretion event. Paleoproterozoic porphyry deposits are very rare since they form at shallow depths and, therefore, are very sensitive to erosion. Nevertheless, the high Re and radiogenic Os contents, together with the low common Os contents of the dated pyrites and molybdenites, argue for the reliability of the data.

FT-ICR Mass Spectrometric and Density Functional Theory studies of Solvated Cerium Chloride Clusters

KONO H. LEMKE¹ AND YIN ZHAO¹

¹Department of Earth Sciences, University of Hong Kong,
Pokfulam Road, Hong Kong, SAR, China (kono@hku.hk)

The molecular-scale speciation of cerium in aqueous fluids (bulk liquid and vapor phase) is a primary field of interest with important implications for our understanding of the transport and deposition of REE's in the Earth's crust. Mass spectrometric and quantum chemical studies of cerium chloride solutions can provide important insight into the composition, structure and energetic properties of molecular cerium species, and as such, deliver new information with respect to the distribution and abundance of such materials in aqueous fluids.

Here we present results from electrospray ionization (ESI) Fourier transform ion cyclotron resonance (FT-ICR) mass spectrometric experiments of cerium chloride complexes and clusters in the gas-phase, in particular, clusters of the general form $[\text{Ce}_m\text{X}_n]^+$ ($\text{X}=\text{Cl}, \text{OH}, \text{O}$) and corresponding micro-solvated species. We also report equilibrium geometries and associated energetic properties using M06/cc-pVXZ-PP ($\text{X}=\text{D}, \text{T}$) level theory in combination with quasi-relativistic effective core potentials for Ce. Ion cluster experiments have been conducted on a custom-modified Bruker-Daltonics 7T FT-ICR mass spectrometer with temperature-control, ESI capability and pulsing valves facilitating ion-solvent reactions. Molecular species identified upon electrospray ionization of aqueous CeCl_3 include a) $[\text{CeCl}_2]^+(\text{H}_2\text{O})_n$, $[\text{CeClOH}]^+(\text{H}_2\text{O})_n$ and $[\text{Ce}(\text{OH})_2]^+(\text{H}_2\text{O})_n$ with $n=0-4$; b) polynuclear $[\text{Ce}_m\text{Cl}_{3m-j}]^+(\text{H}_2\text{O})_n$ with $m=1-5$ and $n=0-4$ c) mixed polynuclear $[\text{Ce}_m\text{Cl}_{3m-2}\text{OH}]^+$ and $[\text{Ce}_m\text{Cl}_{3m-3}\text{O}]^+$ with $m=1-5$ and d) larger solvated clusters of the general form $[\text{Ce}_m\text{Cl}_{3m-4}\text{O}]^{+2}(\text{H}_2\text{O})_n$ and $[\text{Ce}_m\text{Cl}_{3m-4}\text{O}]^{+2}(\text{H}_2\text{O})_n$ with $m\leq 6$ and up to six water molecules. We also conducted mass spectrometric experiments in which the concentration-dependence (1-20mM; pH 5.2-6.9) of the cerium cluster distribution was probed. Results from these concentration-dependent experiments demonstrate that cerium chloride clustering increases with CeCl_3 concentration, in other words, at higher CeCl_3 concentrations (lower pH) more cerium chloride is present as polynuclear chlorocerate. With respect to solution pH, it is likely that the emergence of clusters with bridging hydroxo groups, e.g. $[\text{Ce}_m\text{Cl}_{3m-2}\text{OH}]^+$ arises as a consequence of the partial hydrolysis of $[\text{Ce}_m\text{Cl}_{3m-j}]^+$ clusters, in particular, in the acidic pH range. Last but not least, the observed correlation between ion mass spectra and solution content appears to demonstrate that dinuclear clusters are intermediates on the way from the $[\text{CeCl}_2]^+$ complex to the formation of larger "bulk-like" chlorocerate clusters. In conclusion, results from our ESI mass spectrometric and DFT study strongly point toward molecular clustering being an important factor in understanding Ce speciation in aqueous fluids.

Geochemical Sample Analysis by Microwave Plasma Atomic Emission Spectrometry

T. D. HETTIPATHIRANA* AND J-P LENER

Agilent Technologies, 679 Springvale Road, Mulgrave VIC 3170, Australia (*correspondence: terrance_hettipathirana@agilent.com)

We present the results for a wide range of geochemical Certified Reference Materials (CRM) analyzed using a novel Microwave Plasma - Atomic Emission Spectrometer (MP-AES) developed by Agilent Technologies. This instrumental technique uses microwaves to generate an atmospheric pressure N_2 -plasma and a conventional ICP-OES sample introduction system. Emission line measurement is performed using a Czerny-Turner monochromator and charge-coupled device system.

We have successfully analyzed base metals (Ag, Cu, Ni, Mo, Pb, and Zn) and platinum group metals (Au, Pd, and Pt). Figure 1 depicts a comparison of Certified and MP-AES results for the determination of Au in geochemical CRMs.

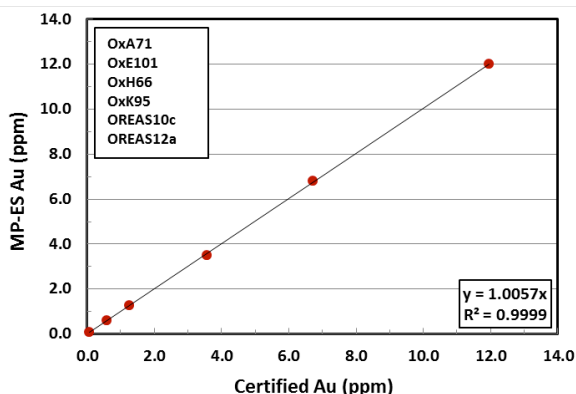


Figure 1 Comparison of Certified and MP-AES results for geochemical CRMs indicates excellent correlation.

The above results indicate that MP-AES is a very powerful technique for a wide variety of geochemical sample analysis. A highly robust atmospheric pressure plasma is generated by using N_2 and therefore the running cost is considerably lower compared with alternative techniques. MP-AES uses no flammable gases making the routine operation much safer than flame atomic absorption spectrometry.

Power of a new ICP-MS, ICP-QQQ: Application of the MS/MS reaction cell to two challenging analysis

LENER JEAN PIERRE¹ AND NAOKI SUGIYAMA²

¹Agilent Technologies (jean-pierre.lener@agilent.com)

²Agilent Technologies (naoki_sugiyama@agilent.com)

A new type of ICP-MS, the Triple Quadrupole ICP-MS (ICP-QQQ) was applied to two challenging analysis. The ICP-QQQ provides MS/MS reaction cell that outperforms existing reaction cell ICP-MS. The MS/MS configuration unique to ICP-QQQ solves a problem of conventional reaction cell, complexity of chemical reaction in cell, allowing use of full potential power of reaction cell to remove spectra interference. The first quadrupole placed in front of cell removes undesired ions, allowing only ions having selected mass to enter the cell. It makes chemical reaction in cell simple and hence consistent regardless of sample matrix.

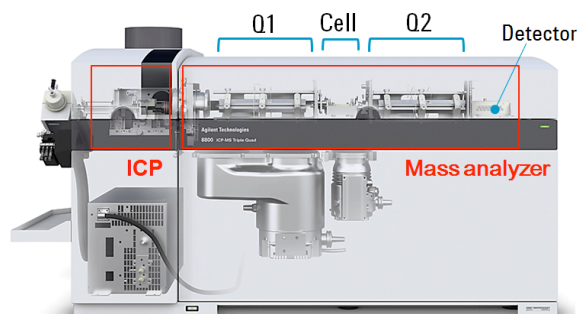


Figure 1: Configuration of ICP-QQQ

One analysis we applied ICP-QQQ is trace rare earth elements (REEs) measurement in REE materials such as gadolinium oxide, where interferences of GdH^+ with Tb^+ and GdO^+ with Yb^+ are problem. The other analysis is trace analysis of noble metals, Ru, Rh, Pd, Ag, Os, Ir, Pt and Au in complex matrix such as Cu, Zn, Ni, Sr, Rb, Zr, Nb, Mo, REE, Ta, W, Hf and Hg. Oxide, argide, atomic and double charged ions of the matrix elements interfere with isotopes of analyte. MS/MS mass shift method was used: analyte ions converted to molecular ions such as oxide ions via chemical reaction is detected on the different mass free from interference. The method successfully measured analyte at trace level in matrix, demonstrating excellent analytical performance of the ICP-QQQ.

Predicting the depth of the lithosphere-asthenosphere boundary from surface heat flow in the Carpathian-Pannonian region: the role of pargasitic amphibole

ISTVÁN KOVÁCS¹, LÁSZLÓ LENKEY², LÁSZLÓ OROSZ¹, JOLÁN ANGYAL¹ AND ZSUZSANNA VIKOR¹

¹ Geological and Geophysical Institute of Hungary, H-1143, Srefánia út 14, Budapest, Hungary
² Eötvös University, Budapest, Hungary, H-1117, Pázmány Péter sétány 1/c

It was shown recently (Green *et al.*, 2010) that pargasitic amphibole is the most important water bearing phase in the upper mantle. Its melting and instability at 3 GPa (~90 km of depth) or ~1050 °C lead to a significant drop in the water storage capacity of the upper mantle. The melt or free fluid forming during the decomposition of pargasite weakens considerably the rheology of the upper mantle resulting in lower seismic velocity, higher conductivity and stronger anisotropy.

If this petrologic model is correct, then we should see geophysical anomalies at ~90 km depth globally, expect places where the heat flow is high. In this areas, where the heat flow is higher than ~60-70 mW/m² -considering an average continental geotherm - the temperature may exceed the pargasite stability at ~1050 °C in a depth shallower than 90 km. The Carpathian-Pannonian region (CPR) which is characterized by high heat flow, and both geophysical and geological data are abundant, is an excellent natural laboratory to test such a petrophysical model. Depth of the 1050 and 1100 °C isotherm was calculated beneath the CPR from heat flow data and compared the depth of major geophysical anomalies indicating the lithosphere-asthenosphere boundary.

Paleoredox chemistry of Cenomanian–Coniacian black shales at high paleolatitudes: Implications for the extent of anoxia during OAE2

M. LENNIGER^{1*}, H. NØHR-HANSEN², L. V. HILLS³ AND C. J. BJERRUM¹

¹ Department of Geosciences and Natural Resource Management and Nordic Center for Earth Evolution (NordCEE), University of Copenhagen, 1350 Copenhagen, Denmark
 (*correspondence: mal@geo.ku.dk)

² Geological Survey of Denmark and Greenland (GEUS), 1350 Copenhagen, Denmark

³ Department of Geoscience, University of Calgary, AB T2N 1N4 Calgary, Canada

Cretaceous oceanic anoxic events (OAEs) have been studied in detail during the last decades. OAE2 is of particular interest as it reflects one of the largest perturbations of the global carbon cycle in the Mesozoic. It is characterised by a widespread deposition of organic rich sediments which is reflected by a positive carbon isotope excursion (CIE) in the terrestrial and marine record. Whereas the paleoredox conditions in low and mid-paleolatitudes are well constrained for OAE2, data from high paleolatitudes are still scarce.

The paleoceanographic response at high paleolatitudes during OAE2 is here characterized by samples from Axel Heiberg Island in Canada. Preliminary palynological analyses indicate a Late Cenomanian–Coniacian age for the section. Bulk organic carbon isotope data have been corrected using the hydrogen index (Rock Eval pyrolysis) to account for changes in organic matter sourcing. Our corrected isotope record correlates in detail with the European carbonate reference curve and confirms our biostratigraphic model. Iron speciation (Fe_{HR}/Fe_T and Fe_{Py}/Fe_{HR}) data point to anoxic but non-euxinic conditions at high paleolatitudes during OAE2. Furthermore the Sverdrup Basin was intermittently suboxic to anoxic (ferruginous) throughout most of the latest Cenomanian–Coniacian. Despite very high TOC (>10%) and hydrogen index values, molybdenum concentrations are relatively low during OAE2 but increase after the event. This suggests a global drawdown of the seawater molybdenum reservoir caused by the widespread extent of ocean anoxia/euxinia in the Cretaceous oceans during OAE2.

Biological controls on oxygenation in the Neoproterozoic and Paleozoic

TIMOTHY M. LENTON¹

¹University of Exeter, Exeter, UK, t.m.lenton@exeter.ac.uk

The deep oceans were finally oxygenated during the Late Neoproterozoic, and this is widely attributed to a rise in atmospheric oxygen. However, existing data suggests there followed a de-oxygenation of the ocean across the Precambrian-Cambrian boundary. Only later in the Paleozoic did the deep ocean recover a fully oxygenated state. What biogeochemical mechanisms could explain these changes?

It is hypothesised that increases in phosphorus weathering, either due to greening of the land [1] or the aftermath of glaciations [2], fuelled organic carbon burial and thus a Neoproterozoic increase in atmospheric oxygen. However, sustained changes in silicate weathering flux are prevented by the well-known regulator of atmospheric CO₂ and temperature. Thus, increases in phosphorus weathering can only be sustained long enough to affect atmospheric oxygen if there is selective weathering of phosphorus relative to bulk rock (by biology) [1], or a shift in the balance of CO₂ sinks from seafloor weathering to continental weathering [3].

Hence it is worth considering if the Neoproterozoic oxygenation of the ocean could have happened without a rise in atmospheric oxygen. A possible scenario invokes the evolution of eukaryotes in the surface ocean producing larger particles that sank faster [4]. This would have shifted oxygen demand away from the bottom waters of continental shelves (where the majority of phosphorus burial and recycling occurs) to greater depth. Oxygenation of the shelves would have increased the efficiency phosphorus removal from the ocean (in organic matter and adsorbed to iron oxyhydroxides) thus lowering global productivity and lowering oxygen demand in the deep ocean, oxygenating it. The net effect on organic carbon burial is uncertain because less export production was counteracted by faster sinking to sediments.

The subsequent early Paleozoic de-oxygenation of the ocean could be explained by the evolution of animal bioturbation lowering the C/P burial ratio of organic matter in sediments and thus lowering atmospheric oxygen [5].

The later rise of land plants, selectively weathering phosphorus and producing recalcitrant high C/P biomass, increased organic carbon burial and atmospheric oxygen, finally producing a persistent oxygenation of the ocean.

[1] Lenton & Watson (2004) *GRL* **31**, L05202. [2] Planavsky *et al.* (2010) *Nature* **467**, 1088-90. [3] Mills *et al.* (submitted). [4] Logan *et al.* (1995) *Nature* **376**, 53-6. [5] Boyle *et al.* (submitted).

Orientation-dependent REE³⁺ luminescence: a possible artifact in luminescence imaging

C. LENZ^{1*}, C. REISSNER¹, D. TALLA^{1,2} AND L. NASDALA¹

¹ Institut für Mineralogie und Kristallographie, Universität Wien, Althanstraße 14, 1090 Wien, Austria

(*correspondence: christoph.lenz@univie.ac.at)

² Institute of Geological Sciences, Masaryk University, Kotlářská 2, 61137 Brno, Czech Republic

Luminescence imaging is a sensitive tool for revealing internal zoning patterns of crystals and other geological samples, especially for species containing rare-earth elements (REE³⁺) [1,2]. In addition to the traditional direct imaging methods, the hyperspectral mapping technique is used increasingly for this [3]. Quantifications of REEs from emission intensities have been proposed for several minerals [3–5]. Note, however, that the orientation-dependence of REE³⁺ emissions is often neglected by Earth scientists [4], even though the phenomenon is well known [5,6].

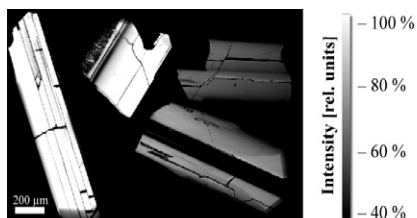


Figure 1: PL map (532 nm excitation with N–S polarisation) of the emission of Nd³⁺, showing clear intensity differences among chemically uniform but randomly oriented crystals.

As an example, we have studied the orientation-dependence of the $^4F_{3/2} \rightarrow ^4I_{9/2}$ emission of trace Nd³⁺ in zircon and xenotime-(Y) and their synthetic analogues. We found once again that the emission intensity depends strongly on the direction of the emitted light being analysed (CL and PL). In PL, the intensities observed are further affected by the polarisation of the incident laser beam relative to the crystal (compare Fig. 1).

[1] Götze (2002) *Anal Bioanal Chem* **374**:703–708. [2] Hanchar & Miller (1993) *Chem Geol* **110**:1–13. [3] MacRea *et al.* (2012) *Microsc Microanal* **18**:1239–1245. [4] Habermann (2002) *Miner Petrol* **76**:247–259. [5] Barbarand & Pagel (2001) *Am Mineral* **86**:473–484. [6] Finch *et al.* (2003) *Phys Chem Miner* **30**:373–38.

Organic biomarkers in sediment from Admiralty Bay, Antarctica

LEONEL, J.^{*1}; ARAÚJO, L. D.¹; AND BÍCEGO, M. C.¹

¹Lab. de Quím. Org. Mar., IO-USP, 05508-120, São Paulo, Brazil.

*corresponding author: juoceano@gmail.com

The use of biomarker data as proxies reflecting recent environmental conditions is a well established geochemical tool. Therefore, this study aimed to get more detailed information on the source and composition of organic matter from surface sediments from Admiralty Bay and adjacent area of Bransfield Strait, Antarctica. Total organic carbon, carbon isotopic composition, *n*-alkanes and fatty alcohols were analyzed in sediment collected in four different isobaths (100m, 500m, 700m, and 1100m). Samples from all isobaths were characterized by low amounts of organic carbon (0.14 – 0.52%) and no significant variation among locations. Values of $\delta^{13}\text{C}$, ranging from -25.9 to -24.7, were similar to those from terrestrial inputs in tropical and subtropical areas. However, the low values of $\delta^{13}\text{C}$ in high latitudes can be related to the higher concentrations of dissolved CO_2 at low surface temperatures and slow growth rates infer small periods of light. In comparison with $\delta^{13}\text{C}$ found in phytoplankton (-28 to -33‰) the values in sediment were higher probably due to the high contribution from krill faeces that are approximately 3-4‰ enriched compared to phytoplankton. Furthermore, the influence of a lateral influx of benthic macroalgae from the nearby shelf areas can also contribute to an enrichment of about 3‰. Average concentrations of *n*-alkanes (*n*-C₁₂ to *n*-C₃₆) were 0.86 $\mu\text{g g}^{-1}$, 0.79 $\mu\text{g g}^{-1}$, 0.67 $\mu\text{g g}^{-1}$, and 0.17 $\mu\text{g g}^{-1}$ at 100, 500, 700 and 1100 m, respectively, and its distribution varied among isobaths. Sediments from 100 m showed more *n*-alkanes with higher molecular weight, dominance of *n*-C₂₉, probably due to the input of *n*-alkanes from terrestrial adjacent areas, especially from grasses, lichens and mosses. On the other hand, at 500, 700 and 1100 m, the lower molecular weight compounds were the predominant *n*-alkanes showing marine influence. Normal alcohols (C₁₂ – C₃₀) concentrations were 25 ng g^{-1} at 100 m, 76 ng g^{-1} at 500 m, 104 ng g^{-1} at 700 m and 158 ng g^{-1} at 1100 m, with predominance of the chain with 16 carbons in all samples. C₁₆ level increased from 100 m to 1100 m, it is considered a typical marine compound since it is the most abundant homologue in phytoplanktons, while C₁₈ appears to be less specific. The ratio low molecular over high molecular alcohols was above 3 in all samples, and also indicates a dominance of autochthonous productivity. The organic matter in the sediment from the Admiralty Bay and adjacent area of Bransfield Strait seems to be a mixture of both terrestrial and marine sources. However, further studies are necessary to fully understand the sources and distribution of organic matter in the region.

Biogeochemical types of lake sapropels in Siberia

G.A. LEONOVA*, V.A. BOBROV, S.K. KRIVONOGOV, A.A. BOGUSH, A.E. MALTSEV AND G.N. ANOSHIN

Institute of geology and mineralogy SB RAS, Koptyug Pr. 3, Novosibirsk 630090, Russia (*correspondence: leonova@igm.nsk.ru)

We recognize three types of lake sapropels based on the paleolimnetic classification taking into account biological and chemical characteristics of sedimentation [1]. Molecular biomarkers were used as additional chemical criteria of origin of organics in sapropels [2]. Biological characteristics imply two types of sapropels: predominately macrophytic and planktonic and macrophytic. Combinations of biological and chemical characteristics imply three types of sapropels. Type 1, macrophytic with high Ca and low Fe, was found in West-Siberian lakes such as the whole Lake Belye (Ca ~ 27%, Fe ~ 1.1%) [3] and near-shore zone of Lake Kirek (Ca ~ 18%, Fe ~ 3%) [4]. Type 2, planktonic and macrophytic with low Ca and high Fe, is characteristic for the central part of Lake Kirek [4]. Type 3, planktonic and macrophytic with low Ca and low Fe, was found in East-Siberian lakes, such as Lake Ochki (Ca ~ 0.43%, Fe ~ 0.67%) and Lake Dukhovoe (Ca ~ 0.86%, Fe ~ 2.7%) [5]. Formation of sapropels in certain lakes mostly depends on physico-chemical characteristics of their waters, i.e., mineralization, chemical class, pH, Eh and on dominated producers of the organic matter [5]. West-Siberian lakes mostly belong to the calcium hydrocarbonate class, have low or medium mineralization and alkaline pH; macrophytes are the main producers of the organic matter. These conditions suggest formation of high-calcic sapropels. East-Siberian lakes show dominated planktonic sapropel production, whereas their hydrochemistry vary from little mineralized calcium hydrocarbonate alkaline (Lake Dukhovoe) to ultra-fresh sulphate Ca-Na highly acidic (Lake Ochki) classes. These conditions suggest formation of low-calcic sapropels. This research was supported by the SB RAS Integration Project no. 125 and RFBR 11-05-00655.

[1] Korde N.V. Biostratigraphy and typology of Russian sapropels (1960), Moscow. [2] Melenevskii *et al.* (2011), *Russian Geology and Geophysics* 52, 583–592. [3] Krivonogov *et al.* (2012), *Palaeogeography, Palaeoclimatology, Palaeoecology* 331–332, 194–206. [4] Bobrov *et al.* (2012), *Russian Poverkhnost'. Rentgenovskie, Sinkhrotronnye i Neitronnye Issledovaniya* 5, 90–96. [5] Leonova, Bobrov (2012), Geochemical role of plankton of continental water basins of Siberia in concentration and biosedimentation of microelements, Novosibirsk, GEO.

Dating the collapse of the Scandinavian Ice Sheet using CH₄-derived carbonate crusts from the Barents Sea

AIVO LEPLAND^{1,2*}, SHYAM CHAND¹, DIANA SAHY³,
STEPHEN R. NOBLE³, DANIEL J. CONDON³, TÖNU
MARTMA², JON HALVARD PEDERSEN⁴, SIMONE SAUER¹,
HARALD BRUNSTAD⁴ AND TERJE THORSNES¹

¹ Geological Survey of Norway, Trondheim, Norway
(*correspondence: aivo.lepland@ngu.no)

² Tallinn University of Technology, Tallinn, Estonia

³ NERC Isotope Geoscience Laboratory, Keyworth, UK

⁴ Lundin Petroleum, Oslo, Norway

Assessment of the potential impact of past CH₄ discharge from CH₄ hydrate reservoirs into the atmosphere is hindered by the lack of robust age constraints on the timing of such fluxes. Authigenic carbonates formed in shallow sediments can be related to CH₄ fluxes to the ocean-atmosphere via stable isotope analyses and can be dated by using U-daughter decay (e.g., Teichert *et al.*, 2003) affording the opportunity to constrain the absolute timing and estimate the rates of CH₄ release.

CH₄-derived carbonate crusts exhibiting characteristic ¹³C-depleted isotopic signatures were collected from several seepage sites of the Barents Sea. The U-Th dating results of early generation aragonite cementing sandy and gravelly sediments constrain the main event of CH₄ discharge and crust formation to a time interval between c. 14 and 11 ka, continuing until c. 9 ka constrained by late stage cavity filling aragonite. These U-Th dates indicate that the carbonate crust formation in the Barents Sea was coincident with the deglaciation of the area and collapse of the Scandinavian Ice Sheet. The CH₄ flux for the carbonate crust formation was likely provided by the dissociation of CH₄ hydrates that extensively formed in underlying sediments during the last glacial period (Chand *et al.*, 2012), but became unstable due to depressuring effects of retreating ice sheet and related isostatic rebound. Ice core records from Greenland and Antarctica demonstrate two CH₄ concentration peaks at ca. 15-13 ka and 11-8 ka, overlapping with the crust formation episode. Such temporal coincidence implies the involvement of destabilised, sediment hosted CH₄ hydrates influencing atmospheric CH₄ and global climate during the last deglaciation.

[1] Chand, S., *et al.*, 2012, Earth and Planetary Science Letters, v. 331-332, p.305-314. [2] Teichert, B. M. A., *et al.*, 2003, Geochimica et Cosmochimica Acta, v. 67, p. 3845-3857.

Coupled isotopic and textural evidence for the biogenicity of 3.4 Gyrs old cell-like structures

KEVIN LEHOT^{1,2}, KENNETH H. WILLIFORD^{1,3}, TAKAYUKI
USHIKUBO¹, KENICHIRO SUGITANI⁴, KOICHI MIMURA⁵,
MICHAEL J. SPICUZZA¹ AND JOHN W. VALLEY¹

¹ NASA Astrobiology Institute, WiscSIMS, Department of
Geoscience, University of Wisconsin, 1215 W. Dayton St.,
Madison, WI 53706, USA

² Université Lille 1, Laboratoire Géosystèmes, CNRS
UMR8217, 59655 Villeneuve d'Ascq, France,
kevin.lehot@univ-lille1.fr

³ Jet Propulsion Laboratory, 4800 Oak Grove Dr., Pasadena,
CA 91109, USA

⁴ Department of Environmental Engineering and Architecture,
Graduate School of Environmental Studies, Nagoya
University, Nagoya, 464-8601, Japan.

⁵ Department of Earth and Environmental Sciences, Graduate
School of Environmental Studies, Nagoya University,
Nagoya, 464-8601, Japan.

The oldest possible morphological evidence for life are 3.4-3.5 Gyr old. Distinguishing geochemical biosignatures in organic matter preserved in such ancient rocks remains difficult due to alteration by deep burial and to the abundance of hydrothermal systems that could have produced abiogenic organics. Microbial morphologies are in general simple and, especially when degraded, can be difficult to distinguish from migrated hydrocarbons precipitated along grain boundaries of variable shapes. Abundant cell-like organic microstructures have been recently reported in the 3.4 Gyr old Strelley Pool Formation from Western Australia. We measured carbon isotope ratios and H/C in situ (with a 15 μm spot) in these organic microstructures using Secondary Ion Mass Spectrometry (SIMS) and characterized the structure of organic matter using Raman spectromicroscopy. Coordinated Raman spectromicroscopy and SIMS carbon isotope measurements distinguished the indigenous cell-like structures and kerogen from late migrated bitumen. SIMS revealed carbon isotopic and H/C heterogeneities between spherical and lenticular cell-like structures and kerogen clots, and internal heterogeneities in lenticular structures. Heterogeneities can be explained by selective diagenetic preservation of the distinct isotopic fractionations inherited from different precursor biomolecules. These results support the interpretation of biogenicity of morphologically cellular structures in the Strelley Pool Formation.

Interactions between chemical inhibitors, scale formation, corrosion and microbes at geothermal plants

LERM, S.¹, WESTPHAL, A.¹, EICHINGER, F.²,
HUENGES E.¹ AND WÜRDEMANN, H.¹

¹ Helmholtz Centre Potsdam GFZ German Research Centre for Geosciences, Telegrafenberg, 14473 Potsdam, Germany. Email: wuerdemann@gfz-potsdam.de

² Hydroisotop GmbH, Woelkestr. 9, 85301 Schweitenkirchen, Germany. Email: fe@hydroisotop.de

Chemical inhibitors are used to prevent scale formation and corrosion that adversely affect the reliability and economic efficiency of geothermal plants. However, knowledge about inhibitor efficiency with respect to chemical fluid composition, temperature and fluid abundant microorganisms is required. In addition, to be sufficiently effective, inhibitors have to be stable in the geothermal plant and the near wellbore area but for ecological reasons also degradable. Since microorganisms, such as sulfate reducing bacteria (SRB), are involved in scaling and corrosion processes, the influence of the inhibitor supply on the microbial community composition should be investigated.

Thus, lab-scale experiments with fluid samples from different geothermal plants in Germany were performed. As fluids from the North German Basin, the Upper Rhine Graben and the Molasse Basin have a significantly different chemical fluid composition that leads to a region-specific formation of scales, different inhibitors were tested. In order to investigate the interactions between microbes and reservoir rock material, fluids were incubated with rock material from outcrop analogues.

First results show the degradability of the supplied inhibitors that was indicated by the production of CO₂ in the gaseous phase of the vessels. Particularly, a correlation between the CO₂ yield and the inhibitor concentration illustrated the substrate-dependent activity of microorganisms.

The influence of inhibitor supply on the microbial community composition in fluids was shown for a bypass system at a geothermal plant in the Styrian Basin. At this plant, supply of a nitrate-based inhibitor led to a reduced diversity and abundance of SRB and a higher abundance of nitrate reducing bacteria. This corresponded to a reduced content of corrosive H₂S in fluids.

3D fluid distribution in subducted slabs: new constraints on H₂O cycling

V. LE ROUX¹, G. GAETANI¹, J. SLAUGENWHITE²
AND K. MILLER³

¹ Woods Hole Oceanographic Institution, 266 Woods Hole road, Woods Hole MA 02543 USA.

vleroux@whoi.edu; ggaetani@whoi.edu

² University of Houston, 4800 Calhoun Rd, Houston TX 77004 USA. jeremy@slaugenwhite.com

³ University of Maryland, College Park MD 20742 USA. kjmiller944@gmail.com

Large amounts of H₂O are carried into trenches via subduction of the sediments, basaltic crust and uppermost mantle that make up the oceanic lithosphere. A major question is how much of this subducted H₂O is released into the overlying mantle wedge, promoting melting, and how much is carried deeper into the mantle. This depends, at least in part, on whether H₂O is able to form an interconnected network among the mineral grains that make up the rock down to very low fluid fractions. In order to achieve connectivity and allow the fluid phase to escape, a minimum amount of fluid (critical porosity) is required when dihedral angles are more than 60 degrees. We investigated the distribution of seawater in simplified sediment analogs (i.e. quartz for siliceous sediments; calcite for carbonate sediments), in natural clays (kaolinite and montmorillonite) and in bulk eclogite. Experiments were performed in a piston-cylinder apparatus at 2 GPa and 650°C. Fluid fractions ranged from ~10% to ~1% to determine the porosity at which connectivity of the seawater network is lost for each rock type.

We used synchrotron X-ray microtomographic techniques (at Argonne National Laboratory, IL) to obtain 3-D images of the pore space network in order to constrain the grain scale distribution of fluids in a subducted slab. This nondestructive 3-D imaging technique has a spatial resolution of 0.7 μm and provides quantitative information on geometrical parameters of fluid topology, such as porosity, dihedral angle distribution, fluid channel sizes and connectivity. The geometrical parameters were extracted using the VSG Avizo® software. This study lays the groundwork for determining the 3-D grain scale distribution of fluids in a range of subducted lithologies. Results from this study provide important new insights into the amount of fluid that can be transported into the deep mantle by subduction.

Influence of surface conductivity on the apparent zeta potential of amorphous silica nanoparticles

P. LEROY^{1*}, N. DEVAU¹, A. REVIL^{2,3} AND M. BIZI¹

¹ BRGM, 3 Avenue C. Guillemin, 45060 Orléans, France
(*correspondence : p.leroy@brgm.fr).

² Colorado School of Mines, Green Center, Department of Geophysics, Golden, 80401 CO, USA

³ ISTerre, CNRS, UMR CNRS 5275, Université de Savoie, 73376 cedex, Le Bourget du Lac, France

Zeta potential is a physico-chemical parameter of particular importance in describing ion adsorption and double layer interactions between charged particles [1]. However, for metal oxide nanoparticles, the conversion of electrophoretic mobility measurements into zeta potentials is a complex problem. This complexity arises because of their high surface electrical conductivity, which is inversely proportional to the size of the particle [2].

To describe the electrochemical properties of amorphous silica nanoparticles, we use a basic Stern model whose parameters are independently adjusted by potentiometric titration and electrophoretic mobility measurements at high salinity (10^{-1} M NaCl) [3]. At low ionic strengths, because of the strong retardation and relaxation effect due to charged counter-ions at the silica/water interface, amplitude of the predicted zeta potential is significantly higher than that of the apparent zeta potential estimated with electrophoretic mobility measurements and Smoluchowski equation. Electrophoretic mobilities are calculated using Henry's electrokinetic model [4] with the predicted specific surface conductivities and zeta potentials. The very good agreement between calculated and measured electrophoretic mobilities confirms that the magnitude of the true zeta potential corresponds to the magnitude of the electrical potential located at the outer Helmholtz plane. Therefore, the assumption of the presence of a stagnant diffuse layer at the amorphous silica/water interface is not required. This study was done within the framework of the NANOMORPH Project (ANR-2011-NANO-008) coordinated by BRGM.

[1] Lyklema (1991) *Academic Press, London*, 736p. [2] Leroy *et al.*. (2011) *J. Colloid Interface Sci.* **356**, 442-453. [3] Sonnefeld *et al.*. (2001) *Colloids Surf. A: Physicochem. Eng. Asp.* **195**, 215-225. [4] Henry (1948) *Trans. Faraday Soc.* **44**, 1021-1026.

Postcards from Mars: Insights into Martian Geochemical Processes from the Curiosity Rover

L.A. LESHIN^{1*}, J.P. GROTZINGER², D.F. BLAKE³, R. GELLERT⁴, P. R. MAHAFFY⁵, R.C. WIENS⁶, S. MAURICE⁷
AND THE MSL SCIENCE TEAM

¹Rensselaer Polytechnic Institute, Troy, NY 12180
(*correspondence: leshin@rpi.edu);

²Caltech, Pasadena, CA;

³NASA/ARC, Moffett Field, CA;

⁴Univ. Guelph, ON Canada;

⁵NASA/GSFC, Greenbelt, MD;

⁶LANL, Los Alamos, NM,

⁷IRAP, Toulouse, France.

With the successful landing of the Mars Curiosity Rover in August 2012, we now have the most capable geochemical laboratory ever to travel to another planet roving Mars' Gale crater. The geochemical instrument suite includes the Chemistry Camera (ChemCam), which uses a laser to vaporize geologic targets and performs atomic emission spectroscopy on the vapor from distances of up to 7m. This provides a geochemical surveying capability that enables rapid identification of unique specimens and accumulation of a large set of rock and fines compositions as the rover traverses. The Alpha Particle X-ray Spectrometer (APXS) provides high quality "bulk" elemental analyses for major, minor and a few trace elements through a touch deployment on the surface of a rock or soil, and is an upgraded version of similar instruments previously flown to Mars. The addition of x-ray diffraction through the Chemistry and Mineralogy (CheMin) instrument and volatile, isotope, and organic analyses with the Sample Analysis at Mars (SAM) instrument suite, give Curiosity the capability to assess the geochemical history of the planet more deeply than previously possible.

Both CheMin and SAM accept sieved fines from either Curiosity's scoop or drill. To date, sampling has occurred at the Rocknest aeolian drift deposit and a fine-grained mudstone called John Klein. At Rocknest, CheMin found a mix of primary igneous minerals and amorphous materials. SAM found that Rocknest fines contain significant bound volatiles that can be released upon heating, largely associated with the amorphous material. Because APXS and ChemCam data support the fines being representative of those found at other sites on Mars, Curiosity results show that martian fines are a good source of water, CO₂ and other volatiles that could be leveraged by living organisms, including future human explorers. At John Klein, early results are consistent with an ancient aqueous habitable environment. Analyses of isotopes and organics also provide exciting windows into martian habitability and volatile evolution. These early geochemical results will be discussed.

Continental lithosphere removal by drip and delamination processes

ALAN LEVANDER^{1*}, MAXIMILIANO BEZADA²,
EUGENE D. HUMPHREYS², JENIFFER MASY¹
AND BRANDON SCHMANDT³

¹ Rice University, Houston Texas, USA 77251

(*correspondence alan@rice.edu)

² University of Oregon, Eugene Oregon, USA 97403

³ University of New Mexico, Albuquerque NM, USA 87131

We present evidence for convective removal of continental lithosphere beneath the western U.S., the western Mediterranean, and the southeastern Caribbean. All three locales are associated with subduction, the first through hydration weakening of overlying lithosphere during Laramide-age flat slab subduction, the latter two by recent or ongoing subduction that includes involvement of the adjacent continental margins. In the western U.S., the Precambrian continental lithosphere beneath the western Colorado Plateau, the Rio Grande Rift, and likely the northern Wasatch Front are experiencing thermo-chemical edge convection that removes most or all of the lithospheric mantle and can reach depths as shallow as the lower crust. Extensive basaltic volcanism accompanies this process, as vertical asthenospheric flow gradients and melt generation help destabilize the lithosphere. In the western Mediterranean, slab rollback and delamination of continental mantle beneath the Alboran crust have also removed the mantle lithosphere beneath the adjacent Iberian and Moroccan margins. Southern Spain and northern Morocco are sites of extensive mid-Cenozoic to modern basaltic volcanism. In the western Mediterranean, however, melt generation may be a consequence of rather than the cause of lithosphere removal. In the southeastern Caribbean, at the southernmost corner of the Antilles subduction zone, Atlantic subduction beneath the Caribbean plate results in a tearing lithosphere that produces a large-scale ocean-continent transform fault system. Deeper levels of the South American continental lithosphere (≥ 75 -100 km depth) south of the surface expression of the plate boundary are dragged along by the subducting Atlantic plate and descend into the mantle. Removal of lithosphere beneath the South American continental margin appears to trigger additional lithospheric instabilities within the continental interior. In contrast to both the western U.S. and the western Mediterranean, this process is almost amagmatic resulting from the relatively thick lithosphere that remains, precluding significant decompression melting. The range of subduction styles in which part or all nearby continental lithosphere is removed suggests a widespread process for recycling continental mantle.

The Effect of Chloride on the Dissolution Rate of Silver Nanoparticles and Toxicity to *E. coli*

CLÉMENT LEVARD^{1,2,4*}, SUMIT MITRA¹, TIFFANY YANG¹,
ADAM D. JEW¹, APPALA RAJU BADIREDDY^{2,3}, GREGORY
V. LOWRY⁴ AND GORDON E. BROWN, JR.^{1,2,5}

¹ Surface and Aqueous Geochemistry Group, Department of Geological & Environmental Sciences, Stanford University, Stanford, CA 94305-2115, USA

² Center for Environmental Implications of NanoTechnology (CEINT), Duke University, Durham, NC 27708-0287, USA

³ Department of Civil and Environmental Engineering, Duke University, Durham, NC, 27708, USA.

⁴ Department of Civil and Environmental Engineering, Carnegie Mellon University, Pittsburgh, PA, 15213, USA.

⁵ Department of Photon Science and Stanford Synchrotron Radiation Lightsource, SLAC National Accelerator Laboratory, 2575 Sand Hill Road, Menlo Park, CA 94025, USA

Pristine silver nanoparticles (AgNPs) are not chemically stable in the environment and react strongly with inorganic ligands such as sulfide and chloride. Understanding the environmental transformations of AgNPs in the presence of specific inorganic ligands is crucial to determining their fate and toxicity in the environment. Chloride (Cl⁻) is a ubiquitous ligand with a strong affinity for Ag(I) and is often present in natural waters and in bacterial growth media. Though chloride can strongly affect toxicity results for AgNPs, their interaction is rarely considered and is challenging to study because of the numerous soluble and solid Ag-Cl species that can form depending on the Cl/Ag ratio. Consequently, little is known about the stability and dissolution kinetics of AgNPs in the presence of chloride ions. Our study focuses on the dissolution behavior of AgNPs in chloride-containing systems and also investigates the effect of chloride on the growth inhibition of *E. coli* (ATCC strain 33876) caused by Ag toxicity. Our results suggest that the kinetics of dissolution are strongly dependent on the Cl/Ag ratio and can be interpreted using the thermodynamically expected speciation of Ag in the presence of chloride. We also show that the toxicity of AgNPs to *E. coli* at various Cl⁻ concentrations is governed by the amount of dissolved AgCl_x^{(x-1)-} species suggesting an ion effect rather than a nanoparticle effect.

Variations in triple oxygen isotopes in precipitation and river waters in the continental U. S.

NAOMI E. LEVIN^{1*}, SHUNING LI¹, J. RENÉE BROOKS²
AND JEFFREY M. WELKER³

¹Department of Earth & Planetary Sciences, Johns Hopkins University, Baltimore, MD 21218, USA
(*correspondence: nlevin3@jhu.edu)

²Western Ecology Division, US Environmental Protection Agency, Corvallis, OR 97333, USA

³Department of Biological Sciences, University of Alaska, Anchorage, AK 99508, USA

The triple oxygen isotope composition of water is an emerging tool in studies of hydrological processes because the $\delta^{18}\text{O}$ - $\delta^{17}\text{O}$ relationship differs during kinetic and equilibrium isotope fractionation such that ^{17}O -excess is sensitive both to humidity at the site of evaporation and to secondary processes during moisture transport [1]. The utility of triple oxygen isotope measurements in hydrological studies is twofold: 1) they provide additional constraints on isotopic fractionation of precipitation when both ^{17}O -excess and *d-excess* can be measured and 2) they provide an additional understanding of hydrologic processes, such as evaporative effects, that are recorded in oxygen bearing minerals (*e.g.*, CaCO_3 , SiO_2) and traditionally investigated with $\delta^{18}\text{O}$ alone.

Most ^{17}O -excess paleoclimate studies are based on high-latitude ice core records [2,3], but there is great potential to apply triple oxygen isotope approaches to climate proxies in low- to mid-latitude settings. A better understanding of ^{17}O -excess in meteoric waters in these settings is thus needed to develop ^{17}O -excess as a tool for probing the modern, past and possibly future hydrological cycle. Here we report ^{17}O -excess values of meteoric waters from the continental U.S. ^{17}O -excess values in weekly precipitation samples vary between -0.01‰ to +0.05‰. The lowest ^{17}O -excess values are from precipitation sourced in the Gulf of Mexico, whereas the highest observed ^{17}O -excess values are from precipitation that originates in the northern Pacific Ocean. ^{17}O -excess values of surface waters are similar to or lower than those of precipitation in the main recharge season. We use our results to demonstrate the role of moisture source, transport effects, and post-precipitation processes on continental-scale ^{17}O -excess variation and to provide a framework for using triple oxygen isotope records as proxies for hydrological change.

[1] Landais *et al.* (2010) *EPSL* **298**, 104-112. [2] Landais *et al.* (2008) *GRL* **35**. [3] Winkler *et al.* (2012) *Clim. Past* **8**, 1-16.

The Formation of the Cores of the Giant Planets

H.F. LEVISON^{1*}, K. KRETKE¹, M.J. DUNCAN²
AND H. NGO^{2,3}

¹Southwest Research Institute, 1050 Walnut St, Suite 400, Boulder, CO 80302, USA

(*correspondence: hal@boulder.swri.edu)

²Department of Physics, Engineering, and Astronomy, Queen's University, Kingston, ON K7L 3N6, Canada

³Division of Geological and Planetary Sciences, California Institute of Technology, Pasadena, CA 91125, USA

It is ironic that the most massive planets in the Solar System had to have formed in the least amount of time. Jupiter and Saturn, for example, which are made mainly of hydrogen and helium, must have accreted this gas before the solar nebula dispersed. Observations of young star systems [1,2] show that gas disks, at least insofar as they are traced by the presence of dust, as well as accretion onto the star, have lifetimes of ~1-10 Myr. So, the gas giant planets had to form before this time.

Thus, one of the most challenging problems we face in our understanding of planet formation is how Jupiter and Saturn could have formed so quickly. In the core accretion model, which envisions that a large planetary embryo formed first by two-body accretion followed by a period of inflow of gas directly onto the growing planet [3,4], the main difficulty is in the first step. The accretion of a massive atmosphere requires a solid core ~10 M Earth-masses in mass [5,4,6].

We will present the most complete models of standard core formation to date and show that it is difficult to construct objects larger than ~2 Earth-masses before the disk dissipates [7]. We will also present some new simulations that include solutions that have previously been suggested, but to have yet been included in full simulations. These include planetesimal-driven migration [8] and pebble accretion [9].

[1] Haisch *et al.* (2001) *Ap.J.* **553**, L153. [2] Hernandez *et al.* (2009) *Ap.J.* **707**, 705. [3] Mizuno *et al.* (1978) *Prog. Theor. Phys.* **60**, 699. [4] Pollack *et al.* (1996) *Icarus* **124**, 62. [5] Mizuno (1980) *Prog. Theor. Phys.* **64**, 544. [6] Hubickyj *et al.* (2005) *Icarus* **179**, 415. [7] Ngo *et al.* (2013) in preparation. [8] Levison *et al.* (2010) *A.J.* **139**, 129. [9] Lambrechts & Johansen (2012) *A&A* **544**, A32.

The relative contribution of sedimentation and diagenesis in colour formation of Quaternary bottom sediments from the southern part of Mendeleev Rise and the continental slope of the East Siberian Sea

M.A.LEVITAN^{1*}, K.V.SYROMYATNIKOV¹,
I.A.ROSHCHINA¹ AND R.STEIN²

¹ Vernadsky Institute RAS, Moscow 119991, Russia
(* correspondence: m-levitan@mail.ru)

² AWI, Bremerhaven 12 01 61 – 27515, Germany

The goal of this study is to determine the relative contribution of both factors based on XRF study of sediments and field colour descriptions of sediment cores using Munsell Soil Colour Chart. Four studied sediment cores are located at the area of Southern Mendeleev Rise and continental slope of the East Siberian Sea. We paid special attention to amounts of Mn, Cu, Ni, Co, As, quartz; Mn/Al and Mn/Fe ratios. Quarts amount mimics the influence of terrigenous matter during glacial/interglacial cycles; As is concentrated in diagenetic Fe sulfides; other abovelisted elements and ratios reflect the relative contribution of sedimentation and diagenesis.

It's important to note that according to V/Cr ratio the studied sediments have been accumulated in the oxic environment. Our study allowed to constrain the consequence of sediment colours reflecting the increasing of diagenesis/sedimentation ratio: dark brown – yellow brown – olive brown – olive grey – grey – dark grey. Pink sediments should be considered separately due to specifics of their composition (abundance of dolomite) but they have been underwent to diagenetic processes as well. The significant role in diagenesis played the type and amount of labile organic matter, sedimentation rates and facies environments of sediments. These conclusions are confirmed by results of dispersion analysis based on 333 samples.

The geochemical history of the Dead Sea from dissolved chemical species and isotopes in pore waters

E. J. LEVY^{1*}, O. SIVAN¹, Y. YECHIELI², I. GAVRIELI², B. LAZAR³ AND M. STEIN²

¹ Dept. of Geology and Environmental Sciences, Ben Gurion University of the Negev, Beer-Sheva, ISRAEL 84105
(*correspondance: elanl@post.bgu.ac.il)

² Geological Survey of Israel, 30 Malkhe Israel St., Jerusalem, ISRAEL 95501

³ Institute of Earth Science, The Hebrew University of Jerusalem, ISRAEL 91904

During the winter of 2010-11 an ICDP-drilling project exposed a 456m long water saturated core from the centre of the hypersaline Dead Sea (Israel). This research provides a unique perspective on the geochemical evolution of the lake from the analysis of dissolved chemical species and isotope proxies within the interstitial water gathered from the samples collected at intervals along the core. In this study we intend to present initial pore water results for major ion concentrations (Na^+ , K^+ , Ca^{2+} , Mg^{2+} , Sr^{2+} , Cl^- , Br^- , SO_4^{2-}) and corresponding ratios (Na/Cl (fig. 1), Mg/Ca (fig. 2), Sr/Ca, Na/K), the carbon system (dissolved inorganic carbon (DIC) and $\delta^{13}\text{C}_{(\text{DIC})}$), $\delta^{34}\text{S}_{(\text{SO}_4)}$ and $\delta^{18}\text{O}_{(\text{SO}_4)}$. Discussion of results will take place during the conference.

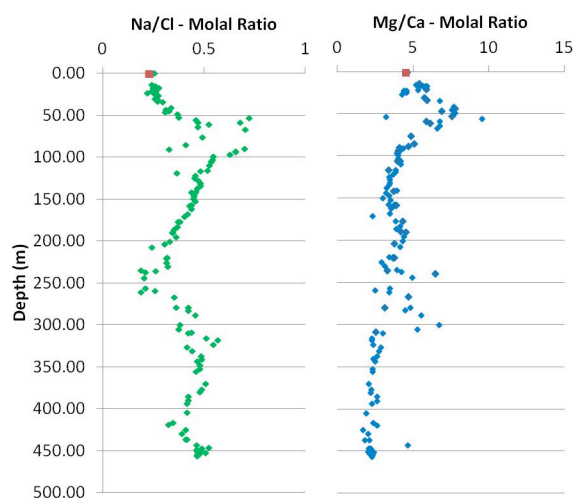


Figure 1 (top left) and figure 2 (top right): Molal ratios for Na/Cl and Mg/Ca from interstitial water concentrations. The depth is the length of the core in meters and the red squares indicate current Dead Sea water molal ratios.

Investigation of groundwater salinity in the Ziz Basin, southeastern Morocco, by using hydrochemical and isotopic tools

Z. LGOURNA¹, N. WARNER², L. BOUCHAOU¹, S. BOUTALEB¹, T. TAGMA³, M. HSSAISOUNE¹, N. ETTAYFI¹ AND A. VENGOSH²

¹Ibn Zohr University, Applied Geology and Geo-Environment Laboratory, Agadir, Morocco (zainabl@gmail.com)

²Duke University, Division of Earth & Ocean Sciences, Durham, NC, USA

³Hassan 1st University of Settat, Polydisciplinary Faculty of Khouribga, Khouribga, Morocco.

This study investigates water quality in Ziz basin, southeastern Morocco.

TDS and majors elements show a linear trend which suggests the coexistence of two end-members: (1) saline end-member dominated by Cl, SO₄ and Na; and (2) fresh end-member dominated by Ca, Mg and HCO₃. The main mechanisms of salinization are evaporation, dissolution of evaporates and carbonate formations within the study area.

Stable isotopes indicate that the High Atlas Mountains with high rainfall and low $\delta^{18}\text{O}$ and $\delta^2\text{H}$ values (-8.64 to -8.31 and -55.76 to -53.88) represent colder climate and constitute the major source of recharge to the basin. Also, the $\delta^{18}\text{O}$ enrichment with respect to the Global Meteoric Water Line (GMWL) confirms that waters from downstream part have been diluted by shallow waters of meteoric origin.

Keywords: *Groundwater quality, Geochemistry, Isotopes, Salinity, Arid area.*

Change of water cycle in the Changjiang (Yangtze river) catchment based on H/O isotopes

CHAO LI*, SHOUYE YANG, KAI DENG, HAILUN WEI, CHENGFAN YANG AND ERGANG LIAN

State Key Lab. of Marine Geology, Tongji Uni., Shanghai 200092, China (*correspondence: cli@tongji.edu.cn)

The effect of the Three Gorge Reservoir on the water cycle and sediment transfer within the Changjiang catchment have been attracting great interests for its environmental significance. Data from Datong hydrologic station indicates the considerable decrease of sediment flux since 2003 due to the water impoundment of the Three Gorge Dam. Nevertheless, the relating water cycle in the catchment over the last ten years has rarely been studied.

H/O isotopes have been regarded as good tracers to identify different water sources for river/ocean, vapour and underground water. This study investigates the H/O isotope composition in the mid-lower Changjiang reaches (from Yichang to Nantong) in 2012 and 2013. The result based on the H/O isotope mass balance equation shows that the river discharge in Datong is roughly equivalent to the total flux of the mainstream at Yichang and of all the tributaries in the mid-lower reaches during the dry season, which means no or minor external input/output (underground water, precipitation) in the lower valley. Thus, the water contribution of each tributary to the Changjiang mainstream at Datong can be estimated quantitatively. The Changjiang upstream (above Yichang) contributes only ~24% to the total fluvial discharge to the East China Sea, while the Dongting Lake and Poyang lake contribute ~68% in together during the dry season. Additionally, a weekly observation near Nantong reveals that the storage and discharge of the Three Gorge Reservoir has exerted a great influence on the water H/O isotope composition in the lower mainstream near the river mouth, while tidal influence is minor. Deuterium excess parameter in the mid-lower Changjiang river water exhibits smaller variability in recent years compared to that observed before the construction of Three Gorge Dam, which implies that the water cycle in the Changjiang catchment has been considerably changed in recent years. Overall, the Dongting and Poyang lakes now play an important role in regulating the Changjiang water discharge to the East China Sea in dry season. The variations of H/O isotopes in the Changjiang river water into the East China Sea clearly indicate the damming effect.

Acknowledgements: This work was supported by NSFC research fund (Grant No: 41076018, 41225020).

Modelling the atmospheric transport distance of PAHs at remote cold regions

CHONGYING LI^{1,2}, MEIHAN LI³ AND CHAOQI YU¹

¹ College of Materials and Chemistry & Chemical Engineering
Chengdu University of Technology, Chengdu 610059,
China, lichy@cdu.edu.cn

² Mineral Resources Chemistry Key Laboratory of Sichuan

³ College of Foreign languages and Cultures, Chengdu
University of Technology, Chengdu 610059,
China, 317292496@qq.com

Long-range atmospheric transport (LRT) of polycyclic aromatic hydrocarbons (PAHs) means the contamination of remote regions such as high mountains. A simple model was developed to estimate the atmospheric transport distance of PAHs at high mountains, especially lighter PAHs like anthracene and phenanthrene.

This model was made by using the OH reaction rate constant difference between PAH isomers (anthracene and phenanthrene) based on considering isomers gas/particle partitioning, reaction with OH radicals, dry and wet deposition, air-surface exchange and dilution of atmospheric dispersion along transport path in atmosphere as follows.

$$D_t (km) = -\frac{6 \times 10^6}{C_{OH} (\text{molecules} \cdot \text{cm}^{-3})} \times \text{wind speed} (\text{ms}^{-1}) \times \ln \left(\frac{C_{st}^A}{C_{st}^P} \times \frac{C_{g0}^P}{C_{g0}^A} \right)$$

Where D_t (km) is the transport distance. C_{OH} is the atmospheric [OH]. *wind speed* is the wind speed of the PAH-containing air masses. C_{g0}^P/C_{g0}^A is the diagnostic ratio (PHEN/ANTH) of anthracene and phenanthrene at emission source, and C_{st}^A/C_{st}^P is the diagnostic ratio (ANTH/PHEN) of anthracene and phenanthrene in snow at sampling location of cold regions.

The model can be used to predict the maximum transport distance and delineate a border of potential emission regions of PAHs at remote sampling sites. The model gave the origin of PAHs in snow at the typically sampling sites in cold regions in Europe and China under a wind speed of 60 m s⁻¹ and 24 h atmospheric average [OH] of 0.3 × 10⁶ molecules cm⁻³ based on some published data. It is concluded that PAHs at the three sampling sites in Europe primarily came from Europe and Northern Africa at a distance of less than 3000 km and PAHs at the two sampling sites in China came from local regions at a distance of less than 1000 km which are similar to the reports in the literatures.

This work was supported by the National Natural Science Foundation of China (41073085) and Construction plan of research innovation team of Sichuan province universities (12TD001).

The marine biogeochemical carbon cycle modeling of Yangtze sea during the Ediacaran–Cambrian transition

DA LI^{1*}

¹ State Key Laboratory for Mineral Deposits Research,
Department of Earth Sciences, Nanjing University,
Nanjing 210093, China (* lida@nju.edu.cn)

Earth's biosphere witnessed a revolutionary change from soft bodied animals to skeletal animals across the Ediacaran–Cambrian boundary and is associated with frequent large oceanic δ¹³C oscillations. The δ¹³C excursions are often interpreted to reflect changes in the global carbon cycle. We have reported a 300m-thick high-resolution carbonate δ¹³C profile for the Ediacaran–Cambrian Xiaotan section, South China, showing a large negative excursion (N1, -12.2‰) in terminal Ediacaran and a sustained pre-‘Tommotian’ positive plateau (P4, up to +7.3‰) which coincides with the occurrence of the *Watsonella crosbyi* Assemblage SSF [1].

Here I used a simple numerical box model to simulate the δ¹³C excursions of Xiaotan section in a straightforward way. Under non-steady-state conditions, the time-dependent changing rate of δ¹³C of marine carbonate is determined by Formula 1. I initiated the forward modeling by giving the uncertain parameters steady-state boundary values (typical Neoproterozoic values). The P4 excursion can be replicated by transiently increasing the amount of organic carbon buried (F_{org}) by 4 fold for a duration of 1 M.yr and keeping for 5 M.yrs and then decreasing back to one tenth of the original F_{org} . These changes in F_{org} could be related to the introduced modern digestion innovations in Phanerozoic time, and the subsequent biological turnover. However, the N1 excursion cannot be replicated by changing F_{org} or M_0 , or both. Instead, it can only be simulated by drastically decreasing δ_w to -13‰. Therefore, we must entertain the possibility that there was an isotopically light source of carbon to the surface ocean during the late Neoproterozoic, which could be the release of methane hydrates from an anoxic dissolved organic carbon-rich ocean or remineralization of old-time organic matters.

$$\frac{d\delta_0^c}{dt} = \frac{F_w^c(\delta_w^c - \delta_0^c) - F_{org}\Delta c}{M_0^c} \quad \text{Formula 1}$$

At the meantime, a backward modeling was tested by starting from the Xiaotan δ¹³C profile. Using the best-fitted curve of the isotopic profile and the first-order derivative curve, unrealistic negative F_{org} values was generated, which also implied normal δ_w value could not generate N1.

[1] Li (2013) *Prec. Res.* **225**, 128-147.

Manganese and cadmium accumulated in tomato under greenhouse conditions

FEI-LI LI¹, ZAN-FANG JIN¹, DANIEL G. SHENG²

¹ Coll Biol & Environ Eng, Zhejiang Univ Technol, Hangzhou 310032, China

² Coll Environ Sci & Eng, Tongji Univ, Shanghai 200092, China

Greenhouse cultivation not only promotes vegetable production, but also alters soil pH, soil aeration, and even root microorganisms in the greenhouse, which affects heavy metal transport in vegetables. Field experiments were conducted. Soils and tomato plants were sampled at harvest and analyzed for concentrations of Mn and Cd as well as other properties.

As compared with open field, greenhouse cultivation significantly decreased soil pH, soil organic matter, and oxidation-reduction potential (ORP) ($p < 0.01$). Total chlorophyll in greenhouse tomato laminae also decreased ($p < 0.01$).

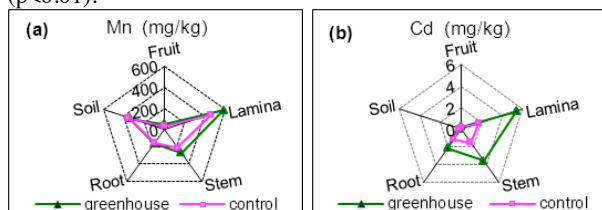


Fig. 1 Comparison of total metals in soil and parts of tomato plant in two cultivations

Mn and Cd concentrations in soil and parts of tomato plant were shown in Fig. 1. Mn and Cd concentrations in two cultivation soils had no significant difference. However, an obvious increase of metal concentrations in greenhouse tomato plant was clearly seen. Specifically, Mn concentrations in tomato root, stem, lamina and fruit increased with greenhouse cultivation by 5%, 27%, 28%, and 50%, respectively; the differences in two parts reached the significant levels ($p = 0.009$ in lamina and $p = 0.029$ in fruit). Cd concentrations in greenhouse cultivation increased in tomato root, stem, lamina, and fruit by 88%, 143%, 216%, and 27%, respectively, with all the differences being significant ($p = 0.001$, $p = 0.000$, $p = 0.000$ and $p = 0.049$, respectively). Lower pH and ORP in greenhouse soil were responsible for enhanced metal accumulation (Wang *et al.*, 2006). Correlation analysis showed that total chlorophyll in lamina was negatively correlated with Cd content, which was in accord with the report of a Cd inhibitory effect on chlorophyll formation (Stobart *et al.*, 1985). Mn and Cd concentrations in tomato fruit were below the limit for safe human consumption.

Greenhouse cultivation promoted heavy metal accumulation in vegetables. In other words, greenhouse cultivation may be a potential remediation of metal pollution.

[1] Stobart A K, *et al.* (1985). "The effect of Cd²⁺ on the biosynthesis of chlorophyll in leaves of barley." *Physiol Plant* **63**: 293-298. [2] Wang A S, *et al.* (2006). "Soil pH effects on uptake of Cd and Zn by *Thlaspi caerulescens*." *Plant Soil* **281**: 325-337.

Seesaw balance of Cenozoic carbon cycle

GAOJUN LI¹

¹MOE Key Laboratory of Surficial Geochemistry, Department of Earth Sciences, Nanjing University, 163 Xianlindao Road, Nanjing 210046, China (ligaojun@nju.edu.cn)

It is generally accepted that decreasing partial pressure of atmospheric CO₂ ($p\text{CO}_2$) has caused the progressive cooling of Cenozoic climate. However, the reason behind the decline of $p\text{CO}_2$ is still unclear. BLAG model (Berner *et al.*, 1983, *Am. J. Sci.* **283**, 641-683) proposes that the decrease of volcanic degassing is the primary driver for the long-term decline of $p\text{CO}_2$ through the negative feedbacks between $p\text{CO}_2$ and silicate weathering. However, the spreading rate of seafloor, which is believed as the major control of CO₂ degassing, seems to have remained relatively constant. The hypothesis of 'uplift driven climate change' proposes that tectonic uplift may have enhanced the sink of atmospheric CO₂ by silicate weathering, and thus produced the decline of $p\text{CO}_2$ (Raymo *et al.*, 1998, *Geology* **16**, 649-653). However, increasing weathering sink of CO₂ could deplete atmosphere all of its CO₂ within several million years while holding volcanic outgassing constant (Berner and Caldeira, *Geology* **25**, 955-956).

The fundamental difference between BLAG carbon model and the 'uplift driven climate change' hypothesis is related to the two extreme mechanisms that control the rate of silicate weathering, i.e., the weathering limited regime in BLAG model and the supply limited regime in 'uplift driven climate change' hypothesis respectively. Since both of the weathering regimes exist on earth, here based on reverse calculation on the major carbon cycle fluxes, a seesaw balance of Cenozoic carbon cycle is proposed by combining the BLAG carbon model and the 'uplift driven climate change' hypothesis following the weatherability idea of Kump and Arthur (1997, Ruddiman, W. (Ed.), *Tectonics Uplift and Climate Change*. Plenum Publishing Co., 399-426). The seesaw balance model could solve both of the driver problem in BLAG model and balance problem in 'uplift driven climate change' hypothesis. Tectonic uplift will enhance the supply limited weathering consumption of atmospheric CO₂ in continents, which initialize the drawdown of $p\text{CO}_2$. The decline of $p\text{CO}_2$ will decrease the weathering consumption of atmospheric CO₂ in weathering limited regions (mainly basaltic islands) until the decrease of weathering limited weathering could compensate the increase of supply limited weathering, then reaches a new steady state.

www.minersoc.org

DOI:10.1180/minmag.2013.077.5.12

Iodine speciation change by a Mn-oxidizing marine bacteria, *Roseobacter* sp. Azw-3k, through the production of reactive oxygen species

HSIU-PING LI¹, DANIELLE CREELEY¹, BENJAMIN DANIEL¹, RUSSELL GRANDBOIS¹, SAIJING ZHANG¹, CHEN XU¹, KATHY SCHWEHR¹, DANIEL KAPLAN², PETER SANTSCHI¹ AND CHRIS M. YEAGER^{3*}

¹Department of Marine Science, Texas A&M University at Galveston, Galveston, Texas

²Savannah River National Laboratory, Aiken, South Carolina

³Los Alamos National Laboratory, Los Alamos, New Mexico

(*Correspondence: cyeager@lanl.gov)

Iodine-129 is one of the most persistent radionuclides released from nuclear reprocessing facilities. With its longevity (half-life: 16 Myr) and biophilic nature (it accumulates in thyroid glands), iodine-129 is a potential human health threat. Thus, it is important to understand the behaviour of iodine in the natural environments. *Roseobacter* spp. are widely-distributed and comprise up to 15~20% of bacterial community in coastal/marine environments, and at least one member of this genus, *Roseobacter* sp. Azw-3k, facilitates extracellular Mn oxidation by releasing superoxide anions (O₂⁻). We hypothesized that *Roseobacter* sp. Azw-3k could mediate iodide oxidation through the production of extracellular superoxide anions and/or biogenic Mn(IV) oxides. Without Mn(II), Azw-3k cultures transformed ~90% of provided iodide (10 μM) into organo-iodine and iodate within 6 days, whereas in the presence of Mn(II), iodide oxidation only occurred after an initial period of Mn(IV) formation (~12 days). Heat-killed cells did not transform iodide. O₂⁻ production rates peaked at day 3, corresponding to early stationary phase of the cultures and the peak of iodide oxidation, and ceased after day 15. The results suggest that biogenic O₂⁻, but not biogenic Mn oxides, were involved in the iodide oxidation process. However, iodide oxidation also occurred in the presence of the O₂⁻ scavengers, Cu²⁺ and superoxide dismutase. Results suggest that Azw-3k-mediated iodide oxidation could be facilitated by two reactive oxygen species, O₂⁻ and its hydrolysis product, H₂O₂.

Poorly-crystalline Fe(Mg) Silicates involved in early fossilization of microbes in modern microbialites

JINHUA LI^{*1}, NINA ZEYEN¹, KARIM BENZERARA¹, SYLVAIN BERNARD² AND OLIVIER BEYSSAC¹

¹IMPMC - ERC Calcyon, CNRS & UPMC, 75005 Paris, France, *correspondence: jinhua.li@impmc.upmc.fr

²LMCM, CNRS & MNHN, 75005 Paris, France

³IMPMC, CNRS & UPMC, 75005 Paris, France

The search for the oldest traces of life has been a long-term challenge partly because of the difficulty to distinguish abiotic artefacts from biogenic traces. One way to improve our capability to detect traces of life is to study the fossilization processes affecting microorganisms in modern environments. Here, we studied the early fossilization of microorganisms in modern microbialites from, hyperalkaline crater lakes in Mexico, which might be good analogues for some Archean deposition environments such as Tumbiana.

Scanning electron microscopy (SEM) and energy dispersive X-ray (EDX) microanalyses on polished petrographic sections showed textures reminiscent of stromatolitic laminations and domal microstromatolites, consisting mainly of alternating aragonite and iron (sometimes magnesium)-rich silicates. Diverse microfossils of unicellular eukaryotes (e.g., diatoms) and prokaryotes were observed to be morphologically well-preserved by the precipitation of iron- or magnesium-rich silicates. The structural and chemical features of these potential fossils were further studied down to the nm-scale using a combination of focused ion beam (FIB) milling, transmission electron microscopy (TEM) and scanning transmission X-ray microscopy (STXM) at the C K-edge and Fe L_{2,3}-edges. The Fe(Mg)-rich silicate was characterized as a poorly-crystalline talc-like phase containing mixed-valence iron. Compared with the aragonite-dominant part, the Fe(Mg)-Si-rich laminations are richer in fossil microbes. Altogether, our results indicate that poorly-crystalline Fe(Mg) silicates can play an important role in the early stages of microbial fossilization.

Uranium transport and deposition in iron oxide copper gold deposits (IOCG's): An experimental approach

KAN LI¹, JOËL BRUGGER^{2,3}, ALLAN PRING², YUNG NOGTHAI¹, BARBARA ETSCHMANN², JING ZHAO¹ AND EDELTRAUD MACMILLAN³

¹School of Chemical Engineering and ³School of Earth and Environmental Sciences, the University of Adelaide, 5005 Adelaide, Australia. Email: kan.li@adelaide.edu.au.

²Mineralogy Department, SA Museum, 5000 Adelaide, Australia.

Iron oxides Copper gold type deposits in southern Australia often contain quantities of uranium, both at economic and the subeconomic level. Olympic Dam (OD) is the largest U resources in the World, but uranium also at Prominent and Moonta where the uranium is subeconomic and a problem in ore concentrates. In South Australian IOCG deposits the ores are unusually oxidised, consisting of hematite, with bornite, chalcopyrite and pyrite as the main sulphide minerals. The uranium occurs in a variety of 'primary' minerals including uraninite and brannerite and these minerals exhibit a remarkably diverse range of textures suggesting extensive remobilization.

We initiated an experimental study of hydrothermal mineral reactions in the Fe-Cu-S-U system, focusing in particular on the fate of U during sulphidation reactions. Much of the U in these IOCG deposits is secondary (either remobilised, or added in hydrothermal events postdating Fe-Cu mineralization). Applying the principles of interface coupled dissolution-precipitation reactions, we were able to reproduce the IOCG mineral assemblages experimentally by reaction of a Cu-rich fluid with hematite. When U is added to the system as uranyl salt or UO₂(s), U precipitates during the sulphidation reaction. Synchrotron experiments were used to characterize the nature of the U in the ores as well as of U precipitated during sulphidation reactions, information critical for deciphering the mechanism of U scavenging. This information improves our understanding reactions at interfaces with conditions far-from-equilibrium in controlling metal endowment.

The characteristics of an old gas reservoir in Sinian strata, central Sichuan basin, south China

L. LI*, Z. C. WANG, T. S. WANG AND H. JIANG

PetroChina Research Institute of Petroleum Exploration & Development, Beijing, China

(*correspondence: liling5551@126.com)

The study region is an important exploration area which has great prospect in Sichuan basin. By analyzing the formation conditions, accumulation periods and characteristics of Sinian gas reservoir in this area, we found that the natural gas is mainly oil cracking gas and the main source rocks were black sapropelic shales at the bottom of Qiongzhusi formation in Lower Cambrian, followed by dark algae dolomite and shale in the third member of Dengying formation. The formation of effective reservoir was controlled by supergene karstification and sedimentary facies. The reservoir was widely distributed with large thickness but strong heterogeneity. The area located at the east high point of an ancient uplift in a long period, whose structural evolution was inherited. It developed large-scale low-amplitude anticline in this region, and the trap formed by top of Sinian System could be 1128km², whose closure was over 200 meters [1]. The trap had strong oil and gas capability.

Analysis of the structural evolution history of the region and thermal history of the source rocks showed that: the source rocks in the 3rd member of Dengying Formation started to generate a large sum of hydrocarbon from the Ordovician to Silurian, the liquid hydrocarbon generated accumulated in top of ancient uplift to form paleo-reservoir; the structural uplift at end of the Silurian terminated the first stage of hydrocarbon generation. They entered the second stage of hydrocarbon generation from the Late Permian. While source rocks in Qiongzhusi formation entered the main phase of hydrocarbon generation from the Triassic to the Middle Jurassic, the hydrocarbon accumulated in the weathered crust of Dengying formation at top of ancient uplift to form paleo-reservoir. They entered the main stage of gas generation from the Late Jurassic to the Early Cretaceous, the liquid hydrocarbon of paleo-reservoir cracked to gas, which accumulated as present gas reservoir [2]. The homogenization temperature of fluid inclusion in Sinian carbonate of this area also supported this view.

[1] Zhang Lin, *et al.* (2004), *Natural Gas Geoscience* 15, 584-589. [2] Yao Jianjun, *et al.* (2003), *Petroleum Exploration and Development* 30, 7-9.

High-precision collision-cell MC-ICPMS analysis of Ca isotopic ratios (including ^{40}Ca)

QIONG LI*¹, MATTHEW THIRLWALL¹
AND WOLFGANG MÜLLER¹

¹Dept. of Earth Sciences, Royal Holloway Univ. of London,
Egham, Surrey, UK. TW20 0EX
qiong.li@rhul.ac.uk

Ca isotopic ratios have traditionally been measured by TIMS due to its high sensitivity and a precision of $\sim 0.1\%$ (2sd) in $\delta^{44/40}\text{Ca}$ has been achieved using double spike techniques [1,2,3]. Compared with TIMS, Ca isotope analysis by MC-ICPMS faces three big challenges: 1) interference of $^{40}\text{Ar}^+$ from the plasma on $^{40}\text{Ca}^+$; 2) high background noise due to scattered ^{40}Ar which can severely affect the low-abundance Ca isotopes; and 3) the presence of hydrocarbon interferences especially for the minor isotopes. Earlier MC-ICPMS work avoided some of these issues by presenting data as $\delta^{44/42}\text{Ca}$, instead of $\delta^{44/40}\text{Ca}$, with 0.1-0.2‰ (2sd) precision using sample-standard bracketing [e.g. 4].

We report Ca isotopic measurements using an IsoProbe MC-ICPMS operated in collision/reaction cell mode using a $10^{10}\Omega$ resistor for ^{40}Ca . A flow of H_2 (0.8 ml/min) through the collision cell eliminates ^{40}Ar interference on ^{40}Ca via charge transfer and enables precise measurements of ^{40}Ca . Blanks (2% HNO_3 , 2×10^{-13} A ^{40}Ca) and Ca samples (1 ppm, 4×10^{-9} A ^{40}Ca) show a residual ^{40}Ar intensity of ca. 4×10^{-14} A, implying negligible Ar interferences on measured ratios.

Internally $^{44}\text{Ca}/^{40}\text{Ca}$ -normalized $^{42}\text{Ca}/^{40}\text{Ca}$ and $^{43}\text{Ca}/^{40}\text{Ca}$ ratios of Ca-isotope standard SRM915b within a day yield 2sd of 72 ppm and 260 ppm respectively after correction for Sr^{2+} interference. Identical normalized $^{42}\text{Ca}/^{40}\text{Ca}$ and $^{43}\text{Ca}/^{40}\text{Ca}$ ratios are obtained for natural apatite and aragonite without chemical separation, and form the basis of an accurate double spike correction. We are currently investigating the use of a ^{43}Ca - ^{46}Ca double spike (DS) for mass bias correction of solution mode analyses, and are comparing results of this with data obtained in both solution and laser-ablation (LA) modes [5] using sample-standard bracketing. Alternating with unknown samples, six sets of measured Ca isotope ratios obtained by laser ablation of a SRM915b pellet agree within the internal error (2se = 0.2‰) over a 6-hour period.

[1] J. Skulan *et al.*, *GCA*, 1997, 61, 2505-2510. [2] A. Heuser *et al.*, *GCA*, 2011, 75, 3419-3433. [3] S. Huang *et al.*, *GCA*, 2012, 77, 252-265. [4] L.M. Reynard *et al.*, *GCA*, 2010, 74, 3735-3750. [5] W. Müller *et al.*, *JAAS*, 2009, 24, 209-214.

Seasonal variations of chemical weathering rates and CO_2 consumption in Yangtze River basin

S.L. LI, Y. CHEN*, J. CHEN, AND J.F. JI

The MOE Key Laboratory of Surficial Geochemistry, School
of Earth Sciences and Engineering, Nanjing University,
Nanjing 210093, China

(*Correspondence: chenyang@nju.edu.cn)

Continental erosion controls atmospheric CO_2 levels on geological timescales through silicate weathering. Rivers play an important role in long-term carbon cycle by transporting rock weathering products to oceans. The Yangtze River (Changjiang) is the largest river in Asian and drains the tectonic uplifted Himalaya and Qinghai-Tibet Plateau which are of especial importance because of the possible connections with late Cenozoic climate change.

In this study, water samples of the Yangtze River were collected at Nanjing twice a month from May, 2010 to April, 2011. Major ions (Cl , SO_4 , NO_3 , Ca , Mg , K , Na , Sr) in the dissolved load were determined. There were linear correlations between Ca/Na , $1000 \times \text{Sr}/\text{Na}$, HCO_3/Na and Mg/Na . Na-normalized ratios of major ions were used in an inverse model to calculate the contribution of the six end-members (i.e. atmosphere, industry pollution, agriculture pollution, carbonates weathering, silicates weathering and evaporates dissolution). Results show that in the monsoon season (May-August) carbonate weathering contributed more to the dissolved load than in the dry seasons. Almost 60% of major ions were derived from carbonates weathering while carbonates contribution reduced to near 40% in dry seasons. The variation of contributions from silicate weathering shows an opposite trend, that means it is low (about 1%) during the monsoon season but can increase astonishingly to 32% in dry seasons. In the whole year, carbonates weathering and silicate weathering consumed 8.32×10^{11} mol and 1.61×10^{11} mol CO_2 , respectively in the Changjiang basin.

Acknowledgment

This study is funded by China Geological Survey (Grant No. 1212011087126).

Late Mesozoic A-type magmatism in Hailar basin, NE China: Constraints on the evolution of the Mongol-Okhotsk Ocean

S.-Q. LI^A, F. CHEN^{A*}, E. HEGNER^B AND J.-D. WU^A

a: Key Laboratory of Crust-Mantle Materials and Environments, School of Earth and Space Sciences, University of Science and Technology of China, Hefei 230026, China

b: Department of Earth and Environmental Sciences, Universität München, Theresienstr. 41, München, Germany

The northeastern China situated between the Siberian and Sino-Korean (North China) cratons was characterized by widespread volcanism and well developed extensional basins in the period of Late Mesozoic. In the north-west of Hailar basin which located west part of NE China there exposes a suit of A-type rhyolitic rocks that had been rarely noticed. Major and trace element, Sr-Nd-Pb and zircon U-Pb data are presented for this special profile. Furthermore general I-type volcanic rocks from mafic to felsic aged 160~120 Ma also selected and performed for comparing.

The first U-Pb Zircon ages that constrains the timing of emplacement of the A-type rhyolites as Early Cretaceous (125±3~136±4 Ma), and the zircon ages range from 158±6~125±3 Ma indicate complicated magma chamber evolution and mixing process. All the volcanic rocks belong to high-K calc-alkaline series. The mafic-felsic rocks show enrichment of LILE and LREE, and depleted in HFSE and HREE compared to the A-type rhyolites with higher HFSE, HREE contents and no negative Nb-Ta anomalies. All the volcanic rocks show slightly depleted to enriched isotopic features. These data suggest that basaltic-andesitic rocks in Hailar basin were generated by fractional crystallization of melts partial melting from the enriched lithospheric mantle which had been metasomatised by previous slab subduction of the Paleo-Asian Ocean and the Mongol-Okhotsk Ocean, whereas the andesitic-rhyolitic magmas were produced by the melting of lower crustal mafic and felsic granulites, respectively. Accordingly we suggest the A-type rhyolites are generated by high-temperature partial melting of lower continental crust which depleted by previous I-type melts extraction and the anhydrous melting with high F contents increased the HFSE contents in the melt. Considering the evolution of the Mongol-Okhotsk Ocean, this A-type magma event provides evidence for the slab break-off process of the Mongol-Okhotsk Ocean.

Incorporation of trace metals into soil microcodium as a novel proxy for paleo-precipitation

TAO LI^{1*} AND GAOJUN LI¹

¹MOE Key Laboratory of Surficial Geochemistry, Department of Earth Sciences, Nanjing University, 163 Xianlindadao Road, Nanjing 210046, China
taoli.es.nju@gmail.com(*presenting author);
ligaojun@nju.edu.cn

Trace element compositions of carbonates have been successfully applied to reconstruct the paleo-environments under which they are precipitated. However, information on the incorporation of trace metals into the authigenic carbonates in soil is rare. Major challenges come from the impurity of soil carbonates and thus contamination of trace metals by other mineral phases.

Here we present trace element compositions of microcodium found in Chinese loess. Microcodium is formed by the replacement of bio-residues by soil solution, which is very easy to identify and pick. We have observed large variation in the Mg/Ca and Sr/Ca ratios of microcodium in the Holocene soils across Chinese Loess Plateau, which reflects large variation in corresponding composition of soil solution. Rayleigh fractionation associated with the precipitation of secondary carbonate is responsible for the compositional variation of soil solution. The extent of Rayleigh fractionation is significantly correlated to precipitation amount (Fig. 1). The incorporation of trace metals in microcodium may serve as a novel proxy for paleo-precipitation. Initial application of the new proxy indicates clear glacial-interglacial changes of precipitation amount on Chinese Loess Plateau.

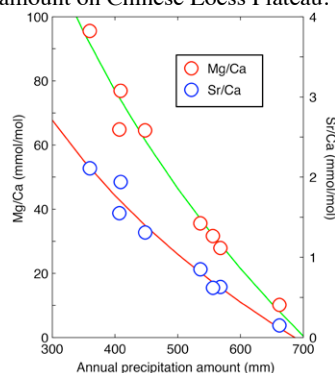


Fig. 1. Holocene calibration curves for the Mg/Ca and Sr/Ca ratios of microcodium as proxies for precipitation amount.

$^{40}\text{Ar}/^{39}\text{Ar}$ Phenocryst-Matrix isochron dating on Quaternary volcanic rocks

WEI-RAN LI^{1*}, JIAN-QING JI¹ AND JING ZHOU¹

¹Peking University, School of Earth and Space Sciences, Beijing, China, *lwr@pku.edu.cn

A big challenge of K-Ar and $^{40}\text{Ar}/^{39}\text{Ar}$ dating is to obtain precise ages of Quaternary volcanic rocks with low K and high Ca content. To date these rocks, isochron method has been widely used on matrix with phenocryst removed. However, if argon isotope concentrations of matrix are too close, isochron ages may be unreliable. To solve this problem, we have developed a Phenocryst-Matrix isochron method to get more reliable results. This method is based on initial $^{40}\text{Ar}/^{36}\text{Ar}$ values of phenocryst and matrix tested uniform. To determine it, we propose to compare the uniformity of initial $^{36}\text{Ar}/^{38}\text{Ar}$ values of phenocryst and matrix before samples are irradiated by neutron. If the initial $^{36}\text{Ar}/^{38}\text{Ar}$ values are uniform, the initial $^{40}\text{Ar}/^{36}\text{Ar}$ values are supposed to be uniform. Here we dated young volcanic rocks from Lei-Zhou area in Southeastern China, and obtained five isochron ages that range from 0.05Ma to 0.35Ma with relatively large error. Considering these unreliable results and tested uniform initial $^{36}\text{Ar}/^{38}\text{Ar}$ values of phenocryst and matrix, Phenocryst-Matrix isochron method was applied for all the samples of this area (shown in the figure below), yielding an age of 0.18 ± 0.03 Ma, which fits well with stratigraphic time.

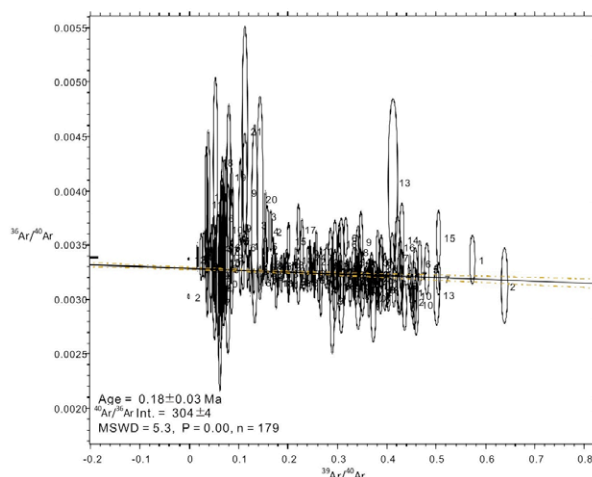


Figure 1: $^{40}\text{Ar}/^{39}\text{Ar}$ Phenocryst-Matrix isochron for all the samples from Lei-Zhou area.

Sulfur isotopic compositions of total suspended particulates (TSP) in Chengdu, Southwest China

X.D. LI^{1*}, Z. YANG^{1,2}, B.J. LIU¹, L.J. WU³
AND B.L. WANG¹

¹Institute of Geochemistry, Chinese Academy of Sciences, Guiyang, Guizhou, PR China

(*correspondence: lixiaodong@mail.gyig.ac.cn)

²Graduate University of Chinese Academy of Sciences, Beijing, PR China

³College of Environment and Civil Engineering, Chengdu University of Technology, Chengdu, Sichuan, PR China

The sulfur isotopic compositions were analyzed to discuss the source and transformation process of sulfur in total suspended particulates (TSP) that collected from a megacity, Chengdu, SW China where atmospheric particulate matters, a major air pollutant, currently affect air quality of this city.

The annual variations of $\delta^{34}\text{S}$ values of TSP from 2005 to 2010 were little and the data were concentrated within 5.3~5.8‰. The seasonal variations of $\delta^{34}\text{S}$ values of TSP were obvious, and the order was winter (6.6‰) > spring (5.2‰) > autumn (5.0‰) > summer (4.5‰) which is similar to the concentrations of sulfate in TSP. The $\delta^{34}\text{S}$ and sulfate content of TSP were higher in winter and spring that probably be associated with high-sulfur coal combustion, and lower in summer and autumn which might be affected by biogenic sulfur which having light $\delta^{34}\text{S}$. Under different weather conditions as foggy, cloudy, sunny and rainy days, the changes of $\delta^{34}\text{S}$ values were not obvious except that higher data in the rainy days, and there is no correlation between the $\delta^{34}\text{S}$ values and sulfate content of TSP. In the rainy days, the gaseous sulfur dioxide having light $\delta^{34}\text{S}$ values dissolved in rain by liquid-phase oxidation reaction, which led to the collected TSP being little affected by gaseous SO_2 and the sulfur in TSP were more from the particulates having heavy $\delta^{34}\text{S}$ values resulted from coal combustion. Consequently, the $\delta^{34}\text{S}$ values of TSP were probably higher in the rainy days.

The mass ratios of $[\text{SO}_4^{2-}]/[\text{NO}_3^-]$ in TSP decreased from 2005 to 2010, which indicated the atmospheric quality in Chengdu would be more affected by vehicle exhaust while the pollution control in coal combustion are stepped up.

This work was supported by the National Natural Science Foundation of China (Grant No. 41173022).

[1] Querol *et al.* (2000) *Atmos Environ* **34**, 333-345. [2] Lee *et al.* (2002) *Tellus B* **54**, 193-200. [3] Guo *et al.* (2010) *J Geophys Res* **115**, D00K07, DOI: 10.1029/2009JD012893.

Controlled bio-inspired synthesis of composites: a close simulation of biomineralization process

XUAN QI LI¹ AND NICO SOMMERDIJK¹

¹Laboratory of Materials and Interface Chemistry
And Soft Matter CryoTEM Research Unit
Department of Chemical Engineering and Chemistry
Eindhoven University of Technology

Many structural biomaterials, biopolymers as well as biominerals, derive their mechanical properties from a complex hierarchical fibrillar organization. An intriguing example is the Stomatopod Dactyl club that consists of an impact resistant calcium phosphate-chitin composite structure. The chitin matrix has a highly expanded helicoidal organization.

In nature, biominerals often grow at controlled reacting conditions, such certain pH value, temperature, concentrations of reactants and also reaction rate. However, most bio-inspired mineralization studies cannot control those parameters during the reaction.

In this study, we investigated self-assembly and reaction process of chitosan and calcium phosphate in water solution, control the reaction parameters, and obtain ordered composite structures in a controlled biomimetic way. In addition, we investigated the interaction rules between biopolymers and minerals during assembly and mineralization process on the molecular level, which will be very helpful for biomineralization research and biomaterials synthesis. A controlled reaction system assisted by a titration setup was built up. The assembly process of chitosan, the nucleation and growth of calcium phosphate, and the formation process of chitosan/calcium phosphate biocomposites were investigated by the cryo-transmission electron microscopy (cryoTEM), Fourier transform infrared spectroscopy (FTIR), X-ray diffraction (XRD) etc.

A theoretical approach of isotope fractionation mechanism for thermal diffusion processes

XUE-FANG LI AND YUN LIU*

State Key Laboratory of Ore Deposit Geochemistry, Institute of Geochemistry, Chinese Academy of Sciences, China.
Correspondence*: Liuyun@vip.gyig.ac.cn

Under thermal gradients, not only chemical compositions of a homogeneous system will be significantly changed between high temperature and low temperature ends, but also its isotopic compositions will be tremendously changed (e.g., Richter *et al.*, 2008, 2009; Huang *et al.*, 2010). However, the isotope fractionation mechanism of such thermal diffusion processes is still under debating. Dominguez *et al.*, (2011) used transition-state theory (TST) model to explain stable isotope fractionations in high-temperature silicate melts. They mainly considered the zero-point vibrational energy (ZPE) of diffusing species with different isotopes. Other kinetic energies were completely ignored even they are important under high temperatures. They also did not consider kinetic energies (ZPE, translational, rotational energies, etc.) for the activated complex at transition state. Their treatment resulted in an unusually large ZPE difference for different isotopologues, which was questioned by Lacks *et al.*, (2012a) for the unusually large wavenumber of a vibration. Lacks *et al.*, (2012b) proposed a new model based on Chapman-Enskog theory to treat the thermal diffusion processes and used a specially designed classical molecular dynamics (MD) method to treat temperature gradients. They concluded that the classical mechanical collisions maybe the essence reason of isotope fractionation, but not the quantum effect suggested by Dominguez *et al.*, (2011). They also found that heavier isotope systems (i.e. Fe, Ca, Mg) can be fractionated to larger extents than those of network formers but lighter isotope systems (i.e., Si, O). Until now, all theoretical studies are focused on high temperature conditions, there is no theoretical framework for systems with temperature gradients at low or medium temperatures.

Here, we propose a new theoretical model for dealing with isotope fractionation by thermal diffusion. We used a newly developed thermodynamic law which directly relates Soret coefficient to entropy (Duhr and Braun, 2006a; Duhr and Braun, 2006b). We have developed its counterpart for isotope fractionation treatment. By following this approach, we provide a unified equation for the calculation of isotope fractionation under thermal gradients for any temperature condition. Using high temperature silicate melts as examples, we test our equation and find out the relationship between isotope fractionation and temperature gradients.

Soil microbial species selection and activity influenced by semiconducting minerals

YAN LI¹ AND ANHUAI LU^{2*}

¹School of Earth and Space Sciences, Peking University, Beijing. (liyan-pku@pku.edu.cn)

²School of Earth and Space Sciences, Peking University, Beijing. (*correspondence: ahlu@pku.edu.cn)

Semiconducting minerals are a unique class that could absorb photons with energy equivalents to or higher than the bandgap to form negatively charged photoelectrons and positively charged photoholes in the conduction band (CB) and valence band (VB), respectively. There is a wide distribution of semiconducting minerals in natural soils, mainly including Fe and Mn oxides [e.g., hematite (Fe₂O₃), goethite (FeOOH), pyrolusite (MnO₂)]. The redox potential of their CB electrons ranges from -1.01 V to 0.28 V (vs. NHE). Natural microbes have evolved various strategies to acquire electron energy for maintaining metabolism. We predicted photoelectrons in the CB of semiconducting minerals is a natural solid phase electron source for microbes and make influences on microbial metabolism. We designed experiments in an electrochemical equipment to simulate the energy of CB electrons by setting the redox potential of electrodes similar to the CB potential of goethite. A natural soil microbial community was inoculated and the microbial community structure were analyzed by *16S ribosomal RNA* gene. The results indicated the soil microbial community at day 0 was diverse, and some species like *Chitinophaga*, *Pseudomonas*, *Alcaligenes* and *Pedobacter* became enriched by day 5. By day 10, the *Alcaligenes* species constituted greater than 70% of the total bacterial population, in marked contrast to < 8% in the control with no applied electrode potential. Then, the growth of a pure *Alcaligenes* strain under three different electrode potential (-0.15 V, -0.06 V and +0.06V) was observed and its denitrification efficiency of nitrate was measured. Both were found to be closely related to the electrode potential. The quantity of the biofilm coated on the electrode and the nitrate reduction efficiency reached the highest at -0.15 V among three electrode potentials. In contrast, no biofilm formation or no reduction of nitrate were observed in the open circuit control. Therefore, photoelectrons probably led to the enrichment and selection of certain microbes such as *Alcaligenes* and also influenced its denitrification activity.

A contrastive study of organic matter influences on the smectite illitization in Dongying Sag, China

YINGLI LI¹, JINGONG CAI^{1*}, SHOUPENG ZHANG² AND JUNFENG JI³

¹State Key Laboratory of Marine Geology, Tongji University, Shanghai 200092, China

(*correspondence: jgcai@tongji.edu.cn)

²Geological Scientific Research Institute, Shengli Oil Field Company, Sinopec, Dongying 257015, China

³State Key Laboratory of Surficial Geochemistry, Nanjing University, Nanjing 210093, China

Many factors such as temperature, pressure and time etc. can affect the smectite illitization in mudstone. Whereas the organic matter which owns important relationship with clay minerals has been easily ignored. For this point, samples respectively representing water-rock interaction system and water-rock-organic interaction system were selected here to make a contrastive study on the influences of organic matter during the smectite illitization in mudstone.

11 red mudstone (RM, 1000m-5300m) and 23 dark mudstone (DM, 2200m-3500m) samples from Dongying Sag were studied with X-ray Diffraction and pyrolytic analysis. Results show that RM had about 0.01-0.14%TOC (0.07% in average) while the latter had 0.17-6.75%TOC (2.16% in average). Obvious smectite illitization differences were also indicated. (1) Above 3100m: Illite proportion of RM (37-60%) was higher than that of DM (31-48%). Mixed-layered illite/smectite of RM was mainly R0, R1 patterns and that of DM was R0 pattern. Illite Crystallinity of RM (Kübler index, 0.40-0.76) was usually higher than that of DM (0.44-0.69). (2) Beneath 3100m: Illite proportion of RM (9-65%) turned significantly lower than that of DM (52-100%). Mixed-layered illite/smectite of RM turned to be mostly R3 pattern, while the DM being R1, R3 pattern. Simultaneously, the RM Illite Crystallinity (Kübler index, 0.61-0.69) got lower than that of DM (0.69-0.90). In short, the three mentioned parameters significantly inverted at the depth of 3100m. Considering their discrepancy in TOC content, it is thought that organic matter not only influenced the smectite illitization but also made this differently above/beneath 3100m. This could stimulate further study of smectite illitization especially under water-rock-organic matter interaction system.

This work was supported by National Natural Science Foundation of China (Grant No. 41072089), National Oil and Gas Special Fund (Grant No.2011ZX05006-001).

Experimental study on gas generation potential of marine source rock with high maturity

LI YONGXIN¹, WANG ZHAOYUN¹, HU SUYUN¹
AND WANG HONGJUN¹

¹ Research Institute of Petroleum Exploration and Development, PetroChina,
*lyxin@petrochina.com.cn (*presenting author)

The ancient marine source rocks in basins of west China have endured lengthy process of thermal evolution, which makes them have a relatively high degree of maturity. According to analysis of available data, a fair number of liquid hydrocarbons, account for 40%-60% of total, still remain in source rocks within oil window. And these hydrocarbons can crack into gas at high mature stage, serving as an important source of some gas pools found in deep formations. In this way, the deep formations will have great resource potential. In order to assess the amount of dispersive liquid hydrocarbons resident in source rocks, a simulation of marine marl with low organic matter abundance under different fluid pressures were carried out.

The sample used in these experiments is from a core of Pando-X1 well from Madre de Dios Basin in Bolivia. It is of Devonian age, and at this locality it is thermally immature in the pre-oil generation. The collected sample is a marine marl with an organic carbon content of 0.95 wt %. The sample was crushed into gravel-sized chips. Reflectance measurements on vitrinite macerals found dispersed in the kerogen gave a mean %Ro of 0.59. All of the experiments were conducted in stainless-steel. The temperature is set at 290°C, 310°C, 330°C, 350°C and 370°C, while the pressure obtained at each temperature was set at 10MPa and 20MPa respectively.

The results indicated that, the peak time of hydrocarbon generation and expulsion was around 310°C under the pressure of 10MPa, with the expulsive oil rate and the total oil yielding rate of 182.5mg/g and 193.4mg/g, respectively. Under 20MPa, the temperature corresponding to the hydrocarbon generation and expulsion peak was about 330°C, with the expulsive oil rate and the total oil yielding rate of 92.4mg/g and 111.4 mg/g, respectively. It has been suggested that, the increase of pressure represses the thermal evolution of organic materials. It enlarges the effective hydrocarbon expulsion stage of source rocks in addition to postponing the major expulsion period. As a result, the residence time of resolvable organic materials with large quantity has been enlarged, which provides material basis for the generation of gas during the high evolutionary phase.

Metal zoning feature and its Genesis of Bairendaba vein type ore forming system in Inner Mongolia, China

LI ZHENZHEN^{1*}, CAI YUQI¹ AND LIU YIFEI²

¹ Beijing Research Institute of Uranium Geology, Beijing, 100029, China

(*correspondence: leemimi@163.com)

² Institute of Mineral Resources, Chinese Academy of Geological Sciences, Beijing, 100037, China

Bairendaba Zn-Pb-Ag deposit is located in Inner Mongolia, China, and is a large scale vein type deposit with more than 4 000 tons of Ag and 2M tons of Zn+Pb.

The deposit is hosted in faults system of Carboniferous quartz diorite. There are More than 68 veins are found in the deposit, most of them are dip to the north. The No. 1 and No. 3 veins are the main orebodies and host more than 77% metal reserves of Bairenda[1]. Hydrothermal alterations closed to orebodies are well developed, including silicification, chloritization, epidotization and minor sericitization. The mainly ore minerals occurred in the deposit are marmatite, pyrrhotite, galena, with minor chalcopyrite, arsenopyrite, pyrite, Ag-bearing tetrahedrite and sulfosalts. The most common gangue minerals are quartz and fluorite.

The orebodies show obvious mineralization zoning feature, with Cu-bearing ores in the center and high grade Ag-bearing ores in the outer of the deposit. There is a systematic variation of metal grades, metal ratios and metal tonnage in the most economic No. 1 vein along its trend as it is divided into equidistant blocks by the cross sections. The tonnage and grade of zinc in each ore block decrease from west to east, the tonnage and grade of lead and silver of each ore block increase first and then decrease gradually. The Ag/Pb ratio of each block decrease first and then increases gradually, while the Ag/Zn and Pb/Zn ratios increase gradually all the time.

We propose that this metal zoning feature and systematic variation of metals is a reflection of decreasing temperature of ore forming system from west to east, and is the consequence of mixture of high temperature ore forming fluid with cold meteoric water in the fault system.

[1] Liu et al. (2012) Journal of Jilin University (Earth Science Edition), 42(4),1055-1068.

Nano-Scale Mineral Protection for Black Carbon Stabilization using Synchrotron-Coupled Transmission X-ray Microscopy for 3-D Tomography

BIQING LIANG^{1*}, CHUN-CHIEH WANG², JOHANNES LEHMANN³, IIZUKA YOSHIYUKI⁴, YEN-FANG SONG⁵ AND CHUNG-HO WANG⁶

¹Institute of Earth Sciences, Academia Sinica, Nangang, Taipei, Taiwan ROC

(*Correspondence: betacau07@gmail.com)

²Biomedical and Molecular Imaging Group, National Synchrotron Radiation Center, Hsinchu, Taiwan ROC (wang.jay@nsrrc.org.tw)

³Department of Crop and Soil Sciences, Cornell University, Ithaca, NY 14853, USA (CL273@cornell.edu)

⁴Institute of Earth Sciences, Academia Sinica, Nangang, Taipei, Taiwan ROC (yizuka@earth.sinica.edu.tw)

⁵Biomedical and Molecular Imaging Group, National Synchrotron Radiation Center, Hsinchu, Taiwan ROC (Song@nsrrc.org.tw)

⁶Institute of Earth Sciences, Academia Sinica, Nangang, Taipei, Taiwan ROC (chwang@earth.sinica.edu.tw)

Black Carbon (BC) encompasses a variety of highly aromatic C forms including biochar, soot and graphite. Black C plays an important role in global warming and carbon cycling, and may act as a significant sink for green-house-gas CO₂ due to its long-term residence in the slower geological C pool. We explore high-resolution 3-D imaging using synchrotron-coupled Nano-Transmission X-ray Microscopy (TXM) and elemental mapping to describe the interplay of BC and mineral. Mineral particles of nano size are found in close association with both fresh and aged BC samples. Mineral of sheet layer is found important for the physical protection of BC. Our study provides the first direct description of BC physical protection by minerals, by far which is considered the most important mechanism for BC stabilization in environment.

Mercury Emission from Coal Fire and Spontaneously-ignited Gangue Hill and Distribution in Local Near-Surface Air in North China

HANDONG LIANG¹ AND YANCI LIANG²

¹State Key Laboratory of Coal Resources and Safe Mining, Beijing, China,

hdl6688@vip.sina.com (*presenting author)

²School of Chemical and Environmental Engineering, China University of Mining and Technology, Beijing

Underground coal fire is a global environmental and ecological hazard [1]. In China alone there are 84 coalfield in 13 provinces currently suffering from coal fire, with coal annual loss over 200 million tons. Coal gangue is a byproduct of coal mining and often piled up on site. There are estimated over 5,000 giant gangue hills located across China, with many of them reported spontaneous ignition [2]. These two source have no control or mitigation method of mercury emission, hence may bring mercury pollution on local environment and further contribute to global mercury inventory.

To study the mercury emission and diffusion pattern, a typical mining area with coal fire and gangue hill in Wuda coalfield, Inner Mongolia was chosen. Atmospheric mercury concentrations were measured at 1.2 m to ground surface by 10 m x 10 m grid in the peripheral area of fire zone and a giant gangue hill 6.7 km apart. Both results gave a prevalent mercury concentration of 40-50 ng/m³, which is 30 times higher than the background level of atmospheric mercury (1.6 – 1.8 ng/m³), and equal to previously reported atmospheric mercury concentration in the vicinity of mercury smelting factory [3]. The mercury concentration of ground vapor in a drilling hole -0.4 m to the surface in the vicinity of the gangue hill also fell in this range. The consistency of mercury content in two areas suggests that the mercury content may be the consequence of long-term accumulation and diffusion of gaseous mercury from multisites and multitype sources in the mining area rather than directly from the source. In addition, few vegetation were found in the mining area, and surface vegetation restored in correlation with the distance from the mining area. The exact influence range, the potential influence on remote populated area, and the potential impact on local vegetation of mercury emission from coal fire and spontaneous-ignited gangue hill still requires further insight.

[1] Stracher (2004) *Int. J. Coal Geol.* 59, 1-6. [2] Zhao *et al.* (2008) *Int. J. Coal Geol.* 73, 52-62. [3] Li *et al.* (2008) *Environ. Chem.* 27, 96-99.

An XPS study on the valence states of arsenic in arsenian pyrite: implications for Au deposition mechanism of the Yangshan gold deposit, Western Qinling Belt, central China

JINLONG LIANG^{1*} AND WEIDONG SUN²

¹Department of Geochemistry, Chengdu Univ. of Technology, Chengdu 610059, China

(*correspondence: richardlj104@yahoo.com.cn)

²Guangzhou Institute of Geochemistry, the Chinese Academy of Sciences, Guangzhou 510640, China

The Yangshan gold deposit is a typical sediment-hosted disseminated type recently exploited in the Western Qinling Orogen, central China. Determination of gold chemical states is difficult due to its low concentrations of ppm level in the major Au carrier, arsenian pyrite. It is well known that the enrichment of Au in pyrite is usually associated closely with the enrichment of arsenic in the mineral.

Here we obtained pristine surfaces of arsenian pyrite from the Yangshan ore by sputtering with Ar⁺ beam in the vacuum chamber of an X-ray photoelectron spectroscopy (XPS). The XPS results indicate that the predominant state of arsenic is As⁻, whereas As³⁺ is the oxidized state likely formed during sample preparation, which only distributed on the surface.

The new observations suggest that the enrichment of Au in arsenian pyrite is not due to the double substitution of As³⁺ + Au⁺ for 2 Fe²⁺ as previously proposed[1], but because significant substitution of As⁻ for S⁻ resulting in structure loosening facilitates Au entering the pyrite lattice[2].

[1]Deditius *et al.*. (2008) *Geochimica et Cosmochimica Acta* 72, 2919-2933. [2]Liang *et al.*.(2013) *Journal of Asian Earth Sciences* 62, 363-372

Spontaneously-Ignited Gangue Hill – a Potential Source for Global Mercury Inventory

YANCI LIANG^{1*} AND HANDONG LIANG²

¹ School of Chemical and Environmental Engineering, China University of Mining and Technology, Beijing.

liangyc08@hotmail.com (*presenting author)

² State Key Laboratory of Coal Resources and Safe Mining, Beijing, China

Coal gangue is a waste mining material mingled with small amount of coal. It is of little value for reproduction and mostly piled up into gangue hills [1]. The total stock of coal gangue in China is documented over 5 billion tons to date with an annual increment of 2,000 million tons [2]. Due to the mingled coal content, gangue hill is believed to share a similar spontaneous ignition process to coal fire. In China, spontaneously-ignited gangue hill cases are quite common in coal mining areas [1,3].

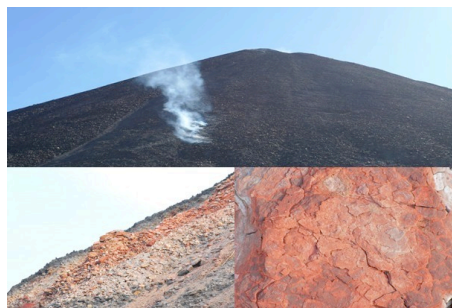


Figure 1: landscapes of spontaneously-ignited gangue hill

This study focused on a giant gangue hill with a height about 50 meters in Wuda coal field, Inner Mongolia. Red clinkers were scattered on the surface, indicating multiple spontaneous ignition in history. Three large burning sites and several vents were around the hillside. Atmospheric mercury concentrations were measured on each burning sites and vents, and the average is 12,438 ng/m³ (min: 319, max: 31,754, n=12), which is around 7,000 times of background level of atmospheric mercury (1.6-1.8 ng/m³).

Gangue hills are prone to intermittent self ignition, which releases mercury both in coal and surrounding clay or rocks. The long-term mercury inventory from gangue hill and potential impact on local environment requires further study.

[1] Pan *et al.*. (2005) *Resources and Industries*. 7, 46-49. [2] Ao *et al.*. (2005) *J. Chin. Coal Soc.* 30, 656-660. [3] Zhang *et al.*. (2011) *Clean Coal Technol.* 17, 97-100.

Molybdenum isotope fractionation in the mantle

Y.-H. LIANG^{1*}, C. SIEBERT², J. G. FITTON³, K. W. BURTON⁴, AND A. N. HALLIDAY¹

¹ Department of Earth Sciences, University of Oxford, South Parks Road, Oxford, OX1 3AN, UK

² GEOMAR, Helmholtz Center for Ocean Research, Wischhofstrasse 1-3, 24146 Kiel, Germany

³ School of GeoSciences, University of Edinburgh, Grant Institute, West Mains Road, Edinburgh EH9 3JW, UK

⁴ Department of Earth Sciences, Durham University, Science Labs, Durham, DH1 3LE, UK

(*correspondence: Yu-Hsuan.Liang@earth.ox.ac.uk)

Molybdenum is a refractory and moderately siderophile element that is highly redox-sensitive and has mainly been used to study changes in marine sedimentary environments [1,2]. So far little is known about mass dependent isotope fractionation of Mo at high temperatures in the Earth, in particular during mantle processes.

We have analyzed 42 mafic (mainly MORB and OIB) and 7 ultramafic rocks from diverse locations, using a double-spike technique and MC-ICPMS. The $\delta^{98/95}\text{Mo}$ values exhibit a significant range from $+0.53 \pm 0.21$ to $-0.56 \pm 0.01\%$ relative to NIST SRM 3134. The compositions of MORB ($+0.03 \pm 0.07\%$, 2s.d.) and ultramafic rocks ($+0.38 \pm 0.15\%$, 2s.d.) are each relatively uniform and distinct from each other, providing clear evidence of fractionation associated with partial melting. In contrast OIBs display significant variability within a single locality. The most extreme values measured are for nephelinites from the Cameroon Line and Trinidad, which also have anomalously high Ce/Pb [3] and low Mo/Pr relative to normal oceanic basalts [4]. The observed relationships between $\delta^{98}\text{Mo}$ and Ce/Pb, U/Pb, and Mo/Pr provide evidence that sulfide plays a critical role, not just in fractionating chalcophile elements [5], but also in preferentially incorporating heavier Mo isotopes. Residual immiscible sulfide liquids lead to the eruption of magmas with relative light Mo isotopes and low Mo/Pr relative to the source composition. Therefore, the Mo isotopic composition of the bulk silicate Earth and mantle will be best represented by values for peridotites.

[1] Colodner, D., *et al.* (1995) *Earth Planet. Sci. Lett.* **131**, 1-15. [2] Morford, J.L., and Emerson, S. (1999) *Geochim. Cosmochim. Acta* **63**, 1735-1750. [3] Halliday, A.N., *et al.* (1995) *Earth Planet. Sci. Lett.* **133**, 379-395. [4] Newsom, H.E., *et al.* (1986) *Earth Planet. Sci. Lett.* **80**, 299-313. [5] Yi, W., *et al.* (2000) *J. Geophys. Res.-Solid Earth* **105**, 18927-18948.

Tectonic control on the distribution of Paleogene deep-lake syn-rift deposits in Qikou sag, Bohaiwan Basin, Eastern China

YUANTAO LIAO^{1,2}, HUA WANG¹ AND WENLI XU¹

¹ Faculty of Earth Resources, China University of Geosciences, Wuhan, China, lyt706@gmail.com

² Key Laboratory of Tectonics and Petroleum Resources, Wuhan, China

The tectonic control on subaqueous sediment routes and stacking patterns is not well understood although the resulting deposits may form potentially important hydrocarbon reservoirs. In this study, an area of lacustrine syn-rift succession in the Qikou sag is examined in detail to unravel the interplay between fault geometries evolution and sediment transport paths and infilling patterns.

Qikou sag is a typical superimposed rift basin at the center of Bohaiwan Basin, Eastern China. Structurally, it is characterized by a linked system deep NEE-SWW striking half-grabens. This study focuses on the eastern part of the Qikou sag and it is bounded to the north by the overlapping Gangdong, Gangxi and Binhai normal faults. Syn-rift succession of the Qikou sag comprises Oligocene Shahejie Formation (EsF), Dongying Formation (EdF) and is mostly dark-grey mudstone interbedded with fine to coarse-grained sandstone deposited by large-scale turbidity currents in deep-lake. Using strata pattern, fault activity history, seismic attribute and heavy mineral analysis based on three-dimensional seismic and well logging data, our study demonstrate that the growth and propagation of main border normal fault segments associated with paleogeomorphology changes (particularly subaqueous relay ramps) have a marked influence on dispersal and localization of the turbidity currents during the syn-rifting phase. The main sediment supply is interpreted to be sourced from the basin marginal Cangxian uplift and the significant coarse-grained materials were transported to the deep-lake over long distance. In subaqueous settings, however, no clear evidence of channel incision on the relay ramp is observed, and turbidity currents are likely to bypass the relay ramp and flow down the inner fault slope directly into the basin. Therefore, Locating subaqueous syn-rift sediment and relating them with evolutionary relay ramps need further investigation.

Acknowledgements

This work is supported by the National Natural Science Foundation of China (NSFC) No. 41102069 and Special Fund for Basic Scientific Research of Central Colleges, China University of Geosciences (Wuhan) No. CUGL110248.

Effects of CO₂ leakage on benthic biogeochemistry – Results from a large scale field experiment

ANNA LICHTSCHLAG^{1*}, DOUG CONNELLY¹, HENRIK STAHL², PETE TAYLOR² AND RACHAEL H. JAMES¹

¹National Oceanography Centre, University of Southampton Waterfront Campus, European Way, Southampton, SO14 3ZH, UK,

correspondence: alic@noc.ac.uk

² Scottish Association for Marine Sciences, Oban, Argyll PA37 1QA, UK

Over the last few decades seafloor Carbon Capture and Storage (CCS) has been recognized as having great potential as an effective and safe method to reduce anthropogenic CO₂ emissions. However, the impact of any CO₂ seepage from a storage site on the marine environment is poorly understood. Released CO₂ will potentially dissolve into sediment pore waters, increasing the concentration of total dissolved carbonate and decreasing pH. As a consequence, metals may be released into pore waters and potentially into the water column. The effects of these changes to pore water chemistry on benthic ecosystems needs to be assessed.

To this end, we have analysed the chemical composition of pore waters, sediments, and the water column during a CO₂ release experiment that we carried out in Ardmucknish Bay, Scotland, as part of the 'Quantifying and Monitoring Potential Ecosystem Impacts of Geological Carbon Storage' (QICS) project. CO₂ gas was injected into the sediment 12m below seafloor at a known flow rate through a borehole drilled through the underlying bedrock. Sediment cores and water column samples were taken before, during and after the CO₂ release from 3 sites, at varying distances from the injection point.

Our data demonstrate that injected CO₂ was detected in the pore waters within 30 cm of the sediment-seawater interface within 33 days after the start of the CO₂ injection, but only at the site located closest to the injection point. As the CO₂ dissolved, concentrations of dissolved inorganic carbon (DIC) and total alkalinity (TA) increased and the δ¹³C of the DIC decreased, reflecting the low δ¹³C value of the injected CO₂ gas (δ¹³C = -26.6 ‰). Highest DIC concentrations (up to 30 mmol L⁻¹, compared with background levels of ~ 2.2 mmol L⁻¹) were observed 5 days after the injection had stopped. Pore waters with highest DIC concentrations also had enhanced concentrations of cations (e.g. iron, calcium) and nutrients. However, concentrations of all pore water constituents had returned to background values 18 days after the CO₂ injection was stopped.

Paired Sr Isotope (⁸⁷Sr/⁸⁶Sr, δ^{88/86}Sr) Systematic of Sulfates and Pore Waters: New Perspectives in Marine Weathering, Seepage Signatures and Fractionation Processes

V. LIEBETRAU^{1*}, M. HAECKEL¹, A. EISENHAUER¹, H. VOLLSTAEDT¹, L. HAFFERT¹ AND C. HENSEN¹

¹Helmholtz Centre for Ocean Research Kiel (GEOMAR), Germany (*vlietrau@geomar.de)

The simultaneous but independent determination of the conventional normalized radiogenic (⁸⁷Sr/⁸⁶Sr) and the fractionation reflecting stable (δ^{88/86}Sr) Sr isotope ratio on pore waters, sediments and precipitates (e.g. carbonates and sulfates) opens a new perspective in the field of marine weathering and Sr contribution to the ocean chemistry.

As established tool in provenance studies on silicates and SIS-geochronology (Sr-Isotope-Stratigraphy) of marine carbonates the radiogenic ⁸⁷Sr/⁸⁶Sr signature is in our approach directly combined with the isochemical stable Sr (δ^{88/86}Sr) fingerprint of isotope fractionation, mainly due to water/rock-interaction and secondary precipitation processes.

One of our initial case studies, includes gypsum bearing sediments of active mud volcanoes (MV) and mounds from the Gulf of Cadiz (GoC). The Mercator MV is characterised by high δ^{88/86}Sr ratios of 0.72‰ for small idiomorphic (mm scale, most probably authigenic) and up to 0.92‰ for large (cm scale) heterogeneous gypsum crystals. The related pore water profile reflects also elevated signatures from around 0.7‰ at the crystals to 0.52‰ close to the sediment surface at ⁸⁷Sr/⁸⁶Sr ratios around 0.7105. Referred to NIST-SRM-987 the IAPSO seawater (SW) standard of this study plots on 0.39‰ (±0.03, 2SD) in δ^{88/86}Sr and on 0.70917(1) in ⁸⁷Sr/⁸⁶Sr.

Potential explanation for the observed trend and PW signatures heavier than SW are (a) strong fractionation processes enriching light isotopes in secondary precipitates and remineralisation products and/or (b) preferential dissolution of mineral phases high in δ^{88/86}Sr.

In order to develop a better understanding of isotope fractionation processes we conducted experiments providing contrary Sr and Ca isotope systematics for the precipitation of gypsum.

Whereas the precipitate is enriched in ⁸⁸Sr by more than 0.1‰ when compared to the initial fluid source, the δ^{44/40}Ca isotope signature is depleted as known for carbonates.

In contrast, Sr of biogenic SrSO₄ dominated sulfates of acantharia follows the Ca fractionation systematic with a strong depletion of 0.3‰ in δ^{88/86}Sr compared to seawater.

Standing on Lal's shoulders: A look back and ahead at *in situ* cosmogenic nuclide production rate scaling

NATHANIEL LIFTON

Department of Earth, Atmospheric, and Planetary Sciences
and Department of Physics, Purdue University, West
Lafayette, IN 47907 [nlfifton@purdue.edu]

Devendra Lal had a profound influence on the development of the field of cosmogenic nuclides – nuclides produced by the interaction of cosmic rays with matter. When he passed away on 1 December 2012 at the age of 83, the scientific community lost a creative and energetic advocate, whose wide-ranging interests led to pioneering atmospheric, terrestrial, and extraterrestrial applications of these nuclides. Although he made significant contributions to many fields, his landmark publication in 1991 (Lal, 1991) presented theoretical underpinnings of key terrestrial cosmogenic nuclide applications in a manner accessible to a broad audience. Lal (1991) thus stands out as the foundation for many of the cosmogenic nuclide techniques now widely used to study rates and magnitudes of geomorphic and geologic processes operating at or near Earth's surface.

A cornerstone of many of these applications is the ability to predict the production rate of a nuclide of interest anywhere on the Earth, through a procedure known as production rate scaling. The scaling model presented in Lal (1991) was a key contribution to this area, and is still among the most widely used. Subsequent studies presenting alternatives have pointed out various discrepancies between that model and measurements of atmospheric cosmic ray fluxes (e.g., Desilets and Zreda, 2003), yet those alternative models appear to have biases as well. A new model based on analytical fits to Monte Carlo simulations of atmospheric cosmic ray spectra, both of which agree well with measured spectra (Sato *et al.*, 2008), enables identification and quantification of the biases in previous models, and allows for a flexible framework for exploring the implications of potential future advances such as nuclide-specific scaling and time-dependent atmospheric reconstructions.

References

[1] Desilets, D., and Zreda, M., 2003. *Earth Planet. Sci. Lett.* **206**(1-2), 21–42. [2] Lal, D., 1991. *Earth Planet. Sci. Lett.*, **104**(2-4), 424–439. [3] Sato, T., Yasuda, H., Niita, K., Endo, A., and Sihver, L., 2008. *Rad. Res.* **170**(2), 244–259.

Compositional zoning of polyphase garnet in pelites as a consequence of three metamorphic events in Precambrian *P-T-t* history of the Yenisey Ridge, Siberia

I.I. LIKHANOV^{1*} AND V.V. REVERDATTO¹

¹Sobolev Institute of Geology and Mineralogy, Novosibirsk, Russia (*correspondence: likh@igm.nsc.ru)

In situ U-Th-Pb geochronology of monazite and xenotime from different growth zones of the garnet porphyroblasts coupled with P-T path calculations derived from garnet zoning patterns records three temporally distinct events in the polymetamorphic history of the rocks, which differ in their ages, thermodynamic regimes and metamorphic field gradients. The first stage occurred as a result of the Grenville orogeny (1050-850 Ma) and was marked by LP zoned metamorphism at c. 4.8-5.0 kbar and 565-580°C with gradient $dT/dH=20-30^{\circ}\text{C}/\text{km}$ typical of orogenic belts. At the second stage, the rocks experienced collision-related (801-793 Ma) MP metamorphism at 7.7-7.9 kbar and 630°C with $dT/dH=10^{\circ}\text{C}/\text{km}$. The final stage evolved as a syn-exhumation retrograde metamorphism (785-776 Ma) at 4.8-5.4 kbar and 500°C with $dT/dH=12^{\circ}\text{C}/\text{km}$ and recorded a relatively fast post-collisional uplift of the rocks to upper crustal levels in shear zones. The duration of thrust exhumation does not exceed 17 My, which implies an exhumation rate of 500-700 m/My. This is consistent with the rate of exhumation (400 m/My) calculated for coeval collision-related metamorphic events in the Yenisey Ridge [1] resulted from crustal thickening due to thrusting [2] and agrees with the results of thermomechanical numerical modeling (350 m/My) [3]. The final stages of collisional orogeny were followed by the development of rift-related bimodal Baikal-Yenisey dyke belt (790-780 Ma) along the western margin of the Siberian craton and the onset of Rodinia's breakup. Post-Grenville episodes of regional crust evolution are correlated with the synchronous succession and similar style of the later tectono-metamorphic events within the Valhalla orogen along the Arctic margin of Rodinia supercontinent [4] and support the spatial proximity of Siberia and North Atlantic cratons at c. 800 Ma, as indicated by the paleocontinental reconstructions of the Rodinia configuration in Neoproterozoic [5].

[1] Likhonov *et al.*,(2011) *Russ. Geol. Geophys.* **52**, 1256-1269. [2] Likhonov & Reverdatto, (2011) *Int. Geol. Rev.* **53**, 802-845. [3] Likhonov *et al.* (2004) *J. Metamorph. Geol.* **22**, 743-762. [4] Cutts *et al.*(2010) *J. Metamorph. Geol.* **28**, 249-267. [5] Dalziel *et al.*(2000) *J. Geol.* **108**, 499-513.

Tracing the fate of endogenous CH₄ in water-logged soil and peat

K. L. H. LIM¹, R. D. PANCOST^{1*}, E. R. C. HORNIBROOK²,
P. J. MAXFIELD³ AND R. P. EVERSHEDE¹

¹ OGU, School of Chemistry, University of Bristol, Cantock's Close, Bristol BS8 1TS, U.K. (*correspondance: r.d.pancost@bristol.ac.uk)

² School of Earth Sciences, University of Bristol, Wills Memorial Building, Queen's Road, Bristol BS8 1RJ, U.K.

³ Department of Applied Sciences, University of the West of England, Coldharbour Lane, Bristol BS16 1QY, U.K.

Anaerobic conditions in soils experiencing water saturation favour the production of methane (CH₄) [1], which may undergo subsequent oxidation by methanotrophs [2]. Here, we combine stable isotope probing and flux methods to trace the fate of ¹³C-labelled methanogen substrates introduced to a peat and organic-rich water-saturated soil, in order to constrain production by methanogenic *Euryarchaeota* and its subsequent utilisation by CH₄-oxidisers. We monitor carbon flow by ¹³C-analysis of *Archaea*-derived intact polar lipids, proposed to serve as a biomarker for extant methanogen biomass in this setting [3], and phospholipid fatty acids (PLFAs), in addition to the isotopic composition and flux of CH₄ and CO₂.

Enrichment in the δ¹³C values of CH₄, and concurrently phospholipid-bound archaeol, confirm the *in situ* production of CH₄ and incorporation of ¹³C into archaeal biomass by predominantly acetoclastic and, to a lesser extent, hydrogenotrophic methanogens. Utilisation of endogenous CH₄ by methanotrophs was traced by incorporation of ¹³C-label in the isotopic values of CO₂. Enrichment of some PLFA lipids was also observed. At present, we are unaware of any other studies which have successfully involved the ¹³C-labelling of intact archaeal lipids in the terrestrial realm.

[1] Peters & Conrad (1996), *Soil Biol. Biochem.* **28** (3), 371-382. [2] West & Schmidt (2002), *Microb. Ecol.* **43** (4), 408-415. [3] Lim *et al.* (2012), *Archaea*, **896727**, 10.1155/2012/896727.

Indium from the Lagoa Salgada Orebody, Portugal

LIMA A.M.C.¹, RODRIGUES B.C.¹, OLIVEIRA A.,²
AND GUIMARAES F.²

¹ Geology Centre of Porto, Porto, Portugal

² LNEG, S. Mamede de Infesta, Portugal

The Iberian Pyrite Belt is one of the most outstanding European ore province, hosting one of the largest concentrations of massive sulphides in the Earth's Crust. Lagoa Salgada orebody, the most northerly of the Iberian Pyrite Belt known so far, is a small massive sulphide deposit with an inferred mineral resource of 3.7 Mt. The orebody has been described as composed of a central stockwork zone – a thick Volcano Sedimentary Complex with more than 700m – and a massive sulphide lens in the northwest. It is covered by more than one hundred meters beneath sediments of the Sado Tertiary basin.

A Junior Exploration Company has implemented an exploration program with recent drilling holes in new areas of the northwest lens of the deposit. Different types of ores have been identified on preliminary metallographic study that have established five basic textural domains: (i) Massif pyrite; (ii) Banded texture with layers of sphalerite and, rarely, of sphalerite and galena; (iii) Secondary transformation of massive pyrite; (iv) Infilling veins texture; (v) Supergenic banded texture.

The ore mineralization assemblage is mainly composed of pyrite with minor sphalerite, tetrahedrite-tennantite, arsenopyrite, chalcopyrite, galena, stannite, cassiterite, and supergene minerals which are in different amounts represented throughout the basic textural domains.

Polished sections of massive sulphide ore samples were studied by Electron-probe microanalyses (EMPA). Most of the minerals phase are behind the detection limit of Indium values, however, related with banded basic textural domain (ii) it was identified one generation of sphalerite, with mean granular dimension of 20 micra included on recrystallized arsenopyrite, that have 23000 ppm of Indium. This value is four times more Indium content than the best average values of other studied sphalerite examples on the same orebody deposit, in recent published results. This discovery proves again the complexity of this deposit and highlights the needed of prospecting new areas inside the ore body with predominance of this generation of sphalerite.

Ongoing works will demonstrate the Lagoa Salgada orebody potential for this rare trace metal, that is used in high-tech applications and is critical for European Industry.

Heavy metal contamination in the semi-urbanised Laurel Creek Watershed, Waterloo (Ontario), Canada

ANA T. LIMA¹, GORDON S. GELLER¹, JON P. JONES¹, PHILIPPE VAN CAPPELLEN¹ AND HANS H. DÜRR¹

¹Department of Earth and Environmental Sciences, University of Waterloo, Canada, hans.durr@uwaterloo.ca

Metal pollution in our watersheds can have numerous and sometimes severe impacts on the health of organisms which interact with the affected water sources. Some metals are required for cellular growth and maintenance as micronutrients, but are toxic at larger doses, while others are not required and are toxic at even low concentrations. Anthropogenic activities provide pathways for these metals to enter waterways, including industrial activities, mining, and transportation. There is currently a limited amount of literature addressing metal budgets and pathways within individual drainage basins, leading to some limitations of the understanding of heavy metal sources and interactions within these basins. Here, we study Waterloo region, and specifically the Laurel Creek drainage basin (80 km² basin area, population 123,500, precipitation 907 mm/year). The Laurel creek watershed has a myriad of land uses that makes it a perfect local setting for our metal budget approach. This tributary to the Grand River is divided in agricultural land (37% basin area), and a mosaic of residential (32% of basin), commercial (4.5% of basin), and industrial land (7% of basin), with some brownfields constituted of previously active tanneries. Extensive datasets, mostly at very high resolution, are available, both historical and current, including climate, GIS data on land use, drinking water, storm water management and sewage system, particulate levels, and measurements of various other factors influencing contaminant pathways, with ongoing sampling for many of these. Using the data available, along with an available water model and GIS processing, the aim is to create a water and metal budget, following the methodology first presented by [1]. The budget will focus on specific target heavy metals, such as copper, nickel, and cadmium. We anticipate that this work will introduce a more detailed conceptual model for heavy metals in urban settings, with a better description of some overlooked sources. This study will serve as a stepping stone for larger watershed studies.

[1] Meybeck *et al.* (2007). *Science of the Total Environment*, 375, 204-231.

Evaporation as the transport mechanism of metals in arid regions

ANA T. LIMA^{1,2}, ZEINAB SAFAR¹
AND J.P. GUSTAV LOCH¹

¹ Department of Earth Sciences, Division of Geochemistry, Utrecht University, PO Box 80.021, 3508 TA Utrecht, The Netherlands

² Ecohydrology, Department of Earth and Environmental Sciences, University of Waterloo, Waterloo, Canada N2L 3G1

Arid regions are wide and vast areas of the globe with a relatively low population density. Arid regions are known for the deserts, the scarcity of fresh water and long periods of draught. The main climatic process that dictates water flow in soils in such areas is evaporation rather than precipitation e.g. [1]. While groundwater protection is a main issue in temperate regions, arid regions do not have such concerns when dealing with soil contamination. Contaminated sites are often not a priority, as its remediation, since there is no real scarcity of land for certain economic activities and overlooking how contamination of desert areas could ever affect human health.

This study tests the hypothesis of heavy metals coupled flow with the evaporating soil water in arid climates. Laboratory tests were performed to study the migration of heavy metals in an artificially spiked soil, using compressed air as evaporation driving force. A loamy and a sandy soil, collected near Al-Hasa, Saudi Arabia, are spiked with a heavy metal solution that is representative of a landfill leachate in developing country [1], and then used in this study. Main results show that while evaporation does transport heavy metals to the surface of a sandy soil, the loamy soil does not show the same trend. Therefore, contaminant accumulation predominates at the surface of sand soils in arid and semi-arid regions. Given that 90% of the land in Saudi Arabia, and for the most of arid regions, is sand, contaminated sand sites can pose a considerable hazard to the environment, especially biota, humans included. Ingestion or inhalation of sand particles from contaminated sites is a public health issue that should be assessed in arid regions. Sand and silt size particles from arid regions do travel long distances and may present an aerosol problem elsewhere. This is a source of atmospheric pollution that has been overlooked.

[1] Elrick & Mermout (1994) *J. Hydrology* **155**, 27-38. [2] Rawat *et al.* (2009) *J. Hazard. Materials* **172**, 1145-1149.

From grains to planetesimals in evolving protostellar disks.

D.N.C. LIN^{1,2,3}, Y. ZHANG², B. DAI³, Y. FENG³, J. AND C. LI³

¹University of California, Santa Cruz, USA

²KIAA and School of Physics, Peking University, China

³Physics Department, Tsinghua University, China

We model the properties of meteorites and protostellar disks in the context of the new planet-formation paradigm that planets and their building blocks may have migrated extensively. We suggest that CAIs condensed, with little age spread in a hot compact nebula formed by the infall of turbulent gas. Hydrodynamic drag led to the accumulation of meter-size particles near the inner boundary disk boundary beyond the stellar magnetosphere where the first generation planetesimals and proto-planetary embryos formed. Earth-mass embryos migrated outwards to and stalled at a few AU's. They promoted the accumulation of later generation grains and planetesimals. In the solar nebula, embryos became cores of gas giants. Strong perturbation by emerging Jupiter and Saturn led to the wide-spread episodic melting and re-condensation of chondrules. In less massive disks, super-Earth embryos formed, and blocked the migration of grains and planetesimals to produce transitional disks. Super-Earths migrate to their present-day compact orbits during the disk depletion.

Electronic Spin Transitions of Iron and Geoelectrons in Earth's Mantle

J.-F. LIN¹

¹Department of Geological Sciences, Jackson School of Geosciences, The University of Texas at Austin, Austin, TX 78712 (*afu@jsg.utexas.edu)

Based on a pyrolytic compositional model, the lower mantle is mainly made of ferroperricite, aluminous silicate perovskite, and calcium perovskite. Silicate perovskite transforms into silicate post-perovskite structure just above the core-mantle region, the D" layer. The existence of iron in the lower-mantle minerals can affect a broad spectrum of the minerals' physical and chemical properties. In this presentation, I will address recent results and current understanding on the pressure-induced electronic spin-pairing transitions of iron and their associated effects on physical properties of host phases in lower-mantle minerals [1]. The spin crossover of Fe²⁺ in ferroperricite occurs over a wide pressure-temperature range extending from the middle part to the lower part of the lower mantle. Furthermore, a high-spin to low-spin transition of Fe³⁺ in the octahedral site of perovskite occurs at pressures of 15-50 GPa [2]. In post-perovskite the octahedral-site Fe³⁺ remains in the low-spin state at the pressure conditions of the lowermost mantle. These changes in the spin and valence states of iron as a function of pressure and temperature have been reported to affect physical, chemical, rheological, transport properties of the lower-mantle minerals. These effects of the spin transition can thus significantly affect our understanding of the deep Earth. I will present and evaluate the consequences of the transitions in terms of their implications to deep-Earth geophysics, geochemistry, and geodynamics [1-3].

The electrons of ferrous and ferric iron ions that occupy some of the lattice sites in mantle minerals become slightly polarized in the presence of the Earth's magnetic field. Using recent deep-Earth geophysics and geochemistry results, we have developed a model of the polarized electron spin density within the Earth. We have examined possible long-range spin-spin interactions between these spin-polarized geoelectrons and the spin-polarized electrons in recent particle physics experiments [4]. Such information might eventually help reconcile seismic observations and mineral physics data with geochemical models.

[1] Lin *et al.* (2013) *Rev. Geophys.* (in press). [2] Lin (2012) *Am. Miner.* **97**, 592-597. [3] Lin *et al.* (2013) *Am. Miner.* **97**, 583-591. [4] Hunter *et al.* (2013) *Science* **339**, 928-932.

Precision mapping and towcam aided study over geochemical anomalies of the Goodweather Ridge, Southwestern Taiwan

SAULWOOD LIN^{1*}, C.-W. HSU¹, I-JY HSIEH¹, HSIU-HUI CHANG¹ AND GERHARD BOHRMANN²

¹Institute of Oceanography, National Taiwan University, Taipei, Taiwan (*correspondence: swlin@ntu.edu.tw)

²MARUM/ Center for Marine Environmental Sciences University Bremen, Germany

Very fine scale and detail bathymetric map could reveal a great deal of processes that may occur near the sea floor. This study used a MARUM SEAL 5000 AUV (Autonomous Underwater Vehicle) to obtain high-resolution depth variations on the sea floor and towcam aided piston coring to facilitate a better resolution of sea floor biogeochemical processes relate to methane gas venting.

Fine scale, high-resolution seafloor structures were obtained on the west of Good Weather Ridge by AUV mapping. A fault scarp previously draw based on seismic data at ridge slope is clearly visible from the AUV map, about 1-3 m deep and extending from south to the north about 4 km long. A series of micro-faulting branch structures appeared away from the ridge slope toward north. Another set of pockmarks, up to 7 m deep, 70 m in diameter, appeared on the surface indicating faulting extended from deep to sea floor. Large scale of authigenic carbonate buildups, and shallow SMI were observed. This study demonstrated that fine-scale mapping and towcam-aided sediment sampling could provide unprecedented details of sea floor features in corresponding to geochemical variations as a result of deep fluid venting.

Two Neo-Tethyan magmatic suites of distinctive geochemical features in Burma and southern Tibet: Zircon U-Pb and Hf constraints with regional tectonic implications

LIN, T.-H.¹, CHUNG, S.-L.¹, MITCHELL, A.H.G.², THURA OO³, TANG, R.-T.¹ AND WU, F.-Y.⁴

¹ Institute of Geosciences, National Taiwan University, Taipei, Taiwan, tehsienlin@ntu.edu.tw

² Consulting Geologist, 20, Dale Close, Oxford OX1 1TU, UK

³ University of Yangon, Kamayut Township, Yangon, Myanmar

⁴ Institute of Geology and Geophysics, Chinese Academy of Sciences, Beijing, China

The Neo-Tethyan subduction that operated before the India-Asia collision resulted in an Andean-type convergent margin in South Asia (Yin and Harrison, 2000; Chung *et al.*, 2005; Kapp *et al.*, 2005; Mo *et al.*, 2005), induced arc magmatism distributing more than ~2,500 km that formed the Transhimalayan batholiths in the Lhasa terrane. Based on the age distribution and geochemical characteristics, the MMB may correlated northward to the Danxi Batholith, western Yunnan (Yang *et al.*, 2006; Liang *et al.*, 2008; Xu *et al.*, 2012), westward to the Bomi-Chayu Batholith (Chiu *et al.*, 2009; Lin *et al.*, 2012) and the Central Lhasa plutonic belt, which is a northern Transhimalayan plutonic suite typically has low and negative $\epsilon_{\text{Hf}}(\text{T})$ values suggesting involvement of old continental crust in the petrogenesis (Chu *et al.*, 2006, 2011; Chiu *et al.*, 2009; Zhu *et al.*, 2011); Comparatively, the Wuntho-Mokapalin arc in West Burma, characterized by high and positive $\epsilon_{\text{Hf}}(\text{T})$ values, with similar age and isotopic characteristics as the Lohit Batholith in the Eastern Himalayan Syntaxis, was proposed as the southward extension of the Gangdese Batholith, in general, has long been regarded as the main arc component produced by northward subduction of the Neo-Tethyan oceanic slab under the Lhasa terrane.

Organic carbon from the Tissint Martian Meteorite: Hints for biogenic origin

Y. LIN^{1*}, A. EL GORESY², S. HU¹, J. ZHANG¹,
P. GILLET³, Y. XU¹, J. HAO¹, M. MIYAHARA⁴,
Z. OUYANG⁵, E. OHTANI⁴, L. XU⁶, W. YANG¹, L. FENG¹,
X. ZHAO¹, J. YANG⁷ AND S. OZAWA⁸

¹ Institute of Geology and Geophysics, CAS, Beijing, China
(*correspondence: LinYT@mail.igcas.ac.cn)

² Bayerisches Geoinstitut, Universität Bayreuth, Germany

³ EPFL, CH-1015, Lausanne, Switzerland

⁴ Tohoku University, Sendai, Japan

⁵ Institute of Geochemistry, CAS, Guiyang, China

⁶ National Astronomical Observatories, CAS, Beijing, China

⁷ Guangzhou Institute of Geochemistry, CAS, China

⁸ National Institute of Polar Research, Tokyo, Japan

Organic carbon was found in Tissint, the new Martian meteorite fall [1], most filling fractures and a few entrained in shock-melt veins. The organic carbon is kerogen-like based on Raman spectra. Some organic carbon inclusions in the veins were transferred to diamond. The organic carbon has been analyzed with NanoSIMS 50L. The abundances of H, N, O, S, P, F and Cl relative to C of the organic carbon are comparable with coal. The organic carbon grains have $\delta^{13}\text{C}$ values of $-13.0 \sim -33.3\text{‰}$, δD values of up to $+1183\text{‰}$ and normal N isotopic compositions.

The organic carbon in Tissint is of Martian origin, based on the presence in the shock-melt veins, the formation of diamond and the D-enrichment. It formed by depositing from organic-rich groundwater on Mars. The petrographic settings and significantly light C isotopes of the organic carbon are consistent with a biogenic origin. Our observations of the organic carbon argue against an igneous origin [2]. The organic carbon couldn't originate from carbonaceous chondrites that impacted on Mars, because the chondritic kerogen has heavier N isotopes and relatively homogeneous H isotopes.

[1] Chennaoui A., H. , *et al.* 2012. *Science* 338: 785-788.

[2] Steele A., *et al.* 2012. *Science* 337: 212-215.

Precise Determination of B Isotopic Compositions in Low Concentration Carbonates and Fluids Using Micro-sublimation MC-ICPMS

YEN-PO LIN¹, CHEN-FENG YOU^{1,2*}
AND CHUAN-HSIUNG CHUNG²

¹Department of Earth Sciences, National Cheng Kung University, Tainan, Taiwan

²Earth Dynamic System Research Center (EDSRC), National Cheng Kung University, Tainan, Taiwan
(*correspondence: cfy20@mail.ncku.edu.tw)

Although the pH-dependence of boron (B) isotopic fractionation in marine carbonates has been widely used for pH reconstruction in ancient seawater, the available analytical techniques still exhibit large discrepancies. In this study, we evaluated systematically the B isotopic compositions in two reference materials, JCp-1 (porites coral) and Jct-1 (giant clam). A low blank boron separation procedure was evaluated using micro-sublimation technique [1], subsequently combined with MC-ICPMS isotopic measurement. The two carbonate standards were treated with oxidative cleaning (NaOCl) and without any prior cleaning for comparison. There is no major B isotopic difference between the two groups; however, the cleaned carbonates show slightly lower $\delta^{11}\text{B}$ with better precision. These $\delta^{11}\text{B}$ results agree well with literature values, but achieve with high throughput and high precision (2SD, 0.2 ‰).

Boron isotopic fractionation during sorption is rather significant in soils and river water. Our $\delta^{11}\text{B}$ technique was applied further for a better understanding of clay adsorption/desorption behaviors of B in aqueous environments, as well as the associated isotopic fractionation during water/rock interaction. The calculated K_p s and the degree of B isotopic fractionation showed significant variation among various minerals.

[1] Wang *et al.*, 2010 *Talanta* **82** 1378–1384

Higher oxygenation level after Sturtian glaciation meltdown despite varying local redox in Nanhua basin

HONG-FEI LING¹, XI CHEN¹, DA LI¹, G.A. SHIELDS², D. VANCE³ AND L. OCH²

¹ Department of Earth Sciences, Nanjing University, China

² Department of Earth Sciences, University College London

³ School of Earth Sciences, University of Bristol

Both of the major two oxygenation events occurred coincidentally with severe glaciations in the early and late Proterozoic. Causal relationship was proposed that enhanced postglacial weathering input caused high rates of productivity and organic carbon burial and thus further oxygenation of the surficial Earth (Planavsky *et al.*, 2010). Here we present data of iron speciation, pyrite sulfur isotopes and Mo isotopes of black shales and Mn-rich carbonates of the basal Datangpo Formation immediately covering the Sturtian diamictite in Tongren County, South China, to constrain the oceanic redox condition in the aftermath of the glaciation. Our iron speciation data show anoxic condition of local seawater within the Nanhua Basin, while published data for samples in Minle County (Li *et al.*, 2012), ~70 km from Tongren, show euxinic condition, indicating heterogeneous redox in the Nanhua Basin. The $\delta^{34}\text{S}_{\text{py}}$ values of our samples are between 20.6‰ and 59.3‰, similar to those of Minle area (38.6-57.3‰). Furthermore, our samples show a negative correlation between $\delta^{34}\text{S}_{\text{py}}$ and pyrite-sulfur contents. Low S_{py} , anomalously high $\delta^{34}\text{S}_{\text{py}}$ and their correlation suggest a very low seawater sulphate content which limited pyrite formation, given ferruginous condition and relatively high organic carbon content. The $\delta^{98}\text{Mo}$ values range between which should be the lower limit of the coeval ocean values as Mo-isotope fractionation may have existed during deposition in ferruginous condition. However, the high end of our data is higher than those of euxinic black shales in mid-Proterozoic ($\delta^{98}\text{Mo} \leq 1.13$, Kendall *et al.*, 2011; and in pre-Sturtian Neoproterozoic ($\delta^{98}\text{Mo} \leq 1.19$ at 750Ma, Dahl *et al.*, 2011), suggesting a higher oxygenation level of the ocean after the Sturtian glaciation.

Destruction of the North China Craton Induced by Ridge Subductions

M.X. LING¹, W.D. SUN¹, F.Z. TENG², Y. LI³, X. DING¹, X.Y. YANG⁴, W.M. FAN¹ AND Y.G. XU¹

¹ Guangzhou Institute of Geochemistry, CAS, Guangzhou 510640, China (mxling@gig.ac.cn)

² Department of Geosciences, University of Arkansas, Fayetteville, AR 72701, USA

³ China Petroleum Pipeline Engineering Corporation Langfang 065000, China

⁴ School of Earth and Space Sciences, University of Science and Technology of China, Hefei 230026, China

The destruction of the North China craton (NCC) has been attributed to a "top-down" rapid delamination or to "bottom-up" long-term thermal/chemical erosions, or hydration by subduction released fluids. Based on the distribution of one Jurassic and two Early Cretaceous adakite belts and the drifting history of the paleo-Pacific plate, here we propose that three ridge subduction events dominated the large-scale decratonization in the NCC. Both physical erosion (delamination) and magmatism (thermal/chemical erosions) induced by ridge subduction contributed to the destruction of the NCC, whereas the last ridge subduction at 130 ± 5 Myrs was the key driving force that led to the final destruction, which mainly occurred in the Cretaceous. Integrated study of mineralogy, major and trace elements, as well as Mg isotopes, was conducted, which supports the ridge subduction model: The flat subduction of a spreading ridge had stronger physical erosion on the thick lithosphere mantle of the NCC. The final decratonization was triggered by the last ridge subduction, with both physical erosion (flat subduction) and thermal erosion (adakitic and A-type magmatisms). Given that ridge subduction occurred throughout Earth's history, the associated decratonization processes are presumably a common phenomenon that modified the chemical compositions of the continental crust.

The related paper was published in *Journal of Geology* (Ling, M.X. *et al.*, 2013. Destruction of the North China Craton Induced by Ridge Subductions. *Journal of Geology*, 121(2): 197-213).

The link between biotic and abiotic systems: How and why does gold accumulate in calcrete (caliche)?

M.J. LINTERN

CSIRO Minerals Downunder Flagship, 26 Dick Perry Avenue, Kensington, WA 6152, Australia (correspondence: lin082@csiro.au)

It is well known to mineral explorers that in drier parts of Australia Au accumulates in calcrete (caliche). Calcrete is a Quaternary aeolian or marine addition to the soil yet it is strongly correlated with Au derived from the weathering of Archean rocks. Why this should be the case is not well understood..

Through a series of recent field observations, laboratory experiments and microanalytical techniques it will be demonstrated that the relationship between gold and calcrete is mediated by both biological and climatic mechanisms. We track the process by which Au becomes adsorbed by plant roots and is translocated to the canopies of large trees. From here the Au is transferred to the soil whereby organic processes involving bacteria, fungi and/or plant roots serve to complex and mobilise Au. Climate affects the uptake of Au in plants and causes it to accumulate in the pedogenic carbonate horizon of soil profiles.

It is important that we elucidate these abiotic-biotic processes if we are to identify the constraints on the Au-calcrete association. Mineral explorers may overlook Au deposits if they fail to understand mechanisms on how soil anomalies form above them.

Geochemical processes during weathering of natural volcanic glasses: comparison with experimental alteration

ANGELO LIOTTA¹, MICHEL DUBOIS¹
AND ARNAUD GAUTHIER¹

¹ LGCgE, Université Lille 1, France
angelo.liotta@ed.univ-lille1.fr

The objective of this research, currently in progress, is to study the weathering processes of glassy silicate materials, in order to understand the geochemical processes involved and the variation of mineral phases as a result of alteration.

The use of samples of natural glass of volcanic origin has allowed to obtain some powder or sections of fresh silicate glass that have been subjected to artificial alteration in the laboratory, in order to model the geochemical processes that have occurred.

Moreover, the study of naturally altered samples has allowed to observe the effects of weathering after a period of time corresponding to the age of the sample. Three samples were collected in the eastern Sicily, Italy. They include the rhyolitic obsidian of historical age coming from the island of Lipari (Aeolian Islands) in the southern Tyrrhenian Sea, connected to a complex subduction-related magmatism. The second one is a glassy salband from a basaltic dike outcropping in the western wall of the Valle del Bove (Etna), having an estimated age between 15 and 60 thousand years. The third sample is a glassy crust of tholeiitic pillow lavas from submarine eruptions of the upper Pliocene in shallow water environment in the northwestern Iblean Mountains.

The characterization of the samples was obtained by Raman spectroscopy, which showed the effects of the devitrification and the presence of some secondary minerals such as phillipsite and offretite, two varieties of zeolite found in the cavities of oldest basalts.

Samples have been altered from 1 to 100 days of experiment. Alteration experiments were conducted in pure water at 90°C; solid modifications were observed by SEM. The analysis showed the formation of an amorphous material surface characterized by a slight decrease in the content of silica, alkali and calcium, and by a marked increase in titanium (up to 3.17%) and iron (up to 16.21 %) contents.

All these results allow to test the geochemical modeling in the long term. Further analysis will be needed to reach a full understanding of the weathering of glassy materials, in order to prevent the environmental pollution caused by the alteration of vitrified metallurgical or radioactive waste.

Sulfur and Chlorine isotopes in volcanic products at Mt. Etna, Italy

M. LIOTTA^{1,2*}, A.L. RIZZO², A. PAONITA²,
J.D. BARNES³, A. CARACAUSI², R. CORSARO⁴
AND M. MARTELLI²

¹Dipartimento DiSTABiF, Seconda Università di Napoli, Caserta, Italy (*correspondence: marcello.liotta@unina2.it)

²Istituto Nazionale di Geofisica e Vulcanologia, Sezione di Palermo, Italy

³Department of Geological Sciences, University of Texas, Austin, Texas 78712, USA

⁴Istituto Nazionale di Geofisica e Vulcanologia, Sezione di Catania, Italy

Mt. Etna volcano is characterized by a persistent volcanic plume and by a complex fumarolic field. Two types of fumaroles were identified: low-temperature fumaroles, which are dominated by CO₂ with minor amounts of SO₂ and H₂S, and negligible chlorine contents, and high-temperature fumaroles, which are strongly air-contaminated and characterized by appreciable amounts of volcanogenic carbon, sulfur, and chlorine [1, 2].

Sulfur and Chlorine isotopic compositions ($\delta^{34}\text{S}$, $\delta^{37}\text{Cl}$) of fumarolic and plume gases collected at Mount Etna volcano during 2008–2011 are compared to those of volcanic rocks. While low-temperature fumaroles are affected by postmagmatic processes that modify the pristine isotopic signature of sulfur and remove chlorine [2], high-temperature fumaroles and plume gases allow to constrain the $\delta^{34}\text{S}$ of magmatic SO₂ to $\sim 0 \pm 1\%$, being systematically 1–2‰ lower than that of S dissolved in Etnean melts [2].

Chlorine dissolved in rocks shows an isotopic composition partially overlapping with that of high-temperature fumaroles and plume gases defining a narrow range of $\delta^{37}\text{Cl}$ range of $\sim 0 \pm 0.7\%$ for magmatic chlorine [3].

While sulfur fractionation ($\alpha_{\text{gas-melt}}$) depends on the speciation of sulfur, thus providing a useful information on the redox conditions of the Etnean plumbing system, chlorine exhibits negligible fractionation during degassing of magmatic bodies. Accordingly, isotopic fractionation model for sulfur and chlorine during magma degassing provide inferences on the mantle source of Etnean magmas and physico-chemical conditions in the shallower system.

[1] Martelli *et al.* (2008) *Geophys. Res. Lett.* **35**, L21302. [2] Liotta *et al.* (2010) *Chem. Geol.* **278**, 92-104. [3] Liotta *et al.* (2012) *Geochem. Geophys. Geosyst.* **13**, Q05015. [4] Rizzo *et al.* (2013) *EPSL in press*.

BC/OC ratios : A new metrics to mitigate Emissions, Health and Radiative Impacts. Focus on African megacities.

C. LIOUSSE¹, DOUMBIA T.^{1,2}, ASSAMOË E.¹,
GALY-LACAUX C.¹, BAEZA A.³, PENNER J.E.⁴, VAL S.³,
CACHIER H.⁵, XU L.⁴, CRIQUI P.⁶
AND ROSSET R.¹

¹Laboratoire d'Aerologie, UMR 5560, CNRS/Université de Toulouse, France

²Université C. A. Diop, Dakar, Sénégal

³RMX Université Paris Diderot-Paris 7, France

⁴University of Michigan, Ann Arbor, USA

⁵LSCE, Gif sur Yvette, France

⁶LEPHEO Grenoble, France

Fossil fuel and biofuel emissions of particles in Africa are expected to significantly increase in the near future, particularly due to rapid growth of African cities. Air quality degradation is then expected with important consequences on population health and climatic/radiative impact.

In this work, we show the central role of black carbon to organic carbon ratios (BC/OC) to characterize African anthropogenic emissions and impacts:

- a new BC and OC African anthropogenic emission inventory adapted to regional specificities has been constructed for the years 2005 and 2030.

- BC and OC radiative impacts in Africa have been modeled with TM5 model and Penner *et al.* (2011) radiative code for these inventories for 2005 and 2030 and for two emission scenarios: a reference scenario and a ccc* scenario including regulations. In this study we will show that enhanced heating is expected with the ccc* emissions scenario in which the OC fraction is relatively lower than in the reference scenario.

- results of short term POLCA intensive campaigns in Africa in terms of aerosol inflammatory impacts on the respiratory tract through in vitro studies. In this study, organic carbon particles appear more biologically active than BC particles.

Quite importantly, air quality improvement obtained through regulations in the ccc* scenario with higher BC/OC ratios are accompanied by stronger heating impact. BC/OC ratio variations may be considered as a standard reference index to study air quality, health and climatic impacts.

Geochemistry and crystal preferred orientation of upper mantle peridotite xenoliths from the Nógrád-Gömör Volcanic Field (Northern Pannonian Basin)

N. LIPTAI^{1*}, L. PATKÓ¹, L. E. ARADI¹, CS. SZABÓ¹,
I. J. KOVÁCS², K. HIDAS³, GY. FALUS², O. VASELLI⁴,
A. TOMMASI⁵ AND F. BAROU⁵

¹Lithosphere Fluid Research Lab, Eötvös University,
Budapest, Hungary (*correspondence:
n.liptai.elte@gmail.com)

²Geological and Geophysical Institute of Hungary

³Instituto Andaluz de Ciencias de la Tierra, Consejo Superior
de Investigaciones Científicas, Granada, Spain

⁴Department of Earth Sciences, Florence, Italy

⁵Geosciences Montpellier, University of Montpellier,
Montpellier, France

Information on the physical and chemical properties of the subcontinental lithospheric mantle can be obtained by the study of mantle rocks outcropped on the surface mostly as xenoliths or massive peridotite bodies. The Nógrád-Gömör Volcanic Field (NGVF) is one of the five occurrences in the Carpathian-Pannonian region where Plio-Pleistocene alkali basalts host upper mantle peridotite xenoliths. There is only a limited number of publications that provide basic petrographic and geochemical data about xenoliths in the area [e.g. 1, 2], and none of these contains analyses of crystal preferred orientation (CPO), which can be an important key to gain insight into the rheological conditions of the given mantle domain, and thus, the evolution of the Pannonian Basin.

Here we present major and trace element contents and CPO data of representative lherzolite xenoliths collected from different parts of the NGVF. The major goal is to depict an overall picture of CPO in olivines in the studied area and look into geochemical data to see if there is any link between them. Our results show that the xenoliths are geochemically similar, however, three types of olivine CPO can be distinguished, which correlate with localities, xenolith fabrics, and calculated equilibrium temperatures. This suggests that the studied xenoliths recorded the presence of various types of deformation events in the upper mantle beneath the NGVF, which occurred most probably during the Neogene evolution of the Pannonian Basin.

[1] Szabó *et al.* (1992) *Tectonophysics*, **208**, 243–256.

[2] Konečný *et al.* (1995) *Acta Vulcanologica*, **7**, 241–247.

Chemical composition of apatite as a tool for modeling composite-pluton evolution using Polytopic Vector Analysis (PVA)

LISOWIEC K.¹, SŁABY E.¹, FÖRSTER H.-J.², GÖTZE J.³
AND MICHALAK P.P.³

¹ING PAN, Warsaw, PL klisowiec@twarda.pan.pl

²GFZ, Potsdam, DE, forhj@gfz-potsdam.de

³TUBAF, Freiberg, DE, goetze@mineral.tu-freiberg.de

Composite plutons are common constituents of the continental crust, therefore identification of their evolution path is crucial. Polytopic Vector Analysis (PVA) is used to define the number and composition of end-members from a data set representing a system formed by mixing of several different components. This approach is routinely applied to study whole-rock composition. We verified its applicability for mineral compositions. Apatite grains from a composite granitic pluton were studied with FE-EPMA and CL. The pluton formed by mixing of mantle- and crust-derived melts influenced by late-magmatic fluids, thus being a suitable example for a heterogeneous system. Apatites exhibit complex zoning in BSE and CL, pointing to rapid changes in melt composition. Variation in trace-element content demonstrates distinct trends that changed over time of formation of the pluton.

Polytopic Vector Analysis was applied to the whole rock and apatite major and trace-element compositions, in order to verify the record of a common differentiation path. The results of the PVA study performed for the whole rock are consistent with previous studies employing other modeling approaches and are in accord with the supposed magma-mixing model. Apatite composition does not reflect operation of this mixing model, especially in the case of REEs which exhibit chaotic distribution, likely resulting from local saturation of the melt. The results of the PVA of apatites from every stage of magma differentiation will be presented and the advantages and limitations of this approach will be shown.

Chalcophile and Highly Siderophile Element systematics in Mid-Ocean Ridge Basalts

MORITZ LISSNER^{1*}, STEPHAN KÖNIG¹, AMBRE LUGUET¹,
PETRUS LE ROUX² AND ANTON LE ROEX²

¹Steinmann Institut für Mineralogie, Universität Bonn,
Germany mlissner@uni-bonn.de (* presenting author)

²Department of Geological Science, University of Cape
Town, South Africa

Mid-Ocean ridge basalts (MORBs) constitute an exceptional window to investigate the chalcophile element (S, Se and Te) and the highly siderophile element (HSEs: Os, Ir, Ru, Pt, Pd, Re) signatures of the depleted MORB mantle (DMM), provided that the behavior of these elements during MORB evolution is entirely understood. Hence, we analyzed S, Se, Te, HSEs and ¹⁸⁷Os in 20 Southern Mid-Atlantic Ridge (SMAR) MORBs, which range in composition from typical N-MORBs to plume-overprinted E-MORBs [1].

All samples display positively-sloped CI-normalized HSE patterns ($Pt_N/Ir_N=2.8-88.3$, $Pd_N/Ir_N=3.1-17.3$, $Re_N/Pd_N=40-270$), with E-MORBs having higher Pt and Pd contents than N-MORBs. S, Se and Te concentrations range from 715-1143 ppm, 107-242 ppb and 1.63-9.46 ppb, respectively. S contents increase with decreasing Mg# and Se concentrations. Se and Te positively correlate with each other and with incompatible PGEs (Pt, Pd). In addition Se/Te increase with decreasing Te concentrations defining a clear non-linear trend. After filtering out possible effects of seawater alteration, volatilization upon eruption and sulphide fractionation on S, Se, Te and HSE contents, the Se/Te and Pd/Ir ratios appear as indicators of the mantle source composition, correlating with discriminant parameters like La_N/Sm_N and Sr-Nd-Pb isotopic signatures. While both N- and E-MORBs are characterised by supra-chondritic Se/Te and Pd/Ir, N-MORBs generally show higher Se/Te but lower Pd/Ir (Se/Te=51-92 vs. 26-38, $Pd_N/Ir_N=3.1-7.0$ vs. 4.4-17.3). Partial melting modelling [2] performed to reconstruct the DMM composition, predicts an incompatible behaviour of both Se and Te during partial melting as well as chondritic abundances of Se, Pt and Ir but sub-chondritic Pd and Te contents in the SMAR mantle source. This ultimately supports supra-chondritic Se/Te and sub-chondritic Pd/Ir ratios in the MORB mantle source and has important implications on the Se, Te and HSE budget estimate of the Earth's primitive mantle.

[1] le Roux *et al.* (2002) *EPSL* **203**, 479–498. [2] Rehkämper *et al.* (1999) *GCA* **63**, 3915-3934.

Deep melting of subducted carbonate and carbonatite melt diapirs in the Earth's mantle

K.D. LITASOV^{1,2*}, A. SHATSKIY^{1,2} AND E. OHTANI³

¹Sobolev Institute of Geology and Mineralogy, Novosibirsk,
630090, Russia (*correspondence: klitasov@igm.nsc.ru)

²Novosibirsk State University, Novosibirsk, 630090, Russia

³Tohoku University, Sendai, 980-8578, Japan

Minor amounts of alkalis (Na and K) can drastically reduce the solidus temperatures of carbonated silicate mantle, by as much as 400-500°C. Low-degree melting of carbonated peridotite and eclogite at pressures of 3-10 GPa produces Na- and K-bearing carbonatite melt. Mass-balance calculations of samples obtained below apparent solidi show clear deficits of alkalis suggesting the presence of minor alkali-rich liquid or solid carbonate phases. Here we determined the true solidi in Na- and K-bearing carbonated systems and report the stability of new alkaline carbonate phases [1]. Starting materials correspond to Na- and K-bearing Mg-Ca-carbonatite. Experiments were run at pressures from 3-21 GPa and 750-1450°C using multianvil apparatus.

Major carbonate phases in both the Na-carbonatite and K-carbonatite systems are aragonite and magnesite. Magnesite is a liquidus phase together with silicates. Aragonite contains significant amounts of Na₂O (up to 7 wt.%), K₂O (up to 1 wt.%), and MgO (up to 8 wt.%) in the Na-carbonatite system. The solidus temperature is defined by the stability of double carbonate phases. The solidus slope has a significant change between 6 and 10 GPa. Above 10 GPa the solidus becomes flat at a temperature near 1150°C. In the Na-bearing system it may have a slightly negative slope above 15 GPa according to stability of K-Ca carbonate in this system. Several K- and Na-bearing double carbonates were observed in both the Na-carbonatite and K-carbonatite systems. The major phases observed in the experiments are (K,Na)₂Mg(CO₃)₂ and (K,Na)₂Ca₄(CO₃)₅. Low-degree partial melts are Na- and K-rich, for Na- and K-bearing carbonatite, respectively, due to early melting of double alkali carbonates.

According to solidi temperatures significant melting of subducting carbonates would likely occur at the transition zone depths. Taking into account the amount of subducted carbonated (1-2 wt.% CO₂) in the top 500 m of model slab we proposed a model for mobile carbonatite melt diapirs, generating from the slab in the transition zone, migrating upwards, modifying and oxidizing possibly reduced mantle section [2], precipitating diamonds, creating enriched source regions, and initiating volcanism at the surface.

[1] Litasov *et al.* (2013) *Geology* **41**, 79-82. [2] Rohrbach & Schmidt (2011) *Nature* **472**, 209-212.

Calculation of mass (im-)balance in the oceanic cycling of Cu and Zn isotopes

S.H. LITTLE^{1,2*}, D. VANCE^{1,2}, T. W. LYONS³
AND J. MCMANUS⁴

¹Bristol Isotope Group, School of Earth Sciences, University of Bristol, Bristol, UK.

²Now at: Institute of Geochemistry & Petrology, Dept. of Earth Sciences, ETH Zürich, Clausiusstrasse 25, 8092 Zürich, Switzerland. *susan.little@erdw.ethz.ch; derek.vance@erdw.ethz.ch

³Department of Earth Sciences, University of California, Riverside, USA. timothy.lyons@ucr.edu

⁴Oregon State University, College of Earth, Ocean & Atmospheric Sciences, 104 CEOAS Admin. Bldg., Corvallis, OR 97331-5503, USA. mcmanus@coas.oregonstate.edu

The stable isotope systems of the transition metals are increasingly being developed as tracers for the paleoenvironment. However, as yet, controls on their modern cycling in the oceans are little known. In particular, constraints on their modern oceanic mass balance are sparse [1].

We present best estimates for the fluxes and isotopic composition of Cu and Zn for the known oceanic inputs (rivers, aeolian dust) and outputs to sediments (in normal marine and anoxic settings), the latter based on estimates for Mo, with Cu/Mo or Zn/Mo ratios of different types of marine sediments [2, 3]. For both Cu and Zn, the sum of the known input fluxes is greater than that of the output fluxes, i.e. the cycles are out of balance. This imbalance is also observed in the isotope ratios of sources and sinks. For $\delta^{65}\text{Cu}$, we find flux-weighted outputs that are isotopically light (at $\sim 0.3\text{‰}$) compared to the inputs (at $\sim 0.6\text{‰}$). For $\delta^{66}\text{Zn}$ we observe the reverse, with a sink for Zn that is isotopically heavy (at $\sim 0.7\text{‰}$) compared to the input, the latter indistinguishable from detrital sediments (at $\sim 0.3\text{‰}$).

Taken at face value, these calculations require that the Cu and Zn cycles include an unidentified additional sink to achieve flux and isotopic mass balance. For Cu, this sink should be isotopically heavy (at ca. $+2\text{‰}$) while for Zn, a missing sink for light isotopes (at ca. -1‰) is implied. However, we consider these projected missing sink isotopic compositions to be implausible. Instead, we discuss the possibility of (an) additional source(s) of Cu and Zn, the presence of which would reduce the isotopic extremity of each missing sink. We suggest that one such source may be solubilisation of a portion of the large riverine particulate flux at the river-sea interface.

[1] Little, Vance, Landing & Walker Brown (submitted), *GCA*. [2] Morford and Emerson (1999), *GCA* **63**, 1735–1750. [3] McManus, Berelson, Severmann, Poulson *et al.* (2006), *GCA* **70**, 4643–4662.

Differentiation of the mantle ultrabasic-basic magmas and diamond-forming carbonatite melts on experimental evidence

YU.A. LITVIN

Institute of Experimental Mineralogy, Chernogolovka, Moscow Region 142432 Russia (litvin@iem.ac.ru)

Generalized melting diagram-complex of upper-mantle peridotite-eclogite system

The diagram-complex consolidates garnet peridotite Ol-Opx-Cpx-Grt and four eclogitic simplexes. Primary komatiitic magma is formed under control of invariant peritectic Ol+Opx+Cpx+Gr+L linked with olivine eclogite simplex by univariant Ol+Cpx+Grt+L curve. Peridotite and silica-saturated eclogite compositions are separated by Opx-Cpx-Grt plane. Peritectic points of peridotite and Coes-eclogites (Coes+Opx+Cpx+Gr+L) are linked by univariant Opx+Cpx+Grt+L curve. While piercing the Opx-Cpx-Grt plane, the curve has temperature maximum known as thermal eclogitic barrier [1]. The barrier represents an insuperable obstacles for ultrabasic-basic magma both equilibrium and fractional differentiation.

“Peridotite-to-eclogite tunnel” mechanism against the thermal eclogitic barrier

Fractional crystallization of primary komatiitic magma is accompanied by increasing concentration of jadeite component at residual melts. This activates mechanism of ultrabasic-basic magma differentiation with formation of continuous peridotite-eclogite series. By experimental data, the differentiation is controlled by reaction of Ol- and Jd-components above 4.5 GPa [2]. As result Ol is disappeared and Grt formed. Liquidus reaction point Ol+Jd-Cpx = Grt+L operates effectively in Ol elimination along the univariant curve Ol+Cpx+Grt+L that brings residual melts compositions into the Cpx-Grt join. The join is a commonplace for all the peridotite and eclogite simplexes. Here “peridotite-to-eclogite tunnel” mechanism is proved and makes the round the thermal eclogitic barrier. As a result, it paves the way for continuous fractional crystallization of ultrabasic-basic magmas and transfer from Ol-bearing peridotite to Coes-bearing eclogite rocks. Differentiation of the carbonatite melts parental for diamonds and primary inclusions.

By experimental evidence, a changeable composition of the carbonatite parental melts for diamond and inclusions is based on peridotite₃₀carbonatite₇₀-eclogite₃₅carbonatite₆₅-carbonatite system [3]. Differentiation of parental melts is controlled by “peridotite-to-eclogite tunnel” mechanism associated with carbonatization of peridotitic Mg-components. Fractional differentiation is responsible for formation of diamond-hosted mineral inclusions for peridotite and eclogite parageneses. *Support*: RFBR grant 11-05-00401.

[1] O’Hara (1968) *Earth-Sci. Rev* 4, 69-133. [2] Gasparik & Litvin (1997) *Eur. J. Mineral.* 9, 311-326. [3] Litvin *et al.* (2012) *Geochem. Internat* 9, 726-759.

Graphic method for estimating the biological absorption coefficient

YU.S.LITVINENKO

EcoGeoLit Ltd., Moscow, Russia (ecogoelit@mail.ru)

Fixed biological absorption coefficient values (A_x) as in relation of microelement contents in plants ashes to its content in the soil (Perelman, 1975) show overall biophilic qualities of chemical elements but not the accumulation dynamics in plants depending on the concentration of it in soil.

Such dynamics is shown on the plot of element concentration in plants ($\ln C_v$) against its concentration in the soil ($\ln C_s$).

A_x coefficients for selected intervals of Ni concentration in soils are tangents of the angle α between the graph and the x axis (fig. 1).

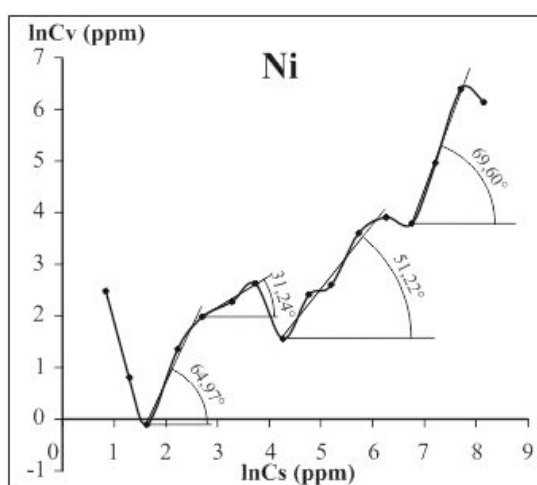


Figure 1: angle α of the plot of Ni concentration in moss against its concentration in the soil.

Cs, ppm	Cv, ppm	angle α	tg $\alpha = A_x$
< 5.2	12.0-0.9	barrier	
5.2-15.0	0.9-7.2	64.97°	2.14
15.0-41.8	7.2-13.7	31.24°	0.61
41.8-71.3	13.7-4.7	barrier	
71.3-524.3	4.7-49.7	51.22°	1.24
524.3-863.5	49.7-44.2	barrier	
863.5-2229	44.2-598.4	69.60°	2.69
>2229	<598.4	barrier	

Table 1: Selected Ni concentration intervals in soil (C_s) in accordance with Ni concentrations in moss (C_v) and A_x coefficients for these intervals.

A_x coefficient calculated on all the data as ratio of average C_v/C_s is equal to 0.2.

Upper Cretaceous Marine Source Rocks and its Contribution to Hydrocarbon Accumulations in Eastern Niger Basin, Niger

LIU BANG^{1*}, WAN LUNKUN², MAO FENGJUN³
AND LIU JIGUO⁴

¹ Research Institute of Petroleum Exploration & Development, PetroChina, Beijing, P.O. Box 910, China
(*correspondence: liubang@petrochina.com.cn)

² Research Institute of Petroleum Exploration & Development, PetroChina, Beijing, P.O. Box 910, China
(wanlunkun@petrochina.com.cn)

³ Research Institute of Petroleum Exploration & Development, PetroChina, Beijing, P.O. Box 910, China
(maofengjun@petrochina.com.cn)

⁴ Research Institute of Petroleum Exploration & Development, PetroChina, Beijing, P.O. Box 910, China
(ljiguo@petrochina.com.cn)

The Eastern Niger Basin is a typical Mesozoic-Cenozoic intracontinental rift basin of the Central and Western African rift system, including Tenere and Termit depression. Using techniques of kerogen maceral analysis, rock pyrolysis and GC-MS for mudstone cuttings from Yogou and Donga formation of the Upper Cretaceous, this study investigates the origin, abundance, type and thermal maturity of organic matter. Kerogen macerals are dominated by amorphinite displaying no or weak fluorescence, and rock extracts have a regular sterane distribution of $C_{29} > C_{27} > C_{28}$. These characteristics suggest that the organic matter of the Upper Cretaceous mudstones originated mainly from land-derived plants. Rock-Eval pyrolysis data reveals that the Yogou Formation of the Upper Cretaceous generally have moderate to good hydrocarbon potential with kerogen predominantly Type II₂-III, while the Donga Formation are mainly bad-moderate source rocks with type III kerogen. T_{max} values indicate that the threshold depth for hydrocarbon generation of source rocks is about 2300m. Three-dimensional modeling of hydrocarbon generation suggests that petroleum in marine source rocks began to be generated in the Early Palaeocene. Peak generation took place from the Late Eocene to Early Miocenes, with thermally mature area covering most of the basin. Geochemical results of crude oils show that the majority of oil samples are characterized by Pr/Ph ratios below 1.5, high relative abundance of β -carotane and gammacerane, and dominance of C_{29} steranes over C_{27} steranes. Geochemical correlation analysis of oil and rock samples indicates that most of oils from the Eastern Niger basin were probably derived from the Upper Cretaceous marine source rocks.

Sr and Mg isotopes of Marinoan Cap dolostones: implication for glacial lake Harland?

CHAO LIU¹, FRANCIS MACDONALD²,
ZHENGRONG WANG¹ AND TIMOTHY RAUB³

¹ Yale University, New Haven, CT, USA, chao.liu@yale.edu, zhengrong.wang@yale.edu

² Harvard University, Boston, MA, USA, fmacdon@fas.harvard.edu

³ University of St. Andrews, St. Andrews, Scotland, UK, timraub@st-andrews.ac.uk

Marinoan cap dolostones have been suggested to be formed in a lid of glacial-melt water on top of normal seawater (i.e., the “glacial lake Harland”, [1]), which needs to be tested geochemically. In this study, Sr and Mg isotopes of the cap dolostones were investigated from three sections of Marinoan cap dolostones: Hay Creek Group (Canada), Ol member (Mongolia), and Nuccaleena formation (Australia). An incremental leaching technique [2] has been applied to these samples, in order to understand their diagenetic history and to constrain the Sr and Mg isotope compositions of penecontemporaneous seawater. Cap dolostones from Nuccaleena formation can be categorized into two groups based on their chemistry. Group-I samples are located in the bottom and top parts of the section, exhibiting $^{87}\text{Sr}/^{86}\text{Sr}$ values (~ 0.7075) similar to previously reported Marinoan seawater values [3], and $\delta^{26}\text{Mg}_{\text{DSM3}}$ increasing upwards from -2.14% to -1.75% . Group-II samples are located in the middle part of the section, with elevated $^{87}\text{Sr}/^{86}\text{Sr}$ values (average of 0.7092 ± 0.0003) and $\delta^{26}\text{Mg}_{\text{DSM3}}$ values (average of $-1.71 \pm 0.05\%$). For Mongolian cap dolostones, all samples exhibit similar $^{87}\text{Sr}/^{86}\text{Sr}$ values (average of 0.7091 ± 0.0001) and $\delta^{26}\text{Mg}_{\text{DSM3}}$ values (average of $-1.63 \pm 0.05\%$) to group-II Australian cap dolostones. For Canadian cap dolostones, more elevated $^{87}\text{Sr}/^{86}\text{Sr}$ values (higher than 0.7200) are observed. However, they share similar $\delta^{26}\text{Mg}_{\text{DSM3}}$ values ($\sim -1.60\%$) to Mongolian samples and group-II Australian samples. These geochemical variations could be explained by glacial lake Harland model, i.e., the cap dolostones from Nuccaleena formation recorded seawater signals before, during and after the stage of glacial lake Harland, whereas those from Mongolia and Canada are formed exclusively during the stage of glacial lake Harland. However, other possibilities cannot be ruled out.

[1] Hoffman (2011) *Sedimentology* 58, 57-119. [2] Liu *et al.*, *Chemical Geology*, under review. [3] Halverson *et al.*, (2007) *PALEO* 256, 103-129.

The Paleoproterozoic basin evolution in the Trans-North China Orogen, North China Craton

CHAOHUI LIU¹ AND GUOCHUN ZHAO²

¹ Institute of Geology, Chinese Academy of Geological Sciences, Beijing 100037, China denverliu82@gmail.com

² Department of Earth Sciences, The University of Hong Kong, Pokfulam Road, Hong Kong, gczhao@icloud.com

The Trans-North China Orogen (TNCO) has been recognized as a continent-continent collisional belt along which the Eastern and Western Blocks amalgamated to form the North China Craton. However, controversy has surrounded the timing and tectonic processes involved in the collision of the two blocks, ranging from the westward-directed subduction with final collision at ~ 2.5 Ga to the eastward-directed subduction with final collision at ~ 1.85 Ga. Detailed lithostratigraphic and geochronological analyses for the low-grade supracrustal successions in the TNCO has been carried out recently, which help us to examine current models. Lithostratigraphic data indicate that the Gantaohu, Jiangxian and Lower Zhongtiao Groups and lower parts of the Hutuo and Yejishan Groups are composed of metaclastic rocks, carbonates and metavolcanic rocks, interpreted as back-arc basin deposits, whereas the Dongjiao, Upper Zhongtiao, Danshanshi Groups and the upper parts of the Hutuo and Yejishan Groups consist only of metaconglomerates and metasediments, interpreted as foreland basin deposits. For the Gantaohu, Hutuo and Yejishan Groups, we found major age U-Pb age peaks of detrital zircons at ~ 2.5 and ~ 2.15 Ga, which are consistent with ages of the lithological units in the middle sector of the TNCO. Besides the age peaks of ~ 2.5 Ga and ~ 2.15 Ga, detrital zircons from the Lower Zhongtiao, Upper Zhongtiao and Danshanshi Groups also gave an older age peak of 2.7 Ga, which is comparable with ages of the lithological units in the Taihua Complex. For the back-arc basin deposits, their maximum depositional ages were constrained at ~ 2.1 Ga, whereas the presence of ~ 1.85 Ga detrital zircons from the foreland basin deposits indicates that they were deposited after this time. At ~ 2.1 Ga, back-arc basins developed behind an “Andean-type” arc that were subsequently incorporated into the TNCO during the later collision. At ~ 1.85 Ga, the two blocks collided along the TNCO, resulting in the crustal thickening followed by rapid exhumation/uplift, which shifted the back-arc basins to foreland basins. Such a shift in the late Paleoproterozoic supports the model that the collision between the Eastern and Western Blocks occurred at ~ 1.85 Ga.

Existence of elevated $\delta^{18}\text{O}$ values in the lithospheric mantle: evidence from olivines in Sailipu mantle xenoliths, Tibet

CHUAN-ZHOU LIU¹, FU-YUAN WU¹ AND QIU-LILI

¹Institute of Geology and Geophysics, Chinese Academy of Sciences, 100029, Beijing.
chzliu@mail.iggcas.ac.cn

In southern Tibet Plateau, post-collisional Sailipu ultrapotassic lavas erupted at ca. 17 Ma entrain peridotite xenoliths of small sizes (<1 cm). It has been suggested that the Sailipu mantle xenoliths were derived from a relic of the thickened Asian lithospheric mantle, the lower portion of which has been delaminated by convective removal [1]. Clinopyroxene trace-element compositions, together with the ubiquitous presence of phlogopite, support that the Sailipu mantle xenoliths have been metasomatized by fluids/melts liberated from the subducted Neo-Tethys Ocean [1].

Olivines separated from Sailipu peridotite xenoliths have been analyzed for oxygen isotope using secondary ion mass spectrometry (SIMS). The studied olivines have Fo contents of 88–91, containing 0.04–0.08 wt.% CaO and 0.38–0.55 wt.% NiO. Such compositional characteristics are in stark contrast with olivine phenocrysts crystallized from the host lavas (Fo_{69–81}, 0.14–0.47 wt.% CaO and 0.13–0.28 wt.% NiO). Olivines in each sample display homogeneous oxygen isotope compositions, as both inter- and intra-grain variations are always less than the precision of the method (i.e., ~ 0.5‰). Olivines from eight samples with Fo of 87.7–89.1 have similar $\delta^{18}\text{O}$ values ranging from 5.22‰ to 5.41‰, which are well within the range of the upper mantle (5.18 ± 0.28‰) defined by olivines in mantle xenoliths from various settings [2]. In comparison, olivines from one sample with a Fo content of ~ 91.3 has the highest $\delta^{18}\text{O}$ values ranging from 7.42‰ to 8.92‰ (with an average of 8.03 ± 0.28‰), which are remarkably higher than the upper mantle values. Such heavy oxygen isotopes could result from metasomatism by slab-released fluids or melts, which commonly have elevated $\delta^{18}\text{O}$ values. Therefore, our results support the existence of high oxygen isotopes, at least locally, in the lithospheric mantle.

[1] Liu, C.Z. *et al.*, 2011. *Geology*, 39, 923–926. [2] Matthey *et al.*, 1994. *EPSL*, 128, 231–241.

Multiple metamorphic events hidden in zircons from the Sanjiang complex belt, southeastern Tibetan Plateau

F.L. LIU, F. WANG, P.H. LIU AND C.H. LIU¹

¹Institute of Geology, Chinese Academy of Geological Sciences, Beijing, 100037, China

Analyses of mineral inclusions within complexly zoned zircons, combined with SIMS U–Pb ages for various domains within the zircons, provide evidence of the origin and multistage metamorphic evolution of the Sanjiang complex, southeastern Tibetan Plateau. Metamorphic zircons with high-pressure (HP) mineral inclusions in paragneisses, amphibolites and garnet pyroxenites, suggest they are formed at 650–720°C and ~14 kb. These HP zircons yield U–Pb ages of 249–230 Ma, indicating an Early–Middle Triassic HP metamorphic event within the Sanjiang complex belt. Two groups of Eocene–Oligocene metamorphic zircons are also present. One of the groups comprises homogeneous zircons containing medium-pressure (MP) amphibolite–granulite facies mineral inclusions in paragneisses, amphibolites, and marbles. These assemblages are stable at peak P–T conditions of 720°C–760°C and 8.0–9.6 kb, and yield consistent Eocene ages (44–36 Ma). The second group is homogeneous and all zircons contain distinct low-pressure (LP) mineral inclusions in paragneisses, amphibolites and garnet pyroxenites, and marbles, recording post-peak P–T conditions of 700°C–750°C and 5.0–6.5 kb, and yielding younger Oligocene metamorphic ages (32–25 Ma). ⁴⁰Ar/³⁹Ar analyses of biotite, muscovite, and amphibole yield the youngest ages (25–14 Ma, Miocene) related to late cooling during retrogressive metamorphism under conditions of 520°C–620°C and 4.0–4.5 kb. These new data suggest a clockwise P–T–t path for the Sanjiang metamorphic complex, typical of continent–continent collision, indicating collision–subduction tectonism prior to the strong, left-lateral, ductile deformation along the Ailao Shan–Red River (ASRR) shear zone that started at ~32 Ma and lasted until 25 Ma, causing mid-crustal (18–25 km depth) high-temperature metamorphic conditions. Continued uplift, and a slowing of left-lateral ductile shearing occurred at ~25–14 Ma at a depth of 10–15 km and under relatively low-temperature conditions. This temporal and kinematic link between left-lateral shearing along the ASRR and the opening of the South China Sea supports the occurrence of the block extrusion of Indochina from Eurasia along lithospheric-scale strike-up faults.

Oxidization of chalcopyrite Mediated by *Acidithiobacillus ferrooxidans* and secondary minerals

HUAN LIU^{1*}, XIANCAI LU¹, BINGJIE OUYANG¹, XIANGYU ZHU¹, JUAN LI¹ AND JIANJUN LU¹

¹School of Earth Sciences and Engineering, Nanjing University, Nanjing, China, huanliu.earth@gmail.com (* presenting author)

Chalcopyrite is one of the most abundant copper mineral. The microbial oxidization of chalcopyrite in mining wastes is an important pathway for the release of heavy metals into surrounding environments. We performed an bath experiment to disclose the mechanism of chalcopyrite- *Acidithiobacillus ferrooxidans* in this study.

A strain of *Acidithiobacillus ferrooxidans* isolated from acid mine drainage of Shizishan Cu-Au mineral deposit, eastern China, was used to interact with hand-selected chalcopyrite particles from sulfide ores in this study. *A. ferrooxidans* were inoculated into three flasks each contains 300 mL sterilized 9K culture with 17 mM Fe²⁺. Other flasks with same volumetric 9K culture were control groups without inoculation. After reacting for 5 days, 10 days and 20 days, samples were extracted and lyophilized for SEM observation and spectral analysis (FTIR, XRD, Raman and XPS). STXM coupled with NEXAFS analyzed the distribution of Fe and Cu in/on the cell. As for the reacted solution, ICP-OES was employed to determine the concentrations of Cu and Fe, while Ion Chromatography (IC) to measure the contents of S₂O₃²⁻, SO₃²⁻ and SO₄²⁻.

The results reveal the enhancement of oxidation of chalcopyrite by microbial mediation. Surface etching attributed to the adhesion of the cells on chalcopyrite results in various pits on chalcopyrite surface. Jarosite and elemental sulfur were identified as main secondary minerals. The concentration of Cu in solution increased in the beginning reaction days and decreased a little subsequently because of adsorption onto and coprecipitation into Fe(III) sulfate minerals. Base on the depth profiles of XPS analysis of reacted chalcopyrite particles, detailed information of oxidization processes of Cu, Fe and S can be acquired. From the surface to the depth, the content of Fe(III) decreases and Fe(II) increases. S was presented as sulfate and sulfur in the surface, and contents of reduced states increase in the deep. According the variation of their chemical states, the chemical mechanism behind the microbial oxidation was discussed, which will highlight the study on bioleaching technology for the processing of low-grade copper sulfide ores.

Acknowledgement

We appreciate the supports from the National Natural Science Foundation of China (Grant No. 40930742, 41272056).

Control of gypsum-salt rock on source rock and reservoir in the Dongpu depression of Bohai gulf basin, eastern China

JINGDONG LIU^{1*} AND YOULU JIANG²

¹Wuxi Research Institute of Petroleum Geology, SINOPEC, Wuxi 214151, China
(*correspondence: ljd840911@126.com)

²School of Geosciences, China University of Petroleum, Qingdao 266555, China (upcyj@126.com)

Source rocks and gypsum-salt rocks of Dongpu depression distribute alternately in vertical, overlay in horizontal, which have a symbiotic relationship[1,2]. The source rocks in gypsum-salt and sand-shale transition zone have the highest organic matter abundance, and the nearer the distance from gypsum-salt rocks, the higher organic matter abundance the source rocks have. Organic matter types of source rocks in gypsum-salt zone and transition zone are mainly type I and type III Kerogen, while that in sand-shale zone are mainly type II1 and type II2 Kerogen. For the role of high thermal conductivity of gypsum-salt rocks, source rocks in the upper part of which has shallower threshold depth for oil generation, and that in lower part has deeper threshold depth, that effectively expand the scope of the hydrocarbon generation window.

Sandstone in Dongpu depression is interfingered with gypsum-salt rocks in space[1]. By the compactness and high thermal conductivity of gypsum-salt rocks, the porosity of sandstone in the lower part of gypsum-salt rocks has larger porosity than normal sediment stratum. By the carbonate cementation and gypsum and salt rock grain infiltration, the porosity of sandstone in the lower part of gypsum-salt rocks performs first increases and then decreases with increasing depth, and the maximum porosity appears within a certain distance in the lower part of the gypsum-salt rocks..

[1] Du Haifeng, *et al.* (2008) *Journal of Palaeogeography*, 1,53-62. [2] Wang Dongxu, *et al.* (2005) *Natural Gas Geoscience*, 3,329-333.

Age of the Kelameili ophiolite in Eastern Tianshan: LA-ICP-MS U-Pb zircon Dating

JUNFENG LIU* AND YONG LI

School of Earth Science and Resources, Chang an University, Xi'an 710054, China (*correspondence: junfengliu@chd.edu.cn)

Being an important complex unit along the Kelameili default, Kelameili ophiolite mainly consists of serpentized peridotite, pyroxenite, gabbro and silicolite, etc. It is located between the eastern Junggar (the North) and a southward subduction zone beneath the eastern Tianshan; the latter is defined by the Harlik-Danahu arc in the eastern Qinling Mountains, West China [1,2].

Determining the time of the Kelameili ophiolite is very important for understanding the evolution of Eastern Tianshan area. Previous dating results however, range from late Devonian to early Permian, displaying a large span. That led to various models to reconstruct the Tianshan orogenic belt in early Paleozoic.

Here we show LA-ICP-MS dating results for single zircon grains of gabbro from the Kelameili ophiolite, which yield 352 ± 3 Ma. Those zircon grains are small in size (30-100 μ m) and idiomorphic. Cathodoluminescence images show obvious magmatic oscillatory zoning. The U and Th concentrations vary from 30ppm to 278ppm, with high Th/U ratios (> 0.3), also suggesting their typical magmatic origins. The new-determined age definitely indicates that the gabbro from the Kelameili ophiolite was formed in the early Carboniferous, which gives a valid constrain on the formation of the Kelameili ophiolite.

This work is supported by the Fundamental Research Funds for the Central Universities (CHD2010JC042).

[1] Ma *et al.* (1997) *House of Nanjing Univ.*, 2, 25. [2] Xiao *et al.* (2004) *J. Geol. Soc.*, London, 161, 339-342.

Petrology, P-T-t path, and geotectonic significance of high-pressure mafic granulites from the Jiaobei terrane, North China Craton

PINGHUA LIU, FULAI LIU¹, FANG WANG, JIANHUI LIU, HONG YANG, JIA CAI AND JIANRONG SHI

Institute of Geology, Chinese Academy of Geological Sciences, Beijing 100037, China (lph1213@126.com)

High-pressure (HP) mafic granulites in the Jiaobei terrane are composed predominantly of garnet-bearing mafic granulites, garnet-hypersthene granulites, and garnet amphibolites, and they are found as irregular lenses or deformed parallel dykes within tonalitic-trondhjemitic-granodioritic gneisses or granitic gneisses. The HP mafic granulites contain four distinct metamorphic assemblages of which the early prograde assemblage (M_1) is represented by the cores of garnets, together with mineral inclusions of clinopyroxene + plagioclase \pm quartz, and it formed at 740–770 °C and 0.90–1.00 GPa. In contrast, the peak assemblage (M_2) consists of high-Ca cores in garnet, high-Al cores in clinopyroxene, and high-Na cores plagioclase in the matrix, which formed under P-T conditions of 850–880 °C and 1.45–1.65 GPa. The peak metamorphism was followed by near-isothermal decompression (M_3), which resulted in the development of orthopyroxene + clinopyroxene + plagioclase \pm quartz \pm amphibole \pm magnetite symplectites or coronas surrounding some garnet grains with P-T conditions of 780–830 °C and 0.65–0.85 GPa. Surrounding some garnet grains are symplectites of amphibole + plagioclase + quartz \pm magnetite, which formed during a cooling retrograde stage (M_4) with P-T conditions of 590–650 °C and 0.62–0.82 GPa. The combination of petrography, mineral compositions, metamorphic reaction history, thermobarometry, and geochronology defines a near-isothermal decompressional clockwise P-T path for the Jiaobei HP mafic granulites, suggesting that the Jiaobei terrane underwent initial crustal thickening, followed by relatively rapid exhumation, cooling, and retrogression. This tectonothermal path was probably generated by subduction and collision-related tectonic processes.

This study was financially supported by the Nation 973 Project of Chinese Ministry of Science and Technology (grant no. 2012CB416603), the Basic Scientific and Research Foundations of institute of Geology, Chinese Academy of Geological Sciences (grant no. J1212)

Iron isotope systematics of the Baima magmatic Fe-Ti(V) oxide deposit, SW China

PING-PING LIU¹, MEI-FU ZHOU²,
BÉATRICE LUIS³, DAMIEN CIVIDINI⁴
AND CLAIRE ROLLION-BARD⁵

¹The University of Hong Kong, Hong Kong, China,
liupp@hku.hk

²The University of Hong Kong, Hong Kong, China,
mfzhou@hkucc.hku.hk

³CRPG, Nancy, France, luais@crpg.cnrs-nancy.fr

⁴CRPG, Nancy, France, cividini@crpg.cnrs-nancy.fr

⁵CRPG, Nancy, France, rollion@crpg.cnrs-nancy.fr

The Baima oxide-bearing mafic-ultramafic layered intrusion, SW China, provides an excellent opportunity to examine the controls of high temperature fractionation of Fe isotopes. The intrusion consists of a Lower zone of net-textured and disseminated oxide ores, a Middle zone of olivine gabbro and an Upper zone of gabbro. Fe isotopes (IRMM-014-normalized) have been measured by high-resolution MC-ICPMS (Neptune Plus) at the CRPG-Nancy, with a 2 sigma reproducibility of $\leq 0.08\text{‰}$ [1]. Olivine has $\delta^{56}\text{Fe}$ values ranging from -0.01 to $+0.11\text{‰}$, clinopyroxene from $+0.11$ to $+0.22\text{‰}$ and titanomagnetite from $+0.20$ to $+0.51\text{‰}$. In $\delta^{56}\text{Fe}_{\text{Cpx}}-\delta^{56}\text{Fe}_{\text{Ox}}$ diagram, Baima samples plot on the primitive mantle end member of the mantle metasomatism trend, indicating the parental magma of the Baima intrusion is the partial melting equivalent of the mantle rocks. Fe isotopes of titanomagnetite-clinopyroxene and titanomagnetite-olivine pairs do not display linear correlations, strongly against simple fractional crystallization model.

Positive correlations of whole-rock TFe_2O_3 vs. $\delta^{56}\text{Fe}$ values of olivine, roughly constant $\delta^{56}\text{Fe}$ values of titanomagnetite from net-textured and disseminated oxide ores and an abrupt break of TFe_2O_3 content and $\delta^{56}\text{Fe}_{\text{Mt}}$ between oxide ores and mafic rocks would indicate that mechanisms for the Fe-Ti oxide ore genesis depend on the oxidation state of the magma chamber. Oxygen fugacity variations inferred from V contents of titanomagnetite indicate that the crystallization of low $\delta^{56}\text{Fe}$ titanomagnetite occurred firstly from a high $f\text{O}_2$ liquid, followed by the $f\text{O}_2$ dropped to the lowest with crystallisation of high $\delta^{56}\text{Fe}$ titanomagnetite on olivine gabbro and gabbro.

These results indicate the strong control of redox state of the magma on Fe isotopic signatures.

[1] Johanna (2011), *Chem. Geol.* **285**, 50-61

Anharmonic effects of equilibrium clumped isotope signatures for H_2O , H_2S , SO_2 , NH_3 and CH_4

QI LIU AND YUN LIU*

Institute of Geochemistry, Chinese Academy of Sciences
(*correspondence: liyun@vip.gyig.ac.cn)

Geological application of clumped isotope techniques has been broadened, but the studied objects mainly remain CO_2 , or O_2 . There is an urgent need to include other species into the inventory of clumped isotope geochemistry. In this study, we provide equilibrium Δ_i values of several common gaseous molecules which can be potential targets for the clumped isotope study in future. For improving the calculation accuracy, theoretical treatments beyond the harmonic level by including several higher-order corrections to the Bigeleisen-Mayer equation are used. We have evaluated contributions from many higher-order corrections (e.g., AnZPE, AnEXC, VrZPE, VrEXC, QmCorr and CenDist) to calculate the anharmonic effects of vibration, vibration-rotation coupling, quantum mechanics and centrifugal distortion for rotation, etc., which are ignored in the Bigeleisen-Mayer equation for the calculation of reduced partition function ratios. All calculations are performed at MP2/aug-cc-pVTZ level and no frequency scale factor has been used. The computational details of these higher-order corrections can be found in [1].

Our results provide detailed temperature dependencies of clumped isotope signatures of those molecules. We also find AnZPE is the most significant correction at room temperature. VrZPE plays second important role at room temperature, but may contribute equally important to AnZPE at higher temperature. Other corrections can contribute a little only if hydrogen atom is involved. With the increase of temperature, contributions of AnEXC, VrEXC and CenDist will become larger; contributions from AnZPE and QmCorr will become smaller. Our results suggest anharmonic corrections can significantly improve the estimation of clumped isotope signatures especially when hydrogen atom is in the clumps (e.g., H_2O , H_2S , NH_3 and CH_4). Higher-order anharmonic corrections are therefore recommended to the theoretical study of clumped isotope fractionations.

[1] Liu, Tossell and Liu (2010) *Geochim. Cosmochim. Acta* **74**, 6965-6983.

Which ligand is the most important for gold transport in hydrothermal fluids? An *in situ* XAS study in mixed-ligand solutions

WEIHUA LIU¹, BARBARA ETSCHMANN^{2,4},
DENIS TESTEMALE⁵, YUAN MEI^{1,3},
JEAN-LOUIS HAZEMANN⁵, KIRSTEN REMPEL⁶,
HARALD MÜLLER⁷ AND JOËL BRUGGER^{2,3}

¹ CSIRO Earth Science and Resource Engineering, Australia, (weihua.liu@csiro.au)

² South Australian Museum, Australia

³ School of Earth and Environmental Sciences and ⁴School of Chemical Engineering, University of Adelaide, Australia

⁵Institut Néel, Département MCMF and FAME beamline, ESRF, France

⁶Department of Applied Geology, Curtin University, Perth, Australia

⁷ESRF, Grenoble, France

Gold transport and deposition in hydrothermal ore fluids is dependent on the identity and stability of predominating aqueous gold complexes. Gold(I) bisulfide (e.g., Au(HS)₂) and in some instances Au(I) chloride complexes are widely acknowledged to account for Au transport in ore fluids.

This study investigates the potential of the unconventional ligands Br⁻ and NH₃ to increase Au mobility. This was achieved by determining the predominant Au species in hydrothermal fluids with binary mixed ligands (Br⁻ - Cl⁻, Br⁻ - HS⁻, HS⁻ - NH₃), and measuring their structural properties using *in situ* Synchrotron X-ray Absorption Spectroscopy (XAS). The capacity of XAS to follow the progress of ligand exchange reactions was demonstrated at room temperature, where the Au(III)Br₄⁻ complex was found to predominate in mixed Br⁻/Cl⁻ solutions (Br⁻/Cl⁻ = 0.1-1), with average ligand numbers derived from XAS in good agreement with a recent UV-Vis study (Usher *et al.*, 2009, *Geochim. Cosmochim. Acta* 73, 3359-3380). At temperatures up to 400 °C and at 600 bar, the XAS measurements show that Au(I) - HS⁻ complexes are the only stable Au species in mixed HS⁻/Br⁻ and HS⁻/NH₃ fluids (HS⁻/Br⁻ = 0.1; HS⁻/NH₃ = 0.2), indicating that hydrosulfide is the most important ligand for Au transport in the hydrothermal fluid under our experimental conditions, i.e., hydrosulfide complexes outcompete bromide and ammine complexes in S-bearing fluids. These results are comparable to solubility and speciation calculations based on the available thermodynamic data.

Li isotope geochemical study on weathering of granite in Longnan, Jiangxi Province, South China

W.J. LIU¹, C.Q. LIU^{1,2*}, Z.Q. ZHAO², T. ZHAO¹,
Z.F. XU¹, T.Z. LIU² AND L. HUANG²

¹Institute of Geology and Geophysics, Chinese Academy of Sciences, Beijing 100029, China

(*correspondence: liucongqiang@vip.skleg.cn)

² Institute of Geochemistry, Chinese Academy of Sciences, Guiyang, Guizhou, 550002, China

Li isotope has been newly demonstrated to be a powerful tool in studying silicate weathering in a weathering profile, catchment, and even continental scale. In this study, we focus on variation in Li isotope geochemical features along soil and weathering profiles of three sites along a mountain ridge slope, which was developed on granite in Longnan, Jiangxi Province, South China. The studied profiles include JLN-S4 (mountain top, 120 cm deep soil profile); JLN-S3 (middle slope, 120 cm deep soil profile); and JLN-S1 (valley floor, about 1100 cm deep weathering profile). Li content and δ⁷Li of bulk samples, along with major element composition and CIA (chemical index of alteration) values of the bulk samples from weathering and soil profiles were determined.

JLN-S4 profile samples have CIA values between 97.63 and 98.32, with δ⁷Li values from -2.50‰ to -3.90‰; JLN-S3 profile samples have CIA values varying from 94.42 to 96.12 and δ⁷Li values from -0.73‰ to -1.55‰; The weathering profile JLN-S1 at valley floor has a generally descending CIA values (57.77~92.44) with increasing depth. Its δ⁷Li values vary with CIA, showing a two stage relationship: persistent increase from -14.92‰ to 0.66‰ when CIA increasing from 57.77 to 74.56, and δ⁷Li variation in a range of -4.74~3.62‰, with no obvious relationship with CIA change. Li contents in JLN-S4 vary between 3.84 and 15.03 µg/g, in JLN-S3 between 1.43~8.03 µg/g, and in JLN-S1 between 6.95~22.27 µg/g. In JLN-S1, Li contents decrease with increasing CIA (57.77~74.56), no regular tendency in Li abundance was observed in samples with higher CIA values. Two granite bedrock samples have δ⁷Li value of -0.23 and 0.39‰, Li abundances of 38.58 and 34.22 µg/g, respectively.

The Li isotope geochemical features of the profiles in this study indicate that Li isotope behavior was dominantly determined by weathering extent during incipient weathering of granite, while much complicated factors, such as mineral phases, adsorption and desorption of different clay minerals control Li isotope geochemical features as weathering and pedogenesis progressing.

pH-Eh diagram of ore-forming elements from first principles molecular dynamics simulations

XIANDONG LIU^{1,2}, MICHIEL SPRIK², JUN CHENG²,
XIANCAI LU¹ AND RUCHENG WANG¹

¹ State Key Laboratory for Mineral Deposits Research, School of Earth Sciences and Engineering, Nanjing University, Nanjing 210093, P. R. China

² Department of Chemistry, University of Cambridge, Cambridge CB2 1EW, United Kingdom

pH-Eh diagram maps out the stable species of an aqueous electrochemical system with respect to the activity of proton and electron under a certain T-P condition. Such diagram presents the fundamental properties of aqueous species, which is very useful for understanding numerous natural processes, such as transport and enrichment of elements. Research of aqueous speciation has heavily relied on solubility experiments and related thermodynamics calculations. Due to the experimental difficulty in high T-P conditions, first principles molecular dynamics (FPMD) simulations have been attracting more and more attentions.

FPMD based vertical energy gap method was an advanced technique developed recently by our group (Adriaanse *et al.*, 2012; Costanzo *et al.*, 2011), which combines electronic structure calculation, MD and free energy perturbation theory. With this method, one can evaluate the ingredients for making pH-Eh diagrams of aqueous complexes: acidity (pKa) and redox potential (pE). In this presentation, we will show the results of important ore-forming elements. The pKa case studies include $\text{H}_2\text{S}_0/\text{HS}_n^-$, Zn^{2+} and Cu^{2+} . The calculated redox couples are $\text{Cu}^+/\text{Cu}^{2+}$ and $\text{Fe}^{2+}/\text{Fe}^{3+}$. Comparisons between the calculated and experimental values indicate a reasonable accuracy. Origins of the error such as density functionals and finite size effects will be discussed.

[1] Adriaanse C., Cheng J., Chau V., Sulpizi M., VandeVondele J. and Sprik M. (2012) Aqueous Redox Chemistry and the Electronic Band Structure of Liquid Water. *Journal of Physical Chemistry Letters* **3**: 3411-3415. [2] Costanzo F., Sulpizi M., Della Valle R.G. and Sprik M. (2011) The oxidation of tyrosine and tryptophan studied by a molecular dynamics normal hydrogen electrode. *Journal of Chemical Physics* **134**.

Roles of NH_4NO_3 and secondary organics in growing > 10 nm new particles to cloud condensation nuclei size in marine atmosphere

XIAOHUAN LIU, YUJIAO, ZHU, HE MENG,
GAO HUIWANG AND YAO XIAOHONG

¹ Key Laboratory of Marine Environment and Ecology, Ministry of Education of China, Ocean University of China, Qingdao 266100, China

A Fast Mobility Particle Sizer was used to investigate new particle formation events over the marginal Sea in China during two cruise experiments in the falls of 2010 and 2011. New particles cannot grow over 30 nm in three out of four new particle formation events in 2010. The air quality modeling results showed that formation of secondary organics (SO) occurred through the events, formation of NH_4NO_3 was thermodynamically forbidden. SO was likely the major contributor to the growth of > 10 nm new particles. In one event, new particles grew over 50 nm (the threshold of particle acting as cloud condensation nuclei (CCN)) and the modeling results showed formation of NH_4NO_3 and SO being concurrently with the growth of > 10 nm new particles. However, the formation rate of SO in the event was significantly less than that in one out of the three events. Formation of NH_4NO_3 was probably the key factor in growing > 30 nm new particles to CCN size and formation of SO may play an important role in growing particles <30 nm. In 2011, a regional nucleation event was observed in the marine and coastal atmosphere and formation of NH_4NO_3 was identified from the modeling and was probably the key factor in growing > 30 nm new particles to CCN size.

A mineralogical record of metallogeny associated with supercontinent assembly

XIAOMING LIU¹, ROBERT M. HAZEN¹,
ROBERT T. DOWNS², JOSHUA GOLDEN²,
EDWARD S. GREW³, GRETHE HYSTAD⁴
AND DIMITRI A. SVERJENSKY^{1,5}

¹Geophysical Laboratory, Carnegie Institution of Washington,
5251 Broad Branch Rd NW, Washington DC 20015 USA.
E-mail: xliu@ciw.edu

²Department of Geosciences, University of Arizona, 1040 East
4th Street, Tucson, Arizona 85721-0077, USA.

³Department of Earth Sciences, University of Maine, Orono,
Maine 04469, USA.

⁴Department of Mathematics, University of Arizona, Tucson,
Arizona 85721-0077, USA

⁵Department of Earth & Planetary Sciences, Johns Hopkins
University, Baltimore, Maryland 21218, USA.

Analyses of temporal and geographic distributions of the minerals of beryllium, boron, copper, mercury, and molybdenum reveal episodic deposition and diversification [1-4]. We observe statistically significant increases in the number of reported mineral localities and/or the appearance of new mineral species at ~2.85-2.6, ~1.95-1.80, ~1.10-0.90, ~0.60-0.50, and ~0.43-0.25 Ga—intervals that correlate with presumed episodes of supercontinent assembly and associated collisional orogenies of Kenorland (Superia), Columbia (Nuna), Rodinia, Godwana (Pannotia), and Pangea, respectively. In contrast, few deposits or new mineral species containing these elements have been reported from the intervals of supercontinent stability and breakup at ~2.5-1.9, ~1.8-1.2, 0.9-0.6, and 0.50-0.43 Ga. Variations in the details of these trends may reveal changing near-surface environments, including those associated with ocean chemistry and biological influences. For example, no mercury mineral localities or new Hg minerals are documented from 1.8-0.6 Ga. By contrast, we observe pulses of 14 new beryllium minerals associated with peralkaline complexes in southwest Greenland at 1.16 and 1.27 Ga.

[1] R.M.Hazen *et al.* (2012) Mercury (Hg) mineral evolution. *American Mineralogist* 97, 1013-1042. [2] E.S.Grew & R.M.Hazen (2010) Evolution of boron minerals. *Geological Society of America Abstracts with Programs* 42, 92. [3] E.S.Grew & R.M.Hazen (2013) Evolution of the minerals of beryllium. Stein, in press. [4] J.Golden *et al.* (2013) Rhenium variations in molybdenite. *Earth and Planetary Science Letters*, in press.

The Study of Metallogenic Model of Super-Thin Alteration-Type Gold Deposit on XiongEr Mountains in Western Henan Province, China

YAJIAN LIU¹, YUNKE CHEN² AND WANSHAN LEI^{2,3*}

¹Department of mineral exploration, Henan Huatai Zijin Mining Industry Co., Ltd, LuoYang, 471700, China
(*correspondence: liu_yajian@yahoo.com.cn)

²College of Earth Science and Land Resources, Chang'an University, Xi'an 710054, China
(*correspondence: lws198255@gmail.com)

³Key Lab of Western China's Min Resources and Geological Engineering, Ministry of Education, Xi'an 710054, China

The gold deposit is on the north hillside of Xiong'er mountain in Luoning county, Henan province, which belongs to the southern margin of north China platform. Taihua mountain group in Archeozoic is crystalline basement, both Xiong'er mountain group and Nantianmen mountain group are sedimentary cover. Glided detachment faults formed between them. Super-Thin alteration-type gold deposit mainly distributed in the glided detachment tectonic zone. Metallogenic period is Yanshanian, and the characteristics of single ore veins are generally small in size, thin thickness and high grade. Generally they appear in groups. The formation of gold deposit closely connected with the detachment tectonic. The main metallogenic activities are controlled of the detachment faults' three cycle: 1. The stage of thrust napping structure from north to south. The crust in the southern margin of north China platform was under the intensively constricting environment, developed a series of large scale overlap thrust napping structure and arose acidic magma's activity, at the same time, the thickness of crust became thicker, mantle material with high temperature and low density formed in upper mantle, they transported in the plastic state and arched up along upper mantle and lower crust; 2. NS tensional rifting stage. The crust was on the tension releasing stage, the early thrust napping structure system and compressive detachment fault obtained a little tensional stress, brittle ductile occurred on the superficial crust. Mantle-derived mineral upwelling slowly along the detachment fault and secondary ore-transmitting structure. Thus large and super-large golden deposit formed in PDZ (Principal displacement zone), such as Kangshan, Hongzhuang and Shangong golden deposits etc; 3. WE thrust shear stage. At this stage brittle ductile broke and the crust shrank. Relative to superficial crust, pressure became bigger and temperature higher in the deep crust. Mantle-derived mineral accumulated rapidly along the gradient zone of pressure and temperature. At the same time, under the effect of atmospheric precipitation and retrograde metamorphism on the superficial crust, Ore mineral rapidly migrated, enriched, mineralized, and finally formed super-thin alteration-type gold deposit, such as Tantou, Nanping and Luyuan-Gou gold deposits, etc. This research is financially supported by the special Fund Basic Scientific Research of Central Colleges and the Special Fund of Basic Research Support Program of Chang'an University (Grant No. CHD2009JC159).

www.minersoc.org

DOI:10.1180/minmag.2013.077.5.12

The heavy oil accumulation characteristics and exploration potential of Orinoco heavy oil belt in East Venezuela Basin

LIU YA MING

Research Institute of Petroleum Exploration and Development, Petrochina, Beijing, China

(*correspondence: liuyaming-hw@petrochina.com.cn)

The parte knowledge of no exploration needed in Orinoco heavy oil belt is popular. In fact its resource isn't distributed omnipresent, and the accumulation recognition need to be enhanced. Based on the theory of hydrocarbon accumulation, the heavy oil accumulation conditions and characteristics of Orinoco heavy oil belt are analyzed, and the exploration direction is pointed out in this paper.

Orinoco heavy oil belt is located in the foreland slope region with weak structural affection. The main source rocks are the neritic mudstone of upper Cretaceous Guayuta group, with a thickness of more than 500m, rich in organic matter (TOC weight of 0.25-6.6%) and high hydrocarbon potential. The main reservoirs are the Delta sandstones of Oficina formation in Miocene and the Merecure formation in Oligocene, sandstones distributed widely in the shape of sheet, reservoir thickness keep stable on the east-west direction, and thinning to the south gradually. The reservoir capability is excellent for shallow burial(200-2000m, average of 900m), high porosity(10-32%, average of 21%), and high permeability(20-5000mD, average of 430mD). The regional shale, intrabed shale, bitumen and underlying basement are sealing layers. The main trap type are lithologic stratigraphic traps. Faults, unconformities and connective sandstones formed excellent combination of oil migration pathways. biodegradation ocured during the long distance migration (50-200km) period in the late Miocene and main accumulation period in the Pliocene-Pleistocene are the main viscosifying factors. The gas chromatography analysis of saturated hydrocarbon components (C10+) of heavy oil from many samples showed the n-paraffins and isoprenoid have different degrees of consumption due to high level of biodegradation.

The accumulation model is long distance migration biodegradation and concentrated shallow burial. Source rocks, migration pathways and viscosifying mechnism controlled the heavy oil accumulation. The western part, the Oficina formation and stratigraphic related traps are the key points for exploration.

Stable isotope analysis of carbonates using Isoprime MultiFlow-IRMS

YAN LIU^{1,2}, JINCAI TUO^{1*}, CHENJUN WU²
AND D RU CHEN²

¹ Key Laboratory of Petroleum Resources Research Institute of Geology and Geophysics Chinese Academy of Science Lanzhou, 730000, China

(correspondence: jctuo@lzb.ac.cn)

² Graduate School of the Chinese Academy of Science, Beijing, 100039, China (yanliu@lzb.ac.cn)

Isoprime MultiFlow is the pretreatment device which can connect with Isoprime 100 (IRMS) for carbonates analysis. We found that the $\delta^{18}\text{O}$ values decreased when the CO_2 sample peaks increased higher in our experiments. The empirical linear regression of the $\delta^{18}\text{O}$ value was a function of the CO_2 quantity, which was useful to correct the deviation caused by the decreasing trend of $\delta^{18}\text{O}$ value. In addition, we tested the analysis linearity of IRMS and the fractionation of other interfaces. The results showed that the temperature of GC column in MultiFlow was significant factor for the variation of $\delta^{18}\text{O}$ value. Although the user guide recommended that 100°C was a sufficient setting for separating the gas species of interest, we found that 60°C for GC column was better to adjust the decreasing of $\delta^{18}\text{O}$ value. We inferred that the high temperature would cause the oxygen isotope exchange between CO_2 and the filler inside the GC column.

Research supported by Key Laboratory of Petroleum Resources Research, Institute of Geology and Geophysics, Chinese Academy of Sciences and NSFC(41202093).

Fluid electrolytes of Mohailaheng Pb-Zn deposit in Tibetan plateau

YINGCHAO LIU¹, ZENGQIAN HOU¹, ZHUSEN YANG²
AND SHIHONG TIAN²

¹Institute of Geology, CAGS, Beijing 100037, China
(lychappy@126.com)

²Institute of Mineral Resources, CAGS, Beijing 100037, China

The Mohailaheng deposit, located in the north eastern margin of Tibetan collisional orogen, is a MVT-like Pb-Zn deposit controlled by thrust nappe structures [1] in the 'Sanjiang' metallogenic belt. Ore bodies in this deposit are stratabound and hosted by Early Carboniferous limestone in the hanging wall of a Cenozoic thrust fault system. Five mineralization stages are recognized, including minerals such as sphalerite, galena, dolomite, barite, calcite and fluorite.

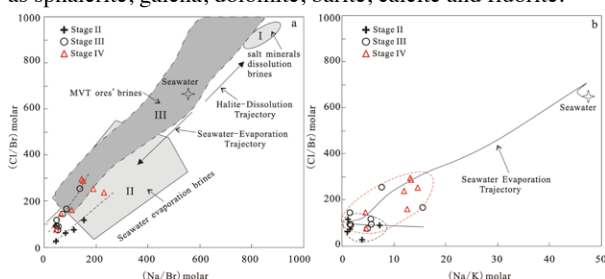


Fig.1 Binary plots of fluid inclusion electrolytes from the Mohailaheng deposit. (The field of I form [2], of II from [3], and of III from [4]. Seawater evaporation curves from [5].)

The solute compositions of ore-forming brines for the Mohailaheng deposit were measured from bulk extraction of fluid inclusions in barite, calcite and fluorite in different mineralization Stages. The Cl/Br and Na/Br molar of the solutes plot close to seawater evaporation line (Fig. 1a) and constrain the source of the ore-forming brine to evaporate seawater. Some Cl/Br and Na/K plot along but slightly above the seawater evaporation line (Fig. 1b) indicating seawater was evaporated beyond halite saturation. Some data in Fig. 1a plot in the compositional field for MVT basinal brines suggesting they all share a common origin. Other data out of MVT field in Fig. 1a may indicate other origins such as regional metamorphic fluid suggesting by microthermal work.

This work was supported by grants (Contract No. 2009CB421007, 2011CB403104 and J1314).

[1] Hou *et al.*. (2008) *Mineral Deposits* 27, 420-441. [2] Heijlen *et al.*. (2001) *Miner Deposita* 36, 165-176. [3] Kesler *et al.*. (1996) *Geochim Cosmochim Acta* 60, 225-233. [4] Leach *et al.*. (2005) *Econ Geol* 100th Anniversary Volume, 561-607. [5] Fontes & Matray. (1993) *Chem Geol* 109, 149-175.

Boron isotopic composition in *Arctica islandica* shell: a potential historical, prehistorical and geological seawater pH indicator

YI-WEI LIU^{1*}, SARAH M. ACIEGO¹, ALAN D.
AND WANAMAKER JR.²

¹Earth and Environmental Sciences, University of Michigan,
1100 N. University Avenue, Ann Arbor, MI 48109, USA
(*correspondence: liuyiwei@umich.edu;
aciego@umich.edu)

²Department of Geological and Atmospheric Sciences, Iowa
State University, Room 12, Science I, Ames, IA 50011-
3212, USA (adw@iastate.edu)

Research on the ocean carbon cycle is vitally important due to the projected impacts of atmospheric CO₂ on global temperatures and climate change, but also on ocean chemistry. The actual influence of this CO₂ rise on the pH of North Atlantic seawater is largely unknown because of the dearth of instrumental records or reliable proxies. The long-lived bivalve mollusk *A. islandica*, common in the shelf seas of the temperate to sub-polar North Atlantic, is an excellent high-resolution marine archive with great potential for monitoring pH as well as other seawater properties. Boron isotopic composition ($\delta^{11}\text{B}$) in aragonite biogenic carbonate has been suggested to trace ambient seawater pH because marine carbonates will primarily incorporate $\text{B}(\text{OH})_4^-$ into the carbonate structure during growth, in which the $\delta^{11}\text{B}$ is pH dependent. Here we aim to develop a $\delta^{11}\text{B}$ -pH transfer function in *A. islandica* to reconstruct mid to high latitude seawater pH record. An improved rapid throughput microsublimation technique coupled with Total Evaporation NTIMS method was conducted so that <1 ng boron could be measured. Reproducibility of boron isotopic composition of better than $\pm 0.3\%$ (2SE, $n > 10$) was achieved for a variety of isotopic standards and natural samples. We analyzed boron isotopic composition in the living shells reared at the Darling Marine Center, Maine, USA in which seawater temperature, salinity and pH were carefully monitored. During the experimental period (January 2010 to August 2010), the temperature raised from 2 to 18°C, with a 3 ppt salinity variation and a 0.2 pH unit change. Our pilot data suggest the the $\delta^{11}\text{B}$ value reflects the ambient seawater pH. This study will form the basis for reconstructing high-resolution seawater pH in the mid to high latitudes of the Atlantic Ocean through the living and fossil history of *A. islandica*.

On the test of a new volume variable cluster model method for stable isotope fractionation of solids: Equilibrium Mg isotope fractionations between minerals and solutions

YUN LIU

State Key Laboratory of Ore Deposit Geochemistry, Institute of Geochemistry, Chinese Academy of Sciences, China. (Liuyun@vip.gyig.ac.cn)

There is a tremendous interest in developing a cluster-model-based method of isotope fractionation calculation for solids because most of new techniques developed in modern quantum chemistry are for molecules which usually are represented by cluster models. The reason we developed this method is to remedy problems raised from a similar method used by Rustad and co-workers (e.g., [1]), especially to enhance its implementation on isotope fractionation calculations between solids and aqueous species.

For the test of this so-called volume variable cluster model method (VVCMM), we estimated Mg isotope fractionations between various silicate and carbonate minerals. We also study the Mg isotope fractionations between minerals and solutions. These cases usually are thought as the confusing part for isotope fractionation calculations because large disagreements exist among different theoretical groups (e.g., [1] and [2]).

Our results are very close to existing Mg and O isotope experimental data. Especially, for those mineral vs. solution cases, our results are better than previous theoretical estimations, suggesting very useful applications of this method in future.

[1] Rustad *et al.* (2010) GCA, 74, 6301-6323. [2] Schauble (2011) GCA, 75, 844-869.

Grow and Die: The Microbial mud mound and Its Sedimentary Environments of the Middle Permian, Sichuan Basin

LIU ZHICHENG¹, ZHANG TINGSHAN^{2*}, WANYAN QIQI³ AND CANG YAN⁴

- 1) State Key Lab. of Oil & Gas Reservoir Geology and Exploitation Engineering, Chengdu, Sichuan, 610500; rex_swpu2005@126.com.
- 2) State Key Lab. of Oil & Gas Engineering, Chengdu, China zhangtingshan@swpu.edu.cn (* presenting author).
- 3) Research Institute of Petroleum Exploration & Development-Langfang, PetroChina, Langfang, Hebei, 065007; Wanyanqiqi@petrochina.com.cn.
- 4) Shunan Gas District of Southwest Oil and Gas Company, PetroChina, Luzhou, Sichuan, 646000, China. snyangyang@petrochina.com.cn

A Microbial mud mound in the Middle Permian Qixia Fm. in Sichuan basin, is first found. This mud mound belongs to Waulsortion and is supported by mud, the primary builder is fungi. The species diversity is low, high species richness. The main lithology including bioclastic micritic limestone and thrombolite. The mud mound can be divided into mound-core, mound-flank, mound-base. Through a multidisciplinary approach, including carbonate petrology and geochemistry of the mud mound and unground, we reconstruct the development history of the Microbial mud mound and characterize the formation and the evolution of the eastern portions of Sichuan basin. The results of geochemical analysis of the Qixia Fm. show: all of the paleosalinity Z value greater than 122, $\delta^{13}\text{C}$ compositions range from 1.84‰ to 4.58‰ (VPDB); $\delta^{18}\text{O}$ compositions range from -6.33‰ to -4.42‰ (VPDB); the Ancient water temperature values range from 33.60°C to 24.26°C; $V/(V+Ni)$ values range from 0.51228 to 0.77795. It shows that the environment of Qixia period were relatively deep water, hydrodynamic weaker, higher temperature, high salinity and anoxic. According to geochemical analysis, the Microbial mud mound growth environment is low dissolved oxygen content, the higher water temperature and the salinity is higher. After it died, the water temperature was reduced and salinity began to increase which became a stable super salty hypoxia environment.

Origin and implications of $^{238}\text{U}/^{235}\text{U}$ variations in CAIs

B. D. LIVERMORE¹, J. N. CONNELLY¹
AND M. BIZZARRO¹

¹Centre for Star and Planet Formation, Natural History Museum of Denmark, University of Copenhagen, Copenhagen 1350 DK. Email: bettina@livermore.dk

Calcium-aluminum rich inclusions (CAIs) are submillimeter- to centimeter-sized inclusions that condensed from gas in the hot, inner region of protoplanetary disk and are a major constituent of carbonaceous chondrites. Believed to be the first formed solids in our Solar System, they have been a prime target for absolute Pb-Pb geochronology to establish the age of the Solar System [eg. 1] as well as a time anchor for several relative chronometers. It is now known that CAIs display significant variations in their $^{238}\text{U}/^{235}\text{U}$ ratio [2], a critical parameter in all Pb/Pb age calculations. Whereas this variation was first attributed to the decay of the short-lived radionuclide ^{247}Cm to ^{235}U [2], it is likely at least part of this variation is due to mass dependant fractionation that occurred during the CAI forming process [1]. Therefore, beyond the importance of this ratio for geochronology, understanding the origin of uranium isotopic variations in CAIs may offer insights into CAI forming processes and conditions.

Ten large CAIs have been selected for this study from the pristine carbonaceous chondrite (CV3) NWA 3118 [3], all with sizes large enough for accurate determination of their $^{238}\text{U}/^{235}\text{U}$ ratios. The sample has been cut dry into 3 mm slabs using a diamond wire saw and CAIs selected on the basis of their size have been imaged using a scanning electron microscope. Using the procedure of [1], U is separated from the samples and measured by HR-MC-ICP-MS using a Thermo-Fisher Neptune Plus. To determine the degree of mass-dependent isotope fractionation experienced by individual inclusions, stable Mg and Nd isotope composition are measured for each CAI and compared to the uranium isotopic ratios. Correlations between the Mg, Nd and U isotope ratios will support a model of mass-dependent fraction of U to explain the isotopic variations observed in CAIs from CV chondrites. A lack of correlation will support ^{247}Cm as the primary cause of U isotopic variability. In addition, the CAIs measured for U isotopes will also be dated using the Pb-Pb system based on the Pb step-wise dissolution procedure by [1].

[1] Connelly *et al.*. (2012) *Science* **338**, 651. [2] Brennecka *et al.*. (2010) *Science* **327**, 449. [3] Russel *et al.*. (2005), *MAPS* **40**, A201.

The relationship of goethite surface structure, habit and adsorption capacity

K.J.T. LIVI¹, M. VILLALOBOS², M. VARELA³, M. VILLACÍS-GARCÍA², K. VACA-ESCOBAR²
AND D. A. SVERJENSKY⁴

¹HRAEM Facility, Dept. of Earth and Planetary Sciences, Johns Hopkins University, Baltimore, MD 21218 USA

²Environmental Bio-Geochemistry Group, Geochemistry Dept. Geology Inst., UNAM, CU México 04510, D.F.

³Oak Ridge National Laboratory, Oak Ridge TN 37831 USA

⁴Dept. of Earth and Planetary Sciences, Johns Hopkins University, Baltimore, MD 21218 USA

It is well established that the adsorption capacity of goethite ($\alpha\text{-FeOOH}$) per m^2 increases significantly with decreasing specific surface area (SSA, determined by N_2 -adsorption). For example, the adsorption of chromate increases three-fold as SSA decreases from 94 to 50 $\text{m}^2\cdot\text{g}^{-1}$ [1]. This has led to recent explanations postulating the possible roles of different faces with different surface site densities and affinities [1-3]. The current model assumes that small particles with $\text{SSA} > 80 \text{ m}^2/\text{g}$ are “ideal” prismatic crystals elongated parallel to the **b**-axis (Pnma setting) with {101} and/or {001} forms [4]. It is assumed that the more reactive goethites, which have larger particles and $\text{SSA} < 80 \text{ m}^2/\text{g}$, may have different crystal face distributions to the “ideal” crystals.

We report electron microscopy observations on a suite of synthetic goethites with SSA ranging from 40 to 100 $\text{m}^2\cdot\text{g}^{-1}$. Transmission Electron Microscopy (TEM) confirms that the crystals are well-formed elongate blades: the 40 $\text{m}^2\cdot\text{g}^{-1}$ and the 100 $\text{m}^2\cdot\text{g}^{-1}$ crystals have length modes of about 1 μm and 100 nm, respectively. The 40 $\text{m}^2\cdot\text{g}^{-1}$ sample has single-domain crystals elongated parallel to the **b**-axis as expected. However, the 100 $\text{m}^2\cdot\text{g}^{-1}$ sample contains numerous crystals that have mosaic-domain structure and are instead elongated parallel to the [610] direction. Atomic-Resolution Scanning TEM analysis of the steps on the long edges of two crystals of the 40 $\text{m}^2\cdot\text{g}^{-1}$ sample revealed only 66% terraces parallel to either {001} or {101} forms and 33% parallel to {210}. In contrast, steps on two crystals of the 100 $\text{m}^2\cdot\text{g}^{-1}$ sample with [610] habit were 96% {210}-type and 4% {110}. The change in habit and increase in {210}-type steps in high SSA samples, although surprising, must now be taken into account in assessing the adsorption behavior of goethites.

[1] Villalobos & Pérez-Gallegos (2008) *J. Colloid Interface Sci.* **326**, 307-323. [2] Villalobos *et al.*. (2009) *J. Colloid Interface Sci.* **336**, 412-422. [3] Salazar-Camacho & Villalobos (2010) *Geochim. Cosmochim. Acta* **74**, 2257-2280. [4] Schwertmann (1984) *Thermochim Acta* **78**, 39-46.

Photoferrotrophy and Fe-cycling in a freshwater column

LLIRÓS M^{1,2}; CROWE SA³; GARCÍA-ARMISEN T⁴;
DARCHAMBEAU F⁵; MORANA C⁶; BORREGO CM^{7,8};
TRIADÓ-MARGARIT X⁹; BOUILLON S⁶; BORGES AV⁵;
SERVAIS P⁴; CANFIELD DE³ AND DESCY JP¹

¹ University of Namur, Belgium. jpdscy@fundp.ac.be

² Universitat Autònoma de Barcelona, Spain.
marc.lliros@uab.cat

³ University of Southern Denmark, Denmark.
sacrowe1@gmail.com; dec@biology.sdu.dk

⁴ Université Libre de Bruxelles, Belgium. tgarciaa@ulb.ac.be;
pservais@ulb.ac.be

⁵ Université de Liège, Belgium. alberto.borges@ulg.ac.be;
Francois.Darchambeau@ulg.ac.be

⁶ Katholieke Universiteit Leuven, Belgium.
Cedric.Morana@ees.kuleuven.be;
Steven.Bouillon@ees.kuleuven.be

⁷ University of Girona, Spain. carles.borrego@udg.edu

⁸ Catalan Institute for Water Research, Spain.

⁹ Centre d'Estudis Avançats de Blanes, Spain.
xtriado@ceab.csic.es

Ferruginous (anoxic and iron-rich) conditions dominated ocean chemistry throughout much of the first 3.5 billion years of Earth history. Modern ferruginous water masses are rare, but detailed examination of these oddities, especially of photoferrotrophs and their Fe-reducing respiratory counterparts, could yield important insights into the early evolution of life on Earth. Here, we report pelagic photoferrotrophs from Kabuno Bay, DR Congo. Based on 16S rDNA, the Kabuno Bay photoferrotrophs are similar to laboratory cultures of *Chlorobium ferrooxidans*, the only member of the Chlorobi previously known to conduct photoferrotrophy. Photoferrotrophs comprised up to 38.3%, of the total microbial community and exhibited high rates of phototrophic ferrous Fe oxidation. Up to 60% of total depth integrated bacterial production was carried out at depths where photoferrotrophic GSB dominate. Microbial groups involved in methanogenesis and Fe-reduction also comprised large fractions of the microbial community within depth intervals dominated by photoferrotrophs. Microorganisms typically implicated in the sulfur cycle were only present at low relative abundances, and this is consistent with low measured rates of sulfate reduction and sulfide oxidation. Our findings in Kabuno Bay support models for early ocean ecosystems with primary production driven by photoferrotrophy and organic matter degradation channeled through both Fe-reduction and methanogenesis.

A meta-analysis reveals biases in methods to quantify marine microorganisms

KAREN G. LLOYD¹, MEGAN MAY², RICHARD KEVORKIAN¹ AND ANDREW D. STEEN¹

¹University of Tennessee, Knoxville, TN, USA

²Depauw University, Depauw, Greencastle, IN, USA

There is no universally-accepted method for quantifying specific microbial taxa in the marine subsurface, but this is a crucial first step in any analysis of sedimentary microbial ecology. The two most common methods are fluorescent in situ hybridization (FISH), often with catalyzed reporter deposition (CARD-FISH), and quantitative PCR (qPCR). We compiled sediment cell quantifications from published papers and defined yield as the sum of bacterial and archaeal FISH/CARD-FISH counts divided by total cell counts. We found that permeabilization with proteinase K results in higher yield, as well as higher percent archaea, than permeabilization with lysozyme or other methods, which may be explained by the fact that lysozyme hydrolyses peptidoglycan, which does not exist in archaeal cell walls. Studies in which the absence or near-absence of archaeal CARD-FISH signals have been used to argue for the dominance of bacterial activity in the deep subsurface (e.g. [1], [2]) used lysozyme, suggesting that the low abundance of Archaea in those studies may be artifactual. The ratio of qPCR-determined 16s rDNA copy numbers to directly-counted cells is highly variable, and is often outside of physiologically reasonable range of 1-10, suggesting that qPCR does not provide absolute quantification of specific taxa.

[1] Schippers, *et al.* (2005), *Nature*, 433: 861-864. [2] Webster, *et al.*, (2009), *Environmental Microbiology*, 11:239-257.

Improved multi-ion-counting capabilities for high sensitivity U-Pb LA-MC-ICP-MS zircon geochronology

N. S. LLOYD^{1*} AND C. BOUMAN¹

¹ Thermo Fisher Scientific, Bremen, Germany.
(*correspondence: nicholas.lloyd@thermofisher.com)

The Thermo Scientific NEPTUNE *Plus* with Jet Interface option has been shown to significantly enhance LA-MC-ICP-MS sensitivity for hafnium isotope ratio analyses [1, 2], allowing precise and accurate Hf ratios to be determined from 25 μm diameter laser ablation spots (within 100 ppm 2RSD). The high sensitivity Jet and X-cones have also been used to enhance Hf isotope ratio sensitivity on a NEPTUNE *Plus*, whilst U-Pb ratios were analysed from a split flow to a Thermo Scientific ELEMENT XR [3].

In this poster we present U-Pb data from the NEPTUNE *Plus* with Jet Interface option. The sensitivity enhancement can be used to collect U-Pb ratios on Faraday cups from larger ablation spots, or for small spot sizes using multi-ion-counting. We use an array of new Compact Discrete Dynode (CDD) electron multipliers in combination with classical large-scale Secondary Electron Multipliers (SEM). The new CDDs have the same performance characteristics as the classical SEMs used in the NEPTUNE *Plus* and TRITON *Plus*.

The multi-ion-counting package allows for simultaneous analysis of ²⁰²Hg, ²⁰⁴Pb, ²⁰⁶Pb, ²⁰⁷Pb, ²⁰⁸Pb and ²³⁸U on the electron multipliers. If desired, also ²³²Th and ²³⁵U can be detected along on additional CDD multipliers. The detector catching ²⁰⁶Pb is a dual detector; ²⁰⁶Pb can be detected in either an SEM or Faraday. This setup gives full flexibility for the analysis of zircons, where ²⁰⁶Pb is the most abundant Pb isotope.

This contribution will present U-Pb data on zircon standards as well as analytical and instrumental challenges relating to the laser ablation process, the plasma interface and the multi-ion-counting detectors will be discussed.

[1] Lloyd *et al.* (2011) *Min. Mag.* **75**(3), 1351. [2] Hu *et al.* (2012) *J. Anal. At. Spectrom.* **27**, 1391-1399. [3] Tollstrup *et al.* (2012) *Geochem. Geophys. Geosyst.*, **13**.

Arsenic release from red mud affected soil-water systems

CINDY L. LOCKWOOD^{1*}; ROBERT J. G. MORTIMER¹;
DOUGLAS I. STEWART²; WILLIAM M. MAYES³
AND IAN T. BURKE¹

¹School of Earth and Environment, University of Leeds, LS2 9JT, UK (*correspondence: ee09cll@leeds.ac.uk)

²School of Civil Engineering, University of Leeds, LS2 9JT, UK

³Centre for Environmental and Marine Sciences, University of Hull, Scarborough, YO11 3AZ, UK

Red mud is a highly alkaline waste product from bauxite ore processing. It contains elevated concentrations of several oxyanion forming elements such as Al, As, V and Mo that are mobilised at high pH. The tailings dam breach at Ajka, western Hungary, released ~1 million m³ of toxic red mud into the Torna and upper Marcal valleys. As part of the initial clean-up, some thinner red mud deposits (< 5 cm) were ploughed into fields to prevent dust formation and some wetland areas were left untreated.

We used anaerobic microcosm experiments to determine the mechanisms of As release from red mud mixed with uncontaminated soils. Soils from unaffected locations in the Torna and upper Marcal valleys were mixed with Ajka red mud at two different ratios (9 % and 33 % red mud), with soil only incubations as controls. XAS spectroscopy and HPLC-ICP-MS was used to determine changes in As oxidation state.

After 180 days the water in soil-only control microcosms contained ~ 200 $\mu\text{g L}^{-1}$ As, of which ~50% had been converted to As(III) as a result of microbial As(V) reduction. However, dissolved As concentrations in red mud effected systems reached only 100 $\mu\text{g L}^{-1}$ after a similar time period, all as As(V), despite microbial Fe(III)-reduction being observed. When red mud is added to soils there is an initial rapid increase in dissolved As concentrations that correlates with microcosm pH. However, concentrations at equilibrium are independent of both microcosm pH and red mud loading and are ultimately controlled by the dissolution of inorganic-arsenate host phases from the red mud.

This study shows that although As in red mud is not bioavailable, the slow leaching of As from red mud / soil mixtures at circum-neutral pH will in time result in an overall increase in the amount of aqueous As(V) present in affected environments. In addition, the use of red mud as a soil amendment should be carried out with caution as even low loadings of red mud may result in As-release at problematic concentrations.

Mass Transfer of Fluids and Metals in the Deep Earth

M. LOCMEELIS^{1*}, M. L. FIORENTINI¹, T. RUSHMER², J. ADAM², F. ZACCARINI³, G. GARUTI³, M. TURNER² AND S. TURNER²

¹CET/CCFS, The University of Western Australia, Perth, Australia (*Marek.Locmelis@uwa.edu.au)

²Dept. Earth and Planetary Sciences and CCFS, Macquarie University, Sydney, Australia

³University of Leoben, Austria

Mantle-derived fluids are generally considered to be involved in the transport and distribution of trace elements in the deep Earth. However, we lack a robust understanding of the processes that lead to mass transfer of fluids and metals between the mantle and the crust. In this study, we integrate a series of volatile- and S-bearing high P/T experiments with the analysis of rock samples collected from one of a series of Ni-Cu-PGE mineralized alkaline ultramafic pipes in the Ivrea-Verbano Zone (IVZ). This exhumed section of the critical crust-mantle interface shows tantalizing relationships between ultramafic fluid-rich rocks and metal-rich sulfide mineralization. Geothermometry suggests that the Valmaggia pipe was emplaced at a temperature of ~900-950°C, close to the water-saturated peridotite solidus. The high P/T experiments support this observation, based on an H₂O-saturated run at 950°C and 2 GPa that yielded a mineral assemblage remarkably similar to the pipe. High H₂O contents in the melt are also supported by SHRIMP-SI analysis of pyroxene that yielded 550 ppm H₂O, which corresponds to ~4 wt% H₂O in the melt. Whole-rock and laser ablation ICP-MS data of silicate phases from the pipe suggest that a juvenile, sulfur- and metal-bearing mantle fluid refertilized a depleted harzburgitic source at depth, causing partial melting. The evolving, volatile-rich melt then intruded the IVZ, most likely as a series of open-system feeder conduits and/or chonoliths that subsequently reached sulfide saturation and formed widespread Ni-Cu-PGE mineralization. This hypothesis is supported by isotopic data, which indicate that this alkaline pipe was emplaced slightly after the voluminous mafic magmatic event that underplated the lower crust in the IVZ during the late Carboniferous. The significant difference in epsilon Nd values between whole-rock (-3.1) and amphibole-phlogopite concentrates (respectively -1.0 and -1.6) at ca. 290 Ma indicates that multiple metasomatic events may have been responsible for the establishment of open conduits and the transfer of fluids and metals between the metasomatized lithospheric mantle and the lower crust.

Cation adsorption, hydrogen bonding structure and dynamics at the clay-water interface: MD simulations with new models of muscovite and montmorillonite

NARASIMHAN LOGANATHAN.^{1*}, BRICE F. NGOUANA W.¹ AND ANDREY G. KALINICHEV¹

¹Laboratoire SUBATECH (UMR-6457), Ecoles des Mines de Nantes, 4 Rue Alfred Kastler, La Chantrerie, 44307, Nantes Cedex 3, France (*loganath@subatech.in2p3.fr)

The structure of water films at charged clay surfaces is crucial factor in understanding and predicting the physico-chemical properties of the adsorbed aqueous species which can provide fundamental insights into mobility of contaminants in soils and subsurface environments. Concurrently, the ion-water interactions strongly depend upon both the nature of the charge-compensating ions and the clay substrate structure. Classical molecular dynamics (MD) computer simulations using CLAYFF forcefield [1] were performed for a series of monovalent cations at the surfaces of newly developed models of muscovite and montmorillonite. Atomic density profiles, near-surface atomic distribution maps and the structure and dynamics of the interfacial H-bonding network were analyzed in detail for both clay substrates. The energetics of surface complexation was quantified via the calculation of potentials of mean force for the adsorption processes. Only one stable adsorption site for cations is observed at the muscovite surface in contrast to two different adsorption sites in the case of montmorillonite. The local structural disorder of the substrate charge distribution is clearly responsible for the significant redistribution of water molecules at the interfacial region.

The lateral diffusion of H₂O molecules is 35% reduced at the surface of muscovite in comparison with the bulk liquid state. The diffusion rate of aqueous species in disordered montmorillonite structure is similar to that in the ordered structure. The calculated hydrogen bond lifetimes between H₂O-H₂O pairs are lower than between H₂O and the bridging oxygens of the muscovite surface. The simulation results are compared with available experimental data and other simulations [2,3] to provide a reliable comprehensive molecular view of the structure and aqueous ion at the clay-water surface.

[1] Cyan, R.T., *et.al.* (2004) *J.Phys.Chem B.* **108**, 1255-1266.

[2] Wang, J., *et.al.* (2005) *J.Phys.Chem B.* **109**, 15893-15905.

[3] Lee, S. S., *et.al.* (2012) *Langmuir.* **28**, 8637-8650.

A new benthic Mg/Ca temperature calibration to reconstruct thermocline temperature variability in the Indonesian archipelago

E. LO GIUDICE CAPPELLI¹*, A. HOLBOURN¹, W. KUHN¹
AND M. REGENBERG¹

¹ Institute of Geosciences, Christian-Albrechts-University,
Kiel, Germany
(*correspondence: elgc@gpi.uni-kiel.de)
(ah@gpi.uni-kiel.de)
(wk@gpi.uni-kiel.de)
(regenber@gpi.uni-kiel.de)

23 Multi-corer core tops representing a range of modern bottom water temperature (BWT) between 3°C and 8°C and covering a water depth between 500 and 2000 m were retrieved from the Makassar Strait (Indonesia) and the Timor Sea to produce a regional BWT calibration. Mg/Ca ratios of the benthic foraminifer *Hoeglundina elegans* show an exponential relation with temperature ($\text{Mg/Ca} = 0.21e^{(0.23\text{BWT})}$, $R^2 = 0.91$). This relationship differs significantly from previous calibrations [1, 2], but shows similarity to a later re-calibration [3]. We applied our calibration to sediment core SO18471, retrieved within the lower thermocline of the Indonesian Throughflow (ITF) outflow into the Timor Sea (9°21.987' S, 129°58.983' E, 485 m water depth, 13.5 m length). In core SO18471, we measured Mg/Ca ratios in ~10 tests of *H. elegans* in 10 cm intervals (~1-2 kyr time resolution) to reconstruct thermocline temperature variability. We based the age model on 5 AMS ¹⁴C dates and on correlation of our benthic oxygen isotope curve to the Antarctic EDML1 ice core [4]. Preliminary results show that BWT varied from 5 to 10°C over the last 140 kyr (present day BWT is 8°C). During periods of relatively high sea level, thermocline waters cooled and freshened, suggesting a gradual shift from surface to thermocline dominated ITF. In contrast, during sea level lowstands, thermocline temperatures increased, supporting the hypothesis of a reduced thermocline flow during glacials. Although sea level variations appear to be the main control on ITF variability, changes in the global thermohaline circulation and the Australian-Asian monsoon were also influential. Our data suggest that cooling events in the Northern Hemisphere during MIS 3 led to a reduction in ITF intensity, resulting in higher thermocline temperatures in the Timor Strait.

[1] Rosenthal *et al.*. (2006) *Paleoceanography* **21**, PA 1007.
[2] Reichert *et al.*. (2003) *Geology* **31**, 355-358. [3] Ní Fhlaithearta *et al.*. (2010) *Paleoceanography* **25**, PA4225. [4] Ruth *et al.*. (2007) *Clim. Past Discuss.* **3**, 349-574.

Biogeochemical cycle of dissolved zinc and cobalt in the South Atlantic

M.C LOHAN¹*, N.J. WYATT¹, A.MILNE²
AND E.M. WOODWARD³,

¹Marine Institute, University of Plymouth, Plymouth, PL4 8AA, U.K. (*correspondence: maeve.lohan@plymouth.ac.uk

²SoGEES, University of Plymouth, Plymouth, PL4 8AA

³Plymouth Marine Laboratories, Plymouth, PL1 3DH, U.K.

We report the first comprehensive dataset of dissolved zinc and cobalt along the South Atlantic 40°S transect as part of the UK GEOTRACES programme. To date there is little understanding of the supply of Zn and Co which are essential requirements for phytoplankton growth, to this highly productive region. Surface concentrations of zinc and cobalt were extremely low with a pronounced subsurface minima (25pM and 10pM respectively) reflecting the biological uptake in this highly productive region. *Prochlorococcus* has an absolute cellular requirement for cobalt. Where the phytoplankton biomass was dominated by *prochlorococcus*, highest concentrations of cobalt were observed below chlorophyll max, indicating a biological control on the vertical flux of cobalt.

The vertical distributions of Zn and Co were similar to soluble reactive phosphorus. The ecological stoichiometry for dissolved Co and Zn ($\text{Co:PO}_4^{3-}/\text{Zn:PO}_4^{3-}$ ratio 1:1) suggests that both Zn and Co are influencing phytoplankton diversity.

A strong correlation was observed between zinc and silicate across the entire study region ($R^2 = 0.97$, $n = 460$). By utilizing Si* as a tracer for Subantarctic Mode Water, our data indicate that the preferential removal of Zn in the Southern Ocean prevented a direct return path for dissolved Zn to the surface waters of the South Atlantic at 40°S, and potentially the thermocline waters of the South Atlantic subtropical gyre.

Diversity of microbial communities in sites of discharges gas-and-oil containing mineralized fluids in Lake Baikal

A.V. LOMAKINA^{1*}, T.V. POGODAEVA¹, I.V. MOROZOV²
AND T.I. ZEMSKAYA¹

¹Limnological Institute, Siberian Branch of the Russian Academy of Sciences, Ulan-Batorskaya Street 3, Irkutsk, 664033, Russia (*correspondence: lomakina@lin.irk.ru)

²Institute of Chemical Biology and Fundamental Medicine SB RAS, 8, Lavrentiev Ave., Novosibirsk, 630090, Russia.

Natural discharges gas-and-oil containing mineralized fluids have been identified in different parts of the South and Central Baikal using different methods (De Batist *et al.*, 2002; Klerx *et al.*, 2003; Khlystov 2006; Khlystov *et al.*, 2007; Kontorovich *et al.*, 2007; Granin *et al.*, 2010) have been found in. We study microbiol community in deep-water sediments of sites with high concentration of ammonium (up to 20 mg/L), bicarbonate ions (up to 183 mg/L), total Fe (4.7 mg/L) and methane. For detection representatives *Planctomycetes*, ANAMMOX group, methanotrophs bacteria and methanogenic archaea, and other bacteria degrading oil in surface and deep-water sediments of cold seeps with different hydrocarbon structure we using methods of molecular biology (PCR analysis, FISH, pyrosequencing). Comparative analysis of nucleotide sequences of Bacteria and Archaea of 16S rRNA gene fragments from the site of natural oil discharge, Gorevoi Utes (Central Baikal), has indicated different microbial composition in the studied samples. We have identified representatives of the phyla *Bacteroidetes*, *Proteobacteria* (β , γ , and δ), *Verrucomicrobia*, *Nitrospirae*, *Chloroflexi*, *Planctomycetes*, *Acidobacteria*, *Chlorobi*, and *Actinobacteria*. Using *Planctomycetes*-specific primers, we have obtained various representatives of the phylum, including the ANAMMOX group in sites of discharge gas-and-oil containing mineralized fluid: cape Gorevoi Utes and Posolskaya Shoal (South Baikal). Fluorescent in situ hybridization (FISH) with labeled oligonucleotide probes has confirmed the presence in the microbial community site of Posolskaya Shoal of *Planctomycetes* and the ANAMMOX group. Using *pmoA*-gene specific primers was obtained in surface sediments representatives of types I, II methanotrophs.

Therefore, at the sites with cold seeps in Lake Baikal we have detected bacteria participating in methane (methanotrophs) and oil oxidation, and utilize ammonium.

This work supported by the Integration Project No.82, the RFBR Grant No.12-04-31031 мол_a.

Molecular scale speciation of U(VI) association with clay bacterial isolates

M. LÓPEZ-FERNÁNDEZ¹, I. SÁNCHEZ-CASTRO¹, A. AMADOR-GARCÍA¹, M. ROMERO GONZALEZ²
AND M.L. MERROUN^{1*}

¹Department of Microbiology, University of Granada, Spain (*correspondence: merroun@ugr.es)

²Department of Civil and Structural Engineering, University of Sheffield, Sheffield, UK

Clay deposits have been studied in recent years as potentially host rock for deep geological disposal of radioactive wastes. A reliable performance assessment of these systems depends on better knowledge on the interactions of actinides with host rock natural microorganisms. The present work aims to characterize the speciation of U(VI) associated with highly U resistant bacteria isolated from Spanish clay deposits. The U(VI) bacterial interaction experiments were performed under physiological conditions. The speciation of U(VI) in U-loaded culture medium is complex and dominated by $(\text{UO}_2)_2\text{CO}_3(\text{OH})_3$. Several spectroscopic and microscopic techniques indicated that the speciation of U(VI) changed drastically upon the addition of bacterial cells to U-loaded culture medium. Infrared spectroscopy analysis revealed that bacterial phosphate groups are involved in the coordination of U(VI) at these neutral conditions. X-ray absorption spectroscopy and time resolved laser induced fluorescence spectroscopy showed that U phosphate precipitation is the main interaction process. The U precipitates are localized at the cell surface as was demonstrated by TEM analysis. The biomineralization of U(VI) phosphates is seen as a detoxification mechanism of the cells to overcome the toxicity of this radionuclide. The results of this work will help in understanding the role of microbiological process in the chemical behavior of actinides in geological and environmental context for future nuclear waste disposals.

^{129}I concentrations in surface and deep seawater from the Irish Sea and the Atlantic Ocean

J.M. LÓPEZ-GUTIÉRREZ^{1,2}, M. VILLA-ALFAGEME³,
J.I. PERUCHENA², CH. SCHNABEL², CH. MARCINKO⁴
AND P. MCGINNITY⁵

¹Universidad de Sevilla, Departamento de Física Aplicada I, c/ Virgen de África, 7, 41011 Sevilla, Spain (correspondence: lguti@us.es).

²Centro Nacional de Aceleradores. Junta de Andalucía, CSIC, Universidad de Sevilla. c/Thomas Alva Edison N° 7, 41092 Sevilla, Spain (jiperuchena@us.es, schnabel@btinternet.com).

³Universidad de Sevilla, Dpto. Física Aplicada II, Av. Reina Mercedes, 4A. 41012 Sevilla, Spain (mvilla@us.es).

⁴National Oceanography Centre, University of Southampton Waterfront Campus, European Way, Southampton SO14 3ZH, United Kingdom (c.marcinko@noc.ac.uk).

⁵Radiological Protection Institute of Ireland, Clonskeagh Square, Dublin 14, Ireland, Ireland (pmcginnity@rpii.ie).

In this work, ^{129}I concentrations in seawater samples from the Irish coast and from the Extended Ellet Line (from Scotland to Iceland) are presented, including both surface samples as well as two depth profiles at the Atlantic Ocean. The results aim to increase and update the information on the presence of this radionuclide in the Atlantic waters.

Surface water ^{129}I along the Irish coast, directly affected by Sellafield discharges, is 3.2×10^{10} at./kg in average. Measured ^{129}I concentrations along the EEL are typically in the order of 10^8 at./kg, slightly over the results obtained by Alfimov *et al.* [1] in waters sampled nearby in 1999. Also, our results are about one order of magnitude lower than those previously found in the Irminger Basin [2] and in the Arctic Oceans [3].

The two EEL depth profiles show different shapes, as shown in figure 1. Profile 1 decreases with depth, due to dilution. However, profile 2 shows the highest ^{129}I levels in the deepest waters. The North Atlantic Deep Waters current from the Arctic Ocean Profile and enriched in ^{129}I was probably sampled in Profile 2

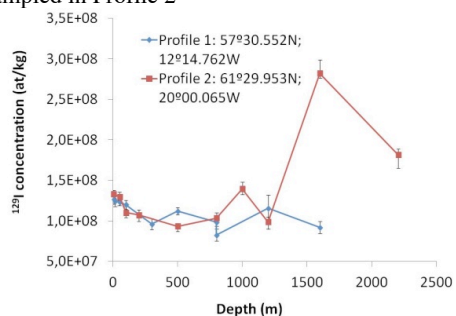


Figure 1.

[1] Alfimov *et al.* (2004). Nucl. Instr. Meth. Phys. Res.B **223–224**, 446–450. [2] Gómez-Guzmán *et al.* (2013). Nucl. Instr. Meth. Phys. Res.B **294**, 547–551. [3] Alfimov *et al.* (2013). Nucl. Instr. Meth. Phys. Res.B **294**, 542–546.

The platinum behavior in the North Atlantic Ocean

DANIEL EDUARDO LÓPEZ SÁNCHEZ,
ANTONIO COBELO GARCÍA

¹[Grupo de Bioquímica Mariña, Instituto de Investigacións Mariñas de Vigo C/Eduardo Cabello, 6. C. P.: 36208. Vigo, Pontevedra, Spain]

We studied the water mass influence over the dissolved platinum levels and its behavior in the North Atlantic. 24 profile stations were sampled during the GEOTRACES cruise in early-spring 2010. 5 water mass were found in the profile: the North Atlantic Deep Water, Denmark Strait Overflow Water, Labrador Sea Water, Iceland and Scotland Overflow Water and Western North Atlantic Central Water. We found different platinum concentration within the different water masses. Platinum concentration increased with depth. The intermediate Atlantic water formation should have an influence on the higher platinum concentration, and could be used as a tracer. However, no significant statistical differences were observed.

A potential geothermometer for antigorite serpentinite

LÓPEZ SÁNCHEZ-VIZCAÍNO V.¹, PADRÓN-NAVARTA J.A.^{2,3}, HERMANN J.³, CONNOLLY J.A.D.⁴, GARRIDO C.J.⁵, GÓMEZ-PUGNAIRE M.T.⁶ AND MARCHESI, C.⁵.

¹Dpt. Geología, Universidad de Jaén, Linares, Jaén.

²Géosciences Montpellier, CNRS-UM2, Montpellier, France.

³Research School of Earth Sciences, ANU, Australia.

³Swiss Federal Institute of Technology, Zurich, Switzerland

³Instituto Andaluz Ciencias de la Tierra, Granada, Spain.

³Dpt. Mineralogía Petrología, Universidad de Granada, Spain

Geothermobarometry in antigorite serpentinite is traditionally hampered by the lack of assemblages buffering the antigorite composition, and customarily relies on the conditions at which breakdown reactions occur of phases like brucite, diopside or titanian clinohumite and/or alternatively on associated mafic assemblages. The aluminium-content in antigorite may provide an independent constraint of the pressure-temperature conditions for serpentinite phase equilibria. Such information would permit a more precise estimation of the conditions for the subduction and exhumation structures recorded in serpentinite during orogenic cycles. Additionally, the relation between the Al-content and the modular structure in antigorite could be investigated more precisely without the need of indirect temperature constraints based on associated mafic rocks.

A model for the incorporation of alumina in FeO-MgO-Al₂O₃-SiO₂-H₂O (FMASH) serpentinites has been developed by considering ideal Tschermak (Al₂Mg₁Si₁) solid solution in antigorite [1]. In the assemblage antigorite-olivine-chlorite-fluid the Al-content of antigorite is buffered and temperature sensitive. This temperature sensitivity is the basis for a serpentinite geothermometer at greenschist, amphibolite and eclogite facies conditions. The buffer assemblage is stable in harzburgite bulk compositions for relatively moderate amounts of Al₂O₃ (> 1.8 wt. %) and is widespread in lherzolites protoliths, where it occurs together with diopside or, in a narrow higher temperature field, with tremolite.

The utility of the Tschermak solid solution model in antigorite has been applied to serpentinite samples from the Betics (Cerro del Almiraz, Spain) and the Western Alps (Zermatt-Saas). Agreement with previous estimates of metamorphic PT conditions supports the reliability of this new geothermometer.

[1] Padrón-Navarta *et al.*, 2013 Tschermak's substitution in antigorite and consequences for phase relations and water liberation in high-grade serpentinites. *Lithos* (in press)

Quantifying effective ferric iron content in hematite-rich metapelites through phase equilibria modelling

D. LO PÒ^{1*} AND R. BRAGA¹

¹University of Bologna, Piazza di Porta San Donato 1, 40126, Bologna, Italy

(*correspondence: deborah.lopo@unibo.it)

Iron is a common element in metapelites and is usually approximated to be entirely ferrous. Underestimating the ferric iron (Fe³⁺) content, however, may result in erroneous whole-rock compositions and thus incorrect P-T estimates when dealing with Fe³⁺-oxides-rich metapelites. A geothermobarometric-based approach to infer the rock Fe₂O₃ content is here presented using hematite-rich metapelites from Palaeozoic basement of the Pisani Mts. (Northern Apennines, Italy) as example. The paragenesis is represented by phengitic white mica, chlorite (X_{Fe²⁺} = Fe²⁺/(Fe²⁺+Mg) = 0.54), chloritoid porphyroblasts (X_{Fe²⁺} = 0.86), quartz and rutile. Hematite is widespread in the matrix and locally forms mm-thick layers. Because of the lack of reliable Fe³⁺ recalculation scheme for major rock-forming minerals, thermodynamic modelling was first attempted assuming whole-rock total iron as FeO. This assumption failed to reproduce the observed paragenesis and mineral compositions. This mismatch suggested that a certain amount of bulk Fe_{tot} must be converted into Fe³⁺, which is mainly contained in hematite. In order to calculate the Fe₂O₃ content a P-X_{Fe₂O₃} (X_{Fe₂O₃} = Fe₂O₃/(FeO + Fe₂O₃)) pseudosection was performed at a fixed T = 475 °C, estimated through the chloritoid-chlorite geothermometer [1]. X_{Fe²⁺} in chlorite and chloritoid intersect in the field corresponding to the observed paragenesis, at P ≈ 9-10 kbar and X_{Fe₂O₃} ≈ 0.6, which is the effective Fe³⁺ content needed to stabilise the observed paragenesis. The inclusion of Fe³⁺ in the modelling increases the whole-rock MgO/(MgO+FeO_{tot}) ratio, which in turn affects chloritoid and chlorite X_{Fe²⁺}. The new P-T constraint agrees with available thermobaric conditions for the Alpine metamorphism in Northern Apennines recorded in Triassic metasedimentary cover, especially in the Verrucano facies rocks [2]. Our modelling suggests that the generally overlooked Northern Apennine Palaeozoic basement was deeply involved during the Paleogene collision between the Adria and Corsica-Sardinia microplates.

[1] Vidal *et al.* (1999) *Journal of Metamorphic Geology* **17**, 25–39. [2] Franceschelli *et al.* (2004) *Periodico di Mineralogia* **73**, Spec. Issue 2, 43-56.

Highly siderophile elements and mantle heterogeneities: The interplay between accessory sulfides and trace minerals.

LORAND, J.-P.

LPGN, CNRS UMR 6112, University of Nantes, Nantes, France (jean-pierre.lorand@univ-nantes.fr)

Highly siderophile elements (HSE = Platinum-group elements, Au, Re, Se, Te) occur at ppb concentration levels in the Earth's upper mantle. The HSE are now currently used as geochemical tracers, owing to their wide range of compatibility. Accessory (<0.1 vol.%) Fe-Ni-Cu sulfides (BMS) are the main HSE carriers in the fertile upper mantle. In contrast to lithophile elements, the HSE are versatile elements which easily change their host minerals as a function of sulfur-saturation, redox conditions, pressure, fugacity of sulfur, melt compositions. Recent studies put strong effort to unravel which phases control the HSE budget of mantle rocks after partial melting, metasomatism and magmatic refertilization. Each stage generates specific interplay between BMS and a wide range of micron-sized trace platinum-group minerals (PGMs).

By progressively eliminating sulfur, adiabatic partial melting processes and porous flow percolation systems at high melt/rock ratios transfer the HSE systematic of mantle residues from the BMS to refractory monosulfides, and then to PGMs. The HSE may form their own minerals (refractory PGMs, i.e. Os-Ir-Ru alloys/sulfides; Pt-Ir(Os) alloys) which carry the whole-rock HSE budget at the micron scale. The inhomogeneous distribution of these micron-sized PGMs may cause extreme nugget effects in the whole-rock budgets. They may also decouple elements that are usually considered to be proxies in sulphur-saturated conditions (e.g. Se and Te, Pt and Pd).

Magmatic erosion at the lithosphere-asthenosphere boundary and magmas fluxing through the lithospheric mantle may completely rejuvenate the PGE budgets inherited from melting events. Melt/mantle reactions redistribute the HSE systematics into newly formed, metal-rich BMS, while generating a wide variety of Pt-Pd-Te-Bi microphases. Arsenic may also play an important role in the sub-arc mantle or in volatile-rich metasomatic processes, generating immiscible Ni-As-S liquids in the most As-rich environments. Refractory PGMs may survive these rejuvenation, dispersing the Os isotopic compositions of ancient melt depletion events on a regional scale through refertilized peridotites and melt vein-conduits (e.g. chromitites, pyroxenites). Thus, understanding mantle heterogeneities from whole-rock HSE systematics requires appropriate tools for evaluating the different HSE carriers and their origin.

Basalt weathering on Mars: insights from Li-isotope fractionation models

E. LOSA ADAMS^{*1}, C.G. LOZANO¹, P. DIZ¹, L.G. DUPORT¹, A.F. DAVILA² and A.G. FAIREN³

¹ Universidad de Vigo. 36200 Vigo. Spain.

(corresponding author*: elosa@alumnos.uvigo.es)

² SETI Institute, Mountain View, CA 94043, USA.

³ Cornell University. Ithaca, 14853 New York, United States

Lithium is incorporated as trace element in most of basalt bearing minerals, namely olivines, clinopyroxenes and plagioclase feldspars, where Li abundance lies in the order of 1-200 ppm depending on their source area. For modeling purposes, we assume an initial value of ⁷Li = 5 ‰ that corresponds to the average isotopic signature of unweathered MORB basalts [1,2]. It is also assumed that dissolution of basalt leads to release of both isotopes, without significant isotope fractionation. Secondary minerals incorporate a significant fraction of the dissolved Li, with selective uptake of ⁶Li by clays through cation exchange reactions [3].

Modelling clay-water Li isotope fractionation

Geochemical Models dealing with the selective uptake of each Li isotope by clays were achieved by implementing in the *Phreeqc* code a specific algorithm that splits the total amount of sorbed Li between ⁶Li and ⁷Li isotopes under the assumption that fractionation occurs following a Rayleigh distillation process. Li-isotopic signature in H₂O resulting from weathering of basalt was analyzed in two scenarios: (1) at near equilibrium conditions and constant temperature, (2) along simultaneous freezing and evaporation buffered by a CO₂ atmosphere. Resulting models were used to describe possible paths of Li isotopic fractionation and the extent of basalt weathering on early Mars conditions, as a function of supersaturation, temperature and evaporation rates. We suggest, using MSL capabilities for Li detection, to complete an initial screening for targets relevant for an eventual analysis of Li isotopes.

[1] Tomascak, P.B., 2004. Reviews in Mineralogy and Geochemistry. Vol. 55, 153-195. [2] Tang *et al.*, 2007 *Int. Geol. Rev.*, 49, 374-388. [3] James, R.H., Palmer, M., 2000. *Geochim. Cosmochim. Acta* 64, 3111-3122.

Thermodynamic data for cementitious systems: Katoite

B. LOTHENBACH^{1*}

¹Empa, Concrete & Constr. Chem., Dübendorf, Switzerland
(*correspondence: barbara.lothenbach@empa.ch)

The formation of katoite, $3\text{CaO}\cdot\text{Al}_2\text{O}_3\cdot 6\text{H}_2\text{O}$, is observed experimentally in hydrated calcium aluminate cements but generally not in hydrated Portland cements. Thermodynamical modeling of the stable phases in hydrated Portland cements without calcite predicts either the formation of katoite, $3\text{CaO}\cdot\text{Al}_2\text{O}_3\cdot 6\text{H}_2\text{O}$ [1], or monosulfoaluminate, $3\text{CaO}\cdot\text{CaSO}_4\cdot\text{Al}_2\text{O}_3\cdot 12\text{H}_2\text{O}$ [2-4], depending on which thermodynamic data are used.

A recent critical review of the thermodynamic data for katoite resulted in $\Delta_f G^\circ = -5008.2$ kJ/mol and $\Delta_f H^\circ = -5537.3$ kJ/mol [5] using an entropy of 422 J/mol/K and heat capacity of 446 J/mol/K from [6]. It was shown that some of the experimental solubility measurements have been performed on carbonated samples where monocarboaluminate had precipitated [5]. This resulted in too low $\Delta_f G^\circ$ values for katoite in many databases [2-4] and thus to wrong predictions on the stability of katoite as shown in the figure below.

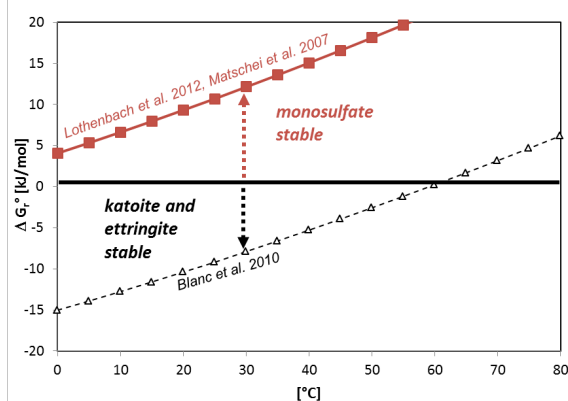


Figure 1: Influence of the stability of katoite on the stability of ettringite and katoite relative to monosulfate in hydrated Portland cements: $3\text{CaO}\cdot 3\text{CaSO}_4\cdot\text{Al}_2\text{O}_3\cdot 32\text{H}_2\text{O} + 2(3\text{CaO}\cdot\text{Al}_2\text{O}_3\cdot 6\text{H}_2\text{O}) \rightleftharpoons 3(3\text{CaO}\cdot\text{CaSO}_4\cdot\text{Al}_2\text{O}_3\cdot 12\text{H}_2\text{O})$.

[1] Matschei *et al.* (2007) *Cem Concr Res* **37**, 1379-1410. [2] P. Blanc *et al.* (2010) *Cem Concr Res* **40**, 1360-1374. [3] Damidot & Glasser (1993) *Cem Concr Res* **23**, 221-238. [4] Lothenbach & Winnefeld (2006) *Cem Concr Res* **36**, 209-226. [5] Lothenbach *et al.* (2012) *Cem Concr Res* **42**, 1621-1634. [6] Geiger *et al.* (2012) *Am Min* **97**, 1252-1255.

Distinctive Composition and Genesis of Copper Ore-forming Arc Magmas

ROBERT R. LOUCKS^{1*}

¹Centre for Exploration Targeting & CCFS, School of Earth and Environment, University of Western Australia, Crawley, WA 6009, Australia
*email: Robert.Loucks@uwa.edu.au

In arc segments undergoing orogenic deformation, magma ascent to shallow depths is inhibited by horizontal compressive stress that hinders dyke propagation and that fosters development of subhorizontal magma chambers deep in the ductile lower crust. Experimental and field evidence shows that distinctive chemical features of Cu-ore-forming arc magmas develop in magma chambers near the Moho where country- rock temperatures on a normal arc geotherm are around 700-800°C, so magma chambers cool slowly and tend to last long enough to experience intermittent influxes of mantle-derived basaltic magmas that mix with residual magma already in the chamber, producing multiple cyclic units in stratified crystal cumulates on the magma chamber floor. Residual dacitic melt fractions eventually acquire extraordinary contents of dissolved H_2O (~10 wt%) and SO_3 and probably Cl by inheritance through many cycles of chamber replenishment and fractional crystallisation. Over many such cycles, residual magmas reach unusually high ferric/ferrous ratios, due to selective segregation of ferrous iron into cumulate silicates. The typically high oxidation states of Cu-ore-forming arc magmas is reflected in part by elevated V/Sc and Eu/Eu^* ratios. This high oxidation state endows the magma with exceptional sulfur-carrying capacity, because sulfate is around 100 times more soluble (at anhydrite saturation) than sulfide (at pyrrhotite saturation) in magmas of dacitic to rhyolitic composition. The effects of high pressure and high content of dissolved H_2O are to retard plagioclase crystallisation and promote early and prolific hornblende crystallisation, which causes the ratios $(\text{Eu}/\text{Eu}^*)/\text{Yb}$ and Sr/Y to increase in residual melt as differentiation proceeds from basaltic to dacitic compositions.

Values of $\text{Sr}/\text{Y} > 35$, $(\text{Eu}/\text{Eu}^*)/\text{Yb} > 2$, and $\text{V}/\text{Sc} > 10$ at 58-70 wt% SiO_2 are typical of arc magmas parental to magmatic-hydrothermal copper ore deposits throughout Phanerozoic time, according to my compilation of compositions of ore-forming intrusives in >135 deposits. These ratios may be used to screen collections of whole-rock chemical analyses to identify igneous complexes that are prospective (fertile) for copper ore genesis. Hundreds of thousands of such analyses are available in published literature. I have compiled many.

Evolution of anthropogenic contamination in the Seine River (France) over the last 15 years revealed by boron isotope ratios

P. LOUVAT¹, D. GUINOISEAU¹, G. PARIS^{1,2}, J.-B. CHEN^{1,3}, B. CHETELAT^{1,3} AND J. GAILLARDET¹

¹Institut de Physique du Globe de Paris, Sorbonne Paris Cité, Univ Paris Diderot, UMR 7154 CNRS, Paris, France

²GPS - Caltech, MC 131-24, Pasadena, CA 91125, USA,

³State Key Laboratory of Environmental Geochemistry, Institute of Geochemistry, CAS, Guiyang 550002, China

Boron is an ubiquitous constituent of plants and materials and is widely used by human activities (borosilicate glasses and ceramics, detergents, fertilizers, cosmetics...). Boron has a relatively conservative behaviour within the hydrosphere, and its isotopic compositions are possible tracers of anthropogenic activities. Following the work by Chetelat and Gaillardet (Env. Sci. Tech. 2005) on boron isotopes as a probe for anthropogenic contamination in the Seine River (France), we investigate 3 other series of water samples collected in Paris (monthly between 2004 and 2007) and on the whole Seine Basin (at high- and low-water stages) between 2004 and 2012 that complement their 1994 series. ¹¹B/¹⁰B ratios have been measured by MC-ICP-MS with d-DIHEN as sample introduction device (Louvat, Bouchez and Paris, Geostand. Geoanal. Res. 2011) after boron extraction on resin Amberlite IRA 743 (adapted from Lemarchand *et al.*, Chem. Geol. 2002). They are expressed in ‰, notation δ¹¹B.

From 1994 to 2007, B concentrations ([B]) have been reduced by a factor of up to 2 for the Seine River in Paris, and the range of δ¹¹B variations restricted (2 to 9 ‰). On the whole Seine River Basin, [B] are the highest downstream from Paris, associated to the lowest δ¹¹B. These characteristics are even more pronounced during low-water stage. There is however no marked evolution of [B] and δ¹¹B between the sampling session of 2004-2007 and the more recent ones of 2009 and 2011-2012.

Low δ¹¹B and high [B] are attributed to anthropogenic sources of boron within the Basin, which are increasing downstream with increasing population density and industrial activities. Two hypotheses are tested to explain the variation of [B] and δ¹¹B in Paris between 1994 and 2006: i/ changing of the δ¹¹B signature for the plant treated waste waters from -10‰ to 0‰, ii/ decrease of the anthropogenic input of boron to the Basin.

A high T cell for the *in situ* study of flux-driven magmatic processes

M. LOUVEL^{1*}, D. TESTEMALE¹, E. LAHERA¹
AND J.-L. HAZEMANN¹

¹ Institut Neel, CNRS-Grenoble, F-38042 - Grenoble, France.
*marion.louvel@grenoble.cnrs.fr

Aqueous fluids and vapors that exsolve from silicate melt as magma rises through the upper crust are of critical importance in volcanic arcs. They can for instance affect the dynamics of magma ascent and trigger eruption or favor the mobilization of metals as Cu, Au and Mo at the origin of the formation of porphyry ore deposits [1, 2]. Up to now, constraints on the nature of these volatile-rich phases and their relation to silicate melts are mainly limited to the chemical analysis of volcanic fumaroles and the study of melt and fluid inclusions [3]. Furthermore, experiments investigating aqueous fluids or vapor phases in complex systems involving both fluids and melts are challenging, scarce and rely either on mass balance calculations [4] or synthetic fluid inclusions [5].

Here, we present an hydrothermal cell [6] developed to achieve P-T conditions relevant to the *in situ* study of magmatic-hydrothermal processes. This device enables visual monitoring of the high P-T sample but also Raman, X-ray fluorescence (SXRF) and X-ray absorption (XAS) measurements up to 950 °C and 1.5 kbar. Preliminary studies focused on determining 1) phase relations, fluid densities and volatiles speciation in H₂O-CO₂, H₂O-CO₂-NaCl and H₂O-CO₂-Hpg melt systems from 200 to 950 °C and 0.5 to 1.5 kbar and 2) the effect of pressure, temperature and fluid composition on the fractionation and speciation of Cu in fluid-melt systems.

[1]Sparks, 1978. *J. Volcanol. Geotherm. Res.* **3**, 1-37.
[2]Hedenquist and Lowenstern, 1994. *Nature* **370**, 519-527.
[3]DeVivo *et al.*, 2005. *Elements* **1**, 19-24. [4]Keppler., 2010. *Geoch. Cosmo. Acta* **74**, 645-660. [5]Simon *et al.*, 2005. *Geoch. Cosmo. Acta* **69**, 3321-3335. [6]Testemale *et al.*, 2005. *Rev. Sci. Instr.* **76**, 043905-5.

Monodentate inner-sphere coordination of arsenate and phosphate anions, stabilized by hydrogen bonding, at the goethite/water interface

LARS LÖVGREN^{*1}, HANNA NELSON¹
AND STAFFAN SJÖBERG¹

¹Department of Chemistry, Umeå University, SE-901 87
Umeå, Sweden (*lars.lovgren@chem.umu.se)

We have previously described adsorption of arsenate to goethite (α -FeOOH) using a simplified surface complexation model including two surface complexes with arsenate anions [1]. ATR-FTIR studies have, however, shown that more than two complexes are formed [2,3]. Supported by this information new models are presented for surface complexation of arsenate and phosphate. Based on data from potentiometric titrations and batch adsorption experiments, combinations of complexes were tested. Different stoichiometries with corresponding charge distributions according to Pauling's valence bond theory were tested. A coordination mode considering monodentate inner-sphere binding to singly coordinated surface hydroxyl groups with hydrogen bonding to neighbouring triply coordinated surface oxygen were assumed. The resulting model consists of six ternary surface species which match data from both wet chemistry and spectroscopy. Four of the complexes involve a hydrogen bond between the arsenate (or phosphate) anion and a neighbouring surface site. In one complex the ligand acts as a hydrogen bond acceptor and in the other three as a hydrogen bond donor. Species with the same overall charge can be regarded as surface isomers.

[1] Nelson *et al.* (2013) *Appl. Geochem.* In press. [2] Loring *et al.* (2009) *Chemistry- a European Journal* **15**, 5063-5072. [3] Persson *et al.* (2012) *J. Colloid Interface Sci.* **386**, 350-358.

Use of mobile laser-based methane analysers to target plume sampling for high-precision isotopic analysis

D. LOWRY¹, R. FISHER¹, J. FRANCE¹, M. LANOISELLÉ¹, G. ZAZZERI¹, E.G. NISBET¹,
A. WELLPOTT² AND S. BAUGUITTE²

¹Greenhouse Gas laboratory, Department of Earth Sciences,
Royal Holloway, University of London, Egham, Surrey
TW20 0EX, UK (d.lowry@es.rhul.ac.uk)

²Facility for Airborne Atmospheric Measurements (FAAM),
Cranfield University, Cranfield, Bedford MK43 0AL, UK

Laser-based analysers are capable of very high precision methane concentration measurements, but are not yet close to matching the precision for isotopic measurement of methane by isotope ratio mass spectrometry. The challenge is even bigger for mobile platforms, such as aircraft, where a plume of methane may be encountered for as little as 5-seconds.

Real-time methane measurements have been made using mobile laser-based spectrometers on land, sea and air platforms, while steel flask and Tedlar bag sampling systems have been used to grab air samples from the identified plumes for later high precision isotopic analysis by IRMS. The rapid-response (1Hz or better) of the methane concentration measurements combined with fast-flow sampling pumps allows narrow plumes to be targeted for sample collection.

A 4WD vehicle is used to detect plumes from landfill sites, gas processing and distribution systems in the UK. A ship-based system is detecting emissions of methane near hydrate dissociation zones in the Arctic and outflow of biological plumes from South America into the Atlantic. The aircraft-based system has been used to target emission plumes from leaking gas rigs, wetlands and forest fires.

The IRMS systems at RHUL are capable of $\pm 0.05\%$ precision or better on triplicates using 75cc of air per analysis. Methane sources have very distinctive $\delta^{13}\text{C}$ signatures around -20% to -40% for combustion sources down to -60 to -80% for biological sources. The further away from the source that a plume is encountered the more diluted toward atmospheric background of -47% is the plume signal. This requires high-precision isotopic measurement to identify the source of the methane increment over background.

Although laser-based isotopic systems are starting to provide useful data at static ground-sites close to source emissions, the combination of laser-based concentration measurements and IRMS provides the best method to identify unknown methane sources, to understand distribution of sources at the regional scale and to tightly constrain the source isotopic signature of known sources.

Are there Unique “Nano” Effects from Exposure to Metal and Metal Oxide Nanoparticles?-Yes and No!

GREGORY V. LOWRY^{1,2}, RUI MA^{1,2}, CLEMENT LEVARD^{3,2}, BENJAMIN P. COLMAN^{4,2}, EMILY S. BERNHARDT^{4,2}, GORDON E. BROWN, JR.^{5,2} AND MARK WIESNER^{4,2}

¹Carnegie Mellon University, Pittsburgh, PA 15213

²Center for Environmental Implications of Nanotechnology

³Centre de Recherche et d'Enseignement de Géosciences de l'Environnement, Aix-en-Provence, France

⁴Duke University, Durham, NC 27708

⁵Stanford University, Stanford, CA 94305

Engineered nanomaterials (ENMs) have novel properties relative to their bulk counterparts. This “uniqueness” is raising societal concerns about their potential for negative environmental effects. However, it is unclear if ENMs result in unique “nano” effects in the environment. Research in the Center for Environmental Implications of Nanotechnology is identifying cases where nanomaterial exposures indeed lead to unique “nano” effects compared to ionic controls, and cases where they do not, i.e. effects are predicted from existing geochemical principles.

The solubility of silver nanoparticles (Ag NPs) was independent of nanoparticle size down to 5 nm. Solubility increased with decreasing size, but in a manner predictable from thermodynamics. This indicated a constant surface energy and an absence of strain on the FCC structure of the particles. This was confirmed with X-ray absorption spectroscopy and by pair distribution function analysis of total X-ray scattering data. The toxicity of Ag NPs to four different organisms was fully explained by the availability of dissolved silver species in the exposure media. Despite the apparent “non-uniqueness” of Ag NPs, application of Ag NPs in biosolids to terrestrial plants resulted in an increase in N₂O flux from the system relative to biosolids and AgNO₃/biosolid controls. This behaviour may be a result of spatial and temporal uniqueness of Ag NPs, i.e. their distribution in the environment and their ability to afford sustained low-level release of Ag ion, rather than from a unique reactivity.

Photoelectrons from minerals and microbial world

ANHUI LU^{1*} AND YAN LI²

¹School of Earth and Space Sciences, Peking University, Beijing.

(*correspondence: ahlu@pku.edu.cn)

²School of Earth and Space Sciences, Peking University, Beijing. (liyan-pku@pku.edu.cn)

The Earth surface is a multiple open system. Semiconducting minerals, including many metal oxides and sulfides, are ubiquitous on Earth's surface and widely participate in redox reactions following photoelectron/photohole pairs excited by solar light. Microorganisms evolve various pathways to utilize extracellular electrons and to get energy. Recently, Lu^[1] presented evidences demonstrating solar energy mediated by semiconducting mineral photocatalysis, promoted the growth of some nonphototrophic bacteria and revealed that the ternary system of microorganisms, minerals and solar light has played a critical role in the life history on Earth. Under simulated sunlight, photoelectrons generated from semiconducting minerals could be used by nonphototrophic microbes to support their metabolisms. The growth of microbe, closely related with the photon quantity and energy, and well fitted the light absorption spectra of the semiconducting mineral. The overall energy efficiency from photon to biomass was 0.13‰ to 1.9‰. Further studies revealed that in natural soil system, semiconducting mineral photocatalysis influenced the microbial community. This solar energy utilization pathway by nonphototrophic microorganisms mediated by semiconducting mineral photocatalysis extends our knowledge on the use of solar energy by nonphototrophic microorganisms, and provides a new concept to evaluate the life origin and evolution. The comprehending of non-phototrophic bacteria solar energy utilization conducted by semiconducting minerals in present environment will greatly help us to better understand the energy transform mechanism among interfaces of lithosphere, pedosphere, hydrosphere and biosphere.

[1] Lu, Li & Jin *et al.* (2012), *Nature Communications* 3, 768-775.

Phases of gold and silver in the sediments in the Jidong gold ore concentration area, China

LU JILONG¹ SHI HOULI¹ HAO LIBO¹ ZHAO YUYAN^{1A} AND LIU HONGYAN²

¹College of GeoExploration Science and Technology, Jilin University, Changchun 130026, China. lujl@jlu.edu.cn

²Center of Testing Science, Jilin University, Changchun 130026, China.

49 samples of sediment in Jidong ore concentration area, located in the subunit of the yanshan fold belt in north China platform - the middle of Malanyu uplift, were sampled and the different phases of gold and silver were analyzed. The results showed that eight phases of gold (soluble facies, surface adsorbing facies, organic facies, carbonate facies, natural gold facies, iron and manganese oxides facies, sulfide facies and residual facies) could be detected in the sediments and seven phases of silver (as same as phases of gold except natural gold facies) could be detected in the sediments. Au of sediments existed mainly in the phases of natural gold facies and sulfide facies in the gold abnormal area, while in the background area, mainly in natural gold facies and organic facies. But to the silver of sediments, both existed mainly in the sulfide facies and residual facies in gold abnormal area and the background area. Thus could be utilized in the evaluation of anomaly and be propitious to gold deposit exploration in the area.

Acknowledgement: The study was supported by SinoProbe-04-05-02.

Pb and Zn Coprecipitation with Iron Oxyhydroxide Nano-Particles

PENG LU,¹ SHELLY KELLY² AND CHEN ZHU,¹

¹Department of Geological Sciences, Indiana University, Bloomington, 1001 E 10th Street, Bloomington, IN 47405-1405, chenzhu@indiana.edu

²Argonne National Laboratory, Biosciences Division, Argonne, IL 60439-4843, United States

Pb and Zn coprecipitation with Fe³⁺ was studied with sorption edge measurements, desorption experiments, paired coprecipitation – adsorption experiments for comparison, sorbent aging, EXAFS, High Resolution Transmission and Analytical Electron Microscopy (HR TEM–AEM), and geochemical modeling. Coprecipitation of Pb with ferric oxyhydroxides occurred at ~ pH 4 [1] and for Zn at pH ~5 [2], about 0.5-1.0 pH unit higher than Fe³⁺ precipitation. Coprecipitation is more efficient than adsorption in removing Pb and Zn from aqueous solutions at similar sorbate/sorbent ratios and pH. HRTEM of the Pb-Fe and Zn-Fe coprecipitates shows a mixture of 2 to 6 nm diameter 2-line ferrihydrite spheres. The co-refinement of the Pb LIII-edge and the Fe K-edge EXAFS spectra suggested that Pb formed a solid solution in the Pb-Fe coprecipitate [3]. Desorption experiments show that more Pb²⁺ was released from loaded sorbents collected from adsorption experiments than from Pb to Fe coprecipitates at dilute EDTA concentrations. Desorbed Pb²⁺ versus dissolved Fe³⁺ data show a linear relationship for coprecipitation desorption experiments but a parabolic relationship for adsorption experiments.

Based on these results, we hypothesize that Pb²⁺ was first adsorbed onto the nanometer-sized, metastable, iron oxyhydroxide polymers of 2-line ferrihydrite with domain size of 2–3 nm. As these nano-particles assembled into larger particles, some Pb²⁺ was trapped in the iron oxyhydroxide structure and re-arranged to form solid solutions.

Our study shows that coprecipitation and adsorption experiments resulted in different Pb and Zn incorporation mechanisms, which could result in different mobility, bioavailability, and long-term stability of trace metals in the environment.

[1] Lu, P., NT Nuhfer, S. Kelly, Q. Li, H. Konishi, E. Elswick, C. Zhu. (2011) Pb²⁺ coprecipitation with iron oxyhydroxide nano-particles. *Geochimica et Cosmochimica Acta* **75**, 4547-456. [2] Martin, S., Zhu, C, Rule, J., Nuhfer, N. T., Ford, R., Hedges, S., Yee, S. (2005) A high resolution TEM-AEM, pH titration, and modeling study of Zn²⁺ coprecipitation with ferrihydrite. *Geochimica et Cosmochimica Acta* **69**, 1543-1553, 2005. [3] Kelly, S., Lu, P., Newville, M.G., Bolin, T., Chattopadhyay, S., Shibata, T., Zhu, C. (2008) Molecular structure of Lead (II) coprecipitated with Iron(III) oxyhydroxide. *In Adsorption of Metals by Geomedia II: Variables, Mechanisms, and Model Applications*. (M. Barnett and D. Kent eds.), pp. 67-94, Developments in Earth & Environmental Sciences 7, Elsevier.

www.minersoc.org

DOI:10.1180/minmag.2013.077.5.12

Preliminary studies on physicochemical characterization of PM_{2.5} collected in underground and ground-level rail systems Shanghai metro

SENLIN LU^{1*} HAO XIAOJIE¹ LIU DINGYU¹ ZHANG RONGCI¹ YI FEI¹ GU YAN¹ LUO WENYUN^{1*} LIN JUN² AND YONEMOCHI SHINICHI³

¹School of Environmental and Chemical Engineering, Shanghai University, Shanghai 200444, China

²Shanghai Institute of Applied Physics, Chinese Academy of Sciences, Shanghai 201800, China

³Center for Environmental Science in Saitama, Saitama 374-0115, Japan

Metro systems are an important transportation mode in megacities across the world. Few works focused on fine particles in the atmosphere of metro. A campaign was conducted to investigate physicochemical characterization of ambient fine particles (PM_{2.5}, D<2.5µm) in the atmosphere of underground and metro station of Shanghai rail system. Proton induced X-ray emission (PIXE) technique, field energy scanning electronic microscopy (FESEM) and synchrotron radiation X-ray absorption fine structure (XAFS) were employed to analyse chemical elements and microscopic characterization of PM_{2.5}. Our results showed that mass level of PM_{2.5} in the air of underground of Shanghai metro system (42.17±23.74 µg/m³) was higher than that of PM_{2.5} collected out of metro station (21.54±6.86 µg/m³). The PM_{2.5} was mainly consisted by fly ashes, mineral particles. Al, Si, Ca, S, Fe, Cu, Na, Mg, K, V, Cr, Mn, Zn, Ba, Re, Ti, Cl could be found in the fine particles. Al, Si, Ca, S and Fe were the main elements. Their mass level followed Si>Al>Ca>S>Fe. Considering speciation of trace elements playing key role in their toxicological effects, speciation of copper was selected to be analyzed by XAFS. The XAFS results demonstrated speciation of Cu in fine particles (PM_{2.5}) is present as Cu (I), while significant amount of Cu is present as Cu (II) in the ultrafine particles (PM_{0.1}). Armed with the above results, cellular toxicity will be carried out to assess health risks induced by fine particles in the atmosphere of Shanghai metro system.

Financial supports from NSFC(grant No. Grant No.41273127, 11005144) were acknowledged.

I/Ca evidence for upper ocean deoxygenation during the Paleocene-Eocene Thermal Maximum

ZUNLI LU^{1*}, ELLEN THOMAS², XIAOLI ZHOU¹, ROSALIND E.M. RICKABY³ AND ARNE WINGUTH⁴

¹Department of Earth Sciences, Syracuse University, Syracuse, NY, 13244, USA. zunlilu@syr.edu

²Department of Geology and Geophysics, Yale University, New Haven, CT, 06511, USA

³Department of Earth Sciences, University of Oxford, South Parks Road, Oxford, OX1 3AN, UK

⁴Department of Earth and Environmental Sciences, University of Texas at Arlington, Arlington, TX 76019, USA

Anthropogenic global warming affects marine ecosystems in complex ways, but the possibility of declining oxygenation is a growing concern. Forecasting the extent, rate and intensity of future ocean deoxygenation and its effects on oceanic biota remains highly challenging because of the complex feedbacks in the earth-ocean-biota system, and the lack of sensitive proxies to reconstruct oceanic oxygen levels of the past². Information from past events such as the Paleocene-Eocene Thermal Maximum (PETM, ~55.5 Ma), possibly the best geological analog for modern global warming, may help in such forecasting. During the PETM, low-oxygen conditions were widespread along continental margins, but there is no evidence that deoxygenation was global and extended into open oceans. We apply a novel paleo-redox proxy, iodine to calcium ratios, in bulk foraminiferal tests (>63µm coarse fraction). The oxidized form of iodine (iodate, IO₃⁻), but not the reduced form iodide, can be incorporated in the calcite structure, thus preserving information about paleo-redox changes. Our results indicate horizontal and vertical expansion of the Oxygen Minimum Zone (OMZ) in the Pacific, Atlantic and Indian oceans following the emission of isotopically light carbon into the ocean-atmospheric system during the PETM.

Source tracing in Li-bearing brines, Salar Pozuelos, NW Argentine

F. LUCASSEN¹, L. KORTE¹, S.A. KASEMANN¹, A. MEIXNER¹ AND R.N. ALONSO²

¹Universität Bremen/MARUM, Isotope Geochemistry, Bremen, Germany, Lucassen@uni-bremen.de

²Universidad Nacional de Salta-CONICET, Salta, Argentina

The source of the spatially restricted Li anomaly and the enrichment processes of Li in the Central Andean salt lakes (salars) are still enigmatic, even though the deposits share common features with other evaporites under arid conditions. A study on chemistry and Li and Sr isotope composition of brines and related salts in a small salar indicates heterogeneous sources of the material ($^{87}\text{Sr}/^{86}\text{Sr} \sim 0.710 - 0.720$), which relates to differences between the principal magmatic, metamorphic and sedimentary rock units. Li contents in brines increases systematically with Mg, K, and Na and is highly variable within the region of NaCl – saturation, where it increases by on-going evaporation and NaCl precipitation. Li isotope variation in the brines is large ($\delta^7\text{Li} \sim +12$ to $+20\text{‰}$), whereas the differences between brine and related salt are $< 1\text{‰}$ with the lower δ - values in the salt. In different sample areas, $\delta^7\text{Li}$ increases with the Li contents, i.e. progressive evaporation. Li concentrations of the brines vary independently of the highly systematic evaporation trend of O and H isotope fractionation, whereas $\delta^7\text{Li}$ shows a general increase with the O and H isotope variation.

A possible path for the Li enrichment in the present salar starts with the dissolution of Li from various rock sources (Sr isotope variability) with low $\delta^7\text{Li}$ (0 to $+6\text{‰}$ for common silicate rocks [1]). These low $\delta^7\text{Li}$ evolve to variably higher values during mineral dissolution and precipitation processes in an aqueous medium. The initially meteoric water changes its O and H isotope signature according to the extent of evaporation on its way from the Li source rock into the salar, e.g., as surface runoff or thermal spring that sample deep sources. Within the salar, the different sources do not mix thoroughly. The dominant process of Li enrichment is evaporation of the brines and halite precipitation. This is accompanied by further but potentially minor fractionation of $\delta^7\text{Li}$, because the ^6Li prefers octahedral coordination in the halite. Complete evaporation leads to layers of high Li halite. Further enrichment of Li by reworking of such layers in dissolution – precipitation cycles, e.g. in pluvial ponds is expected.

[1] Tang *et al.* (2007) *Int. Geology Review* **49**, 374-388

Understanding the impact of Geochemistry: A tribute to Jean Carignan

JOHN N. LUDDEN¹

¹British Geological Survey, Keyworth, Nottingham, NG12 5GG, Jludden@bgs.ac.uk

Jean Carignan, a key scientist in the world of geoanalysis, passed away aged only 48 on the 12th October 2012. Jean started his scientific career as an undergraduate at the University de Quebec a Montreal. With Clement Gariépy he revisited the Pb-isotope signatures of granitoids from the Canadian Superior province. They pioneered the use of Pb-isotopes in minute quantities of separated feldspars for different suites of granitoids. This work underpinned tectonic models for source regions for these rocks, which were integrated into the Canadian Abitibi Grenville Lithoprobe project. As a tireless analyst, always searching for the next improvement that would allow the field of geochemistry to advance, Jean was hired as director of the Centre de Recherche Petrographiques and Geochimiques (CRPG) in Nancy, Service d'Analyses des roches et Mineraux (SARM) on the retirement of Kuppusami Govindaraju. It was here that he developed a mixed array of elemental and isotope analyses for the science community and is used both in France and internationally. In particular, these involved the use of the new generation of ICP-Multi collector Mass spectrometers that were being developed in the late 1990's. This led to a series of research projects in coupled trace element and isotope tracers in environmental processes ranging from Cu, Zn, Fe etc. to Hg and Pb. Jean and his team introduced a number of analytical improvements and focussed on the environmental impact of atmospheric pollutants using novel approaches with samples such as epiphytic lichens as samplers of atmospheric components of the Kola Peninsula.

In this talk I will investigate some of the impacts of his science.

BGS©NERC 2013

The Geochemistry of London

JOHN N. LUDDEN, DENIS W. PEACH AND DEE FLIGHT

¹British Geological Survey, Keyworth, Nottingham, NG12

5GG Jludden@bgs.ac.uk

²British Geological Survey, Keyworth, Nottingham NG12

5GG dwpe@bgs.ac.uk

³British Geological Survey, Keyworth, Nottingham NG12

5GG dmaf@bgs.ac.uk

The population of the Greater London area is expected to grow from 8.2 million in 2013 to >9 million in 2020. London sits on complicated Quaternary superficial deposits including gravels and sands of the Thames and older deposits such as the London Clay, which overlie the chalk basement, the major aquifer of SE England. The superficial deposits include a legacy of pre- and post-industrial hazardous waste and there is also local chemical contamination in groundwater.

As geochemists we must identify and provide workable solutions to removing legacy pollutants and more importantly industrial infrastructure and agricultural development of the UK and worldwide must increasingly be underpinned by solid baseline data in order to provide solutions to environmental issues.

BGS has undertaken a systematic high-density geochemical soil survey of the Greater London Area the "London Earth" project aiming to give insight into the environmental impacts of urbanisation and industrialisation as well as to characterise the geochemical baseline of the Europe's most populous city. We must communicate to councils, developers and the general public of any environmental or health risks. It is urgent that as geochemists we assess these baselines and monitor the subsurface using new sensor networks.

BGS@NERC 2013

Experimental partitioning behavior of MORB in subduction zones at 2 and 3 GPa

STEFANIE LUGINBUEHL^{1*}, PETER ULMER¹

AND THOMAS PETTKE²

¹Dept. Earth Sciences, ETHZ, 8092 Zurich, Switzerland

(*correspondence: stefanie.luginbuehl@erdw.ethz.ch)

²University of Bern, Institute of Geological Sciences, 3012

Bern, Switzerland

Arc volcanic rocks show a typical geochemical signature of fluid-mobile trace element enrichments such as LILE (K, Rb, Cs, Ba). It is assumed that there is an apparent correlation between the structure and composition of the subducting oceanic lithosphere and the composition of subduction zone magmas. The slab components contributing most to the metasomatism of the wedge peridotite are the hydrated igneous oceanic crust and the sediment layer overlying it with notably high trace element concentrations. The mobility of these elements depends on both the nature and composition of the transfer agent and the phase assemblage of the residue.

To investigate the major and trace element budget within subduction zones, we conducted piston cylinder experiments at 2 and 3 GPa and 700 to 1200°C on a K-free, water-saturated and trace element-doped basaltic (pristine) MOR composition. Mobile phases are collected by the employment of diamond traps and subsequently analysed by the cryogenic LA-ICP-MS technique [1] to quantify major and trace element compositions of fluids and melts.

For K-free MORB compositions we find that the solidus lies between 800 and 850°C at 2 and 3 GPa, subsolidus phase assemblages consist mainly of the hydrous phases amphibole and epidote. Garnet, clinopyroxene and rutile, a typical eclogitic phase assemblage, is stable at higher, supersolidus temperatures. We present new results on the trace element partitioning behavior between liquids and mineral phases. In agreement with previous studies, we find that garnet is strongly controlling Heavy REE, while rutile and titanite (2 GPa, 700°C) hold back HFSE ($D^{\text{solid/fluid}} \geq 10$). Additionally we find staurolite being stable at 3 GPa and 700°C that incorporates HFSE as well as Th. Epidote is an abundant phase at PT-conditions where we suggest an aqueous fluid being released from the dehydrating slab, it strongly incorporates Light REE, Th and to a lesser extent U ($D^{\text{solid/fluid}} \geq 100$). These new experimental results are utilized in forward modelling to quantify element mobility in subduction zones.

[1] Kessel K. *et al.* (2004) *Am. Mineralogist*, **89**, 1078-1086.

Experimental and modelling studies of nuclear materials

G.R. LUMPKIN^{1*}, R.O. AUGHTERSON¹, D.J. GREGG¹,
E.Y. KUO¹, S.C. MIDDLEBURGH¹, M.J. QIN¹,
M. DE LOS REYES¹, G.J. THOROGOOD¹, Y. ZHANG¹,
Z. ZHANG¹, M. ROBINSON² AND N.A. MARKS²

¹ANSTO, Locked Bag 2001, Kirrawee DC, 2232, NSW, Australia (*correspondence: grl@ansto.gov.au)

²Curtin University of Technology, Perth, WA, Australia

Advanced nuclear fuel cycles offer considerable promise for improvements in safety, performance, actinide management, and provide opportunities for associated methods of energy production (e.g., hydrogen based systems). In general, the proposed reactor systems require new materials capable of performing under the extreme conditions imposed by temperature, radiation fields, and corrosive media. Here we present a comparison of the results obtained from minerals with laboratory observations using ion irradiation methods. The results generally set out the groups of potential actinide host phases in terms of those with intrinsic radiation tolerance due to recovery of damage on picosecond time scales (e.g., fluorite), those with favorable kinetics for longer term damage recovery (e.g., monazite), and many others with unfavorable kinetics. We have also conducted atomistic modelling studies of some of these minerals and other materials of interest. Together with information from the literature, the results are briefly summarized in terms of structure, bonding, and the energetics of defect formation and recovery. We briefly report on the effects of decay of Tc to Ru in rutile.

Figure 1: Atomistic simulations using empirical potentials showing the total Frenkel defect formation energies from the lanthanide, titanium, and oxygen atoms in the orthorhombic Ln_2TiO_5 compounds.

The role of Th-U minerals in assessing the performance of nuclear waste forms

G.R. LUMPKIN^{1*}, R. GIÈRE², C.T. WILLIAMS³
AND T. GEISLER-WIERWILLE⁴

¹ANSTO, Locked Bag 2001, Kirrawee DC, 2232, NSW, Australia (*correspondence: grl@ansto.gov.au)

²University of Freiburg, 79104 Freiburg, Germany

³The Natural History Museum, Cromwell Road, London, UK

⁴University of Bonn, D-53012 Bonn, Germany

A number of alternative crystalline nuclear waste forms have been proposed for deployment in geological repositories. Materials range from general purpose polyphase waste forms for high level wastes to highly specialized waste forms designed specifically for actinides and certain fission products. Here we review the information available from natural systems relevant to the performance of candidate waste form phases. Observed mineral transformations include (approximately) constant volume chemical changes and breakdown to new phase assemblages, with or without loss of Th and U. Together with laboratory experiments, the geochemical data indicate that zirconolite is a promising host phase for actinides and certain fission products. Pyrochlore has a slightly higher dissolution rate in the laboratory and is generally more susceptible to geochemical alteration. Monazite also has low dissolution rates in laboratory experiments, favorable geochemical behavior, and minimal physical property changes due to retention of crystallinity over geological time scales. Although zircon has been studied extensively, the 17-18 % volume expansion due to alpha decay continues to be a major issue for application as an actinide host phase in nuclear waste forms.

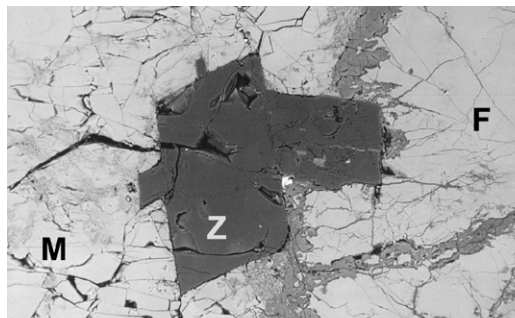


Figure 1: Monazite (M), zircon (Z), and fergusonite (F) from the Rutherford #2 pegmatite ($t = 289$ Ma), Amelia, Virginia. These ABO_4 minerals have reacted differently in the presence of late stage granitic pegmatite fluids. Altered areas are darker gray and most prominent in fergusonite. Image width ~ 1 mm.

Photochemistry of dissolved combined amino acids

RACHEL A. LUNDEEN, JEREMY SCHAECHLI
AND KRISTOPHER MCNEILL*

Institute of Biogeochemistry and Pollutant Dynamics, ETH
Zurich, Universitaetstrasse 16, 8092 Zurich, Switzerland,
kris.mcneill@ethz.ch, rachel.lundeen@env.ethz.ch,
sjeremy@student.ethz.ch

Amino acids are an significant, identifiable portion of the dissolved organic nitrogen pool of natural waters, and are important substrates for microbes at the base of the food web. A portion of the naturally occurring amino acids are photoreactive, which means that photochemistry could play a significant role in the modulation of the microbial utilization of DON. While most research in this area has centered on dissolved free amino acids, most amino acids are present in natural waters as combined amino acids.

The purpose of the present study was to examine the differences in photoreactivity of dissolved free and combined amino acids. Specifically, this work focused on the oxidation of histidine residues in an intact protein (GAPDH) by singlet oxygen.

The results indicate that the reactivity of histidine residues is decreased when in the context of an intact protein, and that the decrease is due to decreased accessibility to the oxidant. The differential reactivity of near-surface and buried residues led to a sensitive method for tracking the intactness of the folded protein during the photolysis.

Return of Archean low sulfate levels during the earliest Mesoproterozoic Oceans

GENMING LUO^{A,C}, SHUHEI ONO^B, JUNHUA HUANG^C,
CHAO LI^A, JIANGSI LIU^A AND SHUCHENG XIE^A

- a. State Key Laboratory of Biogeology and Environmental Geology, China University of Geosciences, Wuhan 430074, China
- b. Department of Earth, Atmospheric, and Planetary Sciences, Massachusetts Institute of Technology, 77 Massachusetts Avenue, Cambridge, MA 02139, USA
- c. State Key Laboratory of Geological Processes and Mineral Resources, China University of Geosciences, Wuhan 430074, China

Sulfate, the second abundant anion in the modern ocean (~28mM), plays an important role in the present biogeochemical cycle of C, S and O. It has been shown that more than 50% of organic matter is remineralized through microbial sulfate reduction and as high as 80% of methane was oxidized by anaerobic methane oxidation archaea coupled with microbial sulfate reduction (Jørgensen, 1982; Valentine, 2002). Furthermore, oceanic sulfate concentration is an important proxy for oxidation state of Precambrian atmosphere and ocean. Therefore unraveling the variation pattern of oceanic sulfate concentration in geological history is very important scientific issue.

A number of studies have shown that oceanic sulfate concentration varied distinctly and periodically in Phanerozoic (e.g., Lowenstein *et al.*, 2003). However, the details of the evolution history of the Precambrian oceanic sulfate concentration are unclear beyond the general increasing trend (Kah *et al.*, 2004). Here we analyzed sulfur isotopic composition of carbonate associated sulfate ($\delta^{34}\text{S}_{\text{CAS}}$) and corresponding disseminated pyrite ($\delta^{34}\text{S}_{\text{py}}$) at the 1.6 Ga Gaoyuzhuang Formation in the North China Craton. The results show that both the $\delta^{34}\text{S}_{\text{CAS}}$ and $\delta^{34}\text{S}_{\text{py}}$ are relatively constant, varying around $13.0\text{‰} \pm 1.8\text{‰}$ and $8.0\text{‰} \pm 2.3\text{‰}$, respectively over 200 m stratigraphic sections. Therefore the sulfur isotopic fractionation ($\Delta^{34}\text{S}$) between the sulfate and pyrite at this time was ~5‰. The relative uniformity in the $\delta^{34}\text{S}_{\text{py}}$ implicates that the pyrite was formed in the water column, and the small $\Delta^{34}\text{S}$ implicates that the sulfate concentration in the earliest Mesoproterozoic ocean would have been extremely low, probably far less than 1 mM. Our identification of extremely low oceanic sulfate concentration in the earliest Mesoproterozoic points to a distinct perturbation in ocean chemistry, which might be related to the decline of coeval atmospheric O_2 concentration.

[1] Jørgensen, B.B. (1982) . *Nature* 296, 643-645. [2] Kah, L.C., Lyons, T.W., and Frank, T.D. (2004) *Nature* 431, 834-838. [3] Lowenstein, T.K., Hardie, L.A., Timofeeff, M.N., and Demicco, R.V. (2003) *Geology* 31, 857-860 [4] Valentine, D.L. (2002) *Antonie van Leeuwenhoek* 81, 271-282.

Petrography and geochronology of the Xianshi uranium deposit in Xiazhuang ore field of South China

JINCHENG LUO^{1*}, RUIZHONG HU¹, XIANWU BI¹,
YOUWEI CHEN¹ AND XIAOYAN JIANG²

¹State Key Laboratory of Ore deposit Geochemistry, Institute of Geochemistry, Chinese Academy of Sciences, Guiyang, Guizhou, 550002, China

(*correspondence: luojincheng027@126.com)

²Institute of Geology and Geophysics, Chinese Academy of Sciences, Beijing 100029, China

South China is rich in numerous U deposits that provided the dominantly U source for the country in the past several decades. Xianshi U deposit is one of very particular deposit in Xiazhuang ore field, situated in southeast Guidong composite granite pluton, Guangdong province is directly associated with hosted-granite and diabase dike and the intersection part between trend and silicification zone. Additionally, the netlike diabase dikes seemingly intrude the main U mineralization of massive uraninite, based on the relatively close contacts between diabase dikes and the high-grade U mineralization. We present detailed petrography, mineral paragenesis and geochronology characteristics of the Xianshi U deposit. Four distinct types of U mineralization have been identified by cross cutting relationships and textures observed in thin sections and BSE images. Alteration is well developed, mainly including pyritization, silicification, carbonation and hematitization. The latter two types are closely related to the high-grade U mineralization. *In-situ* SIMS U-Pb dating of the different type uraninites firstly yield three group ages of 134.6 ± 4.4 , 113.4 ± 2.1 and 103.7 ± 1.8 Ma, respectively. The major U mineralization event occurred at ~ 135 Ma, closely related to the emplacement of diabase dykes and the crust extensional tectonic regime. It appears to represent the oldest U mineralization event observed in Xiazhuang ore field. Stage 2 and stage 3 of U reconcentration generated at 113.4 ± 2.1 and 103.7 ± 1.8 Ma, respectively and appeared as veined uraninite associated with calcite vein. Two ages are consistent with hydrothermal fluid events correlated well with that of diagenetic age of diabase dykes, likely representing the age of two resetting events. Therefore, there are indications that uraninite from Xianshi U deposit has experienced at least three episodes of U concentration associated with the intrusion of local mantle-derived diabase dykes, and is likely to be interpreted to be the hydrothermal origin during Cretaceous crustal extension in South China.

Behaviors of Pb, As and Cd in the Mining Impacted Farmlands

LIQIANG LUO*, BINBIN CHU, YING LIU, XIAOFANG WANG, TAO XU, YING BO AND JIANLIN SUN

National Research Center of Geoanalysis, Beijing, China, 100037(* Correspondence, luoliqiang@cags.ac.cn)

Behaviour and correlations of Pb, As, Cd, Cr, Cu, Zn and other trace elements in farmlands near a Pb-Zn mine were investigated and evaluated. Some of the water and soil quality in the farmlands exceeded permitted standards. The highest concentration of Pb in irrigation water system was over 10 times that of the standards. The minimum, average and maximum, concentrations of Pb in farmland soils were 3.3, 14 and 35 times higher, respectively, than the environmental quality evaluation standards for farmland of edible agricultural products. The minimum concentrations of As and Cd were beyond the standards, while the average and maximum concentrations of As were 4.5 and 11 times higher than the environmental quality evaluation standards. For Cd they were 9 and 34 times higher than the standards. The concentrations of Pb, As and Cd in aerosols and dusts were extremely high and the maximum concentrations of Pb, As and Cd were 10296, 114, and 76 mg/kg, respectively.

The Pb isotope data reveals that the sources of lead in the soils around the Pb-Zn mine were a mixture of lead minerals and ores, current vehicle exhaust particles and deposits of vehicle exhaust particles before unleaded gasoline became available, and even some coal ash.

Correlations between element concentrations in water and soils in the farmlands were very strong. For example, the correlation coefficient of Pb and Cd concentrations in water was 0.944, and in vegetable farmland soils, the correlation coefficients between Pb and As, Pb and Cu, Cd and Mn and Zn concentrations, as well as between Mn and Zn exceeded 0.9. The correlation coefficients between Pb concentrations in soil and water were 0.679, and for As and Cd, they were 0.717 and 0.611, respectively. The element correlations between water and soils were rather strong and may indicate direct impacts on each other. The element concentrations in the aerosols were correlated strongly. For example, the correlation coefficients of Pb and Cd, as well as with Mn, Cu and Zn, were over 0.9 in aerosol samples.

The investigation reveals that the major sources of the pollution in the irrigation water systems and farmland soils were mining activity and vehicle exhaust particles. The contaminants from mining activities have impacts on surrounding environments and may be transported to wide ranges.

Pockmark activity inferred from pore water geochemistry in shallow sediments of the pockmark field in southwestern Xisha Uplift, northwestern South China Sea

MIN LUO¹ AND DUOFU CHEN^{1*}

¹Key Laboratory of Marginal Sea Geology, Guangzhou Institute of Geochemistry of Chinese Academy of Sciences, Guangzhou, China (*correspondence: cdf@gig.ac.cn)

Pockmarks are widespread on the seabed off southwestern Xisha Uplift, northwestern South China Sea. Some of them are enormous that are rarely observed worldwide, but their activities are poorly known up to now. We collected three gravity-piston cores from this pockmark field, one (C9) from outside but in close proximity to a giant pockmark and the other two (C14 and C19) from inside of two giant pockmarks. The sulfate concentration-depth profiles of C9 and C19 pore water are dominantly in response to organoclastic sulfate reduction (OSR), while the sulfate concentration of C14 pore water exhibits three zones of different concentration gradients resulting from various contribution of OSR and anaerobic oxidation of methane (AOM). The depth-profiles of sulfate $\delta^{34}\text{S}$ values of C9 and C14 pore water are in accordance with their sulfate concentration-depth profiles. The relatively low sulfur isotope fractionation in C14 pore water suggests a higher microbial sulfate reduction rate as a possible consequence of AOM than that in C9 pore water. The depth of sulfate-methane interface (SMI) and methane diffusive flux of C14 are estimated to be ~ 14.3 mbsf and ~ 0.0144 mol·m⁻²·yr⁻¹, respectively, based on the sulfate concentration gradient below 3.7 mbsf. Pore water Mg/Ca and Sr/Ca weight ratios imply that high Mg-calcite precipitated in C14. $\delta^{13}\text{C}_{\text{DIC}}$ values of C9 and C19 pore water are inferred to derive from a binary mixing between $\delta^{13}\text{C}$ of organic matter and $\delta^{13}\text{C}_{\text{DIC}}$ of bottom water, while DIC of bottom water, organic matter, methane, and ¹³C-enriched DIC from below SMI possibly all contribute to the DIC pool below 0.66 mbsf in C14. The integrated analysis of pore water geochemistry suggests that the pockmark where C19 was collected may be inactive while the pockmark where C14 was obtained may be presently in sluggish activity with methane-bearing fluid weakly seeping from subsurface sediments.

Acknowledgements: This study was supported by NSFC (91228206), CAS (KZCX2-YW-GJ03) and GIGCAS 135 project Y234021001.

Study of geogas nano-particles of metal deposit in Inner Mongorlia plateau, China

SONGYING LUO^{1,2}, JIANJIN CAO^{1,2*}
AND ZHENGQUAN WU¹

¹Department of earth sciences, Sun Yat-sen University, Guangzhou 510275, China

² Guangdong Provincial Key Lab of Geological Process and Mineral Resources Survey, Guangzhou 510275, China (*Corresponding: eescjj@mail.sysu.edu.cn)

Geochemistry and nano-scale science were adopted in exploration for deep and concealed mineral deposits. The nano-particles in the ascending flow from the concealed ore-bodies are closely to the deposit, and full of the ore-forming information of the type of the deposit. Also modern testing technology can provide a high sensitivity and high resolution method to observe and measure the geogas nano-particles. In our present studies, the static methods of geogas prospecting are used to capture the geogas nano-particles overlying the concealed metal deposit, that are three different types of vegetation form, climate and soil environment in Inner Mongolia plateau, China. The three concealed metal deposits are Dongshengmiao polymetallic pyrite deposit, where is located in Gobi in Hetao Plain of the Yellow River Basin, might be hydrothermal mineralization, Kaxiutata iron deposit is located on the edge of Badanjilin desert, and Bairendaba Ag polymetallic deposit is located in grassland, might be an epithermal silver deposit or a silver orogenic deposit, or of both. The samples are measured by using the TEM technique. The results showed that, the geogas nano-particles may be used as indicators for prospecting the deep concealed ore-bodies, the characteristics and concentrations of the geogas particles is closely related to the type of the ore-bodies and bedrock, not the type of vegetation form, climate or soil environment. It is suggested that geogas prospecting is feasible and applicable to prospect many different types of metal deposit, even other minerals resources.

The research of this dissertation is supported by the National Natural Science Foundation of China (Grant No. 41030425).

Water Quality Simulation in reservoirs in series on the Maotiao River, Southwest China

WENYUN LUO, JING ZHANG, MING YANG,
ZHENG JIAO AND FUSHUN WANG*

School of Environmental and Chemical Engineering, Shanghai University, Shanghai 200444, China
(*correspondence: fswang@shu.edu.cn)

The construction of dams in series has a great impact on the quality and structure of aquatic ecological system of river basin. In this study, we investigated six reservoirs in series on the Maotiao River, southwest China. A monthly sampling strategy was performed in these reservoirs, during year of 2006 to 2007. Nutrients concentration and other parameters, such as DO, T and pH along the river reach and water column in reservoirs were determined. The results showed that seasonal DO and thermal stratification were developed obviously in the Baihua Reservoir and the Hongfeng Reservoir. In addition, we used WASP software to simulate the water quality of these six reservoirs. By comparison, simulated value fitted well with the monitoring values, especially the DO. In the Baihua Reservoir, serious pollution was frequently occurred in October, and DO concentration was extremely low, due to the water overturn. Based on our monitoring and simulating results, we tried to adjust the inflow discharge, and we found that the simulated value of DO in epilimnion in the Baihua Reservoir can be increased by 1.3 mg/L in October. This result indicates that the discharge regulation in upstream reservoirs is a potential method to mitigate the water pollution in downstream reservoir.

Financial supports from NSFC (Grant No. 41273128) were acknowledged.

Geoelectrochemical anomaly, mechanism and exploration of copper and nickel deposit, Hongqiling, Jilin, China

X.LUO¹, M.WEN^{1*} AND F.OUYANG^{1,2}

¹Guilin University of Technology, Guilin, 541004, China
(*meilanwen112@126.com)

²China University of Geosciences, Beijing 100083

The geo-electrochemical study of Hongqiling Cu-Ni deposit resulted in a significant understanding of the geo-electrochemical feature of this copper nickel ore deposit, such as finding the ore-forming halo mechanism of the electrochemistry, which can be used for exploring the concealed ore deposits. This exploration method, called geo-electrochemical extraction, was successfully applied in the area of the Hongqiling mining area, Jilin province, China. The geo-electrochemical result shows that there exist geochemical anomalies of Cu, Ni, Co, Pt, Cr, Sr over the ore bodies. These anomalies, with synchronous vertical feature, are characterized variable value order from high to low: Cu>Ni>Co>Pt>Cr>Sr. The study of the electrochemical dissolution of Cu- Ni ores shows that after 24-hour, 2.2×10^{-6} of Cu^{2+} , 1.8×10^{-6} of Ni^{2+} , and 1.5×10^{-6} of Co^{2+} dissolved from the ores appear in the solution. This experimental work proves that the Cu-Ni ores can be dissolved by using electrochemical method, and thus the geo-electrochemical extraction is feasible in searching for concealed ore deposits. The success of this exploring technique in the exploration for concealed ore deposits has been demonstrated in the subsequent exploration activities in the Hongqiling area, and resulted in discoveries of 3 areas of geo-electrochemical anomaly.

Helium Isotope and $C^3\text{He}$ Signatures in the Northern Lau Basin: Distinguishing Arc, Backarc, and Hotspot Affinities

J. LUPTON¹, M. LILLEY², D. BUTTERFIELD³, J. RESING³,
R. ARCULUS⁴, K. RUBIN⁵, D. GRAHAM⁶, N. KELLER⁷,
E. BAKER³ AND R. EMBLEY¹

¹NOAA/PMEL, Newport, OR 97365 USA

²School of Ocean., Univ. of Washington, Seattle, WA, USA

³NOAA/PMEL, Seattle, WA, USA

⁴RSES, Australian National Univ., Canberra, Australia

⁵SOEST, Univ. Hawaii, Honolulu, HI, USA

⁶COEAS, Oregon State Univ., Corvallis, OR, USA

⁷IES, Univ. of Iceland, Reykjavik, Iceland

Helium isotope and $C^3\text{He}$ ratios have proven useful for differentiating between various mantle reservoirs such as mid-ocean ridges, arcs, backarcs, and mantle hotspots. True back-arc systems are similar to mid-ocean ridge (MOR) systems with $^3\text{He}/^4\text{He}$ of $\sim 8 \text{ Ra}$ ($R = ^3\text{He}/^4\text{He}$ and $\text{Ra} = \text{Rair}$) and $C^3\text{He}$ of $\sim 10^9$. In contrast, arc volcanoes have lower $^3\text{He}/^4\text{He}$ and higher $C^3\text{He}$ ratios ($\geq 10^{10}$), presumably due to carbon addition by the downgoing slab. Hotspots typically have elevated $^3\text{He}/^4\text{He}$ (12 - 30 Ra) and $C^3\text{He}$ similar to MORBs ($\sim 10^9$). We have applied this approach to the northern Lau Basin, which is host to a complicated pattern of volcanic activity, with the NE Lau Spreading Center in the west, the volcanoes of the Tofua Arc in the east, and various other volcanic centers in between. Farther west along the NW Lau Spreading Center, elevated $^3\text{He}/^4\text{He}$ ratios in the seafloor lavas suggest that an OIB or mantle plume component, possibly from Samoa, has influenced this extensional zone. This paper will discuss how these volcanic centers and spreading zones show varying degrees of influence from arc, MOR, and hotspot components based on their $^3\text{He}/^4\text{He}$ and $C^3\text{He}$ fingerprints.

Characterization of transport parameters during limestone dissolution experiments

LINDA LUQUOT^{1*}, TOBIAS RÖTTING^{1,2}
AND JESUS CARRERA¹

¹Institute of Environmental Assessment and Water Research
(IDAEA, CSIC) Barcelona, Spain

²GHS, Departement of Geotechnical Engineering and
Geosciences, Technical University of Catalonia (UPC-
BarcelonaTech), Barcelona, Spain

(* linda:luquot@idaea.csic.es)

CO_2 sequestration in deep geological formation is considered an option to reduce CO_2 emissions in the atmosphere. After injection the CO_2 will slowly dissolve into the pore water producing low pH fluids with a high capacity for dissolving carbonates. Limestone rock dissolution induces geometrical parameters changes such as porosity, pore size distribution, or tortuosity which may consequently modify transport properties (permeability, diffusion coefficient). Characterizing these changes is essential to model flow and CO_2 transport during and after the CO_2 injection.

Here we report experimental results from the injection of acidic fluid into limestone core samples of 25.4 mm diameter, 12.5 mm length. Experiments were realized at room temperature. Before and after each acidic rock attack, we measure the sample porosity, the diffusion coefficient and the pore size distribution. During percolation experiments, the permeability changes are recorded and chemical samples taken to evaluate calcite dissolution. Several dissolution-characterization cycles are performed on each sample in order to study the evolution and relation of the different parameters.

These experiments show that far from the well injection site (i.e. intermediate pH solution (4-5)), dissolution processes are characterized by slow mass transfers. We measure a permeability decrease during the different experiments. Nevertheless, we observed a porosity increase in the sample inlet with higher pore diameters. In the opposite, we measured smaller pore sizes near the core sample outlets. These results indicate that some fine particles move from the sample inlet towards the outlet. Due to the low fluid acidity, these fine particles are not dissolved inside the samples and are transported inside. Consequently, these particles can locally clog the porous space and decrease the permeability.

Role of carboxylates released by microorganisms and roots of alpine pioneer plants in mobilising phosphorus and metal cations during early soil formation

JÖRG LUSTER^{*1}, HANS GÖRANSSON²,
HARRY OLDE VENTERINK³, IVANO BRUNNER¹
AND BEAT FREY¹

¹Swiss Federal Research Institute WSL, CH-8903
Birmensdorf, Switzerland

(*correspondence: joerg.luster@wsl.ch;
ivano.brunner@wsl.ch, beat.frey@wsl.ch)

²Inst. of Forest Ecology, BOKU, A-1190 Vienna, Austria
(hans.goeransson@boku.ac.at)

³Inst. of Integrative Biology, ETHZ, CH-8092 Zurich,
Switzerland (harry.oldeventerink@env.ethz.ch)

In the framework of an interdisciplinary study on initial soil formation along a deglaciation chronosequence, we examined the role of carboxylates in mobilising P and metal cations, in particular at the early stages of soil development, where no or only little soil organic matter has built up.

At selected sites with 6, 70 and 128 year old soils, soil solution was collected in-situ using micro suction cups, differentiating between the rhizosphere of specific plants and bulk soil. At the youngest site, carboxylates were enhanced in all rhizospheres exhibiting plant specific patterns, while phosphate and metal concentrations were increased in rhizospheres at all soil ages. Overall and independent of soil age, soil type and sampling date, net mobilisation of P and metals correlated with the net production of carboxylates, with malate, tartrate, oxalate and citrate playing specific roles.

A comparison with laboratory experiments on P mobilisation by plants and on granite dissolution by bacterial and fungal isolates, suggests that both bacteria and fungi are important for initial nutrient mobilisation. Bacteria, releasing mainly oxalate, are efficient in mobilising metals, while fungi, releasing mainly citrate and malate, are able to mobilise both phosphate and metals [1,2]. Once first plants appear, they seem to strongly increase nutrient release from minerals in their rhizosphere with root exudation of carboxylates probably playing a two-fold role. On one hand it stimulates microbial activity, on the other hand contributes directly to weathering, in particular by means of ligands that are not produced by microorganisms such as tartrate.

[1] Frey, Rieder, Brunner, Plötze, Koetzsch, Lapanje, Brandl & Furrer (2010), *Appl. Env. Microbiol.* 76, 4788-4796. [2] Brunner, Plötze, Rieder, Zumsteg, Furrer & Frey (2011), *Geobiology* 9, 266-279.

Carbonate, not carbonatite, at Villamayor volcano (Calatrava Volcanic District, Central Spain)

M. LUSTRINO¹, S. AGOSTINI², L. S. CAPIZZI¹,
M. PSARAKIS¹ AND D. PRELEVIĆ³

¹Dipartimento di Scienze della Terra, Università degli Studi di Roma La Sapienza, Roma, ITALY

²CNR – Istituto di Geoscienze e Georisorse, Pisa, ITALY

³Geocycles Research Centre and Institute of Geosciences, University of Mainz, Mainz, GERMANY

The Villamayor Volcano (~9 Ma) represents the oldest volcanic activity in the Calatrava Volcanic field, Central Spain. The products of this activity have been classified in literature as leucitites despite a minor presence of modal leucite (<5 vol. %), the low K₂O content (<4.3 wt) and the low K₂O/Na₂O ratio (<1.8). The lava flows of this small volcano are strongly porphyritic with the presence of subhedral to euhedral olivine phenocrysts. A recent paper (Humphreys *et al.*, 2010) classify these rocks as leucitites and considers the olivine phenocrysts as mantle debris. The carbonate inclusion is considered to represent the relict of Ca-carbonatitic magma crystallizing calcite and, in one single case, aragonite. We challenge the Humphreys *et al.* (2010) hypothesis for several reasons:

1) The olivine crystals cannot be considered mantle xenocrysts because of their low Forsterite content (72-89 mol% Fo) and euhedral to subhedral shape..

2) The rare mica associated with carbonate within hollow olivine has relatively low Mg# (73-84 vs. 89-95).

3) The carbonate present in the Villamayor mantle sources, in equilibrium with the leucititic magma cannot be Mg-free as the Ca-carbonate (calcite and aragonite) found within the hollow olivine crystals. The calculated leucite composition (obtained subtracting 30% olivine, considered xenocrysts by Humphreys *et al.*, 2010) is MgO-poor (0.52 wt%). This is not compatible with a mantle melt.

4) The SrO content of the carbonate inclusions is generally low (generally <0.20 wt) and never exceeding 0.54 wt%, values, compatible with sedimentary carbonates.

We propose a sedimentary source for the carbonate inclusions. In our model sedimentary carbonate is scraped off the country rocks and partially digested by the ultrabasic melt. When in contact with the carbonate xenocrysts the olivine growth is stopped, producing the typical hollow body euhedral shape of the Villamayor olivine.

[1] Ref: Humphreys *et al.* (2010) *Geology*, 38, 911-914.

Driving mineral dissolution studies in a new direction

ANDREAS LÜTTGE^{1,2,*}, CORNELIUS FISCHER^{1,2},
ROLF S. ARVIDSON¹ AND INNA KURGANSKAYA¹

¹Marum, Univ. Bremen, 28359 Bremen, Germany

(*correspondence: c.fischer@uni-bremen.de)

²Rice University, Houston, TX 77005, USA

Recent studies by [1] have demonstrated that intrinsic rate variations in mineral dissolution are common and of up to 2.5 orders of magnitude. As a major consequence, we have abandoned the concept of simple closed-form rate equations. Instead, we have introduced the concept of rate spectra. Such rate spectra are the direct result of the fact that dissolution rates depend critically on surface energy distribution. This alternative avoids the highly problematic use of concepts such as reactive surface area that have proven to be mainly not quantifiable.

It is not sufficient to just criticise the existing approach that has certainly produced a sound large data base and many valuable observations. However, we are increasingly skeptic that we will gain much new insight from this approach. Instead we would like to encourage a competition for a new, more powerful approach. As a start, we suggest here one possible method that consists of experiments with analytical tools such as atomic force microscopy, RAMAN-coupled vertical scanning interferometry, among others, and comprehensive theoretical methods such as kinetic Monte Carlo (KMC) calculations. The latter tool provides the capability of predicting crystal dissolution mechanisms and rates. As an example, we will discuss a couple of two recent studies by [2,3] that have focused on phyllosilicates and quartz. In these studies, we demonstrate that complex KMC models which are parameterized with results from *ab initio* and DFT calculations can indeed successfully predict the behavior and development of dissolving crystals.

[1] Fischer *et al.* (2012) *Amer. J. Sci.* **312**, 885-906. [2] Kurganskaya & Lüttge (2013a) *GCA*. [3] Kurganskaya & Lüttge (2013b).

Contamination of DM-sourced magmas produced diverse flood basalts in the Karoo province?

LUTTINEN A.V.¹ AND HEINONEN J.S.¹

¹Finnish Museum of Natural History, P.O.Box 17, FIN-00014 University of Helsinki, Finland

Continental flood basalt (CFB) provinces represent large emplacements of mantle-derived magmas that frequently exhibit incompatible element and isotopic affinity to silicic continental crust. Whether or not this affinity stems from predominantly lithospheric mantle sources rather than crustal contamination of hotspot magmas has remained controversial.

The Middle Jurassic lavas and dikes of Vestfjella were generated during the breakup of Gondwana and represent remnants of the Karoo CFB province in Antarctica. The Vestfjella CFBs record notably diverse geochemical compositions (e.g., initial ϵNd from -15 to +8). The well-exposed 1-km-thick lava succession and the crosscutting dike swarm are dominated by three variably enriched geochemical types (CT1, CT2, and CT3), but the dikes also include rare lamproitic, ferropicritic, and MORB-like (initial $\epsilon\text{Nd} = +8$) types. The Sr, Nd, Pb, and Os isotopic compositions of the MORB-like dikes overlap with those of modern Southwest Indian Ridge MORB, but the trace element compositions indicate melting at high pressures (below thick Gondwanan lithosphere).

Our calculations using the energy-constrained assimilation and fractional crystallization (EC-AFC) model demonstrate that the diverse CFB types could have been derived from a single MORB-like parental magma type by contamination. Importantly, calculations using Archean and Proterozoic granitoids and local lamproite as crustal and lithospheric mantle contaminants infer that even the most enriched CFBs of Vestfjella contain >90% of a depleted sublithospheric mantle-derived component.

These results lend support to the view that lithospheric contamination of voluminous sublithospheric mantle-derived melts may be chiefly responsible for the predominance of enriched magma types in CFB provinces.

Snow and ice algae rock - Cryo-Life habitability in an extreme environment

STEFANIE LUTZ¹, ALEXANDRE M. ANESIO²
AND LIANE G. BENNING¹

¹School of Earth & Environment, University of Leeds, LS2
9JT, UK (*correspondance: s.lutz@leeds.ac.uk)

²Bristol Glaciology Centre, School of Geographical Sciences,
University of Bristol, BS8 1TH, UK

Snow and glacial ice surfaces cover about 10% of Earth's surface and despite being extreme environments they are colonised by a plethora of organisms [1]. On an ecosystem scale, snow and ice algae are the crucial primary colonisers and producers [2]. They evolved a suite of protective biomolecules (e.g., pigments), are well adapted to cold, UV and nutrient stress [2] and dominate the organic and inorganic carbon flux on glaciers. This may also imparts them a central role in controlling the diversity and structure of other communities in glacial ecosystems, yet so far little is known about this. Microbial cryo-adaptation and preservation of life and geochemical signals also have clear implications for the life detection on other icy planets (e.g., Mars, Europa).

Here we show how assessing a variety of physico-chemical (T, melting and transition from snow to bare ice habitats, UV/PAR radiation) and biogeochemical (nutrient and trace metal scarcity, pigment and lipid compositions, and structure) parameters in varied cryogenic glacial habitats (e.g., snow, ice and cryoconites) can be used to define cryo-life habitability at a whole ecosystem scale of a glacier (~ 1 km² of Mittivakkat glacier, SE-Greenland). We found that by far the snow and ice algae dominate the glacial C cycle and the primary production on a glacial scale. The low nutrient (< 1 ppm) and trace metal (< 100 ppb) contents combined with slowly weathering and nutrient-scarce minerals provide an extreme setting for algae growth. Nevertheless, spectroscopic and chromatographic analyses of cells revealed a broad and, rapidly changing cryo-organic inventory during the melting season. The spatial and temporal heterogeneity in pigment composition and abundance between samples correlated well with the functional group distributions showing a clear trend among microbial communities and their adaptation strategies. These findings together with metagenomic diversity and functional gene analyses provide a first comprehensive insight into the ecology of an entire glacial surface ecosystem.

[1] Anesio & Laybourn-Parry (2011) *Trends in ecology & evolution* **27**(4), 219-225. [2] Remias *et al.* (2005) *European Journal of Phycology* **40**(3), 259-268.

The MUSIC model over the years from a personal point of view

J. LÜTZENKIRCHEN¹

¹Institut für Nukleare Entsorgung, Karlsruher Institut für
Technologie (KIT), Hermann-von-Helmholtz-Platz 1,
76344 Eggenstein-Leopoldshafen, Germany;
johannes.luetzenkirchen@kit.edu

The first MUSIC papers were revolutionary: explicit consideration of distinctly different sites on a single face of a mineral based on structural considerations vs. previously used generic sites; fractional (Pauling) charges in surface chemical reactions vs. text-book integer charges; prediction of proton affinity constants vs. numerical fitting. The failure of MUSIC to describe goethite surface charge for updated particle morphology required inclusion of further details of the mineral water interface, such as the effects of H-bonds on predicted affinity constants. Fractional charges were now based on Brown-Altermatt. Up to this point basic charging was the major issue treated by MUSIC. Completion of the framework by introducing charge distribution (CD) allows modeling the adsorption of dissolved pollutants to minerals by combining macroscopic with atomistic level data. CD-MUSIC (to my mind still the most advanced model for this purpose) is heavily cited, but comparably few CD-MUSIC applications from outside Wageningen appeared, maybe related to its incompatibility with common speciation codes or due to other shortcomings of the few codes permitting fractional charges. Fortunately, popular tools like Phreeqc now include CD-MUSIC. Model calculations will exemplify recent developments and associated problems. Experimental model systems will be discussed that strongly support the MUSIC approach, but at the same time hint to limitations arising from effects that CD-MUSIC was never supposed to handle. Grateful for having met Willem van Riemsdijk early on I will surely miss discussions with him and his continued encouragement over the years.

Climate and topographic controls on soil organic carbon cycling in southern Arizona, USA

R. LYBRAND^{1*}, K. HECKMAN² AND C. RASMUSSEN¹

¹Dept of Soil, Water & Environmental Science, University of Arizona, Tucson, AZ [*correspondence:

rlybrand@email.arizona.edu, crasmuss@ag.arizona.edu]

²Northern Research Station, USDA Forest Service, Livermore, CA [kaheckman@fs.fed.us]

The objective of this research was to understand how climate and topography control soil organic carbon (SOC) sequestration across the Santa Catalina Mountain Critical Zone Observatory in southern Arizona, USA. The CZO spans significant range in mean annual temperature (>10°C) and precipitation (>50 cm yr⁻¹). SOC distribution was examined using density and aggregate separations to obtain the free, occluded, and mineral SOC pools for surface and subsurface granitic soils from divergent and convergent landscape positions. Radiocarbon analyses demonstrated that free fractions typically contained the youngest and the mineral or occluded the oldest C depending on the ecosystem. Desert scrub soils sequestered relatively little (<1%), dominantly fast-cycling SOC where the oldest C was mineral associated, indicating organo-mineral interactions as the dominant sequestration mechanism. In contrast, the conifer systems stored more SOC (>3%) and preserved the oldest C through physical occlusion mechanisms. Conifer SOC was 2x greater in the convergent site versus the adjacent divergent site. The age and chemistry of SOC in conifer convergent landscapes suggest downslope transport and burial of SOC in convergent surface soils as an important topographic control on SOC cycling. Bulk soil measurements at the mixed conifer convergent soil-weathered rock interface (~120 cm in depth) indicated a modern $\Delta^{14}\text{C}$ signal (0.0‰, -16.3‰), suggesting downward transport of dissolved organic carbon in the soil pedon. The data confirms shifts in SOC sequestration mechanisms across climatically distinct ecosystems of the southwestern U.S.

O-MIF and S-MIF effects in photolysis of CO and SO₂

J. LYONS¹, G. STARK², D. BLACKIE³, H. HERDE²
AND N. DE OLIVEIRA⁴

¹SESE, Arizona State Univ., james.r.lyons@asu.edu

²Physics Dept., Wellesley College, gstark@wellesley.edu

³Physics Dept., Imperial College,

douglas.blackie01@imperial.ac.uk

⁴Soleil Synchrotron, nelson.de.oliveira@synchrotron-soleil.fr

CO Photolysis

O-MIF during CO photolysis in the solar nebula has been suggested as the origin of the slope-1 solar system O isotope line. Photolysis experiments have demonstrated a wavelength-dependence to the $\delta^{17}\text{O}/\delta^{18}\text{O}$ ratio of photoproduct O that seems to rule out a slope-1 trend. Simulations of the experiments using synthetic isotopic CO spectra and ALS synchrotron spectra reproduce the data well, but require an isotope dependence in the dissociation probability, ϕ , such that $\phi_{\text{C180}} \sim 0.5 * \phi_{\text{C170}}$ for the CO E(0) band at 107 nm. Solar nebula model calculations of CO photolysis using OB stellar spectra, synthetic CO spectra, and the new values for ϕ for the E(0) band yield $\delta^{17}\text{O}/\delta^{18}\text{O}$ values close to unity, so that inclusion of the revised ϕ value improves the agreement between the nebular photolysis model and the solar system O isotope line. Direct evidence for a reduced value for ϕ_{C180} can be made by high-resolution linewidth measurements of the E(0) band for C¹⁸O. The cause of the isotopic differences in ϕ are the mismatch of energy levels in an indirect predissociation process, such as occurs in CO photolysis.

SO₂ Photolysis

Could isotopic dissociation probability effects play a role in S-MIF generation during SO₂ photolysis? Self-shielding has been shown to be important in photolysis experiments in optically-thick SO₂ columns, but a pressure effect is also seen such that the S-MIF signature in photoproduct sulfur is reduced at pressures approaching ~1 atmosphere. The pressure effect could arise from either 1) pressure broadening of the SO₂ rovibronic lines in the dissociation regions, or 2) from collisional deactivation of coupled (bound) SO₂ excited states. At the Soleil synchrotron we have measured pressure broadening in ³²SO₂, and see broadening ~ 0.2 – 0.3 cm⁻¹ atm⁻¹ for N₂ and CO₂ gases. Such broadening appears to be insufficient to explain the pressure effect seen in photolysis experiments. We therefore consider it possible that isotopic variations in dissociation probability also occur during SO₂ photolysis. Optically-thin model simulations for the known non-unity dissociation probability region for SO₂ (~210-220 nm) show that maximum $\Delta^{33}\text{S}$ values of ~ 10‰, with $\Delta^{36}\text{S}/\Delta^{33}\text{S} \sim -1$ for elemental sulfur are possible (but far from proven) for this mechanism.

Behaviour of anthropogenic radionuclides in the proglacial environment

E. ŁOKAS^{1*}, P. WACHNIEW², M. GAŚSIOREK³
AND P. BARTMIŃSKI⁴

¹Institute of Nuclear Physics PAS, Krakow, Poland
(*correspondence: Edyta.Lokas@ifj.edu.pl)

²AGH University of Science and Technology, Krakow, Poland
(wachniew@agh.edu.pl)

³University of Agriculture in Krakow, Krakow, Poland
(rrgasior@cyf-kr.edu.pl)

⁴Maria Curie-Skłodowska University, Lublin, Poland
(piotr.bartminski@umcs.pl)

Retreating Arctic glaciers uncover areas that are sites of intense biogeochemical and geomorphic activity. Analyses of fine-grained deposits from proglacial zones of two Spitsbergen glaciers revealed unexpectedly high concentrations of fallout radionuclides reaching 3000 Bq/kg, 1 Bq/kg and 20 Bq/kg for ¹³⁷Cs, ²³⁸Pu and ²³⁹⁺²⁴⁰Pu, respectively. Airborne anthropogenic radionuclides are efficiently retained in cryoconites – accumulations of dust and organic matter on glacier surfaces. This highly active material is washed down as melting of glacier surface proceeds and may be redeposited in the proglacial zone. Upon entering the subglacial drainage system the cryoconite material becomes diluted with large volumes of water carrying fine-grained mineral material derived from weathering of rocks. Therefore, the extremely high activities of fallout radionuclides might be found only in those parts of the proglacial zone that receive direct runoff from glacier surface. Activities measured at other sites were similar to values reported for Arctic soils. Granulometric, mineralogical, and chemical properties showed no significant vertical variability in the collected proglacial deposits. The observed distribution of radionuclides with depth in the deposits must thus reflect changes in their delivery to particular sites. Finally, development of vegetation on these hot-spots of radioactivity will lead to introduction of fallout radionuclides into the Arctic food web.

This study was supported by the Foundation for Polish Science PARENT-BRIDGE Programme co-financed by the EU European Regional Development Fund.

www.minersoc.org
DOI:10.1180/minmag.2013.077.5.12

Nanomineralogy of gemstones: From genesis to discovery

CHI MA* AND GEORGE R. ROSSMAN

Division of Geological and Planetary Sciences, California
Institute of Technology, Pasadena, CA 91125, USA.
*Email: chi@gps.caltech.edu

Nanomineralogy is the study of Earth and planetary materials at nanoscales, focused on characterizing nanofeatures (like inclusions, exsolution, zonation, coatings, pores) in minerals and rocks, and revealing nanominerals and nanoparticles [1]. With advanced high-resolution analytical scanning electron microscope, we are now capable to characterize solid materials easier and faster down to nanometer-scales. During our nanomineralogy investigation of gemstones, nanofeatures are being discovered in many common gems, which cause color and other optical effects, and provide clues to genesis. Presented here are a few colorful projects demonstrating how nanomineralogy works and plays a unique role in gemstone and geomaterial research.

Rose quartz contains nanofibers of a dumortierite-related phase that is pink, which is the true cause of rose color and optical star effects [2,3]. Sub-micrometer inclusions of ilmenite are the cause of color in blue quartz.

Why is obsidian black? Because most obsidians contain nano-inclusions of magnetite. 'Fire' obsidian, a variety of obsidian from Oregon, has thin layers showing various colors. The layers, 300 to 700 nm thick, consist of concentrated nanocrystals of magnetite, giving rise to brilliant colors in reflection due to thin-film interference [4]. Whereas 'rainbow' obsidian from Mexico contains oriented nanorods of hedenbergite, which cause the rainbow effects via thin-film interference [5].

During a study of benitoite, the state gemstone of California, new mineral barioperovskite (BaTiO_3) and two more new barium titanate minerals BaTi_2O_5 and BaTi_3O_7 were discovered to occur in a tubular inclusion within one benitoite crystal [6].

- [1] Ma (2008) *Eos Trans. AGU*, 89, abs MR12A-01.
- [2] Goreva *et al.* (2001) *American Mineralogist*, 86, 466-472.
- [3] Ma *et al.* (2002) *American Mineralogist*, 87, 269-276.
- [4] Ma *et al.* (2007) *Canadian Mineralogist*, 45, 551-557.
- [5] Ma *et al.* (2001) *Canadian Mineralogist*, 39, 57-71.
- [6] Ma and Rossman (2008) *American Mineralogist*, 93, 154-157.

Granite compositions: Source vs. process, revisited. An isotopic traverse across SE Australia

ROLAND MAAS¹ AND IAN NICHOLLS²

¹School of Earth Sciences, University of Melbourne, Australia,
maasr@unimelb.edu.au

²School of Geosciences, Monash University, Melbourne,
Australia

Granite compositions are determined by source characteristics, by details of melting, melt extraction and transport through the crust, by magma mixing and assimilation at various scales and depths, and by magma chamber processes. The importance of each factor is often difficult to ascertain. We examine this issue using Sr-Nd-O isotope data for 430-370 Ma granites across the Paleozoic Lachlan Orogen (LO), SE Australia.

S-types granites in the eastern LO show strong isotopic links with Lower Paleozoic low- ϵ_{Nd} meta-turbidites which dominate the mid crust. Further west, geophysical data suggest the presence of a greenstone-dominated, lower/mid-crustal Neoproterozoic block with a thickness of 25 km above Moho, the Selwyn Block. S-type granites in this area have higher ϵ_{Nd} , $\delta^{18}\text{O}$ and lower $^{87}\text{Sr}/^{86}\text{Sr}$ than those in the eastern LO, and links to the meta-turbidites – present above the block – are weak. In the far western LO where the mid crust comprises thick, imbricated Cambrian metabasalts overlain by meta-turbidites, S-types show the widest isotopic range (ϵ_{Nd} -2 to -9), consistent with links to both metabasalts and turbidites.

I-type granites in the eastern LO show strong Sr-Nd isotope covariation; their large range in ϵ_{Nd} (+6 to -8) could reflect source rock heterogeneity (e.g. Cambrian greenstones underlying the meta-turbidites have a similar isotopic range), syn-magmatic mixing (crustal assimilation), or both. I-types in the western part of the orogen are isotopically diverse, with distinct trends in Sr-Nd-O isotope plots in the various structural zones, but links to known lower crustal features appear to be weaker than for the S-types.

The data from this example suggest that heterogeneity in source (isotopic) compositions is transferred to S-type granite/volcanic compositions with little disturbance by post-melting processes, at least at an orogen-wide scale. I-type petrogenesis appears to be more complex and probably involves mixing processes (mixed sources, syn-magmatic mixing).

Temporal variations of atmospheric helium isotopes

J.C. MABRY^{1*}, T.F. LAN¹, P. BURNARD¹ AND B. MARTY¹

¹CRPG-CNRS, 54501 Nancy, France (*correspondence: jmabry@crpg.cnrs-nancy.fr)

The isotopic composition of the atmosphere ($^3\text{He}/^4\text{He} = 1.382 \pm 0.005 \times 10^{-6}$) is distinctly different from crustal helium ($^3\text{He}/^4\text{He} \sim 10^{-8}$). Several authors [e.g. 1, 2, 3] have proposed that the amount of excess crustal helium entering the atmosphere due to modern fossil fuel extraction may be enough to upset the balance of the helium composition in the atmosphere on a timescale short enough to detect with modern measurement techniques. Previous attempts failed to detect variations beyond the measurement precision [3, 4]. However, recent measurements by [5] from the Cape Grim Air Archive (CGAA) found a decrease of the atmospheric $^3\text{He}/^4\text{He}$ of 0.23–0.30‰ per year over the period 1978 to 2011. We will attempt to replicate these results using a high-precision helium isotope measurement system we have devised.

Air samples are collected in copper tubes which are sealed with steel clamps. Each sample is approximately 15–20 cm³ of air which is purified all at once and then measured in 11 standard-bracketed aliquots. The amount of helium in each sample aliquot is matched to the amount in an aliquot of the standard to minimize pressure effects. Measurements are made on a Thermo Helix Split Flight Tube (SFT) multi-collector noble gas mass spectrometer. With this system we have a long-term reproducibility of sample air of 0.05% (2 σ).

Our initial measurements of the $^3\text{He}/^4\text{He}$ in CGAA samples do not reproduce the results of [5]. They are consistent with no change in the helium composition over time with an upper limit (2 σ) of 0.16‰ per year decrease in $^3\text{He}/^4\text{He}$. We will make further measurements of the CGAA samples.

Sample	$R_{\text{air}}/R_{\text{std}}$ (2 σ)	# analyses
CGAA 1978	1.0402 (0.0027)	3
CGAA 1979	1.0386 (0.0010)	7
CGAA 2008	1.0387 (0.0004)	4
CGAA 2011	1.0389 (0.0014)	4

[1] Oliver *et al.* (1984) *GCA* **48**, 1759–1767. [2] Pierson-Wickman *et al.* (2001) *EPSL* **194**, 165–175. [3] Sano *et al.* (2010) *GCA* **74**, 4893–4901. [4] Lupton and Evans (2004) *GRL* **31**, L13101. [5] Brennwald *et al.* (2013) *EPSL* **366**, 27–37.

Application of clumped isotope thermometry to subsurface dolostone samples

J. M. MACDONALD^{1*}, C. M. JOHN¹ AND J. P. GIRARD²

¹Carbonate Research, Dept. Earth Science and Engineering, Imperial College London, SW7 2AZ (*correspondence: john.macdonald@imperial.ac.uk; cedric.john@imperial.ac.uk)

²TOTAL, CSTJF, Ave Larribau, 64018 Pau (jean-pierre.girard@total.com)

Platform carbonates are a major hydrocarbon reservoir setting, and are often dolomitized. An important parameter in characterising these reservoirs is the palaeotemperature of the various carbonate phases during burial diagenesis. Clumped isotope analysis of CO₂ from acid digestion of carbonate phases may offer the best route to accurately and precisely determining this temperature. We apply the clumped isotope palaeothermometer to natural dolostone samples from the Northern Marion Platform (NMP, offshore NE Australia) and to dolostone samples from other subsurface locations.

Initially, five dolostone samples from the NMP collected between ~100–160 metres below sea floor (mbsf) were analysed. Petrographic analysis revealed that these samples were all pervasively dolomitized: planar-s to planar-e dolomite forms 100% of the modal mineralogy. Initial clumped isotope analysis (triplicate analyses; reaction at 90°C for 45mins; acid and non-linearity corrections applied; data transferred to universal reference frame [1]) yielded temperatures of 22 °C to 31 °C using the calibration of Ghosh *et al.* [2].

As a second step, we analysed samples from subsurface wells where independent constraints using fluid inclusion thermometry exist. By testing clumped isotope thermometry on these well-constrained natural reservoir samples, we hope to show that clumped isotope thermometry is an ideal technique to determine burial temperatures in carbonate reservoir rocks, as it overcomes some of the problems inherent in fluid inclusion and conventional $\delta^{18}\text{O}$ thermometry.

[1] Dennis *et al.* (2011) *Geochim. Cosmochim. Acta* **75**, 7117–7131. [2] Ghosh *et al.* (2006) *Geochim. Cosmochim. Acta* **70**, 1439–1456.

Hot CD-MUSIC

M. L. MACHESKY^{1*}, D. J. WESOŁOWSKI², M. K. RIDLEY³, M. PŘEDOTA⁴, Z. ZHANG⁵, P. A. FENTER⁵
AND J. D. KUBICKI⁶

¹Univ. of Illinois, Illinois State Water Survey, Champaign IL, USA, (*correspondence: machesky@illinois.edu)

²Oak Ridge National Laboratory, Oak Ridge, TN, USA (dqw@ornl.gov)

³Texas Tech Univ., Dept. of Geosciences, Lubbock, TX, USA, (moira.ridley@ttu.edu)

⁴Univ. South Bohemia, České Budějovice, Czech Republic (predota@prf.jcu.cz)

⁵Argonne National Laboratory, Argonne, IL 60439, USA (zhazhang@anl.gov, Fenter@anl.gov)

⁶The Pennsylvania State Univ., University Park, PA 16802, USA, (jdk7@psu.edu)

Among the many seminal contributions of Professor van Riemsdijk is the CD-MUSIC model, which was developed in collaboration with Professor Hiemstra, and has remained the state-of-the-art Surface Complexation Model since its publication in 1996[1]. Also in the mid-1990's our group began investigating ion adsorption phenomena (primarily cations) over a wide range of temperatures extending into the hydrothermal regime (10-250°C), mostly on rutile, but also on several other metal oxides[2]. More recently, we have also complimented these macroscopic data with a variety of molecular-level information, including X-ray synchrotron experiments, and static DFT as well as classical molecular dynamics (MD) simulations. CD-MUSIC has proven to be a sturdy framework within which we have been able to coherently interpret this assortment of data[3,4].

This contribution will summarize our efforts to rationalize adsorption data for rutile to 250°C within the CD-MUSIC model framework with particular focus on Sr²⁺ and Zn²⁺. Our classical MD simulations suggest that the enhanced adsorption observed macroscopically as temperature increases is due to adsorbed cations moving closer to the surface and shedding more bulk hydration water in the process. CD-MUSIC can mimic this behavior although the agreement is not perfect, suggesting extensions to CD-MUSIC may be warranted.

[1] Hiemstra & van Riemsdijk (1996) *JCIS* **179**, 488-508.

[2] Machesky *et al.* (2006) *Interface Sci. Tech.* **11**, 324-358.

[3] Ridley *et al.* (2009) *GCA* **73**, 1841-1856.

[4] Ridely *et al.* (2012) *GCA* **95**, 227-240.

Geochemical variations of basalts from petit-spot volcanoes in the northwestern Pacific

S. MACHIDA^{1,2*}, N. HIRANO³, Y. KATO², A. TAMURA⁴
AND S. ARAI⁴

¹ School Creative Sci. Engineer., Waseda Univ., Tokyo 169-8555, Japan (*correspondence: m-shikit@aoni.waseda.jp)

² School of Engineer., Univ. of Tokyo, Japan

³ Center NE Asian Studies, Tohoku Univ., Japan

⁴ Grad. School of Sci., Kanazawa Univ., Japan

Petit-spot, new type young volcanoes discovered on the old Pacific plate, originate from melting in the uppermost mantle asthenosphere, and that the magma exudes where the plate flexes and fractures before subducting [1]. Our recent studies defined that alkaline basalt lavas from petit-spot show (1) high concentrations of incompatible trace elements indicating extreme enrichment in highly incompatible elements (e.g., Rb, Ba, U, Th, and Nb) and REE, and depletion in heavy REE [1], and (2) extreme EM-1-like, Sr, Nd, and Pb isotopic compositions [2]. These results indicate that melting of small-scale recycled plate material produces petit-spot magma [2]. Thus, detailed geochemical investigation for these petit-spot volcanoes will provide key constraints on our understanding of the nature of heterogeneity of the northwestern Pacific upper mantle.

Basalts were collected from twelve petit-spot volcanoes at a site in the Japan Trench (Site A), a site approximately 600 km ESE of the Site A (Site B), and a site approximately 200 km S of the Site A (Site C). Five distinct compositional groups are identified on the basis of their major and trace element compositions. The Group 1 basalts (G1), from the Sites A and C, are enriched in LILEs and LREEs. Then, they show negative U, Th, Nb, and Ta anomalies. The Group 2 basalts (G2) from the Site A show negative U, Th, Nb, Ta, Zr, and Hf anomalies, and higher alkali contents than G1. However, on the basis of other major element characteristics, G2 are further subdivided into three groups. G2-2 have lower SiO₂ and higher FeO*/MgO than G2-1 (and G1). G2-3 show a similar major element signature to G2-2, except for lower CaO. The Group 3 basalts, obtained from Site B, show lower SiO₂ and higher FeO*/MgO than G2-2, and negative Zr and Hf anomalies. Variation of Ba/Nb of basalts from all groups correlates to Sr and Nd isotopic compositions. These observations suggest that the source heterogeneity for petit-spot magma is regulated by degree of contributions of LILEs and LREEs-enriched material.

[1] N. Hirano *et al.* (2006) *Science*, **313**, 1426-1428. [2] S. Machida *et al.* (2009) *GCA*, **73**, 3028-3037.

Using noble gases for real-time tracing of oxygen turnover in aquatic systems

LARS MÄCHLER¹, MATTHIAS S. BRENNWALD
AND ROLF KIPFER^{1,2}

¹Eawag, Dep. of Water Resources and Drinking Water, Swiss Federal Institute of Aquatic Science and Technology, Switzerland

²Institute for Geochemistry and Petrology, Swiss Federal Institute of Technology Zurich, Switzerland

Our recent experimental developments on membrane inlet mass spectrometric systems allow the quasi-continuous measurements of dissolved gas concentrations in natural waters under field conditions. Dissolved He, Ar, Kr, N₂, O₂, and CO₂ concentrations can be quantified within minutes with high precision [$\pm 1\%$, 1].

The method was employed in a peri-alpine river to analyze the temporal and spatial dynamics of oxygen turnover during bank infiltration.

During *low* river discharge, the measurements indicated that aeration of groundwater is dominated by direct hyporheic exchange, and that the transport of solutes and heat are decoupled. The combined Ar-O₂ analysis allowed the in-situ oxygen consumption rate and its dependence on the water temperature to be determined. During *high* river discharge after a flood event, we found that significant amounts of excess air were produced in the vicinity of the studied groundwater wells. The formation of excess air and the corresponding oxygen input into the groundwater varied according to the confining conditions within the aquifer and therefore also co-varied with different ecological process zones.

Our results show that the combined analysis of noble and biogeochemically active gases yields valuable information on the dynamics and the importance of different gas exchange mechanisms in aquatic systems with respect to biogeochemical oxygen turnover and thus groundwater quality

[1] Mächler *et al.* ES&T, 46, 7927-8522, 2012.

Co-evolution of the ocean-atmosphere-sediment system through Phanerozoic time

FRED T. MACKENZIE*¹ ROLF ARVIDSON²
AND MICHAEL W. S. GUIDRY¹

¹University of Hawaii, Dept. of Oceanography, Honolulu, HI, USA *correspondance: fredm@soest.hawaii.edu, mguidry@soest.hawaii.edu

²Universität Bremen, MARUM/Fachbereich Geowissenschaften (FB5), Bremen, Germany
rsa4046@uni-bremen.de

Attempts to unravel the history of seawater chemistry go back as far as E. Halley [1] and J. Joly [2] and more recently W. W. Rubey [3] and H. D. Holland [4] among others. We have shown previously [5] that seawater chemical changes on the multi-million year time scale through Phanerozoic time reflect the essential state of the ocean-atmosphere-sediment system with respect to major lithophile and organic component fluxes constrained by a number of observations from the sedimentary rock record.

Despite relatively rapidly changing periods like the end Permian and PETM episodes, the system appears homeostatic and self-regulating and produces two dominant chemostatic modes despite apparent time lags among various variables that suggest different biogeochemical pathways leading to the modes: (Mode I) elevated atmospheric CO₂ and depressed seawater Mg/Ca and SO₄/Ca ratios, pH and carbonate saturation states (the calcite-dolomite seas) versus (Mode II) depressed atmospheric CO₂ and elevated seawater Mg/Ca and SO₄/Ca ratios, pH and carbonate saturation states (the aragonite seas). Transitions between the two modes are modified and overprinted by irreversible evolutionary and ecosystem changes. One example involves the shift of the locus of biogenic carbonate sediment deposition through radiation of pelagic calcifiers and the expansion of dolomite deposition enabling development of Mode I seawater chemistry in the Mesozoic. In addition, Paleozoic deep seas might have been sites of inorganic carbonate accumulation "lost" via subduction. Without this accumulation it is difficult to account for high atmospheric CO₂ concentrations and Mode I seawater chemistry during much of Paleozoic time.

[1] Halley (1715) *Phil. Trans.* **29**, 296-300. [2] Joly (1899) *Sci. Trans. Royal Dublin Soc.* **7**, 23-66. [3] Rubey (1951) *Geol. Soc. Am. Bull.* **62**, 1111-1148. [4] Holland (1972) *Geochim Cosmochim. Acta* **36**, 637-651. [5] Arvidson *et al.* (2006) *Am. J. of Sci.* **306**, 135-190. Guidry *et al.* (2007) In: *Evolution of Primary Producers in the Sea*, 377-403. Mackenzie *et al.* (2008) *Mineral. Mag.* **72**, 329-332. Arvidson *et al.* (2011) *Aquat. Geochim.* **17**, 735-747.

Alunite-Turquoise occurrence from Ali-Abad porphyry copper deposit, Central Iran

M. A. MACKIZADEH^{1*}, B. TAGHIPOUR² AND L. GORGI¹

¹Department of Geology, Isfahan University, Isfahan, Iran
(ma_mackizadeh@yahoo.com)

²Department of Earth Sciences, Shiraz University, Shiraz, Iran
(taghipour@shirazu.ac.ir)

The Ali-Abad porphyry copper deposit is situated in Central Iranian volcano-plutonic arc belt. The oldest rocks in the area are conglomerate and sandstones of Sangestan formation (late Cretaceous). They have been intruded by Oligocene to Miocene porphyritic granitoids.

The widespread hydrothermal alteration has been taken place in conglomerate and sandstones including: Quartz-sercite, argillic, advanced argillic, silicification and skarn formation. The following mineral assemblage has been detected:

Alunite+ turquoise + pyrite+ sercite+ garnet+ quartz+ goethite + epidote+ calcite+ jarosite

According to field and mineralogical investigations the close associate of alunite-turquoise is well established in alteration zones. Probably, the turquoise is formed in charge of alunite or other Al-rich mineral phase during latest stage of alteration process. It seems that oxidation of sulphide minerals (supergene environment) its responsible for generation of all chemical reactions necessary for alunite-turquoise formation.

[1]Taghipour, B., Moore, F., Mackizadeh, M. A., and Taghipour, S (2013) Hydrothermal garnet in porphyry copper related skarn deposits, Ali-Abad, Yazd Province, Iran, Iranian J. Scie. Tech. accepted paper.

Metal precipitation mechanisms in, “low sulfide,” magmatic Cu-Ni-PGE mineralization at Sudbury, Canada: First constraints on oxygen fugacity

MATTHEW A. MACMILLAN¹, JACOB J. HANLEY²
AND DOREEN E. AMES³

¹Saint Mary's University, Halifax, NS, B3H 3C3

(*correspondence: macmillanmatt41@gmail.com)

²Saint Mary's University (jacob.hanley@smu.ca)

³Geological Survey of Canada (dames@nrcan.gc.ca)

The Sudbury Igneous Complex (SIC), Ontario, Canada, is a large (~60km x 30km), elliptical mass of layered igneous rock situated along the contact between the Superior & Southern provinces of the Canadian Shield. The SIC is widely accepted to have been produced by melting of lower crust and upper crustal veneer due to meteorite impact at ~1850 Ma [1], and is remarkably associated with world-class Cu, Ni & PGE mineral deposits. Along the North Range of the SIC, “footwall-type,” deposits are subdivided into sharp-walled vein and low sulfide PGE rich Cu-Ni-PGE mineralization.

Low sulfide mineralization occurs as ≤decimetre-scale blebs, disseminations & stringers of sulfide minerals that generally comprise <3% of any sample and are mined due to their anomalously high concentrations of precious metals compared to other deposit styles at Sudbury. Sulfides in these samples are intergrown with each other, and consist of bornite, chalcopyrite & millerite, and, as a result of their textural equilibrium with a variety of hydrothermal phases (Qtz, Cal, Ep, Chl, Ttn, Grt), are inferred to have precipitated from a hydrothermal fluid.

Hydrothermal garnets, which are rare in the footwall systems, were separated from a sulfide-bearing Qtz-Cal-Ep vein (also containing a CuO phase – tenorite) within the deep 153 ore body at the Coleman Mine and allow constraints to be placed on the formation conditions of low sulfide mineralization in this area of the SIC footwall. Garnets have been studied using include fluid inclusion methods, LA-ICPMS mapping, Lu-Hf/Sm-Nd isotopes and EMP (epidote-garnet equilibria oxythermobarometer) [2]. The results address the chemistry of fluids from which low sulfide mineralization formed, and will constrain P, T & fO_2 – conditions that have not been reported for low sulfide-style mineralization within the SIC footwall.

[1] Krogh *et al.* (1984), *The Geology and Ore Deposits of the Sudbury Structure: Ontario Geological Survey*, 431-447. [2] Donohue & Essene (2000), *Earth and Planetary Science Letters* 181, 459-472.

Arc lithosphere imposes segmented, great circle volcano distribution in the central Sunda Arc, Indonesia

COLIN G MACPHERSON¹, ADAM PACEY^{1,2}
AND KEN JW MCCAFFREY¹

¹Department of Earth Sciences, Durham University, Durham, UK, DH3 1LE. colin.macpherson@durham.ac.uk

² Department of Earth Science & Engineering, Imperial College London, South Kensington, London SW7 2AZ, UK

The term island arc betrays the common assumption that subduction zone magmatism occurs in curved zones, which can be expressed by approximating arcs as segments of small circles on a spherical surface. Such observations are used to relate arc volcano locations to their vertical separation from seismicity in the subducted slab and to conclude that the primary control on loci of magmatism lies in the slab or mantle wedge.

The small circle approximation ignores longstanding, empirical observations that magmatic centres in many subduction systems describe linear features i.e. segments of great circles. The Sunda Arc, Indonesia, is one system that has proved difficult to accommodate in small circle models. We applied an objective line-fitting protocol; Hough Transform image analysis, to explore the distribution of central Sunda Arc volcanoes. This shows that volcano distribution in the central Sunda Arc is best described as an echelon, great circle segments each of 500 – 750km length, rather than as small circles.

Central Sunda Arc segmentation reflects weakness of the arc lithosphere resulting from tectonic forces generated close to the plate margin and/or by arc lithosphere flexure. To the east of our study area the arc has collided with Australian continental crust while highly oblique convergence to the west has produced the Great Sumatran Fault. In both cases volcano locations can be related to stress imposed upon the arc lithosphere by these specific features. Furthermore, changing locations, petrography and geochemistry of central Sunda magmatism since the late-Pliocene can also be attributed to evolving stress in the upper plate.

We conclude that the arc lithosphere stress field is the primary control on distribution of Sunda Arc volcanoes. Interplay between this stress field and the arc crust will provide a major control upon pathways of magma from the mantle wedge to the surface.

Micro-Chronology of the Earliest Solar System: Challenges for the Future

GLENN J. MACPHERSON*

*Dept. Of Mineral Sciences, Smithsonian Institution, Washington, D.C. USA 20560
(correspondence: macphers@si.edu)

During the first ~1-2 Ma of our Solar System's history, as the Sun evolved from a Class 0 to a Class II protostar, solid matter in the innermost disk was heated, evaporated and recondensed, and extensively reprocessed (including melting). Such solids are preserved in chondrites as calcium-aluminum-rich inclusions (CAIs) and amoeboid olivine aggregates (AOAs). Evidence for the original evaporation and condensation is preserved mainly in the form of characteristic chemical and isotopic signatures, but rarely in the physical properties (e.g. textures) of the objects. In contrast, evidence for repeated melting and re-heating is everywhere in the petrology of most CAIs and AOAs. Advances in the analytical precision of mass spectrometry (MS), especially secondary ionization (SIMS), thermal ionization (TIMS), and inductively-coupled plasma (ICP-MS), now permit extraordinary time resolution of early solar system events that are recorded in the petrologic properties of CAIs and AOAs. Pb-Pb ages of CAIs yield a precision of < 500 Ka. ICP-MS measurements of the ²⁶Mg-²⁶Al isotope system demonstrate that the primary fractionation (presumably via condensation) of Al from Mg took place within 20 Ka. SIMS determinations of internal ²⁶Mg-²⁶Al extinct isochrons confirm that CAI precursors formed within a very short time consistent with that determined by ICP-MS, but remelting and reprocessing of CAIs continued for at least 200 Ka and possibly as long as 600 Ka. The time resolution of such SIMS internal isochrons is now better than 50 Ka. The challenge now is to identify the nature of the processes that are recorded in this chronology. For example, the original fractionation event that made the CAI precursors apparently was singular and of short duration whereas remelting occurred as a result of a process that happened repeatedly over 200 Ka or more. Nor is it clear if the formation of Wark-Lovering rims was a singular event affecting all CAIs simultaneously or a repeating event over time. Finally, there is as yet no anchor that ties Solar chronology with CAI chronology. One recent suggestion is that the last (or nearly so) FU-Orionis flare in the early Sun was responsible for making the generation of CAIs we now see, but earlier generations were destroyed. Such linking of solar processes and chronology with nebular products is a major challenge for the future.

Soluble Manganese(III) and a revised Sedimentary Redox Cycle

A. S. MADISON¹*, A. MUCCI², B. SUNDBY², B. M. TEBO³
AND G. W. LUTHER¹*

¹ School of Marine Science and Policy, College of Earth, Ocean and Environment, University of Delaware, Lewes, DE 19958, USA (*correspondence: luther@udel.edu); present address Golder Associates Inc., 200 Century Parkway, Mt. Laurel, NJ, USA 08054 (Andrew_Madison@golder.com)

² Department of Earth and Planetary Sciences, McGill University, Montreal, QC, Canada H3A 2A7 (alfonso.mucci@mcgill.ca; bjorn_sundby@uqar.ca)

³ Division of Environmental and Biomolecular Systems, Oregon Health and Science University, Beaverton, OR 97006, USA (tebo@ebs.ogi.edu)

Recent field studies have confirmed the presence of soluble manganese(III) or [Mn(III)]_{aq}, which along with Mn(II) passes through a 0.2 μm filter, in natural waters of the Black Sea, the Baltic Sea and Chesapeake Bay. This species can account for a large fraction (up to 100%) of the dissolved Mn pool at the oxic/anoxic interface. We have applied a spectrophotometric method to determine the concentration and speciation of Mn in sediment porewaters of the St. Lawrence Estuary collected during cruises in 2009 and 2010. In all samples, [Mn(III)]_{aq} accounts for up to 80% of the total dissolved Mn pool in the vicinity of the oxic-suboxic boundary, with concentrations ranging from the detection limit of 50 nM to 80 μM. We use flux calculations and a diagenetic model to explore the interaction of Mn(III) with other element cycles.

Data collected along the Laurentian Trough of the St. Lawrence Estuary demonstrate that the reduction-oxidation capacity of the soluble Mn pool has been underestimated since Mn(III) can act as either an electron acceptor or an electron donor during interactions with the C, N, S, O and Fe cycles. In these (hemi)pelagic sediments, our data suggest that a significant fraction of the porewater Mn(III) is produced through the oxidation of Mn(II) by O₂. Soluble Mn(III) intermediates are also produced during dissimilatory MnO₂ reduction upon organic matter mineralization and abiotic reduction of MnO₂ by reductants such as Fe(II), FeS and H₂S. Finally, our results reveal that soluble Mn(III) is likely ubiquitous in porewaters, and, as such, is a key redox species in the global sedimentary cycles of carbon, oxygen, iron and sulfur.

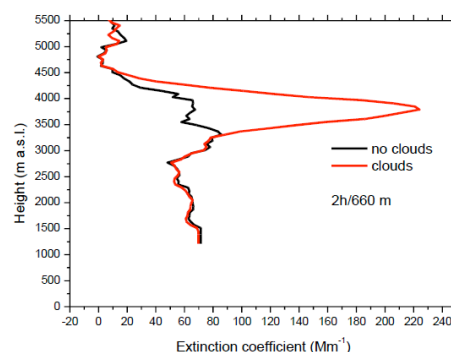
Study of droplet activation in thin broken clouds

F. MADONNA¹, M. ROSOLDI¹ AND G. PAPPALARDO¹

¹Consiglio Nazionale delle Ricerche - Istituto di Metodologie per l'Analisi Ambientale, Tito Scalo, Potenza, I-85010, Italy

fabio.madonna@imaa.cnr.it

The impact on climate of thin clouds is one of the most uncertain. Their importance is related to their global mean cloud fractional coverage [1]. Moreover, they provide significant information about the mechanisms leading to clouds formation. Thin clouds are difficult to observe accurately and large discrepancies exist among different observation techniques [2]. A study to assess the behaviour of macrophysical and microphysical properties of thin clouds is proposed. The study takes advantage of multi-wavelength lidar and microwave radiometer measurements performed at CIAO (CNR-IMAA Atmospheric Observatory), in Potenza, Italy. Particular attention has been paid to optically thin broken stratocumulus where it is possible to investigate the fast change between non-saturation and saturation conditions in an aerosol layer and the droplet activation.



In the plot, it is reported the profiles of aerosol extinction coefficient integrated over 2 hours obtained including (black) or excluding (red) clouds. The plot shows the separation between the region where droplets are activated from that where aerosol particles seems to be not affected by nucleation processes. The results of the mentioned study over two years of data, including aerosol, water vapour and liquid water measurements, will be presented.

[1] Rossow, W. B., and R. A. Schiffer (1999) ISCCP. Bull. Amer. Meteor. Soc., 80, 2261–2287. [2] Turner, D. D., and Coauthors (2007), Bull. Amer. Meteor. Soc., 88, 177–190.

Geochemical and mineralogical characteristic of current roadside pollution from experimental monitoring plots located in different countries

TADEUSZ MAGIERA¹, MARIOLA JABŁOŃSKA², MARZENA RACHWAŁ¹ AND MAŁGORZATA WAWER¹

¹Institute of Environmental Engineering, Polish Academy of Sciences, 34 M. Skłodowskiej-Curie Str., 41-819 Zabrze, Poland (*correspondence:

tadeusz.magiera@ipis.zabrze.pl)

²The Faculty of Earth Sciences, University of Silesia, 60 Będzińska Str., 41-200 Sosnowiec, Poland (Mariola.Jablonska@us.edu.pl)

The aim of the study was characterisation of current particulate pollutants emitted by traffic sources and deposited on roadside topsoil. For this purpose 7 cm of topsoil were removed and replaced by 30 plastic boxes filled with pure quartz matrix. Such experimental monitoring plots were installed in Poland, Germany, Finland, Tadjikistan, Greece and China close to arteries with high traffic volume. Geochemical analyses of some heavy metals (HM) were conducted by AAS (Fe, Mn, Zn, Pb, Cu) and ICP (Cd, Co, Mo and W) after extraction in aqua regia. Additionally SEM and X-ray diffraction analyses were conducted in soil layer removed from monitoring place and in sand matrix after 1 and 2 years of exposition.

Chemical analyses of removed topsoils have shown that the highest contents of Fe, Mn, Zn, Pb, Cu were noted in Poland and Germany, but the highest amount of W was detected in Finland. After 1 and 2 years of exposure a big changes in HM content in quartz sand were observed. Contents of Fe, Mn, Zn and Pb in most monitoring plots were even three times higher after 2 years than after 1 year of exposure. There was significant increase of W in sand matrix after 2 years' exposure in samples from Finland.

Mineralogical analyses revealed different iron forms: metallic iron (α -Fe), Fe oxides (mostly magnetite and hematite), Fe-Zn and Fe-Cu oxides (ferrites) and other mineral components as: barite, aluminosilicates glassy phases and different kinds of spinels. In matrix from Finland plot tungsten carbide particles were also commonly observed.

Lithium isotope evidence for pervasive metasomatism of sub-continental lithospheric mantle

T. MAGNA¹, L. ACKERMAN^{1,2} AND P. ŠPAČEK³

¹Czech Geological Survey, Klárov 3, CZ-11821 Prague, Czech Republic; tomas.magna@geology.cz

²Inst. Geology, Academy of Sciences CR, Rozvojová 269, CZ-16500 Prague, Czech Republic

³Inst. Geophysics, Academy of Sciences CR, Boční II, CZ-14134 Prague, Czech Republic

We present Li contents and isotope compositions in a suite of spinel peridotite/harzburgite xenoliths, enclosed in Tertiary alkaline lavas from three volcanic centres in the western part of the Eger rift, Bohemian Massif, belonging to the European Cenozoic Rift System. Secondary features were observed in subset of xenoliths implying metasomatism by alkali-rich melts with carbonate affinity [1]. Whole-rock xenoliths show no to slight Li enrichment (1.4–5.8 ppm) coupled with extreme ⁷Li depletion in some samples ($\delta^7\text{Li}$ from -9.7 to 2.5‰), attesting to dramatic departure from $\delta^7\text{Li}$ of pristine mantle ($\delta^7\text{Li}=3\text{--}4\text{‰}$). More complex co-variations are observed for bulk $\delta^7\text{Li}$ and modal olivine, clinopyroxene and orthopyroxene for the three volcanic centres. $\delta^7\text{Li}$ values do not correlate with parameters of magmatic fractionation and/or fluid activity and are thus regarded as independent parameter of secondary metasomatism. However, carbonate-rich metasomatism does not impart specific Li signature to xenoliths that carry distinctive Nb–Ti enrichments in melt pockets [2]. On the contrary, relics of oceanic crust preserved as eclogites are ubiquitous in the wider area which may carry strongly negative $\delta^7\text{Li}$ values [3]. Their melts can metasomatize the sub-continental mantle and erase its intrinsic Li signature [4]. Therefore, we propose a scenario whereby xenoliths from the sub-continental mantle beneath central Europe were invaded by eclogitic melts formed at lower temperatures that carry distinctively light Li isotope compositions from earlier subduction of Saxothuringian lithosphere, operating in the area during the Devonian/Carboniferous although timing of the metasomatic imprint remains uncertain. Host alkaline basalts always have higher $\delta^7\text{Li}$ than the xenoliths, as also reported for xenoliths with mantle $\delta^7\text{Li}$ signature [5], implying uniform relationship of basalt–xenolith systems in continental settings.

[1] Špaček *et al.* (2013) *J Petrol*, in press; [2] Ackerman *et al.* (2013) *J Petrol*, under review; [3] Magna *et al.* (2004) *IJMS* **239**, 67-76; [4] Tang *et al.* (2012) *Lithos* **149**, 79-90; [5] Magna *et al.* (2008) *EPSL* **276**, 214-222

Arsenic methylation in the bedrock aquifer of the Willamette Basin, Oregon, USA

SCOTT C. MAGUFFIN¹ AND QUSHENG JIN¹

¹1272 University of Oregon Eugene, OR, USA

Groundwater arsenic contamination is a significant threat to human health in many regions of the world. In aquifers, arsenic typically exists as arsenate or arsenite. Methylated arsenic, such as monomethylarsonate (MMA), dimethylarsinate (DMA), and trimethylarsenate, are less abundant and often overlooked as potentially significant species of arsenic. Identifying biogeochemical processes that control arsenic speciation is critical for developing remediation strategies and for predicting the mobility of arsenic in groundwater.

We analysed arsenic speciation in the bedrock aquifer of the Willamette Basin, Oregon, USA. Our results show that arsenite is the main species, with concentrations up to several parts per million (ppm); DMA is the main methylated species, with concentrations up to 20 ppb. Significantly, the concentrations of DMA correlate linearly with those of arsenite. Based on these observations, we hypothesize that in the aquifer 1) methylated arsenic species are produced from inorganic arsenic by prokaryotic methylation; and 2) prokaryotic methylation can be a significant process in the cycling of arsenic.

To test our hypotheses, we incubated aquifer sediments in reactors and monitored arsenic speciation over time. We also included sterilized sediments as a biological control. We observed the accumulation of MMA and DMA in all but the sterilized control. To determine the *in situ* rate of arsenic methylation, we conducted a push-pull test in the bedrock aquifer. Based on the field observations, we calculated that DMA accumulated at a rate of 1 to 3 ppb per day. Because DMA is produced and consumed simultaneously, this value represents the minimum rate of DMA production in the aquifer.

Our results demonstrate that DMA is produced *in situ* at a significant rate by indigenous aquifer prokaryotes. The results suggest that arsenic methylation is an important factor in evaluating the occurrence and mobility of arsenic in groundwater. Because of the volatility of many methylated arsenic species, arsenic methylation may also constitute a significant pathway in the global cycling of arsenic.

Structure, dynamics, and spectroscopy of metalloproteins from methanogenic and hydrocarbonoclastic microbes

JOHN S. MAGYAR^{1*}, WEI TING CHEN¹, CHRISTINA L. CLEVELAND¹, PAUL B. HARVILLA¹
AND VICTORIA F. OSWALD¹

¹Barnard College, Columbia University, New York, NY
10027, USA

(*correspondence: jmagyar@barnard.edu)

The increasing scarcity of conventional, easily accessible petroleum sources leads to an increasing dependence on hard to reach petroleum in deep, cold offshore waters. These extraction processes lead to significant environmental challenges, including unprecedented spills in deep water. Here, we report progress toward an understanding of molecular adaptations for life at low temperatures, based on our study of cytochrome *c* from *Colwellia psychrerythraea*, a psychrophilic, hydrocarbonoclastic marine bacterium responsible for a large portion of the early bioremediation of the 2010 *Deepwater Horizon* oil spill in the Gulf of Mexico. Although surface oil spill bioremediation is well-established, the biogeochemistry of deep marine oil spills is not yet well understood. An understanding of psychrophilic metalloprotein dynamics and thermodynamics is essential to a full understanding of biogeochemical cycling in these environments.

Further insights into microbial metal uptake processes are gained from our parallel studies of a putative metalloregulatory protein from the methanogenic archaeon *Methanocorpusculum labreanum*. We suggest that this protein is involved in regulation of nickel uptake, which is essential for methanogenesis. In addition, we have determined that this protein is an iron-sulfur cluster-binding flavoprotein, suggesting a role in electron transfer processes as well.

For both *Colwellia* and *Methanocorpusculum*, we have used genomic information to identify specific proteins of interest. The genes are either synthesized chemically or amplified from genomic DNA by PCR and cloned into *E. coli*. The proteins have been overexpressed and purified, and we are currently characterizing them by a wide variety of spectroscopic and other techniques, including UV-vis absorption, circular dichroism, fluorescence, atomic absorption and NMR spectroscopies; X-ray crystallography; differential scanning calorimetry; electrochemistry; and analytical HPLC.

Isotopologue effects in the generation and consumption of nitrous oxide

PAUL M. MAGYAR^{1*}, SEBASTIAN KOPF¹,
VICTORIA J. ORPHAN¹ AND JOHN M. EILER¹

¹California Institute of Technology, Pasadena, CA 91125,
USA (*correspondence: pmagyar@caltech.edu)

Nitrous oxide in air and natural waters is produced and consumed by chemical and biochemical reactions that fractionate isotopes by a variety of equilibrium and kinetic mechanisms. Previous measurements of $\delta^{15}\text{N}$, $\delta^{17}\text{O}$, $\delta^{18}\text{O}$, and position-specific ^{15}N incorporation ('site preference') have identified characteristic fractionations for many of these processes. In particular, site preference measurements have successfully distinguished between N_2O produced by bacterial nitrification and denitrification. But there remain too few constraints to fully characterize the sources and sinks of pools of N_2O in complex natural settings, and no existing isotopic tools distinguish among some biological sources, e.g., archaeal and bacterial nitrification. It is possible additional progress could be made by adding new constraints from the study of the multiply substituted isotopologues of N_2O [1].

We use high resolution multi-collector gas source mass spectrometry to measure the relative proportions of six singly and doubly substituted isotopologues of nitrous oxide, including $^{14}\text{N}^{15}\text{N}^{16}\text{O}$, $^{15}\text{N}^{14}\text{N}^{16}\text{O}$, $^{14}\text{N}^{15}\text{N}^{18}\text{O}$, $^{15}\text{N}^{14}\text{N}^{18}\text{O}$, $^{14}\text{N}_2^{17}\text{O}$, and $^{14}\text{N}_2^{18}\text{O}$ [2]. Each of these species has unique chemical and physical properties that potentially lead to distinctive isotope fractionations. Here, we describe the measurement of N_2O produced by diffusion through a pinhole, which produces an isotope effect dependent only on molecular mass. This tests our ability to accurately determine the 6-dimensional isotopic 'fingerprint' of a given fractionation. For the mass 47 species, $^{14}\text{N}^{15}\text{N}^{18}\text{O}$ and $^{15}\text{N}^{14}\text{N}^{18}\text{O}$, our measured result are within 0.1‰ of the expected value. In addition, we have analyzed N_2O produced by pure cultures of a denitrifying bacterium that lacks a N_2O reductase enzyme. It has a site preference consistent with the expectation for denitrifiers [3]. Measurements of site preference and of multiply-substituted isotopologues are both consistent with a kinetic isotope effect produced at the catalytic center of the nitric oxide reductase enzyme and distinct from the predicted equilibrium fractionation [4].

[1] Kaiser *et al.* (2003) *Geophys. Res. Lett* **30**, 1046, doi:10.1029/2002GL016253. [2] Eiler *et al.* (2013) *Int. J. Mass Spectrom.* **335**, 45-56. [3] Ostrom *et al.* (2007) *J. Geophys. Res.* **112**, G02005, doi:10.1029/2006JG000287. [4] Wang *et al.* (2004) *Geochim. Cosmochim. Acta* **68**, 4779-4797.

Coupling fluid residence times, erosion rates and weathering fluxes to evaluate the operation of a hydrologic thermostat

K. MAHER^{1*} AND C.P. CHAMBERLAIN²

¹Department of Geological and Environmental Sciences,
Stanford University, Stanford, CA, 94305,
kmaher@stanford.edu

²Department of Environmental Earth System Science,
Stanford University, Stanford, CA 94305,
chamb@stanford.edu

The Earth's thermostat is thought to be a negative feedback between atmospheric CO_2 levels and chemical weathering of silicate rocks that keeps temperatures relatively moderate over geologic time scales. To evaluate the operation of this thermostat, we relate the weathering flux per area of continent to the cooperation between runoff and tectonic processes. The two are linked here by the balance between the time that water spends in the weathering zone (which depends on runoff, hydraulic conductivity and the length of the flow path) and the kinetics of mineral weathering (which depend on composition, temperature and erosion rate). We use two types of equations: (1) a reactive transport equation that quantifies weathering-derived solute as a function the fluid residence time; and (2) an equation that relates erosion to the abundance of fresh minerals in the soil. We calculate the weathering-derived solute concentration (C) as a function of the Damköhler number (Da), which is modified to account for the effect of erosion on the supply of fresh minerals. This approach requires that as fluid residence time becomes shorter than the equilibrium time, solute concentrations decrease and solute fluxes plateau. This relationship is observed in modern rivers draining tectonically inactive areas whereas solute fluxes are smaller and Damköhler numbers lower, because reduced supply of fresh lengthens the equilibrium time. In contrast, in active mountain ranges, high relief and rapid supply of fresh minerals result in long fluid residence times and short equilibration times such that solute concentrations and fluxes are high. This approach allows weathering rates to increase asymmetrically between tectonically active and inactive areas in response to changes in climate, to create a bimodal hydrologic thermostat. However, to fully evaluate this model for weathering fluxes requires improved understanding of the reactive flow paths in large catchments and how they are moderated by physical/chemical erosion, the underlying causes for variations in concentration-discharge relationships and the biogeochemical factors that influence the equilibrium time.

Iron speciation and aging in organic-rich aquatic systems

P. MAHESHWARI^{1,2}, Y. WANG² AND T.D. WAITE^{2*}

¹Civil Engineering, Indian Institute of Technology
Gandhinagar, Ahmedabad 382424, India

²Water Research Centre, School of Civil & Environmental
Engineering, University of New South Wales, Sydney
2052, Australia (*correspondence: d.waite@unsw.edu.au)

Iron is ubiquitous in natural environments and used widely in engineered treatment systems as a coagulant or adsorbent. These systems typically contain dissolved organic matter which may influence both speciation and time- dependent transformation of iron species present. In an attempt to understand the speciation and transformation of iron in organic-rich systems, a ferric salt was added in a controlled way to supernatant from a bench-scale membrane bioreactor high in soluble microbial products (SMP) and the system allowed to age and the reductive reactivity of Fe examined. In particular, for each aging time, ascorbate was added to these samples in varying concentrations. The formation of Fe(II) upon reduction of Fe(III) species by ascorbate was measured using ferrozine colorimetry [1].

Following Wang and Waite [2], we assumed the Fe(III) to be present as either weakly bound Fe(III)SMP, strongly bound Fe(III)SMP and AFO. The relative distribution of iron into these forms and their rate constant for ascorbate reduction are shown in Figure 1. It was observed that despite AFO being the most stable form, dissolved Fe(III) mainly exists as strongly bound SMP complexes with weakly bound Fe(III)SMP turning negligible after extended aging.

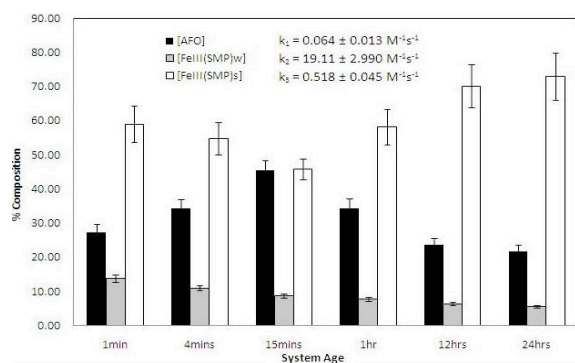


Figure 1: Relative composition of Fe(III) species and their corresponding ascorbate reduction rate constants.

[1] Viollier *et al.* (2000) *Appl. Geochem.* **15**, 785-790. [2] Wang & Waite (2010) *Water Research* **44**, 3511-3521.

Microbial communities colonising bedrock outcrops in a Swedish forest

S MAHMOOD*, A EKBLAD, D BYLUND AND RD FINLAY

Uppsala BioCenter, Department of Forest Mycology and Plant
Pathology, Swedish University of Agricultural Sciences,
Box 7026, SE-750 07, Uppsala, SWEDEN

(*correspondence shahid.mahmood@slu.se)

We are using mor-layer covered bedrock outcrops as a model system to study patterns of microbial colonisation of rocks and biogeochemical processes that lead to mobilisation of mineral nutrients essential for plant growth and ecosystem function. The nutrients released from the bedrock are utilised by the microbial community, taken up directly by roots or transported to roots via mycelia of ectomycorrhizal fungi that form symbiotic associations with tree roots. We are testing the following hypotheses: (1) Microbial communities that have the ability to weather minerals or capture mobilised nutrients will increase in relative abundance or activity on the rocks compared to the overlying organic mor-layer. (2) Ectomycorrhizal fungal communities make a major contribution to the biological weathering of minerals/bedrocks in forest ecosystems. Bedrock outcrops colonised by ectomycorrhizal fungal mycelia/tree roots should therefore have a relatively higher concentration of organic acids than the rocks colonised by mosses or apparently bare rocks. (3) Since the organic sources of C tend to have a very low $\delta^{13}\text{C}$, we expect that the rock surfaces that exhibit varying degrees of biological weathering would also reflect differences in their $\delta^{13}\text{C}$ signatures depending on the level of biological activity (deposition of C in the form of organic acids/microbial biomass, root exudates and solubilised organic matter etc). To test hypothesis 1, we are analysing fungal and bacterial communities colonising rocks using 454- pyrosequencing. To test hypothesis 2, the rock surface minerals are being used for analysis of organic acids using LC-MS/MS. To test hypothesis 3, the rock surface minerals are being used for analysis of $\delta^{13}\text{C}$ using IRMS.

Effect of N on microbially mediated weathering of primary minerals

S. MAHMOOD¹, C. MARTINS¹, M OLOFSSON²,
D. BYLUND² AND RD. FINLAY^{1*}

¹ Uppsala BioCenter, Dept Forest Mycology & Pathology, Swedish University of Agricultural Sciences, Box 7026, Uppsala SE-750 07, Sweden. (*roger.finlay@slu.se)

² Dept Natural Sciences, Technology & Mathematics, Mid Sweden University, SE-85170 Sundsvall, Sweden.

The aim of this study was to determine whether N addition affects: (a) composition of microbial communities in forest soil responsible for mobilization of nutrients from primary minerals, (b) kinetics of organic acid production, (c) rate of nutrient release from primary minerals and uptake by plants, and (d) C allocation patterns in the rhizosphere. We used microcosms with pine seedlings growing in mor layer soil from granite outcrops in a mixed pine-spruce-birch forest. Fungal mats often observed at the mor layer-rock interface harbor microbial communities that mobilize mineral nutrients from granite rocks and/or capture and transport the mobilized nutrients to tree roots via mycelial networks of ectomycorrhizal fungi. The growth substrate was amended with quartz, apatite, biotite or no minerals and two concentrations of a slow release N fertilizer in factorial combinations. Microcosms were sampled destructively after 0, 6, 12 & 60 weeks. Bacterial and fungal communities were analysed by DGGE & 454 pyrosequencing and soil solutions sampled to study kinetics of organic acid production (LC-MS) and for elemental analysis (ICP-AES) to determine weathering rates. C allocation patterns were studied using ¹³C-RNA based stable isotope probing (SIP) of rhizosphere microbial communities. After 12 weeks there were only small changes in rhizosphere bacterial communities in response to N application and/or mineral amendments but fungal community structure exhibited larger changes. N had a negative effect on mobilization of nutrients from these minerals into the soil solution, and also reduced plant nutrient uptake. Seedlings in apatite-amended substrates had higher biomass compared to those grown in biotite-treated substrates and also higher P concentrations.

Contemporaneous crustal records in the eastern and western Dharwar craton: Evidence from U- Pb and Lu - Hf isotope sytematics

B. MAIBAM^{1*}, A. GERDES² AND J.N. GOSWAMI³

¹Department of Earth Sciences, Manipur University, Imphal, India, e-mail: bmaibam@yahoo.com (*Presenting author)

²Institute of Geosciences, Goethe-University Frankfurt, Germany, e-mail: gerdes@em.uni-frankfurt.de

³Physical Research Laboratory, Ahmedabad, India, e-mail: goswami@prl.res.in

Combined U - Pb and Lu - Hf isotope systematics of detrital (metasedimentary) and magmatic (orthogneissic) zircon grains from the eastern and western Dharwar craton provide new insight on the tectonomagmatic evolution of this ancient crust in the Indian shield. This data set establish the antiquity and nature of the source magma (juvenile or recycled) sampled by the analyzed zircon grains and provide a better understanding of the Archean crustal evolution in the Indian shield. For this study we have selected five samples (three from the western and two from the eastern block) that yielded reasonable number of zircon grains.

U - Pb ages for detrital zircon grains suggest presence of ≥ 3.4 Ga crustal components in both the western block and the eastern block of the Dharwar craton. Zircon from magmatic rocks of the western block yielded ages ranging between 3.1 - 3.2 Ga, while those from the eastern block show a bi-model distribution with records of older components (3.0 - 3.2 Ga) and presence of younger events (overgrowth at 2.7 and 2.5 Ga). Magmatic and detrital zircon grains of western Dharwar block exhibit $\epsilon_{\text{Hf}}(t)$ of +1 to +5 and Hf model ages of 3.25 - 3.45 Ga suggesting formation of juvenile crust during this epoch. A predominant phase of crustal reworking during 2.85 - 3.1 Ga could be inferred from the subchondritic ϵ_{Hf} values (-5 to -0.9) for detrital zircon grains.

The age data for majority of the detrital and few magmatic zircon grains from the eastern Dharwar craton suggest formation of juvenile crust (ϵ_{Hf} of +1 to +4) during 3.2 to 3.6 Ga. A crustal reworking phase during 2.5 to 3.0 Ga could be inferred from the ϵ_{Hf} ranging from +4 to -16 in majority of the magmatic and some detrital grains. The combined U-Pb-Hf isotope data is consistent with the idea that crust formation processes took place contemporaneously in both western and eastern blocks of the Dharwar craton.

Effects of aqueous phosphate on U(VI) sorption

F. MAILLOT¹*, V. MEHTA², J.G. CATALANO¹,
D.E. GIAMMAR² AND Z. WANG³

¹Earth & Planetary Sciences, Washington Univ., St. Louis,
MO 63130, USA, (*correspondence:
fabien.maillot@wustl.edu)

²Energy, Environmental and Chemical Engineering,
Washington Univ., St. Louis, MO 63130, USA

³Pacific Northwest National Lab., Richland, WA 99352 USA

Uranium contamination of soils and groundwater has resulted from past mining, processing, and waste disposal activities. Among the in-situ remediation strategies for oxic subsurface environments, phosphate-based treatments have generated significant interest [1]. The soluble uranyl ion [U(VI)O₂²⁺], stable in oxidizing environments, has a strong affinity for phosphate, which can potentially reduce its aqueous concentrations by promoting the nucleation of low-solubility U(VI)-phosphate minerals or by enhancing U(VI) sorption to subsurface minerals.

We investigated the effect of aqueous phosphate on U(VI) sorption on montmorillonite (Clay Mineral Society source clay SWy-2) and goethite. Both minerals are important components in the reactive fine fraction of soils and sediments at sites contaminated with uranium [2]. We determined U(VI) adsorption isotherms at several pH conditions and initial [PO₄³⁻]. Uranium speciation was further investigated using U L_{III}-edge EXAFS and Time Resolved Laser Fluorescence spectroscopies.

A series of possible competing and cooperating reactions may occur in the presence of U(VI) and phosphate, including the formation of U(VI)-phosphate precipitates, U(VI)-phosphate ternary surface complexation [3], and surface site competition between U(VI) and phosphate. Formation of uranyl-phosphate minerals was observed in the presence of either goethite or montmorillonite. Before the onset of precipitation however, our results show contrasting behavior between these two systems. While phosphate does not substantially influence the extent of U adsorption on montmorillonite, it was found to enhance U sorption on goethite at pH 4 and to inhibit it at pH 8. These observed differences indicate that the specific mineralogy of a contaminated field site could greatly influence the applicability of phosphate-based uranium remediation.

[1] Vermeul *et al.* (2009) *300 Area Uranium Stabilization Through Polyphosphate Injection: Final Report*. [2] Stubbs *et al.* (2009) *Geochim. Cosmochim. Acta* **73**, 1563-1576. [3] Singh *et al.* (2012) *Environ. Sci. Technol.* **46**, 6594-6603.

The effect of Alkali-Feldspar composition on mineral-melt partitioning of Trace Elements

M. MAIMAITI¹*, F. ARZILLI² AND M.R. CARROLL³

¹Geology Division, University of Camerino, Via Gentile III da Varano Camerino (MC) Italy, 62032

(*correspondence:maierziyaguli.maimaiti@unicam.it)

²Geology Division, University of Camerino
(arzilli.Fabio@gmail.com)

³Geology Division, University of Camerino
(michael.carroll@unicam.it)

The aim of this work is to better understand how variations in Alkali-Feldspar composition can influence trace elements substitution and mineral-melt partitioning. Feldspars are a group of very common and important rock-forming minerals. Moreover Trace elements are useful as they are much more sensitive to partial melting, crystal fractionation and magma mixing, contamination processes, and thus Trace elements can provide geochemical and geological information out of proportion to their abundance.

To investigate systematically the trace element partitioning between alkali feldspar and silicate melt, this study examines Ba, Rb, Sr partition coefficient variations with feldspar Or, Ab, An content by using experimental data from Arzilli (2012), Mahood and Stimac (1990) and London (1996). We have discovered that for our experimental data, exponential model fits better than simple linear regression model. We suggest that the relationship between partitioning of Ba, Rb, Sr and feldspar Or, Ab, An content is not well produced by a simple linear model and better results are obtained with an exponential model involving feldspar Or content.

We are currently working more on the effect of Alkali-Feldspar crystal growth rate on trace elements partitioning as when the growth rate is fast, the crystal can be less selective in allowing trace elements to enter their structure.

[1] Lofgren *et al.* (2006) *American Min.* **91**, 1596-1606.

Pseudomorphic replacement of diopside during interaction with (Ni,Mg)Cl₂ aqueous solutions

A. S. MAJUMDAR*, H. E. KING, T. JOHN,
C. KUSEBAUCH AND A. PUTNIS

Institut für Mineralogie, Universität Münster, Corresstraße 24,
48149 Münster, Germany

*correspondance: asmajumdar.min@uni-muenster.de

Alteration of peridotite, including serpentinization, has a special place among fluid rock interaction that not only drastically changes rock properties at the ocean floor but also leads to rich ore deposits worldwide. During peridotite serpentinization, olivine and orthopyroxene are more reactive than clinopyroxene. Hence, it may be reasonable to assume that after initial serpentinization of olivine and orthopyroxene, the hot hydrothermal solution rich in metal ions (e.g. Ni) can open further possibilities for relict clinopyroxene to react.

We present a hydrothermal experimental study of diopside-(Ni,Mg)Cl₂ solution interaction to clarify the replacement mechanism and pattern of element mobilization during alteration. Different chloride solutions were used with Ni/Mg ratios of 0, 0.5 and 1. Experiments were carried out in cold seal pressure vessels at 300-600 °C and 1 kbar pressure for 15 days in gold capsules. For 500-600°C NiCl₂ experiments solutions were also spiked with 50% H₂¹⁸O to study the behaviour of isotopic exchange, hence, the replacement mechanism. Raman, SEM and microprobe analyses were performed on reactive samples to identify the phases and to observe textural and compositional features.

The reactive samples show a sharp compositional and structural interface between diopside and the pseudomorph phases. A complex rim of Ni poor and Ni rich regions are present in NiCl₂ and (Ni,Mg)Cl₂ experiments. Here, the precipitated phases are willemseite and/or nepouite. For MgCl₂ experiments, only talc was detected. The experiment with ¹⁸O-enriched solution documents a shift in the Si-O(bridging)-Si band of willemseite towards lower wavenumbers confirming that diopside pseudomorphism occurs via an interface coupled dissolution-precipitation, where the spatial coupling between dissolution-precipitation is dependent on temperature. The study also shows evidences for Ca transport in the opposite direction to Ni and/or Mg during alteration. This may be important as a geochemical tracer for economic Ni deposits and Ca mobilization during serpentinization.

Mineralogy and thermodynamics of secondary arsenic phases

JURAJ MAJZLAN¹, PETR DRAHOTA² AND MICHAL FILIPPI³

¹ Institute of Geosciences, Friedrich-Schiller-Universität Jena, Germany, Juraj.Majzlan@uni-jena.de

² Institute of Geochemistry, Mineralogy and Mineral Resources, Charles University, Prague, Czech Republic, drahota@natur.cuni.cz

³ Institute of Geology, Academy of Sciences of the Czech Republic, Prague, Czech Republic, filippi@gli.cas.cz

Arsenic is an integral part of the toxic load of many types of mining waste. The parageneses of arsenic minerals in the primary assemblages (rocks, ores) and the secondary assemblages (oxidation zones, polluted soils, waste forms) are quite variable. In this contribution, we will describe different mineral assemblages found at sites polluted by arsenic, including naturally polluted soil profiles, rocky mine dumps, tailings, underground spaces, and caves. Here, the mineralogy is not only dictated by the bulk chemical composition but also by the local conditions and shows surprising variations. For example, although mining waste is commonly dominated by arsenic-rich hydrous ferric oxide and scorodite (FeAsO₄·2H₂O), polluted soils contain more commonly pharmacosiderite [(K,Na,Ba)Fe₄(AsO₄)₃(OH)₄·6-7H₂O] and Ca-Fe arsenates such as arseniosiderite. This difference could arise from different availability of element due to different time scales. If so, such differences could suggest how the waste forms could react and transform in the future. In waste forms from material processed by pressure oxidation contain yet different types of ferric arsenates, not known as minerals. Little is known about their solubility and reactivity. The chemical composition of the whole system influences, of course, the nature of the secondary arsenic minerals, and the link between the two can be easily established.

In addition to the crystalline arsenate phases, As(V) can be also incorporated into the crystal structure of iron oxides, especially hematite, as epitaxially intergrown clusters with angelellite-like local structure. This mode of occurrence may be found especially in older systems with relatively low pollution loads.

Thermodynamic data suggest, not surprisingly, that scorodite is the most stable phase in the system Fe₂O₃-As₂O₅-H₂O. Kaňkite, bukovskýite, As-rich hydrous ferric oxide, FeAsO₄, and presumably also zýkaite are metastable. The data for more complex ferric arsenates (pharmacosiderite, arseniosiderite, yukonite) are missing; this work is in progress and could reveal interesting relationships between the simpler and more complicated ferric arsenates.

Cathodoluminescence of barytocalcite $\text{CaBa}(\text{CO}_3)_2$

M. MAKIO¹, H. NISHIDO², N. KUSANO²
AND K. NINAGAWA²

¹Graduate School of Social and Cultural Studies, Kyushu University, 744 Motoooka, Nishid-ku, Fukuoka, 819-0395, Japan

²Department of Biosphere-Geosphere Science, Okayama University of Science, 1-1 Ridai-cho, Okayama 700-0005, Japan (correspondence: nishido@rins.ous.ac.jp)

Anhydrous double salts of CaCO_3 and BaCO_3 have not been investigated with respect to CL properties up to date. In this study we have characterized CL emissions in barytocalcite $\text{CaBa}(\text{CO}_3)_2$, of which structure is different from rhombohedral-calcite type.

Single crystals of three barytocalcite (Blagill, UK; Fosters, UK; Langban, Sweden) were selected for CL spectral measurements at various temperatures.

CL spectra of barytocalcite at room temperature have a pronounced emission peak at around 600 nm in red region. It can be assigned to an impurity center of divalent Mn ion (4G-6S) as an activator, which occupies Ca site in barytocalcite structure, where the centered wavelength is appreciably smaller than the value of calcite (620 nm) due to different crystal field. Barytocalcite has aragonite-like structural configuration rather than calcite-like one. Therefore, various types of Ca sites substituted with Mn ions can be suggested for this Ca-Ba series carbonates, which might modify the strength of crystal field around activated Mn ions. Temperature controlled CL measurements reveal that the CL intensity of Mn activated emission in barytocalcite decreases in an increase of sample temperature, suggesting a temperature quenching effect especially pronounced in the range of $-50\sim 25$ °C. The intensity at -189 °C is twice as much as that at room temperature. Furthermore, an increasing temperature results in a shift of the emission peak to shorter wavelengths, which might be attributed to an increase in the distance between Mn ion and adjacent ligand.

Hematite scalenohedra –ancient jewelry and a problem of sedimentary mineralogy

EMIL MAKOVICKY, MATTEO PARISATTO AND
FLEMMING HØJLUND^{1,2,3}

¹Institute for Geoscience and Natural Resource Management, University of Copenhagen, Østervoldgade 10, 1350 Copenhagen, Denmark, emilm@geo.ku.dk

²Department of Geosciences, University of Padova, Via Gradenigo 6, 35131 Padova, Italy, matteo.parisatto@unipd.it

³Moesgaard Museum, Moesgaard Allé 20, 8270 Højbjerg, Denmark, farkfh@hum.au.dk

In 1964 a scalenohedron of hematite was found in archaeological excavations of the bronze-age layer (1980-2020 BC) of the Tell of Qala'at al-Bahrain on the shores of the Persian Gulf, together with faience and carnelian beads. We subjected the scalenohedron to X-ray tomographic investigation using a Bruker microCT-Skyscan 1172 high resolution scanner. The system has a polychromatic microfocus X-ray source with a tungsten anode; it was run at 100 kV and 10 W. 2000 radiographs were acquired over 360° , 9 radiographs were averaged for each angular position.

Scanning revealed considerable internal porosity of the 'crystal', with a preferential concentration of small pores in the central portions and with larger, elongated pores in the subsurface portions. The internal structure reveals that it is a pseudomorph after a scalenohedral carbonate, composed of an intergrowth of hematite tablets and grains. Its geometry coincides with that of calcite {21-34} scalenohedron, with minor presence of {10-10} and {02-24}.

Mineral trade knows such 'hematite scalenohedra' from the Arzanah and Hormuz Islands in the Persian Gulf. Both are top portions of tall salt diapirs occluding fragments of Precambrian Hormuz Formation: blocks of various volcanic rocks, sediments and even iron ore, forming a jumbled mass. Specularite is reported in geological descriptions but not the hematite pseudomorphs which look very much like our specimen. Our research revealed an extensive replacement of well-crystallized carbonates by hematite (may-be in relation to the formation of large hematite masses which in this pre-iron-age society were polished into hematite weights) but it leaves open the question at which geological stage the evaporite sequence produced perfect carbonate crystals and when were they pseudomorphosed by hematite. This may have practical importance, a number of these diapirs being connected with the Gulf gas and oil occurrences.

Fluid-induced redox processes at the slab-mantle interface: insights from ultrahigh-pressure garnet peridotites

NADIA MALASPINA¹, FALKO LANGENHORST²
AND STEFANO POLI³

¹Università degli Studi di Milano Bicocca, Milano, Italy
(nadia.malaspina@unimib.it)

² Universität, Jena, Germany (falko.langenhorst@uni-jena.de)

³Università degli Studi di Milano, Milano, Italy
(stefano.poli@unimi.it)

The slab-to-mantle volatile transfer is related to the fluid speciation, which in turn is a function of fO_2 , in a system buffered by equilibria involving redox-sensitive elements. The redox processes taking place in the portion of mantle wedge on top of the subducting slab is poorly investigated and the oxidising power of fluids is still unknown.

A case study is represented by grt-orthopyroxenites and peridotites from Dabie-Shan (China) hosted by grt-coe gneisses which contain an association of $opx + grt \pm cpx \pm ol$, formed at the expenses of a previous grt-peridotite. Grt includes primary polyphase inclusions corresponding to a solute-rich aqueous fluid enriched in LILE and LREE. Orthopyroxenites represent metasomatic layers produced after the reaction of mantle peridotites with a Si-saturated fluid phase sourced by the associated crustal rocks. The trace element pattern of this fluid shows a peculiar LILE signature which is recorded by subduction grt-peridotites from Sulu (China). These samples show porphyroclastic grt, cpx and phl, and a younger paragenesis of fine-grained $ol + cpx + opx + phl \pm magnesite$ equilibrated with neoblastic grt.

We measured the Fe^{3+} distribution of the major phases of orthopyroxenite and peridotite with Flank Method electron probe microanalyses and EELS. Pyrope-rich metasomatic grt presents a complementary decrease in Al_2O_3 , relative to the increase of Fe_2O_3 . Diopsidic cpx contains $Fe^{3+}/\Sigma Fe$ up to 0.51 and high Na, requiring the incorporation of an aegirine component. The coupled Na- Fe^{3+} enrichment in cpx suggests a corresponding enrichment in the whole rock and could be favoured by the influx of alkali-rich metasomatic fluid phases. To investigate the role of deep fluids in the redox processes of the suprasubduction mantle we also measured the Fe^{3+} in the microprecipitates of polyphase inclusions using EELS on a TEM. The solute content of slab fluids may contain high Fe^{3+} concentrations and surprisingly inclusion phases such as phl may contain up to 0.70 of $Fe^{3+}/\Sigma Fe$. If net bulk rock oxidation can be demonstrated, silicate-alkali-rich C-bearing fluids could be regarded as potential carriers of oxidising components to the suprasubduction mantle.

Timing and distinct magma sources in ultramafic-mafic intrusions of the Taimyr Peninsula (Russia)

K.N. MALITCH¹, I.YU. BADANINA¹
AND A.P. ROMANOV²

¹Institute of Geology and Geochemistry of the Uralian Branch of Russian Academy of Sciences, Ekaterinburg, Russia
(*correspondence: dunita@yandex.ru)

²Krasnoyarsky Research Institute of Geology and Mineral Resources, Krasnoyarsk, 660049, Russia

It is commonly assumed that ultramafic-mafic intrusions and associated PGE-Cu-Ni sulphide deposits of Northern Siberia represent a small component of a major episode of mafic activity at ~250 Ma, which included formation of the most extensive flood-basalt province on Earth [1]. Recent studies, however, advocated protracted evolution of the ore-forming magmas parent to the Noril'sk-type intrusions [2-4].

This report presents the results of uranium-lead ages of zircons and whole-rock Nd-Sr isotope data for the same suite of lithologies from the Binyuda and Dyumtalei ultramafic-mafic intrusions located in the limits of the Taimyr Peninsula (Russian Arctic). The rocks investigated comprise sulphide-rich varieties of (1) melanotroctolite and (2) ferrogabbro (i.e. gabbro abnormally high in iron) occurring in bottom parts of the Binyuda and Dyumtalei intrusions, respectively.

Zircons are characterized by similar U-Pb ages (248.5±11 Ma at Binyuda and 244.4±2.4 Ma at Dyumtalei). In contrast, silicate material show distinct Sr-Nd isotope signatures ($\epsilon Nd = 3.5 \pm 0.7$ and $^{87}Sr/^{86}Sr_i = 0.70493 \pm 0.00021$ at Dyumtalei, $\epsilon Nd = -3.4 \pm 0.3$ and $^{87}Sr/^{86}Sr_i = 0.70585 \pm 0.00004$ at Binyuda). The determined Nd-Sr variability is interpreted to represent a primary source signature of the lithological units. An important role of the juvenile component is clearly defined for the Dyumtalei intrusion, whereas a major contribution from a SCLM source is inferred for the Binyuda intrusion.

These signatures clearly manifest deviation from those typical for the ore-bearing intrusions of the Noril'sk Province, characterized by a significant time span of zircon and baddeleyite U-Pb ages (from ca. 350 to 230 Ma), relatively constant ϵNd values (+1.0±0.5) and heterogeneous radiogenic $^{87}Sr/^{86}Sr_i$ (from 0.70552 to 0.70798).

The study was supported by RFBR (grant 13-05-00671) and the Uralian Division of Russian Academy of Sciences (grant 12-5-9-019-Arctic).

- [1] Campbell *et al.* (1992) *Science* **255**, 1760-1763. [2] Malitch *et al.* (2010) *Contrib. Mineral. Petrol.* **159**, 753-768. [3] Malitch *et al.* (2012) *Russ. Geol. Geophys.* **53**, 123-130. [4] Malitch *et al.* (2013) *Lithos* **164-167**, 36-46.

Effect of variable CO₂ on andesite-lherzolite reaction: Implications for mantle hybridization and generation of alkalic basalts

ANANYA MALLIK *¹ AND RAJDEEP DASGUPTA¹

¹Rice University, Houston, TX, USA (*am33@rice.edu)

Presence of recycled oceanic crust, a major heterogeneity in the Earth's mantle, is invoked in the source of many ocean island basalts (OIBs) [1]. However, andesitic partial melts derived from oceanic crust, upon reaction with subsolidus peridotite, produce basanites [2] but cannot form strongly alkalic lavas such as nephelinites. In this study, we evaluate whether such an andesite, with dissolved CO₂, can evolve to more Si-deficient magma due to partial reactive crystallization in subsolidus peridotite.

We performed piston-cylinder experiments at 1375 °C, 3 GPa with homogenous mixtures of 25% or 33% of an andesite and lherzolite KLB-1 with 1 to 5 wt.% CO₂ in the starting melts (0.25 to 1.62 wt.% bulk CO₂). Upon reaction, with increasing CO₂ in the reacting melt: a) modes of reacted melt, opx and garnet increased while that of olivine and cpx decreased b) the andesite evolved from basanite to nephelinite c) the residual melts, on a volatile-free basis, showed variation in SiO₂ from 44-40 wt.% and 45-43 wt.%, TiO₂ from 6-5 wt.% and 7-6 wt.%, Al₂O₃ from 14-11 wt.% and 13-10 wt.%, MgO from 13-17 wt.% and 12-17 wt.%, CaO from 8-11 wt.% and 8-11 wt.% and Mg# from 68-75 and 69-73, for 25% and 33% melt-added series, respectively and d) FeO* and Na₂O did not show significant variation.

Our results show that with increasing CO₂ in the andesite, its reaction with lherzolite yields greater degree of Si-undersaturation owing to dilution of melt SiO₂ by CO₂ and lowering of melt SiO₂ by enhanced crystallization of opx at the expense of olivine. Increased precipitation of garnet lowers Al₂O₃ in the reacted melts. Increased CaO and MgO and no significant trend of FeO* and Na₂O with greater bulk CO₂ content confirm propensity of Ca²⁺ and Mg²⁺ over Fe²⁺ and Na⁺ in entering silicate melt as carbonates. Residues show more opx-enrichment with greater CO₂ in the system. We have developed a model for quantitative prediction of mineral modes in hybrid residues as a function of melt-rock ratio and dissolved CO₂ in the reacting melt. At a given MgO, the CO₂-bearing reacted melts are better match for alkalic OIBs in terms of SiO₂, Al₂O₃, CaO, Na₂O and CaO/Al₂O₃ than their volatile-free analogs.

[1] Hofmann & White (1982), *EPSL* 57, 421-436. [2] Mallik & Dasgupta (2012), *EPSL* 329-330, 97-108.

Use of uranium, thorium and carbon isotopes for thermal groundwater and travertine dating

MALOV A.I., BOLOTOV I.N., ZYKOV S.B., DRUZHININ AND S.V., POKROVSKY O.S.

Institute of the Ecologic Problems of the North, UB RAS, Naberezhnaya Severnoi Dviny, 23, Arkhangelsk, 163061, Russia
malovai@yandex.ru

The use of ¹⁴C dating in groundwater in some cases, is facing serious difficulties. It first of all - reducing the specific activity of ¹⁴C in groundwater due to dissolution of carbonate host rocks, overstates age, and mixing with younger water, substantially understates it. In this regard, we propose the sharing of ¹⁴C and ²³⁴U-²³⁸U for dating. However, ²³⁴U-²³⁸U method now not enjoys great popularity. This is due to the need to determine a large number parameters. It should be noted difficulty in defining SSA, and respectively, α -recoil loss factor. For practical use of the ²³⁴U-²³⁸U method, we offer to introduce in the calculation the generalized parameter (probability of the transfer of ²³⁴U into water, or "effective α -recoil loss factor") derived empirically from geological benchmarks, hydrodynamic calculations, and paleo-hydrogeological reconstructions [1]. For hydrothermal system located within mainland European Subarctic ¹⁴C age of thermal waters is 9-12 ka, ²³⁴U/²³⁸U age - 6-11 ka. Calibrated $\delta^{13}\text{C}$ age of travertine - to 3 ka. U-Th age of travertine -- up to 1.5 ka. Assessment calculations show that when dating groundwater isotope of uranium, 10% admixture of young water (up to 100 years) reduces the age of ancient water (11 ka) by 11%. Joint dating of the groundwater and from them formed travertine possible to estimate the velocity of the groundwater in the hydrothermal system and the speed of neotectonic uplift of the area.

[1] Malov (2013) *Lithol. Miner. Resour.* **48**, 254-265.

Biogeochemistry of the Big Toroki sapropel lake, Western Siberia

A.E. MALTSEV*, G.A. LEONOVA, S.K. KRIVONOGOV,
AND V.A. BOBROV

Institute of geology and mineralogy SB RAS, Koptyug Pr. 3,
Novosibirsk 630090, Russia
(*coresspondence: maltsev@igm.nsk.ru)

We investigated a 1.8 m long sediment core of Lake Big Toroki (N 55° 24', E 80° 36'). The lake has a closed basin of 9.57 km² in area and a 1 m in depth and is overgrown by macrophytes [1]. Its water is low-mineralized (845 mg/l), and belongs to the hydrocarbonate Na-Mg class according to [2]. The sediments are organic-mineral sapropels (C_{org} 45.4 %) according to [3]. Water macrophytes are the main producers of the organic matter. The sediment sequence consists of a substrate, bluish-gray sandy silts (180–160 cm), blackish peat (160–120 cm), coarse peaty sapropel with abundant mollusk shells (129–122 cm), blackish peaty sapropel with random gastropod shells (120–75 cm) and greenish macrophytic sapropel with random bivalve shells (75–0 cm).

Total organics, C_{org} and carbonates vary along the core in compliance with its sediment units. Total organics is 40–50% in the sapropel, 60–61% in 120–130 cm and sharply declines below 140 cm. C_{org} is 14–18% in 0–70 and 120–135 cm intervals, 9–13% in the middle and sharply declines from 6.4 to 0.47 % in 140–180 cm interval. Carbonates are low, 3–4 %, in the upper 0–75 cm and progressively increases to 14–16 % below.

The sediment pore waters showed variations in Fe, Mn, Cu, Zn, Pb and Cd. Sharp peaks of Fe and Mn are in the lower middle (90–130 cm), Cu, Zn and Cd in the upper middle (60–80 cm) and Pb in the top (0–40 cm) parts of the core. Changes of H, N and S, which mostly compose the organic matter, match variations of C_{org}.

This research was supported by the SB RAS Integration Project no. 125.

[1] Agricultural organic-mineral materials in the Novosibirsk Region (1990), Novosibirsk. [2] Alekin O.A. (1948), General hydrochemistry. Leningrad, Gidrometeoizdat. [3] Korde N.V. (1960), Biostratigraphy and typology of Russian sapropels, Moscow, USSR Ac. Sci.

What causes the rapid change of Cenozoic magma sources in the Pamir?

N. MALZ*¹, L. RATSCHBACHER¹, J. A. PFÄNDER¹
AND C. MÜNKER²

¹Institut für Geologie, TU Bergakademie Freiberg, Germany
(*correspondence: malz@geo.tu-freiberg.de)

²Institut für Geologie und Mineralogie, Universität zu Köln, Germany

The Pamir mountains, building the western elongation of the Tibet plateau, were formed by the India-Asia collision ~55 Ma ago. Extreme shortening resulted in extremely thickened crust making the Pamir an ideal natural laboratory to study crustal melting processes.

After the India-Asia collision, post-collisional granitoids appear at ~46 Ma and the magmatic activity in the Pamir was rather sparse until ~33 Ma. During this time, Sr- and Nd-isotope compositions (initial ⁸⁷Sr/⁸⁶Sr: 0.7223 to 0.7067 and initial εNd: -10.3 to -2.6) indicate a gradually increasing amount of mantle components, coupled with decreasing SiO₂ contents (77 to 62 wt.%). At ~29 Ma, this trend reverses with an increasing crustal component up to ~14 Ma; initial ⁸⁷Sr/⁸⁶Sr compositions increase again from 0.7064 to 0.7203 and initial εNd decrease from -3.7 to -8.4. Apart from these highly evolved granitoids, basaltic magmatism occurred contemporaneously. The youngest samples at ~11 Ma from the easternmost region of the Central Pamirs are ultrapotassic tephrites to tephriphonolites, showing some of the least radiogenic Nd isotopic compositions (initial εNd: -9.6 to -12.3) together with rather radiogenic Sr isotope compositions (initial ⁸⁷Sr/⁸⁶Sr: 0.7100-0.7104).

What triggers the variable proportions of mantle and crustal components in the the sources of Cenozoic igneous rocks over such short time intervals? The post-collisional magmatism in the Tibetan Plateau is supposed to be influenced by a slab break-off at 55-40 Ma [1], leading to the ascent of asthenospheric material, thus triggering partial melting in the ascending mantle and the lower crust. Such a scenario provides a viable explanation for the increasing amount of mantle component in the 46-33 Ma igneous suites of the Pamir. The ongoing (crustal) shortening led to an extremely thick crust, in which anatexis caused the 29-14 Ma magmatism. Moreover, the subducting cold Indian slab interrupted the asthenospheric upwelling. We will further test this genetic model by combined Lu-Hf and U-Pb measurements on igneous zircons.

[1] e.g. Kohn and Parkinson, 2002, *Geology*, 30, 591-594

The Eastern Rift Zone through time: A record of plume pulsing or magma plumbing evolution?

CHRISTINA J MANNING^{1*} AND MATTHEW THIRLWALL¹

¹Department of Earth Science, Royal Holloway University of London, Egham, Surrey. TW20 0EX

(*correspondence: c.manning@es.rhul.ac.uk)

Lavas from Öraefajökull volcano, SE Iceland, exhibit isotopic compositions distinct from normal Icelandic enriched mantle, attributed to the presence of recycled sediment in their source [e.g.1, 2]. This distinctive source has recently been recognized in postglacial Eastern Rift Zone (ERZ) lavas [3], indicating the source is more widespread, as well as in the East Iceland Tertiary lavas (~13 Ma) [4], indicating that it is also long lived.

A comprehensive suite of lavas from the ERZ; Sida and Fljótshevrí Groups (0.7 - 3 Ma) and Tertiary lavas from Skaftafell (3-5 Ma) have been analysed for Sr-Nd-Pb isotopic ratios along with major and trace elements. Whilst both Skaftafell and ERZ lavas lie on correlations trending towards an enriched end-member similar to the Öraefajökull source, the Skaftafell lavas trend to an end-member which has lower $^{143}\text{Nd}/^{144}\text{Nd}$ for a given $^{87}\text{Sr}/^{86}\text{Sr}$ and more positive $\Delta^{207}\text{Pb}$ and $\Delta^{208}\text{Pb}$. This suggests a temporal change in the composition of the enriched mantle source in the past 5 Ma. Further, the Sida and Fljótshevrí lavas (0.7 - 3 Ma) show more depleted and less variable isotopic compositions suggesting the transition was not gradual, but that there was a distinct break in the supply of enriched mantle at ~3 Ma. Possible mechanisms for this could be: 1. Supply of discrete blobs of enriched mantle from the plume [4], 2. Changes to the magma plumbing regime resulting in a reduced contribution from the enriched source and greater homogenisation of melts between 3 and 0.7 Ma.

[1] Prestvik *et al.* (2001), *EPSL* 190, 211-220 [2] Kokfelt *et al.* (2006), *J.Pet* 47, 1705-1749 [3] Manning and Thirlwall (2013), *CMP* in review [4] Kitagawa *et al.* (2008), *J.Pet* 49, 1365-1396.

Fluids, subduction, and deep carbon

CRAIG E. MANNING^{1*}, YUAN LI² AND JAMES EGUCHI¹

¹Department of Earth and Space Sciences, University of California, Los Angeles, CA 90095, USA

(*correspondence: manning@ess.ucla.edu)

²Bayerisches GeoInstitute, Universität Bayreuth, 95440 Bayreuth, Germany

Studies of the deep carbon cycle have concluded that the mantle is gaining C because more carbon is subducted than is degassed by volcanism [1]. This relies on the assumption that all CO_2 lost from slabs is degassed at arc volcanoes, which is problematic because arc crust is permeable [2] and arc magmas may attain deep fluid saturation [3]. Support has also been drawn from models showing that slab fluids possess low X_{CO_2} [4]. But new theoretical and experimental results show that C solubilities are likely higher than these models predict. Total dissolved carbon depends on the solubilities of all C species (e.g., $\text{CO}_{2\text{aq}}$, HCO_3^- , CO_3^{2-} , etc), which are controlled by pH, $f\text{O}_2$, halogens, and dissolved cations. Controls on these variables in subduction zones are likely to combine to elevate carbonate mineral solubility. For example, the calculated pH of model slab mineral assemblages of jadeite, white mica and quartz [5,6] along the top of the Costa Rica slab [7] indicate that the CaCO_3 solubility is higher at mineral-buffered pH than at the more alkaline pH of otherwise pure H_2O saturated only in CaCO_3 , or than in molecular mixing models. Carbonate solubility is also enhanced by salts. At a given P-T, calcite solubility increases in proportion to the square of NaCl mole fraction [8]. Our studies in KCl, LiCl, and their mixtures have similar form and, at fixed P, T and X_{salt} , solubility decreases as $\text{LiCl} > \text{NaCl} > \text{KCl}$, consistent with Pearson Hard-Soft Acid-Base rules. Metal-carbonate ion pairing and reduction of carbonate or CO_2 to CH_4 during mantle-wedge serpentinization will further increase solubility. Models including the above effects yield ≥ 1 wt% total C in some slab fluids. C carried by subduction-zone fluids and deep degassed magmatic volatiles likely play important roles in the deep carbon cycle, and must be taken into account in assessing the gain or loss of carbon by the mantle.

[1] Dasgupta & Hirschmann (2010) *Earth Planet. Sci. Lett.* **298**, 1-13. [2] Ingebritsen & Manning (2002) *PNAS* **99**, 9113-9116. [3] Blundy *et al.* (2010) *Earth Planet. Sci. Lett.* **290**, 298-301. [4] Gorman *et al.* (2006) *Geochem. Geophys. Geosys.* **7**, Q04007. [5] Manning *et al.* (2010) *Earth Planet. Sci. Lett.* **292**, 325-336. [6] Wohlers *et al.* (2011) *Geochim. Cosmochim. Acta* **75**, 2924-2939. [7] Syracuse *et al.* (2010) *Phys. Earth Planet. Int.* **183**, 73-90. [8] Newton & Manning (2002) *Am. Min.* **87**, 1401-1409.

A new lithospheric model for southeastern Sicily (Italy)

F.C. MANUELLA¹, A. BRANCATO¹, S. CARBONE¹, S. GRESTA¹

¹Dipartimento di Scienze Biologiche, Geologiche e Ambientali, Sezione di Scienze della Terra, Università di Catania, Corso Italia 57, 95129, Italy (correspondence: abranca@unict.it), fmanuella@alice.it, carbone@unict.it, gresta@unict.it

An interdisciplinary approach for a new lithospheric model for southeastern Sicily and the Sicily Channel has been recently proposed by Manuella et al. [1], as retrieved from the integration of published petrologic and geophysical data.

The model elaborated by Manuella et al. [1] points out the existence of a Permo-Triassic oceanic lithosphere that broadens from the Hyblean Plateau to the Sicily Channel, underlying a thick Mesozoic-Cenozoic sedimentary and volcanic sequence, in continuity with the adjacent Mesozoic Ionian-Tethys ocean, thus confirming the hypothesis of Scribano et al. [2]. The Permo-Triassic basement consists of a level of peridotites, affected by different degrees of serpentinization (35–100 vol.%) ranging to a depth of 8–19 km, and a remarkable anomaly occurs at 19 km, corresponding to the Moho discontinuity, which has been considered as a serpentinization front.

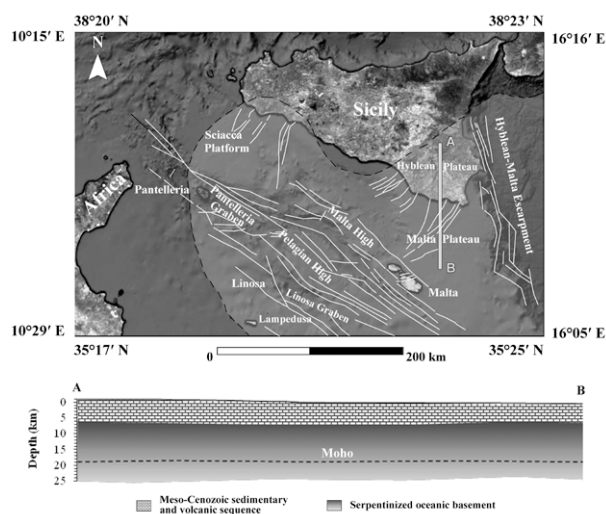


Figure 1. A schematic view of the new lithospheric model

[1] Manuella *et al.* (2013), *J. Geodyn.* 66, 92–102. [2] Scribano *et al.* (2006), *Miner. Petrol.* 86, 63–88.

Spatial and temporal variability in clay mineral and iron (oxyhydr)oxide minerals of the Changjiang (Yangtze) River suspended sediment: Monsoon controlling weathering

CHANGPING MAO^{1,*}, JUN CHEN², XUYIN YUAN¹,
YINXIAN SONG² AND JUNFENG JI²

¹ Institute of Isotope Hydrology, School of Earth Sciences and Engineering, Hohai University, Nanjing 210098 China (*correspondence: maochangping@hhu.edu.cn)

² Institute of Surficial Geochemistry, School of Earth Sciences and Engineering, Nanjing University, Nanjing 210093

Clay mineral assemblages and iron (oxyhydr)oxide are sensitive to bedrock geology and chemical weathering, and therefore have long been regarded as a powerful indicator of the nature of the source areas. The goal of the present work is to show quantitative spatial distribution and seasonal variability pattern of clay mineral assemblages and iron (oxyhydr)oxide in river suspended sediments for the entire Changjiang (Yangtze) basin.

The Changjiang (Yangtze) River originates on eastern periphery of the Tibetan Plateau and causes large continental masses from Tibet to the oceans. A large part of the Changjiang Basin has a subtropical monsoon climate. The suspended sediments of Changjiang River drainage basin were collected during the flood (July–August 2007) and dry (December 2007, January 2008) seasons.

In the present work, river suspended sediment was investigated by quantitative mineralogical, geochemical analyses of bulk samples and single particles. The results indicate that an increasing trend of hematite% and goethite% were observed in the main channel from the upper to middle reaches. The concentration of illite has a ranges from 60% to 80% in summer and 40% to 60% in winter, both with a decreasing trend from the upper to lower reaches. The kaolinite contents of the lower stream abruptly increased from 10% to 30% in the dry seasons (winter) relative to the flood seasons (summer). This peak is probably associated with strong inputs of suspended material from the Poyang lake and its tributaries (located between middle and lower reaches of the Changjiang River).

Our results suggest that spatial and temporal variations in clay mineral and iron (oxyhydr)oxide minerals primarily reflect variations in the intensity of the monsoon, and which is the principal forcing factor on the mechanical and chemical weathering processes between the different sub-catchments of Changjiang River.

Element mobility from seafloor serpentinitization to high-pressure dehydration of antigorite in subducted serpentinite: insights from Cerro del Almiraz (southern Spain)

CLAUDIO MARCHESI^{1*}, CARLOS J. GARRIDO¹,
JOSÉ ALBERTO PADRÓN-NAVARTA², VICENTE LÓPEZ
SÁNCHEZ-VIZCAÍNO³
AND MARÍA TERESA GÓMEZ-PUGNAIRE⁴

¹IACT, CSIC-UGR, 18100 Armilla (Granada), Spain

(*correspondence: claudio@iact.ugr-csic.es;

carlos.garrido@csic.es; teresa@ugr.es)

²Géosciences Montpellier, UMR 5243, CNRS-UM2, 34095
Montpellier, France (padron@gm.univ-montp2.fr)

³Departamento de Geología, Universidad de Jaén, 23700
Linares (Jaén), Spain (vlopez@ujaen.es)

⁴Departamento de Mineralogía y Petrología, UGR, 18002
Granada, Spain (teresa@ugr.es)

The Cerro del Almiraz massif is composed of antigorite serpentinite and chlorite harzburgite separated by a transitional zone that marks the front of prograde serpentinite-dehydration at high pressure in a paleo-subduction setting. Concentrations of Sc and V indicate that the peridotite precursor of serpentinite experienced up to 20% partial melting in the spinel stability field at $-2 < \Delta \log fO_2^{FMQ} < 0$. Peridotites underwent intense seafloor serpentinitization in a fluid-dominated system. Olivine hydrolysis at ~ 200 °C and pyroxene serpentinitization at > 350 -400 °C remobilized Ca and REE (especially LREE and Eu) and caused the progressive enrichment of Cs, Rb, Ba, U and Pb and locally the crystallization of talc by silica fluid addition. Transformation to antigorite serpentinite upon subduction led to Sr depletion, and Ti, Tm, Yb and Lu were remobilized at the sample scale during fluid-assisted crystallization of titanian clinohumite. The high-pressure prograde breakdown of antigorite to chlorite harzburgite preserved the REE fractionations and the characteristic negative Eu anomaly of precursor serpentinites. Relative enrichment of Th-U-Nb-Ta-Pb-Sr in chlorite harzburgite cannot be balanced by closed-system dehydration of serpentinite indicating that dehydration occurred in an open system involving external fluids equilibrated with crustal sources. Open-system fluid flux in the subducted slab results in the recycling into the deep convective asthenospheric mantle of prograde harzburgite enriched in Th, U, HFSE and Pb relatively to oceanic depleted peridotite.

Isotopic composition of precipitation in Ferrara Province

MARCHINA C.¹, VACCARO C.^{1*}, FAZZINI M.¹,
DI ROMA A.¹ AND BIANCHINI G.¹

¹Dip. Fisica e Scienze della Terra, Università di Ferrara, Italy
(*vcr@unife.it)

Ferrara province is located in the Po valley, a flat low-land surrounded by the Alps and the Appennines. The particularity of this area is represented by the proximity to the Comacchio Valleys and the Adriatic Sea. It is interesting to note that, in spite of the vicinity to the sea, the area is characterized by continental climatic characteristics. Stable hydrogen and oxygen isotope ratios are dynamic tracers for the cycling of atmospheric moisture as influenced by water vapour advection, condensation, and evaporation [1].

The stations selected for this study include various sectors of the Ferrara province and allow to characterize the isotopic fingerprint of the local meteoric water. The recorded $\delta^{18}O$ values ranging between -6.95 and -5.19, and δD values ranging between -46.21 and -31.82 are compared with Northern Meteoric water Line [2].

These data will be implemented with the investigation of further local events in the selected stations in order to create an hydro-archive, i.e. a data-set of stable isotope of meteoric water in Ferrara province. This is important considering that the stable isotopes provide a snapshot of the current climatic conditions to be compared with the literature data and with the future composition, as a proxy to evaluate on-going climatic changes.

[1] H.Fudeyasu, *et al.* (2008) *J. Geophys. Res.*, **113**. [2] Longinelli and Selmo (2003) *Jour. Hydrol.* **270**, 75-88]. [3]Zuppi and Sacchi, (2004) *Global Planet. Change* **40** 79–91].

Bacterial phosphate acquisition from minerals in ultra-oligotrophic, ferruginous environments

JULIA A. MARESCA^{1,*}, MENGYIN YAO¹, CARRIAYNE JONES², SEAN A. CROWE², EDWARD F. DELONG³ AND DONALD E. CANFIELD²

¹Civil and Environmental Engineering, University of Delaware, Newark, DE USA.

²NordCEE, University of Southern Denmark, Odense, Denmark.

³Civil and Environmental Engineering, Massachusetts Institute of Technology, Cambridge, MA USA.

*Correspondence: jmaresca@udel.edu

Although ancient ferruginous environments were likely primarily anoxic, the abundant Fe²⁺ could have been oxidized to form iron oxyhydroxides by abiotic processes, iron oxidizing microbes, or free oxygen produced by oxygenic photosynthesizers within oxygen "oases". Iron oxyhydroxides are known to be strong adsorbents of phosphate. Thus, microbes in ferruginous environments would have had to contend with high Fe concentrations and low, sometimes vanishingly low, dissolved inorganic P concentrations. Lake Matano, on Sulawesi Island, Indonesia, is a stratified ferruginous lake with less than 15nM soluble inorganic phosphate. We have isolated 9 heterotrophic bacterial strains from this lake, and most are capable of solubilizing phosphate from Fe oxyhydroxide minerals. All strains grow when provided with low concentrations of soluble inorganic phosphate, but some cannot tolerate high phosphate concentrations (30 mM). When goethite with adsorbed phosphate is provided as the sole P source, all strains grow quite well, and P is released into the medium. Measurements of pH changes in unbuffered medium suggest that some isolates produce acids that contribute to P desorption, though the variability in the amount of phosphate solubilized, consumed, and released suggests that these isolates have multiple mechanisms for P acquisition from Fe particles and subsequent intracellular storage. In addition to the physiological data from these isolates, metagenomic data from Lake Matano surface water indicates that a variety of phosphorus sources can be used, including inorganic phosphates, organophosphates, and phosphonates. These data from Lake Matano use extant pelagic bacteria to characterize microbial pathways for P acquisition from sinking Fe particles, how these pathways affect rates of growth, and how different P acquisition strategies may have regulated biological activity in ancient ferruginous oceans.

The energy budget of the mantle

JEAN-CLAUDE MARESCAL¹, CLAUDE JAUPART², STEPHANE LABROSSE³ AND FRANCIS LUCAZEAU²

¹GEOTOP, University of Quebec, Montreal, Canada

²Institut de Physique du Globe de Paris, Paris, France

³Ecole Normale Supérieure de Lyon, Lyon, France

We have estimated the present total energy flow of the Earth to be 46 +/- 3 TW. The heat loss through the continents and their margins was obtained by integrating the available heat flux measurements which yields 14TW. For the oceans, we have used a cooling plate model for the seafloor with parameters constrained by heat flux and bathymetry data (29TW), and we used the buoyancy flux to estimate the hotspots contribution (3-4TW). After removing the radiogenic heat production in the continental crust and lithosphere (7-8TW), the total heat loss from the convecting mantle is 38+/-3 TW. The mantle energy loss must be balanced by radiogenic heat production in the Earth's mantle, heat flow from the core, and secular cooling of the mantle. All the other possible sources (tidal dissipation, differentiation of the crust from the mantle, gravitational energy released by thermal contraction) account for < 1TW. Geochemical and cosmochemical estimates of the concentration in radioactive elements in bulk silicate earth (crust and mantle) yield values in the range 13-24 TW, i.e. ~5-17TW for the heat production of the Earth mantle. For our preferred estimate of 11TW, the mantle Urey ratio is 0.29. Recent measurements of the thermal conductivity of the core have led to a re-evaluation of the core heat flow with a lower bound of 9TW and a range 9-17TW. Subtracting the mantle heat production and the core heat flow from the mantle energy loss, we obtain that the present cooling rate of the mantle is ~16 TW with a very wide range (1-33TW). This represents a cooling rate of ~100 K/Gy (7-220K/Gy), much higher than long term cooling rates obtained from petrological estimates of Archean mantle temperature (~70K/Gy).

$^{206}\text{Pb}/^{238}\text{U}$ matrix induced bias in LA-ICP-MS: A multivariate study

E. MARILLO-SIALER¹, J. D. WOODHEAD¹ AND J. HERGT¹

¹School of Earth Sciences, The University of Melbourne, Victoria, Australia
e.marillosialer@student.unimelb.edu.au

Many studies acknowledge the occurrence of systematic discrepancies between the $^{206}\text{Pb}/^{238}\text{U}$ ratios measured by LA-ICP-MS and TIMS across different reference materials (e.g. [1, 2]). In order to investigate these effects further high-precision morphology and volume determinations of laser ablation pits, obtained in several zircon materials under varying ablation conditions, have been achieved by confocal laser scanning microscopy (CLSM 700, Carl Zeiss). These provide detailed information on subtle differences in ablation behaviour between different zircon matrices. We demonstrate that small but significant differences in pit dimensions and laser penetration rates exist between zircons. Subsequent evaluation of the $^{206}\text{Pb}/^{238}\text{U}$ values reveals an association between ablation behaviour and deviations in the $^{206}\text{Pb}/^{238}\text{U}$ downhole fractionation patterns observed during ablation - a finding that has major ramifications for studies of U-Pb geochronology employing laser ablation.

The differences in ablation behaviour between zircons, however, cannot be ascribed to a single variable. Based on our initial observations the measured laser penetration rates may also be partially dependent on the crystallographic orientation of the crystals. Multivariate analysis of all possible parameters involved in the ablation process (zircon chemistry, crystallographic orientation, accumulated radiation damage, topographical and morphological data, and ablation cell spatial variations) will be used to identify the most important causes of these artifacts, and thus hopefully provide a means of correcting the results. Our ultimate goal is to offer researchers a method for producing high-accuracy U-Pb ratio measurements by LA-ICP-MS.

[1] Klötzi *et al.* (2009) *Geostand. Geoanal. Res.* 33, 5-15. [2] Allen & Campbell (2012) *Chem. Geol.* 332-333, 157-165.

Fe, S isotope systematics of the 3.24 Ga old Mendon-Mapepe Formations, Kaapvaal Craton, South Africa

JOHANNA MARIN-CARBONNE¹, ELODIE MULLER¹, VINCENT BUSIGNY¹, CLAIRE ROLLION-BARD² AND PASCAL PHILIPPOT¹

¹Institut de Physique du Globe de Paris, Sorbonne Paris Cité, Université Paris 7 Diderot, UMR 7154 CNRS, France
mcarbonne@ipgp.fr

²Centre de Recherches Pétrographiques et Géochimiques, Université de Lorraine, UMR 7358, 15 rue Notre Dame des Pauvres, F-54500 Vandoeuvre-lès-Nancy, France

Variations of Fe and S isotope compositions of sedimentary pyrites have placed important constraints on the chemistry and redox evolution of the Earth's ocean and atmosphere over geological time. In order to better constrain the paleo-environmental conditions and potential biological role on these pyrite formations, we developed coupled Fe and S isotope and trace element compositions analyses in 28 samples from the Barberton Barite Drilling Project (BBDP). The BBDP intercepted the transition from deep-water black cherts and komatiitic basalts of the Mendon Formation to shallow-water sulfate deposits and terrigenous and volcanoclastic sediments of the 3.24 Ga old Mapepe Formation. In situ Fe and S isotope compositions of pyrite were measured with ims 1280 HR2 at CRPG, with a reproducibility better than 0.2 ‰ (2σ) in both $\delta^{56}\text{Fe}$ and $\delta^{34}\text{S}$. Iron and S isotopes of bulk-rocks were analysed at IPGP, with a reproducibility better than 0.1 ‰ (2σ) in $\delta^{56}\text{Fe}$, $\delta^{34}\text{S}$ and $\Delta^{33}\text{S}$.

In situ and bulk-rock analyses reveal a large range of variation from -4.3 ‰ to +3.2‰ for $\delta^{56}\text{Fe}$, from -6.6 ‰ to +3.5 ‰ for $\delta^{34}\text{S}$ and from -3.5‰ to 1.8‰ for $\Delta^{33}\text{S}$. Although mean in situ pyrite Fe and S isotope compositions are generally well correlated with bulk-rock values, there are some offset depending on the presence of other Fe and S mineralogical phases (sulfates, carbonates, clays). This is well illustrated by co-variations between Fe and S isotope compositions with some major and trace elements (SiO₂, Al, U...). Pyrites of all samples show a clear correlation between in situ $\delta^{56}\text{Fe}$ and $\Delta^{33}\text{S}$ values. Pyrite from sedimentary rocks display a rough trend between negative $\delta^{56}\text{Fe}$ and $\Delta^{33}\text{S}$ values and positive $\delta^{56}\text{Fe}$ and $\Delta^{33}\text{S}$ values (mostly in BIFs). These large Fe and S isotope variations may reflect a mixing between different sources and record pyrite formation pathways. Coupled S and Fe isotope composition at μm-scale provides new insights into the origin of isotope variations in Archaean pyrites and its link to ocean chemistry.

Mineralogical and geochemical zoning at high-temperature contacts as a function of CO₂ pressure: An example from Romanian skarns

STEFAN MARINCEA^{1*}, DELIA-GEORGETA DUMITRAS¹,
ANGELA MARIA ANASON¹, CRISTINA GHINET¹
AND AURORA MARUTA IANCU¹

Geological Institute of Romania, 1, Caransebes Str.,
Bucharest, Romania, RO-012271. (*correspondence:
marincea@igr.ro)

Obviously mineral zoning occurs in two high-temperature skarn deposits: Cornet Hill and Măgureaua Văței (Metaliferi Massif, Apuseni Mountains, Romania). In both occurrences, an extensive metasomatism affected Tithonic - Kimmeridgian reef limestones of the Căpâlnaș-Techereu unit. The magmatic Upper Cretaceous intrusions at the contact are monzodioritic to quartz-monzodioritic.

The metasomatic mineral zoning is defined by the predominance of a mineral species and is, from the outer to the inner part of the metasomatic area: (1) calcite (marble) / tilleyite / spurrite + perovskite / wollastonite + gehlenite + vesuvianite / wollastonite + grossular / quartz monzonite at Cornet Hill (CH) and (2) calcite (marble) / wollastonite + titanian andradite + vesuvianite / gehlenite + grossular at Măgureaua Văței (MV). Differences in mineral zoning and in crystal chemistry of mineral species are principally due to the different pressures of volatile components (i.e., CO₂, SO₃, H₂O) which are higher at MV and lower at CH. Silicate-carbonates (e.g., spurrite, tilleyite) and hydrous or hydroxyl-bearing silicate-carbonates (e.g., scawtite, fukalite) are restricted to the CH skarn area. Sulfate-bearing mineral species (i.e., ellestadite-OH, thaumasite) are more common at CH, whereas a silicate-bearing apatite occurs at MV.

The hydrothermal alteration results in a restricted association of hydroxyl-bearing minerals at MV (i.e., xonotlite, hibschite, thomsonite), whereas at CH the association also includes afwillite, gismondine, tobermorite, riversideite.

Chemical geothermometry of geothermal fluids: past, present, and future

LUIGI MARINI

Consultant in Applied Geochemistry, I-55049, Viareggio
(LU), Italy (luigimarini@appliedgeochemistry.it)

Most water geothermometers, including the Na-K and silica functions were initially derived on a purely empirical basis. Long ago, geochemists observed a general decrease in Na/K ratio and a general increase in SiO₂ concentration of thermal waters with increasing temperatures. The first geothermometers were based on these empirical correlations. Studies of hydrothermal alteration mineralogy developing in high-temperature hydrothermal systems as well as modeling of both mineral-solution equilibria and irreversible mass transfer taking place during water-rock interaction suggested that geothermometers are governed by equilibrium reactions between hydrothermal minerals and the aqueous solution under reservoir conditions. A new generation of geothermometric techniques was consequently proposed and a theoretical justification for water geothermometers was found.

Moreover, a different approach to geothermometry, based on speciation-saturation calculations carried out at different temperatures, was also suggested. It was shown that the saturation indexes with respect to a number of plausible hydrothermal alteration minerals converge to 0 at the equilibrium temperature, if the geothermal water is in equilibrium with the considered minerals.

Also gas geothermometers were initially empirical or partly empirical and were later improved by introduction of vapor-liquid distribution coefficients into equilibrium relations. The importance of addition to or removal from equilibrium liquids of equilibrium vapors was thus demonstrated. This approach was later extended to fumarolic gas discharges. Besides, geothermometric functions involving the H₂/Ar and H₂/N₂ ratios were proposed, based on the hypothesis that Ar and N₂ are present in hydrothermal fluids in relative contents close to those of air-saturated groundwater.

In addition to provide a condensed history of chemical geothermometry, this presentation also intends to review main geothermometers and related graphical tools, trying to emphasize advantages and limitations and to give practical hints to the user. Future developments are also briefly considered.

How to protect geochemists working on environmental issues from litigation?

LUIGI MARINI

Consultant in Applied Geochemistry, I-55049, Viareggio (LU), Italy (luigimarini@appliedgeochemistry.it)

Four researchers working on environmental geochemistry at the Dept. of Env. Sciences of Siena University are involved in litigation. In December 2002, their institution was entrusted by the Italian Ministry of Defense to perform a geochemical-environmental study of two Sardinian firing ranges, due to their experience on the environmental impact of Depleted Uranium (DU) gained through previous investigations carried out in Kosovo. The geochemical-environmental study was focused on the distribution of U and other toxic heavy elements in soils, but active stream sediments, natural waters, and wild and cultivated plants were also investigated. Unfortunately, in contrast with the expectations of several inhabitants of the area, the Siena researchers did not find any evidence on the presence of DU in the surveyed area. The study of the Siena researchers was harshly criticized by the public prosecutor of Lanusei, technically advised by a full professor in physics of Brescia University, who is also member of the CERN of Genève. The crime of aggravated intentional omission of precautions against accidents and disasters was ascribed to the Siena researchers. In particular, they have been charged with: (a) not denouncing the danger of anomalous concentrations of Th present in the firing range; (b) using the knowledge gained in Kosovo to select methods that prevented to highlight the possible presence of DU. Actually, for what concerns point (a), there is no Th anomaly as Th contents in local soils are comparable with the values found in other areas of the Sardinia Region and elsewhere. For what concerns point (b), it is totally different, in terms of adopted investigation tactics, to study a small area, in which one knows that DU-shell were used and see the explosion craters (like in Kosovo), and to investigate a large area, in which one does not know if DU-shell were used or not (like in the Sardinian firing ranges). These facts demonstrate that technical advisors must be selected among experts in geochemistry to ensure a fair trial. The international geochemical community is urged to play an active role on this crucial point.

Radionuclides (^{10}Be , ^{210}Pb , ^{137}Cs and ^7Be) to Determine Anthropogenic Impact on Erosion Rates

J. MARQUARD^{1*}, R.E. AALTO¹ AND T.T. BARROWS¹

¹College of Life & Environmental Sciences, Univ. of Exeter, EX4 4RJ, UK (*correspondence: jm459@exeter.ac.uk)

Short lived radiometric isotopes (^{210}Pb , ^{137}Cs and ^7Be) have been used widely for determining sediment sources and deposits [1-3]. However, little research has combined short and long term radiometric isotopes for this purpose. Here we combine short lived radionuclides with the long lived meteoric ^{10}Be to evaluate anthropogenic impacts on sediment erosion and redistribution during American colonial times (late 16th century) and longer timescales (within the Pleistocene). This research is based in the Christina River Basin, Pennsylvania (USA) within the Critical Zone Observatory (CRB-CZO). Anthropogenic impacts are being evaluated on soil redistribution and river channel development by using fallout radionuclides. Pre-colonial soil profiles and erosion rates are being quantified to gain information about natural erosion in the catchment. Sediment redistribution during colonial settlement is being evaluated to see the effects of land clearing and stream damming for mill use. Floodplain development within the last century is being investigated to identify changes in the source of sediment erosion due to afforestation and mill dam breaching. In addition, suspended loads in the streams from various storm events are being analysed to determine the present main source of erosion.

Initial results show changes in the concentration of the meteoric ^{10}Be tracer in river sediment of different ages. Millpond deposits that were in the streams at colonial times have a relatively high ^{10}Be concentration. Floodplain sediment that was deposited within the last century and present suspended loads have a lower ^{10}Be concentration. This clearly indicates a response of the erosional source in the streams to the environmental changes in the watershed. Deforestation and the increase in agricultural land-use enhances sediment surface erosion with high ^{10}Be and therefore lead to high ^{10}Be sediment deposits from that time. Afforestation and the increase in urbanisation in the catchment within the last 200 yrs in turn led to a decrease in upland erosion.

- [1] Wallbrink & Murray (1996) *Water Res* **32** (2), 467-476.
 [2] Zapata (2003) *Soil Till Res* **69**, 3-13. [3] Aalto & Nittrouer (2012) *Phil. Trans.* **370**, 2040-2074.

Ni diffusion in small angle grain boundaries of forsterite

MARQUARDT, KATHRINA¹ AND DOHMEN, RALF²

¹Deutsches GeoForschungsZentrum Potsdam

²Institut für Geologie, Mineralogie und Geophysik, Ruhr Universität Bochum

Defects such as grain boundaries and interfaces are potent pathways for the transport of elements in rocks [1]; therefore they strongly affect large-scale physical properties of rocks, e.g. viscosity, electrical conductivity and bulk diffusivity. Yet data for geo-relevant materials are rare. The dependence of diffusion on the grain boundary structure e.g. defined by the lattice misfit, in silicates is unknown [p.954, 2]. Limited experimental studies in material sciences indicate major effects of grain boundary orientation on diffusion. Lately, synthetic georelevant bicrystals became available. Thus only now, first diffusion data on single grain boundaries have been produced [e.g. 3].

The effect of grain boundary orientation on diffusion in forsterite tilt grain boundaries (misorientations of 17° and 11°) was characterized by transmission electron microscopy (TEM). The site specific TEM-foils were cut using the focused ion beam technique (FIB). To study diffusion we prepared amorphous thin-films of Ni₂SiO₄ composition perpendicular to the grain boundary using pulsed laser deposition. Annealing (800-1000°C) leads to crystallization of the thin-film and Ni-Mg inter-diffuse into the crystal volume and along the grain boundary. The interdiffusion profiles were measured using the TEMs energy dispersive x-ray spectrometer standardized using the Cliff-Lorimer equa. and EMPA measurements.

We obtain volume diffusion coefficients that are consistent with earlier studies of Ni-Mg interdiffusion in forsterite at comparable temperatures. Contrasting to [4] our volume diffusion data are about an order of magnitude slower, while having similar activation energies. Grain boundary diffusion perpendicular to the dislocation lines of the small angle grain boundaries proved to be max. an order of magnitude faster than volume diffusion. The difference decreases markedly at temperatures above 1000°C.

[1] Hartmann, Wirth & Markl (2008) *Contributions to Mineralogy and Petrology* 156, 359-375. [2] Dohmen & Milke (2010), *Reviews in Mineralogy and Geochemistry* 72, 921-970. [3] Marquardt, Petrishcheva *et al.* (2011), *Contributions to Mineralogy and Petrology*. 162, 739-749. [4] Ito, Yurimoto, *et al.* (1999). *Physics and Chemistry of Minerals* 26, 425-431.

Magma Signatures in the Terceira Rift Azores: a melt inclusion study

A FILIPA A MARQUES¹, ZOLTAN ZAJACZ², PEDRO MADUREIRA³ AND STEVEN D SCOTT⁴

¹CREMINER (LARSyS), University of Lisbon, Portugal

²ETH Zürich, Switzerland

³EMEPC & University of Évora, Portugal

⁴University of Toronto, Dept. Earth Sciences, Canada

The Terceira Rift (TR) is a 550km long ESE trending line of volcanic reliefs (Graciosa Island, Terceira Island, D. João de Castro Bank, S. Miguel Island) alternating with deep basins (e.g. E of Terceira, Hirondelle) that define the plate boundary between the European and African plates on the Azores plateau [1]. Seismic tomography suggests that the Azores plume is centered NE of Terceira supplying upwelling plume material SW of Terceira (e.g. Faial) [2].

Melt inclusions (MI) are small portions of melt trapped during crystal growth. Their study allows the characterization of the composition of primary melts, mantle heterogeneity, magma sources and timescales. This study presents the first geochemical dataset of olivine-hosted unexposed MI sampled from submarine and subaerial lavas along the TR. Plots of incompatible trace element ratios (Fig.1) confirm the presence of distinct mantle signatures showing a mixing trend between two end-members that represent extreme topographic domains: Terceira and Hirondelle Basin. These findings will be discussed considering recent geophysical and geochemical data obtained in the area.

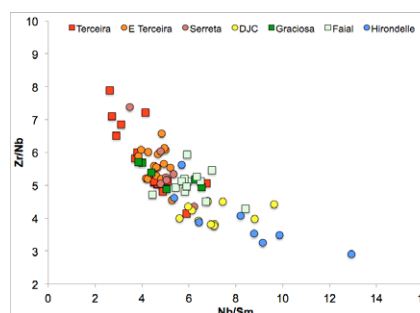


Fig. 1 Incompatible trace element plots of olivine-hosted MI from the TR. (square symbols: aereal lavas; circles: submarine lavas)

AFA Marques research is funded by CREMINER/LA UI101 POSC (co-financiado FEDER) and FCT's project TerRiftic (PTDC/MAR/111306/2009). Steve Scott's research is funded by the NSERC. [1] Vogt PR, Jung WY (2004) *EPSL* 218:77-90. [2] Yang T, Shen Y, van der Lee S, Solomon SC, Hung SH (2006) *EPSL* 250:11-26

Buried lava paleosol in NW Fogo island (Cape Verde) – chemical and mineralogical evolution

R. MARQUES^{1,2}, M.I. PRUDÊNCIO^{1,2}, J. C. WAERENBORGH^{1,3}, J. T. COUTINHO¹, F. ROCHA^{2,4}, E. FERREIRA DA SILVA^{2,4} AND M.I. DIAS^{1,2}

¹Campus Tecnológico e Nuclear, IST/UTL, EN10, Sacavém, Portugal (rmarques@ctn.ist.utl.pt)

²GeoBioTec, Univ. Aveiro, Aveiro, Portugal

³Centro de Física da Matéria Condensada - Univ. Lisboa, Portugal

⁴Dep. de Geociências, Univ. de Aveiro, Aveiro, Portugal

In Fogo island (Cape Verde archipelago), buried paleosols developed between alkaline lava flows occur. Six samples (from parent rock to paleosurface) were collected from a 1 m thick profile. Weathered samples vary in colour from dark brown to yellowish. Chemical and mineralogical analyses were performed by instrumental neutron activation analysis, Mössbauer spectroscopy and X-ray diffraction.

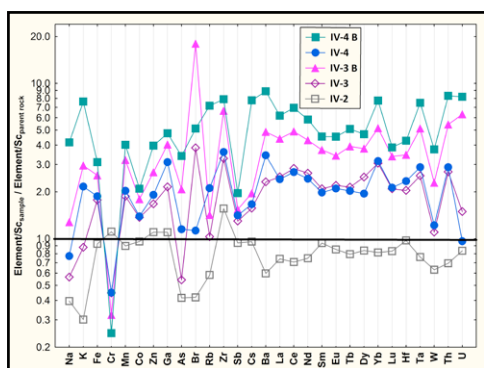


Fig. 1 – Chemical variations with depth/weathering degree (after normalization to Sc)

The main minerals of the parent rock identified by XRD are pyroxenes, olivines and phyllosilicates. In the paleosol only pyroxenes, quartz, phyllosilicates and in the most weathered/surficial samples hematite, were clearly identified.

Except for Cr a general enrichment of the studied chemical elements occurs with increasing weathering (Fig.1). The ancient surficial level has a significant enrichment in Na, K, Rb, Cs, Ba, REE, Ta, Th and U. Bromine variations may be mainly related with the presence of fluorapatite detected by XRD. Iron has a conservative behaviour. As the weathering degree increases the Fe^{3+}/Fe^{2+} ratio increases from 35% up to 85% and hematite is formed.

Bottom up approach for the predictive modelling of sorption isotherms on argillaceous rocks

M. MARQUES FERNANDES^{1*}, R. DAEHN¹, N. VER² AND B. BAEYENS¹

¹Paul Scherrer Institut, CH-5232, Villigen, Switzerland

(*correspondence: maria.marques@psi.ch)

²Hungarian Academy of Sciences, H-1525, Budapest, Hungary

Sorption in natural argillaceous rocks is inherently too complex and multi-faceted to be mechanistically predicted. The so-called “bottom up” approach for argillaceous rocks is based on the hypothesis that the uptake of sorbates in such complex systems can be quantitatively described based on the understanding of the sorption mechanisms on 2:1 type clay minerals [1]. Illite and illite/smectite mixed layers are the major clay mineral components of many argillaceous rocks, and their properties are supposed to be responsible for the radionuclide uptake in these systems.

The aim of this work is to test the capabilities of the 2SPNE SC/CE sorption model [2] and of the generalised sorption model for Cs [3] to make blind predictions of the sorption isotherms in two argillaceous rocks, Boda Clay Formation (BCF) and Opalinus Clay (OPA). As a complementary tool Extended X-ray Absorption Fine Structure (EXAFS) spectroscopy is used to verify the assumptions made in this approach.

Sorption isotherms of Cs(I), Ni(II), Co(II) and Eu(III) were measured on BCF and OPA rock samples in their respective pore-waters. The sorption prediction on these argillaceous rocks was then carried out using the mechanistic sorption models developed for illite [2, 3], and the results scaled over the illite and illite/smectite weight content in the sample. Generally a good agreement between the measured data and the predicted values was found. However, some discrepancies were observed, e.g. for Ni(II) on BCF at higher Ni(II) equilibrium concentrations. EXAFS was therefore used to verify the sorption mechanisms along the isotherm at the molecular level. In the isotherm region, where prediction and measurement coincide, sorption was in fact the only uptake-controlling mechanism. In contrast, EXAFS showed precipitation as additional uptake processes in the isotherm regions where prediction and measurement deviated.

[1] Bradbury & Baeyens (2000) *Appl. Clay Sci.* **52**, 27-33. [2] Bradbury & Baeyens (2009) *Geochim. Cosmochim. Acta* **73**, 1004-1013. [3] Bradbury & Baeyens (2000) *J. Contam. Hydrol.* **42**, 141-163.

Open-pit coal mining effects on rice paddy soil composition and metal bioavailability to *Oryza sativa* L. plants in Cam Pha, northeastern Vietnam

J. EDUARDO MARQUEZ, RAUL E. MARTINEZ HOÀNG THI BÍCH HÒA AND RETO GIERÉ

Institut für Geo- und Umweltwissenschaften, Albert-Ludwigs-Universität, Albertstraße 23b, D-79104 Freiburg, Germany.

This study quantified Cd, Pb, and Cu content, and the soil-plant transfer factors of these elements in rice paddies within Cam Pha, Quang Ninh province, northeastern Vietnam. The rice paddies are located at a distance of 2 km from the largest Coc Sau open-pit coal mine. Electron microprobe analysis and energy-dispersive spectroscopy revealed a relatively high proportion of carbon particles rimmed by an iron sulfide mineral in the quartz-clay matrix of rice paddy soils at 20-30 cm depth. Bulk chemical analysis of these soils revealed Cd, Pb, and Cu in concentrations exceeding calculated background concentrations by 2500, 1226, and 979 %, respectively. Metals and metalloids in Cam Pha rice paddy soils, including As, Cd, Cr, Cu, Hg, Mn, Ni, Pb, and Zn, ranged from 0.2 ± 0.1 to 140 ± 3 mg/kg, in close agreement with toxic metal contents in mine tailings and Coc Sau coal. Native and model *Oryza sativa* L. rice plants were grown in the laboratory in presence of 1.5 mg/kg of paddy soil from Cam Pha to investigate its effects on plant growth. A decrease in growth of 60% with respect to a control was found for model plants, whereas a decrease of only 10% was observed for native rice plants. This result suggests an adaptation of native Cam Pha rice plants to toxic metals in the agricultural lands. The Cd, Cu, and Pb contents of the native rice plants from Cam Pha paddies exceeded permitted levels in foods. Cadmium was highest in the rice-grain endosperm at 0.09 ± 0.01 mg/kg, compared to the allowed content in foods of 0.05 mg/kg. Along with rice plant adaptation to contaminated soils, bioaccumulation of trace metals, such as Cd and Pb, poses a severe health risk to the population of Cam Pha. The adaptation of native rice plants, combined with bioaccumulation ratios of 1 ± 0.6 to 1.4 ± 0.7 calculated for Cd transfer to the rice-grain endosperm, strongly suggest a continuous input of toxic metals from coal-mining to agricultural lands in Cam Pha. In addition, our results imply a sustained absorption of metals by native rice plant varieties, which may lead to metal accumulation (e.g. Cd) in human organs and in turn to severe disease.

Sectoral contributions to black carbon concentrations and radiative forcing in Delhi

PALLAVI MARRAPU^{1,2}, YAFANG CHENG², GREGORY R. CARMICHAEL^{1,2}, GUFRAN BEIG³, SCOTT SPAK², MICHAEL DECKER⁴, MARTIN G SCHULTZ⁴ AND SAROJ K. SAHU³

¹ Chemical and Biochemical Engineering, The University of Iowa, Iowa city, IA, United States.

² Centre for Global and Regional Environmental Research, The University of Iowa, Iowa city, IA, United States.

³ Indian Institute of Tropical Meteorology, Pune, Maharashtra, India.

⁴ Forschungszentrum Juelich GmbH, Juelich, Germany.

In this study we evaluate the air pollution levels in Delhi and their impacts on weather and climate. The two way interactions between pollution and meteorology are evaluated using the WRF-Chem model. The analysis period is focused on October 2010, the time period of the Commonwealth Games. The model is compared to BC and PM_{2.5} measurements at 11 sites. A sector based analysis is performed to assess the contributions to pollution and direct radiative forcing from transport, residential, power and industrial emissions. The contributions from emissions outside of Delhi are also evaluated to see the extent that regional emissions need to be controlled to meet air quality targets in Delhi. Results of simulations for emission scenarios for 2030 generated by the GAINS model that address air quality and climate strategies are also discussed.

Competitive effect of Al(III) on Eu(III) sorption to illite

R. MARSAC*¹, A. SCHNURR¹, T. KUPCIK¹, T. RABUNG¹,
T. SCHÄFER¹, N.L. BANIK¹, C.M. MARQUARDT¹,
M. MARQUES-FERNANDEZ², B. BAEYENS²,
M.H. BRADBURY² AND H. GECKEIS¹

¹Karlsruhe Institute for Technology, Institute for Nuclear Waste Disposal, D-76021 Karlsruhe, Germany. (*correspondence: remi.marsac@kit.edu)

²Paul Scherrer Institut, Laboratory for Waste Management, 5232 Villigen PSI, Switzerland

Clay rock formations present low permeability and strong sorption capabilities for cations, two properties that make them suitable as host rocks for nuclear waste disposal. Accurate description of radionuclide sorption onto clay rock based on geochemical sorption modelling is required to assess radionuclide migration properly. Examining published studies on trivalent actinide/lanthanide (An/Ln(III)) sorption to Illite batches (Illite du Puy) reveals data sets showing different metal ion sorption behavior [1-3] (and own experimental data). Surface complexation constants can differ by more than one order of magnitude ($\log^s K_1=1.9$ vs. 3.1).

Comparing Eu sorption data implies that in one case (stronger sorption) [3] the description of isotherms by the 2 SPNE SC/CE model requires the consideration of strong and weak sites, where binding to strong sites prevails at low $[Eu]_{tot}$ and sorption to weak sites at higher $[Eu]_{tot}$. In the other cases Eu(III) sorption appears to be linear over a wide range of $[Eu]_{tot}$, suggesting strong sites being absent or blocked. We explain this observation by slightly different Illite purification procedures notably by the effect of an acid washing step [1-3]. If Illite batches are washed at pH=3.5 with HCl during 1 week before Eu addition, we exclusively found weaker Eu sorption. A possible explanation for this observation is the incongruent Illite dissolution resulting in the release of Al(III), which in turn can compete with Eu(III) for sorption sites. In order to confirm this hypothesis we contacted Illite during 1 week with a solution containing 10^{-4} M of Al(III) (i.e. equal to [Al] due to illite dissolution at pH=3.5) at different pH. Again, we found Eu sorption behaviour similar to that of the acid treated clay. Taking the competing effect of Al(III) species into account can explain the different Eu(III) sorption data sets.

[1] Gorgeon (1994) Ph.D. thesis University Paris 6. [2] Bradbury & Baeyens (2009) *Geochim. Cosmochim. Acta* **73**, 990-1003. [3] Bradbury *et al.* (2005) *Geochim. Cosmochim. Acta* **69**, 5403-5412.

Deep ingression of meteoric water in late-metamorphic veins: a LA-ICPMS fluid inclusion study from the Rhenish Massif, Germany

A. MARSALA^{1*}, T. WAGNER² AND M. WÄLLE¹

¹ETH Zurich, Department of Earth Sciences, Institute of Geochemistry and Petrology, Clausiusstrasse 25, 8092 Zurich, Switzerland (*correspondence: achille.marsala@erdw.ethz.ch)

²Division of Geology, Department of Geosciences and Geography, University of Helsinki, P.O.Box 64 (Gustaf Hällströmin katu 2a), FI-00014 Helsinki, Finland

The fluid evolution of late-metamorphic quartz vein systems in the fold-and-thrust belt of the Rhenish Massif has been investigated by microthermometry and LA-ICPMS microanalysis. The quartz veins are hosted in very low-grade organic-matter-rich metapelites of the Hunsrückschiefer and record two major stages of textural evolution: (1) a massive vein filling assemblage with elongate-blocky quartz, chlorite, albite and apatite, and (2) an open space filling assemblage with euhedral crystals of quartz, ankerite/dolomite and minor calcite and sulfides. The euhedral quartz crystals host well preserved fluid inclusion assemblages and permitted to reconstruct the evolution of the fluid system with time. The fluid inclusions, all aqueous two-phase with low salinity, belong to three successive generations. They show a systematic decrease in salinity from 4.7-5.3 to 3.1-3.9 and 1.4-1.7 wt.% eqv. NaCl, and a decrease in homogenization temperatures from 210-225 °C to 148-164 °C and 124-139 °C. LA-ICPMS microanalysis of individual fluid inclusions yielded reproducible concentrations of Li, Na, K, Rb, Cs, Mg, Ca, Ba, Sr, B, Al, As, Sb, S, Cl and Br. Alkali metals and boron, arsenic and antimony are correlated with the fluid salinity. Element concentrations are highest in the early fluid generation and decrease systematically in the latter two generations. Changes in salinity, homogenization temperature and elemental concentrations are explained by fluid mixing between a hot metamorphic fluid (moderate salinity and elevated concentrations of B, As and Sb) and a cooler dilute meteoric fluid during late-metamorphic exhumation and uplift. Cl/Br ratios of the fluid inclusions extend from close to seawater to values that are substantially below seawater. Because evaporitic rocks are absent in the shallow-water marine sequence of the Rhenish Massif, the elevated Br concentrations and Cl/Br ratios below seawater are best explained by fluid-rock interaction and uptake of Br from the organic matter in the metasediments.

Mélange formation, mantle-wedge diapirs and subduction zone magmatism

HORST R. MARSCHALL¹ AND JOHN C. SCHUMACHER²

¹ Dept Geology & Geophysics, WHOI, Woods Hole, MA, USA, hmarschall@whoi.edu

² Dept Earth Sci., University Bristol, Bristol, UK, j.c.schumacher@bristol.ac.uk

Components derived from the subducting slab contribute to the source region of magmas produced at convergent plate margins. The characteristic range of compositions of these magmas is commonly attributed to three-component mixing in the source regions of these magmas: hydrous fluids derived from subducted altered oceanic crust and components derived from the thin sedimentary veneer are added to the depleted peridotite in the mantle wedge, where melt is produced. We recently proposed an integrated physico-chemical model of subduction zones that includes mélange formation at the slab-mantle interface as the dominant physical mixing process, as well as low-density mantle-wedge diapirs that transport the well-mixed materials into the hot corner of the mantle wedge beneath arcs [1].

The strong petrologic and chemical contrast at the slab-mantle interface leads to the production of hybrid rock compositions by metasomatic reactions, diffusion and mechanical mixing. The rise of low-density plumes in the mantle wedge provides a mechanism to transport these buoyant hybrid rocks from the slab-mantle interface toward the source region of arc magmas. The mélange plumes may partially melt in the hot corner of the mantle wedge due to heating and decompression, or their interior parts may dehydrate and flux-melt the overlying mantle-wedge harzburgite. The combination of these processes may produce the large range of major and trace-element compositions found in modern island arc volcanic rocks.

Consequences and predictions from our model include the following: low-velocity zones at the slab-mantle interface and in the mantle wedge may represent layers and diapirs of fluid-rich mélange material instead of hot, melt-bearing mantle. The slab components are transported as solid matter into the source region of arc magmas rather than through the classically invoked fluids and melts. The temperatures and timescales for the generation of arc magmas determined from isotope and trace-element ratios need to be revisited, as these may reflect processes in the head of the mélange diapirs rather than in the subducting slab or the harzburgitic mantle wedge.

[1] Marschall, Schumacher (2012) *Nature Geosci.* 5: 862–867

Raman hyperspectral imaging of carbonaceous materials and hematite: potential misinterpretations

CRAIG P. MARSHALL¹ AND ALISON OLCOTT MARSHALL¹

¹Department of Geology, University of Kansas, Lawrence, KS, 66045, USA cpmarshall@ku.edu and olcott@ku.edu

Raman hyperspectral imaging is becoming increasingly popular in geoscience applications, as geologists, paleontologists, and planetary and space scientists discover the wealth of non-destructive mineral data that Raman spectroscopy can provide. One common application of Raman hyperspectral imaging is identification of optically similar minerals within thin sections and their spatial distribution. For example, hematite, disordered sp^2 carbonaceous material, and graphite can co-occur within a sample and often appear as black opaque minerals that are challenging to distinguish optically [e.g., 1,2]. In order to distinguish between these three minerals geologists will typically collect a Raman spectrum in the carbon first-order region between 900–1800 cm^{-1} . Coincidentally the hematite 2LO (which appear due to point defects of the α - Fe_2O_3 lattice) at ca. 1320 cm^{-1} is located in the same frequency region of the disordered sp^2 carbonaceous material D band (A_{1g} mode active due to disorder and decreasing crystallite size) at ca. 1350 cm^{-1} . While some geologists are cognizant of the overlap between the broad 2LO hematite mode and the broad D band of disordered sp^2 carbon, many however remain unaware [e.g., 3,4,5,6], identifying hematite by examination of the mineral fingerprint region (200–800 cm^{-1}) only [e.g., 7]. We suggest that rather than examining the mineral fingerprint region and the carbon first-order region separately for hyperspectral 2D and 3D imaging, the entire spectral region from 200–1800 cm^{-1} should be used in order to eliminate further false identification of these two minerals. Furthermore we suggest caution when interpreting the carbon first-order region as the G band (E_{2g2} mode in-plane C-C stretching LO phonon mode of an infinite crystal) from carbon is always present whatever the degree of structural order that the carbon sp^2 lattice has.

[1] Marshall *et al.* (2011) *Nat Geosci.* 4, 240–243. [2] Marshall and Olcott Marshall (2011) *Spectrochimica Acta.* 80, 133–137. [3] Lu *et al.* (2007) *Adv. Funct. Mater.* 17, 3885–3896. [4] Lu *et al.* (2008) *J. Phys. Chem. C.* 112, 7069–7078. [5] Torporski *et al.* (2004) *GIT Imaging Microsc.* 4, 38–40. [6] Schopf *et al.* (2005) *Astrobiology.* 5, 333–371. [7] Schopf *et al.* (2010) *Precamb Res.* 179, 191–205.

A new model for emerald mineralisation and boiling as a mechanism for emerald zoning and colouration.

DAN MARSHALL^{1*}, LARA LOUGHREY²,
MEGHAN HEWTON³ AND GABRIEL XUE⁴

¹Earth Sciences, Simon Fraser University, Burnaby, BC, Canada (correspondence: marshall@sfu.ca)

²Teck Resources Ltd., 550 Burrard St, Vancouver, BC, Canada (laraloughrey@gmail.com)

³Teck Alaska Inc., Red Dog Mine Anchorage, AK, USA (mlhewton@gmail.com)

⁴Callinex Mines Inc., Vancouver, B.C., Canada (gabe@callinex.ca)

Emerald forms in a number of geological environments [1] from a wide variety of fluids, dominated by water, generally comprising a variety of salts, and compressible gases [2]. Geological environments are variable but unique in that they offer mechanisms that allow for the combination of beryllium-rich fluids to interact with chromium- and vanadium-bearing fluids or rocks. Our more recent work has concentrated on a relatively new occurrence of emerald in the Northwest Territories of Canada. Emerald from this deposit has precipitated from saline brines via inorganic sulphate reduction.



Figure 1. Zoned emerald from the Byrud deposit.

Zoned gem emerald occurs in a number of deposits worldwide. The best known occurrences of zoned emerald are the Emmaville-Torrington in Australia, Erongo in Namibia, and the Byrud deposit in Norway. Recent fluid inclusion studies indicate that the zebra striping or zoned emerald (Fig. 1) is related to alternating precipitation of clear beryl and emerald in the vapour and liquid conjugates of (two-phase) boiling systems respectively.

[1] Groat *et al.* (2008) *Ore Geol. Rev.* 34, 87-112.

[2] Roedder (1972) *U.S.G.S. Prof. Paper* 440 JJ, 164 p.

Crustal evolution during granite emplacement: inheritance and development of heat-producing element enrichment

V. MARSHALL^{1,2*}, K. KNESEL², S. E. BRYAN³,
C. M. ALLEN⁴ AND I. T. UYSAL¹

¹Queensland Geothermal Energy Centre of Excellence, v.marshall@uq.edu.au (*presenting author)

²School of Earth Sciences, The University of Queensland

³Earth, Environmental & Biological Sciences, Queensland University of Technology

⁴Institute of Future Environments, Queensland University of Technology

The Big Lake Suite (BLS) granite in central Australia is one of the most prospective hot-dry rock geothermal resources worldwide. We have undertaken LA-ICP-MS ²⁰⁶Pb/²³⁸U dating of ~500 spots in 431 zircons across two plutons to shed new insights into petrogenesis and the relationship between emplacement age and elemental enrichment; heat-producing element (HPE) enrichments vary from 144–28 ppm Th and 30–8 ppm U between plutons.

New emplacement ages were obtained for drill holes Big Lake 1 (299 ± 6 Ma, MSWD 1.6, n=33) and Moomba 1 (324 ± 5 Ma, MSWD 0.71, n=42) in the southwest pluton, and Habanero 1 (315 ± 5, MSWD 1, n=38), Jolokia 1 (319 ± 13, MSWD 0.75, n=5) and McLeod 1 (306 ± 5 Ma, MSWD 1.8, n=74) in the northeast pluton. ²⁰⁶Pb/²³⁸U ages suggest protracted magmatism ~325–300 Ma, reinforcing the idea of piecemeal accumulation of granitic bodies.

Inherited 427–414 Ma ages for igneous zircons were identified in all wells (except Jolokia 1) indicating a recycled Silurian magmatic component in the BLS. Although there is overlap, inherited zircons have (on average) lesser trace-element enrichment (~250 ppm U) than emplacement-aged zircons (~870 ppm U). This suggests the emplacement-aged magma had undergone a greater degree of differentiation, thereby enriching it in HPE relative to magma compositions from which the inherited zircon population crystallised.

Protracted magmatism over ~25 Myr, and differences in emplacement history, can help explain variations in U and Th enrichment across the two plutons. Samples from the southwest pluton exhibit a difference in emplacement age of ~25 Myr, yet exhibit similar maximum Th and U enrichment implying initial elemental composition and differentiation controls allowed the magma to differentiate to the same level. Comparatively, in the northeast pluton, greater variability in final Th and U enrichment suggests slight differences in source controls over the crystallisation history of the pluton.

Magmatic volatiles and mantle source lithology in the Hawaiian Plume: a view from olivine-hosted melt inclusions, glasses, and osmium isotopes

JARED MARSKE¹, ERIK HAURI¹, MICHAEL GARCIA²
AND AARON PIETRUSZKA³

¹5241 Broad Branch Rd, Washington DC, marske@ciw.edu

²5241 Broad Branch Rd, Washington DC, ehauri@ciw.edu

³1680 East-West Rd, Honolulu HI, mogarcia@hawaii.edu

⁴Box 25046 DFC, Denver, CO, apietrusza@usgs.gov

Variations in radiogenic isotopes (e.g. Pb,Nd) and magmatic volatiles (e.g. CO₂,H₂O) in Hawaiian volcanoes reveal important processes (i.e. source heterogeneity, melting, magma degassing). Shield-stage lavas likely originate from a plume source containing peridotite and ancient recycled oceanic crust (pyroxenite). The source region may also be heterogeneous with respect to volatile concentrations. However, shallow degassing makes it difficult to determine if there is a link between mantle source composition and volatile budget. Here we present Os isotopic ratios and volatile contents on olivines and glasses for 33 samples from Koolau, Mauna Kea, Mauna Loa, Hualalai, Kilauea, and Loihi to determine if volatiles in magmas correlate with geochemical tracers of source lithologies. For a given volcano, most osmium isotopic compositions of olivines are similar to the whole-rock values, yet some Mauna Loa and Loihi olivines display the significantly low 187Os/188Os values (~0.117) that may reflect partial melts of ancient recycled mantle lithosphere. SIMS analyses on Hawaiian glasses reveal a range in abundances of CO₂ (10-251 ppm), H₂O (0.2-1.2 wt.%), S (38-2960 ppm), and Cl (39-2960 ppm). However, most samples have low CO₂ contents (<100 ppm) indicating they experienced degassing. Olivine-hosted melt inclusions may better preserve pre-eruptive concentrations and we will present new volatile contents on Hawaiian melt inclusions from the same olivines analyzed for Os isotopes.

Helium isotopes signature of mafic volcanics at Stromboli (Italy) during its magmatic evolution.

M. MARTELLI¹, A. RIZZO¹, A. RENZULLI², F. RIDOLFI², I. ARIENZO³ AND A. ROSCIGLIONE⁴

¹Istituto Nazionale di Geofisica e Vulcanologia, Sezione di Palermo, Palermo, Italy, m.martelli@pa.ingv.it

²Dipartimento di Scienze della Terra, della Vita e dell'Ambiente - University of Urbino, Italy

³Istituto Nazionale di Geofisica e Vulcanologia, Sezione di Napoli Osservatorio Vesuviano, Napoli, Italy

⁴Dipartimento DiSTeM, Università di Palermo, Italy

A study on fluid inclusions of mafic minerals from selected volcanics is conducted to characterize the He and Ar isotopes of Stromboli. We also measured trace element in clinopyroxenes of selected samples and Sr-Nd isotopes. The samples belong to (i) the present-day activity of Stromboli; (ii) the extreme terms among the magmatic series erupted (calcalcaline CA and potassic KS); (iii) the ultramafic xenoliths outcropping in the island. The gas content trapped in mafic crystals is consistent with magma crystallization and fluid entrapment from mantle depths to progressively shallower conditions. All samples have ³He/⁴He in the range 4.0-4.9 Ra, except the KS (³He/⁴He < 3.5 Ra), associated to higher Sr and lower Nd isotope ratio. Overall, He isotopes are well associated to lithophile element isotopes. The whole set of helium isotope data indicates ratios lower than those measured in the most uncontaminated Aeolian lavas (i.e., Alicudi, ~ 7 Ra) and in common volcanic arcs, due to subduction-related contamination beneath Stromboli. ³He/⁴He from mafic minerals are compared to those of currently geothermal fluids, with the latter ranging between 3.9 and 4.5 Ra. The maximum ³He/⁴He ratio measured in LP fluid inclusions (i.e., 4.6 Ra) would thus correspond to the upper limit that should be expected for surface gases during or before high-intensity eruptive events, when a deep gas component is released from the magma.

Developing the comminution age technique: Isolating the detrital minerals

A.N. MARTIN* AND A. DOSSETO¹

¹Wollongong Isotope Geochronology Laboratory, School of Earth and Environmental Sciences, University of Wollongong. (*correspondence: anm724@uowmail.edu.au)

The uranium-series isotopes can be used to quantify the timescales on which Earth-surface processes operate; this is essential before we can begin to try to understand how the erosion of the Earth's surface responds to climate change.

The traditional uranium-series methodology analyses the isotopic composition of the bulk sediment; however, this requires complex modelling to account for the variable isotopic composition of authigenic phases, such as carbonates and organic material [1]. The accuracy of the calculated ages can be improved by focussing on the isotopic evolution of only the detrital minerals. One such example is the emerging *comminution age* technique which calculates a radiometric age by relating the (²³⁴U/²³⁸U) of the detrital minerals to the surface area [2].

Sequential extraction procedures are currently used to remove the non-detrital fraction but these procedures are unreliable and suffer from a lack of reproducibility and completeness. To overcome this, the isolation of the detrital minerals can be monitored by analysing the (²³⁴U/²³⁸U) of the sediment throughout the procedure. This is possible as there are three domains of (²³⁴U/²³⁸U) in sediment: 1. (²³⁴U/²³⁸U) = 1 for the inner-core of detrital minerals, (²³⁴U/²³⁸U) < 1 in the outer-rind (ca. 50 nm) of sediment due to the effects of alpha-recoil, and (²³⁴U/²³⁸U) > 1 for the non-detrital fraction [3]. The minimum (²³⁴U/²³⁸U) of the sediment therefore represents the optimum isolation of the detrital minerals.

This study evaluates existing sequential extraction procedures and proposes an *optimised* procedure based on the above methodology. This will be presented in addition to the implications of the results upon ages calculated using the comminution age technique.

[1] A.J. Plater, M. Ivanovich, R.E. Dugdale (1992), *Applied Geochemistry*, 7 101-110. [2] D.J. DePaolo, K. Maher, J.N. Christensen, J. McManus (2006), *Earth and Planetary Science Letters*, 248 394-410. [3] V.E. Lee (2009), "Radiogenic Isotope Geochemistry and the Evolution of the Earth's Surface and Interior", PhD Thesis, University of California, Berkeley.

Fayalite oxidation processes at Obsidian Cliffs, Oregon

A.M. MARTIN^{1*}, E. MÉDARD², B. DEVOUARD², L.P. KELLER¹, K. RICHTER¹, J.-L. DEVIDAL² AND

Z. RAHMAN¹

¹Johnson Space Center, 2101 NASA Parkway, Houston, TX 77058 USA (*correspondence: aud.martin23@gmail.com)

²Clermont Université, UBPCNRS/IRD, Laboratoire Magmas et Volcans, 5 rue Kessler, 63038 Clermont-Ferrand, France

Fayalite Fe₂²⁺SiO₄, the ferrous end-member of olivine, is present in terrestrial rocks and in primitive meteorites [1]. A ferric fayalite, laihunite Fe²⁺Fe³⁺₂□(SiO₄)₂, has also been reported in terrestrial [2, 3, 4, 5] and martian [6] samples. In order to constrain the oxidation processes of fayalite, we have studied crystals found in lithophysae from the Obsidian Cliffs rhyolite using EMPA and SAED+EELS on a TEM, and made thermodynamic modelling.

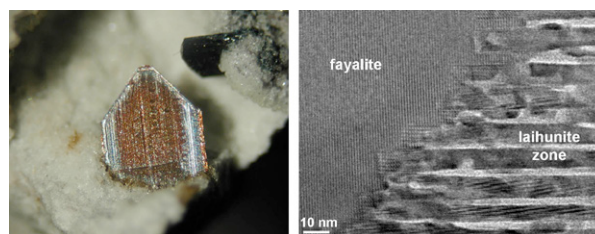


Figure 1: (a) picture of an oxidized fayalite crystal (approx. 1.6 mm tall) (©B.Lechner) (b) HRTEM image of the fayalite/laihunite interface.

Fayalite crystallized at 800-900°C and low p_{H₂O}. Temperature decrease to 650°C induced the oxidation of fayalite into a "laihunite" zone Fe²⁺Fe³⁺₂□(SiO₄)₂ composed of nano-lamellae of various oxidation phases (Fig.1). Further cooling, H₂O exsolution from rhyolite lava and/or infiltration of meteoric water caused the oxidation of the "laihunite" zone into an "oxyfayalite" zone Fe²⁺_{0.26}Fe³⁺_{1.16}□_{0.58}(SiO₄) also made of nano-lamellae.

Fayalite oxidation reactions can be used to constrain the emplacement and cooling history of the lava flow. Our data also hint at the existence of a ferric fayalite phase that is more oxidized than laihunite.

[1] Jogo *et al.* (2009) *EPSL* 287, 320-328 [2] *Laihunite* Research Group (1982) *CJG* 1, 105-115 [3] Schaefer (1983) *Nature* 303, 325-327 [4] Kitamura *et al.* (1984) *AmMin* 69, 154-160 [5] Shen *et al.* (1986) *AmMin* 71, 1455-1460 [6] Noguchi *et al.* (2009) *JGR* 114, E10004.

Heating from within and without, tales of contrasting long-lived crustal hot spots

M. HAND¹

South Australian Centre for Geothermal Energy Research,
University of Adelaide, S.A., 5005 Australia.
(correspondence: martin.hand@adelaide.edu.au)

High thermal gradient conditions in the crust can be generated by a number of mechanisms: direct advection of heat via magmatism, high basal heat flow associated with extension/removal of lithospheric mantle, rapid exhumation of deeply buried rocks and high rates of internal heat generation. While each of these mechanisms may have characteristic time and length scales, the duration of metamorphism as perceived by geologists is generally controlled by the exhumation potential in the system which determines the thermal record of an individual rock. Therefore long-lived high-T metamorphism generally points to thermally anomalous conditions in crust with low exhumation potential where material stays within the system for an extended period of time (e.g. orogenic plateaus).

More intriguing is apparently long-lived (~ 100 Ma) high-T “hot-spot” metamorphism that appears to have operated on a sub-orogenic (~ 100km) scale length scale. This sub-orogenic scale means that rocks can potentially easily move out of the high-T region curtailing the duration of their high-T history. Such systems can be plausibly driven by high rates of internal radiogenic crustal heat generation in chemically anomalous crust undergoing limited deformation. For example in parts of central Australia, crustal heat generation rates are regionally in excess of $8\mu\text{Wm}^{-3}$, and are spatially associated with high-T low-P granulite metamorphism.

“Long-lived crustal “hot spots” can also be generated in highly localised rift basins developed in thick continental lithosphere. Continental rift basins may accumulate in excess of 25km of sediment fill associated with voluminous mafic magmatism. This creates a logical setting for high-T, medium P metamorphism associated with on-going basin development, including high-grade intrabasinal deformation.

We discuss salient features of internally and externally driven crustal “hot spots”.

Carbon budget during alteration of the oceanic crust

I. MARTINEZ*¹, S. SHILOBREEVA², V. BUSIGNY¹,
C. LAVERNE³, J. ALT⁴ AND P. AGRINIER¹

¹ IPGP, PRES Sorbonne Paris Cité, Paris, France (*
correspondence: martinez@ipgp.fr).

² Vernadsky Institute, Moscow, Russia.

³ Univ. Aix-Marseille III, Marseille, France.

⁴ Univ. of Michigan, Ann Arbor MI, USA.

Although it is largely accepted that volatile elements are incorporated into the oceanic crust during alteration, the flux of carbon involved in this transfer remains poorly known. The detailed study of altered rocks is a key to better constrain the C uptake during alteration. In this work, we studied carbon concentrations and isotopic compositions in altered basaltic samples drilled from 2 different sites. We first selected a young section of altered oceanic crust (15 Ma): the ODP/IODP Hole 1256D, providing a large variety of rocks from lavas down to the gabbroic rocks. The second set of samples, which is of Jurassic age (Site 801, 150 Ma), was selected to evaluate C uptake variations during aging of the crust. All samples are enriched in carbon relative to fresh basalts. For 1256D samples, total CO₂ ranges between 564 and 2823 ppm with $\delta^{13}\text{C}$ values from -14.9‰ to -26.6‰. The carbon isotope compositions are interpreted in terms of a mixing between two components: (1) carbonate with $\delta^{13}\text{C} = -4.5‰$ and (2) organic compound with $\delta^{13}\text{C} = -26.6‰$ representing more than 75% of the total C in most of the samples. Jurassic samples are enriched in carbon relative to 1256D samples (with total CO₂ between 0.3 and 2wt%). Although the organic carbon concentration and isotope composition remains constant in these samples, the carbonate concentration strongly increases. A possible explanation is that higher atmospheric CO₂ in the Mesozoic [1] may have led to higher carbonate contents in the old 801 basement. Alternatively, we propose a two-step model for carbon cycling during crustal alteration: (i) organic compounds are formed close to ridge axis, either through recycling of biogenically-derived material or Fischer-Tropsch-type reactions; (ii) away from the ridge axis, the organic production decreases and carbon uptake is dominated by carbonate precipitation from seawater. The total flux of C stored in the altered oceanic crust, as carbonate and organic compounds, is estimated at $2.9 \pm 0.4 \cdot 10^{12}$ molC/yr with a mean $\delta^{13}\text{C}$ of -4.7‰.

[1] Gillis & Coogan (2011) *EPSL* **302**,385-392.

Modelling of rare earth element sorption to *Bacillus subtilis* bacteria

RAUL E. MARTINEZ¹, OLIVIER POURRET²
AND YOSHIO TAKAHASHI³

- ¹ Institut für Geo- und Umweltwissenschaften, Albert-Ludwigs Universität, Albertstraße 23b, D-79104, Freiburg, Germany. raul.martinez@minpet.uni-freiburg.de
- ² HydrISE, Institut Polytechnique LaSalle Beauvais, 19 rue Pierre Waguet, 60026 Beauvais Cedex, France.
- ³ Department of Earth and Planetary Systems Science, Hiroshima University, Higashi-Hiroshima, Hiroshima 739-8526, Japan.

In this study, rare earth element (REE) binding constants and site concentration on the Gram+ bacteria surfaces were quantified using a multi-site Langmuir isotherm model, along with a linear programming regression method (LPM). This approach found one discrete REE binding site on the Gram+ *Bacillus subtilis* surface for the pH range of 2.5 to 4.5. Average log REE binding constants from 1.08 ± 0.04 to 1.40 ± 0.04 for the light REE (LREE: La to Eu), and from 1.36 ± 0.03 to 2.18 ± 0.14 for the heavy REE (HREE: Gd to Lu) at 1.3 g/L of *Bacillus subtilis* bacteria. Similar values were obtained for bacteria concentrations of 0.39 and 0.67 g/L. Within the experimental pH range in this study, *Bacillus subtilis* was shown to have a lower affinity for LREE (e.g. La, Ce, Pr, Nd) and a higher affinity for HREE (e.g. Tm, Yb, Lu) suggesting an enrichment of HREE on the surface of Gram+ bacteria. Total surface binding site concentrations of 6.73 ± 0.06 to 5.67 ± 0.06 and 5.53 ± 0.07 to 4.54 ± 0.03 moles/g of bacteria were observed for LREE and HREE respectively, and a log $K_{\text{REE},j}$ of 1.46 ± 0.02 for a biomass content of 1.3 g/L. The difference in these values (e.g. a lower affinity and increased binding site concentration for LREE, and the contrary for the HREE) suggests a distinction between the LREE and HREE binding modes to the Gram+ bacteria reactive surface at low pH. A multisite Langmuir isotherm approach along with the LPM regression method, not requiring prior knowledge of the number or concentration of cell surface REE complexation sites, were able to distinguish between the sorption constant and binding site concentration patterns of LREE and HREE on the Gram+ *Bacillus subtilis* surface. This approach quantified the enrichment of Tm, Yb and Lu on the bacteria surface and it has proven to be a useful tool for the study of natural reactive sorbent materials controlling REE partitioning in the natural environment.

The conditions of formation of the Castro de Rei reduced W-skarn

I. MARTÍNEZ-ABAD^{1*} AND A. CEPEDAL¹

- ¹Department of Geology, University of Oviedo, Arias de Velasco s/n, 33005, Oviedo, Spain.
(*correspondence: iker@geol.uniovi.es)

The reduced W-skarn of Castro the Rei (Villalba Gold District, NW Spain) is hosted by marbles and calc-silicate hornfels of the contact aureole of a blind poskinematic Variscan granitoid [1, 2]. A hornblende-hornfels facies metamorphism is related to these granitoids, at pressures up to 2 kb [3]. Prograde skarn developed in marble is characterized by garnet (Gr₄₁₋₇₇), pyroxene (Hd₃₃₋₁₀₀), quartz and calcite with minor scheelite, K-feldspar and apatite. Locally, it can be formed by wollastonite, garnet (Gr₆₂₋₈₂) and piroxene (Hd₄₃₋₇₀). Prograde skarn and calc-silicate hornfels were overprinted by two stages of retroskarn. The first stage consists of ferrotremolite, epidote (Ps₁₉₋₃₁), zoisite (Ps₀₋₁₉), quartz, calcite, K-feldspar and sulfides and the second stage is characterized by prehnite or chlorite, quartz, calcite and sulfides. Based on mineral associations, fluid inclusion and stable isotope studies, a T-X(CO₂) isobaric (2kb) diagram with selected phase equilibria [4] was used for establishing the conditions of the skarn formation.

Fluid inclusions in garnet and quartz indicate that the prograde skarn was formed from a low-CO₂ (<0.06 mole fraction) aquocarbonic fluid. At this X(CO₂) the minimum formation temperature of the wollastonite-bearing skarn is 555°C. For the garnet (Gr₄₁₋₇₇) and pyroxene (Hd₃₃₋₁₀₀) skarn, the formation temperature is above 520°C, in agreement with the ¹⁸O fractionation between quartz and garnet that yields a temperature of 534°C. Ferrotremolite, epidote (Ps₁₉₋₃₁) and zoisite (Ps₀₋₁₉) from the first stage of retroskarn are formed at lower X(CO₂) (<0.04 mole fraction) and a temperature below 450°C. For the second stage of retroskarn, fluid inclusions and occurrence of prehnite indicate near 0 X(CO₂) and temperatures below 385°C. This is consistent with the maximum formation temperature calculated for the chlorite [5], up to 325°C.

- [1] Martínez-Abad *et al.* (2011) In: Ediciones Universidad Católica del Norte. Antofagasta, Chile, 2, 550-552. [2] Martínez-Abad *et al.* (2012) *Geo-Temas*, 13, 414. [3] Bellido-Mulas *et al.* (1987) Memoria del IGME. 157 pp. [4] Berman (2007) *Geol. Surv. Can. open file rep.*, 5462, 41pp. [5] Cathelineau, M (1988) *Clay Minerals*, 23, 471-485.

Surface ocean $\delta^{11}\text{B}$ -pH reconstructions and insights into the ocean-atmosphere carbon exchange during the last deglaciation

M.A. MARTÍNEZ-BOTÍ^{1*}, G. MARINO², G.L. FOSTER¹,
P. ZIVERI², M.J. HENEHAN¹, P.G. MORTYN^{2,3}
AND D. VANCE⁴

¹ Ocean and Earth Science, National Oceanography Centre Southampton, University of Southampton, Southampton SO14 3ZH, UK (*correspondence: M.A.Martinez-Boti@noc.soton.ac.uk)

² Institut de Ciència i Tecnologia Ambientals, Universitat Autònoma de Barcelona, 08193 Bellaterra, Barcelona, Spain

³ Department of Geography, Universitat Autònoma de Barcelona, 08193 Bellaterra, Barcelona, Spain

⁴ Institute of Geochemistry and Petrology, ETH Zürich, Zürich, Switzerland

There is a long-standing debate about the causes of the glacial-interglacial fluctuations in atmospheric CO_2 concentrations (pCO_2). One of the most established hypotheses involves the “storage” of CO_2 in the deep ocean during glacial periods, and the subsequent re-communication of this deep carbon reservoir with the surface ocean and atmosphere during deglaciations (mainly via upwelling in the Southern Ocean), thereby causing atmospheric pCO_2 to increase [1-3]. Yet direct evidence for carbon leakage from the ocean into the atmosphere during deglaciations is currently lacking.

Boron isotopes ($\delta^{11}\text{B}$) in planktic foraminifera are a proven proxy for past surface oceanic pH [4,5], which has provided valuable insights into past changes in the ocean carbonate system, and ultimately into past atmospheric pCO_2 . Here we will present new planktic foraminifera $\delta^{11}\text{B}$ results from sediment cores retrieved from the Eastern Equatorial Pacific and Subantarctic Atlantic Ocean that yield novel insights into the causes and mechanisms of pCO_2 rise during the last deglaciation.

[1] Anderson *et al.* (2009) *Science* **323**, 1443-1448. [2] Skinner *et al.* (2010) *Science* **328**, 1147-1151. [3] Burke & Robinson (2012) *Science* **335**, 557-561. [4] Sanyal *et al.* (2001) *Paleoceanography* **16**, 515-519. [5] Foster (2008) *EPSL* **271**, 254-266.

Elemental ratios as proxies for paleoclimate reconstruction in the western Mediterranean

F. MARTINEZ-RUIZ^{*1}, M. RODRIGO-GAMIZ², V. NIETO-MORENO³, F. J. JIMENEZ-ESPEJO¹, D. GALLEGO-TORRES¹ AND M. ORTEGA-HUERTAS⁴

¹Instituto Andaluz de Ciencias de la Tierra (CSIC-UGR), Spain (*correspondence: fmruiz@ugr.es)

²Royal Netherlands Institute for Sea Research, NIOZ, The Netherlands (Marta.Rodrigo@nioz.nl)

³Biodiversität und Klima Forschungszentrum BiK-F, Germany (Vanessa.Nieto-Moreno@senckenberg.de)

⁴Dept. Mineralogía y Petrología (UGR), Spain (mortega@ugr.es)

The western Mediterranean region has provided excellent marine archives for paleoclimate reconstructions. In particular, the Alboran sea basin where exceptional high sedimentation rates allowed high-resolution analyses for reconstructing past climate variability. Elemental ratios have revealed as reliable proxies for such reconstruction and have served to characterize arid/wet fluctuations, intensity of atmospheric fluxes and dust deposition, as well as bottom-water oxygen conditions. Over the past 20,000 cal yr BP, ratios mirroring eolian input (Zr/Al , Ti/Al and Si/Al) evidenced a major input of dust from the offset of the Last Glacial Maximum to the Oldest Dryas. Mg/Al , K/Al and Rb/Al ratios have provided information on fluvial contribution, and record humid conditions during the subsequent Bolling-Allerød warm period, further supported by the decrease of Zr/Al ratio. These ratios have also allowed a detailed reconstruction of paleoclimate conditions during the Younger Dryas and the Holocene. Ratios of redox sensitive elements such as U/Th , Zn/Al , Cu/Al , and V/Al ratios have also supported fluctuations in oxygen conditions at time of deposition, although these elements are particularly susceptible to diagenetic remobilization that could alter the original records. Regarding productivity fluctuations, reconstructions based on Ba proxies, including Ba/Al ratios, have shown a significant increase in the Ba/Al ratio during cold periods, i.e., H1 and Younger Dryas (derived from authigenic marine barite) evidencing enhanced marine productivity. In contrast, during the early Holocene the Ba/Al ratio indicate decreasing productivity. However, the biogeochemistry of Ba is not yet fully understood and mechanisms for barite precipitation in the water column still require further investigation.

Isotope geochemistry in waters affected by mining activities in Portman bay (Spain).

M.J. MARTÍNEZ-SÁNCHEZ¹; M.L. GARCÍA-LORENZO²; C. PÉREZ-SIRVENT^{1*} AND M. HERNANDEZ-CORDOBA³.

¹Department of Agricultural Chemistry, Geology and Pedology. Faculty of Chemistry, University of Murcia, Murcia, Spain. melita@um.es
(*presenting author García-Lorenzo, M.L. mglorenzo@geo.ucm.es)

²Department of Petrology and Geochemistry. Faculty of Geology, Unibersity Complutense of Madrid, Madrid (Spain)

³Department of Analytical Chemistry. University of Murcia.

The objective of this work was to characterize processes affecting waters from Portman bay by way of isotopic analysis, particularly H and O stable isotopes from water molecule and S and O from dissolved sulfates were studied.

Portman bay is situated close to the mining region of La Unión and was subject to mining from the time of the Roman Empire to 1991, when the activity ceased. From 1957 to 1991, the Peñarroya Mining and Metallurgical Society performed ore extraction on a large scale. From Lavadero Roberto, the waste materials were discharged directly into the sea in the inner part of the bay, and later they were also discharged to sea at a distance of the shore. These wastes mainly consisted in ore materials (sulfides as galena, pyrite and sphalerite), phyllosilicates in addition to siderite, iron oxides and sometimes alteration products such as jarosite, alunite, kaolinite and greenalite.

Mining activities have produced great amount of wastes, characterized by high trace elements content, acidic pH and minerals from weathering processes. According to the isotopic analysis, the origin of waters from Portman Bay is not marine, they are meteoric waters subjected to evaporation except for two superficial samples from Portman Bay, where seawater remained stagnated in impermeable sediments. The possible marine infiltrations only take place in the deepest layers (>17 m) because below this depth materials showed low permeability. Superficial waters from Portman bay have undergone evaporation while deep waters showed no evidence of this process. The isotopic results suggested that the sulfates mainly come from sulfide oxidation and transport of produced sulfosalts. The oxygen isotopes of water and sulfates were used to indicate the mechanisms of this oxidation, being Fe³⁺ the principal oxidant of pyrite. Moreover, there is evidence showing that sulfate oxygen is derived from water under aerobic and anaerobic conditions. Isotopic data also suggested that a reduction process is taking place under anaerobic conditions, favored by the depth.

Limestone-based technosols. A remediation technique for sediments contaminated by heavy metals.

M.J. MARTÍNEZ-SÁNCHEZ¹; M.L. GARCÍA-LORENZO²; C. PÉREZ-SIRVENT^{1*}; E. GONZÁLEZ¹; V. PÉREZ¹; S. MARTÍNEZ¹; M.D. BELANDO¹, L. MARTINEZ¹ AND C. HERNANDEZ¹.

¹Department of Agricultural Chemistry, Geology and Pedology. Faculty of Chemistry, University of Murcia, Murcia, Spain. mjose@um.es (*presenting author)

²Department of Petrology and Geochemistry. Faculty of Geology, Unibersity Complutense of Madrid, Spain.

The aim of this work was to assess the suitability of limestone-based technosols for decreasing the toxicity of the leachates caused by rain in sites contaminated by heavy metals. For such a purpose, 64 technosols were prepared in containers of 0.75m³, filled with 4 types of sediments collected from Portman Bay and subjected to different stabilizer proportions (limestone filler), different thickness of a drainage layer and presence/absence of a topsoil cover. The technosols were then submitted to different humidity/dryness cycles simulating the usual rain conditions in the zone and percolates were analyzed using a battery of bioassays.

Portman bay is situated close to the mining region of La Unión. The entire area around the bay was subject to mining from the time of the Roman Empire to 1991. Since 1957, the wastes from mining operations were discharged directly into the sea in the inner part of the bay, while later on, they were also discharged to sea at a distance of the shore. These wastes mainly consisted in ore materials (galena, pyrite and sphalerite), phyllosilicates, in addition to siderite, iron oxides and sometimes alteration products such as jarosite, alunite, kaolinite and greenalite. These materials have suffered a concentration process by floatation with sea water and as a result of the discharge, the whole of the bay has filled up with wastes which also extend into the Mediterranean Sea.

The obtained results suggest that selected remediation technique reduces significantly the toxicological effect of the percolate to the tested organisms. The ecotoxicological testing may be a useful approach for assessing the toxicity as a complement to chemical analysis. In addition, the use of a battery of bioassays allows diminishing problems related to false positive results. The use of limestone filler constitutes an excellent option in sediments polluted by trace elements, because of risk for human health or ecosystems does not exist after the intervention. In addition, the designed experience allow to optimize stabilizer quantities, and may suppose a big cost-saving project in areas affected by mining activities.

The composition of zircon in peraluminous Variscan granites from Northern Portugal

HELENA C.B. MARTINS^{1*} AND JOANA ABREU¹

¹DGAOT, Centro de Geologia, Faculdade de Ciências
Universidade do Porto, Portugal, hbrites@fc.up.pt (*
presenting author)

A group of peraluminous Variscan plutons were selected from the study of zircon composition. The selected plutons are: the post-D₃ Vila Pouca de Aguiar and the Lavadores plutons [1, 2] and the late-D₃ Vieira do Minho pluton [3]. The zircons occur as euhedral to subhedral crystals and exhibit finely concentric oscillatory zoning in BSE imaging. Internal zoning is mainly related to variations of Hf, Y, U and Th concentrations. Compositional ranges in zircon from all granites are present in Figure 1.

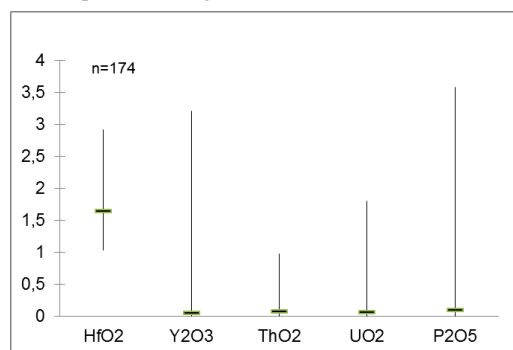


Figure 1: Compositional variation of zircons. Bar shows the complete range of zircon composition (vertical line), including the median (short horizontal line).

The zircon crystals have Zr/Hf ratio varying between 29 to 56, with no significant differences between the different granites. These values are in the same range of other peraluminous granites [5] and are in accordance with a crustal signature of zircon as suggested by several authors [4, 5]. The range of Zr/Hf values in zircon crystals of the studied granite plutons overlaps with that of the potential protholites proposed in the genesis of these peraluminous granites, namely meta-igneous crustal sources at different levels [1, 3].

[1] Martins *et al.* (2009) *Lithos* **111**, 142-155 [2] Martins *et al.* (2011) *CR Geoscience* **343**, 387-396 [3] Martins *et al.* (2013) *Lithos* **162-163**, 221-235 [4] Pupin (2000) *Trans. R. Soc. Edinb.: Earth Science* **91**, 245-256 [5] Pérez-Soba *et al.* (2007) *The Canadian Mineralogist* **45**, 509-527.

This work has been financially supported by PTDC/CTE-GIX/099447/2008 (FCT-Portugal, COMPETE/FEDER).

Sr and Pb isotopes in surface water and bottom sediments from a public water supply reservoir, São Paulo, Brazil

V.T. S. MARTINS^{1*}; C. S. D. MURAKAMI²
AND C. H. GROHMANN³

¹ Institute of Geosciences, University of São Paulo, São Paulo, SP, 05508-080, Brazil (*correspondence: veridian@usp.br)

² cintia.murakami@usp.br

³ guano@usp.br

São Paulo is the biggest city of South America, with almost 20 million people living in its metropolitan area (MASP) of almost 6000 km². This population is mainly supplied by public surface water reservoirs, one of them being the Guarapiranga Dam, which provides water to 3,7 million people that live in the southeast of MASP. The Guarapiranga Dam surroundings are occupied by more than 800 thousand people that may compromise the quality of its waters. In order to investigate the existence of anthropogenic influences on the surface water of Gurapiranga Dam, the chemical composition of water and the surroundings rocks and sediments, as well as the Sr and Pb isotopic ratios of them, were analysed.

The results obtained from samples of water and sediment (bottom or margins), indicate that the water collected in only one point showed evidence of sewage contamination with the presence of high nitrate (>20 mg/L). In the sediments and bottom margin appeared high concentration of copper in the closest points of catchment water by the supply company. The presence of copper may be associated with the use of copper sulfate as algicide to prevent the eutrophication process of the reservoir and occurs mainly in the deepest parts of the dam.

The Sr isotope data indicated as well as the Pb isotopes, that the surface waters isotopic ratios are similar to the leachate (nitric and hydrochloric acids 3.5 M) from the bottom and margins sediments, that exhibited high content of copper (0.717) and organic matter, or with higher clay content. Furthermore, the Sr isotope ratios are also similar to those of rainwater (0.715). As for the Pb isotopes, the Sr isotopes do not clearly distinguish anthropogenic sources from natural sources, since both sources have similar ratios to surface waters in this case. Further studies should indicate that isotopes can be used as monitors of safe drinking water.

Emerging organic pollutants removal from water using high silica zeolites

A. MARTUCCI¹, L. PASTI², E. SARTI² AND R. BAGATIN³

¹Dept. of Physics and Earth Sciences, Univ. of Ferrara, 44100 Ferrara, Italy; (*correspondence:mrs@unife.it)

²Dept. of Chemistry and Pharmaceutical Sciences, Univ. of Ferrara, 44100 Ferrara, Italy; psu@unife.it

³Eni Donegani Env. Technologies, San Donato Milanese 20097, Italy, roberto.bagatin@eni.com

Zeolites are environmentally compatible crystalline aluminosilicates, which have well defined micropore dimensions and composition in a rigid crystal lattice. The shape of their internal pore structure can strongly affect their adsorption selectivity toward host molecules [1-3]. In the present work, organophilic synthetic zeolites which are cheap and available on the market, differing in topology, channel systems and free window apertures, and emerging organic contaminants (i.e. pharmaceuticals, fuel-based-pollutants) differing in chemical properties and molecular dimensions, were tested. A combined diffractometric, thermogravimetric, and gas chromatographic study was used to: (i) measure the sorption capacity of hydrophobic zeolite materials weighed against organic pollutants dissolved in water; (ii) quantify aspects of their removal efficiency for potential use in wastewater and groundwater remediation; (iii) understand zeolite structural features for the adsorption of emerging organic pollutants from aqueous solutions. Coupling the information gathered from these approaches can help in selecting adsorbent materials for water treatment.

[1] D. Löffler *et al.* (2005) *Environ. Sci. Technol.* **39**, 5209-5218. [2] A. Martucci *et al.* (2012) *Micropor. Mesopor. Mater.* **148**, 174-183. [3] L. Pasti *et al.* (2012) *Micropor. Mesopor. Mater.* **160** 182-193. [4] B.A. De Moor *et al.*, *J. Phys. Chem. C* (2011) **115**, 1204-1219.

Nitrogen isotopes in lunar soils: A record of contributions to planetary surfaces in the inner solar system

B MARTY¹, M. CHAUSSIDON¹, E. FÜRI¹, K. HASHIZUME², F. PODOSEK³, R. WIELER⁴ AND L. ZIMMERMANN¹

¹CRPG-CNRS, Université de Lorraine, Vandoeuvre, France, bmarty@crpg.cnrs-nancy.fr

²Osaka University, Japan

³Washington University, St Louis, USA

⁴ETH, Zürich, Switzerland

The nitrogen isotope composition of inner planets ($\delta^{15}\text{N} = 0\text{‰}$ for the terrestrial atmosphere) and meteorites (between -40‰ and $+40\text{‰}$ for most meteorite clans) differs drastically from both Solar ($\delta^{15}\text{N} = -386\text{‰}$ [1]) and Cometary ($\delta^{15}\text{N} \approx +800\text{‰}$ for CN and HCN) values. On Earth, $^{15}\text{N}/^{14}\text{N}$ ratios span over less than 40‰ . In contrast, values measured in lunar soils and rocks vary by up to 400‰ . Since trapped lunar noble gases are exclusively sourced by the solar wind, these variations were initially interpreted as a temporal evolution of the solar wind N isotope composition [2]. Ion probe measurements and N-Ar systematics of soil grains have shown that these N isotope variations instead result from mixing between light N from the solar wind and a ^{15}N -rich component of non-solar origin [3,4]. The latter could have originated from implantation of ancient atmospheric N from the Earth, when the terrestrial magnetic field was weaker than Today [5]. However, the analysis of fluid inclusions in 3.5 Ga-old quartz is consistent with a N content and isotopic composition of the Archean atmosphere comparable to modern values [6], which suggests that the terrestrial magnetic field was strong enough to retain atmospheric N since at least 3.5 Ga. Thus escape of atmospheric N should have occurred before 3.5 Ga ago, e.g., in the Hadean, which is difficult to reconcile with the exposure ages and antiquities of lunar soils generally lower than 2-3 Ga. The secular variations of the N isotope composition of lunar soils are better accounted for by mixing solar wind N with asteroidal (IDPs, micrometeorites, meteorites) nitrogen, and temporal N isotope variations are consistent with a marked increase of the meteoritic flux in the last few hundreds of Ma. The N isotope systematics of lunar soils permit to constrain the fraction of cometary impactors to less than 13%, and the water flux to the lunar surface to about 600 tons/yr [7].

[1] B. Marty *et al.*, *Science*, **332**, 1533 (2011). [2] J.F. Kerridge, *Rev. Geophys.* **31**, **423** (1993). [3] Hashizume *et al.*, *Science* **290**, 1142 (2000). [4] R. Wieler *et al.*, *EPSL* **167**, 47 (1999). [5] M. Ozima *et al.*, *Nature* **436**, 655 (2005). [6] B. Marty *et al.*, submitted. [7] E. Fueri *et al.*, *Icarus* **218**, 220 (2012).

The composition of the Archean atmosphere as a tracer of volatile exchange between the mantle, the surface and the outer space

B. MARTY¹, M. PUJOL^{1,2}, R. BURGESS³, E. HEBRARD¹,
L. ZIMMERMANN¹ AND P. PHILIPPOT⁴

¹CRPG-CNRS, Université de Lorraine, Vandoeuvre les
Nancy, France. bmarty@crpg.cnrs-nancy.fr

²Present address : Total E&P, Pau, France

³Manchester University, UK

⁴IPG Paris, France

The terrestrial atmosphere evolved through time as a result of exchanges of volatile elements with the mantle, the crust, and the outer space. Measurements of noble gases and nitrogen in Archean rocks (barite, hydrothermal quartz, cherts) give insights into the composition of the atmosphere at the time of rock formation. Trapped fluids consist of a mixture of one or several hydrothermal component(s) with an atmospheric end-member, presumably contributed as atmospheric gases dissolved in fresh- or sea-water. The isotopic compositions of Archean neon, argon and krypton appear similar to the present-day ones for radiogenic or fissionogenic isotopes. Compared to extraterrestrial precursors, Archean atmospheric xenon is enriched in its heavy isotopes by 1-2 ‰, and intermediate between chondritic and modern atmospheric [1]. We interpret this difference as resulting from a preferential escape of Xe backwards through time [1,2], due to its increasing photoionization by hard UV light from the young Sun deep into the atmosphere and a more efficient trapping interaction with the primitive organic haze [3]. 3.5 Ga ago, the ⁴⁰Ar/³⁶Ar ratio was 143±24, which, when integrated into a 3-box (mantle, crust, atmosphere) K-Ar model, is consistent with a significant volume of felsic crust between 30% and 55% of its present-day volume at that time [4]. The partial pressure of atmospheric N₂ was similar to, or lower than, the present-day one, and the Archean N isotopic composition was similar within 2-3‰ to the modern one [5]. These results indicate efficient magnetic shielding of the atmosphere since 3.5 Ga, and, together from estimates of the density of the Archean atmosphere [6], set constraint on the P_{CO2} in the Archean atmosphere at <0.7 bar.

[1] M. Pujol *et al.*, *EPSL* **308**, 298 (2011). [2] B. Marty, *EPSL* **313**, 56 (2012). [3] E. Hébrard & B. Marty, AGU Fall meeting (2012). [4] M. Pujol *et al.*, *Nature*, in the press. [5] B. Marty *et al.*, submitted. [6] S.M. Som *et al.*, *Nature* **484**, 359 (2012).

Ectomycorrhiza-bacterial interactions in weathering

MARUPAKULA S*, MAHMOOD S AND FINLAY RD

Uppsala BioCenter, Dept Forest Mycology & Pathology,
Swedish University of Agricultural Sciences, Box 7026,
Uppsala SE-750 07, Sweden.

(*srisailam.marupakula@slu.se)

The role of ectomycorrhizal fungi in mobilising nutrients from organic polymers is widely accepted but the function of mycorrhizal fungal mycelia in mobilising and transferring nutrients from mineral substrates to the host trees is less well understood [1]. In addition to increasing the nutrient absorbing surface area of their host plant root systems, the extraradical mycelia of ectomycorrhizal fungi also provides a direct pathway for translocation of photosynthetically derived carbon to microenvironments in the soil. The continuous provision of energy-rich compounds, coupled with the large surface area of the mycelium, suggests that it may constitute an important niche for bacterial growth and colonization, however the role of these microbial interactions in weathering is still poorly understood. It has been shown that different soil horizons harbour different ectomycorrhizal fungi [2] and that the ectomycorrhizal fungi allocate organic acids to mineral substrates. In this study we use high-throughput sequencing to study the distribution of different bacterial and fungal taxa in O, E or B-horizon soil from a podzol collected from Jädraås, Sweden. Bacterial microbiomes from single mycorrhizal root tips colonised by different fungi were also examined to determine whether distinct bacterial communities were associated with particular mycorrhizal fungi.

[1]. Finlay RD, Wallander H, Smits M, Holmström S, van Hees PAW, Lian B, Rosling A. (2009). *Fungal Biology Reviews* 23: 101-106. [2]. Rosling A, Landeweert R, Lindahl BD, Larsson K-H, Kuyper TW, Taylor AFS, Finlay RD. (2003). *New Phytologist* 159: 775-783.

Simulating magma ascent: An experimental challenge

H. MARXER*, P. BELLUCCI, S. ULMER AND M. NOWAK

University of Tuebingen, Department of Geosciences

*correspondence: holger.marxer@uni-tuebingen.de

Isothermal decompression experiments with H₂O-bearing phonolitic melt (synthetic Vesuvius AD 79 “white pumice” composition) were conducted at super-liquidus T (1323 K) in an internally heated argon pressure vessel. The samples were decompressed from 200 MPa at true and interpolated decompression rates (DRs) of 0.0028–4.8 MPa·s⁻¹, applying a novel continuous decompression (CD) [1] as well as former stepwise decompression (SD) techniques to investigate the effect of decompression path on melt degassing. At target P the samples were quenched rapidly.

The comparison of the vesiculated glass products in terms of bubble number density (BND), size distribution of bubbles and residual H₂O-content in the glass reveals a massive influence of the applied decompression path on the degassing behavior of the melt. Decompression of the H₂O-bearing melt induces supersaturation with H₂O. At a certain ΔP , bubbles will nucleate homogeneously within the melt and grow by H₂O diffusion into the bubbles to regain equilibrium. The extent of supersaturation is controlled by the actual decompression rate, because the diffusion distance of H₂O is limited within a certain time. The experiments have shown that the BND increases with decompression rate, whereas average size decreases. At low CD rates of ≤ 0.024 MPa·s⁻¹ only few bubbles nucleate in the melt, because the decompression rates provide sufficient time for H₂O diffusion into existing bubbles. Bubble growth is the predominant degassing process. Residual H₂O-contents in the glasses indicate that an equilibrium degassing path can be simulated at low decompression rates. In comparison to CD, all corresponding SD run products feature higher BNDs and smaller bubble diameters for low decompression rates. SD results in instantaneous supersaturation due to rapid P drop, which can only be reduced by a massive nucleation event. The differences between the decompression techniques decrease with increasing nominal decompression rate due to the effect of a rapid P drop, enhancing bubble nucleation.

SD techniques are not suitable to investigate the dynamic processes during continuous magma ascent, at least at low nominal decompression rates. Ongoing experiments with CD will give new insights into the dynamic processes within ascending magma prior to eruption.

[1] Nowak *et al.* (2011): *Am. Mineral.*, 96, 1373–1380.

Direct link between end-Triassic CAMP volcanism, C-cycle perturbation and mass extinction

ANDREA MARZOLI^{1,2}, JACOPO DAL CORSO¹, FABIO TATEO², HUGH C. JENKYN³, HERVÉ BERTRAND⁴ AND NASRRDINE YOUBI⁵

¹Dipartimento di Geoscienze, Università di Padova, Italy – e-mail: andrea.marzoli@unipd.it, jacopo.dalcorso@unipd.it

²IGG-CNR, Padova, Italy; tateo@igg.cnr.it

³Department of Earth Sciences, University of Oxford, UK; hughj@earth.ox.ac.uk

⁴ Université Lyon1 and Ecole Normale Supérieure de Lyon, France; herve.bertrand@ens-lyon.fr

⁵Department of Geology, Cadi Ayyad University, Marrakech, Morocco; youbi@uca.ma

The eruption of continental flood basalts of the Central Atlantic Magmatic Province (CAMP) is coeval with mass extinction at the Triassic–Jurassic (Tr–J) boundary. In order to define the role of CAMP volcanism in triggering the biotic turnover, it is crucial to define whether or not onset of CAMP preceded the main end-Triassic climate disruption marked by a significant negative Carbon isotope excursion (CIE) of up to -8 ‰. However, the temporal relationships between volcanism and CIE still remain circumstantial due to the difficulty in correlating a continental event (volcanism) with one recorded in marine sediments (CIE). Sediments underlying CAMP basalts in Morocco are characterized by high contents of MgO (10–32 wt.%) and of mafic clay minerals (11–84%). This geochemical signature must be linked to deposition of mafic clay minerals derived from early-erupted CAMP basalts. The measured C-isotope compositions of bulk organic matter show marked negative CIEs (up to -6 ‰) in association with the highest MgO peaks. This geochemical anomaly can be readily correlated with the initial negative CIE shortly preceding the Tr–J boundary. Our data show that the end-Triassic CIE and associated mass extinction occurred when CAMP had already been active and supports the hypothesis that the cause of the mass extinction was CAMP volcanism.

Interaction of nanoparticles with microorganisms

S. MASAKI¹, H. SHIOTSU¹, F. SAKAMOTO², T. OHNUKI²
AND S. UTSUNOMIYA¹

¹ Department of Chemistry, Kyushu University, Fukuoka 812-8581, Japan (utsunomiya.satoshi.998@m.kyushu-u.ac.jp)

² Advanced Science Research Center, Japan Atomic Energy Agency, Tokai, Ibaraki 319-1195, Japan

Due to ubiquitous and abundant occurrence of nanoparticles (NPs) and microorganisms in the surface and subsurface environments, they encounter and interact in aqueous systems. Microorganisms can also form NPs on the cell surfaces by uptaking or releasing ions from/to solutions. Despite numerous studies reported biomineralization of NPs, knowledge on the interaction between microorganisms and NPs is still limited. Here we report the response of microorganisms to NPs using *S. cerevisiae* (yeast) and CeO₂ NPs (CeNPs).

Yeast was harvested in a YPD media prior to the experiment or a YPD media containing 250 ppm CeNPs (7 nm). The yeast was then contacted with a 1 mM NaCl solution (P-free) for 0-120 h at four pHs: 2, 3, 5 and 7. A variety of analytical techniques have been employed to investigate substances released from the cells, including inductively coupled plasma mass spectrometry (ICP-MS), ion chromatography (IC), high performance liquid chromatography (HPLC) and total organic carbon analyzer (TOC). The cytotoxicity of CeNPs was determined by the classical methylene blue straining technique and the mutated proteins were identified by peptide mass fingerprinting (PMF) analysis.

The solution analysis revealed that yeast released orthophosphate, organic phosphorous compound and various organic matters (<3 kDa) in all solutions. Phosphate released from the cells adsorbed on CeNPs at greater extent than inorganic phosphate by a factor of two. Although dissolved organic carbon (DOC), in general, inhibits phosphate adsorption to mineral surfaces, the released organic substances enhanced anion adsorption in the present study and possibility changed surface property of CeNPs. No cytotoxicity of CeNPs was detected; however, CeNPs induced an excess expression of two proteins: Eno2p and Rps24bp. In addition, the abundance and type of released substances were modified by CeNPs. Because Eno2p is related to the glycolytic system, CeNPs can affect the yeast's metabolism. That is, stimulating glycolytic system, which is the fastest step in the energy production process, lead to the decrease of tricarboxylic acid cycle via the electron transport chain, resulting in the modification of the released substances. The phenomena elucidated in the present study provided new insights to the fundamental process in the interaction between microorganisms and NPs in the Earth surfaces.

Characterization of woody biomass ashes and their utilization potential

CHRISTOPH MASCHOWSKI¹, RETO GIERÉ¹
AND GWENAELE TROUVÉ²

¹ Albert-Ludwigs-Universität Freiburg, Germany
(maschowski@minpet.uni-freiburg.de)

² Université de Haute-Alsace, Mulhouse, France,
(gwenaelle.trouve@uha.fr)

Ash from biomass combustion is typically considered a waste product. Bottom ashes, however, are sometimes used as source of nutrients in fertilizer additives. Fly ashes may be enriched in hazardous constituents (e.g., heavy metals, dioxins, and chlorides). Therefore, they should not be distributed into the environment but rather be land-filled.

In this study, bottom and fly ashes from two different types of solid biomass fuel, wood chips and Miscanthus grass, were sampled on site at a district heating plant and a power plant, respectively. These ashes were investigated by using X-ray diffraction and subsequent pattern analysis by Rietveld refinement method to gain semi-quantitative results for crystalline phases. The results were compared with those from analogous ashes, which have been produced under controlled laboratory conditions from pellets of wood and Miscanthus. Furthermore, the samples were characterized by laser diffraction to determine their particulate size distribution.

The main focus was put on the calcium oxides (mainly lime), which are present in both types of ashes and could bear utilization potential as CO₂-neutral clinker substitution in cement production. Main sources of lime in the ashes of both fuel types are extraneous calcite (present as grains in the fuels and then decomposed during combustion) as well as biogenic Ca phosphates and oxalates, as indicated by SEM/EDX analysis and elemental maps. The Miscanthus fuel used in the power plant, however, was co-combusted with 2 wt% of limestone in order to minimize fouling and slagging and certainly contributed to the lime content of the Miscanthus ashes. Another component of the ashes is SiO₂, mainly under quartz specie. In the wood fuel, the silicon originates from extraneous quartz grains, whereas in Miscanthus it is probably also of biogenic origin.

The second focus of this study was on alkali and alkaline earth metal species. They can help to classify the fuel type. Potassium contents were relatively low for both fuel types, indicating a diminished fouling and slagging potential on combustor walls and convection tubes.

Both ash types contain similar crystalline phases, and our data are close to literature. These results may be used to evaluate the potential of such ashes as secondary raw materials.

The influence of the elemental composition on the cubanite mineralization

A. V. MASHUKOV*, V. G. MIKHEEV
AND A. E. MASHUKOVA

Siberian Federal University, Krasnoyarsk, Russia,
(*correspondence: AVMashukov@sfu-kras.ru)
(VMicheev@sfu-kras.ru)
(AMashukova@sfu-kras.ru)

Using the methods of X-ray and Mössbauer spectroscopy, scanning electron microscopy, there were studied the samples of Norilsk ore types in order to identify compounds containing cubanite. Depending on elemental composition there were singled out sample series.

The concentration of selected elements varied from sample to sample and reached maximum values in percent age: for Cu - 23.0, Fe - 41.7, S - 34.0, O - 1.1. The relative magnetization (I/I_0) of the samples at different temperatures are shown in Table 1

t°C	20	200	240	300	400	500	560
1	0.67	0.61	0.84	0.38	0.14	0.06	0.02
I/I_0	0.67	0.40	0.15	0.12	0.08	0.03	0.02

Table 1: The temperature dependence of the relative magnetization, for I/I_0 line 1 - heating, line 2 - cooling.

The samples have a complex and diverse composition of a wide range of values having the remanent magnetization and its resistance to various demagnetizing factors.

Magnetization changes irreversibly with the change of temperature. This fact, as well as the discrepancy of Curie temperature in the cycle «heating - cooling», indicates the presence of a mechanical mixture, consisting of two and more ferromagnetic phases.

The magnetic phase has the spectrum composed of two six-linear spectrums. The peaks on the spectrum borders show the iron oxide presence. The sample magnetism is caused by the presence of the minerals of sulphide and oxide groups, containing Fe^{2+} and Fe^{3+} as the main components.

Phases containing Cu, Fe, S have complex composition: cubanite I (36,1% $CuFe_2S_3$), cubanite II (54,8% $CuFe_2S_3$), chalcopyrite (5,0% $CuFeS_2$), magnetite (2,22% Fe_3O_4), magnetite (1,64% Fe_2O_3). The position of the absorption lines in the magnetically ordered areas indicates the presence of $CuFeS_2$. Some of the samples of this group have broadened lines, indicating the existence of various positions of the Fe ions in the sublattices. Intergrowths of chalcopyrite ($CuFeS_2$) are characterized by the isomer shift of 0,058 mm/s and the absence of quadrupole splitting.

Thus, the presence of the characteristic structures of the solid solutions decomposition shows a wide temperature range of sulphide crystallization.

Long-term effects of CO₂-charged brine on caprock integrity and existing heterogeneities within the Entrada Sandstone, Green River, Utah

ALEXANDRA MASKELL¹, NIKO KAMPMAN¹, MIKE BICKLE¹, HAZEL CHAPMAN¹, KATHERINE DANIELS¹, ANDREAS BUSCH², MORGAN SCHALLER^{5,6} AND JAMES P. EVANS⁷

¹Department of Earth Sciences, University of Cambridge, Downing Street, Cambridge CB2 3EQ, UK

²Shell Global Solutions International, Kessler Park 1, 2288 GS Rijswijk, The Netherlands

³British Geological Survey, Keyworth, Nottingham, NG12 5GG, UK

⁵Department of Earth and Planetary Sciences, Rutgers University, 610 Taylor Road, Piscataway, NJ 08854-8066

⁶Department of Geological Sciences, Brown University, 324 Brook St., Providence, RI 02912

⁷Department of Geology, Utah State University, 4505 Old Main Hill Logan, UT 84322-4505 16

Natural CO₂ has been escaping through geysers related to fault zones at Green River, Utah for at least 400 ka [1]. A scientific drilling project in 2012 to sample the CO₂ system, showed that the uppermost formation, the Entrada Sandstone, contained zones with high CO₂ pressures, despite this unit being exposed at surface. Core revealed that The Entrada sandstone comprised bleached sandstone layers interbedded with variably bleached and carbonated thin siltstone layers which have acted as aquitards.

Results from mineralogical, petrological, and geochemical analysis of the CO₂-reservoir rocks and sealing siltstone layers from the Entrada Sandstone core are presented together with a reactive transport model of the mineralogical changes. We determine the length scales and mechanisms of CO₂ penetration of the sealing siltstone caprocks, and especially the significance of carbonate precipitation on its sealing properties.

[1] Burnside *et al.* (2013). *Geology*. **41**, 471–474.

Mineral and chemical evolution of fragmental massive sulfide ores

V.V. MASLENNIKOV^{1*}, R.R. LARGE²,
S.P. MASLENNIKOVA¹ AND L.V. DANYUSHEVSKIY²

¹Institute of Mineralogy UB RAS, Miass, Russia
(correspondence: mas@mineralogy.ru)

²CODES, Tasmania University, Hobart, Australia
(Ross. Large@utas.edu.au)

The styles of mineral and chemical evolution of fragmental massive sulfide ores at the Urals and Rudny Altai VMS deposits depends on the primary composition of sulfide clasts and impurity of adjacent sediments.

In the early diagenetic stage, pyrrhotite fragments are replaced by sooty pyrite with increasing grades of Au, Ag, V and U. Pseudomorphic chalcopyrite-2 and sphalerite-2 have inherited Ni, Mn, As, Pb, Tl, Au, Ag, and Te from replaced colloform pyrite fragments. In the submarine supergene zone, chalcopyrite-2 may be partly replaced by bornite or tennantite enriched in Ag and Bi. In pyrite-rich fragmental ores, sphalerite-1,2 is commonly dissolved, but in sphalerite-rich clastic sediments, sphalerite-2 is a dominant product of the sulfide evolution. In submarine supergene zones, all sulfides can be replaced by oxyhydroxides and then transformed to hematite and magnetite in later metamorphic stages. In the last stage of diagenesis, fine grained pyrite is overgrown by pyrite euhedra while chalcopyrite-2 and sphalerite-2 are recrystallized to twin crystal aggregates depleted in most of the trace elements. These mineral consequences are typical of clastic sulfides associated with jasper at the margins of the massive sulfide. In calcareous and serpentinite-rich clastic sulfide sediments, pyrite nodules are commonly the products of diagenesis. In carbonaceous clastic sulfide sediments, diagenesis results in nodular as well as framboidal pyrite. Fine grained diagenetic pyrite inherits high contents of trace elements from ore clasts. In the metamorphic stage, the diagenetic pyrites are replaced by pyrrhotite and euhedral pyrite. The range of submarine supergene and metamorphic alteration assemblages of fragmental massive sulfide ores is due to dissolution of clastic and diagenetic sulfides or their recrystallization and refining.

This mineral research was supported by Program N23 of Presidium RAS (project 12-P5-1003) and LA-ICPMS analyses of sulfides were carried out at CODES, University of Tasmania [1].

[1] Danyushevsky, Robinson, Gilbert, Norman, Large, McGoldrick, Shelley (2011) *Geochim Explor Environm Anal* 11: 51–60.

Accurate measurement of diffusion profiles in altered wellbore cement using XMCT

HARRIS E. MASON^{1*}, WYATT L. DUFRANE¹,
STUART D.C. WALSH¹ AND SUSAN A. CARROLL¹

¹Physical and Life Sciences Directorate, Lawrence Livermore National Laboratory, 7000 East Ave, Livermore, CA 94551

(*corresponding author: mason42@llnl.gov)

Recent, intense effort has been focused on characterizing and modeling the degradation of wellbore cements exposed to CO₂-rich brines due to their role in geologic carbon storage. Scanning electron microscopy (SEM) and micro X-ray computed micro-tomography (XCMT) show the development of three discrete alteration layers in the reacted wellbore cement: a portlandite depleted zone, a Ca-carbonate zone, and an amorphous zone. Alteration models have assumed discrete, sharp contacts between these layers where the chemistry and mineralogy change drastically. Despite the power of XCMT to provide detailed 3D images of these alteration zones, little has been done to refine the geometrical models of wellbore cement alteration using these data.

Interpretation of XCMT images of wellbore cement can be problematic given the large distribution in grain and pore sizes as well as similarities of the mineral compositions and densities. Application of simple grayscale thresholds to XCMT data to identify alteration zones is problematic because of the zones span a narrow range in composition and density. Instead of thresholding, we rely on an advanced user-guided segmentation method which extracts the reaction zones by looking for not only differences in greyscale, but also in texture. This method allows us to more accurately define reaction boundaries and their extent in three dimensions.

With the reaction zone extents as guides, we take the analysis a step further and build 3D maps of mineral and elemental abundances. Using the geochemical model [1] and specific mineral linear X-ray attenuation coefficients we calculate what phases are present and their relative abundances in each zone. The end result shows that the reaction regions are defined by rather diffuse regions where multiple reactions can occur simultaneously, rather than by sharp regions.

[1] H.E. Mason *et al.*, *Environ. Sci. Technol.* 2013: 47, 1745

This work was performed by LLNL under Contract DE-AC52-07NA27344.

Hydrocarbon Source Appraisal in PM_{2.5} in Rio de Janeiro

C. MASSONE,^{1,2} A. WAGENER^{1*}, A. GIODA¹
AND A. SCOFIELD¹

¹Chemistry Department, PUC-Rio, 22453-900 RJ, Brazil
(*correspondence: angela@puc-rio.br) (agioda@puc-rio.br)
(scofield@esp.puc-rio.br)

²IEAPM, 28930-000 RJ, Brazil (cgmassone@gmail.com)

The work aimed at characterizing hydrocarbons present in atmospheric particulate matter (2.5 µm) in urban and rural areas. For this HV sampling of PM_{2.5} over 24h occurred weekly along 12 months. Determination included 45 PAHs, n-alkanes, UCM, hopanes and steranes. Amongst the 16 USEPA PAH *m/z* 252 and 276 predominated, however in urban centers alkylated homologues were as well important (Fig 1). The presence of mature hopanes (Fig 2) and homologue n-alkane series confirm the petrogenic component derived from vehicular emission of unburned fuel. The ratio B(a)Py/(B(a)Py+B(e)Py) near 0.5 indicates moderate fotodegradation of B(a)Py independently of the season. Acephenanthrylene, Bz(c)phenanthrene, diBz(a,j)chrysene, pentaphene, Bz(a)chrysene, picene and indene(7,1,2,3-cd)chrysene were also found and used for source appraisal.

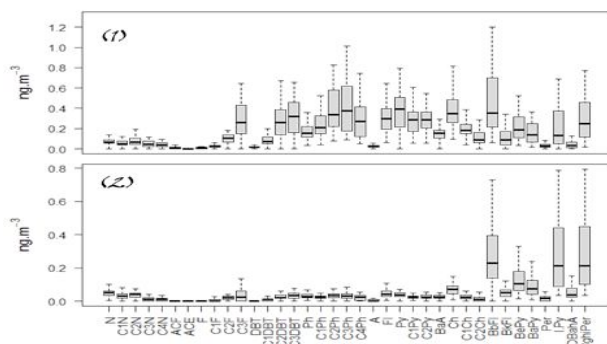


Figure 1. (1) City center; (2) rural area

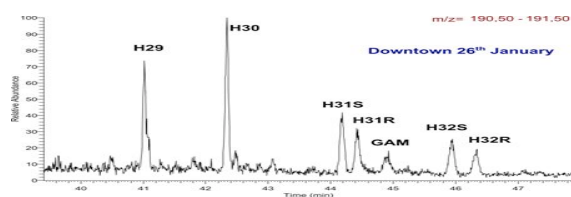


Figure 2. Mature hopanes and Gamacerene

A physicochemical approach to the early generation of continental crust by melting of oceanic crust

H.-J. MASSONNE¹

¹Universität Stuttgart, Azenbergstr. 18, D-70174 Stuttgart, Germany (h-j.massonne@mineralogie.uni-stuttgart.de)

The phase relations of three rocks (basalt, Archaean greywacke, and quartz diorite) each with different H₂O contents were studied by thermodynamic calculations for the P-T range 0.5-4.5 GPa and 550-1300°C using the computer program PERPLE_X [1] and the haplogranitic melt model by Holland & Powell [2]. The obtained P-T pseudosections were contoured by the following parameters: volume, K/(Na+Ca), Na/Ca and Si/Al of melt, and density of the total rock and restite. The melt and restite formed in the three studied rocks could be reasonably well characterized with these parameters and the obtained phase relations. For instance, melts representing TTGs are generated in the basaltic protolith in the pressure range 1.2-2.0 GPa between temperatures of 600-1000°C. The restite shows densities above 3.3 g/cm³ at pressures in excess of 1.3 GPa when more than 5 vol.% of melt has formed in a low-H₂O basaltic composition and at >1.0 GPa and with >20 vol.% melt (T > 850°C) in a more hydrated basalt. TTG melts can also form in the two other studied rocks at a slightly elevated pressure range compared to the basaltic compositions. However restite densities exceed 3.3 g/cm³ only in the stability field of coesite.

The obtained calculation results suggest the following geotectonic scenario which is capable to form considerable volumes of continental crust in Archaean times. The formation of relatively thick plates of oceanic crust, the hydration of their surface and final collision leads first to thickened oceanic crust and the generation of a granitic protocrust by partial melting in the hydrated realm of the underthrust oceanic plate during the collisional process. Subsequently, the protocrust is, in fact, further thickened by this process, but TTG melts are predominantly formed in the underthrust oceanic plate at a later stage. The restites in this partially melted regime reach densities above those of the mantle to be delaminated. The suggested crust-forming process could have occurred until late Proterozoic times.

[1] Connolly, J.A.D. (2005) Earth Planet. Sci. Lett. 236, 524-541. [2] Holland, T.J.B. & Powell, R. (2001) J. Petrol. 42, 673-683.

A multi-component model for the partial melting in presence of CO₂ and H₂O in the mantle

MALCOLM MASSUYEAU¹, YANN MORIZET²
AND FABRICE GAILLARD¹

¹ ISTO CNRS- Univ. Orléans, ORLEANS, France

(*correspondence: malcolm.massuyeau@cnsr-orleans.fr)

² Université de Nantes, Nantes Atlantique Universités,

Laboratoire de Planétologie et Géodynamique de Nantes (LPGN), UMR CNRS 6112, NANTES, France

The link between volatiles and mantle melting has so far been illuminated by experiments revealing punctually, at a given P-T condition and under a specific chemical system, properties such as solubility laws, redox equilibria, and phase equilibria. The aim is to establish a multi-component model describing the Gibbs free energy of melt produced by mantle melting in presence of CO₂-H₂O: Carbonatite-carbonated melt and basalts.

Near solidus melts are dominated by carbonate-rich compositions, evolving towards basaltic compositions at higher temperatures. However, this carbonate-silicate transition is complex, abrupt, and dependent on temperature, pressure and the chemical composition of the system. In order to simulate partial melting in a variety of mantle conditions, we established a parameterization of the mixing properties allowing the complex activity-composition relationships for multi-component hydrated carbonated melts to be accounted for. Using the Margules formalism, this parameterization is calibrated on crystal-liquid, redox, fluid-liquid and liquid-liquid equilibria obtained by experimental studies in the P-T range 1-10 GPa and 900-1800°C (more than 500 data points). We so far adjusted the activity of the SiO₂ and CO₂ melt components which constitutes the main part of the silicated and carbonated frameworks. The SiO₂-CO₂ interaction reveals a strong non-ideality requiring a strongly asymmetric Margules formulation. We also determined the standard thermodynamic properties for the CO₂ melt component.

As applications, we define the composition of incipient melts as a function of depth underneath MORs and Hot-Spots and identify regions of CO₂ saturation for kimberlitic melts.

Multiple sulfur isotopic evaluation of porewater sulfate profiles

ANDREW L. MASTERTSON¹, WILL BERELSON²
AND DAVID T. JOHNSTON¹

¹Dept. of Earth and Planetary Sciences, Harvard University,
Cambridge MA 02138: amasters@fas.harvard.edu

²Dept of Earth Sciences, USC, Los Angeles CA

Modern marine sediment porewater sulfate concentration profiles provide information about total and depth dependent rates of organic carbon remineralization. These profiles only provide net rates, however, as oxidative sulfur cycling is a challenge to uniquely quantify. Researchers have demonstrated active oxidative sulfur cycling in organic rich sediments (where sulfate reduction otherwise dominates) using the δ¹⁸O of porewater sulfate. The utility of this approach, which still carries great promise, relies on a robust understanding of *in situ* sulfur oxidation processes. Furthermore, recent work targeting the oxygen isotopic consequences of the sulfate reduction network, and experimental work on oxygen isotope exchange with sulfur intermediates, demonstrates a complexity to interpreting these records that is to date not fully explored.

Aimed at improving the estimates of net and gross sulfate reduction derived from porewater sulfate profiles in organic rich sediments, we present multiple S (³⁴S/³²S & ³³S/³²S) and sulfate oxygen (¹⁸O/¹⁶O) isotopic profiles from 5 anoxic basins within the California Borderlands and Mexican Margin (Alfonso, Mazatlan, Soledad, Santa Monica, San Blas). All sites exhibit linear sulfate concentration profiles that are used to infer rates of methanotrophy using simple flux balance models, and thus extracting rates of sulfur recycling complements those estimates. We discuss the utility of applying coupled minor sulfur isotope (³³S/³²S) and ¹⁸O/¹⁶O systematics in improving estimates of sulfur recycling processes in these oxidant limited systems, and their implications for improving early diagenetic models of sulfur mediated remineralization reactions.

Groundwater chemistry in 2012 in Miyagi Prefecture including Tsunami affected area

HARUE MASUDA¹, SHINJI NAKAYA², REO IKAWA³
AND NAOATSU MARUI⁴

¹Osaka City University, harue@sci.osaka-cu.ac.jp

²Shinshu University, nakayas@shinshu-u.ac.jp

^{3,4}AIST, reo-ikawa@aist.go.jp, marui.01@aist.go.jp

Geochemical characteristics of the surface and ground waters (total 238 samples) in Miyagi Prefecture, of which coastal area was damaged by Tsunami occurred in association with the giant earthquake on the 11th March, 2011, was documented to figure out the situation of aqueous environment in 2012 and assess the future risk of groundwater by the Tsunami deposits and Fukushima-Daiichi nuclear disaster.

Anthropogenic impact on the studied water was not obvious for whole studied area, and all the studied waters were free from radiogenic Cs. Salinization is prominent in the groundwaters located in the Tsunami affected area, especially the shallow well waters from <10m depths in the southern part of the prefecture. The highest Cl concentration is 14000 mg/L, while the rate of seawater is commonly less than 3 % (500 mg/ L) one year after the Tsunami. Fe and Mn are occasionally higher than the standards of drinking water (0.3 and 0.05 mg/L respectively) in the Tsunami affected groundwaters, while, minor toxic element concentrations (As, Cd, Se, Pb, Cr^{VI}, Zn, F-) are generally lower than the standard values for drinking water. Those elements were released from the host sediments probably due to the reduction of groundwater in association with seawater contamination by the Tsunami, and Tsunami deposits do not seriously cause the contamination at present. However, the groundwater chemistry must be monitored in the future to assess the groundwater as water resources since the recharging age of the studied groundwaters are generally 20 to 50 years.

A model study on the effects of polyacrylic acid added in geothermal water on the growth of silica scale at a geothermal power plant

SACHI MASUNAGA^{1*}, MAYUMI ETOU¹,
YOSHIHIRO OKAUE¹ AND TAKUSHI YOKOYAMA¹

¹Faculty of Science, Kyushu University, Fukuoka,
812-8581 Japan

masunaga@chem.kyushu-univ.jp (*presenting author)

Polyacrylic acid (PAA) has been added as an inhibitor of calcium carbonate scale at the Takigami geothermal power plant, Oita prefecture, Japan. In the geothermal power plant, since the addition of PAA, the amount of silica scale formed from geothermal water has been reported to increase compared with that before the addition.

Aluminum (Al) is extremely concentrated into the silica scales in spite of its low concentration in geothermal water. Therefore, it is considered that Al plays an important role for the formation of silica scale from geothermal water[1]. Moreover, Al forms a stable Al-PAA complex[2]. As a result, it is necessary to consider the interaction among Al, PAA and silicic acid in geothermal water.

In this study, some model experiments were carried out to elucidate whether PAA accelerates the growth of silica scale in geothermal water containing Al, PAA and silicic acid.

At pH 8.5, which is pH value of the geothermal water, PAA didn't affect the polymerization of silicic acid, while Al and Al-PAA inhibited the polymerization between monosilicic acid and polysilicic acid (M-P reaction). From ²⁷Al NMR, we found that 4-coordinated Al in supersaturated silicic acid solution can convert into 6-coordinated Al by the addition of PAA, indicating the formation of Al-PAA complex. The Al-PAA complex adsorbed on the surface of silica gel and retarded the dissolution of the silica gel. It can be deduced that the growth of silica scales from geothermal water is accelerated due to the inhibitions of M-P reaction and of dissolution of silica by the Al-PAA complex.

[1]Takushi Yokoyama *et al.*, (1993) *Geochem. J.*, **27**, 375-384

[2]Mayumi Etou *et al.*, (2011) *Anal. Sci.*, **27**, 111-115

Iron mobilisation from volcanic ash/glass by atmospheric processing

E. MATERS^{1*}, P. AYRIS², C. JACQUES¹, A. GUEVARA¹, R. HENLEY³, S. OPFERGELT¹ AND P. DELMELLE¹

¹ Earth and Life Institute, Université catholique de Louvain, Louvain-la-Neuve, Belgium
(*correspondence: elena.maters@uclouvain.be, caroline.jacques@student.uclouvain.be, alicia.guevara@epn.edu.ec, sophie.opfergelt@uclouvain.be, pierre.delmelle@uclouvain.be)

² Department of Earth and Environmental Science, Ludwig Maximilian University, Munich, Germany
(paul.ayris@min.uni-muenchen.de)

³ Research School of Earth Sciences, Australian National University, Acton, Australia
(r.143.henley@gmail.com)

Deposition of volcanic ash can provide a source of bioavailable Fe to remote regions of the ocean where Fe deficiency limits primary production. Understanding controls of ash Fe solubility is essential for assessing volcanogenic Fe input to the marine environment. It is well known that interaction with acids (e.g., H₂SO₄, HNO₃) and exposure to cloud condensation/evaporation cycles during transport increase Fe solubility in mineral dust. Airborne volcanic ash particles, which act as cloud condensation nuclei and are co-emitted with volcanic acids (e.g., H₂SO₄, HCl, HF), are similarly expected to undergo atmospheric processing. We investigated the influence of such processing on ash Fe solubility by i) exposing six ash samples (57-74 wt.% SiO₂) to pH 1 H₂SO₄ for 336 h to mimic contact with acid during transport, and ii) subjecting a glass sample (58 wt.% SiO₂) to three 12-h cycles of alternating pH 2 and 6 H₂SO₄ to simulate pH changes during cloud evaporation and condensation, respectively. Solution sub-samples were analysed for Si, Al, Fe, Mg, Ca, Na and K concentrations by ICP-AES. Changes in sample surface compositions were assessed by X-ray photoelectron spectroscopy, and untreated ash surfaces were examined by scanning electron microscopy. Results suggest that surficial Fe salts do not constitute a significant fraction of the soluble Fe mobilised from ash in acid. The Fe release trend is consistent with leaching/dissolution of silicate components in the ash. We propose that ash surface properties imparted by eruption plume processing, including oxidation in a water- or HCl-rich environment or interaction with HF, are key in governing ash Fe release. The preliminary findings of the pH cycling experiment suggest that Fe release over 36 h is driven by dissolution and precipitation of Fe(III) at pH 2 and 6, respectively. Acid mobilisation of Fe does not appear to increase significantly over multiple cycles.

Volcanic ash and aerosol

TAMSIN A. MATHER¹

¹Dept. Earth Sciences, University of Oxford, South Parks Road Oxford OX1 3AN, UK, tamsinm@earth.ox.ac.uk

Volcanoes are an important source of silicate particles (e.g., ash) and aqueous aerosol (e.g., sulphate) to the Earth's atmosphere and environment. Persistent emanations represent a key background flux to the atmosphere maintaining its characteristics and composition, while sporadic large-scale eruptions have the potential to perturb the atmosphere's chemical and radiative balance as well as having other direct effects on the Earth's environment. The recent travel chaos in Europe during the Icelandic eruptions of Eyjafjallajökull and Grimsvötn in 2010 and 2011 has also brought into sharp focus the vulnerability of highly developed societies, remote from volcanoes, to their far-flung effects.

In this talk I will explore some of the nature and impacts of volcanic ash and other volcanic particles and how volcanologists study them. I will cover topics such as the generation of particles during volcanic activity, their effects in the plume (e.g., lightning generation and the scavenging of gases), their fall out and their environmental effects (e.g., the potential of volcanic ash to fertilize the oceans). Recent work has also shown the importance of understanding the relationship between volcanic emissions and cloud properties in order to understand the perturbation that anthropogenic emissions represent in terms of the Earth's radiative budget via the indirect aerosol effect.

High Cesium Concentrations in Groundwater in a Coastal Granitoidic Fracture Network

F. MATHURIN^{1*}, H. DRAKE¹, B. KALINOWSKI²,
AND M. ÅSTRÖM¹

¹Linnaeus University at Kalmar, Sweden,

(*presenting author: frederic.mathurin@lnu.se)

²Swedish Nuclear Fuel and Waste Management Co, Sweden

This study aims to increase the understanding of the sources and mechanisms by which elevated Cs concentrations build up naturally in deep and low temperature (<20°C) groundwater residing in fractured crystalline bedrock.

The hydrochemical monitoring program carried out by the Swedish Nuclear Fuel and Waste Management Co (SKB) revealed that high variability in natural Cs concentrations, with values up to several µg/L (Fig. 1), occurs in fracture groundwater at the Äspö Hard Rock Laboratory (Äspö HRL) and the nearby Laxemar area (Sweden) down to 1155m depth. Related to the various types of water residing into the bedrock [1], the highest Cs concentrations were found in both old deep-seated saline and marinogenic groundwater (Fig. 1). The SEM-EDS and XRD analyses of fracture coatings reveal that high Cs concentrations (>50 ppm) in the bulk fracture coatings correlate with a mineral enrichment in illite, together with mixed-layer clays and chlorite. Based on hydrochemical modelling, intrusion of Baltic Sea water (K and NH₄ rich water), together with cation exchange, constitute a consistent explanation for the high Cs concentrations observed in the marinogenic groundwater at the Äspö HRL.

The Cs sorption mechanism and results presented here are relevant for recognition of conditions of importance in term of bedrock disposal of toxic waste materials as fractured bedrock constitutes the last retention barrier separating radionuclides (including ¹³⁴Cs and ¹³⁷Cs) from the biosphere if the release of radionuclides in the repository occurs.

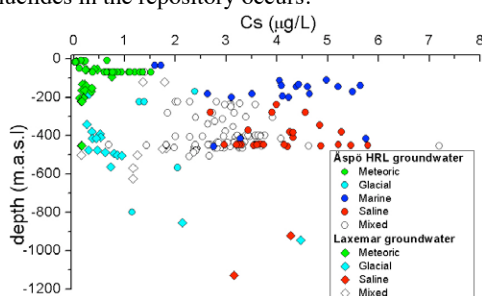


Fig. 1. Vertical distribution of the Cs concentrations in the fracture groundwater.

[1] Mathurin *et al.* (2012) *EST journal* **46**, 12779-12786.

Control of oxygen fugacity in piston cylinder experiments

V.MATJUSCHKIN^{1*}, B.TATTITCH¹ AND J.D.BLUNDY¹

¹ University of Bristol, Wills Memorial Building,

Quenn's Road, Bristol, BS8 1RJ, United Kingdom

(*vladimir.matjuschkin@bristol.ac.uk)

Controlled oxygen fugacity experiments in a piston cylinder apparatus can be carried out using a double capsule technique and different solid oxygen buffers as suggested by Eugster (1957) and Jakobsson (2012). However both the capsule designs used in these studies as well as the choice of the spacer in the piston cylinder assemblage can affect the fO_2 in the experimental charge. The main goal of our study was concentrated on minimizing variability in fO_2 by testing different types of spacers, capsule materials and filling materials. In order to control and/or read the achieved fO_2 in the capsule we have examined the reaction of 3 different fO_2 sensors: NiPd, CoPd and magnetite-ilmenite. All experiments were carried out at 1GPa and 1000°C using the same piston cylinder apparatus.

The results show that use of Al₂O₃ as spacer material in combination with noble metals such as Pd and Pt can lead to oxidation of experimental charge up to $\Delta NNO+5$ as Pd or Pt do not prevent enough hydrogen loss during experiment. Alternatively, using wet spacer materials (e.g pyrophyllite) may reduce the experimental by diffusion of hydrogen into the capsule. Applying MgO spacer with Pt and AuPd (80/20) capsules we could achieve consistent fO_2 between $\Delta NNO+2.5$ and $+3.5$ for experiment durations up to 72 hours. In contrast, the use of pyrex (borosilicate glass) sleeve as spacer material in combination with AuPd capsules showed minimal loss of hydrogen (water) as well as no detectable boron diffusion through the capsule walls. As result, both NiPd and CoPd internal sensors indicated consistent fO_2 values of $\Delta NNO+1$ (± 0.2) for experiments tested up to 26 hours.

A further important factor we tested is the reaction of different solid buffers depending on the fO_2 we aspire to achieve. The metal sensors such as NiPd or CoPd are suitable for short and long time experiments (given the presence of an appropriate amount of water) and are able to register the changes of fO_2 already after first 12 hours of experiment. In contrast, magnetite-ilmenite oxide sensor needs more time for equilibration showing consistent results only after 24-72 hours runs.

[1] Eugster (1957) *J. Chem. Phys.* **26**: 1760-1761

[2] Jakobsson (2012) *Contrib. Mineral. Petrol.* **164**: 397-406

Geomicrobiology of ancient polymetallic Kupferschiefer black shale - minireview

R. MATLAKOWSKA* AND A. SKŁODOWSKA

Laboratory of Environmental Pollution Analysis, Faculty of Biology, University of Warsaw, Miecznikowa 1, 02-096 Warsaw (*correspondance: rmatlakowska@biol.uw.edu.pl)

The highly mineralized upper Permian Kupferschiefer black shale located in the Fore-Sudetic Monocline (SW Poland) is a polymetallic, organic-rich sedimentary rock. It belongs to one of the largest copper and silver deposits in the world but it contains also large amounts of precious and rare elements such as nickel and platinum.

Indigenous microorganisms occurring in the black shale play a role in the biotransformation of the rock. The significant impact of heterotrophic bacteria represented by *Pseudomonas* sp. *Acinetobacter* sp. *Bacillus* sp. and *Microbacterium* sp. [1] includes such activity as: (i) degradation of sedimentary organic matter and metalloorganic compounds [2], (ii) bioweathering of rock-forming and ore minerals [3, 4], (iii) complexation of elements by bacterial extracellular metabolites such as siderophores and organic acids. All these activities strongly influence redistribution of carbon and other elements in the rock and are of environmental significance of the global biogeochemical cycle of elements in deep underground environment.

[1] Matlakowska & Skłodowska (2009) *J Appl Microbiol* **107**, 858-866. [2] Matlakowska & Skłodowska (2011) *Chemosphere* **83**, 1255-1261. [3] Matlakowska *et al.* (2012) *FEMS Microbiol Ecol* **81**, 99-110. [4] Matlakowska *et al.* (2010) *Environ Sci Technol* **44**, 2433-2440.

Chemical composition of chromian spinel of Podiform chromitite, Sangun Zone, southwest Japan.

ICHIRO MATSUMOTO

¹ Faculty of Education, Shimane University, Matsue, Japan. chromim@edu.shimane-u.ac.jp (corrspondence)

There are many chromitite pods in the Sangun zone belongs to inner zone of Southwest Japan. Most many chromitite pods enclosed by dunite rich ultramafic portion were discovered and outpitted in this Zone, in Japan. Maximum size of chromitite-pod called "Nanago-ore body" which is 40*210*25m (2.1*10⁵m³) in size from Wakamatsu chromite mine of the Tari-Misaka ultramafic complex. In this study, I summarized the relationships between chromian spinel in chemistry and size of chromitite-pods for its origin which controls a size.

Chromitite-pods are divided into two groups by Cr# (Cr/(Cr+Al)) of chromian spinel from chromitite that are relatively high-Cr# (Cr#: 0.55<) group and low-Cr# (Cr#: 0.47-0.55) group. High-Cr# groups are from "Nanago-ore body" and "10th ore body" of Wakamatsu mine from Tari-Misaka ultramafic complex and chromitite pods from Takase and Ashidachi ultramafic complexes. Low-Cr# groups are from 51st, 52nd, 53rd, 54th, 55th, and 56th ore bodys of Wakamatsu mine from Tari-Misaka ultramafic complex and chromitite-pods from Inazumiyama, Mochimaru, Yagami, Ashidachi, and Yanomine ultramafic complexes.

Cr# of chromian spinel in dunite-harzburgite host rock of chromitite varies from 0.45 to 0.65 in "Nanago-ore body" and "10th ore body" of Wakamatsu mine and 0.40 to 0.60 in the other chromitite-pods.

Relationships Cr# of chromian spinel from chromitite-pods and from dunite-harzburgite indicated that it was a relatively large-scale chromitite which shows high Cr# of chromian spinel in this area. The results of above characteristics clearly show that spinel precipitation and concentration are more intense at "Nanago-ore body" than at the other chromitite bodies of the Wakamatsu mine and the other chromitite-pods of other ultramafic complexes. That is supposing the origin of chromitite is the magma mixing which continues with melt and the reaction of a wall rock ultramafic rocks [1], the reaction ratio and reaction stage are important. Matsumoto *et al.*, (2002) [2] also pointed out this importance by resarch of Wakamatsu chromitie mine. This study support the idea.

[1] Arai and Yurimoto (1994): *Econ. Geol.*, 89, 1279-1288.
[2] Matsumoto *et al.* (2002): *Shigen-Chishitsu*, 52, 135-146.

Ion irradiation experiments to olivine: Comparison with space weathering rims of Itokawa and lunar regolith particles

T. MATSUMOTO^{1*}, A. TSUCHIYAMA², A. TAKIGAWA², K. YASUDA³, Y. NAKATA³, N. WATANABE⁴, A. KOUCHI⁴, M. NAKAMURA⁵, A. MIYAKE² AND M. OHTAKE⁶

¹Department of Earth and Space Science, Osaka University, Machikaneyama-cho 1-1, Toyonaka, Osaka, Japan.

(*correspondence: tmatsumoto@kueps.kyoto-u.ac.jp)

²Division of Earth and Space Science, Kyoto University.

³The Wakasa wan Energy Reserch Center, Japan.

⁴Institute of Low Temperature Science, Hokkaido University, Japan.

⁵Department of Earth Science, Tohoku University, Japan.

⁶ISAS/JAXA, Sagamiara, Japan

Surface morphologies of regolith particles of asteroid Itokawa recovered by the Hayabusa missions have important information about phenomena on the surface of an airless celestial body. In previous studies, space weathering rims were found on Itokawa particles by TEM and STEM [1, 2]. Especially, vesicles were identified in thick space weathering rims probably caused by solar wind He⁺ implantation [2]. Blister structures corresponding to the vesicles were also observed on the particle surfaces by FE-SEM [3].

In this study, we carried out ion irradiation experiments to olivine particles (Fo₇₀) at the Wakasa Wan Energy Research Center and Institute of Low Temperature Science in order to understand relationship between space weathering processes and surface nano-morphological changes of Itokawa particles. The fragments were irradiated by H⁺, H₂⁺ and He⁺ ions at 4 to 50 keV with fluences of 1 × 10¹⁶ to 1 × 10¹⁸ ions/cm². Irradiated samples were observed by FE-SEM. Ultra-thin sections of the samples prepared by FIB were observed by TEM and STEM. Lunar regolith particle surfaces were also observed by FE-SEM for comparison. Blister structures and numerous bubbles, which have silimar structures to the Itokawa particles, were observed on the irradiated olivine samples. The blister structures were also observed on the lunar particles. The mean size and number density of blisters on lunar and Itokawa regolith particles are within almost the same range, suggesting that blisters formed on lunar and Itokawa particles by the same process.

[1] Noguchi *et al.* (2011) *Science*, **333**, 1121-1125. [2]

Noguchi *et al.* (2013) *Met. Planet. Sci. accepted*. [3]

Matsumoto *et al.* (2013) *LPSC XLIV*, 1441.

Improved understanding of sources and processes of metal mobilization from sulfidic mine wastes through the application of post-transition stable isotopes

MATTHIES, R^{1,2*} AND BLOWES, D W¹

¹Department of Earth and Environmental Sciences, University of Waterloo, 200 University Avenue West, Waterloo, ON Canada N2L 3G1 (*correspondence: romy_matthies@gmx.net)

²School of Civil Engineering and Geosciences, Newcastle University, Newcastle upon Tyne, NE1 7RU, UK

The generation of metalliferous mine waters can result in potentially harmful impacts on environmental receptors. We conducted a 30 week lab-scale humidity cell test with sulfidic tailings from the Kidd Creek massive sulfide deposit, Canada. In 7-day cycles, the mine waste was exposed to three days of dry and moisturized air to accelerate sulfide-mineral oxidation. On day seven, metals were mobilized through flushing with deionized water. For the first time, we combined this prediction technique with a detailed study on the fractionation of stable zinc isotopes to i) identify principal metal sources and ii) improve understanding of the geochemical processes leading to metal mobilization. The dissolution of secondary and tertiary oxyhydroxysulfates at the beginning of the study led to considerable changes in zinc isotope ratios, potentially indicating kinetic fractionation of zinc isotopes. Thereafter, zinc was primarily mobilized through the oxidation of primary sulfide minerals with little or no change in δ⁶⁶Zn values. The limited isotope fractionation observed may assist in the use of zinc isotopes as a tracer of anthropogenic, metal mine sources in future studies.

Inter-laboratory calibration of Zn isotopic compositions for organic and inorganic reference materials

N. MATTIELLI^{1*}, A. E. SHIEL^{2,3}, K. GORDON², D. WEIS²,
J. PETIT⁴ AND E. COUDER¹.

¹G-Time, Université Libre de Bruxelles, 1050 Brussels, Belgium (*nmattiel@ulb.ac.be)

²PCIGR, EOAS, University of British Columbia (UBC), Vancouver, B.C. Canada

³Dept. of Geology, University of Illinois at Urbana-Champaign, Urbana, IL USA

⁴UMR 5805 EPOC-OASU, TGM, Université de Bordeaux1, 33405 Talence cedex, France

Significant inaccuracy in MC-ICP-MS measurements of Zn isotopic composition may be caused by inorganic and organic resin-derived components added to samples during column chemistry or/and to incomplete separation of the analyte from the sample matrix [1]. In addition, previous studies [1, 2] have shown that mass bias corrections, using sample-standard bracketing and external normalization, fail to accurately correct for these matrix effects.

The present work aims to calibrate several organic and inorganic reference materials to assess the accuracy of Zn isotopic measurements. Analyses of a broad compositional range of USGS rock reference materials, including the basalts BCR-2 and BHVO-2 and the gabbro HRM-27, and organic reference materials, including the lichen BCR-482, the rye grass BCR-281, the San Joaquin soil SRM 2709, the light sandy soil BCR-142 and the lobster hepatopancreas TORT-2, have been systematically performed on two Nu Plasma MC-ICP-MS (Nu 015 at ULB and Nu 021 at PCIGR).

Two anion exchange chromatography procedures have been compared for Zn isolation using 0.2 mL or 2 mL of AG 1-X8 resin. Elemental concentrations were determined by ICP-MS for each digested sample and Zn eluate cut to monitor both Zn recovery and the presence of potential matrix interferences. Zn isotopic ratios have been corrected both by external normalization using Cu and by sample-standard bracketing with IRMM 3702 and Lyon JMC Zn standard solutions. The lightest and heaviest $\delta^{66}\text{Zn}$ values ($\pm 2\text{SD}$; relative to Lyon JMC) of the study are exhibited by the lichen BCR-482 ($+0.09 \pm 0.06\%$) and the lobster hepatopancreas TORT-2 ($+0.49 \pm 0.07\%$), respectively.

[1] Shiel, A.E., Barling, J., Orians, K.J. & Weis, D. (2009). *Analytica Chimica Acta* 633, 29–37. [2] Petit J.C.J., Taillez, A. & Mattielli, N. (2013). *GGR*. DOI: 10.1111/j.1751-908x.2012.00187.x.

Across-arc geochemical variations in Central America subduction zone: evidences from Honduras basalts

MICHELE MATTIOLI¹, SAMUELE AGOSTINI²
AND ALBERTO RENZULLI¹,

¹ Dipartimento di Scienze della Terra, della Vita e dell'Ambiente, Università di Urbino "Carlo Bo", Campus Scientifico "Enrico Mattei", 61029 Urbino (PU), Italy

² Istituto di Geoscienze e Georisorse, Consiglio Nazionale delle Ricerche, Area della Ricerca di Pisa, Via G. Moruzzi, 1, 56124 Pisa (PI), Italy

The across-arc geochemical data on the subduction zone of Central America are relatively scarce in Honduras where the active volcanic front does not occur inland but few km offshore the Pacific Ocean coast. In order to fill this gap we selected quaternary basalts from a arc to back-arc transect, enclosing (i) El Tigre, a stratovolcano in the Gulf of Fonseca, (ii) Yojoa Lake and Sula Graben back-arc volcanism, and (iii) Utila, a quaternary volcanic island near the strike-slip boundary between the North-American and Caribbean plates, about 200 km behind the front.

We found systematic variations in trace elements and isotopic compositions of basalts across this Honduras transect. Lavas from El Tigre are calc-alkaline with a significant LIL enrichment and Nb depletion, a strong slab signature and incompatible element contents similar to those in the main front of the adjacent volcanoes from El Salvador and Nicaragua (e.g. Ba/La up to 80). The back-arc quaternary volcanism of Yojoa Lake, Sula Graben and Utila is Na-alkaline, with a wide range of composition at Yojoa (basalts, hawaiites, mugearites, benmoreites, trachytes) and a more restricted, mafic composition at Sula and Utila (basalts and hawaiites). The back-arc basalts have similar major-trace element compositions to OIBs, such as relative enrichment in Nb and Ta, depletion in Pb and no pronounced peaks of fluid-mobile incompatible elements (Ba/La < 20).

The Sr and Nd isotopic data show a clear systematic variation passing from arc to back-arc, with El Tigre lavas characterized by higher $^{87}\text{Sr}/^{86}\text{Sr}$ (≈ 0.7038), and lower $^{143}\text{Nd}/^{144}\text{Nd}$ (≈ 0.51301), Utila basalts having typical values of a Depleted Mantle unaffected by any subduction imprint (≈ 0.7028 and 0.51310 , respectively), whereas Sula and Yojoa have intermediate values.

$^{208}\text{Pb}/^{204}\text{Pb}$ and $^{206}\text{Pb}/^{204}\text{Pb}$ isotope ratios of El Tigre are very similar to arc volcanoes of El Salvador and Nicaragua (38.2 and 18.5, respectively), whereas back-arc samples have higher $^{206}\text{Pb}/^{204}\text{Pb}$ (18.6–18.7 for Sula and Yojoa, 18.7 for Utila island).

Modal metasomatism in upper mantle from Eastern part of Central European Volcanic Province (SW Poland).

MAGDALENA MATUSIAK-MAŁEK¹, JACEK PUZIEWICZ¹, THEODOROS NTAFLIS² AND MICHEL GRÉGOIRE³

¹University of Wrocław,
magdalena.matusiak@ing.uni.wroc.pl

²University of Vienna, Austria

³University Toulouse III-CNRS, France

Cenozoic volcanic rocks of mafic affinity occur abundantly in central Europe forming the Central European Volcanic Province. The ascending magmas intensively sampled upper mantle peridotites. Mantle xenoliths from the Eastern part of CEVP (SW Poland) are in general strongly depleted and nominally anhydrous.

Small amounts of hydrous phases (mostly pargasitic amphibole) in xenoliths from Lutynia and Wilcza Góra were reported in literature (Blusztajn and Shimizu, 1994, Chem.Geol; Matusiak-Małek *et al.*, 2010, Lithos). The first locality with significantly higher amounts of amphibole was described by Nowak *et al.* (e.g. 2010, EGU2010-9299) from Wotek Hill.

Mafic and ultramafic xenoliths from Wilcza Góra basanite form four compositional groups. Almost half of the xenoliths contain pargasitic amphibole with modal compositions up to 5%. Amphibole forms: (1) intergranular grains; (2) amphibole-spinel-clinopyroxene clusters in host peridotite; (3) cores of clinopyroxene II; (3) lamellae in pyroxenes and (4) amphibole-olivine vein. Composition of amphibole follows compositional variations of host peridotite. The mg-number in amphibole occurring in peridotitic xenoliths is 0.910, the TiO₂ content is 0.262-0.413 wt.%. Amphiboles in xenoliths affected by "Fe-metasomatism" have mg-number from 0.892 to 0.852, while in cumulative xenoliths the latter is 0.854-0.734. The TiO₂ content is 0.533-2.220 and 2.915-3.508 wt.%, respectively. One xenolith contains vein formed of high mg-number 0.860-0.908 and TiO₂-rich (3.253-3.705 wt.%) amphibole. The REE pattern of the vein amphibole is LREE-enriched with negative inflection from Nd to La. It perfectly mimics REE composition of coexisting clinopyroxene.

Amphibole in Wilcza Góra xenoliths stands for local modal metasomatism in upper mantle beneath SW Poland. Composition of the amphibole suggest that it was introduced to the host peridotite together with clinopyroxene I due to reaction with hydrous mafic alkaline melt(s).

Oxidation state of iron in a primary Martian basaltic melt

A. K. MATZEN^{1*}, J. R. BECKETT², A. B. WOODLAND³ AND B. J. WOOD¹

¹Oxford Department of Earth Sciences, UK, OX1 3AN
(*correspondence: andrew.matzen@earth.ox.ac.uk)

²California Institute of Technology, Pasadena, CA 91125

³Goethe-Universität, D-60438, Frankfurt am Main

Olivine is an extremely important mineral in the generation and evolution of basaltic melts. Roeder and Emslie [1] concluded that the olivine (ol) silicate liquid (liq), exchange coefficient, $K_{D,Fe^{2+}-Mg} = (FeO/MgO)^{ol}/(FeO/MgO)^{liq}$ (by weight), is 0.30 ± 0.03 , independent of temperature (*T*) and liquid composition. An accurate $K_{D,Fe^{2+}-Mg}$ is predicated on a precise measurement, or calculation, of the abundances of Fe²⁺ and Fe³⁺ (expressed as Fe³⁺/ΣFe) in the liquid. It is well known that major-element composition can affect Fe³⁺/ΣFe [e.g., 2], and very few measurements have been made on primitive liquid compositions relevant to Martian petrogenesis. We measured the Fe³⁺/ΣFe ratios of a series of experimentally-produced glasses to better constrain the appropriate $K_{D,Fe^{2+}-Mg}(s)$ to use for Martian systems.

One-atmosphere, super-liquidus (1450°C) experiments were performed on a synthetic basalt modeled after the primitive magmas found near Home Plate (50% SiO₂; 10% Al₂O₃; 18% FeO*; 12% MgO) [3] at log fO_2 s ranging from -10 to -0.68. Fe³⁺/ΣFe of the resulting glasses were measured using Mossbauer and XANES spectroscopy. Fe³⁺/ΣFe vary from 0.06 to 0.68, and compare favorably with estimates based on terrestrially-relevant experiments [4]. Our results appear to contrast with much lower Fe³⁺/ΣFe reported for similar experiments on a Zagami bulk composition [5].

One-atm experiments on model Martian compositions provide the tightest constraint on $K_{D,Fe^{2+}-Mg}$ because *T* and fO_2 are well known, allowing us to use [4] to predict the amount of Fe²⁺ present in each liquid. The median of 17 published 1-atm experiments yields $K_{D,Fe^{2+}-Mg} = 0.354 \pm 0.008$ (error is one mean absolute deviation). Applying this $K_{D,Fe^{2+}-Mg}$ to the ol-phyric shergottites, leads to the possibility that Y980459, NWA 5789 and 2990 are liquid compositions (others appear to have accumulated olivine), identical to the results of [3].

[1] Roeder & Emslie (1970) *CMP* **29**, 275-289. [2] Sack *et al.* (1980) *CMP* **75**, 369-376. [3] Filiberto & Dasgupta (2011) *EPSL* **304**, 527-537. [4] Jayasuriya *et al.* (2004) *Am. Miner.* **89** 1597-1609. [5] Righter *et al.* (2013) *Am. Miner.* **98** 616-628.

Geochemistry of rare earth element (REE) in weathered crust from the granitic rocks in Sulawesi Island, Indonesia

ADI MAULANA^{1*}, KOTARO YONEZU², AKIRA IMAI³
AND KOICHIRO WATANABE⁴

¹ Faculty of Engineering, Kyushu University, Fukuoka 819-0395, Japan (*correspondence: adi-m@mine.kyushu-u.ac.jp)

² Faculty of Engineering, Kyushu University, Fukuoka 819-0395, Japan (yone@mine.kyushu-u.ac.jp)

³ Faculty of Science, Akita University, Japan (akira@gipc.akita-u.ac.jp)

⁴ Faculty of Engineering, Kyushu University, Fukuoka 819-0395, Japan (wat@mine.kyushu-u.ac.jp)

We report for the first time the geochemistry of rare earth elements (REE) in weathered crusts of I-type and calc-alkaline to high-K (shoshonitic) granitic rocks at Mamasa and Palu region, Sulawesi Island, Indonesia. The weathered crusts can be divided into horizon A (lateritic profile) and B (weathered horizon) in the Mamasa region with the present of horizon C (weathering front) in the Palu region. Quartz, K-feldspar, kaolinite, halloysite and montmorillonite with Ca-amphibole prevail in the weathered crust. The total REE content of the weathered crust are relatively elevated (40 to 75%) compared to the parent rocks, particularly in the lower part of horizon B in Mamasa profile and in horizon C in Palu profile. This suggests that REE-bearing accessory minerals may be resistant against weathering and may remain as residual phase in the weathered crusts. The mass transfer illustration using isocon diagram shows a different transfer trend from Mamasa and Palu weathering profile. The positive Ce anomaly in the horizon A of Mamasa profile indicated that Ce is rapidly precipitated during weathering and retain at the upper soil horizon, suggesting the occurrence of redox-controlled process which leading to the CeO₂ precipitation.

Bioavailability of metals associated with aquatic natural organic matter

PATRICIA A. MAURICE^{1*}, KESHIA KUHN¹,
LISA NEUBAUER², THILO HOFMANN²
AND FRANK VON DER KAMMER²

¹Civil & Environmental Engineering & Earth Sciences, Univ. of Notre Dame, Notre Dame, IN 46556 USA

*corresponding: pmaurice@nd.edu

²Dept. of Environmental Geosciences, Univ. of Vienna, Vienna, Austria

This research focused on the bioavailability of trace metals associated with natural organic matter (NOM) to aerobic bacteria, using abiotic experiments with the siderophore desferrioxamine B (DFOB) and live-culture experiments with aerobic *Pseudomonas mendocina*. Trace metal contents and distributions in reverse osmosis, XAD-8 and XAD-4 isolates from the Suwannee River (SR), were measured prior to and following reaction with DFOB using field flow fractionation (FFF) with in-line UV/vis, fluorescence, and ICP detection. Results showed that Fe is preferentially associated with intermediate to high molecular weight (MW) components at both the native pH of the SR (3.4) and pH 7, Al is fairly uniformly distributed, and Cu is preferentially associated with lower MW components. Reaction of SR XAD-8, XAD-4 and RO samples with excess of the microbial siderophore DFOB removes ~75% of Fe within 1 hour. Al and Cu are also decreased, but not as efficiently. Upon reaction with DFOB, loss of some higher MW components and addition of more low to intermediate MW components suggests that Fe, and perhaps also Al, likely bridges organic components. Live-culture experiments showed that while siderophores are useful for Fe acquisition from NOM by *P. mendocina*, they are not required. Overall, our research shows that metals bound to NOM are likely highly bioavailable, and further emphasize that trace metals need to be considered in any study of aquatic NOM.

Linking soil chemistry, treeline shifts and climate change: a scenario

CHRISTIAN MAVRIS^{1,*2,5}, SUSANNE P. ANDERSON²,
MARKUS EGLI¹, ALEX E. BLUM³, GERHARD FURRER⁴
AND DENNIS DAHMS⁵

¹Dept. of Geography, University of Zurich, CH-8057

(*correspondence: christian.mavris@geo.uzh.ch)

²INSTAAR, University of Colorado, Boulder, CO 80301, USA

³US Geological Survey, Boulder, CO 80303, USA

⁴Inst. Biogeochemistry & Pollutant Dynamics, ETH Zurich, CH-8092

⁵Dept. of Geography, University of Northern Iowa, Cedar Falls, IA, USA

Global warming can destabilize our fragile ecosystems. As cold areas become warmer, both flora and fauna must adapt to new conditions [1]. It is widely accepted that climate changes deeply influence the treeline shifts. But there is little knowledge about what happens to the soil chemistry when ecosystems tend to replace each other. Will elemental availability become a crucial factor in progressively warming conditions?

The Sinks Canyon and Stough Basin - SE flank of the Wind River Range, Wyoming, USA - offer a case study to answer these questions. Conceptually, the areas were divided into three main subsets: tundra, forest and subarid environment, all with soils developed on granitoid moraines. From each subset, a liquid topsoil extract was produced and mixed with the solid subsoil samples in batch reactors at 50 °C. The batch experiment was performed over 1800 h, and the progress of the dissolution was regularly monitored by analysing liquid aliquots with IC and ICP-OES.

The nutrients are released within the first hours of the experiment. Si and Al are continuously released into the solution, while some alkali elements - i.e. Na - show a more complex trend. Organic acids (acetic, citric) and other ligands produced during biodegradation play an active role in mineral dissolution and nutrient release. Furthermore, the mineral colloids detected in the extract (X-ray diffraction) can significantly control surface reactions (adsorption/desorption) and contribute to specific cationic concentrations. The experimental set up is then compared to a computed dissolution model using SerialSteadyQL and PHREEQC software.

Decoding the mechanisms driving mineral weathering is the key to understand the main geochemical aspects of landscape adaptation during climate changing conditions.

[1] Burga *et al.* (2010) *Flora* **205**, 561-576

Mg isotope fractionation during hydrothermal carbonation of serpentine

V. MAVROMATIS^{1,*}, A. BEINLICH², H. AUSTRHEIM³ AND
E.H.OELKERS¹

¹ GET, CNRS, UMR 5563, Toulouse, France,

mavromat@get.obs-mip.fr(*), oelkers@get.obs-mip.fr. ²

MDRU, EOS, University of British Columbia, Canada,

abeinlic@eos.ubc.ca. ³ PGP, University of Oslo, Norway,

h.o.austrheim@geo.uio.no

As (i) the Mg isotope composition of seawater is lighter than that of the mantle and (ii) Mg isotopic composition of the mantle is considered homogeneous [1], significant fractionation processes must be occurring during the alteration of the continental crust [2,3]. This study has been initiated to explore possible processes accounting for this fractionation.

Here we present new observations of Mg isotope fractionation during the carbonation of the Linnajavri Ultramafic Complex, N-Norway. Carbonation of the serpentinite in this complex occurred at closed system conditions (except for the volatiles) at ~275 °C resulting in the formation of mainly magnesite and talc [4]. Textural observations and reaction path considerations indicate that mineral replacement began with magnesite precipitation resulting in an increasing Si activity in the alteration fluid eventually saturating talc. The original serpentine has an isotopic composition of $\delta^{26}\text{Mg}$ (DSM3) = -0.11±0.05, whereas talc is enriched in ^{26}Mg with average $\delta^{26}\text{Mg}$ = 0.17±0.08 and magnesite is depleted in ^{26}Mg with average $\delta^{26}\text{Mg}$ = -0.95±0.15. These observations indicate that Mg isotopes are efficiently fractionated at mid-crustal PT conditions.

The observed fractionation has significant implications for the Mg isotope distribution in natural waters due to the large difference of the dissolution rates of Mg bearing silicates relative to Mg-bearing carbonates - the dissolution rates of magnesite are ~3 orders of magnitude faster than that of talc at 25 °C and pH=8 [5,6]. Our observations suggest that Mg isotope fractionation during carbonate formation and their faster erosion rates at Earth's surface conditions may explain the enrichment of seawater in ^{24}Mg compared to that of fresh mantle Mg and that Mg-bearing hydrous silicates may represent the missing sink for residual the ^{26}Mg .

[1] Teng *et al.*, (2007) *EPSL* **26**, 84-92. [2] Tipper *et al.*, (2006) *EPSL* **247**, 267-279. [3] Wimpenny *et al.*, (2010) *GCA* **74**, 5259-5279. [4] Beinlich *et al.* (2012) *Terra Nova* **24**, 446-455. [5] Saldi *et al.* (2007) *GCA* **71**, 3446-3457. [6] Pokrovsky *et al.*, (2005) *Chem. Geol.* **217**, 239-255.

Tracing the movement and fate of injected CO₂ in a mature oil field using geochemical, isotopic and modeling approaches

B. MAYER¹, G. JOHNSON^{1,2}, C. DALKHAA¹, M. SHEVALIER¹, M. NIGHTINGALE¹ AND I. HUTCHEON¹

¹University of Calgary, 2500 University Drive NW, Calgary, Canada, T2N 1N4.

²Midland Valley, 144 West George St, Glasgow, UK, G22HG

*Correspondance: bmayer@ucalgary.ca

Carbon capture and geological storage is a potential technology to reduce CO₂ emissions into the atmosphere. Monitoring of CO₂ storage sites is required by many of the emerging regulations with specific interest in accounting of injected CO₂ in various target reservoirs. At the Pembina Cardium CO₂ Monitoring Project in central Alberta (Canada), we have used chemical data and carbon and oxygen isotope ratios of produced water and gases sampled repeatedly from various observation wells to trace the movement of injected CO₂ and assess pore space saturation with CO₂. The distinct carbon isotope ratios of injected CO₂ in association with gas compositional and flux data were used to determine the percentage of injected CO₂ produced at several observation wells using two end-member mixing calculations [1]. Changes of δ¹⁸O values of produced water of up to 4 ‰ were caused by oxygen isotope exchange between CO₂ and H₂O following CO₂ injection [2]. The changes in the δ¹⁸O values of water were used for a quantitative assessment of CO₂ dissolved in the fluids and of free phase CO₂ in the pore space of the reservoir. Subsequently, we combined seismic and geochemical information with reservoir modeling approaches in an attempt to determine a carbon budget for injected CO₂ in the mature oil field. Results of partitioning calculations indicate that two years after commencement of CO₂ injection the majority of the CO₂ remained in a free phase within the reservoir, while smaller amounts of injected CO₂ were dissolved in water and oil. In April 2010, CO₂ injection at this pilot site was stopped but geochemical monitoring commenced for an additional 2 years until June 2012. We observed continued increases of δ¹⁸O values of formation water suggesting increases in CO₂ pore space saturation in the vicinity of two observation wells. The obtained results indicate that chemical and isotopic techniques can play a crucial role in monitoring the movement and the fate of CO₂ in geological reservoirs during and after CO₂ injection.

[1] Johnson *et al.* (2011), IJGGC 5, 933-941;

[2] Johnson *et al.* (2011), Chem Geol 283, 185-193.

Adsorption of ¹⁰⁹Cd onto metaloxide nanoparticles

NATALIA MAYORDOMO^{1*}, JUAN-LUIS LOPEZ-GOMEZ¹,
URSULA ALONSO¹ AND TIZIANA MISSANA¹

¹CIEMAT, Avenida Complutense, 40. C.P 28040 Madrid (Spain) *natalia.mayordomo@ciemat.es

To reduce the environmental impact of hazardous pollutants, as the highly toxic metal Cd, geochemical barriers providing confinement are required. To enhance contaminant retention in geochemical barriers, different nanoparticles (NPs) are being analysed, taking into account their inherent retention properties, either single or combined with other materials.

To assess which NPs better prevent the risk of contaminant leakage, detailed experimental and theoretical sorption studies in a wide range of geochemical conditions, are demanded. The stability of the NPs, upon contaminant adsorption in different environments, is an aspect that must be also evaluated.

In this study, the retention capability of two metaloxide NPs (Al₂O₃ and CuO) as candidate sorbents for Cd immobilisation in geochemical barriers was analysed.

Sorption experiments have been carried out in different electrolytes (NaNO₃, NaHCO₃, Na₂SO₄ and NaClO₄) and in a wide range of pH and ionic strengths, to simulate different environmental and salinity conditions. Sorption isotherms at different Cd concentration were also performed.

In addition, particles size and surface charge were systematically measured in all experiments to assess NPs stability, essential to predict their performance.

Geochemical modelling of a wide set of experimental sorption data contributes to probe the capability of selected NPs as ¹⁰⁹Cd adsorbents in geochemical barriers and contamination risk assessment.

Acknowledment: The research leading to these results has received funding form the Spanish Government under the project NANO BAG (CTM2011-27975). N. Mayordomo acknowledges the FPI BES-2012-056603 grant from MINECO (Spain).

Paleo-methane emission events in Krishna-Godavari basin, Bay of Bengal: Geochemical signatures

ANINDA MAZUMDAR

Gas Hydrate Research Group, Geological Oceanography, National Institute of Oceanography, Goa - 403004, India

Marine cold seep associated authigenic carbonates are known from modern and past geological records. Cold seeps are characterized by expulsion of fluid enriched in methane, hydrogen sulfide, and bicarbonate from the seafloor that results in the precipitation of calcium carbonates and pyrite at or below the sediment-water interface, often associated with a proliferation of chemosynthetic communities. Cold seeps are known to be associated with methane hydrate deposits. Methane hydrate, a crystalline, ice-like form of methane and water (molar ratio 1:6) exists within the marine sediments at suitable temperature-pressure conditions [1]. In the Krishna-Godavari (K-G) Basin (Bay of Bengal), seismic data show the regional presence of gas hydrates manifested in the form of a bottom simulating reflector (BSR). BSRs represent a phase boundary where low-velocity gas-charged sediments occur below the hydrate stability zone. Recent drilling and logging activities on-board JOIDES Resolution in the Indian margin under the aegis of Indian National Gas Hydrate Program (NGHP) have confirmed the existence of massive gas hydrate deposits in the K-G Basin [2]. Extensive fault and fracture zones in K-G basin sediments are apparently responsible for the advective transportation (focussed flow) of methane rich fluid from the base of gas hydrate stability (BGHSZ) to the sediment water interface. The sharp perturbation in sulfate, sulfide and bicarbonate concentrations at the sediment-water interface is attributed to the anaerobic oxidation of methane (AOM) performed by a syntrophic consortium of CH₄-oxidizing archaea and sulfate-reducing bacteria [3]. Here we report repeated evidence of such methane expulsion events in K-G basin in the quaternary period. Highly ¹²C enriched authigenic carbonates in the form of chimneys, massive crusts, chemosynthetic clams and other faunal records indicate cold seep events [3]. Destabilization of deep seated methane hydrate is one possible cause for these sudden methane pulses. Shale tectonics induced fault and fracture opening and change in geothermal gradient could be one of the plausible reason for focussed gas emission events.

[1] Kvenvolden (1988) *Chem. Geol.*, **71**, 41-51. [2] Ramana *et al.* (2004) *International Jour. Environmental Studies* **64**, 675-693. [3] Boetius *et al.* (2000) *Nature*, **407**, 623-626. [4] Mazumdar *et al.* (2009) *Geophy. Geochem. Geosys.*, **10**, 1-15.

Thermal structure of the Sgurr Beag thrust, NW Scotland

S.E. MAZZA^{1*}, R.D. LAW¹ AND M.J. CADDICK¹

¹ Dept. of Geosciences, Virginia Tech, Blacksburg, VA 24061, USA (*correspondence: mazza@vt.edu)

In the Caledonides of NW Scotland, well-understood metamorphic temperatures (*T_m*) and deformation temperatures (*T_d*) [i.e. 1, 2] progressively increase up structural section in the Moine thrust sheet at the foreland edge of the orogenic wedge. However, the thermal history of the hinterland thrust sheets is less well-constrained [3]. This study focuses on determining *T_d* and *T_m* for the Sgurr Beag thrust sheet in the hinterland of the Scottish Caledonides, to test whether potentially thrust-related inversion continues into the structurally higher thrust sheets that are penetratively deformed at higher (upper amphibolite) temperatures.

Preserved microstructures imply a wide range of possible deformation temperatures, which are quantified with the quartz c-axis fabric opening angle thermometer [4]. *T_d* from quartz opening angle thermometry increases up section, ranging from 395°C to 583°C ± 50°C. This indicates that if the isothermal surfaces dip towards the hinterland, thrust-related thermal inversion continues into the Sgurr Beag nappe. This study also presents new metamorphic *P-T* constraints for the Sgurr Beag nappe, based on garnet-biotite thermometry and GASP barometry, indicating *T_m* of ~620°C at 5.8 to 7.4 kbar. Together, *T_d* and *T_m* indicate that deformation continued past peak metamorphic conditions in the Sgurr Beag thrust sheet.

[1] Read (1931) *B.G.S Memoir*, **238**. [2] Johnson & Strachan (2006) *JGS*, **163**, 579-582. [3] Thigpen *et al.* (submitted) *JMG*. [4] Kruhl (1998) *JMG* **16**, 142-146.

New applications of dissolved gallium in the oceans: Promoting increasingly routine measurement

JASON A. MCALISTER^{1*} AND KRISTIN J. ORIAN¹

¹ University of British Columbia, Vancouver, Canada
(*Correspondence: jmc alister@eos.ubc.ca)

Dissolved gallium (Ga) is present in the oceans at picomolar concentrations, consistent with more routinely measured dissolved trace metals such as iron and aluminum, yet Ga exhibits comparatively less contamination risk, therefore easing sample collection and analysis. Shown here are three applications utilizing dissolved Ga concentrations in the ocean to study carbon dynamics, climate change, and mechanisms controlling sources and sinks of trace elements and isotopes (TEIs) in the ocean. Dissolved Ga is applied to 1) development of a model utilizing dissolved Ga profiles to estimate particulate abundance, 2) utilization of dissolved Ga as a new parameter differentiating Pacific and Atlantic source waters to the western Arctic Ocean, and 3) identification of differentially sourced plume waters of the Columbia River. Particulate abundance is vital to estimates of carbon flux and drawdown of CO₂ from the atmosphere. Dissolved Ga profiles are utilized here to model relative particulate abundance of CaCO₃ and opal, complimenting established sediment trap and U-Th methods, and providing potential for particulate abundance to be estimated on an increasingly routine basis. Arctic inputs from the Atlantic, identified by a strong dissolved Ga gradient, represent comparatively warm waters that threaten sea ice melt and CO₂ release if able to permeate Pacific source water stratification via upwelling over the extensive shelf area of the Arctic Ocean. Finally, the Columbia River plume provides a spatially and temporally unique environment, combining the plume induced salinity gradient with dynamic winds resulting in upwelling and downwelling conditions oscillating on the order of days. A plume endmember mixing model developed here utilizes dissolved Ga to identify offshore waters associated with formation under divergent wind conditions, influencing scavenging reactions and therefore concentrations of dissolved TEIs. Oceanographic study of complex multiparameter problems such as climate change requires a broad suite of variables including trace elements and isotopes. Results of this work encourage increasingly routine measurement of dissolved Ga concentrations and application to oceanographic research, including future GEOTRACES cruises.

Experimental dissolution of FeCO₃ under controlled sulfidic conditions

ALISON MCANENA^{1*} AND SIMON W. POULTON²

¹Institute of Marine and Coastal Science, Rutgers, The State University of New Jersey, New Brunswick, 08901 NJ, USA (*correspondence: amcanena@marine.rutgers.edu)

²School of Earth and Environment, University of Leeds, Leeds, LS2 9JT, UK

In modern sedimentary environments, reduced Fe minerals (e.g. siderite; FeCO₃) tend only to precipitate under anoxic conditions in environments where high Fe(II)_{aq} pore water concentrations are accompanied by low rates of sulfide fixation. In contrast, siderite-rich sediments are extensively observed throughout the Precambrian rock record, both in marine shales and banded iron formations. However, rising atmospheric oxygen and the gradual rise in oceanic sulfate concentrations through time ultimately led to the increased sulfidation of reactive Fe minerals, and hence less preservation of siderite in marine sediments. Nevertheless, high concentrations of siderite, particularly during the Precambrian, persist in sediments that contain pyrite, likely due to sulfate limited conditions during diagenesis. However, the reactivity of siderite towards dissolved sulfide is currently unknown.

We investigate the kinetics of siderite dissolution in the presence of sulfide under varying conditions. The rate of Fe(II) carbonate dissolution was measured experimentally on samples of synthetic and natural FeCO₃, under controlled initial sulfide concentrations, mineral surface area and pH. We propose a reaction mechanism where carbonate species undergo direct substitution with dissolved sulfide on the mineral surface, ultimately producing FeS as a major reaction product. The rate constant (k_{Fe}) determined by the sulfidation of siderite is similar to other highly reactive Fe minerals, such as ferrihydrite, but up to 5 orders of magnitude faster than more crystalline Fe(III) oxides; with complete siderite dissolution occurring over just tens of minutes.

Our data suggest siderite in marine sediments is highly reactive towards dissolved sulfide, even in the presence of low sulfide concentrations. FeS formation is limited by sulfide (and hence, initial sulfate) availability, with experimental results explaining the stability of co-precipitating FeS and FeCO₃ species observed within some sedimentary environments. We therefore conclude that the remobilization of reduced Fe(II) minerals by sulfide may have contributed greatly to Fe cycling in both modern and ancient anoxic environments.

Chromium isotope fractionation during pedogenesis: Influence of redox recycling

C.N. MCCLAIN*, K. MAHER, K.L. WEAVER
AND J.L. DRUHAN

Department of Geological and Environmental Sciences,
Stanford University, Stanford, CA 94305, USA
(*correspondence: cynthia.mcclain@stanford.edu)

Tracking the fate of Cr and $\delta^{53}\text{Cr}$ during physical and chemical weathering of soils is central to investigating both naturally occurring Cr(VI) drinking water contamination and the use of Cr as a paleoredox proxy. Cr is a unique system to study because it is possible to monitor variations of both the fluid $\delta^{53}\text{Cr(VI)}$ as well as the solid $\delta^{53}\text{Cr(III)}$ in space and time to interpret modern and ancient (bio)geochemical cycling. However, determining fractionation factors from observed isotope patterns is difficult due to multiple transformation pathways, recycling, and inherent heterogeneity in soils. The coupling of Cr-, Fe- and Mn- cycling and the presence of secondary minerals such as Fe-Cr-oxyhydroxides and Mn-oxides in soils indicates that Cr(III) available for oxidation may have been recycled (oxidized and reduced multiple times). Here we present a theoretical study that quantitatively tracks Cr isotopes during pedogenesis by modeling oxidation, reduction, fluid flow and physical denudation. We apply the model to a corresponding field study of solid and fluid speciation, isotope composition, physical and chemical gradients occurring in a modern serpentine mollisol developed on ultramafic bedrock in the Putah Creek watershed of the northern California Coast Range. The model is parameterized using both field and published data. Results demonstrate that increased recycling changes apparent fractionation, depending on fractionation factors assumed. These simulations show that it is difficult to attribute in-situ fractionation factors to specific reactions without careful evaluation of phases, mechanisms and rates. Our modeling methods can also be applied to other elements (such as Fe) and environments (such as groundwater aquifers) to evaluate the spatial variability in isotopic composition imposed by redox recycling.

Seafloor massive sulfide exploration in SW Pacific - A commercial perspective

TIMOTHY F. MCCONACHY¹

¹SVP Science & Exploration, Neptune Minerals, Inc., Suite 3,
Level 7, North Tower, 1-5 Railway Street, Chatswood,
NSW, 2067, Australia
tim.mcconachy@neptuneminerals.com

The discovery and recovery of seafloor massive sulfides near Galapagos and black smokers at 21°N on the East Pacific Rise in the late 1970s is arguably one of the great natural science discoveries of the 20th Century. Since then, black smokers have been found in all the world's oceans. Because of the high concentrations of copper, lead, zinc, silver and gold associated with seafloor massive sulfides, they have gone, in the space of less than 30 years, from being a scientific curiosity to a potential new source of metals for commercial use, attracting significant speculative investment by private and public companies and state-owned enterprises. One commercial Mining Licence has been granted in the Bismarck Sea by the Government of Papua New Guinea and further mining licences are likely to follow in other countries' waters along the SW Pacific Ring-of-Fire.

The SW Pacific region is attractive to explorers for two main reasons: firstly, it has convergent plate boundaries with associated volcanic arcs and back arcs which host deposits of massive sulfide that generally contain superior metal grades due to complex crustal melting and fractionation processes; and secondly, countries in the region are able to grant secure title to explore within their territorial waters and Exclusive Economic Zones under existing legislation.

Land-based explorers are finding that new deposits are hard to discover and difficult to permit; and drilling, feasibility, construction and stripping typically takes 10 years or more. By contrast, on the seafloor, new deposits are relatively easier to find, they are high grade, have no or little overburden and mining does not require high levels of infrastructure or capital; and mine scheduling is flexible.

Neptune Minerals holds granted licences and licence applications in seven countries in the SW Pacific. It has completed exploration programs using a combination of hydrothermal plume survey, moderate to high-resolution acoustic seabed mapping, ROV mapping and sampling, geophysics, drilling and spot sampling, making and assessing a number of new discoveries. The company's 'baby step' approach to its exploration, environment and social licences is akin to adopting a precautionary approach.

Black carbon concentrations and fluxes during recent millennia from a developing array of Arctic ice cores

J.R. MCCONNELL^{1*}, D. DAHL-JENSEN², D. FRITZSCHE³,
M. NOLAN⁴ AND M. SIGL¹

¹Desert Research Institute, Reno, NV 89509, USA

(*correspondence: Joe.McConnell@dri.edu,
Michael.Sigl@dri.edu)

²University of Copenhagen, Copenhagen Denmark
(ddj@gfy.ku.dk)

³Alfred Wegener Institute, Potsdam, Germany
(Diedrich.Fritzsche@awi.de)

⁴University of Alaska, Fairbanks, AK, USA
(matt2013@drmattnolan.org)

Short-lived aerosols such as black carbon (BC) and dust are important components of climate forcing, although warming from increased carbon dioxide and other greenhouse gas concentrations is the long-term driver of climate change. With their short lifetimes in the atmosphere, aerosol concentrations and deposition rates are dominated by regional – rather than global – sources and intra- and inter-annual variability is high. Such aerosols in snow are especially important in the high latitudes because of their strong impact on albedo.

Because most BC aerosols in high latitudes originate in lower latitudes, changes in long range transport processes and pathways may dominate over changes in source strength in determining concentrations and deposition rates in these regions. However, detailed understanding of past and present concentrations, deposition rates, sources, and transport pathways of BC to and within the Arctic is lacking. Here we present and discuss detailed records of BC measured in a developing array of ice cores widely distributed around the Arctic. We use a range of elemental and chemical tracers measured in the same ice cores to identify likely sources and to investigate spatial and temporal patterns of BC deposition during recent centuries and millennia.

Transformational science with a new global volcanic gas emissions database

B. MCCORMICK¹, E. COTTRELL¹, T. FISCHER²,
G. CHIODINI³ AND C. CARDELLINI⁴

¹Department of Mineral Sciences, National Museum of Natural History, Smithsonian Institution, Washington, DC, USA

²Department of Earth and Planetary Sciences, University of New Mexico, Albuquerque, NM, USA

³Istituto Nazionale di Geofisica e Vulcanologia, Osservatorio Vesuvio, Napoli, Italy

⁴Dipartimento di Scienze della Terra, Università di Perugia, Perugia, Italy

Volcanic degassing is regularly monitored at many volcanoes worldwide, with direct sampling and both ground- and satellite-based remote sensing techniques. Recent years have seen a sea-change in instrument sophistication and capability. The literature contains a wealth of additional data arising from campaign measurements of degassing. However, there is currently no existing inventory of volcanic gas emission measurements in an easily accessible form, such as an online relational database.

Inspired by the Deep Carbon Observatory's DECADE initiative to estimate global volcanic CO₂ flux, we are building a new database incorporating all published degassing and volatile data for Earth's volcanoes. Appropriate metadata will be carefully defined and attention paid to data quality. Numerous factors influence the accuracy of gas emission measurements, and some categorisation or quantification of the uncertainty present in each data entry is crucial. Emissions fluxes and relevant metadata will be incorporated into the database of Smithsonian's Global Volcanism Program as we aim to directly link gas emissions to volcanic activity. Gas compositions will be incorporated into the EarthChem database with the intent to make these two databases interoperable.

Our vision is for the database to become an essential tool of the volcanological community, and we seek close collaboration with the volcanic emissions community from the onset. Close consultation with gas geochemistry and monitoring experts will ensure that the data and metadata types defined and implemented in the database are fit-for-purpose, and that the proposed database search capabilities, visualisation schemes and output standards meet the user needs of these researchers. We will build on lessons learned from the Italian volcanic gas database, GOOGAS. We are also working closely with cyber-infrastructure specialists to ensure the new database is fully inter-operable with existing online resources (e.g. EarthChem, WOVOdat, Global Volcano Model, GOOGAS, IRIS) and can be extended beyond gas emissions into other monitored parameters in the future.

HIMU lithospheric mantle in the Southwest Pacific: Tracing the roots of Zealandia

ALEX J. MCCOY-WEST^{1*}, VICKIE C. BENNETT¹
AND YURI AMELIN¹

¹Research School of Earth Sciences, Australian National University email: alex.mccoywest@anu.edu.au

The existence of a widely sampled HIMU reservoir in the Southwest Pacific is well documented from the Pb isotopic compositions of intraplate basalts with $^{206}\text{Pb}/^{204}\text{Pb} > 19.5$. The origin of this signature however, remains controversial with proposed sources including metasomatised subcontinental lithospheric mantle and ancient oceanic lithosphere stored in the deep mantle [e.g. 1-3]. Here we further investigate the origin of HIMU characteristics through a combined petrologic and Sr-Nd-Pb isotopic study of a suite of mantle xenoliths assembled from 12 localities throughout New Zealand. Prior Re-Os isotopic study of this suite [4] demonstrated that a substantial portion of the lithospheric mantle underlying southern New Zealand is Paleoproterozoic in age (c. 1.7 Ga) and thus > 1 b.y. older than the oldest overlying crustal rocks.

For this investigation Sr, Nd and Pb isotopic compositions were determined from leached clinopyroxene mineral separates of the xenoliths using ID-TIMS methods. Pb isotopic compositions were determined using a ^{202}Pb - ^{205}Pb double spike. Initial results show a narrow range of measured $^{206}\text{Pb}/^{204}\text{Pb}$ between 19.5-21.1 and with no simple correlation with $^{238}\text{U}/^{204}\text{Pb}$ or with Os isotopic composition. $^{87}\text{Sr}/^{86}\text{Sr}$ isotopic compositions show a narrow range centered about 0.7025-0.7028, with $^{143}\text{Nd}/^{144}\text{Nd}$ isotopic data having more variability. The CPX leachates had lower $^{206}\text{Pb}/^{204}\text{Pb}$, showing that the HIMU signature does not result from contamination by the host basalts.

The Pb isotopic results are consistent with a widespread HIMU component residing in the lithospheric mantle beneath Zealandia. The homogeneous measured Pb isotopic compositions and lack of correlation with Os model ages imply a multi-stage history for lithosphere development in the region, with Paleoproterozoic melt extraction as reflected in Os isotopic signatures followed by an extensive, but much younger metasomatic event generating the Pb isotopic characteristics.

[1] Panter *et al.* (2006) **JPet** 47, 1673-1704. [2] Timm *et al.* (2009) **JPet** 50, 989-1023. [3] McCoy-West *et al.* (2010) **JPet** 51, 2003-2045. [4] McCoy-West *et al.* (2013) **Geology** 41, 231-234.

Abundance and ubiquity of H₂O in the martian interior

FRANCIS M. MCCUBBIN*

Institute of Meteoritics, 1 University of New Mexico, MSC03-2050, Albuquerque, NM 87131, USA
(fmccubbi@unm.edu)

There is substantial evidence supporting the past existence of abundant flowing water on the martian surface, however the source for this water remains elusive. Earlier studies of martian meteorites resulted in estimates of less than about 35 ppm H₂O [1], which is incompatible with an internal source for the surface water. These earlier studies primarily relied upon bulk rock water contents of the meteorites and were likely affected by magmatic degassing [2]. Even modern efforts to estimate H₂O abundances in martian melt inclusions likely suffer from volatile loss [i.e., 3].

We have revisited the abundance and distribution of H₂O in the martian interior through studies of volatile bearing mineral phases in martian meteorites [4-5], which are more likely to retain their OH components during magmatic degassing. There are water contents available for amphibole and biotite in the Chassigny meteorite [5-7] and apatite in a number of enriched and depleted shergottites [4]. If the water in these minerals was primary to the parental melts, the magmatic source regions from which the parental melts were derived likely have 70-300 ppm H₂O. This would imply that both geochemically depleted and enriched sources on Mars have elevated H₂O abundances and Mars' ancient surface water could be internally derived.

[1] Mysen, B.O. (1998) *Am Min.*, 83, 942-946. [2] McSween H. *et al.* (2001) *Nature*, 409, 487-490. [3] Usui T. *et al.* (2012) *EPSL*, 357-358, 119-129. [4] McCubbin, F.M. *et al.* (2012) *Geology*, 40, 683-686. [5] McCubbin, F.M. *et al.* (2010) *EPSL*, 292, 132-138. [6] McCubbin, F.M. *et al.* (2013) *MAPS*, In Press, DOI: 10.1111/maps.12095. [7] Watson, L.L. *et al.* (1994) *Science*, 265, 86-90.

Bio-calcification and its response to ocean acidification: new insights from boron isotopes

M.T. McCULLOCH^{1,2}, J.A. TROTTER¹, M. HOLCOMB^{1,2}
AND P. MONTAGNA³

¹ Oceans Institute and School of Earth and Environment, The University of Western Australia, Crawley 6009, Australia.

² ARC Centre of Excellence in Coral Reef Studies, UWA.

³ ISMAR-CNR, via Gobetti 101, I-40129 Bologna, Italy.

Bio-calcification is not only responsible for building the majestic coral reefs of the tropics, but is also a determinant of the oceans carbonate chemistry and ultimately the CO₂ content of the biosphere upon which life depends. By its very nature, biomineralisation occurs within a restricted, physiologically controlled environment, whose connectivity to external seawater is poorly known. Understanding these factors is thus fundamental to quantifying the response of this key group of organisms to CO₂ driven climate change and ocean acidification. Boron isotopes are an ideal tool to interrogate these processes, as its speciation is pH dependent, and biocalcifiers specifically incorporate the isotopically distinct borate species into their carbonate skeleton.

Using boron isotope systematics we show how biological up-regulation of the pH of the calcifying fluid is a characteristic of both azooxanthellate and zooxanthellate aragonitic corals. Scleractinian corals up-regulate pH at their site of calcification such that internal changes are approximately one-half of those in ambient seawater [1]. Although the absolute magnitude of the pH-buffering capacity is species-dependent, it provides a mechanism to raise the saturation state of the calcifying medium, thereby potentially increasing calcification rates at relatively little additional energy cost. This is especially evident in deep-sea corals where high degrees of pH up-regulation has facilitated calcification at, or in some cases below, the aragonite saturation horizon. Models [2] combining biologically induced pH regulation with abiotic calcification, (IpHRAC) now make it possible to unravel the effects of increased temperature and reduced seawater saturation states on bio-calcification. Up-regulation of pH is not however ubiquitous among all calcifying organisms; those lacking this ability may undergo severe declines in calcification as CO₂ increases.

[1] Trotter *et al.*, (2011) *Earth Planet. Sci. Lett.* 303,163-173.

[2] McCulloch *et al.* (2012) *Nature Climate Chg.* 2, 623-627.

Continuous measurement of methane emissions from a landfill using a new laser-based open path instrument

DAYLE MCDERMITT^{1*}, LIUKANG XU¹, XIAOMAO LIN²,
JIM AMEN³, KARLA WELDING³, TYLER ANDERSON¹
AND ANATOLY KOMISSAROV¹

¹LI-COR Biosciences, Lincoln, NE USA 68504

*correspondence: dayle.mcdermitt@licor.com,

liukang.xu@licor.com, jim.amen@licor.com,

tyler.anderson@licor.com, anatoly.komissarov@licor.com

² Dept. Of Agronomy, Kansas State Univ., Manhattan, KS
USA xlin@ksu.edu

³ Bluff Road Landfill, City of Lincoln, Lancaster County, NE
USA 68517 kwelding@lincoln.ne.gov

A new laser-based open path methane analyzer (LI-7700, LI-COR Biosciences) was used to measure methane emission rates by eddy covariance from June to December 2010 at the municipal landfill in Lincoln, NE USA. The instrument provides continuous measurements at 10 Hz with minimal maintenance and can operate on solar power. High frequency corrections for effects of temperature and water vapor on methane absorption spectra, and operation in dusty environments present special challenges that will be discussed. Methane concentrations varied sharply from near background to more than 60 ppm. Methane emission rates varied as much as 35-fold from day to day and depended strongly on changes in barometric pressure (P), increasing with falling P and decreasing with increasing P. Emission rates were systematically higher in December than during the summer period. Higher rates were associated with changes in P that were larger in magnitude and longer in duration in winter than in summer, and with lower mean temperatures, which appeared to reduce methane oxidation rates. Power spectrum and ogive analysis showed that 10 days of averaging were required to capture 90% of the variance in emission rate. Implications of these results for estimating landfill emission rates will be discussed.

The Earth and its building blocks

W. F. McDONOUGH¹

¹ Dept of Geology, University of Maryland, College Park, MD, 20742-4211, USA.

The composition of the Earth was shaped by the chondritic building blocks that most likely populated the inner solar system. The observed isotopic composition of the *available* chondrites, which are few and only recently (<10⁵ years) delivered, reveal an enstatite chondrite (EC) match, or similarity, to that of the Earth. However, and in stark contrast, the Earth does not match EC for their volatile element abundances, nor their mineralogical attributes. Based on the planetary mass fraction of Fe in the Earth's core, the planet is strongly reduced, intermediate in redox potential between ordinary (OC) and EC. Increasingly, it is observed that the niningerite and oldhamite in EC, as well as other phases, is the alteration product of sulfidation of ferromagnesian silicates and not a primary feature [1].

The ¹⁴²Nd isotope data [2] has opened up a new vista in revealing aspects of solar system history and the nature and distribution of the early building blocks. A fundamental observation from this isotope system is that the three dominant classes of chondrites, CC, OC and EC, have clear differences in their average ¹⁴²Nd/¹⁴⁴Nd compositions and the Earth is most similar to the EC class [3]. Interpretation of the ¹⁴²Nd signature of the Earth include a deep hidden reservoir [4] or loss of the equivalent reservoir to space by an ablation process [5]. Alternatively, the data are consistent with early solar system heterogeneity [6].

Neutrino geoscience, the detection of electron anti-neutrinos from beta-decays of Th and U series, is now providing data on the amount and distribution of U and Th inside the Earth. The latest results from the KamLand and Borexino experiments were reported earlier this year [7,8] and demonstrate that the Earth contains a considerable amount of primordial heat and favors both cosmochemical [9] and geochemical models [10]. Combined with data for the composition of the continental crust, these models will be interpreted in terms of the residual amount of heat producing power left in the mantle needed for mantle convection and driving plate tectonics.

[1] Lehner *et al.* 2013, GCA 101; [2] Boyet & Carlson 2005, Science 309; [3] Gannoun *et al.* 2011, PNAS 108; [4] Boyet & Carlson 2006, EPSL; [5] O'Neill & Palme 2008, Phil. Trans. R. Soc. A 306; [6] Qin *et al.* 2011, GCA 75; [7] Bellini *et al.* 2013, arXiv:1303.257; [8] Gando *et al.* 2013, arXiv:1303.4667v2; [9] Javoy *et al.* 2010, EPSL 293; [10] McDonough and Sun 1995, CG 210.

Remarkably hot quartz in resurgent intrusions associated with the 18.8 Ma Peach Spring Tuff supereruption

S.M. McDOWELL^{1*}, C.F. MILLER¹ AND J. WOODEN²

¹Vanderbilt University, Nashville, TN 37235, USA

(*correspondence: susanne.m.mcdowell@gmail.com)

²Stanford University, Palo Alto, CA 94305

(jwooden@stanford.edu)

The Silver Creek caldera (southern Black Mountains, western Arizona) is the source of the 18.8 Ma, >700 km³ Peach Spring Tuff (PST), the only supereruption deposit in the Colorado River Extensional Corridor (CREC) [1]. A 30 km² intrusive complex within the caldera records ~200 ka of post-PST resurgent magmatism and consists of two primary units: the intermediate to felsic Moss porphyry (62-68 wt% SiO₂; 18.81 ± 0.09 Ma [TIMS U-Pb zircon age]) and the felsic Times porphyry (>72 wt% SiO₂; 18.63 ± 0.08 Ma) [2]. Both units intrude trachytic, densely welded intracaldera PST.

To investigate epizonal magmatic processes during and immediately after the PST supereruption, and to constrain the thermal history of the PST magmatic center, we applied Ti-in-quartz thermometry [3] to two samples of Moss, one sample of Times, and one sample of a younger (18.21 ± 0.07 Ma) crosscutting quartz porphyry dike. Quartz in the Moss yields conspicuously high Ti concentrations (~60 to 340 ppm; avg. 160 ppm), corresponding with Ti-in-qtz temperatures of ~730-980°C (avg. 840°C, $a_{\text{TiO}_2} = 0.7$). Ti-in-qtz concentrations for the Times (~45-150 ppm; avg. 95 ppm) and quartz porphyry dike (~50-110 ppm; avg. 70 ppm) give mean Ti-in-qtz temperatures of 780°C and 745°C, respectively. Quartz temperatures are broadly consistent with trends in zircon saturation and Ti-in-zircon temperatures for the same units. Moss temperatures are higher than those for all other units in the CREC except intracaldera PST, which yields comparable Ti-in-zircon temperatures [4, 5].

Mineral thermometry suggests that the Moss records a brief period of exceptionally hot magmatism that coincides temporally and spatially with the PST eruption. Quartz data are consistent with the hypothesis that influx of anomalously warm and/or voluminous mafic magma led to rapid production and accumulation of massive, high-T PST magma [6]. Temperatures of successive post-PST intrusions fell at a rate of ~0.25°C/k.y.

[1] Ferguson *et al.* (2013) *Geology* **41**, 3-6. [2] McDowell *et al.* (2012) *GSA AbsProg* **44**, 320. [3] Watson & Wark (2006) *ContribMinPet* **152**, 743-754. [4] Claiborne *et al.* (2010) *ContribMinPet* **160**, 511-531. [5] Pamukcu *et al.* (2013) *JPet.*

Not so hot and not so salty microbes and their role in oil recovery and corrosion

MICHAEL J. MCINERNEY¹

¹Department of Microbiology and Plant Biology, University of Oklahoma, Norman, OK 73019 USA; mcinerney@ou.edu

Diversifying the global energy portfolio with carbon-free or carbon-neutral fuels is critically needed. However, fossil fuels will likely be the dominant energy source for several decades. Significant amounts of oil remain entrapped in oil reservoirs, many of which are not too hot (30 to 50°C), but are salty (salinities ranging from 2 to 19%). We conducted a test of a microbial plugging process in a hypersaline oil reservoir (14-19% salinity; 35°C). The injection of molasses and nitrate stimulated *in situ* microbial growth and metabolism, which blocked a major water channel and corrected interwell permeability heterogeneities. The efficacy of biosurfactant-mediated oil recovery was tested in a control field trial. Two wells received an inoculum of biosurfactant-producing *Bacillus* species and 67 cubic meters of nutrients (glucose, sodium nitrate, and trace metals); two wells received just nutrients; and one well received only formation water. The lipopeptide biosurfactant was detected only in the produced fluids from the inoculated wells. A year later, the two wells that received an inoculum were treated with the same two strains and 670 cubic meters instead of 67 cubic meters of nutrients. The lipopeptide biosurfactant concentration was about 20 mg/L and about 330 barrels of additional oil were recovered. Most probable number analysis showed that heterotrophic, thiosulfate-reducing bacteria related to *Anaerobaculum* species were the most numerous sulfide producers in a corroding oil production facility (marine salinity; 55°C). Enrichments containing *Anaerobaculum* species caused significant corrosion of metal coupons when yeast extract and thiosulfate were present. Our work shows that microbial permeability profile modification and *in situ* biosurfactant production are possible. Fermentative thiosulfate users are important mediators of corrosion in some oil production facilities

RESOChron: ELA-ICP-He-MS instrument for *in situ* U-Th-Pb-He geothermochronology

BRENT IA MCINNES¹, NOREEN J EVANS¹, MIKE SHELLEY², BRAD McDONALD¹, DAVID GIBBS³, ASHLEY NORRIS⁴, ED ROBERTS³, CLIFF GABAY⁴ AND DES PATTERSON⁵

¹AuScope GeoHistory Facility, John de Laeter Centre for Isotope Research, Applied Geology, Curtin University, Perth WA Australia; b.mcinnnes@curtin.edu.au

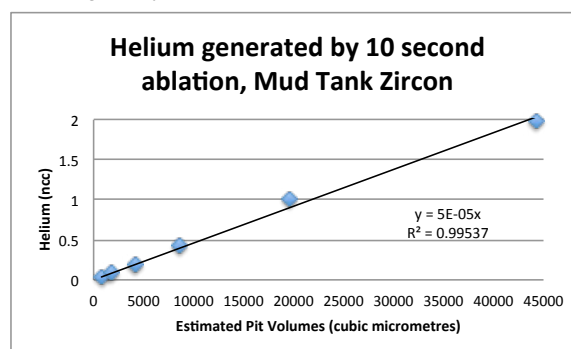
²Laurin Technic Pty Ltd., Canberra ACT, Australia

³Australian Scientific Instruments Pty Ltd, Canberra ACT

⁴Resonetics Ltd, Nashua NH, USA

⁵Patterson Instruments Ltd, USA

The development of an *in situ* microanalytical instrument capable of rapid automated U-Th-Sm-Pb-He isotope analysis of multiple grains will permit a more detailed interrogation of the time-temperature history of apatite, zircon, rutile, titanite and other accessory phases. Previous work¹⁻³ has demonstrated the technical feasibility of this approach, while this project advances the field via the development of a prototype system that integrates four existing commercial components: (i) a helium mass spectrometry module based on the Alphachron™ design, (ii) an ICP-MS module (Agilent 7700), (iii) an excimer laser ablation module based on the RESOLution design, and (iv) swappable ultra-high vacuum and flow-through analytical cells designed by Laurin Technic.



Initial *in vacuo* laser ablation testing on a large Mud Tank zircon indicate that: (i) the DL for radiogenic ⁴He, is exceeded when ablation volumes are >780 μm³ corresponding to a 10 μm deep ablation pit with 5μm radius; (ii) U-Th-Pb-He mapping/profiling is feasible with this new approach.

[1] Boyce J. W. *et al.*, 2006, GCA 70, 3031–3039; [2] Boyce J. W. *et al.*, 2009, G-cubed 10. doi:10.1029/2009GC002497; [3] Vermeesch, P. *et al.*, 2012, GCA 79, 140-147.

Evaluating the role of arc volcanism on Neoproterozoic to Early Paleozoic climate

N. RYAN MCKENZIE^{1*}, NIGEL C. HUGHES², BENJAMIN C. GILL³ AND PAUL M. MYROW⁴

¹Department of Geological Sciences, Jackson School of Geoscience, University of Texas at Austin, Austin TX, 78712

²Department of Earth Sciences, University of California, Riverside, Riverside CA, 92521

³Department of Geosciences, Virginia Polytechnic Institute & University, Blacksburg VA, 24061

³Department of Geology, Colorado College, Colorado Springs CO 80903

*Corresponding author: rmckenzie@jsg.utexas.edu

Identifying the driving mechanisms for major climatic shifts deep in Earth history is challenging. Here we use a global compilation of detrital zircon age data to evaluate spatiotemporal variation in continental arc volcanism and tectonic outgassing of CO₂ to the atmosphere during the Neoproterozoic and Early Paleozoic. This data set reveals a direct link between tectonically driven CO₂ emissions and the dramatic episodes of climate change observed in this interval: the Cryogenian “Snowball Earth” and the “hothouse” world of the Cambrian. Importantly, these climatic events had profound affects on early animal evolution. Specifically, our data show the following trends: (1) a global reduction in continental arc volcanism occurred around the transition into the “Snowball Earth” whereas widespread arc systems initiated near the terminal Cryogenian and its glacial interval; (2) Continental arc systems stayed active and further expanded dramatically during the Ediacaran and into the Cambrian. This corresponding to an extreme greenhouse climate and protracted interval of global environmental stress; and (3) A global reduction in arc volcanism during the early Ordovician is associated with a period of global cooling and the onset of the Great Ordovician Biodiversification Event (GOBE). These data demonstrate that global variation in plate tectonic regimes plays a major role in steering Earth’s climate and evolutionary patterns on million year time scales.

Initiation and 35 Myr duration of S-type granitic magmatism in an accretionary orogen

SEANN J. MCKIBBIN¹, BILL LANDENBERGER², WILLIAM J. COLLINS³ AND C. MARK FANNING⁴

¹Vrije Universiteit Brussel, Brussels, Belgium; seann.mckibbin@gmail.com;

^{2,3}University of Newcastle, Newcastle, Australia;

bill.landenberger@newcastle.edu.au;

bill.collins@newcastle.edu.au

⁴Australian National University; mark.fanning@anu.edu.au

Granites in circum-pacific igneous provinces can often be divided into ‘S-’ and ‘I’-types on the basis of elemental and isotopic characteristics [e.g. 1]. This division reflects a dominance of sedimentary or igneous source components, and dating of granites allows tracking of the relative contributions to growing batholiths in accretionary orogens. In the Lachlan and New England Orogens of Eastern Australia, a progression from S-type through I-type to A-type granites occurs repeatedly over ~100 Myr periods. S-type intrusion occurs during the first major extensional event following major compression, while later I-type intrusion reflects a diminished sedimentary source and increasing mantle contribution. The timing of S- and I-type granites is therefore related to the tectonic evolution of orogens [2].

The S-type phase of intrusion in the New England accretionary orogen (~300-280 Ma) records an environment switching from compression to extension and back to compression as part of this process. We have undertaken U-Pb dating of zircons extracted from small (~backarc) gabbroic and dioritic bodies (Bakers Creek Supersuite), recalculated the ages of S-type granites (Hillgrove Supersuite), and compiled chronological data for the New England Orogen in order to investigate the establishment of magmatism in this area. We find a progression through: (1) diverse magmatism involving gabbroic, dioritic, S- and I-type during establishment of magmatism (305-295 Ma); (2) a major pulse of S-type magmatism (295-285 Ma), ending with; (3) I-type and HREE-depleted (deep crustal) magmatism around the time of the Hunter-Bowen orogenic event (~285-266 Ma).

Magmatism occurs over a ~35 Myr period in the region of most voluminous intrusion, but timing varies along-strike and may reflect asymmetric rifting of the orogen. Together, these data time the heating, melting, depletion, and exhaustion of the S-type magma source.

[1] Kemp, A. I. S. & Hawkesworth, C. J., 2003. *Treatise on Geochemistry* 3, 349-410. [2] Collins, W. J. & Richards, S. W., 2008. *Geology* 36, 559-562.

Identifying the sources of iron in reservoir fluids at a CO₂ injection pilot in Alberta, Canada

BREEGE MCKIERNAN^{1*} MICHAEL WIESER¹
MICHAEL NIGHTINGALE^{2A} AND BERNHARD MAYER²

¹Department of Physics and Astronomy, University of Calgary, 2500 University Drive NW, Calgary, AB, T2N1N4, Canada (bmckiern@ucalgary.ca (*presenting author))

²Department of Geoscience, University of Calgary, 2500 University Drive, NW Calgary, AB, T2N1N4, Canada (night@earth.geo.ucalgary.ca, bmayer@ucalgary.ca)

The Pembina oil field is situated in western-central Alberta, Canada. After decades of water-flooding, a CO₂ injection pilot project was constructed to enhance tertiary oil recovery. A detailed geochemical monitoring program was conducted to study the impact on the geochemistry of reservoir fluids and rocks [1]. Increased iron concentrations, up to 144 µg/g, were measured at observation wells in the vicinity of the two CO₂ injectors after CO₂ injection commenced.

Iron isotopic compositions were measured and two possible sources of iron were investigated: leaching from the production pipes and siderite dissolution. Iron isotope data are summarized in Figure 1.

Data suggest that neither siderite dissolution nor iron leaching are the only processes occurring at the site. Either a third source of iron or BSR are responsible for the measured iron delta values.

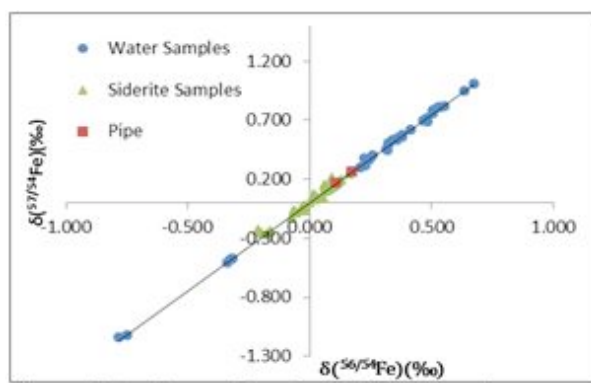


Figure 2: Iron isotope data obtained for reservoir water obtained from observation wells, siderite samples from the reservoir and production the pipe.

[1] Michael Nightingale (2010). Unpublished MSc. Thesis. University of Calgary.

EARTHTIME: Past, Present, and Future

NOAH MCLEAN¹

¹NERC Isotope Geosciences Laboratory, Keyworth, Nottingham, UK
noahm@bgs.ac.uk

The last ten years have seen a revolution in geochronology. Recognizing that the apparent precision achievable by a new generation of mass spectrometers and laboratory techniques outstripped inter-laboratory agreement and revealed unrecognized inter-chronometer biases, the EARTHTIME initiative was formed to move science forward through community engagement and collaboration. A series of inter-related experiments in the U-Pb and Ar-Ar communities, including inter-lab comparisons, community tracer calibration and distribution, and adoption of software and data reduction norms, have been broadly successful, in large part due to international cooperation.

The success of the U-Pb and Ar-Ar experiments have since inspired the same approach from other chronometers whose increasing measurement precision and proliferation of laboratories has elicited the same questions. The U-series community is now embarking on a large international inter-laboratory comparison, in conjunction with first-principles calibration efforts; the LA-ICP-MS U-Pb community has completed an inter-laboratory comparison and is presently engaged in software package comparison and development of data reduction norms; and the EarlyTime initiative, focused on geochronology of meteorites, is organizing an inter-laboratory comparison. These efforts seek to replicate, and strive to be informed by, the progress made by EARTHTIME.

As these parallel projects advance and the accuracy of each system improves, it is worthwhile considering both the limiting uncertainties and the ultimate goals involved. Minimizing and correctly estimating inter-laboratory biases by measuring multiple 'secondary' standards across many laboratories yields a community-wide measure of the external reproducibility of each method. As measurement uncertainties and internal repeatability improve, along with our ability to estimate them, this external reproducibility and the ability to tie each system back to first principles measurements define accuracy and precision for each system.

These uncertainties also determine how well we can compare between isotopic systems, an ultimate goal of EARTHTIME and the larger geochronology community. Decay constant uncertainties dominate our ability to combine data from multiple chronometers, and active research and debate is focused on inter-relating these decay constants through geologic comparisons, for instance dating the same discrete event in time with multiple chronometers.

Did the Moon Form at 4.36 Ga?

CLAIRE L. MCLEOD^{1*} AND ALAN BRANDON¹

¹Department of Earth and Atmospheric Sciences, University of Houston, Science and Research Building 1, Houston, TX, 77204, *clmcleod@central.uh.edu

Magma ocean crystallisation is an important stage of early planetary differentiation and evolution. Estimates for the timing of lunar magma ocean (LMO) crystallisation, and consequent formation of the lunar crust (ferroan anorthosites; FANS, and the Mg suite), is not well constrained with ages spanning from 4.57 Ga to 4.18 Ga^[1,2,3,4]. More recent studies^[5,6] on lunar crustal samples are consistent with a late *c.* 4.36 Ga age for the moon from Sm-Nd, Rb-Sr and Lu-Hf isotopes. The Sm-Nd isotopic systematics of KREEP samples and lunar mare basalts constrains the age of LMO crystallisation from 4.49 Ga to 4.31 Ga^[7], while the Lu-Hf system suggest that the KREEP reservoir also formed *c.* 4.36 Ga^[8]. The U-Pb ages of lunar zircons indicate a potentially older age for LMO solidification at *c.* 4.42 Ga^[9].

To further examine LMO crystallisation and its relationship to the timing of lunar formation, a suite of mare basalts that span the range of petrologic types from the Apollo collection will be evaluated for their Sm-Nd systematics. High-precision ¹⁴²Nd/¹⁴⁴Nd to date indicate a closure age of *c.* 4.34±0.04 Ga for the Sm-Nd mare basalt source reservoirs^[7,10]. With the additional new ¹⁴²Nd/¹⁴⁴Nd data presented here, we will test whether the previously obtained correlation with ¹⁴³Nd/¹⁴⁴Nd represents an isochron with an age *c.* 4.36 Ga, the implication of this being that the mantle source closure time for the basalts is consistent with a rapid LMO solidification following a late lunar formation time. Alternatively, if these new data do not lie on a coupled ¹⁴²Nd-¹⁴³Nd isochron, this would indicate multistage histories for their lunar mantle sources^[11]. In the latter case, the coupled ¹⁴²Nd-¹⁴³Nd data for lunar basalts implies a more protracted differentiation history and are likely more consistent with an early formation time of the Moon.

^[1]Papanastassiou & Wasserburg (1976) *7th LSC* 2035-2054; ^[2]Carlson & Lugmair (1988) *EPSL* 90, 119-130; ^[3]Alibert *et al.* (1994) *GCA* 58, 2921-2926; ^[4]Borg *et al.*, (2011) *Nature* 477, 70-72; ^[5]Borg *et al.* (2013) *LPSC #1563*; ^[6]Carlson *et al.* (2013) *LPSC #1621*; ^[7]Boyett and Carlson (2007) *EPSL* 262, 505-516; ^[8]Gaffney *et al.* (2013) *LPSC #1714* ^[9]Nemchin *et al.* (2009) *NatureGeo* 2, 133-136; ^[10]Brandon *et al.* (2009) *GCA* 73, 6421-6445 ^[11]Munker (2010) *GCA* 7340-7361.

Magma-mixing processes recorded in compositionally zoned titanite from the Ross of Mull Granite, Scotland

G. W. MCLEOD^{1*} AND T. J. DEMPSTER²

¹Earth & Environment, University of Leeds, Leeds, LS2 9JT, UK (*correspondance: g.w.mcleod@leeds.ac.uk)

²Geographical and Earth Sciences, University of Glasgow, G12 8QQ, UK (tim.dempster@ges.gla.ac.uk)

Accessory minerals play a significant role in the control of trace element behaviour and consequently may be crucial in deciphering magma genesis and crystallization histories. Titanite is characterised by slow diffusion of trace elements, and as such may preserve magmatic zoning. The incorporation of REE and HFSE within titanite makes it ideal for assessing petrogenetic processes.

In plutonic environments the detail of petrogenesis is often lost as slow rates of cooling allow minerals to chemically re-equilibrate during sub-solidus diffusion. The Ross of Mull Granite displays a variety of plutonic level magma-mixing phenomena and represents an excellent site to test the potential of titanite to preserve geochemical fingerprints of its genesis. A textural and geochemical investigation of titanite from the pluton reveals that zoning in trace elements strongly correlates with field evidence of magma-mixing processes. Diorite enclaves contain a range of textures indicative of variable states of interaction with the host granite and suggest that a number of discrete mixing events have occurred, both prior to emplacement at the present level and in situ.

Titanites from both the enclaves and the host granite show compositional zoning dominated by fine-scale oscillatory types as well as major discontinuities linked to dissolution events associated with changes in titanite, and associated ilmenite, stability. The zones reflect growth during changing melt chemistry and correlate with variations in REE and HFSE. Introduction of fresh diorite magma into the granite host, and the subsequent mixing processes, induced compositional, temperature and oxygen fugacity changes to which titanite responded. Processes recorded by titanite zoning include; (i) homogenisation of crystal free melts; (ii) crystal transfer and scavenging between partially crystallised magmas; (iii) melt segregation and transfer from crystalline enclaves; and (iv) late-stage diffusive exchange. Titanite thus records both localised and distal mixing activity and is capable of revealing many otherwise hidden events within the magma chamber.

Trace element partitioning between carbonate globules and silicate glass in volcanic carbonatites

S. C. MCMAHON^{1*}, E. R. HUMPHREYS-WILLIAMS², C. E. L. GILDER¹, R. A. BROOKER¹, T. E. JEFFRIES²
AND M. J. WALTER¹

¹School of Earth Sciences, University of Bristol, BS8 1RJ, UK (correspondence: sorchamcmahon@bristol.ac.uk)

²Department of Earth Sciences, Natural History Museum, Cromwell Road, London, SW7 5BD, UK (E.Williams@nhm.ac.uk)

The origin of globular-shaped carbonate in silicate glass in carbonatites is subject to much debate. Whether such 'globules' represent immiscible carbonatite melts or rounded calcite crystals has important implications for calcio-carbonatite genesis. Here we present major and trace element analyses of carbonate and silicate glass from volcanic carbonatites in the Calatrava Volcanic Province (CVP), Spain and the Auvergne, France, as well as new experiments reproducing the CVP textures.

Compelling textural evidence for liquid immiscibility includes curved menisci against silicate melt, and budding of globules (suggestive of coalescence) [1]. However, experiments have shown that similar globules can form as solid carbonate crystals in equilibrium with silicate melt [2]. Experimentally produced immiscible carbonate melts also do not reproduce the stoichiometric calcite and dolomite compositions observed in the natural volcanic carbonatites.

One way to resolve whether the globules formed as melts or solids in natural and experimental samples is to investigate the way elements are distributed between the two phases. LA-ICP-MS has been employed for *in-situ* trace element analysis of both carbonate and glass. Partitioning into a crystalline phase is controlled by the characteristics of the lattice site where the element resides, subject to strictly defined constraints related to the element size (ionic radius) and the charge. Classic Onuma parabolae are observed, suggesting a crystal control over the partitioning in some volcanic carbonatites, with calcite globules representing crystalline carbonate crystallised from carbonate-rich silicate melt. Experimentally we have reproduced these pure calcite 'globules', as well as more complex immiscible alkali-bearing carbonate melts. We report on the partitioning characteristics for both and draw comparisons with the natural samples in order to elucidate their origin as solids or melts.

[1] Bailey *et al.* (2005) *Min Mag* **69**, 907-915 [2] Brooker & Kjarsgaard (2011) *J. Pet* **52**, 1281-1305

Iron supply and cycling on the Oregon-California shelf: Comparisons with the Gulf of Mexico hypoxic zone

JAMES MCMANUS^{1*}, MOUTUSI ROY², SILKE SEVERMANN³, ZANNA CHASE⁴, WILLIAM BERELSON⁵, CLARE REIMERS¹, MIGUEL GOÑI¹, APRIL ABBOTT¹
AND JESSE MURATLI¹

¹Oregon State University, CEOAS, 104 CEOAS Admin Bldg, Corvallis, OR, 97331 (*correspondence: mcmamus@coas.oregonstate.edu,

creimers@coas.oregonstate.edu, mgoni@coas.oregonstate.edu, aabbott@coas.oregonstate.edu, jmuratli@coas.oregonstate.edu)

²Arizona State University, Tempe, AZ, 85287 (Moutusi.Roy@asu.edu)

³Rutgers University, New Brunswick, NJ, 08901 (silke@marine.rutgers.edu)

⁴University of Tasmania, AU (Zanna.Chase@utas.edu.au)

⁵University of Southern California, Los Angeles, CA, 90089 (berelson@usc.edu)

The riverine supply of fine-grained sediment to coastal regions along the Northeast Pacific margin generates a patchy "depositional" setting with sediments containing varying amounts of sands and muds. The mid-shelf adjacent to the Umpqua River, features a mud-rich sediment patch that is relatively rich in operationally defined reactive iron. Reactive iron concentrations here covary with the distribution of organic material, suggesting that there may be a coupling between their delivery and burial.

Downcore profiles of dissolved iron from a number of locations along the Oregon margin shows that sediments can range from being relatively enriched to depleted in dissolved iron concentrations. Although this pattern may point to a connection between the diagenesis of continentally derived sediment and the iron supply to coastal waters from the sediments, other factors such as rates of fluid advection, bottom water dissolved oxygen contents, and the availability of fresh organic material likely influence net iron transport across the sediment-bottom water boundary. In an effort to separate some of the factors that might influence dissolved iron input to the overlying water column, we compare iron benthic fluxes along the Oregon and California margin with fluxes from the "hypoxic" shelf region in the Gulf of Mexico. Our results do not suggest significantly greater benthic iron fluxes within the Gulf of Mexico compared to the Oregon and California margins.

Materials from geochemically inspired studies : from Titan's tholins to extremophile bacteria

PAUL F MCMILLAN¹

¹Dept. of Chemistry, University College London, 20 Gordon St., London WC1H 0AJ, UK

Geochemistry and experimental geology studies have long been linked to the identification and processing of new materials with great technological importance and high societal impact. Examples range from hydrothermal and sol-gel synthesis of ceramics to development of techniques for *in situ* studies of functional materials under extreme conditions. New research extending from planetary sciences to deep life geochemistry are leading to new developments in nanomaterials technology and biochemical processing with medical and forensic applications. Here we describe and discuss recent results that extend from fundamental studies and interplanetary based observations of Titan's atmospheric aerosols to new materials being developed for efficient charge storage and energy use applications on Earth, to the involvement of new studies of extremophile bacteria in the deep Earth environment to development of nanotechnology and biomedical applications. These examples will illustrate the continued and emerging links between geochemistry, advanced materials science and biology, with enormous benefits to society.

Secondary organic aerosol formation in aerosol water: Impact on aerosol physical properties

V. FAYE MCNEILL¹

¹Department of Chemical Engineering, Columbia University, New York, NY, USA 10027 vfm2103@columbia.edu

The chemistry of atmospheric aerosols influences their direct and indirect effects on climate. Inorganic aerosols may acquire an organic component via *in situ* interactions with volatile organic compounds (VOCs), a family of processes known as secondary organic aerosol (SOA) formation. SOA formation is one of the greatest sources of uncertainty in estimations of aerosol climate forcing. Pathways for aqueous-phase SOA formation have been identified in which water-soluble VOCs dissolve into cloud droplets or wet aerosols, followed by aqueous-phase reactions which lead to the formation of SOA material. Our recent laboratory studies show that particle-phase chemical reactions between organics and inorganic salts can lead to secondary organic products which absorb light in the UV and visible, thus changing the optical properties of the particle. We have also shown that aqueous-aerosol SOA products may be surface-active, therefore potentially enhancing the ability of small particles to nucleate cloud droplets (CCN activity). In addition to these bulk surfactant effects, our work demonstrates that the surface adsorption of methylglyoxal and acetaldehyde from the gas phase can depress aerosol surface tension and increase CCN activity. Finally, I will introduce a photochemical model of coupled gas and detailed aqueous aerosol chemistry that we have developed in order to study the formation of secondary organic aerosol material in aerosol water and the associated changes in aerosol physical properties. I will present results for atmospheric scenarios and highlight needs for additional experimental work.

Production of archaeal lipid biomarkers in stable isotope labeled incubations of MCG-rich sediments

T. B. MEADOR^{1*}, G. KUIPPERS¹, C. LAZAR^{1,2}, M. KÖNNEKE¹, A. TESKE² AND K.-U. HINRICHS¹

¹MARUM Center for Environmental Sciences and Department of Geochemistry, University of Bremen, 28359 Bremen, Germany (*correspondence: tmeador@marum.de)

²Department of Marine Sciences, Univ. North Carolina at Chapel Hill, Chapel Hill, NC 27599-3300, USA

The Miscellaneous Crenarchaeota Group (MCG) exhibit a global-distribution in anoxic, aquatic sediments and occur throughout a variety of distinct geochemical sediment regimes [1]. Several researchers have proposed that MCG live heterotrophically on organic carbon sources that are buried in the seafloor [1, 2], and Lloyd *et al.* [3] recently identified peptidases within the MCG genome; however, there is still no direct evidence of the metabolic strategy employed by these archaea. We incubated MCG-rich sediments from the White Oak River estuary anaerobically with deuterated (D) water and ¹³C-bicarbonate [cf. 4], and determined the growth response of the MCG community in response to the addition of various organic substrates by quantifying the production of archaeal intact polar lipid (IPL) biomarkers, including compounds thought to be specific for MCG.

After a period of 145 days, evidence of D uptake into IPLs containing crenarchaeol indicated that several substrates stimulated benthic Crenarchaeota, which was supported by increases in the relative abundance of MCG clones in archaeal 16s rRNA clone libraries by up to 30%. The incubations amended with monosaccharides, peptone, or with yeast extract and acetate showed the highest label incorporations, translating into an ~ 5-fold increase in cell production rate, relative to a control incubation with no substrate amendment. Given that only minimal ¹³C was incorporated into archaeal lipids, our data are consistent with heterotrophic growth by MCG. Furthermore, these findings provide new evidence for the benthic production of crenarchaeol, likely by MCG, which is in conflict with the presumed planktonic source of this biomarker [e.g., 5].

[1] Kubo *et al.* (2012) *ISME J.* **10**, 1949-65. [2] Biddle *et al.* (2006) *PNAS* **103**, 3846-51. [3] Lloyd *et al.* (2013) *Nature* doi.10.1038/nature12033. [4] Wegener *et al.* (2012) *Environ. Microbiol.* **14**, 1517-27. [5] Sinninghe-Damsté (2002) *J. Lipid Res.* **43**, 1641-51.

Reconstructing the magma feeding system of the Cappadocian ignimbrites (Turkey) through amphibole thermobarometry

E. MEDARD¹, J.-L. LE PENNEC¹, J.E. FRANCOMME¹
A. TEMEL² AND F. NAURET¹

¹Clermont Université, UBP/CNRS/IRD, Laboratoire Magmas et Volcans, 5 rue Kessler, 63038 Clermont-Ferrand, France (E.Medard@opgc.univ-bpclermont.fr)

²Hacettepe University, Faculty of Engineering, Department of Geological Engineering, 06800, Beytepe-Ankara, Turkey

The Cappadocia area of Central Turkey superbly exposes a succession of Neogene dacitic to rhyolitic ignimbrites and fallout deposits, recording 10 Ma of magmatic activity. This provides an excellent example of long-lived, relatively low frequency magmatic system, with a low average magma production rate (about 10⁻³ km³/a), but short-lived large eruptions (up to 300 km³ for the Cemilköy ignimbrite). Most of the ignimbritic and fallout units share a very similar, low-variance, phenocryst mineralogy (plagioclase + biotite + amphibole + magnetite + quartz), which makes them perfect targets for Al-in amphibole barometry.

An accurate Al-in hornblende barometer has been recalibrated from literature data and new experiments on the Kızilkaya ignimbrite. This new barometer takes into account the effect of both edenite and Tschermack substitutions on Al concentrations. Our data, combined with existing literature data, show a very good pressure-dependence of the Tschermack substitution (correlation coefficient of 0.95) for amphibole in equilibrium with biotite, plagioclase and quartz. Our new barometer reproduces experimental pressures with an average error of 36 MPa in the 100-400 MPa range. More experiments are underway to improve the barometer's accuracy.

Pre-eruptive temperatures are relatively stable for most units, between 700 and 760 °C. Amphiboles crystallized in the upper crust, between 9 and 14 km depth, hinting at a constant depth of magma storage beneath the Cappadocian ignimbrite field. Detailed investigation of one of the youngest unit, the Kızilkaya ignimbrite, produces a tight unimodal pressure distribution at 260 ± 20 MPa (9.8 ± 0.8 km depth), with a maximum data dispersion lower than the 2σ uncertainty of the barometer. If the erupted reservoir was homogeneous, as suggested by the absence of magma mixing, and amphibole was present in the entire reservoir, the aspect ratio of the magma chamber would be relatively low, with a minimum diameter of 7.5 km and a 1.5 km maximum height.

From small-scale chemical processes to long-term (radioactive) contaminant migration predictions

JOHANNES C.L. MEEUSSEN¹, THOMAS J. SCHRÖDER¹
AND JORIS J. DIJKSTRA²

¹Nuclear Research and Consultancy Group Petten, The Netherlands. (* Correspondence: meeussen@nrg.eu)

²Energy Research Centre of the Netherlands, Petten The Netherlands(j.j.dijkstra@ecm.nl)

Migration rates of (radioactive) contaminants in porous materials, such as soil rock and concrete, are dominated by distribution of ions over pore solution and solid phase. Precipitation and adsorption are small-scale chemical processes that determine the distribution and in this way control migration rates at larger scales. The often multicomponent nature of such interactions results in a strong dependence of single element behaviour on chemical conditions, which complicates the translation of experimental results to field conditions. Credible contaminant migration predictions require a model that contains the major soil reactive phases / surfaces, e.g. the different oxide and organic matter surfaces, dissolved organic carbon, including their mutual chemical interactions in a thermodynamic consistent way[1]. The combined CD-MUSIC model for oxides, the NICA-DONNAN model for organic matter, and the LCD model go a long way achieving this. To accommodate these combined models an advanced numerical framework is required[2]. It is, however, important to realize that whatever the assumed sophistication of the conceptual- or numerical model, careful evaluation of model accuracy is essential for its usefulness in practice. Such an evaluation can only be done by testing the model on truly independent data [3].

[1] Schröder et al. (2005), *Environmental Science & Technology* 39, 7176-7184. [2] Meeussen, (2003), *Environmental Science & Technology* 37, 1175-1182. [3] Dijkstra, et al. (2009) *Environmental Science & Technology* 43, 6196-6201.

The structural determinants of silicon fractionation properties of silicate minerals: a First-Principles Density Functional Study

M. MÉHEUT^{1*} AND E. A. SCHAUBLE²

¹GET, Université Paul Sabatier, Toulouse, France

(*correspondence: meheut@get.obs-mip.fr)

²ESS Dept., UCLA, Los Angeles, USA

Silicon is among the new isotopic systems that are emerging due to recent analytical progress in mass spectrometry. Thorough understanding of the parameters influencing natural Si-isotope variation is therefore of great importance to assess potential geochemical applications.

Ab initio methods based on density functional theory have proven successful in predicting equilibrium fractionation factors as a function of temperature (e.g., 1). We use the PBE functional, combined with norm-conserving pseudopotentials and plane wave basis sets. We focused on phyllosilicate minerals: kaolinite, lizardite, talc and pyrophyllite, which appear to span a wide range in fractionation properties despite having the same basic silicate polymerization. In this family of silicates, calculated Si isotope fractionation appears to be correlated with chemical composition:

$$\Delta^{30}\text{Si}(\text{min, quartz}, T) = \sum a_X(T) \frac{X^{\text{eq}}}{\text{Si}^{\text{eq}}} \quad (1)$$

with X^{eq} representing the cation equivalents of $X=\text{Al, Mg, Si}$, i.e. the number of $\frac{1}{2}(\text{SiO}_2)$, $\frac{1}{3}(\text{Al}_2\text{O}_3)$, (MgO) units in the mineral, and $a_X(T)$ is a parameter depending on temperature. Further analysis leads us to interpret this relationship as an electron donation effect, such that $a_X(T)$ should increase with decreasing electronegativity of X. To assess the generality of this relationship, we computed fractionations for a more diverse suite of minerals. Within the $\text{MgO-Al}_2\text{O}_3\text{-SiO}_2$ system, relation (1) continues to hold for quartz, pyrope and enstatite ($R^2 = 0.99$, $n=7$), but forsterite is strongly anomalous. To assess the effects of Ca^{2+} , Na^+ , K^+ and tetrahedral Al^{3+} on Si fractionation, we computed the properties of albite, anorthite, microcline, diopside, wollastonite, jadeite, grossular, and the three Al_2SiO_5 polymorphs. Preliminary results suggest almost all of these minerals follow relation (1) reasonably well (excepting wollastonite), if tetrahedral Al^{3+} is assumed to have no effect on Si fractionation ($\Delta^{30}\text{Si}(\text{Al}^{3+})=0$).

These results suggest that particular attention should be given to chemical compositions in Si isotope studies.

[1] Meheut et al. (2009) *Chem. Geol.* **258**, 28

Speciation and thermodynamic properties of palladium chloride and bisulfide complexes: insights from experiments and *ab-initio* molecular dynamics simulations

YUAN MEI^{1,2}, T. M. SEWARD³, JOËL BRUGGER^{1,4},
STEPHEN J. BARNES² AND MARCO L. FIORENTINI⁵

¹School of Earth and Environmental Sciences, The University of Adelaide, Australia (yuan.mei@adelaide.edu.au)

²CSIRO Earth Science and Resource Engineering, Australia

³Victoria University of Wellington, New Zealand

⁴South Australian Museum, Australia

⁵CET/CCFS, The University of Western Australia, Perth, Australia

Characterising the speciation and solubility of platinum group elements (PGE) in hydrothermal fluids is useful in understanding the formation of PGE deposits, and for supporting the development of new exploration tools for high value magmatic nickel sulfide deposits, whose small footprints may be extended by hydrothermal remobilisation of PGE. A number of experimental studies have investigated Pd speciation and solubility in hydrothermal chloride solutions, with reasonable agreement over the nature and stability of Pd(II) chlorocomplexes (Barnes and Liu, 2012). In contrast, there are significant discrepancies among the available thermodynamic properties for the predominant Pd bisulfide species. This uncertainty severely hinders numerical modelling of PGE mobility in hydrothermal fluids.

Ab-initio molecular dynamics (MD) simulations were performed to investigate the stability of possible Pd-Cl and Pd-HS complexes in hydrothermal fluids. The simulations revealed the preference of four-fold square planar structures of both chloride and bisulfide complexes at high P,T (300 °C, 500 bar). We are building a geochemical model for Pd transport via thermodynamic integration (Mei *et al.*, 2013). The species geometry and thermodynamic properties derived from the MD simulations will be compared with the existing thermodynamic properties (Boily and Seward, 2005) and with new EXAFS measurement of Pd chloride complexes in hydrothermal brines up to 340 °C.

[1] Barnes and Liu (2012) *Ore Geol. Rev.*, **44**, 49–58. [2] Boily and Seward (2005) *Geochim. Cosmochim. Acta.*, **69**, 3773–3789 [3] Mei, Sherman, Liu, Brugger (2013) *Geochim. Cosmochim. Acta.*, **102**, 45–64.

Protein-silica interactions: The effect of lysozyme on the structure of amorphous silica

D.B. MEIER^{1*}, D.J. TOBLER², C.L. PEACOCK¹
AND L.G. BENNING¹

¹ School of Earth and Environment, University of Leeds, United Kingdom (*correspondence: eedbm@leeds.ac.uk)

² Nano-Science Center, Department of Chemistry, University of Copenhagen, Denmark

Amorphous silica is one of the two dominant biominerals in the world's oceans where it is precipitated by diatoms, radiolarians or siliceous sponges. Furthermore, in geothermal settings microorganisms can become quickly silicified through the precipitation of silica from under- or oversaturated geothermal waters. In both cases, the interaction between amorphous silica and cell internal or cell wall macromolecules, like proteins, are crucial for templating the siliceous structures or for enhancing microbial silicification [1, 2]. However, how and if proteins affect the structure, composition and morphology of amorphous silica at the molecular level is only poorly understood

Here, we quantified the effect a typical protein (lysozyme) has on the atomic structure and composition of amorphous silica that was precipitated from supersaturated aqueous solutions in the absence or presence of variable lysozyme concentrations (0 – 10'000 ppm).

Synchrotron-based pair distribution function (PDF) analyses showed only a minor change in the short range ordering (>15 Å) of amorphous silica precipitated in the presence of ≥ 1000 ppm lysozyme. This suggests limited structural interactions and hardly any incorporation of the lysozyme within the amorphous silica structure. Fourier Transform Infrared (FTIR) spectroscopic analyses however, indicate significant incorporation and surface interaction between lysozyme and amorphous silica at all lysozyme concentrations.

Further PDF and FTIR experiments are underway to test for artifacts and to confirm the findings reported above. Moreover, thermogravimetric analyses, X-ray diffraction, total carbon analyses and high resolution microscopy will help to quantify the ratio of incorporated to adsorbed protein contents, the water contents, and the morphology of amorphous silica as a function of protein content.

[1] Perry & Keeling-Tucker (2000), *Journal of Biological Inorganic Chemistry*, **5**, 537-550. [2] Tobler, Stefansson & Benning (2008), *Geobiology*, **6**, 481-502.

Multi-element 2D analysis of drilling cores containing mining residues using LIBS and chemometric analysis

J.A. MEIMA

Bundesanstalt für Geowissenschaften und Rohstoffe (BGR)
Hannover, Germany (jeannet.meima@bgr.de)

Laser-induced breakdown spectroscopy (LIBS) is a type of atomic emission spectroscopy that uses a laser-generated plasma to ablate, atomize, and excite material from a sample surface. LIBS has potential for rapid non-destructive and in-situ geochemical analysis. However, quantitative analysis with LIBS, especially of heterogeneous materials, is very challenging; matrix effects and plasma variations influence the LIBS signal. These limitations have successfully been overcome using multivariate chemometric methods and repetitive measurements in other applications [e.g. 1].

This study tries to estimate limits of detection and accuracy for multi-element LIBS analysis of drilling cores containing mining residues (Harz, Germany) with the LIBS system described below. The LIBS system uses a Nd:YAG 50 mJ 1064 nm laser and an Echelle spectrograph with CCD detector (285-960 nm, resolution 28-94 pm). On the drilling cores, nine meter in total and each one cut in halve, 1000 x 12.5 mm large surface strips were measured, representing 20000 individual (5 accumulated laser shots each) LIBS measurements. Over 100 alternating layers consisting of sludge, Pochsand or wall rock were found; all layers were sampled and analysed by XRF as reference samples. A calibration model was developed with Partial Least Square Regression (PLSR) analysis.

A qualitative LIBS analysis based on characteristic emission lines for heavy metals and major elements has shown, that significant chemical differences may exist between layers. Inside a layer of sludge or wall rock, the LIBS signal appears to be relatively constant. On the other hand, Pochsand layers that consist of very coarse sand appear to be very heterogeneous; heavy-metal enrichment is clearly related to distinct particles. Multivariate chemometric analysis on the relatively homogeneous layers is currently applied to build and test calibration models for a quantitative interpretation of the LIBS measurements.

[1] Sirven *et al.* (2006) Anal. Chem. 78, 1462-1469.

H₂O-adsorption at the (100)-pyrite surface: Forcefield simulation studies supporting GIXRD-experiments

S. MEIS^{1*}, U. MAGDANS², X. TORRELLES³ AND H. GIES¹

¹Institute of GMG, Ruhr-University Bochum, 44780 Bochum, Germany, (*correspondance: sandrina.meis@rub.de)

²IA Physics, RWTH Aachen, 52056 Aachen, Germany, (magdans@physik.rwth-aachen.de)

³ICMAB-CSIC, Campus de la UAB, 08193 Bellaterra, Spain, xavier@icmab.es

It is of great importance to study mineral-adsorbate interfaces, because in natural processes mineral surfaces are able to function as templates for the ordering of organic molecules and water. The periodically ordered surface atoms induce an ordering of the adsorbates, so that specific chemical reactions can take place near surfaces. The (100)-pyrite (FeS₂) surface plays an important role in many environmental, biological and mineralogical processes, e.g. in acid mine drainage processes and in the Iron-Sulphur world scenario, that describes one possibility for the origin of life [1].

The structure of the (100)-FeS₂-H₂O interface was determined with grazing incidence X-ray diffraction experiments under environmental conditions, previously [2]. An adsorption model for H₂O at the (100)-FeS₂ surface was determined including three adsorption layers in a distance of 1.9(1)Å, 3.0(3)Å and 5.4(4)Å to the surface, a transitional zone of partial ordered H₂O molecules and H₂O molecules that occupy vacancies of the topmost FeS₂-layer.

Here we report about molecular dynamic (MD) simulations of the H₂O-adsorption on the (100)-FeS₂ surface, carried out with the program package Materials Studio 5.0, particularly the program "Adsorption locator", from Accelrys Inc. Using the forcefield COMPASS27 we confirmed the experimental achieved adsorption model of H₂O. Additionally we determined the orientation of H₂O-molecules within the adsorption layers, the exact positioning of the H-atoms and we get information about the influence of the H₂O-density on the ordering within the adsorption layers. The comparison of the experiment and different MD simulations is well suited to get detailed information about the atomic structure of the (100)-FeS₂-H₂O-interface and to get information about interface systems under perfect adsorption conditions compared to interface systems exposed to higher entropy.

[1] G. Wächtershäuser, C. Huber (1998), Science 281 670-672. [2] S. Meis, U. Magdans, X. Torrelles (2011), Acta Cryst. A67, C338-C339.

Osmium isotope and PGE reference materials OKUM and MUH-1

T. MEISEL^{1*}, O.M. BURNHAM², C. KRIETE³
 SYED N. H. BOKHARI¹ AND T. SCHULZ⁴

¹Montanuniversität, 8700 Leoben, Austria (*correspondence: thomas.meisel@unileoben.ac.at)

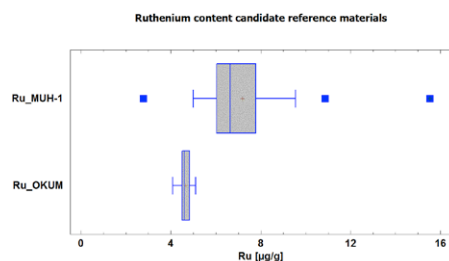
²Geoscience Laboratories, Ontario Geological Survey, Sudbury, ON Canada P3E 6B5

³Federal Institute for Geosciences and Natural Resources, 30655 Hannover, Germany

⁴University of Vienna, Austria

As for many isotope systems, certified reference materials (CRM) of *real* samples are very sparse. Solutions with known isotopic composition exist for QA/QC purposes, but for the evaluation of the combined standard measurement uncertainty *matrix matched* CRM need to be applied. For method validation, calibration and verification purposes of Os isotopic composition and platinum group element content (PGE) two ultramafic RM with different matrices have been prepared. OKUM, an ultramafic komatiite and MUH-1, a depleted harzburgite (Kraubath, Austria) have been prepared and are already certified for major and trace elements by an interlaboratory certification process lead by the International Association of Geoanalysts (IAG). Whereas the dominant PGE bearing phases in lherzolites are sulfides, the dominant phases in harzburgites are alloys and laurites. As a result, the homogeneity of harzburgites with respect to PGE distribution is generally much worse than for lherzolites and komatiites.

Initial homogeneity tests with 2 g and smaller test portion sizes demonstrate this significant difference.



This test already demonstrates that validated methods with lherzolithic RM such as UB-N cannot be applied to harzburgites as these are generally heterogeneous.

Both RM show PGE distributions typical for mantle restites and komatiite melts with ¹⁸⁷Os/¹⁸⁸Os of 0.127 and 0.27 respectively and thus ideal matrix RM for mantle studies.

Early diagenetic quartz formation at a deep iron oxidation front in the Eastern Equatorial Pacific

P. MEISTER^{1*}, B. CHAPLIGIN², A. PICARD³, H. MEYER²,
 C. FISCHER⁴, D. RETTENWANDER⁵, G. AMTHAUER⁵,
 C. VOGT⁴ AND I.W. AIELLO⁶

¹Max-Planck Institute Marine Microbiology, 28359 Bremen, Germany (*correspondence: pmeister@mpi-bremen.de)

²Alfred Wegener Institute, 14473 Potsdam, Germany

³Eberhard Karls University, 72076 Tübingen, Germany

⁴University of Bremen, 28359 Bremen, Germany

⁵University of Salzburg, 5020 Salzburg, Austria

⁶Marine Laboratories Moss Landing, CA 95039-9647, USA.

Diagenetic quartz formation at low temperature is still not well understood. Lithified chert consisting of microcrystalline quartz was recovered at ODP Site 1226 in the Eastern Equatorial Pacific [1] near the base of a 420 m thick Miocene-Holocene sequence of nanofossil and diatom ooze. Precipitation temperatures calculated from oxygen isotope values in the cherts are near to present porewater temperatures, and a sharp depletion in dissolved silica occurs at 385 m, indicating that silica precipitation is still going on.

It has been observed that quartz forms in experiments in the presence of fresh precipitated iron oxyhydroxides [2]. Indeed, a deep iron oxidation front occurs above 400 m sediment depth, which is caused by upward diffusing nitrate from an oxic seawater aquifer in the underlying basaltic crust. Sequential iron extraction and analysis of the X-ray absorption near-edge structure (XANES) revealed that iron in the cherts predominantly occurs as illite and amorphous iron oxide, whereas iron in the nanofossil and diatom ooze occurs mainly in smectites. Mössbauer spectroscopy confirmed that the amorphous iron in the cherts is largely oxidized.

Two possible mechanisms may be operative during early diagenetic chert formation at iron oxidation fronts: (1) quartz precipitation may be initiated by adsorption of silica to freshly precipitated iron oxides. (2) Iron oxidation lowers the pH, which brings the reactive surfaces of iron oxides closer to the zero point of charge, facilitating the binding of SiO₂. We suggest that the formation of early-diagenetic chert at iron oxidation fronts is an important process in suboxic zones of silica-rich sediments. The largest iron oxidation front ever occurred during the great oxidation event ca. 2.5 Ga ago, when large amounts of iron and chert beds were deposited.

[1] D'Hondt *et al.* (2002) *Proc. ODP, Init. Repts.* **201**. [2] Harder & Flehmig (1970) *Geochim. Cosmochim. Acta* **34**, 295-305.

B content and $\delta^{11}\text{B}$ from cultured diatoms (*Thalassiosira weissflogii* & *T. pseudonana*): Relationship to $\text{pH}_{\text{seawater}}$ and diatom C acquisition

*L.M. MEJÍA¹, J. FIETZKE², K. ISENSEE¹, A. MÉNDEZ¹, J. PISONERO¹, N. SHIMIZU³, C. GONZÁLEZ¹, B. MONTELEONE³ AND H. STOLL¹

¹Universidad Oviedo, C/ Arias de Velasco s/n, 33005 Oviedo, Spain. *correspondence: [luzmamera2@yahoo.com]

²Helmholtz Centre for Ocean Research Kiel, Wischhofstr. 1-3, 24148 Kiel, Germany

³WoodsHole Oceanographic Institute, Woods Hole, USA

Despite the importance of diatoms in regulating climate, most geochemical records are based on carbonates. Among them, B content and $\delta^{11}\text{B}$ has been widely used to reconstruct pH from foraminifera and coral fossils. We present preliminary results of $\delta^{11}\text{B}$ on diatom opal and compare them to $\delta^{11}\text{B}$ on inorganically precipitated opal. We measured B content in opal with the aim of determining if [B] can be used as a pH proxy or to identify physiological responses to acidifying pH.

Thalassiosira pseudonana and *Thalassiosira weissflogii* were cultured at varying pH and Si and C quotas were determined. Frustule B content was measured by LA-ICPMS and ion probe. Cells of both species grown at higher pH have higher [B] and higher Si requirements per fixed C. If this trend is representative of diatom silicification in a future more acidic ocean, it could contribute to changes in the efficiency of diatom ballasting and C export, as well as changes in the diatom abundance in the phytoplankton community in Si-limited regions. If B enters the cell through the same transporter employed for HCO_3^- uptake, an increased HCO_3^- requirement with decreasing CO_2 concentrations, and higher $\text{B(OH)}_4/\text{HCO}_3^-$ ratios would explain the observed increase in frustule B content with increasing pH.

With current analytical precision, frustule [B] is unlikely to resolve ocean pH with a precision of paleoceanographic interest. However, if B content was controlled mainly by HCO_3^- uptake, then B content measurements might reveal the varying importance of active HCO_3^- acquisition in the past. Though as occurs with B content, $\delta^{11}\text{B}$ may depend either on seawater pH and/or biomineralization processes, preliminary $\delta^{11}\text{B}$ results show very low values, which agrees with the very low pH at the site of silicification (~5). At this acidic pH, it is very unlikely that $\delta^{11}\text{B}$ provides enough sensitivity to reconstruct $\text{pH}_{\text{seawater}}$. Conversely, $\delta^{11}\text{B}$ in diatom opal may be used to constrain $\delta^{11}\text{B}_{\text{seawater}}$, which is very important for foram-based pH reconstructions.

Investigation of the processes of organic matter diagenesis in sediments of Lake Beloye, West Siberia, by the pyrolytic methods

V.N. MELENEVSKY^{1*}, G.A. LEONOVA², V. A. BOBROV², A.S. KONYSHEV⁴ AND A.E. MALTSEV⁵

^{1,4}A.A. Trofimuk Institute of Petroleum Geology and Geophysics, Siberian Branch of the Russian Academy of Sciences, Russia (*correspondence: vmelenevsky@yandex.ru)

^{2,3,5}Institute of Geology and Mineralogy, Siberian Branch of the Russian Academy of Sciences, Russia

During diagenesis, biopolymers (proteins, fats, carbohydrates, lignin, etc. synthesized by animals and plants) of organic matter (OM) transform into a geopolymer - the so-called kerogen composing most of the OM of ancient sediments. Starting from the sedimentation and deposition of OM of plant and animal genesis, many biochemical and chemical reactions run in it.

Study of the Holocene sediments of Lake Beloye (West Siberia) in the depth range 0 – 137 cm gave an insight into the transformation of organic matter (OM) at the early stages of diagenesis. Analysis of OM was performed by pyrolytic methods (Rock Eval (RE) and pyrolysis + gas chromatography-mass spectrometry (Pyr-GC-MS)). RE pyrolysis is intended for the identification of oil source rocks, but owing to its simplicity and reliability, this method has been widely used for the study of immature OM in soils and recent lacustrine and marine sediments [1, 2]. The Pyr-GC-MS is the main method for the study of the molecular composition of protokerogen. It consists in conducting the flash-pyrolysis at >600 °C with a subsequent gas chromatography-mass spectrometry analysis of the products [3]. Using RE and Pyr-GC-MS methods, 15 and 8 samples have been studied, respectively. The results of the work are presented in detail in [4].

The work has shown that the macromolecular aliphatic structure of the kerogen and the precursors of sterane and hopane geomolecules – sterenes and hopenes – form at the early stages of diagenesis. We suggest that macrophytes and bacteria are the main sources of OM for the studied lacustrine sediments.

[1] Disnar *et al.* (2003) *Org. Geochem.* **34**, 327–343. [2] Sebag *et al.* (2006) *European J. Soil Sci.* **57**, 344–355. [3] Jocteur- Montrozier and Robin, (1988). *Revue d'Ecologie et de Biologie du Sol.* **24**, 203–214. [4] Melenevskii *et al.* (2011) *Russian Geology and Geophysics* **52**, 583–592.

Geochemistry of the Salma eclogites (Belomorian mobile belt, Baltic Shield)

A.E. MELNIK

Institute of Precambrian geology and geochronology RAS,
St. Petersburg, Russia (meliks1@yandex.ru)

In the north-western part of the Belomorian mobile belt were found numerous bodies of an eclogitic rocks, which were named Salma eclogites [1]. Salma eclogites include two types of eclogitic rocks (after basic and after ultrabasic rocks) which occur as tectonic blocks of various size and shape in gneisses. Sm-Nd (grt-cpx-wr) and a local zircon U-Pb dating give the eclogites ages of 1.9 Ga [2]. The data have not proved previously published the Archean values of eclogite metamorphism age. The eclogites are variably affected by overprinted amphibolization. So, rims of Salma eclogite bodies are commonly strongly amphibolized and also some bodies are completely replaced by amphibolites. Geochemistry of REE and trace elements in the eclogites and garnet amphibolites (completely retrogressed eclogites) were investigated using ICP-MS. Both basic and ultrabasic less retrograded eclogitic rocks have an almost flat chondrite-normalised REE patterns (YbN/LaN – 1,15-1,96) (Fig. 1). Retrogressed Salma eclogites and garnet amphibolites after eclogites in comparison with fresh rocks are enriched in REE (especially in LREE) and trace elements (U, Th, Nb, Ti, Zr). The enrichment in REE and high field strength elements is caused by fluid affection during retrograde metamorphism.

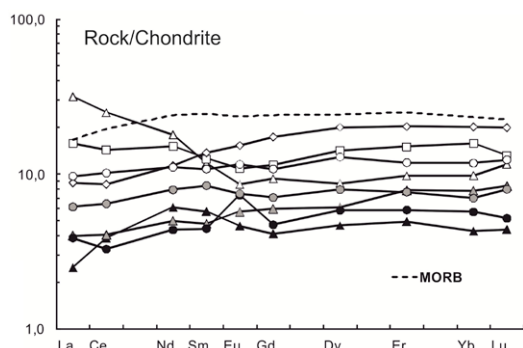


Figure 1: REE distribution in Salma eclogites (solid symbols - ultrabasic eclogites; gray symbols - basic eclogites; open symbols - retrogressed eclogites and garnet amphibolites after eclogites).

[1] Konilov *et al.* (2004) 32nd IGC Abstracts (pt. 1) 108.

[2] Skublov, Berezin, Melnik (2011) *Petrology* 19, 470-495.

Geochemical characteristics of volcanic and plutonic rocks in the 36 Ma Organ Mountains caldera, USA: Are they telling the same story?

V. MEMETI^{1*} AND J. DAVIDSON¹

¹Durham University, Dept. of Earth Sciences, Durham, DH1
3LE, UK, (email: valbone.memeti@durham.ac.uk)

Volcanic and plutonic rocks are often studied as separate magma systems as they naturally represent different crustal depth levels. Results from such studies have often led to inconsistent interpretations regarding the geochemical processes and the time scales responsible for the compositional variations. This has resulted in a blurred understanding of the connection between these two sub-systems and how magma plumbing systems operate over time.

We are examining the ~36 Ma Organ Mountains caldera in New Mexico, USA, where contemporaneous volcanic and plutonic rocks of the same arc magma system are juxtaposed due to extensional tectonics along the Rio Grande Rift. Detailed geologic and structural mapping [1] and high precision ⁴⁰Ar/³⁹Ar ages of both volcanic and plutonic rocks [2] provide an excellent framework to study the geochemical evolution and connection of both rock types for >2.5 myrs of active magmatism. Three caldera-forming ignimbrites erupted within 600 kyrs [2] from this system with a total erupted volume of 500-1,000 km³ next to less voluminous pre- and postcaldera trachyte and andesite lavas. The ignimbrite sequence is zoned from a crystal-poor, high-SiO₂ rhyolite at the base to a crystal-rich, low-SiO₂ rhyolite at the top. This compositional zoning pattern of increased silica is also seen from the top downward in the main intrusion, the Organ Needle batholith, which has been interpreted to be the source for the ignimbrites [1]. The plutons are composed of granodiorite and syenite, and minor diorite and leucogranite.

We will present major oxide, trace element and Sr, Nd and Pb isotope analyses of whole rocks for all plutonic and volcanic units as well as CL images and electron microprobe analyses on individual minerals and discuss 1) the geochemical relationship at rock and mineral scales of all rocks including pre- and postcaldera forming units, 2) the magmatic process(es) responsible for the compositional variations in both rock types, and 3) the possible cause(s) for the large ignimbrite eruptions as well as the smaller sized lava flows if they were derived from the underlying intrusions.

[1] Seager (1980), NM Bureau of Mines and Min. Res. Memoir 36, 97 p. [2] Zimmerer & McIntosh (2013) *Journal of Geophysical Research*, v. 93, p. 4421-4433

Insights into boron volatility in magmatic systems

G. MENARD^{1*}, I. VLASTELIC¹, E. F. ROSE-KOGA¹, J. L. PIRO¹ AND C. PIN¹

¹Laboratoire Magmas et Volcans, Université Blaise Pascal, Clermont-Ferrand, France

(*correspondence : g.menard@opgc.univ-bpclermont.fr)

It is generally accepted that boron behaves as a volatile element in magmatic systems but the amount of B leaving magma (i.e. the absolute volatility) is poorly known [1]. In the aim to quantify the losses due to magmatic degassing, B concentration of recent (1977-2010) lavas from Piton de la Fournaise volcano (Réunion Island) were measured by isotope-dilution ICP-MS, using a new method avoiding sample evaporation. Twenty-three samples were selected based on three criteria: 1) samples are highly fresh and not contaminated; 2) they are cogenetic (they show tiny variations in Pb-Sr-Nd isotopes); 3) samples cover a wide range of eruption and degassing conditions, with an order of magnitude variation in magma effusion rate. Samples include massive basalts with variable amounts of cumulative olivine and naturally quenched samples (including Pélé's hairs and scoria).

B content varies from 1.15 to 3.98ppm. B behaving as a highly incompatible during magmatic processes, ratios involving B and another highly incompatible elements such as B/Nb have to be constant in our suite of cogenetic lavas [2]. However, while most samples show uniform B/Nb of 0.14, few samples show anormalous high (quenched samples) or low (first lavas of April 2007) B/Nb ratios. Because the samples are fresh and unaltered and do not include exotic minerals potentially holding B, we interpret these subtle variations as related to degassing processes. The amount of B loss in each sample has then been estimated taking the composition of a primitive olivine-hosted melt inclusion as representative of the undegassed melt composition. Boron loss varies between 10% for less-degassed samples to almost 30% for the first lavas of the April 2007 eruption. Moreover, the knowledge of eruptive history allows us to distinguish B loss during 1) continuous open-system degassing in the magma chamber (10%), 2) lava emplacement and cooling (4-10%) and 3) shallow closed-system degassing due to a vapor accumulation at the top of the magma chamber prior to the April 2007 eruption (5-8%) [3].

[1] Rubin (1997) *Geochim. Cosmochim. Acta* 61, 3525-3542.

[2] Hofmann *et al.* (1986) *Earth Planet. Sci. Lett.* 79, 33-45.

[3] Vlastelic *et al.* (2013) *J. Volcanol. Geotherm. Res.* 254 94-107.

Early diagenesis of sulfur and trace element pyritization in sediments of a tropical upwelling system: Cabo Frio, southeastern Brazil

U. MENDOZA^{1*}, R. DIAZ¹, M. MOREIRA¹, N. AMORIM¹, M.E. BÖTTCHER², W. MACHADO¹, S.R. PATCHINEELAM¹, R. CAPILLA³ AND A.L. ALBUQUERQUE¹

¹Geoquímica Ambiental, Universidade Federal Fluminense, RJ 24020-150, Brazil (*correspondence: ursmendoza@geog.uff.br)

²Marine Geology, Leibniz Institute for Baltic Sea Research Warnemünde, D-18119 Warnemünde, Germany

³Petrobras-Cenpes, RJ 21941-915, Brazil

The early diagenesis of sulfur and the potential effects of sedimentary pyrite re-oxidative cycling on the degree of trace metals pyritization (DTMP) were assessed in short sediment cores from the continental shelf under the influence of a tropical upwelling system (Cabo Frio, Brazil). Under these depositional conditions, the degree of reactive iron pyritization was limited by both dissolved sulfide availability and pyrite oxidation events. Textural analyses of pyrite framboids provide evidence of re-oxidation processes, reflecting dynamic redox conditions in the sediments. The total sulfur, the chromium reducible sulfur (CRS), and degree of pyritization (DOP) values are relatively low, and showed an increase with depth at all stations. The isotope composition of pore-water sulfate (+18.7‰ to +23‰) remained close to the seawater value, but very light stable sulfur isotope signatures of the CRS fraction (-25.2‰ to -40.8‰) are found that reflect intense bioturbation-induced sulfur re-cycling. Relations between DTMP and stable isotope signals are found, suggesting high (Pb, As, Cd and Mn), low (Zn and Cu) or negligible (Cr and Ni) influences by iron sulfide re-oxidation. Pyrite-richer sediments provide an apparent threshold for intense pyrite re-oxidation, while CRS generally becomes more depleted in ³⁴S with increasing depth. This depletion was greatest and becomes less variable when CRS contents exceed ~0.1 wt% (with δ³⁴S values averaging -40‰ ± 1‰), after which most trace elements (Pb, As, Cd, Mn and Zn) presented more accentuated DTMP values. Before the stabilization of the pyrite re-oxidation, the release of Mn and Fe into pore water was evidenced, indicating reduction of these elements. Sulfur isotope signatures of pyrite formed under the oxic bottom water conditions at Cabo Frio are similar to those observed in euxinic sedimentary environments, as the modern Black Sea. It is also indicated, that a superimposition of sulfate reduction and intense oxidative sulfur cycling leading to pyrite re-cycling can affect benthic trace element fixation.

Essential aqueous geochemistry of Pb(II) solid formation

A. MENDOZA-FLORES¹ AND M. VILLALOBOS^{1*}

¹Environmental Bio-Geochemistry Group, Geochemistry Department, Geology Institute, UNAM, Coyoacan, CU, Mexico 04510, D.F. (*correspondence: mariov@geologia.unam.mx)

Lead is a biologically non-essential toxic metal whose biogeochemical cycle has been affected considerably by anthropogenic activities [1]. Its mobility in aqueous environments is determined by its ability to form soluble complexes with organic matter [2], adsorbed complexes on Fe, Mn and Al oxide surfaces [3], and most of all a great variety of solids with major anions such as O²⁻, hydroxyl, carbonate, sulfate, and nitrate [4]. However, the essential aqueous geochemistry of lead has serious gaps of knowledge. In particular, a dubious Pb(OH)₂ solid phase has been proposed [4,5], but never identified, and solubility product constant values with up to four orders of magnitude differences have been reported [6] and incorporated in the databases of the different geochemical speciation codes available. The goal of this work was to test the existence of this hydroxide phase and the validity of its solubility constants.

The solids formed in perchlorate and nitrate electrolyte systems, under closed and open atmospheric CO₂ conditions, were identified by X-ray diffraction and other spectroscopies. We show that no solid phase of Pb(OH)₂ is formed at any pH value, and thus the concentrations of aqueous Pb(II) are controlled by the solubilities of solid oxide phases and combinations of carbonates and hydroxi-carbonates, depending on the conditions imposed on the system. Therefore, widespread geochemical databases must be corrected to exclude Pb(OH)₂ as an actual Pb(II) solid phase forming, to yield more accurate aqueous Pb(II) solubility behavior predictions.

[1] Boutron *et al.* (1983) *Geochim. Cosmochim. Acta* **47**, 1355-1368. [2] Pinheiro *et al.* (1999) *Environ. Sci. Technol.* **33**, 3398-3404. [3] McKenzie *et al.* (1980) *Aust. J. Soil Res.* **18**, 61-73. [4] Elkhatab *et al.* (1991) *Environ. Pollut.* **69**, 269-276. [5] Liu *et al.* (1989) *J. Colloid Interface Sci.* **130**, 101-111. [6] Liu *et al.* (2003) *J. Colloid Interface Sci.* **268**, 266-269.

Evaporation of Mg- and Si-rich melts: evolution of chemical and isotopic compositions of FUN CAIs

R.A. MENDYBAEV^{1*}, F.M. RICHTER¹, F.-Z. TENG², R.B. GEORG³ AND A.V. FEDKIN¹

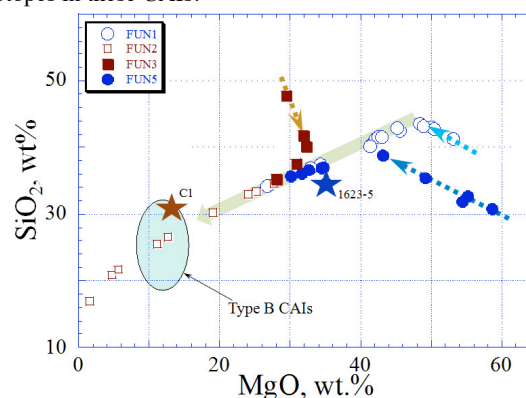
¹University of Chicago, IL, USA (*ramendyb@uchicago.edu)

²University of Washington, Seattle, WA, USA

³Trent University, Peterborough, ON, Canada

Extremely large mass-dependent fractionations of Si, Mg and O isotopes in FUN CAIs suggest that their precursors lost significant amount of matter by evaporation. Chemical and Mg, Si and O isotopic compositions of the residues produced by evaporation of forsterite-rich melts (FUN1 and FUN2) in vacuum at 1900°C suggest that the evaporating component is Mg₂SiO₄ [1]. The evaporation trajectories of FUN1 and FUN2 pass close to the compositions of C1 and Vig1623-5 FUN CAIs, and the measured Mg and Si isotopic compositions of most natural FUN CAIs also plot close to the correlation lines established by the evaporation residues [1].

To test if evaporation of melts with compositions different from the forsteritic melts would result in residues with chemical and isotopic compositions of C1 and 1623-5, we conducted new sets of experiments in which FUN3 and FUN5 melts were evaporated at the same conditions as earlier. Starting FUN3 and FUN5 compositions were obtained by adding MgO and SiO₂ to the C1 (FUN3) and 1623-5 (FUN5) in the amounts required by enrichments in heavy Mg and Si isotopes in these CAIs.



After initial predominant loss of Si (FUN3) or Mg (FUN5), further evaporation results in loss of Si and Mg in forsteritic proportions (constant $a_{\text{MgO}}/a_{\text{SiO}_2}$ in the melt) and the evaporation trajectories are the same as established by FUN1 and FUN2 melts.

[1] Mendybaev *et al.* (2013) *44th LPSC*, Abstract #3017.

The microbial compelling attraction for hydrogarnets in the oceanic crust

B. MENEZ¹; V. PASINI^{1,2}; D. BRUNELLI^{2,3}; C. PISAPIA¹, P. LE CAMPION¹, C. LAVERNE⁴ AND E. GERARD¹

¹ Institut de Physique du Globe de Paris, 1, rue Jussieu - 75238 Paris cedex 05, France (menez@ipgp.fr; pasini@ipgp.fr; pisapia@ipgp.fr; emgerard@ipgp.fr)

² Università di Modena e Reggio Emilia, L.go St. Eufemia 19, 41100 Modena, Italy (valerio.pasini@unimore.it; danielle.brunelli@unimore.it)

³ Istituto di Scienze del Mare – CNR, Via Gobetti 101, 49100 Bologna, Italy

⁴ Laboratoire de Pétrologie Magmatique, Université Paul Cézanne Aix-Marseille III, Faculté des Sciences et Techniques, Avenue Escadrille Normandie-Niemen, 13397 Marseille cedex 20, France (christine.laverne@univ-cezanne.fr)

Microbial life appears to develop deep in the oceanic crust, taking advantage of the redox gradients locally generated during hydrothermal alteration of the crystalline rocks. Nonetheless everything does not seem to be everywhere and habitats are proving to be highly specific, mineralogically¹ speaking. Notably, hydrogarnets were recently shown to represent microbial niches hosted in serpentinized mantle-derived rocks from the Mid-Atlantic ridge. These hydroandraditic garnets ($\text{Ca}_3\text{Fe}_2^{3+}(\text{SiO}_4)_{3-x}(\text{OH})_{4x}$ with trace amounts of Al, Ti, Cr) serve as metabolic substrates likely providing oxidized iron and calcium to the attached microbial community². Far from being anecdotic, such occurrences can be found in other geographically-distant locations along the ridge system as for example in the South Western-Indian ridge, likely signing an extensive process. In addition, the extent does not appear to be limited to the peridotitic portion of the oceanic crust. We present here results obtained on hydroschorlomite, a Ti-, Ca-, Fe-rich andraditic garnet hosted in altered basalts drilled in Hole 1256D during ODP Leg 206 (Equatorial East Pacific)². In situ characterization of the organic carbon speciation at the microscale reveals the presence of microbiologically-derived material in close association with the hydrogarnets found in the deepest cores of basalts (661–749 mbsf). The specificity of these microhabitats will be discussed and compared in terms of chemical and mineralogical characteristics, inferred hosted metabolisms along with their potential as shaping low temperature alteration processes.

[1] Ménez *et al.*, 2012, *Nature Geoscience*, 5: 133-137. [2] Laverne *et al.*, 2006, *Geochemistry, Geophysics, Geosystems*, 7(10), doi:10.1029/2005GC001180.

Protolith and tectonic implications of the Changhai metamorphic supracrustal sequence in southeast Liaoning Province, NE China: Constraints from zircon U–Pb and Lu–Hf isotopic and whole-rock geochemical evidences

E. MENG¹, F.L. LIU¹, J. CAI¹, Y. C²

¹ Institute of Geology, Chinese Academy of Geological Sciences, Beijing 100037, China (mengen0416@126.com; lfi0225@sina.com; caijia91052@126.commailto:)

² School of Earth and Space Sciences, Peking University, Beijing 100871, China (cuiying0430@126.com)

The Changhai metamorphic supracrustal rocks, located in the eastern-central part of the Jiao–Li–Ji Belt in the North China Craton, are mainly composed of various types of garnet–mica schists, along with minor quartzites and marbles. Geochemical results indicate that the source rocks were mainly granitoids with a possible minor contribution from clastic sediments with an active continental margin signature. Detrital zircons have U–Pb age peaks at approximately 1887, 2174, 2552, 2765, and 3212 Ma, ϵHf values of –11.1 to +13.0, and three major time windows of average continent crustal model ages (T_{DM}) of 2.04–2.33, 2.48–2.56, and 2.72–2.93 Ga. These results suggest that sediments of the Changhai metamorphic supracrustal rocks were mainly sourced from nearby basement granitoid rocks and, to a lesser extent, from Paleoproterozoic metamorphosed strata such as the North and South Liaohe groups. Furthermore, the source rocks of the magmatic zircons analyzed in this study appear to have originated from interaction between old continental crust and juvenile material. The youngest concordant zircon age peak at 1879 Ma coincides with the timing of formation of regionally widespread granitoids, mafic igneous rocks, and metamorphism of the South Liaohe and Ji'an groups in the Jiao–Liao–Ji Belt, and requires the sedimentary protoliths of the Changhai metamorphic supracrustal rocks to have been deposited after this time. The results regarding lithostratigraphy, provenance, and depositional age indicate that the Archean Northern Liaoning–Southern Jilin Complex in the north, and the southern Liaoning–Nangrim Complex in the south were already a single continental block by 1887 Ma, and that the Changhai metamorphic supracrustal rocks was deposited at an active continental margin.

This research was financially supported by research grants from the Natural Science Foundation of China and Chinese Geological Survey Program (Grants 41202136 and 1212011120150).

Multimodal and multiscale microscopies to study biomineralization and crystallization processes

NICOLAS MENGUY^{1*}, KARIM BENZERARA¹, JINHUA LI¹,
LAURENT CORMIER¹, OLIVIER DARGAUD¹
AND GUILLAUME RADTKE¹

¹Institut de Minéralogie et de Physique des Milieux Condensés (IMPMC), UMR 7590 CNRS–UPMC–IRD, 4 place Jussieu, 75252 Paris Cedex 05, France, Nicolas.Menguy@upmc.fr (* presenting author)

For years, imaging and spectroscopic methods have been intensively used to obtain information on properties of minerals present on Earth and the processes involved in their formation. Recently, dramatic improvements have been made in terms of spatial and spectral resolutions. For instance, a resolution better than 0.1 nm may now be achieved on crystalline compounds using Z-contrast on STEM-HAADF imaging mode. It is also possible to combine both high spectral (0.1 eV) and spatial resolutions (20 nm for STXM, better than 1 nm for EELS). Moreover, owing to the FIB sample preparation method, these highly local techniques can be associated with complementary large scale analytical methods allowing a multi-scale approach.

Here, we shall present recent studies focused on the nm-scale processes involved in the formations of (i) aragonite in corals, (ii) intra-cellular magnetite in magnetotactic bacteria and (iii) crystal nucleation in glasses. For coral biomineralization, combined nano-diffraction studies, HRTEM and polarization-dependent synchrotron-based STXM imaging, have evidenced the biological control exerted by the organism leading to a hierarchically structured solid material [1]. Concerning the intracellular magnetites, we focused on asymmetric crystals formed by bacteria belonging to the *Nitrospira* phylum [2]. Atomic scale processes and crystal shape control involved during crystal growth will be discussed on the basis of ultra-high resolution observations performed on an aberration corrected STEM. In addition, we will present some results related to nanoscaled heterogeneities in glasses leading to the crystal nucleation [3]. The ability to identify directly the crystallized phase from the image will be also addressed.

[1] Benzerara *et al.* (2011) *Ultramicroscopy*, **111**, 1268 - 1275. [2] Li *et al.* (in prep) [3] Dargaud *et al.* (2012) *J. of Non-Cryst. Solids*, **358**, 1257–1262

Application of a novel microfluorination technique to quantify biogenic opal $\delta^{18}\text{O}$

ANTHONY J. MENICUCCI¹, HOWARD J. SPERO²
AND JOY MATTHEWS³

¹Department of Geology, University of California Davis, Davis CA USA (amenicucci@ucdavis.edu)

²Department of Geology, University of California Davis, Davis CA USA (*correspondence: hjspero@ucdavis.edu)

³Department of Plant Sciences, Stable Isotope Facility, University of California Davis, Davis CA USA (jamathews@ucdavis.edu)

$\delta^{18}\text{O}$ data from organisms that precipitate biogenic silica, such as diatoms or grass phytoliths, are relatively rare in the literature. The paucity of opal $\delta^{18}\text{O}$ data is due to the difficulty in isolating, purifying, and analyzing the covalently bound oxygen for geochemical analysis, which typically involves dangerous fluorination reagents and/or IR laser systems. We have developed a new microfluorination technique for opal and quartz analysis that utilizes polytetrafluoroethylene powder (PTFE, C_2F_4 , Teflon) as a fluorine source. Cleaned and purified samples are dehydrated-dehydroxylated at 1060°C in vacuum prior to analysis and 0.4 mg of sample is then mixed with PTFE and graphite in silver foil capsules. Samples are analyzed at 1450°C with a vario PYRO cube TC/EA and IRMS in continuous flow mode. All data are calibrated to VSMOW using NBS-28 quartz. Acceptable data were obtained when sample yields exceeded 88% (>80% of >300 samples analyzed), yielding replicate precision better than $\pm 0.4\text{‰}$ (1σ).

Utilizing this method we analyzed a suite of diatom samples from a sediment trap time series collected in the Gulf of California, Guaymas Basin. Samples were collected in the late fall/early winter during three different years (1993, '94, '96). Diatom $\delta^{18}\text{O}$ ranged between 35 and 36.2‰ (VSMOW) ($n=7$). Five samples span a single fall through early winter period and when converted to temperature using the Labeyrie (1974) relationship, record surface water temperatures between 25-27°C that are in good agreement with temperatures during the peak fall opal flux. These data suggest sinking diatom frustules remain suspended in the deep pycnocline through early winter and data from sediment cores are likely to be seasonally biased.

[1] Labeyrie (1974), *Nature* 248, 40-42.

U-series isotope composition of primary minerals to determine regolith production rates on three different lithologies

D. MENOZZI¹ AND A. DOSSETO¹

¹Wollongong Isotope Geochemistry Laboratory; GeoQuEST Research Centre, School of Earth and Environmental Science, University of Wollongong, Wollongong, NSW, Australia. (dm791@uowmail.edu.au; tonyd@uow.edu.au)

The complex interaction between weathering, erosional and biological processes converts bedrock into regolith, namely the ensemble of soil and saprolite. Assessing rates of regolith formation is necessary to evaluating soil sustainability and investigating landscape's past history and future evolution.

Recently, uranium-series isotopes have been used to quantify independent time-integrated regolith and soil production rates [e.g. 1, 2, 3]. This is because their abundance in regolith is function of time and weathering. However, until now this method has been applied to bulk material, without distinguishing among primary minerals, secondary phases and other soil components. The overall research goal is to improve the U-series method accuracy, measuring regolith production rates on primary mineral phases in place of bulk material.

Three weathering profiles developed over basalt, granite and sandstone in NSW, Australia, have been sampled from flat-topped areas characterized by comparable climatic regime and low erosion. Separation of primary minerals along the weathering profiles and their uranium-thorium isotopic composition will provide rates of regolith production. This will contribute to improving U-series technique and will emphasize the role of parent material in determining soil formation rates.

[1] A. Dosseto, H.L. Buss, P. Suresh, *Earth and Planetary Science Letters* 337 (2012) 47-55. [2] A. Dosseto, S.P. Turner, J. Chappell, *Earth and Planetary Science Letters* 274 (2008) 359-371. [3] L. Ma, F. Chabaux, E. Pelt, E. Blaes, L. Jin, S. Brantley, *Earth and Planetary Science Letters* 297 (2010) 211-225.

Superheating water to model soil “immobile” water

LIONEL MERCURY^{1,*}, KIRILL I. SHMULOVICH², AND PATRICK SIMON³

¹ Institut des Sciences de la Terre d'Orléans, UMR 7327 Université d'Orléans-CNRS-BRGM, 45071 Orléans Cedex, France (* lionel.mercury@univ-orleans.fr).

² Institute of Experimental Mineralogy, Russian Academy of Science. 142432 Chernogolovka, Russia.

³ CEMHTI, UPR3079 CNRS-Université d'Orléans, 45071 Orléans Cedex 2, France.

Superheating

The superheated liquids are less stable than their vapour, while their criteria of internal stability are met. They can be produced when an increasing T or a decreasing internal P (including negative pressure, or liquid tension) beyond the stable values is produced in liquid in such conditions that vapor does not nucleate. This nucleation suppression can be reached in nature either during a short time by a very rapid P or/and T variation (phreatomagmatism, for instance), or by decreasing the air humidity at a liquid-air interface located in infra-micronic container (soil capillarity, for instance). The method of choice to experimentally probe superheating is the micro-thermometry of fluid inclusions [1], that can be designed in terms of composition and density of occluded liquids (in quartz). Their volumes are intermediate between macro-systems, in which superheating is restricted to low tensions with very short lifetime, and nanosystems, wherein the host matches the size of the critical vapor nucleus.

Properties and behaviours of interest

The first property available from the present experiments are the surface of the metastable PT domain available for aqueous solutions, that depends on the liquid composition and densities [2]. A second property of interest is the ability of this in-pores tensioned liquids to change the mechanical tensor in the surrounding solid, by recording the SiO₂ Raman bands in quartz during a microthermometric cycle. The third property is the transmission of the liquid tension to the dissolved solutes, again through recording characteristic Raman shifts of solutes with known liquid tension. Consequently, the solubility of gases and minerals in such superheated mixtures changes, and in general increases, with consequences on weathering and external gas cycles. At last, the superheating lifetime, the energy of the critical boiling, and the direct consequences of this return-to-equilibrium to local parageneses are explored.

[1] Roedder (1967) *Science* 155, 1413-1417. [2] Shmulovich K.I., Mercury L., Thiéry R., Ramboz C., and El Mekki M. (2009) *Geochim. Cosmochim. Acta* 73, 2457-2470.

Crustal sources of peraluminous granites: the Montes de Toledo batholith, Iberian Hercynian Belt

MERINO, E.^{1*}, VILLASECA, C.¹, PÉREZ-SOBA, C., OREJANA, D.¹, BELOUSOVA E.² AND ANDERSEN, T.³

¹ Facultad CC. Geológicas, Univ. Complutense de Madrid, Spain (*correspondence: enriqmer@geo.ucm.es)

² GEMOC, Macquarie University, NSW, Australia

³ Dpt. of Geosciences, Univ. of Oslo, Blindern, Oslo, Norway

The Montes de Toledo batholith (MTB) is a composite Hercynian plutonic array (~ 200 km long) located within the Central Iberian Zone (CIZ). The MTB magmatism lasted from 316 to 297 Ma with prevailing monzogranitic to leucogranitic compositions and a marked S-type character. Two contrasted segments are distinguished according to their geochemical and isotopic signatures: the eastern (E-MTB) and the western (W-MTB; Villaseca *et al.* [1]). Restitic and metamorphic enclaves are commonly found, though in the E-MTB are also frequent mafic microgranular enclaves. The E-MTB granites are enriched in Ca, Fe, Na, Sr and Y-HREE, whereas the W-MTB granitoids display higher ACNK ratios and higher P, K, Rb and LREE contents. The wide whole-rock ($^{87}\text{Sr}/^{86}\text{Sr}$)₃₀₀ isotopic variation (0.706 – 0.723) and the abundance of inherited Neoproterozoic zircons in the granitoids imply the involvement of a heterogeneous crustal source. ϵHf values of the Neoproterozoic zircons from the W-MTB granites overlap those from the Schist-Greywacke Complex (ϵHf up to +10 and +11, respectively), suggesting a major contribution of these metasediments to the granite source. This is also supported by the similar range of their ϵNd whole-rock isotopic composition (from -3 to -6) and Nd model ages (1.3 – 1.4 Ga). In contrast, the Neoproterozoic zircons of the E-MTB granites show lower ϵHf values (< +5) suggesting a different protolith. A meta-igneous source is consistent with the common presence of inherited zircons in those granites with the same Ordovician age range as in the outcropping CIZ peraluminous augen orthogneisses (i.e., from 460 to 480 Ma).

[1] Villaseca *et al.* (2008). *J Geosci* **53**, 263-280

Rates of Natural silica precipitation through time

R.MERLE¹, A.NEMCHIN¹, S. SIMONS¹, F. TOMASCHEK², AND T. GEISLER²

¹Curtin University, Department of applied geology, Perth Australia [a.nemchin@curtin.edu.au; r.merle@curtin.edu.au]

² Universitat Bonn, Steinmann Institut, Bonn, Germany [tgeisler@uni-bonn.de; ftom@uni-bonn.de]

Significant deposits of amorphous and cryptocrystalline silica (opal) in the Northern Yilgarn Craton are closely associated with the formation of calcrete. Precipitation of this calcrete occurs in the areas of summer rainfall, where rapid water infiltration and high evaporation rates limit prolonged periods of dampness and plant respiration. The high U concentration accompanied by low initial Pb and Th concentrations shown by some common varieties of opal facilitates the application of the U-Pb and U-series techniques for high precision age determination of opaline silica.

We used SHRIMP (sensitive high resolution ion microprobe) U-series dating of two common opal samples found in calcretes from the weathering profile in the Yilgarn Craton (Western Australia) to determine the timing of one of the latest silicification events in the area and to investigate variations of silica precipitation rates during the late Pleistocene. All analyses indicate that ^{238}U , ^{234}U and ^{230}Th are not in secular equilibrium, allowing the calculation of $^{230}\text{Th}/^{238}\text{U}$ - $^{234}\text{U}/^{238}\text{U}$ ages.

An apparent symmetrical decrease of ages from centre of the opal veins towards their contacts with the calcrete suggests that the precipitation of silica did not take place in an open space fissures, but rather as replacement of carbonate. The opal growth rate was not constant during the entire time interval between 150 and 40 kyr recorded by the two samples and the age patterns can be interpreted to represent several episodes of very fast growth of opal interrupted by periods of absence or relatively slow silica precipitation. The estimated precipitation rate variation obtained from both opal samples shows three maxima with one near 90 kyr that is visible in both samples. In addition, we found increased precipitation rates at about 135 kyr and 117 kyr in one sample, whereas in the other samples the highest precipitation rates occurred at about 70 and 45 kyr.

These rates appear to exhibit systematic variations through time that can be linked to the major orbital cycles of the Earth, suggesting that silica precipitation rates in the Yilgarn craton and perhaps in whole Australia are controlled by climate variations.

Shells of *Corbicula fluminea* mussels and the bioavailability of anthropogenic Rare Earth Elements in river water

GILA MERSCHEL¹ AND MICHAEL BAU^{1,2}

¹Earth and Space Sciences Program, Jacobs University
Bremen, 28759 Bremen, Germany

²Integrated Environmental Studies Program, Jacobs University
Bremen, 28759 Bremen, Germany

Rare Earth Elements (REE) of anthropogenic origin can be found in river water and drinking water all around the world [1]. The Rhine River and the Weser River in Germany both carry an anthropogenic Gd anomaly that results from the use of Gd in MRI contrast agents that are introduced into the rivers with the effluents from waste water treatment plants [2,3]. In addition, the Rhine River also carries an anthropogenic La anomaly (and most recently an anthropogenic Sm anomaly [4]), downstream of the Town of Worms, where industry effluents with high concentrations of La (and Sm) are discharged into the river [3]. The shells of invasive freshwater mollusk *Corbicula fluminea* were collected from both rivers to investigate the bioavailability of these anthropogenic REE. As the aragonite shell of *Corbicula* grows from the epithallial fluid of the mussel, anthropogenic metals have to be taken up by the mussel organism in order to eventually be available for incorporation in the shell. *Corbicula* shells from the Weser River and from the upper Rhine River incorporate the geogenic REE from the river water, with slight preferential incorporation of LREE over HREE. Anthropogenic La is readily incorporated into the shells, reflecting La-REE relationships in ambient river water. In contrast, anthropogenic Gd could not be detected in any of the *Corbicula* shells. These results show that anthropogenic Gd is not bioavailable, probably due to the persistence of the highly stable Gd-DTPA complex that is used as MRI contrast agent. Potential effects of high doses of REE should be investigated, because fish are known to bioaccumulate REE [5] and anthropogenic REE have been found in tap water [2].

[1] Kulaksız & Bau (2011) *Appl Geochem* **26** 1877-1885 [2] Kulaksız & Bau (2007) *EPSL* **260** 361-371 [3] Kulaksız & Bau (2011) *Environ Intern* **37** 973-979 [4] Kulaksız & Bau (2013) *EPSL* **362** 43-50 [5] Sun *et al.* (1996) *Chemosphere* **33** 1475-1483

Time resolved monitoring of Uranium contamination of oak trees

DIRK MERTEN^{1*}, DIETRICH BERGER¹, ARNO MÄRTEN¹,
AND MIRKO KÖHLER²

¹Friedrich-Schiller-University, Institute of Geosciences, 07749
Jena, Germany (*correspondence: Dirk.Merten@uni-
jena.de, Dietrich.Berger@uni-jena.de,
Arno.Maerten@uni-jena.de)

²Wismut GmbH, 09117 Chemnitz, Germany
(M.Koehler@wismut.de)

Monitoring organisms such as higher plants are used for qualitative and quantitative detection of contaminants in the environment because they take up nutrients and contaminants via air, water and soil. Since trees in temperate regions form annual rings, chronological records of environmental pollution for the near vicinity of the trees can be obtained by spatially resolved analysis of the tree rings.

In the current work a simple and minimal-destructive method for sampling and the spatially resolved (about 200 μm resolution) analysis of trees was developed. Concentration of nutrients and pollution of trees with U and other heavy metals was measured by laser ablation-inductively coupled plasma-mass spectrometry (LA-ICP-MS) in annual rings of oak trees grown in a former uranium mining area in Thuringia. The area was contaminated with heap material during active mining and was elaborately remediated by Wismut GmbH in 2002 after termination of mining.

For quantification the standard reference material Virginia Tobacco Leaves CTA-VTL-2 was pressed and used for calibration while C was used as internal standard. Thus, it was possible to deduce a temporally resolved depiction of the element concentrations reflecting the history of uranium contamination for the last 50-60 years and also to indicate remediation success.

The U concentrations in the analyzed tree cores could be directly related to mobile U concentrations in the substrate thus verifying the applied method as a successful biomonitoring tool for U contamination in soils.

The physical and chemical characteristics of marine primary organic aerosol

MESKHIDZE, N. AND B. GANTT

North Carolina State University, Raleigh, NC, USA,
nmeskhidze@ncsu.edu, bdgantt@gmail.com

Knowledge of the physical characteristics and chemical composition of marine organic aerosols is needed for the quantification of their effects on solar radiation transfer and cloud processes. This presentation examines research pertinent to the chemical composition, size distribution, mixing state, emission mechanism, photochemical oxidation, and climatic impact of marine primary organic aerosol (POA) associated with sea spray. Numerous measurements have shown that both the ambient mass concentration of marine POA and size-resolved organic mass fraction of sea spray aerosol are related to surface ocean biological activity. Recent studies have also indicated that fine mode (smaller than 200 nm in diameter) marine POA can have a size distribution independent from sea-salt, while coarse mode aerosols (larger than 1000 nm in diameter) are more likely to be internally-mixed with sea-salt. Modeling studies have estimated global submicron marine POA emission rates of $\sim 10 \pm 5 \text{ Tg yr}^{-1}$, with a considerable fraction of these emissions occurring over regions most susceptible to aerosol perturbations. Climate studies have found that marine POA can cause large local increases in the cloud condensation nuclei concentration and have a non-negligible influence on model assessments of the anthropogenic aerosol forcing of climate. Despite these signs of climate-relevance, the source strength, chemical composition, mixing state, hygroscopicity, cloud droplet activation potential, atmospheric aging, and removal of marine POA remain poorly quantified.

The current presentation will also summarize results from the recent marine aerosol workshop held in Raleigh, NC [1], where workshop participants identified the most critical open questions regarding sea spray aerosol and developed a list of priorities for conducting and facilitating novel research. The rankings of the most pressing science questions based on their feasibility impact on reducing the current uncertainty ranges for different processes will also be discussed. The workshop presentations are available online at: http://www4.ncsu.edu/~nmeskhi/Marine_Aerosol_Workshop/WEBSITE.html.

[1] Meskhidze *et al.* (2013) *Atmos. Sci. Lett.*, in review.

Effect of atmospheric organics on iron bioavailability

MESKHIDZE, N.¹, M. S. JOHNSON², D. HURLEY¹,
AND M. D. PETERS¹

¹North Carolina State University, Raleigh, NC, USA
nmeskhidze@ncsu.edu, dlhurley@ncsu.edu,
mdpeter@ncsu.edu

²NASA Ames Research Center, matthew.s.johnson@nasa.gov

Iron (Fe) delivered to the surface ocean through atmospheric pathways is of specific interest for the marine environment and plays a vital role in the earth's biogeochemical cycle. The deposition of atmospheric Fe to the ocean's surface may be an important control on primary productivity in vast areas of the global oceans. Mineral Fe at the source regions is primarily in the form of Fe-oxyhydroxides and aluminosilicate minerals. Once airborne, Fe can be mobilized from the minerals through the effect of acids, organics, and sunlight initiating a complex cycling between ferric (Fe(III)) and ferrous (Fe(II)) forms of Fe.

Here mineral dust and dissolved Fe (Fe_d) deposition rates are predicted using GEOS-Chem with a comprehensive dust-Fe dissolution scheme. The model simulates Fe_d production during the atmospheric transport of mineral dust taking into account inorganic and organic (oxalate)-promoted Fe dissolution processes, Fe(II)/Fe(III) photochemical redox cycling, dissolution of Fe-containing minerals (hematite, goethite, and aluminosilicates), and detailed mineralogy of wind-blown dust. Calculations suggest that during the yearlong simulation $\sim 0.26 \text{ Tg}$ of Fe_d was deposited to global oceanic regions [1]. Compared to simulations only taking into account proton-promoted Fe dissolution, the addition of oxalate to the dust-Fe mobilization scheme increased total annual model-predicted Fe_d deposition to global oceanic regions by $\sim 75\%$. During the daytime, a large fraction of model-predicted fluxes of Fe_d are in the Fe(II) form, while nocturnal fluxes of Fe_d are largely in the Fe(III) form [1].

In addition to model simulations, laboratory experiments were also conducted to quantify the effects of atmospheric organics on Fe bioavailability after deposition to the surface ocean. Fe(II) was detected by absorbance spectrophotometry using the Ferrozine technique and total soluble iron was determined by addition of hydroxylamine to reduce Fe(III) to Fe(II). This presentation will refine the concept of what constitutes soluble Fe in atmospheric waters and bioavailable Fe in the oceans. The important role of atmospheric organics for marine biogeochemistry and carbon cycling will also be discussed.

[1] Johnson, M.S. and N. Meskhidze (2013), *Geosci. Model Dev. Discuss.*, 6, 1901-1947.

It's getting hot on Earth - The Middle Eocene Climatic Optimum in a terrestrial sedimentary record

K. METHNER^{1,2}, U. WACKER², J. FIEBIG^{1,2}, A. MULCH^{1,2,3}
AND C. P. CHAMBERLAIN⁴

¹ Biodiversity and Climate Research Centre, Frankfurt am Main, Germany; katharina.methner@senckenberg.de

² Goethe Universität, Frankfurt am Main, Germany

³ Senckenberg Research Institute and Natural History Museum, Frankfurt am Main, Germany

⁴ Stanford University, Stanford, CA, USA

The Middle Eocene Climatic Optimum (MECO) is an enigmatic global warming event interrupting the protracted Cenozoic cooling. It is marked by a negative shift in marine oxygen isotope records that indicate an increase of water temperatures by up to 5 to 6 °C and thus, documents an increase in temperatures on top of the warm Eocene climate. This makes the MECO one of the hottest phases during Earth's climate history, but the questions, if and how the MECO affected continental sites are still unresolved.

Here, we present a stable isotope record ($\delta^{18}\text{O}$) and clumped isotope (Δ_{47}) temperatures from an Eocene mammal fossil locality in southwestern Montana, USA. The sampled section (Upper Dell Beds, Sage Creek Basin) comprises about 60 m of stacked paleosols that were correlated to Chron C18r by paleomagnetic and biostratigraphy. The oxygen isotopic record of pedogenic carbonates range from -12 to -18 ‰ (SMOW) and reveals prominent shifts of oxygen isotope ratios of up to 6 ‰ within 3 m of section. The associated Δ_{47} -temperatures indicate an increase in temperatures of about 5 °C, reaching peak temperatures of 31 ± 2 °C, and a rapid drop in temperatures of about 9 °C. Thus, we think that this record has the potential to (1) document the MECO in a terrestrial record, (2) yield realistic temperature changes between the MECO event and the post-MECO cooling phase, and (3) help to track the isotopic evolution of precipitation during a short term climatic event in continental interiors.

Stability behaviour of silver nanoparticles in different aqueous media

G. METREVELI* AND G. E. SCHAUMANN

Universität Koblenz-Landau, Institute of Environmental Sciences, Environmental and Soil Chemistry, Landau, Germany (*correspondence: metreveli@uni-landau.de)

Due to the wide application of engineered nanoparticles (ENP) in different industrial products, in the last years, the risk potential for their release in the environment is increased as never before. Mobility and toxicological behaviour of ENP in aquatic systems is strong depending on their stability and aggregation properties [1]. Furthermore, the changes in the chemical composition of the aqueous phase can influence the aggregation reversibility [2], which can lead to the remobilisation of previously aggregated and immobilised nanoparticles. Despite the increasing amount of studies on the environmental behaviour of ENP, there is a lack of information about reversibility of the aggregation.

In this study, aggregation of citrate stabilised silver nanoparticles (Ag NP) was investigated in synthetic aqueous media and natural river water (Rhine). The influence of pH value, sodium and calcium cations and humic acid (HA) on the stability of Ag NP was characterised. The reversibility of the aggregation was studied after reducing of ionic strength (by centrifugation and washing) and applying of ultra sound at different energy levels.

Ag NP showed high aggregation at high sodium and calcium concentrations ($c(\text{Na}^+) > 40$ mmol/L, $c(\text{Ca}^{2+}) > 0.5$ mmol/L), at low pH values (pH <3) and in river water. HA stabilised Ag NP and the stabilisation effect was much higher for pH induced aggregation than for sodium and calcium cation induced aggregation. After reducing of ionic strength, the aggregation of Ag NP was reversible especially after applying of shear forces, but the disaggregation was not fully complete. After treatment, small aggregates remained in the dispersions, which were more stable, than the big aggregates.

The results of this study show that the reduction of ionic strength and the presence of shear forces can lead to the partial disaggregation of previously aggregated nanoparticles. As a consequence, the probability of nanoparticle remobilisation can be increased.

[1] Morones *et al.* (2005) *Nanotechnology* **16**, 2346-2353. [2] Fabrega *et al.* (2009) *Environ. Sci. Technol.* **43**, 7285-7290.

Artificially induced migration of redox layers in Adriatic sediment

E. METZGER^{1*}, D. LANGLET¹, E. VIOLLIER², N. KORON³,
B. RIEDEL⁴, M. ZUSCHIN⁴, M. STACHOWITZ⁴,
J. FAGANELI³, M. THARAUD²,
E. GESLIN¹ AND F. JORISSEN¹

¹ LUNAM Université, Université d'Angers, UMR CNRS 6112
LPGN-BIAF, Angers, France (*edouard.metzger@univ-angers.fr)

² Université Paris Diderot, Sorbonne Paris Cité, UMR CNRS
7154 LGE-IPGP, Paris, France

³ Marine Biology Station, National Institute of Biology, Piran,
Slovenia

⁴ Department of Marine Biology, University of Vienna,
Vienna, Austria

Long term experimental studies suggests that, under anoxic transient conditions, redox fronts within the sediment shift upwards causing sequential rise and fall of benthic fluxes of reduced species (Mn(II), Fe(II) than S(-II)) (e.g; Kristiansen *et al.*, 2002). In order to study such processes in a more realistic system, benthic chambers were deployed on the seafloor of the Northern Adriatic and sampled after 9, 30 and 315 days of incubation. High resolution porewater profiles were sampled by DET probes and redox sensitive species were analysed (Alk, SO₄²⁻, Mn²⁺, Fe²⁺).

Results show that anoxia was reached after 7 days. Mn and Fe started diffusing towards the water column giving a rusty color to the seafloor. Infaunal species appeared at the surface. After 20 days (fig. 1), all macro-organisms were dead. Porewater chemistry showed expected redox shifts. However, bottom water chemistry followed a peculiar evolution: after 1 month, sulfide had a higher concentration in the overlying water than in the porewater leading to a diffusional flux into the sediment. The source of sulfide was attributed to the decomposition of dead macroorganisms laying on the seafloor. Our results suggest that the sulfide rise in the water column in coastal waters is strongly controlled by the biomass of benthic macrofauna and can be decoupled from sedimentary geochemical processes.



Figure 1: left: chamber after 20 days of incubation; right: chamber after 10 months of incubation.

Lateral carbon isotope homogeneity in a Late Ordovician epeiric sea

J. GARRECHT METZGER^{1*} AND DAVID A. FIKE¹

¹Washington University, St. Louis, Missouri 63130, USA
(*correspondence: gmetzger@levee.wustl.edu)

Carbon isotope ratios of marine carbonate rocks ($\delta^{13}\text{C}_{\text{carb}}$) can be used to correlate coeval ancient strata. Detailed correlation requires that the carbon isotopes of the carbon source, the oceanic dissolved inorganic carbon pool ($\delta^{13}\text{C}_{\text{DIC}}$), be homogenous on the mixing time of the ocean, (~1,000 years). Previous reports have suggested that apparent large ($\geq 1.5\text{‰}$) offsets in $\delta^{13}\text{C}_{\text{carb}}$ observed for Late Ordovician carbonate strata of North America are the result of large scale (i.e., 100s-1000s km) lateral gradients in the isotopic composition of DIC in the surface ocean (e.g., from the open Iapetus Ocean to shallow Laurentian epeiric seas [1,2]. An alternative interpretation is that apparent offsets in $\delta^{13}\text{C}_{\text{carb}}$ are in large part the result of the differential admixture of secondary carbon incorporated into the rocks resulting in variable and lower $\delta^{13}\text{C}_{\text{carb}}$ values in diagenetically altered locations [3].

Here, we present Late Ordovician $\delta^{13}\text{C}_{\text{carb}}$ data covering >1,400 km and spanning multiple depositional environments, from shallow cratonic sea to deeper foreland basins. Multiple transects through the same interval across the study area reveal no systematic $\delta^{13}\text{C}_{\text{carb}}$ gradients (maximum offsets between any coeval strata are ~0.6‰). Detailed sampling has identified discrete stratigraphic intervals with characteristic $\delta^{13}\text{C}_{\text{carb}}$ values resolvable at sub-permil levels. The work discusses the stratigraphic as well as biogeochemical implications of these findings.

[1] Holmden *et al.* (1998) *Geology* **26**, 567-570. [2] Panchuck *et al.* (2006) *J. Sed. Research* **76**, 200-211. [3] Metzger and Fike (2013) *Sedimentology* **in press**; doi: 10.1111/sed.12033.

The contribution of phytoliths in improving the understanding of Si cycling

J.D. MEUNIER*, AND C. KELLER

Aix-Marseille Université, CNRS, IRD, CEREGE UM34,
13545 Aix en Provence, France (*correspondance:
meunier@cerege.fr)

The Si cycle is remarkably affected by biomineralisation processes through the formation of diatoms and other microorganisms in aquatic systems, and through the formation of phytoliths that constitute the main form of Si storage in terrestrial plants. After translocation from the roots to the shoots as silicic acid, the main form of Si in soil solutions, Si is polymerized through the elimination of water by evaporation and the formation of phytoliths occurs. Phytoliths are composed of opal A (XRD-amorphous phase) particles although some authors have suggested the presence of crystalline silica. Contrary to many nutrients, Si cannot be subsequently redistributed within the plant because the phytoliths remain insoluble until the litter falls and decomposes. The beneficial effects of Si have been demonstrated by many studies using pots, hydroponic and field experiments and are particularly remarkable in plants exposed to biotic or abiotic stresses.

During litter decomposition phytoliths are either dissolved and constitute a source of recycled Si for plants or preserved from weathering and their morphoscopy may then be helpful for reconstructing the past vegetation. After presenting some evidences that phytoliths can control the biogeochemical cycle of Si at ecosystem or watershed levels, several issues concerning phytolith research are discussed. A few recent studies have provided some evidences that agriculture practices can deplete ASi pools of soil. Because phytoliths constitute one of the most rapidly bio available source of Si for crops, the consequence of soil erosion and straw exportation on crop yield should be more studied in cultivated areas. In order to better integrate the phytoliths in the global models of Si cycling there is a need for a better quantification of soil phytolith pool (ASi). Extraction using gravimetric methods are time consuming and poorly correlated with extractions using alkaline dissolution protocols such as the DeMaster's (1981), initially used for diatom test quantification in aquatic systems. We have recently shown that alkaline extraction may not be strong enough to dissolve aged phytoliths, and may underestimate ASi by a factor of 4.

Laboratory Study of Nitrate Photolysis in Antarctic Snow: Quantum Yield, Mechanism, Isotope Effects and Wavelength Dependence

CARL MEUSINGER^{1#}, TESFAYE A. BERHANU^{2#},
JOSEPH ERBLAND², JOEL SAVARINO²
AND MATTHEW S. JOHNSON^{1*}

¹Copenhagen Center for Atmospheric Research, CCAR,
Department of Chemistry, University of Copenhagen,
Copenhagen, Denmark

²Laboratoire de Glaciologie et Géophysique de
l'Environnement, CNRS/Université Joseph Fourier-
Grenoble 1, Grenoble, France

[#]CM and TAB contributed equally to the work.

*Corresponding author msj@kiku.dk

Post-depositional processes alter the nitrate concentration and isotopic composition at low accumulation sites. Available nitrate ice core records can only provide input for studying past atmospheres and climate if such processes are fully understood. Reported quantum yields for the main reaction differ by orders of magnitude. The experimental system included a Xe lamp with optional UV filters, an environmental chamber with temperature control and a N₂ flow system to flush gas phase products and used natural snow from Dome C, Antarctica. Irradiated snow was sampled in 1 cm sections and analyzed for nitrate concentration and isotopic composition ($\delta^{15}\text{N}$, $\delta^{18}\text{O}$ and $\Delta^{17}\text{O}$). Observed values for the quantum yield lie in the middle of the range of previously reported values and can be explained using two types of nitrate: one easily accessible (photolabile) and one of trapped or buried nitrate. The quantum yield changes from 0.45 to 0.05 within what corresponds to weeks of UV exposure in Antarctica. An average photolytic isotopic fractionation of $^{15}\epsilon = -15 \pm 0.01 \text{‰}$ was found for the experiments without a wavelength filter. These results are ascribed to excitation of the intense absorption band of nitrate around 200 nm. No fractionation was observed in the oxygen isotopes. An experiment with the 305 nm UV filter, close to the actinic flux spectrum in Dome C, showed a photolytic isotopic fractionation of $^{15}\epsilon = -38 \pm 2.2 \text{‰}$ slightly more positive than the fractionation determined in the field (-40 to -74.3‰, Erbland *et al.*, In review). We demonstrate that the photolytic fractionation of nitrate isotopes in snow is very sensitive to the actinic flux spectrum, leading to the reinterpretation of previous laboratory studies. In order to directly apply results from laboratory studies to ambient conditions the wavelength of irradiation has to match that in the field, as the photolytic fractionation changes significantly depending on the impinging spectrum.

The biological pump and evolution of marine animal ecosystems

K.M. MEYER^{1*}, A. RIDGWELL² AND J.L. PAYNE¹

¹Department of Geological and Environmental Sciences, Stanford University, Stanford, CA 94305, USA
(*correspondence: meyerk@stanford.edu)

²School of Geographical Sciences, University of Bristol, Bristol, BS8 1SS, UK (andy@seao2.org)

The export of organic matter from the surface ocean and its respiration at depth creates gradients in nutrient and oxygen availability that influence the structure and distribution of marine ecosystems. Today the strength of the biological pump is strongly influenced by mineral-ballasted phytoplankton. In Earth's past, however, mineralized phytoplankton were less common and, consequently, the biological pump was likely weaker. Here we use the GENIE model to explore the impact of a changing biological pump on marine chemistry and ecosystem structure. We find that under a weaker biological pump likely typical of the Paleozoic and early Mesozoic, the position of the oxygen minimum zone shallows and anoxia is more prevalent near the surface. In this scenario, less oxygen is available to benthic ecosystems on shelf environments. If so, these results imply that the mid-Mesozoic radiation of phytoplankton with mineralized tests spread oxygen demand more evenly through the oceans and reduced the spatial extent of anoxic regions. Thus, we hypothesize that the Phanerozoic trend toward greater animal abundance and metabolic demand was driven more by increased oxygen availability than by greater food availability. In fact, a reduction in productivity may have been required to generate sufficient oxygen availability in the shallow oceans to make the oceans more habitable for animals.

Preliminary U-series dating results from the GISP2 ice core

K.W. MEYER AND S.M. ACIEGO

University of Michigan, Ann Arbor, MI 48109-1005, USA
(*correspondence: meyerkw@umich.edu)

Ice core climate proxy records often lack precise age constraints on the geochemical variations they record in trapped gases and/or dust inclusions. Currently, few geochronological methods exist to determine the age of the disturbed sections of deep and basal ice. Recent work on material from the Antarctic EPICA Dome C core has demonstrated advances in a radiometric dating method based on $^{234}\text{U}/^{238}\text{U}$ measurements and dust surface area [1]. Our work has focused on applying these same methods to ice samples from the Greenland Ice Sheet Project (GISP2) drill core. Given that the bottom 10% of the GISP2 core consists of disturbed deep ice argued to be 240 ka or older, external dating methods are necessary for confirming the absolute age of these samples and to further extend Northern Hemisphere climate reconstructions [2].

The U-series method depends on determining three variables: (1) the initial concentration of ^{234}U in the soluble fraction of the ice, (2) the parent concentration (^{238}U) in the dust and (3) the precise surface area of the dust grains to account for the loss of ^{234}U from the grain by α -recoil.

One of the critical assumptions of the dating method is that the dust is of marine origin, possessing an initial $^{234}\text{U}/^{238}\text{U}$ activity ratio of 1.14 ± 0.01 [3]. Other studies have determined that there is a significant presence of soluble dust from sea salt deposition on the Greenland Ice Sheet by $^{87}\text{Sr}/^{86}\text{Sr}$, $^{234}\text{U}/^{238}\text{U}$, and ϵ_{Nd} measurements [4]. Our initial measurements yielded $^{87}\text{Sr}/^{86}\text{Sr}$ values ranging between 0.709439 ± 0.00002 and 0.711007 ± 0.00003 . These values are in agreement with the average global $^{87}\text{Sr}/^{86}\text{Sr}$ composition of seawater, given possible interaction with the insoluble fraction. Therefore, our underlying assumption for the source of the soluble dust fraction is plausible. Initial $^{234}\text{U}/^{238}\text{U}$ activity ratios for the soluble fraction increase from 1.178 to 1.229 with depth, suggesting that the daughter excess of ^{234}U correspond to resolvable ages. Surface area and ^{238}U measurements of the insoluble fraction will be presented in the context of the uranium age equation.

[1] Aciego et al. (2011) *Quaternary Science Reviews* **30**, 2389–2397. [2] Suwa et al. (2006) *Journal of Geophysical Research* **111**, D02101. [3] Henderson (2002) *Earth and Planetary Science Letters* **199**, 97–110. [4] Lupker et al. (2010) *Earth and Planetary Science Letters* **295**, 277–286.

Metamorphic evolution and tectonic implications of carbonate-bearing mafic boudins and surrounding metasediments of the Tianshan Mountains (NW China)

MELANIE MEYER*

GeoZentrum Nordbayern, Friedrich-Alexander-Universität
Erlangen-Nürnberg, Schlossgarten 5a, D-91054 Erlangen,
Germany

(*correspondence: melanie.meyer@gzn.uni-erlangen.de)

The metamorphic belt in the southern Tianshan Mountains of NW China provides the opportunity to investigate both the metamorphic evolution of mafic rocks (upper oceanic crust with rarely preserved pillows) during subduction and the exhumation mechanisms in a subduction channel (mafic rocks as boudins enclosed in metasediments). The (U)HP-LT rocks (blueschists, eclogites and metasediments; as in many (U)HP terranes, voluminous schists enclose rare eclogite lenses and layers [1]) are interpreted to represent part of a tectonic mélange formed along a suture zone between the Yili-central Tianshan and Tarim plates ([2],[3]).

This study provides detailed information on the metamorphic evolution of both metasedimentary host rocks and mafic boudins of the (U)HP-LT metamorphic belt. Profiles across different mafic boudins and enclosing metasediments were investigated (whole rock major and trace element geochemistry by XRF and LA-ICP-MS, mineral chemistry by EMPA, thermobarometry, P-T pseudosection modeling using PerpleX) in order to constrain potential protoliths and differences in peak P-T conditions between distinct mafic boudins, and also between metasediments and mafic boudins. Furthermore, metasomatism of the subducted rocks was investigated. This study aims to increase our understanding of the metamorphic evolution of mafic rocks during subduction, the detachment from the subducted slab and the mixing of different materials and metamorphic reactions in the subduction channel during exhumation.

All eclogites investigated contain a variable amount of carbonate minerals. Thus, in addition the carbon cycle in subduction zones is addressed in the context of the P-T evolution.

[1] Lü *et al.* (2012) *J. Metamorph. Geol.* **30**, 907-926. [2] Gao *et al.* (1999) *J. Metamorph. Geol.* **17**, 621-636. [3] van der Straaten *et al.* (2008) *Chem. Geol.* **255**, 195-219.

The Joy of Making Planets in Disks: Dynamical and Chemical Recipes

MICHAEL R. MEYER¹

¹Institute for Astronomy, ETH Zurich, mmeyer@phys.ethz.ch

Circumstellar disks are an outcome of the star formation process, and their physical properties set the initial conditions of planet formation. Yet the total mass, orbital radius, mean density, and composition of planets formed in these disks depends critically on dynamical processes and the transmutation of the initial ingredients (gas and dust from the interstellar medium) through chemistry. Here we review some of the key physical and chemical processes in disks that dictate the composition of forming planets. In particular we focus on new observational results that constrain theories of planet formation.

Deep fast-spread Oceanic Crust - Fluid Interactions: Petrography and Volatiles from IODP Expedition 345 Hess Deep Plutonic Crust

R. MEYER¹, R.P. WINTSCH², T. NOZAKA³, K. M. GILLIS⁴, J.E. SNOW⁵, AND IODP EXPEDITION 345 SHIPBOARD SCIENTIFIC PARTY

¹ University of Bergen, Norway; Romain.Meyer@geo.uib.no

² Indiana University, Bloomington IN, USA

³ Okayama University, Japan

⁴ University of Victoria, B.C., Canada

⁵ University of Houston, Houston TX, USA

IODP Expedition 345 returned to the Hess Deep Rift almost exactly 20 years after ODP Leg 147. Here we report preliminary results of the recent expedition (Dec. 2012 - Feb. 2013) in the Eastern Pacific Ocean. The Hess Deep Rift exposes a dismembered, but nearly complete lower crustal section of fast-spread East Pacific Rise (EPR) plutonic crust. Recovered core includes high Mg# (79-89) olivine gabbros, gabbros, gabbro-norites and troctolites. Due to the scarcity of in-situ rocks from these depths alteration processes within such deep parts of the oceanic crust are still ambiguous. However, such data are essential to better understand global crustal mass balance, tectonics, hydrothermal processes, and cast light on deep crustal biosphere conditions. Shipboard petrography has revealed that high-temperature tremolite-chlorite replacement of olivine + plagioclase is less abundant at deeper levels, in contrast to the dominance of background greenschist/subgreenschist-facies serpentinisation of olivine in addition to prehnite +/- chlorite formation after plagioclase. Shipboard C, H and S measurements define H₂O as major volatile component (0.95 – 9.57 wt.%) in the sampled plutonic rocks. Water abundance within these rocks correlates with the degree of alteration, Ni, and modal olivine contents. The H₂O/MgO ratio of the troctolites (0.31) is consistent with that of serpentine (0.32) and indicates the importance of serpentinisation within the sampled lowest EPR oceanic crust. Localized low-temperature alteration is possibly due to Cocos-Nazca rifting associated with cataclastic deformation.

Glaciers and floodplains controls on weathering fluxes deciphered from two glacial-interglacial Nd isotopes records on both sides of New Zealand

LAURE MEYNADIER¹, ANTOINE COGEZ¹ AND CLAUDE ALLÈGRE¹

¹Equipe de Géochimie et Cosmochimie, Institut de Physique du Globe de Paris – Sorbonne Paris Cité, UMR 7154, Université Paris Diderot

A wide variety of climatic, tectonic or chemical factors can influence weathering intensity and/or fluxes. The interest of studying time series relies on the fact that some of these parameters varied through time and other remained constant : it is then possible to unravel informations “all other things being equal” about controls on weathering mechanisms.

We studied Nd isotopes (ϵ_{Nd}) in two DSDP sites (593 and 594) both in the detrital and authigenic fractions. These sites were collected on the large continental shelf, on both western and eastern side of New Zealand. The sediment covers the last 3 glacial-interglacial cycles (300 kyrs). The interest of this area is linked to the rather uniform lithology, and to the contrasts between the western and the eastern sides of NZ, introduced by the Alpin Chain topography. The Main Divide of the Alpin Chain separates the eastern side with steep slopes and high pluviometry, and the western side with small floodplains and lower pluviometry. In addition climatic forcing factors, such as the glacier extent, did vary through the glacial to interglacial periods.

Our results show ϵ_{Nd} variations in phase with the climatic fluctuations on both cores, but with a much lower amplitudes on the western core than on the eastern one. Given the various paleoceanographic informations available in the area we are able to demonstrate that the ϵ_{Nd} signal can not be explained by variations of the mixing contributions of the different ocean masses surrounding New Zealand. The ϵ_{Nd} signal has clearly a continental and local origin.

Using mixing calculations we show that the weathering Nd fluxes could have been up to 2 to 3 times higher during glacials than during interglacials. This result is explained by the control of glacial erosion that deliver higher amount of fine and fresh materials, easily weatherable. Moreover the lower amplitude of the variations on the western site suggests that floodplains play a key role in the chemical maturation of these fresh and fine grounded minerals delivered from the higher relief. Finally the relationship between our ϵ_{Nd} record and the $\delta^{18}O$ record suggest a non linear response (hysteresis like relation) of the erosion and weathering processes to climatic forcings.

Sr-Nd and Pb isotopic portray of the Crozet plume

C. M. MEYZEN^{1*}, A. MARZOLI¹, G. BELLINI¹
AND G. LEVRESSE²

¹ Università degli Studi di Padova, Via G. Gradenigo, 6, 35131 Padova, Italia (* correspondence: christine.meyzen@unipd.it, andrea.marzoli@unipd.it, giuliano.bellieni@unipd.it)

² Centro de Geociencias, Universidad Nacional Autónoma de México (UNAM), Blvd. Juriquilla No. 3001, Querétaro, 76230, México (glevresse@geociencias.unam.mx)

New Sr, Nd and Pb isotope data are presented for alkali basalts of the sub-aerial eruptive stage of East Island. This landmass is the second largest of the easternmost and oldest island group of Crozet archipelago. Its lavas are remarkably isotopically homogeneous in spanning a narrow range of isotopic variability. They occupy an intermediate position among the isotopic variability spectrum defined by Earth's oceanic island basalts. They fall in a mixing triangular shape formed by the end-member mantle components: a Depleted Mantle (DM) component, an Enriched Mantle (EM) component and a common component. The mixture domination by a large fraction of the common component suggests an isolation of the East island mantle source from homogenizing effects of convection mixing and recycling processes for Ga timescales. A possible inter-island source heterogeneity, such as those identified in the Pacific and Atlantic oceans, could exist at Crozet islands, as the younger western group is more isotopically depleted in Sr-Nd than the eastern one. Overall, lavas from Crozet islands share Pb-Sr-Nd isotopic affinities with their Reunion-Mauritius counterparts, but differ from those of Marion-Prince Edward and Kerguelen volcanoes. However, we cannot reject the seismic inference that Crozet volcanism is a secondary expression of Kerguelen hotspot, if its compositional bottom layer is heterogeneous. Finally, the Sr-Nd-Pb isotopic signatures of basalts north of the Crozet Bank along the Southwest Indian Ridge show no affinity with those of East island. The seismically rideward flow identified must thus be composed of isotopically distinct material from that of feeding East island volcanism.

Convergence in chemical compositions between aqueous fluid and silicate melt in the peridotite-H₂O system

KENJI MIBE^{1*}, TATSUHIKO KAWAMOTO²
AND SHIGEAKI ONO³

¹Earthquake Research Institute, University of Tokyo, Tokyo 113-0032, Japan (*correspondence: mibe@eri.u-tokyo.ac.jp)

²Institute for Geothermal Sciences, Graduate School of Science, Kyoto University, Kyoto, 606-8502, Japan (kawamoto@bep.vgs.kyoto-u.ac.jp)

³Institute for Research on Earth Evolution, Japan Agency for Marine-Earth Science and Technology, Kanagawa, Japan. (sono@sono@jamstec.go.jp)

In order to understand the magma genesis and chemical differentiation in the Earth's interior, we have been investigating the stability fields and chemical compositions of aqueous fluid, silicate melt, and supercritical fluid magma in the peridotite-H₂O system. Mibe *et al.* [1] found that the second critical endpoint occurred at around 3.8 GPa in the system peridotite-H₂O. Using the quenched recovered samples obtained by Mibe *et al.* [1], we determined the chemical composition of aqueous fluid, silicate melt, and supercritical fluid in the vicinity of the second critical endpoint in the system peridotite-H₂O by EPMA analyses. A 10- to 30-um diameter electron beam was used to obtain the composition of quenched materials from aqueous fluid, silicate melt, and supercritical fluid.

In the run at 3.3 GPa, the composition of aqueous fluid was high-Mg dacitic, whereas the composition of silicate melt was peridotitic. In the run at 3.6 GPa, the composition of aqueous fluid was high-Mg andesitic, whereas the composition of silicate melt was komatiitic. At 4 GPa (i.e., above the second critical endpoint), the composition of supercritical fluid magma was basaltic. Our results clearly indicate that the compositions of aqueous fluid and silicate melt converge at around 3.8 GPa, which is consistent with the results by Mibe *et al.* [1].

[1] Mibe *et al.* (2007) *J Geophys Res* **112**:B03201.

Concentration and Behavior of CO₂ in MORB and OIB: a reevaluation

PETER J. MICHAEL^{1*} AND DAVID W. GRAHAM²

¹Dept. of Geosciences, Univ. Tulsa, 800 S. Tucker Dr., Tulsa, OK, 74104, USA (*correspondence: pjm@utulsa.edu)
²CEOAS, Oregon State Univ., Corvallis, OR, 97331, USA (dgraham@coas.oregonstate.edu)

Estimation of initial magmatic CO₂ contents in basalts is hindered by degassing and loss of CO₂ during magma ascent. The most widely accepted estimates of CO₂ flux are derived from ultra-depleted ([Nb]<1.5ppm) mid-ocean ridge basalts (MORB) and melt inclusions from Siqueiros region of the East Pacific Rise that did not exsolve CO₂ [1], and from highly vesicular Mid-Atlantic Ridge (MAR: 14°N) “popping rocks” that did not lose bubbles because they ascended quickly [2,3]. These data indicated that that CO₂/Nb was roughly constant at 239±46 for MORB and that CO₂ behaves incompatibly like Nb during melting and source enrichment [1]. A correct recalculation of the CO₂/Nb in popping rocks from 14°N, and new data from popping rocks at 34°N MAR, showed that their CO₂/Nb is much higher: closer to 576 [4]. These authors proposed that the low CO₂/Nb values for ultra-depleted MORB [1] are unrepresentative of the mantle. Their higher CO₂/Nb estimate [4] yields higher estimates of CO₂ flux from the mantle, in line with estimates from helium.

We have analyzed a larger set of ultra-depleted MORB glasses from the mid-ocean ridge system. Most erupted undersaturated in CO₂, have few or no vesicles, and yield extremely low CO₂ when crushed *in vacuo*. Their CO₂/Nb is 250±50, showing that this ratio [1] is widely applicable to ultra-depleted mantle. We also compiled published data for enriched submarine basalts including ridge popping rocks [4], and basalts from North Arch, Hawaii. The latter have up to 57% vesicles, suggesting two samples lost no bubbles [5]. Their CO₂/Nb is 1125 and 1216, similar to ratios for some popping rocks from 34°N. For the data set as a whole, CO₂/Nb is positively correlated with La/Sm. We propose that CO₂ is more incompatible than Nb, behaving geochemically more like Ba or Rb. CO₂/Ba is 114±43 for most ultra-depleted through highly enriched MORB. Rb and Ba should be better proxies for CO₂ because, unlike Nb, they are not retained in subduction zones during magma genesis. Thus, Rb and Ba more closely follow CO₂ during subduction and recycling into deep mantle. A Ba proxy for CO₂ suggests a MORB CO₂ flux that is ≈40% higher than [4] and ≈3x higher than [1].

[1] Saal et al. 2002 Nature 419. [2] Sarda & Graham 1990 EPSL 97. [3] Javoy & Pineau 1991 EPSL 107. [4] Cartigny et al. 2008 EPSL 265. [5] Dixon et al. 1997 J. Petrol. 38.

‘Freiberg Strategy’ for obtaining matrix-matched reference materials for resource-related microanalytical methods technology

P.P. MICHALAK¹, A.D. RENNO², S. MERCHEL², F. MUNNIK², J. GUTZMER², R. UECKER³, Z. GALAZKA³, H-P. HELLER¹, M. RADTKE⁴ AND U. REINHOLZ⁴

¹TU Bergakademie Freiberg, DE (Przemyslaw-Piotr.Michalak@student.tu-freiberg.de)
²HZDR, Dresden, DE, ³IKZ, Berlin, DE, ⁴BAM, Berlin, DE,

Quality assurance of natural raw materials (e.g. ores) requires thorough studies on concentration and spatial distribution patterns of technologically relevant trace elements within the mineral matrix at the microscale. Obtaining such a goal is yet only possible with the use of beam-based microanalytical methods and a proper set of homogeneous, matrix-matched reference materials (RMs) doped with trace elements relevant to resource technology.

Natural minerals usually exhibit chemical heterogeneity at µg/g sampling masses and are unsuitable as RMs for in-situ chemical microanalysis. On the other hand, available synthetic RMs (e.g. glasses, pressed pellets) fail to satisfy matrix-match criterion.

A collaboration involving several German scientific institutions centered around TU Bergakademie Freiberg proposed a novel strategy for obtaining such RMs through the synthesis of multi trace element doped mineral matrices subsequently tested for chemical and structural homogeneity with both microscopic and spectroscopic (RMs-dependent and absolute) microanalytical methods.

Three mineral matrices vital to resource technology applications – pyrite, tantalite and feldspar – have been synthesized using flux method, Czochralski method and alkoxide-based sol-gel synthesis, respectively and doped with various sets of technologically important trace elements at the concentration range found in corresponding natural minerals. Their spatial chemical micro-homogeneity has been investigated using light and electron microscopy as well as RMs-dependent (EPMA, LA-ICP-MS) and absolute (PIXE, PIGE) analytical methods.

Quantitative and qualitative elemental spatial distribution maps have been obtained for major and trace elements for each matrix. Homogeneity of the matrices was evaluated using petrologically sensitive statistical analysis.

Established homogeneity testing protocol will be employed in the next stages of the project.

Biomass combustion – a possible source of environmental pollution?

M. MICHALIK^{1*}, M. POGRZEBA², AND W. WILCZYŃSKA-MICHALIK³

¹Jagiellonian University, Institute of Geological Sciences, ul. Oleandry 2a, 30-063 Kraków, Poland (*correspondence: marek.michalik@uj.edu.pl)

²Institute for Ecology of Industrial Areas, ul. Kossutha 6, 40-844 Katowice, Poland (mag@ietu.katowice.pl)

³Pedagogical University, Institute of Geography, ul. Podchorążych 2, Kraków, Poland (wanda.michalik@post.pl)

The content of selected elements in biomass (virginia fanpetals; cup plant; switchgrass; eastern cordgrass; miscanthus) grown on contaminated experimental field and in low-temperature ash obtained in 475°C was studied. The soil is enriched in various elements (e.g. Zn up to 2000 ppm, Pb up to 430 ppm, Cd up to 19 ppm) and contains numerous components of anthropogenic origin (spherical dust particles from high-temperature industrial processes, fragments of various types of metallurgical slag, coal ash, etc.).

The content of potentially toxic elements determined in biomass is relatively high (e.g. Zn up to 545 ppm, Cd up to 8,5 ppm, Pb up to 115 ppm, Hg up to 24 ppb). The content of these elements in low-temperature ash is very high (Zn from 4100 to >10 000 ppm, Cd from 30 to 207 ppm, Pb from 380 to 2870 ppm, Ag from 171 to 1048 ppb, As from 9 to 22.5 ppm, Hg below 0.5 ppb).

Detailed study of dry biomass indicates that high content of various elements is related partly to dust particles deposited on its surface (e.g. Pb, Cd and Zn sulphides, Zn containing clay minerals, Ca and Ba sulphates, particles rich in Fe, Cr, Ni, etc.) and partly to accumulation of various elements (e.g. Zn) in plant tissue.

Results indicate that in the case of biomass cultivated on the polluted sites risk of emission of elements characterized by low values of boiling point during fuel combustion or leaching of potentially toxic elements from ash to the environment is probable.

Study was supported by NCN grant No. 579/B/P01/2011/40.

Linking reactive silica with organic matter burial in Mississippi delta sediments

P. MICHALOPOULOS * AND K. PARINOS

Institute of Oceanography, Hellenic Center for Marine Research, Anavyssos, 19013, Greece

Deltaic sediments account for ~40% of organic carbon burial in the oceans. Furthermore poorly crystalline Al-Si-(Fe)-phases precipitate on biosiliceous and clastic particles as a result of reverse weathering reactions in deltaic sediments [1]. Amorphous biogenic silica and poorly crystalline Al-Si-(Fe) precipitates are quantified as reactive silica (RSi). This study examines the links between RSi and sedimentary organic matter in Mississippi delta sediments and the implications for organic matter burial and preservation. Suspended matter and sediment samples from the Mississippi river and seven delta stations were analyzed for reactive silica (RSi), total organic carbon (TOC), total nitrogen (TN) and stable isotopes ($\delta^{13}\text{C}$, $\delta^{15}\text{N}$).

Top (>50cm) and bottom sediments from delta sites close to the river mouth have identical $\delta^{13}\text{C}$, $\delta^{15}\text{N}$ values, indicating similar OM sources. In top sediments RSi is not related to TOC or TN. Below 50cm, RSi correlates with TOC, TN suggesting a diagenetic control. Correlations in mid-shelf stations show that TOC:Si, TN:Si ratios decrease from top to bottom, indicating preferential loss of TOC and TN relative to RSi. Stronger coupling between RSi and preserved residual OM is found in mid-shelf sites where sediments are more diagenetically altered. We propose that formation of Al-Si coatings on biosiliceous particles [2-3] may also partially inhibit the decomposition of diatom-bound OM. During burial, ~34% of residual sedimentary OM appears related to RSi in nearshore and mid-shelf deposits.

[1] Michalopoulos *et al.* (2000) *Geology* **28**:1095-1098 [2] Lucaides *et al.* (2010) *Chemical Geology* **270**:68-79 [3] Presti and Michalopoulos (2008) *Cont. Shelf Res.* **28**:823-838

Chemical and isotopic features of mafic granulites from Serre massif (Calabria-Italy)

F. MICHELETTI¹*, A. FORNELLI¹, A. MUSCHITIELLO¹
AND G. PICCARRETA¹

¹Earth science and geo-environmental Dep., Bari University
Italy, francesca.micheletti@uniba.it

Different types of mafic granulites characterize the lower crust of the Serre Massif (Calabria, Southern Italy). They consist of: layered metagabbros (Pl+Opx+Amph±Cpx±Bt±Qtz±Grt) and metric bodies of meta-monzogabbros (Pl+K-feld+Opx+Cpx+Bt±Qtz±Grt) at the base of the lower crust and lenses or layers of metabasites (Pl+Opx+Cpx±Bt±Amph±Qtz±Grt) interleaved with migmatitic metapelites and felsic granulites overlying the metagabbros. The magmatic protoliths are Neoproterozoic (~570 Ma), whereas the granulite-amphibolite facies metamorphism took place in Variscan times [1]. Metagabbros and metabasites are sub-alkaline (Na₂O+K₂O=1-5%) with K₂O<1%, whereas meta-monzogabbros show alkaline character (Na₂O+K₂O=5-7%) with K₂O around 3% reflecting the contents of biotite.

The meta-monzogabbros showing enrichment of incompatible elements are interpreted as derived from small degree of partial melting of enriched mantle, probably as underplating magma in Neoproterozoic times. Subsequent or incremental mantle partial melting events produced melts with tholeiitic and calc-alkaline affinities forming the protoliths of metagabbros and metabasites.

The isotopic features (Sm-Nd, Rb-Sr) of metabasites reflect some crust contamination assisted by fluids derived from host metasediments. On the other hand, also the participation of biotite in the partial melting could account for the variation of Rb-Sr characteristics within the metagabbros and metabasites (Fig. 1).

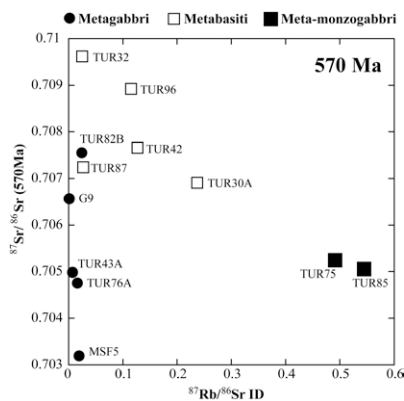


Fig. 1 Rb-Sr isotopic compositions of mafic granulites.

[1] Fornelli *et al.* (2011) *Mineral Petrol* **103**, 101-122.

Crustal evolution of the intracontinental Warburton–Cooper–Eromanga Basin system, central Australia

A. W. MIDDLETON^{*1}, I. T. UYSAL¹ AND S. D. GOLDING¹

¹University of Queensland, Queensland 4072, Australia
(*correspondence: alexander.middleton@uqconnect.edu.au)

The Warburton–Cooper–Eromanga basins host one of the most prospective hot dry-rock geothermal resources (Big Lake Suite granite; BLS) that stems from unusual enrichment in radiogenic elements (up to 144 ppm Th and 30 ppm U). The overlying Eromanga Basin is also endowed with substantial hydrocarbon reserves. Despite these attributes, holistic basin analysis has not been attempted leaving much of central Australia's crustal evolution poorly constrained. By conducting geochemical and geochronological analyses of primary, vein-hosted and authigenic phases, this study elaborates on its crustal evolution throughout the Palaeozoic and the influences on basin thermal and fluid flow events.

U–Pb (420 ± 6.7 Ma) and U–Th–total Pb (407 ± 16 Ma) of granite-hosted primary zircon and uraninite, respectively, provide coincident ages with Sm–Nd of carbonate veins (437 ± 17 Ma) of Warburton vein carbonates. Authigenic illite from Warburton sediments produce a Rb–Sr isochron age of 323.3 ± 9.4 Ma, consistent with previous U–Pb zircon ages estimating emplacement of the Big Lake Suite (Marshall *et al.* unpublished). Rb–Sr of granite-hosted clay fractions yield ages of 87.4 ± 4.9 Ma and 101.1 ± 6.4 Ma, in agreement with quartz encapsulated Ar–Ar total-gas ages of the same clay separates. Isotopically more robust Sm–Nd dating, however, produces older ages of 128 ± 16 Ma. Calculated δ¹⁸O and δD fluid isotopic values are compatible with an influx of meteoric waters in an extensional environment.

Multifaceted analysis of primary and secondary phases produced geologically significant ages attributed to substantial thermal events throughout basinal evolution. Warburton Basin dates provide evidence of episodic magmatic activity associated with relaxation-related and back-arc extension. Dating of illite from the Cooper–Eromanga constrains intra-cratonic basin formation consistent with episodic rifting of Gondwana and opening of the Tasman Sea along the eastern margin of Australia [1]. Such consistency suggests plate-wide transmission of tensional stress to intra-continental crust weakened by abnormally high geothermal gradients, associated with the BLS, and preceding basinal tectonism [2].

[1] Bryan *et al.* (2012) *Episodes* **35**, 142–152. [2] Friedmann & Burbank (1995) *Basin Res.* **7**, 109–127.

Potential of uranium removal from post-uranium mining heaps by indigenous bacteria

S. MIELNICKI^{1*}, L. DREWNIAK¹, M. SZYMKIEWICZ¹,
B. REWERSKI¹ AND A. SKŁODOWSKA¹.

Laboratory of Environmental Pollution Analysis, Faculty of Biology, University of Warsaw, Warsaw, Poland
(*correspondence: smielnicki@biol.uw.edu.pl)

In Poland until 1925 there was no information about existence of uranium ore. First uranium mine was established in Kowary in 1948 and after that uranium ore exploitation in Poland had lasted to 1967. Nowadays low-grade uranium heaps exist in Southern Poland posing potential danger to surrounding environment and human beings. The traditional methods of bioremediation are well known but they are costly and inefficient, moreover they require the use of large volumes of acids which can cause irreversible environmental damages.

Alternative environmental friendly methods can be developed. Indigenous microorganisms can participate in pollution mobilisation and the resulting leak can be collected into the drainage system. Identification of indigenous microorganisms existing in the environment of piles is the first step in the assessment whether the process can take place.

Five sites containing waste with uranium concentration in the range from 112.75 to 2986 mg/L were chosen as a potential places for isolation of microorganisms, metagenomic DNA and *16S rRNA* gene analysis to define microbiological potential. Bacteria from the genus of *Halothiobacillus*, *Sphingomonas*, *Pseudomonas* and *Acidithiobacillus* were found as dominant. They are well known as microorganisms able to indirect transformation of uranium compounds.

After 14 days of incubation, indigenous bacteria in acidic conditions (starting pH 2.5) mobilized 0 - 60% of uranium (depending of the type of waste) in comparison to sterile control in which 0-50% of uranium was mobilized respectively.

These preliminary results clearly show that construction of passive bioremediation system is possible and may be efficient.

Gaussberg leucites – new data on mineralogical and geochemical composition

N.A. MIGDISOVA^{1*}, N.M. SUSHCHEVSKAYA¹,
B.V. BELYATSKY² AND D.V. KUZMIN³

¹Vernadsky Institute for Geochemistry, RAS, Moscow, Russia
(*correspondence: nat-mig@yandex.ru)
²IPGG, St.Petersburg, Russia
³Max-Planck Institute für Chemie, Mainz, Germany

New geochemical data on Quaternary magmatism of the Gaussberg volcano (Antarctica) confirms the unique features of ultra-potassium alkaline magmatism developed under exclusively continental conditions. Volcanic cone is located on the within Gaussberg rift zone possibly being a part of Lambert fracture zone. The crystallization sequence of Gaussberg volcano lavas is $Ol \rightarrow Ol + Cpx \rightarrow Ol + Cpx + Lc$. Two different types of clinopyroxene phenocrysts were detected: high TiO_2 , low Al_2O_3 group (1) and high Al_2O_3 and low TiO_2 group (2). Rare element patterns for whole-rocks are similar to [1]. Rare element distribution for Cpx 1 demonstrates specific signature showing higher LILE values and appreciably lower $D^{Cpx/L4}$ (two orders of magnitude) then in [2]. These features can be a result of fluid impact on magmatic system. Gaussberg volcano mantle source is enriched in $^{207}Pb/^{204}Pb$ and $^{208}Pb/^{204}Pb$ while it has low $^{206}Pb/^{204}Pb$ (≈ 17.5) value. High $^{87}Sr/^{86}Sr$ ($\approx 0.707-0.710$) taken together with low $^{143}Nd/^{144}Nd$ (≈ 0.5119) ratios suggest LOMU-type of primary mantle source.

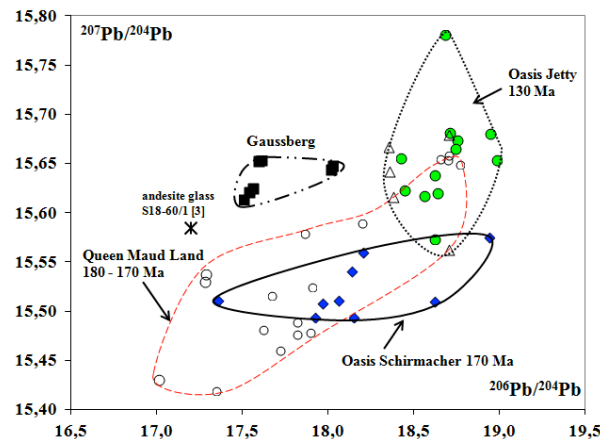


Figure 1: Isotopic data reveal that Gaussberg volcano melts source was the ancient Gondwana lithosphere but not the Antarctic mantle source (Mesozoic plumes)

[1] Murphy D.T. *et al.* (2002) *J.Petrology*, **43**, 6, 981-1001. [2] Foley S.F. & Jenner G.A. (2004) *Lithos*, **75**, 19-38. [3] Kamenetsky V. S. *et al.* (2001) *Geology*, **29**, 3, 243-246.

Kinetics of arsenic sorption on aquifer sediment from Bangladesh imaged by XRF microprobe in flowing columns

I. MIHAJLOV^{1*}, B.C. BOSTICK¹, M. STUTE^{1,2},
I. CHOUDHURY³, K.M. AHMED³ AND A. VAN GEEN¹

¹Lamont-Doherty Earth Observatory of Columbia University, Palisades, NY, USA

(*correspondence: mihajlov@ldeo.columbia.edu)

²Barnard College, New York, NY, USA

³Dhaka University, Dhaka, Bangladesh

To avoid groundwater arsenic (As) contamination, much of the population of Bangladesh depends on deeper wells that are low in As. Pumping these wells could draw high-As groundwater into currently As-safe aquifers. This research examines the mechanisms of As adsorption on natural aquifer sediments that can help retard the migration of As.

Freshly collected sediment from a low-As aquifer in Bangladesh was used for sorption kinetics studies in low-O₂ batch reactors set up in the field with *in situ* (unoxidized) groundwater, as well as in two small columns run under a synchrotron beam for ~20 hrs. Sorption of As onto column sediments was monitored by continuous X-ray fluorescence (XRF) imagery at 2 or 3 μm resolution, and Fe mineralogy was assessed by XANES at several representative points.

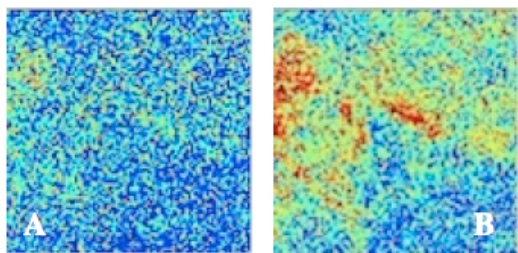


Figure 1: Same-scale and co-located XRF images of As on column sediment at time 0 (A) and after 16 hrs of continuous flow (B). Warmer colors indicate higher concentrations.

Results from both batch and beam column experiments consistently indicated that As adsorption proceeded at a high initial rate ($k \sim 0.5 \text{ hr}^{-1}$) over the first 1-3 hrs, after which it progressively slowed down by 1-2 orders of magnitude. Sites responsible for rapid initial adsorption varied widely in mineralogy and reactivity, while later adsorption rate was more uniform and focused on sites correlated to Fe concentrations. Microscale measurements supplement the macroscopic data and indicate that As transport is kinetically limited by diffusive processes on the grain scale or smaller.

Copper and lead isotope ratios as tracers of soils pollution from the Kombat mining area, Namibia

MARTIN MIHALJEVIC^{1*}, VOJTECH ETTLER¹, BOHDAN KRIBEK², VLADISLAV CHRASTNY, ALES VANEK³
AND VIT PENÍZEK³

¹Institute of Geochemistry, Mineralogy and Mineral Resources, Charles University in Prague, Albertov 6, 128 43 Prague 2, Czech Republic

(*correspondence: mihal@natur.cuni.cz)

²Czech Geological Survey, Geologicka 6, 152 00 Prague 5, Czech Republic

³Department of Soil Science and Soil Protection, Czech University of Life Sciences Prague, Kamycka 129, 165 21, Prague 6 – Suchbát, Czech Republic

Copper (Cu) and lead (Pb) concentration, isotopic composition (⁶⁵Cu/⁶³Cu, ²⁰⁶Pb/²⁰⁷Pb) were studied in contaminated and non contaminated luvisols and mollisols from the Kombat mining area, Namibia. The Cu and Pb concentrations in the studied soils ranged between 21 mg/kg – 757 mg/kg, and 19 mg/kg – 815 mg/kg respectively. Concentration of both metals increased with increasing soil depth. The Pb isotopic signatures (²⁰⁶Pb/²⁰⁷Pb) in soils ranged between 1.15 – 1.21. In most of soil samples, surface horizons exhibited lower ²⁰⁶Pb/²⁰⁷Pb ratio, which originates from the slime dust pollution (²⁰⁶Pb/²⁰⁷Pb ~ 1.15) compared to deeper soil horizons, with lithogenic Pb signatures. Isotopic composition of Cu differs on contaminated and uncontaminated sites and cultivated and non-cultivated sites. The $\delta^{65}\text{Cu}$ in the studied soil horizon ranged between -0.373 ‰ and 0.561 ‰ . The most pronounced variations occurred in contaminated non cultivated soils (0.529 ‰). The contaminated surface horizons are enriched in isotopically heavier Cu (tailing materials), and $\delta^{65}\text{Cu}$ decreased with depth. Fractionation of Cu isotopes in soils is attributed to mobilization of lighter isotope, and preferential binding of heavy isotopes on secondary soil components. This study was supported by the Czech Science Foundation (project P210/12/1413) and IGCP project no. 594.

Ar-Ar and U-Pb isotopic ages of Early Caledonian granulites from the Svyatoy Nos Peninsula (Transbaikalia)

E.I. MIKHEEV¹, A.G. VLADIMIROV^{1,2,3}, A.V. TRAVIN¹, T.B. BAYANOVA⁴ AND N.I. VOLKOVA¹

¹IGM SB RAS, Novosibirsk 630090, Russia
(mikheev@igm.nsc.ru, travin@igm.nsc.ru)

²Novosibirsk State University, Novosibirsk 630090, Russia
(*correspondence: vladimir@igm.nsc.ru)

³Tomsk State University, Tomsk 634050, Russia

⁴GIN KSC RAS, Apatity 184209, Russia
(tamara@geoksc.apatity.ru)

Metamorphic rocks of Svyatoy Nos Peninsula (Transbaikalia) are basic granulites, graphitic marbles, diopside plagioclites and quartzites. The P-T metamorphic conditions are estimated to be 815-860°C and 7.9 to 8.3 kbar. The granulites are intruded by abundant veins of syntectonic granites and granitic pegmatites attributing to Barguzin Complex of the Angara-Vitim batholith (280-298 Ma) [1]. The U-Pb zircon dating of single grains indicates age of granulite metamorphism at 495 ± 5 Ma.

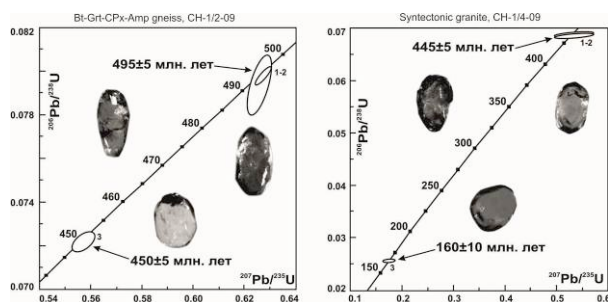


Figure: U-Pb dating of single zircon grains from Svyatoy Nos Peninsula granulites.

Syntectonic granosyenite-granites connecting with intense strike-slip deformations gave ages of 450 ± 5 and 445 ± 5 Ma. Ar-Ar ages on amphibole (256 - 245 Ma) probably date a thermal effect from the Angara-Vitim Batholith.

The sponsorships are the the Earth Sciences Department of SB RAS (IP ONZ-10.3, IP №77) and Federal Grant Programme of Russia (project № 2012-1.2.1-12-000-2008-8340).

[1] Cygankov et al. (2007), Russian Geology and Geophysics **48**, 156-180.

Multiphase inclusions with kokchetavite and K-cymrite in UHP calc-silicate rocks from Kokchetav massif

ANASTASIA O. MIKHNO^{1*}
AND ANDREY V. KORSAKOV¹

¹V.S. Sobolev Institute of Geology and Mineralogy SB RAS, Novosibirsk 630090, Russia
(*correspondence: mao14@list.ru)

Ultrahigh pressure (UHP) rocks of the Kokchetav massif are of particular interest as they were exhumed from at least 120 km depth [1] and experienced peak metamorphic conditions of approximately $T = 1000-1100$ °C and $P = 6-7$ GPa [2].

Here we present findings of K-cymrite ($KAlSi_3O_8 \cdot H_2O$) and kokchetavite ($KAlSi_3O_8$) in association with muscovite/phengite, lollingite, calcite and α -cristobalite in multiphase mineral inclusions in ultrapotassic clinopyroxene (K-Cpx) porphyroblasts of calc-silicate rocks (Kokchetav massif, Northern Kazakhstan). These inclusions were interpreted to be melt at peak metamorphic conditions [3]. Findings of K-cymrite and kokchetavite in polyphase inclusion along with experimental data on K-cymrite calcination [4] proves model of kokchetavite formation through the dehydration of K-cymrite. Presence of K-cymrite in multiphase inclusions in K-Cpx porphyroblasts testifies for high K_2O -content which should be nearly equimolar to H_2O -content in melt [5]. Korsakov *et al.* [6] supposed that gneisses underwent melting to form K_2O -rich melt which migration and further reaction with the carbonate interlayers caused the formation of the calc-silicate rocks with K-Cpx. Neither kokchetavite, nor K-cymrite were reported in gneisses. This fact could imply that melt in gneisses should contain less amount of K_2O , than that in calc-silicate rocks. Therefore we assume that K-rich melt was formed during the prograde metamorphic stage at low melting degrees and then migrated to calc-silicate rocks protholith to form K-Cpx. During peak metamorphic conditions gneisses underwent extent melting which decreased K_2O -content in melt.

This study was supported by MD-1260.2013.5 and RFBR grants no.12-05-31431 and no.13-05-00367.

[1] Sobolev & Shatsky (1990) *Nature* **343**, 742-746. [2] Mikhno & Korsakov (2013) *Gondwana Research* **23**, 920-930. [3] Korsakov & Hermann (2006) *EPSL* **241**, 104-118. [4] Thompson *et al.* (1998) *Contrib.Min.Petrol.* **130**, 176-186. [5] Harlow & Davies (2004) *Lithos* **77**, 647-653. [6] Korsakov *et al.* (2004) *Terra Nova* **16**, 146-151.

Transmission electron microscopy of iron metal in Almahata Sitta ureilite

T. MIKOUCHI^{1*}, K. YUBUTA², K. SUGIYAMA²,
Y. AOYAGI¹, A. YASUHARA³, T. MIHIRA³,
M.E. ZOLENSKY⁴ AND C.A. GOODRICH⁵

¹Dept. Earth & Planet. Sci., Univ. of Tokyo, Tokyo 113-0033, Japan (*correspondence: mikouchi@eps.s.u-tokyo.ac.jp)

²Inst. for Materials Res., Tohoku Univ., Sendai, Miyagi 980-8577, Japan

³JEOL Ltd., Akishima, Tokyo 196-8558, Japan

⁴ARES, NASA-JSC, Houston, TX 77058, USA

⁵Planet. Sci. Inst., Tucson, AZ 85719, USA

Almahata Sitta (AS) is a polymict breccia mainly composed of various ureilite lithologies with lesser chondritic lithologies [1]. Fe metal is a common accessory phase in ureilites, but our earlier studies on Fe metals in one of AS fragments (#44) revealed unique features never seen in other ureilites [2,3]. In this abstract we report detailed transmission electron microscopy (TEM) on these metal grains to better understand the thermal history of ureilites.

We prepared FIB sections of AS#44 by JEOL JIB-4000 from the PTS that was well characterized by SEM-EBSD in our earlier studies [2,3]. The sections were then observed by STEM (JEOL JEM-2100F).

One of the FIB sections shows a submicron-sized intergrown texture composed of Fe metal (kamacite), Fe carbide (cohenite), Fe phosphide (schreibersite), and Fe sulfide (troilite). Probably, this eutectic-looking texture was formed by shock re-melting of pre-existing metal + graphite + phosphates (phosphide?) + sulfides with various amounts.

The other FIB section is mostly composed of homogeneous Fe metal (93 wt% Fe, 5 wt% Ni, and 2 wt% Si), but BF-STEM images exhibited the presence of elongated lathy grains (~2 μm long) embedded in an interstitial matrix. The SAED patterns from these lath grains could be indexed by α-Fe (*bcc*) while interstitial areas are γ-Fe (*fcc*). The elongated α-Fe grains show tweed-like structures suggesting martensite transformation. Such a texture can be formed by rapid cooling from high temperature where γ-Fe was stable. Subsequently α-Fe crystallized, but γ-Fe remained in the interstitial matrix due to quenching from high temperature. Presence of C may have enhanced its stability. This scenario is consistent with very rapid cooling history of ureilites suggested by silicate mineralogy.

[1] Zolensky *et al.* (2010) *MAPS*, **45**, 1618-1637. [2] Goodrich *et al.* (2010) *MAPS*, **45**, A66. [3] Mikouchi *et al.* (2011) *MAPS*, **46**, Suppl., 5409.

Structure of Amorphous Ferric Arsenate from EXAFS Spectroscopy and Total X-ray Scattering

CHRISTIAN MIKUTTA^{1*}, F. MARC MICHEL², PETAR MANDALIEV¹ AND RUBEN KRETZSCHMAR¹

¹Institute of Biogeochemistry and Pollutant Dynamics, ETH Zurich, Switzerland (*christian.mikutta@env.ethz.ch)

²Virginia Tech, Blacksburg, USA

Amorphous ferric arsenate ('AFA', FeAsO₄·*n*H₂O) is a secondary As precipitate frequently encountered in acid mine-waste environments. Its structure has been proposed to resemble that of scorodite (FeAsO₄·2H₂O) in which isolated FeO₆ octahedra share corners with four adjacent arsenate (AsO₄) tetrahedra in a three-dimensional framework (framework model). Conversely, AFA was postulated to consist of single chains of corner-sharing FeO₆ octahedra being bridged by arsenate (chain model). In order to test the accuracy of both structural models, we synthesized AFAs and analyzed their structure by As and Fe *K*-edge extended X-ray absorption fine structure (EXAFS) spectroscopy and total X-ray scattering. We found that both As and Fe *K*-edge EXAFS spectra were most compatible with isolated FeO₆ octahedra being bridged by AsO₄ tetrahedra ($R_{\text{Fe-As}} = 3.33 \pm 0.01 \text{ \AA}$). Wavelet-transform analyses of the Fe *K*-edge EXAFS spectra of AFA complemented by shell fitting confirmed Fe atoms at an average distance of 5.3 Å, consistent with crystallographic data of scorodite and in disagreement with the chain model. Reduced pair distribution functions, $G(r)$, provided unequivocal evidence for the absence of single corner-sharing FeO₆ linkages in AFA. Analyses of radial distribution functions, $R(r)$, additionally indicated that in AFA each As atom has on average about four nearest Fe neighbors, in accordance with the framework model. In summary, our findings imply that scorodite formation from AFA in mining environments proceeds via growth of small clusters with a scorodite-type local structure.

Unconventional generation of hydrocarbons in petroleum basin: the role of siderite/water interface

V. MILESI^{1*}, A. PRINZHOFER², F. GUYOT^{1,3}, F. BRUNET⁴,
LAURENT RICHARD⁵, J. DAIROU⁶
AND M. BENEDETTI¹

¹ Univ Paris Diderot, Sorbonne Paris Cité, IPGP, UMR 7154 CNRS, Paris, France (*correspondence : milesi@ipgp.fr)

² HRT, Av. Atlantica 1130- Copacabana – Rio de Janeiro

³ IMPMC UMR 7590 CNRS, UPMC

⁴ ISTERre, Université Joseph Fourier, Grenoble, France

⁵ Geoquímics dels Àngels, Carrer dels Àngels 4-2-1, 08001 Barcelona, Spain

⁶ BFA, CNRS EAC 4413, Univ Paris Diderot, Paris, France

Hydrocarbons in the petroleum basin of Solimões in Northern Brazil show isotopic trends similar to those of abiotic hydrocarbons observed in oceanic hydrothermal systems.

High concentrations of ferrous iron in the brines indicate a highly reduced environment. Such redox conditions are consistent with the large amount of siderite FeCO_3 in the sediments. The capacity of siderite-water interactions to generate unconventional hydrocarbons has been tested experimentally.

Synthetic FeCO_3 and water were reacted in gold containers at 500 bars, 200°C and 300°C. Siderite dissolution led to reducing conditions due to magnetite formation. In addition, at 200°C, TEM showed the precipitation of a nanometric layer of amorphous carbon covering magnetite grains. At 300°C, H_2 was produced and reacted with CO_2 to generate organic compounds such as methane and carboxylic acids [1]. The dissolved organic compounds concentrations are consistent with a cascade of reduction from CO_2 to CH_4 [2].

Alternatively, CH_4 could form through the hydrogenation of the amorphous carbon coating observed on magnetite grains. This latter mechanism is more consistent with the isotopic data from the Solimões basin where, in addition, senile kerogen and H_2 -rich fluids coexist. Experimental validation is currently underway.

[1] McCollom (2003), *Geochim. Cosmochim. acta*, **67**, 311-317. [2] Seewald *et al.* (2006), *Geochim. Cosmochim. acta*, **70**, 446-460.

A new calibration of the carbonate clumped isotope thermometer based on synthetic calcites

I. MILLÁN*, S. BREITENACH, N. MECKLER, M. ZIEGLER
AND S. M. BERNASCONI

ETH Zürich, Geologisches Institut, Sonneggstrasse 5, 8092 Zürich, Switzerland.

(*correspondence: isabel.millan@erdw.ethz.ch)

Previous calibrations of the clumped isotope thermometer based on synthetic calcites differ in the inferred relationship between isotopic ordering in the carbonate and temperature [1, 2]. The “absolute reference frame” proposed by Dennis *et al.* [3] improved the interlaboratory comparison but did not eliminate the discrepancies between the laboratories. It is clear that especially for inorganically precipitated carbonates more experimental data are needed. Here we present a new calibration on synthetic calcites and compile all published calibration data available to date.

Our new calibration is based on 11 synthetic calcites precipitated at known temperatures between 4°C and 80°C. CaCO_3 was precipitated inorganically by mixing solutions of NaHCO_3 (0.1M) and CaCl_2 (0.1M) at the desired temperatures. The solutions were kept at known temperatures in incubators for 5 days before starting the experiments. Analyses were conducted at ETH on small carbonate samples (ca. 170-220 μg) using a Kiel IV Carbonate Device coupled to a Thermo Finnigan MAT 253 Mass Spectrometer [4]. The samples were measured multiple times on different days, with each measurement consisting of 9-15 analyses of separate aliquots. Data are presented relative to the “absolute reference frame” [3].

We find a robust linear relationship between Δ_{47} and temperature of precipitation. We discuss several issues related to the slope of the linear regression through Δ_{47} plotted against solution temperatures and the compilation of previous calibrations in the absolute reference frame.

[1] Ghosh *et al.* 2006. *Geochim Cosmochim Acta* 70, 1439-1456 [2] Dennis and Schrag, 2010. *Geochim Cosmochim Acta* 74, 4110-4122 [3] Dennis *et al.*, 2011. *Geochimica Et Cosmochimica Acta* 75, 7117-7131 [4] Schmid and Bernasconi, 2010. *RCMS* 24, 1955-1963.

Hot/cold, wet/dry, big/small, erupt/stall, juvenile/anatectic? – Multiple personalities of felsic magmatism

C.F. MILLER^{1*}, S.M. MCDOWELL¹, T.L. CARLEY¹, W.O. FRAZIER¹, A.S. PAMUKCU¹, A.DEJ. PADILLA¹, L.L. CLAIBORNE¹, D.M. FLANAGAN¹, G.A.R. GUALDA¹, J.S. MILLER², J.L. WOODEN³ AND R.W. MAPES⁴

¹Vanderbilt Univ, Earth & Environmental Sciences, Nashville USA, calvin.miller@vanderbilt.edu (* presenting author)

³Stanford U, Geol & Env Sci, Stanford USA, jwooden@stanford.edu

²San Jose State U, Geology, San Jose USA, jonathan.miller@sjsu.edu

⁴ExxonMobil, Houston TX USA, russmapes@gmail.com

Felsic magmas are linked by qtz-feldspar-melt equilibria that limit their range of major element compositions. Crustal processing is thus clearly a common factor in production of all such magmas, but this does little to resolve – and in fact obscures – longstanding and recent controversies concerning sources, generation and emplacement processes, evolution, and relationships between felsic plutonism and volcanism.

Field, geochemical, and geochronological characteristics of similarly silicic rocks from a variety of environments we have investigated* reveal remarkable diversity:

- Scales: small (~10³ km³ - increments in some plutons, small eruptions) to giant (10³ km³ supereruptions)
- Initial temperatures: ~700 C to near 1000 C
- Zircon inheritance: negligible to dominant
- Entrained crystal fractions: negligible to near lock-up
- Initial water contents: ~dry to wet (≤3 to near 10 wt%)
- Clear volcano-pluton connections, as well as plutons unlikely to have erupted counterparts and eruptions unlikely to have left appreciable plutonic residue
- Isotopically juvenile to ancient crust-dominated
- Involvement of mafic magma: obvious in some, apparently limited in others, absent or occult in yet others

Characteristics generally correlate and suggest that (1) cool, wet, crystal-rich magmas, largely anatectic, are doomed to stall without eruption; (2) very large magma volumes ('big tanks') may reflect unusual thermal input, either initially producing huge volumes or mobilizing stagnant mushes. Intriguing departures from simple relationships warrant further consideration – e.g. large variations in T and magma volumes in closely associated magma systems, isotopically primitive granitoids with abundant ancient zircon inheritance, very hot felsic magmas with no obvious mafic input.

[*Deep-seated to very shallow plutons, convergent and extensional settings, southern Appalachians, SW USA, Iceland; small to supereruption volcanic deposits, subduction, extension, hot spot settings, Cascades & SW USA, Iceland]

Chalcopyrite in the R chondrite PRE 95411

K.E. MILLER^{1*}, M.S. THOMPSON¹, T.J. ZEGA¹ AND D.S. LAURETTA¹

¹Lunar and Planetary Laboratory, Dept. of Planetary Sciences, University of Arizona, Tucson, AZ 85721
(*correspondence: kemiller@lpl.arizona.edu)

The R chondrites record petrologic grades from 3 to 6, suggesting parent-body histories from unaltered to nearly equilibrated. However, a growing body of evidence suggests the group may have experienced hydrothermal alteration. Reports of amphibole, biotite, and chalcopyrite in the R chondrites all support aqueous processes [1-3]. Recent observations of hydrous minerals in a second R chondrite and other indications of aqueous alteration appear to corroborate the earlier results [4, 5]. Here we expand on these efforts and report an investigation of chalcopyrite in a sulfide assemblage in the R3 chondrite PRE 95411.

Electron microprobe analysis indicates the assemblage is primarily composed of pyrrhotite with minor pentlandite, troilite, and chalcopyrite. Based on previously described methods [6], we used focused ion beam scanning electron microscopy (FIB-SEM) to prepare an electron-transparent cross section of the assemblage for transmission electron microscope (TEM) analysis [7]. Selected-area electron-diffraction confirms the presence of chalcopyrite and troilite. Energy-dispersive X-ray spectrometry shows that the chalcopyrite and troilite grains are bifurcated by an Fe-Ni-O-rich vein. The vein center contains a linear domain of Fe-rich, Ni-poor nanocrystalline material. In comparison, the material around the domain is amorphous and relatively Ni-rich and Fe-poor. Chemical mapping also reveals that the grain boundary between troilite and the chalcopyrite is enriched in Cu. These microstructural features are reminiscent of those associated with a cubanite grain in the Orgueil CI chondrite [8], suggesting hydrothermal alteration.

These results indicate that the R chondrites experienced volatile-rich conditions. Improved understanding of the distribution of volatiles provides important constraints on the formation and evolution of the solar system.

[1] McCanta *et al.* (2008) *Geochim. Cosmochim. Ac.* **72**, 5757-5780. [2] Schulze *et al.* (1994) *Meteoritics* **29**, 275-286. [3] Jackson and Lauretta (2010) *Meteorit. Planet. Sci.* **45**, A94. [4] Gross *et al.* (2013) *44th LPSC*, #2212. [5] Ruzicka *et al.* (2013) *44th LPSC*, #1168. [6] Zega *et al.* (2007) *Meteorit. Planet. Sci.* **42**, 1373. [7] Zega and Floss (2013) *44th LPSC*, #1287. [8] Berger *et al.* (2011) *Geochim. Cosmochim. Ac.* **75**, 3501-3513.

Significant observed copper isotopic abundance variations in biological materials.

KERRI MILLER^{1*}, TYLER COPLEN²
AND MICHAEL WIESER¹

¹Department of Physics and Astronomy, University of Calgary, 2500 University Drive NW, Calgary, AB, T2N 1N4, Canada, kamiller@ucalgary.ca (*presenting author)

²US Geological Survey, 12201 Sunrise Valley Drive, Reston, VA, 20192, USA

Copper is an essential nutrient in both flora and fauna and has proven to be critical in maintaining homeostatic balance by participating in many metabolic processes. Copper has two naturally occurring stable isotopes, ⁶³Cu and ⁶⁵Cu. The ratio between the amounts of these two isotopes can be used to indicate the source of copper to an organism, give insight to cycling processes as well as metabolic pathways. Natural variations in copper isotopic composition have a measured range of 9 ‰ in geological materials and 3 ‰ in water samples [1, 2]. Recent evidence has shown that the assimilation and subsequent use of copper in an organism may cause further fractionation. This has been demonstrated in mice where it was shown that modified gene expression caused a shift in isotopic composition of copper in the brain [3]. In a recent study, participants with Parkinson's disease demonstrated differences in the metabolism of copper isotopes [4].

In order to explore the copper isotope variability in living systems, select samples were analyzed: exotic wood samples, wild animal hair, and hair and fingernails samples from local Calgary residents. Wood samples were analyzed as part of an ongoing project to determine if isotopic systems can be used to identify the geographic origins of the wood in an effort to prevent illegal trading. Hair samples from wildlife in Alberta were analyzed to determine if copper isotopes can be used to identify the dominant source of food. Hair and nail samples from local Calgary residents were also analyzed and compared to the local drinking water. A range in $\delta^{65}\text{Cu}$ of over 20 ‰ was observed.

[1] Larson, P.B., Maher, K., Ramos, F.C., Chang, Z., Gaspar M., Meinert, L.D. (2003) *Chemical Geology* **201**; 337–350. [2] Borrok, D.M., Nimick, D.A., Wanty, R.B., Ridley, W.I. (2008). *Geochim Cosmochim Acta* **72**; 329–344. [3] Büchl, A., Hawkesworth, C.J., Ragnarsdottir, K.V., Brown, D.R.; (2008) *Geochem. Trans.* 1-7. [4] Lerner, F., Sampson, B., Rehkamper, M., Weiss, D.J., Dainty, J., O'Riordan, S. (2013) High precision isotope measurements show poorer control of copper metabolism in parkinsonism. *Metallomics*, **5**; 125-132.

Construction of high-resolution trace element time-series in slow growth speleothems by ELA-ICP-MS: Challenges, new approaches and validation strategies

NATHAN R. MILLER* AND JAY L. BANNER¹

¹Department of Geological Sciences, The University of Texas at Austin, Austin, TX 78712-1722, USA

(*correspondence: nrmiller@jsg.utexas.edu)

Speleothems hold important potential to record terrestrial paleoclimate variations over millennial scales, as increasingly supported by monitoring studies of modern karst systems. Trace element variations in drip waters and corresponding plate calcite samples demonstrate the potential for subannual resolution in settings having well-expressed seasonality (rainfall, temperature). The high sensitivity and rapid peak-hopping capabilities of quadrupole ICP-MS, integrated with the superior coupling capacity and high spatial accuracy of modern excimer 193 nm laser ablation systems (ELA-ICP-MS line scans), offers an efficient means for constructing high-resolution chemical time-series in growth-banded speleothem calcite. However, application of the technique becomes increasingly challenged with decreasing speleothem growth rates, a factor that has relegated most high-resolution trace element studies to growth rates exceeding 100 $\mu\text{m}/\text{yr}$. Slow-growth speleothem records (< 50 $\mu\text{m}/\text{yr}$) present three significant challenges to ELA-ICP-MS, namely: (1) growth banding is often not visible by standard petrographic techniques, let alone via imaging of the laser ablation system; (2) the crystallographic fabric comprising growth bands develops as successions of rhombohedral overgrowths, the scale and geometry of which can compromise the goal of obtaining unaliased stratigraphic sampling; and (3) achieving counting statistics capable of resolving subannual chemical signals is more difficult due to the need for small apertures (lower signal-to-noise) and because of more limited “dwelling” time within growth band intervals associated with rapid chemical gradients. Parallel-offset line traverses, a well-established approach for evaluating reproducibility of chemical signals, often do not show high correspondence due to such localized sample aliasing – raising the question “We know what we are targeting, but do we know what we are hitting? We reiterate the importance of locating laser ablation line scans from the informed perspective of oriented growth band fabric imagery, and developing analytical validation strategies that demonstrate the capacity to resolve slow-growth chemical waveforms.

Geochemical stratigraphy and correlation within the Faroe Islands Basalt Group: Temporal and Spatial Evolution of Mantle Sources during Continental Rupture

MILLETT, J. M.^{1*}, HOLE, M. J.¹, JOLLEY, D. W.¹
AND PASSEY, S. R.²

¹Department of Geology & Petroleum Geology, Meston Building, Kings College, University of Aberdeen, Aberdeen, AB24 3UE UK (*correspondence: j.millett@abdn.ac.uk)

²CASP, West Building, 181A Huntingdon Road, Cambridge CB3 0DH, UK

The geochemical signatures recorded during periods of Large Igneous Province (LIP) volcanism provide important evidence as to mantle sources and magmatic evolution through time. Our understanding of the temporal development of these provinces relies on both accurate stratigraphical sampling constraints of flood basalt sequences along with the integration of available age-dating methods. In this contribution we present new major, trace and mineralogical element data for the Faroe Islands Basalt Group (FIBG), NE Atlantic. The FIBG records a near continuous ~6.6km composite eruptive succession of the Palaeogene aged North Atlantic Igneous Province. All the data is stratigraphically constrained within a GIS database and has been compared to biostratigraphic and sedimentary inter-bed geochemical data which allows high resolution inference into the timing of eruption events during continental rupture. Distinct mantle source variations occur at a number of intervals through the stratigraphy including N-MORB-like and enriched 'Icelandic' sources. The integration of the new flow by flow data for the lower Beinissvørð and upper Enni Formations helps constrain the timing and the nature of these transitions. A distinct transition from Nb-depleted N-MORB-like to a Nb-enriched 'Icelandic' source is recorded in the last few flows of the first major phase of FIBG volcanism. This transition immediately precedes the regional hiatus recorded by the Prestfjall Formation before renewed N-MORB-like source volcanism. The timing of this hiatus, directly after the short lived onset of 'Icelandic' source volcanism implies a potential link between magma plumbing and tectonic reorganisation at the time. The Enni Formation at the top of the FIBG encompasses at least two inter-digitating flow fields sourcing separate high-TiO₂ enriched sources and a low-TiO₂ MORB-like source. The distribution of distinct geochemical lava groups on the Faroe Islands are demonstrated to overlap both in space and time. The present results have important implications to correlation attempts involving lava geochemistry on both the local and regional scale.

Lithium isotopes in surficial waters: examples from rivers and peatlands

ROMAIN MILLOT^{1*}, PHILIPPE NÉGREL¹,
ANNE-MARIE DESAULTY¹ AND AGNÈS BRENOT²

¹ BRGM, Laboratory Division, Orléans, France
(* correspondence : r.milloy@brgm.fr)

² BRGM, Territorial Activities Division, Lyon, France

In the present work, we report data for lithium and its isotopes in two different hydrosystems in France: the Loire River basin and the Sauvetat peatland system within the Massif Central (part of the Loire catchment).

Assessing the behaviour of lithium and the distribution of Li isotopes during weathering is of major importance for studying water/rock interactions at the surface of the Earth. This is because lithium (⁶Li ~ 7.5% and ⁷Li ~ 92.5%) is a fluid-mobile element and, due to the large relative mass difference between its two stable isotopes, it is subject to significant low temperature mass fractionation which provides key information on the nature of weathering processes.

The Loire River in central France is approximately 1010 km long and drains an area of 117 800 km². Lithium concentrations in river waters of the Loire River main stream and the main tributaries span a wide range from 3.4 to 46.5 μg/L, whereas δ⁷Li are between +5.0 and +13.3‰. There is a clear contrast between the headwaters upstream and rivers located downstream in the lowlands, with a significant decrease of the δ⁷Li with the distance from the source. In addition, one of the major tributaries in the Massif Central (the Allier River) is clearly influenced by inputs from mineralized waters resulting of hydrothermal activities having lower δ⁷Li values.

Concerning the peatland system in the Sauvetat area, we explore the use of Li and its isotopes as a proxy of ground-to-surface water exchanges in a peatland from a mire-lake complex in the French Massif Central, with the aim to investigate the capability of Li isotopes as hydrogeological tracers. Variations in δ⁷Li values can be used to distinguish between precipitation, groundwater and anthropogenic inputs (significantly enriched in ⁷Li) in peat lands, providing a unique perspective on the hydrologic dynamics of the system.

These two examples reveal important information about lithium and its isotopes but, considered together, provide a more integrated understanding of the factors controlling lithium isotopic distribution in surficial waters.

Global silicate weathering: not always in control of climate, and not required to balance global degassing

BENJAMIN MILLS¹, ANDREW J. WATSON¹
AND TIMOTHY M. LENTON²

¹School of Environmental Sciences, University of East Anglia, Norwich, NR4 7TJ, U.K.

²College of Life and Environmental Sciences, University of Exeter, Exeter EX4 4PS, UK.

Silicate weathering and carbonate deposition allows for net transfer of CO₂ from the atmosphere to the crust, and dependence of the rate on local temperature and CO₂ concentration stabilizes long term climate [1].

However, the operation of this process is considerably more complex than the simple kinetic relationships employed in current models. Limitation at the global scale via transport of cations is possible either under very high temperature/CO₂, such as following a snowball Earth event [2], or under very low erosion rates, such as during the Mesozoic. In both of these cases, climate stability may have been unattainable for long periods.

In the Precambrian, smaller continental area and lack of biotic soils likely provided harsh limitation of the silicate weathering flux, requiring the operation of an additional stabilizing mechanism to counter the higher degassing rates expected. Seafloor carbonatization appears to be a likely candidate [3], and additional climate regulation via this process decouples the the global silicate flux from CO₂ degassing rates.

The action of two independent stabilizing mechanisms allows for the global silicate weathering rate to increase permanently in response to biological or tectonic enhancements. We suggest that increasing rates of organic carbon burial over time (leading to planetary oxygenation), as well as changes in CO₂ dynamics, may be linked to a progressive increase in terrestrial chemical weathering rates.

[1] Walker, J.C.G., P.B. Hays, and J.F. Kasting (1981), *J. Geophys. Res.* **86**, 9776-9782. [2] Mills, B., *et al.* (2011), *Nature Geosci.* **4**, 861-864. [3] Caldeira, K. (1995), *Am. J. Sci.* **295**, 1077-1114.

Experimentally verifying the low oxygen demands of primitive animals

D.B. MILLS^{1*}, L.M. WARD², C. JONES¹, M. FORTH¹, B. SWEETEN¹, A.H. TREUSCH¹ AND D.E. CANFIELD¹

¹Nordic Center for Earth Evolution, Institute of Biology, Univ. of Southern Denmark, 5230 Odense M, DK

(*correspondence: daniel.brady.mills@gmail.com)

²Department of Geological and Planetary Sciences, Caltech, Pasadena, CA 91125, USA (lward@caltech.edu)

A rise of oxygen in the atmosphere and oceans is one of the most popular explanations for the relatively late and abrupt appearance of animal life on Earth [1, 2]. Multiple lines of geochemical evidence support an oxygenation and ventilation of the Ediacaran ocean (635–542 Ma), corresponding with the diversification of complex life, and supporting oxygen's role as the driving environmental factor behind the rise of metazoans [3, 4, 5, 6]. However, the critical concentration of oxygen required for primitive animals remains ambiguous. Therefore, in order to evaluate the oxygen-trigger hypothesis for animal origins, the minimum oxygen concentration supportive of animal life, in general, needs to be experimentally determined.

Our experiments show that modern demosponges, serving as analogs for early animals, can survive under low-oxygen conditions of 0.5-4.0% present atmospheric levels. Given that the last common ancestor of metazoans likely exhibited a physiology and morphology very similar to those of modern sponges [7, 8], its oxygen demands may have been met well before the marine redox shifts of the Ediacaran Period. Therefore, while animals certainly require oxygen, their origination did not necessarily require a contemporaneous rise in the oxygen content of the atmosphere and oceans. Our results, overall, suggest that the relatively late origination of animal life on Earth was not due to restrictively low levels of environmental oxygen that were finally lifted during the Neoproterozoic Era.

[1] Nursall (1959) *Nature* **183**, 1170-1172. [2] Knoll (1992) *Science* **256**, 622-627. [3] Fike *et al.* (2006) *Nature* **444**, 744-747. [4] Canfield *et al.* (2007) *Science* **315**, 92-95. [5] Scott *et al.* (2008) *Nature* **452**, 456-459. [6] Sahoo *et al.* (2012) *Nature* **459**, 546-549. [7] Sperling *et al.* (2009) *Mol. Biol. Evol.* **26**, 2261-2274. [8] Erwin *et al.* (2011) *Science* **334**, 1091-1097.

Fluid flow and redox metal cycling in Cayman Trough hydrothermal sediments

RACHEL A. MILLS^{1*}, WILLIAM B. HOMOKY¹
AND THE DEEPESTVENTS SHIPBOARD SCIENTIFIC TEAM

¹Ocean and Earth Science, University of Southampton,
National Oceanography Centre Southampton, SO14 3ZH,
UK (*correspondence: rachel.mills@soton.ac.uk,
w.homoky@soton.ac.uk)

Metalliferous sediments accumulate adjacent to active hydrothermal vent sites via mass wasting of mound debris and fall-out of particles from hydrothermal plumes. Continued redox reactions at the limit of oxygen penetration lead to 'zone refining' of the sediment pile and metal enrichment around the active redox front [1]. Diffusive processes and active circulation of dilute hydrothermal fluids through the sediments may lead to significant fluxes of some elements into and out of the seafloor, though this is poorly constrained and not included in evaluations of ocean budgets for these elements.

We present dissolved micro-nutrient trace metal pore-fluid data for representative sediments from the Beebe Vent Field [2]. The Beebe Vent Field fluids are extremely deep (5000 m), high temperature (>400°C) and metal-rich. Fragile sulfide chimneys topple readily to form metalliferous sediments which are oxygen depleted within 3-7 mm of the seawater interface. The deep sedimentary setting precludes significant carbonate accumulation at the seafloor and pelagic sedimentation is minimal leaving weathered sulfide exposed to seawater. Primary chimney mineral phases which dominate the sediment, break down during seafloor weathering and there is a flux of reduced metals to the overlying water column associated with this sedimentary reprocessing. Therefore, secondary processing of hydrothermal material during active weathering of seafloor deposits can lead to enhanced fluxes of trace metals to the ocean which are then transported out of the benthic boundary layer via plume entrainment and dispersal over significant distances.

[1] Severmann, S., *et al.*, (2006) *Geochim. Cosmochim. Acta*, 70, 1677-1694. [2] Connelly, D.P. *et al.*, (2012) *Nature Comms.*, 3, doi:10.1038/ncomms1636.

Biomass residues from different classes of soil microorganisms are a significant source of soil organic matter

A. MILTNER*, J. ACHTENHAGEN, C. HOFFMANN-JÄNICHE, M. SCHWEIGERT, M. BRAECKEVELT, F.-A. HERBST, J. SEIFERT, T. FESTER AND M. KÄSTNER
UFZ - Helmholtz Centre for Environmental Research, Leipzig,
Germany (*correspondence: anja.miltner@ufz.de)

Introduction

Cell envelope fragments originating from soil microorganisms were demonstrated to contribute significantly to the formation of soil organic matter (SOM) [1]. This hypothesis was supported by chemical and microscopic analyses [1] as well as by NMR spectroscopy [2]. Different classes of soil microorganisms have different chemical compositions of their cell envelopes and thus may contribute to SOM formation to a different extent. We compared the fate of *Escherichia coli* (Gram-negative bacterium), *Bacillus subtilis* (Gram-positive bacterium) and *Laccaria bicolor* (ectomycorrhizal fungus) in soil to estimate their relative contributions to SOM formation.

Material and Methods

¹³C-labeled organisms produced by culturing them on labeled glucose were mixed with soil and incubated for up to 224 days. Isotopic data of soil and CO₂ released by respiration were used to set up mass balances. Additional information about the fate of the biomass C was derived from quantitative and isotopic analyses of fatty acids and amino acids. Selected samples were also analysed by scanning electron microscopy.

Results and Discussion

For all classes of microorganisms, substantial amounts of the label remained in the soil. Fungal biomass was mineralised slower than bacterial biomass, with Gram-negative bacteria being mineralised slightly slower than Gram-positive ones. The amount and isotopic composition of the biomolecules showed that substantial amounts of the bacterial biomass-derived C were incorporated into non-living SOM. Proteins seemed to be particularly prone to stabilisation in soil: Highly labeled *B. subtilis* proteins were detected until the end of the experiment. Biomass residues of all types of soil organisms thus contribute to SOM formation, and proteins seem to be involved significantly in this process.

[1] Miltner *et al.* (2012) *Biogeochemistry* **111**, 41-55. [2] Simpson *et al.* (2007) *Environ Sci Technol* **41**, 8070-8076.

Role of zero-valent sulfur in marine methane oxidation

J. MILUCKA^{1*}

¹Max Planck Institute for Marine Microbiology, 28359 Bremen, Germany (*correspondence: jmilucka@mpi-bremen.de)

Sulfate is the main oxidant for seafloor methane, and the transition zones of methane and sulfate thus play a key role in the biogeochemical carbon cycling in methane-bearing marine sediments. Our recent results¹ suggest that the impact of anaerobic oxidation of methane (AOM) on the marine sulfur cycle might be just as important.

Using a suite of microbiological and experimental biogeochemical approaches, such as cultivation, stable- and radio-isotope labelling experiments and single-cell-based techniques, we have investigated microbial sulfur cycling associated with marine methane oxidation in microbial enrichment cultures. We could show that during AOM sulfate is only partially reduced to zero-valent sulfur, which is stored intracellularly as a mixture of cyclo-octasulfur and soluble polysulfides. The release of the produced sulfur from the cells provides a local source of zero-valent sulfur in sulphidic marine sediments. Furthermore, we could show that the produced zero-valent sulfur in a form of disulfide can be further disproportionated to sulfate and sulfide by bacteria associated with the methane-oxidizing archaea.

Our observations show an unexpectedly diverse metabolic potential of the AOM microorganisms and expand the physiological diversity of known microbial sulfur metabolisms. Moreover, our results suggest a solution to the long-standing mystery of a missing intermediate in AOM by suggesting a key role of zero-valent sulfur in this process. These new insights have important implications for the biogeochemical carbon and sulfur cycling in marine sediments.

[1] Milucka *et al.* (2012), *Nature* 491, 541–546.

Record of bacterial sulfate reduction during 50~210 kyr ago in the submarine hypersaline Meedee Lake, off Crete Island, Eastern Mediterranean Sea.

H. MINAMI^{1*}, K. E. YAMAGUCHI^{1,2}, H. NARAOKA³, M. MURAYAMA⁴, M. IKEHARA⁴ AND H. TOKUYAMA⁴

¹Dept. Chem., Toho Univ. (6113023m@nc.toho-u.ac.jp); ²NASA Astrobiology Inst. (NAI); ³Dept. Earth & Planet. Sci, Kyushu Univ. ⁴Ctr for Adv. Marine Core Res. (CMCR), Kochi Univ.

Meedee Lake (2920m deep) is a submarine, hypersaline lake with its salinity >10 times higher than that of normal seawater, due to elution of submarine evaporites formed during Messinian Salinity Crisis 5.33 to 6 Ma ago. The density-stratified lake water has been kept anoxic due to consumption of dissolved O₂ by decomposition of organic matter sinking from the overlying water.

In order to understand changing redox state and microbial activity in the submarine extreme lake environment, sediment core was collected from the margin of the lake. The core shows alternation of pyrite-bearing light- and Fe-oxide-bearing dark-colored layers reflecting fluctuating redox during deposition [1]. The sulfate-rich lake hosted sulfate-reducing bacteria.

To obtain insight into biogeochemical S cycling in the lake, we measured abundance of S-bearing species by sequential extraction method. Five phases were separately quantified: (1) AVS (acid volatile sulfide), (2) pyrite, (3) sulfate, (4) organic-S, and (5) elemental S, by using a method of [2], a combination of [3, 4, 5]. Isotopic compositions of these phases were measured by EA-IRMS at Kyushu University.

Sulfate was found to be the most abundant species, accounting for 90% in both light and dark layers. The isotopic compositions ($\delta^{34}\text{S}_{\text{SO}_4}$ vs. VCDT) vary greatly from +16‰ to +32‰. Such large fluctuations are most likely due to variable (a) degrees of sulfate utilization by sulfate-reducing bacteria (SRB) and/or (b) sulfate concentration. When activity of SRB was not enhanced, sulfate utilization by SRB was not complete, and/or sulfate concentration is reasonably high, then the $\delta^{34}\text{S}_{\text{SO}_4}$ values would not have much changed from their original seawater value (+21‰). Contrary, when activity of SRB was enhanced and sulfate utilization was near complete, then the $\delta^{34}\text{S}_{\text{SO}_4}$ values would have progressively increased from ~21‰ (i.e., Rayleigh fractionation).

Bacteriogenic pyrite would have gone by oxidation due to lowering of lake water level and invasion of oxic seawater, while sulfate minerals would have been preserved. This study demonstrates utility of sulfur isotope compositions of sulfate minerals in sediments to uncover past activity of SRB, even if bacteriogenic pyrite was not well preserved.

[1] Izumitani (2010) M.Sc., Kochi Univ. [2] Kobayashi (2011) Senior Thesis., Toho Univ. [3] Canfield *et al.* (1986) *Chem, Geol*, 54, 189, [4] Buckland & Boman. (2005). *Agricul, Food Sci*, 14, 70.

www.minersoc.org

DOI:10.1180/minmag.2013.077.5.13

Geochemical map of $^{87}\text{Sr}/^{86}\text{Sr}$ ratios using stream sediments is useful for detection of food-producing areas and human migration?

M. MINAMI^{1*}, Y. JOMORI² AND A. OHTA³

¹Center for Chronological Research, Nagoya University, Nagoya 464-8602, Japan

(*correspondence: minami@nendai.nagoya-u.ac.jp)

²Graduate School of Environmental Studies, Nagoya University, Nagoya 464-8601, Japan

³Geological Survey of Japan, AIST, Ibaraki 305-8567, Japan

Geochemical map of $^{87}\text{Sr}/^{86}\text{Sr}$ ratios is needed for multiple purposes of detection of food-producing areas, tracing of patterns of ancient human migration, and culture change in earlier times, as well as environmental applications. We have started a nationwide geochemical mapping of $^{87}\text{Sr}/^{86}\text{Sr}$ ratios using catchment outlet stream sediments (<180 μm) in Japan. The $^{87}\text{Sr}/^{86}\text{Sr}$ spatial distribution in Shikoku Island and the Kii Peninsula in Japan largely reflected underlying $^{87}\text{Sr}/^{86}\text{Sr}$ bedrock distribution [1]. The result shows that $^{87}\text{Sr}/^{86}\text{Sr}$ map using stream sediments is useful for investigating the geochemical and geological features of bedrocks. Meanwhile, $^{87}\text{Sr}/^{86}\text{Sr}$ values of stream sediments might not be indicative of biological $^{87}\text{Sr}/^{86}\text{Sr}$ values of vegetation and fauna. In this study, therefore, we investigated relationship between $^{87}\text{Sr}/^{86}\text{Sr}$ ratios in biological samples and in stream sediments collected around the sampling points. The samples used are rice-plants, animal bones, paddy water and soil, and stream water and sediments collected from an area distributing of granite bedrocks in Toyota, Japan. For soil and stream sediments, bulk Sr and ammonium acetate extractable Sr (exchangeable Sr) fractions were both analyzed. $^{87}\text{Sr}/^{86}\text{Sr}$ ratios were measured with thermal ionization mass spectrometer (TIMS; VG Sector 54) at Nagoya University.

The bulk Sr fractions in soil and stream sediments showed larger $^{87}\text{Sr}/^{86}\text{Sr}$ ratios than the exchangeable Sr fractions and biological samples. The $^{87}\text{Sr}/^{86}\text{Sr}$ ratios of exchangeable Sr fractions were in agreement with the $^{87}\text{Sr}/^{86}\text{Sr}$ ratios in biological samples within analytical errors. The results suggest that the $^{87}\text{Sr}/^{86}\text{Sr}$ ratio of biological samples is constrained by the $^{87}\text{Sr}/^{86}\text{Sr}$ ratio of catchment outlet stream sediments, that is, underlying bedrocks upstream of the sampling points, and that the $^{87}\text{Sr}/^{86}\text{Sr}$ map using stream sediments can be an important database for identifying food-producing areas and ancient human migration in archaeology.

[1] Jomori *et al.* (2013) *Geochem. J.* **47**, 321-335

Tectonic and geothermal significance of thermal springs of Sicily Isl. (southern Italy)

ANGELO MINISSALE¹, SALVATORE GIAMMANCO², DOMENICO MONTANARI³, SALVATORE MONTELEONE⁴ AND MARCO DOVERI³

¹ Institute of Geosciences & Earth Resources, Italian Research Council (CNR), Via La Pira 4, 50121 Florence (Italy), e-mail: *minissa@igg.cnr.it*

² Italian National Institute for Geophysics and Volcanology, Piazza Roma 1, 95125 Catania (Italy), e-mail: *salvatore.giammanco@ct.ingv.it*

³ Institute of Geosciences and Earth Resources, National Research Council of Italy (CNR), Via Moruzzi 1, 56124 Pisa (Italy), e-mail: *d.montanari@igg.cnr.it*; *doveri@igg.cnr.it*

⁴ Department of Geology, University of Palermo, Via Archirafi 20, 90100 Palermo (Italy), *salvatore.monteleone@unipa.it*

Rough morphology, thick (>5km) buried, trusted sequences of Mesozoic platform limestone and active faulting, in a very dynamic context at the boundary between the African and Eurasia plates, make Sicily a perfect place for the emergence of deep circulating waters as thermal springs. Most of them are located in its western sector (west Sicily springs=WSS); a few are related to the presence of the Etna and Iblei Mts Quaternary volcanics in eastern Sicily (ESS). Most of WSS are located along the seashore, or anyhow near the coast; others emerge inland at relatively higher elevations, but always at the edges of outcrops of the limestone sequences. The chemistry of springs suggests that the main circuit of WSS is inside the Mesozoic limestone, and the relative composition is: i) $\text{Ca-SO}_4(\text{HCO}_3)$ for those located inland, ii) markedly Na-Cl for those emerging along the sea, respectively. The $\delta^{18}\text{O}$ and δD composition of most of them suggests meteoric origin, with average recharge elevations at 700 m. Among WSS, the springs from Sciacca are the most promising for geothermal prospecting, since they seem to be a mixing between meteoric water and high temperature oxygen-shifted Mediterranean seawater. Moreover, they also have a CO_2 dominated associated gas phase suggesting the presence of a degassing hydrothermal system in the deep reservoir. Excluding the Sciacca springs in southern Sicily and some mud volcanoes at the foot of the Etna Mt., strongly CO_2 -dominated and high in $^3\text{He}/^4\text{He}$ ratio, suggesting the presence of a mantle gas component, the gas phase associated to the carbonate WSS is N_2 -dominated, reflecting the atmospheric recharge areas more than any deep hydrothermal systems.

Interaction of ions at the surface of soil components

BABAK MINOFAR^{1,2}

¹Institute of Nanobiology and Structural Biology of Academy of Sciences of the Czech Republic

²Faculty of Science, University of South Bohemia Branisovska 31 Ceske Budejovice, minofar@nh.cas.cz

Complex structure of soil makes it interesting for both experimental and theoretical studies. One of most important components of soil, which has strong effect and play important role in the process of adsorption of different elements to the plants and complex formation process of many metal ions in the environment is natural organic matter (NOM).

Solvation structure and dynamics of building blocks of NOMs in aqueous solution studied and surface propensity to the air/aqueous interface observed and decrease of surface tension measured¹ which is supported by surface sensitive (VSFG) spectroscopy².

Also we have used the Temple-Northeastern- Birmingham (TNB)³ model of humic acid which was proposed by Sein *et al.* for complex formation with different ions such as carbonate and iodate ions. We have observed that strong interactions between carboxylate groups of model humic acid take place both in protonated and not protonated humic acids. Moreover, hydrogen bonding and complex formation are two main factors which influencing the aggregation of model humic acid in aqueous solutions. Moreover, we studied the surface propensity and interaction of TNB with different organic contaminants such pesticides by classical molecular dynamics (MD) simulations and revealed that the hydrophobic interaction between organic contaminants and hydrophobic parts of humic acid is one of the most important factor for interactions and surface propensity to the air/aqueous solution interface.

[1] Minofar, B.; Jungwirth, P.; Das, M. R.; Kunz, W.; Mahiuddin, S.; Jungwirth, P.: *Journal of Physical Chemistry C*, 111 (2007) 8242. [2] Yi Rao, Mahamud Subir, Eric A. McArthur, Nicholas J. Turro, Kenneth B. Eisenthal, *Chemical Physics Letters* 477 (2009) 241–244 [3] Sein LN, Varnum JM, Jansen SA. Conformational modeling of new building block of humic acid: approaches to the lowest energy conformer. *Environ Sci Technol* 1999;33:546–52.

Textural control over electron transfer and reaction with Li⁺ of biomineralized Fe-oxides

J. MIOT^{1,2,3,4*}, N. RECHAM^{1,4}, D. LARCHER^{1,4}, F. GUYOT^{2,5} AND J.M. TARASCON^{1,4}

¹LRCS/CNRS, Univ. Picardie J.Verne, 80039 Amiens, France

²IMPMC/CNRS, UPMC, 75252 Paris, France

³LMCM/MNHN, 75005 Paris, France (*correspondence : jmiot@mnhn.fr)

⁴RS2E, CNRS 3459, France

⁵Univ. Denis Diderot, Sorbonne Paris Cité, IPGP/CNRS, 9Paris, France

The capacity of biominerals, in particular Fe-bearing minerals, to conduct electrons is increasingly studied with the aim of understanding the mechanisms by which bacteria can retrieve electrons from minerals [1,2] and designing electricity providing [3] or energy-storing devices [4]. Here, we present a two-step biomineralization pathway using the anaerobic Fe-oxidizing bacteria *Acidovorax sp.* strain BoFeN1 leading to the formation of α -Fe₂O₃ that was used in Li-ion batteries. Biomineralization of γ -FeOOH within the 40-nm thick cell wall of the bacteria [5], followed by a short heat treatment provided an alveolar material consisting of hollow rod-type shells made of an assemblage of nanometric and oriented α -Fe₂O₃ particles (Fig. 1A, B). This material exhibited enhanced electrochemical properties compared to abiotic controls, which relies on its specific texture at the μ m- and nm-scales allowing increased electronic transfer and sustained reaction with Li⁺ ions. These results have implications for energy storage and for understanding the mechanisms of electron/ion transfer through biominerals.

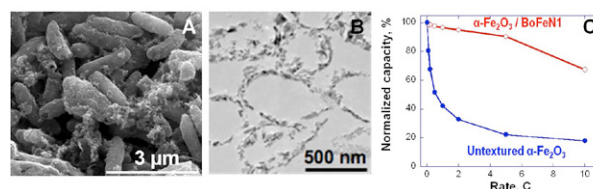


Figure 1: Texture of α -Fe₂O₃ bacteriomorphs biomineralized by BoFeN1 observed by SEM (A) and TEM in thin section (B). Electrochemical capacity-power (vs. Li⁰) for textured and untextured materials (C).

[1] Kato *et al.* (2012) *PNAS* **109**, 10042-46. [2] Pfeffer *et al.* (2012) *Nature* **491**, 218-221. [3] Lovley (2011) *Env. Microb. Reports* **3**, 27-35. [4] Miot *et al.* (submitted) *En. & Envir. Science*. [5] Miot *et al.* (2011) *Geobiology* **9**, 459-470.

The effect of light elements on metal/silicate partitioning

FRANCESCA MIROLO¹, EKATERINA S. KISEEVA¹, JON WADE^{1*} AND BERNARD J. WOOD¹

¹University of Oxford (*correspondence:

Jon.Wade@earth.ox.ac.uk, francesm@earth.ox.ac.uk,
Kate.Kiseeva@earth.ox.ac.uk, berniew@earth.ox.ac.uk)

The accretion of the Earth was marked by the high-pressure segregation of most of its core, accompanied by dissolution of about 10% of one or more “light” elements into the metallic phase. Various light elements have been proposed including S, Si, C and O, with each having an effect on the partitioning behaviour of the trace elements. Metallurgical data indicate that dissolution of even small amounts of light elements in liquid Fe can have profound effects on the activities of some trace components. For instance, significant partitioning of Si into the core of the growing Earth should have affected the observed Mo¹ content of the mantle.

Here, we use the epsilon model of non-ideal interactions in Fe liquids (ϵ)². We present interaction parameters (ϵ), derived from 1.5GPa, 1650°C metal-silicate equilibration experiments, for W, Ni, Co and Mo in liquid Fe alloyed with C, S and Si.

At oxygen fugacities above IW-3, we can safely assume a 6+ valence for W and 4+ for Mo³. In the system Fe-S we can then derive Ni, Co, W and Mo interaction parameters. For example, our W interaction parameter (e_{W}^{S}) is 8.4(±1), as opposed to the literature value of 6.1⁴. This means that at fixed oxygen fugacity, W becomes less siderophile with increasing metallic S content. However, for Mo in the same system we derive $\epsilon_{\text{Mo}}^{\text{S}}$ to be 0.5 (±1.7); the partitioning behaviour of Mo is therefore significantly less sensitive to the S content of the metallic phase. In contrast to W, the metal-silicate partitioning of Ni and Co are relatively insensitive to both S and C contents of the metal. Mars is proposed to possess a sulphur rich core, which would imply the primitive martian mantle possesses a higher W/Mo ratio than Earth's if the core's S content is taken into account.

[1] Ono-Nakazato *et al.* (2007) *ISIJ Int* **47**, 365-369 (2007).

[2] Wagner. *Thermodynamics of Alloys* (1962). [3] Wade *et al.* (2012) *Chem Geol* **335**, 189-193. [4] Steelmaking, J. S. f. t. P. o. S. a. t. t. C. o. *Steelmaking Data Sourcebook* (1988).

Reconstruction of Holocene climate variability using stalagmites from the Herbstlabyrinth, central Germany

SIMON MISCHEL^{1*}, DENIS SCHOLZ¹, CHRISTOPH SPÖTL² AND KLAUS PETER JOCHUM³

¹Institute for Geosciences, University of Mainz, J.-J.-Becherweg 21, 55099 Mainz, (*correspondence: simon.mischel@uni-mainz.de)

²Quaternary Research Group, Innrain 52a, A-6020 Innsbruck, Christoph.Spoetl@uibk.ac.at

³Max Planck Institute for Chemistry, Hahn-Meitner-Weg 1, 55128 Mainz, k.jochum@mpic.de

The Herbstlabyrinth cave system lies at an elevation of 435 m asl in a small limestone area in Central Germany. The cave has a length of about 7 km and is well decorated with speleothems.

The chronology of two Holocene stalagmites is established by precise ²³⁰Th/U dating using a NU Plasma MC-ICPMS at the Max Planck Institute for Chemistry, Mainz. The age model is constructed using StalAge [1]. Trace element concentrations and stable isotope ratios have been analysed at a temporal resolution of ~50 years.

In order to support the interpretation of the proxies in terms of past climate variability, we set up an extensive cave monitoring program to understand the processes occurring in the cave system.

In both stalagmites, P, Ba and U are positively correlated with each other and negatively correlated with $\delta^{13}\text{C}$. This suggests that these proxies reflect the productivity of the vegetation above the cave. In contrast, Mg, which is interpreted as a proxy for effective precipitation above the cave [2], is negatively correlated with P, Ba and U. This indicates that the vegetation is more productive during more humid phases.

The $\delta^{18}\text{O}$ values of precipitation in the research area show a strong positive correlation to the winter North Atlantic Oscillation (NAO) index [3]. Due to strong evapotranspiration during summer months, summer precipitation does not contribute to the recharge of the cave system. Thus, the $\delta^{18}\text{O}$ values of the dripwater and speleothem calcite reflect winter precipitation. Therefore, the $\delta^{18}\text{O}$ values recorded in the speleothems from Herbstlabyrinth may give us the opportunity to reconstruct the NAO, with more positive values reflecting NAO+ conditions and vice versa.

[1] Scholz & Hoffmann (2011), *Quaternary Geochronology* **6**, 369-382 [2] Fairchild & Treble (2009), *Quaternary Science Reviews* **28**, 449-468 [3] Baldini, McDermott, Foley & Baldini (2008), *Geophysical Research Letters* **35**, L04709

Multiple sulfur isotope geochemistry of Dharwar Supergroup, Southern India: Late Archean record of changing atmosphere

KAORU MISHIMA^{1*}, RIE YAMAZAKI², M. SATISH-KUMAR³, TOMOKAZU HOKADA⁴, AND YUICHIRO UENO^{1,5}

¹Department of Earth & Planetary Sciences, Tokyo Institute of Technology, Tokyo, Japan. mishima.k.ab@m.titech.ac.jp

²Institute of Geosciences, Shizuoka University, Shizuoka, Japan

³Department of Geology, Faculty of Science, Niigata University, Niigata, Japan

⁴National Institute of Polar Research, Tachikawa, Tokyo, Japan

⁵Earth-Life Science Institute, Tokyo Institute of Technology, Meguro, Tokyo, 152-8551, Japan

Sulfur isotope mass-independent fractionations (S-MIF) in sedimentary sulfides and sulfate provide strong constraints on the evolution of the early Earth's atmosphere. In the late Archean, the S-MIF signature changed dramatically: minimum $\Delta^{33}\text{S}$ at around 2.9 Ga, subsequent large $\Delta^{33}\text{S}$ variation culminated at 2.5 Ga and its sudden drop at the end of Archean. Moreover, $\Delta^{33}\text{S}$ - $\Delta^{36}\text{S}$ relation shows characteristic slope of around -0.9 in the Archean period [1]. The change of $\Delta^{33}\text{S}/\Delta^{36}\text{S}$ slope may reflect perturbation of atmospheric chemistry, though the mechanisms of the large $\Delta^{33}\text{S}$ variations and the $\Delta^{33}\text{S}$ - $\Delta^{36}\text{S}$ relation is still a matter of debate. We report multiple sulfur isotope data for sedimentary pyrite derived from the Dharwar Supergroup in the Western Dharwar craton, southern India. The lower unit (post-3.0 Ga) of the Dharwar Supergroup consists of basal conglomerate, stromatolitic carbonate, silici-clastics with diamictite, chert/BIF and pillow basalt in ascending order. The upper unit unconformably overlies the pillow lava, and consists of conglomerate/sandstone with ~ 2.6 Ga detrital zircons, komatiite lava, BIF and silici-clastic sequence with mafic volcanics. Sulfur isotope analysis of extracted sulfide of these sedimentary rocks display clear MIF record of high $\Delta^{33}\text{S}$ values up to +3.9‰. The $\Delta^{33}\text{S}/\Delta^{36}\text{S}$ slope changes from -1.52 to -0.96 in ascending stratigraphic order. The lowest slope value of -1.52 from Bababudan Group is stratigraphically just below the Talya diamictite, implying the link between shift of atmospheric chemistry and climatic system. On the other hand, carbonate rocks from Bababudan Group show very large variation $\delta^{34}\text{S}$ values up to +19.4‰ with negative $\Delta^{33}\text{S}$, whereas other sedimentary rocks show near 0‰ $\delta^{34}\text{S}$ value. The observed lithologic control possibly reflect geographical heterogeneity of S-MIF and sulfate reducing activity in the late Archean ocean.

[1] Farquhar (2000) *Science*, **289**, 756-758.

Determination of U, Cs and Sr isotopes and their distribution coefficients in soil affected by Fukushima daiichi nuclear power plant accident

S. MISHRA^{1,2}, A. TAKAMASA¹, H. ARAE¹, W. MIETELSKI³, Y. WATANABE¹, S. YOSHIDA¹ AND S.K.SAHOO⁴

¹National Institute of Radiological Sciences, 4-9-1 Anagawa, Inage-ku, Chiba 263-8555, Japan

²Bhabha Atomic Research Centre, Mumbai – 400 085, India

³The Henryk Niewodniczanski Institute of Nuclear Physics, Polish Academy of Sciences, Krakow, Radzikowskiego 152, Poland (sahoo@nirs.gov.jp)

Isotopic determination of U (^{238}U , ^{235}U and ^{234}U), Cs (^{137}Cs and ^{134}Cs) and Sr (^{90}Sr) were carried out in soil samples around Fukushima daiichi nuclear power plant (FDNPP) to find out source and extent of contamination due to fallout activity resulted as a consequence of the nuclear accident caused due to a severe earthquake followed by tsunami. ^{137}Cs activity was found to vary from 930 ± 20 Bq/Kg to $62,200\pm 900$ Bq/Kg which is much higher than the global fallout in Japan. $^{134}\text{Cs}/^{137}\text{Cs}$ activity ratio was found to vary from 0.84-0.87, comparable with other reported values. ^{90}Sr activity found to vary from 8.4 ± 1.5 Bq/Kg to 21.2 ± 2.6 Bq/Kg. Distribution coefficients (K_d) were measured using laboratory batch method to establish transfer of radionuclides. K_d values for U, Cs and Sr were found to be $\log U-K_d \approx 3 > \log Cs-K_d \approx 2 > \log Sr-K_d \approx 1-2$ (Fig.1). Chemical characterization with respect to different soil parameters like particle size distribution, pH, organic content, cation exchange capacity, CaCO_3 , elemental and oxide composition of soil has been carried out to understand the geochemical behavior of these radionuclides. A good correlation was observed for $U-K_d$ with Fe and organic content of soil. Similarly $Cs-K_d$ and $Sr-K_d$ show good correlation with cation exchange capacity and fine particle concentration respectively.

Site specific K_d values can be used for contaminant transport model to predict the radionuclide migration and also the relationship between soil parameters and sorption behavior of radionuclides will be helpful for soil remediation and dose assessment.

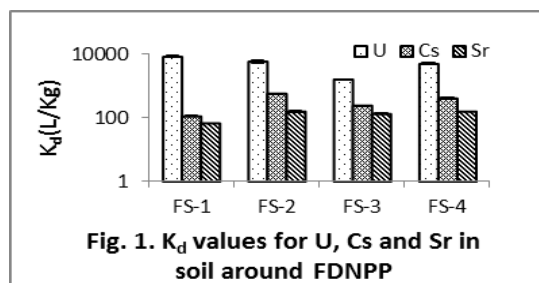


Fig. 1. K_d values for U, Cs and Sr in soil around FDNPP

Glass forming ability of sub-alkaline silicate melts

VALERIA MISITI¹, FRANCESCO VETERE^{2,3}, GIANLUCA IEZZI^{1,2}, HARALD BEHRENS³, FRANCOIS HOLTZ³, GUIDO VENTURA¹, ANDREA CAVALLO¹, MARCEL DIETRICH³ AND SILVIO MOLLO¹.

¹Istituto Nazionale di Geofisica e Vulcanologia, Via di Vigna Murata 605 00143 Rome, Italy

²Dipartimento di Ingegneria & Geologia, Università G. d'Annunzio, Via dei vestini 30, 66100 Chieti, Italy

³Institute for Mineralogy, Leibniz University of Hannover, Callinstr. 3, Hannover, D-30167, Germany

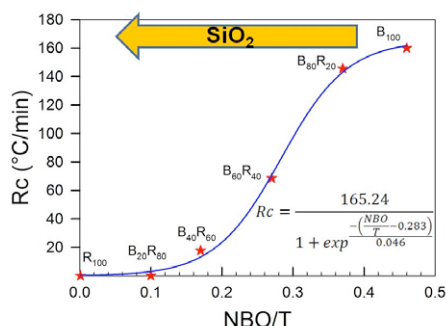
The glass forming ability (GFA) of six sub-alkaline silicate melts is quantified *via* the experimental determination of their critical cooling rate R_c (the minimum rate at which a liquid can be frozen to a solid with crystals < 2 vol.%). The selected compositions vary from basalt (B) to rhyolite (R) (B_{100} , $B_{80}R_{20}$, $B_{60}R_{40}$, $B_{40}R_{60}$, $B_{20}R_{80}$ and R_{100}).

For each composition, six cooling rates (150, 30, 3, 1, 0.116 and 0.0167 °C/min) are investigated between 1300 °C (liquidus region) and 800 °C (quenching temperature).

The crystallized phases and their contents are determined by image analysis on backscattered SEM pictures and include glass, pyroxene, spinel, plagioclase and, occasionally, olivine and melilite.

The estimated R_c values are 0.02, 0.12, 10, 50 130 and 160 °C/min for R_{100} , $B_{20}R_{80}$, $B_{40}R_{60}$, $B_{60}R_{40}$, $B_{80}R_{20}$, and B_{100} respectively.

R_c increases by 4 order of magnitude from R_{100} to B_{100} and can be related to the NBO/T (non bridging oxygen per tetrahedron) parameter as shown by the following figure:



Our results on the crystallization kinetics of the most abundant and common silicate melts in nature can be applied to retrieve solidification conditions of volcanic rocks as well as to design glass-ceramics with inexpensive starting materials.

Lithium Isotope History of Cenozoic Seawater: Changes in Silicate Weathering and Reverse Weathering

SAMBUDDHA MISRA^{1,*} AND PHILIP N. FROELICH²

¹Department of Earth Sciences, University of Cambridge, CB2 3EQ, UK, *correspondence: sm929@cam.ac.uk

²Froelich Education Services, 3402 Cameron Chase Dr., Tallahassee, FL, 32309. USA.

Weathering of uplifted continental rocks plays a central role in controlling both climate and seawater chemistry by consuming CO_2 and releasing cations to the ocean. Lithium isotopes provide a unique record of these changes because Li, unlike other tracers of ocean chemistry change, is hosted entirely in silicates. The isotopic composition of dissolved Li in seawater ($\delta^7Li_{SW} \sim 31.0\text{‰}$) reflects a balance between river dissolved Li inputs ($\delta^7Li_{Riv} \sim 23\text{‰}$), hydrothermal Li input ($\delta^7Li_{HT} \sim 8.4\text{‰}$) and large fractionation ($\Delta_{SW-SED} \sim 15\text{‰}$) during seawater-Li removal into marine authigenic clays via reverse weathering ($\delta^7Li_{SED} \sim 16\text{‰}$). A geologic record of δ^7Li_{SW} change is sensitive to the very large Li-isotope fractionation factors and to changes in silicate sources and sinks on time scales of the Li residence time in seawater ($\tau_{Li} \sim 1.5$ Ma). From the Paleocene (60 Ma) to the Present δ^7Li_{SW} rose 9‰, requiring large changes in continental forward weathering and seafloor reverse weathering consistent with pulsed tectonic uplift, more rapid continental denudation, increasingly incongruent continental weathering and more rapid CO_2 drawdown.

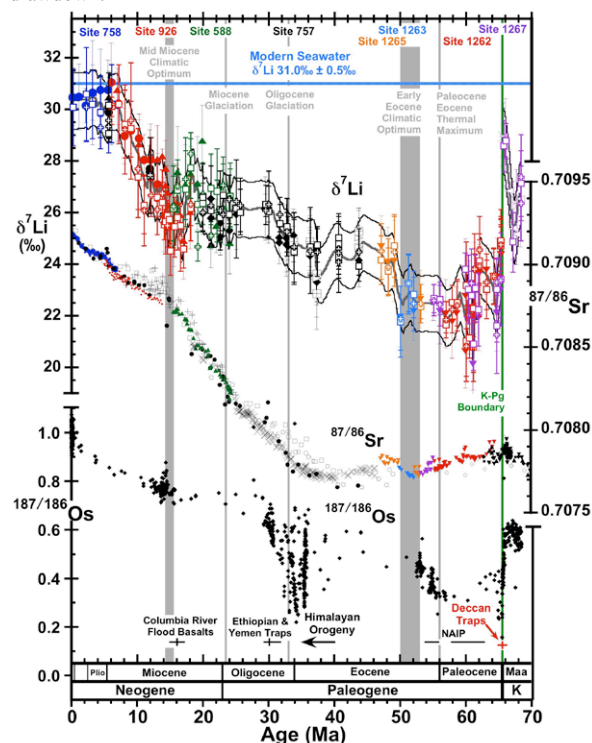


Figure: Li-, Sr-, and Os-isotope records over the past 68 Ma [1]. [1] Misra and Froelich, *Science*, 2012

Analysis of anion adsorption and its effects on alumina nanoparticles stability

TIZIANA MISSANA, ANA BENEDICTO, NATALIA MAYORDOMO AND URSULA ALONSO

¹CIEMAT, Avenida Complutense, 40. C.P 28040 Madrid (Spain)

Nanoparticles may enhance contaminant transport in groundwater provided the contaminant is irreversibly adsorbed onto their surface and they are stable and mobile. Colloid-driven contaminant transport is an issue of concern associated to hazardous waste repositories, because many uncertainties still exist.

The chemistry of the groundwater mainly determines the size and charge of the particles and has a large impact on particles stability and mobility but the colloidal properties can also be affected by the contaminant adsorption itself. This is a point potentially very relevant on the overall colloid-driven transport, but scarcely considered.

The stability of colloidal systems is generally evaluated by studying the aggregation kinetic after the change of a specific chemical condition, generally pH or ionic strength of the aqueous solution. Often, the effects of divalent cations, especially Ca^{2+} , are evaluated. On the other hand, the effect of anion adsorption on colloid stability is mostly neglected.

In this work, the effects of Se(IV) (selenite) adsorption on alumina (Al_2O_3) nanoparticles were analysed. Selenite adsorption was studied in a wide range of pH (2-12) and ionic strengths ($5 \cdot 10^{-4}$ - $1 \cdot 10^{-1}$ M in NaClO_4) and the effect of the adsorption on the main properties of the colloids (size and charge) were analysed. Similarly, the effects of SO_4^{2-} competitive adsorption were studied.

Adsorption on Al_2O_3 was almost independent of the ionic strength and decreased with increasing pH, as expected for anions. The set of adsorption data was successfully fit by surface complexation modeling.

It was clearly shown that the anion adsorption (at medium-high surface occupancies) affected alumina nanoparticle stability. A clear shift of the isoelectric point towards more acid pH and enhancement of colloid aggregation, even at low ionic strength, were observed.

The presence of anions in the chemical composition of natural water, frequently not accounted for in stability studies, will be discussed, as well as the implications on possible colloid-driven contaminant transport in the environment.

ACKNOWLEDGMENT: The work has been partially supported by the project NANOBAG (CTM2011-27975).

Coupled μ -XAFS-FISH technique for direct observation of the microbe-metal-mineral interaction

S. MITSUNOBU^{1*} AND F. SHIRAISHI²

¹Institute for Environmental Sciences, University of Shizuoka, Shizuoka 422-8526, Japan (*correspondence: mitunobu@u-shizuoka-ken.ac.jp)

²Department of Earth and Planetary Systems Science, Hiroshima University, Hiroshima 739-8526, Japan (fshirai@hiroshima-u.ac.jp)

Many geochemically important redox reactions are largely associated with microbial activity and are energy sources for microorganisms. For instance, recent studies suggest a significant relationship between Fe(II)-oxidizing bacteria and ancient Banded Iron Formation, one of the large geochemical events [1]. However, the detailed mechanisms of environmental biogenic reactions are largely unknown, because there are few adequate analytical techniques to observe it in high spatial resolution.

Here, we directly coupled synchrotron microprobe (μ -XAFS) with *in situ* phylogenetic analysis, fluorescence *in situ* hybridization (FISH), to determine simultaneously the chemical species and distributions of microbial community at micrometer scale (Fig. 1), which leads to better understanding of the microbial reaction in the environment. We applied the coupled μ -XAFS-FISH to one of the most ubiquitous environmental biomineralizations, Fe mineral deposition by Fe(II)-oxidizing bacteria (FeOB).

In situ visualization of microbes by FISH revealed that *Betaproteobacteria* (presumably revealed to FeOB, *Gallionella* spp.) were localized within 10 μm of the Fe mat surface. Furthermore, *in situ* mineralogical characterization by μ -XAFS suggested that Fe local structure at the FeOB accumulating parts was dominantly composed of secondary short-ordered Fe-O₆ linkage, which is normally not observed in synthetic Fe oxyhydroxides [2]. The present study indicates that the coupled XAFS-FISH technique could be a potential technique to provide direct information on specific biogenic reaction mediated by specific microbes.

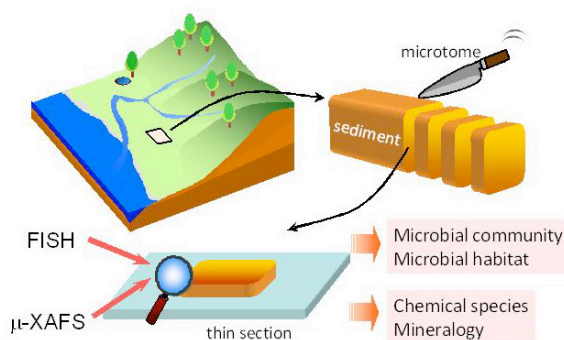


Fig. 1 Schematic figure showing coupled μ -XAFS-FISH technique.

[1] Kappler *et al.* (2005) *Geology* **33**, 865. [2] Mitsunobu *et al.* (2012) *Environ. Sci. Technol.* **46**, 3304.

Similarities between discordant chromitites from northern Oman ophiolite and chromitite xenoliths from Takashima alkali basalt, southwest Japan arc

MAKOTO MIURA¹, SHOJI ARAI¹, MARIE PYTHON² AND AKIHIRO TAMURA¹

¹Dept. Earth Sci., Kanazawa Univ., Kanazawa 920-1192, Japan (*correspondence: mimk1214@stu.kanazawa-u.ac.jp)

²Dept. Natural History Sci., Hokkaido Univ., N10W8, Sapporo 060-0810, Japan

We examined some discordant podiform chromitites in the mantle section of northern Oman ophiolite along Wadi Hilti, Fizh and Rajmi, to consider their origin. They are clearly discordant to the foliation of the surrounding mantle harzburgite. In outcrops, they show various texture (layered, massive, schlieren, anti-nodular and rarely nodular texture). Chromian spinels from all chromitites examined are full of minute orbicular inclusions of hydrous (pargasite and Naphlogopite) and anhydrous (pyroxenes) silicates. They usually show a concentric distribution indicating a primary origin.

Their chromian spinels in all discordant chromitites show a relatively high Cr# ($=Cr/(Cr+Al)$ atomic ratio), 0.7 to 0.8, and a low TiO₂ content, 0.15 to 0.2 wt%. The Oman discordant chromitites are comparable in chemical characteristics of chromian spinel with some arc-related plutonic rocks [1].

Their chromitite xenoliths from Takashima alkali basalt, southwest Japan arc, are similar to the Oman chromitites in spinel chemistry and texture [2]. In addition, we found laurite, one of platinum-group minerals, in the Takashima chromitite. The Takashima laurite is included in the compositional range of laurites in Oman chromitite [3]. Chondrite-normalized PGE pattern of the Takashima chromitite shows a slightly negative slope from Ru to Pt, which is also analogous to that of some chromitites from Oman.

These similarities between the Oman discordant chromitite and Takashima chromitite xenoliths, strongly suggest that some ophiolitic podiform chromitites are of sub-arc origin.

[1]Arai *et al.* (2011) *Island Arc* 20, 125-137. [2]Arai and Abe (1994) *Mineral Deposita* 29, 434-438. [3]Ahmed and Arai (2002) *Contrib Mineral Petrol* 143, 263-278.

Discovery of coesite and stishovite from eucrite

M. MIYAHARA¹, E. OHTANI¹, A. YAMAGUCHI², S. OZAWA², T. SAKAI³ AND N. HIRAO⁴

¹ Graduate School of Sci., Tohoku Univ., Sendai 980-8578, Japan. miyahara@m.tohoku.ac.jp

² NIPR, Tokyo 190-8518, Japan.

³ GRC, Ehime Univ., Matsuyama 790-8577, Japan.

⁴ JASRI, 1-1-1 Kouto Sayo, Hyogo 679-5198, Japan.

The existence of a high-pressure polymorph in a meteorite is a critical evidence for a dynamic event occurred on its parent-body. It is expected that HEDs meteorites originate from an asteroid, 4 Vesta. Although recent Dawn mission clarified that 4 Vesta suffered from heavy meteorite bombardments, a high-pressure polymorph has not been found in HEDs meteorites so far. We got one of eucrite samples, Béréba. Béréba sample studied here has several shock-melt veins, implying that it was heavily shocked. We investigated Béréba using a laser micro-Raman spectroscopy, FEG-SEM and FIB-TEM techniques to clarify a record of a dynamic event and its possible parent-body.

We focused our interests on a silica phase of Béréba in this study. Raman spectroscopy analyses showed that silica grains in the host-rock of Béréba are quartz and minor cristobalite. Most quartz grains entrained in the shock-melt veins transform to coesite. Some silica grains entrained in or adjacent to the shock-melt veins have network-like and/or lamellae-like textures. Raman spectroscopy and TEM observation indicate that such silica grains include coesite, stishovite and silica glass along with quartz. This is the first report of a high-pressure polymorph in HEDs meteorites.

The existence of stishovite indicates that pressure condition recorded in Béréba should be ~8 GPa at least based on a phase diagram obtained from static high-pressure and high-temperature synthetic experiments. U-Pb radio-isotope age of apatite entrained in the shock-melt vein is ca 4.2 Ga [1], which is relatively younger than bulk-rock Pb-Pb radio-isotope age (ca 4.5 Ga) [2]. The young U-Pb radio-isotope age of apatite would be due to disturbance by a thermal event such as a dynamic event. When a high-pressure polymorph is heated under ambient condition, it vitrifies easily. Accordingly, a dynamic event formed coesite and stishovite in Béréba occurred at least after ca 4.2 Ga ago.

[1] Zhou Q. *et al.*, 42nd LPSC., 2575pdf (2011). [2] Carlson R.W., *et al.*, 19th LPSC., 166-167 (1988).

Evaluation on reactivities of metal ions with hard ligands having oxygen donor

A. MIYAJI* AND Y. TAKAHASHI

Hiroshima University, Higashi-Hiroshima 739-8526, Japan
(*correspondence: asa-miyaji@hiroshima-u.ac.jp)

Complexation of metal cations by ligands such as hydroxide ion, carbonate ion, carboxylate ion, and phosphate ion is one of the most important factors to control behavior of metal ions in natural environment. Previous study showed that these ligands were classified as intermediate hard ligands having oxygen donor, which favors to form the ionic bond [1]. However, it was found that the reactivity of each ligand greatly depends on ionic radius and that there is a great difference of the reactivity between hydroxide ion and other ligand such as carbonate and carboxylate. For example, among the divalent alkaline earth metal ions, Mg^{2+} mainly precipitates as hydroxide (brucite), while Ca^{2+} prefer to form carbonate (calcite) or phosphate (apatite) minerals than hydroxide. However, quantitative discussion on the selectivity of metal cations is not quantitatively performed.

In this study, we evaluated the standard Gibbs free energy (ΔG_R^0), enthalpies (ΔH_R^0) and entropy (ΔS_R^0) for the complex formation of hydrated metal cations with these ligands based on a critical thermodynamic database including ΔG_R^0 , ΔH_R^0 , and ΔS_R^0 . As a result, we found that the entropic contribution to the free energy was large in the case of hydroxide complex of small radius cation. In contrast, the entropic contribution to the free energy was small in the case of hydroxide complex of large radius cation and other complex. In addition, the enthalpy contribution was not significant in the reaction. In the aqueous complexation reaction, ΔS_R^0 was controlled by the number of water molecules replaced by the ligand, suggesting that hydroxide complex for large cation was not stable due to the small effect of dehydration.

[1] D. Turner *et al.* (1981) *Geochim. Cosmochim. Acta* **45** 855-881

Progress of serpentinization reactions triggered by silica addition: Petrological evidence from Iwanai-dake ultramafic body, Hokkaido, Japan

A. MIYOSHI AND T. KOGISO¹

¹Graduate School of Human and Environmental Studies,
Kyoto University, Kyoto 606-8501, Japan.
kogiso@gaia.h.kyoto-u.ac.jp

Transformation of peridotite into serpentinite in the mantle wedge is one of the key processes that influence geodynamic regimes of subduction zones, because serpentinization changes the physical properties of peridotite, such as density, magnetic susceptibility, electric conductivity and rheology. Recent petrologic studies have proposed that serpentinization reactions proceed via a two-stage process involving the early formation of serpentine + brucite and subsequent magnetite formation. Magnetite, which is the key mineral controlling magnetic properties, electrical conductivity and density of peridotite as well as the efficiency of hydrogen generation, is thought to be formed by the second-stage reaction, but there has been little consensus among researchers regarding what factor promotes the formation of magnetite during serpentinization. We investigated successive changes in mineralogical textures associated with the progress of serpentinization observed in serpentinized harzburgite and dunite samples from Iwanai-dake ultramafic body (Hokkaido, Japan), which probably derived from a mantle wedge. Two kinds of mesh rim types were observed in the serpentine mesh texture of serpentinized harzburgite: a rim consisting of both serpentine and brucite (type-A rim) and a rim consisting solely of serpentine (type-B rim), which are always accompanied by brucite-magnetite veins. The formation of type-B rims and brucite-magnetite veins appears to have occurred concurrently with the serpentinization of orthopyroxene, suggesting that serpentinization reactions of harzburgite took place in two stages, with magnetite being formed by the second-stage reactions, which were triggered by a supply of silica component from serpentinization of orthopyroxene. In the case of serpentinized dunite, type-A rim was predominant and the fraction of magnetite does not increase with the progress of serpentinization. These observations suggest that silica supply is the trigger for the second-stage serpentinization reactions, in which magnetite and hydrogen are generated.

Effect of grid resolution and permeability anisotropy on mineral trapping for CO₂ disposal in the saline aquifer of Subei Basin, China

S.X. MO¹, F. ZHENG¹, S.M. JIANG², X.Q. SHI^{1,*},
L. ZHAO¹ AND Y. CHEN¹

¹School of Earth Sciences and Engineering, Nanjing University, China

²Department of Hydraulic Engineering, Tongji University, Shanghai 200092, China

(*correspondence: shixq@nju.edu.cn)

A vertical 2-D numerical model is built to study the interactions between water and minerals after supercritical CO₂ is injected into the saline aquifer of Yancheng Formation in Subei Basin, China using the parallel reactive transport modelling code TOUGHREACT-MP. The result shows that the carbonate minerals (e.g., calcite, siderite and dawsonite) significantly precipitated due to the dissolution of epidote, chlorite and albite. The total amount of CO₂ mineral trapping was as high as 34.0% after 5000a. The results of sensitivity analysis show that the volume of epidote significantly affects the CO₂ storage capacity. Three scenarios for the same conceptual model with different grid resolution are carried on to analysis the effects of numerical resolution. The results show that grid resolution has little impact on the reaction path of minerals dissolution and precipitation, however, the total amount of CO₂ mineral trapping using coarser grid is overestimated comparing to that with finer grid. The influence of the ratio of permeability anisotropy is also compared using another three scenarios corresponding to large, moderate and small vertical permeability, respectively. The results indicate that reduction of the vertical permeability results in more solubility and mineral trapping for a short period of time (e.g., 1000 a). However, more CO₂ is stored in minerals for the model with a moderate vertical permeability after 1000a, which implies that convective mixing process may significantly enhance mineral trapping.

Acknowledgement: This research was supported by the Natural Science Foundation of Jiangsu Province (BK2012313) and NSFC No. 41172206.

Reconstructing past organic matter fluxes from δ¹⁵N records

J. MÖBIUS*, B. GAYE, N. LAHAJNAR AND K.-C. EMEIS

Center for Earth System Research and Sustainability (CEN),
University of Hamburg, Bundesstrasse 55,
D-20146 Hamburg, Germany

(*correspondence: juergen.moebius@zmaw.de)

Organic matter fluxes from mixed layer to sea floor are hard to quantify from sediment records. Remineralization in the water column and in the sediment extinguishes the primarily produced signal to different degrees. As the reliability of biogenic barium as a proxy for primary production turned out questionable during the past decade, the quantification of organic matter fluxes is open again. In a recent study, we demonstrate that in certain settings stable isotopes of nitrogen (δ¹⁵N) may provide a tool to reconstruct past organic matter fluxes.

Stable isotope ratios of nitrogen are indicative for N sources, availability and cycling in the water column. The δ¹⁵N signal can be transferred to the sea floor by sinking particulate organic matter and further archived in the sediments. Interpretation of sedimentary δ¹⁵N records is usually complicated by an early diagenetic isotopic enrichment that mainly occurs during particle sinking and at the sediment water interface. However, we discovered that isotopic enrichment proceeds systematically due to organic matter remineralization and follows Rayleigh type fractionation logics. Accordingly, if isotopic enrichment is known, we can recalculate the amount of organic N that has been remineralized.

Our study has been carried out on Eastern Mediterranean Sea sediments from Holocene to Pleistocene sapropels and their remnants after post-depositional remineralization. The data set further comprises recent to subrecent sediments as well as sediment trap samples. Reconstructed N fluxes from recent and past sediment samples match fluxes reported in sediment traps and seem to validate our approach. Similar coincidence has been obtained for Arabian Sea core record and sediment traps. Hence, the new application of δ¹⁵N possibly is appropriate in a wider range of marine settings.

New tool for the direct isotopic dating of PGM (^{190}Pt - ^4He method): new constructions on the timing of Pt mineralization in Kondyor and Galmoenan massifs, Russian Far East

MOCHALOV A.G.¹, YAKUBOVICH O.V.^{1,2}, BRAUNS M.³
AND SHUKOLYUKOV YU.A.^{1,2,*}

¹ IPGG RAS, Makarova nab., 2, Saint-Petersburg, Russia
[correspondence: mag1950@mail.ru]

² Saint-Petersburg State University, Saint-Petersburg, Russia

³ Institute of archaeometry, Mannheim, Germany

* deceased

New ^{190}Pt - ^4He method of isotope geochronology for the native minerals of platinum is based on the α -decay of ^{190}Pt isotope. Radiogenic helium in crystal structures of native metals tends to form atomic clusters that appear as nanoscale “bubbles”. Therefore the stability of ^{190}Pt - ^4He isotope system in native minerals of platinum is rather high [1].

By the novel ^{190}Pt - ^4He method we have determined age of Pt>Ir fluid-metamorphogenic, Pt>Os magmatogenic-fluid-metasomatic, and Pt magmatogenic-fluid-metasomatic types of platinum mineralization of alkaline-ultramafic massifs Kondyor (Aldanian Shield, Russia) and gabbro-dunite-pyroxenite Galmoenan massif (Koryak-Kamchatka belt, Russia).

Obtained age of isoferroplatinum for Pt>Ir fluid-metamorphogenic, and Pt>Os magmatogenic-fluid-metasomatic types of platinum mineralization of Galmoenan massif is 63 ± 3 Ma (average from 10 samples). The data are in good agreement with relevant geological observations. Obtained age of isoferroplatinum for Pt>Ir fluid-metamorphogenic, and Pt magmatogenic-fluid-metasomatic types of platinum mineralization of Kondyor massif is 123 ± 6 Ma (average from 20 samples). The data are also in excellent agreement with relevant geological observations and other existing geochronological determinations. Noteworthy that the age of Pt>Ir fluid-metamorphogenic and Pt>Os magmatogenic-fluid-metasomatic types of platinum mineralization doesn't have any significant discrepancy.

Conducted ^{190}Pt - ^4He dating experiments also let us to separate a new young type of Pt mineralization on the Kondyor massif. ^{190}Pt - ^4He ages for fine cubic crystals of isoferroplatinum turned out to be around 8 Ma. The same young age for these crystals was also obtained by the independent ^{190}Pt - ^{186}Os method. These data may indicate formation of these Pt minerals under surface conditions.

[1] Shukolyukov (2012) *Petrology*, **20.6.**, 491-505

Barium stable isotope fractionation during diffusion through silica hydrogel: Experimental determination of kinetic isotope effects at low temperatures

K. MOELLER^{1*}, T.F. NÄGLER¹, M. DIETZEL²
AND M.E. BÖTTCHER³

¹Institute of Geological Sciences, University of Bern, Bern, Switzerland

(*correspondence: kirsten.moeller@geo.unibe.ch)

²Institute of Applied Geosciences, Graz University of Technology, Graz, Austria

³Leibniz-Institute for Baltic Sea Research, Warnemünde, Germany

Only very few studies have so far focussed on barium (Ba) stable isotope fractionation in nature. Many questions thus still remain regarding the direction and extent of isotope fractionation in physical and (bio)geochemical reactions. To date, experimental studies of Ba isotope fractionation are limited to precipitation of Ba-carbonates and -sulphates [1,2] and adsorption of Ba onto Mn-oxides and clay minerals [3].

Here, we investigated Ba isotope fractionation during diffusion of Ba through a silica hydrogel. The gel was prepared in 15 cm long glass U-tubes. A concentration gradient was established by applying a BaCl_2 solution (0.1 and 1.0 mol/l, respectively) on one side of the gel and deionised water on the other side. Diffusion experiments were run at two different temperatures (10 and 25°C) over 2, 6, 12, 20 and 27 days, respectively.

The rates of Ba diffusion through the silica hydrogel correlate positively with initial BaCl_2 concentration and temperature. Ba isotope fractionation, however, appears to be independent from both boundary conditions. Initially, diffused Ba was found to be fractionated by as much as -2.2‰ in $\delta^{137/134}\text{Ba}$ relative to the BaCl_2 stock solution. With continuing duration of the experiments, the $\delta^{137/134}\text{Ba}$ values increased rapidly to about -0.6‰ after 27 days. We hypothesise that initial kinetic isotope fractionation caused by Ba diffusion switched to a later control via adsorption of Ba onto the silica hydrogel. Our experiments thus show that fractionation of Ba isotopes of more than 2‰ in $\delta^{137/134}\text{Ba}$ ($\sim 0.7\text{‰/amu}$) are possible under experimental conditions and that the light Ba isotopes are favoured substantially during Ba diffusion through an aqueous medium.

[1] von Allmen *et al.* (2010) *Chem Geol* **277**, 70-77. [2] Böttcher *et al.* (2012) *Isot En Health Stud* **48**, 457-463. [3] Böttcher *et al.* (2012) *Mineral Mag* **76**, 1495.

Geochemistry and petrogenesis of Hassan Salaran granitoid complex in SE Saqqez, western Iran

FAKHRADDIN MOHAMMAD ABDULLAH^{1*}, ALI A. SEPAHI² AND SHELER. S. AHMAD¹

¹ University of Garmian, Kalar, Kurdistan Region, Iraq, (*correspondence: fakhraddin.mohammad@gmail.com)

² Bu Ali Sina University, Hamadan, Iran (sepahi@basu.ac.ir)

The Hassan Salarn granitoid complex is located 20km to southeast of Saqqez city in Kurdistan Province, western Iran. It is composed of two distinct granitic rock suites that have various petological and geochemical characteristics. They also have different origins and petrogenesis. G₁ granitoids comprise alkali feldspar granite, syenogranite and quartz alkali feldspar syenite, whereas G₂ granitoids are composed of monzogranite, granodiorite and tonalite. Geochemically, G₁ granitoids are peralkaline, A-type and aegirine-normative but G₂ granitoids are subalkaline (calc-alkaline), metaluminous, I-type and diopside-normative. G₁ granitoids are also ferroan alkali and ferroan alkali-calcic whereas G₂ granitoids are magnesian and calcic.

According to tectonic discrimination diagrams [1], G₁ granitoids plot in the field of the within plate granites whereas G₂ granitoids plot in the field of volcanic arc granites. Considering the method for classification of granites setting [2], G₁ granitoids plot in the post-orogenic field but G₂ granitoids plot in the field of mantle fractionated rocks. G₁ granitoids contain higher concentrations of alkalis, Zr, Rb, Nb, Y, Th, Ce, high FeO/MgO ratios and lower concentrations of Mg, Ca and Sr, resembling post-orogenic A-type granites. It is possible that heat from a mantle-derived magma which intruded into the lower crust, and/or rapid crustal extension have been essential generation of appropriate melts producing G₁ granitoids. Thus we can conclude that G₁ granitoids were generated from a mixed mantle-crust source. Negative Nb anomalies and low contents of Ti and P probably indicate a subduction-related origin for protolith of G₂ granitoids. Negative Nb anomalies and enrichment in Ce relative to its adjacent elements can be related to involvement of continental crust in magmatic processes. G₂ granitoids are also enriched in Rb, Ba, K, Th, Ce and depleted in Nb, Zr and Y, indicating that they have had interacted with crust. G₂ granitoids may result from contamination of mantle-derived magmas by continental crust during a subduction event.

[1] Pearce *et al.* (1984) *Journal of Petrology* **25**, 956-983.

[2] Batchelor & Bowden (1985) *Chem. Geol.* **84**, 43-55.

Comparing MSW landfill sites of Ottawa (capital of Canada) and Mashhad (the 2nd biggest city of Iran)

HOSSEIN MOHAMMADZADEH

Groundwater research center (GRC), Faculty of science, Ferdowsi University of Mashhad, Iran, P.O.B, 91775-1436 (mohammadzaddeh@um.ac.ir)

Waste disposal is an important issue in almost all cities and landfilling of municipal solid waste (MSW) is the most widely used disposal method in all over the world. In big cities like Mashhad (cultural capital of Iran) and Ottawa (capital of Canada), in spite of waste composting and recycling, considerable amount of MSW is disposed in landfill sites. In this study, the Mashhad municipal landfill (ML) and Ottawa municipal landfill (OL) sites which are owned and operated by the Cities of Mashhad (Iran) and Ottawa (Canada), respectively, have been investigated. The ML and OL sites were compared by looking at 1) site characterization of ML and OL; 2) waste composition and the geochemical composition of leachate in both ML and OL sites; and 3) the environmental impacts of both sites.

Landfilling in OL and ML sites began in 1960s and 1975, respectively. Both sites accept residential, industrial, commercial/institutional, and construction/demolition MSW material. However, ML is receiving about 584000 tons MSW annually (with dial average of 1600 tons), which is much more than that of OL landfill (355070 tons annually). At Ottawa landfill site, both the shallow and deep aquifers have been impacted by the landfill leachate infiltrating from the unlined portions of the landfill site. The presence of methane, DIC and the enriched d13C-DIC values at some monitoring wells, in comparison with pristine groundwater, provide evidence for leachate impact on groundwater at OL site [1, 2]. The detailed description of sampling procedures, analytical techniques, leachate composition, and leachate impact on the environment is given by Mohammadzadeh and Clark [3]. The ML site, with an elevation of 1080 a.s.l., is located on an igneous bedrock covered with alluvial deposit. Since the covered soil is not that much thick and there is fractured network in granitoid bedrock, it is suspected that ML leachate have had an impact on groundwater resources.

[1] Mohammadzadeh, H., I.D. Clark, M. Marschner, and G. St-Jean. (2005). Compound specific isotopic analysis (CSIA) of landfill leachate DOC Components. *Chemical Geology* 218: 3-13. [2] Mohammadzadeh, H., and I.D. Clark. (2008). Degradation pathways of dissolved carbon in landfill leachate traced with compound-specific 13C analysis of DOC. *Isotopes in Environmental and Health Studies* 44: 267-294. [3] Mohammadzadeh, H., and Clark, I.D. (2011). Bioattenuation in a groundwater impacted by landfill leachate traced with d13C, *Ground Water*, 49 (3).

Evolution of neodymium isotopic signature of seawater during the Late Cretaceous: new insights on oceanic circulation changes

M. MOIROUD^{1*}, E. PUCÉAT¹, Y. DONNADIEU², G. BAYON³ AND J.-F. DECONINCK¹

¹UMR CNRS, Université de Bourgogne, 21000, Dijon, France
(*correspondence: mathieu.moiroud@u-bourgogne.fr)

²UMR CEA/CNRS, Laboratoire des Sciences du Climat et de l'Environnement, 91191, Gif sur Yvette Cedex, France
(yannick.donnadieu@lscce.ipsl.fr)

³Département Géosciences Marines, Ifremer, 29280 Plouzané, France (germain.bayon@ifremer.fr)

Changes in oceanic circulation during the Late Cretaceous have been inferred from the neodymium isotopic composition (ϵ_{Nd}) of fish remains, which reflects the signature of past seawater [1, 2]. However the nature of these changes remains controversial, mainly due to insufficient temporal and spatial coverage of Nd isotope data. Data from continental margins in particular remain scarce for the Cretaceous [3, 4].

This work aims at reconstructing the signature of neritic and oceanic water ϵ_{Nd} during the Late Cretaceous/Early Paleogene in potential areas of deep water sinking and seaways linking different oceans. For this purpose, samples of fish remains, foraminifera and detrital fraction have been recovered in Late Cretaceous to Paleocene sediments from both oceanic (DSDP/ODP sites 152, 258, 323, 690 and 700) and neritic (Wyoming, Texas, New Jersey, Chile, Seymour Island, Egypt and Hokkaido) sites.

The results primarily point out a decreasing trend after the Cenomanian-Turonian interval, previously observed in the Atlantic and the Indian sector of the Southern Ocean [5, 6] and a general increasing trend during the Maastrichtian and the Paleocene, but also document the first Cretaceous ϵ_{Nd} data for the Southern Pacific, the continental margins of North America and Japan, and the Panama and Drake passages. Nevertheless, further comparisons with ϵ_{Nd} data available in the literature and climate modelling are required to tentatively explain the oceanic circulation during the Late Cretaceous.

[1] Robinson *et al.* (2010) *Geol. Soc. of Am.* **38** (10), 871-874.
[2] MacLeod *et al.* (2011) *Nat. Geosci.* **4**, 779-782. [3] Pucéat *et al.* (2005) *EPSL* **236**, 705-720. [4] Soudry *et al.* (2006) *Earth-Sci. Rev.* **78**, 27-57. [5] Murphy *et al.* (2012) *Paleoceanography* **27**, PA1211. [6] Robinson & Vance (2012) *Paleoceanography* **27**, PA1102.

Water quality and human health in relation to aquatic environment pollution by metals

T.I. MOISEENKO¹, N.A. GASHKINA¹
AND V.V. MIGORSKY²

¹ V.I. Vernadsky Institute of Geochemistry and Analytical Chemistry, RAS, Kosygin 19, Moscow 119991, Russia
(*correspondence: moiseenko.ti@gmail.com)

² Institute of the North Eco-Industrial Problems, Kola Science Center of RAS, Fersman 14, Apatity 184200, Russia

The assessment of the ecological consequences of element geochemical cycle changes due to the impact of mining and the metallurgical industry is of great importance for the health of the environment. This study collates published data concerning surface water contamination by metals, bioaccumulation and health of humans and fish within the Euro-arctic region of Russia (Murmansk region), in order to investigate their relationship. The results of metal concentration analysis of water from the sites of surface water intake for five cities and towns, as well as from pipe systems supplying drinking water to the public, show that industrial water treatment fails to remove toxic metals from the water. Fish were used as a biological indicator to show the impact of the pollution on living organisms. Renal disorders prevailed among the observed diseases within human populations. Statistical analysis demonstrated that human populations in those cities which are located in close proximity to smelters show the highest incidence of disease. The highest accumulation of metals within the kidney and liver were recorded in inhabitants of Monchegorsk, where the concentrations of many metals, especially, nickel, copper, chromium, cadmium, and lead, are 2–10-fold higher compared the normal. The highest concentrations within the kidney tissue were recorded for chromium and cadmium. Kidney pathologies are abundant within the population using the contaminated water supply for drinking water. The correlation between the content of this chemical element in water and pathology of kidney and liver of those patients who were examined postmortem was significant. Statistical analysis demonstrated that human populations in those cities which are located in close proximity to smelters show the highest incidence of disease. The highest content of toxic metals, especially cadmium, was found in the liver and kidney organs. The burden of evidence of the disorders observed in fish and in human populations indicates that there is a high probability of prolonged water contamination having a negative influence on the health of human populations.

New U-Pb ages for syn-orogenic magmatism in the SW sector of the Ossa Morena Zone (Portugal)

P. MOITA^{1*}, J.F. SANTOS², M.M. COSTA² AND F. CORFU³

¹Centro de Geofísica de Évora, Universidade de Évora, Portugal, pmoita@uevora.pt

²Geobiotec, Dep. Geociências, Universidade de Aveiro, Portugal

³Geology Department, Oslo University, Norway

The Ossa-Morena Zone (OMZ) is a major geotectonic unit within the Iberian Massif (which constitutes an important segment of the European Variscan Belt) and one of its distinguishing features is the presence of a noteworthy compositional diversity of plutonic rocks. In the SW sector of the OMZ, the tonalitic Hospitais intrusion (located to the W of Montemor-o-Novo) is considered a typical example of syn-orogenic magmatism, taking into account that both the long axis of the plutonic body and its mesoscopic foliation are oriented parallel to the Variscan WNW-ESE orientation. Another relevant feature of the Hospitais intrusion is the occurrence of mafic microgranular enclaves within the main tonalite. In previous works (Moita *et al.*, 2005; Moita, 2007), it was proposed that: (1) the Hospitais intrusion is part of a calc-alkaline suite, represented by a large number of intrusions in this sector of the OMZ, ranging from gabbros to granites; (2) the enclaves are co-genetic to the host tonalite in the Hospitais pluton.

In this study, zircon populations from one sample of the main tonalite (MM-17) and one sample of the associated enclave (MM-17E) were analysed by ID-TIMS for U-Pb geochronology. In each sample, three fractions of nice glassy, euhedral, long prismatic and inclusion free crystals were analysed. The results from the three fractions of MM-17 yielded a weighted average ²⁰⁶Pb/²³⁸U age of 337.0 ± 2.0 Ma. Similarly, for the enclave MM-17E a weighted average ²⁰⁶Pb/²³⁸U zircon age of 336.5 ± 0.47 Ma was obtained. These identical ages, within error, are in agreement with a common parental magma for the tonalite and mafic granular enclaves.

Similar U-Pb ages have been reported in previous works for plutonic and metamorphic events in this region (e.g.: Pereira *et al.*, 2009; Antunes *et al.*, 2011). Furthermore, also in the SW sector of the OMZ, palaeontological studies (Pereira *et al.*, 2006; Machado & Hladil, 2010) carried out in Carboniferous sedimentary basins containing intercalated calc-alkaline volcanics (Santos *et al.*, 1987; Chichorro, 2006) have shown that they are mainly of Visean age. Therefore, magmatism displaying features typical of continental arc setting seems to have been active in this part of the OMZ during the Lower Carboniferous times.

Funding: FCT through projects Petrochron (PTDC/CTE-GIX/112561/2009) CGE PEst-OE/CTE/UI0078/2011 and Geobiotec (PEst-C/CTE/UI4035/2011).

Water on the primordial Earth

S.J. MOJZSIS^{1*}, A. MORBIDELLI², K. PAHLEVAN³ AND E.A. FRANK¹

¹ Geological Sciences, CLOE, University of Colorado, USA

² Observatoire de la Cote d'Azur, CNRS, Nice, France

³ Geology and Geophysics, Yale University, USA

(*mojzsis@colorado.edu)

Water is the medium for life; it facilitates the long-term carbon cycle and aids in plate tectonics by modulating key geophysical parameters such as the mechanical strength of crust. Earth's surface hydrosphere totals 2.8×10⁴ M_e, and the mantle may contain 2.7(±1.3)×10³ M_e of water [1], approximately its storage capacity [2]. Ancient rocks show the hydrosphere existed in the first 700 Myr, and Hadean zircons extend this to about 180 Myr after solar system formation [3]. Earth has retained its volatiles since primary accretion [4], but H- and N-isotopic compositions are chondritic rather than cometary [5]. As such, water may have arrived late in the accretion epoch *viz.* the *Grand Tack* model [GT; 6] or even later via a *Late Veneer* [LV; 7]. The *Late Heavy Bombardment* [LHB] was not significant: it delivered too little (0.1% of the LV's mass), too late. Whether the LV mass (~5×10³ M_e) was brought in by many small undifferentiated planetesimals or a small number of large differentiated bodies is still an open issue, and we discuss advantages and disadvantages of both options. Such a mass was insufficient to deliver all the water even assuming CI composition. Earth-Moon O-isotopes exclude a CM, CI, or OC composition for the LV; EC composition would be possible but they are so water poor that they cannot explain Earth's water abundance whatever the LV mass. Volatiles were delivered towards the end of Earth accretion rather than via an LHB, LV, or Moon-forming event. This view is consistent with the latest dynamical models provided that Moon formation was fortuitously late [8].

[1] Hirschmann & Dasgupta (2009); [2] Smyth & Jacobsen (2006); [3] Harrison (2009); [4] Albarède *et al.* (2013); [5] Marty (2011); [6] Walsh *et al.* (2011); [7] Albarède (2009); [8] Halliday (2013).

The geochemical evolution of clinopyroxene in the Roman Province: A window on decarbonation from wall-rocks to magma

S. MOLLO¹ AND A. VONA²

¹Istituto Nazionale di Geofisica e Vulcanologia, Via di Vigna Murata 605 00143 Rome, Italy (*correspondance: mollo@ingv.it)

²Dipartimento di Scienze, Università degli Studi Roma Tre, L.go San Leonardo Murialdo 1 00146 Rome, Italy

We present results from atmospheric pressure experiments conducted at 1140, 1160 and 1180 °C under the buffering conditions of air, MH and NNO. The starting materials were a shoshonite and a phonotephrite from the Roman Province. These natural samples were doped with variable amounts of CaO and CaO+MgO whose stoichiometric proportions reproduced the assimilation by magmas of calcite and dolomite, respectively.

Results underline that, during magma-carbonate interaction, the oxygen fugacity exerts a primary control on clinopyroxene composition. With increasing fO_2 , the content of Tschermak molecules, i.e., CaAlAlSiO₆, CaFeAlSiO₆, and CaTiAlSiO₆, in clinopyroxene significantly increases at the expenses of hedenbergite and enstatite components.

The compositional variation of clinopyroxene described by our experiments is compared with the chemical analyses of natural crystals found in skarns and lavas at the Roman Province. This comparison provides that the simple ingestion of carbonate by magmas cannot explain the geochemical evolution of clinopyroxene in the Roman Province. At the periphery of magma chamber, the decarbonation reaction proceeds with the highest efficiency producing high CO₂ emissions. This causes extreme oxidizing conditions that, in turn, control the geochemical evolution of clinopyroxene in skarns. However, the oxidative capacity of CO₂ fluxing progressively decreases from the skarn shell to the interior of the magma. Consequently, the chemical analyses of clinopyroxenes found in lavas testify to laterally variable lower redox conditions in the magma chamber.

Lithospheric mantle connection of clinopyroxene inclusions in chromites from the Archean Nuasahi ultramafic-mafic complex (India)

SISIR K. MONDAL^{1*}, SHOJI ARAI², BETCHAIDA D. PAYOT² AND AKIHIRO TAMURA²

¹Department of Geological Sciences, Jadavpur University, Kolkata-700032, India

(*correspondence: sisir.mondal@gmail.com)

²Department of Earth Sciences, Kanazawa University, Kanazawa 920-1192, Japan

The 3.1Ga Nuasahi igneous complex in India is a sill-like layered intrusion within the early Archean greenstone belt of the Singhbhum craton. The igneous complex consists of a lower ultramafic unit (~ 400m thick) containing three chromitite ore bodies and an upper gabbroic unit containing magnetite bands. In between the lower ultramafic unit and the upper gabbro a PGE-rich discordant breccia zone is present. The main rocks of the lower ultramafic unit are orthopyroxenite, harzburgite, dunite and chromitite. Chromites from the massive chromitites contain numerous independent clinopyroxene (cpx) inclusions (> 95% of total inclusion populations) along with tiny phlogopite (<1%). The cpx inclusions are of variable sizes and shapes (rounded, elliptical and euhedral crystals), and in places they mimic the shape of the host chromite grain, and appear as the seed and negative crystals. In addition, few opx and olivine grains are identified in net-textured chromitites. Major element analysis by EPMA confirms that the cpx inclusions are Cr-diopside in composition which suggest a lithospheric mantle origin of the inclusions. Phlogopites are K-rich and compositionally similar to mantle phlogopite. *In situ* trace element analyses by laser ablation ICP-MS show that the chondrite-normalized REE patterns for the cumulus cpx in the upper gabbro and the cpx inclusions in chromites from the massive chromitites from the Nuasahi complex are different. Previous studies showed that the chromitite-bearing sill-like ultramafic-mafic complex in Nuasahi was formed from a boninitic parental magma in a supra-subduction setting. Previous Os isotopic study of the unaltered chromites indicated melt extraction as early as 3.7Ga from a subchondritic Os isotopic source implying derivation from a subcontinental lithospheric mantle. The high-Mg parental magma of the Nuasahi igneous complex may have originated in the deeper parts of the metasomatized lithospheric mantle wedge from where the cpx xenocrysts (along with phlogopite) were collected and transported to the crustal magma chamber where it had been entrapped by the growing chromite crystals.

Natural uranium ores host iron-reducing and iron-oxidizing bacteria as demonstrated by high throughput sequencing and cultural approaches.

L. MONDANI¹, K. BENZERARA², M. CARRIERE³, R. CHRISTEN⁴, L. FEVRIER⁵, W. ACHOUAK⁶, P. NARDOUX⁷, C. BERTHOMIEU¹ AND V. CHAPON^{1*},

¹LIPM, UMR 7265/CEA/CNRS/Aix –Marseille Univ., Saint-Paul-lez-Durance, France.

(*correspondence: virginie.chapon@cea.fr)

²IMPMC, CNRS UMR 7590, Univ. Curie, Paris, France.

³LLAN, CEA, Grenoble, France.

⁴Univ. Nice Sophia-Antipolis/CNRS, UMR 6543, Nice, France.

⁵IRSN, SERIS, L2BT, Saint-Paul-lez-Durance, France.

⁶LEMIRE, UMR 7265/CEA/CNRS/Aix –Marseille Univ., Saint-Paul-lez-Durance, France.

⁷SEPA, AREVA NC, Bessines-sur-Gartempe, France.

We investigated the influence of uranium on the indigenous bacterial communities in natural uranium ores by conducting an in-depth analysis of soil samples collected in the region of Bessines, one of the most important natural uranium deposits in France. Soil samples exhibiting 1.5 to 25.5% U in mass were compared with nearby control soils containing trace uranium. EXAFS and XRD analyses of soils revealed the presence of U(VI) and uranium-phosphate mineral phases, identified as sabugalite and meta-autunite.

A comparative analysis of bacterial diversity using DGGE [1] and high throughput pyrosequencing of 16S rRNA genes revealed the presence of complex populations in both control and uranium-rich samples. Among the 232,000 reads analyzed by pyrosequencing, 23 bacterial phyla were detected with *Proteobacteria*, *Acidobacteria* and *Chloroflexi* being predominant. Statistical analyses of the DGGE fingerprints and pyrosequencing data showed that bacterial communities of uranium-rich samples differ from that of controls. An enrichment of sequences related to iron- and uranium-reducing bacteria as well as iron-oxidizing species in uranium-rich samples was evidenced by both methods. Several iron-reducing anaerobic isolates related to *Pelosinus*, *Clostridium* and *Enterobacter* were cultured from the uranium-rich soil samples and characterized.

Taken together, these results demonstrate that uranium shapes bacterial diversity and suggest the existence of an iron and/or uranium redox cycle mediated by bacteria in the soil.

[1] Mondani *et al.* (2011) *PLoS ONE* 6(10): e25771. doi:10.1371/journal.pone.0025771

Towards Understanding Magnetite Biomineralisation: The Effect of Short Chain Peptides on the {100} and {111} Magnetite Surfaces

AMY E. MONNINGTON* AND DAVID J. COOKE

Department of Chemical & Biological Sciences, University of Huddersfield, Queensgate, Huddersfield, HD1 3DH, (*correspondence: amy.monnington@hud.ac.uk, d.j.cooke@hud.ac.uk)

Biomineralisation is the process by which living organisms form minerals. The earliest known example of biomineralisation is that of the biosynthesis of magnetite [1]. A major step forward in understanding the principles of magnetite biomineralisation occurred with the discovery of Magnetotactic bacteria (MTB) [2]. Despite this, much of the detailed atomistic mechanism by which the process occurs is unknown.

Numerous commercial applications for bacterial MNPs have been suggested, including the removal of radionuclides and heavy metals from waste water, MRI contrast agents, magnetic antibodies and drug and gene delivery. However, such applications are not commercially viable at present. In order to produce MNPs more economically the biomineralisation processes need to be further understood. Therefore, we are developing an atomistic model for the system, in an attempt to understand the processes involved.

Magnetite formation within *Magnetospirillum magneticum* AMB-1 occurs under the influence of the Mms6 protein. It was previously discovered that the Mms6 protein was linked to the control of the morphology and size of the magnetite crystals within the *M. magneticum* AMB-1 [3]. The acidic C-terminal region of this sequence is of particular interest due to its potential linkage to iron binding. It is hypothesised that if key iron binding sites within the C-terminus of the Mms6 protein are substituted for alanine, the protein's overall iron binding ability is diminished.

In this study, an atomistic model of Mms6-driven magnetite formation was developed, using molecular dynamics (based on classical atomistic potentials), to study the attachment of a series amino acid repeats (alanine-alanine, alanine-glutamic acid & glutamic acid-glutamic acid) to the {100} & {111} magnetite surfaces and investigate the effect on iron binding ability.

[1] J.W. Schopf *et al.*, *Science*, 1965, 149, 1365, [2] R. Blakemore, *Science*, 1975, 190, 377, [3] A. Arakaki *et al.*, *J. Colloid Interface Sci.*, 2010, 343, 65.

Time scales of mingling in shallow reservoirs.

C. P. MONTAGNA¹, P. PAPALE² AND A. LONGO³

¹Istituto Nazionale di Geofisica e Vulcanologia, via della Faggiola 32, 56127 Pisa, Italy; montagna@pi.ingv.it

²Istituto Nazionale di Geofisica e Vulcanologia, via della Faggiola 32, 56127 Pisa, Italy; papale@pi.ingv.it

³Istituto Nazionale di Geofisica e Vulcanologia, via della Faggiola 32, 56127 Pisa, Italy; longo@pi.ingv.it

Arrival of magma from depth into shallow reservoirs has been documented as one of the possible processes leading to eruption, e.g. for the recent eruption of Eyjafjallajökull [1], or for most eruptions at Campi Flegrei [2]. Magma intruding and rising to the surface interacts with the already emplaced, degassed magmas residing at shallower depths, rejuvenating them and causing intense mixing and mingling. These processes can cause pressure variations in the reservoirs and eventually lead to eruptions. The chemical signatures of such processes are often identifiable in eruptive products.

We performed two-dimensional numerical simulations of the arrival of gas-rich magmas into shallow reservoirs. We solve the fluid dynamics for the two interacting magmas evaluating the space-time dependent evolution of the physical properties of the mixture, including density and viscosity. Volatile exsolution is computed self-consistently as well.

Our results show that patterns of convection and mingling develop quickly into the chamber and feeding conduit/dike, leading on longer time scales to a density stratification whereas the lighter, gas-richer magma, mixed with different proportions of the resident magma, rises to the top of the chamber due to buoyancy. Over time scales of hours, the magmas in the reservoir appear to have mingled throughout, and convective patterns become harder to identify.

Our simulations have been performed changing the geometry of the shallow reservoir, and the gas contents of the initial end-member magmas. Both parameters play an important role in determining the efficiency of the mixing processes. Horizontally elongated magma chambers favour mixing, while vertically elongate, dike-like reservoirs inhibit efficient convection. Higher density contrasts between the two magmas cause faster ascent velocities and increase mixing efficiency as well.

Petrological evidence suggests for Campi Flegrei residence and mixing times of few days, from the arrival of fresh magmas to eruption, supporting our findings [3].

[1] Moune *et al.* (2012) *J. Geophys. Res.* **117**, B00C07. [2] Arienzo *et al.*, (2010) *Chem. Geol.* **270**, 135-147. [3] Perugini *et al.* (2010) *Bull. Volc.* **72**, 431-447.

Do amino acids inhibit calcite growth?

G. MONTANARI*, N. BOVET, AND S. L. S. STIPP

Nano-Science Center, Department of Chemistry, University of Copenhagen, Denmark (*giulia.montanari@nano.ku.dk)

The organic matrix that regulates growth of biogenic calcium carbonate contains high concentrations of acidic amino acids. They can form long macromolecules, which bind to surface sites and inhibit growth of the mineral. In this study, we investigated the effect of single amino acid units on calcite crystal growth, to determine how their structure is related to inhibition. We tested glycine (Gly), the smallest amino acid, and aspartic acid (Asp), with concentration range from $8 \cdot 10^{-6}$ to $4 \cdot 10^{-4}$ M. Both have an amino group but they differ in the number of carboxylic groups. To quantify their impact on crystal growth rates, we undertook calcite precipitation experiments, using the constant composition method [1]. XPS (X-ray photoelectron spectroscopy) of calcite exposed to amino acid bearing solutions revealed that both molecules adsorbed. Calcite morphology was observed with SEM (scanning electron microscopy); rough corners and step edges indicate blocking of surface sites (Figure 1).

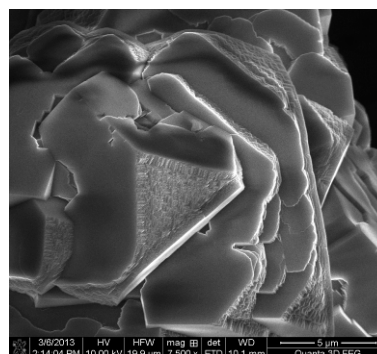


Figure 1: SEM image of calcite crystal exposed to Aspartic acid. Rounded and roughened corners and serrated edges are clearly visible.

Asp is a better inhibiting agent than Gly, which is active only for the highest concentrations investigated. The extra carboxylic group and the particular conformation of Asp can be the main factors promoting the interaction with surface sites. These results shed light on the parameters to take into account to predict or design a good scale inhibiting molecule.

[1] Lakshmanan *et al.* (2011) *GCA* **75**, 3945-3955.

Highly siderophile and chalcophile element systematics of crust-derived Ligurian garnet pyroxenites

ALESSANDRA MONTANINI^{1*}, AMBRE LUGUET², STEPHAN KÖNIG² AND RICCARDO TRIBUZIO³

¹¹ Dip. Fisica e Scienza della Terra, Università di Parma, Italy (alessandra.montanini@unipr.it).

² Steinmann Institut, Universität Bonn, Poppelsdorfer Schloss, 53115 Bonn, Germany

³ Dip. Scienze della Terra e dell'Ambiente, Università di Pavia, Italy

There is growing evidence from major, trace elements and isotopic systematics (e.g. Nd, 187Os, 186Os) that pyroxenites are significant constituents of OIB and MORB sources. Although pyroxenites probably play an important role in the recycling of crustal 187Os and 186Os signatures within the mantle, their highly siderophile and chalcophile element signatures are not well constrained. Here, we present platinum group elements (PGE: Os, Ir, Ru, Pt, Pd), Re, Se, Te and 187Os compositions of nine garnet pyroxenites and two peridotites from the External Ligurian ophiolites (Italy). On the basis of their mineralogical, geochemical and Nd-Hf isotopic features, the pyroxenites (HREE-depleted Type A, HREE-enriched Type-B and retrogressed) were correlated with partial melting of an eclogite source derived from gabbroic protoliths [1]. Whereas the host peridotites exhibit typical mantle-like concentrations and a relatively flat CI-chondrite-normalised HSE patterns, the pyroxenites show large concentration ranges, reaching up to 46 ppb Pd, 538 ppb Se and 81 ppb Te. Their HSE patterns display a positive slope from Os to Re, but with significant differences between the pyroxenites. Type-A pyroxenites show lower Os, Ir, higher Pt, Pd concentrations and flatter Pd-Re segments than Type-B pyroxenites. The retrogressed pyroxenites show mixed signatures with Os-Ir contents similar to Type-B pyroxenites but Pt, Pd concentrations as well as Pd-Re segments similar to Type-A. Selenium and Te are significantly enriched in all the pyroxenites but independently of the pyroxenite groups. The ¹⁸⁷Os/¹⁸⁸Os ratios vary from unradiogenic in the peridotites (0.1257) to highly radiogenic in the pyroxenites (0.2649-2.4748). Here we show that crust-derived mantle pyroxenites show a large range of highly siderophile and chalcophile elements signatures, which could likely contribute to geochemical and isotopic heterogeneities of the Earth's mantle.

[1] Montanini *et al.* (2012) *EPSL* 351-352, 171-181.

New insights on the nucleation and growth of chrysotile, magnesite, goethite and calcite

G. MONTES-HERNANDEZ¹

¹ISTERRE, University of Grenoble I and CNRS, BP 53, 38041 Grenoble Cedex 9, France
german.montes-hernandez@ujf-grenoble.fr

Chrysotile, magnesite, goethite and calcite are widespread minerals in Earth systems and other telluric planets. These minerals play an important role on the fate and transport of several trace elements (including the so-called strategic elements or rare-Earth elements of economic interest) and organic molecules at the mineral-fluid interfaces. Particularly, carbonate minerals plays also a crucial role on the global carbon cycle. In general, their formation and textural properties have already been investigated in the past. However, various questions still remain unanswered concerning their formation in natural systems as well as their production at laboratory and industrial scales. In this way, various new results on the nucleation and growth processes of these minerals from macroscopic to nanoscopic scales are summarized in this meeting contribution. In last six years, independent semi-continuous or batch experiments under specific physicochemical conditions were carried out to precipitate chrysotile nanotubes via dissolution of so-called proto-serpentine precursor [1], micro-crystals of magnesite via simultaneous dehydration and carbonation of brucitic layer of dypingite precursor [2], acicular nanocrystals (in width) of goethite from ferric hydroxide gel [3] and nanosized calcite via aqueous or gas-solid carbonation of portlandite [4-5]. I note that the nucleation and growth mechanism routes of these common minerals are still debated, for example, the role of so-called precursor formation and/or pre-nucleation existence addressed in the recent years are not clear at the present time, opening a broad spectrum of experimental and modeling possibilities to decipher this fundamental scientific obstacle.

[1] R. Lafay, G. Montes-Hernandez *et al.* *Chemistry – A European Journal* (2013) DOI: 10.1002/chem.201204105

[2] G. Montes-Hernandez *et al.* *Crystal Growth & Design* 12 (2012) 5233-5240. [3] G. Montes-Hernandez *et al.* *Crystal Growth & Design* 11 (2011) 2264-2272. [4] G. Montes-Hernandez *et al.* *Chemical Geology* 290 (2011) 109-120.

[5] G. Montes-Hernandez *et al.* *Crystal Growth & Design* 10 (2010) 4823-4830.

Peering into the Cradle of Life: Multiple sulfur isotopes reveal insights into environmental conditions and early sulfur metabolism some 3.5 Ga

A. MONTINARO¹*, H. STRAUSS¹, P. MASON²
AND A. GALIĆ²

¹Westfälische Wilhelms-Universität Münster, Münster,
Germany (*correspondance:amont_01@uni-muenster.de)

²Utrecht University, Utrecht, The Netherlands

Multiple sulfur isotopes have been used successfully for constraining Earth's early sulfur cycle, prevailing overall environmental and redox conditions in particular, as well as for tracing life on Earth. ICDP project "Peering into the Cradle of Life" aims at investigating the environmental conditions that existed when life emerged and evolved on our planet. Samples stem from the Barberton Greenstone Belt in South Africa (3.55–3.23 Ga), one of the oldest well preserved rock successions from the earliest part of Earth history. This study centers on core BARB5, comprising carbonaceous shale, interbedded sandstone and conglomerate and volcanoclastic rocks from the middle Mapepe Formation of the Fig Tree Group. Total sulfur abundance ranges between 0.01 and 3.03 wt.% and total carbon abundances between 0.15 and 10.29 wt.%. The carbonaceous shale displays $\delta^{34}\text{S}$ values between -0.99 and 3.33‰; volcanoclastic rocks between -6.57 and 2.32‰; sandstone and conglomerate between 0.37 and 3.44‰. Similar to the $\delta^{34}\text{S}$ values, $\Delta^{33}\text{S}$ values are different for each lithofacies. Samples from the carbonaceous shale yielded a range between 0.41 and 2.33‰; volcanoclastic rocks between -0.32 and 0.20‰; sandstone and conglomerate between 0.14 and 0.61‰. Some preliminary conclusions can be drawn. Each lithofacies is characterized by a different isotopic composition. Clearly, $\Delta^{33}\text{S}$ values in carbonaceous shale reflect mass-independent isotope fractionation, hence an atmospheric signature. In contrast, volcanoclastic rocks display rather small $\Delta^{33}\text{S}$ values but substantial variability in $\delta^{34}\text{S}$, that could reflect solely mass-dependent isotopic fractionation, hence a terrestrial signature. However, alternatives have been proposed.

THEREDA – Thermodynamic Reference Database

HELGE C. MOOG¹ AND FRANK BOK²

¹Gesellschaft für Anlagen- und Reaktorsicherheit (GRS) mbH,
Theodor-Heuss-Straße 4, 38122 Braunschweig, Germany,
helge.moog@grs.de

²Helmholtz-Zentrum Dresden-Rossendorf e.V., Institute of
Resource Ecology, Surface Processes Division (FWOG),
Bautzner Landstraße 400, 01328 Dresden (Germany),
f.bok@hzdr.de

THEREDA was founded by five institutions in Germany and Switzerland. Our main objectives are

- To ensure that equilibrium calculations for nuclear disposal issues are consistent among different institutions
- To save basic thermodynamic data in a way which renders them usable on a long term
- To have a technical platform which facilitates the decentralized editing of data
- To provide users with ready-to-use parameter files for the most widely used geochemical codes
- To make sure that each datum can be traced back to its original source
- To classify the entered data in order to inform the user about the quality of the data and hence his calculations

Following these objectives THEREDA has evolved into a web-based platform for a common thermodynamic database. The main focus lies on providing a database for high-saline systems. However, some efforts have been made to design THEREDA as flexible as possible for future demands, as necessity arises, namely: other models for the aqueous solution, non ideal gas and solid phases, etc.

Backbone of the whole database is a Pitzer-consistent set of phase constituents along with equilibrium constants and Pitzer coefficients for the basic hexary system Na-K-Mg-Ca-Cl-SO₄-H₂O. The set is at present being extended to be valid for temperatures between 120 and 200°C, depending on the particular system. At the same time data are added to extend the database for polythermal, in parts even polybaric equilibria with HCO₃⁻/CO₂(g).

Consistently to the above mentioned backbone, other joint members of THEREDA collaborate to extend the database for actinides, activation- and fission products, and heavy metals. Another string of endeavour is targeted towards geothermal applications.

The THEREDA team welcomes colleagues from other database projects to discuss or collaborate on specific subjects of common interest.

Reactive transport of common hydrological tracers in porous media – an experimental study

PRATHAP MOOLA¹, BERGUR SIGFÚSSON²
AND A. STEFÁNSSON¹

¹Institute of Earth Sciences, University of Iceland, Sturlugata 7, 101 Reykjavík, Iceland (snp3@hi.is)

²Reykjavík Energy, Baejarhálsi 1, 110 Reykjavík, Iceland

Groundwater flow is commonly studied by means of tracer tests. The tracers commonly used involve inorganic salts and organic compounds. The results of such tests in porous rocks are based on the assumption that the tracers are inert, i.e. do not react with the solutions and/or minerals of the groundwater system.

In this study the chemistry of commonly used organic hydrological tracers were studied experimentally upon flow in porous rocks. The tracers studied included Fluorescein, Rhodamine B, Sodium Naphthionate, Pyranine, Amino Rhodamine G and Amino G in solutions of pH 3, 6 and 9 with three types of porous sand, quartz, rhyolitic and basaltic sand. The experiments were conducted using a Teflon flow-through reactor packed with the sand of interest. Experimental solutions with and without the tracers were alternatively pumped at fixed flow rates through the reactor and the tracer concentration at the outlet of the reactor continuously monitored spectrophotometrically. The major chemistry of the outflow solution was further studied. The experimental results were supported by 1-D reactive transport simulations conducted with the aid of the PHREEQC program. In the simulations, dissolution of the solids and formation of secondary minerals was taken into account as well as possible sorption processes. According to the experimental results and the reactive transport simulations the primary rocks alter to form secondary minerals and solutes that are partially transported out of them column (system). Some of the hydrological tracers studied were observed to be non-reactive, however, others seem to be affected by processes like adsorption and desorption. The results imply that simulation of groundwater flow in porous rocks based on tracer tests may not be valid in some cases without considering reactive transport and incorporating sorption reactions of the tracer used.

Melt inclusion constraints on the origin of the Peridot Mesa phonotephrite, San Carlos, Arizona

G. MOORE

Department of Earth and Environmental Sciences, University of Michigan, Ann Arbor, MI, 48107, USA

(*correspondence: gm Moore@umich.edu)

The Peridot Mesa vent in San Carlos, Arizona, USA, is known for its striking array of upper mantle xenoliths, and the gem quality peridot that is mined from them. While many studies have been conducted on the xenoliths, surprisingly little is known regarding their host magma. Our previous petrographic, analytical, and experimental work [1, 2] showed that the Peridot Mesa lava is not a basanite as previously thought [3], but an evolved phonotephrite, and that the phenocrysts are consistent with crystallization of anhydrous magma during rapid ascent. Phase equilibrium experiments on the lava composition failed to reproduce the observed phenocryst assemblage however, regardless of a variety of pressures, temperatures, and volatile contents [2].

Given the energetic magmatic environment required to entrain and erupt such large (up to 50 cm dia) mantle xenoliths on the surface, one hypothesis for the inability of phase equilibrium experiments to crystallize the observed assemblage is that the erupted lava is the final product of mixing of two or more magmas that had different crystallization paths. This possibility is supported by the observation that there are several older occurrences of eruptions with similar characteristics in the area [4], indicating a well-developed pathway for such magmas.

As this mixing hypothesis must be ruled out before further phase equilibrium experiments are considered, an effort has been undertaken to identify and measure the composition of melt inclusions in the phenocrystic phases found in rapidly quenched scoria. Preliminary results from the electron microprobe on the bulk composition of the melt inclusions show that, similar to the residual glass, there is not significant variation in the liquid composition, suggesting that magma mixing and/or assimilation of xenolithic material is not an important process, or is extremely rapid and efficient, resulting in a homogeneous magma.

[1] Gullikson *et al.* (2010) *AGU Fall Meeting Abstracts*, 2263.

[2] Gullikson *et al.* (2012) *Mineralogical Magazine* **76**, 1790.

[3] Frey & Prinz (1978) *E.P.S.L.* **38**, 129–176. [4] Wrucke *et al.*, (2004) *Geological Investigation Series*, U.S.G.S., **I-2780**.

Detection of non-stoichiometric silicate mineral dissolution in rivers draining alpine glaciers using $\delta^{44/40}\text{Ca}$

J. MOORE^{1,2}, A. D. JACOBSON², C. HOLMDEN²
AND D. CRAW³

¹ Department of Physics, Astronomy, & Geosciences, Towson University, Towson, MD 21252 USA (*correspondence: moore@towson.edu)

² Department of Earth and Planetary Sciences, Northwestern University, Evanston, IL 60208 USA (adj@earth.northwestern.edu)

³ Saskatchewan Isotope Laboratory, Department of Geological Sciences, University of Saskatchewan, Saskatoon, Canada SK S7N 5E2 (ceh933@mail.usask.ca)

⁴ Geology Department, University of Otago, Dunedin, New Zealand (dave.craw@stonebow.otago.ac.nz)

Rivers draining glaciers frequently have high Ca concentrations, which have been attributed to the dissolution of carbonate minerals, even in predominantly silicate watersheds. Apportioning riverine Ca between silicate and carbonate weathering is typically done with the “Ca/Na method,” which assumes that plagioclase is the dominant source of silicate Ca and that Ca and Na are released in stoichiometric proportions. Here, we tested whether high-precision Ca isotope measurements ($\delta^{44/40}\text{Ca}$ by MC-TIMS, $2\sigma_{\text{SD}}=\pm 0.07\text{‰}$) could track Ca sources to non-glacial and glacial rivers draining the Southern Alps of New Zealand. The mountain range consists of schist and greywacke containing trace hydrothermal calcite (1-3%). Hydrothermal calcite and silicate rocks are isotopically distinct. The Ca isotope composition of rivers is consistent with mixing between calcite and silicate sources. Glacial rivers are statistically different than non-glacial rivers ($p < 0.001$) and have more negative $\delta^{44/40}\text{Ca}$ values. The glacial rivers plot closer to the silicate end-member. We observe no evidence for isotopic fractionation as a factor controlling the variability in stream water $\delta^{44/40}\text{Ca}$ values. For non-glacial rivers, carbonate weathering provides ~50 – 90% of the riverine Ca, and more importantly, the Ca/Na and Ca-isotope source apportionment methods yield the same results within 2%. However, for glacial rivers, the Ca-isotope method yields 25% more Ca from silicate weathering compared to the Ca/Na method. Taken together, the data point to the enhanced release of silicate Ca in glacial watersheds. We attribute the effect to non-stoichiometric release of Ca from silicate mineral surfaces damaged by glacial grinding. One implication is that alpine glacial watersheds may consume atmospheric CO_2 at higher rates than previously realized.

Recent Changes in Coastal Aquifers: Local effects expressed globally

WILLARD S. MOORE¹

¹Department of Earth and Ocean Sciences, University of South Carolina, Columbia, SC USA, moore@geol.sc.edu

Coastal populations are increasing rapidly, while potable water supplies are decreasing due to over-pumping and sea water intrusion into coastal aquifers. This problem has affected almost all coastlines during the past century. Here I focus on biogeochemical consequences of sea water intrusion into coastal aquifers, systems we call subterranean estuaries.

Oxygen is the most powerful oxidizing agent in most waters. However, its oxidizing capacity is limited by solubility (maximum ~0.28 mmol/L). Once dissolved oxygen is depleted, sulfate ion (~29 mmol/L in seawater) becomes the electron acceptor of choice to facilitate carbon oxidation. Thus seawater has a great deal more oxidizing capacity than fresh water. The reaction products of sulfate oxidation of organic matter include both inorganic and organic forms of dissolved N, P, and C as well as sulfide. Additionally, reducing conditions in the aquifer lead to reduction of iron and manganese oxides. This increases concentrations of Fe^{2+} and Mn^{2+} as well as other metals, plus ions that were absorbed onto the oxides. As this chemically-altered seawater exchanges into coastal waters as submarine groundwater discharge, it carries high nutrient, carbon, metal, and sulfide concentrations.

Continued seawater intrusion will lead to greater inland expansions of subterranean estuaries. This expansion may produce greater total SGD fluxes of nutrients, carbon, and metals because the biogeochemical reactions that affect their concentrations will operate over larger spatial scales and affect portions of aquifers that have not been in contact with seawater for thousands of years.

Insights into glacial weathering from a new hydrochemical database from 95 glaciated catchments

NILS MOOSDORF¹, JENS HARTMANN¹
AND JOSHUA A. WEST²

¹ University of Hamburg, KlimaCampus, Bundesstraße 55,
20146 Hamburg, Germany (nils@moosdorf.de)

² University of Southern California, Department of Earth
Sciences, Los Angeles, CA 90089, USA

Chemical rock weathering in glaciated areas is involved in several feedback loops in the earth system. The fluxes and geochemical characteristics of glacial weathering have been assessed at many single locations, but only a few studies have compared multiple sites [e.g. 1] to draw broader conclusions.

Here we present a new database compiled from 95 glaciated catchments, published by 46 sources. This database allows to analyze general patterns associated with the effect of glaciers on chemical weathering.

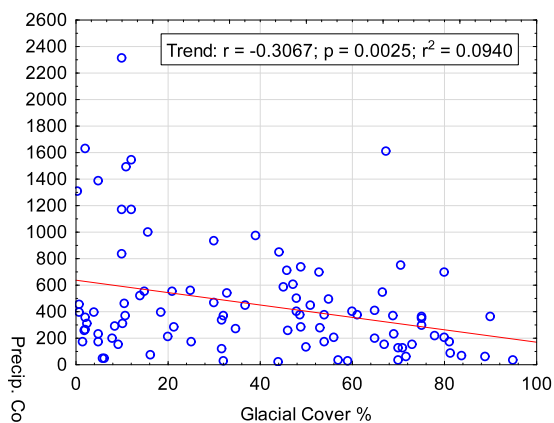


Figure 1: Precipitation corrected cation concentrations against glacial cover. Each point represents one catchment.

The first analysis of the database shows that cation concentrations decrease with increasing glacial cover (Figure 1). Mean concentrations are below the global average of 875 $\mu\text{Mol/L}$ [2], but cation denudation rates are on average 21.4 $\text{t km}^{-2} \text{a}^{-1}$, above the global average of 10 $\text{t km}^{-2} \text{a}^{-1}$ [3].

The database will be analyzed in depth to identify relations between ion concentrations, weathering rates, stoichiometry and seasonality with potential influencing factors (e.g. dominating lithology).

[1] Anderson *et al.* (1997) *Geology* **25**, 399-402. [2] Livingstone (1963) In: Fleischer (Ed.), *Data of Geochemistry*, Sixth Edition. USGS Professional Papers, pp. 1-61. [3] Hartmann *et al.* (in prep).

Dust direct radiative forcing and the complex refractive index of hematite

H. MOOSMÜLLER* AND J. P. ENGELBRECHT

Desert Research Institute, Nevada System of Higher
Education (NSHE), Reno, NV 89512, USA
(*correspondence: Hans.Moosmuller@dri.edu)

Ambient light absorption of entrained mineral dust in the visible and near-visible spectral region is generally dominated by iron oxides, in particular by hematite ($\alpha\text{-Fe}_2\text{O}_3$) [1, 2]. Therefore, sign and magnitude of mineral dust direct radiative forcing are critically dependent on the complex refractive index spectrum of hematite, especially its imaginary part. Here, we discuss the sensitivity of mineral dust shortwave radiative forcing on the imaginary part of the hematite refractive index.

Spectra of the imaginary part of the hematite refractive index have been reported in more than 15 publications. Unfortunately, these literature values vary greatly, between one and nearly five orders of magnitude for different parts of the spectrum (Fig. 1). In addition, virtually all of these publications fail to give an error estimate for their results.

Here, we review these published values together with the respective methods of determination, attempting to give a recommendation for values and errors that should be used. Furthermore, we estimate the error in dust radiative forcing originating from the uncertainty in hematite refractive index.

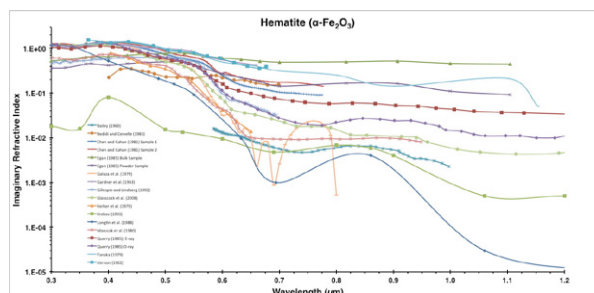


Figure 2: Imaginary part of the hematite refractive index as function of wavelength as obtained from 15 different publications.

[1] Lafon *et al.* (2006) *J. Geophys. Res.*, **111**, doi:10.1029/2005JD007016. [2] Moosmüller *et al.* (2012) *J. Geophys. Res.*, **117**, doi:10.1029/2011JD016909.

Composition of the Earth's core from density measurements of liquid iron alloys at megabar pressure

G.MORARD^{1,*}, D.ANTONANGELI¹, J.SIEBERT¹,
D. ANDRAULT², N.GUIGNOT³, F.GUYOT^{1,5}
AND G.GARBARINO⁴

¹Institut de Minéralogie et de Physique des Milieux

Condensés, Univ. Pierre et Marie Curie, Paris, France

*correspondence: guillaume.morard@impmc.jussieu.fr

²Laboratoire Magmas et Volcans, Clermont-Ferrand, France

³Synchrotron SOLEIL, Gif-sur-Yvette, France

⁴European Synchrotron Radiation Facility, Grenoble, France

⁵ Institut de Physique du Globe de Paris, France

The liquid core of the Earth extends between 2900 km and 5150 km depth accounting for 18% of the total planetary volume. Although mostly composed of iron, it contains impurities that lower its density and its melting temperature with respect to pure Fe. Knowledge of the nature and content in light elements (O, S, Si, C) in the core has major implications for establishing the bulk composition of the Earth and for building models of Earth's differentiation.

Angle dispersive X-ray diffraction experiments in double-sided laser heated diamond anvil cell (LH-DAC) were performed at ID27 beamline at the European Synchrotron Radiation Facility (ESRF) in Grenoble. *In situ* investigations enable determination of melting temperature and structural and density properties of the Fe-based alloys. Experiments were performed on an Fe-Ni-S alloy up to 94 GPa and 2800 K and on an Fe-Ni-Si alloy up to 91 GPa and 3200 K. New results on Fe-O and Fe-C liquid alloys will be also presented.

The appearance of a diffuse X-ray scattering signal at wavevectors of about 30 nm⁻¹ was used to determine the onset of melting. Extrapolations of measured melting curve up to the core-mantle boundary pressure yielded values of 3,600–3,750 K for the freezing temperature of plausible outer core compositions. We extracted densities and compressibilities from the diffuse X-ray signal scattered by the liquid up to megabar conditions, using a method developed for diamond anvil cells by Eggert and collaborators [1]. The obtained equations of state parameters indicate that sulfur, and not silicon, can more easily account for the differences in density and bulk modulus between pure iron and a reference Earth seismic model. This challenges traditional Earth's accretion and differentiation models, that do not foresee S as major light element in the core. These results thus rather argue for strong disequilibrium Earth formation mechanisms.

[1] Eggert, Weck, Loubeyre and Mezouar (2002), *Phys RevB*, 2002, **65**, 174105

Origin of noble gases on Earth: a mixture of Solar, solar wind implantation and phase Q

MOREIRA MANUEL¹ AND CLAIRE ROUBINET²

¹moreira@ipgp.fr

²roubinet@ipgp.fr

The origin of noble gases on Earth is debated since more than 70 years and the observation that the noble gas elemental relative abundances are not solar [1]. Mantle and atmospheric noble gas isotopic compositions are neither chondritic nor solar, at the exception of the neon isotopic ratio that shows a value intermediate between the chondritic components and the solar value, wclose to the neon B value. Since the works of Cafee *et al.* [2] and Holland *et al.* [3], the question of the terrestrial primordial isotopic composition of the Kr and Xe is discussed. They show that the primordial mantle might have been chondritic instead of atmospheric. In addition to that, Pujol *et al.* [4] have shown that the archean atmosphere might have been chondritic, suggesting a xenon loss fractionation accompanied with mass fractionation. A major implication of these observations is the massive subduction of atmospheric xenon in the whole mantle.

We show in this study that the Ne and Ar were added to the parent bodies of the Earth by solar wind implantation. Atmospheric Kr isotopes, on contrary, suggest a late veneer of cometary material with a solar composition added to the chondritic krypton degassed from the mantle. The primordial noble gas compositions on Earth are therefore a mixture between the chondritic, solar, and implanted solar wind. An unknown isotopic fractionation has modified the isotopic composition of the xenon of the atmosphere, without affecting the other noble gases. Subduction of atmospheric Kr and Xe into the whole mantle is required in such a model.

[1] Brown, H. (1949). In *The Atmospheres of the Earth and Planets*. E. G. Kuiper. Chicago, University of Chicago Press: 258-266. [2] Cafee, M. W., G. P. Hudson, et al. (1999). *Science* 285: 2115-2118. [3] Holland, G. and C. J. Ballentine (2006). *Nature* 441: 186-191. Holland, G., M. Cassidy, et al. (2009). *Science* 326: 1522-1525. [4] Pujol, M., B. Marty, et al. (2011). *Earth and Planetary Science Letters* 308: 298-306.

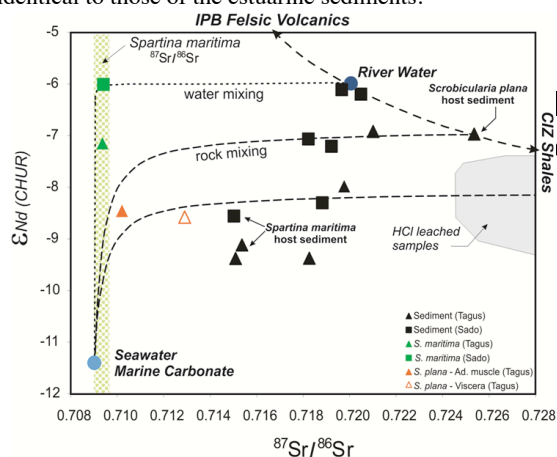
Nd and Sr isotope geochemistry of sediments and associated biota from Tagus and Sado estuaries (Portugal)

S. MOREIRA^{1*}, M.C. FREITAS¹, J. MUNHÁ¹, C. ANDRADE¹ AND C. TASSINARI²

¹Universidade de Lisboa, Fac. Ciências, Departamento de Geologia, Centro de Geologia. 1749-016 Lisboa, Portugal. (*correspondence: scmoreira@fc.ul.pt)

²Universidade de São Paulo, Centro de Pesquisas Geocronológicas. CEP 05508-080 - São Paulo, Brasil.

This study reports on Nd and Sr isotopes and elemental geochemistry of sediments and associated biota (*Spartina maritima*; *Scrobicularia plana*) collected in the intertidal domain of Sado and Tagus estuaries. Sediments display UCC type REE patterns, but variable $^{143}\text{Nd}/^{144}\text{Nd}$ (0.512171–0.512325) and $^{87}\text{Sr}/^{86}\text{Sr}$ (0.715367–0.725351) isotopic ratios, which tend to decrease with increasing Ca/Al and Si/Al values. The observed variations of isotopic ratios suggest that Nd and Sr in the Tagus and Sado estuarine sediments were mainly derived from an heterogeneous UCC source (e.g., old recycled CIZ shales + juvenile IPB volcanics) with variable inputs from relatively unradiogenic, Ca, Si – rich, marine components. *S.maritima* and *S.plana* tissues have $^{143}\text{Nd}/^{144}\text{Nd}$ isotopic ratios (0.512272–0.512330 and 0.512197–0.512204, respectively), which are similar to those of their host sediments; however, $^{87}\text{Sr}/^{86}\text{Sr}$ values (0.709193–0.709408 and 0.709321–0.710204, respectively; excepting viscera of *S.plana* bearing lithic particles = 0.712855) are much lower than those of their sedimentary substrate. These results indicate that Sr and REE in *S.maritima* and *S.plana* tissues had distinct sources; metabolic Sr was mostly derived from seawater, whereas REE were bio-processed from sources identical to those of the estuarine sediments.



Speciation study in the sulfamethoxazole-copper-pH-soil system: Implications for antibiotic retention prediction in soils

M.-C. MOREL, L. SPADINI*, K. BRIMO AND J.M.F. MARTINS

LTHE Laboratory., UMR5564 CNRS, University of Grenoble 1, BP 53, 38041 Grenoble Cedex 09, France

(*correspondence lorenzo.spadini@ujf-grenoble.fr) (marie-christine.morel@ujf-grenoble.fr, jean.martins@ujf-grenoble.fr)

Most antibiotic substances are acid-base reactive and metal complexing. These characteristics determine specific chemical relationships for the prediction of their retention in soils, aquifers, and suspended matters. The results for Sulfamethoxazole (SMX), a persistent sulfonamide antibiotic commonly found in natural waters, is presented. The speciation of the SMX - Cu(II) - H⁺ system in solution and the combined sorption of these components on a natural vineyard whole soil were investigated by acid base titrimetry and Infrared Spectroscopy. Cu(II) is considered to represent a strongly complexing trace element cation (such as Cd²⁺, Zn²⁺, Pb²⁺, Ni²⁺, etc.) in comparison to major but more weakly binding cations (such as Ca⁺⁺ and Mg⁺⁺). The analysis showed that SMX is a medium to weak copper complexing agent and it also qualifies as a weak to medium soil sorbate at pH 6. However, the sorption of SMX in soil increases strongly in the presence of copper. This strongly supports the hypothetical formation of ternary SMX-Cu-soil complexes, especially when considering the almost quantitative sorption of the strongly sorbing copper. The data were successfully modelled with the assumption of the existence of binary and ternary surface complexes in equilibrium with aqueous Cu, SMX and Cu-SMX complexes. It is thought that other strongly complexing cations such as Cd(II), Ni(II), Zn(II), Pb(II), Fe(II/III), Mn(II/IV) and Al(III) present on the surface of reactive organic and mineral soil phases affect the solid/solution partitioning of SMX, and that the sorption strength may be estimated from existing sorption constant relationships. This study thus suggests that the state of surface-adsorbed cations significantly affects the sorption strength of SMX, and that the interactions may be predicted by combining equilibrium analysis and modeling studies.

Arsenic-chloride exchange in the Pecora River Valley (Southern Tuscany, Italy)

G. MORELLI^{1*}, M.GASPARON^{1,2}, P.COSTAGLIOLA³, V. RIMONDI³, M.BENVENUTI³, F.DI BENEDETTO³, P.LATTANZI³, AND M.PAOLIERI³

¹School of Earth Sciences, The University of Queensland, Brisbane, Qld, 4072, Australia (*g.morelli@uq.edu.au)

²National Centre for Groundwater Research and Training, Australia

³Dipartimento di Scienze della Terra, Università degli Studi di Firenze, Florence, Italy

High concentrations of As have been documented in large aquifers (e.g. Bangladesh, China, India -West Bengal [1]) and coastal Holocene/Quaternary alluvial plains where fresh groundwater mixes with intruding seawater [2]. Very high As concentrations have been measured in the alluvial sediments (As>500mg/kg) of the Pecora River (Southern Tuscany, Italy; [3]). As concentrations exceeding 10 µgL⁻¹ [4] have been recorded in some of the groundwaters potentially exposed to seawater intrusion caused by aquifer overexploitation. To quantify how the ionic exchange between As oxianions (adsorbed on minerals' surfaces) and seawater Cl⁻ may contribute to the release of As in groundwater, desorption kinetic experiments were carried out on three samples from this alluvial deposit. After 24 hours, desorption experiments using four aqueous solution with different salinity extracted between 20 and 80 µgL⁻¹ of As, with the highest levels extracted by seawater. For longer desorption periods (~20 days), the samples were saturated with the same solutions to constrain the timing of the As-Cl reaction. The solutions with Cl⁻<2000 mgL⁻¹ extracted <20 µgL⁻¹ of As after at least 8 days, while the extracted As using seawater varied between 20 and 60 µgL⁻¹. Compared to other experimental studies [5], the percentage of extracted As is much lower (< 0.04% of the total) because the mobile (and thus potentially bioavailable) As is only 9-11% of the total As, which is mainly associated with relatively stable Fe-oxides and sulphides. This study demonstrates the importance of a rigorous mineralogical characterization for a prediction of potential As release from coastal aquifers following seawater intrusion.

[1] Smedley and Kinniburgh (2002) *App. Gechem* **17**, 517–568. [2] Liu *et al.* (2003) *Sc.Tot.Envir.* **313**, 77–89. [3] Costagliola *et al.* (2008) *App. Gechem.* **23**, 1241–1259. [4] Rossato and Tanelli (2009), *Rendiconti Online Soc. Geol. It.*, **6**, 404–405. [5] Goh and Lim (2005) *App. Gechem.* **20**, 229–239.

Cyclic subduction of the Aeolian Arc: Evidence from Salina.

MORETTI, H.C.^{1*}, GOTTSMANN, J.C.,¹ BLUNDY, J.M.¹ AND SULPIZIO, R.²

¹Department of Earth Sciences, University of Bristol, BS8 1RJ, hm12523@bristol.ac.uk

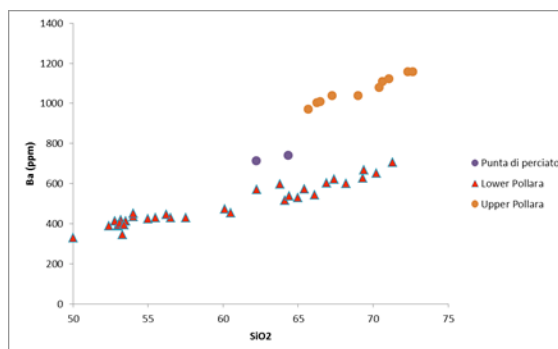
(j.blundy@bristol.ac.uk), (j.gottsmann@bristol.ac.uk)

²Università di Bari A. M., 70125, (roberto.sulpizio@uniba.it)

The island of Salina is part of the Aeolian Arc of Italy, located in the southern Tyrrhenian Sea. It occupies a central position at the junction of a sub-arcuate chain of seamounts and volcanic islands with a linear belt of volcanic islands defined by the Tindari-Letojanni fault and is related to a steeply dipping Beniof zone. Volcanic activity on Salina has stretched from 430ka to 13ka, initially consisting of mafic lavas and concluding with more evolved, mingled, basaltic andesite and rhyolite explosive eruptions.

Geochemical evidence from basalts across the Aeolian Arc suggests that whilst Panarea, Salina and Lipari have a strong signature of fluid metasomatism from a subducting slab, the outlying islands of Alicudi and Stromboli have a more complex genesis with evidence of slab sediment melting, inflowing mantle and crustal assimilation [1].

A temporal trace element analysis for Salina shows the amount of Barium, for example, varies across eruptions; some more evolved eruptions have significantly higher barium for similar levels of silica and suggest a marked cyclicality that may not be driven by fractionation alone. The variations are examined to determine the degree to which they are driven by changes in subduction fluid metasomatism as opposed to increased assimilation of crustal materials or changes in the style of fractionation.



[1] Francalanci *et al.*, in Beccaluva, Bianchini and Wilson, *Cenozoic volcanism in the Mediterranean Area*, p235-264, (2007).

Pathways of redox state and sulfur release track the shift from low-energy to highly-explosive basaltic eruptions at Mt. Etna

MORETTI R.^{1,2}, MÉTRICH N.³, ALLARD P.³, AIUPPA A.⁶,
ARIENZO I.² AND DI RENZO V.¹

¹ DICDEA, Seconda Università degli Studi di Napoli, Aversa (CE), Italy

² INGV, sezione Osservatorio Vesuviano, Napoli, Italy

³ IPGP, Sorbonne-Paris Cité, Univ. Paris Diderot, UMR 7154 CNRS, Paris France

⁴ DiSTeM, Università di Palermo, Palermo, Italy

Basaltic magmas can transport and release large amounts of volatiles into the atmosphere, especially in subduction zones, where slab-derived fluids enrich the mantle wedge. Mt. Etna in Sicily, is one typical basaltic volcano where the volatile control on variable activity (effusive to Plinian) can be investigated. Based on a melt inclusion study of sulfur in products from Strombolian or lava-fountain activity to Plinian eruptions, here we show that different eruptive styles correspond to distinct sulfur degassing paths. Depending on their initial water content, oxidation state, and extent of CO₂-fluxing, Etnean magma batches can soon reach the limit of sulfide saturation or get rid of sulfur on degassing only. Melt inclusion data indicate that the magma involved in the powerful 122 BC Plinian eruption is richer in sulfate ($S^{6+}/S_{\text{tot}} > 0.65$) than the magmas erupted during less energetic explosive February 1999 and Strombolian effusive 1997-98 eruptions. We propose a direct relationship between the high sulfate (SO₄²⁻) content in melts and hence high oxidation state of the melts and the magnitude of an eruption. Highly oxidized conditions ($[S^{6+}/S_{\text{tot}}]_{\text{melt}}$ and $SO_{2,\text{gas}}/[H_2S+SO_2]_{\text{gas}} > 0.6$) in Etnean magma batches enhance the probability of violent explosive eruptions, such as the 122 BC Plinian event. The different patterns of sulfur release (oxidized vs reduced) of Etnean magmas are discussed and modeled.

Bend-Faulting, Serpentinization, and Mantle Recarbonation at Trenches

JASON P. MORGAN¹

¹Earth Science Department, Royal Holloway Univ. London, Runnymede, Surrey, TW20 0EX
(jason.morgan@rhul.ac.uk)

It is well known that mid-ocean ridges are a key site for chemical interactions between oceanic crust and the hydrosphere, and that these interactions modulate the chemistry of the oceans. Subduction forearcs are also key sites of chemical fluid-rock exchanges. These fields are likely to still have many surprises to reveal, but are relatively mature. However, it is becoming increasingly evident that the oceanic lithosphere may also strongly interact with the hydrosphere during plate subduction, as it bends — by bend-faulting — when it enters a trench. I briefly review recent seismic evidence collected by the SFB574 and others that suggests that bend-faulting is associated with ~10-20% serpentinization in a layer extending at least 5km below the Moho. If this serpentine forms with a 1% carbonate fraction (note that at least this degree of carbonitization occurs during mid-ocean-ridge serpentinization processes), then bend-faulting-linked serpentinization will consume an atmosphere's worth of CO₂ every 40,000 years, and it is likely that the carbonate storage in serpentinized subducting lithosphere exceeds that in overlying oceanic crust and sediments. This poorly-understood geological process clearly merits further study, with significant potential implications for the global carbon cycle, for the geochemical evolution of the mantle, and for human exploitation for potential carbon sequestration at oceanic trenches. CO₂-rich fluids released by deserpentinization reactions may even play a role in 'lubricating' the subduction channel, and in the volatilization of the forearc. While bend-faulted Moho lies within the potential drilling window for the Chikyu marine drilling platform, it may prove to be much easier to gain constraints on bend-fault-related serpentinization from observations on Alpine serpentinites. Another critical observation to begin to document this interaction would be to find and study an active site of bend-fault fluid venting at the seafloor — with candidate sites evident in swath-mapping and deep-bottom photos offshore Central America.

Potassium stable isotopic compositions measured by high-resolution MC-ICP-MS

L.E. MORGAN¹, N. LLOYD², R. ELLAM¹, J. I. SIMON³,
AND M. TAPPA⁴

¹Scottish Universities Environmental Research Centre,
Rankine Ave., East Kilbride, G75 0QF, UK
(*correspondence: leah.morgan@glasgow.ac.uk)

²ThermoFisher Scientific, Hanna-Kunath Str. 11, 28199
Bremen, Germany

³Center for Isotope Cosmochemistry and Geochronology,
ARES, NASA JSC, Houston, TX 77058, USA

⁴JE-23 ESCG/Jacobs Technology, Houston, TX 77258, USA

Potassium stable isotopic (⁴¹K/³⁹K) compositions are notoriously difficult to measure. TIMS measurements are hindered by variable fractionation patterns and too few isotopes to apply an internal spike method for instrumental mass fractionation corrections. Internal corrections via the ⁴⁰K/³⁹K ratio can provide precise values and are appropriate in some cases (e.g. identifying excess ⁴¹K [1]) but not others (e.g., determining fractionation effects and metrologically-traceable isotopic abundances). SIMS analyses have yielded results with 0.25‰ precisions [2]. Previous studies have not resolved isotopic variation in terrestrial materials.

We measured ⁴¹K/³⁹K ratios on NIST K standards with < 0.07‰ precisions (1σ) on the Thermo Scientific NEPTUNE Plus MC-ICP-MS. ³⁹K and ⁴¹K were sufficiently resolved from the interfering ³⁸ArH⁺ and ⁴⁰ArH⁺ peaks in wet cold plasma and high-resolution mode. Measurements were made on narrow but flat, interference-free, plateaus (ca. 50 ppm by mass width for ⁴¹K). Although ICP-MS does not yield accurate ⁴¹K/³⁹K values due to significant instrumental mass fractionation (ca. 6%), this bias is sufficiently stable that relative ⁴¹K/³⁹K values can be precisely determined via sample-standard bracketing. Measurement tolerances on matrix effects that are amplified by the cold plasma were tested; the use of clean samples and standards is critical.

On the Thermo Scientific TRITON TIMS, using a co-loaded Rb standard to normalize for fractionation, accurate but less precise ⁴¹K/³⁹K ratios have been measured. Differences in ⁴¹K/³⁹K between NIST K standards identified via MC-ICP-MS are also apparent in the TIMS data. Combined, these approaches yield more reliable K isotopic measurements than were previously possible and may allow for the identification for the first time of sub-permil terrestrial variations in ⁴¹K/³⁹K.

[1] Wielandt and Bizzarro, 2011. [2] Humayun and Clayton, 1995.

Diffusion of Helium in the mantle: an explanation for MORB-OIB patterns of 3He/4He ratios

W. JASON MORGAN¹, AND JASON P. MORGAN²

¹Earth Science Department, Harvard Univ., Cambridge, MA, USA (wjmorgan@princeton.edu)

²Earth Science Department, Royal Holloway Univ. London, Runnymede, Surrey, UK (jason.morgan@rhul.ac.uk)

OIBs have a wide range of 3He/4He ratios, MORBs have a much narrower range peaked at 3He/4He ≈ 8 Ra. In addition, the ratio of 3He/20Ne (both stable isotopes) is significantly higher in MORB than in OIB, likewise the ratio of 4He/21Ne (both daughter isotopes produced by U and Th decay) are similarly higher in MORB than OIB. (Stable 3He/36Ar and radiogenic 4He/40Ar have the same pattern as the He/Ne plots, only with more scatter.) [See Honda and Patterson, GCA 63, 1999.] To explain this, we assume that rising mantle plumes are 'lumpy'; a mixture that includes lumps of primordial mantle (which will be rich in 3He, 20Ne, 22Ne, 36Ar, etc.) as well as lumps containing the EM1, EM2, HIMU components, all in a general matrix of relatively-barren, previously-melted 'harzburgite'. When the rising lumps (plums) melt, the He, Ne, Ar, and most of the other incompatible elements will go into the melts that are known as OIB. But not all of the lumps melt (near the cooler edge, some don't rise shallow enough to pressure-release melt); those that don't melt go into the asthenosphere, flowing horizontally away from the rising column. At a spreading center, this asthenosphere contributes the 'plums' left over from OIB partial melt-extraction but also some of the more barren matrix that the plums are embedded in becomes part of the melt because of the higher extents of partial melting that occur when making MORB. What is the effect of diffusion? If the helium, because of its small size, can diffuse a distance of 100 m or 1000 m in a billion-plus years (the 'age' of a lump) whereas neon or argon diffuse only decimeters or centimeters in this time because of their larger radii (i.e., not much more than non-noble incompatible elements like K, Rb, or U can diffuse), then the 3He and 4He (and H) can diffuse far out into the 'barren harzburgite' matrix. Thus when the lumps in a plume melt there will be a shortage of 3He and 4He relative to the 20Ne, 21Ne, or argon. With the extensive melting that occurs to make MORB, fluxing causes some of the barren matrix to contribute its 3He and 4He to the MORB melt which results in an excess of helium relative to neon and argon. This extraction of helium from the longtime-diffused-into barren matrix also can explain the uniformity of the 3/4 ratio in MORB as opposed to the variability of 3/4 in OIB.

Structure and reactivity of nanocrystalline iron oxides in the environment

GUILLAUME MORIN¹, FABIEN MAILLOT¹, AREEJ ADRA¹,
MARC BLANCHARD¹, GEORGES ONA-NGUEMA¹,
YUHENG WANG¹, NICOLAS MENGUY¹
AND GORDON E. BROWN JR².

¹Institut de Minéralogie et de Physique des Milieux Condensés (IMPMC), Environmental Mineralogy, UMR 7590 CNRS – UPMC – IRD, 4 place Jussieu, 75252 Paris cedex 05, France

²Department of Geological & Environmental Sciences, Stanford University, Stanford, CA 94305-2115, USA

Iron (oxyhydr)oxides are widespread minerals in Earth's surface environments. They exhibit a large variety of polymorphic structures that can be used as tracers of physicochemical conditions of formation, especially redox and pH. Moreover, structural defects and inorganic and organic impurities are also potential indicators of formation pathways, either biotic or abiotic. When formed at ambient temperature, iron oxide minerals usually have sub-micron size, which enhances their surface reactivity. Although the properties and occurrences of iron oxide minerals have been studied for several decades, recent advances have been made in understanding the structures of nanocrystalline iron oxyhydroxides as well as their surface reactivity.

In the present communication, we will review recent spectroscopic investigations of ferrihydrite [1], schwertmannite [2], and nanomagnetite [3] that play a key role in iron and trace element cycling in the environment and in water treatment technologies. Local structures of these mineral phases, including the status of sorbed or coprecipitated impurities, will be discussed based on Extended X-ray Absorption Fine Structure (EXAFS) analyses. Implications for the remediation of arsenic contaminated waters in mining environments will be especially addressed. In addition, we will present specific properties of nanomagnetites for scavenging pollutants such as arsenic via precipitation, sorption, and redox reactions. Spectroscopic results will be interpreted in light of theoretical calculation for arsenic sorption onto the surface of the reference mineral, hematite.

[1] Maillot *et al.* 2011 GCA 75, 2708-2720. ; [2] Maillot *et al.* 2013 GCA 104, 310-329 ; [3] Wang *et al.* 2011 ES&T 45, 7258-7266 ; [4] Blanchard *et al.* 2012 GCA 86, 182-195

Light hydrocarbons and dissolved organic carbon in shallow aquifers of the St. Lawrence Lowlands: Concentrations and $\delta^{13}\text{C}$ signatures

ANJA MORITZ¹, JEAN-FRANCOIS HELIE², DANIELE PINTI², MARIE LAROCQUE², DIOGO BARNETCHE²
AND YVES GELINAS¹

¹Concordia University, 7141 Sherbrooke West, Montreal, QC, H4B 1R6, Canada

anjamoritz@hotmail.com, yves.gelinas@concordia.ca

²UQAM, 405 rue Sainte-Catherine East, Montreal, QC, H2L 2C4, Canada

helie.jean-francois@uqam.ca, pinti.daniele@uqam.ca,

larocque.marie@uqam.ca, barnetche.diogo@gmail.com

Recent field studies identified a new source of natural gas in Quebec: shale gas. These gases are mainly found in the Utica Shale and result from kerogen cracking. Gases formed from kerogen cracking are referred to as thermogenic gases and are mainly composed of methane, ethane and propane. Due to the presence of natural faults in the bedrock above the Utica Shale, these gases can migrate and contaminate the shallow aquifers that are exploited for human consumption. Contamination of the aquifers can also be caused by the migration of biogenic gases formed by methanogenic bacteria in surface wetlands and lake sediments. As part of an effort initiated by the Québec *Commission d'étude environnementale stratégique* on shale gases, the project consists in the development and implementation of the methods and the analysis of the concentration and the isotopic signature of these light hydrocarbons and dissolved organic carbon (DOC) in groundwater samples. The stable isotope analyses will help determine the origin of the gas and DOC in these samples, including the discrimination between Utica shale gas and conventional gas. Water samples have been collected from >100 wells in the St. Lawrence Lowlands (Québec, Canada).

Seasonal distributions of archaeal membrane lipids and TEX₈₆ thermometry in the modern shallow coastal ocean

MORIYA, K.*¹, KUWAE, M.², YAMAMOTO, M.³, KUHINIRO, T.⁴, ONISHI, H.², HAMAOKA, H.⁵, SAITO, M.², SAGAWA, T.², FUJII, N.⁶, YOSHIE, N.², OMORI, K.² AND TAKEOKA, H.²

¹ Fac. of Natural System, Kanazawa Univ., Japan.

(*correspondence: kmoriya@staff.kanazawa-u.ac.jp)

² Center for Marine Environ. Studies, Ehime Univ., Japan.

³ Div. Earth System Science, Hokkaido Univ., Japan.

⁴ Royal Netherlands Inst. for Sea Res., Yerseke, Netherlands.

⁵ National Res. Inst. of Fisheries and Environ. of Inland Sea, Fisheries Research Agency, Japan.

⁶ Inst. Lowland and Marine Rese., Saga Univ., Japan.

While a large number of studies have documented rapid increase in the annual sea surface temperature (SST) and global mean sea level rising, global warming effect on enclosed coastal seas, such as Seto Inland Sea or Chesapeake Bay, is less understood. For understanding historical SST records in these shallow basins, we need to utilize a certain SST proxy preserved in sediments. However, paleothermometry in the shallow coastal basin is rather difficult because carbonate microfossils typically used for paleotemperature proxies are practically absent in the shallow ocean. On the hand, it is expected that organic compound based paleo-temperature proxies, such as TEX₈₆, can be utilized even in the shallow coastal sea. However, since TEX₈₆ thermometry has rarely been used for such shallow marine sediments, applicability of TEX₈₆ in the coastal ocean is still uncertain.

Here we test potential ability of TEX₈₆ paleothermometry in shallow coastal anoxic basin. We collected particulate organic matters from the water column of Beppu Bay (Seto Inland Sea) (~70m deep) at every 10 m. The vertical depth profile of glycerol dialkyl glycerol tetraethers (GDGTs) distribution within the anoxic and oxygen-enriched water columns was determined. We also calculated TEX₈₆ values, TEX₈₆^H and TEX₈₆^L temperatures which were compared with the in situ measurements of water temperatures.

Comparing total GDGTs in the anoxic water mass to those of the oxygen-enriched water mass, those are significantly abundant in the anoxic bottom water. TEX₈₆^{H/L} derived temperatures correlate with the in situ measurements of water temperatures. Therefore it is expected that temperatures delivered from TEX₈₆^{H/L} represent in situ water temperatures in Beppu Bay.

Technological challenges for the advanced study of seafloor life

YUKI MORONO^{1*}, TAKESHI TERADA², MOTOO ITO¹ TATSUHIKO HOSHINO¹ AND FUMIO INAGAKI¹

¹Kochi Institute for Core Sample Research, Japan Agency for Marine-Earth Science and Technology (JAMSTEC), Monobe B200, Kochi 783-8502, Japan. (*correspondence: morono@jamstec.go.jp)

² Marine Works Japan Ltd., Oppamahigashi 3-54-1, Yokosuka 237-0063, Japan.

During the past decades, scientific ocean drilling has explored the seafloor biosphere at some representative drilling sites: on the ocean margins, organic-rich anaerobic sedimentary habitats (e.g., Shimokita coalbeds) harbor sizable numbers of microbial cells over 1,000 meters below the seafloor whereas microbial populations in ultra-oligotrophic aerobic sedimentary habitats of the oceanic gyre (e.g., South Pacific Gyre) are several orders of magnitude lower. Molecular analysis at the community level demonstrates the occurrence of seafloor microbial ecosystems that consist of phylogenetically diverse microbes; however, metabolic functions of individual microbial components and strategies for long-term survival under the energetically and geophysically severe condition have remained largely unknown. To address these issues, analytical developments customized for seafloor life are of our essential challenges for the advanced microbiological and biogeochemical analyses.

One of the most fundamentally significant techniques is the precise detection and enumeration of indigenous seafloor life. Recently, we have standardized an improved cell separation method, which effectively detached the cells from mineral grains of the sedimentary habitat, by applying multiple density gradient layers. Based on the cell-derived fluorescent wavelength pattern [1], the detached cells can be precisely enumerated using an automated fluorescent microscopic system [2] and/or a flow cytometry. The combined use of this technique with a cell sorter allows us to separate the cells for single cell genomics and mass spectrometry (e.g., NanoSIMS) analyses. The systematic analytical scheme currently applies to some representative deep-biosphere samples such as the South Pacific Gyre and Shimokita coalbeds (i.e., IODP Expedition 329 and 329, respectively), from which results may open a new window to the study of seafloor life.

[1] Morono *et al.* (2009) *ISME J.* **3**, 503-511. [2] Morono *et al.* (2010) *Sci. Drilling* **9**, 32-36.

Characterization of the deep microbial life at different CCS sites

DARIA MOROZOVA^{1*}, DOMINIK NEUMANN¹, MICHAEL ZETTLITZER² AND HILKE WÜRDEMANN¹

¹ Helmholtz Centre Potsdam GFZ, International Centre for Geothermal Research, Hermannswerder 15, 14473 Potsdam, Germany. *Correspondence: Hilke.Wuerdemann@gfz-potsdam.de

² RWE Dea AG, Laboratory Wietze, Industriestraße 2, 29323 Wietze, Germany

Deep subsurface formations like subsurface saline aquifers or depleted gas reservoirs are candidate sites for the carbon capture and storage (CCS) technology. Since the Earth subsurface is known to be a major habitat for a high number of different groups of microorganisms, our working group aims at microbial monitoring at different CCS-sites in Germany (a 650m-deep saline aquifer and a 3.5km-deep depleted gas reservoir). Both sites are characterized by high salinity (325 g/l and up to 420 g/l) and relatively high TOC content (up to 150 mg/l and up to 300 mg/l). In order to characterize the microbial life in extreme habitats we aim to localize and identify microbes including their metabolism influencing mineral creation and dissolution. The ability of microorganisms to speed up dissolution and formation of minerals might result in changes of the local permeability and the long-term safety of CO₂ storage. Genetic fingerprinting (PCR SSCP, DGGE), qPCR and FISH are applied for identification and quantification of changes in deep microbial community caused by the injection of supercritical CO₂.

Although saline aquifers could be characterized as an extreme habitat for microorganisms due to high pressure and salinity, a high number of diverse groups of microorganisms were observed with molecular biological methods in downhole samples from the injection and observation wells at a depth of about 650m depth. Of great importance was the identification of the sulfate reducing bacteria, which are known to be involved in corrosion processes. Microbial monitoring during CO₂ injection has shown that both quantity and diversity of microbial communities were strongly influenced by the CO₂ injection.

First results of the sequence analyses from a 3,5km-deep, 120-130°C hot reservoir indicate the presence of several H₂-oxidizing bacteria, thiosulfate-oxidizing bacteria and biocorrosive thermophilic microorganisms. Due to the hypersaline and hyperthermophilic reservoir conditions, and therefore low cell numbers, the quantification of those microorganisms was not yet possible.

Crystal-chemical analyses of soil and drilled rock in Gale crater, Mars

S.M. MORRISON^{1*}, R.T. DOWNS¹, D.F. BLAKE², D.L. BISH³, D.W. MING⁴, R.V. MORRIS⁴, A.S. YEN⁵, S.J. CHIPERA⁷, A.H. TREIMAN⁶, D.T. VANIMAN⁷, R. GELLERT⁸, C.N. ACHILLES⁴, E.B. RAMPE⁴, T.F. BRISTOW², J.A. CRISP⁵, P.C. SARRAZIN⁹, J.M. MOROOKIAN⁵ AND THE MSL TEAM

¹ U. Arizona, Tucson, AZ 85721, USA (*correspondence: shaunnamm@email.arizona.edu)

² NASA ARC, Moffett Field, CA 94035, USA

³ Indiana U., Bloomington, IN 47405, USA

⁴ NASA JSC, Houston, TX 77058, USA

⁵ JPL-Caltech, Pasadena, CA 91109, USA

⁶ LPI, Houston, TX 77058, USA

⁷ PSI, Tucson, AZ 85719, USA

⁸ U. Guelph, Guelph, ON N1G 2W1, Canada

⁹ SETI Institute, Mountain View, CA 94043

The CheMin instrument on the Mars Science Laboratory Rover *Curiosity* performed X-ray diffraction analyses in Gale crater on both martian soil at Rocknest [1] and drilled rock at John Klein. Crystalline phases were identified and their abundances and unit-cell parameters were refined with the Rietveld method [2]. Crystal-chemical systematics, using data from the literature, were developed for the observed phases and were used to estimate the chemical compositions of the martian minerals.

Estimated Rocknest soil mineral compositions:

olivine: (Mg_{0.63(3)}Fe_{0.37})₂SiO₄

plagioclase: (Ca_{0.57(13)}Na_{0.43})(Al_{1.57}Si_{2.43})O₈

augite: [Mg_{0.87(10)}Fe_{0.40}Ca_{0.73(4)}]Si₂O₆

pigeonite: [Mg_{1.13(9)}Fe_{0.70(10)}Ca_{0.17}]Si₂O₆

In addition to the crystalline component, there is also an amorphous component. Subtracting the weighted chemistry of the crystalline component from the bulk composition, determined by APXS [3], provides an estimate of the amount and chemical composition of the amorphous component.

Currently, the analysis of the John Klein drilled rock sample continues. Preliminary data indicate the presence of smectite(s), sulfates, and igneous minerals similar to those found in Rocknest soil, representing the mineralogy of a potentially habitable environment. These data facilitate determination of comparable crystal-chemical systematics and comparisons with Rocknest soil.

[1] Blake *et al.* (2013) *LPS XLIV*, Abstract. [2] Bish *et al.* (2013) *LPS XLIV*, Abstract. [3] Yen *et al.* (2013) *LPS XLIV*, Abstract.

Atomic Views of Martian Evolution

D.E. MOSER^{1*}, D. A. REINHARD², D. OLSON², P. H. CLIFTON², D. J. LARSON², J.R. DARLING³, K.T. TAIT⁴, M. BUGNET⁵, B. GAULT⁵ AND I.R. BARKER¹

¹Univ. of Western Ontario, London, Ont., CAN N6A 5B7
(*correspondence: desmond.moser@uwo.ca); ²CAMECA, Madison, WI 53711, USA; ³University of Portsmouth, UK; ⁴Royal Ontario Museum, Toronto, Ont. CAN M5S 2C6; ⁵CCEM, McMaster University, Hamilton, Ont. CAN

The extremely sluggish volume diffusion rates of U and Pb in minerals such as baddeleyite and zircon, together with their resistance to breakdown during shock metamorphism, make them ideal recorders of inner Solar System evolution. In the case of highly shocked basaltic shergottite NWA5298, our discovery of igneous (187±33 Ma) micro-baddeleyite, with micron-wide reaction rims of much younger launch-generated zircon, promises further information on young Mars evolution if afforded high spatial resolution techniques.

Here we present the first atomic resolution STEM (HAADF detector) imaging of baddeleyite and zircon microstructure, and our progress toward their combination with atom probe tomography (CAMECA LEAP[®]) results for extraterrestrial phases. Conventional EBSD analysis indicates that euhedral baddeleyite CL zones are now amorphous at 50 nm length-scales, whereas high resolution STEM results reveal a mosaic of slightly misoriented nanocrystalline domains overgrown by unshocked zircon in single orientation. Rare dislocation trains in zircon are perhaps due to thermal stress on transit to outer space and Earth. Atom probe results for terrestrial reference zircon BR266 reveal a generally homogeneous distribution of radiogenic Pb²⁺. The goal of LEAP analyses is to map Pb and trace element distribution in martian ejectic zircon rims, the age of which is constrained to lie between the youngest shocked baddeleyite date of 22±2 Ma [1] and the cosmic ray exposure ages of ~3 Ma for similar shergottites [2]. These techniques open the door to direct analysis of atom-scale mineral records of the evolution of Mars and the interplanetary travel of martian crust.

[1] D.E. Moser *et al.* (2012) Microstructure and U-Pb dates of martian baddeleyite rimmed by zircon indicate a 'young' igneous and metamorphic history for shergottite NWA 5298. *Lunar Planet Sci Conf. XLIII* Abs. 2173. [2] O. Eugster *et al.* (1997) Ejection Times of Martian Meteorites. *Geochim.Cosmochim. Acta.* **61**, 2749–2757.

Effect of the isotopic composition of nitrite on the enrichment factor during benthic denitrification

AURELIE MOTHET^{1*}, MATHIEU SEBILO¹, ANNIET M. LAVERMAN², VERONIQUE VAURY¹
AND ANDRE MARIOTTI¹

¹UPMC Univ Paris 06, UMR Bioemco, 4 place Jussieu, 75252 Paris Cedex 05, France, aurelie.mothet@upmc.fr (*presenting author)
²UPMC Univ Paris 06, UMR Sisyphe, 4 place Jussieu, 75252 Paris Cedex 05, France

Mediated by denitrifying bacteria under anoxic conditions, denitrification plays an important role reducing nitrate pollution in surface and groundwater. Denitrification can be traced by isotopic biogeochemistry; the isotopic enrichment factor associated with denitrification may vary significantly (i.e. for nitrogen, ϵ vary from -30 to 0‰). This large range might be due to the presence of nitrite, an intermediate during denitrification, not accounted for in the enrichment factor. The presence of nitrite, either transient or continuous, during denitrification is regularly observed. Variations in nitrite concentrations (production and/or reduction), depleted in ¹⁵N and ¹⁸O could modify the enrichment factor for nitrate, when the isotopic composition of nitrite and nitrate are measured together.

Therefore, the objective of this study was to determine the nitrogen and oxygen isotopic fractionation ($\epsilon^{15}\text{N}$, $\epsilon^{18}\text{O}$) associated with both nitrate and nitrite during denitrification by environmental benthic denitrifying communities. Denitrification rates were determined in sediments from four different locations in the Seine bassin (France). Nitrate reduction rates as well as nitrite production and reduction rates were determined and the ¹⁵N and ¹⁸O of both compounds were analysed. As expected, our results show that the isotopic composition of nitrite (¹⁵N and ¹⁸O) is depleted. With a maximum nitrite concentration of about 1% of the initial nitrate concentration, the isotopic enrichment factor shows a significant isotopic shift (-2‰ for nitrogen and oxygen). This indicates the importance of considering a correction of the enrichment factor for denitrification taking into account nitrite.

Calculating rates of ductile thrusting

MOTTRAM, C.M.^{1*}, PARRISH, R.R.², WARREN, C.J.¹,
HARRIS, N.B.W.¹ AND ARGLES, T.W.¹

¹Dept. of Environment, Earth and Ecosystems, The Open University, Walton Hall, Milton Keynes, MK76AA, U.K.

²NERC Isotope Geosciences Laboratory, British Geological Survey, Keyworth, Nottingham NG12 5GG, United Kingdom

*correspondence: catherine.mottram@open.ac.uk

The ductile interiors of mountain belts, key to our understanding of orogenic processes, are often exhumed from mid-crustal levels by ductile shearing. The Sikkim Himalaya presents some of the best exposures of a ductile shear zone in the world. The Main Central Thrust (MCT) is a major Himalayan structure that has accommodated a large amount of movement during India-Asia convergence. In Sikkim, a duplex beneath the thrust has folded the MCT into a dome. This structural configuration allows a novel method for determining rates of processes by exploiting the late-stage folding of the MCT (figure 1).

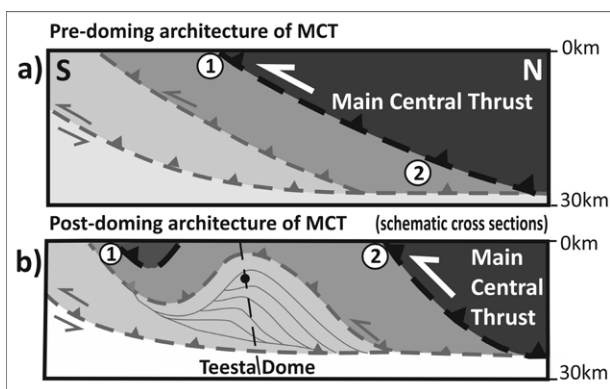


Figure 1. Illustrates a schematic cross-section before (a) and after (b) folding of the MCT. Both the two marker locations (1 and 2) are currently at the surface (b), prior to folding location 2 lay at depth (a). Therefore the age of peak metamorphism at 2 is likely to be younger than at 1, assuming metamorphism is contemporaneous with thrusting. The age difference between samples taken from locations 1 and 2 can be used to calculate a rate of thrusting.

The timing of metamorphism of rocks formed at equivalent metamorphic grades across the MCT (1 and 2 on figure 1) has been determined from U-Th-Pb monazite geochronology. The data show significant differences in the timing of metamorphism in the northern and southern exposures of the MCT in Sikkim, consistent with the figure 1 model. Rates of thrusting from initial calculations (~1cm/yr) appear slower than reported in earlier studies. This approach is the first to exploit folding of a major fault to calculate rates of ductile thrusting at a mid-crustal level.

Geochemistry of Nowdoz potassic volcanic rocks, the sample for early cenozoic potassic magmatism in NW Iran

SEYED ZAHED MOUSAVI¹

¹Basic science department, Meshkinshahr branch, Islamic Azad University, Meshkinshahr, Iran, (zahedmousavi@gmail.com)

The studied area is situated at 47°16'– 47°23' East and 38°20'– 38°23' North between Meshkinshahr and Ahar cities, NW Iran. Despite the importance of the potassic volcanic in geology of Iran and good studies done on it, yet there is no clear information from the history of the this volcano rocks. In this article we will attempt a review of past research results, new data (field, petrography and geochemical). In addition by using the geo-chemical data, we discuss the origin and tectonic position. This area is part of Azarbaijan structural zone. High intensity alteration systems have effected on this rocks that argilice and silica zones are importance of them. Geochemical characterization and magma series show that composition on Nowdoz volcanic rocks are basalt, leucitite, tephrites and phonolitic tephrites. Many samples are in alkalic range. A general trend are observed toward increasing alkalinity with decreasing of SiO₂ Main oxides and rare earth element characterization confirm the fractionation of assemblage of olivine, pyroxin, plagioclases based on the decreasing of MgO, CaO, FeO_t and MnO with decreasing of SiO₂ and increasing of Rb/K, Sr and also decline of Sc with increasing of SiO₂. Fairly regular linear trends in major and trace elements in SiO₂ represent the same magma reservoir for rocks of this area. Although there is a enrichment of Large Ion Lithophile Elements and depletion in High Field Strength Elements. However with survey of geodynamical models for potassic magmatism, it seems that this area, based on idea of Arabian plate sub ducting under Iranian plat in late cretaceous and geochemical feature, are comparable with postcollosion related magmatism patterns.

Archaean granites: classification, origin and tectonic implications

JEAN-FRANÇOIS MOYEN^{1,2}

¹Université Jean-Monnet, Saint-Etienne, France.

Jean.francois.moyen@gmail.com

²CNRS UMR6524

The Archaean continental crust is dominated by granitoids, covering a large range of compositions and rock types. While several classification schemes exist for modern granitoids, there is relatively little application to Archaean rocks and a comprehensive terminology is lacking.

Similar to modern granitoids, Archaean rocks fall under three main groups: peralkaline granites; metaluminous granites and related rocks (granite to diorite); and metaluminous to peraluminous granites. Archaean peralkaline granites, although superficially similar to their modern counterparts, are mostly magnesian and lack the enrichments in trace elements that reflect, in the modern Earth, an origin related to fractionation of mafic melts derived from enriched mantle sources. Metaluminous granites (including sanukitoids) are, in some respect, similar to modern arc granites; but are no exact match to modern rocks, most likely pointing to different mantle enrichment processes in Archaean “subduction” environments. Metaluminous to peraluminous granites are formed by dehydration melting of mafic hydrous silicates and include potassic rocks, very similar to modern rocks and similarly generated by biotite dehydration melting; as well as sodic rocks (TTGs and low-pressure sodic granitoids), related to breakdown of amphibole (or of an equivalent eclogitic assemblage). Sodic granitoids can further be subdivided in low-pressure rocks (similar to rare, oceanic-plateau related granites, with the same apparent “arc” signature); medium-pressure TTGs; and high-pressure TTGs, that do not have a modern counterpart, suggesting some uniquely Archaean petrogenetic process, involving deep (> 15–20 kbar) melting of metamafic rocks.

The differences between Archaean and modern granitoids reflects similar differences observed in mafic rocks: Archaean mafics lack the clear dichotomy observed in the modern record between arc and non-arc samples; and do not show any evidence for strongly depleted or enriched mantle sources. Likewise, Archaean granites reveal a tectonic system with a near-primitive mantle; more common melting of oceanic plateaus; some continental collision; deep melting of mafic rocks, with no modern equivalent; and lacking modern-style subductions (with water fluxed melting of the mantle wedge), although some rocks record melting of a mantle enriched by buried surface matter.

Applications of Absorption Spectroscopy for Water Isotopic Measurements in Cold Clouds

ELISABETH MOYER^{1*}, LASZLO SARKOZY¹,
KARA LAMB^{1*}, BEN CLOUSER¹, ERIC STUTZ¹,
BENJAMIN KÜHNREICH², JANEK LANDSBERG³,
JAN HABIG⁴, NARUKI HIRANUMA⁴, STEVEN WAGNER²,
VOLKER EBERT⁵, ERIK KERSTEL³, OTTMAR MÖHLER⁴
AND HARALD SAATHOFF⁴

¹Department of the Geophysical Sciences, University of Chicago, Chicago, IL, USA (*correspondence: moyer@uchicago.edu)

²Center of Smart Interfaces, Technische Universität Darmstadt, Darmstadt, Germany

³Laboratoire Interdisciplinaire de Physique, J. Fourier University of Grenoble, Grenoble, France

⁴Institute for Meteorology and Climate Research, KIT, Karlsruhe, Germany

⁵Physikalisch-Technische Bundesanstalt, Braunschweig, Germany

While mass spectrometry has been the measurement technique of choice for environmental water isotopic studies, absorption spectroscopy is becoming increasingly competitive for many applications. Advances in instrument sensitivity allow extending the use of isotopic measurements beyond tracing large-scale water transport, an application with relatively loose measurement requirements, to microphysics studies in cirrus and convective clouds in the dry upper troposphere. We outline measurement requirements for science applications in cold cirrus clouds, describe the development of isotopic instrumentation for microphysics studies at the AIDA aerosol and cloud chamber, and present isotopic measurements from the 2012-2013 ISOCLOUD campaign. ISOCLOUD adiabatic expansion experiments from 233-190 K produced the first direct measurements of isotopic fractionation factors at temperatures applicable to cirrus clouds and suggest the feasibility of field studies using water isotopologues as microphysical tracers.

www.minersoc.org

DOI:10.1180/minmag.2013.077.5.13

Heterogeneous distribution of Zn stable isotopes in mice

FREDERIC MOYNIER¹, TOSHIYUKI FUJII²,
ANDREY S SHAW³ AND MARIE LE BORGNE³

¹Department of Earth and Planetary Science and McDonnell Center for Space Sciences, Washington University in St Louis. moynier@levee.wustl.edu

²Research Reactor Institute, Kyoto University, 2-1010 Asashiro Nishi, Kumatori, Sennan, Osaka 590-0494, Japan. tosiyuki@rri.kyoto-u.ac.jp

³Department of Pathology and Immunology and Howard Hughes Medical Institute, Washington University School of Medicine in St Louis. shaw@pathology.wustl.edu; mleborgne@pathology.wustl.edu

Zinc is required for the function of more than 300 enzymes involved in many metabolic pathways, and is a vital micronutrient for living organisms. To investigate if Zn isotopes could be used to better understand metal homeostasis, as well as a biomarker for diseases, we assessed the distribution of natural Zn isotopes in various mouse tissues. We found that, with respect to Zn isotopes, most mouse organs are isotopically distinct and that the total range of variation within one mouse encompasses the variations observed in the Earth's crust. Therefore, biological activity must have a major impact on the distribution of Zn isotopes in inorganic materials. The most striking aspect of the data is that red blood cells and bones are enriched by ~0.5 per mil in ⁶⁶Zn relative to ⁶⁴Zn when compared to serum, and up to ~1 per mil when compared to the brain and liver. This fractionation is well explained by the equilibrium distribution of isotopes between different bonding environments of Zn in different organs. Differences in gender and genetic background did not appear to affect the isotopic distribution of Zn. Together, these results suggest that potential use of Zn isotopes as a tracer for dietary Zn, and for detecting disturbances in Zn metabolism due to pathological conditions.

Cd mobility in anoxic Fe-mineral-rich environments – potential use of Fe(III)-reducing bacteria for soil remediation

E. MARIE MUEHE^{1*}, IRINI J. ADAKTYLOU¹, MARTIN OBST², CHRISTIAN SCHRÖDER¹, SEBASTIAN BEHRENS¹,
ADAM P. HITCHCOCK³, TOLEK TYLSIZCZAK⁴,
UTE KRÄMER⁵ AND ANDREAS KAPPLER¹

¹Geomicrobiology, University of Tuebingen, Germany, eva-marie.muehe@uni-tuebingen.de (* presenting author)

²Environ. Anal. Microscopy, University of Tuebingen, Germany

³Chemistry and Chemical Biology, McMaster University Hamilton, Canada

⁴ALS, Lawrence Berkeley National Laboratory, Berkeley

⁵Plant Physiology, University of Bochum, Germany

Agricultural soils worldwide are increasingly burdened with heavy metals such as Cd from industrial sources and impure fertilizers. Metal contaminants potentially enter the food chain via plant uptake from soil and may affect human and environmental health negatively. New remediation approaches are needed to diminish soil metal contents, but in order to apply them it is necessary to understand how soil microbes and minerals interact with these toxic metals.

Here, we show that microbial Fe(III) reduction leads to Cd immobilization in Cd-bearing anoxic soils. To understand how microbial Fe(III) reduction influences Cd mobility, we isolated a new Cd-tolerant, Fe(III)-reducing *Geobacter sp.* strain Cd1 from a heavily Cd-contaminated soil in Germany. In lab experiments, this *Geobacter* strain first mobilized Cd from Cd-loaded Fe(III) (oxyhydr)oxides followed by precipitation of Cd-bearing mineral phases. Using Mössbauer spectroscopy and Scanning Electron Microscopy, the original and newly formed Cd-containing Fe(II) and Fe(III) mineral phases, including Cd-Fe-carbonates, Fe-phosphates and Fe-(oxyhydr)oxides, were identified and characterized. Using Energy Dispersive X-ray spectroscopy and Synchrotron-based Scanning Transmission X-ray Microscopy, Cd was mapped in the Fe(II) mineral aggregates formed during microbial Fe(III) reduction.

Microbial Fe(III) reduction mobilizes Cd prior to precipitation of the Cd as Cd-bearing mineral phases. On the one hand, the mobilized Cd could potentially be taken up by phytoremediating plants, resulting in a net removal of Cd from contaminated sites. On the other hand, Cd precipitation could immobilize Cd more strongly and reduce Cd bioavailability in the environment, causing less toxic effects to crops and soil microbiota. However, the stability and therefore bioavailability of these newly-formed Fe-Cd mineral phases needs to be assessed thoroughly. Whether phytoremediation or immobilization of Cd in a mineral with reduced Cd bioavailability are feasible mechanisms to reduce the toxic effects of Cd in the environment still remains to be determined.

Sequestration of labile organic carbon in Alaskan permafrost soils

MUELLER CARSTEN W.¹; KAO-KNIFFIN JENNY²;
RETHEMEYER JANET³; LÖPPMANN SEBASTIAN¹; HINKEL
AND KENNETH⁴; BOCKHEIM JAMES⁵

¹Lehrstuhl für Bodenkunde, TU München, Freising-
Weihenstephan, 85356 Germany,
carsten.mueller@wzw.tum.de

²Cornell University, Department of Horticulture, Ithaca, NY
14853, USA, jtk57@cornell.edu

³University of Cologne, Institute of Geology and Mineralogy,
Cologne, 50674, Germany, janet.rethemeyer@uni-
koeln.de

⁴University of Cincinnati, Department of Geography,
Cincinnati, Ohio, 45221, USA, hinkelkm@ucmail.uc.edu

⁵University of Wisconsin-Madison, Department of Soil
Science, Madison, WI 53706, USA, bockheim@wisc.edu

Permafrost affected soils of the Northern circumpolar region represent 50% of the terrestrial soil organic carbon (SOC) reservoir and are most strongly affected by climatic change. Although a large number of studies revealed the overall C cycles in this region, there is only scarce knowledge about the quantitative and qualitative properties of organic matter compartments and their potential stability. To unravel chemical and physical properties of SOC in permafrost soils we combined the physical soil fractionation with the evaluation of the chemical composition using nuclear magnetic resonance spectroscopy (NMR) and microscopic techniques as nano-scale secondary ion mass spectrometry (NanoSIMS).

Approximately 50-75% of Alaska's Arctic Coastal Plain is covered with thaw lakes and drained thaw lakes that follow a 5,000 yr cycle of development (between creation and final drainage), thus forming a natural soil chronosequence. The drained thaw lakes offer the possibility to study SOM dynamics affected by permafrost processes over millennial timescales. In April 2010 we sampled 16 soil cores reaching from young drained lakes (0-50 years since drainage) to ancient drained lakes (3000-5500 years since drainage).

We can show that up to over 25 kg SOC per square meter were stored as mostly labile organic matter particles rich in carbohydrates. In contrast only 9.7 ± 2.3 kg OC per square meter were sequestered as presumably more stable mineral associated OC dominated by aliphatic compounds. The formation of soil aggregates, comparable to soil aggregation in temperate soils, was proved by physical fractionation and microscopic evidence. Here we show that significant amounts of labile SOC are stored in permafrost soil layers which soon could be degraded due to the deepening of the active layer resulting from climatic change.

Unraveling cooling histories using Fe-Mg zoning of exsolution lamellae in a garnet pyroxenite from the Granulitgebirge, Saxony, Germany

THOMAS MUELLER¹, HANS-JOACHIM MASSONNE²
AND ARNE P. WILLNER²

¹Institut für Geologie, Mineralogie und Geophysik; Ruhr-
Universität Bochum; D-44801 Bochum; Germany;
thomas.mueller-1@rub.de

²Institut für Mineralogie und Kristallchemie; Universität
Stuttgart; D-70174 Stuttgart, Germany

The exchange of elements such as Fe-Mg between co-existing ferromagnesian minerals is a consequence of changing external (intensive) variables, such as temperature and/or pressure and proceeds via a series of kinetically controlled processes. Compositional zoning patterns of co-existing mineral pairs can thus be used to model the incomplete diffusive equilibration process if diffusive parameters and the partition coefficient are known as a function of P and T. Unraveling such zoning patterns is the key tool to decipher the nature of measured temperatures using geothermobarometry and are thus potential recorders of cooling and exhumation processes on various timescales.

The studied sample is a garnet pyroxenite from the Granulitgebirge, Germany. The rock contains remarkable exsolution textures from former megacrysts that produced up to mm-wide, alternating lamellae of garnet (grt) and clinopyroxene (cpx). Compositional profiles of Fe and Mg measured with the electron microprobe perpendicular to the grt-cpx interfaces reveal almost flat, but often slightly zoned patterns with increasing Fe from the grt center towards the interface and decreasing Fe (from core to rim) in the adjacent cpx.

We present data from a numerical finite difference scheme that simulates diffusive exchange between grt and cpx along a virtual cooling path. The model assumes local equilibrium at the interface and diffusive fluxes are constraint by mass balance. Preliminary modeling results suggest very efficient compositional resetting even for very fast cooling rates at temperatures above 1000 °C, so that no record of the growth of the lamellae is preserved. Nevertheless, the presence of slight chemical zoning can successfully be used to estimate P-T conditions of lamellae formation as well as cooling / exhumation rates in the temperature range between 700 – 1000 °C. Finally, modeling results indicate fast cooling rates of $\gg 100$ °C/Ma in agreement with published estimates for the crystalline complex of the Granulitgebirge based on geochronology.

Dating deposition and low-grade metamorphism by in situ U-Pb geochronology of titanite

J.R. MUHLING^{1,2*}, B. RASMUSSEN² AND I.R. FLETCHER²

¹CMCA, The University of Western Australia, Stirling Highway, Crawley, WA 6009, Australia

(*correspondence: janet.muhring@uwa.edu.au)

²Dept of Applied Geology, Curtin University, Kent Street, Bentley, WA 6102, Australia

Titanite (CaTiSiO₅) is a widespread accessory mineral, composed of major rock-forming elements, that incorporates sufficient U into its structure for U–Pb geochronology. It occurs in felsic to intermediate igneous rocks, in very low to high-grade metamorphic rocks, in sedimentary rocks and in hydrothermal ore deposits. Because titanite can form at temperatures below 700°C, its closure temperature for the diffusion of Pb, it can provide ages for a wide range of low- to moderate temperature geological processes. Although titanite forms detrital and authigenic grains in sedimentary rocks, it has rarely been used to date deposition, diagenesis or low-grade metamorphism.

Two generations of titanite are preserved in tuffaceous rocks of the Paleoproterozoic Timeball Hill Formation, southern Africa: euhedral, brown crystals with apatite inclusions, and colorless, pore-filling cement. The brown titanite has elevated U, Th and Fe and low Al, consistent with a magmatic origin, whereas the colorless titanite has high Al and F and low Fe contents, suggestive of a diagenetic or metamorphic paragenesis. In situ SHRIMP geochronology of brown titanite from a tuff bed gives a weighted mean ²⁰⁷Pb/²⁰⁶Pb age of ~2275 Ma and is interpreted to provide a reliable estimate for depositional age.

Authigenic titanite has been reported as pore-filling cement in a number of sandstone units worldwide but has not previously been dated. Fe contents vary widely, and some examples have elevated amounts of high-field-strength elements. The compositions may reflect local metamorphic or hydrothermal fluid compositions. In situ U–Pb dating of intergranular titanite from a tuffaceous sandstone in the Timeball Hill Formation yields an age of ~2145 Ma, which corresponds with previous estimates for a low-grade tectonothermal event in southern Africa.

Our results demonstrate that titanite is a versatile chronometer that can be used to constrain depositional ages, and those of diagenesis and low-grade metamorphism. It has the potential to increase the number of sedimentary rock units that can be dated, and to elucidate the histories of low-temperature geological processes in depositional basins.

An EBSD study of textural evolution across a shear zone in the Bergen Arcs, Western Norway

HIROKI MUKAI^{1*}, HÅKON AUSTRHEIM² AND ANDREW PUTNIS¹

¹ Institute for Mineralogy, University of Münster, Münster, Germany (*correspondence: hmukai001@uni-muenster.de)

² Physics of Geological Processes, University of Oslo, 0316 Oslo, Norway

The interaction between fluid infiltration, mineral reactions and rock deformation has been the subject of much debate and raises fundamental issues such as the mechanism of fluid transport in nominally impermeable rocks. Localisation of deformation in shear zones provides an opportunity to study the textural and mineralogical evolution from relatively undeformed wall rocks through to the highly strained shear zone and to evaluate the various mechanical and chemical processes which result in rock weakening. Rock strength or rheology is a critical parameter in geodynamic models for collision and subduction zones.

The present study was carried out from cross sections through an amphibolite facies shear zone associated with the Caledonian Orogeny (~420Ma) that transects older anorthositic granulite facies rocks (~930Ma) in the Bergen Arcs, western Norway. In this region, it is possible to study the textural and chemical changes from the relatively unaltered granulites which retain the high grade mineralogy and texture, through to highly strained and hydrated minerals within the shear zones.

Our SEM observations of the cross sections showed that the granulite facies rock is composed of plagioclase (An₅₀), garnet and an Al-rich clinopyroxene, with minor scapolite. Closer to the shear zone, the original granulitic plagioclase is replaced by a 2-phase feldspar intergrowth composed of an Na-rich and Ca-rich network where the Na-rich domains (composition ~An₂₄) are surrounded by thinner "veins" of Ca-rich plagioclase (An₆₄). At the same time the garnet grains develop Fe-richer rims of variable width and involve the production of amphibole crystals at the boundary with the plagioclase. Lastly, in the shear zone, polygonal plagioclase retaining the 2-phase structure and foliated amphibole crystals were observed.

In the present study, we investigated in detail the evolution of the microtextures by electron back scattered diffraction (EBSD). Especially, we focused on their crystal preferred orientations (CPOs) which can be related to the deformation mechanisms.

Relationship Between Volatiles and Noble Gases in Icelandic Lavas: Evidence for Crustal Recycling

S. B. MUKASA¹, L. C. LOUDIN¹, M. PETERSON²
AND E. T. DIXON³

¹Department of Earth Sciences, University of New Hampshire, Durham, NH 03824, USA

²Department of Geological Sciences, Brown University, Providence, RI 02912, USA

³US Department of Energy, 1000 Independence Ave, SW, Washington, DC 20585-0420, USA

The anomalously high volume of magma erupted on Iceland relative to elsewhere along the Mid-Atlantic Ridge historically has been attributed to an unusually hot mantle. More recently, compositional gradients in the underlying mantle, established during much earlier melting events, have also been invoked. We propose a third alternative, namely, significant quantities of volatiles in the melt source. Olivine-hosted melt inclusions from Miðfell in Iceland's Western Volcanic Zone have major oxide compositions that place them among the most primitive lavas (highest MgO and lowest SiO₂) on the island. Trace-element-abundance patterns for these inclusions define two end-member compositions – depleted and enriched mantle sources – suggesting intimate spatial association between the two. These end-member compositions are observed even between melt inclusions from the same individual hand sample, indicative of the survival of mantle heterogeneity within an incompletely mixed magma chamber.

Although degassing is common among the inclusions, some have exceptionally high H₂O concentrations of up to 3.0 wt. %, by far the highest water concentrations ever reported in basalts from an ocean island. A subset of the olivine separates from Miðfell and Eldborg, previously analysed for Ne and He isotopic compositions, have melt inclusions which show that when ²⁰Ne/²²Ne and ³He/⁴He R/R_a in the host olivine are relatively low (10.39 and 18 R/R_a, respectively), the H₂O, CO₂, F, S and Cl concentrations are all elevated. In contrast, when ²⁰Ne/²²Ne and ³He/⁴He are high – 11.10 and 29 R/R_a, respectively – the concentrations of the five volatiles are low. This suggests that crustal recycling was an important process in mantle melting beneath Iceland.

Exceptionally high-water concentrations in some of the melt inclusions suggest that part of the uniqueness of Iceland's geochemistry and eruptive nature is due to a hydrated source rather than solely the presence of a large thermal anomaly. This has important implications for the concentration of water in mantle materials, and thus the geophysical properties that govern the nature of flow in the mantle and the magma generation that produces ocean islands.

The results of metal mercury solubility in water study

RENATA V. MUKHAMADIYAROVA^{1*}
AND YURY V. ALEKHIN¹

¹ Geochemistry Department, Faculty of Geology, Lomonosov Moscow State University, 119991 Moscow, Russia
(*correspondence: rinutiya@mail.ru)

Correctly determine of the metal mercury solubility in the form of Hg⁰(aq) results [1,2] have set us the task to adjust the Henry's constants for a wide range of temperatures and in accordance with our published data. It is well known that the process of dissolution for inert and unhydratable gases in water temperature dependence of the Henry's coefficients has an extreme [3].

For Hg⁰ temperature dependence of the Henry's constant has a distinct, but little extreme at the temperature range 120-130 °C, which is close to the position of extrema in systems with inert gases (Ar, Kr). We considered our new results, data of Sorokin *et al.* [4] for Hg⁰ and to compare - data for such hydratable gases like CO₂ and H₂S [3].

Thus, we see that the dissolution of elemental mercury vapor in water has an extreme by temperature, and, obviously, their interaction with water is very similar to that of the inert gases, but at lower equilibrium partial pressure of the vapor. This fact provides a virtually constant value of Henry's law constant in the range $\log K_H = -2,40 \div -2,43$ in a wide temperature range.

The obtained values of the Henry's constants for Hg⁰ show that these values are close to the values characteristic of weak hydratable gases as Ar, CH₄, CO, H₂, N₂, O₂, etc. [3]. Obviously, the data presented in [4] characterize Henry's Law constant, calculated based on the total concentrations of mercury, including the dominant to 100-150 °C oxidized forms.

[1] Alekhin, Zagrtzenov, Mukhamadiyarova (2011) Mos. Univ. Geol. Bul., 66(6), pp. 439-441. [2] Alekhin, Zagrtzenov, Mukhamadiyarova (2011) Goldschmidt Conf. Abst., p. 421. [3] Naumov, Rygenko, Khodakovskiy (1971) Thermodynam. database directory. – 240 p. (in Russ.) [4] Sorokhin, Pokrovskiy, Dadze (1988) Physicochemical conditions of mercury-antimony mineralization formation. - 144 p. (in Russ.).

The research has realized by supporting of RFFI (№11-05-93107-CNRS-a; №12-05-31155).

Trace-element fingerprints of chromites and sulfides from the Archean Nuggihalli greenstone belt, western Dharwar craton, India

RIA MUKHERJEE^{1,2*}, SISIR K. MONDAL¹,
 JOSÉ M. GONZÁLEZ-JIMÉNEZ², WILLIAM L. GRIFFIN²,
 NORMAN J. PEARSON² AND SUZANNE Y. O'REILLY²

¹Department of Geological Sciences, Jadavpur University, India (*correspondence: ria.mkj@gmail.com)

²ARC Centre of Excellence for Core to Crust Fluid Systems (CCFS) and GEMOC, Macquarie University, Australia

The Nuggihalli greenstone belt hosts discontinuous lens-shaped bodies of 3.1Ga plutonic ultramafic-mafic rocks (chromitite-bearing serpentinite and tremolite-chlorite-actinolite schist, pyroxenite, anorthosite, magnetite-bearing gabbro), that are conformably surrounded by a contemporaneous unit of metavolcanic schists (komatiite-komatiitic basalt), encompassed within the tonalite-trondhjemite-granodiorite suite of rocks. Trace-element compositions analyzed by laser ablation ICP-MS on unaltered chromites ($Cr\# [100Cr / (Cr+Al)] = 79-87$, $Mg\# [100Mg / (Mg+Fe^{2+})] = 45-55$) show enriched values for Ti (1766-3277 ppm), Mn (2037-2615 ppm), Zn (382-763 ppm), Co (197-257 ppm) and lower values of Ga (21-27 ppm), Ni (660-1202 ppm), V (475-682 ppm) and Sc (3.99-7.14 ppm) relative to MORB. In chromite/MORB multi-element plots the trace-element patterns of the unaltered chromites resemble Archean chromites from Ni-sulfide unmineralized komatiitic rocks. Compositionally zoned chromites have modified core ($Cr\# = 65-73$, $Mg\# = 7-15$, $Fe^{3+}\# [100Fe^{3+} / (Cr+Al+Fe^{3+})] = 5-12$, $Ga = 10-29$ ppm, $Ti = 839-1680$ ppm, $Zn = 7098-9188$ ppm, $Sc = 2-7$ ppm, $Mn = 1701-5554$ ppm, $Ni = 113-570$ ppm, $V = 538-893$ ppm, $Co = 520-866$ ppm) with rims of ferritchromit and rare magnetite ($Cr\# = 72-99$, $Mg\# = 2-32$, $Fe^{3+}\# = 23-77$, $Ga = 1.5-43$ ppm, $Ti = 544-8929$ ppm, $Zn = 578-13039$ ppm, $Sc = 0.62-30.69$ ppm, $Mn = 1284-25176$ ppm, $Ni = 200-3584$ ppm, $V = 157-2837$ ppm, $Co = 112-2255$ ppm). The altered chromites show inter-sample, intra-sample, and intra-grain heterogeneity in trace-element distribution owing to hydrothermal alteration. Minor sulfides represented by millerite and niccolite (~2 modal%, 20-40 μm) occur in the interstitial spaces within massive chromitites. Disseminations (5-8 modal%, 20-50 μm) of chalcopyrite, pyrite and Ni-Co bearing sulfides occur in magnetite in the interstices and as inclusions. The platinum group elements are below the detection limits of laser ablation ICP-MS for all the sulfide occurrences in the Nuggihalli greenstone belt.

A Mesoarchean Paleosol from eastern India—the second oldest paleosol on Earth

JOYDIP MUKHOPADHYAY^{1#}, QUENTIN CROWLEY²,
 GAUTAM GHOSH¹, SAMPA GHOSH¹,
 KALYAN CHAKRABARTI¹, B. MISRA¹
 AND SANKAR BOSE¹

¹Department Of Geology, Presidency University, Kolkata, India, E-Mail: Joydip17@Gmail.Com

²Department Of Geology, School Of Natural Sciences, Trinity College, Dublin, Ireland

The Keonjhar paleosol, in the southern part of the Singhbhum craton has long been identified [1] but its age has not previously been well constrained. The paleosol occurs between the Singhbhum Granite and supracrustal siliciclastics unconformably overlying the granite, along the western margin of the pluton. The paleosol is locally mined for pyrophyllite. Recently, the paleosol has been classified as a vertisol [2]. The Singhbhum Granite on which the paleosol has been developed has been dated at ca. 3.33 Ga (U-Pb zircon LA-ICPMS) [3]. Here we report detrital zircon U-Pb LA-ICPMS ages from overlying sandstones covering a wide geographic locality from Pal Lahara in the west to Mahagiri hills in the east. U-Pb detrital zircon ages from four samples and more than 120 concordant or near concordant analyses indicate that the youngest grains cluster between 3.0 and 3.3 Ga, and none of the zircons are younger than 3.0 Ga. Our data suggest that the depositional age of the sandstones is ca. 3.0 Ga and thus constrain the age of formation of the paleosol between 3.0 Ga and 3.3 Ga. The Keonjhar paleosol is therefore the second oldest known paleosol on Earth, after the Pilbara paleosol (ca. 3.4 Ga) [4] and provides an excellent opportunity to study the Earth's Mesoarchean atmosphere directly from the rock record.

[1] Saha (1994), *Geol. Soc. Ind. Mem.* **27**, 341p. [2] Bandopadhyay *et al.* (2010) *Precamb. Res.* **177**, 277-290. [3] Tait *et al.* (2011), *Geol. Mag.*, **148**, 340-347. [4] Johnson *et al.* (2009), Goldschmidt Conference Abstract, A601.

Probing the Hadean world with noble gases

SUJOY MUKHOPADHYAY¹

¹Dept. of Earth and Planetary Sciences, Harvard University, Cambridge, MA 02138, USA; sujoy@eps.harvard.edu

Earth's violent accretion likely generated multiple magma oceans. In particular, the Moon-forming giant impact is often thought to have produced a whole mantle magma ocean, which would have homogenized any pre-existing chemical heterogeneity within the mantle. The ratio of primordial ³He to primordial ²²Ne in the mantle preserves a record of magma oceans on the early Earth. Importantly, the ³He/²²Ne ratio of the Earth's shallow depleted mantle is significantly higher than the deep mantle. To explain this observation, I propose that at least two giant impact-induced atmospheric blow-off and magma ocean degassing episodes are required and that the last giant impact did not generate a whole mantle magma ocean. Accordingly, if plumes are derived from Large Low Shear Wave Velocity Provinces (LLSVPs) at the base of the mantle, then LLSVPs (i) are not remnants of crystallization of a global magma ocean associated with the last giant impact; and (ii) are not dense cumulate piles that crystallized from the last magma ocean at shallow depths and were subsequently gravitationally overturned to the core-mantle boundary, as shallow cumulates would be the most degassed (with the highest ³He/²²Ne ratios). LLSVPs either correspond to crystallization products from an earlier magma ocean or are produced through a mechanism not associated with magma oceans.

Mantle Xe isotopic constraints indicate that the final mantle outgassing and atmospheric blow-off events inferred from ³He/²²Ne ratios were accomplished between ~30 to 65 Myrs after the start of the Solar System. Therefore, catastrophic outgassing associated with giant impacts, including the Moon-forming impact, must have occurred within this time window. Previous calculations of impact-induced atmospheric erosion have, however, found that it is difficult to completely remove the atmosphere from a body as large as Earth by a giant impact. The need for atmospheric loss inferred from the noble gas data can be reconciled with the dynamics of giant impacts by considering the new high-spin Moon formation hypothesis. I will discuss the origin of Earth's early atmosphere in light of the new high-spin model for Moon formation and new noble gas data from mantle-derived rocks. I propose that major differences in the noble gas signatures of terrestrial planetary atmospheres reflect the diverse outcomes of late impact events on each planet.

Of ancient reservoirs and recycled noble gases

S. MUKHOPADHYAY, R. PARAI, J. M. TUCKER AND M. K PETŐ¹

¹Dept. of Earth & Planetary Sciences, Harvard University, Cambridge, MA 02138, USA; sujoy@eps.harvard.edu

The noble gases provide important constraints on planetary volatile cycling and our understanding of mantle structure and dynamics. For example, OIBs have ¹²⁹Xe/¹³⁰Xe ratios closer to the atmospheric ratio than MORBs, which could either reflect a higher proportion of recycled Xe in the OIB source or the sampling of an ancient, less-degassed reservoir (>4.45 Ga, since ¹²⁹I, which produces ¹²⁹Xe, is extinct after ~100 Ma). However, measurements of mantle-derived noble gases indicate that OIB sources do not have a higher proportion of recycled atmospheric Xe relative to MORB sources. The observation that the differences in the Xe isotopic composition of MORBs and OIBs cannot be attributed solely to recycling requires that OIBs sample a reservoir that evolved with a lower I/Xe ratio than the MORB source. Thus, differences in the degree of outgassing between the MORB and OIB sources must have been established by 4.45 Ga and subsequent mixing between the two reservoirs must have been limited. As a result, if OIBs are derived from the large low shear wave velocity provinces (LLSVPs) at the base of the mantle, then the Xe data require these features to be at least as old as 4.45 Ga.

Although the differences in MORB and OIB Xe isotopic composition cannot be solely due to recycling, new high-precision Xe measurements in MORBs and OIBs indicate that ~80-90% of the Xe in the MORB and OIB sources could be attributed to recycled atmospheric Xe. Thus, recycling of atmospheric noble gases is a process important to mantle volatile budgets. Our ability to constrain mantle source ¹²⁹Xe/¹³⁰Xe and ⁴⁰Ar/³⁶Ar ratios through multiple step crushing experiments now reveals significant heterogeneities in these ratios among mantle sources. For example, along 500 km of the Southwest Indian Ridge, in a region removed from any known plume influence, we observe ~50% and ~80% of the total mantle variation in ⁴⁰Ar/³⁶Ar and ¹²⁹Xe/¹³⁰Xe, respectively. Such large variations indicate a MORB source that has experienced heterogeneous recycling and mixing of material metasomatized by subduction zone fluids carrying recycled atmospheric Ar and Xe. Thus, a more complex picture emerges from new high-precision noble gas data, of a planetary interior that has both retained broad ancient degassing features and developed fine-scale heterogeneity from a chaotic, integrated history of volatile cycling.

Nitrogen and oxygen isotopic composition of atmospheric nitrate near the highways

ARATA MUKOTAKA*, SAKAE TOYODA
AND NAOHIRO YOSHIDA

Tokyo Institute of Technology, Japan
(*correspondence: mukotaka.a.aa@m.titech.ac.jp)

Nitrogen isotope ratio ($\delta^{15}\text{N}$) and conventional oxygen isotope ratio ($\delta^{18}\text{O}$) in atmospheric nitrate has been used to estimate the NO_x sources and its oxidation pathways. Recently, ^{17}O -excess ($\Delta^{17}\text{O} \approx \delta^{17}\text{O} - 0.52 \times \delta^{18}\text{O}$) is known to be more robust indicator of atmospheric nitrate formation pathways than $\delta^{18}\text{O}$ value. Although the $\delta^{15}\text{N}$, $\delta^{18}\text{O}$ and $\Delta^{17}\text{O}$ values in atmospheric nitrate have been studied in various regions [e.g. ref.1 and references therein], only a few observations of the oxygen isotope ratios in urban area have been reported. In this study, we collected precipitation and atmospheric particles near the highways located in Yokohama, Japan from January 2012 to December 2012, and measured $\delta^{15}\text{N}$, $\delta^{18}\text{O}$ and $\Delta^{17}\text{O}$ values in nitrate.

Precipitation samples were collected using a funnel and plastic bottle. The atmospheric particle samples were collected on quartz filters using high-volume air sampler. The filters were replaced every week. The stable isotope ratios of nitrate were measured by GC-IRMS after converting nitrate to N_2O .

The $\delta^{15}\text{N}$ and $\delta^{18}\text{O}$ values in precipitation, and the $\delta^{15}\text{N}$ values in particle showed a temporal variation similar to the previously reported values ($-2.2\text{‰} < \delta^{15}\text{N} < 13.6\text{‰}$ and $52.6\text{‰} < \delta^{18}\text{O} < 83.4\text{‰}$) [2, 3]. The variation of $\delta^{18}\text{O}$ values in particulate nitrate was similar to that of precipitation, but extremely low values (26.2‰ to 39.7‰) were observed from the end of August to the end of November. The low $\delta^{18}\text{O}$ values cannot be explained by typical nitrate formation processes that involve ozone, and imply that isotopically light oxygen, such as O_2 ($\delta^{18}\text{O} = 23.5\text{‰}$) played a key role in NO_x oxidation process in the period [4, 5]. Implication from $\Delta^{17}\text{O}$ data will be also discussed.

[1] Savarino *et al.*, (2013) *Proc. Natl. Acad. Sci. USA.*, doi: 10.1073/pnas.1216639110. [2] Kaiser *et al.* (2007) *Anal. Chem.*, 79, 599-607. [3] Michalski *et al.* (2003) *Geophys. Res. Lett.*, 30(16), 1870. [4] Kroopnick and Craig (1972) *Science*, 175, 54-55. [5] Proemse *et al.* (2012) *Atmospheric Environment*, 60, 555-563.

Anoxic geothermal fields and the early life

ARMEN Y. MULKIDJANIAN^{1,2}, ANDREW YU. BYCHKOV³,
DARIA V. DIBROVA^{1,2}, MICHAEL Y. GALPERIN⁴
AND EUGENE V. KOONIN⁴

¹University of Osnabrück, Germany (amulkid@uos.de),

²School of Bioengineering and Bioinformatics, and ³School of Geology, Moscow State University, Russia

⁴National Center for Biotechnology Information, NLM, NIH, Bethesda, Maryland 20894, USA

We have reconstructed the 'hatcheries' of the first cells by combining geochemical analysis with phylogenomic scrutiny of the inorganic ion requirements of universal components of modern cells [1]. These ubiquitous, and by inference primordial, proteins and functional systems show affinity to and functional requirement for K^+ , Zn^{2+} , Mn^{2+} , and phosphate. Thus, protocells must have evolved in habitats with a high K^+/Na^+ ratio and relatively high concentrations of Zn, Mn and phosphorous compounds. Geochemical reconstruction shows that the ionic composition conducive to the origin of cells could not have existed in marine settings but is compatible with emissions of vapor-dominated zones of inland geothermal systems. Under anoxic, CO_2 -dominated atmosphere, the elementary composition of pools of condensed vapor at anoxic geothermal fields would resemble the internal milieu of modern cells.

The scientists who address the origin of life problem from a purely chemical viewpoint argue that specific formation of activated, cyclic ribonucleotides with a potential for polymerization could take place in formamide-rich solutions, particularly under the action of UV light and in the presence of borate and phosphorous compounds [2, 3].

The exhalations of even modern geothermal fields contain high amounts of ammonia, phosphate, borate and hydrocarbons, so that the anoxic geothermal fields should have been conducive for formation of simple amides and nitrogen-containing organic molecules, including activated nucleotides.

Hence, the anoxic geothermal fields, which we identified as tentative cradles of life by using the top-down approach and phylogenomic analysis, could provide exactly those geochemical conditions that were suggested as most conducive for the emergence of life by the chemists who pursued the complementary bottom-up strategy.

[1] A.Y. Mulkiidjanian, A.Y. Bychkov, D.V. Dibrova, M.Y. Galperin, E.V. Koonin (2012) Origin of first cells at terrestrial, anoxic geothermal fields, *Proc Natl Acad Sci U S A*, 109: E821-830. [2] S.A. Benner, H.J. Kim, M.A. Carrigan (2012) Asphalt, water, and the prebiotic synthesis of ribose, ribonucleosides, and RNA, *J. Am. Chem. Sci.* 45: 2025-34. [3] R. Saladino, G. Botta, S. Pino, G. Costanzo, E. Di Mauro (2012) Genetics first or metabolism first? The formamide clue, *Chem Soc Rev*, 41: 5526-5565.

Mantle compositional gradients in a hot subduction setting, the Garibaldi Volcanic Belt, northern Cascade Arc

EMILY K. MULLEN* AND D. WEIS

PCIGR, University of British Columbia, Vancouver, Canada
(*correspondence: emullen@eos.ubc.ca)

Hot subduction zones challenge the dehydration melting model for primary arc basalt generation, as hot slabs may liberate water at depths too shallow to trigger mantle melting. The Garibaldi Volcanic Belt (GVB), the northernmost segment of the Cascade Arc, extends from Glacier Peak in the south to Bridge River Cones in the north and is one of the hottest subduction zones globally [1, 2]. The age of the subducting plate decreases from ~10 Ma in the south to ~5 Ma in the north at the trench [3], resulting in a northerly increase in slab temperature beneath the arc axis [1]. Together with a decrease in magmatic productivity, basalts grade progressively from typical calc-alkaline arc basalts in the south to alkalic basalts in the north, reflecting reduced melt fractions due to low slab input [4]. Both basalt varieties occur at Mt. Garibaldi. Gradual northerly decreases in La/Nb, $^{87}\text{Sr}/^{86}\text{Sr}$ (0.70318 to 0.70298) and Pb isotope ratios are consistent with the hypothesis of decreasing slab input. In addition, decoupling of ϵ_{Hf} from ϵ_{Nd} indicates sediment input as a fluid. The most alkaline basalts record minimal slab input, with Pb isotope ratios lower than in other Cascade Arc basalts and similar to Explorer MORB. However, Zr/Nb, $^{208}\text{Pb}^*/^{206}\text{Pb}^*$, ϵ_{Nd} (+8.9 to +7.1) and ϵ_{Hf} (+13.3 to +8.5) decrease to the north, indicating an arc-parallel gradient in mantle source enrichment that is unrelated to slab input. The alkaline basalts tap a mantle source more incompatible element enriched and isotopically distinct from the depleted mantle that produces calc-alkaline basalts. The enriched mantle is also hotter (~1500°C) than the sub-arc mantle wedge (max ~1350°C) [2], consistent with upwelling asthenosphere, possibly at the slab edge [5]. Arc-parallel mantle flow may draw the upwelling mantle into the arc, generating a compositional gradient upon which slab input is superimposed. The influx of this upwelling mantle may have far-reaching effects, as the $^{208}\text{Pb}^*/^{206}\text{Pb}^*$ trend begins as far south as Mt. Adams and continues to the end of the GVB.

[1] Harry & Green (1999) *Chem. Geol.* 160, 309-333. [2] Syracuse *et al.* (2010) *Phys. Earth Planet. Interiors* 183, 73-90. [3] Wilson (2002) *USGS Open-File* 02-328. [4] Green (2006) *Lithos* 87, 23-49. [5] Long & Silver (2008) *Science* 319, 315-318.

Multiple sulphur isotope analyses of sulphate deposits from the Sargur Group, Dharwar Craton, India.

E. MULLER¹, P. PHILIPPOT¹, C. ROLLION-BARD²
AND D. S. SARMA³

¹Institut de Physique du Globe, Paris, France, emuller@ipgp.fr

²CRPG-CNRS, Vandoeuvre-les-Nancy, France

³CSIR-NGRI, Hyderabad - 500 007, India

Sulphides from sedimentary rocks older than 2.45 Gyr old define a positive $\delta^{34}\text{S}$ - $\Delta^{33}\text{S}$ correlation called the "Archean Array". In contrast, Archean sulphates were deposited during short periods of times between 3.5 and 3.2 Gyr ago and define a narrow isotopic range that is not correlated with the Archean Array. Sulphide associated with the sulphate deposits form a specific isotopic domains characterized by ^{34}S -depleted values with both positive and negative $\Delta^{33}\text{S}$. These sulphides were interpreted to reflect a combination of UV-photochemical processes in optically-thick volcanic plumes combined with terrestrial processes of biologic and/or non biologic origin. Here we present S isotope systematics of the 3.2 Ga sulfate deposit of the Sargur Group near Ghattihosahalli (Dharwar Craton, India).

The rocks investigated consist of a meter-scale layer of barite interbedded within different types of quartzites and micaschists grading towards the west into Cr-micaschists, ultramafic volcanics and felsic gneiss. Bulk and in situ S-isotope analyses were measured with IRMS in dual-inlet mode at IPGP and ims 1280 HR2 at CRPG, respectively, both with a reproducibility better than 0.2 ‰ (2 σ) in $\delta^{34}\text{S}$ and 0.1 ‰ in $\Delta^{33}\text{S}$.

S-isotope compositions of barites ($\delta^{34}\text{S} = 3.19$ to 4.35 ‰ and $\Delta^{33}\text{S} = -0.49$ to -0.47 ‰) fall within the range of other Archean sulphates. Pyrites in sulphates and other rock types show a narrow range of $\Delta^{33}\text{S}$ values between -0.70 and $+0.37$ ‰ but a larger range of $\delta^{34}\text{S}$ values between -12.21 and $+0.27$ ‰ in barite, -4.12 and $+0.63$ ‰ in micashists and quartzites, -6.96 and -2.43 ‰ in Cr-micaschists, and 1.83 and 5.99 ‰ in surrounding gneisses. These results are consistent with previous data obtained in other Archean sulphate deposits from the Pilbara Craton and Barberton Greenstone Belt, thus arguing for a common origin. Different from other deposits, however, is the relative small range of both $\delta^{34}\text{S}$ and $\Delta^{33}\text{S}$ values, which suggests that the isotopic imprint inherited from atmospheric and microbial/hydrothermal processes have been reequilibrated in part during greenschist/amphibolite facies metamorphism and pervasive ductile deformation.

Vibrational spectroscopic study of Np(V) sorption on mineral oxides

KATHARINA MÜLLER, JULIA BERGER, MAXENCE
CORDIEZ, ANNETT GRÖSCHEL,
AND HARALD FOERSTENDORF

Helmholtz-Zentrum Dresden-Rossendorf, Institute of
Resource Ecology, Dresden, Germany
(*correspondence: k.mueller@hzdr.de)

Mineral oxides play a decisive role in regulating the mobility of contaminants in the environment because of their widespread occurrence in rocks and soils, their tendency to form coatings on mineral surfaces and their wide-ranging technical applications [1].

Due to its long half-life and its toxicity, Np-237 is considered as a major contaminant of the ecosystem in the long-term safety assessment of nuclear waste repositories. The pentavalent state is environmentally most relevant [2].

For the first time, in-situ Np(V) sorption is comparatively studied on the oxyhydroxides of Fe, Mn, Si and Ti by ATR FT-IR spectroscopy under a variety of environmentally relevant sorption conditions. From the results, the formation of binary inner-sphere complexes on oxides of Si, Mn, Fe and Ti can be derived [3]. In case of ferrihydrite, the formation of an additional ternary Np-carbonato surface species is assumed. In addition, time resolved spectra provide kinetic information on the surface reactions.

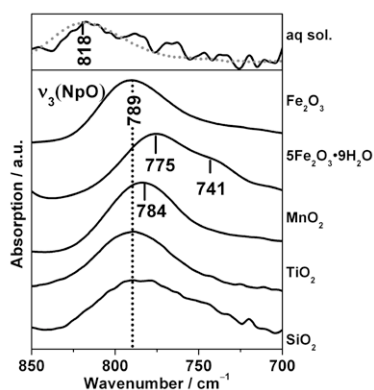


Fig. 1: IR spectra of an aq. Np(V) solution and of the sorption complexes formed onto several mineral oxides (50 μ M Np(V), 0.1 M NaCl, pH 7, 60 min sorption, 0.1 mg mineral oxide/cm², N₂).

[1] Dixon J. B. *et al.* (1989) *Minerals in soil environments*. Madison, Wis.: Soil Science Soc. of America. 1244. [2] Kaszuba J. P. *et al.* (1999) *Env. Sci. & Techn.* **33**(24), 4427-4433. [3] Müller K. *et al.* (2009) *Env. Sci. & Techn.* **43**(20): p. 7665-7670

Nano-particulate pressed powder tablets for LA-ICP-MS

S. MÜLLER¹ AND D. GARBE-SCHÖNBERG^{1*}

¹CAU Kiel, Institut für Geowissenschaften, 24098 Kiel,
(*correspondence: dgs@gpi.uni-kiel.de)

The accurate determination of ultra-trace elements in geological samples containing refractory minerals - e.g., zircon in plutonic rocks and sediments, spinel in ultramafic rocks and eclogites - is a challenge. While standard table-top or microwave-assisted digestion protocols fail in completely dissolving these minerals, alternative procedures also show shortcomings: (i) pressurized bomb digestion yields accurate results but is time-consuming; (ii) preparation of fused glasses with, and without, addition of a flux for subsequent analysis by either LA-ICP-MS or after re-dissolution with ICP-MS suffers from contamination from heterogeneously distributed impurities in lithiummetaborate, and strong memory for Li, B; (iii) shock melting using a strip-heater produces glasses contaminated with strip material. Ultrabasic or evolved rocks cannot be melted without matrix modification. All fusion techniques bear the risk of volatile losses, and glass beads typically show significant inhomogeneity of trace elements if not thoroughly homogenized during melting.

Pressed powder tablets have repeatedly reported as a means for the direct analysis of solids by laser ablation. Analytical results, however, were not convincing in terms of detection limits, accuracy, and precision if compared to results obtainable with solution analysis or homogeneous glasses. Here we show that undiluted pressed powder tablets can be successfully used for ultra-trace element analysis of granitoid, gabbroic, and ultrabasic rocks from the Oman ophiolite (Wadi Gideah reference profile) after pulverisation to nano-particle grain size. More than 40 trace elements have been analysed in a series of rock CRMs with average RSDs of 1-3% and excellent accuracy for most elements incl. HFSE. Detection limits are in the low ppb range.

Downhole Fluid Analysis coupled with Asphaltene Nanoscience for Reservoir Evaluation

OLIVER C. MULLINS

Mullins1@slb.com

For condensates, the most important compositional variation is GOR, and the cubic equation of state (EoS) treatment of GOR variations is well developed and successful. Consequently, key reservoir attributes such as vertical and lateral connectivity, extrapolating gradients to obtain contacts for reserves estimation, and properties of the produced fluids are addressed by Downhole Fluid Analysis (DFA) on the MDT measuring GOR and light end compositional variations. In contrast, black oils are generally defined as having low GOR; while black oils can exhibit GOR variations, the most important compositional variation of black oil and heavy is the asphaltene concentration. However, there had been no predictive equation of state for asphaltene gradients because the (colloidal) size of asphaltene particles in crude oils had been unknown. Consequently, the gravity term was unknown. Without knowing the gravity term, modeling of reservoir fluids is precluded.

In recent years, the molecular and colloidal size of asphaltenes in crude oils – from condensates to mobile heavy oil – has been resolved and codified in the Yen-Mullins model. These scientific advances have led to the first predictive equation of state (EoS) for asphaltene gradients, the Flory-Huggins-Zuo EoS. By coupling this new science of the FHZ EoS with the new technology of DFA, a powerful new method of reservoir evaluation has been developed leading to myriad applications. Establishing thermodynamic equilibration of asphaltenes strongly implies reservoir connectivity as proven in published case studies involving light condensates to mobile heavy oil. Huge asphaltene and viscosity gradients are obtained in mobile heavy oil columns around the world in agreement with simple application of the FHZ EoS, and where conventional modeling fails miserably. Two mechanisms of tar mat formation are seen to be a natural process readily accounted for by the FHZ EoS and resolving a long standing enigma in the oil industry. Disequilibrium has become much easier to identify using DFA & the FHZ EoS in conjunction with the cubic EoS. Methods for production optimization and risk management are identified.

The confluence of advanced asphaltene science with the third generation of DFA tools, the IFA, enables a powerful new approach to address many complexities in reservoir dynamics.

A secular solution to a diabolical problem: Porphyry vs. iron oxide-copper-gold deposits

A. HAMID MUMIN¹ AND JEREMY P. RICHARDS²

¹Dept. Geology, Brandon University, Brandon, Manitoba, Canada, R7A 6A9, mumin@brandonu.ca

²Dept. EAS, University of Alberta, Edmonton, Alberta, Canada, T6G 2E3 Jeremy.Richards@ualberta.ca

Porphyry Cu±Mo±Au (porphyry) and magmatic-hydrothermal iron oxide-copper-gold deposits (IOCG) are distinct in being dominated by Fe±Cu-sulfide minerals in the former and Fe-oxides in the latter. Most of the largest IOCG deposits formed in the Precambrian, whereas porphyry deposits occur most commonly in late Phanerozoic rocks and are rare in the Precambrian. Despite these major differences, they share many similarities: associated magma composition (calc-alkaline to mildly alkaline); tectonic setting (orogenic to post-orogenic), depth of formation (≤ 5 km from surface), major metal inventory (Cu, Au), and hydrothermal alteration styles (albeit with wider development of high-T near-neutral alteration, and more restricted development of low-T hydrolytic alteration in IOCG deposits).

We conclude that fundamentally similar tectonomagmatic and hydrothermal processes give rise to these two distinct deposit types. We link the key differences in mineralization style (Fe-sulfide vs. Fe-oxide) and temporal prevalence to oxidation of the deep oceans during the Neoproterozoic Oxidation Event. Following this event, sulfate concentrations in deep ocean waters, seafloor sediments, and seawater-altered oceanic crust increased dramatically, and for the first time in geological history abundant sulfur and sulfate were introduced into subduction zones and arc magmas. Phanerozoic arc magmas were thereafter significantly richer in S than in the Precambrian (Prouteau & Scaillet, 2013) and, combined with their relatively high oxidation state, were ideal transportation agents for Cu and Au into upper crustal magmatic-hydrothermal systems.

In contrast, S-poor Precambrian arc and derivative magmas formed S-poor IOCG deposits in orogenic, and post-orogenic settings, while S-rich conditions were relatively rare (leading to a dearth of porphyry-type deposits). Higher geothermal gradients in the Precambrian, combined with the lower acid-generating potential of S-poor hydrothermal fluids may explain the greater extent of high-T near-neutral pH alteration in IOCG deposits compared to porphyries.

[1] Prouteau & Scaillet, 2013: *J. Petrology*, v. 54, p. 183–213.

The role of mesoscale ocean eddies in the glacial cycle of atmospheric pCO₂

DAVID R. MUNDAY*¹, HELEN L. JOHNSON²
AND DAVID P. MARSHALL¹

¹Department of Physics, University of Oxford, Oxford, UK
(*correspondence: munday@atm.ox.ac.uk)

²Department of Earth Sciences, University of Oxford, Oxford, UK

The close relationship between Antarctic temperature and atmospheric pCO₂ suggests an important role for the Southern Ocean in glacial cycles. Recent high-resolution model results indicate that the sensitivity of Southern Ocean upwelling and global stratification to changes in Southern Ocean wind stress may be low [1]. This may limit the sensitivity of the climate system as a whole to changes in Southern Ocean wind stress, by limiting the change in ventilation of abyssal carbon reservoirs.

We use MITgcm in an idealised configuration to investigate the changes in circulation that occur at both coarse (climate model) resolutions and higher, eddy-permitting, resolutions as the applied wind stress is changed. At coarse resolutions, the mesoscale eddy field is represented by the Gent & McWilliams parameterisation. However, at eddy-permitting resolutions, large geostrophic eddies are well represented by the model. By coupling these physical circulations to MITgcm's simple biogeochemistry package, we are able to elucidate the effect that changes in the mesoscale eddy field, and/or its representation, have on atmospheric pCO₂.

We find that the use of an eddy-permitting ocean model reduces the sensitivity of atmospheric pCO₂ to both increasing and decreasing wind stress. A carbon pump decomposition indicates that the 4 main reservoirs of carbon in the ocean (saturation state, disequilibrium, soft tissue carbon, and hard tissue carbon) vary quite differently when the model is eddying, as opposed to the eddy field being parameterised.

[1] Munday, D. R., H. L. Johnson, and D. P. Marshall, 2013: Eddy saturation of equilibrated circumpolar currents. *J. Phys. Oceanogr.*, **43**, 507–532.

Lithospheric mantle heterogeneities beneath Southern Patagonia

A. MUNDL^{1*}, T. NTAFLS¹, E.A. BJERG²,
L. ACKERMAN³ AND C.A. HAUZENBERGER⁴

¹Department of Lithospheric Sciences, University of Vienna, Austria (*correspondence: andrea.mundl@univie.ac.at)

²CONICET-Universidad Nacional del Sur, Departamento de Geología, Bahía Blanca, Argentina

³Institute of Geology v.v.i., Academy of Sciences of the Czech Republic, 165 00 Praha 6, Czech Republic

⁴Institute for Earth Sciences, University of Graz, Austria

Thirty samples from Pali Aike Volcanic Field (PAVF) and Tres Lagos in Southern Patagonia comprise Sp-lherzolites, Sp-harzburgites, Sp-Gt-lherzolites and Sp-Gt-harzburgites.

According to Cpx REE and other trace element patterns, the samples can be divided in 3 Groups within Sp-peridotites and 3 within Sp-Gt-peridotites. Group I Sp-peridotites show a depletion in LREE reflecting different degrees of partial melting. Group II shows flat REE patterns from HREE to MREE with an enrichment in LREE indicating metasomatic overprint. Group III samples show an enrichment in MREE over LREE and HREE suggesting basaltic melt percolation. While Group I Sp-Gt-peridotites represents slightly depleted samples with typical REE patterns of Cpx in equilibrium with Gt, Group II Cpx REE patterns show LREE enrichments reflecting metasomatic event(s). The garnets in this group exhibit wide kelyphitic rims that have been formed according to the reaction of Gt+Ol to Sp+Cpx+Opx. Primary Sp inclusions in Gts of Group I and II indicate transitions from spinel to garnet stability field. Group III of Sp-Gt-peridotites is represented by highly depleted samples showing REE patterns otherwise typical for Cpx coexisting with Gt. However, an entire absence of Gt suggests that all Gt has been consumed during partial melting event(s).

Re-Os analyses of unmetasomatized Sp-peridotites reveal highly variable T_{RD}. While T_{RD} at Tres Lagos range from 1 to 1.6 Ga, samples from PAVF yield ages from 0.3 to 2.3 Ga. A depletion in Pt, Pd and Re reflects different degrees of partial melting. Depleted Os compared to other IPGEs (Ir, Ru) can be connected to sulfide breakdown upon eruption, while a general depletion in IPGEs in comparison to PM is suggested to be due to melt percolation processes.

Trace element patterns, samples showing highly different degrees of partial melting, as well as transition reactions from spinel to garnet stability field reflecting a multi-stage thermal history, suggest a very heterogeneous SCLM beneath S-Patagonia.

Mantle-crust fractionation of the platinum-group elements

JAMES E MUNGALL¹ AND JAMES M BRENNAN¹

¹Department of Earth Sciences, University of Toronto,
Toronto ON; mungall@es.utoronto.ca;
brenan@es.utoronto.ca

We use new sulfide melt/silicate melt partition coefficients $\sim 10^6$ to develop a fully constrained model of PGE behavior during melting to predict the abundances of PGE in mantle-derived magmas and their restites, including mid-ocean ridge basalts, continental picrites, and the parental magmas of the Bushveld Complex of South Africa. Our model constrains mid-ocean ridge basalt (MORB) to be the products of pooled low and high degree fractional melts. A significant control on PGE fractionation in mantle-derived magmas is exerted by residual alloy or platinum group minerals in their source. Within-plate picrites are pooled products of larger degrees of fractional melting in columnar melting regimes. At low pressures (e.g., MORB genesis) the mantle residual to partial melting retains primitive mantle inter-element ratios and abundances of PGE until sulfide has been completely dissolved but then evolves to extremely high Pt/Pd and low Pd/Ir because Pt and Ir alloys form in the restite. During melting at high pressure to form picrites or komatiites Ir alloy continues to appear as a restite phase but Pt alloy is no longer stable due to the large effect of pressure on fS_2 , which causes large increases in alloy solubility. Magmas parental to the Bushveld Complex of South Africa appear to be partial melts of mantle that has previously been melted to the point of total sulfide exhaustion at low pressure, closely resembling mantle xenoliths of the Kaapvaal craton. Using the new extremely large D_{PGE}^{sul} the Merensky Reef and UG2 Pt deposits of the Bushveld Complex can be modeled as the result of sulfide saturation due to mixing of magmas with unremarkable PGE contents, obviating the need to postulate anomalously PGE-rich parent magmas or hydrothermal inputs to the deposits.

An extraterrestrial cause for the Silicate Earth's Nb paradox?

C. MÜNKER¹, R.O.C. FONSECA² AND T. SCHULZ³

¹Institut für Geologie und Mineralogie, Universität zu Köln,
Germany, c.muenker@uni-koeln.de
²Steinmann Institut, Universität Bonn, Germany
³Dept. für Lithosphärenforschung, Universität Wien, Austria

Although both elements are considered lithophile, the silicate Earth exhibits a marked Nb deficit relative to its geochemical twin Ta, when compared to chondrites [1]. This feature is commonly referred to as “terrestrial Nb paradox”. Many explanations for this paradox that favour the presence of hidden silicate reservoirs cannot explain the observation that the Early Archean silicate Earth was already depleted in Nb. This would leave core formation at high pressures in a reduced early Earth as the only viable explanation for the terrestrial Nb paradox [2].

In a combined geochemical and experimental study, we investigated, whether low pressure metal segregation on small planetesimal precursors can also account for the Nb deficit. We performed high precision measurements of HFSE concentrations employing isotope dilution and ion exchange separation on representative groups of iron meteorites, their sulfide inclusions and achondrites. This protocol avoids molecular interferences on many HFSE, in particular for iron meteorites and sulfides rich in transition metals. Our results indicate that reduced achondrites exhibit strongly subchondritic Nb/Ta (as low as 1), whereas more oxidised achondrites (e.g., eucrites) exhibit near chondritic Nb/Ta. As expected, iron meteorites exhibit extremely low Nb-Ta concentrations (<1 ppb), whereas Nb can be strongly enriched relative to other HFSEs in sulfides (to ppm levels).

To simulate metal-sulfide segregation on small planetesimals, we performed experiments at $\sim 1300^\circ\text{C}$ and 10 kbar using a piston cylinder apparatus. Measured sulfide-silicate partition coefficients for Nb are ca. 2 orders of magnitude higher than for Ta. At fO_2 lower than IW-3, Nb becomes chalcophile while Ta remains lithophile, and the silicate melt is thus depleted in Nb, as found in our study for more reduced achondrites.

Collectively, our results reveal that Nb may be sequestered into planetesimal cores at low pressures and low fO_2 , provided that immiscible sulfide and metal liquids were segregated. Therefore, the silicate Earth's Nb deficit may be a feature inherited from differentiated planetesimals that did not fully equilibrate with the proto-Earth upon their accretion.

[1]Münker *et al.* (2003) *Science* **301**, 84-87 [2] Wade & Wood (2001) *Nature* **409**, 75-78.

Pb, Zn and Cd dynamics in mining areas under Mediterranean climate and carbonated geologic context: northern Tunisia example

MUNOZ MARGUERITE¹ AND GHORBEL MANEL²

¹GET, Observatoire Midi Pyrénées, Université de Toulouse, CNRS, IRD, 14 avenue E. Belin, F-31400 Toulouse, France. margot.munoz@get.obs-mip.fr

²RME, Faculté de Sciences de Tunis el Manar, 2092 Tunis, Tunisia. manel.ghorbel@get.obs-mip.fr

Maghreb countries, particularly Tunisia contain large amounts of mining wastes rich in metals such as Pb, Cd and Zn. Wastes are located in active or abandoned mining sites. Metals can diffuse to all environment compartments: water, air and soil.

In wastes, due to carbonated geology, calcite is dominant and metals are mainly associated with carbonates (cerussite, smithsonite and hydrozincite), in addition to silicates (hemimorphite and willemite) and sulphides (galena and sphalerite). Cd substitutes Zn in zinc-carbonates, silicates and sphalerite where it can reach 0.98wt%.

In this carbonated context, drainage water display a basic pH and metals are fixed by precipitation of stable minerals under oxidizing conditions (cerussite, hydrozincite, smithsonite and hemimorphite). Equilibrium between water and secondary minerals in mining drainage controls concentrations of metals at low values.

Ore treatment wastes are fine grained (silt and clay). Their cohesion is variable (15 and 124 kPa) and their permeability is low (10^{-6} - 10^{-9} m/s) and limits infiltration process. These features, under Mediterranean climate, promote mechanical erosion of wastes during brief and intense rainfall events. However, the low density of water runoff makes the impact of particulate transport often limited, but highly concentrated, in soils around the waste dumps. Thus, maximum concentrations in soils have been measured up to 2% Pb, 3% Zn and 200 mg.kg⁻¹ Cd.

This climate, also characterized by a long dry season, allows contaminated dust emissions from dumps especially in summer. Maximum emission flux of dust was estimated to 88.2 g/s of PM10. Resulting concentrations of airborne Pb and Cd exceeded WHO guidelines for air quality, up to 1km from the source in the dominant wind direction (Ghorbel, 2012).

Remediation is intended to support natural processes using phytostabilisation of wastes by covering them with native metal-resistant plants.

[1] Ghorbel, M (2012). Contamination métallique issue des déchets de l'ancien site minier de Jebel Ressayas : modélisation des mécanismes de transfert et conception de cartes d'aléa post-mine dans un contexte carbonaté et sous un climat semi-aride. Evaluation du risque pour la santé humaine. PhD thesis of Toulouse and Tunis El Manar Universities. 231p.

Structure and thermal property of dense silicate glasses under high-pressure

MOTOHIKO MURAKAMI¹

¹Department of Earth and Planetary Materials Science, Tohoku University, 6-3 Aoba, Sendai, Miyagi 989-8578, Japan motohiko@m.tohoku.ac.jp

The current structure of Earth's interior is believed to have formed through dynamic differentiation from a global magma ocean in the early Earth. Elucidation of the structural changes and heat transport properties of silicate melts in the deep Earth is fundamental to understanding the evolution and structure of Earth's interior. The possible presence of dense, gravitationally stable, silicate melts at the bottom of the current mantle as a remnant of a deep magma ocean has been proposed to explain observations of anomalously low seismic velocities above the core-mantle boundary. However, the nature of silicate melts under such extreme pressures is poorly understood. Direct measurements of structural changes or thermal properties on silicate melts under ultrahigh-pressure conditions remain a great challenge and are currently beyond experimental capabilities. Silicate glasses have alternatively been extensively studied as analogues for quenched silicate melts, to simulate the high-pressure behavior of silicate melts. Previous experimental works on silicate glasses have, however, been still limited to lower pressure condition, which is far below the pressure condition of the bottom of the mantle.

To address this issue, we have conducted several series of ultrahigh-pressure experiments on silicate glasses with chemical compositions ranging from pure silica to more complex system up to ~200 GPa using combined spectroscopic techniques including Brillouin scattering, optical absorption (from visible to near-infrared) and synchrotron Mössbauer measurements in the energy domain. The results based on sound velocity data reveal the possible densification mechanism of silicate glasses above ~100 GPa that is likely associated with the onset of a change in Si-O coordination number to higher than sixfold. Optical and synchrotron Mössbauer data show a significant change in the absorption coefficients of the iron-bearing silicate glasses with pressure, most likely due to their gradual electronic structural changes. Based on the present results, we will discuss the possible implications for the densification mechanisms and heat transport property of the silicate melts at the base of the mantle.

Reconstruction of the accident-derived I-131 deposition in Fukushima through the analysis of I-129 in soil.

YASUYUKI MURAMATSU^{1*}, HIROYUKI MATSUZAKI²,
TAKESHI OHNO¹, NAOYA INAGAWA¹
AND CHIAKI TOYAMA¹

¹ Department of Chemistry, Gakushuin University, Mejiro,
Tokyo, Japan, 171-8588;

*Correspondence: yasuyuki.muramatsu@gakushuin.ac.jp

² Department of Nuclear Engineering and Management, The
University of Tokyo, Tokyo, Japan, 113-8656.

Large quantities of radionuclides were released during the accident at Fukushima Daiichi Nuclear Power Plant which occurred during March of 2011. We have carried out intensive studies on the distribution and behaviour of radioiodine and radiocesium in the environment following the accident. Special attention was paid to I-131 (half-life: 8 days) because of its affinity to thyroid glands and because, at the time of the Chernobyl accident, an increase of thyroid cancer for infants and children was observed as a result. Although the amount of I-131 released from the Fukushima accident is about one tenth of that released from the Chernobyl accident, it is necessary to obtain information on the deposition density of this nuclide in different locations surrounding the nuclear power plant at the time of the accident. However, most of it decayed away after some months due to its short half-life and there were not enough data to construct a deposition map for I-131.

In order to estimate the deposition of I-131, we focused on I-129 (half-life: 15.7 million years) which was also co-released during the accident and deposited in soils across the region. Surface soil samples collected from different places in Fukushima Prefecture were analyzed for I-129 by AMS (accelerator mass spectrometry) after the chemical separation. Soil samples that had been determined for I-131 were used to estimate I-131/I-129 ratio. A good correlation was found between the concentration of I-131 and that of I-129 in soil. This finding suggests the possibility to estimate the I-131 deposition through the analysis of I-129 in soil. We also analyzed soil samples collected from different locations of Fukushima Prefecture within a project organized by MEXT (Ministry of Education, Culture, Sports, Science, and Technology, Japan) for reconstructing the deposition density of I-131.

Heterogeneous melt involved in formation of a thick Moho transition zone in northern Oman ophiolite: implications for MORB evolution

R. MUROI^{1*}, S. ARAI¹, H. NEGISHI¹ AND A. TAMURA¹

¹Dept. Earth Sci., Kanazawa Univ., Kanazawa 920-1192,
Japan

(*Correspondence: halcyons@stu.kanazawa-u.ac.jp)

The evolution process of MORB from depleted melts in equilibrium with abyssal peridotites has been unclear. Here a melt with gentle REE pattern like the ordinary MORB is referred to "Melt 1", and a melt with steeply LREE-depleted pattern like ultra-depleted MORB [1] to "Melt 2". CPXs (clinopyroxenes) in dunites and wehrlites in the Moho transition zone of Oman ophiolite were generally in equilibrium with Melt 1 [2]. We found dunites-wehrlites containing CPXs in equilibrium with Melt 2 in predominant Melt-1 related dunites-wehrlites from a thick Moho transition zone of Wadi Thuqbah, northern Oman ophiolite [3]. Some of the Melt-2 related dunites-wehrlites contain relic OPX (orthopyroxene) partially replaced with olivine: other Melt-1 related ones are free of OPX, and occasionally contain sulfides [3]. The Fo content of olivine is higher in the Melt-2 related rocks (around 91) than in the Melt-1 related ones (88-90). The Cr₂O₃ content in CPX is higher in the former (1.1-1.3 wt%) than in the latter (0.9-1.1 wt%). The OPX in the former is similar in chemistry to that in the mantle harzburgite downsection.

These features possibly indicate chemical evolution of Melt 1 from Melt 2 through reaction with the mantle peridotite (consumption of OPX combined with olivine production). The Moho transition zone dunites and wehrlites are cumulates from melts enriched with olivine crystals (crustal mush) [3]. The Melt-2 related rocks sometimes with OPX were formed from an incomplete melt-peridotite reaction product, and the Melt-1 related rocks, from a melt-peridotite reaction product, where OPX digestion was completed. This suggests a possibly important role of the Melt 2-peridotite reaction in formation of ordinary MORB (Melt 1) in the upper mantle [cf.4,5].

[1] Sobolev & Shimizu (1993) *Nature* **363**, 151-154. [2] Akizawa *et al.* (2012) *Contrib. Mineral. Petrol.* **164**, 601-625. [3] Negishi *et al.* (2013) *Lithos* **164-167**, 22-35. [4] Kelemen *et al.* (1995) *Nature* **375**, 747-753. [5] Arai & Matsukage (1996) *Proc. ODP, Sci. Results* **147**, 135-155.

The coupling of particle acidity and gas phase ammonia in the biosphere-atmosphere system

JENNIFER MURPHY¹ AND ALEXANDRA TEVLIN¹

¹Department of Chemistry, University of Toronto, Toronto ON, Canada

Ammonia is the most important gas phase base in the atmosphere and is known to influence the formation and growth of atmospheric particles. While the magnitude and trends of ammonia emissions are highly uncertain, it is likely that a legacy of synthetic fertilizer application has led to an increased potential for ammonia emissions from many ecosystems. We have obtained observational evidence for the bi-directional exchange of ammonia between the surface and the atmosphere, and the coupling of this process to gas-particle partitioning. From intensive field campaigns in urban and rural environments, simultaneous measurements of particle composition and gas phase ammonia permit the calculation of particle acidity, which affects gas-particle partitioning of ionizable species and may influence toxicity and secondary organic aerosol formation. In a complementary analysis, we use long-term measurements (1990-2010) of particle composition from Canada's Chemistry and Precipitation Monitoring Network (CAPMoN) to calculate trends in strong acidity and infer trends in gas phase ammonia.

Fractionation of ²³⁸U/²³⁵U by reduction during low T uranium mineralisation processes

MELISSA J. MURPHY^{1*}, CLAUDINE H. STIRLING², ANGELA KALTENBACH², SIMON P. TURNER¹ AND BRUCE F. SCHAEFER²

¹GEMOC, Department of Earth and Planetary Sciences, Macquarie University, Australia (*Correspondence: melissa.murphy@mq.edu.au)

² Centre for Trace Element Analysis and Department of Chemistry, University of Otago, New Zealand

Investigations of 'stable' uranium isotope fractionation during low temperature, redox transformations may provide new insights into the usefulness of the ²³⁸U/²³⁵U isotope system as a tracer of palaeoredox processes. Sandstone-hosted uranium deposits accumulate at an oxidation/reduction interface within an aquifer from the low temperature reduction of soluble U(VI) complexes in groundwaters, forming insoluble U(IV) minerals. This setting provides an ideal environment in which to investigate the effects of redox transformations on ²³⁸U/²³⁵U fractionation. Here we present coupled measurements of ²³⁸U/²³⁵U isotopic compositions and U concentrations for groundwaters and mineralised sediment samples collected in the vicinity of the high-grade Pepegooona sandstone-hosted uranium deposit, Australia.

The mineralised sediment samples display extremely variable ²³⁸U/²³⁵U ratios, spanning a 5 ‰ range. The groundwaters show a greater than 2 ‰ variation in their ²³⁸U/²³⁵U ratios, and exhibit a clear systematic relationship between ²³⁸U/²³⁵U isotopic composition and U concentration; samples with the lowest U concentrations have the lowest ²³⁸U/²³⁵U ratios. The preferential incorporation of ²³⁸U during the precipitation of uranium minerals leaves the groundwaters enriched in ²³⁵U, resulting in a progressive shift in ²³⁸U/²³⁵U towards lighter values in the aqueous phase as U is removed. Previous studies on the same groundwaters have shown significant disequilibrium between ²³⁴U and ²³⁸U. ²³⁸U/²³⁵U ratios however, show a poor correlation with (²³⁴U/²³⁸U) activity ratios, which suggests that mineral leaching during weathering is unlikely to control the observed uranium ²³⁸U/²³⁵U isotopic variability within this low temperature, redox-controlled mineralised system. Rather, the results imply that ²³⁸U/²³⁵U fractionation may be controlled by the nuclear field shift effect during the reduction of U(VI) to U(IV) during mineralisation processes. The findings of this study support the use of the ²³⁸U/²³⁵U isotopic system as a palaeoredox tracer to constrain the nature and timing of palaeoredox conditions.

www.minersoc.org

DOI:10.1180/minmag.2013.077.5.13

Stabilising a craton: The 3.1 Ga Mpuluzi batholith (Swaziland / RSA)

R.C. MURPHY^{1*}, W.L. GRIFFIN¹, N.J. PEARSON¹
AND SUZANNE Y. O'REILLY¹

¹GEMOC/CCFS, Earth and Planetary Sciences, Macquarie University, NSW 2109 Australia

(*correspondence: rosanna.murphy@mq.edu.au)

The Barberton Greenstone Belt and Ancient Gneiss Complex in Swaziland and adjacent South Africa are some of the most-studied Early- to Mid-Archean (3.6 to 3.2 Ga) crustal remnants. The granite-greenstone belt is surrounded and overlain by several large granitoid bodies (Mpuluzi, Piggs Peak, and Nelspruit batholiths), all emplaced ~3.1 Ga, and marking the end of TTG magmatism and regional metamorphism in the area.

The granitoids were emplaced as extensive, km-thick sheets and extend over more than 10,000 km². Zircon U-Pb ages range from ~3.08 to ~3.15 Ga; emplacement may have occurred over as much as 70 Ma. Some samples also have a minor inherited population at ~3.5 Ga, implying the involvement of older crustal material. Zircon Hf-isotope data show a range of up to 15 epsilon units within each sample, but little variation between samples. Average model ages of the 3.1-Ga zircons are ~3.5 Ga, corresponding to the age of the inherited population. These older grains commonly have model ages back to 4 Ga.

Whole-rock Sr and Nd isotopic data yield isochron ages of 3.022 Ga for both systems, and the initial ratios yield model age of 3.11 Ga for each system, perfectly consistent with the U-Pb data. The tight isochrons for both systems (r^2 for Sr = 0.9974, Nd = 0.9615) strongly suggest that the whole mass formed and cooled together, and the small time gap between the isochron and model ages suggests rapid cooling.

These 3.1 Ga granitoids therefore represent the final stage in the cratonisation of the region; this could represent the "draining" of fusible material from the lower crust, increasing its rigidity and limiting further tectonism. The unusual emplacement style, the large volume of magmas involved and the apparently short timescale of emplacement raise several important questions about the processes involved in the stabilisation of the eastern Kaapvaal Craton in particular and ancient crust in general: (1) What was the heat source for the magmas, and what was the source material? (2) How were these volumes of magma extracted from the deep crust? (3) What controlled the emplacement style as sheets rather than deep-rooted batholiths? These problems will now be addressed by dynamic and thermodynamic modeling.

Zinc Melanterite Formation from Acid Mine Drainage in Pan de Azúcar Mine (Zn-Pb-Ag), Northwest Argentina

JESICA MURRAY¹ ALICIA KIRSCHBAUM²
AND BERNHARD DOLD³

^{1,2} IBIGEO-CONICET jesimurray@yahoo.com.ar; alikir2002@yahoo.com.ar ; ³Bernhard Dold Sustainable Mining Research & Consult (SUMIRCO), Bernhard.dold@gmail.com

Melanterite formation in Pan de Azúcar Mine: Evaporation of acid mine waters formed by oxidation of sulfide rich tailings in Pan de Azúcar Mine (Zn-Pb-Ag) favors the formation of soluble sulfates as Melanterite ($\text{Fe}^{2+}\text{SO}_4 \cdot 7\text{H}_2\text{O}$), which is one of the most common ferrous sulfates in nature and one of the first phases to precipitate from evaporation of acid mine drainage. One of the most important characteristic of these phases is their ability to store metals as Ni(II), Cu (II), Zn (II) [1] Zn-Melanterite: Acid mine drainage (139 g/L SO_4^{2-} ; 8960 mg/L Zn; 99.7 mg/L Cd; 47 mg/L Fe (total); 44 mg/L As; 10 mg/L Cu; 1.4 mg/L Pb) seeps from one of the tailings impoundments during dry season. High evaporation rates and high concentration of sulfate and iron favors the precipitation of melanterite at pH=2.1. Some preliminary SEM-EDS studies show high Zn concentrations in melanterite crystals, which indicates its ability to capture this metal in their structure instead of Cu or Ni, probably due to the Zn excess in the acid water. XRD and field observation suggests that during the dry season, melanterite dehydrates and changes to rozenite ($\text{Fe}^{2+}\text{SO}_4 \cdot 4\text{H}_2\text{O}$) as has been described by Nordstrom [1, 2]. In the following rainy season that phases dissolves and metals are again available to the hydrological cycle. This process has an important influence on temporal variation of metals in surface waters.

[1] Sulfate Minerals, Crystallography, Geochemistry and Environmental Significance (2000). Reviews in Mineralogy and Geochemistry, V 40. [2] Nordstrom (1982). Acid Sulfate Weathering: Soil Science Society of America Spec. 10, 37-56

Application of Clumped Isotopes to the Dolomite Problem

MURRAY, SEAN T.¹, PETER K. SWART²
AND MONICA M. ARIENZO³

^{1,2,3}4600 Rickenbacker Causeway, Miami FL 33149

¹smurray@rsmas.miami.edu

²pswart@rsmas.miami.edu

³marienzo@rsmas.miami.edu

The measurement of clumped isotopes has been applied to Miocene to late Pliocene dolomites from San Salvador, Bahamas. These dolomites formed as recently as 500 ky BP, yet are texturally mature and display near perfect stoichiometry (46-48% MgCO₃). They were proposed to have formed at low temperatures (20-28°C) and from normal to slightly evaporated sea water¹. Given the well constrained environmental conditions, these dolomites offer the opportunity to test the application and accuracy of the various calibrations for relating Δ_{47} and temperature. Accurate temperatures of formation can then be used to determine which of the multitude of formulas for determining the fractionation of $\delta^{18}\text{O}$ between the dolomite and the fluid is most accurate.

The dolomites returned Δ_{47} values from 0.64‰ to 0.68‰. Based on the analysis of these samples and the application of the various formulas for relating Δ_{47} to temperature, we propose a modified Dennis *et al.* (2011)² method which takes into account the temperature difference between the theoretical calibrations for dolomite and calcite proposed in Guo *et al.* (2009)³. This method produced temperatures ranging from 23.3°C to 41.5°C. All other methods proposed in the literature produced temperatures that were considered too high considering the well constrained depositional and diagenetic setting of these samples.

Using the modified Dennis *et al.* (2011)² method, it has been concluded that the $\delta^{18}\text{O}_{\text{dolomite-fluid}}$ fractionation equation of Sheppard and Schwarcz (1970)⁴ produces the most reasonable water $\delta^{18}\text{O}_{\text{water}}$ values considering our interpretation of the temperatures.

¹Swart, Ruiz, & Holmes (1987), *Geology* 5, 262-265.

²Dennis, Affek, Passey, Schrag, & Eiler (2011), *Geochimica et Cosmochimica Acta* 75, 7117-7131. ³Guo, Mosenfelder, Goddard III, & Eiler (2009), *Geochimica et Cosmochimica Acta* 73, 7203-7225. ⁴Sheppard & Schwarcz (1970), *Contr. Mineral and Petrol.* 26, 161-198.

Helium isotope compositions of geothermal fluids and alkaline volcanics in Turkey: A comparative assessment for crust-mantle dynamics

HALIM MUTLU¹, ERCAN ALDANMAZ², FIN M. STUART³,
DURU ARAL¹, NILGÜN GÜLEÇ⁴ AND DAVID R. HILTON⁵

¹Eskişehir Osmangazi Univ., 26480, Eskişehir, Turkey
(*correspondence: hmutlu@ogu.edu.tr)

²Kocaeli University, 41380, Izmit, Turkey

³SUERC, Glasgow, G75 0QF, Scotland

⁴Middle East Technical Univ., 06531, Ankara, Turkey

⁵Scripps Inst. of Oceanography, CA, 92093, USA

As a part of the Alpine-Himalayan orogenic belt, the Anatolian land has experienced a series of volcanism, plutonism and active tectonism since the Neogene. This unique geologic disposition facilitated occurrence of vast number of fossil and modern geothermal systems which are closely associated with Neogene-Quaternary volcanism in areas of seismic unrest. He-CO₂ systematics of geothermal fluids in Anatolia has been the subject of several studies over the last decade. He-isotope compositions, reported as R/Ra values, vary over a wide range from 0.27 to 7.76 (Nemrut caldera-eastern Anatolia). The mantle-derived helium component, which is likely transferred to the crust beneath Turkey by recent magmatism, constitutes up to 96% of the total He composition in fluids. CO₂/³He ratios varying from 2.4x10⁵ to 26x10¹³ encompass the range of island arcs (~2.0x10¹⁰) and continental fluids (>10¹¹). Additionally, in this work new helium isotope data are presented for mantle-derived xenolith-bearing basaltic lavas from the Thrace basin in NW Turkey as well as olivine-bearing volcanic rocks from western and southern Anatolian regions. The peridotite xenoliths from the Thrace alkaline volcanic suite are composed of spinel-harzburgites and dunites. Homogenous ³He/⁴He ratios (6.7-7.1 Ra) of harzburgites are very close to that of MORB-type mantle. One dunite sample from the same region is represented by a lower helium isotope composition (3.0 Ra). Alkaline basalts from Kula (western Anatolia) and Osmaniye (southern Anatolia) areas have ³He/⁴He ratios of 7.9 Ra which is coincident with values typical of upper mantle. Olivine in basalt sample from the Söke area in western Anatolia yielded lower helium composition (1.9 Ra). Our ongoing survey on isotope compositions of noble gases in Turkish volcanics, will lead to a better understanding of these apparent anomalies in regard to temporal changes in crust-mantle dynamics in the eastern Mediterranean.

A bond valence approach to surface energy and crystal morphology

ANDREAS MUTTER¹ AND MARTIN T. DOVE²

¹Department of Earth Sciences, University of Cambridge,
Downing Street, Cambridge CB2 3EQ, UK.
am2100@cam.ac.uk

²School of Physics and Astronomy, Queen Mary University of
London, Mile End Road, London E1 4 NS, UK.
martin.dove@qmul.ac.uk

The aim of our research is to provide a methodology, which can be applied to investigate the interaction and the reactivity of mineral interfaces with the environment. The underlying principle of our approach is to define the interaction between internal structural parameters and surface parameters in order to obtain an ideal abstract crystal morphology. This abstract crystal morphology can then be used as a reference morphology to different growth morphologies or crystal morphologies predicted by other atomistic simulations.

The internal parameters chosen on behalf of our model are the number of atoms per surface area (reticular density) and the lattice density. The surface parameters are the number of dangling bonds (bond valence deficiency) per surface area or their corresponding surface energy. The internal parameters are determined by the crystal structure type and therefore are invariable. In contrast, the surface parameters are variable due to differences in the chemical compositions of different minerals, even though they may agree in their crystal structure type.

In order to obtain the surface energies of different crystal interfaces, our model uses the bond valence approach of Brown [1]. First we calculate the surface specific bond valence deficiency, then we assign to each bond via its bond length a certain bond energy, which then in its summation over the surface area gives us the surface energy. The main advantage of this approach is, compared to other atomistic simulations, that it does not demand for charged neutral surfaces to obtain the surface energy. Therefore, naturally charged and charged neutral surfaces can be compared likewise, which is a major advantage while comparing different growth morphologies in variably composed solutions.

This performance of our model, its combined approach of internal and interfacial parameters, not only gives results which are in good agreement with literature data, but also enables us to discuss the importance and the occurrence of naturally polar surfaces on behalf of the crystal morphology.

[1] Brown, I.D. (2002), *The chemical bond in inorganic chemistry*. Oxford Science publications.

Gold in sulfide wastes - peat system

I.N. MYAGKAYA*, E.V. LAZAREVA, M.A. GUSTAYTIS
AND S.M. ZHMODIK.

Institute of Geology and Mineralogy SB RAS, Pr. Koptug, 3,
Novosibirsk, 630090, Russia (*i_myagkaya@mail.ru)

Carbonaceous matter is an effective concentrator of precious metals. We study gold partitioning between sulfide material and peat in a halo around the Ursk tailing pit (Kemerovo region, Russia) with ore cyaniding wastes. The wastes of processed primary ore and ore from the oxide zone are piled up in two 10-12 m piles. Being not fastened, the material has been washed out by floods and rainfalls for more than 50 years. The swampy area downstream of the tailings is burnt by acid mine drainage (AMD) and covered by shed material, with remains of peat mounds rising above.

The shed wastes and peat have been sampled in test pits to 20 cm deep. The gold contents are 0.1 to 3.8 ppm (mean 0.6 ppm) in all wastes, and 1.2 ppb in AMD nearby.

Gold in peat varies broadly, from 0.18 to 155 ppm, mostly 0.18 to 19 ppm. The mean and median values are different (5 and 2 ppm). There are three Au zones in the Ursk halo peat: (1) near the piles and mainstream AMD where the primary and oxide zone ore wastes interlayer (max. 40 ppm); (2) same as (1) but farther from the piles and with higher gold (max. 60 ppm); (3) a perennially wet zone 200 m far from the oxide zone wastes with extremely high gold (40 to 155 ppm).

Peat along the oxide zone wastes bears secondary minerals, namely concentric aggregates of Fe(III) compounds, gypsum, Na-jarosite, framboidal pyrites; barite druses and globules; zinc sulfide; euhedral Hg selenides and sulfides: timmanite (HgSe), onofrite (Hg(S,Se)), cinnabar (HgS).

Gold is high (80 ppm) in material rich in Hg sulfides with Cu, Ag, I, and Se impurities. Submicron and nanoparticles of gold largely cover organic detritus and locally form sheaths over bacterial cells. Native Au particles (to 1.5 μm in diameter, purity 947-1000 ‰), at Cu impurity of 7.5-53 ‰, occur in material cemented with secondary Fe(III) compounds. Cu-gold formation may be mediated directly by bacteria. This process in peat was reproduced in laboratory [1]. Formation of secondary Au in the presence of sulfides is mediated first by iron- and sulfur-oxidizing bacteria and then by thiosulfate oxidizers and sulfate reducers [2].

The study was supported by Grant 11-05-01020 from RFBR and an 2012-2013 OPTEC grant for young scientists, and was run as part of SB RAS Integration Project #94

[1] Kuimova et. al. (2011). *Lithosphere*. **4**. 131-136. (Published in Russian). [2] Southam et. al. (2009). *Elements*. **5(5)**. 303-307.

Structures of weakly binding anions at the interfaces of Fe-polymers and Fe-oxides: Evidence from X-ray and infrared spectroscopic studies

SATISH C. B. MYNENI AND NYSSA CROMPTON¹

¹Departments of Geosciences and Chemistry, Princeton University, Princeton, NJ 08544, USA.
smyneni@princeton.edu

Halides and oxoanions (e.g. CO_3^{2-} , NO_3^-) are common in all aquatic systems, and play an important role on the interfacial reactions of both cations and anions. Several of these ions (e.g. Cl^- , Br^- , NO_3^- , SO_4^{2-}) are considered to interact weakly at the mineral-water interfaces, and thus are used as inert-electrolytes in aqueous geochemical studies for decades. However, our X-ray and infrared spectroscopic data suggest that these ions form strong complexes at the interfaces of Fe-oxides, and play an important role in Fe-oxide transformations.

We examined the reactions of Cl^- , NO_3^- , SO_4^{2-} , and SiO_4^{4-} with soluble Fe-polymers, and freshly prepared Fe-oxhydroxides. The coordination environments of several of these ligands are highly disputed, and experimental evidence was presented for the formation of both inner- and outer-sphere complexes using different macroscale and molecular methods. We examined the coordination environments of these ions using the X-ray and vibrational spectroscopy techniques. We found that these ions exhibit a variety of complexes at the Fe-oxide-water interfaces; however, H-bonded complexes are identified as the predominant complexes for these ligands at the Fe-oxide-water interfaces.

Differences in the molecular structures of these ions at the Fe-oxide-water interfaces are attributed to the rates at which freshly prepared Fe-oxides transformed to goethite. Our studies indicate that goethite appeared first in freshly precipitated Fe-oxides in the presence of SO_4^{2-} and NO_3^- , when compared to that of Cl^- . However, the rate at which the concentration of goethite increased was much lower in the presence of SO_4^{2-} . In addition, the crystallinity of goethite was affected significantly in the presence of these ligands indicating that these weakly coordinating ligands play a central role on the stability and crystallinity of Fe-oxides. Details of these interactions will be presented.

Strontium Isotope Anomalies and ^{26}Al - ^{26}Mg Chronology in CAIs from CV Chondrites

K. MYOJO¹, T. YOKOYAMA¹, Y. SANO², N. TAKAHATA², N. SUGIURA³, H. IWAMORI¹ AND M. UNO¹,

¹Department of Earth and Planetary Sciences, Tokyo Tech, myojo.k.aa@m.titech.ac.jp

²Atmosphere and Ocean Research Institute, Univ. of Tokyo

³Department of Earth and Planetary Science, Univ. of Tokyo

Many nucleosynthetic isotope anomalies have been documented in calcium and aluminum rich inclusions (CAIs). Recently, Moynier *et al.* [1] found positive $^{84}\text{Sr}/^{86}\text{Sr}$ anomalies in Allende CAIs, suggesting excess of the p-process component or deficit of the r-process component in the CAIs. In contrast, Brennecke *et al.* [2] measured Ba, Nd and Sm isotopic compositions in Allende CAIs and discovered that the CAIs have r-process excesses only for Ba isotopes. If these anomalies in CAIs were caused by the injection of refractory materials via a nearby supernova, isotopic anomalies could vary due to difference in time and/or location. To reveal the timing of injection toward the early solar system or processes that caused excesses of nucleosynthetic isotope anomalies in CAIs, we first measured Al-Mg ages in type B CAIs from Allende and NWA 2364 and type C CAI from Allende, then we measured Sr isotopic anomalies in the same CAI. For Al-Mg ages, we used NanoSIMS at the AORI, the Univ. of Tokyo, and for Sr isotopic analysis, we used TIMS, Triton plus at Tokyo Tech.

Al-Mg internal isochrones of type B CAIs yielded initial $^{26}\text{Al}/^{27}\text{Al}$ ratio which are consistent with the canonical value of 5.11×10^{-5} [3]. Two Allende CAIs show $^{84}\text{Sr}/^{86}\text{Sr}$ anomalies of 187 ppm (type B) and 46 ppm (type C) higher than terrestrial standard, whereas the CAI from NWA 2364 has no anomalies. In addition, we also measured $\delta^{88}\text{Sr}/^{86}\text{Sr}$ ratio to trace the degree of mass dependent isotope fractionation. Allende type B CAI has 0.3 ‰ higher and other two CAIs have values lower than terrestrial standard. These results suggest that Sr isotope signatures in individual CAIs inherited isotope signatures of their formation locations. The excesses of a p-process nuclide (^{84}Sr) in CAIs are most likely caused by irradiation from the proto-sun, and their heterogeneous isotope signature is attributed to the distance from proto-sun to formation region of individual CAIs.

[1] Moynier *et al.* (2012) *Astrophysical Journal*, 758:45, [2] Brennecke *et al.* (2011) *LPSC Abstract #1302* [3] Jacobsen *et al.* (2008) *EPSL* 272, 353-364.

Impact of crustal elements on global atmospheric deposition of Nitrogen

STELIOS MYRIOKEFALITAKIS¹, NIKOS DASKALAKIS¹ AND MARIA KANAKIDOU¹

¹ Environmental Chemistry Processes Laboratory, Department of Chemistry, University of Crete, P.O. Box 2208, 71003 Heraklion, Greece; stelios@chemistry.uoc.gr; nick@chemistry.uoc.gr; mariak@chemistry.uoc.gr

Nitrogen (N) deposition plays a significant role in ecosystem functioning and particularly in ocean productivity. Reactive nitrogen also impacts on tropospheric chemistry driving tropospheric ozone production, and on atmospheric acidity. A large number of compounds consist the reactive N pool, like nitrogen oxides, ammonia, nitric acid, organic nitrates, amines, amino-acids etc. Chemical transformations occurring in all phases present in the atmosphere, affect the solubility of reactive nitrogen pool and thus of N-deposition. A significant fraction of N-deposition occurs in the form of particulate matter (PM) deposition. Atmospheric PM is composed of water, inorganic salts, crustal material, organics and trace metals. Important contributors to the dry fine PM are inorganic compounds like ammonium (NH_4^+), and nitrate (NO_3^-), sodium (Na^+), sulfate (SO_4^{2-}) and bisulfate (HSO_4^-). Crustal species like Ca^{2+} , K^+ , Mg^{2+} are major components of dust and can neutralize part of the acidity of the atmosphere (e.g. NO_3^- , SO_4^{2-}). Their presence is thus affecting the partitioning of NO_3^- , SO_4^{2-} and NH_4^+ on atmospheric PM as well as N-solubility and deposition, especially in areas where dust comprises a significant portion of total PM such as the Mediterranean region.

The effect of crustal material on N-containing species deposition is here investigated using the global TM4-ECPL global chemistry-transport model (Myriokefalitakis *et al.*, ACP, 2011; Kanakidou *et al.*, GBC, 2012 and references therein). The model is able to simulate oxidant chemistry, accounting for non-methane volatile organic compounds and all major aerosol components, including secondary aerosols like sulfate, nitrate and secondary organic aerosols. It also accounts for multiphase chemistry in clouds and aerosol water. Gas-particle partitioning of inorganic and crustal components is solved using the ISORROPIA II aerosol thermodynamics model (Fountoukis and Nenes, ACP, 2007). Global simulations have been performed considering and neglecting crustal material for the partitioning of $\text{HNO}_3/\text{NO}_3^-$ and $\text{H}_2\text{SO}_4/\text{SO}_4^{2-}$. Differences between the N-deposition amounts and their solubility are presented and thoroughly discussed.

www.minersoc.org
DOI:10.1180/minmag.2013.077.5.13

Evaporitic sulfate concretions, Moodies Group (~3.2 Ga, Barberton Greenstone Belt, South Africa)

SAMI NABHAN¹, CHRISTOPH HEUBECK¹
AND MARTIN HOMANN¹

¹Freie University Berlin, Institute of Geological Sciences,
Malteserstr. 74-100, 12249 Berlin (sami.nabhan@fu-
berlin.de; christoph.heubeck@fu-berlin.de;
martin.homann@fu-berlin.de)

Quartz-rich sandstones of fluvial to supratidal facies in the Archean Moodies Group (~3223 Ma, Barberton Greenstone Belt, South Africa) include several regionally traceable beds with common to abundant nodular concretions of chert and megaquartz pseudomorphs after gypsum and barite. Electron microprobe analyses show remnants (<20 μm) of these minerals within the concretions but not in the host rock. Petrographic thin sections show characteristic mottled extinction of poikilotopic gypsum cement, now silicified.

Concretions reach up to 8 cm in diameter, are stratiform and commonly associated with aqueously reworked fine-grained tuffaceous sediment of rhyodacitic composition. Detailed geological mapping indicates a braided fluvio-deltaic setting, transitional to sandy supratidal flats which were colonized by microbial mats and occasionally underwent desiccation; the setting is clearly nonmarine. Gypsum pseudomorphs commonly grew inward into concentric hollow or fluid-filled cavities, suggesting mantling followed by dissolution of an unknown precursor mineral, but also grew displacively outward. Nodule growth apparently took place under early diagenetic conditions in unconsolidated sediment in the vadose zone dominated by frequent capillary rise of groundwater brine under mildly evaporative conditions. Partially reworked rhyodacitic tuffs may have delivered alkali cations such as Ca, Na, Ba, and K while carbonates were supplied by atmospheric silicate weathering of mafic to ultramafic volcanic rocks. The provenance of sulphate ions is unknown but may have included microbial and/or abiotic disproportionation of volcanic S or SO₂.

Nodular concretions of the Moodies Group may represent the oldest terrigenous evaporites known to date. Their chemical and isotopic composition constrains the occurrence of sulfate in the atmo- and hydrosphere of the Early Earth, its interaction with the emerging biosphere, Archean weathering, possibly local climatic conditions, and vadose-zone hydrodynamics of the world's oldest well-preserved siliciclastic shoreline system.

Petrosomatic Evolution of Montviel Alkaline System and Rare Earth Carbonatites, Abitibi, Canada

O. NADEAU*, R. STEVENSON AND M. JÉBRAK

*(correspondence: nadeau.olivier@uqam.ca) Geotop,
Université du Québec à Montréal, Québec, Canada

Montviel is a Paleoproterozoic alkaline complex intruding the Archean TTG and volcanic rocks of the Northern Abitibi Zone, Quebec, Canada. It consists of a series of ultramafic to carbonatitic peralkaline bodies. According to field relations, intrusions of peridotites and pyroxenites were followed by melteigites / ijolites / urtites, syenites, sodic granite, and comagmatic silicocarbonatites, calciocarbonatites and ferrocarnatites [1]. The magmatic evolution appears to have ended with a major explosive event which formed carbonatite-bearing polygenic breccia. The carbonatites and the breccia are hosts of one of the largest rare earth element (REE) and niobium mineral deposits being developed in Canada [2]. Detailed petrographic work indicates primary mineralization was partly magmatic, hosted in carbocernaite (REE carbonate) and partly carbothermal, recrystallizing carbocernaite to cebaite and kukharenkoite (REE fluorocarbonates). A second carbothermal event enriched specific parts of the system in heavy rare earths, crystallizing ewaldite (heavy REE carbonate) and heavy REE-enriched qaqarsukite (a fluorocarbonate). A third metasomatic event preferentially remobilized the light REE, further enriching the heavy REE in the areas that were first enriched. Preliminary analyses suggest that the fluorocarbonic stages were followed by an aqueous, hydrothermal stage. The final explosion stage of mineralization preferentially remobilized the light REE enriching the breccia in heavy REE. Trace element concentrations and ¹⁴³Nd/¹⁴⁴Nd ratios are used to investigate the petrogenesis of the system, trace the source(s) of the rare earths and study their behavior in this complex magmatic-carbothermal system.

[1] Goutier, J., 2005. Géologie de la région du lac au Goéland (32F15). Ministère des ressources naturelles et de la faune du Québec. Report RG 2005-05. 44 page. [2] Desharnais, G., Duplessis, C., 2011. Montviel Core Zone REE Mineral Resource Estimate, Professional Report 43-101, Quebec, Canada, 74 pp.

Guyana: The Lost Hadean crust of South America?

S. NADEAU^{1*}, W. CHEN², J. REECE¹, D. LACHHMAN¹,
R. AULT¹, T. FARACO³, L. FRAGA⁴, N. REIS⁵
AND L. BETIOLLO⁶.

¹Guyana Geology and Mines Commission, Georgetown,
Guyana goldenserge@hotmail.com (* presenting author)

²State Key Laboratory of Mineral Deposit Research, Nanjing,
China: nmgchenwei@163.com

³CPRM Belém, Brazil: telma.faraco@cprm.gov.br

⁴CPRM Rio de Janeiro, Brazil: leda.fraga@cprm.gov.br

⁵CPRM Manaus, Brazil: nelson.reis@cprm.gov.br

⁶CPRM Boa Vista, Brazil: leandro.betiollo@cprm.gov.br

U-Pb age dating of zircons was conducted on eighteen rocks from Southern Guyana (Guiana Shield). These were collected by geologists of the geological surveys of Guyana and Brazil during a joint geological and geo-diversity mapping project along their common border. A total of 447 U-Pb age determinations in zircons were obtained by Laser ICP-MS at the State Key Laboratory of Mineral Deposit Research, Nanjing, China.

The rocks were taken from the three main stratigraphic units present in Southern Guyana, where little age dating existed and will be presented south to north:

1) The zircons of granitic rocks of the Southern Guyana Granite Complex (most southerly) yielded the youngest age ca 1925-1984 Ma. These rocks contain only a few older zircon xenocrysts clustering at ca 2086 Ma, ca 2138 Ma, ca 2261 Ma and ca 2297 Ma.

2) The metamorphic age of zircons from the Kanuku Complex (centrally located) is estimated at ca 1956-1968 Ma and obtained from one S-type granite and one paragneiss sample. Moreover, several paragneiss samples contain significant proportions of detrital zircons with older age values clustering at ca 2200-2269 Ma, ca 2450 Ma, ca 2520 Ma, ca 2635 Ma and ca 2707-2721 Ma.

3) The rocks of the Iwokrama Formation (most northerly) display the largest range of age due to the presence of numerous zircon xenocrysts. Minimum age of crystallization of the volcanic and subvolcanic granitic rocks is ca 1981-1986 Ma. Older zircon xenocrysts cluster at ca 2196-2202 Ma, ca 2395-2417 Ma, ca 2487-2489 Ma, ca 2852-2882 Ma, ca 2949 Ma, ca 3701 Ma, ca 3778 Ma and ca 4218 Ma. The oldest age obtained is from a zircon core with a concordant age of 4219 Ma +/- 19 (1s). A second zircon core determination from the same crystal yielded a slightly discordant age of 4210 Ma +/- 19 (1s). The rim of the same zircon gave an age of 3733 Ma +/- 23 (1s).

The zircon xenocrysts in the range ca 2520-3811 Ma in the Iwokrama Formation overlap with Archean age of rocks of the Imataca Complex in Venezuela and of the Amapa Complex of northern Brazil dated between ca 2500 and 3700 Ma. The subvolcanic granite and felsic volcanic rocks of the Iwokrama Formation appear to contain zircons from a "Lost Hadean Crust" representing the oldest component of the Guiana Shield and of South America.

Hydrothermal magnetite from the Grasberg porphyry and Ertsberg East skarn Cu-Au deposits

PATRICK NADOLL¹ JOHN WALSHE¹ DAVID FRENCH² AND
CLYDE LEYS³

¹CSIRO, Australian Resources Research Centre, PO Box
1130, Bentley, WA 6102, Australia

²CSIRO, Energy Technology, PO Box 52, North Ryde, NSW
1670, Australia

³Freeport McMoRan Indonesia, Jakarta 12310 Indonesia

Recent years have seen an increased interest in the use of hydrothermal magnetite as a pathfinder mineral for exploration. Ongoing research puts further constraints on systematic compositional patterns in hydrothermal magnetite that can help to target deeply covered and remote deposits. We present preliminary data for hydrothermal magnetite from the Grasberg porphyry and the Ertsberg East Skarn System Cu-Au deposits. Both are among the biggest deposits of their types in the world and occur within the Ertsberg mineral district in Papua, Indonesia. Magnetite of igneous and hydrothermal origin is a widespread mineral phase in intrusive rocks and hydrothermal veins as well as in associated skarns. A total of 892 electron microprobe analyses of hydrothermal magnetite have been obtained. The main elements that can be used to characterize and discriminate hydrothermal skarn and porphyry magnetite are Mg, Al, V, Mn, and Zn. Titanium, Cr, Co, and Ni show little to no distinct variation between these two types of magnetite (Figure 1). Magnesium and Mn contents are comparable with concentrations found in hydrothermal magnetite from other skarn deposits. Titanium on the other hand appears to be characteristically enriched in hydrothermal skarn magnetite from the Grasberg deposit compared to skarn magnetite from other deposits.

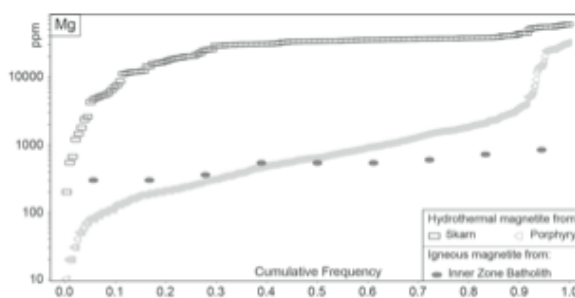


Figure 1 Probability plot for Mg concentrations in hydrothermal magnetite from the Grasberg deposit. Igneous magnetite from the Inner Zone Batholith, Japan is plotted as a reference.

Large scale material transport in the protoplanetary disk and its relevance to the “planetary” oxygen isotopic composition

H. NAGAHARA¹ AND K. OZAWA²

¹Dept. Earth Planet. Sci., The Univ. Tokyo, Hongo, Tokyo 113-0033, Japan. hiroko@eps.s.u-tokyo.ac.jp

² (ozawa @eps.s.u-tokyo.ac.jp)

Protoplanetary disk evolves basically due to the change of the accretion rate with time, of which most significant consequence is the change of temperature as a function of the location within the disk and time. Despite most physical models and astrophysical observations, meteoritic and planetary evidence strongly suggest the presence of high temperature stage at least in the early stage that resulted in isotopic homogenization of the inner solar system. Furthermore, the inner edge of the disk was faced to the proto-Sun for a long duration, where condensation /evaporation of planet-forming minerals should have occurred, and it is now well known that some of condensates were transported to the asteroid belt or even the comet regions. Oxygen isotope is one of the exceptions that retained isotopic heterogeneity in chondrites but approximate homogeneity in planets.

Large scale material transport was investigated by using the model by Ciesla (2011; ApJ 740) and the possibility of homogenization by oxygen isotopic exchange during drift of grains within the disk. The basics of the model is the radial advection and diffusion equation, where the stochastic diffusion term is introduced by the Monte Carlo method. The evolution of temperature and density radial profiles were described as a function of distance from the proto Sun, and therefore the trajectory of grains enables us to evaluate the thermal history. The disk is in a steady state, number of grains were 10000, oxygen isotope of dust formed in the inner edge is assumed to be -50 permils and ice from outside is +100 permils. We assume that $T \sim 1000\text{K}$ is the boundary when grains exchange oxygen isotopes with the ambient gas.

The calculation results show that the average position moves inward with time, and grains larger than cm in order fell quickly to the Sun, but smaller grains remain in the disk, although large fraction of the grains fell into the Sun in 10^6 years with some grains experiencing $T > 1000\text{K}$. If the viscosity of the disk is as small as $\alpha = 0.0001$, most grains remain after 10^6 years. The results suggest that it is impossible to change oxygen isotopic composition of all the dust grains in the inner disk, and therefore, oxygen isotopes homogenization took place at the very early stage and that was retained through the disk evolution.

Molybdenum Isotopic Compositions in Allende Chondrules

Y. NAGAI^{1*}, T. YOKOYAMA¹ AND W. OKUI¹

¹Department of Earth and Planetary Sciences, Tokyo Institute of Technology (Tokyo Tech), 2-12-1 Ookayama, Meguro, Tokyo 152-8551, Japan

(*correspondence: yuichiro.nagai@geo.titech.ac.jp)

Chondrules are primordial materials formed in the early Solar system. They have various characteristics of the texture and petrography as well as $\Delta^{17}\text{O}$ values that generally correlate with the classes of their host chondrites. It is argued that chondrules have formed in multiple reservoirs separated in time and space in the early Solar System. This is also supported by variable $^{84}\text{Sr}/^{86}\text{Sr}$ ratios in chondrules from different chondrite groups [1]. However, there still remains unclear how individual chondrules have obtained the nucleosynthetic Sr isotope anomalies, nor is clear the linkage between isotope anomalies and the other characteristic properties of chondrules. In this study, we focus on Mo isotopes in chondrules to further constrain their formation processes. Molybdenum has seven isotopes produced by different nucleosynthetic processes (s-, r- and p-process). The Mo isotope anomalies recorded in bulk meteorites and CAIs would provide a clue to decode the material transport in the solar nebula [2], yet no Mo isotope data are available regarding chondrules.

Chondrules samples prepared by the freeze-thaw method. were dissolved using a mixture of HF-HNO₃ (3:1) in Teflon vessels at 180 °C. After drying at 120 °C, they were dissolved in 0.5M HF and centrifuged for several hours. Mo was purified by a two-step anion exchange column chemistry employing HCl-HF-HNO₃ (modified from [3]). Molybdenum isotopic compositions in the chondrules were measured by N-TIMS (TRITON *plus* at Tokyo Tech).

Allende chondrules are found to have Mo isotope anomalies (e.g., $\mu^{95}\text{Mo}/^{96}\text{Mo} = 94 \pm 27$ ppm) that are resolvable from those in bulk Allende [4] and Allende CAIs [2]. The anomalies in Allende chondrules are also distinctive from bulk Murchison [2,4], which has an s-process deficit in Mo isotopes. Thus, it is conceivable that chondrite matrices, CAIs and chondrules are formed from separated, isotopically distinctive reservoirs at least for Allende. Our result is consistent with Sr isotope anomalies observed in Allende meteorite [1].

[1] Okui & Yokoyama (2013). *LPSC*, **44th**, #2776. [2] Burkhardt *et al.* (2011). *EPSL*, **312**, 390-400. [3] Nagai *et al.* (2012). *Goldschmidt*, **22nd**, #4414. [4] Nagai & Yokoyama (2013). *LPSC*, **44th**, #2373.

Development of Large-Scale Apparatus for Gas Production from Methane Hydrate Layer

JIRO NAGAO*, YUSUKE JIN AND YOSHIHIRO KONNO

ProTech/MHRC, National Institute of Advanced Industrial Science and Technology (AIST), Sapporo 062-8517, Japan (correspondence: jiro.nagao@aist.go.jp)

Background

To utilize methane hydrate as valuable natural gas resources, a suitable gas production technique and conditions should be established. Experimentally the production method and suitable conditions have been investigated using the core samples. The reproducible results on how methane hydrate dissociates under various conditions could be presented from core-sample experiments. Whereas a core-scale experiments in a laboratory can demonstrate the heat transport process, a dissociation of methane hydrates in an actual reservoir is dominated by the material flow process. In order to couple data obtained from core-scale experiments with the results of field-scale production tests, a large-scale gas production apparatus was conducted at the AIST [1], financially supported by MH21 Research Consortium.

Certification of Apparatus

A large-scale production system for methane hydrate production tests can perform the dissociation experiments under the similar conditions of the actual reservoir under a deep sea floor. Developed large-scale apparatus is shown in Fig.1. The steel vessel has an inner diameter of 1000 mm, a height of 1500 mm and a volume of 1710 L. An overburden pressure of up to 16.5 MPa can be applied for sandy sample. The temperature of the vessel can be controlled from -5 to 20°C . A production well of a steel pipe with a diameter of 100 mm and a length of 1000 mm with holes is connected to a gas and water separator. Holes in the side and bottom of vessel are provided to allow the insertion of gas, water and temperature/pressure sensors. Real-time observations of the rate of the production of gas and water can be performed.



Fig.1 Developed large-scale apparatus

[1] Nagao (2012) *Synthesiology* 5, 89-97.

Microbially mediated redox processes in lactate stimulation with sedimentary rock and groundwater

T. NAGAOKA^{1*}, T. NAKAMURA¹, Y. SASAKI², T. ASANO², T. ITO², Y. AMANO³, T. IWATSUKI³ AND H. YOSHIKAWA²

¹Bioengineering sector, Environmental Science Research Laboratory, Central Research Institute of Electric Power Industry, 1646 Abiko, Chiba, 270-1194, Japan (*correspondence: nagaoka@criepi.denken.or.jp)

²Geological Isolation Research and Development Directorate, Japan Atomic Energy Agency, Tokai, Ibaraki, Japan

³Geological Isolation Research and Development Directorate, Japan Atomic Energy Agency, Horonobe, Hokkaido, Japan

It is significant to investigate the geochemical groundwater evolution around the nuclear waste repository, because geochemical condition could influence the radionuclide migration behavior and corrosion of barrier materials in the repository. Therefore, a laboratory jar experiment was conducted with deep subsurface sedimentary rock and groundwater, in order to assess the response of the geochemical and microbial communities toward redox processes. The redox process was induced by exposure to air and discontinuation to sediment suspension, which simulated the process occurring during operation of nuclear waste repositories, i.e., tunnel excavation, transport of waste containers, and final backfilling. During the experiments, redox potential, dissolved oxygen, and pH in the suspension were measured, and the concentrations of dissolved ions concentration, HCl-extractable iron, and also head space gasses in the jar were analyzed. Moreover, microbial DNA was extracted from the suspension, and PCR-DGGE analysis was performed to analyze the response of microbial communities toward the geochemical changes. As a results, after discontinuation of air exposure with lactate amendment, redox potentials decreased from ca. $+100$ mV to -600 mV (vs. Ag/AgCl), and some sequential terminal electron-accepting process (TEAPs) was observed with the reactions of aerobic respiration, iron reduction and hydrogen fermentation. The related species of the microbes along with TEAPs, e.g., *Pseudomonas sp.* for aerobic respiration and *Shewanella sp.* for iron reduction, was also detected. These results indicated that the microbial activities would affect the geochemical changes in nuclear repositories.

This study was performed as a part of "Project for Assessment Methodology Development of Chemical Effects on Geological Disposal System" funded by Ministry of Economy, Trade and Industry, Japan.

Mineralogy, petrology, O and Mg-isotope compositions of AOAs from CH carbonaceous chondrites

KAZUhide NAGASHIMA¹, ALEXANDER KROT^{1*} AND CHANGKUN PARK¹

¹HIGP/SOEST, University of Hawai'i at Manoa, Honolulu, HI, 96822, USA. *(kazu@higp.hawaii.edu)

Amoeboid olivine aggregates (AOAs) in CH chondrites are texturally and mineralogically similar to those in other carbonaceous chondrite groups. They show no evidence for thermal metamorphism or alteration in an asteroidal setting and consist of nearly pure forsterite (Fa₂₃), anorthite, Al-diopside, Fe,Ni-metal, spinel, ±low-Ca pyroxene (Fs₁Wo₂₃) and CAIs. The CAIs inside AOAs are composed of Al,Ti-diopside, spinel, perovskite, melilite (Åk₁₃₋₄₄), anorthite, hibonite, and grossite. The CH AOAs, including CAIs within AOAs, have isotopically uniform ¹⁶O-rich compositions ($\Delta^{17}\text{O} = -23.5 \pm 2.2\%$) and on a three-isotope oxygen diagram plot along ~slope-1 line. The only exception is a low-Ca pyroxene-bearing AOA that shows a range of $\Delta^{17}\text{O}$ values, from -24.3% to -15.2% . Melilite, grossite, and hibonite in four CAIs within AOAs show no evidence for radiogenic ²⁶Mg excess ($\delta^{26}\text{Mg}^*$). In contrast, anorthite in 5 out of 6 AOAs measured has $\delta^{26}\text{Mg}^*$ corresponding to (²⁶Al/²⁷Al)₀ of $(4.4 \pm 0.6) \times 10^{-5}$, $(4.2 \pm 0.6) \times 10^{-5}$, $(4.0 \pm 0.6) \times 10^{-5}$, $(1.7 \pm 0.2) \times 10^{-5}$, and $(1.7 \pm 0.2) \times 10^{-6}$. Anorthite in another AOA shows no resolvable $\delta^{26}\text{Mg}^*$: (²⁶Al/²⁷Al)₀ < 2×10^{-6} . We infer that CH AOAs formed by gas-solid condensation, aggregation of the condensates mixed with the previously formed CAIs, thermal annealing, and possibly melting to a small degree in a ¹⁶O-rich gaseous reservoir during a brief epoch of CAI formation. The lack of resolvable $\delta^{26}\text{Mg}^*$ in melilite, grossite, and hibonite in CAIs within AOAs reflects heterogeneous distribution of ²⁶Al in the solar nebula during this epoch. The observed variations of the inferred initial ²⁶Al/²⁷Al ratios in anorthite of the mineralogically pristine and uniformly ¹⁶O-rich CH AOAs could have recorded (i) admixing of ²⁶Al in the protoplanetary disk during the earliest stages of its evolution and/or (ii) closed-system Mg-isotope exchange between anorthite and spinel+forsterite+Al-diopside during subsequent prolonged (days-to-weeks) thermal annealing at T>1000°C and slow cooling rates (~0.01 K hr⁻¹) that has not affected their O-isotope systematics. The proposed thermal annealing may have occurred in an impact-generated plume invoked for the origin of non-porphyrific magnesian chondrules and Fe,Ni-metal grains in CH and CB carbonaceous chondrites about 5 Ma after formation of CV CAIs.

Rare-earth element speciation in ferromanganese oxides from the Indian Ocean

B. NAGENDER NATH¹, T.C.VINEESH² AND G. PARTHIBAN³

¹CSIR-National Institute of Oceanography, Goa-403004, India, nagender@nio.org

²Faculty of Maritime Studies, King Abdulaziz University, Jeddah, Saudi Arabia, vineeshtc@gmail.com

³CSIR-National Institute of Oceanography, Goa-403004, India, parthi@nio.org

Oceanic ferromanganese oxides are major sinks for rare-earth elements (REE); hydrogenous oxides being especially suitable for cerium enrichment. Deep-sea muds and ferromanganese nodules and encrustations are considered as potential future sources of REEs. There are differing views on the relative importance of two oxides of Fe and Mn as the REE carriers. Here we present results from sequential leaching experiments performed on different types of ferromanganese oxides from the Indian Ocean in order to quantify the amount of REE associated with the hydrous Mn oxides and Fe oxides. A four-step sequential leaching method is employed here, which is intended to selectively leach metals that are surface adsorbed/loosely bound, Mn-oxide bound, Fe-oxide hosted or held in aluminosilicate residue respectively. Results of this sequential extraction experiment work have revealed that nearly all REEs are closely associated (above 95%) with Fe-bearing phase. The shale-normalized patterns of iron-oxide bound fraction show a distinct similarity in shape and magnitude with the bulk REE patterns except for Ce. Similar magnitude suggests that much of the REEs are hosted by iron-oxyhydroxide phase. Likewise, ~90% of cerium is bound to iron oxide phase and this phase displays a positive Ce anomaly which is typical of low temperature ferromanganese oxides. In contrast, Mn-oxides exhibit a weak positive Ce fractionation. A pronounced positive cerium anomaly in the iron oxide phase suggests an important role of Fe-oxide in acquiring positive Ce anomaly. Enrichment of other tetravalent elements such as Zr, Th and Hf in this phase suggests that the Ce-oxidation must have taken place before the adsorption.

A distinct europium positive anomaly and depleted HREE is seen in the manganese oxide phase in many of the samples. Fractionation of Eu from other REEs and reduction of Eu⁺³ to Eu⁺² can only occur at temperatures above 200–250°C and characteristic of hydrothermal plume particulates and seawater. This is interesting and may pose a question as to whether the hydrothermal sources are contributing Mn to the CIB nodules.

Mollusc clumped isotope thermometry using a new approach

PRASANNA NAIDU K.^{1A} AND PROSENJIT GHOSH²

¹(prasanna@ceas.iisc.ernet.in)

²(pghosh@ceas.iisc.ernet.in)

We present a new approach of calibrating clumped isotope thermometry for mollusc. In our study we sampled growth bands from live mollusc specimens (*Villorita cyprinoides* var. *cochinensis*) collected from Cochin back water estuary in India. The growth bands represent seasonal carbonate deposition at different temperatures during a year. Simultaneous collection of water samples and co-existing carbonate allowed calculation of temperature using Epstein thermometry [1]. The temperature estimated using this approach showed seasonal range of 20° C to 42 °C.

The Δ_{47} values are derived using the method described in Ghosh *et al* 2006 [2] where heated gas equivalent together with carbonate standards (like NBS-19 and MAR J1) are analysed. The approach in producing this calibration curve varies from Henkes *et al.*, 2013 [3] where bulk samples of mollusc species collected from natural marine setup across latitudes along with specimens grown under monitored conditions were analysed for Δ_{47} using carbon dioxide equilibrium scale. Our relation obtained as a function of temperature (in kelvin) is

$\Delta_{47} = 0.055 \times 10^6/T^2 + 0.02$ ($r^2 = 0.8996$), which matches well with the inorganic calcite precipitation curve. We are monitoring the similar specimens at laboratory condition at different temperatures to further evaluate the thermometry equation.

[1] Kim, S.-T. & O'Neil, J.R. (1997) *Geochim. Cosmochim. Acta*, **61**, 3461-3475. [2] Ghosh *et al* (2006), *Geochim. Cosmochim. Acta* **70**(6), 1439-1456. [3] Henkes *et al* (2013), *Geochim. Cosmochim. Acta* **106** (2013) 307-325.

A first look at boron isotope based pCO₂ values from the eastern Arabian Sea for the last 22 kyr

S. S. NAIK^{1*}, P.D. NAIDU¹, S. N. NAIK¹
AND G. L. FOSTER²

¹CSIR-National Institute of Oceanography, Goa, India 403004
(*correspondence: sushant@nio.org)

²Ocean and Earth Science, National Oceanography Centre
Southampton, University of Southampton, SO14 3ZH,UK
(Gavin.Foster@noc.soton.ac.uk)

The Arabian Sea is an unique region with semi-annual reversal of surface water circulation between southwest (SW) and northeast (NE) monsoons. The pCO₂ in the Arabian Sea is always in excess of that in the atmosphere, and the EAS is found to serve as a significant source of carbon dioxide to the atmosphere [1]. However nothing was known up to today about the past pCO₂ variations of the EAS.

We present here for the first time pCO₂ values from the eastern Arabian Sea for the last 22 kyr. We have used planktonic foraminifera species *Globigerinoides ruber* (*sensu stricto*) from a sediment core AAS9/21, collected at 1807m water depth (14°30.539'N, 72°39.118'E). We have analysed boron isotopes on a MC-ICPMS at the University of Southampton, UK. pH and pCO₂ were calculated from the boron isotopic values. Results show that pCO₂ varied from ~200 to ~440ppmv during the study period. A comparison with atmospheric CO₂ data from Antarctic ice core [2] suggest that the EAS seems to have fluctuated between a source and sink of atmospheric CO₂ in the past, with significant excess (w.r.t. the atmosphere) during the deglacial. Further comparison with western Arabian Sea (WAS) pCO₂ values [3] for the similar period reveals that during most of the time the WAS pCO₂ values were much higher as a result of intense upwelling which brings CO₂-rich sub-surface waters to the surface. The large variations in pCO₂ from the EAS are probably be due to a combination of physical processes such as moderate upwelling, influx of freshwaters from rain and rivers, and winter convective mixing processes.

[1] Sarma V.V.S.S. *et al.* (1998)*Tellus*,**50B**, 179-184. [2] Monnin E. *et al.* (2004) *Earth Plan. Sci. Lett.*,**224**, 45-54. [3] Palmer M.R. *et al.* (2010) *Earth Plan. Sci. Lett.*,**295**, 49-57.

Cerium stable isotope fractionation as a potential paleo-redox proxy

RYOICHI NAKADA^{1*}, YOSHIO TAKAHASHI^{1,2}, AND
MASAHARU TANIMIZU^{2,1}

¹ Hiroshima University, Higashi-Hiroshima, Hiroshima, ryo-
(nakada@hiroshima-u.ac.jp)

² Japan Agency for Marine-Earth Science and Technology
(JAMSTEC), Nankoku, Kochi 783-8502, Japan

Cerium (Ce) has anomalously high or low concentrations relative to its neighboring elements, lanthanum (La) and praseodymium (Pr), because of its chemical properties; this phenomenon is known as the Ce anomaly. This redox-sensitive property of Ce allows the estimation of the redox state of paleo-ocean environments and the evolution of the atmosphere. However, a consideration of only the relative abundance of Ce may lead to an incomplete understanding of its oxidation process. In the current study, three important geochemical parameters, namely, abundance, stable isotope ratio, and chemical speciation, were obtained for Ce to derive more information from the Ce anomaly. Assuming equilibrium isotopic fractionation, the mean isotopic fractionation factors between the liquid and solid phases (α_{L-S}) of (i) Ce adsorbed on ferrihydrite, (ii) spontaneous precipitation of Ce, and (iii) Ce adsorbed on δ -MnO₂ were 1.000145 (± 0.000022), 1.000196 (± 0.000031), and 1.000411 (± 0.000079), respectively. These results indicate that the degree of isotopic fractionation of Ce between the liquid and solid phases becomes larger as the redox condition becomes more oxic in the following order: adsorption without oxidation < spontaneous precipitation < oxidative adsorption. Previously, the appearance of the Ce anomaly and/or XANES analysis constituted the only tool available for exploring the redox state. This study, however, suggests that the degree of mass-dependent fractionation of Ce can be used to clearly distinguish spontaneous precipitation from oxidative adsorption on δ -MnO₂, that occurs under more oxic conditions than the Ce(III)/Ce(IV) boundary. Our results suggest that the combination of the stable isotope ratio and chemical state of Ce can be used to classify the redox condition into the three stages based on Ce geochemistry, thereby offering a powerful tool for exploring redox conditions in paleo-ocean environments.

[1] R. Nakada, Y. Takahashi, and M. Tanimizu, Isotopic and speciation study on cerium during its solid-water distribution with implication for Ce stable isotope as a paleo-redox proxy. *Geochim. Cosmochim. Acta* 103 (2013) 49-62.

Stable isotopes of heavy elements in the modern ocean

YUSUKE NAKAGAWA, SHOTARO TAKANO
AND YOSHIKI SOHRIN*

Institute for Chemical Research, Kyoto University, Gokasho
Uji, Kyoto 611-0011, Japan (*correspondence:
sohrin@scl.kyoto-u.ac.jp)

Stable isotopes of heavy elements are now emerging as powerful tracers in the modern ocean and proxies in the paleocean (Tanimizu *et al.*, 2013). Mass fractionation of heavy elements in marine environments is expected to provide unique information on a number of processes. The isotopic compositions of dissolved heavy metals in seawater are fundamental data for stable isotope marine chemistry. However, the precise analysis of seawater is highly challenging (Boyle *et al.*, 2012). The target elements occur at nmol/kg to pmol/kg in seawater. For the precise isotopic ratio determination using MC-ICPMS or TIMS, we have to preconcentrate the analytes quantitatively with a 50-1000-fold enrichment factor from a kg scale sample. It is also important to chemically separate the analytes from interfering major and minor constituents. In addition, it is critical to avoid contamination of the analytes through the sampling, pretreatment, chemical separation, and measurement. Preconcentration using chelating resins seems promising for this purpose.

We have developed a new method for the precise determination of Mo isotope ratios in seawater on the basis of preconcentration using the TSK-8HQ chelating resin and measurement by MC-ICPMS (Nakagawa *et al.*, 2008). Using this method, we have analyzed 172 seawater samples obtained from the Pacific, Atlantic, and Southern Oceans, with an oxygen concentration of 16–373 $\mu\text{mol/kg}$ (Nakagawa *et al.*, 2012). The average isotope composition in δMo (relative to a Johnson Matthey Mo standard solution) was as follows: $\delta^{92/95}\text{Mo} = -2.54 \pm 0.16\text{‰}$ (2SD), $\delta^{94/95}\text{Mo} = -0.73 \pm 0.19\text{‰}$, $\delta^{96/95}\text{Mo} = 0.85 \pm 0.07\text{‰}$, $\delta^{97/95}\text{Mo} = 1.68 \pm 0.08\text{‰}$, $\delta^{98/95}\text{Mo} = 2.48 \pm 0.10\text{‰}$, and $\delta^{100/95}\text{Mo} = 4.07 \pm 0.18\text{‰}$. These results demonstrate that Mo isotopes are uniformly distributed in the modern oxic ocean, strongly supporting the possibility of seawater as an international reference material for Mo isotopic composition.

Recently we have developed a new method for the isotopic analysis of dissolved Cu in seawater (Takano *et al.*). We are now studying the isotopic composition of Cu of the modern ocean. Our data suggest that the combination of concentration and isotopic composition of Cu would be useful to evaluate relative significance of biogeochemical processes.

Nature of transition metals on fine and ultrafine particles and the cytotoxicity

Y. NAKAMATSU, T. AOKI AND S. UTSUNOMIYA

Dept. Chemistry, Kyushu University, Fukuoka 812-8581, Japan (utsunomiya.satoshi.998@m.kyushu-u.ac.jp)

Despite of mounting evidence indicting adverse health effects of ultrafine particle (UFP; <100 nm in diameter), it is difficult to appropriately evaluate the toxicity because of the small size, various shape, mixed chemical state and complicated crystal structure. Transition metals are known to be a factor that causes damage by inducing reactive oxygen species (ROS). The aim of this study is to systematically understand the nature of UFP associated with transition metals and the adverse health effects on lung cells based on the rigorous investigation of crystallo-chemical property of individual UFP in the urban atmosphere and the cytotoxicity assessment.

Inductively coupled plasma mass spectrometry (ICP-MS), X-ray absorption near-edge structure (XANES), scanning and transmission electron microscopy (SEM and TEM) have been employed to rigorously characterize particulate matters collected at urban areas of Fukuoka and Tokyo, and at remote area of Nagasaki. Epithelium cells and macrophage cells were exposed to 0.5-50 ug/ml of SRM 1649a, magnetite nanoparticle, and heavy metal ions, Fe, Mn, Ni and Cr, for 12 hours-26 days in a humidified atmosphere at 37 °C and 5% CO₂. Cytotoxicity assessment was performed using WST assay. Statistic analysis was carried out based on analysis of variance (ANOVA).

All samples revealed that the dominant Fe speciation of the size fraction >1 µm was Fe-bearing aluminosilicate, while that in submicron-size fraction was ferric Fe oxides. In the urban UFP, major Fe species was spinel-structured Fe oxides such as magnetite or maghemite, and some of them were mixed with Mn, Cr and Ni. In addition, sulfate and SiO₂ coating were identified in some of those particles.

Both urban UFPs and magnetite nanoparticles did not reveal an acute health effects on the lung cells; however, an exposure to aqueous Mn²⁺ significantly decreased the viability. Ni²⁺ also revealed the cytotoxicity in less extent. These results suggest that the speciation of heavy metals in the solution determine their toxicity, and protein and amino acid may decrease the toxicity of heavy metals by forming complexes. Because Fe-bearing nanoparticles did not decrease the viability, the soluble species of the other toxic metals, namely Mn and Ni, are the primary factor determining the acute cytotoxicity. On the other hand, long life-time of magnetite nanoparticles in alveoli solution resulted in the phase transformation from spherical magnetite to needle-shaped oxyhydroxide, which may result in an increase in the toxicity.

Non-ideal fluid geometry in the mantle and lower crust

M. NAKAMURA^{1*}, S. OKUMURA¹, T. YOSHIDA¹, O. SASAKI², AND E. TAKAHASHI³

¹Dept. Earth Sci., Tohoku University, Aobaku, Sendai 980-8578, Japan (*correspondence: nakamm@m.tohoku.ac.jp)

²Tohoku University Museum, Aobaku, Sendai 980-8578, Japan (sasaki@museum.tohoku.ac.jp)

³Dept. Earth Planet. Sci., Tokyo Institute of Technology, Tokyo 152-8551, Japan (etakahas@geo.titech.ac.jp)

Fluid phases characterize the physical and chemical processes in subduction zones. The conventional view on grain-scale fluid distribution is based on dihedral angle between minerals and fluids in isotropic monomineralic rocks (i.e. ideal “equilibrium” geometry). Natural rocks are, however, composed of anisotropic multiple phases and undergo textural adjustment to minimize interfacial and strain energy such as grain growth and dynamic recrystallization, which results in microstructural complexity. To understand real fluid distribution in deep-seated rocks, we conducted an X-ray CT study of xenoliths from the lower crust and uppermost mantle from Ichinomegata-Maar, NE Japan. All the observed spinel lherzolite, hornblendite, and hornblend gabbro xenoliths contained upto a few vol% of intergranular pores, indicating that the rocks were saturated with a free-fluid phase (Figure 1). The imaged pore fluids are typically polyhedral and tens–hundreds of micrometers in scale; this suggests that they were formed via coalescence of smaller pore fluids. The fluids are localized in interphase boundaries (between different mineral phases), while most of the monomineralic triple junctions lack pore fluids. All these characteristics are consistent with the results of grain-growth experiments in a fluid-bearing bimineralic system[1]; in other words, the role of interfacial energy anisotropy and grain growth are crucial in determining fluid distribution in nature. The geometry, distribution and thus connectivity of fluids cannot be assessed simply from dihedral angles.

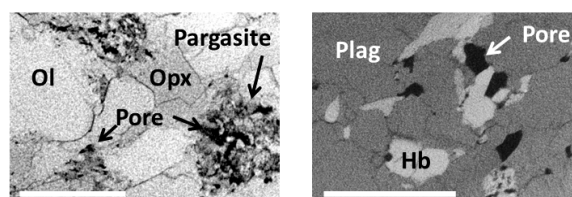


Figure 1: Typical CT images of pores in the lherzolite (left) and hornblende gabbro (right) xenoliths. Scale bars, 500 µm.

[1] Ohuchi and Nakamura (2005) *J. Geophys. Res.* **111**, B01201, doi:10.1029/2004JB003340.

***In situ* observation of electrical current generation in deep-sea**

HASHIMOTO⁴ KEN TAKAI^{2,3} AND HYDROTHERMAL ENVIRONMENTS RYUHEI NAKAMURA¹, MASAHIRO YAMAMOTO^{2,3}, KAZUMASA OGURI², SHINSUKE KAWAGUCCI^{2,3}, KATSUHIKO SUZUKI³, AND KAZUHIITO

¹RIKEN Center for Sustainable Resource Science, Wako, Saitama 3510198, Japan, (ryuhei.nakamura@riken.jp)

²Institute of Biogeosciences, Japan Agency for Marine-Earth Science and Technology (JAMSTEC), Yokosuka, Japan

³Submarine Resources Research Project, JAMSTEC, Yokosuka, Japan

⁴Department of Applied Chemistry, School of Engineering, The University of Tokyo, Japan

Deep-sea hydrothermal vents discharge subsea floor hot and reductive fluids into cool and oxidative seawater. The inter-fluidal oxidation-reduction potential substantially drives various abiotic and biotic oxidation-reduction reactions and supports chemosynthetic ecosystems in the mixing zones. It is predicted that electric current is generated if the two solutions are connected by conductor with electrodes [1]. Here we conducted *in situ* electrochemical analyses of high temperature of hydrothermal fluids and ambient seawater. We succeeded in measurement of the oxidation-reduction potential as about -39mV at high temperature about 309°C in deep-sea hydrothermal fluid. The voltammetry analyses indicated that the open circuit voltage between the hydrothermal fluid and ambient seawater bridged by platinum electrodes was up to 0.74 V but the average current density generated in the seawater cathode was much lower than that in the hydrothermal-fluid-anode. By harvesting the natural setting of potential steep, we for the first time show proof of *in situ* generation of electricity in a newly developed fuel cell installed in deep-sea hydrothermal vents and witness light emitting diode lamp lighting in dark deep-sea environment. The results provide important clues not only to understanding of extracellular electron transports in the deep-sea vent microbial communities but also to future development of *in situ* electric power plants that will supply the electricity for the exploration of deep-sea resources and the following observatories of the deep-sea environments and ecosystems.

[1] R.Nakamura *et al.* *Angew. Chem.* 2010 **49**, 7692.

Millennial-scale wet and dry climate changes during the last glacial maximum in the south Siberia

F.W. NARA^{1*}, T. WATANABE^{1*}, T. KAKEGAWA², K. MINOURA², S. YAMASAKI¹, N. TSUCHIYA¹, T. NAKAMURA³ AND T. KAWAI⁴

¹Graduate School of Environmental Studies, Tohoku University, Sendai 980-8579, Japan. (narafumi@m.tohoku.ac.jp)

²Department of Earth and Planetary Materials Science, Graduate School of Science, Tohoku University, Sendai, 980-8578, Japan

³Center for Chronological Research, Nagoya University, Nagoya, 464-8602, Japan

⁴Association of International Research Initiatives for Environmental Studies, Tokyo, Japan

To investigate the millennial-scale wet and dry climate changes in the south Siberian region for the last 33 kyr, the centennial scale analysis (less than 70 years) of the inorganic elements (e.g. K and Ti) for the Lake Baikal sediment core (VER99G12) were carried out. The fluctuation of the K/Ti ratio during the last glacial maximum period (LGM; 26–19 cal kyr BP) was observed (Fig. 1). Because of the susceptible to water leaching of K comparing to Ti in soil environment, this fluctuation indicates the millennial-scale wet and dry climate changes during the LGM in the south Siberian region. Also, the increase in the precipitation at the climate transition period between OIS2 and 1 (OIS2/1, 11.5 cal kyr BP) was indicated by the significant decrease in the K/Ti ratio. The result of the grain size distribution of the same core is also discussed as well.

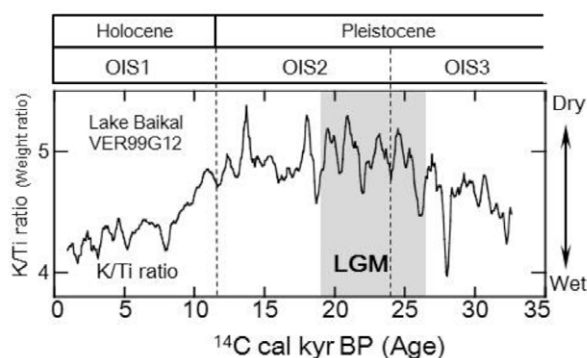


Figure 1. Vertical profile of the K/Ti ratio of the Lake Baikal sediment core (VER99G12). OIS; Oxygen isotope stage

Mass-independent fractionation of sulfur isotopes for all S-bearing components of Archean sediments

HIROSHI NARAOKA¹, EMI MORIWAKI¹ AND SIMON R. POULSON²

¹Dept. Earth & Planet. Sci., Kyushu Univ., Japan
(naraoka@geo.kyushu-u.ac.jp)

²Dept. Geol. Sci. & Engineer., Univ. Nevada-Reno, USA
(poulson@mines.unr.edu)

Mass-independent isotope fractionation of sulfur (MIF-S) signatures in Archean sediments have been often used to infer the presence of an O₂-poor atmosphere, as UV photolysis of atmospheric SO₂ can produce MIF-S in the absence of an ozone layer [e.g. 1]. However, recent theoretical [2] and experimental [3,4] studies have shown that non-photochemical processes can also produce MIF-S. Hence, key factors controlling the production of MIF-S signatures in Archean sediments remain unclear. In this study, we performed δ³⁴S-δ³³S analyses of S-bearing fractions and bulk samples of ~2.7 Ga black shales from drill core from the Jeerinah Formation, Western Australia. Elemental sulfur (S⁰), sulfate (water-soluble and HCl-soluble fractions), pyrite and organic-bound sulfur (kerogen-S) fractions were obtained by solvent extraction and gravity separation.

A slope of ~1 is observed for many bulk samples in a plot of δ³³S vs. δ³⁴S, but also for the S-bearing fractions (Fig. 1). The S-bearing fractions show large intra-sample heterogeneity (up to 8‰ for δ³⁴S), and positive Δ³³S values for all fractions (up to 6‰). The presence of MIF-S for all S-bearing fractions indicates multiple sulfur sources throughout the Archean sulfur biogeo-chemical cycles, and suggest that possible modern weathering has had little impact upon S-isotope signatures.

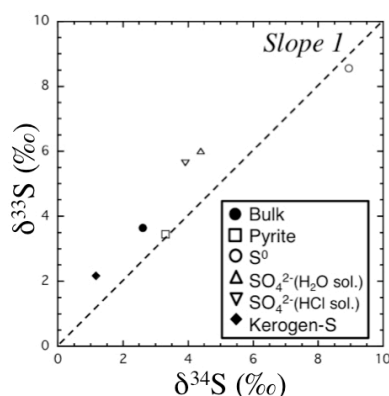


Figure 1. Intra-sample δ³⁴S-δ³³S heterogeneity in Archean sediment.

[1] S. Ono *et al.*, *EPSL* **213**, 15 (2003) [2] A.C. Lasaga *et al.*, *EPSL* **268**, 225 (2008) [3] Y. Watanabe *et al.*, *Science* **324**, 370 (2009) [4] H. Oduro *et al.*, *PNAS* **108**, 17635 (2011).

Use of homogenized sediment in experimental set up: Re-stabilization of redox fronts and artifacts due to sieving methods

M.P. NARDELLI^{1*}, E. METZGER¹, C. BARRAS¹, F. JORISSEN¹ AND E. GESLIN¹

¹ LUNAM University, Université d'Angers, UMR CNRS, 6112UMR, LPGN-BIAF, Angers, France.

(*correspondence: mariapia.nardelli@univ-angers.fr)

In experimental microcosms where the addition of marine sediments is needed to mimic natural benthic systems, sieved and homogenized natural sediment is often used (e.g.[1]), but the consequences of sieving methods on early diagenetic processes and their possible effects on experimental results are often neglected.

Our experiment investigated the effects of two different sieving methods on organic matter concentration and mineralization, exchanges at water/sediment interface and geochemical steady state reaching times for the main chemical species (O₂, Fe²⁺, PO₄²⁻, NH₄⁺, ΣNO₃, H₂S, SO₄²⁻).

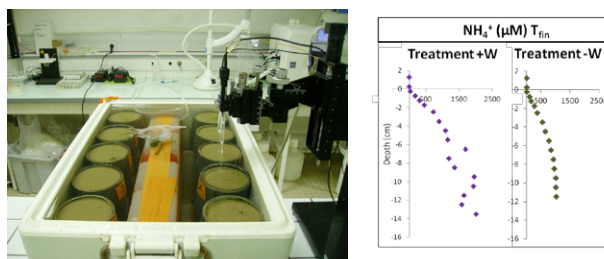


Figure 1 Experimental set up

One set of sediment samples was sieved (<38μm) with natural seawater (+W). The other was sieved without additional water (-W). The results show that while oxygen penetration depth in both treatments is stable within 7 days, the other chemical species show higher concentrations and longer time to reach steady state after the -W sieving treatment compared to the other sieving method. This is suggested to be due to the removal of organic matter during the +W treatment.

[1] Koho *et al.* (2011), *FEMS Microbiol. Ecol.* **75**, 273–283.

Granite compositions in a veined-lower mantle, as indicated by mineral inclusions in diamonds from Juína deposits, Brazil

NARDI, L.V.S.^{*1}; PLÁ CID, J.²; PLÁ CID, C.C.³; GISBERT, AND P.E.⁴; BALZARETTI, N.M.⁵.

¹Instituto de Geociências, Universidade Federal do Rio Grande do Sul, Brazil. (lauro.nardi@ufrgs.br)

²Departamento Nacional de Produção Mineral (DNPM), Brazil. (jorge.pla@bol.com.br)

³Universidade Federal de Santa Catarina, Brazil.

⁴Facultad de Geología - Universidad de Barcelona, Spain. E-mail: (pedro@natura.geo.ub.es)

⁵Instituto de Física - Universidade Federal do Rio Grande do Sul, Brazil.

The mineral inclusions of diamonds are the only natural samples from lower mantle. Recent studies of the inclusions in the alluvial diamonds from Juina province, Brazil, which are believed to be formed in the lower mantle and in the transition zone, have shown the presence of K- and Na-bearing inclusions with structures corresponding to hollandite and composition equivalent to those of alkali feldspars. Compositional determinations were obtained with electron microprobe, and structural information from RAMAN microspectroscopy. Hollandites, stichovite, phengite, CAS-phase, titanite and Na-Ca-garnet/cpx are in composite inclusions with hydrous MgFeAl-perovskite and almandine-grossularite garnet; isolated inclusions of ferropericlaase, ilmenite and pigeonite-augite clinopyroxene were also observed. Na- and K-hollandite can also occur as isolated inclusions. K- and Na-hollandite + SiO₂ in the same diamond grains indicate the presence of melts crystallizing, at the lower mantle, products with compositions corresponding to granitic rocks. The association with abundant inclusions of ferropericlaase and MgFeAl-perovskite suggests a highly heterogeneous mantle, probably with a 'veined'-structure similar to that suggested by Foley⁽¹⁾, but, with veins of granite composition. The growth of diamonds in the parts of mantle where melting occurred and these veins were formed, is consistent with high concentrations of volatiles, probably originated from subducted oceanic lithosphere.

⁽¹⁾ Foley, SF (1992) *Lithos* 28:435-453.

Crystal-melt partitioning of REE and evolution of Martian melts

W. NASH^{1,*} AND B. WOOD¹

¹Department of Earth Science, Oxford University, Oxford, UK, (*correspondence: william.nash@earth.ox.ac.uk)

REE concentrations in the SNC (Shergottite-Nakhilite-Chassignite) meteorites preserve information about the nature of their source regions, now widely believed to be the Martian mantle [1]. In particular, the influence of major phases on partial melting and fractional crystallisation can be inferred from REE concentrations in the meteorites, provided mineral-melt partition coefficients are known for each element under the appropriate conditions, and provided the REE concentrations (assumed chondritic) of the source region are known. Such information may then be combined with knowledge of the pressure-temperature-dependences of the inferred phase's stability to yield constraints on the depth of melting within the Martian mantle.

We have experimentally determined mineral-melt partition coefficients for a wide range of trace elements, between a synthetic Martian primary melt [2] and each of the conjectured major mantle-forming minerals (olivine, orthopyroxene and clinopyroxene) [3]. Experiments were conducted in a piston-cylinder apparatus at 15 kbar pressure, 1340°C, in graphite capsules. The fO_2 conditions approximate those anticipated during melting of Mars' mantle [4]. The new data have relevance for questions concerning the degree of relatedness among the SNC meteorites, and by extension the extent of heterogeneity within the Martian mantle.

In addition to their application to Mars specifically, these new partitioning data provide a test of the Wood and Blundy partitioning model [5] for iron-rich systems, and of its extension to similar situations for which experimental data are not currently available. Data for clinopyroxene in particular show close agreement with the model (for trivalent cations occupying the M2 site), with a maximum partitioning value (D_o) of 0.31, and an ideal radius (r_o) 0.97Å similar to the values reported for terrestrial clinopyroxenes under similar conditions [5].

[1] Treiman *et al* (2000). *Planetary and Space Science*, 48(12-14), 1213-1230. [2] Bertka and Holloway (1993a). *Contributions to Mineralogy and Petrology*, 115(3), 313-322. [3] Bertka and Holloway (1993b). *Contributions to Mineralogy and Petrology*, 115(3), 323-338. [4] Filiberto, *et al* (2010). *Geophysical Research Letters*, 37(13). [5] Wood and Blundy (1997). *Contributions to Mineralogy and Petrology*, 129(2-3), 166-181.

Geochemical modelling of salt systems: Case study Sebkhia Om lekhiolate

NASRI N.¹, BOUHLILA R.², SAALTINK M. W.³ AND GAMZO P.⁴

¹Laboratory of Modelling in Hydraulic and Environment National School of Engineering of Tunis, (nasri.hydro@gmail.com)

²National School of Engineering of Tunis, (bouhlila.rachida@enit.rnu.tn)

⁴GHS, Dept Geotechnical Engineering and Geosciences, Universitat Politècnica de Catalunya, UPC- Barcelona,

³Water Department, University of the Republic, Uruguay

The process of evaporation constitutes very important phenomena in formation of salt system in arid environment [1]. Based in hydrogeochemical modeling, CHEPROO and PROOST using data base Pitzer [2] elaborate the evolution of the salt sequence minerals according to the time and along the distance.

The center of sabkha in characterized by enrichment in mirabilite ($\text{Na}_2\text{SO}_4 \cdot 10\text{H}_2\text{O}$) and depletion of calcium in clay formation.

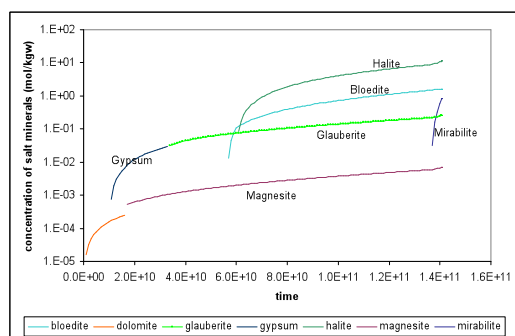


Fig. Salt minerals according to the time

[1] Bouhlila 1999 thesis ENIT. [2] Pablo *et al.* 2011 Journal of Hydrology **401** 154–164

Chromium mobility in Tuscan serpentinite bodies: Inferences from rodingitization and carbonation

C. NATALI^{1*}, C. BOSCHI¹, I. BANESCHI¹, A. DINI¹, AND L. CHIARANTINI¹

¹CNR-Istituto di Geoscienze e Georisorse, Pisa, Italy
(*correspondence: c.natali@igg.cnr.it)

The natural heavy metal enrichment of Tuscan ultramafic rock bodies and derived soils represents an important environmental concern for the area in which they outcrop. Moreover, most of them are superficial aquifers due to their high level of fracturing, thus representing an ideal study case to evaluate the mobility of heavy metal. Despite a comparable whole rock geochemistry, the heavy metal content of spring waters outpouring from the various ophiolitic outcrops reveals significant differences. The highest level of total chromium are detected in spring waters circulating in naturally carbonated serpentinites whereas very low chromium amount is recorded in non-carbonated serpentinite aquifers. Moreover, beside the total chromium content, also the CrVI in the most enriched waters exceed the maximum allowed from the Italian regulation and has therefore monitored and evaluated [1]. The key factors controlling both chromium mobility and carbonation potential have to be referred to the different oceanic history of these rock bodies that led in some occurrences to the alteration of the primary Cr-bearing phases. In particular, in the ophiolitic outcrop of Montecastelli Pisano (PI), serpentinitisation and subsequent modal Ca-metasomatism affecting serpentinite promoted the spinel re-equilibration and Cr transfer from Mg-Al-chromite (and chromite) to adjacent newly formed silicate phases (Cr bearing garnet and Cr-chlorite) whose are significantly more sensible to weathering. The intense Fe-brucite (and serpentine) vein crosscutting the whole serpentinites should provided a viable pattern for the CO₂-rich fluids circulating in these rocks to leach out Cr, and other elements, from alteration minerals. The carbonation of the serpentinite body, mainly affecting Fe-brucite vein, led to an increase of the porosity and therefore enhancing the mineral weathering. In addition, the massive Fe-brucite dissolution controlling carbonation, led to the formation of Mg-Fe-carbonates and Mg-Fe-Layered Double Hydroxydes (LDH) in the carbonated veins, in which CrIII can substitute FeIII and potentially oxidized to CrVI [2].

[1] Chiarantini *et al.*, (2013) *Geo. Res. Abs.* **15**, EGU2013-8839. [2] Radha & Vishnu Kamath (2004) *Bul. Mater. Sci.* **27**, 355–360.

High precision determination of the terrestrial ^{40}K abundance

M.O. NAUMENKO^{1*}, K. MEZGER¹, T.F. NÄGLER¹ AND I.M. VILLA^{1,2}

¹Universität Bern, Institut für Geologie, Baltzerstrasse 3, CH-3012 Bern, Switzerland. (correspondence: naumenko@geo.unibe.ch)

²Università di Milano Bicocca, Piazza della Scienza 4, 20126 Milano, Italy

^{40}K is one of the important constituents of the age equation used for K-Ar and K-Ca dating systems. The main sources of the uncertainty in K-Ca, K-Ar and ^{39}Ar - ^{40}Ar ages are the branching ratio of the ^{40}K decay, the total decay constant and the abundance of ^{40}K . The most recent reports [1] imply that the least precisely known term in the K-Ar age equation is the abundance of ^{40}K . A ^{40}K abundance of $(1.1672 \pm 41) \times 10^{-4}$ was measured on terrestrial material [2], which is to this day the basis of the IUPAC recommendation of the terrestrial K isotope composition. Its uncertainty of 0.35% is much higher than the goal of the EARTHtime initiative, i.e. a total absolute uncertainty of 0.1% on the absolute age.

In order to improve on this situation we measured the abundances of the K isotopes in terrestrial standards NIST SRM 918b and 985 by thermal ionisation mass-spectrometry on a Finnigan TRITON instrument. Three measurement protocols combined with two amplifier set-ups were applied: (A) dynamic measurement with in-run normalisation to the IUPAC value $^{41}\text{K}/^{39}\text{K}=0.072168$; (B) a simple total evaporation procedure; (C) the "NBL-modified" total evaporation [3]. Two loading techniques and two types of filaments (tantalum and rhenium) were tested. The total ion yields (ionisation+transmission) were tested for the evaporation procedures (B) and (C) and ranged up to 48%. Isobaric interferences of Ca on K were tested and were not observed.

The results all agree with the terrestrial $^{40}\text{K}/^{39}\text{K}$ ratio recommended by IUPAC, but have much higher precision. The most reliable results were obtained with the total evaporation protocol with an amplifier configuration that uses 10^{10} , 10^{11} and 10^{12} Ω resistors on Faraday cups. The uncertainty of K-Ar and K-Ca dating systems contributed by the uncertainty of the ^{40}K abundance are now reduced from 0.35% to 0.05%.

[1] Renne P.R. *et al.* (2010) *Geochim. Cosmochim. Acta* **74**, 5349-5367. [2] Garner E.L. *et al.* (1975) *J. Res. Natl. Bur. Stand.* **79A**, 713-725. [3] Richter S., Goldberg S.A. (2003) *Int. J. Mass Spect.* **229**, 181-197.

Re-Os isotope systematics of sulfides from Olympiada gold deposit (Yenisei Rige, Russia)

NAUMOV E.A.,^{1*} TESSALINA S.,² BORISENKO A.S.¹, NEVOLKO P.A.,¹ AND KOVALEV K.R.¹

¹ Institute of geology and mineralogy SB RAS, Novosibirsk, Russia, 630090, (*correspondence: naumov@igm.nsc.ru)

² John de Laeter Centre, Curtin University, Perth, Australia

The Olympiada Au deposit is located within the Yenisei Ridge in Central Siberia, along with a number of other Au and Au-Sb deposits. The Olympiada deposit occurs in metasedimentary terrigenous-carbonate rocks of Paleoproterozoic to Mesoproterozoic age, metamorphosed to amphibole-epidote greenschist facies. This deposit contains about 550–600 t of Au with the average grade of 3–4 ppm Au in primary sulfide ores and 10 ppm in supergene ores.

The Au mineralisation occurs in the contact zone between quartz-mica and carbonate-quartz-mica schists, and is controlled by a district-scale anticline, incorporating bedding-subparallel fractures and transverse fault zones. The orebodies are composed of carbonate-quartz-mica metasomatites containing 3–5 vol% sulfides (mostly arsenopyrite, pyrite, pyrrhotite, stibnite) and scheelite. Minor chalcopyrite, sphalerite, galena, tennantite-tetrahedrite and Bi-minerals are locally present.

Arsenopyrite is the main Au-bearing mineral and can be subdivided into 2 types according to mineralogical and chemical specific features: coarse-crystalline (Type 1) and acicular aggregates (Type 2), which represent distinct ore forming events differing by Au contents. First type is characterized by elevated contents of Au averaging 330 ppm, whereas Type 2 arsenopyrite contains only about 30 ppm of Au.

Both type of arsenopyrite were studied for isotopic composition of Re and Os. Type 1 arsenopyrite contains 3 ppb of Os and 20 ppb of Re and characterised by high $^{187}\text{Os}/^{188}\text{Os}$ ratio up to 14. Type 2 arsenopyrite has lower Os and Re contents up to 0.5 ppb and 5 ppb correspondingly, together with low $^{187}\text{Os}/^{188}\text{Os}$ ratio of 0.3.

This difference implies different sources for these 2 stages of ore-forming process. Ore-forming fluids which forms gold-bearing arsenopyrites of the first type possibly have some crustal source. Origin of arsenopyrite of the second productive stage requires a source with mantle-like Os isotope signatures.

CO₂ induced geochemical reactions at the pore scale

NAVARRE-SITCHLER, A.^{1,2}, MOUZAKIS, K.², ROTHER, G.³, BANUELOS, J.L.³, WANG, X.⁴, KASZUBA, J.⁵, AND MCCRAY, J.²

¹Department of Geology and Geological Engineering, Colorado School of Mines, (asitchle@mines.edu)

²Hydrologic Sciences and Engineering, Colorado School of Mines

³Chemical Sciences Division, Oak Ridge National Laboratory

⁴Chinese University of Petroleum

⁵Geology and Geophysics, University of Wyoming

In many geologic systems pore space is conceptualized as a containment and delivery system for fluids, not unlike a pipe network that delivers water through a city. However, in rocks exposed to reactive fluids, pore networks are not static. The pore network undergoes constant reshaping as minerals dissolve and precipitate. Despite the importance of pore network structure on many fundamental geologic processes, the physical characteristics of pore networks in rocks are poorly understood, in part due to their dynamic nature. Sub-micron sized pores in fine-grained rocks, such as shales and mudstones, require advanced techniques for quantification and characterization. Small angle neutron scattering, a technique that provides statistical data on the topology and architecture of pore networks, was combined with high-resolution imaging, and gas sorption measurements to characterize and quantify the pore network structure in 5 fine-grained rocks. In these rocks a large fraction (up to 80%) of the pore volume and surface area is contained within pores <20 nm in diameter. When two of these rocks were reacted with CO₂ under conditions relevant to CO₂ sequestration or enhanced oil recovery, mineral dissolution and precipitation changed the structure of the pore network with an overall loss of pore connectivity. This study demonstrates the application of neutron scattering to the study of pore networks in fine-grained rocks and the reshaping of these pore networks by mineral reaction.

The Río Mundo dolostones (Spain): Implications for MVT and hydrocarbon formation

D. NAVARRO-CIURANA^{1*}, R. CODINA-MIQUELA¹, E. CARDELLACH¹, E. VINDEL², D. GÓMEZ-GRAS¹, A. GRIERA¹, L. DANIELE¹ AND M. CORBELLA¹

¹Dept. de Geologia, Universitat Autònoma de Barcelona, Campus UAB, Edifici C, 08193, Bellaterra, Spain.

(*correspondence: didac.navarro.ciurana@gmail.com)

²Dpt. de Cristalografía y Mineralogía, Facultad de Ciencias Geológicas, Universidad Complutense de Madrid UCM, 28040, Madrid, Spain.

Dolomitic rocks constitute a potential natural resource as they may host base-metal and hydrocarbon deposits. The study of the dolomitization associated with a Zn-(Pb) Mississippi Valley-type (MVT) deposit in the Río Mundo area (Albacete, SE Spain) may be a breakthrough for mining and hydrocarbon companies, as it is an excellent example to unravel relationships between dolomitization, fluid flow, fractures, host-rock porosity, ore deposition and hydrocarbon accumulation. Petrographical and C/O stable isotope data from carbonates (dolomites and calcites) have been used in order to study these associations. The MVT mineralization consists of sphalerite with hydrocarbon fluid inclusions, galena, pyrite and marcasite. It is hosted by Middle Jurassic dolostones, which are found below Upper Cretaceous age rocks. The hydrothermal dolomitizing event was essential for the ore genesis as it increased the rock porosity up to ~25%. Host limestones have $\delta^{18}\text{O}$ values between +27.55 and +27.83‰ (SMOW) and $\delta^{13}\text{C}$ from +2.32 to +3.16‰ (PDB). Pervasive dolomitization resulting from interaction with hydrothermal fluids have $\delta^{18}\text{O}$ values between +25.07 and +26.89‰ and $\delta^{13}\text{C}$ from -0.53 to +0.61‰. The limited $\delta^{18}\text{O}$ shift may be explained by interaction of regional limestones with a ¹⁸O-enriched dolomitizing fluid at low fluid/rock ratio and constant temperature. $\delta^{13}\text{C}$ values indicate that hydrothermal fluids were enriched in ¹²C, compatible with the presence of hydrocarbons trapped in sphalerite and porosity-filling organic matter. Although part of the ore is disseminated within dolostones ($\delta^{18}\text{O}$: +25.85 to +26.34‰; $\delta^{13}\text{C}$: -2.31 to -0.15‰), most massive brown to reddish sphalerite zoned crystals appear associated with vein-dolomite ($\delta^{18}\text{O}$: +25.13 to +26.93‰; $\delta^{13}\text{C}$: -0.75 to +0.59‰) filling fractures. The overlap of the different dolomite isotopic signature ranges suggests an isotopic resetting or the occurrence of a single dolomitizing event. The mineralization and hydrothermal dolomitization event must have occurred during Upper Jurassic to Lower Cretaceous times.

The compared reactivity of different organic matters and clay in the whole soil and at the microscale: Unraveling the reactivities by combining chemical analysis and physical fractionation

A. NAVEL¹, L. SPADINI^{1*}, I. LAMY², E. VINCE¹ AND JEAN M.F. MARTINS¹

¹LTHE Laboratory, UMR5564 CNRS, University of Grenoble 1, France (*correspondence: lorenzo.spadini@ujf-grenoble.fr) (aline.navel@ujf-grenoble.fr, , jean.martins@ujf-grenoble.fr)

²INRA, UR251, PESSAC Physico-chemistry and ecotoxicology of soils from contaminated agrosystems - RD10 -F78026 Versailles Cedex, France (isabelle.lamy@versailles.inra.fr)

Organic carbon is one of the most reactive, often the most reactive component of common soils. Despite this, describing inside a complex soil matrix the reactivities of the different habits of organic matter (bioclasts, bacteria, degraded solid and dissolved organic matter) and the relative contribution to reactivity of mineral compounds is still a challenging task. The study focus on the reactivity determination of metals, protons, and generally complexing compound. A procedure is presented based on 'soft' granulometric fractionation separating coarse soil aggregates (>250 and 250-63 μ m), silty (63-20 μ m) and fine (20-2 and <2 μ m) soil fractions. The whole-fraction reactivity toward protons and Cu(II) (taken as example of complexing trace elemental cations) is compared to the fraction-specific total organic carbon (T_{OC}) and aqua regalis extracted Al (E_{Al}) content. T_{OC} varies in the soil fractions dependent on 20 years lasting organic amendments in the studied silty-loam soil. E_{Al} content represents the acid, and consequently the relative water accessible clay content in each fraction. Combining linearly these reactivities descriptors allows accessing to the reactivity contribution of different soil organic matters, soil clay and a residual phase. The comparison with referenced reactivity knowledge shows that this method allows accessing representative reactivities of studied components. With this method the soil aggregates are preserved. They are known to represent specific microbial habitats. This opens interesting perspectives relative to the study of biogeochemical site effects in the complex soil matrix.

Thermodynamic Constraints on Stability of Ceramics under Extreme Conditions – Phase Change and Amorphization from Chemical Effects of Radioactive Decay

ALEXANDRA NAVROTSKY¹²³

(¹anavrotsky@ucdavis.edu)

In addition to radiation damage, ceramics in a nuclear reactor or waste form undergo chemical changes as a result of fission and radioactive decay. Because ceramics are typically ionic solids with stringent requirements to maintain appropriate cation size and charge balance on various sublattices, and such transmutations change both the size and charge of ionic species, one can expect phase change, exsolution, and/or vitrification arising from these chemical changes as well as from radiation damage. Two examples are discussed: the incorporation of rare earth fission products in UO₂ and the effect of the decay of Sr to Y to Zr and of Cs to Ba in titanate waste forms incorporating these short-lived fission products. In the former case, rare earths are accommodated by creation of oxygen vacancies, which change ionic and thermal conductivity and, in many cases, stabilize the fluorite phase. In the latter, using perovskite, pollucite, and fresnoite as examples, a general trend of destabilization is seen, with exsolution of new phases and extensive vitrification arising from the violation of charge balanced substitution within the initial structures. Such behavior has the potential to diminish waste form durability

Bio-influence on the metal precipitation in ferromanganese nodules of the Central Indian Ocean Basin

B. NAYAK*, S.K. DAS AND P. MUNDA

CSIR National Metallurgical Laboratory, Jamshedpur-831007, INDIA (*correspondence: brn69@rediffmail.com)

In deep-sea ferromanganese nodules metals can precipitate by chemical oxidation and/or by microbial enzymatic processes [1-4]. Using high resolution FEG-SEM we have documented varieties of ultra-microfossils in the ferromanganese nodule samples of the Central Indian Ocean Basin (CIOB) (e.g., Fig. 1).

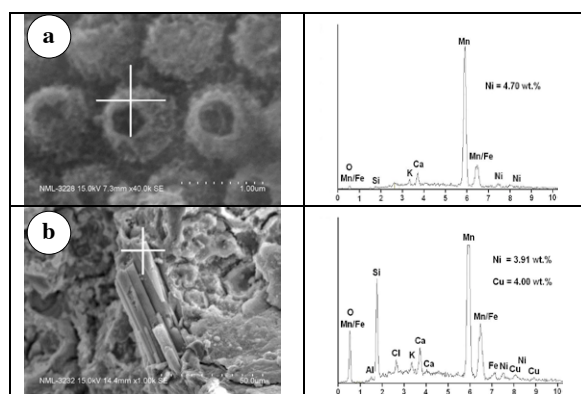


Figure 1: Fossilized microbes with their corresponding EDAX analysis at marked cross points; (a): clumpy microbes; (b): rod-shaped bacteria.

These fossilized microbes are mostly protozoa belonging to varieties of bacteria, diatoms and foraminifera. The chemical compositions of these ultra microfossils indicate a high-level of manganese precipitation in and around them. While clumpy microbes are enriched with Ni, the rod shaped bacteria are rich in Cu. Up to 4.7 wt.% Ni and 5.3 wt.% Cu have been recorded in the fossilized microbe bodies. The high abundance of ultra-microfossils and their chemical compositions indicate that microbes played a major role in the precipitation of metallic elements in the ferromanganese nodules of the CIOB.

[1] Graham & Cooper (1959), *Nature* **183**, 1050-1051. [2] Greenslate (1974), *Nature* **249**, 181-183. [3] Roy (2006), *Earth Sci. Rev.* **77**, 273-305. [4] Wang *et al.* (2009), *Mar. Biotech.* **11**, 99-108.

Characterization of Diagenetically Altered Carbonate Reservoirs, Asmari Formation, Dezful embayment, SW Iran

P. NAZARIAN SAMANI^{1*}, M. MORADPOUR¹ AND S. A. MOALLEMI¹

¹ Research Institute of Petroleum Industry-14665, 137-Tehran-Iran (*correspondence: samanip@ripi.ir)

The Oligocene-Miocene Asmari carbonate Formation is wellknown as a major hydrocarbon reservoir in southwestern Iran. Determining the Asmari Formation reservoir quality based on defining diagenetic evolution were deduced from microscopic description of thin sections. Development of reservoir quality appears to be controlled effectively by diagenesis. Investigations reveal that diagenetic factors including compaction, cementation (by anhydrite, calcite and dolomite), dolomitization, dissolution and their effect on porosity changed the reservoir quality. Compaction and significantly cementation reduced the porosity however; this effect was healed by later dissolution and leaching processes. Dolomitization in this Formation enhanced the original porosity in depositional textures and protracted dolomitization created intercrystalline porosity, creating the best reservoir facies in SW Iran [1]. Two kind of distinct dolomitic textures involve fine to medium dolomite crystals (20-100 μ) increased the intercrystalline porosity while the other, coarse mosaic of dolomite crystals (>100 μ) especially associated with mud residuals are shown degradation effect on reservoir quality. It will be appeared that rock-water interaction lead to dissolution and dolomitization phenomenon which are the most important processes fortify pore spaces and controlling the reservoir quality in the Asmari Formation of SW Iran.

[1]Aqrawi *et al.* (2006) *Journal of Petroleum Geology*, **29**, 381-401.

Synchrotron FTIR on melt inclusions, clinopyroxene and olivine from Mt Etna recent explosive eruptions

SABRINA NAZZARENI¹, MASSIMO POMPILIO², HENRIK SKOGBY³, ANDERA PERUCCHI⁴ AND PAUL DUMAS⁵

¹Dip. Fisica e Geologia, Università di Perugia, Italy
(sabrina.nazzareni@unipg.it)

²Istituto Nazionale di Geofisica e Vulcanologia, Sez. di Pisa, Italy

³Dept. of Geosciences, Swedish Museum of Natural History, Stockholm, Sweden

⁴SISSI, Elettra, Trieste Italy

⁵SMIS, Soleil synchrotron, Paris, France

The volatile budget of magmas from active volcanoes are crucial in developing volcanological models. The solubility of H₂O in silicate melts is, on the whole low, and strongly dependent on pressure. As a consequence magmatic melts reaching the surface have lost most of their original volatile contents.

We studied the volatile content of recent eruptions of Mount Etna (the 3930 BP picritic eruption and Cono del piano - 2001 and 2002 eruptions), to reconstruct a model for the ascent and degassing of these magmas. We determined the volatiles content by FTIR techniques measuring the hydrogen content of clinopyroxene phenocrysts and the H₂O and CO₂ contents of melt inclusions entrapped in the same clinopyroxenes (cpx) as well as in olivine (ol) phenocrysts.

Synchrotron FTIR experiments were conducted at SMIS (Soleil, Paris) and SISSI (Elettra, Trieste) beamlines. FTIR spectra were collected in the 900-8000 cm⁻¹ range with 4 cm⁻¹ resolution using scanning areas of variable size (200-400 μm-long and 200-400 μm-wide) following a regular grid of square-aperture dimension of 10 μm. Thus we measured high resolution chemical maps of H₂O and CO₂ distribution and speciation on melt inclusions to study the diffusion of H between the inclusions and cpx- or ol-host mineral. Line transect across chemical zonations in cpx (from the outer edge to the core of the crystal) showed details on the H₂O distribution with a more water rich core (PDL2001: 214 ppm H₂O; TEF2002-2:204 ppm H₂O) and a more "dry" (PDL2001: 138 ppm H₂O; TEF2002-2: 109 ppm H₂O) rim as detected by polarised FTIR spectra of oriented single-crystals. The water content of the Etna cpx phenocrysts is quite high suggesting a water rich magmatic system and showed only minor variations from the different eruptions: 254 ppm H₂O for 3930 BP picritic eruption; 214 ppm H₂O for 2001 eruption; 161-254 ppm H₂O for 2002 eruption.

Amber and amber-like materials on the Romanian market

ANTONELA NEACȘU^{1*}, DELIA GEORGETA DUMITRAȘ², MIHAELA ELENA CIOACĂ² AND ANGELA MARIA ANASON²

¹University of Bucharest, Faculty of Geology and Geophysics, 1, N. Bălcescu Ave., 010041 Bucharest, Romania.

(*correspondence: antonela.neacsu@gmail.com)

²Geological Institute of Romania, 1, Caransebes Str., Bucharest, Romania, RO-012271.

Amber is a natural fossil resin with a controversial paleobotanical origin and is a mineraloid for mineralogists. The final internal structure and chemical composition of amber depend on light and oxygen exposure, on temperature and humidity differences, also on the biologic agents that characterized the environment, including the geological one, after resinosis (a large, unrepeatably secretion of resin by some Conifers and flowering trees, during Cretaceous and Tertiary periods). The oxidizing processes into the depositional context are important for the gemological properties of amber (color, cracks and transparency).

There are few amber varieties used for manufacturing, including jewelry: the Baltic amber with its variety succinite (Poland, Russia, Baltic Countries, Ukraine, Germany), the amber of Dominican Republic, the Chinese amber, the Burma amber (burmite), the amber from the Romanian Carpathians (rumanite or romanite). In Romania amber is treated as gemstone, including the risk of fake industry, that uses both natural substances (e.g., actual resins, copal and pressed amber), and synthetic polymers (glass and plastics). A distinction between amber and imitations could be made applying Fourier-transform infrared spectroscopy (FTIR) and X-ray diffractometry (XRD) targeting the natural inclusions or proving an internal organizing tendency of material. FTIR curves of amber-like samples found ourdays in gem exhibitions organized by the Geological Institute of Romania are similar to those of romanite samples are similar to those of romanite, succinite, Dominican amber, burmite and copal. On the contrary, plastics, synthetic resins and modern resin of Rosaceous are found on the Romanian market, used as imitations or sometimes sold as genuine amber.

The effect of AFC processes and source oxidation on Fe isotopes in evolved Banda Arc lavas

O.NEBEL¹, R.J.ARCULUS¹, M.WILLE² AND P.Z.VROON³,

¹Research School of Earth Sciences, The Australian National University, Canberra, Australia

²Mineralogie und Geodynamik, Eberhard Karls Universität Tübingen, Germany

³Department of Petrology, VU University Amsterdam, The Netherlands

Igneous rocks, ranging in composition from mafic to felsic, show resolvable variations in their stable Fe isotope compositions [1]. These variations are closely related to the oxidation state of Fe in igneous systems, i.e., Fe²⁺ and Fe³⁺, with heavy Fe isotope compositions predominately associated with the more oxidized species. Reported Fe isotope variations ($\delta^{57}\text{Fe}$ relative to IRMM-014) in island arc basalts (IAB) span a range from negative to positive values [2], and are on average systematically lighter than those reported for mid ocean ridge basalts (MORB) [3], a fact that is seemingly opposing their expected oxidation state.

Here we present the stable Fe isotope composition of 13 IAB and 8 subducting sediments sampled along the active Banda Arc (East Indonesia). All samples are well characterised for their Sr-Nd-Pb-Hf-O isotope composition, which record progressive sediment melt contribution along the arc from NE to SW. We find that crystal fractionation increases $\delta^{57}\text{Fe}$ and identify this process as the dominant factor controlling the Fe isotope composition of this evolved arc suite. The opposite effect is observed upon magnetite saturation at ~4 wt.% MgO. Arc crust assimilation has also a strong influence driving the IAB towards heavier Fe isotopes. Sediment melting appears to have little or no effect on the Fe isotope composition in contrast to signatures for most radiogenic isotope tracers.

We imply that Fe in the sediment melt fully equilibrates with the mantle wedge either prior to or during wedge melting. As a consequence, if it is assumed that sediment melts carry more Fe than aqueous fluids, the slab agent has little or no affect on the redox state of IAB sources. Instead we propose that progressive wedge depletion has the potential to harvest Fe³⁺ and this lowers $f\text{O}_2$ (and $\delta^{57}\text{Fe}$). If $\delta^{57}\text{Fe}$ monitors the redox conditions of evolving arc rocks, then crystal fractionation is the driving force in elevating $f\text{O}_2$ in subduction zones.

[1] Dauphas and Rouxel, Mass Spectrometry Reviews, 2006;

[2] Dauphas *et al.*, EPSL, 2009, [3] Teng *et al.*, GCA 2013

Geochemical features of granitoid Central Siberia magmatism in the Permian-Triassic

T.S. NEBERA, AND N.N. BOROZNOVSKAYA

Tomsk State University, Tomsk, Russia (tsnebera@mail.ru)

The granitoids of the Kolyvan-Tomsk folded zone, part of the western segment of the Altai-Sayan region, are the youngest magmatic formations of Late Hercynian tectogenesis. Developing the geochemical criteria of granitoid classification is an important perspective for geodynamic interpretation of the granitoids. The studied rocks are characterized peraluminiferous and have converged features granite S-and I-types. I-granites have a more mafic composition with a high content of calcium amphibole and accessors in the form of magnetite and allanite. They are characterized by a high oxidation of iron and oxygen fugacity, appreciable concentrations of Ba (~ 800-1200 g / t), Sr (~ 1200-2000), and calcium. Derived from the granite-granodiorite -granosyenite series, geochemically similar to rocks of I-type. They can be attributed to the products of latite-type magmatism with $\text{K}_2\text{O} > \text{Na}_2\text{O}$, high the K/ Rb ratios, Mg, high Ni concentrations. Breed from leucogranit series are rather consistent with S-type characteristics. They have a relatively high concentration of Rb in the background of a sharp decrease in the content Ba (up to ~ 120 g / t) and Sr (up to ~ 40 g / t) are enriched in Be and Cs, which makes them similar to Li-F granites. The results of luminescent analysis of the granitoids studied (intensive X-ray luminescence of Fe³⁺ in feldspars) indicates also that they were formed from a high-alkaline melt. The geochemical differences (characteristics) discovered for the granitoids allow us to assume that they were formed under complicated geodynamic conditions from the high alkalinity melt. This study was funded by the Russian Ministry of Education and Science (projects 5.3143.2011, 14.B37.21.0686, 14.B37.21.1257).

Cadmium sorption by green rust

S. NEDEL*, K.N. DALBY, K. DIDERIKSEN,
B.C. CHRISTIANSEN, AND S.L.S. STIPP

Nano-Science Center, Department of Chemistry, University of
Copenhagen, Denmark (*correspondance:
sorin@nano.ku.dk)

Cadmium pollution, released into soils from agricultural and industrial activities, is considered a potential threat to biota. As with other pollutants, Cd mobility and bioavailability in soils largely depend on sorption-desorption processes at the interface between soil solution and mineral surfaces. Fe (oxyhydr)oxides are ubiquitous in soils. They have a large surface area and can adsorb and incorporate metals, meaning that these minerals are likely to affect Cd migration. The interaction of Cd with soil minerals has been investigated thoroughly but we know of no study on Cd interaction with green rust (GR). GR consists of brucite like layers of Fe(II),Fe(III) hydroxide separated by interlayers of water molecules and anions. These minerals are highly redox active, can form both by biotic and abiotic processes, and are likely to be present in soils and groundwater. The aim of this work was to determine if Cd can be sorbed and effectively immobilized by GR.

GR was synthesised at circumneutral pH by two methods: transformation of ferrihydrite in an Fe(II) solution and oxidation of an Fe(II) solution. Cadmium was added, at a series of concentrations either in the initial Fe(II) solution or in suspensions with preformed GR. X-ray diffraction (XRD) and transmission electron microscopy (TEM) showed that Cd²⁺ was not reduced by preformed GR nor incorporated in freshly forming GR. However, GR₅₀₄ partially sorbed the divalent heavy metal, with higher sorption occurring at lower Cd concentrations. Upon oxidation of GR, Cd²⁺ remained associated with the Fe(III) solid. X-ray photoelectron spectroscopy (XPS) showed that it was sorbed by newly formed lepidocrocite.

These results contribute to fundamental understanding of contaminant interaction with green rust and can be implemented in current reactive transport models. We also demonstrated that Cd²⁺ mobility will be affected to some extent by sorption to GR, which can be present naturally in soil and form from iron corrosion, for example in permeable reactive barriers or pipes.

Zircon U-Pb-ages, Hf isotope and trace element composition in the evolution of the IVAC Complex (Urals, Russia)

I.L. NEDOSEKOVA^{1*}, E.A. BELOUSOVA²,
B.V. BELYATSKY³ AND N. PEARSON²

¹Zavaritsky IGG UB RAS, Ekaterinburg, Russia
(*correspondence: vladi49@yandex.ru)

²GEMOC/CCFS, Macquarie University, Sydney, Australia
(elena.belousova@mq.edu.au)

³IPGG RAS, St.Petersburg, Russia (bbelyatsky@mail.ru)

It has been widely accepted that Hf isotope composition of zircon is relatively stable and is not affected by significant alteration due to influence of the hypogenic processes [1]. We have studied Hf isotope composition (coupled with U-Pb-age) in different populations of zircon from Ilmeny-Vishnevorsky Alkaline Complex (IVAC), Uralian Fold Belt.

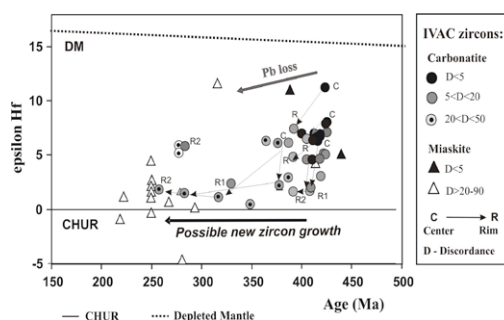


Figure: Hf isotope composition of the IVAC zircons (calculated for individual zircon ages) plotted against U-Pb ages, where D presents percentage of their age discordance.

The results indicate that the early zircons I from IVAC carbonatites and miaskites form concordant age cluster (U-Pb-age 410-424 Ma, D<5) and displays moderately depleted isotope Hf composition ($\epsilon_{\text{Hf}}=11.7-4.7$), where variations plausibly reflect primary heterogeneity of the magma source(s). The outer zones of the zircon I grains are characterized by disturbed U-Pb systems ($5 < D < 20$) and lower ϵ_{Hf} values (shifting by 3-4 units in regard to the central parts of grains). These shifts do not correspond to the lines of Hf isotope evolution of zircons compositions or radiogenic Pb loss trends (Figure). The later newforming zircons II dated at T=250-320 Ma (frequently $D > 50-90$, $\epsilon_{\text{Hf}} = -5$ to $+11$).

Both, the disturbance of U-Pb-system and formation of zircons with distinct, less radiogenic Hf-isotope composition could be related to the later ca 250 Ma metamorphic event.

[1] Patchett *et al.* (1981) *ContrMinPet* **78**, 279-297.

Biological fractionation of molybdenum isotopes: Lake Mývatn, Iceland

REBECCA NEELY*¹, CHRISTOPHER SIEBERT², KEVIN BURTON³, EYDÍS SALOME EIRIKSDÓTTIR¹ AND ÁRNI EINARSSON¹

¹* Institute of Earth Sciences, Sturlugata 7, 101 Reykjavík, Iceland (correspondence: ran6@hi.is)

²GEOMAR, Helmholtz Centre for Ocean Research, Germany

³Department of Earth Sciences, Durham University, UK

Molybdenum (Mo) is an essential enzyme cofactor in nearly all organisms and has been known to be of biological importance for some time [1]. Such biochemical ubiquity may come as a surprise given the relative scarcity of Mo at the Earth's surface. However, its unreactive, conservative behaviour in oxygenated, aqueous solutions makes it the most abundant transition metal in the oceans.

Laboratory based studies have shown that certain soil bacteria and cyanobacteria all favour light isotopes during Mo assimilation, thus causing measurable fractionations [2]. This study aims to bridge the gap between these laboratory experiments and the natural environment. Lake Mývatn is an ideal location to investigate these processes. Located on young, porous lava of the Icelandic rift zone it is almost exclusively sourced by groundwater flow and has only one riverine output, making it a perfect natural "box-model". Groundwater and outlet samples were analysed for Mo isotopes over the course of one growing season.

There are two distinctive groundwater inputs; $\delta^{98}\text{Mo}_{\text{hot}}$: 0.57 ‰ and $\delta^{98}\text{Mo}_{\text{cold}}$: 0.35 ‰ (0.1 2s.d.). The Mo concentration of the lake waters is described by simple, proportional mixing of these inputs. However, the Mo isotope value of the lake is heavier than the mixed inputs, consistent with a preferential uptake of light Mo isotopes by *Anabaena* (cyanobacteria), known to bloom in the lake in the summer months. Over the course of the year the outlet varied systematically between $\delta^{98}\text{Mo}$ 0.36 ‰ and $\delta^{98}\text{Mo}$ 0.66 ‰ with a signal predicted by a concentration driven model and biological fractionation of between - 0.2 ‰ and - 0.4 ‰. These results represent the first measurements of biological fractionation of Mo in the natural environment and have implications for our understanding of Mo systematics and its potential as a proxy in a geological context.

[1] Howarth & Cole (1985) *Science* 229. 653-655. [2] Zerkle, Scheiderich, Maescam, Liermann & Brantley (2011) *Geobiology* 9 (1): 94-106

XAFS analysis of C-S-H formed by cement-bentonite interaction

KUMI NEGISHI¹, HIROYUKI SKAMOTO¹, TOMOKO ISHI², DAISUKE HAYASHI², NAOKI FUJII², HITOSHI OWADA², AND HIROAKI NITANI³

¹Taiheiyō Consultant Co., Chiba pref., 285-0802, Japan

²RWMC, Tokyo, 104-0052, Japan

³KEK, Ibaraki pref., 305-0801, Japan

The analysis of long-term alteration of engineered barriers to be used for the disposal of TRU waste predicted precipitation of calcium silicate hydrate (C-S-H) minerals in the bentonite along the interface with the cement. In order to quantitatively measure the C-S-H predicted to form as a secondary mineral in the bentonite, the authors used XAFS analysis technique. The XAFS analysis which provides information around the concerned element regardless of the crystallinity of the mineral was assumed to be an effective mean to analyze poorly crystallized C-S-H. The local structural environment of calcium in the C-S-H with different Ca/Si ratio was also evaluated based on the EXAFS spectra in this study.

A test piece prepared by contacting a compacted bentonite and a hardened cement paste was immersed in the simulated fresh, reducing and high pH (FRHP) groundwater. The calcium K-edge XAFS measurement was conducted for the compacted bentonite. A synthetic C-S-H with high Ca/Si ratio was prepared and dissolved to generate low Ca/Si ratio C-S-H. These C-S-H minerals were subjected to the XAFS analysis.

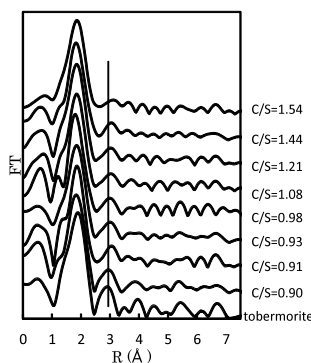


Fig.1 Radial structure function of C-S-H

The XAFS measurement allowed for evaluation of the variation of the quantity of the C-S-H in the bentonite. No significant difference was observed in the EXAFS spectra and conditions around the calcium among C-S-H minerals with different Ca/Si ratio. Conditions around the calcium in the C-S-H were similar to those in the tobermorite (Fig. 1).

This research is a part of "Development of the technique for the evaluation of long-term performance of EBS (FY2007-2012)" funded by the ANRE, METI of Japan.

A new model for biomineralization and trace-element signatures of foraminifera tests

G. NEHRKE^{1*}, N. KEUL², G. LANGER³, L. DE NOOIJER⁴,
J. BIJMA¹ AND A. MEIBOM⁵

¹Alfred Wegener Institute, Bremerhaven, Germany

(*correspondence: gernot.nehrke@awi.de)

²Lamont-Doherty Earth Observatory, Columbia University, Palisades, New York, USA (nkeul@ldeo.columbia.edu)

³Department of Earth Sciences, Cambridge University, Cambridge, UK (gl345@cam.ac.uk)

⁴Department of Marine Geology, Royal Netherlands Institute of Sea Research, Horntje, The Netherlands (Lennart.de.Nooijer@nioz.nl)

⁵Laboratory for Biological Geochemistry, School of Architecture, Civil and Environmental Engineering (ENAC), Ecole Polytechnique Fédérale de Lausanne, CH-1015 Lausanne, Switzerland (anders.meibom@epfl.ch)

The Mg/Ca ratio of foraminifera calcium-carbonate tests is used as proxy for seawater temperature and widely applied to reconstruct global paleo-climatic changes. However, the mechanisms involved in the carbonate biomineralization process are poorly understood. The current paradigm holds that calcium ions for the test are supplied primarily by endocytosis of seawater. Here, we combine confocal-laser scanning-microscopy observations of a membrane-impermeable fluorescent marker in living benthic species *Ammonia tepida* with dynamic ⁴⁴Ca-labeling and NanoSIMS isotopic imaging of its test. We infer that Ca for the test in *A. tepida* is supplied primarily via trans-membrane transport, but that a small component of passively transported (e.g. by endocytosis) seawater to the site of biomineralization plays a key role in defining the trace-element composition of the test. Our model accounts for the full range of observed Mg/Ca and Sr/Ca benthic foraminifera test compositions and predicts the effect of changing seawater Mg/Ca ratio.

Re-Os-PGE constraints on the evolution of backarc oceanic mantle

WENDY R NELSON¹ JONATHAN E SNOW¹ ALAN D BRANDON¹ YASUHIKO OHARA^{2,3} AND CIN-TY LEE⁴

¹Dept of Earth and Atmospheric Sciences, University of Houston, Houston, USA (wrnelson2@uh.edu, jesnow@uh.edu, abrandon@uh.edu)

²Hydrographic and Oceanographic Dept of Japan, Tokyo, Japan (yasuhiko.ohara@gmail.com)

³Japan Agency for Marine Earth Science and Technology, Yokosuka, Japan

⁴Dept. of Earth Science, Rice University, Houston, USA (ctlee@rice.edu)

Our direct understanding of the evolution of oceanic mantle during backarc extension is limited to exposures of abyssal peridotite and ophiolites. Few direct comparisons of ophiolite and backarc peridotite have been made due to the small number of documented exposures and limited in situ samples from backarc settings. Here we report Re-Os and PGE data for backarc abyssal peridotites from the Godzilla Megamullion (GM), a massive ~9000 km² oceanic core complex located in the Parece Vela Basin (Philippine Sea). The distal portion of GM records early, magmatically productive extension marked by moderately depleted spinel peridotites. This transitions into a less melt-productive medial region characterized by more fertile peridotite. The proximal region represents the most recently exhumed portion of the megamullion. Isotopically, the regions are indistinguishable, with whole rock ¹⁸⁷Os/¹⁸⁸Os = 0.1174-0.1704. Elevated ¹⁸⁷Os/¹⁸⁸Os values correlate with MgO loss, suggesting the influence of sea floor weathering. While spinel grains in proximal samples record high TiO₂ and Cr# indicative of melt-rock interaction, PGE abundances are not strongly affected; distal samples record stronger depletions in Pt-Ru-Pd than proximal samples, consistent with higher degrees of melt extraction. In all samples, Re abundances are low (2-107 ppt) and are positively correlated with TiO₂ abundances in spinel, suggesting that Re is mildly influenced by melt-rock interaction. However, ¹⁸⁷Os/¹⁸⁸Os ratios are not correlated with Re concentration, demonstrating that modest Re addition occurred recently. As a whole, the ¹⁸⁷Os/¹⁸⁸Os data suggest that the backarc oceanic mantle in this region did not experience significant ancient melt depletion. Instead, the geochemical and isotopic signatures of the GM were generated during backarc extension associated with the Izu-Bonin-Mariana subduction zone.

Evolution of the Lower Crust in the Point of View of Fluid-Rock Interaction Under the Bakony-Balaton Highland Volcanic Field

BIANCA NÉMETH^{1,2}, KÁLMÁN TÖRÖK¹,
ISTVÁN KOVÁCS¹ AND CSABA SZABÓ²

¹ Geological and Geophysical Institute of Hungary, H-1143, Srefánia út 14, Budapest, Hungary

² Lithosphere Fluid Research Lab, Institute of Geography and Earth Sciences, Eötvös University, Budapest, Hungary, H-1117, Pázmány Péter sétány 1/c

Plio-Pleistocene alkali basalt hosted mafic garnet granulite xenoliths were studied from the Bakony-Balaton Highland Volcanic Field (Hungary). Two particular samples were chosen for analyses (optical microscopy, microthermometry, major and trace element geochemistry, Raman and IR spectroscopy), which contain primary silicate melt inclusions (SMI) in the rock-forming minerals. The samples have non-equilibrium texture in contrast with majority of known mafic garnet granulite xenoliths. SMI were observed in plagioclase, clinopyroxene and ilmenite in both xenoliths. The major element geochemistry of the glass of SMI suggests the presence of a silica rich melt at relatively high temperatures (830-920 °C). The origin of the melts could have been derived by the melting of biotite-gneiss or quartz-amphibolite. Our data suggest that the SMI derived from partial melting of different lower crustal rocks having mafic and metasedimentary origin with an occasional presence of C-O-H±S±N fluids. Petrography suggests at least five fluid events in the lower crust. The IR study of the water content in the rock-forming minerals and in the host minerals, including SMI and fluid inclusions, suggest that the acidic melt contained relatively high amounts of water. The observed SMI and fluid inclusions locally rehydrated the originally dry minerals.

The research was supported by OTKA to Kálmán Török, project number: NN79943 and a MC IRG (NAMs-230937) to István Kovács.

When do insoluble particles act as good CCN?

A. NENES^{1,2*}

¹School of Earth and Atmospheric Sciences, Georgia Institute of Technology, Atlanta GA, USA (correspondence: athanasios.nenes@gatech.edu)

²School of Chemical And Biomolecular Engineering, Georgia Institute of Technology, Atlanta GA, USA

The ability of dust particles to serve as CCN under atmospherically relevant supersaturations depends on their mineralogy, size, morphology, and atmospheric processing. Most studies to date focus on the soluble fraction of aerosol particles when describing cloud droplet nucleation, and overlook the interactions of the hydrophilic insoluble fraction with water vapor. A new approach to include such interactions is presented, by combining multilayer Frenkel-Halsey-Hill (FHH) physical adsorption isotherm, Kohler theory and curvature (Kelvin) effects.

The importance of adsorption activation theory (FHH-AT) is demonstrated by measurements of CCN activity of mineral aerosols generated from clays, calcite, quartz, and desert soil samples from Northern Africa, East Asia/China, and Northern America. Based on the dependence of critical supersaturation with particle dry diameter, it is found that the FHH-AT is a better framework for describing fresh (and unprocessed) dust CCN activity than classical Köhler theory (KT). Ion Chromatography (IC) measurements performed on fresh regional dust samples indicate negligible soluble fraction, further supporting FHH-AT.

The results presented reshapes the conventional model of CCN activity, as it demonstrates that dust particles do not require deliquescent material to serve as atmospheric cloud nuclei. A droplet parameterization framework for large scale models that includes the new CCN activation physics is also developed and constrained by laboratory measurements. The framework accounts for aging of dust (via deposition of hygroscopic material), and is included within a global model framework to assess the impact of dust on warm cloud droplet number.

Crystallographic relationships between diamond and its olivine inclusions. An update

F. NESTOLA^{1*}, P. NIMIS¹, S. MILANI¹, R. ANGEL¹,
M. BRUNO² AND J.W. HARRIS³

¹Dipartimento di Geoscienze, Università di Padova, Italy
(*correspondence: fabrizio.nestola@unipd.it,
paolo.nimis@unipd.it, sula.milani@studenti.unipd.it,
rossjohn.angel@unipd.it)

²Dipartimento di Scienze della Terra, Università di Torino, Italy (marco.bruno@unito.it)

³School of Geographical and Earth Sciences, University of Glasgow, UK (Jeff.Harris@glasgow.ac.uk)

We have investigated the crystallographic relationships between olivine inclusions and their diamond hosts by in-situ single-crystal X-ray analysis. We studied 21 diamonds, all from the same kimberlite source (Udachnaya, Yakutia), containing a total of 51 olivine inclusions with diamond-imposed morphology. Each diamond contained up to nine individual olivines. On a statistical basis, no preferential orientation could be found. In particular, only 3 olivines showed an orientation comparable to that found by Mitchell & Giardini [1], i.e. (101)oli // (101)dia and (010)oli // (111)dia, which is believed to be the most favourable in the case of epitaxy. Based on our data, such orientation cannot be considered as “typical” of olivines included in diamonds. Although olivines in different diamonds showed random crystallographic orientations, multiple olivines within the same diamond often showed very similar orientations. Up to three sets of iso-oriented inclusions have been found within a single diamond. Our unprecedented data set clearly refutes the long assumed existence of a systematic crystallographic relationship for olivine inclusions in diamonds [1, 2]. The implications in terms of syngensis vs. protogenesis of the inclusions will be discussed.

[1] Mitchell & Giardini (1953), *Am. Mineral.* **38**, 136-138. [2] Futergendler & Frank-Kamenetsky (1961), *Zapisky Vsesoyuznogo Mineralogicheskogo Obshestva* **90**, 230-236.

Colloid-associated iron and arsenic transport in streams

ELISABETH NEUBAUER¹, FRANK VON DER KAMMER¹,
KLAUS-HOLGER KNORR², STEFAN PEIFFER²,
MARTIN REICHERT², STEPHAN J. KÖHLER³,
HJALMAR LAUDON⁴ AND THILO HOFMANN¹

¹University of Vienna, Department of Environmental Geosciences, Austria (elisabeth.neubauer@univie.ac.at)

²University of Bayreuth, Department of Hydrology, Germany

³Swedish University of Agricultural Sciences, Department of Aquatic Sciences and Assessment, Uppsala, Sweden

⁴Swedish University of Agricultural Sciences, Department of Forest Ecology and Management, Umeå, Sweden

Significant correlations between concentrations of arsenic (As), iron (Fe), and natural organic matter (NOM) are often observed in wetland draining streams. However it is not yet understood how the transport of Fe and As along with NOM and iron hydroxide colloids is affected under variable hydrological and hydrochemical conditions.

Analysis with Flow Field-Flow Fractionation coupled to UV-Vis spectroscopy and inductively coupled plasma mass spectrometry revealed that As was associated with NOM and, if present, Fe-organo-mineral colloids in the size range below 25 nm.

The colloid composition in the studied streams was highly variable on a temporal and spatial level: Short-term groundwater level fluctuations affected the release of Fe, NOM and As, and colloid composition with respect to NOM and Fe-hydroxides changed within hours. This is due to changing flow paths of the groundwater that feeds the stream as well as the chemical composition of the hydraulically active soil layers. Under all conditions, 25 to 50% of the total As was associated with NOM. However, the mass of As exported per mass of NOM was considerably higher under baseflow conditions.

The colloid composition was also affected when stream water moved from first order, acidic streams to more basic, larger streams. Fe was mainly transported as Fe-NOM complexes in acidic first order streams. In contrast, in the more basic higher order streams, Fe-hydroxide colloids and particles were present. The amount of colloid-associated As decreased from 75% to 26% with increasing pH, and As in the colloidal size range was mainly associated with NOM.

There is growing interest in quantifying the riverine fluxes of Fe to the oceans. Association with NOM enhances the Fe mobility in streams. Concentrations of NOM bound Fe in the studied catchments were high compared to literature data. In conclusion, wetland-draining catchments are of special importance for riverine Fe and trace element transport.

Nickel and methanogens

A. NEUBECK^{1*} AND M. IVARSSON²

¹Department of geological sciences, Stockholm University, Stockholm, Sweden

²Department of Paleobiology and the Nordic Center for Earth Evolution (NordCEE), Swedish Museum of Natural History, Stockholm, Sweden

Methanogens require Ni for their growth and as a consequence the microbial fractionation of Ni isotopes can be used as a biomarker for activity of methanogenic communities [1]. Anaerobic laboratory experiments were performed using methanogens to investigate methanogenic growth in a modified nutrient media [2] with olivine Fo91 (5g/l) added as an additional mineral nutrient source and as the only H₂ provider. One of the investigated methanogens showed an increased growth in the experiments with added olivine. There was also a close relationship between the mobilized Ni and the growth of the methanogen. This is the first experimental evidence of a close methanogen-mineral interaction. Ni is an element that previously has been neglected in the study of fossilized microorganisms and their interaction with mineral substrates and, thus, there are no records or published data of Ni in association with microfossils. However, we have detected enrichments of Ni in fossilized microorganisms and ichnofossils, respectively, from three separate locations. Ni is not present in the host rock in none of the samples, thus, it is more probable that the Ni content is primary, a remnant of the live microorganisms. More extensive analysis is required to understand the uptake, preservation and fractionation of Ni by methanogens as well as the preservation and magnitude of Ni in microfossils.

[1] Cameron V, Vance D, Archer C, House CH. A biomarker based on the stable isotopes of nickel. *Proceedings of the National Academy of Sciences*. 2009 Jul 7;106(27):10944–8.

[2] Westerholm M, Roos S, Schnürer A. *Syntrophaceticus schinkii* gen. nov., sp. nov., an anaerobic, syntrophic acetate-oxidizing bacterium isolated from a mesophilic anaerobic filter. *FEMS Microbiology Letters*. 2010.

Characterization of microbial diversity of a geothermal plant after long-term shutdown periods

DOMINIK NEUMANN¹, DARIA MOROZOVA¹,
JULIA SCHEIBER², SEBASTIAN TEITZ¹
AND HILKE WÜRDEMANN^{1*}

¹ Helmholtz Centre Potsdam GFZ, International Centre for Geothermal Research, Hermannswerder 15, 14473 Potsdam, Germany. *(Correspondence: Wuerdemann@gfz-potsdam.de)

² GEIE Exploitation Minière de la Chaleur, Kutzenhausen, France.

The geothermal plant in Soultz-sous-Forêts, located at the western part of the Upper Rhine Graben, is running as an EGS, including four wells ranging to a depth of 5 km. By long-term circulation of deep brines in the reservoir geothermal fluids with a total dissolved solid content of 97 g/L, a temperature around 160°C and a pH around 4.5 are produced. In order to characterize the microbial diversity and its potential involvement in scaling and corrosion processes after long-term shutdown periods, a series of fluid samples from the production well GPK2, taken during two plant restarts, were analyzed. Characterization of the microbial community was done by genetic fingerprinting (PCR DGGE) and qPCR.

Results indicate a diverse microbial community in the fluid of the production well after shutdown periods. In both sampling campaigns a clear shift in the Bacteria community composition was visible after the restart, which could be explained by the increasing temperature and the increasing amount of reservoir fluid. The diversity of the Archaea was not affected.

Sulfate reducing Bacteria (SRB), as indicated by the presence of their 16S rRNA gene and *dsr* genes, were found only until a produced fluid volume of 260 m³ (Two borehole volumes) during the first sampling campaign. This indicates the growth of these microorganisms and biofilm formation on the well casing during the shutdown period and their removal after restart of the fluid production. Preliminary quantification results underline this assumption: highest levels of DNA, 16S rRNA gene copies and *dsr* gene copies were found in the first samples after the restart, while in later samples values were lower or below the detection limit.

The results, as well as further analyzes like the creation of clone libraries or the detection of cell numbers will contribute to characterize the potential involvement of the found microorganisms in corrosion processes and enhance the understanding of the microbial community associated with geothermal plants.

Effect of Al/B substitution on structure and properties of silicate glasses and melts

D. R. NEUVILLE

CNRS-IPGP, Géochimie&Cosmochimie, Paris Sorbonne Cité,
1 rue Jussieu, 75005 Paris, France.

The relationship between physical properties and structure of glasses and melts in the system $MO-T_2O_3-SiO_2$ (with $M=Na_2, Ca$ and $T=Al, B$) are technologically and geologically important, in particular to understand the microscopic origin of the configurational thermodynamic properties. The connection of these network former is fundamental to understand the physical properties of magmatic liquids.

The configurational properties of melts and glasses provide fundamental information needed to characterize magmatic processes. A principal difficulty, however is to link the "macroscopic" configurational entropy with the structure of melts. This has been done by combining viscometry with Raman and NMR spectroscopy studies. From the viscosity measurements at low and high temperatures, we have obtained the configurational entropy, S_{conf} ($\log \eta = Ae + Be/TS_{conf}$, where η is the viscosity, T the temperature and Ae, Be two constants).

Silicon, aluminum, and boron are 3 network formers playing different role on the silicate network, whereas Si is the strongest network former in coordination 4, 5 or 6 as a function of T, P ; Al can play different function as a network former in 4- or 5-fold coordination and probably as a network modifier in 6 fold coordination. Boron observed in 3 or 4 fold coordination is always a network former but for very "fragile" glasses.

For the glass the Al/B substitution produce a small decrease of the molar volume while this substitution produced a strong decrease of viscosity and glass transition temperature while the fragility of the network is less affected by this chemical change. Raman spectra show significant change in the D1 and D2 bands. NMR spectroscopies show also significant change as a function of chemical change and temperature. All this observations will be discussed and interpreted in order to link microscopic versus macroscopic changes.

Historical deposition of Polycyclic Aromatic Hydrocarbons in an Amazon estuary

P.A. NEVES*¹, S. TANIGUCHI¹ AND M.C. BÍCEGO¹

¹Laboratório de Química Orgânica Marinha, Instituto Oceanográfico da Universidade de São Paulo, 05508-120, São Paulo, Brazil. *(correspondence: ticinev@yahoo.com.br)

Polycyclic aromatic hydrocarbons (PAHs) are ubiquitously distributed in the aquatic environments, coming from natural and anthropogenic sources. PAHs can accumulate in sediments and their historical deposition can show source alterations throughout time. The study area, Guajará Bay, is located in northeastern Amazon and Belém (one of Amazon's biggest cities) is located in its margins. To evaluate the temporal changes of PAHs in Guajará Bay a sediment core was collected in 2010. Total PAH concentration (ΣPAH) ranged from 46.9 to 595 $ng\ g^{-1}$ (dry weight) along the core. The core can be divided in two periods regarding PAHs sources to the area. In the first period, corresponding from 1900's to the early 1960's, ΣPAH remained constant, with an average of 79 $ng\ g^{-1}$ (d.w.), possibly characterizing base levels of PAHs for this region. Composition of individual PAH showed a predominance of alkyl-PAH over its parental compound such as methylphenanthrene over phenanthrene. Usually, these PAHs are associated with petrogenic inputs, however, there is no evidence of oil during this period in the region. Thus, the higher proportions of alkyl-PAHs could be related to natural sources, such as organic matter diagenetic transformation or biogenic synthesis. During the second period, which starts in the late 1960's, ΣPAH increases, reaching its maximum value at the top of the core. Diagnostic ratios showed a predominance of pirolitic PAH in the area, suggesting that this input is probably related to the intensification of the urban and industrial development, encouraged by the government since 1950's. The variation of PAH contents was closely related to the changes in the environment of the Amazon area evaluated.

www.minersoc.org

DOI:10.1180/minmag.2013.077.5.14

Establishment of euxinic oceanic conditions following the Lomagundi Event

L. NGOMBI-PEMBA^{1*}, D. E. CANFIELD²,
E. U. HAMMARLUND^{2,3}, S. BENGTSON^{2,4},
A-C. PIERSON-WICKMAN⁵, F. GAUTHIER-LAFAYE⁶,
O. ROUXEL⁷ AND A. EL ALBANI¹

¹UMR 7285, Univ. Poitiers, 86022 Poitiers, France
(*lauriss.ngombi.pemba@univ-poitiers.fr)

²Nordic Center for Earth Evolution (NordCEE), Box 50007,
105 05 Stockholm, Sweden

³Southern University of Denmark, Institute of Biology,
Campusvej 55, Dk-15 5230 Odense M, Denmark

⁴Swedish Museum of Natural History, Department of
Palaeozoology

⁵Département Géosciences, UMR 6118, Université de
Rennes, 35042 Rennes, France

⁶Laboratoire d'Hydrologie et de Géochimie de Strasbourg,
UMR 7517-UdS-CNRS, 67084 Strasbourg, France

⁷IFREMER, Département Géosciences Marines, 29280
Plouzané, France

Following the great oxidation event (GOE), the isotope record of marine carbonate rocks suggests a massive burial of organic carbon in an event known as Lomagundi excursion (LE). It is estimated that during this period atmospheric oxygen attained levels much higher than during GOE [1]. It is proposed that as the LE declined, oxygen dropped to lower levels [1, 2], but the direct geochemical evidence for the state of atmospheric and ocean oxygenation both during and after the LE is missing. This time window is also represented by the 2.2-2.0 Ga Francevillian group of Gabon, well known for the earliest large colonial organisms [3]. In order to investigate the nature of marine water-column chemistry, samples representing the entire section were subjected to multielement (C, S, Fe, Mo, U) biogeochemical study.

Geochemical data show deep water oxic conditions during deposition of the lower part of the section in agreement with the LE. Nevertheless the interlayered Mn deposits occurred in ferruginous anoxic conditions reflecting sea-level changes. The upper part of the section reflect euxinic conditions, and together with $\delta^{98}\text{Mo}$ values, these data confirm a significant decrease in the oxygenation of ocean water in the aftermath of the Lomagundi Event.

[1] Bekker & Holland (2012), *Earth and Planetary Science Letters* **317-318**, 295-304. [2] Planavsky *et al.* (2012), *PNAS* **109**, 18300-18305. [3] El Albani *et al.* (2010) *Nature* **427**, 100-104.

Hydration, structure and mobility of Cs⁺ and Sr²⁺ in montmorillonite and muscovite clay minerals

BRICE F. NGOUANA W.^{1*}, NARASIMHAN L.¹ AND
ANDREY G. KALINICHEV

Laboratoire SUBATECH (UMR-6457), Ecoles des Mines de
Nantes, 4 Rue Alfred Kastler, La Chantrerie, 44307,
Nantes Cedex 3, France (* ngouana@subatech.in2p3.fr)

Clay minerals used as natural and engineered barriers in geological nuclear waste repositories are able to considerably reduce the mobility of radionuclides in the environment. The radionuclide retention happens through a combination of various physical and chemical processes taking place at the clay-water interface, but their molecular mechanisms are still insufficiently understood.

To obtain detailed microscopic scale information on the structure, dynamics, and energetics of Cs⁺ and Sr²⁺ ions at the surfaces of model illite and smectite clays (muscovite and montmorillonite, respectively) we have performed a series of classical molecular dynamics (MD) computer simulations using the CLAYFF force field [1]. New sets of structural models with different degrees of compositional disorder in the octahedral and tetrahedral layers of clay were constructed and investigated in order to quantify the effects of such disorder on the properties of the adsorbed ions.

The structural properties were probed in terms of the atomic density distributions in the direction normal to the clay surfaces, along the planes parallel to the clay surfaces, atom-atom pair correlation functions, and coordination numbers. The 2-dimensional and 3-dimensional diffusion coefficients were calculated to probe the ionic mobility at the clay surfaces and in the interlayer space. In the case of montmorillonite (a swelling clay), the hydration energetics was also systematically investigated by determining the hydration and immersion energies [2].

The atomic density profiles vary with the charge and size of the ions and show a significant layering at the interfacial regions of both studied clays. Pair correlation functions and coordination numbers indicate only one stable adsorption site for cations on the basal surface of muscovite (ditrigonal) in contrast to two adsorption sites on a similar montmorillonite surface (ditrigonal and triangular). Cs⁺ and Sr²⁺ mobility is considerably reduced by substrate adsorption, but the diffusion coefficients tend to get closer to bulk solution values when the ions are removed from the surface.

[1] Cygan, R.T. *et al.* (2004), *J.Phys.Chem B*, **108**, 1255-1266.
[2] Smith D. E. (1998), *Langmuir*, **14**, 5959-5967.

Constraining OH diffusivity in silicate melts

HUAIWEI NI^{1,2}, ZHENGJIU XU³ AND YOUXUE ZHANG³

¹CAS Key Laboratory of Crust-Mantle Materials and Environments, School of Earth and Space Sciences, University of Science and Technology of China, Hefei 230026, China (*Correspondence: hwni@ustc.edu.cn)

²Bayerisches Geoinstitut, Universität Bayreuth, 95440 Bayreuth, Germany

³Department of Earth and Environmental Sciences, University of Michigan, Ann Arbor, MI 48109, USA

The transport of water in silicate melts is mostly dominated by molecular H₂O (H₂O_m) diffusion. Diffusivity of hydroxyl (OH), the other water species, has not been well quantified. It has been previously assumed that OH diffusivity is close to the Eyring diffusivity (i.e., inversely proportional to melt viscosity), or essentially approaches zero. However, in our experimental study of water diffusion in an Fe-free andesitic melt, we found that these assumptions do not hold.

Diffusion experiments were performed at 1 GPa in a piston-cylinder apparatus using a double diffusion couple technique. One couple contained a dry glass (with 0.01 wt% water) and a hydrous glass (with ~3 wt% water), and the other contained the same dry glass and a different hydrous glass (with ~6 wt% water). Both couples experienced the same pressure and thermal history, which is crucial for constraining the dependence of H₂O diffusivity on water content. Diffusion profiles preserved in the quenched products were analyzed with both FTIR and confocal Raman microspectroscopy. Nearly identical profiles were obtained from the two methods for profile length > 1 mm (produced at 1619-1842 K), but for profile length < 0.1 mm (produced at 668-768 K) FTIR analysis showed marked convolution effects due to its spatial resolution being inferior to that of Raman.

Previous models neglecting OH diffusivity cannot satisfactorily reproduce the measured profiles. We developed a new fitting procedure that simultaneously fits both diffusion profiles from a single experiment and also accounts for the role of OH diffusion. With the new model, OH diffusivity is constrained to be 10%-20% of H₂O_m diffusivity at 1619-1842 K as total water content approaches zero. The obtained OH diffusivity is much higher than the Eyring diffusivity, indicating that in melt structure OH is not necessarily bonded with network-forming cations, such as Si. On the other hand, OH diffusivity is close to reported F diffusivity (both the size and the valence of OH and F are comparable).

Research on heavy metal environmental geochemistry in urban soils in Haikou, China

QIAN NI¹, ZHENGYU BAO² AND CHUNYAN WANG³

¹ State Key Laboratory of Biogeology and Environmental Geology, (niq1981@163.com)

² Faculty of Material science and Chemistry, (zybao@263.net)

³ Faculty of Engineering, (1239901602@qq.com)

China University of Geosciences, Wuhan 430074, China

Soil heavy metals constitute serious environmental hazards from the point of view of polluting the soils and adjoining streams and rivers. Therefore, a series of investigations were performed to provide heavy metal signatures of urban soils and to evaluate pollution level. Concentrations of Cd, Zn, Ni, Cr, Cu, Pb, Hg and As were measured on 70 topsoil samples and 16 deep-soil samples collected from green areas in Haikou city, capital of Hainan province. The results indicate that, in comparison with Chinese Environmental Quality Standard II for Soils (CEQSSII), urban soils in Haikou have lower metal concentrations as a whole, especially Hg, As, Cu, Pb and Zn (except one maximum) lower than the Chinese Environmental Quality Standard II (CEQSSI). These concentration levels are comparable to those in other studies, such as London, Hong Kong, Shanghai, and so on, we found that these values are lower in Haikou except Cr and Ni. Histograms of distributions of these concentrations show "double peak" or "long tailed", which may be related to soil parent material types and anthropic contributions. Pollution evaluations of single factor index and comprehensive index indicate that soils in study area are unpolluted by most heavy elements, except that Hg and Cd are medium polluted elements which should be noticed. Speciation analyses show that Zn, Ni, Cr, Cu, Pb and As are mainly in the residual and Fe-Mn oxide phases, while Hg is associated with the organic, humic and residual fractions. The high exchangeable Cd (about 24%) in urban soils need further investigation for ecological and health implications.

Keywords: Heavy metals, Urban soils, Pollution evaluation

Alteration at bentonite-cement interfaces – An experimental approach

CLAUDIA NICKEL^{1,2}, ANDRE BALDERMANN¹, MARTIN DIETZEL¹, GEORG H. GRATHOFF² AND LAURENCE N. WARR²

¹Institute for Applied Geosciences, Graz University of Technology, Rechbauerstraße 12, 8010 Graz, Austria; (claudia.nickel@tugraz.at)

²Institute for Geography and Geology, Ernst-Moritz-Arndt Universität Greifswald, Friedrich-Ludwig-Jahn-Str. 17a, 17487 Greifswald, Germany

The identification of alteration processes at the interface of clay and contacting cement is crucial for ensuring the long-term stability of underground nuclear waste repositories, i.e. the Aspö field test site (Sweden).

In order to investigate alteration features directly at the bentonite-cement interfaces, three flow-through laboratory experiments were realized. Differences in the water uptake behavior and related changes in the mineralogy and chemistry of Portland cement clinker and air-dried MX-80 bentonite were monitored using wet-cell X-ray diffraction (XRD) and transmission electron microscopy analyses, covering an experimental period of 1 year.

The water uptake rate was ~44-times higher in the clay-cement experiments than that of the pure MX-80 bentonite reference experiment, and the steady state was reached after ~22 and ~963 h, respectively. XRD data display progressive hydration of the Na-montmorillonite interlayer sites, as expressed by the stepwise increase of the water layers (WL) from 12.4 Å (1 WL) and 15.7 Å (2 WL) to 18.6-19.1 Å (3 WL). *CALCMIX* modeling of the montmorillonite revealed 65 ± 2% 3 WL and 35 ± 2% 4 WL at the steady state, suggesting complete hydration of the cement and bentonite was reached in the less altered zone. In contrast, cation exchange of Na⁺ (0.36 to 0.08 a.p.f.u.) for Ca²⁺ (0.08 to 0.12 a.p.f.u.) was recognized in the montmorillonite interlayer sites close to the clay-cement contact, corresponding with a general depletion in CaO of the contacting Portland cement by a factor of 2.5. In addition, various of original cement phases were preserved, and only minor proportions of C-S-H phases were found.

Cation exchange within the clay and the preservation of original cement phases suggests that intense alteration processes occurred at the bentonite-cement contact. The Ca for Na substitutions strongly reduced the smectites swelling pressure and inhibited the formation of stable cement phases, by quantitative removal of CaO. These processes destabilized the clay-cement buffer and need further investigation for long-term nuclear waste disposal in sustainable underground repository sites that require clay-cement sealings.

Coupled spectromicroscopic investigations for improved conceptual models of soil carbon cycling

PETER S. NICO¹, MARCO KEILUWEIT^{1,2,3}, JENNIFER PETT-RIDGE², PETER WEBER² AND MARKUS KLEBER³

¹Earth Sciences Division, Lawrence Berkeley Laboratory, One Cyclotron Rd, Berkeley CA 94720

²Chemical Sciences Division, Lawrence Livermore National Laboratory, 7000 East Avenue, Livermore CA 94550

³Crop and Soil Science, Oregon State University, Corvallis, OR 97331

Useful numeric models can only be constructed from accurate conceptual models. Biogeochemical interfaces or hotspots result from the spatial and temporal convergence of two or more different materials or processes. A comprehensive understanding of interfaces requires analytical techniques that complement each other in spatial, temporal, and elemental sensitivity. Our team has built expertise in the application of multiple (spectro)microscopic techniques to laboratory investigations of soil carbon cycling. We have sought to understand the interface between inorganic mineral phases, organic compounds, and biological organisms occurring at the micron scale. We have made particular use of synchrotron based (spectro)microscopic techniques such as SR-FTIR, STXM/NEXAFS, hard X-ray microprobe, and X-ray microtomography as well as high resolution secondary ion mass spectrometry (NanoSIMS). This presentation will include technical considerations and challenges associated with sample preparation and handling required for successful application of multi-modal imaging analysis. In addition, the specific findings from several different investigations and the associated insights will be presented. The data shown will illustrate the challenges associated with obtaining statistically robust and quantitative measurements with this approach along with its' power for improving conceptual mechanistic models.

Leucosome formation by disequilibrium melting and melt loss: Perspectives from the South Marginal Zone (SMZ) of the Limpopo Belt, South Africa

G. NICOLI^{1*}, G. STEVENS¹, J-F MOYEN², AND J. TAYLOR¹

¹Stellenbosch University, PB X1, Matieland 7602, South Africa (*correspondence: gnicoli@sun.ac.za)

²UMR 6524 CNRS, Université Jean Monnet, 23 rue du Dr Michelon, 42023 Saint-Etienne, France

This study investigates the details of the anatexis process which result in the formation of dm- to m-scale, markedly low K₂O content leucosomes during biotite incongruent melting.

Two hypotheses exist for the origin of such leucosomes; that they represent the products of fractional crystallization of plagioclase and quartz [1]; and, the redistribution of K₂O and H₂O from the segregated melt back into the residuum [2]. Evidences from metapelites in the SMZ do not support either hypothesis. The peritectic assemblage is well preserved in zones of residua adjacent to leucosomes [3]; leucosomes are characterised by strong positive Eu anomalies, whilst the gneisses from which they were derived have insignificant Eu anomalies; Na:Ca ratios in the leucosomes are similar to those in their source rocks; field-based XRF profiles of K₂O content across leucosomes and their hosting gneisses does not show substantial K₂O enrichment in the gneisses adjacent to the leucosomes. In addition, leucosomes formed by biotite + sillimanite melting are shown to have become rheologically solid prior to the occurrence of biotite melting in the absence of sillimanite at higher temperature.

These findings suggest that the leucosomes formed by biotite fluid-absent melting involving disequilibrium behaviour of plagioclase. Such a mechanism fits with the entire spectrum of field, textural and chemical data from the SMZ and open new perspectives on the role played by disequilibrium processes during S-type granite genesis. The results argue that the melt leaves the source instantaneously, that individual leucosomes are constructed incrementally; that leucosome volumes do not represent the volume of melt present at any time; and the leucosomes in such granulites constitute part of the residuum after partial melting.

[1] Brown (2002), *J. metamorphic Geol.*, **20**, 25-40. [2] Kreisman (2001), *Lithos*, **56**, 75-96. [3] Stevens and van Reenen. (1992) *Precambrian. Research*, **55**, 303-319.

Changes of magma geochemistry at Mt. Etna during the last 45ka due to sampling of a variegated mantle

EUGENIO NICOTRA^{1,2*}, MARCO VICCARO², RENATO CRISTOFOLINI² AND SANDRO CONTICELLI³

¹Università della Calabria, Via P. Bucci 15/B, 87036, Arcavacata di Rende (CS), Italy, (eugenio.nicotra@unicit.it)

²Università di Catania, Corso Italia 57, 95129 Catania, Italy

³Università di Firenze, Via G. La Pira 4, 50121, Firenze, Italy

Mt. Etna magmas show long- and short-term variations especially for K contents, some LILEs and HFSEs as well as Sr-Nd-Pb-Hf isotope ratios, a feature increasingly more evident during the last four decades of activity. Nonetheless, magma source characteristics are still debated. Contributions to this discussion arise from focusing the attention on volcanic products of Etna of the last 45 ka of activity, belonging to the “*Ellittico*” and “*Recent Mongibello*” volcanic successions. Incompatible trace elements for mantle-equilibrated compositions of the most basic products reveal that the Etnean magmas under consideration can be produced by rather low partial melting degrees of a peridotite variably enriched by metasomatic phases such as amphibole and/or phlogopite. Sr-Nd-Pb-Hf isotopes suggest that recycled and altered oceanic lithosphere is a dominant component in the Etnean mantle source. A dominant FOZO reservoir has been inferred [1], although not sufficient to satisfactorily explain the observed isotopic variations. Addition of variable proportions of an EM1-type component (up to 10%) has been then suggested. Hf isotopes provide further evidence that the enriching component at Mt. Etna could be related to the metasomatizing action of high-T fluids (i.e., silicate melts), which may be frozen in the form of pyroxenite veins at mantle conditions. Our calculations confirm that involvement of variable amounts of this enriched component in magma genesis is able to explain the long- and short-term geochemical and isotopic variations observed throughout the last 45 ka.

[1] Viccaro M., Nicotra E., Cristofolini R., Millar I.L. (2011), *Chemical Geology* 281, 343-351.

Gas geochemistry of spring waters along the Alpine Fault, NZ

S. NIEDERMANN¹, M. ZIMMER¹, J. ERZINGER¹, S.C. COX², C.D. MENZIES³ AND D.A. TEAGLE³

¹Deutsches GeoForschungsZentrum GFZ, Telegrafenberg, D-14473 Potsdam, Germany (nied@gfz-potsdam.de)

²GNS Science, Private Bag 1930, Dunedin 9054, New Zealand

³School of Ocean and Earth Science, University of Southampton, Southampton SO14 3ZH, United Kingdom

The Alpine Fault on the South Island of New Zealand is one of the longest, straightest, and fastest-moving transform faults, with oblique-slip at rates that accommodate over half of the Australia-Pacific plate motion and cause rapid uplift of the Southern Alps. No major earthquakes have occurred on the fault in historic time, but it last ruptured around 1717 AD and is thought to fail in large moment magnitude ($M_w > 7$) to possibly great ($M_w > 8$) earthquakes at ~330 yr recurrence intervals. Rocks southeast of the Alpine Fault are exhumed at rates faster than they can cool, resulting in a 63°C/km geothermal gradient, convective circulation and warm springs without related volcanic activity. Because the seismic cycle is fundamentally controlled by fluids, improved knowledge of fluid circulation in the shallow crust is paramount to understanding earthquake processes on the Alpine Fault.

In the context of the Deep Fault Drilling Project (DFDP), we have investigated gas compositions and noble gas isotopic abundances in spring waters from the vicinity of the fault. Free gas was sampled at four springs, while nine other springs provided water samples that were degassed in the lab. N₂ is commonly the most abundant gas, CO₂ concentrations vary widely from <0.1% to >96%, and CH₄ contributes up to 13%. He concentrations are up to ~500 ppm. ³He/⁴He ratios are generally highest (up to 0.81 Ra) close to the fault and decrease to radiogenic values (<0.04 Ra) towards the southeast at distances of a few kilometers from the fault, with two exceptions: Copland Spring (0.42 Ra) is located ~12 km from the fault and exhibits the highest gas flow and the highest CO₂ content of all springs studied in this work. Kotuku Spring, the only location available for sampling on the Australian plate, yields a particularly high ³He/⁴He ratio of ~3.1 Ra despite low gas flow and ~17 km distance from the fault. Obviously, mantle fluids can penetrate the thick crust beneath the Southern Alps directly at the fault and may be diverted away from it only where major passageways through the crust exist. It remains to be seen whether the high ³He/⁴He ratio of Kotuku indicates a distinct fluid origin on the northwest side of the fault in general or is just a local feature.

Calcium and Oxygen Isotope Fractionation during Precipitation of Calcium Carbonate Polymorphs

A. NIEDERMAYR^{1,2}, A. EISENHAEUER³, F. BÖHM³, B. KISAKÜREK³, I. BALZER¹, A. IMMENHAUSER¹, S.J. KÖHLER⁴ AND M. DIETZEL²

¹Institute of Geology, Mineralogy and Geophysics, Ruhr University Bochum, Germany (andrea.niedermayr@rub.de).

²Institute of Applied Geosciences, TU Graz, Austria.

³GEOMAR, Helmholtz Centre for Ocean Research Kiel, Germany.

⁴Department of Aquatic Sciences and Assessment, University of Agricultural Sciences Uppsala, Sweden.

Different isotopic systems are influenced in multiple ways and amounts by the crystal structure, surface properties, hydration and dehydration processes, deprotonation, adsorption, desorption, isotope exchange and diffusion processes. Herein we studied the structural and kinetic effects on fractionation of stable Ca- and O-isotopes during CaCO₃ precipitation in order to evaluate processes controlling their fractionation.

Calcite, aragonite and vaterite were precipitated using the CO₂ diffusion technique¹ at a constant pH of 8.3, but various temperatures (6, 10, 25 and 40°C) and precipitation rates (10^{1.5} to 10⁵ μmol h⁻¹ m⁻²).

The precipitation rate effect on fractionation of Ca-isotopes is mainly influenced by the precipitated polymorph. The calcium isotope fractionation between calcite/vaterite and aqueous Ca²⁺ increases with increasing precipitation rate. In contrast the fractionation of Ca-isotopes between aragonite and aqueous Ca²⁺ decreases with increasing precipitation rate. Hence, the influence of precipitation rate on the fractionation of calcium isotopes of aragonite is reverse compared to that of calcite and vaterite. The fractionation of ¹⁸O/¹⁶O between CaCO₃ and H₂O decreases with increasing precipitation rate. The latter behaviour is - in contrast to calcium isotope fractionation - similar for all three polymorphs.

Vaterite formation induces lower fractionation of calcium isotopes ($\Delta^{44/40}\text{Ca}_{\text{CaCO}_3\text{-aq}} = -0.10$ to -0.55 ‰) compared to calcite (-0.69 to -2.04 ‰) and aragonite (-0.91 to -1.55 ‰). In contrast the fractionation of oxygen isotopes is highest for vaterite, followed by aragonite and calcite at similar precipitation rates and temperatures. Although fractionation of oxygen isotopes is mainly dominated by temperature in our experiments with constant pH, whereas fractionation of calcium isotopes is dominated by polymorphism and kinetic processes.

¹A. Niedermayr, S.J. Köhler and M. Dietzel (2013), *Chemical Geology*, 340, 105-120.

How sandstone mineral surfaces interact with Ca^{2+} and Cl^- ions

A.R. NIELSEN*, K.N. DALBY, N. BOVET, AND S.L.S. STIPP

Nano-Science Center, Department of Chemistry, University of Copenhagen, Denmark (*skrupsax@hotmail.com)

Sandstone oil reservoirs form an important global resource. Production with the highest possible yield would extend the resources that are currently accessible with existing infrastructure and postpone the need for developing more risky deep water and high Arctic fields. Enhanced oil recovery (EOR) methods, including flooding with low salinity water, have increased oil recovery rates for sandstone reservoirs, even though the mechanisms responsible are not yet fully understood. Linking reservoir scale studies with investigations carried out at the molecular scale would increase our understanding of such mechanisms and allow EOR methods to be optimised.

In this work, we examined the change in surface composition of two natural sandstones (SS1 and SS2) and the associated extracted clay, during exposure to calcium chloride (CaCl_2) solutions at a variety of concentrations. For investigating surface uptake, we used X-ray photoelectron spectroscopy (XPS) on fast frozen samples [1]. The sandstones and extracted clay have been thoroughly characterised with X-ray powder diffraction (XRPD) and scanning electron microscopy (SEM) with energy dispersive X-ray spectroscopy (EDXS).

The ratio of Ca/Si and Cl/Si , derived from XPS spectra, show which ions stick to the surface at various Ca concentrations (Figure 1). The SS2 sandstone adsorbed more chloride than calcium, no matter what solution concentrations were used, whereas the opposite was observed for SS1. SS2 also had a higher affinity for adsorption in general than SS1. XRPD patterns confirmed a difference in mineral composition.

We are using the information about responses from natural sandstone and natural clay minerals to design model systems for determining the mechanism behind the oil release that is observed on the reservoir scale in response to low salinity water injection.

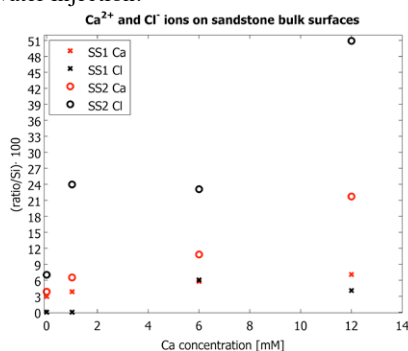


Figure 1: The ratio of Ca/Si and Cl/Si for the two bulk sandstones presented as a function of the calcium concentration of the solution.

Calcite scaling: Growth inhibition by Mg^{2+} , SO_4^{2-} and $\text{Mg}^{2+} + \text{SO}_4^{2-}$

M. R. NIELSEN*, K. K. SAND AND S. L. S. STIPP

Nano-Science Center, Department of Chemistry, University of Copenhagen, Denmark (*mia.rohde.nielsen@nano.ku.dk)

Calcite precipitation in wells, pipes, boilers and the like causes problems for industry. Effective inhibition would save huge amounts of energy and money. Magnesium (Mg^{2+}) is known to poison calcite growth [1-3], so better understanding of how it works could lead to improved scale inhibitors. It has recently been shown that adsorption of both Mg^{2+} and sulfate (SO_4^{2-}) changes calcite surface tension [4-5].

We investigated the effect of each ion singly and in combination by precipitating calcite at room temperature in a constant composition reactor [6]. Calcite precipitated at constant rate, then ions were added and the change in growth rate was monitored with time.

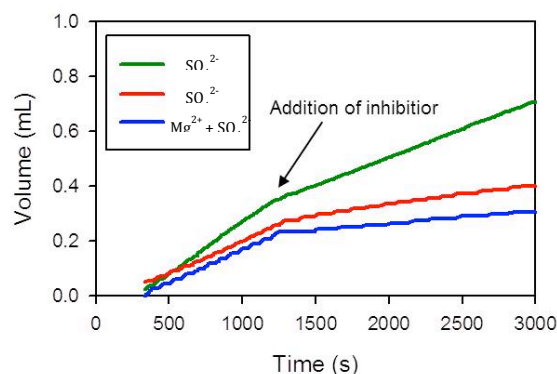


Figure 1. Typical plots for reagent addition versus time. Concentration of the inhibitors was 7.4 mM in all cases

Growth rate for pure calcite ranged from $1.8 \cdot 10^6$ to $6.0 \cdot 10^6$ $\text{mol s}^{-1} \text{m}^{-2}$, consistent with previous data. Increased Mg^{2+} concentration correlated directly with increased inhibition. Dissolved Mg^{2+} decreased with growth, suggesting incorporation into the newly formed calcite. Although there is less inhibition by SO_4^{2-} alone than Mg^{2+} alone, when the two are present together, inhibition is strongest (Figure 1).

[1] Berner (1975) *Geochim. Cosmochim. Ac.* **39**(4) 489-494. [2] Deleuze & Brantley (1997) *Geochim. Cosmochim. Ac.* **61**(7) 1475-1485. [3] Davis *et al.* (2000) *Science* **290**, 1134-1137. [4] Sakuma H. *et al.* (2013) abstract, Goldschmidt Conference, this volume. [5] Zhang, P.; *et al* *Colloid Surf. A-Physicochem. Eng. Asp.* 2007, **301**, 199. [6] Lakshtanov *et al.* (2011) *Geochim. Cosmochim. Ac.* **75**(14) 3945-3955.

Toxic effects of butyl elastomers on aerobic methane oxidation

HELGE NIEMANN¹, LEA I. STEINLE^{1,2}, JAN H. BLEES¹,
STEFAN KRAUSE², INGEBORG BUSSMANN³, TINA
TREUDE² AND MORITZ F. LEHMANN¹

¹University of Basel, Dept. of Env. Geosciences, CH
(helge.niemann@unibas.ch)

²Helmholtz Centre for Ocean Research (GEOMAR), DE

³Alfred Wegener Institute, Messtation Helgoland, DE

Large quantities of the potent greenhouse gas methane are liberated into the water column of marine and lacustrine environments where it may be consumed by aerobic methane oxidising bacteria before reaching the atmosphere. The reliable quantification of aerobic methane oxidation (MOx) rates is consequently of paramount importance for estimating methane budgets. A widely used set of methods for measuring MOx rates is based on the incubation of water samples during which the consumption of methane is monitored. Typically, incubation vessels are sealed with butyl rubber stoppers because these elastomers are essentially impermeable for gases at the relevant time scales. We tested the effect of different stopper materials (unmodified- and halogenated butyl rubber) on MOx activity. MOx rates in samples sealed with unmodified butyl rubber were > 75% lower compared to parallel incubations with halogenated butyl rubber seals, suggesting inhibiting/toxic effects associated with the use of unmodified butyl elastomers. In aqueous extracts of unmodified butyl stoppers, we detected various organic compounds including potential bactericides such as benzyltoluenes, phenylalkanes and benzothiazoles. The inhibition of MOx is most probably caused by organic contaminants that bleed off from the unmodified butyl elastomer into the incubation water.

Multidisciplinary geophysical-geochemical analysis for qualitative renovation by artificial recharge of aquifers (WARBO LIFE)

NASSER ABU ZEID¹, DANIEL NIETO^{2*}, ALESSANDRO
AFFATATO², LUCA BARADELLO², FLAVIO ACCAINO²
SALVATORE PEPI¹, SABRINA RUSSO¹ AND CARMELA
VACCARO¹

¹Dip. Fisica e Scienze della Terra, Università di Ferrara, Italy

¹OGS (Istituto Nazionale di Oceanografia e di Geofisica
Sperimentale) Borgo Grotta Gigante 42/C - 34010 -
Sgonico (TS) – Italy * (dniето@ogs.trieste.it)

Large areas of the Po Valley proximal to the delta show serious problems related to salinization of the superficial aquifers which are vital for the sustainability of the agricultural activities in the area. Since 2012 the EU life WARBO project activities regards the application of integrated direct and indirect technologies aiming at the monitoring of the possibility to enhance ground water quality in two test sites. One test site is located few km's to the south of the Po River and about 40 km on-shore the western margin of the Adriatic Sea, Northern Italy. In this area, the artificial recharge shall be initiated by flooding an existing lake formed after the termination of pre-existing quarry.

Subsurface geological and hydrogeological model of this test site have been constructed based on through analysis of existing information about surface and subsurface lithology. These were integrated by the acquisition of new geophysical data employing surface and borehole geoelectromagnetic and seismic techniques. The geophysical results helped in the definition of the geohydrogeological conceptual model. This model, together with the geochemical data, aided in the definition of the possible interactions between surface and ground water bodies. Moreover, the outcomes of the integrated analyses helped in the optimization of the monitoring network.

One of the expected results of this project is to succeed in diluting the high salinity of fossil ground water whose presence, surely, contrasts the natural recharge from the Po River. This may be possible by accumulating fresh water in the existing lake. Monitoring activities shall aid in defining the rate of salinisation attenuation in aquifers characterised by modest to low average permeability. Understanding the advantages and drawbacks of artificial recharge activities shall help in defining its usefulness or its applicability in other sites having similar characteristics.

Carbon isotope fractionation of injected CO₂ in carbonate reservoirs: Comparison of results from the laboratory and enhanced oil recovery field sites in Alberta, Canada

M. NIGHTINGALE^{1*}, B. MAYER¹, M. SHEVALIER¹
C. DALKHA¹ AND V. BECKER¹

¹University of Calgary, Calgary, Canada, T2N 1N4.

(*correspondance: night@earth.geo.ucalgary.ca)

Much of what can be surmised about the geochemical reaction of injected CO₂ when sequestered in geological formations has been gleaned from the chemical and isotopic analysis of produced fluids during CO₂ enhanced oil recovery (CO₂-EOR). Carbon isotopes of produced CO₂ have been shown to be a valuable tool for tracing the fate of injected CO₂ [1]. When CO₂ is injected into water bearing carbonate rock, carbon from four distinct sources: 1) injected CO₂, 2) in-situ CO₂, 3) dissolved inorganic carbon (largely bicarbonate) and 4) dissolution of carbonate minerals in carbonic acid, can be expected to contribute to the overall “carbon pool” and may have an impact on the equilibrium carbon isotope ratios of both the produced CO₂ and dissolved inorganic carbon (DIC). We present the results of chemical and isotopic analyses of produced CO₂ and DIC before and after the initiation of CO₂ injection at two carbonate hosted CO₂ enhanced oil recovery projects in Alberta, Canada. Results suggest carbon isotope equilibrium is established in a fashion similar to open system carbonate dissolution in shallow environments [2]. In spite of large increases in dissolved bicarbonate attributed to carbonate mineral dissolution, the equilibrium carbon isotope values of the bicarbonate appear to be controlled largely by the injected CO₂ and system temperature. Field observations were verified via a series of laboratory experiments using artificial brines and isotopically distinct CO₂ ($\delta^{13}\text{C} = -37.5\text{‰}$) and carbonate rock ($\delta^{13}\text{C} = +1.2\text{‰}$). Observed increases in dissolved calcium up to 575 mg/l, and dissolved bicarbonate up to 1500 mg/l, can be attributed to the dissolution of added calcite. The $\delta^{13}\text{C}_{\text{HCO}_3}$ of -28.1‰ at the end of the experiment demonstrates the dominance of the CO₂ and system temperature (20°C) in determining the $\delta^{13}\text{C}$ values of DIC under equilibrium conditions and the “overprinting” of the isotopic signature of the carbon contributed through calcite dissolution.

[1] Johnson *et al.* (2011), IJGGC 5, 933-941. [2] Clark, I.D. & Fritz, P. (1997) *Environmental Isotopes in Hydrogeology*. Lewis Publishers, Boca Raton, FL.

Magma sources within the Armenian territory since the Jurassic

I. NIKOGOSIAN¹, KH. MELIKSETIAN², M.J VAN BERGEN¹,
P.R.D. MASON¹ AND G. NAVASARDYAN²

¹Department of Earth Sciences, Utrecht University,
Budapestlaan 4, the Netherlands, (iniki@geo.uu.nl)

²Institute of Geological Sciences, ANA of Sciences, Yerevan,
Armenia, (km@geology.am)

The Armenian Highland forms part of the intensely deformed central segment of the Alpine-Himalayan belt, where fragments of continental blocks of Gondwanaland origin, Mesozoic Tethian island arcs and Late Cretaceous ophiolite sequences constitute a complex geological mosaic. Extensive magmatic activity between the Early Jurassic and Holocene developed under a diversity of geological regimes, ranging between rift and post-collisional settings.

We undertook a detailed geochemical and petrological study of representative, MgO-rich igneous products to explore relationships between magmatism and geodynamics in key areas of the Lesser Caucasus. Samples cover the entire Jurassic-Quaternary time interval, and include picrites, ophiolites, subalkaline and alkaline basalts, dolerites, and shoshonitic-high-K calcalkaline basalts.

Early liquidus assemblages in most of the samples virtually always include high-Fo (>88) olivine that presumably crystallized from (near-)primary mantle-derived melts. Exceptions are low-Fo olivines from the Quaternary Aragats, Gegam and partially Syunik volcanoes that probably crystallized from crust-contaminated AFC melts and/or mixtures of mantle and crust-derived (adakite-type) melts. Spinel inclusions trapped in high-Fo olivines contain variable amounts of Ti, Al, and Cr, that enable us to distinguish the nature of mantle sources involved (MORB-type, OIB-type, subduction-type).

Geochemical signatures of the parental melts were obtained for all studied samples using LA-ICP-MS analysis of melt inclusions trapped in the high-Fo olivines. A wide diversity of (near-) primary melts was found within and between distinct magmatic systems. Where partial melting and secondary effects can be ruled out, much of this variation reflects the amalgam of different mantle-lithosphere domains, which were mobilized in response to the changing geodynamic conditions that have affected the region since Jurassic times.

Multiple origins of carbon in Italian kamafugite melt

I. NIKOGOSIAN, M.J. VAN BERGEN AND S. CHANEVA

¹ Department of Earth Sciences, Utrecht University, The Netherlands (m.j.vanbergen@uu.nl)

Despite ongoing discussion on magmagenesis and geodynamic controls, there are compelling indications that small volumes of kamafugitic magma in the Intra-Appennine Volcanic Province of peninsular Italy were derived from sources that had been affected by (past) subduction of the Adriatic lithosphere. A close association with carbonatitic rocks has posed the question concerning the origin of carbon, which may have been derived from the mantle sources or from interaction with Mesozoic carbonates residing in the crust. We explored the crystallization history of olivines and their melt inclusions, separated from a representative specimen from San Venanzo, which enables us to (1) determine the primary composition(s) of mantle-derived kamafugite melt and (2) to trace the effects of crustal interaction on melt composition and magma evolution. Complex textures of olivine phenocrysts and their trace element compositions provide a framework for the sequence in which melt evolved within a single plumbing system.

Pristine core parts, characterized by high Fo_{93-90} , low CaO, (0.2-0.3 wt.%) and Cr-spinel inclusions ($Cr\# \sim 0.7$) are considered to have crystallized from primary mantle-derived melt. Compositions of melt inclusions in these cores are consistent with mantle derivation (8-12 wt.% MgO), but span a continuous range between 3 and 9 wt.% K_2O . The K-richest MI have compositions are relatively enriched in Na_2O , P_2O_5 and TiO_2 , while the K-poor endmember is characterized by very high CaO contents (up to 21 wt.%). Rim parts show a strong compositional gradient of decreasing forsterite (down to Fo_{70}) and increasing CaO (up to 1.8 wt.%). Profiles of phosphorous contents in the olivines point to steep increases in the rim parts, indicating that they originated as rapid overgrowths onto phenocryst cores. The combined signatures suggest that the rim parts crystallized from an evolved melt that was contaminated through interaction with carbonate-rich lithologies. Fluid inclusions indicate that this interaction occurred at relatively shallow crustal levels (2 – 10km).

From major and elements contents of core-hosted MI we infer that the kamafugite represents an assembly of primary melts with differentiated compositions, controlled by low-degree melt extraction from a mantle source with mineralogical variations. Our observations are consistent with a mantle source affected by siliceous K-rich and carbonate/apatite-rich metasomatic agents derived from subducted carbonate-bearing metapelites.

Modeling soil structure and nutrient dynamics using the 1D-Integrated Critical Zone Model

N. P. NIKOLAIDIS^{1*}, J. VALSTAR², E. ROWE³,
K. MOIROGIORGOU¹ AND F.E. STAMATI¹

¹Department of Environmental Engineering, Technical University of Crete, Chania 73100, GREECE

(*correspondence: nikolaos.nikolaidis@enveng.tuc.gr)

²Deltares Soil and Groundwater Systems, Utrecht, The Netherlands

³NERC Center for Ecology and Hydrology, Bangor, UK.

Model Development

Soil structure has a strong influence on the physical, chemical and biological processes that take place within the soil, and these processes can in turn influence soil structure. The aim of this work was to develop a tractable and defensible mathematical model, the 1D Integrated Critical Zone (1D-ICZ) Model, that links soil aggregate formation and soil structure to nutrient dynamics and biodiversity. Models of flow and transport (Hydrus 1D); bioturbation; Chemical equilibrium, weathering (SAFE); C/N/P dynamics and soil structure, CAST; and vegetation dynamics, PROSUM, were integrated to formulate the 1D-ICZ Model. This model can simulate and quantify the dynamics of C, N and P sequestration in soils in relation to soil structure and organic matter protection, the effects of exudates and mycorrhizae on nutrient mobilisation and acquisition, above and below ground C stocks including microorganisms, fungi and consumers, and water transformation and filtration in soils.

Model Application Results

Theoretical model simulations will be presented to illustrate the sensitivity of nutrient dynamics to dynamic changes of soil structure due to carbon amendments in the system. The inter-relationships between nutrient dynamics and soil structure dynamics will be elucidated. Soil structure and nutrient content data from cropland to set-aside land conversions will be used to validate the 1D-ICZ model. It will be shown that the 1D-ICZ model can quantify four of the most important soil functions: biomass production, C sequestration, water filtration, and biodiversity and thus be an integral component of soil Life Cycle Assessments and Ecosystem Valuation Analyses by linking inventory data to midpoint indicators for soil functions and services.

Fe³⁺ partitioning systematics between orthopyroxene and garnet in well-equilibrated mantle xenoliths

P. NIMIS^{1*}, A. GONCHAROV² AND D. IONOV³

¹ Dipartimento di Geoscienze, Università di Padova, Italy
(*correspondence: paolo.nimis@unipd.it)

² Faculty of Geology, Saint-Petersburg State University, Russia (aleksey.g.goncharov@gmail.com)

³ Université J. Monnet and UMR6524-CNRS, Saint Etienne, France (dmitri.ionov@univ-st-etienne.fr)

Ferric iron to total iron ratios in coexisting orthopyroxene and garnet from eighteen mantle xenoliths from Siberia (Udachnaya, Obnazhennaya) and Mongolia (Dariganga) were measured by ⁵⁷Fe Mössbauer spectroscopy at room temperature. The xenoliths include both coarse and sheared types and were checked for equilibrium based on textural and compositional criteria. A further check was made through cross-evaluation of thermometric estimates using internally consistent thermometers (cf. [1]). Thermobarometric estimates encompass a large P–T field (1.9–6.4 GPa; 740–1295 °C) relevant to Earth's upper mantle in both on-craton and off-craton settings. The Mössbauer data show that the partitioning of Fe³⁺ between orthopyroxene and garnet is essentially independent of the temperature of equilibration, but varies significantly with pressure. The $(\text{Fe}^{3+}/\text{Fe}_{\text{tot}})_{\text{Grt}}/(\text{Fe}^{3+}/\text{Fe}_{\text{tot}})_{\text{Opx}}$ ratio increases with pressure and is lower than unity at P < ca. 3.5 GPa and higher than unity at higher pressure. These partitioning systematics imply that thermometers based on Fe–Mg exchange equilibrium between orthopyroxene and garnet will fail at very low and very high pressure if redox conditions in the natural rocks are different from those in the experiments that were used to calibrate the thermometer. In particular, increased bulk Fe³⁺ contents due to more oxidized conditions will lead to over-estimated Opx–Grt temperatures at low P and under-estimated temperatures at high P. Conversely, decreased bulk Fe³⁺ contents due to more reduced conditions will lead to under-estimated Opx–Grt temperatures at low P and over-estimated temperatures at high P. The observed Fe³⁺ systematics may in part explain recognized inconsistencies between two-pyroxene and Opx–Grt thermometry of mantle xenoliths (cf. [1]).

[1] Nimis & Grütter (2010), *Contrib. Mineral. Petrol.* **159**, 411–427.

Dynamical and isotopic perspectives on accretion and core formation

FRANCIS NIMMO¹

¹Dept. Earth & Planetary Sciences, University of California Santa Cruz, CA 95064, USA (fnimmo@es.ucsc.edu)

Numerical modelling of accretion suggests the following characteristics: Mars-sized bodies can form fast (~1 Myr) but completing an Earth takes longer (10–100 Myr); late-stage impacts can remove (or add) material in a stochastic fashion; the “feeding zone” of a growing planet expands with time. All these characteristics can potentially be quantified using cosmochemical measurements.

Isotopic systems such as Hf–W [1], Pd–Ag [2] and Fe–Ni [3] provide constraints on the timing of core formation. The biggest challenge is to better understand the degree of mantle re-equilibration during large impacts [4]. Re-equilibration occurs at cm-scales during impacts involving Mm-scale objects; it is thus hard to model numerically, but can perhaps be better quantified via laboratory experiments [5]. The effective conditions under which core formation occurred can also be probed with stable Fe or Si isotopes, though the presence of S complicates matters [6].

The bulk compositions of planets may have been affected by late-stage removal of material [7], and spall fragments such as the Moon produced [8]. Models show that smaller surviving bodies show more variability in bulk chemistry and isotopic signatures [9]; larger bodies experience more averaging and are harder to fragment. Stochastic late impacts may be responsible for the variable amount of “late veneer” apparently added to the terrestrial planets [10].

Feeding zone expansion and the Pd–Ag [2] and I–Xe systems [11] both suggest late impactors are more volatile-rich. Later impactors may also have been more oxidized [12], but recent high-P partitioning experiments suggest this is not required [13].

Late-stage impacts probably caused several episodes of regional if not global melting. For both Earth and Mars, mantle convection subsequent to these magma ocean episodes has not been able to erase initial heterogeneities [11,14].

[1] Kleine *et al.* *GCA* 73, 2009 [2] Schonbachler *et al.*, *Science* 328, 2010 [3] Dauphas *et al.*, *LPSC* 44, 2013 [4] Daphuas & Pourmand, *Nature* 473, 2011. [5] Deguen *et al.* *EPSL* 310, 2011 [6] Shahar *et al.*, *LPSC* 44, 2013 [7] O'Neill & Palme, *PTRSL-A* 366, 2008. [8] Cuk & Stewart, *Science* 338, 2012 [9] Dwyer *et al.*, this meeting [10] Bottke *et al.*, *Science* 330, 2010 [11] Mukhopadhyay, *Nature* 486, 2012 [12] Rubie *et al.* *EPSL* 301, 2011 [13] Siebert *et al.* *Science* 339, 2013. [14] Halliday *et al.* *Space Sci. Rev.* 96, 2001.

Influence of gelatin hydrogel porosity on the formation of calcite mesocrystals

F. NINDIYASARI¹, L. FERNÁNDEZ-DÍAZ^{2,3*}, E. GRIESSHABER¹, J. M. ASTILLEROS^{2,3}, N. SÁNCHEZ-PASTOR² AND W. W. SCHMAHL¹

¹ Department für Geo- und Umweltwissenschaften, Ludwig-Maximilians-Universität München, München, Germany

² Department of Crystallography and Mineralogy, Complutense University, Madrid, Spain. (correspondence: *lfidiaz@geo.ucm.es)

³ Institute of Geoscience (CSIC, UCM), Madrid, Spain

The formation of biological hard tissues occurs in confined environments within organic matrices and involves the oriented attachment of nanoparticles. Similarities between hydrogels and organic matrices make hydrogels an adequate support for studying biomineralization. In this work the crystallization of CaCO₃ in gelatin hydrogels with solid contents ranging between 2.5 and 10 wt% was investigated at 15°C. Changes in the gelatin concentration correlated with changes in the characteristics of the CaCO₃ precipitates, with heavier hydrogels leading to smaller nucleation densities, diminishing proportions of vaterite with respect to calcite and calcite crystals showing smaller sizes, progressively rougher surfaces and more complex morphologies. Moreover, the calcite crystals grown in heavier hydrogels were identified as mesocrystals consisting in assembled nanometric basically equally-oriented rhombohedral subunits separated by small amounts of gelatine (Fig. 1a). Hydrogels with higher gelatin contents were characterized by more complex porosities, which correlated with lower ion diffusivities through the hydrogel and higher supersaturations at nucleation (Fig. 1b). These results highlight the connection between medium porosity, supersaturation and mesocrystals formation.

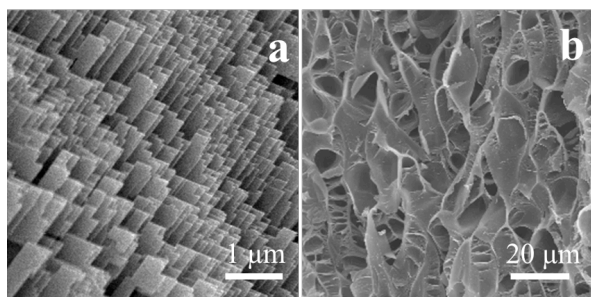


Fig 1. (a) Surface of calcite mesocrystal (10 wt% gelatine hydrogel)
(b) Porous structure of a 10 wt% gelatine hydrogel

A Modeling Framework to Predict Changes in Soil Chemistry and Agricultural Return Flow in Seawater Farming of Halophytes

*QINGQIAN NING¹, WAN ABDUL-MATIIN¹ AND FARRUKH AHMAD¹

¹Bio-Energy and Environmental Laboratory (BEEL), Water and Environmental Engineering, Masdar Institute of Science and Technology, PO Box 54225, Abu Dhabi, United Arab Emirates. (qing@masdar.ac.ae)

Growing halophyte plants using Integrated Seawater Energy and Agriculture Systems (ISEAS) offers a sustainable solution for the generation of biomass feedstock for carbon neutral biofuels; halophytes neither enter the foodchain, nor do they compete with food-crops for natural resources. One such field demonstration of ISEAS for biomass production to generate aviation biofuels, is planned for the coastal regions of Abu Dhabi, UAE, where it will likely face a number of region-specific soil chemistry and hydrogeology challenges not encountered in past demonstrations in Mexico and Eritrea. The unique soil chemistry (evaporite deposits, especially gypsum), and hypersaline coastal hydrogeology of Abu Dhabi will affect long-term halophyte agricultural productivity when Arabian Gulf seawater is applied to coastal soils as part of ISEAS. As an initial phase of the demonstration project, a salt deposition numerical modeling framework was developed to test different seawater loadings onto coastal soils. The aim of this exercise was to predict changes in irrigation return flow and soil chemistry over time in order to establish salt and water balances for sustained operation of the site. These modeling results will be further validated with laboratory lysimeter studies and with field monitoring data collected during one year of ISEAS operation. The results from this study could be used to (i) determine the optimal saline water loading correlating with peak soil salinities that selected halophytes can tolerate, (ii) potential for sodicity of the soil with saline water application, (iii) impacts of land application of saline water on underlying coastal groundwater, and (iv) develop strategies to control soil water activities in favor of halophyte agricultural productivity at ISEAS sites.

Can modern methane events and $\delta^{13}\text{CH}_4$ measurements say anything about glacial/interglacial transitions?

EUAN G NISBET¹, DAVID LOWRY¹, REBECCA E. FISHER¹,
JAMES L. FRANCE¹ AND REBECCA BROWNLOW¹

¹Dept. Earth Sciences, Royal Holloway, Univ. of London,
Egham TW20 0EX, UK. (n.name@rhul.ac.uk)

Over the past decade several major excursions, in the southern tropics, mid-latitudes and Arctic, have occurred in the atmospheric methane record. These recent growth rates, though short-lived, are comparable to those seen in the glacial-interglacial transitions. In the tropics recently, transient growth rates in excess of 10 ppb/yr have been observed, with sustained though lower growth rates through 2007-late 2012. This southern tropical event was apparently driven by increased rainfall, not directly by anthropogenic emissions as in the high CH_4 -growth events in the 1980s. A brief strong growth event occurred in the Arctic in 2007/8, while high growth in the northern mid-latitudes occurred in 2003 and again in 2009. These latter events may have been partly driven by anthropogenic inputs.

$\delta^{13}\text{CH}_4$ studies of sources and polar flights suggest that Arctic and boreal wetlands, not hydrates, have been the dominant regional summer CH_4 source in recent years. Hydrate-fed submarine plumes occur but their main near-future impact may be local ocean acidification and deoxygenation. In winter, Arctic anthropogenic emissions likely dominate. These modern changes, and their rapid fluctuations, suggest boreal and tropical wetland emissions, responding very quickly to warming or cooling, could have dominated the increase in CH_4 at glacial terminations. Modern Atlantic transects and observations also show the importance of distinct air masses in shaping the annual average record.

Temperature effects on cathodoluminescence of calcite

H. NISHIDO¹, S. NISHIZAWA¹ AND N. KUSANO¹

¹Department of Biosphere-Geosphere Science, Okayama
University of Science, 1-1 Ridai-cho, Okayama 700-0005,
Japan (correspondence: nishido@rins.ous.ac.jp)

Cathodoluminescence (CL) of calcite has been extensively investigated by many researchers, and used for a wide range of geoscientific applications. The CL features are affected by many factors such as activator, sensitizer and quencher of transition metal elements. However, the temperature effects on calcite CL have not been precisely clarified so far. In this study we have quantitatively evaluate temperature quenching effects on calcite CL with various activator concentrations.

Six calcite samples with Mn concentrations of 13, 129, 1259, 3520, 9170, 66500 ppm were selected for CL spectral measurements at various temperatures from $-190\sim 25\text{ }^\circ\text{C}$.

CL intensity of low-Mn calcite increases with an increase in sample temperature, but the intensity of medium-Mn calcite shows almost unchangeable at a wide range of temperature. In contrast CL intensity of high-Mn calcite decreases with increasing temperature. These facts imply that temperature effects on calcite CL depend on activator concentrations in calcite, whereas luminescence efficiency generally decreases with rising temperature due to an increase in non-radiative transitions, which has been known as temperature quenching.

A least-square fitting of the Arrhenius plot by assuming a Mott-Seitz model provides an activation energy of 0.04~0.07 eV for high-Mn calcite in a temperature quenching process. These values correspond to lattice vibration energy, suggesting that the energy of non-radiative transition might be transferred to lattice as phonon. The result leads that activator (Mn ion) concentration considerably affects temperature quenching effect on CL of calcite.

***In situ* observation of dehydration and incongruent dissolution of Serpentine (Antigorite) into aqueous fluids**

RYO NISHIZAKI AND TATSUHIKO KAWAMOTO¹

¹ Inst. Geothermal Sci., Graduate School of Science, Kyoto Univ. Kyoto 606-8502, Japan (ryo.nishizaki@gmail.com)

Serpentine plays important roles as triggering earthquakes through its dehydration and controlling the rheological coupling between slab/mantle. We heated a natural polycrystalline antigorite ($\text{Mg}_{51}\text{Si}_{36}\text{O}_{90}(\text{OH})_{66}$) in H_2O in the Basset-type externally heated diamond anvil cell [1]. During 600–620°C, we observed that antigorite slightly dissolved into aqueous fluids and then forsterite started crystallizing under a pressure range from 0.27 to 0.64 GPa. The forsterite grew up to about 30 μm across in an hour. According to the previous studies, a dehydration reaction of antigorite = forsterite + talc + H_2O [2] can occur under the present experimental conditions. Nevertheless, talc was not found in our experiments during 1–4 hours. The experimental duration may be too short for antigorite to dehydrate and nucleate talc. Alternatively our observation indicates that antigorite dissolves incongruently into aqueous fluids at the dehydration reaction in the presence of aqueous fluids.

Takahashi *et al.* [3] conducted shear-sliding tests on antigorite gauge at temperature higher than the stability of antigorite under constant pore water pressure of 30MPa at confined pressure of 0.1GPa. They observe forsterite using SEM and trace amounts of talc using XRD in shear-localized zones. The incongruent dissolution of antigorite in our experiments can explain that the dehydration of antigorite forms forsterite, which can cause strengthening and embrittlement of the gouge even at constant pore water pressure. The talc-dissolved aqueous fluids can be silica-rich, and such fluids can migrate upwards to precipitate talc in the plate boundary [4].

[1] Bassett *et al.* (1993) *Rev. Sci. Instrum.* [2] Evans *et al.* (1976) *Schweiz. Mineral. Petrogr. Mitt.* [3] Takahashi *et al.* (2011) *J. Geophys. Res.* [4] Hirauchi *et al.* (2013) *Geology*

Physiological and isotopic characteristics of nitrogen fixation by hyperthermophilic methanogens: Implication for nitrogen anabolism of the seafloor microbial communities on the early Earth

MANABU NISHIZAWA¹, JUNICHI MIYAZAKI^{1,2}, AKIKO MAKABE³, KEISUKE KOBAYASHI³, AND KEN TAKAI^{1,2}

¹ Precambrian Ecosystem Laboratory, JAMSTEC (e-mail: m_nishizawa@jamstec.go.jp)

² SUGAR Program, JAMSTEC

³ Tokyo University of Agriculture and Technology

Hyperthermophilic hydrogenotrophic methanogens are considered to represent one of the most important classes of primary producers in hydrogen (H_2)-abundant hydrothermal environments throughout the history of Earth. Despite extensive studies of methanogenesis, comprehensive research on nutrient anabolism in hyperthermophilic methanogens is limited. This study first investigated the physiological properties and isotopic characteristics of experimental cultures of hyperthermophilic methanogens during the fixation of dinitrogen (N_2), an abundant but less-bioavailable compound in hydrothermal fluids. We found that these hyperthermophilic methanogens actively assimilated N_2 via molybdenum (Mo)-iron (Fe) nitrogenase under broad ranges of Mo and Fe concentrations relevant to present and past oceanic and hydrothermal environments. Furthermore, the methanogens produced more ^{15}N -depleted biomass than that previously reported for diazotrophic photosynthetic prokaryotes. These results indicate that diazotrophic methanogens can be broadly distributed in seafloor and subseafloor hydrothermal environments, where the availability of the transition metals is variable and organic carbon and nitrogen compounds and ammonium are extremely scarce. This perspective may provide key clues to understanding the geological and evolutionary history of the global nitrogen cycle if the nitrogen isotopic ratios of organic matter in the geological records associated with seafloor and subseafloor hydrothermal activities are linked to the potential functions of diazotrophic hyperthermophilic methanogens. The possible emergence and function of diazotrophy coupled with methanogenesis 3.5 billion years before the present may be inferred from the nitrogen and carbon isotopic records of kerogen and fluid inclusions from hydrothermal deposits.

Acid water problem: Mining districts from Tuscany (central Italy)

B. NISI^{1*}, B. RACO¹, O. VASELLI², T. ABEBE³,
R. BATTAGLINI³, G. MASETTI¹, F. TASSI², M. LELLI¹
AND M. DOVERI¹

¹CNR-IGG Institute of Geosciences and Earth Resources, Via Moruzzi 1, 56124, Pisa, Italy; (*correspondence: b.nisi@igg.cnr.it; b.raco@igg.cnr.it; masetti@igg.cnr.it; m.elli@igg.cnr.it; m.doveri@igg.cnr.it)

²Department of Earth Sciences; Via G. La Pira 4, 50121 Florence, Italy; (oraldo.vaselli@unifi.it; franco.tassi@unifi.it)

³MASSA spin-off, largo G. Novello 1c, 50126, Florence; Italy; (t.abebe@massaspinoff.com; r.battaglini@massaspinoff.com)

Acid mine drainage (AMD) is a major source of water contamination in metal- and coal-mining districts worldwide. AMD is a natural consequence of mining activity where the excavation of mineral deposits (metal bearing or coal), below the natural groundwater level, exposes sulphur-bearing compounds to atmospheric O₂ and water. The most common reactions that lead to the production of AMD involve the chemical and biological oxidation of metal sulfides contained in mine waste heaps, active or abandoned mine workings, or in tailings piles left over from the processing of sulfide ores. Chemicals used for treating AMD after formation are hydrated lime, pebble quicklime, caustic soda, soda ash briquettes, and ammonia. Each chemical reacts differently with a specific AMD. Therefore, it is essential that each AMD source has been treated and evaluated chemically/physically to determine which is most environmentally sound, efficient and cost effective. In this study a geochemical survey of mine waters discharging in the main mining districts of Tuscany (central Italy) was carried out to establish their geochemical features to provide information on AMD processes at mining-impacted sites in order to supply a background information necessary to the scientists responsible for assessing remediation technologies.

The composition of Mercury's crust from MESSENGER observations

LARRY R. NITTLER^{1*}, SHOSHANA Z. WEIDER¹
AND SEAN C. SOLOMON²

¹Carnegie Institution of Washington, Washington DC 20015 USA (*lnittler@ciw.edu)

²Lamont-Doherty Earth Observatory, Columbia University, Palisades, NY 10964, USA

The MERCURY Surface, Space ENVIRONMENT, GEOchemistry, and Ranging (MESSENGER) spacecraft has returned a wealth of data since it began orbiting the innermost planet more than two years ago. Imaging observations reveal a surface shaped by widespread volcanism that produced both flood lavas and pyroclastic deposits [1]. Geochemical measurements from X-ray and gamma-ray spectroscopy show Mercury's crust to be chemically distinct from those of the other terrestrial planets and rich in volatile elements [2-4]. Mg/Si ratios are generally higher, and Al/Si and Ca/Si ratios lower than typical crustal materials on other planets; there is no evidence for a lunar-like, feldspar-rich crust. The abundance of sulfur is surprisingly high (~1-4 wt %), which most likely indicates that Mercury formed under highly reducing conditions, and is consistent with the low total surface Fe abundance (1-2 wt %) [4,5]. Correlations between Mg/Si, Ca/Si, and S/Si suggest that MgS and CaS are important crustal minerals. The average K/Th ratio and Na abundance are similar to those of other terrestrial planets, ruling out some high-temperature models of Mercury's formation. The high abundance of volatiles likely plays a key role in the formation of "hollows", enigmatic shallow depressions observed only on Mercury [6]. Substantial chemical heterogeneity is also observed [7,8]: high-reflectance smooth volcanic plains are, on average, enriched in Al, Na, and K and depleted in Mg, Ca, and S, relative to older, darker terrains. The observed compositional variations most likely reflect intrinsic differences in the magmas that produced the surface materials, as well as possible thermal redistribution of K and Na from hot surficial regions to colder ones. The Fe abundance also appears to be heterogeneous on 1000-km scales and is uncorrelated with other elements [5].

- [1] Head J. W., *et al.* (2011) *Science*, **333**, 1853-1856.
[2] Nittler L. R., *et al.* (2011) *Science*, **333**, 1847-1850.
[3] Peplowski P. N., *et al.* (2011) *Science*, **333**, 1850-1852.
[4] Evans L. G., *et al.* (2012) *JGR*, **117**, E00L07. [5] Weider S. Z., *et al.* (2013) *LPSC*, **44**, abstract 2189. [6] Blewett D. T., *et al.* (2011) *Science*, **333**, 1856-1859. [7] Weider S. Z., *et al.* (2012) *JGR*, **117**, E00L05. [8] Peplowski P. N., *et al.* (2012) *JGR*, **117**, E00L04.

Arsenic mobility in limestone and fertiliser-amended tailings

TARYN L. NOBLE^{1,3} AND BERND G. LOTTERMOSER^{2,3}

¹School of Earth Sciences, University of Tasmania, Private Bag 79, Hobart, 7007, TAS (Taryn.Noble@utas.edu.au)

²Environment and Sustainability Institute, University of Exeter, Cornwall Campus, Penryn, Cornwall, TR10 9EZ, UK (B.Lottermoser@exeter.ac.uk)

³Cooperative Research Centre for Optimising Resource Extraction (CRC ORE), Australia

Remediation of acid rock drainage (ARD) through the addition of limestone results in the removal of deleterious metals (e.g. Cd, Cu, Pb) from solution, by mineral precipitation and adsorption reactions as the pH increases. However, arsenic (As) can be mobilised under neutral to alkaline pH conditions due to desorption reactions from different mineral surfaces. Also, the mobility of As is complicated by fluctuations in redox chemistry as well as As desorption in the presence of competitive anions. We investigated the mobility of As at a historic cassiterite tailings deposit (Royal George, Tasmania), where recent remediation efforts by statutory authorities included the application of crushed limestone and phosphate fertiliser pellets to the tailings surface.

Scorodite and iron oxide phases were identified to be the main As-host phases in non-amended tailings. Leaching experiments using different extraction solutions were conducted on amended and non-amended tailings. Results show that As mobility was considerably reduced in near neutral pH, low sulphate extraction solutions for both amended and non-amended tailings. However, a significant proportion of As was mobilised in the amended tailings relative to non-amended tailings, when extraction solutions with high sulphate concentrations were used. Since high dissolved sulphate (>1000 mg/L) waters are present in ARD environments, the application of phosphate fertiliser, in addition to limestone as an amendment strategy, may mobilise As from waste rocks and tailings in the long term. Rehabilitation efforts of As-rich wastes need to consider both the mineralogical siting of As and porewater chemistry.

Trace Element and Isotope Geochemistry of Cretaceous Basalts from Axel Heiberg Island, Arctic Canada

INÊS G. NOBRE SILVA^{1*}, VICTORIA PEASE¹
AND GEORGE MORRIS²

¹Dept. of Geological Sciences, Stockholm University, SE-106 91, Stockholm, Sweden (*inobre@geo.su.se)

²Geological Survey of Sweden, Box 670 SE-751 28 Uppsala

Cretaceous volcanic rocks related to the High Arctic Large Igneous Province (HALIP) in the Canadian Arctic Islands comprise dykes, sills and lava flows emplaced within the Sverdrup Basin. During an expedition to northwestern Axel Heiberg Island in the summer of 2007, a suite of 114 - 130 Ma basaltic rocks was recovered from the Bukken Fiord region. We present the first geochemical study on 11 of these basalts, including isotopic compositions by MC-ICP-MS (Pb) and TIMS (Sr and Nd).

All samples are tholeiitic. They cover a narrow range of MgO (3.2 to 7 wt%) and SiO₂ (45 to 54 wt%) contents and have high TiO₂ contents that range from 2 to 4 wt%. Trace element ratios of immobile, alteration resistant elements (e.g., Th/Nb, Th/Ta, La/Yb, Zr/Y, Nb/Y) suggest interaction and incorporation of crustal material by an enriched mantle source. The preliminary isotopic compositions of these basalts also support contamination by a crustal component. This is evidenced by their high ⁸⁷Sr/⁸⁶Sr (0.7036 to 0.7084), ²⁰⁶Pb/²⁰⁴Pb (18.5 to 19.1) and ²⁰⁸Pb/²⁰⁴Pb (38.2 to 38.9) values despite the acid leaching treatment prior to isotopic analyses to remove the disturbance effects of post-magmatic alteration.

Additional isotopic analysis will further constrain the mantle-crustal components involved in the formation of these basalts and the extent of contamination or assimilation. Integration of these new data with prior HALIP studies will contribute to a better understanding of Cretaceous magmatism during the opening of the Canada Basin.

XAS crystal-chemistry of Fe in mangrove sediments from New Caledonia. Implication for iron biogeochemical cycling

V. NOËL^{1,3*}, C. MARCHAND², F. JUILLOT^{1,2}, G. ONA-NGUEMA¹, G. MARAKOVIC³ AND G. MORIN¹

¹IMPMC, Université Pierre et Marie Curie, 75005 Paris, France (*correspondence: Vincent.Noel@impmc.upmc.fr, Farid.Juillot@ird.fr, Georges.Ona-Nguema@impmc.upmc.fr, Guillaume.Morin@impmc.upmc.fr)

²IRD, 98848 Noumea, New Caledonia (Cyril.marchand@ird.fr)

³KNS, 98860 Kone, New Caledonia (GMarakovic@koniambonickel.nc)

Mangrove forests are the dominant intertidal ecosystem of tropical coastlines and play a fundamental role in the ecological balance of these areas. They strongly influence the transfer of trace metals between land and sea. In New Caledonia, mangroves act as a buffer zone between massive Fe lateritic deposits and a lagoon registered as an UNESCO World Heritage site. Mangroves are composed of different stands, each dominated by a botanical species. Mangrove zonation mainly results from difference in soil elevation, and length of tidal immersion, and induces different ecosystem productivity, and redox conditions {1}. As a consequence, it may be responsible for differences in sediment geochemistry, and thus differences in metal speciation and bioavailability {2}.

In the present study, we have determined the distribution and speciation of iron in mangrove sediments in relation with organic content, redox, salinity and botanical gradients. Chemical and mineralogical analyses of mangrove sediment core samples were complemented by direct speciation of Fe using EXAFS spectroscopy. The results obtained show that crystal-chemistry of Fe strongly follows the marked change in sediment redox conditions that range from oxic in surface horizons to anoxic in deep horizons. The Fe-bearing minerals (mainly goethite, with minor amounts of Fe-phyllsilicates) are major phases in the upwards horizons and are inherited from lateritic, then progressively disappear from the surface horizons towards deepest horizons where pyrite forms.

{1} Marchand (2012) *Chemical Geology* 300-301, 70-80. {2} Otero (2009) *Geoderma* 148, 318–335.

Back to basics: Boron isotopic fractionation in synthetic calcite and aragonite

J. NOIREAUX^{1*}, V. MAVROMATIS², J. SCHOTT², J. GAILLARDET¹, V. MONTOUILLOUT³, P. LOUVAT¹ AND D. R. NEUVILLE¹

¹IPGP, Univ Paris Diderot, Paris, France, (*correspondence: noireaux@ipgp.fr)

²GET, Univ Paul Sabatier, Toulouse, France

³CNRS-CEMHTI UPR3079, 45071 Orléans France

Boron isotopic fractionation in marine carbonates, such as foraminifera and corals, is dependent on the pH of the seawater in which they form, allowing boron isotopes to be used as a proxy of the ocean-pH. The pH-dependency of the boron isotopic composition in organic calcium carbonates has been confirmed in laboratory environment. This behavior of boron isotopes is classically explained by the incorporation of the borate ion from seawater, whose isotopic composition is a function of its abundance and hence of pH. Modern biologically-precipitated calcium carbonates however display widely spread boron isotopic compositions which can be partially explained by vital effects but do not fit the simple model of preferential incorporation of the borate ion.

In order to better understand the mechanisms responsible for boron isotopic fractionation in calcium carbonates, we precipitated, in laboratory, inorganic calcite, Mg-calcite and aragonite over a wide pH range and performed both isotopic and ¹¹B MAS NMR (Magic Angle Spinning Nuclear Magnetic Resonance) analyses on the solids. Results show that, although $\delta^{11}\text{B}$ rises with pH for all crystal types, calcite and Mg-calcite display a smaller fractionation (more marked for calcite) with respect to the precipitation solution and a much lesser sensitivity to solution pH than expected. NMR spectra show almost exclusively tetrahedral boron in aragonite but highly variable proportions of trigonal and tetrahedral boron in calcite. We therefore suggest that both borate ion and boric acid are incorporated in calcite and Mg-calcite and that boron is present in both crystalline and non-crystalline sites whereas in aragonite the borate ion is the dominant species, representing over 90% of the total boron. These results overall suggest that aragonite-based calibrations should be favoured in future paleo-pH reconstructions. Calcite-based calibrations require a rigorous characterization via NMR spectroscopy of boron speciation and site occupancy in the crystals.

Impact of calcite precipitation on flow alteration in porous media

CATHERINE NOIRIEL¹, CARL I. STEEFEL², LI YANG² AND DOMINIQUE BERNARD³

¹Géosciences Environnement Toulouse, Université Paul Sabatier, CNRS, IRD, 14 av. Edouard Belin, F-31400 Toulouse, (catherine.noiriel@get.obs-mip.fr)

² Earth Sciences Division, Lawrence Berkeley National Laboratory, Berkeley, CA 94720, (CISteeffel@lbl.gov, lyang@lbl.gov)

³Institut de Chimie de la Matière Condensée de Bordeaux, CNRS, 87, av. du Dr Schweitzer F-33608 Pessac, (bernard@icmcb-bordeaux.cnrs.fr)

One of the major challenges associated with sequestration of carbon dioxide, given the complexity and range of coupled thermal, hydrological, mechanical, and chemical processes involved, is the understanding of geochemical reactivity in the case of long-term sequestration. Mineral trapping involves precipitation of minerals like calcite, which can cause a significant reduction in permeability of reservoirs by altering the shape, size and connectivity of the pores, the roughness of their surface, or by plugging the pore throats.

The effects of calcite precipitation in porous media are evaluated through an experimental and modeling study. Two experiments using cylindrical core packed with glass beads and calcite (Iceland spar) or aragonite (Bahamas ooids) were injected with a supersaturated mixture of CaCl_2 and NaHCO_3 to induce calcite growth. Bulk rates of precipitation based on the change in aqueous chemistry over the length of the columns are compared with spatially resolved determinations of carbonate precipitation using X-ray synchrotron microtomography with a resolution of $4.46 \mu\text{m}$. The new crystals are shown to be very different according to the initial mineral surface on which they grow. Results are compared in terms of growth rate, crystal shape, surface area and pore roughness. The impact of crystal distribution on roughness increase and on pore scale flow and permeability is evaluated through numerical modeling. The results are compared with results for several model porous media for which different crystal growth rates were implemented. The effect of differing calcite growth rate laws and surface roughness are compared for cases in which the total porosity change is comparable.

Ten years of ground deformations monitored by the ground-based SAR system on Stromboli volcano and its use in forecasting intense volcanic activity

TERESA NOLESINI¹, FEDERICO DI TRAGLIA^{1,2}, EMANUELE INTRIERI¹, FEDERICA BARDI¹, FEDERICA FERRIGNO¹, SARA FRANGIONI¹, WILLIAM FRODELLA¹, CARLO TACCONI STEFANELLI¹, LUCA TANTERI¹, CHIARA DEL VENTISETTE¹ AND NICOLA CASAGLI¹

¹Dip. Scienze della Terra, Università di Firenze, Via La Pira 4, Firenze

²Dip. Scienze della Terra, Università di Pisa, Via Santa Maria 53, Pisa

A Ground Based Interferometric Synthetic Aperture Radar (GBInSAR) system has been installed on Stromboli Volcano since 2003, when on the 30 December 2002, after a major eruption a subsequently large landslide occurred on the NW flank (Sciara del Fuoco, SdF) of the volcano. This GBInSAR is a remote sensing technique based on microwaves interferometry that permits the production of 2D displacement maps, called interferograms, with millimetre precision. The apparatus installed on Stromboli, exploits a metric spatial resolution and acquisition frequency of about 11 min. Only the component of the displacement vector to parallel to the line of sight can be assessed.

The investigation conducted by analysis of the GBInSAR data, has permitted to divide the crater area and the SdF area in five different sectors, to better analyze and understand the behaviour of the volcano flank dynamics.

The GBInSAR installed at Stromboli volcano has been used as a remarkable early-advice tool for mass and gravitative movements on the Sciara del Fuoco. GBInSAR monitoring highlights different deformation patterns, related to the imminent new vent openings. The analysis of the displacement rates in the summit crater area has been used as early warning signal before the occurrence of major explosions and lava emission. Changing in displacement rate registered by the GBInSAR system in the upper part of the volcano, corresponding to the external flank of the summit craters and at the base of the summit area, has been used to forecast the change in the pressure conditions in the shallow plumbing system and the lateral propagation of the conduit-dike system of Stromboli volcano.

Low core-mantle boundary temperature inferred from the solidus of pyrolite

R. NOMURA^{1*}, K. HIROSE^{1,2,3}, K. UESUGI⁴, Y. OHISHI⁴
AND A. TSUCHIYAMA⁵

¹Tokyo Institute of Technology (Titech), Tokyo 152-8551, Japan (*correspondence: nomura.r.ab@m.titech.ac.jp)

²Earth-Life Science Institute/Titech, Tokyo 152-8551, Japan

³IFREE/JAMSTEC, Kanagawa 237-0061, Japan

⁴JASRI/SPring-8, Hyogo 679-5198, Japan

⁵Kyoto University, Kyoto 606-8501, Japan

The solidus of a pyrolite-like composition plays a fundamental role for understanding structure and evolution of the deep Earth, such as temperature profile in the lowermost mantle and melting in the early Earth. Fiquet *et al.* [1] determined the solidus of a pyrolitic composition up to 120 GPa with X-ray diffraction (XRD) measurements using laser-heated diamond anvil cell techniques (LH-DAC). They identified melting by the disappearance of Debye rings of CaSiO₃-rich perovskite and/or ferropericlase, however, this melting criteria has a potential to overestimate the solidus temperature due to high temperature gradient along X-ray transmitted axis in LH-DAC.

Solidus temperatures of pyrolitic mantle material were determined by discerning a melting texture from synchrotron dual-energy three-dimensional micro-tomographic images measured at BL47XU of SPring8 [2]. The melting was identified by the existence of (a) round-shaped and (b) iron-enriched region at the hottest part of the sample. The measured solidus temperature of the pyrolitic material was 3700 K at 135 GPa, which is extensively lower than that of 4200 K at 135 GPa measured by XRD [1]. Since seismic observations suggest that melting of the current lowermost mantle is very localized [3], the solidus of pyrolite set an upper limit to the present temperature at core-mantle boundary below 3700 K.

The subsolidus phase assemblage and the phase transition boundary between MgSiO₃-rich perovskite and post-perovskite were also determined near the solidus temperature on the basis of high *P-T* XRD measurements in LH-DAC.

These results have great significance for understanding temperature profile in the lowermost mantle and melting in the early Earth such as volume of basal magma [4] remnants, since these remnants should have lower solidus temperature than that of pyrolite.

[1] Fiquet *et al.* (2010) *Science* **329**, 1516-1518. [2] Tsuchiyama *et al.* *GCA in press*. [3] Williams & Garnero (1996) *Science* **273**, 1528-1530. [4] Labrosse *et al.* (2007) *Nature* **450**, 866-869.

A practical constraint on entrainment and condensate evaporation and from aircraft and satellite observations of isotope ratios of water

DAVID NOONE¹

¹Department of Atmospheric and Oceanic Sciences and Cooperative Institute for research in Environmental Sciences, University of Colorado, Boulder, CO, 80309-USA (*correspondence: dcn@colorado.edu)

Convective clouds play a significant role in the moisture and heat balance of the tropics. The dynamics of organized and isolated convection are a function of the background thermodynamic profile and wind shear, buoyancy sources near the surface and the latent heating inside convective updrafts. The stable oxygen and hydrogen isotope ratios in water vapour and condensate can be used to identify dominant moisture exchanges and aspects of the cloud microphysics that are otherwise difficult to observe. Aircraft observations show that there is significant disequilibrium between the cloud core and the ambient environment, which allows an estimate of exchange at cloud boundaries that lead to condensate evaporation. Indeed, the mechanisms for condensate evaporation gives a basis for using satellite profiles of D/H isotope ratios to yield estimates of the rate of moistening of the troposphere above the boundary layer. In the western tropical Pacific and over tropical continents in excess of 60% of condensate evaporates into the environment, and is the principal moisture source for tropospheric water. The success of the calculation relies on both an adequate parameterization of the mechanisms driving the water budget, and the use of isotope ratio data to satisfactorily constrain the parameters. The unique information on moisture history provided by the isotope ratio measurements allows assessment of moisture transport that is not otherwise easily observed.

Au mineralization and its relationship with shear zones in senjedeh gold deposit

ZAHRA NOORIAN RAMSHEH* AND MOHAMMAD YAZDI

Department of Geology, Shahid Beheshti University, Tehran Iran* (zn5562@yahoo.com)

Senjedeh gold deposit is located in middle part of the Sanandaj-Sirjan zone, central Iran. It consists of several gold deposits such as Chah-katoom, Dareh Ashky and Senjedeh. Lithological and stratigraphic investigations show that the geological units in this area include metamorphic rocks (different facies of greenschist to amphibolite schist), silicified and mineralized veins and granitic intrusions. These series have been deformed in effect of tectonic alternating phases and lost their primary sequence and order during late Cretaceous-Tertiary continental collision between the Afro-Arabian and the Iranian micro continent. As a result of these tectonic activities, different rock fabric has been formed. Based on structural studies, major tectonic structure in this area is shear zones. According to oriented sample studies, some of the fabric features related to shear zone. Ore-mineral assemblages mainly include pyrite and chalcopyrite. Gold mineralization in Senjedeh area occurred in relation to hydrothermal alterations in metamorphic units during to normal faulting. The pervasive alterations in this area are silicification and sulfidation which are responsible of gold mineralization. The field and petrographic studies show a direct relationship between structures and gold mineralization. The petro fabric studies and correlation mineralization direction show that Senjedeh Gold deposit can be an example of orogenic gold deposit in Iran.

Key words: Senjedeh gold deposit, shear zone, Sanandaj-Sirjan zone

Structure-property relationship of Na/Ca silicate liquids under pressure by molecular dynamics simulation

FUMIYA NORITAKE¹* AND KATSUYUKI KAWAMURA¹

¹ Okayama University, Okayama, 700-8530, Japan.

(*Correspondence: f.noritake@s.okayama-u.ac.jp)

Peculiar behaviours of physical properties of silicate liquids under high pressure are long standing issue in high pressure earth science. For instance, it is well known that shear viscosities of acidic silicate liquids decreases with increasing pressure [1, 2]. In order to explain the softening of silicate liquids at high pressure, several mechanisms have been proposed by various researchers [1, 3]. To investigate the relationship between structure and properties of silicate liquids, we apply the molecular dynamics method to obtain precise information on structures of silicate liquids under high pressure.

Molecular dynamics simulations of $\text{Na}_2\text{O}\cdot n\text{SiO}_2$ and $\text{CaO}\cdot n\text{SiO}_2$ liquids were performed using the MXDORTO code. The simulated pressure range is from 0.1 MPa to 6 GPa with NPT ensembles and the potential model which well reproduces structures various silicate crystals [4].

In the compression, Si-O and M-O distance remains constant, however Si-Si distances shorten and coordination numbers of O atoms around M atom increase. Adding to those, 3 and 4 membered rings in -Si-O- network decrease with increasing pressure. Those suggest that densification of silicate liquids consist of increasing of flexibility of -Si-O- network, bending of Si-O-Si and increase of coordination number of M atoms. Up to 6 GPa, the decrease of Si-O-Si angle and distortion of SiO_4 tetrahedra in acidic silicate liquids ($n < 3$) are obviously confirmed. Decrease of Si-O-Si angle by densification causes distortion of SiO_4 tetrahedra and weakening of Si-O bonding [5]. These structural change might cause the softening of silicate liquids under high pressure. Differences between Na and Ca was observed in structure, properties and behaviours of those at high pressure.

[1] Kushiro (1976), J.G.R. **81**, 6347-6350, [2] Scarfe *et al.* (1979) Y.B.Carnegie Inst. Wash. **78**, 547-551. [3] Xue *et al.* (1989) Science **275**, 962-964, [4] Noritake *et al.* (2012) J.Non-cryst. Sol. **358**, 3109-3118. [5] Newton and Gibbs (1980), Phys. Chem. Minerals **6**, 221-246.

Montmorillonite colloid size heterogeneity – Fractionation and Characterization

K. K. NORRFORS^{1*}, M. BOUBY², S. HECK², N. FINCK², R. MARSAC², T. SCHÄFER² AND H. GECKEIS², S. WOLD¹

¹Department of Chemistry/Applied Physical Chemistry, KTH Royal Institute of Technology, Teknikringen 30, SE-100 44 Stockholm, Sweden (*correspondence: norrfors@kth.se, wold@kth.se)

²Institute for Nuclear Waste Disposal (INE), Karlsruhe Institute of Technology (KIT), P.O. Box 3640, D-76021 Karlsruhe, Germany (muriel.bouby@kit.edu, stephanie.heck@kit.edu, nicolas.finck@kit.edu, remi.marsac@kit.edu, thorsten.schaefer@kit.edu, horst.geckeis@kit.edu)

Highly compacted bentonite is planned to be one component of the engineered barrier system in many spent nuclear fuel final repository designs. The potential release of montmorillonite colloids, acting as carriers, may enhance the transport of radionuclides in case of a leaching canister. During transport, size exclusion/filtration may occur, resulting in migration of specific size fractions only. Therefore, it is necessary to determine the size heterogeneity of the mobile bentonite clay colloid and its radionuclide association.

In this study, unpurified MX-80 bentonite consisting mainly of smectite with impurities of quartz, plagioclase, orthoclase, muscovite as well as calcite/dolomite, gypsum and pyrite, was sedimented in low ionic strength carbonated synthetic ground water (SGW) at 10g/L. Thereafter, seven colloidal suspensions of various size fractions were obtained by sequential and direct centrifugation. Their particle size distributions were measured by PCS and AsFIFFF/UV-Vis/LLS/ICP-MS. The concentrations of colloids and other elements present in the suspensions were measured by IC and ICP-OES. The mineralogical composition was analyzed by XRD.

The mean particle size is decreasing with the number of fractionation steps, from ~500 down to ~50 nm. The presence of predominantly montmorillonite colloids is confirmed by: i) XRD results, for all colloidal fractions and ii) the Si/Al and Al/Mg mole ratios. There is an instant release of Na and SO₄²⁻ to the SGW while adding the bentonite indicating the dissolution of accessory minerals and cation exchange processes. An increasing release of natural ²³⁸U with decreasing size fractions (i.e. larger exposed surface area) is evidenced. The results are discussed with respect to the implication on radionuclide speciation and transport.

Activities and volatilities of trace components in CaO-MgO-FeO-Al₂O₃-SiO₂ melts

C.ASHLEY NORRIS AND BERNARD J.WOOD

University of Oxford, U.K.,
(ashley.norris@earth.ox.ac.uk;berniew@earth.ox.ac.uk)

Knowledge of the activities of trace components in silicate melts is extremely important for addressing such problems as (a) degassing in volcanic systems (b) volatilities in protoplanetary systems and (c) the effect of melt composition on trace element partitioning. Nevertheless these activities are very difficult to measure by conventional phase equilibrium techniques except under circumstances where the metallic element is stable in a readily accessible f_{O_2} range¹. We have modified the “metal-saturation” approach by measuring the partitioning of a large number of elements (V, Cr, Cu, Zn, Ga, Ge, Mo, Ag, Cd, In, Sn, Sb, W, Tl, Pb and Bi) between liquid Fe alloys and liquid silicate at 1.5 GPa and 1650°C. The data provide activity coefficients for oxide components relative to the activity of FeO, whose partitioning between metal and silicate is also measured. Use of graphite capsules means that the silicate melt composition can be varied over a wide range, but also means that the metal is carbon-saturated, a factor which has a profound effect on the activities of some components (e.g Pb, Ag, W) in the liquid metal.

We find that the activity coefficients of a number of the most important trace components, notably WO₃, MoO₂, GeO₂, TiO_{0.5}, GaO_{1.5}, BiO_{1.5} and SbO_{1.5} are strongly dependent on melt composition each showing variations of 1-2 orders of magnitude over the accessible range of silicate melt compositions. Values for CuO_{0.5} are in excellent agreement with previous experimental data² on Cu-saturated compositions which shows that the method is viable. When combined with thermodynamic data on the gas species we find that volatilities under solar nebula conditions are displaced relative to those of the “conventional” condensation sequence³.

[1] O'Neill, H. S. C. & Eggins, S. M. *Chemical Geology* **186**, 151-181 (2002). [2] Holzheid, A. & Lodders, K. *Geochimica et Cosmochimica Acta* **65**, 1933-1951 (2001). [3] Lodders, K. *Astrophysical Journal* **591**, 1220-1247 (2003).

Geochemical characterization of uranium mill tailings

J. NOS^{1*}, A. BOIZARD², C. PEIFFERT²,
V. PHROMMAVANH¹, M. CATHELINÉAU² AND
M. DESCOSTES¹

¹AREVA Mines – DR&D, 92084, Paris La Défense, France

(*correspondence: jeremy.nos@areva.com)

²CREGU, 54500, Vandoeuvre-lès-Nancy, France

In France, uranium mines were exploited between 1945 and 2001, leading to the production of 76,000 t of U and 50 Mt of mill tailings stored on 16 storage sites. Studies are being performed to determine the long term behaviour of these storage sites, focusing on the mobility of U and ²²⁶Ra.

Following previous work [1] on mill tailings issued from dynamic treatment, coring and sampling were performed in four storage sites, including heap leaching tailings. All the tailings studied come from sulphuric acid treatment of granitic ore. Radio-geochemical variations were assessed through analyses on 10 to 20 samples for each site. Focus was put on the mobility of U and ²²⁶Ra by characterizing their granulometric distribution and performing sequential leachings. Concurrently, water-rock interactions were constrained by pore water sampling on one site.

Samples issued from each site feature strong similarities, typical of a mix of tailings and water treatment sludges. Three main mineralogical families are identified: “inherited minerals”, initially present in the granitic rock (quartz, micas, K-feldspars, ancillary minerals such as sulfides and oxides), “refractory” U-bearing minerals (uraninite, coffinite) and newly formed minerals. The latter are clay minerals and Fe^{III} oxy-hydroxides (from the alteration of the granite host rock), gypsum (due to reagents input during the ore treatment) and U-phosphates (both inherited and newly formed). Geochemical modellings indicate the presence of soddyite controlling the [U] in the porewater.

The average U content is 100 ppm. The ²³⁸U/²²⁶Ra disequilibrium is constant in dynamic treatment tailings, consistent with a homogeneous ore treatment and a limited migration of U and Ra. This ratio is more variable in heap leaching tailings, suggesting a heterogeneous ore treatment.

All these results are considered in the modelling of the long term evolution of mill tailings, taking into account the sorption properties of the newly-formed minerals.

[1] Somot *et al.* (2000) *Tailings and Mine Waste '00*, 343-352.

The importance of dry deposition in estimating nitrogen input in peat bogs

M. NOVAK^{1*}, L. BOHDALKOVA¹, D. FOTTOVA¹,
J. CURIK¹, M. STEPANOVA¹, M. DARMOVZALOVA¹
AND F. VESELOVSKY¹

¹Czech Geological Survey, Geologicka 6, 15200 Prague 5,

Czech Republic (*correspondence:

martin.novak@geology.cz)

It has been recently reported that rain-fed peat bogs in pristine areas store more nitrogen (N) than the amount of N that could have been supplied by atmospheric deposition. In such calculations, cumulative input of nitrate and ammonium are compared with the total N content in ²¹⁰Pb-dated peat cores. We have performed a similar comparison in N-polluted Central Europe. Four sites exhibited 2 – 3 times higher N pool size in *Sphagnum* peat since 1880 than cumulative atmospheric input. This discrepancy might be explained by a large contribution of dry deposition. Dry deposition depends on the surface roughness (leaf area index) and is extremely difficult to measure directly in peatlands. In a first approximation, we have used data on spruce canopy throughfall as a proxy for *Sphagnum* interception of airborne N. At 6 sites of the monitoring network GEOMON, N input via spruce throughfall was smaller than via open area deposition. At another 7 sites, N input via spruce throughfall was slightly higher than via open area deposition (59 vs. 26 kg N ha⁻¹ yr⁻¹ in Orlicke Mts. was an extreme). It appears that dry deposition may not fully explain excess N in wetland ecosystems.

Comparison of $\delta^{53}\text{Cr}$ ratios between geogenic and anthropogenic chromium in Central European waters

M. NOVAK^{1*}, V. CHRASTNY¹, J. FARKAS¹,
T.D. BULLEN², E. CADKOVA¹, Z. SZURMANOVA³,
J. TYLCER³, L. ERBANOVA¹, E. PRECHOVA¹
AND J. PASAVA¹

¹Czech Geological Survey, Prague, Czech Republic
(*correspondence: martin.novak@geology.cz)

²U.S.Geological Survey, Menlo Park, Ca., U.S.A.

³AQD-envitest, Ostrava, Czech Republic

$^{53}\text{Cr}/^{52}\text{Cr}$ isotope ratios can be used to distinguish between geogenic and anthropogenic sources of chromium in surface waters and groundwaters. Often, a multiple-tracer approach is needed. Since 2011, we have monitored Cr concentrations and $\delta^{53}\text{Cr}$ values in seven different areas of the Czech Republic, Central Europe. At two sites, we sampled first-order streams on ultrabasic (serpentinite) bedrock. At five sites, we sampled shallow groundwater in the vicinity of Cr-processing industrial operations. Water samples were complemented with globally distributed minerals and whole-rock samples. So far, we have isotopically analyzed 110 samples. Mean Cr concentrations were 6500 ppb in industrial waters, and 20 ppb in geogenic waters. The range of $\delta^{53}\text{Cr}$ values increased from minerals/rocks to geogenic and industrial waters. The $\delta^{53}\text{Cr}$ of solid samples was close to 0 per mil, with isotopically slightly heavier Cr in some serpentinites (+1.1 per mil). The range of $\delta^{53}\text{Cr}$ of geogenic waters was 4.0 per mil (from -0.1 to +3.9 per mil). The range of $\delta^{53}\text{Cr}$ of anthropogenic waters was 4.6 per mil (from +1.2 to + 5.8 per mil). In general, Cr in anthropogenic waters was isotopically heavier than Cr in geogenic waters. None of the industrial waters had a $\delta^{53}\text{Cr}$ close to 0 per mil. So far, we have not observed C-isotope indices of natural attenuation of the anthropogenically polluted groundwaters.

Fluvial sediments: Assessment of contamination by trace metals respecting natural variability

TEREZA NOVAKOVA^{1,2}, TOMAS MATYS GRYGAR²,
MARTIN MIHALJEVIC¹ AND LADISLAV STRNAD¹

¹Charles University, Faculty of Science, Albertov 6, 128 43 Prague (*correspondence: Tereza.Novakova@natur.cuni.cz, Mihal@natur.cuni.cz, Lada@natur.cuni.cz)

²Institute of Inorganic Chemistry AS CR, 250 68, Rez (Grygar@iic.cas.cz)

According to the latest studies, proper assessment of trace metal contamination levels in fluvial sediments of different rivers necessarily requires individual approaches for each river, according to the local geological proveniences and individual river sedimentation dynamic characteristic.

Such special approach includes sampling respecting floodplain architecture, use of different normalisation elements for each trace metal (e.g., Al, Ti, Rb, Fe) to eliminate highly possible dependence of natural lithogenic background values on lithofacies and finally also use of sufficient method for contamination level assessment.

In this study, comparison of trace elements contamination level (Pb, Zn, Cu, Cr and Ni) of floodplain sediments of five different rivers in Czech Republic (the Berounka, the Jizera, the Morava, the Ohře and the Ploučnice) was done. Floodplain sedimentary profiles were obtained from hand drilled cores, elementary analysis was done by energy dispersive X-ray fluorescence (ED XRF) and by inductively coupled plasma mass spectrometer (ICP MS); cation exchange capacity measurement (CEC) was used for determination of expandable clay mineral content.

Regional lithogenic background values were obtained from "safe" parts of profiles (uniform facies, i.e. no sandy strata, unaffected by reductimorphic processes, unpolluted) and were further used for revelation of potential post-depositional trace elements migrations within profiles and also for determination of anthropogenically contaminated layers.

Elimination of potential influences of lithofacies and also elimination of different provenience influences was allowed by using of carefully chosen normalisation elements for trace elements in the rivers (e.g., Rb normalisation was used for all trace metals in the Morava River sediments or in the case of the Jizera River, Ti normalisation was used for Pb, Zn, Cr and Ni and Rb normalisation for Cu).

The only exception was the upper part of the Ohře River, where no normalisation element was yet established, due to the different proveniences influence and hence simple normalisation could not be used.

The formation of low degree hydrous melts in the Earth's upper mantle

D. NOVELLA^{1*}, D.J. FROST¹ AND E.H. HAURI²

¹Bayerisches Geoinstitut, Universitaet Bayreuth, Germany

(*correspondence: davide.novella@uni-bayreuth.de)

²Carnegie Institution of Washington, DC, USA

Melting processes in the Earth's interior play a crucial role in the chemical evolution of our planet. The presence of low degree, volatile-bearing melts in the deep mantle is supported by the occurrence of volatile-bearing minerals in xenoliths and by geophysical observations. In order to quantify the proportion of melts formed as a function of mantle water content, we have performed a series of crystallization experiments, following a similar methodology to the sandwich technique, where large pools of hydrous melt composition were equilibrated with a complete mantle peridotite phase assemblage. In particular, we determined the chemical composition of these incipient hydrous melts forming at pressures above 3 GPa. Following this approach, we assessed the water content of the low degree melts by mass balance calculation, based on accurate chemical analyses performed on the large portions of melt. The H₂O concentration of the peridotite mineral phases was determined by NanoSIMS analyses in order to obtain information on the partitioning of water between mantle minerals and low degree hydrous melts.

Based on some estimates of the water content of the mantle, a deep onset for the inception of adiabatic melting can also be implied. However, accurate information regarding the chemistry of low degree H₂O-bearing melts is limited to pressures below 3 GPa. This is a consequence of a number of experimental challenges encountered in performing experiments at high pressure within complex systems, such as quench crystallisation and loss of H₂O and FeO from charges. In addition, the small volume of hydrous melts created by plausible mantle H₂O contents at depth creates challenges even for the analysis of major elements. Sandwich experiments are very useful because they permit large proportions of low degree composition melts to be equilibrated with mantle residual assemblages. Large amounts of melt promote crystal growth and facilitate melt analyses.

Using these results the H₂O contents of mineral and melt phases can be addressed as a function of mantle H₂O content. Our results indicate H₂O concentrations in mineral phases that are significantly greater than previous studies performed at similar pressure, temperature and low degree of melting conditions.

Origin of two different zircon types in metabasite veins from the Izera metagranites, West Sudetes, Poland

I. NOWAK^{1*} AND M.J. WHITEHOUSE²

¹Institute of Geological Sciences, Polish Academy of Sciences
INGPAN, Podwale 75, 50-449 Wrocław, Poland

(*correspondence: izanowak@twarda.pan.pl)

²Swedish Museum of Natural History, Stockholm, Sweden

In the northern part of the Izera-Karkonosze Massif, which represents the passive margin of the Saxothuringian terrane, c. 500 Ma granites were intruded by a swarm of the WNW-trending subvertical basic veins and then deformed and metamorphosed. Two types of zircon, types I and II, that differ in colour, size, habit and internal structure were identified in six metabasite veins. Colourless, transparent and euhedral, 300 μm sized, CL-bright zircon of type I display inherited old cores as well as c. 500 Ma oscillatory zoned rims. Their U-Pb ages are almost identical with the previously determined intrusion age of a protolith for the Izera metagranites (U-Pb, zircon, 515-480 Ma). Grains of type I show $\delta^{18}\text{O}$ (6.2-9.1‰) values and Ti-zircon temperatures (600-780°C) similar to the data from the Izera gneiss zircons. Their REE patterns exhibit a narrow range. Such coincidence indicates that the zircons of type I are probably inherited xenocrysts incorporated into the basic magma via assimilation of material of local granitic crust. Type II zircons, which yield ages of c. 370 Ma, are brown, turbid, subhedral crystals up to 600 μm size, and dark in CL. Their large (c. 2/3 of the grain size), almost homogeneous and microinclusion-rich inner parts are surrounded by thinner oscillatory zoned rims. They display a wide range of Ti-zircon temperatures (630-800°C), variable REE contents and $\delta^{18}\text{O}$ (4.5-8.9‰) values. The origin of these brown zircons is ambiguous. Their homogeneous interiors and oscillatory zoned rims indicate growth in a magmatic melt. Grains showing $\delta^{18}\text{O}$ from 5.1-5.5‰ present coherent magmatic-style REE patterns with positive Ce and negative Eu anomalies, also indicative of their magmatic origin. However, dark and inclusion-rich centres of type II grains suggest precipitation from hydrothermal fluids, while low $\delta^{18}\text{O}$ (4.5-5.0‰) values, incoherent REE patterns, LREE enrichment and a lack of Ce anomaly in many grains suggest interaction of the metabasites with hydrothermal fluids during crystallization of the brown zircons. The results are consistent with type II zircon of crystallizing from a fluid-saturated residual melt or more likely representing magmatic crystals hydrothermally altered by fluids coming from the surrounding metagranites.

Delaminated Lithospheric Mantle and exotic metasomatism beneath East Russia

NTAFLOS TH¹, ASCHCHEPKOV I.², KOUTSOVITIS P.¹, HAUZENBERGER A.³, PRIKHODKO V.⁴ AND ASSEVA A.⁵

¹Dept. of Lithospheric Research, University of Vienna, Austria (theodoros.ntaflos@univie.ac.at)

²RAS, Institute of Geology and Mineralogy, Novosibirsk, Russia

³Institute für Erdwissenschaften, University of Graz, Austria

⁴RAS, Far-Eastern Branch, Institute of Tectonics and Geophysics, Khabarovsk, Russia

⁵RAS, Far-Eastern Branch, Geological Institute, Vladivostok, Russia

In the back-arc environment of Far East Russia, mantle xenoliths from Sikhote-Alin(KO) and Primorie (SV), Far East Russia are fertile spinel lherzolites with amphibole, phlogopite armalcolite, fassaite and röhnite in some of the studied samples. Though samples from both localities are fertile there is a systematic difference in their fertility. The KO samples have mg# varying from 0.891 to 0.899 and are slightly more fertile than the SV samples that have mg# ranging from 0.898 to 0.904. The cpx REE confirm this trend as the $(La/Yb)_N$ in KO samples range from 0.10 to 1.00 and in SV samples from 0.15 to 1.73.

The clinopyroxene Sr and Nd isotopic ratios range from 0.702599 to 0.703567 and 0.512915 to 513153, respectively, resembling Pacific MORB isotopic ratios.

En route breakdown of disseminated amphibole produces second generation of cpx and olivine and traces of glass as well fassaite and röhnite indicating crystallization at very shallow depths. Melt pockets consisting of Ca-rich glass plagioclase rutile, ilmenite and armalcolite suggest introduction of small amount of an unusual Ti-Ca-rich anhydrous silicate melt at mantle depths.

The lithospheric mantle beneath the studied area represents the residue after partial melting of up to 5% of a primitive mantle. Despite the fact that the studied area experienced several subducting episodes, the lithospheric mantle appears to be unaffected from the upwelling fluids/melts of the subducted slab(s). Since there is no indication for plume activity, and/or evidence for refertilization, it is likely that the lithospheric mantle has been delaminated as the result of tectonic events (lithospheric attenuation, inverse tectonic) associated with the subduction processes and that the studied spinel lherzolites represent upwelling asthenosphere.

Resilience Biomimcry model for natural disturbance scenarios

NUNES L¹ AND NAROG M²

¹Luisa Nunes, ESACB/CEABN, Qta Sra Mercules, 6000 Castelo Branco Portugal, (lfnunes@ipcb.pt)

²Marcia Narog, USDA Forest Service, Pacific Southwest Research Station, Riverside, CA, mnarog@fs.fed.us

Mobile links are 'keystone' organisms that move among habitats and provide essential ecosystem functions such as pollination, seed dispersal, or nutrient translocation. After disturbance, some ecosystem functions may become disrupted or may disappear altogether. Much like similar habitats joined by corridors, the mobile links connect areas that may be widely separated spatially or temporally. Species strategies and interactions must be reconfigured after disturbance based on residual organisms and any altered environmental constraints. Reassembly of organisms might be based on an ecological memory that contributes and leads to the recovery of the affected area. This ecological memory is the complex network of species and their relations with each other and the environment.

Based on the renewal cycle of Holling, we developed a biomimcry resilience model that identifies recovery strategies inspired by opportunistic species colonization, their accumulation and storage of resources and the reorganization phases to a new stability.

We studied and characterized which interactions take place within and between disturbed and undisturbed areas that facilitate proliferation, regeneration and nutrient translocation. The resilience model also considered limitations such as distance from source areas, availability of dispersal agents and suitability of the disturbed environment.

This resilience model was created to help understand natural recovery processes that can be emulated after disturbances and applied to human community disaster planning.

Probing paleoearthquakes with *in situ* U-Pb SHRIMP-RG analyses of fault-related opals

PERACH NURIEL^{1*}, KATE MAHER^{1J}
AND DAVID M. MILLER²

¹ Department of Geological and Environmental Sciences,
Stanford University, CA 94305, US (*correspondence:
perach@stanford.edu, kmaher@stanford.edu)

² U. S. Geological Survey, 345 Middlefield Road, MS-973,
Menlo Park, CA 94025, USA (dmiller@usgu.gov)

In the past decade U-Pb and U-series dating techniques have been successfully applied to opals from arid regions, providing important temporal constraints on paleohydrology, paleoclimate, and depositional environments. In particular, the use of *in situ* SHRIMP-RG (Sensitive High Resolution Ion Microprobe – Reverse Geometry) dating techniques has been demonstrated to resolve mixed multiage problems that arise from slow-growth or multi-stage growth at the sub-millimeter scale. Building upon these advances, we apply *in situ* SHRIMP-RG dating methods to fault-related opal precipitates taken from seismically active fault zones with the aim of dating brittle deformation events. The Mojave Desert fault segments within the Eastern California Shear Zone (ECSZ) are ideal faults to investigate the long-term history because of the need for improved constraints on the timing of fault initiation and the observed discrepancy between long-term and short-term estimates for strain accumulation rates.

We analyzed fault-related opal samples from five different fault exposures within the Camp Rock and the Cave Mountain fault systems. Millimeter size fragments of fault-related opal, occurring as fault coating, filling or fault-breccia cement, were imaged using cathodoluminescence and backscattering electron microscopy in order to identify distinct phases of opal associated with specific syntectonic microstructures. Sub-samples within each phase are then targeted with multiple SHRIMP-RG analyses (<50 µm in diameter) to allow the construction of ²³⁸U/²⁰⁸Pb-²⁰⁶Pb/²⁰⁸Pb and/or Tera-Wasserburg U-Pb isochrons. Of the 30 distinct phases that were identified, 10 were successfully dated, providing U-Pb ages with 2σ ≤ 10% and MSWD between 0.42 and 1.8. The most important factors for successful age determinations were low amounts of common Pb, high U concentrations (between 50 and 1300 ppm) and heterogeneities within each phase. Ages range from 1.45 to 0.58 Ma and coeval ages are clustered into several periods during this time interval, suggesting periods of enhanced fault activity. Additional analyses of syntectonic opals, taken from several sites and from additional faults segments can constrain the long-term deformational history and contribute to our understanding of how strain is distributed both locally (within a specific structure) and regionally (within different fault systems) over a geological time scale.

U-series isotopes as tracers of particles fluxes and deposition rates of Heinrich layers H2 and H1 from a core raised off Hudson Strait

L. NUTTIN* AND C. HILLAIRE-MARCEL

GEOTOP research centre, Université du Québec à Montréal,
Montreal, Canada (correspondence: lanuttin@gmail.com)

A ~9 m-long core was retrieved from the lower Labrador Sea slope (2674 m water-depth), approximately 180 km off the Hudson Strait shelf edge. It yielded a high resolution record of recent detrital carbonate (DC) sedimentary pulses from the Hudson Strait outlet of the Laurentide ice sheet, assigned to "Heinrich events" H2 and H1. These fine carbonate-rich layers (calcite/dolomite ~ 2.5) originated from glacial erosion of Paleozoic rocks in Hudson Strait and Ungava Bay. The coarse sediment fraction content of the layers suggest intense iceberg calving at the ice-stream edge, while sub-glacial meltwater flushing over the Hudson Strait sill carried fine silt-sized, carbonate-rich glacial flour to the shelf edge. Such suspended sediment pulses led to the spreading of turbidites into the deep Labrador Sea. These layers are characterized by a ²³⁴U deficit (vs ²³⁸U) and by very low ²³⁰Th excesses corrected from decay to the time of deposition (²³⁰Th_{xs})₀. These low values indicate extremely fast deposition. Inventories of (²³⁰Th_{xs})₀ were used to estimate durations of ~1.28 and ~1.99 ka respectively for H2 and H1, relative to estimates of ~1.15 and ~2.12 ka from calibrated ¹⁴C ages on planktic foraminifers. Another DC-layer was deposited at ~8.3 cal ka BP, during the final drainage of Lake Agassiz. Above, high (²³⁰Th_{xs})₀ activities but low ²³⁰Th_{xs}-fluxes point to some ²³⁰Th-focussing with enhanced biogenic carbonate fluxes, under a stronger Western Boundary Undercurrent influence leading to the winnowing of slope sediments, thus reduced sedimentation rates at the site. ²³¹Pa/²³⁰Th ratios are used to further document sedimentary regimes at the site.

www.minersoc.org

DOI:10.1180/minmag.2013.077.5.14

Carbonate mineralization in shallow Lake Balaton

I. NYIRÓ-KÓSA¹, É. TOMPA¹, Á. ROSTÁSI¹, T. CSERNY²
AND M. PÓSFAI^{1*}

¹Dept. of Earth & Env. Sci., Univ. Pannonia, Veszprém, 8200
Hungary, (*correspondence: mihaly.posfai@gmail.com)

²Geol. Geophys. Inst. Hungary, Stefánia 14, H1143 Budapest

Calcite precipitates in hardwater lakes as a result of CO₂ consumption by algae through photosynthesis. Lake Balaton has a large surface area (~600 km²) but an average depth of only ~3.5 m. Its sediment is dominated by carbonate minerals, including Mg-calcite that precipitates from lakewater, aragonite from shells, diagenetic 'protodolomite' and allochthonous calcite and dolomite [1]. We studied various aspects of carbonate formation relevant for the biogeochemical cycles in the lake: the relationships between Mg-content, crystal structure, particle size and morphology, the potential autochthonous formation of dolomite, the roles of organisms in nucleating and reprocessing mineral matter, and the association of P with the carbonate minerals.

Both sediment cores and freshly precipitated material were collected, either by placing sediment traps under the ice (in order to avoid the resuspension of sediments by wind-driven turbulence) or by filtering lakewater. Mg incorporation into calcite was studied by X-ray powder diffraction analysis of d(104) spacings. Particle morphologies, microstructures and compositions were observed using scanning and transmission electron microscopies. The Mg content of calcite increases from west to east in the lake, reflecting a gradient in water composition. Mg-calcite particles are elongated, few µm-large aggregates in which the crystallites occur in a consensus crystallographic orientation. Smaller, euhedral dolomite crystals also occur in the sediment traps; in places their cell parameters slightly differ from those of stoichiometric dolomite. Concerning the roles of organisms in mineral precipitation, no evidence has been found for the microorganism-assisted nucleation of Mg-calcite; however, the reprocessing of mineral matter by filtering organisms (zooplankton and mussels) typically produces pellets of several hundred µm in size that are major constituents of the sediment. Studies are in progress to map the distribution of P in the various carbonate minerals, and to explore the origin of the dolomite that has anomalous lattice parameters [2].

[1] Müller & Wagner (1978) *Spec. Publ. Intl. Assoc. Sed.* **2**, 57-81. [2] This study was supported by a joint EU-European Social Fund grant (TÁMOP-4.2.2.A-11/1/KONV-2012-0064).

www.minersoc.org

DOI:10.1180/minmag.2013.077.5.14

Paleoclimatic changes across the Cretaceous-Paleogene boundary: Geochemical reconstructions from Seymour Island, Antarctica

CHARLOTTE L. O'BRIEN^{1*}, STUART A. ROBINSON¹,
DAVID B. KEMP^{1,2}, J. ALISTAIR CRAME³, JANE E.
FRANCIS⁴, DANIEL J. LUNT⁵, JON R. INESON⁶,
ROWAN J. WHITTLE³ AND VANESSA BOWMAN⁴

¹Department of Earth Sciences, University College London, London, UK (*correspondence: c.l.obrien@ucl.ac.uk)

²Earth, Environment and Ecosystems, Open University, Walton Hall, Milton Keynes, UK

³British Antarctic Survey, High Cross, Cambridge, UK

⁴Earth Sciences, School of Earth and Environment, University of Leeds, Leeds, UK

⁵BRIDGE, School of Geographical Sciences, University of Bristol, Bristol, UK

⁶Geological Survey of Denmark and Greenland, Copenhagen, Denmark

The Cretaceous-Paleogene (K-Pg) boundary, ~66.0 Ma, marks the most catastrophic global extinction event of the past 100 Myr and is well documented in both terrestrial and marine biotic records. Although the K-Pg mass extinction occurred at a time when the Earth's climate operated under greenhouse conditions, the specific climatic and environmental changes associated with this event remain poorly understood. Shallow marine sediments exposed on Seymour Island, Antarctica (paleolatitude ~65°S) provide one of the most expanded K-Pg successions known. Moreover, the high latitudes represent areas of significant climatic importance due to polar amplification of global warming.

We first present a low resolution MBT/CBT (methylation of branched tetraethers/cyclisation of branched tetraethers) continental temperature reconstruction that indicates a persistent cool temperate climate (11.4 ± 5 °C) on the Antarctic Peninsula during the latest Cretaceous to early Paleogene. The addition of a higher resolution study across the K-Pg boundary is then used to investigate short-term paleoclimatic and paleoenvironmental perturbations, using MBT/CBT, BIT indices and biomarker abundances. Integration of these data with paleontological and paleobotanical datasets allows us to reconstruct the response and recovery of high latitude terrestrial and marine environments to the K-Pg global extinction event.

Reaction mechanisms, pathways, and transport in anaerobic abiotic and microbial U(IV)-oxide dissolution studies

PEGGY A. O'DAY^{1*}, MARIA P. ASTA¹,
MASAKAZU KANEMATSU^{1,2}, CARL STEEFEL²
AND HARRY R. BELLER²

¹University of California, Merced, CA 95343 USA

(*correspondence: poday@ucmerced.edu)

²Lawrence Berkeley National Laboratory, Berkeley CA USA

Applications of combined thermodynamic-kinetic descriptions to mineral-water interface processes that include chemical reactivity, microbial metabolism, and physical transport are challenged by the need to bridge differences in spatial and temporal scales for multiple, competing reactions. Even in simplified systems, formulation of reactive-transport model descriptions requires parameterization that must aggregate the details of molecular-scale reactions and microbial catalysis to some extent. Investigations of the oxidative dissolution of biogenic U(IV)-oxide (nominally UO₂(s)) under anaerobic conditions by either chemical oxidants (nitrate or nitrite) or by *Thiobacillus denitrificans*, a chemolithoautotrophic bacterium that catalyzes anaerobic, nitrate-dependent U(IV) and Fe(II) oxidation, are used to examine coupled and competing oxidation-reduction processes in flow-through column experiments. Abiotic oxidation of UO₂(s) in the presence of nitrate under anaerobic conditions is slow but faster than control experiments of non-oxidative dissolution. Abiotic UO₂(s) oxidation by nitrite is significantly faster by several orders of magnitude. In the presence of *T. denitrificans* and dissolved nitrate, higher rates of dissolved U release were observed compared with abiotic controls, suggesting that *T. denitrificans* catalyzed the oxidative dissolution of UO₂(s) in addition to the abiotic oxidation pathways. X-ray spectroscopic characterization of reaction products indicates solid-associated oxidized U(VI) that is retained in the column. Analysis of local atomic structures shows formation of U-oxo molecular moieties within or on particle surfaces that are similar but not identical to aqueous or sorbed uranyl species, suggesting mostly surface particle oxidation rather than detachment and re-adsorption of uranyl in the column. Reactive transport modeling incorporating thermodynamic solubility, irreversible overall abiotic and biotic kinetic reactions, and uranyl sorption can simulate effluent U concentrations for a small amount of UO₂(s) oxidation relative to total mass, but calculations are sensitive to particle surface area.

Remediation Strategies for Redox-Active Elements Using Combined Experimental, Spectroscopic, and Computational Approaches

PEGGY A. O'DAY^{1*}, SUSANA SERRANO¹
VIRGINIA ILLERA¹ AND DIMITRI VLASSOPOULOS²

¹ School of Natural Sciences, University of California,
Merced, CA 95343, USA

(*correspondence: poday@ucmerced.edu)

² Anchor QEA, LLC. Portland, OR 97204, USA

Contaminants such as arsenic (As), mercury (Hg), and other redox-active elements pose particular challenges to remediation because of their ability to readily change oxidation state and speciation at surface conditions from coupled microbial-abiotic processes that are spatially and temporally dynamic. A variety of *in situ* sediment or soil amendment treatments, whether added directly to geomeedia or emplaced within barriers or caps, can sequester and stabilize contaminants in place in order to reduce their ability to partition to water or biota, their toxicity, and their potential for transport. Computational approaches such as thermodynamic-kinetic reaction path and reaction transport models capable of simulating biogeochemical, speciation, partitioning, and transport processes are valuable tools for assessing remediation effectiveness when constrained by spectroscopic and experimental investigations of laboratory and field systems. The contrasting chemical behavior and exposure pathways of As and Hg illustrate how remediation approaches using amendments or sediment caps can be optimized by minimizing the concentration of specific chemical species associated with maximum health risk. For As, inorganic arsenite ($\text{As}^{\text{III}}(\text{OH})_3$) is the most toxic form and human exposure is typically through drinking water. Combined field, laboratory, and modeling studies show that sorption or amendment sequestration of arsenate (As(V)) under oxic conditions, or precipitation of solid As sulfides under anaerobic conditions, are most effective for limiting concentrations of dissolved arsenite. For Hg, remediation should target reduction of net methylation of inorganic Hg to methylmercury, which results primarily from bacterial sulfate reduction in anaerobic environments and is the first step in Hg bioaccumulation. Approaches such as sediment chemical amendments or caps can reduce methylation by limiting bioaccessibility of inorganic Hg through solid encapsulation or irreversible sorption, reducing the total concentration of dissolved sulfide species, buffering system oxidation potential above sulfate reduction, and/or buffering pH at circumneutral or above.

Biogenic Influence on Sea-Spray Aerosol and its Impacts

C.D. O'DOWD*, A. VAISHYA, J. OVADNEVAITE, J. BIALEK, S.G. JENNINGS AND D. CEBURNIS

School of Physics and Centre for Climate and Air Pollution Studies, Ryan Institute, National University of Ireland Galway, University Road, Galway, Ireland
(*correspondence: Colin.Odowd@nuigalway.ie,
aditya.vaishya@nuigalway.ie,
jurgita.ovadnevaite@nuigalway.ie,
jakub.bialek@nuigalway.ie,
gerard.jennings@nuigalway.ie,
Darius.Ceburnis@nuigalway.ie)

Marine aerosol, whether primary or secondary, comprises both inorganic and biogenic organic components. Although primary sea-spray mass is dominated by super-micron sea-salt, the sub-micron sizes dominate the sea-spray number concentration leading to important contributions to both direct and indirect radiative effects [1,2]. The relative contributions of sea-salt and primary organic matter to sub-micron sea-spray has been shown to be influenced by biogenic productivity in oceanic waters, with the organic mass fraction ranging from 10% under low biological activity, to 90% under high activity [3, 4]. The organic enrichment reduces the spray's hygroscopicity [4]; however, there is a dual-state effect leading to hygroscopicity flipping between a high hygroscopicity to low hygroscopicity as the organic matter volume fraction exceeds ~50%. The effect leads to a ~3-fold reduction in scattering enhancement as a function of increasing relative humidity and potentially a reduction in the radiative impact of sea-spray from -6.5 Wm^{-2} to -1 Wm^{-2} under wind speeds of 20 m s^{-1} .

Acknowledgments

This work was supported by the HEA-PRTLI4, EC IPs EUCAARI & GEOMON, EPA-Ireland, ESA (SToSE: OSSA), EC ACTRIS.

[1] O'Dowd *et al.* (1999) *Q. J. Roy. Met. Soc.*, 125, 1295-1313. [2] Mulcahy *et al.* (2008) *Geophys. Res. Letts.*, 35, L16810, doi:10.1029/2008GL034303. [3] O'Dowd *et al.* (2004) *Nature* 431, 676-680. [4] Ovadnevaite *et al.* (2011) *Geophys. Res. Letts.* 38, L21806.

Effects of subduction-related melt extraction on Iapetus Ocean mantle

B.O'DRISCOLL^{1*}, R.J. WALKER², J.M.D. DAY³
AND J.S. DALY⁴

¹School of Physical and Geographical Sciences, Keele University, Keele, UK (*correspondence: b.o'driscoll@keele.ac.uk)

²Department of Geology, University of Maryland, College Park, MD, USA

³Geosciences Research Division, Scripps Institution of Oceanography, La Jolla, CA, USA

⁴UCD School of Geological Sciences, University College Dublin, Dublin, Ireland

Ophiolites enable assessment of the causes and length-scales of mantle compositional heterogeneity because field-based observations can be coupled with geochemical investigations of upper mantle lithologies resolved relative to the petrological Moho. The ~497 Ma Leka Ophiolite (Norway) comprises a section of early-Palaeozoic (Iapetus) oceanic lithosphere with well-exposed mantle and lower crustal sections and remarkably low degrees of serpentinisation ($\geq 20\%$). The Leka upper mantle section is heterogeneous at the cm-to-m scales, manifested by abundant dunite lenses and sheets in harzburgitic host-rock, especially within ~500 m below the Moho. Abundant chromitite (≥ 60 vol.% Cr-spinel) and pyroxenite lenses and layers also occur in the uppermost 200-300 m of the mantle section.

The array of mantle lithologies on Leka is considered to have developed during fluid-assisted melt extraction in a supra-subduction zone (SSZ), offering an opportunity to interrogate the nature of Os isotope and HSE abundance heterogeneities developed in such rocks and circumventing, at least in part, the effects of serpentinisation. Initial results show that the Os isotope compositions of the Leka peridotites are quite consistent, with a range of $\gamma_{Os,497Ma}$ of -1.57 to +4.43, and Os concentrations ranging from 1.4-24.8 ng g⁻¹ Os, for eleven harzburgites and dunites. Given the similarity between Leka peridotites and estimates of Os isotopic composition and HSE abundances in the oceanic mantle (e.g., from abyssal peridotites), we see scant evidence for modification of these elements by SSZ fluid or melt-rock interactions. Comparison of the Leka data with mantle peridotite data from the (~492 Ma) Iapetan ophiolite exposed on the Shetland Islands (Scotland) [1] implies that on ocean-basin scales, SSZ fluid/melt interactions may only play a limited role in processing the HSE in already strongly depleted mantle.

[1] O'Driscoll *et al.* (2012) *EPSL* **333-334**, 226-237.

Earth's Hadean crust: Insights from the Nuvvuagittuq Greenstone belt

J.O'NEIL¹, R.W. CARLSON² AND M. BOYET³

¹Depart. of Earth Sciences, Univ. of Ottawa, Ottawa, Canada

²Carnegie Institution of Washington, Washington DC, USA

³Laboratoire Magmas et Volcans, Clermont-Ferrand, France

The Hadean Eon is still poorly understood due to the scarcity of preserved samples. Most of what we know of early crustal evolution comes from the Hadean Jack Hills detrital zircons. Despite the fact that their host rock has been destroyed, the isotopic composition of these zircons points to a basaltic protocrust reworked to form multiple generations of TTG-like crust. With a minimum age of 3.8 Ga, the Nuvvuagittuq Greenstone Belt (NGB), represents an ideal terrain to investigate early Earth's crustal evolution. Rocks from the NGB show considerable variability in ¹⁴²Nd/¹⁴⁴Nd ($\mu^{142}Nd = +8$ to -18) that can only be produced during the Hadean. The correlation observed between the ¹⁴²Nd/¹⁴⁴Nd and the Sm/Nd ratios of the dominant mafic lithology called the Ujaraaluk unit is consistent with their formation between 4.3 and 4.4 Ga. This age, however, has been challenged because the oldest U-Pb ages on zircons from the NGB felsic rocks are ~3.8 Ga. An alternative model suggests mixing of mantle-derived melts in the Eoarchean with some hypothesized reservoir enriched in incompatible elements during the Hadean to produce the ¹⁴²Nd deficits of the NGB rocks. This conclusion, however, is not supported by our latest ¹⁷⁶Lu-¹⁷⁶Hf / ¹⁴²Nd data. Here we present a summary of the geology and geochronology of the NGB and discuss the alternative models of Eoarchean or Hadean age for the belt. We used long-lived and short-lived isotopic systematics (^{147,146}Sm-^{143,142}Nd, ¹⁷⁶Lu-¹⁷⁶Hf) for all NGB lithologies including mafic and felsic rocks as well as combined Pb-Hf in zircons to understand the evolution of the NGB and the formation of Earth's early crust. Our data suggest that the protolith of the Ujaraaluk unit includes both tholeiitic and calc-alkalic mafic volcanic rocks originally erupted in the Hadean. Reworking of this basaltic precursor over several hundred million years in the Eoarchean produced TTG-type magmatism. If the Ujaraaluk unit is interpreted as Eoarchean, then one must hypothesize the existence of a Hadean enriched component that has identical compositional and isotopic characteristics to the Ujaraaluk as the source of the low ¹⁴²Nd in both some Ujaraaluk and the NGB TTG suite. We suggest instead that the Ujaraaluk unit is a Hadean mafic protocrust and may therefore represent the first crust to stabilize after the moon-forming impact and be the closest analogue to the primordial crustal source of the Jack Hills zircons.

What does Hadean mantle mixing tell us about Hadean geodynamics?

CRAIG O'NEILL¹, VINCIANE DEBAILLE²
AND BILL GRIFFIN³

¹CCFS, Macquarie University, (craig.oneill@mq.edu.au)

² Université Libre de Bruxelles, (vdebaill@ulb.ac.be)

³CCFS, Macquarie University, (bill.griffin@mq.edu.au)

A hot Hadean mantle is suggested from high internal heat production, high rates of impact bombardment, and significant primordial heat from accretion. Consequently, extremely high internal temperatures argue for low internal viscosities, and extremely vigorous mantle convection. Mixing in such high-Rayleigh number convective environment should have efficiently remixed or erased chemically heterogeneous mantle anomalies on timescales of less than 100Myr.

However, platinum group elements concentrations in Archaean komatiites, purported due to the later veneer of meteoritic addition on the Earth, only achieve current levels at 2.7Ga – indicating a time lag of almost 1-2Gyr in mixing this material thoroughly in the mantle. ¹⁴²Nd and ¹⁸²W isotope studies also indicate that heterogeneous mantle domains survived, without mixing, for over 2Gyr – at odds with mixing rates expected.

Here we suggest the surface tectonic regime may have significantly retarded mixing efficiency in the Hadean. A number of lines of evidence suggest episodic resurfacing in the Archaean, and extrapolating back to Hadean times implies the Hadean was characterized by long periods of tectonic quiescence (albeit violently volcanic). We explore mixing times in 3D spherical-cap models of mantle convection, which incorporate vertically stratified and temperature-dependent viscosities. We show that mixing in stagnant lid regimes can be over an order of magnitude less efficient than mobile lid mixing, and for plausible Rayleigh numbers and internal heat production, the lag in Hadean convective recycling can be explained. This explanation not only explains the long-lived ¹⁴²Nd and ¹⁸²W anomalies, but also 1) posits an explanation for the delay between accretion of the late veneer – between 4.5-3.8Ga on a stagnant surface – and its fully mixed signature apparent in elevated PGEs in 2.7Ga komatiites, and 2) provides an explanation for the 400Myrs of immobility of the mafic protolith from which the Jack Hill zircons were sourced, and 3) retards early heat loss from the mantle, providing a solution to the “Archaean thermal catastrophe” of parameterized Earth evolution models.

The effects of silicate melt composition and sulfur on the solubilities of PGEs in silicate melts

HUGH ST. C. O'NEILL¹

¹Research School of Earth Sciences, The Australian National University, Canberra, ACT 0200, Australia
(hugh.oneill@anu.edu.au)

Experimental studies of PGE solubilities at conditions directly relevant to natural basaltic melts are difficult because the low solubilities are often masked by variable amounts of micronuggets suspended in the melts. Experiments in simple haplobasaltic melts appear to establish that solubilities at low pressures are less than ~1 ng g⁻¹ at typical terrestrial oxygen fugacities and temperatures, raising questions as to how PGEs are transported from the mantle and concentrated into economic ore deposits. The applicability of the simple system experiments is sometimes queried because, it is claimed, missing ingredients like Fe or S might enhance solubilities. To address this issue directly, the effect of melt composition on Ir and Pd solubilities has been determined at ambient pressure. Samples were equilibrated in a 1-atm. gas-mixing furnace using Ir and Pd metal loops, quenched to glasses and analysed by laser ICP-MS (detection limits < 1 ng g⁻¹), with EMPA for major elements and sulfur. The compositional dependence was studied first at high temperatures (1500°C for Ir and 1400°C for Pd), which reduces the micronugget problem, and compositions least affected by micronuggets were then selected to measure the effects of T and fO₂. For Ir, ~40 melt compositions in CaO-MgO-Al₂O₃-SiO₂±FeO±Fe₂O₃±Na₂O±TiO₂ were investigated. The results show that Ir dissolves only as Ir³⁺ over the experimentally accessible range of fO₂, and solubilities are simply related to the melt composition through its optical basicity. The effects of FeO and Fe₂O₃ are small but individually resolvable: fO₂-corrected solubility decreases as Fe₂O₃ replaces FeO. High Fe or Ti suppresses micronuggets. As regards sulfur, Ir solubility is too low for any effect to be seen at the fO₂s needed to achieve measurable S²⁻ in the melt in 1-atm experiments. Pd dissolves as Pd¹⁺ with some Pd²⁺ at higher fO₂, in agreement with literature results. The effect of melt composition on Pd solubility is much less than for Ir, and is not related to any simple compositional variable. To investigate the effect of S quantitatively, experiments on the solubility of Ru (as Ru³⁺), which is ~50 times more soluble at a given fO₂ than Ir, were undertaken using a high Fe-Ti picritic composition at 1500°C to eliminate micronuggets, in olivine capsules. Only a small effect was observed despite ~1000 μg g⁻¹ S²⁻ in the melt.

Archean lithospheric mantle: The fount of all ores?

*SUZANNE Y. O'REILLY¹, W.L. GRIFFIN¹, G.C. BEGG^{1,2}, N.J. PEARSON¹ AND J.M.A. HRONSKY^{1,3}.

¹CCFS/GEMOC, Macquarie University, Sydney, Australia
(*correspondence: sue.oreilly@mq.edu.au)

²Minerals Targeting Intl., 17 Prowse St., W. Perth, Australia

³Western Mining Services (Aust.) Pty Ltd, 17 Prowse Street, W. Perth, WA 6005, Australia

Magma-related ore systems form economic deposits that underpin our human civilisation. The magmas related to metallic element redistribution derive from the asthenosphere, then traverse and interact to varying degrees with the subcontinental lithospheric mantle (SCLM). Convergent geochronology datasets of Hf isotopic model ages for zircons and Re-Os model ages for mantle sulfides, reinforced by other geochemical and tectonic criteria, indicate that over 70% of the SCLM and its overlying crust (now mostly lower crust) formed at about 3.5 Ga, probably in a global overturn event that marked a change in Earth's fundamental geodynamic behaviour. This primitive SCLM, the roots of the Archean cratons, was geochemically highly depleted, and subsequently played a major role in crustal metallogeny for many ore types. *Firstly*, the high degree of buoyancy of this ancient SCLM relative to the asthenosphere, due to the Mg-rich and Fe-poor composition, results in persistence today of low-density, rheologically coherent Archean domains (including relict blobs in rifted ocean basins [1]) and commonly, preservation of old crustal domains (the "life-raft" model). *Secondly*, the enduring (and volumetrically dominating) Archean lithospheric mantle domains represent a reservoir for metasomatic enrichment over their 3.5 billion year history, creating a potentially metallogenically fertile mantle impregnated with critical elements (including Au, Cu, Ni? and platinum group elements [2]). *Thirdly*, the formation of Archean cratons provide an architectural lithospheric mantle-scape of regions with contrasting rheology, composition and depth penetration. The cohesive Archean domains control magma and fluid pathways around their margins, and may act as both sinks and sources for ore-forming elements depending on the geodynamic evolutionary stage. *Fourthly*, if this first stabilisation of lithospheric mantle at 3.5 Ga signalled the end of an overturn regime (either uniquely, or intermittent with subduction), then long-lived tectonic regimes conducive to mineralising systems (e.g. back-arc basins, passive margins, cratonic boundaries) became available.

[1] O'Reilly *et al.* (2009), *Lithos*, 112, 2, 1043-1054. [2] Zhang *et al.* (2008), *E. Sci Rev* 86, 145-174.

P-T modeling reveals juxtaposition of units within the Gruf Complex (Central Alps) during orogenesis.

J. OALMANN¹, A. MÖLLER² AND R. BOUSQUET³

^{1,2}Department of Geology, University of Kansas, USA,
(joalman@ku.edu, amoller@ku.edu)

³Institute of Geosciences, Christian-Albrechts-Universität zu Kiel, Germany, (bousquet@min.uni-kiel.de)

Equilibrium assemblage diagrams calculated with Theriak-Domino are used to constrain peak P-T conditions of sapphirine granulites and migmatitic paragneisses. Residual orthopyroxene + garnet + sapphirine + sillimanite granulites record peak conditions of 900–960°C at 8–10 kbar. Subsequent UHT decompression to <8 kbar produced cordierite coronae around peak minerals. Complex compositional zoning patterns in garnet porphyroblasts suggest no diffusional equilibration at peak conditions and thus a short-lived UHT event. Muscovite-bearing and muscovite-free paragneisses reached peak conditions of 650–700°C and 700–750°C, respectively, at ≤7.5 kbar. The paragneisses contain no evidence for UHT metamorphism. The different peak conditions suggest that peak metamorphism of the granulites and paragneisses occurred at different crustal levels. The granulites and associated charnockites were subsequently juxtaposed against the paragneisses and associated orthogneisses along mylonitic shear zones.

Ages of zircon rims in granulites suggest they underwent UHT metamorphism at ≥32.7±0.5 Ma (Liati & Gebauer, 2003, *SMPM*). Variably deformed aplite and pegmatite dikes crosscut all other rock types and are deformed within the mylonitic contacts between the granulite–charnockite and paragneiss–orthogneiss units (Galli, 2010, PhD thesis, ETH Zürich). The dikes crystallized at ≤30 Ma, suggesting juxtaposition occurred between 33 and 30 Ma, coeval with crystallization of the Bergell tonalite–granodiorite. By c.24 Ma, the granulites and thus the entire Gruf Complex cooled below the U-Pb closure temperature of rutile (Oalman *et al.*, 2011, Goldschmidt abstract), coinciding with crystallization of the Novate S-type leucogranite and the latest, undeformed dikes.

UHT metamorphism coincides with the transition from (U)HP to Barrovian metamorphism in the Central Alps. Therefore, heat for UHT metamorphism likely resulted from asthenospheric upwelling after slab breakoff. Exhumation and juxtaposition of units within the Gruf Complex was likely related to the emplacement of the Bergell intrusion.

Isotope effect in the formation of solid water by surface reactions at 10 K

YASUHIRO OBA, NAOKI WATANABE
AND AKIRA KOUCHI

Institute of Low Temperature Science, Hokkaido University,
JAPAN. e-mail:(oba@lowtem.hokudai.ac.jp)

D/H ratio of water in molecular clouds (MCs) is often 2-3 orders of magnitude higher than that of terrestrial ocean water ($D/H \sim 1.56 \times 10^{-4}$). Such a significant deuterium enrichment often observed not only for water but also organic compounds like formaldehyde and methanol in MCs [1] cannot be explained by the gas-phase fractionation only. It is at present widely recognized that grain-surface reactions are crucial for the formation and deuterium enrichment of those molecules.

Among various reactions proposed, the reaction $OH+H_2 \rightarrow H_2O+H$ is considered to have a significant contribution (>70%) to H_2O formation in dense MCs [2] where the typical temperature is ~ 10 K. It is therefore reasonable to assume that deuterated water like HDO could also be formed by the similar surface reactions such as $OH+D_2 \rightarrow HDO+D$ and $OD+H_2 \rightarrow HDO+H$. In the present study, we performed laboratory experiments on the formation of water (H_2O , HDO, or D_2O) by reactions of OH/OD with $H_2/HD/D_2$ on a solid substrate at 10 K.

Experiments were performed under ultra-high vacuum conditions ($\sim 10^{-8}$ Pa). OH or OD radicals were produced by the dissociation of H_2O or D_2O in microwave-induced plasma and cooled to 100 K. Each radical was codeposited with H_2 , HD, or D_2 on a substrate at 10 K.

We found that all reactions studied occur on the substrate at 10 K. However, the reaction efficiency was clearly different between H- and D-atom abstraction reactions from H_2 , HD, or D_2 . The former reactions (e.g. $OH+H_2 \rightarrow H_2O+H$) were about 10 times more efficient than the latter (e.g. $OH+D_2 \rightarrow HDO+D$). The difference in efficiency is derived from the different effective masses of reactions. The efficiency does not depend on the kind of hydroxyls (OH or OD) but only on that of atoms abstracted.

The present study suggests that one of the important factor to control the D/H ratio of water in MCs is OD/OH ratio. If OD and OH were produced by D- and H-addition to O atoms on grains, respectively, atomic D/H ratio in MCs would be crucial for constraining the D/H of water in MCs.

[1] Roueff & Gerin (2003) *Space Sci. Rev.*, **106**, 61–72. [2] Cuppen & Herbst (2007) *Astrophys. J.*, **668**, 294–309.

Distribution of iron (II) in the Northwestern Pacific

H. OBATA¹, S. TAKAHASHI¹, T. GAMO¹
AND J. NISHIOKA²

¹ Atmosphere and Ocean Research Institute, University of
Tokyo, Chiba 277-8564, Japan

² Institute of Low Temperature Science, Hokkaido University,
Hokkaido 060-0819, Japan

Iron is an essential micronutrient for marine phytoplankton and its availability affects marine primary production in the ocean. Among iron species in seawater, Fe(II) is readily bioavailable form for phytoplankton, but its distribution is not clearly revealed. In this study, the distribution of Fe(II) along the 160° E line in the Northwestern Pacific was investigated. Seawater samples were collected during the R/V Hakuho-maru cruise (6 July – 3 August, 2012) with acid cleaned X-Type Niskin samplers deployed onto a CTD-CMS. Dissolved Fe(II) was determined quickly after sampling onboard the ship with luminol chemiluminescence method [1].

We observed the Fe(II) maximum (6 – 54 pM) in the oxygen minimum zone (OMZ) commonly. Dissolved oxygen concentrations were 14 – 58 μ M in the OMZ, where in-situ Fe(III) reduction did not occur. During the remineralization process of biogenic particles, Fe(II) was probably released and / or produced in the reducing conditions within the settling particles [2].

[1] King *et al.* (1995) *EST* 29, 818-824. [2] Kondo & Moffett (2013) *DSR-I* 73, 73-83.

Ions, vapors and/or nanoparticles penetrating volcanic edifices?

J.H. OBENHOLZNER (1), J. L. PARKS (2),
M. EDWARDS(2) AND P. FULIGNATI(3)

¹NHM/Volcanology, Postfach 417, A-1014 Vienna,
Austria/Europe; (obenholtzner@a1.net)

²Virginia Polytechnic Institute And State University, 418
Durham Hall, Blacksburg, VA 24061-0246, USA;
(jparks@vt.edu; edwardsm@vt.edu;)

³Dipt. di Science della Terra, University of Pisa, Via S. Maria,
53, 56126 Pisa, Italy;(fulignati@dst.unipi.it.

A top-sealed plastic tube with a diameter of ca. 15 cm had been buried ca. 70 cm deep vertically at the base of La Fossa volcano, Vulcano island, Italy, next to the front of the obsidian flow. The tube had been filled with layered rock and quartz wool to condense vapors emanating from the soil. At ca. 75 cm below the surface the sample had been exposed to vapors from Sept. 2005 to April 2006. The leached sample had not been in touch with the ground. 2 other glass wool cushions (ca. 10 cm thick, uncompacted) had been underneath to minimize capillary effects. A rock wool layer not touching ground revealed nucleated sylvite (KCl ~10 μm in size) and barite (BaSO_4 ~5-10 μm in size) crystals by SEM/EDS in its basal portion. Other very small (< 2 μm) particles were observed on the rock wool fibers but we could not identify them because they were suddenly volatilized by the electron beam. The bright appearance in backscattered images suggests that these particles may be metal compounds. The nucleation of sylvite and barite documents the presence of ions. Leaching of the quartz wool at room temperature with deionized H_2O and ICP-MS analysis documented 4 groups of elements: 1. positive signal: Mg, K, Ca, Cr, Mn, Ni, (Ba); low to moderate volatility at magmatic conditions. 2. unclear signal: Al, Si, P, Fe; low volatility at magmatic conditions. 3. no signal: V, As, Se, Mo, Co. As, Se, Mo, V are considered to be highly volatile, Co got a low volatility. 4. positive signal: Cu, Zn, Cd, Sn, Pb, W; high volatility at magmatic conditions. Leaching with nitric acid documented also V and Fe, and produced higher values for all elements, except K and Sn. This experiment documents for the first time an unknown element transport by vapors/gases through a volcanic edifice interacting with hydrothermal and magmatic gases. More information can be found at <http://www.iugg2007perugia.it/webbook/>

Volatiles in arrojadite: combining single-crystal XRD and FTIR microspectroscopy

R. OBERTI ^{1*}, G. DELLA VENTURA², F. BELLATRECCIA²
AND F. RADICA²

¹ CNR-IGG, UOS Pavia, Italy,(oberti@crystal.unipv.it)

² University of Roma Tre, Rome, Italy

Arrojadites are complex phosphates typically found in granitic pegmatites or hydrothermal veins, although their occurrence in metamorphic rocks suggests wider conditions of formation. Re-examination by EMP, LA-ICP-MS and single-crystal XRD analysis of a set of samples from various occurrences lead to revise the structure, the formula and the nomenclature of the group [1,2]. The correct structural model for arrojadite implies three OH-groups: two of these (W1 and W2) have similar local environment (they bridge three octahedra), crystallographic orientation and hydrogen-bond system. W3 is connected with the apical oxygen of a newly defined tetrahedron in the structure, and is involved in a bifurcated hydrogen bridge with surrounding oxygen atoms. Raman spectra reported in [1] show two higher-frequency, intense and convoluted bands which were assigned to specific local environments of W1 and W2; an additional low-frequency, broad and weak feature in the spectra could not be assigned with certainty. We report in this work on a FTIR study of various samples studied in [1,2]. Chemical zoning of the volatile components was checked by FTIR imaging using an FPA detector fitted on a Bruker Hyperion 3000 microscope. In contrast with the Raman spectra, the FTIR patterns show a very intense and broad absorption extending from 3500 to 2900 cm^{-1} . Single-crystal XRD has shown that F is ordered at the W1 site, and this generates a significant modification of the FTIR pattern, as observed on holotype fluoro-arrojadite-(BaFe) from Sidi Bou Kricha (Morocco).

The FTIR spectrum of holotype arrojadite-(KNa) from Rapid Creek shows also an intense doublet at 3190-3087 cm^{-1} which can be assigned to NH_4^+ groups, as later confirmed by EMPA. The orientation of the absorber (i.e. the O-H bond) with respect to the crystallographic axis can be determined from polarized-light measurements along the principal optical direction [4]. In all the samples, no evidence of molecular water is present in the NIR 4000-6000 cm^{-1} region.

[1] Cámara *et al.* (2006) *Am. Mineral.* **91**, 1249-1259.
[2] Chopin *et al.* (2006) *Am. Mineral.* **91**, 1260-1270. [3] Libowitzky & Rossman (1996) *Phys. Chem. Miner.* **23**, 319-327.

Rare Earth Elements in the sediments of Lake Baikal

L. M. OCH^{1*}, B. MÜLLER¹, A. ULRICH^{2†}, A. VOEGELIN³,
A. WICHSER², E. A. VOLOGINA⁴ AND M. STURM³

¹Eawag, Swiss Federal Institute of Aquatic Science and Technology, CH-6047 Kastanienbaum, Switzerland (*correspondance: lawrence.och@eawag.ch)

²Empa, Materials Science and Technology, CH-8600 Dübendorf, Switzerland (†passed away)

³Eawag, Swiss Federal Institute of Aquatic Science and Technology, CH-8600 Dübendorf, Switzerland

⁴Institute of the Earth's Crust, Siberian Branch of the RAS, Irkutsk, 664033, Russia

Lake Baikal is the deepest and oldest lake on Earth. However, the biogeochemical cycling of major and trace elements in this oligotrophic lake and its watershed have received relatively little scientific attention. The Rare Earth Elements (REEs), in particular, have gained importance as powerful tracers of chemical processes on the Earth's surface as they form a relatively coherent group of elements with, nonetheless, sensible differences among them. Cerium (Ce) and Europium (Eu), for example, are the only REEs which exhibit redox-sensitivity. The present study offers an overview over the REE chemistry in Lake Baikal and its catchment area and more specifically their distribution in five short sediment cores distributed across the Lake at different depths whereby we analysed and discussed normalised REE patterns and their consequential Ce, Eu and gadolinium (Gd) anomalies. We found that, while particulate REE concentrations are mainly influenced by processes above or near the surface of Lake Baikal, such as the development of a widespread negative Ce anomaly, early diagenetic chemical activity is best reflected in the dissolved fraction of the REEs, where their complexation with inorganic and organic ligands plays an important role in addition to adsorption onto metal oxides and clay minerals. A further extraordinary feature found within the lake's sediments are highly positive Eu anomalies, which are otherwise rare in sedimentary systems, in particular within Fe- and Mn-oxide accumulations buried within the reducing part of the sediment. Eu anomalies correlate with elevated barium (Ba) contents which are likely associated with phosphates and/or manganese oxides and we argue that Eu substitutes for Ba. Furthermore, while the Ce and Eu anomalies are formed within the watershed and the sediment respectively, the omnipresence of positive Gd anomalies in the sediment and the pore waters can be traced back to the atmospheric input into the lake.

Uptake of radiocesium by crops from soils contaminated by the Fukushima Accident

K. ODA^{1*}, Y. MURAMATSU^{1*}, T. OHNO¹, T. KOBAYASHI²
AND S. FUJIMURA²

¹Department of Chemistry, Gakushuin University, Mejiro 1-5-1, Toshima, Tokyo, 171-8588, Japan

(*correspondence: 12142005@gakushuin.ac.jp, yasuyuki.muramatsu@gakushuin.ac.jp)

²Fukushima Agricultural Technology Centre, Koriyama, Fukushima, 963-0531, Japan

Cs-137 ($T_{1/2}$: 30.1 y) and Cs-134 ($T_{1/2}$: 2.06 y) were released by the accident of Fukushima Daiichi NPP and agricultural fields in Fukushima prefecture were widely contaminated. More than 2 years after the accident, some crops exceed the guideline for radiocesium (100 Bq/kg) and the mechanism of higher uptake is poorly understood. We investigated radiocesium and stable element concentrations in rice plants and komatsuna (a leafy vegetable) grown in soils which were collected from the contaminated fields in Fukushima Prefecture. We discuss mechanisms of radiocesium transfer with special reference to the soil characteristics in this study.

Cultivation experiments using soil that was contaminated with radiocesium were carried out in Fukushima Agricultural Technology Centre and the radiocesium concentrations of both soil and plant samples were determined by a Ge-detector at Gakushuin University. The plants were cultivated in Wagner pots (3 L) in a greenhouse.

As a results, the highest values for transfer coefficient were observed in crops grown in brown forest soils, while the plants cultivated in gray lowland soil showed the lowest values. In order to compare soils with different radiocesium levels, we collected them from the top layer with high radiocesium concentrations (upper 5 cm) and from the underlying soil with lower concentrations (5–15 cm). We cultivated komatsuna and found that the transfer coefficients of plants grown in the underlying soils are greater than those of komatsuna planted in the surface soils. This might be related to the speciation of radiocesium in the soils. Deeper layers may have more labile, plant-available radiocesium, while less labile particulate-bound radiocesium from the accident may be more common in the surface soils.

Additionally, we have also carried out stable element analysis (including Cs) in crops and soil extracts to examine whether there is any correlation between the transfer factor of radiocesium and that of stable elements.

Assessment of Groundwater Quality in some parts of Southwestern Nigeria

*ODUKOYA ABIODUN MARY¹
AND LANIYAN TEMITOPE²

¹Department of Geosciences, University of Lagos, Nigeria
(*correspondence: mabiiodun@unilag.edu.ng)

²Department of Geology, Olabisi Onabanjo University, Ago
Iwoye, Nigeria.

One hundred and twenty samples from groundwater were collected at Ago Iwoye, Oru and Ijebu Igbo, Southwestern Nigeria. The purpose was to establish preliminary baselines for these constituents in the ground water of the study area and also to determine the quality. The analysis of trace elements and cations in water were carried out using inductively coupled plasma optical emission spectrometry (ICP-OES at Acme, Ontario Canada. Concentrations of 34 elements which include trace and major elements such as Al, As, B, Ba, Be, Ca, Cd, Ce, Co, Cr, Cu, Fe, K, Li, Mg, Mn, Mo, Na, Ni, P, Sb, Se, Si, Te, Ti, Tl, U, V, W and Zn were determined. Trace elements like Si, Bi and Ti were below detection level of 0.05ppb, 0.05ppb and 10ppb respectively for all the samples. As, Be, Cd, Cr, Cu, Mn, Se and Zn were below Maximum Contamination Level (MCL) of EPA 2012 for all the samples. Al, Br, Fe, Mn, Ni, Pb, Sb were above the standard and generally pose health or environmental hazard for most of the samples with the following ranges <1-2686ppb, 5.48-2199.35ppb, <10-22450ppb, <0.05-52.8ppb and 0.09-11.64ppb respectively. The pollution index among all sites varied from 0.075 to 6.26 and exceeded the acute and chronic effect levels proposed by the United States Environmental Protection Agency in 2007.

Production of S-MIF Signatures during Photochemistry of Biogenic Volatile Sulfur Compounds: A Potential Marker for Marine Stratospheric Sulfur Aerosol Layer

HARRY ODURO¹ AND SHUHEI ONO¹

¹Department of Earth, Atmospheric, and Planetary Sciences,
MIT, 77 Massachusetts Avenue, Cambridge, MA 02139-
4307, USA. E-mail: (Hoduro@mit.edu)

Sulfur mass-independent fractionation (S-MIF) has been reported for UV-photochemistry SO₂ and CS₂ but not for OCS and H₂S. These experimental observations have been linked to S-MIF signatures observed in sedimentary sulfides and sulfates of Archean and Early Palaeoproterozoic age, and have been used as evidence for a low-pO₂ atmosphere on the Early Earth. Although biogenic methylated sulfur compounds is important in atmospheric sulfur cycles today, multiple-S isotope effects of photochemistry of dimethylsulfide (DMS), dimethyldisulfide (DMDS), dimethyltrisulfide (DMTS), and episulfides (e.g., ethylene sulfide (ES)) have not been reported. Characterizing multiple sulfur isotope effects during photochemistry of these organic sulfur compounds may be used to study the fate for marine biogenic sulfur, particularly DMS photochemistry, which is the most abundant biogenic sulfur gas in our present atmosphere.

We will report that broadband UV-photolysis of DMS, DMTS, and ES using a Xenon-Arc lamp produced S-MIF signals with magnitudes of Δ³³S up to +2.9‰ and Δ³⁶S up to +0.9‰ for the solid aerosol sulfur products with significant changes in δ³⁴S fractionations up to +7.1‰. UV-photolysis experiments with water vapor produced relatively small to no S-MIF signals in some of their oxidation products (e.g., sulfate and sulfonic), which may likely result from HO_x oxidation reactions via direct or indirect photodissociation reactions of: O₂ → O + O, and H₂O + O → 2HO. These biogenic gases undergo a rapid oxidation when emitted to the present day atmosphere, and its oxidation products can be transferred above the tropopause and contribute to stratospheric cloud-condensation nuclei (CCN). Our results suggest that the production of S-MIF could be potentially possible even in today's atmosphere containing biogenic sulfur gases. We hypothesize that these S-MIF signals can be used as a marker to identify the source of sulfur aerosols where biogenic sulfur constituents affect radiative forces.

What can spectral properties of SNCs and Martian surface tell us about crust-mantle system evolution?

A. ODY^{1*}, F. POULET², D. BARATOUX³, J.-P. BIBRING²,
M. TOPLIS³ AND C. QUANTIN¹

¹LGLTPE, 69622 Villeurbanne, France (*correspondence: anouck.ody@ias.u-psud.fr)

²IAS, 91405 Cedex Orsay, France

³Observatoire Midi-Pyrénées, 31400 Toulouse, France

The SNC meteorites are the only samples of Mars available for analysis on Earth, providing unique insights into the formation and evolution of the Martian crust-mantle system. However, the absence of identified source regions and the debate surrounding the age of shergottites limits exploitation of the mineralogical and geochemical information provided by these rocks. With this in mind, a comparison between the near-infrared (NIR) spectral properties of the SNCs and spectra of the Martian surface from the NIR imaging spectrometer OMEGA/MEx has been made. We show that shergottite spectra are comparable to those of early Hesperian volcanic provinces such as Syrtis Major, consistent with an age of these meteorites more ancient than the Amazonian [1]. This result is largely controlled by the fact that the pyroxene mineralogy inferred for Hesperian terrains is comparable to that of the basaltic shergottites.

Additional constraints on the formation and evolution of the crust-mantle system can be provided by the study of olivine, which is a precious marker of magmatic processes. The global distribution of olivine as seen with OMEGA shows that olivine is mainly associated with three different geological settings [2]: (1) ejecta around the Hellas basin with an intermediate to forsteritic composition suggesting a Mg# >50 for the excavated upper mantle, (2) large impacts and crustal outcrops that argue for olivine in deeper sections of the crust in the form of cumulates or alternatively in a global layer of older (early Noachian) rocks, (3) early Hesperian lava flows throughout the Martian surface suggesting a planetary event of olivine-enriched fissural volcanism. In contrast, olivine is not detected in Noachian terrains that formed the major part of the southern highlands. This fact could be related to an evolution in magma composition or in the degree of olivine fractionation between these two epochs.

These results will be discussed in light of the predictions of petrologic models for the formation and evolution of the Martian crust-mantle system [3,4].

[1] Bouvier *et al.*, 2009, *EPSL*, 280, 285-295. [2] Ody *et al.*, 2013, *JGR*, 117, E00J14. [3] Elkins-Tanton *et al.*, 2005, *JGR*, 110, E12. [4] Baratoux *et al.*, 2013, *JGR*, 118, 1-6.

Reversibility of calcium and magnesium isotopic signatures during ambient temperature fluid-carbonate mineral interaction

E. H. OELKERS^{1*}, P. POGGE VON STRANDMANN², U.-N. BERNINGER¹ AND V. MAVROMATIS¹

¹GET, CNRS, UMR 5563, Toulouse, FRANCE

(* corresponding author, oelkers@get.obs-mip.fr)

²Earth Sciences, University of Oxford, Oxford OX1 3AN UK

The interpretation of mineral isotopic signatures in low temperature fluid-rock systems commonly relies on the assumption that they remained unchanged since their precipitation over geologic time, despite potentially being out of isotopic equilibrium with their co-existing fluids (e.g. the use of carbonate isotopic compositions to deduce paleo temperatures). Similarly, fluid compositions are frequently interpreted assuming that isotopes are conservatively transferred from minerals to fluids as they dissolve.

In an attempt to test such assumptions, we have dissolved both calcite and hydromagnesite ($\text{Mg}_5(\text{CO}_3)_4(\text{OH})_2 \cdot 4\text{H}_2\text{O}$) in closed-system reactors from far to near to equilibrium conditions in aqueous $\text{NaHCO}_3/\text{Na}_2\text{CO}_3$ solutions at constant pH from 6.5 to 9. Ca and Mg were strongly fractionated during the stoichiometric dissolution of these minerals; in each case the fluid is significantly isotopically heavier than the dissolving mineral. For example, calcite dissolution at pH ~6.8 yielded a fluid phase that was ~0.65‰ heavier than the dissolving mineral during the 3 days required to attain equilibrium. Correspondingly, the calcium in the solid phase became ~0.14‰ higher during this experiment. Isotope fractionation during stoichiometric dissolution is interpreted to stem from the two way transfer of material to and from the mineral as equilibrium was approached, consistent with the concept of microreversibility. Preliminary mass balance calculations suggest that more than 20% of the Ca contained in the calcite present in this experiment must have passed through the fluid phase to attain this degree of fractionation. Similarly, hydromagnesite dissolution at ~pH 8.4 yielded a fluid phase that was ~0.3‰ heavier than the dissolving mineral during the 3 days required to attain equilibrium. In some cases, the isotopic composition of the fluid continues to evolve after the mineral attained elemental equilibrium. These observations clearly contravene the concept of conservative isotopic mass transfer during mineral dissolution and questions the degree to which mineral isotopic signatures can be preserved in low temperature systems.

Using coupled Fe-Mg chemical and isotopic diffusion profiles to model magma residence times of crystals

M. OESER^{1*}, S. WEYER¹, R. DOHMEN², I. HORN¹
AND S. SCHUTH¹

¹Leibniz Universität Hannover, Institut für Mineralogie,
Callinstr. 3, 30167 Hannover, Germany (correspondence:
m.oeser@mineralogie.uni-hannover.de)
²Ruhr-Universität Bochum, Institut für Geologie, Mineralogie
und Geophysik, Universitätsstr. 150, 44780 Bochum,
Germany (ralf.dohmen@rub.de)

Recent studies have shown that chemical diffusion at magmatic temperatures generates Fe and Mg isotope fractionation in olivine that exceeds potential equilibrium isotope fractionation by an order of magnitude [1,2]. Accordingly, diffusion-generated Fe-Mg chemical zoning in olivine should be coupled with Fe-Mg isotopic zoning. In this case, magma residence times of crystals can be derived by adequate modeling of both, chemical and isotopic zoning.

This approach has been tested on olivine grains in basaltic rocks from the Massif Central volcanic region (France). Large, chemically zoned olivines were analyzed by femtosecond laser ablation MC-ICP-MS. With this technique an external precision of $\pm 0.10\%$ (2 SD, based on replicate analyses of glass standards) can usually be achieved for both $\delta^{56}\text{Fe}$ and $\delta^{26}\text{Mg}$.

Several olivines show significant Fe-Mg isotopic zoning (of up to 1.5‰ for $\delta^{56}\text{Fe}$ and up to 0.8‰ for $\delta^{26}\text{Mg}$) that is coupled with the chemical zoning (i.e. Mg#). Furthermore, the zoning profiles of $\delta^{26}\text{Mg}$ and $\delta^{56}\text{Fe}$ are negatively correlated. This strongly indicates that the observed zoning was generated by diffusion of Fe into and Mg out of the olivine during magma evolution (e.g. [3]). Simplified and independent modeling of Fe- and Mg- chemical and isotopic zoning was used to estimate the duration of Fe-Mg inter-diffusion between crystal and melt, which may reflect the residence time in a magma chamber before eruption [4]. Our results point to minimum magma residence times between 0.5 and 10 years, which is similar to the short timescales determined by diffusion modeling of chemical gradients in olivines hosted in basaltic lava flows from Mt. Etna [5].

A major focus of our project is to apply our developed technique to olivine crystals in MORBs to improve our knowledge on magma evolution at mid-ocean ridge settings. Olivines from the Mid-Atlantic Ridge and the Costa Rica Rift show both normal zoning and reverse zoning of forsterite (up to 4 mole percent). Fe-Mg isotopic profiles will be determined to prove whether the chemical zoning was generated by diffusion and thus provides information on magma residence times of these olivines.

[1] Teng *et al.* (2011) *EPSL* **308**, 317-324. [2] Weyer & Seitz (2012) *Chem. Geol.* **294-295**, 42-50. [3] Dauphas *et al.* (2009) *EPSL* **288**, 255-267. [4] Costa *et al.* (2008) *Rev. Mineral. Geochem.* **69**, 545-594. [5] Kahl *et al.* (2011) *EPSL* **308**, 11-22.

The transport of toxic elements in river affected by acid thermal water and effect of dam against elemental distributions

Y. OGAWA¹, D. ISHIYAMA¹, N. SHIKAZONO²
AND N. TSUCHIYA³

¹ Center for Geo-Environmental Science (CGES), Graduate
School of Engineering and Resource Science, Akita
University, Akita010-8502, Japan (*correspondence:
y_ogawa@gipc.akita-u.ac.jp)
² Department of Applied Chemistry, Faculty of Science and
Technology, Keio University, Kanagawa 223-8522, Japan
³ Graduate School of Environmental Studies, Tohoku
University, Miyagi 980-8579, Japan

Acid waters accompanied by mining activities commonly cause environmental problems worldwide. The same is true for the acid thermal waters. The Shibukuro and Tama rivers in Akita Pref., northeast Japan, were one of the most contaminated river system in Japan due to discharge of the the Tamagawa thermal water. This thermal water has being neutralized before inflowing into this river system. The Tamagawa Dam was constructed, and the man-made lake is also contributing dilution of acidic river water. In this study, we investigated the changes in physico-chemical status of As, Cd and Pb originated from the Tamagawa thermal water and their fractionation during river transport.

The geochemical behaviors of As and Pb are mainly controlled by the pH-dependent sorption onto ferric and aluminum solid materials. At upstream region, As tends to be sorbed onto bedrocks and the suspended hydrous ferric oxide (HFO) during river transport. The suspended HFO sorbing As is transported to man-made lake, and the most As originated from the Tamagawa thermal water settled onto the lakebeds. Due to the pH increase, Pb is considerably removed at this lake, although the Pb spread toward the downstream is not completely suppressed. On the other hand, Cd sorption onto both Fe and Al solid phases is not observed in the entire study reach, but Cd concentration is diluted at the lake.

Downstream from the Tamagawa Dam, paddy fields are widely distributed. Accordingly, it is concluded that the Tamagawa Dam plays environmentally important role for not only the neutralization of acid thermal water but also the dilution of toxic elements and/or suppression of their spread.

Biomineralization of jarosite by *Purpureocillium lilacinum*, an acidophilic fungi isolated from Río Tinto

M. OGGERIN^{1*}, F. TORNOS¹, N. RODRÍGUEZ¹, C. DEL MORAL², M. SÁNCHEZ-ROMÁN¹ AND R. AMILS^{1,2}

¹ Centro de Astrobiología, INTA-CSIC, 28850 Torrejón de Ardoz, Madrid, Spain (*presenting author: oggerinom@cab.inta-csic.es)

² Centro de Biología Molecular Severo Ochoa, CBMSO (CSIC-UAM), Madrid, Spain (correspondence: ramils@cbm.uam.es)

Río Tinto (Huelva, Southwestern Spain) is an extreme environment with a remarkably constant acidic pH and a high concentration of heavy metals, conditions generated by the metabolic activity of chemolithotrophic microorganisms thriving in the rich complex of the Iberian Pyrite Belt (IPB).

In this study, we report the specific biomineralization of (hydronium)-jarosite, an iron sulfate mineral that appears in abundance on Río Tinto banks by an acidic fungal isolate, *Purpureocillium lilacinum*. Different fungal species were isolated from Río Tinto; characterized, cultured and tested for their ability to promote the formation of jarosite. Of the 10 strains tested, only *P. lilacinum* was able to produce jarosite. The biomineral was characterized by X-Ray Diffraction (XRD) and its formation was observed with high-resolution transmission electron microscopy (TEM) and scanning electron microscopy (SEM) coupled to Energy-dispersive X-ray spectroscopy (EDX) microanalysis.

Jarosite began to nucleate on the fungal cell wall, even on dead cells (although with much less efficiency). Also extracellular polymeric substances (EPS) released by the fungus could serve as nucleation sites for this biomineralization process. Our model proposes the creation of Fe³⁺/Fe²⁺-rich microdomains in the cell walls of *P. lilacinum* that induce the supersaturation and precipitation of jarosite. This change in the proportions of reduced and oxidized iron species, can be produced by the electrostatic interaction between soluble ferric iron and the negatively charged groups of the fungal cell wall, acting as nucleation sites for mineral precipitation according to previous studies [1].

The occurrence of *P. lilacinum* in an ecosystem with high concentrations of jarosite strongly suggests that might participate actively in the formation of this mineral in the river banks.

[1] Konhauser (1998) *Earth Sci Rev* **43**, 91-121

The biological control on the atmospheric *p*CO₂ level through geologic time

HIROSHI OHMOTO¹ AND ANTONIO C. LASAGA²

¹NASA Astrobiology Institute and Dept. of Geosciences, Penn State University, University Park, PA 16802, USA. (hgo@psu.edu); ²Geokinetics, 213 E. Mitchel Av., State College, PA 16803, USA; (hjb2@psu.edu)

Here we constrain the atmospheric *p*CO₂ levels during the evolution of the Earth's biosphere through pre-biotic, anaerobic, pre-plant aerobic, and plant stages based on the BLAG-type geochemical modeling of CO₂ cycling. We have developed a new set of equations considering: (i) the flux and fate of CO₂ and reduced volcanic gases; (ii) the biological influence of soil formation; (iii) the cycling of phosphorus-bearing compounds; (iv) the C/P ratios of kerogen; (v) the burial efficiency of organic matter in sediments; (vi) the weathering efficiency of kerogen; (vii) the production efficiency of biogenic CH₄; and (viii) the formation of organic haze in the atmosphere and the deposition of haze-C in sediments. Our modeling suggests that the atmospheric *p*CO₂ remained at >100 PAL during most of the pre-biotic-, anaerobic-, and pre-plant aerobic stages. No additional greenhouse gases (e.g., CH₄, H₂) were necessary to maintain a warm Earth under a faint young Sun. A transition of the biosphere caused a drastic change in the atmospheric *p*CO₂ level: a drop from >1,000 to ~100 PAL due to the development of an anaerobic world; a rise from ~100 to ~1,000 PAL during the anaerobic to aerobic transition; and a drop from ~20 to ~2 PAL due to the development of the plant world. Fluctuations in the soil-forming land area profoundly affect the climate of the Earth. Continental breakup would result in a global cooling event, while the formation of supercontinents would result in global warming.

Ocean-pH evolution and weathering conditions during the Ediacaran: Insights from B, Sr & Li isotopes at the Gaojiashan Section, South China

FRANK OHNEMUELLER^{1,*} ANETTE MEIXNER¹ ANTONIA GAMPER² AND SIMONE A. KASEMANN¹

¹ Dept. of Geosciences, University of Bremen, Leobener Str., D-28359 Bremen, *(fohnemue@marum.de)

² Museum für Naturkunde, Invalidenstr. 43, D-10115 Berlin

The Ediacaran to Cambrian transition was a decisive time in Earth history since substantial changes in ocean-atmosphere interactions, climate, tectonics and bio-geochemical processes catalyzed the advent and radiation of metazoa. In this study, we investigate the boron, strontium and lithium isotope records of the Algal Dolomite, Gaojiashan and Beiwan Members (all Dengying Formation) at the Gaojiashan section (551-542 Ma) in south-western Shaanxi, South China to gain detailed insights into changing ocean-pH and weathering conditions. The 65 m thick carbonate-siliciclastic Gaojiashan Section is located at the north-western margin of the Ediacaran Yangtze-platform. Sedimentary data suggest a near shore shallow water setting that is exceptionally well preserved and only present in this part of the platform. Carbonate sedimentation is influenced by continuous detrital input presumably from a pro- and retrograding delta front.

In the upper part of the Gaojiashan Member, a negative $\delta^{13}\text{C}$ and $\delta^{11}\text{B}$ anomaly is unveiled with nadirs down to $\sim -7\text{‰}$ for carbonate carbon and -2‰ for boron, respectively. In total, the excursion comprises a shift of -13‰ for $\delta^{13}\text{C}$ and -12‰ for $\delta^{11}\text{B}$ which equals a decrease of ~ 1.5 pH units. At the same time, Sr isotopes display a positive excursion ($^{87}\text{Sr}/^{86}\text{Sr}$ 0.7085 to 0.7110) indicating a time of enhanced weathering through relative sea-level fall. To further assess the continental silicate weathering flux, Li isotopes have been analysed.

If we accept that those changes in the isotope pattern and ocean geochemistry are of primary origin, it needs to be discussed whether a (temporarily) restricted environment or open-ocean conditions are recorded. In view of the pronounced negative $\delta^{13}\text{C}$ anomaly it must also be considered that the Precambrian-Cambrian boundary interval is recorded in the uppermost Gaojiashan Member and the overlying sediments already belong to early Cambrian strata.

Determination of ^{129}I by ICP-MS/MS; it's application to Fukushima soil samples

TAKESHI OHNO¹, YASUYUKI MURAMATSU¹, SHOICHI TOYODA¹ AND HIROYUKI MATSUZAKI²

¹ Department of Chemistry, Faculty of Science, Gakushuin University, Mejiro 1-5-1, Toshima-ku, Tokyo, Japan, 171-8588, (takeshi.ohno@gakushuin.ac.jp)

² Department of Nuclear Engineering and Management, School of Engineering, The University of Tokyo, 7-3-1 Hongo, Bunkyo-ku, Tokyo, Japan, 113-8656

The accident at the Fukushima Daiichi nuclear power plant (FDNPP) resulted in a substantial release of radioiodine and radiocesium into the environment. The distribution of radiocesium has been studied. On the other hand, ^{131}I could only be determined within a couple of months, due to its short half-life (8 days), resulting in a lack of data on the deposition of this nuclide. Another iodine isotope, ^{129}I (half-life: 1.57×10^7 y), was released simultaneously with ^{131}I . To reconstruct the early distribution of ^{131}I , ^{129}I has been used as a tracer. The determination of ^{129}I in Fukushima soils is of importance to investigate the distribution of radioiodine released from the FDNPP.

Recent advances in ICP-MS/MS (Agilent 8800) have enabled us to determine the long-lived radionuclide ^{129}I in soil samples. The ICP-MS/MS has an additional quadrupole mass filter, situated in front of the reaction cell, which allows only the analyte mass to enter the cell. Therefore, polyatomic interferences, such as $^{127}\text{IH}_2^+$ generated in the cell, can be reduced. In this study, we measured ^{129}I in samples collected from an orchard in Koriyama-shi (about 60 km from the FDNPP). The measured $^{129}\text{I}/^{127}\text{I}$ ratios in the samples by ICP-MS/MS are consistent with the value determined by AMS within the analytical error, suggesting the applicability of this method to measurements of ^{129}I in Fukushima soils. We also examined the depth distributions of radioiodine and radiocesium in the orchard. Sampling was carried out in April 2011 and July 2012. Our results demonstrate that, in April 2011, more than 80% of the radioiodine was distributed in the upper 4 cm of the soil column in the orchard. About one year after the accident, the proportion of the inventory in the upper 4 cm was about 60%, indicating 20% of the radioiodine had transferred to the lower part of the column. On the other hand, no significant change was observed in the depth distribution of radiocesium. This result suggests that it is difficult to use radiocesium as a tracer of ^{131}I released from the FDNPP.

Influence of depth on soil organic matter characteristics: An ultrahigh resolution mass spectrometry study

TSUTOMU OHNO^{1*}, IVAN J. FERNANDEZ², RACHEL L. SLEIGHTER³ AND PATRICK G. HATCHER³

¹Department of Plant, Soil, & Environmental Sciences, University of Maine, Orono, ME 04469-5722.

*(correspondence: ohno@maine.edu)

²School of Forest Resources, University of Maine, Orono, ME 04469-5722.(ivanjf@maine.edu)

³Department of Chemistry and Biochemistry, Old Dominion University, Norfolk, VA 23529.(rsleight@odu.edu.) (phatcher@odu.edu).

The characterization of soil dissolved organic matter (DOM) is a fundamental challenge given its diversity, chemical complexity, and importance in many vital ecosystem processes. We analyzed podzolic B horizon soil collected at multiple depths from the Bear Brook Watershed in Maine (U.S.A.) to study changes in soil DOM chemical properties with depth using ultrahigh resolution mass spectrometry.

The results show that for the B horizon-derived DOM, the Aromaticity Index (A.I.) decreases with depth, indicating that the more aromatic components of DOM are preferentially being removed either through sorption with surface functional groups and/or microbial processes. Also with increasing B horizon depth, the van Krevelen diagram classified protein- and lipid-like DOM components (those that are aliphatic) increase in relative content. Increases in these chemical classifications have been linked to microbial processes.

Soil Horizon	A.I. > 0.5	A.I. > 0.67	VKD % Proteins	VKD % Lipids
B 0-5 cm	19.5	5.3	24.0	0.2
B 5-10 cm	14.3	2.5	26.0	0.4
B 10-15 cm	11.2	1.2	26.9	0.7
B 15-20 cm	11.2	1.8	29.0	0.6
B 20-25 cm	9.1	0.6	30.9	0.8
B 25-50 cm	9.2	0.7	31.8	1.2

Table 1: Influence of soil depth on DOM chemical properties of soils from a reference hardwood stand.

The results are consistent with the hypothesis of Kaiser and Kalbitz [1], who suggested that near-surface DOM is more related to plant-derived molecules, while DOM at depth has a greater content of microbially-derived molecules.

[1] Kaiser & Kalbitz (2012) *Soil Bio. Biochem.* **52**, 29-32.

Autoradiography analysis on local area distribution of radiocesium in trees from FDNPP

T. OHNUKI^{1*}, F. SAKAMOTO¹, N. KOZAI¹, S. YAMASAKI¹, Z. YOSHIDA² AND K. NANBA³

¹ Japan Atomic Energy Agency, Tokai, Ibaraki 319-1195, Japan(ohnuki.toshihiko@jaea.go.jp)

² ATOX, Tokai, Ibaraki, 319-1112, Japan

³ Fukushima U., Fukushima, Fukushima 960-1296, Japan

The nuclear accident at the Fukushima Daiichi Nuclear Power Plant (FDNPP) occurred as a consequence of the massive earthquake and associated tsunami that struck the Tohoku and north Kanto regions of Japan on 11 March 2011. A series of hydrogen explosion was occurred from 13 March to 15 March at the units 1, 2, and 3. The release rate of ¹³⁷Cs on 15 March is estimated between 10¹² and 10¹⁵ Bq/h [1]. This fallout radioactive Cs were dispersed from FDNPP to ocean [1,2] and land [1]. Some of the released radiocesium was deposited on the area located north-west direction from FDNPP. We should elucidate the migration behavior of radiocesium in environments.

Local area distribution and relocation of radiocesium in trees has been studied by measuring its spatial distribution on/in trees using autoradiography analysis. The samples of trees were collected on the places located between 4 and 55 km from FDNPP at approximately 2, 8, 20, and 22 months after the accident. The autoradiography analyses of *Cryptomeria japonica*, *Torreya nucifera*, and *Thujaopsis dolabrata* var. *hondae* collected on approximately 2 and 8 months after the accident showed that radiocesium was mainly distributed as like spots on the branches and leaves of the trees emerged before the accident, and was little detected in new branch and leaves emerged after the accident. On the contrary, radiocesium was detected at the outermost tip of branches in the trees collected after 20 months of the accident. *Morus alba* collected after 22 months contained radiocesium in and outside of the stem, even though no radiocesium was detected in the root, strongly suggesting that some radiocesium was translocated from the outside stem to inside. These results indicate that distribution of radiocesium deposited on/in the trees has been gradually changed with time in the scale of the year.

[1] M. Chino, *et al.*, *J. Nucl. Sci. Technol.*, 48, (2011) 1129-1134. [2] H. Kawamura *et al.*, *J. Nucl. Sci. Technol.*, 48, (2011) 1349-1356.

Leakage behavior of gases to bottom water through sediment layers with gas-hydrate stable conditions

T. OHSUMI^{1*}

¹Dept. Chem., Tokai University, Kita-Kaname, Hiratsuka 259-1292, Japan (*correspondence: ohsumitk@ohsumi-jp.com)

The water under the main thermocline in the Japan Sea is a single water mass referred to as the Japan Sea Proper Water (JSPW). It can be defined as having temperature below 2.0°C, salinity above 34.0. It is known that wintertime air-sea interaction in the Japan Sea, enhanced by outbreaks of dry and cold air masses from the Eurasian continent, generates the JSPS characteristic water mass through deep convection.

Below 10 °C, carbon dioxide hydrate is stable over the pressure of 4.4 MPa. In the Japanese archipelago side of the Japan Sea basin, the area with a water depth from 200 m to 1000 m is several tens thousand square kilometers, which is attractive for the CO₂ storage in the sub-seabed geological formations with at least 10¹¹ tons of CO₂ storage capacity; in the process of upward migration, the leaked CO₂ would have much chance of hydrate formation reaction *in situ*.

While the most famous natural analog is the CO₂ seepage in mid-Okinawa Trough backarc basin found by Sakai *et al.* [1], the recently-found seafloor methane hydrate outcrops occurring on the top of the CH₄ plume in the sediment layers [2] also provides an insight into the leakage mechanism for liquid CO₂.

Gaseous CH₄ plume will be self-sustaining by its dry-out effect in the sediment and be hence developing its size as large as of several hundred meters in diameter [2], which would enhance the mixing of gas with the ambient water to make hydrate crystal growing effectively. The key is the low density of CH₄ hydrate (less than 1.0) that brings about buoyant behavior of the hydrate solid out of the bottom sediment into the overlying water column in the long run. On the contrary, liquid CO₂ might not make a gaseous plume due to its higher solubility in water and small upward migration driving force. The upward migration path could be like a dispersed mesh network in shape, partly due to the increased density of the interstitial water in contact with liquid CO₂ (*i.e.*, partial molar volume of CO₂ gas in aqueous solution is *ca.* 32cm³/mol). Self sealing of the leaked CO₂ *in situ* is probably effective, if there exist no fractures or conduits in the sediment layers.

[1] Sakai *et al.* (1990) *Science* **248**, 1093-1096. [2] Matsumoto (2013) personal communication.

The spatial distribution of chalcophile elements in terrestrial and marine areas of Japan

A. OHTA^{1*} AND N. IMAI¹

¹Geological Survey of Japan, AIST, Tsukuba 305-8567, Japan; a.ohta@aist.go.jp

The Geological Survey of Japan, National Institute of Advanced Industrial Science and Technology, has conducted research on the spatial distribution of 51 elements (Geochemical Maps) both in terrestrial and marine environments [1]. Japan is surrounded by vast sea, so it is important to know the spatial distribution patterns of elemental concentrations comprehensively in land and sea. This project is intended: 1) to elucidate background of elemental abundance in terrestrial and marine areas; 2) to find mass transport from land to sea or in marine environment; and 3) to estimate diffusion processes of pollutants.

Chalcophile elements such as Cu, Zn, As, Cd, Sb, Hg, and Pb are highly enriched in stream sediments associated with metalliferous deposits and anthropogenic activity. However, coastal seas sediments that were supplied by rivers flowing through metalliferous province are not significantly enriched in these elements. We assumed that the sulfide ores are oxidized, consequently releasing heavy elements in river water during transportation. However, Zn and Pb are exception. The high concentration areas of these elements are found both in terrestrial area associated with metalliferous deposits and the adjacent coastal sea area. It is possible that aqueous Zn and Pb released through oxidation process of sulfide are derived to coastal seas and sorbed on the sediment surface.

The influence of anthropogenic activity on geochemical maps is different from the case of metalliferous deposit. The concentrations of chalcophile elements are elevated in both the metropolitan area and adjacent inner bay. Chalcophile elements are enriched in the inner bay but poor in the outer bay. The spatial distributions suggest that the contaminated materials remain in the bay without extending to the outer sea. It is probable that the estuarine circulation prevents fine particles associated with chalcophile elements from reaching the outer sea because it flows from the outer sea to the bays.

[1] Imai, N. *et al.* (2010) Elemental distribution in Japan – Geochemical map of Japan. GSJ, AIST.

[2] Ohta, A. and Imai, N. (2011) *Advanced Topics in Mass Transfer*. (Mohamed El-Amin, ed.), pp. 373-398, InTech.

Modeling fluid migration in deep crust with modeled permeability based on wettability and energy consideration

J. OHTA^{1*} AND T. TOKUNAGA²

¹Department of Systems Innovation, University of Tokyo, Tokyo 113-8656, JAPAN (*correspondence: 7394793531@mail.ecc.u-tokyo.ac.jp)

²Department of Environment Systems, University of Tokyo, Chiba 277-8563, JAPAN

Under the high-temperature and high-pressure system in deep crustal setting, it is considered that fluid flows through deformatively polycrystalline solid [1]. Here, the solid–liquid dihedral angle which express the wettability of the system is considered to be an important factor in determining internal pore structure, and hence, permeability [2, 3]. The pore structure is formed so as to satisfy texturally and energetically stable conditions under certain dihedral angle and fluid fraction [2, 3].

We constructed a permeability model to formulate a relationship among dihedral angle, permeability and fluid fraction by taking into consideration the textural and energetic conditions. The model is based on the assumption that there exists a fluid fraction to minimize grain boundary interfacial energy under certain dihedral angle [3]. We calculated the fluid fraction and the permeability under the “minimum” interfacial energy condition as a function of dihedral angle. The generalized permeability was described as functions of the permeability and the fluid fraction under the “minimum” interfacial energy condition.

We numerically calculated fluid migration processes by applying the modeled permeability to the governing equations formulating both solid deformation and fluid flow through polycrystalline solid. We found that fluid fraction increased with decreasing permeability in the case that the change of dihedral angle was inversely proportional to depth. By setting the solid bulk/shear viscosity to be 10^{20} Pa·s, fluid fraction showed repeated fluctuation. Consequently, intervals with relatively high fluid fraction were formed. Moreover, flow regime drastically changed depending on the solid bulk/shear viscosity. Our result emphasizes the importance of wettability and spatial heterogeneity of deep crust on the fluid flow processes.

[1] Stevenson & Scott (1991) *Annu. Rev. Fluid Mech.* **23**, 305–339. [2] VonBargen & Waff (1986) *J. Geophys. Res.* **91**, 9261–9276. [3] Park & Yoon (1985) *Metall. Trans. A* **16**, 923–928.

A new mechanism for transport of water into CMB

E. OHTANI¹, I. OHIRA¹, T. SAKAI², M. MIYAHARA¹, N. HIRAO³, Y. OHISHI³ AND M. NISHIJIMA⁴

¹Department of Earth and Planetary Material Sciences, Tohoku University, Sendai 980-8578, Japan (correspondence: ohtani@m.tohoku.ac.jp)

²Geodynamics Research Center, Ehime University, Matsuyama 790-8577, Japan

³Japan Synchrotron Radiation Research Institute, Sayo, Hyogo 679-5198, Japan

⁴Institute for Material Research, Tohoku University, Sendai 980-8577, Japan

Water circulation in global Earth is one of the most important issues in geodynamics, because water can affect the physical properties including rheological property of the Earth's materials [1]. Several hydrous minerals in subducting slabs work as water carriers or reservoirs under the conditions of the upper mantle and transition zone [2]. However, it has been debated whether water can be transported into the lower mantle and core [2]. Dehydrated water in subducting oceanic crusts by decomposition of lawsonite may be trapped as a pore fluid because of a high wetting angle between garnet and water, thus resulting in coexistence of water and aluminous MgSiO_3 perovskite, which is the major mineral in the subducting oceanic crust [3]. Here we report a new mechanism for water transport into the lower mantle and core, i.e., a reaction between aluminous perovskite and water to form alumina-depleted perovskite and $\delta\text{-AlOOH}$ [4] along the slab and mantle geotherms under the lower mantle conditions. $\delta\text{-AlOOH}$ coexists with the aluminous MgSiO_3 perovskite and post-perovskite phases in the $\text{MgSiO}_3\text{-Al}_2\text{O}_3\text{-H}_2\text{O}$ system along the slab and mantle geotherms in the lower mantle. Chemical analysis of these phases revealed that the perovskite and post-perovskite phases were depleted in Al_2O_3 . Our results demonstrate the coexistence of alumina-depleted MgSiO_3 perovskite or post-perovskite phase and Mg, Si-bearing $\delta\text{-AlOOH}$ phase in wet slabs subducting in the lower mantle. Thus, Mg, Si-bearing $\delta\text{-AlOOH}$ phase thus formed transports hydrogen into the core-mantle boundary (CMB) region.

[1] Schmidt & Poli (1998) *EPSL*, 163, 361–379. [2] Ohtani *et al.* (2004) *PEPI*, 143–144, 255–269. [3] Ono *et al.* (2002) *EPSL* 203, 895–903. [4] Suzuki *et al.* (2000) *PCM* 27, 689–693.

Micro-scale sensor array-enabled hot spring mapping

J. OILER^{1*}, E.L. SHOCK¹, H.E. HARTNETT¹ AND H. YU¹

¹Arizona State University, Tempe, AZ 85287, USA

(*correspondance: joiler@asu.edu)

Micro-scale temperature and electrical conductivity sensor arrays were fabricated. The linear temperature array consisted of 15 temperature sensors with separations of 1 cm. The linear conductivity array consisted of 5 conductivity sensors with separations of 1 cm. Both arrays were deployed in hot springs at Yellowstone National Park, USA. At one site, two geochemically different hot spring outflow channels converged. One channel was acidic (pH ~3.3, temperature ~36 °C, conductivity ~900 μ S/cm). The second channel was alkaline (pH ~7.8, temperature ~60 °C, conductivity ~4200 μ S/cm). Where the two streams mixed, visually distinct bands of photosynthetic pigments were observed that were not seen elsewhere in either stream.

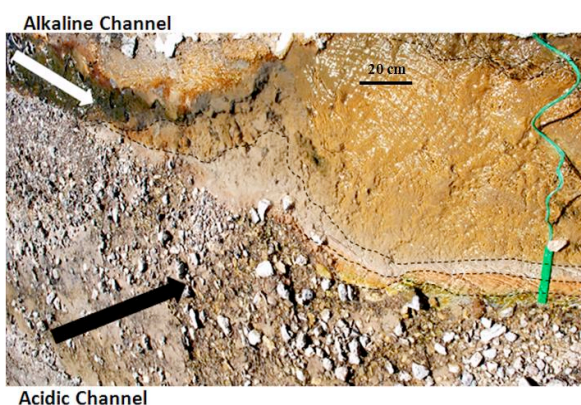


Figure 1: Photograph showing the confluence of two hot spring outflow channels. Where the alkaline channel (top – white arrow) and the acidic channel (bottom – black arrow) mix, bands of color are observed. The location between colors is assisted with dashed lines.

More than 700 temperature and 90 conductivity measurements were taken within the mixing zone using the arrays. Extremely high spatial resolution mapping of temperature and conductivity in the mixing zone was performed. The temperature color map traces out distinct regions that match the shape and width of many of the photosynthetic pigment bands. Furthermore, the temperature data were used to predict the conductivity at a higher sampling density than was measured, providing a new technique for mapping conservative constituents at high spatial resolution in mixing zones.

Development of ETV-MC-ICPMS technique for W isotope analysis

*SATOKI OKABAYASHI¹, SHUHEI SAKATA¹
AND TAKAFUMI HIRATA¹

¹Laboratory for Planetary Sciences, Kyoto University, Kyoto, Japan, (correspondance: okabayashi-s-aa@kueps.kyoto-u.ac.jp)

Hf-W chronometer is based on the negative beta-decay of r-process nuclide ¹⁸²Hf to ¹⁸²W with a half-life of 8.9 ± 0.1 Myr [1]. Hafnium is strongly lithophile elements, whereas W is moderately siderophile elements, and therefore, it has been well recognized that the Hf-W age provided critical information about the timing of metal-silicate differentiation (core formation) processes at the early stage of the planetary formation. Moreover, both the Hf and W is strongly refractory elements, the Hf-W age can reflect the timing of condensation or segregation of the metallic nuggets from chondritic reservoir at the early sequence of the solar system.

In this study, we have developed a new sample introduction system using an electrothermal vaporization (ETV)-MC-ICPMS technique in order to measure the isotope ratio from ng-amount of W. Compared to the conventional nebulization sample introduction technique, the ETV technique has significantly higher sample introduction efficiency. ETV-ICP technique has been accepted as a one of the most powerful tool to measure the small sample sizes[2]. With the conventional ETV system, despite the better sample introduction efficiency could be achieved, signal stability for the refractory elements, including W, was deteriorated. To obtain stable signal intensity profiles for W isotopes, He, instead of Ar, was used as carrier gas.

In our experiments, W sample in 0.5 - 1.0 μ L of 2wt% HNO₃ solution was loaded onto a Re filament. The filament was set into the small glass chamber (~25 mL), and then, temperature of the Re filament is controlled by the incident current (0 - 4 A) under the He gas. W signal was observed at ~1100°C. Compared to Ar gas environment, W signal stability was dramatically improved under the He gas condition. W standard solution (JMC22841) was measured several times, and the obtained ¹⁸²W/¹⁸⁴W ratios were 0.864691 ± 0.000024 from 75 ng W (n = 9) and 0.864693 ± 0.000044 from 25 ng W (n = 9) (corrected using exponential law using ¹⁸⁶W/¹⁸³W = 1.9859 [3]). In this presentation, ¹⁸²W/¹⁸⁴W ratios obtained from meteorite samples will be discussed.

[1] Vockenhuber *et al.* (2004) Phys. Rev. Lett., 93, 172501.

[2] Nixon *et al.* (1974) Anal. Chem., 46, 210-213. [3] Kleine *et al.* (2004) Geochim. Cosmochim. Acta, 68, 2935-2946.

Laboratory experiments on the effect of microbial activities on iodine speciation in seawater

N. OKABE^{1*}, Y. MURAMATSU¹ AND S. AMACHI²

¹Gakushuin University, 1-5-1 Mejiro, Toshima-ku, Tokyo 171-8588, Japan

(*correspondence:12242003@gakushuin.ac.jp)

²Chiba University, 648 Matsudo, Matsudo-shi, Chiba 271-8510, Japan

In seawater, iodine concentration is relatively constant (0.3 – 0.5 micro M). However, chemical forms of iodine are known to be variable and there are species of iodide (I⁻), iodate (IO₃⁻) and organic iodine. Due to the oxic condition in seawater, iodate is thermodynamically stable and it is dominant. In surface seawater, iodide which is a reduced form, also exists, due to presence of microorganisms, e.g. nitrate-reducing bacteria which reduce iodate to iodide (Tsunogai and Sasa, 1969; Amachi *et al.* 2007). In our previous study on the speciation of iodine in pore water of marine sediments, we found the dominant species was iodide. This was explained by the anoxic condition created by the effect of microorganisms in the sediments.

In this study, we used seawater samples collected from site on Pacific Coast such as Numadu (Suruga Bay) and Odaiba (Tokyo Bay). The samples were introduced into 50 ml glass vials after following treatments; autoclaving, filtering or addition of antibiotic substances together with unfiltered fresh samples. They were incubated under light and dark conditions at 25 °C in a laboratory. The chemical forms of iodine were determined over time using HPLC-ICP-MS.

Analytical results showed that the concentration of iodide increased and that of iodate decreased with time under light condition. This result agrees with increased iodide proportion reported in the euphoric zone. However, under dark condition, no obvious changes of iodine chemical forms were observed.

In seawater samples that were either sterilized by autoclaving or filtering, chemical forms of iodine did not change as much. These findings indicate the role of microorganisms on the transformation of iodine species.

Calcite and Chalk: Differences in Vapour Adsorption Behaviour

D.V. OKHRIMENKO*, K.N. DALBY, L.L. SKOVBJERG, N. BOVET, M.P. ANDERSSON, M.H.M. OLSSON AND S.L.S. STIPP

Nano-Science Center, Department of Chemistry, University of Copenhagen, Denmark (*denisokr@nano.ku.dk)

Calcite is a common mineral, widely used in industry and important in environmental processes. It is the main component of chalk and limestone, which serve as natural reservoirs for water and oil. Understanding adsorption energetics and wetting properties of calcite surfaces is important for developing remediation strategies for aquifers, for improving oil recovery, for minimising risk in CO₂ storage and for optimising industrial processes. We have compared the adsorption properties of synthetic calcite with those of chalk samples, composed of biogenic calcite.

We measured the heat of adsorption for water and several alcohols, from the gas phase, and determined the surface energy in order to learn more about the surface properties of these samples. XPS (X-ray photoelectron spectroscopy) was used to monitor changes in chalk surface composition when the organic content was decreased by extraction with CH₂Cl₂/CH₃OH. The affinity for vapour of polar longer chain organic compounds (e.g. alcohols) was higher for synthetic calcite than for chalk, giving enthalpies of adsorption typical for chemisorption (~100 kJ/mole). DFT/MD (density functional theory and molecular dynamics) simulations showed that the alcohols formed structured monolayers on calcite and that dispersive lateral interactions between the CH₂ tails of the adsorbed molecules contributed as much as 60% of the overall adsorption energy. Such behaviour was not observed for the chalk samples. Alcohol vapours adsorbed to chalk with lower binding energy (~80 kJ/mole), showing a distribution of adsorption energies typical for heterogeneous surfaces. After partially removing organic contamination by extraction, water and ethanol adsorption experiments showed that surface energy, mainly the dispersive component, increased. This increase might be a response to the low polarity of surface sites generated during extraction and could be connected to the presence of nanoscale clay lamellae, already seen using AFM (atomic force microscopy) chemical force mapping [1]. However, the response could also result from increased lateral interactions between the CH₂ tails of alcohols adsorbed on the calcite surface of the chalk.

[1] Skovbjerg *et al.* (2012) *Geochim. Cosmochim. Acta* **99**, 57-70

Theory on thermodynamic constraints on biogeochemical diversity

J.G. OKIE^{1*}, P. CANOVAS¹ AND E.L. SHOCK¹

¹School of Earth and Space Exploration, Arizona State University, P.O. Box 8714004, Tempe, AZ 85287. USA.
(correspondence: Jordan.Okie@asu.edu)
(Peter.Canovas@asu.edu, Everett.Shock@asu.edu)

Understanding geographic patterns of biological and geological diversity is central to ecology, evolution, biogeography, and many areas of geology. The number of energy-yielding reactions—geochemical catabolic richness—imposes fundamental constraints on the number of energy-yielding reactions harnessed by a living system—the biogeochemical catabolic richness—which in turn can influence organism and ecosystem function and taxonomic diversity. Theory on geochemical and biogeochemical catabolic richness is lacking, despite its relevance to understanding evolutionary and macroecological patterns of functional and metabolic diversity. A system's potential biogeochemical catabolic richness is the number of chemical reactions having energy-yields above some A_{\min} required to make the reaction useful as an energy source. We develop general mathematical theory based in thermodynamics and theoretical geochemistry showing how potential biogeochemical catabolic richness of a reaction system involving a given chemical species depends on temperature, pressure, concentration, A_{\min} , and the frequency distribution of the species' stoichiometric coefficients for the reactions. We then apply the theory to reactions involving H⁺ to provide mathematical predictions of how the community's potential biogeochemical catabolic richness is a function of temperature, pH, and A_{\min} . We find that the theoretical predictions closely matched empirical richness patterns of hot springs at Yellowstone National Park. The developed theory elucidates the degree to which various physicochemical variables can influence biogeochemical richness, and may have implications for patterns of functional, taxonomic and phylogenetic diversity in microbial communities.

H₂, CH₄ and NH₄ formation through low temperature water-rock reactions in ultramafic rock

OKLAND, I., THORSETH, AND I.H., PEDERSEN, R.B.

Centre for Geobiology/ Department of Earth Science, University of Bergen, Allegaten 41, N-5007 Bergen, Norway. e-mail:(Ingeborg.Okland@geo.uib.no)

H₂, CH₄ and NH₄ are electron donors potentially important for chemolithotrophic microorganisms in subsurface endolithic communities. High-temperature formation of H₂ and CH₄ in ultramafic systems is well studied. Knowledge of low-temperature processes, and the effect of ferrous secondary minerals are however limited. Here we explore the formation of these species during experimental low temperature (25°C) alteration unaltered, medium altered and highly altered dunite from continental sites.

H₂, CH₄, NH₄ and NO₃ were detected in the fluids in all three setups. We suggest that H₂ results from reduction of water due to oxidation of Fe(II) released from olivine in unaltered dunite, from brucite and olivine in medium altered dunite, and from brucite and serpentine in highly altered dunite. CH₄ may result from abiotic methanogenesis or dissolution of CH₄ containing fluid inclusions. The N-species were most likely absorbed to serpentine in the altered dunite, while the source for unaltered dunite is probably explosives used during mining.

The results indicate that water-rock reactions in medium and highly altered ultramafic rocks can provide reduced species potentially supporting microbial communities in low-temperature subsurface environments in ophiolites and near seafloor parts of ultramafic oceanic lithosphere.

Ore Mineralization Processes in the Greater Caucasus Kakheti Segment, Georgia

OKROSTSVARIDZE A.¹ AKIMIDZE K.²
AND GAGNIDZE N³

¹Iliia State University, Georgia. (okrostsva@gmail.com)

²Tbilisi State University, Georgia. (kaqimidze@tsu.ge)

³Tbilisi State University, Georgia. nonagagnidze@gmail.com)

The Greater Caucasus represents a Phanerozoic collisional orogen which is formed along the Euro-Asian continent South margin and is extended over 1200 km between the Black and Caspian Seas. The Kakheti segment is located on the eastern part of the Greater Caucasus southern slope and is mainly formed of folded Lower Jurassic clay-shales and basic volcanic-sedimentary formations, which according to geophysical data, are located on oceanic or transitional crust (Morariu, Nouval, 2009). The complex of these rocks is intersected by Middle-Upper Jurassic gabbroic, dioritic, quartz- dioritic and felsitic intrusions which caused intensive hydrothermal silicification, sericitization and ore mineralization of the fractionated host rocks (Okrostsvardize *et al.*, 2012).

The above mentioned ore mineralization was studied by supported of Georgian National Science Foundation grant (#GNSF/ST09-1071-5-150). Metals chemical analyses more than 300 ore samples were carried out in the laboratory of ACMELABS (Canada, Vancouver), using ICP-MS, by 3B, 14B, F5 and 1F15 methods.

Our research showed that ore mineralization processes genetically are related to postmagmatic events of Middle-Upper Jurassic intrusive magmatism in the Caucasus Kakheti segment. Two mineralization zones - the Northern and the Southern are distinguished here. The Northern one is mainly distinguished by pyrite-polymetallic mineralization, where content of Pb and Zn sometimes is >10000 g/t, Co - varies between 40-295 g/t, and Ag - 5-95 g/t intervals. Au doesn't have an industrial concentration (0.01-0.05g/t) in this zone. The Southern mineralized zone is represented by copper-pyrrhotitic ores, where Cu concentration sometimes is >10000 g/t, and Au reaches industrial concentrations (0.1-3.1 g/t). At the last stage of ore mineralization, at some areas of the South mineralized zone Th and Bi concentrations are detected, which genetically should be related to carbonate hydrotherms. In these rocks Th content varies from 40 to 120 g/t, and Bi - from 200 to 800 g/t, but near the Gelia ore zone concentration of Th reaches 3842 g/t, and Bi - 4806 g/t (Okrostsvardize *et al.*, 2011).

Sr stable isotopic anomalies in primitive meteorites and chondrules

WATARU OKUI^{1*}, TETSUYA YOKOYAMA¹, MASAOI UNO¹, HIKARU IWAMORI¹ AND EIICHI TAKAHASHI¹

¹Department of Earth and Planetary Sciences, Tokyo Institute of Technology. (*:okui.w.aa@m.titech.ac.jp)

Chondrules are one of the main constituents of chondrites (CC: 15-60 vol.%, OC: 60-80 vol.%, EC: 60-80 vol.%). The identification of chondrule formation mechanism is an important clue to understand how Solar System precursor solids formed, were transported, and mixed in the nebula. Interpretations of chondrules' origins are still controversial, however, particularly because chondrule bulk compositions have a large variation in their chemical composition. In this study, we tackle this issue by analyzing highly precise Sr isotope compositions in chondrules with a variety of chemical compositions that were separated from multiple chondrites.

Chondrules were separated by a freeze-thaw method or sampled from sliced specimens by using a micro milling system (Geomill 326, Izumo) [1]. We followed the sample digestion procedure of [2]. Sr isotopic measurements were carried out by TIMS (Triton plus at Tokyo Tech). The ⁸⁴Sr/⁸⁶Sr ratios are reported in μ^{84} Sr units, which are 10⁶ relative deviations from the average of NIST 987 Sr.

The μ^{84} Sr values in two Allende (CV3.6) chondrules (+140 ppm, +130 ppm) are greater than those of bulk Allende (+70 ppm). This result suggests that the matrix components have μ^{84} Sr values lower than bulk Allende, because CAIs also have μ^{84} Sr values greater than the bulk. This is supported by a previous study [3] reporting that Allende acid leachate #1, where matrix component is dominant, had a μ^{84} Sr value lower than the bulk Allende (+35 ppm). Our new data would suggest that Allende chondrules are also isotopically distinctive carriers for Sr along with presolar grains and CAIs. This strongly argues against the genetic linkage between chondrules and matrix components in a single meteorite. On the contrary, μ^{84} Sr values in chondrules from Sahara 97072 (EH3) and Sahara 98175 (LL3.5) are not resolvable from those in the bulk rock of their host meteorite.

For Allende, we propose that X-wind model is one of the conceivable processes to concurrently induce large scale migration of chondrules and Sr isotopic anomalies between chondrules and matrix. In contrast, chondrules from ordinary and enstatite chondrites have formed locally and did not undergo large scale migration in the solar nebula before they formed parent body with matrix.

[1] Sakai and Kodan, (2011) Rapid Commun. Mass Spectrom 25, 1205. [2] Yokoyama *et al.*, (1999) Chem. Geol. 157, 175. [3] Yokoyama *et al.*, (2012) Goldschmidt.

Delineating biotic and abiotic carbonaceous material in the Apex chert

ALISON OLCOTT MARSHALL^{1*}, JAN JEHLICKA², JEAN-NOEL ROUZAUD³ AND CRAIG P. MARSHALL¹

¹ Department of Geology, University of Kansas, Lawrence, KS 66045, USA

(* Correspondance: (olcott@ku.edu)

² Institute of Geochemistry, Mineralogy and Mineral Resources, Charles University in Prague, Albertov 6, 128 43 Prague 2, Czech Republic

³ Laboratoire de Géologie, UMR CNRS 8538, Ecole Normale Supérieure, 24 Rue Lhomond, 75231 Paris Cedex 5, France

The Apex chert in Western Australia has been the center of many debates about whether these rocks contain unambiguous evidence of the early biosphere. Originally, these rocks were described to contain cyanobacterial microfossils [1] although later studies have described these features as having a morphology [2] and mineralogy [3] inconsistent with life. Additionally, these rocks contain carbonaceous material (CM) of unknown origin. This CM as been described by some as being of abiotic catalytic origin [2], and by others as biogenic [4]. Although Raman spectroscopy is not sufficient in and of itself to determine the source of CM, including whether it is biogenic [5], we recently used Raman spectroscopy in a paragenetic framework to demonstrate that the CM is from at least two separate populations [6]. Here we show using high-resolution transmission electron microscopy (HRTEM) that the CM found in the Apex chert exhibits at least four different microtextures. As different types of CM have different carbon crystallinities, the sources of these microtextures can be determined, revealing CM produced by processes such as abiotic catalytic synthesis, meteoritic input, and biological synthesis. These four populations of CM, combined with the geological history of the area, reveals over a billion years of fluid mixing and CM redeposition. Our study reveals that while care should be taken when interpreting bulk chemical data in samples from the Apex chert, HRTEM can offer the ability to delineate biogenic CM from abiotic CM in Archean sedimentary sequences.

[1] Schopf and Packer (1987) *Sci* **237**, 70-73. [2] Brasier *et al.* (2002) *Nat.* **416**, 76-81. [3] Marshall *et al.* (2011) *Nat. Geosci.* **4**, 240-243. [4] Schopf *et al.* (2002) *Sci* **416**, 73-76. [5] Marshall *et al.* (2010) *Astrobio* **10**, 229-243. [6] Olcott Marshall *et al.* (2012) *Astrobio* **12** 160-166.

Mg-isotopic evidence for CBb chondrule formation by condensation from an impact plume

M. B. OLSEN¹, M. SCHILLER¹ AND M. BIZZARRO¹

¹Centre for Star and Planet Formation, National History Museum of Denmark, University of Copenhagen, Copenhagen 1350 DK. E-mail: (mia.b.olsen@snm.ku.dk)

Chondrules are millimeter-sized spherules formed as molten droplets and are a major constituent of chondrite meteorites. Using U-corrected Pb-Pb dating, it has been shown that chondrule formation started contemporaneously with calcium-aluminium-rich inclusions (CAIs) and lasted several Myr [1]. Of interest are chondrules from the CB group, which in contrast to typical chondrules have exclusively non-porphyrific textures and magnesium-rich compositions. Their formation is believed to have occurred >5 Myr after CAIs, that is, much later than most chondrules. Based on these observation, it has been suggested that CB chondrules formed from a plume produced by an impact between planetary embryos after dust in the protoplanetary disk had largely dissipated [2]. However, late formation of these objects in a disk environment cannot be excluded [3]. Here, we use high-resolution Al-Mg isotope measurements to explore the formation mechanism(s) of CBb chondrules.

We selected ten skeletal chondrules from the CBb chondrite Hammadah al Hamra 237 and determined their Mg isotope compositions and ²⁷Al/²⁴Mg values using methods described in [4]. The chondrules show variability in the mass-dependent $\mu^{25}\text{Mg}$ component (from -86 ± 15 ppm to 292 ± 7.1 ppm relative to Earth's mantle) that is correlated to their ²⁷Al/²⁴Mg ratios in a manner consistent with a condensation origin. Using a kinetic fractionation law ($\beta=0.511$) to determine the mass-independent $\mu^{26}\text{Mg}^*$ values results in a negative correlation in $\mu^{26}\text{Mg}^*$ and ²⁷Al/²⁴Mg space, establishing that the $\mu^{25}\text{Mg}$ variability was not imparted by kinetic processes. Instead, using the experimentally determined fractionation factor of $\beta=0.514$ [5] returns a single $\mu^{26}\text{Mg}^*$ population with an uncertainty that is comparable with the external reproducibility of our method (~2.5 ppm). These data indicate that CBb chondrules formed by condensation from a isotopically homogeneous reservoir >4.7 Myr after formation of canonical CAIs. The Mg-isotope composition of CBb chondrules are thus supportive of the giant impact scenario for the the formation of CB chondrites.

[1] Connelly *et al.* (2012) *Science* 338, 651 [2] Krot *et al.* (2005) *Nature* 436, 989 [3] Gounelle *et al.* (2007) *EPSL* 256, 521 [4] Bizzarro *et al.* (2011) *JAAS* 26, 565 [5] Davis *et al.* (2005) *LPSC#36*, 2334

Effects of pH and ionic strength on the surface charge density of self assembled monolayers (SAM)

M.H.M. OLSSON*, M.P. ANDERSSON, J. MATTHIESEN
AND S.L.S. STIPP

Nano-Science Center, Department of Chemistry, University of
Copenhagen, Denmark (*mats.olsson@nano.ku.dk)

The properties of a surface depend very much on its surface charge density and polarity. Charged or highly polar surfaces are usually water wet and interact strongly with polar molecules. In some cases, such surface-organic affinities enhance organic compound adsorption. Surface charge density is therefore also important in making our society more sustainable through, for example, designing new material properties, filtering drinking water, ensuring safe CO₂ storage and enhancing oil recovery. We used ionizable COOH-terminated self assembled monolayers (SAM) to investigate the effect of solvent pH and ionic strength on surface charge density. We set up three different models for the effective charge-charge interaction between neighboring COO⁻ groups and calculated the fraction of deprotonated SAMs for various ionic strengths (figure).

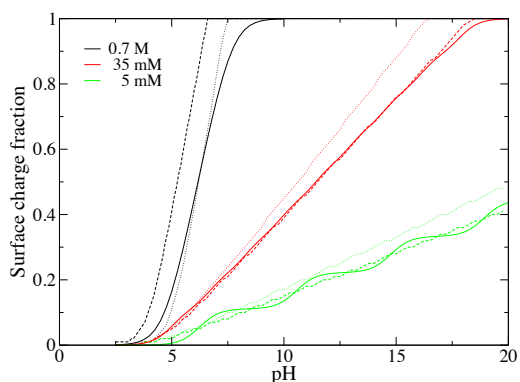


Figure: Titration curves predicted using the three models for three values of ionic strength.

The effective pK_a value of the SAM increases substantially from the monomer value at low salinity because of the increased charge-charge interaction between neighbors. As ionic strength decreases, the titration curves become flatter and deviate significantly from the standard Henderson-Hasselbalch expression. With these simulations, we obtain contour plots of the surface charge density at any pH and ionic strength. The simulations are nicely consistent with data from atomic force microscopy (AFM) chemical mapping.

Biogeochemistry of Acidic lakes in the Iberian Pyritic Belt

E. O. OMOREGIE^{1*}, E. SANTOFIMIA², E. LÓPEZ-PAMO²,
G. WEGENER³, M. E. BÖTTCHER⁴, P. ESCHER⁴, U.
STRUCK⁵, Á. AGUILERA¹ AND R. AMILS^{1,6}

¹ Centro de Astrobiología (CSIC/INTA), Madrid, Spain
(*Correspondence: omoregie@cab.inta-csic.es)

² Instituto Geológico y Minero de España, Madrid, Spain
(e.santofimia@igme.es, e.lopez@igme.es)

³ Max Planck Institute for Marine Microbiology, Bremen,
Germany (gwegener@mpi-bremen.de)

⁴ Leibniz IOW, Warnemünde, Germany
(michael.boettcher@io-warnemuende.de, peter.escher@io-
warnemuende.de)

⁵ Naturkunde für Museum, Berlin, Germany
(ulrich.struck@mfn-berlin.de)

⁶ CBM-SO, Autonoma University of Madrid, Spain
(ramils@cbm.uam.es)

The Iberian Pyritic Belt is one of the largest pyrite deposits on Earth. The exposure and subsequent oxidation of sulfide containing ores, resulting from mining activities, has led to the formation of acid mine drainage (AMD) in this region. Acidic, metal contaminated lakes, which often form as result of the inundation of mine pits are a substantial hazard in this region. For this reason the hydrochemistry of these systems has been the subject of several studies. However, there is very little known about the sediments in these lakes and the role of benthic-pelagic coupling for these systems. We conducted an interdisciplinary study that combined geochemical, stable isotope (H, O, C, S), and microbiological tools to develop a biogeochemical model for three pit lakes: Concepción, Nuestra Señora del Carmen, and Tharsis Filón Centro.

Consistent with the oxidation of sulfide minerals, mixolimnion pH of these lakes ranged between 2 and 3, with enhanced concentrations of dissolved elements, such as SO₄²⁻, As, Fe, Al, Mn, and Zn. ORP ranged from +600 to +400 mV and Fe(III) dominated iron speciation within these zones. In general, Fe(II), CO₂, CH₄ and pH increased in the monimolimnion of all lakes. Additionally, Eh decreased in these zones. In the sediments, pH ranged from 4 to 6 and ORP from -200 to +100 mV. Moderate sulfate reduction rates of up to 60 nmoles SO₄²⁻cm⁻³d⁻¹ were measured in the sediments. CO₂ and CH₄ concentrations were enhanced compared to the water column. 16S rRNA gene analysis revealed the presence of sulfate reducing bacteria as well as a broad spectrum of other bacteria, and archaea commonly associated with acidic sedimentary environments. Our results indicate that the sediments act as concentrators for organic material, resulting in microbial activity that enables the increase in pH of the sediments and bottoms waters of the lakes.

Effect of hydroxycarbonate green-rust particle size on ferrous denitrification

G. ONA-NGUEMA¹, D. GUERBOIS¹, P. MAFFIOLI¹,
V. NOEL¹, J. BREST¹ AND G. MORIN¹

¹Institut de Minéralogie et de Physique des Milieux Condensés (IMPMC), Environmental Mineralogy group, UMR 7590 UPMC-CNRS, Campus de Jussieu – 4 place Jussieu 75005 Paris (*correspondence: georges.ona-nguema@impmc.upmc.fr, delphine.guerbois@impmc.upmc.fr, priscilla.maffioli@impmc.upmc.fr, vincent.noel@impmc.upmc.fr, jessica.brest@impmc.upmc.fr, guillaume.morin@impmc.upmc.fr)

Green-rusts are mixed Fe(II,III) layered double hydroxides commonly found in anoxic zones of natural environments such as sediments and hydromorphic soils, in which they control the concentration of dissolved iron in the soil solutions. In such anoxic environments, green-rust minerals play an important role in the biogeochemical redox cycling of Fe, and can affect the speciation and mobility of many organic and inorganic contaminants. Therefore, an improved understanding of the processes and/or parameters controlling the formation and growth, the particle sizes and reactivity of green-rust in natural and engineered systems may help to better managing contaminant fate. Indeed, previous laboratory studies have reported that synthetic green-rusts are capable of reducing for instance nitrate [1] and nitrite [2], selenate [3], chromate [4], Ag(I), Au(III), Hg(II) [5] and halogenated hydrocarbons [6].

In the present study, we have prepared synthetic Fe(II,III) hydroxycarbonate green-rusts [GR(CO₃)] under various conditions, using various chemical procedures. Among the abiotic GR(CO₃) obtained from these synthesis pathways, the most stable were aged, leading to significant particle growth. The reactivity of nano-sized and micro-sized GR(CO₃) was studied in the presence of either nitrite or nitrate. X-ray diffraction and scanning electron microscopy were used to characterize solid phases of time-series samples obtained after interaction with nitrite or nitrate and show major influence of the particle size on the mass balance and the kinetics of the redox reactions investigated.

[1] Hansen, H.C.B *et al.* **1994**, *Geochim. Cosmochim. Acta* **58**, 2599-2608.; [2] Hansen, H.C.B *et al.* **1996**, *Environ. Sci. Technol.* **30**, 2053-2056.; [3] Myneni, S.C.B. *et al.*, **1997**, *Science*, **278**, 1106-1109.; [4] Loyaux-Lawniczak, S. *et al.* **2000**, *Environ. Sci. Technol.* **34**, 438-443.; [5] O'Loughlin, E.J. *et al.* **2003**, *Chemosphere* **53**, 437-446.; [6] Erbs, M. *et al.* **1999**, *Environ. Sci. Technol.* **33**, 307-311.

Quantitative color mapping of a brown altered granite by means of dark field reflection visible micro-spectroscopy

C. ONGA^{1*} AND S. NAKASHIMA¹

¹Department of Earth and Space Science, Osaka University, Toyonaka, 560-0043, Japan
(*correspondence: chieonga@ess.sci.osaka-u.ac.jp)

Reddish brown zones often extend from fractures toward interiors of granites (Fig.1a). Such colored zones are considered to be due to the presence of iron (hydr)oxides formed by weathering and/or hydrothermal alteration. However, their chemical forms and distributions have not been well characterized by conventional analytical methods.

In this study, microscopic visible dark field reflectance spectroscopy equipped with a color mapping system has been developed and applied to a brown-colored Rokko granite sample (Fig.1b). Sample reflectance spectra show similar features to goethite, lepidocrocite and ferrihydrite. Raman micro-spectroscopy on the granite sample surface confirm the presence of these minerals. L*a*b* color values (second CIE 1976 color space) were determined from the sample reflection spectra.

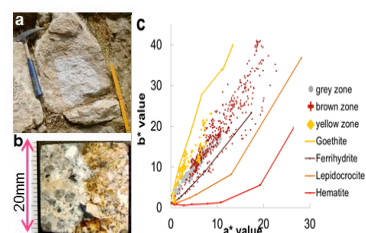


Figure 1: Brown-colored Rokko granite (a) and its hand specimen with a brown front (b). Color values by microscopic visible reflectance spectra in the a*-b* diagram (c).

Grey, yellow and brown zones of the granite show different L* a* and b* values. In the a*-b* diagram (Fig.1c), a* and b* values in the grey and brown zones are between the goethite and ferrihydrite trends, but their values in the brown zone are larger than those in the grey zone. The yellow zone shows data points close to the goethite trend. Iron (hydr)oxides rich areas can be visualized by means of large a* and b* values in the L*, a* and b* maps. The visible dark field reflectance spectroscopy with the color mapping system can be an useful method for studying distribution of colored-minerals such as iron (hydr)oxides.

Phase transformation in Fe₂SiO₄ at high pressure and high temperature

S. ONO¹

¹JAMSTEC., Yokosuka 237-0061, Japan
(sono@jamstec.go.jp)

Olivine, (Mg,Fe)₂SiO₄, is the most abundant mineral in the upper mantle. The iron content in olivine varies with depth because of chemical interactions with other mantle phases and determining the phase diagram of the polymorphs of the Fe₂SiO₄ end-member is important for precise modeling of the Mg₂SiO₄-Fe₂SiO₄ system. With pressure and temperature increase, Fe₂SiO₄ fayalite transforms into a spinel phase. The transition pressure from olivine to spinel phase has been confirmed to be around 5 GPa at high temperatures by previous experimental studies. However, the values of these dP/dT slopes scatter from 2.5 to 4.5 MPa/K. This phase boundary has been used as a pressure calibration point at high temperatures in high-pressure experiment. Therefore, the precise phase boundary of Fe₂SiO₄ needs to be determined.

The starting material was Fe₂SiO₄ fayalite, synthesized from a starting mixture composed of finely powdered Fe₂O₃ and SiO₂. High-pressure X-ray diffraction experiments were performed using a multi-anvil high-pressure apparatus, and was combined with a synchrotron radiation source located at the KEK and SPring-8 facilities in Japan. In our experiments, pressure was applied to the sample by generating a press load. The sample was then quickly heated until it reached the desired temperature for a given press load. After reaching the required temperature, we performed *in situ* measurements using the synchrotron X-rays and the heating temperature was maintained for 1-3 h. At the end of the experimental runs, the sample was quenched by cutting off the electrical power. This heating procedure was the same as that used in typical quench experiments.

We report on the disputed issue of the dP/dT slope of the olivine-spinel transition in Fe₂SiO₄, and establish the phase boundary with improved accuracy using our pressure and temperature data. We performed approximately 25 experimental runs to investigate the phase boundary between the olivine and spinel structures. The gradient of dP/dT of the phase boundary was positive.

$$P \text{ (GPa)} = 0.5(3) + 0.0034(3) \times T \text{ (K)}.$$

The boundary determined in this study is in general agreement with those reported in previous quench or *in situ* high-pressure experiments. However, the dP/dT slope was more positive than that in the previous *in situ* experiment.

Clumped Methane Isotopologue (¹³CH₃D) Thermometry of Geological Methane by Tunable Mid-Infrared Laser Spectroscopy

SHUHEI ONO¹, BARBARA SHERWOOD LOLLAR², ELIZA HARRIS¹, BARRY MCMANUS³, MARK ZAHNISER³
AND DAVID NELSON³

¹Department of Earth, Atmospheric and Planetary Sciences, Massachusetts Institute of Technology, Cambridge, MA.
(sono@mit.edu)

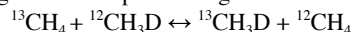
²Department of Earth Sciences, University of Toronto, Toronto, ON, Canada

³Center for Atmospheric and Environmental Chemistry, Aerodyne Research, Inc., Billerica, Massachusetts, USA

We have developed a tunable laser mid-infrared spectroscopy instrument to measure four isotopologues of methane including clumped isotopologue, ¹³CH₃D. Precise measurements of ¹³CH₃D abundance will add another critical dimension to resolve biogenic and abiogenic sources of methane in the marine and continental deep subsurface, and the atmosphere.

The new spectrometer houses two quantum cascade lasers that are tuned to a series of well resolved fundamental absorption lines in the 8 μm wavelength region. One laser measures absorption lines for ¹²CH₃D, ¹²CH₄, and ¹³CH₃D, and the other ¹²CH₄ and ¹³CH₄. Precisions (1σ) are 0.1‰ for the ratio ¹³CH₄/¹²CH₄ and ¹²CH₃D/¹²CH₄, and 0.3‰ for the ratio ¹³CH₃D/¹²CH₄, evaluated by comparing two methane cylinder samples. Accuracy of the technique is assured by comparing δ¹³C and δD values measured by a conventional isotope-ratio mass spectrometer.

The abundance of ¹³CH₃D is expected to reflect the temperature at which methane is thermally equilibrated, according to the isotope exchange reaction:



The equilibrium constant for this reaction approaches unity at very high temperatures (>1,000K). At low temperature, the above equilibrium constant deviates from unity, reaching values of 1.0066, 1.0050, 1.0011 at 0, 100 and 400 °C, respectively. Therefore, the precision of 0.3‰ would permit a temperature estimate of ±10°C for methane formed or scrambled at 25°C. The measured 'clumped isotope temperature', however, is expected to be biased when mixing of two or more sources of methane occur due to some non-linearity in the ratio ¹³CH₃D/¹²CH₄ upon mixing. We will discuss some preliminary data and the potential of this new approach to delineate deep subsurface methane sources and their role in the deep carbon cycle.

Meteorite impact, volcanism, and radiolarian faunal turnover recorded in the Upper Triassic of Japan

T. ONOUE^{1*}, H. SATO², T. NOZAKI³, J. KURODA³
AND K. SUZUKI³

¹Kumamoto University, Kumamoto 860-0862, Japan
(*correspondence: onoue@sci.kumamoto-u.ac.jp)

²Kyushu University, Fukuoka 812-8581, Japan
(3SC12024G@s.kyushu-u.ac.jp)

³Japan Agency for Marine-Earth Science Technology (JAMSTEC), Yokosuka 237-0061, Japan

The Late Triassic was characterized by several marine and terrestrial biotic turnover events prior to the end-Triassic mass extinction. The causes of the end-Triassic mass extinction and these Norian to Rhaetian biotic turnover events are still the subject of debate. Catastrophic processes such as widespread eruption of the Central Atlantic Magmatic Province (CAMP) flood basalts and extraterrestrial impacts have been proposed to account for the biotic turnover events [1, 2]. Here, we report a marine osmium (Os) isotope record reconstructed from an Upper Triassic bedded chert succession in Japan, which accumulated on the paleo-Pacific deep seafloor. We also analyzed the extinction patterns of Late Triassic radiolarian species from the bedded chert succession with the marine Os isotope record.

The Os isotope data show an abrupt and marked negative excursion from an initial Os isotope ratio of ~0.477 to unradiogenic values of ~0.127 in a claystone layer within a middle Norian bedded chert (~215 Ma), indicating the input of meteorite-derived Os into seawater [3]. A gradual decrease in ¹⁸⁷Os/¹⁸⁸Os ratio during the Rhaetian (201–210 Ma) is considered to have been closely linked to the CAMP volcanic event [4]. An analysis of radiolarians provides no indication of a mass extinction event across the claystone layer and during the CAMP volcanic phase. However, a significant faunal turnover occurred at ~1 Myr after the impact event. Biostratigraphic analysis shows that 20 radiolarian species became extinct at this level in the chert. It is possible that the impact triggered the extinction of these 20 species, though the direct cause of their extinction remains uncertain.

[1] Marzoli *et al.* (1999) *Science* **284**, 616-618. [2] Spray *et al.* (1998) *Nature* **392**, 171-173. [3] Sato *et al.* (2013) *MinMag*, this volume. [4] Kuroda *et al.* (2010) *Geology* **38**, 1095-1098.

The influence the stoichiometry of arsenopyrite on the impurity density

V. ONUFRIENOK *, A. SAZONOV AND A. NIKIFOROV

Siberian Federal University, Krasnoyarsk, Russia

(*correspondence: VOnufriynok@yandex.ru)

The chemical composition of arsenopyrite FeAsS may differ in detail from one deposit to another, from one deposition stage to another in a given deposit, and even from the outer parts of a single grain towards its interior. Based on a comprehensive analysis of the crystal structure, chemical and phase composition of the analytical expressions for the calculation of the impurity density in the arsenopyrite received. The algorithm for calculating the impurity density structures such as NiAs proposed Onufrienok (Onufrienok *et al.*, 2012). To calculate the density impurities into arsenopyrite was amended. The impurity density for the impurity atoms cobalt Co, copper Cu, nickel Ni and gold Au is calculated separately. Specimens for investigated from the deposit Panimba Krasnoyarsk region. Studies have been conducted on ~65 samples from different mines. One such series is presented in Table 1

(S/Fe) + (As/Fe)	cobalt Co		nickel Ni		copper Cu		gold Au	
	α , %	β , $\square 10^{-2}$	α , %	β , $\square 10^{-2}$	α , %	β , $\square 10^{-3}$	α , %	β , $\square 10^{-3}$
1.9627	0.16	0.547	0.021	0.069	-	-	0.002	0.026
1.9467	0.18	0.613	-	-	0.007	0.216	0.061	0.792
1.9328	0.30	0.996	0.076	0.251	-	-	0.011	0.142
1.9690	0.18	0.621	0.006	0.019	-	-	0.045	0.592
1.9552	0.17	0.578	0.012	0.039	0.014	0.433	0.007	0.091
1.9866	0.83	2.746	0.016	0.053	0.058	1.795	0.008	0.105
1.9646	0.52	1.716	-	-	0.019	0.588	0.040	0.521
2.0020	0.51	1.694	0.436	1.444	0.017	0.527	0.027	0.361
2.0106	0.25	0.832	0.328	1.086	-	-	-	-
2.0157	0.28	0.954	0.209	0.692	-	-	-	-
2.0340	0.45	1.490	-	-	0.013	0.403	0.010	0.136

Table 1: Results of the microprobe analysis (α) and the results calculations of the density impurity (β) into the arsenopyrite.

Because of the large scatter of the experimental points should speak not about dependencies but only a trend. As it is shown in the table, tendency to increasing of the density impurities with increasing nonstoichiometry is installed. Stoichiometric composition should be considered when the ratio (As + S)/Fe is equal to two. Decreasing this ratio impurity density tends to decrease. Statistical analysis of all samples (~65) confirmed the findings.

[1] Onufrienok *et al.*, (2012): Proceedings of the 10th International Congress for Applied Mineralogy, 487-495

Marine Cements and the Late Cretaceous to Cenozoic History of Magnesium, Strontium, and Calcium in the Ocean

BRADLEY OPDYKE¹, RYAN OWENS¹, JEREMY CAVES²,
PAUL WILSON³ AND ANDRE DROXLER⁴

¹The Research School of Earth Sciences, The Australian National University

²Environmental Earth System Science, Stanford University

³Ocean & Earth Science, National Oceanography Centre, Southampton University of Southampton

⁴Earth Science, Rice University

Relatively unaltered 'pristine' marine cements from neritic environments are recognised as some of the best known proxies for recording marine chemistry through geologic time. Unfortunately, due to their metastable nature they are rarely preserved in the rock record. We have been fortunate enough to recover two examples of such cements from ancient reef environments; one from Site 877 of Leg 144 of the Ocean Drilling Program and one from a RV Melville survey in the Gulf of Papua in 2004. Both were preserved because they were tightly cemented on rapidly subsiding reef platforms and not subject to meteoric diagenesis.

The ODP sample is Maastrichtian in age and the Gulf of Papua sample is from the Early Miocene. These two time intervals represent extremes in the history of strontium incorporation into shallow water depositional environments. During the Late Cretaceous scleractinian corals (which take up large quantities of strontium into their skeletons) were relatively rare, whereas the Early Miocene represents the acme of modern style coral reef growth, with scleractinian corals abundant.

The marine cements record an Early Miocene strontium concentration that is a third of the Late Cretaceous value. Strontium concentrations are similar to or lower than comparable Holocene cements. Magnesium-calcium ratios drop to approximately 3.6 for the Early Miocene and near 2 in the Late Cretaceous. Mass balance of calcium fluxes through over the past 100 million years indicate that the alkalinity has not changed dramatically over this interval. If we hold this total relatively constant then these data confirm previously documented trends in magnesium calcium ratios and for the first time document a significant increase in strontium concentrations in the oceans of the Late Cretaceous relative to the late Cenozoic values.

Changing riverine silicon isotope delivery to the ocean over glacial-interglacial intervals? Evidence from glaciated basaltic terrains

OPFERGELT S.^{1,2}, BURTON K.W.^{1,3}, POGGE VON STRANDMANN P.A.E.¹, GISLASON S.R.⁴ AND HALLIDAY A.N.¹

¹Department of Earth Sciences, University of Oxford, United Kingdom

²Earth and Life Institute, Université catholique de Louvain, Belgium (sophie.opfergelt@uclouvain.be)

³Now at Department of Earth Sciences, Durham University, United Kingdom

⁴Institute of Earth Sciences, University of Iceland, Iceland

The marine primary production is dominated by diatoms which largely depend upon the riverine silicon delivery to the ocean. In paleoreconstruction of Si utilisation by diatoms, a constant Si isotope input from the continent to the ocean is generally assumed. In this study, glacier-fed and direct runoff rivers draining basaltic catchments in Iceland display significantly different dissolved Si isotope compositions, with lighter values ($\delta^{30}\text{Si} = +0.17 \pm 0.18\text{‰}$) associated with the high physical erosion rates in glacial rivers, and heavier values ($\delta^{30}\text{Si} = +0.97 \pm 0.31\text{‰}$) associated with lower physical erosion rates and enhanced formation of secondary minerals in direct runoff rivers. The riverine Si isotopic compositions correlate with those of Li and provide evidence of a climatic dependence that is likely to have led to glacial-interglacial differences in the isotopic composition of Si delivered to the oceans. Based on existing $\delta^{30}\text{Si}$ from diatoms in a sediment record from the Southern Ocean, the interpretation of changes in Si utilisation between the Last Glacial Maximum (LGM) and the early Holocene is revisited accounting for changing Si isotope delivery to the ocean over glacial-interglacial intervals. The results are consistent with a lower Si utilisation during the LGM ($53 \pm 5\%$) relative to the Holocene ($88 \pm 5\%$). During the LGM, Si utilisation values are slightly higher when allowing for changing Si isotope input to the ocean ($53 \pm 5\%$), than when a constant Si isotope input is considered (42 to $47 \pm 5\%$). This study suggests that changes in Si isotope delivery to the ocean should be accounted for in the precise reconstruction of ocean Si utilisation and primary productivity over glacial-interglacial timescales.

Cold-water coral biomineralization in high resolution

OPPELT, A.^{1*}, AND ROCHA, C.¹

¹ Biogeochemistry Research Group, Department of Geography, School of Natural Sciences, Trinity College Dublin, Ireland (*correspondence: oppelta@tcd.ie)

Deep-sea scleractinian skeletons are primarily precipitated along a longitudinal growth axis but also expand radially forming layers. A LA-ICP-MS track at a resolution of 15 μm across radial layers revealed sharp peaks in U^{238} concentrations and almost perfect antithetical behaviour of Mg^{25} and U^{238} (fig. 1). The peaks are preceded by slightly offset minima in Ba^{137} which generally follows Mg for most of the growth. Uranium peaks align with the last precipitates of visible layers before the onset of the next (often white) layer and increase of U^{238} values.

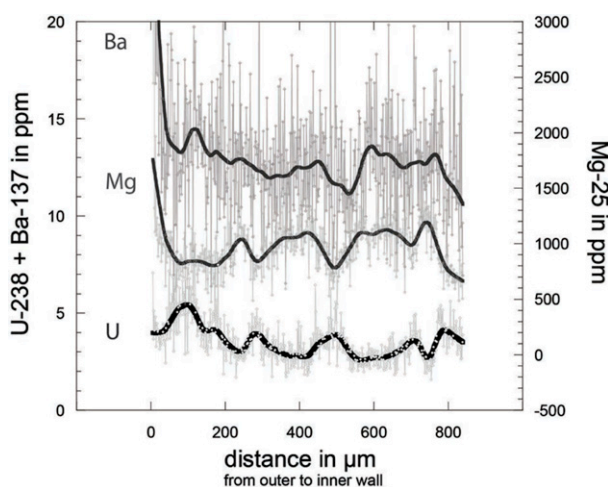


Figure 1: Ba, Mg and U concentrations (weighted at 8%) across the coral wall from outside (left) to inside (right).

The strong antithetical behaviour of U^{238} and Mg^{25} and the known negative correlation of U/Ca concentrations in corals and CO_3^{2-} in seawater [1] invite an interpretation as variations in growth rates in the corals. The short steep increases in U^{238} concentrations will be discussed as phases of low CO_3^{2-} and Mg^{2+} availability, and accordingly lower growth rates. The U peaks are preceded by minima in Ba^{137} which functions as a nutrient proxy [2]. Repeating peaks in Barium might connect variations in growth rate with regular nutrient input from surface primary production or nepheloid layers. $\delta^{13}\text{C}$ ratios will be included in those discussions.

[1] Anagnostou *et al.* (2011) *Geochim. Cosmochim. Ac.* **75**, 2529-2543. [2] Lea *et al.* (1989) *Nature* **340**, 373-376.

Oxygen and carbon cycling in basaltic crust

BETH ORCUTT¹ WOLFGANG BACH² KATRINA J. EDWARDS³ PETER GIRGUIS⁴ AND C. GEOFF WHEAT⁵

¹Bigelow Laboratory for Ocean Sciences, East Boothbay, ME, USA; (borcutt@bigelow.org)

²University of Bremen, Bremen, Germany; (wbach@uni-bremen.de)

³University of Southern California, Los Angeles, CA, USA; (kje@usc.edu)

⁴Harvard University, Cambridge, MA, USA; (pgirguis@oeb.harvard.edu)

⁵Global Undersea Research Unit, University of Alaska Fairbanks, Monterey, CA, USA; (wheat@mbari.org)

Oceanic crust is the largest potential habitat for life on Earth and may contain a significant fraction of Earth's total microbial biomass, yet little is known about the form and function of life in this vast seafloor realm that covers nearly two-thirds of the Earth's surface. A deep biosphere hosted in seafloor basalts has been suggested from several lines of evidence; yet, empirical analysis of metabolic reaction rates in basaltic crust is lacking. The first measure of oxygen consumption in young (~ 8 Ma) and cool (<25 °C) basaltic crust is calculated from modeling oxygen and strontium profiles in basal sediments collected during Integrated Ocean Drilling Program (IODP) Expedition 336 to 'North Pond', a sediment 'pond' on the western flank of the Mid-Atlantic Ridge (MAR). Dissolved oxygen concentrations increased towards the sediment-basement interface, indicating an upward diffusional supply from oxic fluids circulating within the crust. Furthermore, evidence of biological carbon fixation in basalt biofilms comes from stable isotope incubations, with implications for carbon cycling in oceanic crust. Long-term microbiology experimentation in crustal seafloor observatories at the Juan de Fuca Ridge flank and at North Pond are poised to yield exciting new discoveries about the dynamics of microbial activity and community structure in the crustal subsurface.

Newly revealed NNW shift of granitic magmatism during Mid-Miocene period, Kyushu, Japan

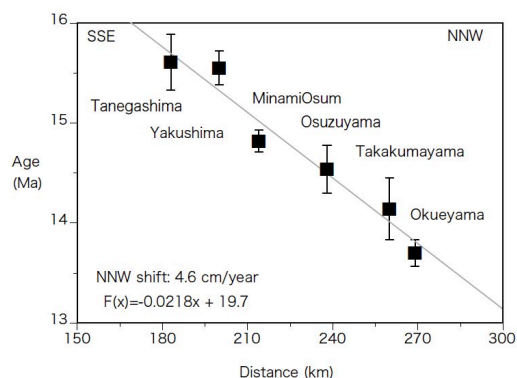
YUJI ORIHASHI¹, HIRONAO SHINJYO² AND RYO ANMA³

¹Earthquake Research Institute, the University of Tokyo
(oripachi@eri.u-tokyo.ac.jp)

²Tokyo Keizai University (shinjoe@tku.ac.jp)

³Graduate School of Life and Environmental Sciences,
University of Tsukuba (ranma@sakura.cc.tsukuba.ac.jp)

Mid-Miocene granitic plutons, related to subduction of young Shikoku Basin of the Philippine Sea (PS) plate after immediate clockwise rotation of SW Janpa, are spodadically but widely distributed along the Nankai Trough in the outer zone of SW Japan (e.g., [1]). Kyushu Island is located on western part of the outer zone. This study newly determined precise U-Pb ages for felsic dikes and granitic bodies of six locations; Tanegashima, Yakushima, MinamiOsumi, Osuzuyama, Takakumayama and Okueyama, by using LA-ICPMS technique [2]. The obtained U-Pb ages ranged from 15.6 Ma to 13.7 Ma and showed negative correlation to their distances from the Nankai Trough (see below figure). Shift rate of the granitic magmatism is 4.6 cm/year with NNW direction, which is almost same to that of recent plate movement of the PS plate (4.8 km/year). Considering that the shift rate is reflected to the subduction of the PS plate, the subduction angle in Mid-Miocene is estimated as ca. 17 degree, which is almost same to that of recent PS plate on Shikoku Island. In Kyushu Island, however, the recent angle becomes max. 60 degree and Plio-Quaternary arc volcanism makes apparent volcanic front. This suggests that the PS plate during Mid-Miocene period has been shallowly subducted and subsequently slab rollback has been occurred due to slab-pushing caused by lateral flow of athenospheric upwelling of the Ryukyu Trough [3] and/or other unknown tectonic events.



[1] Nakada and Takahashi (1979) J. Geol. Soc. Japan, 85, 571-582. [2] Oriha-shi *et al.* (2008) Res. Geol., 58, 101-123. [3] Seno (1999) Island Arc, 8, 66-79.

Authigenic carbonates as dynamic microbial ecosystems: expanding views of methane cycling in the deep sea

VICTORIA J ORPHAN^{1*}, JEFF MARLOW¹, DAVID CASE¹,
JOSH STEELE¹, WIEBKE ZIEBIS², SHAWN MCGLYNN¹,
GRAYSON CHADWICK¹, ANDREW THURBER³
BEN GRUPE³ AND LISA LEVIN³

¹Division of Geological and Planetary Sciences, California
Institute of Technology, 1200 E. California Blvd,
Pasadena, CA 91125 USA (vorphan@gps.caltech.edu)

²University of Southern California, Los Angeles, CA USA

³Scripps Institute of Oceanography, University of California,
San Diego, CA, USA

Sulphate-dependent anaerobic oxidation of methane (AOM) is the dominant sink for methane along continental margins, oxidizing significant fraction of methane in anoxic sediments prior to its release to the hydrosphere. The alkalinity generated during this process frequently results in the precipitation of $\delta^{13}\text{C}$ -depleted authigenic carbonates, which vary in morphology, size, and mineralogy, ranging from micritic cements and cm-sized concretions to massive 'chemoherm' structures, mounds, and pavements that can cover hundreds of square meters. These methane-derived structures often persist long after the flux of methane subsides, with remnant methanotrophic biomarkers recovered from paleo-seep carbonates dating back to the Paleozoic. While these authigenic carbonates have long served as important indicators of methane seepage, they are frequently discussed as passive recorders of prior seep activity, rather than an active microbial habitat. Using a combination of molecular and geochemical analyses, rate measurements, stable isotope labelling experiments and nanoscale secondary ion mass spectrometry (nanoSIMS), we examined the potential for these systems to sustain active methanotrophic microorganisms and documented changes in the microbial community associated with areas of active methane venting and sites of low methane flux. Here we demonstrate that authigenic deep-sea carbonates 1) host abundant methanotrophic archaea and sulphate-reducing bacterial consortia, 2) are actively oxidizing methane 3) are capable of growth and incorporation of methane into biomass 4) provide a unique habitat and food source for seep-associated meio- and macrofauna. Seafloor calcite and dolomite incubations, transplant experiments and *in situ* collections of carbonates show differences in the dominant methanotrophic archaea (ANME-1 vs. ANME-2) and methane-oxidation rates related to levels of methane seepage and possibly mineralogy, with viable endolithic methanotrophic archaea and above background levels of methane-oxidation documented in authigenic carbonates well outside areas of visible methane seepage. Together, this data indicate that authigenic carbonates are living and actively evolving ecosystems and represent a previously underappreciated sink for methane.

www.minersoc.org

DOI:10.1180/minmag.2013.077.5.15

Measurement of light extinction by single aerosol particles

A.J. ORR-EWING*, J.S. WALKER, A.E. CARRUTHERS,
B.J. MASON AND J.P. REID

School of Chemistry, University of Bristol, Bristol BS8 1TS,
UK (*correspondence: a.orr-ewing@bris.ac.uk)

Cavity ring-down spectroscopy (CRDS) is increasingly being used to determine extinction of light by ensembles of aerosol particles, either in the laboratory or in field measurements. Under controlled laboratory conditions, with size-selection of the aerosol particles prior to CRDS detection, extinction efficiencies and refractive indices can be determined. However, the precision and accuracy of such ensemble measurements are limited by a number of factors inherent in the experiments [1,2]. One significant source of uncertainty is the distribution of sizes of the aerosol particles passing through the differential mobility analyser employed as the size-selecting device.

We have therefore developed a CRDS-based method to determine the optical cross sections and extinction efficiencies of *single* aerosol particles of diameter $\sim 1 \mu\text{m}$ or less. A Bessel beam optical trap is used to confine and manipulate the position of the single aerosol particle. Particles smaller than $1 \mu\text{m}$ can be captured indefinitely and we have demonstrated the ability to study processes that change the size or refractive index, such as the evaporation of volatile components or the uptake of water. The measured extinction induced by the particle depends on the position of the particle within the cavity [3,4], so fine positional control is required. Results will be presented for a number of aerosol particle compositions. For example, the variation in extinction efficiency of a single trapped sodium chloride droplet with relative humidity agrees very well with predictions from Mie scattering theory. The advantages of single-particle over ensemble measurements will be discussed.

[1] Miles *et al.* (2011) *Aerosol Sci. Tech.* **45**, 1360-1375. [2] Mason *et al.* (2012) *J. Phys. Chem. A* **116**, 8547-8556. [3] Butler *et al.* (2007) *J. Chem. Phys.* **126**, 174302. [4] Miller *et al.* (2007), *J. Chem. Phys.* **126**, 174303

Temperature reconstruction for the last 1000 years at WAIS-Divide, Antarctica, from inert gas isotopes and borehole temperature.

ANAIS J. ORSI¹ AND JEFFREY P. SEVERINGHAUS²

¹Scripps Institution of Oceanography, UCSD, 9500 Gilman Drive, La Jolla, CA 92093-0244, USA, (aorsi@ucsd.edu)

²Scripps Institution of Oceanography, UCSD, 9500 Gilman Drive, La Jolla, CA 92093-0244, USA, (jseveringhaus@ucsd.edu)

West Antarctica is warming, but it is not clear yet whether it is abnormal, in the context of natural background variability. The amplitude of natural climate variability on multi-decadal timescales remains poorly quantified, but it is essential to our understanding of the significance of the warming of the last 50 years.

Here, we present a 1000-year temperature record at WAIS-Divide, in the center of West Antarctica, reconstructed from the combination of inert gas isotopes from the ice core and borehole temperature measurements. Borehole temperature provides an absolute estimate of long-term trends, while noble gases track decadal to centennial scale changes. This method provides a temperature reconstruction that is independent of the water isotope of the ice, and allows us to improve our understanding of water isotopes as a temperature proxy at this site.

We found that the "Little Ice Age" cold period of 1400-1800 was 0.52°C colder than the last century, and that 50 to 100 year variability is on the order of 0.5 to 1°C .

Gene expression in the deep biosphere

WILLIAM D. ORSI¹, VIRGINIA P. EDGCOMB², GLENN D. CHRISTMAN³ AND JENNIFER F. BIDDLE³

¹ Department of Geology and Geophysics, Woods Hole Oceanographic Institution: (william.orsi@gmail.com)

² Department of Geology and Geophysics, Woods Hole Oceanographic Institution: (vedgcomb@whoi.edu)

³ College of Earth, Ocean, and Environment, University of Delaware: (jfbiddle@udel.edu)

Microbial community metabolism in the marine subsurface likely plays an important role in global biogeochemical cycles but deep biosphere activities are not well understood. Illumina sequencing of community messenger RNA was performed to obtain the first subsurface metatranscriptome from anaerobic Peru Margin sediment up to 159 meters below seafloor. Metabolic reconstruction indicates anaerobic metabolism of amino acids, carbohydrates, and lipids are dominant processes, and profiles of dissimilatory sulfite reductase transcripts are consistent with sulfate concentration profiles. Moreover, cell division transcripts across all three domains of life increase where peaks in microbial abundance are observed in subsurface sulfate-methane transition zones. These data support calculations and models of subsurface microbial metabolism, and represent the first holistic picture of deep biosphere activities. Furthermore, an investigation of eukaryotic 18S rRNA revealed active Fungi across a range of marine subsurface provinces. Subsurface fungal populations exhibit statistically significant correlations with total organic carbon, nitrate, sulfide, and dissolved inorganic carbon suggesting environmental selection of active Fungi in the marine subsurface.

Raman Spectra And Microhardness Of Sphalerite Solid Solutions ZnS·FeS

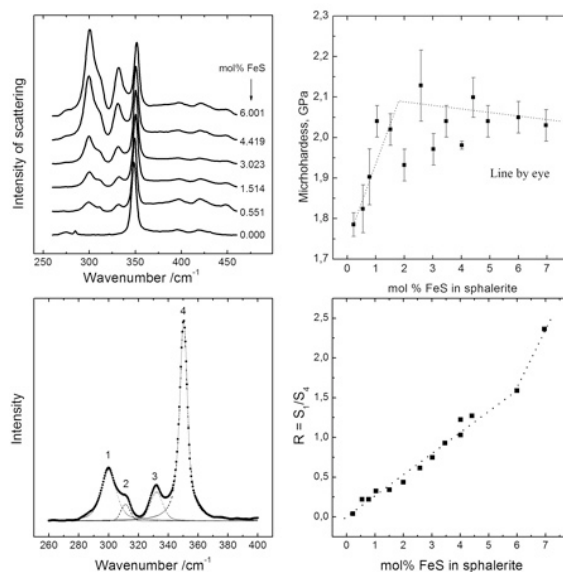
OSADCHII E.G.^{1*}, BONDARENKO G.V.¹, CHAREEV D.A.¹ AND OSADCHII V.O.²

¹ Institute of Experimental Mineralogy RAS, Chernogolovka, Russia (*correspondence: euo@iem.ac.ru)

² Moscow State University, Geological Department

Synthesized sphalerite solid solutions ($\text{Fe}_x\text{Zn}_{1-x}\text{S}$) in the range $0 < \text{mol \% FeS} < 50$ with compositional step 5 have been studied with the use of Raman spectroscopy. The main objective of these experiments was to learn how the iron content of sphalerite affects the Raman spectra [1].

Raman intensities over the whole range of concentrations suggest a structure change in the rather narrow region of mole fractions of FeS between 0.15 and 0.25. Currently special attention was paid for compositions $0 \leq \text{mol \% FeS} \leq 6$ (15 samples, gas transport and average diameter of crystals 1 mm) where microhardness (HV) grows extremely from 1.7 to 2.1 GPa. In this composition area additional peak 310 cm^{-1} appears that might be due to cluster forming process in sphalerite lattice. The ratio of intensities of Raman lines 295 and 345 cm^{-1} can be used for the compositional analysis of sphalerite.



This study was supported by Grant RFBR 13-05-00405.

[1] Osadchii E.G. and Gorbaty Y.E. (2010) *Geochim. Cosmochim. Acta* **74**, 568-573.

Vertical transport of black carbon over East Asia during the A-FORCE aircraft campaign

N. OSHIMA^{1*}, M. KOIKE², Y. KONDO², H. MATSUI², N. MOTEKI², H. NAKAMURA³, N. TAKEGAWA³
AND K. KITA⁴

¹ Meteorological Research Institute, 1-1 Nagamine, Tsukuba, Ibaraki, 305-0052, Japan (*correspondence: oshima@mri-jma.go.jp)

² Department of Earth and Planetary Science, Graduate School of Science, University of Tokyo, 7-3-1 Hongo, Bunkyo-ku, Tokyo, 113-0033, Japan

³ Research Center for Advanced Science and Technology, University of Tokyo, 4-6-1 Komaba, Meguro-ku, Tokyo, 153-8904, Japan

⁴ Faculty of Science, Ibaraki University, 2-1-1 Bunkyo, Mito, Ibaraki, 310-8512, Japan

The Aerosol Radiative Forcing in East Asia (A-FORCE) aircraft campaign was conducted over East Asia in March-April 2009 [1]. We examined vertical transport mechanisms of black carbon (BC) aerosols and their transport pathways over East Asia in spring using the modified version of the CMAQ model and simulating the A-FORCE aircraft campaign. Comparisons of the model results with the A-FORCE observations show that the model reproduces relatively well the vertical distributions of mass concentration and transport efficiency of BC, including their latitudinal gradients and dependences on precipitation that air parcels had been experienced during transport. During the A-FORCE period, we find two types of pronounced upward mass fluxes of BC from the planetary boundary layer (PBL) to the free troposphere (FT) over northern-eastern and inland-southern China. The major uplifting mechanism of BC over northern-eastern China is the cyclones with modest amounts of precipitation. Cumulus convections and orographic lifting along the high-altitude mountains play an important role for the upward transport of BC to the FT over inland-southern China, in spite of the large amounts of precipitation. In addition to the outflow in the PBL over the midlatitude, the upward transports over northern-eastern and inland-southern China, followed by the westerly transports in the lower and the middle FT, respectively, make major contributions to the exports of BC from East Asia to the Pacific in spring.

[1] Oshima *et al.* (2012) *J. Geophys. Res.*, **117**, D03204, doi:10.1029/2011JD016552.

Precipitation and stability behaviour of calcium sulfate: the role of salinity temperature and reaction time

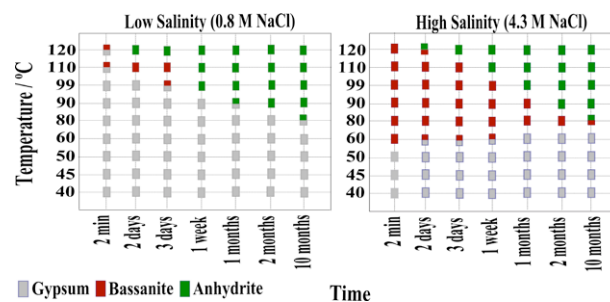
M. OSSORIO¹, A.E.S. VAN DRIESSCHE¹, P. PÉREZ²
AND J.M. GARCIA-RUIZ¹

¹ IEC, IACT, CSIC-U.Granada, Spain. (mercedes@lec.csic.es, sander@lec.csic.es, jmgruiz@ugr.es)

² Depart. Física general, U. Habana, Cuba, (pvperéz@uci.cu)

A marked inconsistency exists between the phase diagram of calcium sulfate and its crystallization behaviour [1]. To gain a better understanding on the precipitation dynamics and stability region of each phase (gypsum, bassanite and anhydrite), a series of precipitation experiments were carried out from 40 to 120 °C, at three salinities (0.8, 2.8 and 4.3 M NaCl) and different reaction times (from 2 min up to 10 months).

Salinity and temperature strongly influence the type and stability of the precipitate. No primary anhydrite precipitation occurs and with increasing salinity bassanite precipitation prevails and its stability is strongly enhanced (up to 10 months at 80 °C). Phase transition occurs through dissolution of the less stable phase and subsequent recrystallization of the more stable phase. This process is controlled by the differences in surface free energy and step kinetic coefficients between the three phases [2-4].



[1] Van Driessche *et al.*, *Science* 336, 2012 [2] Van Driessche *et al.*, *Cryst. Growth Des.* 10, 2010 [3] Morales *et al.*, *Am. Min.* 97, 2012. [4] Morales *et al.*, *Cryst. Growth Des.* 12, 2012.

Testing the “deep-basin high-rank gas machine” hypothesis

CHRISTIAN OSTERTAG-HENNING¹

¹Federal Institute for Geosciences and Natural Resources,
Hannover, Germany (correspondence: (Christian.Ostertag-
Henning@bgr.de)

During the past decade the interest in a more detailed understanding of processes during gas and oil formation has been spurred by growing importance of gas and oil from unconventional reservoirs, e.g. shale gas and shale oil as well as deep basin-centered gas. In addition to the classical view of mainly first-order reactions for the inorganic formation of hydrocarbon gases by thermal cracking of bitumen or kerogen, several researchers have put forward avenues to explain some not accounted for observations in hydrocarbon occurrences, molecular or isotopic compositions. These hypotheses always include a geologic component not considered in most kerogen/bitumen pyrolysis studies: The presence and role of water [1], the possible catalytic activity of mineral surfaces [2], the importance of metals in aqueous fluids, the metastable equilibria of hydrocarbons and more oxidized organic compounds in pore-fluids in the subsurface – and the role of minerals as part of pore-fluid redox- or pH-buffers [3]. Price [4] combined many of the aforementioned hypotheses in calling for a “deep-basin high-rank gas machine”.

A broad study to produce a consistent data set of HC formation rates and elemental transfer reactions in the gas-fluid-rock system at elevated pressures and temperatures is ongoing at the BGR. By using different experimental facilities for maturation of organic matter from small gold capsules to Dickson-type flexible gold-titanium cells in high-pressure reactors to large diameter high pressure reactors for heating/expulsion tests on core material several key questions are being addressed.

The experiments with source rock material of natural maturity series allowed the detailed comparison of effects of natural medium-temperature/high-pressure maturation in the sedimentary basin to artificial high-temperature/high-pressure maturation in the lab. Interestingly, a clear depiction of the predominance of different processes – e.g. thermal cracking, oxidation reactions to less reduced organic compounds, dehydrogenation by cyclization and aromatization - is visible in the data sets. The comparison of sets of experiments with the identical amounts of source rock material with/without the admixture of different mineral standards – e.g. carbonate, pyrite, montmorillonite – yielded clues about the role of certain mineral surfaces for catalytic oxidation/dehydrogenation/hydrogenation and fluid buffering. Using organic model compounds with isotope labels added to the source rocks clearly identified pathways of hydrocarbon gas formation – and the production of more oxidized organic compounds.

[1] Lewan (1997) *Geochim. Cosmochim. Acta* **61**, 3691-3723. [2] Mango *et al.* (1994) *Nature* **368**, 536-538. [3] Seewald (1994) *Nature* **370**, 285-287. [4] Price (1997) USGS DS **67**, H.

Anaerobic methane oxidation in the water column of the eutrophic sub-alpine Lake Zug (Switzerland)

K. OSWALD^{1,2*}, J. MILUCKA³, M.M.M. KUYPERS³, B. WEHRLI^{1,2} AND C.J. SCHUBERT¹

¹ Swiss Federal Institute of Aquatic Science and Technology (Eawag), CH-6047 Kastanienbaum, Switzerland

(*correspondence: kirsten.oswald@eawag.ch)

² Swiss Federal Institute of Technology (ETH), CH-8092 Zürich, Switzerland

³ Max Planck Institute for Marine Microbiology, 28359 Bremen, Germany

Anaerobic oxidation of methane (AOM) remains only partially understood in freshwater environments. Water column field investigations suggest that AOM could be mediated via other pathways, i.e. denitrification or metal oxide reduction, in lakes [1, 2], as opposed to its marine counterpart, where AOM proceeds via SO_4^{2-} reduction [3].

The potential for AOM was assessed in the water column of the eutrophic sub-alpine Lake Zug, situated in Central Switzerland. Through geochemical profiling and flux calculations of the relevant factors, the oxic/anoxic transition zone and anoxic depths, showing favorable conditions for AOM, were identified. At these selected depths, incubation experiments were carried out with ^{13}C -labelled methane to determine methane oxidation rates, simultaneously in-situ available electron acceptors were monitored. Fluorescence in-situ hybridization targeting Group I and II as well as anaerobic methanotrophs was carried out at the incubation depths. Furthermore, functional gene analysis for particulate (*pmoA*) and soluble methane monooxygenase (*mmoX*), both essential for aerobic methanotrophs, and methyl coenzyme M reductase (*mcrA*), an indicator for anaerobic methanotrophs, was completed.

Preliminary experiments show that AOM rates are one order of magnitude higher ($\sim 600 \text{ nM}\cdot\text{d}^{-1}$) than aerobic rates ($\sim 40 \text{ nM}\cdot\text{d}^{-1}$). Highest rates occur at depths, which are devoid of oxygen. First results are still inconclusive as to which electron acceptor is responsible for AOM, however, SO_4^{2-} does not appear to contribute substantially. Hybridization techniques confirm the presence of Type II alpha-proteobacterial methanotrophs as well as Group I and II methanotrophs.

[1] Schubert *et al.* (2010) *Aquatic Sciences* **72**, 455-466. [2] Crowe *et al.* (2011) *Geobiology* **9**, 61-78. [3] Boetius *et al.* (2000) *Nature* **407**, 623-626.

www.minersoc.org

DOI:10.1180/minmag.2013.077.5.15

Chromium Enrichment in sedimentary rocks deposited in shallow water in the 3.2 Ga Moodies Group, South Africa

T. OTAKE^{1-1*}, Y. SAKAMOTO²⁻¹, S. ITOH³⁻¹, H. YURIMOTO³⁻² AND T. KAKEGAWA²⁻²

¹Division of Sustainable Resources Engineering, Hokkaido University, Sapporo, Japan

*(correspondance: ¹⁻¹totake@eng.hokudai.ac.jp)

²Department of Earth Science, Tohoku University, Sendai, Japan,

²⁻¹(yu.sakamoto12@gmail.com),

²⁻²kakegawa@m.tohoku.ac.jp)

³Department of Natural History Sciences, Hokkaido University, Sapporo, Japan.

³⁻¹(sitoh@ep.sci.hokudai.ac.jp),

³⁻²(yuri@ep.sci.hokudai.ac.jp)

Although the temporal change in trace element concentrations in Banded Iron Formations (BIFs) can be useful in reconstructing Earth's Precambrian surface environments and associated biological activity, BIFs from various sedimentary settings, particularly of Archean age, will be investigated to increase our understanding of these environments. In this study, we investigated geological, petrographic and geochemical characteristics of ferruginous rocks deposited in a shallow water environment in the Moodies Group, in the Barberton Greenstone Belt, South Africa. Samples were obtained from an outcrop in the Moodies Hills Block and at a cross cut in the Sheba mine.

The petrographic relationships between hematite and magnetite in the samples resemble those observed in typical oxide-type BIFs. Geochemical data show that Fe and Cr are enriched relative to Ti in the ferrous rocks. Although various detrital minerals are observed, including detrital quartz, the proportion of refractory elements and rare earth element (REE) patterns show that the sediment was predominantly derived from felsic rocks. Therefore, the results of geochemical analyses of these rocks indicate that both Fe and Cr are chemical precipitates or of an early diagenetic origin. Oxygen isotope analyses of individual chromite grains by Secondary Ion Mass Spectrometry (SIMS) reveal they are depleted in ¹⁸O compared to previously reported values for magmatic chromite, indicating that the chromite was formed under sub-magmatic temperatures (e.g., hydrothermal). Therefore, our detailed petrographic and geochemical investigations of the chemical and clastic sedimentary rocks show that some geochemically important elements (i.e., Fe, Cr, and U) were already mobile and fixed in a shallow water environment at 3.2 Ga.

Dissolution of Amorphous Silica in the Presence of Ca²⁺ and Mg²⁺ at pH 6 and 9

EMI OTSU, MAYUMI ETOU, YOSHIHIRO OKAUE AND TAKUSHI YOKOYAMA*

¹Department of Chemistry, Faculty of Science, Kyushu University, 6-10-1, Hakozaki, Higashi-ku, Fukuoka, 812-8581, Japan

Takushi Yokoyama: (yokoyamatakushi@chem.kyushu-univ.jp)

Silica dissolves into natural waters as monosilicic acid (Si(OH)₄) through an break of siloxane bonds by attack of water molecule. Factors controlling the silica dissolution reaction are important subject in geochemistry to elucidate circulation of silicon in hydrosphere. Especially, because an alkaline and alkaline earth metal ions exist abundantly in natural water, the effect of these metal ions on the dissolution of silica has been investigated and the acceleration of the dissolution of silica has been reported¹⁻⁴). However, the acceleration mechanism of dissolution of silica by cations has been uncertain even at present. In the previous studies, only the variation of silicic acid concentration was mainly examined. No researcher has been investigated quantitatively the behavior of cations during the dissolution reaction. The purpose of this study is to elucidate the effect of Ca²⁺ and Mg²⁺ on the dissolution of silica from both the variation of silicic acid concentration with time and behavior of Ca²⁺ and Mg²⁺.

From the behavior of Ca²⁺ and Mg²⁺ during the dissolution of silica, it was revealed that the acceleration mechanism of each metal ion was clearly different by reaction pH. At pH 9, the dissolution of silica is controlled by the interaction between Ca²⁺ and Mg²⁺ and silicic acid: the formation of Ca²⁺-silicic acid complex and of an insoluble magnesium silicate-like structure. Although no adsorption of Ca²⁺ and Mg²⁺ ions occurred at pH 6, the dissolution of silica was accelerated. This may be caused by attack of water molecules to siloxane bonds hydrated to Ca²⁺ and Mg²⁺ ions due to fast exchange reaction with the bulk water near the surface of silica.

[1, 2] Dove *et al.*, *Geochim. Cosmochim. Acta*, (1997 and 1999), [3] Tanaka and Takahashi, *J. Soln. Chem.*, (2005), (4) House, *J. Coll. Interface Sci.*, (1994).

CSD, crystal shape and connectivity in synthetic basalt from 3D reconstruction by X-ray CT image

E. OTSU PUIER^{1,2}, B. DARDÉ¹, L. MONNIER¹, M. NAKAMURA², S. OKUMURA², A. TSUCHIYAMA³
M. UESUGI⁴ AND K. UESUGI⁵

¹ LaSalle Beauvais, Géosciences, France (*correspondence : els.ottavi-pupier@lasalle-beauvais.fr)

² Dept. of Earth Science, Tohoku University, Japan

³ Dept. of Geology and Mineralogy, Kyoto University, Japan

⁴ JSPEC/JAXA, Japan

⁵ SPring-8/JASRI, Japan

In-situ observation of plagioclase crystals in synthetic basalt by using micro-tomography beam lines at SPring-8, is supported from two previous experimental studies realized on same run charge [1,2]. It is here proposed to quantify crystal agglomeration and connectivity (touching crystals/non touching crystals) during crystallization and also to improve corrections applied in 2D CSD. By using micro-tomography beam lines and softwares (©Slice and ©Blob3D), three-dimensional images of the run products at a resolution of 2.74 μm are created. Size and shape evolution during cooling are clearly outlined by variation of the shape factor. A first comparison between 2D/3D CSD shows similarity in the CSD morphology. The connectivity (Fig. 1) between plagioclase crystals increases very rapidly with a ratio of 0.2 to 0.4 in the early stages of crystallization (5% plagioclase crystals) to 1 for 20-25 % of plagioclase crystals in the late stages. Processes of crystals agglomeration do not appear of major importance compared to connected crystals that form a continuous 3D network. This early crystal network strongly influences magma rheology.

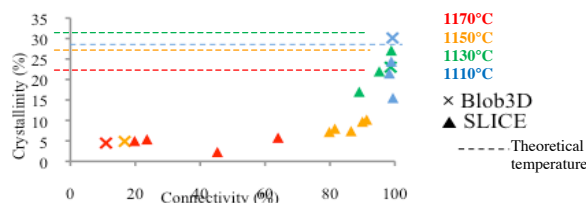


Fig. 1: Plagioclase crystallinity function of plagioclase connectivity

[1] Pupier *et al.* (2008) *Cont. Min. Pet.* **155**, 555-570. [2] Duchêne *et al.* (2008) *Am. Min.* **93**, 893-901.

Marine aerosol activation to CCN and cloud formation

J. OVADNEVAITE*, G. MARTUCCI, D. CEBURNIS,
J. BIALEK AND C.D. O'DOWD

School of Physics and Centre for Climate and Air Pollution Studies, Ryan Institute, National University of Ireland Galway, University Road, Galway, Ireland
(*correspondence: jurgita.ovadnevaite@nuigalway.ie; giovanni.martucci@nuigalway.ie, Darius.Ceburnis@nuigalway.ie, jakub.bialek@nuigalway.ie, Colin.Odowd@nuigalway.ie)

Marine aerosol occurring in cloud condensation nucleus (CCN) sizes suggest that it may contribute notably to the CCN population [1, 2], but further cloud droplet number concentration (CDNC) would strongly depend on the ambient (cloud) conditions, such as available water content, supersaturation and competition between the CCN of different composition [3]. Since the global importance of marine aerosol particles to the cloud formation was postulated several decades ago [4], it has progressed from the evaluation of the nss-sulphate and sea salt effects to an acknowledgement of the significant role of organic aerosol [5]. It was demonstrated that primary marine organics, despite its hydrophobic nature, can possess the high CCN activation efficiency, resulting in the efficient cloud formation [6]. Here we show the relationship between the marine boundary layer aerosol composition, CCN activation and CDNC for different aerosol and ambient conditions. We investigate the activation of sea spray composed of the sea salt and externally mixed with nss-sulphate as well as the sea spray highly enriched in organics, stressing the importance of the latter to the formation of the cloud droplets. We also explore the suitability of existing theories to explain the different composition marine aerosol activation to CCN and resulting CDNC.

Acknowledgments

This work was supported by the SFI, HEA-PRTL14, EC IP EUCAARI, EPA-Ireland, ESA (SToSE: OSSA), EC ACTRIS.

[1] Meskhidze & Nenes (2006) *Science* 314, 1419-1423. [2] Sorooshian *et al.* (2009) *Global Biogeochemical Cycles* 23, GB4007. [3] O'Dowd *et al.* (1999) *Quarterly Journal of the Royal Meteorological Society* 125, 1295-1313. [4] Charlson *et al.* (1987) *Nature* 326, 655-661. [5] O'Dowd *et al.* (2004) *Nature* 431, 676-680. [6] Ovadnevaite *et al.* (2011) *Geophysical Research Letters* 38, L21806.

Dating zircons from volcanic ash beds in sedimentary successions: magmatic crystallization vs. ash deposition

M. OVTCHAROVA^{1*}, U. SCHALTEGGER¹,
N. GOUEMAND² AND H. BUCHER²

¹Earth and Environmental Sciences, University of Geneva, Switzerland, (maria.ovtcharova@unige.ch*)

²Institute and Museum of Paleontology, Zurich, Switzerland

Detailed calibration of the Late-Middle Triassic time-scale requires precise and accurate age determinations from volcanic ash beds within biostratigraphically well dated marine sedimentary sections. High precision CA-ID-TIMS U-Pb zircon dates on volcanic zircon have been used to quantify and calibrate different stratigraphic schemes across the Early-Middle Triassic boundary in South China. Despite an optimal control on the continuity of the stratigraphic record and on the accuracy of analytical procedures, some single ash-beds from the Monggan Wantuo section (Luolou Fm., NW Guangxi, S. China) yield ages that are too old and contradict the stratigraphic succession. How can we improve the confidence in the interpretation of zircon dates as proxies for the age of deposition of these ash beds?

We dated 15 individual ash beds within the 15m Wantuo Mongan section, applying CA-ID-TIMS techniques on a number of single grains for each sample. In 13 out of 15 ash beds zircon dates are following the stratigraphic succession within analytical uncertainty (from the late Early Triassic Luolou Formation – 248.08 ± 0.12 Ma. to the Middle Anisian Transition Beds – 246.43 ± 0.17 Ma). The zircons from two intermediate volcanic ash beds within the Transition Beds at the Early/Middle Anisian boundary yield well clustering ²⁰⁶Pb/²³⁸U dates at 247.10 ± 0.15 and 247.35 ± 0.11 Ma, clearly indicating that the zircons in this magma batch were crystallizing over a long period of time or remobilized from deeper levels within the same magmatic system. The problem of recurrent zircon dates in a sedimentary succession is common and can only be discovered by sufficiently dense sampling and a sufficient number of data for each ash bed.

We have to keep in mind that for the correct interpretation of dates in stratigraphic sections interlayered with fossil-bearing rocks we need; i) at least one single well preserved stratigraphic section with sufficient chronological control (biochronology and/or chemiostratigraphy) to guarantee that the stratigraphic succession is accurately known; ii) volcanic ash beds that are undisturbed (no volcanosedimentary material, no sedimentary reworking); (iii) sufficient sample and data density to be able to distinguish between magmatic and sedimentary signals coded in the crystallization ages of zircon.

The Thrym Complex of southeastern Greenland: Evolution of Ni-Cu-sulfide mineralization in the lower crust

J. OWEN^{1*}, L. BAGAS¹, J. KOLB², M. L. FIORENTINI¹, B.
M. STENSGAARD² AND N. THEBAUD¹

¹CET/CCFS, The University of Western Australia, Perth, Australia (*owenj03@student.uwa.edu.au)

²Geological Survey of Denmark and Greenland, Copenhagen, Denmark

The Thrym Complex of southeastern Greenland forms part of the North Atlantic Craton and is characterized by migmatitic orthogneiss, narrow bands of mafic granulite, ultramafic rocks, paragneiss, and alkaline-carbonatitic intrusive rocks. The narrow bands of mafic granulite are interpreted as tectonically emplaced gabbroic rocks exposed from the lower crust.

The two main styles of mineralization locally observed in the Thrym Complex are: (1) disseminated sulfides associated with mafic and ultramafic locally granoblastic-decussate rocks; and (2) remobilised sulfides concentrated in amphibolite-greenschist facies shear zones. This mineralization observed differs from typical orthomagmatic Ni-Cu-sulfide occurrences common in the upper crust in that there is no evidence for significant contamination by a crustal sulfur source. Furthermore, no trans-lithospheric structure for the emplacement of the mineralization is apparent.

The sulfide mineralization in the Thrym Complex may represent the root of such a system or the result of a similar magma being emplaced in the lower crust in an area lacking such a fluid-pathway. Mantle-sourced magma emplaced at pressure-temperature conditions in the lower crust would maintain or achieve sulfur-saturation more easily than magma emplaced in the upper crust [1]. As such, there may be no need for interaction with crustal material for the formation of sulfide mineralization in lower crustal settings.

[1] Mavrogenes & O'Neill (1999), *Geochimica et Cosmochimica Acta* **63**, 1173-1180.

Trace metal drawdown during a Cretaceous oceanic anoxic event: Implications for global redox conditions

J.D. OWENS^{1*}, C.T. REINHARD² AND T. W. LYONS¹

¹University of California, Riverside, Riverside, CA, USA, (jowens@student.ucr.edu, timothy1@ucr.edu (* presenting author))

²California Institute of Technology, Pasadena, CA, USA, (reinhard@caltech.edu)

The global redox state of the oceans during periods of widespread organic-carbon deposition is an essential part of our understanding of Earth's important climatic feedbacks. The Cretaceous is renowned for several global organic-carbon burial events marked by coeval positive carbon isotope excursions now widely known as oceanic anoxic events (OAEs). Here we present a high-resolution compiled data set from Demerara Rise spanning the Cenomanian-Turonian boundary event (~93.9 Ma) or OAE 2, which shows a dramatic drawdown of redox sensitive trace elements. Organic carbon contents are high throughout the entire section analyzed, and, importantly, Fe speciation implies the locality was dominantly euxinic (i.e., anoxic and sulfidic bottom waters) before, during, and after the event. Molybdenum (Mo) and vanadium (V) are effective paleoredox proxies for tracing oceanic euxinia and anoxia, respectively. The drawdown of Mo coincides with the onset of OAE 2, suggesting a global expansion of reducing and sulfidic conditions. Significantly, though, the drawdown of these two redox sensitive elements is offset by 100 kyr, with V preceding Mo. The decline in V enrichment prior to Mo implies an expansion of low oxygen but non-euxinic conditions prior to the OAE. Numerical geochemical box modeling for Mo suggests that euxinia must have covered >2% but <10% of the global seafloor to explain enrichments that were only 25% of those seen before and after the event. Mo and V drawdown may have impacted the nitrogen cycle and thus patterns of primary production, and this feedback may have contributed to the termination of the OAE.

Chemical compositions of soluble aerosols around the last termination in the NEEM (Greenland) ice core

I. OYABU^{1,2,3*}, Y. IIZUKA³, T. KARLIN¹, M. FUKUI³, T. HONDOH³, D. LEUENBERGER⁴, H. FISCHER⁴, G. GFELLER⁴, S. SCHÜPBACH⁵, R. MULVANEY⁶ AND M. HANSSON¹

¹ Department of Physical Geography and Quaternary Geology, Stockholm Univ., SE-10691, Sweden

(*correspondence: oyabu@lowtem.hokudai.ac.jp)

² Graduate school of Environmental Science, Hokkaido Univ., Sapporo, 060-0810, Japan

³ Institute of Low Temperature Science, Hokkaido Univ., Sapporo, 060-0819, Japan

⁴ Univ. of Bern, CH-3012 Bern, Switzerland

⁵ University of Venice, I-30123 Venice, Italy

⁶ British Antarctic Survey, Cambridge, CB3 0ET, UK

The polar ice cores provide us with reconstruction of past atmospheric aerosols. Soluble aerosols in both Arctic and Antarctic ice cores are well discussed by using the proxy of ion concentration/flux, however, there are few studies about chemical compositions of soluble aerosols in ice cores. Using sublimation method [1], here we show differences in the compositions of sulfate and chloride aerosols around the last termination in the NEEM ice core.

A total of 43 samples were distributed from NEEM ice core section from 1280 to 1580 m. Soluble aerosols were extracted from the samples by sublimation system [1]. Constituent elements and diameter of each non-volatile particle were measured by SEM-EDS. By using a method in ref. [2], we assumed chemical compositions of sulfate and chloride aerosols.

We divided the last termination into 4 stages by focusing on the temperature; Holocene, Younger Dryas (YD), Bølling-Allerød (B-A) and Last Glacial Period (LGP), and compared the mass ratio of sulfate and chloride aerosols in each stage. During the cold stage in YD and LGP, CaSO₄ accounted large percentage of sulfate aerosols. On the other hand, during the warm stage in Holocene, Na₂SO₄ accounted large percentage of sulfate aerosols. In B-A, percentage of Na₂SO₄ is almost as same as that of CaSO₄. Since CaSO₄ is considered to be formed at first among sulfate salts in the atmosphere, these results is probably controlled by Ca²⁺ concentration. Mass ratio of NaCl/Na₂SO₄ decreased from LGP to Holocene (Fig. 2f), which indicate that sulfatization of NaCl increased toward Holocene.

[1] Iizuka *et al.* (2009) *J. Glaciol.* **55**, 552-562. [2] Iizuka *et al.* *J. Geophys. Res.* **117**, D04308.

Geochemistry and Petrology of the Timar basaltic volcanism in the northeast of Lake Van

VURAL OYAN^{1*} MEHMET KESKIN^{2,A}
AND YAVUZ ÖZDEMİR³

¹Yüzüncü Yıl University, Faculty of Architecture and Engineering, Department of Mining Engineering Van, Turkey.

²Istanbul University, Faculty of Engineering, Department of Geological Engineering Istanbul, Turkey.

³Yüzüncü Yıl University, Faculty of Architecture and Engineering, Department of Geological Engineering Van, Turkey.

Timar Pliocene basaltic volcanism in the northeast of the Lake Van Basin erupted from local central eruption centers. Products of basaltic volcanism in the Timar region are covered by younger lavas of Late Pliocene Etrüsk volcanics and Quaternary basalts in age. Available K-Ar ages [1] indicate that basaltic volcanism observed in north and southeast of the Etrüsk volcano erupted in a period between 4.90 and 4.50 Ma corresponding to Zanclean (Pliocene). Alkaline-subalkaline basalts and hawaiites consist of olivine, augite, titanomagnetite and plagioclase phenocrysts and micro-phenocrystals. The groundmass of these lavas contains the microcrystals of the same mineral assemblages and volcanic glass. They display porphyritic, glomeroporphyritic, intersertal and hyalopilitic textures.

Results of our FC, AFC and EC-AFC modelings indicate that the Timar basaltic lavas were slightly influenced by crustal contamination and fractional crystallization. MORB patterns of corrected data to MgO 9% show that some HFS elements such as Nb and Ta are depleted relative to LIL and LREE (La-Ce). This findings imply that Timar basaltic volcanism could have been derived from a mantle source with a distinct subduction component.

Results of our melting models indicate that the Timar basaltic rocks were derived from both shallow and deep mantle sources with different melting degrees ranging between 0.8 - 5 %. The percentage of spinel seems to have increased in the lherzolitic mantle source of the basaltic lavas. Accordingly, chemical character of the lavas turned from alkaline to subalkaline in time. We argue that the temporal increase of spinel contribution and the melting degree in the mantle source region was responsible for transition from alkaline to subalkaline character in the lava chemistry in time.

[1] Lebedev, A.V., Sharkov, E.V., Keskin, M., Oyan, V., 2010. Doklady Earth Science, (433): 1031-1037.

Conditions for Proterozoic anoxic and non-sulfidic ocean: Constraints from a marine biogeochemical cycle model

K. OZAKI^{1*} AND E. TAJIKA²

¹Atmosphere and Ocean Research Institute, University of Tokyo, Chiba 277-8561, Japan

(*correspondence: ozaki@aori.u-tokyo.ac.jp)

²University of Tokyo, Chiba 277-8561, Japan
(tajika@k.u-tokyo.ac.jp)

Understanding the Earth's oceanic redox evolution in response to several environmental conditions is one of the fundamental topics in the Earth science. Accumulating geochemical records, such as iron speciation and molybdenum geochemistry, reveal large spatial heterogeneity of Proterozoic ocean redox chemistry; anoxic and non-sulfidic (i.e., ferruginous) conditions had been prevailed throughout the Proterozoic, and sulfidic conditions might have covered only a small portion of the seafloor. However, the atmospheric oxygen level (pO_2) in the Proterozoic has not been well constrained, and it remains unclear exactly what biogeochemical conditions are necessary to explain such redox structure in the Proterozoic ocean interior.

Here, we try to constrain the conditions for Proterozoic ocean redox structures by use of a marine biogeochemical cycle model in which C-N-P-O-S coupled biogeochemical cycles are taken into account. The results of systematic sensitivity experiments regarding pO_2 and chemical weathering rate on land demonstrate that the conditions for pervasive euxinia are very limited, and widespread ferruginous condition would be an inevitable consequence of low pO_2 and high pyrite burial efficiency during the Precambrian. Sulfidic waters would be restricted in near-shore regions where riverine sulfate flux is sufficient to stimulate the sulfate reduction. We also found that other environmental factors affecting long-term oceanic redox state (e.g. sea-level stand, settling rate of marine snow in water column) do not change above biogeochemical consequences.

These quantitative results would provide insight into further understanding of the Earth's redox history and its stabilization mechanism(s) from a perspective of the biogeochemical dynamics. We also propose that shelf euxinia still has a significant impact on the availability of redox-sensitive, bioessential trace metals, and therefore would provide a linkage between evolution of ocean oxidation state and biological innovation.

Igneous and impact processes on a ureilite parent body inferred from Y-983890 polymict ureilite

SHIN OZAWA¹, AKIRA YAMAGUCHI¹
AND HIDEYASU KOJIMA¹

¹National Institute of Polar Research, Tokyo 190-8518, Japan
(ozawa.shin@nipr.ac.jp)

Ureilite is the second largest group of achondrites. They are largely divided into two types: monomict and polymict. Most ureilites are monomict ureilites, whereas polymict ureilites are relatively rare. Polymict ureilites are polymict breccias containing lithic clasts and mineral fragments of various lithologies [1]. Therefore, it provides valuable information about igneous and collisional processes on ureilite parent bodies. Yamato (Y-) 983890 is a recently classified new polymict ureilite [2]. In this study, we conducted careful petrographic observations on this new polymict ureilite.

Y-983890 consists of lithic clasts and mineral fragments which show a large variety of lithologies. Most of them are monomict ureilite-like materials. They consist of coarse-grained (up to 1 mm) olivine and/or pyroxene (pigeonite, orthopyroxene, and minor augite) with interstitial dark carbonaceous materials and/or graphite. The chemical compositions and Fe/Mg-Fe/Mn relations of olivine and pyroxene are consistent with those of monomict ureilites [3].

Non-monomict ureilite-like materials include feldspathic clasts, dark clasts, a chondrule fragment, and others. We identified several distinct feldspathic clasts. They show different igneous textures and different chemical compositions of constituent minerals (feldspar and pyroxene). Some of the feldspathic clasts are considered to be basaltic counterparts complementary to monomict ureilites (ultramafic residues). The dark clasts consist of fine-grained phyllosilicate-rich matrices with variable amounts of opaque minerals such as magnetite and sulfides (pyrrhotite, pentlandite). These dark clasts mineralogically resemble the matrices of CI carbonaceous chondrites. A chondrule fragment was also identified. It shows a barred olivine chondrule texture. The chemical composition of the olivine is in the range of that of H chondrite. The dark clasts and the chondrule fragment are considered to be fragments of impactors collided with the parent body of Y-983890.

- [1] Goodrich C. A. *et al.* (2004) *Chemie der Erde*, 64, 283–327. [2] Yamaguchi A. *et al.* (2012) *Meteorite Newsletter*, 21. [3] Goodrich C. A. (1992) *Meteoritics*, 27, 327–352.

Organic geochemical characteristics of the coaly Miocene units in the Şahinalı (Aydın) region, Büyük Menderes Graben, Turkey

ORHAN ÖZÇELİK^{1*}, MEHMET ALTUNSOY¹,
SELİN HÖKEREK¹, NESLIHAN ÜNAL¹
AND NAZAN YALÇIN ERIK²

¹Department of Geological Engineering, Akdeniz University, 07058 Antalya, Turkey
(*correspondence: oozcelik@akdeniz.edu.tr);
(altunsoy@akdeniz.edu.tr; selinhokerek@akdeniz.edu.tr;
nunal@akdeniz.edu.tr)

²Department of Geological Engineering, Cumhuriyet University, 58140 Sivas, Turkey (nyalcin@gmail.com)

In the Şahinalı (Aydın-Turkey) region the Miocene units consist of conglomerate, coal, clayey coal, sandstone, siltstone, claystone, clayey limestone and silicalimestone. Total Organic Carbon (TOC) values in these units range between 0.11–38.13 %. Rock-Eval analyses on core samples with the highest TOC values give hydrogen index (HI) values from 60–566 mgHC/gTOC and oxygen index (OI) values from 31–245 mgCO₂/gTOC. The organic matter can be classified as Type II and III kerogen on the modified van Krevelen diagram. Tmax values vary between 338 and 429 °C, with an average of 413 °C indicating the diagenesis stage. Based on the microscopic studies, organic matter is composed of predominantly autochthonous algal and amorphous material, with a minor contribution of terrestrial material. The average vitrinite reflectance value is 0.35 %. Vitrinite reflection index and Tmax values indicate that the organic matter is immature. Biomarker characteristics also verify these results. 8 α (H)-22, 29, 30-trisnorhopane Ts/(Ts+Tm) ratio is 0.85. This value indicates immature (Ts/Tm>1) organic matter, while C32 22S/(22S+22R) ratio is determined to be 2.56. Diasterane/sterane ratio is generally low in immature sediments - between 0.08–0.71 in the samples- in spite of the lithology effect. The thermal process is evaluated through the biomarker data during the coalification, and the moretane/hopane ratio shows immaturity and early maturity. One of the maturity parameters derived out of C29 regular sterane is 5 α (H), 14 β (H), 17 β (H) C29 sterane and 5 α (H), 14 α (H), 17 α (H) C29 sterane ($\alpha\beta\beta/\alpha\beta\beta+\alpha\alpha\alpha$) ratio which is less than 1 in the samples (0.23–0.31). C23/C24 and C28/C29 ratios are between 0.61–2.86 and 0.71–2.95 respectively. 20(S)/(20S+20R) and $\beta\beta/(\beta\beta+\alpha\alpha)$ sterane ratios indicate immature stage. Oleananes type biomarkers were determined to be 5.52–6.51 derived from the angiosperms. This might indicate angiosperm abundance under deposition conditions.

Effect of Magma Mixing on the evolution of the intermediate members of Süphan Volcanics: Eastern Turkey.

YAVUZ ÖZDEMİR¹* NİLGÜN GÜLEÇ²
AND JON BLUNDY³

¹Yüzüncü Yıl University, Department of Geological Engineering Van, Turkey.

²Middle East Technical University, Department of Geological Engineering, Ankara, Turkey.

³University of Bristol, Department of Earth Sciences, Bristol BS8 1 RJ, UK

The Süphan stratovolcano, representing one of the major eruption centers of the post-collisional volcanism in eastern Anatolia, Turkey, consists of lava flows, domes and pyroclastics ranging in composition from basalts to rhyolites. Geochemical data reveal transitional mildly alkaline to calc-alkaline character for the eruptive products. Ar-Ar age data and published K-Ar data from different levels of the volcanostratigraphic succession yield a range of 0.76-0.06 Ma. Mineral chemistry and textures indicate that magma mixing played an important role on the chemical diversity of Süphan volcanics [1]. Intermediate members of the volcanism show a wide range of mineral compositions, for pyroxenes, olivine and plagioclase, that are intermediate between those of basalts and rhyolites. Mineral thermometry of these rocks also yields a wide range of temperatures intermediate between rhyolite (~750 °C) and basalt (~1100 °C). Geochemical modeling [2] of major element compositions suggests that relatively mafic (SiO₂ ≤ 55wt %) and SiO₂ rich (SiO₂ > 65 wt %) members of the Süphan volcanics evolved at moderately hydrated (H₂O=1 wt %) and QFM (quartz-fayalite-magnetite) conditions at 2-4 kbar pressure. On the other hand, most of the lavas with SiO₂ contents between ~ 57 - ~65 wt % are products of isobaric-isenthalpic mixing of 70% basaltic trachyandesitic magma (at 1100 °C) and 30 % rhyolitic magma (at 900 °C) at a crustal pressure of 0.5 kbar.

[1] Özdemir, Y., Blundy, J.D., Güleç, N. (2011). Contributions to Mineralogy and Petrology, (162) : 573-597.

[2] Ghiorso, M. S. & Sack, R. O. (1995). Contributions to Mineralogy and Petrology, (119): 197-212.

Trace Elements in the Environment at the Site of probable Underground Building in the Nizhnekansky Rock Massif (Siberian Craton)

ANDREY OZERSKIY¹ AND DMITRIY OZERSKIY²

^{1,2}Krasnoyarskgeologia Co., Carl Marx Str., 62, Krasnoyarsk, Russia, 660049 (ozerski@krasgeo.ru)

Trace elements were investigated along with geological exploration of the rock massif for underground isolation of radioactive wastes. Perspective site of rock massif is mainly formed by archaean gneisses with dykes of gabbros or dolerites. Exploration methods included well boring up to 700 m in depth, hydrogeological pumping, geophysical and environmental surface researches etc. Bedrocks (205 samples), soil (50), subsoil (50), bottom sediments (25), and natural taiga's vegetation (15) were sampled for environmental analysis. The samples were tested by atomic absorption spectroscopy (AAS), ICP MS and partially chemical methods.

Searching correlations between different environmental systems and spatial distribution we defined two main types of trace elements, that differ on its' origin. The first type named as *autochthonous* originated from parent bedrock. The second type named as *allochthonous* derived to industrial emissions. In turn, both types are subdivided into some groups that are characterized by different conditions of migration and concentration.

Inert elements (Be, Ga, Mo) have approximately equal concentrations in all searched systems. Cerium and lithium form a group named *immobile in bedrock*, both two elements were detected only in bedrock. A more widespread group, *passive migrating to soil*, is characterized by largest concentrations in rocks. Ba, Co, Cu, La, Pb, Sc, Sn, Ti, Y, Yb, Zn form this group.

The group of elements *active migrating to soil* has two sources of its origin: autochthonous and allochthonous. These elements have the largest concentrations in soils. Autochthonous elements derived from bedrocks are Ag, B, Cr, Ge, Nb, Ni, V, Zr. The source of Mn, Sr, and P is a fly ash, emitted by power and heating plants of the Krasnoyarsk, situated about 60-80 km to southwest.

Only one element, cadmium, is *accumulated in surface landscapes*. It was found in vegetation and bottom sediments but never in bedrock and soils. It may be also the result of industrial emission.

Primordial noble gas in the Solar System

M. OZIMA¹ AND B. MARTY²

¹University of Tokyo, Tokyo 113-0033, Japan

(*correspondence: ezz03651@nifty.ne.jp)

²CRPG-CNRS, Université de Lorraine, BP 20, 54051,

Vandoeuvre, France (bmarty@crpg.cnrs-nancy.fr)

The solar noble gases, especially their isotopic compositions, are crucial reference parameters in discussing planetary evolution. Either Solar wind noble gas (SW) or Q-component in primitive meteorites, both widely occurring in the early solar system with very uniform isotopic composition (except for Q-Ne), has been regarded to represent the primordial solar noble gases. Current conventional practice is to assume the SW noble gases as the proxy of the solar noble gas [e.g.1]. However, on the basis of noble gas isotopic systematics based on noble gas isotopic data in various planetary objects, Ozima *et al* [2] concluded that Q-noble gas represented the solar noble gas, from which SW-noble gas was fractionated (30.3%/amu at mass number 16). Here, we propose a new noble gas isotopic reference parameters for the primordial solar system with special reference to the neon isotopic ratio in the Earth, and discuss their implications on the evolution of terrestrial planets.

The primordial ²⁰Ne/²²Ne value in the Earth is still an enigma, but a common assumption is to assign the SW ratio of ²⁰Ne/²²Ne = 13.8 [e.g.1]. However, we infer from the above noble gas systematics [2] that ²⁰Ne/²²Ne in Q-noble gas, namely the solar ²⁰Ne/²²Ne, was close to 13.0. The ratio is almost identical with the in-situ observed ratio in the Jovian atmosphere [4], a likely locale for the primordial noble gas in the early solar system. Moreover, recent Ne isotopic ratios deduced from some mantle-derived materials such as basaltic glasses from Iceland [1] and Devonian plutonic rocks [5] showed the indigenous mantle component of ²⁰Ne/²²Ne = 13.0. The result would require revision of some of widely held Earth evolution models based on the conventional noble gas reference.

[1] Mukhopadhyay (2012) *Nature* **486**, 102-104. Holland *et al.* (2009) *Science* **326**, 1522-1525. [2] Ozima *et al.* (2012) *MAPS*. **47**, 2049-2055. [3] Busemann *et al.* (2000) *MAPS* **35**, 949-973. [4] Mahaffy *et al.* (2000) *JGR* **105**,15061-15071. [5] Yokochi & Marty (2004) *EPSL* **225**, 77-88.

Heavy and Precious Metal Prospecting Using With Geophysical Methods in The Ophiolitic Rocks Exposed Bozkır (Konya-Turkiye) and Hatıp-Çayırbağı (Meram-Konya-Turkiye) Regions.

ALICAN ÖZTÜRK^{1*} AND AHMET. BAYKAL²

¹ Selcuk University, Geological Engineering Department, Konya, Turkey (correspondence: acan@selcuk.edu.tr)

² Yapiray Railway Construction Systems Industry&Trade Inc.

In this study, ore deposit prospecting on the ophiolitic rocks exposed in the Bozkır (Konya) and Hatıp-Çayırbağı (Meram-Konya) regions were realized using with the geological, geophysical and geochemical methods.

In the Bozkır region; emplacement age is Upper Cretaceous of Bozkır Unit and located as allochthonous on the underlying rocks. Bozkır Unit is represented by mainly Bozkır Ophiolitic Melange and Boyalıtepe Group. Although Bozkır ophiolitic Melange consist of serpentinite, gabbro, dunite, diabase, spilitic basalt and deep-sea sediments, Boyalıtepe Group made up of different lithological featured limestones (Mahmuttepe, Kuztepe, Soğucak and Erenlerstepe limestones). In the Miocene time Kızıltepe Volcanics cuts and exposes above mentioned units. Gündüğün formation placed unconformably over all of the older units at the topmost of the sequence.

In the Hatıp-Çayırbağı Region; basement of the sequence is represented by Upper Triassic- Upper Cretaceous aged Lorasdağı Formation and Midostepe Formation. These units were covered Upper Cretaceous Hatıp Ophiolitic Complex and Çayırbağı Ophiolite. Upper Miocene-Lower Pliocene Ulumuhsine Formation unconformably lies over the older units.

Chemical analysis of the rock and plaser samples derived from both two areas were run on the major oxides, trace elements, platinumium group metals and rare earth elements and statistical interpretations were performed.

Different units of both two areas were tried to be determined by using resistivity as an electrical geophysical method. With this aim three-point in the Bozkır region and four-point in the Hatıp-Çayırbağı region investigated using with vertical electrical sounding (VES). As a result of the obtained data of VES in the Bozkır Region; hydrothermal permeable metal-rich and magnetite-rich altered gabbro and spillite siliceous levels were determined formations. In the Hatıp Region silica levels and also magnetite and chromite-rich serpentinite formations have been identified [1].

[1] Öztürk, A. and Baykal, A. (2011), Heavy and Precious Metal Prospecting Using With Geophysical Methods in The Ophiolitic Rocks Exposed Bozkır (Konya) and Hatıp-Çayırbağı (Meram-Konya) Regions. S.R.P.C. p.101.

The geochemical evolution of lateral and vertical direction of Delihalil volcano (Yumurtalık, Turkey)

ALI ÖZVAN^{1*}A AND VURAL OYAN²

¹Yuzuncu Yil University Department of Geological Engineering 65080 Van, Turkey

(*Correspondance:aliozvan@yyu.edu.tr)

²Yuzuncu Yil University Department of Mining Engineering 65080 Van, Turkey

The study area, located between Ceyhan and Osmaniye in Southerh Turkey, is surrounded by pyroclastics and lavas of Delihalil volcano. The lateral and vertical composition of these lavas are different. Basaltic lavas have different shapes as porous and masive in this region. Generally, porous basalt is seen on surface. Geochemical evolution of the Delihali basaltic volcanism in the vertical direction was investigated in this study.

Delihalil volcano and other young volcanics in study region erupted from late Pliocene to historical time along the NE-SW trending left lateral Yumurtalık fault zone in southern Turkey which is characterized by alkali olivine basalts on surface [1]. These lavas were drilled up to 20 m depth at different points. Core samples were taken to determine the vertical compositon of lavas.

These lavas are composed of olivine, plagioclase, augite and titanogaugite crystals and display porphyritic to aphyric textures. The basaltic lavas display transitional characteristics from alkaline to subalkaline and are basanite, alkali basalt and subalkali basalt. MORB pattern of the basaltic lavas imply that basanitic and basaltic lavas erupted from Delihalil volcano could have been derived from a mantle source like within plate. LREE of the most primitive lavas display strong enrichments relative to HREE and MREE on Chondrite-normalized spider diagrams. This finding indicates the presence of garnet in the mantle source.

A partial melting model was conducted to evaluate partial melting processes in mantle source of the basanites and basalts in the Delihalil volcano alkaline volcanism. Results of this study suggest the presence of both strongly garnet and slightly spinel peridotite in the source, a partial melting degree of 0.1-3 % and mixing of the derivative melts from them in the genesis of the mafic basanitic and basaltic lavas.

[1] Parlak, O., Delaloye, M., Kozlu, H., Fontgnie, D., 2000. Bulletin of Earth Sciences Application and Research Centre of Hacettepe University, 22: 137-148.

Synthesis and characterization of K-zeolites by the use of a diatomite

C. PACE¹, D. NOVEMBRE^{1*} AND D. GIMENO²

¹Dipartimento di Ingegneria e Geologia, Università degli Studi G. D'Annunzio, Chieti Scalo 66100, ITALY
(*correspondence: dnovembre@unich.it)

²Depart. de Geoquímica, Petrologia i Prospecció Geològica, Facultat de Geologia, Universitat de Barcelona, 08028, SPAIN (domingo.gimeno@ub.edu)

Hydrothermal crystallization of K-zeolites (K-F and W-Merlinoite type) from gels obtained by the use of k-aluminate and naturally derived k-silicate is here achieved. The use of an inexpensive natural rock ("Tripoli" siliceous rock from Crotona, Italy) reduces the high costs of the usual industrial synthesis protocols and favours the exploiting of the same natural material. Chemical treatments were performed on the opaline siliceous rock, whose composition resulted in quartz, amorphous opaline silica, clay minerals and a minor amount of calcite [1], in order to obtain k-silicate. A first attack with nitric acid to eliminate the calcitic and carbonatic fraction and Fe and Mn oxides, was followed by a treatment in an alkaline bath (KOH 10%) to induce the solubilization of the siliceous fossil fraction and the production of the K₂SiO₃ solution. The second reagent, potassium aluminate, was achieved by the mixing of potash

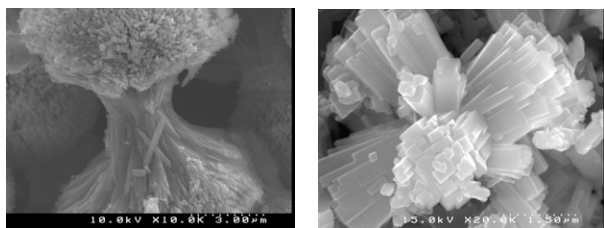


Figure 1: Left: W-Merlinoite type zeolite; right: K-F zeolite.

(20%) with Al(OH)₃ (65%). Five series of synthesis were performed inside autoclaves at a temperature of 150°C and ambient pressure by varying the ratio of the silicatic and aluminatic solutions. Infrared and X-ray spectroscopy, thermo diffraction, nuclear magnetic resonance ²⁹Si, structural refinement together with high temperature diffraction textural, chemical, and physical characterization give values comparable to those proposed by literature.

[1] Novembre *et al* (2004) *Microp. and Mesop. Mat.* **75**, 1-11.

Environmental diversity of denitrification

LAURA A. PACE¹, JAMES HEMP², RANJANI MURALI³, ROBERT B. GENNIS³ AND WOODWARD W. FISCHER²

¹University of Utah (laura.a.pace@gmail.com)

²California Institute of Technology (jim.hemp@gmail.com)

³University of Illinois at Urbana-Champaign

The modern nitrogen cycle is a complex web of microbially mediated redox reactions found in both oxic and anoxic environments. Recently, the breadth of microbial roles in the nitrogen cycle has expanded substantially, with the discovery of both new metabolisms (ANAMMOX; anaerobic oxidation of methane coupled to denitrification), and novel organisms performing known reactions (ammonia oxidation in Archaea). Here we use metagenomics, coupled with biochemical and physiological experiments, to identify new enzyme families able to catalyze nitric oxide reduction. These results greatly expand the known diversity of organisms capable of performing denitrification, suggesting also that this metabolism is more widespread than previously recognized.

Nitric oxide reduction is catalyzed by enzymes from the heme-copper oxidoreductase (HCO) superfamily. The superfamily is extremely diverse, with members playing crucial roles in both aerobic and anaerobic respiration. It is currently divided into two reaction classes; oxygen reductases and nitric oxide reductases. The oxygen reductases are terminal enzymes in aerobic respiratory chains, and are able to conserve energy in a proton electrochemical gradient. The nitric oxide reductases (NOR) catalyze the reduction of nitric oxide to nitrous oxide ($2\text{NO} + 2\text{H}^+ + 2\text{e}^- \rightarrow \text{N}_2\text{O} + \text{H}_2\text{O}$) in microbes capable of denitrification, and are not known to conserve energy.

The HCO superfamily currently consists of three oxygen reductase families (A, B and C) and two NOR families (eNOR and qNOR). We used metagenomics and comparative genomics to discover at least seven new families capable of nitrogen cycle reactions. Five of these families (eNOR, bNOR, sNOR, gNOR, nNOR) catalyze nitric oxide reduction. The two other families are predicted to perform reactions new to the superfamily; nitric oxide dismutation ($2\text{NO} \rightarrow \text{O}_2 + \text{N}_2$) and nitrous oxide reduction ($\text{N}_2\text{O} + 2\text{H}^+ + 2\text{e}^- \rightarrow \text{N}_2 + \text{H}_2\text{O}$). All sequenced ammonia-oxidizing bacteria have the sNOR family, whereas the gNOR family is specifically found in environments where sulfide oxidation is coupled to denitrification. The eNOR and bNOR families have proton channels, which allow them to conserve energy, enabling these microbes to extract more energy from denitrification. Significantly, according to metagenomic data, the eNOR family appears to be the most common NOR found in Nature.

Hydrogen diffusion in Ti-bearing forsterite

PADRON-NAVARTA J.A.^{1,2}, HERMANN J.³,
AND O'NEILL H.S.C

¹Géosciences Montpellier, CNRS-UM2, Montpellier, France.

³Research School of Earth Sciences, ANU, Australia.

Migration of point defect in ferromagnesian silicates controls the transport properties of the Earth's mantle. The geodynamic and chemical evolution is dictated by the influence of "water" (more specifically hydrogen) on the physical properties of olivine (Fe,Mg)₂SiO₄, which dominates the mineralogy of the upper mantle. The presence of hydrogen significantly modifies the timescale of diffusion, plastic deformation and other transport properties in olivine such as electrical conductivity or the attenuation of seismic waves. In order to understand all these processes it is essential to unravel the diffusivity of hydrous defect in nominally anhydrous minerals (NAMs). We report a new experimental approach to study hydrogen diffusion in forsterite containing key hydrous defects relevant for the upper mantle.

Synthetic titanium-bearing forsterite crystals containing 308 ± 20 ppm wt. H₂O were heated at 1273 K, 1173 K and 1073K during 296, 432 and 1304 h (ca. 1.8 months) respectively. The temporal evolution of individual peak heights related to hydroxyl (OH) stretching vibration in the infrared spectra was measured. OH-stretching bands assigned to titanium clinohumite point defects, silicon and magnesium vacancies and defects associated to trivalent cations show contrasting behaviors with time. Two different parts are distinguished during the dehydroxylation process: (1) hydrous defects related to trivalent cations and Mg-vacancies early disappear followed by hydrous defects related to Ti and Si-vacancies with a diffusion coefficients one order of magnitude slower than previously reported. The first part of the dehydroxylation is associated to the precipitation of an oriented Ti-rich phase; (2) In the second part of the dehydroxylation process, a concentration of 39-46 ppm wt. H₂O (exclusively related to Si-vacancies) is reached and remains constant until the end of the experiment. We suggest that this is related to a very slow diffusivity of Si-vacancies when other type of defects are lacking. Hydrogen extraction in forsterite and likely in other NAMs is thus far more complex than previously assumed. Unraveling these complex processes are crucial to understand the deep Earth's water cycle.

Fluorine, Cl, Br & I in serpentinites

LILIANNE PAGE* AND KEIKO HATTORI¹

¹Dept. Earth Sci., Univ. Ottawa, Ottawa, Canada, K1N 6N5

(*correspondance: lpage097@uottawa.ca)

The abundance of F, Cl, Br and I in serpentinites were examined to evaluate their behaviour in subduction zones. Samples include (1) unmetamorphosed, obducted hydrated abyssal peridotites, (2) subducted abyssal peridotites to depth of ~30 km, (3) forearc mantle serpentinites from shallow depth (<30 km) and (4) mantle wedge serpentinites from ~140 km depth in the Himalayas. Samples (1,2,3) from Dominican Republic are composed of lizardite (low temp. serpentine). The Himalayan samples consist of antigorite (high temp. phase). Abyssal peridotites contain high (<530 ppm) Cl but they lose Cl during their subduction. In the mantle wedge, elevated (<880 ppm) Cl in shallow serpentinites suggests transfer of Cl from subducting slab to the overlying mantle wedge. Lower Cl values (≤50 ppm) in deep mantle wedge serpentinites indicate loss of Cl either by pressure increase or transition from lizardite to antigorite. The Br/Cl ratios for obducted abyssal peridotites are comparable to that of seawater, confirming their serpentinization on or near the ocean floor. Bromine appears to mimic Cl in its behaviour; abyssal peridotites partially lose Br during subduction and there is high Br content in shallow mantle wedge serpentinites. However, the degree of Br loss is less than that of Cl with increasing depth, as illustrated by the elevated Br/Cl ratio (<12 × 10⁻³) in the deep mantle wedge. Hydrated abyssal peridotites contain relatively high I/Cl ratios up to 240 times seawater. Our results are consistent with data from sea floor serpentinites [1]. The content of I remains relatively constant during their shallow subduction. In the mantle wedge, shallow and deep forearc serpentinites contain similar amounts of I, indicating retention of I during the lizardite to antigorite phase transition.

Fluorine shows significantly different behaviour from the other halogens. The content of F is low (≤20 ppm) in abyssal peridotites, as expected from low F content in seawater. Upon shallow subduction, F content increases in hydrated abyssal peridotites, likely incorporated from shallow water sediments. Similar F-enhancement is observed for shallow forearc peridotites. Fluorine is further enriched in deep mantle wedge peridotites (<160 ppm) by incorporating F released from slabs and sediments.

Serpentinites likely contribute to the transfer of F and I into the deep mantle, whereas Br and Cl likely have shallow cycles in subduction zones.

[1] Kendrick *et al* (2013) *Earth Planet Sc. Lett.* **365**, 86-96.

Primary and secondary biomass burning aerosols determined by factor analysis of H-NMR spectra

M. PAGLIONE^{1*}, S. DECESARI¹, L. GIULIANELLI¹,
E. TAGLIAVINI², R. HILLAMO³, S. CARBONE³,
S. SAARIKOSKI³, E. SWIETLICKI⁵, S. FUZZI¹
AND M.C. FACCHINI¹

¹CNR-Institute of Atmospheric Sciences and Climate (ISAC),
Bologna, Italy (*correspondence: m.paglione@isac.cnr.it)

²Dept. of Chemistry, University of Bologna, Bologna, Italy
(emilio.tagliavini@unibo.it)

³Finnish Meteorological Institute, Air Quality Research,
Helsinki, Finland (risto.hillamo@fmi.fi)

⁴Div. of Nuclear Physics-Dept. of Physics, Lund University,
Sweden (erik.swietlicki@pixe.lth.se).

Discovery of Secondary Organic Aerosol (SOA) formation in biomass burning plumes leads to the question whether oxidized fraction of biomass burning aerosol is rather of secondary instead of primary origin and what are chemical compositions of oxidized biomass burning POA and SOA.

In the frame of EUCAARI project proton-nuclear magnetic resonance (H-NMR) spectroscopy was applied to investigate the functional group composition of fresh and aged biomass burning aerosols during an intensive field campaign carried out in spring 2008 at a Po Valley rural station, Italy. Factor analysis applied to set of NMR spectra was used to apportion wood burning and other OC source contributions, including aliphatic amines. Comparison between NMR results and those from parallel high resolution aerosol mass spectrometry (HR-Tof-AMS) measurements shows only a partial overlap between NMR and AMS factors relating to fresh biomass burning. The comparison between the two techniques substantially improves when adding factors tracing possible contributions from biomass burning SOA. The chemical composition of such secondary combustion aerosols was shown to be markedly different from that of the corresponding POA and, at the same time, was not represented by most common organic tracers used to apportion biomass burning POA. NMR results, in fact, show that fresh wood burning is composed of polyols and aromatic compounds, with a sharp resemblance with wood burning POA obtained from smoke chambers, while aged samples are depleted of alcohols and are enriched in aliphatic acids with a smaller contribution of aromatics. Factor analysis applied to NMR proven to be able to overcome the main drawbacks of methodologies relying on molecular tracer analysis and could be profitably used for the identification of SOA fractions.

Loss of Volatile Elements After the Moon-Forming Giant Impact

K. PAHLEVAN¹, S. KARATO¹ AND B. FEGLEY²

¹Dept. of Geology and Geophysics, Yale University, USA

²Dept. of Earth & Planetary Sciences and McDonnell Center
for Space Sciences, Washington U. St. Louis, USA

Among the most striking observations made of the Apollo samples is the relative dearth of volatile elements observed in the lunar material [1], including moderately volatile elements that condense from the solar nebula at relatively high ($T > 1,000$ K) temperatures. Although such an observation is generally thought to be consistent with the energetic events associated with a giant impact, no quantitative chemical and dynamical scenario has been put forward to explain it.

The energy released in the Moon-forming giant impact is sufficient to melt and partially vaporize both the Earth and the impactor. The timescale to eliminate this heat by radiation is $\sim 10^3$ years [2]. Hence, the Earth-Moon system is expected to be in a molten, partially vaporized state for the first thousand years after the giant impact. This stage of the evolution may permit the loss of volatile elements via selective partitioning of elements into a vapor phase followed by phase separation of the lunar material. It has been known for decades that H – in molecular form – is gravitationally unbound in the circumterrestrial lunar disk [2]. However, no process is known that can separate the light, unbound vapor species from the heavier molecules of the silicate vapor atmosphere on the relevant timescales.

Here, we investigate a new possibility: redistribution of elements in the proto-lunar disk. Because the Moon accretes from the outermost regions of the proto-lunar disk, it may inherit a composition distinct from that of the inner disk which accretes back onto the Earth. We will present model calculations that explore physical and chemical conditions necessary for the Earth-ward transport of volatile elements in the proto-lunar disk and present the consequences of such a redistribution process. Such an approach has the potential not only to explain the abundances and isotopic composition [3] of lunar volatiles but also to permit the observed abundances to be used to yield insight into the largely unknown processes accompanying lunar origin.

[1]. Ringwood, A.E. (1979), *Origin of the Earth and Moon*. Springer-Verlag, New York. [2]. Stevenson, D.J. (1987), *Annu. Rev. Earth Planet. Sci.* **15** 271-315. [3]. Humayun, M., Clayton, R.N. (1995), *Geochim. Cosmochim. Acta* **59** 2131-2148.

Distribution of dissolved neodymium isotopes across the southern South Pacific

KATHARINA PAHNKE* AND CHANDRANATH BASAK

Max Planck Research Group for Marine Isotope Geochemistry, Institute for Chemistry and Biology of the Marine Environment (ICBM), University of Oldenburg, Oldenburg, Germany (*correspondence: kpahnke@mpi-bremen.de)

The South Pacific is an important area of bottom and intermediate water formation, and a key location for the communication of the Pacific with the Indian and Atlantic Ocean basins. Despite its importance for the global ocean, the South Pacific is largely understudied with respect to the distribution of trace elements and their isotopes, and in particular neodymium isotopes ($^{143}\text{Nd}/^{144}\text{Nd}$, expressed in ϵ_{Nd}), for which only a limited database exists in the southeast Pacific [1].

Here we present dissolved Nd isotopes from 11 stations across the South Pacific between South America and New Zealand and between 46°S and 69°S. The transect samples South Pacific water masses east and west of the Pacific-Antarctic Ridge and north and south of the circum-Antarctic frontal system, affording insight into the spatial variation of the Nd isotopic composition of different water masses. We observe a clear difference in ϵ_{Nd} between bottom waters in the western basin within the Deep Western Boundary Current ($\epsilon_{\text{Nd}} = -9$) and the eastern basin just north of the Ross Sea ($\epsilon_{\text{Nd}} = -7$), suggesting that Antarctic Bottom Water from different source regions carries different isotopic signatures. Notably, bottom water formed in the Ross Sea (RSBW) can also be distinguished from overlying Circumpolar Deep Water, making ϵ_{Nd} a useful tracer for past changes in RSBW export into the southeast Pacific. Most profiles further show a shift towards less radiogenic ϵ_{Nd} at the depth of Upper Circumpolar Deep Water (UCDW) that is associated with a salinity maximum in the Southern Ocean. This negative shift is consistent with a higher component of unradiogenic North Atlantic Deep Water ($\epsilon_{\text{Nd}} \approx -13$) in UCDW. The results provide a good basis for an improved understanding of the distribution of Nd isotopes in the Pacific Ocean, and for the use of ϵ_{Nd} as a tracer of past circulation changes.

[1] Carter *et al* (2012), *Geochim. Cosmochim. Acta* **79**, 41-59.

High Precision measurements of sub nanogram levels of neodymium measured as NdO⁺ using Phoenix X62 Thermal Ionization Mass Spectrometer

ZENON PALACZ¹, DAVID BURGESS AND JEREMY INGLIS¹

¹Isotopx, Unit 1A Milbrook Court, Middlewich, Cheshire, CW10 0GE.

We have analysed sub nanogram amounts of the JNd-I Neodymium standard as NdO⁺ using the Phoenix X62 TIMS. Samples were loaded on single Re filaments with a TaF₅ activator. Ion/Atom detection efficiency increases with decreasing sample size, with efficiencies of up to 30% attained for sample sizes between 500 and 50pg. For sample sizes of 1-10ng efficiencies are about 10%. Similar efficiencies are also observed for Sr. The maximum detection efficiency is close to the transmission of the spectrometer, and that the TaF₅ activator is producing nearly 100% ionization off the filament for small samples of Sr and Nd, which have similar ionization potentials of 5.2 and 5.5eV respectively. This is much higher (by more than an order of magnitude) than Sr and Nd⁺ without the TaF₅ and probably indicates an increase due to close coupling with the very high work function fluorine atom. Using static multicollection and 1e¹¹ ohm resistors, the reproducibility of $^{143}\text{Nd}/^{144}\text{Nd}$ remains better than 20ppm 1RSD for sample sizes down to 100pg. It is possible that using a higher gain resistor will improve this since ion intensities for $^{143}\text{Nd}^{16}\text{O}$ are only 50mv.

Soil aggregate-scale chemical gradients resulting from coupled biogeochemical and transport processes

CÉLINE PALLUD^{1*} AND MATTEO KAUSCH¹

¹Environmental Science, Policy and Management (ESPM), University of California, Berkeley, USA (*correspondence: cpallud@berkeley.edu)

A continuing challenge in environmental science is to understand and predict how concentrations of nutrients and contaminants vary over space and time in natural systems. Within soils, biogeochemical processes controlling elemental cycling are heterogeneously distributed owing partly to the physical complexity of the media. Structured soils are composed of individual aggregates that form a network of interconnected microenvironments. The aggregate scale (mm-cm) is of particular interest due to the sharp transition in pore size between the aggregates themselves and the macropores surrounding them. The objective of this study is to investigate the coupling of physical (transport) and biogeochemical processes that affect small-scale iron transformations and that control selenium sequestration within soils.

We present a combined experimental and modelling study on single artificial soil aggregates assessing the biogeochemical processes governing transformations of redox sensitive elements (iron and selenium) in a complex but controlled setting representative of natural systems. Circumventing byproduct accumulation and substrate exhaustion common in batch systems and avoiding the poor physical analogy to aggregated soils of homogeneously packed columns, our novel experiments mimic soils using constructed cm-scale aggregates in flow-through reactors, which results in diffusively and advectively controlled regions. A newly developed reactive transport model is used to delineate transport regimes, identify reaction zones, and estimate kinetic parameters and reaction rates at the aggregate scale.

Overall, our findings demonstrate significant aggregate-scale variations in biogeochemical processes and consequent distribution patterns of solid phases within soils. We show that those chemical gradients are mainly controlled by diffusive mass-transfer limitations of both solute delivery to the aggregates and metabolite removal from the aggregates. This highlights the importance of appreciating the spatial connection between reaction and transport fronts and of obtaining information on transport-limited, intra-aggregate biogeochemical dynamics to better understand reactive transport of redox-sensitive species in structured soils.

Formation of chondritic meteorites

H. PALME

Sektion Meteoritenforschung, Forschungsinstitut und Naturmuseum Senckenberg, Senckenberganlage 25 D-60325 Frankfurt, Germany
(palmehbert@googlemail.com)

More than 99% of the mass of the solar system is in the Sun. The chemical composition of the Sun and similar stars is well known from absorption line spectroscopy. The Sun has about equal numbers of Mg, Si and Fe atoms. Planetesimals with these characteristics are parental to primitive, undifferentiated or chondritic meteorites. Bulk Earth, Venus and Mars also have approximately solar ratios of Mg, Si and Fe. CI-chondrites match solar abundances to within a few percent. Small deviations from solar abundances in other groups of chondritic meteorites reflect nebular processes prior to accretion to larger objects: (a) Loss or gain of refractory phases (Ca, Al, Ti), (b) variable accumulations of forsteritic olivine and (c) of metallic FeNi and (d) incomplete sampling of volatile elements. In addition, large variations in oxygen contents are observed. Each chondrite group is formed from a comparatively small isolated nebular reservoir [1].

On a cm scale chondritic meteorites are chemically uniform [2]; on a mm scale and below they are extremely variable. Chondrules, mm sized once molten silicate droplets, and fine grained matrix are two major components of chondrites. They are chemically complementary: The low average Fe/Mg and Si/Mg of chondrules is balanced by higher atomic ratios in matrix yielding the chondritic bulk composition. Both components must have formed from a single solar-like reservoir [3]. This is an important often neglected constraint for chondrule formation models. The reason for the enormous chemical variability of chondrules is unclear. Yet, the bulk composition of primitive chondrites requires that it must have been established in a closed reservoir of chondritic composition.

Each chondrite group has its own stable isotope signature [4]. The Earth and the other planets were built of a series of chondritic planetesimals. But stable isotopes indicate that the presently known population of chondrite parent bodies did not significantly contribute to the Earth [5].

Lit.:

- [1] Palme H. and O'Neill H.St.C. (2003) in: *Treatise on Geochemistry, Volume 2-The Mantle and Core*, ed: Carlson, R.W., Elsevier-Pergamon, Oxford, pp. 1-38. [2] Stracke A. *et al* (2012) *Geochim.Cosmochim. Acta* **85**, 114-141. [3] Hezel D.C. and Palme H. (2010) *Earth Planet. Sci. Lett.* **280**, 85-93 [4] Warren P. (2011) *Earth Planet. Sci. Lett.* **311**, 93-100.

The chemical composition of the Earth

H. PALME¹ AND H.ST.C. O'NEILL²

¹Sektion Meteoritenforschung, Forschungsinstitut und Naturmuseum Senckenberg, Senckenberganlage 25, 60325 Frankfurt /Main, Germany, (palmeherbert@googlemail.com),

²Research School of Earth Sciences, Australian National University, Canberra ACT, 0200 Australia

The composition of the Earth is derived from ultramafic rocks, samples from the Earth's mantle in a variety of geologic settings [1]. The high Mg, Ni and PGE contents, chondritic Ni/Co ratios, unfractionated compatible refractory elements (Yb/Sc), chondritic Na/Mn ratios etc. support a primitive mantle origin, affected only by core formation and loss of a small fraction of partial melt, which may have occurred before final accretion of the Earth [2,3]. From a detailed comparison with chondritic meteorites it is concluded that the bulk Earth composition is not CI chondritic (i.e. precisely solar) but has similarities to the chemical composition of the CV group of carbonaceous chondrites: (a) Enrichment of refractory elements, (b) bulk Earth Mg/Si ratio, assuming 7 % Si in the core, (c) similar patterns of moderately volatile elements as CV (d) depletion of Mn and other moderately volatile elements shortly after the first solids had formed in the solar nebula (based on ⁵³Cr). Despite chemical similarities Earth does not match CV precisely: (a) Earth has excess Fe, (b) Earth is more depleted in volatiles than CV chondrites (d) the stable isotopic composition of several elements in the Earth is similar to ordinary chondrites and even closer to enstatite chondrites but different from carbonaceous chondrites [4]. However, enstatite chondrites have very different chemistry and are not good candidates for the Earth. It seems impossible to make the primitive upper mantle from a high Si, low Al source. As chemistry and stable isotopes are decoupled similarities of in stable isotopes have limited significance: Isotopically main group pallasites fit with the non-carbonaceous chondrites while Eagle Station pallasites are close to carbonaceous chondrites [4]. Considering chemistry and stable isotopes one has to conclude that Earth is made of a variety of chondritic meteorites, different from known groups of chondrites.

Lit.: [1] Palme H. and O'Neill H.St.C. (2003) in: *Treatise on Geochemistry, Volume 2-The Mantle and Core*, ed: Carlson, R.W., Elsevier-Pergamon, Oxford, pp. 1-38. [2] O'Neill H.St.C. and Palme H. (2008) *Phil. Trans. R. Soc. A* **366**, 4205-4238. [3] Campbell I.H. and O'Neill H.St.C. *Nature* **483**, 533-558. [4] Warren P. (2011) *Earth Planet. Sci. Lett.* **311**, 93-100.

The role of tephra diagenesis in the carbon cycle

M.R. PALMER^{1*}, T.M. GERON¹ AND SHIPBOARD SCIENTISTS OF IODP LEG 340²

¹School of Ocean & Earth Science, University of Southampton, European Way, Southampton SO14 3ZH, UK (*correspondance: pmrp@noc.soton.ac.uk)

²(http://iodp.tamu.edu/scienceops/expeditions/antilles_volcanism_landslides.html)

Most volcanoes are located close to the oceans. Hence a high proportion of the 10¹⁵ g/yr of tephra that is created by subaerial volcanism ends up in marine sediments, such that tephra comprises ~25% of Pacific Ocean sediments. In addition, individual massive explosive eruptions have covered large areas of the globe during Earth history. Given that fresh tephra is highly reactive when exposed to seawater it is important to consider the implications of this flux of material to the oceans.

We hypothesise that tephra deposition in the oceans may influence the ocean-atmosphere carbon cycle through the following mechanisms: (1) Leaching of tephra deposited in surface waters may cause increased productivity (and drawdown of atmospheric CO₂) via addition of nutrients to Fe-limited areas. (2) Deposition of tephra in sediments leads to rapid depletion of dissolved O₂ in pore waters, thus enhancing organic carbon preservation in underlying sediments. (3) After tephra deposition, bioturbation mixes the upper tephra surface with background sediments. Tephra contains reactive Fe phases that are known to complex organic carbon in non-volcanic sediments and enhance organic carbon preservation. (4) As the tephra layer is buried deeper, it moves into zones of CH₄ and alkalinity production. Alkalinity (and oxidised CH₄) diffuses into the overlying tephra where it encounters high dissolved Ca levels from Ca-Mg exchange during tephra diagenesis, leading to precipitation of calcite cements that effectively sequester CO₂ produced from organic carbon and form a further barrier to downwards diffusion of oxidising species.

We review here the evidence supporting each of these processes and indicate times and places in Earth history when they have played a particularly important role.

Coherent pyroxene-akimotoite phase transformation in NWA 5011 shocked chondrite

E. PÁL-MOLNÁR^{1*}, SZ. NAGY¹, K. FINTOR¹, I. GYOLLAÍ²
AND ZS. BENDŐ³

¹University of Szeged Department of Mineralogy,
Geochemistry and Petrology, Szeged, Hungary
(*correspondence: palmolnare@gmail.com)

²University of Vienna, Vienna, Austria

³Eötvös Loránd University, Budapest, Hungary

Introduction

Akimotoite is a major constituent phase through Earth's transition zone [1]. Up to now this phase transition has been observed as incoherent nucleation and growth in and around opaque shock melt veins [2]. In this abstract we are reporting the possible first coherent pyroxene-akimotoite transformation along the cleavages of pyroxene.

Results and Discussion

The NWA 5011 shocked chondrite consists of shock veins in various thickness and chondrules. A mixed-type pyroxene chondrule (approx. 1 mm in diameter) contains numerous subchondrules observed in the sample. One of the subchondrules exhibits dense cleavage network in which the angle between two cleavage plains is nearly right (87°). Therefore this orientation of crystal face is $\{110\}$. The BSE-images revealed that plain of cleavages enriched in Fe and it shows microgranular texture. However, the microgranular character is slightly overhanging from the original boundary of cleavages to the host grain area. The thickness of "overhanged" transition area is observed up to $0.5\mu\text{m}$, and parallel to the direction of cleavages. In some areas between the cleavages incoherent pyroxene-akimotoite phase transformation occurs. Raman spectra have been collected along the cleavage, which confirmed the pyroxene-akimotoite phase transition. The Fe-enrichment in cleavage is possible due to weathering processes, or melting and subsequent metal-sulfide formation. The most characteristic feature of the Raman spectra is the presence of main vibrations of ringwoodite and stishovite besides akimotoite peaks. This feature confirms that inside the fragments far from boundary of shock melt veins lower P - T regime transformation products in the $\text{Mg}_4\text{Si}_4\text{O}_{12}$ - $\text{Mg}_3\text{Al}_2\text{Si}_3\text{O}_{12}$ system can survive due to the fast temperature drop. This suggests subsequent evidence for high P - T regime change in shock melt veins within a small affected area.

[1] Tomioka & Fujino (1999) *Am. Min.* **84**, 267-271. [2] Hu *et al* (2012) 43rd LPSC, abs#2728.

Single crystal elasticity of the $\text{Na}_{1.07}\text{Mg}_{1.58}\text{Al}_{4.91}\text{Si}_{1.26}\text{O}_{12}$ NAL phase and seismic heterogeneity in the deep mantle

M. G. PAMATO^{1*}, A. KURNOSOV¹, T. BOFFA
BALLARAN¹, D. M. TROTS¹, R. CARACAS²
AND D. J. FROST¹

¹Bayerisches Geoinstitut, Universität Bayreuth, Germany
(*correspondence: martha.pamato@uni-bayreuth.de)

²Laboratoire de Sciences de la Terre, Ecole Normale Supérieure de Lyon, France

Subducted mid-oceanic ridge basalts (MORB) are likely to be important components of the lower mantle. As a consequence of plate tectonics, basaltic oceanic crust is subducted into the mantle introducing chemical heterogeneity. Compared to average peridotitic mantle, MORB are enriched in silicon, aluminium, calcium and alkalis. At lower mantle conditions, experimental studies have shown that subducted MORB comprises more than 20 % of an aluminium rich phase, the so called NAL (new aluminium phase) phase. Evidence for the existence of the NAL phase has been observed in sublithospheric diamonds, where composite multiphase inclusions have been found with similar bulk compositions to NAL. If present, NAL will be a contributor to the bulk elastic properties of the lower mantle and knowledge of its elasticity is crucial for investigating the consequences of subducted crust for the seismology of the mantle.

NAL crystallising in MORB form complex solid solutions and have the general formula $\text{XY}_2\text{Z}_6\text{O}_{12}$ where X is a large monovalent or divalent cation (Ca^{2+} , K^+ , Na^+), Y a middle-sized cation (Mg^{2+} , Fe^{2+} or Fe^{3+}), and Z a small sized cation (Al^{3+} and Si^{4+}). Here we report the crystal structure refinement of NAL synthesized at lower mantle conditions with a composition close to that expected to crystallise in a subducting slab. We also report for the first time its full elastic tensor experimentally determined by Brillouin scattering spectroscopy at room and high pressure. We complement these experimental results with first-principles calculations, performed using density-functional theory and density-functional perturbation theory.

Impact of suspended inorganic particles on phosphorus cycling in the Yellow (Huanghe) River

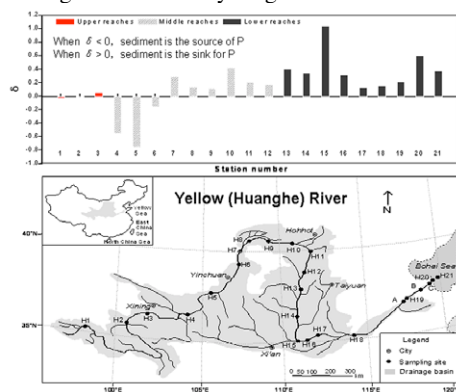
GANG PAN^{1*}, MICHAEL D. KROM^{2,3}, MEIYI ZHANG¹,
XIANWEI ZHANG¹ AND ROBERT J.G. MORTIMER²

¹Research Center for Eco-Environmental Sciences, Chinese Academy of Sciences, Beijing 100085, China,
(*correspondence: gpan@rcees.ac.cn)

²Earth and Biosphere Institute, School of Earth and Environment, University of Leeds, Leeds LS2 9JT, UK

³Charney school of Marine Sciences, Haifa University, Haifa, Israel

While the importance of phosphorus (P) as a limiting nutrient is well established, the understanding of global scale control on P cycling in continents and how these affect riverine P fluxes is still incomplete. P in water and sediment in the Huanghe was measured for 21 stations from the source to the Bohai Sea. The average total particulate matter (TPM) increased from 40 mg/L (upper reaches) to 520 mg/L (middle reaches) and 950 mg/L in lower reaches of the river. Although there was considerable nutrient pollution, the dissolved PO₄ concentration remained low (0.32-0.58 μmol/L) due to adsorption on particles. The P removed was mainly due to the high TPM rather than the surface activity of the particles since they had low labile Fe and low affinity for P. The sediment was a major sink for P in the middle to lower reaches but not in the initial upper to middle reaches. TPM has been reduced by more than 10-fold due to artificial dams over the last decades. Experimental modeling revealed that TPM of 1 g/L was a critical threshold for Huanghe below which most of the P input to the river can no longer be removed by the particles where eutrophication may occur. These findings provide realistic representations of particle control on riverine P fluxes which can be used in coupled land-ocean modeling in global biogeochemical P cycling.



Nd-Sr Isotopic Constraints on the Source of the Hexi Corridor Loess

PAN YAODONG¹ RAO WENBO¹ AND WU WEIHUA²

¹Institute of Isotope Hydrology, Hohai University, Nanjing, 210098, China.(Panyadong612@163.com)

²Institute of surficial geochemistry, Nanjing University, Nanjing, 210093, China

Analysis and Comparison

The loessial soil is very important for habitants in the Hexi Corridor, North China. However, knowledge on the loess source of this region is uncertain till now. In order to answer this question, Sr-Nd isotopic comparisons between the loess of the Hexi Corridor and surface sediments of surrounding areas are conducted in this study.

River sediments from the Qilian mountain are collected for isotopic analysis of their fine-grained fractions in this study. The measured $\epsilon_{Nd}(0)$ values vary from -11.84 to -11.95 with $^{87}Sr/^{86}Sr$ ratios from 0.7196 to 0.7388 □As listed in Table 1 □.

According to topographical and meteorologic data, the Badain Jaran desert, the Qaidam desert, the Taklimakan desert, the Gurbantunggut desert and Rivers of the Qilian mountains might be potential sources to supply fine-grained fractions for the loess formation in the Hexi Corridor. $\epsilon_{Nd}(0)$ values and $^{87}Sr/^{86}Sr$ ratios of fine-grained fractions vary from -7.4 to -10.2 and from 0.7132 to 0.7174 for the Badain Jaran Desert, from -10.0 to -10.5 and from 0.7166 to 0.7187 for the Qaidam Desert, from -9.5 to -11.7 and from 0.7136 to 0.7171 for the Taklimakan Desert, from -1.2 to -3.3 and from 0.7113 to 0.7136 in the Gurbantunggut Desert, respectively [2].

Results and Conclusion

Isotopic compositions of the Hexi Corridor loess are distinctly different from those of the Badain Jaran Desert, the Qaidam Desert and the Gurbantunggut Desert, but are roughly similar to the Taklimakan Desert and river sediments of the Qilian mountain. Due to the stability of Sr-Nd isotopes in the surficial process [3], the geochemical similarity of the loess in the Hexi Corridor with the fine-grained fractions of the Taklimakan Desert and river sediments of the Qilian mountain indicates the two areas might be main sources of the Hexi Corridor loess.

Region	Type	Grain size	$\epsilon_{Nd}(0)$	$^{87}Sr/^{86}Sr$
Qilian Mts.	River sediment	<75μm	-11.84	0.7335
			-12.95	0.7338
			-12.15	0.7196
			-11.96	0.7222

Table 1 Isotopic features of river sediments of the Qilian mountain

[1] Nakano *et al* (2004) *Atmospheric Environment* **38**, 3061-3067.

[2] Chen *et al* (2007) *Geochimica et Cosmochimica Acta* **71**, 3904-3914. [3] Rao *et al* (2011) *Geomorphology* **132**, 123-138.

Molecular level characterization of methyl sugars and other carbohydrate compounds in marine high molecular weight dissolved organic matter (HMWDOM)

C. PANAGIOTOPOULOS^{1,2*}, D.J. REPETA³, L. MATHIEU^{1,2}, J-F. RONTANI^{1,2} AND R. SEMPERE^{1,2}

¹Aix-Marseille Université, Mediterranean Institute of Oceanography (MIO), 13288, Marseille, Cedex 9, France;

²Université du Toulon, CNRS/INSU, IRD, MIO UM 110, 83957 La Garde, France

(*correspondance: christos.panagiotopoulos@univ-amu.fr)

³Department of Marine Chemistry and Geochemistry, Woods Hole Oceanographic Institution, Woods Hole, MA 02543, USA (drepet@whoi.edu)

Dissolved organic matter (DOM) is an active component of the carbon cycle however its chemical composition, fate, and sources are poorly understood. Approximately 30% of surface DOM can be sampled by ultrafiltration, and thereby concentrates the high molecular weight DOM fraction (HMWDOM > 1kDa)[1]. Previous studies have shown that most HMWDOM is comprised of carbohydrates (acylated carbohydrates or APS), but only a minor fraction of the carbohydrate has been identified at the “molecular level” (as monosaccharides after hydrolysis, *i.e.* fucose, rhamnose, arabinose, galactose, glucose, mannose, and xylose). The discrepancy between NMR derived estimates of HMWDOM carbohydrate (50-70% C) and molecular level analyses (10-20% C) has not been explained, and no new sugars have been identified in HMWDOM in about 10-15 years[2].

Here using ultrafiltration, silver cation preparative chromatography, and GC-MS we identified 50 novel sugar compounds after hydrolysis of the HMWDOM. Sugars were identified using chemically synthesized sugar standards and mass spectra data available in literature. Our results showed that mono- and di- methylated hexoses; mono- and di- methylated pentoses; mono- and di- methylated 6-deoxysugars, as well as heptoses, methylated heptoses, 3,6-dideoxysugars and 1,6 anhydrosugars (*i.e.* levoglucosan, galactosan, and mannosan) are components of HMWDOM, which may explain in part the low apparent yields of sugars recovered by molecular level (HPLC) analyses compared to NMR estimates.

Our results also indicated that the above compounds accounted 2-3% of the APS in surface/deep waters and their diversity decreased with depth. The high diversity of mono- and di- methylated hexoses in the surface sample most likely suggests an algal and/or bacterial source, while the high abundance of methylated 6-deoxy hexoses in the deep sample points toward a important bacterial contribution.

[1] Benner *et al* (1992) *Science* **255**, 1562-1564. [2] Aluwihare *et al* (1997) *Nature* **387**, 166-167.

Multiple pools of reduced carbon can be released during hyperthermals

R.D. PANCOST^{1*}, M.P.S. BADGER¹, B. D. A. NAAFS¹, S. FROEHNER¹, J.M. CASTRO², G.A. DE GEA², M.L. QUIJANO³, R. AGUADO³, C. LOWSON¹ AND A. RIDGWELL⁴

¹Organic Geochemistry Unit, Chemistry, University of Bristol, UK (*corr author: r.d.pancost@bristol.ac.uk)

²Depto. Geologia, Univ. Jaén, E-23071, Spain

³Depto. Química Inorgánica y Orgánica, Univ. Jaén, E-23071, Spain

⁴BRIDGE, Geographical Sciences, University of Bristol, UK

Numerous transient hyperthermals have been identified in Earth history, and most are associated with a sharp negative carbon isotope excursion (CIE). The CIEs indicate that rapid global warming was at least partly caused by the release of reduced carbon, with methane hydrates, peat deposits and permafrost all being proposed as sources. Much work on hyperthermals, and especially the Paleocene-Eocene Thermal Maximum (PETM), illustrates that rapid global warming caused dramatic changes in the hydrological, erosional and weathering regime. These changes were associated with a marked increase in the mobilisation and transport of soil and terrestrial vegetation, and it is likely that under a warmer climate state at least some of this OM was oxidised, providing a positive feedback on global warming. Here, we present evidence that even reduced carbon reservoirs that are generally perceived as recalcitrant (*i.e.* kerogen) are also mobilised during such events.

Kerogen inputs to marginal marine sediments increased dramatically during both OAE1a and the PETM. This is documented by a shift in biomarker (sterane and hopane) assemblages from thermally immature to mature signatures over short stratigraphic scales. This is indicative of mixing of two distinct organic matter sources, most likely a source contemporaneous with sediment deposition and another older, reworked source. These observations confirm that an increase in hydrological energy during hyperthermals was sufficient to markedly and widely increase sedimentary rock erosion. We suggest that this strong response was particularly due to rapid deviation from steady state conditions. Moreover, erosion and chemical weathering are generally coupled and even ancient kerogens have been shown to be highly oxidisable during shale weathering; thus, these events were likely associated with kerogen oxidation. Although unlikely to have been a major source of additional reduced carbon (<10% of the CIE), this work highlights the potential lability of all organic matter pools during rapid climate change events.

Anomalous lithospheric and geodynamical evolution of the southern part of Vindhyan basin, central India

O.P. PANDEY, NIMISHA VEDANTI*
AND RAVI PRAKASH SRIVASTAVA

CSIR-National Geophysical Research Institute, Hyderabad,
India (*correspondence: nim.ved@gmail.com)

Introduction

Tectonically active sickle shaped Vindhyan basin is considered the largest intra-cratonic Proterozoic sedimentary basin in peninsular India that covers an area of about 200,000 sq.km. It is well known for diamond occurrences. Possibility of hydrocarbon potential has led to a surge in various kinds of geological and geophysical investigations during recent times. An attempt has been made here to synthesize seismic, gravity [1,2] magnetotelluric, geothermal and borehole geological data, which throws a new light into the crustal and upper mantle evolution of this basin.

Significant Results

The southern part of this basin appears to have undergone episodic thermal interactions between crust and hot underlying mantle, which induced magmatism, upwarping and erosion followed by crustal rifting and sedimentation. Seismic data reveals that as much as 10-15 km crustal exhumation may have taken place beneath this region. Almost 5 to 6 km thick Proterozoic sediments have deposited over exhumed high velocity middle crust in the Jabera basin. A high heat flow of almost 80 mW/m² has also been estimated for this region, which indicates presence of extremely high Moho temperature and mantle heat flow. Lithosphere has been found to be extremely thin at about 50 Km below Jabera basin. In some geo-tectonic segments, granitic-gneissic upper crust has been totally eroded due to sustained exhumation of deep seated mafic rocks. A 5-10 km thick retrogressed metasomatically altered layer with significantly reduced velocities consequent to interaction with hydrothermal and other mantle fluids, has also been delineated at around mid to lower crustal transition. There is a possibility that this region may have been under the influence of a super mantle plume around 1.1 Ga.

[1] Srivastava et al (2007), *Pure and Applied Geophys* **164**,1-14. [2] Srivastava et al (2009), *J.Geol.Soc.India* **73**,715-723.

Atmospheric Evolution and Chemical Aging of Combustion Organic Particulate Matter

SPYROS N. PANDIS¹, NEIL M. DONAHUE²
AND ALLEN L. ROBINSON³

¹Department of Chemical Engineering, University of Patras,
Greece (spyros@chemeng.upatras.gr)

²Department of Chemical Engineering, Carnegie Mellon
University, USA (neil.donahue@andrew.cmu.edu)

³Department of Mechanical Engineering, Carnegie Mellon
University, USA (allen.robinson@andrew.cmu.edu)

Organic particulate material has been traditionally classified as either primary or secondary with the primary component being treated as nonvolatile and inert. Laboratory and field studies during the last decade, demonstrate that primary combustion aerosol is highly dynamic, consisting of mostly semi-volatile material that moves between the gas and particulate phases in the atmosphere and at the same time is oxidized forming a variety of oxygenated products. This oxidation can lead to both lower volatility material through functionalisation but also to smaller lower volatility molecules through fragmentation. A unifying framework for the description of all organic components based on their volatility distribution and oxygen content (the two-dimensional volatility basis set) can be used for the treatment of a wide range of processes affecting organic aerosol loadings and composition in the atmosphere. This modeling framework is combined with emission characterization studies, laboratory smog chamber studies, and field measurements to simulate the atmospheric evolution of these organic emissions. Applications of this modeling framework to major urban areas (Paris and Mexico City) and continental Europe, where major field campaigns have recently taken place are used to provide insights about our understanding (or lack thereof) of the corresponding physical and chemical processes.

Ore genesis of the Longshan Sb-Au deposit, Hunan, China: Evidence from fluid inclusions

M. ZHANG¹, B. PANG^{1*}, D. YANG², X. LIU¹
AND B. WANG¹

¹Guilin University of Technology, Guilin, 541004, China

(*correspondence: pbc@glut.edu.cn)

²Guangzhou Institute of Geochemistry, Guangzhou, 510640, China (yds1019@gig.ac.cn)

The Longshan gold-antimony deposit is one of the typical Sb-Au associations in Hunan province, China. The mineralization is related to NWW and NNE trending fault systems and hosted within gravel sandy slate in Jiangkou Formation of Sinian System. Gold occurs mainly in cracks in stibnite, pyrite and arsenopyrite, or in the contact area of these three minerals and gangue minerals, or enclosed by stibnite. From a limited number of hydrogen and oxygen isotope data, some previous workers proposed that the ore-forming fluid was predominantly meteoric in origin. In contrast, we argued that metamorphic fluid is an alternatively likely source of the ore-forming fluid based on a preliminary study of fluid inclusion microthermometry and Raman spectrum.

Mineralization and paragenesis of the Longshan deposit can be divided into three stages as follows based on geology and petrography of the deposit: Qz + Py +Asp +Au (stageI); Qz + Py +Asp + Sb + Au (stageII) ; Qz + Sb + Cal (stageIII). StageII is the mainest ore-forming stage accounting for approximately 82% of ore reserves. Primary inclusions in quartz from stageII ores are mainly mixed aqueous-gaseous fluid inclusions (H₂O–NaCl–CO₂–other gases). Pure liquid and pure gaseous can be occasionally observed. For mixed aqueous-gaseous fluid inclusions, two or three phases can be observed at room temperature: a bubble of carbonic vapor suspended in aqueous liquid, or a double bubble in which a bubble of carbonic vapor is enclosed by a bubble of carbonic liquid suspended in aqueous liquid. The size of inclusions ranges from 2.31µm to 12.89µm, mainly 3µm to 7µm. These inclusions exhibit relatively variable vapor to liquid ratios (5-25%, mostly 10-15 percent vapor by volume), and have homogenization temperatures ranging from 235°C to 320°C. Two-phase inclusions show a wide salinity range of 0.18-9.85wt% NaCl equiv, with most data clustering around 3-8 wt% NaCl equiv. By contrast, three-phase inclusions have a lower range in salinity (1.42-2.2 wt% NaCl equiv). Trapping pressure estimated from three-phase inclusions is up to 135MPa, suggesting that antimony-gold mineralization occurred at the depth of approximately 7.7km. Laser Raman Spectrum analysis for two-phase of CO₂-H₂O inclusions indicate the existence of minor N₂ and C₂H₆ besides CO₂. Physical and chemical characteristics of fluid inclusions suggest that the Longshan Sb-Au deposits may have resulted from metamorphic fluids.

Acknowledgments This project is supported by NSFC (no.40772056) and the Foundation of Guangxi Key Lab of HMODE (no.11-031-20)

Mafic potassic volcanics from the Altiplano, South America: Indication of a dynamic A-type magma source under construction?

M. J. PANKHURST^{1,2*}, B. F. SCHAEFER²
AND S. P. TURNER²

¹School of Earth and Environment, University of Leeds,

Leeds,UK (*correspondence: m.j.pankhurst@leeds.ac.uk)

²GEMOC, Macquarie University, Sydney, Australia

Small volume monogenetic mafic volcanoes, erupted onto the Altiplano (active orogenic plateau) during the Neogene to Quaternary, display high K, F, Ga/Al and low Ca relative to typical basalts. These characteristics match key chemical affinities of post-orogenic A-type granite magmas.

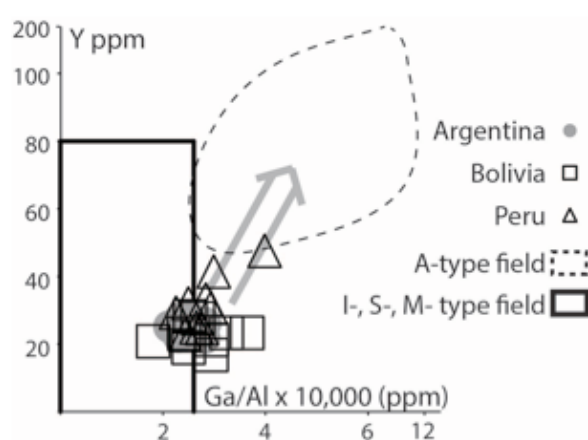


Figure 1. Geochemical affinities between orogenic mafic volcanics and A-type granites. Arrow indicates liquid evolution involving plagioclase and clinopyroxene from a deep crustal reservoir stacked with mantle-derived, low degree partial melts into the A-type field.

New geochemical data and Sr, Nd and Hf isotopic ratios of these Altiplano volcanics are consistent with a petrogenetic model that involves iterative low-degree partial melting regimes within underlying metasomatised asthenospheric and lithospheric mantle. We consider generation of such melts to be widespread and significant, since the same signatures are observed across ~1750 km of strike length and are not restricted to a specific time period. Their small individual erupted volumes suggest ascending batches are subject to efficient cooling and stalling at deeper levels. Therefore it is plausible they may be vastly underrepresented at the surface, and difficult to directly detect by geophysical methods. Second order convections within the mantle during downwelling/delamination of lithosphere may account for the production and emplacement of these magmas. We propose that the generation of these melts during orogenesis contributes chemical and isotopic signatures to subsequent post-orogenic magmas, via their iterative pooling and crystallisation within the lithosphere.

LREE-rich beach sands from Sithonia Peninsula (Chalkidiki, Greece)

A. PAPAPOULOS^{1*}, G. CHRISTOFIDES¹,
G. PE-PIPER² AND A. KORONEOS¹

¹Department of Mineralogy, Petrology, Economic Geology, Aristotle University of Thessaloniki, 54124, Thessaloniki, Greece (*correspondence: argpapad@geo.auth.gr, christof@geo.auth.gr, koroneos@geo.auth.gr)

²Department of Geology, Saint Mary's University, Halifax, Nova Scotia, B3H 3C3, Canada (gpiper@smu.ca)

Beach sands, being the weathering products of the adjacent Sithonia Plutonic Complex [1], have been studied for their heavy mineral and LREE content. For the mineral separation, the 125-500 μm grain-size fraction, accounting for 90.6-95.4 wt % of the whole sample, was used. Among the samples collected, three are particularly enriched in heavy minerals.

Heavy liquid (tetrabromoethane, 2.967 g/mol) and a magnetic separator were employed to determine the wt % heavy fraction and the heavy magnetic and non-magnetic fractions of the whole sample (Table 1). The heavy magnetic fraction (<0.8 amp at cross and longitudinal settings of 10°) contains epidote, allanite, biotite and hornblende, while the heavy non-magnetic fraction (>0.8 amp at same settings) contains zircon, monazite, apatite and sphene.

	Heavy fraction	Heavy magnetic fraction	Heavy non-magnetic fraction
S1	85.3	50.6	34.7
S2	26.8	16.0	10.8
S3	56.4	51.6	4.8

Table 1: Heavy, heavy magnetic and non-magnetic content (wt % relative to the bulk sample).

The content of the studied samples in LREE and Y is particularly high (Table 2). This is attributed mainly to the presence of monazite, allanite and to a lesser extent epidote.

	Y	La	Ce	Pr	Nd	Sm
S1	452	1430	2720	305.0	1030	171.0
S2	126	409	768	81.9	284	46.3
S3	213	371	730	84.2	307	62.4

Table 2: Content of the bulk samples in selected LREE (ppm).

[1] Christofides *et al* (2007) *Lithos* **95**, 243–266.

Organic matter oxidation and authigenic rhenium in late Eocene pelagic sediments

FRANCOIS PAQUAY*¹ AND GREG RAVIZZA¹

¹Geology & Geophysics, SOEST, University of Hawaii, Manoa, Honolulu HI 96822 USA. ravizza@hawaii.edu, (correspondance: paquay@hawaii.edu)

Poor organic carbon preservation in the deep sea during Eocene warmth suggests an important change in the carbon cycle during greenhouse episodes [1]. An expected consequence of this phenomenon is that Eocene pelagic sediments should be more reducing than similar modern sediments. Measured Re concentrations demonstrate significant authigenic Re-enrichment, up to 30X average crustal concentrations, associated with very low total organic carbon (TOC; <0.2%) in late Eocene sediments from ODP Site 1090 (42°54.8' S, 8°53.9' E) on the Agulhas Ridge in the South Atlantic. Using measured ¹⁸⁷Re/¹⁸⁸Os ratios to correct for ¹⁸⁷Re decay since sediment deposition yields initial ¹⁸⁷Os/¹⁸⁸Os ratios that are similar to contemporaneous seawater, requiring that Re enrichment occurred during or soon after sediment deposition. Therefore these data provide strong evidence of a brief episode (a few hundred kyr) of reducing conditions. Integrating Re-Os results with previously published data [2,3] constraining paleoredox (U, U/Al) and paleoproductivity (biogenic Ba, organic carbon and reactive phosphorus) highlights several important aspects of the reduced interval of this record. Re (ppb)/TOC % (up to 55) are among the highest reported to in recent marine sediments. The zone of elevated Re is not clearly associated with evidence of elevated paleoproductivity, suggesting that decreased in oxygen penetration depth is more likely to be due to lower bottom water oxygen, than an episode of elevated organic matter flux to the sediment water interface. Although U/Al ratios are modestly elevated across the interval with elevated Re, average Re/U (15 ng/ μg) ratios are much higher than in most modern reducing sediments and higher than expected if both elements are enriched via diffusion across the sediment water interface and reductively fixed at the same depth. We suspect that elevated Re/U is the result differing reduction mechanisms within sediment pore waters. In total, these results provide empirical evidence that Re is a uniquely powerful paleoredox tracer in organic-poor, pelagic sediments.

[1] Oliveras-Lyle and Lyle (2006) *Paleoceanog.* **21**, doi:10.1029/2005PA001230. [2] Anderson and Delaney (2005) *Paleoceanog.* **20**, doi:10.1029/2004PA001043. [3] Diekmann, *et al* (2005) *Global Planet. Change* **40**, 295-313.

Major and trace elements composition of basalts from ultramafic and volcanic seafloor. Southwest Indian Ridge (61 to 67°E)

MARINE PAQUET^{*1}, MATHILDE CANNAT¹, CÉDRIC HAMELIN², MANUEL MOREIRA¹ AND DANIEL SAUTER³

¹Institut de Physique du Globe de Paris, France

(*paquet@ipgp.fr)

²Centre for Geobiology, University of Bergen, Norway

³Institut de Physique du Globe de Strasbourg, France

Our study area is located on the ultra-slow Southwest Indian Ridge, east of the Melville Fracture Zone, between 61 and 67°E. This part of the SWIR has a very low magmatic supply, and the axial lithosphere is thick. The melt distribution is very heterogeneous with volcanic areas and areas of ultramafic seafloor where plate separation is accommodated by large offset normal faults [1]. The ultramafic rocks are locally overlain by a thin veneer of basalt. Basalts samples have been dredged on these two types of seafloor during the EDUL (1997) and SMS (2010) cruises. We use the major and trace elements composition of these basalts to discuss the magmatic plumbing system of this very low melt supply ridge.

Most basalts from ultramafic seafloor areas have higher Na₂O and TiO₂ contents at a given MgO, and higher Zr/Y and Sr than those from volcanic seafloor. These differences could be explained [2] by a lower degree of partial melting of the mantle source for ultramafic seafloor basalts. However, the lower CaO content of most ultramafic seafloor basalts suggests larger amounts of early fractionation of clinopyroxene [3] from the melts feeding ultramafic areas. This early clinopyroxene fractionation could also partly explain the Na₂O and TiO₂ trends, but not the Zr/Y trend. Our data therefore suggest that both the melting regime and the magma plumbing system producing the two groups of basalts are different. (La/Sm)_n ratio and REE spectra point to a similar source for the two groups of basalts, possibly a refertilized depleted mantle [4]. One dredge in volcanic seafloor stands out with a depleted LREE spectrum, low (La/Sm)_n and very high MgO content. This dredge could be interpreted as resulting from very low degree of melting of a non-refertilized residual mantle domain.

[1] Sauter, Cannat, *et al* (2013). *Nat. Geo.*, 6(4), 314-320.

[2] Klein, Langmuir (1987). *JGR: Solid Earth (1978–2012)*, 92(B8), 8089-8115. [3] Langmuir, Klein, Plank (1992). *Geophysical Monograph Series*, 71, 183-280. [4] Meyzen, *et al* (2003). *Nature*, 421(6924), 731-733.

Early Solar System ⁸⁷Rb-⁸⁷Sr Chronology

R. PARAI^{1*}, S. HUANG¹ AND S. B. JACOBSEN¹

¹Dept. of Earth and Planetary Sciences, Harvard University, 20 Oxford St., Cambridge, MA 02138, USA. (*email: parai@fas.harvard.edu)

The long-lived ⁸⁷Rb-⁸⁷Sr system provides a useful chronometer for early Solar System events. Due to differences in the volatility of Rb and Sr, ⁸⁷Sr/⁸⁶Sr ratios record information about condensation and volatile depletion in the early Solar System. Thus, high-precision analysis of Rb-Sr systematics in Solar System materials such as calcium-aluminum inclusions (CAIs), meteorites and lunar rocks provide insight into processes that shaped the early Solar System, including the formation of Earth's Moon.

Recent studies have argued for a late formation of the Moon based on Sm-Nd and U-Pb systematics [e.g., 1-2], but have avoided use of Rb-Sr chronometry due to possible disturbance of the Rb-Sr system. However, a chronology may be constructed based on relative variations in initial ⁸⁷Sr/⁸⁶Sr in Solar System materials, rather than absolute ages derived by the Rb-Sr isochron method. For Rb-poor samples such as Moore Co. plagioclase, Angra dos Reis, Juvinas and the lunar anorthosite 60025, corrections for radiogenic ingrowth are small, and variations in resulting initial ⁸⁷Sr/⁸⁶Sr may be interpreted to reflect differences in the timing of separation from an evolving solar nebula [e.g., 3-5]. Based on a compilation of literature Rb-Sr data measured in various laboratories over the course of decades, Halliday and Porcelli [6] computed a young Sr model age for lunar formation of 90±20 Myr after the formation of CAIs. However, from the fact that 60025 has an initial ⁸⁷Sr/⁸⁶Sr between the basaltic achondrite best initial and Angra dos Reis [3-4], it appears that 60025 must be essentially as old as these meteorites, requiring a very old age for the Moon (<30 Myr after CAIs).

In order to determine an internally-consistent Sr model age of lunar formation, we undertake precise Sr isotopic measurements in a comprehensive suite of early Solar System materials in a single laboratory. We also develop a Sr double spike method to distinguish any non-radiogenic isotopic anomalies [e.g., 7,8] and thus further refine our chronology.

[1] Borg *et al* (2011) *Nature* **477**, 70-72; [2] Norman *et al* (2003) *MAPS* **38**, 645-661; [3] Papanastassiou and Wasserburg (1969) *EPSL* **5**, 361-376; [4] Wasserburg *et al* (1977) *EPSL* **35**, 294-316; [5] Brannon *et al* (1988) *Proc 18th LPSC* 555-564; [6] Halliday and Porcelli (2001) *EPSL* **192**, 545-559; [7] Moynier *et al* (2010) *EPSL* **300**, 359-366; [8] Moynier *et al* (2012) *ApJ* **758**:45.

Pore scale heterogeneity in the reactive surface area of rocks

ALICIA PARBHOO^{1*}, PETER LAI^{1,2}
AND SAMUEL KREVOR^{1,2}

¹Department of Earth Science & Engineering, Imperial College London, London UK (*correspondence: ap3409@ic.ac.uk)

²The Qatar Carbonates and Carbon Storage Research Centre at Imperial College London, London UK

There are major knowledge gaps in the ability to characterize reactive transport in porous media at scales larger than individual pores. This precludes prediction of the field-scale impact of geochemical processes on fluid flow [1]. This is a source of uncertainty for CO₂ injection, which results in a reactive fluid-rock system, particularly in carbonate rock

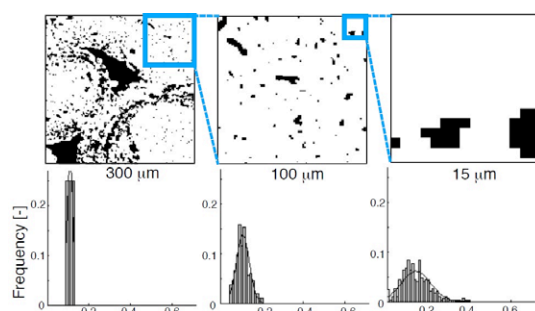


Figure 1: Ratio of surface area to pore volume [m^2/m^3] in an Indiana limestone at various length scales.

reservoirs. A potential cause is the inability of the continuum approach to incorporate the impact of heterogeneity in pore-scale reaction rates. This results in part from pore-scale heterogeneities in surface area of reactive minerals [2,3].

In this study we have created μm resolution 3D images of 3 sandstone and 4 carbonate rocks using x-ray microtomography. Using in-house image processing techniques we quantified the surface area from the images. This quantification was validated against N₂ BET surface area and He porosity measurements of the imaged samples. Distributions in reactive surface area were constructed by calculating surface areas in thousands of randomly selected subvolume images of the total sample (Fig. 1), each normalized to the pore volume in that image. Berea sandstone was far less heterogeneous and has a characteristic pore size at which a surface area distribution may be used to quantify heterogeneity. In carbonates, heterogeneity is more complex and surface area must be characterized at multiple length scales for an accurate description of reactive transport.

[1] Maher *et al* (2006) *Geochimica et Cosmochimica Acta*, **70**, 337-363. [2] Landrot *et al* (2012) *Chemical Geology* **318-319**, 113-125. [3] Li *et al* (2007) *American Journal of Science* **307**, 1146-1166.

Termination and hydration of Forsterite (010) and Diopside (010) surfaces

CHANGYONG PARK AND HONGPING YAN¹

¹HPCAT, Geophysical Laboratory, Carnegie Institution of Washington, Argonne, IL 60439, USA, (cpark@ciw.edu)

The hydrous alteration of ultramafic rocks has been paid much attention for its attribution to the abiogenic hydrocarbon generation from crystalline rocks. The molecular processes at the interface of water and those mineral surfaces, however, have not been described. We use in-situ high-resolution X-ray reflectivity to examine the forsterite (010) and diopside (010) surfaces in water. By modelling the electron density profile in the surface normal direction and fitting the measured data with least-square method, the atomic structures of hydrated single crystal surfaces could be depicted. We found, for the forsterite surface polished with alumina colloidal suspension under acidic environment (pH 3.5), a homogeneous termination with about half of the surface magnesium depleted and replaced with possibly a water species. In contrast, the forsterite surface polished with silica colloids under basic condition (pH 9-10) does not show such homogenous surface, but substantial morphological difference from the alumina-polished surface is observed by Atomic Force Microscopy measurement. The difference indicates the importance of solution chemistry to constrain the surface reactivity and dissolution mechanism. On the other hand, the diopside (010) surface is a naturally grown surface, which shows qualitatively identical features in its termination plane and the first adsorbed water electron density profile compared to those of the forsterite (010) surface. This similarity indicates common features in the hydration structure of these mineral surfaces, although the silicate compositions and structures are quite different.

Quantifying trace element distributions in agate banding by LA-ICP-MS

C.-S. PARK^{1*}, Y. KIM², H. S. SHIN¹, K. YI¹ AND H. OH¹

¹Korea Basic Science Institute, Ochang 368-883, Korea

(*correspondence: cspark@kbsi.re.kr)

²Chungbuk National University, Cheongju 361-763, Korea

Samples

Agates are banded forms of microcrystalline chalcedony often forming spectacular, colorful geodes or veins. Two analyzed agates are characterized by the rhythmic banding of redish and bluish layers, respectively, ranging in width about 50 mm. Boundaries between each layer are well distinguished by the slight contrasting in color. The color of agates can vary with the species and concentration of trace elements. Agates thus can provide direct visual evidence for correlations in concentrations among trace elements and between trace element concentrations and color contrasts.

Analytical methods

X-ray mapping was carried out using a Shimadzu EPMA 1600. Subsequent quantitative mapping was performed using a NewWave 213 nm Nd:YAG laser ablation system attached to a Thermo X2 quadrupole ICP-MS, with instrument settings at 11 J/cm² for energy density, 10 Hz repetition rate, 55 μm beam size, 60 μm spacing between adjacent line scans, and 10 μm/s scan speed. The oxidation rate was controlled below 1%. NIST612 glass was used as the external standard, and ²⁹Si as the internal standard, assuming stoichiometric quartz. Data reduction was carried out using Iolite software.

Results

Among 9 trace elements including Al, Ca, Co, Fe, Ti, Cr, Mn, Cu and Ni. Al and Fe are the most abundant, up to ~5000 ppm in red agate and up to ~500 ppm in blue agate, whereas concentrations of other elements are less than 400 ppm. All the quantitative elemental maps except Cr and Ni show that trace elements are concentrated in the boundaries between each layer. Quantitative Al and Fe maps show a harmonious behaviour of Al and Fe in red agate, but an antithetic relationship in blue agate. The Al and Fe distribution patterns in red agate are reproduced in the Al Kα and Fe Kα X-ray maps, but not clear in blue agate. All the above results suggest that quantitative elemental maps using LA-ICP-MS are privileged to visualize trace elements distributions.

Pb and stable Pb isotopes in sediments of the eastern coast of the Yellow Sea

JONG-KYU PARK¹, MAN-SIK CHOI¹, Dongjun Chang¹, Sojeong Park¹ AND DHONG-IL LIM²

¹Chungnam National University, Daejeon, Korea

(aska4332@naver.com), (mschoi@cnu.ac.kr),

(zzung1009@nate.com)

²Korea Institute of Ocean Science and Technology, Geoje, Korea. dlim@kiost.ac

In order to investigate the distribution and sources of Pb in coastal sediments in the Yellow Sea, 88 surface sediments were collected and analysed for Pb concentration (1M HCl leached and residual fractions) and stable Pb isotopes (²⁰⁷Pb/²⁰⁶Pb, ²⁰⁸Pb/²⁰⁶Pb) using MC-ICP-MS.

Leached Pb concentration varied in the range of 3.8-28.8mg/kg (mean 11.3mg/kg) and showed the highest concentration in the fine-grained sediments and seemed to be associated with Fe oxide/hydroxide. Pb concentration in the residual fraction showed 2.6-18.1mg/kg (mean 11.1mg/kg) range and higher concentration in coarse-grained sediments, which indicated that high Pb were resulted from K-feldspar abundant in sand, which were consistent with the previous study[1].

²⁰⁷Pb/²⁰⁶Pb and ²⁰⁸Pb/²⁰⁶Pb varied in the range of 0.844-0.851 and 2.102-2.118, respectively. Pb isotope ratios decreased from the northern part toward the southern part. Based on the ratio-ratio plots and ratio- the inverse of Pb concentration plots, the spatial distribution of isotopes were responsible for the mixing between materials borne from Korean rivers (the Han and Geum)[2] in the northern part, and the mixing between the Geum River borne sediments and offshore sediments [2]in the southern part.

[1] Kim *et al* , (2001) JKSO, **35**, 179-191 [2] Choi *et al* , (2007) Mar. Chem. **107**, 255-274

An investigation of transboundary particulate matter over northeast Asia

M. E. PARK¹, C. H. SONG^{1*}, R. S. PARK¹, J. LEE²,
S. J. LEE¹ AND J. KIM³

¹School of Environmental Science and Engineering, Gwangju Institute of Science and Technology, Gwangju, Korea (*correspondence: chsong@gist.ac.kr)

²Goddard Space Flight Centre, NASA, Greenbelt, MD, USA

³Department of Atmospheric Science, Yonsei University, Seoul, Korea

CMAQ modeling was conducted for a period of 1 April to 31 May, 2011, in order to assess the impacts of Long-Range Transport (LRT) events on the particulate matter (PM) concentrations over northeast Asia. Meanwhile, a Korean geostationary satellite, Communication, Ocean, and Meteorological Satellite/Geostationary Ocean Color Imager (COMS/GOCI)-retrieved data were also used in this study to overcome the temporal limitation of the Low Earth Orbit (LEO) satellites. The LEO pass over the region of interest once a day (or several days), although these has been mainly applied to investigate the characteristics of AOD over northeast Asia. The GOCI-retrieved AOD products were obtained through Yonsei aerosol retrieval algorithm and CMAQ model simulations considered dust and biomass burning emissions and their transports. The CMAQ-calculated AOD was then improved by integrating hourly GOCI-retrieved AOD via a data assimilation technique for the purpose of producing more accurate AOD products over northeast Asia. It clearly showed the several long-range transport events of the small- and large-scale AOD plumes from Central East China (CEC) to the Korean peninsula. In addition, according to statistical analysis of the assimilated AOD for the LRT and non-LRT events at five AERONET sites, the average AOD increased by LRT events was found to be 0.40 above the background AOD value of 0.24.

Contribution of ammonium nitrate to aerosol optical depth and direct radiative forcing by aerosols over East Asia

RAE S. PARK, SO J. LEE, SUNG-K. SHIN
AND CHUL H. SONG*

School of Environmental Science and Engineering, Gwangju Institute of Science and Technology (GIST), Gwangju, 500-712, Korea (rspark28@gmail.com, *correspondence to chsong@gist.ac.kr)

This study focused on the contribution of ammonium nitrate (NH_4NO_3) to aerosol optical depth (AOD) and direct radiative forcing (DRF) by aerosols over an East Asian domain. In order to evaluate the contribution, CTM-estimated AOD was combined with satellite-retrieved AOD, utilizing a data assimilation technique, over East Asia for the entire year of 2006. Using the assimilated AOD and CTM-estimated aerosol optical properties, the DRF by aerosols was estimated over East Asia via a radiative transfer model (RTM). Both assimilated AOD and estimated DRF values showed relatively good agreements with AOD and DRF by aerosols from AERONET. Based on these results, the contributions of NH_4NO_3 to AOD and DRF by aerosols (Φ_{AOD} and Φ_{DRF}) were estimated for four seasons of 2006 over East Asia. Both Φ_{AOD} and Φ_{DRF} showed seasonal variations over East Asia within the ranges between 4.7% (summer) and 31.3% (winter) and between 4.7% (summer) and 30.7% (winter), respectively, showing annual average contributions of 15.6% and 15.3%. However, these contributions can be even larger in the locations where NH_3 and NO_x emission rates are strong like the Central East China (CEC) region and Sichuan basin. For example, both Φ_{AOD} and Φ_{DRF} over the CEC region range between 6.9% (summer) and 47.9% (winter) and between 6.7% (summer) and 47.5% (winter), respectively. Based on this analysis, it was concluded that both Φ_{AOD} and Φ_{DRF} cannot be ignored in East Asian air quality and radiative forcing studies, particularly during winter.

Keywords: Ammonium nitrate (NH_4NO_3); Aerosol optical depth (AOD); Direct radiative forcing (DRF) by aerosols; Assimilation; AERONET; EANET

Tracking changes in ocean redox during the PETM using Cr isotopes

I.J. PARKINSON^{*1,2}, S.K. DIXON², P. SEXTON², M.A. FEHR², R.H. JAMES³ AND C.L. PEACOCK⁴

¹School of Earth Sciences, University of Bristol, BS8 1RJ, UK. (*correspondence: Ian.Parkinson@bristol.ac.uk)

²Department of Environment, Earth and Ecosystems, The Open University, MK7 6AA, UK.

³School of Earth and Environment, University of Leeds, LS2 9JT, UK.

⁴Marine Geosciences, National Oceanography Centre, Southampton, SO14 3ZH, UK.

Previous deoxygenation events in the geological record may provide insight into the dynamics of changing oxygen levels in the Earth's oceans already underway¹. The Palaeocene-Eocene Thermal Maximum (PETM) at ~55Ma is a ~150 kyr period of intense global warming with evidence for at least local-scale, ocean oxygen depletion^{2,3}. To track seawater oxygenation during the PETM, we use the stable Cr isotope composition of marine carbonates, a new palaeo-redox proxy, which has shown potential when applied to modern and ancient carbonates^{4,5}.

Here we present $\delta^{53}\text{Cr}$, trace element and REE data of foraminifera through the PETM interval from DSDP Site 401 (North East Atlantic), hosting exceptionally well-preserved foraminifera. ~150 mg of foraminifera were taken from the 63-150 μm size fraction and species count data indicate that the relative proportions of dominant species do not change significantly over the event⁶. Systematic changes occur in Cr concentration and $\delta^{53}\text{Cr}$ throughout the event with a positive $\delta^{53}\text{Cr}$ excursion of 1.7‰ coincident with the onset of the negative $\delta^{13}\text{C}$ excursion. This reflects an increased reduction of Cr(VI) and thus a change to more reducing conditions in the water column at the onset of the event. Chromium concentrations of the foraminifera decrease leading into the PETM, and do not recover, indicating either a reduction in seawater Cr concentrations, a change or a change in Cr geochemical cycling during the event.

[1] Stramma *et al* (2008). *Science*, **320**, 655-658. [2] Dickson *et al* (2012). *Geology*, **40**, 639-642. [3] Dypvik *et al* (2011). *P-cubed*, **302**, 156-169. [4] Bonnand (2011). PhD thesis, The Open University. [5] Frei *et al* (2011). *Earth and Planet. Sci. Lett.*, **312**, 114-125. [6] Pardo *et al* (1997). *Marine Micropaleon.*, **29**, 129-158.

New Zircon U-Pb and Hf-isotope data of the Birimian Terrane of the West African craton

LUIS A. PARRA^{1*}, MARCO L. FIORENTINI¹, ELENA BELOUSOVA², ANTHONY I. S. KEMP¹, JOHN MILLER¹, T. CAMPBELL MCCUAIG¹ AND NURU SAID¹

¹Centre for Exploration Targeting, ARC Centre of Excellence for Core to Crust Fluid Systems, School of Earth and Environment, The University of Western Australia., Perth, WA, Australia.

(*Correspondance:20835812@student.uwa.edu.au)

²ARC National Key Centre for Geochemical Evolution and Metalogeny of Continents, ARC Centre of Excellence for Core to Crust Fluid Systems, Department of Earth and Planetary Sciences, Macquarie University NSW, Australia.

In order to explore whether the West African Craton was formed by the accretion of Archean terranes [1], zircons from 22 igneous rocks collected from across SW Mali and Burkina Faso were recently dated using SHRIMP and analysed for in-situ Lu-Hf isotopes by laser ablation MC-ICPMS. The SHRIMP ages for the samples range from 2195 Ma to 2074 Ma. The intrusion ages suggest two domains: (1) SW Mali where the dated samples range between 2130-2074 Ma; and (2) Burkina Faso with ages between 2195-2100 Ma.

The ϵHf in zircons at the inferred emplacement age ranges between 0 and 7.5. Three ϵHf groups can be broadly correlated with age groups: (1) $\epsilon\text{Hf} < 3$, ages 2130-2074Ma; (2) $3 < \epsilon\text{Hf} < 5$, ages 2170-2115 Ma; and (3) $\epsilon\text{Hf} > 5$, with ages 2195-2140 Ma. Combined, the U-Pb and Hf isotope data define two major periods: (1) an alternation between increasing and decreasing Hf values with decreasing U-Pb ages between 2195-2140 Ma; this reflects periods of addition of juvenile magmas and reworking of slightly older crustal material; and (2) falling Hf values with decreasing U-Pb ages 2140-2074 Ma. Slightly higher ϵHf values are observed towards the end of this period. These trends imply the dominance of reworking of slightly older crustal material.

This new insight into the architecture and evolution of the WAC suggests that the craton was formed mainly by the assembly of juvenile material with sporadic episodes of reworking. This conclusion, along with that of a study conducted in the northern portion of the craton [2], helps to constrain the poorly understood tectonic history of the Birimian period of West Africa.

[1] Begg *et al* (2009) *Geosph* **5**:25-50 [2] Abati *Et Al.* (2012) *Precam Res* **212-213**:263-274

In situ U-Pb dating of carbonate by LA-ICP-(MC)-MS and ID-TIMS

R.R. PARRISH¹, M. HORSTWOOD², W. AUSTIN-GIDDINGS³, N.M.W. ROBERTS⁴, D. CONDON⁵
AND T. RASBURY⁶

¹Dept Geology U. Leicester, UK and NIGL, British Geol Survey, Keyworth, Notts, *corresp: rrp@nigl.nerc.ac.uk

²NIGL, British Geological Survey, Keyworth, Notts, NG12 5GG(msah@bgs.ac.uk)

³Institute of Geography and Earth Science, Aberystwyth University, Aberystwyth, Wales wea2@aber.ac.uk

⁴affiliation and address as in ²: nirob@bgs.ac.uk

⁵affiliation and address as in ²: (dcondon@bgs.ac.uk)

⁶Dept of Geosciences, Stony Brook University, Stony Brook, New York, 11794-2100(troy.rasbury@stonybrook.edu)

An easily applicable method to provide absolute age constraints in carbonate has proved elusive except in unusually favourable materials. U-Pb dating of carbonate has so far been restricted to ID-TIMS methods that involve analysis of larger volumes. Unfortunately there is currently no a priori way to know if a sample has a viable U/Pb ratio, and many carbonates are not datable. The challenge is to find a rapid method to date materials in situ by identifying suitable materials (low common Pb, >0.3ppm U), finding the higher-U and highly radiogenic subzones zones that are key to precise ages, so that a substantial robust age on material can be put in a sedimentary or other geological context. Materials of interest include calcite veins in structurally relevant fractures, cements, diagenetic calcite, primary biogenic carbonate, speleothems, lake sediments, tufas and paleosols, etc.

We have successfully adapted LA-ICP-(MC)-MS zircon methods by using a well characterized 254±6 Ma (95% confidence) calcite standard (dated by ID-TIMS at NIGL and Stony Brook) to correct the measured U/Pb ratio for matrix effects. This approach allows in situ U-Pb dating with uncertainties as little as ±4% at 95% confidence with minimal sample consumption, supplemented by ID-TIMS data as appropriate. We have dated samples with average uranium concentrations (0.4-5 ppm) such as speleothems, paleosols, tufa, marine cements (in ammonite chambers), calcite veins from fractures etc. The age of dated materials is as young as 250ky, the latter U-Pb dates agreeing with U-series dating after correcting for U activity. For Quaternary materials beyond the range of U-series, we measure residual disequilibrium of U to make corrections for initial U activity ≠ 1. We have found that our LA-ICP-MS in situ method has distinct advantages over ID-TIMS in its sub-sampling power. Examples of these applications will be presented. This new area of geochronology is likely to grow rapidly in the future.

Long-term residual alteration rates of synthetic basaltic glass

B. PARRUZOT*, P. JOLLIVET AND S. GIN

CEA Marcoule, DEN/DTCD/SECM/LCLT, BP 17171, 30207 Bagnols sur Cèze CEDEX, France.

(*correspondence: benjamin.parruzot@cea.fr)

Laboratory measured residual rates

Basaltic glasses are considered as good analogues to nuclear glasses [1]. However, if forward alteration rates and mechanisms are well-known [2], long-term alteration rates need to be determined in order to deepen this analogy.

We performed batch experiments at high surface-to-volume ratio (high reaction progress) on a Li- or B-doped synthetic tholeiitic basaltic glass at 90°C and 30°C during 1000 days. After 182 days, the rates did not evolve significantly. When considered constant with respect to time, the mean residual rates were $1.2 \times 10^{-5} \text{ g.m}^{-2}.\text{d}^{-1}$ and $3.9 \times 10^{-6} \text{ g.m}^{-2}.\text{d}^{-1}$ at 90°C and 30°C, respectively.

The alteration layer was a dense amorphous gel in which some crystalline clayey sheets may be found. Its porosity was sufficient to allow water and Si to pass through. At the alteration layer/solution interface, low density poorly crystalline clays had precipitated.

Comparison to naturally altered samples

The measured alteration rates indicate a drop of 4 to 5 orders of magnitude when compared to forward alteration rate and 1 order of magnitude inferior to the rates at higher progress of reaction reported by Técher *et al* [3]. This is 10 times higher than the drop between initial and residual rates observed on the SON68 nuclear glass [4].

These values were extrapolated both in temperature (to 5°C with an Arrhenius law) and in time resulting in a value comprised between 0.1 and $0.6 \mu\text{m}/10^3 \text{ y}$. This result is comparable to naturally altered samples showing a similar alteration layer (i.e. non-zeolitized samples) whose alteration rate is comprised between 0.1 and $10 \mu\text{m}/10^3 \text{ y}$ [3].

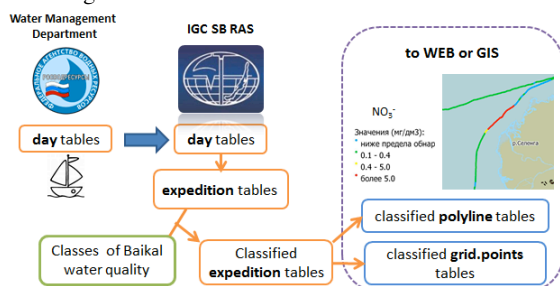
[1] Ewing (1979) *Scientific Basis for Nuclear Waste Management I*, 57-68. [2] Crovisier *et al* (2003) *J. Nucl. Mater.* **321**, 91-109. [3] Techer *et al* (2001) *Chem. Geol.* **176**, 235-263. [4] Gin *et al* (2012) *J. Non Cryst. Sol.* **358**, 2559-2570.

Spatial database for the hydrochemical monitoring of Lake Baikal

A. PARSHIN, S. SHESTAKOV AND K. CHUDNENKO

Vinogradov Institute of Geochemistry SB RAS, Russia.
(correspondence: sarhin@geo.istu.edu)

Lake Baikal is a unique geosystem requiring its preservation in its original form. Since 1965, environmental monitoring of Baikal water is based on researching physical and chemical parameters. Currently used two types of sensors: ship-based measurement systems and analysis of water samples in chemical laboratories. To solve the problems of environmental control, the investigators from IGC SB RAS in cooperation with specialists of Russian Water Management developed a distributed spatial database, to provide the task of collecting, storing, analyzing, interpreting and reporting monitoring data.



In the ship-based part of the database is stored the information coming from the chemical analyzers. This data aggregates with the coordinates in the tables "day", which are transmitted to the data center IGC SB RAS. "Day" tables forms the "expedition" tables. After that, the data is subjected to automatic classification based on the tables of regional classes of water quality "background concentrations-MPC" [1]. Classes are the result of specialized four-year study of Lake Baikal hydrochemistry.

Collected database currently contains more than 2.5 million georeferenced sampling points. For fast display of such data on the web and GIS interfaces require additional treatment. Geodata are transformed into two types of tables: the point of sampling, calculated on the regular network, and sample profiles presented in the form of classified polylines. These tables are linked to the thematic geoportals intended for informing involved agencies, interested professionals and ordinary citizens.

[1] Parshin *et al* (2013) ISSN 2072-8158, 4.

Dissolution of Arsenopyrite under Geologic Carbon Storage Conditions

H.PARTHASARATHY^{1,2*}, D.DZOMBAK²
AND A.KARAMALIDIS^{1,2}

¹National Energy Technology Laboratory-Regional University Alliance (NETL-RUA), Pittsburgh, PA 15236

²Carnegie Mellon University, Department of Civil and Environmental Engineering, Pittsburgh, PA 15213
(*Correspondence: hparthas@andrew.cmu.edu)
(dzombak@cmu.edu),(akaramal@andrew.cmu.edu)

Geologic carbon storage (GCS) in saline formations may induce increased dissolution of many metals including arsenic from reservoir rock minerals and from caprock and overlying rock minerals, in case of leakage of CO₂ or CO₂-saturated brine. Preliminary experiments on metal mobilization on carbonate rocks upon contact with CO₂-saturated brine have indicated arsenic release in excess of the U.S. EPA standards for drinking water. The most common sources of arsenic in sedimentary geologic formations are arsenopyrite (FeAsS) and arsenian pyrite. This study aims to determine the maximum long-term dissolution rates of arsenopyrite under a range of conditions representative of deep and shallow geologic formations. For this purpose, a small-scale flow-through system was developed and used to simulate the dissolution of arsenopyrite under a wide range of temperature, pressure and solution chemistry conditions. The effects of flow rate, pressure and different oxidants on arsenopyrite were separately tested. The dissolution studies focused on determining the mineral dissolution rate based on total As release with the system at steady state operation. However, measurements of Fe and S were also collected for comparison with previous studies. The dissolution rate computed from steady state As concentrations resulting from reaction of the mineral with 10⁻⁴ M Fe³⁺ as oxidizing agent at ambient conditions was 10^{-8.3} mol/m²s, which is comparable to reported rates of arsenopyrite dissolution rates under similar conditions. Ongoing dissolution experiments with CO₂-saturated NaCl solution at high pressure and temperature show the effect of CO₂ and brine on the release of As.

Dissolution of Arsenic and Iron from Reservoir and Cap-Rocks of Geologic Carbon Dioxide Storage Sites

H.PARTHASARATHY^{1,2}, C.LOPANO³, A. HAKALA³,
D.DZOMBAK² AND A.KARAMALIDIS^{1,2*}

¹National Energy Technology Laboratory-Regional University Alliance (NETL-RUA), Pittsburgh, PA 15236

²Carnegie Mellon University, Department of Civil and Environmental Engineering, Pittsburgh, PA 15213

³National Energy Technology Laboratory, U.S. Department of Energy, Pittsburgh, PA 15236

(*Correspondence: akaramal@andrew.cmu.edu)

Dissolution of geologically stored CO₂ in brines of saline geologic formations may lead to a change in pH and brine composition which may subsequently increase the dissolution rates of reservoir and cap rocks. Dissolution of minerals induces the release of various metals that may participate in subsequent dissolution and precipitation reactions, and that may be of concern if reacted formation fluids migrate out of the target storage zone. The objective of this study is to study the release of As and Fe, present in the reservoir and cap rocks of the Lower Tuscaloosa reservoir. XANES analysis of the samples indicated a relationship between As and Fe in these samples. To assess the potential release of As and Fe, and to measure the effect of CO₂ on their release rates, dissolution experiments were conducted with caprock and reservoir rock samples obtained at different depths. The dissolution was studied at representative conditions of the reservoir (i.e. 60 °C, 100 bars, synthetic brine of 1.4M NaCl) utilizing a small-scale flow-through system. The dissolution was conducted with deoxygenated 1.4M NaCl solution for 10 hours prior to CO₂ injection into the NaCl solution. The solution chemistry was defined pre- and post-CO₂ injection by ICP-MS analysis. Accordingly, rock samples were analyzed pre- and post-CO₂ injection by XRD and SEM. Preliminary dissolution experiments showed that upon CO₂ injection, rates of metal release increased significantly before reaching a new equilibrium (Figure 1).

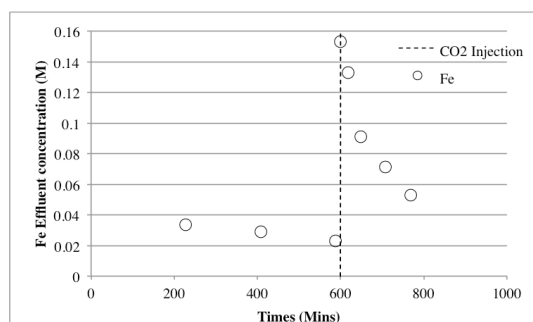


Figure 1. Effluent Fe concentration (M) with time at T=60 °C, P= 100 bar with 1.4 M NaCl. CO₂ injection after 10 hours.

Filling in the juvenile magmatic gap: evidence for continued Paleoproterozoic plate tectonics during the Great Oxidation Event

C.A. PARTIN^{1*}, A. BEKKER¹, P.J. SYLVESTER², N. WODICKA³, R.A. STERN⁴, T. CHACKO⁵
AND L.M. HEAMAN⁵

¹Dept. of Geological Sciences, University of Manitoba, Winnipeg, Manitoba R3T 2N2, Canada

(*correspondence : umpartin@cc.umanitoba.ca)

²Dept. of Earth Sciences, Memorial University, St. John's, Newfoundland A1B 3X5 Canada

³Geological Survey of Canada, 601 Booth Street, Ottawa, Ontario K1A 0E8, Canada

⁴Canadian Centre for Isotopic Microanalysis, University of Alberta, Edmonton, Alberta T6G 2E3, Canada

⁵Dept. of Earth and Atmospheric Sciences, University of Alberta, Edmonton, Alberta T6G 2E3, Canada

Despite several decades of research on the growth of the continental crust, it remains unclear whether the production of juvenile continental crust has been continuous or episodic in the early Precambrian. Models for episodic crustal growth have gained traction recently through compilations of global U-Pb zircon age abundance spectra interpreted to delineate peaks and lulls in crustal growth through geologic time. One such apparent trough in zircon age abundance spectra between ~2.45 and 2.22 Ga is thought to represent a pause in crustal addition, resulting from a global shutdown of magmatic and tectonic processes [1]. The ~2.45 - 2.22 Ga magmatic shutdown model envisions a causal relationship between the cessation of tectonism and accumulation of atmospheric oxygen over the same period. Here, we present new coupled U-Pb, Hf, and O isotope data for detrital and magmatic zircon from the western Churchill Province and Trans-Hudson internides of Canada, covering an area of approximately 1.3 million km², that demonstrate significant juvenile crustal production during the ~230 million-year interval, and thereby argue against the magmatic shutdown hypothesis. Uninterrupted plate tectonics between ~2.45 and 2.22 Ga would have contributed to efficient burial of pyrite and organic matter and the consequent rise in atmospheric oxygen documented for this time interval.

[1] Condie *et al* 2009 *EPSL* **283**, 294-298.

Microthermometric and Raman analysis of fluids that interacted with variably graphitic pelitic schist in the Dufferin Lake zone, south-central Athabasca Basin: Implications for graphite loss and uranium deposition

MARJOLAINE PASCAL^{1*}, KEVIN ANSDSELL¹,
IRVINE R. ANNESLEY¹,
MARIE-CHRISTINE BOIRON², TOM KOTZER³,
DAN JIRICKA⁴ AND MICHEL CUNEY²

¹University of Saskatchewan, Saskatoon, Canada,

(* presenting author: mjp313@mail.usask.ca,
kevin.ansdell@usask.ca, ira953@mail.usask.ca)

²Georessources, Vandoeuvre-lès-Nancy, France,

(marie-christine.boiron@univ-lorraine.fr,
michel.cuney@univ-lorraine.fr)

³Cameco Corporation, Saskatoon, Canada,

(Tom_Kotzer@cameco.com)

⁴D.E Jiricka Enterprises, (djiricka@sasktel.net)

The Athabasca Basin (Canada) contains the highest grade unconformity-type uranium deposits in the world. Underlying the sedimentary rocks of the basin in the Dufferin Lake zone are variably graphitic pelitic schists; altered to chlorite and hematite, and locally bleached near the unconformity (Red/Green Zone: RGZ) during paleoweathering or later fluid interaction.

Fluid inclusions (FI) were examined in quartz veins, using microthermometry and Raman analysis, to characterize and compare the different fluids that have interacted with the RGZ and the graphitic pelitic schist. The inclusions appear to be secondary, which is compatible with quartz veins from deformation zones.

Monophase vapor are the dominant type of FI in the graphitic pelitic schist, whereas aqueous two-phase (L+V) and three-phase (L+V+Halite) FI occur in the RGZ. The temperature of ice melting of aqueous fluid inclusions from the RGZ are between -23 and -26°C, which suggests a salinity of 34wt% using the H₂O-NaCl-CaCl₂ system. The temperature of homogenization (TH) varies mainly between 90 and 170°C. The temperature of dissolution of halite (190-200°C and 210-220°C) yields a salinity of about 32wt% eq. NaCl for the paleofluid. In the graphitic pelitic schist, all FI homogenize into the vapor phase. The CH₄ dominant fluid has a TH between -81 and -74°C. The N₂ dominant fluid has a TH between -152 and -100°C. Some contain CO₂ and traces of H₂S. The aqueous fluid is interpreted to be the regional basinal fluid. The monophase vapor FI could be the break down of graphite to CH₄ and associated feldspars/micas to NH₄ and N₂; three possible reductants for uranium mineralization.

Zn-Pb-Fe sulfide formation in Grieves Siding peat, Tasmania

R. PASCUAL^{1*}, V. KAMENETSKY¹, K. GOEMANN²,
T. NOBLE¹ AND N. ALLEN³

¹School of Earth Sciences and CODES, University of
Tasmania, Hobart, Tasmania 7001

(*correspondence: Richelle.Pascual@utas.edu.au)

²Central Science Laboratory, University of Tasmania, Hobart,
Tasmania 7001

³14 Station Lane, Exton, Tasmania

Aqueous aluminosilicate colloids in mineral formation had been studied in hydrothermal systems, but little is known in low temperature environments. The Grieves Siding Zn-Pb rich peat was investigated to understand the role of organic matter and colloids in the transport and formation of metal-bearing minerals at ambient conditions. The peat samples revealed pronounced enrichment in Zn (up to 28.6 wt%), Pb (up to 3.8 wt%) and other metals. Highly unusual assemblages of sulfides, carbonates, phosphates, oxides, sulfates, silicates, native metals and inorganic carbon were identified in addition to the ubiquitous organics. Dominant sulfide is ZnS with minor PbS and FeS₂. ZnS commonly exhibits colloform texture appearing like schalenblende at smaller scale. The banded ZnS incorporates O (up to 18.5 wt%), Al (up to 4 wt%) and Pb (up to 2.3 wt%), as well as minor (<0.5 wt%) Si, Cd, Fe, As, Ag, and Ni. Carbon is also present. The banding indicate variability in the distribution of Al, O and occasionally C, relative to Zn and S. Dark bands corresponds to an elevated concentration of Al, O and C whereas light bands are linked to diminishing abundance of Al-O-C and prevalence of Zn-S. Sulfate reduction by bacterial action is implicated in the formation of the sulfides. Metal-rich aqueous aluminosilicate colloid precursor to colloform ZnS is possibly produced from the bioweathering of silicates. Organics may also have participated in the transport, deposition and retention of the metals in the peat.

Thermogenic hydrocarbons in Mid Ocean serpentinites

V. PASINI^{1,2}; D. BRUNELLI^{1,3} AND B. MÉNEZ²

¹Università di Modena e Reggio Emilia, L.go St. Eufemia 19, 41100 Modena, Italy.

²Institut de Physique du Globe de Paris, 1, rue Jussieu - 75238 Paris cedex 05, France

³Istituto di Scienze del Mare – CNR, Via Gobetti 101, 49100 Bologna, Italy

The progressive hydration of mantle-derived peridotites is known to support deep microbial ecosystems unrelated to photosynthesis. Relics of endogenic, microbiologically-driven, carbon accumulations have been recently discovered strictly associated to hydrogarnet minerals in serpentinitized rocks coming from the MAR 4-6 °N region [1]. The presence of this colonization suggests that the serpentinitization byproducts can constitute a valuable source of carbon and metabolic energy for microorganisms held deep in the oceanic lithosphere. We have decided to re-investigate the recently described relics of deep microbial ecosystems to study its fate through ageing and thermal degradation. A set of high resolution micro-imaging techniques (HRTEM, Raman and Fourier-transform infrared microspectroscopy, and STXM at the carbon K-edge) have been applied to characterize the organic carbon speciation and its spatial distribution at the micrometer scale. Our data show that the biologically derived organic matter colocalized with the hydrogarnets has experienced thermal degradation and aromatization while a light fraction consisting of C₆-C₁₀ aliphatic compounds associated to carboxylic functional groups wet the surrounding bastite and the late vein network. Ecosystem-hosting serpentinites can thus be seen as source rocks generating deep thermogenic hydrocarbons which then migrate upward and mix with the complex pool of organic compounds discharged at hydrothermal vents. This work shows how a combination of complex biological and geochemical processes contribute to the hydrothermal carbon cycle at Mid Ocean Ridges.

[1] Ménez, B., Pasini, V., Brunelli, D., 2012. Life in the hydrated suboceanic mantle. *Nature Geoscience* 5, 133–137.

Novel Method for Compound Specific Stable Isotope Analysis of contaminated groundwater across the sediment-water interface

ELODIE PASSEPORT¹, KATRINA CHU¹, GEORGES LACRAMPE COULOUME¹, RICHARD LANDIS², EDWARD J. LUTZ², E. ERIN MACK², KATHRYN WEST³, AND BARBARA SHERWOOD LOLLAR¹

¹Dept. of Earth Sciences, University of Toronto, 22 Russell Street, Toronto, ON M5S 3B1, Canada

²Dupont Corporate Remediation Group, Glasgow 300, Newark DE 19714-6300, USA

³URS Group, Newark DE 19714-6300, USA

Chlorinated benzenes are toxic contaminants frequently identified in groundwater. Because a variety of bacteria are able to conduct reductive dehalogenation of these compounds, Monitored Natural Attenuation (MNA) is a potentially effective technique for groundwater remediation. Here, we evaluate the potential for Compound Specific Isotope Analysis (CSIA) to detect *in situ* biodegradation of chlorinated benzenes in a historically contaminated site. Groundwater samples were collected during three sampling campaigns in 2009 and 2012 along a contaminant plume that discharged to surface water until a sheet pile barrier was installed in December 2008 and controlled the release. A passive sampling “peeper” method for conducting microscale CSIA sampling at the groundwater - sediment pore water interface, was also tested for its suitability for CSIA.

In the highest concentration zone, the most ¹³C-depleted carbon isotopic signatures for dichlorobenzenes (DCBs) and 1,2,4-trichlorobenzene (1,2,4-TCB) were measured ranging from $-32.4 \pm 0.5\text{‰}$ to $-29.6 \pm 0.5\text{‰}$. Downgradient of the plume, moderate (2 to 4 ‰, 1,4-DCB and 1,2,4-TCB) to large (10 ‰, 1,2-DCB) enrichments in the heavy stable carbon isotope were observed with values as enriched as $-27.9 \pm 0.5\text{‰}$ (1,4-DCB), $-20.5 \pm 0.5\text{‰}$ (1,2-DCB), and $-28.2 \pm 0.5\text{‰}$ (1,2,4-TCB) in 2009. A similar trend was confirmed in 2012. The most enriched values were measured close to the groundwater / sediment pore water interface where high microbial activity may have been responsible for biodegradation. A novel method for sampling for CSIA via peeper diffusion sampler with a polysulfone membrane showed promise for collecting chlorinated benzene-bearing water samples without significantly affecting contaminant isotope signatures. This new approach will be used to extend the current field investigation by measuring CSIA trends at a fine spatial resolution across the sediment - pore water interface.

Triple oxygen isotope compositions of late Cretaceous dinosaur eggshells and implications for atmospheric carbon dioxide

BENJAMIN H. PASSEY^{1*}, HUANTING HU¹,
SHAENA MONTANARI², SHUNING LI¹
AND NAOMI E. LEVIN¹

¹Johns Hopkins University, Department of Earth and Planetary Sciences, Baltimore, MD 21218, USA

²American Museum of Natural History, Sackler Institute for Comparative Genomics, New York, NY 10024, USA
*(correspondence: bhpassey@jhu.edu)

It has recently been proposed that the triple oxygen isotope composition of minerals that incorporate oxygen from atmospheric O₂ is related to atmospheric carbon dioxide levels [1,2]. The mechanism is mass independent transfer of ¹⁷O and ¹⁸O from O₂ to O₃ and CO₂ during photochemical reactions in the stratosphere, leading to negative Δ¹⁷O(O₂) values, and positive Δ¹⁷O(O₃) and Δ¹⁷O(CO₂). The effect is enhanced by the carbon cycle: the residence time of O in the CO₂ reservoir is far shorter than that of O in the O₂ reservoir, leading to preferential sequestration of positive Δ¹⁷O(CO₂) anomaly to the biosphere + hydrosphere, and hence buildup of negative Δ¹⁷O(O₂) anomaly in the atmosphere. This effect increases with increasing atmospheric CO₂ concentration.

Biominerals forming in equilibrium with body water sample the atmospheric Δ¹⁷O(O₂) signal owing to metabolism (CH₂O + O₂ → CO₂ + H₂O) [2]. We have developed a method that allows for high precision measurement (±0.02‰ 1σ) of Δ¹⁷O of CO₂ (and hence CaCO₃, including eggshell) using a scheme where O in CO₂ is converted to O in H₂O by reduction with H₂. The H₂O is then fluorinated to yield O₂ suitable for mass spectrometry. We apply the method to late Cretaceous (Campanian and early Maastrichtian) dinosaur eggshell from Mongolia [3], as well as modern ostrich eggshell. The Δ¹⁷O values of CO₂ extracted from dinosaur eggshell, ~ -0.15 to -0.27‰ (relative to λ = 0.528), are similar to the observed range for modern ostrich (~ -0.21 to -0.25‰), suggesting that atmospheric CO₂ levels, or operation of the global carbon cycle and stratospheric photochemistry, or both, were not drastically different during the late Cretaceous compared to today. This generally agrees with results from the paleosol carbonate CO₂ barometer [4] and carbon cycle models [5].

[1] Bao *et al* (2008) *Nature* **453**, 504-506. [2] Pack *et al* (2013) *GCA* **102**, 306-317. [3] Montanari *et al* (2013) *Palaeo-3* **370**, 158-166. [4] Ekart *et al* (1999) *Am. J. Sci.* **299**, 805-827. [5] Royer *et al* (2007) *Nature* **446**, 530-532.

Determination of probabilistic Kd values for radionuclides in French rivers using a speciation code

L. MARANG (1), P. CIFFROY(1), AND L.PASTOR⁽¹⁾

⁽¹⁾ EDF, Division Recherche et Développement, Département Laboratoire National d'Hydraulique et Environnement, 6 quai Watier, 78401 Chatou, France (Lucie.pastor@edf.fr)

Environmental risk assessment of radionuclides (RN) depends to a great extent on modelling their fate and mobility based on solid-liquid partition coefficient (Kd). To take into account the variability of many environmental factors that influence the Kd value (pH, nature of particles...), Kd can be expressed as a probability density function (PDF). Several databases containing Kd values have been referenced and a weighted bootstrapping procedure was set up in order to built PDF for environmental conditions. However the relevance and robustness of PDF depends on the number of Kd values in the database. Also, different values of Kd can be used for a specific RN at a specific site (depending on the database used), which can indeed lead to major differences in the results.

The objective of this study is to define a new methodology to calculate site specific Kd values for French rivers. This is particularly interesting when a limited number of Kd value is available in the literature (chromium and nickel for instance). This method is based on a predictive chemical speciation calculation. So far, multi-linear regression models were favoured to predict Kd values. The observed field-based partition coefficient can be counter-intuitive because of the competing roles played by the solid and dissolved organic matter. Recently, new models have become available that can adequately describe metal ion binding to DOC, POC, clays and oxides: the NICA-isotherms [1], the CD-Music model. These new models have been shown to give good predictions of the behaviour of contaminants even in heterogeneous systems characteristics of the natural environment.

To validate this approach, *in-situ* experiments will be conducted as part of the COPA project (funded by NEEDS Environnement), focussing on the major RN released by the French nuclear power plants (NPP) (^{110m}Ag, ⁵⁸Co, ⁶⁰Co, ⁵⁴Mn, ⁶³Ni, ¹³⁴Cs, ¹³⁷Cs, ¹²⁵Sb). First, a steady-state approach will consist in studying the suspended particulate matter and the dissolved fractions collected at the SORA station on the Rhône River (France) since 2005 to extract annual averages or change in compartment during hydrological events (floods, low water periods, controlled released by NPP). Then, a specific and planned release from a NPP will be studied to better assess the non steady-state behaviour of a chosen RN through time and distance from the source.

The detailed methodology as well as preliminary results will be presented here.

[1] Kinniburgh, D.G., et al (1999). Colloids and Surfaces A: Physicochemical and Engineering Aspects, **151**(1-2): p. 147-166.

Extraterrestrial mechanism of kimberlite emplacement

MARIUSZ PASZKOWSKI¹ AND JERZY W. MIETELSKI²

¹Institute of Geological Sciences PAN, Senacka 1, Kraków, Poland, ndpaszko@cyf-kr.edu.pl

²Institute of Nuclear Physics PAN, Radzikowskiego 152, Kraków, Poland, jerzy.mietelski@ifj.edu.pl

The most popular model of kimberlite formation combines “magma needle” concept with massive degassing which is supposed to form extremely narrow and long pipe which is then filled up with kimberlite matter originating from the mantle and some xenoliths dropped into formed vein from the surface. This class of models left some researchers unconvinced. The pipe must be formed rather rapidly, otherwise it will be blocked in the deep rocks due to high pressure there, moreover there will not be diamonds present since in slow decompression they will go into graphite. The energy which forms the pipe in thermodynamic process must be also dispersed. Thus some other models are formed which include explosion of reactive gases or electrical force as an additional factor, including near passage of extraterrestrial charged body. We propose another concept: the kimberlite pipe is formed by an impact of small, macroscopic, ultra dense object which existence was proposed in 1984 as a kind of dark matter. Such objects can be present in jets of accretion discs of a black hole and originate from destruction of neutron star during its impact onto black hole or are remains from Big Bang era. The 1 mm³ volume of such matter can have mass of 10³t. If it has speed of 400 km/s the kinetic energy is 8*10²¹J. On the other hand, the energy which is needed to heat up a 1 m² surface tunnel across whole globe to the temperature of about 1 million K is on the order of magnitude of 10²⁰J. This shows that such ultra dense object may have enough kinetic energy to cross whole globe. At such speeds crossing will take several seconds. The shock wave will heat up the formed plasma tunnel but the degassing will remove all materials from it leaving relatively cold straight vein which can be filled by mantle material and xenoliths. We propose that reality of such scenario can be verified by measurements of the isotopic abundances of the elements in the walls of kimberlite on the side of country (host) rock: the neutrons produced from nuclear reactions during whole process will influence the isotopic abundances, and this influence will decrease with the distance from the center of the pipe. Therefore we propose undertaking of such isotopic studies outside the kimberlite pipes in host rocks.

The stable isotopic composition of carbon monoxide from Greenland firn air samples collected at NEEM

SUPUN PATHIRANA^{1*}, PATRICIA MARTINERIE²,
EMMANUEL WITRANT³, JAN KAISER⁴,
CARINA VAN DER VEEN¹ AND THOMAS RÖCKMANN¹

¹Institute for Marine and Atmospheric Research Utrecht (IMAU), Utrecht University, Princetonplein 5, 3508 TA, Utrecht, Netherlands (*correspondence: s.l.pathirana@uu.nl)

²UJF – Grenoble 1/CNRS, Laboratoire de Glaciologie et Géophysique de l'Environnement (LGGE) UMR 5183, Grenoble, 38041, France (patricia@lgge.obs.ujf-grenoble.fr)

³UJF – Grenoble 1 / CNRS, Grenoble Image Parole Signal Automatique (GIPSA-lab), UMR 5216, B.P. 46, F-38 402 Saint Martin d'Hères, France

⁴School of Environmental Sciences, University of East Anglia, Norwich, NR4 7TJ, U.K. (j.kaiser@uea.ac.uk)

CO plays an important role in tropospheric chemistry. Precise measurement of its isotopic composition from the past is useful in constraining individual source and sink processes and thus its global cycle. High volume air samples from the NEEM EU 2008 S4 & NEEM 2009 S2 boreholes were measured for mole fractions, $\delta^{13}\text{C}$ and $\delta^{18}\text{O}$ of CO on a continuous-flow isotope ratio mass spectrometric (CF-IRMS) system. This system extracts the CO from the air sample (100 mL–200 mL of air required), converts the CO to CO₂ using Schütze reagent and transfers the CO₂ (derived from CO) via an open-split to the IRMS for isotope analysis. The results are qualitatively similar to the ones published in Wang *et al* [1] but also show differences that will be investigated by firn modelling.

[1] Wang *et al* (2012) *Atmos. Chem. Phys.*, **12**, 4365–4377.

Wehrlitization processes within the upper mantle beneath the Northern Pannonian basin (Hungary)

LEVENTE PATKÓ^{1*}, LÁSZLÓ ELŐD ARADI¹, NÓRA LIPTAI¹, ROBERT J. BODNAR², LUCA FEDELE², ZOLTÁN KOVÁCS¹, BERNARDO CESARE³, ORLANDO VASELLI⁴, ANNA MARIA FIORETTI⁵, TERESA JEFFRIES⁶ AND CSABA SZABÓ¹

¹Lithosphere Fluid Research Lab, Eötvös University, Hungary
(*correspondence: patkolev@gmail.com, http://lrg.elte.hu)

²Virginia Polytechnic Institute and State University,
Department of Geosciences, USA

³Department of Geosciences, Padua, Italy

⁴Department of Earth Sciences, Florence, Italy

⁵CNR, Padua, Italy

⁶Natural History Museum, Earth Sciences Department, UK

Plio-Pleistocene alkaline basalts have brought upper mantle xenoliths to the surface at five different locations within the Carpathian-Pannonian region.

After a thorough sampling and detailed petrographic examination, in addition to the dominant lherzolite xenoliths, several wehrlite xenoliths were recognized that show unique modal composition and textural characteristics. Based on the major element geochemistry of the rock-forming minerals, significant Fe and Mn enrichment in olivines, Ti, Al and Fe enrichment in clinopyroxenes, and Fe and Ti enrichment in spinels was observed compared to compositions of common lherzolite xenoliths.

Many silicate and sulfide melt inclusions were observed in the clinopyroxene and olivine from the wehrlite xenoliths. The sulfide mineralogy was consistent with other sulfides found in the upper mantle, however, sulfides in these wehrlite xenoliths show higher Fe and lower Cu concentrations relative to the lherzolite hosted sulfides.

Five representative wehrlite xenoliths from different localities have been selected for a detailed silicate melt inclusion analysis using LA-ICP-MS. The results show an incompatible element enrichment compared to the host mineral, especially in LIL elements (e.g. Ba, Sr, Pb) and in HFS elements (e.g. Th, U, Nb, Ta, Zr, and Ti).

Based on this detailed study, wehrlite xenoliths are interpreted to be products of a process called stealth mantle metasomatism, whereby the metasomatizing agent is a mafic melt with high MgO/FeO ratio, which is different from the host alkaline basalt.

Resolving s- and r-process presolar carriers using Ba-isotope anomalies in FUN CAIs, bulk meteorite samples, and Ivuna acid leaches

C. PATON*, M. SCHILLER AND M. BIZZARRO

Centre for Star and Planet Formation, Natural History Museum of Denmark, University of Copenhagen, Copenhagen DK-1350 Denmark (*Correspondence: chadpaton@gmail.com)

Resolvable nucleosynthetic anomalies are well documented for a number of nuclides (e.g., ⁵⁴Cr, ²⁶Al; ⁸⁴Sr; [1,2,3]). Remarkably, correlations exist between a number of these nuclides [1,2], despite originating from different stellar sources and being hosted in multiple presolar carriers. Such correlations are most readily explained by one of two contrasting processes: Variability due to incomplete mixing of differing components, either because of a late injection of anomalous material [4] or physical differences such as grain size; or alternatively a process that unmixed carriers in a previously homogenised disk (e.g., thermal processing) [1]. Understanding the cause of these correlations is thus a necessary step in deciphering the information they preserve.

We have developed protocols for high-precision Ba-isotope measurement on a Triton thermal ionisation mass spectrometer. Barium has the advantage of having pure p-process (130 and 132), pure s-process (134 and 136), and mixed s- and r-process isotopes (135, 137, 138). By using protocols that allow measurement of the p-process isotopes (despite their very low abundances), we are thus able to identify distinct s- and r-process carriers.

Results from an acid-leach of the Ivuna CI chondrite and two newly measured FUN CAIs (KT-1 and STP-1) allow us to clearly distinguish separate s- and r-process carriers. Our leaching experiment indicates an acid resistant host for the s-process (presumably SiC), whereas the r-process carrier is not resolved by leaching, suggesting parent-body alteration of the original carrier. Despite these physical differences, our FUN CAI data indicate an absence of both carriers, which is difficult to reconcile with a late injection scenario. In combination with data from "canonical" CAIs and chondrites it can be shown that these two carriers behaved independently during early solar system formation.

[1] Trinquier *et al* (2009) *Science* **324**, 374–376. [2] Larsen *et al* (2011) *The Astrophysical Journal* **735**, L37. [3] Paton *et al* (2013) *The Astrophysical Journal* **763**, L40. [4] Chen *et al* (2011) *The Astrophysical Journal* **743**, L23.

Deepwater Horizon spill effects on fish otoliths by LA-ICP-MS

W. PATTERSON III¹ K. MCLACHLIN² R.W. HUTCHINSON^{3A} AND C.J.P O'CONNOR¹

¹University of South Alabama and Dauphin Island Sea Lab, 101 Bienville Blvd, Dauphin Island AL 36528

²ESI Inc, 685 Old Buffalo Trail, Bozeman MT 59718 (mclachlink@esi.com)

³ESI Europe LTD, 8 Averro Court, Ermine Business Park, Huntingdon Cambridgeshire PE296SX

The Deepwater Horizon oil spill that occurred in 2010 released an estimated 4.9 million barrels of oil into the Gulf of Mexico. This study uses laser ablation mass spectrometry (LA-ICP-MS) to measure the effects on the otoliths of multiple populations and species affected by the spill to different degrees. Otoliths are often used as ecological markers due to their fast speed of growth, which makes them sensitive to environmental changes.

LA-ICP-MS offers a precise means of directly measuring elemental heterogeneity across a sample that is impossible with aqueous methods. This study utilizes an XYR shutter to further increase the spatial resolution. A NWR193 laser ablation system fitted with a fast washout TruLine cell and attached to an Agilent 7700s is used to track elemental tracers such as V and Ni from the oil through the otolith to determine how the oil was incorporated and test for earlier exposures.

Reactive transport modeling to assess geological CO₂ storage via mineral carbonation in peridotite

AMELIA PAUKERT^{1*}, JUERG MATTER^{1,2}, PETER KELEMEN¹ AND ERIC SONNENTHAL³

¹Lamont-Doherty Earth Observatory, Columbia University, Palisades, NY, USA (* apaukert@ldeo.columbia.edu)

²Ocean and Earth Science, National Oceanography Centre Southampton, University of Southampton, UK

³Earth Science Division, Lawrence Berkeley National Lab, Berkeley, CA, USA

In situ mineral carbonation is a mechanism for safely and permanently storing CO₂ by converting it to carbonate minerals in geologic formations. Reactive silicate formations with high concentrations of divalent cations (e.g., Mg²⁺, Ca²⁺, or Fe²⁺) have an enormous capacity to sequester CO₂: the mantle peridotite in the Samail Ophiolite, Oman alone could sequester 30x10¹² tons of CO₂ [1]. However, the accessible capacity may be much lower, as CO₂-water-rock interaction is limited by porosity, permeability, and reactive surface area, which are relatively low in fractured-rock aquifers such as in peridotite. Sustained mineral carbonation will also depend on how these hydrogeological factors evolve with reaction progress- carbonating peridotite involves a volume increase of over 40%, so secondary mineralization could clog the existing porosity and permeability, and could armor unreacted peridotite from further carbonation. Alternatively, stresses from volume increase could cause fracturing, creating new permeability, porosity, and reactive surface area. This reactive cracking would allow the carbonation front to continue propagating into the formation. Completely carbonated peridotites in Oman are proof that the carbonation reaction can proceed to completion, given the right conditions [1].

Here we present a reactive transport model of *in situ* mineral carbonation in peridotite to help determine ideal carbonation conditions and how they can be met within the confines of an engineered geological CO₂ storage project. The model is constrained by geochemical and hydrogeological data for peridotite aquifers in the Samail Ophiolite collected over five field seasons. It includes reaction kinetics, non-isothermal multiphase flow, and CO₂ injection scenarios to evaluate how to optimize carbonation by adjusting different parameters (formation temperature, fluid pCO₂, injection rate and temperature, etc.), and estimate what extent of carbonation is realistic for a CO₂ storage project employing *in situ* mineral carbonation in peridotite.

[1] Kelemen *et al* (2011). *Ann. Rev. Planet. Sci.* **39**, 545-576

Simulating Arctic Mixed-Phase Clouds with Aerosol-Dependent Ice Nucleation and Ice Nuclei Depletion

M. PAUKERT* AND C. HOOSE

IMK-AAF, Karlsruhe Institute of Technology (KIT), 76344 Eggenstein-Leopoldshafen, Germany (*correspondence: marco.paukert@kit.edu)

Arctic stratus clouds frequently consist of long-lived supercooled liquid layers which precipitate ice. Depending on the partitioning of liquid water and ice, they modify the radiation budget at ground levels [1].

In semi-idealized simulations with a cloud-resolving model, we investigate for which concentrations of ice nucleating aerosols (here: mineral dust and ice-active bacteria) a stratiform supercooled liquid cloud remains stable, i.e. maintains an approximately constant liquid water path and ice water path over several hours. For this purpose, the ice nucleation scheme in the COSMO model has been replaced by an ice nucleation active site density approach for immersion freezing [2], relating the ice nuclei number to the temperature and to the aerosol surface area based on results from laboratory experiments. In addition, depletion of ice nuclei is taken into account, assuring that only entrainment of fresh aerosol particles or further cooling of an air parcel leads to the formation of ice crystals. The model is applied to the simulation of a cloud which was observed during the ISDAC campaign [3].

The evolution of the liquid/ice partitioning in the cloud is highly sensitive to both the vertical velocity distribution, the ice crystal growth parameterization and the ice nuclei concentration. It is found that both dust and bacteria concentrations need to be several orders of magnitude higher than our initial assumptions based on typical background values to reach the transition from the growing to the glaciating state through immersion freezing.

[1] Shupe & Intrieri (2004), *J. Clim.* **17**, 616-628. [2] Niemand *et al* (2012), *J. Atmos. Sci.* **69**, 3077-3092. [3] Ovchinnikov *et al* (2012), *ISDAC LES intercomparison*, https://engineering.arm.gov/~mikhail/ISDAC_case_description.pdf.

Annual Rainfall Proxy Records from Soda-straw Stalactites

BENCE PAUL^{1*}, HELEN GREEN¹, RUSSELL DRYSDALE², JON WOODHEAD¹, JANET HERGT¹, JOHN HELLSTROM¹ AND JOL DESMARCHELIER³

¹School of Earth Sciences, The University of Melbourne, Parkville, VIC Australia, (*correspondence: bpaul@unimelb.edu.au)

²Melbourne School of Land and Environment, The University of Melbourne, Parkville, VIC Australia

³Glass Expansion 15 Batman Street, West Melbourne, VIC Australia, (jdesmarchelier@geicp.com)

We present a reconnaissance study of the use of soda-straw stalactites (straws) as palaeoclimate proxies. Straws are a previously under-utilised, yet potentially promising, source of such data that may provide intra-annual rainfall records of up to 1000 years, depending on growth conditions. In this contribution we investigate the structure and formation of straws and look at some issues that may affect the reliability of these records. We use laser ablation-inductively coupled plasma-mass spectrometry (LA-ICP-MS) trace element analysis to document surface contamination features that have the potential to obscure annual trace element variations, and discuss a simple method to reveal the underlying layering. We also use LA-ICP-MS to map the two-dimensional trace element distribution in straws. This internal structure reveals broad layers with relatively higher Sr, Mg and Ba contents, compared to narrow, trace-element-poor winter layers. These layers are widest at the outside edge of the straw, narrowing and becoming almost parallel on the interior of the straw.

Based upon these observations, we present a model for the formation of visibly layered straws, where rapid degassing of CO₂ from the drip extending below the straw forms the wider outer layers. In the example presented, summers are defined by increased layer widths and higher trace element contents relative to winter layers. In palaeoclimate studies, where such annual variations can be used to construct time-lines, we suggest that, ideally, the outer-most surface of the straw be analysed where the trace element content difference is greatest and layering is widest.

We also present the trace element profile of the terminal phase of a straw, where layer widths decrease and trace element contents increase. The features described are likely representative of soda-straw responses to drought-induced decreases in percolation water, and may be used to recognise droughts from the pre-instrumental period. We also discuss initial modelling of results from another straw that records annual layers from 1996 to 1780.

Lead isotopes and concentrations in the South Atlantic from the UK GEOTRACES transect along 40°S

M. PAUL¹, T. VAN DE FLIERDT¹, M. REHKÄMPER^{1,2}, D. WEISS¹, M. LOHAN³ AND G. M. HENDERSON⁴

¹Imperial College London, London, SW7 2AZ, UK
(m.paul@imperial.ac.uk)

²Natural History Museum, London, SW7 5BD, UK

³University of Plymouth, Plymouth, PL4 8AA, UK

⁴University of Oxford, Oxford, OX1 3AN, UK

Documenting the distributions of trace elements and their isotopes (TEIs) in the ocean and understanding the processes responsible for these distributions is one of the overarching goals of the ongoing GEOTRACES program [1]. The marine geochemical cycle of lead (Pb) has been extensively influenced by anthropogenic activities since the mid-19th century and, in particular, by the use of leaded gasoline [2]. The characteristic isotope fingerprint of different anthropogenic sources, combined with the short residence time of Pb in the ocean, makes the Pb isotope system a unique source tracer and monitor of ocean circulation [3].

We here present new results from two UK GEOTRACES cruises (D357 and JC068), forming a South Atlantic transect along 40°S. Seawater samples were analysed using a TIMS double spike methodology developed at Imperial College London. This method allows precise measurements for small seawater samples (2L) of both Pb concentrations and isotopic ratios, including the minor isotope ²⁰⁴Pb.

Lead concentrations are generally higher in surface waters (15 to 35 pmol/kg) than in deep water (5 to 15 pmol/kg), and are higher in water depths associated with North Atlantic Deep Water (NADW) than in intermediate waters sourced from the south. The highest Pb concentrations can be found in surface waters close to the South African continent. Lead isotopic compositions clearly support the identification of the major water masses in the region. Excluding coastal areas, surface waters are characterized by ²⁰⁶Pb/²⁰⁴Pb ratios of 18.15 to 18.30, which is distinct from the ²⁰⁶Pb/²⁰⁴Pb ratios of 17.95 to 18.05 characteristic of AAIW. Deep waters usually display higher isotopic ratios with the most radiogenic ²⁰⁶Pb/²⁰⁴Pb ratios of 18.54 being observed at 4500 m depth (Antarctic Bottom Water).

[1] Anderson, R. F. *et al* *Chemie der Erde-Geochemistry* **67**, 85–131 (2007). [2] Ruer *et al* *Chem. Geol.* **200**, 137–153 (2003). [3] Véron *et al* *Deep Sea Res. Part II Top. Stud. Ocean.* **46**, 919–935 (1999).

Searching radiation-resistant microorganisms in high-Mn sites

IVAN G. PAULINO-LIMA^{1*}, KOSUKE FUJISHIMA², JESICA U. NAVARRETE³ AND LYNN J. ROTHSCHILD⁴

¹NASA Ames Research Center

(*correspondence: ivan.g.paulinolima@nasa.gov)

²NASA Ames Research Center [kosuke.fujishima@nasa.gov]

³University of California Santa Cruz [junavarr@ucsc.edu]

⁴NASA Ames Research Center [lynn.j.rothschild@nasa.gov]

Recently, several physiological parameters have been described to play a role on radiation resistance [1, 2]. In particular, a strong positive correlation has been demonstrated between intracellular accumulation of manganese and high resistance to radiation in several biological models [3]. However, the question of the evolution of radiation resistance has never been studied using an approach of environmental microbiology. In order to tackle this problem, soil samples were collected from different locations: (i) a manganese mine in Arizona, (ii) the Atacama desert, Chile, and (iii) the Moffett Field campus, CA. Samples were submitted to UV-C irradiation (300 J/m²) and resistant microorganisms were selected from three different culture media: Marine Agar, LB (Sigma) and R2A (Difco). All isolates were molecularly identified by PCR of the 16S rRNA gene. Each isolate was then subjected to another round of UV-C irradiation and classified according to their tolerance. Survival curves were performed in triplicate for the most resistant isolates and their intracellular Mn/Fe ratio was determined by ICP-MS. UV-resistant isolates have Mn/Fe ratios around two orders of magnitude higher than UV-sensitive ones. Three isolates are more resistant than *Deinococcus radiodurans* to UV-C irradiation, and show a higher Mn/Fe intracellular ratio. A better characterization of these isolates is currently in progress. Access to microbial resources in soils enriched in manganese will be essential for the development of new products and processes for application in various fields of knowledge. The discovery of radiation-resistant microorganisms naturally occurring in manganese-enriched sites will have a profound impact on several lines of research, including future space exploration.

[1] Daly (2012) DNA Repair 11, 12–21. [2] Venkateswaran *et al* (2000) Appl Env Microbiol 66(6) 2620–2626. [3] Daly *et al* (2004) Science 306, 1025–1028.

Dolomite in microbial mats from sabkha (Qatar): insights from combined Raman-Atomic Force Microscopy study.

C. PAULO¹ AND M. DITTRICH¹

¹University of Toronto Scarborough, 1265 Military Trail, Toronto, ON, Canada, M1C 1A4
(*correspondence: mdittrich@utsc.utoronto.ca)

The formation of dolomites has been reported in the extreme environment of Arabian Gulf sabkhas (Illing, Wells *et al* 1965). Many of the sites are characterized by extensive growth of cyanobacterial mats. Carbonates precipitation at low-temperature appears to be impacted by microbial extracellular polymeric substances (EPS) (Dupraz *et al* 2005). Cyanobacteria are key producers of EPS, but so far no information has been gathered on their involvement in dolomite precipitation.

The first objective of this study was to gain insights into the spatial distribution of cyanobacterial EPS and dolomite in different sediment layers of Khor Al-Adaid sabkha (Qatar). Secondly, this project aims to characterize microbial mats in respect of organic and inorganic components on a molecular level. For this purpose, *in-situ* 2D Raman spectroscopy and Atomic Force Microscopy (AFM) were used. Additionally, samples have been analysed with scanning electron microscopy (SEM) and X-ray diffraction (XRD).

Our results showed that Raman fingerprints of dolomite (~1098, ~725 and 300cm⁻¹), cyanobacterial EPS (~1130-1148 cm⁻¹) and carotenoids (1507 and 1000cm⁻¹) are widely distributed in the top 2 cm of the sabkhas sediments. The mineralized EPS have been observed by SEM analysis, and dolomites have been identified by means of XRD.

2D chemical imaging of sediment layers, spectroscopically characterized minerals and organic matter of microbial origins at high spatial resolution. Raman mapping identified small dolomite clusters (<2µm) embedded in a dense cyanobacterial EPS matrix. Therefore, our data provide evidence for an interaction between cyanobacterial molecules, especially EPS, and dolomite in the sabkhas top sediments. This study demonstrated that Raman mapping is a robust and sensitive technique for acquisition of *in situ* information from complex biofilm-minerals samples.

[1] Illing *et al* (1965). Dolomitization and Limestone Diagenesis. Ed. by Lloyd Pray and Raymond Murray. 13:89-111. [2] Dupraz *et al* (2009). *Earth-Science Reviews* **96**:141-16.

High-pressure amphibolite facies metapelites of Carrancas *Klippe*, Southern Brasília Belt, Brazil

M. PAVAN^{1,2A} AND R. MORAES¹

¹Geosciences Institute, University of Sao Paulo, Brazil
(mauriciopsilva@usp.br; moraes@igc.usp.br)

²CPRM – Geological Survey of Brazil, São Paulo, Brazil

The Carrancas *Klippe*, is composed from base to top by a pure to micaceous quartzite, grading vertically to a staurolite-garnet-chloritoid-chlorite phyllite or porphyroblastic kyanite-staurolite-garnet schist, depending on the conditions of metamorphism. The metamorphism recorded in these rocks increases to the southeast, from upper greenschist facies to transition of amphibolite to eclogite facies, as a result of the development of Brasília Belt. Metamorphism was modeled using THERMOCALC, via pseudosections and optimal geothermobarometry. In Estancia Hill, rocks of top portion had peak metamorphic conditions calculated as 10.0 ± 1.7 kbar and 577 ± 8 °C and for Bicas Hill, lower rocks, metamorphic peak conditions were attained at 12.9 ± 1.0 kbar and 608.5 ± 19.5 °C, with retro-metamorphism taking place at 7.0 ± 2.2 kbar and 541.5 ± 25.5 °C. The mineral paragenesis of the studied samples are typical of the greenschist and upper amphibolites facies, respectively. However, the modeling indicates these rocks were exposed to higher-pressure conditions, reaching the transition to eclogite facies. The restricted bulk compositions of these true pelites allow the mineral associations to persist through conditions of higher pressure, as pointed in some theoretical studies.

Increasing metabolic activity of clams and brachiopods over the past 500 million years: A consequence of the changing biological pump?

JONATHAN L. PAYNE¹, NOEL A. HEIM¹,
MATTHEW L. KNOPE¹, KATJA MEYER¹
AND CRAIG R. MCCLAIN²

¹Dept. of Geological & Environmental Sciences, Stanford University, Stanford, CA 94304, USA; (jlpayne@stanford.edu)

²National Evolutionary Synthesis Center (NESCent), 2024 W. Main St., Suite A200, Box 104403, Durham, NC 27705

Numerous indirect lines of evidence suggest a long-term increase in the metabolic activity of marine animals. However, the timing and magnitude of this increase remain poorly quantified, preventing detailed testing of hypothesized controls. Here we use newly compiled body size data for 6834 genera of brachiopods and bivalves, two of the most abundant and diverse clades of marine animals, to show that mean per taxon, per occurrence, and per capita metabolic rates of primary consumers have increased by approximately two orders of magnitude from the Cambrian to the present day, with most of this increase occurring between Cambrian and Jurassic time (540-140 Mya). Secular trends in the thickness of shellbeds, prevalence of fossils, and intensity of bioturbation indicate that this increase in per capita metabolic activity was not offset by a decrease in the number or total biomass of benthic animals, whether bivalves, brachiopods, or other taxa. Biogeochemical modeling suggests that secular variation in the strength of the biological pump may account for the magnitude and timing of this trend in animal community metabolism.

A forward modelling approach to understanding continental growth

J.L. PAYNE¹, K.M. BAROVICH¹, N.J. PEARSON²
AND M. HAND¹

¹Centre for Tectonics, Resources and eXploration (TRaX), University of Adelaide, S.A., 5005 Australia.

(*correspondence: justin.payne@adelaide.edu.au)

²ARC Centre of Excellence for Core to Crust Fluid Systems (CCFS), Macquarie University, NSW 2109 Australia.

The rapid expansion of global datasets of U-Pb and Lu-Hf (\pm O) isotopic data in detrital zircon has provided an avenue to address the questions of the timing and rates of continental growth. Any model suggesting significant growth of the continents in early earth history has dramatic implications for the rate and mechanisms of crustal growth and recycling throughout Earth history. Recent studies using Hf model ages obtained from detrital zircon have suggested 60-65% of the current volume of continental crust existed by the late Archean^{1,2}.

Studies using Hf model ages for continental growth must deal with the issue of Hf model ages that result from the mixing of melts derived from the mantle and crust and/or multiple crustal sources. Studies commonly assume the consistency of mixing across Earth history will average out any short-term bias or else employ O-isotope data to identify mixed model ages. Each of these approaches has shortcomings that may compromise the robustness of the final continental growth model.

Estimates of the proportion of juvenile crustal addition using the ratio of Hf model ages to model ages plus U-Pb ages in a 100 Myr time slice can be reproduced using synthetic Hf data randomly generated from detrital U-Pb age distributions. The use of O-isotopes to remove mixed Hf model ages also seems to be at odds with studies of granite genesis that suggest a larger proportion of granites contain both mantle and crustal components than interpreted from the use of Hf and O isotope data in detrital zircon datasets.

We propose the use of a forward modelling approach to resolve continental growth. This approach uses a priori geologic information to produce models of continental growth that are testable against the detrital zircon and geological records.

1. **E. A. Belousova *et al***, (2010). The growth of the continental crust: Constraints from zircon Hf-isotope data. *Lithos* 119, 457.

2. **B. Dhuime *et al***, (2012). A Change in the Geodynamics of Continental Growth 3 Billion Years Ago. *Science* 335, 1334.

Methane transport and release to the atmosphere in permafrost areas via subterranean groundwater discharge

ADINA PAYTAN¹, ALANNA LECHER¹, NATASHA DIMOVA¹, JOHN KESSLER², AND KATE SPARROW²

¹University of California Santa Cruz, Santa Cruz, CA 95064

²University of Rochester Rochester, NY 14627

Methane release to the atmosphere in permafrost regions of the Arctic is exacerbated by global warming. This may result in a positive feedback effect, as methane is a powerful greenhouse gas. Accordingly, it is important to gain a good understanding of the processes that contribute methane to the atmosphere, particularly in this region. Large quantities of methane are stored in the Arctic in natural gas deposits, permafrost, and as submarine clathrates. Releases from these sources arising from warming have been reported, however, there are still considerable gaps in our understanding of the methane cycle at present and particularly how predicted climate changes will impact the methane cycle.

Subterranean groundwater discharge (SGD) has been recognized as an important conduit for transport of nutrients, metals, methane and other pollutants from land to receiving water bodies throughout the world, and could be a potential important, yet not quantified, source of methane in the Arctic. SGD can be quantified using geochemical tracers such as Ra and Rn and when combined with methane measurements can elucidate the role SGD has in transporting methane from groundwater to surface water bodies such as Arctic lakes and the coastal ocean, from which this methane will be released to the atmosphere.

We have used Ra and Rn along with analytical calculations and methane concentration and isotope analyses in order to determine the contribution of SGD to the methane budget in areas of different hydrological and permafrost conditions in Alaska. Our results indicate that SGD is a major conduit for methane release contributing significant amounts of methane to surface waters particularly in areas where permafrost is abundant and impacted by seasonal temperature changes.

Bioessential metal sorption at ferrihydrite-bacteria interfaces

CAROLINE L. PEACOCK¹ AND ELLEN M. MOON²

¹School of Earth and Environment, University of Leeds, Leeds, UK. (C.L.Peacock@leeds.ac.uk)

²ANSTO Minerals, Australian Nuclear Science and Technology Organisation, Locked Bag 2001, Kirrawee D.C., NSW 2234, Australia. (ellenm@ansto.gov.au)

The association of organic matter with mineral surfaces can exert a profound effect on the behaviour of both the mineral and organic phases. It is becoming apparent that a direct relationship exists between minerals and organics whereby organic matter acts to significantly modify mineral surface physiochemistry and may help preserve mineral reactivity during diagenesis, while minerals similarly help preserve organic carbon leading to burial and long-term carbon storage [e.g., 1]. This relationship is particularly apparent for organics associated with iron (hydr)oxides like ferrihydrite. In these composites the unique surface physiochemistry also produces a complex sorbent with metal sorption properties very distinct from pure iron (hydr)oxides [e.g., 2]. Despite the wide occurrence of iron (hydr)oxide – organic composites, and the major control on metal cycling exerted by the pure end-member components, metal sorption at the composite-water interface is poorly understood.

Here we present the results of on-going research to determine the molecular-level sorption behaviour of bioessential metals with ferrihydrite-bacteria composites. We will show directly for the first time that Cu binds to each of the composite fractions, via the same molecular mechanisms as to the end-member components; namely, a bidentate edge-sharing complex on the ferrihydrite fraction and a monodentate complex to carboxyl functional groups on the bacterial fraction [3]. The presence of the carboxyl groups significantly modifies Cu sorption behaviour on the composites compared to pure ferrihydrite [3,4]. We find that for composites composed predominantly of ferrihydrite this modified behaviour can be modelled in a thermodynamic surface complexation framework by adopting a linear additivity approach, where sorption on the composites is the sum of the pure end-member Cu sorptivities [4]. However, composites composed mainly of bacteria behave in a non-additive manner, which we can explain as a result of their unique surface charge [4]. Modelling and thus predicting metal sorption on these composites is a new challenge.

[1] Lalonde *et al* (2012) *Nature* **483**, 198. [2] Small *et al* (1999) *ES&T* **33**, 4465. [3] Moon and Peacock (2012) *GCA* **92**, 203. [4] Moon and Peacock (2013) *GCA* **104**, 148.

Understanding electron transfer at Fe-bearing mineral surfaces to optimize contaminant remediation

C.I. PEARCE^{1*}, J. LIU¹, B.C. KABIUS¹, A. ARENHOLZ² AND K.M. ROSSO¹

¹Pacific Northwest National Laboratory, Richland WA, USA
(correspondence: *carolyn.pearce@pnnl.gov)

²Advanced Light Source, Lawrence Berkeley National Laboratory, Berkeley, CA 94720, USA

In order to use natural or engineered materials for contaminant sequestration, it is necessary to fully characterize the material in terms of its structure and reactivity. Even within a nanoparticle, elemental distribution can vary from the interior to the surface, thus surface sensitive techniques must be employed to probe mechanisms of interaction between the mineral phase and chemical/biological components present in the subsurface environment.

Here, we present the use of model materials, as well as field samples, in combination with high-resolution spectroscopic and microscopic capabilities, to interrogate interfacial reactivity of Fe-bearing minerals with redox-active contaminants and electron-transfer proteins. A novel and well-characterized set of Fe_{3-x}Ti_xO₄ titanomagnetite nanoparticles was selected as the model mineral system. Replacement of Fe(III) by Ti(IV) in the lattice yield a naturally “tunable” solid-state Fe(II)/Fe(III) ratio, which in principle controls the thermodynamic reduction potential of the mineral phase. Also, the high specific surface area of the nanoparticles greatly improves experimental sensitivity to contaminant/protein interaction and accompanying changes to the solid surface. Nanoparticle properties such as size, morphology, crystallinity, element and valence distribution are characterized by STEM-EELS and micro-XRD. X-ray magnetic circular dichroism (XMCD) is used to distinguish between Fe oxidation states and crystallographic sites at the reactive surface with a probing depth of ~4.5 nm (~5 unit cells).

The mechanism and rate of heterogeneous electron transfer from Fe_{3-x}Ti_xO₄ nanoparticles, microparticles, and natural materials, isolated from Hanford nuclear reservation sediments, to Tc(VII) is investigated. Electron transfer at microbe-nanomaterial interfaces is characterized by examining the oxidation of Fe_{3-x}Ti_xO₄ nanoparticles by the bacterial electron transfer enzyme MtoA, a decaheme *c*-type cytochrome.

Cr isotope fractionation in reducing continental margin sediments

CHRISTOPHER R. PEARCE^{1*}, RACHAEL H. JAMES¹, IAN J. PARKINSON², DOUGLAS P. CONNELLY¹ AND HÉLÈNE PLANQUETTE³

¹National Oceanography Centre Southampton, European Way, Southampton, SO14 3ZH, UK.

²School of Earth Sciences, University of Bristol, Wills Memorial Building, Queens Road, Bristol, BS8 1RJ, UK.

³UMR 6539, LEMAR, Institut Universitaire Européen de la Mer, Place Nicolas Copernic, 29280 Plouzané, France.*
Corresponding author:((c.r.pearce@soton.ac.uk)

Sedimentary records of redox sensitive metals are commonly used to assess the availability of dissolved oxygen in seawater. However the interpretation of such records is complicated by the fact that metal concentrations can also be influenced by factors such as the detrital flux and primary productivity. Redox sensitive isotopic variations may therefore provide a more robust means of assessing seawater oxygenation. The chromium (Cr) isotope system has considerable promise in this regard as the reduction of soluble Cr(VI) to insoluble Cr(III) has been shown to be associated with resolvable isotopic fractionation [1]. Determining when and how Cr isotopes are fractionated in marine sediments will improve our understanding of the mechanisms that control Cr removal from seawater, and will provide a framework for interpreting redox-related variations in the δ⁵³Cr composition of seawater [2].

In order to evaluate the sensitivity of the Cr isotope system to variations in sedimentary conditions we present δ⁵³Cr data from continental margin sediments deposited under a range of redox settings. Oxic samples come from MANOP site H in the eastern Pacific Ocean, where a down core profile is used to assess the behaviour of δ⁵³Cr through the Mn reduction zone. Suboxic samples are analysed from sites along the Californian margin, while anoxic samples come from surface sediments deposited off the coast of Mexico. Previous characterisation of sediment properties at these localities enables variations in δ⁵³Cr to be compared to the behaviour of other redox sensitive metals such as molybdenum (Mo) and uranium (U) [e.g. 3, 4], and helps validate the utility of the Cr isotope system as a tracer of dissolved oxygen in seawater.

[1] Ellis *et al* (2002), *Science* **295**, 2060-2062. [2] Frei *et al* (2009), *Nature* **461**, 250-253. [3] Poulson-Brucker *et al* (2009), *G-Cubed* 10(6), Q06010. [4] McManus *et al* (2006), *GCA* **70**, 4643-4662.

SO₂ and O₂ co-injection with potential carbon storage target sandstone from a fresh-water aquifer.

J.K. PEARCE^{1,2*}, G. DAWSON^{1,2}, S. FARQUHAR²
AND S. GOLDING^{1,2}

¹Cooperative Research Center for Greenhouse Gas Technologies, Canberra, Australia.

²School of Earth Sciences, University of Queensland, Australia. Correspondence*: (j.pearce2@uq.edu.au.) (susan.farquhar@uqconnect.edu.au.) (G.Dawson@uq.edu.au, s.golding1@uq.edu.au.)

CO₂ and associated co-contaminant gases such as SO₂, NO_x, and O₂ are present in gas streams from coal fired power stations.[1] The cost of carbon capture and storage (CCS) may be reduced if CO₂ can be stored safely together with the co-contaminants.[2] Reservoir and sealing cap-rock samples from a potential carbon geosequestration site in the Surat Basin, Queensland, Australia, have been subjected to laboratory-scale experiments at simulated in situ CO₂ storage conditions. Water-rock-supercritical CO₂ reactions with co-injected SO₂ gas were performed and compared with pure CO₂ reactions on sister rock samples. Reactions with co-injection of SO₂ indicate heightened divalent cation release from carbonates and silicates (5 – 20 times the reactivity with pure CO₂) (Fig.1.) suggesting potential for enhanced long term mineral trapping of CO₂. Extensive surface corrosion of carbonates and silicates was also observed with the co-injection of SO₂ and a resulting pH of 2-3.

New experiments including the co-contaminant O₂ are expected to significantly stimulate redox reactions and will also be presented.

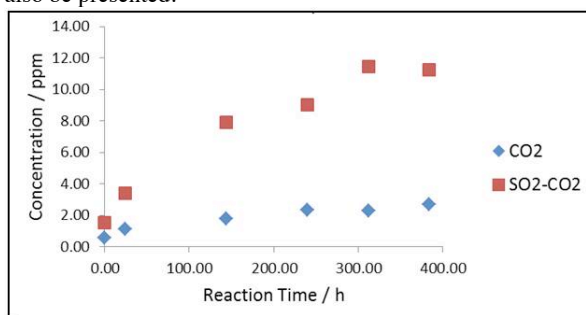


Fig.1: Enhanced evolution of dissolved iron in solution from reservoir rock with SO₂ co-injection (red squares) vs. pure CO₂ storage in situ conditions (blue diamonds).

[1] Xu *et al* (2007) *Chemical Geology* **242**, 319.[2] Glezakou *et al* (2012) *Geochimica et Cosmochimica Acta* **92**, 265.

Microstructural Constraints on Porosity Evolution During Carbonate Replacement Reactions

MARK A. PEARCE^{1*}, NICHOLAS E. TIMMS², ROBERT M. HOUGH¹ AND JAMES S. CLEVERLEY¹

¹CSIRO Earth Science and Resource Engineering, Australian Resources Research Centre, 26 Dick Perry Avenue, Kensington, WA 6151, Australia

²Department of Applied Geology, Curtin University, GPO Box U1987, Perth, WA 6845, Australia

*(correspondence: mark.pearce@csiro.au)

Volume change during formation and modification of carbonate minerals can lead to significant changes in rock porosity and permeability. In gold mineralising systems these reactions have the potential to enhance wall rock permeability leading to dissemination of gold away from the main fracture-derived fluid pathways. We present quantitative electron backscatter diffraction data combined with spatially referenced major and trace-element chemistry to investigate how porosity evolves during reactions that produce and modify carbonate minerals. Data are presented showing the chemically driven recrystallisation of large (several mm across) calcite grains to produce aggregates of iron-rich carbonate and dolomite. Recrystallisation of calcite by siderite occurs by nucleation of new grains that are in low energy crystallographic orientations with respect to the host, preferentially along pre-existing twin interfaces. Dolomite replaces calcite by nucleation on Fe-rich calcite domains in the host grains. Iron in the recrystallised carbonates is sourced from the breakdown large biotite and ilmenite grains (which now form fine grained polycrystalline aggregates as a result of carbonate metasomatism). Gold grains are found at the reaction interface between biotite (reactant) and muscovite (product). Further experimental data will allow kinetics of these reactions to be established, facilitating integration of these reactions with large-scale mineralisation models.

The hole story about laser ablation ICP-MS

N.J. PEARSON¹, W. J. POWELL¹, K.J. GRANT¹,
J.L. PAYNE², R.C. MURPHY¹, E. BELOUSOVA¹,
W.L. GRIFFIN¹, SUZANNE AND Y. O'REILLY¹

¹CCFS/GEMOC, Macquarie University, Sydney, Australia

²TRAX, University of Adelaide, Adelaide, Australia

(*correspondence: norman.pearson@mq.edu.au)

Down-hole laser-induced fractionation is one of the largest contributions to the uncertainty budget of LA-ICP-MS measurements of trace elements and isotope ratios. Efforts to improve the accuracy of analyses and to reduce the size of the uncertainty associated with laser-induced fractionation have been divided between developments in laser hardware and data reduction software. Advances in cell design have improved the quantitative transport of material from the ablation site to the ICP and contributed to increased sensitivity and reduced fractionation. Procedures involving rastering the laser or short acquisition times are also commonly adopted to minimize downhole fractionation, but these compromise spatial resolution and depth information. Linear [1], [2] and exponential [3] down-hole models are used in many data reduction software packages and reflect the basic fractionation response for a wide range of laser specifications and operating conditions. In the majority of models the fundamental assumption made is that matrix-matched standards and samples ablate similarly with consistent time-depth relationships [1]. However, further software advances are limited by our current understanding of the fundamental processes of ablation. Here we present the results of a study of the ablation characteristics of zircon using various combinations of laser wavelength, pulse-width, spot size and fluence, in conjunction with laser cell design (New Wave, HelEx) and gas composition and flow. The results are used to identify the optimum set of hardware parameters and operating conditions to maximise spatial resolution, and minimize ablation rate and U-Pb fractionation. A comparison will also be presented between the effects of mass response (instrument mass bias) of a quadrupole (Agilent 7700) and magnetic sector ICP-MS (Nu Attom) on time-dependent fractionation.

[1] Jackson *et al* (2004), *Chem. Geol.*, **211**, 47-69. [2] Kosler & Sylvester (2003), *Rev. Mineral. Geochem.*, **53**, 243-275. [3] Paton *et al* (2010), *Geochem. Geophys. Geosyst.*, **11**, Q0AA06.

Hydrogen isotope systematics of leaf wax *n*-alkanes in *Betula*, *Pinus*, and *Salix*: Spatio-temporal investigation

N. PEDENTCHOUK^{1*} AND Y. ELEY¹

¹School of Env. Sciences, University of East Anglia, Norwich, UK (*contact: n.pedentchouk@uea.ac.uk)

The use of D/H composition of *n*-alkyl lipids from leaf waxes as a palaeohydrological proxy depends on a thorough understanding of the factors that control D/H fractionation ($\epsilon_{l/w}$) between these compounds and the source water. The issue becomes particularly important when sedimentary organic compounds are sourced by only a few species with very different $\epsilon_{l/w}$ values. This project investigates the magnitude and mechanisms that control $\epsilon_{l/w}$ in several higher plant species that dominate Northern Eurasian forests and thus contribute a significant amount of biomass to soils and sediments in these ecosystems.

First, we measured the δD values of leaf wax *n*-alkanes from *Betula*, *Pinus*, and *Salix* as well as the δD values of tap water in 11 locations from the UK to central Siberia. Second, we measured the δD values of leaf wax *n*-alkanes and leaf water in the same species that were sampled in Norwich, UK throughout the growing season in April, May, July, and September.

The *n*-alkane δD values of the individual genera correlate very strongly with those of tap water along the transect from the UK to central Siberia – the R^2 values calculated for *Betula*, *Pinus*, and *Salix* are 0.95, 0.97, and 0.82, respectively. However, their $\epsilon_{l/w}$ values are characterized by consistent differences that are independent of the location along the transect: *Betula* *c.* -85‰, *Pinus* *c.* -120‰, *Salix* *c.* -140‰.

Our time-series $\epsilon_{l/w}$ data calculated from *n*-alkane and leaf water δD values of Norwich trees sampled from April to September show the same pattern among these genera. Even though the magnitudes of the differences among them are not as large as in the transect data, *Betula* $\epsilon_{l/w}$ values are consistently more positive than those of *Pinus* (by *c.* 5 to 20‰) and *Salix* (by *c.* 20 to 30‰).

Integration of our spatial and temporal δD data provides strong evidence that the processes that lead to the differences in the $\epsilon_{l/w}$ values are not limited to the physical processes that control source water δD . We hypothesize that D/H fractionation during leaf water photolysis and biosynthesis plays a major role in determining $\epsilon_{l/w}$ values in these plants. Our results suggest that leaf-wax-based palaeohydrological studies in northern forest ecosystems may require quantitative analysis of the amount of biomass sourced by common plants with very different $\epsilon_{l/w}$ values.

Volcanic CO₂ flux measurements by Tunable Diode Laser absorption Spectroscopy

M. PEDONE^{1*}, A. AIUPPA^{1,2}, G. GIUDICE², F. GRASSA²,
AND G. CHIODINI³

¹DiSTeM, Università di Palermo, via Archirafi, 36, Palermo 90123, Italy (*correspondence: pedone_maria@libero.it)

²Istituto Nazionale di Geofisica e Vulcanologia, Sezione di Palermo, via Ugo La Malfa, 153, Palermo 90146, Italy

³Istituto Nazionale di Geofisica e Vulcanologia, Osservatorio Vesuviano, via Diocleziano, 328, Napoli 80126, Italy

In the last decades, the use of near-infrared room-temperature diode lasers for gas sensing has grown significantly. The use of these devices, for instance in combination with optical fibers, is particularly convenient for volcanic monitoring applications [1,2]. Here, we report on the first results of the application of an open-path infrared tunable laser-based at Campi Flegrei (Southern Italy). Such Diode-laser-based measurements were performed, during two field campaigns (October 2012, and January 2013), in the attempt to obtain novel information on the current degassing unrest of Solfatara and Pisciarelli fumarolic fields.

At each site, we used an ad-hoc designed measurement geometry, using a TDLs (a Gas Finder unit) and several differently positioned retroreflectors (mirrors), to scan the fumaroles' plume from different angles and distances. From post-processing of the data (acquired at 1 Hz), we derived tomographic maps of CO₂ concentrations in the plume and, by integration and combination with plume transport speed (from video cameras), we inferred the CO₂ flux directly. The so-calculated fluxes, the first ever obtained at Campi Flegrei, average of ~500 tons/day, and support a significant contribution of fumaroles to the total CO₂ budget. The cumulative (fumarole [this study] +soil [3]) CO₂ output from Campi Flegrei is finally evaluated at 1600 tons/day.

[1] Gianfrani L. *et al* (2000). *Appl. Phys. B-Rapid Commun.* **70**, 467-470. [2] Richter D. *et al* (2002), *Optics and Lasers in Engineering*, Volume 37, Issues 2-3, Pages 171-186. [3] Chiodini G. *et al* (2010), *Journal of Geophysical Research*, Volume 115, B03205, doi:10.1029/2008JB006258.

Why was Rodinia underendowed? Comparing the effects of paleogeography versus lithosphere thickness on secular ore deposit preservation

SALLY PEHRSSON*, BRUCE EGLINGTON,
DAVID HUSTON, AND DAVID EVANS¹²³⁴

¹Geological Survey of Canada, Ottawa, Canada;

*correspondence:((pehrsson@nrcan.gc.ca)

²University of Saskatchewan, Saskatoon, Canada;
(bruce.eglington@usask.ca)

³Geoscience Australia, Canberra, Australia,
(David.Huston@ga.gov.au)

⁴Yale University, Connecticut, US, (dai.evans@yale.edu.)

An empirical observation from the Meso- to Neoproterozoic geologic record is that this period, spanning the assembly and tenure of the supercontinent Rodinia, is one of the least endowed in mineral deposits. This underendowment is puzzlingly at odds with models that suggest peaks in contraction-related deposit formation associated with the supercontinent cycle.

The current model suggests change in lithospheric thickness (more negatively buoyant with time) would result in a lack of preservation of deposits, due to enhanced uplift and erosion. With nearly 30% of VMS and Sedex deposits hosted in high grade terrains irrespective of lithospheric age, Rodinia's high grade belts still are underendowed, hence an alternative explanation must be sought.

New models for the transition from breakup of the Paleoproterozoic supercontinent Nuna to assembly of Rodinia highlight the influence of accretion style and paleogeography in deposit preservation. Rodinia extroverted, hence was dominated by subduction of old oceanic lithosphere and strong advancing accretion. This doomed preservation of its VMS deposits, which must accrete quickly to be preserved. Rodinia's long-lived, and latitudinally disposed, peripheral orogen setting, with limited back-arc development, meant that open ocean circulation was enhanced, further diminishing potential for VMS and lode gold deposits. Where Nuna evolved from interior to peripheral orogenic settings a similar deposit decline is observed, suggesting that ultimately paleogeography and style of accretion play a significant role in mineral deposit preservation. Hypothetically running geologic history forward in time suggests that the future supercontinent Amasia is destined to be another Rodinia.

Fe, Al and Ti variations in marine sediment: implications in provenance and paleoclimatic analyses

A. PEKETI AND A. MAZUMDAR

National Institute of oceanography, Dona Paula,
Goa-India 403004, (adipeketi@gmail.com)

Krishna-Godavari basin (K-G basin) is a pericratonic rift basin, formed during 130-134 Ma ago (lower cretaceous) as a consequence of rifting and subsequent drifting of India from the contiguous Antarctica–Australia land mass [1]. Krishna and Godavari are the major rivers that bring the sediment load to the K-G basin. 80% of the catchment area of Krishna river is occupied by Archean and younger crystalline rocks and the remaining 20% comprises of Tertiary Deccan traps (basaltic) and recent sediments [2]. The drainage basin of Godavari river includes Deccan traps (48%), Archean Granites (39%), Precambrian and Gondwana sedimentary rocks (11%) and recent alluvial cover (2%) [3]. Temporal variations in the Fe_T/Al ratio of a sediment core (MD161/8) from K-G basin indicate the relative contributions of terrestrial load from Deccan basalts and granitic rocks [4]. Good correlation ($r^2=0.673/0.74$) between Al/Ti and Fe/Ti suggest a common source and geochemical pathways for Fe_T and Al transportation and accumulation in the sediments [5]. Further studies (Sr-Nd isotope studies) are ongoing to quantify the relative contributions of Deccan basalts and Granitic rocks.

Variations in the Fe_{HR}/Fe_T (highly reactive iron/total iron) ratios normalized with respect to the source indicates the weathering/monsoon intensity. Fe_{HR}/Fe_T ratios are closely related to the runoff as high runoff results in increased content of poorly crystalline iron hydroxides/oxides in the suspended load which constitutes the Fe_{HR} content of the suspended particulates [6].

[1] Ramana *et al* (2001) *EPSL* **191**, 241-255. [2] Ramesh & Subramanian (1988) *JHyd* **98**, 53-65. [3] Biksham & Subramanian (1988) *JHyd* **85**, 515-524. [4] Peketi (2012) Ph.D thesis. [5] Latimer *et al* (2006) *Geology* **34**, 545. [6] Canfield (1997) *GCA* **61**, 3349-3365.

Experimental Evolution of Dissimilatory S Isotope Fractionation

ANDRÉ PELLERIN¹, NADIA MYKYTCZUK², REBECCA AUSTIN¹, GRANT M. ZANE³, LYLE WHYTE², JUDY D. WALL³, BOSWELL AND A. WING^{1,4}

¹Earth and Planetary Sciences, McGill University, Canada, (andre.pellerin@mail.mcgill.ca)

²Natural Resource Science, McGill University, Canada

³Biochemistry, University of Missouri, USA

⁴Weizmann Institute of Science, Israel

Sulfur isotope fractionation during microbial sulfate reduction is controlled by the energy metabolism of sulfate reducing microorganisms. While this metabolism responds to variability in the local environment, it is ultimately dependent on the underlying genotype. Since genotype and environment have both changed throughout Earth's history, the geological record of biogenic S isotopes reflects the influence of environmental and evolutionary change. However, the basic interplay between microbial evolution and S isotope fractionation has not been examined.

We investigated the evolutionary response of S isotope fractionation in *Desulfovibrio vulgaris* Hildenborough (DvH) and *Desulfomicrobium baculatum* (Dbac) through experimental evolution. Twelve replicate lines of DvH and three replicate lines of Dbac were serially transferred in batch cultures of defined media at 33°C. After 1000 generations, the descendant DvH strains were markedly more fit, with relative growth rates increasing by $\approx 20\%$. Fitness improvements were even more pronounced for descendant Dbac strains, with 300% enhancement in growth rates after only 200 generations. In both DvH and Dbac lines, the descendant strains have a clear selective advantage over their ancestors, and have undergone evolutionary adaptation to the constant environmental conditions of the experiment.

The ancestral cultures of DvH and Dbac produced sulfide depleted in $^{34}S/^{32}S$ relative to the sulfate of $-6.8\pm 1.0\text{‰}$ and $-15.4\pm 0.7\text{‰}$ respectively. When the assay was repeated on the evolved lines, Dbac reproducibly showed a lower $^{34}S/^{32}S$ fractionation of $-12.3\pm 0.4\text{‰}$ whereas DvH displayed the same fractionation as its ancestor. These observations suggest that evolutionary trajectory of S isotope fractionation correlates with the magnitude of evolutionary adaptation to a specific environment. As these evolutionary changes in the isotopic phenotype mimic, in a broad sense, known physiological responses of dissimilatory sulfate reducing bacteria, it may be possible to disentangle the metabolic and environmental histories imprinted in the S isotope record..

Sorption of Cobalt and Nickel by Biogenic Birnessite

JASQUELIN PEÑA^{1*}, ANNA A. SIMANOVA¹, JOHN R. BARGAR³, AND GARRISON SPOSITO²

(*correspondence: jasquelin.pena@unil.ch)

¹University of Lausanne, Switzerland, jasquelin.pena@unil.ch, (anna.simanova@unil.ch)

²Lawrence Berkeley National Laboratory, Berkeley, USA (gsposito@berkeley.edu)

³Stanford Synchrotron Radiation Lightsource, Menlo Park, USA, (bargar@slac.stanford.edu)

Birnessite minerals (layer-type MnO₂) produced by bacteria and fungi participate in important biogeochemical processes, particularly trace metal scavenging. Biogenic birnessite, which is enmeshed in a matrix of bacterial cells and extracellular polymeric substances (biomass), has nanoparticulate dimensions and significant structural disorder created by Mn(IV) vacancies. Trace metals tend to adsorb at vacancy sites or become incorporated into the MnO₂ sheet. Thus, the additional sorption sites presented to the solution by the biomass and the mineral particle edges may have a lower affinity for metals than the vacancy sites. In this study we use extended X-ray absorption fine structure (EXAFS) spectroscopy to investigate the mechanisms of Co and Ni sorption in slurries containing Co, Ni and Co + Ni at pH 6 to determine whether metal ions partition to non-vacancy binding sites in the presence of a competing metal. We expect that Co binds strongly to vacancy sites, out-competing Ni, and thus forcing Ni to bind to particle edges or biomass.

In Co-only and Co + Ni samples, we observed similar sorption mechanisms: significant incorporation of Co into the MnO₂ sheet as Co(III) and adsorption at vacancy sites as Co(II). In addition, the fraction of adsorbed Co(II) increased with surface loading. Time-resolved Co K-edge EXAFS spectra acquired from a biomass-free MnO₂ suspension (δ -MnO₂) suggest that adsorbed Co(II) precedes Co(III) incorporation. In contrast to Co sorption, Ni sorption in the Co+Ni samples differed significantly from the Ni-only samples [1]. In the presence of Co, Ni sorption at vacancy sites was markedly reduced, with Ni partitioning to the biomass and birnessite particle edges. Our results indicate that Co uptake into biogenic MnO₂ effectively reduces the proportion of vacancy sites available for Ni sorption, whereas Co uptake is not impacted by Ni sorption. This research is relevant to polluted environments where the attenuation and bioavailability of competing metals may be determined by their affinity to the available sorption sites.

[1] Pena, J., Kwon, K. D., Refson, K., Bargar, J. R., Sposito, G. (2010) *Geochim. Cosmochim. Acta* 74, 3076-3089.

The study on the solubility of the vanadium system focused on Panzhihua, China

Y. PENG^{1,2}, Y. ZENG^{1,2*}, J. J. LI¹, S. FENG^{1,2} AND X. D. YU¹

¹College of Materials and Chemistry & Chemical Engineering, Chengdu University of Technology, Chengdu, 610059, P. R. China;

²Mineral Resources Chemistry Key Laboratory of Sichuan Higher Education Institutions, Chengdu, 610059, P. R. China

(* correspondence: zengyster@gmail.com)

In recent years, the interest of the relationship between microelement and human health increased. Vanadium absence may have negative effects, and it also can be toxic if exposure occurs at high enough levels. It has strong transfer ability in environment. This ability related to the solubility of vanadium in soil solution.

Panzhihua, Sichuan is an important production base of vanadium and titanium magnetite. The vanadium storage is 64% of the total vanadium in China. The vanadium mining and smelting accelerated the vanadium diffusion in soil and water. It causes special environmental problems of vanadium in Panzhihua. Different surface soil in the region, the average mass fraction of vanadium is over 100×10^{-6} . [1] far exceeding the background values of Chinese soil vanadium 86×10^{-6} . [2] The amount of vanadium in the soil surrounding smelter is 16.5 times of contrast values. The amount of vanadium in the plant samples is 6.6 times of contrast values. [3]

The solubility of vanadium in soil solution is effected by coexisting ions in soil, such as potassium, sodium, phosphorus and so on. In order to investigate the relationship of solubility between vanadium and the other co-existing ion in soil, the phase equilibria of the quinary system $\text{NaVO}_3 + \text{KVO}_3 + \text{NaH}_2\text{PO}_4 + \text{KH}_2\text{PO}_4 + (\text{NH}_2)_2\text{CO} + \text{H}_2\text{O}$ and its five quaternary sub-systems were studied at 298 K with isothermal dissoluble method. According to the experimental results, the crystallization form of metavanadate is polyoxovanadate in the weakly acid system. The dissolution and migration of vanadium in aqueous solution has negative correlation with H_2PO_4^- and $(\text{NH}_2)_2\text{CO}$. The existing of K^+ has little effect on the solubility of vanadium. This suggest that in similar soil environment, the solubility of vanadium was restrained by the increase of H_2PO_4^- and $(\text{NH}_2)_2\text{CO}$, which can affect the transfer ability of vanadium.

The Research Fund from the Sichuan Provincial Education Department (11ZZ009).

[1] Teng, Tuo & Ni. (2003) *Chinese Journal of Geochemistry*, 22, 253-262. [2] Wei, Chen & Zheng. (1991) *Environmental Science*, 12, 12-19. [3] Wang & Wei. (1995) *Element Chemistry of Soil Environment*, 231-241.

Mineralogy and boron geochemistry of mud volcanoes from Northern Apennines (Italy)

MADDALENA PENNISI^{1*}, STEFANO BATTAGLIA¹
AND GIOVANNI MARTINELLI²

¹Istituto di Geoscienze e Georisorse, CNR, Via Moruzzi 1,
56124, Pisa, Italy (m.pennisi@igg.cnr.it)

²ARPA Emilia Romagna, Via Amendola 2, 42100, Reggio
Emilia, Italy

Mud volcanoes and associated waters of the Emilia-Romagna Apennines were sampled at Rivalta, Montegibbio, Regnano, Nirano, San Clemente and Bergullo localities and analysed for mineralogy and geochemistry. Mud consists of sandy and clayey silt, composed by quartz, calcite, dolomite, feldspar and phyllosilicates. The separated clay fraction (< 2 μm , about 20%) is represented by illite - smectite (I-S, 29 to 53%) and illite (I, 30 to 49%), with subordinate chlorite, smectite and kaolinite. Boron concentration varies in the range 100 - 400 $\mu\text{g/g}$ in mud samples, and 5 - 80 $\mu\text{g/ml}$ in waters. The mineralogical assemblage of the clay fraction is investigated together with the $\delta^{11}\text{B}$ signature of mud (5.3 to 13.2‰) and waters (17.8 to 43.1‰). These preliminary results allow to investigate: a) the variation of the $\delta^{11}\text{B}$ signature in mud samples as compared to the inverse correlation observed between I-S vs I; b) the relationship between the boron content and the mud - water isotopic fractionation.

Coupling mineralogical and geochemical data, this research was aimed to investigate the roots of the studied mud volcanoes within the Apennine sedimentary pile.

Energy Metabolism in Sulfate Reducing Bacteria

INÉS A. C. PEREIRA^{1*}, ANA RAQUEL RAMOS¹
AND SOFIA S. VENCESLAU¹

¹Instituto de Tecnologia Química e Biológica, Universidade
Nova de Lisboa, Oeiras, Portugal

(*correspondence: ipereira@itqb.unl.pt)

The metabolic pathway involved in dissimilatory sulfate reduction has long been known to involve the activation of sulfate by reaction with ATP to form adenosine-5'-phosphosulfate (APS) performed by the ATP sulfurylase, the reduction of APS to sulfite by the APS reductase (AprBA), and the reduction of sulfite to sulfide by the dissimilatory sulfite reductase (DsrAB). However, how this pathway is associated to energy conservation in sulfate reducing organisms (SRO) has not been clearly established. Our team has characterized several new membrane respiratory complexes from SRO, including the QmoABC and DsrMKJOP complexes involved in the electron transfer pathways to AprBA and DsrAB, respectively [1]. These two complexes are specific to sulfur-metabolizing organisms (sulfate/sulfite/organosulfonate reducers and sulfur oxidizers), and both have subunits that are closely related to subunits of the heterodisulfide reductases from methanogens. I will present recent results on the role of the QmoABC and DsrMKJOP complexes in sulfate reduction, and discuss possible mechanisms of energy conservation associated with both APS and sulfite reduction by the AprBA/QmoABC and DsrAB/DsrC/DsrMKJOP proteins, including an electron confurcation hypothesis involving menaquinone [2].

[1] Grein, Ramos, Venceslau & Pereira (2013) *Biochim Biophys Acta -Bioenergetics* 1827, 145-160. [2] Ramos, Keller, Wall & Pereira (2012) *Front. Microbiol.* 3:137 (open access)

Rocas Atoll, a promising site of climate oscillation record in the South Atlantic: ENSO event register in C and O-isotopes from corals

N.S. PEREIRA^{1,3*}, A.N. SIAL¹, R.K.P. KIKUCHI²,
AND V.P. FERREIRA¹

¹NEG-LABISE, Federal University of Pernambuco, Recife, 50670-000, Brazil (*correspondence: nspereira@uneb.br)

²RECOR, Institute of Geosciences, Federal University of Bahia, Salvador, 40210-340 Brazil

³LAGES, Bahia State University, Paulo Afonso, 48608-240, Brazil

Coral skeleton records isotope ratios, minor and trace element fluctuations as a response to environmental conditions while it grows in shallow tropical oceans. C- and O-isotope ratios from corals are extensively used as proxies to identify environmental factors in tropical shallow water. The Rocas Atoll is an isolated oceanic reef located in the western part of the South Atlantic and offers a great opportunity to investigate global and local phenomena. Being a pristine reef, as this atoll does not undergo terrestrial outputs, most chemical information from the Rocas Atoll corals portrays ocean-atmosphere interaction. Two colonies of *Porites sp.* (PC2 and PT2) were collected in tidal pools in this atoll. The colonies were cut in slabs and X-radiographed. Sclerochronology was done in scanned X-ray negative images using the software CoralXDS. C- and O-isotope analyses were done along the growth axis of each colony. Both *Porite* colonies display anomalous negative $\delta^{18}\text{O}$ (up to -1‰ over the mean value) and slightly positive $\delta^{13}\text{C}$ (up to +0.4‰, PC2 and +1‰, PT2 above the respective mean values). Sclerochronology indicated the anomalous values as coincident with the ENSO event of 2009/2010 that led to a coral bleaching event worldwide [1]. Also, a signal of endolithic algae bloom is imprinted in PC2 where anomalous values of $\delta^{18}\text{O}$ occurs. This is highly related to loss of zooxanthellae (coral bleaching) caused by stress events [2], in this case, probably a thermal stress, since $\delta^{18}\text{O}$ depletion points out to an increase of sea-surface temperature. The observed anomalous behavior of carbon and oxygen isotopes in this study makes the Rocas Atoll a promising place for monitoring major climate oscillation in the Tropical South Atlantic Ocean.

[1] Krishnan *et al* (2012) *Current Science*, **100**:111–117. [2] Hartmann *et al* (2010) *Coral Reefs* **29**:1079–1089.

Impact of organic acids and siderophores on dissolution of basaltic glasses in ultrapure water at 25°C and pH 6.3

ANNE PEREZ.¹, STÉPHANIE ROSSANO¹, NICOLAS TRCERA², DAVID HUGUENOT¹, ERIC VAN HULLEBUSCH¹, AURÉLIE VERNEY-CARON³ AND LOLA SARRASIN¹

¹Université Paris-Est, Laboratoire Géomatériaux et Environnement (EA 4508), UPEMLV, 77454 Marne-la-Vallée, France (anne.perez@univ-mlv.fr)

²Synchrotron Soleil, ligne Lucia, 91190 Gif-sur-Yvette, France

³Université Paris-Est Créteil Val de Marne, Laboratoire Interuniversitaire des Systèmes Atmosphériques (UMR CNRS 7583), UPEC, 94010 Créteil, France

Although microorganisms seem to play an important role in the alteration processes of basaltic glasses in solution, the elementary mechanisms leading to silicate phases alteration remain unclear as well as the respective role of organic acids, siderophores, water chemistry. In order to link the observed degradations to microbial activities or to the bulk solution properties, abiotic and biotic alteration experiments of synthetic basaltic glasses have been performed. Monolithic and powdered samples were placed in 40mL flasks of buffered solution (pH=6.3) containing additionally oxalic acid (0.01M), pyoverdine (Pvd), or microorganisms (the heterotrophic bacterial strain *Pseudomonas aeruginosa* was chosen) during various alteration times ranging from a few hours to 25 days. Elements release from the glass into the solution was measured by Inductive Coupled Plasma Optic Emission Spectroscopy analysis and their distribution was studied regarding the structure of the alteration layer with Scanning Electron Microscopy coupled to an Energy Dispersive X-Ray Detector. Oxalic acid and Pvd are both able to form water-soluble or -insoluble metallo-organic complexes. Organic acids and siderophores (two bioproducts from bacteria) have been shown to dissolve framework ions of several minerals 10 to 1000 times more readily than water does. Measuring their impact on dissolution in abiotic conditions without any secondary interactions between glass and bacteria allowed to quantify more precisely and for each bioproduct separately this improvement in terms of dissolution rates and to define how their presence can impact on dissolution mechanisms already established for ultrapure water. Finally, experiments involving bacteria allowed to complete those results in more complex systems and to identify the distinctive surface pattern of bioalteration.

Constraining the mineral and elemental composition of dust aerosol

C. PÉREZ,¹ R. MILLER¹, J.P. PERLWITZ
AND S. RODRÍGUEZ

¹NASA Goddard Institute For Space Studies, New York, USA,
(carlos.perezga@nasa.gov)

²Izaña Atmospheric Research Centre, Spain

The climate effect of soil dust aerosols depends upon the particle mineral composition. Dust radiative forcing is related to the presence of iron oxides like hematite. Structural iron within clays makes an additional contribution to marine productivity and carbon uptake. Here, we discuss how to constrain the regional distribution of various iron-bearing minerals using measurements of mineral and elemental composition along with information about soil weathering.

We present a prognostic model of aerosol mineral content, based upon previous work relating the soil fraction of each mineral to the soil type. The model is embedded with the NASA GISS Earth System Model and predicts the regional distribution of illite, kaolinite, smectite, calcite, quartz, feldspar, iron (hydr)oxide, and gypsum. Evaluation of the predicted mineral content is challenging because this quantity is infrequently measured. Elemental composition is more commonly available but does not uniquely constrain the mineral distribution, partly because the modeled minerals are only a subset of those contributing to observed elemental composition. We use mineral content and elemental composition within the same measured samples to derive a likely chemical composition for each modeled mineral. This can be applied to the model for comparison to the observed elemental composition.

An additional challenge is predicting the size distribution of each mineral at the time of emission. Previous work prescribes the mineral fraction in each of the soil clay and silt size categories. One challenge is that the clay and silt amount is biased by disturbance and disaggregation of larger particles during size characterization of soils. This leads to predictions of excessive structural iron within the clay size at the expense of aggregates in the silt size. We describe how sparse measurements of the mineral size distribution can be used to constrain the emitted size distribution.

The iron-bearing minerals are related to soil weathering that can be related to various measured quantities such as the Parker index. Using published soil measurements, we evaluate the representation of soil weathering in the model, which provides an independent constraint upon the iron-bearing minerals within the soil that are transported by the model.

Oxidation of Cu(I) in Seawater at Low Oxygen Concentrations

NORMA PÉREZ-ALMEIDA,
MELCHOR GONZÁLEZ-DÁVILA, J. MAGDALENA
SANTANA-CASIANO, ARIDANE G. GONZÁLEZ
AND MIGUEL SUÁREZ DE TANGIL

Departamento de Química, Universidad de Las Palmas de
Gran Canaria, Campus Universitario Tafira S/N, 35017,
Las Palmas, Spain. Email: (mperez@dqui.ulpgc.es)

The oxidation of nanomolar copper(I) at low oxygen ($6\mu\text{M}$) concentrations was studied as a function of pH (6.7–8.2), ionic strength (0.1–0.76 M), total inorganic carbon concentration (0.65–6.69 mM), and the added concentration of hydrogen peroxide, H_2O_2 (100–500 nM) over the initial 150 nM H_2O_2 concentration in the coastal seawater. The competitive effect between H_2O_2 and O_2 at low O_2 concentrations has been described. Both the oxidation of Cu(I) by oxygen and by H_2O_2 had a reaction order of one. The reduction of Cu(II) back to Cu(I) in the studied seawater by H_2O_2 and other reactive oxygen intermediates took place at both high and low O_2 concentrations. The effect of the pH on oxidation was more important at low oxygen concentrations, where $\delta \log k / \delta \text{pH}$ was 0.85, related to the presence of H_2O_2 in the initial seawater and its role in the redox chemistry of Cu species, than at oxygen saturation, where the value was 0.6. A kinetic model that considered the Cu speciation, major ion interactions, and the rate constants for the oxidation and reduction of Cu(I) and Cu(II) species, respectively, was applied. When the oxygen concentration was lower than 22 μM and under the presence of 150 nM H_2O_2 , the model showed that the oxidation of Cu(I) was controlled by its reaction with H_2O_2 . The effect of the pH on the oxidation rate of Cu(I) was explained by its influence on the oxidation of Cu(I) with O_2 and H_2O_2 , making the model valid for any low oxygen environment.

The role of groundwater in the formation of the giant nitrate deposits of Atacama: Iodine-129 and stable chromium isotopic evidence

A. PEREZ FODICH^{1*2}, F. ALVAREZ¹, G.T. SNYDER³,
R. SCHOENBERG⁴ AND M. REICH^{1,2}

¹Dept. of Geology, University of Chile, Santiago, Chile (*correspondence: aliperezfodich@gmail.com)

²Andean Geothermal Center of Excellence (CEGA), University of Chile, Santiago, Chile

³Dept. of Earth Science, Rice University, Houston, TX, USA

⁴Dept. of Geoscience, University of Tuebingen, Germany

The nitrate deposits of the hyperarid Atacama Desert are a complex mineral association of nitrates, chlorides, sulfates, perchlorates, iodates and chromates. Recent studies have focused mainly on the nitrate, sulfate and perchlorate components and despite the fact that the atmospheric influence is indeed recognized, the formation of these extensive deposits still remains highly controversial.

Here we focus on the so far poorly studied iodine and chromium components of nitrates, and we present the first iodine-129 (¹²⁹I) and stable chromium isotopic ($\delta^{53/52}\text{Cr}$) data for these deposits. Stable iodine in the nitrates is high (10's of ppm to >2000 ppm), exceeding the iodine content of the average continental crust by 3 to 4 orders of magnitude. Furthermore chromium is enriched in the nitrate deposits in its oxidized state Cr(VI), forming chromate minerals, a rare phase of chromium under natural and surficial conditions. Iodine isotopic ratios of nitrate samples are generally low ($^{129}\text{I}/^{127}\text{I} \sim 200\text{-}600$) and similar to deep marine sediment reservoirs and shales. Stable chromium isotopes of nitrates have positive and highly fractionated values ($\delta^{53/52}\text{Cr} \sim +1$ to $+3\text{‰}$), showing that the chromium signal is highly distinct compared to most chromium terrestrial reservoirs.

The isotopic signatures of iodine and chromium in the nitrates is consistent with a groundwater source rather than an atmospheric one. Therefore, and considering that: (i) low iodine-129 ratios are indicative of deep sedimentary sources and (ii) chromium data reveal significant redox-cycling, most probably related to groundwater transport, we suggest a genetic model where iodine, chromium and eventually other chemical components (e.g. part of the nitrate and sulfate) were sourced from Jurassic marine shales found upstream in the Precordillera. The formation of nitrate deposits would then be the result of a unique combination of multiple sourcing, groundwater transport processes, and wet and dry (atmospheric) deposition under conditions of increasing desiccation.

Isotopic fractionation of Cu in biofilms from a historic mining site

NATHALIE PÉREZ RODRÍGUEZ^{1*}, WOLFRAM ADLASSNING², ILIA RODUSHKIN³, LENA ALAKANGAS¹,
AND BJÖRN ÖHLANDER¹

¹Division of Geosciences and Environmental Engineering, Luleå University of Technology, Sweden. (nathalie.perez@ltu.se)

²Core Facility Cell Imaging and Ultrastructure Research, University of Vienna, Austria.

³ALS Laboratory Group, ALS Scandinavia, Luleå, Sweden.

The environmental development of historical mine sites offers a good opportunity to study the metal cycle processes within the system. One of those sites is the spoil heap area of Schwarzwand in Salzburg, Austria. In this location a constant bluish precipitation -composed of Cynaobacteria and secondary copper minerals- in the creeks is present. In this study, the Cu concentration and isotope composition ($\delta^{65}\text{Cu}$) in selected samples from biofilm, stream water and heap rocks from Schwarzwand was measured.

Results show a variability towards the heavier Cu isotope from rocks, to water to biofilm samples. An interesting observation is the fact that regardless the Cu concentration in the biofilm that ranges from 100 ppb to 5%, its isotopic signature remains constant, with values from 0.3435‰ to 0.6984‰. Contrary to the expected behaviour of bacterias to be a sink for the lighter Cu isotope [1], the biofilm has a heavier Cu isotope signature compared to the rock and stream water from the site. This biofilm comprises several species of *Phormidium* (Cyanobacteria) embedded in a matrix of organic polymers and detritus. This result implies that in a bulk result the processes that occur in the matrix such as mineral precipitation and adsorption can count in a larger extent to the total Cu isotope in the biofilm system. In addition, the presence of plants such as copper mosses (*Pohlia* spp.) in the biofilm can also isotopically fractionate the Cu available to the biofilm, as it has been seen before in plant systems [2].

The results shown can be of importance in the potencial use of such metal-tolerant biofilms for remediation purposes by pointing out the main processes that can cause a fractionation of metals such as Cu and Fe.

[1] Navarrete *et al* (2011) *Geochim. Cosmochim. Acta* **75**, 784-799. [2] Weinstein *et al* (2011) *Chem. Geol.* **286**, 266-271.

Hg isotope fractionation among atmospheric mercury species above a coastal suburban environment (Pensacola, Florida, USA)

VINCENT PERROT¹, VIRGINIA ELLER²,
WILLIAM, M. LANDING³ AND VINCENT SALTERS⁴

¹National High Magnetic Field Laboratory, Florida State University, Tallahassee, Florida, (perrot@magnet.fsu.edu)

²NHMFL, FSU, Tallahassee, Florida, (eller@magnet.fsu.edu)

³Department of Earth, Ocean and Atmospheric Science, FSU, Tallahassee, Florida, (wlanding@fsu.edu)

⁴NHMFL and Dept. EOAS, FSU, Tallahassee, Florida, (salters@magnet.fsu.edu)

Mercury is a pervasive global pollutant that bioaccumulates in aquatic food webs after being methylated in the anoxic zones of aquatic systems. Atmospheric deposition of Hg from local, regional and global is the main contributor to Hg in ecosystems. The fate of Hg in the atmosphere is controlled by multiple processes. We measured the Hg isotopic composition of gaseous elemental Hg (GEM, gold coated quartz sand traps), reactive gaseous Hg (RGM, KCl soaked quartz fiber filters, QFF) and particulate aerosol Hg (Hg_p, QFF) in the atmosphere above the coast near Pensacola, Florida, during summer 2012. 4 rain samples were also collected. Both mass-dependent (MDF) and mass-independent (MIF) signatures of GEM were significantly different than those of Hg(II) species. GEM, more than 99% of the total Hg at this site, displayed positive $\delta^{202}\text{Hg}$ (0.7 to 1.2‰) whereas both RGM and Hg(p) had negative $\delta^{202}\text{Hg}$ (-2.4 to -0.1‰). On the other hand, GEM (n=14) had slightly negative $\Delta^{199}\text{Hg}$ and $\Delta^{200}\text{Hg}$ average values $-0.26\pm 0.09\text{‰}$ and $-0.07\pm 0.03\text{‰}$, respectively, whereas Hg(p) (n=17) has slightly positive values ($0.33\pm 0.13\text{‰}$ and $0.10\pm 0.04\text{‰}$, respectively). RGM displays no significant MIF ($\Delta^{199}\text{Hg}=0.02\pm 0.14\text{‰}$ and $\Delta^{200}\text{Hg}=-0.02\pm 0.10\text{‰}$). We suggest, in agreement with previous studies, that both oxidation and reduction processes are responsible for the patterns in the isotopic composition of RGM and Hg(p). Preferential scavenging of RGM and Hg(p) (rather than GEM) in wet and dry deposition result in significant variability of the isotopic composition deposited in coastal environments due to seasonal and sporadic changes in air mass trajectories and atmospheric physico-chemistry.

Molecular properties of anion-mineral surface complexes probed with infrared desorption and temperature-excursion experiments

PER PERSSON^{1,2}

¹Centre for Environmental and Climate Research, Lund University, Sweden

²Department of Chemistry, Umeå University, Sweden (correspondence: per.persson@cec.lu.se)

Surface complexation theory provides a framework to conceptually describe molecular-level interactions at water-mineral interfaces [1]. Central to this theory is the formation of local molecular entities (surface complexes) with well-defined structures and compositions. Typically, under a given experimental condition several surface complexes co-exist and a challenge in this research is to determine the molecular properties of the individual species. We need this information to make connections between the properties of these species and their influence on, for instance, surface catalytic, dissolution, and redox processes. Previously, mixtures of surface complexes have been disentangled via pH and ionic strength dependence experiments, thereby exploiting differences in the stability of different protonation states and surface bonding interactions. Here we will introduce infrared desorption and temperature-excursion experiments and their potential to differentiate between and characterize anionic surface complexes. For a series of carboxylic acids we will show that differences in desorption rates separate protonated and deprotonated surface complexes. We will also show that the number of bonds between the carboxyls and the surface is the decisive factor determining desorption rates, and not so much the character of the bond i.e. whether these are inner sphere or hydrogen bonded structures. Infrared temperature-excursion experiments distinguish surface complexes based on their fundamental thermodynamic properties. We will show how this approach helps to shed light on the controversy surrounding surface complexes of sulfate.

[1]. Stumm W. (1992) *Chemistry of the Solid-Water Interface*. Wiley, Inc., New York.

The space and time complexity of chaotic mixing of silicate melts: implications for igneous petrology

PERUGINI D.¹, DE CAMPOS C.P.², ERTEL-INGRISCH W.²
AND DINGWELL D.B.²

¹Department of Earth Sciences, University of Perugia, Italy
(diegop@unipg.it)

²Department of Earth and Environmental Sciences, Ludwig-Maximilian-University, Germany

We present new experimental results on the study of the space and time modulation of compositional fields during chaotic mixing between mafic and felsic silicate melts. The experimental strategy was planned using numerical simulations performed using the experimental geometry. These mixing experiments were performed using a recently developed experimental apparatus, which is capable of mixing high-viscosity silicate melts at high temperatures and under precisely controlled conditions of fluid-dynamics and strain. The compositional variability produced by the mixing process was investigated both along linear analytical transects and on high-resolution 2D X-ray maps, covering the mixing patterns.

Our results indicate that chaotic flow fields represent very powerful dynamics to blend silicate melts, even under laminar fluid dynamic conditions (Reynolds number ca. 10^{-7}) and for dissimilar melts with high viscosity ratios (on the order of 10^3). The repetition of stretching and folding processes between the two melts induced a strong increase of contact interfaces thus favoring efficient chemical exchanges. As a result the initial mafic composition is no longer detectable in the mixing system after ca. 2 h (i.e. the duration of the experiment). A further important result is the observation of highly non-linear patterns in inter-elemental plots produced by the onset of diffusive fractionation processes. This is contrary to common thinking that magma mixing should always produce linear trends between pairs of chemical elements.

A new measure, the “concentration variance”, is proposed to quantify chemical element mobility during the mixing process. This measure is statistically robust and can be quantitatively used to measure chemical element mobility independently of the geometry in which the compositional variation (i.e. transects, areas, etc.) is embedded or the local strain history of the mingling.

Our results highlight concentration variance as a robust probe of the as yet poorly-understood processes involved in the common petrological process of magma mixing.

Concentration variance decay during magma mixing: a volcanic chronometer to measure magma ascent velocity during explosive eruptions

PERUGINI D.¹, DE CAMPOS C.P.² AND DINGWELL D.B.²

¹Department of Earth Sciences, University of Perugia, Italy
(diegop@unipg.it)

²Department of Earth and Environmental Sciences, Ludwig-Maximilian-University, Germany

The ability of chemical elements to diffuse in silicate melts controls the rates of crystal growth and dissolution kinetics, the rate of homogenization of compositional gradients generated by fractional crystallization and assimilation of country rocks as well as one of the most intriguing processes of all, magma mixing. In the context of mixing the time dependence of mass transfer processes constitutes a powerful tool to define geochemical clocks to estimate timescales of magma dynamics and eruption.

Here we aim to understand the timescale of chemical element mobility during mixing to define a chronometer to decipher the ascent velocity of magmas during explosive volcanic eruptions. The mixing process was induced experimentally using a high-temperature centrifuge apparatus under controlled thermal and rheological conditions.

Using this novel laboratory-based time-series experiments, we show that the Concentration Variance Decay (CVD, an inevitable consequence of magma mixing) is exponential with time and represents a powerful geochronometer to measure the time from mixing to eruption/quenching.

The mingling-to-eruption time of some explosive volcanic eruptions from Campi Flegrei (Italy) yield durations on the order of tens of minutes. These imply very rapid ascent velocities of 5-8 meters per second.

Application of the CVD geochronometer to the eruptive products may provide unprecedented information about transport of magmas in active volcanoes and could be decisive for the preparation of volcanic hazard mitigation during volcanic unrest.

Electrical conductivity of partially molten CI-chondritic mantle at high pressures

GIACOMO PESCE¹, GEETH MANTHILAKE²
AND DENIS ANDRAULT³

¹g.pesce@opgc.univ-bpclermont.fr

²g.manthilake@opgc.univ-bpclermont.fr

³d.andrault@opgc.univ-bpclermont.fr

In a primitive Earth scenario, large scale impacts are believed to be responsible of the formation of magma oceans. Such catastrophic events have produced a temperature increase above the mantle liquidus up to a few hundred kilometers depth or more. At present day, the Earth's mantle may also undergo small degree of partial melting at greater depths, but this time the temperature should be just above the solidus. Such partial melting is expected to produce major chemical segregation between the different Earth's reservoirs, which could affect the physical properties of the mantle.

Electrical conductivity is highly sensitive to the presence of melt, and it is one of useful tool to detect melting and its distribution within the mantle. Electrical conductivity of partially molten materials can be accurately determined at high pressures and temperatures using multi anvil apparatus. Our experimental goals are two folds. First, we aim at tracking the onset of melting *in situ* by using electrical conductivity. This will help not only to synthesize samples with well controlled degree of partial melting, but also to refine the sequence of crystallisation of a chondritic mantle for mantle depth up to ~700 km. Second, we aim at determining the effect of partial melting on electrical conductivity in a wide range of mantle pressures. It will therefore provide new clues to localize regions where mantle undergoes melting.

Our preliminary results on chondritic material at shallow mantle conditions (5 GPa) show that, at increasing temperature, electrical conductivity values increase considerably as soon as we reach the solidus temperature, indicating the onset of melting. Cross sections of the recovered samples were investigated using scanning electron microscope and electron microprobe. We aim at determining the solid-liquid phase relations at temperatures intermediate between solidus and liquidus and reconstruct the sequence of phase crystallization.

Water content of the oceanic lithosphere at Hawaii from FTIR analysis of peridotite xenoliths

ANNE H. PESLIER^{1,2} AND MICHAEL BIZIMIS³

¹Jacobs Technology, JETS, Houston, TX 77058, USA;

(anne.h.peslier@nasa.gov)

²NASA Johnson Space Center, Houston, TX 77058, USA

³Earth and Ocean Sciences, University of South Carolina, Columbia, SC 29208, USA; mbizimis@geol.sc.edu

Although water in the mantle is mostly present as trace H dissolved in minerals, it has a large influence on its melting and rheological properties. The water content of the continental mantle lithosphere is starting to be well constrained thanks to the abundance of mantle xenoliths [1,2], but that of the oceanic mantle lithosphere is mainly inferred from MORB glass data. Using Fourier transform infrared (FTIR) spectrometry, we determined the water content of olivine (Ol), clinopyroxene (Cpx) and orthopyroxene (Opx) in spinel peridotite xenoliths from Salt Lake Crater, Oahu, Hawaii, which are thought to represent fragments of the Pacific oceanic lithosphere that was refertilized by alkalic Hawaiian melts [3,4]. Only Ol exhibits H diffusion profiles, evidence of limited H loss during xenolith transport to the surface. Water concentrations (Ol: 9-28 ppm H₂O, Cpx: 246-566 ppm H₂O, Opx: 116-224 ppm H₂O) are within the range of those from continental settings [1,2] but are three times higher than those from Gakkel ridge abyssal peridotites [6]. The Opx H₂O contents are similar to those of abyssal peridotites from Atlantic ridge Leg 153 but ten times higher than those from Leg 209 [5].

The calculated bulk peridotite water contents (50 to 110 ppm H₂O) are in agreement with MORB mantle source water estimates [7] and lower than estimates for the source of Hawaiian rejuvenated volcanism (~525 ppm H₂O [8]). The water content of Cpx and most Opx correlates negatively with spinel Cr#, and positively with pyroxene Al and HREE contents. This is qualitatively consistent with the partitioning of H into the melt during partial melting, but the water contents are too high for the degree of melting these peridotites experienced. Melts in equilibrium with xenolith minerals have H₂O/Ce ratios similar to those of OIB [9].

[1] Peslier (2010) *JVGR* **197**, 239-258. [2] Peslier *et al* (2012) *GCA* **97**, 213-246. [3] Sen *et al* (1993) *EPSL* **119**, 53-69. [4] Bizimis *et al* (2007) *EPSL* **257**, 259-273. [5] Schmädicke *et al* (2011) *Lithos* **125**, 308-320. [6] Peslier *et al* (2007) *Goldschmidt*. [7] Dixon *et al* (1988) *EPSL* **90**, 87-104. [8] Dixon *et al* (1997) *JP* **38**, 911-939. [9] Dixon & Clague (2001) *JP* **42**, 627-634.

Tourmaline breakdown in high-grade metamorphic rocks from the Alamo Complex (Central Iberian Zone, Spain): Implications for evolution of boron during crustal anatexis

PESQUERA A.¹, TORRES-RUIZ J.², GIL-CRESPO P.P.¹
AND RODA-ROBLES E¹.

¹Departamento de Mineralogía-Petrología, Universidad del País Vasco, PO Box 644, E-48080 Bilbao, Spain

²Departamento de Mineralogía-Petrología, Universidad de Granada, Campus Fuentenueva, E-18002 Granada, Spain

The Alamo Complex comprises a set of structural-metamorphic domes alternating with low-grade metasedimentary rocks of Upper Proterozoic to Lower Cambrian age in the northern part of the Schist-Greywacke Complex (Central Iberian Zone). Tourmaline is a widespread mineral within the domes, which occurs in clastic metasedimentary rocks, tourmalinites, gneisses, migmatites, leucogranites and pegmatites. Tourmaline composition from metamorphic rocks, with $Mg/(Mg+Fe) = 0.35-0.73$ and $X/(X+Na) = 0.10-0.56$ ($X = X$ -site vacancy), as well as the bulk-rock B contents (generally < 100 ppm) do not show systematic variations with increasing metamorphic grade. Large tourmaline crystals occur in the transition from biotite-cordierite-sillimanite-plagioclase gneisses to migmatites. Generally tourmaline is scarce or absent in stromatic migmatites. It appears as subhedral crystals in leucosome layers associated with quartz, plagioclase and biotite. Textural evidence for breakdown of tourmaline is provided by the occurrence of crystals in melanosome domains displaying corroded edges and deep embayments. Boron liberated by destabilization of tourmaline would incorporate into associated melts and fluids and play a significant role in controlling the behaviour of boron during anatexis. Tourmaline-bearing leucogranite sheets and dikes can be found within the migmatite zone, suggesting a genetic relationship between leucogranites and migmatites. The high B contents of the leucogranites (up to 1.2% B₂O₃), in conjunction with the low B contents of the migmatites, suggest that anatexis was an open system process with significant circulation of B-rich fluids. These may have important implications on the melt generation and rheology of the rocks. The activity of B-rich fluids during metamorphism, anatexis and segregation of granitic melts would account for the multistage B-metasomatism that occurred in the Alamo complex during the Variscan orogen.

Geochemical and multiple sulfur isotope study on tap and river water quality in the Beijing urban area

MARC PETERS^{1*}, QINGJUN GUO^{1*}, HARALD STRAUSS²,
AND GUANGXU ZHU¹

¹Center for Environmental Remediation, Institute of Geographic Sciences and Natural Resources Research, Chinese Academy of Sciences, Beijing 100101, China (*correspondence: mpeters@igsrr.ac.cn, guojq@igsrr.ac.cn)

²Institut für Geologie und Paläontologie, Westfälische Wilhelms-Universität Münster, Corrensstrasse 24, 48149 Münster, Germany

Deterioration of tap and surface water quality in urban areas has become a major environmental concern worldwide. This study presents the first results of a pilot study on tap and river water in Beijing, China, using multiple sulfur isotopes ($\delta^{34}S_{SO_4}$, $\Delta^{33}S_{SO_4}$) in addition to a large number of physico-chemical and chemical parameters. The concentrations of most inorganic compounds (e.g. SO₄²⁻, NO₃⁻, As, heavy metals) analyzed for 59 tap water samples comply with the drinking water guideline limits as suggested by the WHO. In addition, the majority of 65 river water samples meet the national standards for surface water. However, NO₃⁻ shows concentrations between 50 and 97mg/L in 15.4% of the river water samples exceeding the maximum standard value of 44 mg/L. SO₄²⁻ concentrations are all below the guideline value of 250 mg/L for both tap and river water, although clearly higher compared to rivers in South China due to a drier climate with less precipitation coupled with urban pollution in the Beijing area. Similarly, $\delta^{34}S$ ranges from +6.4 to +15.4‰ for the vast majority of the tap and river water sulfates suggest urban sewage and chemical detergents as well as atmospheric deposition as the main sulfate sources in Beijing waters. $\Delta^{33}S$ values from -0.061 to -0.006‰ for tap water and between -0.061 and -0.017‰ for river water sulfate show no indication for microbial sulfur metabolism (e.g. sulfate reducers, sulfur disproportionators). In summary, the analyzed dissolved inorganic compounds in Beijing tap and river water do not cause a relevant decline in water quality. Forthcoming isotope data for NO₃⁻ ($\delta^{15}N$ and $\delta^{18}O$) and SO₄²⁻ ($\delta^{18}O$) will further strengthen the conclusions.

Acknowledgements: Financial support by the One Hundred Talents Program of the Chin. Acad. of Sciences, NSFC (No. 41250110528) and the fellowship for young international scientists program of the Chin. Acad. of Sciences.

^{184}Os - ^{180}W decay: a new chronometer in geocosmochemistry

STEFAN T.M. PETERS^{1,2*} CARSTEN MÜNKER^{1,2}
HARRY BECKER³ AND TONI SCHULZ⁴

¹Institut für Geologie und Mineralogie, Universität zu Köln, Germany (correspondence: *stefan.peters@uni-koeln.de)

²Steinmann-Institut, Universität Bonn, Germany

³Institut für Geologische Wissenschaften FU Berlin, Germany

⁴Dep of Lithospheric Research, Universität Wien, Austria

Alpha decay of ^{184}Os to ^{180}W has been theoretically predicted, but was previously not observed in particle counting experiments [1]. Sufficiently precise measurements to detect ^{184}Os -decay in natural materials have long been impossible due to the low abundance of ^{180}W (~0.12%). However, recent advances in ICP mass spectrometry have permitted measurements at precisions better than one part in 10,000, by which non-terrestrial abundances of ^{180}W in some iron meteorites could be resolved [2]. Here, we investigate whether these ^{180}W -anomalies can be explained by α -decay of ^{184}Os , by using combined ^{180}W and Os-W concentration measurements. Osmium and W concentrations were determined by isotope dilution in 11 iron meteorites and in one H5 ordinary chondrite (Pultusk). Tungsten isotope compositions were analysed on splits of the same samples by the Neptune multi-collector ICPMS at Cologne-Bonn (for details of the analytical procedure, see [3]). The abundances of ^{180}W in our samples correlate significantly with $^{184}\text{Os}/^{184}\text{W}$ ratios (MSWD = 1.3) with a slope of $m = 0.000295 \pm 0.000060$. We propose that this correlation represents a combined isochron for iron meteorites and ordinary chondrites (age: ~4.565 Ga). The slope of this isochron corresponds to a decay constant value for $\lambda^{184}\text{Os}(\alpha)$ of $6.46 \pm 1.34 \times 10^{-14} \text{ a}^{-1}$. The calculated half-life is $1.12 \pm 0.23 \times 10^{13}$ years. This value is in good agreement with theoretical predictions (e.g., [4,5]), and is only slightly lower than the minimum estimate from particle counting.

Importantly, the now confirmed ^{184}Os - ^{180}W decay system may constitute a viable new chronometer and tracer for geological processes that fractionate Os from W, such as core formation and silicate differentiation. This is illustrated by a measured ^{180}W -deficit in terrestrial basalts relative to chondrites by 1.16 ± 0.69 parts in 10,000, consistent with core formation ~4.5 Ga ago.

[1] Sperlein and Wolke (1976) *J. Inorg. Nucl. Chem.* **38**, 27-29. [2] Schulz et al (2012) *EPSL* **362**, 246-257. [3] Peters et al (2013) *LPI* 1719, 2073. [4] Medeiros et al (2006) *J. Phys. G: Nucl. Part. Phys* **32** B23 [5] Gangopadhyay (2009), *J. Phys. G: Nucl. Part. Phys.* **36**, 095105.

Deglacial change in terrestrial carbon storage estimated by benthic $\delta^{13}\text{C}$

C.D. PETERSON^{1*} AND L.E. LISIECKI¹

¹Department of Earth Science, University of California, Santa Barbara, CA, 93106-9630, USA (*correspondence: carlye@umail.ucsb.edu, lisiecki@geol.ucsb.edu)

Terrestrial carbon storage is dramatically decreased during glacial periods due to cold temperatures, increased aridity, and the presence of large ice sheets on land. Most of the carbon released by the terrestrial biosphere is stored in the glacial ocean, where the isotopic signature of terrestrial carbon ($\delta^{13}\text{C}$ terrestrial carbon = -25‰) is observed as a 0.32-0.7‰ depletion in benthic foraminiferal $\delta^{13}\text{C}$. The wide range in estimated $\delta^{13}\text{C}$ change is due to different subsets of benthic $\delta^{13}\text{C}$ data and different methods of weighting the mean $\delta^{13}\text{C}$ by volume. We estimate the glacial-interglacial $\delta^{13}\text{C}$ change of marine DIC using benthic *Cibicides* spp. $\delta^{13}\text{C}$ records from 486 core sites (seven to twelve times as many as previous studies). We divide the ocean into eight regions to generate linear regressions of regional $\delta^{13}\text{C}$ versus depth (0.5-5 km) for the late Holocene (0-6 ka) and Last Glacial Maximum (18-21 ka) and estimate a mean $\delta^{13}\text{C}$ decrease of 0.39 \pm 0.05‰ (2 σ). Assuming an isotope change of 0.04‰ in the surface ocean (0-0.5 km), we estimate a whole ocean $\delta^{13}\text{C}$ change of 0.33‰, equivalent to a terrestrial biosphere decrease of ~500 Pg C. If we account for uncertainty of \pm 0.05‰ in our deep ocean estimate and a range of 0.34‰ for possible surface changes, we estimate a terrestrial biosphere decrease of 360-600 Pg C. Our estimate is smaller than a vegetation reconstruction estimate of 750-1050 Pg C [1] and within the uncertainty range of a recent dynamic global vegetation model estimate of 550-694 Pg C [2]. Additionally, our estimate falls in the middle of previous whole ocean $\delta^{13}\text{C}$ estimates of 0.32‰ [3] and 0.46‰ [4].

[1] Crowley, (1995), *Global Biogeochemical Cycle*, **9**, 377-389. [2] Prentice et al, (2011), *New Phytologist*, **189**, 988-998. [3] Duplessy et al, (1988), *Paleoceanography*, **3**, 343-360. [4] Curry et al, (1988), *Paleoceanography*, **3**, 317-341.

Volatile Budget of the Galapagos Plume

M. PETERSON^{1*}, A. SAAL¹, E. HAURI², M. KURZ³,
R. WERNER⁴, F. HAUFF⁴, D. GEIST⁵ AND K. HARPP⁵

¹Brown University, Providence, RI, 02912, USA

(*correspondence: mary_peterson@brown.edu)

²DTM CIW, Washinton DC, 20015, USA

³WHOI, Woods Hole, MA, 02543, USA

⁴GEOMAR, Kiel, 24148, Germany

⁵University of Idaho, Moscow, ID, 83844, USA

The study of volatiles (H₂O, CO₂, F, S, and Cl) is important because volatiles influence melting and crystallization, as well as the rheology of the mantle. New volatile data obtained from 89 submarine glass chips collected from the Galapagos show variations between regional mantle sources forming the Galapagos Archipelago.

The concentration of volatiles can be affected by degassing, sulfide saturation, and assimilation of hydrothermally altered material. We use ratios between volatile and refractory elements that have similar incompatibilities to account for melting and crystal fractionation. Degassing has affected the concentration of CO₂ of the samples, but has had a minor impact on the concentration of H₂O, F, Cl and S. Our samples are sulfide undersaturated. Assimilation of hydrothermally altered material is assessed using Cl/K ratios and the magnitude of the Sr anomaly (Sr/Sr* > 1), which can indicate plagioclase assimilation. Samples depleted in trace elements (TE) have Cl/K ratios greater than the 0.01 expected for a depleted source. They also show a positive correlation between Sr/Sr* and volatile/refractory ratios, indicating assimilation has affected all of the volatile concentrations of these depleted samples. Intermediate to enriched TE samples have been less affected by contamination.

Within our sample suite there are 3 end-member compositions; a high ³He/⁴He group (>20*Ra), a TE-enriched group similar to Pinta Is., and a TE-depleted group. The S/Dy ratios for the sample suite cluster around a mean value of 220±41. Between the high ³He/⁴He group and the TE-enriched group, H₂O/Ce ranges from 160±33 to 146±28 and the F/Nd varies from 19±1 to 25±2 respectively. The H₂O/Ce ratios of TE-depleted samples are significantly contaminated, but the F/Nd ratio is 16±2. The high ³He/⁴He and TE-enriched samples are significantly degassed but the TE-depleted have CO₂/Nb ratios up to 400, slightly higher than expected for undegassed MORB. Uncontaminated Cl/K ratios are defined as the lowest ratios at a given TE enrichment (Nb/La). Our uncontaminated values are consistent with those previously reported for MORB and OIB.

U-Pb-Hf – isotopes of zircon from the eastern part of the Sveconorwegian Orogen, SW Sweden: Implications for the growth of Fennoscandia

ANDREAS PETERSSON¹, ANDERS SCHERSTÉN¹,
JENNY ANDERSSON² AND CHARLOTTE MÖLLER¹

¹Department of Geology, Lund University, Sölvegatan 12, SE-223 62 Lund, Sweden. (andreas.petersson@geol.lu.se;

anders.schersten@geol.lu.se; charlotte.moller@geol.lu.se)

²Geological Survey of Sweden, Box 670, SE-751 28 Uppsala, Sweden. (jenny.andersson@sgu.se)

Models for the growth of Fennoscandia, including the crust in the eastern part of the Sveconorwegian orogen, have largely been based on U-Pb data and do not discriminate between juvenile and reworked crust. These growth models also stand in contrast with current estimated reworking rates of the Palaeoproterozoic. The present comprehension of the growth of southwestern Fennoscandia involve ~330 million years of semi-continuous, subduction-related magmatism. We present new combined U-Pb and Hf isotopic data, from the Eastern Segment and the Idefjorden terrane of the Sveconorwegian Province, and suggest a revised model of crustal growth. Most of the crystalline basement in this part of the shield formed by mixing of a 2.1 to 1.9 Ga juvenile component and Archaean crust. Our combined U-Pb-Hf data reveal that Archaean reworking decreased between 1.9 and 1.7 Ga and a mixed Svecofennian crustal reservoir was generated. Succeeding magmatism between 1.7 and 1.4 Ga involved reworking of this reservoir with little or no crust generation. An influx of juvenile magma is recorded at c. 1.2 Ga by granite to quartz-syenite magmatism with mildly depleted (εHf_(1.18 Ga) of c. 3) signatures. The amount of recycled crust in the 1.9-1.7 Ga arc system as recorded by the U-Pb-Hf system is thus in contrast to previously proposed models for the growth of the southwestern part of the Fennoscandian Shield. Our data agree with the proposed long-term subduction along the western margin of Fennoscandia, but suggest substantial reworking of existing crust and minor amounts crustal growth after 1.9 Ga.

Mercury speciation in a historic Hg-mining and smelting area, Apuseni Mts., Romania

L. PETRESCU*¹, D. JIANU¹ AND C. MILU¹

¹Bucharest University, Faculty of Geology and Geophysics, Bucharest, Romania (*lucpet@geo.edu.ro)

Few published data exist on mercury content in mine waste dumps from Romania, although mercury contamination in soil is a problem found at many production (active and inactive) sites. The Izvorul Ampoiului abandoned mercury mine is connected with the Neogene vulcanite from the Apuseni Mts. Mercury generally appears in the form of cinnabar (HgS), though native Hg is also occasionally found. Hg mining has been active from the 16th century till 1968. During this period, Izvorul Ampoiului deposit constituting the first productive mine in Romania. An Hg ore smelter located close to the mine had been in operation from 1925 since 1968. The waste material from the mine and the roasting site was dumped in close vicinity of the mine. There is no exact information available on the total production, but in 1967 the plant were processed 18000 tons of ore with a content of 0.468% Hg and were extracted 8434 kg of Hg. A total of 32 minesoils was sampled from the top 15 cm. Concentration of total Hg was determined using an AMA-254 (LECO). In addition from the total Hg determinations, waste samples were also submitted to a sequential extraction procedure (i.e. Kingston method) to remove mobile Hg (leaching with 2% HCl+10% ethanol solution), semimobile Hg (leaching with 33% HNO₃ solution) and nonmobile Hg (leaching with 1:6:7 HCl:HNO₃:H₂O solution). The XRD analysis revealed that the sampled waste material consisted mainly of kaolinite, muscovite, calcite, quartz, halloysite and goethite. Presence of clay minerals and Fe-oxyhydroxides suggested relatively favourable conditions for Hg adsorption to the mineral surfaces. Hg associated with mineral surfaces may undergo methylation processes, and thus, may represent a potential long-term environmental risk. Mercury concentrations in the mine waste samples were highly variable. Total Hg concentrations vary from 3.7 to 27.85 ppm with a mean of 14.03 ppm. These concentrations exceeded the guideline value of 1.0 ppm established by the Romanian Legislation. The sequential extraction shows that the semimobile fraction yielded the highest concentration of Hg, being about 50–57% of total mercury. Contents in the non-mobile fraction were about 30%. Although mobile Hg fraction represents only ~10% of total Hg, this fraction contains the most available Hg, including methylmercury content, not to be overlooked. Subspeciation by solid phase extraction showed that the mobile organic Hg concentration is less significant (approximately 4%). Mobile organic mercury subfraction corresponds, according to the reference method, to the most toxic and bioavailable fraction. These data could not be confirmed with others since there are no existing data about organic mercury content in this area. Further investigations will be carried out in order to elucidate the factors affecting mercury mobility in surrounding soils.

Intrusion mechanisms of mafic plutons in the middle crust: Insights from the Permian Sondalo gabbroic complex (Central Alps)

B. PETRI^{1*}, M. MATEEVA¹, G. MOHN²,
G. MANATSCHAL¹, K. SCHULMANN^{1,3}
AND E. SKRZYPEK⁴

¹EOST, Université de Strasbourg, France (*Correspondance : bpetri@unistra.fr)

²Département Géosciences et Environnement, Université de Cergy-Pontoise, France

³Center for Lithospheric Research, Czech Geological Survey, Praha, Czech Republic

⁴Uniwersytet Wrocławski, Wrocław, Poland

Across Europe, Late-Carboniferous – Permian bimodal magmatism is one of the last manifestation of the Variscan orogenic cycle. Whereas acid magmatic bodies are mostly restricted to upper and middle crustal levels, mafic intrusions are emplaced through the entire continental crust. The reason for such shallow intrusion levels for basic magmas still remains enigmatic, as buoyancy shall not be the main driving force. In order to understand the emplacement of mafic magmas in rather uncommon levels (< 20km), we characterized the structure of the intrusion of the Sondalo gabbroic complex, exposed in the Austroalpine Campo unit (N-Italy).

Macroscopic foliations, anisotropy of magnetic susceptibility (AMS) data and lithological mapping allow to subdivide the pluton into three concentric areas. From the core composed of Ol-Gabbro to the dioritic rim, the mean magnetic susceptibility (Km) decreases from $1.43 \cdot 10^{-3}$ S.I. to $8.42 \cdot 10^{-4}$ S.I., and the mean anisotropy (P) from 1.073 to 1.044. These data reveal the existence of a vertical magnetic and magmatic foliation associated with a vertical magnetic lineation in the centre of the pluton composed of gabbro and Ol-bearing gabbro. The foliation is parallel to both the large granulite-facies metapelitic septa and the surrounding host-rock foliation. In contrary, the more dioritic external facies develops a moderately dipping magnetic fabric roughly parallel to the margins of the pluton.

Our data and field observations suggest that magma ascent was probably facilitated by the mechanical anisotropy provided by the steep fabric in the metapelitic host-rock. The assimilation of H₂O-rich melts derived from the surrounding metapelites also made the magma buoyant enough to reach shallower crustal levels.

Using CO₂ flux to constraint a 3D physical model of the Campi Flegrei caldera geothermal system

Z.PETRILLO^{1*}, G.CHIODINI¹, A.MANGIACAPRA¹, S.CALIRO¹; P. CAPUANO², G. RUSSO³, C. CARDELLINI⁴ AND R. AVINO¹

¹Istituto Nazionale di Geofisica e Vulcanologia, Osservatorio Vesuviano, Via Diocleziano 328, Napoli, Italy

(*correspondence: zaccaria.petrillo@ov.ingv.it)

²Università degli Studi di Salerno, Dipartimento di Fisica, Salerno, Italy

³Università degli Studi di Napoli Federico II, Dipartimento di Scienze Fisiche, Napoli, Italy

⁴Università di Perugia, Dipartimento di Scienze della Terra, Italy

Fluids release at depth has a primary role in generating volcanic unrest periods at Campi Flegrei (CF). According to [1] 5000 ton/day of a CO₂ - H₂O gas mixture is released in the Solfatara area (~1.4 km²). Heat flux associated to this degassing process was estimated to be ~100MW, representing the most important term in the energetic balance of the whole caldera. We have developed a 3D physical model of the CF geothermal system which accounts for the caldera rocks physical properties, bathymetry and water table topography. The new model, developed by using the TOUGH2 code simulator, was constrained by density values obtained by tomographic inversion of gravity data collected both onshore and offshore the caldera. Empirical relations between density and porosity and between porosity and permeability, derived by published data on samples cored in deep wells or collected in outcrops, allowed us to characterize the main rocks physical parameters controlling the dynamic of the CF geothermal system. We have investigated the effects of the injection at depth, in axis with Solfatara crater, of a hot gaseous mixture rich in CO₂ (5800 ton/day), according with the estimated mass flux released in the area through diffuse degassing. We show that the effects of the water table topography together with the bathymetry and the heterogeneous distribution of the rocks physical properties, lead to important differences in the hydrothermal circulation of fluids at CF. These constraints allow the activation of convective cells with different behaviour, which produce variable pattern of temperature inside the hydrothermal system. As a consequence, the predominant effect is again represented by a central plume below the Solfatara crater, but with a non-axisymmetric structure and a wider extension. Additionally, high temperature zones are present near the coastline and the in the middle part of the submerged area of the caldera with a SE-NW alignment.

[1] Chiodini *et al* (2001) *JGR* **106**, 16216-16221

Composition-dependent anisotropic interdiffusion tensor obtained from cation exchange between alkali feldspar and NaCl-KCl salt melt

E. PETRISHCHEVA, R. ABART AND A.-K. SCHAEFFER

University of Vienna, Department of Lithospheric Research, Vienna, Austria (elena.petrishcheva@univie.ac.at)

While homogeneous diffusion is fully described by a scalar diffusivity, diffusion in anisotropic crystals requires a tensor describing transport in each direction and correlations between different directions. Reconstruction of the scalar diffusion coefficient is an important inverse problem, which is addressed using backward integration of the concentration profile from a known solution of the diffusion equation. Moreover, by adjusting an experimental setup, even a composition-dependent diffusion coefficient can be reconstructed from the self-similar solution of the nonlinear diffusion equation.

We demonstrate that this method can be naturally generalized for an anisotropic system. The generalization is then applied to quantify the full composition-dependent anisotropic diffusion tensor for Na-K interdiffusion in alkali feldspar. Composition profiles obtained from cation exchange at 850°C and 1 bar between oriented cylinders and plates of sanidine with $X_{Or} = 0.84$ and a KCl salt melt show a plateau of compositions in equilibrium with the salt melt at the crystal surfaces separated from the unaffected interior regions of the crystals by a transition zone that is sharp in the *b*-direction and comparatively shallow in all directions lying in the *a-c* plane. Given that a 40 fold molar excess of alkali cations in the salt mixture relative to the feldspar was applied, the composition of the salt remained essentially constant during cation exchange. The presence of an inflection point in the composition profiles can thus only be explained by a composition dependent Na-K interdiffusion coefficient.

For 850°C we show that the Na-K interdiffusion coefficient is by a factor of about 10 larger in the *a-c* plane than in *b*-direction. There is only a weak composition dependence in the range $0.86 < X_{Or} < 0.95$. Only at $X_{Or} > 0.95$ the interdiffusion coefficient increases by about a factor of 10. These results were thoroughly tested by obtaining numerical solutions of the nonlinear diffusion equation with the reconstructed diffusion tensor and the initial conditions describing the experimental setup. Thereafter the numerical results were compared with the actually observed concentration profiles. Good agreement was found.

Mixing, mingling and enclave crumbling in the post-Minoan dacitic magmas of Santorini volcano, Greece

PETRONE CHIARA MARIA^{*1}, FRANCALANCI LORELLA²,
AND VOUGIOKALAKIS GEORGIOS E.³

¹The Natural History Museum, Dept. Earth Sciences,
Cromwell Road, SW7 5BD London, UK,
(*correspondence: C.Petrone@nhm.ac.uk)

²Dipt. Scienze Terra, Università degli Studi di Firenze, Italy

³I.G.M.E., 3rd Entrance Olympic Village, Athens, Greece

The post-caldera islets of Palea- and Nea-Kameni formed as a result of nine eruptive events from A.D. 46-47 to 1950 in the center of the Santorini Minoan caldera. The erupted products are represented by dacitic lava flows and domes hosting basaltic to andesitic mafic enclaves. Dacitic rocks have low porphyritic index that increases with time, whereas their degree of evolution decreases pointing to the composition of the mafic enclaves. Enstatite contents of pyroxene and anorthite contents of plagioclase decrease from mafic enclaves to host lavas. Sr isotopes systematically increase with time and toward the less evolved composition of lavas and mafic enclaves, whereas Nd isotopes decrease. Whole rocks and mineral separates of mafic enclaves from the younger events are more Sr-radiogenic than their host lavas, the opposite occurs in the A.D. 46-47 lavas and enclaves.

Mixing and mingling processes between dacitic and mafic magmas, along with crumbling of the mafic enclaves in the host lavas are responsible for the observed textural and geochemical characteristics of the dacitic host lavas. The variations of Sr-Nd isotopes with time in the enclave magmas seem to indicate assimilation of limestone from the basement by the most mafic magmas; this process is associated to new mafic magma inputs and femic phase crystallization. A shallow layered reservoir with dacitic magmas overlaying lower mafic magmas is supported by our data. Crystal fractionation and cumulitic processes affect the lower part of the plumbing system allowing further layering of the mafic magmas, generating the variable and complex textures shown by the mafic enclaves. Different portions of the layered reservoir were frequently and variably sampled during time, as testified by variable types, compositions and distributions of mafic enclaves in the different eruptions. All this allows us to suggest periodic arrivals of mafic magmas in the post-Minoan plumbing system of Santorini, also implying for a still active magmatic system whose behaviour needs to be fully evaluated, also in the light of the 2011-2012 unrest.

A novel 2D LA-ICP-MS data analysis and visualization solution

JOSEPH A. PETRUS^{1*} AND BALZ S. KAMBER²

¹Laurentian University, Department of Earth Sciences,
Sudbury, Ontario, Canada (*correspondence:
jpetrus@laurentian.ca)

²Trinity College Dublin, Department of Geology, Dublin,
Ireland, (kamberbs@tcd.ie)

Microscale mapping of geochemical data, both isotopic and trace elemental in nature, by LA-ICP-MS has become tremendously popular in recent years [1]. Typically, such maps are produced by continuously analyzing the elements of interest while rastering a laser over an area and periodically monitoring gas blanks and standards. In order to properly interpret the resulting data, sophisticated processing, visualization and analyses are usually required. Although software packages exist to help with the aforementioned tasks [2,3,4], they tend to emphasize data processing and visualization, but quantitative analysis remains difficult.

Here we report the capabilities of a new LA-ICP-MS mapping tool that focuses on visualization and analysis by leveraging Iolite's [2] extensive data processing capabilities. It is written in Python and makes use of the matplotlib plotting library to produce publication quality figures. The key features include map-wide multi-phase internal standard corrections, extracting traverses, integrating arbitrarily shaped two-dimensional regions, and inspecting regions on the map *via* standard diagrams (*e.g.*, concordia or REE). Furthermore, the package can be integrated with Iolite to provide a convenient workflow.

Examples of zoned igneous phenocrysts from historic lava flows, zoned Precambrian pyrite of a sulfur reducing bacteria origin, reaction textures in spinel peridotite, and complex zircon will be provided to demonstrate the functionality and strengths of this new mapping tool.

- [1] Woodhead *et al* (2007) *Geost. Geoanal. Res.* **31**, 331-343.
[2] Paton *et al* (2011) *J. Anal. At. Spectrom.* **26**, 2508-2518.
[3] Paul *et al* (2012) *J. Anal. At. Spectrom.* **27**, 700-706. [4] Rittner & Müller (2012) *Computers & Geosciences* **42**, 152-161.

The influence of functional groups on organic aerosol hygroscopicity

M. D. PETTERS¹, S. R. SUDA¹, G. YEH², A. MATSUNAGA²,
C. STROLLO², P. J. ZIEMMANN²
AND S. M. KREIDENWEIS³

¹Department of Marine Earth and Atmospheric Sciences,
North Carolina State University, Campus Box 8208,
Raleigh, NC

²Air Pollution Research Center, University of California,
Riverside, CA 92521-0001, USA.

³Department of Atmospheric Science, Colorado State
University, Fort Collins, CO 80523-1371, USA.

Organic aerosols in the atmosphere are composed of a wide variety of species, reflecting the multitude of sources and growth processes of these particles. Especially challenging is predicting how these particles may act as cloud condensation nuclei (CCN). Köhler theory relates the particle's dry diameter to its critical supersaturation. A hygroscopicity parameter, kappa, parameterizes this relationship in terms of the particle's chemical composition. Previous studies have characterized kappa values for a range of organic model compounds. Here we extend these studies by designing new model systems that allow systematic investigation of the influence of the number and location of particular functional groups on the organic aerosols' kappa value. Organic compounds were synthesized via gas-phase and liquid-phase reactions. Aerosol products from gas-phase reactions were collected on filters, extracted using ethyl acetate, and fractionated by reversed-phase high-performance liquid chromatography using gradient elution with acetonitrile and water. The eluate was atomized, the solvent was removed by evaporation, and the residual aerosol particles were analyzed as a function of retention time using high-resolution scanning flow CCN analysis. Individual organic compounds eluting from the synthesized mixture were identified using thermal desorption particle beam mass spectrometry. These experiments yielded changes in kappa that can be attributed to the addition of one or more hydroxyl, nitrate, carboxyl, aldehyde, hydroperoxide, and methylene functional groups while otherwise maintaining the structure of the organic molecule. Our results show that the addition of hydroxyl and carboxyl groups can significantly increase a particle's kappa value, while the addition of hydroperoxide, nitrate, and methylene groups does not. We anticipate that our results contribute to a mechanistic understanding of chemical aging and will help to guide input and parameterization choices in models that rely on simplified treatments such as the atomic oxygen-to-carbon ratio to predict the evolution of organic aerosol hygroscopicity.

LA-ICP-MS: a success story of in-situ element & isotope ratio analysis

T. PETTKE

University of Bern, Institute of Geological Sciences, CH-3012
Bern, Switzerland (pettke@geo.unibe.ch)

LA-ICP-MS has become the method of choice for in-situ trace element analysis, recently expanding into applications traditionally dominated by other analytical techniques. In its beginning ~30 years ago [1], fundamental problems arising from poorly controlled LA of material to element ionization from dry particles orders of magnitude larger than dried liquid aerosol to sensitive and representative transient signal recording dominated research initiatives (Longerich and co-workers [2]). High-UV LA combined with MS detection has since become the preferred instrumental combination [3].

And where are we today? Studies on technical parameters have greatly improved our understanding of fundamental processes occurring at various sites in the instrumentation. Hand in hand goes prominent progress achieved in "fitting LA-ICP-MS for purpose", by developing new or significantly refining analytical protocols. However, praised seminal instrumental developments have not resulted in quantum leaps; hence, neither LA-ICP-MS analytical protocols nor instrumentations have changed radically in the past decade.

This contribution outlines the interplay between fundamental instrumental parameters for successful LA-ICP-MS measurement of element concentration and isotope ratio data and addresses components critical to analytical accuracy, including calibration materials [4]. Emphasis will be put on the quantification of the bulk composition of phase mixtures (e.g., fluid inclusions [5,6]) for which LA-ICP-MS is the undisputed analytical instrument of choice. Precise and accurate isotope ratio and radiometric age determinations are now feasible from ever decreasing sample amounts, emphasizing the relevance of analytical sensitivity.

Common perception is that instrumental possibilities (e.g., sensitivities, resolution in space and time, signal detection, element and isotope ratio fractionation) dictate the progress in LA-ICP-MS applications. However, no modern equipment can compensate for lack of sound instrumental and geoscientific understanding of how to employ LA-ICP-MS for solving analytical problems.

[1] Gray (1985) *Analyst* **110**, 551-556. [2] Jackson *et al* (1992) *Can. Min.* **30**, 1049-1064. [3] Günther *et al* (1997) *JAAS* **12**, 939-944. [4] Eggins & Shelley (2002), *Geostand. Newsletter* **26**, 269-286. [5] Günther *et al* (1998) *JAAS* **13**, 263-270. [6] Heinrich *et al* (2003) *GCA* **67**, 3473-3497.

Mapping soil carbon from cradle to grave: C transformations from roots to organo-mineral associations

JENNIFER PETT-RIDGE^{1*}, MARCO KEILUWEIT^{1,2},
SHENGING SHI³, ERIN NUCCIO³, JEREMY BOUGOURE¹,
PETER K. WEBER¹, EOIN BRODIE⁴, XAVIER MAYALI¹,
MARKUS KLEBER², PETER S. NICO⁴
AND MARY FIRESTONE³

¹Chemical Sciences Division, Lawrence Livermore National Laboratory, 7000 East Avenue, Livermore CA 94550

²Crop and Soil Science, Oregon State University, Corvallis, OR 97331

³Environmental Science, Policy and Management, University of California, Berkeley, CA 94702

⁴Earth Sciences Division, Lawrence Berkeley Laboratory, One Cyclotron Rd, Berkeley CA 94720

Carbon cycling in the rhizosphere is a nexus of biophysical interactions between plant roots, microorganisms, and the soil organo-mineral matrix. Plant roots provide 30-40% of soil organic C inputs, accelerate the rate of organic matter mineralization by ~10X, and support an active microhabitat for microbial transformation of soil C. Our research on how roots influence decomposition of soil organic matter in both simplified and complex microcosms uses geochemical characterization, molecular microbiology, isotope tracing, metabolomics and novel imaging approaches ('ChipSIP' and 'STXM-SIMS') to trace the fate of isotopically labelled root exudates and plant tissues. Our work in synthetic rhizospheres suggests root exudates drive O₂ limitation, alter metal chemistry and mineralogy, and influence the availability of SOM. Using a combination of X-ray spectromicroscopy and NanoSIMS, we have imaged the deconstruction of ¹³C/¹⁵N-labeled ligno-cellulose in model plant cells *in situ*, and mapped associations of plant cell-derived decomposition products with specific soil minerals. In the more complex rhizospheres surrounding roots of the annual grass *Avena fatua*, the microbial community undergoes a compositional succession as the plant grows, senesces, and dies. We have developed an isotope array that allows us to follow root C into bacterial, fungal, and microfaunal communities. The presence of root detritus significantly alters the soil microbial community over short time spans, leading to a higher proportion of eukaryotic microbes and Bacteroidetes. Finally, we have characterized the molecular cocktail of compounds exuded by *Avena* roots, and showed that increased belowground C allocation and root biomass driven by elevated CO₂ correspond to a greater amount of root-derived ¹³C in the 'heavy' soil fraction, commonly assumed to reflect longer term stabilization.

CO₂ mineralization in percolated olivine-rich rocks: Control of olivine crystallographic orientation and fluid flux

S. PEUBLE^{1,*}, M. ANDREANI², M. GODARD¹, B. VAN DE MOORTELE² AND P. GOUZE¹

¹Géosciences, CNRS-Université Montpellier 2, France

*(peuble@gm.univ-montp2.fr)

²Laboratoire de Géologie de Lyon, France

In situ carbonation of ultramafic rocks is potentially an effective means for mitigating atmospheric CO₂ concentrations. CO₂ mineralization reactions in sub-surface conditions are controlled by the coupling of flow and transport processes and of chemical reactions occurring at the mineral-fluid interfaces. To better understand the roles of the structure of rocks and of fluid fluxes on the reactivity of ultramafic systems, we performed a reactive percolation experiment using a sintered olivine core (ø 6.35 mm × L 13 mm) in which CO₂-rich fluid was injected at P-T conditions similar to that expected for *in situ* storage. The sample was then characterized by EBSD and FIB-TEM.

EBSD analyses indicate a weak crystal preferred orientation (CPO) of the olivine (ol) aggregate resulting from sintering, with [010]_{ol} parallel to the axis of cylinder. We observe the development of a dense network of microcracks parallel to (100)_{ol}. Symmetrical etch pits indicating olivine dissolution are observed on (010)_{ol} surfaces. Two reaction products were identified: dolomite (dol) and magnesite (mgn). EBSD analyses revealed a statistical relationship between the olivine fabric and the direction of carbonate (carb) growth, marked by (10-14)_{carb}: (10-14)_{mgn} is parallel to (001)_{ol} and (10-14)_{dol} is parallel to (100)_{ol}. FIB-TEM analyses indicate however that carbonate growth is non-topotactic.

At all scales, [10-14]_{carb} is systematically oriented parallel to the main direction of fluid flow. In our sample, sintering induced the localization of (001)_{ol} and (100)_{ol} and the development of microcracks parallel to the cylinder axis, which is also parallel to the main direction of fluid fluxes. As a consequence, fluid fluxes and chemical transport were promoted and the olivine-fluid surface area was larger in that direction compared to that perpendicular to fluid fluxes. In turn, these conditions facilitated the development of local concentration gradients and the growth of carbonates at the olivine surface, where local fluid velocity tends toward zero, thus explaining that (10-14)_{carb} is statistically parallel to (001)_{ol} and (100)_{ol}.

Our results suggest that carbonate growth is controlled by the hydrodynamic conditions rather than by the olivine CPO during *in situ* carbonation of ultramafic rocks.

Crustal evolution determines seawater Sr and Nd isotope records

BERNHARD PEUCKER-EHRENBRINK¹

¹Woods Hole Oceanographic Institution, Woods Hole, MS 25, MA 02543, USA, (behrenbrink@whoi.edu)

Radiogenic isotope ratios record time-integrated parent-daughter ratios, and are thus sensitive to the chemical composition and time. The oceans receive the integrated runoff from the continental surface and preserve these signals in marine sedimentary records. Radiogenic isotope records of seawater and marine sediments have been reconstructed over the past five decades for many of the radiogenic isotope systems. For some systems (Sr) excellent records do exist that integrate seawater signals for the entire ocean, whereas global records of radiogenic isotopes with short marine residence times are much more difficult to establish (Nd, Pb).

Here, I attempt to link long-term (Phanerozoic) records of marine radiogenic isotope systems to records of the evolution of the continental surface that interacts with the hydrologic cycle. For the present we can show that the dissolved and particulate loads from the continents integrate different portions of the continental surface (Peucker-Ehrenbrink *et al.*, 2010). For instance, the areas generating dissolved loads are characterized by significantly older bedrock (~400 Myr) than those generating particulate loads (~320 Myr), with both being younger than the mean bedrock age of the non-glaciated, exorheic portion of the continental surface (~450 Myr). This age bias reflects the disproportionate role active margins and high-standing ocean island play in exporting sediment to the oceans.

Using present-day systematics as a guide, I argue that the first-order trough-like shape of the Phanerozoic marine Sr isotope record reflects the rejuvenation of the continental surface involved in exporting Sr to the ocean from the early Phanerozoic to the mid Jurassic that is followed by an "aging" that continues into the Quaternary. This long-term evolution of the continental surface is mirrored by a similar, though much less well-constrained, record of rejuvenation affecting areas involved in exporting Nd to the oceans. As Nd export to the ocean is overwhelmingly tied to export of the detrital load to the ocean, the first-order co-evolution of both records is suggestive of underlying trends in the evolution of the continental surface that connects the terrestrial hydrologic cycle with the oceans.

Peucker-Ehrenbrink *et al.* (2010), *G-cubed* 11 (3), Q03016, doi: 10.1029/2009GC002869.

Fertile magmatism in a changing compression and extension regime on the Central Balkan Peninsula

I. PEYCTHEVA^{1,2}, ST. GEORGIEV¹, V. GROZDEV¹, P. MARCHEV¹ AND A. VON QUADT²

¹Geological institute, BAS, Sofia, peyctheva@erdw.ethz.ch

²IGP, ETH-Zurich, (quadt@erdw.ethz.ch)

The Balkan Peninsula is one of Europe's mineralized regions with world-class ore deposits. Numerous Cu-(Au-Mo) porphyry and Au-(Cu) epithermal deposits are formed during the oblique Late Cretaceous northward subduction of the Tethys beneath the European continent and the Palaeogene postcollisional extension. Integrated U-Pb zircon, Sr-Nd-Hf isotope and geochemical analyses on Palaeogene rocks in W Bulgaria, SE Serbia and eastern FYR Macedonia aim to constrain the temporal and tectono-magmatic evolution of the region that favour significant ore-formation.

After the cease of the subduction at ~70 Ma and the accretion of the Morava-Rhodope/Getic units the region is marked by a collision/compression and break of magmatism till ~60 Ma when rift-like alkaline basalts in eastern Serbia formed. Their trace-element and isotope signature define a depleted source, similar to the European Asthenospheric Reservoir (Cvetkovic *et al.*, 2004). It is followed by Na-calc-alkaline rhyolites at ~45 Ma, displaying typical adakitic signature. Sr-Nd whole rock and Hf-zircon isotope data define a mantle dominated source ($^{87}\text{Sr}/^{86}\text{Sr}_{(i)}$ 0.7047-0.7051; ϵNd between -0.2 and +2.4; ϵHf -zircons of +4 to +10). Eocene adakite-like magmatic rocks can be traced further to S-SE in the Rhodopes and to Turkey, and are likely related to subduction-enriched lithospheric mantle but asthenospheric OIB-like mantle source could be an alternative option.

The Cenozoic magmatism in W-SW Bulgaria and E Macedonia changed to normal crustal-dominated granitic composition (33-30 Ma, $^{87}\text{Sr}/^{86}\text{Sr}_{(i)}$ 0.709-0.716; ϵNd -6 and -10; ϵHf -zircons -2 to -8), but was more mantle influenced in Surdulitsa (SE Serbia) at 34 Ma. The magmatism migrated further to SW and show magmatic ages at 29-24 Ma in Kratovo-Zletovo and the Buchim-Borov dol. Less radiogenic strontium ratios 0.7060 and slightly negative ϵNd -2.6 to -3.1 define an increase of mantle input from a subduction-enriched mantle lithosphere.

Tectonic reconstructions suggest a repeated change of compression/collision and extension episodes that were plausible for the generation of fertile magmatism. The latter reveal signature of subduction-enriched mantle source but magma composition was additionally crustal modified and controlled by the crustal composition and thickness.

Biological Diversity and Potential in Geothermal Systems

BRENT PEYTON¹ AND HOPE LEE²

¹Director, Thermal Biology Institute, Montana State University, Bozeman, MT 59717 USA
(bpeyton@coe.montana.edu)

²Pacific Northwest National Laboratory, Richland WA 99352 USA (hope.lee@pnnl.gov)

Geothermal environments are very small in size and distribution on Earth, however, they play strategic role in the pursuit of novel microbial activity for industrial and energy related processes. Hot springs are natural ecosystems where microorganisms have adapted to high temperatures and unique geochemical environments, over centuries, making them ideal to study for understanding extreme ecosystems. Thermal features are also "target" environments for isolating novel and robust microorganisms for biotechnology and energy applications.

Thermal environments have been a source of beneficial microorganisms, including the discovery of unique microorganisms and thermostable enzymes (e.g., Taq polymerase), for the degradation of biomass, and the production of lipases, and for algal biofuels. This presentation will include a brief overview of Yellowstone thermal areas, and results of interdisciplinary geochemical and microbial investigations in the Heart Lake Geyser Basin focused on characterization of unique microbial communities, microbes for enzyme discovery, and for algal biofuels applications.

Correlated chemical and temporal evolution of Cenozoic magmatism in SE-Germany (Heldburg region)

J.A. PFÄNDER*¹, A. KLÜGEL², S. JUNG³
AND J. ROHRMÜLLER⁴

¹TU Bergakademie Freiberg, Germany. ²Universität Bremen, Germany. ³Universität Hamburg, Germany. ⁴Bayerisches Landesamt für Umwelt, Hof, Germany.
(*correspondence: pfaender@tu-freiberg.de)

Detailed petrogenetic models on the causes and sources of Cenozoic magmatism in Central Europe have been developed based on a large number of trace element and isotope data. Due to only sparsely available geochronological data, however, the timescales of the underlying processes (e.g. mantle convection and regional "plume" activity) often remain unclear.

Here, we present new high-resolution ⁴⁰Ar/³⁹Ar ages along with major and trace element data from a series of basanites and melilitites from SE-Germany (Heldburger Gangschar) in order to constrain the temporal and chemical evolution of magmatism in this region. This, in turn, provides information on the temporal evolution and dynamics of the underlying melting processes.

The ages indicate two magmatic events, an older one between ~40 and ~25 Ma, and a younger one from ~17.6 to ~13.1 Ma. The older group comprises mostly melilitites, the younger group are basanites. Although incompatible trace-element patterns (REE and multi-element diagrams) of both groups are similar and indicate enriched mantle sources, specific geochemical tracers indicate different processes involved during magma genesis. For example, the older melilitites differ from the younger basanites by having higher and more variable Nb/Ta (17.7 - 20.7 vs. 18.3 - 19.4), higher Sm/Yb, Ho/Lu and CaO, and more pronounced negative Rb and K anomalies in primitive mantle-normalized trace element diagrams. This indicates a stronger influence of residual amphibole on magma genesis during the earlier stage of magmatism, possibly in the lithospheric part of the mantle, and is consistent with the higher variability in Nb/Ta in the older rocks. La/Yb is high in the melilitites (47 - 63) and unrelated to their ages, but is inversely correlated with age in the basanites (26 to 47). This indicates (i) low degrees of partial melting during the first magmatic event, and (ii) higher but gradually decreasing degrees of partial melting over time and/or a different mantle source during the second stage of magmatism. The second event can be interpreted as a waning pulse of ascending mantle beneath the Heldburg region, active until magmatism ended at about 13 Ma.

www.minersoc.org

DOI:10.1180/minmag.2013.077.5.16

Distribution of metabolic activity and current production along conductive cable bacteria

C. PFEFFER^{1,*}, S. LARSEN¹, L. RIIS DAMGAARD¹,
L.P. NIELSEN^{1,2} AND N. RISGAARD-PETERSEN¹

¹Center for Geomicrobiology, Department of Biological Sciences, Aarhus University, 8000 Aarhus C, Denmark
(*correspondence: christian.pfeffer@biology.au.dk)

²Section for Microbiology, Department of Biological Sciences, Aarhus University, 8000 Aarhus C, Denmark

Centimetre long bacterial filaments belonging to the Desulfobulbaceae family mediate electric coupling of oxygen reduction and sulfide oxidation in spatially separated regions of marine sediments [1,2]. Their cell numbers are equal throughout the few millimetres of oxic and the underlying 2-3 cm of anoxic sediment. Thus, only about 10% of the cells are responsible for the reduction of oxygen for the entire filament, using the electrons produced by sulfide oxidation of all connected cells below. As a consequence, a much higher electron turnover per cell must be assumed for those cells with access to oxygen.

In this study, we evaluated whether the higher metabolic rate in the oxic zone coincides with increased energy conservation. Our experimental approaches involved comparison of carbon and ammonia incorporation rates in different filament sections by using stable isotope labelling and nanoSIMS. Moreover, we estimated the vertical distribution of current production by microprofiling electric fields and conductivities in artificial sediment systems.

Our preliminary data suggests that the highest metabolic activity is indeed exhibited by cells in the oxic zone, where excess energy seems to be conserved in storage components rather than used for cell growth. Furthermore, we found that current production, and thus sulphide oxidation, takes place throughout the top 2-3 cm of the anoxic sediment zone, which includes a zone where no free sulphide is detectable.

[1] Nielsen *et al* (2010), *Nature* 463, 1071–1074.

[2] Pfeffer *et al* (2012), *Nature* 491, 218–221.

High-precision tantalum isotope measurements by MC-ICPMS

M. PFEIFER^{1,2,*}, C. MÜNKER^{1,2} AND S.T.M. PETERS^{1,2}

¹Institut für Geologie und Mineralogie, Universität zu Köln, Germany (*correspondence: m.pfeifer@uni-koeln.de)

²Steinmann-Institut für Geologie, Mineralogie und Paläontologie, Rheinische-Friedrich-Wilhelms-Universität Bonn, Germany

Tantalum-180(m) is the rarest observationally stable nuclide in the solar system and has a relative abundance of $0.01201 \pm 8\%$ [1]. Furthermore, ^{180m}Ta is the only nuclide that is stable in an excited state, whereas in ground state it undergoes decay to ^{180}Hf and ^{180}W with a half-life of 8.1h. Therefore, the nucleosynthetic origin of solar system ^{180m}Ta and the relative contributions from s-process branching at ^{179}Hf and from neutrino process in core-collapse supernovae are uncertain [2]. Isotope analyses on natural materials may provide a clue to the source of this nuclide. However, the extremely low $^{180m}\text{Ta}/^{181}\text{Ta}$ ratio challenges sufficiently precise measurements. Here we present a high precision method as well as first data on extraterrestrial material.

Tantalum from two basalts (La Palma, Canary Islands) and one L6 chondrite (Wagon Mound) was separated by anion exchange chromatography modified after [3,4]. Measurements were conducted with a Neptune MC-ICPMS using $10^{12}\Omega$ amplifiers on masses 180 (Ta, Hf, W) and ^{178}Hf for monitoring the large isobaric interference by ^{180}Hf (rel. ab. 30.64%). ^{183}W was monitored for correction of the minor ^{180}W interference (rel. ab. 0.12%). ^{181}Ta was tuned to 40-45V to achieve optimum precision. Instrumental mass bias was corrected for externally by doped Yb, using different ratios between masses 171 to 176 and the exponential law. This protocol enables more precise measurements than using doped Re [4], and the external reproducibility (2σ) was typically better than $\pm 7 \epsilon$ -units for ca. 80ng of sample

We found that our anion exchange chromatography procedure can efficiently separate interfering Hf and W from Ta. Measured solutions had both Hf/Ta and W/Ta of less than 0.00002, sufficiently low to measure $^{180m}\text{Ta}/^{181}\text{Ta}$ ratios accurately. First results for the L6 chondrite and the La Palma basalts are indistinguishable from the terrestrial isotopic value defined by the Alfa AesarTM standard solution.

[1] de Laeter & Bukilic (2005) *Phys. Rev. C* **72** (2), 025801.

[2] Travaglio *et al* (2011) *ApJ* **793** (2), 93. [3] Münker *et al* (2001) *Geochem. Geophys. Geosyst.* **12** (2), 2001GC000183.

[4] Weyer *et al* (2002) *Chem. Geol.* **187**, 295.

Uranium partitioning and isotope composition in shales of the Middle Devonian Marcellus Formation

THAI T. PHAN^{1,*}, ROSEMARY C. CAPO¹², BRIAN W. STEWART¹², SHIKHA SHARMA¹³ AND JAIME TORO³

¹National Energy Technology Laboratory - Regional University Alliance, 626 Cochran Mill Rd., Pittsburgh, PA 15236, USA

²Department of Geology and Planetary Science, University of Pittsburgh, PA, 15260, USA (*correspondence: thaiphan@pitt.edu)

³Department of Geology and Geography, West Virginia University, Morgantown, WV, 26506, USA

Natural gas extraction from the Middle Devonian Marcellus Shale has raised interest in investigating the distribution and behaviour of NORM (naturally occurring radioactive material) associated with both produced water and drill cuttings from this unit. The Marcellus is a variably calcareous shale with intercalated limestone. Based on core extracted in Greene County, southwestern Pennsylvania, uranium (U) concentrations in Marcellus Formation samples range from 3 to 47 ppm. Sequential extraction experiments indicate that 30 to 95% of the U is held in the silicate fraction. Although there is a positive correlation of whole rock U concentration with TOC as observed by others, U associated with the oxidizable (organic) fraction contributes less than 25% (and usually <10%) of the total. Up to 64% of the U was found in the 1.0 N acetic acid leachate, which has implications for uranium release into the environment from relatively soluble carbonate minerals in drilling waste. The source of NORM in Marcellus produced water is primarily radium [1], the daughter product of U and Th. The low U concentrations measured in produced water samples from three Marcellus Shale gas wells (0.1 to 0.5 µg/L) may result from U reduction and precipitation as UO₂ or U₃O₈, consistent with relatively high Mn²⁺ (1-8 g/L) and Fe²⁺ (20-120 g/L) concentrations.

²³⁸U/²³⁵U ratios of Marcellus shale obtained by MC-ICPMS using the double spike method fell in a narrow range of 137.80 to 137.85, similar to other black shales. ²³⁸U/²³⁵U ratios in the carbonate fraction of calcareous shale units were in the range of marine carbonate; however carbonate cements extracted from black shale units were isotopically heavier by an average of 0.7 ‰. ²³⁸U/²³⁵U ratios in the organic matter and silicate fractions generally overlap and are lower than coexisting carbonate cement by about 0.3 ‰.

[1] Rowan *et al* (2011) USGS SciInvestRep **2011-5135**.

Isotopic and mineralogical evidence for atmospheric oxygenation in 2.76 Ga old paleosols

P. PHILIPPOT^{1*}, Y. TEITLER¹, M. GERARD², P. CARTIGNY¹, E. MULLER¹, N. ASSAYAG¹, G. LEHIR¹ AND F. FLUTEAU¹

¹Institut de Physique du Globe, Sorbonne Paris Cité, Univ Paris Diderot, CNRS, Paris, France (philippot@ipgp.fr)

²Institut de Minéralogie et de Physique de la Matière Condensée, Univ Paris Jussieu, IRD, 75252 Paris, France

Recent chemical and isotopic data from Archean marine sediments indicates that alteration of continental surfaces have contributed a substantial fraction of the flux of redox-sensitive elements (S, Cr, Mo) to the ocean several hundreds of millions of years prior to the Great Oxidation Event (GOE; between 2.45 and 2.32 Ga). However, controversies regarding the factors controlling these deliveries (increase of atmospheric oxygen, acid rock drainage, microbial activity on land) have highlighted the problems of identifying a reliable proxy of continental surface alteration during the Archean. Unlike marine proxies, which are indirect climatic records, paleosols, which form at the atmosphere-lithosphere interface, can provide direct constraints on the weathering processes at the time of formation. Here we present new sulfur isotope and mineralogical data from the reference 2.76 Ga old Mount Roe Basalt paleosols at Whim Creek (Western Australia). The data are from new lithofacies that were not documented in previous studies. These lithofacies contain a Fe³⁺-montmorillonite, calcite and sulfate mineralogical assemblage and display enrichments in Cr and Mo compared to the original basalt. Sulfur isotope analysis of microscopic sulfate inclusions preserved in Fe³⁺-montmorillonite and calcite yielded δ³⁴S, Δ³³S and Δ³⁶S values that are different from the field of mass independent (MIF) Archean sulfates. Δ³³S values overlap the field of post-Archean, mass dependent (MDF) terrestrial materials. In a Δ³³S-Δ³⁶S diagram, sulfates plot away from the MIF slope ~-1 defined by Archean samples and overlap the MDF slope of ~-7 defined by post-2.32-Ga old sulfides. The large range of δ³⁴S (up to 20‰) between different samples indicates that S-isotope heterogeneities are preserved on a small scale. Such heterogeneities are best explained by repeated cycles of microbial sulfate reduction producing sulfides followed by the re-oxidation of sulfides into sulfates during oxidative weathering and/or microbial oxidation of microbially-derived ³⁴S-depleted sulfides. These results suggest that the concentrations of free oxygen in the Late Archean climate system has increased, at least transiently, to levels similar to the GOE.

New generation multi-collector mass spectrometers require new $^{40}\text{Ar}/^{39}\text{Ar}$ standards

D. PHILLIPS^{1*} AND E. MATCHAN¹

¹School of Earth Sciences, The University of Melbourne, Parkville, VIC, 3010, Australia (*correspondence: dphillip@unimelb.edu.au)

The accuracy of $^{40}\text{Ar}/^{39}\text{Ar}$ ages is dependent on the availability of mineral standards of known age. Popular standards include Fish Canyon Tuff sanidine (FTCs) [1], Alder Creek Rhyolite sanidine (ACRs) [2] and Mt Dromedary biotite (GA1550) [3]. Despite common usage, the ages of these standards is contentious, with published values varying by >2% [4, 5]; well beyond the $\pm 0.1\%$ goal of EARTHTIME.

In this study, we report ultra-high precision, $^{40}\text{Ar}/^{39}\text{Ar}$ analyses of FTCs, ACRs and GA1550 biotite aliquots, using a multi-collector ARGUSVI mass spectrometer. Step-heating results resolve distinct (~1%) age gradients for all samples, attributed to argon loss and/or extraneous argon contamination. This discordance complicates efforts to assign accurate ages to these standards, with different heating protocols also likely to cause inter-laboratory bias.

These data suggest that these minerals are non-ideal as high precision $^{40}\text{Ar}/^{39}\text{Ar}$ standards. In broader terms, the results mandate a re-evaluation of high precision $^{40}\text{Ar}/^{39}\text{Ar}$ ages referenced to these standards, including the astronomically calibrated ages for FTCs [6], and $^{40}\text{Ar}/^{39}\text{Ar}$ ages used to define new decay constants [4].

[1] Cebula *et al* (1986) *Terra Cognita*, **6**, 139–140. [2] Turrin *et al* (1994) *Geology*, **22**, 251–254. [3] McDougall & Roksandic (1974) *J. Geol. Soc. Austr.*, **21**, 81–89. [4] Renne *et al* (2010) *Chem. Geol.*, **145**, 117–152. [5] Spell & McDougall (2003) *Chem. Geol.*, **198**, 189–211. [6] Rivera *et al* (2011) *Earth Planet. Sci. Lett.*, **311**, 420–426.

Lack of isotopic exchange between organics and clays in Semarkona chondrite: submicrometer scale heterogeneity of the D/H ratio.

PIANI, L. ^{*1,2}, ROBERT, F. ¹ AND REMUSAT, L. ¹

¹LMCM, UMR CNRS 7202, MNHN, Paris, France. ²CRPG, UMR 7358, CNRS-Université de Lorraine, France. *(correspondence: piani@crpg.cnrs-nancy.fr)

Organics and clays are the main hydrogen bearing phases in non-equilibrated chondrites. These primitive solid reservoirs recorded the signatures of the early solar system. While organics are formed prior to accretion of the parent body, clays are thought to have formed during its aqueous alteration. As a consequence, clays may contain the H isotopic signature of the hydrothermal fluids and may provide the composition of the ice accreted on the parent body. Both phases can exhibit highly heterogeneous D/H ratios depending on the chondrite [1–4]. However, their intimate mixing within the chondrite matrix [5] makes it difficult to investigate possible interactions between clays (water) and organics, because local isotopic measurements are not possible with current analytical techniques.

An analytical protocol was developed using the nanoscale secondary ion mass spectrometer NanoSIMS 50. D/H and OD/OH ratios were deconvoluted to allow localized semi-quantitative information on the isotopic composition of organics and clays to be obtained [6]. Using this protocol, measurements were carried out on Au-pressed matrix pieces of the Semarkona unequilibrated ordinary chondrite.

No isotopic equilibrium was observed between organics and clays. Relatively isotopically homogeneous organic matter ($\delta\text{D} \sim 2000\text{‰}$) is mixed with extremely heterogeneous clays (with δD from 0 to more than 10,000‰), attesting to a lack of global isotopic exchange between organics and water. Moreover, micrometer-size areas of exceptionally D-rich inorganic material were identified and these are surrounded by D-poor material (mostly clays and/or organics). The origin of the most D-rich inorganic material remains puzzling, however, the observations demonstrate the limited extent (few μm) of aqueous alteration on the Semarkona parent body and suggest that the parent body accreted ice from several regions of the solar system.

[1] Remusat *et al* 2010 *Astrophys J*, **713**, 1048–1058. [2] Deloule and Robert 1995 *GCA*, **59**, 4695–4706. [3] Bonal *et al* 2013 *GCA*, **106**, 111–133. [4] L. Remusat and L. Piani 2013 *LPSC #1401* [5] Le Guillou *et al* 2011 *LPSC #1996*. [6] Piani *et al* 2012 *Anal chem*, **84**, 10199–206.

Site-specific carbon isotope measurement of organics by gas source mass spectrometry

ALISON PIASECKI¹, JOHN EILER¹, ALEX SESSIONS¹,
JOELMA P. LOPES², JULIANA A. LEMINI²
AND LUIZ C. S. FREITAS²

¹Caltech Pasadena, CA, USA (piasecki@gps.caltech.edu)

²Petrobras, Brazil

Most isotopic measurements constrain the bulk compositions of molecules or minerals, averaging over non-equivalent sites. Site-specific isotope measurements potentially could add new constraints regarding the sources and reaction histories of molecules. For example, previous studies demonstrate that biosynthetic reactions, such as decarboxylation of pyruvate, lead to even/odd ordering and more complex patterns of ¹³C enrichment within fatty and amino acids, with differences of up to 30‰ between adjacent C positions. Such variations are potentially preserved in the products of thermal degradation of biomolecules (e.g., propane). And isotopic structures of these products may also reflect the mechanisms and conditions of the ‘cracking’ reactions by which they are produced from larger biomolecules at elevated temperatures, and/or measure their later consumption by thermal or bio-degradation.

We have developed a new mass spectrometric technique for measuring the difference in ¹³C enrichment between the terminal central C position in propane. Our measurement based on comparison of the δ¹³C values of one- and two-carbon fragment ions, each of which is analyzed using a new high resolution mass spectrometer, the MAT 253 Ultra. We applied this technique to a sample suite of wet (i.e., ethane and propane-rich) natural gases. Conventional interpretations of δ¹³C values of these components of these gases suggest they are a single suite that varies only in its level of thermal maturity. However, we find these samples can be divided into two populations that differ by 5‰ in the δ¹³C of their central carbon position. Within each of these populations, the δ¹³C of the terminal carbon position can vary by up to 7‰. Several interpretations of these data are possible; a simple hypothesis we suggest is that the central carbon position samples the δ¹³C of the source rocks (which are known to be a mix of lacustrine and marine rocks in this suite), whereas variations in δ¹³C of the terminal carbon within any set of samples from a given source increases with increasing thermal maturity. We are now exploring this and other hypotheses through experiments, modeling, and measurements of other suites. More generally, this work suggests a path toward site-specific measurements of a variety of organic molecules.

Evaluating the fossilization potential of Fe(II)-oxidizing bacteria

AUDE PICARD¹, MARTIN OBST¹ AND ANDREAS KAPPLER¹

¹Center for Applied Geoscience, Eberhard Karls University
Tübingen, Tübingen, Germany (aude.picard@uni-
tuebingen.de ; martin.obst@uni-tuebingen.de ;
andreas.kappler@uni-tuebingen.de)

The hunt for microfossils in the rock record has been pursued for several decades to reconstruct the individual steps in life evolution as well as the appearance of microbial metabolisms [1]. Given the small cell size and the limited morphological diversity in the microbial world, the biogenicity of microbial-like structures has always been questioned. Fossilization experiments have shown that microorganisms can be well preserved in silica [2]. However the presence of Fe³⁺ appears essential during the fossilization process in silica [3, 4]. In this study, we investigate the fossilization potential of Fe(II)-oxidizing bacteria after exposition to pressure (P) and temperature (T) conditions simulating diagenetic processes during sediment burial and rock formation. Within this project we seek to propose a “biosignature” for microbial Fe metabolism to be compared to the rock record. *Gallionella*-like microorganisms produce twisted stalks – structures made of a polysaccharide bone and coated with Fe(III) oxyhydroxides – as a result of growth and Fe(II) oxidation [5]. A Fe(II)-oxidizing microbial mat containing twisted stalks was collected at the Segen Gottes mine (SW Germany) and incubated at various P/T conditions in a hydrothermal autoclave. Twisted stalks were preserved at the highest P/T conditions tested (1 week at 250°C/140 MPa) and after the longest incubation (4 months at 170°C/120 MPa). Fe(III) minerals evolved from ferrihydrite to hematite with increasing P/T conditions. Polysaccharidic and peptidic components were altered at the highest P/T conditions tested. However organic carbon was relatively well preserved. It seems that Fe(III) oxyhydroxides covering the organic carbon are acting as a protectant to maintain the morphology and organic components of the twisted stalks and might be able to preserve these structures over geological times.

[1] F. Westall (2008) *Space Sci. Rev.* 135: 95-114. [2] J.K.W. Toporski, A. Steele, F. Westall, K.L. Thomas-Keptra, D.S. McKay (2002) *Astrobiology* 2: 1-26. [3] F. Orange, J.R. Disnar, F. Westall, D. Prieur, P. Baillif (2011) *Paleontology* 54: 953-964. [4] F.G. Ferris, W.S. Wyfe, T.J. Beveridge (1988) 16: 149-152. [5] C.S. Chan, S.C. Fakra, D. Emerson, E.J. Fleming, K.J. Edwards (2011) *The ISME J.* 5: 717-727.

Effect of Hafnium on Glass Structure and Dissolution

EM PIERCE^{1*}, SN KERISIT², F ANGELI³,
T CHARPENTIER³, JP ICENHOWER⁴, J HOPF¹

¹Oak Ridge National Laboratory, (pierceem@ornl.gov)

²Pacific Northwest National Laboratory

³Commissariat à l'Énergie Atomique ⁴Lawrence Berkley National Laboratory

Reactions that occur at the solid-water interface control the composition of the world's fresh water, soil development and nutrient distribution, the cycling of elements in the Earth's Critical Zone, and to predict the impact from the disposal of vitrified nuclear waste [1]. Recently, multi-scale or hybrid models, which capitalize on advancements in the understanding of solid-water interfacial reactions, have been used to better describe the macroscopic interactions occurring in the systems [2]. However, knowledge gaps in the fundamental understanding of solid-water reactions impede the ability to accurately describe microscopic processes (e.g., sorption, surface layer formation, etc.) that represent the underlying phenomena controlling macroscopic reaction kinetics.

An important step in improving our ability to accurately forecast radionuclide release from vitrified waste is to establish a link between the glass atomic-level structure and macroscopic dissolution behavior. This study extends the previous work by Pierce et al. [3], by evaluating the effect the high-valence cation hafnium has on the structure and chemical durability of alkali aluminoborosilicate glass.

Results from flow-through experiments show a ~100× decrease in the dissolution rate with increasing Hf content from 0 to 20 mol% HfO₂. The results also reveal a divergence in the magnitude between the average steady state rates measured in dilute and near-saturated conditions. Monte Carlo simulations indicate that the divergence in glass dissolution behavior results from the formation of a low coordination Si sites when Si from the saturated solution adsorbs to Hf on the glass surface. The residence time of the low coordination Si site is longer at the glass surface and increases the density of anchor sites from which altered layers with higher Si densities can form than in the absence of Hf. These results illustrate the importance of understanding solid-water/solid-fluid interactions by linking macroscopic reaction kinetics to nanometer scale interfacial processes.

[1] Brown and Calas (2012), *Geo. Perspec.*, **1**. [2] Steefel and Maher (2009), *Rev. Min. & Geo.* **70**, pp485-532. [3] Pierce et al. (2010), *GCA*, **74**, 2634-2654.

Back to the future: high-sensitivity noble gas mass spectrometers with modern electronics.

J. PIERONEK^{1*}, W. HAMES², T. BECKER³, P. RENNE³,
M. BILLOR² AND A. ILLIES⁴

¹JVP Systems, 3525 Del Mar Heights Rd., San Diego, CA, 92130, USA (*correspondence: jvp@jvpsystems.com);

²Geology, Auburn University, Auburn, AL 36849, USA;

³Berkeley Geochronology Center, Berkeley, CA 94709, USA;

⁴Chemistry, Auburn University, Auburn, AL 36849, USA.

Spectrometers designed 30 years ago, operated in a single-collector mode, remain capable of routinely measuring argon isotopic ratios that may vary over five orders of magnitude, with precisions better than 0.2% for gas species in quantities of ~ 10⁻¹⁶ mol. Aging electronics are the Achilles heel of these systems. A focus of our activities is to develop a new generation of novel electronic device upgrades for the control of typical noble gas mass spectrometers (e.g., the MAP-215 and similar instruments). Over the past 30 years, most analog circuits have been redesigned to use MOS (Metal Oxide Semiconductor) technologies that consume less power, are smaller, and allow more circuitry to improve the performance of a given device. Such devices can incorporate circuitry to protect against external or internal transients. For example, a newly designed emission regulator is able to sustain leakage (as caused by the slow deposition of filament metal on the insulating components of the source) between the source, half-plates, filament and repeller without damage. Considering electromagnet and filament control, stability to within 1 to 2 parts per million can be achieved. The use of 24-bit analog to digital converters coupled with more powerful, responsive power supplies will result in significantly reduced electromagnet settling time. The thermal stability of these devices is enhanced by using state of the art, low power, enclosed circuitry with convective cooling. Multiple sensor inputs are incorporated to allow monitoring and logging of environmental conditions such as temperatures and humidity. All critical voltages and currents are controlled, and monitored over an Ethernet interface. This control eliminates noise from potentiometers and other moving electromechanical components, and permits full logging of parameters useful in automatic tuning algorithms. This level of control also will permit expedient changes and tuning of source parameters for analysis of different isotope groups (He, Ar, etc.). It is possible to completely control all of these electronics remotely through a standard web browser. Test data generated in this effort are presented in this forum for analytical standards and geologic samples of varying age and context.

Anomalous CO₂ contents in a shallow aquifer of the Mt.Amiata geothermal area, Italy

L.PIEROTTI^{1*}, G.CORTECCI¹, G.FACCA²
AND F.GHERARDI¹

¹CNR-Istituto di Geoscienze e Georisorse, Pisa, Italy

(*correspondence: l.pierotti@igg.cnr.it)

²Instruments Care, Pisa, Italy

In the framework of a project funded by Seismic Service of the Tuscany Region [1], the Bagnore thermal spring (Mt.Amiata geothermal area) has been selected as a suitable site to identify possible hydrogeochemical anomalies related to seismic activity. Since 2004, the Bagnore spring ($T_{\text{WATER}} = 21.5^{\circ}\text{C}$) has been monitored in continuous (more than 8×10^5 data available today) with an automatic station equipped for the measurement of temperature, pH, EC, Eh, and the dissolved content of CO₂ and CH₄. During the period 2004-2012, 68 discrete sampling campaigns for the determination of selected chemical-physical parameters in situ (T, pH, EC, alkalinity), and chemical parameters in the laboratory (Na, K, Ca, Mg, Cl, SO₄, NO₃, B), have also been performed. From all these data, it emerges that the low salinity (240 mg/l) waters of the Bagnore spring belong to the Ca-SO₄ chemical type, and are characterized by a background P_{CO2} value of about 0.04 bar. Significant H₂S and H₃BO₃ anomalies have been also detected, suggesting that the shallow aquifer feeding the Bagnore spring effectively absorbs gases diffusing from below. Isotopic analyses on TDIC ($\delta^{13}\text{C} = -7.8$ and -11.6‰) and dissolved SO₄ ($\delta^{34}\text{S} = -6.9\text{‰}$) point to exclude the hypothesis of a prevalently magmatic origin for the gases interacting with waters in the shallow volcanic aquifer. TDIC is thus interpreted as the result of the mixing between CO₂ of metamorphic origin and soil-derived CO₂. Low, basically radiogenic ³He/⁴He ratios in gas vents of the area [2], further support this hypothesis. The $\delta^{34}\text{S}$ -SO₄ signature possibly indicates that H₂S absorbed in the shallow aquifer derives from thermochemical reduction of Triassic anhydrite ($\delta^{34}\text{S} = 15.5\text{‰}$) in the geothermal reservoir, at an estimated temperature of about 300°C.

During the last three years, two anomalous, progressive increases in P_{CO2} (up to 0.07 bar) and SO₄ concentration (up to +10%), correlated with a measurable decrease in pH (up to -0.3 pH units, down to 5.6) and HCO₃ concentrations, have been observed over several months. These trends ended just a few days before two seismic events of magnitude 2.5 and 2.7.

[1] Cioni R. *et al* (2007) *NHESS* 7, 405-416. [2] Minissale *et al* (1997) *JVGR* 79, 223-251.

Origin of the chemical and U-Sr isotopic variations of soil solutions, stream and source waters at a small catchment scale (the Strengbach case; France)

¹PIERRET M.C.,¹ STILLE P.,¹⁻²PRUNIER J.
AND ^{1A}CHABAUX F.

¹Laboratoire d'Hydrologie et de Géochimie de Strasbourg, EOST, Université de Strasbourg et CNRS, 1 rue Blessig 67084 Strasbourg, France

²Université Paul Sabatier, CNRS et IRD, Observatoire Midi-Pyrénées, 14, avenue Edouard Belin, 31400 Toulouse, France

This is the first comprehensive study dealing with major and trace element data as well as ⁸⁷Sr/⁸⁶Sr isotope ratios and (²³⁴U/²³⁸U) activity ratios (AR) determined on the totality of springs and brooks of the Strengbach catchment. It shows that the small and more or less monolithic catchment drains different sources and streamlets with very different isotopic and geochemical signatures. Different parameters control the diversity of source characteristics. Of importance are especially the hydrothermal overprint of the granitic bedrock, which was stronger on the granite from the northern than from the southern slope, and the different meteoric alteration processes of the bedrock causing the formation of 0.5 to 9 meter thick saprolite and above the formation of an up to 1m thick soil system. The chemical compositions of the source waters in the Strengbach catchment are only to a small extent the result of alteration of primary bedrock minerals and rather reflect dissolution/precipitation processes of secondary mineral phases like clay minerals.

The (²³⁴U/²³⁸U) AR however, are decoupled from the ⁸⁷Sr/⁸⁶Sr isotope system and reflect to some extent the level of altitude of the source. In addition, the important thickness of the saprolite allows to explain the low (²³⁴U/²³⁸U) AR <1, which are uncommon for surface waters. Preferential flow paths along constant fractures in the bedrocks might explain the over time homogeneous U AR of the different spring waters.

At the soil scale, the geochemical signatures of soil solutions result mainly from biological impact (recycling, degradation and exudation), weathering of secondary phases and atmospheric inputs.

This study further highlights the fact that processes controlling the chemical and isotopic water signatures are different at the soil and catchment scales.

Characterisation of cronstedtite synthesized by iron clay interaction in a cooling procedure

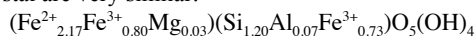
I. PIGNATELLI^{*1}, E. MUGNAIOLI², J. HYBLER³,
R. MOSSER-RUCK¹ AND M. CATHELINÉAU¹

¹GeoRessources UMR-CRNS 7359, Université de Lorraine, Faculté des Sciences et Technologies, Campus Aiguillettes, BP 70239, 54506 Vandoeuvre-lès-Nancy, France (* correspondence : isabella.pignatelli@univ-lorraine.fr).

²Institut für Physikalische Chemie, Johannes Gutenberg-Universität Mainz, Welderweg 11, 55128 Mainz, Germany.

³Institute of Physics, Academy of Science of Czech Republic, Cukrovarnicka 10, 16253 Prague 6, Czech Republic.

The cooling of steel containers in radioactive waste storage has been simulated by an original step by step experiment from 90°C to 40°C. Among newly formed clay minerals observed in run products, cronstedtite has been undoubtedly identified by different analytical techniques (XRD, TEM and SEM). This is the first time that cronstedtite is so abundant and well-crystallized in an iron-clay interaction experiment. The formation of cronstedtite is favoured by the release of Fe and Si in solution after the dissolution of quartz, T-O-T phyllosilicates and iron metal. Cronstedtites are characterised by various morphologies: pyramidal (truncated or not) crystals have been observed from 90°C to 60°C experiments, whereas conic crystals with a rounded or hexagonal cross-section occur only in 90° and 80°C experiments. The mean formulae of pyramidal and conic crystal are very similar:



Pyramidal crystals are, thus, more frequent and show different polytypic sequences as well as various degree of disorder. Polytypes $2M_1$, $1M$ and $3T$ have been identified thanks to TEM investigations. The two monoclinic polytypes are very rare in nature, at the contrary of $3T$ polytype (Hybler *et al* 2008). Thanks to the cooling procedure, the stability range of cronstedtite with respect to the temperature is determined. Between 90°C to 60°C cronstedtite appears to be stable and 50°C corresponds to the lower limit of cronstedtite stability as confirmed by crystal alteration. The occurrence of cronstedtite seems to be favored both by temperature range (90°-60°C) and by the progressive temperature decrease, as shown by the comparison of our results with those of previous studies carried out on the same starting claystone but with slightly different experimental conditions (duration time, liquid/rock or iron/clay ratios).

Evidence for global metasomatic enrichment in oceanic lithosphere

S. PILET¹, N. ABE², L. ROCHAT³, D. BUCHS⁴
AND P.O. BAUMGARTNER⁵

¹University of Lausanne, CH, Sebastien.Pilet@unil.ch

²Jamstec, Yokosuka, JP, abenatsu@jamstec.go.jp

³University of Lausanne, CH, Laetitia.Rochat@unil.ch

⁴Cardiff University, UK, BuchsD@cf.ac.uk

⁵University of Lausanne, CH, Peter.Baumgartner@unil.ch

Oceanic lithosphere is generally interpreted as mantle residue after MORBs extraction. However, some models [1, 2] suggest that this lithosphere could be re-enriched by metasomatic processes in the periphery of ridges. Xenoliths from OIBs could not be used to confirm or invalidate this hypothesis because the metasomatism observed in these xenoliths is likely to be related to the hot spot activity itself. Direct evidence for refertilization of oceanic lithosphere at a global scale is thus missing. Here we used Petit-spot lavas and their enclosing xenocrysts to suggest that oceanic lithosphere is likely to be metasomatized before its recycling in subduction zones.

Petit-spot lavas are interpreted as the surface expression of low degree melts extracted from the base of the lithosphere by plate flexure or crack propagation [3]. Petit-spot lavas accreted in the north of Costa Rica [4] show the presence of cpx xenocrysts similar to cpx observed in metasomatic veins worldwide. The composition of these cpx xenocrysts suggests crystallization at high pressure (15-25 km) in a differentiated liquid percolating across the lithosphere. Similar liquids are identified in Petit-spot lavas sampled on the Pacific plate in front of Japan [5]. These rocks do not contain high-pressure cpx xenocrysts, but contain low-Mg# cpx interpreted as cpx crystallized at low pressure in a liquid similar in composition to that from which cpx xenocrysts observed in Costa Rica petit-spot lavas crystallized. These different observations suggest that the lithosphere is re-enriched by metasomatic process before its subduction. Plate flexure allows low degree melts present at the base of the lithosphere to percolate and differentiate across the oceanic lithosphere, producing a refertilisation of this lithosphere, and in some cases the emission of Petit-spot lavas at the surface. Modelling of the effect of this metasomatic enrichment on the composition of the lithosphere suggests that portions of recycled oceanic lithosphere could correspond to an enriched mantle component rather than depleted mantle.

[1] Halliday *et al* (1995) *EPSL* **133**, 379-395; [2] Niu and O'Hara (2003), *JGR* 108; [3] Vallentine & Hirano (2010), *Geology* **38**, 55-58; [4] Buchs *et al* (2013), G3 [5]. Hirano *et al* (2006), *Science* **313**, 1426-1428.

Study of surfaces of Al_2SiO_5 minerals by Lateral Force Microscopy

CARLOS PIMENTEL^{1,2}, CARLOS M. PINA^{1,2}
AND ENRICO GNECCO³

¹Departamento de Cristalografía y Mineralogía, Universidad Complutense de Madrid, Spain,

(cpimentelguerra@geo.ucm.es, cmpina@geo.ucm.es)

²Instituto de Geociencias UCM-CSIC (IGEO)

³IMDEA Nanociencia, Madrid, Spain.

(enrico.gnecco@imdea.org.)

Kyanite, sillimanite and andalusite (Al_2SiO_5) are polymorphic minerals which traditionally have been used as geobarometers and geothermometers. However, P-T determinations using Al_2SiO_5 minerals are problematic. Transformations between Al_2SiO_5 polymorphs involve breaking strong Si–O and Al–O bonds. This, combined with the small free energy differences between polymorphs, makes difficult to determine the P-T fields of these minerals, which usually persist as metastable phases [1].

The aim of this work is to study the nanotribological properties of kyanite, sillimanite and andalusite surfaces and their relationship with different Si–O and Al–O bonds schemes. We measured friction on Al_2SiO_5 cleavage surfaces immersed in water using a lateral force microscope (LFM) at RT. Lateral deflection signals along different crystallographic directions were measured and converted into frictional forces after an adequate calibration [2]. While frictions measured at the microscale on different Al_2SiO_5 surfaces were compared, $10 \times 10 \text{ nm}^2$ frictional maps provided detailed structural information (see Figure). The methodology and preliminary results presented here represent a new approach to the study of the Al_2SiO_5 polymorphs.

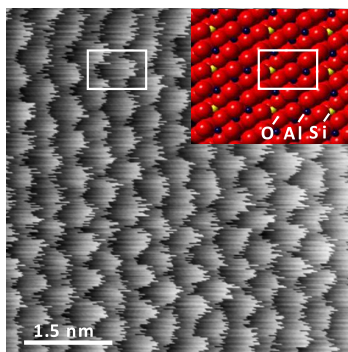


Figure: LFM image of kyanite (100) face showing the surface lattice. The inset shows the kyanite surface structure.

[1] Putnis, A. (1992) *Introduction to mineral sciences*. 457 pp.

[2] Noy et al (1995) *J. Am. Chem. Soc.* **117**, 7943.

Nanotribology of mineral surfaces in aqueous environments

CARLOS M. PINA^{1,2}, CARLOS PIMENTEL^{1,2}
AND ENRICO GNECCO³

¹Departamento de Cristalografía y Mineralogía, Universidad Complutense de Madrid, Spain, cmpina@geo.ucm.es;

(cpimentelguerra@geo.ucm.es.)

²Instituto de Geociencias UCM-CSIC (IGEO)

³IMDEA Nanociencia, Madrid, Spain.

(enrico.gnecco@imdea.org.)

Investigations on the structure of mineral surfaces are fundamental to gain a better understanding of their reactivity. The latest developments in surface sensitive techniques and, in particular, in atomic force microscopy (AFM), have provided interesting information on the terminations of mineral faces at the nanoscale. Despite this, nanotribology studies of mineral surfaces are still scarce. Recent works have, however, demonstrated that friction measurements performed with lateral force microscopy (LFM) can be used to obtain detailed crystallochemical and crystallophysical information on mineral surfaces [1-3].

Here we present friction measurements conducted on carbonate, sulphate and silicate mineral surfaces using LFM operating in water. Measured friction forces at the nanoscale are typically in the range of 10 nN and they were found to vary with the crystallographic direction. In all cases, crystal lattices could be resolved and the surface unit cells were measured. On the surfaces studied no reconstruction nor relaxation phenomena were observed.

Our LFM measurements were extended to study epitaxial overgrowths on mineral surfaces [4]. Frictional maps allowed us to resolve substrate and overgrowth surface lattices and to determine epitaxial relationships. Furthermore, by increasing the vertical force of the LFM, we removed overgrown islands attached on the substrates. Depending on the mismatch between overgrowth and substrate lattices, different shear strengths for overgrowth detachment in the range of 5 to 150 MPa were calculated.

The results that we present here demonstrate that LFM in liquid is a very suitable technique to study mechanical properties of mineral surfaces and epitaxial phenomena at a molecular scale.

[1] Shindo *et al* (1999) *Physical Chemistry Chemical Physics*, **1**, 1597-1600. [2] Pina *et al* (2012) *Physical Review B*, **85**, 073402 [3] Cubillas & Higgins (2009) *Geochemical Transactions*, **10**,7. [4] Pina *et al* (2012) *Mineralogical Magazine*, **76**, 2235.

Equilibrium isotope fractionation factors in liquids from path integral molecular dynamics simulations

C. PINILLA*¹, M. BLANCHARD¹, G. FERLAT¹,
E. BALAN¹, R. VUILLEUMIER² AND F. MAURI¹

¹IMPMC, Université Pierre et Marie Curie, CNRS, IRD, 4
Place Jussieu, 75252, Paris Cedex 05, France

²Ecole Normale Supérieure, Département de Chimie, UMR
CNRS-ENS-UPMC n° 8640, 24 Rue Lhomond, F-75231
Paris Cedex 05, France

The equilibrium fractionation factor between two phases is of importance for the understanding of many planetary and environmental processes. Although thermodynamic equilibrium can be achieved between minerals at high-temperature, many processes in Earth and environmental sciences involve reactions between liquids or aqueous solutions and solids [1]. In crystals, the fractionation factor α is theoretically modelled using a statistical thermodynamic approach to calculate the equilibrium constants of isotope exchange reactions from the vibrational energy levels of the phases [2]. These calculations are mostly based on empirical or ab-initio description of the systems to extract the harmonic vibrational information. In the case of a periodic systems such as liquid phases and solutions, further approximations are however required and could include the use of finite-size molecular clusters or the use of relaxed configurations taken from molecular dynamics (MD) runs.

In this work we present a systematic study of the calculation of the D/H and ¹⁸O/¹⁶O equilibrium fractionation factor in water for the liquid/vapour and ice/vapour phases using several levels of accuracy within the simulations. Namely, we use MD in combination with an empirical potential model for water. The exact fractionation factor for this potential is obtained from thermodynamic integration using Path Integral MD calculations. Compared with standard MD, this method makes it possible to take into account quantum effects in the thermodynamic modelling of liquids. We compare these results with those of the modelling strategies usually used, which involve the mapping of the quantum system on its harmonic counterpart. Accordingly, we discuss the implications of these approaches for the calculation of fractionation factors in liquid systems.

[1]Hoefs (1997) *Stable Isotope Geochemistry* (Springer, Berlin). [2] M. Blanchard *et al* (2009) *Geochim. Cosmochim. Acta* **73**, 6565-6578

* Carlos Pinilla, pinilla@impmc.upmc.fr (presenting author)

Insights into a volatile rich subcontinental lithospheric mantle: Iherzolite xenoliths from the Cameroon Volcanic Line, Africa

ZSANETT PINTÉR^{1,2}, ISTVÁN KOVÁCS², ZOLTÁN KONC³,
MÁRTA BERKESI¹, CSABA SZABÓ¹, ANDREA PERUCCHI⁴,
AND LEVENTE PATKÓ¹

¹Lithosphere Fluid Research Lab, Eötvös University, Hungary
(zsanett.pinter.hu@gmail.com)

²Geological and Geophysical Institute of Hungary, Budapest

³Laboratoire Magmas et Volcans, UBP-CNRS-IRD, Clermont-Ferrand, France

⁴ELETTRA Synchrotron Light Laboratory, Trieste, Italy

We have carried out detailed petrographic, petrophysical (EBSD), geochemical and fluid inclusion study (e.g. Raman, FTIR coupled synchrotron radiation, FIB) on spinel Iherzolite xenoliths from Barombi Mbo (BM) and Nyos Lake coupled with study of the H₂O content of their nominally anhydrous minerals (NAMs). Results indicate that the BM protogranular xenoliths provide a characteristics of a juvenile subcontinental lithospheric mantle suffered low degree partial melting and record deformation regime governed by combination of simple and pure shear. The NAMs in BM xenoliths show moderate bulk water content (100-130 ppm). Their fluid inclusions consist of high-density CO₂-H₂O(-H₂S) system, which also contain phlogopite as a step-daughter mineral. The porphyroclastic Nyos xenoliths preserve a transpressional deformation regime and metasomatism indicated by the presence of pargasite. Nyos xenoliths have low bulk NAMs H₂O content (10-60 ppm) and their fluid inclusions also contain high-density CO₂-H₂O(-H₂S) fluids with phlogopite and pargasite step-daughter minerals.

Helium isotopic gradients in a catchment basin: Constraining groundwater flow patterns and residence times

D. L. PINTI^{1*}, G. VAUTOUR¹, E. ROULLEAU²,
M. C. CASTRO³ AND Y. SANO²

¹GEOTOP, Université du Québec à Montréal, QC, Canada, (* correspondence: pinti.daniele@uqam.ca)

¹GEOTOP, Université du Québec à Montréal, QC, Canada

²AORI, The University of Tokyo, Kashiwanoha, Chiba 277-8564 Japan

³Earth and Environmental Sciences, University of Michigan, Ann Arbor, MI 48109-1005, USA

Fifty-six groundwater samples were collected for noble gases analysis from Ordovician fractured aquifers and Quaternary granular aquifers at the Bécancour Basin. This is one of several basins collecting waters from the Appalachian Mts and discharging into the St. Lawrence River, between Montreal and Quebec, eastern Canada. Multiple goals were at the origin of this extensive survey. The main goals of this study were to identify groundwater flow paths and to estimate groundwater residence times. In particular, helium was coupled to alkanes (CH₄, C₂H₆, C₃H₈) to identify gas seepage potentially originating in the deeper Utica shales, a local target for shale gas exploration.

Helium isotopic data show the occurrence of three components: atmospheric, i.e., an air saturated water (ASW) origin, tritogenic and terrigenous. Tritogenic helium is found both in Quaternary granular and Ordovician fractured aquifers. In the eastern border of the basin, a helium isotopic gradient with depth is observed, from values close to atmospheric ³He/⁴He (R) ratio of 1Ra at the surface up to 4.5Ra at 60 m depth. Preliminary minimum ³H-³He ages range from modern to 32 yrs. Waters show radiogenic ⁴He concentrations from 10⁻⁷ to 10⁻⁵ ccSTP/g, i.e., up to three orders of magnitude higher than ASW. Interestingly, some of these samples contain tritium suggesting that these are young waters enriched by extraformational ⁴He (⁴He excess). In these two areas, concentration gradients with depth are apparent, suggesting vertical migration of He from deeper horizons. Using an advective-diffusive model, ⁴He fluxes were estimated and range from 3.2 x 10⁻¹⁰ to 1.2 x 10⁻⁹ mol m² yr⁻¹, flux values that are smaller than the average crustal flux of 1.7 x 10⁻⁶ mol m² yr⁻¹ but closer to a pure flux from *in situ* production of 2 x 10⁻⁹ mol m² yr⁻¹.

Mineralogy and distribution of Indium and Selenium metals within zinc-rich ore types of the Neves Corvo deposit, Portugal

ÁLVARO MM PINTO^{1,2}, JORGE MRS RELVAS²,
JOÃO RS CARVALHO², NELSON PACHECO³
AND YANAN LIU⁴

¹MUHNAC, Museu Nacional de História Natural e da Ciência, University of Lisbon, Portugal

²CREMINER (LARSyS), University of Lisbon, Portugal

³SOMINOR, Sociedade Mineira de Neves-Corvo, Portugal

⁴University of Toronto, Dept. Earth Sciences, Canada

The Neves Corvo deposit is located in the Portuguese segment of the Iberian Pyrite Belt (IPB). The deposit is hosted by an upper Devonian to lower Carboniferous Volcanic-Siliceous Complex and embraces six orebodies: Graça, Corvo, Neves, Zambujal, Lombador and Semblana.

The Neves Corvo deposit has important contents of a wide range of high-tech elements, which can be profitable commodities such as the case of Indium (In) and selenium (Se). Indium average grades deposit ranges in between 30 to 215 ppm. Graça, Lombador and Zambujal orebodies have the higher average grades on indium, respectively 215, 152 and 150 ppm. These higher indium grades were observed within zinc-rich ores (MZ) at the Graça and Lombador orebodies and in the copper-zinc-rich ores (MCZ) of the Zambujal orebody. Indium is present as minor element in the structure of major minerals such as chalcopyrite, sphalerite, stannite group minerals and fahlores. Selenium average grades vary in between 10 and 3220 ppm. Lombador and Zambujal orebodies have the highest selenium average concentration, showing 2560 and 3220 ppm, respectively. At the Zambujal orebody the high selenium grades occur in the lead-zinc-rich ores (MZP), while in the Lombador orebody the highest selenium grades were detected at the copper-zinc rich ores (MCZ). Selenium occurs both as Se-minerals and as minor element in the structure of major sulfide minerals. Selenium mineralogy is represented by selenium-bearing galena containing up to 30% of clausthalite (PbSe) end member and junoitite (Pb₃Cu₂Bi₈[S,Se]₁₆), which is described here for the first time either at the Neves Corvo deposit, or the Iberian Pyrite Belt. Selenium also occurs as minor element in fahlores group minerals and sphalerite.

This is a contribution to project ZHINC (PTDC/CTE-GIX/114208/2009; Foundation for Science and Technology (FCT-MCTES)).

Constraining the Nd isotopic composition of Antarctic Bottom Water formed in the Weddell Sea

ALEXANDER M. PIOTROWSKI¹, CLAUS-DIETER HILLENBRAND², CLAIRE S. ALLEN², EUGENE DOMACK³, AND ANDREAS MACKENSEN⁴

¹Department of Earth Sciences, University of Cambridge, Cambridge, CB2 3EQ, UK

²British Antarctic Survey, Cambridge, CB3 0ET, UK

³Department of Geosciences, Hamilton College, Clinton, N.Y. 13323, U.S.A.

⁴Alfred Wegener Institute, Bremerhaven, Germany

The Southern Ocean is a key region linking ocean circulation and global climate. Antarctic Bottom Water (AABW) ventilates much of the world's deep ocean as it propagates, together with Circumpolar Deep Water, via the Antarctic Circumpolar Current (ACC) from the Atlantic sector of the Southern Ocean into the Indian and Pacific sectors, and spreads northwards into deep basins. Proxy data from sediment cores suggest that during Late Quaternary glacial periods, increased volumes of AABW filled the deep ocean, perhaps enlarging the carbon reservoir of the world ocean and lowering atmospheric carbon dioxide. Much of the evidence for glacial circulation of deep and bottom water masses is based on stable carbon isotope ($\delta^{13}\text{C}$) records from benthic foraminifera. This proxy, however, can be interpreted as either indicating changes in water mass sources, biological productivity or air-sea gas exchange. This is especially problematic in the glacial Southern Ocean where all three of these controls are likely to have been dramatically different than today. Thus Nd isotopes have been utilized as a deep water source tracer to reconstruct the balance of North Atlantic Deep Water (NADW) and AABW in the global deep ocean. Here we constrain the Nd isotopic composition of AABW formed in the Weddell Sea, allowing us to more accurately determine past changes in the mixing ratio of NADW and AABW at other coresites. The Nd isotopic composition of reductive sediment leaches, foraminifera, and Holocene Fe-Mn coatings on dropstones were analysed from cores located along the flowpath of the clockwise flowing Weddell Sea gyre. These allow us not only to constrain potential temporal variability in the Nd isotopic composition of newly-formed AABW, but also to show how it acquires this Nd isotopic composition as it flows northwards along the Antarctic Peninsula.

Organomineralization drives early chimney edification at the hyperalkaline hydrothermal field of the Prony Bay (New Caledonia)

PISAPIA C.^{1*}, GERARD E.¹, GERARD M.², MENEZ B.¹ AND THE HYDROPRONY TEAM

¹IPGP, 75238 Paris Cedex 05, France (*correspondence: pisapia@ipgp.fr, emgerard@ipgp.fr, menez@ipgp.fr)

²IMPMC, 75005 Paris, France (martine.gerard@impmc.upmc.fr)

The serpentinization process of ultra-mafic rocks by hydrothermal fluids at ultra-slow spreading ridges is recognized as a potential energy source for the development of (sub)surface lithoautotrophic microbial ecosystems. The hydrogen generated by the hydration of Fe²⁺-bearing silicates can reduce CO₂ coming either from mantle degassing or seawater forming methane and other light hydrocarbons similarly to methanogenesis. In the 2000's the discovery of the Lost City Hydrothermal Field (LCHF) hosted on ultramafic substratum near the Mid-Atlantic ridge changed our vision of how and where life can have emerged on Earth and on other planets [1]. It highlighted the importance of serpentinization for the abiotic production of prebiotic molecules and for the sustaining of deep microbial life.

The Prony Bay Hydrothermal Field, discovered in New Caledonia, presents strong mineralogical, geochemical and microbiological similarities with the Lost City Field. The low-temperature (40°C) hyperalkaline springs (pH 11) rich in hydrogen and methane discharge at shallow depth (0-50mbsl) forming carbonated chimneys that host peculiar microflora.

We used a combined geomicrobiological approach (SEM, XRD, Q-ICP-MS, CLSM and FISH) to track microbial cells within the mineralized edifice and to evaluate their impact on the carbonation and (bio)mineralization processes. Similarly to the LCHF [2] the mineralogy is here dominated by brucite and aragonite being replaced by calcite when ageing signing seawater incursions. Filamentous bacteria belonging to the Firmicutes phylum were found to initiate the mineral nucleation through organomineralization processes in active discharging conduits. Mineralized filaments appear ubiquitous in the early stages of the chimney formation, then being consolidated as the mineralization proceeds. It leads to peculiar morphologies whose diagenesis need to be further investigated to be then searched for in the rock record as biosignatures of primitive serpentinization-based ecosystems.

[1] Kelley *et al* (2001), *Nature* **412**, 145-149. [2] Ludwig *et al* (2006), *GCA* **70**, 3625-3645.

Evidence for crustal contribution to recent compositional changes at Mt. Etna volcano

BRADLEY PITCHER^{1*}, WENDY A. BOHRSON²
AND MARCO VICCARO³

¹Oregon State University, Corvallis, OR, USA

(*correspondence: pitcherb@onid.orst.edu)

²Central Washington University, Ellensburg, WA, USA

(bohrson@geology.cwu.edu)

³Universita di Catania, Catania, Italy (m.viccaro@unict.it)

Numerous studies have shown that lavas erupted in the last 4 decades at Mt. Etna are characterized by abrupt geochemical changes. Recent (post-1971) lavas are enriched in some alkali elements, have higher $^{87}\text{Sr}/^{86}\text{Sr}$, and have lower plagioclase to clinopyroxene modal abundance ratios than historic eruptions (i.e. 1329-1971). *In situ* plagioclase compositional and isotopic data provide crucial insights into possible causes for these changes. Core to rim electron microprobe transects were performed on 133 plagioclase crystals from 11 different samples with eruption dates between 1329 and 2005. Plagioclase An (mol%) ranges from 32 to 92, and cores of recent plagioclase tend to exhibit higher An than historic cores. Core and rim $^{87}\text{Sr}/^{86}\text{Sr}$ for 87 of these crystals, collected by LA-ICP-MS, augment TIMS whole-rock and groundmass data. Plagioclase $^{87}\text{Sr}/^{86}\text{Sr}$ range from 0.7030 to 0.7036, and with the exception of 7 analyses, are less radiogenic than whole rock $^{87}\text{Sr}/^{86}\text{Sr}$ (0.7033 and 0.7036), which, in turn, are less radiogenic than groundmass values (0.7035-0.7037). While a majority of crystals from all samples exhibit core to rim increases in $^{87}\text{Sr}/^{86}\text{Sr}$, recent rims have higher $^{87}\text{Sr}/^{86}\text{Sr}$ and larger Sr isotope gaps between rim and whole rock compared to their historic counterparts. In addition, recent plagioclase exhibits more potassic rims for a given An % than the rims of historic crystals, despite having similar core values; this indicates that potassium enrichment must occur during the timeframe of plagioclase crystallization. We propose that an increase in H₂O content of recent parental magmas suppressed plagioclase crystallization to shallower depths, yielding lower plagioclase to clinopyroxene modal abundance ratios and higher An cores. This delayed crystallization enhanced production of latent heat at shallow depths, causing a higher degree of contamination by sedimentary country rock. The Sr isotope disequilibria among plagioclase, whole-rock and groundmass, along with the K enrichment documented in recent rims, strongly suggest that late-stage crustal assimilation, together with other differentiation processes and features inherited from the source, contributed to generate the final signature of recent magmas at Mt. Etna.

Impact of Saharan dust and polluted aerosol on the microbial food web of the Eastern Mediterranean – a mesocosm approach

PITTA P.¹, KROM M.D.², TSAGARAKI T.M.¹,
GIANNAKOUREOU A.³, GOGOU A.³, LAGARIA A.¹,
MIHALOPOULOS N.⁴, PANAGIOTOPOULOS C.⁵, PARINOS
C.³, RAHAV E.⁶, SHI Z.⁷, TSAPAKIS M.¹, TSIOLA A.¹,
VIOLAKI K.⁴ AND HERUT B.⁶

¹Oceanography Inst., Hellenic Centre for Marine Research, Crete, Greece

²School of Earth Sciences, Leeds University, Leeds, UK

³Oceanography Inst., Hellenic Centre for Marine Research, Athens, Greece

⁴Chemistry Department, University of Crete, Greece

⁵Aix-Marseille Univ., Med. Inst. of Oceanography (MIO),

UMR 7294, CNRS/INSU, UMR 235, IRD, Marseille

⁶Universite Sud Toulon-Var (MIO), La Garde cedex, France

⁷Israel Oceanographic & Limnological Research, Haifa, Israel

⁷School of Geography, University of Birmingham, UK

The impact of Saharan dust and polluted aerosol on the microbial food web of the oligotrophic Cretan Sea was studied during a mesocosm experiment that took place at the mesocosm facility of HCMR in Crete (<http://mesoaqua.eu/cretacosmos>), in May 2012, in the framework of the projects ATMOMED-MESOAQUA and ADAMANT-THALIS. "Pure" Saharan dust (1.6 mg/l) and mixed aerosols (1 mg/l), collected in Crete and elsewhere, were each added to 3 mesocosms of 3 m³, while 3 more mesocosms were used as control (no addition). Preliminary results of primary production and phytoplankton biomass (mainly *Synechococcus*) indicate a net response of the autotrophic community to both Saharan dust and mixed aerosol additions between days 1 and 4. The response of the heterotrophic bacterial community to both treatments was also clear but was faster than the one of the phytoplankton and lasted only from day 0 to day 2. The above-mentioned biological parameters were related to the temporal distributions of numerous chemical species, such as inorganic and organic nutrients, total proteins, total mono- and poly-saccharides and their molecular composition profiles, in order to highlight the production and degradation dynamics of organic matter.

Fluid geochemistry and Natural Gas Hazard (CO₂, Rn) in the urban area of Rome (central Italy)

L. PIZZINO AND A. SCIARRA

Istituto Nazionale di Geofisica e Vulcanologia, Rome, Italy

(*correspondence: luca.pizzino@ingv.it)

The city of Rome is located in the Roman Comagmatic Province, where large sectors experience a huge degassing both from soils and aquifers [1, 2]; gas composition is dominated by CO₂, that can act as a carrier for other minor components such as N₂, CH₄, H₂S and Rn. Gases are produced at depth (throughout mantle degassing and/or decarbonation processes) and upraise towards surface through fault and fracture systems, thus characterising well defined enhanced permeability belts. Gases exhaled from soils and aquifers can enter houses, potentially reaching harmful indoor levels [3]. Indeed, some gases (CO₂, H₂S) can have a short-term toxicity, while others (i.e. radon) can cause lung cancer at prolonged exposures. As a consequence, an evaluation of the level of Natural Gas Hazard (NGH) to which these areas are exposed, is required. By now, detailed information on CO₂ and Rn distribution in ground waters was assessed for the volcanic complexes around Rome [1, 4], allowing to discriminate areas where deep fluid upraise and where analysis of indoor-gas levels has to be carried out, in order to lessen their impact on human health. Such an investigation is still lacking for the urban sector of the Italian capital, where about 2500000 people habitually live.

A detailed geochemical study in ground waters started in 2011 and is currently going on in the roman area; 128 water wells and 16 springs were investigated for their chemical and isotopic composition. The preliminary investigation allowed us to recognise and mark off areas in which deep fluids upraise, generally characterised by the presence of hypothermal and CO₂-rich waters. In particular, the role of deep CO₂ as a sound marker of deep tectonic structures in this sector of central Italy, is emphasised. Waters rich in deep CO₂ are located in the southern and in the north-eastern sectors of Rome, that can be considered as potential NGH-prone areas; hypothermal waters have been found in the south-western part of Rome. Radon-rich waters roughly mimic the CO₂ distribution and circulate mainly in the southern sectors of Rome. So far, no H₂S-rich groundwater has been found.

[1] Pizzino *et al* (2002) *Nat. Haz.* **27**: 257–287. [2] Frondini *et al* (2008) *Glob. and Plan. Change* **16**: 89–102. [3] Annunziatellis *et al* (2003) *J. Geochem. Explor.* **77**, 93–108. [4] Cinti *et al* (2010) *Chem. Geol.* **284**: 160–181.

Petro-geochemical evidence for vapour transport in andesite shear fractures

M. PLAIL^{1*}, M. EDMONDS², J. BARCLAY¹,
M. C. S. HUMPHREYS³ AND R. A. HERD¹

¹School of Environmental Sciences, University of East Anglia, UK (*correspondence: m.plail@uea.ac.uk)

²Department of Earth Sciences, University of Cambridge, UK

³Department of Earth Sciences, University of Oxford, UK

The andesitic Soufrière Hills Volcano (SHV), active since 1995, emits large fluxes of volcanic gases (dominantly H₂O, CO₂, SO₂, HCl). The gas is largely decoupled from the flux of magma to the surface, indicating efficient magma-vapour segregation. Effective open-system degassing at dome forming eruptions may control eruption style. However, evidence for vapour transport through magma is not often preserved in the erupted rocks. We present the first petro-geochemical evidence for metal-bearing vapour transport in shear zones in SHV andesite and a model for their formation.

Andesite blocks in deposits from SHV contained narrow shear zones (2 m x 2–10 cm), with alternating low porosity, fine-grained (~30–70 μm) and higher porosity, coarser-grained (~100–350 μm) bands. The higher porosity (7–19% vol) bands consist of broken and comminuted crystals compositionally identical to mineral compositions in the SHV andesite. However, the low porosity (~1%) bands have elevated zones of oxides (<8% vol) and cordierite. Bulk ICP-MS analyses indicate that metal concentrations (Cu, Ni, Pb, Au, Ag and Zn) are greatly enhanced relative to the surrounding andesite. For example, Cu and Au concentrations are >10 times higher than in the andesite host. Cu is present as Cu-Fe sulphide inclusions in Ti-magnetites and plagioclase phenocrysts. We also demonstrate that trends in metal enrichment in the shear zones match well with published experimental metal vapour/melt partition coefficients.

The enhanced metal and volatile concentrations in the shear zones indicate that these zones acted as permeable pathways for metal-bearing gas in the shallow volcanic system. The shear fractures formed in response to brittle failure at high magma strain rates and viscosity, along which metal-bearing vapour or fluid was transported. The gas pathway survived until frictional heating at the slip surface created a partial melt upon which volatiles and metals were resorbed, thus preserving the geochemical signature of the magmatic gases. The subsequent recrystallization of the peraluminous partial melt on cooling resulted in the highly unusual presence of volcanic cordierite.

www.minersoc.org

DOI:10.1180/minmag.2013.077.5.16

Earth surface redox constraints from the ancient Cr cycle

NOAH J. PLANAVSKY¹, CHRISTOPHER T. REINHARD¹,
XIANGLI WANG², WOODWARD W. FISCHER¹, THOMAS
M. JOHNSON² AND TIMOTHY W. LYONS³

¹ California Institute of Technology (planavsky@gmail.com)

² University of Illinois, Urbana Champaign

³ University of California, Riverside

Stable Cr isotope ratios of sedimentary rocks provide a historical record of large kinetic isotope fractionations associated with redox reactions at the Earth's surface. Cr in most igneous phases exists as Cr(III), which remains stable/immobile during terrestrial weathering under reducing conditions. Furthermore, both theoretical and experimental studies indicate that Cr will undergo limited fractionation during non-redox-dependent transformations. In marked contrast to non-redox processes, the oxidation and reduction of Cr induce large isotope fractionations. Therefore, Cr isotopes are ideally suited to track redox processes.

To date, iron formations have been the most utilized Cr isotope archive. Iron formations, as chemical precipitates, have the potential to trap an aqueous Cr isotope signature, rather than carrying a predominantly detrital Cr load. Further, iron oxides sorb significant amounts of Cr. And therefore iron oxide-rich rocks have a much higher potential than other chemical precipitates (e.g., cherts and carbonates) to have Cr isotope signatures that are rock buffered during burial alteration.

Based on previous work and our new results, the Archean iron formation Cr isotope record is generally characterized by near-crustal $\delta^{53}\text{Cr}$ values suggesting a lack of significant Cr redox cycling. In stark contrast, Neoproterozoic iron formations and Phanerozoic ironstones exhibit large and variable Cr isotope fractionations—a clear signal of substantial Cr redox cycling. Rather surprisingly, we found four mid-Proterozoic ironstones with limited Cr isotope variability despite having significant authigenic Cr enrichments. *In situ* Cr abundance work confirms that Cr in the examined samples is present in depositional phases (e.g., iron ooids) rather than in detrital Cr-rich phases (e.g., chromite). Our new results fill in a previously existing billion-year gap in sedimentary Cr isotope data and suggest that, in the Neoproterozoic, there was a permanent switch to a more oxidative Cr cycle. These results suggest limited Cr isotope fractionations due to low (relative to standard models) environmental oxygen concentrations for intervals of the mid-Proterozoic.

Modelling scavenged ocean tracers: Rare earth element transport and fractionation

YVES PLANCHEREL¹, XINYUAN ZHENG¹, PETER SCOTT¹,
SAMAR KHATIWALA² AND GIDEON M. HENDERSON¹

¹ University of Oxford, Earth Sciences Department, Oxford,
OX1 3AN, (yvesp@earth.ox.ac.uk)

² Lamont-Doherty Earth Observatory, Columbia University,
New York, USA

Insoluble metals such as rare-earth elements (REEs), Al, and Th have not been so widely studied as nutrients or dissolved gases as tracers of ocean process, but are seeing increasing interest driven by extensive new datasets and by a desire to understand the cycling of micronutrient metals (e.g. Fe, Cu) which are critical for biology and have a component of insoluble behaviour. Insoluble tracers have spatial oceanographic gradients dominantly controlled by their propensity to attach to particles (scavenging). In the ocean, REEs are interesting because, when normalized to their source composition (i.e. continental inputs), they show a systematic and relatively smooth (except Ce) progression from the light to the heavy REEs. The shape of this REE-pattern, which is the macro-scale representation of the lanthanide contraction, varies spatially in the ocean as a function of source proximity, water-mass mixing, water mass age and particle concentration. Because source types are similar for most REE (mostly rivers and dust), and REEs do not influence the particle field, the slight differences amongst the source-normalized dissolved REE concentrations in the ocean interior reflects the balance between physical transport and scavenging. Light REE (LREE) scavenge more readily than heavy REE (HREE) so HREE are more sensitive to transport than LREE.

In this study we exploit the LREE-to-HREE progression and explore the value of a new tracer (REE*) defined by the incremental differences between REEs in the pattern. We first present the large scale distribution and mean gradients of REE from the analysis of a global REE data set assembled from published historical values and new GEOTRACES measurements. Secondly, we discuss results from a set of sensitivity modeling experiment, based on the transport matrix formalism, designed to better understand controls on the distribution of REE in the ocean, the potential value of REE* as a water mass tracer, and the use of REEs to understand scavenged elements more generally.

Did thioarsenates start off the early arsenic cycle?

BRITTA PLANER-FRIEDRICH¹

¹Bayreuth University, Environmental Geochemistry Group,
Universitätsstrasse 30, 95440 Bayreuth, Germany,
(b.planer-friedrich@uni-bayreuth.de)

Arsenic is known as a poison, but there is a diversity of microorganisms that can conserve energy from oxidation or reduction processes in the As cycle. Two inorganic species are commonly thought to exist: Arsenite and Arsenate. Chemolithotrophic arsenite oxidation requires strong oxidants, such as nitrate or oxygen as electron acceptors. That means arsenate production could have only taken place after the onset of oxygenic photosynthesis about 2.5 billion years before present. Dissimilatory arsenate reduction with organic carbon or sulfide as electron donors completes the As cycle.

However, it has been suggested that arsenite could be oxidized in the absence of oxygen, by anoxygenic photosynthesis (1) which is known for Sulfide or Fe²⁺, but was unsuspected for As. It would enable a full As cycle already 3-3.5 billion years ago. Evidence for anoxygenic As photosynthesis came from two hot springs in Mono Lake, a saline lake in California, USA. The hot springs contain 100-130 μM As, supposedly all arsenite, 5000 μM Sulfide and are dominated by *Oscillatoria*-like cyanobacteria and an *Ectothiorhodospira* strain. Incubations of slurried biofilms showed arsenite oxidation in the light with CO₂ fixation (1).

We re-analyzed As speciation in these hot springs by our IC-ICP-MS method (2) and discovered that arsenite actually is only a minor species (<3%). Instead, thioarsenates (AsS_nO_{4-n}³⁻) dominate (78-95%). The observed anoxygenic production of arsenate (from thioarsenates, instead of arsenite!) could thus be a novel microbial metabolism. An alternative explanation is that there is no anoxygenic arsenic photosynthesis, but arsenite oxidation occurs as an abiotic follow-up to sulfide oxidation. Laboratory experiments show that monothioarsenate forms from arsenite and S⁰, an initial product of anoxygenic sulfide photosynthesis. Upon depletion of the S⁰ reservoir, monothioarsenate is desulfidized and forms arsenate. Thioarsenates might thus have been key reactive intermediate As species to help kick off a full As cycle before the advent of free oxygen by abiotically freeing the microbially catalyzed S cycle.

(1) Kulp *et al* (2008) *Science* **321**, 967 (2) Planer-Friedrich *et al* (2007) *Environ. Sci. Technol.* **41**, 5245.

Short Timescales of Magma Ascent Recorded in Melt Inclusion Diffusion Profiles

TERRY PLANK¹, ALEXANDER S. LLOYD¹,
PHILIPP RUPRECHT¹, ERIK HAURI² AND YOUXUE ZHANG³

¹Lamont-Doherty Earth Observatory, Palisades, NY, USA,
(tplank@ldeo.columbia.edu), (alloyd@ldeo.columbia.edu)

²Department of Terrestrial Magnetism, Carnegie, Washington,
DC, USA, (ehauri@ciw.edu)

³Dept of Earth & Environmental Sci., Univ of Michigan, Ann
Arbor, MI, USA, (youxue@umich.edu)

The rate of magma ascent is a primary proposed control on the eruptive vigor of volatile-rich magmas. Yet, very few quantitative estimates exist, in part because few geochronometers work at such short timescales (minutes to days). Here we present results of two different diffusion clocks, both of which record the minutes prior to and during eruption. The first involves diffusion of volatile species along melt embayments, as the partially-enclosed melt strives to equilibrate with surrounding degassing melt during magma ascent. NanoSIMS analysis (~5 micron spots) provides profiles of H₂O, CO₂, S, Cl and F along 100-300 micron tubes hosted in olivine from the 1974, sub-Plinian eruption of Volcan de Fuego in Guatemala. Fully-enclosed melt inclusions from the same samples constrain the initial volatile contents, and the decompression-degassing path followed by the melt exterior to the embayments. Despite very different diffusivities and solubilities, H₂O, CO₂ and S profiles all yield a consistent ascent rate in three different ash and lapilli samples: 13-16 m/s. Such rapid ascent, 8-9 km in 9-10 minutes, may contribute to the explosivity of this eruption.

Fully-enclosed melt inclusions from the same samples preserve major element profiles (MgO, CaO, Al₂O₃) that derive from olivine-growth on the inclusion rim and diffusion within the inclusion. We fit profiles using a coupled diffusion-growth model, where olivine growth is limited by both the rate of undercooling and the supply of MgO to the interface. While multiple cooling histories are possible, a constant cooling rate of 0.3-0.5K/s fits diffusion profiles across the ~ 50 micron diameter inclusions, with growth of ~ 0.4 microns of olivine in ~ 10 minutes. The similar timescales (~ 10 min) for both chronometers point to rapid decompression and cooling in the run-up to this explosive eruption. Extension of these melt inclusion clocks to other volcanic systems should provide new data on ascent, degassing and cooling rates, and their relationships to eruptive magnitudes.

On the hunt for a Gondwanan suture zone in South India

DIANA PLAVSA^{1*}, ALAN S. COLLINS¹, JOHN F. FODEN¹
CHRIS CLARK² AND M. SANTOSH³

¹Centre for Tectonics, Resources and Exploration (TRaX),
University of Adelaide, Australia

²The Institute for Geoscience Research (TIGeR), Curtin
University of Technology, Australia.

³School of Earth Sciences and Resources, China University of
Geosciences Beijing, China

The Southern Granulite Terrane (SGT) of India is located at the apex of the Indian subcontinent and is a Proterozoic mobile belt that was involved in the amalgamation of the Gondwana supercontinent. The tectonic evolution and geochemical characterization of individual crustal domains within the SGT is rendered difficult due to the intensity of metamorphism (ultra-high-temperature conditions) associated with the ca. 550–500 Ma collision between Neoproterozoic India and the African continents.

Here, we use Sm–Nd isotopes, U–Pb zircon geochronology and whole-rock geochemistry of the basement rocks combined with the Lu–Hf and U–Pb isotopic systems in detrital zircons from the overlying Neoproterozoic sequences to define Indian versus African affinities of the rock packages. The results are used to place constraints on the spatial distribution of individual crustal domains during the Proterozoic. Our results show that the metasedimentary rock packages north of the proposed suture zone (Palghat Cauvery Shear Zone) have Palaeoproterozoic maximum depositional ages and detrital signatures typical of Indian basement rocks, while those to the south have Neoproterozoic maximum depositional ages and probable African sources.

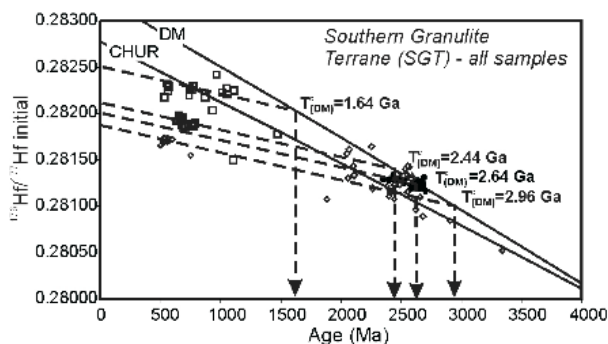


Figure 1: Initial $^{176}\text{Hf}/^{177}\text{Hf}$ vs. Age (Ma) evolution plot of detrital zircons from across the SGT.

Self-organizing reactive porosity waves allow large-scale fluid escape from subducting oceanic lithosphere

OLIVER PLÜMPER¹, TIMM JOHN², YURI Y.
PODLADCHIKOV³ AND MARCO SCAMBELLURI⁴

¹Department of Earth Sciences, Utrecht University, The
Netherlands (o.plumper@uu.nl)

²Institut für Mineralogie, University of Münster, Germany

³Institute of Earth Sciences, University of Lausanne,
Switzerland

⁴Dipartimento per lo Studio del Territorio e delle sue Risorse,
Università di Genova, Italy

At subduction zones seawater-altered oceanic lithosphere is returned to the Earth's mantle, where increasing temperatures and pressures results in the progressive destabilization of the hydrous minerals to release large amounts of aqueous fluids. This cycling of volatiles is one of the most distinctive features of subduction zones and has fundamental consequences for Earth's geodynamics and chemical cycles. Fluids released from the subducting slab trigger sub-arc mantle melting leading to explosive volcanism and induce petrophysical changes during dehydration that are thought to be the principal source of intermediate-depth intra-slab earthquakes. In all these cases large-scale transport systems need to form where fluids can escape from the subducting slab to either migrate up-dip along the plate interface or into the overlying mantle wedge. However, permeability is minimal at the depths and confining pressures relevant to subduction settings, thus insufficient to allow for pervasive fluid flow with high enough fluxes to efficiently drain the subducting oceanic plate. Evidence of the volatile cycle indicates that a fluid extraction mechanism is required that can keep pace with the slab descent velocity of cm/year to avoid the fluid being lost to the mantle. The tendency of fluid flow to occur channelized in space and time, illustrated in nearly all high-pressure terrains as vein networks, points to a potential mechanism. Channelized fluid flow would enable efficient fluid release rates with high local fluid fluxes over long distances. However, how a dehydrating system with an initially low, pervasive fluid production develops into channelized fluid extraction network is largely unknown. By using an interdisciplinary approach of field observations, reaction microstructures and numerical modeling we investigate the most prominent devolatilization reaction for the deep volatile cycle, the breakdown of serpentine phases within the subducting oceanic mantle. Based on our findings we formulate a fully consistent mechanistic model of metamorphic fluid escape during mineral dehydration.

Formation conditions of sapphirine-bearing assemblages from some complexes of Siberia

K.K.PODLESSKII

Institute of Geology of Ore Deposits, Petrography, Mineralogy and Geochemistry (IGEM), Russian Academy of Sciences, Staromonetny per. 35, 119017 Moscow, Russia (kkp@igem.ru)

Samples of granulites containing sapphirine-bearing assemblages from the Sutam, Chogar and Sharyzhalgay complexes, Siberia have been investigated with the microprobe, and their formation conditions have been estimated both with conventional thermobarometry and, where possible, with thermometry based on Ti contents of quartz [1]. With the estimates based on different methods showing good agreement, anomalously low temperature of $700\pm 50^\circ\text{C}$ has been obtained for the sapphirine + quartz bearing assemblages from the Sharyzhalgay complex (figure below), while metamorphic conditions estimated for the samples from other complexes correspond to conventional high-temperature ranges. Textural relations in the studied samples show that in many cases sapphirine formed due to retrograde reactions after spinel, aluminous orthopyroxene or sillimanite.

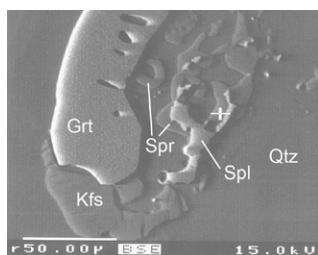


Figure 1, BSE image of Grt+Spr+Spl+Qtz assemblage in sample B-125 from the Sharyzhalgay complex.

Comparison of calculated stability fields of sapphirine-bearing assemblages with the estimates of temperature and pressure based on the mineral compositions indicate relatively low water activity in the course of metamorphism. However, lack of reliable experimental data on changes in composition of sapphirine with temperature and pressure inevitably requires considerable ambiguity in modeling reactions involving this mineral [2].

[1] Wark & Watson (2006) *CMP* **152**, 743-754. [2] Podlesskii (2010) *Petrology* **18**, 350-368.

Fe K-edge XANES of synthetic and natural silicate glasses: composition and $f\text{O}_2$ dependent structural properties

BT POE¹, C ROMANO², G CIBIN³, DB DINGWELL⁴, K-U HESS⁴ AND M POTUZAK⁵

¹Dipartimento INGEO, Università G. D'Annunzio, Chieti Italy (poe@ingv.it)

²Dipartimento di Scienze, Università degli Studi Roma Tre, Roma Italy (claudia.romano@uniroma3.it)

³Diamond Light Source Ltd., Oxfordshire UK (giannantonio.cibin@diamond.ac.uk)

⁴Department for Earth and Environmental Sciences, Ludwig-Maximilians University, Munich Germany (dingwell@lmu.de, hess@lmu.de)

⁵Corning Inc., New York, USA (potuzakm@corning.com)

The pre-edge region of the Fe K-edge x-ray absorption spectrum is well known to be sensitive to both local structural order (coordination number, polyhedral type) and valence state of iron. We have examined several Fe-bearing silicate glasses, both synthetic and remelted natural samples with wide-ranging chemical compositional characteristics, quenched from superliquidus temperatures and oxygen fugacities ranging from air to ca. 10^{-8} . Their Fe K-edge spectra were acquired on the GILDA beamline (BM08) at ESRF using a Si (311) monochromator. The pre-edge region of the spectra of all glasses were background subtracted and then normalized before being fit to the sum of two Lorentzian-shaped peaks. The energies of these two peaks remained nearly independent of glass composition and $f\text{O}_2$ whereas intensities and linewidths varied. For individual series of samples having the same chemical composition and varying oxygen fugacity, we observe a smoothly varying centroid position as a function of $\log f\text{O}_2$, consistent with changes in $\text{Fe}^{3+}/\text{Fe}^{2+}$ observed in many previous studies of this type, and verified for several samples using wet chemical analyses. Differences in the behavior of the centroid vs $\log f\text{O}_2$, however, from one series to another can be traced to compositional parameters such as degree of polymerization of the melt (e.g. NBO/T). We also observe systematic variations in total integrated intensities as a function of both $f\text{O}_2$ and chemical composition, allowing us to predict the degree to which Fe gradually transforms from a network former to a network modifier as oxygen activity decreases. The subtle differences applied to the structural role of a single chemical component in a multicomponent natural silicate melt could result in important differences in its physical properties and dynamic behavior.

Expanding hypoxia challenging marine life: Metazoan adaptations and limitations revisited

HANS-O. PÖRTNER¹

¹Integrative Ecophysiology, Alfred-Wegener-Institute, Am Handelshafen 12, 27570 Bremerhaven, (correspondence: Hans.Poertner@awi.de)

Expanding hypoxia in the world's oceans has led to renewed interest in the adaptation of organisms to life in hypoxic waters and to quantifying their sensitivity. The paper will discuss concepts and present understanding of hypoxia effects in the context of other marine drivers, predominantly temperature, and CO₂, which may combine with further anthropogenic stressors such as pollutants. In animals the concept of oxygen and capacity dependent thermal tolerance (OCLTT) has been proposed as a suitable integrator of various effects, from molecular to ecosystem level of biological organisation. Recent studies confirm applicability of the concept to climate related phenomena in the field. It has successfully explained effects of climate-induced temperature changes on species abundance and biogeographical ranges and appears applicable to climate related shifts in species distribution, temperature related phenology and predominance based on differential temperature dependent performance ranges which are sensitive to hypoxia. Focusing on various degrees of hypoxia, the paper will discuss the living conditions in hypoxic zones and which life forms those conditions can or do not support. Furthermore, it will be investigated how interactions of hypoxia with temperature and CO₂ may have played a key role in metazoan evolution during climate oscillations in earth history.

Li and Ca isotope evidence for continental weathering as a driver of End-Ordovician glaciation

PHILIP POGGE VON STRANDMANN¹, ANDRE DESROCHERS² AND TONU MEIDLA³

¹Department of Earth Sciences, University of Oxford, UK, (philipvs@earth.ox.ac.uk)

²Department of Earth Sciences, University of Ottawa, Canada

³Institute of Geology, University of Tartu, Estonia

The end-Ordovician Hirnantian interval (~445Ma) represents one of the largest mass extinctions in Earth history, and coincides with low temperatures, a major glaciation, and a significant drop in sealevel. However, this time period is also characterised by relatively high pCO₂ levels, and therefore the processes that triggered the glaciation, and its consequences for marine chemistry and life, are not well understood. Proposed causes include an increase in marine productivity and burial of organic carbon (causing a positive C isotope excursion), leading to drawdown of CO₂ [1], but also oscillations in silicate weathering (as a major sink of atmospheric CO₂), potentially due to continental movement and later ice-sheet coverage [2].

Lithium isotopes are a relatively novel tracer of continental weathering. Li is almost entirely situated in silicates, rather than carbonates, and its isotopic fractionation in rivers is demonstrably due to the intensity of silicate weathering. In addition, Li isotope fractionation remains constant in marine carbonates, regardless of changes in temperature or type of skeletal calcite. Calcium isotopes yield information on the balance of continental weathering vs. carbonate precipitation in the oceans, and hence the combination of Li and Ca isotopes can be used to examine CO₂ removal and sequestration processes.

We have determined Li and Ca isotope ratios through multiple marine carbonate sections from Anticosti Island in Canada and Inju in Estonia. The sections show an increase in δ⁷Li, reaching its peak slightly earlier than the peak in the C isotope excursion caused by the glaciation. This suggests that silicate weathering intensities decreased, while silicate weathering fluxes increased, in the run-up to the glaciation. We further investigate this with a series of dynamic models, using changes in ocean chemistry (Li, Ca, Sr and Os isotopes) to constrain the evolution of continental and marine processes through this period of extreme climate change.

[1] Brenchley *et al* , 1995, *Mod. Geol.* **20**, 516-519 [2] Kump *et al* , 1999, *Palaeo* **152**, 173-187

Variability of biogeochemical characteristics of bottom sediments near the B.Goloustnoe seep (Lake Baikal)

T. POGODAEVA^{1*}, O. PAVLOVA¹, G. KALMYCHKOV², O. SHUBENKOVA¹ AND T. ZEMSKAYA¹

¹Limnological Institute SB RAS, Ulan-Batorskaya St., Irkutsk 664033, Russia (*correspondence: tatyana@lin.irk.ru)

²Vinogradov Institute of Geochemistry SB RAS, 1 Favorsky St., Irkutsk 664033, Russia

In order to assess the short-term activity, we studied the area near the methane seep B.Goloustnoe within two winter expeditions, during the ice period, and three summer expeditions. Bottom sediments in the area are saturated in methane (99.3vol.%) of mixed (biogenic + thermogenic) genesis [1]. Methane concentrations in the studied sediments reached 70 mL/L of sediments. Bottom sediments indicated fresher calcium bicarbonate waters, with salinity of up to 100 mg/L, than the water in Lake Baikal. At the same time, bicarbonate ion concentration in the surface layer was less than 1.2 mM. We have determined a temporal variability in chemical composition of pore waters and methane concentrations. Additionally, we have identified the variability in the distribution and number of hydrocarbon oxidizing aerobic and anaerobic microorganisms (HCOM). Trends in concentration profiles of bicarbonate ions consistently changed the directions, from horizontal to left and right inclined. In the surface sediment layer, sulfate ions occurred (being absent), accumulated (up to 0.15 mM), and disappeared again. The profiles of methane curves showed decrease in methane concentration in the near-surface layers of the sediments indicating its consumption. Using pmoA-gene specific primers was obtained in surface sediments representatives of types I, II, X methanotrophs. Size of the consumption zone was inversely proportional to the methane concentration in the core. At moderate concentrations of methane in sediments, thickness of the consumption zone in the methane seep B.Goloustnoe reached 1.2 m.

These factors suggest the situation variability at this site: change, termination, and renewal of gas flows; and gas discharge is accompanied by the discharge of low-salinity waters. Underlying gas hydrates may be the source of these waters. Intensity of gas-containing fluids changes chemical environment causing fluctuations in the development of aerobic and anaerobic microorganisms.

[1] Hachikubo *et al* (2010) *Geo-Mar Lett* **30**, 321–329.

Tracing industrial atmospheric emissions using radiogenic isotopes

A. POIRIER¹, J. GOGOT¹ AND A. BOULLEMANT²

¹Geotop-UQAM, CP8888, Succ. Centre-ville, Montréal, QC, H3C 3P8, Canada

²RioTintoAlcan, 1188 rue Sherbrooke Ouest, Montréal, QC, H3A 3G2, Canada

Large industrial complexes are generators of large economic boost in the area where they establish themselves. But a big industry, such as an aluminium smelting complex inevitably has some environmental impact on its immediate surroundings.

Our study aims at monitoring one aspect of such impact, namely the dispersion of particulate matter in the atmosphere, and their eventual fallout on the regional level. Two radiogenic isotope systems were used in order to do so: osmium (Os) and lead (Pb). These metals were found to be present as traces in the carbon anodes, one of the main raw materials to be used in such Al-smelting industrial process. These anodes are consumed during the electrolytic process and produce CO₂ when reducing Al₂O₃ to liquid metallic Al. Large gas emissions so formed entrain some particulate matter at the stacks, despite the use of high efficiency gas and dust scrubbers.

From our results of osmium content and lead isotopic composition, the main conclusion of our study is that some of the dust generated by this type of industry does escape to the atmosphere, but seems to be falling back very close to its source (e.g. nearby the emitting chimneys) and in this specific case stays nearly completely within the boundaries of the industrial complex.

Comparison of the Fe isotope composition of unfiltered waters, dissolved and particulate fraction of the Amazon River and its tributaries

F. POITRASSON^{1,2*}, L.C. VIEIRA¹,
G.M. DOS SANTOS PINHEIRO^{1,2}, D.S. MULHOLLAND^{1,2},
P. SEYLER^{1,2}, F. SONDAG^{1,2}, G.R. BOAVENTURA¹
M.M. PIMENTEL¹

¹Instituto de Geociências, Universidade de Brasília, Campus Darcy Ribeiro, 70904-970 Brasília-DF, Brazil.

²Laboratoire Géosciences Environnement Toulouse, IRD-CNRS, 14-16, av. E. Belin, 31400 Toulouse, France.

*corresponding author: Franck.Poitrasson@get.obs-mip.fr

Pioneering studies revealed that for some river waters, large $\delta^{57}\text{Fe}$ fractionations are observed between the suspended and dissolved load, and isotopic variations were also recognized on the suspended matter along the hydrological cycle. On land, soil studies in various locations have shown that $\delta^{57}\text{Fe}$ signatures depend mostly on the weathering regime. It thus seems that Fe isotopes could become an interesting new tracer of the local interactions between soils, rivers and the biosphere.

We therefore conducted Fe isotope surveys through multidisciplinary field missions on rivers from the Amazon Basin. It was confirmed that acidic, organic-rich black waters show strong Fe isotope fractionation between particulate and dissolved loads. Furthermore, this isotopic fractionation varies along the hydrological cycle, like previously uncovered in boreal waters suspended matter. In contrast, unfiltered waters show very little variation with time.

It was also found that Fe isotopes remain a conservative tracer even in the case of massive iron loss during the mixing of chemically contrasted waters such as the Negro and Solimões tributaries of the Amazon River. Given that >95% of the Fe from the Amazon River is carried as detrital materials, our results lead to the conclusion that the Fe isotope signature delivered to the Atlantic Ocean is undistinguishable from the continental crust value, in contrast to previous inferences.

The results indicate that Fe isotopes in rivers represent a promising indicator of the interaction between organic matter and iron in rivers, and ultimately the nature of their source in soils. As such, they may become an interesting tracer of changes occurring on the continents in response to both weathering context and human activities.

Probing gold and sulfur geological fluids at extreme conditions by in-situ spectroscopy

G.S. POKROVSKI^{1*}, A. BORDAGE², J. DUBESSY³,
L. DUBROVINSKY⁴, D. GUILLAUME¹, J.-L. HAZEMANN²,
N. JACQUEMET¹, M.A. KOKH¹, K. KOUZMANOV⁵
AND A. ZWICK⁶

¹GET, CNRS, University of Toulouse, France
(gleb.pokrovski@get.obs-mip.fr)

²Institut Néel, ESRF, Grenoble, France

³G2R-Géoresources, Vandoeuvre-lès-Nancy, France

⁴Bayerisches Geoinstitut, Bayreuth, Germany

⁵University of Geneva, Switzerland

⁶CEMES, CNRS, Toulouse, France

Although aqueous fluids account for a tiny fraction of our planet, they play a key role in chemical elements transfer on Earth. These fluids dissolve and precipitate minerals, form economic ore deposits, and control geochemical cycles of metals and volatiles. Knowledge of the chemical status of dissolved elements - their speciation, and the solubility of minerals is the key to quantifying the geological impact of such fluids operating at 'extreme' conditions of high pressure and temperature in Earth's interiors. Because these milieus are not accessible to direct observations, their study requires in-situ spectroscopic approaches.

In this contribution, we report on our recent findings on the behavior of sulfur and gold in hydrothermal-magmatic fluids, revealed by in-situ Raman and X-ray absorption spectroscopy coupled with thermodynamic and molecular modeling. Results challenge the long-standing paradigm that sulfate (HSO_4^- , SO_4^{2-}) and sulfide (H_2S , HS^-) are the two major forms of sulfur in terrestrial fluids [1]; they demonstrate that in the liquid and supercritical fluid phase in addition to these two common sulfur redox states, the trisulfur ion, S_3^- , forms in significant amounts above $\sim 300^\circ\text{C}$ and over a range of depth (to ~ 100 km) [2]. The S_3^- ion binds gold in hydrothermal fluids, forming stable $[\text{HS-Au}^{(0)}\text{-S}_3]$ complexes largely enhancing the metal solubility; thus, S_3^- is likely to be an important carrier of sulfur and associated metals (Au, Pt, Cu, Mo) for magmatic-hydrothermal deposits in subduction zones [3]. The formation of S_3^- requires a revision of metal speciation models in S-rich aqueous and carbonic fluids [3, 4, 5] and, potentially, silicate melts, operating in the Earth's crust and upper mantle.

[1] Ohmoto & Lasaga (1982) *GCA* **46**, 1727-1745. [2] Pokrovski & Dubrovinsky (2011) *Science* **331**, 1052-1054. [3] Kouzmanov & Pokrovski (2012) *SEG Special Publication* **16**, 573-618. [4] Pokrovski *et al.* (2009) *GCA* **73**, 5406-5427. [5] Kokh *et al.* (2013) *MinMag*, this volume.

Carbonatites out of a subducted altered oceanic crust? Experimental evidences for epidote-dolomite eclogite melting at 3.8–4.2 GPa

S. POLI

Dept. of Earth Sciences, University of Milan, 20133 Milan, Italy (stefano.poli@unimi.it)

Current knowledge on the solidus temperature for carbonate-bearing rocks suggests that carbonatitic magmas should not at the slab-mantle interface, unless thermal relaxation is promoted by a variety of possible tectonic scenarios. For a mildly warm subduction path, COH-bearing altered MOR basaltic eclogites are expected to lose all H₂O component at epidote breakdown, located at approx. 2.8–3.0 GPa. Above this pressure limit, the solidus of a carbonated basaltic eclogite has a minimum temperature of approx. 1000 °C at 4.0–4.5 GPa. However, the oceanic crust includes a range of gabbroic rocks, altered on rifts and transforms, with An-rich plagioclase abundances from 50% to 80% in volume. It has been shown that epidote disappearance with pressure depend on the normative anorthite content of the bulk composition considered, we therefore expect that altered gabbros might display a much wider pressure range where epidote affects solidus relationships.

New experimental data from 3.8 to 4.2 GPa, 750 °C to 1000 °C are intended to unravel the effect of variable bulk and volatile compositions in model eclogites, enriched in the normative anorthite component (An₃₇ and An₄₅). Experiments are performed in a piston cylinder and multi-anvil machines apparatus.

At 3.8 GPa, 800 °C, fluid saturated conditions, garnet, omphacite and kyanite coexist with epidote, dolomite and magnesite. At 900 °C, fluid-rich conditions, garnet and Na-poor clinopyroxene coexist with a silicate fluid/melt of granitoid composition, a carbonatitic melt and a Na-carbonate. Close to fluid-saturation, 4.2 GPa, 900 °C, garnet and Na-rich clinopyroxene coexist with a carbonatitic melt and dolomite. The carbonatitic melt is richer in Ca compared to dolomite, consistently with phase relationships in the model system MgCO₃-FeCO₃-CaCO₃. The H₂O-component deriving from a fluid-absent melting of epidote, enlarged in its pressure stability in An-rich gabbros, promotes melting of carbonates.

The possibility of extracting carbonatitic melts from a variety of gabbroic rocks in a subducting slab, at depths in the order of 120–130 km, offers new scenarios on the metasomatic processes in the lithospheric wedge of subduction zones and a new mechanism for recycling carbon.

Impact of climate change on soil microorganisms and carbon cycling in an arable ecosystem

CHRISTIAN POLL, SVEN MARHAN
AND ELLEN KANDELER¹

¹Institute of Soil Science and Land Evaluation, Soil Biology Section, University of Hohenheim, Emil-Wolff-Str. 27, D-70593 Stuttgart

Carbon cycling in terrestrial ecosystems provides a feedback mechanism to climate change by releasing or sequestering additional atmospheric CO₂. However, the role of soil microorganisms as key players in this feedback mechanism is still unclear. The Hohenheim Climate Change (HoCC) experiment was established in summer 2008 to manipulate soil temperature and precipitation on an arable field. Soil temperature is increased by 2.5 °C in 4 cm and is combined in a factorial design with the following precipitation manipulation treatments: a) ambient, b) precipitation amount decreased by 25% during summer and increased by 25% during winter, c) drought periods increased by 50% during summer, d) combination of b and c. The experimental plots were planted with spring wheat (*Triticum aestivum*, 2009), spring barley (*Hordeum vulgare*, 2010), oilseed rape (*Brassica napus*, 2011) and winter wheat (*Triticum aestivum*, 2012). Soil samples (0–5 cm, 5–15 cm and 15–30 cm depth) were taken at four occasions in 2009 and 2010 and at three and two occasions in 2011 and 2012, respectively. Data of aboveground biomass, soil organic carbon, soil microbial biomass, ergosterol content, hydrolytic enzyme activities and CO₂ fluxes (weekly measurements) will be presented. Results from 2009 and 2010 indicate that changes in soil temperature and precipitation differently affected aboveground biomass and that these effects depended on the crop. Effects of elevated soil temperature on microbial biomass and CO₂ fluxes were related to moisture conditions during the different seasons of the year in 2009 but not in 2010 [1]. First evaluation of ergosterol contents and enzyme activities from 2009 to 2012 indicate that soil warming increases fungal biomass and microbial activity depending on the time of sampling. Overall, the presentation will give insight into the complex interactions between climate change, soil moisture and soil microorganisms as key players of carbon cycling in the investigated arable ecosystem.

[1] Poll, Marhan, Back, Niklaus & Kandeler (2013), *Agriculture, Ecosystems and Environment* 165, 88–97.

Fe β -factors for sulfides from NRIXS synchrotron experiments

V.B. POLYAKOV^{1*}, E.G. OSADCHII¹, D.A. CHAREEV¹,
A.I. CHUMAKOV I.A. SERGEEV³

¹Institute of Experimental Mineralogy, RAS, Chernogolovka,
142432, Russia

(*correspondence: polyakov@iem.ac.ru)

²European Synchrotron Radiation Facility (ESRF), BP 220, F-
38043 Grenoble, France

³Forschungszentrum Juelich GmbH.

We obtained equilibrium Fe isotope fractionation factors (β -factors) for troilite pyrrhotites, sphalerite, pyrite, and chalcopyrite nuclear inelastic x-ray resonant scattering (NIXRS) experiments performed in ESRF (Fig. 1).

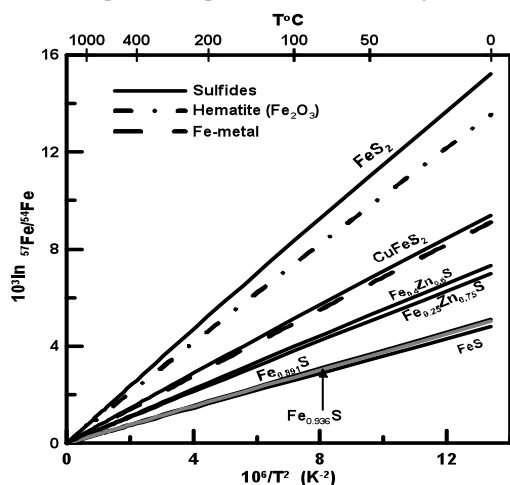


Figure 1: NRIXS-derived β -factors of sulfides.

The β -factor for troilite from our experiment coincides with that obtained in [1] from NRIXS data [2]. β -factors for pyrrhotites and sphalerite are quantified first time. The Fe β -factor for pyrite agrees excellently with DFT calculations [3] and deviates significantly from the Mössbauer-derived β -factor [4]. The β -factor for chalcopyrite agrees with those calculated in [5] based on data in [6]. Our experiments with chalcopyrite, performed at different temperatures, revealed that anharmonicity may effect on the NRIXS spectrum and lead to overestimating the NRIXS-derived β -factor.

[1] Polyakov *et al* (2007) *GCA* **71**, 3833-3836. [2] Kobayashi *et al* (2004) *Phys. Rev. Lett.* **93**, 195503. [3] Blanchard *et al* (2009) *GCA* **73**, 6565-6578. [4] Polyakov and Mineev (2000) *GCA* **64**, 849-865. [5] Polyakov & Soultanov (2011) *GCA* **75**, 1957-1974. [6] Kobayashi *et al* (2007) *Phys. Rev. B* **76**, 134108

Thermochronological estimates of uplift and cooling rates of the Bodonchin metamorphic wedge

O.P. POLYANSKY* AND V.P. SUKHORUKOV

V.S. Sobolev Institute of Gology and Mineralogy, SB RAS. Pr.
Ac. Koptuyug 3, Novosibirsk, 630090, Russia

(*correspondence: pol@igm.nsc.ru)

Reconstructing the tectonic history of the structures of the Irtysh-Bulgan lineament (SW Mongolia) is of interest for solving the problem of continental crust formation. Based on the new thermochronological and geothermobarometric data, we analyze the metamorphic conditions and tectonic evolution of the Bodonchin zonal complex in the Mongolian Altay [1]. A crustal fragment exposed on the southern slope of the Mongolian Altay consists of isoclinal-folded rocks, over 20 km thick, and shows a continuous metamorphic zoning from greenschist facies to migmatites. Using THERMOCALC P-T estimates we calculated the thermal state of the crust beneath Mongolian Altay during terrane collision and reconstructed the paleogeotherm at the peak of syn-collisional metamorphism. The thermal state of the crust was characterized by high radiogenic heat production (1.66 $\mu\text{W}/\text{m}^3$) and elevated heat flow (45 mW/m^2). The estimated P-T conditions in two zones (staurolite-kyanite schists and migmatites) of the Bodonchin complex correspond to the paleogeotherms with average temperature gradients of $\partial T/\partial z = 25.5$ and $27.2^\circ\text{C}/\text{km}$. The data from isotope dating of zircon and other metamorphic minerals (Bt, Ms, Amp) were used to construct a thermochronological model for the retrogressive stage of polymetamorphic evolution. The uplift rates of metamorphic rocks as a result of thrusting within the Bulgan Fault zone were estimated at 315–1010 m/Myr .

[1] Polyansky *et al* (2011) *Rus. Geol. Geophys* **52**, 991-1006.

Magma dynamics at Etna before the 122BC Plinian eruption: Constraints from plagioclase zoning profiles

MASSIMO POMPILIO^{1*} AND PAOLA DEL CARLO¹

¹Istituto Nazionale di Geofisica e Vulcanologia, Sez. di Pisa, Italy (*correspondence: pompilio@pi.ingv.it)

The 122 BC Plinian eruption of Etna is one of the best studied highly-explosive basaltic eruption since detailed stratigraphic, textural, and compositional data, including pre-eruptive volatile content, are available. Former studies [1] proposed an eruption model in which an abrupt decompression event triggered a sudden bubble nucleation allowing the magma to develop rapidly into a microvesicular foam or alternatively the attainment of some critical threshold in rheology of foam-like magma was invoked and the occurrence of special external forces was excluded [2]. The above mechanisms, both feasible, still don't consider adequately the state and the evolution of the magmatic plumbing system before the eruption. To fill this gap we measured zoning profiles in plagioclases of different size (from large megacrysts to microphenocrysts) belonging to the Plinian deposit and plagioclase phenocrysts erupted during the Strombolian activity that preceded the paroxysmal phase. To detail the whole temporal evolution of the system we assumed that megacrysts found in Plinian products have recorded the whole pre-eruptive history, while phenocrysts and microphenocrysts account only for the final phases. Similarly, we considered the zoning of plagioclases of the Strombolian activity as representative of the state of the magmatic system before the climatic phases. Plagioclase zoning has been interpreted by comparison with synthetic profiles obtained from the thermodynamic modelling of different magmatic processes that involved single/multistage and open/closed-system paths [3]. Results indicate that the magmatic system underwent a complex evolution that entails: i) existence of at least two distinct magmatic environments; ii) progressive migration of magmas between these two environments iii) progressive overfilling and destabilization of the shallow plumbing system before the Plinian phase. This picture emphasizes the active role of the magma transfer in determining the eruptive style and allows to identify what is the combination of factors that can favour the development of such a large explosive event.

[1] Coltelli, Del Carlo & Vezzoli (1998) *Geology* **26**, 1095–1098. [2] Goepfert & Gardner (2010) *Bull. of Volcanol.* **72**, 511–521. [3] Ghorso and Sack (1995) *Contrib Mineral Petr* **119**, 197–212.

Leucoxene Photoactivity in the Water – Mineral System

A. PONARYADOV^{1*}, O. KOTOVA¹ AND YU. RYABKOV²

¹Institute of Geology Komi SC UB RAS, Syktyvkar

(*correspondence: alex401@rambler.ru)

²Institute of Chemistry Komi SC UB RAS, Syktyvkar

The photocatalytic activity of leucoxene in the water – mineral system was studied. Leucoxene was extracted from samples of titaniferous sandstones taken from quarry of Pizhemscoe deposit (Russia) (malorucheiskaya suit, Devonian). Mineral composition is presented by quartz, leucoxened ilmenite, zircon, tourmaline, amphibole. Samples KAH-1, KAH-1-2 and KAH-1-3 were studied (Table 1).

Grain-size analysis was carried out and the TiO₂ content was measured for each grain-size fraction. Fractions with the highest TiO₂ content are shown in Table 1.

Sample	Fraction, mm	TiO ₂ content, wt. %
KAH-1	-0.315+0.25	10.60
KAH-1-2	-0.25+0.2	12.25
KAH-1-3	-0.05	14.91

Table 1: TiO₂ content in studied samples.

Photocatalytic activity of the samples was studied using test reaction of degradation of 2, 4, 6-trichlorophenol (TCP) in water.

According to the obtained results photocatalytic activity of leucoxene samples is in direct relation with TiO₂ content and specific surface area.

The project was done under the financial support of projects 12-5-6-016-ARKTIKA and 12-M-35-2055.

Inter- and intra-specific variability of trace metals in shells of *Mytilus* sp., *Serripes* sp., and *Arctica* sp.

A. PONNURANGAM^{1,2*}, A. KOSCHINSKY¹, M. BAU¹,
T. BREY² AND J. BIJMA²

¹School of Engineering and Science, Jacobs University,
Bremen, Germany
(*correspondence: a.ponnurangam@jacobs-university.de)

²Alfred Wegener Institute for Polar and Marine Research,
Bremerhaven, Germany

Bivalve shells contain within their structure a record of their past growth in the sea due to the sequential deposition of layers of mineralised material, laid down according to the organism's growth rate. For this reason, the importance of bivalve shells as proxy archives for changes in environmental conditions like ocean acidification, is increasingly recognized. However, data for trace metal concentrations in bivalve shells are quite scarce and underrepresented.

The incorporation of trace metals, including rare earth elements and yttrium (REY), as well as uranium in shells of *Mytilus* sp., *Serripes* sp. and *Arctica* sp. was investigated through bulk trace metal analysis. The chemistry of these trace metals in terms of speciation and complexation, makes them particularly useful in acting as geochemical proxies of oceanic change. We looked at the availability and variability of trace metals in shells from different locations and at the extent to which these shells reflect the ambient seawater trace metal content.

Differences in element concentrations were found within and between species. Clear-cut differences in concentrations of REY were observed between the different species of bivalves. Shells of the same species from different sampling locations were found to be enriched differently. Some shells exhibited more seawater-like signatures while others reflected signature patterns of particulate matter. Furthermore, major trace elements like uranium, also varied within species obtained from different locations. *Serripes* sp. from Svalbard were found to contain higher concentrations of uranium than those from Alaska.

Our findings demonstrate the extent of within-species spatial biomineral variability and provide hints as to how shells may or may not reflect characteristics of ambient seawater. If the incorporation of trace metals in biominerals is indeed sensitive to environmental condition, these elements may add to proxy based reconstruction of environment history.

Whether graphites is able to reflect an economical aspect of metalliferous strata

V.A.PONOMARCHUK^{1,2*}, T. N. MOROZ¹,
A.N. PYRYAEV¹, A.V. PONOMARCHUK¹
AND D.V. SEMENOVA¹

¹Institute of Geology and Mineralogy, 630090 Novosibirsk,
Russia;

²Novosibirsk State Universitet
(*correspondence: ponomar@igm.nsc.ru)

A carbon situated in numerous of Au-, Pt-, Pd-ore and other metals deposits. Carbon-metal correlation is wide discussed and contrary points of view are exist: active (metalorganic+transport) and passive (reducing environment) role of carbon. In order to understand correlation described above comparative study have ben performed. It include morphological (scanning microscopy), microelemental (synchrotron radiation –X-Ray fluorescence), isotopic composition investigations and carbon ordering degree analysis (Raman spectroscopy) of Malomyr, Suhoy Log (Russia) and Suzdal (Kazakhstan) black shale deposits. Moreover, graphites in Pt–Low_Sulfide Ores of Verhnetalnahsk intrusion have ben studied [1,2].

The main propeties of the black shale deposit graphites are moderate generation temperature (200–400°C), low degree of carbon ordering (I_{D1}/I_G – from 0.6 to 1.2) and wide range of carbon isotopic composition (generally from -18 to -28 ‰). Graphites in Pt–Low_Sulfide Ores of Verhnetalnahsk intrusion characterized by nanostructured topology (Fig.), high generation temperature (450 - 750°C), high Pt content (less than 50 ppm), high degree of carbon ordering (I_{D1}/I_G – from 0.02 to 0.2) and short range of carbon isotopic composition (fron -13.5 to -15 ‰). Preliminary conclusion: only nanostructured graphite is able to reflect economical characteristics of metalliferous strata.

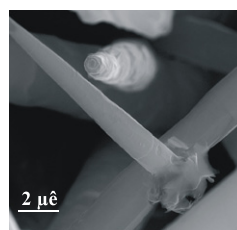


Figure. Scan-image of nanostructured graphite: "T"-joint nano- and microtubes.

[1] Ryabov, Ponomarchuk, Titov & Semenova (2012) *Doklady Earth Sci.* 446, 1193–1196; [2] Ponomarchuk V., Kolmogorov, Ryabov, Titov, Moroz, Pyryaev & Ponomarchuk A. (2013) *Bul. of the Russian Academy of Sci. Physics* 77, 203–206.

Isotopes of elemental carbon in the Chelyabinsk meteorite

V.A. PONOMARCHUK^{1,2*}, N.M. PODGORNKYKH¹,
A.N. PYRYAEV¹ AND A.V. PONOMARCHUK¹

¹Institute of Geology and Mineralogy, 630090 Novosibirsk, Russia;

²Novosibirsk State Universitet

(*correspondence: ponomar@igm.nsc.ru)

Isotope composition of elemental carbon in Chelyabinsk meteorite fragments (date of iron-fall – 15 February 2013) was studied. A fragments covered by dark fusion crust with thickness about 1 mm had amorphous or sometime roundish shape with size about 0.7-1.5 cm. Outer crust and traces of silicate material melting were removed mechanically. Mineralogical composition of fragments under investigation was reported by [1,2]. The meteorite previously classified as LL5 chondrite (S4, W0) [GEOKHI RAS].

Analytical procedure includes advance warming-up (1000°C) of samples in helium continuous flow during two hours. Then the samples were combusted in oxygen (950°C) during 40 minutes. Carbon isotope composition were determined using Thermo Finnigan 253 mass spectrometer and GasBanch with specially-constructed line [3]. Table exhibit obtained data.

Table. Carbon content and isotopic composition of elemental carbon in Chelyabinsk meteorite. Variation of given isotopic composition values not exceed ~1,5 ‰ within at least two measurements.

Sample	Weight mg	Content C, ppm	Carbon-13 (PDB)
2.36	29.2	340	-24,5
2.55	7.51	1270	-23.6
3.14	7.15	6710	-22.7
2.73	8.91	2120	-16.8
4.03	10,8	3700	-17,9

Thus carbon content and $\delta^{13}\text{C}$ values remains in usual order for CO-type meteorites [4].

[1] Sharygin, Karmanov, Timina, Tomilenko, Podgornykh, <http://www.igm.nsc.ru/Menu/NewsDetails.aspx?newsid=44>;

[2] Sharygin, Timina, Karmanov, Tomilenko & Podgornykh (2013) *Min Mag*, this volume; [3] Semenova & Ponomarchuk (2009) *GCA* 73, A1193; [4] Pearson, Sephton, Franchi, Gibson & Gilmore (2006) *Meteoritics & Planetary Science* 41, 1899–1918.

The results of preliminary study of magnetic fabric in the Panj-Kuh granitoid, SE Damghan - Iran

M. POORALIZADEH MOGHADAM*¹, M. SHEIBI²
AND H.GHASEMI³

¹MSc. student of Petrology, Department of Geology, Shahrood University of Technology, Shahrood, Iran

(*correspondence: Mahdokht.p.petro@shahroodut.ac.ir)

^{2,3}Faculty Member, Department of Geology, Shahrood University of Technology, Shahrood, Iran

(sheibi@shahroodut.ac.ir and

h_ghasemi@shahroodut.ac.ir)

Panj-Kuh pluton (15 km²) is located in the most northern part of Central Iran structural zone, SE Damghan. The pluton intruded in Eocene volcanic - sedimentary rocks and compositionally ranges from monzonite to syenite. It is I-type granite, calc-alkaline and metaluminous in nature and it's associated Fe oxide deposit created by sodic-calcic and potassic alteration [1].

Magnetic fabric on the Panj-Kuh granitoid carried out by (MFK1-FA) Kappbridge susceptometer (AGICO, Brno) operating at low field ($4 \times 10^{-4}\text{T}$; 920 Hz) at Geomagnetic Lab of Shahrood University of Technology. According to the determined measurements (41 stations and 262 fragments), mean values of the magnetic susceptibility (K_m) for syenite and monzonite are 37880 and 22713 μSI , respectively. The rocks due to the relatively high average magnetic susceptibility ($K_m > 400 \mu\text{SI}$) belongs to ferromagnetic granites and the magnetite is the main iron bearing mineral carrying magnetic susceptibility. Where the Na-Ca alteration - characterized by the partial or full absence of magnetite and biotite and appearance of albite and scapolite – is intensified, magnetic susceptibility magnitude is decreased. The main identified microstructural types in the studied pluton is magmatic. The percentage of anisotropy (P%) values vary from 1 to 1.2 and show positive correlation with degree of deformation. Shape parameter of magnetic ellipsoid (T) values varies from 0.93 to -0.48 and most of magnetic ellipsoids are oblate.

[1] Sheibi & Esmaeily (2004) in 5th international symposium on Eastern Mediterranean Geology, 1242-1243.

Estimates of REE distribution in the hydrothermal ore forming fluid of the Iul'tin and Svetloe deposits

J.A.POPOVA¹, A.YU.BYCHKOV^{1,2}, S.S.MATVEEVA¹
AND T.M. SUSHCHEVSKAYA²

¹Moscow State University, Moscow, Russia

julka_p@rambler.ru

²Vernadsky Institute of Geochemistry RAS, Moscow, Russia

Two Sn-W deposits, Svetloe and Iul'tin (Chukotka Peninsula, Russia) take place within the Iul'tin ore district. Both deposits belong to the cassiterite-quartz formation, are confined to an intersection of deep-seated faults, have spatial and genetical relation to the Upper Cretaceous granitic magmatism and show similar sequences and composition of mineral assemblages.

REE content in single grains of fluorite, wolframite and scheelite was measured by ICP-MS at the Element-2 instrument. REE concentrations in the hydrothermal fluid were obtained based on the distribution coefficients of mineral/fluid [1].

REE content in Svetloe and Iul'tin wolframites allows to suggest that for the wolframites the fluid was magmatic one. This magmatic fluid was enriched by Sm, Gd, Tb, Dy and was characterized by Eu minimum. Regularities of REE spectra changes indicate the presence of two generations of fluorite in the deposits. For the first fluorite generation the fluid is magmatic one, its composition corresponds to the wolframite magmatic fluid. For the second fluorite generation the fluid is exogenous, the Eu minimum is absent or indistinct, these fluorites are enriched in light REE.

The content of the REE were determined in fluid inclusions using aqueous extracts from quartz. This method shows lower REE concentrations than calculated ones based on mineral composition, but the regularities of REE spectra changes also correspond to the presence of two fluid sources (exogenic and magmatic).

The evolution of fluid was calculated based on thermodynamical model of ore deposition for Iul'tin deposit. Modeling demonstrated that the REE content changes due to both mixing of two different fluids and minerals (wolframite and fluorite) deposition.

This study was supported by RFBR 13-05-00954.

1.Raimbault L. Bull. Mineral, V. 108, P.737-744, 1985.

Primary and secondary biogenic aerosols

ULRICH PÖSCHL

Max Planck Institute for Chemistry, Multiphase Chemistry
Department, Mainz, Germany; (u.poeschl@mpic.de)

Biogenic aerosols comprise primary biological particles (PBAP) such as bacteria, spores and pollen emitted from the Earth surface as well as secondary organic matter (SOA) formed by reaction and condensation of gaseous precursors in the atmosphere. PBAP are essential for the spread of organisms in the biosphere, and numerous studies have suggested that PBAP and SOA can be important for atmospheric processes, including the formation of clouds and precipitation.

The sources and diversity, atmospheric abundance and transport, physicochemical properties and transformation of biogenic aerosols, including their activity as cloud condensation and ice nuclei (CCN, IN), however, are not yet well characterized. Thus, their actual influence on the evolution, present state and future development of the Earth system, the hydrological cycle and other biogeochemical cycles is not yet well constrained. General perspectives and recent advances shall be outlined and discussed.

[1] Burrows, Elbert, Lawrence, & Pöschl (2009), *Atmos. Chem. Phys.* **9**, 9263-9280. [2] Despres *et al* (2012), *Tellus B* **64**, 15598. [3] Fröhlich-Nowoisky, Pickersgill, Després, & Pöschl (2009), *Proc. Natl. Acad. Sci.*, **106**, 12814-12819. [4] Fröhlich-Nowoisky *et al* (2012), *Biogeosci.* **9**, 1125-1136. [5] Fuzzi *et al* (2006), *Atmos. Chem. Phys.* **6**, 2017-2038. [6] Elbert, Taylor, Andreae & U. Pöschl (2007), *Atmos. Chem. Phys.* **7**, 4569-4588. [7] Huffman, Treutlein, & Pöschl (2010), *Atmos. Chem. Phys.* **10**, 3215-3233. [8] Huffman *et al* (2008), *Atmos. Chem. Phys.* **12**, 11997-12019. [9] Huffman *et al* (2013) *Atmos. Chem. Phys. Discuss.* **13**, 1767-1793. [10] Pöhlker *et al* (2012), *Science* **337**, 1075-1078. [11] Pöschl (2005), *Angew. Chem. Int. Ed.*, **44**, 7520-7540. [12] Pöschl *et al* (2010), *Science*, **429**, 1513-1516. [13] Pöschl (2011), *Atmos. Res.* **101**, 562-573. [14] Shiraiwa, Ammann, Koop & Pöschl (2011) *Pro. Natl. Acad. Sci.*, **108**, 11003 - 11008. [15] Shiraiwa *et al* (2011) *Nature Chem.* **3**, 291-295.

Silicon diffusion in liquid iron: Kinetic implications for metal-silicate equilibration

ESTHER S. POSNER*, DANIEL J. FROST
AND DAVID C. RUBIE

Bayerisches Geoinstitut, Universität Bayreuth, Germany
(*correspondence: esther.posner@uni-bayreuth.de)

Silicon is a likely light element in the Earth's core on the basis of Si depletion in the mantle relative to primitive chondrite compositions. Previous studies reveal Si solubility in liquid iron to increase at elevated pressures, which implies that Si would partition from the basal region of a magma ocean into metallic cores of impacting bodies during accretion. The core-mantle boundaries (CMBs) of differentiated bodies are characterized by chemical disequilibrium implying ongoing transport of primary elements, such as Si, between a liquid outer core and the base of silicate mantle. We are conducting a series of high *P-T* experiments to constrain the diffusivity of Si in liquid iron in order to understand the kinetics of chemical transport and equilibration during core formation and processes occurring at CMBs.

Experimental diffusion couples comprised of highly polished cylindrical disks of 99.97% Fe and metallic Fe₆Si were contained in an MgO capsule and annealed within the *P-T* range 2023–2523 K and 7–25 GPa in a multi-anvil apparatus. To minimize the occurrence of diffusion prior to reaching the target temperature, a rapid heating rate of 20°C/sec was used to ramp the temperature to the required value. Experimental durations were very short (< 30 sec) and terminated by quenching at ~500°C/sec by switching off the electrical power. Recovered capsules were cut and polished parallel to the axis of the cylindrical sample and measured using EMPA 10 µm-step line scans. The data were fit to the error-function solution to the diffusion equation in accord with “zero-time” initial condition profiles.

Preliminary results indicate that silicon diffuses in liquid iron at least one order of magnitude slower than Fe self-diffusion [1], which could influence the viscosity of the outer core if silicon is present.

[1] Dobson (2002) *PEPI* **130**, 271-284.

The bacterial C-isotope archive: modern anoxygenic phototrophs elucidate past processes in S and Fe- rich systems

N.R. POSTH¹, L.A. BRISTOW¹, K.S. HABICHT¹, R.P. COX
AND D.E. CANFIELD¹

¹Nordic Center for Earth Evolution (NordCEE), Institute for
Biology, University of Southern Denmark, Campusvej 55,
5230 Odense M, Denmark
(*correspondence: nicolep@biology.sdu.dk)

Anoxygenic phototrophic bacteria oxidizing sulfide, thiosulfate, elemental sulfur or Fe(II) are considered to be among the earliest organisms on Earth. As sulfur and iron were abundant on early earth, Fe and S oxidation states and isotopic signatures in the rock record are routinely utilized as markers for the rise of oxygen. In another approach, studies of modern S and Fe-oxidizing anoxygenic phototrophs afford us the opportunity to investigate how these organisms may have influenced the geochemical evolution of our planet.

Sulfide-rich, meromictic, Lake Cadagno (Switzerland) is an ideal location to study purple and green sulfur anoxygenic phototrophic bacteria as analogues of ancient systems (e.g., Tonolla *et al*, 2003; Canfield *et al*, 2010). The stable chemocline allows for the development and maintenance of a geochemical gradient and S-cycling microbial community.

We present work carried out on the C-isotopic signatures imparted by S-metabolizing anoxygenic phototrophic bacteria both in pure culture and in the lake waters to understand how C-fixation pathways, water column cycling, sedimentation and diagenesis can influence the isotope record. Combining ¹³C/¹²C analysis of field and pure culture POM and DIC, FISH-SIMS and eco-physiological studies, we aim to elucidate the C-isotope signature of the microbial carbon lifecycle. Part of our focus is to clarify whether the isotopic biosignature is a combination of all bacterial community members or dominated by a single member. Future work will compare this S-rich system to Fe-rich analogues.

[1] Tonolla, M., Peduzzi, S., Hahn, D., Peduzzi, R. (2003). *FEMS Microbiology Ecology* **43**, 89-98. [2] Canfield, D.E., Farquhar, J., Zerkle, A.L. (2010) *Geology* **38**, 415-418.

The uranium mineralization of Pen Ar Ran (Armorican Massif), France: An atypical "vein type" deposit

POUJOL, M.^{1*}, BALLOUARD, C.¹, BOULVAIS, P.¹, CUNNEY, M.², CATHELIN M.² AND GAPAIS, D.¹

¹UMR CNRS 6118, Géosciences Rennes, OSUR, Université Rennes 1, 35042 Rennes Cedex, France.

(*Correspondence: marc.poujol@univ-rennes1.fr)

²UMR CNRS 7566 G2R, Université de Lorraine, 54506 Vandoeuvre-lès-Nancy, France

Twenty percent of the uranium produced in France was extracted in the Armorican Massif, in three different locations (Pontivy, Guérande et Mortagne) which belong to the "High Heat Production Belt", a 100 km wide NW-SE zone characterized by elevated contents in radioactive elements present in most of the geological formations [1], including 320 to 315 Ma old peraluminous granites [2].

In the Guérande uranium district, the Pen Ar Ran deposit is located in a deformed zone, at the contact between porphyroids and quartzitic black schists. This deformed zone corresponds to an E-W shear zone that affected both the metamorphic formations (porphyroids and black schists) and the intrusive Guérande leucogranite, during its emplacement. Mineralization is under the form of massive veins carrying pechblende and sulphide that are spatially associated with the leucogranite. However, this uranium deposit is different from the other "vein type" known in France because of the unusual nature of its uranium oxides (between pechblende and uraninite). Furthermore, the fluids responsible for this mineralization are hotter (350-400°C) than elsewhere.

The question of the source of the uranium is also complex. The uranium content of the metamorphic formations is rather low (around 3 ppm) but it is also low in the leucogranite (max. 9 ppm). It is however possible that the uranium was leached out of the granite by surface derived oxidizing fluids while the granite was still at depth [3]. Therefore, the leucogranite could represent the source of the uranium. In order to test this hypothesis, we performed a comprehensive petrological, geochemical, and geochronological study of the Guérande granite and compared these data to the available data from the porphyroid and the uranium mineralization.

[1] Vigneresse, J.L., Cuney, M., Jolivet, J., Bienfait, G. (1989). *Tectonophysics*, **159**, 47-60. [2] Tartèse, R., Ruffet, G., Poujol, M., Boulvais, P., Ireland, T.R. (2011). *Terra Nova*, **23**, 390-398. [3] Tartèse, R., Boulvais, M., Poujol, M., Gloaguen, E., Cuney, M. (2013). *Economic Geology*, **108**, 379-386.

Controls on redox-nutrient cycling in the Cretaceous greenhouse ocean: Insights from S isotope systematics

SIMON W. POULTON¹, SUSANN HENKEL², CHRISTIAN MÄRZ³, HANNAH URQUHART³, SASCHA FLÖGEL⁴, SABINE KASTEN⁵, JAAP S. SINNINGHE DAMSTÉ⁶ AND THOMAS WAGNER³

¹School of Earth & Env., Uni. of Leeds, Leeds LS2 9JT, UK

²Inst. of Geology and Mineralogy, Uni. of Cologne, Germany

³School of Civil Eng. & Geosci., Newcastle Uni., UK

⁴IFM-GEOMAR, Kiel, Germany

⁵Alfred Wegener Inst., Bremerhaven, Germany

⁶NIOZ, NL-1790 AB Den Burg, The Netherlands

Oceanic anoxic events (OAEs) were a frequent occurrence in the Cretaceous greenhouse ocean. Based on a variety of paleoredox indicators, euxinic water column conditions are commonly invoked for these OAEs. However, in a high resolution study of OAE3 deep sea sediments [1], revised paleoredox indicators suggest that euxinic conditions fluctuated with anoxic ferruginous conditions on orbital timescales. Building upon this, we here present new data for a continental shelf setting at Tarfaya, Morocco, that spans a period prior to, and during, the onset of OAE2. We again find strong evidence for orbital transitions from euxinic to ferruginous conditions. The presence of this distinct cyclicity during OAE2 and OAE3 in shallow and deep water settings, coupled with its occurrence on the anoxic shelf prior to the global onset of anoxia, suggests that these fluctuations were a fundamental feature of anoxia in the Cretaceous ocean.

The observed redox cyclicity has major implications for the cycling of phosphorus, and hence the maintenance and longevity of OAEs. However, despite this significance, controls on the observed redox cyclicity are essentially unknown. Here, we utilize S isotope measurements (pyrite S and carbonate-associated S) from the deep sea and shelf settings to model oceanic sulphate concentrations across the redox transitions. Perhaps surprisingly, we find no evidence to suggest that ferruginous conditions arose due to extensive drawdown of seawater sulphate (as pyrite-S and organic-S) under euxinic conditions. Instead, S isotope systematics in the deep sea imply increased sulphate concentrations during ferruginous intervals. Based on these observations and other major element data, we infer that the redox cyclicity instead relates to orbitally-paced fluctuations in continental hydrology and weathering, linking the redox state of the global ocean to climate-driven processes on land.

[1] März *et al* (2008) *GCA*, **72**, 3703-3717.

Introducing a comprehensive data reduction algorithm for high-precision U-Th geochronology with isotope dilution MC-ICP-MS

ALI POURMAND^{1*}, FRANÇOIS L.H. TISSOT²,
MONICA ARIENZO¹, DAVID MCGEE³ AND ARASH SHARIFI¹

¹Neptune Isotope Lab., University of Miami - RSMAS, Miami, FL, USA, apourmand@rsmas.miami.edu

²Origins Lab., Department of Geophysical Sciences, University of Chicago, Chicago, IL 60637, USA

³Department of Earth, Atmospheric and Planetary Sciences, MIT, Cambridge, MA 02139

Multi collector inductively coupled plasma mass spectrometry (MC-ICP-MS) is being increasingly utilized for U-Th geochronology of carbonate deposits with comparable precision to thermal ionization mass spectrometry (TIMS) [1, 2]. While attention has been paid to propagation of uncertainties for U-Th-Pb analysis by TIMS and the isochron technique [3,4], a comprehensive data processing scheme is lacking for MC-ICP-MS. To address this need, we have developed an algorithm in Mathematica application to allow for step-by-step monitoring of the data reduction process. The program is flexible and affords the user easy control over input variables. Adjustments for background and spike isotope contributions, abundance sensitivity and instrumental mass bias are implemented through the code, followed by age calculation and propagation of uncertainties with Monte Carlo simulation. A rigorous standard bracketing procedure was adopted using Uranium (CRM-112A) and Th (IRMM-035) standard solutions, doped with IRMM-3636a ²³³U/²³⁶U “double-spike”, to account for deviations of isotope ratios from certificate values and improve accuracy. Following a single U/TEVA extraction chromatography step to separate U from Th, ten replicate ages from a speleothem in Cathedral Cave (CC), Utah showed excellent agreement ($R^2 = 0.999$) with results previously measured at the University of Minnesota by single collection ICP-MS [5]. The external reproducibility of our analytical technique was evaluated by analyzing six aliquots of an in-house standard, prepared by homogenizing a piece of the CC speleothem, which returned a mean age of 21468 ± 120 y (2SD). A limited amount of the standard powder is available upon request for interlaboratory calibration. We have successfully dated 36 samples from caves in the Bahamas, the Dominican Republic and Iran.

[1] Fietzke *et al* (2005) *J Anal Atom Spectrom* **20**, 395-401. [2] Hoffmann *et al* (2007) *Int J Mass Spectrom*, **264**, 97-109. [3] Ludwig & Titterton (1994) *GCA* **58**, 5031-5042 [4] McLean *et al* (2011) *G3*, **12**. [5] McGee *et al* (2012) *EPSL* **351-352**, 182-194.

Carbon mineralization in artificial wetlands

I. M. POWER^{1*}, J. MCCUTCHEON², A. L. HARRISON¹,
G.M. DIPPLE¹ AND G. SOUTHAM³

¹The University of British Columbia, Vancouver, BC V6T 1Z4, Canada (*correspondence: ipower@eos.ubc.ca; aharriso@eos.ubc.ca, gdipple@eos.ubc.ca)

²The University of Western Ontario, London, ON N6A 5B7, Canada (jmccutc3@uwo.ca)

³The University of Queensland, St Lucia, Brisbane QLD 4072, Australia (g.southam@uq.edu.au)

Carbon mineralization is a promising strategy for mitigating global climate change. We have extensively studied the microbiology, geochemistry, and mineralogy of alkaline wetlands found in hydromagnesite [$Mg_5(CO_3)_4(OH)_2 \cdot 4H_2O$] playas as a biogeochemical analogue for carbon mineralization [1]. These wetlands are fed by Mg-HCO₃ groundwaters and are unique habitats for carbonate precipitating microbes, including cyanobacteria and algae. Growth of these phototrophs within pond systems has also been proposed for producing biofuel [2]. Carbonate precipitation and biomass production could be facilitated using specially designed artificial wetlands that receive waters rich in dissolved cations (e.g., Mg²⁺ and Ca²⁺). This offers a low energy strategy for sequestering carbon dioxide (CO₂) within carbonate minerals and biomass. Utilization of phototrophs is advantageous in that many species are halophilic and can be grown on non-arable land such as mine sites [3]. As a potential application, we consider mine tailings facilities that produce Mg-rich leachate waters. In microcosm experiments, a phototrophic consortium was able to induce carbonate precipitation from leachate waters, yet precipitation was limited by the availability of CO₂. A larger-scale (10 m long) flow-through wetland fed by Mg-HCO₃ waters demonstrated that a carbon sequestration rate of 120 t CO₂/ha per year could be achieved. Geochemical modeling using mine site water budgets also indicates that up to 17% of a mine's annual greenhouse gas emissions could be sequestered [4]. Coupling of carbonate precipitation and biomass production in artificial wetlands may represent an economically efficient alternative to other technologies currently under development for CO₂ sequestration.

[1] Power *et al* (2009) *Chem. Geol.* **260**, 286-300 [2] Mata *et al* (2010) *Renewable Sustainable Energy Rev.* **14**, 217-232 [3] Jansson & Northen (2010) *Curr. Opin. Biotechnol.* **21**, 365-371. [4] Power *et al* (2011) *Env. Sci. Technol.* **45**, 9061-9068.

Anomalous abundances of He and mobile metals in surface media over the deeply buried Millennium U deposit, Athabasca Basin, Canada

MICHAEL J. POWER^{1*}, KEIKO HATTORI¹, DANIELE L. PINTI² AND ERIC G. POTTER³

¹Department of Earth Sciences, University of Ottawa, Ottawa, Canada (correspondence: mpowe102@uottawa.ca)

²GEOTOP, Université du Québec à Montréal, Montréal, Canada

³Geological Survey of Canada, Ottawa, Canada

We examined soil and noble gas geochemistry over the Millennium uranium deposit, Athabasca Basin, SK, Canada. It has indicated resources of 68.2 million lbs U₃O₈ at ~750 m depth, along a major fault in granites & metamorphosed pelites of Archean to Paleoproterozoic age below the Athabasca sandstones.

110 soil samples along two transects 503 and 333 m long over the deposit yielded anomalous values in U (≤ 0.6 ppm), Pb (≤ 35 ppm) and Cu (≤ 15 ppm) in aqua regia digestion of humus, when compared to the $\mu \pm 2\sigma_x$ for metal values. Anomalous values were also detected for U (≤ 102 ppb) Pb (≤ 2100 ppb), and Cu (≤ 220 ppb) in B-horizon soils leached by ammonium acetate compared to the $\mu \pm 2\sigma_x$ of metal values. Most anomalies were directly above the ore zones and surface traces of major faults, including the ore-hosting Marker fault. Gas samples were collected in monitoring wells and drill holes by submerging diffusion samplers at 10 to 42 m below the surface for 3 days. The ⁴He, ²²Ne, ³⁶Ar, ⁴⁰Ar, ⁸⁴Kr and ¹³²Xe were measured by quadrupole mass spectrometry at GEOTOP. Analytical uncertainties range from 1.5 to 4.6% of the measured amount. Measured ⁴He concentrations in water ranges from 6.89×10^{-8} to 4.23×10^{-5} ccSTP/g. The lower amount is identical to that expected by equilibration with the atmosphere (Air Saturated Water value or ASW). The higher amount is clearly related to radiogenic ⁴He produced by the U ore and released in the water. Indeed, three samples yielded anomalous ⁴He/³⁶Ar ratios, 715, 239 and 108 times the ASW value, clearly indicating the addition of radiogenic ⁴He. Ratios of ⁴He/²²Ne (790, 340 and 130 times ASW value), ⁴He/⁸⁴Kr (690, 240 and 110 times ASW), and ⁴He/¹³²Xe (580, 210 and 95 ASW) were also observed, confirming the results.

Broad geochemical anomalies in soil and gas at the property show that fault-controlled redistribution of elements and gases possibly exists over the deposit. Our results suggest upward migration of metals and He to surface through these geological features – detectable by geochemical exploration methods for U using two different surface media.

Isotope geochemistry of Wayang Windu geothermal field, Indonesia

R. PRASETIO^{*1}, B. WIEGAND¹, M. SAUTER¹ AND D. MALIK²

¹GZG, Universität Göttingen, Goldschmidt Str. 3, 37075 Göttingen, Germany (* rasi_prasetio@yahoo.com)

²Star Energy, Ltd. Jl. Letjen S. Parman Kav. 62-63, 11410 Jakarta, Indonesia

Wayang Windu geothermal field is located in West Java, Indonesia, associated with Quaternary active volcanoes. The geothermal system is transitional between liquid and vapor dominated systems [1]. Naturally occurring isotopes, i.e. δD , $\delta^{18}O$ and ⁸⁷Sr/⁸⁶Sr were combined with gas compositions and chemical data of the fluids to characterize fluid-rock interaction and properties of the reservoir. Several samples were collected from thermal manifestations and deep wells.

Most of the thermal manifestations and deep well fluids are bicarbonate type and have neutral pH values, except for steam heated waters, which are acid sulphate type waters. Deep brine fluids are of mature chloride type. Gas-mineral (i.e. pyrite and iron oxides [2]) equilibria indicate that reservoir temperatures vary between 230-300°C. δD and $\delta^{18}O$ compositions suggested that although fluids from thermal manifestations and deep fluids are of meteoric origin, deep fluids may have recharged from a lower elevation than fluids of the thermal manifestations. Furthermore, deep fluids show a strong oxygen shift, indicating water-rock interaction, while $\alpha_{D_{L-V}}$ and $\alpha_{^{18}O_{L-V}}$ model calculations indicate steam separation (boiling) at ~200°C. ⁸⁷Sr/⁸⁶Sr ratio vary between 0.7046-0.7058 and are similar to ⁸⁷Sr/⁸⁶Sr ratio of Sunda arc calc-alkaline volcanic rocks [3].

[1] Bogie *et al* (2008), *Geothermics* **37**, 347-365 [2] Abrenica *et al* (2010), Proceedings World Geothermal Congress 2010 [3] Whitford (1975), *Geochim. Cosmochim. Acta* **39**, 1287 – 1302

Geochemical constrains and tectonic significance of Late Cretaceous mafic dykes from the Bhavani shear zone, South India

P.PRATHEESH* AND V. PRASANNAKUMAR

Department of Geology, University of Kerala, Trivandrum
695 581, India (*Correspondence:
pratheeshponline@gmail.com)

South Indian Granulite Terrain (SIGT), a composite crustal unit, comprises multiply deformed litho-blocks dissected by crustal-scale shear zones with the history of multiple phases of reactivation. The Palaghat-Cauvery Shear System (PCSS), the prominent among these, is an Archaean crustal boundary with repeated reactivation and is believed to have an integral role in the modeling and reconstruction of Gondwana supercontinent. This terrain bears significant evidences of extensive magmatic activity in the form of dyke swarms, puncturing the granulites as well as the shear zone rocks. Mafic dyke swarms of varying composition and age are common in all the lithological units of the Palaghat-Cauvery Shear System (PCSS). The present study is an attempt to discuss the characteristic geochemical signatures and the tectonic background of the probably late Cretaceous mafic dykes which have important relations to the timing and tectonics of amalgamation of the Gondwana supercontinent. The mafic dykes, occurring at different parts of the Bhavani Shear Zone (BSZ), a constituent of the PCSS, are relatively fresh and have distinguishing structural relations and geochemistry. Geometrical analysis of joint patterns in these dykes suggest both predefined and self generated path for emplacement, the strain localised domains in the shear zone exerting a spatial control.

Geochemical studies indicate sub-alkaline tholeiitic basalt nature for these dykes with both high-Mg and high-Fe tholeiitic characters. Incompatible elements modeling suggests a depleted mantle source for these dykes and the average REE distribution in these dykes indicate considerable fractionation and possible crustal contamination as well as probable elemental mobility. Tectonic discriminations imply MORB characteristics as well as oceanic island affinity. Correlation of geochemical characteristics with other coeval units in the similar tectonic environments suggests an affinity to Marion Hotspot. In general comparison, these basalts are similar to the 45° E Indian Ocean ridge basalts and the basaltic rocks of eastern Madagascar volcanic province. The characteristic features of these dykes are discussed in terms of late Cretaceous Indian ocean tectonics and Gondwana reassembly.

Computational Study of Rutile and Quartz Interfaces with Aqueous Solutions

M. PŘEDOTA¹, O. KROUTIL^{1,2}, Z. CHVAL² AND S. PAŘEZ³

¹Faculty of Science, University of South Bohemia, České Budějovice, Czech Republic (predota@prf.jcu.cz)

²Faculty of Health and Social Studies, University of South Bohemia, České Budějovice, Czech Republic

³Institute of Chemical Process Fundamentals, Academy of Sciences of the Czech Republic, Prague, Czech Republic

In the past, we have obtained numerous simulation and experimental results of the TiO₂/aqueous solution interface including structure of adsorbed water and ions [1], hydrogen bonding and profiles of distance-dependent viscosity and diffusivity [2]. Here we will present our results on prediction of zeta potential (ζ) from molecular dynamics simulations and determination of dielectric properties of the interface. Our results show that the molecular nature of water and specific interactions of ions with the surface are key phenomena giving rise to the observed behavior.

In contrast to our works on TiO₂ and SnO₂ interfaces, our modelling of quartz (101) interface has been initiated only recently [3]. We have developed a model of negatively charged quartz, necessary for modeling of quartz surfaces above its point of zero charge ($\text{pH}_{\text{pzc}} \approx 2-4.5$), by a modification of the ClayFF force field [4], keeping the simple form of interaction potentials and introducing modified *ab initio* derived charges for a limited number of surface atom species. We present results of interactions of quartz (101) surface with aqueous solutions of NaCl and small organic molecules representing basic building blocks of larger biomolecules and functional groups of organic matter. As model molecules, benzoic acid, phenol, and salicylic acid were chosen. We studied interactions of molecules with surface for a set of surface charge densities 0.00, -0.03, -0.06 and -0.12 C/m², approximately corresponding to pH values 4.5, 7.5, 9.5 and 11.

[1] Předota *et al* (2014) *J. Phys. Chem. B* **108**, 12061-12072.

[2] Pařez & Předota (2012) *Phys. Chem. Chem. Phys.* **14**, 3640-3650. [3] O. Kroutil *et al* "Computer simulations of quartz (101)-water interface over a range of pH values", submitted.

[4] Cygan *et al* (2004) *J. Phys. Chem. B*, **108**, 1255-1266.

This research is primarily sponsored by the Czech Science Foundation (No. 13-08651S).

Os-isotopes constraints on the dynamics of orogenic mantle: the case of central Balkans

D. PRELEVIĆ¹, G. BRÜGMANN¹, M. BARTH¹,
M. BOŽOVIĆ¹, V. CVETKOVIĆ² AND S.F. FOLEY¹

¹Geocycles Research Centre, University of Mainz, Becherweg 21, 55099 Mainz, Germany

²Faculty of Mining and Geology, University of Belgrade, Djušina 7, 11000 Belgrade, Serbia

The origin and evolution of Phanerozoic SCLM during orogenesis is a puzzling issue because of its multi-episodic and time-integrated melting and enrichment history. This is especially so in the Alpine-Himalayan accretionary orogen, which formed at a diffuse and long lived convergent boundary between Eurasia and Gondwanaland. The accretion of thin continental slivers and numerous oceanic island arcs resulted in a complex collage of continental blocks intercalated with ophiolitic terrains. The net effect of this accretion is mingling of severely mismatched geological and geochemical compositions.

We aim to monitor lithospheric mantle development under the Balkan part of the Alpine-Himalayan belt. In our holistic approach we combine Os isotopic and HSE as well as whole rock and mineral compositions of a number of mantle xenoliths in Palaeocene alkaline basalts, Mesozoic ophiolites and Oligocene-Miocene lamproitic lavas sourced within the lithospheric mantle.

Both ophiolitic peridotites and lithospheric mantle of the Balkan sector of the Alpine-Himalayan belt demonstrate similarly high extents of the previous melt extraction. Further resemblance is seen in the Os isotopic variation observed in ophiolites and in the Serbian lithospheric mantle, implying fluid-induced enrichment of a depleted Proterozoic/Archaean precursor, whereby the enriched component had suprachondritic Os isotopic composition. The ultimate source of this component is attributed to the subducting oceanic slab. We tentatively propose a two-stage scenario connecting lithospheric mantle with ophiolites and lamproites in a geologically reasonable fashion: i) the first stage took place in a suprasubduction oceanic environment, and it is responsible for the fluid-related enrichment of depleted mantle; ii) the second-stage connects the lithospheric mantle and lamproites during the partial melting that generated lamproitic melts. This is in accordance with the recent model¹ proposing that the part of the lithospheric mantle under the Balkans has seen oceanic lithosphere development.

[1] .Prelević, D. *et al* , EPSL,2013. **362**: p. 187-197.

Effect of surface heterogeneity and interfacial water on surface potential

T. PREOČANIN¹, D. NAMJESNIK¹, M. SAPUNAR¹,
J. LÜTZENKIRCHEN² AND N. KALLAY³

¹Faculty of Science, University of Zagreb, Horvatovac 102a, Zagreb, Croatia, tajana@chem.pmf.hr

²Institut für Nukleare Entsorgung , Karlsruher Institut für Technologie (KIT), Hermann-von-Helmholtz-Platz 1, 76344 Eggenstein-Leopoldshafen, Germany

At the metal oxide crystal plane, exposed to the electrolyte aqueous solution, one or more amphoteric surface groups could be present. Different surface groups could be regularly distributed according to crystal structure, but also on two or more distinct surface patches.

The stability of surface groups depends on their thermodynamic and kinetic properties. If more than one kind of surface group is present at the crystal plane the surface potential, as well as the other surface properties, would depend on surface concentrations of each surface sites, their thermodynamic equilibrium constants, and potential interactions between them. It is expected that the most stable surface species predominates at the surface and determines the overall surface properties. Different surface areas at the same crystal plane are in direct electrical contact through the bulk of the crystal, and consequently they are affected by same surface potential if the solid is conductive. The resulting surface potential is influenced by equilibrium at all surface patches, and will be somewhere between two extreme values characterized individual surface areas.

The effect of two different surface sites and surface transformations of hematite 001 surface [1] were measured by means of single crystal electrode [2]. The results are interpreted by surface complexation model using the general model of electrical interfacial layer.

The measured $\Psi_0(\text{pH})$ function is nonlinear with a broad zero-potential region around the point of zero potential. Electrokinetic measurements of the same crystal planes give the clear isoelectric points and higher values of the zeta potential with respect to surface potentials. This unexpected behavior could be explained by considering pH dependent charging of the interfacial water layer affecting electrokinetic behaviour but not the surface potential [3].

[1] J. Lützenkirchen *et al* (2013) *Geochimica et Cosmochimica Acta*, submitted. [2] N. Kallay *et al* (2005) *J. Colloid Interface Sci.* **286**, 610-614. [3] N. Kallay *et al* (2012) *J. Colloid Interface Sci.* **375**, 167-171.

New Frontiers in Natural and Chemical Tracers monitoring for Reservoir management

HUGUES PREUD'HOMME¹

¹LCABIE – UMR5254 – IPREM, 2 avenue Angot 64053 PAU cedex 9, FRANCE

Tracing test campaign in oil or gas reservoir is one of the most powerful techniques to obtain experimental data for a better description and understanding of the reservoir, interwell connectivity, multilevel/allocation approach or to design a future Enhanced Oil Recovery. It's also a useful tool to modelize the water flow in simulation models of porous media/rocks, laboratory core test or just to estimate the residual oil saturation. After decades of use of radionuclides, this time is over, new frontiers in analytical sciences are benefit to direct multi-monitoring of ultra-trace element (natural tracers) or ultra trace of chemical/geothermal such as halogenated or fluorescent tracers. Simple (no sample preparation), sensitive (ppt or ng.L⁻¹ level), rapid (less than 6') and robust (direct analysis even in brine or high salinity reservoir water (150g.L⁻¹).

We will discuss here of the analytical development story and we highlight with figures of merit obtained along reservoir monitoring. We will finish with a few perspectives offered by the techniques such as well integrity and geological storage monitoring.

[1] Direct sensitive simultaneous determination of fluorinated benzoic acids in oil reservoir waters by ultra high-performance liquid chromatography-tandem mass spectrometry, Serres-Piole, C., Moradi-Tehrani, N., Lobinski, R., Preud'homme, H. (2011) *Journal of Chromatography A* 1218, 5872-5877.

[2] New passive water tracers for oil field applications, Serres-Piole, C., Commarieu, A., Garraud, H., Lobinski, R., Preud'Homme, H., (2011) *Energy & Fuels* 25, 4488-4496.

[3] Water Tracers in Oil Field Applications: A Guideline, Serres-Piole, C., Moradi-Tehrani, N., Allanic, C., Lobinski, R., Preud'homme, H., (2011) *Journal of Petroleum Science and Engineering* 98-99, 22-39.

Simulation of magma ascent prior to the high risk caldera forming eruptions of Campi Flegrei

O. PREUSS¹ AND M. NOWAK¹

¹University of Tuebingen, Department of Geosciences, Wilhelmstr. 56, 72074 Tuebingen, Germany

The dynamic magmatic processes prior to the 39 ka Campanian Ignimbrite (CI) eruptions at Campi Flegrei (CF), occurring during magma ascent, cannot be observed directly in nature. Therefore, experimental simulations of CI magma ascent are necessary and will give detailed insight into the mechanisms of CF super eruptions.

A pressure decrease during magma ascent accompanied with fluid oversaturation in the melt initiates bubble nucleation, growth, coalescence and segregation, and possible partial crystallization, which lead to a substantial density decrease and a change in viscosity. These processes may act as driving forces for increased ascent rates and may lead to catastrophic eruption styles.

Discrepancies of previous studies demonstrate that the *P-T-t* conditions and volatile contents (H₂O, CO₂, Cl) of the primitive melt prior to the eruption, generating the CF volcanic products are not well constrained. This study is focused on the conduction of continuous decompression experiments [1] using a trachytic CI composition [2] to gain insight into the dynamic degassing processes. First isothermal decompression experiments, above the liquidus at 1050 °C, are performed using a starting pressure of 200 MPa and H₂O content of 5 wt% and a continuous decompression to 75 and 50 MPa with different decompression rates. Additionally, two different types of sample material (glass cylinders / glass powder) are used.

Changes in decompression rate and type of starting material lead to significantly different degassing behavior of the melt. Fast decompression rates lead to massive volatile oversaturation, thus bubble nucleation is the predominant mechanism. In contrast, bubble growth is the preferred mechanism at slow decompression rates to reequilibrate the system. In ongoing experiments, additional volatiles (CO₂, Cl) will be added to simulate conditions closer to the CF volcanic system. To investigate heterogeneous bubble nucleation caused by decompression induced crystallization processes, experiments will be performed at lower temperatures below the liquidus.

[1] Nowak, M. *et al* , 2011, *Am Mineral*, 96: 1373-1380 [2] Civetta, L. *et al* , 1997, *J Volcanol Geoth Res*, 75(3-4): 183-219.

Crystallization temperatures of carbonate phases at Kennecott, Alaska based on clumped isotope thermometry

JASON B. PRICE* AND JOHN M. EILER

Division of Geological and Planetary Sciences, California Institute of Technology, Pasadena, CA 91125, USA
*jprice@caltech.edu

We measured growth temperatures of eight carbonate phases from the Bonanza Cu-(Ag) mine, Kennecott, Alaska, using the clumped isotope paleothermometer. A comparison of these data with independent geologic constraints, including phase equilibria of hydrothermal silicates and sulfides, suggests measured temperatures reflect carbonate growth conditions (Fig. 1). This method provides a means to document the low-temperature histories of ore bodies and to clarify ambiguous paragenetic positions of unmineralized carbonate phases. Clumped isotope measurements are accompanied by $\delta^{18}\text{O}$ measurements, which together with measured temperatures, are used to calculate $\delta^{18}\text{O}_{\text{water}}$ values for the mineralizing fluids; this helps to constrain the fluid source(s) and genetic model for the Kennecott deposits.

Calcite phases that predate Cu deposition grew at low temperatures (43-71°C); carbonate phases associated with copper deposition are much warmer (89-157°C); postmineral calcite phases are again cool (38-59°C). Limestone wallrock adjacent to the orebodies displays the largest temperature range of any subset (79-164°C) and may reflect burial diagenesis, metamorphism, and/or metasomatism. Premineral baroque dolomite, including zebra dolomite, grew at 102-142°C. Calcite veins containing Cu-sulfides grew at 89-157°C. Synmineral dedolomitization formed in the range 98-109°C. Only one calcite sample crystallized within the stability field of djurleite (<93°C), a volumetrically important component of the ore. Calculated compositions for $\delta^{18}\text{O}_{\text{water}}$ support a fluid mixing model to form the Cu deposits, whereby a 0‰ fluid carrying sulfide mixed with a metamorphogenic, Cu-bearing fluid of 5-8‰ derived from the Nikolai Greenstone.

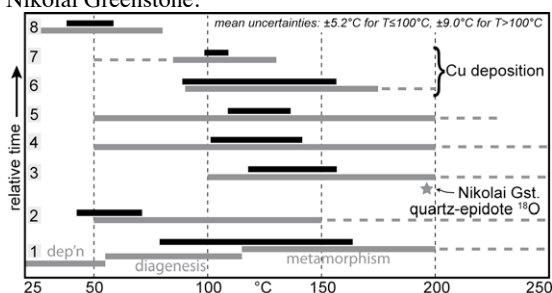


Fig. 1: Independently constrained temperature ranges (grey) and measured temperature ranges from clumped isotope paleothermometry (black) for carbonate phases at Kennecott, Alaska. 1) limestone wallrock, 2) premineral cal. 3) cal. in epidote-quartz veins in Nikolai Greenstone, 4) hydrothermal baroque dol., 5) cal. infilling dol. breccia, 6) Cu-bearing cal. veins, 7) dedolomite selvages, 8) postmineral cal.

Microbial diversity in an arsenic-rich shallow-sea hydrothermal system undergoing phase separation

ROY E. PRICE^{1,*}, RYAN LESNIEWSKI², AND JAN P. AMEND^{1,2}

¹Dept. of Earth Sciences, University of Southern California, Los Angeles, USA

²Dept. of Biological Sciences, University of Southern California, Los Angeles, USA

*Corresponding author: royprice@usc.edu

Phase separation is a ubiquitous seafloor process in hydrothermal vent systems, yet investigations of how this process affects microbial ecology are rare. We evaluated prokaryotic diversity in arsenic-rich shallow-sea vents off Milos Island (Greece) by comparative analysis of 16S rRNA clone sequences from two vent sites with similar pH and temperature but marked differences in salinity. Clone sequences were also obtained for arsenic functional genes (AFGs) involved in arsenite oxidation (*aioA* -like). Bacteria in the surface sediments (0 to 1.5 cm) at the high salinity site consisted of mainly *Epsilonproteobacteria* (*Arcobacter sp.*), which transitioned to almost exclusively Firmicutes (*Bacillus sp.*) at ~10 cm depth. On the other hand, the low salinity site consisted of Bacteroidetes (Flavobacteria) in the surface and predominantly *Epsilonproteobacteria* (*Arcobacter sp.*) at ~10 cm depth. Archaea in the high salinity surface sediments were dominated by the orders Archaeoglobales and Thermococcales, transitioning to Thermoproteales and Desulfurococcales (*Staphylothermus sp.*) in the deeper sediments. In contrast, the low salinity site was dominated by Thermoplasmatales in the surface and Thermoproteales at depth. The abundance of free and dissolved gases, and other redox couples, were similar at the two sites, suggesting that salinity and/or arsenic concentrations may select for microbial communities that can tolerate these parameters. Many of the archaeal 16S rRNA sequences contained inserts, possibly introns, including members of the Euryarchaeota, something not reported previously. Clones containing *aioA* -like genes affiliated with either *Alpha*- or *Betaproteobacteria*, although most were only distantly related to published representatives. Most clones (93 out of 105) originated from the deeper layer of the low salinity, higher arsenic site, which is also the only sample with overlap in AFG and 16S rRNA gene data, suggesting arsenotrophy as an important metabolism.

CO₂-olivine interaction in porous media - an experimental study

J. PŘIKRYL¹, A. STEFÁNSSON¹ AND B. SIGFÚSSON²

¹Institute of Earth Sciences, University of Iceland, Sturlugata 7, 101 Reykjavík, Iceland (jap5@hi.is)

²Reykjavík Energy, Baejarhalsi 1, 110 Reykjavík, Iceland

Increased anthropogenic CO₂ emissions have caused an imbalance in the CO₂ cycle and resulted in climate change. One potential way to reduce CO₂ is to convert it to carbonate minerals. Mafic and ultramafic rocks provide good candidates for such carbonate sequestration due to high availability of divalent cations like Mg²⁺, Ca²⁺ and Fe²⁺. Such permanent CO₂ storage in basalts has recently received considerable attention.

In order to study the mineralization reactions upon continuous injection of aqueous CO₂ solutions into porous media containing Mg-Fe rich rocks, reaction transport experiments and simulations were conducted. The system studied involved reacting olivine (93 % forsterite) with aqueous solutions containing CO₂ and NaCl at acid to alkaline pH values. The experiments were conducted using a 1-D flow-through reactor at 70°C. Using the solution chemistry, the reaction progress, carbonate mineralization rate and porosity changes were studied as a function of time. The experimental results were supported by 1-D reactive transport simulations conducted with the aid of the PHREEQC program. According to the experimental results and the reactive transport simulations olivine progressively dissolves forming secondary minerals and solutes that are partially transported out of the column (system). The exact reaction path was found to depend on solution composition and pH and reaction progress (time). The mass movement of the system at a particular steady state as well as porosity changes may be divided into three stages. Stage I is characterized by initial olivine leaching, stage II is characterized by mineralization formation and decrease in porosity and stage III is characterized by remobilization of the previously formed secondary minerals and eventual increase in porosity. The results of this study have important implications on the continuous CO₂ injection and potential carbonate sequestration into porous rocks.

Redox state during core formation on planetesimals

E. A. PRINGLE^{1*}, P. S. SAVAGE¹, J. BADRO², J.-A. BARRAT³ AND F. MOYNIER¹

¹Washington Univ., St. Louis, MO 63130, USA

(*correspondence: eaprangle@wustl.edu, savage@levee.wustl.edu, moynier@levee.wustl.edu)

²IPGP, Paris, France (badro@ipgp.fr)

³Université de Brest, I.U.E.M., Plouzané, France (barrat@univ-brest.fr)

Formation of the terrestrial planets likely involved accretion of planetesimals large enough to have previously differentiated metallic cores. However, the physicochemical conditions prevailing during planetesimal differentiation remain poorly understood. The asteroid 4-Vesta is the smallest extant planetary body known to have differentiated a metallic core. HED (Howardite, Eucrite, Diogenite) meteorites, which are thought to sample 4-Vesta, provide us with an opportunity to study core formation in planetary embryos.

Partitioning of elements between the core and mantle of a planet fractionates their isotopes according to formation conditions. One such element, silicon, shows large isotopic fractionation between metal and silicate, and its partitioning into a metallic core is only possible under very distinctive conditions of pressure, oxygen fugacity and temperature. Therefore, the silicon isotope system is a powerful tracer with which to study core formation in planetary bodies.

Here we show through high-precision measurement of Si stable isotopes that HED meteorites are significantly enriched in the heavier isotopes compared to chondrites ($\Delta^{30}\text{Si} = 0.1 \pm 0.06 \text{‰}$). This is consistent with the core of 4-Vesta containing at least 1 wt.% of Si, which in turn suggests that 4-Vesta's differentiation occurred under more reducing conditions ($\Delta\text{IW} \sim -4$) than those previously suggested from analysis of the distribution of moderately siderophile elements in HEDs.

Is oxygen-17 of atmospheric nitrate a tracer of industrial pollution?

B. PROEMSE¹, B. MAYER¹, M. FENN² AND C. ROSS²

¹University of Calgary, 2500 University Drive NW, Calgary, Alberta, Canada, T2N 1N4.

²USDA Forest Service, Pacific Southwest Research Station, 4955 Canyon Crest Drive, CA 92507, USA

*Correspondence: bcpromse@ucalgary.ca

The oxygen isotopic composition of atmospheric nitrate ($\Delta^{17}\text{O-NO}_3$, $\delta^{18}\text{O-NO}_3$) provides useful information about the oxidation pathways of nitrogen compounds in the atmosphere resulting in the formation of nitrate. Oxygen-17 contents (expressed as $\Delta^{17}\text{O}=\delta^{17}\text{O}-0.52*\delta^{18}\text{O}$) may be anomalously enriched in atmospheric nitrate as a result of the interaction with ozone (O_3), whereas other oxidants (OH , HO_2 , NO_3) contribute insignificant amounts of $\Delta^{17}\text{O}$. We postulate that in addition to the ability of $\Delta^{17}\text{O}$ as a proxy of oxidation pathways in the atmosphere, $\Delta^{17}\text{O}$ may also constitute a potential tracer for industrially derived atmospheric nitrate in close proximity of some anthropogenic emission sources.

The Athabasca Oil Sands Region (AOSR) in northeastern Alberta, Canada, holds one of the World's largest heavy oil reserves. The processing and upgrading of oil sands has raised concerns about potential environmental impacts of industrial nitrogen (N) emissions on neighbouring aquatic and terrestrial ecosystems. Stable isotope techniques may help to assess such impact in the case where industrial emissions are isotopically distinct from background values. Atmospheric nitrate in bulk deposition and throughfall was collected using ion exchange resins over ~6 months time periods from summer 2007 to summer 2011. Nitrate deposition rates, nitrogen and the triple oxygen isotopic compositions ($\delta^{15}\text{N}$, $\delta^{18}\text{O}$, and $\Delta^{17}\text{O}$) of atmospheric nitrate in bulk deposition and throughfall were determined. Nitrate emitted in $\text{PM}_{2.5}$ (particles with a diameter $<2.5 \mu\text{m}$) from one of the major emission stacks was also analyzed for $\delta^{15}\text{N}$, $\delta^{18}\text{O}$, and $\Delta^{17}\text{O}$ and was not anomalously enriched in oxygen-17 ($\Delta^{17}\text{O-NO}_3 \approx 0\text{‰}$), providing a potential tracer of industrially derived nitrate [1]. $\delta^{18}\text{O}$ and $\Delta^{17}\text{O}$ values of atmospheric nitrate deposition showed distinct trends towards lower values with increasing nitrate deposition rates in all sampling periods. This relationship between the oxygen isotopic composition and atmospheric nitrate deposition rates allowed for the estimation of industrial contributions to atmospheric nitrate deposition in the AOSR [2].

[1] Proemse, Mayer, Chow & Watson (2012), *Atm. Env.* 60, 555-563. [2] Proemse & Mayer (2012), in: K. Percy (Ed) *Developments in Environmental Science*, 11, 243-266.

Gas-solutions interaction in hydrothermal ore forming processes

V.YU. PROKOFIEV¹, S.L.SELECTOR²
AND N.N. AKINFIEV¹

¹IGEM RAS, per. Staromonetny 35, Moscow, 119017 Russia, vpr@igem.ru

²IPCHE RAS Leninsky pr., 31-4, 119071, Moscow, Russia, sofs@list.ru

The heterogenic fluid participates in the ore forming process at many hydrothermal deposits. The origin of such a fluid is usually explained by the phase separation of a homogeneous gas-saturated water-salt fluid. An alternative model of ore-forming process in which a heterogeneous fluid occurs by mixing a water-salt solution and the gas fluid is discussed in this report.

A thermodynamic modeling of the adiabatic process of interaction of water-salt fluid (1M NaCl) with gaseous CO_2 at 350o C, 1 kb was carried out. According to this model the process of increasing of carbon dioxide amount in the system accompanied by the gas phase appearance at CO_2 concentration of about 3m. The gas volume increases with the addition of CO_2 to the system up to 8 m. Meanwhile the water proceeds into the gas phase, the salt concentrations and ionic strength of the solution increase. Synchronously gold solubility decreases by about 20%.

Thermodynamic modeling characterizes only one aspect of the process of aqueous fluid with the gas mixing, but this process is much more complex.

The process of gas passing through the liquid increases the interphase, which leads to a number of inter-fluids border effects. Such process is called "barbotage", it is easy-to-realize technically and it is used in series of technological processes.

Barbotage is broadly used in technologies for heating and mixing of aggressive liquids, as well as for solutions scavenging. Barbotage generates the gas emulsions and leads to formation of large interfacial area at liquid - gas interphase boundary. It promotes the intensifications of heat- and mass-exchange processes and deeper gas-liquid chemical interaction. Spontaneous formation of scores of small bubbles can cause a cavitation. Barbotage facilitates also the flotation process.

The signs of the barbotage participation in some natural hydrothermal ore-forming systems are demonstrated in the report. The gas-liquid interaction must be considered upon the study of hydrothermal ore deposits.

This work was carried out within the framework of the Russian Foundation for Basic Research (projects 12-05-01083-a).

An abrupt change in the Nitrogen cycle and redox conditions of surface environments in Ediacaran-Cambrian as recorded in Carbonate Associated Nitrate (CAN)

M.G. PROKOPENKO^{1,2}, F. CORSETTI², R.G. GAINES¹,
S. LOYD³, J. KAUFMAN⁴ AND W.M. BERELSON²

¹Dept. of Geology, Pomona College, Claremont, CA, 91767, USA (prokopen@usc.edu)

²Dept of Earth Sciences, USC, Los Angeles, CA, 90089, USA

³Dept. of Earth and Space Sciences, UCLA, Los Angeles, CA, 90095, USA

⁴Dept. of Geology and Earth System Science Interdisciplinary Center, Univ. of Maryland at College Park, College Park, MD, 20742, USA

The Ediacaran-Cambrian transition witnessed a major restructuring of the planetary biota, however the accompanying changes in major biogeochemical cycles, including that of O₂, are less well constrained. We developed a novel approach of determining nitrate content in carbonates as a proxy for the availability of dissolved O₂ and applied it to investigate changes in O₂ and nitrogen cycles through this important transition in Earth history. Nitrogen (N) may be present in the environment in six different oxidation states, from N³⁻ in ammonium to N⁵⁺ in nitrate, with the oxidation state dictated by the ambient environmental redox state: under anoxic conditions, fixed inorganic N is likely to be stable in form of ammonium, while in the presence of dissolved O₂, the main form is nitrate. Therefore, the abundance of nitrate should reflect availability of dissolved O₂, but geologic records of oceanic nitrate have not been previously explored.

We surveyed the concentrations of CAN in carbonates from the ~2.3 Ga year old Deutschland Formation (South Africa), the ~1.4 Ga year old Belt Supergroup (Montana, USA), a series of deep and shallow water limestones spanning ~ 800 to 540 Ma years from Death Valley (California, USA) and north-western Mexico, as well as a set of early to late Phanerozoic carbonates. We found a distinct step function increase in the levels of measured CAN between 600 and 540 Ma. We argue that a sharp nitrate increase, recorded in these carbonates may reflect a rapid increase in atmospheric O₂ through this time period, which would have led to rapid transformation of fixed N to oxidized forms (from ammonium to nitrate). In the Deutschland Formation, which has been suggested to contain a geochemical record of the first transient O₂ “whiffs” in Earth history, we found evidence for a transient presence of CAN between 2.2 and 2.4 Ga. However, a significant degree of dolomitization of many samples calls for further investigation of CAN dynamics with respect to this common diagenetic process.

Impact of basalt weathering and plant recycling on Mg transport from the soil to the river under permafrost environment: A stable Mg isotope study in Central Siberia.

PROKUSHKIN A.S.¹, MAVROMATIS V.²,
POKROVSKY O.S.² AND VIERS J.²

¹V.N. Sukachev Institute of Forest, SB RAS, Akademgorodok, Krasnoyarsk, Russia, prokushkin@ksc.krasn.ru (*)

²GET, CNRS, UMR 5563, Toulouse, France, mavromat@get.obs-mip.fr, oleg@get.obs-mip.fr, viers@get.obs-mip.fr

To unravel the different sources of Mg generated by basalt weathering in Central Siberia under permafrost conditions and larch deciduous forest, we measured the Mg isotopic composition of large rivers (Nizhnaya Tunguska and Kochechum, tributary of Enisey) and a small stream, snow, surface flow, interstitial soil solutions, plant biomass, litter and soils. During winter baseflow, the dissolved Mg isotope composition of large rivers is significantly lighter compared to the source basaltic rocks and atmospheric deposition, suggesting a deep underground source such as sedimentary carbonate rocks. During spring flood and in the summer-fall season, $\delta^{26}\text{Mg}$ increases by 0.3-0.2 ‰ and approaches the Mg isotope composition of ground vegetation (dwarf shrubs, mosses) and soil organic horizon. Overall riverine waters are 0.6-1.0 ‰ lighter than the unaltered bedrock and deep minerals soil horizon.

Despite low variability of Mg isotopic composition between *Larix gmelinii* organs (i.e. stem wood, roots, needles etc.), there is a 0.2-0.3 ‰ enrichment in $\delta^{26}\text{Mg}$ of larch needles in the course of growing season, from June to September. It likely demonstrates plant uptake of isotopically heavier Mg along with the progressive thawing of mineral soil (deepen soil active layer). Taken together, Mg isotope approach indicates the important contribution of vegetation (larch needles, mosses and dwarf shrubs) in riverine Mg isotope signature and help to reveal the contribution of isotopically light carbonates or sedimentary rocks in large rivers of Central Siberian Plateau.

Interaction of organic matter with different minerals in an artificial soil incubation experiment

GEERTJE JOHANNA PRONK^{1,2}, KATJA HEISTER¹
AND INGRID-KÖGEL-KNABNER^{1,2}

¹Lehrstuhl für Bodenkunde, Technische Universität München,
85350 Freising-Weihenstephan, Germany

²Institute for Advance Study, Technische Universität
München, Lichtenbergstrasse 2a, 85748 Garching,
Germany

The interaction between minerals, organic matter (OM) and microbes leads to the formation of complex biogeochemical interfaces in soil. It is challenging to characterize these interactions in natural soils, where environmental conditions are highly variable. Therefore, we performed an incubation experiment with so-called 'artificial soils' composed of mixtures of clean model materials, where the development of organic matter (OM) was followed in a simplified system. The artificial soils were composed of 8 different mixtures of quartz, illite, montmorillonite, ferrihydrite, boehmite and charcoal, manure as OM source, and a microbial inoculant extracted from a natural arable soil. They were incubated up to 18 months. Development of OM during incubation was determined from CO₂ respiration, C and N content, and particle size and density fractionation. The OM composition was determined by e.g. solid-state ¹³C nuclear magnetic resonance (NMR) spectroscopy and acid hydrolysis.

The artificial soil mixtures developed quickly into aggregated materials, and nitrogen-rich, proteinaceous material, originating from microbial debris, accumulated in the <20 μm size fraction. Furthermore, density fractionation showed an increasing association of OM with minerals. There was no effect of mineral composition on the respiration rate. However, the presence of a clay mineral led to a higher content of non-hydrolysable N, indicating that interactions took place between N-containing OM and clay mineral surfaces. Contrary to expectations, the presence of ferrihydrite had no effect on OM. We conclude that OM preferentially interacted with the clay minerals in this system.

Overall, the artificial soil incubation experiment provided a system, where the turnover of the original manure substrate could be studied in a simplified system. Due to the well-defined composition of the artificial soils, this experiment gives us new insight into the dynamics of interactions between specific minerals and charcoal, OM and a microbial community during the turnover of organic matter in a soil-like system.

Carbon isotope analysis in conglomerates of the Cambro-Ordovician Cow Head Group, western Newfoundland as a proxy for the origin of carbonate cements

SARA B. PRUSS¹, DAVID A. FIKE²
AND KATIE A. CASTAGNO³

¹Department of Geosciences, Smith College, Northampton,
MA USA, spruss@smith.edu

²Department of Earth and Planetary Sciences, Washington
University, St. Louis, MO USA 63130,
dfike@levee.wustl.edu

³Department of Marine Affairs, University of Rhode Island,
Kingston, RI USA 02881, katie@castagno.com

The radiation of complex skeletal organisms in the Upper Cambrian to Middle Ordovician interval is preserved in the Cow Head Group at Cow Head, western Newfoundland, in approximately 255 m of deep-water slope deposits. Conglomerate beds are a ubiquitous feature of the Cow Head Group and span Upper Cambrian through Middle Ordovician stratigraphy. To determine the source of carbonate cements and the relationship between clast and matrix in individual samples, conglomeratic samples were microdrilled in several places for carbon isotope analysis. Generally, clasts showed the most consistent isotopic variability within a single sample, but individual matrix values could vary by as much as 3.5. The large variability of carbon isotope values in individual samples, particularly in the matrix, suggests some role for local organic matter remineralization, perhaps in the presence of low oxygen which may enhance precipitation, and that these samples may not be recording DIC. Additionally, the low variability in some beds and the overlapping values of both clast and matrix carbonate indicates that clasts were occasionally sourced locally and that these values might best be approximating DIC. This study, along with complementary trace element analyses, provide important constraints on the possible sources of carbon in cements for allodapic conglomerate deposits that straddle this Cambro-Ordovician interval.

Oxygen fugacity vs. mineralogical control on transition metal (Fe, Cr, V) stable isotope compositions of Mariana forearc peridotites

J. PRYTULAK^{1*}, P. BONNAND²³ AND I.J. PARKINSON²⁴

¹Department of Earth Science and Engineering, Imperial College London, UK. (*j.prytulak@imperial.ac.uk)

²Depart. Environ., Earth Ecosys., The Open University, UK

³Department of Earth Sciences, Oxford University, UK. pierre.bonnand@earth.ox.ac.uk

⁴School of Earth Sciences, University of Bristol, UK. Ian.Parkinson@bristol.ac.uk

Controversy surrounds the oxygen fugacity (fO_2) of subduction zones. Emerging redox-sensitive stable isotope systems may provide an independent assessment if their isotopic fractionation can be linked to fO_2 . However, other factors such as mineral coordination number can also influence stable isotope fractionation. Here we present the first investigation of combined Fe, Cr and V stable isotope compositions. We investigate peridotites from two forearc seamounts drilled on ODP Leg 125. The studied peridotites have been characterised for major and trace elements, modal mineralogy and fO_2 (ranging from FMQ -0.7 to +1.8) [1]. We find no correlation between Fe, Cr, or V isotopes and fO_2 . Iron isotope compositions are generally heavier than the terrestrial mantle [e.g., 2], but show significant scatter. Chromium and V isotopes are positively correlated with V isotopes displaced to heavier values than comparably depleted peridotites [3]. Chromium isotope compositions are within the range published for mantle xenoliths [4]. However, Cr isotopes correlate with modal clinopyroxene in forearc harzburgites. These results suggest that Cr and V isotopes may be more robust to secondary processes than Fe isotopes and that mineralogy may have a greater influence on Cr and V stable isotope fractionation than oxygen fugacity.

[1] Parkinson and Pearce, 1998. *JPet*, **39**, 1577-1618. [2] Craddock *et al* 2013. *EPSL*, **365**, 63-76. [3] Prytulak *et al* 2013. *EPSL*, **365**, 177-189. [4] Schoenberg *et al* 2008. *Chem. Geol.*, **249**, 294-306.

Radiogenic heat potential of the Sardinian Variscan crust

A. PUCCINI^{1*}, G. XHIXHA^{2,3}, S. CUCCURU¹, G. OGGIANO¹, M. KAÇELI XHIXHA¹, F. MANTOVANI², C. ROSSI ALVAREZ⁴ AND L. CASINI¹

¹University of Sassari, Department of Science of Nature and Environmental Resources, Via Piandanna, 4 - 07100 Sassari, Italy (*correspondence: apuccini@uniss.it)

²University of Ferrara, Physics Department, Via Saragat, 1 - 44100 Ferrara, Italy. Istituto Nazionale di Fisica Nucleare (INFN), Ferrara Section, Via Saragat, 1 - 44100 Ferrara, Italy

³Agricultural University of Tirana, Faculty of Forestry Science, Kodër Kamëz - 1029 Tirana, Albania

⁴Istituto Nazionale di Fisica Nucleare (INFN), Padova Section, Via Marzolo, 8 - 35131 Padova, Italy

The ⁴⁰K, ^{238,235}U and ²³²Th composition of the Variscan crust is derived from *in-situ* radiological characterization using a portable gamma-ray spectrometer [1]. Details about the analytical procedure and statistical processing of spectrometric data is given in [2]. A total of 400 measurements were performed in Sardinia, because of excellent exposure and detailed geologic information on the architecture of the Corsica-Sardinia Batholith and its country rocks [3].

The results of gamma-ray spectrometry measurements indicate that most granitoids have potential heat production rate between 0.49 and 6.92 $\mu\text{W m}^{-3}$. Both migmatites and low-grade metasediments are characterized by lower values in the range 1.3 – 3.1 $\mu\text{W m}^{-3}$. The U-Th-K abundances in the Sardinian Variscan crust are 1283^{+340}_{-463} Bq kg⁻¹, 47^{+18}_{-29} Bq kg⁻¹ and 67^{+21}_{-31} Bq kg⁻¹ respectively for ⁴⁰K, ²³⁸U and ²³²Th. These values are slightly higher than those typical for the upper continental crust [4]. However, the average heat production rate of the Variscan crust of northern Sardinia is about half of that inferred in the Bohemian Massif [5]. Therefore, we argue that selective enrichment of heat-producing elements in the crust cannot account for early Permian HT metamorphism in this part of the Variscan chain.

[1] Caciolli *et al* (2012) *Sci. Total Environ* **414**, 639–645. [2] Puccini *et al* (2013) *Environ. Earth Sci* in press, doi: **10.1007/s12665-013-2442-8**. [3] Casini *et al* (2012) *Tectonophysics* **544**, 31–49. [4] Rudnick & Gao (2003) *Treatise on geochemistry: meteorites, comets and planets*, vol 1, Elsevier Ltd., Oxford. [5] Lexa *et al* (2011) *J. Metamorphic Geol* **29**, 79–102

Isotopic and Elemental Evidence of Magma Ocean Processes Recorded in Early Archean Komatiites

IGOR S. PUCHTEL¹, RICHARD J. WALKER¹,
MATHIEU TOUBOUL¹ AND JANNE BLICHERT-TOFT²

¹Dept. of Geology, Univ. of Maryland, College Park, MD
20742, USA (correspondence: ipuchtel@umd.edu)

²Ecole Normale Supérieure de Lyon, 69007 Lyon, France

Isotopic and elemental data for well-characterized Archean komatiite systems from around the globe provide critical new insights into early-Earth processes. Combined new ^{142,143}Nd, ¹⁸²W, ¹⁷⁶Hf, and ^{186,187}Os isotopic data for early Archean komatiite systems are consistent with formation, followed by long-term isolation, of deep-seated mantle domains with fractionated time-integrated Sm/Nd, Hf/W, Lu/Hf, and Pt/Os ratios at ca. 4400 Ma. These domains were likely generated as a result of crystallization of a primordial magma ocean, with Mg-perovskite, Ca-perovskite, and Fe-Pt alloy acting as the fractionating phases [1]. The inferred mantle domains were largely mixed away by 2.7 Ga on the scale of mantle reservoirs sampled by late Archean komatiite lavas emplaced worldwide, as evidenced by uniform time-integrated Sm/Nd, Lu/Hf, Re/Os, and Pt/Os ratios in late Archean komatiite systems. The total HSE abundances present in the sources of early Archean komatiite systems, corrected for the inferred Pt fractionation during crystallization of the terrestrial magma ocean, are 70–75% of those in estimates of the modern PM, and are within the range of the total HSE abundances present in the sources of late Archean komatiite systems, indicating little change in HSE abundances in the Archean mantle between 3.5 and 2.7 Ga.

Higher Pt abundances in late Archean komatiites compared to their early Archean counterparts have been taken as evidence for sluggish, downward mixing of late accreted material into the mantle [2]. Our ^{142,143}Nd, ¹⁸²W, ¹⁷⁶Hf, and ^{186,187}Os isotopic and HSE abundance data for early Archean komatiite systems are inconsistent with such a scenario; instead, our data require that late accretion of HSE to Earth was largely complete by the time the terrestrial magma ocean had crystallized. Rather than downward mixing of an HSE-rich late veneer, the Pt concentration variations observed in Archean komatiites [2] may reflect sluggish mixing of diverse post-magma ocean domains characterized by variably fractionated HSE abundances.

[1] Puchtel I.S. *et al* (2013) *GCA* 108, 63-90. [2] Maier W.D. *et al* (2009) *Nature* 460, 620-623.

Chemical reactions of hydrogen in depleted gas reservoirs – a major research topic of the H₂STORE project

D. PUDLO¹, S. HENKEL¹, R. GAUPP¹ AND THE H₂STORE TEAM²

¹Friedrich-Schiller-University Jena, Institute of Geosciences,
Burgweg 11, D-07749 Jena, Germany (*correspondence:
dieter.pudlo@uni-jena.de)

²German Research Centre for Geosciences, Potsdam (GFZ) &
Clausthal University of Technology & Centre National de
la Recherche Scientifique, Université de Lorraine

The collaborative project H₂STORE (= Hydrogen to Store) investigates the feasibility of hydrogen underground storage in porous sandstones. Thereby a special emphasis is given to depleted gas reservoirs and gas storage sites, which commonly are comprised of reservoir sandstone layers and sealing mudstone cap rocks.

The most fundamental study on interaction of hydrogen with reservoir sandstones was given by Foh *et al* [1]. However there, only specific single mineral behaviour with hydrogen were regarded not taking into account the chance of complex interactions with further reservoir compounds. The complexity of potential reactions of hydrogen within depleted gas reservoirs arises from (a) reactions of hydrogen with the total mineral assemblage and thereby generated most variable reaction components, which might react quite different, than assumed monomineralic systems, (b) reactions with (commonly) high saline formation water, present in the pore space of the reservoir sandstones, (c) reactions with the residual remnants (e.g. crude oil, bitumen) of the HC-sites, and (d) reactions with microbiological organisms (e.g. bacteria) present at depths.

Thus, reactions in depleted gas/oil reservoirs and hydrogen are highly complex and asks for detailed investigations.

In the H₂STORE project several kinds of laboratory experiments at reservoir conditions and numerical simulation approaches are planned to investigate reactions given above. The relevance of these regards for hydrogen underground storage in porous media is that by these mineralogical, geo-, hydro-, and biochemical interactions the reservoir quality (e.g. porosity, permeability) can be strongly affected and an impact on the recharge rate for injected hydrogen and on the potential of green methane (“power-to-gas”) production is most reasonable.

[1] Foh *et al* (1979) *Underground hydrogen storage. Final report. Brookhaven National Laboratory, p. 145.*

Carbonate biomineralization under aerobic and anaerobic conditions by a novel deep subsurface bacterial isolate

FERNANDO PUENTE-SÁNCHEZ¹, MÓNICA SÁNCHEZ-ROMÁN¹, NURIA RODRIGUEZ^{1,2}, DAVID FERNÁNDEZ-REMOLAR¹, VÍCTOR PARRO¹ AND RICARDO AMILS^{1,2}

¹Centro de Astrobiología (INTA-CSIC), 28850 Madrid, Spain.

E-mail: puentesf@cab.inta-csic.es

²Centro de Biología Molecular Severo Ochoa (CSIC-UAM), 28049 Madrid, Spain.

The Iberian Pyritic Belt (IPB), one of the largest massive sulphide deposits on the world, is considered to be a Martian analogue.

A recent study [1] has shown the occurrence of micro-scale iron bearing carbonate minerals in sediments from the acidic Tinto River (IPB, Huelva, Spain) as well as in its subsurface. Even though microbial agents responsible for iron and carbonate precipitation in the river sediments are being identified, the specifics on subsurface biomineralization in Martian analogue environments are still poorly understood.

In order to further elucidate this and other open questions, the Iberian Pyritic Belt Subsurface Life (IPBSL) project is currently in progress. In that context, two boreholes (BH11 and BH10) of 339m and 613m depth were drilled into the IPB subsurface.

In this study we report the ability of the novel actinobacteria isolate NR2A-C7, obtained from a 297m deep sample from the IPBSL BH11, to mediate the precipitation of iron and carbonate under aerobic and anaerobic conditions. The minerals formed included crystalline iron phosphates and iron-calcium carbonates with similar composition to minerals identified in core samples from the same borehole.

[1] Earth Planet Sci Lett 351, 13-26, 2012

Calcium carbonate precipitation by CO₂ uptake in alkaline solutions

B. PURGSTALLER¹, A. NIEDERMAYR² AND M. DIETZEL¹

¹Graz University of Technology, Institute of Applied Geosciences, Graz, Austria
(purgstaller@student.TUGraz.at)

²Ruhr University Bochum, Institute of Geology, Mineralogy and Geophysics, Bochum, Germany

The uptake of CO₂ in Ca²⁺ ion bearing alkaline solutions causing subsequent precipitation of CaCO₃ is valid for many natural and man-made environments, e.g. formation of travertine and scaling [1, 2]. However, significant gaps of knowledge exist in respect to combined CO₂ uptake and CaCO₃ precipitation kinetics.

In the present study CO₂ uptake and CaCO₃ precipitation mechanisms and rates were experimentally studied by diffusion of CO₂ through a polyethylene membrane (0.2 mm) from an inner to an outer solution containing 10 mM of CaCl₂ (25°C). The pH was kept constant during two analogous sets of experiments at 8.3, 9.0, 10.0, 11.0 or 11.5 by titration using 500 mM NaOH solution.

By exceeding a supersaturation threshold CaCO₃ is formed in the outer solution. (Micro)Raman and XRD pattern as well as SEM images clearly reveal the formation of calcite and vaterite at all pH values, whereas at pH ≥ 10.0 aragonite additionally occurs. NaOH titration curves and [Ca²⁺] reflect CO₂ uptake rates (∝ ACAR: aqueous CO₃²⁻ accumulation rate [3]) and precipitation rates of CaCO₃ (R). At elevated pH of the outer solution the ACAR is significantly higher and less time for nucleation of CaCO₃, t_{fc}, is required compared to lower pH conditions (e.g. pH 8.3 and 10.0 result in ACAR = 10 and 122 μM h⁻¹ l⁻¹ and t_{fc} = 7.8 and 1.6 h, respectively). At the given total experimental time of 20 h the amount of precipitated CaCO₃ was similar for all 10 experiments. This can be explained by the significantly higher R values subsequent to nucleation at low versus high pH (e.g. pH 8.3 and 10.0 with R = 645 and 178 μM h⁻¹ l⁻¹, respectively) which correlates with a general decrease of [CaHCO₃⁰] at the CaCO₃ surface [4]. Finally, the R values decrease to a nearly constant value of 93 ± 10 μmol h⁻¹ l⁻¹ in all experiments.

[1] Clark, I.D., Fontes, J.-C., Fritz, P., 1992. *Geochim. Cosmochim. Acta* **56**, 2041-2050. [2] Dietzel, M., Usdowski, E., Hoefs, J., 1992. *Applied Geochemistry* **7**, 177-184. [3] Niedermayr A., Köhler S.J. and Dietzel M., 2013. *Chemical Geology* **340**, 105-120. [4] Ruiz-Agudo, E., Putnis, C.V., Rodríguez-Navarro, C., Putnis, A., 2011. *Geochim. Cosmochim. Acta* **75**, 284-296.

In-situ pH and carbon dioxide solubility in NaCl fluids

G. PURSER*, C.A. ROCHELLE AND L. JONES¹

¹British Geological Survey, Environmental Science Centre, Keyworth, Nottingham, NG12 5GG, UK.

pH measurements give crucial insight to processes taking place during CO₂-water-rock reactions both in the laboratory and the field. The pH will govern the chemical species present and subsequent chemical reactions. Accurate determination of pH is important in the laboratory for a detailed understanding of the state of experiments and to test/validate predictive computer simulations. Degassing of samples on depressurisation changes solution pH, hindering accurate assessment of in-situ pH. We have used a commercially available high-pressure pH probe, coupled with high pressure fluid preservation methods to determine CO₂ solubility and pH at elevated temperatures and pressures relevant to geological storage conditions. Measurements were made at a range of salinities from deionised water to 2M NaCl, over temperatures of 40°C to 80°C, and pressures of 50 bar to 200 bar. Results show pH to decrease with increasing salinity, increasing pressure and decreasing temperature. For a subset of the conditions we have also measured pH associated with impurities of SO₂ and NO₂. Our experiments were constrained by the working pressure limits of the commercially available pH probes used, and we are developing different techniques to potentially extend the measuring capabilities up to 500bar.

⁸¹Kr concentrations in deep fracture waters of the Withwatersrand Basin, South Africa

R. PURTSCHERT¹, T.C. ONSTOTT², W. JIANG³, Z.-T. LU³, P. MÜLLER³, E. VAN HEERDEN⁴, M. ERASMUS⁴, G. BORGONIE^{4,5}, B. LINAGE⁴, O. KULOYO⁴, R. KIPFER⁶, M.S. BRENNWALD⁶, B. VISSER⁷, S. MAPHANGA⁷ AND L. JOUBERT⁷

¹University of Bern, CH-3012 Bern, Switzerland

²Princeton University, Princeton, NJ 08544, USA

³Argonne National Laboratory, Argonne, IL 60439, USA

⁴Uni. of the Free State, Bloemfontein 9300, South Africa

⁵Ghent University, Gent 9000 Belgium

⁶Swiss Federal Institute of Aquatic Science and Technology, CH-8600 Dübendorf, Switzerland

⁷Star Diamond, Beatrix & Masimong mines, South Africa

⁸¹Kr has been proposed since many years an ideal tracer for dating subsurface fluids on timescales up to 2 million years. However, only recently the method became practicable for real case investigations due to significant analytical improvements [1]. In this study radioactive noble gas isotopes (⁸¹Kr, ⁸⁵Kr and ³⁹Ar) were applied for the characterisation of fracture waters in the deep gold mines of the Witwatersrand Basin, South Africa [2]. Those waters catalyzed interest because of deep microbial communities that persists to depths of over 3 km [3]. The key objective of the present study is to further constrain the origin of the fluids, to determine the timing of deep subsurface life and to test the ⁸¹Kr method in all kinds of environments. In contrast to expectations [4] we discovered that underground production of ⁸¹Kr is a significant process in the rocks of the Withwatersrand and Ventersdorp Supergroups. All measured ⁸¹Kr activities from fracture water were significantly higher than in atmospheric equilibrium. This is most likely related to elevated U/Th concentrations in the rock strata. Radiometric decay dating is complicated in such cases

[1].W. Jiang *et al* , *Geochim. Cosmochim. Acta* **91**, 1 (2012). [2].T. C. Onstott *et al* , *Geomicrobiology J.* **26**, 269 (2009). [3].G. Borgonie *et al* , *Nature* **474**, 79. [4]. B. Lehmann *et al* , *WRR*. 29, 2027 (1993).

High pressure garnet-bearing ultramafites and basites from the Main Uralian Fault: Comprehension of the Uralian mantle composition

E.V. PUSHKAREV

Institute of Geology and Geochemistry Ural Division of RAS,
Pochtovy str. 7, Yekaterinburg, 620075, Russia
(pushkarev@igg.uran.ru)

Three types of high pressure (HP) garnet-bearing rocks associated with the lherzolite massifs have been distinguished in the Main Uralian Fault (MUF) zone (Southern Urals, Russia): 1) olivine-spinel-pyroxene websterite ($Mg\# = 0.91-0.83$), 2) garnet clinopyroxenites ($Mg\# = 0.85-0.72$), 3) amphibole-pyroxene-ilmenite-garnet basites ($Mg\# = 0.91-0.65-0.45$). The comparison with HP rocks from the orogenic lherzolite complexes gives some similarities only for garnet pyroxenites. But the most Uralian HP rocks have $CaO/Al_2O_3 > 1$. It is much higher than those in primary mantle and in rocks from ophiolites ($CaO/Al_2O_3 = 0.8-0.9$). It indicates these rocks could not be the source or protolith of the Uralian HP rocks. It is supposed, that mantle source must be enriched in clinopyroxene and probably had a wehrlite composition. Perhaps, the most magnesium-rich high-pressure ultramafites in the MUF are relicts of such Paleozoic metasomatized mantle. Some of the garnet-bearing rocks could be the melts crystallized at the deep level close to the boundary between garnet and spinel facies. The study is supported by RFBR grants 13-05-00597, 13-05-96031, and scientific programs 2-C-5-1004 and 12-5-008-NDR

Coupled dissolution and precipitation at mineral – fluid interfaces

ANDREW PUTNIS¹, CHRISTINE VETA PUTNIS¹ AND ENCARNACIÓN RUIZ-AGUDO²

¹Institut für Mineralogie, University of Münster, Germany.
putnis@uni-muenster.de; putnisc@uni-muenster.de

²Department of Mineralogy and Petrology, University of Granada, Spain. encar Ruiz@ugr.es

When a mineral reacts with an aqueous solution with which it is out of equilibrium the first step of any reaction sequence is the dissolution of the mineral surface. The dissolution of even a few monolayers of the parent surface may result in a fluid boundary layer that is supersaturated with respect to a more stable solid phase. Nucleation of this product phase on the parent surface will depend on nucleation kinetics and will be enhanced if there is a degree of epitaxy (i.e. structure matching) between the two solids. The nucleation of the product on the surface of the dissolving parent enhances the dissolution rate of the parent that in turn increases the growth rate of the product. Such an autocatalytic reaction leads to a feedback mechanism between dissolution and precipitation such that their rates become equal.

Continuation of the transformation (replacement) reaction depends on keeping open fluid transport pathways to the reaction interface between the parent and product solids. In other words porosity must be generated in the product phase. The generation of porosity depends on two factors: the relative molar volumes of the two solid phases, and even more importantly, the relative solubilities of the two phases in the fluid i.e. their relative stabilities under the relevant physico-chemical conditions.

These simple ideas, encompassed in the term “interface-coupled dissolution-precipitation” have very wide application to mineral-fluid reactions in the earth as well as in industrial processes. Central to the whole concept is the importance of the mineral-fluid interface. The fluid at this interface can become supersaturated while the “bulk fluid” away from the interface plays no direct role in the reaction except as a fluid reservoir, i.e. it can remain undersaturated with respect to the reaction products.

Examples of mineral-fluid reactions will be given, starting from direct in situ observations by Atomic Force Microscopy and their relevance to mechanisms of incongruent dissolution and “leaching”, to hydrothermal experiments of mineral replacement mechanisms and their relevance to mineral-fluid interaction in rocks.

An example of CO₂ sequestration: Direct nano-scale observations of brucite [Mg(OH)₂] dissolution

CHRISTINE V. PUTNIS¹, JÖRN-ERIK HÖVELMANN²,
ENCARNI RUIZ-AGUDO³ AND HÅKON AUSTRHEIM⁴

¹Institut für Mineralogie, University of Münster,
Corrensstrasse 24, 48149 Münster, Germany

²Fachbereich Geowissenschaften, Universität Bremen,
Postfach 330440, 28334 Bremen, Germany

³Department of Mineralogy and Petrology, University of
Granada, Fuentenueva s/n 18071 Granada, Spain

⁴Department of Geosciences, University of Oslo, PO box 1047
Blindern, 0316 Oslo, Norway

The dissolution and carbonation of brucite on (001) cleavage surfaces was investigated in a series of *in situ* and *ex situ* Atomic Force Microscopy (AFM) experiments at varying pH (2–12), temperature (23–40°C), aqueous NaHCO₃ concentration (10⁻⁵–1 M), and PCO₂ (0–1 atm).

Dissolution rates increased with decreasing pH and increasing NaHCO₃ concentration.

Simultaneously with dissolution of brucite, the growth of a Mg-carbonate phase (probably dypingite) was directly observed. In NaHCO₃ solutions (pH 7.2–9.3), precipitation of Mg-carbonates was limited. Enhanced precipitation was, however, observed in acidified NaHCO₃ solutions (pH 5, DIC ≈ 25.5 mM) and in solutions that were equilibrated under a CO₂ atmosphere (pH 4, DIC ≈ 25.2 mM). Nucleation predominantly occurred in areas of high dissolution, such as deep step edges, suggesting that the carbonation reaction is locally diffusion-transport controlled within a fluid-mineral boundary layer and is the result of interface-coupled dissolution-precipitation. More extensive particle growth was also observed after *ex situ* experiments lasting for several hours. This AFM study contributes to an improved understanding of the mechanism of aqueous brucite carbonation at low temperature and PCO₂ conditions and has implications for carbonation reactions in general.

Different styles of metasomatism in lithospheric mantle beneath Central Europe

JACEK PUZIEWICZ¹, MAGDALENA MATUSIAK-MAŁEK¹,
THEODOROS NTAFLOS² AND MICHEL GRÉGOIRE³

¹University of Wrocław, Poland,
jacek.puziewicz@ing.uni.wroc.pl

²University of Vienna, Austria

³University Toulouse III, France

The lithospheric mantle beneath Central Europe (SE Germany, SW Poland, W Czechia) was sampled by many eruption of alkaline lavas forming the Central European Volcanic Province. The volcanic activity was concentrated in the Eger (Ohře) Rift in the western part of Czechia and its surroundings. The investigated mantle xenoliths show that this lithospheric mantle is mostly harzburgitic and widely affected by cryptic metasomatism.

The study of Księginki xenolith suites (mantle peridotites and pyroxenites) shows that the lithospheric mantle beneath the Eger Rift was – at least in places – extensively chemically rejuvenated and thermally homogenised by alkaline lavas on their way to the surface. The xenoliths representing the mantle located outside the rift evidence significant variability. The “Fe-metasomatism”, leading to slight decrease of Mg/(Mg+Fe) ratios in olivine, ortho- and clinopyroxene is common in lithospheric mantle located outside the Rift. This metasomatism is usually melt-induced and probably related to Cenozoic alkaline magmas moving pervasively through the harzburgites. The metasomatic events caused by CO₂-bearing silicate melt or by different agents were also deciphered in the region. A metasomatic high-Mg and very low Al clinopyroxene occurring in strongly depleted harzburgites was recently discovered in some localities. Its REE patterns as well as major element composition suggest that it might have originated from fluids generated in a supra-subduction (Alpine orogeny related?) setting. This demonstrates that the Central European lithospheric mantle recorded not only young metasomatic events related to Cenozoic rifting and alkaline melts.

Carbon isotopes and microelements distribution in fractions of brown coals

A.N. PYRYAEV* V.A. PONOMARCHUK
AND D.V. SEMENOVA

Institute of Geology and Mineralogy, 630090, ac. Koptuga st.
3., Novosibirsk (*correspondence: pyrayev@gmail.com)

Pyrolysis of coals [1, 2 etc] and element emission in a coal combustion process [3 etc] has been extensively investigated in many studies. Unfortunately, isotopic and microelement composition of extracted coal fractions and relationship of this parameters was not investigated carefully.

Pyrolysis (500°C) of three brown coals (1, 2 and 3) of varying R_{vt}^0 (0.77, 0.49 and 0.41 %, respectively) have been carried out in close isothermal vacuum (5 millibar) system. Two/tree fractions of pyrolyzed coals were collected: A - transparent high-volatile distillate; B - viscous oligomeric (probably) distillate; C - ash that remains after pyrolysis of coal. Yield of the distillates (25-70 wt. %) depends on coal type. Carbon isotope composition were determined using Thermo Finnigan 253 mass spectrometer and GasBanch. Difference in isotopic composition of fractions of one coal reaches 5.4‰.

Pyrolysis of coals lead to partial transfer of microelements from a coals to a distillates. Microelemental composition (25 elements) of initial coals and they fractions were determined using SR-XRD-analysis. Microelement content in distillates decreases from 1100 ppm (Ca) to 0.4 ppm (Y). Such microelements as V, Nb, Th and U was not transferred at all. Some microelements were transferred to a distillates almost totally (Pb, As, Zn).

The major conclusions: 1 - vacuum pyrolysis of brown coals lead to decomposition of coals in distillates and ash that differs in carbon isotopic compositions; 2 - distillates contains some microelements and may be considered as transfer agents of microelements in coals. This point is able to explain formation of polymetallic ores in the neighborhood of coal basin; 4 - it may be suggested occurrence of correlation between isotopic and microelemental composition of coal fractions.

[1] Senneca, Uriciolo, Chirone & Cumbo (2011) *Fuel* **90**, 2931-2938; [2] Krzesinska, Szeluga, Czajkowska, Muszynski, Zachariasz, Pusz, Kwiecinska, Koszorek & Pilawa (2009) *Int. J. of Coal Geol.* **77**, 350-355; [3] Xu, Yan, Zheng, Qiao, Han & Sheng (2003) *Fuel Processing Technology* **85**, 215-237.

Polymetamorphic complexes of the Urals as indicators of formation of the Ural part of the East European Craton

A. M. PYSTIN

Institute of Geology KSC UB RAS, Syktyvkar,
Russia, Syktyvkar State University pystin@geo.komisc.ru

Archean and Paleoproterozoic formations are known in the section of the Ural Lower Precambrian. They are high-temperature and complicatedly dislocated polymetamorphic complexes. There are enough strong reasons to interpret these complexes as tectonically displaced fragments of the crystalline basement, adjacent to the west of the platform.

The lowest age of metamorphic processes in granulite complexes (gneiss-granulite and granulite-metabasite) is limited by 2.8-2.7 Ga. Dynamic regimes of this metamorphic phase varied from moderate (gneiss-granulite complexes) to relatively high (above 10 kbar, granulite-metabasite complexes). Considering the various material composition of granulites of different pressure, we can assume that they were formed in Wilson's cycle.

Gneiss-migmatite complexes were formed under sequential manifestations of the granulite metamorphism which was replaced by the amphibolite facies metamorphism of moderate pressures and accompanying granitization. The lowest age limit of this metamorphic stage is ca. 2.1 Ga. The time of the amphibolite facies metamorphism in the gneiss-migmatite complexes is estimated as 1.95-1.75 Ma.

Eclogite-gneiss and eclogite-schist complexes, obviously, also belong to the Lower Proterozoic. Eclogite formation could take place synchronously with the granulite metamorphism, ca. 2.1 Ga in the lowest age.

Thus, it is reasonable to assume that in the Early Proterozoic metamorphic processes occurred under sharply different dynamic conditions, typical of subduction-collision systems.

The evolution of ultra-high-temperature and high-pressure metamorphic processes in the Ural polymetamorphic complexes generally correlates with the metamorphic development of the Early Precambrian complexes, adjacent to the west of the platform area. Thus, accretion-collision complexes formed 2.88 to 2.58 Ga in the Fennoscandian Shield (Fennoscandia) were revealed. The granulite and eclogite metamorphism correlates in time with uniting of Volga-Ural region and Sarmatia (ca. 2.1 Ga), and more recent amphibolite facies metamorphism and associated granitization - with merging of these two megablocks and Fennoscandia (1.8-1.7 Ga).

The work was supported by the Program of Basic Researches of RAS № 12-I-5-2022.

Zircon as an indikator of metamorphic conditions

YU. I. PYSTINA

Institute of Geology KSC UB RAS, Syktyvkar, Russia,
yktyvkar State University yuliya_pystina@mail.ru

For many years, studying the material composition of the Uralian polymetamorphic complexes with intent to reconstruct metamorphism and to determine the conditions of rock formation, we have been typing zircons [1,2]

We conducted a comparative study of irregularly-shaped zircons (the third morphotype) from two polymetamorphic complexes: the Parikvasshor and Selyankin in the Polar and Southern Urals, accordingly.

In the Parikvasshor complex zircon is represented by colorless or pale grains. Its content in zircon fraction is 55-65%. Optical heterogeneity of zircons is confirmed by microprobe studies. The central part of crystals is enriched in Hf and Fe, and the edge in Th and U; Th/U and Zr/Hf increase from the crystal center to its edge (0.3 to 0.8 and 57.5 to 105.4, respectively). ZrO_2/HfO_2 also increases from the center to the edge.

Irregularly-shaped zircons from plagiogneisses of the Selyankin complex are pale. Crystal sizes are 0.1-0.25 mm, the surface is smooth and shiny. The central part of crystals is enriched in U and Fe, and the edge in Th and Hf; Zr/Hf increases from the crystal center to its edge (102.5 to 337.5). Th/U and ZrO_2/HfO_2 , on the contrary, decrease from the center to the edge (from 5.06 to 0.44 and from 1384.6 to 692.5) correspondingly.

The Selyankin complex is composed of rocks that consistently undergone metamorphism of the granulite and amphibolite facies. Irregularly-shaped zircons indicate the decrease of crystallization temperature to lower stages of the amphibolite facies. The regressive character of the process is confirmed by the decrease of ZrO_2/HfO_2 from the center to the periphery of crystals. As it is known, such a decrease points out to crystallization of the mineral at the fall of temperature and pressure [3]. Rocks of the Parikvasshor complex were subjected to progressive metamorphism of low to medium levels of the amphibolite facies. This is reflected in the geochemical composition of zircon of the third morphotype. ZrO_2/HfO_2 in them increases from the center to the periphery of the

The work was supported by the Program of Basic Researches of RAS № 12-I-5-2022.

1. Pystina Yu. I., Pystin A. M. (2002) Zircon chronicle of the Uralian Precambrian. Ekaterinburg: UB RAS, **159**. 2. Pystina Yu. I., Pystin A. M. (2009) Collection of articles № 7. Syktyvkar: KSC UB RAS, **25–29**. 3. Xuezhao B., Songnian L., Xiaochun G., Huiming L. (1996) IGC 30th, **342**.

www.minersoc.org

DOI:10.1180/minmag.2013.077.5.16

Environmental degradation and health risks in Pearl River Delta, China

J. QI

South China Normal University, Guangzhou 510631, PR China (jungzh@163.com)

With the rapid process of industrialization and urbanization, cities have multiplied and expanded rapidly over the past 2 decades. Cities are sources of creativity, technology, and engines for economic growth. However, they are also sources of health hazards from the changed society, degraded environment and regional climate change.

The Pearl River Delta, including 9 cities (Guangzhou, Shenzhen, Foshan, Zhuhai, Dongguan, Zhongshan, Huizhou, Jiangmen, Zhaoqing), covers an area of 24437 km² and a large population of 42.8 millions. The unprecedented environmental degradation in the region, accompanied by complex interaction between urbanization and global environmental change, which places human health at risk on a large spatial and temporal scale. A range of urban health hazards and associated health risks in the Pearl River Delta result from a variety of factors including heat islands, air pollution, water crisis, soil pollution, infectious diseases, and urban consumerism; in addition, some hazardous health conditions are associated with inequality in living and working conditions. For sustainable development on environment and human health in the Pearl River Delta, it is urgent to understand the possibilities of health problems resulting from environmental changes related with urbanization. The author suggest 3 main areas for policy action and research direction: (1) the need to get full-scale information related to environmental monitoring data and health data, (2) the need to discuss the relationship among economic development, natural resources, environmental pollution and human health, (3) the need to provide new methodological approaches and techniques to implement interventions for sustainable development in the Pearl River Delta.

⁴⁰Ar/³⁹Ar geochronology of phengite from blueschist facies rock of the Myanmar and its implication

MIN QI¹, ZEMING ZHANG¹, HUA XIANG¹, ZENGQIU ZHONG² AND HUANING QIU³

¹Institute of Geology, Chinese Academy of Geological Sciences, No. 26 Baiwangzhuang Road, Beijing 100037, China, minqiqi@gmail.com

²China university of Geosciences, No. 388 Lumo Road, Wuhan, 430074, China

³Guangzhou Institute of Geochemistry, Chinese Academy of Sciences, No. 511 TianHe Area, Guangzhou, 510640, China

High-pressure (HP) low-temperature (LT) metamorphic rocks (blueschist and eclogite) in orogenic belts provide valuable information related to subduction processes of oceanic lithosphere. The blueschist together with garnet amphibolite, marble, quartzite are the associated rocks of the Myanmar jadeitite occurred in ultramafic rocks of the east ophiolite belt along the eastern margin of the Indian plate. The blueschist is composed mainly of glaucophane, phengite, albite, quartz, epidote with minor of actinolite and sphene. Among them glaucophane occurs as large grains whereas actinolite is fine hair-like in the matrix. The amphiboles in blueschist show variable compositions. Phengites in blueschists are characterized by a high Si content of 3.35–3.37 pfu, Mg content of ca. 0.27 pfu, Fe content of ca. 0.17pfu. The ⁴⁰Ar/³⁹Ar dating performed on phengite from the blueschist obtained an age of 147.0 ± 1.5 Ma, representing the metamorphic event during the subduction of oceanic crust. This age is older than ⁴⁰Ar/³⁹Ar ages of 123.9 ± 3.4 Ma of jadeite and 134.8 ± 1.4 Ma of sodic amphibole from the Myanmar jadeitite, and also older than the 100–80 Ma ages of high-pressure metamorphism of the blueschist derived from the subduction of the Neo-Tethys in the Western Himalayan orogen. To our knowledge, the 147 Ma age is probably the earliest time for the initial subduction of the Neo-Tethys beneath the Eurasian continent.

Cr isotopic evidence of enzymatic reduction of Cr(VI) catalyzed by a sulfate-reducing bacterium

LIPING QIN^{1,2}, RUYANG HAN², ROMY CHAKRABORTY², JOHN N. CHRISTENSEN² AND HARRY R. BELLER²

¹Key Laboratory of Crust-Mantle Materials and Environments, University of Science and Technology of China, Hefei, 230026, China (lpqin@ustc.edu.cn)

²Lawrence Berkeley National Laboratory, 1 Cyclotron Rd., Berkeley, CA 94720, USA

Several studies have suggested that Cr isotopic signature could be used for distinguishing between different Cr(VI) reduction pathways [1,2]. We previously showed distinct Cr isotopic fractionation behavior under aerobic versus denitrifying conditions with a single bacterial species, *Pseudomonas stutzeri* strain RCH2, even though the Cr(VI) reduction rates were comparable under those two conditions [3].

To further evaluate Cr fractionation mechanisms associated with enzymatic Cr reduction, in the current study, we used the sulfate-reducing bacterium *Desulfovibrio vulgaris* strain RCH1 isolated from DOE's Hanford 100H site. We found significant Cr(VI) reduction with lactate as the electron donor either in the presence or absence of sulfate; thus, the Cr isotopic signature was examined with and without sulfate. Under both conditions, Cr isotopic fractionation followed the same Rayleigh fractionation with an α value of 0.99806. This value is significantly smaller than the abiotic fractionation factors observed previously and is also smaller than the values from experiments with *Shewanella oneidensis* MR-1 using much lower electron donor concentrations [2], but is very similar to values from experiments with higher electron donor concentrations with either *P. stutzeri* RCH2 under aerobic conditions [3] or *S. oneidensis* MR-1 [1]. Since abiotic reduction of Cr(VI) by sulfide and Fe(II) could also have been involved in these experiments, abiotic reduction experiments with these reagents were conducted. The α values in these experiments were very different from 0.99806, implying that enzymatic reduction was dominant under the conditions tested with strain RCH1.

[1] Ellis *et al.* (2002) *Science* **295**, 260-262. [2] Sikora *et al.* (2008), *Geochim. Cosmochim. Acta* **72**, 3631-3641. [3] Han *et al.* (2012) *Appl. Environ. Microbiol.* **78**, 2462-2464.

Petrology and geochemistry of the Mesozoic potassic and sodic volcanic rocks in the Yishu deep fault zone, Shandong Province, eastern China: Petrogenesis and inferences on the evolution of the mantle sources

JIAN-SHENG QIU*, LIANG LIU AND YOU-LIAN LI

State Key Lab for Mineral Deposits Research, School of Earth Sciences and Engineering, Nanjing University, Nanjing 210093, China (*correspondence: jsqiu@nju.edu.cn)

Late Mesozoic potassic volcanic rocks are widespread along the Yishu deep fault zone and its both sides, but some sodic volcanic rocks are also developed in several parts of this region, especially in the interior of the fault. These rocks provide important constraints on the nature and evolution of the Late Mesozoic lithospheric mantle beneath the region. LA-ICP-MS zircon U-Pb dating yields ages of 124.0~118.7 Ma for the potassic rocks, and of 106.4~96.5 Ma for the sodic ones. Both the potassic and the sodic volcanic rocks show similar trace element features of LILE and LREE enrichment and HFSE depletion. However, the sodic volcanic rocks have lower REE (especially LREE) contents, lower Rb/Sr and La/Nb ratios, and display somewhat Pb depletions in the spidergram profiles. All the rocks have enriched Sr and Nd isotopic compositions, but the sodic volcanic rocks have slightly lower I_{Sr} ratios and higher $\epsilon_{Nd}(t)$ values with respect to the spatially coexisted potassic volcanic rocks, e. g., the I_{Sr} and $\epsilon_{Nd}(t)$ values of the coexisted sodic and potassic rocks in Tangtou basin are 0.7097~0.7100, -10.0~-11.8 and 0.7100~0.7106, -15.5~-17.0, respectively. Zircon $\epsilon_{Hf}(t)$ values of the sodic rocks are also higher than that of the potassic rocks (specially -4.2~-16.6 for the sodic rocks and -13.2~-24.3 for the potassic rocks). The elemental and isotopic systematics indicates that the potassic volcanic rocks were generated by melting of enriched lithospheric mantle which was most likely induced by hybridism of foundering lower crust of the North China Craton at mantle depths, but the magma source of the sodic volcanic rocks contain some proportions of depleted asthenosphere mantle components. Based on a synthesis of the geology and geochemistry, it is suggested that the continued extension thinned the lithosphere and induced the upwelling of asthenospheric melts which mixed with previously enriched lithospheric mantle. Decompression partial melting of the mixed mantle source produced the sodic volcanic rocks.

Experimental study of the reaction kinetics between CO₂-bearing solution and olivine

LIN QIU^{1*}, ZHENGRONG WANG¹, SHUANG ZHANG¹,
SHUN-ICHIRO KARATO¹, JAY J. AGUE¹,
MICHAEL ORISTAGLIO¹, EDWARD BOLTON¹
AND DAVID BERCOVICI¹

¹Department of Geology and Geophysics, Yale University,
New Haven, CT, USA

(*correspondence: lin.qiu@yale.edu)

Olivine, as one of the main constituents in mafic/ultramafic rocks, has been suggested as a promising candidate for trapping anthropogenic CO₂ permanently as carbonates because of its high dissolution and carbonation rates. In this study, we employed an experimental approach to quantitatively evaluate the carbonation reaction kinetics as CO₂-rich solution interacts with olivine (Fo₉₀).

Gem-quality olivine grains and olivine powders (<30µm or 50µm) reacted with CO₂-containing solutions (e.g., 0.25 to 3M NaHCO₃ solutions, fluid/rock mass ratio 5 to 10) in gold capsules placed in a hydrothermal autoclave over durations of 1-14 days at 200 °C and 150 bar. The carbonation fraction (CF, the percentage of carbonated olivine over original olivine) was determined by comparing the concentration of dissolved-inorganic-carbon (DIC) in the solution before and after carbonation reactions.

Our results show that the CF could increase by ~20 times using fine olivine powders (<30µm) relative to the larger grains (~0.18 g/each), and the CF has a positive linear correlation with the concentration of NaHCO₃. The maximum CF in our study reaches ~45%, obtained using <30µm olivine powders and 3M NaHCO₃ solutions within one day of the reaction. Further increase of experimental time, however, will not improve the CF, but result in the precipitation of secondary minerals (including talc), and sometimes the decomposition of the carbonates (i.e., magnesite). However, this scenario could be prevented by using less amount of solutions (fluid/rock_{mass} = 1); in which case, the carbonation reaction is much faster as SiO₂ precipitates as amorphous Si-layer without the formation of secondary minerals. The amorphous Si layers still have voids and channels for the fluid/rock interactions. These observations help constrain the kinetics of the olivine carbonation reactions.

Triplite in Baxiannao W deposit, southern Jiangxi, and its geological significance

QIU LIWEN¹ AND LI GUANGLAI²

¹State Key Laboratory for Mineral Deposits Research, Nanjing University, Nanjing 210093, China

²College of Earth Science, East China University of Technology, Fuzhou 344000, China

A pink mineral was newly found in the Baxiannao tungsten deposit, southern Jiangxi province, China. Analytical results from Laser Raman spectra shows that its Raman shift (425.34, 454.64, 601.12, 981.97, 1040.50, 1073.1 cm⁻¹) is in good concordance with that of sample Triplite R050186 from the ruff data base (432.08, 453.29, 611.42, 981.69, 1043.40, 1072.33 cm⁻¹). The d values of high peak of powder XRD analysis are 1.639, 1.759, 2.032, 2.110, 2.221, 2.517, 2.602, 2.690, 2.735, 2.864, 3.038, 3.278, 3.442, 3.660, 4.299, 5.668, respectively, which well fit the standard 25-1080 triplite. Chemical composition from electron-microprobe analysis is MnO 50.19%~50.96%, FeO* 7.74% ~7.78%, MgO 2.75%~2.89%, CaO 1.75%~2.12%, P₂O₅ 30.95%~31.51%, F 7.21%~7.94%, and H₂O 0.45%~1.02%, and hence the calculated chemical formula is (Mn, Fe, Mg, Ca)₂PO₄(F, OH). All these data prove that the mineral is triplite, the manganese end-member of triplite-zwieselite series. It occurs in the wolframite-bearing quartz vein and associated with quartz and fluorite, which indicates that the ore-forming fluid was rich in phosphor and fluorine. The triplite contains a lot of fluid inclusions of two phases. Almost all the fluid inclusions are aqueous-rich and many of them are larger than 150µm. Raman spectra show that the liquid phase is water while the gas phase contains not only H₂O, but also CH₄ and CO₂. The discovery of triplite together with quartz and fluorite in the tungsten deposit suggests that the related granite is most likely attributed to the fluorine-rich category.

Geology and geochemistry of the Fenghuangshan skarn Cu deposit at Tongling area, Anhui Province, East China

HONGYING QU^{1*}, RONGFU PEI¹, HONGCAI FEI²,
JINWEN LI¹, YONGLEI WANG¹ AND HAOLIN WANG¹

¹MLR Key Laboratory of Metallogeny and Mineral Assessment, Institute of Mineral Resources, Chinese Academy of Geological Sciences, Beijing 100037, China (*correspondence: hongyingqu@126.com)
²ACTA Geological Sinica (English Edition), Beijing, 100037, China

The Fenghuangshan skarn Cu deposit at Tongling area, Anhui Province, is a component of the Middle-Lower Yangtze River metallogenic belt. The Xinwuli quartz monzodiorite and granodiorite related to mineralization at Fenghuangshan are intermediate-acidic intrusive rocks derived from alkali basalt of upper mantle and contaminated by crust materials during magma evolution. We carried out key study for this deposit. Geochemical features, ore-forming fluids and chronology have been studied to understand ore-forming mechanism. Carbon, hydrogen and oxygen isotopes indicate that ore-forming fluids in the deposit mainly are derived from the magma with input of minor amount of meteoric water at the late stage of the mineralization. Sulfur and lead isotopic analysis indicate that ore-forming materials are from the mantle source. Re-Os isotopic dating of molybdenite from the Fenghuangshan Cu deposit yielded an isochronal age of 141.1±1.4 Ma with the model ages ranging from 139.1±2.4 to 142.0±2.2 Ma, which is consistent to zircon SHRIMP U-Pb ages of the related quartz monzodiorite and granodiorite. Dating analysis yielded ages of 136.0±2.0 to 143.0±2.4 Ma for the quartz monzodiorite (a weighted average of 139.4±1.2 Ma) and ages from 136.7±2.0 to 145.3±2.4 Ma for granodiorite (a weighted average of 141.0±1.1 Ma). These studies discuss that the relationship between mineralization and intrusion, helping to understand other skarn Cu deposits which have similar ore-forming settings.

Classification of gemstone tourmalines from Central Brazil by chemistry nomenclature

H.A. QUEIROZ¹ AND N.F. BOTELHO²

¹University of Brasilia, Brazil
(¹hudsonq@gmail.com, ²nilsonfb@unb.br)

Several handpicking mines were important gemstone sources, mainly tourmalines, during the 1970's and 80's in Tocantins State, Central Brazil.

The studied tourmalines exhibit a wide range of colours, black, dark and light blue, dark and light green, pink, purple and colourless, sometimes exhibiting zonation. Classification of tourmalines based on colour, for instance rubellite, indicolite, verdelite, was substituted by chemical nomenclature accordingly Henry *et al.* [1], based on crystal microprobe analysis and the cation distribution.

In colored crystals there are solid-solutions between four species, schorl, elbaite, liddicoatite and rossmanite. Dark-blue and dark-green crystals are examples of schorl-elbaite series; light green, pink and colourless are either elbaite-rossmanite or elbaite-liddicoatite series. Apparently, the calcic tourmaline liddicoatite occurs more frequently in pegmatites hosted in Ca-rich rocks, in a similar way of those from Anjanabonoina, Madagascar [2].

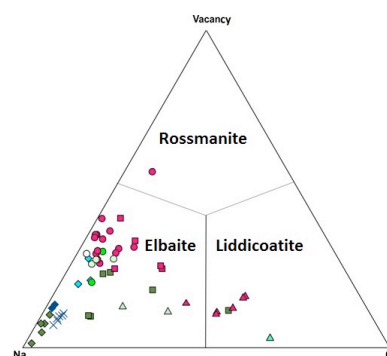


Figure 1: Colored tourmaline species by X site occupancy. The color of each data point is indicative of the color of tourmaline.

[1] Henry *et al.* (2011) *American Mineral.*, **96**, 895-913. [2] Dirlam *et al.* (2002) *Gems & Gemology*, **38**, 28-53.

Levels and geochemistry of urban and rural atmospheric particulate matter in Spain

X. QUEROL, A. ALASTUEY, T. MORENO AND M. VIANA

Institute of Environmental Assessment and Water Research, IDAEA, CSIC, Barcelona, Spain

A review of PM₁₀, PM_{2.5} and PM₁ geochemistry data collected in 1999–2011 from 40 air quality monitoring data, each with 1 to 10 years of data coverage, is presented with the aim of describing major features of urban, industrial and rural source contribution, as well as describing the major concentration trends and their causes.

Ambient air PM levels have markedly decreased in the last decade by around 35%. Although EC limit values are exceeded only in a few hotspots, urban PM levels still exceed by far the WHO guidelines. Causes accounting for these trends are discussed according to geochemical data.

Spatial gradients are very clear across Spain, especially levels of sulphate, nitrate, ammonia and mineral matter. Different emission patterns and climate features may account for these gradients. The incidence of African dust outbreaks on PM levels is also briefly described. Levels of carbonaceous aerosols are mostly influenced by vehicle exhaust emissions. Ranges of concentrations of levels of around 30 trace elements in the 40 sites are presented and discussed. The influence of major industrial hotspots is evidenced, but also the impact of vehicle wear emission in ambient levels of a number of relevant metals is evidenced. Results point to the very high impact of vehicle exhaust and road dust emissions on levels and composition of PM in urban areas. Biomass burning emissions may have local impact but not much at urban scale in the largest urban agglomerations in Spain. Finally, the relevance of specific industrial hotspots is also shown.

Multi-Wavelength Raman survey of IOM from primitive meteorites

E. QUIRICO^{1*}, F-R ORTHOUS-DAUNAY¹, P. BECK¹, L. BONAL¹, R. BRUNETTO², E. DARTOIS², T. PINO², G. MONTAGNAC³, JN ROUZAUD⁴, C. ENGRAND⁵ AND J. DUPRAT⁵

¹IPAG UJF France (correspondence eric.quirico@obs.ujf-grenoble.fr)

²Institut d'Astrophysique Spatiale Orsay France

³Laboratoire de Géologie de Lyon, ENS/UCLB France

⁴Laboratoire de Géologie ENS-Paris France

⁵CSNSM IN2P3/Université Paris Sud Orsay France

We report a survey of the structure of Insoluble Organic Matter (IOM) of a series of 27 CR, CM, CI and ungrouped C2 carbonaceous chondrites by means of Infrared and Multi-Wavelength Raman micro-spectroscopy (244, 514 and 785 nm laser excitations). The IOM in some of these chondrites displays Raman and Infrared signatures that point to the past action of short duration thermal metamorphism, presumably triggered by impacts (e.g. PCA 91008, QUE 93005, Tagish Lake). Interestingly, IOM from other chondrites also display Raman characteristics consistent with a thermal processing. In this regard, IOM and Soluble Organic Matter (SOM) could be considered as two byproducts of organic precursors decomposed by thermo-degradation. The place where this process occurred, within parent body or protosolar disk prior accretion, cannot be firmly identified given the lack of precise knowledge on the nature of the organic precursors and of the time-temperature history of the parent asteroid. Our data also confirm that IOM is structurally more homogeneous in chondrites than in stratospheric IDPs and Antarctic Micrometeorites (AMMs). This suggests IOM contained in these particles was formed under more varying conditions. However, other mechanisms as ions irradiation or atmospheric heating/oxidation cannot be fully excluded for accounting for these variations.

Los Morros olivine basalts from the Domeyko Cordillera in the Antofagasta region, northern Chile

O.M. RABBIA^{1*}, C. JARA², L.B. HERNÁNDEZ¹
AND E. ARAGÓN³

¹Instituto GEA, Universidad de Concepción, P.O. Box 160c, Concepción, Chile

*correspondence: rabbia@udec.cl)

²Cía. Minera Barrick Ltda. Barrio Industrial Alto Peñuelas Sitio 58, Coquimbo, Chile (cjara@barrick.com)

³Centro de Investigaciones Geológicas (UNLP-CONICET), La Plata, Argentina (earagon@cig.museo.unlp.edu.ar)

In the eastern flank of the Domeyko Cordillera at 23°45' S two types of olivine basalts crop out as lava flows covering the Permian crystalline basement and as sills in Jurassic limestones. The basalts lay on an uplifted crustal block within the transpressional Domeyko fault system (DFS).

One type is an olivine-phyric alkali basalt, with Mg# 62-67, Ni 120-190 ppm and Cr 205-338 ppm. The Ta/Hf (>0.4); La/Nb (<2) and Ba/Nb (12-31) ratios suggest an intraplatelike affinity (OIB-type mantle source).

The other, is an olivine-clinopyroxene-phyric transitional basalt (in TAS diagram), with high Ba/Nb (90-100) and Th/Nb (>0.2) ratios indicating an arc affinity. A primitive character is suggested by: Mg# 70-74; Cr 870-1100 ppm, Ni 220-300 ppm and olivine phenocryst with core compositions (2300-3200 ppm Ni and Fo₈₈₋₉₂) in the range of mantle olivines. Its source is more refractory than that of the alkali basalt.

New ⁴⁰Ar/³⁹Ar step-heating ages ranging from 55.6±1.4 to 56.7±1.0 Ma (this work) place the alkaline magmatism in the Palocene-Eocene transition. These ages are close to, but slightly older than the 52.5±1.8 Ma (K/Ar, [1]) for the spatially associated transitional basalts with arc-affinity.

The nature and close relationship in space and time of these basalt types is consistent with short crustal residence time and deep major-faults in extensional zones. The Los Morros basaltic magmatism may imply that the inverse structures of the DFS associated to these mafic rocks may represent step-inverted normal faults inherited from Paleocene and/or previous extensional episodes, later reactivated by the transpressional Incaic tectonic event, which uplifted the Domeyko Cordillera during the Eocene-Oligocene time.

[1] Mpodozis et al (1993) Ser.Nac.Geología & Minería, 282.

Metal isotope fractionation during microbial processes in the Critical Zone

K. RABE^{1*}, A. SCHIPPERS², S. WEYER¹, S. SCHUTH¹
AND M. LAZAROV¹

¹Leibniz Universität Hannover, Institut für Mineralogie, Callinstr. 3, 30167 Hannover, Germany

(*correspondence: k.rabe@mineralogie.uni-hannover.de)

²Bundesanstalt für Geowissenschaften und Rohstoffe, Stilleweg 2, 30655 Hannover, Germany

(Axel.Schippers@bgr.de)

Oxidation of sulfide minerals (e.g. pyrite) in sulfidic mine waste leads to the formation of acid mine drainage [1]. Herbert and Schippers (2008) found large Fe isotope fractionations ($\Delta^{56}\text{Fe}$: -1.4‰ to -2.4‰) between pore water and Fe(oxy)-hydroxides in mine tailings and concluded that this was the product of microbially catalyzed iron cycling [2].

In this study the potential of Fe and Cu isotope fractionation analysis is investigated to fingerprint microbial oxidation of metal sulfides in mine tailings. We focus on the investigation of the metal isotope fractionation between the sulfides and the metal(oxy)-hydroxides. We tested the selectivity of a sequential extraction method consisting of six extraction steps, to distinguish between sulfates, carbonates, Fe(oxy)-hydroxides, oxides, sulfides and silicates [3, 4]. For this test we used a synthetic test sample with known Fe isotope ratios of the components. The first results show that for Fe isotopes no significant isotope fractionation occurs during the extraction.

In the next steps we will adopt this sequential extraction method to natural samples from a porphyry copper mine tailings in Chile [5, 6] and determine the Fe and Cu isotope compositions of the particular fractions. In addition, we will perform laboratory experiments of microbial mineral oxidation and compare the isotope fractionation with that in the mine tailings.

[1] Dold & Fontboté (2001) *J. Geochem. Expl.* **74**, 3-55. [2] Herbert & Schippers (2008) *Environ. Sci. Technol.* **42**, 1117-1122. [3] Dold (2003) *J. Geochem. Expl.* **80**, 55-68. [4] Mehra & Jackson (1960) *Clays Clay Min.* **7**, 317-327. [5] Dold (2006) *Environ. Sci. Technol.* **40**, 752-758H. [6] Korehi *et al.* (2013) *Environ. Sci. Technol.* **47**, 2189-2196.

Groundwater Resource Management of Rampurbaghelan Area, Satna District, Madhya Pradesh India

RABINDRA N. TIWARI

Department of Geology, Govt. P.G. Science College Rewa, Madhya Pradesh (email : geogppandey@gmail.com)

The paper deals with management of groundwater resource of Rampurbaghelan area Satna district, Madhya Pradesh. Geologically, the area is a part of Bhandar Group of Vindhyan Supergroup. The limestone and shale are the main aquifers of the area. For the assessment of groundwater resource, groundwater recharge, groundwater development stage, water table trends, water table fluctuation etc. have been studied. The Pre and Post monsoon water tables are falling. The calculated stage of groundwater development suggests that the area falls in semicritical category. However due to decline in water level, quality and quantity of groundwater have been adversely affected. For scientific management, utilization and augmentation of groundwater resource, the following suggestions have been recommended:

Artificial recharge structures like percolation pond, check dam and contour trenches should be preferred at suitable sites with the help of geological and geomorphological data.

The area having moderate slope can be utilise for contour bunding. The soil taken from the trenches may be placed down the hill in the form of bund. The soil erosion and vegetal. cover can be controlled by growing such seeds of grasses and shrubs on the bunds which are suitable to the area.

Recharge augmentation is positive way, while pumpage control is negative way of management. In extreme cases, when pumpage control is to be observed in the area, the best way of monitoring is at the level of Gram Panchayat.

The groundwater management policies and practices should transcend from academic echelon to actual field implementation. All the related departments publics, stake holders and research institution should be jointly initiate the sustainable action plan with short term and long term plan strategy. Besides these, NGO's may play vital role to conserve the groundwater resource of the area.

The awareness programme is honestly and urgently needed.

Proteogenomic insights into completely oxidizing sulphate reducers (*Desulfobacteriaceae*)

RALF RABUS¹

¹Institute for Chemistry and Biology of the Marine Environment (ICBM), University Oldenburg, Oldenburg, Germany; rabus@icbm.de

Sulfate-reducing bacteria are pivotal to carbon turnover in marine sediments, as Jørgensen (1982) demonstrated in his seminal work on organic carbon rich shelf sediments. The observed high in situ activities could concurrently be explained best by the key properties of newly discovered sulphate reducers belonging to the family *Desulfobacteriaceae* (Widdel 1988): (i) capacity to completely oxidize organic carbon to CO₂, and (ii) broad nutritional versatility spanning from simple fermentation end-products to less well degradable substrates such as aromatic compounds. These early findings and concepts motivated more recent genomic and proteomic investigations to further our molecular understanding of this group's physiological capacity. The first published genome of a *Desulfobacteriaceae* member was that of *Desulfobacterium autotrophicum* HRM2 (Strittmatter *et al.* 2009), which degrades long-chained fatty acids and is capable of chemolithoautotrophy (with H₂ and CO₂). The 5.6 Mbp genome displayed an unusually high degree of plasticity and contains a large suite of genes for regulation and electron transport. The recently completed genome of *Desulfobacula toluolica* Tol2 (Wöhlbrand *et al.* 2012) in combination with sub-proteomics and metabolite analysis allowed a detailed reconstruction of the catabolic network for aromatic-compound utilization and discovery of new degradative capacities. Taken together first genome-based insights are emerging that causally explain the ecosystems function of *Desulfobacteriaceae*.

[1] Jørgensen BB (1982) *Nature* **296**: 643-645 [2] Strittmatter AW *et al.* (2009) *Environ Microbiol* **11**: 1038-1055. [3] Widdel F (1988) In *Biology of Anaerobic Microorganisms*. Munich, Germany: Carl Hanser Verlag, pp. 469-585 [4] Wöhlbrand L *et al.* (2012) *Environ Microbiol* doi:10.1111/j.1462-2920.2012.02885.x

Sedimentary and diagenetic features of the Oolithe Blanche formation (Middle Jurassic): New contribution from Ca, Sr, C, O isotopic compositions

SETAREH RAD¹, YASIN MAKLOUFI²,
CATHERINE GUERROT¹, CHRISTINE FLEHOC¹
AND PIERRE-YVES COLLIN³

¹BRGM, 3, avenue Claude-Guillemain, Orléans, France

²UPMC Univ. Paris 06, UMR 7193, IStEP, Paris, France

³Université de Bourgogne, UMR CNRS 5561, Dijon, France

The Oolithe Blanche formation is present in the Paris Basin at more than 1500 m depth in the middle of the basin and on outcrops at the basin edges. This Bathonian formation (Middle Jurassic) is composed of very shallow marine oolitic and bioclastic limestones, located within a shoreface depositional environmental (Casteleyn *et al.*, 2010).

Calcium, strontium, carbon and oxygen isotopes have been analysed both in ooids and interparticular cement directly extracted from the limestone in order to study sedimentary and diagenetic environment.

The ⁴⁴Ca/⁴⁰Ca ratios (expressed as $\delta^{44/40}\text{Ca}_{\text{SW}}$) were measured by TIMS using a ⁴²Ca-⁴⁸Ca double-spike. Carbon and oxygen isotopic ratios were measured by IRMS.

Preliminary results show a range of $\delta^{44/40}\text{Ca}_{\text{SW}}$ from -0.74‰ to -1.09‰ in the cement and from -0.85‰ to -1.05‰ in ooids. Carbon isotopic signature show a range of $\delta^{13}\text{C}_{\text{vs PDB}}$ range from 1.5‰ to 2.7‰ in the cement and from 1.5‰ to 2.4‰ in ooids while $\delta^{18}\text{O}_{\text{vs SMOW}}$ vary from 21.5‰ to 23.9‰ in the cement and from 21.2‰ to 24.9‰ in ooids.

This first multi-isotopic approach on Oolithe Blanche formation seems to be consistent with the diagenetic evolution of Paris Basin. Effects of diagenesis on the isotopic signatures will be discussed.

Casteleyn, L., Robion, P., Collin, P.Y., Menendez, B., David, C., Desaubliaux, G., Fernandes, N., Dreux, R., Badiner, G., Brosse, E., Rigollet, C., 2010. *Sedimentary Geology* 230, 123–138.

Role of small urban reservoirs in regulating watershed quality

L.K. RADEMACHER^{1*} AND K.L. FAUL²

¹University of the Pacific, Stockton, CA, 95211, USA

(*correspondence: lrademacher@pacific.edu)

²Mills College, Oakland, CA, 94613, USA (kfaul@mills.edu)

Many coastal creeks in California drain small upstream reservoirs. These reservoirs were originally created to store drinking water, but many are currently maintained for recreation, irrigation, and other purposes. More than 200 of these reservoirs are located within the San Francisco Bay (SFB) area, which is western North America's second largest urban area. As a result, these small individual reservoir/creek systems contribute a significant proportion of pollution to the coastal ocean. Understanding modern and historic biogeochemical cycling in urban watershed/reservoirs systems provides new insight into anthropogenic influences on the function of these systems, how differing management strategies in these systems may mitigate or exacerbate contaminant discharge to the urban-influenced coastal ocean, and how best to manage these systems for improved water quality and beneficial use in the future.

The present study investigates three watershed/reservoir systems in the east SFB region to better understand biogeochemical cycling in disturbed urban environments. For example, Lion Creek/Lake Aliso is an acid mine drainage impacted system and the Don Castro/San Lorenzo Creek system is influenced by freeways and residential land uses. In comparison, the relatively undeveloped Lake Anza/Wildcat creek is primarily surrounded by parkland. Water quality data (including standard geochemistry, as well as nutrient and trace element concentrations) from reservoir inlets and outlets at each of these systems is collected biweekly. Depth profiles of pH, conductivity, temperature, and dissolved oxygen within each lake are also collected biweekly. In addition, sediment cores from multiple locations in each lake were collected and analyzed for nutrient and trace element concentrations.

Preliminary results indicated urban reservoirs play an important role in biogeochemical cycling in urban watershed and downstream water quality. Lake water column structure varies over the course of a year with reducing conditions prevailing during warm summer months and more oxidizing conditions occurring during more winter months. The oxygenation state of these lakes ultimately plays a significant role in whether metals and nutrients are mobilized or retained. In addition, sediment cores from each of the lakes indicate changes in how these lakes cycle elements has changed through time in response to differing managing strategies.

FTIR imaging of carbon dioxide diffusion in cordierite-like structures

F. RADICA^{1*}, F. BELLATRECCIA¹, G. DELLA VENTURA¹,
C. FREDA², G. CINQUE³ AND M. CESTELLI GUIDI⁴

¹Università degli Studi Roma Tre, 00146 Rome, Italy
(*correspondence: fradica@uniroma3.it,
bellatre@uniroma3.it, dellaven@uniroma3.it)

²INGV, 00143 Roma, Italy

³INFN-LNF, 00044 Frascati (Rome), Italy

⁴Diamond Light Source, OX11 0DE Didcot, UK

Cordierites and beryls are isostructural minerals that may diffuse significant amounts of H₂O and CO₂ through their structural channels, running along the *c* axis, [1]. Experimental introduction of CO₂ in cordierite-like structure was studied by several authors [2, 3], who pointed out the extreme difficulty to reach sample saturation and homogenization.

In this work we treated cordierite and beryl volatiles-free

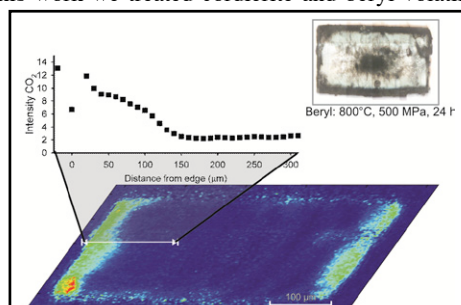


Figure 1 - FPA image and single spot IR transect of a

single-crystals in CO₂-saturated environment at different PT conditions. The run products were analyzed via micro-FTIR spectroscopy in order to quantify the CO₂ content and its distribution across the sample.

Preliminary results show that pressure plays a major role in diffusing gaseous CO₂ across both cordierite and beryl, whereas the effect of temperature is less pronounced. Detailed FPA (focal-plane-array of detectors) imaging shows that the diffusion occurs along the structural channels starting from the basal pinacoids along the *c*-axis direction. As expected, no diffusion occurs perpendicularly to the *c*-axis. The diffusion path of CO₂ does not exceeds 200 µm even after 10 days. Sample cracks formed during the experimental runs speed up diffusion; measured CO₂ contents along these cracks are even 4 times higher than in the rest of the sample.

[1] Goldman *et al.* (1977) *Am. Mineral.* **62**, 1144-1157. [2] Armbruster and Bloss (1982) *Am. Mineral.* **67**, 284-291. [3] Le Breton (1989) *Contrib. Mineral. Petrol.* **103**, 387-396.

Glacial-interglacial changes in ocean carbonate chemistry constrained by boron isotopes, trace elements, and modelling

JAMES W.B. RAE¹, JESS F. ADKINS¹, ALAN FOREMAN²,
CHRISTOPHER CHARLES², ANDY RIDGWELL³, GAVIN L.
FOSTER⁴, DANIELA N. SCHMIDT³ AND TIM ELLIOTT³

¹Geological and Planetary Sciences, Caltech, Pasadena, USA
jamesrae@caltech.edu

²SCRIPPS Institution of Oceanography, UCSD, La Jolla, USA

³University of Bristol, Bristol, UK

⁴School of Ocean and Earth Science, National Oceanography Centre, University of Southampton, Southampton, UK

Deep ocean carbon storage and release is commonly invoked to explain glacial-interglacial CO₂ cycles, but records of the carbonate chemistry of the glacial ocean have, until recently, been scarce. Here we present new boron isotope ($\delta^{11}\text{B}$) data from detailed depth profiles and time series, that record the pH of the deep ocean at the last glacial maximum (LGM), and how it evolved over the deglaciation. We examine these data using a recently developed tracer fields modelling approach [1]. This has previously been applied to $\delta^{18}\text{O}$ data to investigate changes in circulation at the LGM. Here we extend this method to the non-conservative tracers $\delta^{11}\text{B}$ and $\delta^{13}\text{C}$, allowing us to constrain the roles of circulation, the biological pump of organic carbon and CaCO₃, and carbonate compensation, in setting deep ocean carbon storage at the LGM. Finally, we show how deep ocean carbon storage evolved over the deglaciation, with pulses of stratification breakdown in the Southern Ocean and North Pacific causing CO₂ release from the deep ocean to the atmosphere.

[1] Lund, D. C., J. F. Adkins, and R. Ferrari (2011), Abyssal Atlantic circulation during the Last Glacial Maximum: Constraining the ratio between transport and vertical mixing, *Paleoceanography*, **26**, PA1213, doi:10.1029/2010PA001938.

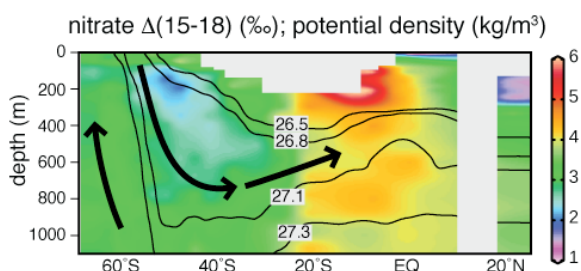
Revealing Pacific Ocean organic matter remineralization and circulation using the dual isotopic composition of nitrate

PATRICK A. RAFTER¹ AND DANIEL M. SIGMAN¹

¹Department of Geosciences, Princeton University

Here we show that the difference between the N and O isotopic composition of nitrate, or $\Delta(15-18)$, is sensitive to organic matter remineralization and largely reflects known patterns of surface ocean nitrogen cycling. For example, incomplete nitrate consumption in high latitude surface waters and N fixation in the subtropical North Pacific lowers subsurface $\Delta(15-18)$, while complete consumption in the lower latitudes elevates subsurface $\Delta(15-18)$ (see Figure 1 below). This sensitivity is exploited to estimate the $^{15}\text{N}/^{14}\text{N}$ of sinking organic matter and to track the modification of nitrate as it passes from the deep Pacific Ocean, through the Southern Ocean surface, and into intermediate-depth waters—a pathway that is necessary for resupplying the low latitude surface ocean with nutrients (Figure 1).

Figure 1: Nitrate $\Delta(15-18)$ along $\approx 150^\circ\text{W}$ in the Pacific Ocean (see colour bar) and potential density (lines). Deep-sea nutrients are brought to the high latitude surface ocean and transported to lower latitudes within the potential density range of 26.5 to 27.1 kg/m^3 (arrows). Changes in nitrate $\Delta(15-18)$ along these isopycnals largely result from organic matter remineralization.



Growth medium and carbon source of unusual rounded diamonds from alluvial placers of the North-East of Siberian Platform

A.L. RAGOZIN^{1*}, V.S. SHATSKY^{1,2}, D.A. ZEDGENIZOV¹
AND W.L. GRIFFIN³

¹V.S. Sobolev Institute of Geology and Mineralogy SB RAS,
Koptuyuga Ave. 3, Novosibirsk 630090, Russia,

(*correspondence: ragoz@igm.nsc.ru)

²A.P. Vinogradov Institute of Geochemistry SB RAS,
Favorsky str. 1a, Irkutsk 664033, Russia

³CCFS/GEMOC, Macquarie University, NSW 2109, Australia

About 70% of diamond placer deposits of the Siberian platform are concentrated in the northeastern part. Primary sources of diamonds of these placers have not yet been established. Some diamonds are neither characteristic to the pipes located nearby nor to any of the known kimberlite pipes of Yakutia. A significant part of the diamonds belongs the variety V [1]. These diamonds are characterized by rounded morphology and radial mosaic-block internal structure. The diamonds are enriched in isomorphous nitrogen (up to 3500 ppm) and have light carbon isotopic composition ($\delta^{13}\text{C}$: -19.6‰ to -24.1‰). The Coe inclusions suggest eclogite paragenesis also supported by the light carbon isotopic composition. Moreover, diamonds contain numerous microinclusions (<1 μm). Rt, Grt, Ap, Kfs, Dy, Omph and Jd have been identified among microinclusions associated with fluid (or melt) inclusions of composition varied from carbonatitic (enriched in Ca, Mg, Fe, Cl, Ba and Sr) to silicic (enriched in Si, Al, Ti, K). Bulk trace element patterns of microinclusions as determined by LA-ICP-MS are similar to that observed in cuboid diamonds from Siberian Platform. Fluid inclusions have demonstrated that growth environment involved H_2O , CO_2 , N_2 , CH_4 and heavier hydrocarbons [2]. The compositions of fluid inclusions in one crystal could change from CO_2 to essentially hydrocarbons from center to the periphery.

Thus the obtained data for unusual rounded diamonds (variety V) indicates the possible connection between the formation of diamonds and subduction events. Variations of the growth media composition may be caused by the interaction between the metasomatizing fluids and silicate substrate.

[1] Orlov Yu.L. (1977) *The Mineralogy of the Diamond*. Wiley and Sons, New York, 1977, 235 p. [2] Tomilenko A.A. *et al.* (2001) *Doklady Earth Sciences* **379**, 571–574.

Petrological and Geochemical Evidences for the Origin of the Neyriz Ophiolites, SE Zagros, Iran

MOHAMMAD RAHGOSHAY¹
AND IMAN MONSEF^{2*}

¹Shahid Beheshti University, Earth Sciences Faculty, Tehran, Iran (M-Rahgoshay@sbu.ac.ir)

²Industrial and Mining Research Center, ZaminOmran, Shiraz, Iran,

(*Correspondance: Iman_monsef@yahoo.com)

The Late Cretaceous Neyriz ophiolites in south eastern of Zagros are a remnant of Neo-Tethyan oceanic lithosphere with nearly continuous NW-SE-trending belt. The ophiolite consists chiefly of mantle (ultramafic) and crustal (cumulates, volcanic and sub-volcanic rocks) sequences.

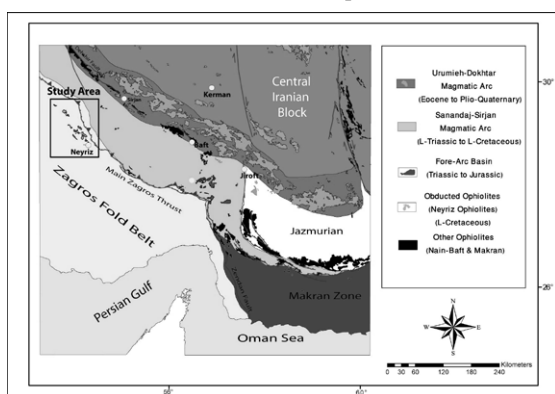


Figure 1: Structural sketch map of Iran with Neyriz ophiolites

The mantle sequences consist of harzburgite, dunite, pyroxenite, gabbroic pockets, diabasic dykes and chromitite presented by mantle deformation conditions. Chromitite ore deposits with podiform and lenses structures are located in dunitic envelope of ultramafic host rocks. The chromitites are alpine type with high values of Cr#, Mg# and Fe²⁺/Fe³⁺ ratio and low values of Al₂O₃ and TiO₂.

The crustal sequences consist of layered gabbros, isotropic gabbros, plagiogranites, sheeted dykes, and pillow lavas. Most of the mafic rocks have flat chondrite-normalized REE patterns and are strongly depleted in incompatible elements (negative Ta-Nb anomalies), similar to depleted tholeiites affinity.

The Neyriz oceanic lithosphere was probably formed within marginal basin system that was later accreted to the northern margin of the Arabian plate.

[1] Sachan (2001) *Ophioliti* **26**, 23–32. [2] Tamura & Arai (2006) *Journal of Asian Earth Sciences* **90**, 43–56. [3] Godard *et al.* (2008) *Earth and Planetary Science Letters* **267**, 410–425.

Tracing the time-resolved magmatic evolution of the Hegau volcanic field (Southern Germany) through apatites

MEINERT RAHN¹² AND ANETTE VON DER HANDT²³

¹Swiss Federal Nuclear Safety Inspectorate, Brugg, Switzerland, meinert.rahn@ensi.ch

²Albert-Ludwigs-Universität, Freiburg, Germany

³University of Minnesota, Department of Earth Sciences, avdhandt@umn.edu

Major outcrops of Tertiary–Quaternary mafic alkaline volcanic rocks form the Central European Volcanic Province (CEVP). The Hegau volcanic field is found at the southern periphery of the CEVP, around 60–70 km to the east of the Upper Rhine graben. Age dating suggests a period of volcanic activity between 15 and 7 Ma [1–3]. Three main lithological units can be distinguished, i.e. from old to young: (1) tuff layers (so-called “Deckentuff”) intercalating with surrounding Miocene sediments, (2) olivine melilitites forming cones, but no lava flows, and (3) isolated phonolite peaks. Carbonatites occur subordinately in the Hegau province, mostly evidenced by calcite-apatite-magnetite aggregates, but suggesting the coexistence of silicate and carbonate melts in the source area.

We investigated apatites from Deckentuffs and phonolites, as their composition is expected to reflect whole rock compositional variation and in particular any changes between silicate and carbonate melt origin [4]. Apatites are often the only fresh remnants of the associated volcanic products; they occur in all lithological units and commonly display a complex internal growth pattern. EPMA and SIMS techniques are applied to decipher the major and trace element compositional evolution. The combination of fission track age dating with chemical composition allows a time-resolved investigation of the evolution of the Hegau volcanic field and its relation to the Kaiserstuhl volcanism.

In addition, apatites with Hegau compositional patterns can be found as thin tuff layers intercalated with sediments as much as 60 km away from the Hegau volcanic field. This suggest a more explosive volcanism which is corroborated by the occurrence of diatreme breccias in the Hegau. Multiple magmatic cycles can be discerned on the basis of apatite composition.

[1] Schreiner (1992) *Geol. Landesamt BW*. [2] Rahn & Selbekk (2007) *Swiss J. Geosci.* **100**, 371–381. [3] Zaugg *et al.* (2008). *Geol. Atlas* **112**, swisstopo. [4] Wang *et al.* (2013) *ChemGeol*, *subm.*

Journal paper isotopic composition as climate proxy

P RAHUL¹, P GHOSH^{1*} AND SNEHA SURESH²

¹Centre for Earth Sciences, Indian Institute of Science, Bangalore (* pghosh@ceas.iisc.ernet.in)

²Pondicherry University, Pondicherry

The increasing use of fossil fuels mainly due to burning of coal and petroleum since the beginning of industrial revolution has caused steady rise in CO₂ concentrations in the atmosphere. CO₂ is well mixed in global atmosphere through general circulation. There is a consistent pattern observed between concentration rise and carbon isotopes in atmospheric CO₂. The isotopic signature seen in CO₂ of atmospheric air is transferred to the biosphere through exchange mechanisms. The $\delta^{13}\text{C}$ signature of fossil fuel derived CO₂ being lighter than other natural sources and preferential uptake of ¹²CO₂ from atmosphere by plants, provide us an opportunity to understand its fluctuations over time through stable isotopic analyses of plant materials [1]. In the present study we investigated the transfer of $\delta^{13}\text{C}$ signal from raw plant material to paper in archives of periodicals and magazines. Study by Yakir (2011) [2] shows a depleting trend in $\delta^{13}\text{C}$ of paper cellulose through time and linked it to global-scale increases in plant intrinsic water-use efficiency. In our study we have investigated the $\delta^{13}\text{C}$ of paper produced from Europe and America capturing atmospheric CO₂ trends mimicking the rise in global temperature for time period of last 100 years. The representative samples of journal papers are retrieved from the library at four to five year resolutions avoiding any ink contamination. We recorded a sudden drop in $\delta^{13}\text{C}$ value (-22.9‰ to -24.39‰) in cellulose composition coinciding with the time period from 1920 to 1925. The global temperature anomalies for the same period ranges from -0.25°C to -0.14°C. Detailed examination of $\delta^{13}\text{C}$ variability revealed impacts of historically important events on atmospheric CO₂ via cellulose in paper. Analyses performed on archives of a regionally published journal confirms global patterns and along with the capturing signatures of regional industrial revolution. Analyses of $\delta^{18}\text{O}$ in the cellulose further confirm the signature of global climatic events due to its linkage with the hydrological cycle. The study identified a potential new reliable archive which can supplement proxy records at much higher time resolutions.

[1] Francey and Farquhar(1982) *Nature* **297**, 28–31.[2]Yakir(2011) *Environ. Res. Lett.* 6 034007

Crustal structure beneath the Dharwar craton, India

S. S. RAI*, KAJALJYOTI BORAH, S. GUPTA AND K. S. PRAKASAM

National Geophysical Research Institute, Hyderabad-50007 India

(*Correspondence: shyamsrai@gmail.com)

We report significant lateral variability in shear wave velocity and Moho depth in the Archean crust beneath the Dharwar craton, India using earthquake waveform data recorded over 50 broadband seismographs (Figure a). The craton is a continuously exposed Archean continental fragment from north to south, and divided into the west Dharwar craton (WDC) of age 2.7-3.36 Ga, and the east Dharwar craton (EDC) of age, dominantly, 2.5 Ga. The craton progressively transition into the Southern Granulite Terrain (SGT) with age of metamorphism around 2.6 Ga.

The inversion of receiver function data reveals significant variation of Moho depth, viz., 38-54 km in the WDC, 40-46 km in SGT, and 32-38 km in the EDC. The average shear wave velocity of crust beneath the WDC is ~3.85 km/s as compared to ~3.60 km/s in the EDC. We infer highly variable thickness (16-30 km) of mafic cumulate ($V_s \geq 4.0$ km/s, $V_p \geq 7.0$ km/s) beneath the WDC, in contrast with a thin one (<5 km) beneath the late Archean EDC. The 3.36 Ga greenstone belt in WDC has maximum basal layer thickness of ~30 km. The result suggest the mafic crust and exceptional thickness of crust beneath the WDC (>50 km) as compared to felsic to intermediate composition for the EDC crust with almost flat Moho (~36 km) (Figure b). Considering the surface exposure of 15-20 km crust, based on P-T condition, in the southern segment of WDC, we speculate a Himalaya-like crustal thickness (50-70 km) beneath the mid-Archean crust pointing towards a plate-tectonic like scenario at ~3.0 Ga. In contrast, the EDC is possibly evolved as a consequence of subduction and delamination that led to a felsic crust with a nearly flat Moho.

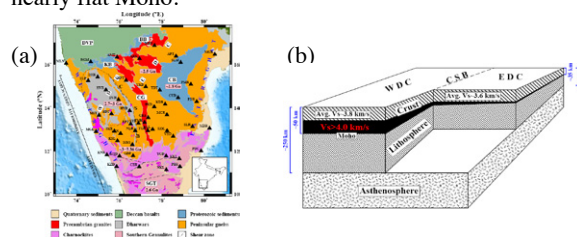


Figure:(a) Tectonic map of Dharwar craton. Seismic stations are shown as black triangles (b) Schematic showing distinct crust-mantle character of the WDC and EDC.

Kinetic parameters of pelagic nitrifying communities: consequences on nitrite dynamics in the Seine River downstream of Paris

M. RAIMONET¹, L. VILMIN², N. FLIPO², T. CAZIER¹,
V. ROCHER³ AND A. M. LAVERMAN¹

¹UMR 7619 Sisyphe, Université Pierre et Marie Curie, 4 place Jussieu, 75252 Paris, France (melanie.raimonet@upmc.fr)

²Centre de Géosciences, MINES ParisTech, 77300 Fontainebleau, France

³SIAAP-Direction du Développement et de la Prospective, 82 avenue Kléber, 92700 Colombes, France

Elevated nitrite concentrations are observed in the Seine River downstream of Paris and its main waste water treatment plants (WWTP). In order to understand the persistence of nitrite in the Seine, we determined kinetic parameters of pelagic ammonia- and nitrite-oxidizing communities. *In situ* ammonia- and nitrite-oxidation rates were deduced by determination of the kinetic parameters of the two processes combined with modeling. We compared the *in situ* rates and kinetic parameters upstream and downstream of the WWTPs during different seasons. The results showed both spatial and temporal variations of the *in situ* nitrification rates and kinetic parameters (e.g., maximal oxidation rate, half-saturation constant). At each given site and season, the *in situ* ammonia- and nitrite-oxidation rates were however similar, most likely resulting in little changes in water column nitrite concentrations. The results confirm that the elevated nitrite concentrations monitored in the Seine River are due to high nitrite released by the WWTP. In addition, the low nitrification rates and the equilibrium between ammonia- and nitrite-oxidation rates appear to prevent the elimination of nitrite from the system, leading to its persistence over more than 100 kilometers. The spatial and temporal variations of kinetic parameters reflect the dynamic microbial community structure and activity and may have implications on biogeochemical models.

Computer simulations of carbonates in water

PAOLO RAITERI^{1*}, RAFFAELLA DEMICHELIS¹ |
AND JULIAN D. GALE¹

¹Nanochemistry Research Institute and Department of Chemistry, Curtin University, Perth WA 6845, Australia (*correspondence: p.raiteri@curtin.edu.au)

Over the last thirty years a lot of effort has been made to understand the structural, surface and crystal growth properties of carbonates in aqueous environments, both experimentally and computationally. The ever increasing resolution of experimental techniques and power of supercomputer are rapidly closing the gap between what the two approaches can achieve. Arguably calcium carbonate is among the most studied minerals, but while there is a general consensus that its crystalline phases grow via an amorphous precursor, there is still much debate about the existence of pre-nucleation clusters and whether the nucleation follows a classical or non-classical pathway. Moreover, other carbonates are comparatively less studied and less understood.

Here we will present a recent force field developed to reproduce the thermodynamic properties of the alkaline-earth carbonates X-CO₃ (X=Mg, Ca, Sr and Ba). This force field is used to study the different stages of the crystallisation mechanism, from isolated ions in solution to pre-nucleation clusters, nanoparticles and the growth of fully developed crystals. These studies include the calculation of reaction free energies (Figure 1), IR spectra and both structural and dynamical properties, and they demonstrate that carefully developed computational models are capable of quantitatively reproducing experimental observations.

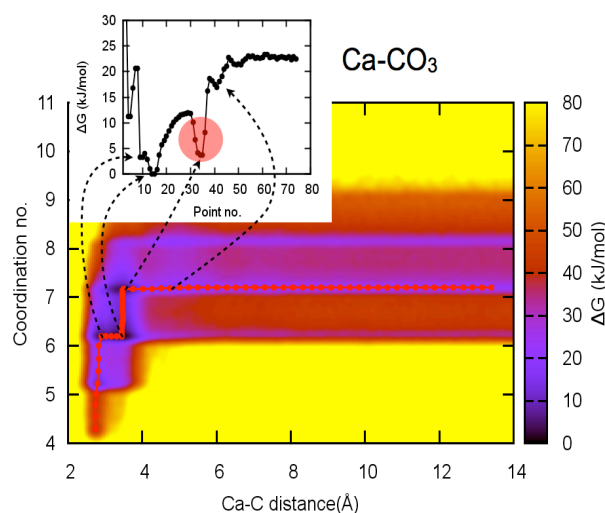


Figure 1 Ca-CO₃ pairing free energy calculated using the metadynamics technique with 2 collective variables.

Presence of > 3.3 Ga old crust and Neoproterozoic juvenile magmatic accretion in eastern most part of the Dharwar craton: Evidence from Peddavura greenstone belt.

M.RAJAMANICKAM¹ AND S.BALAKRISHNAN^{1*}

¹Department of Earth Sciences, Pondicherry University, Puducherry- 605014

(*correspondence: balakrishnan.srinivasan@gmail.com)

Neoproterozoic witnessed rapid growth and stabilization of continents. The Dharwar Craton had significant addition of juvenile material and consequent crustal growth during 2.9 to 2.5 Ga ago in greenstone-granite terrains. [1, 2, 3]. Rocks of Peddavura greenstone belt in eastern Dharwar craton was studied for Rb-Sr and Sm-Nd systematics to understand crustal growth in the Dharwar Craton.

Peddavura greenstone belt consists of pillowed basalt, basaltic andesites and rhyolites inter-layered with ferruginous chert. Basalt and basaltic andesites define a Rb-Sr isochron age of 2551±19 Ma (MSWD=1.16), whereas, rhyolites were scattered and do not show any age. Sm-Nd system also does not yield any age for both the rock types.

The Rb-Sr age could represent time of thermal event that was strong enough to completely reset the Rb-Sr isotopic system in the basaltic rocks. The scattering of samples in Sm-Nd evolution diagram could be due to either low-temperature alteration or heterogeneity in their sources. The basalt and basaltic andesites show variation in their ϵ_{Nd} values, whereas they have similar ϵ_{Sr} . This implies that magmas representing these rocks might have derived from variably LREE enriched and depleted mantle sources. Rhyolites show larger variation in their ϵ_{Nd} as well as in ϵ_{Sr} which are negatively correlated. Parental magmas of rhyolites derived by partial melting of short-lived basaltic rocks were contaminated with older crustal rocks similar to the Gorur-Hasan gneisses. Thus, we infer presence of older crust, > 3.3 Ga, in the eastern most part of the Dharwar Craton.

[1] Balakrishnan *et al.* (1999) *J. Geol.* **107**, 69–86. [2] Krogstad, *et al.* (1989) *Science* **243**, 1337–1340. [3] Jayananda *et al.* (2013) *Precambrian Research* **227**, 55-76.

Microbial mobilization of arsenic for bioremediation of contaminated soils

LIWIA RAJPERT^{1,2}, ŁUKASZ DREWNIAK²,
ALEKSANDRA SKŁODOWSKA² AND MARKUS LENZ^{1,3*}

¹Institute for Ecopreneurship, School of Life Sciences, University of Applied Sciences and Arts Northwestern Switzerland, Gründenstrasse 40, CH-4132 Muttenz, Switzerland (*correspondence: markus.lenz@fnw.ch)

²Laboratory of Environmental Pollution Analysis, Faculty of Biology, University of Warsaw, 03-982 Warsaw, Poland

³Sub-Department of Environmental Technology, Wageningen University, 6700 EV Wageningen, The Netherlands

Arsenic contamination of soil and drinking water is a serious problem of worldwide concern [1, 2]. The efficiency of a novel combined strategy relying on enhancing microbial As mobilization with subsequent immobilization on nanosized iron phases for the treatment of mining impacted soil (As >2000 ppm; Lower Silesia, Poland) was evaluated.

Three bioreactors were operated in parallel assessing 1) inherent As reducing capacity of the soil; 2) biostimulation with external electron donor and 3) bioaugmentation with dissimilatory arsenate reducing microorganisms. Mobilization rates of As, Fe, Mn were analyzed using ICP-MS, whereas aqueous As speciation was analyzed by LC-ICP-MS. Potentially formed hazardous As volatiles were trapped in 1% H₂O₂ (Fig.1). Addition of an external electron donor resulted in both lower total and bioavailable As fraction in soils. Different iron phases were evaluated for their As sorption/desorption capacity of different As species following microbial mobilization. Nanosized ferrihydrite proved to be the most effective and cheap As sorbent evaluated.

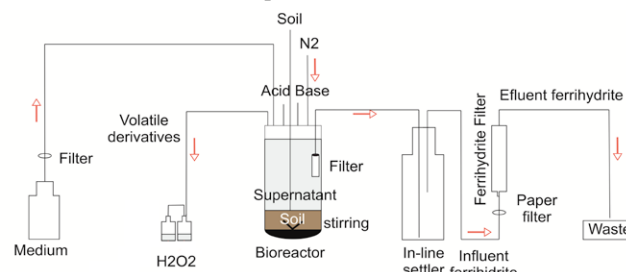


Figure 1: Scheme of bioreactor design.

[1] Camacho LM *et al.* (2011) *Chemosphere* **83**, 211-25. [2] Mukherjee A *et al.* (2006) *J Health Popul Nutr.* **24**,142-63.

Elevated pressure of carbon dioxide affects growth of thermophilic *Petrotoga* sp.

JANA RAKOCZY^{1*}, CLAUDIA GNIESE², AXEL SCHIPPERS¹,
MICHAEL SCHLÖMANN² AND MARTIN KRÜGER¹

¹Bundesanstalt fuer Geowissenschaften und Rohstoffe (BGR),
Stilleweg 2, D-30655 Hannover

²Institut für Biowissenschaften, TU Bergakademie Freiberg,
Leipziger Str. 29, D-09599 Freiberg

Carbon capture and storage (CCS) is considered a promising new technology which reduces carbon dioxide emissions into the atmosphere and thereby decelerates global warming. However, with CCS being a very young technology, there are yet a number of factors that need to be investigated before declaring CCS as being safe. Our research investigates the effect of high carbon dioxide concentrations and pressures on an indigenous microorganism that colonises a potential storage site.

Growth experiments were conducted in liquid culture using the thermophilic thiosulphate-reducing bacterium *Petrotoga* sp., isolated from formation water of the gas reservoir Schneeren (Lower Saxony, Northern German Plain). Growth (OD₆₀₀) was monitored over 10 days at different carbon dioxide concentrations (50%, 100%, and 150% in the gas phase), and was compared to cultures grown with 20% carbon dioxide. An additional growth experiment was performed over a period of 145 days with repeated subcultivation steps to detect long-term effects of carbon dioxide. Short-term cultivation at 50% and 100% carbon dioxide slightly reduced cell growth. In contrast, long-term cultivation at 150% carbon dioxide reduced cell growth and finally led to cell death. This suggested a more pronounced effect of carbon dioxide at prolonged cultivation and stresses the need for closer consideration of long-term effects.

Experiments with supercritical carbon dioxide at 100 bar completely inhibited both growth of a freshly inoculated culture and a pre-grown culture demonstrating the lethal effect of supercritical carbon dioxide. This effect was not observed in control cultures with 100 bar of hydrostatic pressure.

Evaluating the Role Mafic Crustal Assimilation in the Generation of Western US Continental Basalts

RAMOS, FRANK C., GLADISH, E., SLATER, N.
AND PALIEWICZ, C.¹

¹New Mexico State University, Las Cruces, NM 88003 USA

Western US continental basalts are generally thought to reflect pristine geochemical and isotopic signatures inherited from heterogeneous mantle sources. Such thoughts rely on a lack of magmatic interactions with crustal sources. Assessments for the role of potential crustal interactions typically focus on modifications expected for Si-rich materials such as increased SiO₂ or highly elevated trace elements such as Ba. In contrast, mafic crustal assimilation may impart only limited SiO₂ and trace element variations depending on the exact nature of the mafic crust and the degree to which the mafic materials are melted. Tholeiites and alkalic basalts erupted along and the Colorado Plateau-Rio Grande rift transition zone and within the Rio Grande rift itself retain geochemical and isotopic variations that are similar to those expected to result from mafic crustal assimilation. Results allow for the possibility that asthenospherically derived magmas assimilated variable amounts of mafic crust resulting in a range of isotopic and geochemical characteristics that are similar to those expected for trace element enriched heterogeneous subcontinental lithospheric mantle sources. Whole rock isotope signatures in a few of the younger flows (e.g., Bandera and McCartys flows, Zuni Bandera volcanic field, and the Carrizozo flow, Rio Grande rift) vary extensively (e.g., 87Sr/86Sr of 0.7028 to 0.7035 for the Bandera flow, 0.7037 to 0.7084 for the McCartys flow, and 0.7044 to 0.7052 for the Carrizozo flow) and are consistent with more complicated petrogenetic histories involving a range of potential mantle and crustal sources. Here, we present phenocryst and melt inclusion major and trace element compositions to identify and track chemical variations retained in whole rocks and melt inclusions and integrate isotopic signatures of these components imposed during crystallization. Additional mineral signatures of plagioclase and xenocrystic materials will be discussed and the petrogenetic histories of selected young alkalic and tholeiitic basaltic from the Rio Grande rift and Zuni-Bandera volcanic field will be assessed to evaluate the potential role of mafic crustal assimilation in the genesis of respective trace element and isotopic signatures of these continental basalts.

Melt-rock reaction in oceanic troctolites (Ligurian ophiolites, Italy) as revealed by trace element chemistry of olivine

E.RAMPONE^{1*}, G.BORGHINI^{1,2}, L.CRISPINI¹, M.GODARD³, B.ILDEFONSE³ AND P.FUMAGALLI²

¹DISTAV, University of Genova, I-16132 Genova, Italy

(*correspondence: betta@dipteris.unige.it)

²University of Milano, I-20133 Milano, Italy

³UMR CNRS, Universite Montpellier 2, Montpellier, France

Several recent studies have documented that reactions between melt and crystal mush in primitive gabbroic rocks (via reactive porous flow) has an important control in the formation of the lower oceanic crust and the evolution of MORBs. In this context, an open issue concerns the origin of olivine-rich rocks, whether they formed by fractional crystallization of primitive melts or by open system reactive percolation of pre-existing (possibly mantle-derived) olivine matrix. To address this topic, we performed high-quality *in-situ* trace element analyses (by LA-ICP-MS) of olivine in the ideal study case of the Erro-Tobbio ophiolite Unit (Ligurian Alps), where mantle peridotites show gradational contacts with an hectometer-scale body of troctolites and plagioclase wehrlites, and both are cut by later decameter-wide lenses and dykes of olivine gabbros. Previous studies [1] inferred that they represent variably differentiated crystallization products from primitive MORB-type melts. Olivines in the three rock types (mantle peridotites, troctolites, ol-gabbros) exhibit distinct geochemical signature and well-defined elemental correlations. As expected, compatible elements (e.g. Ni) show the highest contents in peridotites (2580-2730 ppm), intermediate in troctolites (2050-2230 ppm) and lowest in gabbros (1355-1420 ppm), whereas moderate incompatible elements (e.g. Mn, Zn) show the opposite behaviour. By contrast, highly incompatible elements like Zr, Hf, Ti, HREE are variably enriched in olivines of troctolites and the enrichment in absolute concentrations is coupled to development of significant HFSE/REE fractionation (Zr_N/Nd_N up to 80). Preliminary AFC modeling show that such large Zr_N/Nd_N ratios in olivines are consistent with a process of olivine assimilation and plagioclase crystallization at decreasing melt mass, in agreement with textural observations. *In-situ* trace element geochemistry of olivine, possibly combined with CPO measurements, thus appears a powerful tool to investigate reactive percolation and the origin of olivine-rich rocks in the lower oceanic crust.

Quantification of the *in situ* heterogeneity of RMs for microanalytical methods

MICHAEL H. RAMSEY¹ AND MICHAEL WIEDENBECK^{2*}

¹University of Sussex, UK; (m.h.ramsey@sussex.ac.uk)

²Helmholtz Zentrum Potsdam, Germany (*correspondence: michael.wiedenbeck@gfz-potsdam.de)

A range of laboratory techniques is available for the geochemist wishing to characterize the chemical and/or isotopic compositions of solid materials at the nanogram or smaller sampling mass range. Examples of widely available techniques are based on the electron probe, laser ablation ICP-MS and secondary ion mass spectrometry (SIMS).

When operating at such small test portion masses there are three fundamental requirements that a reference material (RM) should enable: (1) method calibration, which is typically based on one or a few discrete fragments of the RM, (2) evaluation of method repeatability, which is commonly based on multiple analyses on a single RM fragment, and (3) method development and validation. An additional consideration is that most such materials must necessarily be characterized using laboratory methods operating at the milli-gram or larger sampling scale.

In order to meet all of these requirements it is evident that a microanalytical RM must be assessed for heterogeneity *in-situ* at a variety of scales, and that the corresponding heterogeneity component must be considered for each application being undertaken. When calibrating an instrument it is essential to know the likely variation between the mean content of individual sample aliquots (chips or fragments). This information can commonly be obtained from "bulk sample" analyses conducted on mm-sized units, be it via wet chemical, gas source mass spectrometer or other methods. For evaluating the repeatability of a microanalytical method it is necessary that the *in situ* heterogeneity of the material be quantified at the equivalent sampling scale. For method development and validation a detailed knowledge of a RM's major element composition, as well a knowledge of its heterogeneity at the given sampling scale, are both necessary.

Our work focuses on developing experimental and mathematical tools that will quantify *in situ* heterogeneity at the various sampling scales while taking into account the analytical uncertainties intrinsic to the laboratory method being used to characterize such variations. The ultimate goal of our work is to enable SIMS to assess in detail the isotopic characteristics of candidate RMs at sampling masses well below 1 ng and with overall heterogeneity being evaluated at the < 0.1 ‰ level.

Cryo-XPS monitoring of cell wall compositional changes for *Bacillus subtilis* as a function of pH and Zn²⁺ exposure

MADELEINE. RAMSTEDT*, LAURA. LEONE,
ANDREY. SHCHUKAREV AND PER. PERSSON

Department of Chemistry, Umeå University, 90187 Umeå,
Sweden,
correspondance: madeleine.ramstedt@chem.umu.se

Bacteria such as *Bacillus subtilis* and *Escherichia coli* adjust and alter their gene transcription and protein production depending on the environment they are exposed to. For example, membrane-bound protein complexes are up-regulated at high pH in *B. subtilis* and several enzymes that reduce acidity and transport metals out of the cell are up-regulated at low pH [1]. It has also been reported that building blocks in the cell wall change with varying pH.

X-ray Photoelectron Spectroscopy (XPS) is a surface sensitive analysis method that has been used by several researchers to successfully analyze the chemical composition of bacterial cell walls [e.g. 3,4,5]. In this presentation we will show how we have used cryo-XPS together with a recently developed curve fitting model to predict the chemical composition of the surface of bacterial cells [2]. We have used this to study changes in the surface composition of *B. subtilis* exposed to environments with varying pH and/or Zn²⁺ content. We will also compare the obtained ratios of different substances with ratios obtained using previously published methods based on equation systems [3,4,5].

[1] Wilks, Kitko, Cleeton, Lee, Ugwu, Jones, BonDurant & Slonczewski, (2009) *Applied and Environmental Microbiology* **75**, (4), 981-90. [2] Ramstedt, Nakao, Wai, Uhlin & Boily, (2011) *Journal of Biological Chemistry* **286**, (14), 12389-12396 [3] Dufrière, van der Wal, Norde & Rouxhet, (1997) *Journal of Bacteriology*, **179**, (4), 1023-1028 [4] Rouxhet & Genet, M., (2011) *Surface and Interface Analysis* **43**, (12), 1453-1470 [5] van der Mei, de Vries & Busscher, (2000) *Surface Science Reports*, **39**, (1), 3-24

Alkenones and hydrogen stable isotopic composition of n-alkane as indicators of past temperature and salinity in Lake Van sediments

M.È. RANDLETT^{1*}, M. J. L. COOLEN², A. BECHTEL³,
M. STOCKHECKE¹, O. KWIECIEN¹, Y. TOMONAGA¹,
B. WEHRLI¹ AND C. J. SCHUBERT¹

¹Swiss Federal Institute of Aquatic Science and Technology
EAWAG, Switzerland

²Woods Hole Oceanographic Institution (WHOI), MA 02543,
United States

³Montanuniversität Leoben, Leoben A-8700, Austria
(*correspondence: marie-eve.randlett@eawag.ch)

The successful drilling operations of the International Continental Scientific Drilling Program (ICDP) PaleoVan project allowed the recovery of 220-m long sediment cores, which represents approximately the last 600 ka. This exceptional climatic archive was investigated for two relevant organic molecular proxies; alkenones and hydrogen stable isotopic composition of n-alkanes C₂₉ (δD of n-C₂₉). The potential of unsaturation patterns in alkenones for reconstructing past temperatures in Lake Van was assessed through investigation of algae types responsible for alkenones biosynthesis using ancient DNA stratigraphy. The diversity of alkenones producers within the core hampered the use of a single calibration curve for reconstructing temperature based on alkenone unsaturation patterns, as found elsewhere [1,2]. On the other hand, the δD of n-C₂₉ co-vary with the salinity of the pore water profile in Lake Van. The latter organic proxy therefore seems to be a promising tool for reconstructing changes in the source water salinity due to variable precipitation/evaporation ratio, as previously suggested [3].

[1] Coolen, M.J.L. et al. (2009) *Earth and Planetary Science Letters*, **284**, 610-621 [2] Theroux et al. (2010) *Earth and Planetary Science Letters*, **300**, 311-320 [3] Sachse et al. (2012) *Annual Review of Earth and Planetary Sciences*, **40** (1), 221-249

$\Delta^{17}\text{O}$, $\delta^{17}\text{O}$, $\delta^{18}\text{O}$ variation in precipitated water at Jungfrauoch (3571 m) - relation to meteorological parameters and low altitude stations

S. RANJAN¹ AND M. LEUENBERGER¹

¹Climate and Environmental Physics, Physics Institute and Oeschger Centre for Climate Change Research University of Bern, Bern, Switzerland
shyam@climate.unibe.ch (* Presenting Author)

We have analysed precipitated water sample of seven stations from high altitudes Jungfrauoch (3571 m) to low altitudes Basel (292 m). $\Delta^{17}\text{O}$, $\delta^{17}\text{O}$, $\delta^{18}\text{O}$ was analysed for Jungfrauoch (A) from 1983 to 2011 and Grimsel (B), Guttanen (C), Meiringen (D), Locarno (E), Bern (F) and Basel (G) from 2003 to 2005. pH, temperature, relative humidity, air pressure and precipitation data was available through MeteoSwiss. $\Delta^{17}\text{O}$, $\delta^{17}\text{O}$, $\delta^{18}\text{O}$ and pH variations were analysed by using the conventional CO_2 -equilibrium method and a pH sonde with a repeatability of $\pm .01$ pH unit. Positive correlation were found between $\delta^{18}\text{O}$ & $\delta^{17}\text{O}$, temperature and relative humidity, while poor correlation were found between $\Delta^{17}\text{O}$ & $\delta^{18}\text{O}$, $\Delta^{17}\text{O}$ & $\delta^{17}\text{O}$, pH & relative humidity, air pressure and precipitation of all station. Year 2003, one of the hottest period of Europe and at the same period, highest $\Delta^{17}\text{O}$ values were observed at station A, C, D, G but not at station B, E & F which require further in-depth research. Interestingly, the decreasing trend of pH was observed at all stations. Except at the station G, highest pH of all stations was greater than 10 pH unit while lowest pH was less than 3 units at station A. Only station A is mostly exposed to the free troposphere and receive signals at a continental scale. Contrary to all others stations, low pH was observed mainly during 1991 to 1993 period at station A, which is originating most probably from multiple large volcanic eruptions (Pinatubo, which was 2nd largest eruption of 20th century). Increasing concentration of atmospheric CO_2 have only a small effect on pH changes in precipitated water compared to the results we have observed. Further explanations will be given in the presentation.

U-Pb Dating of Carbonates and Fluorite: Prospects for Understanding Fluids from Deposition Through Burial

E. T. RASBURY¹, R. R. PARRISH², W. AUSTIN-GIDDING³, A. LANZIROTTI⁴, P. TOMASCAK⁵ AND J. R. KYLE⁶

¹Department of Geosciences, Stony Brook University, Stony Brook NY, *corresp: troy.rasbury@stonybrook.edu

²Dept Geology U. Leicester, UK and NIGL, British Geol Survey, Keyworth, Notts, rrp@nigl.nerc.ac.uk

³Institute of Geography and Earth Science, Aberystwyth University, Aberystwyth, Wales wea2@aber.ac.uk

⁴Center for Advanced Radiation Sources, University of Chicago, lanzirrotti@uchicago.edu

⁵Department of Earth Sciences, SUNY Oswego, Oswego, NY, paul.tomascak@oswego.edu

⁶Dept Geological Sciences, Jackson School of Geosciences, University of Texas at Austin, rkyle@jsg.utexas.edu

Minerals such as carbonates and fluorite record information about the fluids from which they formed such as the salinity, temperature, degree of rock-water interaction, as well as details of the source(s) of these fluids. The U and Pb concentrations, U oxidation state and molecular speciation and Pb isotope compositions in these minerals may reveal important information about the nature of the fluids and, in favorable cases, can be used to date the time of mineral formation. The application of emerging *in situ* microbeam analytical techniques such as synchrotron XRF, LA-ICP-MS, and SIMS offers the possibility of tracking the mineralogical and geochemical evolution of these minerals from the time of deposition of limestones through burial diagenesis, faulting and vein formation. Dating of the time of deposition provides a framework for understanding the climate history and fossil information encoded in the rock. Key genetic aspects for ore and hydrocarbon deposits could be provided by a more thoroughly dated history of formation. The timing of tectonic events may be constrained by dating vein fillings of associated fault and fracture systems.

Studies have shown great potential for U-Pb and U-series dating of carbonates precipitated from meteoric fluids and for dating of vein calcite, associated with faulting and with ore mineralization. We will review these studies with insights based on synchrotron and laser ablation work, and present new work on the application of U-Pb dating of fluorite and calcite from a variety of settings, and discuss the expanding applications of these methods to geological problems.

The selective sorption of K⁺ from water solutions by Ca-zeolites

SERGEY V. RASHCHENKO^{1,2*}
AND LIDIA K. KAZANTSEVA¹

¹Sobolev Institute of Geology and Mineralogy SB RAS, 3
Koptuyug Avenue, 630090 Novosibirsk, Russia
(*Correspondence: rashchenko@igm.nsc.ru)

²Novosibirsk State University, 2 Pirogov Street, 630090
Novosibirsk, Russia

The geochemistry of potassium during subduction-related processes does not seem to be a solved problem yet. The important role of subducted oceanic lithosphere as a potassium source for alkali-rich subduction magmatism was repeatedly discussed [1]. However, MORB basalts contain less than 0.16% of K₂O [2] and so cannot be considered as important source of this component. To avoid such discrepancy, some authors consider terrigenous sediments to enrich subducting lithosphere in K₂O [3]. We suggest the alternative mechanism of this enrichment consisting in cation exchange between seawater and zeolitized rocks of the ocean floor. To prove the probability of such process we carried out the experimental modeling of interaction between Na⁺/K⁺ water solutions and Ca-zeolites as common secondary minerals appearing during hydrothermal alteration of basalts.

The water solution with Na⁺/K⁺ molar ratio close to that of seawater (0.06) was used in our experiments. The obtained results for laumontite and stellerite are given in the Table 1.

%	Laumontite	Stellerite
CaO	7.34 → 5.51	8.03 → 2.27
Na ₂ O	1.56 → 2.67	0.14 → 4.71
K ₂ O	0.47 → 1.43	0.05 → 2.46

Table 1: The change in the cation composition of Ca-zeolites due to 30 days of hydrothermal treatment by Na⁺/K⁺ solution.

As one can see, a significant change in cation composition of Ca-zeolites occurs after interaction with Na⁺/K⁺ water solution. Moreover, the K⁺/Na⁺ molar ratio of alkali cations absorbed by laumontite (0.58) and stellerite (0.35) clearly demonstrates the selective sorption of K⁺ from solution with low K⁺/Na⁺ ratio (0.06). Such phenomenon caused by features of zeolites crystalline frameworks probably plays an important role in interaction of zeolitized rocks of ocean floor with seawater and enriches the sedimentary part of oceanic lithosphere in potassium.

This work was supported by the Russian Foundation for Basic Research (grants #12-05-31431 and #13-05-00185).

[1] Schmidt (1996) *Science* **272**, 1927-1930. [2] Melson *et al.* (1976) *J. Am. Geophys Union Trans.* **4**, 351. [3] Konzett & Fei (2000) *J. of Petrology* **41**, 583-603.

Integrated geo-microbial and adsorbed soil gas studies with seismic data interpretation for successful evaluation of Hydrocarbon Resource Potential

M. A. RASHEED*, SANTOSH DHUBIA., SYED ZAHEER
HASAN., B.KUMAR AND P.H.RAO

Petroleum Research Wing, Gujarat Energy Research and
Management Institute, Gandhinagar, Gujarat, India.
abdul@germi.res.in

The hydrocarbon microseepage of light hydrocarbon gases (C1 – C4) can be identified using geochemical means, which provides evidence of charge traps and structures. These light hydrocarbon microseepage gases likewise directly influence shallow anaerobic soil and sediment environments, creating a spectrum of microbial activity. The indicator light hydrocarbon oxidizing bacteria are isolated and enumerated using microbial techniques. Therefore, an integrated and complementary microbial microseepage signature can identify gaseous hydrocarbon microseepage, which occurs directly above charged oil and gas reservoirs in on/offshore region. Present day exploration for oil and gas requires a coordinated effort based on the synergy of geophysics, geology, and geochemistry. The proposed study aims at integrated approach interpreting the geochemical and seismic data to understand the mechanism of hydrocarbon seepage and to evaluate the hydrocarbon potential as well. The main objective of the study is to integrate the seismic and the geochemical data. The seismic gives a clear picture of subsurface tectonics, structures, faults, fractures and reservoir distribution and extension (Attributes) Integrating the subsurface with the surface geochemical data, helps to know the seepage pattern and type of system. Such a study, will lead to the successful exploration. It will be more useful in the virgin areas, and also during Exploration and Development of the fields.

Keywords: Hydrocarbons, Geochemical, Seismic

Algal biofuels: A sustainable pathway to mitigate energy demand

MOHAMMED ABDUL RASHEED*, SYED ZAHEER HASAN
AND B.KUMAR

Petroleum Research Wing, Gujarat Energy Research and
Management Institute,
Gandhinagar, Gujarat, India.

*(Correspondence: abdul@germi.res.in)

Algal fuels are generating considerable interest around the world. These fuels may represent a sustainable pathway for helping to meet the energy demand. Algae is a preferred biodiesel base because algae grow more rapidly and occupy less space compared to other plants used for biodiesel such as corn, soy, canola and other lipid producing organisms. The algae strain, *Chlorella vulgaris*, contains 30% lipids by mass. Thus, a common goal is to create a manageable and cost effective process for manufacturing biodiesel on a large scale. Microalgae are single-cell, photosynthetic organisms known for their rapid growth and high energy content. Some algal strains are capable of doubling their mass several times per day. In some cases, more than half of that mass consists of lipids or triacylglycerides—the same material found in vegetable oils. These bio-oils can be used to produce such advanced biofuels as biodiesel, green diesel and green oil^[1]. Algae consume carbon dioxide as they grow, so they could be used to sequester CO₂ being released from power stations and other industrial plant that would otherwise go into the atmosphere. Meeting the world's fastly growing energy demands will require a multitude of sources. Several private and government agencies are putting efforts to reduce capital and operating costs and make algae fuel production commercially viable. The challenges that need to be addressed are, the exploitation of naturally occurring photosynthetic microalgae, which provides a green and renewable resource of feedstock biomass to meet increasing energy needs and especially the demand for liquid fuels thereby isolation, screening and evaluation of naturally occurring algal strains which exhibit high growth rate and large-scale photo bioreactor design and optimization, to outdoor mass culture and downstream processing. Challenges to be addressed include refinement of the cultivation process, downstream processing of biomass, and development of an economic feasibility model for commercialization of algae-based biofuels and biomaterials.

[1]. Lianna Costantini, Ellie Johnson and Haley London. Report on Micro Algae-Based Biodiesel. Rose-Hulman Institute of Technology, Terre Haute, Indiana, by Group 1, July 1, 2010.

Evidence for increased Southern Ocean waters in the tropical intermediate Indian Ocean during the last deglaciation

HARUNUR RASHID^{1*}, HARRY ELDERFIELD², ALEXANDRA GOURLAN³ AND MARY SMITH⁴

¹Memorial University of Newfoundland, Corner Brook,
Canada hrashid@grenfell.mun.ca*

²University of Cambridge, Cambridge, UK, he101@cam.ac.uk

³Maison des Geosciences, Grenoble, France
alexandra.gourlan@ujf-grenoble.fr

⁴Indiana State University, Terre Haute, USA,
msmith157@sycamores.indstate.edu

Oxygen isotopes ($\delta^{18}\text{O}$) and Mg/Ca in the *Globigerinoides ruber* (w) are analysed from the Bay of Bengal and Andaman Sea sediments. Mg/Ca, Cd/Ca and B/Ca are also determined in *Cibicides wuellerstorfi* and *Uvigerina peregrina* in two cores from the same basins. Furthermore, neodymium isotopic ratios (ϵ_{Nd}) of seawater in two sediment cores are determined. Our results show that seawater oxygen isotope values were most enriched between 17.8 and 14.6 ka. We also find coincidence between the onset of intermediate water warming at 17.8 ka, and the onset of increase in atmospheric CO₂. In the tropical Indian Ocean, the deep water (>2,200 m) warmed after the surface, in sharp contrast with the warming found in the intermediate water which occurs earlier. Furthermore, an inverse relationship between the intermediate and surface waters is also found during the Bolling-Allerod and Younger Dryas periods in which surface water warmed (cooled) and intermediate water cooled (warmed). We hypothesize that the cause of warming of the northern tropical Indian Ocean intermediate water does not lie within the tropics, rather an increase in Southern Hemisphere spring insolation combined with sea-ice albedo feedbacks, consistent with the hypothesis suggested earlier. The hypothesized mechanism involves an increase in upper circumpolar deep-water circulation into the Indian Ocean.

Nitrate- and nitrite dependent anaerobic oxidation of methane

OLIVIA RASIGRAF¹, BAOLI ZHU¹, DORIEN M. KOOL²,
MIKE S. M. JETTEN¹ AND KATHARINA F. ETTWIG¹

¹Department of Microbiology, IWW, Radboud University Nijmegen, The Netherlands

²Royal NIOZ, Department of Marine Organic Biogeochemistry, Texel, The Netherlands

The first described enrichment culture capable of anaerobic oxidation of methane (AOM) coupled to nitrite and nitrate reduction was a consortium of *Methyloirabilis oxyfera* bacteria (80%) and archaea (10-20%) [1], the latter later named AOM-associated archaea (AAA) [2]. However, after prolonged incubation (several months) with elevated nitrite the AAA disappeared from the enrichment culture, and *M. oxyfera* bacteria were shown to oxidize methane without an archaeal partner. Subsequent isotope labeling studies with *M. oxyfera* showed that it can produce oxygen from nitric oxide, which is then used for methane oxidation via a monooxygenase reaction [3]. The isotope fractionation factors for carbon and hydrogen during methane oxidation by *M. oxyfera* were determined, and were in the same range as previously reported for aerobic methanotrophs [4]. Recently we investigated the capacity of *M. oxyfera* bacteria to fix CO₂ via the Calvin-Benson-Bassham cycle and their unusual lipid composition. Furthermore, based on the genomic information and physiological studies, the AAA were shown to possess the capacity for reverse methanogenesis and nitrate reduction. AOM by both *M. oxyfera* and AAA is of great interest for the understanding of and the linkage between the biogeochemical cycles of methane and nitrogen.

[1] Raghoebarsing *et al.* (2006) *Nature* **440**, 918-921. [2] Knittel & Boetius (2009) *Annual Review of Microbiology* **63**, 311-334. [3] Ettwig *et al.* (2010) *Nature* **464**, 543-548. [4] Rasigraf *et al.* (2012) *Geochimica et Cosmochimica Acta* **89**, 256-264.

Deposition of the precursor sediments of banded iron formations

B. RASMUSSEN^{1*}, B. KRAPEZ¹, J.R. MUHLING^{1,2}
AND D.B. MEIER³

¹Dept of Applied Geology, Curtin University, Kent Street, Bentley, WA 6102, Australia

(*correspondence: b.rasmussen@curtin.edu.au)

²CMCA, The University of Western Australia, Stirling Highway, Crawley, WA 6009, Australia

³School of Earth and Environment, The University of Leeds, Leeds, LS2 9JT, United Kingdom

Banded iron formations (BIFs) are derived from iron-rich chemical sediments whose composition is used to make inferences about the early Precambrian ocean, atmosphere and biosphere. Before geochemical information from BIFs can be reliably interpreted, their origin and post-depositional history must be understood. However, the identity of the original sediments and how those sediments were deposited is contentious due to a long history of post-depositional overprinting and the absence of direct modern analogues. Most depositional models are based on the interpretation that the initial precipitate comprised ferric oxyhydroxides that formed when ferrous iron was oxidized in the water column and settled on the seafloor. The lack of well-defined grain-shapes and current-generated structures has been used to infer a pelagic origin for the primary sediments.

New sedimentological and petrographic studies of well-preserved intersections of BIF in the 2.63-2.45 Ga Hamersley Group, Western Australia, show the presence of abundant silt-sized spherical particles (or microgranules) in mm-thick chert microbands. The microgranules are most common in the least-altered BIF where they define sedimentary laminations, implying a depositional origin. They were deposited in lamina sets comprising a basal microgranule-rich lamina overlain by amorphous mud with dispersed microgranules. Seafloor silicification is interpreted to have preferentially replaced the amorphous clay matrix, implying that the precursor sediment must have comprised two particle sizes: silt and clay. Micrograding is interpreted to record plane laminations resulting from deposition of iron-rich muds entrained in dilute turbidity currents. The presence of micrograded structures in other BIFs, implies that re-sedimentation of precursor sediments was common.

A model is proposed in which ferruginous oceans with elevated silica favoured the growth of iron-silicate minerals proximal to active ridge systems. The hydrothermal muds accumulated on a sloping seafloor and were re-sedimented by dilute turbidity currents, and deposited on the basin floor as thin, laterally extensive sheets.

Mantle Source Characteristics and Petrogenesis in the Lunar Crater Volcanic Field

C. RASOZANAMPARANY¹, E. WIDOM^{1*}, J.A. CORTES², E.I. SMITH³, G.A. VALENTINE², D. KUENTZ¹
AND R. JOHNSEN³

¹Department of Geology, Miami University, Oxford, USA, widome@muohio.edu (*presenting author)

²Department of Geology, State University of New York, Buffalo, USA, gav4@buffalo.edu

³Department of Geoscience, University of Nevada, Las Vegas, USA, gene.smith@unlv.edu

The nature of the mantle sources and the role of lithospheric assimilation in producing compositional variations in basaltic monogenetic volcanic fields remains controversial. To address these issues, we have performed major and trace element and Sr, Nd, Pb, Hf and Os isotope measurements on 19 mafic lavas from 4 volcanic centers in the northern Lunar Crater Volcanic Field (LCVF), Nevada. Three eruptive centers (Giggle Springs, <100 Ma; and Hi Desert and Mizpah, ~620-740 Ma) are located within ~500 m of each other; the Marcath volcano (~40 ka), the youngest eruptive center in the field, is located ~6 km SW of these cones. The lavas have essentially constant Nd and Hf isotope ratios, but significant heterogeneity in Sr and Pb isotopes, and superchondritic Os isotope ratios. The older Mizpah and Hi Desert lavas exhibit HIMU-like trace element and Sr-Pb isotope signatures, with Nb-Ta enrichment, Rb, Cs and K depletion, and high ²⁰⁶Pb/²⁰⁴Pb but low ⁸⁷Sr/⁸⁶Sr. In contrast, the younger Marcath and Giggle Spring lavas have enriched mantle (EM) type signatures with high Ba, Rb and Cs, and lower ²⁰⁶Pb/²⁰⁴Pb and higher ⁸⁷Sr/⁸⁶Sr. Together, the LCVF lavas produce a negative correlation between Sr and Pb isotopes that could be attributed to lower crust assimilation. However, the lack of correlation of isotopes with indices of fractionation, OIB-like Nb/U ratios, and a positive correlation of ¹⁸⁷Os/¹⁸⁸Os with Nb/U argue against an important role for crustal assimilation. Instead, the compositional variations are attributed to heterogeneous mantle sources. Mixing models indicate that incorporation of ~18% of 0.8Ga recycled oceanic crust into a depleted mantle source can explain the trace element and isotopic signatures of the HIMU lavas. Subsequent addition to the HIMU-like source of minor (~1%) hydrous fluid derived from subducted oceanic crust could account for the chemical and isotopic compositions of the EM lavas. Our data indicate that the mantle source region in the LCVF is characterized by chemical and isotopic heterogeneity over a very small spatial scale (<500m), and that the nature of the mantle source and the depth of melt generation has changed systematically with time.

Compositions and zoning of coexisting minerals in alkaline-ultrabasic rocks, phoscorites, and carbonatites from the Kovdor Complex, Kola Peninsula

I. RASS AND E. KOVALCHUK

Institute of Geology of Ore Deposits, Petrography, Mineralogy & Geochemistry, Russ. Acad. Sci., 35 Staromonetny, 119017 Moscow, e-mail: rass@igem.ru

The compositions of coexisting pyroxene, magnetite, perovskite, schorlomite, titanite, and apatite in silicate and carbonate rocks were studied by electron-probe microanalysis (EPMA) techniques. The principally different major- and trace-element compositions and zoning of the above minerals from magmatic and metasomatic rocks reflect their different crystallization circumstances (*P*, *T*, *f*O₂, *p*CO₂, *a*SiO₂) in the Earth's crust. Magnetite in silicate rocks is noticeably richer in Ti than this mineral in carbonatites and phoscorites. The Ti content decreases from the cores to rims of magnetite crystals in any magmatic rock but shows the opposite tendency in magnetite of metasomatic Ne-Px rocks. A higher proportion of the magnesioferrite component in magnetite from phoscorites compared to that in silicate rocks is likely attributed to higher oxygen fugacity during the crystallization of the former. Apatite in younger derivatives of silicate rocks bears higher Sr concentrations. Its crystals exhibit core-to-rim variations in the contents of F (by up to 3.2 wt.%), REE, and SiO₂. The F content increases in apatite from magmatic rocks and decreases in that mineral from metasomatic ones. The SiO₂ content of apatite in silicate rocks reaches ~1 wt.% and shows a core-to-rim increase, whereas its concentrations in carbonatitic and phoscoritic rocks are noticeably lower. The presence of Si-rich apatite suggests its crystallization at shallower depths, at which CO₂ activity is lower. The occurrence of Ti-rich andradite and titanite in Px-Ne rocks instead of perovskite is due to a higher *a*SiO₂.

Supported by RFBR13

Diurnal Chemical Characteristics of PM_{2.5} over a Source Region of Biomass Burning Emissions in the Indo-Gangetic Plain

RASTOGI N¹, SINGH A² AND SINGH D²

¹Geosciences Division, Physical Research Laboratory, Ahmedabad, India

²Department of Physics, Punjabi University, Patiala, India
nrastogi@prl.res.in

Wintertime haze/fog has been observed every year over the Indo-Gangetic Plain (IGP); however, the understanding on corresponding particulate composition is meager. The diurnal chemical characteristics of PM_{2.5} were investigated during October-2011 to March-2012 at a site (Patiala, 30.2 °N, 76.3 °E; 250 m amsl) located in the source region of biomass burning emissions over IGP. The study period covers characteristic emissions from post harvest paddy-residue burning during October-November (P1), from fossil, wood, and bio-fuel burning during December-February (P2), and from variable regional sources during March (P3).

A striking diurnal variability was observed in PM_{2.5} mass, SO₄²⁻, NO₃⁻, NH₄⁺, K⁺, OC, EC, and WSOC during P1 with ~30 to 300% higher concentrations of species in nighttime samples. The averaged WSOC/OC ratios for daytime and nighttime samples were ~0.65 and 0.47, respectively in all seasons, suggesting the enhanced daytime secondary organic aerosols formation. The NO₃⁻ was comparable and OC was higher than SO₄²⁻, indicating their importance as scattering species over IGP. The averaged (OC + SO₄²⁻ + NO₃⁻)/EC ratios for the daytime samples were ~12, 15 and 5.5, and for the nighttime samples were ~18, 14, and 6 during P1, P2 and P3, respectively, indicating the dominance of scattering type species in all the seasons with noticeable diurnal difference during P1, and the contribution of absorbing species (EC) increases from P1 to P3. A strong linear correlation ($r^2 = 0.86$) has been observed between all daytime and nighttime OC and K⁺, suggesting that the K⁺ can be used as a tracer for biomass burning emissions over IGP with the OC/K⁺ characteristic ratio of ~16. Water-soluble species were dominant (≥55%) in PM_{2.5} during winter (P2), and could be the major contributor to fog formation over IGP under favourable meteorological conditions. This study has implications in understanding the effects of biomass burning emissions on regional air quality and climate over IGP, and designing appropriate mitigation strategies.

Isotopic evidence for a crustal Pb source in the giant Broken Hill Pb-Zn-Ag deposit, NSW, Australia

MASSIMO RAVEGGI^{1*}, DAVID GILES², JOHN FODEN², SEBASTIEN MEFFRE³, MIKE RAETZ¹ AND IAN NICHOLLS¹

¹School of Geosciences, Monash University, Melbourne, Australia.

(*correspondence:Massimo.Raveggi@monash.edu)

²School of Earth and Environmental Sciences, The University of Adelaide, Adelaide, Australia
David.Giles@adelaide.edu.au

²School of Earth and Environmental Sciences, The University of Adelaide, Adelaide, Australia
John.Foden@adelaide.edu.au

³CODES, The University of Tasmania, Hobart, Australia.
smeffre@utas.edu.au

The Paleo to Meso-Proterozoic Willyama Supergroup, together with the Broken Hill Pb-Zn-Ag deposit, hosts a wide variety of unusual rocks with mineralogical compositions comprising various proportions of quartz ± Fe-oxide ± garnet ± accessories (QFeGA), as well as mafic and felsic orthogneisses that intruded at ca. 1685 Ma. Major, trace, REE and U/Pb zircon geochronology data suggests that the QFeGA lithologies are syn-sedimentary, hydrothermal meta-sediments with limited detrital input, similar to hydrothermal sediments forming at present day spreading centers. Neodymium isotope data suggests that the hydrothermal fluids responsible for their deposition were in equilibrium with the Willyama Supergroup (meta)sedimentary sequences.

Lead isotope data from the mafic and felsic orthogneisses lie within error on the same 1685 Ma ²⁰⁷Pb/²⁰⁶Pb reference isochron with an initial Pb isotope composition of Broken Hill orebody (galena). This is inconsistent with independent geochemical evidence showing that the mafic and felsic orthogneisses were derived from end-member mantle and crustal sources respectively. It is inferred that Pb isotope data is the result of a period of regional homogenisation due to pervasive crustal hydrothermal flux at the time of emplacement of the mafic and felsic rocks (ca. 1685 Ma). This is coincident with formation of the QFeGA rocks and the Broken Hill deposit. It is interpreted that the Pb (and other metals) scavenged by this hydrothermal system from the Willyama Supergroup (meta)sedimentary sequences, provided the metals for the Broken Hill orebody

Field evidence, modeling results, and new investigative strategies shed light on the timing and amplitude of sea level change during past interglacials

M.E. RAYMO¹, A. ROVERE¹, J.X. MITROVICA²,
M. O'LEARY³, P. HEARTY⁴ AND J. INGLIS⁵

¹Lamont-Doherty Earth Observatory of Columbia University,
raymo@ldeo.columbia.edu

¹Lamont-Doherty Earth Observatory of Columbia University,
rovere@ldeo.columbia.edu

²Harvard University, jxm@eps.harvard.edu

³Curtin University, Perth, mickoleary.sci@googlemail.com

⁴University of North Carolina, Wilmington,
kaisdad04@gmail.com

⁵University of North Carolina, Chapel Hill,
jezinglis@gmail.com

Oscillations of sea level, whether rapid or gradual, influence the degree and style of shoreline formation including reef framework construction, destruction, and preservation. Using insight from modern shoreline systems, members of the PLIOMAX project have mapped mid-Pliocene, MIS11, and MIS5e shorelines at numerous localities around the world and modeled the effects of subsequent glacial isostatic adjustment (GIA) on their current position. For both MIS5e and MIS11 we conclude that an ice sheet stability threshold was crossed in the last few kyr of each interglacial resulting in the catastrophic collapse of polar ice sheets with a rise in eustatic sea level to ~9m or more above present. We further show that dynamic topography, supported by convectively maintained stresses generated by viscous flow in the mantle and associated buoyancy variations in the lithosphere, plays a significant role in the post-depositional displacement of Pliocene and even much younger Pleistocene shorelines. We will discuss how we are using predicted global patterns of GIA and dynamic topography to guide field efforts aimed at extracting the eustatic component of sea level change during past warm climates. We also discuss how our field data is helping, in turn, to constrain uncertainties in models of both GIA and the long-term convective evolution of the Earth (uncertainties in mantle viscosity, for instance).

Giving microbial communities a solar supercharge: does the transition to photosynthesis in extreme environments drive taxonomic, biochemical, and metabolic novelty?

JASON RAYMOND, ERIC ALSOP AND MATTHEW KELLOM
School of Earth & Space Exploration, Arizona State Uni.

A combination of prolific biological diversity and steep physical and geochemical gradients make hydrothermal ecosystems outstanding environments for understanding the dynamic interplay between life and environment. Our work investigates taxonomic (e.g. 16S rRNA), metagenomic, and transcriptomic profiling of microbial communities in extreme environments. One such study focuses on communities occurring along a 40+ degree C temperature gradient in a geochemically well-characterized alkaline hot spring in Yellowstone National Park (YNP). The communities along this single outflow channel show changes in community organization, metabolism, and (taxonomic) biodiversity that can be directly related to changes in the geochemistry of their aqueous environments.

One unexpected result of this work comes at the so-called photosynthetic fringe, where “hot” chemotrophic metabolism gives way to “cool” phototrophy. This transition occurs between 55 and 73 degrees C in alkaline YNP springs—an apparent upper temperature limit on photosynthesis that is still poorly understood. While in general, biodiversity increases as temperature decreases, 16S analysis reveals that community diversity—quite unexpectedly—peaks not below but rather just above the onset of photosynthesis, tapering off at both higher and lower temperatures. This increase in biodiversity is not simply the union of lower T photosynthetic and higher T chemotrophic communities; intriguingly, new species not observed in any other communities occur only at this intersection.

We are integrating molecular genetic data with geochemical analyses to investigate several plausible hypotheses for this boost in diversity. Furthermore, this integrated approach provides unprecedented resolution of how the onset of photosynthesis in complex, natural communities results in a dramatic shift not only in the overall numbers but also in the distinct types of biomolecules able to be synthesized by the community at large. Whereas taxonomic diversity is at a maximum above the photosynthetic fringe, biochemical and metabolic diversity is highest below the fringe, where the energetic supercharge provided by photosynthesis makes accessible new and otherwise costly metabolic capabilities.

Finally, we hypothesize that the transitions associated with the photosynthetic supercharge may provide important insights into how the invention of photosynthesis (oxygenic photosynthesis in particular) provided the molecular underpinnings for early life on Earth to achieve new levels of complexity and stands as the single most important biological innovation since the origin of life itself.

www.minersoc.org

DOI:10.1180/minmag.2013.077.5.18

STXM characterization of fossil organic matter from the Montceau-les-Mines Lagerstätte (France)

A. RECANATI¹, S. BERNARD¹, D. GERMAIN²,
S. CHARBONNIER² AND F. ROBERT¹

¹LMCM, UMR 7202, MNHN and CNRS, Paris, France

(arecanati@mnhn.fr, sbernard@mnhn.fr, robert@mnhn.fr)

²CR2P, UMR 7207, MNHN and CNRS, Paris, France

(scharbonnier@mnhn.fr, germain@mnhn.fr)

The fossil record contains key information regarding the evolution of life and environment on Earth. However, decoding this record can be quite challenging as biogenic organic matter (OM) is inevitably altered during fossilization processes. The combination of transmission electron microscopy (TEM) with synchrotron-based scanning transmission X-ray microscopy (STXM) and X-ray Absorption Near Edge Structure (XANES) spectroscopy now offers valuable capabilities for the *in situ* characterization of heterogeneous and organic-rich samples such as fossilized remains [1]. TEM provides spatially-resolved information on organic constituent texture at the sub-nanometer scale, and allows for crystallographic determination. STXM and XANES enable spatially-resolved characterization of organic constituent speciation at the 15 nanometer scale.

Here we report the multiscale characterization of exceptionally preserved soft-bodied plants and animals fossilized within carbonate concretions from the Carboniferous Montceau-les-Mines Lagerstätte [2]. SEM and TEM investigations have revealed mineralogical and textural heterogeneities at all scale of observations, likely explaining the exceptional morphological preservation of the investigated fossils. STXM experiments (performed using the 5.3.2.2. ALS STXM Polymer beamline [3]) have allowed to evidence the similar molecular signatures of the OM composing the vegetal and the animal remains. We interpret this surprising homogeneity as resulting from the replacement of the initial biogenic OM by newly condensed recalcitrant geopolymer compounds during early diagenesis. Altogether, this study illustrates the capabilities of synchrotron-based STXM and XANES spectroscopy to provide molecular-level information on natural OM.

[1] Bernard S. *et al.* (2009) *Review paleobot palyno* **156**, 248-261 [2] Charbonnier S. *et al.* (2008) *Palaios* **23**, 210-222 [3] Kilcoyne A.L.D. *et al.* (2003), *J. Synchrotron radiat* **10** (2), 125-136.

On some feedback-coupling relations between fluid flow, igneous Intrusion, metamorphic / metasomatic events and deformation during low-P high-T regional thermal metamorphism. An example from the Osor high-grade complex (Catalan Coastal Ranges. NE Iberia)

JOAN RECHE¹ AND FRANCISCO J. MARTÍNEZ¹

¹Departament de Geologia. Universitat Autònoma de Barcelona, 08193 Bellaterra (Cerdanyola del Vallés) Barcelona, Spain. (joan.reche@uab.cat)

Bulk composition (BC) controls assemblages and rheology of metamorphic rocks. BC changes are expected in deep crustal levels due to advective phenomena such as pervasive to channelized fluid or melt flows. Imperatively the following coupled phenomena should be investigated: a) How BC changes influence mineral assemblages b) How resulting rheological changes influence deformation regimes, and c) How subsequent P-T evolution occurs.

In the Osor complex we found evidence for sin-D2 fluid flow during a LP/HT thermal metamorphic event at c. 320 my (age of syn-D2 Susqueda diorite) and also retrograde fluid flow related to leucogranite crystallization at c. 300 my. Prograde flow may have produced modal depletion in q and K-Na phases (μ or pl), and modal increase in fibrolite giving sil-enriched D2 foliation planes, through carrying away SiO₂ and alkalis. Local migmatization and genesis of peraluminous granitoid melts probably contributed also to the silica and alkalis depletion. Retrograde fluids from crystallization of sin-D3 granitoid veins recycled silica and alkalis back to the series and produced growth of blastic μ , bi and Na-rich pl. The recycled silica is found as sets of late q-rich veins. The final result are altered surmicaceous, q-poor rocks with different rheological properties with respect to the original metapelites. The genesis of this rheologically weak lithology would have enhanced late gravitational instability [1] during the final stages of D2. Subsequent deformation (D3) shows SCC foliation planes, fish-like micas and porphyroclastic albite, which are features related to uplift-exhumation of the Osor high-grade core.

[1] Gerya et. al. (2004). *Geol. Soc. of Am. Spec. pap.*, **380**, 97-115.

A Simple Method to Filter Arsenic From Water using CuO Nanoparticles

K.J. REDDY AND K.J. McDONALD¹

¹Department of Ecosystem Science and Management, University of Wyoming, Laramie, WY 82071, USA (katta@uwyo.edu)

A continuous flow-through reactor with CuO nanoparticles (NPs) was developed to filter arsenic (As) from groundwater samples. Natural groundwater samples as well as spiked with 100 µg/L of As were passed through (1L per hr) the flow-through reactor to filter As. Samples from the flow-through reactor were collected at a regular interval and analyzed for As and other chemical components (e.g., pH, major and trace elements). The CuO NPs adsorbed with As were regenerated with a sodium hydroxide (NaOH) solution and tested again in the flow-through reactor. The continuous flow-through reactor was effective in filtering As from spiked or natural groundwater samples. The regenerated CuO NPs were also effective in filtering As from groundwater. The CuO nanoparticle treatment did not show any discernible effects on the chemical quality of groundwater samples. Results of this study suggest that CuO NPs show potential for developing a simple process for field applications to remove As from water (Table 1) [1].

Time (min)	Volume (L)	CuO NP (As, µg/L)	RegenCuO NP (As, µg/L)
0	Control	109	110
5	0.1	1.5	<1.0
30	0.5	2.5	<1.0
180	3.0	3.0	<1.0
600	10.0	12.5	5.0
900	15.0	19.0	10.0
1200	20.0	23.0	14.0
Composite		12.5	6.0

Table 1. Effect of CuO NPs in removal of As from groundwater samples with continuous flow-through system.

[1] Reddy, K.J (ed.) (2013) A novel arsenic removal process for water using cupric oxide nanoparticles. *Journal of Colloid Interface Science*, 397:96-102.

Geochemical proxy nanostructure of foraminifera by X-ray imaging: STXM and tomography

SIMON A T REDFERN^{1§}, OSCAR BRANSON¹, HENRY ELDERFIELD¹, TOLEK TYLISZCZAK² AND CHRISTOPH RAU³

¹Department of Earth Sciences, University of Cambridge, Downing Street, Cambridge, CB2 3EQ, UK

²Advanced Light Source, Lawrence Berkeley National Laboratory, Berkeley, CA 94720, USA

³Diamond Light Source, Rutherford Appleton Laboratory, Didcot, OX11 0QX, UK

§satr@cam.ac.uk

Empirical palaeoceanographic proxies typically exploit geochemical signatures in biominerals, such as the shells ('tests') of foraminifera. Correlations between quantities such as Mg-content of the whole shell and the physico-chemical environment in which the shell was laid down by the planktonic organism are used to chart, for example, ocean temperature. Data off tests obtained from ocean floor sediment cores allow the proxy measurement of paleotemperatures back through geologic time.

Implicit here is the assumption that Mg substitutes into the calcite lattice of the shell. Links between XRD results for high-Mg-calcites of foram tests and inorganic high-Mg-calcites lend support to his assumption, but are, of necessity, made from crushed and averaged powder samples of whole shells. The Mg-contents of most foraminifera (0-10 mmol/mol Mg/Ca) are lower than the detection limits of XRD, however. Furthermore, previous LA-ICP-MS and nanoSIMS mapping of elemental concentrations in foram tests indicate banding and chemical heterogeneity.

We have exploited the nanometre scale resolution of STXM methods at the ALS, Berkeley, to determine elemental concentrations and chemical environments (coordination states) of key targets, such as Mg, B and S in foraminifera test. STXM and related methods, such as PEEM, (potentially) ptychography provide unique insights into the chemical state of important geochemical proxies within mineral lattices. We find that Mg is indeed incorporated into the crystalline lattice of CaCO₃, but with some potential indication of clustering. Results show that compositional banding in one element can be compared directly with other key elements.

The role of diagenetic alteration in old foram tests has been explored through synchrotron tomography at Diamond Light Source. Additional capabilities such as coherent diffraction imaging techniques offer future prospects for further exploring the relationship between proxy element distributions and mineral nanostructure.

Partial melting and melt loss: Migmatites from Val Strona di Omegna (Ivrea Zone, NW Italy)

CHARLOTTE REDLER¹

¹Institute of Earth and Environmental Sciences, Mineralogy-
Petrology-Geochemistry, University of Freiburg,
Albertstrasse 23b, D-79104 Freiburg, Germany
(charlotte.redler@minpet.uni-freiburg.de)

The mid to lower crustal field gradient through amphibolite to granulite facies rocks in the Ivrea Zone [1] offers the potential to study classical high-grade metamorphic processes such as partial melting and melt loss. Metapelitic rocks in Val Strona di Omegna show a progressive development in structures, starting with typical amphibolite facies mica-schists at lowest grades that change to metatexites with rare isolated leucosome veins at medium grades and diatexites in high-grade granulite facies rocks.

The first field evidence for partial melting is given by narrow discontinuous leucosomes that coincide with the fluid-absent breakdown of muscovite and the prograde appearance of K-feldspar. Towards high grades the consumption of biotite lead to more extensive melting and the formation of garnet-bearing leucosomes. Zones of diatexite in the highest-grade rocks indicate that melt loss was inefficient and/or accumulation of melt occurred. These zones are common at boundaries between diatexitic metapelitic rocks and metatexitic metagreywacke and may indicate that the metagreywacke formed a low-permeability barrier that restricted melt flow.

Field and petrographic evidence for melting can also be seen by crossing the position of the modelled wet solidus, which is consistent with the small amounts of melt predicted to occur by H₂O-saturated melting. In addition, calculated *P-T* pseudosections show that the metapelitic rocks have produced up to 30-40 mol.% melt at peak metamorphic conditions of around 11 kbar and 900°C. Modelling of granulite facies samples suggest a significant melt loss prior to cooling by showing elevated solidi. This is consistent with a depletion in SiO₂, Na₂O and K₂O and an enrichment in FeO, MgO and TiO₂ relative to amphibolite facies samples.

[1] Redler *et al.* (2012) *J. metamorphic Geol.* **30**, 234–254.

Peloid mud maturation, a mineralogical and health hazard point of view.

MARCO REDOLFI^{1*}

¹Dipartimento di scienze, Univ. Roma3, Roma 00146 Italia
(*correspondence: marco.redolfi@uniroma3.it)

One of the main topic in medical spa is understanding the health hazard correlated to the presence of heavy metal cations in the thermal mud that can be absorbed by the skin associated with the more desirable cations who have beneficial property for some chronic diseases. I develop a standard protocol for analysis of the thermal mud during the maturation for better understanding the characteristic and eventually change in mineralogical and metal available parameter.

I used a maturation protocol developed at Salsomaggiore Terme [1] Italy, mixing a common clay, obtain in Tor Caldara Regional park, Anzio with 11 thermal water collected in the Lazio region in Italy plus distilled water. These mud has been put at 40°C in sealed container for all the maturation period.

After one month and three month of maturation I sample the mud for XRD analysis and heavy metal sequential extraction plus “sweat” extraction [2] to understand the change in these parameter with the progress of the maturation process. These parameter were compered each other, to see the modification of the mineralogy and heavy metal availability during the different stage of mud maturation.

The first data are under integration with new data obtain in these days. But avaiable data demonstrate the formation of gypsum inside the clay, and the partial reduction of some more complex mineral, like plagioclase. The data of the metal and “sweat” extraction are under processing phase and will be ready for the end of June.

[1] Veniale, *et al.* (2004). Formulation of muds for pelotherapy: effects of “maturation” by different mineral waters. *Appl. Clay Sci.* **25**, 135–148.

[2] Tateo F, *et al.* (2009). The in-vitro percutaneous migration of chemical elements from a thermal mud for healing use. *Applied Clay Science*, vol. 44, p. 83-94

Active and Total Microbial Community Structure in relation to Metal Availability within Subsurface Sediments

BRANDI KIEL REESE¹, LAURA ZINKE², HEATH J. MILLS³
AND KATRINA EDWARDS¹

¹Department of Biological Sciences, University of Southern California, Los Angeles, CA (brandi.reese@usc.edu)

²Department of Earth Sciences, University of Southern California, Los Angeles, CA (laurazinke@neo.tamu.edu)

³Department of Oceanography, Texas A&M University, College Station, TX (hmills@ocean.tamu.edu)

To understand the role of biology over geologic time scales and to appreciate past, current and future processes, the total microbial community (including metabolically active and dormant populations) must be characterized. The total microbial community is composed of varying metabolically active and dormant populations based on geochemical conditions. While metabolically active populations change the current geochemical conditions, understanding the total community structure can determine the potential processes available when geochemical conditions change in the future or when geochemical conditions were different in the past. Unlike surface populations that may experience rapid geochemical shifts, timescales for change in the deep subsurface may be over geologic time scales. Thus, dormant populations may become members of a seed bank, which can contribute to the diversity of future microbial communities while remaining examples of past conditions.

Sediment was collected during IODP Expedition 336 on the western flank of the mid-Atlantic ridge (North Pond) and was immediately cryogenically frozen. DNA and RNA were simultaneously isolated from the same sample at eight depths downhole using a uniquely developed extraction method. The V1-V3 region of the 16S gene and gene transcript was targeted using universal *Bacteria* specific primers. This approach targeted the active microbes via rRNA transcripts and the total population (live, dormant, dead) via DNA targets. X-ray Absorption Spectroscopy (XAS) was also used to map elements within the sediment samples chosen for molecular analysis. 16S rRNA gene transcripts extracted were quantified using quantitative rt-PCR. Greater microbial activity was observed at the sediment surface and diversity decreased with depth into the sediment. A majority of the lineages detected were heterotrophic, despite reduced metal species being present, suggesting the overall influence of very low carbon concentrations on community structure and function.

Holocene climate variability from Rio Martino Cave (Western Alps, northern Italy)

REGATTIERI E.*^{1,6}, ZANCHETTA G.^{1,2,6},
ISOLA I.², DRYSDALE R.N.³, ZANELLA E.⁴, LANZA R.⁴,
HELLSTROM J.C.⁵, DALLAI L.⁶, PERRETTE Y.⁷,
COUCHOUD I.⁷, MAGNY M.⁸
AND VANNIERE B.⁸, LANCIL⁹

¹Department of Earth Sciences, University of Pisa, Italy. (regattieri@dst.unipi.it)

²Istituto Nazionale di Geofisica e Vulcanologia, Pisa, Italy.

³School of Earth Sciences, University of Melbourne, Australia.

⁴Department of Earth Sciences, Università degli Studi di Torino, Italy.

⁵Department of Resource Management and Geography, University of Melbourne, Australia.

⁶Istituto di Geoscienze e Georisorse, CNR- Pisa, Italy.

⁷EDYTEM, CNRS, Université de Savoie, France.

⁸Chrono-Environment CNRS, Besancon, France.

⁹Department of Earth Sciences Università degli Studi di Urbino, Italy.

The Alpine region of Europe currently experiences complex climatic conditions and this is also apparent during the Holocene. With this in mind, several flowstone cores were retrieved from Rio Martino Cave (Piemonte, Northern Italy, ca. 1530 m a.s.l.) in the western Alps, where the climate is dominated by North Atlantic synoptic systems. U/Th dating of several flowstones indicates that deposition started at the beginning of the Holocene. One core has been intensively studied using a multi-proxy approach (stable isotopes and rock magnetism). The $\delta^{18}\text{O}$ record show substantial variability through the Holocene, which is interpreted as changes in rainfall $\delta^{18}\text{O}$ recharging the cave catchment. Variations in $\delta^{13}\text{C}$ instead are interpreted as different degrees of soil development. A long-term trend in $\delta^{18}\text{O}$ is apparent, with relatively low values persisting from the commencement of deposition until ca. 6 ka. From 6 to 3 ka the $\delta^{18}\text{O}$ increases gradually before decreasing again from 3 ka onward. $\delta^{13}\text{C}$ shows a good degree of correlation with $\delta^{18}\text{O}$. This long-term trend may be related to changes in the seasonal patterns of precipitation. Superimposed on this trend there are numerous centennial scale oscillations which may reflect alternating periods of drier and wetter conditions.

Both stable isotope records and magnetic susceptibility, which mainly depend on the detrital content, show good correlations with lake level record and flood events in Lake Ledro.

Results of an Interdisciplinary Research Project on Soil Aggregate Formation in CZO's

INGE REGELINK^{1*}, GEORG LAIR², TARU LEHTINEN^{2,3}, JEROEN VAN LEEUWEN¹, BAS VAN DER ZAAAN⁴, JASMIN SCHIEFER², SVETLA ROUSSEVA⁵, AIMERIC BLAUD⁶, MENOJ MENNON⁶ AND STEVE BANWART⁶

¹Wageningen University, Wageningen, The Netherlands, (*correspondence: inge.regelink@wur.nl)

²University of Natural Resources and Life Sciences, BOKU, Vienna, Austria

³University of Iceland, Reykjavik, Iceland

⁴Deltares, Utrecht, The Netherlands

⁵Nikola Poushkarov Institute of Soil Science, Sofia, Bulgaria

⁶University of Sheffield, Sheffield, UK

Soil physical properties such as aggregate stability and porosity are crucial for the soil's agricultural productivity, carbon sequestration capacity and water holding capacity. The formation of soil aggregates is the result of complex interactions between biological, chemical and physical soil processes. Therefore, multi-disciplinary research on Critical Zone Observatories (CZO's) is needed to unravel the key-factors controlling aggregate formation [1].

We will discuss the role of soil chemical and biological processes in the formation of soil aggregates. These data are the result of the joined efforts from soil chemists and biologist collaborating within the SoilTrEC project [2]. We show that organic-mineral interactions and solution chemistry are important for formation of primary soil aggregates. Especially Fe-(hydr)oxides play a crucial role because of their strong interactions with organic substances in the soil [3]. Macro-aggregates are formed when both organic matter, clay minerals and Fe-(hydr)oxides are present in sufficient amounts. These soil macro-aggregates act as habitats for micro-organisms which may in turn alter the organic substances within the soil aggregates. The microbial communities within the macro-aggregates are affected by the land use. Furthermore, land use shows pronounced effects on the structure of the pores within the soil macro-aggregates.

Overall, we want to highlight the importance of multi-disciplinary research in understanding the complex interactions between chemical and biological processes within the critical zone.

[1] Banwart (2011) *Nature*. **474**, 151. [2] Banwart *et al.* (2012) *C R Geosci.* **344**, 758. [3] Regelink *et al.* (2013) *Geoderma*. In press.

Reconstructing subducted sediment fluxes using ancient arc lavas

MARCEL REGELOUS¹, CHRISTOPH BEIER¹ AND KARSTEN HAASE¹

¹GeoZentrum Nordbayern, Universität Erlangen-Nürnberg, Schlossgarten 5, 91054 Erlangen, Germany (correspondence: marcel.regelous@fau.de)

Previous studies have shown that there exists a relationship between the fluxes of trace elements contained in subducting sediments at active subduction zones, and the trace element composition of the associated arc lavas, after correction for melting and fractionation effects [1]. This relationship apparently holds despite the wide range in thermal structure of present-day subduction zones resulting from variations in subduction rate, slab dip and the age of the subducting plate and could be used, together with trace element analyses of ancient arc lavas, to estimate past sediment fluxes at former subduction zones.

This method might be used to test the hypothesis that high atmospheric CO₂ concentrations in the late Mesozoic-early Cenozoic was maintained by subduction and decarbonation of large volumes of carbonate-rich sediment deposited in the former Tethys Ocean [2-4]. If this were the case, then ancient arc lavas from the margins of Tethys would be expected to have relatively high Sr and Ba, and low Th normalised concentrations. The approximate mass of carbonate subducted could be estimated from the Sr concentration of Tethyan carbonate.

The volume and average composition of deep-sea sediment available for subduction at ancient subduction zones has likely varied over time-scales that are long compared to the average age of the oceanic crust (~60 Ma) [5]. Biogenic sediments, which are important hosts of some trace elements, would not have been available for subduction before 500 Ma. The mid-Mesozoic proliferation of planktic calcifiers resulted in a larger carbonate component in deep-sea sediments available for subduction. If carbonate makes up 7-15% of average subducting sediment and has Sr contents an order of magnitude higher than the detrital fraction, then sedimentary Sr fluxes into subduction zones may have been ~50% lower than present before 500 Ma (i.e. for much of Earth's history).

[1] T. Plank, C. Langmuir (1996) *Nature* **362**, 739-743. [2] K. Caldeira (1992) *Nature* **357**, 578-581. [3] D. Kent, G. Muttoni (2008) *PNAS* doi:10.1073/pnas.0805382105. [4] F. Johnston *et al.* (2011) *Earth Planet. Sci. Lett* **303**, 143-152. [5] J. Ludden (2009) *Appl. Geochem.* **24**, 1052-1057.

Occurrence and distribution of natural occurring radioactive materials at a geothermal facility in the North German Basin

SIMONA REGENSPURG¹, JÖRG DILLING²,
JÜRGEN MIELCAREK², RUDOLF NAUMANN¹
AND UWE-KARSTEN SCHKADE²

¹Helmholtz Centre Potsdam, German Research Centre for Geosciences, Telegrafenberg, D-14473 Potsdam, Germany; regens@gfz-potsdam.de

²Federal Office for Radiation Protection, Köpenicker Allee 120-130, D-10318 Berlin, Germany

The occurrence of mineral precipitates with elevated activity concentrations of radionuclides of natural origin is a well known observation from wells of the oil and gas industry. Similar natural occurring radioactive materials (NORM) were found at some deep geothermal facilities. Presumably, these radionuclides are transported with the geothermal fluids and co-precipitate upon change of thermodynamic conditions with the respected oversaturated mineral.

On the one hand, the occurrence of NORM offers the identification of geochemical processes, but on the other hand elevated activities might lead to an enhanced exposure due to radiation. At the geothermal research facility in Groß Schönebeck (North German Basin) the mobility of potassium (⁴⁰K) and radionuclides of the natural uranium- and thorium decay series was intensively monitored. Radionuclide concentrations were measured by gamma-ray spectrometry in samples from reservoir rocks, scalings, filter residues and fluids. Additionally the ambient gamma dose rate of several plant components was monitored. It was found that the content of natural radioactivity in the reservoir rocks is relatively low, whereas a strong enrichment was detected for ²¹⁰Pb and especially for the radium isotopes ²²⁶Ra and ²²⁸Ra in the filter residues of the plant. Filter residues and fluid samples were not in equilibrium with respect to these nuclides.

Since these residues consist mainly of the mineral barite (BaSO₄) and Ra is known as substitute for barium in minerals, barite precipitates apparently act as scavenger for these radionuclides. Further, it was found, that in sandstone reservoir rocks the radionuclides ²²⁶Ra and ²¹⁰Pb are in deficiency compared to their parent ²³⁸U.

REE mobility in carbonatites: insights from the trace-element composition of dolomite

E.P. REGUIR* AND A.R. CHAKHMOURADIAN

¹Department of Geological Sciences, University of Manitoba, Winnipeg, MB, Canada, R3T 2N2 (*correspondence: umreguir@cc.umanitoba.ca)

Dolomite is a principal constituent of many carbonatites. Whereas the major-element chemistry of this mineral has been studied reasonably well, its trace-element variations have not. Here, we examined the trace-element composition of dolomite from carbonatites at Aley (British Columbia, Canada) to improve the current understanding of the processes that affected these rocks after their emplacement.

The examined dolomite shows extremely variable levels of Mn, Co, Sr, Ba, Sc and REE (900-13500, 0-15, 22-7000, 0-600, 0-60 and 0-400 ppm, respectively). Late-stage rhombohedral dolomite associated with quartz and chlorite (\pm REE minerals) is consistently enriched in REE relative to the groundmass. The pattern of enrichment varies from light-REE dominated to heavy-REE dominated. The former type correlates with enrichment in Mn, Sr, Co and Ba. Late-stage dolomite enriched in heavy REE contains lower levels of these elements. There is a general increase in REE content from the core of rhombohedral crystals toward their rim. The groundmass dolomite is characterized by relatively flat chondrite-normalized profiles, which are, in some cases, interrupted by a small negative Y anomaly. With the exception of one sample, REE patterns of the late-stage dolomite show appreciable positive Eu and Y anomalies.

The observed trace element characteristics of dolomite indicate an influx of REE, possibly scavenged from fluorapatite and transported by F-bearing crustal fluids under reducing conditions. The trace-element composition of the late-stage dolomite was further influenced by the precipitation of other associated phases, such as monazite and chlorite.

Crustal thickness estimation from GOCE satellite mission gravity data

M. REGUZZONI¹ AND D. SAMPIETRO^{2*}

¹DICA, Politecnico di Milano, Piazza Leonardo Da Vinci, 32
20133, Milano, Italy
(mirko.reguzzoni@polimi.it)

²GReD - Geomatics Research & Development srl, via
Valleggio 11, 22100, Como, Italy
(*correspondence: daniele.sampietro@g-red.eu)

The boundary between Earth crust and mantle, the so called Moho, is commonly estimated by means of seismic or gravimetric methods. The former methods can be locally very accurate since seismic profiles give an almost direct observation of the actual crustal structure, but can be quite far from reality in large regions where no data are available. The latter methods, although often based on simplified hypotheses to guarantee the uniqueness of the solution, are nowadays becoming more and more important thanks to the improved knowledge of the gravitational field. In particular satellite gravity missions, like the European Space Agency mission GOCE (Gravity field and steady-state Ocean Circulation Explorer) [1], provide a very accurate and spatially homogeneous dataset that can be used to validate the existing global crustal models or to estimate a new one by constraining the relation between Moho depth and crustal density.

In this work a new crustal model (GEMMA model) with a spatial resolution of 0.5°x0.5° and constrained with GOCE observations is computed. For this purpose several additional external information has been used, such as topography, bathymetry and ice sheet models from SRTM, a recent 1°x1° sediment global model and some prior hypotheses on crustal density. In particular the main geological provinces, each of them characterized by its own relation between density and depth, have been considered. A model describing lateral density variations of the upper mantle is also taken into account. Starting from this prior information, an inversion algorithm is applied to the GOCE space-wise grid of second radial derivatives of the gravitational potential [2] to estimate the bottom of the crust. The computed Moho global model is well consistent not only with other global/regional models, but also with the actual gravity field, thus overcoming the main limitation of seismic Moho models (e.g. CRUST2.0).

[1] Drinkwater *et al.* (2007) ESA Special Publication, **627**, 1-8

[2] Reguzzoni & Tselfes (2009). *J Geod*, **83**, 13-29.

Stable Isotope Tracing of Manufactured Nanoparticles

M. REHKÄMPE^{1,2}, A. LAYCOCK^{1,2}, F. LARNER^{1,3},
A. DYBOWSKA², Y. DOGRA⁴, B. STOLPE⁵,
M. DIEZ ORTIZ⁶, J.R. LEAD^{5,7}, C. SVENDSEN⁶,
E. VALSAMI-JONES^{2,5}, C.Z. TYLER⁴
AND T.S. GALLOWAY⁴

¹Department of Earth Science & Engineering, Imperial
College London, London SW7 2AZ, UK

²Life Sciences, Natural History Museum, London SW7 5BD,
UK

³Earth Sciences, Univ of Oxford, Oxford OX1 3AN, UK

⁴Biosciences, University of Exeter, Exeter EX4 4QL, UK

⁵School of Geography, Earth & Environmental Sciences,
University of Birmingham, Birmingham B15 2TT, UK

⁶Centre for Ecology and Hydrology, Wallingford OX10 8BB,
UK

⁷Center for Environmental Nanoscience and Risk, University
of South Carolina, USA

Studies of biological uptake and environmental fate of manufactured nanoparticles (NPs) are often hampered by the difficulty of distinguishing these materials from the normal background levels of elements and natural NPs in environmental samples. Needed are methods for tracking engineered NPs in bulk samples from exposures that are carried out at realistic particle concentrations rather than the much higher levels that are often dictated by the lack of suitable analytical protocols. For metal and metal oxide NPs, this can be achieved by stable isotope tracing, employing NPs that are prepared from a single isotope of the target element.

We are currently investigating stable isotope labeling and tracing for ZnO, CeO₂ and Ag NPs, all materials that have a wide range of applications in industrial and consumer products. Using suitable isotopes and NP preparation methods, stable isotope labeling is cost-effective for these elements. When combined with high precision mass spectrometry for detection, the methodology provides unprecedented sensitivity for NP tracking. For example, biological uptake of ZnO NPs can be detected even at Zn background levels, which exceed the NP concentrations by more than a factor of 10,000.

The application of such methods enables accurate tracing of NP fate and transfer in a wide range of exposure systems and biota. Importantly, the results are able to directly address the key question of whether organisms take up nanoparticles directly or whether the elements are taken up only after particle dissolution.

Quality control for novel isotope analyses

M REHKÄMPER¹, F WOMBACHER², S NIELSEN³, M SCHÖNBÄCHLER⁴, M FEHR⁵, T GOLDBERG¹, F LARNER⁶, A LAYCOCK¹, M PAUL¹ AND T VAN DE FLIERDT¹

¹Dept of Earth Science & Engineering, Imperial College London, London SW7 2AZ, UK

²Institut für Geologie und Mineralogie, Universität zu Köln, D-50674 Köln, Germany

³Dept of Geology and Geophysics, WHOI, Woods Hole, MA 02543, USA

⁴Institut für Geochemie und Petrologie, ETH Zürich, CH-8092 Zürich, Switzerland

⁵Dept of Environment, Earth and Ecosystems, The Open University, Milton Keynes MK7 6AA, UK

⁶Dept of Earth Sciences, University of Oxford, Oxford OX1 3AN, UK

Research in isotope geo- and cosmochemistry is often driven ahead by investigations that interrogate novel isotope systems or particularly ‘difficult’ sample types, whereby analytical challenges are frequently addressed by the use of advanced instrumentation and/or new techniques of sample preparation and data acquisition. Testament to this are the numerous isotopic ‘methods’ articles that are published by geochemists and the even more frequent contributions that present and discuss novel data from, prominently, studies of (still) ‘non-traditional’ stable isotope systems, extinct radionuclides and nucleosynthetic isotope anomalies.

Such leading edge work faces similar but distinct analytical difficulties and additional metrological challenges. In particular, it cannot rely on well-characterized pure-element isotope standards and geological or environmental reference materials (RMs), for evaluation and documentation of data quality. The geochemical community has, however, been very adept in finding pragmatic solutions to such challenges in quality control, through innovative work of individual laboratories, critical peer review of journal articles and, most importantly, generally good-natured competition and extensive collaboration, both formal and informal, between research groups.

With regard to reference materials and method validation, geochemists and metrologists share a common interest in improving data quality and intercalibration but communication and collaboration between these communities on isotopic research is often limited. This is unfortunate because both sides could readily profit from improved interaction, for example in the preparation, characterization and distribution of RMs.

Field Sampling for Porewater Mercury and Methylmercury using DGT

DANNY REIBLE^{1*}, PAUL BIRETA², ARIETTE SCHIERZ¹, JAMES GRUNDY² AND RICH LANDIS³

¹Center for Research in Water Resources, University of Texas at Austin, Austin, TX, USA, reible@mail.utexas.edu (*presenting author)

²Civil, Architectural and Environmental Engineering Department – EWRE, University of Texas at Austin, Austin, TX, USA

³DuPont, 974 Centre Road, Wilmington, DE, USA

Dissolved porewater concentrations have the potential to better relate to mercury methylation rates than bulk mercury sediment loadings. The diffusive gradient in thin film (DGT) technique is applied to determine aqueous mercury and methyl mercury vertical porewater concentration profiles. DGT probes were deployed in the South River (Virginia, USA) where previous industrial activities had led to mercury contamination. The river is primarily a sand and gravel stream with limited microbial productivity. The DGTs were used to evaluate methylation rates and extent and identify locations contributing significantly to methyl mercury. A potential remedial option of biochar amendment was evaluated in a small floodplain pond. The DGTs were used to measure the performance of the sediment amendment including changes to available mercury and methyl mercury. Sampling of bulk sediment, surface water, porewater, and biota was carried out in parallel. Specific redox couples were also measured over depth using cyclic voltammetry. Conclusions were drawn as to the sources of significant methylation and relationship to sediment geochemistry.

The microstructure and trace metal geochemistry of pyrite from porphyry Cu deposits

M. REICH^{1,2,*}, A. DEDITIUS³ AND F. BARRA^{1,2}

¹Dept. of Geology, University of Chile, Santiago, Chile
(*email: mreich@ing.uchile.cl)

²Andean Geothermal Center of Excellence (CEGA),
University of Chile, Santiago, Chile

³Graz University of Technology, Graz, Austria

Porphyry copper deposits (PCDs) are currently the world's largest source of copper and molybdenum, and are also among the largest reservoirs of gold in the upper crust. Despite the fact that pyrite is a ubiquitous mineral phase in these deposits, the major and trace element chemistry of pyrite from PCDs remains poorly understood.

Here we report the first comprehensive trace element database of pyrite from the Dexing deposit, China's largest porphyry Cu deposit, determined using a combination of electron microprobe analysis (EMPA) and secondary-ion mass spectrometry (SIMS). Results show that the concentrations of precious metals (e.g., Au, Ag), metalloids/chalcogens (e.g., As, Sb, Se, Te), and base/heavy metals (e.g., Cu, Co, Ni, Zn, Hg) in pyrite from a PCD are more significant than previously thought (e.g. ~6 wt.% Cu, ~3 wt.% As, ~0.25 wt.% Au, and ~0.2 wt.% Ni).

EMPA-WDS elemental mapping and SIMS depth profiling reveal that some of these metals occur exclusively in solid solution in the pyrite structure (e.g., As, Ni) or are present in solid solution and also in micro- to nano-sized inclusions (e.g. Cu and Au). The mineralogical occurrences are associated with complex textural and chemical features such as oscillatory growth zoning and sector zoning with variable porosity, where Cu-rich, As-(precious metals)-poor zones alternate with As-(precious metals rich)-rich, Cu-poor zones, and with barren pyrite zones.

These observations point toward a decoupled behavior of Cu and As in this porphyry system, strongly suggesting that selective partitioning of metals into pyrite is most likely the result of changes in fluid composition, probably caused by fluid mixing and repeated and intermittent pulses of Cu and As-bearing fluids of magmatic/ hydrothermal origin. Despite the fact that more studies are needed to increase our knowledge about metal partitioning in sulfides during the hydrothermal stages of PCDs formation, the observations and data presented here support an important role of pyrite as a record of fluid variations, and as a host of precious and base metals, metalloids/chalcogens and potentially PGEs.

The disparate crystal records of the Youngest Toba Tuff, Indonesia

M.R. REID^{1,*} AND J.A. VAZQUEZ²

¹Northern Arizona University, Flagstaff, Arizona 86011, USA
(*correspondence: Mary.Reid@nau.edu)

²U.S. Geological Survey, Menlo Park, California 94025, USA

The 74 ka Youngest Toba Tuff (YTT) is the product of a giant eruption (>2800 km³) from the Toba Caldera Complex of Sumatra, Indonesia. The YTT sample suite spans the compositional range of 63-75 wt.% SiO₂, with most >68.8 wt.% SiO₂. The narrower compositional range of quartz-hosted melt inclusions suggests that YTT compositional heterogeneity may reflect a spectrum of crystal-liquid mixtures [1]. Quartz from high silica rhyolites are relatively unzoned whereas those from low silica rhyolites have Ti, and therefore temperature, reversals late in their crystallization history. Limited diffusional relaxation across these bands suggests rim crystallization within a few ka of eruption [2]. In contrast, allanite from a high silica rhyolite grew extensively over >35 ka and are not reversely zoned at the rims [3]. ²³⁸U-²³⁰Th-²⁰⁶Pb zircon crystallization dates range to even older ages but mainly predate eruption by <400 ka. Despite the strong crustal signature of the YTT (⁸⁷Sr/⁸⁶Sr ~ 0.714), bonafide xenocrysts are relatively rare. Growth on individual zircon grains occurred over a protracted time interval (>100-500 ka), and was likely episodic. Zircon ages in high silicic rhyolites may span a more limited range. Zircon from individual rocks exhibit a significant Th/U compositional range and evidently crystallized from a plumbing system with a wider range in thermochemical conditions than those characterized by YTT matrix glasses. Cores nucleated over at least a 300 ka interval, often from relatively unevolved magmas. Zircon rims grew from host melts and yield ages that range from ~80 ka to ~115 ka. Compositional reversals are recorded by rims in zircon from low silica rhyolite but not high silica rhyolite. Considered collectively, ages and age ranges obtained from YTT phases decrease in the order zircon > allanite > quartz, a sequence that parallels that for attainment of phase saturation conditions. Minerals stable in more diverse magmatic compositions apparently persisted longer. Crystals were apparently remobilized intermittently by magmatic rejuvenation rather than being incorporated by foundering of roof rocks at the time of eruption. Domains that ultimately erupt as low silica rhyolites were remobilized beginning 40 ka before eruption – based on the zircon/allanite ages – with the most recent reheating occurring within a few thousands years of eruption [2].

[1] Chesner and Luhr (2010), *JVGR*; [2] Matthews *et al.*, (2012) *J Pet*; [3] Vazquez and Reid (2004) *Science*

Assessment of a gold absorbing resin in natural groundwaters for mineral exploration

N. REID^{1*}, D.J. GRAY¹ AND A. LUCAS²

¹ Deep Exploration Technologies Cooperative Research Centre, CSIRO Earth Science and Resource Engineering, Kensington, Western Australia, Australia
(*correspondence: nathan.reid@csiro.au)

² School of Earth and Environment, University of Western Australia, 35 Stirling Highway, Crawley 6009, Western Australia

One of the most important elements for mineral exploration is gold, and yet it is one of the hardest to accurately measure in groundwater. Recent successes in regional hydrogeochemistry in Australia [1] has highlighted the potential of using activated carbon via both grab sampling and a newly modified Diffusive Gradients in Thin films (DGT) technique [2] to gain low level detection of Au (and other elements) as increasing concentrations of Au can vector to large mineral systems. A question we are addressing is whether the Au signal can be concentrated and/or improved by the use of specific Au absorbing resins.

We used Micro-CT tomography to determine how a specific resin, Purolite A100, absorbs both ionic and metallic Au from solutions, and precipitates it both on and within the resin structure.

Preliminary results show that Purolite A100 absorbs more Au (and also Ag, Bi, Pt and Pd) than activated carbon and gives more consistent results at higher concentrations.

Further research is still required for improving the absorbance of Au at lower Au concentrations.

[1] Gray *et al.* (2009) *Geological Survey of Western Australia Record* 2009/21, ISBN 978-1-74168-280-9. [2] Lucas *et al.* (2012) *Anal. Chem.* **84**: 6994-7000.

Investigating the physicochemical gradients in oil sands wastes

THOMAS REID^{1*}, RYAN BOUDENS¹
AND CHRIS WEISENER¹

¹GLIER - University of Windsor, Windsor, Ontario, Canada
*(reid11c@uwindsor.ca)

The Athabasca Oil Sands contain one of the world's largest oil reserves consisting of approximately 178 billion barrels of oil [1]. With 20% recoverable through open pit mining methods, this extraction process produces a considerable amount of fluid fine tailings (FFT) waste material, which must be deposited on site in tailings ponds. These ponds allow the waste sands, clays, residual bitumen and water to settle out, allowing for the water to be recycled for use again in the extraction process. It is vital to understand the physicochemical gradients which form in these tailings ponds over time, with the goal of remediation once the ponds are no longer needed.

To study the influences of biotic and abiotic processes on fresh and mature FFT, sensitive microsensor profiling techniques are being used to measure hydrogen sulphide (figure 1), oxygen, Eh, and pH profiles over a 1 year period. These profiles are accompanied by pore water extraction methods to analyse cation, anion and pore water gas expression. To compliment these static experiments, dynamic simulations will investigate shear forces (wave action and turbulence) on the water-sediment interface in each of the biotic and abiotic microcosms, under controlled atmospheric conditions.

This holistic study provides insight regarding biotransformation and physicochemical controls effecting sediment oxygen demand associated with remediated wetlands & end pit lake development.

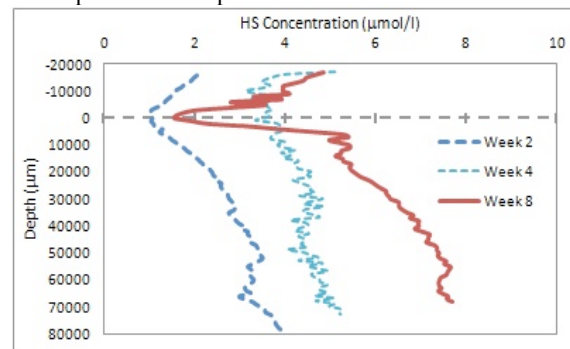


Figure 1: HS⁻ concentration profiles of mature FFT at 2, 4, and 8 weeks, extending from cap water down into the FFT sediment; dashed line is the sediment-water interface

[1] Canada National Energy Board. Canada oil sands: opportunities and challenges to 2015. An energy market assessment. Calgary: Publications Office, National Energy Board; 2004.

Adoption of Eu(III) onto minerals in the presence of humic acids: effects of various solution parameters and sorptive fractionation on modelling and spectroscopy

P.E. REILLER,¹ N. JANOT² AND M.F. BENEDETTI²

¹CEA/DEN/DANS/SEARS/LANIE, Gif-sur-Yvette, France

³Institut de Physique du Globe de Paris, Université Denis Diderot, Paris, France
pascal.reiller(at)cea.fr

Adsorption of metals on minerals with humic acids is always under predicted [1]. The case of Eu(III) in ternary system including purified Aldrich humic acid (PAHA) and α -Al₂O₃ was measured, modelled and probed using time-resolved laser-induced luminescence spectroscopy (TRLS). Each binary system was studied independently [2,3,4], and the luminescence properties of Eu(III), luminescence spectra and decay times (τ), were acquired and compared [5]. Influence of ionic strength and PAHA concentration was also evaluated. The typical luminescence behaviour of Eu(III)-HA system, showing a bi-exponential decay, was also found in the ternary system Eu(III)/PAHA/ α -Al₂O₃, but with marked differences. Luminescence spectra and faster decay τ_1 are the same in both system at pH < 6, but with higher τ_2 indicating a rigid environment for Eu(III). For pH > 6, modifications of Eu(III) luminescence spectra and decrease of τ_2 are showing a progressive influence of α -Al₂O₃. The non-variation of τ_1 suggests the on-going influence of PAHA, notwithstanding its progressive desorption.

Comparing with previous data on sorptive fractionation of PAHA [2,3,6], and with the TRLS evolution of the system [5], an operational modelling was proposed [4], which implies that alumina-sorbed PAHA is showing a stronger interaction towards Eu(III) compared with non-sorbed PAHA even at pH > 7. This stronger interaction is due to the sorptive fractionation which reveals stronger binding sites [1,4,7].

[1] Reiller (2012) *Miner. Mag.* **76**, 2643-2658; [2] Janot, Reiller, Korshin, Benedetti (2010) *Environ. Sci. Technol.* **44**, 6782-6788; [3] Janot, Reiller, Zheng, Croué, Benedetti (2012) *Water Res.* **46**, 731-740; [4] Janot, Reiller, Benedetti (2013), *Colloids Surf. A*, DOI: 10.1016/j.colsurfa.2013.02.052.; [5] Janot, Benedetti, Reiller (2011) *Environ. Sci. Technol.* **45**, 3224-3230; [6] Reiller, Amekraz, Moulin (2006) *Environ. Sci. Technol.* **40**, 2235-2241; [7] Tipping, Griffith, Hilton (1983) *Croat. Chim. Acta* **56**, 613-621.

Geochemistry of European bottled water

CLEMENS REIMANN¹, MANFRED BIRKE²
AND ALECOS DEMETRIADES³

¹Geological Survey of Norway, P.O. Box 6315, Sluppen, 7491 Trondheim, Norway

²Federal Institute for Geosciences and Natural Resources, Wilhelmstrasse 25 – 30, 13593 Berlin, Germany

³IGME, 1 Spirou Louis Street, Entrance C, Olympic Village, 136 77 Acharnae, Athens, Hellas

To obtain a first impression of the geochemistry and quality of ground water at the European scale bottled mineral water was used as a sampling medium. In total, 1785 bottled waters were purchased from supermarkets of forty European countries, representing 1247 wells/drill holes/springs at 884 locations. All bottled waters were analysed for 72 parameters at the laboratories of the Federal Institute for Geosciences and Natural Resources (BGR) in Germany. The result provide a first impression of the natural variation of chemical elements in ground water at the European scale. Maps demonstrate that geology is one of the key factors influencing the observed element concentrations for a significant number of elements. Examples include high values of (i) Cr clearly related to the occurrence of ophiolites; (ii) Li (Be, Cs) associated with areas underlain by Hercynian granites; (iii) F (K, Si) related to the occurrence of alkaline rocks, especially near the volcanic centres in Italy, and (iv) V indicating the presence of active volcanism and basaltic rocks. The natural variation of element concentrations in the bottled water covers usually between three to four orders of magnitude and reaches up to 7 orders of magnitude for a few elements (e.g., Li, U). A comparison with the chemistry of European tap water, surface water and Norwegian ground water shows surprising similarities in terms of median and variation. This proves that bottled water can be taken as a proxy for European ground water quality for the majority of elements/parameters. The bottled water samples showed, however, exceptionally high concentrations for a few elements typical for deep, hydrothermal sources (e.g., B, Be, Br, Cs, F, Ge, Li, Rb, Te and Zr).

Fortunately less than one percent of all samples returned values that were above the currently valid European maximum admissible concentrations (MACs) for drinking and/or bottled water (e.g., for As, Ba, F, Se, NO₃ and NO₂). It is, however, an important observation that currently there exist no water action levels for some of the elements that show an exceptionally high natural variation (e.g., Li and U).

www.minersoc.org

DOI:10.1180/minmag.2013.077.5.18

Chemistry of Europe's agricultural soils - the GEMAS project

CLEMENS REIMANN¹, ALECOS DEMETRIADES²
AND MANFRED BIRKE³

¹Geological Survey of Norway, P.O. Box 6315, Sluppen, 7491 Trondheim, Norway

²IGME, 1 Spirou Louis Street, Entrance C, Olympic Village, 136 77 Acharnae, Athens, Hellas

³Federal Institute for Geosciences and Natural Resources, Wilhelmstrasse 25 – 30, 13593 Berlin, Germany

Geochemical Mapping of Agricultural and grazing land Soil (GEMAS) is a cooperative project between the Geochemistry Expert Group of EuroGeoSurveys and Eurometaux. During 2008 and until early 2009, a total of 2108 samples of agricultural (ploughed land, 0-20 cm) and 2023 samples of grazing land (0-10 cm) soil were collected at a density of 1 site/2500 km² each from 33 European countries, covering an area of 5,600,000 km². All samples were analysed for 52 chemical elements following an aqua regia extraction, 41 elements by XRF (total), and soil properties, like CEC, TOC, pH (CaCl₂), following tight external quality control procedures. In addition, the agricultural soil samples were analysed for 57 elements in a mobile metal ion (MMI[®]) extraction, Pb isotopes and magnetic susceptibility. The GEMAS project thus provides for the first time fully harmonised data for element concentrations and soil properties known to influence the bioavailability and toxicity of the elements at the continental (European) scale. The provided database is fully in compliance with the requirements of the European REACH Regulation (Registration, Evaluation, Authorisation and Restriction of Chemicals). It also provides valuable information for other European pieces of legislation related to metals in soil.

The results demonstrate that robust geochemical maps of Europe can be constructed based on low density sampling. At the European scale element distribution patterns are still governed by natural processes, most often a combination of geology and climate.

An Iceland-like Setting for Generation of Earth's Earliest Known Crust

REIMINK, J.R.,^{1*} CHACKO, T.,¹ STERN R.A.^{1,2}
AND HEAMAN, L.M.¹

¹Department of Earth and Atmospheric Sciences, University of Alberta, Edmonton T6G 2E3, Canada
(reimink@ualberta.ca)

²Canadian Centre for Isotopic Microanalysis, University of Alberta, Edmonton T6G 2E3, Canada

The Acasta Gneiss Complex (AGC) contains the oldest rocks on Earth with U-Pb zircon ages indicating crust formation between 3.6-4.03 Ga [1-3]. Here we report whole rock geochemistry along with SIMS U-Pb, trace element, and O-isotope compositions of zircon from a >4.0 Ga tonalite unit identified during detailed mapping of the AGC.

Unlike typical Archean TTGs [4], this unit is characterized by moderate silica contents (58-62 wt % SiO₂), strong Fe-enrichment (12-15 wt% FeO), and low Mg numbers (13-18). REE patterns are relatively unfractionated (La/Yb_N ~2.5) and contain a significant negative Eu anomaly. These features strongly suggest that, unlike deep-seated Archean TTG magmas [4], the evolution of this AGC tonalite was dominated by shallow-level fractionation processes involving plagioclase.

Zircons from this well preserved unit document complex morphological patterns, very similar to previously described pre-4.0 Ga zircons from the AGC [1]. Two phases of igneous zircon growth, centers and mantles, are compositionally distinct but record indistinguishable U-Pb ages >4.01 Ga. Oxygen isotopic compositions from zircon centers and mantles document a decrease in δ¹⁸O from a mean of 5.6±0.1‰ to a mean of 4.7±0.1‰. This center to mantle decrease in δ¹⁸O can be explained by late-stage assimilation of hydrothermally altered crust.

Collectively, these data for the >4.0 Ga AGC tonalite are strikingly similar to those reported for intermediate rocks from Iceland (e.g., icelandites), which are thought to have formed by a combination of shallow-level basaltic magma fractionation and assimilation of surface-water altered crust [e.g., 5]. Thus, Iceland may serve as a suitable analogue for the generation of Earth's earliest proto-continental crust.

[1] Bowring & Williams, (1999) *Cont. Min. Petro.* **134**, 3-16.
[2] Stern & Bleeker, (1999) *Geosci Can* **25**, 28-31. [3] Iizuka *et al.*, (2007) *Precambrian Research* **153**, 179-208. [4] Moyen & Martin, (2012) *Lithos* **148**, 312-336. [5] Wood, (1978) *Journal of Petrology* **19**, 393-436

Toward an *in-situ* bioremediation strategy for acidic *in-situ* leach uranium mining

B.C. REINSCH^{1*}, M. DESCOSTES²,
R. BERNIER-LATMANI¹ AND P. ROSSI¹

¹École Polytechnique Fédérale de Lausanne, Lausanne, Switzerland,

(*correspondence : brian.reinsch@epfl.ch)

²AREVA, Paris, France

In Kazakhstan, *in-situ* leach (ISL) mining of uranium utilizes the oxidizing power of pH < 2 sulfuric acid solutions to liberate and mobilize uranium from the ore's naturally reducing conditions. Although ISL has the potential to be less environmentally impactful than physical mining techniques, it includes the risk of groundwater contamination. A detailed geochemical and microbiological analysis and comparison of pre-, mid-, and post-mining conditions is warranted in order to assess and potentially mitigate that risk.

A theoretically ideal remediation strategy for ISL would be one that re-equilibrates the pH, immobilizes uranium as U(IV) precipitates, and does not require physical disruption of the surface. The strategy proposed here is *in-situ* biostimulation. The injection of carbon-based electron donors into the subsurface would, in theory, promote the growth of indigenous bacterial communities able to reclaim the subsurface. The proposed mechanism is that stimulated sulfate and/or iron reducing bacteria can return the pH to its original value and re-establish reducing conditions more rapidly than the commonly practiced strategy of natural attenuation. Biostimulation could also utilize the existing configuration of pumps and pipes, originally used to inject acid.

The objectives of this study are: 1) to characterize the impact of the injection of sulfuric acid on the subsurface geochemistry, 2) to probe changes in the subsurface microbial communities as a result of mining operations, 3) to identify through laboratory-based studies which electron donors may promote Fe- and/or sulfate-reducing microbial communities post-mining, and 4) to ascertain the composition of the microbial community post-remediation. The results presented here represent the initial stages of a pioneering study to understand the effects of uranium ISL on the environment and to design and implement an *in-situ* bioremediation strategy in Southern Kazakhstan.

Geochemistry of Biotite of The Vila Nova Plutonite (Central Portugal)

A.I.M. REIS¹

¹Department of Earth Sciences, University of Coimbra, 3000-272 Coimbra, Portugal (aimreis@gmail.com)

The Vila Nova plutonite intruded phyllites and metagraywackes of Neoproterozoic-Cambrian Beiras Group in Central Iberian Zone of Iberian Massif which is the SW segment of the European Variscan Belt and occurs in a group of seven plutonites of similar age and particular features related to a major strike slip shear zone.

The Vila Nova plutonite has a compositional variability of tonalite-granodiorite-granite. Its a rock of fine to medium grained, muscovite>biotite. The $\delta^{18}\text{O}$ values are 11.09_{tn}-11.54_{gd}-12.65_{gt} ‰. The plagioclase An(%) contents are 13.2_{tn}-13.6_{gd}-14.6_{gt} and feldspar Or(%) contents are 86.2_{gd}-93.2_{gt}. The tonalitic lithotype do not contain feldspar.

Biotite is often altered to chlorite associated with acicular rutile and opaque minerals such as pyrite and is absent in granitic composition with tourmaline.

They are magmatic except in microgranular enclaves where they are reequilibrated, the X_{FeO} is 0.74_{Tn} - 0.71_{Gd} - 0.73_{Gt}[1] and are ferriferous biotites[2] with aluminopotassic trends[3] evidence of peraluminous magma.

The biotite in surmicaceous xenolithes, stretched on alternated reeds with muscovite, occur in the tonalitic composition and have less content of Si, Ca, Na and higher content of Al^{IV} and Zn and, in the microgranular enclaves in the granodioritic composition the dispersed and subhedral biotite have less content of Ti, Zn, K and higher contents of Fe³⁺, Ca and Na than others biotites. In these textural heterogeneities some elements have opposite behavior from center to rim. The biotites in the evolutionary trend have a decrease of Fe³⁺, Fe²⁺, Mn, Li, Ca, Rb, OH, Li/Mg, Rb10³/K and Fe²⁺/Mg and an increase of Mg, Na, Cs, F, Si/Ca.

[1]Nacht, H.; Ibhi, A.; Abia, E. H.; Ohoud, M. B. (2005) Discrimination between primary magmatic biotites, reequilibrated biotites and neofomed biotites. *C.R. Geoscience*, 337, 1415-1420. [2]Tischendorf, G.; Förster H.-J. and Gottesmann, B. (1999a) The correlation between lithium and magnesium in trioctahedral micas: Improved equations for Li₂O estimation from MgO data. *Mineralogical Magazine*, 63, 57-74. [3]Nacht, H.; Razafimahefa, N.; Stussi, J.M.; Carron, J.P.; (1985) Composition chimique des biotites et typologie magmatique des granitoïdes. *C. R Acad. Sc. Paris*, 301 (11), 813 – 818.

Chromitites from the Andriamena greenstone belt, Madagascar: Hints of a mid-Archean ophiolite?

LAURIE REISBERG^{*1}, MARYSE OHNENSTETTER²
AND CATHERINE ZIMMERMANN¹

¹Centre de Recherches Pétrographiques et Géochimiques, UMR 7358, CNRS, Université de Lorraine, BP 20, 54501 Vandoeuvre-lès-Nancy, France. (*correspondence: reisberg@crpg.cnrs-nancy.fr)

²GéoRessources, UMR 7359, CNRS, Université de Lorraine, BP 70239, 54506 Vandoeuvre-lès-Nancy, France

The Andriamena greenstone belt of Madagascar contains massive chromitite bodies of likely ophiolitic affinity, composed of about 90% chromite and 10%, mostly secondary, gangue minerals (talc, green amphibole, orthopyroxene, Ca and Mg carbonate). Arguments in favor of an ophiolitic origin for the chromitite include the high Cr# (0.67-0.74), coupled with relatively high Mg# (0.6-0.78) of the constituent chromite. In addition, these phases display very low TiO₂ contents (<0.25%), which are also characteristic of ophiolites and possibly suggestive of an arc environment. Though in most places the chromitite is in tectonic contact with a variety of igneous lithologies, remnants of apparently cogenetic ultramafic rock types, including dunites, harzburgites, and some pyroxenites are sometimes immediately juxtaposed with the chromitite. The very high Fo content of the olivine in the dunite, as high as 0.95, also attests to an ophiolitic provenance.

Platinum group element (PGE) and Os isotopic analyses were performed on several chromitite samples. Chondrite normalized PGE spectra display marked depletions in PPGE relative to IPGE, with (Pt/Ir)_N ranging from ~0 to 0.09, though Pd contents are somewhat less depleted than those of Pt. The observed PPGE depletion is another feature characteristic of ophiolitic chromitites. The IPGE enrichment is consistent with the presence of laurite microinclusions in the chromite revealed by SEM. Os isotopic compositions are tightly clustered, with ¹⁸⁷Os/¹⁸⁸Os ranging from 0.1057 to 0.1059, corresponding to T_{RD} model ages of ~ 3.2 Ga, assuming primitive upper mantle parameters [1]. ¹⁸⁶Os/¹⁸⁸Os measurements are in progress.

If the ophiolitic nature of the chromitites is confirmed, our results might imply that mechanisms similar to present-day tectonic processes may already have been active in the mid-Archean.

[1] Meisel, Walker, Irving & Lorand (2001), *Geochim. Cosmochim. Acta* **65**, 1311 – 1323.

Biogeochemical cycling of Au and Pt - Integrating field studies, micro-analyses and molecular biology

FRANK REITH^{1*}, CARLA ZAMMIT¹, DIETRICH H. NIES,
GORDON SOUTHAM³ AND JOËL BRUGGER¹

¹The University of Adelaide, School of Earth and Environmental Sciences, Adelaide SA5005, Australia (*correspondence:frank.reith@csiro.au)

²Martin-Luther University Halle-Wittenberg, Institute of Biology/Microbiology, Halle, Germany.

³The University of Queensland, School of Earth Sciences, Brisbane, QLD 4072, Australia

The biosphere catalyzes a variety of biogeochemical reactions that transform Au and Pt. Studying these interactions from the nano- to the macro-scale requires a well-integrated set of tools ranging from field studies to micro-analytical, synchrotron- and omic approaches. Gold and Pt grains are rare, hard to find and getting access to prospecting sites often requires a great deal of 'field diplomacy'. To study biofilms living on grain surfaces, Au and Pt grains need to be collected under field-sterile conditions and frozen, refrigerated or fixed immediately after collection for genomic-, culturing- or electron microscopic studies, respectively. In particular, FIB-SEM-EBSD/EDXA has been useful in understanding the distribution and structure of biominerals and biofilms, as well as their effect on the (trans)formation of Au and Pt grains. In addition, FIB-SEM has been used to study analogue Au and Pt biominerals formed in laboratory experiments by organisms (i.e., *Cupriavidus metallidurans*) identified on Au grains. Synchrotron spectroscopy techniques (μ XRF, μ XANES and μ EXAFS) allow us to map the distribution and speciation of Au and Pt in individual *C. metallidurans* cells. This has led to an understanding of the fate of environmentally important mobile Au- and Pt-complexes (identified with HPLC-ICP-MS), upon contact with cells. To understand the reaction of cells to the toxic complexes transcriptome microarrays and 2-D SDS-PAGE was used. Important determinants of Au and Pt resistance and sensitivity were studied using deletion mutagenesis and (LA)-ICP-MS analyses of cells and proteins enriched in Au. Specific Au-binding proteins have been identified with MALDI-TOF-TOF, and can be used as biosensors for in field quantification of Au. To investigate the distribution of these important determinants in surface to depth environments high-density phylogenetic and functional microarrays (e.g., PhyloChip, GeoChip) are used. Understanding the determinants of biogeochemical cycling of Au and Pt may explain the formation of large supergene deposits have formed, and provide the basis for novel approaches in exploration, bio-hydrometallurgy and bio-remediation.

Quantifying the relative contribution of natural gas fugitive emissions to total methane emissions in Colorado, Utah, and Texas using mobile $\delta^{13}\text{CH}_4$ analysis

CHRIS W. RELLA^{*1}, RENATO WINKLE¹, ERIC CROSSON¹,
GLORIA JACOBSON¹, ANNA KARION²³,
GABRIELLE PETRON²³ AND COLM SWEENEY²³

¹Picarro Inc., 3105 Patrick Henry Drive, Santa Clara,
California 95054 USA. *correspondence:
rella@picarro.com

²National Oceanic and Atmospheric Administration, Earth
System Research Laboratory, Global Monitoring Division,
Boulder, CO, USA

³University of Colorado, Cooperative Institute for Research in
Environmental Sciences, Boulder, Colorado

Fugitive emissions of methane into the atmosphere are a major concern facing the natural gas production industry. Because methane is more energy-rich than coal per kg of CO_2 emitted into the atmosphere, it represents an attractive alternative to coal for electricity generation, provided that the fugitive emissions of methane are kept under control. A key step in assessing these emissions is partitioning the observed methane emissions between natural gas fugitive emissions and other sources of methane, such as from landfills or agricultural activities. One effective method for assessing the contribution of these different sources is stable isotope analysis, using the $\delta^{13}\text{CH}_4$ signature to distinguish between natural gas and landfills or ruminants. We present measurements of mobile field $\delta^{13}\text{CH}_4$ using a spectroscopic stable isotope analyzer based on cavity ringdown spectroscopy, in three intense natural gas producing regions of the United States: the Denver-Julesburg basin in Colorado, the Uintah basin in Utah, and the Barnett Shale in Texas. Mobile isotope measurements of individual sources and in the nocturnal boundary layer have been combined to establish the fraction of the observed methane emissions that can be attributed to natural gas activities. The fraction of total methane emissions in the Denver-Julesburg basin attributed to natural gas emissions is 78 +/- 13%. In the Uintah basin, which has no other significant sources of methane, the fraction is 96% +/- 15%. In addition, preliminary results in the Barnett shale, which includes a major urban center (Dallas), are presented.

Experimental characterization of replacement symplectites: The influence of temperature and small amounts of water on microstructure evolution

PATRICK REMMERT^{1*}, BERND WUNDER¹, LUIZ MORALES¹, WILHELM HEINRICH¹ AND RAINER ABART²

¹GFZ Potsdam, Telegrafenberg, 14473 Potsdam, Germany
(*patrick.remmert@gfz-potsdam.de)

²University of Vienna, Althanstrasse, 1090 Wien, Austria

Symplectite microstructures are a widespread phenomenon in a multitude of different parageneses in metamorphic rocks. The aim of this study is to characterize the formation of symplectites and to investigate experimentally the influence of temperature and water content on the evolution of symplectite microstructures.

Synthetic monticellite (Mtc) crystals with an excess forsterite (Fo) component of about 8 mole% were annealed in a piston-cylinder apparatus at 1.2 GPa, 950 - 1200°C, run durations of 5min - 24h and water contents of 0 - 1.0 wt.% H_2O using Al_2O_3 as a pressure medium. At these conditions Mtc breaks down into two types of fine-grained symplectite microstructures.

The two symplectite microstructures can be explained by two types of cellular segregation reactions: (a) The Mtc precursor phase (Mtc I) is replaced by a symplectite (type I) consisting of Fo rods in a Mtc matrix without excess Fo component (Mtc II). (b) A symplectite (type II) consisting of a lamellar intergrowth of merwinite (Mw) and Fo is formed. In both cases replacement of the Mtc precursor phase by the symplectite implies chemical diffusion within the advancing reaction front.

The lamellar spacing of both symplectites shows a strong temperature dependence. At identical run durations the spacing of Sy I increases from 450 nm at 1000°C to 1200 nm at 1100°C, whereas the Sy II spacing increases from 250 to 400 nm. Both symplectite microstructures could only be produced in experiments with at least minute amounts of water. Adding H_2O to the experiment strongly increases the reaction rate of the symplectite formation.

Applying the formalism introduced by Degi *et al.* [1] yields a diffusion coefficient for MgO and CaO within the reaction front of around $7 \cdot 10^{-13} \text{ m}^2/\text{s}$ for the formation of the Sy II indicating very fast diffusion inside the reaction front.

[1] Degi *et al.* (2009), *Cont. Min. Pet.*, **159**, 293–314

The vapour-brine partitioning of uranium in boiling ore systems

KIRSTEN U. REMPEL^{1*}, WILHELM HEINRICH²,
AXEL LIEBSCHER³ AND PETER DULSKI⁴

¹Dept. of Applied Geology, Curtin University, Australia
(*correspondence: kirsten.rempel@curtin.edu.au)

^{2,3,4}GFZ GeoForschungsZentrum, Potsdam, Germany

²(whsati@gfz-potsdam.de); ³(alieb@gfz-potsdam.de)

⁴(dulski@gfz-potsdam.de)

Uranium is found in ore systems associated with high-temperature H₂O-CO₂ fluids of probable magmatic origin, such as skarns and iron oxide-Cu-Au-U deposits. At P-T-X conditions of vapour-liquid (V-L) coexistence, the exsolved magmatic fluids undergo boiling, so uranium mobility in the ore fluid is dependent on its partitioning between V and L. In an experiment using a pressure vessel equipped with dual sampling lines, we have determined the partition coefficients ($D_{V/L}$) for U at 400°C between coexisting CO₂-rich vapour and NaCl brine. $D_{V/L}$ increases linearly from 1.5×10^{-4} to 2.0×10^{-1} , with increasing P from 263-356 bar.

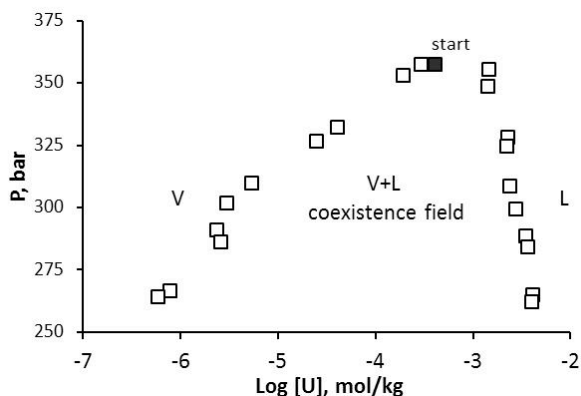


Figure: Uranium concentrations in vapour and liquid sample pairs taken at equivalent P, from a starting P-T-X of 356 bar, 400°C, and bulk composition of 4.2×10^{-4} m (100 ppm) U, 2.3 m CO₂ and 0.5 m NaCl (filled square).

The results of this study suggest that boiling may be instrumental to the production of zoned uranium orebodies, as the majority of U is carried in the denser brine rather than in the coexisting CO₂-rich vapour. However, at conditions approaching the critical curve, increasing concentrations of U are partitioned into the vapour (e.g., 1% of the total U at 325 bar, rising to 20% at 357 bar). This study presents the first experimental data on the V-L partitioning of U and its mobility in H₂O-CO₂ vapour.

Different D-rich organic reservoirs in unequilibrated ordinary and carbonaceous chondrites

LAURENT REMUSAT¹, SYLVAIN BERNARD¹,
LAURETTE PIANI², JEAN-YVES BONNET³
AND ERIC QUIRICO³

¹LMCM, UMR CNRS 7202, MNHN, Paris, France

²CRPG, UMR CNRS 7358, Université de Lorraine, France

³IPAG, UMR CNRS 5274, UJF, Grenoble, France

Insoluble organic matter (IOM) contained in chondrites is known to host large D-enrichments [1]. The distribution of D in carbonaceous chondrites (CC) appears to be heterogeneous at the sample, micrometer and molecular scales [1-3]. The isotopic signature is influenced by primary (pre-accretional) processes, including low temperature chemistry occurring in the outer protosolar nebula or in the parent molecular cloud [4] and secondary processes during the evolution of the parent body [1]. On the other hand, the distribution of D in the IOM of ordinary chondrites (OC) remains cryptic. Most of the OC have been subjected to thermal metamorphism. Surprisingly, the D-content of IOM in OC and CC exhibit an opposite evolution with increasing temperature of the parent body [1]. While more high temperature CC have a lower D/H compared to pristine or hydrated CC, the D/H ratio of OC IOM increases with increasing temperature.

To better understand this striking observation, we have subjected the IOM of Orgueil (CC) and GRO 95502 (OC) to thermal heating without oxygen (pyrolysis). Then, we have evaluated the evolution of each IOM upon heating by NanoSIMS (to assess the D/H distribution), STXM (molecular structure) and Raman (organization degree). In CC, the D-content decreases, while in the meantime the IOM undergoes the carbonization process (loss of heteroatoms and formation of larger aromatic structures). In OC, the D/H ratio increases likely due to the loss of a D-depleted organic component.

We conclude that in CC the D-rich organic component is thermally sensitive whereas in OC it is thermally refractory. This clearly indicates different organic moieties that may have distinct origins. Organic radicals were suggested to be the carrier of the D-excess in CC [3]. In OC, another organic component, yet unidentified has to be invoked. It might have been formed in the interstellar medium [4]. The opposite behavior of the organic D-rich component in CC and OC may induce distinct evolutions of the D/H of their IOM upon thermal metamorphism.

[1] Alexander *et al.* 2010 *GCA*, **74**, 4417-4437. [2] Remusat *et al.* 2006 *EPSL*, **243**, 15-25. [3] Remusat *et al.* 2009 *ApJ*, **698**, 2087-2092. [4] Aléon 2010 *ApJ*, **722**, 1342.

Groundtruthing the nitrogen isotopic composition of planktonic foraminifera as a paleobiogeochemical proxy

H. REN^{1*}, D.M. SIGMAN², K.K. ELLIS², M.A. WEIGAND², R.F. ANDERSON³, A.C. RAVELO⁴, M.A. ALTABET⁵, S.E. FAWCETT² AND P.A. RAFTER²

¹RCEC, Academia Sinica, Taipei 115, Taiwan

(*correspondence: abbyren@gate.sinica.edu.tw)

²Dept. of Geosciences, Princeton Uni., Princeton, NJ 08544, USA (sigman@princeton.edu)

³LDEO, Columbia Uni., Palisades, NY 10968, USA (boba@ldeo.columbia.edu)

⁴EPS, Univ. of California, Santa Cruz, CA 95064, USA (acr@es.ucsc.edu)

⁵DEOS, Uni. Of Massachusetts, Dartmouth, New Bedford, MA 02744-1221 (maltabet@umassd.edu)

The nitrogen isotopic composition of the organic matter trapped within the calcite shells of planktonic foraminifera (FB- $\delta^{15}\text{N}$) has been explored as a new proxy in ocean sediment records to reconstruct past changes in the marine nitrogen cycle, but information on its generation and preservation is so far minimal. In this study, we report measurements of the $\delta^{15}\text{N}$ of foraminiferal biomass from Sargasso Sea net tow material and shell-bound N from shallow sediments collected in different open ocean regions. The annual average biomass $\delta^{15}\text{N}$ of three euphotic zone dwelling species, *G. ruber*, *G. sacculifer*, and *O. universa* in the Sargasso Sea surface is around 2‰, similar to but slightly lower than the thermocline nitrate $\delta^{15}\text{N}$, as well as their shell-bound $\delta^{15}\text{N}$ in the surface sediment. We observe large seasonal variations in the biomass $\delta^{15}\text{N}$. $\delta^{15}\text{N}$ is lowest in fall to winter, followed by a $\delta^{15}\text{N}$ rise during the spring bloom. Our global data set of FB- $\delta^{15}\text{N}$ from surface sediments in the oligotrophic regions shows a strong correlation between FB- $\delta^{15}\text{N}$ and changes in the subsurface nitrate $\delta^{15}\text{N}$, which is the dominant source of new N to the euphotic zone. In the subarctic North Pacific and the eastern equatorial Pacific, where nitrate is abundant at the surface, FB- $\delta^{15}\text{N}$ in the surface sediment closely tracks changes in surface nitrate $\delta^{15}\text{N}$ and is thus anticorrelated with nitrate concentration. These results are strong evidence that FB- $\delta^{15}\text{N}$ is a reliable proxy for tracing the $\delta^{15}\text{N}$ of the N supply to surface waters in oligotrophic regions and for reconstructing surface nitrate utilization in high-nutrient regions. We will also examine the interspecies differences in terms of depth habitat and trophic level.

Heavy metal availability in contaminated soils: complementary insights from isotopic exchange, DMT, and sequential extractions

Z. L. REN^{1,2}, J. DAI², Y. SIVRY¹ AND M. F. BENEDETTI^{1*}

¹Université Paris Diderot- Sorbonne Paris Cité - IPGP, UMR CNRS 7154, Paris, France 75205 (*correspondence: benedetti@ipgp.fr)

²College of Resources and Environment, South China Agricultural University, Guangzhou, China 510642

Contaminated calcareous topsoils were sampled from paddy fields around a lead/zinc mine in Lechang, Guangdong Province, South China. The soil pH was 7.8, total heavy metal contents were 768 mg Pb kg⁻¹, 715 mg Zn kg⁻¹, 58.7 mg Cu kg⁻¹ and 22.6 mg Ni kg⁻¹.

Donnan membrane technique (DMT) and stable isotopic exchange kinetic (SIEK) technique were performed to determine the concentration of free metal ion (FMI) in soil solution and the available metal pool (isotopically exchangeable metal, *E* value) in soil. Traditional sequential extractions were also used to assess the metal distribution among the geochemical compartments of soil solid phase.

DMT results showed that quite few FMIs were presented in the soil solutions. At soil:solution ratio = 100 g L⁻¹, the total dissolved Pb, Zn, Cu, Ni were only 0.91, 3.29, 3.34, 0.07 µg L⁻¹, while large proportion of Pb, Cu and Ni were complexed. A good agreement was found between the FMIs concentration measured by experiments and calculated by NICA-Donnan model.

However, multi-SIEK results indicated that the isotopically exchangeable pool of Pb, Cu and Zn were large. After 12-day equilibrium, E_{Pb} , E_{Cu} , and E_{Zn} value were 302, 13, and 106 mg kg⁻¹, which were up to 39%, 22% and 15% of metal total content, respectively. In contrary, E_{Ni} value was only 1 mg kg⁻¹ (i.e. 1.5% of total Ni).

Combined with the metal distribution in solid phases given by sequential extractions, the larger Pb available pool may be attributed to the high carbonate-bound and Mn oxides-bound fractions. A large proportion of Ni in the so-called residual fraction (i.e. 75% of total Ni) may explain the lower E_{Ni} .

Therefore, such combination of different techniques can give a more comprehensive insight into the heavy metal availability, thus it can provide implications to risk assessment and long term remediation.

Broader impacts of geochronology

PAUL R. RENNE*^{1,2}

¹Berkeley Geochronology Center, 2455 Ridge Rd., Berkeley, CA 94709, USA (*correspondence: prene@bgc.org)

²Dept. Earth and Planetary Science, Univ. California, Berkeley, CA 94720, USA

Few Earth and/or planetary scientists need convincing that geochronology is fundamentally important to quantitative knowledge of planetary and biotic evolution. However, to non-scientists or even scientists from other disciplines, geochronology may be perceived as an esoteric or arcane pursuit with little “practical” value. On the contrary, geochronology plays a vital role in mineral and petroleum resource exploration. Perhaps less well-known outside the Earth science community are applications to natural hazard evaluation, particularly those due to volcanism and seismicity. In validating the cyclic orbital forcing of earth’s climate, geochronology facilitates the discrimination of anthropogenic versus endogenous climate change, and permits quantification of the rate of change. Geochronology has even played a critical role in nuclear forensics. It is fair to anticipate that technological innovations will continue to improve the precision and scope of various geochronometric techniques in the future. Consequently, geochronology will likely have increasing importance to societal issues in addition to underpinning new discoveries about how the Earth works and interacts with the rest of our Solar System.

Stepwise calibration of the Alder Creek sanidine ⁴⁰Ar/³⁹Ar dating standard to the historical 79 CE eruption of Vesuvius

RENNE*^{1,2}, PAUL R. AND DEINO², ALAN D.

¹Berkeley Geochronology Center, 2455 Ridge Rd., Berkeley, CA 94709, USA (*correspondence: prene@bgc.org)

²Dept. Earth and Planetary Science, Univ. California, Berkeley, CA 94720, USA

Interlaboratory variations in argon isotope data for standards remains a significant problem for ⁴⁰Ar/³⁹Ar geochronology. A bellweather for the problem is the ca. 1.2 Ma Alder Creek sanidine (ACs) standard, for which a range of ca. 2 % in ⁴⁰Ar*/³⁹Ar_K has been reported by various laboratories. To address this problem we are calibrating ACs against sanidine (79Vs) from the 79 CE eruption of Vesuvius, whose age is known from analysis of the writings of Pliny the Younger and other sources to within 3 months [1] in 1934 years, i.e., a relative uncertainty of ±0.013%. Direct calibration of ACs against 79Vs involves measuring a ratio of ⁴⁰Ar/³⁹Ar (R'-ACs/79Vs) between the two samples of ca. 600, which admits the possibility of bias from detector non-linearity and differential sensitivity to memory. Hence we use a third sample (X) of intermediate age to provide a stepping stone between ACs and 79Vs and make use of the fact that (R'-ACs/79Vs) = (R'-ACs/X) × (R'-X/79Vs). Neglecting atmospheric ⁴⁰Ar, the optimal values of (R'-ACs/X) = (R'-X/79Vs) = 24, corresponding to an age of ca. 46 ka. Accordingly, we have selected sanidine from the ca. 40 ka Campanian ignimbrite (CIs) in the Campi Flegrei as the stepping stone. Previous studies of CIs have yielded satisfactory reproducibility and no evidence of extraneous argon. Preliminary data suggest that this approach will yield a value of (R'-ACs/79Vs) with <2% relative uncertainty, hence will contribute to clarifying the absolute age of ACs.

[1] Rolandi *et al.* (2007), *JVGR* **16**, 87-98.

A new Cenozoic Record of Sulfur Isotopes from Foraminiferal Calcite.

VICTORIA RENNIE^{1*}, GUILLAUME PARIS²,
JESS F. ADKINS² AND ALEXANDRA V. TURCHYN¹

¹Department of Earth Sciences, University of Cambridge,
Cambridge CB2 3EQ, UK, vcr22@cam.ac.uk (*presenting
author)

²Dept. of Geology and Planetary Sciences, Caltech, Pasadena,
CA, USA

The sulfur isotope composition of marine sulfate ($\delta^{34}\text{S}_{\text{SO}_4}$) reflects the balance between the weathering and burial fluxes of both evaporite minerals and pyrite, and their isotopic composition. These are the dominant fluxes into and out of the marine sulfur cycle, and thus a change in the seawater $\delta^{34}\text{S}_{\text{SO}_4}$ would reflect a change in the global sulfur cycle. The importance of the sulfur cycle lies in its potential to help elucidate the subsurface remineralization of organic carbon and, indirectly, the oxidation state of Earth's surface environment.

Reconstructions of seawater $\delta^{34}\text{S}_{\text{SO}_4}$ have previously been made using marine barite (limited to the past 130Ma) and discontinuous evaporite deposits. However, carbonate-associated sulfate (CAS), sulfate that has been incorporated into the carbonate lattice, has potential to act as an alternative archive for seawater S-isotope history and can provide information on regional and global variations in the S-cycle over geological time.

We present CAS $\delta^{34}\text{S}_{\text{SO}_4}$ results from single species foraminifera, using a new sulfur isotope analytical technique optimised for mass limited samples [1]. We report an interspecies variability of up to 1‰ in planktonic forams and a large decrease in $\delta^{34}\text{S}_{\text{SO}_4}$ variability upon the choice of shell cleaning. This method also allows us to identify contaminant phases with greater ease than in bulk studies. Our $\delta^{34}\text{S}_{\text{SO}_4}$ record for the Cenozoic, using a species-specific approach, is in agreement with the coeval barite $\delta^{34}\text{S}_{\text{SO}_4}$ record, engendering confidence in CAS as a proxy for $\delta^{34}\text{S}_{\text{SO}_4}$.

[1] Paris *et al.* (2013) *Chemical Geology*, **345**, 50-61.

Past and present impact of mining activity on metal and metalloid contamination in sediments of the Gardon River watershed (France)

ELEONORE RESONGLES^{1*}, CORINNE CASIOT¹, REMI FREYDIER¹, LAURENT DEZILEAU², JEROME VIERS³
AND FRANÇOISE ELBAZ-POULICHET¹

¹Hydrosociences UMR 5569, CNRS Universités Montpellier I and II IRD, Montpellier, France,
eleonore.resongles@univ-montp2.fr (* presenting author)

²Géosciences UMR 5243, CNRS Université Montpellier II,
Montpellier, France

³Géosciences Environnement Toulouse UMR 5563,
CNRS Université Paul Sabatier IRD, Toulouse, France

Contamination of river sediments by metal(loid)s originating from mining activity is a worldwide problem. Because the transport of metals associated with sediments can represent more than 90% of the total flow of metals in rivers, identify their sources and evaluate their potential mobility are particularly important.

The purpose of this work was to assess past and present influence of mining activity on metal(loid) enrichment in sediments of a former mining watershed now industrialized and urbanized, the Gardon River watershed (France).

Samples of a sedimentary archive and current sediments of the Gardon River and its tributaries were characterized combining geochemical analyses, zinc isotopic analyses and sequential extractions.

Considering metal(loid) concentrations in sediments upstream from the mining sites and in bottom sediments of the archive, natural background values were proposed. Based on these values, enrichment factors (EF) were calculated. Several tributaries were highly impacted by old mining sites (EF values up to 250 for Pb, 160 for Cd, 60 for Zn, 70 for As and 1850 for Sb) and by industrial activity. These polluted tributaries impacted metal(loid) content of the main stream sediments. EF values increased in Gardon River sediments downstream from old Pb/Zn mines about 3-fold for Pb, Cd and 2-fold for Zn, As and downstream from old Sb mines about 5-fold for Sb. Interelement relationships were used to distinguish the main contaminant sources. Although Zn isotopic signatures differed significantly for mining impacted tributaries ($\delta^{66}\text{Zn} \sim 0.08\text{‰}$) and for industrial impacted tributary ($\delta^{66}\text{Zn} \sim 0.31\text{‰}$), Zn isotopic composition remained homogeneous in the main stream sediments of the Gardon River watershed ($\delta^{66}\text{Zn}$ values around 0.20‰). Finally, the percentage of metal(loid)s present in the "mobile" pool, as estimated by sequential extraction, was: Sb (1-5%) < As (1-22%) < Zn (10-65%) = Pb (15-68%).

Quantification of the role of orbital and millennial timescale processes on $\delta^{18}\text{O}$ and $^{17}\Delta$ signals

CORENTIN REUTENAUER¹, AMAËLLE LANDAIS²,
MARIE-NOËLLE WOILLETZ³, CAMILLE RISI⁴,
PASCALE BRACONNOT², THOMAS BLUNIER¹, VERONIQUE
MARIOTTI² AND MASA KAGEYAMA²

¹Centre for Ice and Climate, Niels Bohr Institute, University of Copenhagen, Juliane Maries Vej 30, DK-2100 Copenhagen Ø, Denmark (creuten@nbi.ku.dk)

²Institut Pierre-Simon Laplace/Laboratoire des Sciences du Climat et de l'Environnement, LSCE/IPSL, UMR CEA-CNRS-UVSQ 8212, CE Saclay, L'Orme des Merisiers, 91191 Gif-sur-Yvette Cedex, France

³EPHE, UMR CNRS 5805 EPOC - Université Bordeaux 1 Avenue des Facultés, 33405 Talence (France)

⁴Laboratoire de Météorologie Dynamique, Jussieu, Paris, France

The triple isotope composition of atmospheric oxygen ($\delta^{18}\text{O}$, $^{17}\Delta$) integrates the signature of various mass dependent processes associated with hydrological cycle, biological cycle and non mass dependent photochemical reactions in the stratosphere, both on orbital and millennial timescales: changes in global seawater, hydrological cycle, relative humidity, vegetation distribution and C3/C4 plants partition. At the orbital timescale, tropospheric $\delta^{18}\text{O}$ bears a strong orbital precession signal while at the millennial timescale, $\delta^{18}\text{O}$ depicts a clear decrease in phase with Greenland InterStadial events. $^{17}\Delta$ ($\ln(\delta^{17}\text{O}+1) - \lambda * (\delta^{18}\text{O}+1)$) is more directly related to variations in the global biospheric productivity with a main variability associated with the glacial – interglacial changes.

Here we make use of a global model integrating changes in climate, biosphere productivity, water isotopic composition to quantify the contribution of the different processes to $\delta^{18}\text{O}$ and $^{17}\Delta$ signals at relevant orbital periods (snapshots of pre-industrial period, Last Glacial Maximum (LGM), Heinrich event). The model accounts for the latest fractionation ratios between $^{18}\text{O}/^{16}\text{O}$ and $^{17}\text{O}/^{16}\text{O}$ associated with oxygen respiration processes and leaf transpiration, oceanic net primary production (simulated by PISCES model), the spatial and temporal variation of vegetation distribution (simulated by ORCHIDEE model), climatic conditions and isotopic composition of meteoric water and water vapor (LMDZ global circulation model)

Bacterial diversity in Baltic Sea sediments from Skagerrak and Bothnian Bay

CAROLINA REYES^{1*}, OLUWATOBI ONI¹,
OLAF DELLWIG², MICHAEL E. BÖTTCHER²
AND MICHAEL W. FRIEDIRCH¹

¹Leobener Strasse, NW2, D-28359 Bremen, Germany
(*correspondence: reyes@uni-bremen.de)

²Leibniz-Institute for Baltic Sea Research, Seestrasse D-18119 Rostock, Germany

The biogeochemical cycling of iron is a key process in terrestrial and aquatic systems including marine environments. However, limited information exists about the diversity and metabolic pathways of microorganisms linked to the iron cycle in ocean sediments. The goal of this study was to determine the bacterial community diversity in sediment samples from Skagerrak (SK) and Bothnian Bay (BB) using pyrosequencing as a first step in characterizing microorganisms potentially involved in iron reduction at these two sites. DNA was extracted from various depths from sediments collected in SK and BB. Porewater profiles of relevant electron acceptors showed that sulfate was ~28 mM and ~2 mM in SK and BB sediments, respectively. H_2S was below detection in both sediments, and Fe^{2+} and Mn^{2+} levels reached ~140-150 μM in SK sediments between 6-7 cm depth and ~300 μM within the first 2 cm in BB sediments. V1-V3 regions of the 16S rRNA gene were used for 454 titanium pyrosequencing and sequences were analyzed using QIIME (1). Proteobacteria dominated these sediments and potential iron- and manganese-reducing bacteria included *Desulfurmonadales*, *Alteromonadales*, *Geobacteraceae*, *Pelobacteraceae*, *Shewanellaceae*, *Myxococcales*, *Oceanospirillales*, and *Campylobacterales*. Additionally, *Actinobacteria*, and *Bacteroidetes* were also dominant. These results imply that marine systems are likely to harbor more metabolically diverse iron and manganese reducing microorganisms than the traditional *Shewanella* and *Geobacter* model systems.

[1] Caporaso *et al.* (2010). Nature Methods, **7**: 335-336

Igniting flare-up events in Sistan Suture Zone, Iran

M. REZAEI-KAHKHAEI¹ AND F. CORFU

¹Department of Geoscience, Shahrood University, Iran
(*correspondence: Rezaei@shahroodut.ac.ir)

²Department of Geosciences, University of Oslo, PB 1047
Blindern, N-0316 Oslo, Norway
(fernando.corfu@geo.uio.no)

Sistan Suture Zone (SSZ) was undergone a number of important short-lived tectonic events from the middle Cretaceous to recent: (i) rifting of a large continental mass in the middle Cretaceous produced the Lut and Afghan blocks with an intervening marine basin (flysch) accumulated; (ii) northeastward subduction under the Afghan block by the Maastrichtian; (iii) collision between the Lut and the Afghan blocks terminated subduction by the middle Eocene; and continued convergence between the Lut and Afghan blocks resulted in widespread conjugate strike-slip faulting [1]. Zahedan–Saravan granitoides are parts of SSZ and occurred after closure of the ocean with a northwest–southeast trend (figure). The granitoides can be separated into two groups based on detailed age, major and trace-element geochemistry and field work. They are dominated by biotite granites at about 50km away from subduction place (ophiolitic rocks) with ~ 43Ma in age and granodiorites at 70-90km away from subduction place with 30Ma in age. The granitoides were cut by lots of andesitic and rhyolitic dykes at ~ 29Ma before they completely cold. U–Pb dating and geochemical analyses reveal: (1) a shift between the ages of biotite granites near the subduction place and the granodiorites farther than biotite granites from the subduction place; (2) Relative to granodiorites, biotite granites are richer in CaO, MgO, TiO₂, Ni, Cr, Co, Zr, Yb, Cs and Lu; and (3) an apparent flare-up in the SSZ from 43 to 29Ma.

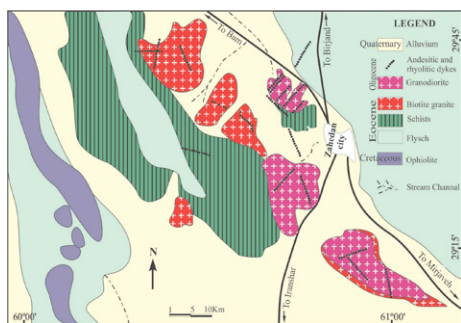


Figure: Geological map of Zahedan–Saravan granitoides.

[1] Tirrul *et al.* (1983) *Geol Soc Am Bull* **94**, 134-150.

Dependence of Sulfur Cycling and Mobility in Peat Soil on the Water Table Regime

F. REZANEZHAD^{1*}, R-M. COUTURE^{1,2},
C. PARSONS¹, R. KOVAC¹, D. O'CONNELL¹
AND P. VAN CAPPELLEN¹

¹Ecohydrology Research Group, University of Waterloo,
Waterloo, Canada (*correspondence:
frezanez@uwaterloo.ca)

²Norwegian Institute for Water Research, Oslo, Norway

Water table fluctuations change the soil redox environment and hence, affect the metabolism of electron donors and acceptors by the native microbial community. To investigate the role of water table dynamics on biogeochemical transformations and fluxes in soils, an automated column system was developed to simulate the interactions between groundwater and surface waters under controlled conditions. In this system, the position of the water table is imposed using a computer-controlled, multi-channel pump connected to a hydrostatic equilibrium reservoir and a water storage reservoir. We compared two water table regimes: i.e., fast (4 days) vs. slow (16 days) water table fluctuations. The pulse of oxygen introduced by lowering the water table caused a partial and temporal oxidation of previously reduced species. As expected, draining and rewetting of the soil columns resulted in a significant re-oxidation of reduced sulfur species, changes in pore water SO₄²⁻ concentration and microbial sulfate reduction rates. However, the dual-porosity structure of the peat soil was found to strongly modulate the sulfur cycling and mobility. This study supports the importance of water table dynamics and soil texture on biogeochemical functioning of peat soil environment.

Caprock's nanoporous structure modification by supercritical CO₂/water interaction: A contribution of adsorption techniques

D. RHENALS^{1,2}, S. LAFORTUNE¹, H. SOULI²
AND P. DUBUJET²

¹French National Institut for Industrial Environment and Risks, Parc Technologique Alata, BP 2, Verneuil-en-Halatte, 60550, France-david-rhenals@ineris.fr

²National School Engineers of Saint Etienne, 58 rue Jean Parot, Saint-Etienne, France

CO₂ storage is envisioned as a technique which reduces large quantities of CO₂ rejected in the atmosphere because of many human activities.

The effectiveness of this technique is mainly related to the storage capacity as well as its safety. The safety of this operation is primarily based on the conservation of petro-physical properties of the caprock, which prevents the transport of CO₂ through it. However when CO₂ reaches the reservoir/caprock interface due to buoyancy effects, the interaction between interstitial fluid and injected fluid creates a series of dissolution/precipitation reactions affecting the properties of containment of the caprock, which is generally characterized by low transport properties.

This study aims to assess the impact caused by CO₂/interstitial fluid interaction on the nanostructure of the caprock under geological storage conditions. In order to do this, degradation experiments in a well characterized shale have been conducted using batch reactors for two months.

Adsorption-desorption isotherms showed an increase in the sorption capacity as well as a variation on pore size distribution. BJH and Dubinin Stoeckli distributions showed an increase in porous density lower than 10 nm, which is mainly attributed to dissolution of carbonates and some aluminosilicates detected initially with XRD techniques. Chemical water analysis showed an increase in Ca, Mg, Na, K, Si concentration, which is consistent with porous structure variation determined by physical adsorption.

Composition of the shallow aqueous fluids released beneath the SE Mariana Forearc Rift

JULIA RIBEIRO¹, ROBERT J. STERN¹,
KATHERINE A. KELLEY², ALISON SHAW³,
FERNANDO MARTINEZ⁴ AND YASUHIKO OHARA⁵

¹Geosciences, University of Texas at Dallas, USA.

²GSO, University of Rhode Island, USA.

³Depart. of Geology and Geophysics, WHOI, USA.

⁴SOEST, University of Hawai'i at Manoa, USA.

⁵Hydrographic and Oceanographic Depart. of Japan, Japan.

Fluids released from subducted slabs are thought to be more aqueous beneath forearcs than are the fluids released beneath arc volcanoes; however, investigating their composition is challenging as the cold forearc mantle generally does not melt. Basaltic lavas of the Southeast Mariana forearc rift (SEMFR) provide an unusual opportunity to examine basalts affected by such fluids. SEMFR extends from arc volcanoes nearly to the Mariana trench and was generated by forearc seafloor spreading ~2.7–3.7 Ma ago. SEMFR basalt compositions are similar to backarc basin basalts and contain olivines with unusually depleted basaltic melt inclusions. These OL-MI were captured by unusually refractory olivines (Fo₉₀₋₉₃), and we interpret them to have formed as hydrous melts trapped in the forearc mantle. Fragments of this mantle (OL xenocrysts and Cr-spinel) were entrained with SEMFR basalt magmas during their ascent. SEMFR glassy rinds and Ol-MI have variable volatile contents (mean H₂O=1.85±0.26 wt%, S=757±109 ppm, Cl=334±169 ppm, F=94±31 ppm, CO₂=144±137 ppm). SEMFR Ol-MI and their host basaltic glassy rinds have unusually high ratios of volatiles and fluid-mobile elements (FMEs; mean H₂O/Ce=10096±3901, Cl/Nb=1238±516, Cs/Th=6±5, Ba/Th=523±203, Rb/Th=79±38 for the Ol-MI; and mean H₂O/Ce=4953, Cl/Nb=838, Cs/Th=0.84±0.66, Ba/Th=265±97, Rb/Th=27±14 for the glassy rinds) ever recorded in the Mariana intraoceanic arc (mean H₂O/Ce=1705±1125, Cl/Nb=429±414, Cs/Th=0.39±0.16, Ba/Th=264±150, Rb/Th=15±3), indicating that the shallow fluids have distinctive FMEs/Th and volatile/incompatible ratios. SE-NW gradient in these ratios demonstrate that the aqueous fluids and the volatile fluxes are the highest at ~50–100 km slab depth, suggesting that hydrous minerals in the subducted slab mostly break down beneath the arc.

Contact-metamorphic effects of the Santa Eulália Plutonic Complex (Southern Portugal): Litological and structural constraints

RIBEIRO, M.A.^{1(*)}, SANT'OVAIA, H.¹ AND CRUZ, C.¹

¹Centro Geologia, Faculdade de Ciências, Univ. Porto R.
Campo Alegre, 4169-007 Porto, Portugal
(*correspondence maribeir@fc.up.pt)

The Santa Eulália Plutonic Complex (SEPC) is a late-variscan granitic pluton in SW sector of the Iberian Orogen. This granite with 400 km² cross-cuts the regional NW-SE variscan structures, namely a major high-grade and high-strain shear zone in the contact between two axial geotectonic zones of the Iberian variscan belt. The host rocks of SEPC are composed by low to high grade metamorphic rocks from Upper Proterozoic to Lower Paleozoic. In the NE-sector of the shear zone a low grade metasedimentary Ediacaran unit (Série Negra) composed by siliciclastic rocks, including black cherts, is located adjacently to a high grade unit (migmatites and gneiss). In the SW-sector of the shear zone, a low-grade metasedimentary and metavolcanic Cambrian sequence has quartz-pelitic, carbonate and volcanic rocks. The lithostratigraphic units are also tectonic units bounded by major high-strain transcurrent faults placing side by side different rock types and different metamorphic grades, but always characterized by a well-developed vertical foliation. Both at east or at west, the host rocks are phyllite and quartz-phyllite, in chlorite zone conditions, without any thermal effects even at short metric distance from the contact. The metapelitic rocks show millimetric veins (2mm thick) with biotite, quartz, chlorite and apatite, concordant with foliation, without exhibiting any thermal effects on the walls. The Cambrian carbonate rocks outcropping in narrow bands near the ESE border of SEPC did not show any post-kinematic thermal effect. Unlike, in the western sector of SEPC the thermal effect is marked in the metasedimentary roof pendants, by metamorphic and metasomatic paragenesies in pelitic and carbonate hornfels, the later with large wollastonite crystals.

Our results highlight that the thermal effects of the SEPC in the host rocks are restricted to the roof pendants and the metasomatic effects are constrained by the carbonate rocks. The shape of the pluton, the absence of lateral thermal effects, the smooth bend of the vertical host rocks around the pluton in eastern border suggest a small thickness of the massif in the western border, and a deep rooting in the major vertical shear zone at the eastern border.

This work has been financially supported by PTDC/CTE-GIX/099447/2008 (FCT-Portugal, COMPETE/FEDER).

Diverse capacity for 2-methylhopanoid production correlates with specific niches

JESSICA N. RICCI¹, MAUREEN L. COLEMAN¹, PAULA V. WELANDER², ALEX L. SESSIONS¹, ROGER E. SUMMONS², JOHN R. SPEAR³ AND DIANNE K. NEWMAN^{1,4*}

¹California Institute of Technology, Pasadena, CA 91125, USA (jricci@caltech.edu, mlcoleman@uchicago.edu, als@gps.caltech.edu, correspondance: dkn@caltech.edu)

²Massachusetts Institute of Technology, Cambridge, MA 02139, USA (welande@standford.edu, rsummons@mit.edu)

³Colorado School of Mines, Golden, CO 80401, USA (jspear@mines.edu)

⁴Howard Hughes Medical Institute, Pasadena, CA 91125, USA

Molecular fossils of 2-methylhopanoids (2-MeBHPs) are important geological biomarkers and have often been interpreted as proxies for cyanobacteria and their main metabolism oxygenic photosynthesis [1]. However, substantial culture and genomic-based evidence indicates that organisms other than cyanobacteria can make 2-MeBHPs [2, 3]. Yet, these lines of evidence do not address which organisms produce 2-MeBHPs in the environment. In this study, we use metagenomic and clone library methods to address the environmental diversity of *hpnP*, the gene encoding the C-2 hopanoid methylase. We show that *hpnP* copies from alphaproteobacteria and unknown origin are found in diverse modern environments, including some representative of those preserved in the rock record, while cyanobacterial *hpnP* genes are more rare and localized to specific habitats. Moreover, *hpnP* diversity in any given locale can be spatially and temporally heterogeneous, stressing the need to sample environments rigorously before drawing general conclusions. Additionally, we asked if *hpnP* is overrepresented in organisms or environments with a specific metabolism or associated with a particular niche. We found the presence of *hpnP* to be significantly correlated with organisms and environments known to support plant-microbe interactions. Our results indicate that 2-MeBHPs can no longer be used as unambiguous biomarkers for cyanobacteria and hints at a potential interpretation for 2-MeBHPs separate from oxygenic photosynthesis that underpins the observed enrichment of *hpnP* in these contexts.

[1] Summons *et al.* (1999) *Nature* **400**, 554-557. [2] Rashby *et al.* (2007) *PNAS* **104**, 15099-15104. [3] Welande *et al.* (2010) *PNAS* **107**, 8537-8542.

Thermodynamic analysis of water-rock-hydrocarbon interactions in petroleum systems

LAURENT RICHARD

Geoquímics dels Àngels, Carrer dels Àngels 4-2-1,
08001 Barcelona, Spain

Throughout their evolution across the crust of the Earth, minerals and organic compounds interact in many geological processes ranging from the low-temperature early diagenesis of marine sediments to the metamorphism of pelitic schists. The geochemical cycles of iron, sulfur or nitrogen (among other elements) are governed by such interactions, which correspond to oxidation-reduction reactions. Well-documented examples include the decarbonation of siderite in the presence of carbonaceous matter [1], the formation of sulfur-rich organic matter in carbonate sediments [2], or the exchange of nitrogen isotopes among petroleum and clays in clastic reservoirs [3].

It is the purpose of the present communication to illustrate how thermodynamic properties published for solid and liquid hydrocarbons and sulfur- and nitrogen-bearing compounds of geochemical interest [4,5] can be used to develop quantitative models for the evolution of water-rock-hydrocarbon systems, as well as to make reasonable estimates regarding the composition of petroleum fluids as a function of temperature, pressure, the fugacities of CO₂, H₂S, NH₃ and H₂, and their mineralogical and aqueous environment. Conversely, I will show how compositional data for crude oils can in some instances be used to evaluate or retrieve thermodynamic data.

[1] French B.M. (1971) *Am. J. Sci.* **271**, 37-78. [2] Gransch J.A., Posthuma J. (1974) *Adv. Org. Geochem.* 1973, 727-739. [3] Williams L.B. *et al.* (1995) *Geochim. Cosmochim. Acta* **59**, 765-779. [4] Helgeson H.C. *et al.* (1998) *Geochim. Cosmochim. Acta* **62**, 985-1081. [5] Richard L., Helgeson H.C. (1998) *Geochim. Cosmochim. Acta* **62**, 3591-3636.

The role of arc magmas and subduction-modified lithosphere in ore formation

JEREMY P. RICHARDS¹

¹Dept. Earth and Atmospheric Sciences, University of Alberta,
Edmonton, Alberta, Canada, T6G 2E3
Jeremy.Richards@ualberta.ca

Arc magmas are a unique source of subduction-derived volatiles (water, sulfur, and chlorine: mostly derived from seawater-altered oceanic lithosphere), plus water-soluble elements (alkalis and large-ion lithophile elements) and chalcophile and siderophile metals. Upon emplacement in volume in the upper crust, these magmas may generate porphyry Cu±Mo±Au and epithermal Au±Cu deposits. However, during their ascent through the upper plate lithosphere, they interact with these rocks to form hybrid calc-alkaline magmas, and fractionate to leave ultramafic to mafic, amphibolitic cumulate residues at the base of the crust (MASH process of Hildreth and Moorbath, 1988).

Over the life of an arc (typically ≤10–15 m.y.), the mantle wedge above the subduction zone becomes increasingly hydrated and oxidized as slab fluids cause progressive metasomatism, leading to partial melts that also increase in water content and oxidation state over time. Early primitive magmatic fluxes entering the upper plate lithosphere may leave considerable amounts of metals behind in cumulate zones as sulfides separated from relatively reduced (ΔFMQ ≈ 0) magmas (Lee *et al.*, 2012). However, increasing oxidation state in later magmas (ΔFMQ ≈ 1–2) suppresses sulfide-saturation, and leads to efficient transport of metals in magma fluxes reaching the upper crust (Botcharnikov *et al.*, 2011). Consequently, major porphyry-forming events are commonly relatively late in the evolution of a given arc.

The deep crustal residues of arc magmatism are relatively fusible (amphibole-rich) and likely contain small amounts of metal sulfides. Re-melting of these residues during later tectonic events, such as collision or rifting, may generate metalliferous magmas with similar chemical and isotopic characteristics to normal arc magmas, which may go on to form post-subduction porphyry Cu±Mo±Au deposits. Their derivation from partial melting of deep crustal garnet-amphibolites gives these magmas adakite-like high Sr/Y and La/Yb ratios, but they are not formed by slab melting.

Botcharnikov *et al.*, 2011: *Nature Geoscience* 4: 112–115.
Hildreth & Moorbath, 1988: *Contrib. Min. Pet.* 98:455–489.
Lee *et al.*, 2012: *Science* 336: 64–68.

Rhizogenic C-Fe Redox Cycling: Sleeping Couple No Longer

D. DEB. RICHTER^{1*}, A.R. BACON¹, M.L. MOBLEY²,
M. OELZE³ AND F. VON BLANKENBURG³

¹Duke University, Durham, NC 27708 USA
(*correspondence: drichter@duke.edu)

²University of Wyoming, Laramie, WY 82072 USA

³German Research Center for Geosciences, D-14473,
Potsdam, Germany

Nearly all soil data derive from bulked collections that homogenize soil heterogeneity [1, 2]. We therefore have limited understanding of biogeochemical processes, properties, and gradients that may contrast greatly amongst the many micro-environments that exist within soil profiles. Rooting can affect the upper several meters of soils and especially subsoil rhizospheres are hotspots of biological and chemical activity. In upland soils, distinctive redoximorphic features often visually illustrate microenvironments that contrast not only in color, but in chemistry, physics, and biology. Such redoximorphic features are often interpreted as being relic features of past ecosystems [3]. We hypothesize that mottles are both relic and active microsites in which organic-reductant enriched rhizospheres are periodically reduced when saturated, when the C-Fe redox cycle is associated with carbon stabilization, FeIII reduction, mineral dissolution reactions, and colloidal translocation.

Depth-dependent sampling of redoximorphic microsites in three upland soils was combined with chemical and physical analyses to investigate processes, properties, and time scales on which these rhizogenic microsites operate. In all three soils, we attribute C enrichment and Fe depletion in rhizospheres to result from electron acceptors periodically switching from O₂ to FeIII and other redox-active species, when subsoils become periodically saturated due to wet conditions and low hydraulic conductivity. Both $\Delta^{14}\text{C}$ and $\delta^{56}\text{Fe}$ [4] data indicate that the rhizogenic C-Fe redox cycle operates in the contemporary forest ecosystem, thus redoximorphic features are both relic and active. Large contrasts in clay and crystalline Fe concentrations among these microsites demonstrate large but local-scale mobility of Fe and colloidal materials. The significance of the upland rhizogenic C-Fe redox cycle is underscored by the deep and extensive rooting and mottling of many upland soils across a range of plant communities, lithologies, and climatic regimes.

[1] Fimmen, Richter, Vasudevan *et al.* (2008) *Biogeochem* **87**, 127-141. [2] Richter, Oh, Fimmen, & Jackson (2007) The rhizosphere and soil formation. pp. 177-198. In Zoe Cardon & Julie Whitbeck, eds. *The Rhizosphere - An Ecological Perspective*. Academic Press, Boca Raton, FL. [3] Jacobs, West, & Shaw (2002) *Soil Sci. Soc. Am. J.* **66**, 315-323. [4] Guelke & von Blankenburg (2007) *Environ. Sci. Technol.* **41**, 1896-1901.

Kinetic isotope fractionation at the frontier of modern geochemistry

FRANK RICHTER

The Univ. of Chicago, Chicago, IL USA
[richter@geosci.uchicago.edu]

Geochemistry can claim a special place in the Earth sciences because it provides distinctive insight into both processes and the time scale over which they operated. I will review recent developments both from experiments and natural settings that illustrate how stable isotope fractionations are being used to identify the process responsible for chemical zoning, and that when the zoning is unambiguously shown to be due to diffusion, can it be used to provide a measure of time. To make this case for the role of stable isotopes the first thing one needs to demonstrate is that mass transport by diffusion in silicate systems is easily recognized by the fact that it produces isotopic fractionations that are large compared to modern analytical methods. The state of affairs in terms of the results of laboratory experiments involving chemical diffusion in melts [1-4], minerals [5], and metal alloys [6] is that in every case so far studied large kinetic isotope fractionations were found and thus they do provide a "fingerprint" with which to distinguish mass transport by diffusion from other mechanisms. What makes this especially relevant is that what has been found in the laboratory experiments has also been found in numerous natural settings ranging from quenched contacts between mafic and silicic melts [7], minerals from mantle xenoliths [8], from lava flows both on Earth and from Mars [9,10] and from a lava lake [11]. A corollary to the above arguments is that when one finds chemical zoning that does not have correlated stable isotope fractionations, one should avoid any temptation to interpret these as providing a measure of time. Thus kinetic isotope fractionations can both give special insight into the causes of chemical zoning, but equally importantly, spare us from the embarrassment of using diffusion kinetics to infer cooling rates from chemical zoning caused by some process other than diffusion.

[1] Richter *et al.* (2003) *GCA* **67**, 3905-3923. [2] Richter *et al.* (2009a) *GCA* **73**, 4250-4263. [3] Watkins *et al.* (2009) *GCA* **73**, 7341-7359. [4] Watkins *et al.* (2011) *GCA* **75**, 3103-3118. [5] Richter *et al.* (2013) unpublished data. [6] Richter *et al.* (2009b) *Chem. Geol.* **258**, 92-103. [7] Chopra *et al.* (2012) *GCA*, **88**, 1-18. [8] Jeffcoate *et al.* (2007), *GCA*, **71**, 202-218 [9] Parkinson *et al.* (2007) *EPSL* **257**, 609-921 [10] Beck *et al.* (2006) *GCA* **70**, 4813-4825 [11] Teng *et al.* (2011) *EPSL* **308**, 317-312.

A history of inhibition: thresholds and echinoderm Mg/Ca

R. E. M. RICKABY¹, M. VICKERS¹, H. C. JENKYN¹,
A. S. GALE², P. BOTS⁴ AND S. SHAW³

¹Department of Earth Sciences, University of Oxford, South Parks Road, Oxford, OX1 3AN; rosr@earth.ox.ac.uk

²School of Earth and Environmental Sciences, University of Portsmouth Burnaby Building Burnaby Road Portsmouth PO1 3QL

³SEAES, University of Manchester, Oxford Rd, Manchester, M13 9PL

Oscillations between an ocean which generates a primary abiotic precipitate of calcite or aragonite have been identified throughout the Phanerozoic and attributed to variability in the major ion chemistry of the ocean (magnesium, calcium and sulphate concentrations as lead candidates). Such variability represents fundamental changes to Earth surface processes, notably the balance among continental weathering, sedimentation, and volcanic activity. These cycles in seawater chemistry and primary mineralogy of marine carbonates have implications for reconstructing the drivers of changes in atmospheric CO₂, for the feedbacks in the global carbon cycle, and for the evolution of biomineralising life. Yet the record of precisely how, when and what these major changes have been is scant at best. Further definition of the chemical thresholds and a quantitative reconstruction and mechanistic understanding of the drivers of these fundamental ocean chemistry changes remains elusive.

First we shall explore how the combined effects of chemical inhibitors can alter the potential thresholds for a change in primary marine carbonate precipitate (Bots *et al.*, 2011). We then employ an established method (Dickson, 2002) to provide insight into refining the Meso-Cenozoic history of the dominant kinetic inhibitor of calcite precipitation, namely magnesium. We demonstrate the utility of a uniquely pristine sample compilation of echinoderm fragments collected from clay hosted sediments to preserve a history of seawater Mg/Ca. Our reconstructed history of seawater Mg/Ca is largely concordant with existing results except for a part of the middle Jurassic which appears to be characterised by much lower Mg/Ca ratios than predicted by most models.

[1] Bots P., L. G. Benning, R. E. M. Rickaby, S. Shaw, 2011, The role of SO₄ in the switch from calcite to aragonite seas, *Geology* **39**, 331-334. [2] Dickson, J. A. D., 2002, Fossil echinoderms as monitor of the Mg/Ca ratio of phanerozoic oceans, *Science*, **298**, 1222-1224.

Boundary addition of Hf and Nd in the Southern Ocean

J. RICKLI¹, M. GUTJAHN², D. VANCE¹,
C.D. HILLENBRAND³, G. KUHN⁴
AND M. FISCHER - GÖDDE⁵

¹ETH Zurich, Institute of Geochemistry and Petrology, Switzerland (joerg.rickli / derek.vance@erdw.ethz.ch)

²GEOMAR Helmholtz Centre for Ocean Research Kiel, Germany (mgutjahr@geomar.de)

³British Antarctic Survey, Cambridge, UK

⁴Alfred Wegener Institute, Bremerhaven, Germany

⁵Westfälische Wilhelms Universität, Münster, Germany

Hf and especially Nd isotopes are increasingly used to reconstruct past ocean circulation. Many of these applications rely on their quasi-conservative behaviour implying that the key process that governs their distribution is circulation. Here, we report new elemental (Hf, Zr, Nd) and isotope data (ϵ Hf, ϵ Nd) from the Pacific sector of the Southern Ocean, which document the relative significance of circulation vs boundary processes on the Hf and Nd distribution adjacent to Antarctica. Seawater depth profiles were sampled in the Ross Sea, along the West Antarctic continental rise and in the vicinity of the Marie Byrd Seamounts offshore the Amundson Sea Embayment (ASE). In addition, several samples were taken within 1.5 m to the seabed in the ASE. The samples were not filtered, which implies that some of the observations may be accentuated by contributions from the leaching of particulates during sample acidification.

The key observations for Nd include (a) the shift to radiogenic ϵ Nd and elevated Nd concentrations in the ASE (ϵ Nd up to -5.4), (b) a gradual increase in ϵ Nd with depth from 1000 m to 3000 m water depth in the open ocean (-9 to -7.8) along the entire West Antarctic margin and (c) distinctly more radiogenic deep waters beneath 3000 m, especially at the Haxby seamount (up to -3.1). (a) is indicative of boundary release of Nd. (b) probably reflects the mixing of freshly forming boundary affected deep waters with circumpolar deep water (CDW) upon sinking. (c) indicates that, in addition to the shelf, the deep ocean floor and basaltic seamounts act as sources of radiogenic Nd.

Hf isotopes are relatively homogenous in the data set (ϵ Hf mostly between +2 and +3.8). Boundary release is, however, evident from elevated Hf and Zr concentrations in the embayment. In addition, distinctly unradiogenic ϵ Hf of -1 are observed in deep waters at the Haxby Seamount. The data thus suggests that relatively unradiogenic Hf is released from Antarctica in the sampling area, which probably also accounts for the slight but systematic difference between measured ϵ Hf of CDW and deep waters of the eastern Pacific compared to the Atlantic sector of the Southern Ocean.

Is this a good time to be burning fossil fuels?

ANDY RIDGWELL¹

¹University of Bristol, Bristol, UK, andy@seao2.org

The basic for any sane analysis and discussion of the biotic response to past ocean acidification is, of course, identifying that there has been ocean acidification in the first place. But outside of the relatively recent geological past, the measurement and interpretation of direct proxies for the key parameters involved – pH and carbonate ion concentration (saturation state) becomes increasingly challenging. This is important as only the closely coupled decline in both these parameters together constitutes a future-relevant marine environmental change. One can resort to analysis of the size and duration of carbon isotopic changes and if really desperate ... models, in order to make estimates of the magnitude of carbon release and perturbation, but often such thinking takes place in a conceptual framework delineated by observations of how the modern carbon cycle works.

What I would like to explore here is whether the sensitivity of ocean chemistry to perturbation could have been much greater earlier in the Phanerozoic compared to today. For instance, following the advent and proliferation of planktic (carbonate) biomineralization during the Mesozoic: did the emergent deep sea carbonate 'buffer' preclude ocean acidification driven mass extinction? And what would it take in terms of fossil fuel CO₂ emissions to overwhelm it today?

Evolution of the oceans biological pump

ANDY RIDGWELL¹

¹University of Bristol, Bristol, UK, andy@seao2.org

Earth history is punctuated by a huge variety of transitions and perturbations in climate and global biogeochemical cycling. These may be linked to major extinctions or evolutionary innovations, and may exhibit evidence for greenhouse warming and CO₂ release and hence potentially hold direct future-relevant information. In interpreting the geological record it is common to assume the presence in the ocean of a strong vertical 'pump' of carbon and associated trace elements and isotopic properties. Proxies for past environments and perturbations are duly interpreted on this basis. However, evolutionary innovations have the potential to change the ground rules and give rise to non uniformitarianism behaviors of the global carbon cycle in deeper time. For instance, the cycle and reservoir of dissolved organic in the ocean may have been dominant in the past and has been invoked to explain a number of prominent features of the geological record. But is even this thinking too constrained by our familiarity with the modern? Just how radically different might the biological pump have been at different times since the advent of photosynthesis? When was a biological pump of any sort first developed?

In this talk I'll start by summarizing the known knowns and known unknowns surrounding the marine carbon cycle as it exists today, as we need to be clear at the outset about what key processes are incompletely understood. I will then piece together a potted history of how today's carbon cycle might have arisen in relation to the various evolutionary developments and transitions over the past ~2 Ga and discuss the implications for how we interpret the geological record.

Surface Complexation Modeling of cation adsorption by TiO₂ nanoparticles

MOIRA K. RIDLEY^{1*}, MICHAEL L. MACHESKY²
AND JAMES D. KUBICKI³

¹Texas Tech University, Dept. of Geosciences, Lubbock, TX, USA, moira.ridley@ttu.edu (* presenting author

²University of Illinois, Illinois State Water Survey, Champaign, IL, USA, machesky@illinois.edu

³The Pennsylvania State University, University Park, PA, USA jdk7@psu.edu

Surface Complexation Models (SCM) provide a means to quantify the specific adsorption of ions, the interaction of electrolyte ions, and the pH-dependent charging at mineral-aqueous solution interfaces. Additionally, SCMs provide a thermodynamic framework for predicting surface protonation equilibria. The charge distribution (CD) and MUSIC model facilitates the integration of molecular-scale information with macroscopic data to describe the interface behavior of ion-mineral systems.

In this presentation, we will discuss the application of the CD and MUSIC model to provide a thermodynamic description of the primary charging behavior of a suite of monodisperse, nanocrystalline anatase particles in NaCl media. Additionally, the CD-MUSIC model has been used to evaluate the interaction of Sr²⁺ and Ca²⁺ ions with the same suite of nano-anatase samples.

The adsorption of cations onto nano-anatase was evaluated over a wide range of pH, surface loading, and ionic strength. Complementary DFT-MD molecular simulations were also completed to evaluate the bonding geometries of all cations on the predominant (101) anatase surface. The adsorption behavior for the two divalent cations onto the anatase surface are broadly similar; although, Ca²⁺ first adsorbs at slightly low pH values and has slightly steeper charging curves than Sr²⁺. The variations in the macroscopic charging curves for the interaction of Sr²⁺ and Ca²⁺ with anatase reflect the differences in binding geometries identified at the molecular-level. The DFT-MD optimizations show inner-sphere binding for all cations; however, the most stable binding geometries are different for each ion. The Na⁺ and Sr²⁺ ions have bidentate coordination geometries, with Na⁺ ions coordinated to two bridging oxygen (BO) surface sites and Sr²⁺ coordinated to two terminal oxygen surface sites. Conversely, Ca²⁺ ions are coordinated to three BO sites. This molecular-scale information was used explicitly to constrain all CD-MUSIC model fits.

Organic carbon and trace element mobilization from a biochar amended arable soil: A soil column study

THOMAS RIEDEL¹, JENNIFER GEILICH¹
AND S ASCHA IDEN¹

¹Technische Universität Braunschweig, Institut für Geoökologie

The addition of charred biomass (biochar) to agricultural soils is currently attracting attention as a means for sequestering carbon and as a potentially valuable method to improve soil fertility. Because some uncertainty remains about the possible impacts of biochar additions on organic carbon and trace element cycling in arable soils we conducted a soil column study to investigate the mobilization of trace elements (Mn, Fe, Cu, Zn) and organic carbon.

Amendments of 1% (w/w) of grounded and finely dispersed biochar resulted in a net reduction of organic carbon, Cu and Zn leaching from the saturated soil columns. The organic carbon leaching from the amended soil was less phenolic indicating that sorption to biochar was compound specific. A more detailed characterization of the organic matter with ultra-high resolution mass spectrometry revealed that the most non-polar compounds detectable with this method were retained by the biochar likely because of hydrophobic interactions.

Cu and (to a lesser extent) Zn were associated with the organic matter retained by the biochar as revealed by gel-permeation liquid chromatography hyphenated with inductively coupled plasma mass spectrometry. Complexation with organic matter may therefore play an important role in the interactions of some metals with biochar in soils. The elution behavior of Fe and Mn was almost unaffected.

After two weeks of flow interruption the water-logged soil columns had turned anoxic. Under these conditions the elution behavior of the trace elements changed markedly. Mobilization of Fe and Mn increased strongly, but the increase was less pronounced for the biochar amended soil indicating that sorption of Fe(II) and Mn(II) to the biochar had occurred. Zn and organic carbon on the other hand showed almost no difference to the oxic elution indicating no redox sensitivity.

Our results show that charred biomass affects the quantity and quality of organic matter as well as the quantity and speciation of trace elements leaching from agricultural soils.

Tectonically enhanced deep subsurface microbial carbon cycling in the Nankai Trough, Japan

N. RIEDINGER^{1*}, M. STRASSER² AND T.W. LYONS¹

¹Dept. of Earth Sciences, Univ. of California, Riverside, CA 92521 USA (*correspond.: natascha.riedinger@ucr.edu)

²Geological Institute, ETH Zurich, 8092 Zurich, Switzerland

The occurrence and activity of microbial communities in deep subsurface environments are highly investigated. However, the abundance of microbial life and the source of energy necessary for these microorganisms remain controversial and under explored.

Here we investigate the impact of depositional and tectonic events on those deep microbial processes in sediments at IODP (Integrated Ocean Drilling Program) Site C0006, drilled and sampled during IODP Expedition 316 at the Nankai Trough, Japan. The observed methane isotope profiles indicate that active microbially mediated methane production occurs in sediments below 450 mbsf. This observation is supported by alkalinity measurements, indicating a source of inorganic carbon into the pore water as a by-product of deep in situ methane production. Thus, our data provide evidence for carbon cycling in these deep subsurface sediments. This is likely related to the highly dynamic tectonic regime at Nankai Trough, where tectonically induced temporary temperature increase can re-stimulate organic matter at distinct depths.

While tectonic activity can lead to the reactivation of recalcitrant organic matter, the variable sedimentary system provides niches for microbial abundance. The newly available/accessible organic carbon compounds fuel the microbial community – resulting in an onset of microbial methane production several hundred meters below the seafloor. This process is also captured in the isotope signal of methane, and thus methane isotopes can help us pin down locations of active microbial processes in deeply buried sediments.

Accurate isotope composition measurements by a miniature LMS system designed for in situ space research

A RIEDO^{1*}, M. NEULAND¹, S. MEYER¹, M. TULEJ¹ AND P. WURZ¹

¹Physics Institute, Space Research and Planetary Sciences, Sidlerstrasse 5, 3012 Bern, Switzerland (*correspondence: andreas.riedo@space.unibe.ch)

A miniature laser ablation reflectron time-of-flight mass spectrometer designed for in situ space research for sensitive and accurate measurements of the elemental and isotopic composition of extraterrestrial material is described and its performance for accurate in situ measurements of isotope composition is demonstrated [1-4]. A ns- (266 nm, 5 ns, 20 Hz) [1-2] and a fs-laser ablation ion source (775 nm, 190 fs, 1kHz) [3] were used to investigate figure of merits (mass resolution, dynamic range, detection sensitivity and accuracy of measurements). The studies are performed with a high spatial resolution by focusing the pulsed laser radiation to spot of about Ø20 and 40 µm, respectively on the sample surface. The measurements are conducted with high dynamic range of at least 10⁸ and a mass resolution (m/Δm) of up to 800-900, as measured at ⁵⁶Fe [1]. High detection sensitivity is achieved in measurements of both, metallic and non-metallic elements (tens of ppb) [1]. While ns-laser ablation ion source have to be calibrated with appropriate NIST standard reference materials (SRM), the relative sensitivity coefficients (RSC) were determined to be close to one when the fs-laser ablation ion source was applied [3]. Hence, the coupling of LMS with a fs laser system is preferable and is of considerable interest for the development of standard-less instruments. We developed a measurement procedure, which will be discussed in detail, that allows LIMS to measure isotope composition of elements, e.g. Ti, Cr, Pb, etc., with a measurement accuracy and precision in the per mille and sub per mille level for the first time and is comparable to the performance of other well-known and accepted measurement techniques (TIMS, SIMS and LA-ICP-MS) [2-3]. High performance of the LMS instrument offers versatile applications regarding in situ investigations of the chemical composition (elemental and isotopic) of extraterrestrial surface material [1-4].

[1] Riedo *et al.* (2013) *J. Mass Spectrom.* **44**, 1-15. [2] Riedo *et al.* (2013) *PSS*, submitted. [3] Riedo *et al.* (2013) *JAAS*, submitted. doi: 10.1039/C3JA50117E. [4] Tulej *et al.* (2012) *Int. J. Spectros.*, doi:10.1155/2012/234949.

Insight into biotite weathering rate using U-series isotopes

S.RIHS*¹, A. GONTIER¹, M.P. TURPAULT²,
D. LEMARCHAND¹, A. VOINOT¹ AND F. CHABAUX¹

¹LHyGeS/Université de Strasbourg (UMR 7517), Strasbourg, France (* correspondence: rihs@unistra.fr)

²Lab. Biogéochimie des Ecosystèmes Forestiers, (UR INRA 1138), Champenoux, France (turpault@nancy.inra.fr)

While the chemical weathering rate of silicates is a key parameter for several geochemical processes, field measurement of these rates remains challenging. Uranium- and Th-series nuclides were used to investigate biotite weathering in a soil profile. Some crystal-habits of biotites (including the alteration products) were hand-picked from five horizons (20 to 140 cm) of a soil profile from the experimental Breuil-Chenu site (France). Additionally, biotites from a seemingly 'fresh' block of the granitic bedrock were also recovered. Chemical analyses and XRD data allow quantifying the fraction of biotite remaining in these crystal-habits (91% to 9%). The extraction of the 'fresh' biotite interlayer demonstrates the lack of U and Th in this interlayer.

Unexpected behaviour of U and Th nuclides was recorded in these biotites. An unambiguous loss of ²³²Th occurs during the transformation of the biotite to its alteration products, whereas little U loss (similar to Fe) was observed, implying an efficient redistribution of U between the primary mineral and the alteration products (mainly kaolinite and vermiculite) within the crystal-habit. The measured U-series activity ratios show a ordered evolution, consistent with an increased weathered stage in these samples. However, this "U-series-derived-weathered-stage" is not always coherent with the location of the sample within the soil profile, i.e.: the 'fresh' biotite from the granite bedrock actually displays some U-series activity ratios typical of significantly weathered samples, suggesting an incongruent leaching of U and Th isotopes. These results highlight that the U- and Th-series nuclides are probing some water-mineral interactions occurring before macroscopic mineral transformation.

Using an open-system leaching model, the coupled (²³⁴U/²³⁸U), (²³⁴U/²³⁰Th), and (²²⁶Ra/²³⁰Th) disequilibria measured in the samples permit to calculate a weathering duration ranging from 12 to 50 ka for the most altered biotite of this soil profile. The biotite weathering rates deduced from these data are consistent with the range of field rates previously reported [1], suggesting a valuable use of U-series isotopes for mineral-weathering field rate determination.

[1] White A. (2002) *Chem. Geol.* **190**; 69-89.

Dissolved Mo, W, V in Atlantic surface water

M. RIMSKAYA-KORSAKOVA*, E. BEREZHNYAYA
AND A. DUBININ

P.P. Shirshov Institute of Oceanology RAS, Moscow, Russia
(*correspondence: korsakova@ocean.ru)

Molar ratio of Mo/W is about 1800:1 in the Pacific Ocean water, while in the Earth's crust Mo/W ratio is close to 1. Tungsten was preferentially scavenged by hydrogenic Fe-Mn oxyhydroxides in oceans relative to Mo, that enriches ocean water. In sediments of South Atlantic one can see gradual decrease of Mo/W ratio in the past. It is not clear what drives the directional changes of Mo/W ratio. To investigate the factors controlling the behavior of these elements in the Earth's history (a record in the sediments), their variations should be studied in the modern ocean water.

The concentration of W in open ocean water is extremely low (about 50 pmol/L). So we developed the technique for solid phase extraction preconcentration of dissolved W together with Mo and V from ocean water with ICP-MS detection. The concentration factor is 50; the detection limits are 0.31 nmol/kg for Mo, 6 pmol/kg for W and 40 pmol/kg for V. The precision of the determination is 2.7% for Mo, 3.4% for W and 3.5% for V in seawater (n=6).

The concentrations of the above mentioned elements in 16 surface water samples of submeridional profile (from 36°N to 36°S) across the Atlantic Ocean have been determined using the developed technique. The ranges of studied elements concentrations were: Mo – 90-110 nmol/kg, W – 54-93 pmol/kg and V – 28-35 nmol/kg along the profile. Concentrations of studied elements are not clearly correlate to salinity. Mo content shows strong correlation with V content. Distribution of W differs from that of Mo and V. The Mo/W ratio in the surface water changes from ca. 1100 to 1800 along the profile in Atlantic Ocean.

Regional scale OA oxidation observed over the Po Valley basin (Italy), at Mt. Cimone (2165 m asl)

M. RINALDI¹, S. GILARDONI¹, S. DECESARI¹, S. FUZZI¹, P. CRISTOFANELLI¹, P. BONASONI¹, S. FERRARI², V. POLUZZI² AND M.C. FACCHINI¹

¹Istituto di Scienze dell'Atmosfera e del Clima, Consiglio Nazionale delle Ricerche, Bologna, 40129, Italy
(*correspondence: m.rinaldi@isac.cnr.it)

²Centro Tematico Regionale Aree Urbane, Arpa Emilia-Romagna, Bologna, 40138, Italy

High resolution time of flight aerosol mass spectrometer (HR-ToF-AMS) measurements have been performed, for the first time, at Mt. Cimone GAW station (44°12' N, 10°42' E, 2165 m asl) from 11 June to 9 July 2012, under the framework of the EU project PEGASOS and the Emilia-Romagna Region project SUPERSITO.

The peculiar character of the site allows the investigation of organic aerosol (OA) ageing occurring at regional scale over the Po Valley. In fact, particles sampled during the day are representative of the early stages of aerosol atmospheric oxidation, comprising processed primary OA and secondary OA formed in the Po Valley basin, being the site within the planetary boundary layer (PBL). During the night, the aerosol sampled at Mt. Cimone is representative of more processed conditions, as the site is in the free troposphere (FT), containing aerosols with an age from several hours to days.

Elemental analysis performed with high resolution mass spectra [1], revealed decreasing average H/C and increasing O/C ratio from PBL to FT samples. As a consequence, the OM/OC ratio passes from 1.83±0.05 in PBL, to 1.94±0.08 in FT samples.

These results evidence the progressive oxidation of OA over the Po Valley basin, from few hours after their emission/formation to one or more days of atmospheric processing. On a Van Krevelen space, the data produce a slope of ~ -1, suggesting that the observed regional scale oxidation processes occur mainly through the addition of carboxylic functional groups [2]. This is further confirmed by the analysis of the HR mass fragments, showing that, from PBL to FT samples, the average contribution of fragments containing carbon, hydrogen and more than one oxygen atom (CHO>1) passes from 25% to 33%, while both CH and CHO fragments decrease their contribution.

[1] Aiken *et al.* (2007) *Anal. Chem.* **79**, 8350-8358. [2] Heald *et al.* (2010) *Geophys. Res. Lett.* **37**, L08803.

Sr²⁺ and Mn²⁺ incorporation during CaCO₃ cementation on calcitic and aragonitic shells

T. RINDER^{1*}, M. DIETZEL² AND A. DEDITIUS²

¹GET/CNRS, 14 avenue Édouard Belin, 31400, Toulouse(*correspondence: rinder.thomas@gmx.net)

²TU Graz, Institute of Applied Geosciences, Rechbauerstr. 12, Graz, Austria

Precipitation of calcium carbonates may cause significant changes in the porosity, permeability and overall physical properties of sedimentary rocks. For instance in sandstone the loss of permeability and porosity negatively influences the potential quality of the hostrock as a hydrocarbon or groundwater reservoir [1]. In recent years more attention to cementation issues is received for the increasing efforts to reduce CO₂ emission into the atmosphere and the possibility of long term storage by means of underground fixation in carbonates [2].

In the present study flow through experiments were carried out to investigate carbonate cementation of primary unconsolidated shell material by investigation of the spatial distribution and trace element incorporation of the precipitated material. NaHCO₃ – Na₂CO₃ – CaCl₂ solutions supersaturated with respect to calcite were pumped through columns packed with shell fragments of a grain size between 0.5 and 1mm. Sr²⁺ and Mn²⁺ addition was used to trace the temporal and spatial evolution of newly formed precipitates in the pore space.

Overall distribution coefficients calculated from aqueous bulk solutions result in a D_{Sr} of 0.68 and D_{Mn} of 6.08 for the precipitated CaCO₃. These coefficients are in good agreement with literature values within the given proportions of precipitated calcite and aragonite. However, apparent measured distribution coefficients in the newly formed CaCO₃ solids derived from electron microprobe analysis are highly heterogeneous and results in a maximum D_{Sr} and D_{Mn} value of 18 and 163, respectively.

Alternating trace element rich and poor growth zones were discovered in our experiments carried out at a constant solution composition, temperature and flow rate. We suggest that the incorporation behaviour depicted by bulk ratios which serve as proxies for the reconstruction of environmental conditions during precipitation of CaCO₃ is not necessarily valid on the microscale. The actual locally occurring trace element incorporation into CaCO₃ can significantly exceed or fall below the average bulk incorporation.

[1] Taylor & Machent (2011), *Marine and Petroleum Geology* **28**, 1461-1474. [2] Matter *et al.* (2009), *Energy Procedia* **1**, 3641-3646.

Using TOF-SIMS isotope mapping for studying dissolution and precipitation processes at mineral grains in an experimental CO₂-sequestration setup

S. RINNEN¹, A. RISSE², C. OSTERTAG-HENNING²
AND H.F. ARLINGHAUS¹

¹Physikalisches Institut, University of Muenster, Wilhelm-Klemm-Str. 10, 48149 Muenster, Germany
(stefan.rinnen@wwu.de)

²Bundesanstalt fuer Geowissenschaften und Rohstoffe, Hannover, Germany

CCS (Carbon dioxide capture and sequestration) is a technique investigated for its possible employment in the reduction of the amount of anthropogenic CO₂ gas emitted into the atmosphere. Deep saline aquifers are one option for storing CO₂ gas streams produced e.g. by the combustion of fossil fuels at power plants. These gas streams contain different impurities depending on their origin, among them O₂, NO_x, SO_x in addition to the CO₂. We have used ToF-SIMS to determine the influence of these impurities on dissolution and precipitation processes at the minerals.

Experiments under in situ pressure and temperature conditions of possible geological storage sites were performed at the German Bundesanstalt fuer Geowissenschaften und Rohstoffe (BGR) in flexible Dickson-type gold-titanium cells and small gold capsules.

Minerals common in the deep saline aquifers (e.g. siderite, calcite) were placed in small reaction cells of thin gold foil in a reactor vessel and exposed to isotopically enriched water (H₂¹⁸O) or carbon dioxide (¹³CO₂) during the experiments.

To facilitate the determination of the amount of dissolved ions incorporated into newly formed precipitates within the reaction chambers, a database of positive and negative ToF-SIMS spectra for a variety of rock-forming minerals were set up to identify minerals and mineral alterations. In addition, preparation techniques were developed for high-resolution measurements of the incorporation of isotope-labeled elements/ions (e.g. ¹⁸O) into mineral precipitates. The results show that ToF-SIMS can simultaneously image the elemental, isotopic, and molecular compositions of these minerals with high spatial resolution. Also, elemental and isotopic distributions as a function of depth can be monitored.

Carbonatitic Magmas? A Mineralogical and Isotopic Approach

DEBORA C. RIOS^{1,2*}, DONALD DAVIS²,
HERBET CONCEIÇÃO³, MARIA DE LOURDES S. ROSA³,
AND CÂNDIDO A.V. MOURA⁴

¹Jack Satterly Geochronological Lab, University of Toronto, Canada, debora.rios@utoronto.ca (* presenting author)

²GPA, CPG em Geologia, UFBA, Salvador-BA, Brazil

³Núcleo de Geologia, UFS, Sao Cristovao-SE, Brazil.

⁴Para-Iso Isotopic Laboratory, UFPA, Belem-PA, Brazil.

Massive deep orange calcites are intensely colored, coarse grained rocks, in contact with silicate rocks that exhibit centimetric crystals of phlogopite, occurs at Serrinha Nucleus (SerN), Brazil. Ocelli are a common feature, composed of euhedral fluorapatite, diopsidic pyroxenes and barite. Associated creamy coloured rocks are composed of >90% calcite, 3-8% green-olivine and diopside, 1-2% euhedral sulphides and well developed crystals of purple-spinel and blue-fluorapatites, as well as rounded mafic enclaves composed of amphibole, biotite and pyrite. Coarse calcite veins and/or dykes also cut the 2.1 Ga syenite-lamprophyre association and the meta-gabbros of Itapicuru Greenstone, demonstrating a clear interrelation between carbonates and silicate minerals including Fe-Mg-Mn calcite, diopside, apatite, quartz and Fe-Ni oxides. Rutile, few zircons and pyrite were described from the heavy mineral concentrates.

C and O preliminary results for δ¹³C (PDB) between +12 e +13 per mil, δ¹⁸O (PDB) of -10 per mil, and V-SMOW of +20, suggest the involvement of different magmatic or hydrothermal phases in these rocks formation. LA-ICP Pb-Pb analyses of calcites yielded model ages of ~1950 Ma and U-Pb ages from 2 zircons are (i) 2.11 Ga, close to that of SerN syenites and lamprophyres, suggesting that these rocks may be comagmatic and (ii) a clear core-border relationship showing ages of 2.7 and 2.5 Ga, respectively, similar to those reported for zircon xenocrysts in syenites and kimberlites.

Our results show that these rocks are calcite carbonatites, fairly well exposed, and that have not been metamorphosed. The ocellar texture suggests liquid immiscibility, indicating silicate magma droplets. Although further work remains to be done, the isotopic data suggest an emplacement age of ~2.0-2.1Ga, coeval with emplacement of the syenites and lamprophyres and to the gold mineralization at Itapicuru Greenstone. This syenite-lamprophyre-carbonatite association is closely related to Au in many Archean cratons worldwide.

Investigation of reactive transport with closed-flow column experiments and parallel factor analysis (PARAFAC) of fluorescence data

THOMAS RITSCHEL* AND KAI UWE TOTSCHKE

Institute of Geosciences, Friedrich-Schiller-University Jena
(*correspondence: Thomas.Ritschel@uni-jena.de)

The study of biogeochemical interfaces is crucial to understand soil functioning [1]. The sorption of solutes and colloids to these interfaces results in the phenomenon of retardation. Besides the interactions at the sorbent-solution-interface, the sorption rate depends also on the spatial structure of the pore network (size distribution, connectivity, topology). Column experiments allow for the consideration of the structure and thus for a quantification of possible rate limitations. We focus on column experiments run in closed-flow mode. There, a typical oscillation in the “breakthrough” of solute concentration, which conveys additional information about the flow regime (dispersivity, water content, immobile water) as well as the effective interaction kinetics, can be observed. Another major feature of the closed flow design is the conservation of tracer mass inside the column setup. Therefore, the investigation of sorption characteristics can be simplified by using mass balances.

Our objective was to study the interaction between different solutes (conservative tracers, e.g., NaCl and reactive tracers, e.g., acetate, oxalate and vanillic acid) and artificial porous media (composed of quartz, illite, goethite and charcoal in a well defined grain size distribution). The reactive tracers were chosen to probe specific reactive surfaces, which allowed for a consideration of involved sorption mechanisms and an estimation of sorbent surface coverage. The concentration-time profile of solutes was measured with non-consuming techniques (fluorescence spectroscopy or electrical conductivity measurements). PARAFAC analysis of fluorescence data was used for the quantification of aromatic compounds in complex background solutions. Since the reconstructed sorption characteristics are influenced by physical and chemical non-equilibrium and possible sorption sites were unavailable due to aggregate formation and immobile regions in the porous medium, we were able to estimate the amount of void volume and the availability of sorption sites of goethite.

[1] Totsche, Rennert, Gerzabek, Kögel-Knabner, Smalla, Spittler & Vogel (2010), *J. Plant Nutr. Soil Sc.* **173**, 88-99.

Hydrogeochemical modeling and noble gas analysis of spring waters from Poços de Caldas, MG-Brazil

RITTER S.M.¹, ISENBECK-SCHRÖTER M.^{1*}, FREUNDT F.², AESCHBACH-HERTIG W.² AND BONOTTO D.M.³

¹Inst. of Earth Sciences, Heidelberg Univ., INF 236, 69120 Heidelberg, Germany

(*corr: Margot.Isenbeck@geow.uni-heidelberg.de)

²Inst. of Env. Physics, Heidelberg Univ., INF 229, 69120 Heidelberg, Germany (aeschbach@iup.uni-heidelberg.de)

³Instituto de Geociências e Ciências Exatas, UNESP- Campus of Rio Claro, Av 24-A, nº 1515 Bela Vista 13506-900 - Rio Claro, SP - Brazil (dbonotto@rc.unesp.br)

Thermal and non-thermal spring water samples from the city of Poços de Caldas were analysed with respect to their chemical composition and dissolved noble gas contents. The objective is a better understanding of the hydrogeochemical evolution, maximum reservoir temperature, groundwater age and possible heat sources of the low-enthalpy thermal system.

The genesis of the thermal alkaline waters (Na-K-(H)CO₃-SO₄-F-type) could be approached by an inverse model of water-rock interactions with PhreeqC. The model favours four main processes to take place in thermal water formation: (I) pyrite oxidation; (II) CaF₂ or NaF dissolution; (III) calcite precipitation; (IV) Na-K-alumosilicate weathering; (V) equilibrium at depth of Na and K with Na-K-alumosilicates (e.g. orthoclase and nepheline). Thoroughly chosen chemical Geothermometers, calculated with the computer program SolGeo [1], indicate maximum equilibrium reservoir-temperatures of 105-130°C, which offer estimates on the circulation depth of 2.6-3.3 km.

Dissolved noble gas contents and their isotopic ratios in the water samples generally support previous assumptions [e.g. 2] of (i) different aquifer sources for the springs; (ii) the occurrence of mixing of thermal and non thermal water during ascent; and (iii) relatively long residence times of the circulating meteoric water in the geothermal system. Further noble gas data examination could lead to obtain age constraints derived by ⁴He accumulation and more information about the heat source of the geothermal system.

[1] Verma, S. P., Pandarinath, K., & Santoyo, E. (2008). SolGeo: A new computer program for solute geothermometers and its application to Mexican geothermal fields. *Geothermics* **37**, p. 597-621. [2] Bonotto, D. M. (2005). The U-isotopes modelling in aquifers from Pocos de Caldas plateau, Brazil. *Environmental Geology* **48**, p. 507-523.

Early mantle composition and evolution inferred from ^{142}Nd and ^{182}W variations in Isua samples

H. RIZO*^{1,2}, M. TOUBOUL², R.W. CARLSON¹, M. BOYET³,
I.S. PUCHTEL² AND R.J. WALKER²

¹Carnegie Institution of Washington, Dept. of Terrestrial Magnetism, Washington DC 20015, USA.

²University of Maryland, College Park, MD 20742, USA

³Universite Blaise Pascal, 63038 Clermont-Ferrand, France

*Correspondence: hrizo@ciw.edu

The composition and evolution of the early terrestrial mantle is largely unknown due to the sparse geological record preserved from Earth's infancy. The short-lived ^{146}Sm - ^{142}Nd chronometer applied to Eoarchean Greenland rocks led to the discovery of the oldest known mantle reservoir. Samples derived from this reservoir have ^{142}Nd excesses of 10-20 ppm compared to modern samples, which combined with ^{147}Sm - ^{143}Nd systematics suggest that their source was depleted in incompatible elements, and formed in the first 150 Ma of Solar System history [1-4]. Recently, ^{182}W excesses of $\sim +13$ ppm relative to terrestrial standards were also detected in rocks from the same area [5], as well as in the mantle sources of 2.8 Ga komatiites [6]. ^{182}W excesses could reflect imperfect mixing of late-accreted materials into the mantle during the period between 4.5 and 3.8 Ga. Given the short half-life of ^{182}Hf , these excesses could instead reflect Hf/W fractionations during the first tens of Ma of the Solar System history. In this case, ^{182}W and ^{142}Nd signatures would indicate that early-formed mantle reservoirs were not erased during the Moon-forming giant impact. Re-mixing of early-formed Greenland reservoirs likely started during the Hadean and the obliteration of these heterogeneities with respect to ^{142}Nd seems to have been completed by 3.3 Ga [7], whereas the ^{182}W anomalies detected in 2.8 Ga komatiites imply that W isotopic heterogeneities persisted in the mantle until at least the late Archean [6]. We present new highly siderophile element and ^{182}W data for 3.8 Ga to 3.3 Ga old Isua samples, previously analyzed for ^{142}Nd . This dataset may help constrain the composition of the Archean mantle as it evolved through time, and may allow modeling the mixing rate of late accreted meteoritic material in the mantle.

[1] Bennett *et al.*, (2007) *Science* **318**, 1907-1910. [2] Boyet and Carlson (2006) *EPSL* **250**, 254-268. [3] Caro *et al.*, (2006) *GCA* **70**, 164-191. [4] Rizo *et al.*, (2011) *EPSL* **312**, 267-279. [5] Willbold *et al.*, (2011) *Nature* **477**, 195-199. [6] Touboul *et al.*, (2012) *Science* **335**, 1065-1069. [7] Rizo *et al.*, (submitted)

Noble gases geochemistry of magma degassing at Santorini (Greece): Inferences on 2011-2012 unrest

RIZZO A.¹, BARBERI F.², CARAPEZZA M.L.³,
FRANCALANCI L.⁴, D'ALESSANDRO W.¹,
DI PIAZZA A.² AND SORTINO F.¹

¹Istituto Nazionale di Geofisica e Vulcanologia, Sezione di Palermo, Via Ugo La Malfa 153, 90146 Palermo, Italy

²Dipartimento di Scienze, Università di Roma Tre, Largo San L. Murialdo 1, 00146 Roma, Italy

³Istituto Nazionale di Geofisica e Vulcanologia, Sezione di Roma1, Via di Vigna Murata 605, 00143 Roma, Italy

⁴Dipartimento di Scienze della Terra, Università degli Studi di Firenze, Via La Pira 4, 50121 Firenze, Italy

We performed a noble gases investigation of fluid inclusions hosted in olivines and pyroxenes from mafic enclaves contained in the 1570 and 1925 A.D. dacitic magmas erupted at Nea Kameni. These enclaves are a portion of mafic magma batches that replenished the shallow chamber of the plumbing system hosting cooler and more silicic melts. Their Sr-Nd isotope ratios are quite similar to those measured in the host dacitic rocks, implying a common parental magma. Therefore, the analysed enclaves may be considered representative of the historic magma erupted at Nea Kameni which could be still present in the volcano plumbing system feeding the crater fumaroles.

Gases extracted from fluid inclusions are affected by an appreciable air contamination, as their $^4\text{He}/^{20}\text{Ne}$ and $^{40}\text{Ar}/^{36}\text{Ar}$ ratios are near to the typical atmospheric signature. The $^3\text{He}/^4\text{He}$ ratios of olivines, once corrected for air contamination (3.1-3.6 Ra), show higher and more reliable values than the cogenetic pyroxenes. These values partially overlap those of the gases (3.5-4.0 Ra) collected from Nea Kameni fumarolic field and from bubbling springs at Palea Kameni. The range of $^3\text{He}/^4\text{He}$ ratios (3.1-4.0 Ra) is appreciably lower than typical arc volcanoes (R/Ra $\sim 7-8$), implying that a contamination by ^4He -rich fluids occurred either directly in the mantle and/or in the plumbing system. Comparison of $^3\text{He}/^4\text{He}$ and $^4\text{He}/^{40}\text{Ar}^*$ ratios measured in enclaves with those of fumarolic gases, as well as long-term monitoring of R/Ra in the latters, coherently indicate that magma involved in the 2011-2012 unrest is likely more primitive and ^3He -rich than the mafic enclaves. This would imply that the Santorini magma presently available for eruption has a lower explosive potential than in the recent historic eruption of Nea Kameni.

F and Cl solubilities in wadsleyite and ringwoodite

M. ROBERGE¹, H. BUREAU¹,
N. BOLFAN-CASANOVA², D. FROST³,
C. RAEPSAET⁴, S. SURBLE⁴, H. KHODJA⁴
AND G. FIQUET¹.

¹IMPMC, UPMC-CNRS, 75252, Paris, France

(*presenting author: mathilde.roberge@impmc.umpc.fr)

²LMV, UBP-CNRS, 63038, Clermont-Ferrand, France

³BGI, 95440 Bayreuth, Germany

⁴LEEL, SIS2M, CEA-CNRS, 91191 Gif-sur-Yvette, France

The relative distribution of volatile elements (e.g. H, C, F, Cl, S) in the different Earth's various reservoirs provides strong constraints on the understanding of the Earth's history. This study aims to access the mechanism and proportion of halogens that may be accommodated in minerals of Earth's Transition Zone (TZ; 410 to 660 km depth). The storage of water in the TZ is thought to be important due to its high solubility (up to 3.3 wt% water [1,2]) in wadsleyite (Wd) and ringwoodite (Rw), the two main phases of the TZ (60 % of its volume). As the halogen and water cycle are often linked (see the review after [3]), we investigate whether the TZ could be a deep reservoir for F and Cl. Therefore, we are measuring the F and Cl solubilities in Wd and Rw. F and Cl doped Wd and Rw samples were synthesized in multi-anvil press to reach the conditions of pressure and temperature of the TZ (14 to 22 GPa; 1100 to 1450°C). The obtained crystal sizes were greater than 10 μm, allowing precise measurement of halogen contents in individual crystals. The synthesis were performed under both anhydrous and hydrous conditions to study the influence of water on the F and Cl solubilities. F and Cl quantification was realized by ion beam analysis: we used μ-PIGE (μ-Particle Induced Gamma Ray Emission) for F; and μ-PIXE (μ-Particle Induced X-ray Emission) for Cl. We show that F and Cl can be incorporated in Wd and Rw in significant amounts. F solubility decreases with the presence of water. This suggests that F (possibly Cl) and water (OH) are accommodated on the same crystallographic sites in Wd and Rw. If we assume that the transition zone would store significant amounts of Cl and F, it means that (1) the TZ has been continuously supplied by Cl and F-bearing subduction materials, or (2) TZ is a hidden deep light halogen elements reservoir which never exchanges with the rest of the mantle. In both cases, F and Cl bulk silicate Earth contents may have been underestimated. If confirmed, the Earth's accretion models may have to be revisited.

[1] Inoue *et al.*, (1995) *JGR* 22, 117-120; [2] Bolfan-Casanova *et al.*, (2000) *EPSL* 18, 2 209-221; [3] Pyle and Mather, *Chem Geol* (2009), 263, 1-4, 110-121.

Mass independent isotope fractionation in Ozone

REINHARDT, P.¹ AND ROBERT, F.²

¹Laboratoire de Chimie Théorique, UMR-CNRS 7616,
UPMC, 4 place Jussieu, F 75252 Paris, France

²Laboratoire de Minéralogie et Cosmochimie du Muséum,
UMR CNRS 7202, MNHN, Paris 75005, France.

We propose that the average lifetime of an activated O₃* complex yielding ozone and formed by collisions involving distinguishable isotopes in the reaction O + O₂, is not equal to the average lifetime of the same complex but formed by collisions involving indistinguishable isotopes. We ascribe the mass independent isotopic fractionation factor η [1] to the average lifetime ratio of complexes formed by reactions involving dis- and indistinguishable isotopes.

Calculated average lifetimes of the O₃* complexes in a thermal gas were obtained by classical trajectories of collisions O + O₂, where all atoms have the same mass (16 amu). Simulations have been carried out in an ab-initio potential surface [2] of three oxygen atoms in a singlet ground state. We derive the mass-dependent fractionation as measured in laboratory experiments [3] by including differences in the zero-point energies of involved O₂ molecules. The numerical results account well for the measured isotopic fractionation in ozone [3, 4], as reported in the Table 1.

Reactions	Complex	ΔZPE	$\alpha(M.D.)$	η	$\alpha(calc.)$	$\alpha(mes.)$	
16	17-18	16-17-18 ^(*)	0	1.00	1.20	1.20	= 1.20 NR+R
16	17-17	16-17-17	11.79	1.13	1.20	1.36	1.23 NR+R
16	18-18	16-18-18	22.76	1.26	1.20	1.51	1.50 NR+R
17	16-16	17-16-16	-11.62	0.87	1.20	1.04	1.03 NR+R
17	18-18	17-18-18	10.80	1.12	1.20	1.35	1.31 NR+R
18	16-16	18-16-16	-22.10	0.75	1.20	0.90	0.92 NR+R
18	17-17	18-17-17	-10.64	0.88	1.20	1.05	1.03 NR+R
18	18-16	18-18-16	-22.76	0.74	1.28	0.95	0.92 I+R
16	16-18	16-16-18	22.10	1.25	1.28	1.60	1.45 I+R
16	18-16	16-18-16		1.00	1.00	1.00	1.08 I
17	17-17	17-17-17		1.00	1.00	1.00	1.02 I
18	18-18	18-18-18		1.00	1.00	1.00	1.03 I
18	16-18	18-16-18		1.00	1.00	1.00	1.04 I

Table 1: ΔZPE the difference in zero-point energies; $\alpha(MD)$ the calculated mass-dependent fractionation factor; $\alpha(calc.)$ the overall calculated isotopic fractionation factor: $\alpha(calc.) = \eta \times \alpha(MD)$ [1]; $\alpha(mes.)$ the measured isotopic fractionation factor as reported by [3]; last column: the type of reaction. R and NR for reactive and non reactive, I for indistinguishable. The reference reaction is shown by a (*).

[1] Gao, Y. Q., Marcus, R.A., 2001. *Science*. 293, 259–263.
[2] Schinke, R., Fleurat-Lessart, P., 2004. *J. Chem. Phys.*, 121, 5789. [3] Janssen, C., *et al.* 2001. *Phys. Chem. Chem. Phys.* 3, 4718-4721. [4] Thiemens, M.H., Heidenreich III, J.E., 1983. *Science*. 219, 1073–1075.

New insights into the evolution of a stagnant magma chamber- magma loss and liquid evolution in the Upper Zone of the Bushveld Complex

R. JAMES ROBERTS¹

¹University of Pretoria; james.roberts@up.ac.za

The Upper Zone (UZ) of the Bushveld Complex is the final magma chamber to be emplaced and crystallised during the evolution of the mafic portion of Bushveld magmatism. Though isotopic evidence indicates that no magma was added to the UZ during its crystallisation history, numerous studies have postulated the loss of large volumes of magma (20-40% of the original volume[1,2]) from the magma chamber. These estimates are problematic in that volcanic material related to the Upper Zone has never been identified. This new study utilises Zr and K bulk rock data to argue that the Upper Zone has experienced little or no magma loss. Previous estimates of Zr abundance have been too low, as researchers have assumed that Zr was incompatible in the UZ; in fact, zircon is a cumulus phase in the UZ, and is especially abundant in the magnetite and nelsonite layers in the sequence. The new estimate of <5% magma missing from the original magma is conformable with global studies on intrusion/extrusion rates for mafic magmas[3], and has consequences for the evolution of the liquid line of descent (LLD) for the UZ. A new multi-part LLD for the UZ was constructed and tested using MELTS. The modelled liquid and the actual sequence of minerals present in the UZ is extremely close, indicating that the UZ separated into a number of separate magma packets which then crystallised independently of one another. It is noted that despite the good correlation between the model and the actual rocks, the high Fe, low Si bulk liquid calculated for the UZ is unlikely to occur in nature, and that a portion of the UZ magmatic sequence is likely to be hidden underneath the roof rocks of the Bushveld Complex.

[1] R. Grant Cawthorn and Feodor Walraven, (1998), Emplacement and Crystallization Time for the Bushveld Complex, *J. Petrology* 39(9): 1669-1687 [2] Van Tongeren J A, Mathez E A, Kelemen P B (2010), A felsic end to Bushveld differentiation, *J. Petrology* (51):1891-1912 [3] White, S. M., J. A. Crisp, and F. J. Spera (2006), Long-term volumetric eruption rates and magma budgets, *Geochem. Geophys. Geosyst.*, 7, Q03010

Distinguishing between advection and source changes recorded by Nd isotopes in the NE Atlantic

N. L. ROBERTS^{1*} AND A. M. PIOTROWSKI¹

¹University of Cambridge, Cambridge, UK,
(*correspondence: nr297@cam.ac.uk)

Nd isotopes, measured on authigenic sediment phases, are a powerful tracer of past changes in ocean circulation [1]. Recent method developments have shown that planktonic foraminifera, which have not been chemically cleaned, preserve the Nd isotope signature of bottom water, and thus are an alternative phase to sediment leachates, avoiding possible contamination by volcanic phases [2, 3]. However, interpretation of downcore changes in Nd isotope records, in terms of past changes in water mass proportion, relies on the accurate reconstruction of the endmember composition of water mass source. Records from Fe-Mn crusts [4] and corals [5] from the NW Atlantic, and a sediment leachate record measured on core ODP 980 in the NE Atlantic [6] suggest the Nd isotope composition of the northern source endmember remained constant between the last glacial and the Holocene. However, a recent study comparing sediment leachate and uncleaned foraminifera Nd isotopes from a core close to ODP 980 indicates that sediment leachate data from this region are not reliable [7], thereby calling into question the invariant nature of the northern source endmember composition.

We present Nd isotope records, measured on unclean planktonic foraminifera, from a depth transect of cores in the northern NE Atlantic, which today are bathed by a mixture of overflow waters and Labrador Sea water. Our records sample Nd isotope composition from 1 – 4 km depth, and from 0 - 30ka. We compare our Nd isotope records with previously published benthic $\delta^{13}\text{C}$ and B/Ca records, measured on the same cores, and used to infer past changes in ocean circulation [8]. We use the observed decoupling between these three proxies to distinguish between endmember source changes in the Nd isotope composition and circulation controlled changes, with implications for interpreting changes in the Nd isotope signatures recorded elsewhere in the N Atlantic.

[1] Piotrowski *et al.* (2005) *Science* **307**, 1933-1938. [2] Roberts *et al.* (2010) *Science* **327**, 75-78. [3] Roberts *et al.* (2012) *GCA* **94**, 57-71. [4] Foster *et al.* (2007) *Geology* **35**, 37-40. [5] van de Flierdt *et al.* (2006) *Paleoceanography* **21**, PA4102. [6] Crocket *et al.* (2011) *Geology* **39**, 515-518. [7] Piotrowski *et al.* (2012) *EPSL* **357-358**, 289-297. [8] Yu *et al.* (2008) *EPSL* **271**, 209-220.

Linking Iron and Nitrogen Cycles in Lake Sediment

ELIZABETH ROBERTSON¹ AND BO THAMDRUP¹

¹Nordic Centre for Earth Evolution, Institute of Biology, University of Southern Denmark, Odense M, Denmark

In anoxic environments, iron reduction can function as a significant pathway for organic matter oxidation, resulting in the production of ferrous iron. This Fe²⁺ can potentially be oxidised by nitrogen species formed in surface sediment (e.g. nitrate; NO₃⁻, nitrite; NO₂⁻). The fate of such oxidized nitrogen compounds is of particular importance to nitrogen availability in microbial communities – determining whether nitrogen is retained in the environment in a bioavailable form (NH₄⁺) or effectively ‘lost’ as N₂. Although both freshwater and marine microbial strains have been isolated which are capable of coupling NO₃⁻ reduction to iron oxidation, the role of such processes for either iron or nitrogen cycling in natural environments is largely unknown.

The potential interactions of iron with NO₃⁻ reduction pathways were investigated in anoxic incubations with iron-rich sediment from a shallow, mesotrophic Danish lake. ¹⁵N tracing methods were used to determine contributions of denitrification and dissimilatory nitrate reduction to ammonium (DNRA) and how Fe²⁺ potentially influences the partitioning between these processes. DNRA was found to be the dominant nitrate reduction process and appeared to be further stimulated by addition of Fe²⁺ to incubations. These results suggest that NO₃⁻ reduction coupled to Fe²⁺ oxidation in this sediment yields NH₄⁺ as opposed to N₂ as previously described in several culture studies; resulting in nitrogen being retained in the system as a bioavailable substrate. Whether our findings are more generally applicable to aquatic systems such as marine sediments and anoxic waters where Fe²⁺ and oxidized nitrogen species co-occur is currently being explored.

Identifying carbon pools in heterogeneous materials: Use of peak fitting and TGA-DSC-MS data

S.A. ROBERTSON^{1*}, E. LOPEZ-CAPEL², D.A.C.MANNING², N. FINLAY¹ AND K.L.JOHNSON¹

¹School of Engineering and Computing Sciences, Durham Univ, DH1 3LE, UK (*correspondence: steven.robertson@durham.ac.uk)

²School of Civil Engineering and Geosciences, Newcastle Univ, NE1 7RU (elisa.lopez-capel@newcastle.ac.uk)

Thermogravimetry-differential scanning calorimetry (TG-DSC) is an effective tool for the analysis of modelable carbon pools (including labile, recalcitrant, resistant and inorganic carbon) in soils [1,2]. Coupling of the TG-DSC instrument with a quadrupole mass spectrometer to give a TG-DSC-MS arrangement allows the temperature dependent evolution of low molecular weight species such as carbon dioxide and methane to be monitored at the same time as mass losses [2].

A TG-DSC-MS analytical run from 100 to 1000 °C in an atmosphere of 20% O₂ 80% He₂ produces data that can be interpreted using GRAMS-AI software (Thermo Scientific). After ruling out potential interferences, monitoring the m/z 44 ion shows the evolution of CO₂ at different temperatures during the TG-DSC-MS run and a semi-automated peak fitting process has been developed, whereby the proportions of labile, recalcitrant, resistant and inorganic carbon in a sample can be estimated. By defining a range of temperatures over which each carbon pool might be expected to thermally decompose, and running multiple iterations of GRAMS-AI's peak fitting algorithm, a composite “best fit” of the four individual carbon pool peaks to the m/z 44 trace can be produced. The relative peak areas indicate the proportion of each type of carbon in the sample and parallel use of an elemental analyser allows estimation of carbon masses.

The approach adds utility to the TG-DSC-MS approach where heterogeneous materials are under investigation and has been used to investigate man-made soils [3] and to study organic rich residuals from the drinking water industry [4]. It appears to have general applicability in cases where rapid estimation of the size of the four carbon pools is required.

[1] Lopez-Capel *et al.* (2005) *Soil Sci. Soc. Am. J.* **69**, 136-140. [2] Lopez-Capel *et al.* (2006) *J Anal. Appl. Pyrolysis* **75**, 82-89. [3] Manning *et al.* (2013) *Int. J. Greenhouse Gas Control*, submitted. [4] Finlay *et al.* (2013) *MinMag*, this volume.

Characterization of Gas-Phase Air Pollutants and their Public Health Impact

ROBERTS-SEMPLÉ D

dawn_semplea@yahoo.com

Air pollution can have deleterious effects on human health. This study examines the role of meteorological factors on air pollution concentrations and their cumulative effects on public health in Hackensack Meadowlands, New Jersey. Ambient concentrations of nitrogen oxides (NO_x) and ground-level ozone (O_3) were measured and meteorological variables were monitored at the Meadowlands Environmental Research Institute (MERI) from June 2007 to May 2008, to characterize the temporal and seasonal variations of gas-phase air pollutants. Health records of respiratory hospital admissions were obtained from the New Jersey Department of Health and Senior Services (NJDHSS). Statistical analyses were conducted by using time series, multiple linear and principal component regression techniques. The meteorological conditions and air pollutants that may be associated with human respiratory health effects were analyzed.

The results show that ambient levels of NO_x and O_3 are influenced by certain meteorological conditions in the Meadowlands, and there is a strong relationship between hospital admission and personal exposure to NO_2 . There is no direct relationship between O_3 and hospital admission ($r=0.092$), whereas hospital admission and NO_x correlate ($r=0.317$) but more strongly with NO_2 ($r=0.359$) at a significance level of 0.01. Hospital admission rates are indirectly affected by relative humidity ($r=-0.077$). The seasonal dependence of pollutants is caused mainly by low wind speed and differences in chemical processing, making them interdependent. Seasonal variations of NO_x were less distinct with strong diurnal patterns of traffic-related peaks during the early morning rush hour. There was a strong association between NO_x and respiratory hospital admissions in the fall, winter and spring seasons. The variability of NO_x and O_3 was altered by distinct atmospheric conditions and chemical inter-conversions of the pollutants. There was an inverse relationship between concentrations of NO_x and O_3 ; the latter was dominant in summer and specific time of the day (early afternoon). For O_3 , association with hospital admissions was strongest at 2 lag days. Both climate-induced and pollution-induced health effects of NO_x and O_3 suggest that current national standards may not adequately provide a safe threshold for air pollutants from a public health perspective.

Uranium isotopes as a novel tracer of paleo-hydrology?

LAURA F ROBINSON¹ JOHN M SWARTZ²
AND WILLIAM G THOMPSON³

¹University of Bristol, BS8 1RJ, Bristol UK
(laura.robinson@bristol.ac.uk)

²Institute for Geophysics | J.J. Pickle Research Campus,
Austin, TX (jmswartz@gmail.com)

³Woods Hole Oceanographic Institution, Woods Hole, MA
02543 USA (wthompson@whoi.edu)

Uranium series isotopes provide unique insights into the rates and amplitude of geologic processes through their range of chemical behaviours in different environments, and their radioactive decay. In this case we use ^{234}U and ^{238}U isotopes to examine and quantify the controls of uranium input to rivers with an emphasis on watershed precipitation and discharge. First we show data from contrasting hydrological zones in two dynamic regions: New Zealand and Chile. After controlling for lithology and physical weathering caused by uplift we show that the strength of the hydrologic cycle plays a distinct role in controlling the $^{234}\text{U}/^{238}\text{U}$ ratio in river waters as they move through a water shed. Hydrothermal systems, subsurface processes and lakes may also act to affect the final ratio as rivers discharge into the ocean. The hydrologic cycle is thought to have changed markedly over millennial and glacial interglacial timescales leading to the possibility of a shift in the $^{234}\text{U}/^{238}\text{U}$ ratio of rivers, groundwater and seawater. Terrestrial speleothem $^{234}\text{U}/^{238}\text{U}$ records appear to provide supporting evidence for a lower regional hydrologic cycles during the last glacial period. By contrast, a compilation of seawater $^{234}\text{U}/^{238}\text{U}$ recorded in corals point to a shift in the opposite direction.

www.minersoc.org

DOI:10.1180/minmag.2013.077.5.18

Structure and Radiation Damage in $Y_2Ti_2O_7$ and Y_2TiO_5

M. ROBINSON¹, N.A. MARKS^{1*}, D.J. CARTER¹, M.J. QIN², S.C. MIDDLEBURGH², G.J. THOROGOOD², E.Y. KUO², R.O. AUGHTERSON² AND G.R. LUMPKIN²

¹Nanochemistry Research Institute, Curtin University, Australia (*correspondence: N.Marks@curtin.edu.au)

²Australian Nuclear Science & Technology Organisation, Locked Bag 2001, Kirrawee DC, 2232, NSW, Australia

Yttrium titanate is a rich solid-state system with important applications in a nuclear context. When it takes the stoichiometry $Y_2Ti_2O_7$ yttrium titanate adopts the pyrochlore form, a crystal structure which has been extensively studied as an immobilization matrix for nuclear waste. Y-Ti-O nanoparticles are also key ingredients in high-performance oxide-dispersion-strengthened (ODS) steels needed for next-generation fission and fusion reactors. The structure of these nanoparticles is complex and not fully clear, spanning a range of possibilities including enriched clusters, defective rocksalt-type TiO phases as well as stoichiometric $Y_2Ti_2O_7$ and Y_2TiO_5 [1,2]. The Y_2TiO_5 structure itself is poorly understood, with the phase diagram thought to comprise a low-temperature orthorhombic phase, a high-temperature cubic phase, and a hexagonal phase at intermediate temperatures [2].

Here we develop a new interatomic potential for yttrium titanate and apply it to both the determination of structure and irradiation response. The potential employs partial charges and is fitted to lattice parameters, internal coordinates and elastic constants obtained from density-functional-theory. For both $Y_2Ti_2O_7$ and orthorhombic Y_2TiO_5 the potential provides a substantial improvement over existing literature models.

Recent experiments [3] have shown that cubic Y_2TiO_5 exhibits a pyrochlore-derived superstructure involving a tripling of the unit cell along 111 directions. To determine its structure, Monte Carlo simulations were performed to order the cations and anions within a large $3 \times 3 \times 3$ tiling of the 88-atom unit cell. Experimental diffraction reflections were used to arrange the cations by calculating the structure factor, while the potential was used to order vacancies on the oxygen sublattice. The potential was also employed in Molecular Dynamics calculations of threshold displacement energies, thermal spikes and radiation damage cascades in $Y_2Ti_2O_7$ and Y_2TiO_5 . Using these simulations we interpret experimental studies of amorphization and quantify the role of anti-sites and structure in radiation response.

[1] Hirata *et al.* (2011) *Nature. Mat.* **10**, 922-926. [2] Jiang *et al.* (2010) *Acta Mater.* **58**, 1536-1543. [3] Whittle *et al.* (2011) *Acta Mater.* **59**, 7530-7537.

A new model for the formation of podiform chromitites in ophiolites

PAUL T. ROBINSON^{1*}, JINGSUI YANG¹, MEI-FU ZHOU² AND FAHUI XIONG¹

¹Chinese Academy of Geological Sciences, Beijing, China (*correspondance: paulrobinson94@hotmail.com)

²Department of Earth Sciences, Univ.of Hong Kong, Hong Kong, SAR, China (mfzhou@hku.hk)

Podiform chromitites occur in the upper mantle sections of ophiolites where they are typically surrounded by dunite envelopes formed by melt-rock reaction. Both high-Cr and high-Al varieties are common, but rarely in the same ophiolite. In contrast, residual chromite grains in the host peridotites and dunites show a wide range of composition. The podiform chromitites are generally thought to be magmatic precipitates from suprasubduction (SSZ) melts migrating through the mantle wedge. However, the recent confirmation of diamonds in both podiform chromitites and peridotites of several ophiolites, and evidence suggesting depths of formation >300 km for some of the chromitites, challenges this model. All UHP minerals would be destroyed if they were exposed to SSZ melts at shallow mantle levels. We suggest that residual chromitites first crystallize as discrete grains in mantle peridotites beneath mid-ocean spreading centers near the top of the transition zone, where they encapsulate diamonds and highly reduced phases carried by fluids from greater depths. These would be high-Al chromitites, indicating relatively low degrees of partial melting of the host peridotites. Some of these chromite-bearing mantle sections in which diamonds occur are eventually trapped in suprasubduction zones where they are infiltrated by hydrous SSZ melts, either arc tholeiitic or boninitic in composition. As these melts migrate through the mantle wedge they react with the host peridotites, dissolving pyroxene, precipitating olivine in dunite 'channels', and becoming progressively enriched in Cr. These melts react with and locally remobilize the 'residual' chromite grains, increasing their Cr#. The residual chromite grains are not melted but become more Cr rich by diffusion. The remobilized chromite grains are carried to shallow levels by the rising melts where they are deposited, along with newly precipitated grains, as podiform chromitites. The UHP minerals within the chromite grains are not destroyed because they are protected from the melts. This model accounts for the fact that podiform chromitites are found only in ophiolites and for the preservation of UHP minerals in both podiform chromitites and residual chromitites within the host peridotites.

The age of the Moon from U-Th-Pb systematics on terrestrial and lunar primitive mantles

KACEM ROCHD

Chouaib Doukkali University, El Jadida, Morocco
rochdkacem@yahoo.com

U-Th-Pb systematics of the primitive mantles reflect early mantle differentiation and core formation processes and may provide key constrain on the genetic relationship between the different planets. Here, we show that the Pb data for the terrestrial and lunar primitive mantles define a system of isochrons centred on unequilibrated primitive meteorites (e.g.; Mezo Madaras meteorite), which suggests that the Earth and Moon were formed at different times by direct accretion from the solar nebula. Following this result, we determine the age of the Moon to be exactly 5.13 Gyr. In principle, this new method of portraying a solar system by secondary isochrons centred on unequilibrated primitive meteorites can be used for precise dating all other objects in the solar system provided they are formed by direct accretion from the collapse of solar nebula and have experienced core-mantle segregation early in their planetary evolution. An other example is Mars whose Pb data for its primitive mantle might be available in the near future.

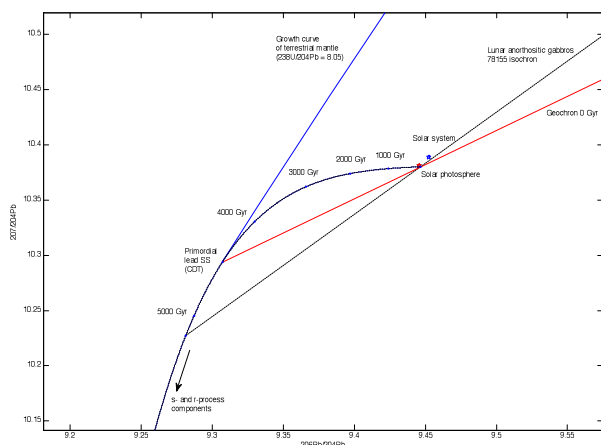


Figure 1: $^{206}\text{Pb}/^{204}\text{Pb}$ vs. $^{207}\text{Pb}/^{204}\text{Pb}$ plot for 4.55 Gyr geochron, including data point of terrestrial mantle calculated with $\mu = 8.05$ (Rochd, 2009), and 5.13 Gyr lunar isochron, including data points of plagioclase ($\rho < 2.89$) from Apollo 17 anorthositic gabbro 78155 (Nunes, 1975).

[1] Nunes, Tatsumoto, and Unruh (1975) Proc. Lunar Sci. Conf. 6th, 1431-1444. [2] Rochd (2009) Geochim. et Cosmochim. Acta, **73**, 13, A1109-A1109.

Carbonation of cement within a repository for radioactive wastes: Impact of CO₂ on cement mineralogy and permeability

C.A. ROCHELLE*¹, G. PURSER¹ AND A.E. MILODOWSKI¹

¹British Geological Survey, Keyworth, Nottingham, NG12 5GG, UK

(*correspondence: caro@bgs.ac.uk)

Large quantities of cementitious materials will be used for radioactive waste repository construction and buffer/backfill. Degradation of organic material within the waste will produce CO₂, leading to cement carbonation. This will reduce its capacity to maintain highly alkaline conditions, thus possibly aiding radionuclide migration. Conversely, some carbonation reactions might improve material properties, e.g. by reducing cement permeability. Currently, it is unclear whether the overall changes due to carbonation will be beneficial or deleterious to long-term radionuclide immobilisation.

As part of the pan-European FORGE project we have undertaken a laboratory study to examine the impact of carbonation on 'Nirex reference vault backfill' (NRVB) cement. Aims for the work were to quantify changes in cement mineralogy, structure, porosity/permeability, and the composition of coexisting aqueous fluids. Lab investigations exposed samples of cement to free phase and dissolved CO₂ under a range of potential *in-situ* conditions; 20°C or 40°C, 4 MPa or 8 MPa, 'young' (Na/K/Ca-rich) or 'evolved' (Ca-rich) cement porewaters. The experiments involved static and flowing experiments lasting 10-365 days.

Reaction was rapid in all experiments, with samples increasing in weight by up to 9% with no change in overall size. Key reactions were breakdown of portlandite and calcium silicate hydrates and formation of carbonates and silica. Reaction fronts moved through the cement over time, demarking regions of low, partial and full carbonation. The fully carbonated zone showed evidence for higher-density carbonate-filled fractures and concentric 'relic' reaction fronts, which separated areas having lower-density and high porosity. Appreciable amounts of a Cl-rich phase formed in the partially carbonated zone.

Controlled flow-rate experiments revealed decreases in overall sample permeability for gaseous, supercritical and dissolved CO₂. Carbonation was fastest with supercritical CO₂, but the greatest permeability reduction occurred with dissolved CO₂. Permeability decreases reflect porosity reduction due to conversion of portlandite and CSH to secondary carbonate minerals. The greatest reductions in porosity and permeability occurred in a very narrow zone at the leading edge of the visible alteration front.

Design Overview of the Potsdam 1280-HR SIMS Instrument

A. ROCHOLL¹* AND M. WIEDENBECK¹

¹Helmholtz-Centre Potsdam, GFZ, German Research Centre of Geosciences, Telegrafenberg, 14473 Potsdam, Germany (*correspondence: Alexander.Rocholl@gfz-potsdam.de)

The Helmholtz Zentrum Potsdam is currently installing a CAMECA 1280-HR SIMS, which will begin producing user data in the autumn of 2013. This state-of-the-art, ultra-high sensitivity and large geometry ion microprobe will function as an open user facility, in accordance with the Helmholtz Society's support of the global scientific community through providing access to top-end infrastructure. The new 1280-HR instrument will be integrated into the Helmholtz SIMS network, whereby the activities in the Potsdam laboratory will be closely coordinated with new SIMS infrastructure currently being installed in both Dresden (accelerator SIMS) and Leipzig (NanoSIMS 50L). While the 1280-HR is intended mainly for geoscience studies, the facility will also support a limited number of well defined material science investigations as well as serving as a platform for instrumentation development work. This abstract provides a brief overview of the new facility's design and operational goals.

The instrument currently being installed consists of the basic 1280-HR design, including the five trolley multi-collection system along with a Resistive Anode Encoder, thus making the system optimized for both low uncertainty isotope ratio determinations (e.g., $\delta^{13}\text{C}$, $\delta^{18}\text{O}$ and $\delta^{34}\text{S}$) as well as quantification and distribution mapping of low concentration elements in minerals, glasses or biological materials. The possibility of very high mass resolution of $M/dM \geq 25,000$ allows the separation of isobaric masses, such as ^{40}Ca and ^{40}K . The sample loading system consists of the standard 2-positron carousel; a high capacity 500 l/s turbo pump with vibration damping provides improved vacuum in the sample source chamber. The most significant design modification unique to the Potsdam instrument is the addition of 5 flanges in the coupling and projection sections of the machine, including one intended for the integration of a total ion current measuring capability. Factory testing has shown a repeatability for $\delta^{18}\text{O}$ determination ($n=10$) of $\pm 0.25\text{‰}$ (1sd) on a quartz disk, with further improvements in analytical uncertainty expected once the instrument enters routine service. Envisioned key analytical topics include H, B, C, O, S and Pb isotopic studies, geochronological applications and the quantification of volatile elements in geological materials.

Trace-elements distribution in tourmaline, micas and K-feldspar from the Berry-Havey pegmatite (Maine, USA): implications for the pegmatitic evolution

E. RODA-ROBLES¹, W. SIMMONS², A. PESQUERA¹, P. P. GIL-CRESPO¹, J. NIZAMOFF² AND J. TORRES-RUIZ³

¹Dpto. Mineralogía y Petrología, UPV/EHU, Bilbao, Spain, encar.roda@ehu.es

²Earth and Environmental Sciences, University of New Orleans, USA. wsimmons@uno.edu

³Dpto. Mineralogía y Petrología, Universidad de Granada, Spain. jotorres@ugr.es

The Berry-Havey pegmatite (Oxford pegmatite field, Androscoggin County, Maine, USA), is a highly evolved pegmatite enriched in Li, F, B, Be and P. The pegmatite has a complex internal structure, with four texturally and compositionally different zones, which show an increasing degree of evolution inwards: wall zone, intermediate zone, core margin and core zone, where gemmy tourmaline-bearing pockets are common. The main minerals are quartz, feldspars, Al-micas (muscovite-lepidolite series), tourmaline (schorl-elbaite-rossmanite), and minor Fe-micas (biotite and zinnwaldite). Garnet, beryl, amblygonite-montebrazite, and apatite are common accessory minerals.

Most trace elements do not show a clear preference for any of the main minerals. However, Li, Cs, Mn, Ba, Nb, and Ta mainly partition into the Fe-mica, whereas Be, Sn, W and Zr partitions preferably into the Al-mica. P and Sr partition into the K-feldspar. Tourmaline is the poorest of the four phases in trace elements. Li content increases from the wall zone to the core in all the phases. Rb, Cs and Ba show a similar trend for micas and K-feldspar, with Rb and Cs increasing gradually from the wall zone to the core zone, simultaneously to the decrease of Ba. In tourmaline Li, Be, Mn, Sn, Nb and Ta contents increase from the wall zone to the core zone, and finally decrease in the gemmy tourmaline from the pockets. Overall, REE contents are very low. The origin of these differences relates to the concentration of the elements in the melt and the variations in the compatibility of these elements between the minerals and melt during fractional crystallization, which in turn depends on the behavior of major elements. Micas, K-feldspar and tourmaline are good geochemical monitors using trace elements such as Li, Rb, Be, Sr and Ba, to understand the petrogenesis of pegmatites.

Chromium isotope record of the Otavi Group, Namibia

A RODLER^{1,2,4}, R FREI^{2,4}, C GAUCHER^{3,4}, AR VOEGELIN^{2,4}, CV ULLMANN^{2,4} AND C KORTE^{2,4}

¹Natural History Museum of Denmark (alexandra.rodler@reflex.at)

²University of Copenhagen (robertf@geo.ku.dk, andrea.voegelin@geo.ku.dk, cu@geo.ku.dk, korte@geo.ku.dk)

³Universidad de la República, Uruguay (gaucher@chasque.net)

⁴Nordic Center for Earth Evolution (NordCEE)

Due to its redox-sensitivity, the chromium isotope system is an interesting paleoclimatic tracer particularly powerful in recording fluctuations of atmospheric oxygenation and continental weathering [1]. Here we seek to investigate detailed $\delta^{53}\text{Cr}$ records associated with intense climatic changes during Neoproterozoic glaciations.

We present a $\delta^{53}\text{Cr}$ record of late Neoproterozoic marine carbonates stretching from the Chuos (746±2Ma[2]) to the the Ghaub Fm (635.6±0.5Ma[3]), exposed in northern Namibia, covering shallow water sedimentation during the Cryogenian glaciations. The $\delta^{53}\text{Cr}$ stratigraphy was complemented with $\delta^{13}\text{C}_{\text{carb}}$ as well as major and trace element concentrations. The Chuos $\delta^{53}\text{Cr}$ signal is close to mantle inventory [4], but recovers rapidly to positive values after the glacial sequence, indicating a sufficiently oxygenated atmosphere. Prior to the Ghaub glaciation, $\delta^{53}\text{Cr}$ values are positively fractionated (+0.12±0.02‰) and correlate to $\delta^{13}\text{C}_{\text{carb}}$, while in post-Ghaub carbonates $\delta^{53}\text{Cr}$ values decrease to ~-0.08‰, similar to drops observed in post-Chuos sediments, and accompanied by increased Cr, Sc, and Ti concentrations. These $\delta^{53}\text{Cr}$ results suggest increased continental-derived detrital input as a consequence of enhanced weathering periods related to rapid climate change, elevated post-glacial $p\text{CO}_2$ [5], proximity to the continent and/or increased hydrothermally-derived Cr input.

The observed $\delta^{53}\text{Cr}$ fluctuations indicate sufficiently high atmospheric oxygen levels to oxidize and mobilize Cr during weathering processes on land prior and after the major Neoproterozoic glaciations. Increased weathering due to rapid post-glacial rise of $p\text{CO}_2$ render the $\delta^{53}\text{Cr}$ signal unfractionated, also potentially indicating the predominance of accumulated hydrothermally-derived Cr in the shallow seawater pool during the Ghaub aftermath.

[1] Frei *et al.* (2012) *Gondwana Research* **23**, 797–811. [2] Hoffman *et al.* (1996) *Communs Geol. Surv. Namibia* **11**, 47–52. [3] Hoffman *et al.* (2004) *Geology* **32**, 817–820. [4] Schoenberg *et al.* (2008) *Chemical Geology* **249**, 294–306. [5] Crowe *et al.* (2013) *EPSL* (in press).

A new experimental approach to silicic magma differentiation

CARMEN RODRIGUEZ^{1*}, ANTONIO CASTRO² AND ANTONIO SÁNCHEZ-NAVAS³

¹University of Huelva Campus El Carmen, 21071 Huelva, Spain (*correspondence: carmen.rodriguez@dgeo.uhu.es)

²Unidad Asociada de Petrología Experimental, CSIC-University of Huelva, Campus El Carmen, 21071 Huelva, Spain (dorado@uhu.es)

³University of Granada Campus Fuentenueva 18071

The separation of fluid and crystals from melt at diverse stages in the evolution of magmatic systems is inferred on the basis of thermomechanical modelling [1], geochemical relations of zoned silicic plutonic bodies [2] and phase equilibrium studies [3]. However, experimental tests dealing with magmatic differentiation of natural magmas at real pressures and temperatures are very scarce [4, 5].

In our laboratory experiments, gravity effects are separated from those imposed by thermal gradients, which simulate natural conditions of crystallization in a cooling magma chamber. Major and trace element distribution profiles result from the thermal gradient for water-bearing magma systems. The observed profiles are exclusively explained by diffusion in the liquid and boiling-assisted crystal-liquid separation, without invoking gravity crystal settling. These experiments confirm the key role of fluids in silicic magma differentiation and their implications on explosive volcanism and ore deposit generation.

[1]Huber *et al.* (2009) *EPSL* **283**, 38-47. [2] Bachmann & Bergantz (2004) *Journal of Petrology* **45**, 1565-1582. [3] Pichavant *et al.* (2002) *Geochimica et Cosmochimica Acta* **66**, 2193–2209. [4] Masotta *et al.* (2012) *Contributions to Mineralogy and Petrology* 163. [5] Huang *et al.* (2009) *Geochimica et Cosmochimica Acta* **73**, 729-749.

Origin of Grande Ronde Basalts, Columbia River Basalt Group

SEDELIA RODRIGUEZ¹ AND GAUTAM SEN²

¹Florida International University, Miami, FL, USA

²American University of Sharjah, Sharjah, UAE, gsen@aus.edu

The Grande Ronde Basalt lavas contain 0-5% phenocrysts of plagioclase, augite, pigeonite, and olivine. Plagioclase hygrometry shows that the erupted lavas contained less than 0.3% dissolved H₂O. The presence of rare An₉₆ plagioclase megacrysts suggests ~4.5wt% dissolved H₂O in some parent magmas. All magmas degassed during ascent and eruption. Size of plagioclase phenocrysts suggests an average phenocryst residence time in magma of 160 years. Ignoring hiatuses between eruptions, we estimate that the 110 flows of the GRB erupted over a cumulative time of 17,600 years, with an average eruption rate of about 8.6 km³/year. The average interval between eruptions is estimated to be 3658 years. Model simulations and petrological reasoning indicate that the primary melts were generated from spinel peridotite at 1.5 GPa, perhaps under hydrous conditions. Extensive melting of lithospheric eclogite may have played a role as well; however, this is not constrained by our simulations. Magmas underwent contamination, mixing, and partial crystallization during and prior to their short residence within shallow (6 km) intrusives. Our petrologic conclusions lead us to present a petrotectonic model that supports the hypothesis that the CRBG magma generation was greatly aided by a thinned lithosphere and H₂O that may have come off the mantle wedge.

The role and effect of Mg on the formation of carbonates

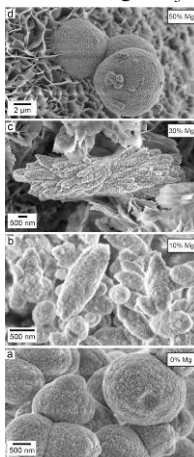
JUAN DIEGO RODRIGUEZ-BLANCO^{1,2*}, SAMUEL SHAW^{1,3}, PIETER BOTS^{1,3} AND LIANE G. BENNING¹

¹School of Earth and Environment, University of Leeds, Leeds LS2 9JT, UK. (* presenting author)

²Nano-Science Center, Department of Chemistry, University of Copenhagen, Denmark.

³School of Earth, Atmospheric and Environmental Sciences, The University of Manchester.

Mg is the most abundant divalent cation in seawater. It plays an important role in the crystallization of CaCO₃-based biominerals that control the marine global carbon cycle. However, the mechanisms of CaCO₃ crystallization from solution in the presence of Mg are still poorly understood. Here we show that a spherulitic growth mechanism often controls the nucleation, growth and crystallization of Ca-Mg carbonate polymorphs produced with variable Mg contents (0-50%) and at different temperatures (7.5-220°C). Combining *in situ* and realtime synchrotron-based diffraction and scattering with time-resolved UV-Vis spectrophotometry and high-resolution imaging we quantitatively evaluated the kinetics and mechanisms of the formation and crystallization reactions in the Ca-Mg-CO₃ system.



Under all conditions an initial, variable Mg containing, poorly-ordered, nanoparticulate precursor (amorphous calcium carbonate, ACC) forms from solution and transforms to various nanocrystalline intermediates via a spherulitic growth mechanism. In turn these intermediates crystallize via a dissolution and reprecipitation mechanisms to end products. The composition, kinetics of formation, local structure and stability of the ACC are dependent on the initial Mg/Ca/CO₃ ratio, the temperature, supersaturation and pH of the reactions. At 0% Mg, pure ACC rapidly (<2 min at 21°C) crystallizes to vaterite via spherulitic growth (image *a*, bottom) and later transforms slower (hours) into calcite through dissolution-reprecipitation [1,2]. With 10% Mg, ACC is ~1 order of magnitude more stable than pure ACC, and transforms to Mg-calcite with no vaterite intermediate [3] (*b*). Higher Mg contents further stabilize the ACC for hours to days. These high Mg-ACC phases crystallize spherulitically either to monohydrocalcite (*c*; Mg/Ca > 0.25; T < 60°C; [4]), dolomite (*d*; at Mg/Ca ~1; T > 60°C; [5]) or various Mg-rich carbonates (e.g., at Mg/Ca > 1 hydromagnesite).

[1] Rodriguez-Blanco *et al* (2011) *Nanoscale* **3**:265-271; [2] Bots *et al* (2012) *Cryst. Growth Des.* **12**:3806-3814 [3] Rodriguez-Blanco *et al* (2012) *J. Alloy. Compd.* **536**:S477-S479; [4]+[5] Rodriguez-Blanco *et al* (2013) *GCA* in review.

www.minersoc.org

DOI:10.1180/minmag.2013.077.5.18

Modeling of enhanced *in situ* biodenitrification in fractured aquifer: Biogeochemical interactions and isotope fractionation

P. RODRÍGUEZ-ESCALES^{1,2,*}, B.M. VAN BREUKELEN³,
G. VIDAL-GAVILAN^{1,2}, A. SOLER² AND A. FOLCH⁴

¹Dept. Geologia. UAB. 08193, Bellaterra, Spain.

(*correspondance: prescales@gmail.com).

²D'ENGINY biorem S.L., C. Madrazo 68, 08006 Barcelona, Spain.

³Dept. Cristal·lografia, Mineralogia i Dipòsits Mineals, UB, Martí Franquès s/n, 08028, Barcelona, Spain.

⁴Dept. of Earth Sciences, VU University Amsterdam, De Boelelaan 1085, NL-1081 HV Amsterdam, The Netherlands.

⁵GHS, Dept. of Geotechnical Engineering and Geo-Sciences. UPC. Jordi Girona 1-3, Mòdul D-2. 08034, Barcelona, Spain.

Enhanced *in situ* biodenitrification (EIB) is a feasible technology to clean up nitrate-polluted groundwater and achieve drinking water standards. We developed a reactive transport model that considers biogeochemical processes as well as isotope fractionation to enable better monitoring and management of this technology. In this work, we applied this model to interpret data from batch experiments on EIB. Furthermore, 2-D simulations at field scale are in progress to model an EIB pilot conducted in a fractured aquifer system. The used codes were PHREEQC for batch scale and PHAST for field scale. The fractured media were modeled as equivalent continuum media with two hydraulic conductivity zones. The flow model was validated with experimental data from a tracer test with bromide. The reactive transport model at batch and field scale was validated with experimental values of Vidal-Gavilan *et al.* (2013) [1]. The preliminary results show that parameters determined in batch experiments can be used as first estimates to reproduce field observations provided groundwater flow is well known. Moreover, the inclusion of isotope fractionation processes allowed to determinate the real scope and exact degree of EIB at field scale.

[1] Vidal-Gavilan, G., Folch A., Otero N., Solanas, A.M., Soler A., 2013. App.Geochem (in press).

Uptake of $Pb^{2+}_{(aq)}$ by baryte-celestine solid-solution crystals

R. M. RODRÍGUEZ-GALÁN, J. CARNEIRO AND M. PRIETO

Department of Geology, University of Oviedo, Spain

The interaction of dissolved toxic metals with minerals frequently leads to dissolution-coprecipitation processes in which the metal ion incorporates into the solid phase substituting for the major ion in lattice positions. The fact that the solubility of a minor constituent in a solid solution is smaller than the solubility of its equivalent pure solid explains the environmental relevance of these coprecipitation reactions. Interaction studies are typically carried out by using stoichiometric minerals as host phases. However, in most cases the effectiveness of this removal mechanism could be significantly increased using suitable solid-solutions instead of pure minerals. In this work we study the interaction of Pb-bearing aqueous solutions with baryte ($BaSO_4$) and intermediate (5-15 % molar Sr) members of the $(Sr,Ba)SO_4$ solid solution.

Compositionally homogeneous crystals of the solid solution were obtained by precipitation & aging in a closed reactor at 90°C. The obtained precipitates were checked for compositional homogeneity by considering the full width at half maximum intensity values (FWHM) of some selected reflections of the XRD patterns. The precipitate compositions were determined by analyzing the remaining solutions by ICP-AES. Moreover, samples of each precipitate were analyzed by SEM-EDS.

The interaction experiments were carried out in closed reactors at 25°C. The aqueous composition was analyzed repeated times during the experiments, which lasted one month. In the case of the interaction with strontian baryte, lead incorporates into the solid phase while some barium and a large proportion of strontium incorporate to the aqueous solution. As result the aqueous solution becomes depleted in lead at a significantly greater extent than during the interaction with pure baryte.

Future work will deal with the implementation of an equilibrium model for the $(Pb,Sr,Ba)SO_4-H_2O$ system. An added implication is related to the effectiveness of Sr-bearing baryte as a sequestering phase for radium. The interaction with baryte leads to a significant removal of dissolved Ra^{2+} , but the depletion could be considerably greater using strontian baryte.

Acknowledgements. This work was supported by the German Federal Ministry of Education and Research (ImmoRad: 02 NUK 019A)

Biom mineralization of Mg-rich Calcite (Mg_xCa_{1-x}CO₃) by *Proteus mirabilis*

YUL ROH^{1*} AND SERKU KANG²

¹Chonnam National University, Gwangju, Korea,
(*correspondence: rohy@jnu.ac.kr)

²Chonnam National University, Gwangju, Korea,
(chodang02@naver.com)

Recently bacterially induced carbonate precipitation has been proposed as an environmentally friendly method to apply CO₂ sequestration and fixation [1]. The objectives of this study were to investigate biom mineralization of the carbonate minerals using microorganisms enriched from rhodoliths and to identify environmental factors that control the formation of calcite by the microorganisms.

Carbonate forming microorganism (CFM) was enriched from rhodoliths using D-1 medium for microbial activity and aerobically cultured at 25°C using D-1 medium with containing 30:30 mM Ca:Mg-acetate concentrations to confirm formation of carbonate minerals. Enriched microorganisms were analyzed by 16S rRNA gene DGGE analysis to confirm microbial diversity. Various ratios of Ca and Mg-acetate concentrations (60:0, 60:20, 20:60, 0:60 mM) were added to D-1 medium to examine how different Ca and Mg ratios affect the biom mineralization of carbonate minerals. Mineralogical characteristics of bio-precipitates were determined by XRD and SEM-EDS analyses.

A 16S rRNA sequence analysis showed the enriched microorganisms contained CFM such as *Proteus mirabilis* [2]. XRD analyses showed that the precipitates were calcite with Ca:Mg-acetate (60:0, 60:20 mM), Mg-rich calcite with Ca:Mg-acetate (30:30, 20:60 mM) and huntite with Ca:Mg-acetate (0:60 mM) were formed, whereas any carbonate minerals were not formed without the microorganisms in D-1 medium. Also, through various ratios of Ca/Mg concentrations, we observed that the formation of Mg-rich calcite and huntite occurred when the level of Mg ion was much higher than that of Ca ion in D-1 medium. SEM-EDS analyses showed that the carbonate minerals formed by the microorganisms were a rhombohedron shape consisted of Ca, Mg, C, and O and irregular shaped extracellular polymeric substance (EPS) with Ca, Si, and Mg component.

These results indicate that the microorganisms induce precipitation of carbonate minerals on the cell walls and EPS via the accumulation of Ca and/or Mg ions on the cells. Therefore, microbial precipitation of carbonate minerals may play one of important roles in metal and carbon biogeochemistry as well as carbon sequestration in natural environments.

[1] Reddy (2012) *J. Cryst. Growth.* **352**, 151-154. [2] Xi *et al.* (2002) *Infect. Immun.* **70**(1), 389-394.

Redox processes in the Earth's mantle

ARNO ROHRBACH¹

¹Institut für Mineralogie, Westfälische Wilhelms-Universität
Münster, Germany, arno.rohrbach@uni-muenster.de

Redox reactions are crucial for many geological processes, but especially how Earth's surface and atmosphere became oxidized enough to form a habitable planet is a key question. To understand redox controls in Earth's mantle is of prime importance, because oxygen fugacity (fO₂) regulates the biogeochemical cycles of volatiles such as C-O-H or S and their respective fO₂-dependent species. These volatiles also link deep mantle reservoirs and Earth's surface because they promote mantle convection and initiate volcanism through solidus depression in various tectonic settings.

The redox state of the mantle may be reconstructed, for instance, by investigating mantle melts. Subduction related basalts (IAB) have higher Fe³⁺-ΣFe ratios than mid-ocean ridge basalts (MORB) or ocean island basalts (OIB) [1]. A matter of debate is, whether these higher redox states are a source signal from the mantle wedge with higher Fe³⁺-ΣFe compared to the MORB source [2], or, if IAB melts are affected by post genetic oxidation at some stage between early crystallization and solidification. Fe³⁺-ΣFe ratios in basalt glasses correlate with H₂O content [1] but differ from results based on other redox proxies such as V/Sc [3,4], Zn/Fe_T [5], or Fe isotopes [6]. Key problems, e.g., if and how subduction related fluids oxidize the mantle, if subduction causes a secular variation in mantle fO₂, or if the mantle is buffered with respect to fO₂ remain highly controversial.

Oceanic crust, lithosphere and overlying sediments are generally more oxidized than the ambient mantle if subducted to depths >100 km, because cratonic lithosphere and potentially also the asthenosphere become increasingly reduced with increasing depth [7,8]. The redox contrast between delaminated oxidized blocks from the slab and reduced ambient mantle sets the frame for hydrous and carbonatitic redox melting processes in the deeper mantle [9,10].

[1] Kelley & Cottrell (2009) *Science* **325**, 605–607. [2] Malaspina *et al.* (2009) *J. Petrol.* **50**, 1533–1552. [3] Mallmann & O'Neill (2009) *J. Petrol.* **50**, 1765–1794. [4] Lee *et al.* (2005) *J. Petrol.* **46**, 2313–2336. [5] Lee *et al.* (2010) *Nature* **468**, 681–685. [6] Dauphas *et al.* (2009) *EPSL* **288**, 255–267. [7] Stagno *et al.* (2013) *Nature* **493**, 84–88 [8] Rohrbach *et al.* (2007) *Nature* **449**, 456–458. [9] Foley (2011) *J. Petrol.* **52**, 1363–1391. [10] Rohrbach & Schmidt (2011) *Nature* **472**, 209–212.

Palaeozoic biosphere and climate: Modes of marine primary production and methane cycling feedbacks

MEGAN ROHRSSSEN¹, GORDON D. LOVE*¹
AND CHRISTOPHER T. REINHARD²

¹Department of Earth Sciences, University of California,
Riverside, CA, 92521, USA; *Correspondence:
glove@ucr.edu

²Department of Geological and Planetary Sciences, California
Institute of Technology, Pasadena, CA, 91125, USA

Lipid biomarker records of microbial community structure during the Late Ordovician through Early Silurian (~449-439 Ma) indicate substantial differences in the balance of bacterial versus algal primary production through the Late Ordovician, largely in response to climatic change associated with the Hirnantian glaciation ([1]). Our biomarker records suggest that these warm Palaeozoic intervals were associated not only with elevated atmospheric $p\text{CO}_2$ (~4-16x preindustrial atmospheric levels, PAL), but also with a higher average flux of oceanic methane, exerting a potential positive feedback on hothouse climates in the Paleozoic. To refine the assessment of a methanotrophic contribution to lipid biomarkers, we have conducted compound-specific carbon isotope analyses on hydrocarbon extracts from Anticosti Island (Canada) the Vinini Formation (USA), the Maquoketa Formation (USA), and OM9 drill core (Estonia).

Recent models have demonstrated that a relatively modest increase of 4-5x preindustrial $p\text{CH}_4$ can generate 2-3°C of warming [2]. Methane cycling feedbacks on climate must have been of similar or greater impact in the Palaeozoic, a period of warm conditions and reduced oxidant availability [3] which may have driven a larger proportion of remineralized organic matter through microbial methanogenesis and attenuated the efficacy of combined anaerobic methane oxidation processes as a throttle for methane fluxes to the atmosphere. Because the loss rate of atmospheric methane scales inversely with atmospheric methane abundance [4], increased fluxes to the atmosphere will often translate into higher steady-state concentrations. We explore the possible effects of this for Palaeozoic times with a series of simple mass balance calculations given a range of carbon flux and anaerobic remineralization scenarios.

[1] Rohrsen, *et al.* (2013), *Geology* 47, 127-130. [2] Beerling, *et al.* (2011), *PNAS* 108, 9770-9775. [3] Luo, *et al.* (2010), *EPSL* 300, 101-111. [4] Schmidt & Shindell (2003), *Paleoceanography* 18, 1-9.

Solubility and TRLFS studies on Nd(III)/Cm(III) complexation with gluconate in NaCl and CaCl₂ media.

H. ROJO^{1,2}, X. GAONA¹, TH. RABUNG¹, M. GARCIA³,
T. MISSANA³ AND M. ALTMAIER¹

¹Institute for Nuclear Waste Disposal, Karlsruhe Institute of
Technology, Karlsruhe, Germany (henar.rojo@kit.edu)

²Laboratory for Waste Management, Paul Scherrer Institut,
Villigen PSI, Switzerland

³CIEMAT, Research Centre for Energy, Environment and
Technology, Madrid, Spain

Radionuclide sorption and solubility in cementitious systems can be affected by the presence of organic ligands. Gluconic acid (GLU) is a poly-hydroxocarboxylic acid expected in repositories for low and intermediate-level radioactive waste as a component of cementitious materials. The formation of very stable An(III)-GLU complexes has been reported in the literature, although in contrast to An(IV) no ternary species Ca-An(III)-GLU have been described so far. These species may play a relevant role in cementitious and saline environments, where high Ca^{2+} concentrations are expected in certain scenarios.

Undersaturation solubility studies with $\text{Nd}(\text{OH})_3(\text{am})$ were conducted in inert gas (Ar) gloveboxes at $22 \pm 2^\circ\text{C}$. Samples were prepared in dilute NaCl (0.1 M) and CaCl_2 (0.1 and 0.25 M) solutions as background electrolytes. Parallel experimental series were prepared with $\text{pH}_c = \text{constant} \sim 12$ and $10^{-6} \leq [\text{GLU}] \leq 10^{-2}$ M, and with $[\text{GLU}] = \text{constant} = 10^{-3}$ M and $9 \leq \text{pH}_c \leq 13$. TRLFS measurements were performed with $\sim 10^{-7}$ Cm(III) per sample, with NaCl (0.1 M) and CaCl_2 (0.1 and 0.25 M) as background electrolytes. In the NaCl systems, three different concentration levels of Ca^{2+} were considered: 0, 10^{-3} M and 10^{-2} M. The initial concentration of GLU in all samples (10^{-6} M) was increased to $3 \cdot 10^{-3}$ M by step-wise additions of NaCl-NaGLU or CaCl_2 -CaGLU₂ solutions of appropriate ionic strength.

The solubility of $\text{Nd}(\text{OH})_3(\text{am})$ remains unaffected by GLU in 0.1 M NaCl solutions. On the other hand, solubility of $\text{Nd}(\text{OH})_3(\text{am})$ in 0.1 and 0.25 M CaCl_2 solutions is clearly increased by GLU under hyperalkaline conditions. The species forming are pH-dependent and unequivocally involve the participation of Ca^{2+} , with the likely formation of a Nd-GLU complex with stoichiometry 1:2. No further increase of Nd(III) concentration is observed at $[\text{GLU}]_{\text{tot}} \geq 10^{-3}$ M, resulting in an upper solubility limit at $[\text{Nd}] \sim 10^{-6.5}$ M which suggest the formation of a new Ca-Nd-GLU solubility limiting solid phase. Consistently with Nd(III) solubility data, TRLFS confirms the key role of Ca^{2+} in the complexation process, with the likely formation of a Ca-Cm(III)-GLU complex with Ca:GLU ratio 1:1. Two Ca-Cm-GLU species are further identified in 0.1 M and 0.25 M CaCl_2 solutions.

Importance of reference materials and of the determination of matrix effects for precise and accurate measurements by SIMS

C. ROLLION-BARD¹ AND NANCY ION MICROPROBE TEAM¹

¹Centre de Recherches Pétrographiques et Géochimiques, Univ. de Lorraine, UMR 7358, 15 rue Notre Dame des Pauvres, F-54500 Vandoeuvre-lès-Nancy, France, rollion@crpg.cnrs-nancy.fr

SIMS technique (Secondary Ion Mass Spectrometer) has been used for several decades to examine element and isotope compositions at micrometer scale in various geological samples [1]. But SIMS measurements are subject to matrix effect at the time of sputtering process. To overcome these matrix effects in the order to achieve precision and accuracy of the analyses, reference materials are needed. These reference materials must have the same chemical composition and mineralogy of the sample, or at best, must be the closest possible.

We will show different examples of determination of matrix effect for oxygen isotopes: in CaCO₃ polymorphs, in different carbonates (magnesite, dolomite, siderite, rhodochrosite and ankerite, [2]), and in a solid-solution, i.e. Fe-Ca-Mg garnets [3,4]. We will highlight the importance of the choice of the reference materials and the determination of possible matrix effect. When all the precautions regarding these effects are taken, a precision better than 0.5 ‰ can be achieved, the more complex the correction, the worse precision is reached.

[1] Shimizu N. & Hart S.R., 1982, *Ann. Rev. Earth Planet. Sci.*, 10, 483-526. [2] Rollion-Bard C. & Marin-Carbonne J., 2011, *JAAS*, 26, 1285-1289. [3] Vielzeuf D. *et al.*, 2005, *Chem. Geol.*, 223, 208-226. [4] Page F.Z. *et al.*, 2010, *Chem. Geol.*, 270, 9-19.

Differentiating magma sources from conglomerate and breccia clasts, IODP Site U1349, Ori Massif, Shatsky Rise Oceanic Plateau

I.V. ROMANOVA* AND D.T. MURPHY

School of Earth, Environmental and Biological Sciences, Queensland University of Technology, 4001, Brisbane, Australia (*correspondence: i.romanova@qut.edu.au)

Shatsky Rise in the northwestern Pacific is one of the largest (~500,000 km²) and oldest (145-135 Ma) Large Igneous Province on the oceanic floor. Studies of magnetic lineations and bathymetry showed that Shatsky has an elongated structure with three edifices (Tamu, Ori, Shirshov) progressively decreasing in age and in volume [1]. Integrated major and trace elements and Sr-Nd-Pb-Hf isotopes for the Shatsky Rise basalts show 4 distinct magma types and MORB-like compositions with trends towards the enriched plume(?) source for Ori and Shirshov Massifs [2-4]. Deciphering deep plume vs. shallow mantle contributions to the Shatsky magmatism remains a fundamental problem.

During the IODP Expedition 324, site U1349A penetrated Ori massif near its summit [5] and recovered volcanoclastic sandstones, volcanic breccia, a clay-rich layer and polymictic volcanoclastic conglomerate (Unit III, ~20 m) between sedimentary layers and igneous basement. The breccia clasts range in size from 2-20 mm and the conglomerate clasts from 2-80 mm. These fragments represent eroded volcanic material originating from locally sourced portions of the Ori Massif.

All clasts are heavily altered picritic and tholeiitic basalts with little or no primary magmatic minerals preserved and significant enrichments in fluid mobile elements (Ca, Na and K). For the fluid immobile element Ti the concentration of TiO₂ ranges from 1.8-4 wt.%, whereas the Shatsky Rise basement lavas have no TiO₂ contents higher than 2.7 wt.%. This implies that the clasts are derived from different lavas with distinct petrogenesis and geochemistry relative to the rest of the basement lavas sampled to date. Thus, at least 5 magma types compose Ori Massif. Trace element and Nd-Hf isotope data on the new High-Ti magma type will allow further investigations into source heterogeneities.

[1] Nakanishi *et al.* (1999) *Journal of Geophysical Research Solid Earth* **104**, 7539-7556. [2] Mahoney *et al.* (2005) *Geology* **33**, 185-188. [3] Sano *et al.* (2012) *Geochemistry Geophysics Geosystems* **13**, 8010-8010. [4] Geldmacher *et al.* (2012) AGU Fall Meeting, D151A-2339. [5] Expedition 324 Scientists (2010) *Proc. IODP*, **324**: Tokyo (IODP-MI).

A 2000-year rainfall record from the Eastern Tropical Pacific and ENSO variability during the Common Era

LIDIA ROMERO VIANA^{1,2}, ULRIKE KIENEL²
AND DIRK SACHSE¹

¹University of Potsdam, Institute of Earth and Environmental Science, Karl-Liebknecht-Str. 24-25, 14476 Potsdam-Golm, Germany

²GFZ German Research Centre for Geosciences, Telegrafenberg, 14473 Potsdam, Germany

The ENSO is the dominant mode of interannual tropical climate variability with widespread global teleconnections. Understanding its natural variability is a key factor to evaluate its effect on the internal variability in the global climate system. We present a 2000-year rainfall reconstruction from the Eastern Tropical Pacific based on a calibrated lipid biomarker ratio, the DiTe index [1], using the annually laminated sedimentary sequence of a crater-lake located in Isabel Island (Mexico). In the region, the highly seasonal rainfall pattern is dominated by ENSO dynamics, resulting in drier/wetter conditions during positive (El Niño)/negative (La Niña) anomalies. Our inferred past rainfall variability shows negative anomalies at millennial and centennial scale coinciding with periods of high frequent and strong El Niño events being coherent with other hydroclimatic records, based on independent proxies within the target region. Our record of subdecadal resolution allows for detailed evaluation of regional rainfall variability during key periods, such as, the Medieval Climate Anomaly and Solar minima and therefore, contributes to the understanding of climatic variability in the Tropical Pacific. [1] Romero-Viana, Kienel & Sachse (2012), *Palaeogeogr. Palaeoclimatol. Palaeoecol.* 350, 49-61.

Are the anhydrite and gypsum carbonation pathways the same?

T. RONCAL-HERRERO¹, P. BOTS^{1,2},
J.D. RODRIGUEZ-BLANCO^{1,3}, J.M. ASTILLEROS^{4,5*},
M. PRIETO⁶, L.G. BENNING¹ AND L. FERNÁNDEZ-DÍAZ^{4,5}

¹School of Earth & Environment, University of Leeds, LS2 9JT, United Kingdom

²School of Earth Atmospheric and Environmental Sciences, University of Manchester, M13 9PL, United Kingdom

³Nano-Science Center, Department of Chemistry, University of Copenhagen, Denmark

⁴Department of Crystallography and Mineralogy, Complutense University of Madrid, Spain. (*correspondence: jmastill@ucm.es)

⁵Institute of Geoscience (CSIC, UCM), Madrid, Spain.

⁶Department of Geology, University of Oviedo, Spain.

Coupled dissolution-recrystallization reactions during interactions between carbonate-bearing fluids and calcium sulphate minerals lead to de novo formation of CaCO₃ polymorphs. The carbonation of anhydrite (ANH, CaSO₄) and gypsum (GYP, CaSO₄·2H₂O) produces dramatic changes in both textural and chemical properties of the starting calcium sulphate phase (e.g., porosity, composition etc.). However, our understanding of such processes is still fragmented.

Here we present an experimental study comparing the carbonation of ANH and GYP at 25 °C. In both cases, the formation of various CaCO₃ polymorphs occurred immediately upon contact between the solid phase and a Na₂CO₃ solution. However, differences in textural features and reaction pathways were observed between both systems. GYP carbonation produces a large volume of porosity with a prominent gap between parent and product phases. Conversely during ANH carbonation such a gap does not form and porosity generation is minimal. Furthermore, the produced CaCO₃ polymorphs are spatially differently distributed on ANH vs. GYP surfaces and within the replaced layer indicating that the nature and reactivity of the parent phases control the CaCO₃ polymorph and the evolution of textural features during carbonation. These results have implications for biomineralization, CO₂ sequestration and industrial applications.

ACKNOWLEDGEMENT. This work was supported by EC under grant MRTN-2006-035488 and MECC-Spain under grant CGL2010-20134-C02-01.

Opal-CT precipitation in a clayey soil explained by geochemical transport model of dissolved Si (Blégny, Belgium)

B. RONCHI^{1*}, A.L. BARAO², F. VANDEVENNE²,
N. VAN GAELLEN¹, D. VERHEYEN¹, R. ADRIAENS¹,
O. BATELAAN¹, A. DASSARGUES¹, E. STRUYF², J. DIELS¹
AND G. GOVERS¹

¹KULeuven, Celestijnenlaan 200E, 3001 Heverlee, Belgium
(*correspondence: benedicta.ronchi@ees.kuleuven.be)

²UA, Campus Drie Eiken, D.C.116, Universiteitsplein 1, 2610 Wilrijk, Belgium

Dissolved Si (DSi) exported by rivers are controlled by geological, hydrological and biological cycle processes [1]. The DSi concentrations measured in a river of an upstream catchment in eastern Belgium (Blégny, Land of Herve) don't vary seasonally ($6.91 \pm 0.94 \text{ mg L}^{-1}$; $n=363$). Si concentrations in pore water are often higher and vary more ($8.65 \pm 3.65 \text{ mg L}^{-1}$; $n=128$). The decrease of DSi along the flowpath of water is due to sink processes, i.e. precipitation, adsorption or uptake by vegetation. As the DSi in the river does not show any seasonal variation, uptake by vegetation can be ruled out [1] whereas precipitation or adsorption can control the DSi drained by the stream water. This hypothesis is confirmed by XRD and DeMaster analysis. At 0.1m depth the soil is constituted of 62% quartz, 7% K-feldspar, 6% plagioclase, 3.2% carbonates, 18.9% Al-clay, 1.47% Kaolinite, 0.63% Chlorite and 0.2% amorphous Si, probably of biogenic origin. At 1.5m depth, the amounts of several minerals (35.8% quartz, 0.6% K-feldspars, 0.9% plagioclase, Al-clay 14.7%) drop drastically. Carbonates, chlorite and kaolinite are absent whereas 40.4% opal-CT appears. The precipitation of opal-CT controls the DSi export of this catchment.

To describe DSi export from a catchment a geochemical transport model is developed in HP1 which couples the water flux model Hydrus with the geochemical model PHREEQC [2]. Our model is based on the conceptual model developed in [3]. First results show different DSi export dynamics in the unsaturated zone than in the aquifer due to different $p\text{CO}_2$ values and varying soil moisture conditions. Further development of the model will help to find out the reason of opal-CT precipitation in this setting.

[1] Fulweiler, Nixon (2005) *Biogeochemistry* **74**:115–130. [2] Simunek, Jacques, van Genuchten, Mallants (2006) *JAWRA* **42**:1537–1547. [3] Ronchi *et al.* (2013). *Silicon*, **5**(1), 115–133.

Constraining the origin of sulfur isotopic variability through the end-Ordovician Hirnantian glaciation and mass extinction

CATHERINE V. ROSE^{1*} AND DAVID A. FIKE¹

¹Department of Earth & Planetary Sciences, Washington University, St. Louis, MO 63130, USA

*(crose@eps.wustl.edu)

Geochemical records of the end-Ordovician Hirnantian Stage show parallel positive excursions in the stable isotope compositions of sedimentary pyrite sulfur ($\delta^{34}\text{S}_{\text{pyr}}$), organic carbon, and carbonate carbon; these isotope excursions coincide with the end-Ordovician glaciation and mass extinction. An increase in pyrite burial attributed to marine anoxia has been proposed to explain the sulfur isotope excursion and link oceanic redox conditions to the extinction of marine fauna. Such an increase in pyrite burial would generate a parallel excursion of equal magnitude in the isotopic composition of coeval marine sulfate. However, paired sulfur isotope data from the Hirnantian Stage of Anticosti Island, Quebec, do not covary, which suggests enhanced pyrite burial is not the cause of the Hirnantian $\delta^{34}\text{S}_{\text{pyr}}$ excursion and questions the role of anoxia in the mass extinction. We present new high-resolution paired sulfur isotope data from carbonate-associated sulfate (CAS) and pyrite during the Hirnantian Stage from the Girardeau Formation, Missouri, USA, to test these hypotheses. The results show a 28‰ enrichment in $\delta^{34}\text{S}_{\text{pyr}}$ but no parallel excursion in $\delta^{34}\text{S}_{\text{CAS}}$, indicating that enhanced pyrite burial did not generate the Hirnantian $\delta^{34}\text{S}_{\text{pyr}}$ excursion. These observations may best be explained by a transient reduction in the expressed isotopic fractionation during microbial sulfate reduction associated with Hirnantian sulfur cycling possibly caused by: a change in actual biological fractionation; a shift in the chemocline leading to restricted exchange of porewater sulfate; or glacio-eustatic sea-level drawdown corresponding to syndepositional sediment reworking and increased oxidation.

Fe Isotope Fractionation During Reduction of Fe(III) to Fe(II)

A.D. ROSENBERG*, C.E. HODIERNE AND S.G. JOHN

Dept. of Earth and Ocean Sciences, University of South Carolina, USA (*correspondence: arosenberg@geol.sc.edu)

Phytoplankton growth, and thereby primary productivity, is limited in many regions of the ocean by insufficient iron (Fe) availability. In seawater iron exists in two different oxidation states – Fe(III) and Fe(II). While Fe(III) is thermodynamically stable in oxic environments, it can be reduced to Fe(II) by photochemical or biological reduction. In the ocean release of Fe(III) from ligands by reduction to Fe(II) is often necessary for Fe to become bioavailable to phytoplankton. Recently, techniques have been developed to measure dissolved Fe stable isotope ratios ($\delta^{56}\text{Fe}$) in seawater and marine plankton, opening the door to using $\delta^{56}\text{Fe}$ as a tracer for biologically important Fe redox cycling in the oceans.

In order to clarify the impact that various reduction pathways have on Fe isotopic fractionation, the natural reduction of Fe(III)-L to Fe(II) was simulated in the lab by the reduction of Fe(III)-EDTA to Fe(II) in three ways: photochemically, chemically, and electrochemically. During photochemical reduction, Fe(III)-EDTA was reduced upon exposure to direct sunlight which promotes ligand-to-metal charge transfer. Chemical reduction was achieved by the addition of a reducing agent such as hydroxylamine hydrochloride. Electrochemical reductions were carried out using a rotating-disc electrode at a variety of overpotentials. Following reduction, Fe(II) was collected and purified for Fe isotope analysis by MC-ICPMS.

The reduction pathway has a large impact on the observed isotope effect. Photochemical reduction produces positive $\delta^{56}\text{Fe}$ values (+0.95 to +1.03 ‰) while chemical reduction produces negative $\delta^{56}\text{Fe}$ values (-1.73 to -2.20 ‰) with electrochemical reduction iron isotope ratios (-0.28 to -0.94 ‰) falling in between the two. Further investigation into isotopic fractionation during reduction of Fe(III) to Fe(II) may provide insight into the pathways by which Fe(III) is reduced and made bioavailable to phytoplankton in the oceans, leading to an overall greater understanding of marine iron cycling.

Linking nutrient and contaminant dynamics in rhizospheres of hyperaccumulators

C.E. ROSENFELD^{1*}, R.L. CHANEY², A. LANZIROTTI³ AND C.E. MARTÍNEZ¹

¹Pennsylvania State University, Department Ecosystem Science and Management, University Park, PA, USA, cer196@psu.edu (* presenting author), cem17@psu.edu
²USDA ARS Environmental Chemistry Laboratory, Beltsville, MD, USA Rufus.Chaney@ars.usda.gov
³Consortium for Advanced Radiation Sources, University of Chicago, Chicago, IL, USA lanzirotti@uchicago.edu

Trace metal contamination in soils is a global problem, causing plant and microbial toxicity, diminished crop production or decreased land cover. Some plants can grow, and even thrive, in heavily polluted soils though it is generally unclear how. Our goal was to elucidate linkages between contaminant and nutrient uptake in plants grown in metal contaminated soil.

We examined two ecotypes (Ganges and Prayon) of the metal hyperaccumulator, *N. caerulescens* (formerly *Thlaspi caerulescens*) grown on field-contaminated soil. Both ecotypes are known zinc (Zn) hyperaccumulators, while only the Ganges ecotype hyperaccumulates cadmium (Cd). At harvest, rhizosphere and plant thin sections were obtained for synchrotron-based μ -X-ray fluorescence (μ -XRF) and Zn- μ -X-ray Absorption Near Edge Structure (Zn- μ -XANES) spectroscopy.

Substantial Zn was accumulated by the plants (1390 mg Zn/kg), though there was no significant difference between ecotypes. Cadmium uptake, was significantly greater in the Ganges ecotype (750 mg Cd/kg) than the Prayon ecotype (90 mg Cd/kg). There was also greater Cd root-to-shoot translocation (root:shoot ratio = 0.13) than Zn (root:shoot ratio = 0.81). The Ganges ecotype took up significantly less Ca, which was also evident by the reduced rhizosphere Ca/Zn correlation in that ecotype. All rhizosphere soil regions investigated contained spectral features consistent with a combination of ZnS and ZnO, while bulk soil regions only occasionally contained such features. Inside the Ganges root, Zn speciation was most consistent with complexation by soft ligands (e.g. cysteine or histidine) while the Prayon roots contained Zn in a combination of mineral ZnO/Zn(OH)₂-like forms and hard-ligand (e.g. organic acids) complexes.

Nutrient biogeochemical cycles are often linked to differential metal accumulation in plants, as nutrient acquisition may be enhanced or inhibited because of contaminant uptake. In our plants, increased Cd uptake was correlated with decreased Ca uptake, decreased Zn-Ca co-location, and altered Zn speciation. On a larger scale, shifting Zn complexation in roots and the rhizosphere may impact Zn bioavailability to other organisms and mobility within contaminated ecosystems.

Particulate Organic Carbon Age Spectra: Evaluating Different Spectra from Different Basin Types

BRAD E. ROSENHEIM¹; VALIER GALY²,
ELIZABETH K. WILLIAMS³; BRIAN J. ROBERTS⁴;
MEAD A. ALLISON⁵; KATHRYN SCHREINER⁶
AND THOMAS S. BIANCHI⁷

¹Tulane University, brosenhe@tulane.edu

²Woods Hole Oceanographic Institution, vgalay@whoi.edu

³Tulane University, ewillia6@tulane.edu

⁴Louisiana Universities Marine Consortium,
broberts@lumcon.edu

⁵The Water Institute and Tulane University,
mallison@thewaterinstitute.org

⁶Northwestern University,
kathryn.schreiner@northwestern.edu

⁷University of Florida, tbianchi@ufl.edu

We compare age spectra from a multi-year sampling effort on the Mississippi-Atchafalaya River System (MARS), in which several different discharge regimes were sampled, the Narayani River in Nepal, and the Colville River Delta, for application of ramped pyrolysis ¹⁴C analysis to samples from different basin types. The emerging picture from the MARS is one of consistency, with some variability related to flood provenance and discharge. Large river systems such as the MARS are integrative of a range of different lithologies and carbon sources. In contrast, the Narayani River, where high incision rates erode old carbonaceous rocks more efficiently during high discharge events, shows more variability and wider overall age spectra. Limited sedimentary storage of watershed primary productivity in the Narayani River watershed results in substantially wider age spectra than from the MARS system. It is likely that the Narayani River is less consistent in time than the MARS as contributions of old carbonaceous material are likely driven by discharge regime. We add to this comparison density-separated fractions from POC samples of the Arctic Colville River to further test a recent conceptual model of basin-control on POC age structure (Blair and Aller, 2012).

The fate and behaviour of volatiles during subduction of oceanic crustal material towards the deep mantle

A. ROSENTHAL^{1*} AND D.J. FROST¹

¹Bayerisches Geoinstitut, University of Bayreuth, 95440
Bayreuth, Germany (*correspondence:
Anja.Rosenthal@Uni-Bayreuth.de)

Knowledge of the abundance and distribution of H₂O in the Earth's deep interior (i.e. mantle and core) remains highly controversial.

The chief means of replenishment of the Earth's interior with volatiles over much of geological time is subduction (i.e. the transport of crustal material into the deep Earth by large-scale tectonic processes) but constraints are very poor as natural samples from the deep Earth's interior subduction zones are inaccessible. High pressure experimental investigations however can overcome that problem by simulating deep mantle conditions and processes.

The aim of this study is to experimentally determine the maximum storage capacity, solubility and behaviour of H₂O in hydrous and nominally anhydrous minerals (NAMs) during subduction of hydrated oceanic crustal material into the deep upper mantle. We apply a novel experimental approach, which will for the first time enable determination of maximum H₂O contents of NAMs (and hydrous phases) in equilibrium with the full phase assemblage in subducted oceanic crust. This was not achieved in numerous previous studies which concentrated on simple, monomineralic systems.

Here, we present first results of experimentally determined melting and phase relations of an altered oceanic basalt composition GA1 [1] containing varying amounts of water (<1 wt%) at varying temperatures (sub-solidus to near solidus) and pressures (6-9 GPa; i.e. ~200 to ~300 km depth) using multi anvil apparatuses at University of Bayreuth, Germany.

Outcomes will allow constraints to be placed on the fluxes of H₂O recycled into the mantle at subduction zones, a critical step in the Earth's overall volatile budget.

[1] Yaxley & Green (1994) *EPSL* **128**, 313-325.

Redox and pressure controls on iron isotope variations in MORBS determined by NRIXS spectroscopy

M. ROSKOSZ^{1*}, N. DAUPHAS², E.E. ALP³, C.K. SIO²,
F. L.H. TISSOT², D.R. NEUVILLE⁴, M. HU³, J. ZHAO³,
L. TISSANDIER⁵, C. CORDIER¹ AND E. MÉDARD⁶

¹*Unité Matériaux et Transformations, Université de Lille,
mathieu.roskosz@univ-lille1.fr

²Origins Laboratory, The University of Chicago,

³Advanced Photon Source, Argonne National Laboratory

⁴Institut de Physique du Globe de Paris

⁵Centre de Recherches Pétrographiques et Géochimiques,
Nancy

⁶Laboratoire Magmas et Volcans, Clermont Université.

Iron isotopic variations are commonly reported in materials produced in high temperature environments such as planetary mantles. However, a reliable database of equilibrium fractionation factors between melts and igneous minerals is still lacking to interpret the rock record. In the case of iron, these factors can be directly derived from Nuclear Resonant Inelastic X-ray Scattering (NRIXS) experiments at a synchrotron facility [1, 2] through the determination of mean force constants. This method is insensitive to kinetic effects during mineral and glass synthesis, contrasting with conventional experimental approaches [3].

Because iron is a multivalent element, its isotopes could be good tracers of redox conditions during melting [4, 5]. To establish Fe isotope systematics as a redox proxy, we used NRIXS to measure mean force constants of synthetic ⁵⁷Fe-labelled olivine and silicate glasses synthesized at different oxygen fugacities in a gas mixing furnace and in piston-cylinders at different pressures with and without dissolved water.

At a given Fe³⁺/Fe²⁺ ratio, the force constants of tholeiitic to andesitic glasses are almost identical. For all samples, the force constant increases linearly with Fe³⁺/Fe_{tot}. The effect of pressure and water content is moderate. Thus, for mafic melts, there is little structural control; redox effects seem to dominate. Our data demonstrate that even at high temperature (1100 °C), the equilibrium δ⁵⁶Fe fractionation between the two oxidation states of iron in MORBS is large (+0.25 ‰). The iron isotopic fractionation factors derived from NRIXS data may explain the heavy iron isotopic compositions measured in MORBS.

[1] Polyakov (2009) *Science* **323**, 912-914. [2] Dauphas *et al.* (2012) *GCA*. [3] Roskosz *et al.* (2006) *EPSL*. [4] Dauphas *et al.* (2009) *EPSL* **288**, 255-267. [5] Dauphas *et al.* (2012) *Goldschmidt Conf.*

Approaching real uncertainty estimates for δ¹¹B data

MARTIN ROSNER¹ AND JOCHEN VOGL²

¹IsoAnalysis UG, martin.rosner@isoanalysis.de

²BAM Federal Institute of Materials and Testing,
jochen.vogl@bam.de

The measurement uncertainty is an indispensable quality criterion of isotope ratio data and sets important limits for the general use and geochemical interpretation of such data. Despite traceability to the International System of Units (SI) or an accepted standard an uncertainty statement allows the direct comparison of isotope data which have been obtained in different laboratories and/or using different procedures. To realise traceability and comparability of isotope data a realistic uncertainty statements should include uncertainty contributions from all influence quantities. In isotope geochemistry, however, often the term uncertainty is used for terms describing the statistical dispersion of measurement results such as precision, repeatability or reproducibility. Because an measurement uncertainty must include all influence quantities even the so-called external precision or reproducibility will underestimate the overall uncertainty. Without uncertainty statement traceability and comparability of measurement results cannot be established. In cases where no uncertainty for isotope ratio data is presented it is highly recommended that at least the measurement results of a quality control sample with known isotope composition are presented which can be used to evaluate the accuracy and roughly estimate uncertainty.

Here we present an approach to calculate uncertainty budgets for δ¹¹B data which can easily be used for other δ-values. Our approach considers uncertainty components from the mass spectrometric isotope ratio determination (repeatability and reproducibility), the chemical preparation (contamination, isotope fractionation) and the isotope reference material (or δ-zero material). Having quantified the single uncertainty components the identification of the most important contributors to the overall uncertainty is possible and strategies to improve the measurement uncertainty can be investigated. The here presented expanded uncertainties for δ¹¹B values between 1.2 and 0.4 ‰ of matrix standards (IAEA B1-3) and processed isotope reference materials (NIST SRM 951, ERM-AE101) show that typically intense sample preparation is the biggest uncertainty contributor. Uncertainties derived from unprocessed reference materials or standards will therefore significantly underestimate the uncertainty of real samples.

Effect of Fluid Salinity on Subcritical Crack Propagation in Calcite

ROSTOM F, RØYNE A, DYSTHE D AND RENARD F

fatma.rostom@ens-lyon.fr

The slow propagation of cracks, also called subcritical crack growth, is a mechanism of fracturing responsible for a ductile deformation of rocks under crustal conditions. In the present study, the double-torsion technique was used to measure the effect of fluid chemistry on the slow propagation of cracks in calcite single crystals at room temperature. Time-lapse images and measurements of force and load-point displacement allowed accurate characterization of crack velocities in a range of 10^{-8} to 10^{-4} m/s. Velocity curves as a function of energy-release rates were obtained for different fluid compositions, varying NH_4Cl and NaCl concentrations. Our results show the presence of a threshold in fluid composition, separating two regimes: weakening conditions where the crack propagation is favored, and strengthening conditions where crack propagation slows down. We suggest that electrostatic surface forces that modify the repulsion forces between the two surfaces of the crack may be responsible for this behavior.

Halogens in the early Solar System inferred from meteoritic phosphates

J. ROSZJAR^{1*}, T. JOHN², M. J. WHITEHOUSE³,
A. BISCHOFF⁴ AND G. D. LAYNE⁵

¹Institut für Geowissenschaften, FSU Jena, Germany

(*correspondence: julia.walter-roszjar@uni-jena.de)

²Institut für Mineralogie, WWU Münster, Germany

³Swedish Museum of Natural History, Stockholm, Sweden

⁴Institut für Planetologie, WWU Münster, Germany

⁵Department of Earth Sciences, Memorial University, St. John's, NL Canada

Although F, Cl, Br, and I are relatively abundant elements in the Solar System, their distribution, abundances and the related fractionation processes in early formed meteoritic material is poorly constrained. Owing to different condensation temperatures, the halogens each have different volatility, which makes them suitable for constraining early Solar System processes such as degassing and fluid-rock interactions. The halogen budget of individual meteorite samples appears dominantly controlled by apatite, which preferentially incorporates halogens. However, merrillite, if present, also contributes to the bulk halogen budget. Although these phases are accessory rock components, they are widely distributed among meteorite classes. Fluorine, Cl, Br, and I concentrations together with the stable Cl isotope composition of individual apatite and merrillite grains were determined in ordinary (OC) and Rumuruti chondrites (RC), primitive achondrites (PA), eucrites (EUC), and silicate-bearing IAB iron meteorites. Petrography and chemistry of phosphate grains were determined using SEM and EPMA. Halogen concentrations and stable $\delta^{37}\text{Cl}$ values were determined using a Cameca IMS 1280. $\delta^{37}\text{Cl}$ values of most meteorite groups are in the range of -0.05 ± 1.20 ‰ (2σ), consistent with results from [1], but with an evolutionary trend from chondritic to more evolved differentiated rocks. The EUC apatite is in the range of -4.49 ± 0.33 ‰ to $+11.93 \pm 0.33$ ‰, similar only to the Moon. For the latter dry fractionation processes were discussed [2]. Thus, the EUC parent body was either as dry as the Moon, or other mechanisms such as metasomatism [3] may fractionate the Cl isotopes. The same evolutionary trend is seen for halogen concentrations, which are dominated by Cl- and Br-rich apatite in OC, and IAB irons, and F- and I-enriched EUC apatite, with PA being intermediate. Compared to apatite, merrillite halogen concentrations are an order of magnitude lower, with limited Cl variation, except for EUC, consistent with a parent body halogen fractionation process.

[1] Sharp *et al.* (2007) *Nature* **446**, 1062-1065. [2] Sharp *et al.* (2011) *Science* **329**, 1050-1053. [3] Barrat *et al.* (2011) *Geochem. Cosmochem. Acta* **75**, 3839-3852.

www.minersoc.org

DOI:10.1180/minmag.2013.077.5.18

Evidence for volatiles on Mercury

D. A. ROTHERY^{1*}, R. J. THOMAS¹ AND L. KERBER²

¹Dept of Physical Sciences, The Open University, Milton Keynes, MK7 6AA, UK

(*correspondence: d.a.rothery@open.ac.uk)

²Laboratoire de Météorologie Dynamique du CNRS, Université Paris 6, Paris, France

Several independent lines of evidence provided by MESSENGER suggest that Mercury is surprisingly rich in volatiles: (i) Gamma-ray spectroscopy reveals a high K/Th ratio in its surface regolith similar to Mars, and very much higher than the Moon [1]. (ii) X-ray spectroscopy reveals 2-5% S in its surface regolith [2]. (iii) It has recognisable pyroclastic deposits around vents, requiring explosive exsolution of an unknown magmatic volatile phase in the range 3600-13,000 ppm [3]. (iv) It exhibits patches of steep-sided, flat-bottomed 'hollows' (10s of m deep and 100s of m to km wide) associated with a spectrally distinct (blue, high albedo) unit that appear to form by sublimation, or some similar process capable of dispersing material to space [4]. (v) Neutron spectrometer measurements [5] show a hydrogen-rich phase, interpreted as water-ice, within permanently-shadowed polar craters [6].

Polar-ice (v) is probably cold-trapped from on-going cometary impacts, but (i)-(iv) are likely to reflect volatiles intrinsic to Mercury. It has been argued [7] that (i) and (ii) could result from low oxygen fugacity affecting geochemical affinities rather than demonstrating volatile-richness on a volumetric planetary scale. Nevertheless it is clear from study of volcanic vent architecture, pyroclastic deposits and hollows that migration of volatile phases from the interior to and through the surface plays a major role in sculpting Mercury's surface. We look forward to enhanced insights when Bepi Colombo achieves orbit.

[1] Peplowski *et al.* (2011) *Science* **333**, 1850-1852. [2] Nittler *et al.* (2011) *Science* **333**, 1847-1850. [3] Kerber *et al.* (2009), *EPSL* **285**, 263-271. [4] Blewett *et al.* (2011) *Science* **333**, 1856-1859. [5] Lawrence *et al.* (2013) *Science* **339**, 292-296. [6] Neumann *et al.* (2013) *Science* **339**, 296-300. [8] Young *et al.* (2003) *EPSL* **213**, 249-259. [7] McCubbin *et al.* (2012) *GRL* **39** L09202

Heavy noble gases in type 3 enstatite chondrites. Implications for the Earth primordial signature and its evolution.

C. ROUBINET* AND M. MOREIRA¹

¹IPGP 1, rue Jussieu 75005 Paris (*correspondence : roubinet@ipgp.fr) (moreira@ipgp.fr)

Enstatite chondrites have often been proposed as possible building rocks of telluric planets and in particular of the Earth [1]. This hypothesis is based firstly on the coincidence of their respective formation zone (inner part of solar system [2]) and also on the similarity of their isotopic composition (O, N, Ni, Mo, Ru, Os, ⁵³⁻⁵⁴Cr...) [1]. Moreover, enstatite chondrites of type 3 in particular are the only chondrites to display close ¹⁴²Nd/¹⁴⁴Nd ratio to Earth [3]. Thus their study may bring information about primordial composition of the Earth concerning noble gases.

Analysis of E3s by mass spectrometry coupled to stepwise heating allows us to highlight that their primordial composition for Xe and Kr is related to phase Q. So, regarding the ubiquity of this phase, its resistance to high temperatures and also its high noble gases content, it seems appropriate to consider it is the most likely primordial signature of the Earth.

We will discuss the possibility of a terrestrial evolution starting with a phase Q composition, as nowadays, Earth's mantle and atmosphere don't display the same isotopic signature. This discrepancy can be due first to fractionation during accretion process as it has been suggested for Nd ([4]) or to post-accretion processes like partial loss of primary atmosphere [5] and also noble gases subduction which can have modified in the long run mantle's signature [6].

[1] Javoy (2010) *EPSL*, **293** (3), 259-268 [2] Kallemeyn (1986) *Geoch. Cosmoch. Acta*, **50**, 2153-2164 [3] Gannoun (2011b) *PNAS*, 108(19), 7693 [4] Caro (2010) *Geoch. Cosmoch. Acta*, **74**, 3333-3349 [5] Pepin (1991) *Icarus*, 92, 1-79 [6] Holland (2006) *Nature*, **441**, 186-191

Decoupling of the sub-basinal CO₂ and He mantle fluxes as evidenced by intense CO₂/³He fractionation of natural gases from Brazilian south Atlantic margin basins

VIRGILE ROUCHON¹, EUGENIO VAZ DOS SANTOS NETO²,
AND ERICA TAVARES DE MORAIS²

¹IFP Energies Nouvelles, Rueil-Malmaison, France.
virgile.rouchon@ifpen.fr

²PETROBRAS R&D Center, Rio de Janeiro, Brazil

Fluxes of mantle CO₂ in sedimentary basins are of present concern regarding deep basin oil and gas exploration. Such degassing of the mantle, although of lower amplitude than that of MOR and convergent margin magmatism, has some influence on the global carbon cycling and on the carbon mass balance of sedimentary basins.

Nearly 150 samples of various basins of the Brazilian Atlantic margin have been analyzed for their molecular composition, stable isotopic ratios of carbon, hydrogen and of the nobles gases (³He/⁴He, ⁴⁰Ar/³⁶Ar). The gases analyzed show a full compositional range corresponding to the mixing of thermogenic gas (average δ¹³C_{CH4-PDB} = -39‰) with inorganic CO₂ (average δ¹³C_{CO2-PDB} = -5.5‰), with CO₂ contents from 0.1 up to 78%. The ³He/⁴He ratio shows a consistent increase with the CO₂ concentration from 3.4e⁻⁷ up to 8.9e⁻⁶. The CO₂/³He ratio of the richest CO₂ samples is reaching that of MORB between 1.2-1.6e⁹. A decreasing trend in the CO₂/³He ratio defined by the whole sample set correlates with decreasing ³He/⁴He ratio and CO₂ abundance. The data support a large scale loss of CO₂ (of up to 99%) from an initial mantle fluid during its ascent towards the surface, in addition to mixing of this fractionated fluid with thermogenic gases from within the basins.

The potential loci and processes of this fractionation are discussed along with their consequence for the relative fluxes of mantle C and He to sedimentary basins.

Interactions of Arsenic and Chromium with Struvite During Mineralization

ASHAKI A. ROUFF* AND NING MA

School of Earth and Environmental Sciences, Queens College,
CUNY, Queens NY 11367, USA

The Graduate Center, CUNY, 365 Fifth Ave., New York, NY
10016, USA

(*correspondence: Ashaki.Rouff@qc.cuny.edu)

Struvite (MgNH₄PO₄·6H₂O, MAP) recovered from wastes may be a viable alternative to phosphate fertilizers [1]. However, the potential for sorption of trace elements in wastes with struvite has not been fully addressed. This study evaluates the sorption of arsenic (As) and chromium (Cr) with struvite as impacted by oxidation state, pH and initial solution concentration [2, 3]. The As content of struvite precipitated in the presence of As(V) as AsO₄³⁻ and As(III) as AsO₃³⁻ increased with pH from 8-11. Struvite recovered from As(V) solutions had As concentrations greater than fertilizer limits over the entire pH range. X-ray absorption fine structure (XAFS) analysis revealed that As(V) was coprecipitated into the struvite structure, and that As(III) was adsorbed to the mineral surface. Oxidation state also dictated Cr sorption with struvite precipitated in the presence of Cr(III) as Cr³⁺ and Cr(VI) as CrO₄²⁻ at concentrations of 1-100 μM. Less Cr was associated with struvite recovered from Cr(VI) solutions compared to Cr(III) solutions over the range of concentrations. For struvite formed in the presence of Cr(III), XAFS confirmed the formation of adsorbates at low initial Cr concentrations, with surface precipitates dominating at higher solution concentrations. Where surface precipitates were detected, the Cr content of struvite exceeded the limit for fertilizers. Fourier transform infrared analysis (FT-IR) suggested that Cr(VI) may be adsorbed and/or coprecipitated with struvite. The extent and mechanisms of sorption for As and Cr have implications for the use of struvite as a fertilizer. Coprecipitated As(V) and precipitated Cr(III) are likely to be delivered to agricultural soils along with struvite, introducing contamination to soils and plants. Conversely, low concentrations of As(III) and Cr(VI) pose less of a risk, and adsorbates may be removed from the struvite surface prior to application.

[1] de-Bashan & Bashan (2004), *Water Res.* **38**, 4222–4246.

[2] Ma & Rouff (2012) *Environ. Sci. Technol.* **46**, 8791-8798.

[3] Rouff (2012) *Environ. Sci. Technol.* **46**, 12493–12501.

A 30ka Sponge-Diatom Silicon Isotope Record of Dissolved Silicon Concentration in Subantarctic Mode Water

J.ROUSSEAU^{1*}, M.J.ELLWOOD¹, H.BOSTOCK², H.NEIL², AND S.FALLON¹

¹Research School of Earth Sciences, Australian National University, Canberra, Australia (*correspondence: u4406548@anu.edu.au)

²National Institute of Water and Atmospheric Research, Wellington, New Zealand

Here we present silicon isotope records for biogenic sponge ($\delta^{30}\text{Si}_{\text{sponge}}$) and diatom ($\delta^{30}\text{Si}_{\text{diatom}}$) silica from Southern Ocean sediments. For two cores located in Subantarctic Mode Waters (SAMW) on the Campbell Plateau, NZ, we observe a decrease in $\delta^{30}\text{Si}_{\text{sponge}}$ values from the late Holocene through to the mid-deglacial period. From the mid-deglacial $\delta^{30}\text{Si}_{\text{sponge}}$ values increase through to the LGM. $\delta^{30}\text{Si}_{\text{sponge}}$ results for a core located within Antarctic Intermediate Waters (AAIW) generally follow the same trend during the Holocene, but are consistently and expectedly more negative than the shallower SAMW values. During the deglacial period the difference between Intermediate Water and Mode Water depth $\delta^{30}\text{Si}_{\text{sponge}}$ is variable suggesting large changes in silicon utilisation within the Subantarctic Zone during this time. A diatom silicon isotope record ($\delta^{30}\text{Si}_{\text{diatom}}$) from the Macquarie Ridge, located further south and upstream of the sponge records, suggests a similar degree of silicon utilisation between the Holocene and the LGM and higher utilisation for a short period during the deglacial.

Modelling dissolved Silicon concentration ([DSi]) in SAMW from a comparison of the Macquarie Ridge $\delta^{30}\text{Si}_{\text{diatom}}$ and Campbell Plateau $\delta^{30}\text{Si}_{\text{sponge}}$ records we find that [DSi] in SAMW may have been 100-150% higher in the LGM compared to the Holocene, which is consistent with the Silicic Acid Leakage Hypothesis. This prediction however is not corroborated by a model using a more distal Indian Ocean $\delta^{30}\text{Si}_{\text{diatom}}$ record for the comparison, pointing towards significant regional differences in SO Silicon dynamics over this period.

Dynamics of chemical characteristics of solubilized organic matter in wetland soils under aerobic or anaerobic conditions.

ASMAA ROUWANE, ISABELLE BOUVEN, MARION RABIET, GILLES GUIBAUD AND MALGORZATA GRYBOS

Groupe de Recherche Eau-Sol-Environnement, Université de Limoges, 123 av. A. Thomas, Limoges, 87060, France.

Soil organic matter plays an important role in the release and potential transport of metal(loid)s^{1,2}. Wetlands are a large terrestrial carbon pool, thus understanding the chemical quality of dissolved organic matter (DOM) in wetland soils is crucial.

Controlled incubations of a wetland soil (Roselle catchment, France) were carried out under aerobic and anaerobic conditions (simulating temporarily and permanently flooded soil). Solubilized organic matter was quantified and characterized. Anaerobic incubation involved strong releases of dissolved organic carbon (DOC) to the soil solution (2 mg of C per g of soil), which was correlated with an increase of solution pH (from 6.0 to 7.3) and Fe reduction. In contrast, aerobic incubation (preventing soil reduction) at pH 6.0 induced a smaller DOM release (0.8 mg of C g per g of soil). Released DOM under both experimental conditions had an increasing trend in aromaticity* with incubation time. Indeed after 500 h of anaerobic incubation, DOM exhibited aromaticity of 60% whereas the aromaticity of DOM released in aerobic experiment was 40%. Using size exclusion chromatography coupled to UV and fluorescence detection, three main size fractions (labeled i, ii, iii) of released DOM were identified. The first fraction (i) with an apparent molecular weight (aMW) >10kDa was constituted of protein-like compounds and had a disappearance trend with incubation time. The second fraction (ii) with an aMW from 1kDa up to 10kDa, exhibited aromatic characters and was composed of a mixture of protein-like and humic substances-like compounds. The fraction (ii) had an increasing trend with incubation time with a higher release of humic substances-like compounds under anaerobic conditions. The third fraction (iii) with an aMW <1 kDa, composed of protein-like and humic substances-like compounds, had a decreasing trend with incubation time whatever experimental conditions.

In conclusion, evolution of DOM solubilization in reduced wetland soils comparing to DOM released under aerobic conditions is different in terms of chemical characteristics and of MW distribution.

¹Frimmel and Huber, 1996; ²Grybos et al., 2009; *calculated according to Weishaar et al., 2003

Non-traditional Stable Isotope Systematics of Seafloor Hydrothermal Systems

OLIVIER ROUXEL¹

¹IFREMER, Centre de Brest, 29280 Plouzané, France

Seafloor hydrothermal activity at mid-ocean ridges is one of the fundamental processes controlling the chemistry of the oceans and the altered oceanic crust. Past studies have demonstrated the complexity and diversity of seafloor hydrothermal systems and have highlighted the importance of water-rock reactions and subsurface environments in controlling the composition of hydrothermal fluids and mineralization types. In addition, the far-field consequences of hydrothermal venting on deep oceanic metal reservoirs, in comparison to other marine sources, is just starting to be recognized.

Isotope ratios of various metals and metalloids, such as Fe, Cu, Zn, Ge, Se, Cd and Sb have recently provided new approaches for the study of seafloor hydrothermal systems. Here, I will present new results of non-traditional isotope systematics of seafloor hydrothermal systems, in particular:

(1) the mechanisms of metal isotope fractionation in hydrothermal chimney environments through paired isotopic analysis of mono-mineralic sulfides in contact with hydrothermal fluid;

(2) the controlling parameters of metal isotope signatures of hydrothermal vent fluids through the study of mid-oceanic and back-arc hydrothermal vent fields, spanning wide ranges of pH, temperature, metal concentrations and contributions of magmatic fluids enriched in SO₂.

(3) the potential role of high-temperature seafloor venting in affecting deep sea metal isotope composition through the investigation of metal isotope systematics in hydrothermal plume.

Ultimately, the use of complementary stable isotope systems should help identify the complex interactions between fluids, minerals, and potentially organisms in seafloor hydrothermal systems and constrain metal sources in marine environments.

Mineral and Melt Inclusion Geochemistry of the Nea Kameni Dacites, Santorini, Greece

ROWE, M.C.¹, ELLIS, B.S.² AND KYRIAKOPOULOS, K.³

¹University of Auckland, School of Environment, Auckland, New Zealand. Michael.rowe@auckland.ac.nz

²ETH Zurich, Institute for Petrology and Geochemistry, Zurich, Switzerland. Ben.ellis@erdw.ethz.ch

³Department of Geology and Geoenvironment, National and Kapodistrian University of Athens, Athens, Greece. ckiriako@geol.uoa.gr

Since the voluminous 3.6 ka Minoan eruption, the Santorini volcano has been periodically erupting small volumes of dacitic magma forming the Kameni islands. This study focuses on variations in mineral geochemistry of lavas spanning from 46-47AD to 1950 to better understand the temporal evolution of silicic magmatism at the Santorini volcano. In addition to feldspar geochemistry, this study utilizes silicate melt inclusion analyses to document melt compositions associated with different feldspar populations. On a bulk level, the dacites of Nea Kameni have remained compositionally homogeneous while containing a mixture of mafic grains and crystal clots. The Kameni dacites contain two populations of feldspar, one An₃₈₋₆₅ interpreted as crystallising from the dacitic liquid and a second An₈₆₋₉₄ derived from a mafic magma. The two feldspar populations are distinct in terms of ⁸⁷Sr/⁸⁶Sr as determined via LA-ICPMS with the higher anorthite plagioclase having higher ⁸⁷Sr/⁸⁶Sr. The same two isotopic populations appear to be contributing to the Kameni magmatic system for the past 1900 years.

Analysis of glassy melt inclusions from the 1940 eruption preserve a similar bimodal distribution of glass compositions consistent with host compositions. Interestingly, despite their assumed cumulate nature, high-An feldspar retain euhedral, undegassed glassy melt inclusions. High-An plagioclase contain mafic melt inclusions whereas the lower An plagioclase contains melt inclusions more similar to the groundmass glass. Pre-eruptive volatiles (S, Cl, H₂O) are maintained in both populations of melt inclusions.

The ⁸⁷Sr/⁸⁶Sr data indicate that the dacitic magmas cannot represent fractionated equivalents of the mafic input to the Kameni system (similar to the Minoan eruption). The presence of abundant glassy clasts of dacite as lithics within the Minoan deposits suggests that prior to the last catastrophic eruption a similar period of relative quiescence may have occurred. Kameni-style volcanism may be a common occurrence at Santorini, just with low preservation potential.

Distribution of ^{230}Th and ^{232}Th along the Bonus GoodHope section in the SouthEast Atlantic Ocean

M.ROY-BARMAN¹, S. MARCHANDISE¹, F. THIL¹, LOUISE BORDIER¹, SOPHIE AYRAULT¹, E. GARCIA-SOLSANA² AND C. JEANDEL²

¹Laboratoire des Sciences du Climat et de l'Environnement, France. (*correspondence : Matthieu.Roy Barman@lscce.ipsl.fr)

²Laboratoire d'Etudes en Géophysique et Oceanographie Spatiale, France.

Dissolved concentrations of ^{230}Th and ^{232}Th have been measured in seawater on 5 profiles along the Bonus GoodHope (GEOTRACES/IPY) section in the SouthEast Atlantic Ocean.

Most dissolved ^{232}Th concentrations range from 5 to 98 $\text{pg}\cdot\text{kg}^{-1}$. There is a general increase of the ^{232}Th concentration from the surface to the deep waters. A strong ^{232}Th gradient exists between the stations located off the African continents (where strong ^{232}Th inputs occur) and the stations located in the middle of the section. A distinctly high ^{232}Th concentration of 283 $\text{pg}\cdot\text{kg}^{-1}$ is found at the bottom of the station closest to the African coast, likely linked to an input from the sediment.

Dissolved ^{230}Th concentrations range from 0.7 to 36.4 $\text{fg}\cdot\text{kg}^{-1}$. The ^{230}Th data of the Bonus GoodHope section compare well with the ^{230}Th data of ANT III section obtained near the Polar Front [1]. There is a general increase of the ^{230}Th concentration with depth. In the Cape basin, concentrations increase linearly, with a lower scavenging rate north of the subtropical front than south of it. At the Polar front level, a distinctly low ^{230}Th concentration is found in the deepest sample (9 $\text{fg}\cdot\text{kg}^{-1}$ at 4300 m against 15 $\text{fg}\cdot\text{kg}^{-1}$ at 3048 m) suggesting occurrence of boundary scavenging. South of the Polar Front, upwelling of deep waters create non linear profiles.

Particulate samples collected with in situ pumps are under process for the determination of ^{230}Th and ^{232}Th .

Rutgers van der Loeff & Berger (1993) *Deep-Sea Res.* **40**, 339–357.

Dissimilatory Sulfate Reduction in Hypersaline Environments: What is regulating sulfate uptake?

A.N.ROYCHOUDHURY^{1*} AND D.PORTER²

¹Dept. of Earth Sciences, Stellenbosch University, Stellenbosch 7602, South Africa (*correspondence: roy@sun.ac.za)

²Department of Genetics, University of Pretoria, Pretoria, South Africa

Microbes in engineered systems such as wastewater treatment facilities and mine tailings are often subjected to extremes of salinities. Little is known; however, about the activity and survival mechanisms of sulfate reducers in such extreme environments. Hypersaline pans, a prototype for engineered systems, are used here to understand sulfate uptake and regulatory mechanisms among sulfate reducers.

Thermodynamic and kinetic parameters for dissimilatory sulfate reduction (DSR) were quantified in five hypersaline coastal salt pans located in South Africa. Compared to normal marine environments, salinity and sulfate concentration at the studied salt pans was higher by up to 10 and 20 times, respectively. Determined apparent activation energies (28 – 62 kJ/mol) and Q_{10} values (2.0 – 2.3) for DSR suggest no gross physiological adaptations in bacteria, such as changes in membrane structure, to temperature.

Sulfate uptake affinity, quantified in terms of apparent half-saturation concentration (K_s); however, indicates adaptation with respect to high ionic status of the salt pans. The K_s values (64 – 780 mM) for sulfate reduction determined for the first time from hypersaline environments are two to three orders of magnitude larger than those determined for normal marine ecosystems. This indicates that in hypersaline environments there exists a third transport mechanism, which attenuates even the low-affinity system observed among marine sulfate reducers. We propose that the observed extremely low-affinity, high accumulation system is a consequence of increased regulation of sulfate uptake and accumulation because of adaptation mechanisms employed by halophiles to survive under extremes of salinity.

Redox chemistry profiling in the Kara sea sediments (from the Ob-river to the Saint Anna trench)

ALEXANDER ROZANOV

P.P. Shirshov Institute of Oceanology, Nakhimovsky prosp.
Moscow, 117997. e-mail: rozanov@ocean.ru

Submeridional redox profile across the bottom sediments of the Kara sea from the Ob' river (71 N) to the St. Anna trench (77 N) was studied in the course of the Russian expedition on the R / V «Akademik Mstislav Keldysh» in September 2007. Redox profile is formed under the influence of diagenetic reactions in sediments with organic matter (OM), produced into the sea and brought from the shore. The main oxidants involving microorganisms consistently are oxygen, nitrates, oxyhydroxides of manganese and iron, sulphates and carbon dioxide, while in the pore water accumulate NH_3 , Mn^{2+} , Fe^{2+} , H_2S and CH_4 . The content of the OM, which is a fundamental characteristic of sediments, is more than 1.5% (dw) Corg in the Ob' delta (71 N), close to 1% in the estuary (72 N), 0.5-0.75% in the sediments of inner and outer shelf (72-75 N), as well as in the slope (75-76 N), 2% in the sediments of the of the St. Anna trench (77 N). OM in the deltaic part is mainly terrigenous, in the northern part of the profile the cause of increased OM content is the primary production of plankton. On the border of the estuary and the shelf there is a sharp decrease of suspended matter in the surface waters (from 7 to 1 mg/l), the Corg and many metals of the river runoff in the sediments reach maximum values (Mn 0.3%, Fe 7% dw). The growth of OM stimulates the reduction processes, as reflected in higher concentrations of the dissolved components in the pore water (Mn^{2+} up to 260, Fe^{2+} to 100 μM) and derivatives of H_2S (up to 0.3 %) in the sediments. Dissolved Mn remove from the sediments to the bottom water, dissolved Fe is oxidized by oxygen of the bottom water and forms a thin oxidized layer on the surface. Recycling of Mn and Fe is accompanied by formation of ferromanganese nodules. Sedimentation in central and northern part of the profile, adjacent to the St. Anna trench are characterized by lower content of Mn due to both long distance from the river outflow and diagenetic removal of Mn from the sediments of higher Corg content. In this part of the profile derivatives of H_2S are mainly represented by organic forms, which are very typical for Arctic sediments in contrast to the bottom sediments of the temperate and tropical zones, in which among H_2S -forms prevails diagenetic pyrite.

Effects of lead and strontium on radium uptake by barite: Atomistic simulations and thermodynamic assessment

K. ROZOV¹, V. L. VINOGRAD^{1,2*}, D. A. KULIK³,
F. BRANDT¹, B. WINKLER² AND D. BOSBACH¹

¹Institute of Energy and Climate Research (IEK-6),
Forschungszentrum Jülich, Germany

²Institute of Geosciences, Goethe University, Frankfurt,
Germany (*correspondence: v.vinograd@fz-juelich.de)

³Nuclear Energy and Safety Research Department, Paul
Scherrer Institute, Villigen, Switzerland

Experimental studies related to safety issues of the long-term disposal of spent nuclear fuel in deep geologic formations suggest that Ra released from the fuel can be efficiently immobilized as a constituent of a barite-rich solid solution (SS) [1,2]. Here the uptake of Ra by barite is investigated using the Gibbs free energy minimization method [3] at variable fractions of PbSO_4 and SrSO_4 in the SS. The SSs were modelled as ternary $(\text{Ba}, \text{Sr}/\text{Pb}, \text{Ra})\text{SO}_4$ regular mixtures. The mixing parameters ($W_{\text{BaPb}} = 5.4$, $W_{\text{PbRa}} = 1.5$, $W_{\text{BaRa}} = 2.5$, $W_{\text{BaSr}} = 8.9$, $W_{\text{SrRa}} = 19.6$, $W_{\text{SrPb}} = -0.3$ kJ/mol) were computed from first principles with the aid of the single defect method [4]. The system contained 0.00214 moles of $\text{Ba}_{1-x}(\text{Sr}/\text{Pb})_x\text{SO}_4$, 0.1 m of NaCl, $5.0 \cdot 10^{-6}$ m of RaCl_2 and 1 kg of H_2O . The concentration of $\text{Ra}(\text{aq})$ decreases with the $(\text{Sr}/\text{Pb})\text{SO}_4$ fraction in the system due to the common anion effect. However, in the SrSO_4 case, after the fraction of SrSO_4 exceeds ~ 0.01 , the concentration of $\text{Ra}(\text{aq})$ starts to grow due to the corresponding increase in the mole fraction of RaSO_4 in barite. This effect is suppressed by the decomposition of the SS in Ba- and Sr-rich phases; the concentration of $\text{Ra}(\text{aq})$ remains less than that in the Sr-free system up to the Sr/Ba ratio of ~ 10 . Therefore, at certain conditions, an admixture of PbSO_4 or SrSO_4 in barite would lead to a more efficient immobilization of Ra. The study is funded by BMBF-IMMORAD project through the grant 02NUK019E.

[1] Bosbach et al. (2010) Techn. Report TR-104. Svensk Kärnbränslehantering AB. [2] Curti et al. (2010) Geochim. Cosmochim. Acta **74**, 3553-3570. [3] Kulik et al. (2013) Comput. Geosciences **17**, 1-24. [4] Vinograd et al. (2013) Geochim. Cosmochim. Acta (submitted)

www.minersoc.org

DOI:10.1180/minmag.2013.077.5.18

Fracture propagation driven by crystal growth and the role of interfacial fluid chemistry

A. RØYNE^{1*}, P. MEAKIN^{1,2}, A. MALTHER-SØRENSEN¹,
B. JAMTVEIT¹ AND D.K. DYSTHE¹

¹Physics of Geological Processes (PGP), University of Oslo
(*correspondence: anja.royne@fys.uio.no)

²Carbon Resource Management Department, Idaho National
Laboratory

Crystals that grow confined in pores and cracks may exert a force on their surroundings and thereby drive crack propagation in rocks and other materials. Of particular importance for engineering and cultural heritage is the degradation of building stones due to salt crystallization. The opening of fractures due to crystal growth may also open new pathways for transport of reactive fluids and therefore serve to accelerate the rate of advancement of weathering or replacement fronts.

In order for a growing crystal to actively displace the walls of the confining pore, there must be a liquid film present between the crystal face and the surface of the pore. This film acts as the transport pathway for growth units to the crystal face. The normal stress between the crystal face and the confining wall is transmitted through the disjoining pressure in the liquid film, and the maximum stress which can be exerted is determined by the fluid chemistry and surface properties. The same confined fluid is also present at the crack tip, where it plays a large role in determining the fracture threshold and velocity at low tensile stresses [1,2].

We use a theoretical model of crystal growth in an idealized crack geometry to study how the kinetics of crystal growth and crack propagation are coupled through the confined fluid and the stress in the surrounding bulk solid [3]. The rate of initial crack propagation is found to be limited by subcritical crack growth, while crystal growth becomes the rate limiting step when the crack has grown to sufficient length. The cross-over length is determined by crystal and crack tip kinetics, fluid supersaturation and elastic properties of the surrounding material.

[1] Røyne *et al.* (2011) *J. Geophys. Res.* **116**, B04204 [2] Rostom *et al.* (2012) *Tectonophysics* **583**, 68-75 [3] Røyne *et al.* (2011) *EPL* **96**, 24003

Integration of U-Pb dating, trace elements and oxygen isotopes at the microscale

DANIELA RUBATTO¹, LAURE GAUTHIEZ-PUTALLAZ¹,
AND KATHERINE BOSTON¹

¹Research School of Earth Sciences, Australian National
University, 0200 Canberra, Australia.
Daniela.Rubatto@anu.edu.au

The U-Pb chronology of metamorphic events has greatly benefited from the high spatial resolution achievable with microbeam techniques that allows to date individual growth zones in accessory phases. The capability to retrieve trace elements and isotopic information at the same scale has allowed relating ages to metamorphic processes. With the newly developed capacity to analyse oxygen isotopes at the same scale as U-Pb ages, the application of this method to metamorphic fluid-rock interaction is particularly exciting.

The robustness of zircon makes it a prime candidate for retrieving the oxygen composition of pre-metamorphic history. Zircon in high pressure rocks of the Western Alps show different degrees of metamorphic recrystallization. Their age and oxygen composition constrain the timing of fluid circulation and offer insight into its origin and degree of fluid-rock interaction.

Monazite is particularly promising as monitor and timer of fluid-rock interaction as experimental and field studies have shown that monazite readily recrystallizes in the presence of fluids. Analytical protocols and standards have been developed for in-situ oxygen analysis of monazite using the SHRIMP ion microprobe. Accurate measurements require an additional correction for matrix effect due to the variable composition of monazite. This effect is found to be proportional to the Th content of monazite and produces a shift of circa in $\delta^{18}\text{O}$ of 1‰ every 10 wt% of Th. Oxygen isotopes combined with trace element analysis to relate monazite to major mineral offer new opportunities for monazite geochronology in metamorphic rocks.

Allanite preserves multiple growth zones and retains its U-Pb age up to temperatures of at least 700°C. Geochronology of allanite requires adequate corrections for initial Pb composition, particularly for metamorphic domains formed in sub-solidus conditions. For ion microprobe data, robust results are obtained with Th-Pb isochrons. Even in allanite with high amounts of initial Pb (60-95%) isochrons return reasonably accurate and robust ages. Oxygen isotope analysis of allanite is still hampered by significant matrix effects for which a correction scheme is work in progress.

Accretion and chemical evolution of the terrestrial planets

D.C. RUBIE^{1*}, D.P.O'BRIEN², A. MORBIDELLI³,
S.A. JACOBSON^{1,3} AND E.D. YOUNG⁴

¹Bayerisches Geoinstitut, Bayreuth, Germany
(dave.rubie@uni-bayreuth.de)

²Planetary Science Institute, Tucson, USA (obrien@psi.edu)

³Observatoire de la Cote d'Azur, Nice, France
(morby@oca.eu)

⁴Dept. of Earth and Space Sciences, UCLA, Los Angeles,
USA

Classical dynamical models of planetary accretion have been successful in reproducing the general characteristics of the terrestrial planets of the solar system [1]. However, they have been less successful in reproducing the small mass of the outermost terrestrial planet, Mars, which appears to require a strong depletion of mass beyond ~1 AU [2]. The recent "Grand Tack" model, based on the early inward and then outward migration of Jupiter and Saturn, provides a solution to this problem [3]. We are using a geochemical approach to test the validity of the Grand Tack and other accretion models. Accretion occurs through impacts between growing planets and smaller bodies. Each impact delivers energy (magma ocean formation) and metal and thus an episode of core formation. The chemical evolution of the mantles and cores of growing bodies is modeled based on the bulk composition of the accreting material combined with a mass balance/element partitioning approach [4]. The main constraint is the composition of Earth's primitive mantle and the FeO contents of the mantles of Mercury and Mars (3-4 wt% and ~18 wt% respectively). Bulk composition is defined in terms of solar system (CI) relative abundances of the non-volatile elements with an oxygen content that determines the metal-silicate ratio. Accretion simulations that produce synthetic planets closely resembling those of the solar system are tested. Model parameters (metal-silicate equilibration pressure, starting compositions of embryos and planetesimals) are refined by a least squares regression in order to produce a synthetic Earth that matches Earth's mantle chemistry.

The mantle chemistries of Earth and Mars can be reproduced well when the compositions of bodies that originate in the inner solar system (<~1.6 AU) are highly reduced and those forming further out are more oxidized. However, the current Grand Tack simulations result in an inner planet ("Mercury") that accretes too much material from the outer regions of the planetesimal disk and is thus too massive and too oxidized.

[1] Raymond *et al.* (2009) *Icarus* **203**, 644-662. [2] Hansen (2009) *ApJ* **703**, 1131-1140. [3] Walsh *et al.* (2011) *Nature* **475**, 206-209. [4] Rubie *et al.* (2011) *EPSL* **301**, 31-42.

Timescale and petrogenesis of 2009 and older W. Mata boninite magmas

K.H. RUBIN^{1*}, P. MICHAEL², J. GILL³, D. CLAGUE⁴,
T. PLANK⁵, S. ESCRIG⁶, S. GLANCY¹, E. TODD³,
L. COOPER⁵, N. KELLER⁷, A. SOULE⁷,
E. HELLEBRAND¹, K. KELLEY⁸, E. COTTRELL⁹, F.
JENNER¹⁰, R. ARCULUS¹⁰, P. RUPRECHT⁵, J. LUPTON¹¹,
C. LANGMUIR⁶, J. RESING¹² AND R. EMBLEY¹¹

¹ GG Dept., Univ. of Hawaii, Honolulu, HI 96822 USA
(*correspondence: krubin@hawaii.edu)

² The Univ. of Tulsa, Tulsa, OK

³ Earth and Planetary Sciences, UCSC

⁴ MBARI, 7700 Sandholdt Road, Moss Landing, CA

⁵ LDEO and Columbia University, Palisades, NY

⁶ Harvard University, Cambridge, MA, USA

⁷ WHOI, Woods Hole, MA, USA

⁸ GSO, Univ. Rhode Island, Narragansett, RI

⁹ NMNH, Smithsonian Institution, Washington DC

¹⁰ RSES, Australian National University, Canberra

¹¹ PMEL, NOAA-Vents, Newport, OR

¹² JISAO, NOAA-Vents, Univ. Washington, Seattle, WA

The first active boninite eruption was observed by ROV in 2009 at West Mata, a small, submarine rear-arc volcano in the NE Lau Basin. Globally, boninite is a rarely erupted, arc-fluid-enriched magma. We examine rates and processes of W. Mata boninite generation, ascent, and storage, with implications for arc magma and volatile source-to-surface transport. A number of characteristics indicate magma differentiation during rapid ascent from the mantle within a poorly developed magma storage system: large, very short-lived ²¹⁰Pb-²²⁶Ra disequilibria of 20-40% in glasses, Ni diffusion profiles in olivine, and a complex range of mineral textures, including rapid crystal growth and magma reactions. Geochemical and petrological studies of fresh-appearing lavas collected in 2009 and on two subsequent cruises indicate limited lithological variability throughout the volcano. W. Mata erupts a highly vesicular, crystal-rich (ca 40%) magma, having opx>>cpx>ol and a continuum of mineral compositions (e.g., opx and ol Mg# 92-82). Whole rocks (WR) are boninite *sensu strictu* but have more evolved coexisting glass (WR and glass have MgO=11-15 and 3.5-6.5 wt%, SiO₂=54-57 and 55-58 wt%, TiO₂=0.3-0.45 and 0.4-0.6 wt%). Older, non-summit lavas define distinct but similar major element trends, with variable radiogenic isotope and trace element ratios. Slab influence is indicated by glasses with extreme ²³⁸U-²³⁰Th disequilibria (40% excess U), high Fe oxidation (Fe³⁺/ΣFe=0.2-0.25), strong fluid-mobile element enrichments (Ba and U to 160 ppm and 0.4 ppm), high Cl/K, plus up to 3 wt% H₂O in melt inclusions.

Itrax™ Core Scanner as a quick screening tool for polluted coastal sediments

B. RUBIO *, D. REY, I. RODRÍGUEZ-GERMADE, P. ÁLVAREZ-IGLESIAS AND A.M. BERNABEU

Research group GEOMA. Departamento de Geociencias Marinas y Ordenación del Territorio, Universidad de Vigo, Vigo (Spain).

*Correspondence: brubio@uvigo.es

The traditional techniques for the study of chemical composition of sediment cores, are, among others, the X-ray fluorescence (XRF) and the spectrometry (ICP) applied on discrete samples. The development of non-destructive continuous analysis as the XRF scanners as the Itrax™ core scanner [1], which analyses humid core-sections with a millimetric resolution, have supposed a great advance in the study of sediments and rocks. These instruments are able to detect the majority of the elements from the Al to the U, in a low concentration, depending on the acquisition conditions. Until now, the majority of the works with these scanners have been focused on palaeoceanographic or palaeoclimatic reconstructions, both in marine and continental sediments, being much more scarce the studies based on discrimination of pollution.

We have analysed with the ITRAX from the University of Vigo and varying time-acquisition conditions, sediment cores from the inner Galician Rías Baixas (NW Spain). These are highly organic, but not very heavily polluted environments, however ITRAX was able to detect Hg concentrations lesser than $0.6 \mu\text{g g}^{-1}$ and Cd concentrations in the order of $1 \mu\text{g g}^{-1}$. These values were confirmed by total digestion and subsequent analysis by ICP and by conventional XRF of pressed pellets, obtaining a good relationship for most of the trace elements (Zn, Pb, Cu, etc.) and confirming the presence of Cd and Hg. Pollution by these elements was restricted to the upper 10-15 cm, approximately ranged between 30-50 yr based on ^{210}Pb and ^{137}Cs datings obtained by gamma spectrometry. Only Pb and Hg showed concentrations above the sediment quality guidelines that could be associated with measures of adverse effects. Several sequential extraction protocols (BCR and NWR) of selected samples were also applied in order to get information about the bioavailability of these elements. The data confirms the predominance of oxides and residual fractions in the case of Pb and oxidizable forms (organic-matter and sulphides) in the case of Hg. Our results confirms that ITRAX represent a fast and high-resolution tool for identify pollution in these environments not heavily affected.

[1] Croudace *et al.* (2006). *Geol. Soc. Spec. Publ.* **267**: 51-63. Contribution to IPT- 310000-2010-17 and 10MMA312022PR projects.

Aerosol ageing and effect on their optical properties by a new broadband aerosols spectrometer

MICHEL FLORES¹, NIR BLUVSHEIN AND YINON RUIDICH^{1,*}

¹Department of Environmental Sciences, Weizmann Institute of Science, Rehovot, 76100 Israel

(Flores@weizmann.ac.il, Nir.bluvshstein@weizmann.ac.il

*correspondence: yinon.ruidich@weizmann.ac.il)

The optical properties of complex aerosols, important in determining their radiative forcing in the atmosphere and, subsequently, their impact on climate, are extensively examined. There is an abundance of natural and anthropogenic organic compounds in the atmosphere that can be released as primary aerosols or form secondary organic aerosols (SOAs) via photochemical reactions with OH, NO₃, and O₃.

Aerosols can undergo further processing in the atmosphere with oxidizing species, changing the chemical, physical, and optical properties of the particles. Particle internal structure and composition have important implications for their optical properties. Despite their acknowledged importance, the internal structures of aerosols, mechanisms of formation, atmospheric aging, and heterogeneous reactivity remain poorly understood and yet their environmental role cannot be quantitatively determined.

In this talk we will describe new studies that investigate the changes in optical properties of different model aerosols. We will describe a new broadband aerosol spectrometer that can retrieve aerosol optical properties between 360 and 420 nm, a less explored wavelength range. As examples, we will present the effect of nitration of organic aerosols on aerosol absorption, and the effect of aging on the optical properties of SOA that form from the ozonolysis of biogenic and anthropogenic VOCs. The effect of structure on the optical properties, and how core/shell structure differs from homogenous structure will be demonstrated.

Glacial tillites reveal temporal evolution of upper continental crust

ROBERTA L. RUDNICK¹, RICHARD M. GASCHNIG¹
AND WILLIAM F. McDONOUGH¹

¹Dept. Geology, University of Maryland, College Park, MD
20782, U.S.A., rudnick@umd.edu

Defining the absolute composition of the continental crust, and its lateral and vertical variations, are essential parameters needed in extracting the geoneutrino signal from the mantle and thereby place constraints on the Earth's present-day radioactive power. K, Th, and U are strongly concentrated in the upper continental crust (UCC) so refining its composition and deriving uncertainties is important to neutrino geoscience.

UCC estimates generally rely on reference suites of shales, pelites, and loess (e.g., Hu and Gao, 2008: HG08). Here we use modern to Archean glacial tills and tillites to determine the average UCC composition through time and then we compare them with HG08. Paleoproterozoic tillites are systematically enriched in transition metals (Sc, Cr, Co, Ni) relative to post-Archean tillites and average UCC, indicating more mafic contribution to the Archean upper crust (as previously documented in shales). However, in contrast to shale data, we find no systematic differences in Th/Sc as a function of age in tillites, implying that Th is not systematically depleted in Archean UCC as sampled by the glaciers. Th/U of the tillites correlates with their age: Th/U ~3 in modern tills, and Carboniferous and Paleoproterozoic tillites, whereas Neoproterozoic tillites and HG08 have Th/U ~6. The high Th/U of the Neoproterozoic tillites can be linked to intense weathering (and U leaching) attending the snowball Earth glaciations. The lack of a significant difference in the abundances of heat producing elements in Archean and post-Archean average UCC may imply that the lower surface heat flow in Archean cratons compared to post-Archean regions may be related to differences in Moho heat flux.

Resolving gas transport through compacted sand/bentonite material by using noble gases

J. RUEEDI¹, R. SENGER², DONATELLA MANCA³,
KARAM KONTAR⁴ AND P. MARSCHALL¹

¹NAGRA, 5430 Wettingen, Switzerland

²Intera Inc., 5408 Ennetbaden, Switzerland

³EPFL ENAC IIC LMS, 1015 Lausanne, Switzerland

⁴Solexperts, 8617 Mönchaltorf, Switzerland

Gases (hydrogen, methane, carbon dioxide) may accumulate in the emplacement caverns of a geological repository for low/intermediate-level waste due to the corrosion and degradation of the wastes. Nagra is evaluating the concept of an engineered gas transport system (EGTS), aimed at providing an additional transport pathway for gas release if overpressures were to be developed. Gas permeable tunnel seals are among the main design elements of the EGTS, consisting of sand/bentonite (S/B) mixtures with a bentonite content of 20% to 30%.

It is expected that material heterogeneities at repository scales will, at least to some extent, lead to a water saturation and a gas invasion behaviour that differs from those observed in small-scale lab experiments. Past applications of probabilistic two-phase flow models tried to assess the influence of material heterogeneities on water and gas transport in clay material. The models revealed complex two-phase flow patterns during gas imbibition and after gas breakthrough. It is thought that these patterns are mainly driven by the material properties and associated heterogeneity. However, there is little experimental evidence to constrain the large number of possible model realisations.

In 2010, a laboratory column was filled with a S/B mixture (80% sand and 20% MX80 bentonite) and compacted to a density of 1.5 g/cm³. The column was then saturated with distilled water for a few weeks and a hydro test was performed to determine the hydraulic permeability of the material and to confirm saturation. A gas test was performed by injecting N₂ at increasing pressures until breakthrough. After breakthrough the gas flow was kept constant and the N₂ gas was replaced by a gas mixture (N₂, He, Ar, Xe, SF₆) and the breakthrough pattern of the different gases was monitored continuously using a mass spectrometer. The choice of the gas tracers was made based on their different physical properties – i.e. solubility in water and diffusivity in both gas and liquid phases.

The observed partitioning of the different gas tracers provides unique experimental evidence for the determining the dominating transport processes within the partially saturated material and thus help constrain probabilistic models for two-phase flow and transport through S/B material.

Large Igneous Province Volcanism, Ocean Anoxia and Marine Mass Extinction

M. RUHL^{1,2,*}, C.J. BJERRUM¹, D.E. CANFIELD³,
C. KORTE¹, L. STEMMERIK⁴ AND R. FREI¹

¹Nordic Center for Earth Evolution (NordCEE), Copenhagen University, Oster Voldgade 10, DK-1350 Copenhagen, Denmark.

²Department of Earth Sciences, University of Oxford, South Parks Road, OX1 3AN, Oxford, UK.

³Nordic Center for Earth Evolution (NordCEE), University of Southern Denmark, Campusvej 55, 5230 Odense, Denmark.

⁴Geological Museum, Natural History Museum of Denmark, Copenhagen University, Øster Voldgade 5-7, DK-1350, Copenhagen, Denmark.

(* correspondence: micha.ruhl@earth.ox.ac.uk)

Past global marine mass extinction events are often linked to terrestrial Large Igneous Province (LIP) volcanism, but exact mechanisms driving extinction are often not well constrained.

We studied two of Earth's largest mass extinction events, at the Triassic-Jurassic (~201.4 Ma) and Permian-Triassic (~252 Ma) boundaries, which coincide with Central Atlantic Magmatic Province (CAMP) and Siberian Trap volcanism, respectively. The Triassic-Jurassic mass extinction is often contributed to carbon release driven ocean acidification while the Permian-Triassic mass extinction is suggested to be related to widespread ocean anoxia.

We compare Permian-Triassic and Triassic-Jurassic ocean redox change along continental margins in different geographic regions (Permian-Triassic: Greenland, Svalbard, Iran; Triassic-Jurassic: UK, Austria) and discuss its role in marine mass extinction.

Speciation of iron [(Fe_{HR}/ Fe_T) and (Fe_{py}/ Fe_{HR})] and redox-sensitive trace element concentrations (e.g. Mo, V etc.) show that the Triassic-Jurassic marine mass extinction directly coincides with a rapid shift to anoxic and euxinic conditions at the onset of CAMP volcanism and increased atmospheric pCO₂. Biotic recovery after the extinction event only commences when redox-conditions return from a euxinic to a ferruginous state and stabilization of marine ecosystems only commences after decreasing atmospheric pCO₂ and a return to more oxic marine conditions.

Iron-speciation at both the Triassic-Jurassic and Permian-Triassic mass extinctions however shows 2 phases of euxinia along continental margins, with an initial short peak at the onset of volcanism followed by a shift to ferruginous conditions, possibly due to a strongly diminished ocean sulphate reservoir because of massive initial pyrite burial. D³⁴S_{pyrite} suggests that following prolonged (several 100kyr) euxinic conditions only commence when the ocean sulphate reservoir is replenished by the release of sulphur from volcanism.

Geochemistry of cassiterite and wolframite from quartz veins in Central Iberian Zone (Spain)

CASILDA RUIZ^{1*} AND CONCEPCIÓN FERNÁNDEZ-LEYVA²

¹Technical University of Madrid (UPM), Spain

(*correspondence: casilda.ruiz@upm.es)

²Geological Survey of Spain, Madrid 28003

(c.fernandez@igme.es)

Sn- and Sn-W-bearing quartz veins in the Central Iberian Zone mainly cut across the granites. Some of these veins were mined during the last century. The paragenetic sequence corresponds to two oxide-silicate stages and a sulfide stage in that order. Massive crystalline quartz is the main mineral of the three stages. Stage 1 consists of muscovite, cassiterite and arsenopyrite, stage 2 of wolframite and arsenopyrite, and stage 3 of small amounts of sulfides: arsenopyrite, pyrite, pyrrhotite, sphalerite and chalcopyrite.

Cassiterite from Sn- and Sn-W-bearing quartz veins shows Ti > Fe > Mn content, and Ti replaces Sn. The chemical variation of cassiterite crystals is controlled by the direct substitution of Sn⁴⁺ by Ti⁴⁺. Cassiterite generally shows lighter and darker zones, and Nb content is higher in darker than in the lighter zones. Wolframite consists almost entirely of FeO, MnO, and WO₃, with less than 1% Ta₂O₅, Nb₂O₅, and TiO₂. It shows Mn and Fe substitution. Wolframite individual crystal shows a decrease in the hübnerite component from core to rim. Likewise, Nb increases toward the rim of the wolframite crystal. Ta content of cassiterite and wolframite is generally higher than Nb content. Cassiterite has a higher Nb and Ta content than wolframite [1].

Tungsten is carried as H₂WO₄, WO₄²⁻ [2] and wolframite can be precipitated by the cooling of an Fe-W-bearing fluid, without wall rock reaction [3]. Mineralizing fluid deposits cassiterite, associated with muscovite selvages in the paragenetic stage 1. This fluid evolves and precipitates wolframite, mainly within quartz veins in stage 2. Tungsten shows different behavior from that of tin and consequently, cassiterite is generally not associated with wolframite.

[1] Ruiz, C., Fernández-Leyva, C. (2009). *Geochim. Cosmochim. Acta.* **73**, 13S, A1132–A1132. [2] Wood, S.A., Samson, I.M., (2000). *Econ. Geol.* **95**, 143–182. [3] Heinrich, C.A., (1990). *Econ. Geol.* **85**, 457–481.

Geochemical modelling of Sn and W in granites from Central Iberian Zone (Spain)

CASILDA RUIZ^{1*} AND CONCEPCIÓN FERNÁNDEZ-LEYVA²

¹Technical University of Madrid (UPM), Spain

(*correspondence: casilda.ruiz@upm.es)

²Geological Survey of Spain, Madrid 28003

(c.fernandez@igme.es)

Field and petrographic observations of the quartz veins mineralization in relation with granites in Central Iberian Zone (CIZ) [1], show that cassiterite and wolframite occur in quartz veins principally. It seems that quartz deposition is before the cassiterite one and wolframite is deposited after cassiterite. Processes that form mineral deposits associated with granitic rocks can have a close relationship with magmatic processes. Geochemical calculations applied to Sn and W have been performed to investigate if magmatic processes have been the mechanism by which the mineralisation was generated in the (CIZ).

Complex linear mixing models show that Sn and W increase their concentration in the fractionation stages while modal extracted muscovite is reduced. Sn and W are concentrated in the residual liquid when the modal quantity of extracted muscovite is $\leq 5\%$. Starting from an initial leucogranitic composition, concentrations of Sn can reach up values over 100 ppm after high degrees of fractionation. On the other hand, the calculated W concentrations are much lower. The same results suggest models for equilibrium and fractional crystallisation [2]. Complex linear mixing models show that crystallisation processes generated mineralizations by concentrations of Sn, whereas W does not reach the levels required for generating ones.

[1] Ruiz *et al.* (2008). *Chem. Erde*, **68-4**, 337-450. [2] Fernández-Leyva *et al.* (2009). *Geochim. Cosmochim. Acta*, **73**, 13S, A368-A368.

The pH influence on barite nucleation and growth

CRISTINA RUIZ-AGUDO¹, CHRISTINE PUTNIS²
AND ANDREW PUTNIS³

¹c_ruiz02@uni-muenster.de

²putnisc@uni-muenster.de

³putnis@uni-muenster.de

Barite (BaSO₄) scale formation is a problem in many industrial processes, especially in oilfields where mixing sea water with reservoir water can result in solid layers of barite scale that can completely block pipes. Organic compounds (e.g. organophosphonates) have been used as inhibitors for barite precipitation. The effectiveness of these compounds is pH-dependent, usually more effective at high pH where they are highly deprotonated. Thus to be able to determine the performance of organic additives as barite scale inhibitors, we have first studied the influence of pH on barite nucleation and growth.

To determine the influence of pH on growth, AFM observations of barite growth on a barite cleavage surface were carried out under conditions of constant supersaturation, temperature, Ba/SO₄ ratio and ionic strength but changing growth solution pH.

The effect of pH on nucleation was studied with turbidimetry and conductivity experiments complemented with FESEM observations to determine changes in morphology and size of the barite precipitated. Induction times were determined by monitoring the variation in absorbance due to barite precipitation and this enabled the estimation of potential changes in interfacial tension. Conductivity experiments allowed us to determine the onset of nucleation (i.e. induction time) as well as the supersaturation reached at that point and how both parameters vary with pH.

It was found that increasing the pH of the growth solution results in shorter induction times and lower values of interfacial tension. These changes can be explained considering the effect of increasing hydroxyl ion concentration on barium hydration.

Porosity development during carbonation reactions

ENCARNACIÓN RUIZ-AGUDO¹, CHRISTINE V. PUTNIS²
AND ANDREW PUTNIS²

¹Department of Mineralogy and Petrology, University of Granada, Granada, Spain. encarui@ugr.es

²Institut für Mineralogie, University of Münster, Münster, Germany. putnisc@uni-muenster.de

The reduction in industrial emissions of CO₂ is one of the major challenges of this century. Anthropogenic CO₂ capture and injection into geological formations is considered a promising strategy for the permanent storage of this greenhouse gas. This process is based on the dissolution of silicate rocks in contact with CO₂-rich fluid and the precipitation of carbonates, so that CO₂ is trapped as a stable mineral phase. The generation of product layers on the surface of the carbonating material occurs by an interface-coupled dissolution-precipitation reaction (Putnis, 2009). The study of the processes of dissolution and carbonation of portlandite, Ca(OH)₂, is crucial due to the great potential of this reaction for CO₂ capture and storage, as well as for understanding the carbonation behavior of artificial mineral associations such as mortars or cements.

A critical aspect to consider in mineral replacement processes described above is the porosity evolution. The porosity created depends on the difference between the molar volumes of reagent and the product as well as the relative solubility of the two phases in the reaction fluid. The generation of porosity enables the progress of the replacement reaction, providing pathways for the fluid to be in permanent contact with the reacting solid. On the contrary, if porosity does not form during the reaction, fluid advancement is hampered and the reaction stopped. The maximum capability of CO₂ storage in a geological formation will thus depend on the porosity generated during the carbonation reaction.

This work is aimed at determining how certain physicochemical parameters of the solutions (hydrodynamic conditions, pH or composition) may affect the development of porosity during replacement reactions. Geochemical modelling and experimental studies of the replacement of wollastonite (CaSiO₃) and portlandite by calcite (CaCO₃) are used for illustrating the influence of such parameters.

Putnis A. (2009) Mineral Replacement Reactions. In: Thermodynamics and Kinetics of Water-Rock Interaction. Oelkers E. H & Schott J (eds). *Reviews in Mineralogy & Geochemistry* **30**, 87-124

Toxic element balances in small scale wood combustion systems

H. RUPPERT* AND T. SEIDEL

Geosciences Center & Interdisciplinary Center for Sustainable Development, University of Goettingen, Goldschmidtstr. 3, D-37077 Goettingen, Germany (*correspondence: hrupper@gwdg.de)

In Europe, wood combustion in stoves and boilers is widely applied for residential heating. In Germany, approximately 15 million of 40 million households own small-scale wood-burning furnaces, which deliver 7% of Germany's heat consumption. Using state-of-the-art small-scale combustion systems, we investigated how the air quality changes due to the emissions of harmful elements and organic pollutants during the combustion of wood and straw.

Beside the fuel, we analysed all the originating ashes – grate ash, heat exchanger ash, and fly ash – to reconstruct element fluxes. As the input/output balance calculations show, some elements – such as cadmium, zinc, tin, thallium, lead, bismuth and antimony – may also be retained within the cooler zones of the furnace, in the chimney, or in the refractory lining material where samples could not be taken (Fig. 1). The elements collected by filters correspondent to the element amount in the flue gas, which is emitted into the ambient air. At most, these element portions represent 30 percent of the amount contained in the fuel [1, 2].

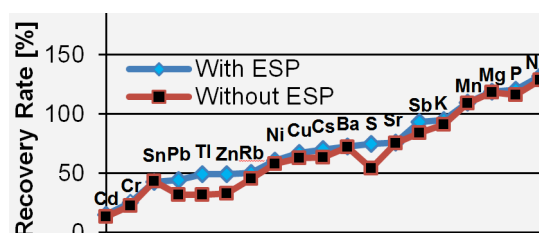


Figure 1: Element recovery rates with and without electrostatic precipitator ESP (combined element amounts in all ashes divided by the amounts contained in the combusted wood)

The pollutants are bound in fine (< 1 μm) particles or gaseous compounds and may enter the lungs' alveoli and contaminate the body. Clearly, effective emission reduction measures are necessary.

[1] Orasche *et al.* (2012) *Energy & Fuels* 26(11), 6695-6704.

[2] Seidel *et al.* (2013) Emissions of Organic and Inorganic Pollutants During the Combustion of Wood, Straw and Biogas. In Ruppert *et al.* (Eds.): *Sustainable Bioenergy Production - An Integrated Approach*. Chapter 13, Springer, Dordrecht, (in print).

The architecture of the intermediate-sized Quizapu magma system

PHILIPP RUPRECHT^{1*}, GEORGE BERGANTZ²,
KARI COOPER³ AND OLIVIER BACHMANN⁴

¹LDEO of Columbia University, Palisades, NY, USA,
(*correspondence: ruprecht@ldeo.columbia.edu)

²Dept. of Earth and Space Sciences, University of
Washington, Seattle, WA, USA

³Dept. of Geology, University of California, Davis, CA, USA

⁴Inst. für Geochemie und Petrologie, ETH Zürich, Switzerland

While high melt fraction magma chambers may be transient features in the crust, magmatic mushes represent the long-lived counterparts of the crustal magmatic factory. Together they source largely variable andesitic to dacitic composite volcanic cones and stratovolcanoes and manifest the continuous presence of silicic magma in the crust above convergent margins. Silicic magmas are ultimately fed and their eruption triggered by magmas generated in the mantle. How intermediate-sized (tens of km³) magmatic systems are assembled and what kind of crustal-scale architecture results from that assembly, requires an integrated approach of crystal-scale geochemistry, petrology, and fluid dynamics.

Utilizing such a combined approach provides tight constraints on the magmatic architecture beneath Volcán Quizapu (Chile), a magmatic system that produced two ~ 5km³ large historic eruptions. The shallowest part of the Quizapu system is dominated by high-melt fraction dacites with minimal evidence for hybridization. This eruptible dacite lense is generated by crystal-melt separation from an andesitic mush of intermediate temperature. Hybridization – common for arc systems – is limited to the andesitic mush, while hot recharge magmas interact only in rare cases directly with the shallow dacite magma [1]. Such mafic recharge leads to mixing and eruption and diffusion modeling of elemental zonation in phenocrysts at Quizapu (e.g., Mg in plagioclase) suggests that recharge, mixing, and eruption occurred within days to a few weeks [2]. Moreover, we consider the thermal effects on the mixing and eruption dynamics associated with hot mafic recharge and find (i) that overall mixing efficiency for the erupted volume is set early during the recharge events – limiting the extent of hybridization [1] – and (ii) that short-term reheating leads to significant viscosity reduction in the resident dacite magma. We argue that late-stage reheating may reduce the potential for Plinian eruptions as water-saturated dacites degas efficiently during ascent [3].

[1] Ruprecht *et al.* (2012), *J. of Petrology* **53**, 801-840. [2] Ruprecht & Cooper (2012), *J. Petrology* **53**, 841-870. [3] Ruprecht & Bachmann (2010), *Geology* **38**, 919-922.

Are long-lived stratovolcanos low-pass filters for magma transport?

PHILIPP RUPRECHT^{1*} AND TERRY PLANK¹

¹LDEO of Columbia University, Palisades, NY, USA,
(*correspondence: ruprecht@ldeo.columbia.edu)

Arc stratovolcanoes localize magmatic activity for 10s to 100s kyr, leading to self-cannibalization and the emergence of polybaric subvolcanic magma storage regions. Partial melts accumulate within mush zones and sills at various levels in the crust. Dense primitive mantle-derived magmas that ascend from mantle source regions encounter those density barriers on their way to the surface, leading to stalling and an evolution to more buoyant magmas through fractionation, mixing, and assimilation. It is therefore not surprising and well-known through geochemical and isotopic studies that primitive magma compositions typically do not reach the surface within voluminous arc magma systems. This view suggests that long-lived arc stratovolcanoes act as low-pass filters for primitive magmas from the mantle, where the frequency of magma addition from the mantle is converted in the crust to a slower integrated ascent rate as magmas stall, evolve and accumulate. Isotope and geochronology studies on crystal cargo provide evidence for such prolonged magma processing. While some stalling and processing in the crust is commonly agreed upon, magma transit times at middle to lower crustal levels are particularly unconstrained. A contrasting view is that magmas rise rapidly (potentially adiabatically), resorb any crystal cargo upon ascent, and crystallize at shallow depth.

Combining geochemical data from primitive crystals (e.g., Fo90), observations of upward earthquake migration beneath long-lived volcanic centers, and thermal constraints on magma transport in the crust, we show that slow processing (low-pass filtering) may not be as ubiquitous as it is assumed for large stratovolcanoes [1]. Instead, a second mode of fast magma transit from the mantle to the surface must coexist. Some phenocrysts in arc magmas record in their crystal zoning mixing episodes of primitive magmas at Moho depth (e.g., >1000 ppm Ni variations in olivines of constant Fo), and provide an upper limit on ascent rates of primitive magmas. In fact, thermal models for dike transport and trace element diffusion calculations for Ni zoning constrains integrated Moho-to-surface ascent rates for the fast mode to ~ 0.1-1 km/day, well in line with seismic observations from migrating earthquake swarms. Such ascent rates require primitive magmas to bypass or transit effectively most middle to lower crust magma storage regions.

[1] Ruprecht & Plank (2013, in press), *Nature*, doi: 10.1038/nature12342

Hydrothermal-sedimentary lithogenesis

V.YU. RUSAKOV

V.I. Vernadskiy Institute Geochemistry and Analytical Chemistry, RAS (rusakov@geokhi.ru)

The model of the hydrothermal-sedimentary lithogenesis rests on data of suspended and settled matter of 'black smokers', proximal and distal metalliferous sediments (MS), as well as the Paleozoic hydrothermal-sedimentary deposits. Recent hydrothermal fields (Broken Spur (<1 kyr), TAG (~40-50 kyr), Krasnov (~120 kyr), Semenov ore cluster (~37-124 kyr)) and ancient VMS deposits of the Urals (Molodezhnoye, Yaman-Kasy, Safiyanovskoe) was selected as an illustration of the model. Moreover, the manganiferous deposits of the Urals (Kyzil-Tash, South-Faizulinskoe, Bikkulovskoe) was also included in this model as an ancient prototype of distal hydrothermal-metalliferous sediments.

On the basis of study of sediment strata on the Krasnov field [Rusakov *et al.*, 2011; 2012] and Semenov ore cluster [Rusakov *et al.*, 2013 in press] was found that epicenter part of the hydrothermal-sedimentary strata in form of ore-bearing sediments, covered ore-bodies, reflects a zone of interrelation between ore-bearing solutions (infiltration-metasomatic processes) and seawater (halmyrolysis). At the distance of the zone the ore-bearing sediments are transformed into proximal MS, ore part of which is completely presented by Fe-oxyhydroxides. Main part of Mn is precipitated on great distance from the hydrothermal field from non-buoyant plumes.

On the basis of study of ferruginous rock around VMS deposits enable to reveal main stages of the meta-sediment formation: (1) sedimentation, (2) infiltration-metasomatic, (3) halmyrolysis, (4) lithification. The infiltration-metasomatic impact of hydrothermal solutions and oxidizing action of seawater leads to copper redistribution within sediment strata and formation of secondary minerals (pyrite is replaced by chalcopyrite, chalcopyrite is replaced by siderite, as well as formation of secondary calcite and chlorites). The main mechanism of lithification of MS is sediment dehydration, expressed in replacement of Fe-oxyhydroxides by hematite and silica by quartz. In spite of such transformations, original lateral zoning of rock is remained indicating on effect of hydrothermal-sedimentary genesis.

Origin of Earth's Earliest Continental Crust: A Combination of Partial Melting and Fractional Crystallization?

T.RUSHMER^{1*} AND J. ADAM¹

¹Department of Earth and Planetary Sciences, Macquarie University, Sydney, AUS (*Tracy.Rushmer@mq.edu.au)

The origin of tonalite-trondhjemite-granodiorite (TTG) plutonic complexes continues to be a major focus of research as these suites make up a majority of Earth's earliest continental crust. Partial-melting experiments were conducted (at 900-1100 °C and 0.5-3.0 GPa) on two greenstones from the Nuvvuagittuq Complex, Quebec, Canada and on PC-103, a 3.66 Ga tonalite that encloses the mafic rocks of the Nuvvuagittuq Complex. At 1.5-3.0 GPa and 950-1100 °C, the experimentally produced melts are compositionally similar to Archean TTGs (including PC-103). But the degree of melting needed to produce these melts is high (> 30 %) and so the relative concentrations of most incompatible elements in the melts are similar to those of their greenstone parent rocks. These greenstones have compositional affinities with modern subduction zone magmas. Thus, arc-like mafic rocks appear to have been selectively involved in TTG formation, implying the involvement of crustal recycling in TTG genesis. The results of experiments on the tonalite PC-103 suggest either equilibrium of its original magma with a garnet pyroxenite residue at ~1050 °C and 3.0 GPa, or compositional control by the plagioclase-pyroxene cotectic at ≤ 900 °C and < 1.0 GPa. The latter option is more consistent with the compositional trends of Archean TTGs. In either case, a high degree of inheritance is involved implying a role for early crustal recycling.

Green River CO₂ natural analogue, Utah: insights into Fe mobilisation from jarosite fracture mineralisation.

J. C. RUSHTON¹, D. WAGNER, G. PURSER, J. M. PEARCE
AND C. A. ROCHELLE

British Geological Survey, Environmental Science Centre,
Keyworth, Nottingham NG12 5GG ¹ jere1@bgs.ac.uk

Outcrop samples of the Jurassic Entrada Sandstone in the Green River area of Utah, USA, have been studied as part of a CO₂ storage natural analogue study (CRIUS consortium). These rocks are locally bleached, the pattern of which is enigmatic but commonly associated with sub-vertical fractures. In some locations these fractures are pathways to recent carbonate travertine deposits. Of key interest is the fate of Fe, whose reduction and mobilisation is implied by the host rock bleaching patterns and which is present in travertine deposits, and CO₂-rich springs and geysers in the area.

Petrographic analysis has revealed a complex and unusual textural and mineralogical assemblage in the fractures. Jarosite (KFe₃(SO₄)₂(H₂O)₆) has been identified; its formation is typically associated with oxidative alteration of sulphide minerals and acid mine drainage^[1]. Cubic pseudomorphs mostly comprising goethite, centrally concentrated in the fractures and containing rare pyrite relics, suggest pyrite was the primary fracture mineralisation, and may indicate that S-bearing reducing fluids are responsible for the host rock bleaching patterns.

Expansive textures associated with the jarosite suggest that it formed with minimal overburden, and that the oxidative fluids were a near-surface episode. Zones of complete and then partial dissolution of diagenetic carbonates in the host sandstones adjacent to the fractures, associated with Al oxide / hydroxide mineralisation, are consistent with low pH fluids resulting from sulphide oxidation. Gypsum- and calcite-cemented fractures cross-cut the jarosite mineralised textures; these later events relate to current CO₂-rich fluid movements since they can be observed to form part of the feeder system linking directly to travertine deposits at some locations. This paragenesis shows that the same fracture flowpaths have been used by several generations of fluids.

Petrographic observations, together with an experimental study of Fe mobilisation from the Entrada Sandstone, suggest that dissolved Fe in the modern regional CO₂-rich fluids is largely derived from the fracture mineral assemblage, rather than through current alteration and leaching of the host rock.

[1] Bigam, J.M. & Nordstrom, D.K. (2000): Iron and aluminium hydroxysulfates from acid sulfate waters. *Reviews in Mineralogy and Geochemistry*. 40, 351-403.

Observed Aerosol Effects on Eastern Pacific Stratocumulus Clouds

LYNN M. RUSSELL^{1*}, ARMIN SOROOSHIAN³,
JOHN SEINFELD², BRUCE ALBRECHT⁵,
ATHANASIOS NENES⁴, W. RICHARD LEITCH⁷,
ANNE MARIE MACDONALD⁷, LARS AHLM¹,
YI-CHUN CHEN², MATT COGGON², ASHLEY CORRIGAN¹,
JILL CRAVEN², RICHARD FLAGAN²,
AMANDA FROSSARD¹, LELIA HAWKINS⁸, HAF JONSSON⁶,
EUNSIL JUNG⁵, JACK LIN⁴, ANDREW METCALF²,
ROBIN MODINI¹, JOHANNES MÜLMENSTÄDT¹,
GREG ROBERTS¹, TAYLOR SHINGLER³, SIWON SONG⁵,
ZHEN WANG³ AND ANNA WONASCHÜTZ³

¹Scripps Institution of Oceanography, UCSD, La Jolla, CA
(*correspondence: lmrussell@ucsd.edu).

²California Institute of Technology, Pasadena, CA.

³University of Arizona, Tucson, AZ.

⁴Georgia Institute of Technology, Atlanta, GA.

⁵Rosenstiel School of Marine Sciences, Miami, FL.

⁶Center Interdisciplinary Remotely-Piloted Aerosol Studies.

⁷Environment Canada, Toronto, Canada.

⁸Harvey Mudd College, Claremont, CA.

Aerosol particles in the marine boundary layer include primary organic and salt particles from sea spray and combustion-derived particles from ships and coastal cities. The Eastern Pacific Emitted Aerosol Cloud Experiment (E-PEACE) 2011 was a targeted aircraft campaign to assess how different particle types nucleate cloud droplets. Particle sources included shipboard smoke-generated particles with 0.05-1 µm diameters (which produced tracks measured by satellite and had drop composition characteristic of organic smoke) and combustion particles from container ships with 0.05-0.2 µm diameters (which were measured in a variety of conditions with droplets containing both organic and sulfate components) [1]. Three central aspects of the collaborative E-PEACE results are: (1) the size and chemical composition of smoke particles compared to cargo ship emissions as well as background marine particles, (2) the characteristics of cloud track formation for smoke and cargo ships, as well as the role of multi-layered low clouds, and (3) the implications of these findings for quantifying aerosol indirect effects. For comparison with the E-PEACE results, the preliminary results of the Stratocumulus Observations of Los-Angeles Emissions Derived Aerosol-Droplets (SOLEAD) 2012 provided evidence of the cloud-nucleating roles of both marine organic particles and coastal urban pollution, with simultaneous measurements of the effective supersaturations of the clouds in the California coastal region.

[1] L.M. Russell et al. (2013)., *Bull. Am. Meteorol. Soc.*

Analogue experiments on volatile escape from crystal-rich magmas

A. RUST¹, K. CASHMAN¹, J. OPPENHEIMER¹
AND I. BELIEN²

¹School of Earth Sciences, University of Bristol, UK
glkvc@bristol.ac.uk

²Exxon Mobil Upstream Research, Houston, TX

The low water content of granitoid bodies requires effective escape of the volatile phase during crystallization of mushy magma. We explore the physical mechanisms for volatile migration in crystal-rich magmas with experiments on three-phase analogue mixtures of syrup, solid particles and gas. The liquid+particles was either placed in a vertical tube or sandwiched between two glass plates; gas was injected into the suspension, or generated throughout the suspension by chemical reaction or by decompression. The proportions of phases, syrup viscosity, particle sizes, and rate of gas injection/expansion were varied. Experiments were videoed and monitored with gas pressure data.

Comparisons with crystal-free experiments indicate that crystals in mushes strongly inhibit buoyancy-driven bubble migration, but can facilitate the formation of temporary connected gas pathways, allow degassing of permeable gas flow at much lower volume fractions of gas than the crystal-free system. The experiments with parallel glass plates facilitate visualization of the gas phase. Three regimes are identified by gas distribution patterns, and are found to be related to the volume fraction of solids: (1) At low particle concentrations the gas forms smooth fingers that intrude steadily; (2) At ~55% particles, the gas penetrates the suspension in bursts, and forms thin "fractures"; (3) At solid fractions sufficient to lock the particles in place, the gas pushes liquid out through the particle network.

In all three regimes the measured gas pressure increases smoothly and does not decrease until, or shortly before, the gas reaches the edge of the liquid+particle mixture. In the fracturing regime, the pressure increase is steady even during bursts of motion; this indicates that the ductile but sudden fracture formation rearranges the gas phase but does not create episodes of pressure buildup and release. Once a fracture has released gas to the outside, however, there are subsequent fluctuations in pressure as the initial fracture heals (viscously) and closes the system until a new fracture reaches the suspension boundary, at which point the process is repeated in a new location (because in heterogeneous suspensions fractures preferentially propagate into areas with relatively high solid contents). This mechanism would allow effective open-system degassing of crystallizing volatile-saturated magma, without leaving textural evidence of the volatile phase.

Calculation of Mass-Dependent Isotope Fractionation in Aqueous-Mineral Systems: In Pursuit of 1-permil Accuracy

JAMES R. RUSTAD¹

¹University of California, Davis, Davis, CA 95615
(correspondence: jrustad@ucdavis.edu)

Calculation of mass-dependent isotope fractionation in geochemical systems is probably the single most successful application of computational chemistry to geochemistry. The accuracy of these calculations is highly system dependent. For heavy isotopes with fractionations between minerals and aquo ions on the 1-2 permil level, first principles calculations are highly challenging, and computational requirements differ considerably between anionic and cationic systems. Aquo ions need large basis sets, particularly anions, which require basis sets of aug-cc-pVTZ (or better) quality. Aquo cations can be represented using continuum solvent models beyond the second shell, while aquo anions cannot. When density functional theory is used, the choice of the exchange-correlation functional has a strong effect on the results. This exchange-correlation variation, together with the basis set variation, can easily result in steps taken through basis-set XC functional that vary over a range of more than ~3 permil, with no apparent consensus on which functionals work best. Thus while past success has often been impressive, reliable prediction of fractionation at the sub-1 permil level will remain a highly challenging, though not unattainable, goal. Examples are taken from $\text{BOH}_3(\text{aq})$ - $\text{BOH}_4(\text{aq})$, $\text{Mg}^{2+}(\text{aq})$ -calcite, $\text{Ca}^{2+}(\text{aq})$ -calcite, $\text{Fe}^{3+}(\text{aq})$ -hematite, $(\text{H})\text{CO}_3(\text{aq})$ -carbonate, perovskite-ferropericline, chlorophyll, and amino acid systems.

Polyoxoions as Model Systems for Mineral Surface Chemistry

JAMES R. RUSTAD¹

¹Corning Incorporated, Sullivan Park Research Center,
Corning, NY 14831, USA
(correspondence: rustadjr@corning.com)

Polyoxometalate ions (POMs) have structures similar to condensed oxide phases and can be used as representative molecular models of the oxide/water interface. Oxygen atoms in POM exchange with water molecules at different rates. At present there is no basis for predicting how the coordination environment and metal substitution influences rates and mechanisms. Lability of oxygen in POMs is governed by low-energy metastable configurations that form from the breaking of weak bonds between metals and underlying highly coordinated oxygen atoms, followed by facile hydroxide, hydronium or water addition. The mediation of oxygen exchange by these stuffed structures suggests a new view of the relationship between structure and reactivity at the oxide/solution interface that de-emphasizes local bond ruptures and activated transition states. Reaction rates are governed by pathways for the formation and destruction of oxygen-stuffed intermediate states, not specific oxygen site chemistry, as has long been assumed. These intermediates form from ring-opening reactions that allow isotopic exchange and, by extension, dissociation and dissolution. As for the Keggin-type polyoxocations, the common feature of these intermediates is the breaking of a weak bond between a surface metal and the deeper, highly coordinated oxygen. The relative energies of the intermediate structures are similar across the range of substituted decaniobates, supporting the experimental observation that metal substitution at a specific site does not change the relative order of reactivity of the different types of oxygen atom. Unlike the Keggin-type polyoxocations, metal substitutions in the decaniobate POMs affect rates mainly by modifying the Bronsted acid/base properties of the molecule.

Combining geochemistry with thermal infrared remote sensing to characterize glacial weathering

A.M. RUTLEDGE*, P. CANOVAS, E. SHOCK
AND P.R. CHRISTENSEN

School of Earth and Space Exploration, Arizona State Univ.,
Tempe, AZ 85281 USA
(*correspondence: allie.rutledge@asu.edu)

Subglacial and englacial weathering of geologic materials contributes to the solute flux in meltwater, provides feedback in the global carbon cycle, and is a potential source of energy to chemotrophic microbes [1]. Thermal infrared (TIR) remote sensing has been used to identify geologic materials and study weathering processes [2]. In this study, we characterize the weathering processes occurring in a glaciated silicate-carbonate system by linking Advanced Spaceborne Thermal Emission and Reflection Radiometer (ASTER) infrared spectroscopy to in-situ rock and sediment samples, and compare our results with aqueous geochemical data. Our major objective is to link *in situ* samples with remote sensing capabilities.

Robertson Glacier (115°20'W, 50°44'N) drains the northern flank of the Haig Icefield in Peter Lougheed Provincial Park, Kananaskis Country, Alberta, Canada. The glacier rests on Upper Devonian impure limestones, dolostones, and shales [3]. Samples of glacially altered rock and sediments were collected at the glacier in 2010 and 2011. TIR laboratory spectroscopy was used to determine the composition and abundance of minerals present. Ice and water samples were also collected at similar locations and analyzed for major and minor elements. TIR imagery of the region was collected with the ASTER satellite instrument.

Dissolved Ca⁺² and SO₄⁻² increase downstream in the outflow channel. This is consistent with earlier studies of this system – these increases are interpreted to be due to acid hydrolysis of calcite fuelled by CO₂ dissolution and by pyrite oxidation [4], which is likely to be microbially mediated. Both ASTER- and lab-scale spectroscopic analyses show evidence for calcite leaching. Lab TIR analyses demonstrate the presence of calcite-depleted weathering rinds on hand samples. ASTER analyses show similar spectra on a regional scale; freshly revealed glacial till is seen to be depleted in calcite relative to the surrounding bedrock. This TIR remote sensing method has wide application to studies of glacial weathering, especially those focusing on less accessible regions of the world.

- [1] Anderson (2007) *Annu Rev Earth Planet Sci* **35** 375-399
[2] Michalski *et al.* (2004) *JGR* **109** E03007 [3] McMechan (1998) *Geological Survey of Canada* **2057** [4] Sharp *et al.* (2002) *GCA* **66** 595-614

Monitoring the $^{40}\text{Ar}/^{39}\text{Ar}$ irradiation parameter 'J' without using geological age standards

DANIEL RUTTE^{*1}, SEPP UNTERRICKER²,
JÖRG A. PFÄNDER¹ AND RAYMOND JONCKHEERE¹

¹Institut für Geologie, TU Bergakademie Freiberg, Germany,
[*daniel.rutte@geo.tu-freiberg.de]

²Institut für Angewandte Physik, TU Bergakademie Freiberg,
Germany

One of the major error components in $^{40}\text{Ar}/^{39}\text{Ar}$ geochronology is the irradiation parameter J. Its associated error is based on the accuracy of the independent age of the geological age standard and the inhomogeneity of the neutron fluence in the irradiation channel. To tackle both problems, we included independent fluence monitors (Ni and Co foil) in two of our irradiation containers, one irradiated under Cd-shielding in the research reactor Geesthacht FRG1 (Germany), the other without Cd-shielding in the research reactor Řez LVR-15 (Czech Republic). The irradiation containers were placed in rotating positions. Based on the activation reaction $^{58}\text{Ni}(n,p)^{58}\text{Co}$, gamma-spectroscopy of the resulting decay of ^{58}Co to ^{58}Fe provided the means to calculate absolute fast neutron fluences. The relative variation of the calculated fast neutron fluence at different points in the irradiation container is in agreement with the J-values measured from geological age standards within 1 sigma errors. For the irradiation in the research reactor LVR-15, the calculated neutron fluence varied systematically by 2.5% over an axial distance of 6 cm and by 1.9% over a radial distance of 3 cm. From the calculated absolute fast neutron fluences we calculated J-values, independent of geological age standards. In a first approach, the calculated J-values are about 12% higher than the J-values determined using geological age standards. The relative 1 sigma errors of the calculated J-values are on average 0.15%, as determined by a Monte Carlo method, which takes into account the weighing error of the Ni- and Co-monitors, as well as counting statistics of the gamma-spectrometer.

Halogen Systematics of the Manus Spreading Center.

L. RUZIÉ^{1,*}, D. CHAVRIT¹, R. BURGESS¹, P. CLAY¹, B. JOACHIM¹, D. R. HILTON², J. M. SINTON³
AND C.J. BALLENTINE¹

¹University of Manchester, UK
(*lorraine.ruzie@manchester.ac.uk)

²Scripps Institution of Oceanography, California, USA

³University of Hawaii, Honolulu, USA

The incompatibility of the heavy halogens (Cl, Br, I) combined with relatively high concentrations and distinct elemental compositions in surface reservoirs makes the halogens good tracers to detect the recycling processes in the different mantle sources. However, the halogen systematics in mantle reservoirs remains poorly constrained mainly because of their very low abundance in materials of interest. An innovative analytical technique, involving neutron irradiation of samples to convert halogens to noble gases then measured using conventional noble gas mass-spectrometry, provides detection limits unmatched by any other technique [1].

We focus on the halogen contents in the glassy margins of basalts erupted along the Manus Spreading Center (MSC), which lies in a back-arc basin setting. Samples consist of both MORB-type lavas and back-arc basin basalts (BABB) [3]. The major and trace elements, as well as $^3\text{He}/^4\text{He}$ ratios, water concentrations and δD have already been determined [2].

The halogen concentration range is between 160 and 1500 ppm Cl, 600 and 5700 ppb Br and 10 and 60 ppb I. The lower concentrations found in MORB-type samples are similar to E-MORB contents from Central Indian Ridge [4]. The higher concentrations are found in BABB samples. A strong negative correlation is apparent between I/Cl and both $\text{H}_2\text{O}/\text{Ce}$ and δD : (1) the lower I/Cl wt. ratios measured in BABB ($4.1 \pm 1.4 \times 10^{-5}$) are associated with the higher $\text{H}_2\text{O}/\text{Ce}$ ratios ($2,150 \pm 580$) and δD ($-52 \pm 15\text{‰}$), (2) the higher I/Cl wt. ratios measured in MORB-type lava ($7.2 \pm 2.5 \times 10^{-5}$) are associated with lower $\text{H}_2\text{O}/\text{Ce}$ ratios (750 ± 130) and δD ($-94 \pm 11\text{‰}$). From these results, we infer that our suite of samples from MSC are explained by mixing a seawater-derived component of the actual slab and the Manus underlying mantle. Considering both the MSC distance to the arc (240 km) and the slab slope, we conclude that a seawater-derived component can be preserved below 100 km depth.

[1] Burgess *et al.* (2002) *EPSL* **197**, 193-203. [2] Shaw *et al.* (2012) *Nature Geosciences* **5**, 224-228. [3] Sinton *et al.* (2003) *J. of Petrol.* **44**, 159-195 [4] Ruzié *et al.* (2012) **V31A-2762**, AGU Fall Meeting.

Ge and Ge-bearing mineral phases in gabbrodolerites of Mt. Ozernaya trap intrusion (Siberian platform)

V.V. RYABOV¹ AND L.V. AGAFONOV¹

¹V.S.Sobolev of Institute Geology and Mineralogy SB RAS, Novosibirsk, 630090, Russia; e-mail: trapp@igm.nsc.ru

Native iron(-platinum) ores [1] are associated with the Mt. Ozernaya trap intrusion, which is a part of the large volcano tectonic structure. Small (5-25 μm) isometric grains and subhedral crystals of Ge and Ge-bearing oxygen-free and oxygen-containing mineral phases are observed in interstices of olivine-bearing gabbrodolerites of this intrusion. The phase composition was determined on LEO 1430VP scanning microscope and on GEOL JXA-8100 electron-microprobe. Because of small sizes of the grains, it was not possible to determine X-ray parameters of the mineral phases. The element composition in Ge and Ge-bearing mineral phases varies within the wide range: Ge (1.0-37.6%), Ni (24.8-72.2%), Co (0.9-5.1%), Fe (1.3-42.9%), Sb (0-20.2%), As (0-39.8%), and S (0-15.7%). Individual grains contain Cu (0.6-5.9%), Pd (4.5-19.9%), and Sn (10.7-18.0%). The ideal formulas of mineral phases are Ni₂Ge, Ni₂(Ge,Sb), Ni₂(S,Ge), and Ni₂(Ge,As).

Three analyses of the oxygen-containing Ge mineral phases show the variation: 41.41, 40.65 and 40.94 GeO₂, 56.98, 51.84 and 51.62 FeO; 0.00, 4.33 and 4.94 MgO; 1.61, 1.65 and 1.61 NiO; 0.00, 0.38 and 0.55 Co; 0.00, 1.12 and 1.08 CuO, respectively. The sums are 100, 99.97 and 100.74, respectively. Their ideal formula is Fe₂GeO₄.

In association with the Ge and Ge-bearing phases, the following constituents are observed in interstices of gabbrodolerites: graphite, iron, cobalt, camacite, taenite, awaruite, NiCoFe-intermetallic compounds, silver, wustite, hercynite, chalcopyrite, cubanite, bornite, pentlandite, heazlewoodite, troilite, acantite, maucherite, nickeline, as well as fayalite, biotite, hastingsite, garnet, demidovskite, breakdown solid solution structure Wo₂En₄₇Fs₅₁ - Wo₄₀En₄₂Fs₁₈, and circon.

Formation of the mineral phases is assumed to occur under highly-reductive conditions involving organoelement compounds. [2]

[1] Ryabov V.V., Lapkovsky A.A. (2010) Austral. J of Earth Sci. **57**, 707-730. [2] Buslaeva E.U. & Novgorodova M.I. (1989) Organoelement compounds in the problem of migration of ore material, 52 p (in Russian).

Variations in modes and rates of long-term denudation in carbonate terrains under Mediterranean to hyper-arid climates

U. RYB^{1*}, A. MATMON¹, Y. EREL¹, I. HAVIV² AND L. BENEDETTI³

¹The Fredy and Nadine Herrmann institute of Earth Sciences, Admond J. Safra Campus, Givat Ram, Jerusalem, 91904, Israel. (*correspondance: uri.ryb@mail.huji.ac.il)

²Ben-Gurion University of the Negev, Be'er-Sheva 84105, Israel

³Aix-Marseille Université, CNRS-IRD-Collège de France, UM 34 CEREGE, Technopôle de l'Arbois, BP80, 13545 Aix-en-Provence, France

Using ³⁶Cl measurements in >100 carbonate bedrock and sediment samples we calculate long-term denudation rates in two drainage basins that drain the western and eastern flanks of the Judean mountain range (central Israel). A sharp climatic gradient from Mediterranean to hyper-arid conditions characterizes the transition from the western to the eastern flank of the range, due to rain shadow effects. Moving from the Mediterranean to the hyper-arid climate zones, denudation rates of interfluvial drop by an order of magnitude from ~20 to 1-3 mm kyr⁻¹ and are linearly dependent on precipitation, indicating that carbonate dissolution is the dominant erosional process. Conversely, denudation rates become increasingly dependent on hillslope gradient only in the dryer climate zone, and thus delineate the dominant control of mechanical processes on denudation within this zone. We demonstrate that the transition between chemically-controlled denudation to mechanically-controlled denudation occurs between mean annual precipitations values of 100 and 200 mm yr⁻¹. The growing contribution of mechanical processes to hillslope erosion is also evident in the increase of denudation rates calculated from sediments, collected from the eastern drainage, between the Mediterranean (16-18 mm kyr⁻¹) and the hyper arid (30-48 mm kyr⁻¹) regions. This study demonstrates that carbonate terrains have the capacity to switch between mechanical and chemical weathering regimes in response to changes in precipitation. Similar transitions in response to changes in temperature or the level of tectonic activity have been reported in the past. It is suggested that the abrupt nature of such transitions is a reflection of the competition between surface and subsurface drainage systems in carbonate terrains, derived from the congruent nature of carbonate dissolution processes.

Sub-sea tailings deposition leach modeling

P. RZEPKA^{1*}, I.F. WALDER¹, P. BOŻECKI²
AND G. RZEPA²

¹Kjeøy Research & Education Center, Kjeøy, 8412 Vestbygd, Norway;

(*correspondence: przemyslaw.rzepka@gmail.com)

²AGH University of Science and Technology, Department of Mineralogy, Petrography and Geochemistry, al. Mickiewicza 30, 30-059 Kraków, Poland.

The sub-sea/deep sea tailings deposition is a controversial method for disposing of mine wastes. Hazardous chemicals used during processing and deposited metal sulfides may dissolve, affecting the sea environment.

The overall objective for this project is to evaluate the copper leaching potential from tailings on the example of the proposed submarine tailing disposal in Repparfjorden discharged from 2 deposits - Nussir and Ulveryggen, mined by Nussir ASA. This experiment gives better understanding of the reactivity of sulfide minerals in saline system during sub-sea deposition.

Several kinetic tests were run based on recirculation of the leachate (batch experiments) using a constant flow rate over the tailings material of 1-2 m/h. The columns were run at approximately 10 °C (Fig. 1).

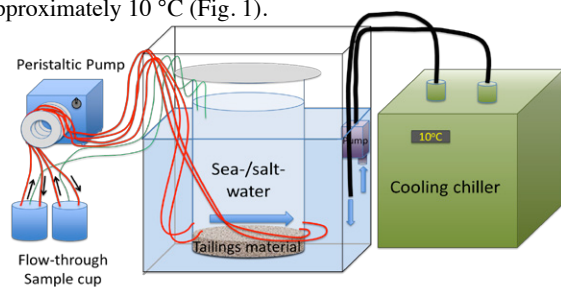


Fig. 1. Scheme of sub-sea tailing deposition leach test model.

There is a distinct increase in copper concentration during the experiments; while other hazardous elements (like Se, As, Ni) do not reveal changes. Copper leaching is a two-stage process: (1) initial rapid dissolution of secondary minerals formed from sulfide oxidation, related to the tailings material disposing period, and (2) long term slow leaching of available surface material of tailings settled on the bottom. Copper concentrations reached 0.02 mg/l after 100 days. Towards the end of experiments (from 70-100 days) the leaching rate leveled off (approximately 2.8 mg/m²/year) with time. Cu content data indicated that there were no further increase or leaching. These experiment results are potentially overestimating sub-sea tailings deposition natural conditions.

δ D in lunar volcanic glasses and melt inclusions: A Carbonaceous chondrite heritage revealed

A.E. SAAL^{1*}, E.H. HAURI², J.A. VAN ORMAN³
AND M.J. RUTHERFORD¹

¹Dept. of Geol. Sc., Brown University, RI, 02912, USA

(*correspondence: asaal@brown.edu)

²DTM, Carnegie Institute of Washington, DC, 20015, USA

³Dept. of Geol. Sc., Case Western Reserve University, OH 44106, USA

Water is perhaps the most significant molecule in the solar system, and determining its origin and distribution in planetary interiors has important implications for understanding the evolution of planetary bodies. Here we present the isotopic composition of hydrogen dissolved in lunar volcanic glasses and in their olivine-hosted melt inclusions to establish the source of the lunar magmatic water. These volcanic glasses, returned by the Apollo 15 and 17 missions, represent some of the best-studied and most primitive magmas generated within the Moon. The D/H ratios and H₂O contents were measured simultaneously in the center of the exposed interiors of individual lunar volcanic glass beads and olivine-hosted melt inclusions, using a Cameca NanoSIMS 50L multicollector ion microprobe. We examined very-low Ti and low-Ti glasses from Apollo 15 15426/27 and high-Ti glasses from Apollo 17 74220. The Apollo 17 high-Ti glasses contain olivine-hosted melt inclusions, small samples of magma trapped within the olivine that grew in the magma before eruption. By virtue of their enclosure within their host crystals, melt inclusions are protected from loss of volatiles by degassing during eruption. After consideration of cosmic ray spallation and degassing processes our results demonstrate that lunar magmatic water has an isotopic composition that is indistinguishable from the bulk water in carbonaceous chondrites and similar to terrestrial water, implying a common origin for the water contained in the interiors of the Earth and Moon. The Moon must have received its water during or shortly after its accretion, before the formation of a robust lunar lithosphere ≤ 100 My. Data for highly siderophile elements [1] suggest that a late veneer of meteoritic material delivered to the Moon was too small to be responsible for the lunar volatile budget. Therefore, the simplest scenario consistent with our observations is that the Earth was wet at the time of the Moon-forming event, as predicted by dynamic models [2,3], and that the water was not completely lost during this giant impact.

[1] Day, J. M. D. *et al.* (2007) *Science* **315**, 217-219. [2] Morbidelli, A. *et al.* (2000) *Meteor. Planet. Sci.* **35**, 1309. [3] Walsh, K.J. *et al.* (2012) *Meteor. Planet. Sci.* **47**, 1941.

Fluid-mineral reactions during CO₂-based geothermal energy extraction

MARTIN O. SAAR, XIANG-ZHAO KONG,
BENJAMIN M. TUTOLO, ANDREW J. LUHMANN AND
WILLIAM E. SEYFRIED, JR.¹

¹Department of Earth Sciences, University of Minnesota, 310 Pillsbury Dr. SE, Minneapolis, MN 55455, USA.
saar@umn.edu

Geothermal energy extraction with groundwater as the subsurface heat extraction fluid can result in substantial scaling (mineral precipitation) in pipes, heat exchangers, power conversion equipment, and the subsurface reservoir. A potential solution to this problem is to utilize carbon dioxide (CO₂) as the subsurface heat extraction fluid. During this approach, CO₂ from an emitter, such as a coal-fired power plant, biofuel plant, or concrete factory, is injected into a geothermal reservoir such as a sedimentary basin or a hydrofractured rock. In the case of the sedimentary basin approach, large amounts of CO₂ are permanently stored underground in the form of a CO₂ plume while a small portion of the geothermally heated CO₂ is circulated back to the surface for power production before reinjection into the reservoir along with the main CO₂ stream. This is referred to as a CO₂-Plume Geothermal (CPG) system.

When CO₂ is injected into deep saline aquifers, the CO₂ largely displaces the brine although there is a small degree of dissolution at the CO₂-brine interface. The result is a multicomponent-multiphase plume environment that ranges from virtually pure CO₂ in the center of the plume to CO₂ with dissolved water on the CO₂ side of the CO₂-water interface, to brine with dissolved CO₂ on the brine side of the interface, to brine with no CO₂ away from the plume.

Here, we present results on the reactions of some of the above described fluid components with various reservoir minerals that are based on flow-through reaction cell experiments under realistic T and P conditions. Pre- and post-experiment X-Ray Computed Tomography analyses provide 3D images of pore-space geometry changes due to the reactions. The 3D images are then used as input in lattice-Boltzmann fluid flow simulations to determine permeability field changes due to the fluid-mineral reactions. The ultimate objective of this work is a parameterization of permeability changes as a function of fluid and mineral chemistry for typical host rocks and T-P conditions which can be included into geothermal reservoir simulators such as TOUGH2.

Evaluation of different RNA preservation methods to study the active microbial communities in oil sand tailings ponds

SABARI PRAKASAN M.R.^{1*}, NADINE LOICK²
AND CHRIS WEISENER¹

¹GLIER, University of Windsor, Windsor, Canada
(*mullapus@uwindsor.ca)

²Rothamsted Research, Hertfordshire, England

Analysis of RNA is the best approach to understand active microbial populations in an environment. In contrast to DNA, which can persist in soil for several days, RNA is an unstable macromolecule making it more suitable to investigate metabolically active microbial communities. Due to its susceptibility to degradation, the preservation of a sample containing RNA is an important step in molecular studies. In the field of Oil Sand Tailings Research sample-preservation is especially important as due to logistical limitations the extraction of nucleic acids may only be possible days after the samples are taken. The aim of this study is to evaluate the ability of different methods to preserve RNA in Oil Sand Tailings samples both short term (5 days) and long-term (30 days). In our study different preservation solutions including LifeGuard™ Soil Preservation Solution (MoBio Laboratories, Inc.), RNAlater® (Ambion), glycerol and liquid nitrogen are compared to find the best preservative method for soil RNA preservation.

Analysis of different RNA samples shows that all four preservation methods provide significant amounts of RNA for further analysis. After cDNA synthesis T-RFLP analysis is used to compare community structure derived from the differently treated samples. Additionally, during RNA-extraction co-precipitated DNA is also analysed. The community structure data derived from cDNA and DNA provides information on the ability and comparability of the different techniques to preserve microbial communities and demonstrates the importance of RNA (cDNA) in microbial ecology.

Interaction of Eu(III) with calcium carbonate: Spectroscopic characterization

A. SABĂU^{1,2}, N. JORDAN³, C. LOMENECH²,
N. MARMIER^{2,*}, V. BRENDLER³, A. BARKLEIT³, S.
SURBLÉ⁴, N. TOULHOAT^{5,6}, Y. PIPON⁵, N. MONCOFFRE⁵,
E. GIFFAUT¹

¹Agence Nationale pour la gestion des Déchets Radioactifs (ANDRA)

²University of Nice - Sophia Antipolis, ECOMERS (*e-mail: nicolas.marmier@unice.fr)

³Helmholtz-Zentrum Dresden-Rossendorf (HZDR)

⁴UMR 3299 CEA/CNRS SIS2M/LEEL

⁵IPNL, CNRS/Université Claude Bernard Lyon

⁶CEA/DEN Saclay, 91191 Gif sur Yvette, France

The present work investigated irreversible sorption processes in the Eu-CO₂-NaCl-CaCO₃ system, by combining macroscopic with TRLFS and RBS spectroscopic studies.

Powders and single crystals were used due to spectroscopic tools requirements. Sorption of europium was investigated by varying the initial concentration in europium concomitant with the contact time (few hours up to 6 months). TRLFS identified two lifetimes and therefore two species at the calcite/water interface. Lifetimes allow an unambiguous discrimination between sorption processes and incorporation. Values of the lifetimes are comparable to the literature [1] and the total loss of water molecules is a distinctive sign of Eu(III) species incorporation.

RBS confirmed that Eu(III) is associated in two different states with calcite:

- (1) heterogeneous (supported by SEM) surface accumulation, i.e. as a surface precipitate, after 1 month contact time
- (2) incorporation up to depths greater than 160 nm after 1 month.

[1] Fernandes, M. M. *et al.*, *J. Colloid Interface Sci.* **321** (2008) 323-331

Monazite anamnesis – providing a quantitative timeframe for metamorphic petrogenetic processes

GAVRIL SĂBĂU¹, ELENA NEGULESCU¹ AND THOMAS THEYE²

¹Geological Institute of Romania, RO-012271 Bucharest, (g_sabau@yahoo.co.uk)

²Institut für Mineralogie und Kristallchemie, DE-70174 Stuttgart, (thomas.theye@imi.uni-stuttgart.de)

Monazite is a privileged phase in metamorphic assemblages, as it has a wide p-T stability field, a complex chemical composition, incorporates high concentrations of radioactive elements and is remarkably refractory to diffusion. Its chemical substitutions represent a very sensitive response to mineral reactions triggered by changing conditions, being recorded and preserved in grain zonations, as well as in regular chemical variations in the monazite populations. Connecting age data with chemical features allows not only dating monazite growth, but also a sometimes surprisingly accurate insight in the concurrent mineral reactions.

We performed several hundred microprobe analyses on monazite in pelitic and gneissic rocks from the South Carpathian basement units, for both chemical characterization and dating. The chemical characterization included structural formulae, ternary plots, normalized plots and elemental ratios therefrom. Relating age point data to compositional trends reveals homogeneous compositional and age domains, as well as regular chemical shifts, having a counterpart in mineral reactions involving monazite, and in variations in the crystallization versus resorption rates of monazite itself.

Monazite acts as a LREE and Th scavenger from decomposing REE-bearing phosphates, carbonates and silicates, and Th (U)-bearing silicates, phosphates and oxides, recording high Th (+Ca, U) and LREE contents in the initial growth stages. Oppositely, monazite resorption is typically indicated by its Nd and Sm enrichment. LREE correlations are variable, reversing differently in different samples with increasing atomic number, whereas the corresponding ratios indicate changes in modal abundance. Y content is buffered by coexisting xenotime and melt, being also markedly fractionated in coexisting garnet, as Y variation strongly and inversely reflects changes in modal garnet abundance. Eu is fractionated in plagioclase (metamorphic or crystallizing from melts) and U in coexisting melts. Heavier MREE are partitioned in xenotime. Monazite chemistry holds thus valuable keys for both identifying and dating thermometamorphic processes, especially those involving melting episodes and garnet growth and decomposition.

Towards Quantitative Paleohydrology: Reconstructing changes in relative humidity from lipid biomarker δD values

DIRK SACHSE¹, OLIVER RACH¹, ANSGAR KAHMEN², HEINZ WILKES³ AND ACHIM BRAUER³

¹University of Potsdam, Institute of Earth and Environmental Science, Karl-Liebknecht-Str. 24-25, 14476 Potsdam-Golm, Germany

²ETH Zurich, Institute of Agricultural Sciences, Universitätsstrasse 2, 8092 Zürich, Switzerland

³GFZ German Research Centre for Geosciences, Telegrafenberg, 14473 Potsdam, Germany

The stable isotopic composition of meteoric waters, recorded through the hydrogen isotopic composition of lipid biomarkers is an integral of a number of hydrological parameters, such as condensation temperature, precipitation amount, evaporation, moisture pathway. It is often difficult to disentangle these parameters for a true quantitative reconstruction of hydrological variables, such as precipitation amount and relative humidity. Here we review the current state of knowledge of the factors driving leaf wax δD values and evaluate how terrestrial plant lipid biomarker δD values in combination with plant physiological modelling can be used to quantitatively reconstruct changes in relative humidity (rH).

We present a proof-of-concept for this approach by estimating relative humidity changes during the Younger Dryas cold period in Western Europe from the analysis of lipid biomarker δD values from the annually varved sediments of Lake Meerfelder Maar. We use the isotopic difference between aquatic and terrestrial lipid biomarkers as a measure of mean leaf water isotope enrichment. We parameterized a Craig-Gordon leaf water isotope model with plant physiological parameters estimated from available vegetation cover information from palynological records and climate proxy data (such as temperature) and solved this model for rH. Our reconstruction of Younger Dryas rH changes documents profound hydrological changes - likely as a consequence of changes in atmospheric circulation due to the position of North Atlantic Sea Ice - which were the ultimate trigger for the observed environmental changes. While supporting previous suggestions of a dry Younger Dryas in Western Europe our new biomarker and modelling approach delivers for the first time quantitative estimates of hydrological changes (i.e. relative humidity changes), which can be directly compared to the output from climate models.

The role of organic matter in genesis of sedimentary-hosted stratiform copper deposits in Nahand-Ivand area, NW Iran

*SADATI N.¹, YAZDI M.¹, BEHZADI M.¹, ADABI M.H.¹,
AND MOKHTARI A.A.²

¹Department of Geology, Faculty of Earth Science, Shahid Beheshti University, Tehran, Iran (*correspondence: sadati_sn@yahoo.com)

²Department of Geology, Faculty of Earth Science, Zanjan University, Zanjan, Iran (² mokhtari1031@gmail.com)

The study area is located in part of Arasbaran- Sabalan zone in the northwestern part of Iran. Cu mineralization in Nahand - Ivand area is observed in sandstone rock units belonging to the Ghom Red beds Formation of Miocene age[1]. The Ghom Red beds Formation include alternations of red oxidized (iron oxide minerals) sandstones and conglomerates that partly convert to reduced clastic such as sandstone, siltstone, shale, conglomerate, limestone, dolomite and marl, which may contain carbonaceous or organic matter. Also Evaporites such as gypsum and salt are commonly associated. In this study, zones of reduction (grey, white, green) within oxidized red-bed sedimentary rocks are the most favored host rocks. The color of the host rocks ranges from light gray to black, reflecting their high organic matter content.

Mineralization is localized in the organic-rich and pyrite-containing gray rocks that replace the red rocks along the vertical and lateral directions[2]. The main ore minerals in the deposit are copper carbonates such as malachite, azurite and some copper sulfides such as chalcocite[3]. During this study 44 samples were collected from the Ghom Redbeds Formation. Host rock and mineralized samples were analyzed for major and trace element contents by Inductively Coupled Plasma–Mass Spectrometry (ICP- MS). The results showed that In addition to copper, precious metals such as silver are less focused. In this area maximum grade of samples are up to 5.2% Cu with an average of 1.4% Cu. Copper precipitation was possibly promoted by reduction zones from organic matter such as woody fragments and plant fossils[4]. It seems that during the formation of the copper deposits, organic matter played an important role in adsorbing and gathering metallic elements [5].

[1] Sadati et al (2012) MINERALOGIA – SPECIAL PAPERS 40, 124. [2] Gablina *et al.* (2008) Lithology and Mineral Resources 43, 136–153. [3] Cox *et al.* (2007) US Geological 03-107, 1- 50. [4] Stensgaard (2011) Geology and Ore 18, 2-12. [5] Jiajun *et al.* (2002) Ore Geology 20, 55–63.

REE contents in soils and sediments from the GEMAS and FOREGS data-bases: comparison between different geological contexts in Italy and Sweden

M.SADEGHI¹, P.PETROSINO², M.ANDERSSON¹,
S. ALBANESE², A.LADENBERGER¹, G. A. MORRIS¹,
J.UHLBÄCK¹, A. LIMA² AND B. DE VIVO²

¹Geological Survey of Sweden, BOX 670, S-75128 Uppsala, Sweden (* correspondance : martiya.sadeghi@sgu.se)

²Dipartimento di Scienze della Terra, dell'Ambiente e delle Risorse, Università degli Studi di Napoli Federico II, L.go S. Marcellino 10, 80138 Napoli

Rare Earth Elements (REEs) are rapidly gaining attention as important chemical resources thanks to the increasing number of high-tech applications in which they are required and, as a consequence, scientific interest on REE-bearing minerals and resources is increasing. In this study, REE data from the FOREGS database of solid media chemistry (topsoils, subsoils, stream sediments, floodplains) have been used to constrain elemental distribution maps. Principal Component Analysis (PCA) has been applied to identify patterns within the data set. Detailed investigation of the distribution of REEs in all media for both countries shows the prominent role played by geogenic components. Despite similar REE concentrations in the underlying bedrocks, several significant differences emerge between the two countries driven by climate, morphology of the territory, age of the deposits, presence of mineralisation, type of soils and presence/absence of till.

The same approach has been applied to the GEMAS database to compare the REE distribution in agricultural and grazing land soils, using the same statistical approach as used for solid media from the FOREGS database. In general, high pH alkaline soils show higher REE concentrations. Certain specific anomalies can be correlated to known phosphate and REE mineralizations. The fingerprint of anthropogenic activity, both agricultural fertilizer use and cattle feed, does not influence the geogenic signal. In both Italy and Sweden, REE concentrations in agricultural and grazing land soils are comparable with those obtained for topsoils sampled from unoccupied and undisturbed areas. The main difference between the elemental distribution of REEs is more closely related to the geochemical behaviour of individual elements and their extractability as affected by the source of the elements in the sample media.

Partitioning behavior of Cs in the matrix of simulated ash residues

A. SAFFARZADEH^{1*} AND T. SHIMAOKA¹

¹Kyushu University, Fukuoka 819-0395, Japan
 (*correspondence: amir@doc.kyushu-u.ac.jp)

Tohoku great earthquake and tsunami of March 11, 2011 caused massive explosions at Fukushima I Nuclear Power Plant. Such incidents led to the dissemination of fission products (such as ¹³¹I, ¹³⁴Cs, ¹³⁷Cs) in a broad geographic area [1, 2]. These radionuclides concentrated in the surrounding natural environments [3] as well as in the debris left from the disaster. Incineration of combustible fraction of disaster debris resulted in the higher level of radioactivity (Cs-related) in the generated ash residues (up to 100,000 Bq/kg in fly ash in some areas), thus banned landfilling.

To model the behavior of radioactive Cs in the ash residues, simulated ash was produced by fusing RDF and Cs salts (non-radioactive) at high temperatures (800-1000 °C). The products mainly consist of glassy matrix (silicate) and a variety of crystalline phases



Fig. 1: SEM image of the ash matrix

(Fig 1). Microbeam analysis indicates that Cs is essentially distributed within the glassy matrix of the ash with little or no partitioning within the crystalline phases (Table 1). Binding of Cs in the silicate structure of the glass is a good evidence for the entrapment of analogous radioactive Cs. Additional experiments are underway to examine the chemical form of Cs and to improve

Phases	Glass		Crystalline				
	1	2	3	4	5	6	7
Cs	1.75	1.51	0.00	0.00	0.00	0.00	0.00
Al	6.16	7.12	4.13	3.71	0.90	0.91	1.14
Si	28.73	28.68	24.53	23.99	16.77	16.92	4.07
Ca	5.30	4.38	20.94	19.38	23.72	23.47	2.01
Fe	15.65	10.70	8.22	9.03	20.96	20.42	60.93
K	2.95	2.76	0.24	0.29	0.18	0.17	0.28

the ash quality in order to meet the standards for landfilling.
Table 1: Chemical composition of the points in Fig 1 (Wt%).

[1] Kato *et al.* (2012) *J. Env. Radio* **111**, 59-64. [2] Hirose (2012) *J. Env. Radio* **111**, 13-17. [3] Yasunari *et al.* (2011) *PNAS* **108**, 19530-19534.

The H₂O-CO₂-(K, Na)Cl fluids, melting of the tonalite gneiss, and the A-type granitic magmas: Experimental evidence for connection

OLEG SAFONOV

Institute of Experimental Mineralogy, Russian Academy of Science, Chernogolovka, Russia, oleg@iem.ac.ru

The A-type (anorogenic) granites, a specific variety of ferroan granitic rocks forming predominantly during crustal extension, are distinct by their medium-to-high peralkalinity (low Al₂O₃ and high K₂O+Na₂O contents), low CaO, elevated contents of F and Cl. Partial melting of the Archean TTGs in the continental basement is discussed among models to explain origin of these granites. However, neither fluid-absent nor hydrous melting of TTGs at pressures up to 15 kbar can fully satisfy the required parameters of the melts. The influx of K and Na seems to be needed for the formation of the A-type granites. Data on the melting of TTGs in presence of the H₂O-CO₂ fluids containing alkali salts are absent, so far. In order to trace variations of mineral assemblages and melt composition in dependence on temperature, concentration of salts and K/Na ratio in the fluids, the experiments on interaction of a biotite-hornblende tonalite gneiss with the H₂O-CO₂-(K, Na)Cl fluids at 5.5 kbar and 750 and 800°C were performed. The H₂O-CO₂-KCl fluids provoke melting only at 800°C. Addition of NaCl assists to melting at 750°C. The increase of the chloride/(H₂O+CO₂) ratio in the fluids results in formation at 800°C of the rhyolitic melts with Al₂O₃ < 13.5 wt. %, CaO < 2 wt. %, K₂O+Na₂O > 7 wt. %, FeO/(FeO+MgO) > 0.8, K₂O/Na₂O > 1, moderately enriched in Cl (0.2-0.6 wt. %). The melt composition correlate with the coexisting mineral assemblages, varying in the sequence Opx+Amp+Pl+Ti-Mt+Ilm → Opx+Cpx+Ilm → Cpx+Kfs+Ilm. Stabilization of Cpx and Kfs at the high chloride/(H₂O+CO₂) ratio in the fluids corresponds to the decrease of CaO and Al₂O₃ contents in the melts, while increase of the Cl content in these melts promotes the FeO/(FeO+MgO) ratio. Stability of pyroxenes at moderate and high chloride/(H₂O+CO₂) ratios in the fluids reflects low a_{H2O} in the melts, i.e. their apparent “dryness”. These characteristics are similar to the A-type granites. At 750°C, the H₂O-CO₂-(K, Na)Cl fluids produce trachytic melts, which model syenites, monzonites and other alkalic basic counterparts of the A-type granitic complexes. The experiments support the model for formation of these complexes by crustal melting during high-grade metamorphism in presence of the aqueous-carbonic-salt fluids fluxing in the extensional environments.

Arsenic contamination in pond sediment of central India

B. L. SAHU¹, K. S. PATEL¹, I. WYSOCKA²
AND I. JARON²

¹School of Studies in Chemistry, Pt. Ravishankar Shukla University, Raipur-492010, CG, India, bharatred007@gmail.com

²Polish Geological Institute, Rakowiecka, Street-00-975, Warsaw, Poland, iwys@pgi.gov.pl

The pond is widely used for the fish culture and other house hold activities in India. The environment of the Kaudikasa, central India is one of the most arsenic contaminated sites in the World [1]. In this work, the contamination of arsenic and other 33 elements in eight pond sediments (N 20°51' and E 80°45') is described. The sediment samples were collected in summer 2012, and the crushed sample (≤ 0.1 mm) was digested in the micro-oven with acids. The acid extracts were analyzed by using techniques: ICP-AES and ICP-MS. Among 34 elements analyzed, eight elements i.e. Na, K, Mg, Ca, Al, S, P and Fe occurred at macro levels, ranging from 0.01 – 0.06, 0.21 – 0.45, 0.17 – 1.08, 0.18 – 0.76, 1.41 – 3.14, 0.01 – 0.06, 0.02 – 0.03 and 2.8 – 6.3% with mean value of 0.01 ± 0.01 , 0.33 ± 0.07 , 0.43 ± 0.30 , 0.38 ± 0.14 , 2.12 ± 0.48 , 0.03 ± 0.01 , 0.03 ± 0.01 and $4.2\pm 0.9\%$, respectively. Twelve metals i.e. As, Ba, Sr, Ti, V, Cr, Mn, Co, Ni, Cu, Zn and Pb was present at milligram levels, ranging from 48 – 256, 129 – 264, 12 – 30, 62 – 735, 38 – 144, 29 – 732, 388 – 1109, 12 – 42, 23 – 108, 35 – 73, 40 – 100 and 17 – 40 mg kg⁻¹ with mean value of 111 ± 52 , 192 ± 32 , 20 ± 5 , 226 ± 151 , 72 ± 25 , 77 ± 49 , 646 ± 177 , 23 ± 8 , 48 ± 21 , 53 ± 9 , 66 ± 17 and 24 ± 6 mg kg⁻¹, respectively. Twelve metals i.e. Li, Rb, Cs, Be, Ga, Tl, Sn, Sb, Bi, Mo, Ag, Cd, Th and U present at lower milligram levels with mean value of 11, 31, 1.3, 1.7, 10, 0.2, 1.5, 0.5, 0.2, 0.8, 0.6, 0.13, 11.7 and 1.24 mg kg⁻¹, respectively. Arsenic content was correlated well with the P, Pb and Zn content. The arsenic concentration was found to be several folds higher than the recommended value of 5 mg kg⁻¹. The arsenic content in the pond sediment of this region was found to be much more higher than other region of the World [2].

[1] Patel *et al* (2005) *Environ. Geochem. Health* **27**,131-145

[2] Durant *et al*. (2004) *Water Res.* **38**, 2989–3000.

Microphysical properties of BC in anthropogenic and biomass burning plumes

L. K. SAHU¹, Y. KONDO², N. MOTEKI², N. TAKEGAWA³,
Y. ZHAO⁴

¹Physical Research Laboratory, Ahmedabad, India, (*correspondence: lokesh@prl.res.in)

²Department of Earth and Planetary Science, Graduate School of Science, The University of Tokyo, Tokyo, Japan, kondo@eps.s.u-tokyo.ac.jp, moteki@eps.s.u-tokyo.ac.jp

³Research Center for Advanced Science and Technology, University of Tokyo, Tokyo, Japan, takegawa@atmos.rcast.u-tokyo.ac.jp

⁴Air Quality Research Center, University of California, Davis, USA, yjzhao@ucdavis.edu

The impact of aerosols on regional air quality necessitates improved understanding of their emission and microphysical properties. The size distributions of black carbon (BC) and light scattering particles (LSP) were measured with a single particle soot photometer on board the NASA DC-8 aircraft during the ARCTAS mission 2008. Air sampling was made in the air plumes of both urban and forest fire emissions over California during the CARB (California Air Resources Board) phase of the mission. Air plumes were identified using tracers for fossil fuel (FF) combustion and biomass burning (BB). Enhancements of BC and LSP in BB plumes were significantly higher compared to those in FF plumes. The average mass concentration of BC in BB plumes was more than twice that in FF plumes. Distinct *emission ratios of BC/CO₂*, *BC/CH₃CN*, *CH₃CN/CO*, and *CO/CO₂* were estimated for the plumes from the two sources. The size distributions of BC and LSP also showed different behaviours. The BC count median diameter of 115 nm in FF plumes was smaller compared to 141 nm in the BB plumes. BC aerosols were thickly coated in BB plumes as the average shell/core ratios were 1.47 and 1.24 in BB and FF plumes, respectively.

U-Th systematics and chronology of CH₄-derived CaCO₃ crusts of the Barents Sea

DIANA SAHY^{1*}, AIVO LEPLAND^{2,3}, STEPHEN R. NOBLE¹, DANIEL J. CONDON¹, HARALD BRUNSTAD⁴.

¹NERC Isotope Geoscience Laboratory, Keyworth, UK

(*correspondence: dihy@bgs.ac.uk)

²Geological Survey of Norway, Trondheim, Norway

³Tallinn University of Technology, Tallinn, Estonia

⁴Lundin Petroleum, Oslo, Norway

CaCO₃ crusts forming due to methane oxidation at seafloor seepage sites serve as archives of past fluid flow and methane discharges into ocean and atmosphere. U incorporation into CaCO₃ during precipitation offers the opportunity to date the crust formation and growth via U-Th systematics (e.g., Aharon et al., 1997; Teichert *et al.*, 2003).

We present U-Th and ⁸⁷Sr/⁸⁶Sr data obtained on such CaCO₃ crusts recovered from the Barents Sea floor using a remotely operated vehicle. CaCO₃ phases occur in different modes within the crusts – disseminated within the siliclastic matrix, porosity- and late cavity- filling. These CaCO₃ domains, sampled by microdrilling, display [²³⁰Th/²³²Th]_{AR} from 0.9 up to ~200 and ²³²Th concentrations from ~10 to 7000 ppb. Intra-crust U-Th dates range from ~13.1 ± 0.4 to 8.9 ± 0.4 ka. Older dates come from CaCO₃ disseminated within the sediment matrix while younger dates are from late cavity filling CaCO₃. Layered cavity fills yield resolvable growth histories on the order of 1.0 kyr. Combined such dating results can be used to constrain the histories of CH₄ seepage in the Barents Sea.

⁸⁷Sr/⁸⁶Sr has been analysed on aliquots drilled adjacent to U-Th sample sites. For the majority of crust samples both ⁸⁷Sr/⁸⁶Sr and δ²³⁴U are close to expected values for modern/Holocene seawater. In addition, a sample of a matrix-dominated tubestone representing a subsurface carbonatized fluid conduit, has more radiogenic ⁸⁷Sr/⁸⁶Sr values and δ²³⁴U closer to secular equilibrium. Such contrasts in ⁸⁷Sr/⁸⁶Sr and initial δ²³⁴U reflect distinctly different fluid chemistries forming surface and subsurface CaCO₃ precipitates. These data, together with crust data from other seeps, demonstrate the utility of U-Th for constraining CH₄ seepage duration and absolute timing.

[1] Aharaon, P., *et al.*, 1997, GSA Bulletin, v. 109, p. 568-579. [2] Teichert, B. M. A., *et al.*, 2003, Geochimica et Cosmochimica Acta, v. 67, p. 3845-3857.

Distribution of Metalloenzymes in Pacific Ocean Environments as Detected by Proteomic Analysis

MAK A. SAITO¹, MATTHEW R. MCILVIN¹, DAWN M. MORAN¹, ALYSON SANTORO², TYLER J. GOEPFERT¹, NICHOLAS HAWCO¹, CARL H. LAMBORG¹

¹Marine Chemistry and Geochemistry Department, Woods Hole Oceanographic Institution, Woods Hole MA 02543 USA

²University of Maryland, Center for Environmental Science, Horn Point Laboratory, 2020 Horns Point Rd Cambridge, MD 21613 USA

*Correspondence to msaito@whoi.edu

The use of mass spectrometry based proteomics has the capability for direct measurement of proteins produced by microbial life. These proteins can include biomarkers for nutrient stress or microbial taxonomy, as well as enzymes that are responsible carrying out biogeochemical reactions. Most biogeochemically-relevant enzymes require one or more metal atoms for catalytic activity. We report on the analyses of samples collected from a range of depths in the Equatorial Pacific and Eastern Tropical South Pacific. Analyses involved total protein extractions, enzymatic digestion, multi-dimensional chromatographic separation, mass spectrometry analyses, peptide mapping by high performance computing, and quantitative estimates. Proteins of interest will be discussed with a particular focus on metalloenzymes that contain nickel, cobalt, copper, and iron.

Origin of atmospheric dust and the associated anthropogenic lead around Omura Bay, West Japan

YU SAITOH^{1*}, YU UMEZAWA², KAZUAKI KAWAMOTO²,
MASAHARU TANIMIZU³ AND TSUYOSHI ISHIKAWA³

¹CAMCR, Kochi University, B200 Monobe, 783-8502, Japan

(*correspondence: jm-yu-saitoh@kochi-u.ac.jp)

²Graduate School of Fisheries Science and Environmental Studies, Nagasaki University

³Kochi Institute for Core Sample Research, JAMSTEC

In order to evaluate the responsibility of the cross-border pollution to the atmospheric environment in West Japan, we measured the trace element concentration and Sr-Pb isotope ratios of aerosol particles collected at the eastern hill of Omura Bay with temporal high resolution from May 2011 to June 2012. The acid-soluble component of the aerosol samples contain more than 10 times the amount of Cd and Pb than the residual dust components contain. This suggests that these elements are mainly of anthropogenic origin. The ⁸⁷Sr/⁸⁶Sr of silicate component is high in winter and spring (0.712-0.714), and is lowest in summer (0.706). These high and low ratios are typical of Asian dust and the local sediment, respectively. The seasonal change is considered to reflect the difference of dominant wind direction between winter and summer. Although the correlation between ⁸⁷Sr/⁸⁶Sr and soluble Cd and Pb ($r > 0.7$) suggests that the anthropogenic components are transported with the Asian dust, the isotope ratios of soluble Pb (²⁰⁶Pb/²⁰⁷Pb: 1.16, ²⁰⁸Pb/²⁰⁷Pb: 2.44) suggest that their origin is Japan in spring, when much amount of Asian dust arrives, while those in fall and winter (²⁰⁶Pb/²⁰⁷Pb: 1.13-1.15, ²⁰⁸Pb/²⁰⁷Pb: 2.42-2.43) suggest far-east Russian and/ or Central Asian origin. Perhaps because dust particles act as adsorbent, lead concentration is highest in the season of Asian dust. Cross-border pollution is highlighted in winter when the coal combustion for heating is at the peak under the wintry atmospheric pressure pattern around East Asia.

Melting history of the Pozanti-Karsanti ophiolite, Turkey: Implications from whole-rock and mineral compositions

SAMET SAKA^{1*}, IBRAHIM UYSAL¹, R. MELIH AKMAZ²
AND MELANIE KALIWODA³

¹Karadeniz Technical University, Trabzon, Turkey

(*correspondence: sakasamet61@gmail.com)

²Bülent Ecevit University, Zonguldak, Turkey

³Mineralogical State Collection Munich, Germany

Pozanti-Karsanti ophiolite, from the eastern Tauride, Turkey, is represented by mantle unit and overlying crustal sections composed of ultramafic to mafic cumulates and isotropic gabbros. Harzburgitic to dunitic mantle peridotites are characterized by low Al₂O₃ (0.11–1.01 wt%) and CaO (0.10–1.07 wt%) contents. The low whole rock Al and Ca values are consistent with their high Cr# of spinel values, ranging between 44 and 78. These spinels are generally have low TiO₂ (<0.06% wt%) contents, although spinel in some samples show enrichment up to 0.25 wt%. Chondrite-normalized whole rock and clinopyroxene REE contents show depletion towards HREE to MREE. However, all peridotite samples show marked enrichment of LREE compared to MREE. Both whole rock and clinopyroxene HREE patterns of some peridotite samples follow the melting residue lines, and are modeled ~25–27 fractional melting in spinel stability field. However, depletion of MREE compared to HREE is stronger in some samples and the HREE to MREE patterns do not follow the melting lines produced by various degree of fractional melting in spinel stability field. These samples can be modeled by 5 to 10% fractional melting started at garnet stability field and followed in spinel stability field with additional 22 to 15% melting. The melting degrees obtained from whole rock and clinopyroxene REE data as well as spinel composition are consistent with each other, and confirm that the mantle unit of the Pozanti-Karsanti ophiolite is represented by up to 27% melting at different pressure conditions. The LREE enrichment observed in whole rock and clinopyroxene as well as higher TiO₂ contents of high-Cr# spinels in some samples do not suggest that the mantle unit of the Pozanti-Karsanti ophiolite is the simple melting residue. However, these feature of the peridotites is suggested to be due to the interaction of LREE and TiO₂ rich melts/fluids with formerly depleted peridotites. This interaction, taking place at suprasubduction zone environment, may increase the LREE contents of the peridotites and also cause the equilibration of Ti-depleted spinel to Ti-richer composition.

Correction of initial-disequilibrium on U-Th-Pb system for dating of young zircons

SHUHEI SAKATA^{1*}, SHINSUKE HIRAKAWA¹,
HIDEKI IWANO², TOHRU DANHARA²
AND TAKAHUMI HIRATA¹

¹Laboratory for Planetary Sciences, Kyoto University, Kyoto, Japan (junchan@kueps.kyoto-u.ac.jp)

²Kyoto Fission Track Co. Ltd., Kyoto 603-8832, Japan

Major analytical problems associated with U-Pb age determination of the young zircons (e.g. < 1 Ma) is the initial-disequilibrium in the U-Th-Pb decay systems through the crystallization of zircon in source magma. To correct the effect of initial disequilibrium, the ratio of the distribution coefficient between source magma and zircon crystal (D) for Th and U ($f_{Th/U} = D^{Th}/D^U$) must be defined [1]. To achieve this, we have determined both the ²³⁸U-²⁰⁶Pb and ²³²Th-²⁰⁸Pb ages obtained for three tephra zircon samples collected from Kirigamine rhyolite (Ar-Ar age is 0.945±0.005 Ma [2]), Bishop tuff (Ar-Ar age is 0.7589±0.0036 Ma [3]) and Toga pumice (Ar-Ar age is 0.42±0.01 Ma [4]) by means of laser ablation-ICPMS technique. The resulting ²³²Th-²⁰⁸Pb ages were 0.940±0.010 Ma for Kirigamine, 0.759±0.016 Ma for Bishop, and 0.4296±0.0066 Ma for Toga, demonstrating that the resulting ages were consistent with the previously reported values. The $f_{Th/U}$ values could be calculated based on the measured ²³²Th-²⁰⁸Pb ages and ²⁰⁶Pb/²³⁸U ratios, and the resulting $f_{Th/U}$ values agreed well within the analytical uncertainties. The disequilibrium-corrected ²³⁸U-²⁰⁶Pb age can be calculated under the assumption that the $f_{Th/U}$ value did not vary significantly among the zircons. To evaluate this, we have measured the ²³⁸U-²⁰⁶Pb and ²³²Th-²⁰⁸Pb ages for zircons from Sanbekisuki tephra [5]. The $f_{Th/U}$ values used for the correction was based on the average of three $f_{Th/U}$ values obtained here ($f_{Th/U} = 0.51 \pm 0.11$). The corrected ²³⁸U-²⁰⁶Pb age was 92.1 ± 8.4 ka, which agreed with the ²³²Th-²⁰⁸Pb age (90.4 ± 9.5 ka) within the analytical uncertainties. The good agreement in the corrected ²³⁸U-²⁰⁶Pb age and ²³²Th-²⁰⁸Pb age demonstrates clearly that the present $f_{Th/U}$ value for the Sanbekisuki zircon was consistent with the averaged $f_{Th/U}$ value calculated above. In conclusion, we can construct more accurate and effective U-Th-Pb dating method based on the $f_{Th/U}$ value defined in this study, especially for the young zircons (0.1 – 1 Ma).

[1] Schärer (1984) *EPSL*, **67**, 191-204 [2] Wadatsumi *et al.* (1994) *Fission Track News Letters*, **7**, 7-8 [3] Sarna-Wojcicki (2000) *J. Geophys. Res.*, **105** 21, 431-21, 443 [4] Uto *et al.* (2010) *Volcano*, **55**, 201-206 [5] Machida and Arai (2003) *Atlas of Tephra in and around Japan*

Application of geochemical and statistical approach to assess metal contamination in marine sediments

FANI SAKELLARIADOU¹

¹University of Piraeus, Dept of Maritime Studies, fsakelar@unipi.gr

The two principal sources for heavy metals at the sea are lithogenic and anthropogenic ones. Sediments are considered as physical traps for many environmental pollutants [1]. At the present study, sediment samples from Lavrio port (located 60km SW of Athens, in Greece) were analyzed for the determination of metal content. The area is well known for the presence of mixed sulphide mineralisation (galena, sphalerite and pyrite) hosted within marbles and limestones. Samples were digested with a mixture of conc. acids at high temperature [2]. Metal contents were measured by AAS. Data set was treated with multivariate and geostatistical approach. The dendograms provided by hierarchical cluster analysis gave the (Zn, Pb, Mn) and (Cu, Cr, Ni) groups reflecting the mineralization clusters (the latter group representing also, to some extent, the ultramafic association) as well as the (Fe, Al) group standing for clays and other alluvial matter. Application of Principal Component Analysis showed that sampling sites have positive scores for Mn, Zn and Pb. Inter-element correlation coefficients corresponded to values greater than 0,92 for the pair (Zn, Fe), greater than 0,84 for the pairs (Mn, Zn), (Zn, Pb), (Mn, Fe), (Pb, Fe) and (Cr, Al), and greater than 0,68 for the pairs (Al, Fe), (Fe, Cu) and (Cu, Zn). The Simple Kriging geostatistical approach was applied allowing data interpolation [3]. Spatial patterns of Pb, Zn and Cu showed the highest enrichment around the new berth (cited at the eastern part of the harbour), with elevated content around the main harbour area.

[1] Burton (2002) *Limnology*, **3**, 65–75. [2] UNEP (1985) *Reference Methods for Marine Pollution Studies*, No 31-39. [3] Cressie (1990) *Mathematical Geology*, **22**, 239-252.

Wettability alteration of calcite surface induced by ion exchange

H. SAKUMA^{1,2}, M.P. ANDERSSON¹ AND S.L.S. STIPP¹

¹Nano-Science Center, Department of Chemistry, University of Copenhagen, Copenhagen, Denmark (*correspondence: sakuma.h.aa@m.titech.ac.jp, ma@nano.ku.dk, stipp@nano.ku.dk)

²Tokyo Institute of Technology, Tokyo 152-8551, Japan

The interaction of water and organic molecules with mineral surfaces controls a range of processes in nature and industry. The thermodynamic property, surface tension, helps describe these interactions. We investigated the change in water affinity for a calcite (CaCO_3) {10.4} surface where Ca^{2+} and CO_3^{2-} ions were sequentially replaced with Mg^{2+} and SO_4^{2-} , in the bulk solid and at the surface, which is a system of broad interest, for biomineralisation, oil production, and many others. We used electronic structure calculations based on density functional theory (DFT).

Mg^{2+} substitution for Ca^{2+} is favored but only when SO_4^{2-} ions are present and MgSO_4 incorporates preferentially as ion pairs at the fluid-calcite interface. Mg incorporation weakens organic molecule adhesion, while strengthening water adsorption (Fig. 1). Thus, Mg^{2+} substitution renders the calcite surface more water wet, or hydrophilic, making it less favourable for organic compound attachment. We estimated the change in calcite surface tension after ion exchange and determined the resulting change in macroscopic wettability. When only 10% of surface Ca is replaced by Mg, contact angle changes dramatically, i.e. 40 - 70°, converting a hydrophobic surface to a mixed wet surface. Producing magnesium calcite is a simple trick organisms can use for controlling calcite growth and the process helps explain why oil recovery from carbonate reservoirs is enhanced when both Mg^{2+} and SO_4^{2-} are present in the pore water.

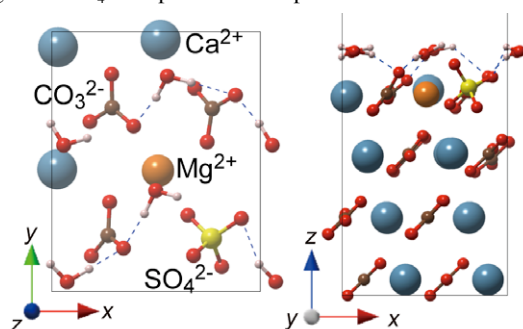


Figure 1: The lowest energy configuration for four water molecules on a calcite {10.4} surface with substitution by a Mg SO_4 ion pair. (Left) Top view. (Right) Side view.

Characterization and Surface Reactivity of Natural and Synthetic Magnetites

C. SALAZAR-CAMACHO¹, M. VILLALOBOS^{1*}
AND M.D.L.L. RIVAS-SÁNCHEZ

¹Environmental Bio-Geochemistry Group, Geochemistry Department, Geology Institute (*correspondence: mariov@geologia.unam.mx)

²Laboratorio de Paleomagnetismo, Geophysics Institute UNAM, Coyoacan, CU, Mexico 04510, D.F.

Magnetite is an Fe(II/III) oxide mineral that occurs naturally and potentially as small particles with significant surface reactivity, and although much work is reported on synthetic material [1,2], little work exists for natural samples. The goal of the present work was to carefully characterize four natural magnetite samples from an iron ore deposit [3] and two synthetic commercial reference samples, and to compare their surface characteristics and reactivity with the aim of evaluating their geochemical behavior towards adsorption of environmentally relevant ions, as well as their potential for use as environmental remediation sorbents. In addition, their As(V) adsorption behavior was determined at pH 6, and was analyzed as related to the surface characteristics and particle aggregation behavior determined.

The analyses revealed high magnetite purity in the natural samples, and specific surface areas (SSA) ranging from 1 to 8 m^2/g . Small alumino-silicate impurities were found in natural magnetites, apparently occurring at the particle surfaces and significantly lowering the magnetite isoelectric point. All samples are composed of aggregates of 39-52 nm magnetite particle units, but highly aggregated with very large size dispersions. The synthetic sample with the smallest particle size (30 nm in average - 39 m^2/g) showed its entire surface area available for adsorption, despite its highly aggregated state observed, suggesting an open and highly dynamic aggregate framework. The other larger samples showed more complex aggregation behavior, which produced: (1) a widely variable As(V) adsorption behavior with no clear predictable pattern among samples; and (2) a large decrease of the As(V) adsorption maxima with increasing solids concentration (Cs) imposed in the experimental set-up for any one particular sample. Therefore, we recommend high caution in using the BET-SSA and Cs parameters when performing experimental adsorption work with micro-sized magnetite.

[1] Das *et al.* (2010) *J. Radioanal. Nucl. Chem* **285**, 447-454.

[2] Ilton *et al.* (2010) *Environ. Sci. Technol.* **44**, 170-176.

[3] Rivas *et al.* (2009) *Earth Planets Space* **61**, 151-160.

U-Pb age of a syn-collisional lower continental crust anatetic event, Socorro-Guaxupé Nappe, SE Brazil

C.A. SALAZAR-MORA^{1*} AND M.C. CAMPOS NETO¹

¹Geosciences Inst., São Paulo Univ., 05508-080, Brazil.

(*correspondance: claudio.mora@usp.br; camposnt@usp.br)

The Southern Brasília Orogen, SE Brazil, occurs along the southern border of the São Francisco Craton and is structured as a pile of Ediacaran syn-metamorphic thickened-skinned nappes that diachronically migrate towards the cratonic margin. The Socorro-Guaxupé Nappe (SGN) is the older and upper allochthon that represents an Andean-type magmatic arc [1]. U-Pb ages in zircon from charnockites, mangerites and Grt-granulites [1] indicate an arc activity around 670 Ma in a subduction-related orogenesis followed by ultra-high-T metamorphism and plutonism lasting until 625 Ma. This age is thought [2] to represent the metamorphic peak of the SGN. In the present study we report on new *in situ* U-Pb and Lu-Hf analysis (both LA-ICP-MS) in zircons from syn-tectonic charnockitic leucosomes that comprise the metatexitic unit of the SGN.

Charnockitic leucosomes were generated under Hbl dehydration melting conditions following the reaction $Hbl + Qtz \rightleftharpoons Opx + Cpx + Pl \pm Melt$, which implies minimum temperatures of 850°C. The leucosomes presented two zircon tipologies. The first comprises bipyramidal-prismatic grains with oscillatory zoning and high luminescence, sometimes preserving low-luminescence cores with 670 Ma. These high luminescence and oscillatory zoning grains show 19 concordant ages at 621 ± 16 Ma. The second tipology of zircons are isometric and *soccer-ball*-type. These grains show sector zoning and a concordia age of 608 ± 4 Ma. Th/U ratios from the *soccer-ball* grains vary from 1.378 to 2.107, whereas prismatic grains vary from 0.118 to 1.774. Some authors also reported high Th/U values from demonstrably syn-metamorphic, high-T melts [3]. ε_{Hf} signatures between -13 and -21 in both tipologies of zircon grains provide evidence of crustal reworking. Despite the 16 Ma error in the age of the prismatic grains, Th/U values clearly separate the two tipologies of zircon. The older prismatic grains may be related to the onset of the metamorphic peak (~625 Ma), whereas the isometric ones provide evidence of long-lived high-T conditions until ~608 Ma.

[1] Campos Neto *et al.*, (2011) *JSAES* **32**, 393-406. [2] Janasi (2002) *Prec. Res.* **119**, 301-327. [3] Hakoda & Harley (2004) *JMPS* **33**, 180-190.

Physico-chemical evolution of Fe-Si-rich interfacial layers during olivine carbonation reactions

G. D. SALDI^{1*}, H. GUO¹, D. DAVAL², J. DAVIS¹
AND K. G. KNAUSS¹

¹Earth Sciences Division, Lawrence Berkeley National Laboratory, 1 Cyclotron Road, Berkeley, CA 94720, USA
gdsaldi@lbl.gov (*presenting author); hguo@lbl.gov;
jadavis@lbl.gov; kgknauss@lbl.gov.

²LHyGeS, Université de Strasbourg/EOST-CNRS UMR 7517,
1 rue Blessig, 67084 Strasbourg, France
ddaval@unistra.fr.

Several recent investigations of mineral carbonation reactions have shown that the formation of Si-rich protective layers at the interface between olivine and aqueous solution can significantly slow down olivine dissolution, thus limiting the rate of conversion to Mg-carbonates.

The experiments conducted on natural Fe-bearing olivine in flexible Au-bags at 90 and 150 °C and with CO₂-saturated fluids show that the presence of Fe in the mineral+fluid system favors the formation of Fe-Si-rich protective layers. The passivating properties of these coatings originate from the strong interaction between Fe(III) and silica and their action is linked to the permanence of oxidizing conditions in the aqueous fluid.

Transmission electron microscope (TEM) analysis of FIB thin sections of the mineral interfacial region allowed us to study the chemical composition and the physical properties of Fe-Si-rich layers as a function of the progress of the carbonation reaction. In particular, a series of batch experiments of different duration was performed on a natural olivine powder (150-300 μm) at 150 °C and $pCO_2=100$ bar to describe the evolution of the olivine/water interface over an overall period of one month. During the initial stage of the reaction, the olivine surface is affected by the incipient precipitation of Fe oxide particles, in association with small amounts of amorphous silica, which cover in a non-uniform fashion the mineral surface and prompts the formation of a Fe³⁺-Si layer. The oxidation of the Fe(II) released by dissolution gradually consumes the oxygen initially dissolved in the aqueous volume, leading to reducing conditions. The change of redox conditions brings about the breakdown of the Fe-Si-rich layer and re-activates the dissolution of the coated olivine surface. Increased concentrations of Fe²⁺ and Mg²⁺ and SiO_(aq) accelerate the rates of the carbonation process by the formation of Mg-Fe carbonate solid solutions which cover the olivine grains on top of a relatively porous (~2 μm thick) residual coating, composed of abundant amorphous silica.

SO₂ camera measurements on Stromboli

GIUSEPPE SALERNO¹, GEORGINA SAWYER² AND MICHAEL BURTON³

¹INGV Osservatorio Etneo, Italy, salerno@ct.ingv.it

²MetOffice, UK, georgina.sawyer@metoffice.gov.uk

³INGV Pisa, Italy, burton@pi.ingv.it

The development of the SO₂ camera, an instrument that allows images of SO₂ amounts to be collected, has opened up new possibilities and insights into degassing behaviour at volcanoes. Here we present recent measurements collected on Stromboli volcano, which reveal patterns in the SO₂ flux emitted from the volcano. Our measurements are compared with the automatic network of scanning spectrometers on the Island which monitor SO₂ emissions. Furthermore we demonstrate a fully integrated retrieval system which takes full account of the light dilution effect, allowing much improved quantification of the measured fluxes.

Quantitative analysis with the Cameca SXFIVE FE at high lateral resolution: Applications to geochronology and mineralogy

P. SALIOT¹ C. HOMBOURGER² AND M. OUTREQUIN³

¹philippe.saliot@ametec.com

²chrystel.hombourger@ametec.com

³michel.outrequin@ametec.com

The development of the Schottky emitter and its implementation as electron source in Electron Microprobe has significantly improved the characterization of materials in earth sciences and in metallurgy.

The strength of an Electron Probe Microanalysis (EPMA) is the ability to accurately measure and quantify element in traces at few 10's ppm level. The Field Emission (FE) Source allows trace element analysis with high beam currents thanks to the high brightness of the source

Analysis at low beam voltage is used in order to take full advantage of the small spot sizes achievable with a Field Emission Source. Thus, the analytical resolution is not limited anymore by the beam diameter but only by the diameter of the X-ray emission volume.

This will be illustrated, in a first example, by measuring different areas in a Monazite grain. U, Pb and Th are quantitatively analyzed with high precision in order to characterize age domains.

In a second example, quantification of small refractory phases (hibonite, grossite, perovskite, ...) formed by gas condensation in the solar nebula will be presented.

Magmatic Epidote in Calcaline tonalite, Dehnow (NW Mashhad, NE Iran)

R. SAMADI¹, S. J. SHEIKH ZAKARIAEE¹
AND N. SHIRDASHTZADEH³

¹Department of Geology, Science and Research Branch,
Islamic Azad University, Tehran, Iran

²Department of Geology, Faculty of Science, University of
Isfahan, Isfahan, Iran

Introduction

The granitoids of Dehnow in NE Iran are part of a calc-alkaline stock (tonalite to granodiorite and diorite) that intruded the remnants of the Paleo-Tethys Ocean in the Triassic [1]. Epidote is commonly known as primary igneous mineral in intermediate plutonic rock [2]. In Dehnow granitoid it occurred as inclusions in the phenocrystic garnet grains or as subhedral grains associated with biotite.

Mineral Chemistry

The major element composition of epidote indicates a Xep (Fe/(Fe+Cr+Al-2)) between 0.43 to 0.65. The average pistacite (Ps) component of the epidote is 0.15 and 0.18 for the inclusions in the garnets and Dehnow granitoid, respectively.

Discussion and Conclusion

Textural criteria may be used to distinguish magmatic and subsolidus (deuteric) epidotes. [3] and [4] argued that euhedral, weakly pleochroic epidote enclosed within biotite is magmatic. The low TiO₂ contents (<0.17%) of most epidote inclusions and epidote in the groundmass suggest that they are primary according to [5], who ascribe TiO₂<0.2% to primary epidote. Based on [6], the Ps values indicate a low *f*O₂ condition but suggesting that the epidote inclusions crystallized under relatively lower *f*O₂ conditions.

[1] Samadi *et al.* (2013) Island Arc (Submitted). [2] Dessimoz & Müntener (2009) Goldschmidt A286. [3] Tulloch (1979) *Con Min Pet* **69**, 105-117. [4] Zen & Hammarstrom (1984) *Geol* **12**, 515-518. [5] Evans and Vance (1987) *Con Min Pet* **96**, 178-185. [6] Sial *et al.* (1999) *Pak J Sci Ind Res* **42**, 342-244.

Geochemical and isotopic studies of the Hooghly River Estuary, India: Natural vs. anthropogenic sources of organic carbon

SAUMIK SAMANTA¹, TARUN K. DALAI^{1*}
AND JITEDNRA K. PATTANAIK¹

¹Department of Earth Sciences, Indian Institute of Science
Education and Research-Kolkata, Mohanpur 741252,
INDIA (*correspondence: dalai@iiserkol.ac.in)

Dissolved, suspended and bed loads have been sampled seasonally from the Hooghly River Estuary, the major distributary of the river Ganga. The samples have been analyzed for pH, temperature, TDS, salinity, major ions, δ¹⁸O of water and δ¹³C of dissolved inorganic carbon (DIC). The results show clear seasonal variations, with lower concentrations of major ions during the monsoon period when the water discharge is the highest. Based on salinity-δ¹⁸O variation trends, which are similar to those observed earlier [1], freshwater can be characterized by δ¹⁸O values of ca. -6‰ and ca. -7‰ during the summer and monsoon periods, respectively. This suggests that overall contributions of rainwater to the Hooghly River dominates over those from snow melt in the upper reaches. Calculations made for mixing of seawater and river water suggest that at Gangasagar where the the river drains into the Bay of Bengal, freshwater constitutes ca. 15% and 30% of the water budget during summer and monsoon periods, respectively.

Salinity shows well correlated linear variations with DIC and δ¹³C_{DIC} which indicate that mixing exerts the major control on DIC abundances. Based on these trends, it is inferred that δ¹³C_{DIC} of freshwater is ca. 1.5‰ lower during monsoon period than in summer. However, δ¹³C_{DIC} values are in general lower than those expected due to conservative mixing. Although calcite precipitation may be one of the underlying causes, this seems unlikely in the Hooghly estuary. A more likely explanation is supply of additional organic carbon to the estuary, oxidation of which could add to DIC pool. The source of such organic carbon is most likely pollution and needs to be assessed. δ¹³C_{DIC} data of this study suggest that processes such as outgassing of CO₂ from the waters and biological productivity are insignificant in regulating the DIC variation in the estuary.

[1] Somayajulu *et al.* (2002) *Mar. Chem.* **79**, 171-183.

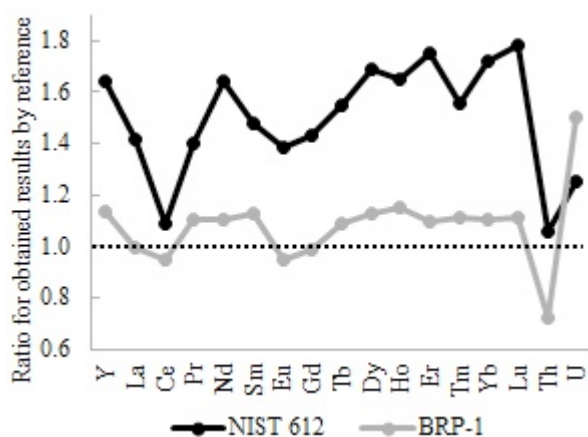
Determination of trace elements in iron formations by LA-ICP-MS

G.M.S. SAMPAIO¹, A.T. DE ABREU¹, H.A. NALINI JR^{1*}
AND C.C. LANA¹

¹Federal University of Ouro Preto, Ouro Preto, MG 35400-000, Brazil (*correspondence: nalini@degeo.ufop.br)

Introduction

Here we present a method to measure trace elements (Y, La, Ce, Pr, Nd, Sm, Eu, Gd, Tb, Dy, Ho, Er, Tm, Yb, Lu, Th and U) in banded iron formation. The samples (XRF fused beads) were ablated (spot and raster) in a Nd:YAG 213 nm New Wave Laser coupled to an Agilent 7700x ICP-MS. Internal standards ²⁹Si and ⁵⁷Fe from the certified reference BRP-1 (in fusion beads) and the glass NIST SRM 612 were used to calibrate the unknowns. We discuss our results based on repeated analyses of the reference material IF-G (GIT-IWG, France).



Results and discussion

The internal standards ²⁹Si and ⁵⁷Fe showed no statistical difference and proved to be suitable for the intended use. Although the slight increase in the instrumental error, the raster pattern showed better mean results than the spot. The calibration with the glass SRM 612 showed a significant bias, as demonstrated in the Figure 1. The best results were obtained by calibration with BRP-1 reducing the matrix effect. Figure 1: Ratio between obtained results using NIST 612 and BRP-1 and values from IF-G certificate.

Acknowledgments

The authors thank the FAPEMIG and VALE that support this study through the project RDP-00063-10.

Microflora of native biofilm on activated carbon under filtration of fulvic acids

O. SAMSONI-TODOROVA*, N. KLYMENKO
AND T. CHEKHOVSKAIA

Institute of Colloid Chemistry and Chemistry of Water, 42 Vernadsky Avenue, Kyiv, 03680, Ukraine
(*correspondence: samsoni@online.ua)

Carbon filters long-term exploitation for drinking water treatment causes the inevitable formation of native biofilms on the surface of porous activated carbon (AC). The aim of this paper was to assess the quantitative and qualitative composition of biofilms microflora that formed spontaneously on AC KAU by filtering of fulvic acids (FC) model solutions in the different conditions. Initial composition of these solutions met Dnieper river water. Filtering time was more than 6 months.

Obtained results are shown in the table 1.

Samples	Microorganisms types and quantity, cells/gAC
AC with native biofilm that was formed by passing of FA solutions (pH 2) and hydrogen peroxide	Yeast; 2.0·10 ²
AC with native biofilm that was formed by passing of FA solutions (pH 2)	Fungi, yeast; 6.0·10 ²
AC with native biofilm that was formed by passing of FA solutions (pH 6) and hydrogen peroxide	Fungi, yeast; 3.5·10 ⁴
AC with native biofilm that was formed by passing of ozonated FA solutions (pH 6)	Fungi, bacteria; 12.1·10 ⁴

Table 1: The qualitative and quantitative composition of native biofilm microorganisms on AC after long-term filtering of FA solutions

Native biofilms were composed from yeast and fungi in the first two cases. This is due to the fact that filtered through charcoal FA solution had low pH, which is more acceptable for the activity of these microorganisms groups. In this case the quantity of microorganisms is lower than by neutral solutions filtering in two orders.

Quantity of live biofilm biomass was about 30% of the total biomass in the biofilm layers near the media and in the outer layers it was about 100%.

Evolution of deep crustal roots of the Arkhangelsk Diamondiferous Province: Evidences from crustal xenoliths and xenocrysts from Devonian kimberlite pipes

A.V. SAMSONOV^{1*}, J.G. GRIBAN¹, YU.O. LARIONOVA¹,
A.A. NOSOVA¹, V.V. TRETYACHENKO²,
E.N. LEPEKHINA³ AND A.N. LARIONOV³

¹ IGEM RAS, Moscow, Russia (*correspondence: samsonovigem@mail.ru);

² NIGP AC "ALROSA", Arkhangelsk, Russia;

³ VSEGEI, St.-Petersburg, Russia

Juvenile continental crust of the Arkhangelsk diamondiferous province (ADP) crystalline basement consists of ca 2.0 Ga calc-alkaline granodiorites, gabbros, metasediments with minor 1.9-1.7 Ga granites. This crust was formed during evolution of the large Lapland-Kola-Dvina orogenic belt [1]. Investigations of crustal xenoliths and zircon xenocrysts from the Devonian kimberlites allow us to recognize several stages in evolution of deep crustal roots of the ADP.

The 2.0 Ga lower-crustal (8-16 kbar) xenoliths of calc-alkaline mafic and intermediate rocks with $T_{DM}(Nd)$ model ages of 2.0-2.2 Ga possibly represent underplated melts of the subduction stage.

The 1.9-1.7 Ga zircon xenocrysts prevail in a whole zircon population of all kimberlite pipes. The zircons probably grew at collisional and post-collisional stages, because of wide range of geochemical features with distinct high-P garnet-equilibrium population.

The 1.5 Ga zircon xenocrysts occur in all kimberlite pipes and might be captured from deep rapakivi granite plutons that are not recognized on the ADP surface.

The 1.2-1.0 Ga zircon xenocrysts were found in all kimberlite pipes and these zircons might be captured from a lower crust reworked during the Grenville Orogeny event which is not revealed on the ADP surface.

The 0.38 Ga Gar-pyroxenite xenoliths ($T_{DM}(Nd)$ model ages of 0.7-0.8 Ga) are common for the V.Griba pipe and might be regarded as a cumulus of Devonian mantle magmas buried (?) beneath the crust.

[1] Samsonov *et al.* (2009) Doklady Earth Sciences, 226–230.

The influence of fault-fracture network activity on fluid geochemistry and mineral precipitation at the Tolhuaca geothermal system, southern Chile

P. SÁNCHEZ^{1,2*}, P. PÉREZ^{2,3}, M. REICH^{1,2},
G. ARANCIBIA^{2,3}, J. CEMBRANO^{2,3}, E. CAMPOS^{2,4}
AND S. LOHMAR⁵

¹ Universidad de Chile, Santiago, Chile (*correspondence: vsanchez@ing.uchile.cl; mreich@ing.uchile.cl)

² Centro de Excelencia en Geotermia de los Andes

³ Pontificia Universidad Católica de Chile, Santiago, Chile (pvperel@uc.cl; garancibia@ing.puc.cl; jcembrano@ing.puc.cl)

⁴ Universidad Católica de Antofagasta, Chile (edcampos@ucn.cl)

⁵ Mighty River Power Chile (silke.lohmar@geotermia.cl)

The nature of the interplay between active tectonics and fluid flow is a key feature to better understand the chemical evolution of fluids in geothermal and hydrothermal systems.

The objective of our current research is to assess the nature of the interplay between brittle deformation and chemical evolution of fluids and mineral paragenesis in the geothermal field of Tolhuaca in the Southern Andes volcanic zone. Tol-1 is a vertical 1.080 m deep borehole which could yield relevant information regarding the evolution of the Tolhuaca geothermal system. The methodology includes the structural and geochemical analysis of oriented faults, fault-veins and veins in the core. Fluid inclusions analysis by microthermometry, LA-ICP-MS and Raman spectroscopy will allow a better understanding of the feedback between the fluid flow episodes and the mineralization. More than 120 structural measurements were performed and 47 samples were taken for thin & fluid inclusions sections.

Our preliminary results show that there is a strong correlation between abundance of structures and rock type. Lava intervals exhibit more intense fracturing and veining than tuff and volcanoclastic intervals. In the upper 300 m of the core, structures are primarily steeply dipping with a dominant normal sense of displacement (some dextral component). Below a cataclastic zone at 300 m, structures are more variable in dip and sense of motion, with some reverse faults. Fluid inclusions petrography reveals the periodically feedback between fault-fractures networks activation and mineral mineralization sealing the conduits for fluid flow.

Changes in bacterial diversity and community structure within a geochemically variable uranium-mine water treatment plant

I. SÁNCHEZ-CASTRO^{1*}, M. LÓPEZ-FERNÁNDEZ¹,
A. AMADOR-GARCÍA¹, V. PHROMMAVANH², J. NOS²,
M. DESCOSTES² AND M.L. MERROUN¹

¹Department of Microbiology, University of Granada, Spain

(*correspondence: sanchezcastro@ugr.es)

²R&D Department, AREVA Mines, France

Monitoring and treatment of mining waters, containing heavy metals and radionuclides, are essential throughout the uranium mining. In order to meet the increasingly demanding regulatory requirements, optimized treatment and remediation strategies must be developed through the use of comprehensive biogeochemical models. Since biotic factors have been described to play a key role in these processes, an exhaustive analysis of the microbial diversity emerges as an important prerequisite.

Therefore, this work aims to assess the bacterial diversity occurring along the drainage treatment settling ponds of a former uranium mine and to link it to the associated geochemical features. A set of four sediment samples were taken along the treatment facility (before treatment, in the two treatment ponds and after treatment).

Highly diverse bacterial communities were observed in all samples by analyzing a total of 400 clones through a PCR-RFLP approach targeting the 16S rRNA gene. The clone libraries were dominated mainly by sequences closely related to the phyla *Acidobacteria*, *Actinobacteria*, *Bacteroidetes*, *Firmicutes*, *Planctomycetes* and specially *Proteobacteria*. Within this predominant phylum, relative abundance of *Alpha*-, *Beta*-, *Delta*- and *Gammaproteobacteria* varied among the different samples indicating specific distribution of the different bacterial populations according to geochemical variations. Links between the bacterial diversity and the geochemistry of the sediments will be discussed. Moreover, detection of sequences affiliated with metal-reducing bacteria (e.g., *Rhodoferrax*, *Ferribacterium*, *Geobacter*, *Geothrix*, *Anaeromyxobacter*) in all four samples, suggests that there is an evident potential for the bioremediation of the studied site.

Raman spectroscopy evidence for the ikaite-calcite/Vaterite transformation

N. SÁNCHEZ-PASTOR^{1*}, M. OEHLERICH²,
J.M. ASTILLEROS¹³, M. KALIWODA⁴, C.C. MAYR²⁵⁶,
W. W. SCHMAHL²⁴⁵ AND L. FERNÁNDEZ-DÍAZ¹³

¹Dpto. Cristalografía y Mineralogía. Universidad Complutense de Madrid, Spain. (*correspondence: nsanchez@ucm.es)

²Dept. Geo und Umweltwissenschaften. Ludwig-Maximilians-Universität, Germany

³Institute of Geosciences. CSIC - UCM, Spain

⁴Mineralogische Staatssammlung München, Germany

⁵Geo-Bio-Center. Ludwig-Maximilians-Universität, Germany

⁶Institut für Geography. Friedrich-Alexander-Universität, Germany

Ikaite ($\text{CaCO}_3 \cdot 6\text{H}_2\text{O}$) is a metastable phase that crystallizes from alkaline waters with high phosphate concentrations at temperatures close to 0°C. Above 4°C ikaite crystals transform rapidly to produce calcite pseudomorphs which are considered a valuable paleoclimatic indicator. In this work synthetic ikaite crystals were grown at near-freezing temperatures using an experimental setup that involved the diffusion of CaCl_2 through a silica gel prepared using natural water from the Argentinian lake "Laguna Potrok Aike". After recovering the crystals from the gel, their transformation was monitored by in situ collecting Raman spectra. The spectra taken in the first stages of the transformation showed the characteristic carbonate vibration modes of ikaite at 1067 cm^{-1} (symmetric CO stretch) and 700 cm^{-1} (in plane band). The second most intense band is due to lattice vibrations and found at 200 cm^{-1} , with secondary peaks at 136, 216 and 265 cm^{-1} . Moreover, the ikaite spectra show good resolved OH modes at 3180, 3240 and 3424 cm^{-1} whose intensity changes could be followed. During the transformation new bands at 1081 and 1085 cm^{-1} , characteristic for vaterite and calcite, appeared in the spectra. After a few hours, the Raman spectrum obtained was identical to that of calcite. However, the external shape of ikaite crystals remained unchanged during the replacement. A mechanism involving the coupling of ikaite dissolution and calcite/vaterite crystallization and the generation of a large amount of porosity is proposed for this transformation.

Acknowledgements: This research was partially funded by DFG-grants in the framework of the ICDP drilling project PASADO and project CGL2010-20134-C02-01 (DGCYT).

Clay-rich sediments injected into clastic dykes during earthquakes in the Galera fault zone (Guadix-Baza basin, Central Betic Cordillera)

CATALINA SANCHEZ-ROA¹, JUAN JIMENEZ-MILLAN^{1*}, FERNANDO NIETO², FRANCISCO J. GARCIA-TORTOSA¹, ISABEL ABAD¹ AND ROSARIO JIMENEZ-ESPINOSA¹

¹Department of Geology and CEACTierra, Associated Unit IACT (CSIC-UGR), Faculty of Experimental Science, University of Jaén, Campus Las Lagunillas s/n, 23071 Jaén, Spain (catasroa@ujaen.es; *correspondence: jmillan@ujaen.es; gtortosa@ujaen.es; miabad@ujaen.es, respino@ujaen.es)

²Department of Mineralogy and Petrology and IACT (CSIC-UGR), Faculty of Science, University of Granada, Avda. Fuentenueva s/n 18002, Granada, Spain (nieto@ugr.es)

The Galera Fault zone is a sinistral fault, which is 23 km long and strikes N48°E [1, 2]. The fault zone is 1.5 km wide with several parallel splays dipping NW between 40° and 60°, although vertical dips have also been noted locally.

During field observations within the area, clastic dikes were identified crosscutting the stratification of the sequence as well as filling spaces in between stratification planes. The clastic dikes are composed of medium sand size grains in a matrix of clay minerals. The mineral species identified through x-ray diffraction include quartz, albite, mica, chlorite and smectite. The SEM study reveals prismatic oriented fragments of diatoms. The muscovite and clinocllore crystals show a larger grain size than smectite which exhibits a flaky morphology and its presence is associated with the diatom fragments.

Injection clastic dikes have been previously described as a form of seismites, and their emplacement corresponds to episodic pulses of increasing hydraulic pressure generated by seismic loading [3]. Given that other co-seismic structures such as globular seismites have been identified in the area [4] and considering the clastic origin of the material we could infer that the sediments were saturated with water as a result of fluid circulation associated with the fault zone and later injected into fractures during seismic events.

[1] García Tortosa *et al.* (2011) *Geomorphology* **125**, 517-529. [2] Sanz de Galdeano *et al.* (2012) *Journal of Iberian Geology* **38**, 209-223. [3] Levi *et al.* (2006) *Geochem. Geophys. Geosyst.* **7**, Q12009. [4] Alfaro *et al.* (2010) *Terra Nova* **22**, 172-179.

Geochemical and microbial signals related to carbonate formation in the subsurface of Rio Tinto

¹SÁNCHEZ-ROMÁN, ¹FERNÁNDEZ-REMOLAR D, ¹PUENTE-SÁNCHEZ F, ¹RODRIGUEZ N, ¹PARRO V AND ¹²AMILS R,

¹Centro de Astrobiología (INTA-CSIC), 28850 Madrid, Spain. E-mail: msanzroman@cab.inta-csic.es

²Centro de Biología Molecular Severo Ochoa (CSIC-UAM), 28049 Madrid, Spain

Rio Tinto is considered a good geochemical terrestrial analogue of Mars due to its high content of iron and extreme acidic pH [1]. The occurrence of carbonates in this extreme environment is very local and they are found to occur under certain conditions of pH and iron concentration [2]. To understand its formation we have recovered and generated samples from cores, taken from wells BH10 and BH11 of depths of 340 and 620 meters, respectively, under anaerobic and sterile conditions. These wells were drilled during the field campaign of the Iberian Pyrite Belt Subsurface Life (IPBSL) project. IPBSL is a drilling project, currently under development, specifically designed to characterize the subsurface ecosystems operating in the Iberian Pyrite Belt (IPB), in the area of Peña de Hierro, and responsible of the extreme acidic conditions existing in the Rio Tinto basin [3]. The present study emphasizes the mineralogical, geological-biochemical and microbial implication for carbonate formation in Rio Tinto. Herein, we show that the formation of carbonate minerals in Rio Tinto is closely related to microbial activity and that can occur under both oxic and anoxic conditions. The formation of carbonates in such extreme environment could explain the occurrence of carbonates on Mars. Finally, this environmental and experimental study provides potential mineralogical biosignatures that may be useful to test life on Mars and other extraterrestrial habitats.

[1] *Planet Space Sci* **55**, 370-381,2007; [2] *Earth Planet Sci Lett* **351**, 13-26, 2012; [3] *Appl Environ Microbiol* **69**, 4853-4865, 2003.

Thermodynamics of carbon-bearing fluids and oxidized carbon speciation equilibria in subduction zone fluids

CARMEN SANCHEZ-VALLE¹, DAVIDE MANTEGAZZI¹ AND THOMAS DRIESNER¹

¹IGP, ETH Zürich, Switzerland

(correspondence: carmen.sanchez@erdw.ethz.ch)

Subduction zones play an important role in the deep carbon cycle as allow the reintroduction of C into the mantle and the recycling through arc magmatism. The occurrence of diamond-bearing fluid inclusions in HP rocks of oceanic origin suggests that C can be efficiently transferred from the slab to the mantle wedge through dissolution reactions driven by slab-derived aqueous fluids (Frezzotti *et al.*, 2011). A better understanding of the role of aqueous fluids on C recycling thus relies on the development of robust thermodynamic models of the properties of C-bearing aqueous species at relevant conditions.

In this contribution, we present first experimental data on the thermodynamic properties of oxidized carbon species at high P-T that have been used to constrain a model of the speciation of oxidized carbon in aqueous fluids at subduction zone conditions. The thermodynamic properties of oxidized C-bearing aqueous fluids were determined up to 650 °C and 4 GPa from acoustic velocity measurements performed on Na₂CO₃ and NaHCO₃ aqueous solutions with various concentrations (0.1 to 1 m). Experiments were conducted on externally heated diamond anvil cells by Brillouin scattering spectroscopy. Densities of the fluids directly obtained from the measured acoustic velocities were used to calibrate an equation of state (EoS) able to predict the thermodynamic properties of carbonated fluids at high P-T conditions. Further, the derived partial molar volume and compressibility of aqueous CO₃²⁻ and HCO₃⁻ ions were used to constrain the effect of P on the equilibrium constant controlling the speciation of oxidized carbon in high temperature fluids: $\text{HCO}_3^- = \text{H}^+ + \text{CO}_3^{2-}$ (Eq.1). The calculated volume of reaction $\Delta\bar{V}_r$ for Eq.1 is negative at the investigated P conditions, indicating that aqueous carbonate ions CO₃²⁻ are the dominant C-species in high P oxidized fluid. This observation is consistent with direct investigations of the speciation of fluids in equilibrium with carbonate minerals by Raman spectroscopy. The predicted stability of aqueous CO₃²⁻ in high P fluids and the enhanced solubility of carbonate minerals under P, indicate that CO₃²⁻ ions may be major components in slab-derived fluids and may thus control the mobility of other rock-forming elements in subduction zones.

Branched tetraethers derived temperature reconstruction from northwestern Black Sea: Proposition of correction and associated sensitivity test

L. SANCHI^{1*}, G. MENOT¹ AND E. BARD¹

¹Aix-Marseille Université, CNRS, IRD, Collège de France, CEREGE UM 34, 13545 Aix-en-Provence, France

(*correspondence: sanchi@cerege.fr, menot@cerege.fr, bard@cerege.fr)

Proxies based on branched GDGT (glycerol dialkyl glycerol tetraether) core lipids are promising tools to reconstruct past continental temperatures. However their use is not always straightforward, notably because of the uncertainties on the source of these biomarkers.

Here we study the relative distribution of branched GDGTs (brGDGTs) in lacustrine sediments from a core retrieved in the northwestern Black Sea (from 40 to 9 cal ka BP). We first discuss the origins of the branched GDGTs. Comparisons to geochemical proxies from the same core support a dominant terrestrial origin of the brGDGTs during the last glacial, and a strong decrease of the soil derived brGDGTs relative proportion toward the Holocene. As this lowering of the soil vs. lacustrine derived brGDGTs is prone to bias the temperature signal reconstructed with a soil calibration, we propose a correction of this signal with a binary mixing model. We further test the sensitivity of this model with a Monte Carlo method. The resulting signals are consistent with (discrete) independent temperature reconstructions from the study area. Moreover the temperature relative evolution provides insights into the millennial scale climate variability in central and eastern Europe. Notably, the imprints of Heinrich event cold spells and late glacial climatic oscillations are in line with other regional paleorecords from the northern hemisphere.

Calcite step growth velocities; a function of saturation index and the Ca^{2+} to CO_3^{2-} activity ratio

K.K. SAND^{1*}, D.J. TOBLER¹, K.K. LARSEN²,
E. MAKOVICKY³ AND S.L.S. STIPP¹

¹NanoScience-Center, University of Copenhagen,
Universitetsparken 5, DK-2100 Copenhagen.
*kks@nano.ku.dk

²Centre for Star and Planet Formation, University of
Copenhagen, Denmark.

³Department of Geography and Geology, University of
Copenhagen, Denmark

Calcite (CaCO_3) growth rate has an impact on many natural and industrial processes, ranging from biomineralisation to carbon storage and pipe scaling. Larsen *et al.* [1] noted that Ca^{2+} to CO_3^{2-} activity ratios in natural waters are rarely unity and demonstrated that growth velocities of the calcite acute and the obtuse steps varied with the Ca^{2+} to CO_3^{2-} ratio at constant states of supersaturation. We have extended the work of Larsen *et al.* to quantify the growth rates for acute and obtuse steps as a function of saturation index (SI) and Ca^{2+} to CO_3^{2-} activity ratios. Microscopic analysis of growth spirals show that absolute growth velocities change with SI. We have also observed that, independent of SI, acute step velocities are higher than obtuse velocities at low Ca^{2+} to CO_3^{2-} ratios, whereas obtuse step velocities are higher at higher Ca^{2+} to CO_3^{2-} ratios (Fig. 1). This shift is certainly related to the different geometries of the acute and obtuse steps.

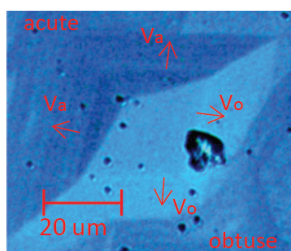


Figure 1. Growth spiral at a $\text{Ca}^{2+}/\text{CO}_3^{2-} = 50$. The obtuse step velocities are faster (V_o) and apex shifts toward the acute corner.

These results have implications for current models of calcite growth and reaffirm that calcite growth cannot simply be described using classical crystal growth theory intended for the high order symmetry of cubic atomic lattices. The rhombohedral symmetry of the calcite atomic structure must be considered.

[1] Larsen *et al.* (2010). *Geochimica et Cosmochimica Acta* **74**, 2099-2109

Quantification of organic matter redox states by mediated electrochemical analysis

M. SANDER¹, L. KLÜPFEL¹, A. PIEPENBROCK²,
A. KAPPLER² AND M. AESCHBACHER¹

¹Institut for Biogeochemistry and Pollutant Dynamics, Swiss
Federal Institute of Technology Zurich (ETHZ),
Switzerland (michael.sander@env.ethz.ch)

²Geomicrobiology Group, Applied Geosciences, Eberhard
Karls University Tübingen, Germany

Electron transfer reactions involving organic matter (OM) play a key role in carbon and element cycling in wetlands. Under anoxic conditions, OM may act as terminal electron acceptor in anaerobic microbial respiration. Reduction of OM may competitively suppress electron transfer to CO_2 and hence methanogenesis. Under oxic conditions, OM is susceptible to enzymatic oxidation, which ultimately leads to OM mineralization and hence CO_2 emissions. Despite the widely recognized importance of OM redox reactions to the biogeochemistry of wetlands, these reactions were difficult to study in past work as direct quantification methods were missing. We recently introduced mediated electrochemical analysis as a novel approach in which water-soluble organic mediator compounds are used to facilitate electron transfer and redox potential equilibration between OM and electrodes. The approach includes two types of measurements: (i) Mediated electrochemical reduction and oxidation directly quantify (changes in) the numbers of electrons that small OM samples accept and donate in electrochemical cells with well defined redox conditions. (ii) Mediated potentiometric redox potential measurements can be used to determine (changes in) the reduction potentials E_h of OM samples and on the thermodynamics of redox reactions involving OM. The unique capabilities of mediated electrochemical analysis for the analysis of OM redox dynamics in wetlands will be highlighted by results of two mechanistic laboratory studies. In the first study, mediated electrochemical analysis was used to quantify changes in the redox states of different OM over successive microbial reduction and O_2 -oxidation cycles. The results demonstrate that electron transfer to and from OM was fully reversible, that system thermodynamics controlled the extents of microbial OM reduction, and that OM accepted electrons over wide E_h ranges. In the second case study, OM oxidation during incubation with phenoloxidases (i.e., laccases) was quantified, and fast, extensive and irreversible enzymatic oxidation of phenolic moieties in OM was demonstrated. Implications for OM redox dynamics in wetlands under anoxic and oxic conditions will be discussed.

Aerosol modifications observed at Mt. Cimone (Italy) during the Eyjafjallajökull eruption in 2010

S. SANDRINI^{1*}, L. GIULIANELLI¹, S. DECESARI¹, P. CRISTOFANELLI¹, A. MARINONI¹, M. CHIARI², G. CALZOLAI², S. CANEPARI³ AND C. PERRINO⁴

¹Institute of Atmospheric Sciences and Climate, National Research Council, Bologna, 40129, Italy
(*correspondence: s.sandrini@isac.cnr.it)

²Italian National Institute for Nuclear Physics, Florence section, Sesto Fiorentino, 50019, Italy

³University of Rome "La Sapienza", Chemistry Department, Rome, 00185, Italy

⁴C.N.R. Institute of Atmospheric Pollution, Monterotondo St., Rome, 00015, Italy

Measurements of physical and chemical properties at the Mt. Cimone GAW-WMO Global Station (2165 m a.s.l.) allowed the detection of two volcanic transports occurred during the Eyjafjallajökull Icelandic volcano eruption in Spring 2010. Both episodes were characterized by an abrupt increase of fine and especially coarse mode particles number, with a consistent ash mode at an optical diameter of about 2.5 μm and an accumulation mode peaking at 0.2 - 0.3 μm . To figure out whether and to what extent the local aerosol mass was influenced by the transported volcanic ash the chemical composition of filter samples was derived from different analytical techniques (Ionic Chromatography, PIXE-PIGE and ICP-OES) showing a fine fraction dominated by sulphates and a coarse fraction of mainly crustal origin with a composition in good agreement with that of volcanic ash collected at the eruption site. The concentrations of selected elements (Ti, Al, Fe, Mn) allowed to estimate a volcanic plume contribution of about 10 $\mu\text{g m}^{-3}$, corresponding to about 40% of the total PM10 mass on 18 May, the most intense of the two events. A comparison with contributions observed in other parts of Europe is presented.

Characteristics and genesis of ion-adsorption type REE ores

K. SANEMATSU^{1,2*} AND Y. WATANABE¹

¹Geological Survey of Japan, AIST, Tsukuba 305-8567, Japan
(*correspondence: k-sanematsu@aist.go.jp)

²CODES, University of Tasmania, Private Bag 126, Hobart, Tasmania 7001, Australia

Ion-adsorption type REE deposits are the predominant source of HREE and Y in the world, and they have been economically mined only in South China. In order to elucidate the genesis of the deposits, we review petrochemistry of parent granites of ion-adsorption ores, and geochemical and mineralogical characteristics of the ores.

The REE deposits in China consist of weathered granites called ion-adsorption ores which have over 50 % of ion-exchangeable REY relative to whole-rock REY [1, 2]. The parent granites of the deposits are generally characterized by metaluminous to weakly peraluminous ($ASI < \sim 1.1$) compositions and low P_2O_5 contents ($< 0.08\%$). The granites contain allanite, titanite and REE fluorocarbonates (e.g., synchysite), which are degraded by chemical weathering, and they are poor in insoluble REE phosphates (monazite and xenotime). The HREE-rich granites are particularly fractionated and underwent deuteric alteration associated with mineralization of REE fluorocarbonates. The LREE/HREE ratios of ion-adsorption ores are constrained by nature and occurrences of these REE-bearing minerals in the granites.

The REE-bearing minerals in granites are degraded by low-pH soil water near the surface, and REE are transported downward in a weathering profile. REE are transported by complexing with humic substances and (bi)carbonate ions or as free ions in soil and ground water at low to near-neutral pH. REE are immobilized by adsorption or incorporation into secondary minerals due to pH increase resulting from the contact of the soil water with rock-forming minerals or higher-pH ground water. Ce is mostly immobilized as CeO_2 by oxidizing from Ce^{3+} to Ce^{4+} near the surface. The other REE^{3+} are most likely to be adsorbed on the surfaces of kaolinite, halloysite and illite because of their points of zero charge and abundances in the ores. As a result, the weathering profile of the deposits is divided into a REE-leached zone of the upper part of the profile with positive Ce anomaly and a REE-accumulation zone (ion-adsorption ores) in the lower part with negative Ce anomaly. The occurrence of ion-adsorption ore is estimated by the negative Ce anomaly which is positively correlated with ion-exchangeable REE [2].

[1] Bao & Zhao (2008) *Ore Geol. Rev.* **33**, 519-535.

[2] Sanematsu et al. (2013) *Miner. Deposita* **48**, 437-451.

Mantle-crust interactions in the oceanic lithosphere: Constraints from minor and trace elements in olivine

A. SANFILIPPO^{1*}, R. TRIBUZIO^{1,2} AND M. TIEPOLO²

¹Dipartimento di Scienze della Terra e dell'Ambiente, Università di Pavia, 27100 Pavia, Italy (*correspondence: alessio.sanfilippo@unipv.it)

²CNR - Istituto di Geoscienze e Georisorse, U.O. di Pavia, 27100 Pavia, Italy

Minor and trace element compositions of olivines are used as probes into the melt-rock reaction processes occurring at the mantle-crust transitions in the oceanic lithosphere. We considered mantle and lower crustal sections from the Alpine Jurassic ophiolites. In particular, we analyzed olivines from plagioclase-impregnated harzburgites and replacive dunites (Fo 91-90 mol%), and olivines from olivine-rich troctolites, troctolites and olivine-gabbros (Fo 88-82 mol%). The olivines from the harzburgites most likely experienced re-equilibration with the impregnating melts, as indicated by Mn, Ti, Y and HREE variations and the low Na concentrations. The olivines from the dunites have: (i) Mn, Ni, Co and Ca compositions similar to the primitive (Fo 91-89) olivine phenocrysts in MORB [1], and (ii) relatively high Y and HREE contents indicating equilibrium with primitive MORB. We thus reinforce the hypothesis [2] that replacive dunites act as conduits for the extraction of MORB. The involvement of MORB-type melts in the formation of the dunites is substantiated by the spinel compositions (Cr# ~35, TiO₂ ~0.3 wt%). Notably, the concentrations of Mn, Ni and Co in the dunites olivines produce positive correlations, in agreement with a formation through melt-harzburgite reactions. The preservation of this geochemical inheritance indicates that the liquids migrating along the dunites may change their compositions in response to the dunite-forming reactions. The olivine-rich troctolites are considered to be hybrid rocks formed by interaction between an olivine-rich matrix and MORB-type melts. The olivine chemistry in these rocks is controlled by the composition of the infiltrating melts and provides little information about the nature of the olivine matrix. Fractional crystallization rules the compositions of the olivines from the troctolites. Furthermore, the olivines from the troctolites have higher Y and HREE, and lower Co than the olivines in olivine-gabbros. These variations show that the troctolite/olivine gabbro transition is partly constrained by melt-rock reaction processes.

[1] Sobolev A, Hofmann A, *et al.* (2007), *Science* **316**, 412

[2] Kelemen P, Shimizu N, & Salters V (1995) *Nature*, **375**, 747-753

Solid - Liquid Equilibria of K₂SO₄-KBr-H₂O System at 373 K

SHIHUA SANG^{1,2*}, TING LI¹ AND YONGXIA HU¹

¹College of Materials and Chemistry & Chemical Engineering, Chengdu University of Technology, Chengdu 610059, China. (sangsh@cdut.edu.cn)

²State Key Laboratory of Oil and Gas Reservoir Geology and Exploitation (Chengdu University of Technology), Chengdu 610059, P. R. China

Massive high-salinity underground brines are frequently met in the exploitation of oil and gas resources. In particular, the underground gasfield brines in Western Sichuan Basin (China), are very rare liquid mineral resources in the world. The B, K, and Br contents of the brines are far beyond the lower grades of the comprehensive industrial utilization. The ternary system K₂SO₄-KBr-H₂O is a subsystem of the underground gasfield brines. The solid-liquid equilibria for the ternary system at 373 K were measured experimentally using the method of isothermal solution saturation. In the phase diagram of the ternary system K₂SO₄-KBr-H₂O at 373 K (Figure 1), there are one invariant point E and two univariant curves DE and CE. Equilibrium solids were KBr and K₂SO₄ in the studied ternary system. The crystallization area of K₂SO₄

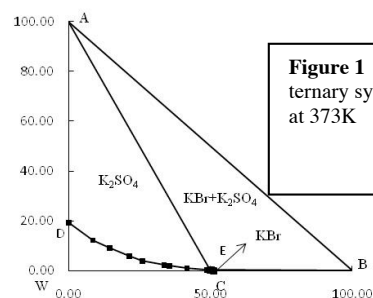


Figure 1 Phase diagram of the ternary system K₂SO₄-KBr-H₂O at 373K

(AED field) in the phase diagram is obviously bigger than that of KBr (BEC field).

Acknowledgements

This work was supported by Open Funds (PLC201204) of State Key Laboratory of Oil and Gas Reservoir Geology and Exploitation (Chengdu University of Technology), the National Natural Science Foundation of China (40973047), the Specialized Research Fund (20125122110015) for the Doctoral Program of Higher Education of China.

Structural change in molten basalt at deep mantle P-T conditions

C. SANLOUP¹, J.W.E. DREWITT¹, P. DALLADAY-SIMPSON¹, D.M. MORTON¹, N. RAI², W. VAN WESTRENNEN², Z. KONOPKOVA³ AND W. MORGENROTH^{3;4}

¹SUPA, Centre for Science at Extreme Conditions and School of Physics and Astronomy, University of Edinburgh, Edinburgh, EH9 3JZ, UK

²Faculty of Earth and Life Sciences, VU University Amsterdam, The Netherlands

³DESY Photon Science, Notkestr. 85, 22607 Hamburg, Germany

⁴Frankfurt University, Germany

In the recent years, structural and density information on silica glass have been obtained up to record pressures of up to 100 GPa¹, a first major step towards obtaining data on the molten state.

In this abstract, the structure of molten basalt is reported up to 60 GPa by means of in situ x-ray diffraction, and structural changes are evidenced. Silicon coordination increases from 4 at ambient conditions to 6 at 35 GPa, similarly to what has been reported in silica glass¹⁻³. Compressibility of the melt after completion of Si coordination change is lower than at lower pressure (P) conditions, implying that a single equation of state can not accurately describe density evolution of silicate melts over the whole mantle P-range. The transition pressure coincides with a marked change in the P-evolution of nickel partitioning between molten iron and molten silicates, indicating that melt compressibility controls siderophile element partitioning.

1. Sato and Funamori, PRL 101, 255502 (2008). 2. Meade *et al.* PRL 69, 1387 (1992). 3. Benmore *et al.*, PRB 81, 054105 (2010).

Ion microprobe U-Pb dating and Sr isotope measurement of a proto-conodont

YUJI SANO^{1*}, KOSAKU TOYOSHIMA¹, KOTARO SHIRAI¹, NAOTO TAKAHATA¹, AKIZUMI ISHIDA¹ TOMOHIKO SATO² AND TSUYOSHI KOMIYA²

¹Atmosphere and Ocean Research Institute, The University of Tokyo, Kashiwanoha, Kashiwa, Chiba 277-8564, Japan (ysano@aori.u-tokyo.ac.jp)

²Department of Earth Science and Astronomy, The University of Tokyo, Komaba, Meguroku, Tokyo 153-8902, Japan

We report here *in situ* ion microprobe U-Pb dating of a protoconodont micro-fossil using a NanoSIMS [1,2]. Twenty-three spots on the single fragment of the protoconodont (size: approximately 850 µm x 250 µm) derived from a sedimentary layer in the Meishucunian formation, Yunnan Province, South China provide a ²³⁸U/²⁰⁶Pb isochron age of 547 ± 43 Ma (2σ, MSWD=1.9), which is consistent with the depositional age of the formation, 536.5 ± 2.5 Ma reported by a zircon U-Pb dating [3]. On the other hand, five spots on the small region in the sample yield the isochron age of 416 ± 73 Ma (2σ, MSWD=0.31), apparently younger than the formation age. The younger age may be attributable to the latter metamorphic event, probably Caledonian orogenic activity recorded in the younger zircon with the age of 420 - 440 Ma [4].

We also measured the ⁸⁷Sr/⁸⁶Sr ratios of the protoconodont by a NanoSIMS [5]. Nineteen spots on the older age region give the ⁸⁷Sr/⁸⁶Sr ratio of 0.71032 ± 0.00023 (2σ) on the weighted mean average, while seven spots on the younger area provide that of 0.70862 ± 0.00045 (2σ), significantly smaller than the older part. This is the first finding of U-Pb age and Sr isotope heterogeneity within a single fragment of micro-fossil, even though there is not a large chemical difference measured by a semi-quantitative SEM-EDS analysis.

[1] Sano *et al.* (2006) *Geochem. J.* **40**, 597-608. [2] Takahata *et al.* (2008) *Gond. Res.* **14**, 587-596. [3] Sawaki *et al.* (2008) *Gond. Res.* **14**, 148-158. [4] Guo *et al.* (2009) *Geochem. J.* **43**, 101-122. [5] Sano *et al.* (2008) *App. Geochem.* **23**, 2406-2413.

On the reliability of paired carbon isotope as a pCO₂ proxy in the Ediacarian Araras platform, Brazil

PIERRE SANSJOFRE^{1,2,3*}, MAGALI ADER¹,
RICARDO I.F. TRINDADE², AFONSO C.R. NOGUEIRA⁴

¹Institut de Physique du Globe de Paris, France (ader@ipgp.fr)

²Universidade de São Paulo, Brazil (rtrindad@iag.usp.br)

³McGill University, Montréal, Canada (*correspondence : pierre.sansjofre@mcgill.ca)

⁴Universidade Federal do Pará, Belém, Brazil (anogueira@ufpa.br)

The snowball Earth model accounts for many of the typical geological and geochemical features of the Marinoan glaciation deposits (~635Ma) and of their overlying cap carbonate [1]. Melting this snowball Earth would have required a massive increase of the atmospheric carbon dioxide content (pCO₂). Recently however, we proposed instead a low atmospheric pCO₂ in the glaciation aftermath [2]. Our interpretation is based on paired carbon isotope data obtained on cap carbonates from Mirassol d'Oeste section (Ediacarian Araras platform, Brazil), together with previous results from cap carbonates of the Doushantuo Fm. and Zhamoketi Fm [3,4]. All three data sets showed low $\Delta^{13}\text{C}_{\text{carb-org}}$ ($=\delta^{13}\text{C}_{\text{carb}} - \delta^{13}\text{C}_{\text{org}}$). We made the case that these anomalously low values result from a decrease in the photosynthetic fractionation factor (ϵ_p), which can be related to pCO₂ lower than 3000 ppmv at the time of cap carbonate deposition.

We performed here a regional study based on 4 other sections sampled along the Araras carbonate platform. This new data set is broadly consistent with a low atmospheric pCO₂ scenario and allow to explore and identify both the local and global carbon isotopic variations of the Araras carbonate platform. In details, some features indicate that the occurrences of the low $\Delta^{13}\text{C}_{\text{carb-org}}$ are restricted to shallow depositional environments. In this present contribution, we discuss two alternate hypotheses that can be invoked to explain the low $\Delta^{13}\text{C}_{\text{carb-org}}$: (i) a shallow water early diagenetic process inducing a $\delta^{13}\text{C}_{\text{org}}$ increase and a $\delta^{13}\text{C}_{\text{carb}}$ decrease or (ii) primary producers presenting lower ϵ_p due to other parameter than pCO₂. In both case, the diagenetic event and the primary producers would remain to be constrained.

[1] Hoffman and Schrag (2002) *Terra Nova* **14**, 129-155. [2] Sansjofre *et al.* (2011) *Nature* **478**, 93-96. [3] Jiang *et al.* (2010) *Earth Planet. Sci. Lett.* **299**, 159-168. [4] Shen *et al.* (2008) *Earth Planet. Sci. Lett.* **265**, 209-228.

Magnetic susceptibility and $\delta^{18}\text{O}$ characterization of granites related with W, Sn, Mo and Bi (Au) hydrothermal vein deposits

HELENA SANT'OVAIA¹, HELENA C.B. MARTINS¹ AND
FERNANDO NORONHA¹

¹DGAOT, Centro de Geologia, F.C. Univ. Porto, Portugal, hstantov@fc.up.pt (* presenting author)

The Northern Portugal mainland comprises an important W-Sn metallogenic province characterized by W-(Mo-Bi), W, W-Sn, and Sn hydrothermal vein deposits related with sinorogenic Variscan granites. These granites are usually classified into two main groups: peraluminous and metaluminous. As the granite rocks reflect redox states of their corresponding melts, the presence of magnetite and/or ilmenite as accessory minerals represent oxidized- and reduced-type respectively. The mineralogical features and magnetic susceptibility (K) of the granites were examined in order to deduce the redox conditions of magma systems, using the magnetic susceptibility data from around 644 sampling stations on different massifs of Variscan Portuguese granites. Whole-rock oxygen-isotope ($\delta^{18}\text{O}$) values were compiled from bibliography [1,2,3,4]. Despite of different petrographic and geochemical characteristics, K values in the majority of the studied granites vary from 20 to 300×10^{-6} SI units corresponding to peraluminous and meta-peraluminous, reduced, ilmenite-type granites. The oxidized or magnetite-type granites are scarce and represented by metaluminous late orogenic with K values ranging from 15 to 20×10^{-3} SI units and low $\delta^{18}\text{O}$ values ranging from 8.9 to 10.3‰ . Major W-Sn ore deposits are related to reduced ilmenite-bearing granites with $\delta^{18}\text{O}$ enriched (9.3 to 13.5‰); W- (Mo-Bi- Au) deposits are related with oxidized granite series (i.e. magnetite or titanomagnetite-bearing granites). Magnetic susceptibility measurements, represent a powerful tool on mineral exploration of deposits related with intrusive magmatism.

[1] Antunes *et al.* (2008) *Lithos* **103**, 445-465. [2] Martins *et al.* (2009) *Lithos* **111**, 142-155. [3] Neiva *et al.* (2009) *Lithos* **111**, 186-202. [4] Sant'Ovaia *et al.* (2011) *Min. Mag.* **76**, 6, 2325.

This work has been financially supported by PTDC/CTE-GIX/099447/2008 (FCT-Portugal, COMPETE/FEDER).

Microbial communities in terrestrial CO₂ springs: Insights into the long-term biogeochemical effects of geologic carbon storage

EUGENIO-FELIPE U. SANTILLAN^{1*}, JONATHAN MAJOR¹
AND PHILIP C. BENNETT¹

¹University of Texas Austin, Austin, TX, USA
(efu.santillan@utexas.edu * presenting author)

During carbon sequestration, CO₂ is stored in subsurface reservoirs such as sandstone and basalt formations perturbing native microbial communities. Useful and accessible natural analogues to study long term effects of CO₂ on these communities are high CO₂ springs. Laboratory cultures have shown CO₂ to be toxic for microorganisms starting at 1 atm. Here we present data indicating microbes that can survive up to 10 times that pressure.

In this study, 16S rRNA gene sequences were used to characterize microbial communities from 3 sequestration analogues at depths where PCO₂ is at approximately 2 atm: from a basalt formation in Klickitat (KT), WA containing approximately 700 ppm of total dissolved solids (TDS); from a sedimentary formation along the Little Grand Wash Fault (LGW), UT containing 15,000 ppm TDS; and from a saline water in Bravo Dome (BD), NM containing 50,000 ppm TDS. Results show that the springs were dominated by a few major organisms but still contained more diversity than was expected at toxic CO₂ pressures. LGW sequences had no archaea and were dominated (>85%) by the genus *Acinetobacter*. KT sequences were more diverse than that of LGW and contain methanogens and methanotrophs suggesting CH₄ cycling. Candidate phyla were also detected in KT such as those from the OP, WS, and SPAM divisions. Sequencing for BD is currently underway.

Laboratory cultures also show bacteria at LGW performing lactate fermentation at 10 atm PCO₂, demonstrating viability at sequestration conditions. This study confirms the presence and viability of microbial communities in CO₂ rich environments that can continue to affect the geochemistry as well as the long-term storage of CO₂.

Bioremediation and soil formation processes in bauxite residue tailings

T. C. SANTINI^{1,2*} AND L. A. WARREN^{1,3}

¹McMaster University, GSB218, Hamilton, ON, L8S4K1, Canada (*correspondence: santini@mcmaster.ca; warrenl@mcmaster.ca)

²University of Western Australia, M087, Crawley, WA, 6009, Australia

³CSIRO Land and Water, Lucas Heights, NSW, 2234, Australia

Bauxite residue is an alkaline, saline-sodic tailings material generated during the Bayer process, in which alumina is extracted from bauxite. Between 3 and 4 billion tonnes of bauxite residue are estimated to be currently stored in facilities worldwide. *In situ* remediation of bauxite residue by application of inorganic and organic amendments, coupled with natural weathering and soil formation processes, is a cost-effective way to decrease alkalinity and salinity such that the tailings can then support a vegetation cover. Very little information on microbial activity and its potential influence on the geochemistry and mineralogy of bauxite residues currently exists, impeding development of effective remediation strategies. Here, a bauxite residue storage facility was investigated after 15 years of weathering to evaluate the effect of amendments on geochemistry and mineralogy of the bauxite residue, and development of microbial communities.

Illage, and the addition of compost and gypsum, significantly decreased pH and salinity of the tailings. Highly diverse microbial communities were detected in these tailings, indicating that endemic organisms adapted to these materials occur *in situ*. Further, microbial community species composition varied with applied treatments and depth below surface indicating microbial selection of different conditions based on aeration, pH, salinity, and carbon availability. Experiments indicated that endemic communities were able to degrade oxalate, and reduce Fe³⁺ and SO₄²⁻, precipitating minerals such as vivianite and siderite; all of which are important steps in the development of soils capable of supporting plant growth. However, the species responsible for carrying out these functions differed between treatments and depths, indicating that knowledge of the specific microbes associated with different conditions is required. Overall, the study demonstrated that microbial communities can influence geochemical cycles and soil formation within bauxite residue deposits, and that the composition and function of microbial communities can be influenced by the application of chemical and physical treatments to bauxite residue.

Acid rock drainage associated with tropical glacier retreat: Nevado Pastoruri, Perú.

E. SANTOFIMIA^{1*}, E. LÓPEZ PAMO¹, J. PALOMINO²
AND A. AGUILERA³

¹Instituto Geológico y Minero de España, Madrid, Spain (*
correspondence: e.santofimia@igme.es)

²Facultad de Ciencias del Ambiente, Huaraz, Perú.

³Centro de Astrobiología, Torrejón de Ardoz, Madrid, Spain.

An important glacier retreat has been registered in the Nevado Pastoruri (Huascarán National Park) from 1962 to 2001, reducing its surface a 60% [1]. This process is frequent in glaciers located at Cordillera Blanca. Occasionally, glacier retreat exposed pyrite-rich rock outcrops of the Chicama formation, causing its alteration and the generation of acid rock drainages (ARDs) [2].

In the case of Nevado Pastoruri, the glacier retreat has left exposed to atmospheric conditions the sandstones and lutites with coal enriched in pyrite of the Chimú formation [3].

The proglacial zone presents a lot of lakes, scant vegetation, and intense fluvio-glacial erosion. On morphologies typically glacier are abundant the ARDs, revealing like springs of underground water, runoff or forming lakes. ARDs are clearly identifiable for the colour and the morphology (terraced iron formations), which is associated with the oxidation of Fe(II).

The water sampling was carried out in the proglacial zone. After cluster analysis using 23 samples, two groups were established. The first group (n=8) gathered the most acidic samples, pH 3, showing also the highest concentrations of elements such as SO₄, Fe, Al, Ca, Mg, Mn and Zn. These samples were directly related to the pyrite alteration (227 mg/L SO₄, 41 mg/L Fe) and aluminosilicate dissolution (10 mg/L Al), showing especially high values. This group is made up by the ARDs. The average concentration of these samples was an order of magnitude higher than the values showed by second group, which showed a scant mineralize (freshwater).

The ARDs geographical distribution is not disperse. These samples are grouped in a band of 600 m length with N-S direction and 250 m wide, between the elevations of 4925 and 5025 m. The mixing of two water types generates the source of River Pachacoto, showing Fe(III) buffer water (pH 3.1, Fe 0.7 mg/L) and several mg/L of dissolved Al (4.5) that confers mineral acidity to water.

[1] Duran *et al.* (2009) *Investigaciones Sociales* **13**, 59-77. [2] Fortner *et al.* (2011) *Applied Geochemistry* **26**, 1792-1801. [3] INGEMMET (1996) *Geología de los cuadrángulos de Huaraz, Recuay, La Unión y Yanahuana*, pp. 292.

Sr and Nd isotope data for arc-related (meta) volcanics (SW Iberia)

J.F. SANTOS¹, J. MATA², S. RIBEIRO¹, J. FERNANDES¹,
AND J. SILVA²

¹Geobiotec/Dep. Geociências, Un. Aveiro, Portugal,
jfsantos@ua.pt

²Fac. Ciências Univ. Lisboa/ CeGUL, Portugal

In the southern sector of the Ossa-Morena Zone (Iberian Variscan Chain), along its boundaries with the Beja-Acebuches Ophiolite and the South-Portuguese Zone, Upper Palaeozoic igneous mafic and intermediate rocks, both intrusive and extrusive, are widely represented. The so-called Odivelas Unit (Andrade, 1983), include (meta-) basalts and (meta-) andesites, which, according with previous studies, display low-K tholeiitic to calc-alkaline signatures and, therefore, are interpreted as remnants of an active margin volcanic arc. Santos *et al.* (1990) subdivided those volcanics into two groups: in Alfândão-Peroguarda, the tholeiitic nature is dominant; in Odivelas-Penique, the calc-alkaline signature becomes more pronounced. Intercalation of limestone layers provided some age constraints, showing that the subduction-related volcanic activity in the studied area began in the Lower Devonian and continued, at least, through the Middle Devonian (Conde & Andrade, 1974; Machado *et al.*, 2010).

In this work, samples previously studied by Santos *et al.* (1990) and Silva *et al.* (2011) were analysed for Sm-Nd and Rb-Sr isotopes. Considering that the volcanics were systematically affected by hydrothermal metamorphism, it is expected that the Sr signatures show significant disturbance. In contrast, Nd isotope ratios probably reflect the primary features. Alfândão-Peroguarda samples show a very limited range of positive initial ϵ_{Nd} , from +5.1 to +4.3 (assuming 400 Ma), showing no evidence for significant crustal assimilation and, therefore, allowing the attribution of negative Nb and Ta anomalies to arc-related processes. On the other hand, $^{87}Sr/^{86}Sr$ varies from 0.7044 to 0.7060 (for 400Ma). These samples rocks define a horizontal trend on the initial ϵ_{Nd} vs. initial $^{87}Sr/^{86}Sr$ plot, typical of co-genetic rocks that underwent interaction with seawater. On the other hand, Odivelas-Penique volcanics show wide spectra for both initial $^{87}Sr/^{86}Sr$ (from 0.7038 to 0.7066) and ϵ_{Nd} (from +4.6 to -4.1). Significantly, the highest ϵ_{Nd} values for this group are within the narrow range defined by Alfândão-Peroguarda tholeiitic basalts, suggesting a common mantle source (or very similar sources) for the most mafic magmas of both sectors.

The whole set of Nd isotope ratios supports the distinction previously proposed between the two groups of volcanics. In addition, the variation from positive to negative initial ϵ_{Nd} values in the Odivelas-Penique suite shows that its geochemical features were likely influenced by assimilation of continental crustal material.

Funding: FCT through projects Petrochron (PTDC/CTE-GIX/112561/2009) and Geobiotec (PEst-C/CTE/UI4035/2011).

Behaviour of rare earth elements (REE) at Funil Reservoir, Southeastern Brazil

J.M.C.O. SANTOS-NEVES¹, M.M. FERREIRA¹, M.S.M. VIDAL¹, A.A. ROCHA² AND S.R. PATCHINEELAM*¹

¹Department of Geochemistry and ²Department of Analytical Chemistry. Institute of Chemistry, Universidade Federal Fluminense, Niterói, Rio de Janeiro State, Brazil.

*sam_pat_br@yahoo.com

Rare earth elements (REE) have specific biogeochemical characteristics, which allow their use as reliable tracers of natural processes at various spatial and temporal scales in aquatic systems [1-3]. This study aims to evaluate the role of Funil Reservoir on REE behaviour. Considering the objectives, water samples were collected in three sample stations, during dry and rainy seasons: (P-01) upstream the Funil reservoir at Queluz, São Paulo State; (P-02) at the reservoir; and (P-03) downstream the Funil Reservoir, at Itatiaia. REE concentrations were determined by ICP-MS.

REE concentrations are presented in Table 1. Calculated ratios from REE normalized by PAAS indicate that values of Gd/Yb > La/Yb, which suggests that there is an enrichment of heavy REE in all sample points in both seasons.

	Rainy season			Dry season		
	P-01	P-02	P-03	P-01	P-02	P-03
ΣREE (ng/L)	72,91	54,14	102,36	77,97	87,71	83,64
La/Yb	0,19333	0,17172	0,05481	0,216	0,212	0,196
Gd/Yb	0,03696	0,3308	0,17023	0,395	0,378	0,395

Table 1: REE concentrations and ratios at study area.

Our results indicate that REE abundance is controlled by weathering in drainage basin. During dry season REE concentrations increased. And during rainy season, REE concentrations before and after the reservoir were greater than concentrations at Funil reservoir (P-02). The distinct behaviour observed between dry and rainy seasons is the Funil Reservoir act as geochemical barrier modifying fluvial transport of REE. Another factor that probably affect REE behavior is algal bloom, with dominance of cyanobacteria which occurs during rainy season, which influence the behaviour of REE through the incorporation and release of these metals.

[1] GOLDSTEIN & JACOBSEN (1987) *Chemical Geology*, **48**, 245-272. [2] ELDERFIELD *et al.* (1990) *Geochimica Cosmochimica Acta*, **54**, 971-991. [3] XU & HAN (2009) *Applied Geochemistry*, **24**, 1803-1816.

Hydromagnesite precipitation in microbial mats from a highly alkaline lake, Central Spain

M. ESTHER SANZ-MONTERO^{1*}, ÓSCAR CABESTRERO¹ AND J. PABLO RODRÍGUEZ-ARANDA¹

¹Petrology and geochemistry Department. Facultad de Ciencias Geológicas (UCM), Madrid, Spain. mesanz@geo.ucm.es (*presenting author)

Microbialites comprised of up to 45% hydromagnesite and 10% of dolomite have been recognized in Las Eras playa-lake, Central Spain. Las Eras is an evaporitic highly alkaline lake, with pH values ranging from 9.4 to 11, that covers an area of 0.1 km² [1]. Mg-enriched groundwater flows into this lake, which is supersaturated in hydromagnesite and dolomite. The hydrous Mg-carbonate precipitation occurs in the uppermost layer of benthic microbial mats. This layer is dominated by *Microcoleus* that consists of trichomes in bundles and diatoms embedded in their EPS. Low-vacuum scanning electron microscopy revealed that hydromagnesite nucleation is initiated on the cells of aerobic heterotrophic bacteria that are responsible for the degradation of the microbial biomass. A progressive mineralization of the heterotroph cells by the deposition of plate-like crystals of hydromagnesite on their surface was observed. This resulting in the entombment of the bacteria and the formation of radiating aggregates of hydromagnesite crystals. The degradation and concomitant Mg-carbonate precipitation, finally, led to the lithification of the microbial mat.

This evolution shows that aerobic heterotrophic bacteria play a crucial role in the formation of microbialites in Lake Las Eras by promoting the Mg-carbonates precipitation. This lake is one of the few modern environments where hydromagnesite is a dominant precipitating mineral in microbialites. Thus, it provides a modern analog to use in the interpretation of saline and/or alkaline environments. In turn, the exceptional preservation of bacteria microfossils clustered into magnesite crystals has been already documented in Miocene saline deposits [2].

The authors greatly appreciate support from MINECO Program (Project CGL2011-26781).

[1] Sanz-Montero *et al.* (2013) *Geogaceta*, **53**, 97-100. [2] Sanz-Montero, M.E and Rodríguez-Aranda, J.P. (2012) *Sedimentary geology*, **263-264**, 6-15.

Unravel the role of lake ice cover on the methane budget: A multi-proxy analysis

C.J. SAPART¹, T. BOEREBOOM², T. RÖCKMANN¹,
H. NIEMANN³, C. VAN DER VEEN¹, J-L. TISON²

¹Institute for Marine and Atmospheric research Utrecht,
Utrecht University, The Netherlands

²Laboratoire de Glaciologie, Université Libre de Bruxelles,
Belgium

³Department of Environmental Sciences, University of Basel,
Switzerland

Large uncertainties exist on the evolution of the atmospheric methane (CH₄) budget in the future. Concern about possible feedbacks of natural sources in a changing climate is growing, especially concerning the role of thawing of permafrost areas in the Arctic regions. Subarctic lakes are considered as “hotspots” for CH₄ emissions, but the role of the ice cover during the winter period is not well understood to date. Different types of gas bubbles with high CH₄ mixing ratios have been identified in lake ice cover. A recent study revealed that the gas composition of those bubbles depends on, inter alia, the bubble type, the lake depth and the hydrological status of the lakes.

Analysing mixing and stable isotope ratios of CH₄ and CO₂ on those bubbles is an efficient tool to identify the mechanisms involved in the release, the oxidation and transport of CH₄ in permafrost lakes and to better constrain the potential influence of lake characteristics. Those analyses together with lipid biomarkers distribution analysis on lake ice samples reveal that different bubble types contain different isotopic signatures and that oxidation of dissolved CH₄ is the most important process determining the isotopic composition of CH₄ in bubbles. This shows that the increased exchange time between gases coming from the sediments and the water column, due to the capping effect of the lake ice cover, reduces the amount of CH₄ released and favours its oxidation into carbon dioxide.

Leaching of Zn, Cu and Pb from oxidised sulphidic mine waste as a function of temperature, L/S ratio and leaching reagents

NAEEM SAQIB¹, MATTIAS BÄCKSTRÖM²

^{1,2}Man-Technology Environment Research Center, Örebro
University, SE-701 82, Örebro, Sweden,

¹(naeem.saqib@oru.se) ²(mattias.backstrom@oru.se)

Formation of low pH drainage from sulphidic mine waste enhances trace element mobility and posing a serious threat to the surrounding environment [1]. A sustainable and cost effective remediation method is therefore desired. Utilization of the sulphidic waste as a secondary source for metals might be a viable alternative. In this laboratory scale study chemical extraction has been employed to assess the potential of metal release and possible metal recovery from oxidised sulphidic mine waste. Waste from an old copper and lead mine in Kopparberg, mid Sweden, was used for the experiments. Mine waste was extracted with four leaching agents: (i) distilled water, (ii) sulphuric acid, (iii) sodium hydroxide and (iv) sodium bicarbonate (0.01 M), at three liquid solid ratios (5, 10, 20) and at four temperatures (25, 45, 65, 85 °C), for a time of 6 hours during intermittent shaking. Generated solutions were analysed with respect to pH, electrical conductivity, acidity and metal concentrations.

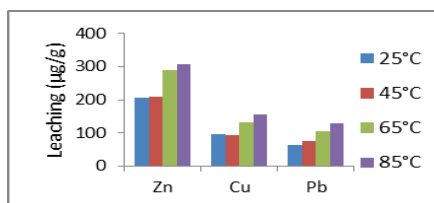


Figure 1. Effect of temperature on metal leaching from sulphidic mine waste using sulphuric acid.

Results indicate that increasing temperature enhances extraction of elements due to increase in reaction rates. Increasing L/S ratio increased extraction only to a certain extent after which it decreased or had no prominent effect. Sulphuric acid proved to be the best extraction media extracting as much as 14 % Zn, 10 % Cu and 3 % Pb of the total content. Leaching of Zn and Pb decreased from acid to neutral pH so it is a very crucial factor governing the extraction. Lead extraction with sulphuric acid is probably limited by anglesite (PbSO₄(s)).

[1] Alena Luptakova, *et al.* (2010) Metals Recovery from Acid Mine Drainage, *Nova Biotechnologica* 23, p 1-10.

Fuzzy Hierarchical Cross-Clustering of Romanian Mineral Waters

C. SĂRBU

¹Faculty of Chemistry and Chemical Engineering, Babeş-Bolyai University, Arany Janos Str., No 11, RO-400028, Cluj-Napoca, Romania *E-mail address:* csarbu@chem.ubbcluj.ro

Cluster analysis is a large field, both within fuzzy sets and beyond it. The application of Fuzzy sets in a classification function causes the class membership to become a relative one and consequently an object or sample can belong to several classes at the same time but with different degrees. In this investigation, Fuzzy hierarchical cross-clustering algorithm has been applied for simultaneous clustering of different Romanian mineral water samples and their chemical characteristics (ions concentration), and the results obtained have been allowing an objective interpretation of their similarity and differences, respectively. This very informative fuzzy approach allows the qualitative and quantitative identification of the characteristics responsible for the observed similarities and dissimilarities between mineral water samples. In addition, the fuzzy hierarchical characteristics clustering and fuzzy horizontal characteristics clustering procedures revealed a high similarity between some ions concentration and other features.

Surfactants from the gas phase may promote aerosol cloud droplet nucleation

NEHA SAREEN¹, ALLISON SCHWIER¹, TERRY LATHAM², ATHANASIOS NENES^{2,3} AND V. FAYE MCNEILL¹

¹Department of Chemical Engineering, Columbia University, New York, NY, USA 10027 vfm2103@columbia.edu

²School of Earth and Atmospheric Sciences, Georgia Institute of Technology, Atlanta, GA, USA 30332

³School of Chemical and Biomolecular Engineering, Georgia Institute of Technology, Atlanta, GA, USA 30332

The uptake of water-soluble volatile organic compounds (WSVOCs) by wet atmospheric aerosols can lead to the formation of secondary organic aerosol material (SOA). We have performed a series of laboratory studies in order to quantify the impact of WSVOC uptake and aqueous-phase SOA formation on aerosol cloud condensation nuclei (CCN) activity. Deliquesced, acidified submicron ammonium sulfate aerosols at >60% RH were exposed to ppb levels of gas-phase methylglyoxal, acetaldehyde in a continuous-flow aerosol reaction chamber (residence time = 3-5 h). Aerosol size and CCN activity was monitored at the reactor outlet via scanning mobility particle sizer (SMPS) and continuous-flow streamwise thermal gradient chamber CCN counter (CFSTGC), respectively.

Methylglyoxal and acetaldehyde are known to form SOA and suppress surface tension in bulk aqueous aerosol mimics, but both of these species have relatively low Henry's Law constants. We found evidence that adsorption of these species from the gas phase to the gas-aerosol interface significantly impacts aerosol CCN activity, by directly altering the aerosol surface tension. Up to 15% reduction in critical dry diameter for activation was observed without any detectable particle growth due to bulk uptake of organics (Sareen *et al.*, Proc. Natl. Acad. Sci. USA, 2013).

Finally, we have developed a general analytical approach for predicting aerosol surface tension based on gas-phase surfactant loadings, taking into account the effects of both bulk uptake and surface adsorption. These predictions allow calculation of the particle hygroscopicity and predictions of cloud droplet formation. We will present results for atmospheric scenarios and highlight needs for additional experimental work.

Immobilization of boron in groundwaters by combination of MgO with woodchips

KEIKO SASAKI¹, XINHONG QIU¹, HITOSHI TAKAMORI³, SAYO MORIYAMA⁴, KEIKO IDETA⁵ AND JIN MIYAWAKI⁶

¹Department of Earth Resources Engineering, Kyushu University, Japan: (keikos@mine.kyushu-u.ac.jp, q-q11@mine.kyushu-u.ac.jp)

³Asahi Kasei E-Materials Co. Ltd., Japan: takamori.hf@om.asahi-kasei.co.jp

⁴Fukuoka Institute of Health and Environmental Sciences, Japan: sayo.moriyama@yahoo.com

⁵Institute for Materials Chemistry and Engineering, Kyushu University, Japan: (keiko@cm.kyushu-u.ac.jp, miyawaki@cm.kyushu-u.ac.jp)

Boric acid is one of the most difficult species to immobilize in aqueous environments, because it predominantly exists as a molecular form. Boron specific resin is widely used and well known to immobilize with N-methyl-glucamate groups. However, it requires alkaline pHs and is unsuitable to apply to contaminant sites in a large scale like groundwaters. In the present work, permeable reactive barrier column tests were conducted to remove boron (B) in groundwaters in a laboratory scale for 11 months by using combination of MgO agglomerates with woodchips instead of boron specific resin. MgO agglomerates are one of engineering-assisted geomaterials for handling and main reactive materials here, while woodchips are natural and supplemental ones. ¹¹B-NMR and XRD results revealed that boron was mainly immobilized as ¹³B by co-precipitation with Mg(OH)₂ through destructive sorption of MgO and as ¹⁴B with woodchips through complexation which is in complementary mechanism and facilitated after alkalization by hydration of MgO. SEM images of solid residues MgO agglomerates after immobilization of B were quite different from without woodchips, suggesting that a variety of organic acids in leachate from woodchips affects to Mg²⁺ species as a precursor for Mg(OH)₂ precipitate. This affected also to increase the permeability because of avoiding the formation of bulky and needlelike-shaped precipitates of Mg(OH)₂. As a result, boron specific resin can be alternatively replaced with combination of engineering geomimetics with natural materials, which improved the efficiency to immobilize boron in groundwaters.

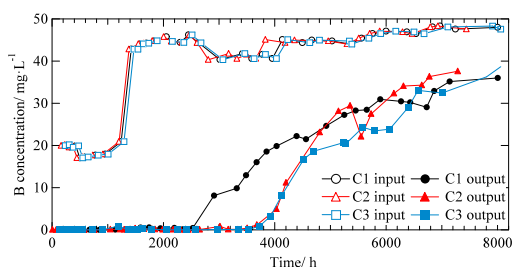


Fig. 1 Changes in B concentrations in input and output solutions with time. C1, MgO; C2, MgO + woodchips; C3, MgO + B specific resin

Investigation of ancient fluid migration in Ordovician carbonates in the Michigan Basin using secondary minerals

J.K. SASO¹, R. CALDAS², L. W. DIAMOND², A. PARMENTER³ AND T. A. AL^{1*}

¹Earth Sciences, University of New Brunswick, Canada (*correspondence: TAL@unb.ca)

²Institute of Geological Sciences, University of Bern, Switzerland (diamond@geo.unibe.ch)

³Nuclear Waste Management Organization, Canada (aparmenter@nwmco.ca)

Investigations of the Upper Ordovician Trenton and Black River group argillaceous limestones in southwest Ontario, Canada, indicate that secondary calcite, dolomite, celestite and anhydrite occur in fracture-filling veins, with dolomite also replacing primary calcite in the limestone. The objectives of this study were to define the paragenetic sequence, identify the source(s) of the fluids, and if possible, place time constraints on the formation of these minerals.

Petrographic studies were conducted by optical and scanning-electron microscopy (SEM). Analyses of $\delta^{18}\text{O}$ and $^{87}\text{Sr}/^{86}\text{Sr}$ were conducted by isotope-ratio and thermal ionization mass spectrometry, respectively. Measurements of $\delta^{18}\text{O}$ were also conducted by ion microprobe. Microthermometric data were collected from doubly-polished 150 μm thick sections.

The paragenetic sequence, from oldest to youngest, is replacement dolomite, vein dolomite, calcite in veins, and late-stage sulphate minerals. Mass-balance calculations indicate that replacement dolomite in the Trenton Group formed under closed conditions, while replacement dolomite in the Black River Group required an external source of Mg. Depth profiles of $\delta^{18}\text{O}$ and $^{87}\text{Sr}/^{86}\text{Sr}$ in vein carbonates suggest they formed as ^{18}O -depleted and $^{87}\text{Sr}/^{86}\text{Sr}$ -enriched fluid ascended from the underlying shield. The $^{87}\text{Sr}/^{86}\text{Sr}$ composition of late-stage sulphate minerals suggests they formed from sedimentary basin brine. Fluid-inclusion investigations of the calcite in veins indicate four fluid migration events with homogenization temperatures in the range of 40 to 90 $^{\circ}\text{C}$. These temperatures are consistent with predictions of temperature associated with peak burial during the Late Carboniferous.

Osmium isotope evidence for a large impact event in the Late Triassic

H. SATO^{1*}, T. ONOUE², T. NOZAKI³ AND K. SUZUKI³

¹Kyushu University, Fukuoka 812-8581, Japan

(*correspondence: 3SC12024G@s.kyushu-u.ac.jp)

²Kumamoto University, Kumamoto 860-0862, Japan

(onoue@sci.kumamoto-u.ac.jp)

³Japan Agency for Marine-Earth Science Technology

(JAMSTEC), Yokosuka 237-0061, Japan

(nozaki@jamstec.go.jp, katz@jamstec.go.jp)

Seawater ¹⁸⁷Os/¹⁸⁸Os ratios reflect contributions to the global ocean from riverine (¹⁸⁷Os/¹⁸⁸Os ≈ 1.4), and hydrothermal and extraterrestrial inputs (¹⁸⁷Os/¹⁸⁸Os ≈ 0.12 - 0.13). Given the distinctive ¹⁸⁷Os/¹⁸⁸Os ratios of these inputs and the relatively short residence time of Os in the ocean, seawater ¹⁸⁷Os/¹⁸⁸Os ratios are highly sensitive to change in these fluxes. Thus, Os isotope has been used to demonstrate the 65 Ma impact event at Chixhulub in Mexico [1, 2], based on an abrupt decline in seawater ¹⁸⁷Os/¹⁸⁸Os ratios during the Cretaceous/Paleogene (K-Pg) boundary.

We report the marine ¹⁸⁷Os/¹⁸⁸Os ratios of the middle Norian bedded chert and claystone succession in Japan to provide new evidence of an extraterrestrial input. These bedded cherts are considered to be deep-sea sediments that accumulated in a pelagic, open ocean setting within the Upper Triassic paleo-Pacific Ocean (Panthalassa).

The initial ¹⁸⁷Os/¹⁸⁸Os ratios exhibit an abrupt and marked negative excursion from 0.477 to unradiogenic values of 0.127 in a claystone layer. The Os concentration of this claystone layer is ca. 3 ppb which is three orders of magnitude higher than those of chert layers. Moreover, a plenty amounts of spherule and Ni-rich spinel granules and extraordinary PGE-enrichment was reported from the claystone [3]. The amplitude of this negative Os isotope excursion is comparable to those of the late Eocene (0.5 to 0.28) [4] and the K-Pg boundary (0.4 to 0.157) [1]. These geochemical lines of evidence strongly suggest that a large, kilometer-sized impactor is requisite to explain high Os concentration and unradiogenic ¹⁸⁷Os/¹⁸⁸Os ratios of the Upper Triassic claystone layer.

[1] Ravizza & Peucker-Ehrenbrink (2003) *Science* **302**, 1392-1395. [2] Luck & Turekian (1983) *Science* **222**, 613-615. [3] Onoue *et al.* (2012) *Proc. Natl. Acad. Sci. USA* **109**, 19134-19139. [4] Paquay *et al.* (2008) *Science* **320**, 214-218.

Let's use metastable geomaterials in environmental protection: An intelligent geotechnology learnt from natural processes

T. SATO^{1*} AND K. FUKUSHI²

¹Faculty of Engineering, Hokkaido Univ., Kita 13 Nishi 8, Kita-Ku, Sapporo 060-8628 Japan

²Institute of Nature and Environmental Technology,

Kanazawa Univ., Kakuma, Kanazawa 920-1192 Japan

*Correspondence: tomsato@eng.hokudai.ac.jp

In order to ensure sustainable development, engineering technologies used in environmental protection (e.g. purification, remediation) must utilize safe, cost-effective and environmentally efficient materials. As such, the use of ubiquitous geomaterials, rather than synthetic materials, is envisioned. The use of geomaterials for environmental applications, referred to as "geotechnology", is based on principles learnt from natural processes. Therefore, naturally occurring physical, chemical and biological processes can serve as useful analogs in designing cost-effective and intelligent geotechnologies to address environmental problems.

Geomaterials such as clays, carbonates and iron minerals, which are generally stable under Earth surface conditions, have been used widely for environmental applications. This is due to their cost-effectiveness and stability over a range of conditions. However, metastable materials widely observed in nature have been found to be more environmentally efficient due to their higher reactive surface areas and reactivity to hazardous contaminants compared to more stable materials. For example, iron oxides such as hematite, goethite, ferrihydrite and schwertmannite are seen as important naturally occurring sorbents of arsenate and phosphate. However, poorly crystalline and metastable ferrihydrite and schwertmannite exhibit higher capacities for arsenate and phosphate adsorption compared to crystalline goethite and hematite. Similarly, metastable aragonite and monohydrocalcite show better anion adsorption capabilities compared to calcite. Recently, it has been found that the stability of these materials can be modified by the adsorption of certain ions. Therefore, the long-term stability and efficient performance of metastable materials can be controlled in order to maximize their effectiveness. In this presentation, intelligent geotechnologies learnt from natural processes using metastable geomaterials will be introduced, with natural iron oxides and calcium carbonates as examples.

Analcime alteration of montmorillonite: Growth rates

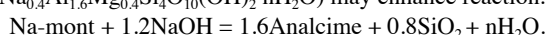
HISAO SATOH^{1,2}, KATSUO TSUKAMOTO², HITOSHI OWADA³ AND TOMOKO ISHII³

¹Mitsubishi Materials Co., Naka 311-0102, Japan

²Tohoku University, Sendai 980-8578, Japan

³RWMC, Tsukishima, 104-0052, Japan

Analcime is very common zeolite as a low-temperature secondary mineral of alkaline alteration. Growth of analcime was previously studied on precursor Na-clinoptilolite^[1] and leucite^[2]. Such an alkaline alteration is predicted in the bentonite barrier of radioactive waste repository by cement-leachates in groundwater^[3]. Chemical similarity between analcime ($\text{NaAlSi}_2\text{O}_6 \cdot \text{H}_2\text{O}$) and montmorillonite ($\text{Na}_{0.4}\text{Al}_{1.6}\text{Mg}_{0.4}\text{Si}_{14}\text{O}_{10}(\text{OH})_2 \cdot n\text{H}_2\text{O}$) may enhance reaction:



We investigated growth kinetics of analcime to evaluate the behavior of bentonite barrier under hyperalkaline condition.

Direct measurements of analcime growth rate on substrate, analcime at 90-120 °C were conducted using in-situ phase-shift interferometer (PSI)^[4]. Supersaturation with respect to analcime was controlled by dissolution of coexisting montmorillonite in the cell with flow of 0.3 M NaOH solution.

The dissolution and growth rates of analcime near equilibrium were observed to be -3.6×10^{-3} and 2.7×10^{-3} nm/s, at ΔG of -11.29 and 8.80 kJ/mol respectively (Fig. 1). Our results agree with previous data^[1], which roughly draws a growth rate curve. We conclude that the key of analcime growth is porewater chemistry in montmorillonite. The dissolution of montmorillonite can be affected by porosity (density)^[5]. Our results can extend the observed alteration towards a mechanistic model involving porosity change.

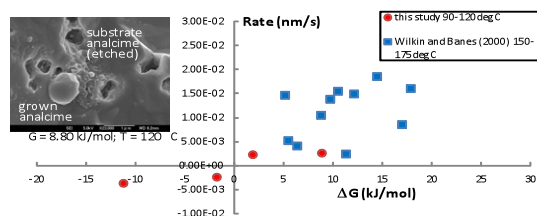


Figure 1: Growth rate curve of analcime and a surface after run showing etch pits and grown grains (FESEM).

[1] Wilkin & Barnes (2000) *Am. Min.* **85**, 1329-1341. [2] Putnis *et al.* (2007) *Am. Min.* **92**, 19-26. [3] Nakayama *et al.* (2004) *Appl. Clay. Sci.* **27**, 53-65. [4] Satoh *et al.* (2007) *Am. Min.* **92**, 503-509. [5] Satoh *et al.* (2013) *Clay Min.* (in press). This research is a part of "Development of the technique for the evaluation of long-term performance of EBS (FY2007-2012)" funded by the ANRE, the METI of Japan.

Heterogeneity of the uppermost mantle in back-arc settings: Insights from trace-element compositions and water contents in Japanese peridotite xenoliths

TAKAKO SATSUKAWA¹, MARGUERITE GODARD², SYLVIE DEMOUCHEY² AND KATSUYOSHI MICHIBAYASHI³

¹ARC Center of Excellence for Core to Crust Fluid Systems (CCFS) and GEMOC National Key Center, Earth and Planetary Sciences, Macquari University, Sydney, NSW 2109, Australia

²Géosciences Montpellier, Université Montpellier 2 and CNRS, Cc 060, Place E. Bataillon, 34095 Montpellier cedex 5, France

³Institute of Geosciences, Shizuoka University, Ohya 836, Shizuoka 422-8529, Japan

The uppermost mantle in the back-arc region of a subduction zone is the site of complex interactions between partial melting and fluid migration. To constrain these interactions and reveal the heterogeneity of the uppermost mantle in back-arc setting, we measured geochemical compositions and water contents of spinel peridotite xenoliths obtained from two back-arc volcanoes; Ichinomegata (NE Japan) and Oki-Dogo (SW Japan). The mineral chemistry of Ichinomegata peridotites shows a typical residual peridotite trend, depleted in light rare earth elements (LREE). Some samples of Oki-Dogo peridotites have lower Mg# in olivine (down to 0.88) and are enriched in LREE, indicating that these are affected by melt-rock interactions. Olivine has low water contents in samples from both Ichinomegata and Oki-Dogo. However, the water contents in pyroxenes in Ichinomegata peridotites are significantly higher than in Oki-Dogo. These differences might be due to the different mobility of water during fluid metasomatism versus melt-rock interaction. The water contents of the pyroxenes suggest interactions with water-rich fluids. Hydration incorporation in Ichinomegata peridotite is proposed to be associated with a water-rich metasomatism, which lead to depleted REE patterns in clinopyroxene, and the REE patterns of orthopyroxene are more depleted than for Oki-Dogo samples. However, the chemical composition of Oki-Dogo peridotites shows that they have experienced melt-rock interactions that have lead to the characteristic flat REE pattern of the clinopyroxene. Furthermore, these variations in chemical characteristics between Ichinomegata and Oki-Dogo might be induced by the changes in the subduction system in the Japan Island arc, such as the age and angle of the subducting slab.

Salt Lakes of Western Australia – Emissions of natural volatile organic compounds

T. SATTLER¹, T. KRAUSE¹, H. F. SCHÖLER¹, K. KAMILLI²,
A. HELD², C. ZETZSCH², J. OFNER³, W. JUNKERMANN⁴
AND E. ATLAS⁵

¹Inst. of Earth Science, University of Heidelberg, Germany;

²Bayreuth Centre of Ecology and Environmental Research,
University of Bayreuth, Germany;

³Vienna University of Technology, Austria;

⁴Inst. for Meteorology and Climate Research, Karlsruhe Inst.
of Technology, Garmisch-Partenkirchen, Germany

⁵Rosenstiel School of Marine and Atmos. Sci., Miami, USA

Western Australia is a semi-/arid region that is heavily influenced by global climate change and agricultural land use. The area is known for its many saline lakes with a wide range of hydrogeochemical parameters. This area has been repeatedly investigated since 2006 and consists of ephemeral saline and saline groundwater sourced lakes with a pH reaching from 2.5 to 7.1. The semi-/arid region was originally covered by natural eucalyptus forests, but land-use has changed considerably after large scale deforestation from 1950 to 1970. Today the region is mostly used for growing wheat and live stock. The deforestation led to a rising groundwater table, bringing dissolved salts and minerals to the surface.

In the last decades, a concurrent alteration of rain periods has been observed. A reason could be the regional formation of ultra-fine particles that were measured with car-based and airborne instruments around the salt lakes in several campaigns between 2006 and 2011. These ultra-fine particles emitted from the lakes and acting as cloud condensation nuclei can modify cloud microphysics and thus suppress rain events [1]. New data from a campaign in 2012 accentuates the importance of these hyper saline environments for the local climate.

Ground-based particle measurements around the salt lakes in 2012 were accompanied by novel chamber experiments directly on the lakes. The 1.5 m³ cubic chamber was constructed from transparent PTFE foil permitting photochemistry within while preventing dilution of the air due to lateral wind transport. This experimental setup allows linking the measured data directly to the chemistry of and above the salt lakes. Another advantage of the PTFE chamber is the enrichment of volatile organic compounds (VOC) that are emitted from salt lakes as possible precursors for the ultra-fine particles.

Chamber air was sampled using stainless steel canisters. Sediment, crust and water samples were taken for investigation of potential VOC emissions in the laboratory using GC-MS technique.

Different VOC and halogenated volatile compounds (VOX), exceeding atmospheric background concentrations, were identified from the sampled chamber air. Their enrichment or depletion over the time in the chamber allows for postulated reaction pathways leading to the formation of ultra-fine particles.

Geochemical and acoustic investigations of hydrocarbon seepage on the continental shelf off northern Norway

S. SAUER^{1*}, J. KNIES¹, C. SCHUBERT², A. LEPLAND¹
AND S. CHAND¹

¹Geological Survey of Norway, Trondheim, Norway

(*correspondence: simone.sauer@ngu.no)

²Swiss Federal Institute of Aquatic Science and Technology (EAWAG), Kastanienbaum, Switzerland

Active natural hydrocarbon seepage in the Hola area along the continental shelf off northern Norway has recently been found by Chand *et al.* 2008 [1]. We conducted acoustic and geochemical investigations to gain a better understanding of the extent and history of this gas seepage. Seismics and water column acoustic data were used to reveal potential hydrocarbon pathways to the seafloor and to locate active gas seepage. Methane concentrations are determined in the water column and in sediment pore waters and geomicrobiological analyses of the sediments from the seepage sites are used to assess microbial processes involved in the methane cycle.

We use sulfate and methane sediment pore water profiles to estimate the anaerobic oxidation of methane and stable isotopic analyses of methane are applied to identify biogenic or thermogenic methane sources. Concentration profiles of dissolved iron, ammonium and phosphate provide information on biogeochemical activity in the sediments.

The results of the geochemical investigations of seawater and sediment pore waters will ultimately be combined with the investigation of methane-derived carbonate crusts whose presence has recently been documented in the Hola area with an AUV based on photo and synthetic aperture sonar images. U-Th dating of these carbonate crusts will provide insights into past methane release and possible links with climate variations.

[1] Chand, S., Rise, L., Bellec, V., Dolan, M., Bøe, R., Thorsnes, T., Buhl-Mortensen, P., 2008. Active Venting System Offshore Northern Norway. *Eos, Transactions American Geophysical Union* 89, 261-262.

Mobility of Au in the mantle

*J. EDWARD SAUNDERS¹, N. J. PEARSON¹, SUZANNE Y. O'REILLY¹, W. L. GRIFFIN¹

¹ARC Centre of Excellence for Core to Crust Fluid Systems (CCFS) and GEMOC, Macquarie University, NSW, 2109, Australia, (*Correspondence: james.saunders@mq.edu.au)

Sulfides are the main host for Au in the silicate earth [1,2], but there are few reliable analyses of Au in mantle sulfides. As both a chalcophile and a highly siderophile element, Au is an important tracer of differentiation/ metasomatism in the mantle. Sulfides melt incongruently in the mantle, and are mobile in a range of melts and fluids; thus this component is readily modified during mantle processes. *In-situ* analyses are important for unravelling these processes, because multiple generations of sulfides are commonly present in mantle xenoliths [2, 3, 4].

We have analysed Au in sulfides hosted in peridotite xenoliths from eastern Australia, southeastern China and Spitsbergen (Arctic Norway). These data have been used to assess the average abundance of Au in mantle sulfides, and investigate how mantle processes affect their Au content. The variety of metasomatic characteristics, in terms of style and strength of metasomatism, in the three sample sets makes it ideal for understanding how Au behaves in the mantle.

The Au content in sulfides in mantle peridotites across all datasets is 1.3 ± 4.1 ppm. This is similar to the limited data in the literature (global average Au = 1.5 ± 4 ppm). Both this study, and the data in the literature indicate that sulfides in the continental lithospheric mantle contain less Au than would be calculated using whole-rock PUM values (~ 2.5 ppm). The pyroxenites studied have even lower Au contents (average Au = 0.08 ± 0.10 ppm). This difference has important implications for the ability of mantle melts to transport Au, and as metasomatic agents.

While globally, mantle sulfides hosted in peridotites have a similar average and range of Au concentrations, there are important differences at local scales. This study shows the relationship between mantle metasomatism, as defined by silicate chemistry, and Au concentration in mantle sulfides. A significant amount of metasomatic sulfides can be introduced associated with the modification of the silicates, and these typically have a reduced Au content, similar to the low concentration observed in the pyroxenite melts analysed.

[1] Mitchell & Keays (1981) *GCA* **45**, 2425-2442. [2] Alard *et al.*, (2000) *Nature* **407**, 891-894 [3] Alard *et al.*, (2002) *EPSL* **203**, 651 – 663. [4] Griffin *et al.*, (2012) *Lithos*, **149**, 115- 135.

Radiolysis and life in deep subseafloor sediment of the South Pacific Gyre

J. SAUVAGE¹, A.J. SPIVACK¹, A. G. DUNLEA², R.W. MURRAY², R. POCKALNY¹, S. D'HONDT¹
AND IODP EXPEDITION 329 SHIPBOARD SCIENTIFIC PARTY

¹Graduate School of Oceanography, University of Rhode Island, Narragansett, RI 02882, USA
(*correspondence :justine_sauvage@my.uri.edu)

²Department of Earth and Environment, Boston University, Boston, MA 02215, USA.

The nature of the energy yielding mechanisms in the low-energy organic-poor sedimentary environment underlying the South Pacific Gyre (SPG) is not fully constrained. We used the approach of Wang *et al.* (2008) to quantify rates of organic-fuelled metabolic activities at most IODP Expedition 329 Sites (U1365 through U1370). At Site U1366 and U1370 net rates of oxygen-reducing organic oxidation averaged 1.77×10^{-2} and 1.64×10^{-3} fmol O₂ cell⁻¹ yr⁻¹, respectively, representing a tremendously low cellular metabolism. At Site U1370, we observe net oxygen reduction throughout the entire sediment column. At Site U1366, statistically significant net oxygen reduction is not detected at depths greater than 11 meters below seafloor. Despite these low rates of organic oxidation, most cell counts are above the minimum detection limit throughout the entire sequence at both sites.

Hydrogen from natural radioactive splitting of water has been hypothesized to be a significant electron donor in organic-poor sediment of the SPG. Because water radiolysis produces H₂ and $\frac{1}{2}$ O₂ simultaneously, oxidation of this H₂ does not contribute to net O₂ reduction in the sediment. Our calculation of radiolytic H₂ production, based on radioactive element content and sediment physical properties, indicate that on average 5.63×10^{-1} and 9.79×10^{-2} fmol H₂ yr⁻¹ cell⁻¹ is available throughout the sequence at Sites U1366 and U1370, respectively. Despite these relatively high production rates, dissolved H₂ abundances are below detection at both sites. These results suggest that H₂ from in situ water radiolysis fuels the predominant energy-yielding pathway for microbes in SPG sediment.

O, Si, Fe isotopes and Ge/Si constraints on the preservation of signatures inherited from the formation of Isua BIFs

LUDIVINE SAUVAGE^{1*}, MARC CHAUSSIDON¹,
BÉATRICE LUIS¹ AND CLAIRE ROLLION-BARD¹

¹CRPG UMR 7358 CNRS-Univ. Lorraine, BP 20, 54501
Vandoeuvre-lès-Nancy, France (*lsauvage@crpg.cnrs-
nancy.fr)

A 5.7 cm long sample, made of 9 alternating magnetite-rich and quartz-rich layers, of the oldest known example of archaean BIF (3.7-3.8 old Isua sample IF-G) was studied by ion microprobe for its O, Si and Fe isotopic compositions, and by laser ICP-MS for its trace element concentrations (Ge/Si ratios). Isotopic profiles across the layers were obtained with a resolution of 50-100 μ m (spot size 25 μ m) to look for systematic isotopic variations (total of 580 $\delta^{18}\text{O}$ data in quartz and magnetite, 441 $\delta^{30}\text{Si}$ in quartz and 641 $\delta^{56}\text{Fe}$ in magnetite). Ge contents in quartz were measured in parallel with a spot size of \sim 120 μ m.

$\delta^{56}\text{Fe}$ values range from -0.1 to +2.4‰ and are quite homogeneous (\pm 0.8‰, 2σ) within a given magnetite layer, with no significant differences between two successive layers, in agreement with previously published values [1, 2, 3]. Up to 3‰ variations in $\delta^{18}\text{O}$ values are present in the magnetite and quartz layers (except one showing larger variations) with an average \sim 8‰ difference in $\delta^{18}\text{O}$ between quartz (either in the quartz layers or in the magnetite layers) and magnetite, in agreement with isotopic equilibration under amphibolite facies metamorphism. In contrast to $\delta^{18}\text{O}$ and $\delta^{56}\text{Fe}$ values, $\delta^{30}\text{Si}$ values show systematic "stratigraphic" isotopic variations (from -3.5 to 0‰) with significant differences between quartz in the quartz-rich and the magnetite-rich layers. Ge/Si ratios vary from 0.6 to 1.2×10^{-5} mole/mole (i.e., 7-14 ppm Ge). There are significantly lower than published data on bulk quartz layers from a Isua sample (Ge/Si $> 2 \times 10^{-5}$ mole/mole [4]) due to the occurrence of Ge-rich amphiboles. Ge/Si variations seem to follow those of $\delta^{30}\text{Si}$. Because quartz is resistant to Si isotopic exchanges, $\delta^{30}\text{Si}$ are likely to reflect variations in the conditions of formation and diagenesis of the Isua BIFs. Ge/Si ratios could trace temperature fluctuations and parent fluids of different origin.

[1] Dauphas, N. et al. (2007) *Geochim. et Cosmochim. Acta* **71**, 4745-4770. [2] Whitehouse M.J. and Fedo C.M. (2007) *Geology* **35**, 719-722. [3] Czaja, A.D. et al. (2013) *Earth Planet. Sci. Lett.* **363**, 192-203. [4] Frei R. & Polat A. (2007) *Earth Planet. Sci. Lett.* **253**, 266-281.

How kimberlites form: Clues from olivine geochemistry

L. SAUZEAT¹, C. CORDIER¹ AND N.T. ARNDT^{1*}

¹ISTerre, Université de Grenoble, France (*correspondence:
Nicholas.Arndt@ujf-grenoble.fr)

The formation of olivine in kimberlites is not well understood. In most kimberlites, olivine occurs as large rounded single or polycrystalline nodules (1-10mm) and as small single crystals in the matrix. It is widely accepted that majority of them are xenocrysts produced by reaction and elimination of minerals from mantle peridotite either within kimberlite melts in transit toward the surface or within the mantle before. The compositions of the cores of olivines in polycrystalline nodules range widely, from about Fo92 to Fo83, whereas the rims have more restricted compositions, usually about Fo88.

In this study, we focus on very well preserved kimberlites from Kangamiut in Greenland. We conducted petrological studies and microprobe analyses along several profiles in one unusual polycrystalline nodule. This nodule is an assemblage of small closely packed fragments, most with the uniform composition Fo92, but some fragments have rims with lower Fo contents. Our results show that the fragment rims are complex and comprise an internal zone with variable forsterite contents (Fo88 to Fo92) but roughly constant minor element contents (e.g. 0.07 wt.% CaO and 0.35 wt.% NiO), and an external zone with near-constant Fo (Fo88) but variable minor element concentrations (0.09-0.41 wt.% CaO and 0.19-0.29% wt. NiO). This external zone is similar to the thin rim surrounding all the polycrystalline nodule. We attribute these compositions to two major processes. The first, which is responsible for the internal zone, occurred before the incorporation of the nodule in the kimberlitic magma and is related to "defertilisation" of peridotite in the lithosphere; i.e. reaction with CO₂-rich fluids that removed pyroxene and garnet to produce a dunitic lithology. The second, which is responsible for the external zone, resulted from crystallization of olivine from the kimberlitic magma.

Agés and deformation of felsic dikes within granulites and gneisses of the Gruf Complex, Central Alps.

J. SAVAGE¹, A. MÖLLER¹, J. OALMANN¹
AND R. BOUSQUET²

¹Department of Geology, University of Kansas, USA,
jsav1013@ku.edu, amoller@ku.edu, joalmann@ku.edu
²Institute of Geosciences, Christian-Albrechts-Universität zu
Kiel, Germany, bousquet@min.uni-kiel.de

Magmatic leucosomes and dikes in metamorphic terranes provide an opportunity to correlate accessory phase crystallization ages with the timing of deformation and metamorphic events as well as larger scale magmatic intrusions.

The Gruf Complex consists of migmatitic gneisses plus scarce charnockites and UHT sapphirine granulites. We identified several mineralogically distinct types of leucosomes and dikes: 1) foliation-defining, biotite-bearing leucosomes that are commonly folded; 2) medium-grained hornblende- and/or biotite-bearing granite pods crosscutting these leucosomes; 3) biotite-bearing pegmatite dikes, boudinaged or crosscutting the main foliation; 4) pegmatitic muscovite-, garnet-, beryll-bearing dikes, crosscutting all other rock types. Field observations indicate changing melt composition during and after regional metamorphism and associated deformation. Zircons from these dikes were dated by LA-ICP-MS to constrain deformation and metamorphism.

All analyzed samples contain oscillatory-zoned zircons with ages of 250–300 Ma. A leucosome within a brecciated metaperidotite enclave contains equant, sector-zoned 32.2 ± 0.2 Ma zircons. Most dike sample zircons have rims of 28–30 Ma. An undeformed muscovite-bearing pegmatite dike crystallized at 25.6 ± 0.3 Ma. Another muscovite-bearing pegmatite dike lacks zircon domains <28 Ma, probably due to insufficient Zr in the melt.

Apparent zircon saturation temperatures (T_{Zrs}) for dike and leucosome samples are 680–890°C and uncorrelated with age. We attribute the wide T_{Zrs} -range to inherited zircon that did not dissolve in the melt. The pegmatite without <28 Ma zircon has a T_{Zrs} of 730°C suggesting its parental magma formed by partial melting of material similar to the deformed dikes, but did not exceed 730°C.

Conclusions: partial melting in the migmatites is coeval with the 30–32 Ma Bergell intrusion and main deformation. Dike emplacement and deformation continued until c. 24 Ma, coinciding with intrusion of the Novate granite and cooling of the granulites below the T_c of rutile at c. 500°C. The presence of 32 Ma zircons in all dikes indicates remelting of older leucosomes and dikes as the mechanism to produce the more fractionated pegmatites.

The copper isotope composition of bulk Earth: A new paradox?

PAUL S. SAVAGE^{1*}, HENG CHEN¹, GREGORY SHOFNER²,
JAMES BADRO² AND FRÉDÉRIC MOYNIER¹

¹Washington University in St. Louis, MO 63130, USA
(*correspondence: savage@levee.wustl.edu,
chenheng@levee.wustl.edu, moynier@levee.wustl.edu)
²IPGP, Paris, France (gshofner@gmail.com, badro@ipdp.fr)

It is estimated that two thirds of terrestrial Cu is held in the core [1]; hence, to constrain the bulk Earth Cu isotope composition, $\delta^{65}\text{Cu}$ estimates for both mantle (BSE) and core are required. By analysing a representative suite ($n \sim 50$) of basaltic samples and their differentiates, we have investigated the behaviour of Cu isotopes during mantle melting and magmatic differentiation, and established a robust $\delta^{65}\text{Cu}$ value for BSE. Our results show that, during fractional crystallisation, Cu isotopes can be fractionated to both lighter and heavier compositions, depending on crystallising phase. However, during partial melting, there is no resolvable fractionation. This implies that primitive basaltic melts are a good proxy for the Cu isotope composition of the mantle. Such analyses give an average $\delta^{65}\text{Cu}_{\text{BSE}}$ value of 0.07 ± 0.12 ‰ (2sd; relative to the standard NIST 976).

To estimate the Cu isotope composition of the Earth's core, we performed a series of piston-cylinder experiments to determine the $\text{Cu}_{\text{metal/silicate}}$ isotope fractionation factor. These show that metal is preferentially enriched in the heavier Cu isotope, which agrees with empirical data from silicate-bearing iron meteorites [2]. Using these data to estimate a $\delta^{65}\text{Cu}_{\text{CORE}}$ value, we calculate the Cu isotope composition of bulk Earth to be $\delta^{65}\text{Cu}_{\text{BE}} \approx 0.16$ ‰. The “paradox” is as such: bulk Earth has a heavier Cu isotope composition than most (if not all) of the thus-far analysed chondritic meteorite groups [3, 4].

Assuming chondrites = bulk Earth, to explain this “missing ^{63}Cu ”, we tentatively propose two possibilities:

- 1) Isotopically light Cu entered the Earth's core as a sulphide phase, or is stored in a thus-far unsampled part of the mantle, again in sulphides.
- 2) The light Cu isotope was preferentially lost as a result of volatile processes during Earth's accretion.

Alternatively, the current $\delta^{65}\text{Cu}$ chondrite dataset does not represent bulk Earth, and further analyses are required.

[1] McDonough, *ToG*, 2003; [2] Williams and Archer, *GCA* **75**, 2011; [3] Luck *et al.*, *GCA* **67**, 2003 [4] Barrat *et al.*, *GCA* **83**, 2012.

Nitrate and its N and O isotopes in a tropical marine boundary layer

J. SAVARINO¹* S. MORIN², J. ERBLAND¹, M. D. PATEY³,
W. VICARS¹, B. ALEXANDER⁴ AND E. P. ACHTERBERG³

¹LGGE/CNRS/UJF, BP 96, 38402 St Martin d'Hères, France
(*correspondance joel.savarino@ujf-grenoble.fr)

²CEN/Météo-France/CNRS, 38402 St Martin d'Hères, France
(samuel.morin@meteo.fr)

³School of Ocean and Earth Science, University of
Southampton, Southampton SO14 3ZH, UK
(eric@noc.soton.ac.uk)

⁴Dept. of Atmospheric Sciences, University of Washington,
Seattle, WA 98195-1640, USA (beckya@uw.edu)

Isotopic investigations are instrumental in deciphering sources and processes affecting atmospheric nitrate. Combining the analysis of the ¹⁷O-excess ($\Delta^{17}\text{O} = \delta^{17}\text{O} - 0.52 \delta^{18}\text{O}$) with the nitrogen stable isotope ratio (¹⁵N/¹⁴N) on the same sample is a powerful tool to reveal unexpected processes happening in the air [1].

Despite recent successes in using the isotope composition of nitrate for deciphering atmospheric chemical processes in polar and mid latitude regions [2, 3], the strong oxidative atmosphere of the sub tropical and tropical regions has been largely forgotten [4]. In order to partially fill this gap, we present a full seasonal cycle of the nitrate isotope systematic at the Cap Verde (Lat 16° 85'N, Long. 24° 87' W, Alt. 20m), characteristic of a tropical marine boundary layer (MBL).

While the concentration of nitrate at this MBL do not show any season variations, the oxygen isotopic characteristics display a pronounced seasonal cycle that is compatible with nitrate formation chemistry, which includes the BrNO₃ sink at a level of ca. 20 ± 10% of nitrate formation pathways. The results also suggest that the N₂O₅ pathway is a negligible NO_x sink in this environment. Observations further indicate a possible link between the NO₂/NO_x ratio and the nitrogen isotopic content of nitrate in this low NO_x environment, possibly reflecting the seasonal change in the photochemical equilibrium among NO_x species.

[1] Thiemens, M. H. (2006) *Annual Review of Earth and Planetary Sciences*, **34**, 217-262. [2] Morin, S. *et al. Science*, **322**, 730-732, doi: 10.1126/science.1161910. Michalski, G. *et al. (2003) Geophys Res Lett*, **30**, 1870, doi: 10.1029/2003gl017015. [4] Alexander, *et al. (2009), Atmos Chem Phys*, **9**, 5043-5056, doi: 10.5194/acp-9-5043-2009.

Experimental modeling of silicates phosphatization in the hypergenesis zone

A.V. SAVENKO

Moscow M.V. Lomonosov State University, 119991, Moscow,
Russia (correspondence: Alla_Savenko@rambler.ru)

Now there was a concept that immobilization of dissolved phosphates on silicate minerals in the hypergenesis zone occurs on the mechanism of superficial adsorption. At the same time it is possible to assume that alongside with it process of silicates phosphatization similar to widespread process of silicates carbonatization proceeds. This hypothesis was verified during the longtime experiments.

The phosphatization of two basic clay minerals (kaolin and montmorillonite) was studied after two-year long interaction with 0.25–5.0 mM orthophosphate solutions under acidity conditions ranged pH 1.8–8.8. The results have shown (figure) that variation of dissolved phosphorus and silicon concentrations at pH 3.7–8.8 is close to equivalent: $\Delta[\text{Si}] \approx -\Delta[\text{P}]$ whereas $\Delta[\text{Si}]$ value at pH 1.8 is in 1.5–2 times exceeds decrease in phosphates concentration. Quantity of phosphorus immobilized by clay minerals is in direct proportion of its equilibrium concentration in the solution: $-\Delta[\text{P}] = k[\text{P}]_{\text{eq}}$. The proportionality factor k is identical to all studied samples and decreases from 0.58 till 0.44 at the pH increase with 1.8 up to 8.8. Quantity of silicon passing in the dissolved forms reaches 6–20% of total amount of silica in the solid phase. It specifies phosphatization of clay minerals which products are dissolved silica and poorly soluble basic aluminium phosphates.

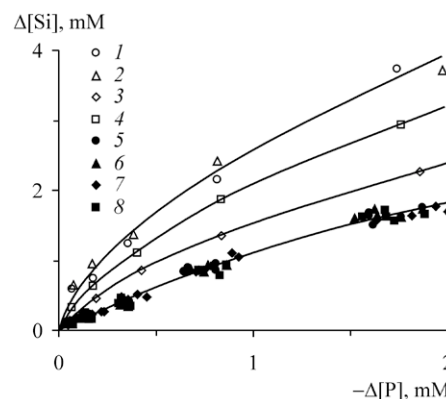


Figure: Relationship between variation of dissolved phosphorus and silicon concentrations at the clay minerals phosphatization. pH 1.8/3.7–8.8: 1/5 – kaolin, Glukhoveck; 2/6 – ditto, Podolsk; 3/7 – montmorillonite, Askanija, sample 1; 4/8 – ditto, sample 2.

Multi-proxy investigation of Holocene climate in West Siberia using peat deposits

YU. V. SAVINYKH,¹ N. PEDENTCHOUK,² YU.I. PREIS³ AND E.V.GULAYA¹

¹Institute of Petroleum Chemistry SB RAS, Tomsk, Russia, yu-sav2007@yandex.ru

²School of Env. Sciences, University of East Anglia, Norwich, UK

³Institute of Monitoring of Climatic and Ecological Systems SB RAS, Tomsk, Russia

West Siberia is a vast region that covers a large part of northern Asia and, in spite of its size, is relatively homogenous in terms of topography and climate. It is an ideal target for studying palaeoclimate, because even a relatively limited number of sites would provide representative data for investigating climate changes that affect large areas of this region. This project uses a multi-proxy approach to study Holocene climate change in West Siberia.

A peat core was obtained from an ombrotrophic bog located in the vicinity of Tomsk. Bog vegetation is dominated by peat moss, but also comprises a substantial number of vascular plant species. The base of the 6.5-m-long core was dated at 10,500 cal yr BP. Organic matter was subjected to palynological, biomarker, and stable isotopic analyses.

Our preliminary testate amoebae (analyst I.V.Kurina) and *n*-C₂₃ alkane (sourced mainly by *Sphagnum* spp.) δ D in the upper 260 cm of the core show the following patterns. The percentage of hydrophilic testate amoebae starts to increase from the background level at 140-135 cm, reaches its peak at 125-115 cm, drops to a minimum at 85-65 cm, and then undergoes an increase towards the top of the core. The δ D values of *n*-C₂₃ decrease from -170‰ at c. 200 cm to -225‰ at 105-100 cm, change sharply to -210‰ at 95-85 cm and then reach -190‰ at the top. Because more negative δ D values of *Sphagnum* spp. could indicate colder or wetter (or a combination of both) climate, we suggest that these two data sets point to a period of wetter climate during the time interval recorded by the peat sequence between 140 and 100 cm. The integration of our data with palynology from previously published reconstructions of West Siberian climate from 500 and 1700 cal yr BP, corresponding to c. 150-50 cm of our core, suggests a period of cold and wet climate. Our ongoing work on biomarker and stable isotopic compositions of various sources of organic matter in this core will allow us to provide more detail with regards to palaeoclimatic changes during this and earlier time intervals in the Holocene.

Boron isotopes in boninites from the Izu-Bonin-Mariana arc system: Insights into subduction initiation

IVAN P. SAVOV¹ AND SAMUELE AGOSTINI²

¹Univ. Leeds, School of Earth & Environment, Leeds LS2-9JT, UK; i.savov@leeds.ac.uk; ²Istituto di Geoscienze

e Georisorse- CNR, Pisa, Italy s.agostini@igg.cnr.it

The origin of boninites has long been debated and several mechanisms for their formation have been proposed [1]. These rocks have both high MgO contents and somewhat LREE+LILE enrichments, thus their genesis should involve large percentage melting of highly melt-depleted but also highly fluid metasomatized mantle sources. One mechanism to explain boninite generation in the Izu-Bonin-Marianas (IBM) arc-basin system invokes sinking of cold Pacific oceanic slabs, trench retreat and intense backarc spreading [1]- all resulting in anomalous mantle melting conditions and voluminous boninite eruptions close in time and space to the oldest mafic volcanic arc rocks in IBM at ~ 51 Ma [2]. Since the mantle is extremely depleted in B and has very negative $\delta^{11}\text{B}$ ratios and the slab fluids have very positive $\delta^{11}\text{B}$ signatures, B and B isotope ratios are able to trace the slab-fluid additions and the resulting boninite generation. We have selected a suite of representative boninites from the the Izu-Bonin (Bonin Ridge) and the Marianas (Guam Island) segments of the IBM. The boninites all have remarkably similar $^{87}\text{Sr}/^{86}\text{Sr}$ (0.7042-0.7049) and $^{143}\text{Nd}/^{144}\text{Nd}$ (0.51283-0.51297) isotope signatures. Interestingly the boninites $\delta^{11}\text{B}$ ranges from +0.9 to +5.1 permil (data always better than ± 1 per mil), supporting models for early slab fluid liberation via dehydration of old foundering Pacific slabs. Such fluid additions are necessary for lowering the melting temperature of the depleted mantle wedge and for boninite generation. Based on the isotope (B, Nd, Sr) and trace element similarities we envision the boninite sources to be chemically similar to blueschist-containing serpentinite muds and serpentinitized peridotites erupted today via mud volcanoes in the IBM forearc and successfully drilled during ODP Legs 195 and 125 [3]. Links between high Mg arc volcanic rocks and serpentinite-derived fluids are becoming increasingly common [4] and we will discuss possible links between metamorphic petrology of the slab inventory, island arc magma generation and the usefulness of B isotopes as tracer.

[1] Leng & Gurnis (2011), *Geochem. Geophys. Geosyst.*,12,Q12018; [3] Ishizuka *et al.* (2011), *EPSL* 306; [3] Savov *et al.* (2007), *JGR-Solid Earth* 112, B09205 [4] Tonarini *et al.* (2007), *Geochem. Geophys. Geosyst.*,8, Q09014.

Stable C and O isotope ranges of African land snail shells

Y. SAWADA^{1*}, D. L. DETTMAN² AND M. PICKFORD³

¹Shimane Univ. 402-1 Fukushima, Kurashiki 710-0048, Japan
(*correspondence: yoshipikotan4306@sky.megaegg.ne.jp)

²Environ. Isotope Lab. Dept. Geosciences, Univ. Arizona,
Tucson, AZ85721 (dettman@email.arizona.edu)

³Muséum National d'Histoire Naturelle, France
(pickford@mnhn.fr)

Cenozoic fossil land snails can be found in many continental sections (Pickford, *J. African Earth Sci.*1995). We show how stable C and O isotope ranges of modern land snail shell from various ecosystems in Africa are related to snail genus, climate, and diet. Sequential powdered samples are drilled following growth lines through multiple years of shell growth to document stable isotope response to seasonal environmental variation. Results are summarized as follows: $\delta^{13}\text{C}$: Variation within one specimen is small. Shell $\delta^{13}\text{C}$ primarily responds to differences in diet, i.e. C3 plants, C4 plants, and the ingestion of carbonate from detritus, bedrock or soil.

$\delta^{18}\text{O}$: (1) Snails of the same genus from same ecosystem have similar values. (2) Oxygen isotope ranges from tropical forest, upland forest, coastal steppe, semi-desert and desert are small, with forest values generally lower than desert or semi-desert. (3) Regions with pronounced dry and wet seasonality (savannah, Mediterranean) can have large seasonal variation in $\delta^{18}\text{O}$. Within one climate type, snails of different genus often have similar ranges, although sometimes ranges are different. Habitat/climate has a stronger control on shell chemistry than taxonomy.

The $\delta^{13}\text{C}$ and $\delta^{18}\text{O}$ ranges of land snail shells reflect ecosystems, diet, and perhaps micro-habitat preference. Land snail fossils are potential targets for paleoenvironmental reconstruction based on a combination of faunal analysis and stable isotope geochemistry. [abbreviation] C: $\delta^{13}\text{C}$ VPDB, O: $\delta^{18}\text{O}$, VPDB.

[Tropical forest: Gabon, Uganda, Tanz.] *Leptocala* C: -11.28 ~ -13.28; O: -0.97 ~ -3.29; *Trochonanina* C: -14.20 ~ -15.56; O: +0.39 ~ -1.74; *Thapsia* C: -11.80 ~ -13.35; O: -1.37 ~ -3.55; *Limicolaria* C: -12.68 ~ -15.36; O: +1.01 ~ -3.85; *Achatina* C: -8.45 ~ -13.02; O: +0.13 ~ -2.83 [Upland forest: Kenya, Ug.] *Limicolaria* C: -9.37 ~ -11.41; O: +1.41 ~ -2.13; C: -7.90 ~ -10.02; O: +3.45 ~ -0.07; C: -8.35 ~ -12.33; O: +2.03 ~ -2.23; *Trochonanina* C: -0.24 ~ -5.22; O: +1.63 ~ -1.25 [Savannah woodland: Namibia, Kenya, Mozambique] *Xeroceratus* C: -6.37 ~ -7.99; O: -2.31 ~ -7.76; *Achatina* C: -5.96 ~ -10.90; O: +5.38 ~ -5.42; C: -4.84 ~ -13.83; O: +5.59 ~ -4.65; C: -8.37 ~ -13.82; O: +1.33 ~ -8.16; *Limicolaria* C: -1.82 ~ -7.92; O: +2.91 ~ -4.64 [Mediterranean: Morocco] *Helicopsis* C: -3.19 ~ -4.62; O: +0.74 ~ -0.99; *Rumina* C: -9.27 ~ -9.80; O: +5.76 ~ -1.08; *Kabyliya* C: -5.31 ~ -7.01; O: +3.48 ~ -0.07 [Coastal steppe: Oman] *Rochebrunia* C: -4.49 ~ -7.67; O: +2.95 ~ +0.92; *Euryptyxis* C: -9.28 ~ -10.88; O: +0.80 ~ +0.37; *Obeliscella* C: -7.88 ~ -9.52; O: +1.42 ~ -1.02 [Semi-desert: Nam. Ug.] *Dorcasia* C: -5.91 ~ -8.58; O: +3.89 ~ -0.12; *Bloyetia* C: -5.96 ~ -7.32; O: +2.79 ~ -1.21 [Desert: Nam.] *Dorcasia* C: -0.18 ~ -1.03; O: +3.37 ~ +1.26; *Trigonephrus* C: -0.20 ~ -2.75; O: +5.70 ~ +3.27.

Seasonal methane fluxes and sulfate reduction rates in a eutrophied Baltic estuarine system

JOANNA E. SAWICKA*, CAMILLA OLSSON AND VOLKER BRÜCHERT

Department of Geological Sciences, Stockholm University
Svante Arrhenius Väg 8, 10691 Stockholm, Sweden
(*joanna.sawicka@geo.su.se)

Estuaries and shelves are thought to be the source of 75% of the oceanic CH_4 emissions to the atmosphere, but to date relatively few data are available that report spatial and seasonal variations in production and emission of CH_4 from sediments in eutrophied coastal settings. Himmerfjärden (Baltic Sea, Sweden) is an estuary with a surface area of 174 km^2 . The estuary has a well-described eutrophication gradient from the inner part of the estuary to the opening, which is due to a sewage treatment plant (STP) in the inner estuary that has been discharging treated sewage since 1973. The sediments in the bay consist of organic-rich postglacial mud, sand, and glacial clay. CH_4 fluxes at sediment/water interface, pore water concentrations of SO_4^{2-} , CH_4 , and H_2S , and ^{35}S -sulfate reduction rates were measured in the spring, summer, autumn, and winter in the estuary at two stations, one close to the STP and one at a reference site outside the estuary. Additionally, sea-air fluxes and CH_4 water column concentrations were measured at the two stations.

Benthic methane fluxes were determined from ex-situ incubations and showed seasonal and spatial variations. The lowest CH_4 flux ($0.1 \text{ mmol m}^{-2}\text{d}^{-1}$) was observed in winter at the reference site and the highest CH_4 flux ($8.74 \text{ mmol m}^{-2}\text{d}^{-1}$) was recorded in the summer in Himmerfjärden sediment. For the other seasons, CH_4 fluxes at both stations were between $1 \text{ mmol m}^{-2}\text{d}^{-1}$ and $2 \text{ mmol m}^{-2}\text{d}^{-1}$. Sulfate reduction rates showed spatial variability and were consistently 10-fold higher in Himmerfjärden ($\sim 0.3 \mu\text{mol cm}^{-3}\text{d}^{-1}$) than at the reference site. There was a distinct zone of organoclastic sulfate reduction in both sediments at 3-7 cm depth. In the contaminated sediments near the STP, the sulphate-methane transition zone (SMT) was observed persistently during the year at depths 12-16 cm, indicating the presence of anaerobic methane oxidation, but was not detected above 40 cm depth at the reference site. Water column CH_4 concentration profiles showed that the sediments are the major source of CH_4 in the water column, as there was a pronounced increase in concentrations towards the bottom. Near-bottom water CH_4 concentrations were between 109 and 131 nmol/l . Concentrations at the surface were generally two-fold lower indicating efficient methane oxidation in the water column. Nevertheless, surface waters at both stations were oversaturated with respect to CH_4 throughout the year indicating that Himmerfjärden is an annual net source of CH_4 to the atmosphere.

www.minersoc.org

DOI:10.1180/minmag.2013.077.5.19

Thermodynamics of the C-H-O fluid at extreme conditions

S.K. SAXENA^{1*}, R. HRUBIAK¹, V. DROZD¹,
A.B. BELONOSHKO², P. SHI³ AND G. ERIKSSON⁴

¹Department of mechanical and materials engineering, Florida International University, Miami, FL 33199, USA (*correspondence: saxenas@fiu.edu)

²Department of Metallurgy, Royal Technical University, Stockholm, Sweden

³Thermo-Calc AB, Stockholm, Sweden

⁴GTT-Technologies, Aachen, Germany

The superfluid model [1] for calculation of high pressure-temperature fluid fugacities builds on the combination of experimental data on pure and mixed fluids at temperatures lower than 1000 K over several kilobars and molecular dynamics generated data at extreme conditions (> 5 kbar and up to 100 GPa and 4000 K). The model is found to be generally consistent with post-publication (since 1992) experimental data. The calculated data on water at low pressure differs significantly from the Brodholt-Wood fluid inclusion data [2] but closely reproduces the densities measured by Abramson and Brown [3]. The superfluid model and the model of Zhang and Duan [4] are closely similar.

We have used the model to calculate high pressure and temperature phase equilibrium in binary (MgO-CO₂, Al-H₂), ternary (Fe-H₂O-C, wustite-H₂O-C) and multicomponent (carbonaceous chondrite) systems. The results show that while a carbonate may be stable over the entire range of the mantle pressures and temperatures, it is not stable if the mantle is chondritic in composition. Iron carbide (Fe₃C), on the other hand, is stable to extreme pressure and temperatures in the ternary as well as in chondritic composition and may be a good candidate to be assimilated in the core. The conclusions are that a) the carbonate may not be the storage for CO₂ in the deep earth and b) carbon is more likely stored in Earth's core as carbide and as diamond in the mantle.

The authors wish to acknowledge the support and collaboration of the Deep Carbon Observatory.

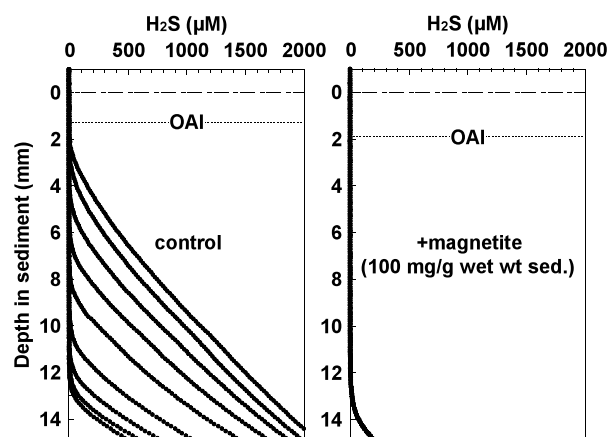
[1] Belonoshko, A.B., Shi, P., Saxena, S.K. (1992) *Computer and Geosciences* **18**, 1267–1269. [2] Brodholt, J.P., Wood, B.J. (1994) *Geochim. Cosmochim. Acta* **58**, 2143–2148. [3] Abramson, E.H., Brown, J.M. (2004) *Geochim. Cosmochim. Acta* **68**, 1827–1835. [4] Zhang, C., Duan, Z. (2009) *Geochimica et Cosmochimica Acta* **73**, 2089–2102.

Effect of magnetite addition on H₂S dynamics in coastal marine sediment

M. SAYAMA

National Institute of Advanced Industrial Science and Technology (AIST), Tsukuba 305-8569, Japan
(m.sayama@aist.go.jp)

It has been well known that magnetite is poorly reactive towards dissolved sulfide (H₂S) on a time scale of hours to days (Canfield *et al.*, 1992; Raiswell and Canfield, 1996; poultou *et al.*, 2004). However, microprofiles of H₂S in experimental sediment cores made with coastal marine surficial sediment showed a dramatic change by the addition of magnetite (Fig. 1). The depth of H₂S front at which H₂S concentration starts to increase stayed at the original even after four days incubation in the core with magnetite addition (Fig. 1, right), whereas the H₂S front moved up quickly and reached to the oxic-anoxic interface (OAI) within 24 hours in the control core (without magnetite addition) (Fig. 1, left). Possible mechanism to explain these results might be electrochemical oxidation of H₂S at deep with long distance electron (e⁻)-transfer through solid state cycling of structural Fe²⁺ and Fe³⁺ in magnetite (Latta *et al.*, 2011).



The partitioning of trace elements between clinopyroxene and trachybasaltic melt during rapid cooling

P. SCARLATO¹, S. MOLLO¹, J. D. BLUNDY², G. IEZZI³
AND A. LANGONE⁴

¹Istituto Nazionale di Geofisica e Vulcanologia, Via di Vigna Murata 605 00143 Rome, Italy (*correspondance: mollo@ingv.it)

²School of Earth Sciences, University of Bristol, Wills Memorial Building, Bristol BS8 1RJ, UK

³Dipartimento INGEO, Università G. d'Annunzio, Via Dei Vestini 30, 66013 Chieti, Italy

⁴C.N.R.- Istituto di Geoscienze e Georisorse, UOS Pavia, via Ferrata 1 27100 Pavia, Italy

Variation of trace element partition coefficients

We present the variation of trace element partition coefficients measured at the interface between rapidly cooled clinopyroxene crystals and co-existing melts. Results indicate that, Ds for REE, HFSE and TE increase with increasing cooling rate, in response to clinopyroxene compositional variations. The entry of REE into the M2 site is facilitated by a coupled substitution where either Na substitutes for Ca on M2 site or Al^{iv} substitutes for Si in the tetrahedral site. Due to the lower concentration of Ca in rapidly cooled clinopyroxenes, LILE on M2 decrease at the expense of monovalent cations. Conversely, higher concentrations of HFSE and TE on the M1 site are facilitated as the average charge on this site increases with the replacement of divalent-charged cations by Al^{vi}. At both equilibrium and cooling rate conditions, Ds for isovalent cations define parabola-like curves when plotted against ionic radius, consistent with the lattice strain model.

Implications

Although crystallization kinetics alter clinopyroxene composition, deviations from equilibrium partitioning are insufficient to change the tendency of a trace element to be compatible or incompatible. Consequently, there are regular relationships between ionic radius, valence of the trace element and D. Under both equilibrium and cooling rate conditions, the partitioning of trace elements is driven by charge-balance mechanisms; cation substitution reactions can be treated in terms of the energetics of the various charge-imbalanced configurations.

A Pilot Br Isotopic Study of Arid Playa Lakes and Ordinary Chondrites

BRUCE F SCHAEFER¹

¹CCFS, Department of Earth and Planetary Sciences, Macquarie University, NSW 2109, Australia
(Bruce.Schaefer@mq.edu.au)

Introduction: Bromine possesses a chemistry broadly comparable to that of Cl and F, however its heavier mass and lower abundance results in slightly different behaviours in geochemical cycling. For example it is disproportionately enriched in sea water with respect to Cl. Br can be considered to be a “hydrophile” element, and hence its behaviour is in governed by that of water. It possesses two isotopes ⁷⁹Br (50.686%) and ⁸¹Br (49.314%).

This study has developed new chemical extraction, and most significantly, new mass spectrometric protocols for Br isotopes on silicates, evaporites and waters using N-TIMS methodologies. Existing CF-IRMS methodologies offer internal precision of ~0.3‰ (1SD, [1]), whereas N-TIMS measurements of laboratory HBr and seawater standards produce external reproducibility of <0.07‰ (1SD) over an 18 month period with internal precision typically <0.06‰ (1SD) on single analyses.

This study presents the first high precision, N-TIMS isotopic data on playa lake evaporites and ordinary chondrites, recording a >5‰ variation in solar system ⁸¹Br/⁷⁹Br.

[1] Shouaker-Stash *et al.*, *Anal. Chem.*, **77**; p4027-4033, 2005.

New data on anisotropy and composition dependence of Na/K-interdiffusion in alkali feldspar

A.-K. SCHAEFFER¹, E. PETRISHCHEVA¹, G. HABLER¹, R. ABART¹ AND D. RHEDE²

¹University of Vienna, Department of Lithospheric Research, Vienna, Austria (anne-kathrin.schaeffer@univie.ac.at)

²GFZ German Research Centre for Geosciences, Telegrafenberg, 14473 Potsdam, Germany

Cation exchange experiments have been conducted using crystallographically oriented plates of gem quality sanidine as starting material.

The observed geometry of the diffusion fronts can be explained by a composition dependence of the interdiffusion coefficient. We extracted the composition dependence of the interdiffusion coefficient from our measured data by use of the Boltzmann transformation in the composition interval between X_{Or} 0.5 and 1 for the directions (001) and (010).

At 850°C the interdiffusion coefficient D is nearly constant at $0.3 \times 10^{-15} \text{m}^2 \text{s}^{-1}$ over the composition range X_{Or} 0.50 to 0.95 and then rises steeply to values of $2.5 \times 10^{-15} \text{m}^2 \text{s}^{-1}$ for profiles normal to (001). Normal to (010) D is nearly constant at $0.03 \times 10^{-15} \text{m}^2 \text{s}^{-1}$ over the composition range X_{Or} 0.5 to 0.97 before, too, rising steeply at higher X_{Or} . Thus interdiffusion normal to (001) is faster by a factor of about ten than interdiffusion normal to (010).

Christoffersen *et al.* [1] measured interdiffusion coefficients in the composition range between X_{Or} 0.1 to 0.8 in diffusion couple experiments. They observed a similar anisotropy but they find a composition dependence of D for intermediate compositions which disagrees with our findings. Also, their absolute values for the interdiffusion coefficient at a given composition are smaller by about a factor of ten.

Comparison with theoretical calculations of the interdiffusion coefficient from self-diffusion data found in literature [2, 3] using the Manning relation for interdiffusion in ionic crystals shows a rough fit for interdiffusion normal to (001) while the slower interdiffusion normal to (010) deviates significantly from what would be expected.

The activation energy also shows an anisotropy; normal to (001) it is about 340 kJ/mole while it is 250 kJ/mole normal to (010).

[1] Christoffersen *et al.* (1983) *American Mineralogist*, **68**, 1126-1133. [2] Foland (1974) *Geochemical Transport and Kinetics*, 77-98. [3] Kasper (1975) *Ph.D. thesis, Brown University*.

The geochronological signal of a dying magma system

U. SCHALTEGGER¹, C. BRODERICK¹ AND J.F. WOTZLAW¹

¹Section of Earth and Environmental Sciences, University of Geneva (urs.schaltegger@unige.ch, joern.wotzlaw@unige.ch, cindy.broderick@unige.ch)

U-Pb dating of zircon is the most commonly used geochronometer for temporal quantification of pluton and batholith forming processes. High-precision zircon $^{206}\text{Pb}/^{238}\text{U}$ dating repeatedly produces a dispersion of ~50-200 ka between the oldest and youngest zircon of the same sample, and of up to 1 Ma within a plutonic unit, pointing to a prolonged magmatic evolution with non-monotonously varying parameters like melt temperature, crystallinity and melt composition. Combining high-precision U-Pb dates with trace element and Hf isotope analysis on the same dated volume of zircon, we are able to trace different processes acting during the assembly of a pluton and quantify their timing: 1) changing melt composition due to fractional crystallization of zircon and of other accessory minerals (e.g., titanite) over time; 2) quantify the evolution of overall crystallinity of a magmatic body over time; 3) changes in magma temperature by identifying periods of enhanced and suppressed zircon crystallization, and correlate them with periods of mafic magma recharge and thermal rejuvenation of the system; 4) changing sources of incoming melts over time by linking initial Hf isotopes to crystallization age.

Probability density functions of $^{206}\text{Pb}/^{238}\text{U}$ zircon dates of a pluton usually point to several peaks of enhanced zircon crystallization during a prolonged period of increasing crystallinity of the magma, leading to stalling of the crystal mush and subsequent complete solidification at upper crustal levels. The non-steady decrease of the volume of potentially eruptible crystal-poor liquid leads eventually to the "plutonic death" of a magmatic system.

Labile structures in organic matter under the influence of multivalent cations – an issue for dynamic interfaces?

GABRIELE ELLEN SCHAUMANN¹

¹University Koblenz-Landau, Insitute for Environmental Sciences, Fortstr. 7, Landau, Germany, schaumann@uni-landau.de

Soil organic matter (SOM) controls large part of the processes occurring at biogeochemical interfaces in soil and may contribute to sequestration of organic chemicals. In this contribution, the idea that sequestration of organic chemicals is driven by physicochemical SOM matrix aging, and its consequences for transport processes will be discussed. In contrast to chemical aging processes, physical matrix aging involves changes in the supramolecular arrangement of SOM molecules and molecule segments. Organic chemicals can be entrapped in nanovoids, which can transform to a semi-persistent cage. Persistence of entrapment directly depends on the rigidity and stability of the cage. Water molecule bridges (WaMB) and cation bridges (CaB) between segments of soil organic matter (SOM) have been found to stabilize the supramolecular SOM matrix and are therefore suspected to control immobilization of organic chemicals in soil. Contaminants sequestered by WaMB or CaB can be immobilized or released suddenly upon changes in environmental conditions like moisture, temperature or melting. Understanding their dynamics is highly important to model the reaction of soil as well as release and transport of organic chemicals on changes in climatic conditions. While the idea of CaB in solid soil organic matter is more and more accepted, there is increasing evidence that such cross-links are not relevant in all types of soil organic matter, depending on the spatial distribution of charged functional groups in the OM. Only if distances between functional groups are sufficient, CaB can form. Larger distances can be bridged by CaB-WaMB associations. Also interfacial properties are dynamic. Soil wettability can with increasing involvement of functional groups in CaB-WaMB associations. In the extreme case, high concentrations of multivalent cations can hydrophobize surfaces of SOM. Associations of CaB and WaMB evolve slowly and form a supramolecular network in SOM. Those dynamic associations can fix molecular arrangements inducing water repellency and increase kinetic barriers for the release and uptake of water and sorption and transport of organic chemicals in soil.

The role of soil Cu in chelate mediated Fe acquisition by plants

W.D.C. SCHENKEVELD^{1*} AND S.M. KRAEMER¹

¹University of Vienna. Dept. of Environmental Geosciences, Althanstrasse 14, 1090 Wien, Austria
walter.schenkeveld@univie.ac.at (* presenting author)

Iron is an essential micronutrient to plants. In soils with a neutral to alkaline pH, the solubility of Fe bearing minerals is very low and can become limiting for plant growth. To avoid Fe deficiency in plants grown on such soils, the solubility of Fe needs to be increased. This can be established by means of chelating agents, which strongly bind Fe and form a soluble Fe complex. These chelating agents can either have a natural or an antropogenic origin.

Grasses (including wheat, barley and rice) are very efficient in preventing Fe deficiency, because their Fe acquisition strategy includes the exudation of chelating agents called phytosiderophores (PS). These PS can dissolve soil Fe and the resulting FePS complex can be taken up by a high affinity membrane transporter. In agricultural practice, plant species that are less efficient in acquiring Fe are commonly supplied with micronutrient fertilizers based on synthetic chelating agents. For Fe fertilization on calcareous soils, FeEDDHA (iron ethylene diamine bis-N,N'-hydroxyphenyl acetic acid) is among the most effective.

Soils contain several metals that can compete with Fe for binding to chelating agents, thereby compromising the efficiency of the chelate mediated Fe uptake mechanism. Cu is among the stronger competitors and occurs in soil in quantities that could substantially compromise Fe uptake.

It will be shown and discussed that the extent to which Cu effectively competes with Fe for complexation under soil conditions is controlled by both thermodynamic and kinetic factors. These factors include the specific affinity of the chelating agent for Fe and Cu, the Fe and Cu activity in the soil, the extent to which metal complexes adsorb to reactive soil components, the mobilization rate of Fe and Cu, and the displacement rate of Fe from the Fe-chelate by Cu. Both with PS and synthetic Fe chelates, Cu may considerably limit the time-span the chelating agent remains effective as Fe transporter.

New insights into simultaneous determination of mass-dependent isotopic fractionation and radiogenic isotope variations of strontium by multi-collector ICPMS

HOWIE D. SCHER¹, ELIZABETH M. GRIFFITH²
AND WAYNE P. BUCKLEY JR.¹

¹Department of Earth and Ocean Sciences, University of South Carolina, hscher@geol.sc.edu

²Department of Earth and Environmental Sciences, University of Texas at Arlington, lgriff@uta.edu

Variability of Sr isotope ratios are due to radioactive decay and mass dependent fractionation through various physiochemical reactions. Radiogenic Sr ratios are used for geochronology and provenance while stable isotope ratios of Sr reveal mechanisms of sample formation and resolve mass balance in geochemical systems.

Accurate and precise measurements of stable Sr isotope ratios (e.g., ⁸⁸Sr/⁸⁶Sr) are possible if the ratio can be corrected for mass-discrimination effects during analysis. Ohno and Hirata (2007) developed a method where Sr solutions were doped with Zr, and measured ⁸⁸Sr/⁸⁶Sr ratios were normalized to ⁹¹Zr/⁹⁰Zr=0.2181, while simultaneously measuring ⁸⁷Sr/⁸⁶Sr. Using standard sample bracketing combined with a Zr correction, we tested three variables that influence the mass-discrimination effect on the multi-collector ICPMS. All stable isotope ratios are reported relative to SRM987.

First, solutions of 500 ppb SRM987 with Ba/Sr from 0.002 to 200 were analyzed by bracketing against a SRM987 solution with no Ba. Deviations from $\delta^{88}\text{Sr}=0\text{‰}$ occur above Ba/Sr ratios of 10. Deviations from our long term ⁸⁷Sr/⁸⁶Sr value also occur above this level of Ba.

Second, seawater was processed through standard microcolumn extraction with SrSpec resin (Eichrom). Eluted Sr was adjusted to 250 ppb and Zr was added so that Sr/Zr was ~1. We repeated the Ba doping experiment using the Zr correction. When Ba/Sr<10 the measured $\delta^{88}\text{Sr}$ is $0.37\pm 0.05\text{‰}$ (2σ , n=28) which is within analytical precision of published values for seawater (0.35 to 0.39). Deviations occur above Ba/Sr = 10.

Lastly we tested the Zr/Sr ratio on the measurements of $\delta^{88}\text{Sr}$ in seawater. We determined that the ideal Zr/Sr ratio is slightly lower than unity, and that high Zr/Sr ratios result in inaccurate $\delta^{88}\text{Sr}$ determinations.

[1] Ohno T., and Hirata T. (2007) *Analytical Sciences*, **23**, 1275-1280

Dahomeyan Neoproterozoic imprint on Eburnean Palaeoproterozoic rocks in southeast Ghana – Rubust Ar, flimsy Pb

ANDERS SCHERSTÉN¹, LAURENCE PAGE¹, PER KALVIG²,
ANDREAS PETERSSON¹ AND SOLOMON ANUM³,

¹Department of Geology, Lund University, Sölvegatan 12, SE-223 62 Lund, Sweden. anders.schersten@geol.lu.se; laurence.page@geol.lu.se; andreas.petersson@geol.lu.se;

²Geological Survey of Denmark and Greenland, Øster Voldgade 10 DK-1350, København, Denmark. pka@geus.dk

³Geological Survey Department, Ghana, P.O. Box M 80 Accra, Ghana. anumsolo@yahoo.com

The Dahomeyan belt formed during Pan-African suture between juvenile island arcs rocks that were amalgamated to the >2.0 Ga West African craton (WAC). Arc accretion and subsequent continent collision is manifested through eclogites and mafic to felsic granulites. Pre-collisional passive margin sediments were thrust westward over the WAC. A combined zircon U-Pb and hornblende/mica ⁴⁰Ar/³⁹Ar profile across the Eburnean-Dahomeyan orogens was made to constrain Dahomeyan imprint on the Eburnean rocks in the WAC. Hornblende ages are 2.06 Ga, while micas yield 2.0 Ga. Zircon U-Pb ages yield igneous crystallisation ages >2.1 Ga, however some samples display significant Pb-loss with lower intercept ages that are consistent with a 0.6 Ga Dahomeyan imprint. This probably reflect fluid induced variable resetting of the zircon U-Pb system, while mica and hornblende remained below their blocking temperatures and where inert to the fluids that affected the zircon. A granulite and a zoned plagioclase porphyritic metavolcanic rock from within the Dahomeyan belt, yield 0.614 and 0.577 Ga zircon ages respectively. The 0.577 Ga population represent igneous crystallisation as represented by prismatic zoned crystals. The 0.614 Ga population is represented by rounded featureless zircon, and date granulite facies metamorphism. Hornblende from the granulite yield 0.59 Ga ⁴⁰Ar/³⁹Ar plateaux, dating post granulite facies cooling through ~525 °C, correspond to a cooling rate of at least 10 °C/Myr.

These result highlights the imprint of the Dahomeyan orogen on the >2 Ga Eburnean rocks of the WAC in southeast Ghana. No resetting of Ar-ages is noted in mica or hornblende in the Eburnean rocks, while zircon is variably reset.

Physical evolution of olivine-hosted melt inclusions during high- T homogenization treatments

F. SCHIAVI*, A. PROVOST, P. SCHIANO AND N. CLUZEL

Laboratoire Magmas et Volcans, Univ. Blaise Pascal, CNRS, IRD, 5 rue Kessler, 63038 Clermont-Ferrand, France

(*correspondence: f.schiavi@opgc.univ-bpclermont.fr)

Silicate melt inclusions (MIs) form in thermodynamic equilibrium with their host mineral. After entrapment, during the ascent of the host magma and its cooling upon eruption, MIs may undergo physical and chemical changes, part of which are irreversible. Thus, to properly interpret petrological information recorded by MIs, a full understanding of their physico-chemical behaviour when submitted to variations of external temperature (T) and pressure is required. Homogenization temperature (T_h) of the inclusion content (gas + glass \pm crystals) is thought to correspond to minimum entrapment temperature (T_e). However, T_h in olivine is observed to increase systematically with time during high- T treatments, thus revealing the occurrence of irreversible physico-chemical changes in the MI-host system.

To figure out what processes are responsible for T_h increase, we performed heating experiments on H_2O -rich (Vulcano Is., Italy) and H_2O -poor (Famous-Zone MORB, East Atlantic) olivine-hosted MIs. Equilibrium between melt and olivine compositions suggests $T_e \approx 1210^\circ\text{C}$ for Vulcano MIs and $\approx 1220^\circ\text{C}$ for Famous-Zone MIs. Each experiment consisted of several heating-cooling cycles performed in a rapid-quench optically-controlled Vernadsky heating stage.

In our experiments large variations of T_h with time were measured, along with high first T_h (1230-1300°C for Vulcano MIs; $T_h \geq 1315^\circ\text{C}$, more often $\approx 1430^\circ\text{C}$ for Famous-Zone MIs), which are inconsistent with calculated T_e . T_h increase from one cycle to the next is associated with an increase of low- T bubble size and a slower reduction of bubble volume at high T . Images taken during the experiments on Famous-Zone MIs allowed us to measure expansions of MI cavities up to ~ 30 vol% of the starting volume. Volume expansion occurred quite rapidly (after 10-80 min at $T > 1100^\circ\text{C}$) and increased with time. Its amount, and the associated first T_h as well, seem to be related with MI size, distance of MI walls from olivine faces, and ratio between bubble and MI volumes. T_h increase essentially results from the plastic deformation of host olivine (elastic deformation and dissolution/precipitation interfere but are reversible). Though diffusive water loss may interfere too during the first hours at high T , it cannot explain the observed cavity expansion nor the large and sustained increase in T_h .

Pace of soil formation based on soil structure indices

JASMIN SCHIEFER¹, GEORG J. LAIR^{1,2}
AND WINFRIED E.H. BLUM¹

¹Institute of Soil Research, University of Natural Resources and Life Sciences, Vienna, Austria

²Institute of Ecology, University of Innsbruck, Austria.

E-mail: jasmin.schiefer@boku.ac.at, georg.lair@boku.ac.at

Clay sized aggregates play a key role in soil formation as they accumulate and preserve organic matter (OM) by physical protection against microbial decomposition [1]. However, the development of microaggregates during soil formation is not well understood. For our study we collected soils of a chronosequence of approximately 10 to 10000 years in an alluvial plain of the River Danube [2]. A- and AC-horizons of Fluvisols and Chernozems under cropland, grassland and forest were sampled. Microaggregates ($< 2\mu\text{m}$), gained by ultrasonic dispersion and centrifugation, as well as bulk soil were physically and chemically analysed.

Microaggregates under semi-natural forest showed a steep increase of OM content and a depletion of amorphous Fe-(hydr)oxides in the first years of soil development. In the soils older than about 350 years, OM content in the clay sized aggregates remain more or less constant over time, indicating a possible saturation of the clay sized particles with OM. In contrast, the initially low OM content in the microaggregates under cropland was continuously increasing with soil age. A characterisation of OM in the microaggregates (e.g. by STA) revealed that with time less degradable compounds are accumulating, especially in the AC-horizon. In the AC-horizon of a 2000 - 3000 year old soil the amount of labile and stable OM in the clay sized aggregates was about the same.

Soil structure build-up was strongly influenced by bioturbation (e.g. earthworms) and plant material inputs (roots, litter). A calculation of the annual soil formation rate, based on the depths of the A-horizons, indicates a very high soil formation rate up to ~ 4 mm/year at the beginning, decreasing to ~ 0.1 mm/year after 2000 years.

[1] Chenu and Plante (2006), *Europ. J. of Soil Science* **57** (4), 596-607. [2] Lair *et al.* (2009), *Quat. Geochr.* **4** (3), 260-266.

Using increment cores of eastern cottonwood trees (*Populus deltoides*) to assess the timing of Cd pollution

JOHAN SCHIJF^{1*} AND MARY C. GARVIN²

¹Chesapeake Biological Laboratory, P.O. Box 38, Solomons, MD 20688, USA (*correspondence: schijf@umces.edu)

²Oberlin College, Department of Biology, 119 Woodland St., Oberlin, OH 44074, USA (Mary.Garvin@oberlin.edu)

We measured the concentrations of 8 trace metals in the trunk wood of ~40 eastern cottonwoods (*P. deltoides*), a fast-growing dioecious angiosperm common throughout much of eastern North America. Large trees were selected more or less at random from an area in northern Ohio (USA) that has a known history of soil pollution with a variety of metals and organic compounds, as well as from an equally sized control area. Two increment cores (L < 40 cm, Ø 5 mm) were taken from each tree at chest level. To avoid contamination, annual growth rings were marked on one core and the markings were used to guide cutting of the sample core with tungsten carbide surgical tools into eight 5-year sections covering the period 1970–2009. The older and younger rings were not analyzed. All sections were completely microwave-digested (10 min at 200°C) in a mixture of 16 M nitric acid and 30% hydrogen peroxide, along with one blank and one pine wood SRM (NJV 94-5). The cooled digests were then weighed, diluted 100-fold, and analyzed by Octopole Reaction System ICP-MS (Agilent) for As, Cd, Co, Cr, Cu, Ni, Pb, and V.

While some metals (As, V) are always below the method detection limit (DL) and others appear to vary arbitrarily, Cd is the only one showing behavior that may be interpretable in terms of both space and time. Blanks were always below the DL (~15 ng Cd per g dry wood), there was no evidence of sample contamination, and analytical recovery of the SRM was excellent (>98%). The ~40 trees fall into three distinct groups: 1. Trees with low mean Cd concentrations (270 ng/g) and little temporal variability ($n = 20$); 2. Trees with a clear maximum or temporal trend in the Cd concentration of up to 1300 ng/g ($n = 14$); 3. Three trees with extremely high Cd concentrations (>2500 ng/g). Replicate cores taken from a single tree as well as from separate trees at a single location yielded satisfactory reproducibility (10–20%). Although the timing of maximum Cd concentrations varies, high amounts are not found in the most recent 10 years of any tree. All trees in group 3 and all but one tree in group 2 are located in the polluted area, whereas all but one tree in the control area are from group 1. A simple statistical test indicates that this distribution has an almost negligible probability of occurring by chance ($\chi^2 = 8.819$, $p = 0.003$).

Mg isotope evidence for ancient magmatic differentiation on the angrite parent body

M. SCHILLER^{1*}, T. MIKOUCHI², J. N. CONNELLY¹
AND M. BIZZARRO¹

¹Centre for Star and Planet Formation, Natural History Museum of Denmark, University of Copenhagen, Copenhagen, Denmark (*email: schiller@snm.ku.dk)

²Department of Earth & Planet. Science, University of Tokyo, Tokyo, Japan

Angrite meteorites are the most alkali-depleted rocks in our solar system and they can be divided into plutonic and volcanic angrites [1]. Of the group of volcanic angrites, NWA 1670 is particularly interesting because it contains significant amounts of olivine xenocrysts of up to 5 mm in size that are chemically distinct from the groundmass [2,3]. The existence of xenocryst olivine not in chemical equilibrium with the groundmass offers the potential for a resolvable temporal difference between both phases. Therefore, considering the old age for this angrite [4], the xenocrysts may reflect an earlier magmatic event.

Here we apply the ²⁶Al to ²⁶Mg ($t_{1/2} = 0.7$ Myr) chronometer to examine the temporal relationship of olivine xenocrysts and basaltic groundmass in NWA 1670. Mg isotope data for individual olivine grains and groundmass separates were obtained using the Neptune MC-ICPMS. All olivine xenocrysts have negative $\mu^{26}\text{Mg}^*$ with a mean of -10.7 ± 3.1 ppm. Measured $\mu^{26}\text{Mg}^*$ of the groundmass ranges from -5.3 to $+4.3$ ppm and are positively correlated with ²⁷Al/²⁴Mg ratios. Both sets of data form an apparent isochron suggesting a similar ²⁶Al/²⁷Al abundance at time of their formation to that of other old angrites. However, the negative intercept of the isochron cannot be reconciled with the low ²⁶Al/²⁷Al abundance and suggests that the correlation is best explained as a two component mixing trend. Model ages for single xenocryst olivine range from 0.36 to 1.18 Myr after CAIs. A model age for the most anomalous groundmass sample yields an age of 3.9 Myr after CAIs, consistent with the Mg isochron ages for other volcanic angrites. These data demonstrate that olivine entrained in NWA 1670 are products of ancient magmatic differentiation on the angrite parent body shortly after solar system formation, which significantly predates the formation of volcanic angrites.

[1] K. Keil (2012), *Chem. Erde-Geochem.*, 72, 191–218. [2] T. Mikouchi *et al.* (2003), *Meteorit. Planet. Sci. Suppl.*, 38, 5218. [3] A. Jambon *et al.* (2008) *Meteorit. Planet. Sci.*, 43, 1783–1795 [4] Sugiura *et al.* (2005), *Earth Planets Space*, 57, e13-e16.

Origin of natural gas-fed “eternal flames” in the Northern Appalachian Basin, USA

ARNDT SCHIMMELMANN¹, GIUSEPPE ETIOPE²
AND AGNIESZKA DROBNIAK³

Department of Geological Sciences, Indiana University, 1001
E 10th Street, Bloomington, IN 47405-1405, USA,
aschimme@indiana.edu

²Istituto Nazionale di Geofisica e Vulcanologia, Sezione Roma
2, via V. Murata 605, 00143 Roma, Italy, and Faculty of
Environmental Science and Engineering, Babes-Bolyai
University Cluj-Napoca, Romania,
giuseppe.etiope@ingv.it

³Indiana Geological Survey, Indiana University, 611 N Walnut
Grove, Bloomington, IN 47405, USA,
agdrobni@indiana.edu

Hydrocarbon gas seeps are surface expressions of petroleum seepage systems, whereby gas is ascending through faults and conduits from pressurized reservoirs that are typically associated with sandstones or limestones. The region around the states of New York and Pennsylvania marks the birthplace of commercial gas production from shales dating back into the 19th century. We sampled two burning seeps in New York and Pennsylvania that had not yet received geochemical scrutiny, including compound-specific stable isotope ratios of hydrogen and carbon. A spectacular “eternal flame” in Chestnut Ridge County Park (Erie County, western New York State) marks a natural gas macroseep of dominantly thermogenic origin emanating directly from deep shale source rocks, which makes this a rare case in contrast to most Petroleum Seepage Systems where gas derives from conventional reservoirs. The main flaming seep releases about 1 kg of methane per day and seems to feature the highest ethane and propane (C₂+C₃) concentration ever reported for a natural gas seep (~35 vol. %). The same gas is also released to the atmosphere through nearby invisible and diffuse seepages from the ground. The synopsis of our chemical and stable isotope data with available gas-geochemical data of reservoir gases in the region and the stratigraphy of underlying shales suggests that the thermogenic gas originates from Upper Devonian shales without intermediation of a conventional reservoir. A similar investigation on a second “eternal flame” near Clarrington in Pennsylvania suggests that gas is migrating from a conventional sandstone pool and that the seep is probably not natural but results from an undocumented and abandoned gas or oil well.

High-precision ¹⁰Be-dating and Little Ice Age glacier advances at Steingletscher (Swiss Alps)

IRENE SCHIMMELPFENNIG^{1,2}, JOERG M. SCHAEFER¹,
NAKI AKÇAR³, SUSAN IVY-OCHS⁴, ROBERT FINKEL⁵,
SUSAN ZIMMERMAN⁶ AND CHRISTIAN SCHLUECHTER³

¹Lamont-Doherty Earth Observatory/Columbia University,
Palisades, NY-10964, USA

²CEREGE, 13545 Aix en Provence, France

³Institute of Geological Sciences, University of Bern,
Switzerland

⁴Laboratory of Ion Beam Physics, ETH, Zürich, Switzerland

⁵Earth and Planetary Science Department, University of
California-Berkeley, Berkeley, California, USA

⁶Lawrence Livermore Natl Lab, Ctr Accelerator Mass
Spectrometry, Livermore, CA-94550 USA

The increase in sensitivity of the cosmogenic ¹⁰Be technique now provides novel insights into glacier and climate change by giving dates throughout the Holocene and up to present day from moraines around the globe.

We show the first ¹⁰Be chronology for Steingletscher in the Central Swiss Alps (47°N, ~2000 m altitude), consisting of 30 boulder ages. The chronology includes early Holocene glacier positions, which most likely reflect glacier responses to abrupt cold spells identified in other Northern Hemisphere paleoclimate records. On the younger inner moraines, fourteen ¹⁰Be boulder ages from individual ridges are in stratigraphic order ranging from 170 to 530 years. We relate these boulder ages to glacier advances during the Little Ice Age (LIA, 14th to 19th century in the Swiss Alps). Two samples from moraine ridges inside the LIA limit of Steingletscher yield ages of 170 ± 10 years and 130 ± 10 years. These latter samples potentially allow for quantification of the amount of ¹⁰Be inherited during prior periods of exposure, on the order of a thousand atoms per gram.

Our ¹⁰Be data from boulders deposited during the last millennium are based on quartz samples as small as 5 g, facilitating routine processing for ¹⁰Be dating even on such young samples. Comparing the Steingletscher data with other emerging ¹⁰Be chronologies of recent glacier advances, we will discuss the current analytical limits of ¹⁰Be dating together with the relevance of cosmogenic nuclide inheritance and other sources of natural uncertainty for the overall sensitivity of ¹⁰Be surface exposure dating.

CO₂ fluxes in the submarine hydrothermal system of Panarea

M. SCHIPEK*, R. SIELAND, D. STEINBRÜCKNER, M. PONEPAL, K. BAUER AND B. MERKEL¹

¹TU Bergakademie Freiberg, Scientific Diving Center, 09596 Freiberg, Germany

(* correspondence: mandy.schipek@gmail.com)

The measurement of CO₂ fluxes in terrestrial and submarine hydrothermal systems is affected by large uncertainties. Different methodologies were applied by scientific divers to estimate areal gas fluxes and determine massive gas discharges in water depths between 8 and 30 m in the hydrothermal system of Panarea, Italy.

Because several hundreds of hydrothermal vents exist in the submerged caldera of Panarea it is impossible to measure each gas discharge directly. Therefore gas discharges were classified in 5 groups with respect to their amount of gas release. Class A to D (0 to < 40 l/min) discharges were measured by displacement of water in a graduated container according to [1].

By visual counting and classifying discharge points within areas of increased hydrothermal activity, a rough estimation of diffuse gas release was realized. Massive gas discharges (class E, 40 – 100 l/min) were determined by means of a device based on impeller and temperature readings [2]. Corrections concerning gas temperature and hydrostatic pressure were performed.

A substantial percentage of the investigated gas discharge points (75 – 95%, n ≈ 700) was classified as weak (class A – D). About 10 fumaroles were identified as very intense gas releases (class E). Small gas discharges had been estimated to release up to 30 ± 14.5 t/d CO₂, while massive outlets account for 5 ± 0.6 t/d CO₂ in the submarine area of the caldera. The total CO₂ flux was calculated by considering the dissolution of CO₂ during the ascent to the sea floor [3]. Assuming 20 – 40% of gas dissolution, the total CO₂ flux in the submarine hydrothermal system of Panarea was estimated to be 47 ± 15.1 t/d CO₂. This is about 26% of the CO₂ emission of the nearby terrestrial volcano Vulcano [4] and <0.47% compared to all Mediterranean hydrothermal emissions [5].

[1] Italiano & Nuccio (1991) *J. Volcanol. Geotherm. Res.* **46**, 125-41. [2] Ponopal *et al.* (2010) *Miscellanea* **7**, 66-70. [3] Caracausi *et al.* (2005) *Geochim Cosmochim Acta* **69**, 3045-59. [4] Baubron *et al.* (1990) *Nature* **344**, 51-53. [5] Dando *et al.* (1991) *Prog Oceanogr* **44**, 333-67.

Structure, evolution and function of the root bacterial microbiota of *Arabidopsis* species

K. SCHLAEPPI^{1,2*}, N. DOMBROWSKI¹, E. VER LOREN VAN THEMAAT¹ AND P. SCHULZE-LEFERT¹

¹Department of Plant Microbe Interactions, Max Planck Institute for Plant Breeding Research, Cologne, Germany

²Swiss Federal Research Institute Agroscope, Reckenholzstrasse 191, 8046 Zurich, Switzerland (*correspondence: klaus.schlaepi@agroscope.admin.ch)

Plants touch with their roots soil - one of the richest microbial ecosystems on earth. At this contact zone, the secretion of poorly characterized root exudates fuels the differentiation of a distinct rhizosphere bacterial microbiota compared to the surrounding soil. Rhizobacteria provide microbial services affecting plant growth and health and contribute to ecosystem functioning. We examined the composition and evolution of the bacterial root microbiota within a phylogenetic framework of host species, including *Arabidopsis thaliana* and its sister species *Arabidopsis halleri* and *Arabidopsis lyrata* and evolutionarily ancient *Cardamine hirsuta* with pyrosequencing of 16S rRNA gene amplicon libraries. The composition of rhizobacterial communities varies most as a function of environmental condition and consists of a taxonomically narrow and evolutionarily conserved core microbiota consisting of Actinomycetales, Burkholderiales, and Flavobacteriales. We identified few root microbiota members that provide unique signatures for each host species, possibly reflecting host-specific requirements in a given environment. Most of these host species-dependent microbiota signatures were found for the phylogenetically oldest *C. hirsuta*, indicating that root microbiota diversification is linked to the evolutionary divergence time of the host species. *A. halleri* is the only plant among the tested species that grows on heavy metal (e.g. Cadmium) contaminated soils, tolerating high levels of Cd and accumulating high levels of Cd in leaves. We have initiated the examination of rhizobacterial communities of *A. halleri* grown in soils with elevated heavy metals coupled with community profiling of enrichment cultures and metal uptake measures in leaves. In this context, first insights into microbiota services will be provided.

Continuous soil gas monitoring related to CCS – Lessons learned from a 5-year case study

SCHLOEMER, S.¹, MÖLLER, I.¹ AND FURCHE, M.¹

¹Federal Institute for Geosciences and Natural Resources, Hannover, Germany, s.schloemer@bgr.de

The development of adequate monitoring strategies for CO₂ storage sites is one of the most vigorously discussed subjects related to carbon capture and storage (CCS), both in the public and in the scientific community. Public acceptance of CO₂ sequestration will only be achieved if secure and comprehensible monitoring methods for the natural environment are applied in a transparent way. Deep geological monitoring is mostly related to large scale migration of injected carbon dioxide in the storage formations. In contrast, detection and quantification of different gas species in the vadose zone of soil column and/or in the atmospheric boundary layer is a key method in many fields of near-surface environmental research and geohazards as well as CCS. As CO₂ soil gas concentrations vary over broad ranges, reliable statements on CO₂ seepage can only be made by using continuous long-term gas concentration measurements. We describe lessons learned from the first continuous monitoring program applied on a proposed CO₂ storage site in the Altmark area (Germany).

We will focus on our technical experiences, data interpretation and recommendations for further monitoring programs related to CCS. The most important topic is the reliability of a single station's data quality. Each selected site needs a thorough pre-investigation, e.g. regarding the depth of the biologically active zone and potential free water level. Based on our long lasting experience from field studies and including recent monitoring programs, we strongly recommend that baseline monitoring schemes for CO₂ storage sites should start at least 3 years before the gas injection into the reservoir. We will show that vadose zone monitoring can be considerably more sensitive to small seepage rates than surface flux measurements under favourable conditions but will also address pitfalls and limitations of the method.

Sorption of uranium and neptunium onto diorite from Äspö HRL

K. SCHMEIDE*, S. GÜRTLER, K. MÜLLER, R. STEUDTNER, C. JOSEPH, F. BOK AND V. BRENDLER

Helmholtz-Zentrum Dresden-Rossendorf, Institute of Resource Ecology, P.O. Box 510119, 01314 Dresden, Germany (* k.schmeide@hzdr.de)

Granitic subsurface environments are considered as potential host rock formations for the deep underground disposal of radioactive waste. The retention behavior of the crystalline rock diorite from the Äspö Hard Rock Laboratory (HRL, Sweden) towards the redox-sensitive actinides U and Np was studied by means of batch sorption experiments. The influence of various parameters, such as grain size (0.063 – 0.2 mm, 0.5 – 1 mm, 1 – 2 mm), temperature (25 and 10°C), atmosphere and sorption time (5 to 108 days) was studied using a synthetic Äspö groundwater (pH 7.8, $I = 0.178$ M) as background electrolyte. For U(VI), sorption isotherms were recorded (5×10^{-9} M to 7×10^{-5} M). Distribution coefficients, K_d values, were determined. The K_d values decrease with increasing grain size of the diorite and with decreasing temperature. The K_d values determined under oxic conditions are lower than those determined under anoxic conditions.

In the U sorption system, the speciation of U(VI) in solution and thus, its sorption onto diorite is strongly influenced by the groundwater composition. It was found by time-resolved laser-induced fluorescence spectroscopy that $\text{Ca}_2\text{UO}_2(\text{CO}_3)_3(\text{aq})$ is the dominating species in solution. Hence, calcium and carbonate ions leached out of diorite significantly affect U(VI) sorption. Kinetic experiments showed that sorption equilibrium ($K_d = 1.44 \pm 0.30$, 1 – 2 mm fraction) is reached relatively fast (after 10 to 20 days). As predominant surface species on diorite, $\text{UO}_2(\text{CO}_3)_3^{4-}$ was identified by in situ time-resolved attenuated total reflection Fourier-transform infrared (ATR FT-IR) spectroscopy. About 50% of the sorbed U can be desorbed with Äspö ground water. This part occurs predominantly as U(VI) (94%) as shown by TTA solvent extraction.

In the Np sorption system, the effect of the groundwater composition on speciation and sorption behavior is weak. By ATR FT-IR spectroscopy, NpO_2^+ was detected in solution. During sorption experiments under anoxic conditions (up to 108 days), Np(V) is reduced to Np(IV) by the Fe(II) of the diorite which leads to a very strong Np sorption (95% sorption for $[\text{Np}]_0 = 1 \times 10^{-6}$ M, S/L = 200 g/L). Consequently, only 5–6% of the sorbed Np can be desorbed with Äspö ground water. This small amount was identified as Np(V) by TTA solvent extraction.

Reactivity of nanoscale zero-valent iron particles used for *in situ* groundwater remediation

D. SCHMID, S. LAUMANN, V. MICIĆ AND T. HOFMANN*

Department of Environmental Geosciences, University of Vienna, Vienna, Austria (*correspondence: thilo.hofmann@univie.ac.at)

Nanoscale zero-valent iron (nZVI) is a powerful reducing agent and has therefore been proposed as a tool for *in situ* groundwater remediation [1]. It has a high potential for transformation of a broad range of contaminants, including chlorinated solvents, redox active toxic metals/metalloids and radionuclides, chemical warfare agents, and pharmaceuticals [2,3,4]. The effectiveness of this remediation technique depends on the reactivity of nZVI particles, which is influenced e.g., by particle properties, hydrochemical conditions, and nature of the contaminants.

The aim of this study is to investigate the reactivity of two commercially available nZVI using iopromide in batch and column reactors under pH values typically found in groundwater (pH 7 and 8). Iopromide is a halogenated X-ray contrast media and serves as a model contaminant.

The investigated nZVI included polyelectrolyte-coated nZVI and non-coated nZVI, both in aqueous suspension (NANOIRON s.r.o., Czech Republic). All experiments were carried out under anoxic conditions with the same molar ratio of Fe⁰ and iopromide.

First results show that the degradation of iopromide with both nZVI studied follows a pseudo-first order kinetics. Non-coated nZVI appeared to be more reactive. Both types of nZVI were able to fully degrade iopromide in nearly ten minutes under the applied laboratory conditions. The surface area normalized reaction rate constant (K_{SA}) depends on the pH value and the type of nZVI. The non-coated nZVI reacted 2–3 times faster than the polyelectrolyte-coated nZVI. At the pH of 7 the K_{SA} increases from 330 L m⁻² h⁻¹ for coated nZVI to 940 L m⁻² h⁻¹ for non-coated nZVI. At a pH value of 8 the K_{SA} values are 3–4 times lower, varying from 110 L m⁻² h⁻¹ for coated nZVI to 240 L m⁻² h⁻¹ for non-coated nZVI.

Further experiments will be conducted in column reactors under similar hydrochemical conditions and iopromide concentrations in order to simulate the nZVI-mediated iopromide reduction in groundwater and to compare the reaction rate constants with these obtained in batch reactors.

[1] Karn *et al.* (2009): *Envir. Health Perspect.* 117, 1823–1831. [2] Zboril *et al.* (2012): *Hazard. Mater.* (211–212), 126–130. [3] Zhang, W. (2003): *J. Nanopart. Res.* 5, 323–332. [4] Stieber *et al.* (2011): *ES&T* 45 (11), 4944–4950.

Alpine metamorphism of the Pan-African gneiss basement in the Menderes/Çine massif, SW Turkey, revealed by garnet Lu-Hf geochronology

ALEXANDER SCHMIDT^{1a} AND ROLAND OBERHÄNSLI^{1b}

¹Institute of Earth- & Environmental Sciences, University of Potsdam, Germany

^aalexander.schmidt@geo.uni-potsdam.de

^broob@geo.uni-potsdam.de

The Menderes Massif is one of the large Alpine metamorphic complexes of Turkey. Its southern part, precisely the Çine submassif, is described as a high-grade gneissic core of Precambrian basement covered by a lower-grade series of Paleozoic schists and Cenozoic-Mesozoic marbles. The geochronology of the gneiss basement in this complex so far highly depends on U-Pb ages of zircons, which yield protolith ages between 560 to 540 Ma. Its metamorphic period has been constrained at Alpine ages between 63 and 25 Ma using Ar/Ar and Rb-Sr geochronology. However garnet, one of the most abundant minerals in schists of this region, has yet to be the focus of geochronological work. Here we present the first Lu-Hf ages of garnet crystals from garnet-biotite schists of the southern margin of the Çine submassif. Lu-Hf analysis have been performed on 4–6 cm sized euhedral garnet crystals by the use of a micro-sampling technique, which permits the analysis of the isotopic composition of cores and rims of garnets, and a set number of intermediate radii. Different zones of these garnet crystals were recognized based on trace element distributions in core to rim profiles. The Lu-Hf results so far reveal at least two events, i.e. the beginning of garnet growth represented by a garnet core age of ca. 60 Ma, and an age of ca. 40 to 38 Ma at an intermediate radius of the garnet crystal ($r \sim 50\%$), which also corresponds to a pronounced change in the distribution of heavy to medium rare earth elements. The Fe, Mg, Mn and Ca as well as the heavy rare earth element distributions in the garnet crystals indicate the preservation of a classical growth zoning pattern, i.e. bell-shaped Mn, constant decrease in Fe/(Fe+Mg), and HREE enrichment in garnet cores. Therefore it is clear that the Lu-Hf analysis yield growth ages rather than retrograde overprinting, hence the evidence for the Alpine metamorphism of the Çine submassif.

Quartz solubility and CO_3^{2-} – HCO_3^- equilibrium in $\text{H}_2\text{O}+\text{Na}_2\text{CO}_3$ and $\text{H}_2\text{O}+\text{NaHCO}_3$ fluids at high P and T

C. SCHMIDT¹

¹Deutsches GeoForschungsZentrum (GFZ), 14473 Potsdam, Germany (Christian.Schmidt@gfz.potsdam.de)

Alkali hydrogencarbonate and carbonate in aqueous fluids may play an important role in the mobilization of the REE and other elements at crustal conditions [1] and in subduction zones [2]. Here, the CO_3^{2-} – HCO_3^- equilibrium and the quartz solubility in aqueous 4.65 molal NaHCO_3 and 1.6 molal Na_2CO_3 solutions were studied to 600 °C and 1.53 GPa using a hydrothermal diamond-anvil cell. The recorded spectra were normalized to the temperature dependence of the Stokes-Raman scattering intensity, the frequency and scattering factor, density, and reflection at the diamond-fluid interface [3,4]. The HCO_3^- (aq) and CO_3^{2-} (aq) concentrations were obtained from the integrated intensities of the Raman bands at ~ 1000 and ~ 1060 cm^{-1} assuming that the ratio of the relative molar scattering factors $J_{1000}/J_{1060}=0.1667/0.2434$ [3] is independent of pressure (P) and temperature (T). In the Na_2CO_3 solution, the fraction of the species CO_3^{2-} (aq) did not show a significant dependence on pressure, but decreased with temperature from ~ 0.77 at 100 °C to ~ 0.69 at 200 °C to ~ 0.41 at 600 °C. Before equilibration at 600 °C, the CO_3^{2-} (aq) fraction at vapor pressure was ~ 0.99 at 100 °C and ~ 0.91 at 200 °C. No CO_2 or CH_4 were detected. In the NaHCO_3 solution, the CO_3^{2-} (aq) fraction increased with temperature and decreased with pressure along all studied isotherms from 200 to 600 °C, e.g. at 600 °C from 0.16 at 0.63 GPa to 0.1 at 1.5 GPa. Thus, HCO_3^- ions can be stable in lower crustal and upper mantle fluids. The only detectable Raman band from dissolved silica was at ~ 770 cm^{-1} , which indicates a predominantly monomeric silica speciation. The calibrated integrated intensity of this band was used to determine the SiO_2 (aq) molality. The quartz solubility in 1.6 molal Na_2CO_3 increased with P and T , but was always much higher than the solubility of quartz in water at the same P - T condition. The quartz solubility in 4.65 molal NaHCO_3 increased with T , decreased with P along the 500 and 600 °C isotherms to values below the solubility in water, and was approximately constant at 300 and 400 °C. For lower pressure isobars, there was a distinct drop in the solubility between 500 and 400 °C.

[1] Thomas *et al.* (2011) *Contrib. Mineral. Petrol.* **161**, 315–329. [2] Martinez *et al.* (2004) *Chem. Geol.* **207**, 47–58. [3] Rudolph *et al.* (2008) *Dalton Trans.*, 900–908. [4] Schmidt (2009) *Geochim. Cosmochim. Acta* **73**, 425–437.

Molecular-level comparison of water-soluble sedimentary organic matter extracted by two methods

FRAUKE SCHMIDT^{1*}, BORIS P. KOCH², MATTHIAS WITT³ AND KAI-UWE HINRICHS¹

¹MARUM – Center for Marine Environmental Sciences, University of Bremen, Leobener Straße, D-28359 Bremen, Germany (*correspondence: frauke.schmidt@uni-bremen.de)

²Alfred-Wegener-Institut Helmholtz-Zentrum für Polar- und Meeresforschung, Am Handelshafen 12, D-27570 Bremerhaven, Germany

³Bruker Daltonik GmbH, Fahrenheitstraße 4, 28359 Bremen, Germany

Organic matter in marine sediments is a complex mixture of numerous individual molecules, which are central reactants in various biogeochemical processes and serve as a substrate for benthic organisms. The fate of organic matter and its bioavailability is largely controlled by composition, size and reactivity of the individual organic molecules. In this study, we aim at a molecular characterization of the easily mobilized and thus accessible fraction of organic matter in marine sediments. We compared the molecular composition of (i) the mobile dissolved organic matter (DOM) pool in interstitial waters, extracted with rhizons, with (ii) the organic matter that was extracted from the associated sediment with water in a Soxhlet apparatus. After solid phase extraction, both DOM fractions were subjected to molecular-level analysis by ultra-high resolution Fourier Transform Ion Cyclotron Resonance Mass Spectrometry (FT-ICR-MS). We selected four different sediment horizons of a core from the Black Sea that represented different ages, depositional and geochemical conditions. FT-ICR mass spectra of the Soxhlet extracted DOM yielded 2- to 3-times higher numbers of molecules compared to the interstitial water DOM, with the former being distributed over a larger mass range and exhibiting higher abundances of heteroatom-bearing molecules. We related the molecular-level differences between both DOM pools to age and sediment geochemistry. The Soxhlet-extractable DOM pool was up to 30-times more concentrated than the DOM pool in the interstitial waters. Soxhlet extraction of sediments in combination with FT-ICR-MS analyses opens a window to studying a so far uncharacterized sedimentary organic matter pool that is potentially the major precursor of “traditional” DOM.

Discrimination scheme for Fe-Mn deposits based on REY, HFSE and Th

KATJA SCHMIDT^{1*}, MICHAEL BAU¹
AND ANDREA KOSCHINSKY¹

¹School of Engineering and Science, Jacobs University
Bremen, 28759 Bremen, Germany, *correspondence:
k.schmidt@jacobs-university.de

Marine Fe-Mn deposits can be distinguished based upon the type of aqueous fluid from which they precipitate and their specific setting: While hydrogenetic crusts slowly precipitate from ambient seawater and attain their constituents from this source, diagenetic nodules form within the sediment, with pore water as major source of elements. In the vicinity of hydrothermal vents, hydrothermal crusts precipitate from both hydrothermal fluid and seawater as possible source fluid. Variable concentrations of economically important elements characterize these groups. The individual groups can be separated using discrimination diagrams such as Ce/Ce*_{SN} vs. Nd, Ce/Ce*_{SN} vs. Y/Ho_{SN}, Nb vs. Ta, and Ce/Ce*_{SN} vs. Th, Zr, Hf, Nb, Ta, which combine the effects of redox, growth rate and mineralogy on the trace metal content of Fe-Mn deposits. The redox-sensitive Ce, and HFSE and Th are continuously scavenged during crust growth, while the other REY are controlled by an exchange equilibrium. In contrast to REY, HFSE and Th are mainly scavenged from the Fe oxide phase relative to the Mn oxide phase, and together with the low mobility of these elements during diagenesis, this can be used to separate the individual groups. Hydrogenetic crusts display positive Ce anomalies, negative Y anomalies and high concentrations of REY, HFSE and Th, reflecting slow precipitation from seawater. Diagenetic nodules differ from hydrogenetic crusts and nodules as they display negative Ce anomalies at lower Nd concentrations, related to the low mobility of Ce⁴⁺ in sub-oxic porewaters. Seawater-dominated hydrothermal crusts differ from hydrogenetic crusts and diagenetic nodules as this is the only group which display positive Y anomalies, together with negative Ce anomalies and low Nd concentrations. This signature reflect the rapid scavenging of REY from ambient seawater on hydrothermal oxide particles, without strong fractionation. In contrast to these hydrothermal crusts, hydrothermal Mn crusts which gained significant proportions of their REY content from the mantle via hydrothermal fluids (up to 30%, based on Nd isotopes), often cover the same regions as diagenetic nodules in Ce/Ce*_{SN} vs. Y/Ho_{SN} and Ce/Ce*_{SN} vs. Nd diagrams. Both groups can be further be separated in Ce/Ce*_{SN} vs. Th and Nb vs. Ta diagrams.

Geochemical diversity and K-rich compositions found by the MSL APXS in Gale Crater, Mars

M.E. SCHMIDT¹, P.L. KING², R. GELLERT³, B. ELLIOTT⁴,
L. THOMPSON⁴, J.A. BERGER⁵, J. BRIDGES⁶, J.L.
CAMPBELL³, B. EHLMANN⁷, J. GROTZINGER⁷, J.
HUROWITZ⁷, L. LESHIN⁸, K.W. LEWIS⁹, S.M.
MCLENNAN¹⁰, D.W. MING¹¹, G.M. PERRETT³, I.
PRADLER³, E.M. STOLPER⁷, S.W. SQUYRES¹², A.H.
TRIEMAN¹³ AND THE MSL SCIENCE TEAM

¹Brock Univ, St. Catharines ON L2S2A1 Canada,
*correspondance: mschmidt2@brocku.ca;

²Aust. Nat. Univ., Canberra ACT 0200 Australia;

³Univ. Guelph, ON N1G2M7 Canada;

⁴Univ. New Brunswick, Fredericton, NB E3B5A3 Canada;

⁵Univ. Western Ontario, London, ON N6A3K7 Canada;

⁶Univ. Leicester, LE1 7RH, UK;

⁷Calif. Inst. Tech., Pasadena, CA 91125, USA;

⁸Rensselaer Polytech. Inst., Troy, NY 121808 USA;

⁹Princeton Univ., NJ 08540, USA;

¹⁰Geosciences, SUNY Stony Brook, NY 11794 USA;

¹¹NASA JSC, Houston, TX 77058 USA;

¹²Cornell Univ., Ithaca, NY 14850 USA;

¹³Lunar Planet. Inst., Houston, TX 77058 USA

Along the Curiosity rover's traverse toward Glenelg (through sol 102) the Alpha Particle X-ray Spectrometer (APXS) analysed four rocks and one soil. Microscopic images and compositions of unbrushed rock surfaces are consistent with 5-20% dust contamination. Nevertheless, the underlying characteristics of these rocks may still be discerned. As a group, they span nearly the entire range in FeO* and MnO of the Martian dataset. In addition, they are particularly enriched in volatile metals (K, Zn, Ge), and these elements do not correlate with Cl or S. One rock, Jake_Matijevic is notably alkaline and evolved; its composition is that of a nepheline-normative mugearite. The other three rocks plot in the basanite field of a TAS diagram, with high K₂O (up to 3.0%) and low SiO₂. These three rocks are otherwise SNC-like (high Fe and low Al). Three out of the four rocks (including Jake_Matijevic) plot along a line in variation diagrams, suggesting mixing of Fe-rich and Al-rich components, likely by sedimentary processes.

With only four rocks analyzed so far and ambiguity as to their geologic context (e.g. outcrop vs. float; igneous vs. sedimentary) additional measurements are needed to fully understand the region. It is nevertheless clear that Curiosity landed in a lithologically diverse, K-rich region of Mars.

The influence of Perchlorate (ClO_4^-) on the sorption behavior of Th(IV) on the Muscovite (001) basal plane

M. SCHMIDT¹, S. S. LEE², R. E. WILSON², K. E. KNOPE², P. FENTER² AND L. SODERHOLM²

¹Karlsruhe Institute of Technology (KIT), Institute for Nuclear Waste Disposal, Karlsruhe, Germany

²Argonne National Laboratory, Chemical Sciences and Engineering Division, Argonne, IL, U.S.A.

In many sorption as well as other geochemical studies the perchlorate anion (ClO_4^-) is used as a constituent of the background electrolyte for its non-coordinating behavior. It is assumed that by restricting the competitive coordination reaction in solution it is possible to study the unperturbed sorption reaction. The adsorption of tetravalent thorium to the muscovite (001) basal plane gives a cautionary example, where the change from a weakly coordinating anion (Cl^-) to a non-coordinating anion (ClO_4^-) has a drastic and unexpected effect on the sorption behavior of the cation.

Results from surface x-ray diffraction techniques in combination with alpha-spectrometry measurements will be presented. On the basis of these results we will demonstrate that Th(IV) exhibits a straightforward sorption behavior driven by electrostatic attraction and, to a lesser degree solution complexation and hydrolysis, when the reaction is studied in NaCl background electrolyte media (Schmidt *et al.*, 2012). Thorium adsorbs up to a slightly higher than charge compensating coverage of 0.4 Th/ A_{OC} predominantly as an extended outer sphere complex with two intact hydration spheres.

By the same method and under the same solution conditions – but with NaClO_4 instead of NaCl – the adsorption behavior changes drastically: no interaction of Th with the interface can be detected under these conditions. The changes in solution chemistry are comparably minor, and it appears unlikely that changes in the complexation behavior can explain this observation. Potential interfacial reaction mechanisms underlying this unanticipated behavior will be discussed.

[1] Schmidt, M., Lee, S.S., Wilson, R.E., Soderholm, L. and Fenter, P. (2012) Sorption of tetravalent thorium on muscovite. *Geochimica et Cosmochimica Acta*, **88**, 66-76.

Distribution and enrichment processes of lithium and other solutes in the Salar de Uyuni brine

NADJA SCHMIDT*, ROBERT SIELAND AND BRODER MERKEL

TU Bergakademie Freiberg, Department of Hydrogeology, D-09599 Freiberg, Germany (*correspondence: Nadja.Schmidt@geo.tu-freiberg.de)

The world's largest salt pan, the Salar de Uyuni, is located in the Bolivian Altiplano, at 3650 masl between the eastern and western cordilleras of the Andes. Although it hosts one of the world's most promising lithium deposits, accumulation and horizontal distribution of lithium and other solutes in the brine are not satisfactorily understood.

During various drilling and sampling campaigns (2009-2012) numerous brine samples were taken from boreholes down to 12 m all over the salt lake. Further brine samples were gained from one meter deep drilling holes along three transects from the center to the border in the northeastern part of the Salar. All samples were investigated by IC and ICP-MS as well as for stable isotopes.

Li concentrations in the brine vary between 200 and 1500 mg/L, whereby a vertical gradient could not be observed in the upper 12 m. Li is peaking near the northeastern and southeastern shore, with concentration gradients of 100 mg/L/km (own data) and 40 mg/L/km [1], respectively. Li peaks match with the delta areas of former and recent inflowing rivers. Hence, more than one major tributary as a source of lithium exist, which is in contradiction to results of former investigations supposing the Rio Grande to be the only feeder of lithium to the salt lake basin [2].

The surface in areas where increased Li concentrations occur is characterized by muddy sediments interspersed with crystals of halite and other evaporites. Because clay is decreasing in direction from the shore a temporary fixation and release of Li on clay is assumed as controlling factor leading to an effective enrichment in the brine.

[1] F. Risacher & B. Fritz (2000) *Chemical Geology* 167: 373-392. [2] S.L. Rettig, B.F. Jones, F. Risacher (1980) *Chemical Geology* 30: 57-79

Calcium isotope fractionations from roots to shoots

SCHMITT A.-D.^{1,2*}, STILLE P.¹, LABOLLE F.³, COBERT F.^{1,4}, BOURGEADE P.², CHABAUX F.¹ AND GANGLOFF S.¹

¹Université de Strasbourg et CNRS-UMR 7517,

LHyGeS/EOST ; 1 rue Blessig, F-67000 Strasbourg

²Université de Franche-Comté et CNRS-UMR 6249, Chrono-

environnement ; 16, route de Gray, F-25000 Besançon

³Université de Strasbourg, Institut de Zoologie et de Biologie végétale, 12, rue de l'université, F-67000 Strasbourg

⁴Université de Liège, Faculté d'agronomie de Gembloux; 27 avenue du maréchal Juin, B-5030 Gembloux

* adschmitt@unistra.fr

Recent studies have shown that Ca isotope ratios have the potential to be important tracers of biological activities in forested ecosystems or more generally in plant physiology and in biogeochemistry.

Field studies performed in forested watersheds point to the importance of Ca isotope fractionations in soil solutions due to biological activity in the surficial soil horizons. Hydroponic experiments, performed on rapid growing bean plants, that allow to have a complete growth cycle, helped to identify the mechanisms responsible for these Ca isotope fractionations (Cobert *et al.*, 2011; Schmitt *et al.*, 2013). Indeed, the adsorption of Ca by lateral roots, that are enriched in ⁴⁰Ca compared to the nutritive medium, follows a closed-system equilibrium fractionation with a fractionation factor of 0.9988, suggesting that Ca forms exchangeable bonds with the RCOO⁻ groups in the cell wall structure of the lateral roots. Two other fractionation levels have been identified within the plant during the Ca transfer from roots to shoots. When the xylem sap goes to the shoots, ⁴⁰Ca is preferentially bound to the polygalacturonic acids (pectins) of the middle lamella of the xylem cell wall. Finally, a third fractionation occurs in the reproductive organs also caused by cation-exchange processes with pectins. The fractionation mechanisms are the same whatever the Ca content and pH of the nutritive solution. Only the bean plants average signature as well as the amplitude of the Ca isotopic fractionation within plant organs are highly dependent on the composition of the nutritive solution. A comparative field study is installed to examine the Ca isotopic fractionation in trees of a forested watershed.

[1] Cobert *et al.* 2011, *GCA* **75**, 5467-5482; [2] Schmitt *et al.*, 2013. *GCA* **110**, 70-83.

Atmospheric CF₄ trapped in polar ice – A new proxy for granite weathering

J. SCHMITT^{1*}, B. SETH¹, P. KÖHLER², J. WILLENBRING³ AND H. FISCHER¹

¹Climate and Environmental Physics & Oeschger Centre for Climate Change Research, University of Bern, CH,

(*correspondence: schmitt@climate.unibe.ch)

²Alfred Wegener Institute Helmholtz Centre for Polar and Marine Research, Bremerhaven, Germany

³University of Pennsylvania, Department of Earth & Environmental Sciences, Philadelphia, USA

The reconstruction of continental weathering rates using trace elements and their isotopes measured on marine sediments and crusts is a vigorously growing field. Here, we use a novel approach using the ppt-level trace gas CF₄, tetrafluoromethane, which can be analysed in air trapped in ice cores. CF₄ is a trace impurity in granites and other plutonic rocks, and during weathering this gas escapes into the atmosphere. In preindustrial times, this release from granitic rocks was the only natural source of CF₄. Because CF₄ is inert to destruction processes in the tropo- and stratospheres, its only sink is destruction by UV radiation and radicals in the mesosphere. This chemical inertness is responsible for an exceptionally long atmospheric lifetime which is expected to range between 50 kyr and 400 kyr. Although the globally integrated CF₄ emission flux from weathering is only a few tons per year, the exceptionally long lifetime allows to establish a long-term atmospheric concentration of about 33 ppt. We developed a vacuum melt-extraction system for ice core samples coupled to a mass spectrometry detector to precisely measure these trace amounts of CF₄ found in past atmosphere and applied this method to ice over the entire Dome C ice core. During the last 800 kyr, atmospheric CF₄ varied in a narrow band between 31 ppt and 35 ppt, i.e. only 10-15 % variability, providing a first estimate of the long-term weathering rate fluctuations. Our record shows that CF₄ increases during interglacials and falls during the coldest, glacial phases. However, our CF₄ record shows also a pronounced shift toward higher CF₄ levels after 430 kyr (the Mid-Brunhes Event). With the beginning of Marine Isotope stage 11, we find a steep rise in CF₄ that probably relates to intense weathering during the first full interglacial after a series of lukewarm interglacials.

CF₄ and CO₂ - coupling weathering and carbon cycle

J. SCHMITT^{1*}, B. SETH¹, P. KÖHLER², J. WILLENBRING³
AND H. FISCHER¹

¹Climate and Environmental Physics & Oeschger Centre for Climate Change Research, University of Bern, CH, (*correspondence schmitt@climate.unibe.ch)

²Alfred Wegener Institute Helmholtz Centre for Polar and Marine Research, Bremerhaven, Germany

³University of Pennsylvania, Department of Earth & Environmental Sciences, Philadelphia, USA

The analysis of CO₂ and its stable carbon isotopes from ice cores revealed large changes of atmospheric CO₂ related to changes in ocean circulation, marine biological processes and contributions from the terrestrial carbon storage. These processes dominate the glacial/interglacial CO₂ variations. Yet, CO₂ is also modulated by the marine alkalinity balance. The net alkalinity influx to the ocean is driven by silicate weathering drawing down atmospheric CO₂. Conversely, alkalinity is lost when CaCO₃ is buried in marine sediments. On orbital time scales, these fluxes are assumed to be almost balanced as atmospheric CO₂ and its climatic effects feedback on the weathering rates providing a negative feedback loop.

Trace elements from marine sediments are widely applied to derive weathering rates or changes in the weathering style for a certain region. Here, we use a novel approach to provide a global weathering estimate using the ppt-level trace gas CF₄ archived in polar ice cores. CF₄ is found as a trace gas in granites, and during weathering it escapes to the atmosphere. Because CF₄ is inert in the lower atmosphere, its only sink is destruction by UV radiation in the mesosphere. This chemical inertness is responsible for an exceptionally long atmospheric lifetime which is expected to range between 50 kyr and 400 kyr. We developed a vacuum melt-extraction system for ice core samples to precisely measure these trace amounts of CF₄ and applied it to ice over the entire Dome C ice core. During the last 800 kyr, atmospheric CF₄ varied in a narrow band between 31 ppt and 35 ppt, i.e. only 10-15 % variability, providing a first estimate of the long-term weathering rate fluctuations. Our record shows that CF₄ increases during interglacials and falls during the coldest, glacial phases. However, our CF₄ record also shows a pronounced shift toward higher CF₄ levels after 430 kyr. With the beginning of MIS 11, we find a rise in CF₄ that probably relates to intense weathering during the first full interglacial after a series of lukewarm interglacials. This dataset lends support to a strong positive coupling of continental weathering and climate.

Multitracer paleoclimate and recharge study of groundwater in the North China Plain

T. SCHNEIDER^{1*}, G. CAO², C. ZHENG^{2,3}
AND W. AESCHBACH-HERTIG¹

¹Institute of Environmental Physics, Heidelberg University, Im Neuenheimer Feld 229, 69117 Heidelberg, Germany (*correspondence: Tim.Schneider@iup.uni-heidelberg.de)

²Center for Water Research, College of Engineering, Peking University, Beijing 100871, China

³Department of Geological Sciences, University of Alabama, Tuscaloosa, Alabama, USA

A multitracer study of groundwater in the North China Plain (NCP) was conducted in the framework of a Chinese-German cooperation project whose main objective is to obtain groundwater ages and recharge rates in order to refine a groundwater flow model of the NCP and to help find ways for sustainable groundwater management [1]. Additionally, the obtained data adds to an existing data set from a previous paleoclimate and groundwater recharge study in the NCP [2][3].

Samples were taken on two sampling campaigns in 2011 and 2012 from 36 wells along a transect in the northern NCP starting at the mountains in the west, passing south of Beijing and leading to the Bohai Sea at Tianjin. In addition, seven wells were sampled on a short transect near Handan, further south in the NCP.

Dating tracers being used are ³H-³He, SF₆ and CFCs 11, 12 and 113 for young ages and ¹⁴C as well as ⁴He for a longer time scale. The climate information is obtained through dissolved noble gases and stable isotopes. The combined use of SF₆ and CFCs allows us to identify and correct for possible SF₆ from natural sources and CFC contamination in the highly industrialized area near Beijing.

Dating results show that the groundwater age mainly increases with depth rather than distance along the transect, with an abrupt rise at a depth of around 100m. Enhanced concentrations of both SF₆ and CFCs are unrelated, indicating different sources. The noble gas temperatures suggest a temperature difference between the Holocene and the last glacial period of about 5°C. Overall, the new data confirm and complement previous results from the NCP [2][3].

[1] Cao *et al.* (2013), *Water Resour. Res.* **49**, 159-175. [2] Kreuzer *et al.* (2009), *Chem. Geol.* **259**, 168-180. [3] von Rohden *et al.* (2010), *Water Resour. Res.* **46**, W05511

²⁴¹Am supporting ²¹⁰Pb and ¹³⁷Cs dating

BERNHARD SCHNETZER¹ KATHARINA HÄUSLER²
AND OLAF DELLWIG²

¹ICBM, Carl-von-Ossietzky University, 26111 Oldenburg, Germany; b.schnetzer@icbm.de

²Leibniz Institute for Baltic Sea Research (IOW), Rostock, Germany; katharina.hauesler@io-warnemuende.de; olaf.dellwig@io-warnemuende.de

²¹⁰Pb dating is usually supported by radioactive ¹³⁷Cs to verify age models. Atmospheric nuclear bomb testing in the 50th and 60th as well as the Chernobyl accident in 1986 has introduced not only measurable amounts of radioactive Cs but also Pu nuclides into the environment. Due to the relatively short half-life of ²⁴¹Pu (14.35 a) measurable activities of the daughter ²⁴¹Am are now present and can directly be analysed by modern gamma-ray detectors (Appleby *et al.* 1991). The advantages of using ²⁴¹Am over ¹³⁷Cs are a) its high particle reactivity causing rapid sedimentary burial and b) its immobile behaviour after deposition minimizing redistribution. While the 1963 peak in ¹³⁷Cs is prone for a large dispersion in the sedimentary environment, ²⁴¹Am forms sharp peaks in undisturbed sediments. Even the frequency of atmospheric nuclear bomb testing can be identified by high-resolution sampling of geological archives resulting in more trustful age determinations. In sediments where both ²¹⁰Pb and ¹³⁷Cs fail to give reliable ages, ²⁴¹Am can be used for a rough age estimation of sediment intervals. In such cases the following ²⁴¹Am time markers can be used: increased activities due to the frequency of atmospheric bomb testing in 1951, first maximum in 1958, second maximum in 1962 and a narrow peak in 1986 (Chernobyl) and possibly in the future 2011 (Fukushima). Between these markers, sediment velocities or sedimentation rates (if dry bulk density is known) can be calculated spanning at least a half century back in time. The sharp peaks originating from accidents can easily be missed by low-resolution sampling. Due to the much longer half-life of ²⁴¹Am (432a) compared to ¹³⁷Cs (30.17a) this tracer can be used when ¹³⁷Cs cannot be detected in the environment any more. For instance, ¹³⁷Cs in 1962 sediment layers will be decayed after app. eight half-lives in 2075. In addition, sediment data from the euxinic Landsort and Gotland Deeps (Baltic Sea) indicate a significant influence on ¹³⁷Cs and ²¹⁰Pb burial over time due to the Mn-pump within the redoxline.

[1] Appleby P.G., Richardson N., & Nolan P.J. (1991): ²⁴¹Am dating of lake sediments. *Hydrobiologia* 214, 35-42.

Cr isotopic variations in Neoproterozoic near-surface chemical sediments

R. SCHOENBERG^{1*}, I.C. KLEINHANN¹, M. WILLE¹,
M. VAN ZUILEN², R.B. PEDERSEN³, V. MELEZHNIK^{3,4}
AND N. BEUKES⁵

¹Dept. of Geoscience, University of Tuebingen, Germany
(*correspondence: schoenberg@ifg.uni-tuebingen.de)

²Institute de Physique de Globe de Paris, France

³Centre for Geobiology, University of Bergen, Norway

⁴Geological Survey of Norway (NGU), Trondheim, Norway

⁵Dept. of Geology, University of Johannesburg, South Africa

Recent studies explored the potential of stable Cr isotopic variations in oceanic sedimentary archives as tracer for atmospheric oxygen levels through Earth's history [1,2]. Thereby, the stable Cr isotopic variations in up to 2.75 Ga old BIFs were interpreted to indicate oxidative chromium weathering on the continents initiated by an accumulation of small levels of free atmospheric oxygen some 350 Ma before the ca. 2.4 to 2.32 Ga great oxidation event (GOE) [1]. This interpretation, however, was challenged by others [3], who propose that the Cr isotopic variations in these predominantly Algoma type BIFs are due to non-redox isotopic effects caused by rapid precipitation from their deep-water hydrothermal source.

In order to shed light on the applicability of stable Cr isotopes as paleo-redox tracer we investigated carbonates from well-defined supra-, intra- and subtidal depositional environments from the ca. 2.55-2.48 Ga old Malmani Subgroup of the Transvaal Basin in South Africa and 2.06 Ga old lacustrine carbonates, marine stromatolites and near-shore jaspilites from the Pechenga Greenstone Belt, as well as 2.0 Ga organic-rich, siliceous deposits from the Onega Basin, both situated in the NW Fennoscandian Shield. The relatively large variations (ca. +1.4‰ to -1.2‰ in $\delta^{53/52}\text{Cr}$) found in post-GOE sedimentary archives from the Fennoscandian Shield support chromium redox-cycling associated with oxidative chromium weathering on the continental surface. Compared to the large Cr isotope variations of these post-GOE deposits, the range in $\delta^{53/52}\text{Cr}$ values of late Archean sedimentary archives appears to be much smaller. Possible scenarios to explain the observed Cr isotopic variations in these sedimentary archives and their implications to the presence of free atmospheric oxygen will be discussed.

[1] Frei *et al.* (2009) *Nature* **461**, 250-253. [2] Frei *et al.* (2011) *EPSL* **312**, 114-125. [3] Konhäuser *et al.* (2011) *Nature* **478**, 369-373.

From date to process: Integrating geochemistry and geochronology on very short and very long timescales

BLAIR SCHOENE

219 Guyot Hall, Department of Geosciences, Princeton University, Princeton, NJ, USA.
(bschoene@princeton.edu)

How continental crust is created, preserved and recycled, and whether or not these processes have changed through Earth history are important for a) understanding the geochemical and petrological stratification of the crust and b) quantifying long term geochemical and isotopic cycling in the Earth's crust and mantle. Developing models for crustal evolution requires robust geochronology on both the short and long timescales, targeting relatively rapid geologic phenomena (e.g. magma production and differentiation) as well as long term secular change. This contribution highlights recent efforts to better apply high-precision U-Pb geochronology to continental magmatic systems and to develop techniques comparing magmatic systems through Earth history.

Models describing the transfer of mass and heat through the crust during orogenesis demand age constraints with increasing precision and accuracy. While modern ID-TIMS U-Pb geochronology can resolve the timescales of zircon crystallization in single pulses of magma, much work is needed to relate dates to processes such as magma production, transport, differentiation, and emplacement. Our recent work focuses on integrating zircon crystallization ages and geochemistry to both understand the growth history of single zircons on <50 ka timescales and to build a framework for longer timescale geochemical evolution of two Alpine magmatic systems.

To compare differences in magmatic differentiation during crustal magmatism from the Archean to present, we develop statistical methodologies for analyzing large geochemical databases (Earthchem, etc.). Substantial differences in both crustal inputs (basalts) and indicators of differentiation to high-Si compositions suggest either secular changes in magmatic/metamorphic processes during crustal genesis and modification, or preservation bias. These results motivate further detailed investigation of Archean terranes, although robust comparison between any number of orogenic belts, Archean or modern, require geochronology with precision that is relevant to tectonomagmatic processes. Sub-million year precision is now achievable in Archean rocks by ID-TIMS U-Pb geochronology, but necessitates careful integration of field, geochemical, and geochronological data with numerical modelling studies.

Evolution of temperature and precipitation during Marine Isotope Stage 5 recorded in speleothems from the Hüttenbläuserschachthöhle, western Germany

D. SCHOLZ^{1,2*}, D. HOFFMANN^{2,3}, C. SPÖTL⁴, Y. KOCOT¹
AND P. HOPCROFT⁵

¹Institute for Geosciences, University of Mainz, Johann-Joachim-Becher-Weg 21, 55128 Mainz, Germany
(*correspondence: scholzd@uni-mainz.de)

²Bristol Isotope Group (BIG), School of Geographical Sciences, University of Bristol, University Road, BS8 1SS Bristol, United Kingdom

³CENIEH, Paseo Sierra de Atapuerca s/n, 09002-Burgos, Spain

⁴Institut für Geologie und Paläontologie, Leopold-Franzens-Universität, Innrain 52, 6020 Innsbruck, Austria

⁵Bristol Research Initiative for the Dynamic Global Environment (BRIDGE), School of Geographical Sciences, University of Bristol, University Road, BS8 1SS Bristol, United Kingdom

We present high-resolution $\delta^{18}\text{O}$, $\delta^{13}\text{C}$ and trace element profiles for two stalagmites from Hüttenbläuserschachthöhle, western Germany, which grew during Marine Isotope Stage (MIS) 5.

HBSH-1 provides a climate record with decadal to centennial resolution between 130 and 80 ka, which shows four growth interruptions coinciding with the Greenland Stadials. This shows that stalagmite growth is a very sensitive proxy for cool and dry conditions in the northern hemisphere.

We interpret stalagmite $\delta^{18}\text{O}$ as a proxy for past temperature changes, whereas stalagmite $\delta^{13}\text{C}$ rather reflects changes in the hydrologic balance. The $\delta^{13}\text{C}$ record shows three pronounced negative peaks during MIS 5, and the timing of those is in agreement with MIS 5e, 5c and 5a. This suggests warm and relatively humid climate in western Germany for these phases.

During the Last Interglacial, the evolution of $\delta^{18}\text{O}$ and $\delta^{13}\text{C}$ is opposite. Whereas the $\delta^{18}\text{O}$ signal suggests the warmest conditions around 125 ka followed by a gradual decrease, the $\delta^{13}\text{C}$ signal indicates wetter conditions towards the end of the Last Interglacial. This 'decoupling' of temperature and humidity during MIS 5e is also visible in a series of snapshot simulations performed with the general circulation model FAMOUS.

Chemical and isotopic composition of soil solutions from cambisols in Styria (Austria) - Seasonality, evaporation and interstitial distribution

W. SCHÖN^{1*}, A. LEIS² AND M. DIETZEL¹

¹Institute of Applied Geosciences, Graz University of Technology, Rechbauerstraße 12, 8010 Graz, Austria, (*correspondence: w.schoen@student.tugraz.at)

²Institute of Water, Energy and Sustainability, Joanneum Research, Elisabethstraße 18, 8010 Graz, Austria

In most natural surroundings soil solutions are primarily gained from the uptake of meteoric water. Subsequently infiltration, capillary exchange, bioresponse, evaporation etc. result in complex and individual gas-water-solid systems. Knowledge on the isotopic and chemical evolution of soil solutions and its interstitial distribution is highly relevant for environmental and forensic studies, but respective systematic and combined field and experimental studies are rare.

Therefore we investigated the composition of solids and interstitial solutions of individual horizons for three cambisols in Styria (Austria). The solutions were separated from the soils by compaction method at hydraulic pressures of 27.4 and 54.9 MPa, corresponding to respective matric potentials (mp).

The soils consist mainly of quartz, chlorite, muscovite, plagioclase with associated silicates like kaolinite and vermiculite, but without a significant vertical variability. The pH of the separated soil solutions typically increases with depths and elevated mp. Concentrations of dissolved ions such as Ca²⁺ and Mg²⁺ increase at high mp, which correspond to higher δD and δ¹⁸O values. Lab experiments for evaporation and wetting indicate a systematic correlation of the combined isotope data and solution chemistry. The field-related and experimental results are discussed in respect to the impact of seasonality, evaporation, and mp-related interstitial distribution of the (isotope) geochemical composition of the separated soil solutions.

X-ray tomography links macroscopic silicate fabric and AMS fabric

A. SCHÖPA^{*1}, D. FLOESS², M. DE SAINT BLANQUAT³, P. LAURNEAU⁴, C. ANNEN¹ AND L. BAUMGARTNER²

¹School of Earth Sciences, University of Bristol, Wills Memorial Building, BS8 1RJ Bristol, UK

(*correspondence: anne.schopa@bristol.ac.uk)

²Université de Lausanne, Batiment Geopolis, 1015 Lausanne, Switzerland

³Géosciences Environnement Toulouse / Observatoire Midi-Pyrénées, 31400 Toulouse, France

⁴Laboratoire de Planétologie et Géodynamique de Nantes, CNRS/Université de Nantes, 44322 Nantes, France

Anisotropy of magnetic susceptibility (AMS) has been widely applied to gain insight into magnetic fabrics in granitic intrusions, basalt lava flows and dikes. In order to draw this generic link, it is assumed that the AMS fabric reflects the silicate fabric and hence gives information about magma flow, emplacement related strain and/or tectonic strain. However, a detailed analysis of this link between macroscopic magmatic fabric and AMS fabric is still lacking.

We present the first comparison between different fabric datasets to show how the macroscopic silicate fabric is linked to the magnetite-controlled AMS fabric on the grain-size scale. Datasets include 1) macroscopic silicate fabric measured directly in the field; 2) macroscopic silicate fabric derived from image analysis of rock slab pictures and sample pictures [1]; 3) shape preferred orientation (SPO) of mafic silicates from X-ray tomography images; 4) SPO of magnetite grains from X-ray tomography images [2]; 5) calculated distribution of magnetite grains from X-ray tomography images; 6) AMS fabric. The data were collected in the granitic intrusion of the Lago della Vacca Complex, Adamello Batholith, Italy.

Macroscopic mineral fabrics measured in the field and obtained with image analysis agree with each other and with the SPO of mafic silicates calculated from the tomography scans. Furthermore, the tomography results show that the SPO of mafic silicates and of the magnetite grains are consistent with the AMS data whereas the distribution of the magnetites is less compatible with the AMS fabric.

The consistent results obtained from a variety of methods demonstrate that the orientation of the AMS ellipsoid coincides with the macroscopic silicate fabric. This enforces the application of AMS as a robust tool to characterise magmatic fabrics in granitic intrusions.

[1] Launeau *et al.* (2010) *Tectonophysics* **492**, 230-239. [2] Ketchum (2005) *J Struct Geol* **27**, 1217-1228.

Controls on the isotope composition of trace metals in calcite - New tools for paleo-reconstructions

J. SCHOTT^{1*}, V. MAVROMATIS¹ AND E. H. OELKERS¹

¹Université de Toulouse & CNRS, GET, Toulouse, France,
(*presenting author jacques.schott@get.obs-mip.fr,
mavromat@get.obs-mip.fr, oelkers@get.obs-mip.fr)

Divalent metals including Ba, Mg, Sr, Cd, Co, Cu, Mn, and Zn exhibit contrasting ion size, diffusivity, hydration energy (or rate of exchange of water molecules in their hydration sphere), and affinity to hydrolyze or form inorganic and organic ligands. A large number of past studies have shown that these contrasting properties affect calcite-fluid partition constants, and how these partition coefficients vary with calcite growth rate.

In an effort to extend these observations to isotopic fractionation we have performed a number of related experimentally studies showing how crystal growth rates, and fluid pH and speciation impact the isotopic composition of the divalent metals incorporated into the calcite lattice. For example, the extent of Mg isotope fractionation between calcite and the fluid phase increases considerably with **decreasing** calcite growth rate¹. In contrast, Ba, Sr, and Zn isotope fractionation increases with **increasing** calcite growth rate. Equally, Ca and Mg isotope fractionation increase with calcite and magnesite growth rate, respectively². The distinct behavior of Mg stems from the reduced lability of water molecules in its coordination sphere compared to Ca, Ba, Sr, or Zn, and provides new insight on carbonate growth mechanisms. Moreover, Mg kinetic isotope fractionation can be quantified using three isotope diagrams³ which allow the precise determination of equilibrium fractionation factors and provides a new tool to quantify the growth rates of calcite precipitated in the deep past. Such tools also provide insight into the saturation state of the fluids present when the calcite precipitated. Similarly, the measurement of Zn and Cu concentration and isotope compositions during calcite growth at fixed rates, pH, saturation state, and concentration of selected inorganic and organic ligands, allow quantification of the equilibrium isotope composition of Zn and Cu incorporated in the lattice and its dependence on the aqueous fluid composition. Such observations provide new insight into the metal incorporation mechanisms during calcite growth. Our experimental calibrations, validated by the quantification of Mg, Zn and Cu chemical and isotope fractionation in calcite-precipitating springs, are providing new and powerful tools to reconstruct paleo-environmental conditions from the isotope compositions recorded in carbonate sediments.

[1] Mavromatis *et al.* (2013) *Geochim. Cosmochim. Acta* (in press). [2] Pearce *et al.* (2012) *Geochim. Cosmochim. Acta* **92**, 170-183. [3] Young *et al.* (2002) *Geochim. Cosmochim. Acta* **66**, 683-698.

Serpentinization, Microbial Activities, and Carbon Flow in the Deep Biosphere

MATTHEW O. SCHRENK¹

¹East Carolina University, Greenville, NC, USA

Serpentinizing ultramafic rocks are conduits for the exchange of carbon and energy between the deep Earth and the surface environment and are ubiquitous, occurring on each of the continents and over vast portions of the seafloor. Serpentinization commonly generates high pH (>11), highly reducing conditions rich in hydrogen and methane that can sustain deep subsurface microbial communities which play important roles in controlling the composition and mobility of carbon-bearing compounds. Due to a complex interplay of nutrient sources and sinks and because they are perched near the limits of life, the significance of microbial processes in serpentinites has proven difficult to constrain. Recently, concerted studies of serpentinites in both continental and marine settings have begun to identify the functional potential of serpentinite-associated microbial communities, their energy sources, and their impacts upon carbon speciation. Metagenomic and functional genomic analyses document evidence of both consumption and production of hydrogen and methane in certain environments and in some cases for microbially-mediated sulfur and iron red-ox transformations. These studies also provide evidence for CO and CO₂ assimilation and the potential for the fermentation of organic matter derived from deep Earth materials. These data provide important targets for quantification of subsurface biogeochemical processes and their impact upon the characteristics of circulating fluids and their host rocks. By linking microbiological data with geochemical data, these studies also provide the opportunity to develop new paradigms for understanding microbial adaptations and evolution in the deep subsurface environment.

Intact polar lipids and diagenetic processes in sub-seafloor sediments in the Black Sea

JAN M. SCHRÖDER^{1*}, IVANO W. AIELLO², TOBIAS GOLDHAMMER¹, VERENA B. HEUER¹, MARCUS ELVERT¹, MATTHIAS ZABEL¹ AND KAI-UWE HINRICHS¹

¹MARUM – Center for Marine Environmental Sciences and Dept. of Geosciences, University of Bremen, Germany (*correspondance: jschroeder@marum.de)

²Moss Landing Marine Laboratories, Moss Landing, CA, USA

The Black Sea is the world's largest anoxic basin where the water column beneath 100 m depth as well as the underlying sediments are devoid of oxygen. FS Meteor cruise M84/1 (DARCSEAS) [1] investigated site GeoB 15105 in the SW Black Sea and obtained an 8 m-sedimentary record of complex Late Pleistocene environmental change due to the transition from a limnic to a brackish marine system. The resulting diagenetic regime in these sediments is unusual and exhibits signals of overlapping sulfate reduction, methanogenesis, and Fe reduction, coupled with variable concentrations of total organic carbon. This is consistent with evidence for abundant sulfate-reducing bacteria in the methanogenic zone [2]. Using a strongly improved set of methods for extraction, preparation and detection of microbial intact polar lipids (IPL), we examined signals of the sedimentary microbial communities in relation to the complex diagenetic regime and sedimentary history as determined by pore-water analysis of electron donors and acceptors and sedimentological examination, respectively.

We found that IPLs were present throughout the whole sediment core with a maximum in a sapropel layer at around four meters. IPL concentrations were highly variable and archaeal glycolipids (e.g., mono- and diglycosidic glyceroldibiphytanyltetraethers) as well as bacterial phospholipids (e.g., diether based phosphatidyl-ethanolamines) were observed down to a depth of eight meters. Furthermore, varying ratios of archaeal to bacterial lipids between 0.1 and 0.6 revealed regional differences of microbial abundance and could also be related to methane oxidation processes. Our study provides new insights into the relationship of microbial communities, diagenetic processes and the sedimentary history in the Black Sea sediments.

[1] Zabel (2011) RV METEOR, *Cruise Report M84/1 2011*, DFG. [2] Leloup *et al.* (2007) *Env. Microbiol.* **9**, 131-142.

Sediment traps in Lake Baikal reveal strong changes in productivity over the last decade

C.J. SCHUBERT^{1*}, J. NIGGEMANN² AND M. STURM¹

¹Surf, Eawag, 6047 Kastanienbaum, Switzerland (*correspondence: carsten.schubert@eawag.ch, mike.sturm@eawag.ch)

²Max Planck Research Group for Marine Geochemistry University of Oldenburg, 26129 Oldenburg, Germany, (jniggema@mpi-bremen.de)

More than 10 years of monitoring

Lake Baikal is one of the largest lakes in the world and with a maximum water depth of ~1640 m also the deepest. This makes it unique and comparable to an ocean also since due to efficient vertical mixing oxygen concentrations are high throughout the water column.

We have moored sediment traps which were recovered and renewed every year since 1999. Up to 18 traps were deployed over the whole water column. Organic carbon and nitrogen concentrations and isotopes as well as chlorin concentrations and chlorin indices were measured to estimate productivity and the composition of the organic material. C/N ratios between 10 and 13 hint to a strong autochthonous together with some allochthonous contribution to the organic material. $\delta^{13}\text{C}_{\text{org}}$ values around -31 ‰ (rather light for freshwater systems) were described before by Qiu *et al* [1] and related to diatom blooms. Chlorin measurements showed very strong, i.e., up to 5-fold variations in productivity. Chlorin indices [2] varied from 0.5 to 1.5 indicating differences in organic material freshness over the years.

[1] Qiu *et al.* (1993) *Geology* **21**, 25-28. [2] Schubert *et al.* (2005) *Geochem. Geophys. Geosyst.* **6**, Q03005, doi:10.1029/2004GC000837

Rn in water detection by LSC – sample volume optimization

MICHAEL SCHUBERT¹ AND JUERGEN KOPITZ²

¹Helmholtz Centre for Environmental Research Leipzig, Germany; (michael.schubert@ufz.de)

²Universitätsklinikums Heidelberg, Germany; (Juergen.Kopitz@med.uni-heidelberg.de)

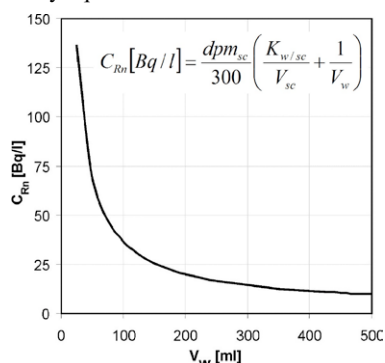
Radon (²²²Rn) is, amongst the noble gases, of particular interest as tracer in groundwater / surface water interaction studies. In related applications radon-in-water concentrations can be detected either directly in the field by using a mobile radon-in-gas monitor or after a water sampling campaign by liquid scintillation counting (LSC) in the laboratory.

If LSC is applied the radon has to be transferred from the water sample of a certain volume V_w [l] into the scintillation cocktail of the volume V_{sc} [l]. Whereas V_{sc} is preset by the size of the LSC vials (usually 20 ml) V_w is not specified. Aim of the presented study is an optimization of V_w .

The equation given in the figure allows calculating the ²²²Rn concentration that was originally present in the water sample C_{Rn} [Bq/l] based on V_{sc} and V_w , on the water/cocktail partition coefficient for radon $K_{w/sc}$ and on the dpm value detected in the cocktail dpm_{sc} . The equation is based on the assumption that dpm_{sc} represents the total dpm of ²²²Rn and its four short-lived progeny (after 3 h equilibration time), i.e. of five radionuclides in decay equilibrium.

Plotting the equation for an exemplary dpm_{sc} value (e.g. 1000), for a $K_{w/sc}$ value of 0.019 (valid for 21°C) and for varying values for V_w and V_{sc} results in a 3D image. Setting V_{sc} to 20 ml (the cocktail volume that is

usually applied) results in the 2D plot for C_{Rn}/V_w shown in the diagram. It becomes obvious that the gradient of the function flattens significantly if V_w increases over about 350 ml. That implies that an increase of the water sample volume over about 350 ml does *not* result in significantly higher counting rates (and neither in better counting statistics). On the other hand, a water volume that is significantly smaller than about 250 ml results in a significantly smaller radon concentration in the cocktail and hence in poorer counting statistics. Thus, water sample volumes of about 250 - 350 ml should be chosen if 20 ml vials are applied for radon-in-water detection by LSC.



Transformational faulting in high pressure polymorphs – two case studies in quartz and olivine

ALEXANDRE SCHUBNEL¹, FABRICE BRUNET², NADÈGE HILAIRET³, JULIEN GASC⁴, YANBIN WANG⁴ AND HARRY W. GREEN II⁵

¹Laboratoire de Géologie, ENS² Paris, France

²ISTERRE, Université Joseph Fourier, Grenoble, France

³UMET, Université de Lille, Lille, France

⁴GSECARS, University of Chicago, Argonne, IL., USA

⁵Dept of Earth Sciences, UC at Riverside, CA, USA

Intermediate and deep focus earthquakes (100 -700 km) occur in a pressure and temperature regime where rocks are expected to deform plastically. The idea that they may be triggered by phase transformations in cold subducting lithosphere is appealing. However, the relationship between phase transformation and faulting remains unclear.

Coesite has been recognized as a reliable marker of ultrahigh-pressure (UHP) metamorphic environments in continental collision zones. Recent careful relocation of subduction-zone earthquakes have also shown that at depths of 100–250 km, seismicity occurs in the uppermost part of the slab, where the former oceanic crust has already been converted to eclogite. In the mantle transition zone, olivine undergoes two phase transformations while deep focus earthquakes locate inside the coldest part of slab, where metastable olivine bodies have sometimes been identified.

Here, we provide experimental evidence that, under differential stress at high pressure and temperature conditions ($\Delta\sigma=2GPa$, $P=2-5GPa$ and $T=1150\pm 50K$), shear fractures nucleate and propagate at the onset of the olivine \rightarrow spinel transition in the Mg_2GeO_4 analogue system. Similar observations were performed for quartz \rightarrow coesite ($\Delta\sigma=4GPa$, $P=3-4GPa$ and $T=1300\pm 50K$) in samples of Arkansas novaculite. In both cases, fracture propagation is sufficiently rapid to radiate energy in the form of intense acoustic emissions. These follow the Gutenberg-Richter law over 4 orders of moment magnitudes and like intermediate and deep-focus earthquakes, require no volumetric strain.

Microstructural analysis shows the development of macroscopic faults, filled with a gouge composed exclusively of the HP polymorph (spinel or coesite). Within the gouge, the material is so fine (1-50 nm) that diffusion accommodated grain boundary sliding may have provided a mechanism viable at “co-seismic” strain rates ($>10^4 s^{-1}$). Our results seem to indicate as a rule that HP polymorphic transformations are mechanically unstable under stress, simply because they are exothermic and induce large negative ΔV . This clearly opens the prospects of revisiting a large number of phase transitions to assess their role in the triggering of deep seismicity.

How mass balance affects isotope ratios in the weathering zone

J.A. SCHUESSLER, J. BOUCHEZ
AND F. VON BLANCKENBURG

GFZ German Research Centre for Geosciences, Helmholtz
Centre Potsdam, Potsdam, Germany
(bouchez@gfz-potsdam.de)

The novel stable isotope signatures in the compartments of the weathering zone are controlled not only by isotope fractionation factors that are characteristic of the chemical processes at play in the weathering zone, but are also controlled by the elemental fluxes between the different compartments, *i.e.* by mass balance effects. To deconvolve these two effects, we designed a steady state, batch reactor, mass balance model representing the weathering zone from the soil scale to the large river scale. We assume the main fractionating processes being formation of secondary precipitates, such as clays, and uptake by plants [1]. The model shows that:

$$\delta_{diss}^X - \delta_{rock}^X = -\Delta^X \cdot \frac{E_{org+sec}^X}{S_{rock+prim}^X} \quad (1)$$

where δ_{diss}^X and δ_{rock}^X are the isotope composition of the metal element X in the dissolved load and in the source rock, respectively, Δ^X the flux-weighted combined isotope fractionation factor, $E_{org+sec}^X$ the export flux of X in isotopically fractionated solids (organics and secondary precipitates), $S_{rock+prim}^X$ the release flux of X to water through primary mineral dissolution.

The main predictions are: (a) For very “soluble” elements (*i.e.* those with a low affinity for secondary precipitates and easily redissolved from plant litter), no fractionated δ_{diss}^X solid is exported, and is likely to be close to the source rock, δ_{rock}^X . Therefore, such elements are not viable tracers of weathering processes. (b) Equation (1) predicts that the largest difference in isotope ratios that can be observed between source rock and dissolved species and is equal to the combined isotope fractionation factor of the processes at play in the weathering zone.

The validity of these predictions are verified using an extensive database of measured water and rock isotope compositions and a compilation of experimentally determined isotope fractionation factors for Li, B, Mg, Si and Ca. It is observed that most $\delta_{diss}^X - \delta_{rock}^X$ data fall indeed between 0 (source rocks) and the best estimate of $-\Delta^X$. Moreover, most of the $\delta_{diss}^{Ca} - \delta_{rock}^{Ca}$ values are small compared to estimates of $-\Delta^{Ca}$, due to its high solubility.

[1] Bouchez *et al.*, *Amer. J. Sci.* **313**, 2013

Early stage Ostwald ripening of submicrometer calcite

L.N. SCHULTZ*, K. DIDERIKSEN, D. MÜTER,
S.S. HAKIM AND S.L.S. STIPP

Nano-Science Center, Department of Chemistry, University of
Copenhagen, Denmark (*correspondence:
lschultz@nano.ku.dk)

Ostwald ripening, also known as grain coarsening, occurs when crystals are at equilibrium with surrounding fluids. Over time, recrystallization favors larger and more thermodynamically stable particles. For calcite (CaCO_3), this affects diagenesis, relevant for aquifers and oil reservoirs and plays a role in industrial products where a thin adsorbed water layer covers crystal surfaces. While saturated conditions are common in nature and industry, rates and consequences of recrystallization at equilibrium are much less known and understood than growth and dissolution far from equilibrium.

We exposed submicrometer scale calcite, with a surface area of $11.8 \text{ m}^2/\text{g}$, to saturated solutions at $23 \text{ }^\circ\text{C}$, $100 \text{ }^\circ\text{C}$ and $200 \text{ }^\circ\text{C}$ and we observed grain coarsening for up to 261 days. Scanning electron microscopy (SEM) showed visible calcite crystal coarsening at $100 \text{ }^\circ\text{C}$ and $200 \text{ }^\circ\text{C}$ (Figure 1) within one day. BET surface area decreased by an order of magnitude and the average diameter grew to $2 \text{ }\mu\text{m}$ or larger. We measured change in particle size distribution and determined that the lognormal shape is indicative of early stage Ostwald ripening, consistent with classical theory.

Coarsening at $23 \text{ }^\circ\text{C}$ was not observable by BET or SEM, but changes in X-ray diffraction peak widths suggest an evolving surface, characterized by crystallite coarsening and fewer defects. These changes affect surface properties during the early stages of Ostwald ripening and have implications in our understanding of Ostwald ripening theories, behaviour in calcitic reservoirs and commercial calcite powder stability.

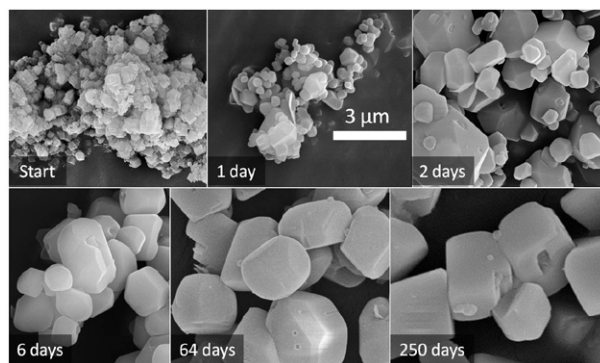


Figure 1. Calcite coarsening at $200 \text{ }^\circ\text{C}$ in saturated solution. The scale bar applies for all images.

Dehydration of metasomatic rocks along subduction and cold diapiric P-T trajectories

JOHN C. SCHUMACHER¹ AND HORST R. MARSCHALL²

¹School of Earth Sciences, University of Bristol, Wills Memorial Building, Queen's Road, Bristol BS8 1RJ, UK
(*correspondence: j.c.schumacher@bristol.ac.uk)

²Department of Geology & Geophysics, Woods Hole Oceanographic Institution, Woods Hole, MA 02543, USA
(hmarschall@whoi.edu)

Material from the subducting slabs is chemically linked to the source region of magmas produced at convergent plate margins. Hydrous fluids and chemical components from (1) subducted altered-oceanic crust and (2) the thin sedimentary veneer are added to (3) depleted mantle-wedge peridotite are invoked as the source of these melts. Exhumed subduction zone mélanges show new rock compositions develop through metasomatism and advection during early subduction where metabasic rocks and other rock types are juxtaposed with serpentinites. In large enough amounts in the source, these new (metasomatic) rock compositions may alter or expand the P-T region over which large amounts of fluid or key trace elements are either retained in or released from the source rocks relative to conditions predicted by the widely applied three-component source models.

This study examines the petrologic changes along a subduction P-T trajectory followed by a cold diapiric rise into the mantle wedge; the high-P, metasomatic rock compositions used for the calculations are from the island of Syros, Greece. These following metasomatic assemblages developed under blueschist-facies conditions and were preserved between garnet-epidote-glaucophane schist and serpentinite:

- (1) glaucophane+epidote+phengite+chlorite;
- (2) glaucophane+epidote+chlorite+omphacite;
- (3) epidote+chlorite+omphacite; (4) chlorite; (5) chlorite+talc.

The calculated phase relations for the metasomatic rocks compositions show that water-rich mineral like chlorite from these rocks could be stable to higher pressures, temperatures, and be more abundant than in hydrated basalt. Chlorite-rich metasomatic compositions produce more garnet than is expected from metabasalts. For example at about 805°C & 21 kbar, metasomatic rock (3) becomes 37 vol% garnet, 19 vol% pyroxene, 37 vol% amphibole; at about 910°C & 20 kbar, metasomatic rock (4) becomes 45 vol% garnet, 15 vol% spinel, 35 vol% olivine.

A decadal lipid biomarker paleohydrological record during the onset of the Younger Dryas from Northeastern Germany

KATHRIN SCHÜTRUMPF¹, ACHIM BRAUER², INA NEUGEBAUER², OLIVER RACH¹ AND DIRK SACHSE¹

¹University of Potsdam, Institute of Earth & Environmental Science, Karl-Liebknecht-Str. 24-25 14476 Potsdam-Golm Germany

(correspondence: k.schuetrumpf@googlemail.de)

²GeoForschungsZentrum Potsdam Section 5.2, Climate Dynamics and Landscape Evolution, Telegrafenberg C109 14473 Potsdam

Regional expressions of global climatic changes, especially their effect on the hydrological cycle, are difficult to predict. However, their impacts, in the form of droughts or extreme precipitation events can be severe for societies and ecosystems. Therefore, a better understanding of the complex hydrological feedback mechanisms during past abrupt climate changes may ultimately lead to better predictions of regional climate changes.

High-resolution proxy data from well dated lacustrine sedimentary archives are particularly well suited for the reconstruction of regional climate changes in the past. Here we are investigating the hydrological impacts of the abrupt climate change during the onset of the Younger Dryas (YD) cold period between 13,000 and 12,400 years BP from the paleolake Rehwiess in Berlin in Northeastern Germany.

We extracted lipid biomarkers from a 122,10 cm sedimentary sequence covering a period of 600 years during the onset of the YD. We identified abundant mid- and long-chained n-alkanes, usually attributed to aquatic macrophytes and higher terrestrial plants, respectively. In addition, we found hopanes of bacterial origin as well as branched alkanes. Dinosterol, a characteristic biomarker for dinoflagellates, was also detected.

Using these samples we construct a record of hydrological changes in decadal resolution. Therefore, we are analyzing the hydrogen isotope composition of lipid biomarkers (D/H). We will evaluate this palaeohydrological record in conjunction with micro-facies, geochemical and palynological data in order to understand the hydrological evolution of regional climate during the onset of the YD in Northeastern Germany.

The Geobiology of Weathering: The 13th Hypothesis

D.W. SCHWARTZMAN^{1*} AND S. BRANTLEY²

¹Department of Biology, Howard Univ., Washington DC 20059, USA (*correspondence: dschwartzman@gmail.com)

²Department of Geosciences, Pennsylvania State Univ., University Park, State College, PA 16802, USA (sxb7@psu.edu)

The magnitude of the biotic enhancement of weathering (BEW) has profound implications for the long-term carbon cycle [1, 2]. The BEW ratio is defined as how much faster the silicate weathering carbon sink is under biotic conditions than under abiotic conditions at the same atmospheric $p\text{CO}_2$ level and surface temperature. Thus, a 13th hypothesis could be added to the 12 outlined by Brantley *et al.* [3] regarding the geobiology of weathering: The BEW factor and its evolution over geological time can be inferred from “meta-analysis” of empirical and theoretical weathering studies. We present estimates of the global magnitude of the BEW drawing from lab, field, watershed and models of the long-term carbon cycle, with values ranging from one to two orders of magnitude.

[1] Schwartzman and Volk (1989) *Nature* **340**, 457-460. [2] Schwartzman (1999 2002) *Life, Temperature, and the Earth: The Self-Organizing Biosphere*. Columbia Univ. Press. [3] Brantley *et al.* (2011) *Geobiology* **9**(2), 140-165.

Serpentinization history of the Santa Elena complex peridotites, Costa Rica

ESTHER M. SCHWARZENBACH^{1*} AND ESTEBAN GAZEL²

Department of Geosciences, Virginia Tech, Blacksburg, VA, United States

(*correspondence: esther11@vt.edu; ²egazel@vt.edu)

Serpentinization is a widespread process where ultramafic rocks react with water or fluids along oceanic ridges or within subduction zones. On the Santa Elena peninsula (Costa Rica) variably serpentinized peridotites outcrop together with layered and pegmatitic gabbros and are intruded by mafic dikes. However, the original tectonic setting of the Santa Elena complex and the origin of the peridotites has not yet conclusively been determined and interpretations range from a supra-subduction zone to an oceanic ridge setting. In this study we identify the alteration history and the sources of the hydrothermal fluids that affected these peridotites by studying the petrology and sulfur geochemistry. Our goal is to contribute to the understanding of the tectonic evolution of Central America.

The Santa Elena ultramafic complex includes lherzolites, cpx-bearing harzburgites and minor dunites. Extent of serpentinization varies between 30 and 100%. Locally clinopyroxene is replaced by amphibole (tremolite, Mg-hornblende, edenite, and pargasite). The peridotites preserve opaque mineral assemblages including pentlandite, awaruite, pyrrhotite, heazlewoodite, magnetite, and locally violarite and smythite. Additionally, most samples contain native Cu and a chemically wide range of Cu-sulfide assemblages including chalcocite, cubanite, bornite, chalcopyrite, samaniite [Cu(Fe,Ni)₈S₈], and sugakite [Cu₂(Fe,Ni)₇S₈]. Elemental mapping revealed that native copper abundantly forms dendritic rims around pentlandite, while pentlandite is variably replaced by Cu-sulfides.

The mineralogical observations and the opaque mineral assemblages of the peridotites generally reflect i) highly reducing conditions during serpentinization and very low water rock ratios ($\ll 1$), ii) that both formation of amphibole and Cu-alteration occurred subsequent to serpentinization, and iii) that serpentinization occurred at $\leq 250^\circ\text{C}$, but that locally fluid temperatures exceeded $300\text{--}350^\circ\text{C}$. Thus, our new data indicates that the peridotites of the Santa Elena complex experienced several stages of hydrothermal alteration and that serpentinization was likely overprinted by a later high temperature hydrothermal event.

Geochemical characterization of thermal springs in the Tete Province, Northern Mozambique

A. SCIARRA*, M. PROCESI, F. QUATTROCCHI
AND D. CINTI

Istituto Nazionale di Geofisica e Vulcanologia, Rome, Italy

(*correspondence: alessandra.sciarra@ingv.it)

A first geochemical survey was carried out in the Northern Mozambique in March-April 2013, with the aim to investigate chemistry and origin of some thermal springs in the Tete Province. The investigated area is located in the East African Rift, adjacent to the marginal sedimentary Mozambique Basin. This area is crossed by the *Rio Zambezi*, one of the main river in Africa and explored during the 19th century by David Livingstone.

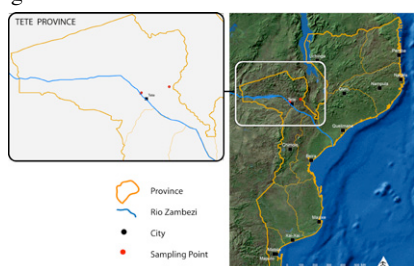


Figure 1: Location of the study area.

Many thermal springs are present in this province due to the proximity with the rift, but considerably little geochemical and geothermal studies have been done, due to the difficulties related both to the site accessibility and social interaction with local tribes. Three thermal springs were sampled close to the *Missao de Boroma*, Tete, crossing the Rio Zambezi by a traditional pirogue. Collected samples are being analysed to determine major, minor and trace elements, $\delta^{18}\text{O}$ and δD , dissolved gas, carbon isotopic ratios of TDIC (Total Dissolved Inorganic Carbon) (expressed as $\delta^{13}\text{C}\text{‰}$ vs. VPDB), the $^3\text{He}/^4\text{He}$ and the dissolved Radon. The measured temperature ranges between 66°C to 42°C and the pH from 7.9 to 8. The conductivity is around 2400 $\mu\text{S}/\text{cm}$ and the Eh is between -208 to -404 mV. The chemical and isotopic analysis are in progress, anyway this first sampling suggests the need to plan and perform a national geochemical survey of the thermal springs in Mozambique. Data should be organized in organic geodatabase and geographic information systems. This information could have a big relevance not only for the geochemical, hydrogeological and geological knowledge of the Country but also for a potential geothermal exploration and exploitation.

Age of the Bird River Sill (Manitoba, Canada) and the Secular Variation of Layered Intrusion-hosted Stratiform Chromite Mineralization

JAMES S. SCOATES¹, R.F. JON SCOATES²
AND COREY J. WALL¹

¹Pacific Centre for Isotopic and Geochemical Research,
EOAS, University of British Columbia, Vancouver, BC,
Canada, (jscoates@eos.ubc.ca, cwall@eos.ubc.ca)

²2502 Holyrood Drive, Nanaimo, BC, Canada,
(jscoates@telus.net)

The Archean Bird River Sill, a 20 km long and up to 800 m thick mafic-ultramafic layered intrusion in the Bird River greenstone belt of southeastern Manitoba, Canada, contains significant resources of chromium and nickel-copper, and locally anomalous concentrations of platinum group elements (PGE). Stratiform chromitite, displaying both remarkable lateral continuity and local irregularities due to synmagmatic disruption, occurs in up to six main intervals over a thickness of ~60 m in the Chromitiferous Zone of the lower ultramafic part of the intrusion. Ni-Cu sulfide mineralization is hosted in ultramafic rocks at the base of, or just below, the sill (e.g., past-producing Maskwa-Dumbarton mines). We report U-Pb zircon ages (chemical abrasion, single grains, ID-TIMS) for cumulates from below and above the Chromitiferous Zone, including (1) a locally pegmatitic, sulfide-bearing, feldspathic peridotite from the PGE Zone beneath the lowermost chromitite horizon (Lower Group) of 2743.72 ± 0.31 Ma ($n=6$), and (2) a leucogabbro in the Lower Gabbro Zone, approximately 35 m above the uppermost chromitite horizon (Upper Paired Group) of 2743.19 ± 0.31 Ma ($n=9$; revised from [1]). These ages are interpreted as the age of crystallization of the sill and they define the timing of the associated Cr-Ni-Cu±PGE mineralization. Other Neoproterozoic mafic-ultramafic intrusions containing economic concentrations of chromite and/or Ni-Cu-(PGE) occur in the northwestern part of the Superior Province in the Canadian Shield (e.g., McFaulds Lake, Big Trout Lake, Puddy Lake, Shebandowan) and share broadly similar geologic relationships. The age of significant intrusion-hosted stratiform chromite mineralization worldwide ranges from Eoarchean (e.g., Akilia, Greenland) to Paleoproterozoic (e.g., Bushveld, South Africa), which is comparable to the range for komatiite-related Ni deposits. This temporal restriction is consistent with both deposit types requiring the involvement of high-MgO, Cr-rich parent magmas produced during large degrees of mantle melting early in Earth history.

[1] Scoates & Scoates (2013) *Econ. Geol.* **108**, 13 p.

Ageing of the Thetyan crust documented by xenoliths from Hyblaean diatremes (Sicily): Implication for crustal assimilation during magma emplacement

VITTORIO SCRIBANO* AND MARCO VICCARO

¹Dipartimento di Scienze Biol., Geol., Amb., Univ. Catania, Corso Italia 55, 95127 Catania, Italy (Correspondence: scribano@unict.it, m.viccaro@unict.it)

Previous study on xenoliths from Miocene diatremes from Hyblaean area (Sicily) suggested that the local Mesozoic sedimentary and volcanic sequence rests upon a fossil oceanic core-complex belonging to the Ionian Thetyan lithospheric domain. Hyblaean xenoliths have also suggested that the postulated core-complex hosted long living hydrothermal systems which have produced diverse geochemical and mineralogical modification to the host ultramafic and gabbroic rocks (e.g. hydration, alkalinization, sulfidization, carbonation) through time, as well the deposition of hydrothermal brines at different crustal levels. The Upper Miocene volcanic rocks cropping out in the Central-Eastern section of the area were erupted after a 50 Ma non-magmatic period (the Eocene hiatus). The interaction between ascending magmas and the fossil hydrothermal system produced dehydration of the serpentinite wall rock with formation of fluidized eruptive systems (i.e. diatremes). The basalt magma assimilated some hydrous peralkaline anatectitic melts thereby attaining a silica-undersaturated, sodic (nephelinitic) character. Magmas that fed the Pleistocene volcanism in the northern margin of the Plateau intersected a section of the fossil hydrothermal system, which was particularly rich in hydrothermal evaporites as testified by the high contents in S, Cl, F, H₂O, Ca, Na, Sr, Ba, relatively high Zr/Hf and occurrence of sodalite series phenocrysts. More in general, we put forward the idea that selective assimilation of hydrothermally altered wall rocks may explain the geochemical paradox of the Hyblaean basaltic lavas, which display Nd-Sr isotope ratios distinctive of MORB-type magmas and distribution of some trace elements more typical of alkaline-series magmas.

Evidence of intergranular melt pools and melt films in lower crustal granite: Products of fluxing by water derived from deformation of nominally anhydrous minerals

S.J. SEAMAN^{1*}, M.L. WILLIAMS, M.J. JERCINOVIC, G.C. KOTEAS² AND L. BROWN

¹Department of Geosciences, University of Massachusetts, Amherst, MA 01003, USA (*correspondence: sjs@geo.umass.edu)

²Department of Geology, Norwich University, Northfield, VT 05663, USA

Water in nominally anhydrous minerals in lower crustal granitoids may move from structural sites and fluid inclusions in nominally anhydrous minerals to grain boundaries during deformation. Along grain boundaries, this water can lower the solidus, facilitating the production of small amounts of partial melt. Outcrops of the 2.6 Ga Stevenson granite, a lower crustal granite in the Athabasca granulite terrane, Saskatchewan, range from K-feldspar megacrystic granite to ribbon mylonite. With increasing deformation, water concentration in quartz and feldspar crystals decreases, and very fine-grained (2-10 micron) brown colored grain boundary films and intergranular pools are progressively developed. The fine-grained multi-phase material on grain boundaries and at grain triple junctions has been interpreted as former melt films and melt pools, respectively. The interpreted melt films have a distinctive pocked texture and a multiphase assemblage with quartz, 2 feldspars and fine (1-2 microns) Fe oxides. Melt films on the grain boundaries of plagioclase, potassium feldspar and quartz are approximately 20 microns wide. Melt pools are up to 100⁺ microns in diameter. In some zones of the rock, melt pools are nearly interconnected, possibly beginning to mobilize, approaching a situation in which a melt conduit would be established. Water in nominally anhydrous minerals has the potential to lower the solidus significantly enough to initiate partial melting in lower crustal granitoids at high ambient temperatures. 3000 ppm water in quartz and feldspars that make up large volumes of lower crustal granitoids would lower the dry solidus of granite by 96°C at 1 GPa, facilitating the production of small volumes of partial melt that wet the grain boundaries along which it is produced.

Tracing denitrification using isotopic composition of nitrogen in soils and plants

MATHIEU SEBILO^{1*}, AURELIE MOTHET¹, LIZ HAMILTON², EDWARD MALONE², VERONIQUE VAURY¹, OLIVIER GROS³ AND GILLES PINAY⁴

¹UPMC Univ Paris 06, UMR Bioemco, 4 place Jussieu, 75252 Paris Cedex 05, France

amathieu.sebilo@upmc.fr (*presenting author)

²University of Birmingham, School of Geography, Earth and Environmental Sciences, Birmingham, B15 2TT, UK

³Département de Biologie, UMR 7138 SAE, Université des Antilles et de la Guyane, 97159 Point à Pitre Cedex, Guadeloupe, France

⁴Observatoire des Sciences de l'Univers de Rennes, UMR Ecobio, Campus Beaulieu, bât. 14. 263 av du Général Leclerc 35042 Rennes Cedex, France.

One of the major challenges of current research on the functioning of the continental ecosphere is to develop integrative approaches allowing scale changes. Isotopic biogeochemistry is an interested integrating tool. The basic idea is that the isotopic composition of a chemical species ($\delta^{15}\text{N}$ for nitrogen) at a definite location reflects (i) its various sources and (ii) processes which affect its concentration. Denitrification generates an isotopic enrichment of ^{15}N and ^{18}O of the residual nitrate in soils or in waters (surface or groundwater).

However, denitrification is intermittent and occurs in hot spots. In order to get insights into this process involved at regional scale, it is important to trace the succession of denitrification in soils and test the hypothesis whether plants could integrate the signal of denitrification occurring in soils. First results show that for a same type of soil, $\delta^{15}\text{N}$ is much higher for agricultural soils than for meadows, forest or mangrove soils. This is mostly likely due to higher gaseous losses processes occurring in agricultural soils such as denitrification.

Moreover, $\delta^{15}\text{N}$ of plants increase with increasing of $\delta^{15}\text{N}$ of soils. This confirms that the $\delta^{15}\text{N}$ of soil organic nitrogen could be an indicator of the intensity of denitrification

Physical and geochemical processes during groundwater replenishment with highly treated wastewater

S. SEIBERT², H. PROMMER^{1,2,3,*}, A. SIADE^{1,3} AND O. ATTEIA⁴

¹University of Western Australia, Crawley, Australia

Henning.Prommer@csiro.au (* presenting author)

²CSIRO Land and Water, Wembley, Australia

³NCGRT, Australia

⁴EGID, Pessac Cedex, France

Decreasing availability of ground and surface water resources in conjunction with increasing water demands has motivated the exploration of unconventional new water sources in Australia and other places. Among possible solutions recycling of municipal wastewater through advanced tertiary treatment techniques presents a promising option to augment existing drinking water supplies. During this treatment process reverse osmosis (RO) plays a critical role in the removal of undesired solutes and results in low ionic strength product water. The purified, desalinated water can be stored underground for protection against evaporation loss and introduce, where required, an additional aquifer treatment step for the removal of trace pollutants (e.g., pharmaceuticals, disinfectant-byproducts). As the recycled low ionic strength water is typically in chemical disequilibrium with the native aquifer conditions, the injection into aquifers often triggers a complex range of coupled physical and geochemical processes that can strongly affect the quality of the groundwater in the recharged aquifer. In this study we present field observations and a model-based interpretation of the data collected during a large-scale groundwater replenishment trial using highly treated waste water in Perth, Western Australia. The trial injection was conducted between November 2010 and December 2012 to clarify the technical feasibility and societal acceptance of a large-scale implementation of this approach. The first phase of the modelling study was dedicated to obtaining an accurate understanding and description of the injectant and temperature propagation within the highly heterogeneous sedimentary aquifer.

The calibrated conservative transport model was then subsequently used to identify and quantify the geochemical reactions that were induced by the injection. In agreement with earlier laboratory results from respirometer tests (e.g., [1,2]) the simulation results show that pyrite oxidation acts as the major driver for reaction-induced concentration changes within the aquifer. Pyrite oxidation showed to cause a rapid removal of oxygen and also the removal of the nitrate contained in the injectant. The acidity produced by the pyrite oxidation showed to be partially buffered by the alkalinity contained in the injected water but also by a range of mineral reactions, including Fe-carbonate and feldspar dissolution. Understanding the nature and longevity of the mineral buffering mechanisms is crucial for the design of future large-scale implementations of groundwater replenishment.

[1] Descourvieres *et al.* (2010a) *Appl. Geochem* **25**, 261–275.

[2] Descourvieres *et al.* (2010b) *Env. Sci. Technol.*, **44**, 6698–6705.

www.minersoc.org

DOI:10.1180/minmag.2013.077.5.19

Competition for sulfide in marine sediments: Electrogenic Filamentous Bacteria versus *Beggiatoa*

DORINA SEITAJ^{1*}, SAIRAH Y. MALKIN², REGINA SCHAUER³ AND FILIP J.R. MEYSMAN^{1,2}

¹Netherlands Institute of Sea Research (NIOZ), Ecosystem Studies Department, Korringaweg 7, 4401 NT, Yerseke, Netherlands (*correspondence: Dorina.Seitaj@nioz.nl)

²Free University of Brussels (VUB), Department of Analytical and Environmental Chemistry, Pleinlaan 2, 1050 Brussels, Belgium

³Aarhus University, Department of Bioscience, Center of Geomicrobiology, Ny Munkegade 116, 8000 Aarhus, Denmark

Recently, a novel mechanism of sulfide oxidation has been described from marine sediments, whereby long filamentous bacteria (ElectroFilaments) couple the reduction of oxygen at the surface to the oxidation of sulfide at centimeters depth via electrical currents. This creates a wide suboxic zone similar to that created by the large sulphur bacteria of the genus *Beggiatoa*. These latter bacteria are motile and capable of intracellular nitrate storage, and in this way, *Beggiatoa* can transport nitrate to deeper sediment layers to oxidize H₂S. In the seasonally hypoxic Lake Grevelingen, The Netherlands, both types of sulfur oxidizing bacteria have recently been observed. This rises the question how these different modes of microbial sulfide oxidation compete?

We conducted a yearlong study of monthly sampling campaigns in Lake Grevelingen. Microsensor profiling of O₂, pH and H₂S revealed the geochemical fingerprint of the dominant microbial process over time (both mechanisms generate a very distinct pH profile). In addition, FISH tagging for *Desulphobulbus* and microscopic counting of *Beggiatoa* allowed to quantify the abundance of the two competing bacteria. Our results show that both modes of microbial sulfide oxidation follow a predictable seasonal succession, where *Beggiatoa* are dominant in autumn right after summer hypoxia, while Electrofilaments become dominant in spring. Field data and additional mesocosm experiments suggest that bottom water oxygenation, nitrate availability and physical disturbance are the main environmental factors controlling the outcome of this microbial competition. These two competing microbial pathways of sulfur oxidation strongly affect the biogeochemical cycling, but in a very different way, and so, the predominance of either mechanism can have a strong impact on the elemental cycling in coastal sediments.

Tracing the origin of sulphur in Darzila karst cave, NE Iraq

A. SEITHER^{1,3*}, K. HEILAND^{2,3} AND S. KUMMER³

¹Norges Geologiske Undersøkelse, 7040 Trondheim, Norway (*correspondence: anna.seither@ngu.no)

²Ingenieurbüro für Grundwasser GmbH, 04229 Leipzig, Germany (k.heiland@ibgw-leipzig.de)

³TU Bergakademie Freiberg, 09596 Freiberg, Germany

Darzila cave, located in the Sangaw district in Northern Iraq, develops by the dissolution of limestone by sulphuric acid through oxidation of H₂S. The hydrogen sulphide may either originate from oil-rich reservoirs, such as the nearby Kirkuk oil field, or from gypsum of the Lower Fars Formation.

Samples from these possible endmembers were subject to isotopic analyses ($\delta^{34}\text{S}$, $\delta^{18}\text{O}$). The water of three prominent floor feeders inside the cave was analyzed for its content of major ions, trace elements, total organic carbon, as well as for the stable isotopic composition of water (δD , $\delta^{18}\text{O}$), dissolved sulphate ($\delta^{34}\text{S}$, $\delta^{18}\text{O}$) and sulphide ($\delta^{34}\text{S}$).

Investigations of water samples pointed towards a potential influence of hydrocarbon-bearing layers at two sites. Indices were significantly elevated SO₄²⁻/Ca²⁺ ratios, an increased content of total dissolved solids (10-31 g/L) and dissolved organic carbon (14-20 mg/L), and relative enrichments of trace elements such as Cr, Be, Ga, Ni, Co, Mn, and V. The isotopic investigations confirmed the influence of H₂S affluxes from hydrocarbons ($\delta^{34}\text{S} \approx -9\text{‰}$ VCDT) at these sites. Further evidence was given by depleted $\delta^{34}\text{S}$ and $\delta^{18}\text{O}$ values in sulphate, small differences between the sulphur isotopic signature of sulphate and sulphide, as well as elevated δD values in ambient water.

The third floor feeder had an entirely different isotopic signature, showing distinct signs of bacterial sulphate reduction and therefore pointing towards primary gypsum from the Lower Fars Formation ($\delta^{34}\text{S} \approx +22\text{‰}$ VCDT) as sulphur source. Main indications were a $\delta^{34}\text{S}$ value of sulphate above that of gypsum and strongly depleted sulphide. However, it appears that sulphate reduction was superimposed by several secondary transformation processes.

Partial melting of rhyolites in the Chaltén Contact Aureole (Patagonia, Argentina)

S. SEITZ^{1*}, B. PUTLITZ¹, L.P. BAUMGARTNER¹,
S. LERESCHE¹ AND P. NESCHER¹

¹Institute of Earth Sciences, University of Lausanne, 1015
Lausanne, Switzerland (* correspondence:
susanne.seitz@unil.ch)

The Chaltén Plutonic Complex (CHPC) consists of mafic and granitic calc-alkaline intrusive rocks emplaced in several successive batches. High-precision U/Pb zircon dating yield ages between 16.9 ± 0.05 Ma and 16.37 ± 0.02 Ma [1]. The host-rocks are formed by a Paleozoic clastic sequence, Jurassic rhyolites and volcanoclastics, and a Cretaceous pelitic sequences. The intrusion of the CHPC post-dates major regional deformation.

Partial melting in the Chaltén contact aureole is limited to small zones at gabbro and tonalite contacts with rhyolites. Partial melting does not occur at the granite-rhyolite contact. The rhyolitic migmatites are characterized by an anastomosing network of veins of quartz, feldspar and almandine-rich garnet. This network is most prominent at 10m to 15m from the contact. Some cm-scale shear zones concentrated partial melt. On a microstructural scale partial melt is segregated along quartz-feldspar grain boundaries. They show typically cusped grain boundaries with melt penetrating along the edges. Petrologic investigations show that melting is to the result of biotite breakdown to cordierite or garnet.

Thermodynamic calculation for these peraluminous rhyolites indicate that first melt occurs at 650-700°C and pressures around 3kbar. Simple thermal calculations yield maximum temperatures of about 550°C at the mafic-rhyolite contact, which is 100-150°C lower than the required temperature for partial melting. Melting in the rhyolitic migmatites was intense enough to partially reset U/Pb ages as indicated by the younging of zircon ages (obtained by laser ablation). We are currently studying the mechanism of partial resetting of the zircon ages, as well as the kinetics of oxygen isotope exchange between quartz phenocrysts and the rhyolite matrix. Preliminary modeling suggests, that oxygen isotopes can be re-equilibrated dominantly by diffusion, while zircon most likely recrystallized.

[1] Ramírez de Arellano *et al.* (2012), *Tectonics* **31**, 1-18

Silicate-natrocarbonate immiscibility in ijolites at Oldoinyo Lengai, Tanzania: Melt inclusion study

V.S. SEKISOVA^{1,2}, V.V. SHARYGIN^{2*} AND A.N. ZAITSEV³

¹Novosibirsk State University, Novosibirsk 630090, Russia
²V.S. Sobolev Institute of Geology and Mineralogy SD RAS,
Novosibirsk 630090, Russia (*correspondence:
sharygin@igm.nsc.ru)

³St. Petersburg State University, St. Petersburg 199034, Russia

Xenoliths of plutonic rocks (ijolite, jacupirangite, etc.) in the Oldoinyo Lengai pyroclastics are considered to be cumulates forming in an intermediate chamber from a parental olivine nephelinite magma [1].

Melt inclusions with silicate-carbonate immiscibility were found in nepheline and Ti-magnetite of olivine-mica ijolite. Other minerals (pyroxene, etc.) contains inclusions without immiscibility; fluorapatite bears natrocarbonate inclusions. Phase composition of inclusions in nepheline (5-100 μ m) is silicate glass + vapor-carbonate globule \pm daughter/trapped crystals \pm sulfide bleb. Vapor-carbonate globule (up to 20 μ m) consists of gas bubble (\approx 60%) and nyerereite-rich carbonate aggregate (\approx 40%). Some inclusions may also contain numerous submicron carbonate globules in glass. Heating experiments with inclusions indicated the following events: (1) carbonate component melted instantaneously at 540-560°C; (2) melting of silicate glass occurred at 580-640°C; (3) all globules gradually coalesced into one large vapor-carbonate globule at 640-800°C; (4) homogenization in this globule occurred at 900-920°C; (5) complete homogenization (miscibility of carbonate and silicate liquids) was not achieved with temperature increase up to 1100°C.

Our study of inclusions advocates very complex history of the Lengai ijolite and evolution of initial silicate melt in an intermediate chamber. Crystallization of ijolites occurred in conditions of silicate-natrocarnatite immiscibility in very broad temperature (540-1100°C). During formation nepheline and other minerals trapped as inclusions at least two immiscible liquids. After entrapment additional carbonate fraction was separated from silicate liquid within inclusion with decreasing temperature. The immiscibility phenomenon was recently recorded in the Oldoinyo nephelinites [2-4].

This work is supported by RFBR (grant 11-05-00875).

[1] Dawson *et al.* (1995) *J Petrol* **36**, 797-826. [2] Mitchell (2009) *Contrib Mineral Petrol* **158**, 589-598. [3] Mitchell & Dawson (2012) *Lithos* **152**, 40-46. [4] Sharygin *et al.* (2012) *Lithos* **152**, 23-39.

Ensemble Simulation of the Atmospheric Radionuclides Discharged by the Fukushima Nuclear Accident

T. T. SEKIYAMA*, M. KAJINO AND M. KUNII

Meteorological Research Institute, Tsukuba 305-0052, Japan

(*correspondence: tsekiyam@mri-jma.go.jp)

Enormous amounts of radionuclides were discharged into the atmosphere by a nuclear accident at the Fukushima Daiichi nuclear power plant (FDNPP) after the earthquake and tsunami on 11 March 2011. The radionuclides were dispersed from the power plant and deposited mainly over eastern Japan and the North Pacific Ocean. A lot of numerical simulations of the radionuclide dispersion and deposition had been attempted repeatedly since the nuclear accident. However, none of them were able to perfectly simulate the distribution of dose rates observed after the accident over eastern Japan. This was partly due to the error of the wind vectors and precipitations used in the numerical simulations. Unfortunately, their deterministic simulations could not deal with the probability distribution of the simulation errors.

Therefore, an ensemble simulation of the atmospheric radionuclides was performed using the ensemble Kalman filter (EnKF) data assimilation system coupled with the Japan Meteorological Agency (JMA) non-hydrostatic mesoscale model (NHM). The JMA-NHM has been used operationally for weather forecasts by JMA. Through this ensemble data assimilation, twenty members of the meteorological analysis over eastern Japan from 11 to 31 March 2011 were successfully obtained. Using this meteorological analysis, the radionuclide behavior in the atmosphere such as advection, convection, diffusion, dry deposition, and wet deposition was simulated. This ensemble simulation provided the multiple results of the radionuclide dispersion and distribution. Because the large (small) ensemble-spread of the multiple results indicates the low (high) accuracy of the numerical simulation, the probability distribution of the simulation errors is obtainable from the ensemble simulation. These statistics can provide information useful for the probabilistic prediction of atmospheric radionuclides.

Numerical simulations are able to collaborate with field observations in depicting the full picture of the radionuclide contamination in Fukushima.

Imaging the reactivity and transport of ⁹⁹Tc through Fe-cement/rock barriers

A. F. SELIMAN¹, J. BRIDGE², S.A. BANWART¹
AND M.E. ROMERO-GONZÁLEZ^{1*}

¹Cell-Mineral Research Centre, Kroto Research Institute, The University of Sheffield, Sheffield S3 7HQ, UK

(*m.e.romero-gonzalez@sheffield.ac.uk)

²School of Engineering, University of Liverpool, Liverpool L69 3GH, UK. (j.brigde@liverpool.ac.uk)

Geological disposal of radioactive waste requires a detailed understanding of the critical processes affecting geochemical transformations at laboratory and field scale. The interfaces between storage containers, repository and geological substrata can be viewed as a series of continuous barriers with varying porosity and chemical composition that governs flow and physical-chemical transformation of radionuclides during their long term transport. Using this approach, we have investigated the mobility of ⁹⁹TcO₄⁻ transport through Fe-cement/sandstone engineered barriers using flow through experiment and gamma imaging of ^{99m}Tc isotope. A flow cell packed with nirex vault reference backfill material (NRVB) containing zero valent iron (ZVI) or magnetite and Sherwood sandstone in a barrier fashion was used. The transport of ^{99m}Tc in synthetic groundwater at pH 10 was imaged using a medical gamma camera at a flow rate of 5.7ml h⁻¹. The Fe-bearing material was prepared to obtain a uniform distribution of 20% ZVI or 10% magnetite representative of steel materials that may create reactive hotspots in the disposal site. The results showed that the unmodified NRBV/sandstone systems have not capacity to retain ^{99m}Tc. In contrast, ^{99m}Tc was not transported through the NRBV containing ZVI and it was retained entirely by the modified barrier. The NRBV/sandstone system modified with magnetite showed retardation of ^{99m}Tc that was overcome over long periods of time, allowing the radionuclide to be eventually transported out of the flow cell. The results showed that ⁹⁹Tc transport is conservative through cement and sandstone. The implication is that this radionuclide will be transported to the outside natural environment surrounding the geological disposal. However, amendment with Fe-bearing materials, especially ZVI increases confinement of the radionuclide within the geological disposal reducing the risk of long term environmental contamination.

Direct observation of gas hydrate formation in a sedimentary matrix on the microscale

K. SELL^{1*}, M. CHAOUACHI², F. ENZMANN¹, W.F. KUHS²,
M. KERSTEN¹, B. PINZER³ AND E.H. SAENGER⁴

¹Gutenberg-University, Mainz 55099, Germany

(*correspondence: sell@uni-mainz.de)

²GZG, University Göttingen 37077, Germany

³PSI, Tomcat Beamline, 5232 Villigen, Switzerland

⁴ETH, Zurich 8006, Switzerland

Gas hydrates (GH) are ice-like solid compounds comprised of gas molecules and water [1]. As it is very difficult to recover natural GH samples due to their fast decomposition under ambient conditions, a lot of open questions are left concerning the microstructure and distribution of hydrates in sediments. This study represents the first direct observation of gas hydrate growth in a sedimentary matrix using time-resolved synchrotron-based tomography leading to first insights on the nucleation and growth of gas hydrates at a high spatial resolution of 740 nm. The time-sequences of the GH formation in the medium reveal that the reaction clearly started at the gas-water interface forming a several μm thick hydrate film (Fig.1). In contradiction to some earlier conjectures a nucleation on the grain surface was not observed. At a later stage the water is replaced by GH of more or less isometric shape with pore space in between. Some of our observations show that water remains as a thin film between grains and hydrate but this needs to be corroborated. Seismic anomalies observed in field studies might be explained by the presence of thin water films in hydrate-bearing sediments. In a next step the full 3D data set will be used as a direct input to model the effective elastic properties.

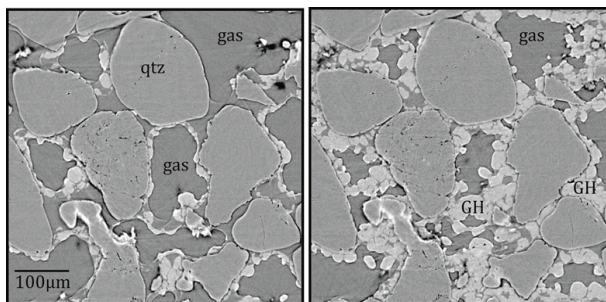


Figure 1: 2D slices depicting the stepwise hydrate growth within the sedimentary matrix.

[1] Sloan & Koh (2008) In: Clathrate hydrates of natural gases. CRC Press, Boca Raton, 752.

Application of mineral thermometers and barometers to shoshonitic-ultrapotassic rocks: The Simav Graben (Western Anatolia, Turkey)

B.SEMİZ

Dep of Geological Engineering, Pamukkale University, 20070, Denizli, Turkey (bsemiz@pau.edu.tr)

The study area is located at the intersection of E–W-trending Plio-Quaternary Simav Graben and NE–SW-trending Neogene Selendi and Uşak-Güre basins in the western Anatolia. Due to their morphological, stratigraphical positions and petrographical features in the field, the investigated shoshonitic-ultrapotassic rocks are called Inceğiz, Gediz, Dereköy, Naşa, Kestel basalts, Saphanedağı and Ilıcaksu Lamproites. All the SHO-UK rocks display similar petrographic characteristics.

Fourteen samples, representing the SHO-UK units in the eastern parts of the Simav Graben have been used for mineral chemical studies and for estimation of the temperature and pressure conditions of magmatic crystallization. These samples are porphyritic, hyaloplitic, pilotaxitic in texture and with the following mineral assemblages; clinopyroxene (En_{40-52} , Wo_{39-48}), olivine (Fo_{63-92}), rarely phlogopite (Mg# 65-91), plagioclase (An_{62-88}), and sanidine (Or_{52-84}). Ti-magnetite, ilmenite and chrome-spinel (5-18% MgO, 39-54% Cr_2O_3) are common accessory minerals.

Application of clinopyroxene [1] and olivine-spinel [2] geobarometric studies for the SHO-UK, equilibrium pressure between ~ 7.6 -10.3 and ~ 16.2 -16.8 kbar has been estimated, corresponding to 25-51 km depth, respectively. Oxygen fugacity ranges from -11.9 and -13.8. Olivine [3], Olivine-spinel [4], clinopyroxene [5] and magnetite-ilmenite pairs [6] geothermometers have been applied for estimating the crystallization temperatures of minerals. Calculated crystallization temperatures are 1193-1262°C for olivines, 1086-1191°C for clinopyroxene and 793-851°C for magnetite-ilmenite pairs. The estimates of magmatic parameters indicate that the magmas forming the SHO-UK rocks crystallized at different levels, from mantle depths toward deep-level magma chambers.

[1] Nimis, (1995) *Contrib Mineral Petrol.* **121**, 115-125. [2] O'Neil, (1981) *Contrib Mineral Petrol.* **77**, 185-194. [3] Putrika, (2008) *Reviews in Mineral. & Geochemist.* **69**, 61-120. [4] O'Neil and Wall, (1987) *J Petrol.* **28**, 1169-1191. [5] Putrika *et al.*, (2003) *Am Mineral.* **88**, 1542-1554. [6] Stomer, (1983) *Am. Mineral.* **68**, 586-594.

Trace element composition of clinopyroxenes from the Kızıldağ ophiolite (S-Turkey): Implication for multi-stage fractionational melting in a SSZ setting

AHMET D. SEN¹, İBRAHİM UYSAL², MARGUERITE GODARD³, SAMET SAKA², RECEP.M. AKMAZ², MELANİE KALIWODA⁴ AND UTKU BAGCI⁵

¹Gümüşhane University, Gümüşhane, Turkey

²Karadeniz Technical University, Trabzon, Turkey

³Géosciences Montpellier, Montpellier, France

⁴Mineralogical State Collection Munich, LMU, Germany

⁵Mersin University, Mersin, Turkey

Trace-element composition of clinopyroxenes from the mantle peridotites of Kızıldağ ophiolite (Hatay, S-Turkey) were determined by laser ablation ICP-MS to better understand the geochemical processes and the formation of the ophiolite. The peridotite sequence is composed of tectonized harzburgite and ultramafic cumulate rocks representing refractory mantle source and Moho Transition Zone (MTZ), respectively. Harzburgites contain spinel with Cr# 47-70 and Mg# 37-66, indicating that they are residue of high degrees of partial melting. Ultramafic cumulates are mainly dunite and wehrlites. Tectonized harzburgites show two different types of compositions. First type of harzburgites are refractory and have primary pyroxene crystals with ductile deformation signs. Second type of harzburgites are more fertile and have interstitial clinopyroxenes showing similar characteristics with rocks from MTZ. Chondrite-normalized rare earth element (REE) patterns of clinopyroxenes from Kızıldağ ophiolite are clearly depleted in light REE (LREE) ($[Lu/La]_N > 100$), and have slightly similar patterns with clinopyroxenes of abyssal peridotites from normal mid-ocean ridges (MOR). Interstitial clinopyroxenes in MTZ dunites have flatter patterns ($[Lu/La]_N \sim 10$) comparable with those from other dunites of all the Tethyan ophiolites (e.g. Oman, Troodos). Clinopyroxenes in tectonized harzburgites having extremely downward REE patterns, characterized by a strong depletion from heavy REE (HREE) to middle REE (MREE), suggest that they are residue of first stage fractional melting in the garnet stability field in a MOR setting. Interstitial clinopyroxene from impregnated harzburgites have more enriched REE patterns than those of depleted harzburgites, indicating spinel field melting in a SSZ setting where melts can percolate within upwelling mantle.

The possible source mantle and magma genesis of basalts from Pitcairn island: Implication from highly siderophile elements and Os isotope ratios

RYOKO SENDA^{1*}, TAKESHI HANYU¹, AKIRA ISHIKAWA^{1,2}, HIROSHI KAWABATA^{1,3}, TOSHIRO TAKAHASHI¹ AND KATSUHIKO SUZUKI¹

¹IFREE, JAMSTEC, Yokosuka 237-0061, Japan

(*Correspondence: rsenda@jamstec.go.jp)

²Earth Science and Astronomy, The University of Tokyo, Tokyo 153-8902, Japan

³Research and Education Faculty, Kochi University, Kochi 780-8520, Japan

It is well known that recycled materials are involved in producing the chemical and isotopic heterogeneities observed in oceanic island basalts (OIB). The type of recycled material present in the Enriched Mantle 1 (EM-1) reservoir has been widely debated. Oceanic crust with pelagic sediment (e.g., Chauvel *et al.*, 1992), delaminated subcontinental lithospheric mantle (SCLM) (e.g., Hauri and Hart, 1993), subducted oceanic plateaus (Gasparini *et al.*, 2000) and just single melting process involving pristine mantle (Collerson *et al.*, 2010) have all been invoked as contributing to EM-1 source. The chemical composition of EM-1 is characterized by radiogenic Sr, unradiogenic Nd, unradiogenic Pb and radiogenic Os isotope compositions compared to the depleted mantle.

We measured Os isotope ratios and highly siderophile elements (HSE) abundances in basalts from Pitcairn Island, south Pacific, which represent strong EM-1 flavor to identify the possible source components of these magmas. The Os isotope ratios (0.138-0.161) have similar to or slightly higher range than, those measured in previous studies on EM-1-type basalts (~0.150). The HSE patterns normalized by chondrites are characterized by fractionation between IPGE (Os, Ir, Ru) and Pd. Among IPGE, Ir abundances of some basalts are depleted compared to Os and Ru. Pt abundances of most basalts also show depleted pattern from Ru and Pd. These characteristics are similar to some picrites from Hawaii (Ireland *et al.*, 2009). However the abundances of HSE in Pitcairn basalts are clearly lower than those of Hawaiian picrites with similar range of MgO. The Os isotope ratios of Pitcairn basalts are higher than those of picrites. We will discuss the components of the source mantle of EM-1 and the magma genesis of Pitcairn Island basalts combining our data with previous studies.

Composition and structure of fresh and aged Fe oxidation products

A.-C. SENN*, R. KAEGI, S.J. HUG,
J.G. HERING AND A. VOEGELIN

Eawag, Swiss Federal Institute of Aquatic Science and
Technology, Überlandstrasse 133, CH-8600 Dübendorf,
(*correspondence: anna-caterina.senn@eawag.ch)

The oxidation of dissolved Fe(II) by O₂ leads to the formation of amorphous to poorly crystalline Fe(III)-precipitates. These precipitates control the fate of major and trace elements at redox-interfaces and play an important role in many natural and technical systems. Dissolved phosphate (P), silicate and Ca are major factors controlling composition and structure of fresh Fe(III)-precipitates [1, 2]. In this study, we therefore investigated (i) the effects of silicate and Ca over a wide range of P/Fe ratios on the composition and structure of fresh Fe(III)-precipitates formed by oxidation of 0.5 mM Fe(II) in bicarbonate-buffered solution at pH 7.0 and (ii) changes in precipitate composition and structure during aging for 30 days at 40 °C.

During Fe(II) oxidation, mostly lepidocrocite (Lp) is formed at initial P/Fe ratios below ~0.1. Phosphate was nearly completely co-precipitated with Fe(III) up to an initial molar P/Fe ratio of ~0.55 in the absence of Ca and ~0.75 in the presence of dissolved Ca. Above these P/Fe ratios, only amorphous Fe(III)-phosphate formed and phosphate removal was incomplete. Enhanced co-precipitation of phosphate and Ca with Fe(III) was attributed to electrostatic effects and to the formation of mixed Ca-Fe(III)-phosphates. Silicate did not interfere with the initial phosphate uptake but inhibited lepidocrocite formation at low P/Fe ratios, instead promoting the formation of hydrous ferric oxide (HFO; ferrihydrite-like polymers with limited corner-sharing linkage of Fe(III)-octahedra). Continuing Fe(III) polymerization during aging led to the remobilization of phosphate, especially in the absence of Ca and silicate. Phosphate remobilization was limited in the presence of Ca, which stabilizes mixed Ca-Fe(III)-phosphate, and especially silicate, which inhibits Fe(III) polymerization into crystalline Fe(III)-precipitates.

The results from this study form the basis for an improved mechanistic and quantitative understanding of Fe(III)-precipitate formation and trace element co-sequestration at aquatic redox-interfaces and in technical systems, for example drinking water treatment for As removal.

[1] Voegelin *et al.* (2010) *Geochim. Cosmochim. Acta* **74**, 164-186. [2] Kaegi *et al.* (2010) *Geochim. Cosmochim. Acta* **74**, 5798-5816.

The occurrence of very high-grade pyrometamorphic xenocrysts/xenoliths in the plutonic rocks of the Alvand plutonic complex, Hamedan, Iran

ALI A. SEPAHI

Department of Geology, Bu-Ali Sina University, Hamedan,
Iran, E-mail: aasepahi@gmail.com, sepahi@basu.ac.ir

The Alvand plutonic complex and a sequence of poly-metamorphic rocks are situated near to Hamedan, Sanandaj-Sirjan zone, Iran. Restites, xenoliths and xenocrysts are abundant in granitoids of the complex but they are rare in gabbroic rocks. Restitic xenocrysts of garnet, sillimanite/andalusite and cordierite which subsequently reacted with granitic magmas are common in granitoids. In gabbroic rocks, especially in a wherlitic olivine gabbro, scarce xenocrysts of andalusite occur which have been converted to sillimanite and a pelitic xenolith in this rocks has been pyrometamorphosed to a very high grade mineral assemblage (e.g. a spinel, sillimanite, mullite and sanidine-bearing assemblage). Thermometric studies have indicated that this very high grade pyrometamorphic assemblage has been formed at peak temperature of more than 1000 °C (up to 1300-1400 °C) when mafic-ultramafic host magma interacted with Al-rich xenoliths.

Tectonomagmatic origin of the Late Jurassic volcanism in the Patagonia Province, Argentina

L. SERRANO^{1,2*}, V. KAMENETSKY², A. MARZOLI¹, M. MARQUEZ³, G. BELLINI¹, H. BERTRAND⁴
AND C. BALLHAUS⁵.

¹*Uni Padua, Italy (linamaria.serranoduran@studenti.unipd.it)

²CODES, University of Tasmania, 7001, Hobart Australia

³Uni Nac. de Patagonia, Comodoro Rivadavia, Argentina

⁴Lab. Géologie, Ecole Normale Supérieure de Lyon, France

⁵Steinman Inst., University of Bonn, 53115, Germany

A thick sequence of the Late Jurassic magmatic rocks in Patagonia (Argentina) extends over 1×10^6 km² from the Atlantic to the Andes [1]. Although bimodal in composition, the Patagonia Province (PP) is one of the largest silicic (felsic) LIPs on Earth. It consists of rhyolites and ignimbrites of the Marifil (~187-177Ma) [2,4] and Chon Aike (~168-151Ma) [2,3] Formations (Fm), with a minor andesitic component represented by the Bajo Pobre (BP) (~164-153Ma) [2,3] and Locontrapial Fm. Thus the total duration of magmatism is ~36 Ma. Our new U-Pb ages on zircons for the Marifil Fm confirm that the first felsic pulse coincided with the Karoo-Ferrar magmatic event (~184-178Ma) [4]. However, the main peak activity in the PP is ~10 Ma younger. Basaltic volcanism of the Cañadon Asfalto (CA) Fm fills an extensional basin contemporaneous with the volcanism of the PP. This magmatism was associated with a complex geodynamic evolution during the Gondwana break-up. The setting comprised continental rifts and a subduction zone in the western continental margin, possibly accompanied by back-arc rifting. Andesites from the BP Fm and basalts from CA Fm are Opx rich rocks with occasional anhedral olivine crystals with Cr-spinel inclusions (Mg# 0.48-0.25; Cr# 0.47-0.37). The most primitive Cr-spinel grains from the BP and CA have contrasting compositions in terms of Al₂O₃ (25-28 and 10-12 wt%) and TiO₂ (1.3-1.4 and 0.4-1.3 wt%, respectively). Accordingly, parental melt compositions can be correlated with MORB for BP and island-arc magmas for CA [5]. Compositions of the Late Jurassic volcanic rocks combined with quartz- and pyroxene-hosted melt inclusion and Cr-spinel study will be discussed and applied to understanding the tectono-magmatic environment of this LIP.

[1] Pankhurst & Rapela (1995) *EPSL* 134, 23-26. [2] Feraud *et al* (1999) *EPSL* 172, 83-96. [3] Pankhurst *et al* (2000) *J. Pet.* 41, 602-625. [4] Jourdan *et al* (2005) *Geology* 33, 745-748. [5] Kamenetsky *et al* (2001) *J. Pet.* 42, 655-671.

Natural and synthetic plagioclases for the interpretation of planetary surfaces

SERVENTI G.¹, CARLI C.², ORLANDO A.³, BORRINI D.⁴, PRATESI G.⁴, SGAVETTI M.¹ AND CAPACCIONI F.²

¹Department of Physics and Earth Sciences, University of Parma (giovanna.serventi@unipr.it)

²Inaf-IAPS Tor Vergata, Roma (cristian.carli@iaps.inaf.it)

³Institute of Geosciences and Earth Resources, C.N.R., Firenze (orlando@igg.cnr.it)

⁴Department of Earth Sciences, University of Firenze

Plagioclase, pl, is an important constituent of planetary surfaces, e.g. Moon and Mercury. Spectrometers detected crystalline pl on the lunar surface [1], with composition of ~An90 and variable FeO content. New data from XRS and GRS on the Hermean surface show contents of Na [2] that are compatible with low-An (<90) pl.

Natural and synthetic plagioclase spectroscopy

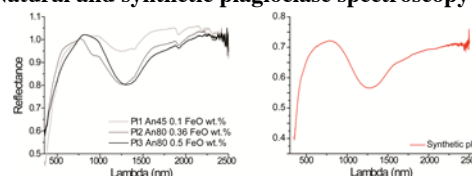


Fig. 1 Natural (left) and synthetic (right) spectra of pl.

Visible and near-infrared reflectance (VNIR) spectroscopy is the most used technique to map the surface of Solar System bodies. Pl, often considered a spectrally neutral phase, shows a clear absorption at ~1.25 μ m, even for very low FeO contents (Fig. 1, left); furthermore, an increase of this component, causes an increase of the absorption band depth, while its position moves to the IR region. We synthesized pl with different An and FeO content, in order to investigate how these parameters control the absorption band in the VNIR. A Pl, An90 with 0.5 wt% FeO, was synthesized from oxides and carbonate at $\log f_{O_2} = -9$; the mixture was first heated at 1600 °C for 15 minutes, quenched and then re-heated at 1400 °C for 24 hours. XRD and EPMA confirmed both the presence of a crystalline phase and its compositional homogeneity. The spectrum is reported in Fig. 1, right.

The synthesis of different pl will allow to create a VNIR spectra database which will be invaluable to better constrain the composition of the crust of Solar System bodies.

[1] Ohtake M. *et al.* (2009) *Nature*, 461, 236-241. [2] Evans *et al.* (2013) *LPSC XLIV*, Abstract #2033.

Bioaerosols in ECHAM5-HAM

ANA SESARTIC¹, ULRIKE LOHMANN¹,
AND TRUDE STORELVMO²

¹ETH Zurich, Institute for Atmospheric and Climate Science,
Zurich, Switzerland (ana.sesartic@env.ethz.ch,
ulrike.lohmann@env.ethz.ch)

²Department of Geology and Geophysics, Yale University,
210 Whitney Ave., USA-06520-8109 New Haven (CT)

Interest in primary biological aerosol particles (bioaerosols) like bacteria and fungal spores is mainly related to their health effects, impacts on agriculture, ice nucleation and cloud droplet activation, as well as atmospheric chemistry [1].

In our study we investigated the impact of bacteria and fungal spores acting as ice nuclei on clouds and precipitation on a global scale. Bacteria [2] and fungal spores [3] as a new aerosol species were introduced into the global climate model ECHAM5-HAM using observational data compiled by [4] for fungal spores and [5] for bacteria.

The addition of bioaerosols into ECHAM lead to only minor changes in cloud formation and precipitation on a global level, however, changes in the liquid water path and ice water path as well as stratiform precipitation in the model were observed in the boreal regions where tundra and forests act as sources bacteria and fungal spores.

This goes hand in hand with a decreased ICNC and increased effective radius of ice crystals. An increase in stratiform precipitation and snowfall can be observed in the model results for those regions as well.

Although bacteria and fungal spores contribute to heterogeneous freezing, their impact in the model was reduced by their low numbers compared to other heterogeneous ice nuclei like mineral dust.

To the best of our knowledge, the influence of bioaerosols on the global climate appears to be small. However, there are still several uncertainties constraining bioaerosol modelling, for example their exact emissions (especially over remote regions and the oceans), the impact of coating and ageing on the bacterial IN-ability, etc. Standardised long-term observations with world-wide coverage of ecosystems, as well as further laboratory data, are therefore necessary for a more precise model evaluation.

[1] Morris *et al.* (2011) *Biogeosciences* **8**, 17-25. [2] Sesartic *et al.* (2012) *Atmos. Chem. Phys.* **12**, 8645-8661. [3] Sesartic *et al.* (2013) *Environ. Res. Lett.* **8**, 014029. [4] Sesartic & Dallafior (2011) *Biogeosciences* **8**, 1181-1192. [5] Burrows *et al.* (2009) *Atmos. Chem. Phys.* **9**, 9281-9297.

N₂O and δ¹⁵N-N₂O data in ice cores: atmospheric versus in situ signal

BARBARA SETH, JOCHEN SCHMITT,
MICHAEL BOCK AND HUBERTUS FISCHER

Climate and Environmental Physics & Oeschger Centre for
Climate Change Research, University of Bern,
Switzerland, (*correspondence: seth@climate.unibe.ch)

N₂O is an important greenhouse gas which has several sources in both terrestrial and marine ecosystems. N₂O mixing ratios and stable isotopes measured from air entrapped in ice cores allow to identify different processes driving changes in these sources. We present a new δ¹⁵N-N₂O record covering the past 15'000 years and discuss possible explanations for the long-term decrease during the Early Holocene.

However, comparative analyses of different ice cores show offsets in the mixing ratios suggesting that elevated mixing ratios are due to in situ production, especially in glacial ice with higher impurity content.

However, the pathways leading to in situ production of N₂O in ice cores are not yet identified. Sowers [1] observes N₂O isotope anomalies in Vostok ice core samples and supposes that microorganisms might use ammonium (NH₄⁺) in ice to produce N₂O. EPICA Dome C (EDC) ice samples suspect to in situ production show fairly heavy δ¹⁵N-N₂O values as well, however, the isotope signature of N₂O produced from ammonium is expected to be rather light. Thus, it is unlikely that in situ produced N₂O in the EDC ice core can be related to NH₄⁺ oxidation.

Alternatively, we propose that in situ N₂O in the EDC ice is produced from nitrate (NO₃⁻). Low accumulation sites like EDC show extremely enriched δ¹⁵N-NO₃⁻ values due to intense post-depositional loss processes [2], while sites with higher accumulation have lighter δ¹⁵N-NO₃ values [3] and we found a lighter δ¹⁵N-N₂O in situ signature for those samples. More knowledge about in situ N₂O could help to verify hidden in situ production or identify ice cores and time intervals suitable to derive the atmospheric history for both mixing ratios and isotopic signature of N₂O.

[1] Sowers (2001), *JGR* **106**, 31903-31914. [2] Blunier *et al.* (2005), *GRL* **32**, L13501. [3] Hastings *et al.* (2005), *GBC* **19**, GB4024.

Competition between microbial and abiotic Fe(II) oxidation: A kinetic modeling approach

M. SETO^{1*} AND P. VAN CAPPELLEN²

¹Dept. of Information and Computer Science, Nara Women's University, Nara 630-8222, Japan, seto@ics.nara-wu.ac.jp (*presenting author)

²Ecohydrology Research Group, University of Waterloo, Waterloo, Canada

Neutrophilic Fe(II) oxidising bacteria (FeOB) are ubiquitous in soils and sediments. It has been proposed that under low oxygen conditions they are able to successfully outcompete abiotic Fe(II) oxidation. Not only do FeOB catalyse Fe(II) oxidation, they may also hinder the autocatalytic growth of Fe(III) oxides, possibly through the binding of Fe(II) and Fe(III) to cell surfaces or extracellular polymeric substances. We present a simple kinetic model of neutrophilic Fe(II) oxidation, which explicitly accounts for the inhibitory effect of FeOB on the autocatalytic Fe(II) oxidation pathway. The model comprises kinetic equations for the different forms of Fe in systems with and without FeOB. The microbial Fe(II) oxidation rate is assumed to be a function of the FeOB cell concentration, the O₂ concentration, and the cell-bound Fe(II) concentration. The latter is related to the aqueous Fe(II) by an isotherm. In the proposed model, cell-bound Fe(II) and Fe(III) are intermediates in the transformation of aqueous Fe(II) to Fe(III) oxides. The validity of the model is statistically examined, using data of Fe(II) oxidation batch experiments in the presence of the bacterium *Leptothrix cholodnii* Appels [1]. The observed microbial Fe(II) oxidation kinetics are well described by the model. Compared to the abiotic experiments, the presence of the bacteria increases the initial Fe(II) oxidation rate by nearly a factor of 3, but decreases the subsequent autocatalytic Fe(II) oxidation rate by about 50%. The results suggest that neutrophilic FeOB may broaden their geochemical niche by slowing down the autocatalytic growth of Fe(III) oxides in low O₂ environments.

[1] Vollrath *et al.* (2012) *Geomicrobiol J.*, **29**, 550-560

Sr-Nd isotope geochemistry of the troctolitic-gabbroic Bell Rock Range, Giles Complex, central Australia

R. E. B. SEUBERT¹, R. R. KEAYS¹, S. M. JOWITT¹
AND A. G. TOMKINS¹

¹School of Geosciences, Monash University, Clayton, VIC 3800, Australia, roland.seubert@monash.edu

The Mesoproterozoic Giles Complex of the Musgrave Province, central Australia, forms part of the c. 1075 Ma Warakurna Large Igneous Province. Here, we provide new Sr-Nd isotope data for a troctolite-gabbro member (Bell Rock Range) of the Giles Complex and compare them with other members of the Giles Complex; these data provide new insights into the formation and evolution of this under-researched magmatic province.

The most primitive melt within the Bell Rock Range is represented by a sample from the top of the intrusion that has an initial ϵNd value of +4.8, higher than the main troctolitic body of the range (ϵNd of -0.3 to +1.3), and ϵNd values of the gabbroic-ultramafic Wingellina Hills, Ewarara, Kalka and Gosse Pile intrusions range from -5.1 to +0.5 [1]. In comparison, the basal part of the Bell Rock Range has ϵNd values of -4 to 1.1, identical to later dykes that cross-cut the range, and indicative of formation from magmas that underwent crustal contamination or were derived from an enriched mantle source. Although the troctolites at Bell Rock Range yield a range of ϵNd and MgO values, they have relatively uniform initial $^{87}\text{Sr}/^{86}\text{Sr}$ values compared to all other lithologies in our database.

These data shed new light onto the petrogenesis of the Giles Complex, and indicate that it is unlikely that any of the the magmas that formed this complex were derived from a depleted region of the mantle. The magmas that formed this complex must have either been sourced from an enriched region of the mantle or have undergone variable crustal contamination, resulting in the range of isotopic compositions observed within this suite of co-magmatic rocks.

The relatively uniform $^{87}\text{Sr}/^{86}\text{Sr}$ compositions of the Bell Rock Range troctolites suggests that they represent an uncontaminated end-member style of Giles Complex magmatism, whereas gabbroic-ultramafic cumulates in the same area represent true mixing between mantle-derived melts and crustal rocks indicative of significant crustal contamination. These findings will contribute to an understanding of the tectonic setting of the Giles Complex.

[1] Wade (2006) PhD thesis, University of Adelaide, Australia.

Iodide Ion Hydration in Aqueous Solution to 360°C: Insight from XAS and Ab Initio MD

T.M. SEWARD¹, HENDERSON C.M.B.², SULEIMENOV O.M.¹ AND CHARNOCK J.M.²

¹Victoria University of Wellington, Wellington 6140, New Zealand; terry.seward@vuw.ac.nz

²University of Manchester, Manchester M13 9PL, UK

The interaction of solute species with solvent molecules is a fundamental aspect of aqueous solutions and changes with increasing temperature and pressure in response to changes in the hydrogen bonding of water solvent. The varying nature of ion hydration in hydrothermal systems plays an important role in many geochemical processes including water stable isotope fractionation, mineral solubility and precipitation, metal complexing and transport reactions.

Anion-solvent interaction is still poorly known at elevated temperatures and pressures and no data exist for iodide solvation above ambient temperatures (Seward and Driesner, 2004). We have therefore studied the first shell hydration of iodide using X-ray absorption spectroscopy from 35 to 350°C at equilibrium vapour pressures. The Exafs of 1.00m RbI as well as 0.10m CsI and SrI₂ was measured using a high temperature X-ray optical cell containing silica glass and/or cvd diamond windows. With increasing temperature from 35 to 350°C, iodide-oxygen(water) distance increased from 3.56 to 3.61Å as the first shell waters are "dragged" away from the iodide ion by expanding bulk water solvent to which they are hydrogen bonded. Over the same temperature range, the number of first solvation shell waters apparently decreases from 7 to 4.

We have also performed ab initio molecular dynamics simulations using the Car-Parinello scheme (Car and Parinello, 1985). The present density functional theory calculations utilised norm-conserving pseudopotentials of Troullier and Martins (1991) to describe the core of all atoms except for hydrogen for which a von Barth-Car analytical pseudopotential was used. The simulation cell was cubic with periodic boundary conditions containing 32 waters and one iodide ion. At 27°C, the iodide-oxygen(water) distance was 3.53Å and increased to 3.59Å at 350°C, in good agreement with our results from XAS.

Car R. and Parinello (1985) Phys. Rev. Lett. 55, 2471.
Seward T.M. and Driesner T. (2004) In: Aqueous Systems at Elevated Temperatures and Pressures (Elsevier), chap. 5.
Troullier and Martins (1991) Phys. Rev. B, 43.

Fluid-mediated re-equilibration and self-irradiation in complex U-Th-rich assemblages of pegmatites: A case from Norway and implications for U-Th-Pb dating of ore deposits.

A.M. SEYDOUX-GUILLAUME*¹, B. BINGEN², C. DURAN³, V. BOSSE⁴, J.L. PAQUETTE⁴, D. GUILLAUME¹, PH. DE PARSEVAL¹ AND J. INGRIN⁵

¹ GET, UMR5563 CNRS-UPS-IRD, Université de Toulouse, 14 av E. Belin, 31400 Toulouse, France

² Geological Survey of Norway, 7491 Trondheim, Norway

³ Département des sciences appliquées, 555 Boulevard de l'Université, Chicoutimi, Québec, Canada, G7H 2B1

⁴ LMV, Université Blaise Pascal, 5 rue Kessler, 63000 Clermont-Ferrand, France

⁵ UMET, UMR 8207 CNRS, Université Lille1, 59655 Villeneuve d'Ascq, France

In most rocks, uranium and thorium are concentrated in favorable crystallographic sites in few minerals such as zircon, monazite, titanite, and rarely uraninite, thorianite, thorite / huttonite, euxenite. These minerals are submitted to intense self-irradiation that can lead to amorphization and also modify their environment by irradiating the host minerals. Here, we focus on accessory minerals in rare-metal-rich pegmatites from southern Norway (Kragere, Iveland-Evje); some of these minerals are rich in U (e.g. up to 15wt % for euxenite). A complex paragenesis of zircon + monazite + xenotime + euxenite was studied by multiple methods including optical and electron microscopy and U-Pb geochronology (SIMS and LA-ICP-MS). Observations show that complex relationships exist between the different minerals (especially zircon-euxenite) and the various processes (alteration by fluids and radiation effects) which have repercussions on the U-Th-Pb geochronology response. Irradiation (self and out), destroy the crystal lattice (amorphization) promoting the alteration of more or less destroyed parts. Amorphization induces volume increase, leading to the formation of cracks which eventually connected into a network through the rock. This fracturing allows fluid circulation, and promotes alteration of source minerals and dispersion of elements (e.g. Pb and U). Our results demonstrate however that monazite and xenotime crystals, even altered, have a greater potential for U-Th-Pb dating [1].

[1] Seydoux-Guillaume *et al.* (2012) *Chem. Geol.* **330-331**, 140-158.

High-spatial resolution imaging of the distribution and inter-element correlation of metals in modern and ancient stromatolites

M.C. SFORNA^{1*}, P. PHILIPPOT¹, M. VAN ZUILEN¹,
A. SOMOGYI², K. MEDJOUBI², P.T. VISSCHER³
AND C. DUPRAZ³

¹ Institut de Physique du Globe de Paris, Sorbonne Paris Cité,
Paris, France (*correspondence : sforna@ipgp.fr)

² Synchrotron Soleil, Saint-Aubin, Gif-sur-Yvette, France

³ Department of Marine Sciences, University of Connecticut,
Groton, Connecticut, USA

Metals, which are widely used by all microorganisms, could act as indicators in the rock record of past microbial activity if we are able to distinguish between biological uptake and late stage contamination associated with diagenesis. Here we present the results of the study of the distribution, inter-element correlation and speciation of trace metals in modern and ancient stromatolites from Big Pond, a hypersaline lake in the Bahamas and the 2.7 Ga-old Tumbiana formation in Western Australia. Results were obtained using synchrotron-based techniques.

In a cm-scale drill core of an extant stromatolite from the Bahamas, the Fe, Ti, Zn, Cu and As contents in the organic fraction of the stromatolite structure increase with depth. We attributed this to metal uptake during early diagenesis. Both in the Bahamas and in the Tumbiana stromatolites, high-spatial resolution imaging at different scales (from the cm- to the nm-scale) reveals different types of metal distribution and inter-element correlations. Although most of the metal enrichments are of diagenetic origin, the occurrence of specific species in isolated organic structures that are preserved in the core of the stromatolite domes most likely reflects remains of past biological activity.

Insights of the Mt. Etna volcanic activity through multiparametric data recorded by the NEMO-SN1 seafloor observatory

T. SGROI*, M. DE CARO, N. LO BUE AND P. FAVALI
Istituto Nazionale di Geofisica e Vulcanologia, Rome, Italy

In the last years the use of seafloor observatories improves the possibility to perform long-term monitoring in abyssal area as far not easily accessible, interested by geophysical processes like volcanism, seismicity or fluid emissions. Presently many programmes to establish permanent underwater networks are launched at global scale (e.g., EMSO in Europe, OOI in USA, NEPTUNE in Canada and DONET in Japan). Recently, a multidisciplinary approach has proven to be a very important tool in the monitoring of volcanic areas. In fact, the different instruments hosted in the seafloor observatory permit to perform multidisciplinary analyses, better focusing on the dynamics of volcanic system.

In the Italian territory, the NEMO-SN1 seafloor cabled observatory is running in the Western Ionian Sea at a depth of 2100 m, about 25 km off-shore Eastern Sicily, as node of EMSO infrastructure (<http://www.emso-eu.org>). Eastern Sicily is of great scientific interest, due to the proximity to seismogenic structures which originated the most destructive earthquakes of the area and to Mt. Etna. The underwater observatory fills the gap in the off-shore sector of the Mt. Etna, focusing on its deeper feeding system. SN1 was able to record also the low-frequency seismic signals linked to Etna volcanic activity, as the volcanic tremor associated to the 2002-2003 eruptive activity. In this work, the joint analyses of seismological, gravimetric and oceanographic data are used to highlight the dynamics of Mt. Etna. The inferences of background noise from volcanic activity and ocean processes are investigated through the cross-analyses of different kind of geophysical data to improve the confidence of volcanic hazard assessment.

Mantle xenoliths from Bir Ali (Yemen)

SGUALDO P.*, BECCALUVA L., BIANCHINI G.
AND SIENA F.

Dip. Fisica e Scienze della Terra, Università di Ferrara
(*sglpla@unife.it)

Mantle xenoliths from the Bir Ali diatrema (southern Yemen) consist of spinel peridotites and clinopyroxenites. In this contribution we present bulk rock (XRF, ICP-MS) and mineral (EMPA, LA-ICP-MS) major and trace element analyses carried out on a collection of 62 samples in order to characterize the lithospheric mantle of the area and constrain its relative petrological evolution. Peridotites are mainly equilibrated at 950-1000 °C and include fertile lherzolites and more refractory harzburgites and dunites, suggesting that partial melting processes variably affected the pristine mantle composition. Subsequent metasomatic reactions are evidenced by: a) glassy films and/or patches; b) interstitial plagioclase; c) rare pargasite amphibole (observed only in one sample). Further evidence of metasomatic interactions is given by anomalously low Fo content (<0.87) of olivine and low Mg# of pyroxene (<0.88). These metasomatic events are confirmed by the bulk rock trace element budget that reveal enrichments in the most incompatible elements, especially in the most refractory dunites (La_N/Yb_N up to 4.1). Coherently, enrichments in the most incompatible elements are also observed in diopsidic clinopyroxene (La_N/Yb_N up to 3.9) and glasses (La_N/Yb_N up to 9.9). Trace element discrimination ratios [1] suggest that the causative metasomatic agents were mainly represented by alkali-silicate melts. Noteworthy, samples characterized by plagioclase impregnation show unfractionated (flat) bulk-rock and clinopyroxene REE patterns suggesting refertilization by subalkaline metasomatic melts. Therefore, the considered lithospheric section appears to be characterized by remarkable heterogeneity, in contrast with what observed in mantle xenoliths collected from the Ethiopian plateau area that display clear evidence of pervasive refertilization by CFB melts [2]. This suggests that the lithospheric mantle of southern Yemen wasn't affected by the thermochemical effects of the Afar plume.

[1] Coltorti *et al.* 2000. *Earth Planet. Sc. Lett.* **183**, 303-320.

[2] Beccaluva *et al.*, 2011. *GSA Special Paper* **478**, 77-104.

Pore-scale simulation of calcite dissolution and precipitation using lattice-Boltzmann method

B. SHAFEI^{1*}, C. HUBER² AND A. PARMIGIANI³

¹School of Earth and Atmospheric Sciences, Georgia Institute of Technology, Atlanta, GA 30332, USA.

babak.shafei@eas.gatech.edu

²christian.huber@eas.gatech.edu

³andrea.parmigiani81@gmail.com

Calcium carbonate dissolution and precipitation plays an important role in the context of CO₂ storage in geologic formation, or as a pH buffer during diagenesis of marine sediments. Using the parallel open-source library palabos (www.palabos.org), we have developed a new multi-species pore-scale model based on the lattice Boltzmann method to investigate the effect of physical and chemical heterogeneities on geochemical behavior of carbonate system in a complex porous media. The model has been successfully applied to study the permeability change of a porous medium associated with a given porosity change during dissolution and precipitation and arsenic sorption on Fe-bearing minerals.

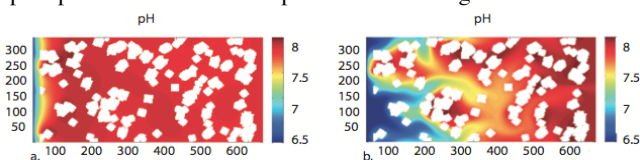


Fig 1. Pore-scale pH distribution at steady-state for a) low Peclet number (Pe=1) and b) high Peclet number (Pe=5).

In this study, we consider standard geochemical pathways for the carbonate system including 7 species (i.e. H⁺, OH⁻, H₂CO₃, HCO₃⁻, CO₃²⁻, Ca²⁺ and CaHCO₃⁺) and 5 mixed kinetic-equilibrium reactions. The focus of our study is to investigate how spatial distribution of the pH is affected by: 1) the kinetic rates of heterogeneous calcite dissolution and precipitation (i.e. pH-dependent vs. pH-independent rate constants), 2) transport regime (i.e. Peclet numbers) and 3) chemical composition of initial and boundary conditions resulting in spatially variable saturation index with respect to calcite. Results showed that the development of pore-scale concentration gradients is a combined effect of heterogeneous reactions and pore-scale flow within the porous medium. In high Pe simulations (Fig 1.a), both depth of penetration and spatial heterogeneity increase compared to low Peclet scenario (Fig 1.b). Calculated minimum, maximum and average pH values in the computational domain are function of Pe, chemical composition of inflow and initial solution in the domain, and type of rate constants.

Geochemistry and petrogenesis of volcanic rocks in the Lahrud region, of the Ardebil province, Iran

HABIB SHAHBAZI SHIRAN

Department of Archaeology, University of Mohaghegh
Ardabili, Ardebil, Iran (Shahbazihabib@yahoo.com)

Compositional analyses of materials from prehistoric contexts have become an important component of most scientifically oriented archaeological projects. Characterizing the elemental signature of materials (obsidian, metals, stones) helps determine provenance and technological production techniques, and therefore is useful for reconstructing trade and interaction between people prehistorically.

Simple petrographic descriptions can provide useful information on raw material provenance, but for some lithic materials more sophisticated techniques are required. Geochemistry can provide this sophisticated tool, trace and interpret the bedrock or the source of the ancient lithic materials. Geochemists have determined the geologic, magmatic and/or tectonic affinities of igneous rocks for decades. This project reports on mineral assemblages and whole-rock geochemistry that mafic rocks used to make lithic artifacts and especially building stones in the Ardebil province, northwestern Iran, have two bedrock sources.

New insights into the isotope exchange reaction between O₃ and CO₂ via O(¹D) from laboratory experiments

ROBINA SHAHEEN¹, THOMAS RÖCKMANN², BELA TUZSON³ AND CHRISTOF JANSSEN⁴

¹University of California at San Diego, Department of Chemistry and Biochemistry, 9500 Gilman Dr, La Jolla, CA 92093 USA, roshaheen@ucsd.edu

²Institute for Marine and Atmospheric Research Utrecht, Utrecht University, Princetonplein 5, 3584 CC Utrecht, The Netherlands, t.roeckmann@uu.nl

³Empa, Swiss Federal Laboratories for Materials Science and Technology, Laboratory for Air Pollution and Environmental Technology, Überlandstr.129, 8600 Dübendorf, Switzerland, Bela.Tuzson@empa.ch

⁴Laboratoire de Physique Moléculaire pour l'Atmosphère et l'Astrophysique, 4 Place Jussieu, 75005 Paris, France, christof.janssen@upmc.fr

Stratospheric CO₂ shows a marked oxygen triple isotope anomaly that is derived from O₃ via O(¹D). So far the precise isotopic composition of the isotope exchange partner of CO₂ has not been identified and it is not clear whether normal mass dependent or anomalous isotope effects contribute during the exchange process. From laboratory experiments using simultaneous mass spectrometric analysis of CO₂ and laser spectroscopy based symmetry selective analysis of O₃ isotopomers, we present experimental evidence that the O(¹D) mediated isotope transfer is coupled to the asymmetric O₃ isotopomers and follows a standard mass dependence. Recently investigated alternative pathways for oxygen isotope exchange between CO₂ and hyperthermal O atoms or O₂ molecules are unlikely to compete significantly with isotope exchange via O(¹D). Existing measurements also indicate unresolved discrepancies for the isotope anomaly of O₃ produced in the laboratory under different photochemical conditions, which may originate from highly energetic oxygen species generated in the photolysis of O₂ and/or O₃. Such variations would be directly transferred to CO₂, and further combined measurements of the isotopic composition of CO₂ and symmetry resolved O₃ are needed to fully unravel all aspects of the isotope exchange.

www.minersoc.org

DOI:10.1180/minmag.2013.077.5.19

Dynamics of H₂O₂ in the external *milieu* of corals – from single organism to the reef

YEALA SHAKED^{1,2*} AND RACHEL ARMOZA-ZVULONI^{1,2}

¹Inst of Earth Sciences, Hebrew Univ., Jerusalem, Israel
(*correspondence: yshaked@vms.huji.ac.il)

²Interuniversity Inst. for Marine Sciences, Eilat, Israel
(rachelar@post.tau.ac.il)

Symbiont-bearing corals are subjected to internal fluxes of reactive oxygen species (ROS) from their symbiotic algae as well as external fluxes from photochemically generated ROS in overlying waters. Here, combining sensitive methods, kinetic approaches and statistical tools, we characterized the dynamics of the membrane permeable ROS - hydrogen peroxide (H₂O₂) - in the external *milieu* of corals in a laboratory setting and in a natural coral reef. On the organism level, we observed flow-induced release of H₂O₂ and antioxidants from intact corals over 2-4 hour periods. In the absence of flow we found that antioxidants associated with the coral quickly degraded externally applied H₂O₂. Scaling up to the ecosystem level, we observed coral-induced changes in H₂O₂ concentrations and elevated antioxidant activities in the proximity of a coral knoll and in the reef lagoon. This newly described ability of corals to change the chemistry of their surrounding water by releasing both H₂O₂ and antioxidants may have important implications for coral physiology and interactions with the environment. External antioxidant activity may enable corals to offset exogenous H₂O₂ whereas the flow induced H₂O₂ release may aid corals in discarding internal H₂O₂.

Traffic-associated heavy metal pollution and source discrimination in Jiangxi Province, China

SHAO LI^{1,2}, XIAO HUAYUN^{3*} AND WU DAISHE¹

¹Environmental and Chemical Engineering College, Nanchang University, Nanchang, 330031, China

²The Key Lab of Poyang Lake Environment and Resource Utilization of Ministry of Education, Nanchang, 330031, China

³State Key Laboratory of Environment Geochemistry, Institute of Geochemistry, Chinese Academy of Sciences, Guiyang, 550002, China

Road traffic is recognized as an important source of heavy metals. In order to identify the levels and sources of heavy metal contamination on three highways in Jiangxi Province, concentrations of Zn, Cu, Pb, Sb, Cd in different chemical forms in airborne particles, road dusts and soils were analyzed. All of the Zn, Cu, Pb, Sb, Cd concentrations in road dusts and soils exceeded background values. And the heavy metal concentrations in road dusts were higher than those in soils. Heavy metal concentrations in airborne particles, road dusts and soils presented similar rules: Zn > Cu, Pb > Sb, Cd. Zinc, Cu, Pb, Sb, Cd concentrations in airborne particles, road dusts and soils were all significantly correlated with vehicle number, indicating that road traffic was one of the main source of these metals. For all these metals, we also found that the ratios were higher near the toll stations than on normal driving road, indicative of an increased heavy metal emission rates under the conditions of low driving velocity and discontinuous movement of vehicles. The sources of the heavy metals were also identified by comparing chemical forms of the heavy metals in airborne particles, road dusts and soils. Lead in airborne particles was dominated by the acid soluble/exchangeable fractions (67%) while that in road dusts and soils was dominated by the residual fractions (45.3% and 43.8%, respectively), which suggested that Pb in airborne particles was derived from traffic, and that in road dusts and soils resulted mainly from the use of leaded gasoline in the past. In raining days, Zn concentrations in PM10 increased possibly because tire abrasion turned to be weak due to the lubrication of rainwater and so more small particles were emitted from the tyre wear. The difference in chemical forms of the heavy metals in airborne particles, road dusts and soils was associated with concentrations of organic matters. Bioavailability of heavy metals in airborne particles was much higher than that in road dusts and soils..

Corresponding author. E-mail: xiaohuayun@vip.skleg.cn.

Redox control on the water column distribution of Ra in a stratified lake - Lake Kinneret, Israel

G. SHARABI^{1,2*}, Y. KOLODNY¹, L. HALICZ¹, A. NISHRI³
AND B. LAZAR¹,

¹ Institute of Earth Sciences, The Hebrew University of Jerusalem, ISRAEL 91904

(*Correspondence: galit@gsi.gov.il)

² Geological Survey of Israel, Jerusalem, ISRAEL 95501

³ Israel Oceanographic and Limnological Research Ltd., P.O. Box 447, Migdal, ISRAEL 14950

The vertical distribution of transition metals in holomictic lakes is controlled by the seasonal mixing/stratification regime that change the redox state in the water column. We studied the control of the Mn redox system on water column distribution of Ra, an element with invariant oxidation state. The study was conducted in Lake Kinneret (The Sea of Galilee), Israel, a warm monomictic lake in northern Jordan valley. Lake Kinneret fluctuates between periods of stratification (spring/summer) and mixing (fall/winter), with full depth mixing (~37 m) in February. The mixed layer (epilimnion) is always well oxygenated while below it (hypolimnion), anoxic conditions prevail.

Vertical profiles of Mn, ²²⁶Ra ($T_{1/2}=1,600$ y) and ²²⁴Ra ($T_{1/2}=3.7$ d) were measured during October 2012. Practically all the Mn in the well-oxygenated mixed layer (0-15 m) was particulate ($10 \mu\text{g}\cdot\text{L}^{-1}$). A large peak of dissolved Mn ($500 \mu\text{g}\cdot\text{L}^{-1}$), appeared at the oxycline ~17.5 m. The reducing hypolimnion, below 20 m, contained ~60 $\mu\text{g}\cdot\text{L}^{-1}$ of dissolved Mn and was virtually deficient of solid Mn-oxides. The water column profile of ²²⁶Ra and ²²⁴Ra were remarkably similar.

Mn speciation along the Kinneret water column is redox sensitive: it appears mainly as solid Mn-oxide in the oxygenated epilimnion, and as dissolved Mn(II) in the anoxic hypolimnion. Hence, the particles of Mn-oxide that sink through the water column, dissolve in the epilimnion-hypolimnion interface and form an extremely large and narrow peak of dissolved Mn(II). The Ra water column profile resembled that of Mn, despite being a redox-insensitive element. This is attributed to adsorption of dissolved Ra on solid Mn-oxides in the epilimnion and its desorption in the hypolimnion. We use the ²²⁴Ra/²²⁶Ra ratios and the large difference in their half-lives to obtain a field estimate of the reduction rate of Mn-oxide.

Magmatic systems of the Paleoproterozoic large igneous provinces: Evidence from the eastern Fennoscandian Shield

E.V. SHARKOV*, M.M. BOGINA AND A.V. CHISTYAKOV
IGEM RAS, Staromonetny per. 35, Moscow, Russia 119017
(sharkov@igem.ru)

It is known that large igneous provinces are usually formed by lava plateaus, dyke swarms and subvolcanic sills, which are united into volcano-plutonic associations. At the same time, rocks within lava plateau were subjected to crystallization differentiation and crustal assimilation, which caused wide variations in their composition. This leaves us with questions where and how this occurred?

For this aim we presented the results of our study of two Paleoproterozoic large igneous provinces in the eastern Fennoscandian Shield: (1) early Paleoproterozoic (2.5-2.35 Ga) province of siliceous high-Mg series, and (2) middle Paleoproterozoic (2.35-1.9 Ga) province composed by high- and low-Ti alkaline and tholeiite basalts. The peculiar feature of these provinces is the presence of layered mafic-ultramafic complexes: dunite-harzburgerite-bronzitite-norite-gabbro-norite-anorthosite (Monchegorsky, Fedorovo-Pansky, Burakovsky, etc.) and wehrlite-clinopyroxenite-gabbro-alkaline gabbro (Elet'ozero and Greymykh-Vyrmes), respectively. The formation of these complexes was controlled by replenishment of fresh magmas in solidified intrusive chambers and impregnation of melts into already solidified rocks (multistage formation). Geochemical data indicate that all rocks of these centers are related in different degree, being often close in major and trace-element composition to volcanics in lava plateaus.

So, we suggest that these layered intrusive complexes represent deep-seated long-lived transitional magmatic chambers where melts, derived from magma-generation zones were accumulated and experienced crystallization differentiation, while evolved melts were mixed with fresh magma portions. Cumulates retained in the crust. Correspondingly, the primary magmas partially lost their components and derived evolved magmas continue their ascent to the surface. The evolved magmas arrived at the surface and formed lava piles of different composition. Thus, it is difficult for primary melts to reach surface; as a rule, they are subjected to transformations in such transitional chambers.

Melting phase relations in Udachnaya-East kimberlite and search for parental melt composition

I.S. SHARYGIN^{1*}, K.D. LITASOV¹, A. SHATSKIY¹,
A.V. GOLOVIN¹, E. OHTANI² AND N.P. POKHILENKO¹

¹Sobolev Institute Geology and Mineralogy, Novosibirsk
630090, Russia (*igor.sharygin@gmail.com)

²Tohoku University, Sendai 980-8578, Japan.

Udachnaya-East kimberlite (UEK) is an unique example of unaltered Group I kimberlites, exhibiting lack of serpentinisation and containing abundant alkaline carbonate and chloride minerals in the groundmass [1]. We studied phase relation in UEK in using multianvil experiments at 3-6.5 GPa and 900-1500 °C [2]. Super-solidus assemblage consists of olivine (Ol), Ca-rich garnet (Gt), Al-spinel (Sp), perovskite (Pv), CaCO₃, and apatite at 3-6.5 GPa with addition of clinopyroxene at 3-4 GPa and Na-Ca carbonate at 6.5 GPa and 900 °C. The subliquidus phase assemblage (Ol + Gt + Sp + Pv) differs from common mantle lithologies, which may be due to unaccounted CO₂ lost during kimberlite degassing at shallow depth. UEK did not achieve complete melting even at 1500°C and 6.5 GPa. This indicates that kimberlite magma below 90 km depth was a mixture of the melt and xenogenic materials (mainly Ol). In the studied *P-T* range, melt has Ca-carbonatite composition (Ca/(Ca+Mg) = 0.6-0.8) with high alkali and Cl contents (2.8-6.7 wt.% K₂O, 7.3-11.6 wt.% Na₂O, 1.2-3.7 wt.% Cl). The K, Na and Cl contents and Ca/(Ca+Mg) ratio decrease with temperature. The SiO₂ content in the partial melt increases with temperature and decreases with pressure (Fig. 1). Consequently, the ascending melt dissolved increasingly more SiO₂ (Fig. 1) and evolved from essentially carbonatite (<5 wt.% SiO₂) toward carbonate-silicate composition (up to 25 wt.% SiO₂).

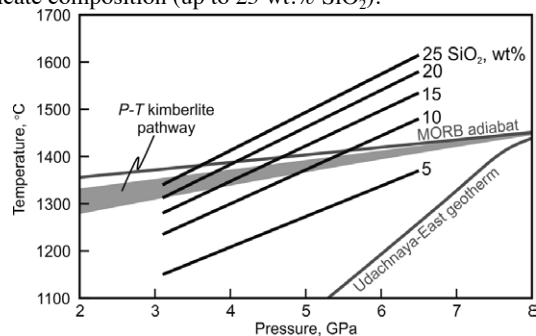


Figure 1: *P-T* plot for UEK melt with SiO₂ isopleths.

[1] Kamenetsky *et al.* (2012) *Lithos* **152**, 173-186. [2] Sharygin *et al.* (2013) *Dokl. Earth Sci.* **448**, 200-205.

Mineralogy of the Chelyabinsk meteorite, Russia

V.V. SHARYGIN^{1*}, T.YU. TIMINA¹, N.S. KARMANOV¹,
A.A. TOMILENKO¹ AND N.M. PODGORNYKH¹

¹V.S. Sobolev Institute of Geology and Mineralogy SD RAS,
Novosibirsk 630090, Russia (*correspondence:
sharygin@igm.nsc.ru)

The entry in the Earth's atmosphere, further blasting and impact of the Chelyabinsk meteor body have been fixed 15 February 2013. We studied small fragments collected in the area of abundant meteorite shower (nearby towns Emanzhelinsk and Korkino, South Urals).

The Chelyabinsk meteorite was classified as an ordinary LL5 chondrite (S4, W0) [GEOKHI RAS]. It is very similar in mineral composition to other LL5 chondrites such as Salzwedel, Hautes Fagnes and Al Zarnkh [1-3]. All meteorite fragments consist of coarse- to fine-grained matrix, rare submillimetre chondrules and thin fusion crust. Some fragments show brecciated texture.

Olivine (Fo₆₈₋₇₂Fa₂₈₋₃₁Ln_{<0.5}), orthopyroxene (En₇₀₋₇₄Fs₂₅₋₂₈Wo₁₋₂), Fe-Ni-metal, troilite, chromite and Na-plagioclase (Ab₇₇₋₈₆An₁₀₋₂₀Or₃₋₁₀) are major primary minerals in the inner part. Ilmenite, Cr-diopside (Wo₄₆₋₄₈En₄₃₋₄₅Fs₁₆₋₁₈, Cr₂O₃ – 0.6-0.8 wt%), chlorapatite, merrillite and feldspathic glass are minor. Coarse- to medium-grained matrix mainly contains primary minerals (olivine, pyroxenes, etc.); some areas show fine recrystallization due to melting and further quenching with formation of skeletal crystals of olivine (Fa₂₉₋₄₆Ln₁₋₃), orthopyroxene, subcalcium pyroxene (Wo₂₂₋₄₂En₄₅₋₆₅Fs₁₃₋₂₂) in feldspathic glass (plagioclase). Metal-sulfide assemblage (up to 10 vol%) is represented by kamasite-taenite intergrowths (or their individuals) and troilite; pentlandite and native copper occur rarely. Chondrules are different in mineralogy. Some of them show well-oriented "barred" texture and consist of olivine and Na-plagioclase (feldspathic glass) with minor chromite and chlorapatite. Other chondrules are similar in mineral composition to the matrix and their oriented texture is less pronounced.

Fusion crust (up to 1 mm) contains relics of primary minerals, mafic-ultramafic brown glass, abundant gas bubbles, newly-formed minerals (zoned skeletal crystals of Cr-Ni-rich magnetite, forsterite-fayalite, wüstite, etc.) and Ni-rich metal-sulfide globules (heazlewoodite, awaruite-taenite, godlevskite, rarely Os-Ir-Pt-Ni alloy).

[1] Matthes (1995) *Chem Erde-Geochem* **55**, 257-261. [2] Gismelseed *et al.* (2005) *Meteorit Planet Sci* **40**, 255-259. [3] Vandeginste *et al.* (2012) *Geol Belg* **15**, 96-104.

Evidence for formation of alluvial diamonds from North-East of Siberian platform in subduction environment

V.S. SHATSKY^{1,2*}, D.A. ZEDGENIZOV², A.L. RAGOZIN²
AND V.V. KALININA²

¹Vinogradov Institute of Geochemistry SB RAS, 1a Favorsky str., Irkutsk, 664033, Russia, (*correspondence: shatsky@igc.irk.ru)

²Sobolev Institute of Geology and Mineralogy SB RAS, 3 Koptyuga ave., Novosibirsk, 630090, Russia

Diamonds from placers show large variability in nitrogen content ranging from below detection to 3500 at.ppm. Nitrogen contents in diamonds with eclogitic inclusions are generally high (average of 950 at.ppm) as compared with diamonds of ultramafic suite (average of 513 at.ppm). $\delta^{13}\text{C}$ values of the diamonds range from -27 to -3‰ (n=28) for eclogitic diamonds and from -7.1 to -0.5‰ (n=16) for peridotitic diamonds. The 265 diamonds were polished to expose their mineral inclusions. Inclusions of eclogite suite are predominant (74%). The diamonds of the eclogitic suite contain garnet, omphacitic clinopyroxene, coesite, K-feldspar, rutile, corundum. The peridotitic diamonds contain olivine, Cr-pyrope garnet, orthopyroxene and chromite. Majoritic garnets of both peridotitic and eclogitic parageneses were identified in 4 diamonds. The olivines have Fo contents between 89.7 and 93.8 mol.% (average – 92.4). Eclogitic garnet and Cpx inclusions are within the range of eclogitic inclusions of worldwide. For an assumed pressure of 5 GPa eclogitic garnet and clinopyroxene gave temperatures in the range 1028-1290°C. The majority of eclogitic diamond show positive Eu-anomalies. High-Ca group garnets are LREE depleted, show strong positive Eu (up to 4.25) and Sr anomalies and have HREE contents that are less than the low- and intermediate-Ca group samples. Eclogitic Cpx inclusions are characterized by convex REE_N patterns with maxima at Nd or Sm. The presence of majorite inclusions indicate that the portion of the diamonds is of sublithospheric origin. Multiple inclusions from diamond and their carbon isotopes composition are consistent with a mixing model in which they result from the interaction of slab-derived melt/fluid with surrounding mantle. The nature of the variations in the carbon isotope composition and the nitrogen contents indicate that the diamonds growth medium have at least two sources (mantle and recycled earth crust via subduction zone). Mantle carbon was involved in the diamond formation process during the final stages of growth.

Telluride-gold-sulfide mineralization in silicification zones of gabbro-dolerite bodies of hengursk complex (Russia, Pay-Khoy)

R.I. SHAYBEKOV

Institute of Geology Komi SC UB RAS, Syktyvkar, Russia, 54 Pervomayskaya st. (*correspondence: shaybekov@geo.komisc.ru)

According to the previous studies gold-telluride mineralization has been found only in the gabbro-dolerite bodies of Pay-Khoy hengursk complex at the districts "Pervyi" and "Savabeytsky" in copper and nickel ores [1]. The studies of sulfide (chalcopyrite highly) mineralization in quartz veins of district "Krutoy" revealed silver-gold-telluride phases with later hydrothermal origin.

Telluride-gold-sulphide mineralization is characterized by a fairly stable composition - chalcopyrite, covellite, wurtzite, gold, silver, coloradoite (found for the first time in Pay-Khoy) and native phase. The composition of coloradoite has minor changes from the classic mineral which could be explained by the specificity of mineral formation or inaccurate analysis due to the small size of the grains. The impurities of silver and lead in insignificant quantities were found, which allowed distinguishing of two kinds - silver-lead and silver. The formation of this type of mineralization occurred in a low-, medium-temperature hydrothermal process in the veins of gold-bearing sulphide mineralization.

The work was made with the support of the program of the presidium RAS №27 (12-П-5-1027) and SC-1310.2012

[1] Shaybekov R.I. Mineral assemblages and genesis of platinum sulphide mineralization in gabbro-dolerite Pay-Khoy (Russia, the Nenets Autonomous District) // Notes RMS, 2011. № 6, pp. 70–86.

Use of passive sampling to measure organic chemicals and metabolites in water and soil: Application to human health risk assessment in developing countries

D. SHEA*, T. HONG, X. XIA, X. KONG, K. O'NEAL, AND P. LAZARO

North Carolina State University, Raleigh, NC 27695-7617
USA (*correspondence: d_shea@ncsu.edu)

Measuring chronic exposure to broad chemical mixtures at trace levels is currently not practical because traditional *grab* samples do not capture temporal variations in exposure and thus provide little information on chronic exposure unless many samples are collected and analyzed. This problem is even greater in developing countries where resources for sampling and chemical analysis can be extremely limited. We will report on the use of passive sampling devices (PSDs) to provide a cost-effective means of estimating chronic exposure and toxic response in water and soil. PSDs sequester and preconcentrate organic chemicals from water and from soil and sediment via desorption to water. Using laboratory-derived and field-verified uptake rates (calibration), PSDs were deployed in the field for a known amount of time (e.g., 1 month), the accumulated chemical residue was measured, and then the average exposure calculated based on the calibration. Extracts of the PSDs also were used in high throughput cell-based assays to measure various toxic endpoints such as genotoxicity and endocrine disruption. We will illustrate the potential utility of PSDs using data from the Red River, Vietnam. In surface waters, we found very good agreement between measured chemicals in the PSDs and synoptically deployed aquatic test organisms, providing strong evidence that PSDs accumulate only the bioavailable fraction of a chemical. In soil, we also found good agreement between PSDs and accumulation in earthworms. In both water and soil, there was generally good agreement between PSD chemical residues and toxic response variables. We will discuss the current utility and limitations for using PSDs for both human and ecological health risk assessments and provide an example of the spatial and temporal variation in human health risk to chemical exposure in the Red River, Vietnam.

Effect of hydrothermal alteration on magnetic susceptibility of Challu Pluton, SE Damghan- Iran

M. SHEIBI^{1*}, P. MAJIDI² AND M. REZAEI KHKHAYY³

^{1,3} Faculty Member, Department of Geology, Shahrood University of Technology, Iran (*correspondence: sheibi@shahroodut.ac.ir, Mehdi.Rezaei@khayam.ut.ac.ir)

² MSc. student of Petrology, Department of Geology, Shahrood University of Technology, Iran (parvinmajidi91@gmail.com)

Challu pluton located in the northern part of Central Iran structural zone, SE Damghan. Based on mineralogy and geochemistry, the pluton is I-type granite and compositionally ranges from monzodiorite and monzonite. The pluton intruded in Eocene volcano-plutonic series of Toroud-Chah Shirin. During the crystallization and cooling, a magmatic-dominated hydrothermal system caused extensive hydrothermal alteration and Fe mineralization.

Challu granitoidic body has been studied using by anisotropy of magnetic susceptibility (AMS). The method carried out by (MFK1-FA) Kappbridge susceptometer (AGICO, Brno) operating at low field (4×10^{-4} T; 920 Hz) at Geomagnetic Lab of Shahrood University of Technology. According to the measurements (32 stations, 96 cores and 384 fragments), the average magnetic susceptibility (K_m , in μ SI) of monzonites and monzodiorites are 9323 and 28776, respectively. Therefore, the rocks belong to the ferromagnetic granitoids (bulk susceptibility $\geq 500 \mu$ SI). Magnetite is the main carrier of the magnetic behavior and pyroxene, biotite and sphene are other carriers. Due to presence of extensive propylitic mineral assemblages (epidote, calcite and chlorite) in the south eastern margin and importance of their effect on AMS, the magnetic susceptibility of some grains of epidotes was determined. The obtained data shows that presence of this mineral has no effect on bulk susceptibility but the grain size of magnetic, its loss and damage during hydrothermal alteration reduced the amount of magnetic susceptibility.

Microbial communities correlate with Lemon Creek Glacier meltwater discharge

CODY S. SHEIK¹, EMILY I. STEVENSON¹, PAUL DEN UYL¹, SARAH M. ACIEGO¹, AND GREGORY J. DICK^{1,2*}

¹Dept. Earth and Environmental Sciences, ²Dept. of Ecology and Evolutionary Biology, University of Michigan, Ann Arbor, MI, 48109, USA. (*Correspondence gddick@umich.edu)

Mineral weathering has long been recognized as an important ecological process that is mediated in part by microorganisms. Recently, microorganisms have been implicated in the weathering of rock in the interstitial waters between bedrock and overlying glaciers (1,2), a process which may directly impact carbon cycling in the the northern Atlantic Ocean (3). Here we surveyed microbial communities associated with sub-glacial meltwaters and mixed sediments over the course of four months as they were discharged from the Lemon Creek Glacier located near Juneau Alaska, USA. Utilizing a high throughput small subunit ribosomal RNA gene sequencing approach, the diversity and structure of microbial communities was quantified and correlated to changes in the water geochemistry.

Microbial communities were consistently dominated by *Proteobacteria* classes *Beta*, *Alpha*, *Gamma* and *Delta* (in descending order of abundance), which accounted for 40-70% of the total community). Many sequences from uncultured groups often associated with anoxic environments were also recovered, including candidate divisions BD1-5, OD1 and TM7 (1-5%) and novel methanogenic Archaea (<0.1%). Phylogenetic richness was high in most samples (15-85 unique lineages) and resembled typical sediment community diversity. Community structure was distinct in each sample and was significantly correlated with time of discharge and sampling location (*e.g.* lower glacial fed lake, glacial outflow channel, and sub-glacial interstitial waters).

Our results suggest that interstitial microbial weathering supports diverse microbial communities that resemble those from anoxic environments, are highly dynamic with respect to time of discharge, yet retain a consistent phylum level taxonomic structure. Furthermore this work highlights ice-water-sediment interfaces as important microbial habitats that are potential analogs for other low temperature geochemically active environments such as the deep subsurface.

[1] Sharp, M., *et al.* (1999) *Geology* 27:107-110. [2] Skidmore, M., *et al.* (2005) *Appl Environ Microbiol* 71:6986-6997. [3] Bhatia, M.P., *et al.* (2013) *Nat Geosci* 6:274-278.

Causes and consequences of low atmospheric pCO₂ in the Late Mesoproterozoic

NATHAN D. SHELDON¹

¹ Department of Earth and Environmental Sciences, University of Michigan, Ann Arbor, MI, USA, (nsheldon@umich.edu)

Based upon various proxy, theoretical, and model constraints, Paleoproterozoic atmospheric pCO₂ [1] was much higher than Phanerozoic levels [*e.g.*, 2]. However, relatively little is known about the transition between the two climate states. Here, geochemical mass-balance from ~1.1 Ga old Midcontinent Rift System (USA) paleosols is used to reconstruct atmospheric pCO₂ during the Mesoproterozoic. The calculations robustly indicate low atmospheric pCO₂ (<10 times Preindustrial levels). Results are consistent between seven paleosols at one site, between paleosols at different Midcontinental Rift sites, and between the new results and previously published pencontemporaneous paleosol [3] and microfossil reconstructions [4-5]. In spite of the lower than expected pCO₂ values, climate models driven by the reconstructed pCO₂ levels predict equable conditions [6]. The newly recognized Mesoproterozoic pCO₂ minimum is best explained as the culmination of a long-term C burial event by the biosphere that is also indicated by marine carbonate δ¹³C changes during the Mesoproterozoic, and which is consistent with changes in the biosphere including increased stromatolite abundance and diversity, evolution of sulfur-utilizing bacteria, and the spread of microbial mats into continental environments. One potential testable consequence of this hypothesis is that it should be accompanied by a gradual rise in atmospheric pO₂ throughout the “boring billion.”

[1] Sheldon (2006) *Precambrian Research* 147, 148-155. [2] Royer *et al.* (2007) *Nature* 446, 530-532. [3] Mitchell and Sheldon (2010) *Precambrian Research* 183, 738-748. [4] Kaufman and Xiao (2003) *Nature* 425, 279-282. [5] Kah and Riding (2007) *Geology* 35, 799-802. [6] Domagal-Goldman and Sheldon (2012) *AGU P13B-1936*.

What caused Mongolian Mesozoic magmatism: Was it crustal or mantle driven?

T. SHELDRIK^{1*}, T.L BARRY¹ AND A.D. SAUNDERS¹

¹University of Leicester, Leicester, LE1 7RH, UK.

(*correspondence: thomassheldrick@gmail.com, tlb2@le.ac.uk, ads@le.ac.uk)

Prior to the Himalayan orogeny, the last major phase of continent collision and amalgamation in mainland Asia was the mid-late Mesozoic closure of the Mongol-Okhotsk ocean. Rapidly following on from the collisional event came extensive and widespread basaltic magmatism that infilled extensional basins across parts of eastern and southern Mongolia, and northern China. The production of voluminous basalts soon after an orogenic event has led some to propose that a mantle plume may have interacted with the crust during this period^[1]. Opposing this theory are suggestions of slab delamination^[2], post-orogenic collapse^[3] or lithospheric overthickening and delamination^[4]. This study aims to assess the plausibility of these models by constraining the mechanisms of magma genesis for these mildly alkali basalts. Then, using these constraints, we plan to test local and regional tectonic syntheses.

To this end, a large suite of basaltic samples have been collected from the most western limit of the Mesozoic volcanism, from the Gobi, Mongolia. Samples have been analysed for major, trace and REE elements (XRF & ICP-MS) with results showing that the basalts are LREE enriched (high La/Ti) and slightly HREE depleted with variable Mg#’s, Pb & Nb anomalies and Th/Nb ratios. The chemistry and a limited amount of isotope data shows that fractionation and crustal contamination processes were important for melt generation. Further sampling and a more extensive isotope study will help to elucidate some of the processes that produced these enigmatic basalts and thereby test models for melt generation.

[1] Yarmolyuk & Kovalenko 2001. *Tectonics, magmatism and metallogeny of Mongolia*, London. [2] Tomurtugoo *et al.*, 2005. *Jour Geol Soc* 162, 125-134. [3] Fan *et al.*, 2005. *Geo Res.* 121, 115-135. [4] Wang *et al.*, 2006. *Earth & Planet papers* 251, 179-198.

Mg isotope evidence for early dolomite formation in a Marinoan cap carbonate

BING SHEN¹, JOSHUA WIMPENNY², QING-ZHU YIN², CINTY LEE³, SHUHAI XIAO⁴ AND CHUANMING ZHOU⁵

¹School of Earth and Space Science, Beijing Univeristy, Beijing, 100871, bingshen@pke.edu.cn

²Department of Geology, University of California, Davis, CA, 95616, jbwimpenny@ucdavis.edu, qyin@ucdavis.edu

³Department of Earth Science, Rice University, Houston, TX, 77002, ctleee@rice.edu

⁴Department of Geoscience, Virginia Tech, Blacksburg, VA, 24060, xiao@vt.edu

⁵Nanjing Institute of Geology and Paleontology, CAS, Nanjing, 210008, cmzhou@nigpas.ac.cn

The global deposition of cap carbonates after the Marinoan glaciation (635Ma) is key evidence supporting the Snowball Earth hypothesis [1]. The cap carbonate is almost exclusively composed of dolostone with rare occurrences of limestone [2]. Thus, this interval is the only time in the Earth’s history when deposition of dolostone occurred globally, suggesting a unique marine geochemistry after the Marinoan glaciation. Here, we report the Mg isotopic composition ($\delta^{26}\text{Mg}$) of the Zhamoketi cap carbonates from two sections in the Quruqtagh area, NW China [3], which contain both limestone and dolostone. Our data show an enrichment of heavy Mg in the cap limestone samples, indicating scavenging of light Mg from seawater consistent with global dolostone precipitation. Compared with their Phanerozoic counterparts, the Zhamoketi cap limestones and dolostones have very similar $\delta^{26}\text{Mg}$ values [4, 5], which may indicate early formation of Marinoan cap dolostone driving seawater to heavier $\delta^{26}\text{Mg}$ values. This study suggests that the sharp transition from extreme icehouse to extreme greenhouse conditions during the meltdown of Marinoan Snowball Earth might have created a suitable environment for global dolostone formation.

[1] P.F. Hoffman, *et al.*, *Science*, 281 (1998) 1342. [2] P.F. Hoffman, *et al.*, *Palaeo, Palaeo, Palaeo*, 277 (2009) 158. [3] S. Xiao, *et al.*, *Precambrian Research*, 130 (2004) 1. [4] A. Galy, *et al.*, *EPSL*, 201 (2002) 105. [5] E.D. Young, *et al.*, *Rev.Mineral.Geoch.*, 55 (2004) 197.

Carbon stable isotope composition in modern snail shell aragonite and its climatic significance

X. F. SHENG, L. L. ZHU AND L. W. LIU

Key Laboratory of Earth Surface Geochemistry, Ministry of Education, School of Earth Sciences and Engineering, Nanjing University, Nanjing 210093, China (shenxuer@nju.edu.cn)

Stable isotope signatures recorded in land snail shells have been widely used to characterize the information of paleo-climate and paleo-environment. $\delta^{13}\text{C}$ values of the land snail shells can be used to discuss and estimate the compositions of local vegetations, namely the ratio of plants C_3 to plants C_4 in the ecosystem, which can examine the drought degree of ancient ecological system.

Here we explored the relationships between the $\delta^{13}\text{C}$ of modern snail shells and associated climatic factors in east part of China in an attempt to develop transfer functions that can be applied to retrieve the climatic information stored in snail shells. Totally 400 $\delta^{13}\text{C}$ values of modern land snail shell aragonite from the field collected were measured from 18 localities in a widely spatial scale, with the result shows the $\delta^{13}\text{C}$ of modern snail shells are obviously related to precipitation, elevation and weakly related to temperature and latitude. The analysis exhibits that the negative correlations between the $\delta^{13}\text{C}$ of shells with the living season precipitation and temperature as the former is robust ($R^2=0.47$) and the latter is weak ($R^2=0.27$). However, correlations between the $\delta^{13}\text{C}$ of shells with elevation and latitude is positive with the former was robust ($R^2=0.48$) and the latter was weak ($R^2=0.34$).

Furthermore, under the condition that the humidity stayed relatively stable, the indoor snail feeding experiment was carried out and the study comes to the conclusion that the food is the dominant factor influencing the $\delta^{13}\text{C}$ of snail shells, and the fractionation value between the diet and snail shells is calculated as 14.72‰. The study simultaneously confirmed that the temperature does not affect the $\delta^{13}\text{C}$ of snail shell under laboratory conditions. In summary, we discussed that the impact effect from the environmental factors on the $\delta^{13}\text{C}$ of snail shells is not a direct action, but through regulating and altering the local vegetation types and compositions in an ecosystem.

The research was financially supported by the NSF of China through Grant 41073065.

A review of radionuclides impact in South Sinai, Egypt: Case study of Sharm El Sheikh area

MAHMOUD I. SHERIF¹, MOHAMED F. GHONEIM¹, MOHAMED TH. S. HEIKAL¹, BOTHINA T. EL DOSUKY¹, MOHAMED M. EL GALY²

¹Geology Department, Faculty of Science, Tanta University, Tanta 31527, Egypt

²Nuclear Material Authority, Cairo, Egypt

The area of Sharm El Sheikh consists mainly of granitic rocks of alkaline type. Alkaline granite is the most favourable host rock for uranium and thorium mineralization. The activity concentration of natural radionuclides (^{238}U , ^{232}Th , ^{226}Ra & ^{40}K) of 100 samples around the studied area, including granites, dikes and stream sediments were investigated using γ -ray spectrometry. The radium equivalent activity (R_{eq}), gamma activity concentration index (I), external hazard index (Hex) internal hazard index (Hin) and annual effective dose rate (AEDR) have been calculated and compared with the internationally approved values.

The permissible values for each index revealed that all exposures of granite and mafic dikes have values below safety limits of radiation. The stream sediments within the major wadis are also safe. However, the felsic dikes that more or less occur far from the inhabited areas of Sharm El Sheikh town exceed the permissible radiation limits indicating their hazardous effect.

Thereby, it was recommended to restrict land use in a buffer zone adjacent to the felsic dikes of very limited distributions. Moreover, a planned major town extension of Sharm El Sheikh area has to be stopped around and within these dikes sites, but alternative future residential areas could be delineated to the northwest of the town.

Electronic structures of transition metal oxides and sulfides: Applications to the physics and chemistry of the Earth

DAVID M. SHERMAN¹

¹School of Earth Sciences, University of Bristol, Bristol BS8 1RJ UNITED KINGDOM (dave.sherman@bris.ac.uk)

A variety of geochemical and geophysical processes result from electronic transitions in minerals and aqueous complexes. In aquatic environments, photochemical excitations on mineral surfaces release dissolved micronutrients and may have played a role in prebiotic synthesis. In the deep Earth, pressure-induced electronic transitions such as spin-pairing, metallization and changes in the band gap/Fermi energies of phases affect the density, transport properties and element partitioning in the core and mantle.

Density functional theory, using approximate exchange-correlation functionals, has enabled us to accurately predict structures and vibrational energies of minerals and aqueous complexes. We can now predict the thermodynamics, phase transitions and seismic properties of minerals in the deep earth and even the thermodynamics of metal complexation in hydrothermal solutions. However, exchange-correlation functionals such as the generalized gradient approximation (GGA) are still based on the local density approximation. Consequently, these functionals still contain an error associated with incorrectly including the electron self-interaction. The self-interaction error yields incorrect electronic structures and band gaps and precludes accurate predictions of electronic transition energies. For the case of a material like FeO, standard GGA functionals incorrectly yield a metallic ground state that becomes Pauli-paramagnetic (rather than a diamagnetic low-spin state) with pressure. Charge-transfer band gaps in Fe₂O₃ are too low. Physicists have addressed this problem using the “Hubbard U” correction to the local density approximation. However the U parameter is an empirical correction. Chemists, however, have recognized that the Hartree-Fock formalism exactly includes the self-interaction correction. A variety of “hybrid” exchange functionals have been developed (e.g., B3LYP) that empirically mix Hartree-Fock exchange with the GGA exchange-correlation functional. Here, I will present several examples to illustrate the application of these functionals to transition metal oxides and sulfides and show how the hybrid functionals predict electronic transitions of importance in geochemistry and geophysics.

Reduced gas flux from Precambrian cratons – Implications for subsurface microbiology

B. SHERWOOD LOLLAR^{1*}, G. HOLLAND², L. LI¹,
G. LACRAMPE-COULOUME¹, G.F. SLATER³,
T.C. ONSTOTT⁴ AND C.J. BALLENTINE⁵

¹Dept. of Earth Sciences, University of Toronto, ON, Canada M5S 3B1 (*bslollar@chem.utoronto.ca)

²LEC, University, Lancaster LA1 4YQ UK

³SGG, McMaster University, Hamilton ON Canada L8S 4K1

⁴Dept. of Geosciences, Princeton University, Princeton, N.J., USA

⁵SEAES, Manchester University, Manchester M13 9PL UK

Quantification of global H₂ flux has to date been based primarily on thermodynamic and geochemical modelling, or on H₂ measurements at a number of marine systems such as the Rainbow and Logatchev hydrothermal vents, the off-axis Lost City field, and more recently, at diffuse vents. H₂ sources from continental systems are significantly less well constrained. Recent exploration of saline fracture waters more than a km below the Earth’s surface in Precambrian continental crust however has identified environments equally as H₂-rich as the hydrothermal vents and spreading centers, and sustaining microbial communities of H₂-utilizing methanogens and sulfate reducers [1]. Here we report on results from > 30 sites and > 250 samples and boreholes in continental Precambrian sites worldwide. Fracture waters accessed via mines and underground research laboratories contain mM concentrations of reduced gases (H₂, CH₄, ethane, propane, butane) as well as high concentrations of noble gases.

First identified in Ne isotope results from the Witwatersrand basin in South Africa [2], novel radiogenic isotope signatures have now been shown to be a consistent feature of these deep waters [3]. Integration of the noble gas signatures with compositional and isotopic information for the reduced gases provide constraints on the residence time of the fracture waters, the degree of interconnectivity of different groundwater systems, and an estimate of the amount of time these waters have been isolated from the surface. This presentation will address the distribution of ancient fluids at selected key reference sites; and the controls of this deep hydrosphere on the biodiversity and distribution of the subsurface microbial biosphere and carbon cycle.

[1] Lin *et al.* (2006) *Science* **314**, 479-482. [2] Lippmann-Pipke *et al.* (2011) *Chem. Geol.* **283**, 287-296. [3] Holland *et al.*, (2013) *Nature*, *in press*.

Geodynamic constraints on the recycling of ancient SCLM and genesis of Tibetan diamondiferous ophiolites

R.D. SHI^{1,2*}, W.L. GRIFFIN², S. Y. O'REILLY², X.R. ZHANG^{1,3}, Q.S. HUANG¹, X.H. GONG¹ AND L. DING¹

¹ Institute of Tibetan Plateau Research, CAS, Beijing 100101 China (*correspondence: shirendeng@itpcas.ac.cn)

² GEMOC/CCFS, Earth and Planetary Sciences, Macquarie University, NSW 2109 Australia

³ Department of Earth Sciences, The University of Hong Kong, Pokfulam Road, Hong Kong, China

Natural diamonds have been found *in situ* in the chromitites and peridotites of Tibetan ophiolites [1,2]. Whole-rock ¹⁸⁷Os/¹⁸⁸Os values of these diamond-bearing peridotites and chromitites vary from 0.1038 to 0.1266, yielding T_{RD} ages back to 3.4 Ga. This suggests that part of the Tibetan Tethys Ocean (TTO) was underlain by a fragment of ancient subcontinental lithospheric mantle (SCLM), left stranded in the oceanic lithosphere during the opening of TTO [3]. However, there has been little geological evidence to support the geodynamics required to recycle ancient SCLM in the Tibetan ophiolites. Here we present the metamorphic ages (peak age: 191 Ma; retrogression age: 181 Ma) of Amdo HP granulites formed by the subduction of TTO crust, the age (184 Ma) of the Naqu ophiolite representing the initial subduction (SI) of TTO at the south margin of the Amdo micro-terrene, and the age (160 Ma) of the Amdo ophiolite, representing the back-arc basin developed by mantle convection in the supra-subduction zone. These ages indicate that TTO in the Amdo area is older than 191 Ma, consistent with a major PGM Os-isotope T_{RD} age peak (243 Ma) [4]. Fig.1 shows the geodynamic situation of the Tibetan Tethys ophiolites, in which the Amdo micro-terrene was isolated in the TTO during the rifting of Gondwana along listric faults, then subducted to >150 km depth, before exhumation.

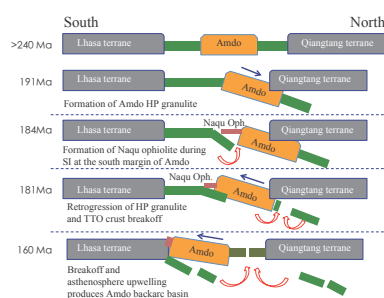


Fig. 1 Recycling of ancient SCLM in the Tibetan ophiolites

[1] Yang *et al.* (2013) *Science* (subm.); [2] Griffin *et al.* (2013) this conference; [3] Shi *et al.* (2012) *Geological Review*, 58(4): 643-652; [4] Shi *et al.* (2007) *EPSL*, 261: 33-48.

This research was funded by the National Natural Science Foundation of China (Grant no. 41172059)

Reconstruction of Oil-filling History by Fluid Inclusion Analysis: A Case Study of Tahe Oil Field, Tarim Basin, NW China

WEIJUN SHI, ZHIRONG ZHANG, JOHN K. VOLKMAN, JIANZHONG QIN AND TENGGER, BINBIN XI

Sinopec Key Laboratory of Petroleum Accumulation Mechanisms, Wuxi Institute of Petroleum Geology, SINOPEC Research Institute of Petroleum Exploration and Production, 100 Jinxi Road, Binhu District, Wuxi, Jiangsu, China. shiwj.syky@sinopec.com

The Tahe oil field in the Tarim Basin of NW China, has Ordovician carbonates as the main reservoir strata. Core samples from the reservoirs in the eastern Tahe oil field were collected for analysis of fluid inclusions (FIs). FIs occurred mainly in calcite and quartz cements and within calcite veins in the carbonate rock matrix. From the homogenization temperatures, molecular compositions obtained by laser ablation and on-line GC-MS analysis, and simulations for fluid pressures and trapping temperature, we determined that 2 types of oil-bearing inclusions representing the 2 main petroleum charging events in the region were present. The early stage of the petroleum-filling occurred about 245 ~ 255 Ma, during the late Permian to early Triassic (late Hercynian). The late charging occurred in the Pliocene (Himalayan Orogeny).

The dominant FIs have blue fluorescence and relatively high maturity (VR of 0.75% R_o from MPI and 1.22% R_o from MPR aromatic maturity parameters). Homogenization temperatures of the associated aqueous inclusions vary from 74 to 92 °C. Results from laser ablation GC-MS analysis showed higher proportions of saturated hydrocarbons and gaseous hydrocarbons. The simulated paleo trapping temperature ranged from 150.6 to 156.9 °C, and fluid pressures ranged from 565.9 to 599.8 bar.

The second type of oil-bearing inclusions displays yellow fluorescence and relatively low maturity (VR of 0.59% R_o from MPI and 1.17% R_o from MPR), and homogenization temperatures from 58 to 113 °C. The yellow fluorescing inclusions contain much more water-soluble aromatic hydrocarbons than in the blue ones. The simulated paleo trapping temperature range from 79.2 to 83.5 °C, and fluid pressures range from 221.8 to 245.3 bar.

Iron dissolution kinetics in mineral dust under more realistic aerosol conditions: Re-considering pH scale

ZONGBO SHI

School of Geography, Earth and Environmental Sciences,
University of Birmingham, B15 2TT, UK Email:
z.shi@bham.ac.uk

Iron (Fe) is a micronutrient that mediates the primary productivity in the global ocean. A significant source of such Fe in the surface ocean is from dust. It is therefore important to quantify the flux of bioavailable Fe from dust, which is strongly dependent on Fe solubility. Fe in dust is mostly insoluble, but such Fe may become soluble after reacting with acidic species during transport. In the last 20 years, many laboratory studies have been conducted to measure the dissolution kinetics of Fe in dust at pH from 1 to 5. It is now known that clouds may actually decrease Fe solubility because of its higher pH, e.g., >4. In contrast, aerosol water can be more acidic but more complicated in composition. However, most of the previous lab studies were conducted under much simplified conditions compared to those in aerosol water. These results, when applied, could lead to large bias in global models. In this work, I measured Fe dissolution kinetics in dust under conditions closer to aerosol water.

The results showed that at the same $[H^+]$ concentration at (1 g dust L⁻¹ solution), (i) (NH₄)₂SO₄ at 1 mol L⁻¹ slows down Fe dissolution; and (ii) NH₄Cl at 1 mol L⁻¹ accelerates the Fe dissolution in dust. Based on these results, I propose to use an effective pH scale for simulating Fe dissolution kinetics in aged dust in models. This pH scale considers the activity of H⁺ ion and [HSO₄⁺], both of which can be predicted by the AIM thermodynamic model (<http://www.aim.env.uea.ac.uk/aim/aim.php>).

In addition, oxalate (0.03 M Na₂C₂O₄) significantly accelerates the dissolution of Fe in dust (1 g dust L⁻¹ solution, 0.1 N H₂SO₄ or 0.01 N H₂SO₄, and 1 M (NH₄)₂SO₄).

Changes in ²³⁸U/²³⁵U associated with reductive immobilization of uranium in groundwater

ALYSSA E. SHIEL^{1*}, CRAIG C. LUNDSTROM¹, THOMAS M. JOHNSON¹, PARKER LAUBACH¹, PHILIP E. LONG² AND KENNETH H. WILLIAMS²

¹Dept. of Geology, University of Illinois at Urbana-Champaign, Urbana, IL USA; ashiel@illinois.edu (*presenting author)

²Lawrence Berkeley National Laboratory, Berkeley, CA USA

The prevalence of groundwater contamination associated with uranium (U) mining and milling activities has driven the need for the development of effective and economically feasible remediation strategies. U is mobile in its oxidized state, U(VI), but immobile and much less toxic in its reduced state, U(IV). Thus, U(VI) reduction to U(IV) is proposed as a remediation strategy for U contaminated groundwaters. The former U mill site in Rifle, Colorado (USA) hosts experiments that investigate the rates and mechanisms of targeted U immobilization techniques. Our research focuses on the development of ²³⁸U/²³⁵U (discussed as δ²³⁸U) as a tool for evaluating immobilization in the subsurface.

U concentrations and ²³⁸U/²³⁵U values have been monitored over the course of three field experiments at the Rifle, CO field site in 2010–11, 2011–12 and 2012–13. These experiments examined changes in U concentrations and ²³⁸U/²³⁵U values associated with biostimulation, desorption and re-oxidation. Large variations accompany acetate-induced biostimulation under both iron reducing and sulfate reducing conditions. In both cases, ²³⁸U is preferentially reduced to U(IV), leaving the remaining groundwater U(VI) relatively isotopically light (Δ²³⁸U = -1.3 and -1.9‰, respectively). Changes in ²³⁸U/²³⁵U accompany changes in the U concentration (dropping from ~150–200 ppb U prior to the acetate injection to ~10 ppb U). During the post-injection phase, as concentrations rebounded, absence of ²³⁸U/²³⁵U greater than pre-injection values implies the primary source of U is advection of U(VI), rather than re-oxidation of U(IV). Bicarbonate-induced desorption, which led to a doubling in the U concentration, has been demonstrated to result in no significant U isotopic fractionation [1].

Our research demonstrates the potential for ²³⁸U/²³⁵U to detect U reductive immobilization in the subsurface and to distinguish between removal by this process and relatively temporary processes such as sorption. U isotopes join the growing number of heavy stable isotopes with demonstrated potential for use in environmental monitoring.

[1] Shiel *et al.* (2013) *Environ. Sci. Technol.* **47**, 2535–2541.

Estimate of residence time of groundwater in Mt. Fuji area, central Japan

N. SHIKAZONO, T. UMEMURA AND T. ARAKAWA

3-14-1, Hiyoshi, Kohoku-ku, Yokohama 223-8522 Japan
(sikazono@applc.keio.ac.jp)

Many groundwater samples were collected from Mt. Fuji area, central Japan which is totally composed of basaltic materials. The samples were analyzed for Na⁺, K⁺, Ca²⁺, Mg²⁺, Si, Al³⁺, Fe²⁺, Fe³⁺, TC (total dissolved carbon), Cl⁻, NO₃⁻, SO₄²⁻. Analytical data plotted against altitude indicate that alkali and alkali earth element and Si concentrations increase with decreasing altitude, indicating that the dissolution of silicates in basaltic materials control the trends. Ca and Mg concentrations positively correlate with each other. This is consistent with CaO/MgO molal ratio of basalt which is 1.47. Therefore, it is inferred that Ca and Mg in groundwater were derived mainly from the congruent dissolution of basalt. Ca/Si concentration ratio determined by the dissolution reactions of basalt accompanied by the precipitation of allophane is 0.29 that is lower than 0.48 estimated from the analytical data on groundwater. This lower value could be due to the precipitation of silica mineral (SiO₂). The agreement between theoretical and analytical results indicate that Ca, Mg and Si concentrations of groundwater are governed by dissolution and precipitation reactions. In order to interpret groundwater chemistry and estimate residence time of groundwater the simplified coupled dissolution kinetics-fluid flow model was used. Assuming reasonable values of parameters (reactive surface area, mass of groundwater, temperature etc) and using rate constant experimentally determined, residence time of groundwater in southeastern and northern part of Mt. Fuji area was estimated to be several years to 30 years. This estimated residence time is consistent with isotope data (beryllium isotope, tritium concentration and CFCs). The calculation indicates that the reasonable residence time (10-30 years) was obtained, if dissolution rate constant of Si for basaltic glass determined by fluid flow experiments but unreasonable one by closed system experiments. It is just conceivable that whether etch pits formed or not and/or heterogeneous dissolution occurred or not has significant impact on dissolution rate of basalt.

Dissolved gallium and gallium/aluminum ratios in the US GEOTRACES North Atlantic zonal section

A.M. SHILLER^{1*}, M. HATTA² AND C.I. MEASURES²

¹Dept. of Marine Science, Univ. Southern Mississippi, Stennis, MS 39529, USA (*correspondence: alan.shiller@usm.edu)

²Dept. of Oceanography, Univ. Hawaii, Honolulu, HI 96822
(mhatta@hawaii.edu, chrism@soest.hawaii.edu)

Gallium has a solution chemistry and geochemical behavior similar to aluminum; however, gallium appears to be less reactive than aluminum. Thus, fractionation of gallium from aluminum has the potential to shed light on aluminum input and removal processes with gallium behaving like a "super-heavy isotope" of aluminum. The 2010/2011 US GEOTRACES North Atlantic zonal section provided an opportunity to create a first detailed ocean section of dissolved gallium. Thirty-two profiles plus ancillary surface water samples were obtained and analyzed for dissolved gallium and aluminum.

In general, this new Ga section is consistent with previous observations: deep and bottom waters ranged between 30 and 35 pmol/kg; a distinct Ga minimum is observed in the Antarctic Intermediate Water; a slight maximum is found in Mediterranean Outflow Water; and, surface waters show a distinct north-westward increase. The surface water trend could be reflective of a residence time effect (i.e., accumulation of dust-derived Ga during North Atlantic gyral circulation) or of greater dust dissolution input. The biggest surprise is the observation of a ~20% increase in Ga in deep waters in the vicinity of the Mid-Atlantic Ridge.

The dissolved Ga/Al ratios are also instructive. Low (i.e., more rock-like) ratios in the Med water and hydrothermally-influenced waters are suggestive of recent inputs of these elements. In contrast, high Ga/Al ratios along the African margin are suggestive of preferential Al scavenging removal. Interestingly, high Ga/Al ratios in Labrador Sea Water along the western margin are actually lower than ratios in the Labrador Sea itself, suggesting accumulation of Al during transit. In surface waters of the eastern part of the section, where there is a significant gradient in chlorophyll fluorescence, the Ga/Al ratio increases with increasing fluorescence. This is consistent with preferential scavenging removal of Al from surface waters.

Spin Transition of Iron in Amorphous Mg-Silicates at Mantle-Related Pressures

S.-H. DAN SHIM¹, C. GU², K. CATALLI³,
B. GROCHOLSKI⁴, L. GAO⁵, E. ALP⁵, P. CHOW⁶,
Y. XIAO⁶, H. CYNN³ AND W. J. EVANS³

¹Arizona State University, SHDShim@asu.edu, USA

²Massachusetts Institute of Technology, USA

³Livermore National Laboratory, USA

⁴Argonne National Laboratory, USA

⁵Smithsonian Institution, USA

⁶Carnegie Institute of Washington, USA

A sharp increase in iron partitioning into melt with respect to mineral phases was reported at 70 GPa in an Al-free system [Nomura *et al.* 2011]. Based on the report, it was proposed that melt may be neutrally or negatively buoyant in the deep mantle. Nomura *et al.* [2011] attributed the iron partitioning change to a sharp high-spin to low-spin change in iron, which was found in their measurements on a Fe-diluted (5%) Mg-silicate glass at a similar pressure. However, Andrault *et al.* [2012] found no sharp change in iron partitioning between silicate melt and minerals in an Al-bearing system up to 120 GPa.

We measured the electronic configuration of iron in two different iron-rich (20%) Mg-silicate glasses at high pressure and 300 K in the diamond-anvil cell combined with X-ray Emission Spectroscopy (XES) and Nuclear Forward Scattering (NFS): Al-free glass up to 135 GPa and Al-bearing glass up to 93 GPa. We found no sharp changes in the spin state of iron up to our maximum pressure. Instead, the population of low-spin iron increases gradually from 1 bar in both glasses, but significant population of iron still remains high spin (40-50%) even at 90-135 GPa. Our observation is consistent with the expectation of gradual response of disordered systems to compression due to the existence of diverse coordination environments for iron in the glasses and continuous structural adjustment of the disordered system with pressure. If our results on Mg-silicate glasses can provide some insights for iron in mantle melts, the spin transition in iron should be gradual and further smeared out at the high temperatures of mantle melts [Sturhahn *et al.*, 2005], and therefore unlikely to induce a sharp change in iron partitioning in the deep mantle.

[1] C. Gu, K. Catalli, B. Grocholski, L. Gao, E. Alp, P. Chow, Y. Xiao, H. Cynn, W. J. Evans, and S.-H. Shim. Electronic structure of iron in magnesium silicate glasses at high pressure. *Geophys. Res. Lett.*, 39:L24304, 2012.

Volatile element content of the mid-ocean ridge mantle

K. SHIMIZU^{1*}, A.E. SAAL¹, E.H. HAURI²,
V.S. KAMENETSKY³ AND R. HÉKINIAN⁴

¹Dept. of Geological Sciences, Brown University, Providence, RI, 02912, USA

(*correspondence: Kei_Shimizu@brown.edu)

²DTM Carnegie Institute of Washington, DC, 20015, USA

³CODES, University of Tasmania, Hobart, Australia

⁴Keryunan, 29290 Saint Renan, France

Volatile element (H₂O, CO₂, F, Cl, S) budget of mid-ocean ridge mantle (DMM) is crucial for understanding mantle melting, rheology, and convection. The isotopic composition of MORB demonstrates that the mantle beneath ridges is heterogeneous. MORB from Garrett transform fault and Macquarie Island defines the depleted and enriched end-members respectively. We have analyzed H₂O, CO₂, F, Cl, S contents of Garrett TF and Macquarie Is. MORB to determine the volatile budget of these end-member components.

28 glasses from Garrett TF [1] and 52 glasses from the Macquarie Is. [2] were analyzed for major, trace, and volatile elements by triplicate analyses. Previous works reported the isotopic composition of a subset of our samples from the Garrett TF [3] (minimum ⁸⁷Sr/⁸⁶Sr = 0.7022) and the Macquarie Is. [2] (maximum ⁸⁷Sr/⁸⁶Sr = 0.7033), which correlates with the degree of trace element enrichment (e.g. Th/La) indicating a long-lived depletion and enrichment of their mantle sources.

We first considered shallow level processes, such as volatile degassing, sulfide saturation and interaction of melt with hydrothermally altered material. Degassing has affected the CO₂ concentration of the glasses except for a few CO₂ undersaturated samples, but it did not affect H₂O, F, Cl, and S. Samples that were sulfide saturated [4] and contaminated by seawater or hydrothermally altered material (high Cl/K) were filtered out.

The CO₂/Nb of the depleted MORB determined using the CO₂ undersaturated Garrett TF glasses MORB is 250, consistent with Saal *et al.* [5]. We use Cl-Nb-CO₂ correlations to determine a CO₂/Nb of ~ 600 for degassed Macquarie Is. MORB, consistent with the work by Cartigny *et al.* [6]. The H₂O/Ce of the depleted and enriched sources are 120 and 170 respectively. The F/Nd, Cl/K, and S/Dy ratios of our samples expand beyond the range of previous reported values.

[1] Hékinian, R. *et al.* (1992) *EPSL* **108**, 259-275. [2] Kamenetsky, V. S. *et al.* (2000) *J. Petrology* **41**, 411-430. [3] Wendt, J. I. *et al.* (1999) *EPSL* **173**, 271-284. [4] Liu, Y. *et al.* (2007) *GCA* **71**, 1783-1799. [5] Saal, A. E. *et al.* (2002) *Nature* **419**, 451-455. [6] Cartigny, P. *et al.* (2008) *EPSL* **265**, 672-685.

Electrochemical Impedance Spectroscopic Study of the Hematite/Water Interface

KENICHI SHIMIZU^{1*} AND JEAN-FRANÇOIS BOILY¹

¹Department of Chemistry, Umeå University, Sweden,
*kenichi.shimizu@chem.umu.se

Hematite is one of the most abundant and stable iron minerals in Earth's upper crust, and thus inevitably plays an important role in various bio-geochemical processes, including mass transport, pollutant migration, and microbial metabolism. This mineral is also a promising material in the search for renewable forms of energy, such as in Li-ion batteries and water splitting. The intrinsic activity of hematite surfaces notably concerns interactions with water and electrolyte ions. Recent cryogenic X-ray photoelectron spectroscopy (XPS) work in our group have addressed such issues by monitoring electrolyte ion loadings and binding mechanisms at nano-sized hematite particle surfaces.[1,2,3]

In an effort to further our understanding of reactions taking place at the hematite/water interface, we used electrochemical impedance spectroscopy (EIS) to extract interfacial properties such as adsorption resistance and electric double layer capacitance using a specially constructed set-up to study surfaces of single body semi-conductive hematite specimens.[4] EIS measurements of crystallographically oriented electrode surfaces contacted with electrolyte solutions (0.1 M NaCl, NaCl/Na₂CO₃, and NH₄Cl) were carried out both in the absence and presence of light in the 4-12 pH range. The resulting spectra were thereafter analyzed using an equivalent electrical circuit model accounting for solution, interface and bulk hematite electrochemical processes. These efforts showed, for instance, that double layer capacitances of the basal (001) plane are insensitive to solution pH and electrolyte type whereas those of the (012) are considerably affected by them. This can be attributed to differences in amphoteric attributes of these two planes. Results revealed that the ammonium ion has a greater influence on charge development than the bicarbonate ion. This finding is consistent with a cryogenic XPS study from our group [3] pointing to hydrogen-bonded interactions between ammonium and hematite surface hydroxo groups.

Photo-irradiation decreased open circuit potentials relative to dark conditions on both (001) and (012) surfaces due to photo-reduction reactions. Impedance spectra show that the (012) is affected more indicating the greater photo-reactivity of this plane. Results also show that the charge transfer resistance within bulk hematite crystal was lower through the (012) plane than on the (001) plane, as can be expected from the anisotropic nature of this mineral.

[1] Shimizu, Shchukarev, Kozin & Boily (2012), *Surf. Sci.* 66, 1005.[2] Shimizu, Shchukarev, Kozin & Boily (2013), *Langmuir* 29, 2623.[3] Shimizu, Shchukarev & Boily (2011), *J. Phys. Chem. C* 115, 6796.[4] Shimizu, Lasia & Boily (2012), *Langmuir*. 28, 7914.

Volatile behavior in an immature subduction zone inferred from boninitic melt inclusions in Cr-spinel

KENJI SHIMIZU^{1,2} AND NOBUMICHI SHIMIZU²

¹Japan Agency for Marine-Earth Science and Technology, Yokosuka, 237-0061, Japan, shimmy@jamstec.go.jp
²Woods Hole Oceanographic Institution, Woods Hole, MA, 02543, United States

Recent studies suggest that boninites formed at the immature stage of subduction zone, whereas related arc tholeiites erupted 0-7 Myrs after boninites at Izu-Bonin-Mariana Arc (e.g. Ishizuka *et al.*, 2011, EPSL), indicating significant changes in conditions of subduction within this period. We have analysed volatile contents and sulfur isotopic compositions of melt inclusions (MIs) in Cr-spinel from beach sands of fore-arc volcanic islands of boninite (Muko, Chichi) and tholeiite (Mukoo and Guam), using secondary ion mass spectrometry (ims-1280). Major element compositions of MIs fully cover compositional ranges of whole-rocks. Some boninitic MIs have MgO higher than 20 wt%, showing that they are very primitive magmas. H₂O and CO₂ contents of MIs are contrasting between boninites and tholeiites, with boninitic MIs are high (up to 4 wt%) in H₂O and low (< 50 ppm) in CO₂, whereas tholeiitic MIs are lower (H₂O ~1-2 wt%) and higher (CO₂ up to ~1300ppm) than boninitic MIs. Except for H₂O, volatiles of boninitic MIs (Cl <500ppm; S ~150ppm) are considerably lower than those in tholeiite MIs (Cl and S up to 3000ppm). $\delta^{34}\text{S}_{\text{VCDT}}$ of boninitic MIs are low (-10 to 0 ‰), whereas those of tholeiite MIs ($\delta^{34}\text{S}_{\text{VCDT}} = +2$ to +7 ‰) are comparable to reported arc tholeiite data. The results suggest that different sources for S were involved in the formation of boninitic and tholeiitic magmas.

Buried ikaite precipitates in Antarctic sediments: Are they fossil indicators of microbial sulfate reduction or AOM?

MEGUMI SHIMIZU^{1*}, MARCOS Y. YOSHINAGA²,
KAI-UWE HINRICHS² AND CINDY VAN DOVER¹

¹Duke University Marine Laboratory, Nicholas School of Environment, Duke University, Beaufort, NC, USA
(*correspondence: megumi.shimizu@duke.edu)

²MARUM Center for Marine Environmental Sciences, University of Bremen, 28334 Bremen, Germany

Ikaite is a calcium carbonate hexahydrate ($\text{CaCO}_3 \cdot 6\text{H}_2\text{O}$) formed at low temperature and high concentration of dissolved inorganic carbon (DIC) in organic-rich sediments [1]. Two microbial processes, bacterial sulfate reduction of organic matter and anaerobic methane oxidation (AOM) by archaeal/bacterial consortia can trigger ikaite precipitation by increasing DIC concentration. To determine which of these processes may contribute to ikaite formation, we studied a 500-cm sediment core from the northern Antarctic Peninsula that contained 4 large ikaite crystals ($\sim 50 \text{ cm}^3$ each) at depths > 300 cm. Apolar (fossil) lipids were extracted from six sediment horizons: at the surface, within the modern sulfate-methane transition zone (85 cm), and the four horizons where ikaite was found (304, 454, 480 and 505 cm). Stable carbon isotopic compositions of bacterial fatty acids (FA), and archaeal biphytanes (BP), archaeol (AR), and hydroxy-archaeol (OH-AR) were analyzed. $\delta^{13}\text{C}$ values of FA and BP ranged from -30‰ to -20‰ (ave = -23 ± 2.3 ‰) from the six sample horizons. AR and OH-AR was extracted from the same horizons, but isotope values were only measurable at the 454 and 500-cm horizons due to low concentrations. In these two horizons, AR was depleted in ^{13}C (ave = -49‰) as well as OH-AR (ave = -87‰). The ^{13}C -enriched values of C_{15-18} FA (bacterial markers for AOM) and of BP (archaeal marker for AOM) suggest they are not derived from AOM because lipids derived from AOM are significantly depleted (-110‰ to -60‰) [2,3]. Although the ^{13}C -depleted AR and OH-AR can from AOM related Archea, they could be also from methanogenic Archaea [4]. $\delta^{13}\text{C}$ in ikaite, DIC and methane will provide a scope on ancient carbon flow and help to reveal ancient microbial activities contributed ikaite formation.

[1] Suess (1982) *Science* **216**, 1128-1131. [2] Elvert (2003) *Geomicrobiology Journal* **20**, 403-419. [3] Hinrichs (1999) *Nature* **398**, 802-805. [4] Londry (2008) *Organic Geochemistry* **39**, 608-621.

Boron and sulfur isotopic variations during subduction of hydrated lithosphere: The Erro Tobbio case

N. SHIMIZU¹, M. SCAMBELLURI², D. SANTIAGO RAMOS³
AND S. TONARINI⁴

¹Woods Hole Oceanographic Inst., Woods Hole, MA, USA

²University of Genova, Genova, Italy

³Amherst College, Amherst, MA, USA

⁴Istituto Geosci. Geores-CNR, Pisa, Italy

Exhumed high-pressure serpentinites provide unique opportunities for advancing our understanding of geochemical changes in hydrated lithosphere during subduction and deep recycling of elements. The Erro Tobbio serpentinitized peridotites represent Jurassic oceanic lithosphere which underwent low-T hydration ($T < 300^\circ\text{C}$) followed by high-T serpentinitization and recrystallization at $\sim 550^\circ\text{C}$, 2 – 2.5 GPa during Alpine subduction. Covariations observed for whole-rock δD , $\delta^{18}\text{O}$, Sr, and H_2O indicate that hydration continued at high temperatures, placing the Erro Tobbio massif in the mantle wedge. During hydration whole-rock boron concentrations varied from 10 to 32 ppm with $\delta^{11}\text{B}$ from +3.8 to +23‰ for low-T serpentinites, and from 12 to 36 ppm with $\delta^{11}\text{B}$ from +17 to +24‰ for high-T rocks. In-situ analysis of sulfur isotopic composition of individual sulfide grains (pentlandite with minor heazlewoodite) has revealed that $\delta^{34}\text{S}$ varies from -2.5 to +4‰ for low-T rocks, consistent with whole-rock data (Alt *et al.*, 2012), while high-T rocks display a much larger range in $\delta^{34}\text{S}$ from -2 to +18‰ with significant increases in modal sulphide. B isotopes, S isotopes, and other geochemical variations observed for the Erro Tobbio peridotites suggest that hydration and mass transfer from slab to wedge occurred at relatively shallow level, resulting in the formation of hydrated mantle wedge with high $\delta^{11}\text{B}$, high $\delta^{34}\text{S}$, enrichment in B, Sr, and other fluid-mobile elements, suitable for the sources for arc magmas and heterogeneous sources for MORB and OIB.

FOZO-HIMU connection: Link to chemical heterogeneity of MORB and variable degree of dehydration

G. SHIMODA*¹ AND T. KOGISO²

¹ Geological Survey of Japan, National Institute of Advanced Industrial Science and Technology, Tsukuba 305-8567, Japan (*correspondence: h-shimoda@aist.go.jp)

² Graduate School of Human and Environmental Studies, Kyoto University, Kyoto, 606-8501, Japan (kogiso@gaia.h.kyoto-u.ac.jp)

It has been considered that source materials of HIMU and FOZO could be recycled oceanic crust. From this perspective, the arising question is what process is responsible for the geochemical difference between HIMU and FOZO. Additionally, coupled production of low Rb/Sr and high U/Pb and Th/Pb ratios of HIMU and FOZO has been controversial. To solve the issue, many studies have been conducted to evaluate the origin of the HIMU source using hydrothermal alteration and/or dehydration reaction. These studies can successfully explain the origin of HIMU and FOZO source. However, they may neglect effect of global chemical trend of MORB composition that should result in variation in isotopic composition of recycled MORB. In addition, variation in condition of subduction process (e.g., amount of dehydrated fluid) should greatly affect the isotopic composition of recycled oceanic crust.

In the present study, geochemical modeling has been conducted to evaluate the origin of HIMU and FOZO reservoirs on the basis of global chemical trend of MORB and variation in subduction processes. For the modeling, MORB compositions from East Pacific rise and Mid-Atlantic ridge are compiled from published data (PetDB: <http://www.earthchem.org/petdb>). The results suggest that crystal fractionation at a mid-ocean ridge can increase U and Th concentrations relative to Pb content, producing high U/Pb and Th/Pb ratios in evolved MORBs. In addition, high degree of dehydration beneath a subduction zone can increase U/Pb and Th/Pb ratios of subducting oceanic crust compared to less dehydrated oceanic crust, suggesting that strongly dehydrated oceanic crust can be a suitable source for HIMU and less dehydrated MORBs can produce material with FOZO isotopic signature. In this context, magma evolution at mid-ocean ridges and variable degree of dehydration beneath subduction zones play an essential role in producing the isotopic variations between HIMU and FOZO.

Occurrence of >3.9 Ga “Nanok” gneiss from Saglek Block, northern Labrador, Canada

M. SHIMOJO^{1*}, S. YAMAMOTO¹, S. AOKI¹, S. SAKATA², K. MAKI², K. KOSHIDA¹, A. ISHIKAWA¹, T. HIRATA², K.D. COLLERSON³ AND T. KOMIYA¹

¹Department of Earth Science and Astronomy, The University of Tokyo, Komaba, Meguro, Tokyo, 153-8902, Japan

(*correspondence: shimojo@ea.c.u-tokyo.ac.jp)

²Laboratory for Planetary Sciences, Kyoto University, Japan

³The University of Queensland, Brisbane Qld 4072, Australia

The Saglek Block is underlain by the Early to Late Archean suites including ca. 3.73 Ga Uivak I Gneiss, ca. 3.62 Ga Uivak II Gneiss, ca. 3.24 Ga Lister Gneiss and ca. 2.5 Ga granite [e.g. 1]. Those rocks underwent high-grade metamorphism, locally reaching granulite facies at 2.8-2.7 Ga [1]. Additionally, presence of over 3.8 Ga, up to 3.91 Ga, zircon cores in the Uivak I Gneiss suggested pre-Uivak I Gneiss rocks [1, 2], named as Nanok Gneiss [2]. However, the origin of the old zircon cores is still unclear: inherited from pre-Uivak I materials or precipitated from an older suite of the Uivak I felsic magma. Thus, we examined the internal structures of zircons using cathodoluminescence (CL) images and conducted laser-ablation ICP-MS U-Pb dating.

The result of the 11 orthogneiss samples from the south of St. John's Harbor is the following. The CL images or microscopic observations clearly display that most of the zircon grains comprise three domains: Zone I to III, respectively. Zone I is located in their central regions, and display clear oscillatory zoning. It is characterized by low U contents and high Th/U ratios. The Zone II lacks obvious oscillatory zoning, and is very dark. It is characterized by high U contents and low Th/U ratio, compared with Zone I. Zone III is a very thin layer in the outermost part of grains or does not exist. The U-Pb ages of Zone I and II shows a peak at 3.96-3.85 Ga and around 2.7 Ga, respectively. Those ages are well-correlated with observations of CL images, U contents and Th/U ratios. The age of the Zone II is in agreement with metamorphic age of previous study. Hence, the age of Zone I can be interpreted lower limit of the magmatic age of the protoliths of the orthogneisses, older than the conventional age of the Uivak Gneiss [1]. We concluded that the granitoid, the precursor of the Nanok Gneiss, were emplaced at 3.96 Ga in the Saglek block, Labrador.

[1] Schiøtte *et al.* (1989) *Can. J. Earth Sci.* **26**, 1533-1556. [2] Collerson (1983) *Lunar planet. Inst. Tech. Rep.* **83-03**, 28-33.

Determination of Boron using Isotope dilution MC-ICP-MS

HYUNG SEON SHIN*, MIN SEOK CHOI, JONG-SIK RYU
AND KWAN SOO HONG

Korea Basic Science Institute, Chungbuk, Korea
(*correspondence: h2shin@kbsi.re.kr)

A new technology applying to the isotope dilution method was used to estimate the amount of B (boron) in geological samples and was determined to be a viable method to minimize naturally occurring B background signals. The B ratios in geological sample (SDC-1 and SGR-1) were measured using a double-focusing multiple collector inductively coupled plasma mass spectrometer (Neptune). High naturally occurring B background signals and $^{40}\text{Ar}^{+4}$ interference were improved using a low RF power technique. A H_3PO_4 in mixed acid ($\text{HNO}_3 + \text{HF}$) was used to reduce the loss of B form (BF_3) in the sample dissolution process.

Boron isotopes were measured using a multi-collector, inductively coupled plasma mass spectrometer (Neptune, Thermo-Finnigan, Bremen, Germany). The present study determined an alternative method to minimize B isotope background signals. The B background signal was improved using a low RF power technique. The 800 W setting represents an excellent compromise between lower interference and the reduced matrix effect experienced at 1200 W. The results at 800 W (SGR: 55.246 ± 0.003 and SDC: 13.273 ± 0.003 mg g⁻¹) were equivalent to the reference values (SGR: 54 ± 3 and SDC: 13 mg g⁻¹). However, the values obtained using 1200 W (SGR: 48.600 ± 0.001 and SDC: 11.127 ± 0.004 mg g⁻¹) were slightly lower than the 800 W values. Furthermore, the addition of H_3PO_4 prevented the loss of boron within the sample dissolution process. The SDC-1 and SGR-1 results obtained by the isotope dilution method were within the range of the reference values. Overall, the high performance of our proposed analytical technique (decreased B background signal under low RF power, H_3PO_4 , isotope dilution method and MC-ICP-MS) makes it suitable for use in the determination of B in geological samples

1. J. K. Aggarwal, D. Sheppard, K. Mezger and E. Pernicka, *Chem. Geol.*, 2003, **199**, 331-342. 2. L. Zhao, Q. Chen, C. Li and G. Shi, *Sol. Energy Mater. Sol. Cells*, 2007, **91**, 1811-1815. 3. T. Fujisakia, A. Yamadab and M. Konagai, *Sol. Energy Mater. Sol. Cells*, 2002, **74**, 331-337. 4. M. Betti, *Int. J. Mass Spectrom.*, 2005, **242**, 169-182.

Boron and other trace element constraints on the slab-derived component in Miocene volcanic rocks from the Setouchi Volcanic Belt in SW Japan

HIRONAO SHINJOE¹, YUJI ORIHASHI²
AND TOMOAKI SUMII³

¹Tokyo Keizai University, Tokyo, JAPAN (*correspondence: shinjoe@tku.ac.jp)

²Earthquake Research Institute, Univ. of Tokyo, Tokyo, JAPAN

³Geological Surv. Japan, AIST, Tsukuba, JAPAN

We present a dataset for boron and other trace element contents for basalts and high-Mg andesites (HMA) obtained from the middle Miocene Setouchi Volcanic Belt (SVB) in SW Japan. SVB was formed along the SW Japan Arc, immediately after the opening of the Japan Sea and clockwise rotation of SW Japan with the subduction of young hence hot Shikoku Basin of the Philippine Sea plate. Previous studies on HMA and basalt of SVB, laid stress on the contribution of subducting sediment, particularly partial melt of terrigenous sediments to the magma source mainly based on their Sr, Nd, Pb isotopic compositions.

Analyzed samples show a large negative Nb and Ta anomalies, and enrichment of alkaline earth elements and Pb, which are features of typical island arc volcanic rocks. Boron content of basalts and HMA is highly variable (7 – 71 ppm).

Trace element compositions of altered oceanic crust-derived fluid, sediment-derived fluid, and sediment melt are modeled, and resultant fluid mobile/immobile element ratios (B/Nb, Ba/Nb, Pb/Nb, and K/Nb) are used to examine slab-derived component to mantle source. Most of element ratios are explained by <5% contamination of sediment melt to depleted mantle except for some HMAs with rather high B/Na ratios. Mantle source for these HMAs may be enriched with some trace elements including boron before the addition of slab-derived melt.

Mechanism and crystallochemical signature of nano-particle formation by microorganisms

H. SHIOTSU¹, M. JIANG¹, Y. NAKAMATSU¹, T. OHNUKI²
AND S. UTSUNOMIYA¹

¹Department of Chemistry, Kyushu University, Fukuoka 812-8581, Japan (utsunomiya.satoshi.998@m.kyushu-u.ac.jp)

²ASRC, Japan Atomic Energy Agency, Tokai, Ibaraki, Japan

Interaction between rare earth elements (REEs) and microorganisms have attracted increasing attention due to the ubiquitous occurrence of microorganisms in the subsurface environment and to implication to the safety assessment of nuclear waste disposal, as REEs are used as a surrogate of trivalent actinides. Post-adsorption nano-mineralization by microorganisms is a key process that can constrain the migration of REEs; however, the mechanisms and factors controlling the process are still unclear. This study demonstrates the REEs (La-Lu) accumulation experiments to understand the effect of pH, coexistent REEs and the functional group of cells surfaces on the crystal chemistry of biogenic nanoparticle formation.

During the exposure of yeast to REE solution at 25 °C, all REEs were removed from the solution by 24 h at pH 4 and 5, while 50 % of the initial amount remained in the solution at pH 3 after 24 h. Deprotonation of the functional groups on the cell surface merely occurs at pH 3 as evidenced by the other experiments at 4 °C. In contrast, 10 % of REEs were adsorbed to the cell surfaces at pH 4 and 5. Particles at the size of ~100 nm precipitated on the cell surfaces at pH 3, while ~30 nm-sized nano-particles were observed at pH 4 and 5 at 25 °C. These nano-particles were characterized as phosphate containing a series of REEs. The nano-particles at pH 3 had monazite structure, while the particles forming at pH 4 and 5 were amorphous, indicating that crystallization took place only at pH 3. REE phosphate inorganically synthesized at room temperature revealed crystalline structure (monazite, xenotime or rhabdophane) depending on the element. Additional inorganic model experiments using the CMC, Ln resin and Cellulose Phosphate, which have the functional groups similar to cell surfaces, demonstrated that the nano-particles precipitated without structure. Based on these data it is suggested that adsorption to the functional groups on the cell surfaces constrain the shape and structure of nanoparticles.

As for the REE pattern, the difference between the distribution coefficient, K_d (ml/g), of LREE and of HREE increased with time increasing. At 24 h, the K_d ratio of Nd to Tm ($K_{d, Nd}/K_{d, Tm}$) is 1.72, 4.61, and 6.86 at pH 3, 4, and 5, respectively. The K_d ratios greater than 1 indicate the preferential uptake of LREE by the microorganisms, which are attributed to the lower solubility products of REE phosphate. As a consequence, the present study underscores the important role of cell surfaces and biological activity on the kinetics, mechanisms and crystal chemistry of nanoparticle formation as well as the physico-chemical properties of nanoparticles.

Sub-daily elemental fluctuation in mussel shell

KOTARO SHIRAI^{1*}, TSUZUMI MIYAJI², BERND R. SCHÖNE³ AND KAZUSHIGE TANABE⁴

¹Atmosphere and Ocean Research Institute, The University of Tokyo, Kashiwa 277-8564 Japan (* correspondence: kshirai@aori.u-tokyo.ac.jp)

²Department of Natural History of Science, Hokkaido University, Sapporo 060-0810 Japan

³Institute of Geoscience, University of Mainz 55128 Mainz Germany

⁴The University Museum, The University of Tokyo, Tokyo 133-0033 Japan

Shells of bivalve mollusks such as mytiloids serve as excellent paleoenvironmental archives. They exhibit a broad biogeographic distribution, occur in large numbers in the fossil record and contain a temporally aligned and highly resolved record of past environmental parameters. For example, Mg/Ca ratios of mussel shells have been explored as a temperature proxy. According to several studies, however, the suitability of the Mg/Ca thermometer is limited by vital effects. In order to extract reliable environmental information from the shell through geochemical analyses it is essential to understand the mechanism of elemental incorporation into the shell during calcification and growth.

In the present study, we have analyzed Mg/Ca Sr/Ca and S/Ca ratios of two shells of the Mediterranean mussel *Mytilus galloprovincialis* collected alive from Tokyo Bay, Japan. Environmental parameters were monitored at the sampling site. The elemental distribution was determined in polished cross-sections by means of electron probe micro analysis. Growth patterns were used to place the geochemical data in a temporal context.

Growth lines (which formed during low tide) showed higher Mg/Ca ratios compared to adjacent growth increments. S/Ca ratios were also high at the growth line. However, the Mg/Ca and S/Ca do not show linear correlation. Both Mg/Ca and S/Ca ratios showed significant periodic fluctuations at the sub-seasonal scale. These fluctuations likely indicate that the shell Mg/Ca ratios primarily reflect biological changes caused by tidal cycle and do not record temperature.

Composition of serpentine after olivine and orthopyroxene: Serpentinized peridotites of Nain ophiolite (Isfahan Province, Iran)

N. SHIRDASHTZADEH¹, G. TORABI¹ AND R. SAMADI²

¹Department of Geology, Faculty of Science, University of Isfahan, Isfahan, Iran

²Department of Geology, Science and Research Branch, Islamic Azad University, Tehran, Iran

Introduction

The Nain ophiolite is one of the most complete ophiolitic suits at the East of Central-East Iranian Microcontinent - ophiolitic belt and it comprises a high proportion of serpentinized mantle peridotites [1]. As a possible alteration product of Nain mantle peridotites, serpentine constructed the veinlets and the mesh texture, characterized with a pale green-white chalky feature. The fibrous serpentine filled the cracks and veinlets are crossing the mesh texture and this indicates their former formation.

Raman Spectrometry and Microprobe Data

Raman Spectrometry of the serpentine suggests that the mesh texture is made of lizardite and the rock veinlets are filled by chrysotile. Based on major element data, lizardite is $Mg_{3.00}Fe_{0.31}Ni_{0.01}Si_{1.84}$, with $Al_2O_3 = 0.00$ wt%, $Mg\# = 0.91$, $Cr\# = 0.00$ in composition and chrysotile is $Mg_{2.14}Fe_{0.10}Al_{0.23}Cr_{0.02}Si_{2.18}$, with $Al_2O_3 = 2.84-5.97$ wt%, $Mg\# = 0.96$, $Cr\# = 0.10$.

Discussion of Results

Lizardite is characterized with higher Mg, Fe and Ni in while chrysotile is higher in Al_2O_3 and Cr#. [2] suggested that serpentine after orthopyroxene (bastite) are generally low in MgO (~ 34–37 wt%), but have silica similar to serpentine after olivine (38–42 wt%). MgO of the studied chrysotile (~ 30–32 wt%), formed after orthopyroxene are generally higher than MgO of lizardite (~ 29 wt%), formed after olivine (i.e. lizardite), but the silica has a similar range (~ 43–54 wt%) in chrysotile and lizardite. The low Mg and high Cr and Al of chrysotile is a consequence of the composition of the original orthopyroxene (e.g., [3]; [4], [2]). Therefore, Al-rich serpentine of chrysotile is found in orthopyroxene bastite with lower MgO and FeO contents, and higher Al_2O_3 and Cr_2O_3 concentrations, while the lizardite is the serpentinization product of olivine.

[1] Shirdashtzadeh *et al.* (2013) *Lithos* (Submitted). [2] Shervais *et al.* (2005) *Inter Geol Rev* **47**, 1-23. [3] Dungan (1979) *Can Min* **17**, 771-784. [4] Wicks & Plant (1979) *Can Min* **17**, 785-830.

Water content of inclusions in superdeep diamonds

S.B. SHIREY¹, E.H. HAURI¹, A.R. THOMSON², G.P. BULANOVA², C.B. SMITH², S.C. KOHN² AND M.J. WALTER²

¹DTM, Carnegie Institution of Washington, Washington DC 20015, USA (shirey@dtm.ciw.edu, hauri@dtm.ciw.edu)

²Dept Earth Sciences, University of Bristol, Queen's Road, Bristol BS8 1RJ, UK (andrew.thomson@bristol.ac.uk)

The water content of the mantle strongly influences mantle convection and partial melting. Previously, direct measurements of mantle water content have been limited to peridotites or inferred from basalts. Superdeep or sublithospheric diamonds from the transition zone and lower mantle carry ultra-high pressure silicate and oxide micro-inclusions that provide an unparalleled opportunity to directly sample the composition, mineralogy and water content of deep mantle minerals.

We measured mineral inclusions in Type II (<20 ppm N) diamonds from the 93 Myr old Collier 4 kimberlite pipe in the Juina field of Brazil for their water content with the DTM NanoSIMS 50L. Studies of these diamonds showed complex growth structures, diverse inclusion assemblages, and heterogeneous C isotopic compositions (-5‰ to -25‰) interpreted as being due to subducted components entrained in the Trinidade plume [1]. Simultaneous scanning ion imaging of ¹²C, ¹⁶O, ¹⁸O, ¹⁹F, ³⁰Si and ⁵⁶Fe was employed and data reduced using the *L'image* (© LR Nittler, DTM) image-processing software. H₂O contents vary from nominally-anhydrous phases such as majorite (30 ppm, J9), walstromite after CaSi-perovskite (74 ppm, J14), and Mg-Al spinel (245 ppm, J2) to more water-rich phases such as Mg-pyroxene (former MgSi-perovskite, 2600 ppm, J2), Fo₉₁ olivine (2300 ppm, J20) and K-feldspar (7800 ppm, J2). Mg-silicate phases along an internal fracture (J9) have 2.3 to 3.8 wt% H₂O and may be epigenetic or compromised.

Inferences on the mineralogy and H₂O contents of the inclusions at the time of trapping depend on identification of retrograde phases, final retrograde pressure, and H₂O storage capacity of the retrograde mineral assemblages. Correspondence of lowest measured water with the most anhydrous phases suggests some retention of original water content, however. Forsteritic olivine with 2300 ppm H₂O, and aluminous Mg-pyroxene with 2600 ppm H₂O, are consistent with H₂O saturation at pressures ≥ 7 GPa [2] and represent lower limits on the original H₂O content of these inclusions if their trapping depths were greater than 200 km.

[1] Bulanova *et al.* (2010) *Cont. Min. Petrol.* 160 489-510. [2] Hauri *et al.* (2006) *Earth Planet. Sci. Lett.* 248, 715-734.

Simultaneous mantle metasomatism, diamond growth and crustal events in the Archean and Proterozoic of South Africa

Q. SHU^{1,2*}, G.P. BREY¹, A. GERDES¹ AND H. E. HOEFER¹

¹Institut für Geowissenschaften, Goethe-Universität, Altenhöferallee 1, D-60438 Frankfurt, Germany; ²China University of Geosciences (Beijing), Xueyuan Road 29, Haidian, Beijing, China. 100083; *shu@em.uni-frankfurt.de

Subcalcic garnets from harzburgites are proxies of the chemical and isotope composition of their bulk rock. The present study and previous work [1,2] on the Sm-Nd and Lu-Hf isotope systematics show that they can be excellent recorders of multiple mantle events. Subcalcic garnets with sinusoidal REE patterns are the results of high degrees of partial melting of their protolith at shallow pressures followed by subduction and re-enrichment by (silico-)carbonatitic melts. Metasomatism in a previously depleted mantle ($\epsilon_{\text{Hf}} = +16$) occurred underneath the crust the East Kaapvaal craton at around 3.2 Ga. Simultaneously, the crust was affected by widespread activity around that time and Sm-Nd model dates of similar age from pooled peridotitic garnet inclusions in diamonds were interpreted as oldest diamond growth ages. Oceanic lithosphere was created between the West- and East-Kaapvaal around 2.95 Ga [2] and subducted underneath the West-block before the collision around 2.88 Ga. This also caused enrichment process in an overlying, highly depleted mantle wedge 2.9 Ga ago [2] and apparently triggered a major growth period of diamonds as demonstrated by similar Re-Os ages from sulfide inclusions in diamonds from Kimberley and Botswana. Further enrichment in the West-Kaapvaal mantle at 2.62 Ga [1] coincides with the 2.6-2.8 Ga Ventersdoorp magmatism and with a 2.6 Ga Re-Os isochron from E-type sulfide inclusions from Koffiefontein. The attachment of the Kheis-Magondi belt to the Kaapvaal craton caused further metasomatism around 1.90 Ga [2] in the mantle along the Western margin of the Kaapvaal craton. The latest stages of mantle metasomatism lie between 0.9-1.3 Ga, coincident with the Namaqua-Natal belt orogeny. Periods of diamond growth younger than 2.6 Ga cannot be related directly to any mantle or crustal event. Major geotectonic events and plume activity episodically remobilized low melting portions in the mantle keel which lead to episodic (auto) metasomatism of the depleted mantle, episodic diamond growth and destruction of the lithospheric keel.

[1] Lazarov *et al.*, 2009, Earth Planet. Sci. Lett. **27**, 1–10.

[2] Shu *et al.*, 2013, Geochim. Cosmochim. Acta, in press

The differentiation mechanism of W and Sn of Qitianling granite in Hunan province, south China

SHUANG YAN^{1,2} AND XIANG XIAOJUN^{1,2}

¹Chongqing Key Laboratory of Exogenic Mineralization and Mine Environment, Chongqing Institute of Geology and Mineral Resources, Chongqing 400042, China;

²Chongqing Research Center of State Key Laboratory of Coal Resources and Safe Mining, Chongqing 400042, China
E-Mail: shy810124@yahoo.com

Both large-scale tungsten and tin mineralization took place mostly in Nanling Mountains, South China. The two elements are usually related and accompanied with granitic rocks. Hua *et al* (2010) proposed that the eastern sector of the Nanling Mountains is characterized by strong and dense W mineralization, while Sn mineralization becomes stronger westwards. This study attempts to discuss reasons that cause the two elements differentiation, in the light of the study on the fluid inclusions of Furong Sn deposit and Xintianling W deposit, of which both have genetic relations to the Qitianling granitic rocks in Nanling Mountains, South China.

According to the study on the fluid inclusions of the two deposits, aqueous two-phase inclusions and daughter mineral-bearing inclusions are found in Furong Sn deposit, located in the south of Qitianling granites. The ore forming fluids have the composition of CaCl₂-NaCl-H₂O system with high salinity (36.99-42.45 wt% NaCl eq.) and temperature (462-494°C). While in the Xintianling W deposit, the CO₂-riched inclusion has been observed as the major inclusion. The ore forming fluids are characterised with low salinity (below 6%) and high temperature (367-392°C). The first melt temperatures of CO₂ range between -66.6~61.1°C.

These findings suggest that CO₂-enriched hydrothermal fluid differentiated from the Qitianling granites is conducive to the separation of W from the granitic magma system. In the later evolutionary tertiary of the magma, the hydrothermal fluid is characterized with high level of Cl⁻, which favor Sn enrichment in the ore-forming fluids. Accordingly, the difference of the ore-forming fluids of the two deposit maybe is the major factors responsible for the differentiation of W and Sn.

This research project was financially supported by the National Natural Science Foundation of China (41003024) and the Open Foundation of the State Key Laboratory of Ore Deposit Geochemistry (201103)

Studies of nuclear waste form glasses with synchrotron radiation

D.K. SHUH^{1*}, W.W. LUKENS¹, J.P. ICENHOWER¹,
J.G. DARAB², T. TYLISZCZAK¹, H. BLUHM¹,
D. A. MCKEOWN, A. C. BUECHELE, I.S. MULLER
AND I.L. PEGG

¹Lawrence Berkeley National Laboratory (LBNL), Berkeley, CA 94720, USA (*correspondence: DKShuh@lbl.gov; WWLukens@lbl.gov, JPIcenhower@lbl.gov, Tolek@lbl.gov, HBlum@lbl.gov)

²J.G. Darab, MEL Chemicals Inc., NJ 08822 USA (JDarab@MEIchem.com)

³Catholic University of America, Washington, D.C. 20064, USA (davidm@vsl.cua.edu, andrewb@vsl.cua.edu, isabellem@vsl.cua.edu, ianp@vsl.cua.edu)

The speciation of several radionuclide and surrogate metal ions in specific formulations of nuclear waste form glasses has been investigated by synchrotron radiation methods. The primary technique to determine the oxidation state and structural information, and chemical behavior in many of these studies has been hard x-ray absorption fine structure (XAFS) [1]. There has been considerable effort utilizing XAFS to understand the conditions under which surrogates, in large part Re for Tc but also including specific metal ions such as Ce and Hf for Pu, are suitable chemical and structural analogs for the actual radionuclides of interest. Similar approaches have been utilized to validate the reliability of surrogates in glass waste form characteristics under processing and alteration conditions [2].

Recently, studies of glass waste form materials have been initiated using new soft synchrotron radiation tools that include the scanning transmission x-ray microscope (STXM) and ambient pressure x-ray photoelectron spectroscopy (APPES) endstations at the Molecular Environmental Sciences Beamline of the Advanced Light Source at LBNL [3]. Spectromicroscopy studies have been conducted using soft x-ray absorption spectroscopy of light atom constituents and metal ions in glasses with STXM, investigating the early stages of the interaction of water with glass surfaces with PES under more realistic conditions of approximately 10 Torr. New opportunities to address critical issues in nuclear waste form glass science with emerging synchrotron radiation methods will be presented and discussed.

[1] Booth *et al.* (1999) *J. Mater. Res.* **14**, 2628-2639.

[2] McKeown, *et al.* (2012) *J. Nucl. Mater.* **429**, 159-165.

[3] Bluhm *et al.* (2006) *J. Electron Spectros. Rel. Phenom.* **150**, 86-104.

A novel ¹⁹⁰Pt-⁴He method of isotope geochronology for the direct dating of native minerals of platinum

YURIY A. SHUKOLYUKOV^{1,2,*}, OLGA V. YAKUBOVICH^{1,2,**}, ALEXANDER G. MOCHALOV¹
AND ALEXANDER B. KOTOV¹

¹IPGG RAS, Makarova 2, 199034, Saint-Petersburg, Russia (** correspondence: olya.v.yakubovich@gmail.com)

²Saint-Petersburg State University, Universitetskaya 7/9, 199034, Saint-Petersburg, Russia

*deceased

Retention of radiogenic ⁴He in crystals of most minerals is very low. Helium can escape easily from minerals in a course of their geological history. However, in a group of minerals, namely native metals, the retention of radiogenic helium is anomalously high [1]. Very low solubility of helium in metals leads to formation of atomic clusters of helium atoms, which manifest themselves as nanometer-scale bubbles. Migration of such "bubbles" in the crystal structure requires relatively high temperature close to the metal melting temperature.

The tendency of helium to form stable bubbles in native metals allows to propose a novel method in isotope geochronology for the direct dating of native minerals of platinum that is based on the α -decay of ¹⁹⁰Pt isotope [2].

We present nuclear-physical, isotope-geochemical and methodological aspects of the novel ¹⁹⁰Pt-⁴He method. We validate the method on a set of new experimental ¹⁹⁰Pt-⁴He dating measurements of four platinum deposits: (i) the Galmoenan massif, a gabbro-dunite-pyroxenite massif in the Koryak Highlands, Russia; the alkaline-ultramafic massifs of (ii) Kondyor, (iii) Inagli and (iv) Chad in the Aldanian shield, Russia. Our experimental measurements confirm the successful applicability of ¹⁹⁰Pt-⁴He for the direct dating of the native minerals of platinum.

[1] Shukolyukov (2012) *Petrology*, **20.1.**, 1-20 [2] Shukolyukov (2012) *Petrology*, **20.6.**, 491-505

Microbial production and transformation of dissolved organic matter in the hydrothermal system

N.A. SHULGA¹, V.I. PERESYPKIN¹ AND I.I. RUSANOV²

¹P.P. Shirshov Institute of Oceanology of the RAS,
Nahimovski prospect 36, Moscow, Russia, 117997,
(nash.ocean@gmail.com)

²Winogradsky Institute of Microbiology RAS, Prospekt 60-
letiya Oktyabrya 7, 117312, Moscow, Russia
(rusanov_igor@mail.ru)

This study was inspired by the lack of information on the microbial production of dissolved organic matter in course of chemosynthesis and methane oxidation at hydrothermal fields: most of studies didn't take into account the production of dissolved organic matter (DOM), considering only formed and consumed microbial biomass in the processes of microbial transformation of endogenous gases coming from hydrothermal solutions.

It is well known that the formation of organic compounds in the zones of hydrothermal activity proceeds under the influence of a number of physicochemical and biogeochemical (extremophile consortiums of bacteria and archaea) factors. We present i) radioisotope measurements of the activity of microbial communities in the hydrothermal fields of the Mid-Atlantic Ridge (MAR) and the East Pacific Rise (EPR), ii) investigation of the rates of microbial CO₂ assimilation, sulfate reduction, methane oxidation, lithotrophic and acetoclastic methanogenesis, and assimilation and oxidation of organic carbon, iii) analysis of samples of sulfide, sulfate, and carbonate hydrothermal deposits of various morphological types. Special attention was paid to the measurement of microbial DOM. We show for deep-sea hydrothermal systems, that in the process of microbial methane oxidation and dark assimilation of carbon dioxide at various temperature gradients of microbial production of DOM in most cases significantly higher than biomass production. Intensities of sulfate reduction and methanogenesis have been measured for the first time at different temperatures and dilution of the hydrothermal solution, not only in anaerobic sediments and solutions, but also in water samples of the contact zone and the plume.

The different content of organic compounds in microbiological samples and ore deposits from hydrothermal systems related to basalt volcanism and serpentinization of ultrabasic rocks testifies the different genesis of DOM.

This work was supported by grant RFBR № 10-05-01116-a, 12-05-31259_МОН-а.

Production and diffusion of cosmogenic noble gases: Using open-system behavior to study surface processes

DAVID L. SHUSTER^{1,2}, MARISSA M. TREMBLAY^{1,2}
AND GREG BALCO²

¹Dept. of Earth and Planetary Science, University of
California, Berkeley, CA 94720 USA

²Berkeley Geochronology Center, Berkeley, CA 94709 USA

We present a new geochemical approach to obtaining information about the temperature and surface exposure history of rocks and sediments. The approach is based on the simultaneous production and diffusion of cosmogenic noble gases in minerals at and near Earth's surface, and aims to take advantage of "open-system" behavior that has previously been viewed only as an undesirable obstacle to surface exposure dating. Given knowledge of diffusion kinetics, the relative abundances of cosmogenic ³He, ²¹Ne and other cosmogenic nuclides in natural samples constrain their temperature histories during surface exposure. When interpreted with a simple theoretical framework, and using laboratory-determined kinetics of He and Ne diffusion [1-3], our preliminary results indicate several pairs of common minerals and easily measureable cosmogenic noble gases that display partial retention at Earth surface temperatures. We focus initially on the minerals quartz and feldspars; these provide sets of nuclide-mineral systems that can be selected and optimized to constrain mean surface temperatures (and changes therein) across a range of climate settings and lithologies over the last few Ma. As an example, we present preliminary results from quartz-bearing Antarctic sandstones that constrain a mean, effective temperature of approximately -15 °C over 5-10 ka of surface exposure. We present the basic theory and fundamental assumptions of this approach, and discuss potential complexity and limitations to the interpretation of these data.

1. Gourbet, L., et al., Neon diffusion kinetics in olivine, pyroxene and feldspar: Retentivity of cosmogenic and nucleogenic neon. *Geochimica et Cosmochimica Acta*, 2012. 86: p. 21-36; 2. Shuster, D.L. and K.A. Farley, Diffusion kinetics of proton-induced ²¹Ne, ³He, and ⁴He in quartz. *Geochimica et cosmochimica acta*, 2005. 69(9): p. 2349-2359; 3. Tremblay, M.M., D.L. Shuster, and G. Balco, Quantifying the open-system behavior of cosmogenic noble gases in quartz. *Goldschmidt 2013* (this meeting).

The Study of Cadmium Accumulation by Floating Macrophytes using Natural Modeling Approach

O.V. SHUVAEVA^{1,2*}, L.A. BELCHENKO²
AND T.E. ROMANOVA^{1,2}

¹Institute of Inorganic Chemistry SB RAS, 3, Ac. Lavrent'ev Pr., 630090, Novosibirsk, Russia, olga@niic.nsc.ru

²Novosibirsk State University, 2, Pirogova, 63090, Novosibirsk, Russia, lab305@lab.nsu.ru

³Novosibirsk State University, 2, Pirogova, 63090, Novosibirsk, Russia, romanova_toma@mail.ru

It is known that phytoremediation technology became an effective method of environment clearing after it has been found the plant's ability to accumulate the contaminants at high concentration level. The floating macrophytes (*FM*) *Eichhornia crassipes* (*EC*) and *Pistia stratiotes* (*PS*) are applied most often to waste waters purification.

The goal of this investigation was to study the efficiency of the metal's bioaccumulation by *EC* and *PS* when exposed to cadmium with an emphasis on the mechanism of transport and transformation of pollutant within the plant and its fate during accumulation act.

To estimate hit consequences of pollutant on ecosystem an experiment was carried out in the conditions close to the natural using an approach of natural modeling consisting in a statement of natural experiments with the use of mesocosms, established directly in a reservoir into which one enters the set portion of pollutant and then supervises the dynamics of its concentration.

As a result it was found that the degree of cadmium extraction by *FM* from contaminated natural water while maintaining the viability of the plants depends on the way of pollutant introducing and the maximum is observed in the case of its gradual entry. Herewith at the first stage of cadmium uptake the sorption of the metal on the surface of the roots takes place where cadmium mainly localized in rhizodermis, and then the pollutant penetrates into the tissues of the stem according to its translocation factor

In contrast to the traditional black-box approach, detailed investigations of pollutant transport and distribution in plant tissues have given sound understanding of the phytoremediation phenomenon. Such advancements could provide a basis for future improving the efficacy of the biological remediation processes.

Modelling fluid-mineral equilibria in two-phase fluid systems

YU. V. SHVAROV¹, E. N. BASTRAKOV^{2*}, T.P. MERNAGH²
AND N. N. AKINFIEV³

¹Moscow State University, Moscow 12345, Russia

²Geoscience Australia, Canberra, ACT 2601, Australia

(*correspondence: Evgeniy.Bastrakov@ga.gov.au)

³IGEM RAS, 119017, Moscow 119017, Russia

There is a demand for modeling fluid-rock interaction in geological systems that contain two fluid phases (e.g., liquid + gas) or experience a transition from supercritical to subcritical state of fluids. The relevant problems include CO₂ sequestration into geological formations; exploitation of gas-rich geothermal systems; quantification of metal transport by low-density fluids in porphyry, epithermal, and lode-gold mineral systems. Modelling of geochemical processes in these systems requires software that allows simultaneous prediction of the accurate phase composition of the fluid part of the system and "conventional" water-rock or gas-rock equilibria. Recent experimental and theoretical studies start to provide thermodynamic models to expand these calculations into the realm of metal bearing fluids [1].

To address these challenges, we employ the HCh software package [2] that uses the Gibbs Free Energy minimization approach for equilibrium calculations. To calculate fluid-fluid equilibria, we have incorporated a customised version of the PRSV equation-of-state [3], where thermodynamic properties of *pure water* at a given temperature and pressure are calculated according to the comprehensive Haar-Gallagher-Kell model [4]. The incorporated algorithms were calibrated and tested against available experimental and theoretical data for the binary H₂O-CO₂ and H₂O-CH₄ systems, and the ternary H₂O-CO₂-CH₄ system.

A practical application of the software to economic geology problems is illustrated by calculation of H₂S concentrations in a supercritical fluid and subcritical gas and liquid phases in equilibrium with mineral assemblages containing iron sulfides and oxides. An equilibrium between pyrite-pyrrhotite mineral pair and the H₂O-CO₂-CH₄-H₂O-H₂S-H₂ fluid offers a plausible explanation of the H₂S concentrations measured in the vapor-rich inclusions from the Missouri lode gold deposit.

- [1] Migdisov & Williams-Jones (2013) *GCA* **104**, 123-135. [2] Shvarov (2008) *Geochem. Int* **46**, 834-839. [3] Stryjek & Vera (1986) *Can. J. Chem. Eng* **64**, 323-333. [4] Kestin *et al.* (1984) *J. Phys. Chem. Ref. Data* **13**, 175-183.

Hg as a proxy for volcanic activity during extreme environmental turnover: the K-T boundary

A. N. SIAL^{1*}, L. D. LACERDA², V. P. FERREIRA¹, R. FREI³, R. A. MARQUILLAS⁴, J. A. BARBOSA¹, C. GAUCHER⁵, C. C. WINDMÖLLER⁶ AND N. S. PEREIRA¹

¹NEG-LABISE and Dept. Geology, UFPE, Recife, Brazil
(*correspondence: sial@ufpe.br)

²LABOMAR, UFC, Fortaleza, Brazil

³Inst. Geogr./Geol., Univ. of Copenhagen, Denmark, 1350

⁴Univ. Salta, Salta, Argentina

⁵Fac. Ciencias, Univ. de La Republica, Montevideo, Uruguay

⁶Dept. Chem., UFMG, Belo Horizonte, Brazil

Hg tends to concentrate in sediments deposited right after major glacial events as a result from leaching of volcanogenic Hg from land surface and accumulation along argillaceous sediments. Low geological background concentrations of Hg makes it suitable for identifying accumulation pulses during sedimentation that can be tentatively related to weathering processes and thus to climatic changes. Intense volcanism was, perhaps, responsible for climatic changes, decrease in biodiversity and mass extinction in the K-T boundary (KTB).

We have used Hg as a proxy for volcanic activity and atmospheric Hg and CO₂ buildup across the KTB in the Yacoraite Fm., Argentina, where Hg up to 250 ng.g⁻¹ has been found. In drill cores across the KTB in the Paraiba Basin, NE Brazil, Hg also increased from late Maastrichtian to early Danian. Hg spikes predating the KTB are, perhaps, the record of volcanic activity very close to this transition. At Stevns Klint, Denmark, Hg contents reached ~ 250 ng.g⁻¹ within a clay layer that comprises the KTB, and exhibits marked ⁸⁷Sr/⁸⁶Sr positive excursion and ²⁰⁶Pb/²⁰⁴Pb and ¹⁸⁷Os/¹⁸⁸Os (t = 65Ma) negative ones. Highest Hg values in the Yacoraite Fm. and at Stevns Klint (~250 ng.g⁻¹) are similar to volcanogenic Hg contents in Neoproterozoic cap carbonates (~ 280 ng.g⁻¹), deposited in the aftermath of Snowball glaciation, a comparative extreme environmental turnover, in absence of meteorite impact. Co-variation between Hg and Al₂O₃ is observed in all studied sections suggesting that Hg is adsorbed onto clays. Thermo-desorption experiments in samples from the Yacoraite Fm. showed Hg²⁺ as the major species present, in agreement with a volcanic origin. Combined Hg and C-isotope stratigraphies may become a powerful tool for the eventual assessment of the role of volcanic activity during extreme climatic and biotic events, such as those during the Cretaceous-Tertiary or Permian-Triassic boundaries.

The age of eclogitisation underneath the Kaapvaal craton – A composite xenolith from Roberts Victor

M. SIEBER*, G.P. BREY, H.-M. SEITZ, A. GERDES AND H.E. HOEFER

Institut für Geowissenschaften, Goethe-Universität,
Altenhöferallee 1, D-60438 Frankfurt, Germany;
*melanie-sieber@stud.uni-frankfurt.de

We have studied a composite, 16x11x5 cm sized, biminerale eclogite xenolith (texturally Type II) from the Roberts Victor diamond mine (South Africa) with a 1 cm thick layer along its longer side of green, Cr-rich cpx with exsolution lamellae (presumably opx which is now completely replaced by calcite) plus a Cr-rich garnet (up to 6 wt% Cr₂O₃) which gradually change into the dark coloured cpx's (without exsolution lamellae and heavily altered in places) and Cr-free garnets in the major part of the eclogite. Electron microprobe traverses across the xenolith show that the individual mineral grains (~4 mm in size) are homogeneous but that there is a gradient of mineral compositions from the Cr-rich layer into the Cr-free part which appears like a diffusional gradient. For example, Al₂O₃ in garnet increases from 18 to a constant level of 23 wt% over a distance of 3 cm and Cr concomitantly decreases from 6 to practically zero wt%. The Mg-value increases over the same distance from 50 to 57. Clinopyroxenes change in composition complementary to the garnets. This concomitant change also holds for the trace elements which were determined by laser ablation ICP MS. The grt-cpx partitioning of the trace elements is the same throughout the xenolith except for a dependency on the Cr-content of garnet.

The temperature of 915 °C of last equilibration were calculated with the Krogh 1988 grt-cpx thermometer at 4.2 GPa.

We interpret the compositional profile as the reflection of the passage of a basaltic melt through peridotite. A contact zone with Cr-rich cpx and a compositional gradient was formed and the whole package was subsequently metamorphosed to eclogite. The aim is to determine the age of eclogitisation with the Sm-Nd and Lu-Hf isotope systems from garnet separates obtained from rock slices parallel to the Cr-rich layer.

Molybdenum isotope fractionation in the Great Artesian Basin, Australia

C.SIEBERT^{1*}, P. POGGE VON STRANDMANN²
AND K. BURTON³

¹GEOMAR, Helmholtz Center for Ocean Research, Kiel, Germany

²Univ. of Oxford, Dept. of Earth Sciences, Oxford, UK

³Univ. of Durham, Dept. of Earth Sciences, Durham, UK

* (correspondence: csiebert@geomar.de)

Over the last decade, Molybdenum (Mo) isotopes have become a valuable proxy for redox conditions in marine sediments. More recently, the behavior of Mo and its isotopes during weathering and erosion have been investigated to constrain inputs to the oceans. This study aims to investigate another aspect of terrestrial Mo cycling, namely its behavior in groundwater aquifers. Recent studies suggest that groundwater input could have a significant impact on oceanic elemental and isotopic budgets. Concentrations and isotope compositions of elements in groundwater are usually controlled by the recharging water (e.g. precipitation) and processes within the aquifer such as chemical weathering. We investigated these processes for Mo in the Australian Great Artesian Basin (GAB), the world's largest confined aquifer underlying ~22% of the Australian continent. The GAB consists of alternating layers of waterbearing sandstone aquifers and non-waterbearing siltstones and mudstones. The thickness of this sequence varies from less than 100 metres at the Basin edges to 3000 metres in the centre. Groundwater in the GAB flows generally west and south with a flow rate between 1 and 5 m/a. Recharge occurs by rainfall into outcropping sandstone along the eastern margins of the Basin. Samples are from the eastern portion of the GAB and range in age from 36 (close to the recharge area) to 700 kyr over a distance of 600 km along the flow of the groundwater.

Molybdenum concentrations and isotopes vary widely throughout the sampled area ([Mo]: 0.4 to 13 ppb and $\delta^{98}\text{Mo}$: -0.2 to 1.4 ‰). The isotopes show correlations with [U] and [SO₄], but are not or only weakly correlated with [Mo], [Mn], [Fe] or $\delta^7\text{Li}$. The observed patterns point to fractionation of Mo isotopes by a sequestering mineral phase. A systematic change of Mo isotope values with distance from the recharge area indicates that the size as well as the processes within the aquifer could impact the isotope composition of groundwater input to the oceans. The results emphasize the role of groundwater processes for the fractionation of Mo isotopes. However, the quantitative impact of this fractionation on the oceanic budget remains to be determined.

Experimental study of accretion and early differentiation of the Earth

JULIEN SIEBERT^{1*}, JAMES BADRO², DANIELE ANTONANGELI¹ AND FREDERICK J. RYERSON³

¹Institut de Minéralogie et de Physique des Milieux

Condensés, Université Pierre et Marie Curie, Paris, France

(*correspondence: julien.siebert@impmc.upmc.fr)

²Institut de Physique du Globe de Paris, Paris, France

³Lawrence Livermore National Laboratory, California, USA

The pattern of siderophile (iron-loving) element abundance in the silicate portion of the Earth is a consequence of metal separation during core formation. Thermodynamic expressions used to constrain the metal-silicate partitioning behavior of siderophile elements are mainly established from large volume press experiments that do not cover the full range of potential P-T conditions for core-mantle equilibrium. Using the laser-heated diamond anvil cell technique, we have extended metal-silicate partitioning measurements to 75 GPa and 4400 K, exceeding the liquidus temperatures for both metal and silicate and, therefore, achieving thermodynamic conditions directly equivalent to the full range of P-T conditions relevant to metal-silicate equilibration at the base of a deep magma ocean. Partitioning results obtained for siderophile elements (Ni, Co, V, Cr, Mn, Nb) and light elements (Si, O) are used to constrain a mechanism for terrestrial accretion and core formation reconciling the observed mantle concentrations of V, Cr and geophysical constraints on light elements in the core. The experiments were performed in the P-T ranges of 35-74 GPa and 3100-4400 K. The metal-silicate partition coefficients for nickel and cobalt decrease with increasing pressure and reach the values required to yield present mantle concentrations at ~50 GPa [1]. Enhanced solubility of oxygen in the metal perturbs the metal-silicate partitioning of V and Cr, precluding extrapolation of previous results (Siebert *et al.* 2013). We will present new continuous core formation models for different redox paths showing that terrestrial accretion under highly reduced conditions as proposed by most core formation models [3, 4] could be reconsidered.

[1] Siebert *et al.* (2012) *EPSL* **321-322**, 189-197. [2] Siebert *et al.* (2013) *Science* **339**, 1194-1197. [3] Wood *et al.* (2006) *Nature* **441**, 825-833. [4] Rubie *et al.* (2011) *EPSL* **301**, 31-42.

Heat producing element enrichment in granitic rocks & zircon Hf isotopic constraints on crustal evolution in NE Queensland, Australia

C.SIEGEL^{1,3*}, S.E. BRYAN^{1,3}, C.M. ALLEN¹, D.J. PURDY²
AND D.A. GUST¹

¹EEBS, Queensland University of Technology, Australia
(*correspondence:c.siegel@qut.edu.au)

²Geological Survey of Queensland, Australia

³QGECE, The University of Queensland, Australia

The primary processes causing enrichment of incompatible Heat Producing Elements (HPE; U, Th & K) in granitic rocks are still poorly understood and are topical in light of increasing interest in engineered geothermal systems. Differentiation of the continental crust, through successive events of granitic magmatism, is expected to lead to a HPE-enriched upper crust and a depleted lower crust. In such a closed system crust model, younger granitic rocks should be more isotopically evolved. Instead, our study of granitic rocks, emplaced within a relatively restricted area (~200x100km), reveals a paradox: isotopic systems become more primitive over time, but HPE concentrations are more elevated. The study area has had ~360 Myr history of granitic magmatism with mainly I- to minor A-type granitic rocks of Carboniferous, Permian, Triassic, Cretaceous & Tertiary age.

Long-term compositional trends are recognised: modal mineralogy and bulk-rock composition record enrichment of K-feldspar and the increase of HPE concentration from the Permo-Carboniferous to the Cretaceous. In contrast, new MC-ICP-MS zircon Hf isotope data indicate secular changes to bulk crustal source compositions. Triassic (ϵHf : +4.9 to +8.5) and Cretaceous (ϵHf : +8.3 to +10.8) zircons are generally more isotopically primitive compared to Permo-Carboniferous (ϵHf : -7.3 to +1.2 & +3.6 to +9.8) and Tertiary (ϵHf : +0.5 to +5.1) zircons. The restriction of more isotopically primitive zircons in Triassic and Cretaceous rocks does not favor the model of a simple differentiated crust but rather an open crust system and progressive basification of the lower crust. Paradoxically, the isotopically primitive Mesozoic intrusions are also the most compositionally evolved, and have the highest HPE enrichments. To explain this, we interpret that fluid fluxing associated with a subduction-related contractional event in the Late Permian-Triassic was important for fertilising the lower crust and enriching it in HPE. This overcame the effects of basification by underplating during earlier back-arc extensional events. Cretaceous-Tertiary intraplate igneous events then provided important catalysts for more typical crustal differentiation.

Hydraulic and geochemical survey of the lithium-resources in the Salar de Uyuni (Bolivia)

ROBERT SIELAND*, NADJA SCHMIDT
AND BRODER MERKEL

TU Bergakademie Freiberg, Department of Hydrogeology, D-09599 Freiberg, Germany

(*correspondence: Robert.Sieland@geo.tu-freiberg.de,
Nadja.Schmidt@geo.tu-freiberg.de,
Broder.Merkel@geo.tu-freiberg.de)

The Salar de Uyuni, located in the southern Altiplano of the Bolivian Andes, is the largest salt flat in the world (10,000 km², 3,653 m a.s.l.). Its alternating sequence of salt, mainly composed of halite, and lacustrine sediments contain a brine which is highly enriched in lithium (up to 4.7 g/L) among other elements [1]. Moreover, it is considered to be the largest lithium-brine deposit in the world.

Between 2009 and 2012 exploration drillings which completely penetrate the upper salt layer (with a maximum thickness of 11 m) as well as brine sampling were conducted at various sites on the salt flat. Porosity measurement of salt cores was realized gravimetrically on dried (70°C, until $\Delta_{\text{weight loss}} < 1\%$) core samples. Additionally, X-ray tomography on selected core samples was used to verify porosity results. Geochemical analyses on brine samples were conducted using ICP-MS.

Porosity data showed large horizontal differences of the salt crust. While the uppermost two meters of the salt are characterized by total porosities between 25 and 40%, deeper parts of the salt crust showed significantly lower porosities between 5 and 18%. Chemical analyses revealed an inhomogeneous distribution pattern for different elements. Among others, highest lithium concentrations were found close to the main tributary in the south as well as in a small fringe in the north of the salt flat.

Using stratigraphic information from drill cores, porosity data as well as the distribution pattern of lithium concentrations in the brine, a conceptual model was developed in order to estimate the total volume of brine occurring in the salt flat as well as the lithium-resource. The total amount of lithium in the Salar de Uyuni is estimated to around 6.6 million tons. This is in contradiction to previous publications [1, 2] which assume the lithium-resources to be about 35% higher.

[1] F. Risacher, B. Fritz (1991) *Chemical Geology* **90**: 211-231 [2] USGS (2012) *Mineral Commodity Summaries 2012*, p. 94-95

Ca, Mo and U isotopes suggest Neoproterozoic-like ocean conditions during the Late Permian Mass Extinction

SILVA-TAMAYO, J.C.¹, PAYNE, J.L.¹, WIGNALL P.B.²,
 NEWTON R.J.², NEUBERT, N.⁴, BRUESKE, A.⁴,
 EISENHAUER A.³, WEYER, S.⁴, FIETZKE, J.³
 AND MAHER, K.¹.

¹Stanford University. cuore@stanford.edu,
 jlpayne@stanford.edu, kmaher@stanford.edu

²University of Leeds. P.B.wignall@leed.ac.uk,
 R.B.newton@leeds.ac.edu

³Helmholtz Center for Ocean Research Kiel
 aeisenhauer@geomar.de, fietzke@geomar.de

⁴Leibniz Universitat Hannover. s.weyer@mineralogie.uni-hannover.de, n.neubert@mineralogie.uni-hannover.de

The most catastrophic extinction event in the history of animal life occurred at the end of the Permian Period, ca. 252 Mya. Ocean acidification and global oceanic euxinia have each been proposed as causes of this biotic crisis, but the magnitude and timing of change in global ocean chemistry remains poorly constrained.

Here we use Ca, Mo and U isotopes applied to globally distributed, well dated late Permian- early Triassic sedimentary sections to better constrain the magnitude and timing of change in ocean chemistry through this interval. All the investigated carbonate successions (Turkey, Italy and China) exhibit decreasing $\delta^{44/40}\text{Ca}$ compositions, paralleling a major decrease in $\delta^{13}\text{C}$ values. These findings support an episode of ocean acidification coincident with the major biotic crisis. The Mo and U isotope records exhibit significant rapid negative anomalies at the onset of the main extinction interval, suggesting rapid expansion of anoxic and euxinic marine bottom waters during the extinction interval. The rapidity of the isotope excursions in Mo and U suggests substantially reduced residence times of these elements in seawater relative to the modern, consistent with expectations for a time of widespread anoxia. The large C-isotope variability during the early Triassic, which is similar to that of the early-middle Cambrian, suggests imply largely biogenetically controlled perturbations of the oceanic carbon cycle. These findings strengthen the evidence for a global ocean acidification event coupled with rapid expansion of anoxic zones as drivers of end-Permian extinction in the oceans.

Shiveluch volcano: Mineralogical records of geodynamic complexity

SIMAKIN A.^{1,2*}, SALOVA T.², GORDEYCHIK B.²
 AND CHYURIKOVA T.³

¹Institute Physics Earth, Moscow Russia, simakin@ifz.ru

²Institute Experim. Mineral., Chernogolovka, Russia

³Inst. Volcanol. Seism., Petropavlovsk-Kamchatskii, Russia

Shiveluch is the most north active andesite volcano on Kamchatka. Several types of magmas mix and interact in Shiveluch magmatic system. There are only two centres of the basaltic eruptions on Shiveluch. Olivine-plagioclase basalts form dyke complex of the NW orientation on the northern edge of caldera. Second centre was found recently on the western slope of volcano. Complex structure of the magma localization in the thick crust of Northern Kamchatka is revealed by the seismic tomography (Lees *et al.*, 2007). Contrasted low Vp zones are traced at the depths 5-7, 13-17, 25-30 km with horizontal dimensions up to 100 km larger than typical intervolcano distances. Results of the magmatic amphibole barometry (new barometer-Simakin *et al.*, 2012a) also clustered around three observed geophysically levels. Detailed mineralogical study of two types of Shiveluch basalts demonstrates heterogeneity of the whole rock and even individual crystals. Oxygen fugacity estimates with clinopyroxene geo-oxobarometer (Simakin *et al.*, 2012b) yield bi-modal distributions with $f\text{O}_2$ around NNO+1(0.5) and NNO+1.6(2.5). Second maximum is close to the high $f\text{O}_2$ estimates (c.a. NNO+2) typical for the high pressure (up to 10-11 kbar) amphiboles.

Compositions of Holocene volcanites around Shiveluch on SiO_2 -Ba diagram are separated into several evolutionary series with different initial Ba content. The upper SiO_2 -Ba set (Sedanka volcanic centre with several Shiveluch compositions) on the Th/Yb – Nb/Yb diagram adjoins decompressional mantle partial melts array. These magmas presumably originate at the mantle upgoing flow near the subducting plate edge. Low Ba basalts (Baidarnaya centre) belong to the Bezymianny-Klyuchevskoy volcanoes compositions set forming on the Nb/Yb – Th/Yb diagram vertical array between normal IAB and N-MORB compositions. Effective melting of the underplated thick continental crust near the Moho depth produces oxidized siliceous amphibole-bearing magmas of adacite affinities. These three components mix and undergo crystallization differentiation before being erupted on Shiveluch.

[1] Lees *et al.*, Geoph. Monograph Series 172, 2007. [2] Simakin A. *et al.*, Earth Science Res., 1(2), 2012a. [3] Simakin A. *et al.*, Petrology, 20(7), 2012b.

Ni sorption at the Particle Edges of Synthetic and Biogenic Birnessite

ANNA A. SIMANOVA^{1*}, SHARON E. BONE², JOHN R. BARGAR³, GARRISON SPOSITO² AND JASQUELIN PEÑA¹

¹University of Lausanne, Switzerland, (*correspondence: anna.simanova@unil.ch, jasquelin.pena@unil.ch)

²Lawrence Berkeley National Laboratory, Berkeley, USA sbone@lbl.gov, gsposito@berkeley.edu

³Stanford Synchrotron Radiation Lightsource, Menlo Park, USA, bargar@slac.stanford.edu

Biogenically produced manganese oxides play an important role in trace metal scavenging in the environment. The metal sorption capacity of the Mn oxides arises mainly from the presence of negatively charged Mn(IV) vacancy sites in the MnO₂ sheets. For example, recent extended X-ray absorption fine structure (EXAFS) studies showed that Ni binds to vacancy sites in biogenic Mn oxides via two preferential coordination geometries: as a triple-corner-sharing complex (Ni-TCS) at circumneutral pH and a mixture of Ni-TCS and Ni incorporated into the MnO₂ sheet at higher pH [1,2]. However, under-coordinated oxygen atoms at particle edges offer additional sites for metal coordination. Metal sorption by particle edges has been reported for chemically synthesized birnessites, but is poorly understood for biogenic minerals where the admixing of organic and mineral functional groups in these microbe-mineral assemblages may modify the reactivity at the particle edges.

In this work, we used δ -MnO₂ as a synthetic analog of biogenic birnessite to study the reactivity of the birnessite edge since it has fewer vacancies and contains no biomass. We studied adsorption of Ni at the surface of δ -MnO₂ as a function of pH and surface loadings using a combination of wet chemistry methods and Ni K-edge EXAFS spectroscopy and compared these data to Ni adsorption at the surface of the biogenic birnessite produced by *Pseudomonas putida* strain GB-1 [1]. At pH 8 the surface speciation and reactivity of δ -MnO₂ was similar to biogenic birnessite, while at lower pH values we detected an additional surface species that likely formed at the particle edges of δ -MnO₂. The absence of this species in biogenic birnessite suggests that the bacterial cells and extracellular substances decrease the reactivity of the the particle edges of biogenic MnO₂.

[1] Pena, J., Kwon, K. D., Refson, K., Bargar, J. R., Sposito, G. (2010) *Geochim. Cosmochim. Acta* 74, 3076-3089. [2] Pena J., Bargar J.R., Sposito G. (2011) *Environ. Sci. Technol.* 45, 7338-7344.

Lithium in HED meteorites – Implications for planetary crusts

M.ŠIMČÍKOVÁ¹, T. MAGNA¹ AND F. MOYNIER²

¹Czech Geological Survey, Klárov 3, CZ-11821 Prague, Czech Republic; tomas.magna@geology.cz

²Dept. Earth Planetary Sciences, Washington University, St. Louis, MO 63130, USA

The Li contents and isotope compositions are presented for a suite of howardites, eucrites and diogenites (HEDs) thought to originate from asteroid Vesta. The Li contents show notable differences between Li-poor diogenites and Li-rich eucrites whereas howardites have moderate Li contents. Contrary to elemental differences, Li isotope compositions are irresolvable among the individual groups of HEDs, attesting to insignificant Li isotope fractionation during formation of thick basaltic crust by melting of Vesta's mantle.

Several observations are derived. (i) All HEDs span an extremely narrow $\delta^7\text{Li}$ range (2.2–4.9‰), except for LAP 03569 and Cachari. This asteroidal homogeneity is surprising provided that Vesta experienced core segregation, magma ocean and solidification, and thermal metamorphism some of which could fractionate Li isotopes. The derived bulk mean $\delta^7\text{Li}$ of Vesta is $3.7 \pm 1.1\text{‰}$ (2σ) which is within the range of the mean $\delta^7\text{Li}$ values derived for the Earth ($\sim 3.3\text{‰}$), Mars ($\sim 4.0\text{‰}$) and the Moon ($\sim 4.1\text{‰}$). (ii) Ordinary chondrites, considered to represent the bulk composition of Vesta, are on average isotopically $\sim 1\text{‰}$ lighter than HEDs while $\delta^7\text{Li}$ values of carbonaceous chondrites fall within the range of HEDs. (iii) Oxygen isotopes in Pasamonte hint to its origin from another parent body than the other HEDs. However, proximity of its $\delta^7\text{Li}$ provides strong evidence for rapid magmatic evolution and basaltic crust differentiation on other bodies akin to Vesta. This implies the existence of planetary embryos in the infancy of the Solar System that were large enough to sustain large-scale magmatism and yet preserving Li isotope compositions intact during their ephemeral magmatic histories. (iv) Unlike Fe isotopes, $\delta^7\text{Li}$ of Stannern-trend eucrites do not differ from the main group eucrites implying no particular Li isotope difference of residual enriched melts that were involved in their genesis. (v) No elemental Li depletion is recorded in HEDs relative to chondrites which is contrary to other volatile elements such as Zn or Cd that experienced massive loss. This suggests effective retaining of Li in Vesta despite its later impact history which is compatible with moderately volatile behavior of Li at high temperatures and/or during planetary melting. Thus, the lack of evolved crustal rocks and prevalence of 'juvenile' basaltic lavas at asteroidal levels may be discerned with Li.

The importance of iron mobility in magmatic-hydrothermal systems

ADAM SIMON^{1*}, LAURA BILENKER¹ AND AARON BELL²

¹Earth & Environmental Sciences, University of Michigan
[*simonac@umich.edu]

²Institute of Meteoritics, University of New Mexico

Iron is a ubiquitous component of arc-related magmas and porphyry-, high-sulfidation, iron-oxide-copper-gold (IOCG), and iron-oxide-apatite (IOA) ore deposits. Iron is present as an essential structural constituent in ferromagnesian silicate minerals, magnetite, sulfide crystals, and sulfide liquids, as well as aqueous fluids that exsolve from silicate melt. The observation that the oxidation state for different arc magma systems varies over approximately five orders of magnitude, from approximately one log unit below the FMQ (fayalite-magnetite-quartz) buffer to the HM (hematite-magnetite) buffer, indicates that iron exists in both ferrous and ferric forms in most arc magmas. The valence of iron is proportionally dominated by Fe²⁺ in most common ferromagnesian silicate minerals, is 2/3 Fe³⁺ and 1/3 Fe²⁺ in magnetite, is Fe²⁺ in sulfides, and is Fe²⁺ in Cl-bearing aqueous fluid. Interestingly, there does not appear to be a sliding scale for the oxidation state of iron in aqueous fluids, in contrast to silicate liquids. The observation that aqueous fluids contain only a single valence state of Fe across five orders of magnitude of fO₂ space is fundamentally different than sulfur, which exists as both H₂S and SO₂ in aqueous fluid and the relative proportion of each is dictated by the fO₂ of the system. These observations have critical implications for magmatic systems.

We continue to investigate experimentally the importance of the mass transfer of iron from melt to aqueous fluid, and the many reactions among aqueous fluid, silicate melt, magnetite, and sulfide phases. Our data confirm field-based hypotheses that the transfer of iron from melt to aqueous fluid increases the ratio of Fe³⁺ / Fe²⁺ in the degassed melt. This has implications for the composition of ferromagnesian silicates and the stability of sulfide phases during degassing. The mass transfer of iron affects the oxidation state of sulfur in the melt, driving sulfur from sulfide to sulfate, which in turn has implications for the mass transfer of ore metals (Cu, Au) from melt to aqueous fluid. This also may affect the fractionation of iron isotopes, and their ability to serve as geochemical fingerprints for source reservoirs of iron in IOCG and IOA deposits. We will present new data and discuss the incredible role that iron plays in moderating phase equilibria of silicate magmas, and the potential use of iron isotopes to assess the evolving oxidation state and source reservoir characteristics of arc magmas.

Insight to the local melt structures and their influence on the fractionation of rare earth elements (La, Gd, Yb, Y)

S.SIMON^{1*}, M. WILKE¹, S. KLEMME², W. A. CALIEBE³, R. CHERNIKOV³ AND K. O. KVASHNINA⁴

¹GFZ, German Research Centre For Geosciences, Potsdam, Germany (*correspondence: ssimon@gfz-potsdam.de)

²Westfälische Wilhelms-Universität, Münster, Germany

³Deutsches Elektronen-Synchrotron, Hamburg, Germany

⁴European Synchrotron Radiation Facility, Grenoble, France

Knowledge of the local structure around rare earth elements (REE) in aluminosilicate melts is of great interest for the geochemistry of magmatic processes, particularly for understanding the partitioning of REE between melt and the coexisting crystals in a more comprehensive way. Several studies already proposed a significant influence of the melt composition on REE fractionation [1 – 4]. In a fundamental study Ponader & Brown [5] showed that the local environment around La, Gd and Yb changes with polymerization of the melt, this was used to explain differences in element partitioning. However, no direct correlation between partitioning data and structural informations was provided.

In this study, melt compositions taken from Prowatke & Klemme [4] and various haplogranitic, -basaltic compositions were doped with La, Gd, Yb or Y and synthesized as glass. EXAFS was used to gather quantitative information on the local environment of Gd, Yb and Y and XANES for qualitative information on the local environment of La in the glasses. Additional high temperature (HT) in situ Y-EXAFS was performed to prove, if the local structure of Y above T_G corresponds to the local structure in the quenched melts. Analysis of the EXAFS data shows that the average bond length, the width and skewness of the REE-O pair distribution function increase with increasing polymerization of the melt for Gd, Yb and Y [6]. XANES spectra confirm a similar trend for La. The HT Y-EXAFS shows no significant change of the local structure above T_G. Finally, correlations of structural parameters and partitioning data from Prowatke & Klemme [4] were obtained.

[1] Blundy & Wood (2003) *Earth Planet. Sci. Lett.* **210**, 383-397. [2] Watson (1976) *Contrib. Mineral. Petrol.* **56**, 119-134. [3] Ryerson & Hess (1978) *Geochim. Cosmochim. Acta* **42**, 921-932. [4] Prowatke & Klemme (2005) *Geochim. Cosmochim. Acta* **69**, 695-709. [5] Ponader & Brown (1989) *Geochim. Cosmochim. Acta* **53**, 2893-2903. [6] Simon et. al. (2012) *Chem. Geol.*, **in press**.

Oxygen isotope fractionation in formation of CO₂

D. SIMONE^{1*}, L.M.T. JOELSSON^{2*}, C. JANSSEN¹
AND M.S. JOHNSON²

¹LPMAA, UMR 7092 UPMC/CNRS, Paris, France
[daniela.simone@etu.upmc.fr]

²Department of Chemistry, University of Copenhagen,
Denmark [joelsson@chem.ku.dk]

*DS and LMTJ contributed equally to the work.

The discovery of mass independent isotope fractionation (MIF) of oxygen isotopes [1] opened a new dimension in environmental research. Much subsequent research has focused on isotope effects in ozone formation [2,3]. Despite the apparent similarity to formation of ozone, relatively little attention has been given to the possibility of MIF in the formation of CO₂ through the reaction CO + O(³P) + M → CO₂ + M [4]. A better understanding of the isotope fractionation in CO₂ may give insights into mechanisms of MIF.

The photochemical reactor at the Copenhagen Centre of Atmospheric Research [5] was used to study the reaction CO + O(³P) + M → CO₂ + M experimentally. O(³P) radicals were obtained from photolysis of O₃ in the visible region. The use of ordinary commercial LED lamps ensured that no O(¹D) and subsequently no OH was formed. An enriched sample of CO (90% ¹³C¹⁶O, 10% ¹³C¹⁸O, trace amounts of ¹³C¹⁷O) was used to distinguish the reaction of interest from possible fluctuations in the background concentrations of ¹²CO and ¹²CO₂ in the reactor. Infrared spectra were recorded with a Bruker IFS 66v/s Fourier Transform Infrared spectrometer. The spectra were analysed using the non-linear least squares algorithm MALT [6]. Experiments were conducted at pressures ranging from 200 to 980 mbar and the isotope chemical kinetics has been modelled using the chemical kinetics software package KPP [7]. Isotope effects were calculated as:

$\alpha_n = \frac{\ln([C^nO]_{t=0}/[C^nO](t))}{\ln([C^{16}O]_{t=0}/[C^{16}O](t))}$. We present first results, which show unusual ratios of ($\alpha_{17}-1$)/($\alpha_{18}-1$). However, as in earlier experiments [4], unambiguous assignment of this MIF is complicated by the presence of side reactions.

[1] Clayton *et al.* (1973), *Science*, 182, 485-488. [2] Brenninkmeijer *et al.*, *Chem. Rev.*, 103(12). [3] Thiemens (2006), *Annu. Rev. Earth Planet. Sci.* **34** 217-62. [4] Pandey and Bhattacharya (2006), *J. Chem. Phys.* 124 234301. [5] Nilsson *et al.* (2009), *Atmos. Environ.* 43 3029-3033. [6] Griffith (1996), *Appl. Spectrosc.* 50 59-70. [7] V. Damian *et al.*: *Comp. Chem. Eng.*, 26, 1567-79, 2002

Estimating uncertainties in base cation weathering rates according to mass balance

MAGNUS SIMONSSON^{1*}, JOHAN BERGHOLM²,
BENGT OLSSON² AND INGRID ÖBORN³

¹Dep. of Soil and Environment, Swedish University of Agricultural Sciences (SLU), P.O. Box 7014, S-750 07 Uppsala, Sweden (*correspondence: magnus.simonsson@slu.se)

²Dep. of Ecology, SLU, Uppsala

³World Agroforestry Centre, Nairobi, Kenya

Because forestry is often allocated to soils with low weathering capacity, intensive harvesting practices may deteriorate plant nutrition. Reliable estimates of weathering rates are therefore crucial in analyses of sustainability of, e.g., whole-tree and stump harvesting. By the mass balance approach present base cation cycling may be estimated from data on leaching, deposition, and accumulation in biomass and soil. Insight in the uncertainties in the weathering estimates is crucial for the interpretation of the data.

Weathering rate of:	Ca	Mg	K	Na
	(kg ha ⁻¹ yr ⁻¹)			
Average	4.0	1.4	3.3	-3.3
Conf. int.	±3.8	±1.6	±4.4	±15

Table 1: Average weathering rates and approximate confidence intervals (ca 95% level) based on spatial variability and uncertainties in allometric functions etc.

Term in balance	Ca	Mg	K	Na
Deposition	8%	43%	2%	26%
ΔK_{exch}	3%	5%	1%	0%
Leaching	4%	28%	0.4%	74%
Biomass accumul	86%	25%	97%	0%

Table 2: Contributions to overall uncertainty in weathering rates according to soil balance.

The present study was carried out in a Norway spruce (*Picea abies* Karst. (L.)) stand on a podzolic soil in SW Sweden. The results pinpoint the difficulty in assessing low weathering rates in general (Table 1), and demonstrates that the influence of the different terms of the balance varies considerably among the different base cations (Table 2). Details of the uncertainty contributions in the different terms of the balance is shown on a poster with the same title.

Assessment and geochemical evolution of springs at Hazaribagh District, Jharkhand, India

HEMANT K SINGH¹, D. CHANDRASEKHARAM², TRUPTI G.³ AND B. SINGH^{4,5,6}

¹Department of Earth Sciences, IIT Bombay, Mumbai, India-400076 and (*correspondence: hemantksingh25@gmail.com)

²Department of Earth Sciences, IIT Bombay, Mumbai, India-400076 (dchandra@iitb.ac.in)

³Department of Earth Sciences, IIT Bombay, Mumbai, India-400076 (trupti@iitb.ac.in)

⁴Department of Earth Sciences, IIT Bombay, Mumbai, India-400076 (banambar.iitb@gmail.com)

⁵IITB-Monash Research Academy, IIT Bombay, Mumbai, India-400076

⁶Civil Engineering Department, Monash University, Clayton, Melbourne, Australia, 3800

Group of thermal and cold springs in Hazaribagh District, Jharkhand with temperatures from 32 to 90 °C and 25 to 27 °C respectively. Three thermal springs and two cold springs are located at Surajkund area, and one thermal spring in Katkamshandi village 15 km from the main town. These springs are located in the Archean Chotanagpur Gneissic Complex (CGC) in the eastern part of Peninsular India. pH of the thermal water ranges from 8.3 to 9, which indicates the springs are alkaline in nature. The water types of thermal springs and cold spring are Na-Cl-SO₄ type. Piper diagram suggests that the geothermal waters circulating through the granitic host rocks have their chemistry compatible with that of the host rock. Since the HCO₃ to Cl ratio is less than one suggest that thermal water is believed to be fast ascending without any major mixing with near surface groundwater but for mild to moderate dilution with groundwater. However anion variation shows sifting toward the SO₄ field suggesting addition of SO₄ from ancient volcanic rocks of the region (Rajmahal volcanics). Mineral saturation index suggest that thermal water is saturated with silica. Two thermal springs of Surajkund area having similar Na/K ratios indicates that they are fed by the same reservoir. Estimated reservoir temperature based on chemical geothermometers is in the range of 150 to 210 °C.

Dissolved barium distribution and cycling in the Bay of Bengal

SATINDER PAL SINGH^{1*} AND SUNIL KUMAR SINGH²

¹Physical Research Laboartory, Ahmedabad, India, satinder@prl.res.in (* presenting author)

²Physical Research Laboartory, Ahmedabad, India, sunil@prl.res.in

Eight depth profiles of dissolved barium concentrations have been measured in the Bay of Bengal (BoB) along the 87°E transect (~6°N to ~21°N) to track the dispersion of its large influx from the Ganga–Brahmaputra (G–B) river system and the outflow to the equatorial Indian Ocean. A typical Ba concentration–depth profile shows relatively higher Ba concentrations in surface waters (depth ≤5 m) followed by a minimum in the depth interval ~50–150 m and a further increase with depth. The Ba data in the upper layers (depth <100 m), excluding a very high Ba ~112.8 nmol/kg at salinity 24.5 near mouth of the Hooghly estuary, show a North–South trend with a strong and significant inverse correlation with salinity ($R^2 = 0.75$; $P < 0.0001$). This indicates the southward flow of dissolved Ba from the G–B river system that also includes its contributions by particle release and SGD. The subsurface Ba minimum is ubiquitous and most probably is a result of Ba uptake on settling particulates. On the other hand, the Ba concentrations in deep waters (depth ≥500 m) is controlled dominantly by water mixing as suggested by a very strong and significant inverse correlation with salinity ($R^2 > 0.95$; $P < 0.0001$). Exceptions to this conservative behavior are the “hot-spots” of dissolved Ba in bottom waters, which are resulted by the dissolution of sediments at and/or below the sediment–water interface.

Attempts were made to budget the Ba abundance in the Bay of Bengal using a two box model approach, surface (top ~100 m) and deep waters (below ~100 m). Under the steady state the annual Ba influx from the Ganga–Brahmaputra river system seems to be balanced through its removal via sinking particulates as a result there is no lateral outflow of dissolved Ba from the G–B to the equatorial Indian Ocean through top ~100 m of the BoB. Most of this sinking particulate Ba (~95 %) is regenerated again in the lower box, preferentially in the intermediate waters ~100–500 m.

Diffusion-driven isotopic fractionations in olivine in laboratory and natural settings

C.K. SIO¹, M. ROSKOSZ², M. CHAUSSIDON³,
N. DAUPHAS¹, R. MENDYBAEV¹, F. RICHTER¹,
AND F.-Z. TENG⁴

¹The University of Chicago, (ksio@uchicago.edu)

²Université de Lille 1, France

³CNRS-CRPG, Nancy, France

⁴University of Washington

Our previous *in situ* measurements of a zoned olivine from Kilauea Iki lava lake revealed large and negatively-coupled Mg-Fe isotopic fractionations [1]. We estimated the relative diffusivities of the isotopes of Mg and Fe in olivine, scaled as $D_1/D_2 = (m_2/m_1)^\beta$, with $\beta_{Fe} \sim 0.25$ and $\beta_{Mg} \sim 0.15$ for an olivine zoned from Fo₈₀ to Fo_{83.6}.

Olivine diffusion experiments were run with the goal to quantify β -values and to compare them with the values estimated from the natural sample. In each experiment, crystallographically oriented Fo₁₀₀ (synthetic) and Fo₀ (Rockport fayalite) crystals were placed in an alumina crucible, held together by gravity, and the rest of the crucible was hand-packed with FeO powder. A total of six crucibles were placed together in the hot spot of a gas-flowing furnace at the Université de Lille 1. Each pair of crucibles were quenched at a time by moving them to a cold spot in the furnace after 10 and 20 days; all crucibles were taken out of the furnace after 30 days. Contacts were made across some Fo₁₀₀-Fo₀ and all Fo₁₀₀-FeO interfaces. The Fo₁₀₀-Fo₀ profiles were fitted using the diffusion equation of [2], while that of Fo₁₀₀-FeO required slower diffusion coefficients.

The longest profile (Fo₁₀₀-Fo₀, 30 days, diffusion along c-axis) was analyzed for its Mg isotopic compositions using SIMS (IMS 1280) at CRPG, Nancy. Matrix standards (Fo# 6, 16, 64, 76, 79, 85, 90, and 95) were previously measured by solution for their $\delta^{26}Mg$, and were used to monitor matrix effects. We find that matrix correction is critical in obtaining accurate β -values and that more matrix standards may be required. Our preliminary data shows > 10% fractionation in $\delta^{26}Mg$, which suggests a β_{Mg} of about 0.1 or less in olivine.

We are currently analyzing more experimental samples and investigating the cause of the apparent discrepancy of the β -value.

[1] C.K. Sio *et al.*, GCA, (in revision). [2] R. Dohmen and S. Chakraborty, (2007). Phys Chem Min. 34, 597-598.

Experimental study of the system Mg₄Si₄O₁₂-Mg₃Cr₂Si₃O₁₂ at 12-25 GPa and 1600 °C

E. A. SIROTKINA^{1*}, A.V. BOBROV¹, L. BINDI²,
AND T. IRIFUNE³

¹Moscow State University, Russia (*correspondence: katty.ea@mail.ru, archi3@yandex.ru)

²University of Florence, Italy (luca.bindi@unifi.it)

³Ehime University, Japan (irifune@dpc.ehime-u.ac.jp)

Pyrope-rich garnets of the ultrabasic paragenesis widely abundant as inclusions in diamonds are characterized by significant admixture of the knorringite, Mg₃Cr₂Si₃O₁₂, end-member. Such garnets often contain majoritic component, (Ca,Fe,Mg)SiO₃, which is an indicator of the sub-lithospheric mantle conditions. Although both components are important for barometry of mantle mineral associations, high-pressure phase relations in the system MgSiO₃-Mg₃Cr₂Si₃O₁₂ have been not studied yet. In this study we report the first results of experiments on the majorite-knorringite join at 12–25 GPa and 1600 °C aimed on investigation of conditions of the formation, structural peculiarities, and evolution of the composition of Cr-bearing majoritic garnets.

We investigated the full range of starting compositions with steps of 10–20 mol% and 2–3 GPa in multi-anvil experiments, which allowed us to plot the preliminary phase diagram for the system MgSiO₃-Mg₃Cr₂Si₃O₁₂ and synthesize garnets of a wide compositional range. The phase assemblages for majorite-rich starting materials (<30 mol % knorringite) include garnet, enstatite, and eskolaite (Cr₂O₃). With the increase of knorringite content in the starting composition, garnet + eskolaite association is formed. Typically synthetic garnets contain significant portion of majorite (>15 mol %) even for pure Mg₃Cr₂Si₃O₁₂ starting composition. The stability of garnet on the phase diagram is limited by pressure: MgSiO₃ ilmenite containing up to 7 wt% Cr₂O₃ appears together with eskolaite at $P > 20$ GPa. Single-crystal X-ray diffraction studies carried out on the produced garnets demonstrated their cubic symmetry in the studied compositional range and allowed us to study structural peculiarities of garnets. The lattice parameter of garnet (in parentheses) linearly increases with increasing the Mg₃Cr₂Si₃O₁₂ component: 11.4725(4) Å (Mg_{3.88}Cr_{0.24}Si_{3.88}O₁₂), 11.5187(6) Å (Mg_{3.58}Cr_{0.84}Si_{3.58}O₁₂), 11.5445(5) Å (Mg_{3.38}Cr_{1.24}Si_{3.38}O₁₂), and 11.5718(1) Å (Mg_{3.21}Cr_{1.58}Si_{3.21}O₁₂).

Characterization of indigenous oil field microorganisms for microbially enhanced oil recovery (MEOR)

J. SITTE¹, E. BIEGEL², A. HEROLD², H. ALKAN³
AND M. KRÜGER¹

¹BGR, Geomicrobiologie, D-30655 Hannover

²BASF SE, GVF/H, D-67056 Ludwigshafen

³Wintershall Holding GmbH, R&D, D-34119 Kassel

Microbial activities and their resulting metabolites became a focus of attention for enhanced oil recovery (MEOR, microbial enhanced oil recovery) in the recent years. In order to develop a strategy for a MEOR application in a German oil field operated by Wintershall experiments were performed to investigate different sampling strategies and the microbial communities found in these samples. The objectives of this study were (1) to characterize the indigenous microbial communities, (2) to investigate the dependency of microbial activity/diversity on the different sampling strategies, and (3) to study the influence of the *in situ* pressure on bacterial growth and metabolite production. Fluids were sampled at the well head (surface) and *in situ* in approx. 785 m depth to collect uncontaminated production water directly from the reservoir horizon and under the *in situ* pressure of 31 bar (subsurface). In the lab the pressure was either released quickly or slowly to assess the sensitivity of microorganisms to rapid pressure changes. Quantitative PCR resulted in higher microbial cell numbers in the subsurface than in the surface sample. Biogenic CO₂ and CH₄ formation rates were determined under atmospheric and high pressure conditions in the original fluids, with highest rates found in the surface fluid. Interestingly, no methane was formed in the native fluid samples. While nitrate reduction was exclusively detected in the surface samples, sulfide formation also occurred in the subsurface fluids. Increased CO₂ formation was measured after addition of a variety of substrates in the surface fluids, while only fructose and glucose showed a stimulating effect on CO₂ production for the subsurface sample. Stable enrichment cultures were obtained in complex medium inoculated with the subsurface fluid, both under atmospheric and *in situ* pressure. Growth experiments with constant or changing pressure, and subsequent DGGE analysis of bacterial 16S rRNA genes, revealed that the pressure treatment did not affect the bacterial community composition. Our results show that bacteria in the enrichment culture can tolerate pressure changes between atmospheric and *in situ* reservoir pressure, which makes them promising candidates for further MEOR tests. Since substantial differences in microbial activities were observed between the surface and subsurface fluids, the selection of the sampling strategy should also be considered for MEOR research and industrial application.

Uranium accumulation by plants covering piles and dumps in uranium post-mining area in SW Poland

A. SKŁODOWSKA^{1*}, D. LECH² AND D. RUSZKOWSKI¹

¹Faculty of Biology, University of Warsaw, Miecznikowa 1, 02-096 Warsaw, Poland; (*correspondence: asklodowska@biol.uw.edu.pl)

²Polish Geological Institute, 4, Rakowiecka Street, 00-975 Warsaw, Poland (dariusz.lech@pgi.gov.pl)

The uranium exploration and exploitation in the South-West Poland (Lower Silesia District) had been carried out since 1925 when the first 9 Mg of uranium ore were mined from which 690 mg of radium was extracted and the mining ceased in 1962 (total amount of 704 Mg of U was derived). Nevertheless the old subsurface mines, piles and dumps are still involved in the geochemical cycle of the area. Leaching of uranium and radionuclides may be a serious environmental problem in many countries.

Investigations of the influence of mining activity on the natural environment revealed the local-scale radioactive contamination limited to the dumps and their nearest vicinity at four localities: Kowary-Podgorze, Radoniów, Kopaniec/Kromnow and Grzmiaca. Standard ecological test "MARA" performed on 54 samples of wastes and water taken in 15 localities showed moderate toxicity in 5 waste samples and 1 water sample. Another standard test MicroTox showed minor toxicity in 2 waste samples and did not show ecotoxicity of any water sample.

Accumulation of uranium by plants covering the surface of 5 piles containing the most radioactive wastes (dose 1.94-97 μSv/h) was examined. Grasses were found as hyper-accumulator of uranium in all examined places. Maximum uranium concentration 817.15 mg/kg d.w. was noted in the roots of fescue (*Festuca* sp.) growing in Kopaniec pile and 178.85 mg/kg d.w. in the roots of meadow grass (*Poa* sp.) growing in Grzmiaca. Aerial parts of these plants contained 10-20 lower concentration of uranium. Dicotyledonous plants accumulate uranium in the roots up to 196.22 mg/kg d.w. and in leaf up to 138.56 mg/kg d.w. (hawkweed in Kopaniec). Hyper accumulation of uranium was noted in mosses (mainly in *Hypnum cupressiforme*) occurring in streams in the nearest vicinity of piles (up to 700 mg/kg d.w. in Kowary).

These results clearly show that plants actively participate in uranium geochemical cycling what is important factor in environmental risk assessment and may be valuable indication for planning remediation processes.

New experimental constraints on slab top conditions

S. SKORA^{1*}, M. MARTINDALE^{1,2}, L. CARTER^{1,3},
J. BLUNDY¹, T. ELLIOTT¹ AND J. PICKLES¹

¹Dept of Earth Sciences, University of Bristol, BS8 1RJ
(*correspondence: Susanne.Skora@bristol.ac.uk)

²Dept of Earth and Ocean Sciences, University of British
Columbia, 6339 Stores Road, Vancouver, BC V6T1Z4

³Dept of Earth Sciences, Rice University, 6100 Main Street,
Houston Texas, 77005

Subduction zones give rise to arc volcanism because fluids and/or hydrous melts that are released from the slowly heating subducted slab trigger melting in the overlying mantle wedge. The arc geochemical signature points towards a ternary mixture of a melt from subducted sediment, fluid from basaltic oceanic crust and depleted mantle peridotite. The use of the arc geochemical signature in combination with experimental petrology on phase relations, melting and trace element behaviour is therefore key for constraining the P,T,fO₂ conditions in subducted slabs. The aim of this presentation is to place such constraints, using our latest experimental results on subducted sediment and basalt.

A nice example is given by the geochemical signal of the Mariana Arc. Here, the pelagic sediments dominate the incompatible trace element budget over volcanoclastics in the sedimentary column, whereas the volcanoclastics are predominant in the arc geochemical signature. Our study on the melting phase relations of natural volcanoclastic sediments at 3-6 GPa and 800-900°C [1] has revealed that biotite control melting at these conditions in this lithology. The vapour-saturated solidus for volcanoclastic sediments is higher (825-850°C) than in other, phengite bearing marine sediments (700-750°C) at 3 GPa. This trend is reversed at high-pressure conditions (6 GPa) where the biotite melting reaction occurs at lower temperatures (800-850°C) when compared to the phengite melting reaction (900-1000°C). This places tight constraints on slab top temperatures beneath the Mariana Arc at 180 km depth (6 GPa). It must be above the biotite melting reaction (>800°C) but below the phengite melting reaction (<900°C), preventing pelagic sediments from releasing all their incompatible elements into the liquid phase. Another set of experiments using natural altered oceanic crust provide further constraints. Here, we find that the elevated Ba/Th ratio characteristic of many (sediment-starved) arc basalts is only generated within a narrow temperature field (800-850°C), above phengite breakdown but below epidote-out.

[1] Martindale *et al.* (2013), *Chem Geol* **342** 94-109.

Micromorphology of diamond resorption at 100 kPa: The role of metal ions

V.L. SKVORTSOVA^{1*}, Y.FEDORTCHOUK²
AND A.A.SHIRYAEV³

¹MSU, Moscow, 119991, Russia (*correspondance:
valskvor@yahoo.com)

²Dalhousie University, Halifax, B3H 4R2, Canada

³IPhCE, RAS, Moscow, 119071, Russia

Natural diamonds show various resorption features produced during ascent in kimberlite magma. Experiments conducted at 100 kPa and 900 °C in KOH melts with constant flow of H₂O vapor or CO₂ gas in the presence of ions of elements common in natural kimberlites (Mg, Ca, Sr, Al, Si, Fe, Cr, Ni, Co, REE) and in mantle minerals (olivine, ilmenite) demonstrated strong catalytic effect of some metal ions on diamond dissolution rate. We report a detailed investigation of micromorphological features induced on diamond surface in these experiments. We examine individually the effects of the oxidizing media, of the catalytic ion, and of the pre-existing defects in diamonds.

The study uses crystals of natural diamonds after loss of 50-80% of the initial weight. Field-Emission SEM and Atomic Force Microscope were used for surface characterisation. It is shown that for the same catalyser ions etching in aqueous fluids leads to smoother surfaces, whereas CO₂-fluids leaves extremely rough surfaces. In presence of the strongest catalysers (Fe, Cr, Ni ions) the {110} faces show rounded steps. Other strong catalysers (Sr,Cr + Si, ilmenite) produce deep positive trigons of various shapes and sizes on {111} faces. The weakest catalysers (Ca, Mg, Si ions, olivine, natural kimberlite) reveal fine details of {110} faces and shallow trigons on {111} even at low H₂O and CO₂ concentrations. In fragmented diamonds severe resorption exhibited internal growth structure and defects. Besides influence of extensive parameters, heterogeneities of internal structure (e.g. growth/resorption features); traces of deformation-related features and other defects play important role in formation of final surface morphology.

Imaging of spatial trace-element distribution in apatite using various X-ray based and spectral analytical methods

SLABY E.¹, LISOWIEC K.¹, MICHALAK P.P.², GÖTZE J.U.², MUNNIK F.³, FÖRSTER H.-J.⁴ AND RHEDE D.⁴

¹ING PAN, Warsaw, PL, e.slaby@twarda.pan.pl

²TUBAF, Freiberg, DE, s.michalak@hzdr.de,

³HZDR, Dresden, DE, f.munnik@hzdr.de

⁴GFZ, Potsdam, DE, forhj@gfz-potsdam.de

Magmatic apatites formed in a composite granitoid pluton usually exhibit distinct zonation patterns caused by changes in trace-element composition, such as REEs and Y. Such compositional variations can be used to describe various petrological and geochemical processes, e.g. mixing of magmas of different composition. Apatites from Karkonosze Massif of Poland were studied using various X-ray-based and spectral analytical methods: FE-EPMA – Field Emission Electron Microprobe (including BSE images), PIXE/PIGE – Particle Induced X-ray/Gamma Emission and CL – Cathodoluminescence. Each method was employed to visualize (mappings) and quantify (spot analyses, line profiles) trace-element distribution patterns in single apatite grains. Slightly different suites of trace elements possessing various detection limits were analyzed with each method, with the largest number of elements measured by EPMA and the lowest detection limits achieved by PIXE. PIGE was proved to be most sensitive for analyzing light elements, such as F and Cl. Cathodoluminescence turned out to be the method best suited for visualizing zonation patterns with subtle, very thin zones not seen either on BSE images or X-ray maps. Because each method has advantages and limitations, their combined application is required to best visualize trace-element variations in apatite, which then can be used for modelling magma- differentiation processes.

Evolution of rhyolite magmas in the Halle Volcanic Complex – A record from Hf and O isotope and Hf concentrations in zircon

SŁODCZYK ELŻBIETA^{1*}, PIETRANIK ANNA¹, BREITKREUZ CHRISTOPH² AND FANNING MARK³

¹University of Wrocław, Geological Sciences, Poland; elzbieta.slodczyk@ing.uni.wroc.pl (* presenting author) anna.pietranik@ing.uni.wroc.pl

²TU Bergakademie Freiberg, Geology and Paleontology, Germany, cbreit@geo.tu-freiberg.de

³The Australian National University, Australia, Mark.Fanning@anu.edu.au

The Halle Volcanic Complex (HVC) is located in the northeastern Saale Basin in NE Germany. The region is underlain by the Mid – German Crystalline Zone. The HVC is dominated by rhyolitic rocks (c. 200 km³), which were mainly emplaced as large laccoliths. The U/Pb age of zircons ranges from 289 to 301 Ma, inherited zircons are scarce [1].

We have chosen four localities within the HVC for detailed isotopic and chemical analyses of magmatic zircon: Spitzberg, Wettin, 1044 and 1390 [1]. εHf, δ¹⁸O and elemental concentrations of Zr, Hf have been measured in previously dated zircons from these localities. On the basis of Hf content we divided zircon in two groups: zoned grains with low Hf core (8 - 9000 ppm) and high Hf rim (10 - 12000 ppm) and unzoned grains with constant low Hf concentration through grains (6 - 9000 ppm). High Hf rims occur also as magmatic overgrowths on inherited cores. Most of high Hf zircon fragments are also characterized by higher εHf compared to low Hf zircon. The diversity in δ¹⁸O (6.3 - 8.1 ‰) does not correlate with Hf concentration and εHf.

Generally, the isotope and chemical characteristic of zircon grains is similar between localities and suggest an input of higher εHf magma towards the late stage of magma evolution, probably shortly prior to the final emplacement. Lack of correlation between εHf and δ¹⁸O implies that at least three sources contributed material [2] to the ca. 300 Ma magmatism contrary to the simple two source contribution observed for the NE German Basin [3].

[1] Breitzkreuz *et al.* (2009), Z. Dt. Ges. Geowiss. 160:173-190. [2] Romer *et al.* (2001), CMP, 141:201-221. [3] Pietranik *et al.* (2013), J. Petrol – in press

The role of ultramafic veins in mafic alkaline magmatism: Contrary evidence from continental intra-plate settings

K.A. SMART^{1*}, S. TAPPE^{1,2}, A. STRACKE³, R. L. ROMER⁴
AND D. PRELEVIĆ⁵

¹University of the Witwatersrand, Johannesburg, South Africa
(*katie.smart2@wits.ac.za)

²De Beers Group Exploration, Johannesburg, South Africa

³Westfälische Wilhelms-Universität, Münster, Germany

⁴GFZ Potsdam, Germany

⁵University of Mainz, Mainz, Germany

Continental and oceanic mafic alkaline magmas have comparable major and trace element compositions that point towards similar P-T and volatile conditions during partial melting of their upper mantle source regions. While it is now widely accepted that OIB source regions must contain small amounts of recycled mafic components that contribute disproportionately to the magmatism, the geochemical and isotopic heterogeneity of equivalent magmas beneath continental interiors are more commonly explained by the contribution of partial melts of ultramafic veins at the base of the lithosphere. Vein-style metasomatism has also been suggested to explain the isotopic heterogeneity observed in OIBs formed on thick oceanic lithosphere, such that recycling of oceanic crust may not be the dominant source of mantle heterogeneity [1].

We analysed a suite of Mesozoic primitive mafic alkaline basalts and Permian alkaline lamprophyres from southern Sweden (Baltic Shield) for their major and trace element, and Sr-Nd-Hf-Pb isotope compositions. Although the Mesozoic alkaline basalts exhibit trace element features typically ascribed to melting of hydrous potassic phases within the mantle lithosphere, relatively homogeneous, moderately depleted radiogenic isotope compositions argue against derivation from old vein-metasomatized lithosphere. Isotopic modelling of hydrous metasomatic veins (represented by the Permian lamprophyres) potentially introduced to the lithospheric mantle beneath the Baltic Shield during Permo-Carboniferous plume magmatism suggests that such vein material, if it persisted to the Mesozoic, did not play a role in later mafic alkaline magmatism. In contrast, our data show that low-volume alkaline basaltic magmas beneath a thick continental lid 'oversampled' recycled oceanic crust from an otherwise highly depleted convecting upper mantle, similar to OIBs and E-MORBs.

[1] Pilet *et al.* (2008). *Science* **320**, 916 – 919.

Wintertime nitrate isotope dynamics in the Atlantic Sector of the Southern Ocean

S.M. SMART^{1*}, D.M. SIGMAN², S.E. FAWCETT²,
S.J. THOMALLA³, M.A. WEIGAND² AND C.J.C. REASON¹

¹Department of Oceanography, University of Cape Town,
Private Bag, Rondebosch, 7700, South Africa
(*correspondence: sandimsmart@gmail.com)

²Department of Geosciences, Princeton University, Princeton,
New Jersey 08544, USA

³Ocean Systems and Climate Group, CSIR, P.O. Box 320,
Stellenbosch, 7599, South Africa

We provide the first data on the wintertime patterns of seawater nitrate isotopes (¹⁵N/¹⁴N and ¹⁸O/¹⁶O) for the region south of Africa. Water column profile and underway surface samples collected in July 2012 span a range of latitudes from the subtropics to 57.8°S, just beyond the Antarctic winter sea-ice edge (56.7°S). The data are used in the context of simple models of nitrate consumption (including the Rayleigh model) to estimate the isotope effect (the degree of isotope discrimination) associated with the assimilation of nitrate by phytoplankton. Within the Antarctic, application of the Rayleigh model to depth profile N isotope data yields lower isotope effect estimates than are derived from the spatial variations within the mixed layer (the latter yielding isotope effect estimates near the commonly observed value of 5‰). The data from the Subantarctic Zone, both profiles and surface variations, also yield markedly low estimates for the assimilation isotope effect when analysed with the Rayleigh model. Similar behaviour observed in the N and O isotopes of nitrate suggest that the isotope effect is underestimated by the Rayleigh model due to mixing of waters across a wide range of nitrate concentrations in this more northern domain of the Southern Ocean. The nitrate N-to-O isotope relationship (i.e. Δ(15-18), defined as δ¹⁵N-δ¹⁸O) is remarkably uniform across the entire sampled Southern Ocean surface; however, there is a measurable Δ(15-18) difference between the surface mixed layer and the underlying deep water. The significance of these observations will be presented.

Unraveling the CaCO₃/PSS Mesocrystal Formation Mechanism by *in situ* TEM and *in situ* AFM

P.J.M. SMEETS^{1,2}, K. R. CHO¹, D. LI¹, M.H. NIELSEN¹,
N.A.J.M. SOMMERDIJK² AND J.J. DE YOREO^{1,3*}

¹The Molecular Foundry, Lawrence Berkeley National Laboratory, Berkeley, CA 94720, USA

²Laboratory of Materials and Interface Chemistry, Eindhoven University of Technology, 5600 MB Eindhoven, Netherlands

³Pacific Northwest National Laboratory, Richland, WA 99352, USA (*James.DeYoreo@pnl.gov)

The interplay between mineral and organic species is central to the control of microbial systems over biomineral formation. Deciphering the underlying mechanisms requires *in vitro* studies in which the physical and chemical parameters can be well controlled.

Using negatively charged polyelectrolyte polystyrene sulfonate (PSS) as a proxy for a bio-organic mediator, we investigate particle-mediated crystallization of CaCO₃, one of the most abundant materials for biomineralization. To induce growth, we use a calcium source in combination with the ammonium carbonate diffusion method. Utilizing similar conditions, Wang *et al.* showed that this approach yielded a family of well-defined calcite-PSS mesocrystals – i.e. 3D regular but porous scaffolds composed of easily distinguished and almost perfectly aligned nanocrystals [1]. Although mesocrystal formation was suggested to proceed via assembly of an amorphous precursor, direct proof of this mechanism is lacking. Here we use *in situ* TEM and *in situ* AFM to follow the formation process. For *in situ* TEM a custom designed fluid cell was utilized, containing two Si/Si₃N₄ wafers with electron transparent Si₃N₄ membranes.

We find that the observed mesocrystal morphology can be obtained merely through CaCO₃ overgrowth in PSS solution on a single crystal seed, and *in situ* AFM demonstrates that the development of this morphology is due to polymer poisoning of atomic steps during classical layer-by-layer calcite growth. However, both *in situ* TEM and AFM reveal a complex pathway during the initial stages of formation. Ca- PSS particles first adsorb onto the substrate. After about 2h of reaction with ammonium carbonate in the TEM fluid cell, these then appear to transform into larger amorphous aggregates. We are now attempting to detail the structural evolution of these initial particles and draw inferences about their formation mechanism and role in crystallization.

[1] Wang *et al.* (2005), *J. Am. Chem. Soc.* **127**, 3246-3247

The Discovery and Role of Non-Stoichiometric Complexes of Calcium Carbonate in the Solution Precipitation of Vaterite

P.J.M. SMEETS¹, W.J.E.M. HABRAKEN^{1,2},
L. BERTINETTI², F. NUDELMAN^{1,3},
AND N.A.J.M. SOMMERDIJK^{1,3*}

¹Laboratory of Materials and Interface Chemistry, Eindhoven University of Technology, 5600 MB Eindhoven, Netherlands

²Max-Planck-Institute of Colloids and Interfaces, 14424 Potsdam, Germany

³SoftMatter CryoTEM Unit, Eindhoven University of Technology, 5600 MB Eindhoven, Netherlands
(*correspondence: N.Sommerdijk@tue.nl)

Calcium carbonate (CaC) is the most abundant biogenic mineral, found in marine organisms and their fossilized deposits. Its crystallization mechanism is heavily debated since recent studies proposed a non-classical crystallization pathway via pre-nucleation clusters [1]. In the present study, we used cryo-TEM in combination with a titration set-up and demonstrated the existence of subnanometer-sized complexes (~0.4-0.6 nm) as prevalent pre-nucleation species in CaC mineralization, even in under-saturated regimes, which persisted after nucleation.

We show that these pre-nucleation species contain only one calcium in the equilibrium structure, which makes them complexes rather than clusters, similar as what was recently shown for calcium phosphate [2]. From a detailed analysis of the titration data we calculated that the average CaC-pre-nucleation complex chemistry represents a Ca/C ratio <<1, contains at least 50 mol% of bicarbonate and has an overall negative charge. This observation is in contrast to the previously proposed neutral CaCO₃ clusters that have been reported to exist under similar conditions [1]. We used *ab-initio* calculations to identify the structure of these complexes.

Furthermore, a dense liquid phase [3] of sub-micron sized assemblies of complexes exist already before the nucleation event. We propose a nucleation mechanism in which a calcium carbonate nucleus forms within these assemblies through a transformation of the complexes, after which the bulk phase (vaterite) propagates by ion growth.

[1] Gebauer *et al.* (2008), *Science* **322**, 1819-1822. [2] Habraken *et al.* (2013), *Nature Communications* **4**, 1507. [3] Bewernitz *et al.* (2012), *Faraday Discussions* **159**, 291-312

Lu-Hf and Sm-Nd garnet geochronology: Closure revisited and new applications in lithosphere studies

MATTHIJS A. SMIT^{1,2,3}, ERIK E. SCHERER²,
KLAUS MEZGER⁴, LOTHAR RATSCHBACHER⁵,
ELLEN KOOIJMAN^{2,6} AND BRADLEY R. HACKER¹

¹Department of Earth Sciences, UC Santa Barbara, USA

²Institut für Mineralogie, WWU, Münster, Germany

³Institute for Geography and Geology, University of Copenhagen, Denmark

⁴Institut für Geologie, Universität Bern, Switzerland

⁵institut für Geologie, TU Bergakademie, Freiberg, Germany

⁶Swedish Museum of Natural History, Stockholm, Sweden

The link between ¹⁷⁶Lu-¹⁷⁶Hf and ¹⁴⁷Sm-¹⁴³Nd dates and *P-T* information from garnet is still subject to uncertainty because closure systematics are not well constrained. To progress in this field, we performed ¹⁷⁶Lu-¹⁷⁶Hf and ¹⁴⁷Sm-¹⁴³Nd geochronology on garnet crystals of different size ($\varnothing = 0.90\text{--}6.2$ mm) from a granulite from the Archean Pikwitonei Granulite Domain, Superior Province, Canada. Metamorphism in this region started at $\sim 2716 \pm 4$ Ma and peak metamorphism (760 °C [1]) occurred at 2639 ± 2 Ma [2].

The ¹⁷⁶Lu-¹⁷⁶Hf dates for the larger size fractions ($\varnothing > 2.5$ mm) yielded 2714 ± 6 Ma, identical to the age of first garnet growth. Smaller grains exhibit slight younging to ~ 2680 Ma. In contrast, the ¹⁴⁷Sm-¹⁴³Nd dates are equal to or younger than the age of peak metamorphism. The age trends cannot be explained by inclusion effects or REE zoning, but instead relate to diffusive loss of radiogenic ¹⁷⁶Hf and ¹⁴³Nd.

The data enable the quantitative evaluation of the closure systematics of the ¹⁷⁶Lu-¹⁷⁶Hf and ¹⁴⁷Sm-¹⁴³Nd chronometers in garnet: ¹⁷⁶Lu-¹⁷⁶Hf dates for garnet of a typical grain size ($\varnothing > 0.5$ mm) represent (re-)crystallization of the phase. The same applies to ¹⁴⁷Sm-¹⁴³Nd, except for UHT rocks and cases where *dT/dt* is much lower than commonly observed in tectonic settings.

These constraints enable the use of garnet geochronology in unravelling prograde histories of deep-crustal rocks. We used this approach to assess the enigmatic history of the deep crust underlying the Pamir-Tibetan Plateau. We obtained a detailed record of near-isobaric heating between 37.0 and 26.5 Ma and relate this directly to high mantle heat flow induced by roll-back or breakoff of the Indian plate.

[1] Kooijman *et al.* (2012) *J. Metamorph. Geol.* **30**, 397-412.

[2] Heaman *et al.* (2011) *Can. J. Earth Sci.* **48**, 205-245.

Geomicrobiological activity in the Mesoarchean Witwatersrand-Mozaan Succession: Evidence from iron formations and shales

A.J.B. SMITH^{1*}, N.J. BEUKES¹ AND J. GUTZMER^{1,2}

¹PPM, Department of Geology, University of Johannesburg, Johannesburg, South Africa (*correspondence: bertuss@uj.ac.za)

²Helmholtz Institute Freiberg for Resource Technology, Halsbruecker Str. 34, 09599 Freiberg, Saxony, Germany

The Mesoarchean ($\sim 2.96\text{--}2.92$ Ga) Witwatersrand-Mozaan Succession of southern Africa is one of the oldest, well preserved supracratonic successions in the world. Numerous iron-rich units occur in this succession in the form of iron formations and iron-rich shales. Detailed studies of multiple deep level drill cores have led to the reconstruction of the lateral facies distribution of these iron-rich units. The iron formations are distal deposits, and change from hematite-magnetite, magnetite, mixed magnetite-carbonate to mixed carbonate-silicate facies towards proximal environments [1]. Proximal to the banded iron formations are iron-rich shales with manganese-rich carbonate concretions, grading into iron-poor shales and eventually sandstones [2]. This facies distribution illustrates that iron deposition only took place below wave base, likely below the photic zone. Distribution of iron was likely controlled by ferrous iron- and reduced manganese-rich hydrothermal plumes with a limited vertical extent due to neutral buoyancy [3]. Chemolithoautotrophic iron-oxidizing bacteria are inferred to have caused the precipitation of iron as ferric oxyhydroxides, with hematite preserved where the plume was not in contact with the sediment. Magnetite and isotopically light iron-rich carbonate, in contrast, formed diagenetically through interaction of the hydrothermal plume and organic carbon sourced from biological activity in the sediment [1]. The manganese-rich carbonate concretions in the more proximal iron-rich shale show evidence for dissimilatory manganese reduction of manganese originally precipitated by manganese-oxidizing bacteria [2]. Microbial oxidation of iron below the photic zone in iron formations and of manganese in shales suggest that free molecular oxygen at micro-oxic conditions were developed at depth in the the Witwatersrand-Mozaan basin since known geomicrobial processes require micro-oxic conditions.

[1] Smith *et al.* (2013) *Ec Geo.* **108**, 111-134. [2] Smith *et al.* (2010) *Geochim Cosmochim* **74** suppl 1, A973. [3] Isley (1995) *J Geol* **103**, 169-185.

Millennial Scale Holocene Climate Variability: Iberian Precipitation Reconstructed from two Speleothems

A.C. SMITH^{1*}, P.M. WYNN¹, P. A. BARKER¹, M.J. LENG² AND S. NOBLE².

¹Environment Centre, Lancaster Univ., LA1 4YQ, UK

(*correspondence: a.smith8@lancs.ac.uk, p.wynn@lancs.ac.uk, p.barker@lancs.ac.uk)

²NERC Isotope Geosciences Laboratory, Nottingham, UK (mjl@bgs.ac.uk, srn@bgs.ac.uk)

Palaeoclimate records from the Northern Iberian Peninsula are ideally suited to provide detailed insight into terrestrial climate change and oceanic variability. However, long duration unaltered palaeoclimate records are rare in this region. Two speleothems from a small cave in Matienzo (Cantabria) have been used in conjunction with cave monitoring to develop a continuous, high resolution isotope and trace element palaeoclimate record, which spans the Holocene and Younger Dryas. This speleothem record is interpreted in terms of changing winter precipitation amount, driven by moisture deliverance from the North Atlantic Ocean [1]. Oxygen isotope maxima occur at 1200, 3100, 4500, 5200, 8000 and 9500 years BP, suggesting significant periods of relative winter aridity throughout the Holocene.

Precipitation minima occur in phase with North Atlantic cold periods marked by IRD and identified by Bond *et al.* 1997 [2]. Concurrent alterations in oceanic and atmospheric circulation are known to cause significant reductions in moisture availability, in this case limiting precipitation in Southern Europe. The high correlation between the timing of North Atlantic cold events and speleothem isotope maxima suggests a rapid atmospheric response to changes in oceanic conditions and strong teleconnections between the northern Atlantic Ocean and mid latitudes. This speleothem offers one of the first high resolution, continuous terrestrial records of North Atlantic Ocean cold SST events. These large-scale oceanic processes appear to have dramatically influenced precipitation in northern Iberia and may have played a decisive role in environmental development in the region.

[1] Drunmond *et al.* (2011) *Climate Res.* **48**,193-201. [2] Bond *et al.* (1997) *Science* **278**, 1257-1266.

Chemostratigraphy of Pennsylvanian Core Shale Cyclothems, Illinois Basin, Southern Indiana

CHRISTOPHER N. SMITH^{1,2*}, CLINTON BROACH², HAMED CHOK¹, WILLIAM S. ELLIOTT JR.³ AND WILLIAM P. GILHOOLY III²

¹Weatherford International Ltd
christopher.smith4@weatherford.com*,
hamed.chok@weatherford.com

²Department of Earth Sciences, Indiana University-Purdue University Indianapolis
cbroach@umail.iu.edu, wgilhool@iupui.edu

³Department of Geology and Physics, University of Southern Indiana
wselliott@usi.edu

Major and trace element data from five Late Middle Pennsylvanian cores (Carbondale Group) were determined to investigate sediment sources and chemical conditions in the water column during organic matter deposition. A series of limestone, gray and black shale (including the Excello Shale), siltstone, sandstone and coals from a coal bed methane exploration well that penetrated the Linton and Petersburg Formations, Vanderburgh County, Southern Indiana were sampled to provide 99 core samples used in this study. These sequences were deposited in a near-shore intracratonic basin flooded by shallow epeiric seas.

Exploratory data analyses including principal component analysis (PCA) and hierarchical clustering analysis (Ward's Linkage HCA) were used to analyze the data for significant groupings of elements by lithology and total organic carbon (TOC) content. Principal component 1 (PC1) accounts for 49% of the total variance in the data and can be used to distinguish between clastic (Si, Al, K, Na, Ti) and carbonate (Ca, Sr) related elements. Principal component 2 (PC2) accounts for 19% of the total variance and is indicative of the presence or absence of redox sensitive trace element proxies for total organic carbon (Mo, U, V, Cr, Ni, Zn and Hg). Clustering analysis of sandstone and siltstones form a largely homogenous grouping for sequences interpreted as marine and non-marine, whereas there is greater heterogeneity in the groupings of both gray and black shales.

The Excello black shale shows the strongest enrichment in redox sensitive trace metal proxies for TOC. Finally, low TOC gray shales exhibit a relative enrichment in rare earth elements relative to the black shales and the North American Shale Composite (NASC), that may also reflect different sediment sources or diagenetic processes.

Adopting a combined U-Th-Pb strategy to date speleothems >200 ka

CHRISTOPHER J.M. SMITH^{1*}, DAVID A. RICHARDS¹, DANIEL J. CONDON², MATTHEW S.A. HORSTWOOD², RANDALL R. PARRISH², JON WOODHEAD³ AND DEREK C. FORD⁴

¹School of Geographical Sciences, University of Bristol, UK
(*correspondence: chris.smith@bristol.ac.uk)

²NERC Isotope Geosciences Laboratory, British Geological Survey, UK

³School of Earth Sciences, University of Melbourne, Australia

⁴School of Geography and Earth Sciences, McMaster University, Canada

Speleothems are widely recognised as valuable records of palaeoenvironmental and landscape change with robust and precise chronologies to ~500 ka, principally based on the U-Th decay scheme. However, the practical upper limit for speleothem dating can be extended by the adoption of U-Th-Pb methodologies that account for disequilibrium in the decay chain, see review by Woodhead & Pickering (2012) [1]. While the range of applications is expanding, widespread adoption of these methods is hampered by the need to accurately predict, with high precision, the initial state of U-series disequilibrium (i.e. $(^{234}\text{U}/^{238}\text{U})_{\text{initial}}$), and also analyse material with a sufficient range of U/Pb to provide high precision isochron age determinations.

For a suite of speleothems spanning the late Pliocene to late Pleistocene exhibiting variable U (1-100 $\mu\text{g g}^{-1}$) and low non-radiogenic Pb (<50 ng g^{-1}), we have adopted a combined U-Th-Pb dating strategy to take full advantage of the sensitivity and spatial resolution of available techniques. For individual growth layers, we have used: (1) rapid in-situ U-Pb LA-MC-ICPMS (193 nm ArF excimer laser) techniques, which enables fast throughput, high spatial resolution and a wide range in U/Pb for individual spots; (2) conventional U-Pb ID TIMS, for high-precision three-dimensional isochrons at lower spatial lower resolution; (3) U-Th MC-ICPMS static Faraday methods, to obtain high-precision estimates of initial $^{234}\text{U}/^{238}\text{U}$ for material ≥ 500 ka.

We discuss the relative merits of each of the above methods and their combined use, focusing in particular on the compromises that have to be made between spatial resolution and age precision for speleothems with different growth rates and ages.

[1] Woodhead & Pickering, (2012) *Chem Geol* **322-323**, 290-299.

Diamond inclusions reveal fugitive mantle nitrogen

E.M. SMITH^{1*}, M.G. KOPYLOVA¹, M.L. FREZZOTTI² AND V.P. AFANASIEV³

¹Department of Earth, Ocean and Atmospheric Sciences, University of British Columbia, 2207 Main Mall, Vancouver, BC V6T 1Z4, Canada (*correspondence: esmith@eos.ubc.ca)

²Department of Geological Sciences and Geotechnologies, University of Milano-Bicocca, Piazza della Scienza 4, 20126 Milano, Italy

³Sobolev Institute of Geology and Mineralogy, Siberian Branch of the Russian Academy of Sciences, pr. Akademika Koptuyuga 3, Novosibirsk, 630090, Russia

Mantle volatiles in mid-ocean ridge basalts and fluid inclusions in mantle xenoliths are dominated by CO₂. Nitrogen generally appears as a trace component. However, we report diamonds from three different localities, the Kaapvaal, Congo, and Siberian cratons, that have N-rich fluid inclusions and melt inclusions.

Nitrogen in the inclusions was analyzed with micro-Raman spectroscopy. Fluid inclusions in the Siberian diamond are CO₂-N₂ mixtures with 40±4 mol% N₂. Melt inclusions in the diamonds from the Kaapvaal and Congo cratons contain exsolved bubbles of volatiles that are nearly pure N₂, with <9 mol% CO₂. At the time of trapping, the silicate melt would have contained ~1 wt% dissolved N₂.

These melt and fluid inclusions are well-preserved samples of mobile, undegassed mantle phases. Such N-rich fluids/melts reveal an unrecognized type of concentrated N flux escaping the convecting mantle. This critical observation casts uncertainty on current flux models, which otherwise suggest considerable net influx to the mantle via subduction that does not return to surface (at mid-ocean ridges, volcanic arcs, back-arc basins, and hotspots).

We propose that the N₂ in our samples was liberated by oxidation from NH₄⁺-bearing silicates. The coexistence of N₂ and oxidized carbon species in fluid/melt inclusions supports the idea that oxidizing conditions help to mobilize N and C. This implies redox conditions control mantle nitrogen behaviour, both in terms of storage and geodynamic cycling.

Additionally, the oxidation of NH₄⁺ to N₂ could be accompanied by isotopic fractionation. This would allow isotopically light N₂ (low ¹⁵N/¹⁴N) to be derived from isotopically heavy subducted or stored NH₄⁺ (higher ¹⁵N/¹⁴N). This isotopic fractionation may explain the gross mismatch between isotopically heavy N influxed by subduction and the isotopically light N effluxed from the mantle, in diamonds and mid-ocean ridge basalts, for example.

An inert desolvating nebulizer system and rapid washout accessory for tungsten isotope measurements with multicollector ICP-MS

F.G.SMITH^{1*}, J. HOLST², C.PATON² AND M. BIZARRO²

¹CETAC Technologies, Omaha, NE 68144 USA
(*correspondence: fsmith@cetac.com)

²Center for Star and Planet Formation, Natural History Museum of Denmark, University of Copenhagen, Copenhagen DK-1350, Denmark

Multicollector ICP-MS instruments are specialized devices for high-precision isotope ratio measurements. Prepared liquid samples may be concentrated (100 to 1000 mg/L) in elements of interest; these higher concentrations can cause longer analyte washout times and signal spikes. This poster will describe an inert, low flow (50 to 200 μ L/min) desolvating nebulizer system with a rapid washout accessory. This nebulizer system can also be equipped with a dedicated autosampler that features a dual-flowing rinse capability to minimize sample carryover. Wetted parts are composed of fluoropolymers such as PFA (perfluoroalkoxy) for lowest trace metal blanks and maximum chemical resistance. Optimum operating conditions for the nebulizer system with a contemporary multicollector ICP-MS for tungsten measurements will be detailed. Figures of merit will include signal enhancement, isotope ratio measurements and long-term (12 hour) ratio stability, and rinse out characteristics with and without the rapid washout accessory [1].

[1] Holst *et al.* (in review), "¹⁸²Hf-¹⁸²W age dating of a ²⁶Al-poor inclusion and implications for the origin of short-lived radionuclides in the early solar system." Proceedings of the National Academy of Sciences.

Biogenic new particle formation and its potential impacts on climate

J. N. SMITH^{1,2*}, M. LAWLER², P. WINKLER³, J. ZHAO⁴, AND P. MCMURRY⁴

¹National Center for Atmospheric Research, Boulder, CO 80307 USA (*correspondence: jimsmith@ucar.edu)

²University of Eastern Finland, 70211 Kuopio, Finland

³University of Vienna, 1090 Vienna, Austria

⁴University of Minnesota, Minneapolis, MN 55455 USA

Observations show that growth rates of freshly nucleated atmospheric nanoparticles are about 5-10 times higher than can be accounted for by sulfuric acid condensation. This additional growth is primarily due to the uptake of organic compounds, often of biogenic origin, by processes that are not yet understood and that might include condensation of low-volatility vapors or reactions that occur on or within particles. If the growth of freshly nucleated atmospheric aerosols is sufficiently fast, these particles can reach sizes required to serve as cloud condensation nuclei (CCN), and may thereby potentially affect the climate.

We have performed laboratory and field measurements focusing on understanding the role of biogenic organic compounds in the formation and growth of atmospheric aerosols. Measurements were made using the Thermal Desorption Chemical Ionization Mass Spectrometer (TDCIMS), an instrument capable of realtime measurements of the molecular composition of ambient aerosols as small as 10 nm in diameter. In recent laboratory experiments of new particle formation from α -pinene ozonolysis, high molecular weight (m/z 430-560) low volatility gases correlated with initial stages of particle formation [1]. Additional work has focused on identifying particle phase compounds present in nanoparticles of varying size during the earliest stages of growth: in those studies organic acids were observed in the smallest particles formed by nucleation [2].

Our laboratory results are also compared to field observations of nanoparticle composition and gas phase precursors at sites in which biogenic emissions dominate. These include an isoprene-dominated region (Columbia, MO), and several sites with a mixture of terpene emissions (Hyytiälä, Finland, Manitou Forest, Colorado). These observations show that atmospheric nanoparticles are often enriched with organic acids and nitrogen-containing compounds. These particles are often quite hygroscopic, and thus may have a far greater effect on cloud formation than previously thought.

[1] Zhao *et al.* (2013) ACPD **13**, 9319-9354. [2] Winkler *et al.* (2012) GRL **29**, L20815.

Western Oregon as a low-sediment end member of particulate organic carbon export from temperate forested uplands

J.C. SMITH^{1*}, A. GALY^{1,2}, N. HOVIUS³ AND A. TYE⁴

¹Department of Earth Sciences, University of Cambridge, Cambridge CB2 3EQ, United Kingdom (*correspondence: jcs74@cam.ac.uk)

²(ajbg2@cam.ac.uk)

³German Research Centre for Geosciences GFZ, 14473 Potsdam, Germany (hovius@gfz-potsdam.de)

⁴British Geological Survey, Keyworth, Nottingham NG12 5GG, United Kingdom (atye@bgs.ac.uk)

The transfer of continental biomass to geological storage has the potential to sequester considerable amounts of carbon dioxide. Despite an initial focus on active mountain belts as prime locations for this erosion, temperate forested uplands might also have a significant role to play.

In some temperate catchments with high connectivity between hillslopes and actively incising channels, clastic yield is high, but soil is preferentially mobilised by overland flow beyond a moderate discharge threshold, resulting in the export of globally significant amounts of biomass [1]. However, these processes are not universal in temperate forested uplands. Using organic carbon and nitrogen elemental and isotopic ratios, we present results revealing contrasting particulate organic carbon dynamics in the headwaters of Western Oregon. Suspended sediment concentrations are typically very low, while organic carbon concentrations frequently reach 30%. A lack of active incision has led to the development of flat, thickly vegetated riparian zones which isolate hillslopes. Nevertheless, considerable amounts of soil and plant material are eroded from the channel and immediately adjacent areas during rain. Such settings export non-fossil organic carbon at rates of $\sim 6 \text{ t km}^{-2} \text{ yr}^{-1}$, around half the rate from the high-sediment temperate end member. Contrasts between the two systems suggest that ecosystem biology is the principal control on POC export style in temperate forested uplands.

Comparison of our results with studies made downstream of these headwaters at their entry to the Pacific Ocean [2, 3] offers new insights into the fate of biomass mobilised in Oregon's uplands and similar settings.

[1] Smith *et al.* (2013), *Earth Planet Sc Lett* **365**, 198-208. [2] Hatten, Goñi & Wheatcroft (2012), *Biogeochemistry* **107**, 3-66. [3] Goñi *et al.* (2013), *J Geophys Res-Bioge* **118**, 1-23.

Helium equilibrium between pore water and quartz: A clever, but limited tool

S.D. SMITH^{1,2*}, G.A. HARRINGTON¹, B.D. SMERDON¹ AND D.K. SOLOMON²

¹CSIRO Water for a Healthy Country Flagship, Urrbrae, SA 5064, Australia

(*correspondence: stan.smith@csiro.au)

(glenn.harrington@csiro.au, brian.smerdon@csiro.au)

²Dept. of Geology and Geophysics, Univ. of Utah, Salt Lake City, UT 84112, USA (kip.solomon@utah.edu)

Pore water helium concentrations calculated from quartz helium concentrations [1] offer a unique tool to determine helium distribution in low permeability formations. Analyses have been carried out on shale and sandstone core samples from the San Juan Basin, USA and the Eromanga and Surat basins, Australia.

Comparing quartz-derived helium concentrations to direct pore water concentrations reveal up to an order of magnitude difference between the two. This uncertainty is unacceptable for modelling vertical helium transport to constrain estimates of fluid flux. However, in the San Juan Basin, ³He/⁴He ratios agree between methods. In the Eromanga Basin, modelling indicates >90% equilibrium is expected, however, when compared with direct pore water measurements [2], as low as 10% of equilibrium is observed. Regardless of present-day equilibrium, the method could be useful for paleohydrology studies, provided the timing of equilibrium can be constrained.

The method appears more promising in deeper (thus hotter) basins where the equilibrium time between pore water and quartz is reduced significantly. In shallow systems, the equilibrium time may greatly exceed the lifespan of shallow, quasi-steady state hydrological systems. Further testing of the method in additional basins may result in an adequate screening method to find where the method is applicable. The possibility exists that this method will not come to fruition as too much uncertainty remains and equilibrium is found in theory instead of in the samples.

[1] Lehmann, Waber, Tolstikhin, Kamensky, Gannibal, & Kalashnikov (2003) *Geophys Res Lett* **30**, 4. [2] Gardner, Harrington, & Smerdon (2012) *J. Hydrol* **468**, 63-75.

Using tephra layers to provide absolute and relative chronologies for sedimentary archives: An example from the Lake Suigetsu SG06 record from Japan

V.C. SMITH¹, R.A. STAFF¹, D. F. MARK²,
S.P.E. BLOCKLEY³, C. BRONK RAMSEY¹
AND T. NAKAGAWA⁴

¹Research Laboratory for Archaeology and the History of Art, University of Oxford, Oxford OX1 3QY, U.K.
(victoria.smith@rlaha.ox.ac.uk)

²Scottish Universities Environmental Research Centre (SUERC), East Kilbride G75 0QF, U.K.

³Centre for Quaternary Research, Royal Holloway University of London, Egham TW20 0EX, U.K.

⁴Department of Geography, University of Newcastle, Newcastle Upon Tyne NE1 7RU, U.K.

The Lake Suigetsu SG06 sedimentary archive from Honshu Island, central Japan, provides a high-resolution palaeoenvironmental record for the last 150 kyrs. The 73 m-long record contains numerous layers tephra (30 visible and numerous cryptotephra) sourced from explosive volcanism from Japan and South Korea. These marker layers can be used for both relative and absolute chronology.

The glass chemistry of these tephra is typically unique, therefore most of the layers can be correlated to those in other archives and to specific eruptions [1]. Since many of these layers are widespread (>600 km from source) these isochrons allow for the assessment of leads and lags in palaeoclimate across the region.

The tephra can also be dated using ⁴⁰Ar/³⁹Ar methods. These ⁴⁰Ar/³⁹Ar ages are crucial for constraining the pre-50 ka SG06 age model. Correlating these distal SG06 tephra layers to proximal deposits is essential as large crystals are required to obtain precise and ⁴⁰Ar/³⁹Ar ages and these are only abundant in the coarser proximal deposits [2].

Precise radiocarbon dates have been obtained for all the post-50 ka visible SG06 tephra layers [1] using the modelled radiocarbon data and varve chronology [3]. These radiocarbon dates and ⁴⁰Ar/³⁹Ar ages of the eruptions can significantly improve the age models of other archives in which the tephra are found.

[1] Smith *et al.* (2013) *Quaternary Science Reviews* **67**, 121-137. [2] Smith *et al.* (2011) *Quaternary Science Reviews* **30**, 2845-2850. [3] Bronk Ramsey *et al.* (2012) *Science* **338**, 370-374.

Molecular simulation of aqueous electrolyte solutions

WILLIAM R. SMITH^{1,2}*, FILIP MOUČKA³
AND IVO NEZBEDA⁴

¹University of Ontario Institute of Technology, Faculty of Science;

²University of Guelph, Mathematics and Statistics,
(william.smith@uoit.ca *presenting author)

³J.E. Purkinje University, Physics, (fmoucka@seznam.cz)

⁴J.E. Purkinje University, Chemistry, (inezbeda@icpf.cz)

We employ the Osmotic Ensemble Monte Carlo (OEMC) algorithm [1] to predict the solute and water chemical potentials in aqueous electrolyte solutions. OEMC implements a Semi-Grand Canonical Ensemble simulation of the solution phase, which can be viewed as an application of the Reaction Ensemble Monte Carlo algorithm [2] to the case of an inter-phase chemical reaction, including speciation reactions as appropriate.

Focusing on aqueous NaCl at ambient conditions, we present the following:

1. An improved electrolyte force field based on SPC/E water and a simple charged Lennard-Jones sphere model, determined by fitting the concentration dependence of the density and chemical potential, and the solubility.
2. Calculations of the concentration dependence of the water chemical potential and demonstration of thermodynamic consistency with the electrolyte chemical potential using the Gibbs-Duhem equation.
3. Electrolyte chemical potentials at finite concentrations for polarizable force fields for water and the electrolyte, using the Multi-Particle Move Monte Carlo method [3].
4. Calculations predicting the onset of homogeneous nucleation in supersaturated aqueous electrolyte solutions.

[1] F. Moučka, I. Nezbeda, W.R. Smith, *J. Phys. Chem.* **B116**, 5468 (2012); *idem*, *J. Chem. Phys.*, in press (2013). [2] W.R. Smith, B. Tríska, *J. Chem. Phys.* **100**, 3019 (1994) [3] F. Moučka, M. Rouha, and I. Nezbeda, *J. Chem. Phys.* **126**, 224106 (2007).

The North Australian Craton: A Palaeoproterozoic accretionary orogen

R.G. SMITS^{1,2*}, W.J. COLLINS² AND M. HAND¹

¹Centre for Tectonics, Resources and Exploration, University of Adelaide, S.A. 5005, Australia, russell.smits@adelaide.edu.au

²School of Environmental and Life Sciences, University of Newcastle, NSW 2308, Australia,

The North Australian Craton (NAC) is 1,830,000 km², making up almost one quarter of Australia. The development of this system has a broad spatial and temporal organization such that sedimentation, magmatism and tectonism generally migrated southward over the interval ~2000 to 1700 Ma, and at least in the northern parts of the craton, appears to have a late Archaean substrate. In most regions, within 10–20 Ma, sedimentation was followed by deformation and granite-dominated magmatism associated with high thermal gradient metamorphism, pointing to a systematic pattern of crustal consolidation as the craton developed.

Detrital zircon spectra, maximum depositional of sediments, distribution of mafic intrusives and Hf isotopes over the NAC indicates a southerly migration of depositional activity from the Pine Creek Orogen in the north to the Arunta Orogen in the south, with two main phases of basin formation between 1880–1850 and 1830–1780 Ma. The sediments of these basins share common zircon detritus populations, particularly Neoproterozoic sources. A general trend toward more primitive Hf values with time is typical for retreating accretionary orogens. The Archean detrital populations recorded in sediments from all regions of the NAC, Hf isotopic data coupled with the systematic spatial and temporal pattern of magmatism and deformation/metamorphism is consistent with an Archean substrate that migrated southwards over a period of ~300 Ma. We can envisage such a migration as being controlled by a long-lived retreating margin, with distinct “pulses” of magmatism related to periods of accelerated extension. This scenario suggests that the NAC developed in an oceanic back arc setting, rather than in an intracratonic setting as has been recently proposed. The model implies that formation of Palaeoproterozoic continental lithosphere can be efficiently achieved in back arc settings, similar to the modern-day western Pacific.

Terrestrial temperature response during Early Eocene hyperthermals

K.E. SNELL^{1*}, H.C. FRICKE², W.C. CLYDE³
AND J. M. EILER¹

¹Div. of Geological and Plan. Sci., Caltech, Pasadena, CA 91125 (*correspondence: ksnell@caltech.edu)

²Geology Dept., Colorado College, Colorado Springs, CO 80903

³Dept. of Earth Sciences, Univ. of New Hampshire, Durham, NH 03824

The Early Eocene is marked by a number of rapid global warming events called hyperthermals that are associated with negative carbon isotope excursions (CIE) in both marine and terrestrial records. Each theory to explain the connection of these hyperthermals with the CIEs predicts a different climatic response. Characterizing the timing, duration and magnitude of temperature change will help establish their cause and possibly establish whether or not they are driven by a single process. It is possible that all share a common underlying cause; if so, we might predict that the temperature change during each hyperthermal is proportional to the magnitude of its associated CIE (and perhaps exhibit other similarities, such as the relative amplitudes of marine and terrestrial temperature change). To our knowledge, the only hyperthermal for which we know the terrestrial temperature change is the Paleocene-Eocene Thermal Maximum (PETM).

Here we use carbonate clumped isotope (Δ_{47}) thermometry of paleosol carbonates from the Bighorn Basin (Wyoming, USA) to produce paleotemperature estimates at high temporal resolution for Early Eocene hyperthermals ETM2 and H2. Average baseline temperatures (which likely reflect near-peak summer ground temperatures) before and after the two hyperthermals are ~28°C and increase to ~38°C during the apex of each CIE; temperatures appear to recover close to baseline temperatures between ETM2 and H2. These data (combined with previous constraints on the PETM) suggest that both the absolute temperatures and the magnitudes of temperature change associated with the PETM, ETM2 and H2 are similar (within error); the magnitudes of temperature change (~10°C) also appear similar to/slightly greater than that found in arctic sediments [1]. In addition, our record shows a cooling interval within the peak of ETM2 that is similar in pattern to an event that is present in the arctic record [1]. These results suggest that the temperature change associated with the hyperthermals does not necessarily scale with the magnitude of the local CIEs from paleosol carbonate nodules (~6‰ for the PETM and ~4‰ for ETM2). For ETM2, the CIE appears to precede warming.

[1] Sluijs *et al.* (2009) *Nature Geoscience*, 2, 777–780.

Dissolution rates and surface chemistry of calcium aluminosilicate glasses in cementitious systems

R. SNELLINGS^{1*} AND K. SCRIVENER¹

¹Institute of Materials, EPFL, Lausanne, Switzerland
(*correspondence: ruben.snellings@epfl.ch)

Waste calcium aluminosilicate (CAS) glasses are widely used as supplementary cementitious materials in Portland-cement based construction materials for environmental, economical and technical reasons. The amount of cement that can be replaced by waste CAS is largely depending on their reactivity and composition. Understanding the reactivity or rates of dissolution of these wastes in typical Portland cement pore solutions of high ionic strength and alkalinity (pH \approx 13) is of great importance to optimise the performance, durability and sustainability of the blended Portland cements.

Water quenched synthetic CAS glasses of selected compositions ranging from pure silica framework to CaO-rich depolymerized glasses were subjected to batch dissolution reactions avoiding hydration product precipitation. The obtained dissolution rates scaled linearly with the Ca/(Al+Si) molar ratio, and showed a large difference in reactivity between framework and partially depolymerised glasses (Fig. 1).

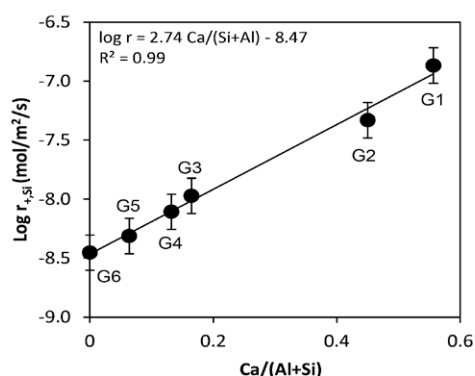


Figure 1: Dependence of glass dissolution rate at pH 13 on the molar Ca(Al+Si) ratio of the glass.

Glass dissolution rates also depended on solution composition. Increasing Al activity decreased dissolution rates of framework glasses, while increasing Ca activity decreased dissolution rates of all glasses. The glass surface chemistry as a function of solution pH and composition was investigated by XPS, zeta potential measurements and surface titrations and lead to a model of CAS glass dissolution for high pH cement type environments.

Isotopic Tomography of Monazite

DAVID R. SNOEYENBOS^{1*}, EMILY M. PETERMAN²,
MICHAEL J. JERCINOVIC³, MICHAEL L. WILLIAMS³ AND
DAVID A REINHARD⁴

¹Box 513, Chesterfield, MA 01012 USA

*correspondence: kyanite@mac.com

²Bowdoin College, Brunswick, ME 04011 USA

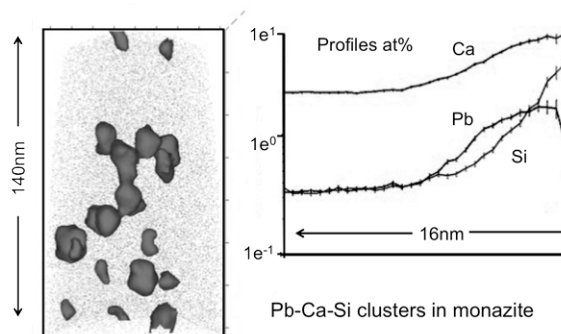
³University of Massachusetts, Amherst, MA 01002 USA

⁴Cameca Instruments Inc., Madison, WI 53711 USA

In Atom Probe Tomography (APT) a specimen is evaporated atom by atom, and the mass/charge and original position (X,Y, Z to 0.2nm) of each detected atom is recorded to produce a quantitative 3-D reconstruction at the atomic scale. APT can also provide *in situ* atomic scale isotopic tomography of U, Th and radiogenic Pb, allowing access to otherwise cryptic thermochronologic information.

A polymetamorphic monazite grain from the Churchill Province, Canada was selected for analysis by APT. Prior EPMA analysis indicates monazite crystallization at 2.55Ga, overgrowth at 2.37Ga, and fracture-infill and further overgrowth at 1.84Ga. Datasets of up to 200 million atoms were collected, sampling the various domains and their mutual interfaces.

Distinct clusters of Pb atoms <10nm dia. and spaced at 20–30nm were observed in the older, reheated domain. These clusters contain up to 1.7 at.% Pb, 4 at.% Si and 7 at.% Ca in a radial structure. These clusters closely resemble those found by APT in reheated zircon [1. Valley *et al.*]. The presence of ²⁰⁸Pb, ²⁰⁷Pb and ²⁰⁶Pb in the clusters indicates post-crystallization segregation of radiogenic Pb from both the Th and U decay chains. Because Th and U enter the monazite structure via coupled substitution (e.g. Th+Ca, Th+Si and U+Si), Si and Ca in the clusters may represent the unpaired atoms after radionuclide decay. To measure an isotopic age at this scale, precise ²⁰⁷Pb/²⁰⁶Pb determination requires a minor correction for interfering species such as (ThPO₃)₃₊.



[1] Valley, J. W. *et al.* (2012) Elemental and isotopic tomography at Single-Atom-Scale in 4.0 and 2.4 Ga zircons. Abstract V12A-05 presented at 2012 Fall Meeting, AGU, San Francisco, Calif., 3-7 Dec.

Potential temperatures of convecting mantle based on Al partitioning between olivine and spinel

A.V.SOBOLEV^{1,2}, V.G.BATANOVA^{1,2}, D.V.KUZMIN³
AND N.T.ARNDT¹

¹ISTerre, University J. Fourier, Grenoble, France,
alexander.sobolev@ujf-grenoble.fr

²Vernadsky Institute of Geochemistry RAS, Moscow, Russia

³Sobolev Inst. of Geol and Min, SBRAS Novosibirsk, Russia

Knowledge of potential temperatures of convecting mantle is required for the understanding the global processes on the Earth [1]. The common way to estimate these is the reconstruction of primary melt compositions and liquidus temperatures based on the Fe-Mg partitioning between olivine and melt. This approach requires knowledge of the compositions of primitive melts in equilibrium with olivine alone as well as composition of olivine equilibrium with primary melts. This information is in most cases unavailable or of questionable quality. Here we report a new approach to obtain crystallization temperatures of primary melts based on the olivine-spinel Al-Cr geothermometer [2]. The advantages of this approach are: (1) common presence of spinel in assemblage with high-Mg olivine and (2) low rate of diffusion of Al in the olivine, which promises to preserve high magmatic temperatures.

We analysed over one thousand spinel inclusions and high-Mg host olivines from different MORB, OIB and Archean komatiites on the JXA-8230 EPMA at ISTerre, Grenoble, France. Concentrations of Al, Ti, Na, P, Zn, Cr, Mn, Ca, Co, Ni were determined with a precision of 10 ppm (2 standard errors) using a newly developed protocol [3]. When available, we also analysed matrix glass and glass inclusions in olivine and found that temperature estimations from olivine-spinel (Al-Cr) and olivine-melt (Fe-Mg)[4] equilibrium match within (+/-30 degree C).

The results show contrasting crystallization temperatures of Mg-rich olivine of the same Fo content from different types of mantle-derived magmas, from the lowest (down to 1220 degree C) for MORB to the highest (up to 1500 degree C) for komatiites. These results match predictions from Fe-Mg olivine-melt equilibrium and confirm the relatively low temperature of the convecting mantle source of MORB and higher temperatures in the mantle plumes that produce the OIB of Iceland, Hawaii, Gorgona, and Archean komatiites.

[1] McKenzie & Bickle, 1988, *J. Petr.* 29, p 625-679. [2] Wan et al, 2008, *Am. Min.* 93, p1142-1147. [3] Batanova & Sobolev, 2013, *Min. Mag.* (this issue). [4] Ford et al, 1983, *J. Petr.* 24, p 256-265.

Crystallization of P-rich minerals from the high phosphorus rare-metal magma of East-Kalguty dyke belt (S.Altay, Russia)

SOKOLOVA E^{1,2*} AND SMIRNOV S.Z.^{1,2}

¹ V.S. Sobolev Institute of Geology and Mineralogy SB RAS, Novosibirsk, Russia

(*correspondence: ekaterina@igm.nsc.ru)

² Novosibirsk State University, Novosibirsk, Russia

High phosphorus content is an important feature of some highly evolved peraluminous Ca-poor granitoids, associated with ore deposits. East-Kalguty dyke belt (South Altai, Russia) is one of the few representatives of rare-metal rich felsic high-phosphorus rocks (avg 0.39 wt % P₂O₅ and ASI=1.23). In this case alkali feldspars (Af) represent significant reservoir of phosphorus, containing 0.14 wt % P₂O₅ in average. Incorporation of P into feldspars involves the substitution $2\text{Si}^{4+} = \text{Al}^{3+} + \text{P}^{5+}$ [1].

Average P-content 0.27 wt % of P₂O₅ in the melt equilibrated with Af phenocrysts from dyke rocks was calculated from dependence $\text{ASI} = 0.7273 * \text{D}[\text{P}]/\text{Af}/\text{melt} + 0.7818$ derived by D.London on the basis of experimental data [1].

Direct measurement of P₂O₅ by EMPA in melt inclusions in quartz phenocrysts showed 0.29 wt %, which is in good agreement with the calculated value. This means that Af crystallized from the same melt with quartz phenocrysts.

Comparison of Ca and P content, and Ca/P ratio in the melt inclusions and rocks shows that apatite crystallized before entrapment of the melt inclusions in quartz. Low Ca content results in excess of phosphorus in the evolved melts, which was later incorporated into feldspars and ambligonite LiAl[PO₄](OH). Main intrusive phase of the Kalguty granite massif, preceding to rare-metal dykes, have P-content close to the clark of felsic rocks [2]. The increase of P in latest dykes, which reaches a maximum in the rare-metal rich dykes is explained by introduction of phosphorus by external fluids into magmatic system with subsequent its accumulation in the course of magma differentiation.

This study was supported by grants RFBR 12-05-31-290 and 13-05-00471.

[1] London (1992), *American Mineralogist* 77, 126-145. [2] Vinogradov (1962), *Geochemistry* 7, 555-565

Reactive transport modeling of cement/concrete – rock interaction: The Tournemire and Maqarin cases

JOSEP M. SOLER¹

¹IDAEA-CSIC, 08034 Barcelona, Catalonia, Spain

In the framework of the GTS-LCS project (JAEA-Japan, NAGRA-Switzerland, NDA-UK, POSIVA-Finland, SKB-Sweden), reactive transport modeling of 2 analogues of cement-rock interaction in a repository is being performed: The DM borehole at Tournemire (France) and the Eastern Springs hyperalkaline system at Maqarin (Jordan). In Tournemire solute transport is dominated by diffusion between concrete and rock (mudstone); in Maqarin there is flow along a fracture zone from a cement-like metamorphic rock body with diffusion between fracture and wall rock (clay-containing limestone). The two cases are examples of diffusion (Tournemire) and fracture-flow (Maqarin) dominated systems. In the modeling presented here, calculations have been performed with the CrunchFlow reactive transport code. Results are compared with observations.

Results for the Tournemire case (concrete-mudstone interaction during 15 years) show sealing of porosity at the rock side of the interface (mm scale) due to the precipitation of C-A-S-H, calcite and ettringite, together with clay dissolution. The location of sealing is influenced by cation exchange. Without exchange, sealing is at the concrete side of the interface.

The hyperalkaline system at Maqarin may have been active for tens or several hundreds of thousands of years. The high-pH solution flows along the full length of the fracture (ca. 80 m), with intense mineral alteration in the wall rock (cm scale). Major secondary minerals include ettringite-thaumasite, C-S-H/C-A-S-H and calcite. C-S-H/C-A-S-H precipitation is controlled by the dissolution of primary silicates. Ettringite precipitation is controlled by diffusion of sulfate and aluminum from the wall rock to the fracture, with aluminum provided by the dissolution of albite. Calcite precipitation is controlled by diffusion of carbonate from the wall rock. Extents of porosity sealing along the fracture and in the fracture-wall rock interface depend on assumptions regarding flow velocity and composition of the high-pH solution. The multiple episodes of fracture sealing and reactivation evidenced in the fracture infills were not included in the simulations.

Financial support from POSIVA and the many discussions with the LCS team are gratefully acknowledged.

Spatial heterogeneity of benthic methane dynamics in the subaquatic canyons of the Rhone River Delta (Lake Geneva)

S. SOLLBERGER^{1,2*}, J.P. CORELLA³, S. GIRARD CLOS³, M.-E. RANDLETT^{1,2}, C.J. SCHUBERT¹, D. SENN^{1,2}, B. WEHRLI^{1,2} AND T. DELSONTRO^{1,2}

¹Eawag, Swiss Federal Institute of Aquatic Science and Technology, CH-6047 Kastanienbaum, Switzerland

²Institute of Biogeochemistry and Pollutant Dynamics, ETH Zurich, CH-8092 Zurich, Switzerland

³Environmental Science Institute (ISE) and Dept. of Geology and Paleontology, University of Geneva, CH-1205 Geneva, Switzerland

* *correspondence*: sebastien.sollberger@eawag.ch

Heterogeneous benthic methane (CH₄) dynamics from river deltas, resulting from variable organic matter accumulation, have been recently reported in various aquatic and marine environments. The spatial heterogeneity of CH₄ sediment release from the Rhone delta of Lake Geneva (Switzerland/France) was thus investigated. Methane benthic dynamics were compared (1) between three underwater canyons of different sedimentation regimes, (2) along a longitudinal transect of the canyon most influenced by the Rhone River, and (3) laterally across a canyon. Results indicate higher CH₄ diffusion rates in the canyon, which continuously receives loads from the Rhone River compared to the other canyons, as well as in intermediate sites instead of proximal and distal reaches of the canyon. The lateral canyon survey results were inconclusive due to the shorter length of the cores. The more allochthonous material is found in higher sedimentation rate environments and partially explained the greater CH₄ diffusion rates. The lower river velocity in the intermediate region characterized by a smaller fraction of coarser sediment allowed more organic matter to settle down and be preserved. This induced higher CH₄ diffusion rates than in the proximal region, where the upper layer of sediments were potentially more disturbed by a stronger river inflow. Total CH₄ sediment release was found to range from 0.9 to 1.2 x 10⁴ t CH₄ yr⁻¹ for the entire delta, although it is most likely oxidized before CH₄ reaches the atmosphere due to the oxic water column. Finally, turbidites were shown to act as sealing layers beneath which CH₄ could accumulate in high amounts and potentially act as source layers for ebullition.

Spatial microbial community structure of a shallow-water hydrothermal system

MIRIAM SOLLICH^{1,2*}, IOULIA SANTI³, PETRA POP RISTOVA¹, THOMAS PICHLER², KAI-UWE HINRICHS^{1,2} AND SOLVEIG I. BÜHRING¹

¹MARUM & ²Dept. of Geosciences, University of Bremen, Bremen, Germany (*correspondence: msollich@uni-bremen.de)

³Max Planck Institute for Marine Microbiology, Bremen, Germany

Marine shallow-water hydrothermal systems are extreme environments, characterized by discharge of hot and often acidic fluids with elevated concentrations of reduced compounds. Steep physico-chemical gradients on small spatial scales lead to the formation of various microniches for microbial communities. In contrast to deep-sea hydrothermal systems, the sun light in shallow systems results in a combination of photoautotrophic and chemoautotrophic primary production. Despite the comparably easy accessibility of shallow-water hydrothermal systems, little is known about the spatial microbial community structure and its relationship to physico-chemical conditions.

Here, we present data for the system off Milos island, one of the most hydrothermally active regions in the Mediterranean Sea. A combined approach of gene- and lipid-based techniques (ARISA and intact polar lipids) with porewater geochemistry data was applied along a temperature gradient to investigate the spatial microbial community structure.

Supported by statistical analyses, ARISA data revealed significant changes of the bacterial community structure along the temperature gradient and depth profiles from hydrothermally unaffected areas towards the vent orifices. Intact polar lipid results are consistent with the ARISA data and clearly differentiate samples from close to the vent outlet from those in less affected areas. Changes from phospho- and betaine lipids within the top layer of the unaffected area to glyco- and ornithine lipids in the hydrothermally influenced sediment layers show a change from photoautotrophic algae to a bacteria-dominated community.

Statistical analyses revealed that changes in the microbial community structure were mostly related to spatial heterogeneity in pH and sulfide and less to temperature.

The innovative approach to combine gene- and lipid-based methods proved to be very useful to describe the spatial microbial structure.

Biogeochemical features of the behavior of arsenic in Sherlovogorsk mining district of the Zabaikalsky Krai (Russia)

M.A. SOLODUKHINA AND G.A. YURGENSON

Federal state budget institution of science, Institute of Nature Recourses, Ecology and Cryology, Siberian Branch of Russian Academy of Sciences, Chita, Russia (mabn@ya.ru, yurgga@mail.ru)

As a result of multiyear research (2002-2012 gg.) conducted in Sherlovogorsk mining district of the Zabaikalsky Krai, the peculiarities of biogeochemical behaviour As in the components of the landscape. Shows the sources of his income, concentration, regularities of the spatial distribution of the soil, especially biological capture and accumulation in plants.

The spatial distribution of arsenic (As) on the territory of the region is due to the regularities of the development of the second phase of formation of Sherlovogorsk of ore-magmatic system, which is associated with the formation of tin-polymetallic Deposit.

All of the components of landscapes Sherlovogorsk ore district has considerably enriched with As. It is established, that in natural soils background of the site content As in 6 times exceeds MPC and in 2 times - soil Clark. On the territory of the fields maximum Clark concentration (CC) in the soil (the ratio of the average content in the soil to the soil Clark) is 1183, and the excess of MPC in 1005 times. In техноземе career-dumping landscape respectively QC=340, and the excess of MPC in 289 times. Sherlovogorsk ore area can be identified as arsenic biogeochemical province.

The main form of location As in soils is the residual. In the permafrost meadow-forest, in gravelly low-power soil, Chernozem without carbonates, in the chestnut carbonate soil more than 50% As fixed in a stationary position in the oxidation products arsenopyrite, first of all skorodit and other arsenates.

Capture As different plants varies considerably. Herbaceous plants and shrubs more intensively involve As in biological Cycling, than shrubland. Of wood and shrub of plants *Crataegus sanguinea* Pallas and *Betula pendula* Roth do not have гипераккумуляцией As, in contrast to the bushes: *Pentaphylloides fruticosus* (L.) O. Schwarz, *Pentaphylloides parvifolia* (Fischer ex Lehm.) Sojak and *Artemisia gmelinii* Weber ex Stechm. In them, just as in the grassy plants of natural-technogenic landscape detected toxic and critical concentration As (more than 5 mg/kg).

For the majority of the studied plants tend maximum capture As roots and leaves, by the end of the vegetation period is marked its accumulation in these bodies. Minimum contents As found in fruits and seeds.

The obvious hubs, As are herbaceous plants: *Potentilla acervata* Sojak, *Aconogonon angustifolium* (Pall.), *Gallium verum* L. and subshrubs - *Artemisia gmelinii* Weber ex Stechm.

Melting and breakdown of MgCO₃ at high pressures

N.A. SOLOPOVA^{1,2,*}, A.V. SPIVAK², YU.A. LITVIN²
AND L. S. DUBROVINSKY¹

¹Bayerisches Geoinstitut, University of Bayreuth, Bayreuth, Germany, (*corresponds: solopenok@yandex.ru)

²Institute of Experimental Mineralogy of the Russian Academy of Sciences, Chernogolovka, Moscow region, Russia

Studies inclusions in ultra-deep diamonds suggest that magnesite can be major stable carbonate in the lower mantle. It can play an important role for the carbon cycle in the Earth's interior. New form of magnesite II was reported at the high-pressure and high-temperature [1]. However, the information about melting of magnesite at high pressure is limited [2].

We study high-pressure high-temperature behavior of magnesite, stability of the melt and its decomposition in static compression experiments between 10 and 60 GPa and temperatures up to 3500 K using diamond anvil cell technique with laser heating. Special methodology was used for determining the melting point. The spherical boron doped diamonds were used as a heat absorber for laser heating.

In accordance with thermodynamic analysis [3] our experimental results showed that magnesite does not decompose to MgO and CO₂ under conditions of the Earth's lower mantle and demonstrate extended field of congruent melting of magnesite. We observed also formation of MgO and diamond or graphite as a result of decomposition of MgCO₃ melt. Formation of diamond and graphite may be explained by a two stage reaction: MgCO₃=MgO+CO₂; CO₂=C+O₂.

The obtained results allow to determine the phase relations of MgCO₃ at high pressures and high temperatures, and important for constraining the conditions of diamond crystallization from the carbonate-bearing parental media in the Earth's lower mantle.

[1] Isshiki, Irifune, Hirose & Ono (2004), *Nature* 427, 60-62.

[2] Katsura & Ito (1990), *Earth and Planetary Science Letters* 99, 110-117. [3] Dorogokupets (2007), *Geokhimiya* 6, 624-631.

This work was funded by grant RFBR 12-05-33044.

Complex C-O-H-N-S fluids and sulphide-silicate melt immiscibility in the upper mantle

I. SOLOVOVA^{1,*}, A. BOUIKINE², L. KOGARKO²
AND A.B. VERCHOVSKY³

¹Institute of Geology of Ore Deposits solovova@igem.ru

²Vernadsky Institute of Russian Academy of Sciences,

³The Open University, Milton Keynes, UK

The minerals (Ol, Opx, Cpx) of metasomatized garnet lherzolite xenoliths from East Antarctica contain diverse microinclusions of melt, fluid, and fluid-silicate-sulphide inclusions with typical liquid immiscibility textures. At room temperature, the fluid inclusions contain one (liquid), two (liquid and gas) or three (H₂O and CO₂ liquids and gas) phases. All the inclusions are CO₂-dominated. The obtained data suggest the existence of two sources of fluids. Fluid of fluid-silicate-sulphide inclusions show homogenization temperatures of up to -64.8°C, and densities of up to 1.17 g/cm³, which correspond to pressures ≥13 kbar at the moment of fluid entrapment (at 1000°C). Phase transitions at -151°C are close to the critical point of N₂ (-147°C). The Raman spectra of fluid inclusions display lines of CO₂, H₂S and N₂. The high-pressure fluid inclusions have low C/N₂ and N₂/Ar, heavy nitrogen isotope compositions and elevated ⁴⁰Ar/³⁶Ar values (up to 530). Second type inclusions have lower densities (≤0.82 g/cm³) and, correspondingly, lower entrapment pressures (≤7 kbar). Their Raman spectra exhibit a distinct H₂O line. Their fluid has higher C/N₂ and C/Ar, lower δ¹³C, and close to atmospheric N₂/Ar and ⁴⁰Ar/³⁶Ar values. It is suggested that the observed fluids are products of mixing between a mantle derived fluid and atmospheric air or/and seawater.

Fe(II) uptake mechanisms on montmorillonite clay minerals: A multidisciplinary approach

D. SOLTERMANN^{1,2,*}, M. MARQUES FERNANDES¹,
B. BAEYENS¹, M.H. BRADBURY¹ AND R. DÄHN¹

¹Laboratory for Waste Management, Paul Scherrer Institut, Villigen PSI, Switzerland, (*daniela.soltermann@psi.ch).

²Institute of Biogeochemistry and Pollutant Dynamics, ETH Zürich, Zürich, Switzerland

Virtually all radioactive waste repository designs contain large amounts of iron (steel canisters) and reducing conditions will prevail in the long-term. Due to the corrosion of steel canisters, high ferrous iron (Fe²⁺) concentrations in the interstitial porewaters in the near- and far-fields might be expected, which could have a significant influence on the sorption behaviour of other radionuclides through sorption competition effects. The best suited approach investigating the sorption of Fe²⁺ on clay minerals and the influence of high aqueous Fe²⁺ concentrations on the radionuclide retention by clay minerals is a multi-disciplinary one, consisting of macroscopic sorption experiments, geochemical modelling and advanced spectroscopic techniques, such as X-ray absorption spectroscopy (XAS). Fe²⁺ uptake on an iron-free synthetic montmorillonite in the absence of any competing metal was measured by batch sorption experiments under anoxic conditions (O₂ <0.1 ppm). A two-site protolysis nonelectrostatic surface complexation and cation exchange sorption model¹ was used to quantitatively describe the uptake of Fe²⁺ on montmorillonite. Two types of clay surface binding sites, so-called strong ($\equiv\text{S}^{\text{S}}\text{OH}$) and weak ($\equiv\text{S}^{\text{W}}\text{OH}$) edge sites, were required to model the Fe²⁺ sorption isotherms. XAS data showed spectroscopic differences between Fe sorbed at low and medium concentrations, which were chosen to be characteristic for uptake on strong and weak sites, respectively. The XAS data analysis indicated that Fe is located in the continuity of the octahedral sheet.²

Sorption competition experiments of divalent metals Fe and Zn were carried out to further elucidate the uptake processes at the clay mineral-water interface. The competition experiments were performed for the combinations of Zn(II)/Fe(II) and Fe(II)/Zn(II), where the former represents the trace index metal and the latter the blocking metal at high concentration. The results of the wet chemistry and XAS measurements indicate that Fe(II) is competing with Zn(II) if the Fe(II) is present in excess (blocking metal). However, no competition effects between Fe(II) and Zn(II) were observed if Zn(II) is the blocking metal. These results can be explained by a selective uptake of trace Fe on montmorillonite due to Fe(II)/Fe(III) redox processes taking place at the clay surface.² The outcome of this study contributes to an improved molecular understanding of the Fe-clay interaction under anoxic conditions in the absence and presence of other divalent metals.

[1] Bradbury&Baeyens. *J. Contam. Hydrol.*, 1997, **27**(3-4), 223-248. [2] Soltermann *et al. Environ. Sci. Technol.*, 2012, doi: 10.1021/es304270c.

Application of portable XRF analyzers in Au and PGE exploration: An example from the Bushveld Complex, South Africa

ALIREZA SOMARIN

Thermo Fisher Scientific, Tewksbury, MA 01876
alireza.somarin@thermofisher.com

Field portable X-ray fluorescence (FPXRF) analyzers are used worldwide in exploration and mining of various types of metallic and non-metallic deposits from base metals to REEs, precious metals and even hydrocarbons. FPXRF application in base metal and REE exploration and mining is relatively easy and straight forward due to their high economic threshold combined with low detection limit of these metals by FPXRF. Application in precious metal projects needs good understanding of the limitations of the technique; however, FPXRF can still be utilized in such cases using pathfinder elements. This paper summarizes one of these cases in Au-PGE exploration in the Bushveld Complex, South Africa.

In this study, the pathfinder elements were defined using lab assays of 63 samples that were collected along a stratigraphic section. Elements with highest correlation with the target metals (Au, Pt and Pd) were classified as pathfinder elements. These elements were Ni and Cu in this case study (Figure 1). Analyzes of the samples (both direct shot and pulp samples) by FPXRF indicate that all anomalous zones of Au, Pt and Pd can be easily identified by locating anomalies of Ni and Cu on prepared (pulp) and even un-prepared samples. Such anomalous samples have target elements lower than detection limit of FPXRF and should be analyzed by laboratory techniques.

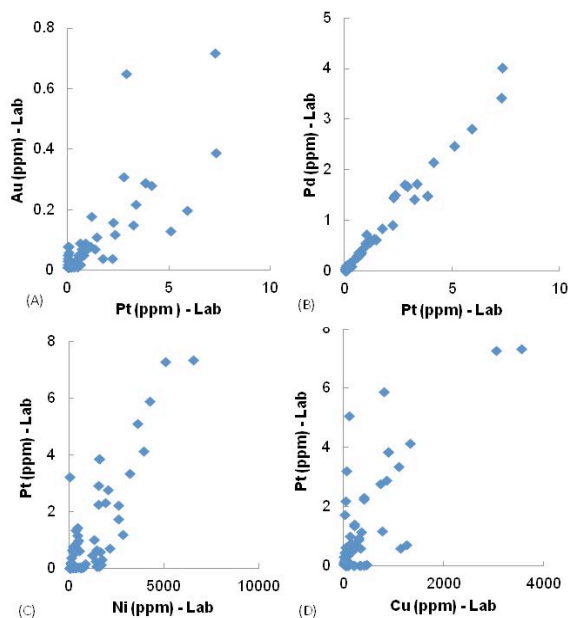


Figure 1: A and B) Correlation between target elements. C and D) Correlation between Pt and pathfinder elements (Ni and Cu).

The Neoproterozoic magmatic evolution in Northern Guangxi, China

SONG HAO^{1,2}, XU ZHENGQI^{1,2*}, NI SHIJUN^{1,2}
AND ZHANG CHENGJIANG^{1,2}

¹ Department of Geochemistry and Nuclear Resources Engineering, Chengdu University of Technology, Chengdu 610059, China (*Correspondence: xuzhengqi@cdu.cn)

² Key Laboratory of Nuclear Techniques in Geosciences of Sichuan Province, Chengdu 610059, China

As a Neoproterozoic giant intrusion, Motianling Pluton in North Guangxi remains a long-standing controversy in the diagenetic age. Based on a series of U-Pb dating in the Motianling Granites, the study of volcanic rocks in the study area mainly aims at retracing the tectono-magmatic evolutionary history in Jinningian epoch of Northern Guangxi. However, the relationship between the Danzhou Group and the Motianling Granites is still in great dispute [1]. This paper attempt to clarify the relationship between Danzhou Group and the Motianling Granites.

With long elongation time in the diagenesis, the Danzhou Group and the Motianling Granites have the time-overlap part and are formed within nearly 100 million years. And the main granite body is formed in the middle-late period of sedimentation of the Danzhou Group, with the later persistent granitic magmatic activity even after the deposition epoch during the formation period of the patched granite body in the Motianling Granites. The severe subsidence of earth surface is resulted from the orogenic extension, which results in the formation of the fine clastic sedimentary of the Danzhou Group (part of Sibao Group can be included). And the partial melting of the crust is resulted from the lithospheric delamination accompanying with the granitic magmatic activity. Through combining the U-Pb dating results with the element geochemistry, the main granite body and the diabase bodies/veins are formed after the Bendong granodiorite, then display the increasing tendency in acidity (SiO₂) and decrease tendency in alkali (Na₂O+K₂O) in the patched granite bodies.

This work is supported financially by the National Natural Scientific Foundation of China (Grants No. 41173059) and the Foundation of China Nuclear Geology (Grants No. 201148 and 200995).

[1] Li Z X *et al.* (1999) *Earth and Planetary Science Letters* **173**, 171-181.

The Triassic Igneous rocks in the Northeastern part of the South Korea

KYO-YOUNG SONG¹

¹Korea Institute of Geoscience & Mineral Resources, Daejeon, Korea (kysong@kigam.re.kr)

The Triassic igneous rocks, gabbroic to granite in composition, occur scattered throughout the Yangyang and Gangneung areas in the northeastern part of the South Korea. The total alkali versus silica composition of these igneous rocks shows a series of differentiation well and large variation from gabbro to alkali granite. So these igneous rocks can be classified to the Yangyang suite on the concept of granite suite.

The Yangyang suite is consist of gabbro, two mica granite, biotite granite, the Namhangjin diorite, the Yangyang syenite, the Yangyang granite and the Hajodae granite. The Yangyang suite is divided into two groups by whole-rock geochemistry analysis, alkali and subalkali rocks group. These means the Yangyang suite is consist of two subsuite. The geochemistry and isotopic composition of these two subsuites indicate that these are thought to be derived from the different granitic magma source. Alkali rocks group contains gabbro, the Namhangjin diorite, the Yangyang syenite and the Yangyang granite, subalkali rocks group contains two mica granite, biotite granite and the Hajodae granite.

The SHRIMP zircon U-Pb ages of the Yangyang suite range from 234±2.9 to 226.5±1.8 Ma.

This Yangyang suite is very important to understand and explain the indentation model which the South China Blocks had collided into the North China Blocks in the Korean peninsula as a wedge-shaped.

Water Vapor Interactions with FeOOH Particle Surfaces

XIAOWEI SONG* AND JEAN-FRANÇOIS BOILY

Department of Chemistry, Umeå University, Sweden *Email: xiaowei.song@chem.umu.se

Iron oxyhydroxide (FeOOH) minerals play important roles in a variety of atmospheric, terrestrial and technological settings. Interactions with water vapor are particularly important given the predominance of water-bearing gases in the environment. In this work, molecular details of water adsorption reactions at FeOOH surfaces were resolved using vibrational spectroscopy, quartz crystal microbalance and molecular dynamics. Acidified and alkalified mineral surfaces were investigated to determine protonation effects on interfacial water loadings and structures. The effects of residual salts on the surfaces were further studied by resolving competitive hydration processes between surface-bound Cl ions and hydroxyl groups.

This work reveals the initial mechanisms of formation of thin water films on mineral surfaces under atmospheric conditions [1]. We show that thin films of adsorbed water display liquid water-like attributes. The affinity of surface (hydr)oxo groups for water molecules is strongly dependent on their abilities at forming hydrogen bonds. Coordination number and site accessibility/steric constraints are main factors. These groups have moreover stronger affinities for water than chemisorbed water ($-\text{OH}_2$) and Cl-exchanged group (e.g. $-\text{Cl}$, $\mu\text{-Cl}$). Finally, we identified a *surface memory effect* showing that original surface protonation states can be retrieved by evacuating surfaces from surface-bound waters. This confirms that the original surfaces were at thermodynamic equilibrium prior water uptake reactions and that all reactions are reversible. This reversibility may further hold in mineral particles undergoing several water condensation-evaporation cycles in nature. This work thus opens a path for understanding water structure as well as condensation reactions on these important mineral particles.

[1] Song X.W., Boily J.-F. (2013), Chem. Phys. Lett. 560, 1-9.

A stable isotope perspective on tracing natural and anthropogenic Hg emissions at the global scale.

JEROEN E. SONKE

Observatoire Midi-Pyrénées, 14 avenue E. Belin 31400 Toulouse, sonke@get.obs-mip.fr

A decade of research on the natural variations in mercury (Hg) stable isotope abundances has shown large variations across biogeochemical reservoirs. These variations result from the gradual separation of heavy/light or even/odd Hg isotopes during the numerous physicochemical processes that shuttle Hg across the Earth's surface. As a result, a Hg isotopic measurement gives rise to four useful isotope fingerprints that may characterize its source, or code for the transformations that Hg has undergone in the past.

Tracing the dominant natural and anthropogenic Hg emissions at the global level is a challenge. The further Hg emissions travel from their source, the more likely it is that oxidation/reduction, sorption or (de-)methylation reactions modify the original source Hg isotope signatures. This presentation illustrates an integrated approach to evaluate Hg isotope tracing at the global scale. Similar to modern and historic Hg emission inventories, a parallel Hg isotope library needs to be built per industrial sector and geographical region. Industrial processes include Hg transformations that may change isotope signatures and need to be understood. Monitoring of the isotopic composition of emitted Hg species and associated Hg deposition at different spatiotemporal scales is necessary. Finally, monitoring of critical receptor environments on continents and oceans and on different time scales (modern, geologic) will tell if globally relevant emission sources can be recognized. All of these tasks are compatible with box and process models of the global Hg cycle, so that Hg isotopic information may in the near future be integrated in global models to help understand Hg cycling.

The approach will be illustrated for coal fired power plant (CFPP) emissions: A coal Hg isotope library, containing ~200 coal samples from historically dominant coal burning regions has been made. A study on two large Chinese coal fired power plants suggests that stack emission Hg isotope signatures are slightly modified from feed coal signatures by emission control technologies. Bi-weekly monitoring of gaseous and particulate Hg isotope signatures in Asian urban-industrial environments is compatible with a dominant CFPP source. Finally, a preliminary attempt to integrate an emission isotope library in a global Hg box model will be compared to historical records of Hg deposition and isotopic variation in peat bogs.

www.minersoc.org

DOI:10.1180/minmag.2013.077.5.19

(Non-?) Traditional Hg stable isotope geochemistry in the early 1920's

J. E. SONKE¹, N. ESTRADE², O.F.X DONARD³
AND J. CARIGNAN²

¹ Observatoire Midi-Pyrénées, CNRS-GET-Université de Toulouse, France, sonke@get.obs-mip.fr

² CRPG, UMR 7358, CNRS-Université de Lorraine, Nancy, France

³ IPREM/LCABIE, UMR 5254, CNRS-Université de Pau et des Pays de l'Adour, Pau, France

In 1919 Sir Francis Aston discovered the multiple stable isotopes of mercury (Hg) using his mass spectrograph. Only one year later Johannes N Brønsted and György de Hevesy used high precision density measurements to prove that liquid Hg distillation into a vacuum fractionates Hg isotopes as a function of isotope mass. In more detailed studies during the 1920's Brønsted and colleagues managed to produce Hg vapors and residual liquids that were heavily fractionated by up to -84‰ and +74‰ on the $\delta^{202}\text{Hg}$ scale. They derived the kinetic isotope fractionation law, and used Rayleigh equations and diagrams to estimate Hg isotope separation factors. They also explored the natural variations in Hg isotope abundances, by converting cinnabar (HgS) into liquid Hg and measuring its density. By sheer coincidence they did not find any density variations for nine global cinnabar deposits, within their measurement uncertainty of 0.4 - 1.2 ‰ on the $\delta^{202}\text{Hg}$ scale. Today we know that the $\delta^{202}\text{Hg}$ of cinnabar may vary by up to 5 ‰ across a single cinnabar deposit.

In 2006 Jean Carignan was interested in the potential isotopic fractionation of volatile metals under natural and industrial conditions. He proposed to examine the distillation of liquid Hg in a vacuum, without knowing that nearly one century before him scientists had looked at the issue. Using MC-ICPMS, we made nearly identical observations as Brønsted and co-workers: a kinetic isotope fractionation factor of 1.0067 for the $^{202}\text{Hg}/^{198}\text{Hg}$ pair (Estrade *et al.*, 2009). We also performed Hg isotope analysis of Hg vapor that is in equilibrium with liquid Hg. Here we observed deviations from theoretical mass dependency for the two odd Hg isotopes, ^{199}Hg and ^{201}Hg , in what has become the first experimental evidence for nuclear volume fractionation of Hg isotopes. This contribution will look back on both the early and more recent measurements.

[1] Estrade, N., Carignan, J., Sonke, J.E., Donard, O.F.X., 2009. Mercury isotope fractionation during liquid-vapor evaporation experiments. *Geochimica et Cosmochimica Acta*, 73: 2693-2711.

Satellite and aircraft views of relationships between particles, cloud water, and rain water

ARMIN SOROOSHIAN^{1*}, ZHEN WANG², GRAHAM FEINGOLD³, TRISTAN L'ECUYER⁴
AND HAFLIDI H. JONSSON⁵

¹ Chemical and Environmental Engineering, University of Arizona, Tucson, AZ, United States

(*correspondence: armin@email.arizona.edu)

² Chemical and Environmental Engineering, University of Arizona, Tucson, AZ, United States
(zhenw@email.arizona.edu)

³ Earth Systems Research Laboratory, NOAA, Boulder, CO, United States (graham.feingold@noaa.gov)

⁴ Department of Atmospheric and Oceanic Sciences, University of Wisconsin, Madison, WI, United States
(Tristan@aos.wisc.edu)

⁵ Center for Interdisciplinary Remotely Piloted Aircraft Studies, Naval Postgraduate School, Monterey, CA, United States (hjonsson@nps.edu)

A poorly characterized process in warm clouds is the conversion of cloud water to rain water especially with regard to the rate by which this complex process occurs. Using a satellite remote sensing data set, this conversion process is examined in a global sense over oceans to identify regional differences and relationships with relevant environmental parameters [1]. We show that a faster conversion process coincides with conditions of reduced atmospheric stability, higher low-level wind speeds, and low aerosol index values. Aircraft measurements are used in a stratocumulus cloud environment to provide more views on relationships between environmental factors influencing water in clouds [2].

[1] Sorooshian, Wang, Feingold & L'Ecuyer (2013), A satellite perspective on cloud water to rain water conversion rates and relationships with aerosol types and atmospheric stability. *Geophys. Res. Atmos.*, 118, doi: 10.1002/jgrd.50523
[2] Sorooshian, Wang, Coggon, Jonsson, Ervens (2013), Observations of sharp oxalate reductions in stratocumulus clouds at variable altitudes: organic acid and metal measurements during the 2011 E-PEACE campaign. *Environ. Sci. Technol.*, doi: 10.1021/es4012383.

Iron isotope geochemistry of the Balmuccia peridotite massif and the composition of the upper mantle

PAOLO A. SOSSI^{1*}, HUGH ST.C. O'NEILL¹
AND MARCO BELTRANDO²

¹Research School of Earth Sciences, Australian National University, Canberra, ACT, 0200

²Dipartimento di Scienze della Terra, Università di Torino, Via Valperga Caluso 35, 10125 Torino, Italy

Extensive work on global, unmetasomatised oceanic and lithospheric mantle-derived peridotites reveals a scatter of $\pm 0.1\%$ $\delta^{57}\text{Fe}$ around the 0‰ value (vs. IRMM-014) [e.g. 1, 2]. Contrastingly, most primitive basaltic lavas cluster about $\delta^{57}\text{Fe} \approx 0.1\%$ [3]. This disparity has typically been ascribed to iron isotope fractionation during partial melting [4]. However, recent studies place the composition of primitive, undepleted mantle at $\approx +0.1\%$, obviating the need for such melting-induced fractionation [5]

In order to constrain the relative effects of partial melting and metasomatism on the iron isotope composition of the upper mantle, we present data from the remarkably fresh and well-characterised Balmuccia orogenic peridotite massif of the Ivrea Zone in northern Italy [6]. A spectrum of cogenetic ultramafic samples were analysed, comprising pyroxenites to lherzolites, harzburgites and dunites, faithfully capturing the variation recorded in the massif.

The starting composition of the Balmuccia lherzolite has about 39% MgO, 3.1% Al₂O₃, 2.9% CaO and 8.3% FeO, which could be explained by the extraction of $\approx 5 \pm 0.33\%$ MORB from primitive mantle. This initial composition has a $\delta^{57}\text{Fe} \approx 0.013\% \pm 0.005\%$ and defines an anchor point from which trends of pyroxene-addition, melt depletion and Fe-metasomatism are identified. Residual harzburgites extend to lighter $\delta^{57}\text{Fe}$ and higher Mg#s, while Fe-enriched harzburgites and dunites are typified by heavier iron isotope compositions and near-constant Mg# with respect to the lherzolites.

Lherzolites with lower MgO contents also exhibit heavier $\delta^{57}\text{Fe}$ values, nearing +0.05‰ at the MgO content of the primitive mantle (36.77%). However, given that MORBs, with $\delta^{57}\text{Fe} \approx 0.15\%$ [3] are derived from depleted mantle, a source of Fe isotope fractionation between partial melting and their eruption onto the ocean floor seems to be required.

[1] Weyer and Ionov, 2007, EPSL; [2] Huang *et al.*, 2011, GCA, 75; [3] Teng *et al.*, 2013, GCA; [4] Dauphas *et al.*, 2009, EPSL; [5] Poitrasson *et al.*, 2013, CMP; [6] Hartmann and Wedepohl, 1993, GCA

Hf isotope systematics of Archean anorthosites: The Manfred Complex, Yilgarn Craton, Western Australia

A.K. SOUDERS^{1*}, P.J. SYLVESTER¹, J.L. CROWLEY²
AND J.S. MYERS³

¹Department of Earth Sciences, Memorial University, St. John's, NL A1B 3X5, Canada (*kate.souders@mun.ca)

²Department of Geosciences, Boise State University, 1910 University Drive, Boise, Idaho 83725-1535 USA

³Department of Applied Geology, Curtin University, Perth, WA 6845, Australia

Archean anorthosite complexes represent a minor, yet distinct rock type found within many Archean terranes. These mantle-derived melts are commonly found in layers with associated leucogabbro, gabbro, and ultramafic units of similar origin. Most Archean anorthosites are intensely deformed and metamorphosed yet preserved igneous minerals have been identified within several complexes. It has become obvious that Archean anorthosites contain zircon crystals, which can be used to establish robust crystallization ages for anorthosite complexes. These minerals are also ideal targets for in situ Lu-Hf isotopic analysis to further characterize the source of Archean anorthosites and provide insight into the formation and evolution of the continental crust during the Archean.

The ca. 3.7 Ga Manfred Complex is exposed northeast of Mount Narryer within the Narryer Gneiss Terrane, Yilgarn Craton, Western Australia. The layered anorthosite-gabbro-ultramafic intrusion outcrops in pods and lenses, engulfed by granitic gneisses [1, 2, 3]. We have sampled anorthosites, leucogabbros and gabbros from the Manfred Complex and determined their age by LA-ICPMS U-Pb zircon geochronology. Zircons separated from these rocks give ages of 3.63 Ga to 3.73 Ga. LA-MC-ICPMS Lu-Hf isotope analyses were performed by focusing the laser spot directly on top of the U-Pb analysis location for each zircon grain. Initial Hf isotope compositions of zircon grains from the Manfred complex range from ca. $\epsilon_{\text{Hf}} +2$ to -3 . This range suggests contributions from both depleted mantle and ancient crustal sources to the parent magma of the Manfred Complex.

[1] Kinny *et al.* (1988) Prec. Res. 38, 325-341. [2] Myers (1988) Prec. Res. 38, 309-323. [3] Williams & Myers (1987) WA Geol. Surv. Rpt. 22, 32 pp.

Secondary Organic Aerosols in the coupled climate aerosol model ECHAM-HAM: Insights into production dependencies and climate impacts

G.SOUSA SANTOS^{1*}, T. STANELLE¹, I. BEY¹
AND U. LOHMANN¹

¹Institute for Atmospheric and Climate Science, ETH Zurich, Universitaetstrasse 16, 8092 Zurich (*correspondence: gabriela.sousa-santos@env.ethz.ch)

Aerosols are an integral part of the climate system, because they play essential roles in the atmosphere's radiation budget and in the hydrological cycle. An important fraction of the aerosols in the troposphere are organic. So far, most models only considered Primary Organic Aerosol (POA) emissions into the atmosphere. However, Secondary Organic Aerosols (SOA) are a non negligible fraction of the total organic.

We aim to investigate SOA processing and impacts on the climate system using two sets of simulations with ECHAM-HAM: two equilibrium simulations for 2000 conditions without SOA and with interactive computation of SOA, and a 50-year hindcast (1960-2010).

The hindcast simulation shows a general increase in SOA burdens in the Northern Hemisphere from 1960 to 2010. SOA production increases from 25 to 30Tg/yr globally and 0.75 to 1.3Tg/yr in Europe. This translates in a increase in SOA surface concentrations of roughly 30% globally and 40% in Europe. In Europe, the reported changes mainly resulted from an increase in biogenic precursor emissions, which are, in turn, most likely connected to changes in anthropogenic land cover and in a lower degree to changes in surface radiation. In other regions of the world other factors like anthropogenic precursor emissions and temperature changes have higher importance. According to the model, SOA has impact on the Earth radiation budget, with a direct radiative effect at the top-of-the-atmosphere (TOA) of -0.35W/m^2 . We will present details of the effect on other climate variables, especially on cloud properties at the conference.

Best practices for reducing energy poverty and (as a result) emissions of methane, carbon dioxide, and black carbon/aerosols

BENJAMIN K. SOVACOOOL

Institute for Energy and the Environment, Vermont Law School, bsovacool@vermontlaw.edu

This presentation demonstrates how small-scale renewable energy technologies such as solar panels, cookstoves, biogas digesters, microhydro units, and wind turbines are helping Asia eradicate energy poverty and (as a result) reduce greenhouse gas emissions. Through an in-depth exploration of case studies in Bangladesh, China, India, Laos, Indonesia, Malaysia, Mongolia, Nepal, Papua New Guinea, and Sri Lanka, the presentation highlights the applicability of different approaches to the promotion of renewable energy in developing countries. It also illuminates how household and commercial innovations occur (or fail to occur) within particular energy governance regimes. It lastly, and uniquely, explores successful case studies alongside failures or "worst practice" examples that are often just as revealing as those that met their targets. Based on these successes and failures, the presentation concludes by presenting twelve salient lessons for policymakers and practitioners wishing to expand energy access and raise standards of living in some of the world's poorest communities.

Benthic fluxes and early diagenesis processes in Adriatic Sea

F. SPAGNOLI^{1*}, G. BARTHOLINI² AND P. GIORDANO³

¹CNR-ISMAR, Largo Fiera della Pesca, 60125, Ancona, Italy

²Università di Bologna, Dipartimento di Scienze Biologiche, Geologiche e Ambientali, Piazza di Porta S. Donato, 1, Bologna

³CNR-ISMAR, Via Gobetti, 101, 40120, Bologna, Italy

During the last decades various researches in the Adriatic and Ionian Sea allowed the individuation of different area characterized by various early diagenesis environments that generate dissolved fluxes at the sediment-water interface with different intensity.

North of the Po River a thin and discontinuous band of terrigenous fine carbonate sediment and with different reactivity of organic matter produces benthic fluxes extremely variable in functions of the fresh organic matter entered by the main rivers

In front of the Po River a limited area, with high sedimentation rate and high continental and autochthonous organic matter inputs, generates high nutrient benthic fluxes.

In the western Adriatic sediments are characterised by progressive southward decrease of sedimentation rate and reactive organic matter that generate decreasing benthic fluxes. The central Adriatic Sea bottom sediment area is characterized by prevalently carbonate sediments and low fluxes of nutrients due to little organic and inorganic inputs and to precipitation of authigenic mineral.

In the Meso-Adriatic and South Adriatic Depression low sedimentation rates and strongly reworked organic and inorganic matter produce very low benthic nutrient fluxes.

In Ionian Sea slope sediments are characterized by very low particulate inputs and by negative fluxes of DIC acting in this way as CO₂ traps while basin sediments show higher benthic fluxes due to increases of organic matter inputs.

AMERIGO: A new benthic lander for dissolved flux measurements at sediment-water-interface

F. SPAGNOLI^{1*}, G. CICERI², G. GIULIANI¹, V. MARTINOTTI² AND P. PENNA¹

¹CNR-ISMAR, Largo Fiera della Pesca, 60125, Ancona, Italy

²RSE SpA, Via Rubattino 54, 20134, Italy

Amerigo is a new autonomous and automatic benthic lander for the measurements of dissolved benthic fluxes at the sediment-water interface. The lander is able to measure fluxes of nutrients such as ammonium, nitrites, nitrates, phosphates and silica, gases such as oxygen, carbon dioxide and methane, trace elements such as heavy metals, and also other dissolved pollutants resulting from human activity. AMERIGO is able to operate from transitional environments to continental shelf and abyssal plain. The Lander can include various components, at present it is equipped with 3 benthic chambers for measuring the fluxes at the water-sediment interface and is prepared to host a microprofiler and other benthic instruments (mini-penetrometer, gravimeter, etc.). The 3 benthic chambers are equipped with a water sampler, which also allows injection of tracers, a system for the refilling of the consumed oxygen (Oxystat) and sensors for pH and dissolved gas monitoring (oxygen, methane and in future CO₂). Outside the benthic chambers a CTD probe for measuring the chemical-physical parameters (temperature, conductivity and pressure) and a niskin bottle for the sampling of the water column are present. The lander is equipped with all mechanisms for the dipping (ballast weights), positioning on the bed, raising (a timed release mechanism (burn-wire type) for the release of the ballast and glass spheres for the flotation) and recovery (radio transmitter, GPS position system and flasher) on board. A useful property of AMERIGO is the modularity and flexibility, that is different components, which can be assembled and programmed on the basis of needs and of the environmental conditions in which it will operate.

After the two first testing cruises early results of the AMERIGO functioning will be presented.

Hydrogeochemical radiation burden in the ambiance of natural radioactivity in the hills of Vršac

¹V. SPASIĆ-JOKIĆ, ²V. GORDANIĆ, ²M. VIDOVIĆ
AND ³D. JOVANOVIĆ

¹Faculty of Technical Sciences, University of Novi Sad,
svesna@uns.ac.rs

²IHTM, University of Belgrade gordanicv@gmail.com,
mivibgd@yahoo.com

³Geological Survey, Belgrade, dragan.jovanovic@gzs.gov.rs

During regional hydrogeochemical prospection (500 km²) samples were collected from surface flows, springs, wells and borings. In water, contents of uranium, radium and radon were determined. Three anomaly zones of radionuclides in water were identified, and their values vary within the interval: 0.1-166 ppb for U, up to 7 Bq for Ra and 2.8-36 Bq. Risk for cancer incidence was calculated using Monte Carlo techniques. Anomalies of radioactive elements are located in the area which is built of granites, gneiss and crystalline schists. According to the available data it is considered that the granites have intruded in the crystalline schists during Hercynian orogeny which is of significance for uranium deposits formation. In the purpose of defining conditions of uranium migration and depositing at favorable geochemical barriers, beside contents of U, Ra and Rn in water, some other parameters (Eh, pH, Ep, content of microelements, etc) were determined. Identification of the areas of hydrogeochemical radiation burden caused by presence of radionuclides (U, Ra, Rn) in water is of special relevance for determination of geopathogenic zones of the influence of natural radioactivity. By applying conversion factors the radiation burden was calculated for each radionuclide. Research results are shown on maps and charts. That results are representing the influence of natural radionuclides in water, which are ingested in the ambient of living environment of rural settlements.

Keywords: hydrogeochemistry, radioactivity, cancer incidence, uranium, radium, radon.

This work has been financed by the Ministry of Science and Technological Development of the Republic of Serbia (project No. 45006).

[1] S. Pavlović *et al.* (1966) Study of Yugoslavian granitoid massifs, fund of Geoinstitute, Belgrade, Serbia.

Mineral Physics in the Terapascal Regime: Dynamic Studies of Planetary Interiors

DYLAN K. SPAULDING

Origins Initiative, Harvard University,
dylanspauling@fas.harvard.edu

Laser-driven shock wave techniques extend the reach of mineral physics to the terapascal regime, permitting unprecedented studies of planetary compositions. Such experiments probe extreme states of matter characteristic of late-stage giant impacts (such as that believed to have formed the moon) as well as the present-day interiors of several Earth-mass exoplanets. Here, I present a suite of recent results on the physical and transport properties of fundamental mineral phases in the Earth's mantle: SiO₂, MgO and MgSiO₃. Experiments on molten MgSiO₃ show the first evidence of a liquid-liquid phase transition with a 6% volume reduction over a wide temperature range, suggesting the potential for unexpectedly complex behavior in silicate liquids at ultra-high pressure. Results on MgO resolve controversial predictions for high-pressure melting and the B1-B2 transition. In addition, data for all three materials reveal thermal and electrical conductivities enhanced by one to two orders of magnitude in the fluid state relative to estimates for the present-day terrestrial mantle. These results underscore the potentially significant role of conductive liquid silicates and oxides in governing the early thermal-chemical evolution of the Earth and other extra-solar 'rocky' planets.

Evidence from fluid inclusions extends the record of seawater chemistry by ~300 million years, from ~544 Ma to ~830 Ma

NATALIE SPEAR^{1*}, H.D. HOLLAND¹,
JAVIER GARCIA-VEIGAS², T.K. LOWENSTEIN³
AND ROBERT GIEGENGACK¹

¹Earth and Environmental Science, Univ. of Pennsylvania, Phila., PA 19014, USA (*correspondence: nahilln@sas.upenn.edu)

²Univ. of Barcelona, Barcelona 08028, Spain

³Department of Geological Sciences, State Univ. of New York at Binghamton, Binghamton, NY 13902, USA

We analyzed primary fluid inclusions in halite from marine evaporites in the ~830-Ma Browne Formation of the Officer Basin in Western Australia by the Cryo-SEM-EDS technique. The parent seawater, calculated from the concentrations measured in those inclusions, contained ~565 mmolal Cl⁻, ~456 mmolal Na⁺, ~50 mmolal Mg²⁺, 9-12 mmolal Ca²⁺, ≥ 3 mmolal SO₄²⁻, and ~1 mmolal K⁺. The concentrations of the major ions, except K⁺ and possibly SO₄²⁻, fall within the known range of Phanerozoic seawater composition. Ours is the first direct measurement of the composition of Mid-Neoproterozoic seawater, and extends direct documentation of seawater chemistry by ~300 Ma.

We sampled the Browne Formation from two cores (Empress 1A and Lancer 1), both from the western Officer Basin, a large intracratonic basin that covers an area of ~525,000 km² in Western and South Australia. In spite of the distance between the two studied wells (~264 km), the lithology and thicknesses throughout the sedimentary succession of the encountered Browne Formation are remarkably similar.

The amount of sulfate in the Mid-Neoproterozoic ocean was closely linked to the amount of oxygen in the atmosphere and deep ocean. Our estimates suggest that Mid-Neoproterozoic marine-sulfate concentrations were considerably lower (≥ 10%) than modern values. By terminal Neoproterozoic time, the composition of fluid inclusions in halite and the mineralogy of evaporite rocks indicate that seawater-sulfate levels rose significantly, to 50 to 80% of modern concentrations, a trend that parallels a similar increase in atmospheric and oceanic oxygen. By imposing a tighter constraint on the sulfate levels of Neoproterozoic seawater, we can define more accurately the circumstances and timing of the oxygenation of the Earth's atmosphere and oceans.

Geochemical evolution of prehistoric magma sources beneath Mt. Etna

E.A. SPENCE¹, H. DOWNES^{1*}, J. BLICHERT-TOFT²,
J.G. BRYCE³ AND E. HEGNER⁴

¹Dept of Earth and Planetary Sciences, Birkbeck University of London, UK (*correspondence: h.downes@ucl.ac.uk)

²Ecole Normale Supérieure de Lyon, Lyon, France.

³UNH Earth Sciences, Durham, New Hampshire, USA.

⁴Dept of Earth and Environmental Sciences, Ludwig-Maximilians Universität, Munich, Germany.

Prehistoric alkalic lavas of Mount Etna representing a ~70 ka time span, sampled from four vertical sections in the southern wall of the Valle del Bove (VdB), exhibit geochemical and isotopic variations distinguishing them as six separate lithostratigraphic and volcanic units within the newly defined framework of Etna [1]. Intersecting geochemical correlations between lavas highlight their stratigraphic relationships, and new isotopic data such as ⁸⁷Sr/⁸⁶Sr (0.7033-0.7036) and ²⁰⁶Pb/²⁰⁴Pb (19.76-20.02), indicate subtle changes in evolution of the magma sources beneath Etna. The alkalic centres of the VdB and modern Etna no longer tap the source(s) of ancient Iblean magmatism (2.6-1.4 Ma) [2]. Isotopic variations indicate that the oldest unit Salfizio-1 (>85 ka) tapped a mantle source similar to present-day Etna (⁸⁷Sr/⁸⁶Sr >0.7035), while four other units relate more closely to the source of historic Etna magmatism (⁸⁷Sr/⁸⁶Sr <0.7035) [3]. The sixth group, part of Piano Provenzana formation (~42-30 ka) of Ellittico, has the most chemically evolved lavas (58-62 wt% SiO₂) and exhibits lower Hf and Nd isotopic ratios and less radiogenic ²⁰⁶Pb/²⁰⁴Pb and ⁸⁷Sr/⁸⁶Sr than the oldest unit, implying that the temporal trend generally observed in the evolution of Nd-Sr isotope systematics breaks down over a ~70 ka period. Mt. Etna's unique position on an accretionary wedge related to the Calabrian Arc, formed during convergence of the African and Eurasian plates and close to the extensional Malta Escarpment [4], presents a complicated tectonic evolution model for Etna magmatism. Subduction processes, slab rollback of Ionian oceanic lithosphere and upwelling asthenospheric mantle are all likely to introduce chemical and isotopic heterogeneities into the convecting mantle.

[1] Branca *et al.* (2011) *Ital. J. Geosci.* **130**, 265-291. [2] Trua *et al.* (1998) *Contrib. Min. Pet.* **131**, 307-322. [3] Viccaro and Cristofolini (2008) *Lithos* **105**, 272-288. [4] Doglioni *et al.* (2001) *Terra Nova* **13**, 25-31.

The isotopic artifacts of enhanced crustal preservation in collisional orogenesis

CHRISTOPHER J. SPENCER^{1*}, PETER A. CAWOOD¹,
CHRIS HAWKESWORTH¹ AND NICK M.W. ROBERTS²

¹Department of Earth and Environmental Sciences, University of St Andrews, North Street, St Andrews KY169AL

²NERC Isotopes Geosciences Laboratory, British Geological Survey, Keyworth, Nottingham, NG12 5GG, UK

*cs207@st-andrews.ac.uk

The generation of felsic crust at accretionary/collisional tectonic boundaries is considered globally to be in steady-state, although the rate of crustal production can vary locally.

U-Pb, Hf, and O isotopic analyses in detrital zircon are widely used to assess the timing and isotopic composition of crustal growth. The age distribution of global detrital zircon record is comprised of “peaks” and “troughs”.

This episodic temporal distribution of zircon crystallization ages has been argued to represent periods of global collisional orogenesis that isolated continental crust formed within accretionary settings within the interior of newly formed supercontinents. This is shown by comparing U-Pb, O, and Hf isotopes in detrital zircons derived from the accretionary, collisional, and post-rift stages of the assembly of the supercontinent of Rodinia based on data from Laurentia and Baltica.

Our results show that continental crust with highly negative ϵHf and high $\delta^{18}\text{O}$ values that formed during the accretionary stage is largely removed from the record preserved in collisional and post-rift stages, probably via sediment subduction, subduction erosion or tectonic delamination. These relations support the hypothesis that detrital zircon age peaks do not represent non-steady state felsic crust formation, but are an artifact of selective preservation during collisional orogenesis.

SCLM super-Si garnet traces the Archaean

DIRK SPENGLER

Institute of Earth and Environmental Science, Potsdam University, 14476 Potsdam, Germany (spengler@geo.uni-potsdam.de)

Sub-continental lithospheric mantle (SCLM) garnet that hosts oriented pyroxene lamellae, that exsolved from former super-Si garnet, have been reported only from the oldest parts of cratons including the Kalahari, Laurentia and Siberia composite cratons [1-5]. Direct implications are: the exsolution microstructure has (1) an Archaean affinity and (2) a global distribution. This study reviews reconstructed and normal garnet chemistries to evaluate proposed garnet origins and exsolution scenarios.

Proportions of pyroxene lamellae in garnet that were quantified using standard techniques range with 0.5-9.6vol.%. Re-integrated garnets have Si+Ti in the range of 2.992-3.086 (median 3.034) cations per 12 oxygen. Maximum values correspond to 7.9 GPa (median 6.4 GPa) [6] that favour a lithospheric origin of all garnet prior to exsolution. Garnet Si isopleths have negative slopes in P-T space [6] suggesting that the above P estimates are overestimated if pre-exsolved garnet formed at high T.

Ti-Na systematics shows a bimodal distribution. The larger fraction of pre-exsolved garnet (G1, G4, G5, G12) has $\text{TiO}_2 > 0.4 \text{ wt.}\%$ and has a positive correlation between TiO_2 and Na_2O with $\text{TiO}_2/\text{Na}_2\text{O} > 10$. These features overlap those of lamellae-free garnet megacrysts [7], consistent with an origin from re-fertilising melts. The other, minor fraction of pre-exsolved garnet (G4, G5) has $\text{TiO}_2 < 0.4 \text{ wt.}\%$ that correlates negatively with Na_2O at dominantly $\text{TiO}_2/\text{Na}_2\text{O} < 2$. Major elements suggest these pre-exsolved garnets to have a pyroxenite/websterite origin. Non-eclogitic lithospheric garnet diamond inclusions from the Siberia, Kaapvaal and Slave cratons include the negative, but not the positive correlation defined by the pre-exsolved garnet chemistry. Thus, low $\text{TiO}_2/\text{Na}_2\text{O}$ garnet (pyroxenitic/websteritic) formed part of Archaean SCLM prior to local lithospheric diamond formation.

In summary, (1) lamellae type pyroxene exsolution in garnet occurred at SCLM depth most likely by cooling and (2) appears to be a tracer of Archaean provinces, (3) high $\text{TiO}_2/\text{Na}_2\text{O}$ pre-exsolved garnet may have formed by infiltrating melts, (4) low $\text{TiO}_2/\text{Na}_2\text{O}$ pre-exsolved garnet is related to the origin of websterite/pyroxenite. Additional REE systematics will be presented to provide constraints on the latter.

[1] Haggerty & Sautter (1990) *Science* **248**, 993-996. [2] Roden *et al.* (2006) *Lithos* **90**, 77-91. [3] Spengler *et al.* (2006) *Nature* **440**, 913-917. [4] Bobrov *et al.* (2012) *Doklady* **444**, 574-578. [5] Alifirova *et al.* (2012) *Int. Geol. Rev.* **54**, 1071-1092. [6] Collerson *et al.* (2010) *GCA* **74**, 5939-5957. [7] Schulze (1997) *Expl. Min. Geol.* **6**, 349-366.

Tracking environmental changes over the past 3000 years in the Region of Ria do Mamanguá, Rio de Janeiro, Southeastern Brazil using molecular organic markers

A. M. SPERA^{1*}, S. TANIGUCHI¹, J. LEONEL¹
AND M. C. BICEGO¹

¹Praça do Oceanográfico, 191, Cidade Universitária, São Paulo – SP, Brazil. 05508-120

(*correspondence: amandaspera@usp.br)

Molecular organic markers (terrestrial *n*-alkanes and alkenones) and other geochemical tracers ($\delta^{13}\text{C}$, $\delta^{15}\text{N}$ and $\delta^{34}\text{S}$) were used to assess changes in rainfall patterns and in the sea surface temperature over the past 3000 years in the Region of Ria do Mamanguá, located on the southern coast of Rio de Janeiro, Brazil. It was possible to identify periods with distinctive contribution from terrestrial organic matter in the sediments cores. The wetter periods between 2733 and 2000 cal years BP and between 1100 and 200 cal years BP presented a higher contribution of terrestrial organic matter to the area. While the dryer period between 2000 and 1100 cal years BP showed a lower input. Furthermore, it was possible to identify the presence of the Little Ice Age event, that was characterized as a period of wetter conditions and with relatively low SST in the Region of Ria do Mamanguá, corroborating with other paleoclimate records in South America. A possible reduction in the termohaline circulation during these cold events may have contributed to the increase in the latitudinal temperature gradient. A lower sea surface temperature in the North Atlantic could have contributed to a displacement in the atmospheric system of the South Hemisphere through a change in the latitudinal position of the Intertropical Convergence Zone (ITCZ). The ITCZ acts as the main source of moisture to the region where the South American Summer Monsoon is formed and consequently the South Atlantic Convergence Zone (SACZ). The SACZ is one of the main features responsible for most of the rain in the Region of Ria do Mamanguá.

The global record of local iron geochemical data from Proterozoic through Paleozoic basins

E.A. SPERLING¹, C. WOLOCK², A.H. KNOLL^{1,2}
AND D.T. JOHNSTON¹

¹Dept. of Earth and Planetary Sciences, Harvard University, Cambridge, MA, USA

(*correspondence: sperling@fas.harvard.edu)

²Dept. of Organismic and Evolutionary Biology, Harvard University, Cambridge, MA, USA

Iron-based redox proxies represent one of the most mature tools available to sedimentary geochemists. These techniques, which benefit from decades of refinement, are based on the fact that rocks deposited under anoxic conditions tend to be enriched in highly-reactive iron. However, there are myriad local controls on the development of anoxia, and no local section is an exemplar for the global ocean. The global signal must thus be determined using techniques like those developed to solve an analogous problem in paleobiology: the inference of global diversity patterns through time from faunas seen in local stratigraphic sections. Here we analyze a dataset of over 4000 iron speciation measurements (including over 600 de novo analyses) to better understand redox changes from the Proterozoic through the Paleozoic Era. As with paleobiological diversity curves, it is expected that a number of biases affect such a dataset, including both spatial and temporal sampling bias and stochastic error.

Preliminary database analyses yield interesting observations. We find that although anoxic water columns in the middle Proterozoic were dominantly ferruginous, there was a statistical tendency towards euxinia not seen in early Neoproterozoic or Ediacaran data. Also, we find that in the Neoproterozoic oceans, oxic depositional environments—the likely home for early animals—have exceptionally low pyrite contents, and by inference low levels of porewater sulfide. This runs contrary to notions of sulfide stress on early metazoans. Finally, the current database of iron speciation data does not support an Ediacaran or Cambrian oxygenation event. This conclusion is of course only as sharp as the ability of the Fe-proxy database to track dissolved oxygen and does not rule out the possibility of a small-magnitude change in oxygen. It does suggest, however, that if changing $p\text{O}_2$ facilitated animal diversification it did so by a limited rise past critical ecological thresholds, such as seen in the modern Oxygen Minimum Zones benthos. Oxygen increase to modern levels thus becomes a Paleozoic problem, and one in need of better sampling if a database approach is to be employed.

Viscosity and structure of fayalite liquid at high pressure up to 9GPa

H. SPICE^{1*}, C. SANLOUP¹, J. DREWITT¹,
C. DE GROUCHY¹, C. CRÉPISSON², Y. KONO³, C. PARK³,
AND C. MCCAMMON⁴

¹Centre for Science at Extreme Conditions, University of Edinburgh, UK (holly.spice@ed.ac.uk) (*presenting author)

²UPMC Univ Paris 06, UMR 7193, ISTEP, Paris, France

³HPCAT, Geophysical laboratory, Carnegie Institution of Washington, USA

⁴Bayerisches GeoInstitut, Universitaet Bayreuth, Germany

Viscosity of magma is a crucial transport property of melts that influences a variety of important igneous processes, both during the evolution of the early Earth and in the present day mantle [1]. Previous experimental work on polymerized silicate melts e.g. [2] show a decrease in viscosity with increasing pressure. Viscosities of depolymerized silicate melts are poorly documented at mantle P-T due to experimental difficulties.

Here we present the results of *in situ* experiments on the viscosity and structure of pure fayalite melt at high pressure. Fayalite consists of isolated silica tetrahedra, so is as depolymerized as possible for a silicate melt. Viscosity measurements were carried out using the falling sphere viscometry technique e.g. [3]. Viscosity was found to decrease along the fayalite liquidus up to ~9GPa.

The structure and compressibility of fayalite melt was studied up to 7.5GPa. The coordination of the Fe-O bond was found to increase gradually from ambient pressure to 7.5GPa [4]. Higher coordination numbers allow for a more densely packed structure, resulting in a longer and hence weaker Fe-O bond, causing a decrease in viscosity [5]. The results suggest that deep Fe-rich melts will have a high density, but will be very mobile due to their low viscosity. Compressibility of the melt is derived from extrapolation of the structure factor to $q=0 \text{ \AA}^{-1}$. This enables the determination of density as a function of P with an unprecedented P resolution. This is a promising method to extract the equation of state of non-crystalline materials at mantle P.

[1] Ghosh and Karki (2011) *Geochim. Cosmochim. Acta.* 75, 4591-4600. [2] Kushiro (1976) *JGR* 81(35), 6347-6350. [3] Liebske *et al.* (2005) *EPSL* 240, 589-604. [4] Sanloup *et al.* *Geochim. Cosmochim. Acta.* Accepted. [5] Reid *et al.* (2003) *Phys Earth. Planet. Inter.* 139, 45-54.

Origin of curved CSDs: Heterogeneous nucleation of crystals in crystallizing magmas

VÁCLAV ŠPILLAR* AND DAVID DOLEJŠ

Institute of Petrology and Structural Geology, Charles University, Albertov 6, 128 43 Praha 2, Czech Republic
(*correspondence: vaclav.spillar@seznam.cz)

Crystal size distributions (CSDs) are becoming a routine method to quantitatively describe textures of plutonic and volcanic rocks. Simple batch or open system crystallization models involving homogeneous nucleation and crystal growth predict linear trends in the logarithmic population density vs. crystal size space. Since numerous magmatic rocks show concave-up curves, their origin was interpreted as due to multiple crystallization stages or population mixing. Many crystal populations in magmatic rocks also have a non-random, clustered, spatial distribution whose origin remains unclear. We show that both curved CSDs and clustering of crystals can be self-consistently explained by crystallization involving heterogeneous nucleation on crystal surfaces.

We performed three-dimensional numerical simulations of melt crystallization by homogeneous and heterogeneous nucleation and crystal growth. The rates of heterogeneous and homogeneous nucleation were coupled in order to simulate texture with a characteristic ratio of heterogeneous to homogeneous nuclei (H). Quantitative parameters describing sizes, contact, and spatial relationships of crystals were evaluated as functions of the H -ratio.

As H increases above ~2, the CSD evolves from straight to progressively curved, the number of neighbors around a crystal increases, and the clustering index, R , decreases below unity. At $H > 10$, the resulting texture gains porphyritic appearance, and for $H > 200$, the crystallization proceeds as radial growth of heterogeneous nuclei on isolated centers and a spherulitic texture develops. Numerical simulations with variable nucleation and growth rate functions indicate that these results are general and robust, thus solely depend on the H -ratio. This approach allows meaningful determination of the role of the heterogeneous nucleation in natural samples without of a detailed knowledge of the underlying kinetics of crystallization.

Our simulations are consistent with the number of heterogeneous nuclei being about an order of magnitude predominant over the number of homogeneous nuclei in ordinary magmatic rocks with curved CSDs, without involvement of mechanical mineral-melt interactions or late magmatic coarsening.

The climate impacts of natural aerosol

DOMINICK VINCENT SPRACKLEN, CATHERINE SCOTT
AND ALEX RAP,

School of Earth and Environment, University of Leeds, Leeds,
UK; dominick@env.leeds.ac.uk

Natural aerosol plays a significant role in the Earth system because climate controls many natural aerosol sources and because natural aerosol alters the radiative balance of the Earth. Here we explore a wide range of interactions and feedbacks between natural aerosol, anthropogenic aerosol and climate.

Firstly, we quantify the direct and first aerosol indirect effect of different natural aerosol sources. We explain the magnitude of these different radiative effects in terms of atmospheric chemistry and aerosol microphysics. Secondly, we quantify the impact of the natural aerosol background on the anthropogenic aerosol indirect effect. We find that a higher natural aerosol background tends to reduce the first aerosol indirect effect attributed to anthropogenic aerosol. Next, we explore the impact of anthropogenic aerosol on natural aerosol – climate feedbacks. We demonstrate that anthropogenic pollution aerosol in the Northern Hemisphere has reduced the climate feedback that occurs due to changes in natural aerosol emissions. Finally, we explore the impact of natural aerosol on diffuse radiation and the impact on the terrestrial biosphere.

Age calibration of geomagnetic polarity reversals around the Cretaceous-Paleogene boundary

COURTNEY SPRAIN^{1*}, PAUL J., RENNE^{1,2}
AND GREGORY P.R. WILSON³

¹Dept. Earth and Planetary Science, Univ. California,
Berkeley, CA 94720, USA (*correspondence:
spra0111@berkeley.edu)

²Berkeley Geochronology Center, 2455 Ridge Rd., Berkeley,
CA 94709, USA

³Dept. Biology, Univ. Washington, Seattle, WA 98195, USA

Improved understanding of the timing of events attending the end-Cretaceous mass extinction is limited by difficulty in correlating marine and terrestrial records. The Geomagnetic Polarity Time Scale (GPTS), if well-calibrated, offers an important means to address this problem. Terrestrial sections in the Hell Creek region of Montana, interbedded with abundant sanidine-bearing tuffs, provide an opportunity to refine the ages of polarity reversals near the Cretaceous-Paleogene boundary (KPB), ultimately providing a test on the accuracy of orbital tuning chronologies e.g. [Ogg, 2012] for these reversals. Variable sedimentation rates often render terrestrial sequences unsuitable for such purposes, but in this case close stratigraphic proximity between reversals and tuffs allows very small fractional interpolations, ranging from 0.01 to 0.25 of the distance between bounding dated tuffs.

Preliminary new ⁴⁰Ar/³⁹Ar ages for 3 tuffs were combined with existing magnetostratigraphic data from two sections [Swisher *et al.*, 1993] to evaluate the potential of these records for time-scale calibration. Magnetic data gaps as large as several meters were used as conservative proxies for the uncertainty in reversal placement. Ages and uncertainties (+/- systematic sources) based on the optimization calibration of the ⁴⁰Ar/³⁹Ar system [Renne *et al.*, 2011] were determined by linear interpolation for the following three polarity reversals immediately following the KPB, and are shown compared with the GTS 2012 values [Ogg, 2012].

<u>Chron boundary</u>	<u>Age (Ma)</u>	<u>±σ (Ma)</u>	<u>GTS 2012</u>
C28r top	64.755	0.028/0.050	64.667
C28r base	64.900	0.044/0.061	64.958
C29r top	65.605	0.080/0.092	65.688

The uncertainties in our ages are dominated by the coarse spacing of samples defining the Chron boundaries. Our modelling indicates that with sampling at the decimeter scale and with age precision demonstrably attainable from these tuffs [Renne *et al.*, 2013], these reversals can be dated with a resolution of ±10 ka, and an absolute accuracy of ±40 ka.

Initial $^{176}\text{Hf}/^{177}\text{Hf}$ of the Earth and early silicate differentiation

P. SPRUNG^{1,2}, T. KLEINE¹ AND E.E. SCHERER³

¹Institut für Planetologie, University of Münster, 48149 Münster, Germany (sprung@uni-muenster.de)

²Institute of Geochemistry and Petrology, ETH Zürich, 8092 Zürich, Switzerland

³Institut für Mineralogie, University of Münster, 48149 Münster, Germany

Investigating silicate differentiation on Earth using the ^{176}Lu - ^{176}Hf system requires knowledge of the $^{176}\text{Hf}/^{177}\text{Hf}$ evolution of the bulk silicate Earth (BSE). The starting point of this evolution is commonly determined by back-calculating the present-day $^{176}\text{Hf}/^{177}\text{Hf}$ of chondrites to the age of the solar system [1]. Relative to this $^{176}\text{Hf}/^{177}\text{Hf}$ evolution, most Hadean zircons exhibit less radiogenic $^{176}\text{Hf}/^{177}\text{Hf}$ and were interpreted in terms of crust extraction from a primordial mantle at 4.4–4.5 Ga [e.g., 2]. However, Bizzarro *et al.* [3] argued that the initial $^{176}\text{Hf}/^{177}\text{Hf}$ of the angrite Sahara 99555, which is ~ 4 ϵ -units below the back-calculated chondrite initial [1], provides a more appropriate initial $^{176}\text{Hf}/^{177}\text{Hf}$ of the BSE. Relative to such a revised $^{176}\text{Hf}/^{177}\text{Hf}$ evolution of the BSE [3], Hadean zircon populations show both enriched and depleted signatures, which was inferred to imply continuous crustal growth throughout the Hadean [3].

To better constrain the initial $^{176}\text{Hf}/^{177}\text{Hf}$ of the BSE we have initiated a Lu-Hf study on primitive meteorites, complemented by investigations of KREEP-rich lunar rocks, which provide the signature of a strongly enriched reservoir that formed at *ca.* 4.4 Ga [4]. Our data for low-Lu/Hf phases in primitive meteorites, which should directly provide the initial $^{176}\text{Hf}/^{177}\text{Hf}$ of the solar system, overlap with the back-calculated chondrite initial [1]. Moreover, we show that the $^{176}\text{Hf}/^{177}\text{Hf}$ of KREEP at ~ 3.9 Ga is ~ 5.5 ϵ -units below the contemporaneous $^{176}\text{Hf}/^{177}\text{Hf}$ of chondrites, yielding a two-stage model age of *ca.* 4.4 Ga, assuming a chondritic Lu-Hf isotopic evolution for the bulk Moon. This Lu-Hf model age of KREEP is fully consistent with other, independent estimates for the age of KREEP. In contrast, the two-stage model age of our KREEP-rich lunar rocks relative to the revised BSE evolution of [3] is *ca.* 4.0 Ga and thus *ca.* 400 Myr too young. Thus, our new data do not support the revised initial $^{176}\text{Hf}/^{177}\text{Hf}$ of the BSE based on Sahara 99555 [3], but rather indicate that the back-calculated chondrite composition [1] is a reliable estimate for the initial $^{176}\text{Hf}/^{177}\text{Hf}$ of the BSE.

[1] Bouvier *et al.* (2008) *EPSL* **273**, 48–57. [2] Kemp *et al.* (2010) *EPSL* **296**, 45–56. [3] Bizzarro *et al.* (2012) *G3* **13**, Q03002. [4] Carlson & Lugmair (1979) *EPSL* **45**, 123–132.

The structural role of iron in pantelleritic glasses

P. STABILE^{1*}, M.R. CICONI¹, G. GIULI¹, H. BEHRENS², J. KNIPPING² AND E. PARIS¹

¹School of Science and Technology, Geology Division, University of Camerino, Via Gentile III da Varano, 62032 Camerino, Italy (paola.stabile@unicam.it)

²Institute of Mineralogy, Leibniz University Hannover, Callinstr.3, D-30167, Hannover, Germany

The main objects of this work are to determine the effect of oxygen fugacity and composition on the structural role of Fe in silicate glasses representative of pantelleritic magmas. Since many studies have investigated melts using glasses as a structural analogue [1, 2, 3], we have focused on the structural environments of Fe and S in synthetic glasses to relate their behaviour to natural magma with the same composition.

Several glasses have been synthesized under controlled oxygen fugacity conditions (from air to iron-wustite buffer) and with different (Na+K)/Al ratios. In fact, alkali content is known to affect strongly the Fe oxidation state in silicate glasses [4], but it is still controversial to which extent alkali can modify Fe structural role in glasses/melts. Hydrothermal syntheses have been carried out at 1.5 kbar and temperatures between 800°C and 1000°C. Additionally, glasses were produced by melting in a Ar/H₂ gas mixing furnace at ambient pressure and at 1250°C.

Water incorporation in the glasses has been characterized by Karl-Fischer titration (KFT) and IR spectroscopy. Additionally, the redox state of iron in the glasses has been determined by colorimetric wet-chemical analyses. Preliminary Fe K-edge X-ray Absorption Spectroscopy data allowed to study the kinetic of Fe reduction under anhydrous conditions. Here we present preliminary results on Fe oxidation state, coordination number and geometry [5]. The results will be useful for understanding the role of Fe in the polymerization of the silicate melt and the interaction Fe-S.

[1] Calas & Petiau (1983) *Solid State Communic.* **45**, 625–629. [2] Mysen *et al.* (1985) *American Mineralogist* **70**, 317–331. [3] Giuli *et al.* (2002) *Geochimica et Cosmochimica Acta* **66**, 4347–4353. [4] Moretti & Ottonello (2003) *Journal of Non-Cryst. Solids* **323**, 111–119. [5] Giuli *et al.* (2012) *American Mineralogist* **97**, 468–475.

First-principles calculations of the lattice thermal conductivity of the lower mantle

STEPHEN STACKHOUSE^{1*}, LARS STIXRUDE²
AND BIJAYA B. KARKI³

¹School of Earth and Environment, University of Leeds, Leeds LS2 9JT, United Kingdom
s.stackhouse@leeds.ac.uk (* presenting author)

²Department of Earth Sciences, University College London, Gower Street, London WC1E 6NT, United Kingdom
l.stixrude@ucl.ac.uk

³School of Electrical Engineering and Computer Science, Department of Geology and Geophysics, and Center for Computataion and Technology, Louisiana State University, Baton Rouge, LA 70803, United States of America
karki@csc.lsu.edu

The rate of loss of heat from Earth's core is controlled by the thermal conductivity of the minerals that comprise the overlying mantle. The heat-flux at the core-mantle boundary has implications for the thermal evolution of both the core and mantle, the size and stability of plumes, and magnetic field generation. As insulators, conduction in lower mantle phases is expected to be dominated by phonon transport. Estimates of the thermal conductivity of MgSiO₃ perovskite, the most abundant phase, at core-mantle boundary conditions, vary significantly, with the phonon contribution reported to lie between 1.6 and 17 Wm⁻¹K⁻¹. In view of this, we have performed ab initio non-equilibrium molecular dynamics simulations to determine the lattice thermal conductivity of MgSiO₃ perovskite at lower mantle conditions, calculating it to be 6.5 ± 0.8 Wm⁻¹ K⁻¹, a value consistent with geophysical constraints on the thermal state at the base of the mantle. Our results suggest that the conductivity depends strongly on pressure, helping to explain the dynamical stability of superplumes, and weakly on temperature and composition, so that lateral variations in thermal conductivity at the base of the mantle are small.

Origin of methane to n-butane in marine sediments of the New Jersey shallow shelf

S. STADLER¹, R. VAN GELDERN² AND S. SCHLÖMER¹

¹Federal Institute for Geosciences and Natural Resources (BGR), Stilleweg 2, 30655 Hanover, Germany,
susanne.stadler@bgr.de, stefan.schloemer@bgr.de

²GeoZentrum Nordbayern, Schlossgarten 5, FAU Erlangen–Nürnberg, 91054 Erlangen, Germany,
robert.van.geldern@fau.de

Concentrations and stable carbon isotope compositions of C₁ to C₄ in pore fluids were measured in three cores (M0027A, M0028A and M0029A) of IODP Expedition 313 that targeted Miocene sedimentary sequences up to 67 km off the coast of New Jersey, USA (Mountain *et al.* 2010), to understand processes related to gas geochemistry and carbon cycling in the investigated shallow shelf. Stable carbon isotope data and C₁/(C₂+C₃) ratios suggest a biogenic origin of methane. If methane is produced by a biogenic process this could in principle also be the case for C₂₊ gases as suggested by Hinrichs *et al.* (2006). An alternative explanation could be low-temperature kerogen cracking (Rowe & Muehlenbachs 1999). Showing first data we discuss gas formation mechanisms including the potential source of the organic material, secondary alteration processes and the role of mixing of gases of different origin (biogenic versus thermal) at the investigated site.

[1] Hinrichs, K.U., Hayes, J.M., Bach, W., Spivackl, A.J., Hmelo, L.R., Holm, N.G., Johnson, C.G. and Sylva, S.P. (2006): Biological formation of ethane and propane in the deep marine subsurface. - Proceedings of the National Academy of Sciences of the United States of America 103:14684-14689. [2] Mountain, G., Proust, J.-N., McInroy, D., Cotterill, C., and the Expedition 313 Scientists (2010): Proceedings of the Integrated Ocean Drilling Program, Volume 313: Tokyo (Integrated Ocean Drilling Program Management International, Inc.). [3] Rowe, D., Muehlenbachs, A. (1999): Low-temperature thermal generation of hydrocarbon gases in shallow shales. - Nature (London) 398:61-63.

High-pressure stability of synthetic $\text{Al}_{63}\text{Cu}_{24}\text{Fe}_{13}$ icosahedral quasicrystal

V. STAGNO¹, L. BINDI^{2*}, C. MURPHY¹, Y. FEI¹,
AND P.J. STEINHARDT³

¹Carnegie Institution of Washington, USA (vstagno@ciw.edu; cmurphy@ciw.edu; yfei@ciw.edu)

²Università di Firenze, Italy (luca.bindi@unifi.it).

³Princeton University, USA (steinh@princeton.edu).

Quasiperiodic crystals are solids characterized by quasiperiodic translational order and a discrete point group impossible for ordinary periodic crystals [1]. Among synthetic quasicrystalline solids, icosahedral- $\text{Al}_{63}\text{Cu}_{24}\text{Fe}_{13}$ is of particular interest since it is representative of icosahedrite, the first quasicrystal found in nature [2, 3]. Although an extraterrestrial origin has been recently established for icosahedrite [4], pressure and temperature conditions at which the mineral would be stable are still not clear. Previous studies showed that synthetic AlCuFe quasicrystals do not undergo any phase transitions over pressures up to 35 GPa (at room temperature) [5] and over a temperature range of 500-870 °C at ambient pressure. However, no data are available for $\text{Al}_{63}\text{Cu}_{24}\text{Fe}_{13}$ quasicrystal at high temperatures and pressures.

We have performed *in situ* high-pressure synchrotron X-ray diffraction experiments under quasi-hydrostatic conditions (neon pressure medium) using diamond anvil cell technique up to 51.5 GPa (in both compression and decompression) to investigate the possible structural evolution of the synthetic analogue of icosahedrite. We also performed a series of quenched experiments with multi anvil to determine the thermal stability of $\text{Al}_{63}\text{Cu}_{24}\text{Fe}_{13}$ at different isobars (between 3 and 20 GPa) and employing different capsule materials to intrinsically buffer the oxygen fugacity.

Preliminary results from *in situ* X-ray diffraction data collected at ambient temperature confirm that the high degree of translational order for the $\text{Al}_{63}\text{Cu}_{24}\text{Fe}_{13}$ icosahedral quasicrystal is retained at much higher pressures than previously reported.

Results from this study will improve our knowledge regarding the origin of icosahedrite in nature and provide constraints on the pressure and temperature conditions for its formation.

[1] Levine, D., Steinhardt, P.J. (1984) *Phys. Rev. Lett.* **53**, 2477-2480. [2] Bindi, L. *et al.* (2009) *Science* **324**, 1306-1309. [3] Bindi, L. *et al.* (2011) *Am. Mineral.* **96**, 928-931. [4] Bindi, L. *et al.* (2012) *PNAS* **109**, 1396-1401. [5] Sadoc, A. *et al.* (1994) *Phil. Mag.* **70**, 855-866.

Impact of anthropogenic land cover changes (ALCC) on dust particle emissions and associated impact on radiation

TANJA STANELLE¹, ISABELLE BEY¹, CHRISTIAN REICK²,
THOMAS RADDATZ² AND INA TEGEN³

¹Institute for Atmospheric and Climate Science & Center for Climate Systems Modeling, ETH Zurich, Switzerland, tanja.stanelle@env.ethz.ch

²Max Planck Institute for Meteorology, Hamburg, Germany

³Leibniz Institute for Tropospheric Research, Leipzig, Germany

Mineral dust particles are usually considered as 'natural' aerosols. Human activities can however affect emission of dust particles by altering land properties or through an increase in desertification associated with climate change. Changes in wind speed due to climate change also alter the amount of dust particles emitted in the atmosphere. The goal of this work is to estimate the extent to which human activities contribute to dust emissions and how this has changed since the pre-industrial time taking into account both climate change and ALCC.

For this purpose, we use the global aerosol-climate model ECHAM6-HAM2.1, in which a new method to calculate potential dust source areas was implemented. This allows us to quantify emissions from agricultural sources and to account for past and future land cover changes. The results from the simulation using the new method compare relatively well to measurements and data available in the literature, indicating that the new approaches allows a reasonable representation of today's dust load and providing confidence into the new method.

In a 'best guess' simulation, where we consider the attempts of farmers to prevent ground erosion, we find that nearly 10 % of today's dust particles are emitted globally from agricultural sources. But agricultural dust sources are not necessarily new dust sources. Often natural grass or shrub land, where emissions of dust particles can take place, were converted into agricultural land. We then account for ALCC between 1850s and 2000s in the model system and simulate emissions under different climate conditions. The contribution of ALCC on changes in dust emissions between pre-industrial times and today is estimated. Further an estimate of the changes in radiative fluxes due to dust particles emitted from agricultural sources including both the direct and indirect aerosol effect is provided.

Geochemical and isotopic monitoring of dissolved carbon dynamic in a karst aquifer, located above the Rouse site test for CO₂ geological storage

Y. STANISZEWSKI¹, A. GROLEAU¹, D. JEZEQUEL¹ AND P. AGRINIER¹

¹IPGP-Paris 7, Institut de Physique du Globe de Paris & Univ. Paris Diderot, Sorbonne Paris Cité, UMR 7154 CNRS, 75005 Paris, France (stanis@ipgp.fr)

A new method for monitoring CO₂ sequestration.

A near surface perched karst aquifer is considered as an integrative system of putative CO₂ leaks above the Rouse site test of CO₂ storage (operated by Total near Pau - France). We develop a low cost and long term geochemical monitoring of spring waters in order to describe the natural forcings that drive the dynamics of the dissolved carbon. Such procedure is mandatory in order to determine dissolved carbon thresholds above which excursions can be anomalies.

The chemical composition of the groundwater is ultra-dominated by calcium and bicarbonate ions. Dataset of 4 main springs is obtained with:

(1) high frequency measurements (15') of conductivity (C₂₅), pH & hydrodynamics (C₂₅ and pH are used to determine the dissolved carbonate system: pH, pCO₂, DIC & alkalinity).

(2) bi-monthly geochemical and isotopic samples which give another appreciation of the dissolved carbon dynamics.

We show that the C₂₅ is a very robust proxy of the alkalinity because a strong linear relation has been established between C₂₅ and carbonate composition in all meteorological conditions. At present, after three years of monitoring, we note that the dominant natural forcing of dissolved carbon is the hydrodynamic which is linked to pluviometry.

Modelisation of the geochemical impact induced by an input of CO₂ in the aquifer is in progress, using thermodem database [1] with the software PHREEQC [2].

Other aquifers will be tested like a typical carbonate karst: "Parc des Grands Causses".

[1] Blanc, P. *et al.* (2012), *Applied Geochemistry* 27, p2107–2116 [2] Parkhurst, D.L., Appelo, C.A.J., (1999) U.S. Geol. Surv. Water Resour. Invest. Rep. 9

Formation mechanism of hematite-rutile pseudomorphs from Mwinilunga (Zambia)

N. STANKOVIĆ*, N. DANEU AND A. REČNIK¹

¹Department for Nanostructured Materials, Jožef Stefan Institute, Jamova 39, 1000 Ljubljana, Slovenia nadezda.stankovic@ijs.si

In geologic environments we often find minerals which formed by replacement reactions from a parent mineral as a consequence of solid-liquid interactions [1]. The newly formed mineral or mineral assemblages retain some characteristics of the parent minerals like their euhedral shape, whereas the chemical composition and texture of the products may be different. The changes are readily used for the interpretation of geological history of the samples.

In our work we studied rutile-hematite intergrowths from the Mwinilunga locality in Zambia. Samples can be described as euhedral hematite crystals intergrown with oriented rutile crystals. The general relationship between rutile and hematite can be determined already by macroscopic observation of hematite crystals and larger rutile crystals on their surface as $\langle 010 \rangle (101)_{\text{RUT}} \parallel \langle 001 \rangle (110)_{\text{HEM}}$. Besides single rutiles, also rutile twins on (101) and (301) planes are found on the surface of the samples [2].

In order to determine the mechanism of ilmenite replacement by hematite and rutile, we analyzed the sample with different methods of electron microscopy. Detailed structural analysis of the sample interior along the $[001]_{\text{HEM}}$ confirmed the macroscopically observed orientation relationship and all six possible orientations of rutile crystals within the single-crystal hematite matrix were found. The stable hematite-rutile interface was determined from the HRTEM images. In the perpendicular orientation, i.e. along the $[100]_{\text{HEM}}$ zone axis, we found nano-sized relicts of parent ilmenite and we observed the diffusion paths of Ti-ions towards the rutile lamellae. The results of our analyses suggest that re-crystallization of ilmenite to hematite and rutile is structurally controlled. The transformation is possible since all three minerals (ilmenite, rutile and hematite) have a common oxygen sublattice which is controlling the re-crystallization to rutile and hematite [3].

[1] Putnis A, (2009) *RevMineralGeochem* 70, 87-124. [2] Daneu *et al.* (2007) *AmMin* 92,1789-1799. [3] Armbruster (1981) *NeuesJbMinerMonat* 7,328-334.

Mg-aenigmatite from the Tazheran massif (East Siberia, Russia)

STARIKOVA A.E.¹ SKLYAROV AND E.V.² KANAKIN S.V.³

¹IGM SB RAS, Novosibirsk, Russia, a_sklr@mail.ru

²IEC SB RAS, Irkutsk, Russia, skl@crust.irk.ru

³Institute of geology SB RAS, Ulan-Ude, Russia, skan_61@mail.ru

Aenigmatite ($\text{NaFe}^{2+}_5\text{TiSi}_6\text{O}_{20}$) occurs usually in high-Na magmatic rocks in association with nepheline, aegirine or augite, arfvedsonite or riebeckite, K-feldspar, sometimes fayalite. Variations of its composition are related mostly to the presence of Fe^{3+} whereas content of MnO and MgO is low (usually < 1 wt%). The Tazheran Massif of alkaline and nepheline syenites (East Siberia, Russia) [2] is the second occurrence of high-Mg aenigmatite (up to 10 wt% MgO, $\text{Mg}/(\text{Fe}+\text{Mg}) = 0.3-0.4$). The only high-Mg variety have been described before in Ne-syenite on Mount Kenia [1]. In the Tazheran massif both high-Mg and typical aenigmatites occur separately at the marginal part of the Ne-syenite veins with Mll-Wo-Cpx-Grt-Ne metasomatic rocks. Both aenigmatite varieties associate with aegirine-augite, nepheline, K-feldspar, sometimes with ilmenite, Fe-olivine and richterite (only with high-Mg aenigmatite) and have low content of CaO (less than 2 wt%) and Al_2O_3 (up to 5 wt%). In Mg-aenigmatite content of MgO varies from 8.5 to 10 wt%, whereas in aenigmatite – from 1 to 2 wt%. There are no transition on composition between the minerals. In most cases aenigmatites as well as Cpx and Amp occur as symplectite with nepheline. According to composition high-Mg aenigmatite does not belong to aenigmatite-rhonite ($\text{Ca}_2(\text{Mg},\text{Fe}^{2+},\text{Fe}^{3+})_5\text{TiO}_2(\text{Si},\text{Al})_6\text{O}_{18}$) series, but is transitional variety of series $\text{Na}_2\text{Fe}^{2+}_5\text{TiO}_2[\text{Si}_6\text{O}_{18}]$ (aenigmatite) - $\text{Na}_2\text{Mg}_5\text{TiO}_2[\text{Si}_6\text{O}_{18}]$ (unknown).

The work was supported by RFBR (№ 12-05-31253, 12-05-00229) and special grant of OPTEC LLC.

[1] Price, R.C., Johnson, R.W., Gray, C.M. and Frey, F.A. (1985) *Contrib. Mineral. Petrol.*, **89**, 394-409. [2] Sklyarov E. V., Fedorovsky V. S., Kotov A. B. *et al.* (2009) *Russ. Geol. Geophys.* **50** (12), 1405–1423.

Fe isotopic composition of sequentially extracted reactive Fe from marine sediments

MICHAEL STAUBWASSER^{1*}, SUSANN HENKEL¹, SABINE KASTEN² AND SIMON W. POULTON³

¹Institute of Geology and Mineralogy, Uni. of Cologne, GER

*correspondence: m.staubwasser@uni-koeln.de

²Alfred Wegener Institute, Bremerhaven, GER

³School of Earth & Env., Uni. of Leeds, Leeds LS2 9JT, UK

The partitioning of Fe in sediments and soils has traditionally been studied by applying sequential leaching methods. These are based on reductive dissolution and exploit differences in dissolution rates between different reactive Fe (oxyhydr)oxide minerals. We used lab-made ferrihydrite, goethite, hematite and magnetite spiked with ^{58}Fe and leached two-mineral mixtures with both phases abundant in excess of the methods dissolution capacity. Leaching was performed with 1) hydroxylamine-HCl and 2) Na-dithionite as the reactive agent. Following Poulton & Canfield (2005) [1], the first dissolution is designed to selectively leach the most reactive Fe-phases, ferrihydrite and lepidocrocite, whereas the second dissolution is designed to leach goethite and hematite. Magnetite would then be dissolved in a third dissolution step with oxalic acid.

First results show that the hydroxylamine-HCl method for ferrihydrite dissolves only insignificant amounts of goethite and hematite. However, magnetite-Fe constitutes about 10% of the total dissolved Fe. The Na-dithionite dissolved Fe from goethite-magnetite and hematite-magnetite mixtures contain about 30% of magnetite-Fe.

We applied selective sequential leaching and Fe isotope analysis to fine-grained marine sediments from a depocenter in the North Sea, which contain abundant reactive Fe (oxyhydr)oxides and show evidence for Fe sulfide formation within the upper 10 cm. Fe isotopes of the hydroxylamine-HCl leach targeting ferrihydrite shows a downcore increase of $\delta^{56}\text{Fe}$ typical for sediments undergoing microbial reductive Fe dissolution, whereas Fe isotopes of the Na-dithionite leach (goethite and hematite) and oxalic acid leach (magnetite) are identical and show no downcore variation in $\delta^{56}\text{Fe}$. This means, that only the most reactive Fe phases participate in the Fe redox cycle in this location. The similar isotopic composition of goethite + hematite and magnetite suggests a detrital source, which is not utilized possibly due to the abundant ferrihydrite and lepidocrocite present.

[1] Poulton & Canfield (2005), *Chemical Geology* 214, 209–221

The Connection Between Life and Oceanic Volcanism: Biosphere Meets Lithosphere

HUBERT STAUDIGEL¹

¹Scripps Institution of Oceanography, UCSD-0225, La Jolla CA 92093-0225, USA; hstaudigel@ucsd.edu

Life and volcanoes have been intimately connected since the beginning of life on Planet Earth. Microbial trace fossils in volcanic glass are amongst the earliest well preserved physical fossils on earth and we can trace the association of microbes with volcanic features throughout the geological record. Interactions between volcanoes and life may occur in diverse settings, in the deep biosphere and hydrothermal systems, in the hydrosphere and at the earth's surface and atmosphere. The total biomass associated directly or indirectly with oceanic volcanoes may comprise a substantial fraction of the total biomass on Earth. Volcanoes are known to impact life, as volcanic aerosols disrupt air traffic, change the earth's radiation budget and cause tsunamis (e.g. Thera and Krakatoa). Consequences for civilization may be substantial, with well documented changes in climate, crop failures and major loss of life and property, including the destruction of an entire culture. Oceanic volcanoes are particularly relevant as the most common and voluminous volcano type and for their immediate interaction with the oceanic/atmospheric systems that control many key global geochemical cycles.

Feedbacks between life and volcanoes are best studied using combined geo- and biological investigations. There is a clear relationship between microbial activity and many types of mineralization. Distinct microbial communities are known to preferentially colonize particular substrates. Their activity may accelerate substrate dissolution processes and distinct microbial dissolution fabrics. There are remarkable similarities in sub-sea basalt-hosted microbial communities with the ones in terrestrial soils, in terms of diversity as well as the relevance of *eukarya*, *prokarya* and *archaea*. We are beginning to understand specific microbial consortia associated with volcanic rock and their main functions such as their capabilities to gain energy from chemolithotrophic reactions and their mechanisms for carbon fixation. We are beginning to explore many details of the genetic underpinnings of microbial function specializing in volcano/ hydrothermal interactions. However, there remains much room for illuminating the geological/ geochemical controls of extremely slow-growing microbial communities, microbial evolution in the geological record and the biological controls of global geochemical cycles, amongst many other issues.

Inert nano-reactors or dynamic micelle interfaces? CaCO₃ precipitation from microemulsions

TOMASZ M. STAWSKI¹ AND LIANE G. BENNING¹

¹Cohen Geochemistry Group, School of Earth and Environment, LS29JT, University of Leeds, Leeds, United Kingdom, (t.m.stawski@leeds.ac.uk and l.g.benning@leeds.ac.uk)

Reverse microemulsions are, thermodynamically stable suspensions of water droplets in oil i.e. micelles that are stabilised by an interface surfactant. Water droplets are typically 1-50 nm in diameters and can carry dissolved salt ions and exchange their content upon collisions, which lead to mineral precipitation. These droplets are believed to act as "nano-reactors" because precipitation occurs in the water pools shielded by the surfactants from the oil phase

Here we show how we can use microemulsions to elucidate the formation of CaCO₃ phases and stabilise initial amorphous stages. Micelles are used to confine volume in which nucleation and growth occurs. Mixing of two distinct microemulsions containing Ca²⁺ and CO₃²⁻ ions leads to a reproducible method to make nano-sized, monodisperse particles. However, there is no correlation between the initial droplet size and the size of solid CaCO₃ particles, which are considerably larger than the original micelles. Therefore, the notion of a "nano-reactor" may in this case be inaccurate, because it implies the formation of an inert, impenetrable water-surfactant-oil interface that limits the growth to a single droplet.

By using time-resolved and *in situ* small and wide-angle X-ray scattering and high-resolution imaging we demonstrated that CaCO₃ grows through a continuous but progressive and slow disintegration of the micelles, rather than precipitation inside of individual droplets. Upon destabilisation of the original salt-ion carrying micelles, new water-mineral-surfactant interfaces are created. These constitute a nucleus and they direct further growth. The formation of this interface is crucial in stabilising amorphous CaCO₃ in the form of nanoparticles (30-100 nm) and this also slows down or prevents further growth and crystallization.

We believe that these findings are relevant for understanding of the CaCO₃ growth mechanisms occurring at water-nonpolar liquid interfaces in natural and industrial environments (e.g. preventing scale formation). Microemulsions could also be a good analogue model system for mineralization of coccolith plates formed within the cell vesicles produced in the Golgi apparatuses of coccolithophores.

Organic Carbon inventory of the Tissint meteorite.

A. STEELE¹, F. MCCUBBIN², L.G. BENNING³,
S. SILJESTRÖEM⁴, G. CODY¹, Y. GOREVA⁵, E. HAURI⁶,
J. WANG⁶, A. KILCOYNE⁷, M. GRADY⁸, C. SMITH¹¹,
C. FREISSINET¹², D. GLAVIN¹², A. BURTON¹³, M. FRIES¹⁴,
J. BLANCO³, M. GLAMOCLJA¹, K. ROGERS¹,
S. MIKHAIL⁶ AND J. DWORKIN¹²

¹University College London, Gower St, London.
(stealie@mac.com.)

²Inst. of Meteoritics, Dept. of Earth and Planetary Sci, Univ.
New Mexico, Albuquerque, New Mexico, 87131 USA

³School of Earth and Environment, University of Leeds,
Leeds, LS2 9JT, UK.

⁴Department of Chemistry and Materials, SP Technical
Research Institute of Sweden, 501 15 Borås Sweden.

⁵Department of Mineral Sciences, Smithsonian Institution,
Washington, DC. 20013-7012 USA.

⁶Department of Terrestrial Magnetism, Carnegie Institution of
Washington, 5241 Broad Branch Rd, Washington DC.
20015 USA.

⁷Advanced Light Source, 1 Cyclotron Road, MS 7R0222,
LBNL, Berkeley, California 94720. USA.

⁸Centre for Earth, Planetary, Space and Astronomical
Research. Open University, Milton Keynes, Walton Hall,
Milton Keynes, MK7 6AA, UK.

⁹Université de Toulouse, UPS-OMP, IRAP, Toulouse, France.

¹⁰CNRS, IRAP, 9 Av. colonel Roche, BP 44346, 31028,
Toulouse Cedex 4, France.

¹¹Department of Mineralogy, The Natural History Museum,
Cromwell Road, London, SW7 5BD. U.K.

¹²NASA Goddard Space Flight Center, Greenbelt Road,
Maryland 20771, USA.

¹³Catholic University of America, NASA Goddard Space
Flight Center, 8800 Greenbelt Road, Greenbelt, Maryland,
20771, USA.

¹⁴Planetary Science Institute, 1700 East Fort Lowell, Suite
106, Tucson, Arizona, 85719 USA

The fall of the Tissint meteorite has provided a unique opportunity to study a minimally contaminated piece of Mars. Martian organic carbon has been detected previously in igneous basalts and the carbonates of ALH 84001. Analysis of sealed maskelynite inclusions using *in situ* techniques including Raman, NanoSIMS, ToFSIMS, STXM and TEM, coupled with whole rock analysis by stepped combustion, GCMS and evolved gas analysis has revealed an inventory of organic compounds containing -CH, -CN, -CNO, -COOH, -CO and aromatic complexes. These are spatially resolved to known inorganic catalysts, i.e. magnetite, pyrite, nickel containing pyrrhotite and clays. Furthermore there is a release of nitrogen containing organics above 600°C, at which temperature $\delta^{15}\text{N}$ is $\sim +40\%$. These results show that Mars has an inventory of organic carbon and nitrogen containing molecules that are probably produced through abiological hydrothermal activity.

PTX properties of FeCl₂-bearing fluids at elevated PT conditions

MATTHEW STEELE-MACINNIS^{1*}, PILAR LECUMBERRI-SANCHEZ¹ AND ROBERT J. BODNAR¹

¹Department of Geosciences, Virginia Tech, Blacksburg VA 24061, USA (*correspondence: mjmaci@vt.edu)

Iron chloride is a significant component of saline aqueous fluids in many ore-forming environments, commonly occurring at concentrations of up to several mass percent [1]. Thus the effect of FeCl₂ on the phase equilibria of aqueous fluids is a significant factor in interpreting fluid evolution in iron-rich systems such as tin-tungsten deposits and some porphyry copper deposits. However, there are few available experimental data on the phase equilibria and thermometric properties of iron-bearing aqueous fluids [2].

We have used the synthetic fluid inclusion technique to investigate the pressure-temperature conditions along the locus of critical points in the system H₂O-FeCl₂, from 0 to 35 wt% FeCl₂. Our results show that the effect of FeCl₂ on the phase equilibria of aqueous fluids is unlike that of other divalent cation chlorides such as CaCl₂ or MgCl₂. Specifically, the locus of critical points for H₂O-FeCl₂ fluids occurs at significantly lower pressure (at a given temperature) compared to the critical curve of the system H₂O-NaCl. For example, at 500 °C the critical point for H₂O-FeCl₂ fluids occurs at 480 bar, compared to about 560 bar for H₂O-NaCl. The low pressure along the H₂O-FeCl₂ locus of critical points implies that immiscibility (boiling) of FeCl₂-rich fluids can occur only at relatively low pressures, or relatively shallow levels in the crust. These results allow us to reinterpret the conditions of mineralization at boiling, Fe-rich hydrothermal systems.

[1] Yardley (2005) *Econ. Geol.* **100**, 613-632. [2] Liebscher (2007) *Rev. Mineral. Geochem.* **65**, 15-47.

IR spectroscopic and quantum chemical study of metal bicarbonate and carbonate interaction in aqueous solutions

ANDRI STEFÁNSSON¹, KONO LEMKE²,
PASCALE PÉNÉZETH² AND JACQUES SCHOTT³

¹ University of Iceland, Sturlugata 7, 101 Reykjavík, Iceland
(e-mail: as@hi.is)

² University of Hong Kong, Pokfulam Road, Hong Kong

³ GET, CNRS/UMR 5563-Université Paul Sabatier, 14 rue
Edouard Belin, 31400 Toulouse, France

Carbonate speciation are among the most important in aqueous systems. Carbonic acid deprotonates to form HCO_3^- and CO_3^{2-} , which further may complex with dissolved cations in solution. In this study, potentiometric and IR spectroscopic measurements were conducted as well as molecular simulation calculations to gain insight into the aqueous speciation of $\text{H}_2\text{O}-\text{CO}_2-\text{NaCl}\pm\text{MgCl}_2$ solutions. In $\text{H}_2\text{O}-\text{CO}_2-\text{NaCl}$ solutions $\text{CO}_2(\text{aq})$, HCO_3^- and CO_3^{2-} predominates, with addition to the $\text{NaHCO}_3(\text{aq})$ and NaCO_3^- ion-pairs. These ion-pairs are weak at low-temperatures but become increasingly important with increasing temperature under neutral to alkaline conditions in moderately dilute to concentrated NaCl solutions. With addition of MgCl_2 , MgHCO_3^- and $\text{MgCO}_3(\text{aq})$ ion-pairs form, these accounting for significant part of the carbonate species concentrations. The combined potentiometric and IR measurements demonstrate that these ion-pairs truly exist in solution and cannot solely be explained by non-ideal ion-ion interaction. Moreover, the coordination number of Mg^{2+} is reduced upon substitution of HCO_3^- and CO_3^{2-} to the hydration shell from six to a maximum number of five. These changes may have profound effects on further reactions of $[\text{MgCO}_3\cdot n\text{H}_2\text{O}]^0$ and $[\text{MgHCO}_3\cdot n\text{H}_2\text{O}]^+$ to form Mg-carbonate and bicarbonate clusters and minerals. No such coordination changes were observed associated with Na^+ HCO_3^- and CO_3^{2-} ion pairing. Based on the experimental results the equilibrium ionization and ion-pair formation constants were retrieved that can be used to calculate aqueous speciation in $\text{H}_2\text{O}-\text{CO}_2-\text{NaCl}+\text{MgCl}_2$ containing solutions.

$\delta^{30}\text{Si}$ in early Archean cherts and implications for the silica cycle

E. J. T. STEFURAK*¹, W. W. FISCHER²
AND D. R. LOWE¹

¹Stanford University, Stanford, CA 94305, USA

(*correspondence: ltrower@stanford.edu)

²California Institute of Technology, Pasadena, CA 91125,
USA

Si isotopes in Archean cherts offer insight into mass fluxes and mechanisms associated with silica concentration, precipitation, diagenesis and metamorphism. Previous studies have used Archean chert $\delta^{30}\text{Si}$ to estimate seawater $\delta^{30}\text{Si}$ [1-4], assuming a simple mass balance model with silica inputs from crustal weathering balanced by outputs of hydrothermal silicification and amorphous silica precipitation from seawater. This model relies on reservoir analogies, even though silicon reservoirs often have broad $\delta^{30}\text{Si}$ ranges resulting from low temperature dissolution and precipitation reactions. We propose that process analogies are more appropriate for the early Archean system.

To connect isotope composition to process, we used secondary ion mass spectrometry (SIMS) to compare $\delta^{30}\text{Si}$ and $\delta^{18}\text{O}$ in distinct silica phases present in cherts, including carbonaceous bands, pure chert bands and grains, early cavity-filling cements and later quartz-filled veins. Our results indicate that low temperature processes fractionated silicon isotopes in early Archean marine basins—behavior that probably precludes the application of chert $\delta^{30}\text{Si}$ as a paleothermometer. Relationships between $\delta^{18}\text{O}$ and petrographic textures are consistent with setting during early burial and diagenesis [5]. The average value we observe for petrographic textures we infer to be primary silica precipitates from seawater, $\delta^{30}\text{Si} +0.6\text{‰}$, is heavier than expected for bulk silicate Earth ($\delta^{30}\text{Si} -0.4\text{‰}$). This constraint is consistent with an isotope mass balance wherein contemporaneous iron formation deposits have negative $\delta^{30}\text{Si}$ composition and form a notable fraction of the mass balance of Si leaving seawater. Precipitation of authigenic clay minerals may have also comprised a large part of the required ^{30}Si -depleted sink, in addition to playing a role as an important non-carbonate alkalinity sink consuming cations released by silicate weathering. We present a new model for the Archean silica cycle based on process analogies and existing data sets.

[1] Robert & Chaussidon (2006), *Nature* **443**, 969-972. [2] van den Boorn *et al.* (2007), *Geology* **35**, 939-942. [3] van den Boorn *et al.* (2010), *Geochim Cosmochim Acta* **74**, 1077-1103. [4] Abraham *et al.* (2011), *EPSL* **301**, 222-230. [5] Lowe & Knauth (2003), *GSA Bulletin* **115**, 566-580.

Impact of Natural Sulfidation of Silver Nanoparticles on Bioavailability and Biouptake

JOHN STEGEMEIER^{1,2}, GREGORY V. LOWRY^{1,2},
AMY DALE^{1,2}, CLEMENT LEVARD^{3,2},
FABIENNE SCHWAB^{4,2}, BENJAMIN P. COLMAN^{4,2},
EMILY S. BERNHARDT^{4,2}, ELIZABETH A. CASMAN^{1,2} AND
MARK R. WIESNER^{4,2}

¹Carnegie Mellon University, Pittsburgh, PA 15213

²Center for Environmental Implications of Nanotechnology

³Centre de Recherche et d'Enseignement de Géosciences de l'Environnement, Aix-en-Provence, France

⁴Duke University, Durham, NC 27708

Engineered silver nanoparticles (Ag NPs), often partially or fully sulfidized, enter the environment. There, sulfidation of Ag NPs greatly decreases the rate of oxidation of Ag⁰ and the release of Ag⁺. We hypothesized that sulfidation of Ag⁰ NPs added to an emergent freshwater wetland mesocosm would greatly decrease silver bioavailability. We dosed a 1.2x1x3m freshwater wetland mesocosm with 30nm PVP-coated Ag NPs (25 mg/L Ag) and then determined the distribution and speciation of Ag NPs after 18 months. A sediment diagenetic model was developed and used to predict the distribution and speciation of Ag in the mesocosms.

Ag⁰ NPs in sediments sulfidized over 18 months. Ag speciation was approximately 50% Ag₂S, 30% Ag-S-R (likely organic matter complexed) and 20% Ag⁰ as determined by X-ray absorption spectroscopy. Sulfidation decreased dissolved Ag concentration in the water column to below method detection (2 µg/L). The sediment diagenetic model could predict Ag distribution and speciation well using parameter values (e.g. bioturbation) and partition coefficients (e.g. Ag-organic matter) in the range expected for freshwater sediment and demonstrated seasonal fluctuations. There was measurable uptake of Ag into several sediment dwelling organisms, suggesting that Ag₂S or Ag-S-R species remained bioavailable. The uptake of Ag₂S in duckweed roots was confirmed with synchrotron based micro-X-ray fluorescence (µ-XRF) and µ-XANES indicates that the silver within the root cortex was predominantly Ag⁰.

Cavity ring-down spectroscopy for the high-precision analysis of the triple oxygen isotope composition of water and water vapor

E. J. STEIG¹, V. GKINIS², A.J. SCHAUER¹, J. HOFFNAGLE²,
S. TAN² JAND S.W. SCHOENEMANN¹

¹Earth and Space Sciences, University of Washington, Seattle, WA 98195, USA, steig@uw.edu

²Institute for Arctic and Alpine Research, University of Colorado, Boulder, CO 80309, v.gkinis@nbi.ku.dk

³Picarro Inc., 3105 Patrick Henry Drive, Santa Clara, CA 95054, jhoffnagle@picarro.com

High precision analysis of the ¹⁷O/¹⁶O isotope ratio is an important new tool in water isotope analysis. The ¹⁷O-excess (= ln(δ¹⁷O+1)-0.528 ln(δ¹⁸O +1)) is sensitive to kinetic fractionation processes and nearly invariant with temperature [1]. For most applications, measurements of ¹⁷O-excess must have a precision of ~5 per meg. This precision is normally obtained by flourination of H₂O to O₂ and analyzed by dual-inlet isotope ratio mass spectrometry (IRMS).

Cavity ring-down spectroscopy (CRDS), commonly used for measurements of δ¹⁸O or δD in water [2, 3], provides several advantages over IRMS, including streamlined sample handling and the ability to measure ambient water vapor in the field. Use of CRDS for ¹⁷O-excess poses unique challenges not addressed by existing commercial instruments. While a H₂¹⁷O absorption region is present in some instruments, the absorbance is influenced by the tail of the H₂¹⁶O spectrum; resulting precision is inadequate for distinguishing samples from the meteoric water line.

We describe a new CRDS system for high precision ¹⁷O-excess measurements. Innovations include i) use of two lasers that measure absorption in different IR regions; ii) sample introduction system for continuous introduction of water vapor over long time periods (similar to [3]); iii) novel improvements to the spectroscopy. Samples can be analyzed with ~5 per meg precision in 60 min. Calibration with respect to VSMOW is achieved using working laboratory standards previously calibrated with IRMS [4]. The results show that both the precision and the accuracy of the new CDRS are competitive with IRMS methods. An additional benefit is improved precision of δ¹⁸O and δD (0.02 ‰, 0.08 ‰).

[1] Luz and Barkan (2005), RCM, 19, 3737-3742; [2] Crosson (2008) Appl. Phys. B, 92, 403-408; [3] Gkinis *et al.* (2011) Atmos. Meas. Tech., 3, 2531-2542; [4] Schoenemann *et al.* (2013) RCM, 27, 582-590.

Eocene hydrocarbon migration, Green River Formation, Utah

HOLLY STEIN^{1,2}, JUDITH HANNAH^{1,2}, GANG YANG¹,
HELGE LØSETH³, LARS WENSAAS³
AND PETER COBBOLD⁴

¹AIRIE Program, Colorado State University, Fort Collins, CO
80523-1482 USA; holly.stein@colostate.edu

²CEED Centre of Excellence, University of Oslo, Norway

³Statoil ASA, Research Centre Rotvoll, Trondheim, Norway

⁴Géosciences, Université de Rennes, France

The renowned Eocene Green River Formation presents a spectacular field setting to study both source rock and migration of hydrocarbon. From the Uinta basin, we combine field observations with Re-Os data from pristine outcrop and drill core samples to interpret hydrocarbon migration history.

To build a meaningful Re-Os data set, we employ our sampling strategy to capture just a few mm of stratigraphic section for each analysis. Larger bulk samples risk homogenization of real variations in the initial Os ratio and any time occupied by non-depositional or erosional intervals. Re-Os data for the Mahogany Bed and the petroliferous Mahogany Zone in Hells Canyon (Utah) are combined with Re-Os data from drill core from the Parachute Creek and Douglas Creek members to provide a compelling story for hydrocarbon migration. Samples from high-TOC “Rich Zones” (local stratigraphic nomenclature; the Mahogany Zone is “Rich Zone 7”) show a narrow range of Re and Os concentrations and a narrow range in ¹⁸⁷Re/¹⁸⁸Os ratios relative to low-TOC “Lean Zones”; this combination can lead to easily misinterpreted Model 1 isochron ages with low MSWDs and large age uncertainties. Such data sets do not provide accurate depositional ages. Rather, these data sets may characterize Re-Os behavior on initiation of hydrocarbon migration. In effect, we may be looking at source rock with incipient migration of its own oil (i.e., unconventional hydrocarbon), with local homogenization of organic matter and the Re and Os it carries. Samples from designated Lean Zones have nearly an order of magnitude lower Re and Os and yield Re-Os scatterchrons of 47-49 Ma. Scatterchrons and variable ¹⁸⁷Os/¹⁸⁸Os ratios are attributed to local migration of oil still mixed with original kerogen.

Our Re-Os data and an interpretation that accommodates the full data set bring new understanding to hydrocarbon systems in lacustrine rocks. In some cases, Re-Os results inform us not just about the shale, but about hydrocarbon generation and incomplete expulsion. Field relationships are used to support this interpretation.

Project initiated and funded by Statoil ASA, including joint field work; additional core samples from USGS library.

Dust transport over the late Quaternary Red Sea - Dead Sea regions from Nd-Sr isotopes in deep- sea cores and lake sediments

M. STEIN^{1*}, D. PALCHAN^{1,2}, A. ALMOGI-LABIN¹,
Y. EREL² AND SL GOLDSTEIN³

¹Geological Survey of Israel, 30 Malkhe Israel St. Jerusalem,
95501 ISRAEL (motistein@gsi.gov.il)

²Institute of Earth Science, The Hebrew University of
Jerusalem, ISRAEL 91904

³Lamont -Doherty Earth Observatory, Columbia University,
Palisades NY 10964, USA

The Red and Dead Seas situated along the African – Syrian Rift valley between the Sahara and Arabia deserts and the subtropical Mediterranean received during the late Quaternary dust particles that were transported from the Sahara-Arabia deserts, Ethiopian Highlands and the Nile delta. Nd and Sr isotope ratios, chemical and mineralogical compositions of fine-detritus particles, that were recovered from the deep-sea cores: KL15, KL11 and KL23 and from Dead Sea and east Mediterranean sedimentary archives were used to determine the particle sources and reconstruct the synoptic conditions responsible for their transport.

The data indicate that during glacial dust was blown to the northern Red Sea and the east Mediterranean- Dead Sea area from the Sahara deserts by winds associated with the strong-glacial Mediterranean winter cyclones. At the same time dust was blown from Sahelian sources by southern winds associated with monsoonal circulation. During the last interglacial and the African Humid Period, monsoonal rains caused erosion and flooding at the ANS margins of the Red Sea, increasing the contribution of granitic ANS material to the Red Sea floor. During the Heinrich events (e.g. H11 and 1), mixed basaltic-granitic dust was blown from all sources reflecting severe regional aridity, when both monsoonal and Mediterranean cyclone activity were weak.

Enhanced ice nucleation activity of soil dust particles

I. STEINKE¹, R. FUNK², A. DANIELCZOK³, K. HÖHLER¹,
N. HIRANUMA¹, N. HOFFMANN¹, M. HUMMEL¹,
S. KIRCHEN⁴, A. KISELEV¹, M. LEUE², O. MÖHLER¹,
H. SAATHOFF¹, M. SCHNAITER¹, T. SCHWARTZ⁴,
B. SIERAU⁵, O. STETZER⁵, E. TOPRAK¹, A. ULRICH²,
C. HOOSE¹ AND T. LEISNER^{1,6}

¹Institute for Meteorology and Climate Research Atmospheric Aerosol Research, Karlsruhe Institute of Technology, Germany

²Institute of Soil Landscape Research, Leibniz Centre for Agricultural Landscape Research, Germany

³Institute for Atmospheric and Environmental Sciences, Goethe University Frankfurt, Germany

⁴Institute of Functional Interfaces, Karlsruhe Institute of Technology, Germany

⁵Institute for Atmospheric and Climate Science, ETH Zürich, Switzerland

⁶Institute of Environmental Physics, Heidelberg University, Germany

Primary biological particles have been identified as very efficient ice nuclei at high sub-zero temperatures. Soil dust particles emitted from agricultural areas contain large amounts of organic material such as fungi, bacteria and plant debris. Thus, soil dust particles may act as a carrier for highly ice-active biological particles. In this work, we present ice nucleation experiments conducted in the AIDA cloud chamber where we investigated the ice nucleation efficiency of three types of soil dust from different regions of the world. Results are presented for the immersion freezing and the deposition nucleation mode of these soil dust samples: all soil dusts show higher ice nucleation efficiencies than desert dusts, especially at high temperatures. In addition, inertially separated ice crystal residuals from these AIDA experiments have been analyzed in order to elucidate the ice nucleation process in more detail. The organic content of the soil dusts is investigated with regard to morphology and composition, hydrophilicity, as well as the diversity and viability of species. These characteristics are then related to the ice nucleation efficiencies of the individual dusts.

Oceanographic control on microbial methane oxidation in the water column offshore Svalbard

LEA I. STEINLE*^{1,2}, CAROLYN GRAVES^{3,4},
CHRISTIAN BERNDT², TOMAS FESEKER⁵,
MORITZ F. LEHMANN¹, TINA TREUDE²
AND HELGE NIEMANN¹

¹University of Basel, Dept. of Env. Geosciences, CH
(*correspondence: lea.steinle@unibas.ch)

²Helmholtz Centre for Ocean Research (GEOMAR), DE

³National Oceanography Centre Southampton, UK

⁴University of Southampton, UK

⁵University of Bremen, DE

A large number of gas flares were recently discovered at the landward termination of the methane gas hydrate stability zone off Svalbard. The gas ebullition is most probably caused by seasonal bottom water temperature fluctuations of 1-2°C, causing periodic methane hydrate formation and dissociation. During summer time, methane concentrations were consistently elevated in bottom waters (up to 825 nM), providing abundant substrate for aerobic methanotrophs. Our investigations on the spatio-temporal variation of aerobic methane oxidation (MOx) rates revealed highest rates (up to 3.1 nM/day) at ~50 m above the sea floor. Despite constant supply of methane, MOx rates displayed a high temporal variability. Comparison of MOx rates and water temperature revealed consistent spatio-temporal patterns that suggest an oceanographic control on the magnitude of MOx: Cool Arctic bottom water contains a comparably large standing stock of methanotrophic bacteria. This water mass is episodically displaced by the warmer W-Spitsbergen current, which is depleted in methanotrophic biomass. CARD-FISH analyses confirmed that high MOx rates are associated with the presence of methanotrophic cell aggregates. Our data thus imply that MOx fluctuations offshore Svalbard are indirectly controlled by ocean circulation patterns rather than methane substrate availability.

Absorption and fractionation of Rare Earth Elements (REE) by plants

M. STEINMANN^{1*}, L. BRIOSCHI¹, E. LUCOT¹,
MC. PIERRET², P. STILLE², J. PRUNIER^{2,3}, PM. BADOT¹

¹ Chrono-Environnement, Univ. Franche-Comté/CNRS,
F-25030 Besançon, France (*correspondence :
marc.steinmann@univ-fcomte.fr)

² LHyGeS-EOST, Univ. Strasbourg/CNRS,
F-67084 Strasbourg, France

³ GET, Univ. P. Sabatier/CNRS, F-31400 Toulouse, France

Rare Earth Elements (REE) are increasingly used by man (electronics industry, medicine, agriculture) and therefore considered as emerging pollutants. The present study documents REE mobility in non-polluted natural soil-plant systems in order to characterize their environmental availability for future anthropogenic pollution.

The study is based on a field approach in non-polluted natural sites with contrasting geological environments (limestone, granite and carbonatite) and highly variable REE contents. The data show that REE uptake by plants is not primarily controlled by the plant itself, but depends on the concentration and the speciation in the soil and the adsorbed soil water pool. REE uptake by plant roots are linked with those of Fe. Roots absorb preferentially the light REE (Fig. 1). Before translocation, REE are retained by the Casparian strip leading to much lower concentrations in the aerial parts. The transport of the REE within the xylem is associated with the general nutrient flux.

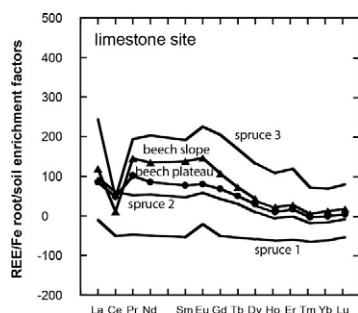


Figure 1: Soil-normalized REE/Fe ratios of plant roots ($([REE/Fe]_{\text{root}}/[REE/Fe]_{\text{soil}})*100$) showing that roots absorb the LREE preferentially with respect to Fe. Figure from [1].

[1] Brioschi *et al.* (2012) *Plant Soil*, DOI 10.1007/s11104-012-1407-0

Late Devonian “Kellwasser-Event” A global mass-extinction equivalent to the Precambrian-Cambrian boundary interval?

YANNIK STEINMANN^{1*}, ULRICH STRUCK¹
AND ANTONIA GAMPER¹

¹Museum für Naturkunde, Invalidenstr. 43, D-10115 Berlin,
(*yannik.steinmann@fu-berlin.de)

The Late Devonian Kellwasser Event characterizes a significant epoch in the evolution of the Palaeozoic ecosphere and hosts one of the five major global mass-extinction events in Earth history. During this period massive continental renovations forced seawater level changes and climate instabilities thus provoking biogeochemical perturbations of the oceans likely comparable to the Precambrian-Cambrian evolution events. Culminating in the extinction of up to 60% of the pelagic biosphere the Kellwasser period is characterized by the deposition of two black shale successions, the so-called Kellwasser horizons (e.g. Germany, France, USA). Well preserved Devonian strata crop out in sections around the Kellwassertal in the central German Harz Mountains. However, geochemical data especially sedimentary bulk nitrogen isotope values from these rock sections are rare.

We determined $\delta^{13}\text{C}_{\text{carb}}$, $\delta^{13}\text{C}_{\text{org}}$ and $\delta^{15}\text{N}$ isotope values from an outcrop near Goslar including the basal cephalopod limestone, the lower and upper Kellwasser horizons and the overlying lower Famennian limestones. The section represents a carbonate-siliciclastic setting in a submarine rise environment permanently connected to the ocean but influenced by multiple trans- and regression events. $\delta^{15}\text{N}$ isotope data from the Kellwasser horizons reveal two major negative excursions, one shift down to -1.2‰ , the latter -1.7‰ . Two positive co-occurring $\delta^{13}\text{C}_{\text{carb}}$ and $\delta^{13}\text{C}_{\text{org}}$ excursions represent the global Kellwasser carbon isotope signal as already reported in other upper Devonian sections worldwide.

Our data represent trustful markers for the marine palaeo-oxygenation state and nutrient availability suggesting that biogeochemical events during the Frasnian-Famennian interval can roughly be compared to the Precambrian-Cambrian boundary interval and may record phases of photic zone anoxia. Scenarios like the stepwise upper Devonian mass-extinction of biota associated with marine transgressive events and negative $\delta^{15}\text{N}$ excursions can be paralleled to the Precambrian-Cambrian event recorded in sections e.g. of South China and Kazakhstan thus enabling new approaches of interpretation.

Mineralogical characterization and crystallization kinetics of fibrous and acicular volcanic orthopyroxenes from Mt. Etna, Sicily, Italy

I. STELLUTI^{1*}, C. VITI², A. GIANFAGNA¹

¹ Dipartimento di Scienze della Terra, Sapienza Università di Roma, Italy (*correspondence: igor.stelluti@uniroma1.it)

² Dipartimento di Scienze Fisiche, della Terra e dell'Ambiente, Università di Siena, Italy (cecilia.viti@unisi.it)

The present study reports mineralogical characterization of unusual acicular and fibrous orthopyroxenes occurred in the autoclastic volcanic products from Santa Maria di Licodia, belonging to "Mt. Calvario Formation", Etna Volcano. The orthopyroxene is associated to Na-feldspar, augitic clinopyroxene, apatite and Fe-Ti oxides and shows variable morphology from prismatic to fibrous, with composition enstatite to ferroan-enstatite. Prismatic and acicular morphologies highlight a composition with high Fe contents (FeO 18-20 wt%) and moderate Ca enrichments (~1 wt %), whereas the fibers present enrichment in Mg contents (FeO < 11%). Fibrous orthopyroxene has been investigated by Transmission Electron Microscopy (TEM), revealing fibers less than 1 μm in diameter, with perfectly euhedral habit, high crystallinity and crystal order. Selected Area Electron Diffraction (SAED) patterns show sharp and intense reflections, with limited streaking effects, probably corresponding to polytypic disorder and twinning. Corresponding HRTEM images confirm the occurrence of rare packing defects and twinning, giving rise to lamellar nanostructures in both parallel and orthogonal orientations with respect to c fiber axis. A remarking feature is represented by the systematic occurrence of a very thin amorphous film that envelops the entire fiber. Focused-beam EDS microanalyses highlighted reverse zoning, with Fe-enriched cores and Mg-enriched rims.

Orthopyroxenes with fibrous morphology are rare [1, 2] and there is no evidence in literature about their presence in volcanic environment. The occurrence of the fibrous orthopyroxene in the volcanic area studied [3] allowed to undertake this detailed mineralogical investigation. The data obtained provide some preliminary constraints on crystallization kinetics pointing to conditions of high temperature crystallization and very fast cooling.

[1] Abu El-Rus et al. (2006) - *Lithos*, **89**, 29-46. [2] Bryant et al. (2007) - *Geochem. Geophys. Geosyst.*, **8**, 24 pp. [3] Gianfagna et al. (2012) *EMC2012* - **1**, 533.

Magmatic evolution at Yellowstone: The role of isotopically juvenile magma inferred from zircon age, trace-element and Hf isotope data

MARK STELTEN^{1*}, KARI COOPER¹, JORGE VAZQUEZ², JOSH WIMPENNY¹, QING-ZHU YIN¹

¹University of California – Davis, Davis, CA, USA (*correspondance: mestelten@ucdavis.edu)

²U.S. Geological Survey, Menlo Park, CA, USA

Yellowstone caldera (USA) is a prime example of a long-lived, large-volume silicic magma system that has produced numerous eruptions of rhyolite and basalt during Quaternary time, including caldera-forming eruptions at ca. 2.1 Ma, ca. 1.3 Ma and ca. 0.640 Ma [1]. The most recent post-caldera eruptive episode at Yellowstone produced the Central Plateau Member (CPM) of the Plateau Rhyolite, which erupted between ca. 170-70 ka. Previous research (e.g., [2]) has documented that the Nd isotopic compositions of the CPM rhyolites lie between that of the local crust and Yellowstone basalts, leading to the hypothesis that both local crust and isotopically juvenile material are required to explain the genesis of the CPM rhyolites. Additionally, it is clear from oxygen isotopic studies that the low $\delta^{18}\text{O}$ values of the CPM rhyolites (~4 to 4.5‰) require some contributions from remelted, hydrothermally altered crustal rocks [3, 4]. Here we use zircon age, trace-element and Hf isotopic compositions to explore the role of isotopically juvenile magma in the generation of the CPM rhyolites.

New Hf isotope data from CPM zircons demonstrate the presence of zircons with juvenile Hf isotope compositions (-4 to 0 ϵ_{Hf}) relative to their host CPM glasses (-5.7 to -6.2 ϵ_{Hf}), which requires that isotopically juvenile silicic magmas contributed mass to the CPM magma reservoir. Local crustal sources and older Yellowstone rhyolites have ϵ_{Hf} values lower than the CPM rhyolites (<-6.5 ϵ_{Hf}) and therefore cannot represent the sources responsible for contributing the high- ϵ_{Hf} zircons observed in the CPM rhyolites. Instead, new Hf isotope data show that the Yellowstone basalts (-0.1 to 5.5 ϵ_{Hf}) are the only source identified to date with an appropriate isotopic composition to account for the Hf isotopic heterogeneity observed in CPM zircons. Thus, these data suggest that 1) the high ϵ_{Hf} CPM zircons crystallized from isotopically juvenile silicic magma that is a hybrid of silicic liquids derived from Yellowstone basalts and local crust and 2) this isotopically juvenile hybrid magma is then added to the CPM reservoir periodically through time. In turn, these data provide direct evidence supporting the concept that both crustal-derived and mantle-derived (i.e., juvenile) components are required to generate Yellowstone rhyolites.

[1] Lanphere et al. (2002), *Geol Soc Am Bull*, **114**, 559-568. [2] Hildreth et al. (1991), *J. Pet.*, **32**, 63-138. [3] Bindeman et al. (2008), *J. Pet.*, **49**, 163-193. [4] Watts et al. (2012), *Contrib. Mineral. Petrol.*, **164**, 45-67.

Biotite is an important host for Nb in the lower crust

STEPANOV A.S.^{1,2}, HERMANN J.¹

¹RSES, Australian National University, Canberra, Australia

²CODES, University of Tasmania, Hobart, Australia
(sasha.stepanov@utas.edu.au)

The trace element-enriched continental crust is a result of partial melting of the mantle, which displays a complementary depleted composition. Nb and Ta are elements regarded as geochemical twins showing very similar properties and they display a strong affinity to Ti minerals. Therefore it is surprising that significant fractionation of Nb and Ta are observed at global scale. The subchondritic Nb/Ta ratio of both the continental crust and the depleted mantle is known as the “missing Nb paradox”.

We present partitioning data between biotite and granitic melt for experimental and natural samples that provide evidence that Nb is compatible in biotite. Nb can thus be enriched in the residue during partial melting of crustal rocks. Additionally, biotite preferentially incorporates Nb over Ta (Stepanov and Hermann, 2013). Hence, incipient partial melting in the lower crust with biotite as residual mineral can result in restites with high Nb contents and super chondritic Nb/Ta.

Data from two key localities of crustal anatexis provide additional evidence for intracrustal Nb and Ta fractionation during partial melting of biotite-bearing rocks. Crustal, granulite facies metapelite encalves from the El Hoyazo (EH) dacite, Spain, contain melt inclusions that have significantly lower Nb and Nb/Ta than the bulk rock composition. In contrast, residual biotite is an abundant phase in the enclaves and has high Nb contents and Nb/Ta significantly higher than the bulk rock. In the classic lower crustal section in the Ivrea Verbano zone, northern Italy, metasedimentary amphibolite grade rocks have typical crustal Nb/Ta ratios, whereas granulite grade restites have higher and partial melts lower ratios. Therefore we suggest that intra-crustal differentiation might be an important process to produce Nb-rich rocks with superchondritic Nb/Ta that represent one of the missing reservoirs to balance the subchondritic Nb/Ta of the upper crust and the depleted mantle.

[1] Stepanov, A.S., Hermann, J., 2013. Fractionation of Nb and Ta by biotite and phengite: Implications for the “missing Nb paradox”. *Geology* 41, 303–306.

The Paleoproterozoic MORB-type tholeiitic dykes as indicators of early continents breakup

A.V. STEPANOVA^{1*}, A.V. SAMSONOV²,
E.B. SALNIKOVA³, YU.O. LARIONOVA²,
A.N. LARIONOV⁴, V.S. STEPANOV¹

¹Institute of Geology, Karelian Research Centre, Russian Academy of Sciences, Petrozavodsk, Russia
(*correspondence: stepanov@krc.karelia.ru)

²IGEM Russian Academy of Sciences, Moscow, Russia

³IPGG, Russian Academy of Sciences, St. Petersburg, Russia

⁴CIR VSEGEI, St. Petersburg, Russia

The time and circumstances of the Precambrian continents fragmentation is usually highly controversial issue because of deep erosion and absence of clear evidences of breakup events. Relics of various igneous provinces occur in Precambrian Shields, but it is difficult to decide which of them is indicator of final continent breakup.

In the Karelian Craton, Eastern Fennoscandian Shield there are a lot of Paleoproterozoic (2.5 -1.97 Ga) mafic dykes that vary in composition from high-Mg to high-Fe-Ti tholeiites [1]. Among them we recognize very specific dykes of age 2.13-2.14 Ga. In spite of intracontinental tectonic setting these dykes are MORB-type tholeiites with flat REE patterns, HFSE enrichment, Nb/Nb* = 0.7-1.6 and ϵ_{Nd} range from +3.0 to +1.4. Geochemical modelling indicates that chemical and isotopic compositions of the dykes are best explained by derivation of their parental magmas from partial melting of depleted mantle sources in the spinel peridotite stability field, followed by fractional crystallization and low (< 6%) extent assimilation of continental crustal material. The latter suggests a rapid rise of mafic melts, accompanied by rapid crust extension, which follows from the morphology of the dykes.

Widespread MORB-type tholeiitic dykes on the Karelian Craton suggest substantial lithosphere thinning accompanied by asthenosphere rising. This allows us to consider MORB-type tholeiitic dykes as indicators of final breakup of the Achaean continent and Lapland-Kola and Svecofennian oceans opening. This statement is supported by strong compositional similarity between studied dykes and syn-breakup basalts in North Atlantic Igneous Province [2], [3] and Afar [4], [5].

[1] Vuollo & Huhma (2005) *Prec. Geol. of Finland*, 195–236.

[2] Søger & Holm (2011), *Chem. Geol.*, 297–313. [3] Waight & Baker (2012), *JP*, 1569–1596. [4] Barrat *et al.* (2003) *Lithos*, 1–13. [5] Daoud *et al.* (2010) *Lithos*, 327–336.

Formation of Se(0) nanoparticles by *Azospirillum brasilense*

R. STEUDTNER^{1*}, A. MAFFERT¹, M. VOGEL¹,
C. FRANZEN¹ AND A.C. SCHEINOST¹

¹ Helmholtz-Zentrum Dresden-Rossendorf e.V.,
Institute of Resource Ecology, P.O. Box 510119, D-01314
Dresden, Germany
(*correspondence: r.steudtner@hzdr.de)

We investigated the reduction of SeO_3^{2-} by *Azospirillum brasilense*. The formation of fairly soluble Se(0) nanoparticles during this process is of interest for both bioremediation of Se-contaminated sites and for nanobiotechnology.

A. brasilense was cultured in 30 mL medium at 30 C in a shaking (100 rpm) incubator for 3 days in the presence of 1 mM Se(IV). The cellular material was then separated from the red Se precipitate by using a modified procedure of Oremland *et al.* [1]. The cleaned precipitate was resuspended in deionized water. For selective Se(IV) quantification in the culture media we used hybrid generation atomic absorption spectrometry (HG-AAS) [2]. The formed Se precipitate was characterized by scanning electron microscopy with energy-dispersive X-ray spectrometry (SEM-EDX), photon correlation spectroscopy (PCS) and zeta potential measurements.

After exposing *A. brasilense* to Se(IV), the bacterial growth continued after an extended lag-phase. After a cultivation time of 3 days, a reddish staining of the sample was observed, indicating the formation of Se(0). SEM coupled to EDX confirmed the formation of nanoparticulate, red Se(0). Only 10 % of the initial Se(IV) concentration could be recovered from the culture media by HG-AAS. The separated Se(0) suspension was stable for several hours, sufficient for the PCS and the zeta potential measurements. In contrast, Se(0) chemically formed by reduction with hydroxylamine solution produced amorphous aggregates with rapidly settled down. PCS and SEM imaging showed that the Se(0) particles had a particle size distribution between 100 and 300 nm with an averaged particle diameter of 200 nm. The isoelectric point of Se(0) particles was at $\text{pH } 2.8 \pm 0.2$. The preference of forming Se(0) particles with a negative charge agree very well with the literature [3].

[1] Oremland *et al.* (2004) Appl. Environ. Microb. **70**, 52-60.
[2] Niedzielski *et al.* (2002) Pol. J. Environ. Stud. **11**, 219-224. [3] Dhanjal & Cameotra (2010) Microb. Cell Fact. **9**, 1-11.

Stable and Radiogenic Strontium isotope behaviour in the subglacial environment

E. I. STEVENSON^{1*}, S. M. ACIEGO¹, I. J. PARKINSON²
K.W. BURTON³, C. ARENDT¹

¹ Earth and Environmental Sciences, University of Michigan,
Ann Arbor, MI 48109 USA, (*correspondence:
emisstev@umich.edu)

² Bristol Isotope Group, School of Earth Sciences, University
of Bristol, Wills Memorial Building, BS8 1RJ, UK

³ Department of Earth Sciences, Durham University, Science
Labs, Durham DH1 3LE, UK

Subglacial hydrology plays a key role in determining the nutrient fluxes from glaciated terrains. Differences in the chemical and isotopic composition of the glacial outflow are controlled by variations in initial inputs, mineralogy, mineral dissolution and residence time. We present geochemical data from the glacial discharge of two geographically, geologically and climatologically distinct glaciers over two field seasons: the Athabasca Glacier, Canada (AG, Precambrian sedimentary bedrock) and the Lemon Creek Glacier, USA (LCG, Southeast Alaska metamorphic belt).

Strontium isotopes are widely utilized in studies of weathering and hydrology. Radiogenic Sr ($^{87}\text{Sr}/^{86}\text{Sr}$) is a good proxy for varying hydrological inputs and weathering reactions, however Sr *stable* isotopes ($\delta^{88/86}\text{Sr}$) can be fractionated by both precipitation and dissolution reactions. A combination of the two strontium systems should therefore provide improved constraints on the weathering environment.

Radiogenic Sr results indicate differences in glacial outflow composition with $^{87}\text{Sr}/^{86}\text{Sr} \sim 0.7142$ and ~ 0.7106 for AG and LCG respectively. Radiogenic Sr data from the AG show clear resolvable seasonal excursions, varying from 0.716 in May to 0.712 in July. By contrast, the meltwater from the Lemon Creek shows little variability in radiogenic strontium with time. The $^{87}\text{Sr}/^{86}\text{Sr}$ in suspended sediments from the LCG are consistently less radiogenic than their water counterparts and show a similar trend toward more radiogenic values as the season progresses.

The $\delta^{88/86}\text{Sr}$ data, however clearly show the difference in the underlying bedrock geology with mean $\delta^{88/86}\text{Sr} \sim 0.19$ and ~ 0.33 for AG and LCG respectively. Analysis of $\delta^{88/86}\text{Sr}$ from suspended sediments from LCG show consistently lighter compositions than the corresponding water sample.

Variations in both $^{87}\text{Sr}/^{86}\text{Sr}$ and $\delta^{88/86}\text{Sr}$ in the meltwater will be analyzed using principle component analysis to reveal relationships with water mass source and elemental fluxes.

Determining the pre-eruptive magmatic conditions and sulfur release of the AD1280 Quilotoa eruption, Ecuador

A-M. STEWART; J. CASTRO

Johannes Gutenberg Universität, 55099 Mainz, Germany
(*stewara@uni-mainz.de, castroj@uni-mainz.de)

Pre-eruptive conditions in the magma storage zone prior to the AD1280 eruption of Quilotoa volcano in Ecuador have been constrained using geothermobarometry; values of 240 MPa average magma pressure and f_{O_2} NNO+1.63 were calculated; a relatively oxidized, shallow magma of 800°C.

Using FTIR and EMPA on glass melt inclusions in quartz phenocrysts, total water dissolved in the melt was determined to be ~6.65 wt% (X_{H_2O} 0.21), of which 5.05wt% exists as H_2O_m while 1.6wt% is OH. CO_2 in the melt is variable. The average, 141ppm, corresponds to X_{CO_2} $1.8e^{-4}CO_2$.

Using CO_2 - H_2O solubility models, a melt X_{H_2O} 0.2 was computed – equal to the value measured in the melt, indicating water saturation at the time of trapping.

A dominance of H_2O over CO_2 is revealed in the vapor phase: 0.98 and 0.02 respectively.

Melt sulfur concentrations are 47-92ppm. Petrologic methods, magma volume- SO_2 degassing correlations and ice core records were combined to estimate values of 969 Mt H_2O and 2.25 Mt SO_2 degassed from the melt during the eruption, from which ≤ 3.4 Mt H_2SO_4 could have been produced (assuming 100% SO_2 -to- H_2SO_4 conversion) and a total of 35-75Mt SO_2 (melt + excess S vapor phase), producing ~52-115 Mt H_2SO_4 .

Origin of dissolved solids in Marcellus shale produced water

BRIAN W. STEWART^{1*}, ELIZABETH C. CHAPMAN²,
ROSEMARY C. CAPO¹, JOSEPH R. GRANEY³
AND JASON D. JOHNSON³

¹Department of Geology and Planetary Science, University of Pittsburgh, Pittsburgh, PA 15217, USA (*correspondence: bstewart@pitt.edu)

²Echelon Applied Geoscience Consulting, 1229 Twelve Oaks Ct. Murrysville, PA 15668, USA

³Department of Geological Sciences, Binghamton University, Binghamton, NY 13902, USA

Hydraulic fracturing of black shales for natural gas production results in large volumes of flowback and produced water, which rapidly (within days to weeks) achieves high levels of total dissolved solids (TDS), sometimes $>2 \times 10^5$ ppm. This highly saline water continues to be produced, albeit at much diminished rates, over the lifetime of the well. This brine could originate from (1) interaction of injected water with salts in the formation, (2) extraction of brine trapped in pores within the shale and/or (3) formation water previously held in fractures, sandy lenses, or adjacent strata. To evaluate the origin of these dissolved solids, we carried out sequential leaching experiments on dry-drilled cuttings from the Middle Devonian Marcellus shale and adjacent units in Tioga County, New York, USA. The samples were treated with ultrapure water to dissolve soluble salts and sulfates, 1N ammonium acetate buffered to pH 8 to extract exchangeable cations, 8% acetic acid to dissolve carbonate minerals and 0.1N HCl to target other acid-soluble phases.

The water leachates had consistently higher Na/Cl and lower Ca/ SO_4 , Na/Ca and Sr/Ca ratios compared to produced water [1, 2]. Ba/Ca ratios were highly variable (as in the produced water) and $>90\%$ of the Ba extracted was in the ammonium acetate fraction, suggesting it is bound in exchangeable sites within the shale. $^{87}Sr/^{86}Sr$ ratios of water-soluble and exchangeable Sr range from 0.7093 to 0.7112, mostly within the range of $^{87}Sr/^{86}Sr$ values measured in produced waters [1], but well above Devonian seawater and well below bulk-shale values (>0.731). Based on the significant differences between the chemistry of the leachates and that of Marcellus produced waters, we suggest that most solutes in the latter are inherited from highly saline formation waters in fractures or adjacent strata. Long-term interaction of these waters with the shale imprinted similar Sr isotope ratios on the water-soluble and exchangeable portions.

[1] Chapman *et al.* (2012) *ES&T* **46**, 3545-3553. [2] Haluszczak *et al.* (2013) *AppGeochem* **28**, 55-61.

Improved boron isotope pH proxy calibration for the deep sea coral *Desmophyllum dianthus* through sub-sampling of fibrous aragonite

J.A. STEWART^{*1}, E. ANAGNOSTOU¹ AND G. L. FOSTER¹

¹Ocean and Earth Science, National Oceanography Centre, University of Southampton, Southampton, UK, (*Joseph.Stewart@noc.soton.ac.uk)

The isotopic composition of boron ($\delta^{11}\text{B}$) in marine carbonates is well established as a proxy for past ocean pH [1,2]; however, its robust application to palaeo-environments relies on the generation of species-specific calibrations. Existing calibrations utilising the deep sea coral *Desmophyllum dianthus* highlight the potential application of $\delta^{11}\text{B}$ measurements of this species to pH reconstructions of intermediate depth waters [3,4]. However considerable uncertainty remains regarding the estimation of seawater pH from these bulk $\delta^{11}\text{B}$ measurements, resulting from sub-structural heterogeneities in $\delta^{11}\text{B}$ of *D. dianthus*. To circumvent this problem, thus improving the reliability of the *D. dianthus* $\delta^{11}\text{B}$ calibration, we present a new $\delta^{11}\text{B}$ calibration of micro-sampled fibrous aragonite from *D. dianthus*. Modern coral specimens recovered from the Atlantic, Pacific and Southern Oceans (depth range of 274–1470 m) were micro-sampled using a MicroMill (New Wave), analysed using multi-collector ICP-MS (Neptune) and the measured $\delta^{11}\text{B}$ was regressed against ambient pH taken from hydrographic data sets (pH range 7.4 to 8.0). $\delta^{11}\text{B}$ values from this new fibre calibration are generally lower than bulk septal measurements [e.g. 3] and suggest a stronger and better-defined dependence on ambient seawater pH. This study confirms the utility of *D. dianthus* as an archive of palaeo-pH, provided suitable sampling strategies are applied.

[1] Sanyal *et al.* (2001) *Paleoceanography* 16, 515–519, [2] Hönisch *et al.* (2004) *EPSL* 68, 3675–3685, [3] Anagnostou *et al.* (2012) *EPSL* 349–350, 251–260, [4] McCulloch *et al.* (2012) *GCA* 87, 21–34.

Dual sources for early Taranaki magmas: The Sr isotope story

R.B. STEWART^{1*}, R.C. PRICE², I. E.M. SMITH³ AND A. ZERNACK⁴

¹Volcanic Risk Solutions, IAE, Massey University, Palmerston North 4442, New Zealand (*correspondence: r.b.stewart@massey.ac.nz)

²Faculty of Science and Engineering, University of Waikato, Hamilton, New Zealand (rprice@waikato.ac.nz)

³School of Environment, University of Auckland, Auckland 1142, New Zealand (ie.smith@auckland.ac.nz)

⁴Tanenuiarangi Manawatu Inc., PO Box 1341, Palmerston North, New Zealand (a.zernack@massey.ac.nz)

Mount Taranaki, located 140 km west of the Taupo Volcanic Zone (TVZ), lies 180 km above the Wadati-Benioff Zone and is the most westerly subduction-related volcanism in New Zealand. Compositions are basaltic andesite to andesite with minor dacite and basalt. Taranaki has erupted episodically for more than 130 ka, generating debris avalanche deposits by catastrophic failure of the edifice. These deposits provide a record of the early magmatic evolution of the Taranaki volcanic system. K_2O and LILE are enriched with time, culminating in Holocene high-K andesites [1]. Pre-100 ka magmas include primitive basalts and basaltic andesites with higher silica compositions in progressively younger units and the appearance of late-stage low pressure mineral phases (high-Ti hornblende, biotite and Fe-rich orthopyroxene) confirms a gradual shift to more evolved magmas with time.

Sr isotope compositions have been constant at around 0.7046; similar to the least radiogenic compositions at Ruapehu, a long-lived active andesite volcano in the TVZ, suggesting a common mantle wedge composition for both Taranaki and the TVZ. However, the Taranaki isotope data set contains evidence for the presence prior to 100 ka of an even less radiogenic source with $^{87}\text{Sr}/^{86}\text{Sr}$ compositions of < 0.7040, mostly in primitive basalts with < 50% SiO_2 . Trace element data for these samples have only weak arc signatures. A similar dual Sr isotope source is evident in the older Pouakai volcano in Taranaki. We suggest that in the early Taranaki magma systems a component of relatively unmodified mantle was present that was eclipsed after c. 100 ka by subduction-modified material. The slab under Taranaki is near-vertical and this slab configuration might allow edge flow to contribute to the Taranaki magma source.

[1] Zernack *et al.* (2012) *J Pet* 53, 325–363.

Rare Earth Elements origin and dynamic in contaminated river basins: Nd isotopic evidence

STILLE P.¹, HISSLER C.² AND CHABAUX F.¹

¹ LHyGeS - UMR 7517 CNRS - EOST/UdS, 1 rue Blessig
F-67084 Strasbourg cedex (pstille@unistra.fr,
fchabaux@unistra.fr)

² GEOSAT/EVA/CRP-GL, 41 rue du Brill L-4422 Belvaux
(hissler@lippmann.lu)

Uncertainties in identifying the origin of pollutants in river systems and in quantifying their impact particularly exist for ecosystems in strongly contaminated river basins. The difficulty of such estimations is based on the relative significance of both anthropogenic and natural sources of trace metals in the environment. The natural geochemical background is characterized by important variations at global, regional or local scales. Moreover, elements currently considered to be undisturbed by human activities and used as tracers of continental crust derived material have become more and more involved in industrial or agricultural processes. The global production of lanthanides (REE), used in industry, medicine and agriculture, for instance, has increased exponentially from a few tons in 1950 to about 150 kt in 2012. Consequently, these contributions interfere in the estimation of natural REE sources.

The application of Nd isotope ratios has very recently been successfully used for the first time for tracing the anthropogenic contribution of atmospheric deposition in urban and industrial areas (Lahd Geagea *et al.*, 2008; Hissler *et al.*, 2008; Guéguen *et al.*, 2012). However, at our knowledge, no study focused on the fractionation of the Nd isotopic ratio due to anthropogenic activity in river systems. For this reason, this work is dedicated to the understanding of processes that control the Nd isotopic fractionation in river waters heavily contaminated by anthropogenic activities.

The upper Alzette River basin, in Luxembourg, suffers from substantial historical and current contamination principally due to the presence of the steel industry, which has been active from 1875 until now. The particulate and dissolved fractions of river waters were monitored using a multitracer approach (including REE and Nd isotopes) during two hydrological cycles (bi-weekly and flood event based sampling). This extensive sampling design allowed to understand the seasonal dynamics of the waters Nd isotopic compositions according to the REE composition of the particulate fraction of the water. Combining REE concentrations and the Nd isotopic information allowed us to quantify the annual anthropogenic fluxes of REE.

A review of CO₂ and O₂ gas dynamics within the sub-surface Critical Zone and implications for early-atmosphere studies using paleosols

G. E. STINCHCOMB^{1*}, S. L. BRANTLEY¹

¹Department of Geosciences, Pennsylvania State University,
University Park, PA 16802

(*Correspondence: ges130@psu.edu, ¹sxb7@psu.edu)

The pCO₂ concentrations of early Earth's atmosphere are a key component for resolving the faint young Sun paradox and have been intensely debated for some time. Regolith models that use mass-balance geochemical arguments, based on the consumption of CO₂ through the neutralization of soil, saprolite and rock, prove to be one of the more reliable methods for estimating atmospheric pCO₂ [1, 2, 3]. Yet, many of the assumptions used to estimate the early atmosphere are difficult to test in the modern biotic Earth. This study serves as a review of modern regolith gas research and explores the potential use of deep weathering profiles for refining paleoatmosphere reconstructions. We compiled 248 soil CO₂ and O₂ assays from 29 regolith studies spanning a range of environments that includes deep (>3 m) profiles. Soil CO₂ values (n=174) range from 0.01 to 15.5% by vol., whereas soil O₂ values (n=74) range from 0.2 to 22.85% by vol. The compilation of regolith gas data shows that only 30% of the assays were collected from a depth >3 m; and few of these studies include both gas and bulk geochemical data. The data that do extend to depths >3 m show O₂:CO₂ ratios that exponentially decline with increasing depth. This deep portion of the modern sub-surface Critical Zone has lower O₂:CO₂ ratios and presumed lower biomass concentrations than the modern surface. These observations suggest that the highly acidic, low-oxidizing soil atmosphere *deep* in modern regolith may be a suitable analogue for Precambrian abiotic *near-surface* weathering. Contemporary deep (> 3 m) regolith studies that include both bulk geochemical and gaseous phase data are not only lacking but could provide a much-needed empirical dataset for refining Precambrian atmosphere estimates using paleosols. [1] Sheldon, 2006, *Precambrian Res* 147, 148-155. [2] Driese *et al.*, 2011, *Precambrian Res* 189, 1-17. [3] Brantley *et al.*, *in press*, *In Treatise of Geochemistry, The Atmosphere – History*.

Environmental parameters that determine distribution coefficients of radionuclides for repositories

M. STOCKMANN^{1*}, V. BRENDLER¹, J. FLÜGGE², S. BRITZ²
AND U. NOSECK²

¹Helmholtz-Zentrum Dresden-Rossendorf, D-01314 Dresden, Germany (*correspondence: m.stockmann@hzdr.de)

²GRS Braunschweig, D-38122 Braunschweig, Germany

In order to treat radionuclide sorption processes in natural systems more realistically, temporally and spatially variable distribution coefficients (smart K_d -values) are calculated as a function of important environmental parameters such as pH, ionic strength (IS), concentration of dissolved inorganic carbon [DIC], calcium [Ca] and radionuclides [RN]. This smart K_d -concept is implemented into the transport code r^3t [1].

As a test of the modified code r^3t and the sensitivity analysis of radionuclide sorption regarding the mentioned environmental parameters, a possible future climate transition (seawater transgression) at Gorleben site / Germany was modelled [2]. Seawater inundation drastically influences the distribution and values of all environmental parameters. Chemical changes cause dissolution or precipitation of calcite and these in turn affect the pH, DIC and Ca concentration. In consequence the K_d -values and therewith the transport of radionuclides is impacted.

The results of the calculations are plausible: environmental parameters follow expected trends and major dependencies. As a consequence of the low Ca and DIC concentration in seawater, calcite dissolves in the aquifer and causes an increase of the pH. The K_d -values change according to the changes in environmental parameters. The pH has the most dominant impact on the smart K_d -values for most of the considered RNs, except for Pu and Th, for which the DIC concentration has the strongest impact. Under the assessed conditions for seawater transgressions the smart K_d -values of Cs, Ni, Am and Np(V) increase, those of Se(VI) and U(VI) decrease with increasing pH. The smart K_d -value particularly of Pu and Th decreases with increasing DIC concentration.

This project is funded by the German Federal Ministry of Economics and Technology (BMWi) under contract no. 02 E 11072A and 02 E 11072B.



[1] Fein (2004) Report GRS-192 [2] Noseck et al. (2012) Report GRS-297

Detrital zircon U/Pb ages on sedimentary rocks from the South Carpathians, Romania and implications for regional tectonic provenance

A. STOICA^{1*}, M. N. DUCEA^{1,2}, D. JIANU¹

¹ Faculty of Geology and Geophysics, University of Bucharest, Bucharest, 010041, Romania

² Department of Geosciences, University of Arizona, Tucson, AZ, 85721, USA

(*stoica.mala@gmail.com)

We present new detrital U/Pb zircon ages on six sands and sandstones collected from the South Carpathians, Romania. The Southern Carpathians have a nappe structure assembled during Middle to Late Cretaceous Alpine continental collision, consisting of several thrust nappes: the Getic-Supragetic nappe system, the underlying Severin complex and the lowermost Danubian nappe system, each composed of several amalgamated blocks of different affinities [1]. The analyzed rocks are: 3 mid-Cretaceous sandstones from Bucegi Mountains, one latest Cretaceous from Cozia Mountains, one Quaternary sandstone and one modern sand from Pianu Valley, north from Sebes Mountains. Our LA-MC-ICPMS U/Pb ages on detrital zircons confirm periods of magmatism in the Neoproterozoic and Cambro-Ordovician, as well as an episode of metamorphism in Late Devonian to Carboniferous documented by high U/Th ratio zircons.

The three early Cretaceous sedimentary rocks, collected from Bucegi Mountains, contain detrital zircons of different crystallisation ages ranging from 2.7 Ga to 340 Ma, but mostly clustering around 500 Ma. The predominant Neoproterozoic (550–850Ma) and Cambro-Ordovician (450-520 Ma) zircons indicate subaerial exposure of Leaota metamorphic unit in Aptian. Precambrian tectonics is documented by inherited zircons (cca. 900-1200 Ma, 1800-2200 Ma, 2600-2800 Ma), most likely recycled from Cumpana metasedimentary rocks due to their similarity in age distribution.

In the other samples, the most prominent population occurs between 450 and 500 Ma, followed by less abundant age group between 550 and 800 Ma. Older ages are also present but less frequent frequencies than in the early Cretaceous samples.

Age distribution patterns from all samples are consistent with derivation from basement rocks of the Getic-Supragetic thrust sheets and no contributions from Danubian units.

[1] Balintoni et al. (2009) *Gondwana Res.* **16**, 119-133.

A coordinated in situ NanoSIMS, HR-SEM and TEM search for presolar grains in an ALHA77307 chondrule rim

A.N. STOJIC^{1*}, F. E. BRENKER¹, J. LEITNER²
AND P. HOPPE²

¹Institute of Geosciences, Mineralogy, Goethe University,
Altenhoferallee 1, 60438 Frankfurt/M., Germany
(*correspondence: stojic@em.uni-frankfurt.de)

²Max-Planck Institute for Chemistry, Hahn-Meitner Weg 1,
55128 Mainz, Germany

Only recently, fine-grained rims around chondrules (FGRs) have been reported to contain presolar grains [e.g., 1, 2]. Competing hypotheses explaining formation history of FGRs are namely formation in the solar nebula or as a result of meteorite parent-body alteration processes [3]. FGRs and interchondrule matrix material do not differ chemically or mineralogically except for the grain size of the respective constituent minerals [4]. From the primitive CO3.0 chondrite ALHA 77307 containing a 390 μm x 300 μm large porphyritic chondrule surrounded by a FGR of 30 μm - 75 μm thickness, a transparent thin film suitable for TEM studies was prepared with a new preparation technique, ArIS [5]. Subsequently, 2,200 μm^2 of the FGR part of the thin film was analyzed with the NanoSIMS 50 ion probe in Mainz to search for O-rich presolar grains. Obtained isotope images, HR SEM images and TEM images of the same area were superimposed to unambiguously relocate the presolar grains among the surrounding solar material in the TEM. We detected 4 oxygen anomalous grains (3 silicates and one oxide), showing excesses in their ¹⁷O/¹⁶O ratio relative to the solar value. These grains represent relative abundances of ~ 70ppm and ~ 33ppm for the silicates and oxides, respectively. All grains are Group I which to date constitute the bulk of identified presolar O-rich species forming around low mass RGB/AGB stars. One presolar silicate is a crystalline fayalitic olivine, 180 nm x 40 nm in size. The grain is embedded in a groundmass comprising fine-grained Fe-rich silicates, refractory silicates, sulfides and Fe-Ni metal. There is no microscopically observable evidence of equilibration and this absence more likely favours the solar nebula accretion hypothesis rather than parent body alteration, a conclusion previously obtained only by SEM and NanoSIMS studies in the case of ALHA 77307 [e.g., 6].

[1] Haenecour & Floss (2012) *LPSC*, XL III, # 1107. [2] Leitner *et al.* (2012) *MAPS*, **47**, A394. [3] Metzler *et al.* (1992) *GCA*, **56**, 2873. [4] Brearley (1993), *GCA*, **57**, 1521. [5] Stojic & Brenker (2010) *EJM*, **22**, 17-21. [6] Davidson *et al.* (2012) *AMM*, **47**, A115.

High-precision LA-ICP-MS analysis of microanalytical reference materials for environmental research

B. STOLL^{1*}, K.P. JOCHUM¹, U. WEIS¹
AND M.O. ANDREAE¹

¹Max Planck Institute for Chemistry, Mainz, Germany
(*correspondence: brigitte.stoll@mpic.de)

The high spatial resolution available with LA-ICP-MS microanalysis of speleothems, biogenic calcium carbonates, bones and teeth holds the promise to improve the understanding of past climate conditions and environmental change. However, there are analytical problems with this method, such as interferences, elemental fractionation and matrix-dependent mass load effects using non-matrix-matched microanalytical reference materials (MRM) [1]. We therefore have investigated new carbonate MACS-1, MACS-3 and phosphate MAPS-4, MAPS-5, STDP5, Durango apatite MRM by a sector-field ICP-MS coupled either with 213 nm or 193 nm Nd:YAG nanosecond (ns) lasers, or a 200 nm Ti-sapphire based femtosecond (fs) laser.

Our studies show that many masses are affected by interferences, such as ²⁴Mg⁺⁺ by ⁴⁸Ca⁺⁺ in the carbonate and ⁴⁷Ti⁺ by ³¹P¹⁶O⁺ in the phosphate matrix. Elemental fractionation and mass-load-dependent matrix effects have been detected for the ns laser systems. They are small for refractory lithophile elements, such as Ba and Sr (< 5 – 10%). For chalcophile/siderophile trace elements with low boiling points (e.g., Pb, Zn) these effects are high (up to 20 - 40%) and different for the NIST silicate glasses, commonly used for calibration and the carbonate and phosphate MRM. Experiments with the femtosecond laser demonstrate that these matrix-related effects are negligibly small with this system [2]. This means that NIST glasses are suitable as calibration material [3] for carbonate and phosphate LA-ICP-MS microanalyses when using fs-UV lasers. They are also appropriate for the determination of lithophile element concentrations in environmental samples when using UV-ns lasers. However, when using ns lasers, matrix-matched calibration is still preferred for an accurate analysis of chalcophile/siderophile and volatile elements.

To further characterize the few available carbonate and phosphate MRM, we have analyzed them using the different laser ablation systems. Overall analytical uncertainties at the 95 % confidence level are about 5 – 10% for most elements. Our fs-UV laser results agree well with available reference values.

[1] Jochum *et al.* (2012) *Chem. Geol.* **318-319**, 31-44. [2] Weis *et al.* (2013) this conference. [3] Jochum *et al.* (2011) *GGR* **35**, 397-429.

Combined ^{13}C -D and D-D clumping in CH_4 : Preliminary results

D.A. STOLPER^{1*}, S.S. SHUSTA², D.L. VALENTINE², A.L. SESSIONS¹, A. FERREIRA³, E.V. SANTOS NETO³ AND J.M. EILER¹

¹Caltech, Pasadena, CA, USA (*dstolper@caltech.edu, eiler@gps.caltech.edu, als@gps.caltech.edu)

²University of California, Santa Barbara, CA, USA (sshusta@uamail.ucsb.edu, valentine@geol.ucsb.edu)

³Petrobras, Brazil (alexandrea@petrobras.com.br, eugenioneto@petrobras.com.br)

Methane is a key component of natural gas reservoirs, biogeochemical cycles and greenhouse gas emissions. Its cycle is often studied with stable isotopes (e.g., δD and $\delta^{13}\text{C}$), which help to distinguish between various environmental sources (e.g., thermogenic vs biogenic) and sinks [1]. However, as many of these processes generate methane with similar isotopic compositions, new measurements can aid in understanding various aspects of the methane cycle.

We present a new mass spectrometric technique that allows for the measurement of isotopologues of methane with more than one rare isotope ('clumped' isotopologues) at natural abundances. Specifically, we simultaneously measure $^{13}\text{CH}_3\text{D}$ and $^{12}\text{CH}_2\text{D}_2$ without interferences from water [2] and with external errors of 0.25-0.3‰ (in the Δ_{18} notation [3]).

Clumped isotopologues can serve as geothermometers for equilibrated systems, quantify kinetic processes and fingerprint different sources and sinks. To better understand the information recorded by the clumped isotopes of methane, we experimentally generated a high-temperature (200-500°C) calibration of equilibrium clumping, including approaches to equilibrium from multiple starting points. Application of this calibration to thermogenic methane samples from natural gas fields generally yields high temperatures ($\sim 190 \pm 65$ °C), which span the range of nominal natural gas formation temperatures, though with one high temperature outlier. The same calibration applied to biogenic gases gives lower temperatures (~ 45 -60°C) that are consistent with their inferred or known formation temperature.

Preliminary results indicate that the temperatures derived from combined $^{13}\text{CH}_3\text{D}$ and $^{12}\text{CH}_2\text{D}_2$ clumping are, in most cases, reasonable formation or storage temperatures. This suggests that methane may achieve internal isotopic equilibrium in both high and low temperature processes and retain that signature during storage. If so, then measurements of methane clumped isotopes will serve as a straightforward way to distinguish sources of methane in nature and give insight into the physics and chemistry of how methane forms.

[1] MJ Whiticar, *Chemical Geology* **161** (1999). [2] JM Eiler *et al.*, *IJMS* **335** (2012). [3] JM Eiler, *EPSL* **262** (2007).

The petrochemistry of Jake_M: A martian mugearite

E.M. STOLPER^{1*}, M.B. BAKER¹, A. COUSIN^{2,3}, M. FISK⁴, R. GELLERT⁵, P.L. KING⁶, S. MAURICE³, S.M. MCLENNAN⁷, M.E. MINITTI⁸, M. NEWCOMBE¹, V. SAUTTER⁹, M.E. SCHMIDT¹⁰, A.H. TREIMAN¹¹, R.C. WIENS² AND THE MSL SCIENCE TEAM

¹Caltech, Pasadena, CA 91125, *correspondence: ems@caltech.edu; ²LANL, Los Alamos; ³Institut de Recherches Astrophys. Planétol., Toulouse, France; ⁴Oregon State Univ.; ⁵Univ. Guelph; ⁶Res. School Earth Sci., ANU; ⁷SUNY, Stony Brook; ⁸APL, Johns Hopkins Univ.; ⁹LMCM, Paris, France; ¹⁰Brock Univ.; ¹¹Lunar & Planet. Inst.

Jake_M (JM), the first rock analyzed by the APXS instrument on the Curiosity rover, is an alkaline igneous rock ($\sim 13\%$ normative nepheline). It differs significantly in composition from other known martian rocks and it is fractionated relative to typical martian igneous rocks (MgO ~ 3.5 wt%; Mg# ~ 0.37 ; Ni < 50 ppm; normative oligoclase and orthoclase [$\sim 13\%$]). JM is compositionally similar to terrestrial mugearites, a magma type typically found on ocean islands and in continental rift zones; indeed, were JM found on earth, we would be hard pressed to tell from its composition that it is a martian rock.

The discovery of this rock type on Mars likely indicates an origin by significant fractional crystallization of a primary alkaline or transitional magma generated by melting a region of the martian mantle compositionally distinct from the sources of other known martian basalts. JM's chemical composition (especially its high Al_2O_3 and low FeO contents) suggest that this fractional crystallization occurred under conditions that suppressed plagioclase crystallization relative to crystallization at 1 atm. Although non-unique, MELTS calculations indicate that a reasonable match to JM's composition can be achieved at 2 kbar (~ 15 km depth on Mars) after $\sim 50\%$ fractional crystallization of an estimated parental composition from St. Helena island containing 1.5 wt% H_2O . This result suggests a possible role for elevated pressure and/or water content in JM's petrogenesis.

The discovery of JM has implications for magmatic and eruptive processes on Mars, for the possibility of primary hydrous minerals in martian igneous rocks and for encountering even more fractionated alkaline magmas such as phonolites and trachytes. JM is also distinctly richer in potassium than other martian basalts, consistent with a metasomatized mantle source, perhaps characteristic of the mantle beneath the Gale Crater region.

A novel approach for determining the rate of organic carbon remineralization in bioturbated marine sediments at the global scale

K. STOLPOVSKY^{1*}, A. W. DALE¹ AND K. WALLMANN¹

¹Helmholtz-Zentrum für Ozeanforschung Kiel (GEOMAR),
Wischhofstr. 1-3, 24148 Kiel, Germany,

* kstolpovsky@geomar.de

The spatial variability in benthic particulate organic carbon (POC) mineralization kinetics throughout the ocean is currently unknown. This creates considerable uncertainties when diagenetic models are used to couple benthic and pelagic biogeochemical cycles in global models. The aim of this study is to derive a predictive algorithm to calculate the depth-dependent rate of POC degradation in bioturbated surface marine sediments.

Our approach first uses measured fluxes of oxygen and nitrate across the sediment-water interface to calculate the total depth-integrated rate of POC degradation [1]. Next, a diagenetic reaction-transport model is used to simulate these fluxes to within a defined tolerance range by optimizing the parameters of a depth-dependent POC decay function. The model describes POC mineralization using oxygen, nitrite and nitrate as electron acceptors and also their transport into and out of the sediments by molecular diffusion, sediment burial and bioirrigation.

We applied this approach to published data from 151 stations around the globe to simulate the fluxes of oxygen and nitrate in the uppermost 50 cm of the sediment including the bioturbated layer. Where published data were available, the modelled and measured oxygen and nitrate concentration profiles were compared. Ongoing work attempts to search for spatial trends in the parameters of the optimized POC degradation model and relate these trends to master variables such as the rain rate of POC to the seafloor (RRPOC). Our over-arching goal is to use these results to better predict the benthic exchange fluxes between marine sediments and the overlying water column in global models. This is especially for the main ocean basins where field data is currently limited.

[1] Bohlen, L., Dale, A. W., & Wallmann, K. 2012 Simple transfer functions for calculating benthic fixed nitrogen losses and C:N:P regeneration ratios in global biogeochemical models. *Global Biogeochemical Cycles* 26, GB3029, doi:10.1029/2011GB004198.

Soil organic matter and microbial activity in critical zones of tropical soils from Luquillo, Puerto Rico

M.M. STONE¹ AND A.F. PLANTE^{1*}

¹Department of Earth & Environmental Science, University of Pennsylvania, Philadelphia, PA 19104-6316, USA

(*correspondance: aplante@sas.upenn.edu)

The Luquillo Critical Zone Observatory (LCZO) is located in northeastern Puerto Rico in the El Yunque National Forest (18.33 °N, 65.73 °W) and seeks to understand the evolution of landscapes over time due to varying critical zone processes occurring in areas with similar climates, land use and geologic history. The critical zone is generally defined as the zone “where rock meets life” [1]. From this perspective, it is interesting to examine how microbial activity declines with depth into the critical zone as energy and substrate supplies decline and how this decline might be affected by various landscape properties.

The LCZO Soil Network consists of 216 quantitative soil pits, stratified across two parent materials (volcaniclastic and granodiorite), three forest types (Tabonuco, Palm and Colorado) and three hillslope positions (ridgetops, slopes, valleys). The current study used a subset of soils sampled to a depth of 140 cm and analyzed for organic C, total N and extractable organic P concentrations. Soil microbial biomass was determined using phospholipid fatty acid (PLFA) total lipid analysis [2] and enzyme activities were assayed according to German *et al.* [3].

All enzyme activities declined exponentially with depth, tracking exponential declines in total organic and microbial carbon. However, these trends differed when normalized by substrate or microbial C (i.e., specific activity). Soil parent material did not significantly affect microbial biomass or enzyme activity, though there were several significant depth × forest type interactions. Taken together, the results indicate that soil depth (as a surrogate for substrate availability) is the main driver of microbial activity in the critical zone of these tropical soils, rather than differences in landscape-scale variables.

[1] <http://criticalzone.org/national/research/the-critical-zone-1national/>. [2] White *et al.* (1979) *Oecologia*. **40**, 51-62. [3] German *et al.* (2011) *Soil Biol. Biochem.* **43**, 1387-1397.

Eliminate the organic nitrogen fraction to perform $\delta^{15}\text{N}_{\text{tot}}-\delta^{15}\text{N}_{\text{bnd}}$ analyses in bulk rocks: Application for Iguanodon-bearing Wealden facies of Bernissart (Belgium)

J.-Y. STORME¹, P. IACUMIN², G. ROCHEZ¹
AND J. YANS^{1*}

¹University of Namur, Department of Geology, 61 rue de Bruxelles, 5000 Namur, Belgium. (*correspondence: johan.yans@fundp.ac.be, jean-yves.storme@fundp.ac.be, gaetan.rochez@fundp.ac.be)

²Earth Sciences, Parma University, Viale G.P. Usberti 157/A, 43100 Parma, Italy (paola.iacumin@unipr.it)

$\delta^{15}\text{N}_{\text{org}}$ on bulk could be a useful proxy for reconstructing paleoclimatic and paleohydrologic conditions of the pre-Quaternary Past [1]. Total nitrogen (N_{tot}) and inorganic nitrogen bound (N_{bnd}) concentrations are automatically determined for each sample, to provide nitrogen isotopes on organics ($\delta^{15}\text{N}_{\text{org}}$) using of a mass balance equation. The inorganic nitrogen bound is deciphered by treating decalcified subsample with KOB_r-KOH solution to eliminate the organic nitrogen fraction [2,3,4]. Here we experienced this procedure on samples from a borehole cutting the lacustrine succession of the Iguanodon-bearing Wealden facies of Bernissart, middle Barremian to earliest Aptian in age [5,6,7]. $\delta^{15}\text{N}_{\text{org}}$ data show positive trend upwards whereas $\delta^{13}\text{C}_{\text{org}}$ show negative trend, suggesting variations in paleoclimatic and paleohydrologic conditions. However samples with relatively high TOC contents, after boiling with KOH-KOB_r solution by ~5 minutes, show chaotic $\delta^{15}\text{N}_{\text{org}}$ values, maybe due to uncomplete extraction of organic nitrogen. Similar analyses are required to understand the extraction of organic nitrogen during preparations. Many tests have to be performed such as: use of HCl or other acid, analysis of the type of organic matter in the sediments, limits of TOC contents, KOH-KOB_r treatment before or after HCl treatment, etc. Matching this with other proxies in other successions will improve our knowledge of $\delta^{15}\text{N}_{\text{org}}$ variations in geological Pre-Quaternary successions.

[1] Storme *et al.* (2012). *Terra Nova* **24**, 114-122. [2] Silva & Bremner (1966). *Soil Sci. Soc. Am. Proc.* **30**, 587-594. [3] Corbeels *et al.* (2000). *Plant and Soil* **218**, 71-82. [4] Schubert & Calvert (2001). *Deep-Sea Res I* **48**, 789-810. [5] Yans *et al.* (2005). *Paleovol* **4**, 135-150. [6] Dejans *et al.* (2007). *Rev. Paleobot. Pal.* **144**, 25-38. [7] Schnyder *et al.* (2009). *Palaeogeogr. Palaeoclimatol. Palaeoecol.*, **281**, 79-91.

Evidence for North to South Progression of Pulsed Intrusion and Metamorphism in the Lower Crust of a Gondwana Arc, Fiordland NZ

H.H. STOWELL¹, C.M. HOUT¹, A.J. TULLOCH²,
K.A. ODOM-PARKER¹, J. SCHWARTZ³
AND K.A. KLEPEIS⁴

¹Geol. Sciences, Univ. of Alabama, Tuscaloosa AL 35487
USA (hstowell@geo.ua.edu)

²GNS Science, Dunedin, NZ

³Geol. Sciences, California State Univ., Northridge, CA, USA

⁴Geology, Univ. of Vermont, Burlington, VT, USA

Exhumed magmatic arcs are critical for understanding subduction processes and the growth and deformation of continents. The duration and rates of tectonic shortening and the transition from over-thickened arc crust to thinned crust and ocean floor spreading are poorly understood. This transition may be related to buoyancy changes and delamination of dense lower crust. The Cretaceous rocks of New Zealand's Median Batholith provide a natural laboratory for understanding these processes because the rocks show evidence for eclogite facies metamorphism, magmatism and granulite-facies metamorphism with local loading during metamorphism. Garnet Sm-Nd ages indicate pulses of metamorphism that closely follow magmatic pulses in the Western Fiordland Orthogneiss suite (WFO). Eclogite facies rocks (Breaksea Orthogneiss) SW of the extensional Resolution Island shear zone (RISZ) juxtaposed these ca. 1.8 Gpa rocks against one (Malaspina Pluton) of three large granulite-facies WFO plutons. Rocks on both sides of the RISZ experienced granulite facies conditions, but those on the NE were metamorphosed at a lower P of 1.2 – 1.4 Gpa. Garnet Sm-Nd ages for peritectic garnet indicate that Malaspina rocks in the hanging wall of the RISZ underwent 116-112 Ma granulite-facies metamorphism shortly after pluton emplacement. Preliminary garnet Sm-Nd ages for eclogite-facies metamorphism SW of the RISZ indicate initial high P at ca. 123 Ma, then high T granulite facies metamorphism that lasted until ca. 108 Ma, following initial extension and collapse of the magmatic arc. Granulite facies metamorphism in the Malaspina and Breaksea postdates similar metamorphism in N Fiordland (Pembroke Granulite) by 10 Ma. Compilation of igneous and metamorphic ages along the lower crust exposed in Fiordland indicates temporal pulses of high-temperature metamorphism which may have progressed from north to south over ca. 15 Ma. preceding extension and continuing during initial extensional collapse of the over-thickened arc crust.

Insights in the methanogenic degradation of BTEX and PAH in different geological systems

N. STRAATEN^{1*}, N. JIMENEZ-GARCIA², F. GRÜNDGER¹,
H. H. RICHNOW², T. LÜDERS³ AND M. KRÜGER¹

¹BGR, Stilleweg 2, 30655 Hannover, Germany

(*Correspondence: Nontje.Straaten@bgr.de)

²UFZ, Permoserstraße 15, 04318 Leipzig, Germany

³GSF, Ingolstädter Landstr. 1, D-85764 Neuherberg, Germany

Biodegraded oil is found in many reservoirs worldwide. The more complex hydrocarbons belonging to the PAH and BTEX groups are harder to degrade by prokaryotes than e.g. alkanes. To understand the degradation processes of these hydrocarbons into simpler components, it is very important to get insight in the microbial communities and metabolic processes involved.

The lack of alternative electron acceptors in many habitats limits the possible anaerobic degradation pathways to methanogenesis, which has been shown to be the most important process in different hydrocarbon reservoirs. The composition of the microbial communities in enrichments from habitats with differing geochemical settings, e.g. shallow and deep subsurface terrestrial and marine systems showed a relatively similar composition, independent of the sampling site. Especially methanogenic Archaea, members of the *Syntrophaceae* and sulfate-reducing Prokaryotes contributed to the community in most enrichments. Moreover, in samples from a Chinese oilfield, the crucial process, the conversion of alcanoic, aromatic and polyaromatic hydrocarbons to methane, was proven in incubations via ¹³C-labeling [1]. The further molecular biological analysis of this habitat confirmed the presence of methanogenic Archaea as well as of different Bacteria capable of hydrocarbon degradation. In the ongoing work ¹³C-labeled substrates combined with SIP of proteins and DNA is used to identify the actively involved microorganisms. Preliminary analyses revealed labeled proteins belonging to methanogens, SRB and *Syntrophus* species thus confirming the 16S results. In addition the results from these enrichments are compared with data from environmental samples of gas, shale and oil reservoirs, to determine the *in situ* importance of the enriched hydrocarbon degraders.

[1] Jiménez, Morris, Cai, Gründger, Yao, Richnow, Krüger (2012) *Organic Geochemistry* 52, 44-54.

Observed large- and meso-scale oxygen changes in the ocean

L. STRAMMA^{1*}, R.A. WELLER², R. CZESCHEL¹,
S. BIGORRE², S. SCHMIDTKO³ AND A. OSCHLIES¹

¹GEOMAR Helmholtz Centre for Ocean Research Kiel, 24105 Kiel, Germany (*correspondance: lstramma@geomar.de)

²Woods Hole Oceanographic Institution, Woods Hole, MA 02543, USA

³School of Environmental Sciences, University of East Anglia, Norwich, NR4 7TJ, UK

Model results predict a decline in ocean oxygen and observations confirmed declines at different locations [1]. Within the research initiative 'Climate – Biogeochemistry Interactions in the tropical Ocean' the temporal-spatial scales of oxygen changes were investigated. Large scale oxygen changes for the world ocean were derived at 300 dbar for the last 50 years and in the South Atlantic Ocean even for a 70 year period [2]. Declining upper-ocean oxygen levels in many regions, especially in the tropical oceans, are dominant, whereas areas with increasing trends are found in subtropical and in a few polar regions. A comparison to a numerical biogeochemical Earth system model reveals that the magnitude of the observed change is consistent with CO₂-induced climate change, however there is a large mismatch between observed and modeled oxygen trends.

In the equatorial Pacific the zonal current bands are important in resupplying oxygen to the oxygen minimum zone in the eastern Pacific. In the Pacific strong oxygen changes are related to the Pacific Decadal Oscillation while oscillations on shorter time scales like an El Nino signal in the upper 350 m are superimposed upon this signal [3].

Meso-scale related oxygen changes are expected to be important on the poleward side of the tropical oxygen minimum zones. Recent measurements of the oxygen distribution of eddies near the Peruvian shelf as well as mooring observations at the Stratus mooring at ~20°S, 85°W show a large expanded low oxygen layer in anticyclonic eddies while in cyclonic eddies the low oxygen layer decreased.

The derived results indicate the importance of a large range of temporal-spatial scales which needs to be investigated further.

[1] Keeling *et al.* (2010) *Annu. Rev. Mar. Sci.*, **2**, 199-229.
[2] Stramma *et al.* (2012) *Biogeosciences*, **9**, doi:10.5194/bg-9-1-2012. [3] Czeschel *et al.* (2012) *J. Geophys. Res.*, **117**, doi:10.1029/2012JC008043.

Photochemistry of arsenite and chromate on iron oxyhydroxide

NARAYAN BHANDARI¹, ELIZABETH CERKEZ¹,
RICHARD J. REEDER² AND DANIEL R. STRONGIN^{1,*}

¹Department of Chemistry, Temple University, Philadelphia,
PA 19122, USA (dstrongin@temple.edu)

²Department of Geosciences, Stony Brook University, Stony
Brook, NY 11794, USA

The (photo)chemistry of arsenite [As(III)] and chromate [Cr(VI)] in the presence of ferrihydrite and goethite was investigated. A variety of techniques, including infrared spectroscopy, X-ray absorption near edge structure (XANES) and solution phase analysis were used to characterize the surface bound and aqueous phase species. The exposure of the iron oxyhydroxides to As(III) in the dark resulted in a adsorbed layer of As(III). Irradiation of the As(III)/ferrihydrite or As(III)/goethite system to simulated solar radiation resulted in the conversion of As(III) to adsorbed and aqueous phase As(V). The relative amounts of adsorbed and aqueous phase As(V) product varied whether ferrihydrite or goethite was present in solution due to differences in the rate of the heterogeneous oxidation of surface Fe(II) on the surfaces by dissolved oxygen. This particular reaction resulted in the formation of reactive oxygen species. Redox reactions of mixtures of As(III) and Cr(VI) in the presence of the two iron oxyhydroxides also were investigated. In this circumstance even in the absence of light, As(III) was oxidized to As(V) (~92% conversion) and Cr(VI) was reduced to Cr(III) if one of the small band gap semiconductor iron oxyhydroxide materials was present. As a comparison nanophase aluminum oxyhydroxide (an insulator) was exposed to As(III) and Cr(VI) under dark conditions. Under these experimental conditions far less As(III) oxidation and Cr(VI) reduction occurred (~50% conversion of As(III) to As(V)) compared to when iron oxyhydroxide was present. Furthermore, the exposure of the As(III)/Cr(VI)/ferrihydrite system to simulated solar light led to additional As(III) oxidation and Cr(VI) reduction (compared to dark conditions) while light had no effect on the As(III)/Cr(VI)/aluminum oxyhydroxide system. In general the results suggested that the semiconducting materials were able to drive the redox chemistry more efficiently due to facile surface mediated electron transfer from As(III) to Cr(VI).

Water mass mixing in the Drake Passage during the last 40 kyrs

T. STRUVE^{1,*}, T. VAN DE FLIERDT¹, L. F. ROBINSON²,
A. BURKE³, K. C. CROCKET⁴, M. LAMBELET¹
AND M.E. AURO⁵.

¹Imperial College London, London SW7 2AZ, UK

(*correspondence: t.struve11@imperial.ac.uk).

²University of Bristol, Bristol BS8 1RJ, UK.

³California Institute of Technology, Pasadena, CA 91125.

⁴DG Research and Innovation, European Commission, Rue de
la Loi, 1049 Brussels, Belgium.

⁵WHOI, Woods Hole Oceanographic Institution, MA 02543.

The modern Southern Ocean is a key area for the global ocean circulation as wind-driven mixing, upwelling and redistribution of water masses in the Antarctic Circumpolar Current (ACC) all have a significant impact on the properties and flow patterns of global water masses. It has been suggested that the Southern Ocean plays a central role in oceanographic and climatic changes observed on glacial-interglacial timescales, in particular with respect to carbon sequestration between the deep ocean and the atmosphere.

For the purpose of unravelling Southern Ocean water mass mixing over the past ~40,000 years, the aragonitic skeletons of solitary deep-sea corals collected from two cruises on the Nathaniel B. Palmer to the Drake Passage are used as archives for seawater Nd isotopes. These corals were collected from water depths between 300 and 1750 m and have previously been directly dated by U-Th and analysed for their radiocarbon content.^[1]

Neodymium was extracted from the wash solution of the U-series anion-exchange chemistry using a two-stage ion chromatography (RE-spec and Ln-spec resins). Subsequent analyses of Nd were performed as NdO⁺ on a Triton TIMS using a TaF₅ activator on W filaments. This method yields within run uncertainties around 10 ppm (2σ SE) and external uncertainties around 20 ppm (2σ SD) for sample loads as small as a few ng of Nd.

Preliminary Nd isotope results on *D. dianthus*, *F. curvatum* and *B. malouinensis* specimen growing during the last 40 kyrs show significant variability at intermediate water depths (εNd of ~-5 to -8) and a more stable Nd isotopic composition in the lower water column (>1000m; εNd ~-8).

We will interpret our unique data set in the context of published glacial-interglacial radiocarbon results and inferred Southern Ocean water mass variability and ventilation rates.

[1] Burke & Robinson (2012), *Science* **335**, 557-561.

Emerging understanding of anthropogenic interferences in the ecosystem silica filter

ERIC STRUYF^{1*} AND DANIEL J. CONLEY²

¹ University of Antwerp, Department of Biology, Universiteitsplein 1C, 2610 Wilrijk, Belgium, eric.struyf@ua.ac.be

² Lund University, Dept. Geology, Sölvegatan 12, 22362 Lund, Sweden

The annual fixation of DSi into terrestrial vegetation is 60 to 200 Tmole, 10–40 times more than the yearly export of DSi from the terrestrial geobiosphere to the coastal zone and 3–6 times more than annual weathering of silicates. Ecosystems form a large filter between mobilization of DSi by silicate weathering and mobilization to rivers. A large reservoir of biogenic amorphous Si (mostly plant phytoliths) and pedogenically reworked amorphous Si (ASi) accumulates in soils. ASi is substantially more soluble than mineral Si. Still, ASi persistence and reactivity in soils, the dependence of the ASi turnover on ecological processes and ultimately the global relevance in Si budgets are poorly constrained [1]. A major challenge is presented by the difficulty to separate pedogenic and biogenic amorphous Si phases in the soil. This hampers quantification of the silicate weathering-related C-sink and accurate modelling of transport of Si to rivers and estuaries, where Si plays a crucial in phytoplankton productivity.

Human land management can cause abrupt shifts to the biogeochemical cycle in terrestrial ecosystems and their ability to sequester Si. Our results from a novel technique that allows for separation of biogenic and pedogenic ASi phases, shows that turnover rates of ASi in temperate cultivated soils are strongly reduced compared to forests and stocks of pedogenic ASi are depleted. Newly acquired analysis of Si isotopes in soil water also show this. This results in timescale dependent, 2–4 fold shifts in terrestrial Si mobilisation [2]. Human harvest of crop ASi has created a parallel anthropogenic Si cycle, which has received virtually no quantification so far [3]. Our observations show that intense domestic reindeer and cattle grazing alters physical and chemical reactivity of biogenic ASi (Si is a defense mechanism against herbivory) and can cause abrupt shifts in ecosystem ASi storage and cycling. The combination of experimental, field and modelling studies shows that land use has strongly altered mineral-soil-plant interactions.

[1] Struyf & Conley (2012), *Biogeochemistry*, 107, 9–18. [2] Struyf *et al.* (2010), *Nature Comm.*, 1, 129 [3] Vandevenne *et al.* (2012), *Front Ecol Environ*, 243–48.

Deep-sea coral amino acids illuminate ecosystem processes on South East Australia seamounts

K.M. STRZEPEK^{1*}, A. REVILL², R.E. THRESHER², C. I. SMITH³ AND S.J. FALLON¹

¹ Research School of Earth Sciences, Australian National University, Canberra, 0200, Australia (*correspondance: kelly.strzepek@anu.edu.au, stewart.fallon@anu.edu.au)

² CSIRO Marine and Atmosphere, Hobart, 7000, Australia (andy.revill@csiro.au, ron.thresher@csiro.au)

³ Faculty of Humanities and Social Sciences, Latrobe University, Melbourne, 3086, Australia (colin.smith@latrobe.edu.au)

South-east Australian seamounts and their associated deep-sea ecosystems, are located in an oceanographically complex and climatically sensitive region. Across this region, Bamboo Corals inhabit a tremendous depth range (600–4000m) archiving surface processes by incorporating raining particulates into their banded skeletons. Bulk organic ¹⁵N has previously been used to substantiate the region's shifting surface regimes in response to current climate change, but trophic enrichment was necessarily approximated, obscuring the ¹⁵N-signal of the producers at the base of the foodweb [1].

In this study, we revisit the ¹⁵N archive, instead using individual amino acids (AA) to reconstruct ecosystem dynamics. We are able to capture and decouple, a centenary of trophic interactions from the ¹⁵N-signal of primary production. Furthermore, as specimens were collected between 1000–3000m, we are able to explore deep-sea particle transformations and microbial heterotrophy that connects surface and deepwater ecosystems. By exploiting previously validated ¹⁵N-AA patterns [2] and considering those in the ¹³C-AA record, we propose likely mechanisms that could support the inexplicably high biomass that has been reported within the local bathyl zone [3].

Our preliminary results indicate that clear distinctions seen between depths in the bulk record naturally reflect the isotopic signature of the most abundant AA, glycine, as well as trophic complexity. Furthermore we find evidence of differing particulate processing histories, provenance and species effects that all have important implications for the future interpretation of records from deep-sea coral organics.

[1] Sherwood *et al.* (2009) *Mar. Ecol. Prog. Ser.* **397**, 209–218. [2] McCarthy *et al.* (2007) *GCA* **71**, 4727–4744. [3] Thresher *et al.* (2011) *Nat. Sci. Reports* **1**, 119.

Constraints on the source of mantle plumes from the first picrites erupted Ethiopian flood basalt province

F. M. STUART^{1*} AND N. ROGERS²

¹Isotope Geosciences, SUERC, East Kilbride G75 0QF, UK
(*fin.stuart@glasgow.ac.uk)

²Department of Earth & Environmental Sciences, Open University, Milton Keynes MK7 6AA, UK

The earliest basalts erupted by largest mantle plumes are typically 200-300°C hotter than those derived from convecting upper mantle at mid-ocean ridges. They originate from a thermal boundary layer deep in Earth that is assumed to be the core-mantle boundary. Consequently the first plume-derived basalts provide constraints on Earth structure and differentiation history. The first picrites erupted by the Iceland plume have a high proportion of primordial He ($^3\text{He}/^4\text{He} \sim 50 R_a$) yet a range in radiogenic isotope and incompatible trace element ratios that overlap the global mid-ocean ridge basalt range [1]. This is difficult to reconcile with pristine mantle dominating the plume head. The simplest interpretation is that the convecting mantle has been polluted by primordial He either at the core-mantle boundary or during ascent, thus still requires the existence of primordial volatile reservoir.

In an attempt to provide better constraints on the deep mantle source of plumes we have analysed the He-Sr-Nd-Pb isotopic composition of the earliest high-Ti picrites (HT2) from the Dilb section of the ~30 Ma Ethiopian flood basalt province. The basalts are characterized by high Fe and Ti contents for MgO = 14-15% that implies the parent magma was derived from a high temperature small melt fraction, likely the plume head. The basalts are characterized by a narrow range of $^{87}\text{Sr}/^{86}\text{Sr}$ (0.70396–0.70412) and $^{206}\text{Pb}/^{204}\text{Pb}$ (18.82-19.01). $^3\text{He}/^4\text{He}$ of olivine never exceeds 21 R_a . The Afar plume was sourced in a discrete mantle reservoir that is less degassed and more enriched than the convecting upper mantle. The source region is significantly more degassed than the mantle sampled by the proto-Iceland plume and more homogenous. Clearly the largest mantle plumes are not initiated in a single deep mantle domain with the same depletion/enrichment history and they do not mix with convecting mantle to the same extent.

[1] Starkey *et al.* (2009) *Earth Planet. Sci. Lett.* 277 91-100.

Oxidative corrosion of uraninite (UO₂) surfaces

JOANNE E. STUBBS^{1*}, PETER J. ENG¹, CRAIG A. BIWER², ANNE M. CHAKA³, GLENN A. WAYCHUNAS⁴ AND JOHN R. BARGAR⁵

¹Center for Advanced Radiation Sources, University of Chicago, Chicago, IL, USA, stubbs@cars.uchicago.edu (* presenting author)

²Department of Computational Medicine and Bioinformatics, University of Michigan, Ann Arbor, MI, USA

³Physical Measurement Laboratory, National Institute of Standards and Technology, Gaithersburg, MD, USA

⁴Lawrence Berkeley National Laboratory, Berkeley, CA, USA

⁵Stanford Synchrotron Radiation Lightsource, Menlo Park, CA, USA

Uraninite (UO₂) is the most abundant uranium ore mineral, the product of proposed bioremediation strategies for uranium-contaminated soils and aquifers and its synthetic analog is the primary constituent of most nuclear fuels. It incorporates interstitial oxygen up to a stoichiometry of UO_{2.25} without disruption of the uranium lattice, but the structural details of the process are the subject of ongoing study and debate. Because the solubility and dissolution kinetics of uraninite depend heavily on the oxidation state of uranium, understanding the mechanisms of UO₂ surface oxidation and corrosion is essential to predicting its stability in the environment throughout the nuclear fuel cycle. To date, however, no study has addressed this process at the molecular scale at atmospheric pressure and room temperature.

We present crystal truncation rod (CTR) x-ray diffraction studies of pristine and oxidized UO₂ (111) and (100) surfaces. The clean (111) surface shows minimal contraction of the uppermost atomic layers and a layer of oxygen or hydroxyl group adatoms above the vacuum-terminated surface. Upon exposure to oxygen, an oxidation front proceeds into the crystal, interstitial oxygen atoms penetrate to depths of 30 Å or more, surface-normal layer distances contract (consistent with bulk uraninite oxidation) and an ordered superlattice forms, commensurate with the underlying bulk. Similar oxygen surface penetration and layer contraction are observed upon oxidation of the (100) surface. These results demonstrate that the solid state diffusion of oxygen into UO₂ and UO_{2+x} surfaces is facile and that ordering kinetics are relatively rapid, even at room temperature.

Ab initio thermodynamics, which combines density-functional theory calculations with macroscopic thermodynamics, provides insight into the energetics, bonding and oxidation processes that occur as oxygen reacts with the surfaces and diffuses into the solid. Subsurface oxidation is predicted to contract surface-normal layers, consistent with experimental observations.

Extraction of paleo seawater Nd isotope compositions: A case study from the Indonesian Throughflow

ROLAND STUMPF^{1,2*}, MARTIN FRANK², BRIAN A. HALEY^{2,3}, STEFFANIE KRAFT² AND WOLFGANG KUHN⁴

¹Imperial College London, Dept. of Earth Science & Engineering, London SW7 2AZ, UK (*presenting author)

²GEOMAR Helmholtz Centre for Ocean Research Kiel, Germany

³Oregon State University, College of Oceanic & Atmospheric Sciences (COAS), USA

⁴Christian-Albrechts-Universität Kiel, Institute of Geosciences, Germany

Over the past decade, radiogenic Nd isotope compositions have increasingly been used as a paleo seawater proxy for the reconstruction of past ocean currents and water mass mixing. For this purpose, the Nd isotopes have been extracted from various marine archives, such as ferromanganese crusts and nodules, Fe-Mn oxyhydroxide coatings on detrital sediment surfaces, as well as in foraminiferal shells, cold water corals and fish teeth. However, it is still under debate if all these archives reliably preserve unaltered paleo seawater Nd isotope compositions.

In this study, the Nd isotope compositions of reductively cleaned foraminiferal shells (bulk planktonic & monospecific), of Fe-Mn oxyhydroxide coatings leached from the decarbonated detrital fraction of the sediment, as well as Nd isotope compositions leached directly from the bulk sediment were extracted from carbonate-rich sediment core MD01-2378 (1783 m water depth) located in the outflow region of the Indonesian Throughflow (ITF) in the eastern Timor Sea. We focus on the comparison of the Nd isotope records from these three archives covering the time period of marine isotope stage 3 (~23 – 64 ka B.P.) in order to reconstruct variations of intensity and the relative contributions from different outflow pathways of the ITF.

A comparison of core top Nd isotope compositions extracted from planktonic foraminiferal shells shows good agreement with water column Nd isotope data [1]. Data from a core top sample at a location close to core MD01-2378 showed that there is no significant difference in Nd isotope composition between monospecific ($\epsilon\text{Nd} = -4.3$) and bulk ($\epsilon\text{Nd} = -4.4$) planktonic foraminiferal samples.

The Nd isotope variability observed in the downcore planktonic foraminiferal records of core MD01-2378 ranged from $\epsilon\text{Nd} = -3.5$ to -5.5 with minimum values occurring during the Last Glacial Maximum and either documents variations between different ITF outflow pathways or variable surface water contributions from Northern Australia or even from the Southern Ocean. These data are compared with bottom water Nd isotope variations newly obtained from oxyhydroxide coatings of the same sediment core.

[1] Jeandel *et al.*, (1998). *Geochim Cosmochim Acta*, 62(15), 2597-2607.

Record of historical mercury trends in sediments from the Laguna del Plata, Córdoba, Argentina

Y.V. STUPAR^{1,2*}, J. SCHÄFER³, M.G. GARCIA², S. SCHMIDT⁴, E. PIOVANO², G. BLANC³, F. HUNEAU⁵ AND P. LE COUSTOMER¹

¹Université de Bordeaux, EA 4592 Géorressources & Environnement, ENSEGID, 1 allée F. Daguin, F-33607 Pessac, France (*correspondance : yohanastupar@yahoo.com.ar)

²Centro de Investigaciones en Ciencias de la Tierra (CICTERRA), CONICET/UNC, Av. Vélez Sarsfield 1611, X5016CGA, Córdoba, Argentina.

³Université de Bordeaux, EPOC, UMR 5805, F-33400 Talence, France

⁴CNRS, EPOC, UMR5805, F-33400 Talence, France

⁵Université de Corse Pascal Paoli, Laboratoire d'Hydrogéologie UMR 6134 SPE, Campus Grimaldi, BP 52, F-20250 Corte, France

Mercury concentrations and main carrier phases were determined in sediments of a 120 cm core from Laguna del Plata (LP). This lake is a part of the Laguna Mar Chiquita (LMC) system as it is connected to LMC itself during water highstands. LMC is one of the largest saline lakes in the world representing a sensitive climatic indicator due to its frequent lake level variations at millennial and interdecadal scales [1], with the most recent major variations during the early 1970s and after 2004. Total mercury (Hg_{TP}) concentrations analyzed by Atomic Absorption spectrometry after sample calcination in an O_2 stream (DMA 80) varied between ~13 and ~131 $\mu\text{g kg}^{-1}$ and reflected changes in water and sediment supply to the LP. Selective extractions performed on the sediments using ascorbate, HCl and H_2O_2 revealed that in the base of the core corresponding to a low water level period, Hg is mainly associated to reactive sulfides. In contrast, in the middle and upper part of the core Hg is rather associated with sedimentary organic matter and was interpreted as reflecting Hg deposition at the watershed scale. Core dating, performed with ^{210}Pb and ^{137}Cs , allowed to determine that the highest Hg peak corresponds to the years 1990-1995. This was attributed to the eruption of Lascar volcano in 1993 in the Central Andes of northern Chile rather than anthropogenic pollution sources.

[1] Piovano *et al.* (2002). *Sedimentology* **49**, 1371-1384. [2] Schäfer *et al.* (2006) *Appl. Geochem.* **21**,515-527.

Tracer applications to verify carbon mineralization in Icelandic basalts

M. STUTE¹, J. HALL¹, J.M. MATTER¹, K. MESFIN²,
S.R. GISLASON², E.H. OELKERS^{2,3}, B. SIGFUSSON⁴,
E. GUNNLAUGSSON⁴, I. GUNNARSSON⁴,
E.S. ARADOTTIR⁴, H. SIGURDARDOTTIR⁴, G. AXELSON⁵
AND W.S. BROECKER¹

¹Lamont-Doherty Earth Observatory, 61 Route 9W, Palisades, NY 10964, USA (martins@ldeo.columbia.edu)

²Institute of Earth Sciences, University of Iceland, Sturlugata 7, 101 Reykjavík, Iceland

³GET, CNRS/URM 5563-Université Paul Sabatier, 14 av. Edouard Belin, 31400, Toulouse, France

⁴Reykjavík Energy, Baejarhálsi 1, 110 Reykjavík, Iceland

⁵Iceland GeoSurvey, Grensásvegur 9, 108 Reykjavík, Iceland

The risks associated with geologic carbon storage can be considerably reduced by subsurface carbon mineralization.

The CARBIFIX project in Iceland is a field scale pilot study where CO₂ and H₂S emissions from the Hellisheidi geothermal power plant are dissolved in groundwater and injected into a permeable basalt formation at ~500 m depth below surface [1]. We are using non-reactive (sodium fluorescein, amidhorhodamine G, SF₃CF₃, and SF₆) and reactive (¹⁴C and ¹³C) tracers in an on-going injection project to characterize subsurface CO₂ transport and in situ CO₂-water-rock reactions. In early 2012, 170 tons of pure CO₂ tagged with ¹⁴C and SF₆ were dissolved in water and injected into a confined basalt aquifer. Samples were collected from injection and monitoring wells in evacuated serum bottles with butyl stoppers and analyzed by AMS and mass spectrometry for carbon isotopes, by fluorometry for Na-fluorescein and by gas chromatography for SF₆ and SF₃CF₃. The multi-tracer approach allows us to separate various injection experiments and differentiate between dilution and reaction. While the bulk of the injected CO₂ has not yet arrived at the monitoring wells, a fraction following a fast flowpath appeared within less than a month. δ¹³C shows an initial rise attributed to dissolution of aquifer carbonates and then a drop due to carbonate precipitation. The ¹⁴C/SF₆ ratio is lower than the injection ratio providing additional evidence for carbonate precipitation. The bulk of the injected CO₂ is expected to arrive by the summer of 2013 and we will extend the time series accordingly. Our study demonstrates the value of tracers as a monitoring, verification and accounting tool in reactive geological carbon storage systems.

[1] Gislason *et al.* (2010), *Int. J. Greenh. Gas Con.* 4, 537–545.

Robust Calibration Systems Based on Syringe Pumps for Water Vapor Isotopologue Measurements

ERIC STUTZ^{1*}, JANEK LANDSBERG², LASZLO SARKOZY¹,
ELISABETH MOYER¹ AND ERIK KERSTEL²

¹ Department of the Geophysical Sciences, University of Chicago, Chicago, IL 60637, USA (*correspondence: ejstutz@uchicago.edu)

² J. Fourier University of Grenoble Laboratoire Interdisciplinaire de Physique, (UMR 5588 CNRS-UJF), 38402 Grenoble, France

Advances in spectroscopic instrumentation mean that laser-based absorption spectroscopy (both direct and cavity enhanced) is increasingly used for isotopic measurements in environmental sciences. For studies involving water, this technique offers the advantages of speed and non-destructive sampling, allowing for new applications in water vapor measurements [e.g. 1] and for the support or replacement of mass spectroscopy in studies of ice cores [e.g. 2]. In both uses, instrument accuracy is tied to instrument calibration and therefore dependent on the availability of suitable calibration systems. We describe here a new calibration technique based on syringe pumps for producing air streams of known and constant water content and isotopic composition. Syringe pumps offer advantages over previous methods such as capillary flash-evaporation, water vapor "bubbling", or microdrop generation [e.g. 2,1,3], including greater control and reliability. We show the stability and time response of two calibration systems, built at the University of Chicago and the J. Fourier University of Grenoble and designed for high and low flow rates (0.1 -10 slm) and a water vapor dynamic range of 3-10,000 ppm. We discuss the optimization of parameters such as pressure, injection rate step shape, temperature and hydrophobic coatings. The designs are robust and readily modified for instrument-specific configurations, suggesting they may find wide use in the community.

[1] Sayres, D. S., *et al. Rev Sci Inst.* **80**, 2009. [2] Gkinis, V., *et al. Atm Meas Tech.* **4**, 2011. [3] Iannone, R. Q., *et al. J. Atmos. Ocean. Tech.* **26**, 2009.

Biogeochemical controls on the product of microbial U(VI) reduction

MALGORZATA STYLO¹, DANIEL S. ALESSI¹, PAUL PAOYUN SHAO¹, JUAN S. LEZAMA-PACHECO², JOHN R. BARGAR² AND RIZLAN BERNIER-LATMANI¹

¹Environmental Microbiology Laboratory, École Polytechnique Fédérale de Lausanne, CH-1015, Lausanne, Switzerland

²Chemistry and Catalysis Division, Stanford Synchrotron Radiation Lightsource, SLAC National Accelerator Laboratory, Menlo Park, CA 94025, USA

Biologically mediated immobilization of radionuclides in the subsurface is a promising strategy for the remediation of U-contaminated sites. During this process, soluble U(VI) is reduced by indigenous microorganisms to sparingly soluble U(IV). The crystalline U(IV) phase uraninite, or UO₂, is the preferable end-product of bioremediation due to its relatively high stability and low solubility in comparison to the non-crystalline biomass-associated non-uraninite U(IV) species. However, non-uraninite U(IV) species have been reported to be a predominant U(IV) product formed under field relevant conditions. Therefore the goal of this study was to delineate the biogeochemical conditions that promote the formation of non-uraninite U(IV) versus uraninite, to decipher the mechanisms of its preferential formation and to apply this knowledge to environmentally relevant cases. Batch experiments as well as biofilm reactors were set up to test the influence of biogeochemical conditions on U(IV) product formation. U(IV) products were analyzed with X-ray absorption spectroscopy (XAS), scanning transmission X-ray microscopy (STXM) and various wet chemical methods. As a result of batch experiments, we report an increasing fraction of non-uraninite U(IV) species with decreasing initial U concentration. Additionally, the presence of several common groundwater solutes (sulfate, silicate and phosphate) promote the formation of non-uraninite U(IV). Our experiments revealed that the presence of specific solutes promotes the formation of bacterial extracellular polymeric substances (EPS) and increases bacterial viability, suggesting that the formation of non-uraninite U(IV) is due to a biological response to the presence of these solutes during U(VI) reduction. Ongoing biofilm studies focus on the characterization and origin of U(IV) species formed under field relevant conditions, i.e., in the flow-through systems, under alternating redox regimes with controlled biotic and abiotic processes.

Arsenic immobilization and transformation by zerovalent iron

CHUNMING SU

National Risk Management Research Laboratory, U.S. Environmental Protection Agency, 919 Kerr Research Drive, Ada, OK 74820

Introduction and Experiments

Both granular [1] and nanosized zerovalent iron (NZVI) [2] are effective in removing arsenic from water. Granular ZVI also has been used as permeable reactive barrier media to intercept and remove As from contaminated groundwater at a smelting site [3] and as a filter material for removing As from Bangladesh tube well water [4]. This study focus on As removal mechanisms by NZVI. Batch tests were conducted using 25-nm NZVI to remove As(V) and As(III) under anaerobic conditions as a function of time and pH with or without phosphate and silicate. Minerals were identified.

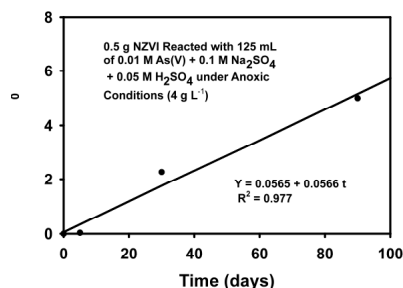


Figure 1. Plot of pseudo-second order removal kinetics for As(V) in the long term test.

Results and Discussion

Both As(V) and As(III) removal increased with increasing time to approach a steady state after 4-5 days in the short-term test. There was generally more removal of As(III) than As(V). Complete or near complete removal of As(V) and As(III) was achieved at pH levels less than 10. Competition of phosphate and silicate against As(V) and As(III) was observed at alkaline pHs. New solid phases formed such as parasymplectite in the As(V) system and vivianite in the phosphate system. This study demonstrated that As(V) removal involves both solid precipitation and adsorption; whereas, As(III) removal only involves surface adsorption.

[1] Su and Puls, (2001) *Environ. Sci & Technol.* **35**, 1487-1492. [2] Kanel *et al.* (2005) *Environ. Sci & Technol.* **39**, 1291-1298. [3] Beak & Wilkin, (2009) *J. Contam. Hydrol* **106**, 15-28. [4] Leupin & Hug (2005) *Water Res.* **39**, 1729-1740.

Evidence of underground water for the forming mechanism of high sulfur condensate reservoirs, Example from the Tazhong area

JIN SU, SHUICHANG ZHANG, GUANGYOU ZHU AND YU WANG

PetroChina Research Institute of Petroleum Exploration and Development, Beijing 100083, China, (susujinjin@126.com)

Condensate gas reservoirs with high content of hydrogen sulfide have been discovered on a large scale in deep marine carbonate formations in the Tarim Basin, which contain formation water with high salinity. Investigations show that, in the Tazhong area, the average negative and positive ion contents in the lower Ordovician to Cambrian formation water are higher than that in the upper Ordovician formation water. Yingshan formation with high-sulfur condensate reservoir is similar to the lower Ordovician to Cambrian formation in water properties, that is to say, the content of Mg^{2+} and SO_4^{2-} and PH value are higher than those in the upper Ordovician formation; these mineral ions and PH are crucial to thermochemical sulfate reduction. Hydrogen sulfide content in Yingshan condensate reservoir and Mg^{2+} content of formation water correlates well in the Tazhong area, which indicates a presumable TSR-origin of hydrogen sulfide according to the reaction theory of contact ion-pair. Besides, the total salinity and pH value of formation water are positively correlated with hydrogen sulfide content in the condensate reservoir, which may indicate that high salinity and pH value are important to activate and maintain TSR reaction. High sulfur condensate reservoirs are all located near the No. I faulted zone and strike-slip faults which are the major pathway for deep fluid migration in the area, showing that the formation water in condensate reservoirs may communicate with high salinity fluid in the lower Ordovician to Cambrian formation and hydrogen sulfide flowed upwards with formation water from deep zones along fractures to form condensate reservoirs with high sulfur content and high salinity. The discovery reveals the forming mechanism of high sulfur condensate reservoirs in the Tazhong area and will be helpful to predict the reservoir fluid properties.

Tectonic setting of the Xigaze ophiolite complex in Tibet based on the characteristics of boninite

SU LI^{1,2}, BAO PEISHENG³, SONG SHUGUANG⁴ AND NIU YAOLING²

¹ Institute of Earth Science, China University of Geosciences, Beijing, 100083, China

² Department of Earth Sciences, University of Durham, Durham, DH1 3LE, UK

³ Institute of Geology, Chinese Academy of Geological Sciences, Beijing, 100037, China

⁴ Department of Earth Sciences, Beijing University, 100871, China

The Xigaze ophiolite complex contains the best preserved ophiolite blocks in the middle section of the Yarlung Zangbo ophiolite belt. It composes of several fragments and extends about 200 km long and ~ 8 km wide. The ophiolite complex consist of five lithologic units, including mantle peridotite, melanocratic to leucocratic cumulates, sheeted dyke complex, pillow lavas and diabase dykes. Most of the basic lava and sheeted dyke complex from the Dejixiang ophiolite are calc-alkaline with variable SiO_2 ranging from basalt to andesite. Their LREE-depleted REE patterns show affinity of N-type MORB (or BAB). The diabase dike samples exhibit low TiO_2 (<0.5%), high MgO (up to 18.24 wt%) and $Mg^\#$ (68.3-83.7) and remarkably high mantle compatible elements Cr, Co and Ni. They exhibit low REE abundances and LREE-depleted REE patterns with $[La/Sm]_n = 0.63-0.90$, which are distinct from the U-shaped REE patterns of typical boninites that occur in forarc settings but similar to the boninites from the back-arc basin ^[1,2,3]. Ol, Sp and Opx were observed in these rocks. We conclude that (1) the Dejixiang ophiolite formed in a backarc basin setting, rather than in the mid-ocean ridge (MOR) or in a fore-arc environment and (2) the boninites are high-Ca type that formed in the late stage of back-arc basin environment during continuous extension of the spreading center that caused further melting of the depleted mantle, these melts intruded as diabase dykes into the former oceanic crust that formed the Dejixiang ophiolite during the early spreading stages of the back-arc-basin. These ophiolite blocks reflect the transition from spreading ridge to arc of the Tethys ocean.

[1] Cameron, 1985, Contrib. Mineral. Petrol. 89, 256–262.

[2] Ishikawa Nagaishi, Umino, 2002, Geology, 30, 899–902.

[3] Xia, Song, Niu, 2012, Chemical Geology, 328, 259–277.

Subducted continental crust materials in the SW Tianshan HP-LTMB

SU WEN, LIU XIN, GAO JUN, LI JILEI AND JIANG TUO

¹Institute of Geology and Geophysics, CAS, Beijing, China

The SW Tianshan HP/UHP-LT metamorphic belt (MB) in NW China occurs along a suture zone between the Yili and the Tarim blocks. It is mainly composed of blueschist, eclogite and greenschist-facies metasediments, metavolcanics, resembling typical *mélange* lithologies. Chemical compositions of mafic rocks are similar to those of typical oceanic basalts, which formed at a seamount setting in the South Tianshan ocean (Gao & Klemd, 2003). The belt has been interpreted as the typical deeper subduction of the oceanic crust in the world (Zhang *et al.*, 2007). Recent 2450-1880Ma age obtained for detrital zircons of metasediments, core of zircons of meta-basalts, implying the SW Tianshan HP/UHP-LTMB may contain subducted continental crust. Here, we therefore performed a geochemical investigation on the intimately associated eclogites and blueschists which may represent continental crust materials.

Both eclogite and blueschist have similar geochemical characteristics: an enriched LREE, flat HREE, weak negative Eu anomalies REE patterns, depleted in Ba, Sr, Nb, Ta, Ti, high Th/Yb, indicating a continental crustal source of the rocks on a Zr/Hf -Nb/Ta diagram (Pfander *et al.*, 2007). Sr-Nd isotopic data of both rocks is relatively constant with $\epsilon_{\text{Nd}}(t) = -7.701$ to -4.55 , whereas $(^{87}\text{Sr}/^{86}\text{Sr})_i = 0.7091$ to 0.7107 . All $\epsilon_{\text{Nd}}(t)$ values and Sr ratios are different with those reported for meta-N-MORBs, E-MORBs, OIBs in the Tianshan HP MB (Ai *et al.*, 2006), but within range of the continental crust. Concerning with tectonic implication for continental crust materials in the HP/UHP-LTMB, two possible mechanisms are proposed here: 1) the fragments of arc basalts derived for a Paleozoic active margin with Precambrian basement have been involved into the subduction process; 2) the continental crust of the Tarim was involved during the collision process. Although present data cannot give a clear explanation to the tectonic background, geochemical and isotopic results demonstrate some continental crust materials have been subducted in formation of HP/UHP-LTMB in the SW Tianshan orogen.

Biochar determination in soils by applying Pyrolysis GC-MS analysis and Black Carbon (BC) concentration through dichromate and permanganate oxidation

MANUEL SUÁREZ-ABELEND¹, JOERI KAAL², HEIKE KNICKER³, MARTA CAMPS-ARBESTAIN⁴ AND FELIPE MACÍAS¹

¹Department of Soil Science and Agricultural Chemistry, Biology Faculty, Santiago de Compostela University, Spain (manuel.suarez@usc.es). ²Instituto de Ciencias del Patrimonio (Incipit), CSIC, Santiago de Compostela, Spain.

³Instituto de Recursos Naturales y Agrobiología de Sevilla (IRNAS-CSIC), Sevilla, Spain. ⁴Institute of Agriculture and Environment, Massey University, Palmerston North, New Zealand.

Distinguishing pyrogenic and non-pyrogenic SOM components is a difficult task as non-selective pyrolysis products such as MAHs, PAHs and phenols can derive from multiple sources. However, black carbon (BC) may contribute significantly to the MAHs and PAHs in a given pyrolysate, especially if BC is more abundant than alternative sources. In this study, samples from a soil rich in pyrogenic material in NW Spain were subjected to $\text{K}_2\text{Cr}_2\text{O}_7$ and KMnO_4 oxidation and the residual SOM was NaOH-extracted and analyzed using analytical Py-GC-MS in order to study the susceptibility of different SOM fractions (fresh, degraded/microbial, aliphatic and specially BC) towards this oxidation agent. Besides solid-state ^{13}C CP MAS-NMR was also performed to support these results. Non-oxidized samples following the same NaOH-extraction procedure were also analyzed. From Py-GC-MS, residual SOM after $\text{K}_2\text{Cr}_2\text{O}_7$ oxidation contained BC, N-containing BC (BN) and aliphatic structures whilst carbohydrate products and lignocellulose were completely oxidized. This was corroborated by a relatively intense resonance of aromatic C and some signal of alkyl C (supporting the presence of a non-pyrogenic fraction mainly consisting of aliphatic structures) in ^{13}C NMR spectra. Thus $\text{K}_2\text{Cr}_2\text{O}_7$ effectively concentrates MAHs, PAHs and BN derived from BC. For KMnO_4 , both techniques indicated that this reagent promotes the oxidation of carbohydrate products, mostly from degraded/microbial SOM but slightly oxidized lignocellulose and aromatic structures (pyrogenic and non-pyrogenic) not providing a good assessment of the BC signal.

Contrasting patterns of bacterial weathering of granite, granulite and gabbro from tropical regions of south India

R. SUBASHRI¹, J. K. DASH², S. BALAKRISHNAN^{2*},
AND N. SAKTHIVEL¹

¹Department of Biotechnology, Pondicherry University,

² Department of Earth Sciences, Pondicherry University,
Puducherry – 605014, India

(*correspondence: balakrishnan.srinivasan@gmail.com)

Bacterial weathering of various rock forming minerals have been studied in detail. Such studies on bulk rocks are essential to better understand bacterial weathering. Results of four different bacterial activity on three different rock types are presented.

Biotite granite, garnetiferous felsic granulite and gabbro from tropical region of south India were collected and powdered to < 120 µm. The bacterial strains, RB 9, 15, 21 and 24, isolated from the rhizoplane of *Ficus* which grew on rocks were identified as *B. multivorans*, *C. malonaticus*, *E. aerogens* and *P. pleccoglossicida* respectively. They were grown for 28 days in a medium containing glucose and rock powder as the carbon and nutrient sources, respectively. Rock and abiotic controls were included. The residual pellets devoid of bacteria and other contaminants were analysed using XRD and ICP-MS.

Bacterial action on the biotite granite weathered biotites completely while microcline and albite were altered to varying degrees by different bacteria. All the major elements were depleted (30-50 %), while 25-40 % reduction of trace elements and REE were observed. P₂O₅ and Ni reduction varied with individual strains.

Felsic granulite showed removal of almandine garnet and reduction in albite and orthoclase to a larger extent. RB15 exerted moderate reduction (10-30 %) and did not fractionate major elements. Whereas, other bacteria showed considerable depletion of MgO (> 60 %). RB24 and RB25 were found to mobilise HREE (~ 30 %) while RB15 released relatively more Eu and trace element release was bacterial dependent.

The gabbro consisting of orthopyroxene, clinopyroxene and plagioclase did not show detectable change in the mineralogy. All the strains enriched Mn while RB9 depleted it. RB25 was found to enrich more HREE compared to LREE and Eu was depleted by RB9. Each bacteria followed unique pattern in release of trace elements.

Microbial weathering of granite, felsic granulite and gabbro show distinct patterns of mineralogical and chemical changes. Each bacterial strain had unique signature in altering the major and trace element abundances of a given rock.

LabData-GC: a database sub-system for post-processing and quality control of CFC and SF₆ measurements

AXEL SUCKOW^{1*}

¹CSIRO Land and Water, Urrbrae, SA 5064, Australia

(*correspondence: Axel.Suckow@csiro.au)

² National Centre for Groundwater Research and Training
(NCGRT), Flinders University, Adelaide

Low-level gas-chromatography measurements, as they are needed for groundwater dating using CFCs and SF₆ often use commercial software for signal detection, peak detection and integration. The raw data and the parameters used during integration as well as the standards and blanks used to determine the absolute concentrations of unknown samples need to be stored for traceability of results.

A database sub-system to the LabData LIMS [1] is presented that covers:

1. storage of all raw data (signal versus time)
2. storage of parameters of peak integration
3. storage of all attribute data of the measurement (sample-ID, origin, project context etc.)

The corresponding graphical user interface and post-processing algorithms allow the calculation of absolute concentrations in water from

1. blank time series
2. sensitivity time series from standard measurements
3. linearity measurements (dependence of sensitivity from peak area)
4. graphical display of all relevant result by export to MS Excel

The database sub system is integrated in a multi-user client server architecture using MS SQL server as back-end and a graphical user interface based on MS Access. The existing modelling capabilities of age distributions using a lumped parameter approach are an add-on. The source code is public domain software and available under the GNU-GPL licence agreement.

[1] Suckow, Dumke (2001): *A database system for geochemical, isotope hydrological and geochronological laboratories*. Radiocarbon 43, No. 2, pp. 325-337.

Abiotic methane formation not from H₂ but from H₂O in the serpentinite-hosted Hakuba Happo hot spring

K. SUDA^{1*}, Y. UENO^{1,2} AND S. MARUYAMA^{1,2}

¹Department of Earth and Planetary Sciences, Tokyo Institute of Technology, Meguro, Tokyo, 152-8551, Japan

(*correspondence: suda.k.ag@m.titech.ac.jp)

²Earth-Life Science Institute, Tokyo Institute of Technology, Meguro, Tokyo, 152-8551, Japan

Serpentinite-hosted hydrothermal system is considered to be important for prebiotic synthesis as well as habitat for the earliest life. Fluids derived from serpentinites are characterized by high concentrations of H₂ and CH₄ [e.g. 1]. It is generally assumed that the methane and hydrocarbons are produced abiotically from the H₂ and CO₂ via Fischer-Tropsch Type (FTT) synthesis [e.g. 1,2]. However, the production mechanism of the methane is not adequately understood yet. We report systematic isotopic study of a new serpentinite-hosted hydrothermal system: Hakuba Happo hot spring in the Shiroumadake area, Japan. The hot spring water was directly collected from 500-1000 m deep two drilling wells that show high pH over 10 and rich in H₂ and CH₄. The δD values of H₂ and H₂O from both wells are almost the same, whereas the δD-CH₄ values are different by approximately 80%. The CH₄-H₂-H₂O hydrogen isotope systematics indicates at least two different mechanisms are required for the methane formation. The higher δD-CH₄ with respect to equilibrium relation is similar to other serpentinite-hosted system reported earlier and demonstrates that the source of hydrogen of CH₄ cannot be H₂ but directly derived from H₂O. This implies that the CH₄ is not produced via the FTT synthesis, but instead, likely produced by hydration reaction of olivine. On the other hand, lower δD-CH₄ with respect to equilibrium relation suggests incorporation of biological methane. Based on the comparison of δD systematics between our result and other serpentinite-hosted hydrothermal system, we suggest that dominant methane formation mechanism in a general serpentinite-hosted system is not FTT reaction. Hydration of olivine may play more significant role for abiotic methane production than previously thought.

[1] Holm & Charlou (2001) *EPSL* **191**, 1-8. [2] Proskurowski *et al.* (2008) *Science* **319**(5863), 604-607.

Organic and inorganic contaminant remediation by biogenic nanopalladium

E. SUJA¹, Y. V. NANCHARAI¹, A. J. FRANCIS^{2,3} AND V. P. VENUGOPALAN^{1*}

¹Biofouling and Biofilm Processes Section, Water and Steam Chemistry Division, Bhabha Atomic Research Centre, Kalpakkam 603102, Tamil Nadu, India

²Division of Advanced Nuclear Engineering, POSTECH, South Korea,

³Brookhaven National Laboratory, USA.

* Corresponding author: E-mail: vpv@igcar.gov.in

Microbial synthesis of nanoparticles is an innovative process for precious metal recovery and preparation of nanocatalysts for transformation of environmental contaminants. Here, we report preparation of microbiologically synthesized palladium (Pd) nanoparticles (Bio-Pd) using *Clostridium* sp. BC1 [1] and microbial granules (MG) under fermentative growth conditions [Fig. 1]. Microbial granules were cultivated in bubble column sequencing batch reactors [2]. Reduction of dissolved Pd (II) to insoluble, black colored Pd (0) by BC1 or MG was instantaneous and complete. Removal of Pd (II) via sorption by BC1 or MG was negligible. Reduction of Pd (II) was mediated by the microbially generated hydrogen and the Pd (0) nanoparticles were predominantly associated with the bacterial cells or MG. The Bio-Pd catalysed the reduction of Cr (VI) to Cr (III) and the transformation of *p*-nitrophenol to *p*-aminophenol [Fig. 2]. Fermentatively produced hydrogen continued to act as the reducing agent for contaminant transformation. Our results demonstrate the potential use of MG for synthesis of Bio-Pd (0), Pd (II) recovery and efficient treatment of toxic contaminants in acidic environment. We also investigated the potential application of Bio-Pd in nitrate reduction.

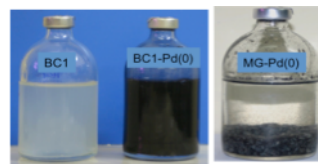


Fig 1. *Clostridium* sp. BC1 culture, Pd (0) nanoparticles associated with BC and microbial granules (MG).

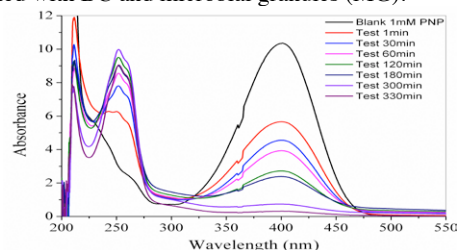


Fig 2. Bio-Pd mediated transformation of *p*-nitrophenol to *p*-aminophenol.

[1] Nancharai and Francis (2011) *Bioresour Technol.* 102(11):6573-8. [2] Suja *et al.* (2012) *Appl Biochem Biotechnol.* 167:1569-1577.

Effect of K₂O Addition on the Viscosity of CaO-SiO₂-Al₂O₃ Melt

S. SUKENAGA^{1*}, T. HIGO², H. SHIBATA¹, N. SAITO² AND K. NAKASHIMA²

¹IMRAM, Tohoku University,

(*correspondance: sukenaga@tagen.tohoku.ac.jp)

²Dept. Mater. Sci. & Eng., Kyushu University

In general, viscosity of silicate melts decreased with the addition of alkali oxides [1], which is due to the depolymerization of the silicate anions. In the case of aluminosilicate melts, the viscosity depends on not only the polymerization degree but also the average bond strength of aluminosilicate framework [2]. Roy and Navrotsky [3] reported that the average bond strength of the aluminosilicate framework could be higher when cations with lower cationic field strength (such as K, Rb, Cs) were present. Therefore, the effect of K₂O on the viscosity of CaO-SiO₂-Al₂O₃ (CAS) melt was investigated to clarify relationship between the viscosity and cationic field strength using rotating cylinder method.

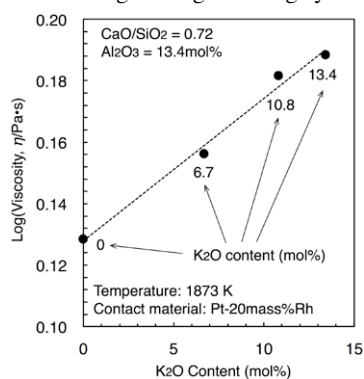


Figure 1: Effect of K₂O addition on the viscosity of the 36.1CaO-50.5SiO₂-13.4Al₂O₃ (mol%) melt at 1873 K. CaO/SiO₂ ratio and Al₂O₃ content were kept constant.

Viscosity of the CAS melt increased with the increase of K₂O. On the other hand, the polymerization degree of aluminosilicate anions should be decreased. (Fig.1) This viscous behavior could be explained by an increase in the average bond strength of aluminosilicate framework with the addition of K₂O.

[1] Mysen & Richet (2005) *Silicate Glasses and Melts*(Elsevier), 191. [2] Dingwell & Virgo (1988) *Geochim. Cosmochim. Acta* **52**, 395-403. [3] Roy & Navrotsky (1984), *J. Am. Ceram. Soc.* **67**, 606-610.

Fluid flow and mineral reaction mechanisms at high pressures: Tauern window, Eastern Alps

MIROSLAV ŠULÁK^{1*} AND DAVID DOLEJŠ¹

¹Institute of Petrology and Structural Geology, Charles University, 128 43 Praha 2, Czech Republic

(*correspondence: miroslav.sulak@natur.cuni.cz)

Aqueous fluids play major role as mass transport agents in the lithosphere but diverse approaches such as direct analysis of fluid inclusions, applications of transport theory to reaction progress, experimental mineral solubilities, time scales retrieved from isotopic tracers and microscale observations of dissolution-precipitation mechanisms still do not provide a self-consistent picture about the fluid flow mode and magnitude of intergrated fluid fluxes. We investigate synmetamorphic hydrothermal replacements, segregations and veins developed in eclogites of the Tauern Window, Eastern Alps, as a model case study to address the conditions and modes of fluid flow and efficiency of fluid-mineral reactions at very high pressures (up to c. 610 °C, 21 kbar). These hydrothermal products record a continuous sequence from volume-conserved rock-buffered replacements to fluid-buffered precipitates in open space with unidirectional growth textures recording local anisotropic stress field at peak pressures. We observe: (1) quartz-kyanite-omphacite-rutile-clinozoisite multicomponent segregations indicating nearly congruent mass transport at local scale, controlled by rheological heterogeneities, where extraction volume for immobile elements (e.g., Ti) does not exceed 2-3 centimeter in size, (2) nearly monomineralic omphacite selvages recording focused fluid flow, (3) extensional quartz veins with euhedral omphacite crystals at the wall contact and (4) large transport veins composed of kyanite and quartz, showing little or no chemical exchange with wall rock. Chemical zoning patterns of garnet and omphacite are texture-independent and indicate local interconnectivity *via* the fluid phase, from low-permeable intergranular replacements to fluid-focusing channels and transport veins. Oscillatory zoning patterns in vein omphacite and kyanite reflect pulsed flushing probably related to pressure fluctuations in crack-seal cycles. Modal variations interpreted by conventional transport theory would yield integrated fluid fluxes reaching c. 10⁵ m³ m⁻² but these will not be required when considering coupling of diffusional and advective mass transfer driven by pressure gradients, where precipitation is controlled by distribution and size of permeability inhomogeneities vs. extensional cavities. The observed phenomena provide a cautionary example against simple inversions of reaction progress to flux estimates.

Using WITCH to quantify landscape and hydrologic controls on solute fluxes in the Critical Zone (Susquehanna Shale Hills Observatory, PA)

PAMELA L. SULLIVAN^{1,2}, YVES GODDÉRIIS³,
YUNING SHI¹, JACQUES SCHOTT³,
CHRISTOPHER J. DUFFY² AND SUSAN L. BRANTLEY¹

¹ Earth and Environmental Systems Institute, Pennsylvania State University, University Park, PA, USA;

pls21@psu.edu, yshi@psu.edu, sxb7@psu.edu

² Department of Civil Engineering Pennsylvania State University, University Park, PA, USA; cxd11@psu.edu

³ Géosciences Environnement Toulouse, CNRS-Observatoire Midi-Pyrénées, Toulouse, France; yves.godderis@get.obs-mip.fr, jacques.schott@lmtg.obs-mip.fr

To investigate the hydrologic and landscape controls on shale weathering and their influence on first-order stream solute fluxes, we coupled a numerical chemical weathering model, WITCH, with a physically-based land surface hydrologic model, Flux-PIHM (Penn State Integrated Hydrologic Model). Using this approach, we were able to simulate vertical water and chemical fluxes across two representative landscape features (planar or swale hillslopes). We extrapolate the results from the soil profiles to estimate the chemical loads to the stream over a 32 year period (1980-2012) at the Susquehanna Shale Hills Critical Zone Observatory (SSH-CZO). Observed soil water (10 cm increments) and stream water chemistry collected between 2006-2011 were used to validate the modelling results. The simulation predicted the saturation state of soil water with respect to illite, smectite and kaolinite. Saturation was driven by seasonal drying, with supersaturated conditions persistent around the rooting zone (25-70 cm) during the summer months. As expected, the modelled weathering rates of illite, chlorite and k-feldspar were elevated near the soil surface where fluids were dilute, especially at the onset of fall when solute fluxes (eg. Mg, Na and Si) reached their maximum. Results from Flux-PIHM suggest a more extensive hydrologic connection between the swale hillslopes and the stream as compared with the planar hillslopes. WITCH then documented the role of this hydrologic connection on the stream water chemistry, with swales contributing bigger solute fluxes.

Sediment phosphorus dynamics in a marine coastal lake: Response to seasonal bottom water anoxia

FATIMAH SULU-GAMBAR¹, DORINA SEITAJ²,
FILIP MEYSMAN² AND CAROLINE P. SLOMP¹

¹Utrecht University, Utrecht, the Netherlands

²NIOZ, Yerseke, the Netherlands

Low-oxygen conditions are expanding in bottom waters of many coastal systems. Increased availability of the nutrient phosphorus (P) is often important in the development and sustainment of hypoxia. However, the controls on the recycling and burial of P in hypoxic and anoxic marine settings are not well understood. Here, we present results of a detailed study of the sediment biogeochemistry and P dynamics at a site in the seasonally anoxic marine Lake Grevelingen, in the Netherlands. Monthly water column and pore water profiles of oxygen and sulphide for 2012 show a short (1 month) but intense period of bottom water anoxia. Strong seasonality in the pore water profiles of dissolved Fe²⁺ and phosphate is seen. In spring, when bottom waters were oxic, our pore water data indicate dissolution of iron sulfides and calcium carbonate due to activity of electrogenic bacteria [1]. Consequentially there is a strong release of Fe²⁺ to the pore water without an associated release of dissolved phosphate. In this period, most released phosphate remains in the sediment. Upon the onset of anoxia, phosphate release from the sediment to the water column is enhanced, both in absolute terms, when compared to the prior oxic period and relative to dissolved inorganic carbon (DIC) and ammonium. With the return of oxic conditions, Beggiatoa establish at the sediment-water interface and the benthic flux of phosphate is again reduced. Sediment P analyses indicate most P in the sediment is present in the form of organic- and iron-bound P, even at depths where sulphide is present at high concentrations throughout the year. This suggests the presence of a reduced Fe-P phase as found recently in euxinic sediments from the Baltic Sea [2]. Further work will focus on the identification of the sedimentary Fe-bound P forms and a reconstruction of the role of the sediment as a P source and sink over past decades.

[1] Risgaard-Petersen *et al.* (2012) *Geochim Cosmochim Acta* 92: 1-13. [2] Jilbert & Slomp (2013) *Geochim Cosmochim Acta* 107: 155-169

Noble gas and halogen recycling at subduction zones

H. SUMINO¹*, M. KOBAYASHI¹, D. CHAVRIT²,
L. JEPSON², A. SHIMIZU³, J.-I. KIMURA⁴,
R. BURGESS² AND C. J. BALLENTINE²

¹GCRC, Univ. Tokyo, Tokyo 113-0033, Japan

(*correspondence: sumino@eqchem.s.u-tokyo.ac.jp)

²SEAES, Univ. Manchester, Manchester M13 9PL, UK

³Tokyo Metropolitan Industrial Technology Research Institute,
Tokyo 135-0064, Japan

⁴IFREE, Japan Agency for Marine-Earth Science and
Technology, Yokosuka 237-0061, Japan

Recent findings of subducted halogens and noble gases with seawater and sedimentary pore-fluid signatures in exhumed mantle wedge peridotites [1], as well as seawater-derived heavy noble gases (Ar, Kr and Xe) in the convecting mantle [2], provide observations that allow us to investigate the processes that control the return of volatile and highly incompatible elements into the mantle. To verify whether and how such subduction fluids modify the composition of the mantle beneath subduction zones, we are investigating noble gas and halogen compositions of olivines and mantle-derived xenoliths in arc lavas from Western-Pacific subduction zones (Izu, Kamchatka and N. Philippines) and those of seafloor sediments and basalts from NW margin of the Pacific plate.

MORB-like ³He/⁴He and halogen ratios of the olivines indicate insignificant contributions to the arc magmas of radiogenic ⁴He and pore-fluid-like halogens, both of which are observed in the subduction fluids released from a slab at a depth of 100 km [1]. In contrast, mantle-derived xenoliths exhibit pore-fluid-like halogens and heavy noble gases but MORB-like He. The high I/Cl ratios of pelagic clays and radiolarian cherts can account for the enrichment of iodine in subduction fluids relative to sedimentary pore-fluids [1], whereas contributions of halogens and noble gases from altered oceanic basalts are limited.

The significantly smaller contributions of subducted noble gas and halogen in the arc magmas relative to those in the mantle wedge peridotites may result from a difference in the P-T condition of the slab in each subduction zone, or from dilution by mantle-derived halogens and He when the subduction fluid induced partial melting. The former implies a relatively small amount of the pore water subduction fluids would be released from a cold slab at a sub-arc depth resulting in further subduction of halogens, heavy noble gases and potentially water, to great depths in the mantle.

[1] Sumino *et al.* (2010) *EPSL* **294**, 163-172. [2] Holland & Ballentine (2006) *Nature* **441**, 186-191.

Formation of Magnetite within aquifer sediments and its effects on Arsenic mobility

JING SUN¹*, STEVEN CHILLRUD², BRIAN MAILLOUX³
AND BENJAMIN BOSTICK⁴

¹Columbia University, New York, U.S.A.,

jingsun@ldeo.columbia.edu

²Lamont-Doherty Earth Observatory, Palisades, U.S.A.,

chilli@ldeo.columbia.edu

³Barnard College, New York, U.S.A., bmaillou@barnard.edu

⁴Lamont-Doherty Earth Observatory, Palisades, U.S.A.,

bostick@ldeo.columbia.edu

One commonly attempted remediation approach for groundwater Arsenic (As) contamination involves stimulating iron (Fe) mineral transformations that affect aqueous As concentration. However, successful strategies are difficult to develop and implement, in part because many Fe minerals are only stable under a narrow window of redox conditions. Magnetite (Fe₃O₄) is a promising target mineral for As remediation due to its stability over a wide range of Eh-pH conditions. Recent studies have found that magnetite is capable of retaining As through surface adsorption and also trapping arsenate As(V) into its structure. However, the factors that promote magnetite formation and As incorporation and adsorption are poorly established.

Here, we did a series of columns, loaded with reduced aquifer sediments from the Dover Landfill Superfund site. We stimulated the formation of As-bearing magnetite, tested its ability of maintaining As retention and evaluated its capability of sequestering additional As. All columns were conducted at circumneutral pH, similar to site conditions but much lower than is normally considered ideal for magnetite formation. The columns were equilibrated with continuous oxygen-free artificial groundwater containing lactate and sodium arsenite As(III), during which As release was observed. Then sodium nitrate and ferrous sulfate were added to the same influent groundwater, which sequestered As on solids quickly and yielded considerable magnetite as suggested by magnetic separations of a sacrificed column. (Synchrotron X-ray absorption spectroscopy as well as sequential extraction will be used to identify and quantify solid-phase Fe and As speciation). These amended columns were able to maintain low aqueous As concentrations even when influent groundwater with high lactate concentration (and no As) were introduced to encourage reduction and also able to continue to retain As after subsequent arsenite and lactate additions.

Porphyry deposits and oxidized magmas

WEIDONG SUN¹, HUAYING LIANG¹, MING-XING LING¹,
HONG ZHANG² AND XIAO-YONG YANG³

¹Guangzhou Institute of Geochemistry, CAS, Guangzhou
510640, China (weidongsun@gig.ac.cn)

²Northwest University, Xi'an 710069, China

³University of Science and Technology of China, Hefei
230026, China

Porphyry deposits supply most of the world's Cu, Mo resources. Here we show that all the porphyry deposits are associated with oxidizing magmas. Oxidation promotes the destruction of sulfides in the magma source and thereby increases initial chalcophile element concentrations [1,2]. Sulfide remains undersaturated during the evolution of oxidized sulfur-enriched magmas where sulfate is the dominant sulfur species, leading to high chalcophile element concentrations in evolved magmas. The final porphyry mineralization is controlled by sulfate reduction, which starts with magnetite crystallization, accompanied by decreasing pH and correspondingly increasing fO_2 . Hematite forms once sulfate reduction lowered the pH sufficiently and the fO_2 reaches the hematite-magnetite oxygen fugacity buffer, which in turn increases the pH for a given fO_2 . In addition to the oxidation of ferrous iron during the crystallization of magnetite and hematite, reducing wallrocks may also contribute to sulfate reduction and mineralization. For porphyry Cu deposits, slab melts (adakite) characterized by high Sr/Y is another controlling factor. Subduction of young ridge forms adakites with high fugacity, such that is the best geological process for porphyry Cu deposits [3,4]. Mo deposits are likely related to Mo-enriched metasediments.

[1] Sun W D *et al.* The link between reduced porphyry copper deposits and oxidized magmas. *GCA*, 2013, 103: 263-275. [2] Sun W D, *et al.* Geochemical constraints on adakites of different origins and copper mineralization. *J. Geology*, 2012, 120: 105-120. [3] Sun W D, *et al.* The genetic association of adakites and Cu-Au ore deposits. *International Geology Review*, 2011, 53: 691-703. [4] Sun W D, *et al.* Ridge subduction and porphyry copper-gold mineralization: An overview. *Science China-Earth Sciences*, 2010, 53: 475-484

The global flux of calcium into and out of marine sediments

XIAOLE SUN^{1*} AND ALEXANDRA V. TURCHYN¹

¹Department of Earth Sciences, University of Cambridge,
Cambridge CB2 3EQ, UK, xs243@cam.ac.uk
(*presenting author)

Fundamental to understanding Earth's climate is an understanding of the removal of carbon from the surface into the rock reservoir. This removal of carbon is achieved through burial of carbon-bearing minerals, both carbonate and organic carbon, in marine sediments. Much of the organic carbon buried in marine sediments is oxidized back to inorganic carbon, which may react with subsurface calcium to precipitate authigenic carbonate, or may return via diffusion to the overlying ocean. The precipitation of authigenic carbonate has recently been invoked as a critical process in the long-term carbon cycle¹.

We use a compilation of 674 pore fluid profiles acquired through the various drilling programs to calculate the flux of aqueous calcium across the sediment-water interface. In coastal regions and other areas of high organic-carbon supply to marine sediments, we calculate a flux of calcium into marine sediments; this calcium consumption is linked to the production of *in situ* authigenic carbonate. Parts of the ocean are dominated by a flux of calcium out of marine sediments, where calcium is produced in the subsurface through carbonate recrystallization, ion exchange, alteration of volcanic ash, or rarely subsurface gypsum dissolution. Our compilation suggests regional heterogeneity in the subsurface calcium (and carbon) cycle, as well as a global flux of calcium between the ocean and marine sediments that is significant in the global calcium cycle.

[1] Schrag *et al.*, (2013) *Science* **339**, 540-544.

Kerogen-generated bitumen as a source of shale gas: Experimental results and mass balance calculation

YONGGE SUN AND LIUJUE XIE

Department of Earth Science, Zhejiang University, Hangzhou 310027, P. R. China. Email: ygsun@zju.edu.cn

It is well known that most of shale gases discovered to date are thermogenetic within the late phase of hydrocarbon generation. This phenomenon was brought into questions with the fact that there is less gas potential of kerogen-cracking throughout the oil & gas window for most type I and II kerogens. Using a high pressure, semi-closed pyrolysis system, one shale from the Songliao basin, NE China with a TOC of 3.29% was selected to probe the gas generation processes throughout the oil & gas window. The results showed that there are at least two processes involved for the gas generation, which were characterized by distinctive characters of dryness ($C_1/\sum C_{1-5}$) and $\delta^{13}C_{\text{methane}}$. The first one is associated with kerogen thermal degradation and occurs at the main phase of oil generation. The second starts at the late phase of oil generation with a decrease of dryness and ^{13}C depleted methane, which is in contrast to the theoretical prediction as the increasing trend of dryness and $\delta^{13}C_{\text{methane}}$ accompanying thermal evolution. It suggests that this process should be mainly related to the cracking of kerogen-generated products retained in shale due to the lack of aliphatic carbon in kerogen at this stage, as evidenced by FTIR and curie Py-GC-MS analyses. A rapid decreasing of polar fraction in retained bitumen could be another indicator of the process. Mass balance calculation using hydrogen content demonstrated that bitumen retained in this shale can contribute 2-3m³HC gas/t rock to shale gas during the stage of 1.3-1.7%Ro and has implications for maturity map-making and shale gas resource assessments before exploration.

Phytoremediation for co-contaminated soils of polycyclic aromatic hydrocarbons and cadmium using willow

Y.Y. SUN¹, H.X. XU^{1*}, J.H. LI², J.C. WU¹

¹School of Earth Science and Engineering, Nanjing University, Nanjing 210093, China (sunyy@nju.edu.cn, *correspondence: hxxu@nju.edu.cn, jcwu@nju.edu.cn)
²Jiangsu Maritime Safety Administrations, Nanjing 210003, China (huadavid2002@163.com)

To investigate the effect of PAHs on the cadmium (Cd) phytoremediation efficiency using willow, field experiments were conducted in the lower reaches of the Yangtze River, China. Based on our previous study, a native willow (*Salix×aureo-pendula* CL 'J1011') was selected, owing to its easy propagation, fast growth, extensive root system, toleration of temporarily waterlogged environments, etc. Results showed that the growth of willow was negatively affected by PAHs (phenanthrene and pyrene) and Cd. The amendment of ethylenediaminetetraacetic acid (EDTA) and ethyl lactate could not only increase the accumulation of Cd in willow tissues, but also promote the degradation of PAHs. After 45 days, the combined treatment willow-EDTA and willow-EDTA-ethyl lactate significantly decreased the concentrations of PAHs and Cd in the soils ($p < 0.05$). Willow could also accumulate phenanthrene (PHE) in tissues, while accumulation of Cd in plants was much higher than that of PHE. The effectiveness of pyrene (PYR) absorption in willow was very weak and there was no detectable PYR in willow shoots. Under the same treatment, the presence of PAHs increased the Cd accumulation in willow shoots, especially for treatment willow-EDTA, while it had no significant influence on the removal of Cd from soils ($p > 0.05$). The results indicate that the native willow *Salix×aureo-pendula* CL 'J1011' together with EDTA and ethyl lactate could be used for phytoremediation of PAHs-Cd co-contaminated soils.

Acknowledgments

This work was supported by the National Natural Science Foundation of China (41102148, 41030746) and the Specialized Research Fund for the Doctoral Program of Higher Education of China (20110091120063).

Chemical and bacteria leaching of a low-grade and high-fluorine uranium ore in column reactors

ZHANXUE SUN*, YAJIE LIU, JIANG LI, XUELI LI AND WEIJUN SHI

East China Institute of Technology, Nanchang, Jiangxi 330013, China (*Correspondence: zhxsun@ecit.cn)

The purpose of the Study and Mineralogy

The purpose of the study is to investigate the technical feasibility of using bioleaching on a low-grade and high-fluorine uranium ore from China, which is not economically exploitable with conventional technologies. The ore contains 0.19% uranium and 1.0% fluorine. Uranium is present primarily as pitchblende and secondarily as coffinite and infrequently as brannerite and uranothorite.

Column Bioleaching Experiments

52-day column bioleaching experiment was conducted with finely ground ore (−0.8 mm) at ambient temperature to study the effect of bacteria on uranium extraction. For the sake of contrast, column chemical leaching experiment was also conducted at same time. The chemical leaching experiment used only sulfuric acid, but the bacteria leaching experiment used sulfuric acid and *A. ferrooxidans* as well.

Results

The leaching rate of U is 91.8% for the bacteria leaching experiment and is only 78.5% for the chemical leaching experiment. The sulfuric acid consumption is 4.73% and 4.97% for bacteria leaching and for chemical leaching respectively. The microorganism used in the bioleaching test resisted high concentration of total fluorine ranging from 1.8g/L to 2.0g/L in the leachate. The experiments suggested the feasibility of bioleaching for extraction uranium from this kind of uranium ore.

This work was financially supported by International Science and Technology Cooperation Project of China (2011DFR60830).

Flow dynamics and $^3\text{H}/^3\text{He}$ ages of deep groundwater at Gardermoen (Oslo Airport, Norway)

A. SUNDAL^{1*}, P. AAGARD¹, B. WEJDEN² AND M.S. BRENNWALD³

¹Dep. of Geosciences, University of Oslo, Norway

*Corresponding author: anja.sundal@geo.uio.no

²Oslo Airport, Water and Soil Dep., Gardermoen, Norway

³Eawag, Dep. of Water Resources and Drinking Water, Swiss Federal Institute of Aquatic Science and Technology, Switzerland

Sandy, quaternary, deposits at Gardermoen constitute the central part of Norway's largest unconfined aquifer. The steady influx of temperate, nutrient rich groundwater is essential for ecology and geomorphology of local conservation areas. The establishment of Oslo Airport (OSL) at Gardermoen in 1998 was therefore approved by the authorities on the condition that the groundwater quality would not be deteriorated. Extensive, continuous monitoring of groundwater quality and fluxes is performed at OSL and numerous research projects have been carried out. Knowledge about the deeper parts of the aquifer, however, is limited.

The total water balance in the study area is well constrained. The sandy deposits form a ridge, with relatively permeable sediments in the North-East and decreasing permeability towards the South-West. The aquifer is solely precipitation fed (40 cm/a net recharge). The groundwater flow is directed towards the North-East (80% of flux) and South-West (20% of flux), away from a crescent shaped groundwater divide and into the effluent rivers Risa and Sogna.

In this study water samples from 20 wells (1.5 – 30m below phreatic groundwater table) have been analyzed for major ions, ^3H and noble gases (He, Ne, Ar, Kr, Xe). The tritium concentrations range from 8–52 TU and the $^3\text{H}/^3\text{He}$ water ages from 1.5–53 years. The water ages generally increase with depth and distance from the groundwater divide. The hydraulic head in some wells deviates from hydrostatic conditions due to underpressure in lower (semi-) confined units. Using water ages in multi-level wells for calibration of flow models (2D grid sections), we investigate different scenarios with respect to flow separation and vertical flow components due to geological heterogeneities. Using ionic content and water ages as tracers is complicated by indication of mixing with fossil seawater (9.5 ka BP) from basal silt deposits.

Interactions between As(V), Fe(III) and natural organic matter

A. SUNDMAN*, T. KARLSSON AND P. PERSSON

Department of Chemistry, Umeå University, SE-901 87

Umeå, Sweden (*Correspondance:

anneli.sundman@chem.umu.se,

torbjorn.karlsson@chem.umu.se,

per.persson@chem.umu.se)

As is naturally occurring mainly as solid $\text{FeAs}_x\text{S}_{2-x}$ and as adsorbed species on Fe and Al hydroxides, but it is also found associated with natural organic matter (NOM) [1]. Under oxic conditions, it has been hypothesized that, ternary complexes of As(V), Fe(III) and NOM are formed and that these play a key role in As biogeochemistry. Recently, spectroscopic evidence for the formation of these complexes in peat humic substances was published [2]. We have further investigated the fundamental properties of the interactions between As(V), Fe(III) and NOM. The experimental range covers different kinds of NOM, concentrations between 6485 and 67 243 ppm Fe, pH 3-7 and Fe(III) to As(V) ratios between 0.5 and 100. Synchrotron based Fe and As K-edge extended X-ray absorption fine structure (EXAFS) spectroscopy in combination with infrared (IR) spectroscopy have been used as molecular probes.

Results and Discussion

The NOM suppressive effect on Fe precipitation [3] is reduced in the presence of As(V). At low pH and Fe concentration, the Fe EXAFS spectrum resembles Fe-NOM reference samples (see Figure 1). At higher Fe concentrations, i.e. 22 916 ppm Fe (or 0.085 mol Fe per mol of carboxylic functional groups), Fe(III):As(V) 1:1 quantitative Fe EXAFS results indicate a precipitated FeAsO_4 phase. As EXAFS and IR data provide further support for these findings. They indicate precipitated FeAsO_4 at high pH and fractions of soluble, unbound H_2AsO_4^- at low pH.

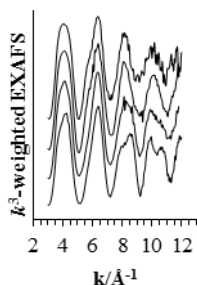


Figure 1. Fe EXAFS data for Suwannee River NOM samples, a) 6489 ppm Fe, pH 5.0, b) 6485 ppm Fe, Fe(III):As(V) 1:1, pH 5.0, c) 22 916 ppm Fe, Fe(III):As(V) 1:1, pH 5.3 and d) precipitated FeAsO_4 .

[1] Redman *et al.* (2002) *Environ. Sci. Technol.* **36**, 2889-2896. [2] Mikutta & Kretzschmar (2011), *Environ. Sci. Technol.* **45**, 9550-9557. [3] Karlsson & Persson (2012), *Chem. Geol.* **322-323**, 19-27.

Coupled radiogenic and stable Sr isotope variations in oceanic basalts

CHELSEA N SUTCLIFFE^{1*}, KEVIN W BURTON²,
IAN J PARKINSON³, DON PORCELLI¹
AND ALEX N HALLIDAY.¹

¹ Department of Earth Sciences, University of Oxford, Oxford, UK. (* presenting author; chelsea.sutcliffe@st-annes.ox.ac.uk)

² Department of Earth Sciences, Durham University, Durham, UK.

³ Bristol Isotope Group, School of Earth Sciences, University of Bristol.

The formation of basaltic crust at mid-ocean ridges and ocean islands provides a window into the compositional variations in Earth's upper mantle. If basalts are in equilibrium with their mantle source, then the composition of long-lived radiogenic isotopes should be identical and unaffected by partial melting or magmatic processes. Consequently, variations in the isotope composition of Sr, Nd and Pb of oceanic basalts are usually attributed to the existence of compositional heterogeneity in the mantle. In contrast, stable isotope variations can arise from mass dependent processes including partial melting, diffusional exchange or fractional crystallisation [1]. Taken together, radiogenic and stable isotopes can be used to unravel source variations from melting and magmatic processes [2].

Radiogenic Sr ($^{87}\text{Sr}/^{86}\text{Sr}$) is a widely used tracer of mantle chemistry and when paired with stable Sr ($^{88}\text{Sr}/^{86}\text{Sr}$) offers a unique opportunity to trace melt compositions. Moreover, using the double spike-TIMS technique, both radiogenic and stable isotopes can be measured to a high precision. However, to date there is little precise data for the stable $^{88}\text{Sr}/^{86}\text{Sr}$ composition of mantle melts and variations cannot be detected at the precisions of existing studies [3]. This study presents high precision DS-TIMS $^{87}\text{Sr}/^{86}\text{Sr}$ and $^{88}\text{Sr}/^{86}\text{Sr}$ data for a geographically widespread suite of young MORBs and OIBs, including MORBs from the FAMOUS ridge section. Resolvable variations in $\delta^{88}\text{Sr}$ of $\sim 0.14\text{‰}$ are found for MORB and within the FAMOUS segment. In contrast, OIB possess a relatively restricted range of compositions from $\delta^{88}\text{Sr} = +0.224 \pm 0.008$ to $+0.280 \pm 0.008 \text{‰}$. The extent to which coupled $^{87}\text{Sr}/^{86}\text{Sr}$ and $^{88}\text{Sr}/^{86}\text{Sr}$ data can be used to disentangle source heterogeneity from variations due to the effects of partial melting and magmatic processes will be discussed, as well as reasons accounting for differences in the trends seen between MORB and OIB.

[1] Teng *et al.* (2013) *Geochim. Cosmochim.* **107**, 12-26 [2] Elliott *et al.*, (2006) *Nature*, **443**, 565-568. [3] Charlier *et al.*, (2012) *EPSL*, **329**, 31-40.

Terrestrial $\Delta^{33}\text{S}$ and the S cycle during the Archean: Evidence from paleosols

SALLY J. SUTTON¹, J BARRY MAYNARD²,
DOUGLAS RUMBLE III³ AND ANDREY BEKKER⁴

¹Department of Geosciences, Colorado State University, Fort Collins CO 80523-1482 USA, ssutton@mail.colostate.edu

²Department of Geology, University of Cincinnati, Cincinnati OH 45221-0013 USA, maynarjb@gmail.com

³Geophysical Laboratory, Carnegie Institution of Washington, 5251 Broad Branch Rd., NW, Washington, D.C., 20015-1305 USA, rumble@gl.ciw.edu

⁴Department of Geological Sciences, University of Manitoba, 125 Dysart Road, Winnipeg, MB R3T 2N2 Canada, bekker@cc.umanitoba.ca

Determination of multiple sulfur isotopes in Archean paleosols and diamictites shows the widespread presence of mass-independently fractionated S in the regolith developed on the pre-2.5 Ga Earth. All values of $\Delta^{33}\text{S}$ are negative, indicating that the Archean surface environments incorporated atmospheric S as SO_4^{2-} , which carried a negative $\Delta^{33}\text{S}$ signal. This S was subsequently converted to sulfide by sulfate reduction, most likely bacterial with terrestrial organic matter as a reductant. Pyrite with similar S isotope systematics has been reported from flood-plain deposits. Grains from these two sources were recycled into detrital pyrites now found in sandstones and conglomerates deposited before the rise of atmospheric oxygen. We suggest that atmospherically-generated S₈ was not similarly contained on the continents, rather was lost to the oceans, creating a continental S reservoir with dominantly negative $\Delta^{33}\text{S}$ values and a predominantly positive S reservoir in marine sediments.

High Energy Synchrotron X-ray Geochemical Probes

S.R. SUTTON^{1,2}, M. NEWVILLE², A. LANZIROTTI²,
M.L. RIVERS^{1,2} AND S. WIRICK²

¹Department of Geophysical Sciences

²Center for Advanced Radiation Sources (CARS) University of Chicago, Chicago, IL USA [sutton@cars.uchicago.edu]

High energy synchrotron facilities produce x-radiation with high brightness making them extremely powerful tools for a wide variety of spatially-resolved geochemical research. The primary techniques, X-ray fluorescence (XRF) analysis, X-ray absorption fine structure (XAFS) spectroscopy, X-ray diffraction (XRD) and computed tomography (CT), are used to determine properties of earth, environmental and planetary materials including chemical and mineralogical compositions, crystallographic and other physical structures, oxidation states and fluid flow characteristics.

These X-ray probes are common instruments at virtually every synchrotron facility, are highly complementary in their capabilities and are typically heavily oversubscribed. Analyses at various spatial scales are required for this research necessitating the availability of a suite of instruments each optimized for analyses at different scales.

Focused X-ray beams can be produced using techniques that rely on collimation, refraction, diffraction, or reflection. The most common devices found in synchrotron X-ray probes are those based on diffraction or reflection. Flood-field modes are also utilized where high spatial resolution is achieved via the detection components. "Fly-scanning" approaches have greatly reduced mapping times.

Research using these X-ray probes has led to important insights into the geochemistry of toxic metals and metalloids in contaminated sediments and tailings, the efficiencies of contaminant remediation strategies, how bio-accumulation processes affect the distribution of trace toxic metal species and manufactured nanoparticles in soils and organisms, flow properties of porous media and valence states of multivalent elements in igneous materials, for example.

This presentation will describe currently operating instruments and recent experiments at some US synchrotron facilities, primarily at the Advanced Photon Source (APS, Argonne National Laboratory, IL USA), as well as new, advanced capabilities soon to be available at the National Synchrotron Light Source (NSLS-II, Brookhaven National Laboratory, NY USA).

Formation of glycine from carboxylic acid and ammonia by shock conditions: Implication to chemical evolution in primitive oceans

C. SUZUKI^{1*}, Y. FURUKAWA¹, T. KOBAYASHI²,
T. SEKINE³ AND T. KAKEGAWA¹

¹Graduate School of Science, Tohoku University, Japan

(*correspondence: b2sm6018@s.tohoku.ac.jp)

²National Institute for Materials Science, Japan

³Graduate School of Science, Hiroshima University, Japan

Origins of amino acids on the early Earth have been debated by many investigators. Previous literatures indicate that intensive impacts of extraterrestrial objects had occurred during 3.8-4.0 billion years ago. These impacts seem to have delivered and produced prebiotic organic compounds including amino acids, amines and carboxylic acids as well as ammonia [1, 2]. However, the variety of biomolecules experimentally formed in the simulation of these processes was limited compared with that of the protein-constituent amino acids. In this study, we focused on the low-molecular-weight organic compounds (LOC) such as amines and carboxylic acids supplied by one impact process. LOC must have experienced further shock wave due to successive impacts in oceans. We demonstrated impact experiments on a solution of formic acid and ammonia to investigate whether amino acids form from LOC by oceanic impacts on the early Earth.

Shock-recovery experiments were performed with a single-stage propellant gun using a sample container. Starting material is a mixture of ¹³C-formic acid and ammonia. After the impact experiments, soluble organic compounds were extracted into water. Then amines and amino acids were analyzed with liquid chromatography-mass spectrometry. Glycine, methylamine and ethylamine whose carbons are composed of ¹³C were identified in all of the samples. The amounts of glycine were almost constant regardless of the impact velocity (0.7-0.8 km/s). The amounts of produced amines increased depending on the impact velocity. These results suggest that shock wave converts a LOC into larger-molecular-weight organic compounds including an amino acid. The successive impacts might have contributed to chemical evolution providing variety in biomolecules on the prebiotic Earth.

[1] Cronin and Pizzarello *et al.* (1988), *Meteorites and the Early Solar System*, pp. 819-857. [2] Furukawa *et al.* (2009), *Nature Geosci.*, **2**, 62-66.

Removal Mechanisms of Silicate in the Wastewater using Aluminum Hydroxide Coprecipitation Method

SHINYA SUZUKI^{1*}, CHIHARU TOKORO²,
DAISUKE HARAGUCHI³, SAYAKA IZAWA⁴
AND SHUJI OWADA⁵

¹Waseda University, Tokyo, Japan, Shinya.

(Suzuki55@gmail.com)

²Waseda University, Tokyo, Japan. (tokoro@waseda.jp)

³Waseda University, Tokyo, Japan,

(d.haraguchi@aoni.waseda.jp)

⁴Waseda University, Tokyo, Japan. (izasaya@uri.waseda.jp)

⁵Waseda University, Tokyo, Japan. (owadas@waseda.jp)

This study investigated removal mechanisms of silicate in the wastewater using aluminum hydroxide coprecipitation method. To investigate detailed silicate uptake mechanism during coprecipitation with aluminum hydroxide, adsorption process and coprecipitation process were distinguished exactly in this study [1].

In adsorption experiment, aluminum hydroxide was previously prepared at pH 9 and combined with silicate solution while pH was strictly controlled at pH 9. All sorption isotherms of silicate in adsorption experiments indicated BET like unsaturation type. Especially, dominant removal mechanisms changed from simple layer adsorption to another sorption phenomena, which was equivalent to multi-layer adsorption when Si/Al molar ratio was 2-5. XRD analysis represented the precipitation of kaolinite, which suggested that silicate uptake during adsorption experiment using aluminum hydroxide consisted of two kinds of mechanisms; one was surface complexation of silicate with aluminum hydroxide and another was precipitation of kaolinite. Results from zeta potential measurement and FT-IR analysis supported these suggestion about silicate uptake mechanism. However, in adsorption experiments, residual concentration of silicate in solution was higher than calculated value from chemical equilibrium of kaolinite precipitation. This results suggested dissolution of aluminum hydroxide to precipitate kaolinite required substantial time.

On the other hand, in coprecipitation experiments, alkaline solution consisted of aluminum and silicate ions was prepared and pH was dropped to 9. In this case, residual silicate concentration gave close agreement with calculated value from chemical equilibrium of kaolinite precipitation. This results suggested coprecipitation process was more appropriate for silicate removal than adsorption process because kaolinite could precipitate rapidly.

[1] C.Tokoro, D. Haraguchi, *Journal of MMIJ* 127(2011), pp. 26-31.

Immobilization of selenium by biofilms of *Shewanella putrefaciens*

Y. SUZUKI^{1*}, H. SAIKI¹, A. KITAMURA²,
AND H. YOSHIKAWA²

¹Graduate School of Bionics, Tokyo University of Technology, 1404-1 Katakura-cho, Hachioji, Tokyo 192-0982, Japan (*correspondence: yosuzuki@stf.teu.ac.jp)

²Geological Isolation Research and Development Directorate, Japan Atomic Energy Agency, 4-33 Muramatsu, Tokai, Naka, Ibaraki 319-1194, Japan

The microbial reduction of the selenite and selenate has been widely studied using planktonic bacteria. Although bacteria are predominantly found within surface-associated cell assemblages, or biofilms in natural settings, there are little information on the interaction between biofilms and selenium. In this study, biofilms of *Shewanella putrefaciens*, which is an iron-reducing bacteria, were formed and their structure was investigated by a confocal laser scanning microscopy (CLMS). Then reduction of selenite by the biofilms was examined.

Biofilms of *S. putrefaciens* were made on circular cover glasses. Formation of biofilms was observed by CLMS. To investigate the reduction of selenite by the biofilms, a solution containing 100 μM sodium selenite as an electron acceptor, 20 mM sodium lactate as an electron donor was added to the biofilms under an anaerobic condition. After 34 h, the selenium concentration in the solution was measured by ICP-AES. Se K-edge XANES spectra of the precipitates appeared on the biofilms were measured at the Beamline 12C, Photon Factory, KEK (Tsukuba, Japan).

The CLMS observation revealed that thickness of the biofilms was about 10-20 μm and the cells were heterogeneously distributed in the biofilms. After 34 h incubation of the biofilms with selenite, the red precipitates were observed at the place where the biofilms were formed. The precipitates were not dissociated from the biofilms by washing with a deionized water indicating that they associated tightly with the biofilms. The selenium concentration in the solution was under detection limit. The Se K-edge XANES spectrum of the red precipitates showed that they were elemental selenium. These results suggest that the biofilms with iron-reducing bacteria in the environment can strongly immobilize the selenium on the biofilms through selenite reduction to elemental selenium.

Prediction of Surface Organic Species at the Mineral-Water Interface vs. Spectroscopy

D.A. SVERJENSKY¹

¹Johns Hopkins University, Baltimore, MD 21218, USA
(*correspondence: cestrada@jhu.edu, sver@jhu.edu)

Surface complexation models have been widely used to model adsorption data for organic species at the mineral-water interface. However, the goal of developing truly predictive models in which the number of surface species, the nature of the surface species attachments and the variations of the proportions of the surface species as functions of environmental conditions such as pH, ionic strength and surface loading has not been reached. Recent advances in the theory and application of the extended triple-layer model (ETLM), in particular taking into account the electrical work associated with desorption of chemisorbed water molecules released during the formation of inner-sphere attachments [1] have enabled substantial progress.

For example, when the ETLM is applied to batch adsorption data referring to a wide range of environmental conditions, typically only a few reaction stoichiometries are able to fit the data. This is in marked contrast to more traditional surface complexation models that lead to highly ambiguous results. From the reaction stoichiometries, model surface species can be inferred. However, few direct *in situ* tests of such results are available. In the present study, two direct tests are described involving experimental adsorption data for the amino acids glutamate and dihydroxyphenylalanine (DOPA) on titanium dioxide. The predicted glutamate surface species and their behavior established using the ETLM [2] were tested with ATR-FTIR spectroscopy and quantum chemical calculations [3]. For DOPA the ETLM results [4] were tested with surface enhanced Raman spectroscopy (SERS) [5]. Excellent agreement is obtained between the number of surface species, the nature of their attachment to the surface and the dependence of the surface speciation on environmental conditions.

[1] Sverjensky & Fukushi (2006), *Env. Sci. & Techn.* **40**, 263-271. [2] Jonsson *et al.* (2009), *Langmuir* **25**, 12127-12135. [3] Parikh *et al.* (2011), *Langmuir* **27**, 1778-1787. [4] Bahri *et al.* (2011), *Env. Sci. & Techn.* **45**, 3959-3966. [5] Lee *et al.* (2012), *Langmuir* **28**, 17322-17330.

Catalytic Structure of the Hammerhead Ribozyme in a Clay Mineral Environment

JACOB B. SWADLING¹, JAMES L. SUTER¹,
DAVID W. WRIGHT¹ AND PETER V. COVENEY¹.

¹Department of Chemistry, University College London, London, WC1H 0AJ.

The hammerhead ribozyme is an RNA molecule that performs self cleavage as part of a replicative cycle [1]. We use the enhanced sampling of replica exchange molecular dynamics (REMD) performed on petascale computers to study the folding pathway and the catalytically active structure of the full-length hammerhead ribozyme in both aqueous solution and a clay mineral environment. We simulated 100 replicas of each system producing a total of 10 μ s of fully atomistic molecular dynamics simulation. Our aim was to understand the solution structure, dynamics and mechanism of the ribozyme in order to resolve hitherto open questions related to the catalytic activity of the ribozyme including the role of metal ions in mediating the reaction and to assess the effect the mineral environment has on the catalytic activity.

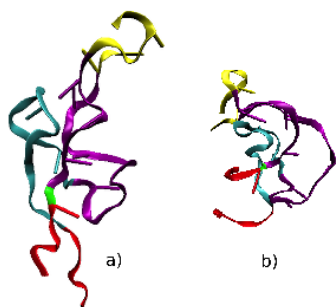


Figure 1. The dominant principal component (PC1) projected

The dominant mode of motion is a junction-bend Figure 1, which alters the availability of the catalytically competent conformations of the active site. We have characterized a set of highly populated structures that reveal a pathway to the native catalytically active site. We show how the montmorillonite clay environment significantly alters the structure and kinetics of the hammerhead ribozyme and discuss the implications this has on the RNA world [2].

[1] W. Scott *et al.* (1995) *Cell* **81**,991-1002. [2] E. Bondi *et al.* (2006) *Gene* **389**,10-18.

¹⁰Be derived catchment denudation rates from the Garhwal Himalaya

ZACHARY SWANDER¹, ANTHONY DOSSETO¹,
DAVID FINK³, JAN HENDRIK MAY¹ AND OLIVER KORUP³

¹Wollongong Isotope Geochronology Lab, University of Wollongong, NSW, Australia (*correspondence to zjs785@uow.edu.au)

²Australian Nuclear Science & Technology Organization, Lucas Heights, NSW, Australia

³Institute of Earth & Environmental Science, University of Potsdam, Potsdam, Germany.

Despite numerous Quaternary paleoclimatic reconstructions based on stable isotope records from ice core, speleothems, etc., relatively little is known about the climatic influence on terrestrial landscape processes beyond the Last Glacial Maximum (LGM). Specifically, how will changes in temperature and precipitation affect erosion rates on orbital and sub-orbital timescales? To address this question, we are measuring the concentration of *in situ* ¹⁰Be, in 15 independently dated Himalayan alluvial terrace samples[1], to quantify paleo denudation rates over the past 50ka.

Within the montane landscape of the Garhwal Himalaya, the Alaknanda River endures extreme monsoon precipitation that totals greater than 2,000mm·a⁻¹ at orographic foci. The intensity of such extreme hydrologic conditions have varied spatially and through time, which should exhibit a quantifiable effect on integrated catchment erosion rates.

This research follows in the fundamental footsteps of Bierman & Steig[2] and Schaller *et al.*[3] who first utilized ¹⁰Be in deciphering paleo-erosion rates from European terrace alluvium. Erosion rates are derived from the inherited TCR concentration integrated over the upstream catchment area and the, which incorporates time spent within the weathering profile, during transit and all other time before compete shielding. When measuring ¹⁰Be within shielded alluvium, subsequent erosion rates may be inferred from the time of burial.

By studying how catchment wide average denudation rates have varied across the LGM transition and correlating this to regional paleoclimatic records; we will be able to quantitatively assess how erosion in the the Himalayan respond to climatic variability. Thus providing geochemically derived evidence linking climatic variability with the geomorphic evolution of Himalayan landscapes.

[1] Ray & Srivastava (2010) *QSR* **29**: 1-24. [1]Bierman & Steig (1996) *ESPL* **21**, 125-139. [2]Schaller *et al.* (2004) *Geology* **112**: 127-144.

The quantitative contribution of oxygenic photosynthesis to Fe(II) oxidation in Precambrian oceans

ELIZABETH D. SWANNER^{1*}, WENFANG WU^{1,2},
BETTINA VOELKER³, RONNY SCHOENBERG¹
AND ANDREAS KAPPLER¹

¹Department of Geoscience, University of Tuebingen, Germany, *elizabeth.swanner@ifg.uni-tuebingen.de

²Institute of Geology and Geophysics, Chinese Academy of Sciences, Beijing, China

³Department of Chemistry and Geochemistry, Colorado School of Mines, USA

Evidence for oxidation of Fe(II) and deposition of Fe(III)-bearing minerals in anoxic or stratified Precambrian oceans has received support from decades of sedimentological and geochemical investigation of Banded Iron Formations (BIF). However, the exact mechanisms by which Fe(II) was oxidized and stabilized in anoxic sediments remain equivocal. The oxidation of Fe(II) by abiotic reaction with O₂ produced by oxygenic photosynthetic cyanobacteria is consistent with evidence for an iron chemocline in some Precambrian BIF basins. However, if oxygenic photosynthesis oxidized Fe in the Archean, O₂ release to the atmosphere must have been minimal, consistent with geochemical evidence for an anoxic atmosphere prior to 2.3 Ga.

We evaluate the hypothesis that Fe(II) oxidation and deposition was mediated by O₂ with laboratory experiments using *Synechococcus* PCC 7002 to represent an early marine cyanobacterium [1]. Our initial results confirm that this strain can grow in Fe(II) concentrations up to 5 mM. The kinetics of Fe(II) oxidation are consistent with an abiotic reaction between Fe(II) and O₂ and not via direct use of electrons from Fe(II) in photosynthesis. We also measured the isotopic fractionation factor between aqueous Fe(II) and precipitated Fe(III) during growth of *Synechococcus* PCC 7002 with Fe(II), which is similar to fractionation factors in abiotic experiments. Microscopic and spectroscopic analysis of the cell-mineral aggregates also inform the location of Fe(II) oxidation and the speciation, mineralogy and spatial relationship of iron to carbon in the resulting precipitates. Our efforts are now focused on quantifying the rates of O₂ production and Fe deposition in a laboratory-scale model of a ferruginous water column where Fe(II) upwells into an engineered photic zone. Our intent is that these results will provide a mechanistic and quantitative framework for evaluating the geochemical consequences of perhaps life's greatest metabolic innovation.

[1] Blank and Sánchez-Baracaldo (2010) *Geobiology*, **8**, 1-23.

Size-dependent reactivity of magnetite nanoparticles: A bridge between lab and field investigations

A.L. SWINDLE^{1*}, A.S. MADDEN¹ AND I.M. COZZARELLI²

¹University of Oklahoma, Norman, OK (*correspondance: aswindle@ou.edu, amadden@ou.edu)

²US Geological Survey, Reston, VA (icozzare@usgs.gov)

Research on nanoparticles has exploded in recent years as we have begun to understand the extensive role these materials play in natural systems as well as their potential benefits and risks to human society. However, the very nature of nanoparticles makes them challenging to study, particularly in a field setting. As a result, many questions remain to be answered concerning how nanoparticles behave in a natural environment and how accurately laboratory results reflect reactions that occur in the field.

In this investigation magnetite nanoparticles with average diameters of 6 nm, 44 nm and 90 nm were synthesized and thoroughly characterized. The nanoparticles were emplaced in the anoxic groundwater zone of the leachate plume in the subsurface of the USGS Norman Landfill Site with custom-built TEM grid-holders. Laboratory analog experiments were also conducted using nanoparticles and synthetic groundwater modeled on the chemistry of the groundwater from the landfill site, but omitted DOC. Finally, a series of magnetite-chromate adsorption experiments was conducted with varying amounts of DOC added to investigate the impact of organics on the surface reactivity of the magnetite nanoparticles.

The field investigation revealed that a thin coating of organics developed on the particles surfaces that occluded the particles from the groundwater and inhibited dissolution. This is supported by geochemical models indicating that magnetite is not thermodynamically stable under the given chemical conditions and by the laboratory analogs which provided evidence of magnetite dissolution in the absence of organics. The chromate adsorption experiments showed that DOC concentrations as low as 1 mg/L can impact the surface reactivity of magnetite even when an excess of mineral surface area is present.

The results of this investigation revealed that under the field conditions, magnetite dissolution decreased as particle size decreased, while this trend was reversed in the laboratory experiments. Adsorption experiments indicate that this reversal is likely due to dissolved and particulate organics. Together, these experiments show that organics play a significant role in the surface reactivity of nanoscale minerals and remain integrally important to understanding the environmental fate of nanomaterials.

U/Pb zircon age of Mistastin Lake crater, Labrador, Canada – implications for high-precision dating of small impact melt sheets and the end Eocene extinction

PAUL J. SYLVESTER¹, JAMES L. CROWLEY²
AND MARK D. SCHMITZ²

¹Department of Earth Sciences, Alexander Murray Building,
Memorial University, St John's NL A1B 3X5 Canada

²Department of Geosciences, 1910 University Drive, Boise
State University, Boise, ID 83725 USA

Accurate and precise dating of the impact cratering record on Earth is important for determining the duration of periods of intense bombardment and their role in causing climatic perturbations and biotic extinctions. Unfortunately only four terrestrial craters are well dated by the U-Pb zircon method; all are large structures, *ca.* 100–300 km in diameter [1]. We investigated the 28-km wide, Mistastin Lake crater [2], Labrador, Canada, in order to determine whether magmatic zircon forms in small-volume impact melt sheets and may be dated precisely and accurately. A sample was collected from Discovery Hill, an 80-meter thick, wedge-shaped butte of columnar-jointed impact melt rock. An age of 36 ± 4 Ma (2σ) for Mistastin was reported by [3] based on $^{40}\text{Ar}/^{39}\text{Ar}$ dating.

In addition to large elongated to equant (~ 100 – $500 \mu\text{m}$) zircon inherited from the country rocks, the melt rock contains tiny, elongate ($\sim 25 \mu\text{m}$ wide \times ~ 100 – $175 \mu\text{m}$ long), prismatic “needle” zircon with narrow, brown-colored melt channel “spines” running through the centers of the crystals. Eleven needles were analyzed by CA-TIMS using the EARTHTIME tracer solution. With only 1–4 pg of radiogenic Pb per needle, it was critical to have low Pb blanks (~ 0.4 pg) for high-precision dating. $^{206}\text{Pb}/^{238}\text{U}$ dates are equivalent with a weighted mean date of 37.83 ± 0.05 Ma (internal error, MSWD = 1.0) that is interpreted as the crystallization age of the impact melt. The results demonstrate that magmatic zircon can crystallize in impact melt from small craters. The new radiometric age for Mistastin makes it now the most precisely and accurately dated small crater on Earth. The Mistastin U/Pb date is significantly older than $^{40}\text{Ar}/^{39}\text{Ar}$ dates for the two largest (~ 100 km) Eocene craters, Popigai (35.7 ± 0.2 Ma, 2σ) and Chesapeake Bay (35.5 ± 0.3 Ma, 2σ) [1] and the end Eocene mass extinction event (~ 34 Ma).

[1] Jourdon *et al.* (2009) *EPSL* **286**, 1–13. [2] Marion & Sylvester (2010) *Planet Space Sci* **38**, 552–573. [3] Mak *et al.* (1976) *EPSL* **31**, 345–357.

Modification of synthetic zeolites and characteristics of their properties

B. SZALA^{1*}, P. TUREK¹ AND T. BAJDA¹

¹Department of Geology, Geophysics and Environmental
Protection, AGH University of Science and Technology,
Krakow, Poland (*bszala@geol.agh.edu.pl)

Synthetic zeolites are increasingly likely to be used in advanced chemical processes and industry due to their attractive properties. Ongoing research is trying to establish a way improve some of their properties, for example, the process of sorption. This process is low because it takes place only on the outer surface of the crystallites. To increase the chemical affinity of the zeolite's surface to the organic compounds, modification of zeolites' surface is necessary. The aim of the study was to perform modifications of a synthetic zeolite and evaluate its sorption properties. The material used was an X-type zeolite prepared from coal fly ash. For modification of the zeolites' surface quaternary, ammonium salts with single or double carbon chain length, such as: dodecyltrimethylammonium bromide (DDTMABr), tetradecyltrimethylammonium bromide (TDTMABr), hexadecyltrimethylammonium bromide (HDTMABr) and octadecyltrimethylammonium bromide (ODTMABr) were used. Surfactants were adsorbed onto a synthetic zeolite in amounts of 1.0 and 2.0 of the external cation exchange capacity (ECEC) in quantities of 24.4 and 48.8 mmol per 100g of zeolite respectively. Quantitative characterization of organo-zeolites and characterization of their properties has been performed. The effectiveness of the modification has been determined based on the content of carbon, hydrogen and nitrogen combined with X-ray Diffraction and IR spectroscopy. Simultaneously, the effectiveness of maximum sorption capacity on organo-zeolites in terms of organic compounds such as benzene, toluene, xylene has been established. The results obtained show an improvement of the sorption properties of the organo-zeolite modified in an amount of 2.0 ECEC in relation to the 1.0 ECEC and unmodified material. Also the carbon chain length surfactants show their importance during the modification. The results of this research can be used in environmental protection and for further studies into the properties of surfactant-modified synthetic zeolites and their potential industrial applications; for example, in petrochemistry.

We gratefully acknowledge the support of NCBiR having provided grant PBS1/A2/7/2012.

Petrogenesis of andesites in Mesoarchaeon supracrustal belts of SW Greenland: Geodynamic implications

KRISTOFFER SZILAS¹ AND J. ELIS HOFFMANN²

¹Lamont-Doherty Earth Observatory, Palisades, New York,
USA

²Institut für Geologie und Mineralogie, Universität zu Köln,
Zùlpicher Str. 49b, 50674 Köln, Germany

We present an overview of geochemical data for the Mesoarchaeon supracrustal belts from the Tasiusarsuaq terrane, SW Greenland. These ultramafic, basaltic and andesitic enclaves are located within younger tonalite-trondhjemite-granodiorite (TTG) orthogneisses and are mainly dominated by tholeiitic basalts. However, calc-alkaline andesites are also present and comprise up to ca. 50% of individual supracrustal belts. These two lithological groups can roughly be divided into tholeiitic and calc-alkaline affinity by having La/Sm ratios less than, or over 3.5, respectively. While the mafic rocks have flat trace element patterns with negative Nb- and Ta-anomalies, the andesitic rocks have strongly fractionated trace element patterns, with distinctly negative Nb-, Ta- and Ti-anomalies, as well as positive Hf- and Zr-anomalies. Thus, they are not related by fractional crystallisation and no gradational transitions between the two groups have been observed. Assimilation of pre-existing continental crust can also not explain the trace element variations of the andesites. Modelling suggests that simple binary mixing of a mafic magma and a TTG-type component in a 1:1 ratio can explain most of the variation that the andesites display. This is confirmed by Hf-isotope modelling that support the large mixing ratio and therefore that actual melting of the local felsic crust must have occurred. We suggest that the hotter conditions during the Mesoarchaeon could explain the significant proportion of melting of the lower crust during addition of juvenile mafic magmas. Overall, the geochemical data are compatible with a modern-style subduction zone environment, for which recent studies have also concluded that substantial magma mixing is a significant process.

www.minersoc.org
10.1180/minmag.2013.077.5.19

Compacted Nanoparticles for Quantification in LA-ICPMS

DANIEL TABERSKY¹, NORMAN LUECHINGER², SAMUEL HALIM², MICHAEL ROSSIER² AND DETLEF GÜNTHER^{1*}

¹ETH Zurich, Department of Chemistry and Applied Biosciences, Laboratory of Inorganic Chemistry (*correspondence: guenther@inorg.chem.ethz.ch)

²Nanograde, Staefa, Switzerland

Gray *et al.* did first studies of LA-ICPMS in 1985 [1]. Ever since, extensive research has been performed to overcome the problem of so-called “non-stoichiometric sampling” and/or analysis, the origins of which are commonly referred to as elemental fractionation (EF). EF mainly consists of laser-, transport- and ICP-induced effects, and often results in inaccurate analyses as pointed out in, *e.g.* references [2,3].

A major problem that has to be addressed is the lack of reference materials. Though the glass series of NIST SRM 61x have been the most commonly reference material used in LA-ICPMS, heterogeneities have been reported for some sample charges [4,5]. In addition, geological relevant elements such as Ti, Fe and Mg are present in very low concentrations only and thus not well suited for calibration. Elements such as Rh, Ru, Pd, Pt and Au (PGEs) are either absent or present in very low concentrations.

The production procedure of glass limits the implementation of these elements into the glass matrix at concentrations required for many applications. Therefore, alternative methods for the production of calibrants were studied concerning the implementation of PGEs into Silicates, Carbonates, and Iron-Sulfides, which are homogeneous at the spatial resolution commonly used in microbeam techniques.

Flame synthesis was used to reproduce the NIST 610 matrix at similar concentrations. Furthermore, PGEs and other elements were added to the matrix. The resulting powder consists of nanoparticles in the size range of 20-50 nm, which is well below the commonly crater diameters used in LA-ICPMS. The PGE concentration is for most of the elements around 500 mg/kg. Multiple analyses of these powders provide a RSD for PGEs in the order of 1-3 %. The difference between the pressed powder analysis and calcinated pellets shows indistinguishable results for most of the elements. The setup of production, preliminary results and first figures of merit will be discussed.

[1] A.L.Gray (1985), *Analyst*, **111**, 551. [2] J. Pisonero *et al.* (2009) *J Anal Atom Spectrom*, **24**, 1145. [3] J. Koch and D. Günther (2009) *Appl Spectrosc*, **65**, 155. [4] P. Sylvester and S.M. Eggins (1997) *Geostandard Newslett*, **21**, 215. [5] S.M. Eggins and J.M.G. Shelley (2002), *Geostand Geoanal Res*, **26**, 269

Evaporation behavior of forsterite (Mg₂SiO₄) in a H₂O-H₂ gas

S. TACHIBANA^{1*} AND A. TAKIGAWA²

¹Department of Natural History Sciences, Hokkaido University, N10 W8, Sapporo 060-0810, Japan. (*correspondence: tachi@ep.sci.hokudai.ac.jp)

²Carnegie Institution of Washington, Department of Terrestrial Magnetism, 5241 Broad Branch Road NW, Washington DC, 20015 USA.

Forsterite (Mg₂SiO₄) is one of the most abundant crystalline silicates in extraterrestrial materials and in circumstellar environments, and its evaporation behavior has been intensively studied in vacuum and in the presence of low-pressure hydrogen gas [*e.g.*, 1-4]. It has been known that the evaporation rate of forsterite is controlled by a thermodynamic driving force (*i.e.*, equilibrium vapor pressure), and the evaporation rate increases linearly with $p\text{H}_2^{1/2}$ in the presence of hydrogen gas due to the increase of the equilibrium vapor pressure. The deviation of the actual evaporation rate from the ideal evaporation rate, which is given by an equilibrium vapor pressure and the kinetic theory of gases, is expressed as an evaporation coefficient (=Actual rate/Ideal rate) ranging from 0 to 1 (a measure of kinetic hindrance for evaporation). The evaporation coefficient is 0.1-0.01 for evaporation of forsterite in vacuum and in hydrogen gas depending on temperature and crystallographic orientation of the evaporating surface [*e.g.*, 1-4]. Besides the free-evaporation dominated regime [FED] (evaporation in vacuum) and the hydrogen-reaction dominated regime [HRD] (evaporation in hydrogen gas), Tsuchiyama *et al.* [5] proposed another evaporation regime called H₂O/H₂ buffer-dominated regime [HBD] as a dominant evaporation regime for forsterite in protoplanetary disks at temperatures of <1400 K and under H₂O-rich conditions. In the HBD regime, the equilibrium vapor pressure of forsterite is not controlled by $p\text{H}_2^{1/2}$, but by the H₂O/H₂ ratio in the ambient gas. In spite of its potential importance, no experimental study has been done to investigate the evaporation kinetics in the HBD regime. We have performed evaporation experiments on forsterite at low pressures with controlled H₂O/H₂ ratios, and have found that the evaporation rates are controlled by the H₂O/H₂ ratio as proposed by [5] and that the evaporation coefficient is consistent with that in FED and HRD regimes.

[1] Hashimoto (1983) *Nature* **347**, 53-55. [2] Nagahara and Ozawa (1996) *GCA* **60**, 1445-1459. [3] Tsuchiyama *et al.* (1998) *Mineral J.* **20**, 113-126. [4] Takigawa *et al.* (2009) *ApJ*, **707**, L97-L101. [5] Tsuchiyama *et al.* (1999) *GCA* **63**, 2451-2466.

Southern Hemisphere orbital forcing and its effects on CO₂ and tropical Pacific climate

K. TACHIKAWA¹, A. TIMMERMANN², L. VIDAL¹,
C. SONZOGNI¹ AND O. ELISON TIMM²

¹ Aix-Marseille Université, UMR7330, CNRS, IRD, CEREGE
UM34,13545 Aix en Provence, France, kazuyo@cerege.fr

² IPRC, SOEST, University of Hawaii, Honolulu, HI 96822,
USA

The western Pacific warm pool (WPWP) is an important heat source for the atmospheric circulation and influences climate conditions worldwide. Understanding its sensitivity to past radiative perturbations may help better contextualize the magnitudes and patterns of current and projected tropical climate change. Here we present a new Mg/Ca-based sea surface temperature (SST) reconstruction over the past 400 kyr from the Bismarck Sea, off Papua New Guinea, along with results from a transient earth system model simulation. Our results document the primary influence of CO₂ forcing on glacial/interglacial WPWP SSTs and secondary effects due to changes in wind-driven tropical boundary currents. In addition to the SST, deep ocean temperature reconstructions from this core are linked with Southern Ocean temperature and sea-ice variations on timescales of ~23 kyr. It is proposed that Southern Hemisphere insolation changes serve as pacemaker for sea-ice variations in the Southern Ocean, which in turn modulate windstress curl-driven upwelling of carbon-rich waters, hence controlling atmospheric CO₂ and tropical WPWP temperatures.

CO₃, OH, and halogen microanalysis in apatite group minerals

R. CHRIS TACKER¹

¹North Carolina Museum of Natural Sciences, 11 W. Jones
St., Raleigh, NC, USA 27601-1029,
christopher.tacker@naturalsciences.org

The last three years have seen a re-evaluation of microanalytical methods for apatite, including standards. This presentation presents new data and reviews recent results for analytical methodology for C, OH, and halogens for apatite minerals.

Initial documentation of anisotropic beam-driven halogen diffusion [1] in apatites, long ignored, has been confirmed and shown to be more complex for varying F and Cl concentrations [2]. Quantitative analysis requires constraints on crystal orientation for *both unknowns and standards*, as well as controlled history under the electron beam. Analytical methods presented here use accelerating voltages <10keV and short analytical durations to clearly define the rise and fall in count rates for zero-time regression. Data in hand show that F and Cl are rapidly lost from the apatite during analysis at 15 and 20 keV in all crystal orientations. Analyses are unlikely to be valid without regression-to-zero techniques for unknown and standard. Uncertainties in electron microprobe halogen analyses are magnified in OH calculated by the difference method.

Problems with FTIR analysis of apatite (strongly polarized OH stretching, crystal size, sample thickness) have been overcome to allow analysis of unpolished mineral separates and experimental products. Polarized radiation is preferred for OH analysis, but unpolarized radiation can be used on (100) sections [3] and euhedral synthetic crystals. The A and B type carbonate substitutions are not strongly polarized, allowing use of unpolarized radiation.

Carbonate and OH standards for apatite are lacking. A large FTIR dataset for naturally occurring apatites shows homogeneities or complexities precluding their use as standards. For example, Durango fluorapatite shows trimodal OH distribution (n=5570). Synthetic standards are under development.

Previously published apatite studies should be carefully evaluated in the light of these results.

[1] Stormer *et al.* (1993) *Am. Miner.* **78**, 641-648. [2] Goldoff *et al.* (2012) *Am. Miner.* **97**, 1103-1115. [3] Tacker (2004) *Am. Miner.* **89**, 1411-1421.

Thermochronological investigation of seismogenic fault zones: an overview and examples from Japanese Islands

TAKAHIRO TAGAMI¹

¹ Division of Earth and Planetary Sciences, Graduate School of Science, Kyoto University, Sakyo-ku, Kyoto, 606-8502, Japan. tagami@kueps.kyoto-u.ac.jp

The timing of faulting episodes can be constrained by radiometric dating of fault-zone rocks. Fault-zone material suitable for dating is produced by tectonic processes, such as (1) fragmentation of host rocks, followed by grain-size reduction and recrystallization to form mica and clay minerals, (2) secondary heating/melting of host rocks by frictional fault motions, and (3) mineral vein formation as a result of fluid advection associated with the fault motions. The thermal regime of fault zones consists primarily of the following three factors: (a) regional geothermal structure across the fault zone and background thermal history of studied province bounded by fault systems, (b) frictional heating of wall rocks by fault motions, and (c) heating of host rocks by hot fluid advection in and around the fault zone. Thermochronological methods widely applied in fault zones are K-Ar (⁴⁰Ar/³⁹Ar), fission-track, and U-Th methods. The thermal sensitivities of individual thermochronological systems are briefly reviewed, which critically control the response of each method against the thermal processes. Based on the knowledge above, representative examples as well as key issues are highlighted to date fault gouges, pseudotachylytes, mylonites and carbonate veins, placing valuable constraints upon geological, geomorphological and seismological frames. Finally, the results from Japanese Islands are presented, including the Shimanto belt, as examples for multiple applications of thermochronological methods.

Geobotany and biogeochemistry of Sungun Copper deposit, northern Iran: An implication to mineral exploration

B. TAGHIPOUR¹ AND M. HEMMATI¹

¹Department of Earth Sciences, Shiraz University, Shiraz, Iran (taghipour@shirazu.ac.ir)

Sungun porphyry copper deposit is located in the east of Azarbaijan, NW of Iran. Geobotany is one of the important methods in mineral exploration. In this method the plants represented paid a heavy metal track. Geochemical prospecting has been carried out on distribution of Zn, Pb, Cu, As, Cd and Mo in the plant species and soil of the Sungun Cu-Mo deposit. Field prospecting has been indicated that *Anthemisnobilis*, *Crepsis sancta* and *Picnomonacarna* are the main plant species in the area. Geochemical results indicated enrichment of Mo, As and Cu (Cu > Mo > As) which is correlated with concentration of the metals in associated soil. *Anthemisnobilis* has been shown the greatest capability for accumulating Cu and Mo in its tissues through soil so it could be used as a bioindicator for mineral exploration. This plant with other plant species such as *Crepsis Sancta* and *Picnomonacarna* have high scavenging ability for Mo and Cu from the soil and could cause serious environmental and health problems in the living organisms of the area.

Density control on formation of crustal magma storage system

BENOIT TAISNE^{1*}

¹Earth Observatory of Singapore, 50 Nanyang Avenue, Singapore 639798
(*correspondance: btaisne@ntu.edu.sg)

Magma reservoirs probably grow by repeated sill-like intrusions. We investigate the conditions for repeated crustal intrusions at the same depth by a feeder dike before a permanent molten reservoir can form. Sill formation requires that magma within a dike develops an overpressure large enough to overcome the strength of surrounding rocks. An efficient mechanism to achieve this involves ascent through layers with decreasing density, such that magma becomes negatively buoyant above some structural interface. To significantly affect dike ascent, the density change in country rock must occur over a thickness of the order of the length-scale for the inflated nose region that develops below the dike tip. This characteristic length depends on the elastic properties of the host rocks, on magma buoyancy and on the flux of magma. It is usually around 1 km for basaltic magmas, comparable to the typical thickness of sedimentary strata and volcanic deposits. The overpressure that develops at the density inversion level is determined by the vertical extent of the inflated dike nose region above that level, and hence is related to the volume of magma in that region. Thus, sill formation also requires that the total volume of magma available in an individual intrusion event exceeds a threshold value.

Pressure variations in metamorphic rocks: Implications for the interpretation of petrographic observations

L. TAJČMANOVÁ

Department of Earth Sciences, ETH Zurich, Switzerland, (lucataj@gmail.com)

During mineral reaction, the overall mechanical state of a rock is very important. Rock strength may control the reaction progress from 0 to 100% which may result in the development of stress, and therefore pressure, variation on all scales. Hence, considering the interplay of metamorphic reaction and mechanical properties is critical for correctly interpreting microstructural observations in metamorphic rocks and correct quantification of the processes.

Stresses that develop during deformation of geologic materials can be responsible for the formation and preservation of GPa-level pressure variations. Considering that the typical value of the lithostatic pressure at the base of the continental crust is ~1 GPa, GPa-level variations make the interpretation of depth from pressure problematic for crustal metamorphic rocks. Such pressure perturbations are more apparent on a small scale (nm to mm), where, in some cases, they can be directly measured by spectroscopic methods. However, the non lithostatic pressure variations can also be relevant to larger (crustal) scales. Schmalholz and Podladchikov [1] have recently shown that even when rocks are deformed in a “weak” crustal-scale shear zone, force balance across the shear zone requires that pressure will not be smoothly varying with depth but it will be paradoxically higher within the shear zone.

The recent microstructural observations and mechanical models question our current quantification approach in metamorphic petrology based on the lithostatic assumption. The recent data have therefore opened horizons for new approaches and new physically rigorous and geologically realistic interpretations of our petrographic observations. Such approaches would contribute to our better understanding the processes in the Earth interior.

[1] Schmalholz & Podladchikov (2013), *Geophys. Res. Lett.*, 10.1002/grl.50417

Structural simulation on silica crystals and glasses

TAKADA¹

¹Research Center, Asahi Glass Co., 1150 Hazawa-cho, Yokohama, 221-8755, Japan (akira-takada@agc.com)

Molecular dynamics simulation has been used to investigate the similarity and dissimilarity in dynamical structural changes between silica crystals and glasses. Many simulation studies have been performed for quartz, cristobalite and silica glasses [1-3], however, there is scarcely any simulation studies on tridymite. The structural building block is the same between in tridymite and cristobalite, nevertheless, structural changes due to the thermal effects is more complex in tridymite than in cristobalite. Such complexity hinders the theoretical study. First, the structural changes of tridymite phase due to thermal effects are investigated by using molecular dynamics simulation. Next, the calculated complex structural changes are compared with those of the other structures such as cristobalite and glasses. Finally, we discuss the similarities and dissimilarities in dynamical structural changes in terms of microscopic structure.

[1] A. Takada, P. Richet, C.R.A. Catlow, G.D. Price (2004) *J. Non-Cryst. Solids* 345&346, 224. [2] A. Takada, P. Richet, C.R.A. Catlow, G.D. Price (2007) *J. Eur. J. Glass Sci. Technol. B* 48, 182. [3] A. Takada, P. Richet, C.R.A. Catlow, G.D. Price (2008) *J. Non-Cryst. Solids* 354, 181.

Ontogenetic stable isotope records of modern planktic foraminifers from Sagami Bay, Japan

H. TAKAGI^{1*}, K. MORIYA^{1,2}, T. ISHIMURA^{3,4}, A. SUZUKI⁴
H. KAWAHATA⁵ AND H. HIRANO¹

¹Waseda University, Tokyo 169-8050, Japan

(*correspondence: harurah-t@fuji.waseda.jp)

²Kanazawa University, Kanazawa 920-1192, Japan

³Ibaraki National College of Tech., Ibaraki 312-8508, Japan

⁴Geological Survey of Japan, AIST, Ibaraki 305-8567, Japan

⁵AORI, The University of Tokyo, Chiba 277-8564, Japan

Stable oxygen ($\delta^{18}\text{O}$) and carbon ($\delta^{13}\text{C}$) isotopes recorded in planktic foraminiferal tests are widely used as proxies for paleoceanography and species ecology. Of such isotopic investigations, ontogenetic isotopic profiles are thought to record foraminiferal ecological information such as depth habitat or symbiotic relationship. Though size-related isotopic series, achieved by analyses of a series of sieved fractions, seem to reflect ontogenetic profiles of species, isotopic profiles through "individual ontogeny" have rarely been examined. In this study, we report ontogenetic isotopic information of individual specimens, together with *in situ* water column oceanographic information ($\delta^{18}\text{O}_{\text{sw}}$, $\delta^{13}\text{C}_{\text{DIC}}$, temperature, salinity, nutrient, and chlorophyll-a).

We examined ontogenetic stable isotopic profiles of planktic foraminifers by performing chamber-by-chamber analyses within a single individual. Each chamber is dissected from an individual and analyzed by specially designed continuous-flow mass spectrometry system [1]. Instead of size-related analyses, this method enables us to reveal individual ontogenetic information free from mixing of seasonal variability. Four modern species, obtained by vertical towing at Sagami Bay, Japan, were analyzed; *Globigerinoides sacculifer*, *Globigerinoides conglobatus*, *Neoglobobadrina dutertrei*, and *Globorotalia inflata*.

The ontogenetic $\delta^{18}\text{O}$ profiles showed overall increase for all species, suggesting the ontogenetic deeper migration commonly found in modern species. While $\delta^{13}\text{C}$ showed steep increase especially in a juvenile stage for all species, the increase continued to the last chambers only in symbiont-bearing globigerinoidid species. $\delta^{13}\text{C}$ of asymbiotic species becomes decrease after the rapid increase in the juvenile stage. Comparing these records to water column chemical and physical data, regardless of their adult habitat depths, all foraminifers analyzed start their calcification, hence their ontogeny, near the thermocline, which corresponds to chlorophyll maxima and nutrient-depleted depth.

[1] Ishimura *et al.* (2004), *RCM*, 22, 1925-1932.

Magma feeding system of Fuji volcano, Japan

E.TAKAHASHI^{1*}, K.ASANO¹ AND J.NAKAJIMA²

¹ Earth and Planetary Sciences, Tokyo Institute of Technology, Tokyo 152-8551, Japan (*presenting author: etakahas@geo.titech.ac.jp)

² Research Center for Prediction of Earthquakes and Volcanic Eruptions, Tohoku University, Sendai, Japan

Fuji volcano is known for its perfect cone shape and it is the largest among Japanese Quaternary volcanoes. In the last 100kya, Fuji has erupted only basalt magma (>>99 vol%), but its eruption style changed (from debris flow and tephra dominant Ko-Fuji or Older Fuji, to lava flow dominant Shin-Fuji or Younger Fuji) at ~15 kya BP. Origin of the voluminous yet monotonous basalt production in Fuji volcano have been discussed but remain unanswered. Here we report the first high-pressure melting experimental results on Fuji basalt (Hoei-IV, AD1707) and demonstrate that its main magma chamber is located at ca.25km depth. We show seismic tomographic images of Fuji volcano for the first time, which reveals the existence of strong upwelling flow in the mantle and its connection to the voluminous lower crustal magma chamber (see Fig.1).

Very frequent low frequency earthquakes just above the magma chamber (open circles in Fig.1) may be due to the injection of basalt magma and/or fluids. The total lack of silica-rich rocks (basaltic andesite and andesite) in Fuji volcano must be due to the special location of the volcano. The plate boundary between the Eurasia plate and the subducting Phillipine sea plate is located just beneath Fuji volcano (~5 km depth). Large tectonic stress and deformation associated with the plate boundary inhibit the survival of a shallow level magma chamber, which would allow the evolution of basalt to silica-rich magma (as observed in all other volcanoes in Japan, e.g., Hakone, Izu Oshima).

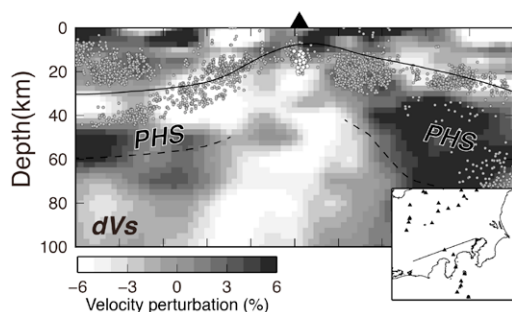


Fig.1 Seismic tomography beneath Fuji volcano. EW section

Migration of radiocesium and radioiodine in soil-water-river system related to Fukushima-Daiichi Nuclear Power Plant Accident

Y. TAKAHASHI*, Q. FAN, A. SAKAGUCHI, YOKO S. TOGO AND K. TANAKA

Hiroshima University, Hiroshima 739-8526, Japan (*correspondence: ytakaha@hiroshima-u.ac.jp)

Radionuclides such as radiocesium and radioiodine were emitted from the Fukushima Daiichi Nuclear Power Plant (FDNPP) accident caused by the Great East Japan Earthquake and Tsunami on March 11, 2011. Highly contaminated areas spread in the northwest direction from FDNPP in Fukushima Prefecture, which mainly resulted from the distribution of the wet deposition on March 15 [1]. After the deposition, vertical profiles of the radionuclides in soil in Fukushima showed that radiocesium and radioiodine have been retained within 5 cm from the surface. Analysis of particulate matters and sediment particles in rivers in the region showed that radiocesium is enriched in finer fractions.

These results suggested that radiocesium and radioiodine have high affinity to soil particles. For radiocesium, adsorption on clay minerals have been indicated. Thus, extended X-ray absorption fine structure (EXAFS) spectroscopy has been used (i) to characterize structure of surface complex of cesium with 2:1 phyllosilicate and (ii) to understand the reduction of the adsorption in the presence of humic substances. We also found a correlation between (i) the fraction of inner-sphere complex among total cesium species adsorbed on the soil particles and (ii) Radiocesium Interception Potential (RIP) value, which suggests that RIP is dependent on the mineral content and humic substances.

About 30% of radioiodine leached by NaOH solution (pH 10.5) from the soil collected one month after the accident [2]. When the NaOH solution was acidified to pH 2, more than 60% of radiiodine in the solution precipitated possibly with humic materials that can bind iodine in the polyorganic structure. This leaching-precipitation behavior suggests that a part of iodine is in the organic form in the soil, which can be a reason for the low leaching rate in the soil by water. The formation of organic iodine in natural soil has been suggested also by XAFS using X-ray microbeam [3]. The formation of organo iodine species proceeds in a relatively short period, such as within a week or a month. Thus, the formation of organo iodine is possible for radiiodine in the soil.

[1] N. Yoshida and Y. Takahashi, *Elements* 8 (1012) 201. [2] K. Tanaka et al., *Geochem. J.* 46 (2012) 73. [3] Y. Shimamoto et al., *Environ. Sci. Technol.* 45 (2011) 2086.

Seasonal change of Iron species and concentration of soluble Iron in the atmosphere in Northwest Pacific region based on the analysis of aerosols collected in Tsukuba, Japan

Y. TAKAHASHI* AND T. FURUKAWA

Hiroshima University, Hiroshima 739-8526, Japan

(*correspondence: ytakaha@hiroshima-u.ac.jp)

Atmospheric iron (Fe) can be a significant source of nutrient for phytoplankton in remote ocean, which in turn has a large influence on Earth's climate. Whether Fe in aerosol can be a bioavailable or not depends mainly on the soluble fraction of Fe. However, factors controlling the soluble fraction of Fe have not been understood fully, since there can be many factors controlling the fraction. In this study, Fe species, chemical composition, and soluble Fe concentration in aerosol collected at Tsukuba through a year were investigated to identify the factors controlling the amount of soluble Fe supplied into ocean. The concentration of soluble Fe in aerosol is correlated with those of sulfate and oxalate which originate from anthropogenic sources, suggesting that soluble Fe is mainly derived from anthropogenic sources. Moreover, the concentration of soluble Fe (%) is also correlated with enrichment factors (EF) of vanadium (V) and nickel (Ni) emitted by fossil fuel combustion. These results suggested that the degree of Fe dissolution is controlled by the magnitude of anthropogenic activity such as fossil fuel combustion. In addition, XAFS was performed in this study to identify the Fe species in aerosols. The fitting of XAFS spectra coupled with micro-XRF showed that main Fe species in aerosols in Tsukuba were illite, ferrihydrite, hornblende, and Fe(III) sulfate. Moreover, soluble Fe fraction to total Fe in each sample measured by leaching experiment is closely correlated with the Fe(III) sulfate fraction determined by XAFS, suggesting that the presence of Fe(III) sulfate is primarily important for the supply of soluble Fe into the ocean. Another possible factor, total concentration of Fe(III) in the atmosphere in terms of the amount of supply of soluble Fe into ocean was high in spring due to the high concentrations of mineral dust in the period in East Asia, but this factor does not contribute to the amount of soluble Fe to a larger degree than the effect of Fe(III) sulfate. Thus, it was concluded that the most significant factor controlling the supply of soluble Fe in North Pacific can be the concentration of anthropogenic Fe species such as Fe(III) sulfate.

[1] Y. Takahashi *et al.*, *Atmos. Chem. Phys.*, 11 (2011) 11237.

[2] Y. Takahashi *et al.*, *Atmos. Chem. Phys. Discuss.* 13 (2013) 7599.

Vertical profiles of copper isotopic composition in the ocean

SHOTARO TAKANO¹, MASAHARU TANIMIZU²,
TAKAFUMI HIRATA³ AND YOSHIKI SOHRIN¹

¹Institute for Chemical Research, Kyoto University, Gokasho Uji, Kyoto 611-0011, Japan (Correspondence: shotaro@inter3.kuicr.kyoto-u.ac.jp)

²Kochi Institute for Core Sample Research, Japan Agency for Marine-Earth Science and Technology, 200 Monobe Otsu, Nankoku 783-8502, Japan

³Division of Earth and Planetary Sciences, Kyoto University, Kitashirakawa Oiwake-cho, Kyoto 606-8502, Japan

Copper is an essential trace metal that shows a vertical recycled-scavenged profile in the ocean. To elucidate the biogeochemical cycling of Cu in the oceans, it is important to determine the profiles of Cu isotopes in the ocean. However, precise isotopic analysis of Cu has been impaired by the low concentrations of Cu as well as co-existing elements that interfere with measurements by multi-collector inductively coupled plasma mass spectrometry (MC-ICP-MS). We have developed a precise and simple method for determining the isotope composition of dissolved Cu in seawater¹. Dissolved Cu was preconcentrated using a Nobias Chelate-PA1 resin and purified using an AG MP-1 anion exchange resin. The concentration and isotopic composition of copper were measured using an Element 2 HR-ICP-MS and a Neptune MC-ICP-MS, respectively. Cu isotopic composition data were expressed as $\delta^{65}\text{Cu}$, where $\delta^{65}\text{Cu}$ (‰) = $[(^{65}\text{Cu}/^{63}\text{Cu})_{\text{sample}} / (^{65}\text{Cu}/^{63}\text{Cu})_{\text{NIST SRM 976}} - 1] \times 10^3$.

We have determined $\delta^{65}\text{Cu}$ in the western North Pacific and Japan Sea. In the western North Pacific, $\delta^{65}\text{Cu}$ values were +0.45–0.53‰ above the thermocline. Below the thermocline, $\delta^{65}\text{Cu}$ values were increased to +0.49–0.71‰. In the Japan Sea, $\delta^{65}\text{Cu}$ values were +0.48–0.57‰ above the thermocline, which were similar to that of the western North Pacific. Below the thermocline, however, $\delta^{65}\text{Cu}$ values were lighter (+0.28–0.56‰) than that of the western North Pacific. We will also reveal the distribution of $\delta^{65}\text{Cu}$ in the eastern North Pacific and central Indian Ocean. We are going to constrain biogeochemical cycles of Cu using $\delta^{65}\text{Cu}$ and Cu concentration data. Our hypotheses at present is that $\delta^{65}\text{Cu}$ above the thermocline is balanced by biological removal of light Cu and aeolian supply of light Cu, and that $\delta^{65}\text{Cu}$ below the thermocline become heavy with the increase in AOU because of preferential removal of light Cu.

[1] Takano, S., Tanimizu, M., Hirata, T., Sohrin, Y., submitted. (2013) *Anal. Chim. Acta*.

Influence of surface condition on data quality of U–Pb zircon dating

M. TAKEHARA^{1*}, K. HORIE², T. HOKADA², H. KAIDEN²
AND S. KIYOKAWA¹

¹Kyushu University, 6-10-1, Hakozaki, Higashi-ku, Fukuoka 812-8581, Japan (*correspondence: 3SC12025R@s.kyushu-u.ac.jp, kiyokawa@geo.kyushu-u.ac.jp)

²National Institute of Polar Research, 10-3, Midoricho, Tachikawa, Tokyo 190-8518, Japan (horie.kenji@nipr.ac.jp, hokada@nipr.ac.jp, kaiden@nipr.ac.jp)

U–Pb zircon dating using microbeam such as SIMS and LA-ICP-MS has played a pivotal role in geochronology. Many analysts empirically believe that accuracy and precision of microbeam analysis strongly depend on surface condition of analytical spots. Especially, existence of cracks within the analytical spots decreases quality of results, but there is no quantitative evidence that the crack decreases the data quality. In this study, we quantitatively discuss influence on the data quality from the surface condition of the analytical spots. AS3 and FC1 zircons collected from gabbroic anorthosites of the Duluth Complex, Minnesota, USA, were used in this study. Previous work reported that some grains in AS3 zircons yield discordant data due to Pb loss caused by thermal diffusion [1].

Observation of thin sections by optical microscope and electron microprobe reveals chloritization of amphibole in AS3, which suggests hydrothermal alteration. U–Pb analyses of some AS3 zircon grains yielded discordant data. The analytical spots that yield discordant data can be classified into (1) altered domains characterized by high contents of LREE and non-formula elements, such as Ca, Al, and Fe, and (2) domains containing undersurface cracks. In the case that analytical depth is close to the undersurface cracks, the second domains also show high LREE contents. When the cracks in zircon worked as channels of hydrothermal fluid [2], there are possibilities that some residuals of the fluid exist in the cracks and/or that areas around the cracks was altered by the fluid. Therefore, selection of the analytical spots for U–Pb zircon dating should be based on observation of cracks not only on the surface but also under the surface. When AS3 and FC1 zircon are used as U–Pb standard material, it is important to carefully choose analytical spots on the basis of the backscattered electron and optical microscope images for achieving more precise analysis.

[1] Schmitz *et al.* (2003) *Geochim Cosmochim Acta* **67**, 3665–3672. [2] Carson *et al.* (2002) *EPSL* **199**, 287–310.

Lower crustal metasomatism of the NE-Japan arc inferred from crustal xenoliths from Ichinomegata crater

MIYUKI TAKEUCHI^{1*} AND SHOJI ARAI¹

¹ Dept. Earth Sci., Kanazawa Univ., Kanazawa 920-1192, Japan (*correspondence: takeuchi-miyuki@stu.kanazawa-u.ac.jp)

Ichinomegata crater, Megata volcano, the NE-Japan arc is a famous locality of ultramafic-mafic xenoliths, and there have been a lot of studies about mantle metasomatism (= metasomatism on mantle-derived ultramafic xenoliths) (e.g., Abe *et al.*, 1992, Abe *et al.*, 1999). However, there have been little documents on metasomatism in crust-derived xenoliths.

Coarse-grained mafic xenoliths from the Ichinomegata crater contain a large amount of pargasite. Some of the pargasite grains are obviously of secondary origin, replacing primary clinopyroxene in hornblende-pyroxene gabbros and pyroxene gabbros. And clinopyroxenes in pyroxene-spinel symplectites, which are a reaction product of olivine and plagioclase, are also replaced with pargasite.

Plagioclase shows a wide range of Ca content (An87-98 in hornblende-pyroxene gabbros, An64-90 in pyroxene gabbros), and are poor in Na around the rim. Pargasites are depleted in TiO₂, but discrete pargasite grains show higher TiO₂ contents (1.0–2.4 wt.%) than secondary grains (0.8–1.7 wt.%). Spinels have been enriched with Ti and Fe (especially Fe³⁺), and separated into two phases, Ti, Fe³⁺-rich magnetite and Al-rich spinel by cooling. Ti has been also added to the minerals in pyroxene-spinel symplectites.

The metasomatic formation of hydrous minerals was accompanied with addition of, at least, Ti, Na and K. Clinopyroxenes contain very low amounts of Rb, Ba, Nb (below detection limits of our LA-ICP-MS). The secondary pargasite is enriched in these elements, but not in HFS elements relative to clinopyroxenes. The hydration is characterized by enrichment of LIL elements but not of HFS elements. This was caused by infiltration of fluids related to hydrous arc magmas.

Hydration and cooling processes observed in the lower crustal gabbros are also recorded in peridotite and websterite xenoliths of upper mantle origin from the Northeast Japan arc. This means widespread modification of mineral chemistry and mineral assemblage from the upper mantle to the lower crust beneath the arc.

Geochemistry of spinel-hosted amphibole inclusions in abyssal peridotite : Embedded evidence for melt-peridotite reaction process?

A. TAMURA^{1*}, T. MORISHITA¹, S. ARAI¹
AND S. ISHIMARU²

¹Dept. Earth Sciences, Kanazawa University, Kanazawa 920-1192, Japan (*aking826@staff.kanazawa-u.ac.jp)

²Dept. Earth and Environmental Sciences, Kumamoto University, Kumamoto 860-8555, Japan

Trace-element compositions of spinel-hosted amphibole inclusions (20–40 μm) were determined by using LA-ICP-MS to more thoroughly understand the melt-peridotite reaction.

Spinel-hosted hydrous minerals (e.g., amphibole and phlogopite) have been documented in ultramafic rocks from the ocean floor and ophiolitic complexes [1, 2]. They are commonly observed in dunite, troctolite and chromitite, to which formation the melt-peridotite reaction contributed significantly. However, the role of formation of the inclusions has been ever constrained well within the framework of melt-peridotite reaction. Arai *et al.* [1] pointed out that the mineral inclusions are formed from a melt enriched in incompatible elements, e.g., TiO_2 and Na_2O , and H_2O , produced by zone refining effects in the melt-peridotite reaction. Until now, trace-element compositions of the inclusions have been rarely examined [2, 3] due to difficulty in establishing their geochemical systematics because of complicated multi-scale uncertainties on the reaction mechanisms, such as melt and rock compositions and geological setting.

A core interval (70 cm) of the residual harzburgite cut by gabbro recovered from the Atlantis Massif, Mid-Atlantic Ridge 30°N shows inhomogeneous compositions caused by reaction with melt forming the gabbro [4]. Pargasitic amphibole inclusions in concentric spinel grains are only observed in the harzburgite near the gabbro contact (10 cm) where depleted residual harzburgite reacted with N-MORB-like melt beneath the ridge. Because the geological and petrological context is well constrained there as above, the pargasite geochemistry will give us a good reference for the systematics of relevant reaction and origin of inclusions. Together with trace-element data of spinel-hosted amphibole inclusions in reacted rocks, we discuss the significances of inclusions on the melt-peridotite reaction processes.

[1] Arai *et al.* (1997) *GCA* 61, 671-675. [2] Schiano *et al.* (1997) *EPSL*, 146, 489-497. [3] Morishita *et al.* (2011) *Geology*, 39, 411-414. [4] Tamura *et al.* (2008) *CMP*, 155, 491-509.

Mission invisible: residual mantle wedge contains phlogopite?

YOSHIHIKO TAMURA¹, OSAMU ISHIZUKA²
AND ROBERT J. STERN³

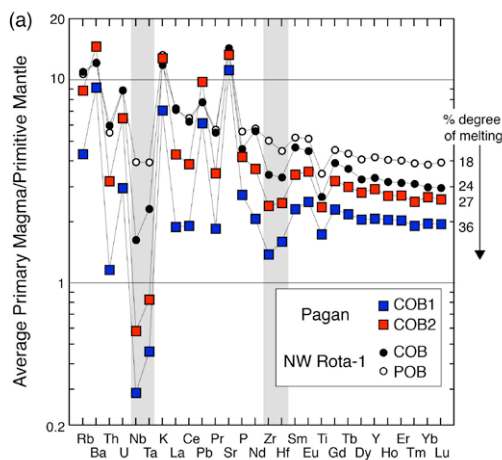
¹IFREE, JAMSTEC Yokosuka 237-0061, Japan,
(tamuray@jamstec.go.jp)

²GSJ/AIST, Tsukuba 305-8567, Japan, (o-ishizuka@aist.go.jp)

³U. Texas at Dallas, Texas 75080, USA,
(rjstern@utdallas.edu)

It is often mentioned that arc basalts are highly depleted in high-field strength elements (HFSE), such as Nb, Ta, Zr and Hf. In the spidergram, which shows four types of primary magmas in the Mariana arc (Tamura *et al.*, 2011; Tamura *et al.*, submitted) (Fig. 1), it is worth mentioning that North West Rota-1 (NWR1) POB, which is the driest and least depleted primary magma type among the four, is not as depleted in Nb, Ta, Zr and Hf as are the other three varieties and contains about 4x more of these HFSE than primitive mantle and are comparable to their HREE contents. On the other hand, the differences in Nb and Ta contents between NWR1 POB and more depleted COB are much larger than those expected from the different degrees of melting. This is also the case for Pagan COB1 and COB2 and comparing Pagan and NWR1. Apparently, Nb and Ta decrease unusually when the fraction of melting increases or when primary magmas become more hydrous from POB through COB and COB2 to COB1.

When the melting conditions are 'dry' as is true for POB,



phlogopite would not be present and Nb and Ta would become highly incompatible. It could be possible that highly depleted hydrous residual mantle wedge of the subduction zone could be phlogopite bearing dunite and harzburgite, which causes depletion of HFSE in wet and depleted arc magmas.

Circulation effect: Response of precipitation $\delta^{18}\text{O}$ to the ENSO cycle in monsoon regions of China

MING TAN

Key Laboratory of Cenozoic Geology and Environment, Institute of Geology and Geophysics, Chinese Academy of Sciences, No.19 Beitucheng West Road, Chaoyang District, Beijing, 100029, China, (tanming@mail.iggcas.ac.cn)

Based on an analysis of the relationships between the time series of amount-weighted mean annual $\delta^{18}\text{O}$ in precipitation ($\delta^{18}\text{O}_w$) and meteorological variables such as temperature, precipitation as well as atmospheric/oceanic circulation indices, it is recognized that the El Niño-Southern Oscillation (ENSO) cycle appears to be the dominant control on the inter-annual variation in $\delta^{18}\text{O}_p$ in the Monsoon Regions of China (MRC). Further analysis shows that the trade wind plays a role in governing $\delta^{18}\text{O}_w$ through affecting the intensity of the different monsoon circulations which are closely linked to the weakening and strengthening of the trade wind and gives the $\delta^{18}\text{O}_w$ different values at or over inter-annual timescales. The southwest monsoon (SWM) drives long-distance transport of water vapor from Indian Ocean to the MRC, and along this pathway increasing rainout leads to more negative $\delta^{18}\text{O}_w$ via Rayleigh distillation processes. In contrast, the southeast monsoon (SEM), which is consistent with the changes in the strength of the West Pacific subtropical high, drives short-distance water vapor transport from the West Pacific Ocean to the MRC and leads to less negative $\delta^{18}\text{O}_w$. Therefore, the $\delta^{18}\text{O}_w$ value directly reflects the differences in influence between the SWM, which is strong when the SE trade wind is strong, and the SEM, which is strong when the SE trade wind is weak. In addition, the South China Sea Monsoon also transports local water vapor as well as plays a role in achieving the synchronization between the $\delta^{18}\text{O}_w$ and ENSO. The author thus terms the $\delta^{18}\text{O}_p$ rhythm in the MRC the “circulation effect”.

Particle-size dependent distribution of radiocesium in river sediments after the FDNPP accident

KAZUYA TANAKA^{1*}, HOKUTO IWATANI², AYA SAKAGUCHI², YOSHIO TAKAHASHI² AND YUICHI ONDA³

¹ Institute for Sustainable Sciences and Development, Hiroshima Univ., Higashi-Hiroshima, 739-8530 Japan (Correspondence: kt0830@hiroshima-u.ac.jp)

² Department of Earth and Planetary Systems Science, Hiroshima Univ., Higashi-Hiroshima, 739-8526 Japan

³ Center for Research in Isotopes and Environmental Dynamics, Univ. of Tsukuba, Tsukuba, 305-8572, Japan

It was reported that most of fallout radiocesium emitted by the Fukushima Daiichi Nuclear Power Plant (FDNPP) accident stayed within 5 cm of surface soil layers [1,2]. Such accumulated radiocesium at the very surface on the ground is possibly being eroded into rivers by surface runoff, and finally goes into the Pacific Ocean. Particle size is an important factor in transportation of radiocesium in river systems. In this study, therefore, we investigated the dependence of radiocesium concentration on particle size and the distribution of particle size in river sediments.

River sediment samples were collected at 8 points in the Abukuma River and Kuchibuto River, which is one of the branches of the Abukuma River. River sediments were divided into 11 fractions with different particle sizes, > 2000 μm , 850 – 2000 μm , 500 – 850 μm , 250 – 500 μm , 125 – 250 μm , 63 – 125 μm , 40 – 63 μm , 20 – 40 μm , 10 – 20 μm , 2 – 10 μm and < 2 μm size fractions. Radiocesium concentration in each fraction was measured with γ -ray spectrometry using a planar type germanium semiconductor detector.

Smaller particle fractions contained a large amount of radiocesium possibly because of the following two factors. One is the specific surface area, and the other is the mineralogy of the sediments. Smaller particles have larger specific surface areas, providing more sorption sites for radiocesium. Also, a large amount of clay minerals, on which radiocesium is strongly sorbed, are contained in smaller fractions. On the other hand, the contribution of each particle-size fraction to radiocesium in bulk sediment is also affected by the mass distribution of sediment particles among different particle sizes as well as radiocesium concentration in each particle-size fraction. In this sense, the contribution of relatively large size fraction to total radiocesium concentration is not negligible in bulk sediment.

[1] Tanaka *et al.* (2012) *Geochem. J.* **46**, 73-76. [2] Kato *et al.* (2012) *J. Environ. Radioact.* **111**, 59-64.

A study on adsorption mechanism of organoarsenic compounds onto ferrihydrite

MASATO TANAKA^{1*} AND YOSHIO TAKAHASHI^{1,2}

¹ Graduate School of Science, Hiroshima University, 1-3-1 Kagamiyama, Higashi-Hiroshima 739-8526,

Japan (*correspondence: tanamasa@hiroshima-u.ac.jp)

² Key Laboratory of Petroleum Resources, Chinese Academy of Sciences, Donggang Road, Lanzhou 730000, China

The inorganic arsenic compounds are cause of groundwater pollution in the world. In addition, organoarsenic compounds also have potential of the water pollution. It is important to know the adsorption structures of arsenic compounds to understand the migration of arsenic compounds in environments. In this study, adsorption structures of methyl and phenyl substituted organoarsenic compounds onto ferrihydrite, one of the most active adsorbents for anions in nature, were studied by the extended X-ray absorption fine structure (EXAFS) measurement and density functional theory (DFT) calculations.

Methylarsonic acid (MMA), dimethylarsenic acid (DMA), phenylarsonic acid (PAA), and diphenylarsinic acid (DPAA) were adsorbed on ferrihydrite at 25 °C, pH 4 and 7. As K-edge EXAFS spectra of organoarsenic solution and adsorbed on ferrihydrite samples were collected by BL01B1 at SPring-8 and BL-12C at KEK Photon Factory (PF).

The EXAFS spectra suggest that all organoarsenic compounds treated in this study form inner-sphere complexes with ferrihydrite regardless of bulky functional groups. The interaction energy analysis using DFT calculations indicate that the steric hindrance between organoarsenic compounds and surface functional groups of ferrihydrite dominate the adsorption structures and adsorption amounts.

Internal ²³⁸U-²³⁰Th isochron method for dating young basaltic eruptions

RYOJI TANAKA^{1*}, TETSUYA YOKOYAMA^{1,2}
AND EIZO NAKAMURA¹

¹PML, ISEI, Okayama Univ., Misasa, 682-0192, Japan
(*correspondence: ryoji@misasa.okayama-u.ac.jp)

²Department of Earth and Planetary Sciences, Tokyo Institute of Technology, Tokyo, 152-8551, Japan

Dating of young (Late Pleistocene to Holocene) volcanic eruption gives valuable information in volcanology, environmentology, and archaeology. Although several geochronological methods such as ⁴⁰Ar/³⁹Ar, (U-Th)/He, and ¹⁴C, and U-series disequilibrium, have been applied for dating, there exist many analytical limitations in these methods especially for young basaltic volcanics.

This study demonstrates the applicability of ²³⁸U-²³⁰Th internal isochron methods for the determination of eruption age from young basaltic volcanics using chemically-separated groundmass phases. Groundmass phases of basaltic lava collected from Laguneta volcano, El Salvador, were separated into several fractions with different magnetic susceptibility, followed by leaching in hydrochloric acid solution. Hydrochloric acid solution congruently dissolves olivine, titanomagnetite, and phosphorous-bearing minerals; incongruently dissolves anorthite-rich plagioclase; and does not dissolve augite, albite-rich plagioclase, and alkali-feldspars in the examined groundmass phases. During acid leaching, the range of (²³⁸U/²³²Th) increased from 0.2 (unleached groundmass fractions) to 1.8 (leachates and residues). No, or little, preferential leaching between U and Th occurs by the acid-leaching treatment. Thus, the linear regression line obtained by leachate, residue, and unleached groundmass fractions can be regarded as an isochron, the slope of which indicates the eruption age. The ²³⁸U-²³⁰Th internal isochron age for two individual samples gave an identical value within the error. Using all the fractions from two samples, the most precise ²³⁸U-²³⁰Th isochron age was determined as 14 ± 1 ka (2σ). This age agrees with the degassing-induced external ²³⁸U-²³⁰Th isochron age obtained by whole rock samples when the error is considered. This study also revealed that acid-leaching preferentially fractionates Ra/Th because of incongruent dissolution of plagioclase. Thus, ²³⁰Th-²²⁶Ra isotope systematics cannot be used for acid-leached samples. The significance of this study lies in the development of precise geochronological method for any type of volcanics which erupted between ~3 and ~300 ky.

Characteristics and driving factors of surface water chemistry of Wujiang watershed

CONG-GUO TANG AND CONG-QIANG LIU

State Key Laboratory of Environmental Geochemistry,
Institute of Geochemistry, Chinese Academy of Sciences,
Guiyang 550002, China

The changes of water chemistry of rivers can reflect influence of anthropogenic activities on water environment in some extent. In order to understand the relationship between the spatial distribution of eco-environment of the watershed and the characteristics of water chemistry and geochemistry of rivers, firstly, the digital Wujiang watershed was built, and then the sub-watersheds were delineated, taking the sample points as sub-watershed outlets based on GIS. Secondly, using the function of spatial analyst of GIS, the statistical features of eco-environment (such as lithology and land use/cover) of each sub-watershed were calculated according to their respective classification. Finally, the correlation between the spatial distribution of lithology of the sub-watersheds and their corresponding $^{87}\text{Sr}/^{86}\text{Sr}$ ratio of river water, the correlation between $\text{NO}_3^-/\text{HCO}_3^-$, $\text{Cl}^-/\text{HCO}_3^-$, $\text{SO}_4^{2-}/\text{HCO}_3^-$ and anthropogenic activities respectively, and the correlation between the fraction of green vegetation of the sub-watershed and their corresponding flux of TDS (total dissolved solids) were analyzed quantitatively. The results justify that the $^{87}\text{Sr}/^{86}\text{Sr}$ ratio of river water is highly dependent on the lithologic feature of the watershed and indicate that anthropogenic activities are one of the main sources of NO_3^- and SO_4^{2-} of river waters, the output of TDS is highly dependent on the percentage of vegetation cover of the watershed.

Evaluation of kinetic effect on clumped isotope fractionation (Δ_{47}) during inorganic calcite precipitation

JIANWU TANG¹, BRAD E. ROSENHEIM²,
MARTIN DIETZEL³, ALVARO FERNANDEZ⁴
AND ARADHNA K. TRIPATI⁵

¹Dept. of Earth & Environ. Sci., Tulane University,
New Orleans, Louisiana 70118, U.S.A.,
(jtang@tulane.edu)

²Dept. of Earth & Environ. Sci., Tulane University,
New Orleans, Louisiana 70118,
U.S.A., (brosenhe@tulane.edu)

³Institute of Applied Geosciences, Graz University of
Technology, Rechbauerstrasse 12, 8010 Graz, Austria,
(martin.dietzel@tugraz.at)

⁴Dept. of Earth & Environ. Sci., Tulane University, New
Orleans, Louisiana 70118, U.S.A., (afernan5@tulane.edu)

⁵Dept. of Earth and Space Sciences, University of California,
Los Angeles, CA 90095, USA
(aradhna.tripati@gmail.com)

To date, published Δ_{47} -temperature calibrations using different inorganic calcite precipitation and biogenic carbonates, as well as obtained by theoretical calculations, are not consistent. Here we present a set of Δ_{47} data measured from inorganic calcites grown at well-controlled experimental conditions. We show that measured Δ_{47} values are strongly influenced by pH during calcite precipitation. When pH is between 8.3 and 9.0, measured Δ_{47} values (1) generally increase with decrease of temperature, (2) are not sensitive to the change of precipitation rate, and (3) are not sensitive to variation in ionic strength. The Δ_{47} -temperature equation calibrated by our Δ_{47} values for inorganic calcite grown at pH between 8.3 and 9.0 can be written as,

$$\Delta_{47} = (0.0367 \pm 0.0033) \times 10^6/T^2 + (0.2743 \pm 0.0376)$$

where Δ_{47} values were reported in the absolute reference frame. The slope of our calibration line is very similar to theoretical line (0.0392, Schauble *et al.*, 2006; Guo *et al.*, 2009). If $\text{pH} \geq 10$, the Δ_{47} values for calcite grown at 5°C significantly drift from the Δ_{47} -temperature line. In this case the comparison of $\delta^{18}\text{O}$ and Δ_{47} values of calcite grown at $\text{pH} \geq 10$ to that grown at $\text{pH} \leq 9$ indicates that every 1‰ depletion in $\delta^{18}\text{O}$ values results in 0.0155‰ enrichment in Δ_{47} values. We argue that any observed kinetic effect on carbonate clumped isotope fractionation is mainly due to isotopic non-equilibrium occurring in the solution during CO_2 - H_2O (de)hydration and (de)hydroxylation.

Geochronology and geochemistry of Early-Middle Triassic magmatism in the Argun Massif, NE China: Constraints on the tectonic evolution of Mongol–Okhotsk suture belt

JIE TANG, WEN-LIANG XU*, FENG WANG, WEI WANG, MEI-JUN XU AND YI-HAN ZHANG

College of Earth Sciences, Jilin University, Changchun 130061, China (893335234@qq.com; (*correspondence: xuwl@jlu.edu.cn)

The Mongol–Okhotsk suture belt is located between the North Asian and the North China cratons and played an important role in the formation and tectonic evolution of eastern part of the Eurasian continent during Mesozoic. However, it remains debated whether the southward subduction of the Mongol–Okhotsk oceanic plate beneath the Argun Massif happened. In this paper, we undertook zircon U–Pb dating and geochemical data of the Early-Middle Triassic intrusive rocks in the Argun Massif which is bounded by the Mongol–Okhotsk suture belt to the northwest, with the aim of addressing the above-mentioned question.

Zircons from five representative intrusions in the Argun Massif are euhedral–subhedral, and display fine-scale oscillatory growth zoning in CL images, implying a magmatic origin. Zircon U–Pb dating demonstrates an Early-Middle Triassic magmatism in the Argun Massif, aged between 241 and 247 Ma. The Early-Middle Triassic rocks are composed of a suite of diorite, granodiorite, monzogranite, and syenogranite. They have $\text{SiO}_2 = 57.71\text{--}72.86$ wt.%, $\text{Mg\#} = 19\text{--}52$, $\text{K}_2\text{O} = 2.39\text{--}5.00$ wt.%, and $\text{Na}_2\text{O} = 3.28\text{--}4.28$ wt.%. Chemically, they belong to the high-K calc-alkaline series. Moreover, they are characterized by enrichment in light rare earth elements (LREEs) and large ion lithophile elements (LILEs), and depletion in heavy rare earth elements (HREEs) and high field strength elements (HFSEs) such as Nb, Ta, and Ti. Their LREEs/HREEs ratios range from 9.68 to 21.56, and their δEu values vary from 0.61 to 1.31. Taken together, these Early-Middle Triassic intrusive rocks are similar to those from an active continental margin setting. Therefore, we conclude that the Early-Middle Triassic magmatism in the Argun Massif could be generated under an active continental margin setting related to the southward subduction of the Mongol–Okhotsk oceanic plate beneath the Argun Massif, which is also supported by the occurrence of the coeval porphyry Cu–Mo deposits such as the Erdenet Cu–Mo deposit in Mongolia and Taipingchuan Cu–Mo deposit in the Argun Massif, NE China.

This research was financially supported by the National Key Basic Research Program of China (Grant 2013CB429803) and the Natural Science Foundation of China (41272077).

Theoretical calibration of Δ_{47} values of ^{13}C - ^{18}O clumps for carbonates

MAO TANG, SI-TING ZHANG AND YUN LIU*

State Key Laboratory of Ore Deposit Geochemistry, Institute of Geochemistry, Chinese Academy of Sciences, China. (Correspondence*: Liuyun@vip.gyig.ac.cn)

Equilibrium clumped isotope distribution has been suggested as a new thermometer for various low temperature systems. With the help of a newly developed cluster-model based method for solids, we re-check equilibrium Δ_1 values of ^{13}C - ^{18}O clumps of those important carbonate minerals: calcite, aragonite, dolomite, nahcolite and magnesite. Although our method is totally different from the method of Schauble *et al.* (2006), our results generally agree with what Schauble *et al.* (2006) predicted except for nahcolite (NaHCO_3). For example, Δ_1 values of ^{13}C - ^{18}O clumps for calcite and aragonite at 25 C degree predicted by Schauble *et al.* (2006) were 0.41 and 0.43 (in per mil), our results are 0.436 and 0.445, respectively. It confirms that the results of calcite and aragonite are close to each other and there is only marginal difference between them. However, the result for nahcolite from Schauble was 0.41, as same as their result for calcite. Our result for nahcolite is 0.454 which is different from the result of calcite.

Furthermore, there are kinetic effects of isotope fractionation during phosphoric acid digestion of carbonates. The calculated kinetic isotope effect on Δ_{3866} was found about 0.22 per mil for acid digestion processes and can be used to explain the offset between theoretical results and the experiments (i.e., Guo *et al.*, 2009). However, the theoretical calibration lines provided by Guo *et al.* (2009) were still different from the experimental calibration line suggested by experiments (e.g., Ghosh *et al.* 2006) in terms of both position and slope. Recently, a new experimental calibration line was suggested (e.g., Dennis *et al.*, 2011). Here, we used higher theoretical levels to re-check the theoretical calibration lines and found deviations from the previous ones. Our kinetic isotope effect results are obviously larger than what Guo *et al.* (2009) predicted. Combining our results of equilibrium Δ_1 values of carbonates and the kinetic isotope effects by acid digestion, we can obtain theoretical calibration lines for Δ_{47} of carbonates. If put our calibration line into the absolute reference frame diagram suggested by Dennis *et al.* (2011), our calibration line is far above the previous theoretical line and falls between the two experimental lines suggested by Caltech and Harvard groups. The slope of our calibration line is smaller than that of Caltech group but very slightly larger than that of Harvard group.

Air-sea fluxes of dimethyl sulfide and acetone in the subtropical and equatorial Pacific Ocean

HIROSHI TANIMOTO^{1*}, YUKO OMORI,
SATOSHI INOMATA, TORU IWATA, SOHIKO KAMEYAMA,
KEN FURUYA, ATSUSHI TSUDA AND MITSUO UEMATSU

¹National Institute for Environmental Studies, Tsukuba, Japan
(*correspondence: tanimoto@nies.go.jp)

²Okayama University, Okayama,

³Hokkaido University, Sapporo, Japan

⁴The University of Tokyo, Tokyo, Japan

⁵The University of Tokyo, Kashiwa, Japan

Fluxes of dimethyl sulfide (DMS) and acetone between the ocean and the atmosphere were measured in the subtropical South Pacific Ocean and the equatorial Pacific Ocean in January-February, 2012. Vertical profiles of these gases were obtained above the ocean surface by measurements at 7 heights from 1 to 1400 cm with a profiling buoy aboard R/V Hakuho-Maru during the KH-11-10 and KH-12-1 (EqPOS) cruises. The concentrations of DMS and acetone in gas samples were monitored by a proton transfer reaction-mass spectrometry (PTR-MS). The concentrations of DMS and acetone in the surface seawater and air were continuously measured with PTR-MS during the cruises. The mean sea surface concentration of DMS in the subtropical ocean (2.1 ± 0.5 nM) was slightly lower than that in the equatorial ocean (3.2 ± 1.0 nM). The DMS fluxes substantially varied in the range of 3.6–13.1 and 0.1–18.9 $\mu\text{mol m}^{-2} \text{d}^{-1}$ in the subtropical and equatorial oceans, respectively. The magnitude of DMS fluxes was dependent of wind speed. The gas transfer velocities of DMS were calculated from the fluxes and the seawater DMS concentrations. We will discuss gas transfer velocities in comparison to previous studies. The air-sea fluxes of acetone will be also presented and discussed.

Partitioning of Nb between rutile and NaAlSi₃O₈-, NaCl- and NaF- aqueous fluids at 1-5 GPa and 300-600°C

E.A. TANIS^{1,2}, A. SIMON¹, O. TSCHAUNER^{2,3} P. CHOW⁴, Y. XIAO⁴, J. HANCHAR⁵, G. SHEN⁵ AND Y. ZHAO⁵

¹Earth & Environmental Sciences, University of Michigan

²HiPSEC, University of Nevada, Las Vegas

³Department of Geoscience, University of Nevada Las Vegas

⁴HPCAT, Carnegie Institute of Washington, Argonne IL

⁵Earth Sciences, Memorial University of Newfoundland

Rutile (TiO₂) has been proposed as an important host for high field strength elements (HFSE) such as Nb and Ta in high-pressure, moderate temperature metamorphic environments, including subduction zone systems. The observed depletion of HFSE in arc magmas can be explained if rutile is chemically inert with respect to aqueous fluids evolved during progressive metamorphism of subducted slab materials. However, both field observations and experimental studies [1] suggest that titanium, as well as HFSE can be soluble in aqueous fluids. Published experimental data were obtained by performing experiments at temperatures >700°C and pressures <2.5 GPa, conditions not entirely relevant to fluid loss in many arc systems. Here, we report new data that constrain directly the partitioning of Nb between fluid and rutile at 1 to 5 GPa and 300-600°C, conditions applicable to fluid evolution during the blueschist to eclogite transition.

We investigated systematically the partitioning of Nb between aqueous fluid and Nb-rutile (1wt% Nb) by adding albite (NaAlSi₃O₈), 10 and 20 wt % NaCl, and 4 wt % NaF to the fluid phase. The concentration of Nb in aqueous fluid was measured directly by using a hydrothermal diamond anvil cell and synchrotron X-ray fluorescence at the HPCAT 16-IDD beamline at the Advanced Photon Source.

Fluid	Pressure (GPa)	Temperature (°C)	Nb Concentration (ppm)
10% NaCl	1.2-2.8	300-700	9-23
20% NaCl	1.7-4.7	300-600	24-86
NaAlSi ₃ O ₈	1.0-5.8	300-600	100-1050
4% NaF	3.0-6.5	300-500	260-1075

Our data indicate that dissolved NaF and albite, relative to pure water and NaCl, have a much greater effect on enhancing Nb concentration and transport in dense, moderate temperature, aqueous fluid. Our findings are consistent field studies such as [1] that document HFSE mobility in aqueous fluids evolved during the blueschist to eclogite transition.

[1] Gao *et al.* (2007) GCA, 71, 4974-4996.

Properties and structural role of iron in silicate melts and glasses

ISABELLE TANNOU^{1,2*}, MARIE JEFFROY¹, DOMINIQUE DE LIGNY³ AND DANIEL R. NEUVILLE²

¹ Saint-Gobain Recherche, 39 quai Lucien Lefranc, 93303 Aubervilliers cedex, France
(correspondence: tannou@ipgp.fr)

² Institut de Physique du Globe de Paris, 1 rue Jussieu, 75238 Paris cedex 05, France (neuville@ipgp.fr)

³ Université Claude Bernard Lyon1, UMR5306 CNRS, 12 rue Ada Byron, 69622 Villeurbanne, France (dominique.de-ligny@univ-lyon1.fr)

Iron is an important element to probe the properties and the structure of silicate melts. In earth science most of lava contain more than 10% of iron whereas the proportion is much smaller in industrial materials. Iron usually occurs in two different valence states (Fe^{2+} or Fe^{3+}), and three coordination: 4, 5 and 6 for these different redox states. Thus, the influence of iron oxide on the melt properties is complicated. Consequently, the redox ratio of silicate glasses and melts is an important parameter which role must be properly studied to understand the physical and chemical properties of these materials.

The coordination of iron may evolve as a function of the redox state. These changes are due to the fact that iron is essentially present in the form of Fe^{3+} in tetrahedral position at lower temperatures whereas it mainly occurs as Fe^{2+} in 6-fold coordination at higher temperatures. These changes in the iron coordination may influence the short range order around network modifier, such as Na or Ca. Our goal is to understand the importance of those coordination modifications caused by the change in iron redox.

X-ray absorption spectroscopy experiments are very valuable to determine short-range order. It should allow us to study the iron valence and coordination, as well as the sodium and calcium environment. However this technique is not always accessible. Therefore, other experimental methods must be used to study the network modifications such as Raman spectroscopy and electron microprobe.

We focused our work on the changes which happen in the glass during the transition between different redox states. Especially with regard to the network structure and the local environment of network-modifier elements.

Temporal variations in the composition and age of terrestrial organic carbon transported by the Yellow River

SHUQIN TAO^{1,2}, TIMOTHY IAN EGLINTON², DANIEL MONTLUCON², CAMERON MCINTYRE² AND MEIXUN ZHAO¹

¹Ocean University of China, Qingdao 266100, China

²ETH Zürich, 8092 Zürich, Switzerland

The Yellow River is the World's highest turbidity major fluvial system, delivering over 1×10^9 t of sediments annually into the Chinese marginal seas, accounting for ~7% global sediment flux to the ocean. Organic carbon carried by the Yellow River therefore may play a significant role in the global and regional organic carbon cycle.

The focus of the present study is to develop an understanding of the sources, composition and age of terrestrial organic carbon that is carried by the Yellow River and supplied to the adjacent Bohai Sea and Yellow Sea. Near-surface suspended particulate matter samples were collected nearby the Lijing Station, ~50 km upstream of the river mouth (Dongying), as part of a sampling campaign between June 2011 and June 2012 in order to assess seasonal variations in fluvial supply. In addition to bulk properties, the abundance and carbon isotopic composition of source-specific biomarkers (fatty acid & alkanes) were measured.

The concentrations of higher plant-derived long-chain ($\geq \text{C}_{24}$) *n*-alkanes, *n*-fatty acids and particulate organic carbon (POC) co-varied with total suspended solid (TSS) concentrations, with peak abundances during summer and early autumn, indicating plant-derived organic carbon is controlled by the overall flux of terrestrial sediments, which in turn is influenced by flood events and human activities.

POC in the Yellow River exhibits relatively uniform $\delta^{13}\text{C}$ values (-23.94 to -24.37‰), and old radiocarbon ages (4000 to 4600 ¹⁴C years). Radiocarbon ages of short-chain (C_{16} , C_{18}) fatty acids were variable but generally modern (from 560 years to greater than modern), suggesting they are sourced from fresh terrestrial debris, but more likely from aquatic productivity during warm and low-turbidity periods. In contrast, long-chain fatty acids display a relatively narrow and pre-aged range from 1550 to 2080 years.

These results, and associated molecular and isotopic information, indicate that the aged OC – likely sourced from soils on the Chinese loess plateau within the drainage basin – contributes significantly to the suspended load of the Yellow River.

Acknowledgements: This study is supported by the China Scholarship Council and the NSFC (grant No. 41020164005).

Linking kimberlite magmatism, transition zone diamonds, and subduction processes

S. TAPPE^{1,2*}, D.G. PEARSON¹, B.A. KJARSGAARD³,
G.M. NOWELL⁴ AND D. DOWALL⁴

¹University of Alberta, Edmonton, Canada

²De Beers Group Exploration, Johannesburg, South Africa
(*sebastian.tappe@debeersgroup.com)

³Geological Survey of Canada, Ottawa, Canada

⁴Durham University, Durham, United Kingdom

The presence of diamonds with transition zone (TZ) inclusion parageneses in a growing number of kimberlites worldwide is generally considered evidence for an ultradeep origin of kimberlites. However, combined geochemical and experimental evidence, including mantle redox constraints, suggests that kimberlite magma formation is best explained by volatile-fluxed melting of refertilized depleted upper mantle domains.

We analysed the Sr-Nd-Hf isotope compositions of fresh hypabyssal kimberlites from the 75-to-55 Ma Lac de Gras (LDG) field of the central Slave craton that contains TZ diamonds. The LDG kimberlites show the most extreme Nd-Hf isotope decoupling reported from global kimberlites. Isotopic modelling suggests that the steep-angled array in Nd-Hf isotope space is best explained by mixing of convecting upper mantle-derived CO₂-rich melt with minor amounts of alkali silicate melt derived from an isolated mantle reservoir with extremely unradiogenic Hf. Our data indicate that OIB-type material stored in the transition zone for >2 Gyr can be the source of the alkali silicate melt component. Given that the nearby 170 Ma Jericho kimberlites contain neither TZ diamonds nor anomalously unradiogenic Hf, we suggest that onset of fast and steep subduction along the western margin of North America at 100 Ma caused significant entrainment of ancient TZ material into the upper mantle beneath the region. Recycled ancient OIB-type material partially melted during the subduction-triggered upward mantle flow, and locally refertilized the depleted convecting upper mantle. Subsequent CO₂- and H₂O-fluxed redox melting of refertilized domains gave rise to kimberlite magma formation beneath the thick cratonic lid in the LDG area starting at 75 Ma. Model calculations indicate that ancient TZ diamonds could have been brought to the Slave craton base by vigorous mantle flow near a subduction zone within <25 Myr, such that they were available for sampling by the ascending upper mantle-derived LDG kimberlite magmas at 75 Ma [1].

[1] Tappe *et al.* (2013), *EPSL*, Vol. **371-372**, 235-251

A Possible Route to K⁺-Enriched Aqueous Solutions on Early Earth

O. TARAN,^{*1} H. LANGE¹ AND G.M. WHITESIDES^{1,2}

¹ Department of Chemistry and Chemical Biology, Harvard University, Cambridge, MA 02138, USA.

² Wyss Institute for Biologically Inspired Engineering, Harvard University, Cambridge, MA 02138, USA.
(correspondence: otaran@gmwhgroup.harvard.edu)

All known living organisms have a K⁺-rich intercellular medium, while usually existing in a Na⁺-enriched environment [1]. High K⁺ concentrations are required for the proper function of numerous essential enzymes and ribozymes [2]. This difference between cation concentrations is translated to potential difference used for energy storage and signalling. Most of the natural terrestrial environments are known to be enriched in Na⁺ due to its higher abundance and high solubility of its salts. The Na⁺/K⁺ mole ratio inside living cells varies around 1/10, which is roughly the opposite ratio of these ions in seawater (47/1). In this work we show that one of the processes leading to the enrichment of groundwaters in K⁺ can occur during acid weathering of Aluminium rich clays and zeolites and the fractional secondary precipitation of alunite and Na-alunite

Zeolites and montmorillonites were treated by acidic (0.1-1M H₂SO₄) solutions (K⁺/Na⁺ mole ratio 1/5) at temperatures 20°-50°C. The clay/acid mixtures were left to evaporate. During the drying process octagonal crystals were formed from coalecent brines on the surface of the clays. The crystals were identified by X-ray diffraction and ICP analysis as KAl(SO₄)₂. The remaining interstitial brine was enriched in Na⁺ and close to saturation with respect to NaAl(SO₄)₂. Fast washing from the final mixture surface leads to the enrichment of K⁺ in the formed solution by orders of magnitude depending on pH, temperature and a mineral type.

This proposed scenario leads to environments rich in potassium and can also be applied for accumulation of other prebiotic components, such as phosphate and small organic molecules. We suggest that acid weathering could be a process to accumulate essential components for the chemical origin of life.

[1] Williams, R. (1970).. *Q. Rev. Chem. Soc.*, 3.[2] Mulkiyanian, A., *et al.* (2012) *PNAS*, 109:E821-E830.

How much magmatic water is transported by volcanic gases?

YURI TARAN¹ MIKHAIL ZELENSKI²
AND ILYA CHAPLYGIN³

¹Institute of Geophysics, Universidad Nacional Autónoma de México, México D.F., 04510, México

²Institute of Experimental Mineralogy, RAS, Chernogolovka, Moscow Dstr.142432, Russia

³Institute of Ore Deposits, RAS, Moscow, 119017, Russia

Gases sampled from volcanic fumaroles and from the surface of lava lakes and lava flows are characterized by temperatures from boiling point of water up to 1100°C. The main component of volcanic gases is water vapor with concentrations from ~50 to 99 vol%. The fraction of magmatic water in volcanic gases is estimated using the isotopic composition of volcanic vapor. For the highest temperature fumaroles of subduction-type volcanoes D/H ratios on average ~ -25‰ (V-SMOW) and ¹⁸O/¹⁶O are close to the corresponding values of the whole rock, usually from +6‰ to +9‰. In many cases volcanic vapors of arc volcanoes with $t > 800^\circ\text{C}$ are represented by almost pure magmatic water. However, there are numerous exceptions from this rule when a $> 800^\circ\text{C}$ volcanic gas is a mixture of magmatic water with up to 50% of meteoric or seawater vapors. Most of the arc fumarolic gases demonstrate a single trend of mixing between magmatic and meteoric end members in their chemical and isotopic compositions. Much more complicated are cases related to volcanic gases from hot spot and rift volcanoes with magmas much less water abundant than arc magmas. Low and medium-temperature fumaroles of Kilauea (Hawaii) and Sierra Negra (Galapagos) discharge gases with a low content of water vapor (50-70 vol%) but all these vapors apparently have meteoric origin and thus the real proportion of magmatic water and its isotopic composition in gases of these hot spot volcanoes is impossible to determine. The new data on the high-temperature ($> 1000^\circ\text{C}$) volcanic gas from a hornito of the Erta Ale lava lake (Zelenski *et al.*, submitted) make possible to estimate the isotopic composition of magmatic water for this continental rift volcano. The Erta Ale volcanic vapor derived from the liquid lava lake seems to be about half diluted by meteoric water and has the isotopic composition between that of local meteoric water and water with $\delta\text{D} < -60\text{‰}$ if to accept $\delta^{18}\text{O} = +6\text{‰}$, like in the Erta Ale whole rock samples. However, this suggestion assumes the absence of the oxygen isotope exchange between CO_2 and H_2O during sampling when the ~1:1 $\text{H}_2\text{O} + \text{CO}_2$ mixture is cooling from the vent to condensate temperature.

Important factors for geochemical research of stream sediments near storm water outflow sites

R. TARAŠKEVIČIUS, R. ZINKUTĖ* AND Ž. STANKEVIČIUS

Nature Research Centre, Akademijos 2, Vilnius LT-08412, Lithuania (*correspondence: zinkute@geo.lt)

Urban storm sewer system is an important pathway of transfer of contaminants to the hydrosphere. Presuming that each storm water outflow (SWO) can increase the content of potentially harmful chemical elements (PHE) in stream sediments, matched pairs of samples can be taken upstream and downstream from SWO. Water flow rate differences lead to variability of lithological composition (from clay to sand) and geochemical changes even within short distance. It is useful to find out the advantageous grain size fraction for revealing the geochemical changes due to influence of SWO.

Thirty nine samples of Neris river sediments including 12 matched pairs of samples near SWO sites of Vilnius city were taken. The contents of Pb, Zn, Cu, Ni, Cr (PHE) and rock forming elements Al, Ca, Mg, Na, K, Fe, Si, P, S, Ti, Mn were determined in the bulk fraction (< 2.0 mm) and fractions < 0.1 mm, 0.1-0.25 mm, 0.25-0.50 mm by x-ray fluorescence.

In most samples the fraction 0.1-0.25 mm (average is ~57%) and < 0.1 mm (30%) prevails. In sequence of fractions < 0.1 mm, 0.1-0.25 mm, 0.25-0.50 mm the contents of most elements decrease due to dilution by quartz and plagioclases.

Using Wilcoxon matched pairs test for the bulk fraction the differences between samples upstream and downstream from SWO are insignificant for all 5 PHE, meanwhile for the < 0.1 mm fraction they are significant for Pb, Zn and Cu. The increase of Cr and Ni contents is insignificant, because they are not the main in pedochemical anomalies of Vilnius.

Analysis of < 0.1 mm fraction seems to have advantages in comparison with the bulk fraction < 2 mm for indicating places of storm water outflow. For refinement of results, not only enrichment factors should be calculated by normalising to clay-related (Al, Mg, K, Ti) or biophilic (S, P) elements, but also the dilution factor by sand (Si) taken into account.

NanoSIMS Pb/Pb dating of tranquillityite in lunar basalts

R. TARTÈSE^{1*}, M. ANAND^{1,2} AND T. DELHAYE³

¹Planetary and Space Sciences, The Open University, Walton Hall, Milton Keynes, MK7 6AA, UK (*correspondence: Romain.Tartese@open.ac.uk)

²Department of Earth Sciences, The Natural History Museum, Cromwell Road, London, SW7 5BD, UK

³Plateforme ONIS/NanoSIMS, Université de Rennes 1, Campus de Beaulieu, 35042 Rennes Cedex, France

Ion microprobe U-Th-Pb geochronology was first carried out three decades ago [1-2] to date phosphates and Zr-rich minerals from lunar samples, but was hampered by the limited mass resolution of the instrument. Subsequent analytical developments improved the accuracy and precision of *in-situ* Pb isotope measurements. In lunar samples, *in-situ* U-Pb dating has mostly been focused on zircon (e.g., [3] and refs therein), which occurs in rock types mainly representing the lunar highlands [3], while it is rare in mare basalts in which U and Th, are mostly hosted by baddeleyite, zirconolite and tranquillityite. This latter group of minerals can also yield precise and accurate Pb/Pb ages [4-9]. However, their small sizes often pose serious challenges to application of *in-situ* dating techniques.

We have used the NanoSIMS 50 at the University of Rennes 1 to carry out high-resolution Pb/Pb dating in tranquillityite in mare basalts. The 120-140 pA primary O⁻ beam produced ~ 3 μm spots. We obtained average ²⁰⁷Pb*/²⁰⁶Pb* dates of 3713 ± 8 Ma, 3769 ± 8 Ma and 3736 ± 10 Ma for samples 10044, 75055 and 74255, respectively, which we interpret as the crystallisation ages of these basalts. These ages are consistent with previous but provide tighter constraints on the crystallisation of these basalts. The high-spatial-resolution achieved in our dating protocol using the NanoSIMS 50 and the common occurrence of tranquillityite in lunar basalts have opened up a new avenue for carrying out rapid, accurate and precise age dating of mare basalts.

[1] Andersen & Hinthorne (1972) *EPSL* **14**, 195-200. [2] Andersen & Hinthorne (1973) *GCA* **37**, 745-754. [3] Nemchin *et al.* (2012) *Aust. J. Earth Sci.* **59**, 277-290. [4] Rasmussen & Fletcher (2004) *Geology* **32**, 785-788. [5] Rasmussen *et al.* (2008) *GCA* **72**, 5799-5818. [6] Schmitt *et al.* (2010) *Chem. Geol.* **269**, 386-395. [7] Wingate & Compston (2000) *Chem. Geol.* **168**, 75-97. [8] Wingate *et al.* (1998) *Precamb. Res.* **87**, 135-159. [9] Yang *et al.* (2012) *J. Anal. Atom. Spectrom.* **27**, 479-487.

Evidences of paleoproterozoic metamorphism in the NW region of the Quadrilatero Ferrifero area, Minas Gerais, Brazil: Implications for gold mineralizations

COLOMBO C. G. TASSINARI^{1*}, MARTA E. VELÁSQUEZ², JOSÉ M. U. MUNHÁ⁴, LYDIA M. LOBATO⁵, ANTONIO M. MATEUS⁴ AND WILLIAM F. CAMPOS⁵

¹Instituto de Geociências da Universidade de São Paulo, Rua do Lago, 562, 05508-900, São Paulo, SP, Brasil, CNPq correspondence: ccgtassi@usp.br

²Departamento de Geologia da Universidade Federal do Amazonas,

³Departamento de Geologia, Faculdade de Ciências, Universidade de Lisboa, Portugal

⁴Instituto de Geociências Universidade Federal de Minas Gerais

⁵Jaguar Mining Group

It was characterized a paleoproterozoic medium-grade metamorphism related to the gold mineralizations in the NW area of the Iron Quadrangle (Quadrilatero Ferrifero), in Minas Gerais State, Brazil. The gold ores are hosted by sericite-chlorite quartz schist from the upper metasedimentary unit of the Rio das Velhas Supergroup. These rocks are metamorphosed under transitional greenschist-amphibolite facies conditions and comprise garnet + staurolite + cummingtonite, biotite + chlorite + plagioclase + quartz; the metamorphic peak is at ca. 600°C and 6.6 kb. The ore consist of arsenopyrite, pyrite, pyrrhotite and free gold in a gangue made of quartz, carbonates, graphite and oxides (hematite, magnetite and ilmenite). The age of the metamorphism was characterized by Sm-Nd ages for garnet-whole rock and Rb-Sr whole rock isochron with an ages around 2.2 Ga. The 1.9 Ga Rb-Sr age of biotite suggest that high geothermal gradients were sustained for a long period of time. The ore minerals are dated by Rb-Sr and Pb-Pb methods, which give an ages of 2.15 and 2.0 Ga. Rb-Sr applied to hydrothermal sericite – whole rock pair, yielded an age of 1928 ± 2.6 Ma. The 2.1-2.0 Ga ages could be related to the first stage of mineralization at 600 °C. The age of 1.9 Ga could be related to the boiling episode that occurs at ~340°C. Pb, Sr and Nd isotopic compositions of the ore minerals suggest that the hydrothermal fluids represents mixing between several reservoirs, like the mantle, lower and upper continental crust. The metamorphism must have sustained elevated crustal geotherms for at least 100 Ma, promoting hydrothermal fluids circulation during the orogenic time.

Mo-W-Re-Au-Cu partitioning between vapor, brine and felsic melt: Super-solidus to sub-solidus

BRIAN TATTITCH^{1*}, JON BLUNDY¹, PHILIP CANDELA²,
AND PHILIP PICCOLI²

¹Bristol Earth Experimental Studies, University of Bristol,
Bristol BS8 1RJ, (Brian.Tattitch@bristol.ac.uk)*

²Laboratory for Mineral Deposits Research, University of
Maryland, College Park, USA

The exsolution of metal-bearing “proto-ore fluids” from magmas initiates at super-solidus conditions and continues throughout cooling and decompression to solidus conditions for the parental magma. The range of exsolution conditions for a particular magma will affect the efficiency by which each ore metal is removed from the melt, the metal ratios in the exsolved fluid(s), the mass of metals available for transport, and ultimately the grade of the deposits.

Experiments performed at a range of P-T conditions across the solidus for a given magma composition provide insight into the behavior of these metals that is not readily accessible by study of natural samples. We have performed exploratory experiments to investigate the effect of the super-solidus to sub-solidus transition on metal partitioning between melt and volatile phases under ore-mineral saturated conditions. These experiments examine Mo-W-Re-Au partitioning, and wolframite-molybdenite solubility, at super-solidus (800°C 100 MPa), near-solidus (725°C 100MPa) and sub-solidus (700°C 75MPa) conditions. New techniques are in development to refine data reduction and account for the complex behavior of our Mo-Fe-W-bearing fluid inclusions. However, the early results may be broadly interpreted as showing that Mo and W partitioning between vapor, brine and melt is strongly influenced by the super-solidus to sub-solidus transition.

The impact of the transition is more pronounced for W ($D^{v/m} = 11 \pm 5$ and 210 ± 120) compared to Mo ($D^{v/m} = 10 \pm 4$ and 50 ± 25) as the temperature drops from 800°C to 725°C. These data are consistent with fractionation of Mo from W across the super-solidus to sub-solidus transition. The molybdenite- and wolframite-saturated fluids have W/Mo ratios that increase from 20 to 30 to 60 in the brine and 15 to 25 to 50 in vapor, for 800°C-100MPa to 725°C-100MPa to 700°C-75MPa, respectively. While these results are tentative, new experiments are in progress that include Mo, W, Re, Au, and Cu. These new experiments and new data analysis techniques will provide further insight into the effect of the super-solidus to sub-solidus transition on the composition and ore-mineral solubility limits of proto-ore fluids.

The silicon isotope record of early silica diagenesis

M. TATZEL^{1*}, F. VON BLANCKENBURG¹,
J. A. SCHUESSLER¹ AND G. BOHRMANN²

¹German Research Center for Geosciences, GFZ Potsdam,
Germany (*correspondence: mtatzel@gfz-potsdam.de)

²Department of Geosciences, Universität Bremen, Germany.
(gbohrmann@marum.de)

During diagenesis, silica is converted to quartz through dissolution-reprecipitation reactions which are likely influenced by isotope fractionation effects.

To assess the impact of diagenesis on the silicon isotope composition of chert, we explored the silicon isotope record of Plio- and Pleistocene siliceous sediments of the South Atlantic that are hosting the youngest products of the incipient stages of silica diagenesis found to date.

High $\delta^{30}\text{Si}$ values of $2.26 \pm 0.18 \%$ (n= 5) and $1.97 \pm 0.06 \%$ (n= 4) characterize two bulk porcelanite (opal-CT) layers found in two drill cores from Maude Rise and the Southwest Indian Ridge, respectively. Bulk $\delta^{30}\text{Si}$ values of surrounding siliceous oozes are lower and range between $-0.34 \pm 0.08 \%$ (n= 4) and $0.60 \pm 0.08 \%$ (n= 7), and $0.16 \pm 0.08 \%$ (n= 4) and $1.45 \pm 0.11 \%$ (n= 6), respectively.

Within these types of siliceous sediments, diatoms constitute both the compartment most prone to dissolution and heaviest in $\delta^{30}\text{Si}$ consistent with [1]. Their dissolution together with isotope fractionation through rapid precipitation of inorganic opal (opal A') during the ascent of pore fluids can produce isotopically heavy diagenetic fluids.

From these fluids porcelanite is precipitated only in narrow ranges of the host sediment characterized by extremely low detrital mineral contents.

High-spatial resolution analyses along profiles through two porcelanite layers by fs LA-MC-ICP-MS show opposing trends of $\delta^{30}\text{Si}$ and Al/Si ratios and indicate a kinetic control on the isotope fractionation factor, varying in response to the chemical composition of the fluid.

We identified processes of fluid generation, isotope fractionation, and chemical controls on precipitation during early stages of silica diagenesis that can well be extrapolated to conditions of ancient chert formation. The understanding of these processes can help discerning diagenetic fingerprints from source signals in the silicon isotope record of chert.

[1] Egan *et al.* (2012) *Geochim. Cosmochim. Acta.* **91**, 187-201.

U-Pb, Lu-Hf and Sm-Nd isotope systematics during polymetamorphism in the Ancient Gneiss Complex, Swaziland

J. TAYLOR*, A. GERDES AND A. ZEH

Institute of Geoscience, Frankfurt University, Altenhöferallee 1, 60438 Frankfurt
 (*correspondence: jeannerocks@gmail.com, gerdes@em.uni-frankfurt.de, a.zeh@em.uni-frankfurt.de)

This study aims to resolve some of the potential complexity associated with Archaean polymetamorphic gneiss terranes, with specific application to high-grade paragneisses from the Ancient Gneiss Complex (AGC) in Swaziland. Archaean zircons and monazites which have experienced multiple growth and/or alteration episodes, typically display a complexity in their zonation and U-Pb ages which is near impossible to resolve. However, Gerdes & Zeh [2] showed that the radiogenic Hf content of zircon, for example, remains constant during alteration, and changes only during new zircon growth; providing a robust tool to constrain the exact number of metamorphic cycles a rock has been through. The Sm-Nd system could provide a similarly useful tool. Monazite, allanite, apatite, rutile and titanite are U, Th and light-REE bearing phases, making them highly amenable for Sm-Nd and U-Pb isotope analysis [1]. This study represents a first attempt at investigating the simultaneous behaviour of the U-Pb, Lu-Hf and Sm-Nd isotope systems in accessory phases during polymetamorphism, by in situ LA-MC-ICP-MS analysis.

We investigate metasedimentary granulites from two separate, spatially related areas of outcrop in south-central Swaziland, which were subjected to multiple high-grade events throughout the Mesoarchaeon [3]. Zircons and monazites from these gneisses are particularly interesting in terms of the complexity in their zonation and U-Pb ages, with dominant age peaks at 3.51 Ga, 3.43 Ga, 3.40-3.39 Ga, 3.35 Ga, 3.33 Ga, 3.23-3.21 Ga, 3.18 Ga, 3.16 Ga, 3.11-3.07 Ga, and 2.99 Ga. The U-Pb, Lu-Hf and Sm-Nd isotope record in these grains may inform on: (1) the provenance of sediments from the south-eastern Kaapvaal Craton and the nature of the Archaean/Hadean hinterland; (2) the number of metamorphic episodes recorded; and (3) Archaean geodynamic processes during key events associated with early lithosphere assembly and crustal differentiation.

[1] Foster & Vance (2006) *JAAS* 21, 288-296. [2] Gerdes & Zeh (2009) *ChemGeol* 261, 230-243. [3] Taylor *et al.* (2012) *GeolSocAmBull* 124, 1191-1211.

Timing of ultra-high temperature (UHT) metamorphism and formation of incipient charnockites in the Kerala Khondalite Belt (KKB), southern India

R. TAYLOR*, C. CLARK AND I.C.W. FITZSIMONS

Dept of Applied Geology, Curtin University, Perth, Australia, (*richard.taylor@curtin.edu.au)

The Kerala Khondalite Belt, also known as The Trivandrum Block (TB), makes up the southernmost tectonic unit of the Indian Subcontinent and the southern extension of the microcontinent Azania. The TB is dominated by high-grade metasedimentary rocks typically either grt-bt felsic gneisses (locally referred to as leptynites) and graphite-bearing grt-crd-sill gneisses (khondalites). The leptynites and khondalites, together with a variety of igneous rocks, have been metamorphosed to granulite facies. Metamorphic conditions vary, with the lowest pressures and temperatures in the centre of the block (5 kbar, ~750°C), and a systematic increase to the north and south up to 8-9 kbar and <1000°C

Charnockites within the Trivandrum block typically form large-scale, orthopyroxene-bearing granitic bodies, such as those seen in the Nagercoil Block at India's southernmost tip. However the appearance of incipient charnockites is more enigmatic, forming metre-scale "patches" within host leptynites, one classic locality being near Kottavattom [1]

Charnockitisation in these rocks is identified as a late stage process related to fluid migration through the host rocks, resulting in some of the youngest ages for accessory phases in the KKB. SHRIMP U-Pb data for both zircon and monazite in the host leptynite and incipient charnockite patches, combined with rare earth elements (REE) in zircon, monazite and garnet have been used to investigate the timing of charnockitisation in relation to the UHT metamorphism in the region.

[1] Raith & Srikantappa (1993). *JMG*. 11. 815-832.

Determination of strontium-90 in seawater using TODGA chelating resin

HIROFUMI TAZOE^{1*}, TAKEYASU YAMAGATA²,
HAJIME OBATA³ AND MASATOSHI YAMADA¹

¹Institute of Radiation Emergency Medicine, Hirosaki University Aomori, Japan (*Correspondence. tazoe@cc.hirosaki-u.ac.jp)

²Atmosphere and Ocean Research Institute, The University of Tokyo, Tokyo, Japan

³College of Humanities and Sciences, Nihon University, Tokyo, Japan

Strontium-90 has been observed maximum values at late 1950s, which originated global fallout from nuclear weapons tests, and gradually reduced to about 1mBq/L in the Pacific Ocean (Pavinec *et al.*, 2012). The accidents of the Fukushima Daiichi Nuclear Power Plant in Japan and the leak of contaminated water released various radioactive nuclides. Casacuberta *et al.* (2012) estimated that amount of Sr-90 release to the sea based on the observed Sr-90/Cs-137 ratio and Cs-137 by modeling data was 90 - 900 TBq. However, Sr-90 data are limited because of its complicated analytical procedure. Determination of Sr-90 in seawater generally requires preconcentration of Sr and separation from Ca and other beta emitters. In this study, rapid and robust purification technique for the daughter radionuclides yttrium-90 of Sr-90 using TODGA chelating resin (Eichrom) without separation of Sr from Ca. TODGA resin shows high distribution coefficient in high HCl and HNO₃ concentrations.

Sr in seawater (20L) was preconcentrated by oxalate coprecipitation. Precipitates was decomposed to carbonate at 550°C and dissolved in HCl and conducted Fe hydroxide coprecipitation. After 2 weeks for ingrowth of Y-90, sample was conducted Fe hydroxide coprecipitation. Precipitate was filtered and redissolved in 7 mL of 12M HCl. Sample solution was flowed to the column combined anion exchange resin (3mL) and TODGA resin (2mL). Most of seawater matrix such as Sr, Ca and Mg were removed by Fe hydroxide coprecipitation and easily eluted 8M HCl from TODGA resin column. Fe and Bi were adsorbed to anion exchange resin. Pb and Bi were also eluted in 8M HCl fraction. Y was eluted by 20 mL of 0.1 M HCl. Y-90 was measured by low background gas flow proportional counter (Canberra LB-4100).

This analytical procedure was applied to seawater from the Pacific Ocean near the Japan Islands in January 2013. Averaged surface Sr-90 concentration was 0.95 ± 0.12 mBq/L, which is comparable to that before the accidents.

Regional modelling of Saharan dust

INA TEGEN¹ AND BERND HEINOLD¹

¹Leibniz Institute for Tropospheric Research, Leipzig, Germany

The Sahara desert in northern Africa is the world's largest source of dust aerosol. Regional-scale models help to understand processes involved in dust emission, transport and deposition, and are suited for comparisons with results of field studies like the SAharan Mineral DUst experiment (SAMUM) that aimed at improving the estimates of Saharan dust radiative forcing, or at understanding of dust deposition in the oceans. Models of modern atmospheric dust still often show considerable deviations from observations. One cause can be inadequacies in simulated meteorological fields that are used to compute dust emission fluxes. In contrast to global-scale dust models, regional dust models are expected to better reproduce individual dust events due to their higher grid resolution. Still, the representation of dust emission events that are related to precipitation events (haboobs, density currents) is problematic at grid resolutions that require parameterization of wet convection processes. New remote sensing products, together with the observations from recent field studies promise an improved understanding of dust regimes and are expected to lead to considerably improved dust models. We summarize findings of recent multi-year regional dust model studies and discuss open questions.

The halogen (F, Cl, Br) budget of continental granitoid plutonic rocks

H. TEIBER^{1*}, M. A. W. MARKS¹, T. WENZEL¹, W. SIEBEL¹,
R. ALTHERR² AND G. MARKL¹

¹Universität Tübingen, Mathematisch-Naturwissenschaftliche Fakultät, FB Geowissenschaften, Wilhelmstrasse 56, D-72074 Tübingen

(*correspondence: holger.teiber@uni-tuebingen.de)

²Ruprecht-Karls-Universität Heidelberg, Institut für Geowissenschaften, Im Neuenheimer Feld 234-236, D-69120 Heidelberg

The main goal of this study is to decipher the contribution of various volatile-bearing minerals to the whole-rock halogen (F, Cl, Br) budget of continental granitoid plutonic rocks and how this budget is governed by primary and secondary minerals. For this purpose, we investigated various granitoids with different volatile-bearing silicate mineral assemblages: (1) hornblende + biotite, (2) only biotite and (3) biotite + muscovite. Furthermore, accessory apatite is present in all samples, whereas fluorite and titanite occur only sporadically.

Halogens (F, Cl, Br) were extracted from the whole-rock powders by Pyrohydrolysis and subsequently analyzed by Ion Chromatography. Volatile-bearing minerals were analyzed for F and Cl by means of Electron Microprobe Analysis and for Br by Total Reflection X-ray Fluorescence.

All the investigated rock samples lie in the range of 500–3000 $\mu\text{g/g}$ F and 50–900 $\mu\text{g/g}$ Cl, respectively. In several samples, F and Cl contents of the whole-rocks roughly correlate with the halogen contents of apatite, biotite and mica and with the presence of fluorite. Br in the whole-rock powders is always $<1 \mu\text{g/g}$ and quantifiable Br concentrations were only found in few hornblende and apatite separates.

Importantly, detailed calculations of the whole-rock halogen budget (based on modal analysis) show strong misfits for many samples and indicate that appreciable amounts of F and Cl are not incorporated in the minerals mentioned before. Indeed, detailed X-ray mapping and short-term leaching experiments (2 minutes) confirm that significant amounts of F and Cl are present (1) in tiny secondary mineral phases, (2) in fluid inclusions and (3) potentially located along grain boundaries. These cannot be accounted for budget calculations based on modal amounts of the various minerals.

Thus, our study shows that great care has to be taken when using the halogen contents of whole-rocks for petrogenetic models, since significant amounts of halogens in whole-rocks might be of secondary origin.

U-Pb geochronology of detrital zircons from metasedimentary rocks from Formation of Desejosa, Serra do Marão, Portugal

R. J. S. TEIXEIRA^{1,2}, C. COKE^{1,3}, M. E. P. GOMES^{1,2}, R. DIAS^{3,4} AND L. O. MARTINS^{1,2*}

¹ Department of Geology, University of Trás-os-Montes e Alto Douro, Vila Real, Portugal, (ccoke@utad.pt, rteixeir@utad.pt, mgomes@utad.pt)

(lisa_martins@hotmail.com) (*presenting author)

² Geosciences Centre, University of Coimbra

³ Centro de Geofísica de Évora, Universidade de Évora

⁴ Universidade de Évora, Escola de Ciências e Tecnologia, Departamento de Geociências, Portugal, rdias@uevora.pt

The Serra do Marão area is located in the Central Iberian Zone and is dominated by an Ordovician sequence that rests on parallel unconformity on Cambrian/Neoproterozoic metasediments, belonging to Group of Douro. Two samples were collected from the upper formation of this Group (Formation of Desejosa): 1) a metapsamite from the top of this formation, which is characterized by a succession of metasilicic and phyllitic layers, and 2) an intraformational metaconglomerate. The U-Pb geochronological data obtained in detrital zircons by Laser Ablation-Quadrupole-Inductively Coupled Plasma Mass Spectrometry will help to constrain their maximum depositional age.

The U-Pb data set (52 detrital zircons with 99–107% and 33 detrital zircons with 85–103% concordant ages for metaconglomerate and metapsamite, respectively, is dominated by Neoproterozoic ages (84.6 % and 57.6 %), but there are few Cambrian (9.6 % and 9.1 %) and Paleoproterozoic (5.8 % and 3.0 %) ages. Mesoproterozoic detrital zircons are also present (6.1 %) in the metapsamite. Furthermore, a cluster of Ordovician ages in the metapsamite (24.2 %) yield a concordia age of $(465 \pm 16 \text{ Ma})$, which may reflect some Pb loss induced by the Early Ordovician felsic volcanism ($470.1\text{--}474.6 \text{ Ma}$) in the area.

The detrital zircon population of both samples record a long-lived Neoproterozoic magmatic episode, probably located near or at the northern Gondwana margin. However, the contribution of other sources containing Mesoproterozoic (1151–1088 Ma) and Paleoproterozoic (2257–1821 Ma) zircons must be considered. The U-Pb concordia age suggest a maximum depositional age of $522 \pm 26 \text{ Ma}$ for the metaconglomerate and an preliminary interval from $537 \pm 22 \text{ Ma}$ to $516 \pm 25 \text{ Ma}$ for the metapsamite.

Acknowledgements: Thanks are due to Petrochron project (PTDC/CTE-GIX/112561/2009).

U-Pb, Nd-Sr and geochemical fingerprints of granitic magmatism inside the Paleoproterozoic Mineiro belt, Southern São Francisco Craton: Evidence from the Ritápolis batholith

¹WILSON TEIXEIRA, ²CIRO A. ÁVILA,
³EVERTON M. BONGIOLO, ¹MARIA H. HOLLANDA ⁴
AND NATALI BARBOSA

¹ Inst. Geociências, USP, wteixeir@usp.br; holland@usp.br

² Museu Nacional, UFRJ, (avila@mn.ufrj.br)

³ Inst. Geociências, UFRJ, (ebongiolo@geologia.ufrj.br)

⁴ PhD program; Inst. Geociências, USP, natali@usp.br

The Mineiro belt (2.45-2.00 Ga) was created through accretionary arcs, ocean closure and eventual continent-continent collision. We document the case of the Ritápolis batholith (RB) – for which the U-Pb and Nd-Sr signatures and geochemistry provide new insights for the evolution of this belt. Dikes of the RB truncate the rocks of the so-called Resende Costa (2.36-2.33 Ga) arc. RB rocks vary from equigranular (fine-medium to coarse grained) to porphyritic with fenocrystals of plagioclase and microcline, showing igneous banding and different types of xenoliths (amphibolite, diorite, gabbro). LA-ICPMS U-Pb zircon dates yielded a crystallization age of 2149 ± 10 Ma (MSWD = 0.8) whereas the analyses from metamorphic rims yielded a lower intercept age of 662 ± 65 Ma, in agreement with the petrographic evidence. Seven Sm-Nd T_{DM} ages fall between 3.5-3.6 and 3.1-3.3 Ga with -4.9 to -7.7 $\epsilon_{Nd(t)}$ values, suggesting that Archean protholiths participated in magma genesis. The RB samples show calc-alkaline and peraluminous to light metaluminous signatures, although a few ones resemble trondhjemites. The observed gaps between the high- and low K_2O phases may be explained either by coeval rocks derived from different batches of at least two magma sources. High- and low K_2O phases show roughly similar chondrite-normalized REE patterns, but with peculiar features (e.g., strong negative Eu anomalies for the high K_2O group like evolved calc-alkaline rocks). This group also has low fractionated patterns in spider diagrams with enriched ratios when one considers the incompatible elements (e.g., Nd, Sm, Dy, Y, Yb and Lu). We conclude that the RB melts were derived in continental arc at 2150 Ma, placed opposite to the Serrinha intra-oceanic arc (2.23-2.20 Ga), as supported by geologic, isotopic and tectonic correlation.

Re-Os isotope and Platinum Group Element composition of Louisville Seamounts Chain, Pacific Ocean

M.L.G. TEJADA^{1*}, T. HANYU¹, A. ISHIKAWA^{1,2}, R. SENDA¹ AND K. SUZUKI¹

¹IFREE, Japan Agency for Marine-Earth Science and Technology, Yokosuka, 237-0061 Japan
(*Correspondence: mtejada@jamstec.go.jp)

²Department of Earth Science and Astronomy, The University of Tokyo, Tokyo, 153-8902 Japan

The Louisville Seamount Chain (LSC) is a ~4300 km-long hotspot trail believed to have been formed by passage of the oceanic lithosphere over a long-lived mantle upwelling in the south Pacific Ocean. Previous dredging on this hotspot chain recovered alkalic basalts that are fairly homogeneous in composition for the last 80 m.y. and geochemical data suggest affinity with the focal zone mantle end-member (FOZO) for the LSC. Recent IODP Expedition 330 recovered transitional to alkalic basalts from the ~50-77 Ma seamounts. This study aims to characterize the mantle source of the LSC in terms of Re-Os isotope and platinum group element (PGE) abundance and to gain knowledge on the temporal geochemical variation.

Our preliminary results from the older, ~65-77 Ma seamounts along the chain suggest that the Os isotopic composition (0.1270-0.1307) of the LSC basalts is close to estimates for the primitive upper mantle (PUM, 0.1262 [1] and 0.1296 [2]) and do not vary with the age of the seamounts sampled. This range of Os isotopic composition is similar to those of Rarotonga (0.124-0.139) and Samoan shield (0.1276-0.1313) basalts and tends to be lower than those of Cook-Austral (0.136-0.155) and Hawaiian shield (0.1283-0.1578) basalts. The PGE concentration in the LSC basalts are less fractionated than the Kilauea basalts but their Pt and Pd contents are much lower for the same range of MgO values. These differences in the relative abundances of the PGE may suggest low-degree melting of a mantle previously depleted of Pt and Pd for the source of the LSC.

[1] Meisel *et al.*, 2001, GCA 65, 1311-1323. [2] Walker *et al.*, 2002, GCA 66, 4187-4201.

Environmental fate and impacts of ceria nanomaterials: Distribution, transformation and bioaccumulation within aquatic mesocosms

M. TELLA^{1,2}, L. BROUSSET^{2,3}, M. AUFFAN^{1,2},
J. ISSARTEL³, C. PAILLES^{1,2}, B. ESPINASSE^{4,5},
E. ARTELLS^{2,3}, A. THIERY^{2,3}, C. SANTAELLA^{2,4},
W. ACHOUACK^{2,4}, A. MASON^{1,2}, I. KIEFFER⁵, J. ROSE¹,
AND J.-Y. BOTTERO^{1,2}

¹ CEREGE, CNRS-Aix Marseille Univ., Aix-en-Provence, France

² ICEINT, Aix-en-Provence, France

³ IMBE, CNRS Aix Marseille Univ., France

⁴ LEMIRE, CNRS Aix Marseille Univ., France

⁵ CNRS, Institut Néel, Grenoble, France

Ceria (CeO₂) NPs are largely used as oxidation catalysts, gas sensor, polishing materials, but also as UV absorber. Their attractiveness comes from the high oxygen storage capacity related to the easy Ce(III)/Ce(IV) redox cycle. The presence of Ce(III) within the structure of CeO₂ NPs enhance reactivity towards living organisms (prokaryotic and eukaryotic cells). Within the ANR-P2N MESONNET project, we determined the behavior of CeO₂-based nanoparticles (NPs) within aquatic mesocosms simulating a pond environment. Another challenge was to work with NPs contamination representative of concentrations expected in natural aquatic environments. Consequently, NPs were chronically applied to water column (0.1 mg L⁻¹ per injection). After 4 weeks, we determined the distribution of Ce in water, sediments and biota, speciation with X-ray absorption spectroscopy and oxidative stress in organisms was measured. Over time, NPs tend to hetero-aggregate and accumulate at the surface of sediments. A partial reduction of Ce from oxidized CeO₂ NPs was observed in the sediment. Bioaccumulation of major Ce(III) was also detected in digestive gland of pond organisms (snail, *Planorbarius corneus*) and correlated with a significant oxidative stress. In addition, using two kinds of CeO₂ NPs for experiments (organic-coated CeO₂-NPs used as paint additives (Nanobyk®), and “bare” CeO₂-NPs (Rhodia®), we highlighted the influence of CeNPs surface formulation on their fate into mesocosms and their reactivity towards organisms.

Effect of solution supersaturation and presence/absence of seeding crystals on the precipitation kinetics of celestite and strontianite

L. TEMGOUA^{1*}, A. CHAGNEAU^{1,2,3}, H. GECKEIS¹
AND T. SCHÄFER^{1,2}

¹ KIT-INE, P.O. Box 3640, 76021 Karlsruhe, Germany.

(*correspondence: louis.temgoua@kit.edu)

(aurelie.chagneau@kit.edu); (thorsten.schaefer@kit.edu)

² Freie Universität Berlin, Berlin, Germany.

³ Brgm, 3 avenue Claude Guillemin, BP 36009, Orléans, France.

In general, precipitation kinetic experiments allow us to determine parameters such as critical saturation index (SI_{crit}), rates of precipitation (R_{precip}) and induction time (t_{ind}) of nucleation. The objectives of this study follow a two-side approach: First we quantify the precipitation kinetics of the isostructural minerals celestite and strontianite over variable saturation indexes (SI) using the method of mixed flow reactors (MFR) in the presence of homogeneous seed crystals. Building on the findings of precipitation kinetics, we will investigate the sorption/incorporation of trivalent actinides/lanthanides in these Sr-minerals under comparable R_{precip} extending the work of [1]. In MFR experiments, equimolar solutions of SrCl₂ and Na₂SO₄ or Na₂CO₃ in 0.1M NaCl (background electrolyte) were fed through separate inlets in the reactor (v_{outflow} = 0.6 ml/min). Solution composition was monitored via ICP-OES and IC. R_{precip} of Celestite were calculated using the mass-balance equation to be ranging from 4*10⁻⁹ to 20*10⁻⁹ mol/ (m²s) for SI's from 0.2 to 1.4, respectively. Plotting R_{precip} vs. SI's showed a parabolic trend suggesting a surface controlled precipitation mechanism at low SI and 2-D nucleation at higher SI. The SI_{crit} was found to be at 0.5 for SrSO₄. t_{ind} between mixing of solutions and formation of the first cluster/colloid were determined by laser-induced breakdown detection (LIBD) in the absence of seeding material. t_{ind} decreased with increasing SI and two linear regressions could be performed with a change of slope at SI ~1.1. This SI is considered as the threshold for the transition between homogeneous and heterogeneous nucleation. The precipitation kinetics of celestite and strontianite will be compared and discussed with respect to nucleation mechanisms and metal uptake.

[1] Holliday, Chagneau, Schmidt, Claret, Schäfer, Stumpf (2012) Dalton Transactions 41, 3642. [2] Delos, Walther, Schäfer, Büchner (2008) J. Colloid Interface Sci. 324, 212.

Elemental sulfur biomineralization and preservation in glacial sulfide springs

TEMPLETON, A.S.^{1*}, LAU, G.², WRIGHT, K.³, WILLIAMSON, C.⁴, SPEAR, J.⁵ AND GRASBY, S.⁶

¹University of Colorado (*alexis.templeton@colorado.edu)

²University of Colorado (graham.lau@colorado.edu)

³University of Colorado (katherine.wright@colorado.edu)

⁴Colorado School of Mines (chawillia@gmail.com)

⁵Colorado School of Mines (jspear@mines.edu)

⁶Canadian Geological Survey (sgrasby@nrcan.gc.ca)

Microbial activity can control the abundance and distribution of sulfur species in environments far from chemical equilibrium, including the precipitation of intracellular and extracellular elemental sulfur in association with organic structures such as surface coatings, cell surfaces, filaments and sheaths. However, the potential for the generation and preservation of S⁰ mineral deposits that could serve as biosignatures of microbial sulfur cycling has not been extensively investigated. We will present a combination of synchrotron based x-ray spectroscopic, Raman, and pyrosequencing-based 16S rRNA and metagenomic data obtained from elemental sulfur deposits produced annually on the ice surface at Borup Fiord Pass in the Canadian High Arctic to define feed-backs between the geochemistry, microbial community composition, gene abundance, production of organic rich matrices and the chemical speciation of S⁰-rich deposits during their rapid precipitation and long-term preservation. This presentation will integrate findings from recently papers by Gleeson *et al.* [1], Wright *et al.* [2], Grasby *et al.* [3], as well as data from sulfur speciation mapping and x-ray absorption spectroscopy of modern sulfur deposits and “paleo” spring systems preserved in permafrost (Lau *et al.*, unpublished).

Gleeson *et al.* (2012) *Astrobiology* **12**, 135-150. Wright *et al.*

(2013) *Frontiers in Extreme Microbiology* **4**, doi: 10.3389.

Grasby *et al.* (2012) *Astrobiology* **12**, 1-10.

Habitability and Hydrogen Generation in Peridotite Aquifers

TEMPLETON, A.S.¹, MAYHEW, L.E.^{1*}, MILLER, H.¹, STREIT, L.² AND KELEMEN, P.²

¹University of Colorado (*lisa.mayhew@colorado.edu)

²Lamont-Doherty Earth Observatory, Columbia University.

The habitability of peridotite aquifers depends upon the rate of generation of energy sources such as H₂ and CH₄ during low-temperature water-rock interactions, as well as the availability of oxidants and nutrients required for microbial growth. Recent work by Mayhew *et al.* [1] suggests that olivine and pyroxene can produce substantial H₂ during water-rock interactions at ≤ 100°C through a surface-promoted mechanism where trace spinel phases such as magnetite, chromite and gahnite mediate electron transfer reactions between adsorbed Fe(II) and water. Mayhew *et al.* [1] also hypothesize microbial activity will be spatially localized to sites of H₂ production adjacent to spinel surfaces.

We will present this conceptual model for H₂-generation during low-temperature peridotite hydration, including synchrotron-based Fe K-edge multiple-energy μXRF and μXANES mapping of altered olivine, pyroxene and San Carlos peridotite before and after H₂ generation. We will also demonstrate that Oman harzburgites, which contain abundant Cr-spinels, produce the highest concentrations of H₂ measured in low-temperature water-rock reactions. Changes in the Fe-speciation associated with experimental H₂ generation by Oman peridotite will be compared against μXRF and μXANES data for samples that have experienced hydration and carbonation at near-surface temperatures in the Oman ophiolite [2]. Altogether, we suggest that extensive hydrogen generation should proceed at temperatures as low as 30°C during modern water-rock interaction in Oman and other peridotite aquifers, giving rise to an enormous potential for subsurface microbial activity when oxidants such as CO₂ are available to sustain microbial growth and methanogenesis.

[1] Mayhew *et al.* (in press) *Nature Geoscience* **6**. [2] Streit *et al.* (2012) *Contributions to Mineralogy and Petrology* **39**, 821-837.

Effect of Solution Chemistry on the Kinetics of Step Growth

H. HENRY TENG AND MINA HONG

Department of Chemistry, the George Washington University, Washington, DC 20052, USA (hteng@gwu.edu)

Crystal growth from solution propagates through the attachment of atoms/molecules (in the classical theory) to the growing surfaces or aggregation of nano building clusters (in the non-classical approach) to each other. While the thermodynamic driving force for the growth is well-understood and can be precisely determined via the saturation level of the solution, our grasp of the effect of other solution chemistry parameters, such as ionic strength and stoichiometry, on the growth kinetics remained loose. In the classical approach, the net growth rate of mono-molecular layers (ie, step velocity v_s) is assumed to be determined by the difference between fluxes of species attaching to and detaching from kinks along step edges. Such treatment leads to the development of the wide used relationship of $v_s = \beta[(a - a_c)/a_c]$ which states that v_s scales linearly with the solute activity a relative to its equilibrium value a_c (the kinetic coefficient β characterizes the enthalpic and entropic barriers for solute incorporation, including desolvation of growth sites and solute particles). It then follows that v_s should be controlled solely by the solution saturation under similar T and P conditions. Yet, literature data from numerous cases argued strongly against this supposition. In this study, we conducted a series of in situ AFM experiments to interrogate the effect of solution chemistry parameters other than supersaturation on step kinetics using calcite as a model system. We found step kinetics were strongly affected by solution pH, ionic strength SI, and the $[Ca^{2+}]/[CO_3^{2-}]$ ratio, and the impact differs in different directions (obtuse vs. acute steps on the $\{104\}$ cleavage faces). For example, while the v_s of acute steps decreased with increasing pH, the obtuse step rate showed little response to pH change. More interestingly, both sides exhibited a sharp trend transition (varied degree of positive $v_s - pH$ dependence) starting at $pH \sim 9.5$. In addition, step velocity in both directions decreased with increasing SI, but the trend became significantly weakened in the acute direction when $SI > 0.1$. The effect of cation-anion ratio on step kinetics appeared to be more complex. A maximum speed was achieved at different values of $[Ca^{2+}]/[CO_3^{2-}]$ for obtuse and acute steps, and the ratio seemed to decrease with increasing pH. These observations strongly suggest that, although supersaturation is the driving force for aqueous phase crystallization, solution chemistry plays critical roles in controlling the actual growth rate and needs to be taken into consideration in kinetic studies of crystallization.

Are molybdenum concentrations and isotopes a tracer for anthropogenic pollution in the atmosphere?

A. TENNANT¹, S. LANE¹, B. PROEMSE² AND M. WIESER^{1*}

¹Department of Physics and Astronomy, University of Calgary, 2500 University Drive NW, Calgary, Alberta, Canada, T2N 1N4

(*presenting author, mwieser@ucalgary.ca)

²Department of Geoscience, University of Calgary, 2500 University Drive NW, Calgary, Alberta, Canada, T2N 1N4

The trace metal molybdenum (Mo) is not very abundant in the environment but has found numerous applications in anthropogenic activities. For instance, in the form of Mo sulphide (MoS_2) it is a component of diesel fuel. Mo is used as a catalyst in many engines and is believed to be the most efficient catalyst for the hydrocracking of bitumen [1]. Molybdenum has even been suggested as a fertilizer additive [2] and has also been found in coal-fired power plant emissions [3]. Hence, anthropogenic activities may release Mo in larger amounts to the environment that may affect terrestrial and aquatic ecosystems (e.g. via its coupling with the N cycle). We have therefore investigated the potential of Mo concentration and isotope ratio measurements as a tracer of anthropogenic emissions.

We measured the molybdenum (Mo) isotopic composition of aerosols collected on Teflon air filters [4]. Airborne Mo was collected at selected locations including a residence in the city of Calgary, Canada, the isotope laboratory at the University of Calgary, the University of Calgary weather station, and the City of Calgary Transit bus garage where the city buses start and idle for extended periods. Concentrations ranged from 0.07 ng/m^3 in the laboratory to 19.0 ng/m^3 in the bus garage. The $\delta^{98/95}Mo$ values measured for the different urban sampling sites (reported relative to SRM 3134) ranged from -0.18 to $+0.94 \text{ ‰}$. The results of this investigation suggest that measurements of Mo concentrations and isotopic compositions have the potential to trace anthropogenic emissions in an urban environment.

[1] Zekel *et al.* (2009), *Solid Fuel Chem.* 43, 290-294. [2] Bandyopadhyay *et al.* (2008), *J. Agric. Food Chem.* 56, 1343-1349. [3] Goodarzi (2006), *Int. J. Coal Geol.* 65, 17-25. [4] Lane *et al.* (2013), *Anal. Bioanal. Chem.* 405, 2957-2963.

Controls on dissolved REE and HFSE in glacial meltwater rivers in southern Iceland

NATHALIE TEPE* AND MICHAEL BAU

Earth and Space Sciences, Jacobs University Bremen, Campus Ring 1, Bremen, Germany,

(*correspondence: n.tepe@jacobs-university.de)

The chemical composition of river waters in southern Iceland is strongly affected by geological events such as volcanic eruptions (e.g., the Eyjafjallajökull in 2010), due to the input of nanoparticles and colloids from volcanic ashes.

In this study, water samples from twelve rivers and volcanic ashes were sampled twice in 2010, and once in 2011 and 2012 to characterize the geochemistry of glacial meltwaters and to investigate the impact of colloids and nanoparticles from volcanic ashes on their chemistry. The REE and other HFSE (e.g., Th, Zr, Nb and Hf) are characterized by low solubilities and high particle-reactivities. In oxic natural waters, therefore, they are not truly dissolved, but typically associated with particulates. In 0.45 μm -filtered water samples they are often well-below the lower limit of determination by analytical techniques such as ICPMS. Comparison of the trace element distribution of river particulates (i.e. filter residues) and volcanic ash to that of the respective 0.45 μm -filtered glacial meltwater (i.e. sum of truly-dissolved trace elements and those that are bound to colloid-/nano-sized particles <0.45 μm) reveals very close similarities.

In 2010, rivers in SW Iceland were affected by the Eyjafjallajökull eruption, while those in the SE were not. $\text{La}_{\text{CN}}/\text{Yb}_{\text{CN}}$ ratios of filter residues in the SW are in a similar range as the Eyjafjallajökull ash (EJ-1: 6.16; EJ-2: 6.58 [1]). River waters, which were sampled in August 2010, show a higher variability in the $\text{La}_{\text{CN}}/\text{Yb}_{\text{CN}}$ ratio and range between 1.46 and 6.96 in the SW and 1.46 and 5.94 in the SE, but the SW rivers, which were sampled 25 days after the Eyjafjallajökull eruptions, show higher $\text{La}_{\text{CN}}/\text{Yb}_{\text{CN}}$ ratios between 7.17 and 9.40. In 2011, an earthquake and a subsequent minor eruption underneath the glacier of Katla volcano caused enhanced glacial flow at the Múlavísl river, which was accompanied by high trace element concentrations. Its $\text{La}_{\text{CN}}/\text{Yb}_{\text{CN}}$ ratio of 13.5 was significant higher in 2011 than in 2010 (2.64) and 2012 (8.73). Moreover, in 2011, the Zr concentration was 222 ppt, which is several orders of magnitudes higher than in 2010 and in 2012.

These results strongly suggest that natural nanoparticles and colloids of a size <0.45 μm control the dissolved REE and HFSE distribution in these rivers.

[1] Sigmarsson *et al.* (2011), *Solid Earth* 2, 271-281.

An improved hot-alkaline DNA extraction method for high cell-lysis efficiency of subseafloor microbial communities

TAKESHI TERADA^{1*}, YUKI MORONO²,
TATSUHIKO HOSHINO² AND FUMIO INAGAKI²

¹Marine Works Japan Ltd., Oppamahigashi 3-54-1, Yokosuka 237-0063, Japan. (*correspondence: teradat@mwj.co.jp)

²Geomicrobiology Group, Kochi Institute for Core Sample Research, Japan Agency for Marine-Earth Science and Technology (JAMSTEC), Monobe B200, Nankoku, Kochi 783-8502, Japan.

One of the prerequisites for DNA-based microbial community analysis is the high cell-lysis efficiency –the critical issue has been long ignored or paid very little attention despite of its significance. In fact, using a commonly used DNA extraction kit, ~80% or more of microbial cells in marine sediment are still remained as the intact form (i.e., DNA-stainable cells), indicating that the large DNA fraction of microbial components are initially biased prior to the subsequent molecular analyses.

To address this technical problem, we standardized a new DNA extraction method with alkaline treatment and heating. First, we attempted to destroy all microbial cells in subseafloor sediment samples from different depths by adding 1 M NaOH at 98 °C for 20 minutes, which treatment disrupted more than 98% of the cells in the examined samples. The DNA integrity test showed, however, that such strong alkaline and heat treatment also destroyed DNA molecules into short fragments, which could not be used for PCR-based molecular analyses. Subsequently, we optimized the alkaline and temperature condition to minimize DNA fragmentation with high cell-lysis efficiency: the best condition we standardized resulted in 50-80% of cell disruption with successfully keeping enough DNA integrity for the amplification of complete 16S rRNA gene (i.e., ~1500 bp). Also, the optimized method yielded higher DNA concentrations than those extracted by a conventional kit-based approach in all tested samples. Consequently, using the newly developed hot-alkaline method, community structure analysis of the extracted DNA assessed by quantitative real-time PCR and pyrosequencing of 16S rRNA genes showed a clear difference to the result using conventional methods, suggesting the better analytical coverage of subseafloor microbial communities than those by the conventional methods.

Sources and concentrations of Highly Siderophile Elements in VHMS deposits through time

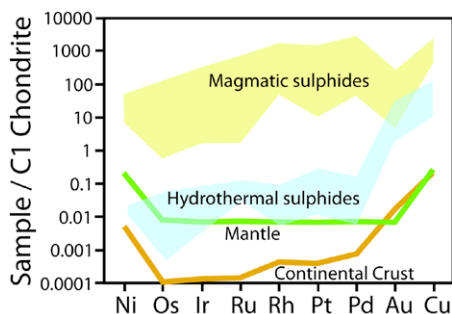
SVETLANA TESSALINA

John de Laeter Centre, Curtin University, Perth, Australia

The seafloor hydrothermal activity is an important mechanism of metals cycling between mantle and continental crust, producing Volcanogenic Hydrothermal Massive Sulphide deposits in various tectonic settings through time.

Concentrations and sources of Highly Siderophile Elements (HSE: Ru, Rh, Pd, Re, Os, Ir, Pt Au) were studied in VHMS deposits from Archean to present using new and published Re-Os isotopic data and the HSE concentrations.

In general, concentrations of HSE, as normalised to C1-chondrite, are situated slightly above the mantle values, with the exception of higher Au contents; and approximately 3 orders of magnitude lower compare to magmatic sulphides.



Remarkably, the Re/(Common Os) ratio significantly increase from Archean deposits in intra-cratonic setting to the Palaeozoic VHMS deposits in island arc setting, reaching the highest values in modern sulphides from MORB setting, with simultaneous decrease in Common Os values. This observations may be related with the change in main metal sources relative to different tectonic settings through time.

Rhenium enrichment in modern VHMS deposits may be also related with higher Re contents in present day seawater, which is along with hydrothermal fluid is one of the main sources of metals in VHMS deposits. Modern seawater is characterised by high Re/Os ratio of ~730, whereas hydrothermal fluid has much lower Re/Os ratio. In general, the Re/Os ratio increases and Os contents decrease by 2 order of magnitude from the stockwork toward the seafloor sulphides, reflecting the fluid - seawater mixing. The same pattern has been observed across hydrothermal chimneys, with higher Re/Os ratio and lower Os contents toward the outer part of chimney. This pattern is confirmed by $^{187}\text{Os}/^{188}\text{Os}$ isotopic mixing between these two end-members, as it was shown for modern and ancient VHMS systems.

Levels and distribution of traffic related metals in Israel; Pb, Zn and platinum group metals (PGM)

N. TEUTSCH*, L. HALICZ AND Y. HARLAVAN

Geological Survey of Israel, 30 Malkhe Israel, Jerusalem, Israel (*correspondence: nadya.teutsch@gsi.gov.il)

Since 1993, automobile exhaust catalysts are compulsory in Israel which obviously lead to a great improvement in the emission of toxic gases to the atmosphere. However, as these converters contain Rh, Pd and Pt, which belong to the platinum group metals (PGM), their utilization has introduced a new contamination source to the environment.

For characterizing the extent of PGM contamination in Israel, road side soils were examined in four locations adjacent to main roads. In all sites, Pt concentrations in soils were relatively low compared to published values [1] (mostly up to 20 ng/g) and could be detected only in top soils. While Rh concentrations were below limit of detection (10 ng/g), high concentrations of Rh and Pt were found in mixed soil and dust surface samples.

Road dust collected along a half km inclined road with heavy traffic yielded very high concentrations of both Pt and Rh (260 to 1480 ng/g and 80 to 440 ng/g, respectively). Remarkable difference was observed between the uphill and downhill at the same location where concentrations uphill were 4-fold higher than downhill direction for both metals, indicating significant PGM emission with increased engine activity.

Elevated trace metal concentrations of traffic related metals (Cr, Cu, Ni, Pb and Zn) were noted for the road dust samples. However, only Zn concentrations exhibit a positive correlation with Pt and Rh concentrations and display a distinct 2-fold enrichment in the uphill direction probably due to tire friction. On a plot of $^{208}\text{Pb}/^{206}\text{Pb}$ vs. $^{206}\text{Pb}/^{207}\text{Pb}$ along with potential Pb sources, all samples are slightly shifted from a mixing line between the known Pb IC petrol values used in Israel and natural sources. No systematic hill slope pattern was observed. The slight shift of data points from mixing suggests an additional yet undefined, anthropogenic source. Hence, while PGM metals and Zn exhibit current contamination, Pb probably represents re-suspension of dust and soil surfaces that still carry the pre-unleaded petrol signature.

[1] Rauch & Morrison (2008) *Elements* 4, 259-263.

Discovery of a "vital" bacterial effect in the formation of biogenic carbonates

CAROLINE THALER^{1*}, MAGALI ADER¹,
BÉNÉDICTE MÉNEZ¹ AND FRANÇOIS GUYOT¹

¹ Institut de Physique du Globe de Paris, Université Paris Diderot, 1, rue Jussieu, 75238 Paris cedex 05, France
(*Correspondence: thaler@ipgp.fr, ader@ipgp.fr, menez@ipgp.fr, Francois.Guyot@impmc.jussieu.fr)

Carbon and oxygen stable isotope compositions of carbonates are widely used to provide information on their conditions of precipitation. However, most carbonates result from a biological activity, which in the case of some skeleton-forming eukaryotic organisms has been shown to lead to isotopic characteristics that differ from those expected for isotope equilibrium. The origin of this difference remains poorly understood and is referred to as the "vital effect". So far, potential microbial vital effects have been overlooked and microbial carbonation is considered from an oxygen isotope perspective as occurring at equilibrium with water. We revisit this assumption by performing an isotope study of carbonates precipitation by the strain *Sporosarcina pasteurii*, a bacterial model of carbonatogen metabolisms. Its ureolytic activity produces ammonia (thus increasing the pH) and dissolved inorganic carbon (DIC) that precipitates as solid carbonates. $\delta^{18}\text{O}_{\text{CaCO}_3}$ results show values up to 20‰ lower than what was expected for carbonate precipitation in equilibrium with water. This demonstrates for the first time that bacteria may precipitate carbonates with a vital effect. The addition of carbonic anhydrase, an enzyme able to equilibrate the oxygen isotopes between DIC and water, yields equilibrium values. This result demonstrates that the vital effect observed in solid carbonates results from disequilibrium between DIC and water, a mechanism also strongly suspected to account for vital effects in skeleton-forming organisms.

X-Ray Spectroscopy and Spectromicroscopy Study of Sulfur Speciation in Urban Soils

J. THIEME¹ AND M. MATHES²

¹ NSLS-II, Brookhaven National Laboratory, Building 743, Upton, NY-11973, USA, e-mail:(jthieme@bnl.gov)
² Institute for X-Ray Physics, University of Goettingen, Friedrich-Hund-Platz 1, 37077 Goettingen, Germany

This study shows the applicability of sulfur x-ray spectroscopy and spectromicroscopy to analytical problems in urban soils.

A combination of x-ray microscopy, elemental mapping and XANES spectroscopy at the K-absorption edge of sulfur was used to analyze the elemental and particulate composition of an urban soil loaded with debris from WWII, exemplarily from Berlin, Germany. The goal was to specify and analyze the sulfur pool of soils with major anthropogenic impact, i.e. the dumping of war debris. This impact obviously influences soil composition and soil formation processes, but may, due to sulfate leaching, also be a substantial risk to urban water quality. The sulfur load of different debris components was studied and the sulfur content of different soil samples was evaluated and correlated to different parameters, such as position of the respective soil horizon within the soil profile or location of the soil profile in the surrounding terrain. With XANES spectroscopy, the averaged sulfur pool of whole soil horizons as well as of single debris components was studied. With X-ray fluorescence imaging and spectromicroscopy, soil aggregates, debris particles, and soil solution were analyzed on the micrometer and sub-micrometer scale. Different soil and debris constituents could be assigned to elemental distribution patterns within collected fluorescence maps, allowing for a detailed analysis of the sulfur pool and release from war debris in subsequent studies. These measurements show highly heterogeneous sample composition and clear gradients in sulfur speciation and oxidation state within single particles. The weathering of the anthropogenic material is therefore directly observable. A detailed understanding of this sulfur lixiviation is central to preserve urban water quality.

Advances in Mass Independent Isotopic Studies

MARK H. THIEMENS¹

¹Departement of Chemistry and Biochemistry 0356
University California, San Diego. La Jolla, CA
(mthiemens@ucsd.edu)

Since the first discovery of a chemically produced mass independent isotopic fractionation process by Thiemens and Heidenreich in 1983 the extent of applications of MIF in nature has expanded across a extensive range of applications that encompass much of terrestrial geochemistry, cosmochemistry, atmospheric science, and climate analysis. Time scales extend from the present to the origin of the solar system, more than 4.5 billion years ago to present. The creation of the INTRAMIF program exemplifies the extent of these investigations.

In the original work on ozone formation, it was shown there is not only a mass independent fractionation that duplicated the pattern observed in meteorites in oxygen and consequently has application in solar system evolution. A major follow up to that work is determining the actual physical chemical mechanism responsible for the effect, which remains elusive to this day. The role of chemical processes in the early solar system for the source of the anomaly in the early solar system is now agreed upon as compared to nuclear processes. Very recent experimental work has deepened understanding of processes will be presented.

The process of formation of isotopically anomalous ozone in the atmosphere has been used to trace chemical and dynamical processes in the atmosphere and has been applied to most major cycles. This includes SO_x, NO_x, CO₂, CO, N₂O, water, carbonates, chlorates, and O₂. The use of high sensitivity analysis of these species has been demonstrated to provide an analytical tool to decipher chemical reaction pathways which are otherwise identifiable by conventional technique as a consequence of using multiple isotope ratio measurements.

Through polar ice studies these processes have been studied through long time scales (present – Holocene). Sulfur isotope measurements have opened a new dimension in tracking the origin and evolution of oxygen in the earth's earliest environment. Recent work has shown that from Mars meteorite oxygen analysis of bulk silicate, water, and secondary minerals that the processes of Mars formation and evolution is less well understood than previously believed and will be discussed.

Modeling non-equilibrium uptake of Se(IV) upon calcite precipitation

BRUNO THIEN¹, FRANK HEBERLING²
AND DMITRII A. KULIK³

¹LES, Paul Scherrer Institut, 5232 Villigen, Switzerland
(bruno.thien@psi.ch)

²INE, Karlsruher Institut für Technologie, 76131 Karlsruhe, Germany (frank.heberling@kit.edu)

³LES, Paul Scherrer Institut, 5232 Villigen, Switzerland
(dmitrii.kulik@psi.ch)

Selenium is relevant as a nutrient or poison for animal and human life, and as long-lived radionuclide ⁷⁹Se in the context of nuclear waste management. We investigated time-dependent Se uptake by growing calcite as a possible way of Se immobilization. Calcite precipitation from aqueous solutions in presence of Se(IV)O₃²⁻ was studied under the surface-controlled steady state conditions at low-to-moderate supersaturation in mixed flow reactor (MFR) experiments [1]. We then simulated MFR experiments using the GEM-Selektor v.3 geochemical code [2].

Calcite precipitation rates predicted using [3] were systematically higher than the rates observed in MFR experiments in Se(IV) - containing solutions. This corroborates the inhibiting effect of aqueous Se(IV) on calcite growth reported before [4]. To account for this effect, an inhibition term involving the Se(IV)O₃²⁻ ion activity was added to the rate equation [3].

Measured amounts of Se(IV) incorporated in calcite overgrowths are substantially higher than those predicted by the atomistic calculations for the solid solution- aqueous solution equilibrium [1]. This can be interpreted by invoking an extremely strong surface growth entrapment mechanism, accounted for in our unified uptake kinetics model [5]. This model was able to describe the observed concentrations of Se(IV) in calcite overgrowths by considering a very high Se surface enrichment factor (1.5·10⁷) with a rather low sub-surface diffusivity (10⁻¹⁰ nm²/s). These parameters for Se(IV) oxyanion differ significantly from those typically used in modeling entrapment effects for cations (Sr, Cd, Co) in calcite [5]. Possible reasons for this difference will be discussed.

[1] Heberling *et al.*, in prep. [2] <http://gems.web.psi.ch>; Kulik *et al.*, this conference. [3] Wolthers *et al.* (2012) *GCA* **77**, 121-134. [4] Renard *et al.* *Chem. Geol.* **340**, 151-161. [5] Thien *et al.*, in prep.

The PSI/Nagra Chemical Thermodynamic Database 12/07: Present status and future developments

T. THOENEN^{1*}, W. HUMMEL¹ AND U. BERNER¹

¹Laboratory for Waste Management, Paul Scherrer Institut, 5232 Villigen PSI, Switzerland (*correspondence: tres.thoenen@psi.ch)

The PSI/Nagra TDB has been updated from version 01/01 [1] to version 12/07 to support the ongoing safety assessments for a deep underground repository for radioactive waste in Switzerland. TDB 12/07 contains three types of data: (1) Core data are widely accepted data of high-quality that are mainly based on the CODATA key values. (2) Recommended data are also of high quality, but they originate from rather active fields in the environmental sciences and may be revised over time. They are mainly based on the critical reviews of data for U, Am, Tc, Np, Pu, Ni, Se, Zr, and Th provided by NEA in their "Chemical Thermodynamics" series. (3) Supplemental data are suitable for scoping calculations. Some estimates are made in cases where their omission would lead to obviously erroneous results. TDB 12/07 is provided for use with the geochemical modeling codes GEMS [2] and PHREEQC [3].

Further development of the database will run along the following lines: (1) Data for Sn will be included from the latest NEA review [4] and for Fe and Mo from forthcoming NEA reviews, as well as data from the IUPAC reviews, e.g. [5], on the chemical speciation of environmentally significant metals (at present Hg, Cu, Pb, and Cd). (2) Since a large part of the data included in TDB 12/07 is applicable only at 25°C, estimation methods [6] have to be considered for extending the application range to the higher temperatures expected in the repository environment. (3) Experimental data were reduced to zero ionic strength by NEA and IUPAC using the specific ion interaction theory SIT [6]. SIT coefficients are not known for many aqueous species (especially in NaCl background media). In order to use the SIT in geochemical modeling of natural systems, estimation methods have to be found to fill these gaps.

[1] Hummel *et al.* (2002) Nagra/PSI Chemical Thermodynamic Data Base 01/01. Nagra NTB 02-16. Nagra, Wettingen, Switzerland. [2] Kulik *et al.* (2013) *Min. Mag.* (this volume). [3] Parkhurst *et al.* (1999) Water-Resources Investigations Report 99-4259, Denver. [4] Gamsjäger *et al.* (2012) Chemical Thermodynamics of Tin. OECD Publications, Paris. [5] Powell *et al.* (2011) *Pure Appl. Chem.* **83**, 1163-1214. [6] Grenthe *et al.* (eds.) (1997) Modelling in Aquatic Systems. OECD Publications, Paris.

Biogeochemical cycling of nitrogen on the early Earth

CHRISTOPHE THOMAZO¹, DOMINIC PAPINEAU²
AND MAGALI ADER³

¹UMR-CNRS 6282 Biogéosciences, Université de Bourgogne, France; (christophe.thomazo@u-bourgogne.fr)

²Geophysical Lab, Carnegie Institution of Washington, USA; (dominic.papineau@bc.edu)

³Institut de Physique du Globe de Paris, France; ader@ipgp.fr

There has been considerable recent interest in variations of the nitrogen isotope composition of ancient organic matter and associated sediments as they provide clues for the early evolution of Earth's atmosphere-ocean-biosphere system. In particular, large $\delta^{15}\text{N}$ isotopic variations recorded from the Mesoarchean to the Paleoproterozoic have been linked to the evolution of the biogeochemical cycle of nitrogen toward its modern –microbially mediated– web of reactions. The biogeochemistry of nitrogen is strongly dependent upon oxidation-reduction reactions, and thus secular variations in $\delta^{15}\text{N}$ most probably underline the protracted oxygenation of Earth's oceans and atmosphere, during a period of roughly 700 Ma between 2.7 and 2.0 Ga.

This contribution provides a synthesis of observations made so far from Archean to Mesoproterozoic sedimentary environments. We present an extensive $\delta^{15}\text{N}$ database: 874 published $\delta^{15}\text{N}$ values measured on various sedimentary lithologies and phases, including kerogen, phyllosilicates, shales, carbonates, cherts, Banded Iron Formations and N_2 -bearing fluid inclusions. The compilation spans from 3.8 Ga to 1.4 Ga and we use statistical methods (Gaussian Kernel functions) applied to geochemical times series for its analysis.

Accordingly, we suggest that the anaerobic process of nitrogen fixation and ammonium assimilation evolved early in biological evolution during the Paleoproterozoic or earlier. Meso- to Neoproterozoic ^{15}N enrichment of +15‰ in average and up to +50‰ most probably record the initiation of the oxidative part of the nitrogen cycle including nitrification and denitrification. A second positive nitrogen isotope excursion is recorded during the Paleoproterozoic at around 2.0 Ga and might reflect the fluctuation of a redox transition zone where NH_4^+ would be present in the deep anoxic ocean and NO_2^- and NO_3^- would accumulate above the oxic-anoxic interface in response to increasing atmospheric and oceanic oxygen concentrations. A complete nitrogen biogeochemical cycle including its oxidative part might thus be recorded since the Paleoproterozoic, in line with the view that free oxygen had stabilized NO_3^- in the surface oceans by that time. Increasing number of $\delta^{15}\text{N}$ measurements through the Precambrian rocks record would help to refine these interpretations.

An experimental investigation of the formation mechanisms of superdeep diamonds

A.R. THOMSON*, M.J. WALTER, S.C. KOHN,
G.P. BULANOVA AND C.B. SMITH

School of Earth Sciences, University of Bristol, Bristol, BS8
1RJ (*correspondence: (andrew.thomson@bristol.ac.uk)

The subduction of oceanic crust is not only a fundamental driving force of mantle convection, but also an integral part of the Earth's deep carbon cycle. Subducted material provides almost all of the return flow of carbon to the earth's interior [1]. Seismic tomography suggests that slabs can penetrate into the deep mantle, thus carbon can potentially be delivered into the transition zone and/or lower mantle and react with ambient mantle [2].

Recent studies of superdeep diamonds from the Collier-4 [3] and Juina-5 [4] kimberlite pipes in Brazil have found direct evidence for such processes. The diamonds show complex growth structures, are composed of isotopically light carbon (ranging up to -25‰) and contain mineral inclusions with compositions expected to form from a mafic protolith in the transition zone and/or lower mantle all of which are consistent with a key role of subducted material in their origin. It has also been observed that former calcium silicate perovskite inclusions have extremely enriched trace element abundances, with REE and HFSE up to 20,000 times primitive mantle [5]. Geochemical modelling suggests that inclusions, and their diamond hosts, crystallised from a low degree carbonated melt of subducted basalt in the transition zone upon reaction with ambient mantle [5].

This study aims to test the model of superdeep diamond growth by experimentally investigating the liquidus phase relations and reactions that occur when an oxidized carbonated melt interacts with reducing mantle peridotite. The bulk composition used to determine the appropriate melt composition represents ODP hole 1256D basalt samples containing 2.5wt% CO₂. Initial multi-anvil experiments at 20 GPa show that two immiscible melts, a Na-rich carbonate melt (~16wt% Na₂O) and a Na-bearing 'granite' melt (>70wt% SiO₂) coexist with majorite at 1400-1500°C. We will report on ongoing experiments in which these melt compositions are reacted with reducing peridotite .

[1] Dasgupta & Hirschmann (2010), *EPSL* 298, 1-13. [2] Rohrbach & Schmidt (2011), *Nature* 472, 209-212. [3] Bulanova *et al.* (2010), *Cont. Min. Pet.* 160, 489-510. [4] Walter *et al.* (2011), *Science* 334, 54-57. [5] Thomson *et al.* (2012), *Min. Mag.* 76(6), 2455.

Bacterial communities inside soil iron nodules

R.L. THORNE¹* A.H. KAKSONEN² AND R. ANAND¹

¹ CSIRO Earth Science and Resource Engineering, ARRC,
Kensington, WA,6151, Australia (*correspondence:
robert.thorne@csiro.au)

² CSIRO Land and Water, Underwood Ave, Floreat WA 6014,
Australia (anna.kaksonen@csiro.au)

Iron nodules are found in a wide variety of surficial environments across the globe [1, 2] and iron spherules of a similar size and morphology are even found within the sediments of Mars [3].

Iron nodules from soils in Western Australia are homogenous, compound and concentric and dominated by hematite and maghemite. Nodule formation has been attributed to weathering and the mobilisation and migration of Fe²⁺ in response to variations in redox potential and differential drying [1].

Bacterial communities within the soil nodules were investigated using cloning and sequencing of polymerase chain reaction amplified 16S rRNA genes. The results showed that the nodules contain a phylogenetically diverse bacterial community dominated by members of *Acidobacteria*, *Actinobacteria* and *Proteobacteria*.

The metabolic potential of uncultivated organisms within the soil nodules can be phylogenetically assessed by a comparison with related sequences from environmental clones or cultured bacteria. The results show that some clone sequences closely resemble cultured Fe-oxidising bacteria and clones from environments with high concentrations of iron. The combination of geochemical and bacterial studies can provide new insights into nodule formation and the role bacteria play in the mineralisation process.

[1] Anand (2002) *Aust. J. Earth Sci* 49, 3-162. [2] Reoloid *et al* (2008) *Sed. Geol* 203, 1-16 [3] Squyres *et al* (2004) *Science* 306, 1709-1714.

Reactive transport modeling of carbon, chlorine, and hydrogen CSIA data to improve monitored natural attenuation for chlorinated ethenes

HÉLOÏSE A.A. THOUMENT^{1*}, MINDY VANDERFORD²,
TOMASZ KUDER³, PAUL PHILP³
AND BORIS M. VAN BREUKELEN¹

¹VU Univ. Amsterdam, De Boelelaan 1085, NL-1081 HV
Amsterdam, The Netherlands,
(*correspondence: h.a.a.thouement@vu.nl)

²GSI Environmental, Inc., Houston, Texas, USA

³Univ. Oklahoma, Norman, OK 73019 USA

Compound-specific stable isotope analysis (CSIA) has been shown to provide an improved insight into the monitored natural attenuation (MNA) of chlorinated solvents. The work presented here focuses on the simulation of carbon (C), hydrogen (H), and chlorine (Cl) isotopes of chlorinated ethenes with a reactive transport model (RTM) calibrated by CSIA data. Such a model allows for the simulation of variations in concentrations and isotope ratios in aquifer systems as result of various degradation pathways and transport processes. The base RTM model was calibrated for C, H, and Cl isotope fractionation observed during complete reductive dechlorination of TCE in a microcosm experiment. Secondly, the Operational Unit 10 at the Hill Air Force Base site (Utah, USA) was intensively sampled. This intricate site presents two plumes of chlorinated solvents (PCE and TCE), which partly mix. Moreover, based on earlier MNA studies, both reductive dechlorination and aerobic oxidation are likely to occur as the aquifer conditions range from oxic to anoxic. The model aids in drawing a better picture of the fate of those plumes, as each transformation process induces distinctive isotope fractionation patterns for the different elements.

Results/Lessons learned

We present (i) the model background, which includes the highlights provided by the microcosm experiment, discuss (ii) the collection of CSIA data at the complex field site, and illustrate (iii) potential applications of the model, notably for the interpretation of the above-mentioned field data. The use of CSIA data at the field site reveals the complexity of the studied aquifer, where degradation is shown to mostly occur in restricted areas.

Relevance of mass transfer processes for the interpretation of stable isotope fractionation

MARTIN THULLNER^{1*}, FLORIAN CENTLER², ANKO
FISCHER³, FALK HESSE⁴, HANS-H. RICHNOW⁵
AND LUKAS Y. WICK⁶

¹Department of Environmental Microbiology, Helmholtz
Centre for Environmental Research – UFZ, Leipzig,
Germany; * (correspondence: martin.thullner@ufz.de)

²Department of Isotope Biogeochemistry, Helmholtz Centre
for Environmental Research – UFZ, Leipzig, Germany

³Isodetect – Company for Isotope Monitoring, Leipzig,
Germany

In recent years, compound specific stable isotope analysis (CSIA) has become an established tool for assessing (bio)degradation of organic contaminants within aquifers. The fractionation of stable isotopes during degradation leads to observable shifts in stable isotope ratios which can serve as a qualitative indicator for in situ contaminant degradation. However, to use stable isotope data to obtain quantitative information on in situ biodegradation requires among others knowledge on the influence of mass transfer processes on the observed stable isotope fractionation.

Mass transfer processes in aquifers range from macroscopic transport including dispersion driven mixing processes to microscopic transport processes controlling the microbial availability of the contaminant. These transfer processes may cause itself an additional fractionation of stable isotopes, but even in the absence of such additional fractionation the mass transfer processes need to be considered for a quantitative analysis of stable isotope signatures [1,2].

This presentation will introduce theoretical and reactive transport modeling concepts on combining mass transfer processes into a quantitative analysis of stable isotope fractionation and the determination of degradation pathways using stable isotope signatures of two different elements. Examples for the verification and application of these concepts will be presented showing the relevance of mass transfer processes at different scales for the interpretation of stable isotope fractionation.

[1] Thullner, Centler, Richnow & Fischer (2012), *Organic Geochemistry* 42, 1440-1460. [2] Thullner, Fischer, Richnow & Wick (2013), *Applied Microbiology and Biotechnology* 97, 441-452.

Lithium and oxygen isotope compositions of basaltic glasses from ridge axes and off-axis seamounts in the northern EPR (10-15°N)

LIYAN TIAN^{1*}, STEVEN B. SHIREY¹, ZHENGRONG WANG²
AND PATERNO R. CASTILLO³

¹Department of Terrestrial Magnetism, Carnegie Institution of Washington, USA (*correspondence: ltian@dtm.ciw.edu)

²Department of Geology and Geophysics, Yale University, USA

³Scripps Institution of Oceanography, UCSD, USA

Geochemical variations in mid-ocean ridge basalts (MORB) have been attributed to the presence of compositionally distinct mantle components in their source, which may include subduction zone processed oceanic sediment, crust and upper mantle material. The light stable isotopes of lithium and oxygen could be potential tracers of the return of the subducted materials to the surface of the earth via basaltic magmatism since these are strongly fractionated by low-temperature water-rock interactions (e.g., seafloor alteration and subduction processes). We present a study of lithium and oxygen isotopes on a group of well-characterized basaltic glasses from both ridge axes and off-axis seamounts in the northern East Pacific Rise (EPR) between 10°N and 15°N. The samples range from normal-MORB to enriched-MORB in composition.

Our results show that the $\delta^7\text{Li}$ values of these glasses vary from 3.1 to 5.2‰, which systematically correlate with other geochemical indices of mantle heterogeneity, forming trends toward a more enriched composition. In detail, heavier Li isotopic ratios are associated with higher highly/moderately incompatible element ratios (e.g., $\text{K}_2\text{O}/\text{TiO}_2$ and Ba/Y), more radiogenic $^{87}\text{Sr}/^{86}\text{Sr}$ and less radiogenic $^{143}\text{Nd}/^{144}\text{Nd}$. On the other hand, the oxygen isotope compositions display a fairly narrow range of 5.44 to 5.68‰ (equal or lower than upper mantle whole rock values), do not correlate with other geochemical indices and, thus, could not provide clear information on the nature of mantle heterogeneity. Previous studies have shown that lateral compositional variability exists in the upper mantle beneath the EPR; this lateral compositional variability is reflected by the lithium isotope variability of axial and off-axis seamount volcanism. Moreover, lithium isotopic data seem to record the incorporation of a heavy-Li-enriched component, most likely a recycled subduction-metasomatized mantle [1], into the suboceanic mantle in the eastern Pacific.

[1]. Elliott *et al.* (2006), *Nature* **443**, 565-568.

Enriched mantle source and petrogenesis of the Miocene ultrapotassic rocks in western Lhasa block, Tibetan Plateau: Lithium isotopic constraints

TIAN SHIHONG^{1,2*}, HOU WENJIE³, HOU ZENGQIAN⁴,
MO XUANXUE², YANG ZHUSEN¹, ZHAO YUE¹,
HOU KEJUN¹, ZHU DICHENG² AND ZHANG ZHAOQING²

¹Key Laboratory of Metallogeny and Mineral Assessment, MLR, Institute of Mineral Resources, CAGS, Beijing 100037, China (correspondence: s.h.tian@163.com)

²School of Earth Science and Mineral Resources, China University of Geosciences, Beijing 10083, China

³Geological Survey of Jiangxi Province, Nanchang 330030, China

⁴Institute of Geology, CAGS, Beijing 100037, China

The authors have successfully applied lithium isotope to the typical study of Sailipu, Dangreyongcuo, Xurucuo and Chazi ultrapotassic rocks in southwestern Tibetan Plateau. Lithium concentrations of 33 whole-rock samples show a range from 11.2 ppm to 46.1 ppm. Lithium isotopic compositions exhibit a variable range of $\delta^7\text{Li}$ values (-3.9 to +3.5‰) with an average $\delta^7\text{Li}$ of 0.1‰ that corresponds to the average of upper continental crust (Teng *et al.*, 2004). Lithium isotopic compositions of UK from SW Tibet do not show any significant correlations with the degree of magmatic differentiation, as inferred from various compositional parameters (e.g., SiO_2 , Li, Rb and Ga). This suggests insignificant Li isotope fractionation during ultrapotassic rock differentiation, reflecting the source characteristics (Teng *et al.*, 2009). Lithium isotopic compositions of these samples vary by 7.4‰ and do not correlate with radiogenic isotopic compositions or chemical and mineralogical parameters. The Li isotopic heterogeneity therefore likely reflects heterogeneous source rocks (Teng *et al.*, 2009). Based on calculation modeling and a comparison with the previous similar results (Agostini *et al.*, 2008; Janousek *et al.*, 2009), the authors hold that the most probable metasomatic agents were melts or fluids derived from subducted Indian crust instead of from Tethyan crust (including sediments). Therefore, the authors put forward a petrogenetic model of ultrapotassic rocks in southwestern Tibetan Plateau.

This work was supported by grants (Contracts No. 12120113016200, 1212011120298, 201011027, 201011011, 41173003, 2011CB403104, 2011CB403102, IGCP/SIDA-600).

On the evolution of the Western Alpine Orogen: U-Pb geochronology and Hf isotopic ratios in zircons from Adamello and Bergell amphibole-rich mafic and ultramafic rocks

M. TIEPOLO¹, R. TRIBUZIO^{2,1}, M. LUSTRINO³
AND F.-Y. WU⁴

¹ CNR-IGG-UOS di Pavia, Pavia Italy,
(tiepolo@crystal.unipv.it)

² DSTA Università di Pavia, Pavia Italy,
(tribuzio@crystal.unipv.it)

³ DST Università La Sapienza, Roma, Italy,
(michele.lustrino@uniroma1.it)

⁴ IGG, CAS, Beijing, China, (wufuyuan@mail.iggcas.ac.cn)

The orogenic belt intrusive rocks are mostly silica-rich products in which the shallow-depth crustal contamination commonly obscures the original mantle geochemical signal. The rare mafic and ultramafic rocks associated with the major intrusive bodies represent a fundamental petrological tool to track back the evolution of the orogen. The reconstruction of the Cenozoic paleogeography and the tectonic evolution of the Western Alps is still matter of debate, with complex geological models involving multiple oceans (i.e., Ligurian-Piedmontese and Valais oceans) incorporating microcontinents (i.e., Briançonnais domain). Also the origin of the Periadriatic magmatism, developed from ~44 to ~31 Ma along the Alpine belt, and its relationship with tectonic evolution of the Alpine Orogeny remains partly unclear.

We carried out U-Pb geochronology and Hf isotopic ratios on zircons from amphibole-rich mafic and ultramafic rocks of the Adamello batholith and the Bergell pluton, the two largest Cenozoic intrusive bodies of the Alpine Orogen. Results show that the Bergell mafic rocks formed ~10 Ma later than the Adamello analogues. In addition, the Bergell gabbros have a more enriched Hf isotopic signature than the Adamello counterparts. We propose that the formation of the oldest mafic rocks from the Adamello batholith is related to the subduction of the Ligurian-Piedmontese oceanic lithosphere. The mafic rocks from the Bergell pluton most likely record the partial recycling in the source of the continental material. These rocks are presumably related to the younger subduction of the Valais basin, which followed that of the Briançonnais continental block.

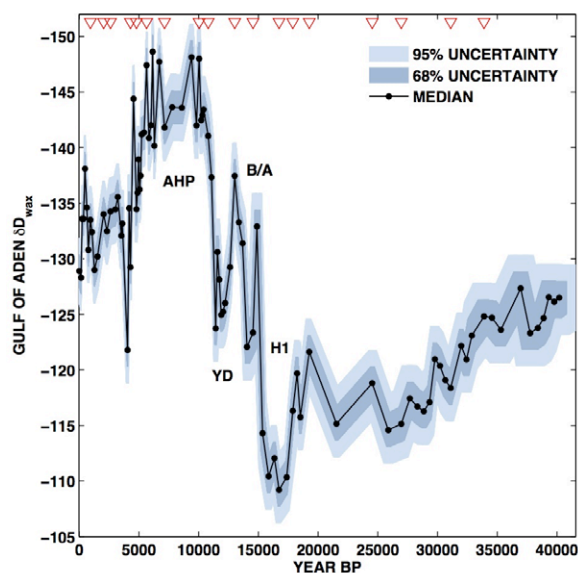
Abrupt shifts in Horn of Africa hydroclimate since the Last Glacial Maximum

JESSICA E. TIERNEY^{1*} AND PETER B. DEMENOCAL²

¹Woods Hole Oceanographic Institution (*correspondence:
tierney@whoi.edu)

²Lamont-Doherty Earth Observatory,
(peter@ldeo.columbia.edu)

The timing and abruptness with which Africa transitioned into and out of the Early Holocene African Humid Period is a subject of ongoing debate, with direct consequences for our understanding of African climate stability, paleoenvironments, and early human cultural development. Here we present a new proxy record of hydroclimate, based on the hydrogen isotopic composition of leaf waxes, from a marine core in the Gulf of Aden that documents rapid, century-scale transitions into and out of the African Humid Period across the Horn of Africa. Similar and generally synchronous abrupt transitions at other East African sites suggest that rapid shifts in hydroclimate are a regionally coherent feature. In addition, the termination of the African Humid Period in East Africa is synchronous with the termination in West Africa. A probabilistic analysis of the abruptness of the transitions in East Africa suggests that they likely occurred within centuries, underscoring the remarkable sensitivity of Northeast African hydroclimate to external forcings. We speculate that the non-linear behavior of hydroclimate in the Horn of Africa is related to convection thresholds in the western Indian Ocean.



Experimental comparison of abiotic and microbial Fe-mineral transformations to identify pathways of magnetic nanoparticle production during pedogenesis

J.L. TILL^{1*}, Y. GUYODO¹, F. LAGROIX², P. BONVILLE³, G. ONA-NGUEMA¹, N. MENGUY¹ AND G. MORIN¹

¹Institut de Minéralogie et Physique des Milieux Condensés
(*correspondance: jessica.till@impmc.upmc.fr)

²Institut de Physique du Globe de Paris, 75238 Paris cedex 05, France

³SPEC, CEA Saclay, F-91191 Gif sur Yvette Cedex, France

We present results from an on-going interdisciplinary experimental study of possible pathways for producing Fe-oxide nanoparticles during pedogenesis of loess-derived soils. The phenomenon of magnetic enhancement in many soil types has been recognized for several years, but the question of whether the enhancement process is primarily driven by microbial activity or abiotic processes is still unresolved. Bioreduction experiments were carried out using the dissimilatory Fe-reducing bacteria *Shewanella putrefaciens* with synthetic nanoparticle preparations of Fe-oxides and oxyhydroxides including goethite, lepidocrocite, ferrihydrite and maghemite. The products of bioreduction are compared with abiotic alteration experiments to examine heating-induced dehydration and redox reactions. Bacterially-mediated re-mineralization of precursor phases produces characteristic high-purity, highly-crystalline euhedral Fe-oxides. Heating-induced dehydration of nanogoethite and lepidocrocite produces topotactic reactions which form pseudo-morphed hematite and maghemite respectively, with distinctive nanostructures containing high concentrations of crystalline defects. However, reduction-heating of dehydrated nanogoethite produces Fe-oxide with non-unique magnetic signatures and morphology that obscure the inorganic origin of the mineral product. The magnetic properties, microstructure, and morphology of the reaction products were characterized with a combination of low-temperature magnetic remanence and susceptibility, high-resolution TEM microscopy, and x-ray diffraction. This study is working toward the identification of magnetic and non-magnetic biosignatures in Fe-oxides that may help elucidate the origins of magnetic minerals in a number of environments, including soils and terrestrial sediments in addition to other planetary settings.

The nature of pyroxenite xenoliths of mantle wedge beneath the Avacha volcano (Kamchatka, Russia)

T.YU. TIMINA^{1*} AND A.A. TOMILENKO¹

¹V.S. Sobolev Institute of Geology and Mineralogy SD RAS, Novosibirsk 630090, Russia (*correspondence: timina@igm.nsc.ru)

Bulk-rock composition determined by XRF for peridotite xenoliths of Avacha volcano shows variations in petrogenic components (in wt.%): SiO₂ (40.5-47), TiO₂ (0.01-0.07), Cr₂O₃ (0.25-1.9), Al₂O₃ (0.3-1.8), MgO (42-48.2), FeO (7.6-10.4), MnO (0.11-0.15), NiO (0.25-0.33), CaO (0.35-1.4), Na₂O (0.1-0.15), K₂O (0.02-0.06). Pyroxenite xenoliths are divided into two groups: orthopyroxenites and clinopyroxenites. In comparison with the harzburgite xenoliths clinopyroxenites are characterized by lower of MgO (17-20.3), NiO (~0.02), Cr₂O₃ (0.12-0.3) contents and by higher SiO₂ (48.6-51), TiO₂ (0.2-0.45), Al₂O₃ (2.6-4.9), CaO (17.3-19) and Na₂O (0.4-0.85) (in wt.%). The bulk-rock composition of orthopyroxenite xenoliths (in wt.) is: SiO₂ (49-54.8), Cr₂O₃ (0.3-1.2), TiO₂ (0.03-0.12), Al₂O₃ (1.2-2.8), MgO (26.6-34.5), FeO (4.7-10) and CaO (1.4-8.5), NiO (0.08-0.15), Na₂O (0.1-0.4). The chemical compositions of peridotitic and pyroxenitic minerals and their primary melt and syngenetic fluid inclusions were described in [1-2].

According to ICP-MS data primary peridotite xenoliths are extremely depleted. Metasomatized peridotite xenoliths, which contain newly formed clinopyroxene, amphibole and sometimes interstitial silicate glasses, differ from primary harzburgites by higher REE contents. Orthopyroxenites have smooth patterns with depletion in LREE ([La/Yb]_n – 0.3-0.7). Clinopyroxenites are the most enriched in trace elements compared to other ultramafic xenoliths ([REE/C₁]_n – 2-5). Their patterns are characterized by high MREE/HREE ([Sm/Yb]_n – 1.5-2.1).

Orthopyroxenites can be considered as derivatives of the metasomatized harzburgites due to their similar bulk-rock composition and features of changes in the mineral composition. Clinopyroxenite xenoliths were formed probably as a result of metasomatic transformation and melting of mantle lherzolites, but not of harzburgites of mantle wedge beneath Avacha volcano.

This work is supported by the grant of President of Russian Federation (No. MK-5459.2013.5), RFBR (grant No. 12-05-00888-a).

[1] Timina *et al.* (2012) *Dokl Earth Sci* **442**, 115-119. [2] Timina *et al.* (2012) *TBG-XV Abst Volume*, 141-142.

Invisible gold in arc volcanic glasses

C. TIMM¹, A. REYES¹, S. GILL², D. LAYTON-MATTHEWS²,
M. LEYBOURNE³, C. DE RONDE¹
AND R. HENLEY⁴.

¹GNS Science, PO Box 30-368, Lower Hutt, New Zealand
(c.timm@gns.cri.nz)

²Department of Geological Sciences & Geological
Engineering, Queen's University, Kingston, Ontario,
Canada

³ALS Geochemistry, 2103 Dollarton Hwy, BC, Canada

⁴Reserach School of Earth Sciences, ANU, Canberra, ACT
0200, Australia

We present new EMPA major and LA-ICPMS trace element data from submarine basaltic to rhyolitic volcanic glasses recovered from the Kermadec arc volcanic centers Monowai, Brothers, Healy, Cotton, Rumble II West, Rumble III and Clark. During time-integrated analyses, invisible nano-sized nuggets rich in Au, Ag, Mo, Sn, Sb and W—mostly located along microlite or microcrystal-glass boundaries—were identified and then mapped using LA-ICPMS. Field and experimental evidence suggest that hot gases exsolve from magmas and accumulate as bubbles, can act as a carrier for metals, including Au and Ag. Mainly due to changes in temperature, pressure, flow regime and melt characteristics (i.e., viscosity, volatile saturation, and so on) during the ascent of the magma and quenching of the lava during eruption, the bubbles become unstable and may collapse, subsequently depositing metal-rich nano-nuggets in the glass. The localised occurrence of the nano-nuggets indicates a heterogeneity in the metal-contents of the gas phases exsolved from the ascending magma. In addition, imperfections, such as microcrystals, may act as nucleation point for nano-nuggets, which can explain their common occurrence along microcrystal-glass boundaries. Furthermore, these nano-nuggets appear to preferentially occur in basaltic glasses rather than in silica-rich glasses, suggesting there is an influence of magma type on the metal-bearing capabilities of the exsolved gases (bubbles). The formation of nano-nuggets in Kermadec arc glasses most likely represents a syn-eruption metal enrichment, possibly representing an indication of the ore forming capabilities of magmatic sources.

Niobium and Tantalum Mineralization in the Nechalacho REE Deposit, NWT, Canada

ALEXANDER TIMOFEEV^{1*} AND A.E. WILLIAMS-JONES¹

¹ Department of Earth & Planetary Sciences, McGill
University, Montreal, Quebec, Canada (*correspondence:
alexander.timofeev@mail.mcgill.ca)

The Nechalacho Layered Nepheline-Aegirine Syenite suite at Thor Lake, North West Territories, situated within the alkaline to peralkaline Blachford Lake Complex, contains substantial reserves of Rare Earth Element (REE), zirconium, niobium, tantalum, and gallium in two ore zones (Upper and Basal zones). Pervasive hydrothermal alteration, involving replacement of primary magmatic mineral assemblages by an assemblage comprising K-feldspar, biotite, zircon and magnetite, influenced the upper 300 m of the layered suite, including the niobium-tantalum mineralization, which occurs in both ore zones. This was followed by albitization.

Previous studies of niobium and tantalum mineralization have focused on pegmatites, in which they occur as magmatic columbite group minerals that vary compositionally due to crystal fractionation. Unlike most pegmatites, niobium and tantalum at Thor Lake are hosted mainly by secondary minerals, i.e., fergusonite-(Y) and columbite group minerals, and as minor components in zircon. In the Upper ore zone, columbite group minerals occur within the altered cores of zircon crystals and immediately surrounding these crystals. Fergusonite-(Y) displays similar textural relationships with zircon in the Basal ore zone. Primary magmatic columbite group minerals have been identified only within drill core intervals of unusually high bulk iron content.

We propose a model in which niobium and tantalum were concentrated at the magmatic stage in a zirconium-silicate, such as eudialyte in the Basal ore zone or within zircon in the Upper ore zone. The zirconium-silicate, eudialyte, was decomposed by hydrothermal fluids, resulting in the formation of zircon with yttrium-rich cores. Fergusonite-(Y) then crystallized during hydrothermal alteration of these zircon cores in the heavy REE-enriched, Basal ore zone. Simultaneously, alteration of yttrium-poor zircon in the heavy REE-depleted Upper ore zone led to the formation of fine-grained columbite group minerals. Locally, primary columbite group minerals crystallized and were later metasomatically altered within iron rich horizons of the ore zones. As opposed to other niobium and tantalum-bearing intrusions, the minerals in the Nechalacho Layered Suite that host these two metals are predominantly of secondary origin.

WHAM- F_{Tox} : An aquatic cation mixture toxicity model

E.TIPPING^{1*}, S.LOFTS¹ AND A.STOCKDALE²

¹Centre for Ecology and Hydrology, Lancaster, LA1 4AP, UK
(correspondence: et@ceh.ac.uk; stlo@ceh.ac.uk)

²Department of Chemistry, University of Manchester, Manchester M13 9PL, UK
(anthony.stockdale@manchester.ac.uk)

An important reason for the development of geochemical models of natural waters is to predict and explain toxic effects towards aquatic organisms. We have extended the WHAM chemical speciation model [1,2] for application in toxicity, by assuming that the binding sites of living organisms can be represented by those of humic acid. The calculated cation accumulation (v_i mol g⁻¹), or “active body burden”, measures the exposure of the organism, and is combined with a cation-specific toxicity coefficient (α_i) to quantify the toxic effect via the combined variable F_{Tox} ($= \sum \alpha_i v_i$).

The toxic response is set to zero when $F_{\text{Tox}} \leq F_{\text{Tox,LT}}$ (lower threshold) and 100% when $F_{\text{Tox}} \geq F_{\text{Tox,UT}}$ (upper threshold) with a linear response in between (Figure 1).

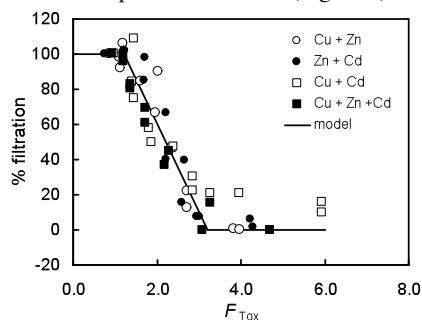


Figure 1: Laboratory toxicity of Cu, Zn and Cd to zebra mussel [3]; data fitted with WHAM- F_{Tox} .

The model has been used to interpret observations of macroinvertebrate species richness in > 400 streams affected by acidification and/or abandoned metal mines [4]. This field application required the use of quantile regression to take into account variations in species numbers due to factors other than the chemical composition of the streamwaters.

[1] Tipping (2002) Cation Binding by Humic Substances, Cambridge University Press. [2] Tipping *et al.* (2011) *Environ. Chem.* **8**, 225-23. [3] Kraak *et al.* (1993) *Ecotox. Env. Safety* **25**, 315-327. [4] Stockdale *et al.* (2010) *Aquat. Toxicol.* **100**, 112–119.

Composition of COH fluids up to 2.4 GPa: A multi-method approach

C. TIRABOSCHI^{1*}, S. TUMIATI¹, P. ULMER², S. RECCHIA³, T. PETTKE⁴, P. FUMAGALLI¹ AND S. POLI¹

¹Dep. of Earth Sciences, University of Milan, 20133 Milan, Italy (*correspondence: carla.tiraboschi@unimi.it)

²Dep. of Earth Sciences, ETHZ, 8092 Zürich, Switzerland

³Dep. of Science and High Technology, University of Insubria, 22100 Como, Italy

⁴Institute of Geological Sciences, University of Bern, 3012 Bern, Switzerland

The mass transfer from the subducting lithosphere to the overlying mantle wedge is mediated by complex solutions resulting from dehydration and decarbonation processes. Compared to H₂O-only and CO₂-only fluid compositions, experiments dealing with mixed H₂O-CO₂ fluids in equilibrium with high-pressure minerals are limited. In order to investigate the speciation and the solute contents of COH fluids in equilibrium with mantle minerals we performed two sets of experiments at identical P , T and fO_2 conditions using a rocking piston cylinder apparatus. Synthetic forsterite with minor enstatite was used as starting material.

In the first set of experiments we investigate the composition of COH fluids by puncturing the capsule in a gas-tight PTFE vessel at $T=80^\circ\text{C}$. Evolved gases were conveyed toward a quadrupole mass spectrometer through a heated line to avoid the condensation of water. Oxalic acid dihydrate and graphite have been used to generate the COH fluid. Experiments were conducted at fO_2 -controlled conditions using NNO, OH (GX, COH) buffer and a double capsule technique. Following thermodynamic modeling we expect in our experiments fluids close to the binary H₂O-CO₂ join.

The second set of experiments was performed to determine the solubility of forsterite in COH fluids. We analyzed the fluid trapped in a diamond layer by the cryogenic laser-ablation inductively coupled plasma-mass spectrometry technique [1]. COH fluids were generated from the addition of graphite, anhydrous oxalic acid and water.

The results will highlight the importance of COH fluids for the mass transport in subduction zones. Comparisons with other experimental systems [2] and with thermodynamic calculations will also be shown.

[1] Aerts *et al.* (2010) *Am. Mineral.* **95**, 1523-1526. [2] Newton & Manning (2002) *Geochim. Cosmochim. Ac.* **66**, 4165-4176.

The distribution of LILE and HFSE in the magmatic hydrothermal systems of mylonites on the example of the detachment-closed metamorphic block (Eastern Trans-Baikalian region, Russia)

TISHIN P.A.¹, BUKHAROVA O.V.¹ AND KREMER I.V.¹

¹ Tomsk state university, Tomsk, Russia, (tishin_pa@mail.ru)

Among the mylonites of the Borschovochny detachment-related metamorphic block with the Early Cretaceous age, simultaneous sills of andesites and dacites are forming. Their intrusion is accompanied by a hydro-thermal change of mylonites. Three main types of metasomatic associations are defined: K (white mica + chlorite + quartz ± adularia), Na-Fe-Ca (chlorite + albite + hematite + epidote + calcite), and K-Ca (quartz + calcite + ankerite + muscovite ± chlorite).

For unchanged metasediment mylonites, the way LILE and HFSE are enriched corresponds to the UK standard with only differences in Cs (7-15 ppm) and Rb (92-135 ppm) enrichment, and low content of Sr (24-133 ppm). Geochemical characteristics of andesites and dacites show their similarity to the volcanites from the island arcs and active continental margins.

Metasomatism stimulates the loss of the most LILE and HFSE. At the same time, Ti is added to the Na-Fe-Ca system (up to 0,8 – 2%) with maintaining the Zr, Hf, Nb Ta, and REE concentrations. It is noted that maximum microelements are removed in the K- and K-Ca systems due to Sr enrichment (150-490 ppm) and inert Ti behavior (to 0,1 – 0,9%). It is obviously demonstrated in geochemistry of the frontal and rare zones, where Th decreases from 2,9 to 0,1 ppm, Zr - from 74 to 3, ΣREE from 79 to 13, La/Yb from 6 to 1,5.

A main mechanism for the extraction of REE is assumed to be the monazite decay, which discovers reaction crown composed by xenotime and galenite when contacting with sulfides.

This study was funded by the Russian Ministry of Education and Science (projects 5.3143.2011, 14.B37.21.0686, 14.B37.21.1257).

Introducing PT-HPLC

FRANÇOIS L H. TISSOT¹, THOMAS J. IRELAND¹, REIKA YOKOCHI^{1,2} AND NICOLAS DAUPHAS¹

¹Origins Lab. Department of the Geophysical Sciences, The University of Chicago, IL. (ftissot@uchicago.edu)

² Department of Earth and Environmental Sciences, University of Illinois at Chicago, Chicago, IL.

High-Performance Liquid Chromatography (HPLC) systems are superior in many respects to gravity-driven open columns commonly used in geochemistry, yet they suffer from several shortcomings that have hampered their adoption in isotope geochemistry (*e.g.* the liquid flow path often contains glass and/or metal parts which are easily corroded/dissolved, electronic controls and housing are often spatially associated with the HPLC unit, shortening the system lifespan [*e.g.* 1])

Here, we present a system developed at the Origins Lab. which addresses many of the shortcomings of commercially available HPLC systems: Pneumatic Teflon-HPLC (PT-HPLC) [2-4]. Development of this system was aided by technologic transfers from the semi-conductor industry and the availability of Teflon-manufactured parts. Its key features are:

1) fully automated elution schemes controlled through LabVIEW software interface, which enables for (i) fresh mixing of reagents for each elution step and (ii) gradient/ramp elutions, while removing the human error/non-reproducibility component, 2) temperature control of the system (up to 80°C) for enhanced chemical separations [5], 3) a modular design making the system adaptable to a variety of separation schemes by quick and inexpensive change of the resin type or column length, and 4) pneumatic actuation, allowing for the electronics to be isolated from the HPLC unit, increasing the lifespan of the system.

To test the PT-HPLC we performed a separation of all REE from each other in one column pass with unprecedented resolution. We used a 70 cm long column ($\phi=0.3$ cm) filled with Ln-resin (25-50 μm resin bead size), a constant temperature of 70 °C, a flow rate of ~0.5 mL/min and a HCl molarity ramp slowly increasing along a convex path from 0.10 M to 10 M HCl. More than 99% of each multi-isotopic REE was separated from its neighbors in one column pass.

This result demonstrates the effectiveness of our system and its great potential to tackle all outstanding geochemical problems that call for demanding separation schemes [6].

[1] Sivaraman *et al.* (2002) *J. Rad. Nucl. Chem.* **252**, 491-495.
[2] Ireland *et al.* (2012) *LPSC* #2141. [3] Tissot *et al.* (2013) *LPSC* #2867. [4] Ireland *et al.* (*Submitted to Chem. Geol.*) [5] Pourmand *et al.* (2010) *Talanta* **81**, 741-753 [6] Tang *et al.* (2012) *EPSL* **359-360**, 248-263.

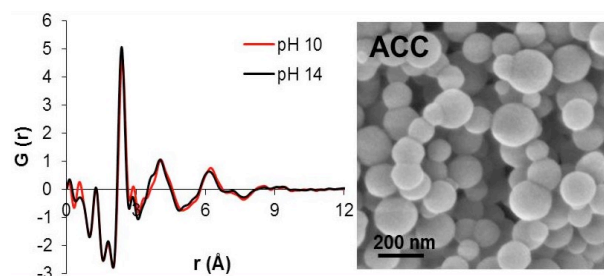
The role of pH and simple organic molecules in amorphous calcium carbonate (ACC) structure

D.J. TOBLER*, K.K. SAND, K. DIDERIKSEN, J.D. RODRIGUEZ-BLANCO, H. O. SØRENSEN AND S.L.S. STIPP

Nano-Science Center, Department of Chemistry, University of Copenhagen, Denmark (*dominique.tobler@nano.ku.dk)

CaCO₃ crystallization controls a large part of the global carbon cycle through fluid-rock interactions, the formation of biominerals and also industrial processes. The initial steps of CaCO₃ crystallization are known to occur via the formation of amorphous calcium carbonate (ACC). The stability of ACC and its crystallization kinetics have been shown to be affected by temperature, pH and (in)organic additives [1]. However, little is known about the effect of these parameters on the structure of ACC at the atomic scale. Obtaining this information would help explain the different stabilities, morphologies, surface properties and formation mechanisms of CaCO₃ biominerals.

We carried out atomic pair distribution function (PDF) analysis using synchrotron radiation to determine the ACC structure formed under various conditions of pH and organic compounds. The results were combined with data from X-ray photoelectron spectroscopy, powder X-ray diffraction, infrared spectroscopy (FTIR) and electron microscopy.



PDF results showed that the short range ordering for ACC (<15 Å) was notably affected by increasing the initial pH of the Na₂CO₃ solution from 10 to 14 (figure left). This difference could indicate an association of the hydroxyl ions with ACC at higher pH, possibly affecting the water content. Conversely, ACC structure remains virtually unaffected when it forms in the presence of several organic compounds (e.g., amino acids, polysaccharides). FTIR revealed small changes in the mode of vibration of carbonate bands and also in water content for certain organic compounds (e.g. citric acid) indicating considerable surface interaction between the organic material and ACC.

[1] Radha *et al.* (2012) *GCA* **90**, 83-95.

Spatial distribution of heavy metals in the urban soils of Chisinau city (Republic of Moldova)

E. TOFAN*^{1,2}, G.O. IANCU¹, GH. JIGAU² AND N. BUZGAR¹,

¹Alexandru Ioan Cuza University, 11, Carol I Bd., 700506, Iasi, Romania (tofanelena@yahoo.com)

²Moldova State University, 60, A. Mateevici, MD-2009, Chisinau, Republic of Moldova

The study area comprised the entire area of Chisinau city and has an approximate dimension of 15/15 km². Soil samples were collected inside the network of 1km/1km², from the depth 0-20 cm. On the grid surface, 120 soil samples have been analyzed. The heavy metal content was analyzed using X-ray Fluorescence Spectrometry (EDXRF Epsilon 5). The analyses for physicochemical parameters were carried out with the following methods: particle size distribution (Kachinsky, 1958), organic matter content (Tiurin, 1965), CaCO₃ (Arunskina, 1970) and the pH was determined using a Corning M-555 pH/Ion Meter. Assessment of anthropogenic contribution in urban soils has been determined by means of enrichment factor (EF), geoaccumulation index (Igeo) and pollution index (PI) [1].

Correlation matrix for analyzed heavy metals and physicochemical parameters was performed to observe relationship between the analyzed parameters. Results presented the chemical association of heavy metals in the study area. The physicochemical properties of urban soils showed a significant positive correlation with each other and with Co, Ni and Cr whose origin is predominantly geogenic. The conclusions highlighted the organic matter has an influence an accumulation of heavy metals. As well is evident that the elements showed a good correlation with each other indicating a common source. The geochemical background range at urban scale has been defined by applying the iterative 2σ technique method. The background geometric mean values for heavy metals (mg/kg) are: Cr (64.2); Co (12.9); Ni (32.7); Cu (28.4); Zn (82.7); Pb (22.8) and As (9.4). The means concentration of analysed chemical elements in Republic of Moldova rocks are Cr (86 mg/kg); Co (11 mg/kg); Ni (38 mg/kg); Cu (22 mg/kg); Zn (83 mg/kg); Pb (17 mg/kg) and As (1.7 mg/kg) [2].

The calculated EF and Igeo results revealed the following order As > Pb > Zn > Cu > Ni > Cr > Co. The PI recorded content from heavily contaminated to uncominated in following order Zn > As > Cu > Pb > Co > Ni > Cr.

[1] C. Reimann and P. de Caritat (2005) *J. Sci. Tot. Env.* 337, 91-107 [2] V.P. Kiriliuk (2011) *Collect. Scient. Art.* 32-35

Fingerprint of last glaciation on ^2H and ^{18}O in groundwater of north-east part of Baltic Artesian Basin

TOKAREV I.V.

tokarevigor@gmail.com

In the northern part of Baltic Artesian Basin (BAB) a groundwater of the multilayered hydrogeological system (mainly the Cambrian and Vendian aquifers) is the principal and most plentiful source for the public water supply in Russia and Estonia. But there are problems with the water quality in many sites due to high salinity and/or the specific components abundance. For example, the natural origin radionuclides (mainly Ra and Rn) and microelements (B, F, Fe, Mn etc.) exceed the sanitary limits.

The BAB is characterized by the limited knowledge about the hydraulic boundaries conductivities of aquifers. Taking into account the complex geological history of the Baltic region in the Pleistocene and Holocene, the isotope archive is significant for the groundwater flow and mass-transport understanding.

The stable isotopes (^2H and ^{18}O) were studied in the aquifers near north-east margin of BAB from a crystalline basement to Earth surface. The fingerprint of the Baltic ice lake is clearly fixed for Cambrian aquifer in Tallinn (Estonia). The lightest stable isotope composition of groundwater for Europe was found here ($\delta^2\text{H}=-160\text{‰}$, $\delta^{18}\text{O}=-21\text{‰}$, Raidla *et al.*, 2009). The isotope composition of water is gradually weighted to the east direction and make up $\delta^2\text{H}=-125\text{‰}$, $\delta^{18}\text{O}=-17\text{‰}$ near the boundary between Estonia and Russia, and $\delta^2\text{H}=-100\text{‰}$, $\delta^{18}\text{O}=-13\text{‰}$ (that is like to modern precipitation) near the Ladoga lake. It seems, a relicts of the Eemian sea water also was obtained in some cases. It is the salty ($M=4-6\text{ g/l}$) and isotopically fractionated water, which have no ^{14}C or have significant ^{14}C age. Isotope composition is weighting, if the water is the thawed permafrost and become lighter, if it is the residual water after sediment freezing.

Clarification of As(V) Sorption Mechanism with ferrihydrite for Quantitative Modelling of Coprecipitation Process in Wastewater Treatment

CHIHARU TOKORO^{1*}, DAISUKE HARAGUCHI², SAYAKA IZAWA³ AND SHUJI OWADA⁴

¹ Waseda University, Tokyo, Japan, tokoro@waseda.jp

² Waseda University, Tokyo, Japan, d.haraguchi@aoni.waseda.jp

³ Waseda University, Tokyo, Japan, izasaya@ruri.waseda.jp

⁴ Waseda University, Tokyo, Japan, owadas@waseda.jp

Coprecipitation method using ferrihydrite has been commonly applied to remove As(V) in wastewater such as acid mine drainage. Objective of this study is to clarify how coprecipitation of As(V) with ferrihydrite occurs in wastewater and quantitative modelling of them.

We investigated the sorption mechanism of dilute As(V) with ferrihydrite using three kinds of experimental studies for an artificial wastewater in which the ion strength was 0.05 and pH was 5 and 7; (i) sorption isotherm formation, (ii) zeta potential measurement and (iii) XRD analysis. We confirmed that As(V) was formed a simple two-dimensional adsorption onto the surface of ferrihydrite when the initial As/Fe molar ratio was less than 0.4, whereas a surface precipitation of amorphous ferric arsenate was formed when the initial As/Fe molar ratio was more than 0.4 [1].

Furthermore, both of XANES and EXAFS analysis on K-edge of As showed As(V) coprecipitates with ferrihydrite was mixture of As(V) adsorbed ferrihydrite and amorphous ferric arsenate. Estimated weight ratio of amorphous ferric arsenate in As(V) coprecipitates became above 0.5 when the initial molar ratio of As/Fe ≥ 0.5 was used. These results corresponded with results by XRD analysis. EXAFS analysis assuming three kinds of surface complexes for As-Fe bond showed the coordination number for 2.85 Å of As-Fe bond increased and it for 3.24 Å of As-Fe bond decreased with increasing the initial As/Fe molar ratio. All experimental data obtained in this study showed As(V) co-precipitation mechanism shifted gradually from As(V) complexation to the surface of ferrihydrite toward amorphous ferric arsenate. Therefore, we constructed surface precipitation model to evaluate quantitatively the coprecipitation process of As(V) with ferrihydrite. Good agreement between experimental and calculated values was observed.

[1] C.Tokoro, Y.Yatsugi, H.Koga and S.Owada (2010) Environment Science and Technology, 44, pp.638-643.

Selenium coprecipitated with barite as a new redox indicator

KOHEI TOKUNAGA^{1*}, YUKA YOKOYAMA¹
AND YOSHIO TAKAHASHI¹

¹ Hiroshima University, Hiroshima, Japan

(*correspondence: ktokunaga@hiroshima-u.ac.jp)

Redox potential (Eh) is an important physico-chemical factor that can affect behaviors of various ions in water. A number of previous studies have suggested that Eh was estimated by the solid-water distribution of redox-sensitive elements based on the effect of change of the oxidation state such as relative enrichment-depletion profiles of particular elements such as iron and manganese. However, the estimation of redox conditions based on these profiles may not be reliable because (i) elemental concentrations are influenced by many factors such as secondary adsorption-desorption reactions and diagenesis and (ii) only the relative evaluation of the redox condition is possible by the depth profile of particular elements. Thus, the aim of this study is to propose a new redox indicator using the oxidation states of redox sensitive element itself in a certain mineral to estimate directly the particular redox condition at the time of the mineral formation. Here, we examined incorporation behavior of selenium (Se) species to barite as a redox indicator for oxic-suboxic condition.

Coprecipitation experiments of Se with barite coupled with determination of Se oxidation state both in barite and water phases were conducted to investigate the influence of the oxidation state on the coprecipitation of Se into barite. The oxidation state of Se in water and barite were determined by HPLC-ICP-MS and X-ray absorption near-edge structure (XANES) at Se K-edge, respectively.

It was found that the Se(VI)/Se(IV) ratio in barite reflects the Se(VI)/Se(IV) ratio in water, which suggests that the oxidization state of Se in barite can work as a redox indicator showing the redox condition at the time of barite formation. Selenium(IV) is incorporated into barite under suboxic condition below the redox boundary of Se(VI)/Se(IV). Selenium(VI), on the other hand, is incorporated under oxic condition above the redox boundary of Se(VI)/Se(IV). Based on the distribution behavior of Se to barite, we conclude that the Se(VI)/Se(IV) ratio in barite can be used as a redox indicator whether barite was precipitated below or above the redox boundary of Se(VI)/Se(IV), the Eh region of which is different from the Fe(III)/Fe(II) and Mn(IV)/Mn(II) boundaries often employed as a signature of redox condition.

Insights into mantle processes from water and trace elements in olivine

P.M.E. TOLLAN^{1*}, J. HERMANN², R.J. ARCULUS²,
H.ST.C. O'NEILL² AND J.P. DAVIDSON¹

¹Department of Earth Sciences, Durham University
(*p.m.e.tollan@durham.ac.uk)

²Research School of Earth Sciences, Australian National University

Olivine continues to be neglected in most trace element studies of mantle rocks. This is in spite of the ability of modern analytical techniques to measure accurately and precisely a diverse and petrologically useful suite of elements and a burgeoning experimental interpretative framework of partition and diffusion coefficients.

We present the results of a detailed study of water and trace elements in olivine as evidence of their utility. Samples chosen for this study are harzburgite xenoliths dredged from volcanic cones close to Ritter Island in the West Bismarck Arc, Papua New Guinea. From textural observations, these samples are assigned to 'residual' or 'reacted' groups. 'Residual' samples display textures indicating an origin through melt extraction and sub-solidus cooling. Olivines have very low concentrations of all incompatible trace elements and water, consistent with the nominally cpx-free mineralogies. Concentrations of Al (0.5-9.1 ppm), Cr (5.0-19.9 ppm) and V (0.09-0.63 ppm) are exceptionally low due to the exsolution of Cr-spinel plates during cooling to temperatures of ~ 600 °C.

'Reacted' samples display textures consistent with melt-rock reaction. Olivines reflect this in significant water and trace element enrichment and disequilibrium, with over an order of magnitude variation in Y (0.08-23.8 ppb), Ca (22.3-793.0 ppm), Na (0.6-22.8 ppm) and Cr (7.2-252.4 ppm) concentrations among crystals in individual samples on a sub-cm scale. These concentrations overlap with and diverge from those measured in 'residual' olivines.

We interpret this as re-equilibration of olivine during percolation of hydrous mantle-derived melts. The extreme trace element disequilibrium requires that this reaction occurred on a very rapid timescale, shortly before magmatic entrainment. Olivine is the only phase that records this late-stage chemical exchange, due to its high modal abundance and more rapid rates of trace element diffusion. Similar studies on olivine from mantle and magmatic rocks can shed new light on the mechanisms and timescales of melt-rock reaction, transport, differentiation and magma mingling.

Two Noble Families display what happened in their early days

I. TOLSTIKHIN

Geological Institute, Apatity, and Space Research Institute,
Moscow, Russian Academy of Sciences, Russia
(igor.tolstikhin@gmail.com)

At the first glance there is nothing similar in behaviour of the refractory highly siderophile noble metals (NM) and the highly volatile inert noble gases (NG). However, all these species are extremely under abundant in the Earth's mantle relative to the solar composition, and this common feature allows them to record processes invisible by other chemical / isotopic systematics.

Since long a post-giant-impact late veneer of chondrite-like material (LV) is widely discussed as a plausible explanation of NM elemental and isotopic abundances in the mantle [1, 2, 3]. Less attention has been attracted to the possibility that this same LV could have delivered to the Earth a volatile-rich material, characterised by, e.g., (almost) solar isotope compositions of He and Ne. Moreover, an enhanced density of this material could also stabilize a noble-species-bearing reservoir (DDP [4]), preventing its intense mixing within the convective mantle.

Chemical transport modeling shows that flux of LV materials from DDP into the mantle could be responsible for chondrite-like relative abundances of NM, solar-like light NG, and contribution of early generated radiogenic Xe isotopes [5]. New results of modeling are presented and discussed.

[1] Wanke *et al.* (1984) *Archaeon Geochemistry*. A. Kroner, *et al.* (eds), Berlin, Springer-Verlag, 1-24. [2] Kramers (1998) *Chem. Geol.* 145, 461-478. [3] Brandon *et al.* (2006) *Geochim. Cosmochim. Acta* 70, 2093-2103. [4] Tolstikhin and Hofmann (2005) *Phys. Earth Planet. Inter.* 148, 109-130. [5] Tolstikhin and Kramers (2008) *The Evolution of Matter*. Cambridge, Cambridge University Press, pp. 520.

Platinum deposits in hardrock of the Konder massif

NADEZHDA TOLSTYKH

Sobolev Institute of Geology and Mineralogy, SB RAS, pr.
Ak. Koptyga, 3, 630090, Novosibirsk, Russia,
(correspondence: tolst@igm.nsc.ru)

The problem of finding of promising ore areas in the bedrock of Ural-Alaska type intrusion, which until recently were considered only as source of placer, is now actual. It is necessary to study the regularities of location of platinum mineralization and to find the new search criteria. Alkaline-ultramafic massif Conder (Aldan Shield, Siberia) is now a major source of mined platinum placers. The rocks, that contain the platinum mineralization, were known until now only in chromitite [1]. Chromite schlieren really are most enriched with platinum (Pt-Fe alloys) and other minerals of platinum group elements (PGM), the content of which is about 0.5 kg/t. Our research has shown the possibility of finding of platiniferous zones unrelated to the chromite ores. Dunites with a rare accessory of chromite also contain platinum grains, ranging in size from 80-120 μm in fine-grained dunites and up to 1 mm – in pegmatoid dunites.

In addition, intensive platinum mineralization was found in the rocks area near a tectonic contact between dunite and clinopyroxenite in the eastern part of the Konder massif. PGMs occur in dunites as well as in clinopyroxenites. A significant part of the Pt-Fe grains are porous. Cooperite amount to about 30% of PGM grains. Iridium, osmium, irarsite, hollingworthite, erlichmanite, laurite, braggite, bowieite, kashinite, ferrorhodsitite, nickel-rich equivalent of cuproiridsite and Pd-Pb-S unnamed phase were found in Pt-Fe alloys as inclusions. Pt-Fe alloys are sometimes partially replaced by tulameenite and Pt-Cu alloys.

Thus, chromite ore is not the only determining criterion in the search for platinum ores. Localization of platinum ore at the contact of dunite and pyroxenite, the presence of numerous sulphide and sulfoarsenidov of PGE, associated with platinum, as well as post-magmatic transformations and replacement of primary Pt-Fe alloys – all indicate the active involvement of S-, As-containing fluids in the formation of these deposits. Such conditions can be created within the permeable dunite, enabling for the migration of fluids- and PGE-rich residual melt and crystallization the platinum ore near the contact with a less permeable pyroxenites.

[1] Rudashevsky *et al.* (1992) *Miner. Journ.* 14(5), 12-22 (in Russian)

Hydrogen isotopic composition of Earth's early ocean estimated from Archean MORB in Barberton Greenstone Belt

FUMIYA TOMIYASU^{1*}, YUICHIRO UENO^{1,2}
AND MAARTEN DEWIT³

¹Department of Earth and Planetary Sciences, Tokyo Institute of Technology, Meguro, Tokyo, 152-8551, Japan (tomiyasu.f.aa@m.titech.ac.jp)

²Earth-Life Science Institute, Tokyo Institute of Technology, Meguro, Tokyo, 152-8551, Japan

³AEON-Africa Earth Observatory Network, and Faculty of Science, Nelson Mandela Metropolitan University, Summerstrand, Port Elizabeth, 6031, South Africa

Origin and evolution of Earth's seawater are still poorly understood. Hydrogen isotopic composition is a key to constrain secular change of seawater volume through time. In Barberton Greenstone Belt, South Africa, the past fragment of Archean oceanic crust is well preserved. We have systematically analyzed hydrogen and oxygen isotopic compositions of sub-greenschist facies pillow basalts in upper part of the Hoogenoeg Complex. Based on petrographic observation together with XRD analysis, almost hydrous mineral in the samples are composed mainly of chlorite with minor amounts of epidote and actinolite. Temperature dependence of isotopic fractionation factor between chlorite and water is weak both for hydrogen and oxygen, thus useful to estimate the δD values of co-existing water. The studied basalt show positive correlation between hydrogen isotopic composition and water content. This relationship is similar to those observed in typical modern basalts hydrated at the seafloor, but systematically offsets to low δD values compared to the modern example. Based on these relationship, we have concluded that the 3.5 Ga seawater and possibly mantle were both depleted in deuterium relative to modern seawater by $24 \pm 5\%$. These results may suggest that Earth's seawater would have been decreased through time due to hydrogen escape rather than increase by degassing of water from mantle imbalanced against subduction.

Tephra from Ischia: dating eruptions and geochemical changes

E.L. TOMLINSON¹, P.G. ALBERT², S. WULF³, L. CIVETTA⁴, R. BROWN⁵, V. SMITH², J. KELLER⁶, G. ORSI AND M.A. MENZIES⁷

¹Geology, Trinity College Dublin, Ireland (tomlinse@tcd.ie)

²RLAHA, University of Oxford, UK

³GFZ, Potsdam, Germany

⁴Istituto Nazionale di Geofisica e Vulcanologia, Napoli, Italy

⁵Earth Sciences, University of Durham, UK

⁶Institut für Geowissenschaften, University Freiburg, Germany.

⁷Earth Sciences, Royal Holloway University of London, UK

Ischia is an active resurgent caldera. Volcanic activity at Ischia began prior to 150 ka, with the largest eruption being the 55 ka, caldera-forming Monte Epomeo Green Tuff (MEGT). Unravelling eruptive history from proximal deposits can be problematic due to burial, resurgent uplift and erosion. In such cases, distal tephra archives can provide valuable information about eruptive frequencies and about the long-term evolution of the volcanic-magmatic system.

Lago Grande di Monticchio (LGdM) lies 140 km east of Ischia. This annually laminated archive contains 64 Ischia tephra layers spanning 132 to 3 ka. These distal layers indicate that Ischia has experienced approximately one eruption every ca. 2100 years. We present major and trace element data for 20 of the layers and correlate 6 of these with glass data for proximal deposits.

Tephra compositions from the pre-MEGT (>55 ka: UMSA to Porticello) period comprise three compositional groups that occur repeatedly in successive eruptions. Tephra from smaller eruptions, e.g. UMSA and Porticello contain just one group, while larger eruptions, e.g. Tisichiello and Olummo record all three compositional groups. Proximal-distal correlations with LGdM indicate these eruptions span the 44 kyrs prior to the MEGT event.

Proximal-distal correlations indicate that the Schiappone eruption occurred 4.5 ka after MEGT. Post-MEGT tephra (<55 ka) record a step to lower FeO and TiO₂ and form compositional groups that overlap with the pre-MEGT but are displaced to lower incompatible element contents.

MEGT tephra spans a wide compositional range, broadly overlapping the three pre-MEGT compositional groups but displaced to higher Nd and Y and containing an additional less evolved glass population. Confirmed distal equivalents of the MEGT include LGdM TM-19, Ionian Sea Y-7, and PRAD 1870 from the Adriatic Sea and probably C-18 in the Tyrrhenian Sea. Therefore, the MEGT was one of the most widely dispersed late Quaternary tephra to source from the Campanian region.

Microstructural development of in situ deformed and heated polycrystalline halite in dependence of silica gel

CATERINA E. TOMMASEO¹

¹Technical university Berlin, department of mineralogy,
ACK9 13355 Berlin
caterina.e.tommaseo@TU-Berlin.de

Our research focused on the influence of silica gel on the texture development and the mechanical behaviour of predeformed polycrystalline halite. In situ experiments help further our understanding of the fundamental mechanisms of the processes taking place during texture development. With different methods both single grain orientation analyses and the texture development in the bulk were successfully obtained.

The results show the influence of silica gel (amorphous phase) either on the texture development and on the physical properties (as stress/ductility behavior) focusing not only on bulk texture but also on the changes in the single grain orientations. The polycrystalline samples doped with silica gel show an increase in the yield strength and a higher Young's modulus (stiffness). In the texture development a preservation of the starting texture is observed, which correlates well with the mechanical behavior. The amorphous phase probably protects the single grains from deformation, preventing strain accumulation by the introduction of defects and thereby preserving the grain shape.

Heterogeneity and anisotropy in the lithospheric mantle

ANDRÉA TOMMASI¹, VIRGINIE BAPTISTE¹,
ERWIN FRETS^{1,2}, KATHERINE HIGGIE¹,
VINCENT SOUSTELLE¹, VÉRONIQUE LE ROUX¹,
DAVID MAINPRICE¹, ALAIN VAUCHEZ¹,
CARLOS GARRIDO² AND JEAN-LOUIS BODINIER¹

¹Géosciences Montpellier, CNRS & Université Montpellier 2,
France

²Instituto Andaluz Ciencias de la Tierra, CSIC, Granada,
Spain

Despite extensive geophysical investigations and studies of xenoliths and peridotite massifs, the lithospheric mantle, in particular beneath continents, remains a 'mysterious' layer. Seismic anisotropy data point to anisotropic physical properties, and hence structures, coherent at scales of 100s km. Receiver functions, in contrast, imply in lateral and vertical heterogeneity at scales < 10km within the mantle lithosphere, but the physical origin of the reflectors are not clear. We will present constraints on the lithospheric mantle seismic properties based on the analysis of an evergrowing database of naturally deformed peridotites and review recent studies of our group on naturally deformed peridotites. These studies highlight the role of reactive percolation of melts and fluids on the evolution of the lithospheric mantle, focusing on the creation of heterogeneity and the feedbacks between melt percolation and deformation. Based on these data, we will discuss the effect of these processes on evolution of the physical properties of the mantle, in particular the rheology. For instance, analysis of naturally deformed shows that static reactive percolation may significantly change the composition, but does not erase the fabrics and hence the anisotropy of physical properties. The latter, which is inherited from the major deformation episodes that shaped the continental plates, may be preserved for very long time spans, playing a major role on the subsequent evolution of continental plates.

Earthquake-driven noble-gas geochemistry in Lake Van (Turkey)

YAMA TOMONAGA¹, MATTHIAS S. BRENNWALD¹, COLIN MADEN², AYŞEGÜL F. MEYDAN³ AND ROLF KIPFER^{1,2}

¹Eawag, Swiss Federal Institute of Aquatic Science and Technology, Water Resources and Drinking Water, Duebendorf, Switzerland, tomonaga@eawag.ch

²Institute of Geochemistry and Petrology, Swiss Federal Institute of Technology, Zurich, Switzerland

³Department of Geological Engineering, Yuzuncu Yil University, Van, Turkey

Terrigenous He release and changes in the He isotope ratio in response to tectonic activity is well known [1,2,3]. However, the very local nature of the He release from the solid earth [4,5,6,7] implies that every system considered has to be addressed as a single and unique entity. Only such case-specific assessment allows to infer possible links between geochemistry and seismic events.

Lake Van (Turkey) is one of the largest terminal lakes and the largest soda lake on Earth. The lake basin is situated in a tectonically active region characterized by the presence of major faults and volcanoes and is known to accumulate mantle fluids [7,8,9]. The societal vulnerability of the area to seismic hazards was dramatically documented by the occurrence of the devastating earthquake of magnitude 7.2 close to the city of Van on Oct. 23rd 2011. This unfortunate and tragic event offers a unique opportunity to study the related emission of fluids from the solid earth. Our research in Lake Van during the last two decades [7,8,9,10] sets a solid experimental basis for understanding possible changes in the noble gas isotope composition in the water column induced by such a major earthquake.

In this work we present the noble-gas concentrations of water samples from Lake Van acquired before and after the earthquake. We compare the new data to our previous measurements and we evaluate the potential of noble gas analysis as geochemical proxy for tectonic activity.

[1] Sano *et al.*, 1998. *Chem. Geol.*, 150(1-2), 171–179. [2] Güleç *et al.*, 2002. *Chem. Geol.*, 187(1-2), 129–142. [3] Fu *et al.*, 2008. *Radiat. Meas.* 43, Suppl. 1, S348–S352. [4] Mamyrin and Tolstikhin, 1984. ISBN 978-0444421807. [5] Oxburgh *et al.*, 1986. *Nature* 324, 632–635. [6] Oxburgh and O’Nions, 1987. *Science*, 237, 1583–1588. [7] Tomonaga *et al.*, 2011. *Geochim. Cosmochim. Acta* 75 (10), 2848–2864. [8] Kipfer *et al.*, 1994. *Earth Planet. Sci. Lett.* 125 (1-4), 357–370. [9] Kaden *et al.*, 2010. *Water Resour. Res.* 46, W11508. [10] Tomonaga *et al.*, 2012. *J. Asian Earth Sci.* 59, 99–107.

Soil Mineralogy, Geochemistry and Trace Element Mobility in the Bitumen Environment of Ondo state, Southwestern Nigeria

TOMORI W.B.¹, YANFUL E.K.¹, FLEMMING R.²; AMOO I.A.³, AIYESANMI A.F.³ AND ADEKOYA J.A.⁴

¹ Department of Civil and Environmental Engineering, Western University, Ontario, Canada; email: tomorifuta97@yahoo.com; eyanful@uwo.ca

² Department of Geology, Western University, Ontario, Canada,

³ Department of Chemistry, Federal University of Technology, Akure, Nigeria; adisamoo@yahoo.co.uk, adisamoo@yahoo.com; demolakt@yahoo.co.uk

⁴ Department of Applied Geology, Federal University of Technology, Akure, Nigeria

Surface and subsurface soil from the bitumen environment of Ondo state was characterized for mineralogy, geochemistry and trace element mobility. Physical, mineralogy and geochemical properties of the soil samples was obtained using standard techniques. The soil in the study area is acidic with low cation exchange capacity. The majority of trace elements reside in residue phase. Hence, trace elements are relatively low mobile. They are therefore of little or no risk to ecosystem health. Major oxides are silica, iron oxide and alumina. Quartz, feldspar and kaolinite are dominant mineral constituting more than 99%.

Biom mineralization and biomimetic synthesis of magnetite nanoparticles

É. TOMPA¹, I. NYIRÓ-KÓSA¹, R. UEBE², D. SCHÜLER²
AND M. PÓSFAL¹

¹Dept. of Earth & Env. Sci., Univ. Pannonia, Veszprém, 8200 Hungary, (*correspondence: mihaly.posfai@gmail.com)

²Ludwig-Maximilians-Universität München, Dept. Biol. I, Biozentrum, D-82152 Planegg-Martinsried, Germany

Ferrimagnetic nanoparticles are used in a wide range of environmental, technical and medical applications, including their use for the transformation and degradation of metallic and organic pollutants, as constituents of magnetic fluids, and as contrast agents for magnetic resonance imaging [1]. Most applications require nanoparticles with highly specific physical properties. While magnetotactic bacteria produce magnetosomes (membrane-bound magnetite nanoparticles) with strictly controlled sizes and shapes, the regulation of these properties is typically much less successful in laboratory syntheses. By using the biom mineralization process in magnetotactic bacteria as a model system, we performed a series of biomimetic synthesis experiments in order to produce magnetic particles with strictly controlled properties.

First, the possible means of control over nanoparticle shapes were explored in abiotic precipitation experiments, by varying the iron source and/or the concentrations and types of organic additives. Depending on the applied conditions, octahedral, disk-like or elongated magnetite particles formed. We also analyzed magnetosomes from the magnetotactic bacterium *Magnetospirillum gryphiswaldense* and studied the effects of growth conditions and genetic modifications on the sizes, shapes and structures of magnetosome particles. Using the available information on the genetic background of magnetite biom mineralization in magnetotactic bacteria [2, 3], we designed a scheme for the bio-assisted synthesis of magnetic filaments. Mutagenized flagellar filaments were produced by inserting part of the gene of the known iron-binding protein Mms6 into the genome of *Salmonella typhimurium*. The mutagenized filaments are being used as stable protein scaffolds for the templated nucleation of magnetite, with the aim of producing magnetic ‘nanotubes’ [4].

[1] Laurent *et al.* (2008) *Chem. Rev.* **108**, 2064–2110. [2] Amemiya *et al.* (2007) *Biomaterials* **28**, 5381–5389. [3] Faivre & Schüler (2008) *Chem. Rev.* **108**, 4875–4898. [4] This study was supported by the EU-FP7 grant “Bio2MaN4MRI”.

Source Controls on the Metal Contents of Mantle-Derived Magmas

N. TONNELIER¹, C.M. LESHER² AND N.T. ARNDT³

¹ Department of Geology, University of Johannesburg, Johannesburg, South Africa

² Mineral Exploration Research Centre, Laurentian University, Sudbury, Ontario Canada

³ Institut des sciences de la Terre, Université de Grenoble 1, St. Martin d’Hères 38400 France

Plume-derived magmas are thought to form by melting of mantle peridotite source but recent studies have shown that ferropicrites and Hawaiian basalts have major and trace elements contents that cannot be explained by this model. Geochemical and petrological studies suggest that their compositions are best explained by melting of olivine-free pyroxenite that formed through reaction between peridotite and melts derived from recycled oceanic crust. Pyroxenite with these composition are minor but ubiquitous component in ultramafic massifs and mantle xenolith. Base and precious metals partition into sulfides, silicates and alloys, and their concentrations provide additional constraints on the lithology of their source. To test this hypothesis, we studied the Ni, Cu, Co, Zn, V, Sc and platinum group elements (PGE) contents of tholeiitic basalts and picrites from Hawaii and ferropicrites from Russia, Canada, and Namibia and compared their compositions with those of peridotite-derived magmas. Hawaiian basalts and ferropicrites have relatively low PGE with respect to Ni and Cu, a characteristic that has been previously attributed to a stage of sulfide saturation during magma ascent or the presence of sulfide in the residue of melting of a peridotite source. However, our study shows that Hawaiian basalts and ferropicrites are enriched in Ni-Co-Cu-Zn and depleted in Pd-Pt, but undepleted in Ru-Ir. These features are inconsistent with previous models but consistent with an olivine-free pyroxene-bearing source formed from recycled oceanic crust.

Our study show that a) the base and noble metal contents of mantle pyroxenite from Beni Boussera (Morocco) is consistent with mixing of eclogite-derived melts and peridotites, and b) the metal content of Hawaiian magmas and ferropicrites can be explained by melting of a mixed peridotite-pyroxenite mantle source. These observations have strong implication on the origin of magmatic ore deposits with mineralization characterized by high Ni-Cu tenors and high Cu/Pd and Ni/Ir ratios (e.g., Voisey’s Bay, Canada; Nebo-Babel, Australia; Eagle, USA, Jinchuan, Limahe, Lengshuiqing, Baimazhai, Jinbulake and Kalatongke, China).

Immobilization of long-lived iodine after incorporation into apatite matrixe

N. TORAPAVA^{1*} AND C. WALTHER¹

¹The Institute for Radioecology and Radiation Protection,
Leibniz University of Hanover, Herrenhäuser Str. 2, 30419
Hanover, Germany

Iodine-129 being long-lived volatile fission product, among with cesium-135 and technitium-99, represents a challenge for the design of repository-suited matrices [1]. The present study investigates a possibility of iodine incorporation in the forms of iodide and iodate into apatite and hydroxalcalite-like matrices. The matrice should meet certain requirements, i.e. being cheap, safe, easy to synthesise, stable and environmental friendly. Optimization of coprecipitation method for synthesis of iodine containing apatite has been done. Obtained matrices will be characterized by SEM and XRD. Stability in the temperature range 100 - 700°C is studied. Leaching experiments in MQ water and brine will be done as well as radiaton damage (α -, γ -) will be studied before the conference.

[1] Watanabe *et al.* (2009) *Appl. Mater. Interf.* **1**, 1579 – 1584.

The study the granitoid rocks in shear zone in SE-Qorveh (Kurdistan, Iran): With emphasis on geochemical behavior of whole-rock and mineral chemistry of Biotite and Feldspar

TORKIAN ASHRAF^{1*} AND REZAIIE MOZHGAN¹

¹Department of Geology, Faculty of Science, Bu-Ali Sina University, Hamedan, Iran. (a-torkian@basu.ac.ir)

²Department of Geology, Faculty of Science, Bu-Ali Sina University, Hamedan, Iran. (rezaiemozhgan@gmail.com)

The studied area is located in NW- Sanandaj-Sirjan belt, between 47° 45' to 48° 00' E-Longitude and 35° 00' to 35° 10' N-Latitude in SE-Qorveh , Iran. The investigation is done on the I-type granitic rocks. Enrichment for LILE & Pb, along with the negative anomaly of HFSE & Ba and low ratios of Nb/Y and Rb/Nb indicate that origin of initial magma is lower continental crust that created in a margin of convergent plate. The deformed granitoid rocks, including protomylonites and mylonites, are investigated in Sangin-Abad, Koh-e-Gazgaz and Poloserkan areas. The deformed rocks show variations in microstructural and mineralogical characterstics. Shear sense indicators (e.g. foliation, lineation, shear folds S-shaped, C-S fabric) suggest dipping slip movement. Petrographic evidence of tectonic activities are including myrmekite, recrystallized and slide alkali feldspars, fractured plagioclases, dynamic quartzes, perthitic orthoclase, and mantled feldspars with Or_{91.19 - 91.54}. Comparing geochemical data of deformed rocks and protolith show that there are varieties in abundances of main elements such as increasing of CaO, MnO, TiO₂ & P₂O₅ in protomylointes and mylonites. The pattern of element variations is consistent with activities of hydrothermal fluids and open system in this zone. Due to thses conditions, feldspars in mylonites and protomylonites are sodic-potsic to sodic in composition. Overall, relationship field, microstructural, textural, geochemical and mineral chemistry characteristics confirm role of the shear zone for formation of these features. Many of researchers have approved relationship between forming of microstructures with stress/strain and hydrothermal fluids. The studied biotite crystals with content of ($\sum \text{FeO} + \text{MnO} \approx 13.4\text{-}42.21$) are neoform crystals. They may be occurred by post-magmatic fluids of the granitoid and have formed in ~550 to ~750 °C which corresponds to this deformation temperature.

Acknowledgment: we thank Dr. Rowe, GeoAnalytical Laboratory Washington State University (USA).

The vulnerability of subsurface soil organic carbon to *in situ* warming and altered root inputs

MARGARET TORN, CAITLIN HICKS PRIES, BIAO ZHU,
JANET JANSSON, EOIN BRODIE, PETER NICO,
DON HERMAN, BRYAN CURTIS AND CRISTINA CASTANH¹

¹Lawrence Berkeley National Laboratory and UC Berkeley,
One Cyclotron Rd, Berkeley, CA, (4720, USA;
mstorn@lbl.gov

Subsurface soils (>30 cm) store more than half of global soil organic carbon (SOC) and the processes governing soil C turnover vary with depth. However, most SOC research has focused on surface soil and controls on subsoil dynamics are poorly understood. We are building a whole soil profile (to 1.5 m) warming experiment in an annual grassland to study the effects of warming and root inputs on SOC dynamics throughout the profile. This presentation will describe the experiment prototype and an initiative for an international consortium of replicated experiments. The soil is heated with resistance heaters inserted to heat the profile to 4°C above ambient while maintaining the natural temperature gradient. Highly ¹³C-enriched *Avena fatua* grass root litter will be added within heated and unheated plots, in a factorial with addition of a DOC mixture to simulate root inputs. A comprehensive suite of measurements—instrumented *in situ* and in the laboratory—will be used to quantify the effect of warming and carbon inputs on soil C and N cycling. To improve predictive understanding and model skill, the experiment is focused on hypotheses concerning: (1) temperature sensitivity of native SOC and new (added root litter or DOC) carbon inputs with depth; (2) the effects of simulated root-input treatments with depth; and (3) interactions between warming and new C inputs. This study is one of the first to study responses of subsurface SOC to global change factors *in situ* and is designed to enhance our understanding of deep SOC stabilization mechanisms and improve predictions of the fate of soil carbon in a changing climate.

Polybaric differentiation within a clinopyroxenite body in the feeder-zone of an ocean island volcano (Fuerteventura, Canary Islands)

TORNARE E.¹ AND BUSSY F.²

¹²Institute of Earth Sciences, Anthropole, University of
Lausanne, CH-1015 Lausanne, Switzerland
levelyne.tornare@unil.ch, 2francois.bussy@unil.ch

It is now widely accepted that fractionation processes and magma differentiation or mixing occur during magma ascent to the surface. However, location of these processes remains a subject of controversy, as are the existence and size of shallow-level reservoirs. This question arises particularly in the case of ocean island volcanoes, which are not supported by a thick crust.

Fuerteventura allows access to the root-zone of an alkaline ocean island volcano. The PX1 pluton is a 22 Ma-old vertically layered mafic intrusion emplaced at shallow level. It consists in a heterogeneous clinopyroxenitic body intersected by dykes of various compositions, often gabbroic, and impregnated by more evolved melts. This clinopyroxenitic body does not show any vertical or horizontal layering. Contacts against the host rock are sharp without any development of a marginal facies. In some areas, the clinopyroxenite mass is modally and texturally highly heterogeneous with numerous enclaves and blobs of wehrlite, dunite and olivine-clinopyroxenite. Enclave outlines are often blurred with progressive transition to the matrix. These features are interpreted as evidence of repeated mingling episodes of crystallizing mushes. Other places are rather homogeneous with interstitial plagioclase occurrence in olivine-clinopyroxenite. Polybaric crystallization within PX1 is inferred from mineralogical assemblages, typically varying from sp-bearing dunite with high mg# (e.g. ol mg#: 82.2 - 83.2 and cpx mg#: 84.1 - 87.3) to plg-ol-clinopyroxenites or krs-clinopyroxenites with lower mg# (cpx mg#: >75.4). Moreover, whole-rock geochemistry indicate a clear differentiation trend among all clinopyroxenite lithologies. In addition cpx frequently display growth zoning with core composition of Cr-diopside evolving towards Ti-augite rims.

We suggest that the PX1 clinopyroxenite body records at least three levels of crystallization/differentiation, i.e. an upper mantle to lower crustal stage at which formed the spinel-bearing dunitic enclaves, a mid-crustal level recorded by the Cr-diopside cpx cores and a shallow-level final crystallization stage during which residual melts were extracted from the system and erupted as subaerial basaltic flows.

Two sources of water and pre-biotic molecules in the inner solar nebula

C. TORNOW^{1*}, P. GAST¹, S. KUPPER¹, I. PELIVAN¹,
E. KÜHRT¹ AND U. MOTSCHMANN^{1,2}

¹ DLR-Institute of Planetary Research, Rutherfordstr. 2, D-12489 Berlin, Germany, (*correspondence: carmen.tornow@dlr.de, philipp.gast@dlr.de)

² Institute of Theoretical Physics, TU Braunschweig, Mendelssohnstr. 2-3, D-38106 Braunschweig, Germany (u.motschmann@tu-bs.de)

Using a multi-stage model of the solar nebula (SN) we derive the chemical abundances and deuterium to hydrogen (D/H) ratios for water and pre-biotic species. The model consists of three consecutive stages described as:

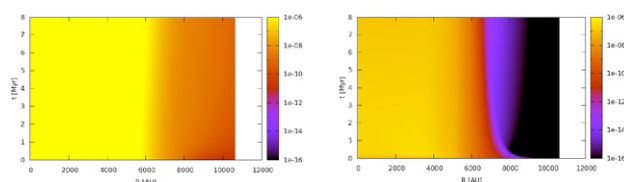
a spherical quasi-stationary core surrounded by the inter-core material of the parental cloud,

a collapsing core forming a proto-stellar source, an extending disk, and a spherical envelope, and

an accreting two-dimensional turbulent disk with gas and dust moving at different velocities

The collapse is simulated by a semi-analytical solution of the magneto-hydrodynamic equations based on a multi-zone mass density. In all stages the same chemical module is used (Semenov & Wiebe [1]).

Large amounts of water and the major pre-biotic molecule H₂CO were produced with relatively high D/H ratios in the dust phase of the first SN stage (source 1, see figure). During the collapse these dust grains flow into the inner nebula being the accretion range of rocky planets. In this range a hot corino forms as a result of the collapse. There, hot neutral gas phase reactions produce H₂O and H₂CO (source 2) along with the equivalent desorbed species but with lower D/H ratios. Thus, this ratio distinguishes molecules originating from different sources (i.e. model stages) of the nebula.



Relative HDO and HDCO abundances w.r.t. total hydrogen.

[1] D. Semenov and D. Wiebe (2011) *Astrophys. J. Supp.*, **196**:25 (37pp)

Metal fluxes at the sediment-water interface in a reservoir affected by AMD

E. TORRES¹, C. AYORA¹, ARIAS, J.L.², GARCÍA-ROBLEDO, E.², PAPANPYROU, S.^{2,3} AND CORZO, A.²

¹ GHS, IDAEA-CSIC, Jordi Girona 18-26, 08034, Barcelona, Spain ² Departamento Biología, Facultad de Ciencias del Mar y Ambientales, Universidad de Cádiz, Pol. Río San Pedro s/n, 11510- Puerto Real, Cádiz, Spain

³ Unidad Asociada de Oceanografía Interdisciplinar. UCA-Instituto de Ciencias Marinas de Andalucía-CSIC, Pol. Río San Pedro s/n, 11510 Puerto Real (Cádiz), Spain

Water reservoirs are a main source of water supply, and knowledge of the metal fluxes at the water-sediment interface is essential to predict their ecological quality. Moreover, redox oscillations promoted by turnover events may significantly alter metal cycling, especially if the reservoir is impacted by acid mine drainage (AMD). Under controlled laboratory conditions, several sediment cores were immersed in a tank of reservoir water and subjected to alternating oxic-anoxic conditions. A detailed sequential extraction was then performed on the sediments to speciate the metals into the solid phases, the pore and tank water was systematically analyzed, and a diffusion-reaction model was calibrated using the experimental results to quantify the reaction rates and the sediment-water fluxes.

The results showed that under oxic conditions, protons, Fe, and As decreased in the tank due to schwertmannite precipitation, whereas Al, Zn, Cu, Ni, and Co increased due to Al(OH)₃ and sulfide dissolution. The reverse fluxes occurred during hypoxia. The model, extended to the complete year, computed that between 25% and 50% of trace metals and less than 10% of Al precipitated under hypoxic conditions re-dissolved during the oxic period, while only 22% and 9% of the Fe and As precipitated under oxic conditions re-dissolved during hypoxia. Consequently, the sediment showed a total acidity neutralization capacity of 3.34 mol/m²/y, with Al, Fe, and proton removal accounting for 55%, 30%, and 13% of this capacity respectively. Compared with coastal marine environments, metal fluxes were up to two orders of magnitude higher, and the sulfur system was the major redox control, meaning that SO₄ was the major oxidant of OM and S(II) was the major O₂ consumer, with values near 90% in both cases.

Potential significance of sulfide mineral oxidation for the Cenozoic carbon cycle

MARK A. TORRES¹ GAOJUN LI² A. AND JOSHUA WEST¹

¹Department of Earth Sciences, USC, 3651 Trousdale Parkway, Los Angeles, CA 90089, USA. (marktorr@usc.edu)

²MOE Key Laboratory of Surficial Geochemistry, Department of Earth Sciences, Nanjing University, Nanjing 210093, China. (ligaojun@nju.edu.cn)

A climatic control on the rate of CO₂ consumption by silicate weathering is thought to stabilize Earth's climate over geologic timescales. At the same time, the observation that tectonic uplift accelerates weathering rates suggests that mountain building can profoundly affect the carbon cycle and global climate. Extensive uplift of mountain ranges during the Cenozoic is thought to have increased silicate weathering rates as evidenced by the marine isotopic records of Sr, Os, and Li, which all show dramatic changes from ~40 Ma to present. Without a corresponding input of CO₂, increased silicate weathering fluxes would deplete the atmosphere of all CO₂ within a few million years, a clearly unreasonable scenario. While a variety of hypotheses have been put forward in order to balance the Cenozoic C cycle, none of them appear to adequately describe the observations. As such, reconciling this "Cenozoic carbon-weathering paradox" has been a major and as yet unresolved challenge in geochemistry and Earth history. We hypothesize that Cenozoic uplift, in addition to increasing rates of CO₂ drawdown by silicate weathering, increased rates of sulfide oxidation coupled to carbonate dissolution. This provided a transient source of CO₂ that contributed, at least in part, to the relative stability of Cenozoic atmospheric pCO₂. The feasibility of this hypothesis is tested in two ways: (1) a simplified mass balance model that constrains the duration of transient CO₂ release in response to increased rates of sulfide oxidation and (2) an inverse isotope mass balance model that uses the Cenozoic isotope records of Sr and Os to reconstruct changes in silicate weathering and sulfide oxidation rates. Together, these models show that the contrasting residence times of DIC and SO₄²⁻ is sufficient to allow for CO₂ release over 40 Myr timescales and that modeled rates of silicate weathering and sulfide oxidation are consistent with independent proxy records of paleo-pCO₂.

On-site porewater measurements of Lake Baikal sediments

NATASCHA T. TORRES^{1,2}, LAWRENCE M. OCH¹, BEAT MÜLLER^{1*}, PETER C. HAUSER², MICHAEL STURM³ AND ELENA G. VOLOGINA⁴

¹Eawag, Swiss Federal Institute of Aquatic Science and Technology, CH-6047 Kastanienbaum, Switzerland

²Department of Chemistry, University of Basel, CH-4056 Basel, Switzerland

³Eawag, Swiss Federal Institute of Aquatic Science and Technology, CH-8600 Dübendorf, Switzerland

⁴Institute of Earth's Crust, Siberian Branch of RAS, Irkutsk, 664033, Russia

* (correspondence: beat.mueller@eawag.ch)

The extraction and analysis of sediment porewater is crucial to investigate the unique early diagenetic processes in Lake Baikal, the world's largest and deepest freshwater source. Investigation of the intricate sedimentary Fe/Mn layers requires porewater sampling and analysis with high spatial resolution and high yield of chemical parameters. Transporting the sediment samples from the field to the laboratory is logistically laborious, and prone to contamination, temperature changes, outgassing, mixing, diffusion and redox changes. Therefore, on-site methods are to be preferred.

Here we present an on-site application of a high spatial resolution porewater sampling and analysing method. The facility, combining filter tube sampler and a portable capillary electrophoresis instrument, was set up in a container on the shore of Lake Baikal for the immediate porewater sampling and analysis after coring from the ice.

The extraction of one porewater sample and the detection of its major inorganic cations and anions including the nutrients P and N could be accomplished in less than 15 minutes. The disturbance of the sediment was minimal and oxygen-sensitive reduced iron (Fe(II)) was detected within the set of cations, including Li⁺, Na⁺, K⁺, Mg²⁺, Ca²⁺, NH₄⁺, and Mn(II) without splitting, acidification or dilution of the sample. The equipment is inexpensive, easy to handle and to transport.



Tungsten isotope Heterogeneities in Archean Komatiites

M. TOUBOUL¹, I. S. PUCHTEL¹ AND R. J. WALKER¹

¹Department of Geology, University of Maryland, College Park, MD 20742, mtouboul@umd.edu

Recent studies demonstrated that the short-lived ¹⁸²Hf-¹⁸²W isotope system ($t_{1/2} \sim 9$ Myr) is a valuable tool for exploring key processes in the early evolution of the Earth, such as mantle differentiation by magma ocean crystallization or crustal extraction and late accretion [1, 2, 3]. The 3.8 Ga Isua rocks [1], the 2.8 Ga Kostomuksha komatiites [2] and the Nuvvuagittuq supracrustal rocks [3] have ~ 15 ppm ¹⁸²W excesses, which is similar to the predicted W isotope composition of the mantle prior to late accretion. However, the mantle source of Kostomuksha komatiites has HSE contents similar to that of the PM estimates, which is inconsistent with preservation of a pre-late accretionary mantle reservoir. Instead, their mantle source must contain an old component, which formed by magmatic differentiation or metal-silicate equilibration and, as a result, inherited a high Hf/W ratio during the lifetime of ¹⁸²Hf.

Here, we present new high-precision W isotope data for 3.3 Ga komatiites from the Weltevreden formation of the Barberton Greenstone belt and 2.4 Ga komatiites from the Vetreny belt. All Vetreny komatiites show small ¹⁸²W excesses that average $+6.2 \pm 4.5$ ppm (2σ SD, $n = 5$). At present, no ¹⁸²W anomaly can be resolved in the Weltevreden komatiites ($\mu^{182}\text{W} = -4.1 \pm 4.7$ ppm, $n = 2$). Similar to 3.5 Ga Komati komatiites [2], the Vetreny and Weltevreden komatiites have W isotope compositions close to that of the modern mantle, consistent with mantle sources having received most of the terrestrial complement of late accreted material, as indicated by the relatively high calculated HSE abundances in their mantle sources ($\sim 80\%$ of the PM estimates, [4, 5]). There is therefore no evidence for a gradual increase of late accreted material contribution in the mantle sources of Archean komatiites from 3.5 Ga to 2.4 Ga, in contrast to earlier conclusions [6]. Our new data rather suggest that most late accreted materials were delivered to Earth and homogenized in the deep mantle prior to 3.5 Ga.

[1] Willbold *et al.*, (2011) *Nature* **477**, 195-199. [2] Touboul *et al.*, (2012) *Science* **335**, 1065-1069. [3] Touboul *et al.* (2013) *EPSL*, submitted. [4] Connolly *et al.* (2011), *EPSL* **311**, 253-263. [5] Puchtel *et al.* (2013) *GCA*, submitted. [6] Maier W.D. *et al.* (2009) *Nature* **460**, 620-623.

Seasonal and interannual evolution of the monoacids organics in the atmosphere of the humid savanna of Lamto

R. PÊLÈMAYO TOURÉ^{1*}, G. KOUADIO¹, V. YOBOUÉ¹ AND C. ROMARIC BEUGRÉ²

¹ Laboratoire de physique de l'atmosphère et de mécanique des fluides (LAPA-MF) Université d'Abidjan- Cocody 22BP 231Abidjan22 Côte d'Ivoire ² Laboratoire de chimie-physique Université d'Abidjan-Cocody 22BP 582Abidjan22 Côte d'Ivoire

*(pelemayo@yahoo.fr)

This work was made within the framework of the network IDAF. It concerns the follow-up of the acidity of the atmosphere of an ecosystem of wet savanna from the organic fraction of the free acidity. It is a question of understanding the major factors which cause the variability of this organic acidity in the interannual and seasonal scales. During ten-year period (1995- 2004) 860 rainy samples were collected in the wet savanna of Lamto. By using Henry's law, we determined the contents in the air of major organic monoacids (HCOOH and CH₃COOH) from the concentrations of these acids measured in rains. The annual partial pressure of organic monoacids on the decade is extremely variable. It is $0,675 \pm 0,56$ ppb and of $0,413 \pm 0,14$ ppb respectively for the formic acid and for the acetic acid. This strong variability is bound to their various sources which are also very variable from one year to the next. The organic acidity varies from 40 % to 60 % on average and almost stable rest from a season to the other one. The seasonal analysis shows that generally the partial pressures of organic acids are of a factor twice as raised in dry season that in wet season. This difference is not inevitably connected to the quantity of haste registered from a season to the other one. But would more be connected to the biomass burning which contribute from 21 % to 51 % to the formation of organic acids in the wet savanna of Lamto.

Reactivity of natural heterogeneous nanoparticles

RAEWYN M. TOWN¹

¹Institute for Physics, Chemistry and Pharmacy, University of Southern Denmark, Campusvej 55, 5230 Odense, Denmark. E-mail:((raewyn.town@sdu.dk

The chemodynamics of metal complexation by humic acid (HA) is not well predicted by molecular concepts. HAs are small permeable particles with radius of a few nm. They carry a significant negative charge at ambient pH and are important complexants of metal ions in the environment. HAs are physically and chemically heterogeneous with distributed thermodynamic and kinetic properties. Recently developed theory for permeable charged nanoparticles [1-3] is applied to interpretation of metal ion binding by HA. Two opposing electric effects are operational with respect to the overall rate of association, namely (i) acceleration of metal ion diffusion from the bulk medium by the negative electrostatic field of the humic particle, and (ii) accumulation of metal ions in the negatively charged particle body by Boltzmann partitioning. The rate-limiting step in the metal-humic complex formation process is identified by comparing theoretical values of the rate constants for outer-sphere and inner-sphere complexation with those derived from measurements of the thermodynamic stability constant (K) and the dissociation rate constant (k_d). The experimentally derived association rate constant, k_a , is found to be practically independent of the degree of metal ion complexation, which confirms previous assumptions that the distribution in K is reflected in that of k_d . For the rapidly dehydrating Cu^{2+} , at an ionic strength of 0.1 mol dm^{-3} , the rate of diffusive supply of metal ions towards the humic particles is comparable to the rate of inner-sphere complex formation, indicating that both processes are significant for the observed overall rate. As the ionic strength decreases, the rate of diffusive supply becomes the predominant rate-limiting process, in contrast with the general assumption made for complexes with small ligands that inner-sphere dehydration is the rate-limiting step. The results are highly significant for interpretation of chemodynamics of metal complexation by HA.

[1] van Leeuwen, Town & Buffle (2011) *Langmuir* **27**, 4514-4519. [2] Duval & van Leeuwen (2012) *J Phys Chem A* **116**, 6443-6451. [3] van Leeuwen, Buffle & Town (2012) *Langmuir* **28**, 227-234.

Halogen ratios in kimberlites and their xenoliths related to their origin

CHIAKI TOYAMA^{1*}, YASUYUKI MURAMATSU¹,
HIROCHIKA SUMINO², JUNJI YAMAMOTO³
AND ICHIRO KANEOKA²

¹Gakushuin University, Tokyo, 171-8588, Japan

(*correspondence: chiaki.toyama@gakushuin.ac.jp,
yasuyuki.muramatsu@gakushuin.ac.jp)

² University of Tokyo, Tokyo, 113-0032, Japan

(sumino@eqchem.s.u-tokyo.ac.jp, ikaneoka@aol.com)

³Hokkaido University, Hokkaido, 060-0810, Japan,

Recently, halogens are revealed to be one of the powerful tracers for water cycling in subduction zones [e.g., 1]. In the previous conference, we reported analytical method and some data for Cl, Br and I in kimberlites from South Africa, Greenland, Canada, Brazil, Russia and China, and found that the I/Br ratios of kimberlites are classified into two groups. In this study, additional samples of kimberlites and mantle-derived xenoliths collected from South Africa and Russia were analyzed to investigate the halogen characteristics and their origins in the kimberlite source regions. We analyzed halogens by using the pyrohydrolysis method [2] combined with ICP-MS and ion chromatography.

The kimberlite and xenolith samples from South Africa, Greenland, Canada and Brazil (Group S) showed high I/Br ratios (about 1×10^{-1}). The value is fairly similar to that of CI chondrite (I/Br ratio: about 1×10^{-1} [3]), suggesting these kimberlites preserve the characteristics of primordial halogen in the mantle from which the kimberlite magmas were formed. In contrast, both Chinese and Russian kimberlite and xenolith samples (Group C) showed low I/Br ratios (about 6×10^{-3}). Similarly low I/Br ratios have been observed in fluid inclusions in eclogites derived from seawater-altered oceanic crust [4] and in seawater associated with halite precipitation [5]. This suggests an involvement of seawater-derived halogens having low I/Br ratios in the source regions of the Group C kimberlites. Low I/Br ratios found in xenoliths also indicate possible subduction-related metasomatism on the halogen composition of the subcontinental lithospheric mantle.

[1] Sumino *et al.* (2010) *EPSL* **294**, 163-172. [2] Muramatsu & Wedepohl (1998) *Chem. Geol.* **147**, 201-216. [3] Anders & Ebihara (1982) *GCA* **46**, 2363-2380. [4] Svensen *et al.* (2001) *J. Metamorphic Geol.*, **19**, 165-178 [5] Zherebtsova & Volkova (1966) *Geochem. Inter.* **3**, 656-670.

Chemical weathering in glacial and proglacial environments

MARTYN TRANTER AND THE BRISTOL GLACIOLOGY GROUP

Bristol Glaciology Centre, School of Geographical Sciences,
University of Bristol BS8 1SS, UK.
(M.Tranter@bristol.ac.uk)

Physical weathering in glaciated environments initially produces debris which is fine-grained (predominantly silt-sized) and coated in microparticles. Geochemically reactive phases, such as carbonates and sulphides, are liberated from the interior of silicate mineral masses and so become more readily available for chemical weathering. Chemical weathering in glacial environments is microbially mediated, since ingress of atmospheric gases to glacier beds and water-laden proglacial sediments is often limited. Instead, the protons required to push chemical weathering beyond simple hydrolysis reactions are generated from the oxidation of sulphides and organic matter. This is the case beneath smaller glaciers, and appears to be the case beneath ice sheets, from waters sampled either directly or indirectly to date. A fundamental difference between the chemical weathering regimes beneath larger and smaller ice masses is the residence time of water beneath the larger ice masses. It is more likely that low oxygen and anoxic conditions are found beneath ice sheets than beneath smaller glaciers. Hence, it is likely that Fe-rich, anoxic waters will be found beneath sectors of the Antarctic and Greenland Ice Sheets. Such waters have the potential to act as fertilisers of Fe-poor circumpolar seas. Chemical weathering is not limited to the aquatic zones that underlie the ice sheets. Movement of ice over bedrock produces localised pressure melting, and the regelation waters produce micro-chemical weathering environments that allow oxidation of sulphides by oxygen, and the formation of nano-particulate iron oxyhydroxides. The refreezing of these waters back onto the glacier sole traps basal debris, which, following ice berg calving at the ice sheet margin, transport potentially labile Fe further afield into the surrounding sea. Glacial debris is also a source of labile P to aquatic ecosystems. Finally, a spectrum and surface and basal processes result in glacial runoff often containing labile DOC and DON. Hence, glaciers and ice sheets are currently being thought of as biogeochemical reactors that convert relatively bedrock into a cocktail of relatively labile, potentially bioavailable, nutrients.

The chemical weathering of proglacial sediments too has potential to effect global nutrient and geochemical cycles. Recent work of potential impacts on the global P cycle is reviewed.

Technetium Reduction and Permanent Sequestration by Formation of Low-Solubility Sulfide Mineral Phases

P.G. TRATNYEK^{1*} AND D. FAN¹

¹Oregon Health & Science University, Beaverton, OR, USA
(*correspondence: tratnyek@ehs.ogi.edu)

Under anoxic conditions, soluble $^{99}\text{TcO}_4^-$ can be reduced to less soluble $\text{TcO}_2 \cdot n\text{H}_2\text{O}$, but the oxide is highly susceptible to reoxidation. One way to minimize the mobility of the Tc^{VII} oxyanion pertechnetate (TcO_4^-) is to effect reduction under sulfidogenic conditions (generated abiotically by Fe^0 or biotically) to form TcS_x , which is significantly slower to oxidize than $\text{Tc}^{\text{IV}}\text{O}_2$. Here we investigate a novel strategy for remediation of Tc-contaminated groundwater whereby sequestration as Tc sulfide is favored by sulfidic conditions stimulated by nano zero-valent iron (nZVI). Fundamental aspects of this hypothesis have been investigated using batch and column experiments under abiotic and biotic conditions.

In the abiotic batch experiments, nZVI was pre-exposed to increasing concentrations of sulfide in simulated Hanford groundwater for 24 h to mimic the onset of aquifer biotic sulfate reduction. Solid-phase characterizations of the sulfidated nZVI confirmed the formation of nanocrystalline FeS phases, but higher S/Fe ratios (> 0.112) did not result in the formation of significantly more FeS. The kinetics of Tc sequestration by these materials showed faster Tc removal rates with increasing S/Fe between $S/\text{Fe} = 0-0.056$, but decreasing Tc removal rates with $S/\text{Fe} > 0.224$. The more favorable Tc removal kinetics at low S/Fe could be due to a higher affinity of TcO_4^- for FeS than iron oxides, and electron microscopy confirmed that the majority of the Tc was associated with FeS phases. X-ray absorption spectroscopy revealed that as S/Fe increased, the pathway for Tc(IV) formation shifted from $\text{TcO}_2 \cdot n\text{H}_2\text{O}$ to TcS_2 . The most substantial change of Tc speciation occurred at low S/Fe, coinciding with the rapid increase in Tc removal rate. This agreement further confirms the importance of FeS in Tc sequestration. The inhibition of Tc removal at high S/Fe appears to have been caused by excess HS^- , which, however, is expected to be mitigated under natural conditions due to the abundance of iron oxides that can scavenge sulfide. The reoxidation kinetics of Tc sequestered under sulfidic conditions was significantly slower than that under non-sulfidic conditions, confirming that Tc(IV) sulfide is more resistant to oxidation than Tc(IV) oxide.

Diagenesis, deformation mechanisms and architecture of the fault zones in the extensional Neogene basins of the northeast Iberian Peninsula.

A. TRAVÉ; V. BAQUÉS; I. CANTARERO; E. PLAYÀ, G. ALÍAS, M. MORAGAS; C. MARTÍNEZ; F. PACHECO; C. J. ZAFRA; AND A. PLATA

Departament de Geoquímica, Petrologia i Prospecció Geològica. Facultat de Geologia. Universitat de Barcelona (UB). c/ Martí i Franquès s/n, 08028 Barcelona, Spain. (atrave@ub.edu)

The faults limiting the Vallès and Penedès basins affect Hercynian crystalline rocks, Triassic, Jurassic and Cretaceous carbonates, and Miocene carbonates, evaporites and detrital rocks. These faults generate gouges, cataclasites, breccias and pseudotachylytes. The main cements are calcite, quartz, laumontite, muscovite, chlorite, albite and iron oxides, depending on the PT conditions. We have established four tectonic events that gather different deformation phases.

Applying geothermobarometers in neofomed chlorites and K-white micas, we have established the PT paths from Hercynian to Neogene. We have observed how the faults have controlled the thickness and distribution of sediments during the first Mesozoic rifting.

Dolomitization and karstification are two widespread diagenetic processes that are recurrent through time and are clearly related to faults.

Trace elements together with radiogenic and stable isotopes of the calcite cements in veins have allowed us to constrain the origin and regime of fluids and the fluid pathways through time.

Isotope characteristics of the Bon Accord oxide body, Barberton greenstone belt, South Africa

M. TREDOUX^{1*}, F. ROELOFSE¹ AND A. SHUKOLYUKOV³

¹Dept of Geology, Univ of the Free State, Bloemfontein, South Africa (*correspondence: mtredoux@ufs.ac.za)

²Scripps Inst of Oceanography, UCSD, La Jolla, USA.

The Bon Accord oxide-silicate body (BAOS) in the the Barberton greenstone terrane is associated with ultramafic igneous rocks. It initially attracted interest because of its extreme whole rock NiO enrichment (>30%) and very unusual mineralogy: In the 1960s, de Waal¹⁻⁵ described several new minerals, including the Ni end-members of magnetite (ferroan Trevorite) and olivine (liebenbergite). De Waal⁶ identified five zones in the semi-circular body, with an increase in hydrous phases from a massive central portion (mainly containing nepouite and Trevorite) to the schistose rim. On the grounds of petrographic information, he proposed that the BAOS represents an altered Archean meteorite.

Tredoux and co-workers⁷ re-examined samples of the BAOS body (sadly no longer *in situ*) in the 1980s, concentrating on its geochemistry. They rejected the meteorite model in favour of a terrestrial model, because of (a) similarities between chromites in the BAOS and those in the host ultramafite, (b) the possibility that this host rock is potentially associated with the basal part of the Jamestown ophiolite⁸ and thus would not have been at surface in the Archean, (c) the high concentrations of platinum-group elements (PGE) which are usually relatively low in Ni-rich irons, and (d) positive (unmeteorite-like) trends of PGE patterns⁷ of many of the BOAS samples.

Radiogenic isotope ratios point to extensive, and variable, degrees of disturbance⁷, but the U-Pb and Sm-Nd data hint at an Archean (3.5 Ga) age. The Cr isotopes, when normalized to a terrestrial standard, yield a value of 1, within analytical error, which points to a terrestrial source for the material.

[1] De Waal (1969) *Am. Min.* 54, 1204-1208; [2] De Waal (1970) *Am. Min.* 55, 1842-1208; [3] De Waal (1971) *Am. Min.* 56, 1077-1081; [4] De Waal (1972) *Am. Min.* 57, 1524-1527; [5] De Waal (1973) *Am. Min.* 58, 733-735; [6] De Waal (1978) *Mineralisation in metamorphic terranes (ed: WJ Verwoerd)*, *Geol. Soc. of South Africa*, 87-98; [7] Tredoux, de Wit, Hart, Armstrong, Lindsay & Sellschop (1989) *J. Geophys. Res.* 94 (B1), 795-813; [8] De Wit, Hart & Hart (1897) *J Afr Ea Sci* 6, 681-730.

Non-Complexing Anions for Raman Microprobes under Hydrothermal Conditions

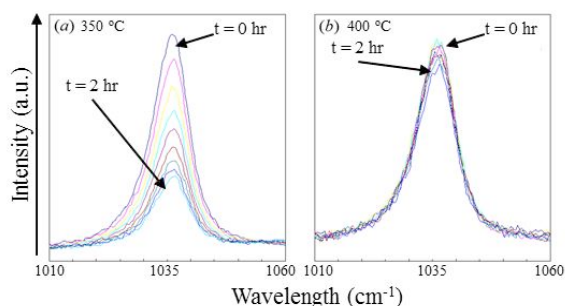
L.M.S.G.A. APPELEGARTH¹, C. ALCORN¹, K. BISSONETTE¹ AND P.R. TREMAINE^{1*}

¹ University of Guelph, Ontario, Canada
(tremaine@uoguelph.ca) (* presenting author)

Small scale techniques based on the use of diamond anvil cells (DAC) and capillary cells (“high pressure optical cells”, HPOC) are being increasingly employed to study subcritical and supercritical solutions using Raman spectroscopy [1]. Quantitative Raman measurements to determine thermodynamic properties and structural information often require the use of internal reference standards. These must be soluble, non-complexing and stable under hydrothermal conditions. The species used for this purpose at ambient conditions are bisulfate (HSO_4^-), perchlorate (ClO_4^-), perhenate (ReO_4^-), and triflate (CF_3SO_3^-).

This paper reports the thermal stability of these internal standards as a function of pH up to 420 °C and 30 MPa. Time-dependent reduced isotropic Raman spectra were obtained using a custom-made LabRamHR 800 spectrometer with quartz HPOC capillary cells at 30 MPa. Typical spectra are shown in Figure 1. In neutral solutions, perchlorate, perhenate and triflate are stable up to 140 °C, 200°C and 400°C, respectively. Simple rate equations, criteria for selecting reference anions, and measurement practices for quantitative hydrothermal studies in Raman microprobes are presented.

Figure 1. Raman spectra showing 0.1 m CF_3SO_3^- decomposition: a) 350°C pH 2 and b) 400°C neutral conditions.



[1] I.M. Cho, R.C. Burruss, W. Lu (2005), in *Adv. in High-Press. Technol. Geophys. Appl.*, J. Chen, Y. Wang, T.S. Duffy, G. Shen, L.F. Dobrzinetskaya, Eds., Chap. 24, pp. 475-485.

Quantifying the open-system behavior of cosmogenic noble gases in quartz

M.M. TREMBLAY^{1,2*}, D.L. SHUSTER^{1,2} AND G. BALCO²

¹Department of Earth and Planetary Science, University of California, Berkeley, Berkeley CA 94720 USA

(*correspondence: mtremblay@berkeley.edu)

²Berkeley Geochronology Center, 2455 Ridge Rd., Berkeley CA 94550 USA

Simultaneous production and diffusion of cosmogenic noble gases in minerals at the Earth's surface offers a potentially powerful tool for reconstructing past Earth surface temperatures. In order to utilize this open-system behavior for paleothermometry, knowledge of both the production rate and diffusion kinetics of a particular cosmogenic nuclide-mineral pair is required. We investigated the diffusion kinetics of ^3He and ^{21}Ne in quartz through a series of stepwise heating and degassing experiments. Natural and synthetic quartz samples were irradiated with protons to produce uniform distributions of ^3He and ^{21}Ne through similar nuclear transmutations as those induced by cosmic rays. Single grains of irradiated natural quartz exhibit two stages of linear Arrhenius behavior for both He and Ne diffusion: one at low temperatures and for gas release fractions of $\sim 75\%$, and one at high temperatures for the remaining $\sim 25\%$. We interpret these two Arrhenian arrays to represent multiple diffusion domain-type behavior in quartz and will discuss the physical meaning of such domains through ongoing experiments on synthetic and natural quartz. Comparison of degassing experiments on vein quartz from the Transantarctic Mountains, conducted using both cosmogenic ^3He from a several-hundred grain aliquot and proton-induced ^3He from a single grain, demonstrates the following: (i) $<6\%$ of the cosmogenic ^3He produced within the low retentivity domain is retained at subzero temperatures over several Myr of exposure, while (ii) $>90\%$ of ^3He is retained within the high retentivity domain. A simple exposure history for this sample using a two-domain diffusion model suggests a maximum effective exposure temperature of -14°C , although ^{10}Be and ^{21}Ne measurements suggest a more complicated history involving both burial and exposure. In contrast, the measured diffusion parameters for Ne from all experiments suggest quantitative retention in quartz over millions of years and at effective exposure temperatures less than 45°C . The ratio of cosmogenic ^3He to ^{21}Ne in quartz may therefore be useful for studying the temperatures of surface processes in polar environments.

Impacts of CO₂ perturbation on well composite samples: experiments and numerical simulations

J. TREMOSA¹, S. MITO², P. AUDIGANE¹ AND Z. XUE²

¹BRGM, 45060 Orléans, France; (j.tremosa@brgm.fr)

²RITE, Kyoto, 619-0292, Japan; (mito@rite.or.jp)

Abandoned wells in the depleted reservoirs envisaged to host CO₂ geological storages are the main possible leakage pathways of CO₂ towards shallow aquifers. Then, for impact assessment, the alteration of well materials with CO₂ in the reservoir conditions requires to be characterized.

Here, the interaction of a composite well sample – formed of steel casing, surrounded by Portland cement, itself surrounded by sandstone – with wet CO₂ and CO₂-saturated brine under pressure and temperature controlled conditions was studied combining a set of batch experiments [1] and reactive transport modeling. In the experiments, lasting up to 8 weeks, noticeable mineralogical changes were observed in the cement, at the interface with the sandstone, leading to a carbonation of the cement. Main mineralogical changes consisted in dissolution of portlandite, replacement of CSH phases rich in Si by Ca-rich CSH phases and precipitation of calcite, amorphous silica and zeolite [1]. Interestingly, no re-dissolution of calcite was observed at the outer boundary of the cement, in relation with the penetration of the carbonation front, as observed in experiments involving only cement and CO₂-saturated brine [2]. For the two other components of the composite well samples, few changes were observed. The steel shown a moderate corrosion with some precipitations of Fe-oxides at its surface. No changes were observed in the sandstone.

These changes in mineralogy were reproduced with the reactive transport model, which highlights the successive dissolution/precipitation reactions. A good agreement was also obtained with the brine composition evolution record during the experiment. It is worth noting that the model suggested slight mineralogical changes in the sandstone consisting in dissolution of carbonates at the boundary of the sample, in direct contact with the CO₂-saturated brine. This observation, in link with the experimental observations in the cement, indicate a buffering effect of the rock on the CO₂ perturbation. This possible buffering was observed by observations at a larger scale on industrial analogue well samples [3] and suggests a preservation of the well integrity.

- [1] Asahara et al. (2013). Energy Procedia, GHGT11. [2] Kutchko et al. (2007). Environ. Sci. Technol., 41, 4787-4792. [3] Carey et al. (2007). Int. J. Greenhouse Gas Control, 1, 75-85.

Benthic nitrogen fixation and Mn/Fe reduction in the Mauritanian oxygen minimum zone: Two overlooked processes?

TREUDE T.^{1*}, BERTICS VJ², GIER J³ AND SOMMER S⁴

¹GEOMAR Helmholtz Centre for Ocean Research Kiel, Wischhofstr. 1-3, 24148 Kiel, Germany, (ttreude@geomar.de)(*presenting author)

²Harvard University, Biological Laboratories, 16 Divinity Avenue, Cambridge, MA 02138, USA, (vbertics@fas.harvard.edu)

³GEOMAR Helmholtz Centre for Ocean Research Kiel, Wischhofstr. 1-3, 24148 Kiel, Germany, (jgier@geomar.de)

⁴GEOMAR Helmholtz Centre for Ocean Research Kiel, Wischhofstr. 1-3, 24148 Kiel, Germany, (ssommer@geomar.de)

Oxygen minimum zones (OMZ) are currently in the focus of many marine biogeochemical studies, especially since their spreading has been discovered and associated with climate change. Understanding element cycling of OMZ is an important key to predict dynamics of this systems as well as feedbacks to environmental changes. Nitrogen and iron are two central elements in cycling processes of OMZ; however, budgeting and following the fate of these elements still remain challenging. Here we present two benthic processes, microbial N₂ fixation and Mn/Fe reduction, from the Mauritanian OMZ, which were measured at six stations along a depth transect between 50 and 1100 m water depth. N₂ fixation was deduced from nitrogenase activity via the acetylene reduction method. Mn/Fe reduction was measured indirectly via total anaerobic production of dissolved inorganic matter after subtraction of sulfate reduction activity. Highest integrated nitrogenase activity (~360 μmol C₂H₄ m⁻² d⁻¹ down to 20 cmbsf) and Mn/Fe reduction (~29 mmol m⁻² d⁻¹ down to 10 cmbsf) was found within low oxygen zones (45 to 56 μM O₂) beneath water depths of 100-240 m. Both processes generally decreased with greater water depths. The percentage of Fe/Mn reduction in total anaerobic organic matter degradation in the top 10 cm increased from ~65% to over 90% downslope. We are convinced that both processes play an important role for element budgeting of OMZ and should be considered in future studies. Especially in developing OMZ featuring terrestrial dust/iron input to the seafloor, such as the Mauritanian OMZ, iron reduction could play a key role for delaying the buildup of sulfidic conditions during organic matter degradation.

Boninite-derived mafic-ultramafic intrusives from Northern Victoria Land (Antarctica): Implications for mantle source metasomatism

R. TRIBUZIO^{1,2*}, F. HENJES-KUNST³, R. BRAGA⁴
AND M. TIEPOLO²

¹ Dipartimento di Scienze della Terra e dell'Ambiente, Pavia, Italy.

² C.N.R. - Istituto di Geoscienze e Georisorse, Pavia, Italy.
(*correspondence: tribuzio@crystal.unipv.it)

³ Bundesanstalt für Geowissenschaften und Rohstoffe (BGR), Hannover, Germany

⁴ University of Bologna, Italy

The Cambrian mafic-ultramafic sequence from Niagara Icefalls area in Northern Victoria Land represents a rare case of boninite-derived intrusive complex. The sequence mostly consists of dunites, orthopyroxenites, melanorites and gabbro-norites, locally associated with hornblende granitoids that were most likely emplaced at upper levels of the continental crust. The mafic-ultramafic sequence was interpreted to be formed by boninite-type melts according to the fractional crystallization evolution: olivine → orthopyroxene → orthopyroxene + plagioclase ± clinopyroxene. The concentrations of incompatible trace elements in the whole sequence are extremely low (e.g., TiO₂ ≤ 0.06 wt%, Y < 3 ppm). The whole-rock REE chondrite-normalized patterns vary from slightly depleted to enriched in the LREE (La_N/Sm_N = 3.5-0.5), in agreement with the REE variations observed for the included clinopyroxenes. The initial ε_{Nd} of the mafic-ultramafic sequence spans one order of magnitude, which roughly decrease with increasing La_N/Sm_N. The granitoids associated with the mafic-ultramafic sequence have nearly homogeneous trace and Nd-Sr isotopic compositions. In particular, the granitoids have high REE amounts, with LREE-enriched patterns (La_N/Sm_N = 4.3-3.4), and highly radiogenic initial Nd-Sr values. The highest initial ε_{Nd} and the lowest initial ⁸⁷Sr/⁸⁶Sr (0.7035) of the mafic-ultramafic sequence document the involvement of isotopically depleted asthenospheric sources. The wide Nd isotopic variations in the mafic-ultramafic sequence could be correlated with the boninite-type parental melts experiencing assimilation of crustal material. However, the most enriched isotopic compositions were found for the most primitive rocks: the dunites and the orthopyroxenites. We thus attribute the enriched isotopic compositions to a mantle source metasomatized by components derived from subducted oceanic metasediments.

High temperature alteration of the gabbroic oceanic crust (Ligurian ophiolites, Italy): Evidence for hydrothermal-magmatic interactions

R. TRIBUZIO^{1,2}, M.R. RENNA³, L. DALLAI⁴
AND A. ZANETTI²

¹ Dipartimento di Scienze della Terra e dell'Ambiente, Università di Pavia, Italy (tribuzio@crystal.unipv.it)

² C.N.R. - Istituto di Geoscienze e Georisorse, U. O. di Pavia, Italy

³ Dipartimento di Fisica e di Scienze della Terra, Università di Messina, Italy

⁴ C.N.R. - Istituto di Geoscienze e Georisorse, U.O. di Pisa, Italy

The gabbroic bodies from the Jurassic Ligurian ophiolites are structurally and compositionally similar to the gabbroic sequences from the oceanic core complexes of the Mid Atlantic Ridge. The high temperature cooling evolution the Ligurian gabbros is locally associated with formation of hornblende-bearing felsic dykes and hornblende vein networks. The hornblende veining is correlated with development of hornblende as coronas/pseudomorphs after the igneous clinopyroxene in the host gabbros. We also found hornblende-rich gabbros as dykes/sills within mantle peridotites.

The hornblendes from the felsic dykes and the hornblende gabbros are characterized by low Mg#, CaO and Al₂O₃, negligible Cl, and high TiO₂, K₂O, REE, Y, Zr and Nb. The whole-rock Sm-Nd isotopic compositions of the felsic dykes and the hornblende gabbros define a Jurassic isochron with a MORB-type initial ¹⁴³Nd/¹⁴⁴Nd ratio. The δ¹⁸O of the hornblendes and coexisting zircons from these rocks do not decipher the presence of a seawater component in these melts. We propose that the felsic dykes and the hornblende gabbros formed by SiO₂-rich silicate melts derived from high degree fractional crystallization of MOR-type basalts.

The vein and the coronitic/pseudomorph hornblendes show high Mg# and CaO, significant Cl and low TiO₂ and K₂O. The coronitic/pseudomorph hornblendes have trace element compositions similar to those of the clinopyroxenes from the gabbros and δ¹⁸O close to that of seawater, thereby documenting an origin by reaction between migrating seawater-derived fluids and the host gabbros. The vein hornblendes commonly show slight LREE enrichment and relatively high values of Nb and δ¹⁸O. The crystallization of these hornblendes most likely required the involvement of both seawater and magmatic components.

FASTREACT – Efficient reactive transport modelling for long-term repository safety assessments

P. TRINCHERO^{1*}, J. MOLINERO¹, G. ROMÁN-ROSS¹,
STEN BERGLUND² AND JAN-OLOF SELROOS³

¹ Amphos 21 Consulting S.L., Passeig Garcia Faria, 49-51, E-08019, Barcelona, Spain

² HydroResearch AB Stora Marknadsvägen 15S SE-18334 Täby Sweden

³ Swedish Nuclear Fuel and Waste Management Company, Box 250 101 24 Stockholm, Sweden

Reactive transport modelling is commonly used to provide support for repository engineering activities and safety assessment studies [1]. Yet, the very large temporal and spatial scales involved in these types of studies along with the non-linearity of the underlying processes pose formidable computational challenges that usually force modellers to simplify the problem.

In this work, we present a numerical tool, denoted as FASTREACT, for the efficient solution of large-scale reactive transport simulations. The tool, which relies on the theory of Stochastic-Convective models [2], decomposes complex three-dimensional geometries into a set of independent streamlines. Reactive transport processes are then solved over the whole set of streamlines using one single reference simulation that incorporates explicitly all the relevant geochemical processes. FASTREACT has been developed for safety assessment calculations of radionuclide transport in fractured rock and thus provides efficient handling of the coupling between advection, reactions and matrix diffusion processes for large amounts of input and output data.

The methodology is tested against a synthetic case study where a radionuclide transport problem is solved over a set of heterogeneous conductivity fields. The results compare favourably with those obtained using an Eulerian approach whereas the computational performance of FASTREACT is proved to be much more efficient when compared with the “traditional” Eulerian 3D simulations.

[1]. Selroos, J.-O. (2008) Site-descriptive modeling of geological repository sites in Sweden International Geological Congress, Oslo (Norway). [2]. Cvetkovic V, Dagan G, 1994. Transport of kinetically sorbing solute by steady random velocity in heterogeneous porous formations. *J. Fluid Mech.*, 265, pp 189-215.

High-precision Neodymium isotope analyses by MC-TI-MS

ANNE TRINQUIER¹, CLAUDIA BOUMAN¹
AND JOHANNES SCHWIETERS¹

¹ Thermo Fisher Scientific, Bremen, Germany,
anne.trinquier@thermofisher.com

Resolving Nd isotope anomalies at the ppm level for materials with a wide range of compositions and Nd concentrations is key to unraveling fundamental relations in geochronology, geochemistry, cosmochemistry and environmental sciences. Nd isotope Thermal-Ionization Mass Spectrometry (TIMS) has proven successful in running Nd both as Nd⁺ on multiple filament assembly (300-500ng) [1] and NdO⁺ on single filament assembly (1-10ng) [2].

The present study on a Thermo Scientific TRITON *Plus* instrument assesses precision and accuracy of Nd analyses adapting the above mentioned protocols on two Nd standards (Merck # 170335 and JNdi [3]) for sample loads ranging from 0.5 µg to the ng range, using 10¹¹ Ω amplifiers, automatized mode and shortened analysis time compared to literature. Nd⁺ analyses of 500ng and 100ng loads on double Re filament assemblies in static mode with rotation of the amplifier-cup association (“virtual amplifier”) yield indistinguishable isotopic ratios. The 1-yr 2RSD reproducibility R_i for ¹⁴³Nd/¹⁴⁴Nd ratios expressed in ppm: R₁₄₃ = 5 and R₁₄₂₋₁₅₀ = 4 to 21 (n=70, 3.6-10V ¹⁴²Nd⁺, 100 or 500 ng). Notably, analyses with 10V ¹⁴²Nd⁺ ion beams could be limited to 1hr. NdO⁺ analysis of 10ng loads on single Re filament assembly, a different ion-beam setting, in static mode, yields Nd isotopic ratios indistinguishable from those obtained in Nd⁺ analyses. This validates the stability of the instrument ion optics, the Faraday cups, and the current amplifier system, as well as accurate oxide interference correction. The 2RSD reproducibility expressed in ppm: R₁₄₃ = 16 (n=13, 1.5V ¹⁴²Nd¹⁶O⁺). Notably, one analysis was limited to 25min.

With acquisition times ≤90min and a reproducibility on ¹⁴³Nd/¹⁴⁴Nd of 5ppm (Nd⁺) and 16ppm (NdO⁺), this study holds promise for achieving highly reproducible results with ever smaller sample amounts. A TRITON *Plus* Nd⁺ study on 100 pg loads using 10¹² Ω amplifiers reported 2RSD reproducibility of 176 ppm on ¹⁴³Nd/¹⁴⁴Nd [4]. Detection limit, precision and accuracy of Nd isotope TIMS analysis are thus expected to be further improved by the combined use of 10¹² Ω amplifiers and NdO⁺ analysis.

[1] Caro et al. (2003) *Nature* 423, 428-432. [2] Harvey and Baxter (2009) *Chem. Geol.* 258, 251-257. [3] Tanaka et al. (2000) *Chem. Geol.* 168, 279-281. [4] Koornneef et al. (2013) *J. Anal. At. Spectrom.*, in press.

Geochemistry and Re-Os age for black shales from the Cambrian-Ordovician boundary, Green Point, western Newfoundland

GYANA R TRIPATHY^{1,*}, JUDITH L HANNAH^{1,2},
HOLLY J STEIN^{1,2} AND GANG YANG¹

¹AIRIE Program, Department of Geosciences, Colorado State University, Fort Collins, CO 80523-1482, USA

(*Presenting author: gyana.tripathy@colostate.edu)

²CEED Centre of Excellence, University of Oslo, P.O. Box 1048, 0316 Oslo, Norway

Chemical and isotopic signatures for black shales can serve as proxies for reconstruction of paleoenvironmental conditions. Here we bring Rock-Eval, major and trace elements and Re-Os isotopic data together to examine the environmental record at the Cambrian-Ordovician Global Stratotype Section and Point (GSSP) at Green Point in western Newfoundland. The Green Point shales are oil mature and contain Type-II organic material of marine origin. A Re-Os isochron for these shales provides the first depositional age for the GSSP boundary at 484 ± 16 Ma (2σ ; Model 3 age; MSWD = 21; $n = 13$), with an initial $^{187}\text{Os}/^{188}\text{Os}$ ratio of 0.74 ± 0.05 .

Factor analysis of the geochemical dataset for Green Point shales shows association of most trace elements with TOC and S contents, ensuring an authigenic origin for most elements and hence, their validity for evaluating paleoredox state. Relatively high enrichment factors for redox-sensitive elements (*e.g.*, Re, U and Mo) compared to average shales, but lower enrichment factors relative to modern Black sea sediments, suggest deposition in anoxic waters. Comparison of global Cambrian-Ordovician shale geochemistry datasets leads us to suggest that anoxic conditions and warm oceanic regimes were restricted to the margins of Laurentia and Baltica whereas depositional basins with colder waters (*e.g.* Avalonia and Gondwana) show geochemically less reducing conditions. These outcomes underscore the important role of paleogeography in regulating ocean conditions and marine life.

Supported by NSF award EAR-0844213 to JLH and HJS; thanks to Jörg Maletz and Sven Egenhoff, co-PIs on the NSF award, for guidance in the field and inspiring conversations.

Nanoparticle interactions with lipid bilayers studied by nonlinear optics

J.M. TROIANO, S.R. WALTER, L.L. OLENICK
AND F.M. GEIGER*

Department of Chemistry, Northwestern University, 2145 Sheridan Road, Evanston, IL 60208, USA

(*correspondence: geigerf@chem.northwestern.edu)

The goal of this work is to understand the fundamental chemistry of how nanoparticles (NPs) interact with biologically relevant interfaces *in situ* at the molecular level. Surface specific nonlinear optical spectroscopies, namely second harmonic (SHG) and sum frequency generation (SFG), are used to investigate the interactions of NPs with lipid bilayers as model cell membranes. Specifically, SHG allows us to probe binding interactions, while SFG allows us to investigate the effect of NPs interactions with the molecular structure of the lipids.

We use resonant and nonresonant SHG to quantify binding constants, adsorption free energies, and interfacial charge densities in real time for gold NPs and quantum dots interacting with bilayers of various lipid compositions. We also examine the relationship between the measured adsorption free energies and the electric double layer interfacial potential to determine the change in the charge state of the NPs during these interactions. Combining this knowledge with the SFG results, detailing molecular structural changes due to the NP-membrane interaction, allows us to predict possible pathways for the molecular level NP-lipid bilayer interactions.

The impact of lipid composition, NP core composition, and capping ligand on the NP-membrane interactions is investigated. Understanding how nanomaterials interact with lipid bilayers at the molecular level is important for predicting and controlling molecular interactions of nanomaterials with living systems as well as designing environmentally and biologically sustainable nanomaterials.

Shallow-level magma-sediment interaction and explosive behaviour at Anak Krakatau

TROLL, V.R.^{1,4}, JOLIS, E.M.¹, DAHRÉN, B.¹, DEEGAN, F.M.¹, BLYTHE, L.S.¹, HARRIS, C.², BERG, S. E.¹, HILTON, D.R.³, FREDA, C.⁴ AND SCHWARZKOPF, L.M.⁵

¹ Dept. of Earth Sciences, CEMPEG, Uppsala University, Sweden

² Dept. of Geological Sciences, University of Cape Town (UCT), Rondebosch, South Africa

³ Geosciences Research Division, Scripps Institution of Oceanography, UC San Diego, La Jolla, USA

⁴ Istituto Nazionale di Geofisica e Vulcanologia (INGV), Rome, Italy

⁵ GeoDocCon, Konradsreuth, Hof, Germany

Crustal contamination of ascending arc magmas is generally thought to be a significant process which occurs at lower- to mid-crustal magma storage levels where magmas inherit their chemical and isotopic character by blending, assimilation and differentiation [1]. Anak Krakatau, like many other volcanoes, erupts shallow-level crustal xenoliths [2], indicating a potential role for upper crustal modification and hence late-stage changes to magma rheology and thus potential eruptive behaviour. Distinguishing deep vs. shallow crustal contamination processes at Krakatau, and elsewhere, is therefore crucial to understand and assess pre-eruptive magmatic conditions and their associated hazard potential. Here we report on a multi-disciplinary approach to unravel the crustal plumbing system of the persistently-active and dominantly explosive Anak Krakatau volcano [2, 3], employing rock-, mineral- and gas-isotope geochemistry and link these results with seismic tomography [4]. We show that pyroxene crystals formed at mid- and lower-crustal levels (9-11 km) and carry almost mantle-like isotope signatures (O, Sr, Nd, He), while feldspar crystals formed dominantly at shallow levels (< 5km) and display unequivocal isotopic evidence for late stage contamination (O, Sr, Nd). This observation places a significant element of magma-crust interaction into the uppermost, sediment-rich crust beneath the volcano. Magma storage in the uppermost crust can thus offer a possible explanation for the compositional modifications of primitive Krakatau magmas, and likely provides extra impetus to increased explosivity at Anak Krakatau.

[1] Annen, *et al.*, 2006. *J. Petrol.* 47, 505-539. [2] Gardner, *et al.*, 2013. *J. Petrol.* 54, 149-182. [3] Dahren, *et al.*, 2012. *Contrib. Mineral. Petrol.* 163, 631-651. [4] Jaxybulatov, *et al.*, 2011. *J. Volcanol. Geoth. Res.* 206, 96-105.

Mixing and progressive melting of deep and shallow mantle sources in the NE Atlantic and Arctic

RG TRØNNES¹, V DEBAILLE², M ERAMBERT³, FM STUART⁴ AND T WAIGHT⁵

¹ CEED and NHM, Univ. Oslo, r.g.tronnes@nhm.uio.no

² Univ. Libre de Bruxelles

³ Dept. Geosciences, Univ. Oslo

⁴ Isotope Geosciences Unit, SUERC, East Kilbride

⁵ Inst. Geography Geology, Univ. Copenhagen

NE Atlantic and Arctic MORB and primitive off-rift basalts in Iceland, Jan Mayen and Spitsbergen (late Quaternary alkaline basalts) record variable geochemical interaction between the asthenospheric mantle (AM), material supplied by the Iceland plume and subcontinental lithospheric mantle (SCLM). The SCLM-component was mixed with the local asthenosphere during and shortly after the continental rifting and ocean basin opening. Using combined Sr-Nd-Pb-Os-He-isotope systematics, the Iceland plume can be modelled as a mixture of 70% refractory/primordial lower mantle (LM) and 30% recycled oceanic crust (ROC). Low-degree melts are preferentially from the enriched ROC and SCLM components, before progressive melting gradually consumes more of the LM and AM components.

The modelled ROC/SCLM-ratio decreases markedly from a maximum of about 2.3 at the Reykjanes Ridge, Reykjanes Peninsula and the Southern Volcanic Flank Zone in Iceland, via 1.2 at the Snæfellsnes peninsula, Western Rift Zone and Mid-Icelandic Belt and 0.7 at Jan Mayen and the Kolbeinsey, Mohns and Knipovich Ridges to less than 0.2 in Spitsbergen and along the Gakkel Ridge. These ratios might be slightly overestimated due to a general background level of ROC (HIMU-component) in an otherwise depleted asthenosphere.

The minor element composition of olivine phenocrysts in primitive off-rift basalts in Iceland and Jan Mayen, sampling preferentially the enriched source components, indicates that the SCLM-lithologies are dominantly peridotitic, in contrast to the ROC-lithologies, recording a higher proportion of eclogites and hybridized pyroxenites. The combined Hf-Nd-isotope systematics also discriminate between these two enriched source components.

The high proportion of the SCLM-component in the asthenosphere along the Kolbeinsey, Mohns, Knipovich and Gakkel Ridges reflects the young, narrow and slow-spreading character of the corresponding oceanic basins. These ridges appear to sample mantle sources with higher proportions of locally derived SCLM-material than other mid-ocean ridges.

Ash-Slag Wastes: the Problem of Recycling

E. TROPNIKOV^{1*} AND O. KOTOVA¹

¹Institute of Geology Komi SC UB RAS, Syktyvkar
(*correspondence: tropnikov.83@mail.ru)

Technogenic materials form separate and the global problem of modern society. They are a special type of raw material from the one hand and an environmental problem from the another. Most urgent part is the recycling of ash and slag.

Coal of Pechora coal-basin (Russia) is characterised with a relatively high ash content. Pechora coal-basin is represented by almost all types of coal, including coke and anthracite at initial stage. Coals are widely used as a fuel, particularly within the boundaries of the coal-basin (Vorkuta, Inta, etc.). Recycling of solid waste from the combustion of fuel is limited to use as a fertilizer rich in trace elements, as well as export them to the so-called ash field, where the above-mentioned products of combustion are stored for later use.

Ash and slag wastes from thermal power plant (Vorkuta coal deposit) were studied.

The composition of the waste was studied and granular iron ore phase was separated. A hierarchy of its globular structure was made. Iron ore pellets are considered as storage of metals. They can be used after the development of appropriate technologies of extraction and enrichment of [1].

The project was done under the financial support of projects 12-5-6-016-ARKTIKA.

[1] Scientific basis of mineral and new materials synthesis, development of new geotechnologies, geomaterials, new analytical methods, geoinformation systems, nanotechnological research / Ed. A.M. Askhabov. Syktyvkar: IG Komi SC UB RAS, 2012. 220 p.

Ce-Monazite and Y-xenotime solubilities in H₂O-NaF at 800°C, 1 GPa: implications for REE transport

P. TROPPEL¹, D.E. HARLOW² J AND C.E. MANNING³

¹Institute of Mineralogy and Petrography, University of Innsbruck, A-6020 Innsbruck, Austria,
(peter.tropper@uibk.ac.at)

²Helmholtz Zentrum Potsdam, Deutsches GeoForschungs-Zentrum, Telegrafenberg, D-14473 Potsdam, Germany

³Department of Earth & Space Sciences, University of California, Los Angeles, CA, 90095-1567, USA

Monazite and xenotime host significant rare earth elements (REE) and are useful for geochronology and geothermometry. Their distribution may be impacted by F-bearing fluids, which enhance solubilities of REE and Y in high-grade metamorphism [1]. To assess this we determined the solubility of synthetic CePO₄ and YPO₄ in H₂O-NaF fluids at 800°C and 1 GPa. We used hydrothermal piston-cylinder and weight-loss methods. Compared to the low solubilities of CePO₄ and YPO₄ in pure H₂O (0.04±0.04 and 0.25±0.04 millimolal, respectively [2]), our results indicate an enormous increase in the solubility of both phosphates with increasing NaF concentration in H₂O: CePO₄ solubility reaches 0.97 molal in 20 mol.% NaF, and YPO₄ shows an even stronger solubility enhancement to 0.45 molal in only 10 mol.% NaF. The greatest relative solubility increases occur at the lowest NaF concentration. The solubilities of CePO₄ and YPO₄ show similar quadratic dependence on NaF, consistent with possible dissolution reactions of: CePO₄ + 2NaF = CeF₂⁺ + Na₂PO₄⁻ and YPO₄ + 2NaF = YF₂⁺ + Na₂PO₄⁻. Solubilities of both REE phosphates are significantly greater in NaF than in NaCl at equivalent salt concentration [2]. A fluid with 10 mol.% NaCl and multiply saturated with fluorite [3], CePO₄, and YPO₄ would contain 1.7 millimolal Ce and 3.3 millimolal Y, values that are respectively 2.1-2.4 times greater than in NaCl-H₂O alone. The results indicate that Y, and by extension heavy rare earth elements (HREE), can be fractionated from LREE in fluorine-bearing saline brines which may accompany granulite-facies metamorphism. The new data support previous indications that REE/Y mobility at these conditions is enhanced by complexing with F in fluids phase associated with metamorphism and subduction [4].

[1] Pan & Fleet (1996) *Contrib. Mineral. Petrol.* **123**, 251-262. [2] Tropper *et al.* (2011) *Chem. Geol.* **282**, 58-66. [3] Tropper & Manning (2007) *Chem. Geol.* **242**, 299-306. [4] Cooper *et al.* (2009) *Geochem. Geophys. Geosys.* **13**, Q03024.

Boron isotope systematics of calcitic gorgonian corals and their response to ocean acidification

J.A. TROTTER^{1*}, R. THRESHER², P. MONTAGNA³,
M. TAVIANI³ AND M.T. MCCULLOCH^{1,4}

¹The UWA Ocean Institute and School of Earth and Environment, The University of Western Australia, Crawley 6009, Australia

²CSIRO Wealth from Oceans Flagship, CSIRO Marine Laboratory, GPO Box 1538, Hobart, Tasmania 7001 Australia

³ISMAR-CNR, via Gobetti 101, I-40129 Bologna, Italy.

⁴ARC Centre of Excellence in Coral Reef Studies, UWA.

Cold-water corals are thought to be especially susceptible to CO₂-driven climate change and ocean acidification given that many live near the aragonite saturation horizon in the deep oceans. Recently, however, boron isotope analysis of aragonitic (scleractinian) cold-water corals revealed their capacity to modulate internal pH and aragonite saturation state at the site of calcification, which enables these species to maintain higher rates of calcification and potentially escape the effects of ocean acidification [1].

Here we investigate the boron isotopic systematics of a suite of calcitic gorgonian corals from a wide range of environments to determine their potential to modulate the pH of the calcifying fluid, their sensitivity to future climate change scenarios, and their utility as archives of seawater pH. These calcitic corals are lower in boron concentration as well as isotopic composition ($\delta^{11}\text{B}$) than aragonitic cold-water corals, with $\delta^{11}\text{B}$ values lying along or near the seawater borate equilibrium curve. This shows that, unlike aragonitic corals, these calcitic species have limited if any ability to modify the calcifying fluid and thereby precipitate their calcitic skeletons close to ambient seawater pH. serve as an archive of continuous seawater pH over centennial to millennial timescales, is especially important given the lack of continuous long-term records and the need to understand the natural variability of seawater pH on longer timescales.

[1] McCulloch *et al.* (2012) *Geochim. Cosmochim.*, 87, 21-34.

Impact of As(V) on abiotic reduction of U(VI) by mackinawite

LYNDSAY D. TROYER¹, JAMES J. STONE²
AND THOMAS BORCH^{1,3*}

¹Department of Chemistry, Colorado State University, Fort Collins, CO, USA 80523-1170

²Department of Civil and Environmental Engineering, South Dakota School of Mines and Technology, Rapid City, SD, USA 57701

³Department of Soil and Crop Sciences, Colorado State University, Fort Collins, CO, USA 80523-1170

(*correspondence: borch@colostate.edu)

Arsenic and uranium are commonly found together in areas of historic uranium mining activity because they can be released during the mining of uranium ore. Studying the behavior of these elements together under anoxic conditions is necessary to understand their mobility in natural sediments. Recent studies have shown that mackinawite produced through activity of sulfate reducing bacteria is one of the major reductants of U(VI) in subsurface environments [1]. Although reduction of uranyl species by mackinawite has been shown to occur, the reduction of U(VI)-carbonates or U(VI)-arsenates has not been investigated. U(VI) and As(V) can form uranyl arsenate mineral precipitates or surface precipitates depending on their relative concentrations [2]. This study examines the reducibility of U(VI)-carbonates and U(VI)-arsenates under varying U/carbonate and U/As ratios in the presence of mackinawite.

Anoxic batch experiments were conducted including mackinawite with U(VI) and As(V) at concentrations ranging between 50 to 500 μM , including treatments with 5 mM and 30 mM dissolved carbonate. After 48 hours, mackinawite was collected for analysis by X-ray absorption fine structure (XAFS) spectroscopy to determine speciation and binding environment of U and As. Results showed that the extent of U(VI) reduction was not affected by the formation of U(VI)-carbonate complexes. U(VI) reduction was only shown to be limited by As(V) at concentrations at or above 500 μM , where the formation of uranyl arsenate mineral precipitates is favored. Although little influence of U(VI)-carbonate and U(VI)-arsenate species was observed on U(VI) reduction, As(V) reduction was limited in the presence of all tested U(VI) concentrations due to preferential reduction of U(VI). When remediating natural environments containing both As and U, As(V) does not prevent U(VI) reduction by mackinawite under environmentally relevant concentrations.

[1] Bargar *et al.* (2013) *PNAS* **110**, 4506-4511. [2] Tang *et al.* (2009) *ES&T* **43**, 4452-4458.

Geochemistry and petrogenesis of a nested granite intrusion – the Sedmihoří composite Stock (Bohemian Massif)

J. TRUBAČ^{1*}, V. JANOUŠEK^{1,2}, J. ŽÁK² AND A. GERDES³

¹Czech Geological Survey, Klárov 3, 118 21 Prague 1, Czech Republic (*correspondence: jakub.trubac@geology.cz)

²Charles University in Prague, Albertov 6, 128 43 Prague 2, Czech Republic

³Institut für Geowissenschaften, Altenhöferallee 1, D-60438 Frankfurt am Main, Germany

Better understanding of how zoned plutons are constructed and for how long the upper crustal magma chambers remain active is crucial to constrain a range of lithospheric processes, including igneous petrogenesis, ore formation, crustal rheology/deformation and volcanism.

The shallow-level Sedmihoří Stock in the southwestern Teplá–Barrandian Unit, Bohemian Massif, provides an excellent case example of a zoned post-tectonic granitic intrusion. It is roughly circular in plan-view and formed by nested intrusions of three magma pulses within a single conduit: (i) less evolved outer porphyritic Bt monzogranite (326.2 ± 1.2 Ma (2σ), LA ICP-MS Zrn), (ii) more fractionated inner Bt–Mu monzogranite (326.6 ± 1.2 Ma), and (iii) innermost minor Mu leucogranite with Tur. All the varieties are siliceous ($\text{SiO}_2 > 71$ wt. %) and moderately peraluminous. While major-element contents do not vary greatly, trace elements display significant differences between the pulses (e.g., $\text{La}_N/\text{Sm}_N = 4.24\text{--}4.45$ outer; $3.38\text{--}3.44$ inner; $2.95\text{--}4.43$ innermost). Still, each of them preserves its remarkable homogeneity.

Field observations, fabric patterns and geochemistry suggest that each pulse represents a single batch of magma with its own geochemical characteristics and potentially also petrogenesis. This rules out a shallow-level fractionation or contamination by the country-rock metasediments, and points to processes deeper in crust or differences in source materials.

The trace-element compositions with evolved crust-like Sr–Nd isotopic signatures show that the granite pulses were derived by anatexis of immature metasediments (Neoproterozoic metasediments of the Teplá–Barrandian Unit; shown by the presence of inherited components in Zrn 2 and 0.6 Ga old). The higher proportion of pelite within the source of the inner Bt–Mu monzogranite is shown by higher Rb/Sr ratios (9–15) as well as more evolved Sr ($^{87}\text{Sr}/^{86}\text{Sr}_{326} = 0.7098\text{--}0.7154$) and less radiogenic Nd ($\epsilon_{326}^{\text{Nd}} = -3.7$) than in the outer facies ($^{87}\text{Sr}/^{86}\text{Sr}_{326} = 0.7067\text{--}0.7076$; $\epsilon_{326}^{\text{Nd}} = -2.5$ to -2.7). Research funding: Czech Science Foundation (GAČR) P210/11/1168.

Using laser-based technology to quantify carbon-13 ratios and fugitive emission CH₄ flux rates quickly and easily

T. TSAI, C. RELLA, AND E. R. CROSSON¹

¹3105 Patrick Henry Dr. Santa Clara, CA 95054 USA

The United States is home to what is estimated to be the largest known shale gas reserves in the world. Often referred to as the “bridge fuel” that will aid in the country’s energy transition from coal to renewable sources like wind and solar, natural gas production is growing at the fastest pace in U.S. history. This expansion involves the introduction of hundreds of thousands of new natural gas wells and processing facilities all across the U.S. Of primary concern is the potentially damaging impact of natural gas drilling on human health due to increase pollution exposure.

Picarro has developed a new instrument (plume scanner) which uses laser-based technology to measure natural gas fugitive emission flux rates from natural gas facilities quickly and easily. As the plume scanner vehicle drives through the plume at the speed of traffic, the air is sampled at 4 different heights along the axis of the vehicle. These gas samples are continuously stored in the vehicle along with wind and vehicle velocity information. When a plume is detected, the stored gas samples are redirected into the inlet of a cavity ringdown spectrometer where concentration and or carbon-13 CH₄ ratio measurements are recorded, synchronized, and/or processed to produce an intensity map or a so-called “scanned” plume image. In this way, fugitive emission flux rates and isotopic measurements of highly localized sources such as natural gas facilities can be made quickly and easily providing greater transparency to stakeholders.

Rare earth element behavior in subduction-zone fluids: the effect of T and ligands

ALEXANDRA TSAY¹, ZOLTAN ZAJACZ¹
AND CARMEN SANCHEZ-VALLE¹

¹IGP, ETH Zürich, Switzerland

(*correspondence: alexandra.tsay@erdw.ethz.ch)

Understanding of rare earth element (*REE*) systematics has a broad application for subduction-zone processes. Particularly, arc-related magmas display a typical trace element abundance spectrum, characterised by the enrichment in light rare-earth element (*LREE*: *La*, *Ce*, *Nd*) and depletion in the heaviest rare earth element (*HREE*: *Yb*, *Lu*) relative to *MORB*. This particular geochemical signature may result from the influx of aqueous fluids and/or silicate melts derived from within the slab. Therefore, investigating the behavior of *REE* in fluids at high *P* and *T* conditions is crucial for constraining the composition of slab fluids, as well as for understanding subduction-zone processes in general.

In this study we present new experimental data on *REE* silicate ($REE_2Si_2O_7$) solubility in aqueous quartz-saturated fluids, containing various ligands (*F*, CO_3^{2-} , SO_4^{2-} , *Cl*), and in hydrous haplogranitic melt at conditions relevant for subducting slab (600-800 °C, 2.6 *GPa*). The experiments were conducted in an end-loaded piston-cylinder apparatus and the fluids were *in situ* sampled at *P-T* in the form of primary fluid inclusions in quartz. Gold capsules were loaded with a chip of synthetic (*La,Nd,Gd,Dy,Er,Yb*)₂Si₂O₇ – phase, various aqueous solutions (~ 20 wt.%) and a piece of natural quartz. In the case of experiments with melt, the capsule was loaded with a piece of $REE_2Si_2O_7$, a synthetic haplogranitic glass and water (~ 15 wt.%). Rb and Cs were added to the solutions as internal standards for LA-ICPMS analyses.

The solubility of *REE* in quartz-saturated H_2O , free of additional ligands, increases more than an order of magnitude as temperature is increased from 600 to 800 °C. Addition of ligands, even in relatively small amounts (0.3-1.5 *m*), promotes *REE* solubility compared to pure H_2O . Each type of ligands leaves a characteristic *REE* pattern, reflecting the preferences of *REE* complexation: *e.g.*, efficient *LREE-Cl* and *HREE-F*, *HREE-CO*₃ complexation. The solubility of *REE* in the melt is moderate, comparable with the solubilities in pure H_2O .

Our results showed that *REE* can be effectively transported by aqueous fluid and the effect of temperature as well as fluid chemistry play an important role in *REE* mobility and *LREE/HREE* fractionation.

3D shapes of regolith particles: comparison between Itokawa and Moon

A. TSUCHIYAMA^{1*}, T. MATSUSHIMA²,
T. MATSUMOTO³, T. NAKANO⁴, D. AMEMIYA¹,
J. MATSUNO¹, T. NAGANO³, A. SHIMADA³,
K. UESUGI⁵, A. TAKEUCHI⁵, Y. SUZUKI⁵
AND M. OHTAKE⁶

¹Grad. School of Sci., Kyoto Univ., Kyoto 606-8502, Japan

(*correspondence: atsuchi@kueps.kyoto-u.ac.jp)

²Grad. School of Systems and Information Engineering, Univ. of Tsukuba, Tsukuba, Japan

³Grad. School of Sci., Osaka Univ., Toyonaka, Japan

⁴AIST/GSJ, Tsukuba, Japan

⁵JARSI/SPring-8, Sayo, Japan

⁶JAXA/ISAS, Sagamihara, Japan

Hayabusa sample analysis elucidated a variety of surface processes on asteroid Itokawa: (1) regolith formation by impact [2], (2) solar wind implantation to uppermost regolith surface [3], (3) space weathering rim formation mainly by solar wind He implantation (~10³ yr) [4,5], (4) grain abrasion probably by grain motion due to impact-induced seismic waves in a regolith layer (>10³ yr) [1,2,6], and (5) final escape of particles from the asteroid by impact (<8 Myr) [3].

The grain abrasion was found based on the 3D shapes and surface morphologies of Itokawa samples using x-ray micro-tomography [2] and FE-SEM observation [6]. The 3D shapes of lunar regolith samples were also examined by tomography [7] but not grain-by-grain as performed for the Itokawa samples. In the present study, the 3D shapes of Apollo 16 highland (60501) and Apollo 11 mare (10084) regolith samples were examined by the same method as the Itokawa particles using micro-tomography at SPring-8.

The shape distribution shows that the lunar regolith is more spherical than the impact fragments although lunar regolith is the product of impact on the lunar surface, suggesting that the regolith was abraded. The cause may be grain motion during gardening by impacts. The degree of abrasion is larger than that of the Itokawa particles due to larger scale of impacts and longer regolith residence time.

[1] Tsuchiyama *et al.* (2013) *LPS XLIV*, #2169. [2] Tsuchiyama *et al.* (2011) *Science*, **333**, 1125-1128. [3] Nagao *et al.* (2011) *Science*, **333**, 1128-1131. [4] Noguchi *et al.* (2011) *Science*, **333**, 1121-1125. [5] Noguchi *et al.* (2012) *Meteor. & Planet. Sci.*, *in print*. [6] Matsumoto *et al.* (2013) *LPS XLIV*, #1441. [7] Katagiri (2010) *Proc. 12th Internat. Conf. Engin., Sci., Constr., Operat. in Challeng. Environ.*, 254-259.

Influence of aerosols on cloud characteristics over Europe: Study with the meteorology-chemistry-radiation eulerian model.

PAOLO TUCCELLA¹, GABRIELE CURCI¹
AND GUIDO VISCONTI¹

¹CETEMPS Centre of Excellence, Dept. Physical and Chemical Sciences, Univ. L'Aquila, L'Aquila, Italy. (¹paolo.tuccella@aquila.infn.it)

Several studies demonstrated that aerosol particles play a crucial role in the climatic system, scattering the incoming radiation (direct effect) and altering cloud properties (indirect effect). Excellent efforts has been done by scientific community to represent the indirect effect in the atmospheric model, but the radiative forcing associated to indirect effect is still very uncertain.

In this study we tried to address the question: how well do the models reproduce the amplitude of aerosol indirect effects? In order to answer to the question, we used WRF/Chem model. A new parameterization for secondary organic aerosol (SOA) yield based on the volatile basis set implemented in WRF/Chem recently, has been coupled with the microphysics of clouds. The effects of this new mechanism is evaluated through the comparison of high resolution simulations on a cloud resolving domain (2 Km of resolution) against the ground-based and aircraft measurements of aerosol chemical composition and particles, and cloud microphysics, issued in the frame of European Integrated project on the Aerosol Cloud Climate and Air Quality Interaction (EUCAARI). The comparison of model results among observations suggest that discrepancies in simulation of chemical fields should be due to errors in simulated meteorological field and uncertainties in horizontal and vertical interpolation of anthropogenic emissions, in their total amount and hourly variations.

The amplitude of indirect has been calculated as $IE = \partial \ln re / \partial \ln N$, where re is the cloud droplet effective radius and N aerosol particle number of each mode of log-normal distribution. Observations attribute the indirect effect to total aerosol particle number with a value of -0.22, very to theoretical value of -0.23. Instead, WRF/Chem reproduces the observed amplitude of IE, but attributes it to the particles of accumulation, while the observations indicate a strong IE due to total particle number.

The reasons of this results are under investigation.

Formation of monazite-(MREE) from paleozoic shales: Role of host rock chemical composition and organic material

JOHANN TUDURI¹, MATTHIEU CHEVILLARD¹,
SÉBASTIEN COLIN¹, ERIC GLOAGUEN¹, JÉRÔME GOUIN¹,
SÉBASTIEN POTEL² AND OLIVIER POURRET^{2*}

¹BRGM, Orléans, France (j.tuduri@brgm.fr)

²LaSalle Beauvais, France

(olivier.pourret@lasalle-beauvais.fr)(* presenting author)

Rare earth element (REE) distributions of stream water, normalized to upper continental crust (UCC), showed, from the source to the catchment outlet, fractionation patterns from heavy REE enriched to more flat and middle REE (MREE) enrichment, together with a progressive disappearance of a negative Ce anomaly. As a consequence, Pourret *et al.* [1] suggest that the continental shelf could be considered as a potential REE trap and thus that shelf sedimentary rocks, similar to metalliferous deep sea sediments, represent a REE potential resource and guide for their exploration. The reassessment of the REE potential of France, led us to discuss the behavior of REEs, from the continental shelf to the basin plain, using authigenic monazite occurrences within ordovician shales and black shales from Brittany (France). Monazite grains (up to 2 mm in diameter) are mostly characterized by their grey color, host-rock mineral inclusions, REE_{UCC} distribution patterns enriched in MREE, low Th and U contents, lack of inherited cores, that strongly suggest authigenic crystallization during diagenesis to low grade metamorphism conditions. Chemical composition highlights zoned crystals with MREE enriched cores (up to: 10 wt% Sm₂O₃; 1.3 wt% Eu₂O₃ and 5 wt% Gd₂O₃) and light REE (LREE) enriched rims. Thus grain cores are characterized by negative and low values of $\log[(La/Sm)_{UCC}]$ and high values of Eu whereas rims have slightly negative to positive values of $\log[(La/Sm)_{UCC}]$ with low Eu concentrations. Grey monazite REE_{UCC} patterns also reflect the abundance of these elements in shales and black shales. Indeed, at near neutral to alkaline pH, monazite evidenced MREE enriched patterns directly linked to organic matter (OM) content, whereas at alkaline pH, REE speciation is mainly driven by carbonate complexation, resulting in the formation of the LREE enriched monazite. This latter hypothesis will be further tested and reinforced by analysing OM fractions of shales and black shales. Eventually, such monazites were later concentrated within placers @ 2 kg/t.

[1] Pourret *et al.* (2012) *Mineralogical Magazine* 76 , 2247.

Nitrogen isotope biogeochemistry of the South Atlantic

ROBYN E TUERENA^{1*}, RAJA S GANESHAM¹, ANTHONY FALLICK², JULIE DOUGANS², ANDREW TAIT² AND E MALCOLM S WOODWARD³

¹University of Edinburgh, School of Geosciences, UK, (r.e.tuerena@staffmail.ed.ac.uk) (* presenting author)

²Scottish Universities Environmental Research Centre, UK

³Plymouth Marine Laboratory, Plymouth, UK

The South Atlantic at 40°S is a highly productive region of the open ocean marking the transition between the Sub Antarctic Zone (SAZ) and the South Atlantic gyre. We present a high resolution depth transect of $\delta^{15}\text{N}_{\text{NO}_3}$ from the subtropical front to elucidate the contrasting nutrient regimes in water masses of subtropical (Agulhas Current, South Atlantic Central Water (SACW)) and Antarctic origin (Antarctic Intermediate Water (AAIW) and Sub Antarctic Mode Water (SAMW)). The preferential uptake of ^{14}N by biota leaves NO_3 enriched in ^{15}N as it is utilised; therefore, $\text{NO}_3/\delta^{15}\text{N}$ relationships in combination with nutrient stoichiometry can describe the history of water mass formation at the surface and transformation during transit [1].

The SAMW supplies high nutrient waters to the low latitude Atlantic, fuelling primary productivity [2]. A greater variation in SAMW NO_3 and $\delta^{15}\text{N}_{\text{NO}_3}$ values compared to previous studies [3,4], may result from incorporation of the underlying AAIW and overlying surface waters during transport. At the surface, we estimate isotope fractionation during NO_3 utilization of $\epsilon \sim 9\text{‰}$, which is consistent with previous SAZ estimates [3]. However, this fractionation effect is diluted in most profiles by the influence of the nutrient poor SACW.

Tropical surface waters are identified between 50-53°W, with $\delta^{15}\text{N}_{\text{NO}_3}$ values in the range of 4-6‰. These depleted $\delta^{15}\text{N}_{\text{NO}_3}$ signatures suggest the influence of N-fixation in this water mass. Similarly, the Agulhas leakage into the South Atlantic is characterised by low $\delta^{15}\text{N}_{\text{NO}_3}$ signatures because it is sourced from the combination of tropical and Southern Ocean water masses of the Indian Ocean. These datasets will be modelled in an attempt to quantify the extent of N fixation, NO_3 utilization and water mass mixing that has occurred in these water masses, to address their role in nutrient transport and productivity within the ocean.

[1] Rafter *et al.* (2012) *Global Biogeochem. Cy.* **26** GB1003. [2] Sarmiento *et al.* (2004) *Nature* **427** 56-60. [3] DiFiore *et al.* (2006) *J. Geophys. Res.*, **C.111** C08016 [4] Sigman *et al.* (2000) *J. Geophys. Res.*, **C.105** 19599-19614.

Volcanism on Mars controlled by early oxidation of the upper mantle

J. TUFF, J. WADE AND B.J. WOOD¹²³

¹²³University of Oxford, U.K., (james.tuff@earth.ox.ac.uk); (jon.wade@earth.ox.ac.uk); (berniew@earth.ox.ac.uk)

We investigated the genetic relationships between Martian meteorites and the surface rocks of the Gusev Crater analysed by MER Spirit. The SNC meteorites, with crystallisation ages mostly in the range 1.4Ga-180 Ma are likely derived from young volcanic regions such as Tharsis Plateau. They are enriched in volatiles and depleted in Ni and other chalcophile elements relative to terrestrial igneous rocks of similar composition¹. Surface rocks from the Gusev crater are much older (~ 3.7 Ga) and are substantially richer in Ni and S with lower Mn/Fe ratios than the meteorites². These observations lead to doubts that surface rocks and SNC meteorites have similar mantle source regions.

We started with the Dreibus and Wänke (DW) estimate of Martian mantle composition and experimentally-produced partial melts of this mantle at 1.5 GPa (^{1,3}). Martian mantle Ni and S contents (up to 3000 ppm) were varied and the Ni and S contents of the melts calculated assuming sulphide saturation at low f_{O_2} (FMQ- 2 log units). The melts were allowed to fractionally crystallise the liquidus mantle phases (olivine, orthopyroxene, clinopyroxene spinel and sulphide), using the crystallisation program 'Petrolog'⁴. This yielded the correct SNC trends of Ni-Mg and Mn-Fe for melts and cumulates with mantle Ni content of 1800 ppm. We repeated the procedure at high f_{O_2} (FMQ+3 log units), conditions where sulphide is unstable. Partial melts are much richer in Ni and S and reproduce the Ni-Mg trend of the Gusev crater rocks. Furthermore, magnetite, found in the recently described "Gusev-like" meteorite NWA7034⁵ becomes the liquidus phase and extracts Mn from the differentiates, consistent with observations of surface rocks. Our results demonstrate that the surface basaltic rocks of the Gusev crater and the igneous SNC meteorites are consistent with partial melting and fractional crystallisation from the same DW-like source but under different f_{O_2} conditions. The implications are that Mars' surface oxidised early in its history and that oxidised material was recycled into the upper mantle.

[1].Dreibus, G. & Wanke, H. *Meteoritics* **20**, 367-381 (1985).[2].McSween, H. Y. *et al.* *Science* **324**, 736-739, (2009).[3]Bertka, C. M. & Holloway, J. R. *Contrib Mineral. Petrol.***115**, 323-338 (1994). [4]Danyushevsky, L. V. & Plechov, P. *Geochem. Geophys.Geosyst.* **12**, Doi 10.1029/2011gc003516 (2011).[5]Agee, C. B. *et al.* *Science* **339**, 780-785 (2013).

A new conceptual model: Reconstruction of freshwater incursions in stratified marine paleoenvironments in Late Devonian extinctions

S. TULIPANI¹, K. GRICE^{1*}, P. GREENWOOD^{1,2},
L. SCHWARK^{1,3} AND R. SUMMONS⁴

¹WA-Organic & Isotope Geochemistry Centre, Curtin
University, GPO Box U1987, Perth, WA 6845, Australia
(*correspondence: k.grice@curtin.edu.au)

²Centres for Exploration Targeting & Biogeochemistry,
University of Western Australia, 35 Stirling Highway,
Crawley WA 6009 Australia

³Institute of Geoscience, Kiel University, Ludewig-Meyn Str.
10, 24118 Kiel, Germany

⁴Department of Earth, Atmospheric & Planetary Sciences,
MIT, E25-633, 45 Carleton Street Cambridge, MA 02139
USA

One of the biggest mass extinctions in Earth's history took place in the Late Devonian. The most well known event occurred at the Frasnian – Famennian boundary, but there were also major biodiversity crises towards the end of the Givetian and Famennian time periods.

Here we present a novel biomarker approach using methyltrimethyltridecylchromans (MTTCs) as indicators of freshwater incursions and terrigenous input to a Late Givetian/Early Frasnian marine palaeoenvironment [1]. The abundance of gammacerane and *Chlorobi* biomarkers furthermore indicated persistent water-column stratification and prevailing photic zone euxinia. MTTCs are isoprenoid substituted aromatic compounds which are established palaeosalinity indicators [2]. Nevertheless, their source and formation pathway remain unknown. Our data would be consistent with an origin from early diagenetic condensation reactions of phytol with alkyl phenols (from higher plant sources) as it has been suggested previously by Li *et al.* [3].

[1] Tulipani *et al.* (2013) *Geology*, in prep. [2] Schwark *et al.* (1998), *Org. Geochem.* 29, 1921-1952. [3] Li *et al.* (1995) *Org. Geochem.* 23, 159-167.

Recent groundwater circulation of U at Forsmark, eastern Sweden

E-L. TULLBORG^{1*}, J. SUKSI², B. SANDSTRÖM³, A. B.
MACKENZIE⁴, J. SMELLIE⁵, L. KRALL⁶
AND I. PUIGDOMENECH⁶

¹Terralogica AB, Gråbo, Sweden, *(evalena@terralogica.se)

²Laboratory of Radiochemistry, Helsinki University, Finland

³WSP Group, Gothenburg, Sweden,

⁴SUERC, East Kilbride, Scotland, UK

⁵Conterra AB, Stockholm, Sweden

⁶SKB, Stockholm, Sweden

Uranium in groundwaters commonly shows a trend of decreasing concentration with depth due to the chemical reactivity of recharging waters, rich in O₂ and CO₂, which promotes U mobility by oxidising U(IV) to U(VI) and by carbonate complexation. Towards depth, the redox potential drops, U is increasingly reduced to the more insoluble U(IV) form, and U concentrations decrease. However, carbonate complexation may enable dissolved U(VI) to exist to greater depths in even mildly reducing conditions. Such is demonstrated in the crystalline bedrock aquifer of the Forsmark area, where elevated U concentrations (10 to 170 µg/L) are found in several borehole sections at depths down to 600 metres. These concentrations are generally associated with Brackish-type groundwaters which are not oxidising but show Eh > -190 mV and bicarbonate contents >30 mg/L. It can, however, be concluded that this water has not transported U into the bedrock aquifer, but rather has mobilised an easily dissolvable uranium phase present along some of the water conducting fractures. The ²³⁴U/²³⁸U activity ratios (AR) in the groundwaters are within the range 2 to 6 and the samples with the highest U contents tend to show the lowest ²³⁴U/²³⁸U AR (≤ 3). Annual sampling (from 2005 to 2012) in some borehole sections with elevated U, has shown the ²³⁴U/²³⁸U AR to be very stable and unique for each specific fracture groundwater and most probably also for the dissolved phase. Because the suspected source is hosted in the fracture fillings, the water/fracture mineral interaction is also studied using U-series measurements on the mineral phase. The results support a complex pattern of leaching and redeposition of U in many of the studied fractures during the last 1.5 Ma, whereas others show only small or insignificant deviations from equilibrium. Together these results support the very inhomogeneous distribution of flow paths typical for crystalline bedrock and previously interpreted in the Forsmark area.

An understanding of the geologically late (<1.5 Ma) behaviour of U in the groundwater can help to interpret the groundwater circulation and find the most important water pathways during this period. The changes in groundwater composition and redox conditions have caused both mobilisation and deposition of U, and it is possible to trace both processes in one and the same fracture sample.

Volatiles released in subduction zones and their role in sustaining magmatism

SIMONE TUMIATI^{1*}

¹Dipartimento di Scienze della Terra, Università di Milano,
20133 Milan, Italy

(*correspondence: simone.tumiati@unimi.it)

It is widely accepted that the generation of arc magmas is triggered by fluids released from the subducting slab and by their interaction with the overlying mantle wedge [1]. The major lithologies involved in devolatilization are pelites, hydrothermally altered basalts, and serpentized harzburgites. Thermodynamic calculations and experiments predict that HP fluids are dominated by H₂O. Nevertheless, the importance of carbon species has been highlighted in the last years because of the relevant CO₂ content of arc magmas and the observation of carbon-bearing phases in mantle-wedge peridotites. Experiments have shown that the release of volatiles extends over several tens of km depths and result from a succession of continuous and discontinuous reactions involving hydrous phases in the subducted lithosphere, such as antigorite and chlorite in ultramafics; amphibole, lawsonite, zoisite, and chloritoid in mafic rocks. Phengite and biotite are involved in melting reactions of a variety of bulk compositions whenever K is available. Carbonates once formed are refractory and stable at very high pressures. Therefore, the transport of carbon in the mantle wedge, via solute species in aqueous fluids or via advecting rock masses in buoyant “cold plumes” have been proposed. In the metasomatized mantle wedge, the stability of hydrous phases depends on bulk alkali content, amount of available fluid and possibly the redox state of the system. In COH-bearing systems, the framework of phase relationships is more complex and the position of the solidus is controlled by a number of factors. In fluid-undersaturated COH-systems, the bulk composition (i.e., X_{Ca}, X_{Mg}, alkalis) and the redox state of the Fe-bearing phases are variables that strongly influence the solidus position. Peridotites saturated in a COH-fluid melt at lower temperatures compared to H₂O-free, CO₂-bearing peridotites. However, the increase of bulk CO₂ shifts the solidus, so that fluid-saturated COH peridotite can eventually melt at higher temperatures compared to fluid-undersaturated COH peridotites. Apparent discrepancies concerning solidus position reflect the variety of experimental strategies adopted, which can be applied to a wide range of geodynamic settings.

[1] Schmidt & Poli (2003) *Treatise on Geochemistry* 3, 567-591.

The formation of elemental sulfur nodules; A modified ‘thiosulfate shunt’ in unique environments

ALEXANDRA V. TURCHYN^{1*}, TOM BISHOP¹
AND ORIT SIVAN²

¹Department of Earth Sciences, University of Cambridge,
Cambridge CB2 3EQ, UK, (avt25@cam.ac.uk)

(*presenting author)

²Department of Geological and Environmental Sciences, Ben
Gurion University, Beer Sheva, Israel

Elemental sulfur, also known as ‘native sulfur’, has been found in a range of natural environments, including marine and lake sediments, often forming large nodules or veins, millimeter to centimeter in size. What governs the formation of elemental sulphur nodules remains enigmatic. While most of the literature suggests it is formed by partial re-oxidation of hydrogen sulphide, elemental sulfur can also form during incomplete bacterial sulfate reduction, during sulfur disproportionation, or even during gypsum metamorphism.

We present sulfur isotope ($\delta^{34}\text{S}$) and major element data from sulfur nodules and surrounding gypsum, from the Lake Lisan formation near the Dead Sea, Israel. The $\delta^{34}\text{S}$ in the nodule is constant between -9 and -11‰, 27 to 29‰ lighter than the surrounding gypsum, consistent with their formation in an ‘open system’. Iron concentrations in the gypsum increase toward the nodule, while manganese concentrations decrease, suggesting a redox boundary at the nodule-gypsum interface during aqueous phase diagenesis. We suggest that sulfur nodules in the Lake Lisan formation are generated through bacterial sulfate reduction, which terminates at elemental sulfur. Sulfate-saturated pore fluids, coupled with the low electron-donor availability, terminate the trithionate pathway before the terminal two-electron reduction, producing thionites, which disproportionate via a modified thiosulfate shunt to form abundant elemental sulfur.

BTX sorption by surfactant-modified synthetic zeolite

P. TUREK¹, B. SZALA^{1*}, J. CZERWIŃSKI²,
T. BAJDA¹ AND J. MATUSIK¹

¹Department of Geology, Geophysics and Environmental Protection, AGH University of Science and Technology, Krakow, Poland (*bszala@geol.agh.edu.pl)

²Environmental Engineering Faculty, Lublin University of Technology, Lublin, Poland

Zeolites are group of aluminosilicate minerals that are distinguishable by their high porosity, high cation exchange capacity and regular cage-like structure. They possess a negative charge that is an effect of heterovalent substitutions of Si⁴⁺ by Al³⁺ in the tetrahedra which are the primary building units of the mineral's framework. Synthetic zeolite was created from fly ash after coal combustion in hydrothermal conditions. Modification of zeolite was conducted with the use of one of the quaternary ammonium salts: hexadecyltrimethylammoniumbromide(HDTMA-Br).

Suspension of synthetic zeolite was mixed with HDTMA solution in high temperature for 24 hours. Surfactant was adsorbed onto a synthetic zeolite in amounts of 1.0 and 2.0 of the external cation exchange capacity (ECEC) in quantities of 24.4 and 48.8 mmol per 100 g of zeolite respectively. Third sample that was used was pure zeolite.

The purpose of this research was to evaluate the difference in sorption of BTX (benzene, toluene, xylenes) on the unmodified zeolite and organo-zeolite modified by HDTMA.

Modification in amount of 2.0 ECEC shows higher sorption of BTX than organo-zeolite 1.0 ECEC. Further still, was the unmodified zeolite. This is caused due to high affinity of apolar BTX to the hydrophobic zone of HDTMA chains. The range of BTX concentrations used in this study was limited by their solubility in water.

Additional objective was to investigate whether FTIR could be used in qualitative and quantitative determination of BTX adsorbed by the zeolite. Our study has provided information on presence of particular spectra that correspond to certain organic compound.

We gratefully acknowledge the support of NCBiR having provided grant PBS1/A2/7/2012.

Three-dimensional distribution of anatectic melt inclusions in garnets by X-ray micro-tomography

TURINA ALICE¹, PARISATTO MATTEO¹,
CESARE BERNARDO¹ AND PERUZZO LUCA²

¹Dipartimento di Geoscienze, Università di Padova, via Gradenigo 6, 35137 Padova, Italy

²CNR-Istituto di Geoscienze e Georisorse, Padova, via Gradenigo 6, 35137 Padova, Italy

(alice.turina@studenti.unipd.it); (matteo.parisatto@unipd.it)
(bernardo.cesare@unipd.it) (luca.peruzzo@igg.cnr.it)

X-ray micro-tomography (μ CT) has been applied to investigate the three-dimensional distribution of primary melt inclusions in garnets from El Hoyazo (Neogene Volcanic Province, Spain). Modeling the distribution density allows a better understanding of the growth and trapping history of peritectic minerals and coexisting fluids and melts during the partial melting of the crust. Glassy inclusions are trapped in nearly all mineral phases in metapelitic enclaves found within El Hoyazo dacites and they have been extensively analyzed. To better investigate their three-dimensional distribution and to understand the relationship between them, other mineral inclusions and the host phase, two garnets have been imaged through μ CT. One of the two was then cut to expose a nearly-equatorial plane to SEM analyses. A preliminary classification based on different absorption coefficients was applied to different inclusions in the tomographic images and then verified by SEM chemical maps. We measured the volume and position with respect to garnet barycenter of glassy melt inclusions and of single-phase inclusions such as monazite, zircon and apatite for a comparison. The modeling reveal a clear peak of melt inclusions density at 1/3 radius distance from the garnet center, while mineral phases are more randomly distributed. Moreover, the type and the size of the inclusions are statistically related to their spatial distribution. There is no evidence of a sharp boundary between inclusion-rich cores and inclusion-free rims. This together with the chemical profile of the garnet composition strongly suggests that the garnet grew in one single event in the presence of anatectic melt. After the maximum, the linear decrease in the density of melt inclusions could indicate trapping at a constantly slowing growth rate of the host mineral or a constant decreasing melt supply. The first hypothesis is less convincing, since mineral inclusions are still trapped after the decrease of melt inclusions, and even seem to increase in density.

Recycling of water between the mantle and crust/hydrosphere

MICHAEL TURNER¹ SIMON TURNER¹ TREVOR IRELAND²
AND JOHN ADAM¹

¹ Department of Earth and Planetary Sciences, Macquarie University, NSW, Australia

² Research School of Earth Sciences, Australian National University, ACT, Australia

Water is added to the mantle via subduction where, due to the break down of hydrous mineral phases, water is released from the subducting slab. Conversely volcanism expels water from the mantle.

To help constrain the water flux of the mantle, we present data from mantle pyroxenes of sub-arc xenoliths and therefore providing estimates of the amount of water recharging the mantle. We have measured the concentration of water within pyroxene phenocrysts from Azores lavas (OIB setting) and the andesitic volcanoes of New Zealand (arc setting).

Preliminary data from pyroxenes of sub-arc metasomatised harzburgite xenoliths reveal varied water concentrations from relatively dry sub-arc mantle regions (Mexico and Kamchatka ~150 ppm) to relatively wet areas (New Ireland and Phillipines >500 ppm). This variation may reflect differences in the petrogenetic history of the xenoliths such as various degrees of metasomatism.

The water content of pyroxenes from Azores lavas vary between 100 and 400 ppm, with the notable exception of relatively hydrous pyroxene cores from Sao Miguel that contain up to 800 ppm.

Preliminary data from pyroxene phenocrysts of Mt Ruapehu and Taranaki (New Zealand) suggest that they also contain a similar variation in water concentrations to that seen within the Azores pyroxenes (between 100 and 450 ppm water). Differences between each andesitic system are also possible with Mt Taranaki (amphibole bearing, back-arc volcanic system) pyroxenes containing relatively low water concentrations (100-250 ppm) compared to the pyroxenes from the volcanic front-arc system of Mt Ruapehu (>300 ppm).

Interestingly pyroxene phenocrysts from OIB and arc magmatism contain a similar range of water contents to pyroxenes from the sub arc mantle.

Extremely young melt infiltration of the continental lithospheric mantle

SIMON TURNER^{1*} AND MICHAEL TURNER¹

¹Department of Earth and Planetary Sciences, Macquarie University, Sydney 2109, Australia
(*simon.turner@mq.edu.au)

It has long been inferred that mantle metasomatism and the incompatible element enrichment of the continents require melts formed by low degree melting of the mantle. Yet establishing the presence of these melts and whether this metasomatism is ongoing and continuous, or spatially and temporally restricted, has proved difficult. Here we report large U-Th-Ra disequilibria in metasomatised, mantle xenoliths from the Newer Volcanics Province in southeastern Australia. The infiltration and passage of carbonatitic ± hydrous silicic melts, combined with crystallization of pargasite can account for the observations. The half-lives of the nuclides indicate that metasomatism was extremely young (≤ 10 kyr) and probably on-going at the time of incorporation in the magmas that transported the xenoliths to the surface. This provides unique evidence for the presence and continuing migration of small melt fractions (~0.02%) in the upper convecting mantle and provides a likely explanation for the seismic low velocity zone. These melts cannot, themselves, be responsible for average continental crust but they could provide an important component for ocean island basalts if returned to the convecting mantle.

Isotopes in vertebrate bioapatite: proxies for climate, pCO₂ and diet

T. TÜTKEN^{1*}, P. HELD² AND S.J.G. GALER²

¹Steinmann-Institut, Rheinische Friedrich-Wilhelms-Universität Bonn, Poppelsdorfer Schloß, 53115 Bonn, Germany (*correspondence: tuetken@uni-bonn.de)

²Max-Planck-Institut für Chemie, Abteilung Biogeochemie, Hahn-Meitner-Weg 1, 55128 Mainz, Germany

Vertebrates integrate bioavailable elements in their skeletal tissues taken up from the environment via air, water and food. Bones and teeth archive isotope signatures of these elements over the timespan of tissue formation and/or remodelling. This enables the reconstruction of diet ($\delta^{13}\text{C}$, $\delta^{44/42}\text{Ca}$), climate ($\delta^{18}\text{O}$), body temperature (Δ_{47}), atmospheric pCO₂ ($\Delta^{17}\text{O}$) and habitat ($\delta^{18}\text{O}$, $^{87}\text{Sr}/^{86}\text{Sr}$) from vertebrate fossils. Bioapatite of fossil hard tissues, especially enamel, can preserve original isotope compositions over geological time scales. The isotopes of the two major elements (Ca, O_(PO₄)) in bioapatite are least biased by diagenetic alteration.

$\delta^{18}\text{O}_{\text{PO}_4}$ of terrestrial and aquatic vertebrates is a proxy for meteoric and ambient water $\delta^{18}\text{O}$ values, respectively. Enamel $\delta^{18}\text{O}_{\text{PO}_4}$ values of fossil large mammals were used to infer the terrestrial palaeoclimate during the last 35 million years for Central Europe. Reconstructed air temperatures agree well with other climate proxy data. The ^{17}O -anomaly ($\Delta^{17}\text{O}$) of air oxygen is a proxy for atmospheric pCO₂. This anomalous $\Delta^{17}\text{O}_{\text{air}}$ is partially recorded in bioapatite $\Delta^{17}\text{O}_{\text{PO}_4}$ of small mammals (<1kg) with a high metabolic rate and thus O₂ consumption. It is preserved in fossil teeth and $\Delta^{17}\text{O}_{\text{PO}_4}$ can be used as a new proxy for palaeo-pCO₂ reconstructions and to monitor diagenetic alteration of bioapatite $\delta^{18}\text{O}_{\text{PO}_4}$ values.

Calcium isotopes ($\delta^{44/42}\text{Ca}$) are a very promising deep time diet proxy for fossil vertebrates with a high preservation potential, even in fossil bones. $\delta^{44/42}\text{Ca}$ values enable us to determine the consumption of plant versus animal tissues and decrease systematically with each trophic level along the foodchain. We found a trophic level effect of $\sim 0.4\text{‰}$ between bones of extant African mammalian herbivores ($-0.46 \pm 0.14\text{‰}$) and carnivores ($-0.89 \pm 0.14\text{‰}$). Ant/termite-feeding mammals ($0.04 \pm 0.16\text{‰}$) have higher $\delta^{44/42}\text{Ca}$ values than both herbivores and carnivores. Whether Ca isotopes are indeed a new geochemical proxy for insectivory is currently being investigated. Using Ca isotopes past diets of extinct vertebrates and fossil food webs can be reconstructed to identify apex predators. T-Rex and sympatric herbivorous dinosaurs display a similar trophic level effect as extant mammals. Preliminary $\delta^{44/42}\text{Ca}$ data for the Eocene terror bird (*Gastornis*) are more in accordance with a herbivorous diet.

Developing speciation codes and thermodynamic data for non-isothermal and non-isobaric systems: applications to CO₂ sequestration

BENJAMIN M. TUTOLO*¹, ANDREW J. LUHMANN¹, XIANG-ZHAO KONG¹, MARTIN O. SAAR¹, AND WILLIAM E. SEYFRIED, JR.¹

¹University of Minnesota Department of Earth Sciences, Minneapolis, MN USA

(*correspondence: tutol001@umn.edu)

Geochemical models typically simulate geochemical processes using thermodynamic data sets of equilibrium constants calculated 0.01-300°C along the steam saturation curve. This approach is sufficient for a broad range of geologic conditions, as long as the data has been calibrated against calorimetric, field, and experimental measurements. However, some commonly utilized data and methods result in unacceptable uncertainties. Notably, longstanding inconsistencies in the aluminum mineral and aqueous species data that are included in many thermodynamic datasets have not been sufficiently resolved. Moreover, simulations of key geologic processes, such as geologic CO₂ sequestration and hydrothermal alteration, are challenging due to the limited T-P range of the data sets.

In this contribution, we correct some of these problems by taking account of recent innovations that enable acquisition of formatted datasets at any T and P within the limits of the thermodynamic equations of state [1]. This is only a short-term measure, however, because modern computers permit development of a new generation of speciation codes that dynamically calculate equilibrium constants at the modeled T-P conditions. These codes will be particularly useful in large-scale, non-isothermal, and non-isobaric reactive transport models. To this end, we develop and use an integrated thermodynamic-speciation code that relies only on standard state thermodynamic properties and equation of state parameters to dynamically calculate mineral-brine-CO₂ interactions. The code incorporates a new, calibrated, internally consistent thermodynamic data set for key aluminum minerals and aqueous species as well as literature data for other minerals and aqueous species. Compared with experiments involving a) thermally-driven dolomite dissolution and precipitation and CO₂ exsolution, and b) arkose alteration under elevated T, P, pCO₂ conditions, the data and integrated speciation code perform well and provide a new opportunity to kinetically evaluate whole-rock dissolution and precipitation reactions.

[1] Kong *et al.* (2013) *Computers & Geosciences* **51**, 415-417.

Rock-Hosted Serpentine Microbiome

K. I. TWING^{1*}, W. J. BRAZELTON¹, D. A. CARDACE²,
T. M. HOEHLER³ AND M. O. SCHRENK¹

¹East Carolina University, Greenville, NC, U.S.A

²University of Rhode Island, Kingston, RI, U.S.A

³NASA Ames Research Center, Moffett Field, CA, U.S.A

*correspondence to KatrinaTwing@gmail.com

Serpentinization is a widespread geochemical process involving the alteration of ultramafic rocks in the presence of water, resulting in a high pH (>10), highly reducing environment containing large quantities of dissolved hydrogen and potentially abiogenic organic molecules, which can serve as energy sources for microbes in the subsurface. Habitability models predict that these environments can sustain microbial life, but little work has been done to directly characterize the microbial communities utilizing the energy generated from this process. Furthermore, prior studies of continental serpentinites have sampled surface seeps that represent an interface between end-member fluids and the atmosphere and may not truly represent the extreme conditions encountered deep within the subsurface.

A recent drilling project at the Coast Range Ophiolite Microbial Observatory (CROMO) in northern California has supplied rock cores from up to 40 m below the surface and provided a window into an actively serpentinizing system. Rock cores from two wells, roughly one mile apart, were sampled at various depths and analyzed for microbial community composition via metagenomics and 16S rRNA tag sequencing, allowing for the comparison of communities within and between rock cores. Additionally, fluid samples from both wells have been sequenced, allowing for the identification of rock-specific microbes within the environment. Preliminary data indicate that communities associated with rocks are lower diversity and different composition than those associated with the surrounding fluids.

To test the question of habitability within the serpentinite subsurface, microorganisms have been cultivated *in situ* within the monitoring wells, showing growth over time, and their diversity is being assessed via 16S rRNA tag sequencing. Future experiments include providing environmentally-relevant mineral substrates *in situ* to determine the extent of microbe-mineral interactions within the serpentinite subsurface environment. This work adds to our growing understanding of the role of microorganisms in this extreme environment.

Pilbara greenstones revisited: a multi-proxy geochemical perspective on Archean crust-mantle interaction

JAN F. TYMPEL, JANET M. HERGT, JON D. WOODHEAD,
ROLAND MAAS AND ALAN GREIG

School of Earth Sciences, The University of Melbourne,
Victoria, Australia

Metabasalt (greenstone) sequences in Archean cratons provide insights into mantle melting and crust formation processes in the Early Earth. The 3.53–3.22 Ga eastern Pilbara Craton, Western Australia, contains large-scale exposures of well-preserved Palaeoarchean supracrustal volcanic sequences, which can be correlated over considerable distances and are characterised by virtually undisturbed immobile element (REE, HFSE) systematics. Previous studies have aimed to establish a stratigraphic and chronological framework, reconstruct the tectonic setting for greenstone emplacement, and determine the composition of sources that may explain the chemical/isotopic signatures in these rocks. The recent suggestion of involvement of a Hadean crustal component, based on distinctly negative ϵ_{Nd} values in metabasalts and cherts within the Warrawoona Group [1], has motivated us to revisit these issues.

Here we present new high-precision trace element and isotopic (Nd-Hf) results for tholeiitic and komatiitic rocks of the Warrawoona Group, the lowermost section of the East Pilbara terrane. Trace element patterns in our samples are characterized by comparatively flat HREE distributions but wide variations in LREE abundances, with mantle-normalized ratios of $(La/Sm)_{PM} < 1$ to > 4 , $(Zr/Y)_{PM} < 1$ to > 5 , $(La/Yb)_{PM} < 1$ to > 20 and $(Nb/Th)_{PM}$ significantly below 1, i.e. from values inferred for mantle-derived melts to values more typical of continental crust. By contrast, HFSE inter-element ratios ($Nb/Ta \sim 16.2$, $Zr/Hf \sim 36.8$) and initial Nd-Hf isotope values are homogeneous ($\epsilon_{Nd} = 1.4 \pm 0.5$; $\epsilon_{Hf} = 2.2 \pm 0.8$), yielding ~ 3.45 Ga isochron ages which are consistent with known emplacement ages.

Our Nd (and Hf) isotope results are consistent with those of Jahn *et al.* [2] and Gruau *et al.* [3] and do not appear to support a significant contribution from assimilated enriched Hadean proto-crust to ~ 3.45 Ga basaltic magmatism. Additional modeling will help to further assess the involvement of potential crustal contaminants.

- [1] Tessalina *et al.* (2010), *Nature Geosci.* **3**, 214-217. [2] Jahn *et al.* (1981), *Geochim. Cosmochim. Acta* **45**, 1633-1652. [3] Gruau *et al.* (1987), *Earth Planet. Sci. Lett.* **85**, 105-116.

Linking noble gas and CH₄ concentrations in the sediment porewater of Lake Lungern, Switzerland

L. TYROLLER^{1,2}, M.S. BRENNWALD¹, C. NDAYISABA¹, Y. TOMONAGA¹ AND R. KIPFER^{1,3}

¹Eawag, Swiss Federal Institute of Aquatic Science and Technology, 8600 Dübendorf, Switzerland
(*correspondence: lina.tyroller@eawag.ch)

²ETH Zurich, Institute of Biogeochemistry and Pollution Dynamics, 8092 Zurich, Switzerland

³ETH Zurich, Institute of Geochemistry and Petrology, 8092 Zurich, Switzerland

Noble gases are powerful tracers for gas transfer processes in lake sediments. They were successfully applied in the sediment of Swiss Lake Sempsee [1] to study CH₄ ebullition in the past. Here, we employed a newly developed method for quantitative sampling of dissolved CH₄ and noble gases [2] to determine both CH₄ and noble gas concentrations in the porewater. In order to assess the depth of active CH₄ production, and to investigate gas transfer processes in the lake sediment we sampled the uppermost metre of the sediments of Lake Lungern, a Swiss hydropower reservoir. This lake is characterised by lake level variations and the formation of CH₄ bubbles in the sediment due to super saturation of dissolved gases in the porewater.

Using the new sampling method, we observed CH₄ concentrations exceeding the in-situ saturation concentration. Compared to the overlying water body, the noble-gas concentration in the sediment porewater showed a depletion of the lighter, more volatile gases relative to the heavier, more soluble gases. This elemental fractionation indicates stripping of noble gases into the CH₄ bubbles released from the sediment. In addition, the absolute noble gas concentrations in the sediment porewater indicate an air excess relative to the concentrations in the overlying water body. We attribute this to the formation of excess air resulting from the dissolution of air bubbles entrapped in the sediment when the lake level falls below the depth of our sampling site. Linking CH₄ and noble gas concentrations in the sediment porewater therefore allows assessing importance of the physical transport processes related to CH₄ emission from the sediments into the water body of the Lake Lungern.

[1] Brennwald *et al.* (2005) *Earth Planet Sc. Lett.* **235**, 31-4.

[2] Tomonaga, Y., Brennwald, M. S., & Kipfer, R. (2011) *Limnol. Oceanogr.: Methods* **9**, 42-49.

What is hidden in a slag heap?

TYSZKA R.¹, KIERCZAK J.², PIETRANIK A.², ETTLER V.³ AND MIHALJEVIĆ M.³

¹Wrocław University of Environmental And Life Sciences, C.K. Norwida 25/27, 50-375 Wrocław, Poland
(rafal.tyszka@up.wroc.pl)

²University of Wrocław, Cybulskiego 30, 50-205 Wrocław, Poland, anna.pietranik@ing.uni.wroc.pl;
jakub.kierczak@ing.uni.wroc.pl)

³Charles University in Prague, Albertov 6, 128 43, Prague 2, Czech Republic (ettler@natur.cuni.cz;
mihal@natur.cuni.cz)

A slag heap after Zn-Pb ore smelting (Świętochłowice, Upper Silesia, Poland) was disturbed during recent slag removal and the freshly uncovered surfaces are examined in this study. The material forming the interior of the slag heap is fine grained (up to 5 cm) and strongly weathered contrary to the large slag boulders on the slag heap surface (up to 2 m), which are only slightly weathered. It is composed of gypsum and hematite plus a mixture of primary and other secondary phases. The weathered material as whole is chemically more homogenous than unweathered slags and has lower Si and higher Fe, Pb (up to 3 wt. %), Cd (up to 560 mg/kg). The examined surfaces are 3 – 4 meters high and 10 – 30 meters wide suggesting that such an extensive slag weathering may have occurred in larger parts of the slag heap.

The implication is that the slag confined in the interior of the slag heap may have extensively reduced grain size and mineralogy dominated by secondary minerals and may contain more potentially toxic elements than the unweathered slag. As such it poses risk to the environment, especially when the slag heap is disturbed.

Radiation damage evolution in nanocomposites

BLAS PEDRO UBERUAGA

Materials Science and Technology Division, Los Alamos National Laboratory, Los Alamos, NM 87545; correspondence: blas@lanl.gov

As nuclear energy systems are taken to higher levels of radiation damage, there is greater need to develop materials that can withstand that damage. Nanocomposites, nanomaterials comprised of both a high density of internal interfaces and second phases, are one promising avenue for such materials. Most work on nanomaterials has focused on the role of the interfaces as sinks of point defects. Here, motivated by a series of experimental studies on oxide composites, we examine the other component of nanocomposites, the dual phase nature of the material without the interfaces acting as defect sinks. We solve a reaction-diffusion model of defect evolution of simple composites under irradiation which depends on defect properties within each phase with no special behavior accounted for at the interface. We identify three regimes of steady-state defect behavior that depend on the relative thermodynamics and kinetics of the defects in the phases comprising the composite. Importantly, in one regime, defect populations are enhanced on one side of the interface and depleted on the other. Further, transient defect populations can exceed steady-state concentrations. We conclude that the evolution of irradiation-induced defects in one phase of the composite is strongly controlled by the defect properties of the other phase, offering a route to controlling defect evolution in these materials.

Magmatic processes revealed by heterogeneous crystal populations in a lamprophyre system

T. UBIDE^{1,2*}, C. GALÉ¹, P. LARREA¹, E. ARRANZ¹, M.LAGO¹ AND J.R. WIJBRANS²

¹Universidad de Zaragoza, Spain (*correspondence: tubide@unizar.es)

²VU University Amsterdam, The Netherlands

Minerals respond texturally and compositionally to changing magmatic environments. We have studied a Cretaceous alkaline lamprophyre intrusion cropping out in the Catalonian Coastal Ranges in NE Spain [1] which includes macrocrysts and microcrysts of clinopyroxene and amphibole with complex zoning patterns. Mineral textures, compositional zoning, barometric estimates and geochronology provide insights into the magma plumbing system.

Macrocryst cores show inverse zoning patterns from more evolved to more primitive compositions. Therefore, they are not in equilibrium with the magma that hosts them and cannot be considered true phenocrysts. Rather, they are classified as antecrysts [2] recycled from earlier stages of the magma system. Macrocryst rims and microcrysts, in contrast, define an evolution from more primitive to more evolved compositions that can be related to progressive fractionation of the magma.

According to clinopyroxene barometry [3], macrocryst cores crystallised in a deep magma chamber (500-800 MPa) whereas macrocryst rims and microcrysts crystallised during the ascent and shallow emplacement of the magma below 50 MPa pressure. ⁴⁰Ar/³⁹Ar ages reveal a short timespan between the crystallisation of macrocrysts and microcrysts.

Our results reveal repeated injection and mixing of batches of a more primitive magma with the resident magma in a deep magma chamber, controlling the crystallisation of macrocryst cores (antecrysts). The last recharge event likely triggered the ascent of the magma to the emplacement level, carrying a significant amount of recycled crystals. The melt underwent fractionation during ascent and emplacement, controlling the composition of macrocryst rims and microcrysts.

This investigation highlights the need to carefully evaluate mineral zoning patterns and mineral-melt equilibrium in apparently simple porphyritic rocks.

[1] Ubide *et al.* (2012) *Lithos* **132-133**, 37-49. [2] Davidson *et al.* (2007) *Annu. Rev. Earth Planet. Sci.* **35**, 273-311. [3] Putirka (2008) *Rev. Mineral. Geochem.* **69**, 61-120.

Sedimentary organic matter variations in the Chukchi Borderland over the last 155 kyr

MASAO UCHIDA¹ AND STEPHAN RELLA²

¹16-2 onogawa tsukuba 305-0044, japan, uchidama@nies.go.jp

²16-2 onogawa tsukuba 305-0044, japan, stephanrella@gmail.com

Knowledge on past variability of sedimentary organic carbon in the Arctic Ocean is important to assess natural carbon cycling and transport processes related to global climate changes. However, the late Pleistocene oceanographic history of the Arctic is still poorly understood. In the present study we show sedimentary records of total organic carbon (TOC, $\delta^{13}C$), $CaCO_3$, benthic foraminiferal $\delta^{18}O$, molecular markers (BIT index) and the coarse grain size fraction from a piston core recovered from the northern Northwind Ridge in the far western Arctic Ocean, a region potentially sensitively responding to past variability in surface current regimes and sedimentary processes such as coastal erosion. An age model based on oxygen stratigraphy, radiocarbon dating and lithological constraints suggests that the piston core records paleoenvironmental changes of the last 155 kyr.

TOC shows orbital-scale increases and decreases that can be respectively correlated to the waxing and waning of large ice sheets dominating the Eurasian Arctic, suggesting advection of fine suspended matter derived from glacial erosion to the Northwind Ridge

by eastward flowing intermediate water and/or surface water and sea ice during cold episodes of the last two glacial interglacial cycles. At millennial scales, increases in TOC might correlate to a suite of Dansgaard-Oeschger Stadials between 120 and 45 ka before present (BP) indicating a possible response to abrupt northern hemispheric temperature changes. Between 70 and 45 ka BP, closures and openings of the Bering Strait could have additionally influenced TOC variability. $CaCO_3$ content tends to anti-correlate with TOC on both orbital and millennial time scales, which we interpret in terms of enhanced sediment advection from the carbonate rich Canadian Arctic via an extended Beaufort Gyre during warm periods of the last two glacial-interglacial cycles and increased organic carbon advection from the Siberian Arctic during cold periods when the Beaufort Gyre contracted.

Exploring fractionation models for some martian primary magmas

A. UDRY^{1*}, H. Y. MCSWEEN¹ AND J. B. BALTA¹

¹Planetary Geosciences Institute, Dept. of Earth and Planetary Sciences, University of Tennessee, Knoxville, TN 37996, USA. (*Correspondence: audry@utk.edu)

The martian surface is mainly composed of tholeiitic basalts [1] as well as some alkaline compositions and sediments derived from basalts. Two hypotheses have been proposed to explain the compositions of martian basalts: 1) melting of martian mantle under various conditions, forming primary magmas with diverse compositions [2], or 2) fractional crystallization of primary magmas, resulting in the various basaltic compositions [3]. On the Earth, the Moon, and the asteroid 4 Vesta, primary magmas are scarce, indicating that most magmas fractionated during ascent. This model should also be applicable for Mars.

We conducted hundreds of fractional crystallization calculations for four different martian primary magmas: 1) Humphrey, 2) Fastball, 3) Yamato-980459, and 4) nakhlite parental melts, using MELTS and pMELTS [4]. Previously, all calculations and experiments have been isobaric. Our results are the first calculations conducted on martian magmas under polybaric conditions. In addition, we investigated isobaric and polybaric calculations at various oxygen fugacities, water contents, and P-T paths for each primary magma. Our study shows that polybaric fractionation of primary magmas (except Y-98) leads to the formation of alkaline compositions if most of the crystallization occurs at high pressures but forms subalkaline compositions if magma undergoes fractionation during rapid ascent.

In addition to examining martian primary magma evolution, we investigated formation of three specific martian alkaline rock compositions: 1) Backstay, 2) Jake Matijevic, and 3) nakhlite intercumulus glass. Backstay and the nakhlite intercumulus glass compositions can be formed through fractional crystallization of tholeiitic primary magmas, with or without water, and with a primary magma held at high pressures. Jake Matijevic [5] likely formed from a metasomatized alkali-rich melt. Our results suggest that alkaline magmas on Mars are formed similarly as on Earth and may be more common than suggested by orbital surveys for alkaline rocks.

[1] McSween *et al.* (2009) *Science*, 324, 736- 739. [2] Baratoux *et al.* (2011) *Nature*, 472, 338-341. [3] McSween *et al.*, (2006) *J. Geophys. Res.* 111, E09S91. [4] Ghiorso and Sack (1995) *Contrib. Min. and Pet.*, 119, 197-212 [5] Stolper *et al.* (2013) LPSC XLIV, Abstract #1685.

Cause of the maximum S-MIF scatter in the late Archean: atmospheric organic sulfur and episodic volcanism

YUICHIRO UENO^{1,2*}, SEBASTIAN O. DANIELACHE³,
MASAFUMI SAITO¹, YOSHIKI ENDO¹
AND MATTHEW JOHNSON⁴

¹Earth & Planetary Sciences, Tokyo Institute of Technology, Japan. (ueno.y.ac@m.titech.ac.jp)

²Earth-Life Science Institute (ELSI), Tokyo Institute of Technology, Japan

³Faculty of Science & Technology, Sophia University, Japan

⁴Copenhagen Center for Atmospheric Research, Department of Chemistry, University of Copenhagen, Denmark.

Sulfur Mass-Independent Fractionation (S-MIF) has been useful to monitor chemistry of the Earth's early atmosphere. In the latest Archean, from 2.7 to 2.5 Ga, $\Delta^{33}\text{S}$ values of sedimentary sulfides exhibit exceptionally large variation compared to older period. The maximum scatter of S-MIF may indicate anomalous chemistry of atmosphere or climatic system of the late Archean Earth, though the primary cause of the large MIF is still poorly understood. We have developed a sulfur isotopic model by improving atmospheric reaction model [1,2]. The improvements to our model includes the addition of hydrocarbon chemistry, chemical formation and deposition of organic sulfur haze, together with newly determined high-accuracy ultraviolet absorption cross sections of SO_2 isotopologues. Our model results suggest that after a volcanic injection of SO_2 into the Archean atmosphere, a significant fraction of the sulfur is converted into organic sulfur and could be accumulated in an atmosphere over a timescale of 10 years, if background atmosphere is reducing enough to yield hydrocarbon haze and volcanic sulfur input is large and episodic. Such model could explain the large $\Delta^{33}\text{S}$ preserved in sedimentary rocks. Moreover, isotopically fractionated two reservoirs (i.e. atmosphere and ocean) can be mixed episodically and thus possible to explain the observed small scale heterogeneity of S-MIF even within a hand specimen level. Preservation process of the S-MIF could have been more dynamical than previously thought.

[1] Danielache *et al.* (2008) *J Geophys Res* **113**, D17314. [2] Ueno *et al.* (2009) *PNAS* **106**, 14784-14789.

The relation between metasomatism and redox state of the upper mantle below the Massif Central, France

LAURA UENVER-THIELE¹, A. B. WOODLAND¹, H. DOWNES² AND R. ALTHERR³

¹ Institut für Geowissenschaften, Universität Frankfurt, Frankfurt, Germany (laura.uenver@online.de),

² School of Earth Sciences, Birkbeck College, University of London, London WC1E 7HX, UK

³ Institut für Geowissenschaften, Universität Heidelberg, 69120 Heidelberg, Germany

Several studies have demonstrated the existence of two geochemically and texturally distinct mantle domains lying north and south of $45^\circ 30'$, respectively [1,2]. These two domains are also reflected by differences in their redox state [3] and record different metasomatic overprints. The aim of this study is to combine redox and trace element data to more closely investigate these metasomatic processes at various length scales.

Preliminary trace element data indicate multiple types of enrichment in LREE, MREE and HSE. These different signatures occur regionally as well as locally, which implies variations in metasomatic style with depth. Most northern domain samples have high La/Nd (>10), but low Sm/Yb (<0.8) and $\log f\text{O}_2$ values $> \text{FMQ}+0.9$. The southern domain appears to have been affected by several different types of metasomatic overprints with variable intensity (e.g. high $(\text{Ce}/\text{Yb})_N$). Oxidation states are also a function of rock type, with harzburgites having $\log f\text{O}_2 \sim \text{FMQ}+1.0$ and lherzolites lying by $\sim \text{FMQ}+0.5$. The harzburgites appear to be more sensitive to changes in oxidation state, presumably due to their generally low spinel contents. The presence of small amounts of amphibole does not correlate with degree of enrichment or the highest $f\text{O}_2$ values. Investigation of how geochemical and redox heterogeneities are influenced by rock type and texture are currently underway.

[1] Downes H. *et al.* (2003) *Chem. Geol.*, 200, 71-87. [2] Lenoir, X. *et al.* (2000) *Earth Planet. Sci. Lett.* 181, 359-375. [3] Uenver-Thiele L. *et al.* (2013) EGU abstract 11398.

Detailed history of atmospheric pollution in South America as recorded by trace elements in the Quelccaya ice core

C. UGLIETTI¹, P. GABRIELLI^{1,2} AND L.G. THOMPSON^{1,2}

¹ Byrd Polar Research Center, 108 Scott Hall, The Ohio State University, 1090 Carmack Road, Columbus, OH 43210, USA (ugliettichiara@gmail.com)

² School of Earth Sciences, The Ohio State University, 125 South Oval Mall, Columbus, OH 43210, USA (gabrielli.1@osu.edu)

Reconstructions of past trace-metal deposition are extremely important to address questions linked to changes in land-use, climate, aeolian dust and to identify spatial patterns and temporal trends in global trace-metal associated with anthropogenic activities. The tropical Andes are particularly interesting because they host a long mining history associated with mineral exploitation and environmental impacts. The glacio-chemical record preserved in the ice of the Quelccaya ice cap, located within the southern Peruvian Andes offers a unique opportunity to geochemically constrain the composition of the tropical atmosphere at sub-annual resolution through time. Two ice cores were retrieved from the ice cap in 2003 (Summit Dome core, (QSD; 5670 m asl, 168.68 m) and North Dome core (QND; 5600 m asl, 128.57 m). Determination of twenty trace elements (Ag, Al, As, Bi, Cd, Co, Cr, Cu, Fe, Mn, Mo, Pb, Rb, Sb, Sn, Ti, Tl, U, V, and Zn) was performed by Inductively Coupled Plasma Sector Field Mass Spectrometry (ICP-SFMS, Element 2) over the first 120 m of the QND core, spanning the time period between 1990 AD and 1500 AD. As, Bi, Cd, Cu, Mn, Mo, Pb and Zn show different increases in concentration and crustal enrichment factors over this time period pointing to varying anthropogenic sources.

Geochemistry of urban soils in Karlstad, central Sweden – preliminary results

J. UHLBÄCK¹, A. LADENBERGER¹, M. ANDERSSON¹ AND M. SADEGHI¹

¹Geological Survey of Sweden, Box 670, S-751 28 Uppsala, Sweden (*correspondence: anna.ladenberger@sgu.se)

As a part of the European project URGE (Urban Geochemistry), in collaboration with EuroGeoSurveys Geochemistry Expert Group (EGS-GEG), surface soils were surveyed in the urban area of the municipality Karlstad in central Sweden to assess geochemical patterns of potentially toxic metals and other elements that can be considered dangerous at elevated concentrations.

306 surface (<10 cm depth) soil samples were collected from Karlstad town and analysed with aqua regia (AR) digestion by ICP-MS. The results show elevated concentrations of Cd, Cu, Pb, Sb and Zn in industrial parts of the town and in the harbour, while playgrounds, residential districts and recreation areas show lower concentrations. Broadly defined greenfields show more variation in metal concentrations, most likely due to the wider spread of potential sample sites in this category. The results display a mixed and complicated relationship between the geological background and anthropogenic overprint, with elevated concentrations in areas with historical and present industrial activity. The geochemical patterns of Ni, Cr and Co are similar and possibly related to the presence of mafic rocks within the extent of the town (especially in the southern part of Karlstad). Elevated As levels occur randomly in greenfield areas indicating a rather natural origin of these anomalies. Higher concentrations of Pb, Cd and Ni in the city centre can be related to traffic. High Cu and Zn contents in the town's central parts point to the long-term use of copper-zinc construction details in buildings, e.g. gutters and roof elements. Elevated Hg concentrations in several places by the Klara river may indicate the pollution related to sewage and fertilizers and affinity of Hg to bind to organic matter-rich bank sediments.

The results from this study can be further used by the local authorities for future planning of the infrastructure and slum-clearance of contaminated land. Potential health risks for inhabitants who reside and work in contaminated areas can also be assessed, with the aim to specify and inform the public about possible precautionary measures.

Structural-diagenetic evolution of fractures in folds: A TGS example from the Alberta Foothills, Canada

E. UKAR*, P. EICHHUBL AND A. FALL

The University of Texas at Austin, Bureau of Economic Geology, PO Box X, Austin, TX 78713

(*correspondence: esti.ukar@beg.utexas.edu)

The late Jurassic-early Cretaceous Nikanassin formation is generally characterized as a tight gas sandstone formation with submillidarcy values of permeability and porosities typically less than 6% [1]. However, the Nikanassin produces gas at commercial rates where it contains a network of open fractures. But exploration and development outcomes are mixed, underlining the necessity for a better understanding and characterization of the more fractured and potentially more productive regions [2].

A unique combined outcrop and core study of fractures associated with three reservoir-scale anticlines reveals the presence of two main fracture sets in all three mesostructures: fracture set one is perpendicular to the fold axis, whereas fracture set two is parallel. Both sets have an associated conjugate oblique fracture set. Scanline data indicate a higher fracture intensity in the steeply-dipping limbs of the folds than in the shallower-dipping limbs. Cathodoluminescence images of cemented fractures reveal several generations of quartz and ankerite cement that are synkinematic and postkinematic relative to fracture opening. Based on homogenization temperatures of two-phase aqueous inclusions in crack-seal cement, synkinematic fracture opening and cement precipitation occurred at or near maximum burial in core samples (190-210°), and during exhumation in outcrop samples (120-160°).

Structural models constructed using MOVE [3] predict a higher strain accumulation in the steep limb of the Sternie Creek Anticline than in the fold hinge and shallow limb. Models also predict an early opening of fracture set 1, which is in accordance with the general observation that set 2 cross-cuts set 1 in outcrop. Opening of most fractures probably occurred during regional folding at the end of the Laramide orogeny.

[1] Solano *et al.* (2011) *SPE Res. Eval. & Eng.* **14**, 357-376

[2] Hayes (2009) *Search and Discovery* article #10182 [3] MOVE *Midland Valley Structural Restoration Software*

Anammox in an ammonium-impacted groundwater aquifer

ANNE ULDAHL^{1*}, BO THAMDRUP²
AND RASMUS JAKOBSEN³

¹DTU Environment, Technical University of Denmark. Miljoevej, Building 113, DK-2800 Kgs. Lyngby. (*correspondence: annu@env.dtu.dk)

²NordCEE and Institute of Biology, University of Southern Denmark. Campusvej 55, DK-5230 Odense M.

³GEUS, Geological Survey of Denmark and Greenland. Oestervoldgade 10, DK-3500 Copenhagen K.

The novel anaerobic ammonium oxidation pathway (anammox) is today recognized as an important sink for reactive N, removing biologically available N in the form of ammonium and nitrite to the gaseous N₂, providing a competition to the dissimilatory nitrite reduction by denitrifiers. Anammox activity and the responsible bacteria are currently demonstrated in a wide range of ecosystems, however; the knowledge about anammox in freshwater systems, like ammonium-impacted groundwater aquifers, is still scarce. With the necessary electron donors and acceptors present in the groundwater system, the activity and abundance of anammox bacteria could be of significant importance since biologically available N, resulting from anthropogenic sources, is a major threat to groundwater quality.

We hypothesize that the anammox process occurs in a contaminated groundwater system, when NO₂⁻ and NH₄⁺ are present under low oxygen conditions. Isotope-based methods were used to quantify anammox activity through the isotope pairing technique: two-meter sediment cores were collected from a groundwater system adjacent to the abandoned landfill site Risby, Denmark; chosen intervals were sectioned and incubated anaerobically as sediment slurries. The production of ²⁹N₂ and ³⁰N₂ was monitored over time after addition of labelled N and unlabelled N as: ¹⁵NO₃⁻ + ¹⁴NH₄⁺ for detecting anammox, denitrification (nitrite reduction to N₂) and DNRA (dissimilatory reduction of ammonium) and with ¹⁵NH₄⁺ + ¹⁴NO₃⁻ for detecting anammox production. Our results show that both anammox and DNRA are active, with denitrification as the dominating pathway.

Preservation potential of $\delta^7\text{Li}$ values in Mesozoic calcite fossils

C.V. ULLMANN^{*1,2}, H.J. CAMPBELL³, R. FREI¹, S.P. HESSELBO², P.A.E. POGGE VON STRANDMANN² AND C. KORTE¹

¹University of Copenhagen, IGN, Øster Voldgade 10, 1350 Copenhagen, Denmark

(*correspondence: c.v.ullmann@gmx.net)

²University of Oxford, Department of Earth Sciences, South Parks Road, Oxford OX1 3AN, United Kingdom

³GNS Science, 1 Fairway Drive, Avalon 5010, New Zealand

Lithium isotopes of fossil carbonates are a promising proxy for determining the intensity of silicate weathering. Here we use elemental and isotopic trends in diagenetically altered Late Jurassic belemnites (*Belemnopsis* sp. and *Hibolithes* sp.) from New Zealand to see if meaningful $\delta^7\text{Li}$ values are preserved in fossil calcites over time spans of > 100 m.y.

The parts of the belemnite rostra that are most altered are characterized by low $\delta^{18}\text{O}$ reaching -12‰ and moderate decreases in $\delta^{13}\text{C}$ (down to -2‰), coupled with high Mn/Ca ratios reaching 4.6 mmol/mol. Both, Sr/Ca ratios and $^{87}\text{Sr}/^{86}\text{Sr}$ ratios were found to decrease with progressive alteration. The direction and magnitude of the trends indicate one main diagenetic phase.

Altered materials show variable $\delta^7\text{Li}$ values between +24 and +40‰, while $\delta^7\text{Li}$ values of the sedimentary matrix are -5‰. $\delta^7\text{Li}$ values of best preserved belemnites are $+27 \pm 1$ ‰ (2 sd, n = 5), pointing to a Late Jurassic seawater $\delta^7\text{Li}$ of ~29-32‰, compatible with the modern value of 31‰. Despite burial down to ~4 km, and thus elevated temperatures, uniform $\delta^7\text{Li}$ values in the well-preserved fossil calcites, and strong isotopic gradients between fossil calcite and sediments have been maintained. This suggests that primary $\delta^7\text{Li}$ values can be preserved over geological timescales.

Recent views on lamprophyric melilitic rocks (polzenites) of the Bohemian Massif

JAROMÍR ULRYCH^{1*} AND LUKÁŠ KRMÍČEK²

¹Institute of Geology v.v.i., Academy of Sciences of the Czech Republic, Rozvojová 269, CZ-165 00 Praha 6, Czech Rep. (*correspondence: Ulrych@gli.cas.cz)

²Brno University of Technology, Faculty of Civil Engineering, Veveří 95, CZ-602 00 Brno, Czech Rep.

The easternmost part of the Cenozoic Volcanic Province of western and central Europe includes rare occurrences of Late Cretaceous to Paleocene (70 to 59 Ma) ultramafic melilitic and melilite-bearing rocks. These rock suites, related to the initial stage of rifting of the Bohemian Massif, occur in the shoulder blocks of the Ohře/Eger Rift zone. Here, in the Ploučnice (Polzen) River area, a group of clinopyroxene-free melilitic rocks - polzenites - was defined by K.H. Scheumann in 1913. He recognized three principal petrographic types of polzenite: Vesec, Modlibohov and Luhov type. Inspecting the petrography of the separate types we find that the Vesec type is represented by polzenite s.s. only (olivine + melilite + nepheline + phlogopite + spinels + calcite ± monticellite, hauyne, perovskite, apatite mineral associations), whereas the Modlibohov type is transitional to the Luhov type representing a clinopyroxene-bearing melilitic rock – alnöite, as defined by H. Rosenbusch in 1887.

Regarding the classification of polzenites, there are currently two petrographic approaches. According to the first view polzenites represent only lamprophyric, i.e. volatile-rich, facies [1] of melilite-bearing group of rocks and can be added as a special petrographic type into this group. According to the second view, polzenites belong to an individual group of ultramafic lamprophyres, however they are considered by some scientists as a more felsic variant of alnöite [2]. With respect to the petrography of clinopyroxene-free polzenite (the Vesec type) for which values of Mg# between 74 and 78 are typical, polzenite can be considered a valid end-member of the ultramafic lamprophyre group.

Acknowledgements. This work was supported by the project "EXCELLENT TEAMS" at BUT; registration number CZ.1.07/2.3.00/30.0005.

[1] Mitchell (1994) *Miner. Petrol.* **51**, 137–146. [2] Tappe *et al.* (2005) *J. Petrol.* **46**, 1893–1900.

Forceful Carbonation of Serpentine

O. I. ULVEN*, H. AUSTRHEIM
AND A. MALTHER-SØRENSSEN

Physics of Geological Processes, University of Oslo, 0316
Oslo, Norway (*Correspondence: o.i.ulven@fys.uio.no)

Mineral carbonation has been suggested as an option for long term sequestration of anthropogenic CO₂[1]. It is in this respect critical to know whether the growth of carbonate minerals will clog pore space, and thus limit further transport of CO₂ into the rock, or whether the carbonate growth will exert enough stress on the host rock to make it fracture, thus making new fluid pathways.

In this work, we perform a numerical study of natural field examples of growth of carbonate minerals in serpentine, and we use a discrete model to reproduce observed structures.

We achieve an improved understanding of the process of mineral carbonation and the feedback on rock deformation, thus improving our ability to determine whether industrial scale mineral carbonation is a viable option for long term storage of CO₂.

[1] Kelemen, P.B, and Matter, J.(2008), Proceedings of the National Academy of Sciences of the United States of America, Vol. 105(45): pp. 17295-17300

Limited releases of U and Tc from Hanford tank residual wastes

WOYONG UM^{1,2,*} AND KIRK J. CANTRELL¹

¹Pacific Northwest National Laboratory, Richland, WA, USA

²Pohang Univ. of Sci. and Technol., Pohang, South Korea
wooyong.um@pnnl.gov (* presenting author)

Most of the Hanford Tank wastes in Washington, USA are expected to be retrieved, stabilized in an appropriate waste form and then disposed in a repository. Small amounts of residual wastes are expected to remain at the bottom of the tanks in a layer no more than 2.54 cm thick as slurry of solid precipitates. The current final stage of tank closure is planned to consist of the addition of cement or grout to stabilize the remaining wastes and tank structure. In this study, three different chemical treatment methods (lime [Ca(OH)₂] addition, an in-situ Ceramicrete based on chemically bonded phosphate ceramics, and a ferrous Iron/Goethite treatment) were tested for their ability to stabilize residual Hanford C-202 tank wastes for reducing contaminant release of Tc and U in particular because they are key groundwater risk drivers.

Leaching tests were conducted using a single-pass flow-through test (SPFT) system with 0.005 M Ca(OH)₂ solution for untreated tank sample and C-202 wastes treated with three different chemical treatments. Technetium concentrations in leachates from tank C-202 residual waste treated with the Ca(OH)₂, Ceramicrete, and Goethite methods are shown in Fig.1. All three treatments methods effectively reduced the leachable Tc concentrations as well as U to well below untreated waste as a result of formation of insoluble secondary precipitates which can behave like mineral coatings.

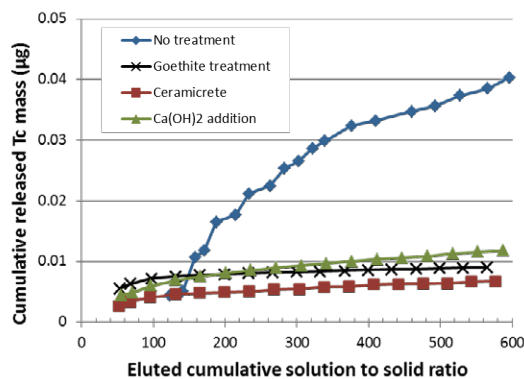


Fig. 1. Released cumulative Tc amounts from the residual wastes.

This innovative approach has the potential to revolutionize Hanford's tank retrieval processes, by allowing larger volumes of residual waste to be left inside tanks while providing an acceptably low level of risk with respect to contaminant release as well as significant cost savings.

Chemical composition of detrital spinel from Eastern Chugoku and Northern kinki of Sangun zone, Southwest Japan.

TOMOYUKI UMEDA¹ AND ICHIRO MATSUMOTO¹

¹Faculty of Education, Shimane University, Matsue, Japan, umedatomoyuki@gmail.com (*presenting author) chromim@edu.shimane-u.ac.jp

Geochemical characteristics of chromian spinel from ultramafic rocks and chromitites in Sangun zone of Central chugoku district have become clear gradually by recent many studies [1,2]. Especially, petrogenesis of chromitite formation [3] and exfoliation for chromitite [4] came to be advanced from these works. However, ultramafic complexes in Sangun zone distribute not only central chugoku district but also from eastern chugoku to northern kinki districts, which are called Wakasa, Sekinomiya, Izushi, Oeyama complexes respectively. Chromitite pods and chromite mines (now closed) also existed in these district. Detailed research of chromian spinel from ultramafic rocks and chromitite in this district is not done sufficiently, and there is the required for a geochemical description for understand origin and petrogenesis of ultramafic rocks and chromitite. However ultramafic rocks in the Sangun zone of these district are also strongly altered and serpentinized. Then we use detrital chromian spinel from the stream sediment, in this study. This is the first report of chemical composition of detrital chromian spinel from ultramafic rocks and chromitite in Sangun zone of from eastern chugoku to northern kinki district.

Cr#(=Cr/Cr+Al) of detrital chromian spinel from Sekinomiya complex varies from 0.43 to 0.56. Cr# of those from Izushi complex varies from 0.36 to 0.56 (mainly 0.43 to 0.50). Cr# of those from Oeyama complex varies from 0.43 to 0.69. That is, Cr# of those from eastern chugoku to northern kinki district overlap with the Cr# (0.4 to 0.6) of detrital spinel from central chugoku district. In addition, We found chromitite boulder in Oeyama complex, and show that Cr# of chromian spinel varies from 0.38 to 0.43, that is the most High-Al podiform chromitite in Japan. This is significant petrological description, indicating involvement of both Al-rich melt and of fertile harzburgite.

[1] Arai (1980): *J. Petrol.*, 21, 141-165. [2] Matsumoto *et al.* (1995): *J.Jpn.Assoc.Mineral.Petrol.Econ.Geol.*, 90, 333-338. [3] Arai and Yurimoto (1994): *Econ. Geol.*, 89, 1279-1288. [4] Matsumoto and Arai (1997): *Resource-Geology*, 47, 189-199.

Petrological Implications of Temporal and Spatial Variations in Magma Chemistry of the Quaternary Tendurek Shield Volcano, Eastern Anatolian Collision Zone, Turkey

E. UNAL^{1*}, M. KESKIN², V.A. LEBEDEV³, ANDREY V. CHUGAEV³ AND E.V. SHARKOV³

¹YYU, Dept. of Geol. Engineering, Zeve Campus, Van, Turkey (*correspondence: esinunal@yyu.edu.tr)

²Istanbul Univ., Dept. of Geol. Engineering, Avcilar, Istanbul, Turkey (keskin@istanbul.edu.tr)

³RAS, IGEM, Staromonetny per., 35, Moscow, Russia

The Quaternary Tendürek Volcano is one of the largest eruption centers of the Eastern Anatolia with a summit elevation of 3538 m and a footprint area of 650 km². It is a shield volcano consisting of lavas ranging in composition from tephrites through benmoreites/phonolites to trachytes. The young volcanism of the region is thought to be related to the continent-continent collision taken place after the closure of the Neo-Tethys Ocean. The Tendürek volcano is of special importance, because it is one of the rare places in Eastern Anatolia where calc-alkaline and potassic alkaline volcanism coexisted.

Lavas of the Tendürek volcano are classified on the SiO₂ versus K₂O diagram as medium K / high K and shoshonitic series. Results of our FC, AFC and EC-AFC modelings indicate that the Tendürek lavas were influenced by crustal contamination and fractional crystallization. Medium to high potassic basalts, trachy-basalts, tephrites and basaltic-trachyandesites basically follow a partial melting trend on La vs. La/Yb diagram in contrast to the trachy-andesites, phonotephrites, tephriphonolites, phonolites, and trachytes of the shoshonitic series aligning along a fractional crystallization trend. The high-SiO₂ phonolitic lavas have a more pronounced enrichment in incompatible elements, such as Rb, Th, La and Nb, in comparison to those in the other shoshonitic rocks. The aforementioned differences in the chemical compositions of these two groups of shoshonitic rocks may reflect variations in the fractional crystallization process which involved clinopyroxene and plagioclase during the petrogenesis of the potassic rocks.

According to our melting model, primitive magma of the Tendürek lavas were derived from mixing of the spinel and garnet peridotite melts with different melting degrees ranging between 1 - 3%.

Possible link between CO₂ degassing and climate change in SW Turkey

E. ÜNAL-İMER^{1*}, I.T. UYSAL¹, J. SHULMEISTER¹
AND J.X. ZHAO¹

¹The University of Queensland, Brisbane, QLD, 4072,
AUSTRALIA (*correspondence: e.unal@uq.edu.au)

High-pressure CO₂-rich fluids can trigger fault activity by reducing the shear stress [1]. Subsurface meteoric water at crustal depths of 10–15 km, mainly contributed by local rainfall sourced groundwater, may be the major fluid source in large-scale continental extensional areas [2]. Carbonate vein deposits could precipitate from such CO₂-rich, deeply circulated overpressurised meteoric water within intensely-fractured/faulted rocks along active normal fault zones, within a rapidly extending region in SW Turkey [3,4,5] sub-samples of such vein calcites were investigated by advanced U-series dating and O-isotope analyses. The U-series ages show that calcite vein formations occurred largely during lower solar insolation (summer) periods in the Late Pleistocene in this region. These are interpreted as the periods of elevated effective precipitation, which could be responsible for fluid overpressures achieved by either increasing absolute or seasonal precipitation or by reducing evapotranspiration. Although full glacial periods are commonly associated with dry climatic conditions, regional conditions can vary. We suggest that the Eastern Mediterranean basin including Turkey was relatively wet under low to transitional insolation regimes, specifically, during the Last Glacial Maximum. This is likely a response to southerly-shifted westerly wind flow in the Northern Hemisphere bringing moisture supply over the study area. Further, the trend of δ¹⁸O values plotted against U-series ages of vein calcites demonstrate possible responses to either climate variability or seismicity-related fluid exchange mechanisms on mm scale.

It is possible to correlate fault activity recorded by co-seismic vein calcites as a product of CO₂ degassing and local climate controlling the effective precipitation. This means that seismic hazard can be linked to changing climatic conditions in the region. Consequently, earthquake clusters in SW Turkey may be considered to be climate-related and a function of the increased availability of fluids during cool to cold climate periods.

[1] Hickman *et al.* (1995) *J. Geophys. Res.* **100**, 12,812–12,831. [2] Wickham *et al.* (1993) *Geology* **21**, 81–84. [3] Uysal *et al.* (2009) *Chem. Geol.* **265**, 442–454. [4] Uysal *et al.* (2011) *EPSL* **303**, 84–96. [5] De Filippis *et al.* (2012) *Geol. Soc. Am. Bull.* **124**, 1629–1645.

Microbial corrosion of steel in Toarcian argillite: Influence of metabolisms and biofilms

L. URIOS^{1*}, A. PEREZ⁴, C. WITTEBROODT³, F. MERCIER⁴,
M. FLACHET², F. MARSAL², D. NEFF, M. MAGOT¹
AND P. DILLMANN⁴

¹Université de Pau et des Pays de l'Adour, IPREM EEM UMR
5254, IBEAS, 64013 PAU, France, (*presenting author,
laurent.urias@univ-pau.fr)

²IRSN, PRP-DGE/SEDRAN/BERIS, B.P. 17, 92262 Fontenay
aux Roses Cedex, France (margot.flachet@irsn.fr)

³IRSN, PRP-DGE/SRTG/LETIS, B.P. 17, 92262 Fontenay
aux Roses Cedex, France (charles.wittebroodt@irsn.fr)

⁴SIS2M/LAPA, CEA/CNRS UMR 3299, 91191 Gif-sur-
Yvette Cedex, France (philippe.dillmann@cea.fr)

In the context of geological disposal of radioactive waste in clayey formations, the consequences of a microbial activity are of concern regarding the corrosion of metallic materials. Actually microbial life has been highlighted in argillaceous formations [1]. Sulfate- and iron-reducing bacteria, as well as bacteria able to develop at high temperatures have been detected in Tournemire¹ (Toarcian argillite) [2]. They can grow at the interfaces between steel and argillite in a short period compared with planned durations of disposal. Such bacteria may influence corrosion [3], that may cause a premature loss of containment of metallic barriers. The formation of biofilms may also lead to environmental modifications at the biofilm/metal interface that may further increase corrosion rates [4]. Thus, an experimental setup was designed to understand the conditions favoring the formation of biofilm and the impact of microorganisms on steel corrosion.

A synthetic solution representative of the Tournemire pore water percolated through cells containing steel coupons placed in contact with Tournemire argillite. Various environmental conditions likely to prevail in a repository were tested (anoxic or oxic conditions, 25°C or 50°C). A mix of strains able to form biofilms and sulfate- and iron-reducing bacteria, each present in Tournemire argillite, has been inoculated. Cells were dismantled after 1, 4 and 8 months to establish a chronology of the involved processes. Analyses of outgoing water chemistry provided indications on mechanisms occurring within the cells. Observations of the steel surface were made using Field Emission Scanning Electron Microscopy and Raman spectroscopy. Molecular characterization of the microbial diversity was used to determine which species are responsible for corrosion.

¹ IRSN's experimental platform

[1] Urios *et al.* (2012) *Appl. Geochem.* **27**, 1442-1450. [2] Urios *et al.* (2013) *Geomicrobiol. J.* **30**, 442-453. [3] Herrera & Videla (2009) *Int. Biodeter. Biodegrad.* **63**, 891-895. [4] Little *et al.* (1991) *Int. Mater. Rev.* **36**, 253-272.

Assesing iron and oxygen isotope homogeneity in garnets

M. UROSEVIC¹, O. NEBEL¹, E.C. PETERSON²,
J.A. PADRÓN-NAVARTA^{1,3} AND D. RUBATTO¹

¹Research School of Earth Sciences, The Australian National University, Canberra, Australia

²Mineralogy, Technology and Innovation, Rio Tinto, Melbourne, Australia

³Géosciences Montpellier, Univ. Montpellier 2 & CNRS, 34095 Montpellier, France

Garnet is a key mineral for (i) dating metamorphic processes in the crust, (ii) tracing P-T conditions in the upper mantle, and (iii) understanding porphyry, skarn and epithermal ore systems. All of these geotectonic settings and associated processes are related to mass transfer of elements in fluids or melts. Detailed knowledge of the redox state under which such processes occur (often referred to as fO_2) and/or the source of fluids is crucial for the study of mass transfer in rock forming processes in crust and mantle.

Here we assess three natural garnets for their major, trace and O-Fe isotope budget in search of suitable standards and constraints on processes controlling their isotope systematics. One garnet from Kakanui, New Zealand (KAK) and two from Erongo, Namibia (ERO-R and ERO-G) are analysed. KAK is a xenocryst pyrope-rich garnet ($Alm_{22-23}Prp_{62-63}Grss_{12}And_2Spss_1$) from mantle-derived alkaline melt. ERO-R is an igneous almandine-rich garnet ($Alm_{64-65}Prp_{6-7}Grss_1And_{<1}Spss_{28-29}$) from a migmatitic vein with negligible proportion of Fe^{3+} . ERO-G is a hydrothermal highly zoned andradite-grossular-rich garnet ($Prp_{<1}Grss_{22-65}And_{32-77}Spss_{1-2}$) with all Fe as Fe^{3+} .

KAK is homogeneous in major and trace elements and in oxygen isotopes at the microscale with $\delta^{18}O \sim 5.3$. Its $\delta^{57}Fe_{(IRMM-014)} = +0.09 \pm 0.01$ is slightly elevated compared to average depleted mantle. Oxygen and Fe isotopes are homogeneous in ERO-R with $\delta^{18}O \sim 8.5$ and $\delta^{57}Fe = +0.11 \pm 0.06$, respectively. ERO-G garnet grains are zoned in oxygen composition with a variation from core to rim between ~ 13 and ~ 11 ‰, which coincides with the growth zoning pattern in Grss-Andr observed in BSE images. Accordingly, their heavy $\delta^{57}Fe$ vary from +0.6 to +0.9. Trace elements composition of ERO-G garnet is highly variable.

Based on our preliminary results KAK and ERO-R appear to be suitable standards for coupled Fe-O isotope analysis. Garnet O isotopes are in line with the source of the sample (mantle versus crust). Fe isotopes strongly correspond to Fe^{3+}/Fe^{2+} and may thus be a sensitive redox proxy in garnet.

Discovery of a Triassic magmatic arc source for the Permo-Triassic Karakaya subduction complex, NW Turkey

P. AYDA USTAÖMER^{1*}, TIMUR USTAÖMER², AXEL GERDES³, ALASTAIR H.F. ROBERTSON⁴
AND GERNOLD ZULAUF³

^{1*}Yıldız Teknik Üniversitesi, ustaomer@yildiz.edu.tr

²Istanbul Üniversitesi, Turkey

³Goethe-University, Frankfurt, Germany

⁴University of Edinburgh, U.K.

The Permo-Triassic Karakaya Complex is well explained by northward subduction of Palaeotethys but until now no corresponding magmatic arc has been identified in the region. With the aim of determining the compositions and ages of the source units, ten sandstone samples were collected from the mappably distinct Ortaoba, Hodul, Kendirli and Orhanlar Units. Zircon grains were extracted from these sandstones and >1300 were dated by the U-Pb method and subsequently analysed for the Lu-Hf isotopic compositions by LA-MC-ICP-MS at Goethe University, Frankfurt. The U-Pb-Hf isotope systematics are indicative of two different sediment provenances. The first, represented by the Ortaoba, Hodul and Kendirli Units, is dominated by igneous rocks of Triassic (250-220 Ma), Early Carboniferous-Early Permian (290-340 Ma) and Early to Mid-Devonian (385-400 Ma) ages. The second provenance, represented by the Orhanlar Unit, is indicative of derivation from a peri-Gondwanan terrane. In case of the first provenance, the Devonian and Carboniferous source rocks exhibit intermediate $\epsilon Hf(t)$ values (-11 to -3), consistent with the formation at a continental margin where juvenile mantle-derived magmas mixed with (recycled) old crust having Palaeoproterozoic Hf model ages. In contrast, the Triassic arc magma exhibits higher $\epsilon Hf(t)$ values (-6 to +6), consistent with the mixing of juvenile mantle-derived melts with (recycled) old crust perhaps somewhat rejuvenated during the Cadomian period. We have therefore identified a Triassic magmatic arc as predicted by the interpretation of the Karakaya Complex as an accretionary complex related to northward subduction (Carboniferous and Devonian granites are already well documented in NW Turkey). Possible explanations for the lack of any outcrop of the source magmatic arc are that it was later subducted or the Karakaya Complex was displaced laterally from its source arc (both post 220 Ma). Strike-slip displacement (driven by oblique subduction?) can also explain the presence of two different sandstone source areas as indicated by the combined U-Pb-Hf isotope and supporting petrographic data.

Multiple fluid events and metal mobility associated with formation of IOCG-type mineralisation in Gawler Craton

Y. UVAROVA^{1,2*}, J. CLEVERLEY^{1,2} AND R. HOUGH¹

¹CSIRO Earth and Resource Engineering, ARRC, Kensington, WA 6151 Australia (*correspondence:

Yulia.Uvarova@csiro.au)

²Deep Exploration Technologies CRC

The Gawler Craton, in South Australia, is host to the giant Olympic Dam deposit and a number of other economic to subeconomic iron oxide-copper-gold (IOCG) prospects including Prominent Hill, Oak Dam, Wirrda Well, Acropolis, Punt Hill, and Carrapateena. Several genetic models have been proposed for the formation of IOCG mineralisation in the Craton, but little is known about the source of metals and sulfur, and mechanisms of their transport and deposition.

Geologic and petrographic studies on IOCG prospects in the Olympic Dam district (Emmie Bluff, Canegrass, Cocky Swamp and Dromedary Dam) indicate several stages of fluid activity. Subeconomic Cu-Au mineralisation at these prospects is associated with the hematite-chlorite-sericite alteration with chalcopyrite commonly replacing pre-existing pyrite. With the use of cutting-edge Synchrotron X-ray Fluorescence Microscopy and Field Emission Gun Scanning Electron Microscopy it was shown for the first time that subeconomic IOCG mineralisation in the Gawler Craton was affected by a late fluid event, which resulted in partial dissolution of Cu mineralisation and transport of Cu in the form of chloride complexes. Patchy chlorite associated with the late alteration of chalcopyrite hosts a previously undescribed in IOCG rocks Cu-Cl phase. This Cu-Cl phase is interpreted to be a by-product of chalcopyrite partial dissolution and contains minor Zr, Y and U. The fluids must therefore have been rich in chlorine to mobilise Cu, and probably fluorine, as they were carrying relatively immobile Zr, Y and U which become mobile in the presence of fluoride complexes. This might be an indication of remobilisation and re-deposition of Cu along with other metals elsewhere in the district and could have implications for a possible metal source for the nearby Cu-Au deposits.

Understanding the role of Phanerozoic and active tectonics in generating geothermal resources in central Australia

I. T. UYSAL^{1*}, U. RING², AND A. W. MIDDLETON¹

¹University of Queensland, Queensland 4072, Australia¹

²Stockholm University, Stockholm 106 91, Sweden

(*correspondence: t.uysal@uq.edu.au)

Central Australia has a significant potential for geothermal development. Recent He and C isotope studies of volatiles from artesian waters suggest mantle-derived fluid reservoirs as a source of the geothermal resources [1], rather than radioactive heat production in the basement granitic rocks as widely believed. In conjunction with isotopic data of the volatiles, our structural geological field observations suggest that geothermal systems in central Australia preferentially occur in areas of deformation-enhanced permeability and deep mantle fluid production. To this end, we performed comprehensive isotopic dating studies (Rb–Sr, Ar–Ar and U-series) to understand the role of Phanerozoic and neotectonic deformations in permeability production and stable isotope tracing to determine the source of fluids in the geothermal reservoirs. Isotopic dating results and stable isotope geochemistry of hydrothermal minerals in basement rocks are interpreted as indicating that Cretaceous extensional tectonic events controlled the thermal history of central-eastern Australian basins and distribution of fracture zones allowing recent uprise of hot mantle fluids. Areas affected by Cretaceous tectonics are characterised by significantly high temperatures (>250°C) at 5 km depth [2] and distinctive geophysical anomalies [3]. Our field studies show that pre-existing faults were reactivated neotectonically and controlled the formation of late Quaternary carbonate vein and breccia deposits, which formed as hydro-fractures during CO₂-rich fluid overpressure, analogous to similar deposits in seismically active geothermal systems worldwide [4]. δ¹³C values of the carbonates are consistent with CO₂ derived from a mantle source. High precision U-series dating of carbonate veins suggests that the release of the pressurised CO₂ occurred intermittently from 35.9 ± 0.15 ka to 1.2 ± 0.02 ka, possibly in association with mantle degassing in response to seismicity.

[1] Italiano. *et al.* (2013), Submitted to *Chemical Geology*. [2] Chopra and Holgate (2005), Proceedings World Geothermal Congress 2005. [3] Saygin and Kennett (2012), *Journal of Geophysical Research* 117, B01304. [4] Uysal *et al.* (2009), *Chemical Geology* 265, 442-454.

Production of The Sodium Sulphate from Acıgöl by Solution Mining Method, Denizli, TURKEY

SERENA UZASCI SULTANYAN¹, SALIH BURAK
KARABEL¹, DEMET KIRAN YILDIRIM¹, MURAT
BUDAKOĞLU¹, MUHITTIN KARAMAN¹
AND MUSTAFA KUMRAL¹

¹Istanbul Technical University, Department of Geological
Engineering, 34469, Istanbul, TURKEY

Sodium sulphate is used widespread in industry. Common usage areas are paper, glass, detergent, textile, and chemical industries. In this study production of the Na₂SO₄ from the lakes by solution mining method has been examined. Evaporites and their usage areas, evaporite deposits in nature and types of it and production types of the sodium sulphate and detailed report about the information about the solution mining method and information of the Acıgöl Lake and production examples in it.

Acıgöl is a lake in Turkey's inner Aegean Region, in a closed basin at the junction between Denizli Province, Afyonkarahisar Province and Burdur Province. The lake attracts attention due to its sodium sulfate reserves. Turkey's largest commercial sodium sulfate production operations are based here. Mirabilite and tenardite are common sodium sulphate minerals that are produced from this lakes.

Sodium sulphate from salty or bitter alkali lakes can be produced in natural and artificial methods. This decision is differs by the facilities production area and capacity. Solution mining method of sodium sulphate is examined in detail. Also, room and pillar method is examined briefly.

By comparing these methods, solution mining step forwards with its advantages. But in salt lakes, where the lake area is wide and weather temperature conditions are optimum for the operation method or where by changing of the seasons last product can be collected by freezers from the lakes surface. Therefore any facility for the production is needed and so in this case solution mining method isn't advantageous.

Neoproterozoic accretion along the southeastern margin of the Eastern Dharwar Craton, India: Evidence from zircon U-Pb ages and their Hf isotopic composition

RAVIKANT VADLAMANI^{1*}, CHIRANJEEB CHATTERJEE¹, WEI-QIANG JI^{2A} AND FU-YUAN WU²

¹Indian Institute of Science Education & Research Kolkata, Mohanpur-741252 (vravikant@iiserkol.ac.in)

²State Key Laboratory for Lithospheric Evolution, Chinese Academy of Sciences, Beijing-100090

Late Mesoproterozoic high-grade tectonothermal event due to collision of the Eastern Ghats Belt [1] with the Eastern Dharwar-Bastar Cratons, is not recorded by the Paleoproterozoic Krishna Province rocks [2] south of the Godavari graben [3]. The Vinjamuru domain represents Paleoproterozoic metaigneous rocks of a continental arc accreted to the margin of the Eastern Dharwar Craton [4] and coeval with the UHT granulite-facies event in the easternmost Ongole domain [2]. Here, we report zircon isotopic data from one critical amphibolite-facies metaandesite sample (VL47) from the central Vinjamuru domain.

The U-Pb zircon ages in this metavolcanic rock record a protracted polycyclic evolutionary history (Fig.1). Derivation of youngest zircons from crustal melts are seen in their negative $\epsilon_{\text{Hf}(t)}$ values at two clusters: 907-1111 Ma ($\epsilon_{\text{Hf}(t)} = -5$ to -7) and 696-810 Ma ($\epsilon_{\text{Hf}(t)} = -21$ to -9). The most likely interpretation of our data is that the Vinjamuru domain rocks also record latest Neoproterozoic accretion (and coeval metamorphism) of the Ongole domain to the Vinjamuru domain, supporting one interpretation of this Eastern Ghats-craton collision at 820 Ma [5].

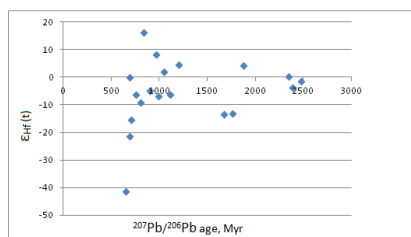


Fig.1. Zircon age vs $\epsilon_{\text{Hf}(t)}$ from metaandesite sample VL47

[1] Bose *et al.*, (2011) *GSA Bull* **123**, 2013-2049. [2] Dobmeier and Raith (2003) *Geol Soc Lond Spl Pub* **206**, 145-168. [3] Mezger and Cosca, (1999) *Precamb Res* **94**, 251-271; [4] Ravikant *et al.* ((2012), *Geol J* doi: 10.1002/gj.2441. [5] Okudaira *et al.* *Geol Mag* **138**, 495-498.

Role of *Bacillus mucilaginosus* at silicon biogeochemical cycle in a system “soil – plant”

O.B. VAISHLYA^{1*}, D.M. AMYAGO¹ AND N.V. GUSEVA²

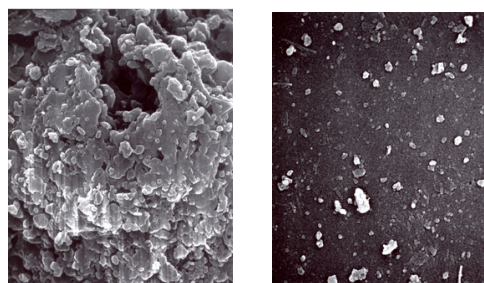
¹National Research Tomsk State University, Lenin av. 36

Tomsk-50 Russia (*correspondence:plantaplus@list.ru)

²National Research Tomsk Polytechnic University, Lenin av.

30 Tomsk 634050 Russia (unpc_voda@mail.ru)

Silicate bacteria *Bacillus mucilaginosus* B-1574 were studied at four steps. First we demonstrated direct evidences that this strain has geochemical activity and is able to leach Si and P from the object of lithosphere - phosphoric ore of Djeroi mining in Uzbekistan, %: P₂O₅-13,6; CaO-44,75; MgO-1,05; CO₂-20,88; Fe₂O₃-3,03; SiO₂-2,7; C_{org}-0,11 (Fig.1, Table 1).



Bacteria of natural biocenosis from Tomsk grey forest soil

Bacteria *Bacillus mucilaginosus* strain B-1574

Figure 1: SEM-photos of fragments of a surface of rock particles after 30-days incubation with bacteria, x5000

Days	N bacteria, x10 ⁸ , cell/ml	SiO ₂ , mg/l		(PO ₄) ²⁻ , mg/l	
		Treatment	Control	Treatment	Control
5	0,00021	5,62	4,75	0,07	0,05
10	0,05	6,62	5,25	0,19	0,06
30	1,25	20,0	6,38	0,32	0,09

Table 1: Transfer of silicon and phosphorus into a solution

Then we revealed in a liquid culture of this strain significant amounts of organic and ketoacids, polysaccharides, IAA, three individual cytokinins. At the third step we made experiments with mineral “Vermiculite” as a model of secondary aluminosilicates. 60 elements were detected in a supernatant by ICP-MS after 50-days incubation with bacteria. Control/Treatment, mg/ml: Mg-84/388; Al- 0.078/2500; Si-26/98; Ca-122/238; Cr-0.054/0.250; Mn- 0.085/3.41; Fe-1.61/36.4; Co-0.015/0.056; Cu- 0.12/0.17; Zn- 0.061/0.390; Mo-0.020/0.031. Then we measured mono-, polysilicic acids and Si-organic compounds in grey forest soil, urbozem and in plants. In both soils we grew *Triticum aestivum* L., *Cucumis sativus* L.: soil polysilicic acids after bacteria activity are the source of plant biolites.

The first data about the REE's contents in new-formed phases (Berezitovoe gold deposit, Priamurye, Russia)

ELENA A. VAKH¹, ALEKSANDR S. VAKH^{2,3}
AND NATALIA A. KHARITONOVA^{2,3}

¹Far East Geological Institute FEB RAS, Russia,
Adasea@mail.ru

²Far East Geological Institute FEB RAS, Russia,
vakh@fegi.ru

³Far Eastern Federal University DVFU, Russia,
tchenat@mail.ru

Here we present the first data on contents and geochemistry of REEs in the secondary new-formed phases from weathering zone of Berezitovy gold deposit hostrocks. Also the analysis of fractionation and migration of REE in single geochemical cycle "bedrock - weathering zone - surface and ground water - secondary new-formed phases" are performed.

The Berezitovy gold deposit located in the northeastern Amur gold province in the downstream basin of the Khaikta River. In 2007, two mining companies: Berezitovy Mine Ltd. and High River Gold Mines Ltd., started to mine this deposit. Geologically, the deposit is localized in a southeast part of the North Asian craton, in a zone of its joint with formations of northern frame Tukuringra-Dzhagdinsky terrain Mongolo-Ohotsky zone. Two formations of sediments (granites and ore-metasomatic rocks) occur in the deposit. Main minerals bearing REEs are allanit, monatsit - (Ce), chervandonit - (Ce).

The preliminarily results of investigation showed, that the content and distribution of REEs in the new-formed phases from weathering zone of deposit. Our data indicate that the content of REEs in new-formed phases of Berezitovoe deposit can reach up to 149 ppm and the content of LREEs is at about 93% of total REEs. All types of new-formed phases display of strong negative Ce and Nd anomalies.

Profiles of distribution of REE of new-formed phases are comparable to bedrock profiles, small difference is observed in distribution heavy groups of elements.

Relation between diatom communities and the degree of AMD affection in selected water dams in Iberian Pyrite Belt

T. VALENTE^{1,2*}, S. ALMEIDA³, M.J. RIVERA^{1,2}, C. DELGADO³, P. GOMES^{1,2}, M.L. DE LA TORRE², M. SANTISTEBÁN^{1,2} AND J.A. GRANDE²

¹CIG-R (PEst-OE/CTE/UI0697/2011) -, Universidade do Minho, Campus de Gualtar, 4710-057 Braga, Portugal (*correspondence: teresav@dct.uminho.pt)

²CIPIMS - Universidad de Huelva, 21819 Palos de la Frontera, Huelva, Spain grangil@uhu.es)

³Departamento de Biologia e GeoBiotec, Universidade de 3810-193 Aveiro, Portugal

In mining regions the presence of water reservoirs affected by AMD is a common problem. This study is part of a project that characterizes the water dams in the Spanish Iberian Pyrite Belt, in order to achieve a classification based on the effects by AMD. This preliminary work presents data from four selected dams: mining dams (Gossan and Águas Ácidas), for industrial use (Sancho), and for human supply (Andévalo). The main objectives are: i) to describe the water and sediment properties; ii) to characterize diatom communities, and iii) to find possible relations between diatoms and the degree of AMD. Chemical composition of water and sediments was determined by AAS and ICP-MS. XRD was performed for mineralogy (bulk and clay fractions). Diatoms were sampled from sediments. Identification and quantification were performed in slides mounted with Naphrax®. Results indicate that the four dams are subject to the effect of metallic loads from polluted rivers, although with different levels: Águas Ácidas>Gossan>Sancho>Andévalo. In accordance, diatom communities have differences in composition and dominant diatom taxa. *Pinnularia acidophila* and *P. aljustrellica* were found dominant in the most acidic dams (Gossan and Águas Ácidas), *Pinnularia subcapitata* was dominant in Sancho and *Eunotia exigua* in Andévalo.

Zirconology of UHP-ultramafic rocks and eclogites from the Maksyutovo complex (South Urals, Russia)

P.M. VALIZER*¹, A.A. KRASNOBAEV², A.I. RUSIN²
AND E.V. MEDVEDEVA¹

¹Ilmeny State Reserve UB RAS, Miass, Russia

(*correspondence: valizer@ilmeny.ac.ru)

²Institute of Geology and Geochemistry UB RAS,
Yekaterinburg, Russia

The U-Pb SHRIMP age of zircons was specified for the UHP-ultramafic rocks (Fo+En+Mgs+Ti-Chu) and jadeite eclogites (Jd+Gr+Alm+Rt±Ph) from the Maksyutovo eclogite-glaucophane schist complex.

The zircon age comprise a range of more than 2 Ga. The most ancient age of 2350±35 Ma corresponds to the primary mantle protolith. The ages of 1644±10, 1492±16 and 1294±64 Ma characterize the different stages of evolution of this mantle protolith.

The Lower Cambrian age of the most crystals from ultramafic rock and eclogite is similar (545.3±5.8 Ma [1] and 533±4.6, respectively). The validity of this age is confirmed by variations of U (113–332 ppm) and Th (41–281 ppm) contents and U/Th ratio (0.43–0.92) that corresponds to the age of the UHP-metamorphism ($P \geq 4.4$ GPa, $T \geq 700$ °C). The ultramafic rocks and jadeite eclogites represent the UHP metamorphosed tectonic mantle-crustal blocks in quartzite-schists of the first unit of the complex.

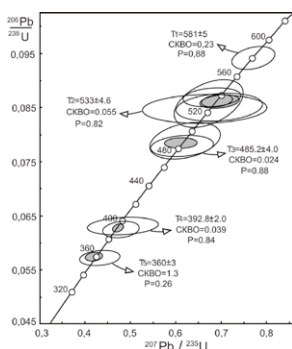


Fig.1 The U-Pb age of zircons from jadeite eclogite.

The Late Devonian (365.3±4.2–360±3 Ma) is the next important stage in the evolution of zircons and rocks. This zircon group is significantly distinct in U content and are characterized by typically magmatic U and Th distribution, which may be interpreted as an index of the progressive stage of HP-metamorphism ($P \geq 1.1$ – 2.2 GPa, $T \geq 450$ – 550 °C). This stage of HP-metamorphism is manifested in all rock associations from the first unit of this complex.

The Early Permian last stage (284.9±7.3 Ma), recording the final transformations of previous generations and appearance of newly formed zircon, was caused by the late shear deformations.

[1] Valizer *et al.* (2011) *Dokl Earth Sci* **441**, 1645–1648.

First results from the Northeast Greenland Ice Stream drilling site

P. VALLELONGA¹, H.A. KJÆR¹, C. TIBULEAC¹,
A. SVENSSON¹, M. KRISTENSEN¹, T. POPP¹, C. HOLME¹,
Y. WENG¹, B. VINTHER¹, D. DAHL-JENSEN¹,
N. KARLSSON¹, S. KIPFSTUHL², L. PETERS³
AND K. CHRISTIANSON⁴

¹Centre for Ice and Climate, Niels Bohr Institute, University of
Copenhagen, Denmark.

(ptravis@nbi.ku.dk)

²Alfred Wegener Institute, Bremerhaven, Germany.

³Penn State, USA.

⁴St Olaf College, Northfield, USA.

The Northeast Greenland Ice Stream (NEGIS) is a fast-flowing outlet stream approximately 1000 km in length, with 4 main glaciers terminating in the Greenland Sea. Radar and seismic surveys were conducted in summer 2012, as well as the drilling of a 70 m firm core at the NEGIS site (75 37.61 N, 35 56.49W). DiElectric Profiling (DEP) analysis was conducted in the field, while density and Electrical Conductivity Measurements (ECM) were conducted after the NEGIS core was transported to Copenhagen for analysis. DEP and ECM measurements were consistent and allowed the identification of several volcanic strata commonly found in Greenland shallow cores. Stable water isotopes have been determined, and allow an evaluation of past variability in deposition and temperature at the site. Continuous Flow Analysis (CFA) measurements comprised of dust particle concentrations, electrolytic conductivity, sodium and ammonium concentrations. Annual cycles were observed for all parameters, allowing the establishment of a seasonally resolved chronology covering the past 400 years.

Tomography at Single-Atom Scale of ^{207}Pb and ^{206}Pb in a 4374 Ma Zircon

J.W. VALLEY¹, T. USHIKUBO¹, A.J. CAVOSIE^{1,2},
D.A. REINHARD³, D.F. LAWRENCE³, I. MARTIN³,
D.J. LARSON³, P.H. CLIFTON³, T.F. KELLY³,
S.A. WILDE⁴, D.E. MOSER⁵ AND M.J. SPICUZZA¹

¹Univ. Wisconsin, Madison, WI 53706 USA;

²Univ. Puerto Rico, Mayaguez, PR 00681 USA;

³CAMECA, Madison, WI 53711 USA;

⁴Curtin Univ., Perth, WA, Australia;

⁵Univ. Western Ontario, London, Ont., CAN N6A 5B7

Local-Electrode Atom Probe (LEAP) tomography can identify and determine the position ($\pm 0.2\text{nm}$) of individual atoms in minerals. These data allow 3-D observations at an unprecedented scale, including new insights on thermal history, radiation damage and element mobility in zircon. "Needles" were milled by FIB ($\sim 150\text{nm}$ dia. $\times \sim 1\mu\text{m}$) and analysed by LEAP from the 4374 Ma core of a zircon from the Jack Hills, WA that has a 3400 Ma magmatic rim. In 3-D, Pb & YREE are co-localized and concentrated in $\sim 5\text{nm}$ clusters, spaced $\sim 20\text{-}50\text{nm}$ apart. The $^{207}\text{Pb}/^{206}\text{Pb}$ ratios (7/6) by LEAP average: 1.23 ± 0.11 inside clusters, 0.32 ± 0.10 outside clusters, and 0.52 ± 0.08 for the full volume of 2 needles ($0.04\mu\text{m}^3$, 6×10^8 ions detected). Significant ^{204}Pb is not detected. U appears homogeneously distributed. Thus Pb in clusters is radiogenic and unsupported by U. LEAP data for other zircons (Valley *et al.* 2012 AGU) suggest that Pb & YREE were concentrated in clusters by diffusion into nanodomains of α -recoil damage. Diffusion distances of $\sim 20\text{nm}$ for these elements in crystalline zircon require temperatures $>700^\circ\text{C}$. In the 4374 Ma zircon, 7/6 by SIMS is 0.5476 in the core and 0.2912 in the rim (3400 Ma) in agreement with LEAP. A model age for LEAP 7/6 = 1.23 in clusters would be older than Earth; however, diffusion during magmatic heating at 3400 Ma (rim age) could produce unsupported Pb clusters with $(7/6)_{3400\text{Ma}}$ of 1.20. Thus, LEAP uniquely explains closed system behavior at the $20\text{-}\mu\text{m}$ -scale of SIMS while documenting Pb mobility at nm-scale. These results refute challenges (based on Pb mobility) to the accuracy of SIMS analyses of age for zircons with similar history and confirm the existence of a population of ~ 4.4 Ga zircons from the early Earth.

Rhenium-osmium dating of Mississippi-Valley-Type ore deposits: The Robb Lake Pb-Zn deposit, British Columbia

D. VAN ACKEN^{1,2}, D. HNATYSHIN¹, S. PARADIS³,
AND R.A. CREASER¹

¹ University of Alberta, Edmonton, Canada

(dh10@ualberta.ca, rcreaser@ualberta.ca)

² Universität Bonn, Bonn, Germany (vanacken@uni-bonn.de)

³ Geological Survey of Canada, Sidney, Canada

(Suzanne.Paradis@NRCan-RNC.gc.ca)

Mississippi-Valley-Type (MVT) ore deposits are formed by fluid flow in sedimentary basins and comprise a large portion of global Pb-Zn resources. Dating the formation of MVT deposits has been attempted by dating their host rocks (Sm-Nd, U-Pb), paleomagnetic measurements or Rb-Sr dating of sphalerite, but all of these methods and results remain inconclusive and controversial to some degree. Pyrite as a major phase in MVT deposits can be dated directly using the long-lived Re-Os isotope system, which has been established to date sulfide formation.

The Robb Lake Pb-Zn deposit in northeastern B.C. is hosted by Silurian-Devonian platform carbonates, and forms part of a sequence of MVT deposits in the northern Rocky Mountains. The timing of its formation is still subject to controversy as two groups of ages are commonly cited. On the one hand, sulfide-forming fluid flow is considered to be associated with the Late Devonian - Early Carboniferous Antler orogeny, based on Rb-Sr studies, fluid inclusion composition, stable isotope data, and ages from other western Canadian MVT deposits along the Presqu'ile Barrier (Pine Point, NWT, [1]). On the other hand, Laramide (~ 65 Ma) ages have been suggested based on numerical modeling of regional fluid flow and paleomagnetism [2].

The Re-Os systematics of pyrite from Robb Lake are quite complex with substantial Re-Os being contained in both the pyrite and the associated dolomite breccia. Leaching of the dolomite using HCl allows for a more reliable age to be calculated from pyrite. A Re-Os isochron for this leached pyrite yields an age of 331 ± 40 (MSWD = 151). Identifying and removing data points that likely still have dolomite contamination produces an age of 351 ± 35 (MSWD = 18). The Re-Os data, although complex, confirm a Carboniferous age for sulfide formation associated with the Antler Orogeny.

[1] Nelson *et al.* (2002) *Econ Geol* 97, 1013-1036. [2] Symons *et al.* (1993) *Can J Earth Sci* 30, 1028-1036

Study of the natural iron fertilization off Crozet and Kerguelen Islands (Southern Ocean) using radium isotopes as tracers

PIETER VAN BEEK^{1,*}, VIRGINIE SANIAL¹,
BRUNO LANSARD¹, MARC SOUHAUT¹,
ELODIE KESTENARE¹, FRANCESCO D'OVIDIO²,
MENG ZHOU³ AND STÉPHANE BLAIN⁴

¹LEGOS (CNRS/UPS/CNES/IRD), Toulouse, France

²LOCEAN-IPSL (CNRS/UPMC/MNHN/IRD), Paris, Fr

³University of Massachusetts, Boston, USA

⁴LOMIC (CNRS/UPMC), Banyuls-sur-Mer, France

The Southern Ocean is known as the largest High-Nutrient, Low-Chlorophyll (HNLC) region of the global ocean. Phytoplankton blooms, however, take place annually off islands and associated plateaus that constitute physical barriers for the Antarctic Circumpolar Current. These phytoplankton blooms were shown to be sustained by natural iron fertilization associated with these topographic features. In the framework of the KEOPS-2 project, we used radium isotopes (Ra) as tracers of iron sources that fuel the phytoplankton blooms around Crozet and Kerguelen Islands, following previous works by [Charette *et al.*, 2007] and [van Beek *et al.*, 2008], respectively. In this work, we report one of the few studies that analyzed all four radium isotopes (²²⁴Ra, ²²³Ra, ²²⁸Ra, ²²⁶Ra) in Southern Ocean waters. Ra isotopes were used i) to trace the input of iron - and other micronutrients - released by the sediments deposited onto the margins and that sustain phytoplankton blooms, ii) to investigate the pathways of the waters that fuel the phytoplankton bloom north of Crozet Islands and east of Kerguelen Island, and iii) to estimate “apparent ages” for offshore waters. When combined to physical observations and modeling, information provided by our geochemical tracers allows us to assess the rates and timescales of the exchange between the islands and offshore waters and to give information on the origin and mechanism of iron fertilization in these areas.

Ocean ridge magma generation rates at slow-spreading ridges favour Hess-type oceanic crust

PETER VAN CALSTEREN^{1*} BRAMLEY MURTON²
AND ROGER SEARLE³

¹ Earth Sciences, The Open University, Milton Keynes MK7 6AA, UK, p.v.calsteren@open.ac.uk

² National Oceanography Centre, Southampton SO14 3ZH, UK, bramley.murton@noc.soton.ac.uk

³ Department of Earth Sciences, Durham University, Durham DH1 3LE, UK, r.c.searle@durham.ac.uk

The widely accepted model for the structure and composition of oceanic crust is based on the ‘Steinmann Trinity’ or Penrose ophiolite stratigraphy. This has an oceanic crust of mafic rocks: basalt pillow lavas with their feeder dykes (sheeted dyke complex) and gabbro plutons, underlain by the ultramafic, peridotite mantle. However, recent work on slow-spreading ridge systems has revealed significant deviations from this simple layered structure[1,2,3].

The thickness of the oceanic crust is derived from geophysical data interpretations assuming that the crust is wholly mafic but a melange of partly serpentinised mantle peridotite and mafic rocks can equally fit the data. If it is accepted that the crust is not completely mafic, then constraints on the amount of generated mafic magma have to be derived elsewhere. The amount of generated magma is determined by the melt generation rate and time, and by the volume of the melt zone.

We have derived melt generation rates for peridotite melting in the garnet stability zone between depths of the solidus at 130Km and 95Km by modelling our U-series data for basaltic glass samples collected by ROV from the Mid Atlantic Ridge slow-spreading centre at 45°N. Our results can be expanded with published results from thermodynamic modelling to estimate total decompression melt generation. We assume that the volume of the melt zone is given by the width of the active volcanicity in the median valley and the depth to the solidus, with 1Km along strike as the distance over which volcanic and tectonic characteristics can be considered as representative. We argue that in an area of tectonic extension, magma ascends vertically and is not focussed.

The our derived magma flux at ‘normal’ slow-spreading ridge segments, contributes <50% of the volume of crust, the remainder probably is serpentinised mantle peridotite. These inferences are agreement with the ‘Hess’ model for oceanic crust.

[1]Cannat (1996), Journal of Geophysical Research-Solid Earth 101(B2), 2847-2857. [2]MacLeod *et al.* (2009), Earth and Planetary Science Letters 287(3-4), 333-344. [3]Minshull *et al.* (1998). Geological Society, London, Special Publications 148, 71-80.

Soil Respiration – A Wetlands Perspective

PHILIPPE VAN CAPPELLEN

Ecohydrology Research Group, University of Waterloo,
Waterloo, Canada (correspondence: pvc@uwaterloo.ca)

Wetlands are an essential part of the Earth's life support system. They provide a wide range of ecosystem services, from food production, via flood protection to pollution abatement. In many parts of the world, however, mounting anthropogenic pressures, for example, water diversion, encroachment, salinization and climate change, are threatening wetlands. Because of their significance, as well as their vulnerability, wetlands are the only class of ecosystems with an international convention dedicated to their protection and sustainable use (the Ramsar Convention). In this presentation I will focus on the biogeochemical functions of wetland soils. As soil biogeochemistry is largely driven by the decomposition of plant-derived organic matter by microorganisms, I will review a number of the physical, biological and geochemical factors that control the turnover of organic matter in wetland soils. Besides the nature of the organic matter itself, key controlling factors include the soil pore network, soil aggregation, water saturation, redox conditions, temperature, and the microbial community structure. I will further discuss the importance of bioenergetic limitations on soil respiration processes. To conclude the presentation, I will highlight a number of areas where I believe geochemists can provide new and timely insights, for example on the effects of redox fluctuations and freeze–thaw cycles on soil organic matter decomposition.

Where Groundwater Meets Surface Water

PHILIPPE VAN CAPPELLEN

Ecohydrology Research Group, University of Waterloo,
Waterloo, Canada (correspondence: pvc@uwaterloo.ca)

Biogeochemical processes at transitions between groundwater and surface waters play a major role in the regional biogeochemical cycles of carbon, nutrients and trace elements. These interfaces occur along the entire aquatic continuum, from headwaters to the coastal zone, and include flood plains, seepage areas, riparian soils and the hyporheic zone. However, while the biogeochemical significance of groundwater–surface water interfaces (GSWIs) is generally recognized, the underlying mechanisms and determining properties have yet to be fully unravelled. GSWIs exhibit unique hydrological, geochemical and ecological characteristics, including variable hydraulic gradients, complex flow dynamics, fluctuating redox conditions and diverse, multifunctional biological communities. In this presentation, I will highlight the biogeochemical functions of GSWIs, with a particular emphasis on the biogeochemical implications of the dynamic redox conditions that characterize many GSWI environments. The key take-home message of the presentation is that observations made under stable, “average” environmental conditions may not be sufficient to predict the fate of nutrients and contaminants at GSWIs. Stated otherwise, rate measurements, chemical speciation, microbial abundance, biodiversity, and other experimental data should be obtained under the dynamic conditions representative of GSWIs, both in the laboratory and in the field.

The oceanic cycles of the transition metals and their isotopes

D. VANCE^{1*}, V. CAMERON², S.H. LITTLE^{1,2}
AND C. ARCHER¹

¹Institute of Geochemistry and Petrology, Department of Earth Sciences, ETH Zürich, Switzerland *Correspondence: derek.vance@erdw.ethz.ch)

²School of Earth Sciences, University of Bristol, UK (glxvc@bristol.ac.uk)

The transition metals show variable behaviour in the oceans, from the conservative but redox-dependent behaviour of Mo, through control by scavenging for Cu, to clearly biologically cycled elements like Ni and Zn. Thus, the abundances of these elements in ocean sediments have been used to understand temporal variability in a variety of key parameters for ocean biogeochemistry. Their isotopic systems are also often now available for study, but much remains to be done to understand the important processes fractionating the isotope systems. Here we assess their oceanic mass balance from an elemental and isotopic perspective.

A common feature of all the elements considered here (Mo, Zn, Cu, Ni) is the fact that the dissolved riverine input to the oceans is isotopically heavier than the continental crust, requiring isotopic fractionation during weathering and riverine transport. Moreover, the oceanic dissolved pool is, in all cases, heavier still. For example, the dissolved phase in rivers has $\delta^{60}\text{Ni} \sim 0.8\text{‰}$, versus silicate rocks at around +0.1 to +0.2 ‰. The dissolved pool in the oceans has $\delta^{60}\text{Ni} = +1.44 \pm 0.15\text{‰}$. Such isotopic data, for Ni and other metals, impose significant constraints on the marine budgets of these elements. There must, for example, be at least one isotopically light sink that renders seawater heavy.

Our approach to elemental mass balance has been to couple the size of the better-known Mo sinks with their metal/Mo ratios. For Cu and Zn the total known outputs are of the same order as, but slightly smaller than, the dissolved riverine input. However, the same approach with Ni highlights a major problem: the output of Ni to Fe-Mn oxides (isotopically close to seawater [1]) is close to an order of magnitude greater than the dissolved riverine input, a finding that is also made for Mn. This imbalance requires a large input for these two elements that is not significant for Mo. One possibility, given the high Ni/Mo and Mn/Mo ratios of riverine suspended load, is that both these elements are mobilised by reduction of oxide coatings in anoxic sediments in estuaries. But either these coatings are isotopically heavy or such a proposal would make simultaneous balancing of the oceanic elemental and isotopic mass budgets impossible.

[1] Gall *et al.* (submitted) *EPSL*.

Isotopic Fingerprint of Ice-Rafted Debris from the Antarctic Margin: A Spatial Record of Initial Ice Growth

T. VAN DE FLIERDT¹, S.-E. KIM¹, C.P. COOK¹,
S.R. HEMMING^{2,3}, T. WILLIAMS³, E.L. PIERCE^{2,4},
S.M. BOHATY⁵, S. PASSCHIER⁶, U. ROEHL⁷,
A.J.P. HOUBEN⁸ AND EXPEDITION 318 SCIENTISTS

¹Imperial College London, London, SW7 2AZ, UK;
tina.vandefliert@imperial.ac.uk

²Columbia University, New York, NY 1094, US

³Lamont-Doherty Earth Observatory, Palisades, NY 1094, US

⁴Wellesley College, Wellesley, MA 02481, US

⁵U Southampton, NOC, Southampton, SO13 3ZH, UK

⁶Montclair State University, Montclair, NJ 07043, US

⁷MARUM, U Bremen, 28359 Bremen, Germany

⁸Netherlands Organization for Applied Scientific Research (TNO), 3584 CB, Utrecht, Netherlands

The onset of widespread Antarctic glaciation across the Eocene-Oligocene transition (~34 Ma) marks one of the most fundamental climate shifts in recent Earth history representing a major step from the greenhouse world of the Cretaceous and early Cenozoic to the icehouse world of today. State-of-the-art climate models suggest that ice expansion initiated at high elevation nucleation points in response to declining atmospheric carbon dioxide concentrations. While marine oxygen isotope records indicate a very rapid ice growth across the Eocene-Oligocene transition, models differ as to which parts of the continent were actually ice covered during the first extensive pulse of glaciation. Such knowledge however may be crucial for understanding important carbon cycle feedbacks in the Southern Ocean.

Here we investigate the geochemical fingerprint of early Oligocene ice-rafted debris (IRD) layers at two locations off East Antarctica: ODP Site 738 (Kerguelen Plateau) and IODP Site U1356 (Adélie Coast). ⁴⁰Ar/³⁹Ar ages of ice-rafted hornblende grains (>150 μm) reveal the tectono-metamorphic age of the grains, and hence provide a way to constrain spatial distribution of the initial ice surges. The first peak of IRD on the Kerguelen Plateau is well characterised and shows a clear Pan-African provenance, with ⁴⁰Ar/³⁹Ar hornblende ages of ~520 Ma, pointing to an origin from the nearby Prydz Bay sector. In contrast, one of the first prominent Oligocene IRD layers offshore the Adélie Coast reveals ⁴⁰Ar/³⁹Ar hornblende ages of ~1500 Ma. Such ages indicate provenance from the local Mertz Shear Zone. We will discuss details of our new data set in the context of model results on initial ice expansion and potential Southern Ocean feedbacks.

Novel method to reconstruct paleopressure: a combined clumped isotope and fluid inclusion technique

V. VANDEGINSTE¹ AND CÉDRIC JOHN¹

¹Department of Earth Science and Engineering and Qatar Carbonate and Carbon Storage Research Centre, Imperial College London SW7 2BP, United Kingdom

Reconstructing the pressure conditions under which diagenetic minerals were precipitated in subsurface can not only enhance our understanding about the burial and diagenetic history of studied rocks, but also bring insight into fundamental processes of mineral precipitation. This novel method is thus relevant for both industrial applications, such as reservoir characterization, as for fundamental research.

We have investigated several carbonate samples from Spain and Oman using both the clumped isotope and the fluid inclusion methods. Clumped isotopes can be used as a paleothermometer, providing a temperature of precipitation of a mineral independent of the stable oxygen isotopic composition of the parent fluid. Hence, both temperature and the stable oxygen isotopic composition of the fluid from which the mineral precipitated are extracted from clumped isotope analysis. The fluid inclusion technique, which is a common technique that has been used for decades, also provides an estimate of the precipitation temperature of a mineral, in addition to information on fluid chemistry and salinity. The estimation of the precipitation temperature of a mineral in this method is based on the temperature of homogenization during cooling-heating experiments. This homogenization temperature is measured at the equilibrium stage between the fluid and the gas bubble. However, at the time of trapping, usually a homogeneous fluid is trapped (and this is a requisite for deriving reliable homogenization temperatures) and a difference between the homogenization and the trapping temperature is expected because of the pressure at trapping conditions and the compressibility of the fluid. Isochores that can be reconstructed based on the density of the fluids, derived from fluid inclusion measurements, can then be combined with the independent temperature data from clumped isotopes, so that both the temperature and pressure conditions during precipitation of the analysed mineral can be reconstructed.

The proposed novel method can thus bring insight into a range of applications, such as prediction of overpressure conditions in the subsurface, fracturing processes, degassing upon pressure drop.

This study is funded jointly by Qatar Petroleum, Shell and the Qatar Science and Technology Park.

Combined Lu-Hf and Sm-Nd garnet-geochronology of lower crustal rocks from Val Strona, Ivrea Zone, Italy

J. VAN DE LÖCHT¹, M. SCHÜNGEL¹,
R. KLEINSCHRODT¹, C. MÜNKER¹,
M. KIRCHENBAUR^{1,2} AND R.O.C. FONSECA²

¹ Institut für Geologie und Mineralogie, Universität zu Köln, Germany; loechtj@uni-koeln.de

² Steinmann-Institut, Universität Bonn, Germany

The Ivrea Zone (IZ, N-Italy) is a key locality to study metamorphic processes in the lower and middle continental crust. The Val Strona section of the IZ is particularly suited to study the timing of metamorphic processes along an increasing temperature gradient, comprising a continuous assemblage of granulite to amphibolite facies rocks. Therefore, three metapelites and one metabasite from the Val Strona section were examined in a combined Lu-Hf and Sm-Nd study, covering both amphibolite-facies and granulite-facies conditions. The samples were also investigated in terms of their petrology and geochemistry, in order to reconstruct the P-T-t path of the IZ rocks. In particular, representative garnets were investigated via electron microprobe (EMP) and LA-ICP-MS, determining their distribution patterns of major and some trace elements (REE, HFSE).

The EMP and LA-ICP-MS profiles in all investigated garnets lack any prograde zonation for 2+ elements (e.g. Mn) and Sm-Nd, whereas for Lu-Hf some growth patterns are preserved. The Lu-Hf ages obtained for the amphibolite-facies metapelites therefore presumably reflect garnet growth (278 ± 3 Ma; MSWD 2.3 and 279 ± 0.9 Ma; MSWD: 0.31). In contrast, the younger Lu-Hf ages obtained for the granulite-facies metapelite (263 ± 0.5 Ma; MSWD 0.9) and for the metabasite (249.6 ± 1.3 Ma; MSWD 2.0) are interpreted to represent cooling ages and document later cooling of the deeper crustal section. All Sm-Nd ages obtained in our study are about 30 Myrs younger than the respective Lu-Hf ages. Hence, the Sm-Nd ages likely represent cooling ages and may indicate retrograde diffusion-controlled re-equilibration processes. In conclusion, the results of this study point to a polyphase metamorphic evolution of the Val Strona section.

Correlation between crystallization patterns and diurnal growth bands in Scleractinian corals

RENÉE VAN DE LOCHT^{1*}, ANDREAS VERCH¹, MARTIN SAUNDERS², KARINA SAND³ AND ROLAND KRÖGER¹

¹University of York, Heslington, York, YO10 5DD, UK

(*correspondence: rvd1500@york.ac.uk)

²CMCA (UWA), Perth, Western Australia 6009, Australia

³University of Copenhagen, DK-1165 Copenhagen, Denmark

Diurnal growth bands are characteristic features of many scleractinian corals [1, 2] and are thought to be linked to the microstructure of the usually aragonite based mineral forming the coral skeleton. To shed light on this correlation we employed focused ion beam to create large (10 x 30 μm) thin lamellae for transmission electron microscopy enabling the detailed study of crystal morphology and orientation in spherulites of *Porites lobata*.

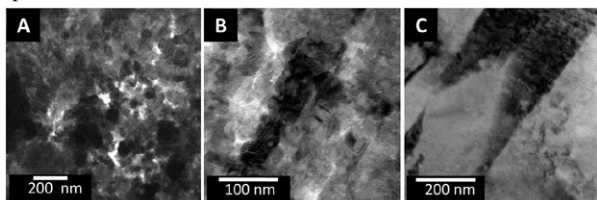


Figure 1: A) Randomly oriented nanocrystals with high porosity. B) Partly oriented nanocrystals with high porosity. C) Large acicular crystals orientated along the [0 0 1] direction (using the Pmcn spacegroup notation).

The investigations show a remarkable sequence of crystal morphology of randomly oriented, partly aligned nanocrystals and acicular crystals (fig 1). Selected area diffraction data shows that the morphology of the partly aligned nanocrystals is polycrystalline at the micrometer scale and no evidence for a non-classical growth mechanism (e.g. self assembly of small units; mesocrystal growth [3]) was found. The overall microstructural sequence is correlated with the observed optical contrast bands associated with a diurnal growth cycle. This is supported by TEM analysis of nanocrystal growth within aragonite needle-like bundles precipitated, using CaCO_3 solutions with organics additives.

[1] Bourne (1887) *Q. J. Microsc. Sci.* **2**, 21-51. [2] Cohen & McConnaughey (2003) *Biom mineralization*, *Min. Soc. Amer.* 151-187. [3] Cölfen & Mann (2003) *Angew. Chem. Int. Ed.* **42** (21), 2350-2365.

Experimental Investigation into the Density, Compressibility, and Phase Equilibria of the Northern Volcanic Plains on Mercury

KATHLEEN E. VANDER KAADEN*, FRANCIS M. MCCUBBIN AND CARL B. AGEE¹

¹Institute of Meteoritics, 1 University of New Mexico, MSC03-2050, Albuquerque, NM 87131, (kvander@unm.edu)

Knowledge of the density, compressibility, and other physical properties of magmas at high pressure is required in order to understand the differentiation of planetary interiors and secondary crust formation. With the recent estimates of Mercury's surface composition from the X-ray spectrometer and Gamma ray spectrometer onboard the Mercury Surface, Space Environment, GEochemistry and Ranging (MESSENGER) spacecraft, we now have our first opportunity to investigate the physical properties of magmas from the planet Mercury [1-3].

The Northern Volcanic Plains on Mercury (NVP) represent, to our knowledge, the most likely example of magmatic liquids that can be compositionally assessed from orbit with relatively high spatial resolution [1-2]. Although these NVP lavas may not represent primary, unfractionated partial melts of the mercurian mantle, they represent our best candidate to experimentally study magmas from the mercurian interior. Our goal is to determine the density and compressibility for a NVP composition using sink/float experiments in order to assess its eruptability onto the surface of Mercury.

We report the sinking of Fo_{100} spheres at 2.5 GPa, 3.5 GPa, and 5 GPa and temperatures of 1973 K, 2048 K, and 2223 K, respectively. We also report the floating of Fo_{100} spheres at 6 GPa and 2323 K. With these results we can place tight constraints on the compressibility of this melt at 0.08 $\text{g/cm}^3/\text{GPa}$. This is slightly more compressible than a komatiite (0.075 $\text{g/cm}^3/\text{Gpa}$) or peridotite (0.065 $\text{g/cm}^3/\text{Gpa}$) melt. Phase equilibria experiments are currently underway to determine a possible depth of origin for this melt. However, given its current density curve, the NVP composition is able to erupt at all pressures relevant to Mercury's mantle as a result of buoyancy alone.

[1] Nittler, L.R. *et al.* (2011) *Science*, **333**, 1847-1850.
[2] Weider, S.Z. *et al.* (2012) *JGR*, **117**, E00L05.
[3] Peplowski, P.N. *et al.* (2012) *JGR*, E00L04.

Triple oxygen isotope composition of photosynthetic oxygen and dissolved oxygen at saturation

A.E. VAN DER MEER AND J. KAISER

Centre of Ocean and Atmospheric Sciences (COAS), School of Environmental Sciences, University of East Anglia, Norwich, United Kingdom

The measurement of biological production rates is essential for our understanding how marine ecosystems are sustained and how much CO₂ is taken up through aquatic photosynthesis. Traditional techniques to measure marine production are laborious and subject to systematic errors. A new biogeochemical approach based on triple oxygen isotope measurements in dissolved oxygen (O₂) has been developed over the last few years, which allows the derivation of gross productivity integrated over the depth of the mixed layer and the time-scale of O₂ gas exchange [1]. This approach exploits the relative ¹⁷O/¹⁶O and ¹⁸O/¹⁶O isotope ratio differences of dissolved O₂ compared to atmospheric O₂ to work out the rate of biological production. Two parameters are key for this calculation: the isotopic composition of dissolved O₂ in equilibrium with air and the isotopic composition of photosynthetic oxygen. Recently, a controversy has emerged in the literature over these parameters [2] and one of the goals of this research is to provide additional data to resolve this controversy. In order to obtain more information on the isotopic signature of biological oxygen, laboratory experiments will be conducted to determine the isotopic composition of oxygen produced by different phytoplankton species. In addition, the isotopic composition of dissolved oxygen at saturation will be measured under different temperature and salinity conditions.

[1] Luz & Barkan (2000) *Science* **288**, 2028–2031. [2] Kaiser (2011) *Biogeosciences* **8**, 1793–1811.

Constraints on the creation of a HIMU-like isotopic reservoir beneath New Zealand

QUINTEN H.A. VAN DER MEER¹ TOD E. WAIGHT¹
AND JAMES M. SCOTT²

¹Copenhagen University, Department of Geosciences and Natural Resource Management, Øster Voldgade 10, København 1350, Denmark
(quinten.vandermeer@geo.ku.dk)

²Department of Geology, University of Otago, Dunedin 9054, New Zealand

The New Zealand microcontinent (Zealandia) formed as the active eastern margin of Gondwana. Upon cessation of subduction at ~110 Ma, extension led to opening of the Tasman Sea at 82 Ma, preceded by the formation of metamorphic core complexes, the opening and filling of half-graben structures and the intrusion of mafic dikes (~88 to 68 Ma). Subsequently, Zealandia has been punctuated by volumetrically minor, intermittent yet widespread intraplate magmatism from ~100 Ma through to recent times. This magmatism has typical OIB-like trace element abundances and radiogenic isotope compositions that trend towards a HIMU (high time integrated U/Pb) end member mantle composition. Recent publications have argued that that the intraplate OIB-like magmatism is not related to a mantle plume but is rather formed by delamination of mantle lithosphere, replacement by asthenosphere and associated partial melting. The variably diluted HIMU signature is interpreted to be the result of mixing between depleted mantle bearing a HIMU component with an Enriched Mantle or continental crust component.

New geochemical and isotopic analyses suggest the dike swarms also have an OIB-like chemistry. Initial Pb isotopic compositions of the dikes however are more similar to Pacific MORB. It is possible that the HIMU-like component in Zealandia is a result of trace element enrichment (with high U/Pb and Th/Pb) of a depleted mantle melt region in the Cretaceous. This source has remained stable beneath Zealandia while Pb ingrowth proceeded rapidly in U-Th rich domains. Repeated melt extraction from this source resulted in the intraplate magmatism with HIMU-like Pb isotopes. Isotopic data from peridotite xenoliths in the Cenozoic intraplate volcanoes reveal that the spinel facies lithospheric mantle beneath Zealandia also has high ²⁰⁶Pb/²⁰⁴Pb ratios. Lithospheric peridotite mantle is a potential source component for the intraplate basalts, which require an additional garnet rich source component.

Biomass burning as a major source of aerosols

G.R. VAN DER WERF¹ AND B.AOUIZERATS²

¹VU University Amsterdam, grvdwerf@gmail.com

²VU University Amsterdam, benjamin.aouizerats@vu.nl

It has been known for decades that biomass burning is a major source of aerosols, but recent advancement in satellite fire detection and biogeochemical modeling enables us better to quantify fire aerosol emissions and resulting concentrations. Here we show recent emissions estimates based on the new version 4 of the Global Fire Emissions Database version (GFED4) modeling framework and explain how climate and humans have shaped spatial and interannual variability in emissions over the past 15 years. We specifically highlight the role of fires not detected by the burned area algorithms but which can be seen in active fire data and occur often close to areas with relatively high population densities. We then focus on Indonesia which has the highest fire emissions density close to populated areas and show the relative importance of secondary aerosol formation on regional air quality.

Assimilation of hydrothermally altered crust at slow spreading ridges

F.M. VAN DER ZWAN^{1*}, C.W. DEVEY¹, N. AUGUSTIN¹,
A. BASAHAM², R.BANTAN², J. FIETZKE¹
AND R.R. ALMEEV³

¹Geomar | Helmholtz Centre for Ocean Research Kiel, Germany, (*correspondence: fzwan@geomar.de)

²King Abdulaziz University, Jeddah, Saudi Arabia

³Institut für Mineralogy, Universität Hannover, Germany

The process of crustal assimilation at mid-ocean ridges is not always obvious as assimilant and assimilator have similar bulk compositions. Hydrothermal alteration of oceanic crust significantly increases its chlorine (Cl) content, making Cl a potentially sensitive assimilation tracer. Although at fast spreading ridges this process has previously been shown [e.g. 1, 2], the intrinsically lower, more constant Cl values (~50-200 ppm) in basalts from slow spreading ridges make the tracing of crustal assimilation more arduous there.

We performed high precision Cl measurements in basalts from 3 slowly spreading ridges: the Southern Mid Atlantic Ridge (SMAR) at 7-10 °S (~3 cm/yr), the Red Sea at 16.5-26.5 °N (max. 1.6 cm/yr) and the Gakkel Ridge at 6 °W - 85 °E (max. 1.5 cm/yr). Chlorine contents vary from 40 to 400, 700 and 1300 ppm respectively, suggesting assimilation is occurring. Generally our Cl contents are higher than for average slow spreading ridges, although the Cl concentrations are not always elevated relative to elements of similar mantle incompatibility (e.g. K, Nb).

In the Red Sea and partially in SMAR samples we see a clear relation between Cl/K (as indicator of assimilation) and the presence of hydrothermal vents sites or tectonic features associated to these. In contrast, the also hydrothermally active [3] Gakkel Ridge has much lower Cl/K values, suggesting that other factors besides hydrothermalism play a role in the visibility of assimilation. The Cl contents of trace-element-enriched magmas (higher primordial Cl) at Gakkel Ridge are less sensitive to assimilation. In contrast, highly saline ocean water, brine pools and the presence of evaporites in the Red Sea make assimilation signals stronger there. Other influencing factors are the spreading rate and the type of rifting, i.e. volcanic or tectonically dominated. Through comparison of ridges with similar spreading rates and tectonic setting, we can examine the factors influencing the susceptibility of Cl concentrations to assimilation of altered oceanic crust.

[1] Michael & Schilling (1989) *Geochim. Cosmochim. Acta* 53, 3131-3143. [2] Gillis *et al.* (2003) *Earth Planet. Sci. Lett.* 213, 447-462. [3] Michael *et al.* (2003) *Nature* 423, 956-961.

Smart air quality policies for a better climate: a regional analysis

R. VAN DINGENEN^{1*}, F. DENTENER¹, G. JANSSENS-MAENHOUT¹, M. MUNTEAN¹, Z. KLIMONT², AND L. HOGLUND²

¹European Commission, Joint Research Centre, Institute for Environment and Sustainability, Ispra (VA), Italy
(*correspondence: rita.van-dingenen@jrc.ec.europa.eu)

²International Institute for Applied Systems Analysis (IIASA), Laxenburg, Austria (klimont@iiasa.ac.at)

Feedbacks of climate policies on air quality (co-benefits as well as trade-offs) are now being recognized and introduced in optimization schemes for air quality policy development. However, also air quality policies can have consequences for climate. Some pollutants are contributing to warming (black carbon (BC), O₃), others are cooling (SO₄, NO₃, organic carbon). Air quality policies are commonly designed without taking into account possible feedbacks on climate, although there is a potential for smart air quality policies that lead to a win-win situation for both climate and air quality.

In this work we evaluate the local and regional benefits of a portfolio of 16 climate-friendly, region-specific air quality measures that were identified in the frame of a recent UNEP-WHO assessment [1] [2]. These measures go beyond the baseline of current legislation and provide a global potential for 0.5K temperature reduction in the coming decades. A first group of measures addresses the reduction of CH₄ emissions (with associated benefits for reduced background ozone), a second group targets BC (with additional benefits for O₃ for those sectors where NO_x and NMVOC are co-emitted species). The portfolio of measures was designed in order to yield a maximal climate benefit worldwide, but the measures also generate clear local and regional air quality and crop production benefits which may help to incentivise the implementation. This local and regional aspect was not explored in the UNEP assessments.

In our analysis we apply a global source-receptor model with a relatively high regional resolution (global coverage with 56 regions) to each of the measures. As a result we provide a region-specific ranking of the most relevant measures in terms of local and regional benefits.

[1] UNEP / WMO (2011) Integrated Assessment of Black Carbon and Tropospheric Ozone. UNEP, Nairobi [2] UNEP (2011) Near-term Climate Protection and Clean Air Benefits: Actions for controlling Short-Lived Climate Forcers. UNEP, Nairobi.

Chemical stabilization of soil thallium using Mn(III,IV) oxide birnessite (δ -MnO₂)

ALEŠ VANĚK^{1*}, MICHAEL KOMÁREK² AND MARTIN MIHALJEVIČ³

¹Department of Soil Science and Soil Protection, Czech University of Life Sciences Prague, Kamýcká 129, 165 21 Praha 6, Czech Republic (* vaneka@af.czu.cz)

²Department of Environmental Geosciences, Czech University of Life Sciences Prague, Kamýcká 129, 165 21 Praha 6, Czech Republic

³Institute of Geochemistry, Mineralogy and Mineral Resources, Charles University in Prague, Albertov 6, 128 43 Praha 2, Czech Republic

The effect of highly crystalline birnessite (δ -MnO₂) on Tl retention and bioavailability in contaminated soils was investigated. The stabilization/immobilization efficiency of the Mn oxide was evaluated on basis of Tl uptake by white mustard (*Sinapis alba* L.), sequential extraction and sorption experiments.

The obtained data clearly demonstrate that the application of birnessite to Tl-rich soils can effectively transform Tl from the labile (easily mobilizable) fraction to its reducible form, thus lowering Tl bioavailability and subsequent accumulation by plants. Substantial reduction of biological uptake of Tl was identified after the oxide application; the Tl levels in mustard tissues decreased by up to 50%, compared to the control treatment (non-amended soil).

The use of birnessite like soil additive might be an efficient and environment-friendly solution for soil systems contaminated with Tl. Nevertheless, further research focused on the long-term stability of the oxide in soil linked with Mn mobilization and potential toxicity for soil microbiota is needed before any general conclusion will be made.

Study of archaeological glass based on elemental imaging by laser ablation ICP-MS

J.T. VAN ELTEREN^{1*}, S. PANIGHELLO², V.S. ŠELIH¹, N.H. TENNENT³, E.F. ORSEGA², A. IZMER⁴, M. ŠALA¹ AND F. VANHAECKE⁴

¹National Institute of Chemistry, Ljubljana, Slovenia
(*correspondence: elteren@ki.si)

²University Ca'Foscari Venezia, Venice, Italy

³University of Amsterdam, Amsterdam, Netherlands

⁴Ghent University, Ghent, Belgium

The study of ancient glass is predominantly focused on retrieval of its chemical composition to trace the provenance of raw materials, to unravel fabrication technologies and to investigate degradation phenomena. Techniques such as laser ablation ICP-MS are frequently used for multi-elemental microanalysis of glass in spot or raster mode. This work focuses specifically on the development of laser ablation ICP-MS techniques for lateral (2D) and volume (3D) imaging of glass to enhance the information retrieval. Spatial distribution analysis offers superior insight into the colocalization of elements to elaborate and advance archaeological hypotheses.

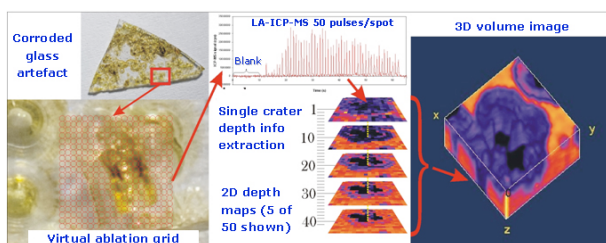


Fig. 1: 3D laser ablation ICP-MS protocol illustrated for imaging of Mg in a corrosion pit of an ancient glass artefact.

Laser ablation ICP-MS imaging techniques will be presented for 2D imaging based on rastering and quantification of the elements in the map using a so-called sum normalization technique which corrects automatically for drift and defocusing issues. Recently an innovative 3D imaging procedure was introduced based on laser drilling on a virtual grid on the surface using a burst of 50 laser pulses on each point of the grid (Fig. 1). After integration of the elemental peak areas, stacks of 50 2D depth maps with a depth resolution of 150 nm were retrieved which could be visualized as volume images. The application of the latter laser ablation ICP-MS imaging procedure will be demonstrated for the study of glass weathering mechanisms involved in the corrosion of some ancient glass artefacts.

Structure of Fe(III) precipitates formed by Fe(0) electrolysis in the presence of groundwater ions

CASE M. VAN GENUCHTEN¹, SUSAN E. AMROSE¹, ASHOK J. GADGIL^{1,2} AND JASQUELIN PEÑA³

¹University of California, Berkeley, USA
cmvanguenuchten@berkeley.edu

²Lawrence Berkeley National Laboratory, USA

³University of Lausanne, Switzerland

Oxyanions and bivalent cations influence the polymerization and precipitation of Fe(III) (oxyhydr)oxides, thus modifying the mineral structure in terms of local coordination environment of Fe, mineral phase, crystallinity, and oxyanion uptake mechanism. Few studies have investigated the interdependent effects of these ions on the formation of Fe(III) precipitates generated from Fe(II) oxidation, despite the co-occurrence of oxyanions and bivalent cations in natural waters. Such studies are essential to understand oxyanion mobility at both natural and engineered redox boundaries.

We combine wet chemical measurements and complementary synchrotron-based X-ray techniques (high energy X-ray scattering and Fe, As, and Ca K-edge X-ray absorption fine structure (EXAFS) spectroscopy) to investigate the interaction between oxyanions (PO_4^{3-} , AsO_4^{3-} , SiO_4^{4-}) and bivalent cations (Ca^{2+} , Mg^{2+}), and their subsequent effect on the formation of Fe(III) precipitates. Fe(III) precipitates were produced by the electrolytic dissolution of an Fe(0) electrode in an electrolyte consisting of oxyanion concentrations ranging from 0.05-0.5 mM and the presence or absence of 1 mM Ca^{2+} or Mg^{2+} .

Our results suggest a systematic decrease in the strength of bivalent cation:oxygen interaction in the order of $\text{Ca} > \text{Mg}$ and $\text{P} > \text{As(V)} \gg \text{Si}$. We find that 1 mM Ca^{2+} enhances the uptake of As(V) (per mass of Fe) more than 1 mM Mg^{2+} . Whereas Fe(0) electrolysis leads to 2-line ferrihydrite-like material in the presence of 0.05 mM As(V) alone (initial $\text{As/Fe} = 0.1$), the presence of 1mM Ca^{2+} with 0.05 mM As(V) promotes the formation of more crystalline lepidocrocite-like material. These results are consistent with a strong Ca-As(V) interaction that can modify the extent of As(V) uptake and the resulting Fe(III) precipitate structure. Ca K-edge XAS data in the Ca:As concentration series display features consistent with second-shell As(V) scattering. No discrete As(V)-Ca surface-precipitate is observed. Our results indicate that direct Ca-As(V) interactions must be considered when assessing iron and arsenic biogeochemistry.

Use of LA-ICP-MS and MC-ICP-MS in a biomedical context

FRANK VANHAECKE^{1*}, MAITE ARAMENDÍA², ANDREI IZMER¹, MARTÍN RESANO² AND LANA VAN HEGHE¹

¹Ghent University, Krijgslaan 281 - S12, Ghent, Belgium

(*correspondence: frank.vanhaecke@ugent.be, andrei.izmer@ugent.be, lana.vanhege@ugent.be)

²University of Zaragoza, Pedro Cerbuna 12, Zaragoza, Spain (maiteam@unizar.es, mresano@unizar.es)

Solution nebulization ICP-MS was exploited since its commercial introduction in the 1980s for the analysis of body fluids. Also elemental speciation using a combination of a chromatographic or electrophoretic separation technique and ICP-MS as a very sensitive and element-specific detector was rapidly deployed in a biomedical context. However, for a long while, both direct analysis of solid materials using laser ablation LA-ICP-MS and isotopic analysis of metallic and metalloid elements using MC-ICP-MS largely remained the domain of geochemical applications. More recently however, also the capabilities of these approaches in a biomedical context are being discovered as will be illustrated in this presentation using applications from the UGent lab.

As a result of the laser beam dimensions (typically from < 5 to > 100 μm diameter) and the sub- μm penetration depth per shot, LA-ICP-MS is also suited for spatially resolved analysis of thin sections of entire small animals and/or selected body parts. By scanning such a section line per line, the distribution of a target element can be visualized in a map. It will be shown how this approach can be used for documenting the distribution of a Br-containing anti-tuberculosis drug across the body compartments of rat or the penetration of a Pt-containing chemotherapeutic drug in cancer tissue after intraperitoneal treatment.

MC-ICP-MS was relied on for isotopic analysis of the essential transition metals Fe, Cu and Zn in human whole blood and/or serum. The isotope ratio results obtained for a reference population were evaluated with the aim of revealing the influence of factors such as gender and feeding habits. A link between the Fe isotope ratio results and the parameters used to describe Fe status (among other, ferritin and transferrin levels) was established. Isotope ratio results obtained for blood from patient groups (e.g., hemochromatosis, anemia of chronic disease ACD, Wilson's disease) were compared to those of the reference population with the aim of investigating the potential of isotopic analysis as a diagnostic tool, capable of revealing diseases that otherwise can only be diagnosed at a later stage or via more invasive methods.

Novel particle method for modelling melt generated heterogeneity in spherical mantle convection models

HEIN VAN HECK AND J. HUW DAVIES

Cardiff University, School of Earth and Ocean Sciences, Cardiff, United Kingdom (vanheckhj@cardiff.ac.uk)

Today there are extensive geochemical databases of surface observations but they lack satisfying geodynamical explanations. Working towards this goal we implement a new way to track chemistry in the well developed mantle convection code TERRA.

The bulk composition and trace element abundance (all isotope of He, Ar, U, Th, Pb, K) are tracked via particles. One value on each particle represents bulk composition, which represents the basalt component. Chemical alteration of bulk composition and trace elements happens at self-consistent, evolving, melting zones. We use a composition dependent solidus, therefore the amount of melt generated depends on pressure, temperature and bulk composition. A novel aspect is that we do not move particles that undergo melting; instead the chemical information carried by a particle is transferred to other particles. Melt is instantaneously transported to the surface, thereby increasing the basalt component carried by the near surface particles and decreasing the basalt component in the residue. As melt arrives at the surface, a fraction of its content of trace elements is moved into separate continent/atmosphere reservoirs. For trace elements in the continent, delayed return to the top of the mantle, simulates erosion and recycling back into the mantle.

Results of our implementation will show the evolution of: 1: bulk composition. 2: melt amount. 3: concentration and abundance of trace elements in the atmosphere, continent, melt and surface layer.

The impact of element speciation on apparent partition coefficients

VINCENT VAN HINSBERG¹* BERNARD WOOD² ANTHONY WILLIAMS-JONES¹ AND ARTASHES MIGDISOV¹

¹Earth and Planetary Sciences, McGill University, Montreal, Canada. (*correspondence: hinsberg@eps.mcgill.ca)

²Earth Sciences, University of Oxford, United Kingdom

Liquids, including aqueous fluids and silicate melts, are strongly underrepresented in the geologic record. This is unfortunate, because fluids and melts play a disproportionately large role in the mobility and cycling of elements, as well as in the rheology of the Earth. To constrain the compositions of these liquids we commonly turn to cogenetic minerals, which are readily available in the geological record, and reconstruct liquid compositions using data on the partitioning of elements among minerals and fluids. Lattice-Strain Theory (LST) provides the reference frame for understanding the systematics of this partitioning, by linking partition coefficients to the extent of charge and/or radius mismatch of an element in the mineral lattice [1]. A large mismatch results in a low partition coefficient and vice versa. This partitioning approach has proven highly successful for silicate melts, and is equally applicable to mineral-aqueous fluid systems [2]. However, partitioning studies are generally mineral-centric and regard the liquid as a passive reservoir from which the mineral selectively incorporates elements depending on their fit. It thereby ignores the variable complexation, or speciation, of elements in melts and fluids.

We have evaluated the impact of speciation on partition coefficients by experimentally determining the trace element partitioning behaviour among minerals and fluids in aqueous solutions with varying ligands. Experimental results, complemented with data from natural systems, show that differences in speciation among the elements change apparent (i.e. measured) partition coefficients by up to 4 orders of magnitude. Speciation exerts control on partitioning by determining the concentrations of the species involved in element uptake [2]. If speciation is known, this effect can be incorporated in LST modelling by correcting concentrations for the proportion of an element present in the species relevant to element uptake.

We conclude that the liquid is not a passive reservoir in element partitioning with minerals. Speciation effects have to be accounted for to accurately reconstruct liquid compositions from minerals. However, if speciation is known, its effects can readily be accommodated in Lattice-Strain Theory.

[1] Blundy & Wood (1994) *Nature* **372**, 452–454; [2] van Hinsberg, Migdisov & Williams-Jones (2010) *Geology* **38**, 847–850.

Aluminium in an ocean general circulation model and observations

M.M.P. VAN HULTEN¹*, H. DE BAAR^{2,3}, R. MIDDAG^{2,4}, A. TAGLIABUE⁵, J.-C. DUTAY⁶, MARION GEHLEN⁶ AND A. STERL¹

¹Royal Netherlands Meteorological Institute, P.O. Box 201, 3730 AE De Bilt, The Netherlands (* corresp.: hulten@knmi.nl)

²Royal Netherlands Institute for Sea Research, P.O. Box 59, 1790 AB Den Burg, The Netherlands

³University of Groningen, P.O. Box 11103, 9700 CC Groningen

⁴University of Otago, Dunedin, Otago, New Zealand

⁵University of Liverpool, 4 Brownlow Street, Liverpool L69 3GP

⁶Laboratoire des Sciences du Climat et de l'Environnement, L'Orme des Merisiers, Bât.712, Gif-sur-Yvette

The distribution of dissolved aluminium (Al) in the ocean is of interest because of the impact of Al on remineralisation of diatom opal and the use of surface ocean Al as a tracer for dust. The main thermocline Al concentration has been simulated reasonably well with only a dust source and scavenging as the removal process [1].

In this study the simulation is significantly improved by the addition of a sediment resuspension source (Fig. 1). This supports the idea that the most significant sources of Al to the ocean are dust deposition and sediment resuspension.

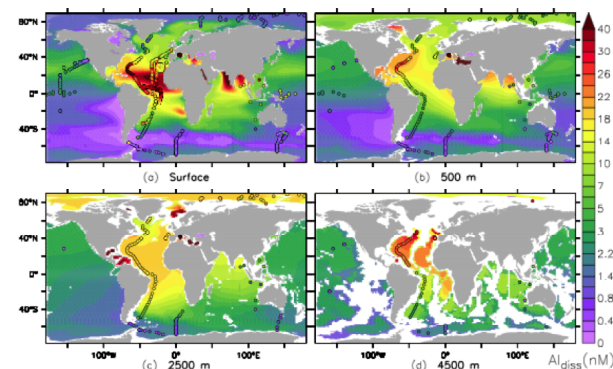


Figure 1: Modelled dissolved aluminium concentration at four depths in the world ocean. Observations as coloured dots. Both simulated and observed concentrations are in nM. Experiments with biological incorporation have been performed as well. These show that this can be an important removal process.

[1] van Hulten, M.M.P., A. Sterl, A. Tagliabue, J.-C. Dutay, M. Gehlen, H.J.W. de Baar, and R. Middag (2012). "Aluminium in an ocean general circulation model compared with the West Atlantic Geotraces cruises". In: *Journal of Marine Systems*. ISSN: 0924-7963. DOI: 10.1016/j.jmarsys.2012.05.005.

Fluid-rock interaction along plate boundary shear zones: insights from modern and ancient examples

VANNUCCHI P

paola.vannucchi@rhul.ac.uk

Field observations and geophysical investigations on modern and ancient plate boundaries reveal that these shear zones are several 100's to 1000's m thick. Marine geophysicists usually see this zone as a low p-wave velocity horizon that implies high fluid content. Onland, ancient plate boundaries are characterized by evidence for incorporation of unlithified, fluid-rich sediments into the fault zone. A better idealization of this dynamic system should consider rock/sediment and fluid supply to the channel, the heterogeneity of deformation, and the evolution of PT conditions as the deeper parts of the shear zones are reached. The upper and lower boundaries of this system can migrate towards the upper or lower plate, defining the main tectonic processes shaping the margin, but also influencing the processes that are responsible for earthquake nucleation, rupture and propagation. Within the shallow, <15 km deep part of the plate boundary shear zone, a gradual change of physical properties defines three subregions; zone 1 of rapid fluid dewatering, zone 2 of overpressure, and zone 3 with metamorphic fluid release. These implications are that a subduction shear zone is a dynamic feature with along-strike and down-dip variations caused by changes in channel material, in trapped fluids, and in interplate boundary geometry.

Release of solid-bound phosphate during the sulfidization of lepidocrocite

K. VAN RIEL¹, T. BEHREND^{1*}, R. T. BUSH²
AND E. D. BURTON²

¹Utrecht University, Faculty of Geosciences, NL-3508 TA Utrecht, The Netherlands (t.behrends@uu.nl)

²Southern Cross GeoScience, Southern Cross University, Lismore, NSW 2480, Australia

Natural ferric iron (oxyhydr)oxides often carry oxyanions such as phosphate or arsenate either adsorbed onto their surfaces or incorporated inside their structure. As a consequence, reductive dissolution of iron (oxyhydr)oxides can lead to the release of the initially solid-bound oxyanions. This link between iron reduction and the mobility and bioavailability of oxyanions is widely recognized but little is known about the kinetic coupling of oxyanion mobilization and iron reduction as well as the underlying mechanisms. Here, we investigated the release of phosphate from lepidocrocite (γ -FeOOH) during its reaction with dissolved sulfide in flow-through reactor experiments at pH values around 7.5 and 8.5. Two types of lepidocrocite were used: One containing structurally bound phosphate, and a second with only adsorbed phosphate. The release of structurally bound phosphate followed the progress of sulfidization and the rates of sulfide consumption were linearly related to the rate of phosphate release. In general, the reaction with sulfide proceeded faster at pH 7.5 than at pH 8.5 and, in turn, phosphate was mobilized faster at pH 7.5. In experiments with adsorbed phosphate, addition of sulfide to the inflow solution led to a pronounced phosphate pulse in the outflow. This quick release can be attributed to ligand exchange reactions in which dissolved sulfide replaces phosphate in surface complexes. However, not all of the adsorbed phosphate was instantaneously removed from the surface. The mobilization of the remaining adsorbed phosphate followed the progress of lepidocrocite sulfidization similar to the behavior of structurally bound phosphate. Furthermore, the fraction of instantaneously released phosphate was smaller at pH 7.5 than at pH 8.5. We propose, that these phenomena can be explained by the different reactivity of bidentate and monodentate phosphate complexes, whereas the latter are more abundant at pH 8.5. That is, phosphate in monodentate complexes readily undergoes ligand exchange with sulfide while bidentate phosphate complexes are relatively inert towards the attack by sulfide. Our results show that the pH effect on phosphate release in anoxic environments can be oppositional depending on the binding form of phosphate.

Formation of the IIE non magmatic iron meteorites

N. VAN ROOSBROEK^{*1}, V. DEBAILLE¹, S. GODERIS², J. W. VALLEY³, M. J. SPICUZZA³ AND PH. CLAEYS²

¹ Lab. G-Time, Université Libre de Bruxelles, 1050 Brussels, Belgium (* nvroosbr@ulb.ac.be, vdebail@ulb.ac.be)

² Earth System Sciences, Vrije Universiteit Brussel, 1050 Brussels, Belgium (stgoderi@vub.ac.be, phclaeys@vub.ac.be)

³ Dept. of Geoscience, Univ. of Wisconsin-Madison, Madison, WI, 53706, USA (valley@geology.wisc.edu, spicuzza@geology.wisc.edu)

The well preserved ~450 kg fragment of the IIE non-magmatic iron (NMI) Mont Dieu II (MDII) meteorite [1] has been investigated to understand the formation of IIE NMI meteorites that are not directly related to core formation [2]. The present study focuses on the abundant large silicate inclusions of MDII, studied under SEM/EDX, and for which major and trace elements were measured by ICP-OES & ICP-MS. Oxygen isotopes were measured by laser-fluorination.

The silicate inclusions are characterized by coarse-grained granular texture, crossed by metal veins. Round structures (~ 1 mm) composed of ferromagnesian minerals are present, interpreted as relict chondrules. Three well-preserved barred olivine chondrules, a feature so far only described for Netschaëvo NMI IIE [3], and glass have been observed. Low Ca-Px, Ol and albitic Pl are the major mineral phases. FeO-rich glass (interpreted as relict from the impacted body), Chr, Tro, Schr, (chlor)Ap and Fe-Ni metal are found as minor phases. The $\Delta^{17}\text{O}$ of MDII is 0.714 ± 0.024 ‰. The Fa and Fs molar contents of the relict chondrules are similar to those observed in H-type OC. The IIE NMI seem also related to OC based on their oxygen isotopic compositions [4], as the $\Delta^{17}\text{O}$ of MDII falls within the range defined for H 3-6 OC [4; 5].

Based on these results, an impact formation model is proposed, where a Fe-Ni impactor collided with an H-chondrite parent body. A position near the edge of the asteroid and at a shallow depth of the magma pool is favored for MDII, because fast cooling is necessary to preserve the chondrules and glass. After this first stage of fast cooling, a second phase involving slower cooling is needed to permit the development of the Windmanstätten pattern.

[1] Van Den Borre *et al.* (2007) *Meteor. Planet. Sci.*, 42:A153.

[2] Haack and McCoy (2004) *Treatise on Geochemistry*, 325-345.

[3] Olsen and Jarosewich (1971) *Science* 174, 583-585.

[4] Clayton and Mayeda (1996) *Geochim. Cosmochim. Acta* 60, 1999-2017. [5] Folco *et al.*, (2004) *Geochim. Cosmochim. Acta* 68, 2379-2397.

The composition of the lower crust of the Oman Ophiolite

J.A. VANTONGEREN¹ AND P.B. KELEMEN²

¹Yale University, jill.vantongeren@yale.edu

²LDEO, Columbia University, peterk@ldeo.columbia.edu

Fundamental questions remain as to where, how, and to what extent chemical fractionation occurs in the oceanic lower crust and upper mantle, prior to eruption of MORB. There is no continuous drill core through oceanic crust *in situ*. Thus, to address these questions, we turn to the Oman ophiolite, where there is a continuous section from residual mantle peridotite to submarine lavas formed at an oceanic spreading ridge.

We present a detailed, stratigraphically-constrained, bulk composition for the lower crust of the Wadi Khafifah section of the Oman ophiolite. Together with sheeted dikes and lavas having trace element contents similar to MORB, the bulk crustal composition meets two fundamental criteria for a mantle-derived melt: (1) It has Mg# in equilibrium with Fo90 mantle olivine; (2) it is multiply saturated in ol+aug+opx±plag/sp at shallow mantle pressures. In addition, clinopyroxene crystallizes early, eliminating the so-called 'pyroxene paradox'. The parent magma – with major element composition indistinguishable from primitive MORB – represents an aggregate produced by polybaric decompression melting of depleted MORB mantle (DMM), which has crystallized approximately 5% olivine – probably by reactive fractionation (Collier & Kelemen, *J Petrol* 2010) in the crust-mantle transition zone – prior to emplacement within the crust. An additional 40-60% fractional crystallization (ol+aug+ plag) in the lower crust is required to produce the observed sheeted dike and lava compositions. Where data are available for comparison, gabbro compositions reported here are similar to analysed samples from modern fast-spreading mid-ocean ridges. Thus, our results are relevant for understanding modern fast-spreading oceanic crust.

Uranyl on Mg-rich minerals: Polarisation Dependent EXAFS

A. VAN VEELLEN¹, R. COPPING², G.T.W. LAW³,
A.J. SMITH¹, J.R. BARGAR⁴, D.K. SHUH²
AND R.A. WOGELIUS^{1*}

¹University of Manchester, SEAES, Oxford Road,
Manchester, M13 9PL, UK (*correspondence:
roy.wogelius@manchester.ac.uk)

²Chemical Sciences Division, Lawrence Berkeley National
Laboratory, MS70A1150, One Cyclotron Road, Berkeley,
CA 94720, USA

³University of Manchester, CRR, School of Chemistry, Oxford
Road, Manchester, M13 9PL, UK

⁴Stanford Synchrotron Radiation Lightsource, PO Box 4349,
Stanford, CA 94309, USA

In the UK, large quantities of intermediate level waste pose complex radiological remediation challenges. Chemical understanding of uranium in these Mg-rich sludges is vital. By applying two EXAFS techniques, we determined: (1) where uranyl (UO₂²⁺) is adsorbed, and (2) how uranyl attaches to the mineral surface. Powder experiments with U(VI) were performed with magnesite [MgCO₃], brucite [Mg(OH)₂], nesquehonite [MgCO₃·3H₂O] and hydromagnesite [Mg₅(CO₃)₄(OH)₂·4H₂O]. K_d values for the Mg-carbonate powders were comparable to or exceeded published results for Ca-carbonates. A second set of experiments (GIXAFS) used single crystals of magnesite (10.4) and brucite (0001). Single crystals were reacted under ambient and reduced PCO₂ ~ -4.5 for 48 hrs. with concentrations of U(VI)-chloride above and below the solubility of schoepite [UO₂(OH)₂·H₂O] (ca. 40% U(VI) adsorbed). GIXAFS measurements were made at $\chi = 0^\circ$ and $\chi = 90^\circ$ relative to the synchrotron beam polarisation. GIXAFS results clearly showed polarisation dependence for both ambient and reduced PCO₂. XANES results showed uranyl is oriented with the axial oxygens perpendicular to the mineral surface. The EXAFS structural model corroborates an uranyl-triscarbonate. This implies local rutherfordine-like [UO₂(CO₃)₃] regions which may polymerise at high uranyl activities into a thin film. These results are useful for predicting uranium behaviour during disposal and remediation. The development of *in-situ* measurements is currently in progress.

Mass-independent sulfur isotope signature in spherule beds of the 3.4- 3.2 Ga Barberton Greenstone Belt, South Africa

M.A VAN ZUILEN^{1*}, P. PHILIPPOT¹, M.
WHITEHOUSE² AND A. LEPLAND³

¹Institut de Physique du Globe de Paris, France
(*correspondence: vanzuielen@ipgp.fr)

²Swedish Museum of Natural History, Stockholm, Sweden

³Norwegian Geological Survey, Trondheim, Norway

Theoretical and experimental studies have shown that atmospheric SO₂ isotopologue self-shielding effects in the 190-220 nm region of the solar spectrum are the likely cause for mass independent fractionation of sulfur isotopes (S-MIF). The main products of this photochemical reaction – SO₃ and S₀ – typically define a compositional array of ca. $\delta^{33}\text{S} = 0.6 \delta^{34}\text{S}$. This is at odds with the generally observed trend in Archean sulfides, which broadly defines an array of $\delta^{33}\text{S} = 1.4 \delta^{34}\text{S}$. Various explanations have been proposed, including a diminution of $\delta^{34}\text{S}$ caused by chemical and biogenic mass-dependent fractionation of sulfur isotopes (S-MDF), mixing with photolytic products produced during felsic volcanic events, or partial blocking of the low-wavelength part of the spectrum due to the presence of reduced atmospheric gases or an organic haze.

Early in Earth's history large meteorite impacts would have ejected dust and gas clouds into the atmosphere that shielded solar radiation and affected global climate. It is thus likely that at certain time intervals of high meteorite flux the atmosphere was significantly perturbed, possibly leaving anomalous sulfur isotopic signatures in the rock record. Here we describe the sulfur-MIF and -MDF signatures in sulfides of spherule beds S2, S3 and S4 of the Barberton Greenstone Belt, South Africa. In particular in spherule bed S3 – and to a lesser extent S4 – a trend of $\delta^{33}\text{S}/\delta^{34}\text{S} = 0.7$ is observed that closely follows the expected trend for SO₂-photolysis in the 190-220 nm spectral range. This suggests that an impact dust cloud (deposited as spherule beds), which sampled the higher region of the atmosphere, specifically incorporated products of SO₂ photolysis in the 190-220 nm range, and blocked photochemical reactions at higher wavelengths (250-330 nm band). By implication, the generally observed Archean trend indeed appears to be the result of additional photochemical reactions that took place in the lower part of the atmosphere.

Geochronology of Weathering and Pedogenesis

PAULO M. VASCONCELOS^{1,2,3}

¹The University of Queensland, School of Earth Sciences,
Brisbane, Qld 4072; paulo@earth.uq.edu.au

The combination of ⁴⁰Ar/³⁹Ar, (U-Th)/He, and U-series dating of weathering-product and pedogenic Mn and/or Fe oxyhydroxides permits determining the chronology and rate of chemical reactions in the weathering crust. These methodologies are complementary and suitable for dating processes spanning from Recent to the earliest preserved weathering profiles on Earth. The application of these methods in weathering geochronology reveals that minerals hosted in pedoliths are invariably much younger than minerals preserved in the underlying saproliths, indicating that the pedolith has a much greater propensity to undergo mineral dissolution-reprecipitation than the remainder of the weathering profile. The greater reactivity of the pedolith appears to be controlled by organic activity, mechanical and chemical, which promotes frequent and recurrent mineral dissolution-reprecipitation. In contrast, the underlying saprolith appears to record the influx of weathering solutions during the early stages of evolution of a weathering profile. Once precipitated, saprolith minerals may remain in metastable equilibrium, sometimes for millions or tens-of-millions of years. Saprolith minerals become more prone to dissolve and reprecipitate when the pedolith front advances into the saprolith. But only during drastic changes in weathering conditions do minerals within the saprolith undergo dissolution-reprecipitation. Identifying and dating the multiple generations of supergene minerals in both the pedolith and saprolith reveal a history of weathering that is protracted and episodic, particularly in the case of deep and stratified lateritic weathering profiles. The major challenges in applying these geochronological approaches to the study of weathering and pedogenesis is the difficulty in identifying and physically sampling distinct generations of supergene minerals. This challenge is particularly acute in the pedolith.

Gas discharges for continental Spain: Geochemical and isotopic features

ORLANDO VASELLI^{1,2}, BARBARA NISI³, FRANCO TASSI^{1,2},
TOM DARRAH⁴, JORDI BRUNO⁵, JAVIER ELÍO⁶,
FIDEL GRANDIA⁷ AND LUIS PEREZ DEL VILLAR⁸

¹Department of Earth Sciences, Florence, Italy
(*correspondence: orlando.vaselli@unifi.it)

²CNR-IGG, Institute of Geoscience & Earth Resources
Florence, Italy

³CNR-IGG, Institute of Geoscience & Earth Resources Pisa,
Italy

⁴Division of Earth & Ocean Sciences, Nicholas School for the
Environment, Durham, USA

⁵Amphos21, Barcelona, Spain

⁶Fundación Ciudad de la Energía (CIUDEN), Ponferrada,
Spain

⁷CIEMAT, Unidad de Integración de Sistemas Geológicos
Madrid, Spain

In this work the results of a geochemical and isotopic survey of 37 gas discharges was carried out in continental Spain are presented and discussed. On the basis of the gas chemical composition, four different areas can be distinguished, as follows: 1) Selva-Emborda (SE) region; 2) Guadalentin Valley (GV); 3) Campo de Calatrava (CC) and 3) the inner part of Spain (IS).

The SE, GV and CC areas are characterized by CO₂-rich gases, while IS has N₂ as main gas compound. The CO₂-rich gases can be distinguished at their turn on the basis on the helium and carbon isotopic composition. The SE and CC areas have a strong mantle signature (up to 3 Ra). Nevertheless, the carbon isotopic composition of CC is within the mantle range and that of SE is slightly more negative (down to -8‰ PDB). The GV gases have a lower mantle signature (≈1 Ra) with respect to SE and CC and more negative carbon isotopes (≈-10‰ PDB). It is worth to mention that the SE, GV and CC areas are related to the youngest volcanic activity in continental Spain, for example the Garrotxa Volcanic Field in Catalonia records the latest event dated at 10,000 years, and the isotopic features, particularly those of helium, are suggesting the presence of magmatic bodies still cooling at depth. The N₂-rich gases, i.e. those from the IS area, has an atmospheric origin, as highlighted by the N₂/Ar ratio that ranges between those of air and ASW (Air Saturated Water). The isotopic composition of carbon is distinctly negative (down to -21‰ PDB) and that of helium is typically crustal (0.02-0.08 Ra), confirming that these gas discharges are related to a relatively shallow source.

The microstructural study of clay minerals - polymer matrix nanocomposites.

A.L.VASILIEV^{1,2*}, ANTON S.OREKHOV^{1,2},
ANDREY S.OREKHOV^{1,2}, S.N.CHVALUN¹
AND S.V.CHERDYNCEVA¹

¹ NRC Kurchatov institute Moscow, Russia (*correspondence: a.vasiliev56@gmail.com)

²Institute of Crystallography RAS Moscow 119454, Russia
orekhov.anton@gmail.com

Clay minerals (layered silicates) have been used as reinforcing filler for polymers. Montmorillonite (MMT) has well-known 2:1 layered structure where the central octahedral alumina sheet is sandwiched by two tetrahedral silicate sheets with cations such as Na⁺ or Ca²⁺, which are present between layers to compensate the net negative charge. The lateral dimensions of MMT particles vary from tens to hundreds of nm. The interlayer cations can be replaced by organic molecules through an intercalation and further exfoliation. Two processes were crucially important: the ability of MMT particles to intercalation and exfoliation and the dispersion of the clay particles in the polymer matrix. The MMT particles, organomodified particles and 1, 3, 5 и 30 wt% MMT filled polymer (polyimide) were studied by transmission electron microscopy and microanalysis. The interplanar distance in the MMT particles determined from the number of high resolution images and electron diffraction pattern was found to be of $c=0.99\pm 0.01$ nm. The edge type dislocation with projection of burgers vector $\mathbf{b}=c[001]$ were observed. The interplanar distance c in the organomodified particles mostly increase to 2.2 – 2.5 nm together with the growth of dislocation density. The study of MMT-polymer nanocomposites demonstrated the enhancement of particles dispersion in the range of 1 to 5 wt% filled polymer with the growth of the exfoliated particles density. Much less exfoliation of the MMT particles were found in 30 wt% filled composite together with formation of high density of pores, observed in these TEM specimens.

The work was supported by grant N 16.253.11.306.

Phase relations of carbonate eclogite during subduction and the effect of redox conditions on diamond – carbonate reactions

PROKOPIY VASILYEV^{1*}, GREGORY YAXLEY¹,
JOERG HERMANN¹, HUGH O'NEILL¹
AND ANDREW BERRY¹

¹Research School of Earth Sciences, The Australian National University, ACT 0200, Australia (*correspondence: prokopi.vasilyev@anu.edu.au)

High pressure experiments are critical to understanding the recycling of carbon into the deep earth during subduction processes [1,2]. Melting and phase relations of carbonate eclogites (former altered oceanic crust) and the effect of oxygen fugacity on diamond versus carbonate stability along deep subduction geotherms are currently very poorly understood.

To investigate this, a series of piston-cylinder experiments was conducted at $P=3.5-6.0$ GPa, and $T=900-1300^\circ\text{C}$. Starting material for the first part of the study models highly carbonated (10% CaCO_3) altered oceanic basalt [1]. Experiments at reduced conditions (using Fe capsules) showed the absence of crystalline carbonate and the presence of siliceous near-solidus melts. In high oxygen fugacity experiments, performed using a Re-ReO₂ buffer at 1000-1100°C, carbon was present as carbonates at high pressure (5.5GPa) and in carbonate-silicate melt at low pressure (3.5 GPa).

The stability of carbon versus carbonate in subducting C-bearing eclogite may be defined by reaction $\text{CaMg}(\text{CO}_3)_2 + 2\text{SiO}_2 = \text{CaMgSi}_2\text{O}_6 + 2\text{C} + 2\text{O}_2$ [3]. This reaction is being investigated in a second series of experiments with compositionally variable carbonate eclogites (mixes of synthetic garnet, clinopyroxene, kyanite, coesite, dolomite and Ir metal as a redox sensor) being used to determine P-T- $f\text{O}_2$ -X phase relations. Garnet Fe³⁺ contents will be determined using the electron microprobe based flank method [4] and the synchrotron based Fe K-edge XANES method [5].

[1] Yaxley & Green (1994) *EPSL* **128**, 313-325. [2] Dasgupta *et al.* (2004) *EPSL* **227**, 73-85. [3] Luth (1993) *Science* **261**, 66-68 [4] Höfer, Brey (2007) *Am.Min.* **92**, 873-885 [5] Berry *et al.* (2010) *Chem.Geol.* **278**,31-37

Petrology of the lamprophyres.

E. VASYUKOV A^{1,2}

¹630090, av. ak. Koptyuga, 3, Novosibirsk, Russia,
lenav@inbox.ru
²630090, Pirogova st., 2, Novosibirsk, Russia

Chuya complex of mica lamprophyres situated in the southeast part of Gornyi Altai and extends to Mongolia. Dikes of this complex are distributed irregularly and form the belts or the areas accompanying fault zones. Lamprophyres from two largest areas, named south-chuya and yustyd respectively, were characterized in geological, petro- and geochemistry terms. Radiological characteristics give evidence of synchronic formation of the dikes from different areas. Bulk-rock analysis indicates, that the rocks are basic to intermediate, calc-alkaline and ultrapotassic. On the most petrochemical and geochemical binary plots the rocks of dykes from different areas fully or partially overlap. The multi-element and rare-earth diagrams of all investigated rocks are equal in the form, at the position of HFSE minima, have high La/Yb (17-62) and Gd/Yb (4-9,7) relations. Geochemistry characteristics allow us to suggest that all rocks were formed as a result of small degrees partial melting of garnet mantle source. However, in our studies, fundamental differences in the isotopic composition of Nd and Sr and some petrochemical features have been established. For the yustyd area rocks the initial isotopic relations are close to BSE. And for the lamprophyres from another area ϵ_{Nd} varies from (-2.84 - -4.05) and $^{87}Sr/^{86}Sr > 0.70858$. In our work we discuss three hypotheses forming the lateral variability in composition of the lamprophyres of the Chuya complex: 1) heterogeneity of the mantle; 2) contamination the rock forming melt by crust material; 3) liquid immiscibility, accompanied by redistribution of some major and trace elements.

The role of fluoride-silicate liquid immiscibility in REE ore genesis

O.VASYUKOVA AND A.E.WILLIAMS-JONES

Department of Earth and Planetary Sciences, McGill University, 3450 University Street Montreal, Quebec, Canada, H3A 0E8, olga.vasyukova@mcgill.ca

The Mid-Proterozoic peralkaline Strange Lake pluton (Québec-Labrador, Canada) hosts potentially economic concentrations of high field strength elements (HFSE), including the rare earth elements (REE), zirconium and niobium in zoned (Zr-rich borders and Ca-F-REE-rich cores) and unzoned pegmatites. Based on bulk rock geochemistry, mineralogy and fluid inclusion data, HFSE enrichment in the pluton has previously been interpreted to be due to extreme fractional crystallization and late hydrothermal alteration. However, recently collected melt inclusion data suggest that a third process, namely melt immiscibility, may have played an important role in the concentration of the HFSE.

Three types of melt inclusion have been identified in quartz from the Strange Lake granite after heating to 900-950 °C and quenching. Type 1 inclusions are composed of silicate glass and display enrichment in Zr, Nb and Ti with increasing alkalinity. Type 2 inclusions also contain silicate glass and, in addition, a globule of a REE-bearing calcium fluoride glass (up to 14 wt.% REE). Type 3 inclusions contain calcium fluoride glass with multiple silicate globules. Calcium fluoride glass in both Type 2 and 3 inclusions in some cases contains a REE fluoride glass globule (up to 50 wt. % REE).

We propose that fractional crystallization enriched the magma in fluorine, leading to silicate-fluoride liquid immiscibility prior to and during emplacement of the pegmatites. This caused partitioning of Zr, Nb and Ti into the silicate melt and F, Ca and REE into the fluoride melt. Further evolution of the melts occurred separately. Quartz, feldspars and arfvedsonite crystallized from the silicate melt, enriching the latter in Zr, Nb and Ti, and fluorite crystallized from the fluoride melt, enriching its residue in REE. The latter melt eventually exsolved a REE-fluoride melt.

The observed zoning of many pegmatites is interpreted to reflect crystallization of the silicate melt, including formation of zirconosilicates in the outer zone, and migration of exsolving or heterogeneously incorporated (prior exsolution) calcium fluoride melt inwards. This latter melt subsequently exsolved a REE-fluoride melt and the two melts crystallized to form the fluorite- and REE mineral-rich pegmatite cores. To our knowledge, this study provides the first example, in which silicate-fluoride liquid immiscibility has been shown to help concentrate the REE to potentially economic levels.

Volatilization of Hg from HgS minerals mediated by the coupled activity of thiosulfate and a sulfur-oxidizing bacterium

A.I. VAZQUEZ-RODRIGUEZ^{1*}, T. ZHANG²,
C.H. LAMBORG², C.M. SANTELLI³, S.C. BROOKS⁴, AND
C.M. HANSEL²

¹School of Engineering and Applied Sciences, Harvard University, Cambridge, MA USA (*correspondence: avazquez@fas.harvard.edu)

²Marine Chemistry and Geochemistry Department, Woods Hole Oceanographic Institution, Woods Hole, MA USA

³Department of Mineral Sciences, Smithsonian Institution, Washington, DC USA

⁴Environmental Sciences Division, Oak Ridge National Laboratory, Oak Ridge, TN USA

Soils and sediments, where mercury (Hg) can exist as the Hg sulfide mineral metacinnabar (β -HgS), represent major Hg reservoirs in aquatic environments. Due to its low solubility, metacinnabar has historically been considered an insignificant source of Hg to the aqueous environment. Our previous work has shown that bacterial colonization of metacinnabar incubated in the shallow sediments of the Hg-contaminated East Fork Poplar Creek (Oak Ridge, TN) is dominated by genera known to use reduced sulfur compounds as electron donors during growth. Based on 16S rRNA pyrosequencing, *Thiobacillus thioparus*, an obligate autotrophic neutrophilic sulfur oxidizer, is among the most abundant colonizers.

Here we show that *T. thioparus* incubated aerobically in the presence of metacinnabar and thiosulfate (0.1-20 mM) results in substantial metacinnabar dissolution and release of Hg. Upon reaction, sulfate concentrations are higher than can be attributed to oxidation of thiosulfate alone, yet aqueous Hg(II) concentrations remain below detection limit. We show that in the presence of live cultures of *T. thioparus* aqueous Hg(II) released following HgS dissolution is rapidly volatilized forming Hg(0). In control incubations (media with thiosulfate and metacinnabar, and no viable cells) thiosulfate concentrations correlate with levels of dissolved Hg(II), suggesting that thiosulfate, a strong Hg-binding ligand, abiotically induces HgS dissolution. *T. thioparus* possesses genes involved in the Mer detoxification pathway, and we are currently investigating *mer* expression in this system.

These findings have important implications for environmental Hg cycling, highlighting the unappreciated potential of Hg release from assumed permanent solid-phase Hg sinks. It further introduces new pathways for solid-phase Hg to enter the global atmospheric mercury pool.

Role of deep carbides in the formation of hydrocarbons?

A VECHT¹ AND ADRIAN P JONES¹

¹Department of Earth Sciences, University College London, WC1E 6BT. email: aron@vecht.com,

Whether hydrocarbons in rocks are inorganic or organic in origin might be evaluated by considering carbides as precursors in the formation of deep hydrocarbons and a range of volatile compounds, since carbide may constitute >2 wt% of the Earth's core [1].

Low pressure carbides can be (a) *Interstitial* (Ti, V, Cr, Zr, Nb, Hf, Ta, W) (b) *Covalent* (B, Si): (c) *Intermediate* (Ti, V, Cr, Mn, Fe, Co, Ni): or (d) *Salt-like* (Groups I, II, and III). In the absence of high-P experimental data, groups (a) (b) and (c) should be included as candidates for carbides found in the inner core, because they are stable at high-T; they also react with water and/or oxygen to form hydrocarbons and CO or CO₂ respectively. Carbides can be described as 'reactive minerals' [2] and react with water to yield hydrocarbons. Hydrocarbon pathways from CH₄ at high-P have started to be explored [3].

Siderophile element carbides (Cr, Fe, Ni, V, Mn, Co) hydrolyse with water to yield "organic matter"[4]. We propose similar reactions based on carbides of Ca and Al for the formation of methane hydrate. The reactions are expected to be of the general type: M_xC_y + nH₂O where M is the metal = Hydrocarbons such as CH₄ + M(OH)₂. In the presence of oxygen such hydrocarbons would react to form CO and ultimately CO₂. Similar reactions could occur with nitrides, sulphides and silicides. These compounds are stable at high-T and would react with water and oxygen at lower temperatures.

Methane hydrates are common in continental shelf sediments and in deep arctic permafrost and occur at depths of around 500m [5]. Methane is found under lakes such as Lake Kivu [6]. It is generally assumed that such deposits are of biological origin. However, no explanation is given as to how complex molecules form organic deposits. Synthesis routes at high-T are well known, but we propose experiments to high-P conditions to test whether deep carbides [7] act as possible precursors in the abiotic synthesis of hydrocarbons and methane hydrates.

[1] Wood (1993) EPSL 117 [2] Vecht (2007) GCA 1060; [3] Cataldo (2003), IntJAstrobiol. 2; [4] Spanu et al (2010) PNAS 10148044108; [5] Kvenvolden (1982) 4th Can Permafrost Conf 305; [6] Deuser et al (1973) Science 181; [7] Oganov et al (2013) *Carbon in Earth* RIMG 75 Ch 3.

Nano and Bulk-Scale Characterization of Biogeochemical Processes: A Case Study

HARISH VEERAMANI¹ AND MICHAEL F. HOCELLA, JR.^{1,2}

¹ Virginia Tech, Blacksburg, VA 24061; harish@vt.edu

² Pacific Northwest National Laboratory

Recent advances in nanotechnology and analytic instrumentation allow biogeochemical processes between microbes, metals and minerals to be probed at remarkable levels of complexity, sensitivity, space and time. One of the dominant trends in geomicrobiology is the detailed characterization and application of biogenic minerals whose characteristic features are at the nanometer scale in at least one dimension. It is therefore important to understand – and ultimately exploit – the unique properties and behavior of a wide range of nanoscale biogenic materials. Central to this trend are the development and application of effective analytic techniques for characterizing the structural and chemical properties of biogenic minerals with (sub)nanometer spatial resolution.

Microbes in the subsurface are involved, directly or indirectly, in a plethora of activities such as metal reduction and oxidation, mineral precipitation and dissolution. These innate capacities of subsurface microbes are often exploited for *in situ* remediation of contaminated sites. During subsurface bioremediation of uranium-contaminated sites, indigenous metal and sulfate-reducing bacteria may produce biogenic minerals such as mackinawite (FeS) which could potentially drive abiotic uranium reduction.

In this work, the propensity of well-characterized biogenic mackinawite to abiotically reduce U(VI) was tested using a suite of electron microscopy and synchrotron based spectroscopy techniques. High-resolution electron microscopy confirmed the formation of nanoparticulate uraninite [UO₂] on the surface of biogenic mackinawite, which was further confirmed with bulk X-ray absorption spectroscopy that revealed the molecular coordination environment of uraninite. X-ray photoelectron spectroscopy confirms that U(IV) reduction was coupled to the oxidation of S²⁻ and not structural Fe(II) within the biogenic mackinawite. The combination of rigorous nano- and bulk-scale characterization provides insights into such biogeochemical processes, that occur during subsurface biostimulation, that are not always possible with bulk-scale analyses alone.

Unravelling complex groundwater recharge and transport of contaminants using combined stable and radioactive isotope tracers

T.W. VENNEMANN^{1*}, C. REYMOND¹, A. BUFFAT¹,
L. DESPOND¹, C. MOREL¹, K. NAUDE², J. MILLER²
AND B. MAPANI³

¹Institute of Earth Sciences, University of Lausanne,
Switzerland (*contact: Torsten.Vennemann@unil.ch)

²Department of Geology, University of Stellenbosch, South
Africa

³Geology Department, University of Namibia, Windhoek,
Namibia

As part of a project assessing the quality and potential of groundwater, a vital resource in the extremely arid but touristic Namib-Naukluft area, a geochemical study of the surface and groundwaters, plants, soil, and rocks was undertaken. The study indicated excessive nitrate concentrations in about 15% of the 70 groundwaters sampled (several 100's of mg/l). While many of these groundwaters with high NO₃⁻ also have high δ¹⁵N and δ¹⁸O values and are from boreholes close to settlements, others are not. Furthermore, the vegetation also has elevated δ¹⁵N values, making it difficult to identify anthropogenic or animal wastes as contaminants. Mean residence times of groundwaters estimated by ¹⁴C measurements of DIC have a wide range (recent as >100% modern carbon to about 14'000 yrs b.p.), and also a wide range of δ¹³C values (−4.6 to −12.8‰) related to infiltration across soils of typical C3 (mountains) and C4 (savannah-desert) type of vegetation and limestone-derived soils and aquifers (δ¹³C of −3 to +2‰). This variation, in addition to drainage across calcrete soils during brief periods of recharge necessitates substantial corrections to the measured ¹⁴C ages, but which can be modelled via the concentrations and stable isotope compositions of DIC. Recharge during decadal “extreme events” is suggested by the H- and O-isotope compositions of the groundwaters with low δ-values compared to normal average annual rainfall. Seasonal variations in H- and O- isotope compositions in combination with modern mean residence times and high high nitrate δ¹⁵N and δ¹⁸O values thus do confirm an anthropogenic/animal-waste origin. The complex recharge of the aquifers across different soils, soil organic matter, can hence be unravelled using a combined isotopic tracing approach. In general, a slow, horizontal flow away from the principal mountain-recharge area, but also with locally important vertical recharge, particularly close to settlements and man-made boreholes, is indicated.

Isotopically light (Solar?) nitrogen associated with the planetary noble gas carrier (Q)

VERCHOVSKY A. B.¹, SEPHTON M. A.³
AND WRIGHT I. P.¹

¹The Open University, Milton Keynes, UK,
a.verchovsky@open.ac.uk

³Imperial College, London, UK

The nature of the planetary noble gas carrier (Q) has remained an intriguing cosmochemical puzzle for decades. Q can be significantly enriched by dissolving all meteoritic silicate minerals to leave behind only carbonaceous material and oxides. However, even after that, the abundance of Q in the residue is much less than 1%. This is the main reason why Q is so difficult to identify. Therefore, Q is characterised indirectly by its properties, such as its susceptibility to oxidation or its resistance to parent body metamorphism compared to macromolecular materials as well as by the noble gas components it contains. Such observations suggest that Q has been formed very early in the Solar System, or may even predate its formation.

Our analyses of a number of CR meteorites using our multi-element isotope analyser, Finesse, in combination with stepped combustion, has revealed a new property of Q – its separation from most of macromolecular carbon and nitrogen. In CR2 and CR3 petrological groups, but not in CR1s, the Q noble gases, are released in a narrow range at a high temperature (~1100°C). It appears that Q somehow becomes isolated within the matrix from direct contact with oxygen gas during stepped combustion. Only when the matrix opens up does oxygen react with Q (oxidising it almost instantly). Since almost no macromolecular C and N remains by the time of Q oxidation, the Q nitrogen dominates the release at these temperatures. And, as such, its isotopic composition is revealed. The lowest measured $\delta^{15}\text{N}$ associated with the noble gas release at the high temperatures is -140‰. And this is only the upper limit since a certain amounts of other (isotopically heavier) N components are also present along with Q nitrogen. We believe that Q nitrogen is likely to have $\delta^{15}\text{N}$ similar to solar composition (-380‰) determined by the Genesis mission. The presence of solar N in Q is also consistent with its He isotopic composition corresponding to pre-deuterium burning era of the early Solar System.

On the importance of ternary alkaline earth carbonate complexes of uranium(VI) in natural waters: a round-robin modeling test

T. VERCOUTER^{1*}, P.E. REILLER¹, E. ANSOBORLO¹,
L. FEVRIER², R. GILBIN², C. LOMENECH³
AND V. PHILIPPINI³

¹CEA, Nuclear Energy Division, France, *correspondence:
thomas.vercouter@cea.fr

²IRSN, Cadarache, France

³University of Nice-Sophia Antipolis, France

The availability of uranium in natural waters is governed by many processes and interactions with chemical compounds. At equilibrium the predominant soluble and solid forms of uranium can be estimated using thermodynamic data and aqueous geochemical speciation codes. The quality of calculations is mainly related to the quality and completeness of the entry data. Within the working group “Speciation” of the CETAMA a round-robin modeling exercise was conducted about the U(VI) speciation in waters of known compositions. The objectives were: i) to test thermodynamic data bases; ii) to compare the modelers’ methods in selecting data; and iii) to evaluate the effect of inorganic species on the U(VI) speciation and solubility.

A recent experimental study on the speciation of uranium in drinking waters have shown that calcium uranium carbonate complexes play an important role [1]. The modeling exercise was build on the basis of water compositions of two of these samples. Other water compositions were derived from these in order to better check U(VI) speciation changes with the bicarbonate content, the saline content and $[\text{Ca}^{2+}]$ and $[\text{Mg}^{2+}]$. The participants of this exercise were asked to provide the distribution of soluble uranium species and evaluate the uranium solubility-controlling solid phase for each water.

The main outcome is on the importance of alkaline earth carbonate ternary complexes such as $\text{Ca}_2\text{UO}_2(\text{CO}_3)_3(\text{aq})$, $\text{CaUO}_2(\text{CO}_3)_3^{2-}$, and $\text{MgUO}_2(\text{CO}_3)_3^{2-}$. These species were reported in recent publications [2], but rarely included in available data bases. As a consequence it emphasizes the necessity of continuous enrichment of data bases with a consistent approach to avoid bias. Moreover, the amount of uranium in solution could be calculated considering various solubility-controlling phases though such estimations definitely requires the expertise of the geochemist.

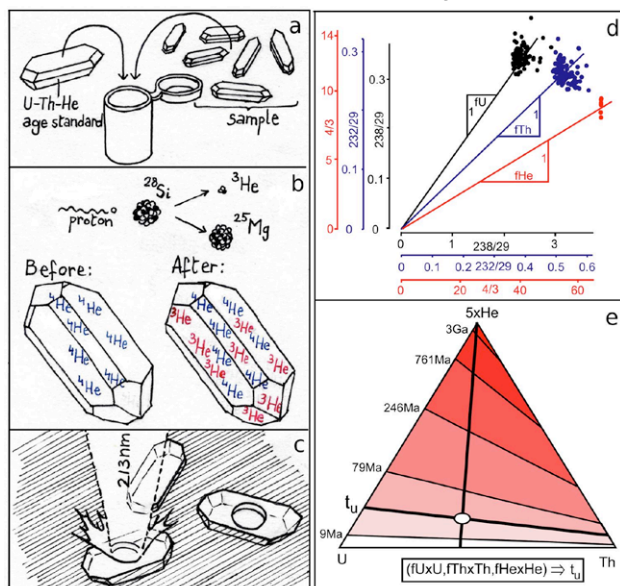
[1] Prat, Vercouter, Ansoborlo, Fichet, Perret, Kurttio, Salonen (2009), *Environ. Sci. Technol.* 43, 3941–3946. [2] Dong, Brooks (2008), *Environ. Sci. Technol.*, 42, 1979–1983.

In situ U-Th-He dating by $^4\text{He}/^3\text{He}$ laser microprobe analysis

PIETER VERMEESCH AND JAMES SCHWANETHAL¹

¹London Geochronology Centre, University College London, p.vermeesch@ucl.ac.uk and j.schwanethal@ucl.ac.uk

We have developed a rapid, flexible and robust method for in-situ U-Th-He dating, in which (a) multiple zircons from the sample are packed together with a standard of known U-Th-He age, (b) these are proton-irradiated to produce spallogenic ^3He , (c) the grains are ablated with a UV laser once to measure the $^4\text{He}/^3\text{He}$ ratios on a noble gas mass spectrometer, and a second time to measure the $^{232}\text{Th}/^{29}\text{Si}$ and $^{238}\text{U}/^{29}\text{Si}$ ratios by ICP-MS. The age of the sample is calculated by comparing the measured isotope ratios of the sample to those of the standard (d), and multiplying the resulting 'scaling factors' (fU, fTh, and fHe) with the normalised (U, Th, He) composition of the standard (e), which can be calculated from the measured U/Th ratio and its age. This method removes the need to know any absolute concentrations or pit volumes and is immune to ICP-MS matrix effects and collateral laser melting.



Thermal history of a Neoproterozoic orogen and A-type leucogranites formation (Yenisey Ridge, Western margin of the Siberian Craton)

A.E. VERNIKOVSKAYA¹, V.A. VERNIKOVSKY^{1,2}, N.YU. MATUSHKIN^{1,2}, I.V. ROMANOVA^{1,3}, I.V. VEYALKO¹, O.P. POLYANSKY⁴, YU.M. LAEVSKY^{2,5} AND K.V. VORONIN^{2,5}

¹Institute of Petroleum Geology and Geophysics SB RAS, Novosibirsk, Russia, (VernikovskayaAE@ipgg.sbras.ru);

²Novosibirsk State University, Novosibirsk, Russia;

³Queensland University of Technology, Brisbane, Australia;

⁴Institute of Geology and Mineralogy SB RAS, Novosibirsk, Russia;

⁵Institute of Computational Mathematics and Mathematical Geophysics SB RAS, Novosibirsk, Russia

Integrated geochemical, petrological and numerical modeling investigations allowed to understand the sequence of thermal events that took place during the formation of Neoproterozoic A-type leucogranites located in the structure of the Yenisey Ridge orogen, south-western framing of the Siberian craton (Vernikovskiy *et al.*, 2011; Vernikovskaya *et al.*, 2013). Two stages of leucogranite formation were distinguished: 1) 750–720 Ma, and 2) 710–630 Ma. The early stage A-type leucogranite plutons are enriched in potassium and were emplaced (≥ 10 km) in the Central Angara terrane during the final phase of its collision with the Siberian craton. This collision was followed by the subsequent accretion of the Yenisey island arc to the Siberian craton in an active continental margin setting during 710–630 Ma. At this time the second stage leucogranite plutons were formed at a shallower emplacement depth (≥ 7 km) within the Tatarka-Ishimba suture zone that was characterized by an elevated heat flow. These leucogranites associate with carbonatites and are characterized by niobium enrichment. The thermal history of the orogen was conditioned by radiogenic heat from the intrusions and their overlapping thermal fields, as well as by elevated heat flow in the suture zone.

Vernikovskiy V.A., Vernikovskaya A.E., Polyansky O.P. *et al.*, (2011), Russian Geology and Geophysics, 52, 1, 24–39. Vernikovskaya A.E., Datsenko V.M., Vernikovskiy V.A. *et al.*, Doklady Earth Sciences, (2013), 448, 2, 161–167.

Pleistocene and Holocene temperature reconstructions using earthworm-produced calcite

EMMA A. A. VERSTEEGH^{1*}, MARK E. HODSON², STUART BLACK³ AND MATTHEW G. CANTI⁴

¹Department of Geography and Environmental Science, University of Reading, Reading RG6 6DW, UK, e.a.versteegh@reading.ac.uk (*presenting author)

²Environment Department, University of York, Heslington, York YO10 5DD, UK, mark.hodson@york.ac.uk

³Department of Archaeology, University of Reading, Reading RG6 6AB, UK, s.black@reading.ac.uk

⁴Centre for Archaeology, English Heritage, Fort Cumberland, Portsmouth PO4 9LD, UK, matthew.canti@english-heritage.org.uk

Although not widely appreciated, many earthworm species are true biomineralisers, producing calcium carbonate (predominantly calcite) granules in specialised glands [1,2]. Granule production in European soils is dominated by two earthworm species, *Lumbricus terrestris* and *L. rubellus*. By means of laboratory experiments, using a wide range of temperatures (3–20 °C) and water compositions, we have established an oxygen-isotope ($\delta^{18}\text{O}$) palaeothermometer for *L. terrestris*. Granules produced by this species are consistently enriched in ^{18}O by 1.5‰ in comparison to equilibrium [3]. Well-preserved earthworm granules are commonly found in archaeological finds and buried soils up to at least ~2 Ma old. In combination with direct U-Th series dating they offer the potential for accurate temperature reconstructions for specific Quaternary time windows.

A selection of earthworm granule samples have been analysed for $\delta^{18}\text{O}$ values and U-Th composition. The samples originate from several interglacials and interstadials (e.g. Weichselian, Hoxnian, Gelasian), as well as Holocene time intervals and well-known archaeological sites (e.g. Silbury Hill, Boxgrove). Temperature reconstructions yield credible values. They show considerable intra-sample variation, which is probably a reflection of seasonal temperature variations. In addition, clear differences can be distinguished between different time intervals. Results will be discussed in context with existing climate reconstructions. We argue that $\delta^{18}\text{O}$ values of earthworm-produced calcite granules provide a useful and reliable terrestrial proxy for palaeotemperature reconstructions.

[1] Canti & Pearce (2003) *Pedobiologia* **47**, 511-521, 10.1078/0031-4056-00221; [2] Lambkin *et al.* (2011) *Pedobiologia* **54**, S119-S129, 10.1016/j.pedobi.2011.09.003; [3] Versteegh *et al.* (in press), *GCA*, 10.1016/j.gca.2013.06.020

2000 yrs of central Mediterranean change – what do proxies tell us?

G.J.M. VERSTEEGH^{1*}, A. LEIDER¹, L. CHEN¹, K.A.F. ZONNEVELD¹, A.-L. GRAUEL², S.M. BERNASCONI², M.-L. GOUDEAU³ AND G.J. DE LANGE³

¹ MARUM, Bremen Univ., 28334 Bremen Germany (*correspondence: versteegh@uni-bremen.de)

² Geological Inst. ETH, 8092 Zurich, Switzerland (stefano.bernasconi@erdw.ethz.ch)

³ Geosciences, Utrecht Univ. 3548CD, Netherlands (gdelage@geo.uu.nl).

The Mediterranean is extremely vulnerable to climate warming through decrease of the critical precipitation - evaporation (P-E) balance. Despite its relevance for society and environment, the natural dynamics of this balance and the human influence thereupon are poorly understood, especially on decadal to millennial time scales.

To increase this understanding we analysed the coastal sediments of the eastern Gulf of Taranto and the Adriatic Mud Belt. The high sedimentation rates, low bioturbation and excellent tephra, ^{14}C , ^{137}Cs and ^{210}Pb and XRF-core scanning-based regional age model allow reconstruction of terrestrial and marine dynamics with a subdecadal resolution.

We present lipid, dinoflagellate and foraminifera-based environmental reconstructions focusing on temperature, the hydrological cycle and human impact during the last two centuries, the Little Ice Age and the Roman Optimum.

The process of regional proxy calibration appeared challenging, not in the least due to having multiple proxies for the “same” environmental variable such as SST (Fig. 1), terrestrial input or productivity. This forced us to reconsider established proxy-environment relations – their accuracy and what they stand for – strongly improving them as sources of knowledge on past environmental change.

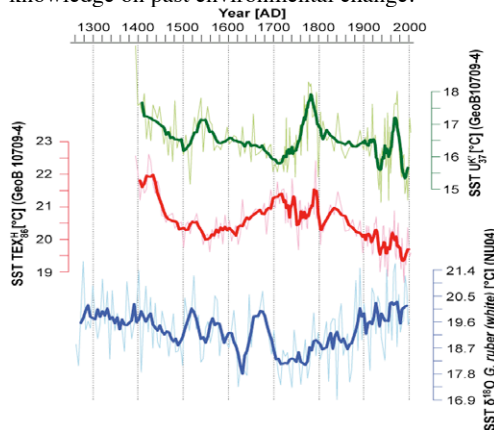


Figure 1: SST: one region, different proxies.

The myth of a highly heterogeneous Hf-Nd Eoarchean mantle and large early crustal volumes

J.D. VERVOORT^{1*}, C.M. FISHER¹ AND A.I.S. KEMP²

¹School of the Environment, Washington State University, Pullman, WA, 99163, USA (*correspondence: vervoort@wsu.edu)

²School of Earth and Environment, University of Western Australia, Perth, 6009, AUS (tony.kemp@uwa.edu.au)

One of the most fundamental and long-standing problems in Earth Sciences is the question of continental growth. Despite decades of work on this problem there is still no consensus on when the continents formed, what were the mechanisms of their formation, and how they have evolved through time. Resolution between the competing models requires insight into the earliest Earth, but the window into this critical time period is far from clear.

One reason for this uncertainty is the lack of old rocks in the geologic record. Crust older than 3.5 Ga constitutes less than 2% globally and the crust that remains is often a complicated mixture of components with different ages and isotopic compositions. Without an accurate integration of age and isotopic composition, analysis of these complicated rocks can yield meaningless information about Earth evolution.

Our solution is to integrate age and Hf isotope data from zircons of the Earth's oldest rocks. We do this using the laser ablation "split stream" technique whereby the aerosol from the zircon laser ablation is split to two mass spectrometers: one to determine U-Pb ages and the other to determine its corresponding Hf isotopic compositions. In this way we can unambiguously determine age and Hf isotopic composition on the same zircon volume.

Using this approach we find that the isotopic record for rocks older than 3.5 Ga is much less variable than has been recently claimed. Two features stand out from these data. First, there are very few samples with ϵ_{Hf} values significantly above zero prior to 3.5 Ga, indicating the lack of a widespread depleted mantle before 3.5 Ga. Second, while there are negative ϵ_{Hf} values for some ancient zircons, consistent with recycling of early-formed crust, the lack of a complementary depleted mantle reservoir from 4.4 to 3.5 Ga indicates that the volume of this early enriched (not necessarily continental) crust was modest. We conclude that widespread continental crust formation did not begin in earnest until ca. 3.5 Ga. This is consistent with both the preserved crystalline rock record and the ages of detrital zircons in the sedimentary record.

Hydrogeochemical study of the multi-aquifer system of the Sibari Plain (Calabria, Southern Italy)

G.VESPASIANO¹, C.APOLLARO¹, A.BLOISE¹, G.CIANFLONE¹, R.DE ROSA¹, R.DOMINICI¹ AND L.MARINI²

¹DiBEST, University of Calabria, I-87036 Arcavacata di Rende (CS), Italy (✉: giovanni.vespasiano@unical.it, apollaro@unical.it, andrea.bloise@unical.it, giuseppe.cianflone@unical.it, derosa@unical.it, dominici@unical.it)

²Consultant in Applied Geochemistry, I-55049, Viareggio (LU), Italy (luigimarini@appliedgeochemistry.it)

The groundwaters hosted in the Sibari Plain multi-aquifer system are heavily exploited through a large number of wells drilled for agriculture. Similar to many other coastal areas, this excessive groundwater extraction has led to intrusion of seawater. To understand the extension of this phenomenon and adopt suitable actions, a multidisciplinary approach was applied in this investigation, which is carried out in the framework of a PON project: "Study for the environmental protection and the mitigation of anthropogenic pollution in the coastal environment of selected areas of Calabria".

Hydrostratigraphic correlations, water level measurements, field determinations (electrical conductivity, temperature, pH) and laboratory chemical and isotopic analyses were carried out for 100 selected wells. In particular, high conductivity values, even >4 mS/cm, and high chloride contents, up to 1,200 mg/l, were measured in several groundwater samples (Figure 1). Interpretation of geochemical data is complicated by both the dissolution of Miocene evaporite deposits, which generates aqueous solutions with characteristics similar to those dictated by seawater ingression, and the occurrence of other processes, such as bacterial sulfate reduction and ion exchange [1, 2].

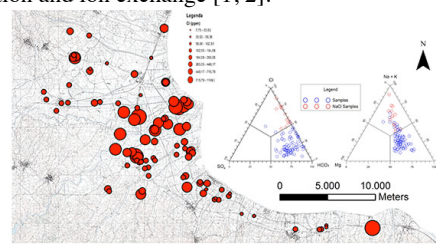


Figure 1. Map of Cl concentrations in the wells of the study area and triangular diagrams of major anions and cations.

[1] Apollaro *et al.* (2012) *Geochemical Journal*, **46** (2), 117-129. [2] Vespasiano *et al.* (2012) In *Rendiconti Online Società Geologica Italiana* **21** (2), pp. 841-842

The role of alkalis in the solubility of H₂O and CO₂ in silicate melts

FRANCESCO VETERE*, HARALD BEHRENS,
ROMAN BOTCHARNIKOV, FRANCOIS HOLTZ
AND SARA FANARA

Institute for Mineralogy, Leibniz University of Hannover,
Callinstr. 3, Hannover, D-30167, Germany

Solubility experiments were performed on phonotephritic compositions in order to investigate the role of alkalis in the behavior of water and CO₂ in magmatic systems. The investigated melt compositions are based on natural phonotephrite from Alban Hills (Ab1) with Na₂O/K₂O (in wt %) = 0.26. Two additional compositions with different Na₂O/K₂O ratios, Ab2 (Na₂O/K₂O=0.98) and Ab3 (Na₂O/K₂O=3.82), were synthesized. Experiments were run at 1250°C and 500 MPa in an internally heated gas pressure vessel. The proportions of water and CO₂ in the systems were systematically varied in the range from 0 to 1. For the calibration of carbon-related IR bands, the total carbon content of the synthesized standards was measured by combustion and subsequent IR spectroscopy using an ELTRA CS800 analyzer. Karl Fischer Titration method was used in order to quantify H₂O content in the melts. Absorption spectra were recorded in the mid-infrared (MIR) using a Bruker IFS88 FTIR spectrometer coupled with an IR-ScopeII microscope.

CO₂ is bound in the investigated glasses as CO₃²⁻ exclusively and its concentration was quantified by the peak height of the 1430 cm⁻¹ band. A drastic change was observed in the absorption coefficients, ϵ , with values of 265 ± 27.2, 228 ± 22.4 L/(mol·cm) and 308 ± 26.6, for Ab1, Ab2, and Ab3, respectively, so that the highest ϵ value is related to the Na-rich composition. There is no detectable effect of the Na/K ratio on the concentrations of dissolved H₂O and CO₂ in the melts. The solubility of CO₂ and H₂O in those melts at 500 MPa is 1.2 wt % and 10.07 wt%, respectively. Results are compared with the existing literature data and models and confirm the very high solubility of CO₂ in phonotephritic melts [1]. Our experimental data indicate that the melt composition in terms of alkali contents influences significantly the extinction coefficient values for CO₂ and that appropriate coefficients must be selected to estimate accurately the amount of dissolved CO₂ in glasses and/or melt inclusions using IR spectroscopy.

[1] H. Behrens, V. Misiti, C. Freda, F. Vetere, R. Botcharnikov, and P. Scarlato (2009). Solubility of H₂O and CO₂ in ultrapotassic melts at 1200 and 1250 °C and pressure from 50 to 500 MPa. *American Mineralogist*, *Volume 94*, pages 105–120.

Magma droplets in coexisting olivine and spinel phenocrysts hosted in the Pohang basalt (South Korea)

ENIKÓ JUDIT VETLÉNYI¹,
LÁSZLÓ ELŐD ARADI¹, CSABA SZABÓ^{1*},
ZOLTÁN ZAJACZ² AND KYOUNGHEE YANG³

¹Lithosphere Fluid Research Lab, Eötvös University,
Budapest, Hungary

²Department of Earth Sciences, Institute of Geochemistry and
Petrology, ETH Zürich, Switzerland

³Department of Geological Sciences, Pusan National
University, Busan, South Korea

*correspondance: eniko.vetlanyi@gmail.com, <http://lrg.elte.hu>

Primary silicate melt inclusions (SMI) in different host minerals provide a unique possibility to reconstruct the evolution path of the host magma. The 2 million years old Pohang alkaline basalt from South Korea contains such silicate melt inclusions hosted in olivine and spinel phenocrysts.

The Pohang basalt has porphyritic texture and contains forsteritic (mg#=0.84-0.88) olivine, Cr-bearing (cr#=0.15-0.24), high Mg (mg#=67.0-69.0) spinel phenocrysts and anorthite-rich plagioclase. The microphenocrystal groundmass consists of olivine, clinopyroxene, spinel, plagioclase and glass. Olivine and spinel phenocrysts have negative crystal shaped or rounded SMIs in size up to 150 microns in diameter. These magma droplets are identified in zoned clinopyroxene, Al-Mg-rich spinel, K-Na-Si-Al-rich residual glass, Ni-Fe-rich sulfide blebs and bubble(s). In addition, olivine daughter minerals occur in the spinel hosted SMIs.

Based on the results of homogenization experiments (with heating-quenching technique) and the equilibrium temperature calculated from olivine–spinel pairs, the homogenization temperatures are in the range of 1050-1240°C in the SMIs irrespectively their host minerals. The estimated oxygen fugacity values are -1.810 to -0.942 log units below the fayalite-magnetite-quartz buffer indicating SMIs entrapment from a relatively reduced magma. Based on geochemical data, it is suggested that the SMIs in both host minerals were entrapped at the very early stages of the crystallization process and it shows the same crystallization sequence: spinel, olivine, sulfide blebs, clinopyroxene, residual glass and bubbles.

The REE patterns of SMIs are flat or slightly decrease from La to Lu, with (La/Lu)_N between 1.6 and 17. The low La/Y and Zr/Nb ratios suggest spinel lherzolite source rock for the Pohang basalt.

Accumulation of trace elements in the Lake Baikal biota

V.A. VETROV

Institute of Global Climate and Ecology, Glebovskaya st.,
Moscow, 107-150, Russia

The objective of the work was to assess accumulation of chemical elements by different hydrobionts' species and to find out a role of biota in removing trace elements from the lake water. Contents of about 30 trace elements were studied in 1979–1987 in plankton, benthos species (hammaridae, polifera, molluscs), most common food fish and in Baikal seal. The full set of AE-, AA- and NA-analytical techniques was used.

Accumulation factors (AF, the ratio of element concentration in dry tissue to that in water dry residue) for 28 metals (Na, Al, Sc, V, Cr, Mn, Fe, Co, Ni, Cu, Zn, As, Se, Br, Rb, Sr, Mo, Ag, Cd, Sn, Sb, Cs, Ba, La, Ce, Hg, Pb, Th, U) and Br showed that there was no regular rise of a metal concentration in dry biomass when going from an initial producent (phytoplankton) up to ultimate consumer (seal). From all 29 considered elements only Rb revealed a tendency to increasing bioavailability from lower trophic levels to upper ones. As a rule, changes in AF's for other elements do not show any certain regularity depending on trophic levels.

The following metals have highest AF: in phytoplankton (AF > 30) – Al, Fe, Pb; in zooplankton (AF > 10) – Al, Fe, Cd, Ce, Hg, Pb; in molluscs (flesh, AF > 100) – Al, Mn, Fe; in seal (flesh, liver, AF > 50) – Al, Fe, Cd. Metal accumulation in fish tissues is relatively low, AF exceeds 5 only for Al, Mn, Fe, Ce.

Estimates of metal flux rates to bottom sediments were calculated on the basis that the input of autochthonic organic matter to sediments was equal to 800.000 ton/year resulting mainly from phytoplankton annual primary produce. These flux rates should be considered as semi-quantitative major estimates which just indicate that uptake of some metals (Na, Cr, u, Zn, Sr, Ag, Cd, Sn, Sb, Hg, Pb, U) by phytoplankton can be a significant route to their removal from the waterbody to the bottom sediments.

Monitoring the stability of scale inhibitors by ATR-FTIR at high pressures and temperatures in synthetic geothermal fluids

ALEXANDRA VETTER¹ AND SIMONA REGENSPURG¹

¹Helmholtz Centre Potsdam, German Research Centre for Geosciences (GFZ), International Centre for Geothermal Research (ICGR), Telegrafenberg, D-14473 Potsdam, Germany

Mineral precipitation (scaling) such as sulfates, carbonates, and oxides are well known phenomena in geothermal plants. These precipitations damage plant equipment (e.g. heat exchangers) or reduce the injectivity of the reservoirs and thus the operation lifetime of such installations. In this context, the use of environmental friendly inhibitors to avoid the formation of these mineral precipitations become attractive.

In this study, scale inhibitors based on ecologically harmless polycarboxylates are examined with respect to their thermal stability by attenuated total reflection - Fourier transform infrared spectroscopy (ATR-FTIR). The spectroscopical device is equipped with to a high pressure - high temperature reaction cell that allows measurements at up to 200 °C 200 bar. In this study, changes in signal intensity and band position for various inhibitors were monitored dependent on temperature and pressure. Additionally, the behavior of scale inhibitors in synthetic fluids at different ionic strenghtes (up to 5M NaCl) is evaluated as a function of temperature and pressure.

Sulfosalt melts from low-grade metamorphic terrains: The case of the Monte Arsiccio mine (Tuscany, Italy)

S. VEZZONI^{1*}, M. D'ORAZIO¹, C. BIAGIONI¹, A. DINI²
AND P. ORLANDI¹

¹Università di Pisa, via Santa Maria, 53, Pisa, Italy

(*correspondence: vezzoni@dst.unipi.it)

²CNR-IGG Pisa, Via Moruzzi, 1, Pisa, Italy

Sulfosalt melts formed during amphibolite/granulite facies metamorphism of pre-existing orebodies have been well documented (e.g., [1]). However, orebodies containing significant amounts of Low Melting Point Chalcophile Elements (LMCE - Ag, As, Bi, Hg, Se, Sb, Sn, Tl, and Te), could experience sulfosalt/sulfide melting at much lower metamorphic temperatures [2]. Up to date, low temperature LMCE sulfide melts have been documented, as inclusions in quartz, only at Lengenbach, Switzerland [3].

A new interesting case study was provided by the barite-pyrite-iron oxide ore deposit from Monte Arsiccio (Apuane Alps, Tuscany, Italy). The deposit originated during a Palaeozoic-Triassic sedimentary-exhalative metallogenic event and was successively metamorphosed and remobilized during the Alpine orogeny [4] under greenschist facies conditions (P = 0.6-0.8 GPa, T = 350-450°C; [5]).

Within these orebodies we discovered an exceptional Tl-Hg-As-Sb-(Ag, Cu)-Pb sulfosalt assemblage embedded in the barite-pyrite ore and in dolostones. Mineralogy is dominated by LMCE-bearing phases, mainly represented by Tl-Hg-Sb-As sulfosalts. The textural features of these assemblages (tiny veinlets pierced along grain boundaries, drop-like internal textures, low interfacial angles between sulfosalts and matrix mineral grains) is interpreted as the result of the mobilization of low-viscosity sulfosalt melts by percolation through the barite-pyrite crystal matrix, and veining in dolostones. Experimental studies (e.g., [6]) support our hypothesis, showing that thallium-bearing polymetallic sulfide systems have liquid phase fields down to very low temperatures (in the range 200-300°C). The physical (low viscosities and high density) and chemical (up to ~20% wt of Tl) characters of the inferred sulfosalt melts suggest that LMCE melt migration can be an effective mechanism of metal mobility in low-grade metamorphic terrains. The Tl-Hg-As-Sb-(Ag,Cu)-Pb sulfosalt assemblage from Monte Arsiccio likely documents the lowest temperature natural sulfosalt melt ever described.

[1] Tomkins *et al.* (2007) *J. Petrol.* **48**, 511-535. [2] Frost *et al.* (2002) *Can. Min.* **40**, 1-18. [3] Hoffman (1994) *Mineral. Deposita* **29**, 439-442. [4] Lattanzi *et al.* (1994) *Mem. Soc. Geol. It.* **48**, 613-619. [5] Fellin *et al.* (2007) *Tectonics* **26**, 1-22. [6] Moh (1991) *N. Jb. Miner. Abh.* **163**, 197-270.

Magma emplacement and sulfide deposition after skarn formation at Campiglia Marittima, Tuscany

S. VEZZONI^{1*}, A. DINI² AND S. ROCCHI¹

¹Università di Pisa, via Santa Maria 53, Pisa, Italy

(*correspondence: vezzoni@dst.unipi.it)

²CNR-IGG, via Moruzzi 1, Pisa, Italy

Most economic skarn deposits are related to magmatic intrusions and a general correlation exists between the composition of igneous rocks and skarn ore type [1]. The Cu-Pb-Zn-Ag skarn deposit of Campiglia Marittima (Southern Tuscany, Italy) is the skarn deposit in which a mineralogical zoning of skarn bodies has been first described [2]. It has been considered as a classic example of exoskarn with an outward zoning sequence developed from a main axial dyke of mafic porphyry: magnetite ⇒ ilvaite ⇒ clinopyroxene ⇒ marble [3]. According to this model, the skarn deposit of Campiglia Marittima represents a key example for the understanding of the spatial and temporal evolution of a metasomatic system, from the local source of ore fluids (mafic porphyry) to the final products (skarn and sulfides).

The new field and laboratory data collected for Campiglia Marittima skarn deposit indicate that this classical model is too simplistic. Geological mapping of about 20 km of tunnels/shafts shows that: 1) mafic porphyry does not form a single axial dyke but small dykelets and pods that crosscut the skarn bodies and fill the skarn pockets; 2) the skarn bodies do not show symmetric, outward growing, mineralogical zoning, but they are formed by several metasomatic units displaying distinct mineral parageneses and growing patterns.

The later intrusion of mafic porphyry heated up the skarn bodies, inducing significant prograde back-reactions on skarn minerals: 1) ilvaite in direct contact with mafic porphyry was replaced by magnetite + hedenbergite; 2) pyrrothite, pyrite and chalcopyrite variably replaced ilvaite for several meters from the contacts; 3) hedenbergite crystals suffered overgrowth of Mg-rich rims.

Thus, a direct causality between magma emplacement, fluid release and skarn/ore formation, at a local scale, is not confirmed and must be searched at a larger, crustal scale. The magmatic source of skarn fluids is inferred to be a deeper, mafic intrusion. The shallow level of emplacement of such intrusion controlled the early exsolution of skarn fluids, and the later extraction of magmas that fed the mafic porphyry system, forming the main sulfide ores.

[1] Meinert *et al.* (2005) *Econ. Geol.* **100/2**, 299-336. [2] Rath (1868) *Deutsch. Geol. Gesell. Zeitschr.* **20**, 307-364. [3] Bartholomé & Evrard (1970) *Int. Union Geol. Sci. (pub.) Ser. A* **2**, 53-57.

Influence of tectonics on magma residence times at Mt. Etna volcano

MARCO VICCARO^{1*}, DONATELLA BARCA², WENDY A. BOHRSON³, MARISA GIUFFRIDA¹, EUGENIO NICOTRA^{1,2} AND BRADLEY W. PITCHER^{3,4}

¹University of Catania, Dept Biol Geol Environ Sci, Corso Italia 57, I-95129, Catania, Italy (*corresponding author: m.viccaro@unict.it)

²University of Calabria, Dept Biol Ecol Earth Sci, Ponte P. Bucci 12B, 87036, Arcavacata di Rende (CS), Italy

³Central Washington University, Dept Geol Sci, Ellensburg, WA 98929, USA

⁴Oregon State University, College Earth Ocean Atmos Sci, Corvallis, OR 97331-5503, USA

Trace element zoning in plagioclase from the historic (pre-1971 AD) and recent (post-1971 AD) activity of Mt. Etna volcano was here used to evidence changes in the feeding system dynamics during the last 250 years. The observed textural characteristics of crystals include both near-equilibrium and disequilibrium textures [1]. The An variation along core-to-rim profiles on selected crystals with different types of textures was evaluated particularly versus the Sr/Ba ratio. At rather comparable average An contents, plagioclase crystals representative of near-equilibrium crystallization from the magma display very distinct Sr/Ba ratios through time (~6 and ~17 in historic and recent lavas respectively). Recent plagioclases also exhibit generally higher potassium contents than the historic ones at the same evolutionary degree. Although contamination due to wall-rock assimilation may have played a role, we suggest here that the features are dominated by input of a K-rich and Ba-poor end-member into the feeding system that becomes evident particularly after the 1971 AD eruption. Magma residence times, which have been calculated through Sr diffusion modeling on plagioclases, are also related to the distinct geochemical signature observed. Calculations give average residence times of ~40 years for crystals of the historic activity and of ~20 years for the post-1971 AD plagioclases. Our estimations strongly agree with geophysical data that highlight an increased E-W directed extension rate within the upper 10 km of the crust before major eruptive events of the last two decades. Differences in the timescales of magma storage observed over the last 250 years can be therefore attributed to the dominant role played by volcano-tectonics on the uppermost part of the feeding system.

[1] Viccaro *et al.* (2010), *Lithos* 116, 77-91.

Insights into the magmatic processes leading to the Holocene caldera eruption of Rinjani, Indonesia

C. M. VIDAL^{1*}, N. METRICH¹, J.-C. KOMOROWSKI¹, I. PRATOMO², F. LAVIGNE³ AND SURONO⁴

¹IPG-Paris, Sorbonne Paris Cité, Univ. Paris 7, UMR-CNRS 7154, Paris, France (*correspondence: vidal@ipgp.fr)

²Museum of Geology, Bandung, Indonesia.

³LGP, Univ. Paris 1, UMR CNRS 8591, Paris, France.

⁴CVGHM, Geological Agency, Bandung, Indonesia.

The cataclysmic caldera-forming eruption at Rinjani volcanic complex (Lombok, Indonesia) ranks among the largest explosive eruptions of the Holocene, and is possibly associated to the largest stratospheric release of volcanic sulfur over the past 7 ka [1]. It produced a succession of plinian fallout and pyroclastic flow deposits. Whole-rock analysis of juvenile pumices from plinian fallout units indicates a range of trachyandesitic to trachytic magma batches (61-64 wt% SiO₂). These magmas display variable enrichments in both major and trace elements indicative of a dominant process of crystal fractionation and of the presence of a zoned (or complex) magma chamber. They also share Nb/Th (0.9) and Nb/Zr (0.04) ratios with those of Rinjani high alumina basaltic scoriae, suggesting that they belong to the same suite. As a whole the compositional range of our samples matches that of the Rinjani calc-alkaline suite [2].

The mineral paragenesis consists of plagioclase (An₄₁ to An₈₀), clinopyroxene (Mg# 0.75), orthopyroxene (Mg# 0.71), amphibole (pargasitic Hbl/magnesio Hbl) and Fe-Ti oxides. Biotite is rarely found. Apatite shows a wide range of volatile contents: F 1.8-0.25 wt%, Cl 0.9-0.45 wt% and S 1300-<100 ppm. Melt inclusions analyzed in plagioclase handpicked from a basal fallout unit represent the most evolved trachytic term (65-70 wt% SiO₂, on anhydrous basis). They contain 3.3-5.1 wt% of H₂O, 2200-3700 ppm of Cl, 440-600 ppm of F, and <100-490 ppm of S. CO₂ is below FTIR detection limit. The erupted magma was thus rich in H₂O and Cl but relatively depleted in sulfur. The estimated P_{H_2O} for this range of water contents is 180-100 MPa [3] that is consistent with prolonged magma ponding at crustal level.

We provide the very first constraints on the pre-eruptive magma conditions and discuss the processes controlling sulfur behavior.

[1] Lavigne *et al.* (2013) *PNAS*, submitted. [2] Foden (1983) *J. Petrol.* 24, 98-130. [3] Moore *et al.* (2008) *Rev. Mineral. Geochem.* 69, 333-358.

Dissolved mercury in Funil reservoir, RJ, Brazil

M. S. M. VIDAL^{1*}, M. M. FERREIRA¹,
S. R. PATCHINEELAM¹, S. SATYRO-FERREIRA²,
T. C. M. SOARES³, I. K. BELMINO³
AND L. D. LACERDA³

¹ Environmental Geochemistry Department, Federal University, Niteroi, RJ, Brazil (*correspondence: celavidal@yahoo.com.br)

² Federal University of Rio de Janeiro, Rio de Janeiro, Brazil

³ Federal University of Ceará, Fortaleza, CE, Brazil

Introduction

Diffuse emissions of several contaminants are linked to water and energy, as the need for these leads to modification of frequency, magnitude and nature of the contribution of water and sediments, mainly due to interventions in the drainage basins such as the reservoirs formation. Among these contaminants is mercury (Hg), which offers known health risk [1]. Therefore, this study evaluated the effect of the Funil dam, located in Resende, RJ, SE Brazil, in the level of Hg dissolved in water at three points of the Paraíba do Sul River (RPS) during 1 year.

Results

Sample	ago/10	set/10	out/10	nov/10	dez/10
Upstream	1,38	0,15	0,13	1,60	1,65
Reservoir	0,59	0,08	<0,05	4,58	0,23
Downstream	0,87	0,11	0,16	3,28	1,61

Sample	fev/11	mar/11	abr/11	jun/11	jul/11
Upstream	5,00	2,70	10,12	2,49	1,16
Reservoir	3,02	4,55	4,92	1,11	26,42
Downstream	9,44	1,87	2,64	3,12	0,98

Figure 1: Hg concentrations in Paraíba do Sul river (ng.L⁻¹).

Samples showed concentrations below the maximum allowed by law [2]. Although the basin RPS has compromised quality of water in several parts, this region does not suffer significant contamination by the element studied.

[1] WORLD HEALTH ORGANIZATION. *Environmental Health Criteria - mercury*. Geneva: WHO, 1992. [2] BRASIL. (CONAMA). *Resolução n. 357*. 17 de março de 2005.

Hydrogeochemical characteristics of water source in the area of Lazarevo village (from the aspect of balneology)

M. VIDOVIĆ¹, V. GORDANIĆ^{2*}, V. SPASIĆ-JOKIĆ³,
A. ĆIRIĆ⁴ AND A. SEKE⁵

¹University of Belgrade, IHTM,
(correspondence: mivibgd@yahoo.com)

²University of Belgrade, IHTM, (gordanicv@gmail.com)

³Faculty of Technical Science, University of Novi Sad,
Belgrade (svesna@uns.ac.rs)

⁴Geological Survey of Serbia, (abciric@eunet.rs)

⁵University of Belgrade, RGF (anaseke@gmail.com)

Geological data obtained from boreholes for oil and gas were used for geological mapping of "Jaša Tomić" sheet 1:100.000, in the area of Pannonian basin represents a special geothermal province (M. Milivojević, 1989) and one complex hydrogeothermal conductive system with four mutually separated reservoirs of underground water. A first hydrogeological system includes Upper Pontian sediments about 2 km thick in Northern Banat and a few tenths of meters in peripheral parts of the basin. In deeper parts clayey-marly sand prevail. In shallower parts larger parts presence of sandy-pebbly sediments of lacustrine and river origin are dominant. Sand water-bearing sediments parts presence vary from 1 to 50 m in thickness. The source of mineral water is located nearby structural boreholes Lazarevo (La-1), Topolovac (Tc-1) and borehole for water supply of village Lazarevo.

HCO ₃	SO ₄	Cl	Na	K	Mg	Ca	Br
569	3655	2744	3076	273	286	118	20
1464	2120	459	1740	1	101	69	5

Table 1: Physical-chemical composition (mg/l) of mineral water in Lazarevo (well) – First raw – data from 1957; second raw – data from 2012

According to results of laboratory researches (2012) water is medium mineralized low alkaline subthermal, Na-Mg-Ca, SO₄-HCO₃-Cl which classifies it as low alkaline saline bitter water. Water which was analysed in the period of 1957 belongs to medium mineralized low alkaline type of water, Na-Mg-Ca, SO₄-Cl-HCO₃ which classifies it as saline-muriatic-bromine-bitter water which is very healing. Variations in chemical composition are obvious, and they depend on the regime of underground water and aquifer type. Researches related to this are planned in the following period.

Acknowledgement: This work has been financed by the Ministry of Science and Technological Development of the Republic of Serbia (project No. OI 176018).

Hf-Nd isotope decoupling in Early Precambrian seawater

S. VIEHMANN^{1,3*}, J.E. HOFFMANN^{1,2}, C. MÜNKER²
AND M. BAU³

¹ Steinmann Institut, Universität Bonn, Germany

² Institut für Geologie und Mineralogie, Universität zu Köln, Germany

³ Jacobs University Bremen, Earth and Space Science Program, Germany

* present address, s.viehm@jacobs-university.de

Banded Iron Formations (BIFs) are Precambrian marine chemical sediments that are archives of the trace element and isotope compositions of ancient seawater. Here we report Hf and Nd isotope data of pure chert and magnetite layers from the ca. 2.7 Ga Temagami BIF (Superior Province, Canada), determined by isotope dilution techniques and MC-ICPMS. Sample aliquots were also analysed for trace element systematics by quadrupole ICP-MS.

Shale-normalised REY patterns of the BIFs are similar to those of modern seawater and other pure Archean seawater precipitates. Enrichment of HREE compared to LREE, positive La and Gd anomalies, and super-chondritic Y/Ho ratios indicate a purely seawater-derived REY composition. Lacking Ce anomalies and strong positive Eu anomalies reveal anoxic conditions (with respect to Ce⁴⁺/Ce³⁺) and REY input into seawater via high-T hydrothermal fluids. Non-chondritic Zr/Hf ratios indicate minor influence of detrital aluminosilicates and a seawater origin of Hf. Samarium-Nd and Lu-Hf isochron ages are within error of the published depositional age of the ~2.7 Ga Temagami IF. Initial $\epsilon\text{Nd}_{2.7\text{Ga}}$ values range from +0.2 to +3.0, but six of the nine samples cluster around +1. In contrast, initial $\epsilon\text{Hf}_{2.7\text{Ga}}$ values point towards heterogeneous, strongly radiogenic compositions (+6.7 to +24.1). In the $\epsilon\text{Hf}-\epsilon\text{Nd}$ diagram, the Temagami BIFs lie well above the 'terrestrial array' and exhibit significantly different $\epsilon\text{Hf}-\epsilon\text{Nd}$ values than Temagami shale and hinterland tholeiites and adakites which tapped the Abitibi mantle [1]. Therefore, Temagami seawater Hf was even more radiogenic than ambient mantle, suggesting that selective weathering processes (including the zircon effect) already operated in the Neoproterozoic, leading to the decoupling of the Hf-Nd isotope systematics, that is well known from modern seawater [2] and Cenozoic FeMn precipitates [3]. This suggests that by 2.7 Ga ago, a significant fraction of evolved continental crust was exposed above sealevel and subject to terrestrial weathering.

[1] Polat & Münker (2004) *Chem. Geol.* **213**, 403-429. [2] Stichel *et al.* (2012) *GCA* **94**, 22-37. [3] Albarède *et al.* (1998) *Geophys. Res. Lett.* **25**, 3895-3898.

Zn isotope fractionation in pristine larch forest developed on permafrost-dominated soils in Central Siberia

VIERS J^{1*}, A.S. PROKUSHKIN², O.S. POKROVSKY¹, A.V. KIRDYANOV², C. ZOUTEN¹, F. CHABAUX³,
P. OLIVA¹ AND B. DUPRE¹,

¹ University of Toulouse – GET laboratory – OMP – Toulouse – France

² V.N. Sukachev Institute of Forestry – SB RAS – Krasnoyarsk – Russia

³ University of Strasbourg – LHyGeS laboratory – Strasbourg – France

*jerome.viers@get.obs-mip.fr

Towards a better understanding of Zn transport and storage in the tree-soil-mineral-river system, stable Zn isotope fractionation was studied in main biogeochemical compartments of a pristine larch forest of Central Siberia developed over continuous permafrost basaltic rock lithology.

It appears that Zn isotopes are not fractionated within the soils compared to the basaltic rocks. By contrast Zn isotope fractionation is observed between plants (larch) and soil and within the plant itself. Among the different habitats of the region receiving different amount of solar radiation and nutrients (South- and North-facing slope, peat bog) we observe systematic habitat-specific differences of Zn isotopic composition between whole plant and soil. As there is no apparently different physiological behavior of Zn within the same species within the different habitats we suggest the key role of Zn speciation in the soil solution to explain these differences. We observe a change of Zn isotopic composition in the larch needles within the course of the growing period suggesting a change in the nutrients source. Although the isotopic measurements do not allow distinguishing between mineral and organic source of Zn in natural waters, it can be concluded that, within the climate evolution and the increase of the thickness of thaw layer in peat bog environments, the global value of $\delta^{66}\text{Zn}$ in Siberian larch forest will increase.

New constraints on K-Pg boundary environmental changes with Li isotopes

N. VIGIER¹, G. RAVIZZA², K. NAGASHIMA²,
R. D. NORRIS³, S. PETIT⁴, D. BEAUFORT⁴
AND A-M KARPOFF⁵

¹CRPG, CNRS, Université de Lorraine, Nancy, France

²University of Hawaii at Manoa, Honolulu, USA

³SCRIPPS, UCSD, La Jolla CA, USA

⁴IC2MP, CNRS, Université de Poitiers, France

⁵IPGS, CNRS, Université de Strasbourg, France

Climatic and oceanic perturbations associated with the Deccan Traps eruption and with the Chicxulub impact are still strongly debated. Because lithium isotopes significantly fractionate during low temperature processes, the composition of mineral phases formed across the K-Pg boundary can provide quantitative information concerning environmental changes at that time. In this study, we investigate in parallel the Li isotope composition of both marine authigenic smectite and benthic foraminifera over a time window of 3 Ma. Comparing both phases is important because the $\delta^7\text{Li}$ of foraminifera may be subject to vital effects during calcification, while authigenic clays are not. The objectives are: 1/ To determine the long-term variation of seawater $\delta^7\text{Li}$ due to changes in continental flux and alteration rate and 2/ To detect short-term variations of the ocean carbon chemistry, recorded by Li isotope fractionation during foraminifera growth.

Li isotopes are measured in clays by MC-ICP-MS, and in benthic foraminifera tests using the ims 1280 ion microprobe, at University of Hawaii. Initial results show a limited variation ($<2\text{‰}$) of clay $\delta^7\text{Li}$ across the Ir-rich layer, indicating little disturbance of the ocean Li at that time. Compared with 0-6 Ma seawater, K-Pg seawater $\delta^7\text{Li}$ was 5.5‰ lower, suggesting a lighter input from continents due to more intensive and more congruent continental alteration.

In contrast, contemporaneous benthic foraminifera tests vary significantly on time scales much shorter than the oceanic residence time of Li (≈ 1.5 Ma), too short to attribute to changes in the $\delta^7\text{Li}$ of the global ocean. Also, these variations precede deposition of the Ir-rich layer. These results strongly suggest changes in Li isotope fractionation through time. The $\delta^7\text{Li}$ of cultured foraminifera indicate a strong dependency on the DIC concentration, but no impact of pH and T on Li isotope fractionation during foraminifera growth. If these data are representative of natural conditions, then our results indicate significant short-term oscillations of ocean DIC before Chicxulub, possibly related to eruption events in the Deccan.

Wild rats as sentinel animals in the assessment of asbestos pollution: a pilot study

R. VIGLIATURO^{1*}, M. ARDIZZONE³, C. VIZIO⁴,
S. CAPELLA¹ AND E. BELLUSO^{1,2}

¹Dip. di Scienze della Terra, Università di Torino, Torino, Italy; ruggero.vigliaturo@unito.it, silvana.capella@unito.it, elena.belluso@unito.it

²IGG CNR, Torino

³via Bligny 4, Casale M.to, Italy; mikeardi@libero.it

⁴reg. Bocca 16/a, Cellamonte, Italy; carlottavizio@yahoo.it

Asbestos fibres are potential carcinogens to humans when reach lungs. Animals can be served as sentinels being exposed like humans to contaminants. Recently investigations on the asbestos burden to evaluate the exposure level in the environment has been successfully carried out on cows [1]. To investigate in towns where these animals don't live, rats as diffused species can be considered. Rats live in colonies in a circumscribed territory. The use of rats as "sentinel animals" would allow to carry out an innovative monitoring method with important practical applications. The aim is to identify the neighbourhoods of the city at risk, by searching for asbestos fibres in the lung tissue of wild rodents captured in specific areas of the Casale Monferrato town. Three kinds of asbestos (crocidolite, chrysotile and asbestos tremolite/actinolite) and five groups of non asbestos fibres (metallic oxides; Al-, Ti-, and vitreous silicates; phyllosilicates) have been detected in the rat lungs by SEM-EDS investigations. These data together with that obtained from positive and negative control rat lungs showed rats are suitable sentinel animals to detect air dispersion hidden sources of asbestos and other inorganic fibres. Regarding the studied area, crocidolite and asbestos tremolite/actinolite are related respectively to anthropogenic and natural sources. Therefore a complete investigation would allow to identify sites of noxious inorganic phase potential dispersion in order to adopt tools to contain or eliminate it before the general population can be damaged.

[1] FORNERO E., BELLUSO E., CAPELLA S., BELLIS D. (2009). *SCI TOTAL ENVIRON*, 407, 1010-1018

Hydrogen mobility in Wadsleyite at low temperatures

E. VIGOUROUX¹, J. INGRIN¹, C. DEPECKER¹,
N. BOLFAN-CASANOVA² AND D. FROST³

- ¹UMET - UMR CNRS 8207 - Université Lille 1 – Cité Scientifique, 59655 Villeneuve d'Ascq, France (eric.vigouroux@ed.univ-lille1.fr, jannick.ingrin@univ-lille1.fr, christophe.depecker@univ-lille1.fr)
²LMV - UMR CNRS 6524 - Université Blaise Pascal – 5 rue Kessler, 63038 Clermont-Ferrand, France (n.bolfan@opgc.univ-bpclermont.fr)
³BGI – Bayreuth University– Universitätsstrasse, 95447 Bayreuth, Germany (dan.frost@uni-bayreuth.de)

Mantle wadsleyite may incorporate large amount of H in its structure (up to several wt % H₂O). A good knowledge of hydrogen diffusion in wadsleyite and its relationship with electrical conductivity is critical to estimate the amount of water present in the transition zone. We present here the results of diffusion experiments realized in deuterium-rich atmosphere at room pressure between 300°C and 450°C. Wadsleyite samples have been synthesized from forsterite powder with a minute amount of water by multi-anvil presses at 16 GPa - 1100°C. The average grain size is less than 5 μm and the water content is around 0.01 wt% H₂O. All samples show major IR peaks at 3372, 3350 and 3322 cm⁻¹ with minor peaks at 3726, 3665, 3615, 3523, 3472 and 3208 cm⁻¹.

We observed the same OH extraction behavior in the three slides annealed: extraction kinetics of bands 3726, 3523, 3372 and 3208 cm⁻¹ is almost 100 times slower than other bands while deuteration affects all the bands in the same way. We obtain an activation energy of 175 kJ/mol for extraction of the “fast” decreasing bands and an activation energy of 202 kJ/mol for H-D exchange.

Our data extrapolated to high temperatures suggest that hydrogen mobility in Mg-wadsleyite is two orders of magnitude higher than extraction kinetics from Hae *et al.* (2006) ($D=8.3 \times 10^{-11}$ m²/s at 1000°C) or it implies an activation volume of 11,3 cm³.mol⁻¹. If we neglect the effect of a potential activation volume, we predict a concentration of hydrogen two orders of magnitude smaller.

[1] Hae *et al.* (2006) *Earth Planet Sci Let* **247**, 141-148.

Half lives of nuclides for geological use: 2012 evaluation for ⁸⁷Rb

I.M. VILLA^{1,3,4}, M.L. BONARDI^{2,5}, P. DE BIÈVRE^{2,6},
N.E. HOLDEN^{2,7} AND P.R. RENNE^{1,8,9}

- ¹International Union of Geological Sciences
²International Union of Pure and Applied Chemistry
³Universität Bern, CH-3012 Bern, Switzerland; igor@geo.unibe.ch
⁴Università di Milano Bicocca, I-20126 Milano, Italy
⁵LASA, Università di Milano; INFN, I-20090 Segrate, Italy
⁶Duineneind 9, B-2460 Kasterlee, Belgium
⁷Brookhaven Natl Laboratory, Upton, NY 11973, USA
⁸BGC, 2455 Ridge Road, Berkeley, CA 94720, USA
⁹EPS, U of California at Berkeley, Berkeley, CA 94720

The IUPAC-IUGS joint Task Group “Isotopes in Geosciences”, TGIG, has evaluated the published measurement results for the decay constant (i.e. half life) of ⁸⁷Rb. A significant part of our evaluation was the effort to follow strict metrological criteria (VIM, 2012) in our assessment of the measurement uncertainties according to GUM (2008).

The ⁸⁷Rb half life was estimated by three groups using totally independent approaches. Kossert (2003) determined the specific activity of Rb salts by liquid scintillation counting. This approach assumes that inter-sample variations are due to stoichiometry. Nebel *et al.* (2011) compared Rb-Sr and U-Pb ages of cogenetic minerals. This approach assumes that certain natural samples behave “ideally”, i.e. all the relevant ages are expected *a priori* to be equal, and relies on control on the samples’ petrology. Rotenberg *et al.* (2012) measured the radiogenic ⁸⁷Sr accumulated in a batch of Sr-free Rb salt over 35 years. This approach relies on having performed precise and accurate measurements of the concentration and isotopic composition of the Sr present in the RbClO₄ at the time of crystallisation. The three sets of experiments yield indistinguishable results, which is a good indication that systematic biases were either coincidentally of the same magnitude and direction in three radically different experimental designs, or negligible after accurate correction. The resulting best estimates are $\lambda_{87} = (1.395 \pm 0.002) \times 10^{-11} \text{ a}^{-1}$ (1s uncertainty), $t_{1/2} = 49.7 \pm 0.1 \text{ Ga}$.

- [1] GUM (2008) Guide to expression of uncertainty in measurement. www.bipm.org/en/publications/guides/gum.html
[2] Kossert K. (2003) *Appl. Rad. Isot.* **59**, 377 [3] Nebel O., Scherer E.E., Mezger K. (2011) *EPSL* **301**, 1-8. Rotenberg E., *et al.* (2012) *GCA* **85**, 41-57. [4] VIM (2012) The International Vocabulary of metrology. <http://www.bipm.org/vim>

Observations and modeling of sinking particle speeds in the Twilight Zone using ^{210}Po - ^{210}Pb deficit

M. VILLA*¹, F. DE SOTO², F. LE MOIGNE³, S. GIERING³, R. SANDERS³ AND R. GARCÍA-TENORIO¹

¹Universidad de Sevilla, Dpto. Física Aplicada II, 41012, Sevilla, Spain (*correspondence: mvilla@us.es)

²Universidad Pablo de Olavide, Dpto. Sistemas Físicos, Químicos y Naturales, Sevilla, Spain

³Department of Ocean Biogeochemistry and Ecosystems, National Oceanographic Centre, Southampton, UK

A one-box model of ^{234}Th uptake and removal in the water column is widely used to calculate downward ^{234}Th and POC flux. The elemental pair of ^{210}Po - ^{210}Pb is an alternative method to estimate carbon fluxes which should offer significant advantages due to its different half-life (138 days) and biogeochemical behaviour. Due to its long half-life, a ^{210}Po deficit is maintained below the euphotic zone and penetrates much further into the twilight zone (100-1000 m) than ^{234}Th . Hence ^{210}Po and ^{210}Pb profiles and ^{210}Po deficit could be used to broaden our knowledge of the twilight zone.

To address this question several water column profiles were sampled during two expeditions of RSS Discovery on the North Atlantic, PAP site (summer 2009) and Irminger Basin (summer 2010). The most important contribution of this work is that ^{210}Po activity down the water column is modelled using a one-box inverse model. Modelled ^{210}Po activities are in very good agreement with the analysed values and the new approach provides information to understand ^{210}Po and ^{210}Pb concentration profiles on the water column. A key output from the model is average downward sinking velocities. Minimum and maximum values range from $20\text{ m}\cdot\text{d}^{-1}$ at 50 m to $150\text{ m}\cdot\text{d}^{-1}$ at 400 m. Averaged values at PAP and Irminger areas do not follow a clear geographical pattern; however, an increase with depth is observed. Finally, the contribution of slow sinking particles into the twilight zone and its implication to the carbon storage is discussed.

Adsorption experiments of arsenic and lead onto barite

F. SAMPERIO JIMÉNEZ¹, R. E. VILLANUEVA-ESTRADA^{2*}, P. VILLANUEVA-GONZÁLEZ³, C. CANET² AND F. MARTÍN-ROMERO⁴

¹ Facultad de Ingeniería, UNAM

² Instituto de Geofísica, UNAM

(*correspondence: ruth@geofisica.unam.mx)

³ Facultad de Química, UNAM

⁴ Instituto de Geología, UNAM

The work consists in the study of the retentions of arsenic and lead onto the barite surface. The barite sample is from a deposit of Múzquiz (Coahuila, México). The batch adsorption experiments using salts of As(III), As(IV), and Pb(II) was according [1]. A measurement of the pHPZC of the barite sample was determined by acid-base titrations.

	As(V)	As(III)	Pb(II)
pH adsorption	8.35	8.55	8.45
$C_{t=0}$ (mg/L)	5.92	9.69	7.07
$C_{t=24\text{ h}}$ (mg/L)	5.08	9.67	< L.D.
Adsorption %	14	0.17	100
R_d (mL/g)	3.6	0.04	2951

Limit of detection (L.D.) for lead is 0.05 mg/L

Table 1. Results of the adsorption experiment. The adsorption was calculated taking account the concentration of the dissolved species. Calculation of the distribution ratio (R_d) between the solutes and barite mineral was calculated as Griffin *et al.* [1].

The determination of the pH_{pzc} of the barite is about 9.8. The present study shows that the barite could be used as adsorbent for Pb(II). Although the adsorption of arsenic is lower, is more effective for As(V) than for As(III). At the pH of adsorption the As(III) the predominant species is not charged (H_3AsO_3), but the As(V) occurs as HAsO_4^{2-} and can be electrostatically attracted to the positive surface of the barite.

[1] Griffin *et al.* (1986) Hazardous and Industrial Solid Waste Testing and Disposal 60, 390-408.

Successive geotherms, Granitic production and evolution of the lower crust in a post collisional context

ARNAUD VILLAROS¹, JEAN-FRANÇOIS MOYEN²
AND MICHEL PICHAVANT¹

¹LabEx VOLTAIRE. IStOrléans, arnaudvillaros@gmail.com

²LMV, université Jean Monnet, St Etienne

Post-collisional context is commonly associated with production of large amount of peraluminous granitic magmas produced from the melting of crustal material. The variability of the produced granite commonly varies from leucogranitic to granodioritic and are mostly peraluminous. The South-Eastern French Massif Central (EFMC) region record several evidence for crustal melting revealed by migmatitic and granitic bodies providing ~30 Ma history of peraluminous granite production. Previous thermobarometric studies provides records for two successive melting event: 1) a biotite stable event at ~314Ma (720°C and 5 kb) 2) a bitotite breakdown melting event constrained at ~301Ma (850°C 4kb) This suggests geotherms evolution from 45 °C/km to 70°C/km in 13Ma.

A thermodynamic modelling approach considering a 20km thick pile of crustal material undergoing successive geotherm evolving from 25°C/km to 70°C/km with starting conditions between 3 and 10 kb. Along this evolution our approach allows successive melt extraction and the monitoring of melt compositional variability, residuum evolution and mineral phases modal and compositional variabilities according to depth, geotherm and composition of the source.

Over the 5 crustal sources used as starting composition for the model, 305 individual partial melting reactions are triggered. Melt and peritectic phases produced provide a variability that suggest the importance of source composition in matter of granite production for some element and ratios (K/Na, X_{Mg}). Compared to regional granites (EMCF). Most of the granites produced in the post collisional context of the EFMC can be reproduced by either melt only (leucogranite) or melt in addition to peritectic material produced along with melt (granite to granodiorite). In the same way, the relative-time constrain provided by the approach shows that it is possible to produce simultaneously heterogeneous granitic magmas in respect to source protolith and depth. Identically, the residual crust undergo a very variable evolution depending on protolith leading to an heterogeneous granulitic lower crust.

Phosphorous Speciation in Atmospheric Deposition Samples in the East Mediteranean

KALLIOPI VIOLAKI¹, MARIA KANAKIDOU¹
AND NIKOS MIHALOPOULOS¹

¹ Environmental Chemistry Processes Laboratory, Department of Chemistry, University of Crete, P.O. Box 2208, 71003 Heraklion, Greece; kviolaki@chemistry.uoc.gr; mariak@chemistry.uoc.gr; mihalo@chemistry.uoc.gr

The interactions between phosphorus-carbon cycles and climate are expected to become an increasingly important determinant of the Earth biogeochemical cycles. The oceans generally act as an important sink of atmospheric CO₂. P limitation of marine primary productivity could play a key-role in this natural process, affecting indirectly the global warming. East Mediterranean Sea (EMS) is P-limited and new knowledge could be arisen by defining the role of organic and inorganic forms of atmospheric P deposition into the marine environment.

This study aims to investigate the sources, the forms and the biogeochemical significance of soluble and insoluble atmospheric P over the EMS. Wet (n=55) and bulk deposition samples (n=76) have been collected during four-year period (2008-2009 and 2011-2012) and analyzed for P speciation. Following the analytical protocol referred in Standard Methods for the Examination of Water and Wastewater (20th Edition), Total Dissolved acid hydrolyzed Inorganic Phosphorous (TDIP) was determined after mild oxidation of sample. Total Dissolved Phosphorus (TDP) was measured after the acid digestion of samples according to Persulfate Digestion Method. Dissolved organically bound phosphates (DOP) were determined by subtracting TDIP from TDP. Disolved Reactive Phosphorous (DRP) was determined as HPO₄²⁻ with Ion Chromatography (IC).

To investigate the role of air mass origin in the P speciation in rainwater, rain samples have been classified in two classes (N/NW and S/SW) corresponding to the main wind sectors influencing the area. DOP is associated with S/SW winds that enrich the atmosphere over the EMS with African dust. N/NW winds transport anthropogenic pollution from N/NW Europe and are associated mainly with DRP. In addition, P solubility changes have been observed and are analysed.

Dry deposition of P is found to be higher than the wet one and is dominated by DRP that is so far known as the most bioavailable form of P and thus is expected to have significant impact on the marine ecosystems.

Modelling carbon cycle and major cations weathering fluxes in a young temperate forest

A. VIOLETTE^{1*}, M. CARNOL², M. AUBINET³,
Y. GODDERIS⁴, M. ERPICUM⁵, B. HEINESCH³
AND L. FRANÇOIS¹

¹UMCCB, Université de Liège, Bât. B5c, 17, Allée du Six
Août, B-4000 Liège, Belgium (*correspondence:
aviolette@ulg.ac.be)

²LEVM, Institut de Botanique, Université de Liège, 27
boulevard du rectorat, B-4000, Belgium

³Unité de Physique des Biosystèmes, GxABT, Université de
Liège, 8 av. de la Faculté, B-5030 Gembloux, Belgium

⁴GET, OMP, 14 avenue Edouard Belin, 31400 Toulouse,
France

⁵Département de Géographie, Université de Liège, Bât. B11,
2, Allée du Six Août 17, B-4000 Liège, Belgium

Chemical weathering provides mineral nutrients to the soil solution. The productivity and resistance of the vegetation is dependent to its capacity to find and adsorb these nutrients. The vegetation itself plays an active role in mineral dissolution by the exudation of organic acids. Indirectly, (i) the nutrient uptake can deplete them in the soil solution and (ii) the soil respiration increases the pCO₂. Both indirect processes also favour the chemical weathering. In poor acid soils, the fertility relies mostly on the organic matter recycling and/or atmospheric inputs. But the biological cycle is not closed and losses by the run off are unavoidable. Moreover, in a young growing forest, the initial pool of mineral nutrients has to be built.

For 20 years, the chemical composition of the streamwater *La Robinette*, in the Belgian Ardennes has been monitored. It initially aimed at the estimation of cations losses due to soils acidification and at the understanding of the forest decline. After a large windfall and a clear-cutting in 1995, spruces were replanted and partially replaced by deciduous species. Since 2006, a flux tower records exchange of carbon between this young ecosystem and the atmosphere (*Jalhay* CarboEurope site). The double monitoring on this site gives the unique opportunity to better explore the relationship between mineral nutrients and organic cycle under a temperate forest. A modelling approach allows deciphering the impact of the two indirect processes cited above on weathering fluxes. We use the vegetation model ASPECTS(1) and the geochemical model WITCH(2) to investigate the origin the drastic pH increase observed these last years in the streamwater (from about 4 to more than 5.5).

(1) Rasse *et al* (2001). *Ecol. Model.* **141**, 35-52. (2) Godderis *et al* (2006). *Geochim. Cosmochim. Ac.* **70**, 1128-1147.

Chemostratigraphy of Paleasian ocean's microcontinent covers

IRINA VISHNEVSKAYA

Sobolev Institute of geology and mineralogy SB RAS,
Novosibirsk, Russia; e-mail:(vishia@igm.nsc.ru)

After the breakdown of the Rodinia super continent the Siberia for a long time was a continent surrounded by the water (700 Ma [1]). The ocean between Siberia continent and others big continent is called Paleasian ocean. Thick carbonate deposits have been accumulated on Siberia passive border and on the microcontinents surrounding in Ediacarian time. This study about investigation of Sr and C isotopic composition of Ediacaran and Cambrian carbonate covers of following microcontinents: Tuva-Mongolian, Zavkhan (both in Mongolia now), Batenev and North-Muya (Russia).

Based on petrographic and geochemical analyses we identified the least altered rock samples. These samples are thought to have primary Sr isotope composition reflecting that of the paleocean. The least altered carbonates of the Tuva-Mongolia terrane have Sr isotope values of 0.7073-0.7086 and δ¹³C values alter from -1.7 to +5.0‰ [2]. The primary ⁸⁷Sr/⁸⁶Sr ratio for Zavkhan carbonate are 0.7072-0.7079 for Tsagaan Oloom Fm (δ¹³C vary from +3 to +14‰) and 0.7084-0.7086 for Bayan Gol Fm. Carbonate cover of Batenev microcontinent is characterized by ⁸⁷Sr/⁸⁶Sr ratios of 0.7075-0.7085 and δ¹³C is -2.5 ...+3.7‰ [3]. The ⁸⁷Sr/⁸⁶Sr ratio from North-Muya microcontinent vary from 0.7085 to 0.7086 and it have δ¹³C about 0.

When compared with the ⁸⁷Sr/⁸⁶Sr ratio variation curve [4] it can be seen that the deposits accumulated asynchronously from the early Ediacaria to middle of Cambrian and cannot be used for lithological correlation of the carbonate successions. *The work was supported by the RFBR (projects nos. 12-05-00569, 12-05-33076).*

[1] Li *et al.* (2008) *Precambrian Res.* **160**, 179–210. [2] Vishnevskaya *et al.* (2013) *Russian Geol. Geophysics* **54** (in press). [3] Letnikova *et al.* (2011) *Russian Geol. Geophysics* **52**, 1154–1170. [4] Halverson *et al.* (2010) *Precambrian Res.* **182**, 337–350.

Global lithium deposits (pegmatites and brines) as indicators of plume-tectonics

A.G. VLADIMIROV^{1,2,3*}, V.E. ZAGORSKY⁴
AND N.I. VOLKOVA¹

¹Institute of Geology and Mineralogy SB RAS, Novosibirsk, 630090, Russia (vladimir@igm.nsc.ru)

²Novosibirsk State University, 630090, Novosibirsk, Russia

³Tomsk State University, 634050, Tomsk, Russia

⁴Institute of Geochemistry SB RAS, Irkutsk, Russia

Spodumene pegmatites. Comparative analysis of geotectonic position of Li-bearing pegmatite deposits of Central Asian Folded Belt and their isotopic ages (U-Pb, Rb-Sr, Ar-Ar, Re-Os) suggests the coincidence of time intervals of the pegmatite formation with main age peaks of plume activity (LIP). The origination of deep-seated granite sources of the pegmatite melts with extremely high lithium contents was stipulated by asthenosphere uplift, and their occurrences was connected with strike-slip deformations in continental lithosphere [1-2].

Salt lakes. Comparative analysis of lithium brine deposits of South America and Central Asia allowed us to conclude that lithium contents in lake waters were determined by lithium concentrations in feeding springs and underground waters, their salinity, tectono-volcanic activity of considered regions, arid climate conditions. The formation of lithium brines of salt lakes is usually connected with leaching of acid tuffs, entering in bimodal volcanic series, which are characteristic for marginal and within-plate riftogenesis [3-4].

The work was supported by the Presidium of SB RAS (projects № 77, 110, 123), FGP "Research and scientific-pedagogical personnel of innovative Russia" (№ 2012-1.2.1-12-000-2008-8340).

[1] Vladimirov A.G. *et al.* (2012), *Chemistry for Sustainable Development* **20**, 3-20. [2] Zagorsky V.E. *et al.* (2013), *Russian Geology and Geophysics* (in press). [3] Volkova N.I. *et al.* (2012), *Chemistry for Sustainable Development* **20**, 21-27. [4] Shvartsev S.L. *et al.* (2012) *Chemistry for Sustainable Development* **20**, 43-49.

Siderite Amendment for *in situ* pH Control in Hyperalkaline Environments

DIMITRI VLASSOPOULOS¹, JESSICA GOIN¹
AND MINNA CAREY¹

¹Anchor QEA, Portland, OR 97204, USA

Remediation of soils and sediments and restoration of sites contaminated by hyperalkaline wastes associated with legacy industrial facilities (e.g. Solvay and chlor-alkali process wastes) present unique challenges and opportunities for geochemical engineering solutions. The feasibility and success of *in situ* treatment strategies such as soil mixing and sediment capping in such settings depends on the use of reactive amendments that can maintain long-term pH neutralization and ultimately lead to establishment of plants and habitat restoration. We present results of extensive experimental and modeling studies carried out to evaluate the reactivity, kinetics, and performance of siderite (FeCO₃) for such applications. Porewater pH neutralization and buffering by natural siderite ore concentrates from Texas was investigated in a series of kinetic batch tests using a hyperalkaline (pH 12) Na-Ca-Cl brine porewater from contaminated lake sediments. In all tests, pH was neutralized and consistently buffered to circum-neutral values within timeframes of weeks to months. The reaction rate was inversely dependent on liquid/solid ratio (varied between 2:1 to 50:1) and only weakly dependent on siderite grain size (from 0.1 to 2 mm), the latter due to the aggregate nature of the siderite ore which consists of individual crystallites <<50 μm in size. Calcite and iron oxides/oxyhydroxides were identified as the main reaction products in the batch experiments. Column testing confirmed the effectiveness of siderite for pH neutralization under dynamic flow conditions representative of field situations with groundwater upwelling through contaminated sediments. A reactive transport model of a siderite-amended sediment cap, incorporating time-dependent porewater upwelling and consolidation following cap construction, siderite dissolution (pH-dependent transition-state theory rate law) and secondary product precipitation kinetics, was developed using PHREEQC with reaction rate constants calibrated to the batch experiment data. The model has been used to simulate pH neutralization under different sediment cap designs, conduct sensitivity analyses to assess potential effects of vertical segregation of amendments during subaqueous cap materials placement, and develop optimal siderite dosing estimates for long-term pH control in support of remedial design for a major sediment remediation project.

Diagenesis affects carbonate $\delta^{53}\text{Cr}$: Evidence from the K-Pg boundary section at Stevns Klint (Denmark)

A.R.VOEGELIN^{1,2,*}, R. FREI^{1,2}, N. THIBAUT¹,
C.V. ULLMANN¹ AND CH. KORTE¹

¹ Department of Geosciences and Resource Management,
University of Copenhagen, DK-1350 Copenhagen,
(*correspondance: andrea.voegelin@geo.ku.dk)

² Nordic Center for Earth Evolution (NordCEE)

The chromium isotopic composition ($\delta^{53}\text{Cr}$) of marine sediments is a valuable tool to detect changes of the redox state of paleoenvironments [1, 2]. Recently, the $\delta^{53}\text{Cr}$ of marine carbonates has shown to be a very sensitive tracer of atmospheric O_2 , weathering and hydrothermal input [3]. We applied this new tracer to the K-Pg boundary sequence at Stevns Klint (Denmark), comprising non-cemented chalk and bryozoan limestones of the uppermost Maastrichtian to lower Danian. The $\delta^{53}\text{Cr}$ data was complemented with other geochemical tracers in order to explore environmental changes before and after the K-Pg extinction event.

We observe a conspicuous 3-step $\delta^{53}\text{Cr}$ evolution from strongly positive values at the base of the section ($\sim +0.7\%$) to intermediate values just below the boundary layer ($\sim +0.3$) and finally to mostly negative $\delta^{53}\text{Cr}$ values (~ -0.07) after the K-Pg event, reflecting mantle inventory [4]. Several lines of evidence suggest that this distinct trend may not reflect a primary oceanographic signal but is the result of post-depositional alteration. A prominent diagenetic component is implied by the Sr concentration and Sr/Ca data, which match the decreasing Cr trends. Increasing Mn and Fe concentrations as well as Mg/Ca ratios further support this interpretation. In addition, the Cr shifts can be linked to lithological changes, controlled by sea-level fluctuations. Differences in primary sediment composition may thus have led to differential diagenetic alteration of the Cr signal.

We hypothesize that the isotopically most positive $\delta^{53}\text{Cr}$ values, preserved in the pure chalks of the lowermost part of the section, reflect a typical marine signal. By contrast, the moderately positive to negative $\delta^{53}\text{Cr}$ values of the more coarse grained limestones in the upper part of the section, reflect removal of heavy $\delta^{53}\text{Cr}$ in an open-system diagenetic regime.

[1] Frei *et al.* (2009) *Nature* **461**, 250–253. [2] Frei *et al.* (2012) *Gondwana Res.* **23**, 797–811. [3] Frei *et al.* (2011) *Earth Planet. Sci. Lett.* **312**, 114–125 [4] Schoenberg *et al.* (2008) *Chem. Geol.* **249**, 294–306.

Arsenic sequestration by fresh and aged Fe oxidation products

A. VOEGELIN*, A.-C. SENN, R. KAEGI AND S.J. HUG

Eawag, Swiss Federal Institute of Aquatic Science and
Technology, Überlandstrasse 133, CH-8600 Dübendorf,
(*correspondence: andreas.voegelin@eawag.ch)

The oxidation of dissolved Fe(II) by O_2 leads to the formation of amorphous to poorly crystalline Fe(III)-precipitates. Because of their high sorption capacity, Fe oxidation products critically affect the fate and impact of trace elements like As in soils and sediments as well as in Fe-based engineered systems for soil, sediment and water remediation or treatment

Related to studies on As and trace metal dynamics in soils and sediments and As removal from drinking water, we perform laboratory experiments to determine how major dissolved species in near-neutral aqueous solution affect the formation, structure and aging of Fe oxidation products. In continuation of earlier work [1,2], we currently explore the effect of molar P/Fe ratio and dissolved Si and Ca on (i) the structure of fresh Fe(III)-precipitates formed by oxidation of 0.5 mM Fe(II) at pH 7.0 and their counterparts after 30 days of aging at 40°C and (ii) the uptake and solubility of co-transformed arsenate (As(V); 500 $\mu\text{g/L}$). Both phosphate and silicate interfere with Fe(III) polymerization. The strong interaction of phosphate with Fe(III) reduces As(V) uptake in fresh precipitates above a P/Fe ratio of ~ 0.55 in the absence and ~ 0.75 in the presence of Ca. The presence of Si (at molar Si/Fe ratio of 2) does not interfere with initial As(V) uptake but effectively reduces As(V) re-solubilisation during aging by inhibiting precipitate crystallisation.

The mechanistic insight gained from well-constrained laboratory experiments helps to rationalize observations from natural and technical systems, for example related to As and Fe co-sequestration at natural redox interfaces or to Fe-based drinking water treatment for As removal. The results are also relevant with respect to the sequestration of other trace elements by fresh and aged Fe oxidation products, a topic that we will address in future experiments.

[1] Voegelin *et al.* (2010) *Geochim. Cosmochim. Acta* **74**, 164–186. [2] Kaegi *et al.* (2010) *Geochim. Cosmochim. Acta* **74**, 5798–5816.

Dark production of reactive oxygen species in freshwaters

B.M. VOELKER^{1*}, R. MARSICO¹, R. SCHNEIDER¹,
C.M. HANSEL² AND T. ZHANG²

¹Department of Chemistry and Geochemistry, Colorado
School of Mines, Golden, CO 80401, U.S.A.
(*correspondance: voelker@mines.edu)

²Marine Chemistry and Geochemistry Department, Woods
Hole Oceanographic Institution, Woods Hole, MA 02543,
U.S.A.

Reactive oxygen species (ROS) superoxide (O_2^-), hydrogen peroxide (H_2O_2) and hydroxyl (OH) can affect metal redox speciation and organic carbon cycling in natural waters. In this study, we focus on hydrogen peroxide, the product of superoxide reduction and the source of strong oxidants including hydroxyl, via Fenton's reaction.

We measured production and decay rates of hydrogen peroxide in dark incubations of freshwater samples from a variety of systems. Dark production was found to be a ubiquitous feature of freshwater environments, and both production and decay rates were generally related to the concentrations of microorganisms in the samples. Production rates ranged from undetectable to greater than 200 nM hr^{-1} , with large temporal fluctuations in two field sites that were sampled repeatedly. Filtering decreased, but did not always eliminate, production of hydrogen peroxide, indicating chemical as well as biological sources of ROS. Our results suggest that metal reactions involving ROS are likely to occur even when photochemical ROS production is minimal.

The dependence of siderophile element partitioning on Pressure, Temperature, fO_2 and S-content

VOGEL, A.K.¹; RUBIE, D.C.¹; FROST, D.J.¹,
AUDÉTAT A.¹ AND PALME, H.²

¹Bayerisches Geoinstitut, Universität Bayreuth, D-95440
Bayreuth, Germany, antje-kathrin.vogel@uni-bayreuth.de

²Forschungsinstitut und Naturmuseum Senckenberg, D-60325
Frankfurt, Germany

The partitioning of siderophile elements between liquid metal and liquid silicate provides information about the conditions that dominated during core formation in the Earth and other terrestrial planets. In particular high pressure – high temperature experiments, performed in a multianvil apparatus, and the quantification of the partitioning behaviour in the form of partition and exchange coefficients yield conclusions about former pressure, temperature and oxygen fugacity conditions.

We have chosen a broad range of elements for our experiments, namely the refractory elements Ni, Co, W and Mo, as well as the moderately volatile elements Ag, As, Au, P, Ge, Cu and Sb and the volatile elements Sn and Pb. We have investigated the partitioning behaviour over the *P-T* range 11-23 GPa and 2200-2800 K respectively. Oxygen fugacities of -2 to -5 log units relative to the iron-wüstite buffer have been determined, enabling us to draw additional conclusions about the valence state of the elements of interest in the silicate melt. In addition, we have investigated the effect of the S content of liquid metal on partitioning because S contents were likely significant, especially during the late stages of accretion.

The most siderophile of the studied elements, gold, exhibits the strongest temperature dependence with exchange coefficients varying over one log unit within a temperature range of 2400-2600 K. Other elements, in particular Pb, show no significant dependence on temperature. The partitioning behaviour of Pb furthermore seems to be unaffected by pressure. With 10 wt% S in the starting material, the exchange coefficient for Sn decreases by 0.5 log units, and converges with the exchange coefficient of Pb, a condition that has to be fulfilled because Pb and Sn are depleted by the same extent in the Earth's mantle.

The results are being incorporated into an accretion/core formation model in order to understand the timing of volatile element addition to the Earth.

Serpentinization, metasomatism and carbonate precipitation in Jurassic mafic and ultramafic sea-floor

M. VOGEL¹, G. L. FRÜH-GREEN¹, C. BOSCHI²
AND E. M. SCHWARZENBACH³

¹ETH Zürich, 8092 Zürich, Switzerland

(*correspondence: monica.vogel@erdw.ethz.ch)

²CNR Pisa, 56124 Pisa, Italy (c.boschi@igg.cnr.it)

³Virginia Tech, Blacksburg, VA 24061, USA
(esther11@vt.edu)

Several Ligurian ophiolitic units are considered to be fragments of heterogeneous Jurassic lithosphere that record tectono-magmatic and alteration histories similar to those documented along the Mid-Atlantic Ridge, such as at the 15°20'N area and the Atlantis Massif at 30°N. We present a petrological and geochemical study of deformation and fluid-rock interaction in the Bracco-Levanto ophiolite complex (BL), which documents a multiphase history of alteration and hydrothermal activity, similar to present-day hydrothermal processes in oceanic core complexes at slow-spreading ridges. A focus is on investigating mass transfer, fluid flow paths, and fluid fluxes during high and low temperature hydrothermal activity, and on processes leading to hydrothermal carbonate precipitation and the formation of ophicalcites, which are characteristic of the BL sequences.

Bulk rock and mineral compositional data allow us to distinguish (1) a widespread phase of Si-metasomatism during progressive serpentinization, and (2) multiple phases of veining and carbonate precipitation associated with circulation of seawater and high fluid-rock ratios in the shallow, ultramafic-dominated portions of the Jurassic seafloor. In general, the ophicalcites have higher Si, Al and Fe concentrations and lower Mg than the serpentinite basement rocks with minimal or no carbonate veins. We interpret the zones of ophicalcites to reflect paleo-pathways for hydrothermal fluids and Si-metasomatism during uplift and emplacement on the seafloor. Bulk rock major and trace element data and Sr-isotope ratios indicate a seawater source of the hydrothermal fluids, and suggest that these fluids had reacted with rocks of mafic composition. We observe regional variations in Mg, Si and Al, which suggest Si-flux towards stratigraphically higher units. Channelling of Si-rich fluids is also indicated by amphibole and talc growth in shear zones. $\delta^{18}\text{O}$ -values of the carbonate veins indicate temperatures up to 150°C and document a decrease in temperature with ongoing veining and carbonate precipitation. Continued pulses of Si-rich fluids upon cooling are indicated by the formation of late-stage calcite-talc druses in the ophicalcites.

Noble gas temperature determination in fluid inclusions - method, tests, future applications

N. VOGEL^{1,2}, M.S. BRENNWALD¹, A. N. MECKLER³,
D. FLEITMANN⁴, C. MADEN², R. WIELER²
AND R. KIPFER^{1,2}

¹Eawag, Swiss Federal Institute of Aquatic Science and Technology, Water Resources and Drinking Water, Dübendorf, Switzerland. nadia.vogel@eawag.ch

²ETH Zurich, Institute for Geochemistry and Petrology, Zurich, Switzerland

³ETH Zurich, Geological Institute, Zurich, Switzerland

⁴University of Reading, Department of Archaeology, Reading RG6 6AB, United Kingdom

Concentrations of dissolved atmospheric noble gases in open water bodies and ground water have successfully been used to reconstruct past climatic and hydraulic conditions [1]. We have developed a combined vacuum crushing and sieving (CVCS) device which allows application of the so-called noble gas thermometer also to samples containing water amounts in the sub-milligram range, such as speleothems [2]. During growth, speleothems trap minute quantities of drip water, whose noble gas concentrations depend on the cave temperature. CVCS enables extraction of this water and the associated dissolved noble gases for analysis without inducing elemental fractionation, and minimizes addition of noble gases from air-filled inclusions. Air-related noble gases do not carry a temperature signal and have hence hampered noble gas temperature (NGT) determination in the past.

CVCS performance has been tested on samples from a stalagmite grown at a known temperature. NGTs deduced from the sieved grain size fractions with the most suitable air/water volume ratios excellently reproduce the expected paleotemperatures [2]. Furthermore, we report NGTs deduced from a stalagmite from Borneo covering two glacial-interglacial cycles (330-460 ka; [3]). These NGTs are compared to a sea surface temperature record from a tropical West Pacific sediment core [4].

We anticipate to apply the CVCS technique also to other fluid-inclusion bearing materials such as organic shells, corals, and consolidated sediments in the future.

[1] Brennwald M.S. *et al.* (2013) In: The noble gases as geochemical tracers, 618 p. [2] Vogel N. *et al.* (2013) G-cubed, submitted. [3] Meckler A.N. *et al.* (2012) Science, 336, 1301-1304. [4] Medina-Elizalde, M. & Lea D.W. (2005) Science, 310, 1009-1012.

Production and certification of Pd and Pt single spikes

JOCHEN VOGL¹

¹BAM Federal Institute for Materials Research and Testing,
Unter den Eichen 87, 12205 Berlin, Germany

So-called spikes are solutions of isotopically enriched elements, which are used in isotope dilution mass spectrometry (IDMS) for the accurate quantification of element concentrations. Based on its proven records, especially in reference material certification IDMS is considered as one of the most powerful and most accurate methods for determining amounts of substance. [1] Contrary to other calibration approaches, IDMS does not directly suffer from long-time changes or drifts in instrument sensitivity. Moreover, provided isotopic exchange between the sample and spike is ensured, losses of analyte do not affect the analytical result. Both advantages are based on the fact that IDMS only requires isotope ratio measurements and isotope ratios are largely unaffected by instrumental drift, setup or by matrix, unless an isobaric interference is present.

IDMS often is applied for quantification of platinum group elements (PGE), either for reference material characterization or for geochemical research. [2] The main reasons for that are the required accuracy and the low PGE mass fractions in the sample. A crucial point in IDMS is, however, the availability of certified spikes. Unfortunately, no such certified spike solutions are available yet for PGE.

To fill this gap, at least partially, two single PGE spikes, one ¹⁰⁶Pd and one ¹⁹⁴Pt spike, have been produced and characterized. The selection of the isotopes, the production of the solutions and the ampoulation will be described in this presentation. Details on the characterization of these spike solutions by reverse IDMS using a primary assay for Pd and Pt will be given offering high purity (> 99.9). All relevant data – mass fraction of the spike isotope, isotopic composition and measurement uncertainties – will be presented. Both spike solutions are intended to become certified reference materials under the ERM® label [3].

[1] Vogl J, *J Anal At Spectrom* 22 (2007) 475-492 [2] Savard D, Barnes SJ, Meisel T, *Geostandards and Geoanalytical Research* 34 (2010) 281-291 [3] European Reference Material, <http://www.erm-crm.org/>

Microbial response on siderophores of heavy metal resistant streptomycetes

A. VOIT*, M. GREYER, T. KRAUBE,
M. GUBE AND E. KOTHE

Institute of Microbiology – Microbial Communication,
Friedrich Schiller Univ., Jena, D 07743, Germany
(*correspondence: Annekatriin.Voit@uni-jena.de)

Large soil contamination by mining activities poses a severe environmental problem. The former uranium mining district Ronneburg (Thuringia, Germany) has been mined for more than 40 years until remediation of the area started in the 1990's. Resulting from mining, the banks of the creeks in the area show high concentrations of Ni, Cu, Mn and Zn and microorganisms have to adapt to these conditions. Thus, the area represents a store to screen for heavy metal resistant strains and their resistance mechanisms, such as the excretion of chelating ligands like siderophores. These mobilise, transport and store Fe³⁺ as well as other (heavy) metals in the environment. This causes a modulation of metal availability to other organisms and may influence motile and growing organisms to perform chemotaxis towards or away from a siderophore gradient to get into better living conditions.

Through the application of a new agar-plate method we were able to investigate chemotactic behaviour of different fungal and bacterial isolates to siderophores. A defined content of siderophores in culture supernatants of three different heavy metal resistant *Streptomyces* strains was supplied with Fe-deficient agar media in divided plates. Streptomycetes as well as fungi were inoculated on the non-siderophore containing side of the plate. Their growth was monitored with respect to effects exerted by the added siderophores.

Fungal strains showed faster growth towards the siderophore-free side while there, changes in morphology to fruitbody producing stages with increased development of aerial mycelium. Expecting a shift in the main area of growth for the whole colony, the tested *Streptomyces* strains displayed negative chemotaxis with siderophores while control showed equal growth. The strains *S. acidiscabies* E13 and *S. tendae* F4 showed lacks of substrate mycelium and a different pigment production indicative of a stress reaction.

Our results suggest that siderophores may play an important role in nature, not only in modulating metal availability, but also as signalling molecules.

Complex urban geochemical analysis of attic dust samples in an industrial area, Ajka, Hungary

PÉTER VÖLGYESI¹, GYOZO JORDAN², DÓRA ZACHÁRY²
AND C SABA SZABÓ¹

¹ Lithosphere Fluid Research Lab, Institute of Geography and Earth Sciences, Eötvös University, Budapest, Hungary, H-1117, Pázmány Péter sétány 1/c

² Research Institute for Soil Science and Agrochemistry, Centre for Agricultural Research, Hungarian Academy of Sciences, Budapest, Hungary, H-1022, Herman Ottó út 15

Recent studies suggest that airborne pollutants can be efficiently studied by the means of attic dust analysis. At Ajka region (Hungary), emissions from mining, coal-fired power plants and alumina industry have left the legacy of contamination. The major objective of this research was to study the geochemical behaviour and distribution of toxic elements in attic dust and to identify contamination source using geochemical, statistical and mineralogical methods. The sampling strategy followed a grid-based stratified random sampling design and 30 samples were collected in 27 houses within the 64 km² project area. The total concentrations of the major and toxic elements (As, Pb, Cd, Cu, Ni and Zn) were measured with ICP-OES and Hg content was analyzed with AAS. Phase analyses of the samples were carried out by the means of scanning electron microscopy (SEM) coupled with energy dispersive spectroscopy (EDS) and X-Ray diffraction (XRD) methods. Results show that the studied attic dust at the Ajka urban area was contaminated mostly by Hg, Pb and Zn with concentrations ranging between 0.1-2 mg/kg, 42.5-881 mg/kg and 90.2-954 mg/kg, respectively. The most frequently identified mineralogical phases were quartz, carbonate, gypsum and Fe- and Al-bearing phases. Based on the SEM and the ICP-OES results, the Power Plant can be considered as the most influential industrial contamination source in the studied urban area.

Halogenated anthropogenic trace gases: The atmospheric imprint and the search for new tracers

MARTIN K. VOLLMER¹, MATTHIAS BRENNWALD²
AND THE AGAGE TEAM³

¹Empa, Swiss Federal Laboratories for Materials Science and Technology, Laboratory for Air Pollution and Environmental Technology, Uberlandstrasse 129, 8600 Dubendorf, Switzerland. martin.vollmer@empa.ch

²Eawag, Swiss Federal Institute of Aquatic Science and Technology, Department of Water Resources and Drinking Water, 8600 Dubendorf, Switzerland. matthias.brennwald@eawag.ch

³URL: Advanced Global Atmospheric Gases Experiment: agage.eas.gatech.edu

The atmospheric burden of anthropogenic long-lived trace gases has produced powerful transient tracers of fluid motion and time-dependent processes in aquatic systems (e.g. CFCs, SF₆). However, for the CFCs, the Montreal Protocol regulations have led to reduced emissions and to atmospheric trend reversal. The resulting ambiguity in the transient signals and the eventual disappearance from the atmosphere launches a search for new tracers. Under this view we present records of atmospheric halogenated trace gases, mainly from the Advanced Global Atmospheric Gases Experiment (AGAGE). Quasi-continuous in-situ measurements of more than 50 compounds are made at several stations around the globe. The measurements track the global atmospheric background as well as signals of regional pollution such as the Asian outflow. The records are completed back in time using air archives such as air stored in canisters and polar firn. The measurements include the major ozone-depletion gases, which are regulated by the Montreal Protocol, and their replacements, most of which are powerful greenhouse gases that are regulated within the framework of the Kyoto Protocol. Chlorofluorocarbons (CFCs) have been replaced by hydrochlorofluorocarbons (HCFCs) and hydrofluorocarbons (HFCs). These trends toward the use of less stable substances is advantageous from the climate perspective but poses difficulties when used as aquatic tracers. Perfluorocarbons (PFCs, e.g. CF₄), which are extremely stable atmospheric compounds (lifetimes are 1000s of years) are another group of potential new tracers. In addition to inertness in air and water, there are numerous additional requirements for the usefulness as tracer, such as atmospheric abundance, history and trend, solubility, and sensitivity to current measurement techniques.

The Phanerozoic $\delta^{88/86}\text{Sr}$ record of seawater: New constraints on past changes in oceanic carbonate fluxes

HAUKE VOLLSTAEDT^{1,*}, ANTON EISENHAEUER¹,
KLAUS WALLMANN¹, FLORIAN BÖHM¹, JAN FIETZKE¹,
VOLKER LIEBETRAU¹, ANDRÉ KRABbenhöFT¹,
JURAJ FARKAS^{2,3}, ADAM TOMAŠOVÝCH⁴,
JACEK RADDATZ¹ AND JÁN VEIZER⁵

¹GEOMAR, Helmholtz-Zentrum für Ozeanforschung Kiel,
hvollstaedt@geomar.de (*Presenting author)

²Department of Geochemistry, Czech Geological Survey

³Department of Environmental Geosciences, Czech University
of Life Sciences

⁴Department of Geophysical Sciences, University of Chicago

⁵Ottawa-Carleton Geoscience Center, University of Ottawa

*Present address: Institut für Geologie der Universität Bern

The isotopic composition of Phanerozoic marine sediments provides important information about changes in seawater chemistry. In particular, the established radiogenic Sr isotope system is a powerful tool for constraining plate tectonic processes and their influence on atmospheric CO₂ concentrations. However, the $^{87}\text{Sr}/^{86}\text{Sr}$ isotope ratio of seawater is not recording temporal changes in the marine Sr output flux, the latter controlled mainly by the burial of CaCO₃ on the ocean floor. Here, we present the first stable isotope record of Sr for Phanerozoic seawater ($\delta^{88/86}\text{Sr}_{\text{sw}}$), which we consider being sensitive to imbalances in the Sr input and output fluxes. This $\delta^{88/86}\text{Sr}_{\text{sw}}$ record varies from $\sim 0.25\text{‰}$ to $\sim 0.60\text{‰}$ with a mean of $\sim 0.37\text{‰}$. Overall, the Phanerozoic $\delta^{88/86}\text{Sr}_{\text{sw}}$ record resembles that of the Ca isotope record ($\delta^{44/40}\text{Ca}_{\text{sw}}$), but differs considerably from the radiogenic Sr isotope record ($(^{87}\text{Sr}/^{86}\text{Sr})_{\text{sw}}$). This implies different controlling mechanisms for the two Sr isotope systematics in the oceans. A new numerical modeling approach, which considers both $\delta^{88/86}\text{Sr}_{\text{sw}}$ and $(^{87}\text{Sr}/^{86}\text{Sr})_{\text{sw}}$, yields improved estimates for Phanerozoic fluxes and concentrations for seawater Sr. During the Phanerozoic, the oceanic net carbonate flux of Sr ($F(\text{Sr})_{\text{carb}}$) varied between an output of $-4.7 \times 10^{10} \text{ mol/Myr}$ and an input of $+2.3 \times 10^{10} \text{ mol/Myr}$ with a mean of $-1.6 \times 10^{10} \text{ mol/Myr}$. On time scales in excess of 100 Myrs the $F(\text{Sr})_{\text{carb}}$ is proposed to have been controlled by the relative importance of CaCO₃ precipitates during the “aragonite” and “calcite” sea episodes. On time scales less than 20 Myrs $F(\text{Sr})_{\text{carb}}$ is likely controlled by short-term variations in carbonate burial rate (linked to ocean acidification or anoxia) and changes in carbonate weathering and recrystallization on the shelf, leading to transient changes in the oceanic carbonate alkalinity budget.

High-temperature rheology of a megacryst-bearing mugearitic magma from Etna (Italy)

ALESSANDRO VONA^{1,*}, ANDREA DI PIAZZA¹,
EUGENIO NICOTRA², CLAUDIA ROMANO¹
AND MARCO VICCARO²

¹Dipartimento di Scienze, Università di Roma Tre, Italy,
alessandro.vona@uniroma3.it (*presenting author)

²Dipartimento di Scienze Biologiche Geologiche e
Ambientali, Università di Catania, Italy

We performed a series of concentric cylinder viscosity measurements at high temperature ($1000 < T < 1400 \text{ °C}$) and high strain rates ($10^{-2} - 10^1 \text{ s}^{-1}$) to investigate the multiphase rheology of a mugearitic lava from Etna volcano. Natural samples exhibit porphyritic index ranging between 30 and 60 vol%. The mineral assemblage is constituted by megacrystic plagioclase (20–50 vol%), phenocrysts of olivine, augitic clinopyroxenes and Fe-Ti oxides, and a microcrystalline groundmass composed prevalently of plagioclase (75 vol%). The knowledge of the rheological evolution during crystallization is paramount in order to understand completely the dynamics of magma transport from the storage zones up to the surface. We have firstly measured the viscosity of the pure liquid phase on both the bulk rock (i.e. initial crystal-free magma) and the separated groundmass (i.e. residual liquid). The slight compositional variation due to crystallization does not affect substantially the viscosity. The contribution of plagioclase megacrysts to magma rheology has been then evaluated through a set of experiments on partially re-melted samples. We defined a temperature-time window in which groundmass is completely melted and different amounts of megacrysts (20–50 vol%) are preserved. Results confirmed the dependence of rheology on the textural features (crystal content, shape, orientation and size distributions) of the crystal-liquid suspension. The characteristics of these samples allowed us to investigate the viscous flow behavior of medium-high concentrated suspensions at strain rates and temperature pertaining to the natural systems. The results of this study were compared with literature models predicting the rheological behavior of crystal-bearing suspensions and were used to constrain the history of storage and transport of these peculiar magmas.

Plagioclase crystallization kinetics in basalts by high-T viscosity measurements

A. VONA¹ AND C. ROMANO^{1*}

¹ Dip. di Scienze, Univ. Roma Tre, Italy,
alessandro.vona@uniroma3.it
claudia.romano@uniroma3.it (*presenting author)

In this study we explore the effect of undercooling and stirring on the crystallization kinetics of remelted basaltic material from Stromboli (pumice from the 15th March 2007 paroxysmal eruption) and Etna (1992 lava flow). Isothermal crystallization experiments were conducted at different degrees of undercooling and different applied strain rate (T=1157-1187 °C and strain rate = 4.26 s⁻¹ for Stromboli; T=1131-1182 °C and strain rate = 0.53 s⁻¹ for Etna). Melt viscosity increased due to decreasing temperature and increasing crystal content and achieved a steady value after 10⁴-10⁵ s. The mineralogical assemblage comprises sp + plg (dominant) ± cpx with an overall crystal fraction between 0.06 and 0.27, increasing with undercooling and flow.

Both degree of undercooling and deformation rate deeply affect the kinetic of the crystallization process. Plagioclase nucleation incubation time strongly decreases with increasing ΔT and flow. Plagioclase growth rates G display relative small variation with Stromboli samples (high strain rate) showing higher values (G=10^{-7.7} m s⁻¹) compared to G values from Etna samples (low strain rate; G=10^{-8.5} m s⁻¹).

G values obtained in this study are generally one or two order of magnitude higher compared to those obtained in literature for equivalent undercooling conditions. Stirring of the melt, simulating flow or convective conditions, facilitates nucleation and growth of crystals via mechanical transportation of matter, resulting in the growth rates observed. Any modeling pertaining to magma dynamics in the conduit (e.g. ascent rate) and lava flow emplacement (e.g. flow rate, pahoehoe - 'a'a transition) should therefore take the effects of dynamic crystallization into account.

Fast hydration of volcanic glass at low temperatures

F. W. VON AULOCK^{1,2} Y. LAVALLÉE²
K.-U. HESS³ S. HENTON-DE ANGELIS²
AND B. KENNEDY¹

¹University of Canterbury (New Zealand);
felixv.aulock@gmail.com

²University of Liverpool (UK); ylava@liverpool.ac.uk

³LMU Munich (Germany); hess@lmu.de

During volcanic eruptions, magma loses most of its volatiles and cools below the glass transition temperature. However, natural volcanic glass is often oversaturated in water. The water often is distributed inhomogeneously and local increases can be observed around textural features such as bubbles, crystals and cracks. The origin of these heterogeneities can either be redistribution of magmatic water or dissolution of meteoric water. However, the processes of dissolution of water in a solid glass and in a silicate melt at elevated temperatures vary significantly and the quantities, timescales and speciation of water dissolution and diffusion remain poorly constrained.

We present preliminary results of water measurements on naturally hydrated volcanic glass and experimentally hydrated silicate glasses. Water heterogeneities in natural, volcanic rhyolitic glass around cracks, bubbles and spherulitic crystals as well as flow banding show increases of up to ~0.2 wt. % above the general water concentrations of ~0.045 to 0.1 wt. %. Textural and numerical proxies based on bulk water diffusion indicate timescales of hydration from hours to months. We propose to adapt these models to consider water speciation and variation with temperature.

To estimate timescales and quantities of hydration, we rapidly hydrated natural and synthetic (Fe-free) glass in a water vapor saturated Argon atmosphere at temperatures below the glass transition while recording enthalpy and gravimetric changes in a simultaneous thermal analysis. Preliminary data shows that a weight gain of 0.15 wt. % in hydration can be reached over 10 h at 400°C.

We evaluate the possibility for glass to physically intrude nanopores and chemically diffuse into the structure. Therefore common models of water dissolution, speciation, and distribution in silicate glasses need to be revised for low temperatures and further experimental and analytical work is needed to create reliable quantitative models.

River denudational transport to the sea using the oceans $^{10}\text{Be}(\text{meteoric})/^{9}\text{Be}$ ratio

F. VON BLANCKENBURG¹ AND J. BOUCHEZ¹

¹GFZ Potsdam, Telegrafenberg, Potsdam, Germany
(*correspondence: fvb@gfz-potsdam.de)

The ratio of the meteoric cosmogenic nuclide ^{10}Be ($T_{1/2} = 1.39$ My) to the stable isotope ^9Be is a proxy of terrigenous input into the oceans. The system combines a tracer of roughly constant flux to the Earth surface (over time scales characteristic of weathering) with one that depends on its release rate from rock by weathering. Using a mass balance model we previously quantified how the $^{10}\text{Be}(\text{meteoric})/^{9}\text{Be}$ traces weathering and erosion from the soil to the river scale [1].

Here we take this tracer further by exploring this isotope ratio when river dissolved and sedimentary material is discharged into the ocean, where meteoric ^{10}Be is added by direct precipitation into the oceans. Using river Be data we first find that the fraction of mobile ^9Be (meaning unlocked from silicate minerals that is now either dissolved or adsorbed onto sedimentary particles) in rivers is globally 20%. We next find that a measured ocean dissolved $^{10}\text{Be}/^9\text{Be}$ ratio of about 1×10^{-7} [2] is satisfied by the mass balance if only 10% of the mobile river Be is eventually dissolved into the oceans by boundary exchange. This number is obtained using the sum of global solid and dissolved river fluxes [3], an average crustal ^9Be concentration of 2.5ppm, and an atmospheric ^{10}Be flux of 1×10^6 atoms g^{-1}cm^2 .

There is good agreement between modeled and measured ocean $^{10}\text{Be}/^9\text{Be}$ ratios when we perform this mass balance for each ocean basin. Only the southern Atlantic deviates from the predicted value, which can be explained by the dominant external deep and bottom water inputs that affect the measured ratio.

We show that the fraction of mobile ^9Be does not change significantly over a large range of global denudation rates. Therefore, the $^{10}\text{Be}/^9\text{Be}$ ratio can serve as a tracer that, unlike radiogenic and stable isotope ratios, truly quantifies past denudation rate and hence terrigenous input into the oceans at a temporal resolution exceeding the residence time of Be in the oceans (ca. 600 years).

[1] von Blanckenburg *et al.* (2012) *EPSL* **351-352**. [2] Kusakabe *et al.* (1990), *Geochemical Journal* **24** [3] Milliman and Farnsworth (2011) Cambridge University Press

Quantification and speciation study of the marine solid-phase iron pool

B.P. VON DER HEYDEN^{1*}, A.N. ROYCHOUDHURY¹
AND S.C.B MYNENI²

¹Dept. of Earth Sciences, Stellenbosch University,
Stellenbosch 7602, South Africa (*correspondence:
bvon@sun.ac.za)

²Dept. of Geosciences, Princeton University, Princeton, NJ
08544, USA

Iron chemistry is tightly linked to marine primary productivity, particularly in High Nutrient Low Chlorophyll (HNLC) regions of the world's oceans, where Fe is commonly the limiting nutrient. Only about one third of the total iron present in the upper 200m of the open ocean water column is present in the smallest 'soluble' size fraction; the remainder is bound to colloidal ligands or incorporated into particles and biology greater than the $0.02\mu\text{m}$ -1000kDa size cut-off. From analyses of a global dataset, colloidal Fe (cFe) behaviour is found to vary between different ocean basins and there is evidence for a seasonal cycle in cFe concentration, associated with depletion during the summer growth season. Controls on distribution and concentration of this (quantitatively more important) larger Fe size class are linked to distance from shore, ambient ligand concentration, and colloid stability and inorganic solubility.

Despite the importance of size-fractionated Fe study, complementary chemical and mineralogical information is required to more fully understand the role of solid phase Fe in the marine system. We have developed a novel Fe L-edge x-ray technique that incorporates both high-resolution (12nm resolution) scanning transmission X-ray microscopy and *in-situ* L₃-edge XANES spectroscopy. Local chemical information derived from the XANES spectra reflect variations in Fe valence state, ligand type and coordination, and the degree of distortion within Fe polyhedra. For use in mineralogical identification of sub-micron sized particles, we present a 2D graphic plot based on variations in the spectral parameters of standard Fe-rich phases. Despite some limitations associated with particle thickness and spectral saturation, this plot has been successfully applied in speciation studies of particles collected from both marine and fluvial systems. A case study is presented highlighting significant chemical differences identified in marine particles (20-700nm in diameter) sampled from the euphotic zone of the different frontal zones of the Southern Ocean. The implications of these differences are discussed in terms of particle solubility and biological availability.

Detection of engineered cerium oxide nanoparticles in the environment

FRANK VON DER KAMMER¹, ELISABETH NEUBAUER¹,
ROBERT B. REED^{1,2}, JAMES F. RANVILLE²
AND THILO HOFMANN¹

¹Department of Environmental Geosciences, University of Vienna, frank.kammer@univie.ac.at

²Department of Chemistry and Geochemistry, Colorado School of Mines

Cerium oxide (CeO₂) nanoparticles are increasingly used in products such as diesel fuel combustion catalysts. CeO₂ nanoparticle emission into the environment is of concern due to potential ecotoxicological effects. The detection of engineered CeO₂ nanoparticles in environmental matrices poses a challenge due to predicted concentrations in the part-per-trillion range and the differentiation from nanoparticulate Ce-containing minerals occurring in nature.

Data provided by the Forum of European Geological Surveys (FOREGS) show La:Ce ratios of 0.50 ± 0.05 in bulk topsoils and stream sediments sampled across Europe, while engineered CeO₂ nanoparticles exhibit La:Ce ratios in the range of 0.001 to 0.002. Therefore, deviations from the “natural” La:Ce ratio may potentially be used for the identification of engineered CeO₂ nanoparticles in environmental matrices.

Sediment and preconcentrated water samples from uncontaminated sites were analyzed by flow field-flow fractionation (FFF) coupled to light scattering detection and inductively coupled plasma mass spectrometry (ICPMS) to determine size distributions and elemental composition of the natural nanoparticles. Preliminary results show that La:Ce ratios are constant at about 0.5 across the natural nanoparticles from unpolluted streams.

By addition of engineered CeO₂ nanoparticles at various concentrations to the natural nanoparticle suspensions followed by FFF analysis, we probe the sensitivity of the size-resolved La:Ce ratios as a tool for determination of engineered CeO₂ nanoparticles. FFF size fractions were collected and analyzed by single particle ICPMS, with the aim of differentiating between natural Ce-containing suspended particulate matter and engineered CeO₂. The results were compared to samples from potentially contaminated road runoff samples.

Preliminary findings on the strengths and weaknesses of these methods for the detection of engineered CeO₂ nanoparticles in environmental matrices will be presented.

Hydrological change in the Turkana Basin through the termination of the African Humid Period: The lacustrine Sr-isotope record

H.B. VONHOF^{1*}, J. KRAUSE¹, A. JUNGINGER², T. JOHNSON³, J. VAN DER LUBBE¹ AND J. JOORDENS¹

¹VU-University Amsterdam, the Netherlands

(*correspondence:h.b.vonhof@vu.nl)

²Potsdam University, Germany

³University of Minnesota Duluth, Duluth USA

At the Termination of the African Humid Period (AHP) important hydrological changes occurred in NE Africa. Lake Turkana in Northern Kenya is one of the larger lakes in the East African Rift Valley and its Holocene history is relatively well studied. The lake dropped by ~ 80 meters at the end of the AHP, presumably caused by a reduced water supply from the Ethiopian highlands, brought to the lake by the Omo River. The Omo River at present supplies more than 80% of the water to Lake Turkana. In the Holocene this situation was different, with significant water supplied to Turkana by two neighbouring Basins: The Chew Bahir Basin to the Northeast and the Suguta Basin to the South.

Here we have analysed the Sr isotope variation of Holocene ostracods and bivalves to identify Holocene changes in water provenance to Lake Turkana. Results show a clear trend in Holocene Sr isotope values. We interpret higher values in the Early Holocene to reflect significantly increased contribution of water from the Chew Bahir Basin. Application of a Sr-isotope mass balance model allowed us to put constraints on the magnitude and rate of hydrological change in Lake Turkana.

The combined signature of Sr- and oxygen isotope variation in Holocene Lake Turkana is in line with a previously postulated increase in rainfall sourced from the Indian Ocean in the Horn of Africa at AHP times.

CA-U-Pb zircon dating obtained by the LA-ICP-MS system: Impact for their interpretations

A. VON QUADT^{1*}, D. GALLHOFER¹, M. WAELLE¹, AND C.A. HEINRICH¹ AND I. PEYTCHEVA^{1,2}

¹ ETH Zurich Inst. for Geochemistry und Petrology, Clausiusstrasse 25, 8092 Zürich, Switzerland

² BAS Sofia Inst. for Geology, 1113 Sofia, Bulgaria

*vonquadt@erdw.ethz.ch

Laser ablation ICP-MS is a powerful method to determine the age of rocks by measuring U/Th/Pb isotopes. The method is fast, cheap and several applications present precise (< 1% ²⁰⁶Pb/²³⁸U age errors) and accurate results using corrections and reference materials [1]. For several years U-Pb zircon analyses by TIMS are using the CA [chemical abrasion] technique to avoid domains that have lost Pb parts [2,3]. In this work we apply the same CA technique for LA-ICPMS analyses, using the Excimer 193nm laser system with a constant geometry ablation cell connected to the quadrupole ICP-MS (PerkinElmer, Elan 6100). The selected target material are zircon grains of intrusive rocks with ages of 24 Ma (Miocene) and 80 Ma (Cretaceous) that show no inherited components.

The analyses we include TIMS and LA-ICPMS measurements of U/Pb ratios of CA- and non CA-treated zircons. All non CA-treated zircon measurements show a broader range of their ²⁰⁶Pb/²³⁸U ages including ratios which refer to recent lead loss or to small inherited Pb components. The CA-treated zircon measurements show a more homogenous age pattern due to the removal of domains with lead loss. In the case of not overlapping concordant ages the cluster with the youngest ages should be interpreted as time of magma crystallization, which is an important advantage of the techniques. Most publications [4] take the 2 sigma error into account for their calculation of ²⁰⁶Pb/²³⁸U ages; following this procedure we can demonstrate that the non CA-treated U/Pb ages are not overlapping with the CA-treated zircon grains measured by LA-ICP-MS and TIMS techniques. The standard error of this mean has even less geological significance if age variations are real [5]; note that the value of the standard error of the mean would decrease if greater numbers of zircons were measured.

[1] Jackson *et al.* (2004) *Chem Geology* **211**, 47-69. [2] Mattison (2005) *Chem Geology* **220**, 47-66. [3] Mundil *et al.* (2004) *Science* **305**, 1760-1763. [4] Jahn-Awe *et al.* (2010) *Tectonics* **29**, TC3008, 1-30 [5] von Quadt *et al.* (2011) *Geology* **39**, 731-734.

Souring control by six years of nitrate injection into a low temperature oil field

G. VOORDOUW^{1*}, A. AGRAWAL¹, HYUNG SOO PARK¹, Y. SHEN¹, T. R. JACK¹, K. MINER² AND A. BENKO³

¹Department of Biological Sciences, University of Calgary, Calgary, Alberta, Canada

² Baker Hughes, Medicine Hat, Alberta, Canada

³ Enerplus Corporation, Calgary, Alberta, Canada

Production of oil by water injection can result in souring by sulfate-reducing bacteria (SRB). Souring can be prevented or reversed by inclusion of nitrate in the injection water, which boosts the activity of nitrate-reducing bacteria (NRB). In the Medicine Hat Glauconitic C (MHGC) field, oil production through water injection was started in 2000. Souring, was noted in 2006. Field-wide injection of 2 mM nitrate was adopted as a souring control strategy in 2007. We have monitored the success of this strategy by monthly sampling of producing wells and analyzing the concentrations of sulfate, sulfide, nitrate and nitrite [1], as well as by determining microbial community composition [2].

Field-wide nitrate injection decreased produced sulfide initially, but this was followed by recovery. Microbial zonation in which NRB grow close to the injection wellbore and SRB deeper in the reservoir was the suggested cause for this. Successful injection of nitrate pulses exceeding the nitrate reduction capacity of the NRB gave credit to this idea [1]. Constant nitrate injection over the past 6 years has given nitrate breakthrough at an increasing number of injection wells. This was associated with removal of sulfide, as well as with breakthrough of sulfate, nitrate and nitrite. Production of oil/water depleted of toluene and other alkylbenzenes and containing increased proportions of the toluene-utilizing NRB *Thauera* were also observed [2].

Long-term injection of nitrate and changes in water management strategy have caused a near complete reversal of souring in the MHGC field. Despite lack of success in the first two years persistence has since paid off.

[1] Voordouw *et al.* (2009) *Environ. Sci. Technol.* **43**: 9512-9518. [2] Agrawal *et al.* (2012) *Environ. Sci. Technol.* **46**: 1285-1292.

Geochemistry of uranium in the reduced carbonaceous sediments of small lakes in Baikal Region

YULIA VOSEL¹, VERA STRAKHOVENKO¹
AND IRINA MAKAROVA¹

¹Sobolev Institute of Geology and Mineralogy Siberian
Branch of Russian Academy of Sciences,
vosel@yandex.ru

The most commonly identified pathway to explain the accumulation of authigenic U in reduced sediments is the microbially mediated reduction of U(VI) to less soluble U(IV) [2]. However previous researchers could not acquire the direct evidence of uranium reduction and formation of its poorly soluble oxides, so the additional investigation of the problem is needed [1]. Our work is aimed at detecting of U reduction process in sediments of two small lakes (fresh and salt) which are located in the Baikal region. To achieve this goal we separated sediments to lithogenic and various authigenic fractions using the method of sequential extraction, which is based on the method of Tessier [3]. According to our research values of activity ratios ($^{234}\text{U}/^{238}\text{U}$) in the insoluble residue significantly differ from 1 in both lakes. This indicates the presence in the residuals not only the lithogenic fraction, but a noticeable amount of UO_2 . Uranium accumulates in lake sediments mainly through chemogenic processes, in different forms (in oxides and hydroxides, organic matter or isomorphic impurities in carbonates). This work was supported by grant RFBR 12-05-31087mol_a

[1]Chappaz, Gobeil, & Tessier (2010), *Geochim. Cosmochim. Acta* 74, 203–214 [2]Klinkhammer & Palmer (1991) *Geochim. Cosmochim. Acta.* 55, 1799–1806 [3] Tessier, Canbell, & Bission, (1979), *Anal. Chem.* 51, 884–851

Volatilization of methylated selenium, sulfur and arsenic from a wetland

BAS VRIENS^{1,2*}, MARKUS LENZ³, LAURENT CHARLET⁴,
MICHAEL BERG¹, LENNY ANDH.E. WINKEL^{1,2}

¹Eawag: Swiss Federal Institute of Aquatic Science and
Technology, Ueberlandstrasse 133, P.O. Box 611, 8600
Duebendorf, Switzerland,
(*correspondence: bas.vriens@eawag.ch),
michael.berg@eawag.ch

²Swiss Federal Institute of Technology (ETH) Zurich, 8092
Zurich, Switzerland, lwinkel@ethz.ch

³University of Applied Sciences and Arts Northwestern
Switzerland, Institute for Ecopreneurship, 4132 Muttenz,
Switzerland, markus.lenz@fnw.ch

⁴Université Joseph Fourier, Grenoble, 1381 rue de la Piscine,
38400 Saint-Martin d'Hères, France,
charlet38@gmail.com

Selenium (Se) is an essential trace element for life. However, it can negatively affect human health due to its narrow range of beneficiary concentration and its unequal distribution in the surface environment. To date, sources, sinks and fluxes in the global Se cycle are poorly understood and quantified. Although methylation and volatilization of Se from terrestrial environments is known to occur (and is studied for e.g. bioremediation purposes), its relevance to the natural global atmospheric Se budget remains unknown.

We applied a novel chemotrapping method in combination with a flow-through chamber system to identify and quantify volatilization of Se, sulfur (S) and arsenic (As) from a minerotrophic peat bog in southern Switzerland. We were able to determine gaseous fluxes of Se ($0.11 \mu\text{g Se}\cdot\text{m}^{-2}\cdot\text{d}^{-1}$), S ($37 \mu\text{g S}\cdot\text{m}^{-2}\cdot\text{d}^{-1}$) and As ($0.16 \mu\text{g As}\cdot\text{m}^{-2}\cdot\text{d}^{-1}$) in the form of non-, mono- and di-methylated species. By comparing these fluxes with total concentrations of these elements in both the peat and surface water, it became evident that Se is approximately 40 to 110 times more efficiently volatilized from the peat bog than As and S, respectively. Furthermore, we observed that elevated temperatures increased volatilization of the investigated elements to a different extent. Our results suggest that Se volatilization from wetlands, and possibly other terrestrial environments, may crucially influence the biogeochemical cycle of Se.

Early Paleozoic intrusives of the Kuznetsk Alatau, Siberia: Isotopic evidence of oceanic lithosphere participation in sources

V.V. VRUBLEVSKII*, I.F. GERTNER
AND A.D. KOTELNIKOV

Tomsk State University, Tomsk, Russia (*vasvr@yandex.ru)

Products of the Early Paleozoic intrusive magmatism are represented in the Kuznetsk Alatau (KA) by granitoid, gabbro-syenite, and alkali basite complexes. They were formed during the period of about 510-490 Ma, which is in the Central Asian fold belt [1]. The magmatic activity implies the presence of multi-component melt sources with age that close to the age of the oceanic lithosphere formation. Nd-Sr isotopic signatures discovered for four studied complexes formed in different ways indicate possible participation of Paleo-Asian Ocean (PAO) lithosphere in the processes of magma generation at the Early Paleozoic stage of this ocean's evolution. The oldest complexes (about 510 Ma) are the differentiated series from gabbro to granodiorite as well as alkaline basic complexes. Despite the petrogenetic differences, these complexes have similar isotopic composition of Nd ($\epsilon_{Nd_T} \sim +4.8 \dots +5.0$). Such values are typical either for magmatic derivatives of moderately depleted mantle, or for mixing products of DMM or PREMA reservoirs with EM-type mantle and continental crust materials. The influence of crust contamination is seen in high ratio of Sr-isotopes in the rocks ($\epsilon_{Sr_T} \sim +1 \dots +28$). Granitoids and gabbro-syenite series with the age of about 500-490 Ma don't have significantly different Nd-isotopic compositions ($\epsilon_{Nd_T} \sim +3.5 \dots +4.6$). Apparently, it is confirmed by narrow range of these $T(Nd)_{DM}$ values ($\sim 0.8-0.9$ Ga). According to different views [2, 3], the beginning of the Rodinia supercontinent's break-up, and following the PAO opening are estimated to be 970-800 Ma. Based on our data, Sm-Nd isotopic age of ultrabasites and gabbroids of the layered series and restite suites varies from 955 to 890 Ma, respectively. Magmatism probably developed under the conditions of plume interacting with active continental margin coupled with MORB+PREMA+EM matter mixing.

This study was funded by the Russian Ministry of Education and Science (projects 5.3143.2011, 14.B37.21.0686, 14.B37.21.1257).

[1] Vrublevskii V.V. *et al.* (2012) *Russ. Geol. Geophys.* **53**, 721–735. [2] Dobretsov N.L. *et al.* (2003) *Gondwana Res.* **6**, 143–159. [3] Li X.Z. *et al.* (2008) *Precambrian Res.* **160**, 179–210.

Mineralogical and geochemical variations in lower Godavari River sediments, Peninsular India: Implications to source rock weathering

SHILPA VUBA*, SADIA FARNAAZ,
NETRAMANI SAGAR AND S. M. AHMAD

CSIR-National Geophysical Research Institute, Uppal Road,
Hyderabad – 500 007, India
(*correspondence:shilpavuba@gmail.com)

Godavari River is the third largest river in the Indian sub-continent, which originates in the Deccan Traps and drains an area of 3.1×10^5 km². The river flows in the east and the south-easterly direction for a distance of 1465 km before discharging into the Bay of Bengal. The major, trace and rare earth elements geochemistry and clay mineral compositions in bed sediments from lower reaches of Godavari River suggest that they are derived from weathering of felsic rocks. Trace and rare earth elemental compositions indicate evidence of sedimentary sorting during transportation and deposition. Lower concentrations of transition elements, such as V, Ni and Cr imply enrichment of felsic minerals in these bed sediments. The REE pattern in lower Godavari sediments is influenced by the degree of source rock weathering. The light rare earth elements (LREE) content are indicating greater fractionation compared to the heavy rare earth elements (HREE). A striking relationship is observed between TiO₂ and Σ REE content suggesting a strong control by LREE-enriched titaniferous minerals on REE chemistry. Shale-normalized REE pattern demonstrate a positive Eu anomaly, suggesting weathering of feldspar and their secondary products, which are enriched in Eu. Chondrite-normalised REE pattern is characteristic of felsic volcanic, granites and gneissic source rocks. Trace elemental compositions in sediments located near urban areas suggest influence of anthropogenic contamination. Chemical Index of Alteration (CIA) is high (avg. 65.76), suggesting a moderate chemical weathering environment. X-ray diffraction analysis in clay fraction shows predominance of clay minerals that are formed because of the chemical weathering of felsic rocks.

CO₂ speciation and transport properties of CO₂-bearing silicate melts from First-Principle simulations

R. VUILLEUMIER^{1*}, A. SEITSONEN², N. SATOR³
AND B. GUILLOT³

¹UMR 8640 CNRS-ENS-UPMC, Département de chimie de l'ENS, 24, rue Lhomond, 75005 Paris, France.

(*correspondence: rodolphe.vuilleumier@ens.fr)

²Physikalisch Chemisches Institut, Universität Zürich, Winterthurerstrasse 190, CH-8057 Zürich, Switzerland (Ari.P.Seitsonen@iki.fi)

³LPTMC, UPMC, UMR CNRS 7600, case courrier 121, 4 place jussieu, 75252 Paris cedex 05, France (sator@lptmc.jussieu.fr, guillot@lptmc.jussieu.fr)

There are growing evidences of the existence of CO₂-rich magmas in the upper mantle [1-3]. So the role of carbon-rich melts at depth is now becoming a credible scenario to explain the extraction of CO₂ from the source region to the surface. During the last three decades many studies have been devoted to measure the solubility of CO₂ in silicate melts of various composition. But due to experimental difficulties these studies were generally restricted to low and moderate pressures (below ~20 kbar). IR spectroscopy has emphasized the importance of CO₂ speciation which may exist either as molecular CO₂ or as carbonate ion (CO₃²⁻), the molecular form being favored in polymerized (silicic) melts while the carbonate ion is dominant in depolymerized (basic and ultrabasic) melts. However it has been suggested recently [4,5] that the CO₂ speciation observed in quenched glasses by IR spectroscopy may not be representative of that in silicate melts equilibrated at high temperature.

To address this issue we have performed First-Principle Molecular Dynamics of CO₂-saturated basaltic and kimberlitic melts. The molecular form is indeed favored in the more polymerized melt. Furthermore, a new transient species is also identified. The electrical conductivity of the CO₂-saturated basaltic and kimberlitic melts has also been evaluated and found in good agreement with experiment. These results have also been used to develop an empirical force field for describing CO₂-rich melts by classical MD simulations.

[1] Dasgupta & Hirschmann (2007) *Nature* **440**, 659-662. [2] Zeng *et al.* (2010) *North China. Chem. Geol.* **273**, 35-45. [3] Helo *et al.* (2011) *Nature Geoscience* **4**, 260-263. [4] Morizet *et al.* (2007) *Eur. J. Mineral.* **19**, 657-669. [5] Spickenbom *et al.* (2010) *GCA* **74**, 6541-6564.

Microstructural control on trace element diffusion in pyrrhotite from komatiite hosted massive Ni sulphides, Yilgarn Craton

Z. VUKMANOVIC^{1,2*}, S. M. REDDY³, B. GODEL²,
S. J. BARNES², M. L. FIORENTINI¹ AND S.-J. BARNES

¹ CET/CCFS, The University of Western Australia, Perth, Australia (*correspondence:

vukmaz01@student.uwa.edu.au;

marco.fiorentini@uwa.edu.au)

²CSIRO, ESRE, Perth, Australia (belinda.godel@csiro.au, stephen.barnes@csiro.au)

³ARC CCTFS, Curtin University, Perth, Australia (s.reddy@curtin.edu.au)

⁴Département des sciences appliquées, Unité d'enseignement en sciences de la Terre, Chicoutimi, Québec, Canada, (sjbarnes@uqac.ca)

Pyrrhotites (Fe₇S₈) from three different komatiite hosted massive nickel sulphide deposits have been analysed with electron backscatter diffraction analysis (EBSD) and laser ablation inductively coupled plasma mass spectrometry (LA-ICP-MS) in order to understand how trace elements behave during deformation.

EBSD data reveals strain localisation microstructures in sample from greenschist facies whereas in sample from mid-amphibolite facies, pyrrhotite contains multiple parallel low angle boundaries and crystallographic preferred orientation. A sample from the upper amphibolite facies, is characterised by very large >2cm grains that contains numerous deformation twins. Laser ablation ICP-MS data reveal increased concentrations of Pb, Bi and Ag along low angle subgrain boundaries and twin boundaries. The increased concentrations of Pb, Bi and Ag are explained by diffusion of the trace elements along fast diffusion pathways (low angle and twin boundaries). Trace element variations are developed at the low-temperature stage of the tectonic history of the three deposits. Diffusion of Pb, Bi and Ag is triggered by their low solubility in sulphide phase, pyrrhotite.

Geochemistry and nano-structure of putative filamentous microbes from the 3.24 Ga Sulfur Springs Group, Pilbara, Western Australia

D. WACEY^{1,2*}, M. SAUNDERS², M.R. KILBURN²,
J.B. CLIFF², C. KONG³, M.E. BARLEY²
AND D. N. MCLOUGHLIN¹

¹University of Bergen, Bergen N-5007, Norway

(*correspondence: David.Wacey@geo.uib.no)

²University of Western Australia, WA 6009, Australia

³University of New South Wales, NSW 2052, Australia

Pyritic filaments from one of Earth's oldest volcanic hosted massive sulfide (VHMS) deposits within the 3.24Ga Sulfur Springs Group, Western Australia, have been interpreted as thermophilic chemotrophic micro-organisms [1]. This interpretation [1] was based upon textural, morphological and inferred behavioral characteristics of the filaments. However, no geochemical evidence for biology has yet been reported, so an alternative explanation as abiotic mineral filaments remains to be discounted.

Here we revisit these putative filamentous micro-organisms, using a suite of high-spatial resolution techniques to investigate their geochemistry and nano-structure.

NanoSIMS elemental mapping reveals occasional enrichments of carbon within some of the pyritic filaments. Similar patterns of carbon enrichment are seen in *bona fide* pyritic filamentous microfossils from the 1.9 Ga Gunflint chert that were also pyritised by hydrothermal fluids.

In situ SIMS multiple sulfur isotope data show small but significant $+\Delta^{33}\text{S}$ (and $-\Delta^{36}\text{S}$) anomalies, consistent with previous bulk data from this VHMS deposit [2], indicating mixing of a hydrothermal fluid containing sulfur of magmatic origin ($\Delta^{33}\text{S}=0$) with circulating seawater containing reduced sulfur derived from atmospheric elemental sulfur ($+\Delta^{33}\text{S}$).

The nano-structure of the filaments was investigated in the TEM using focused ion beam (FIB)-milled ultrathin sections, and by 3D FIB-SEM nanotomography. Notable features include circular to elliptical filament cross sections mostly comprising single pyrite crystals, clustering of filaments in pairs and triplets, and a common preferred orientation of many filaments.

These data provide new insights into one of Earth's oldest black-smoker-type environments and potential associated life. The strength of evidence for the biogenicity of the filaments will be discussed.

[1] Rasmussen (2000) *Nature* **405**, 676-679. [2] Golding *et al.* (2011) in *Earliest Life on Earth: Habitats, Environments and Methods of Detection*, pp. 15-49.

Clumped isotopes, $\delta^{18}\text{O}$, $\delta^{13}\text{C}$, $\delta^{11}\text{B}$, $^{87}\text{Sr}/^{86}\text{Sr}$: A multiproxy approach applied to Silurian brachiopod shells

ULRIKE WACKER¹, JENS FIEBIG¹, AXEL GERDES¹,
AXEL MUNNECKE², MICHAEL M. JOACHIMSKI²
AND BERND R. SCHÖNE³

¹Department of Geosciences, Goethe University Frankfurt, Germany (U.Wacker@em.uni-frankfurt.de; Jens.Fiebig@em.uni-frankfurt.de; gerdes@em.uni-frankfurt.de)

²GeoZentrum Nordbayern, FAU Erlangen-Nürnberg, Germany (axel.munnecke@pal.uni-erlangen.de; michael.joachimski@gzn.uni-erlangen.de)

³Institute of Earth Sciences, Johannes Gutenberg-University, Mainz, Germany (schoeneb@uni-mainz.de)

The geochemical composition of fossil brachiopod shells reveals information about physical and chemical conditions of the paleo-ocean. We studied different stable isotopic systems on Silurian brachiopod shells from Gotland/Sweden to test their resistance against diagenesis and their use for paleoreconstructions.

In general, preanalyses (CL, SEM and trace element concentrations) of more than 60 shells indicate very good preservation. However, SEM investigations show that partial recrystallization occurred resulting in a patchwork of pristine and altered structures. $\delta^{18}\text{O}$ and $\delta^{13}\text{C}$, clumped isotope (Δ_{47}), as well as high resolution (LA-(MC)-ICP-MS) $\delta^{11}\text{B}$ and $^{87}\text{Sr}/^{86}\text{Sr}$ data of several brachiopod shells and their inner fillings (mudstones and sparitic cements) were measured. Clumped isotope temperatures range from 30°C to 70°C, indicating, that Δ_{47} values were partly reset during diagenesis. Because highest shell alteration temperatures correspond to those measured for the cements, we propose that ^{13}C - ^{18}O clumps were reset during cement formation. Since no correlation between Δ_{47} and $\delta^{18}\text{O}$ values is obtained, we conclude that the bulk oxygen isotopic composition was not altered concurrently. Furthermore, $\delta^{11}\text{B}$ and $^{87}\text{Sr}/^{86}\text{Sr}$ values of the brachiopods seem to reflect pristine marine signatures. Therefore we suggest that the alteration of clumped isotope values occurred at low water-rock ratios, not influencing $\delta^{18}\text{O}$, $\delta^{13}\text{C}$, $\delta^{11}\text{B}$ and $^{87}\text{Sr}/^{86}\text{Sr}$ signals.

B-isotope variations in tourmaline in the Varuträsk rare-element pegmatite: the role of mica

THOMAS WAGNER¹, ROBERT. B. TRUMBULL^{2*}, KARIN SIEGEL³, ERIK JONSSON⁴ AND CHRISTOPH A. HEINRICH⁵

¹Division of Geology, University of Helsinki, Finland

²GFZ German Research Centre for Geosciences Potsdam Germany (*presenting: bobby@gfz-potsdam.de)

³Earth & Planetary Sciences, McGill University, Canada

⁴Earth Sciences, Uppsala University, Sweden

⁵Earth Sciences, ETH Zürich, Switzerland

The Varuträsk rare-element pegmatite in northern Sweden is a classic and typical example of highly fractionated LCT-type pegmatites, with a well-developed internal zoning pattern composed of border, wall and intermediate zones and a quartz core. Major and trace element fractionation trends of feldspars, micas, tourmaline, and columbite-tantalite correlate well with the internal zoning pattern. This pegmatite therefore forms a good basis for a case study on the use of boron isotopes in tourmaline to record processes of pegmatite internal evolution.

Early and mid-stage tourmalines from Varuträsk show a systematic increase in $\delta^{11}\text{B}$ values from -14.6 to -6.2 ‰ during crystallization of the primary pegmatite zones. This trend toward ^{11}B -enrichment in the pegmatite magma is opposite to that expected for fluid exsolution or progressive crystallization of tourmaline, and all geochemical and textural evidence suggests a closed-system crystallization without significant influx of external fluids with heavy B-isotope signature. We suggest that crystallization of abundant muscovite in the Varuträsk wall zone depleted the magma in ^{10}B , driving the residual melt toward higher $\delta^{11}\text{B}$ values. Rayleigh fractionation models based on measured B contents of 220 ppm in muscovite and 3.4 wt. % in tourmaline show that the muscovite/tourmaline mass ratio required to explain the observed shift in $\delta^{11}\text{B}$ values is about 200:1, which is consistent with the modal composition of the wall zone assemblage.

The assumption is commonly made that in rocks where tourmaline is present, it plays the dominant role in B-isotope evolution. This assumption is likely to be true for most crystalline rocks but our study shows that it may not be the case for assemblages with a high modal abundance of micas, as in many pegmatites and related rocks such as greisens.

Speleothem reconstruction of sea-level at Bermuda over the last climatic cycles

K. WAINER^{1*}, G.M. HENDERSON¹, A.J. MASON¹, A.L. THOMAS¹, M. ROWE², B. WILLIAMS³, P. J. VAN HENGSTUM⁴ AND R. CHANDLER⁴

¹Dept. of Earth Sciences, Oxford University, South Parks Road, Oxford OX1 3AN, United Kingdom

(*correspondence: karinew@earth.ox.ac.uk)

²Birkbeck College, malet street, London WC1E7HX, UK

³Bermuda Institute of Ocean Sciences, St George's, Bermuda

⁴Woods Hole Oceanographic Institute, Massachusetts, USA

⁵Bermuda Zoological Society, Bermuda

It is now widely accepted that a sea-level rise is associated with global warming [1]. However, its rate, and the height it might reach by the end of the century remain poorly constrained. This study aims to provide better information and precision on the rates and magnitudes of past sea-level change, for periods when sea-level is close to its modern value, using speleothems from Bermudian caves. Speleothems interrupt their growth when they are submerged by sea-water, so U-Th dating periods of growth in coastal sites allows the reconstruction of past sea-level variation versus absolute time [e.g. 2,3,4]. We will present new MC-ICP-MS U-Th ages from a set of speleothems (stalagmites, stalactites, flowstones) collected from -6 to +12 m versus modern sea level from several caves in this northern Atlantic archipelago.

Relative sea-level (RSL) at Bermuda is of particular interest because it is at a distance from northern hemisphere ice sheets where the isostatic response to ice-unloading is uncertain. RSL reconstruction therefore provides both an indicator of possible rates of sea level change, and a test for glacial-isostatic-adjustment (GIA) models.

Our results provide constraint on sea level over the last climatic cycles, and in particular periods when sea level was equivalent or higher than today, at Bermuda which we place in the context of previous assessments of eustatic change, and of GIA models.

[1] Intergovernmental Panel on Climate Change (2007) Contribution of Working Group I to the Fourth Assessment Report, Cambridge Univ. Press. [2] Harmon *et al.* (1981) *Nature* **289**, 357-360. [3] Richards *et al.* (1994) *Nature* **367**, 481-483. [4] Bard (2002) *EPSL* **196**, 135-146.

Sulfide Re-Os Dating in Modally Metasomatised Peridotites, Insights from Letlhakane (Botswana)

A.N. WAINWRIGHT,*¹ A. LUGUET¹, R.O.C. FONSECA¹
AND D.G. PEARSON²

¹ Steinmann Institut, Universität Bonn, Germany

*correspondence: (ashlea.wainwright@uni-bonn.de)

²Department of Earth and Atmospheric Sciences, University of Alberta, Edmonton, Canada

Mantle xenoliths are a geochemist's window into the chemical and mineralogical make-up of the sub continental lithospheric mantle. However, metasomatism can obscure the primary composition and melt depletion history of the xenoliths. Therefore, whole-rock Re-Os age analysis of peridotite xenoliths may provide only a minimum estimate for the age of the lithospheric mantle, and likely reflects the presence of multiple generations of base metal sulfides (BMS) or platinum group minerals (PGM), which differ in age as well as mineralogy and habit. While metasomatic sulphides and/or PGM are likely to yield 'artificially young' Re-Os ages, refractory PGM such as Os-Ir-Ru alloys and refractory sulphides (e.g. laurite) should preserve older ages as a result of their high Os concentrations and resilience to overprinting and isotopic resetting. Together they provide the perfect target to investigate the Os isotopic heterogeneity in mantle samples.

Peridotite xenoliths found associated with the Letlhakane kimberlite (Magondi Belt, Botswana) provide us with a unique opportunity to study modal metasomatic effects on Re-Os and PGE systematics [1]. Whole rock analysis of xenolith samples from Letlhakane show co-variations of Re-Os T_{RD} ages and highly siderophile element fractionations (e.g. Pd/Ir: 0.1, T_{RD} : 2.7Ga – Pd/Ir 1.69, T_{RD} 1.6Ga), due to variable degrees of metasomatic overprint. Three samples that cover the entire metasomatic range were chosen to measure single grain sulfides for Re-Os via micro-distillation. Preliminary results show a wide range in sulfide T_{RD} ages, from future ages to over 3.0 Ga, even in the most metasomatised sample. The habit and structure of the sulfide seems to be the most important factor. Disseminated sulfides occurring in veinlets have the youngest age and most radiogenic $^{187}\text{Os}/^{188}\text{Os}$. On the other hand, discrete interstitial sulfides exhibit unradiogenic ^{187}Os and Archean ages. Our preliminary findings stress the micro-scale heterogeneity of Os isotopic signatures, which likely reflects multiple host mineral generations whose origins are linked to the complex multi-event petrogenetic history of mantle samples.

[1] Stiefenhofer *et al.* (1997) *Contrib. Mineral Petrol.* **127**, 147-158.

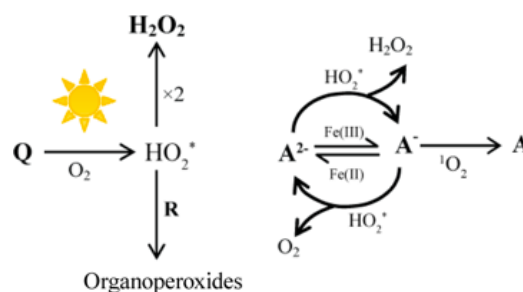
The Role of Reactive Intermediates in Redox Transformations of Iron in Photolyzed Acidic Natural Organic Matter Solutions

T. DAVID WAITE,¹ SHIKA GARG,¹ MARK L. BLIGH¹ AND ANDREW L. ROSE²

¹School of Civil & Environmental Engineering, The University of New South Wales, Sydney; d.waite@unsw.edu.au

²Southern Cross Geosciences, Southern Cross University, Lismore; andrew.rose@scu.edu.au

Recent studies of the dark oxidation of Fe(II) in previously photolysed acidic solutions of natural organic matter (NOM) (Garg *et al.* [1]) suggest the superoxide-mediated formation of semiquinone radicals which act as effective oxidants of Fe(II) (Schematic 1).



Schematic 1. Photolysis of NOM generates HO_2^* which, in turn, oxidize hydroquinone species (A^{2-}) present in NOM to semiquinone radicals (A^-). These radicals are effective oxidants for low concentrations of Fe(II). After Garg *et al.* [1]

In comparison, on continuous photolysis, light-generated singlet oxygen appears to oxidise A^- to the quinone form (A) with short-lived organoperoxy radicals (ROO^*) capable of oxidizing Fe(II) (Garg *et al.* [2]).

[1] Garg, S., Ito, H., Rose, A.L. and Waite, T.D. (2013). *Environ. Sci. Technol.* **47**, 1861–1869. [2] Garg, S., Jiang, C., Rose, A.L. and Waite, T.D. *Environ. Sci. Technol.* (submitted March 2013).

Stable isotopic fractionation of Sr and Eu among igneous rocks

S. WAKAKI^{1,2,3}, M. TANIMIZU¹, T. ISHIKAWA¹
AND T. TANAKA³

¹Kochi Institute for Core Sample Research, JAMSTEC, Kochi
783-8502, Japan. (wakaki(at)jamstec.go.jp)

²Natural History Sciences, Hokkaido Univ., Japan.

³Earth Environmental Sci., Nagoya Univ., Japan.

Sub-permil isotopic variations of Mg, Si, Fe and Sr were observed among igneous rocks, and the possibility of high temperature isotope fractionation during magmatic processes have been documented (e.g.; Charlier *et al.*, 2012; Savage *et al.*, 2011; Teng *et al.*, 2007; Teng *et al.*, 2008). We report sub-permil to permil order stable isotopic variation of Sr and Eu among igneous rocks with various origins.

28 igneous rocks covering a wide range of chemical compositions ($\text{SiO}_2 = 46.7 - 78.2$ wt.%) were analyzed. Samples were decomposed with a mixture of HF, HNO₃ and HClO₄. Granite samples were processed using Teflon bombs. Sr was separated by extraction chromatography using Sr Spec resin (Eichrom). Eu was separated by cation exchange column chromatography using AG 50W-x8 (Bio-Rad) with HCl and α -HIBA. Stable isotopic composition of Sr was analyzed by DS-TIMS technique using ⁸⁴Sr-⁸⁶Sr double spike and VG Sector 54-30 at NU. The results are expressed with relative to NBS 987 as $\delta^{88}\text{Sr} = [({}^{88}\text{Sr}/{}^{86}\text{Sr})_{\text{sample}}/({}^{88}\text{Sr}/{}^{86}\text{Sr})_{\text{NBS 987}} - 1] \times 10^3$. The reproducibility of $\delta^{88}\text{Sr}$ was ± 0.06 . Stable isotopic composition of Eu was analyzed on the Thermo Neptune MC-ICP-MS at JAMSTEC with external normalization using Sm. Potential isobaric interference of BaO was checked and found to be negligible. The results are expressed with relative to an Alfa Aesar Eu₂O₃ reagent as $\epsilon^{153}\text{Eu} = [({}^{153}\text{Eu}/{}^{151}\text{Eu})_{\text{sample}}/({}^{153}\text{Eu}/{}^{151}\text{Eu})_{\text{STD}} - 1] \times 10^4$. The reproducibility of $\epsilon^{153}\text{Eu}$ was ± 0.31 .

The $\delta^{88}\text{Sr}$ and $\epsilon^{153}\text{Eu}$ of the mafic and intermediate samples agreed each other with an average of +0.27 and +0.13, respectively. Felsic samples showed significantly large variations both on $\delta^{88}\text{Sr}$ and $\epsilon^{153}\text{Eu}$ ranging from +0.36 to -0.99 and from +0.20 to -5.73, respectively. Our $\delta^{88}\text{Sr}$ results for six international reference rocks agree well with the previously reported values. The observed variations of both $\delta^{88}\text{Sr}$ and $\epsilon^{153}\text{Eu}$ are correlated with SiO₂ abundances and also with the magnitude of negative Eu anomaly. The correlation between $\delta^{88}\text{Sr}$ and $\epsilon^{153}\text{Eu}$ with negative Eu anomaly indicates that the variation of $\delta^{88}\text{Sr}$ and $\epsilon^{153}\text{Eu}$ was caused by plagioclase fractionation during magmatic differentiation processes. This observation suggests that the melt-plagioclase isotope fractionation factor ($\alpha-1$) of Sr and Eu at magmatic temperature is on the order of 10^{-4} .

Anisotropy: A cause of heat flux variation at the CMB?

ANDREW M. WALKER^{*1}, MICHAEL W. AMMANN²,
STEPHEN STACKHOUSE³, JAMES WOOKEY¹, JOHN P.
BRODHOLT² AND DAVID P. DOBSON²

¹School of Earth Sciences, University of Bristol, Wills
Memorial Building, Queen's Road, Bristol BS8 1RJ, UK
(* correspondence: andrew.walker@bristol.ac.uk)

²Department of Earth Sciences, University College London,
Gower Street, London WC1E 6BT, UK

³School of Earth and Environment, University of Leeds, Leeds
LS2 9JT, UK

We have used atomic scale simulations to determine the thermal conductivity of MgSiO₃ perovskite and post-perovskite under D'' conditions and shown that the thermal conductivity of post-perovskite (~12 W/mK) is 50% larger than that of perovskite under the same conditions (~8.5 W/mK). This finding, in agreement with previous studies on analogue materials, means that the high heat flux into cold regions of D'' where post-perovskite is stable is enhanced relative to a simple single-phase case [1]. Furthermore, we have found that the thermal conductivity of post-perovskite is anisotropic, with conductivity along the *a*-axis being 40% higher than conductivity along the *c*-axis. Thus, – similarly to the lithosphere [2] – there is potential for texturing caused by deformation to modify how the mantle is heated from below. We test this idea by coupling our atomic scale results to previous models of texture in D'' [3] and find that anisotropic thermal conductivity may help to stabilise the roots of mantle plumes (Figure 1).

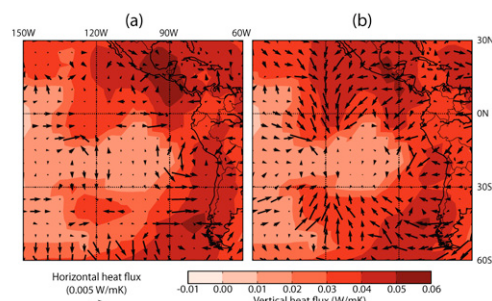


Figure 1: Modelled CMB heat flux at the base of a large plume in the East Pacific. Compared to the isotropic case (a) the horizontal heat flux in the anisotropic textured case (b) feeds heat, and thus buoyancy, into the plume.

[1] Hunt *et al.* (2012) *EPSL* **319-320**, 96–105. [2] Tommasi *et al.* (2001) *Nature* **411**, 783–786. [3] Walker *et al.* (2011) *Geochemistry Geophysics Geosystems* **12**, Q10006.

New Constraints on the Magnitude and Timing of Late Accretion

RICHARD J. WALKER^{1*}, MATHIEU TOUBOUL¹, IGOR S. PUCHTEL¹ AND JINGAO LIU²

¹Dept. of Geology, Univ. of Maryland, College Park, MD 20742, USA (correspondence: rjwalker@umd.edu)

²Department of Earth & Atmospheric Sciences, Univ. of Alberta, Edmonton, Alberta, Canada

Late accretion is defined as continued planetary growth subsequent to the cessation of core segregation. Late accretion was evidently a common, final step in the formation histories of rocky planetary bodies, regardless of size [1]. Evidence for this comes from estimates of planetary mantle compositions for various bodies, projected to contain raised, and broadly chondritic relative abundances of the highly siderophile elements (HSE). Although a ubiquitous process, the proportions of late accretionary mass additions, relative to planetary mass, may have ranged considerably. For example, current estimates suggest the Earth and Mars received proportionally much more late accreted mass than the Moon, perhaps reflecting stochastic late accretionary processes [2]. The timing of late accretion must also have varied considerably, with late accretion evidently occurring on asteroidal-sized bodies within the first 10 m.y. of solar system formation [1], but also acting on late-formed bodies, such as the Moon.

The nature and timing of late accretion to Earth is a particularly important issue, as this process could have delivered considerable water and organics to the mantle. One possibility is that the putative giant impact that generated the Moon was a major clearinghouse event for HSE, and thus, an event that heralded in a final stage of terrestrial late accretion. The long-term preservation of ¹⁸²W isotopic heterogeneities in the mantle [3-4], however, likely indicates that the terrestrial mantle was never completely homogenized, and possibly that the cumulative effects of terrestrial late accretion commensed well before the Moon-forming event. The presence of small enrichments in ¹⁸²W in some early-Earth rocks (Isua [3] and Nuvvuagittuq), coupled with depletions in HSE abundances estimated for their mantle sources, provides some evidence for uneven mixing of late accreted materials into the mantle, although other options to explain the enrichments are also possible. Of note, the magnitudes of ¹⁸²W enrichments are consistent with the mass addition proportions suggested by HSE abundances [3].

[1] Day *et al.* (2012) *Nature Geoscience* **5**, 614-617, [2] Bottke *et al.* (2010) *Science* **330**, 1527-1530, [3] Willbold *et al.* (2011) *Nature* **477**, 195-198, [4] Touboul *et al.* (2012) *Science* **335**, 1065-1069.

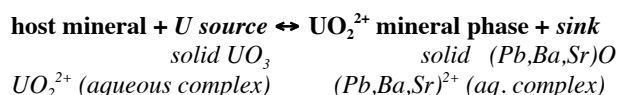
A first principles study of uranyl and neptunyl incorporation into sulfate minerals

S. M. WALKER* AND U. BECKER

Earth and Environmental Sciences, University of Michigan, 2534 CC Little, Ann Arbor, MI 48109, USA

(*correspondence: smwalk@umich.edu)

Solid solution formation at the mineral/water interface occurs when an ion in solution replaces an ion in the lattice; however, experimental observations have not fully decoupled the factors that control this process (*e.g.* ionic radius of foreign ion, coordination environment, molecular orbital interactions, charge compensation). In order to examine the thermodynamics of incorporation, the energies of incorporation of uranyl (UO₂²⁺) into anhydrous sulfate minerals, anglesite (PbSO₄), barite (BaSO₄), and celestine (SrSO₄), are calculated using a quantum mechanical approach. For each mineral, source and sink reference phases are chosen to facilitate the substitution of the uranyl ion with a cation from the host mineral as described by the general equation:



Of the three sulfate minerals, the energy of uranyl incorporation into anglesite was the lowest for solid state oxide reference phases ($\Delta E_{\text{rxn}} = 1.57$ eV). Anglesite also provided the lowest energy of incorporation of an aqueous species (UO₂²⁺_{aq} with the release of Pb²⁺_{aq}). Using aqueous species as source and sink phases but solid incorporation hosts required the combination of periodic and cluster quantum mechanical methods. Incorporation of uranyl was then compared with incorporation of Np(VI)O₂²⁺ and Np(V)O₂⁺ aqueous neptunyl complexes.

Since these static incorporation energies are most closely representative of the enthalpy of incorporation, the free energy was estimated using vibrational entropy values from empirical force field calculations in order to curtail computational expense. These vibrational entropy data tend to make incorporation energy values less energetically uphill. The limits of U- and Np-incorporation were also calculated to predict solid solution behavior.

The geochemistry and mineralogy of responsible mining of rare earths.

FRANCES WALL¹

¹Camborne School of Mines, University of Exeter, Cornwall Campus, Penryn, TR10 9EZ, UK. f.wall@exeter.ac.uk

Responsible mining is often regarded as largely a socio-economic issue but although good behaviour and governance are important, the fundamental ore deposit geochemistry and mineralogy also influence many relevant factors. For example, energy use, water use, resource efficiency, financial profitability, potential environmental contamination, and the health, safety and well-being of the work force are all related to the minerals present; to their compositions, sizes, shapes, textural relations, solubilities, amenability to various beneficiation methods, and how strongly they are held together.

Rare earths, used in many green technologies, are particularly interesting to consider from this point of view. Following the recent supply problems and the designation of rare earths as 'critical' metals, a wide range of rare earth deposits are now under active exploration and development, ranging from fresh and weathered carbonatites and alkaline rocks, to beach sands, ion adsorption clays and even sea floor muds. These diverse deposits have large differences in the characteristics listed above and raise a question about whether some deposits are inherently more environmentally friendly than others.

For example, unconsolidated beach sands, such as those currently mined for monazite in India, do not need comminution and thus can require one third of the energy to process than a hard rock carbonatite deposit. However, the monazite in beach sands is mostly derived from granitic protoliths and contains typically several wt% ThO₂, making it radioactive and problematic to store, ship and process. In contrast, rare earth fluorocarbonates in carbonatite deposits have some of the lowest Th contents of any of the rare earth minerals, and carbonatite monazite is also characteristically low in Th.

In order to make comparisons, metrics are required and it is necessary to balance the various factors, such as energy use, versus the other environmental impacts. The system of apportionment of these impacts when the REE are by-products also makes a large difference to the outcome. Mineral compositions and associations do vary within each deposit type and it is possible to develop a geometallurgical approach to environmental impact early on in an REE exploration project.

Liquid-liquid separation at the onset of CaCO₃ formation

A.F. WALLACE^{1,2*}, L.O. HEDGES^{1,2},
A. FERNANDEZ-MARTINEZ^{1,3}, P. RAITERI⁴,
S. WHITELAM², G.A. WAYCHUNAS¹, J.D. GALE⁴,
J.F. BANFIELD^{1,5} AND J.J. DE YOREO^{2,6}

¹Earth Sciences Division, Lawrence Berkeley National Laboratory, Berkeley, CA 94720, USA (*correspondence: afwallace@lbl.gov, gawaychunas@lbl.gov)

²The Molecular Foundry, Lawrence Berkeley National Laboratory, Berkeley, CA 94720, USA (lohedges@lbl.gov, swhitelam@lbl.gov)

³ISTerre, CNRS & Université de Grenoble 1, 38041 Grenoble, France (Alex.Fernandez-Martinez@obs.ujf-grenoble.fr)

⁴Nanochemistry Research Institute, Department of Chemistry, Curtin University, Perth, WA 6845, Australia (paolo@ivec.org, julian@ivec.org)

⁵Department of Earth and Planetary Science, University of California, Berkeley, CA 94720, USA (jbanfield@berkeley.edu) (jbanfield@berkeley.edu)

⁶Pacific Northwest National Laboratory, Richland, WA 99352 (James.DeYoreo@pnnl.gov)

Recent experimental characterizations of the early stages of calcium carbonate crystallization reveal an abundance of nanometer-sized prenucleation clusters that appear prior to formation of an amorphous intermediate phase. The prevailing interpretation of the clusters as thermodynamically stable suggests that the nucleation of calcium carbonate may follow a non-classical pathway.

This research uses replica-exchange molecular dynamics techniques to probe the initial formation and onset of order within hydrated calcium carbonate cluster species and lattice gas simulations to explore the more general behavior of clusters during phase separation. A two-phase thermodynamic model is also used to determine the free energy of the clusters as a function of size and to enable comparison with classical nucleation theory.

The results suggest that a spontaneous liquid-liquid phase separation may occur within the range of concentrations for which pre-nucleation clusters are observed. Coalescence of the nanoscale droplets results in the formation of a phase whose structure is consistent with that of amorphous calcium carbonate. The significance of these results is discussed within the context of classical and emerging non-classical phase-separation theories.

The potential of using a sector field ICP-MS for analysis of fluid inclusions by laser ablation ICP-MS

M. WÄLLE* AND C.A. HEINRICH

ETH Zurich, Inst. of Geochemistry and Petrology,
Clausiusstrasse 25, 8092 Zurich, Switzerland,
(*correspondence: waelle@erdw.ethz.ch)

Laser ablation inductively coupled plasma mass spectrometry (LA-ICPMS) is a successful technique to measure elemental concentrations in fluid inclusions [1]. Depending on their salinity, inclusions in the size a 10 to several tens of micrometres are needed to determine trace element concentrations reliably. Up to now, quadrupole (Q-) ICP-MS have been used for this kind of analyses due to its ability to switch fast (e.g. within one millisecond) from one mass to another over the entire elemental mass range. Short settling times are required to record the fast changing transient signals obtained by LA-ICPMS analyses of fluid inclusions. Sector field (SF-)ICP-MS would provide a higher sensitivity than Q-ICPMS and, therefore, have to potential to measure smaller inclusion, demand a higher settling time than the latter ones due to changing the magnetic field.

A fast scanning SF-ICPMS was used to explore the potential of this instrument for analysing fluid inclusions. An assemblage consisting of fluid inclusions in the range of a few micrometres up to 150 μm and a salinity of 4wt% NaCl was used to (i) check the accuracy of the fast scanning SF-ICPMS system and (ii) compare the performance of a Q-ICPMS (PerkinElmer, Elan 6100 DRC) and a SF-ICPMS (ThermoFisher, Element XR) coupled to the same laser ablation system. The fast scanning SF-ICPMS system was able to analyse fluid inclusions with a 1.8 to 2 times smaller diameter, i.e. 5 to 8 times in mass, with a similar accuracy, e.g. on elements like Pb, Ba, Sb or Mg, than the Q-ICPMS system measuring the same elements.

[1] Heinrich *et al.* (2003), *Geochim. Cosmochim. Acta* **67**, 3473-3496.

Magma formation in hot-slab subduction zones: Insights from volatile contents of melt inclusions from the southern Cascade arc

WALOWSKI, K.J.¹, WALLACE, P.J.¹, CLYNNE, M.A.², WADA, I.³ AND RASMUSSEN, D.J.¹

¹University of Oregon, Eugene, Oregon 97403, USA
(correspondence: walowski@uoregon.edu)

²USGS Volcano Science Center, Menlo Park, CA, USA

³Tohoku University, IRIDeS, Sendai 980-8579, Japan

Cross-arc geochemical variations can provide insight into dehydration reactions in the subducting slab and magma generation processes in the mantle wedge. In this study, cinder cones were sampled at varying distances from the trench in the Lassen Region, the southern segment of the Cascade Arc, which subducts some of the youngest oceanic crust globally. Olivine-hosted melt inclusions (Fo84-90) from the tephra of 6 calc-alkaline basaltic cinder cones have been analyzed for volatile, major and trace elements.

Using the maximum volatile contents at each cone to represent the undegassed magma, we find values (2.1-3.4 wt% H₂O and 500-1200 ppm CO₂, corrected to be in eq. with Fo90 olivine), slightly higher than primitive melt inclusions from central Oregon [1]. These values from the Cascades overlap with data for other arcs, but are lower on average. We have also analyzed fluid-mobile trace elements to understand the trace element signature of the slab component and the extent of fluid-fluxing across the arc. At the arc axis, (Sr/P)_N values are high, although variable, and they decrease towards the backarc [2]. (Sr/P)_N correlates with other slab-derived fluid tracers such as H₂O/Ce and Cl/Nb, indicating a link between volatile and trace element enrichment of the mantle wedge.

Slab surface temperatures calculated using the H₂O/Ce thermometer [3] range from 740-870±50°C, which is slightly lower than those predicted by new 2D geodynamic models for this region (850-950°C). The similarity of the temperature estimates suggests active fluxing of hydrous material from the slab into the mantle wedge beneath the arc rather than downdragging of hydrous mantle from the forearc region. Both H₂O/Ce and geodynamic model temperatures are at or above the MORB+H₂O solidus [4] suggesting the likelihood of hydrous slab melting beneath the arc. Because high slab temperatures require the slab to largely dehydrate beneath the forearc, our results require either substantial metastability of hydrous phases in altered oceanic crust or serpentinite-derived water from the mantle of the downgoing slab.

[1] Ruscitto(2010) *EPSL* **298**, 153–161. [2] Borg (1997) *Can. Min.* **35**, 425–452. [3] Cooper (2012) *G³* **13**, (3). [4] Schmidt (1998) *EPSL* **163**, 361–379.

World's oldest eclogites? Phase equilibria constraints on 2 Ga metapelitic-hosted eclogites from the Usagaran Orogen, Tanzania

ALEC WALSH*¹, MARTIN HAND¹, ALAN COLLINS¹ AND
RACHEL BRICK¹

¹Centre for Tectonics Resources and Exploration, School of
Earth and Environmental Sciences, University of
Adelaide, Adelaide 5005, South Australia, Australia
(correspondence: alec.walsh@adelaide.edu.au)

Eclogite-facies rocks preserve a record of deep crustal thickening and exhumation. Orogenic belts that contain eclogites generally mark plate collisions and are considered to represent ancient subduction zones. Eclogites from the Paleoproterozoic Usagaran Orogen, which flanks the eastern margin of the Archean Tanzania Craton, yield ages of 2 Ga and are considered to be the amongst the oldest preserved eclogites in the world.

Phase equilibria constraints indicate that metapelitic rocks, which structurally envelop eclogite-facies mafic rocks [1], developed a peak metamorphic assemblage of gt–ky–amph–mus–bi–ru–q at ~12 kbar and 650°C; far lower pressures than previously predicted. Prograde chemical zoning preserved in garnet appears to mitigate against exhumation of the metapelites from eclogite facies conditions. Rather, the petrological and compositional data suggest a steep up-pressure prograde path. Preliminary data suggests that the mafic eclogites underwent metamorphic reworking at around the conditions recorded by the peak assemblages in the enclosing metapelites. If this is correct it implies that the exhuming eclogites became structurally mixed with metasedimentary lithologies located higher in the exhumation channel. Such a scenario is similar to that inferred in modern convergent margin settings, and implies that the Usagaran Orogen is one of the oldest examples of “modern style” plate margin metamorphism.

[1] Möller, Andreas, *et al.* "Evidence for a 2 Ga subduction zone: Eclogites in the Usagaran belt of Tanzania." *Geology* 23.12 (1995): 1067-1070.

Diamonds and their inclusions from Dachine, French Guiana: A record of Paleoproterozoic subduction

M.J. WALTER*¹, C.B. SMITH¹, G.P. BULANOVA¹,
S. MIKHAIL² AND S.C. KOHN¹

¹School of Earth Sciences, University of Bristol, Bristol, BS8
1RJ (*correspondence: m.j.walter@bristol.ac.uk)

²Geophysical Laboratory, Carnegie Institution of Washington,
Washington D.C. 20015, USA

Diamonds and their mineral inclusions provide a record of deep mantle processes. Most diamonds are from the subcontinental mantle lithosphere and record ancient episodes of growth, whereas others form at sub-lithospheric depths and record deep carbon cycling¹. We report new data from a unique suite of diamonds and syngenetic inclusions from the Dachine ultramafic, French Guiana. These samples defy categorisation into traditional diamond groups, but show evidence of originating in a subduction zone environment.

The highly altered Dachine host rock (2.1 Ga) is not kimberlitic, but based on textures and chemical characteristics has been identified as a pyroclastic komatiite². Dachine diamonds also have unique characteristics³ including low N aggregation state (type Ib), a predominance of light C and heavy N isotopes, and complex internal morphologies often showing evidence of deformation. We have located five syngenetic garnet and Cpx inclusions, which are the first reported silicate inclusions in Dachine diamonds. The three garnet inclusions are eclogitic having high Ca and low Cr, and are unusually rich in Mn and Ni but extremely depleted in LIL and LREE. The Cpx inclusions are also extremely depleted in incompatible elements and one is Mn-rich.

The trace element systematics of the silicate inclusions are best matched if the inclusions represent residual phases to either multiple melt/fluid extraction events during subduction, or by a single extraction event involving coexisting trace phases such as epidote and rutile. Temperature constraints from N aggregation are inconsistent with a high-temperature komatiite origin for the Dachine host, whereas trace element systematics can be reconciled with a melt generated in a subduction zone environment, an origin which we presume is cold and hydrous. A model integrating all these observations suggests diamond and inclusion growth, and possibly host magma generation, at the interface between a Paleoproterozoic subducting slab and overlying mantle.

[1]. Shirey *et al* (2013), *RIMG* 75, 355-421. [2]. Capdevila *et al* (1999), *Nature* 399, 456-458. [3]. Cartigny *et al* (2010) *EPSL* 296, 329-339.

New insights on gas storage and transport in shales

CLIFFORD C. WALTERS¹

¹ExxonMobil Research & Engineering, 1545 Rt. 22 E,
Annandale, NJ 08801.
clifford.c.walters@exxonmobil.com

The rapid development of shale gas and liquids has far outpaced our knowledge of how these systems function. Most of the tools and models used on conventional reservoirs are inadequate to characterize tight rocks. Using new methods and techniques, researchers in industry, academia, and government labs have made considerable progress in revealing the underlying processes involved in gas storage and transport.

Although all shales have some inter- and intra-granular mineral porosity, the majority of the gas in mature, carbon-rich shales is stored in porous organic matter. NMR, small angle neutron scattering (SANS), mercury injection capillary pressure (MICP) and gas sorption experiments suggest that shales possess a broad range of pore sizes with an appreciable volume existing in mesopores having diameters of 2 to 50 nm. Unlike conventional reservoirs where pore throats tend to scale with pore size, the connecting pore throats in shales appear to be small (<20 nm). SEM has been extensively used to image pores in shales, but sees only a fraction of the pore network. The Zeiss Helium Ion Microscope has proven to be capable of imaging the nm-scale structures revealing the true nature of gas storage in shales. Local porosity in kerogen can be extremely highly (>30%) and nm-wide conduits for gas migration can be traces over μm distances. These porous networks form late in the oil window, become abundant by the onset of the gas window, and remain relatively unaltered in shales at extremely high maturity.

The nm-scaled features, however, are inadequate to explain the observed rates of gas transport in producing wells. Using micro X-ray CT and NMR, we have measured gas transport in whole cores under reservoir conditions. Rapid transport occurs in high permeability features sub-parallel to bedding, followed by slower transport into the rock matrix surrounding these features. The high permeability features are physical micro-cracks within the mineral matrix and at mineral-organic boundaries. It is impossible to prove that such features exist in undisturbed subsurface shales; however, we find a correlation with their presence and well productivity.

The work being presented was conducted by Max Deffenbaugh, John Dunsmuir, Aaron Eberle, Hubert King, Chris Kliewer, Pavel Kortunov, and Michael Sansone.

Use of sulfur isotopes to quantify biological and abiotic processes contributing to sulfur cycling in an AMD treatment system

EVAN R. WALTERS¹, CHARLES W. PUGH²
KELLY S. BENDER² AND LILIANA LEFTICARIU^{1,*}

¹Southern Illinois University, Department of Geology,
ewalt@siu.edu; lefticar@siu.edu (*presenting author)

²Southern Illinois University, Department of Microbiology,
cpugh13@gmail.com; bender@micro.siu.edu

Untreated drainages from abandoned coal mines are generally low-pH waters that contain high concentrations of dissolved SO_4^{2-} , Fe, Al, Mn and other elements of environmental concern (e.g., As, Se, Zn, Cd and Ni). In the Illinois Basin this has been a significant and costly problem as extensive mining has been carried out during the last century. Currently, treatment systems of coal-generated AMD include the use of bio-induced stabilization of dissolved SO_4^{2-} and metals in sulfides, as the optimal way for effective, long-term treatment. However as AMD systems evolve, fluctuations in physical (e.g., rain induced-dilution, dynamic AMD flow rates), chemical (e.g., precipitation, sorption, desorption, etc.) and biological processes provoke temporal disequilibria within the system. Therefore, it remains challenging to assess the extent of permanent contaminant sequestration and predict long-term treatment viability.

We present a 1-year study of concentrations and $\delta^{34}\text{S}$ values of sulfur compounds in six field-scale column experiments conducted at the Tab-Simco site to constrain the efficiency of various organic substrates in supporting the bio-reduction processes. Our results show: (1) During warm months ($T > 10^\circ\text{C}$) high levels in H_2S in the reactors containing limestone and different combinations of *organic amendments indicate the presence of sulfate reducing bacteria (SRB)*. Analysis of initial microbial community and SRB community via the 16S rRNA and *dsrAB* genes, respectively, suggest the presence of *Desulfotomaculum*, *Desulfomicrobium* and *Desulfococcus*. (2) Sulphur cycling is dynamic and strongly influenced by both biological and abiotic processes. (3) Increasing bacterially-mediated sulfate reduction processes are associated with enrichment of 10-15‰ and precipitation of secondary sulfates is associated with depletion of 1-2‰ in $\delta^{34}\text{S}$ in residual SO_4^{2-} . (4) Isotopic mass balance calculations indicate that abiological sequestration was the dominant mechanism during the initial stage of the experiments and the low-temperature months. Our study demonstrates the applicability of the method to assess the rates, progress and environmental fate of pollutants associated with in AMD treatment processes.

Episodic growth of continental crust: A 3-D geodynamic model

UWE WALZER^{1*} AND ROLAND HENDEL²

¹Institut für Geowissenschaften, F.-Schiller-Univ., Jena,
Germany (*correspondence: u.walzer@uni-jena.de)

²Institut für Geowissenschaften, F.-Schiller-Univ., Jena,
Germany (roland.hendel@uni-jena.de)

The focus of this paper is the question (1) whether the observed zircon age distribution of continental crust (CC) is produced by real crustal growth episodes or is only an artefact of preservation. Question (2): In connection with the second alternative of (1), it has been proposed that there was little episodicity in the production of new CC and that modeling corroborates this opinion. In answer to (1), we conclude that a combination of the two proposals might be possible. In matters of (2), we ascertain that a dynamic modeling of the convection-differentiation system of the mantle reveals the high probability of magmatic episodes. We solve the full set of balance equations in a 3-D spherical-shell mantle. The heat-producing elements are redistributed by chemical differentiation. A realistic solidus model of mantle peridotite is essential. The solidus depends not only on depth but also on the variable water concentration. Furthermore, we introduced realistic profiles of Grüneisen parameter, viscosity, adiabatic temperature, thermal expansivity and specific heat. Our model automatically produces lithospheric plates and growing continents. Regarding number, size, form, distribution and surface velocity of the continents, no rules have been prescribed. Regions of the input parameter space (R_a , σ_y , k , f_3) which are favorable with respect to geophysical quantities show simultaneously not only episodicity of CC growth but also a reproduction of the observed zircon-age maxima referring to the instants of time. Admittedly, we also obtain Archean events for ages greater than 3000 Ma which are not or scarcely visible in the observed zircon ages. Sinusoidal parts of the evolution curve of q_{ob} , U_r and E_{kin} are found superposed with a monotonous decrease. T_{mean} , however, decreases smoothly and slowly, nearly without pronounced variations. Therefore, we can dismiss catastrophic mechanisms which simultaneously incorporate the whole mantle.

Role of exopolymeric substances in dolomite biomineralization by coastal sabkha sulfate-reducing bacteria: an *ex situ* study of microbial community-mineral interactions using solid-support imaging

*WAN ABDUL-MATIIN¹, BILAL MANSOOR², AND FARRUKH AHMAD¹

¹Bio-Energy and Environmental Laboratory (BEEL), Water and Environmental Engineering, Masdar Institute of Science and Technology, PO Box 54225, Abu Dhabi, United Arab Emirates. *wabdulmatiin@masdar.ac.ae

²Advanced Materials and Manufacturing Laboratory, Materials Science and Engineering, Masdar Institute of Science and Technology, PO Box 54225, Abu Dhabi, United Arab Emirates. bmansoor@masdar.ac.ae

While the microbial-mediation model has advanced current understanding of modern dolomite genesis, the exact mechanism remains speculative, especially in the context of microbial community architecture. Here we investigate the biofilm aspect of natural SRB growth within a dolomitizing culture via analysis of media chemistry and surface formations. SRB from a coastal sabkha (western Abu Dhabi) were studied vis-à-vis different quantities of exopolymeric substance (EPS), under simulated sabkha pore water conditions, and using inert solid support materials to capture biofilm/biomineral growth. The experimental reactor with the highest EPS content presented the most significant areal distribution of Mg-rich carbonate phases against reactors of lower/no EPS content (mean Mg/Ca molar ratio of 44.1% vs. 27.9%). More detailed microanalyses of major formations also revealed greater incorporation of Mg^{2+} in saturated, partially degraded EPS aggregates (Mg/Ca molar ratio up to 91.2%) compared to a growing biofilm matrix (Mg/Ca molar ratio up to 41.4%). Furthermore, a variety of mineral morphologies with varying levels of Mg incorporation were observed in inoculated reactors supplemented with EPS, hinting at gradual dolomitization. Strategic nucleating sites for Ca-Mg carbonates appeared to be provided by aged EPS, while actively secreted and extensively growing biofilm EPS instead would initially inhibit mineralization through cation binding. Ca-Mg carbonate biomineralization might hence depend on the dynamic interplay of various physical, chemical and physiological conditions of local EPS that would constitute an optimal nucleating microenvironment.

Thermal evolution of surface silanols and nanopores in silica particles

QUAN WAN*, SHANSHAN LI, ZONGHUA QIN
AND YI XIAO

Institute of Geochemistry, Chinese Academy of Sciences, Guiyang,
Guizhou, 550002, P.R. China

(* Correspondence: wanquan@vip.gyig.ac.cn)

Nanoporous structures have been commonly found in rocks, soils, minerals, and organic matters. It is believed that nanopores are closely related to a range of vital geo-processes and geo-engineering applications, including rock weathering, elemental enrichment and bioavailability, shale gas exploration, carbon cycling and sequestration, etc [1]. Yet knowledge gaps still exist toward understanding fundamental structures and properties of nanopores. Difficulties and inaccuracies in determining nanopore structure and its evolution easily lead to misinterpretation and contradiction of experimental observation [2]. In this study, we used monodisperse, submicron-sized silica particle (synthesized through Stöber process) as our model system, which was subject to dehydration (2hr at 200°C), dehydroxylation (2hr at 400~800 °C) and rehydroxylation (overnight boiling in water). The thermally treated silica particles were subsequently characterized by thermogravimetry (TGA), differential scanning calorimetry (DSC), TGA-IR, pycnometry, elemental analysis and scanning electron microscopy (SEM), etc [3]. Our experimental findings indicated that thermal evolution of surface silanols for Stöber silica (~500nm diameter) accurately fits with the Zhuravlev model for surface chemistry of amorphous silicas [4]. For example, heating at 400°C quantitatively removed all vicinal silanol groups resulting a weight loss (200~1000°C) of ~48.3% (*i.e.*, 1.728/3.574 from TGA data), which was nearly identical to the calculated result using theoretical silanol densities (*i.e.*, 4.6, 2.35, and 0.25 groups/nm² at 200°C, 400°C and 1000°C, respectively; (2.35-0.25)/(4.6-0.25)=48.3%). Our results also indicated a fully reversible recovery of silanol density through boiling in water and a specific surface area (SSA) of ~550 m²/g for silica treated ≤400°C. The large SSA apparently supports a nanoporous structure, which was observed to undergo irreversible pore collapse when heating at above 600°C. This nanopore structure evolution is consistent with the results from density measurements.

[1] Wu *et al.* (2013) *Geochim Cosmochim Acta* **109**, 38-50.
[2] Szekeres *et al.* (2002) *Langmuir* **18**, 2678-2685. [3] Wan *et al.* (2010) *J Therm Anal Calorim* **99**, 237-243. [4] Zhuravlev (2000) *Colloid Surface A* **173**, 1-38.

Late Triassic adakitic rocks formed by partial melting of ancient mafic lower crust in the North China Craton

CHAO WANG¹ AND SHUGUANG SONG^{1*}

¹School of Earth and Space Sciences, Peking University,
Beijing 100871, China

(*correspondence: sgsong@pku.edu.cn)

Adakites were originally defined as partial melts of young subducting oceanic crust [1]. However, based on investigations of adakitic rocks in various settings, several other genetic mechanisms have also been proposed, including partial melting of slab-melt modified mantle wedge [2], assimilation and fractional crystallization of basaltic magmas [3], mixing between felsic and basaltic magmas [4], partial melting of thickened lower crust [5] and partial melting of delaminated lower crust [6].

Here we report the Late Triassic adakitic rocks in the eastern part of the North China Craton. They are granitic gneisses with high SiO₂ (68.87-70.15 %), Sr/Y (118-176) and (La/Yb)_N (54-66) and low MgO (1.30-1.47 %), which are similar to adakitic rocks formed by partial melting of thickened lower crust. In-situ zircon LA-ICP-MS U-Pb dating reveals that they were emplaced in the Late Triassic (218-229 Ma). In-situ Hf isotope data for zircons show that they are characterized by the evolved $\epsilon_{\text{Hf}}(t)$ of -17.4 to -14.6 and T_{DM2} ages of 2.18-2.36 Ga, implying their source materials were extracted from the depleted mantle in the Paleoproterozoic. Trace element modeling suggests that they might be produced by 20-30 % partial melting of the Paleoproterozoic mafic lower crust materials equilibrated with eclogite residues (Grt/Cpx = 30/70).

Based on the above lines of evidence, plus the post-collisional extensional environment in the Late Triassic, we propose that these adakitic rocks in the NCC were produced through melting of the thickened ancient Paleoproterozoic mafic lower crust triggered by upwelling of basaltic magmas. Furthermore, they might be the result of the onset of lithospheric thinning of the NCC initiated in the Late Triassic.

[1] Defant & Drummond (1990) *Nature* **347**, 662-665. [2] Martin *et al.* (2005) *Lithos* **79**, 1-24. [3] Castillo *et al.* (1999) *Contrib. Mineral. Petrol.* **134**, 33-51. [4] Guo *et al.* (2007) *J. Petrol.* **48**, 661-692. [5] Atherton & Petford (1993) *Nature* **362**, 144-146. [6] Gao *et al.* (2004) *Nature* **432**, 892-897.

Biomarker evidence for the Neoproterozoic marine redox condition in South China

CHUNJIANG WANG*, XIAOFENG XIONG, HAIFENG GAI, YUE LIU, BAOGANG LI, XUAN ZHOU AND BO XU

State Key Laboratory of Petroleum Resources and Prospecting, China University of Petroleum, Beijing 102249, China, wchj333@126.com (*presenting author)

An important increase in atmospheric oxygen appears to have taken place during the late Neoproterozoic period [1, 2]. This increase may have stimulated the evolution of macroscopic multicellular animals [1, 3] and may have led to oxygenation of the deep ocean [4].

In order to understand more about the ocean oxygenation process during the Neoproterozoic period, a core spanning 450m of stratigraphic section across Cryogenian Datangpo Fm. and Nantuo Fm., Ediacarian Doushantuo Fm. and Dengying Fm., and early Cambrian Niutitang Fm. (ca. 663–518 Ma), was drilled at Xiushan in South China. The paleogeographic reconstruction suggests that Xiushan region was located at the outershelf margin to slope in the central Yangtze platform of South China [5]. Here we report a secular change in biomarker and C_{org} - and C_{carb} -isotopic compositions based on this drillcore section, which aims to reveal the difference in organic matter sedimentation and marine redox condition between the interglacial Datangpo Fm. and postglacial Doushantuo Fm., and the difference between the outershelf-slope facies Doushantuo Fm. at Xiushan region and the innershelf basin facies at the Jiulongwan section.

Organic geochemical evidence shows that the Datangpo Member I and II could deposit in dysoxic and oxic condition, respectively. It means that the Datangpo Member I black shale was likely not deposited in an anoxic or euxinic condition as suggested before [6]. Obvious difference in Doushantuo biomarker assembly occurs between Xiushan region (outershelf–slope) and the Jiulongwan section (innershelf basin), which may have been caused by differential redox conditions or depositing processes of organic matters. Our data support the idea that the reconstruction of the redox condition in Cryogenian and Ediacaran oceans should be based on approaches from various facies ranging from shallow marine shelf to deep marine basin [5, 7].

[1] Fike *et al.* (2006) *Nature* **444**, 744–747. [2] Canfield *et al.* (2007) *Science* **315**, 92–95. [3] McFadden *et al.* (2008) *PNAS* **105**, 3197–3202. [4] Rothman *et al.* (2003) *PNAS* **100**, 8124–8129. [5] Jiang *et al.* (2011) *Gondwana Res.* **19**, 831–849. [6] Li *et al.* (2012) *EPSL* **331–332**, 246–256. [7] Zhu *et al.* (2007) *PPP* **254**, 7–61.

Interaction of Bioavailability of Soil Heavy Metals in Black Soil Region of Central Jilin Province

D.Y.WANG*, Y.F.LI, Y. Y.YANG AND X.L.YANG

Jilin University, College of Earth Sciences, Changchun, China (wang_dy@jlu.edu.cn*, yuefenyou@163.com, yangyuan52415241@163.com, 33390016@qq.com)

Heavy metal, which endangers ecological environment directly and brings indirect harm by affecting the bioavailability of soil nutrients, is an important substance resulting in soil pollution and degradation. Correspondently, nutrient elements in soil also affect the eco-environmental impacts of heavy metals. Thus, the interaction between heavy metals and nutrient elements, as a new aspect of pollution ecology of heavy metals, is important for maintaining ecological balance.

In present study, it is analyzed that the total and bioavailability contents of heavy metals (Cr, Cd, Cu, Zn, Ni, As) and the contents of major nutrient elements (P, K, Ca, Mg, Fe, B) for 61 surface soil samples in black soil region of central Jilin province, NE China. The bioavailability characteristics of heavy metals are recognized according to the effective coefficients of soil elements (available contents of elements in soil accounting for total amounts). And the effective coefficient correlations for different heavy metal as well as the heavy metals and nutrient elements are calculated by SPSS (Ver. 13.0).

The obtained results indicate that all the following effective coefficient correlations are obvious positive, (1) Cd and Zn with the other heavy metals, (2) Cr with As, Cd, Zn and Ni, (3) Ni with Cr, Cd and Zn, (4) As with the Cr, Cd, Cu and Zn. These findings indicate that the bioavailability conversion of heavy metals have promoting effect to each other in study area.

Remarkably, the effective coefficients of six heavy metals show obvious positive correlations with P, which is consistent with the major standpoint about the interaction between P and heavy metals in soil, implying that the effective content of P plays a role in promoting the activation of heavy metals. Additionally, these results indicate that the following effective coefficient correlations also exhibit obvious positive, (1) micronutrient element B and Fe with As, Cu and Zn, (2) between Fe and Cr, (3) Mg with Cr, Ni and Zn. However, the effective coefficient of Ca has obvious positive correlations with heavy metals except Cu. And the correlations between the effective coefficients of K and As exhibits obviously negative.

In short, study on interaction of bioavailability of elements provides insights to understand the black soil degradation mechanism, prevent heavy metal pollution, balance the nutrients, and strengthen management of the black soil resource.

Petrology, geochemistry and metamorphic evolution of metamorphic rocks in Diancang Shan-Ailao Shan metamorphic complex belt, Southeastern Tibetan Plateau

FANG WANG, FULAI LIU, PINGHUA LIU, JIANRONG SHI AND JIA CAI

Institute of Geology, Chinese Academy of Geological Sciences, Beijing 100037, China
(wangfang_mr@yahoo.cn)

Combined study of petrology, geochemistry and metamorphism of meta-sedimentary rocks and meta-basic rocks, provide clear evidence of metamorphic evolution of Diancang Shan-Ailao Shan metamorphic complex belt. Detailed geochemical analysis in the meta-sedimentary rocks and amphibolites suggest the protoliths of claystone, siltstone, graywacke and island-arc basaltic rock, respectively. Microprobe and mineral inclusions analysis reveals that garnet porphyroblasts in meta-sedimentary rock bear a chemical composition zonation from core to rim. On the basis of paragenesis, mineral transformation and chemical composition zonation of garnets, four metamorphic stages have been recognized, i.e. early prograde metamorphic stage (M_1), peak amphibolite-granulite facies metamorphic stage (M_2), near isothermal decompression retrogression metamorphic stage (M_3), and late amphibolite facies retrograde stage (M_4). The paragenesis of Grt + Pl + Ms + St \pm Ky \pm Bt \pm Kfs + Qz (meta-sedimentary rocks), which formed at 560 ~ 590°C and 5.5 ~ 6.3 kb, is regarded as the M_1 stage mineral assemblage. The typical mineral assemblage of M_2 stage, which constrains P - T condition of 720 ~ 760°C and 8.0 ~ 9.3 kb, contains Grt + Bt + Ky/Sil + Pl + Qz or Grt + Bt \pm Sil + Pl \pm Kfs + Qz (meta-sedimentary rocks) and Grt + Cpx + Pl (meta-basic rocks). The paragenesis of Grt + Bt + Sil + Pl + Qz (meta-sedimentary rocks) and Hbl + Pl \pm Cpx \pm Bt \pm Qz (meta-basic rocks) defines M_3 stage mineral assemblage, occurring at P - T condition of 650 ~ 760°C and 5.0 ~ 7.3 kb. Newly formed intersectional biotite and muscovite, together with the rim of garnet, define the M_4 stage mineral assemblage of Bt + Ms + Pl \pm Kfs \pm Grt + Qz (meta-sedimentary rocks), inferred at 553 ~ 613°C. The metamorphic complex, record a clockwise metamorphic P - T trajectory characterized by near isothermal decompression. The integrated clockwise P - T path established for metamorphic complex in Diancang Shan-Ailao Shan metamorphic complex belt is a potential record of geodynamic process related to subduction-collision-exhumation between Indian and Eurasian plate.

This study was financially supported by the Nation Natural Science Foundation of China (Grant no. 40921001 and 40725007) and by a Chinese Geological Survey Bureau project (Grant no. 1212011121276)

Zircon U-Pb-Hf-O isotopes and REE constrains on the origin of Mesozoic ore-bearing high Mg# adakitic rocks from Ningzhen area of east China: Petrogenesis and tectonic implications

FANGYUE WANG^{1*}, SHUGUANG LIA,^{2*} SHENG-AO LIU² AND SHEMIN AKHTARA¹

¹CAS Key Laboratory of Crust-Mantle Materials and Environments, School of Earth and Space Sciences, University of Science and Technology of China, Hefei 230026, China

²State Key Laboratory of Geological Processes and Mineral Resources, China University of Geosciences, Beijing 100083, China

Cu-Mo-Fe mineralized high Mg# adakitic porphyries intruded in the eastern Lower Yangtze River Belt (LYRB), but the timing and petrogenesis of these adakites are not well constrained. In this study, five samples were collected from the ore-bearing adakites (Anjishan Cu deposit, Tongshan Cu-Mo deposit and Xiangshan Fe deposit) of Ningzhen region, in order to precisely constrain their formation ages, petrogenesis and tectonic settings. Zircon U-Pb ages dated by LA-ICP-MS show that ore-bearing adakite in Ningzhen region are about 110-118 Ma, obviously younger than ore-bearing adakites (140 \pm 5Ma), bimodal volcanic rocks with A-type granites (126-131Ma) along the LYRB. Magmatic zircon Ce⁴⁺/Ce³⁺ of adakites ranges from 4-1615, compatible to those from the older adakites in LYRB. Zircon Hf and O isotopes from Ningzhen adakites show a wide range from -10.58 - -23.35 and 5.74-7.03‰, respectively, fall between those of the LYRB and South Tan-Lu fault zone (STLF). Zircon Ti-thermometry of Ningzhen adakites range from 550-700 °C, averaged at 650 °C, similar to those from the LYRB too. Zircon O-Hf-Ce⁴⁺/Ce³⁺ and Ti-thermometry from the Ningzhen ore-bearing porphyries show their magma source may from an oxidized water-rich sources with continental crust involvement. Genesis of adakites in Ningzhen region is best explained by assimilation between metasomatized mantle and lower continental crust and followed by fractional crystallization. Combined with published ages data of ore-bearing adakites from the LYRB, Mesozoic magmatic activities from LYRB show a younging trend from inland to outland. A slab flat subducting and rolling back evolution model of the LYRB is proposed in this study.

Hydrocarbon Mobility Prediction for lacustrine shale oil plays

WANG, FEIYU¹, WEIPING FENG¹ AND ZHIYONG HE²

¹China University of Petroleum, Beijing, 102249)

²Zetaware Inc., Sugar Land, TX. 77479 USA

Lacustrine shale oil plays or tight oil systems have become the important exploration and development target in China, a great amount residual hydrocarbon exist in the mature organic matter rich lacustrine shale plays, For a shale play to work, it has to have enough original oil in-place volumes and producible, The occurrence and mobility of residual hydrocarbon are key to assessment of shale oil plays.

Residual hydrocarbon can be split into two parts, free oil and adsorbed oil, the former occur in the organic matter rich source rocks intervals and interbedded various scale tight reservoir layers within the shale plays, the latter are mainly located in organic matters in the shale plays. The amount of adsorbed oil for lacustrine shale range from 80 mg/gTOC to 100 mg/gTOC, which will be decreased with maturation increase. The most of adsorbed oil in a shale play are immobile and hard to produce. The free oil appear when residual oil is higher than the adsorbed oil threshold. the more free oil amount correspond to the higher mobility for shale oil. Viscosity is very important to hydrocarbon mobility, but less predictable quantitatively, As maturity or transformation ratio increases, GOR increases four orders of magnitude and viscosity decreases three orders of magnitude in the oil window. The kinetic model of GOR, API and viscosity have been established for the organic rich lacustrine source rock, If maturity or transformation ratio of source rocks can be measured with much greater precision, the viscosity and hydrocarbon mobility will be predicted in reasonable resolution. Vitrinite reflectance data are often problematic for lacustrine shale play when used for the maturity or thermal calibration, a better approach is calibrated with the residual HI of high TOC source rocks. Higher maturity means lower viscosity, maturity map will provide the hydrocarbon mobility trending in the area.

Case studies from the Hataoyan Formation of Biyang basin and Upper Triassic Chang 7 Shale in Ordos basin have been shown the approaches of hydrocarbon mobility prediction in the lake basins. these case studies indicate that the best oil production seems to be from late oil window with vitrinite reflectance equivalent of 0.9 to 1.2 (%Ro).

Neoproterozoic terranes in the NE China and its tectonic implications

FENG WANG, WENLIANG XU*, FUHONG GAO, JIE TANG, AND WENLI HAO

College of Earth Sciences, Jilin University, Changchun 130061, (jlu-wangfeng@sohu.com, * xuwl@jlu.edu.cn)

NE China is located in the eastern section of the Central Asian Orogenic Belt (CAOB), in a region that consists of a collage of several microcontinental massifs (including, from northwest to southeast, the Erguna, Xing'an, Songnen-Zhangguangcai Range, Jiamusi, and Khanka massifs). It has been a controversial issue whether did the Precambrian terranes occur within these microcontinents of NE China, although the geochronological data of the detrital zircons from the Paleozoic strata in NE China display a lot of the information the Precambrian ages. Additionally, the tectonic attribution of these microcontinents is also an unsolved issue.

The Neoproterozoic magmatisms, corresponding to the breakup of the Rodinia supercontinent, have been widely identified in the Erguna Massif [1]. By comparison, no igneous rocks of this age have been identified in the Xing'an, Songnen-Zhangguangcai Range, and Khanka massifs. However, the LA-ICP-MS detrital zircon U-Pb dating for Dongfengshan and Tadong groups indicate that a suite of Neoproterozoic terranes is present along the eastern margin of the Songnen-Zhangguangcai Range Massif (~821–752 Ma, ~752–560 Ma, and ~750–516 Ma)[2]. And Neoproterozoic magmatic zircons (0.75–0.92 Ga) are the most common zircons identified in the Dongfengshan and Tadong groups, suggesting that a Neoproterozoic magmatic event occurred within the Songnen-Zhangguangcai Range Massif. The detrital zircons with similar ages (0.76–0.97 Ga, our unpublished data) have been also identified in the Huangsong Group along the western margin of the Khanka Massif. Additionally, increasing evidence suggests that Neoproterozoic magmatic zircons are present in Paleozoic sedimentary rocks in the Xing'an Massif [3].

The above findings suggest that the Precambrian terranes did occur within the Erguna, Xing'an, Songnen-Zhangguangcai Range, and Khanka massifs, and that these microcontinents have an affinity to the Siberia craton. This research was financially supported by the National Science Foundation of China (Grant 41272075 and 41072038).

- [1] Tang *et al.* (2013) *Precambrian Research* **224**, 597–611.
 [2] Wang *et al.* (2013) *Gondwana Research*, in press. [3] Han *et al.* (2011) *Tectonophysics* **511**, 109–124.

Understanding the sub-surface metabolic activity and pathways of microbial mediated C/N cycling in North Pond, western flank of Mid-Atlantic Ridge

FENGPING WANG^{1*}, XINXU ZHANG², YUEHENG ZHOU^{1,2},
AND THE IODP EXP336 SCIENCE PARTY,

¹State Key Laboratory of Microbial Metabolism and State Key Laboratory of Ocean Engineering, Shanghai JiaoTong University, Shanghai, 200240, People's Republic of China

*Correspondence: fengpingw@sjtu.edu.cn

This project tries to reveal the microbial mediated C/N cycling in the sediments and rocks of North Pond, western flank of Mid-Atlantic Ridge, which represents an ideal model system for studying the biologically mediated oxidative basement alteration. A series of incubations with ¹³C and ¹⁵N labeled substrates including sodium carbonate, acetate, methane, ammonium chloride and sodium nitrate, have been set up onboard. Significant cell growths were observed only when nitrogen substances were supplemented, either alone, or in combination with carbonate or acetate. This data suggests that nitrogen is the limiting nutrient source for cell growth in the North Pond crust biosphere. The microorganisms and their utilized pathways in the assimilation and transformation of C, N are under investigation. In addition, enrichment and isolation of microbial groups involved in iron transformation will also be performed. These integrated studies would give clear clues to understand the underwater microbial activities, key metabolic pathways and their roles in ocean crust weathering.

Seasonal patterns of CO₂ emission from a subtropical reservoir

FUSHUN WANG¹ BAOLI WANG² AND CHENCHEN YAO¹

¹ School of Environmental and Chemical Engineering, Shanghai University, Shanghai 200433, China. fswang@shu.edu.cn

² State Key Laboratory of Environmental Geochemistry, Institute of Geochemistry, Chinese Academy of Sciences, Guiyang 550002, China. baoliwang@163.com

The XinAnJiang River, is the mainstream of Qiantang River, the largest river in Zhejiang Province, China. The XinAnJiang Reservoir, located in Chun'an County, Zhejiang Province, was accomplished in 1959, also known as the Qiandao Lake. Five cruises were carried out along the XinAnJiang Reservoir and its river reach in April, June, August, November 2010 and January 2011, in order to understand the CO₂ emission from this subtropical reservoir. *p*CO₂ of surface water was determined using a continuous measurement system (equilibrator-NDIR system), besides that sampling and analysis of the outflow water and the water column in front of the dam were also conducted in each cruise. The results showed that, *p*CO₂ in the surface water strongly varied during the whole year, ranging from 5 μatm to 1,300 μatm at the inflow reach, from 2 μatm to 1,000 μatm at the central reservoir area, and from 1400 μatm to 3,800 μatm at the outflow water, respectively. In the inflow river reach and central reservoir, the highest values of surface water *p*CO₂ appeared in winter, and the lowest in summer. While the outflow water, has the highest surface *p*CO₂ in summer, and the lowest in spring. Along the water column in central reservoir, *p*CO₂ increased downwardly. In summer, the difference between *p*CO₂ in surface water and bottom water reached to 5,900 μatm, and in spring this difference was only 50 μatm. The annual average *p*CO₂ in inflow waters, reservoir surface and outflow waters were all higher than that of air (380 μatm), and the annual average diffusion flux of CO₂ at water-air interface in these area were 11.37, -0.02 and 345.93 mmol·m⁻²·d⁻¹, respectively, which indicated that the Xin'AnJiang reservoir should be a CO₂ source to the atmosphere. However our result also showed that central reservoir indeed has a role in mitigating the CO₂ emission in this case.

Organic carbon proxies in black shales: strontium

H.J. WANG¹, X.M. WANG¹ AND S.C. ZHANG^{1*}

¹Research Institute of Petroleum Exploration & Development, CNPC, Beijing 100083, China (wanghujian@petrochina.com.cn, wxm01@petrochina.com.cn, *correspondence: sczhang@petrochina.com.cn)

Isotopic and elemental proxies are used to discern the original compositions of ancient sediments, which are subject to later diagenetic/thermal alteration, etc^[1]. Recent work about the Mesoproterozoic (1.36 Ga) black shales in the North China Craton showed a high correlation between total organic carbon (TOC) content and the enrichment factors of Sr normalized to upper crust ($Sr\ EF = (Sr/Al)_{sample}/(Sr/Al)_{upper\ crust}$). No matter which paleoredox conditions is, the relatively low Sr EF (< 1.0) and good positive correlation with TOC (Figure 1), means the uptake of Sr is mainly controlled by the availability of organic substrates, not the solubility at the redox boundary. Besides the isotopic compositions of Sr can reflect the evolution of paleocean^[2], thus jointly estimates of original TOC with the content and isotopic composition of Sr in samples spanning the geologic record, should be useful in estimating the of primary productivity of ancient oceans and the distribution of potential source rocks of petroleum.

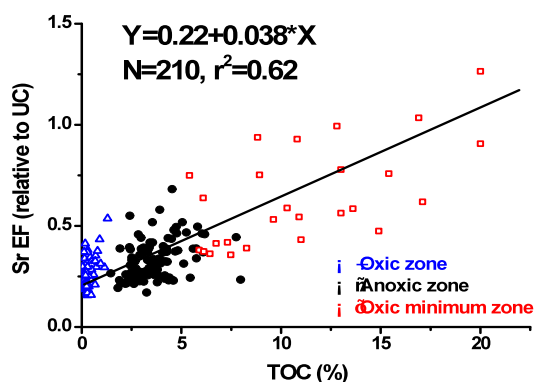


Figure 1: Enrichment factors of Sr (relative to upper crust) versus TOC in Mesoproterozoic sediments.

[1] Wilde *et al.* (2004) *Chem Geol.* **206**, 167-176. [2] Veizer *et al.* (1999) *Chem Geol.* **161**, 59-88.

Simultaneous measurements of C and N Isotopic composition and N abundance in diamonds by NanoSIMS

JIANHUA WANG*, STEVEN B. SHIREY AND ERIK H. HAURI

Department of Terrestrial Magnetism, Carnegie Institution of Washington, 5241 Broad Branch Rd. NW, Washington DC 20015, USA (*correspondence: jwang@ciw.edu)

Diamond, one of the three native carbon minerals on Earth, has been intensively studied for more than 40 years to provide extraordinary information on the cycling of carbon in the Earth's interior. Diamonds are found at the Earth's surface in ultra-high pressure metamorphic terranes, meteorite impact sites, and volcanic eruptions of kimberlite magma or their weathering products. It is the kimberlitic diamonds that provide the largest and deepest specimens - from 150 km to 800 km depth in the mantle. Multi-stage growth patterns are commonly seen in the cathodoluminescence (CL) imaging of diamonds, including those that are large, transparent monocrystals. The SIMS method has been developed to study zonation of carbon and nitrogen isotopic composition and nitrogen abundance in diamonds [1] and is the method of choice for study in the context of the zoning patterns. Separate analytical sessions are required to measure carbon and nitrogen isotopes and nitrogen abundance in the previous method on the Cameca 6f [1] because a single detector must be used at different mass resolution for C and N. We have developed a method to measure both carbon and nitrogen isotopes and nitrogen abundance simultaneously on the same spot using multicollection on the Carnegie NanoSIMS 50L. The NanoSIMS method has a better spatial resolution (15 μ m) with better precisions ($\delta^{13}C$: 2s of $\pm 0.5\%$ and $\delta^{15}N$: 2 σ of $\pm 2.2\%$) and much better transmission of nitrogen ($^{12}C^{14}N$: 1600cts/ppm/nA). We will discuss the details of the NanoSIMS method comparing with the previous method.

Palot *et al.* reported lowest $\delta^{15}N$ values (up to -39.4‰) of terrestrial sample in Kankan (Guinea) diamonds [2]. They interpreted this low N isotopic composition as the primordial heterogeneity preserved in an imperfectly mixed convective mantle [2]. We measured $\delta^{15}N$ value of -29‰ in a peridotite diamond from Liaoning, China. In situ and simultaneous measurements of C and N isotopic composition and N abundance in zoned Liaoning diamonds reveal their complicated growth history and N isotope geochemistry in the deep Earth.

[1] Hauri *et al.* (2002) *Chem. Geol.*, **185**, 149-163. [2] Palot *et al.* (2012) *EPSL*, **357-358**, 179-193.

Multi-scale simulation of structural heterogeneity of swift-heavy ion tracks in complex oxides

JIANWEI WANG*, MAIK LANG, RODNEY C. EWING AND UDO BECKER

Department of Earth and Environmental Sciences, University of Michigan, Ann Arbor, Michigan 48109 USA
(*correspondence: jwwang@umich.edu)

Understanding and prediction of the phase behavior of materials under extreme environments provide a great challenge in the materials' design and engineering in various applications. Swift heavy ion have been used to probe the effect of the high-energy radiation on a wide variety of materials and to explore the complex far-from-equilibrium behavior of the materials under extreme conditions. In this study (J. Phys.: Condens. Matter, 25, 135001), track formation caused by a swift-heavy ion irradiation, 2.2 GeV Au, of isometric $Gd_2Ti_2O_7$ pyrochlore and orthorhombic Gd_2TiO_5 phase was modeled using thermal-spike model combined with a subsequent molecular-dynamics simulation. The thermal-spike model was used to calculate the energy dissipation over time and space. Using the time, space, and energy profile generated from the thermal-spike calculation, the molecular-dynamics simulation was performed to model the atomic-scale evolution of the track. The advantage of combining these two methods, that is using the output from the continuum model as an input for the atomistic model, is that it provides a means of simulating the coupling of the electronic and lattice subsystems and at the same time providing atomic-scale details of the track structure and morphology.

The simulated internal structure of the track consists of an amorphous core and a shell of disordered, but still crystalline, domains. For $Gd_2Ti_2O_7$, the shell region has a disordered pyrochlore with a defect fluorite structure and is relatively thick and heterogeneous with different degrees of disordering. For Gd_2TiO_5 , the disordered region is relatively small as compared with $Gd_2Ti_2O_7$. In the simulation, "facets", that is surfaces with a definite crystallographic orientation, are apparent around the amorphous core and were more evident in Gd_2TiO_5 along the [010] than [001], suggesting an orientationally dependent radiation response of this structure. These results show that track formation is controlled by the coupling of several complex processes, involving different degrees of amorphization, disordering, and dynamic annealing. Each of the processes depends on the mass and energy of the energetic ion, the properties of the material, and its crystallographic orientation with respect to the incident ion beam.

Gallionella-like microorganisms involved in iron oxide formation in groundwater wells across a broad pH range

JUANJUAN WANG¹, MAREN SICKINGER² AND KIRSTEN KÜSEL³

¹Friedrich-Schiller-University of Jena, Dornburgerstr.10
07743 Jena, (juanjuan.wang@uni-jena.de)

²maren.sickinger@uni-jena.de

³kirsten.kuesel@uni-jena.de

Clogging caused by iron ochre incrustations has been a challenge for the functioning of groundwater wells, especially technical wells in mining areas. The formation and dissolution of iron oxides can be mediated by iron-oxidizing and -reducing microorganisms. In this project we studied the potential role of these microbes in the clogging process at three locations in an open-cast mine, comparing a total of 16 wells. The groundwater had pH ranging from acidic (4.5) to neutral (7.5) and relatively high contents of Fe(II) (0.5~7 mM) and DOC (1.4~12.6 mgL⁻¹) at an average oxygen concentration of 3.8 mg L⁻¹. The mineral composition of ochres differed with ferrihydrite being common in circumneutral wells and schwertmannite dominating in the slightly acidic wells. 454 pyrosequencing revealed a high diversity of bacteria in the ochres with a large fraction of *Gallionella*-related sequences. Quantitative PCR suggested that *Gallionella*-related organisms on average accounted for 44 % of the total bacteria. Surprisingly, their abundance was not correlated to any geochemical parameter. *Gallionella*-related organisms were also present in the ground water ranging from 8.4×10^6 to 2.0×10^8 16S rRNA gene copies per L water. Iron reducing bacteria such as *Geobacter*, *Geothrix*, *Rhodoferrax*, were only detected at low abundance, in agreement with a low iron reduction potential. However, the iron reduction potential could be stimulated by the addition of lactate. In conclusion, *Gallionella*-related iron oxidizers dominated ochres and groundwater irrespective of pH, suggesting a major role of these organisms in the formation of ochres across a broad range of geochemical conditions. Deeper insight into the microbiology of the ochre formation process may help to develop strategies for relieving clogging problems in technical wells.

Geochemical fingerprints in Siberian mantle xenoliths reveal progressive erosion of an Archean lithospheric root

KUO-LUNG WANG^{1*}, Y.-H. CHIEN¹, M. I. KUZMIN²,
SUZANNE.Y. O'REILLY³, W.L. GRIFFIN³,
A. VORONTSOV² AND N.J. PEARSON³

¹Institute of Earth Sciences, Academia Sinica, Taipei, Taiwan

(*correspondence: kwang@earth.sinica.edu.tw)

²Institute of Geochemistry, SB RAS, Irkutsk, Russia

³CCFS/GEMOC, Macquarie University, Sydney, Australia

Mantle xenoliths from a microbasalt quarry in Miocene (14 Ma) and Holocene (~0.65 Ma) basalts of the Bulykhta Riverside and Kandidushka volcanoes in the Vitim volcanic plateau, SE Siberia, are dominantly spinel-, garnet-, or garnet-spinel-bearing lherzolites with minor pyroxenites. Equilibrium temperatures and pressures of garnet-bearing lherzolites in the Miocene basalts range from 1110 to 1250 °C and 22 to 28 kbar, whereas those in Holocene basalts have similar temperatures (1110–1180 °C) but lower pressures (20 - 21 kbar). The latter thus yield a hotter geotherm than the former. The Fo contents of olivine in these lherzolites range from 89.1 to 90.6, with most from 89.8 to 90.2. Trace-element patterns of clinopyroxenes (cpx) in the lherzolites can be divided into three types: depleted, enriched and intermediate. The depleted patterns are typical of unmetasomatised, refractory lithospheric mantle. The enriched and intermediate ones provide fingerprints of different metasomatic episodes. Some lherzolites contain amphibole and/or apatite as evidence of modal metasomatism. Whole-rock and cpx Sr–Nd isotopic ratios of lherzolites in Miocene basalts are more radiogenic ($^{87}\text{Sr}/^{86}\text{Sr}=0.70225\text{--}0.70561$ and $^{143}\text{Nd}/^{144}\text{Nd}=0.51288\text{--}0.51303$) than those in Holocene basalts ($^{87}\text{Sr}/^{86}\text{Sr}=0.70244\text{--}0.70374$ and $^{143}\text{Nd}/^{144}\text{Nd}=0.51300\text{--}0.51329$). It indicates the material sampled from the SCLM beneath the Vitim region in Holocene time is more depleted than that sampled in the Miocene. Os isotope compositions of sulfides display similar temporal variation; the lherzolites in the younger basalts have more radiogenic ratios ($^{187}\text{Os}/^{188}\text{Os}=0.1066\text{--}0.1318$) than those in the older basalts ($^{187}\text{Os}/^{188}\text{Os}=0.1168\text{--}0.1350$). Both T_{MA} ages from the least-disturbed sulfides ($^{187}\text{Re}/^{188}\text{Os}<0.07$) and T_{RD} ages from higher-Re/Os sulfides yield model ages ranging from 0.5 to 3.2 Ga, with peaks around 1.4, 1.1, 0.9 and 0.5 Ga. The Miocene basalts sampled a deeper, more refertilised part of the Archean root, compared to the shallower part sampled by the Holocene basalts.

Compositional variation in apatites from carbonatites and associated alkaline silicate rocks: A case study of the Kaiserstuhl complex, Germany

L. WANG^{1,3*}, T. WENZEL¹, A. VON DER HANDT²,
J. KELLER², M. A. W. MARKS¹ AND G. MARKL¹

¹Universität Tübingen, Mathematisch-Naturwissenschaftliche Fakultät, FB Geowissenschaften, 72074 Tübingen, Germany

(*correspondence: lian.x.wang@gmail.com)

²Albert-Ludwigs-Universität Freiburg, Institut für Geowissenschaften-Mineralogie-Geochemie, 79104 Freiburg, Germany

³Faculty of Earth Sciences, China University of Geosciences, 430074 Wuhan, China

In the present study, we investigate textural and chemical signatures of apatites from a series of carbonatites, related alkaline silicate rocks, an unusual carbonate-bearing melilitic dyke rock (bergalite) and a diatreme breccia of the Miocene Kaiserstuhl Volcanic Complex, South Germany.

Significant chemical differences between apatite from carbonatites and associated alkaline silicate rocks exist for Sr, Fe, Mn, Th, U, Nb, Si, S, As, Cl and Br. These differences can be attributed to different partition coefficients, melt compositions, substitution mechanisms and redox conditions.

A systematic and sharp core-mantle-rim zonation is present in apatites from the bergalite sample. The core and mantle zones are compositionally similar to apatites from silicate rocks, whereas the rim compositions correspond to that of carbonatitic apatites. These observations imply that bergalitic apatites initially nucleated in a silicate melt and continued crystallizing from a melt with carbonatitic affinity during later stages. This late-stage carbonatitic melt was interpreted as the protracted fractionation product of the carbonate-bearing nephelinitic melt [1].

Apatites from a diatreme breccia (containing carbonatitic and silicate rock components) comprise three textural and compositional populations: (1) similar to apatites from silicate rocks, (2) similar to apatites from carbonatites, and (3) resembling apatite population (1) partially replaced by population (2). We infer that apatite population (1) derived from silicate rock fragments and apatites (2) crystallized from the later intruding carbonatitic melt causing the formation of the breccia. During ascent of the carbonatitic melt, metasomatic overprint caused the observed replacement textures in apatite population (3).

[1] Keller (1997) *Geol.Ass./Mineral.Ass. Annual Meeting. Abstract*, A77.

Research on the phase composition , expansion property and heavy metals absorption capacity of vermiculite from Yuli Xinjiang Province

L.J. WANG, L.B. LIAO* AND X.X. HUO

School of Material Sciences and Technology, China University of Geosciences, Beijing 100083, China
(*correspondence: lbliao@cugb.edu.cn)

Vermiculite is a kind of natural, non-toxic clay, which was formed from mica weathering or alteration. The Qeganbulak vermiculite ore in Yuli, Xinjiang province is one of the largest vermiculite deposits discovered in China, which is about 90% of the vermiculite reserves in China. Because of its layer ions exchangeability, vermiculites have strong cation exchange capacity, which can be used to remove heavy metals in wastewater.

Under the investigation of X-ray diffraction(XRD), thermogravimetric–differential thermal analysis(TG-DTA), infrared spectroscopy(IR), and chemical analysis etc., vermiculite from Yuli Xinjiang was approved to a mixture of vermiculite, mica, calcite and two kinds of vermiculite-mica mixed-layer minerals Hy-a (vermiculite/mica mole ratio of 6:4), Hy-b (vermiculite/mica ratio of 4:6). Phlogopite was identified as the major type of mica in mica layer in mixed-layer minerals. A small amount of biotite cannot be expelled. Vermiculite are Mg type vermiculite and Na type vermiculite.

Results show that expansion capacity of vermiculite majorly comes from mixing layer minerals(Hy-a, Hy-b), in which Hy-a affect its expansion ability most. The expansion ratio of vermiculite increases with the increase of temperature when the temperature is less than 700 °C, after then it's becoming stable. The expansion ratio of vermiculite reduces with the increase of particle size. The expansion ratio of vermiculite is the highest when its particle size ranges from 1 to 2 mm. When particles are bigger than 2mm, its expansion ratio decreases with the increase of particle size.

Before reaching the absorption/desorption balance of vermiculite towards heavy metal ions like Cd,Cu,Cr etc., the absorption capacity is positive to absorption time, however, after reaching this balance, absorption time won't increase absorption capacity obviously . In addition, the absorption capacity of vermiculite towards heavy metals increases with the increase of concentration of heavy metals. The vermiculite's absorption capacity towards heavy metals can also be phenomenally affected by pH, normally, higher pH can cause higher absorption capacity.

Petrogenesis of Late Permian picritic porphyries associated with Pingchuan iron ores, Emeishan Large Igneous Province, southwest China

MENGWANG¹ AND ZHAO-CHONG ZHANG¹

¹ State Key Laboratory of Geological Processes and Mineral Resources, China University of Geosciences, Beijing, 100083, China (houtong08@gmail.com)

The Pingchuan iron oxide deposit is spatially and temporally associated with the Late Permian picritic porphyries in the Emeishan Large Igneous Province, southwest China. The estimated ore reserve for the Pingchuan deposit is 40Mt at ~60 wt.% Fe. The iron ore bodies are intimately associated with the intrusive masses of picritic porphyry, occurring mainly along the contact zone between the picritic porphyries and the sedimentary country rocks, i.e. limestone. The most important ore types are massive and brecciated ores which together make up 90 vol. % of the deposit. The massive type generally occurs as dykes and large veins consisting predominantly of magnetite with minor calcite and apatite. The picritic porphyries are characterized by a marked range of SiO₂ (37.12-47.39 wt. %) and MgO (19.22-29.08 wt. %), but show a minor variation in Na₂O+K₂O (0.12-1.58 wt. %) and TiO₂ (0.64-1.44 wt. %). The total concentration of rare earth elements (REE) is relatively low (21-83 ppm), and show moderate enrichment in light rare earth element (LREE; [La/Yb]_N=3.01-3.63). The primitive-mantle-normalized patterns of the rocks are comparable to those of ocean island basalt, plausibly indicating a plume source. Petrographic observation suggests the Pingchuan picritic porphyries are virtually cumulus product, and possibly experienced fractional crystallization of Cr-spinel + olivine + clinopyroxene during the magma chamber process. Moreover, the estimated primitive magma composition is picritic which is possibly produced by partial melting of the garnet-facies asthenospheric mantle peridotite. In combination with the available information including field observation and geochemical studies, e.g. fluid inclusions and stable isotope data, we infer that the deposit is hydrothermal in origin and the ore-forming fluids are predominantly primary magma-derived fluids which had been released during the post-magmatic period and mixed with fluids from country rocks.

Carbonate reservoir features and its main control factors in South Slope of Northern Tarim, China

RUIJU WANG, ZHENG HONGJU, JIANG HUA, CHUNMING ZHANG, SUYUN HU, ZECHENG WANG

(PetroChina Research Institute of Petroleum Exploration & Development, Beijing 100083, China)

Good exploration prospects have been shown in carbonate of lower Ordovician, which's depth is larger than 6500m, in south slope of Northern Tarim, but carbonate reservoir features and its attributions have not been completely known. In this research, cores, glass slides, logs, 3-d high resolution seismic, and so on, are used. And researching methods such as tectonic evolution analyzing, reservoir feature depicture, and so on, are applied. Types, periods, distribution and overlapping method of karst were studying in this area. It was recognized that different karsts played the various parts in different areas. North area of Tumuxiuke pinch-out developed potential karst, while most areas on the south side developed alonging-karst. It was particular that Yingmai area developed vertical karst. Complexity of karst reservoir was decided by attribution of high-energy facies and history of tectonic evolution. Research on superimposing pattern of karst and different features was going to help the exploration in the research area.

Geochemical characteristics of sediment of Pearl river estuary and its palaeoenvironmental evolution

WANG SHANSHAN¹ * CAO ZHIMIN² AND LAN DONGZHAO^{2,3}

¹ Zhejiang Institute of Hydraulics & Estuary, Hangzhou, 310020, China (correspondence: shanshwang@gmail.com)
² College of Marine Geosciences, Ocean University of China, Qingdao, 266003, China
³ Third Institute of Oceanography, SOA, Xiamen 361005, China

Data and method

The concentration of metal elements (Co, Cu, Zn, Ni, Cr, Zr, Sr, Ba), total content of organic matter and average grain size were determined from 16 sediment samples in different depth of 3.5m core in Pearl River estuary of China. Three important factors were identified from 160 data, using principal component analysis method.

Discussion of Results

The variance contribution (Tab1) shown the effect for chemical composition of sediment, and after further analysis, We found that, the three factors represented catchment erosion (F1), biogenic deposit (F2) and marine dominated condition (F3) (Tab1) respectively. The factor score curves (Fig1) represented the changes of humidity and temperature and the hydrodynamics in different depth (times).

Factors	Variables and factor loading	Variance contribution %
F1	Co 0.873, Cu 0.906, Ni 0.925, Zn 0.807, Cr 0.628, Average grain size 0.710	42.06
F2	Sr 0.885, Ba 0.949	21.95
F3	Zr 0.748, TOC* -0.937	21.58

*TOC: total organic carbon

Table 1: Result of factor analysis

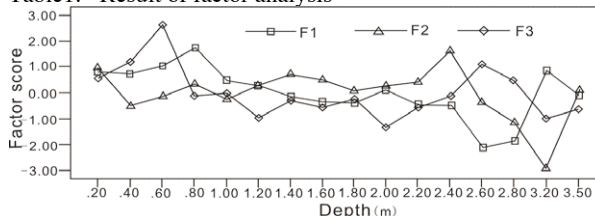


Figure 1. Lines of factor scores in different depth

The study provided an effective approach for palaeoenvironment reconstruction of Pearl river delta. It revealed that the basic palaeoclimate succession in the region of Pear river delta is cool-humid, cool-dry, warm-dry, warm-dry, warm-humid and warm-dry successively.

(This work was funded by National Science Foundation of China (41006052))

Factors influencing methane-derived authigenic carbonate formation at cold seep from southwestern Dongsha area in the northern South China Sea

SHUHONG WANG^{1,2}, WEN YAN^{1,2*}, VITOR H. MAGALHÃES³, ZHONG CHEN^{1,2}, LUIS M. PINHEIRO^{3,A} AND NIKOLAUS GUSSONE⁴

¹CAS Key Laboratory of Marginal Sea Geology, South China Sea Institute of Oceanology, Chinese Academy of Sciences, Guangzhou 510301, China (*wyan@scsio.ac.cn)

²Guangzhou Center for Gas Hydrate Research, Chinese Academy of Sciences, Guangzhou 510301, China

³Centre for Environmental and Marine Studies (CESAM) and Geosciences Department, University of Aveiro, Aveiro 3810-193, Portugal

⁴Institut für Mineralogie, Universität Münster, Corrensstr, 24, 48149 Münster, Germany

The mineral and geochemical studies are carried out on a profile through a diagenetic methane-derived authigenic carbonate sample which was collected from southwestern Dongsha area of the northern South China Sea. The five samples located in the cross-sectional middle mainly consists of dolomite and quartz, and two samples close to surface show small amounts of Mg-calcite. The $\delta^{13}\text{C}$, $\delta^{18}\text{O}$ and $\delta^{44/40}\text{Ca}$ values of the samples range -30.59‰ ~ -0.30‰ VPDB, 3.07‰ ~ 3.59‰ VPDB and 1.35‰ ~ 1.47‰ SRM915a, respectively, indicating a clear contribution of methane oxidation to the carbon pool from which the authigenic carbonates precipitated from. From the isotope signals alone it can not be distinguished if the carbon source is rather thermogenic gas or a mixture of biogenic methane and marine dissolved inorganic carbon (DIC). The $\delta^{18}\text{O}$ values are in general consistent with dolomite precipitation from a fluid similar to present seawater. The observed small variability might be related to fluid oxygen isotope composition. The relative small range in calcium isotope values indicates relatively constant growth conditions and precipitation from seawater like fluid. The central part of the carbonate nodule formed under the strong influence of methane seepage, and the external part is less influenced by methane, either due to reduced methane flux to the surface or caused by erosional exhumation of the carbonate nodule from greater depth to the sediment surface.

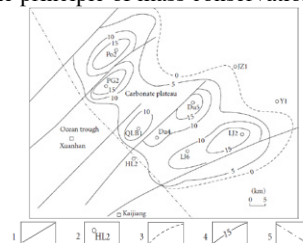
Acknowledgments: This study was supported by CAS (KZCX2-YW-GJ03-01), NSFC (41276050, 41176052), 973 Program (2009CB219502-4).

A Prediction Model of Oil Cracked Gas Resources and Its Application in NE Sichuan Basin, SW China

T.S.WANG*, S.Y. HU AND X. LI

PetroChina Research Institute of Petroleum Exploration & Development, Beijing, China (*correspondence:wts2007@petrochina.com.cn)

The prediction of oil cracked gas resources is necessary and urgent in the gas exploration of these basins at high to over stage in China. A marine crude oil sample was pyrolyzed using sealed gold tubes system in our study. The pyrolysates including gas, liquid, and solid were quantitatively analyzed. Based on the pyrolysis data and kinetic calculation, the yield correlativity among gas, liquid, and solid products was regressed with high correlative coefficients to establish a prediction model suitable for the resource estimation of oil cracked gas. The verification formula for this model was also established on the principle of mass conservation.



1. Fault
2. Well
3. Boundary of sedimentary facies
4. Content contour of solid bitumen in reservoir (%)
5. Distribution area of solid bitumen in reservoir

Fig1. Content contour of solid bitumen in reservoir in NE Sichuan Basin

The affecting factors and the application preconditions of this model were discussed. Finally the model was extrapolated to the prediction of oil cracked gas resources of Feixianguan formation in NE Sichuan basin, SW China[1]. The prediction value of oil cracked resources is about $6.84 \times 10^{12} \text{m}^3$, and generation intensity of oil cracked gas is about $97.5 \times 10^8 \text{m}^3/\text{km}^2$, and the paleo-oil reserves is about $97 \times 10^8 \text{t}$. The verifying value for this prediction is approximately equal to 1, indicating the model is reliable in the resource estimation of oil cracked gas.

It is the first attempt to evaluate oil cracked gas resources through analyzing the increase or decrease of gas, liquid, and solid products in crude oil pyrolysis and the correlativity among the three yields.

Some new ideas are provided for the estimation of natural gas resources and the restoration of paleo-oil accumulations in the areas with high and overmature marine source rocks in south China. It is significant for the decision-making of natural gas exploration in China.

Geochemistry and isotope geochemistry of Upper Cretaceous chalk as equivalent for reservoir chalk of the North sea Basin for EOR

W. WANG¹, M. V. MADLAND¹, U. ZIMMERMANN¹, S.A.R. BERTOLINO², T. HILDEBRAND-HABEL³ AND R. I. KORSNES¹

¹Univ. i Stavanger, IPT, Norway, udo.zimmermann@uis.no

²CONICET-FAMAF, Cd. Universitaria, Córdoba, Argentina

³IRIS, P.O. Box 8046, 4068 Stavanger, Norway

Upper Cretaceous chalk from five exposures (Kansas, USA; Liège and Mons, Belgium; Aalborg and Stevns Klint, Denmark) have been sampled for comparison with reservoir chalk of the North Sea Basin (Tor and Hod Formations at Ekofisk, Brynhild, Enoch, Sleipnir and Jotun fields) of similar porosity in order to understand its reaction in flooding experiments for enhanced oil recovery (EOR). Chalks from Stevns Klint and Mons are very pure and contain like samples from Aalborg only few amounts of clastic material. The latter has abundant diagenetic chert. Liège and Kansas chalk contain the highest amount of clastics. Kansas chalk is particular, as it has reached the highest diagenetic grade, has higher concentrations in trace metals like Fe, Ni, Pb, Zn, Cu than all other chalk types and shows disturbed O-isotopes. This can be explained by abundant secondary micritic and sparitic cement in foraminifer shells. In contrast, C-O isotope values for all other on-shore chalk samples reflect primary seawater composition. This cannot be found in reservoir chalk. Here, O-isotopes are disturbed and similar to samples from Kansas. In some fields (Sleipnir and Jotun fields) trace metal compositions are also enriched and the chalk contains slightly higher amounts of clastic materials (Zr & Rb concentrations 2-5% of typical upper continental crust) and generally higher ΣREE concentrations with lower Y/Ho ratios (29-44) than in all on-shore samples. A post-depositional process affected the reservoir chalk, hence, in disturbing the O-isotope signature and affecting slightly the REE pattern, which is not related to clastic input. Chalk from Kansas shows a higher diagenetic overprint which explains the re-setting of the O-isotopes, but for the re-setting of the O-isotopes in reservoir chalk a reason have still to be found.

Provenance of Eolian Deposits in Desert-Loess Transition, North China by using Nd-Sr isotopic tracers

WANG XIAO*, AND RAO WENBO²,

Institute of Isotope Hydrology, School of Earth Sciences and Engineers, Hohai University, Nanjing, 210098, China
(* correspondence: jswangxiao@126.com)

The desert-loess transition of China is very sensitive to climate change. Many studies on desert evolution and loess formation have been carried out in recent years[1]. However, the provenance of late Quaternary deposits in the desert-loess transition is not yet known. Here, we present Nd-Sr isotopic data of coarse-grained sands in the Dishaogouwan (DSGW) profile in the transition between Ordos deserts and Chinese Loess Plateau to identify the source of eolian deposits during the past 20ka.

The DSGW profile mainly consists of Dishaogouwan (DSGW), Dagouwan (DGW), Chengchuan (CC), Salawusu (SW) and Lishi (LS) Formations. The Salawusu Formation was aqueous but other formations were predominantly of eolian origin. $\epsilon_{Nd}(0)$ values and $^{87}Sr/^{86}Sr$ ratios of coarse-grained fractions vary from -8.4 to -12.5 and from 0.7169 to 0.7199 in DSGW and DGW, from -9.1 to -11.5 and from 0.7179 to 0.7192 in the CC, from -10 to -12 and from 0.7188 to 0.7206 in SW and from -10.5 to -12.7 and from 0.7183 to 0.7190 in LS, respectively.

80% ~ 90% of the eolian deposits developed in different periods were coarse-grained fractions. $\epsilon_{Nd}(0)$ values and $^{87}Sr/^{86}Sr$ ratios of coarse-grained in the Formations which were dominated by eolian deposits vary within a narrow range, implicate for a similar source. Furthermore, the coarse-grained fractions merely sprang and rolled on the earth's surface by the wind[2]. So, eolian deposits in these Formations might be fed by sediment blowing of adjacent highland or mechanical weathering of the sandstones in Ordos. Contrastly, the aqueous deposits of SW was dominated by fine-grained fractions, and water erosion of underlying deposits probably dominated coarse aqueous deposits of sw. $\epsilon_{Nd}(0)$ values and $^{87}Sr/^{86}Sr$ ratios of coarse-grained in SW don't have a obvious difference with the values of eolian deposits. However, there are rarely coarse-grained fractions in Loess plateau from where salawusu valley originated. So underlying eolian deposits with abundant coarse-grained fractions could supply the aqueous deposits with coarse-grained fractions.

[1] Sun *et al.* (1996) Marine Geology & Quaternary Geology 16(1), 23-31 [2] Chen *et al.* (1999) J. Sediment Res. 6, 84-89

In-situ observations of liquid-liquid immiscibility in the system $\text{MgSO}_4\text{-H}_2\text{O}$ (D_2O)

XIAOLIN WANG^{1,2} AND WENXUAN HU^{1,2}

¹School of Earth Sciences and Engineering, Nanjing University, Nanjing, 210093, P.R. China

²Institute of Energy Sciences, Nanjing University, Nanjing, 210093, P.R. China

Liquid-liquid immiscibility has been documented in aqueous UO_2SO_4 solutions at temperatures up to 468 °C [1]. Recently, we reported our observations on the liquid-liquid phase separation in vapor-saturated aqueous MgSO_4 solutions at temperatures up to 350 °C [2]. Under these conditions, we observed that MgSO_4 -rich droplets were separated from the original aqueous MgSO_4 solutions during heating, and these two coexisting liquid phases homogenized during cooling. It has been found that the phase separation temperature decreases from 304.5 °C to 259.5 °C as MgSO_4 concentration increases from 1.19 % to 19.36%. The newly discovered liquid-liquid phase separation in MgSO_4 solutions was characterized by a lower critical solution temperature phenomenon, which was considered to be a macro-scale chemical property of polymeric mixtures.

To further characterize the properties of the immiscible fluids in the system $\text{MgSO}_4\text{-H}_2\text{O}$, we documented in-situ Raman spectroscopic investigations and observed a distinctly new $\nu_1(\text{SO}_4^{2-})$ mode at $\sim 1020\text{ cm}^{-1}$ in the MgSO_4 -rich droplets; the new $\nu_1(\text{SO}_4^{2-})$ mode was predicted to be present in MgSO_4 polymer(s) in aqueous solutions. As mentioned above, both the phase behavior and relevant Raman spectra indicate the existence of polymer(s) in MgSO_4 solutions.

We compared the new $\nu_1(\text{SO}_4^{2-})$ mode with that of MgSO_4 -rich droplets in the system $\text{D}_2\text{O-MgSO}_4$. We found that there was also an $\nu_1(\text{SO}_4^{2-})$ mode at $\sim 1020\text{ cm}^{-1}$. This observation suggests that the polymer(s) in aqueous MgSO_4 solutions is not bonded through H_2O and is probably contact ion pair chain(s), although the exact structure of the polymer(s) is still unknown. In addition, we investigated the hydrogen-bonds in the immiscible fluids. We found that the MgSO_4 -rich fluids has higher potential for the preservation of hydrogen bonds compared with that in the MgSO_4 -poor fluid at the same temperature. This can be ascribed to the formation of hydrogen bonds between SO_4^{2-} and water molecules because the probability of collision of H_2O with SO_4^{2-} in MgSO_4 -rich fluid is higher than that in the MgSO_4 -poor fluid.

[1] Marshall *et al.* (1962) *J. Inorg. Nucl. Chem.* **24**, 889-897.

[2] Wang *et al.* (2013) *Geochim. Cosmochim. Acta* **103**, 1-10.

The distribution of DBT and DBF in Mesoproterozoic (1.36 Ga) sediments

X.M. WANG¹, H.J. WANG¹ AND S.C. ZHANG^{1*}

¹Research Institute of Petroleum Exploration & Development, CNPC, Beijing 100083, China (wxm01@petrochina.com.cn, wanghuajian@petrochina.com.cn, *correspondence: sczhang@petrochina.com.cn)

Previous studies of polycyclic aromatic hydrocarbons considered dibenzofuran (DBF) and dibenzothiophene (DBT) to be derived from phenolic compounds of lignin from woody plants, thus their occurrence was attributed to terrestrial organic matter input^[1]. However, in our recent works in North China Craton, high contents of DBF and DBT were both detected in the Mesoproterozoic (1.36 Ga) low mature mudstones and shales. No matter how high of the total organic carbon contents in the shales, the distribution of DBF and DBT were more likely to be controlled by the paleoredox conditions (Figure 1). DBT had a peak abundance in the anoxic zone, while DBF was enriched in the oxic minimum zone, the transition zone from oxic to anoxic. When the redox conditions changed to oxic, a dramatic decrease was happened in the abundances of DBF and DBT. Thus, we speculated that the abundance and distribution of DBT and DBF in ancient sediments may be controlled by the dynamic sulfic-oxic conditions.

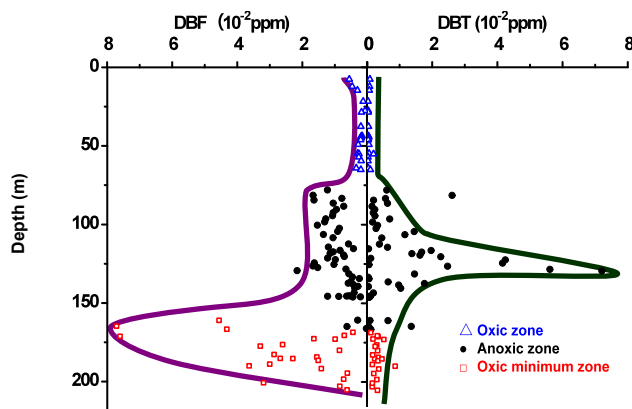


Figure 1: The distribution of DBF and DBT in Mesoproterozoic low mature mudstones and shales.

[1] Fenton *et al.* (2007) *EPSL* **262**, 230-239.

Age, geochemistry, and origin of Proterozoic rapakivi granites in the North Qaidam Orogen, NW China

XIAOXIA WANG¹, NENGGAO HU² AND TAO WANG³

¹ Institute of Mineral Resources, Chinese Academy of Geological Sciences, Beijing 100037, China

² Chang'an University, Xi'an 710054, China

³ Institute of Geology, Chinese Academy of Geological Sciences, Beijing 100037, China

Proterozoic rapakivi granites are mainly distributed within craton in the Northern Hemisphere. However, Proterozoic (ca.1770Ma) rapakivi granites have been recognized from the North Qaidam Orogen, the west segment of the Central Orogenic Systems of China. These granites exhibit typical rapakivi texture. They are A-type granite characterized by high FeOt/(FeOt + MgO) and Ga/Al ratios, and SiO₂, Na₂O + K₂O and rare earth element (except Eu) contents. Their whole-rock $\epsilon_{Nd}(t)$ (-6.09 to -5.74) and zircon $\epsilon_{Hf}(t)$ (-9.4 to -2.8) values, similar to those of the Proterozoic rapakivi granites in North China Craton (NCC), indicate they were derived from old continental crust. These granites contain magmatic microgranular enclaves and are intruded by diabases. The enclaves (more felsic) and granites show a uniform decrease in TiO₂, CaO, Na₂O, K₂O, FeO, and MgO with increasing SiO₂, and similar trace element patterns but different whole-rock $\epsilon_{Nd}(t)$ values. The diabases and other enclaves (more basic) deviate from the trend and have high whole-rock $\epsilon_{Nd}(t)$ values (ca. +4), suggesting their derivation from mantle. All these features indicate that the granites are almost the same as the Proterozoic (ca. 1700 Ma) rapakivi granites in NCC and belong to the Proterozoic rapakivi granite suit in the Northern Hemisphere. They were involved in the Paleozoic North Qaidam orogen. It is first time to recognize Proterozoic rapakivi granites in Phanerozoic orogens. This also reveals that Precambrian craton in North China were strongly destructed and reworked during Phanerozoic.

Rare earth elements in hydrothermal fluids from Kueishantao, off northeastern Taiwan

XIAOYUAN WANG¹ AND ZHIGANG ZENG¹

¹ Key Laboratory of Marine Geology and Environment, Institute of Oceanology, Chinese Academy of Sciences, Qingdao, 266071, China

(*correspondence:wangxiaoyuan@qdio.ac.cn)

The Σ REE concentrations of Kueishantao hydrothermal fluids are 813-1212 ng/L, 1-2 orders of magnitude higher than those of seawater (Σ REE of shallow seawater is 92 ng/L; Σ REE of deep seawater is 14 ng/L), but are lower than they are in most deep-sea hydrothermal fluids [1] and acidic hot waters in continental geothermal fields [2-4]. The difference may be caused by the low leaching efficiency under the seafloor due to the short duration of fluid-andesite interaction in the Kueishantao hydrothermal field [5].

The REE_N distribution patterns of the yellowish fluids (108°C, pH≈2.6, the flux is 35 m³/h) show a slight enrichment of LREE and a slight convex-downward curvature at Eu. The whitish fluids (51°C, pH≈4.9, the flux is 19 m³/h) have REE_N distribution patterns that exhibit a higher enrichment of LREE than those of the yellowish fluids and without Eu anomalies. The REE_N distribution patterns of Kueishantao fluids are different from those of shallow seawater (generally flat with a negative Ce anomaly), deep-sea acid-sulfate fluids, the acid-sulfate fluids in Taiwan Tatun volcanic area and other acid-sulfate hot waters in continental geothermal fields. The Eu anomalies of Kueishantao hydrothermal fluids are controlled mainly by the lower temperature and relative oxidizing conditions. The fractionation between LREE and HREE of the yellowish fluids is influenced mainly by the very low pH and the precipitation of native sulfur. In contrast, the LREE/HREE ratios of the whitish fluids may be related to the adsorption by small sulfur particles.

[1] Zeng (2011) *Beijing: Science Press*, 289-300. [2] Bau *et al.* (1998) *Chem Geol*, 293-307. [3] Sanada *et al.* (2006) *Geothermics*, 141-155.[4] Wood(2006) *J Geochem Explor*, 424-427.[5] Chen *et al.* (2005) *Acta Oceanol Sin*, 125-133.

Nitrogen isotopes of coral skeleton-bound organic matter: Proxy evaluation at Bermuda

XINGCHEN T. WANG^{1*}, ANNE L. COHEN²
AND DANIEL M. SIGMAN¹

¹Department of Geosciences, Princeton University, Princeton NJ 08540, USA xingchen@princeton.edu (*presenting author); sigman@princeton.edu

²Department of Marine Geology and Geophysics, Woods Hole Oceanographic Institution, Woods Hole, MA, 02543, USA acohen@whoi.edu

Nitrogen isotopes of organic matter bound in coral skeleton (hereafter, skeletal $\delta^{15}\text{N}$) have the potential to be a high-resolution proxy for the marine nitrogen cycle. By adapting a previously developed foraminifera-bound $\delta^{15}\text{N}$ method, we have developed a sensitive method for measuring coral skeletal $\delta^{15}\text{N}$, requiring 5 mg of skeleton powder and yielding a precision of $\sim 0.2\text{‰}$. We evaluated the natural variability of this proxy in Bermudan brain corals. Ten live coral colonies (*Diploria labyrinthiformis*) from four locations around Bermuda were collected in 2005 and analyzed for skeletal $\delta^{15}\text{N}$ (Fig. 1). Skeletal $\delta^{15}\text{N}$ showed good reproducibility ($< 0.5\text{‰}$) among different colonies at the same location, suggesting coral skeletal $\delta^{15}\text{N}$ is a reliable proxy for the local nitrogen cycle. Among the four sampling sites, skeletal $\delta^{15}\text{N}$ decreased with distance from the island, from $\sim 6.8\text{‰}$ (inshore, Tynes Bay) to $\sim 3.8\text{‰}$ (offshore, HOG Reef). The annual calcification rate of each colony was estimated from image analysis of 3-D CT scans. Skeletal $\delta^{15}\text{N}$ at each site exhibits a strong, negative correlation with annual calcification rate ($R^2 > 0.9$). We propose that the efficiency of nutrient recycling between the symbionts and coral host is reduced when nutrient concentrations of reef seawater are elevated, resulting in higher skeletal $\delta^{15}\text{N}$ and lower calcification rates at our inshore sites.

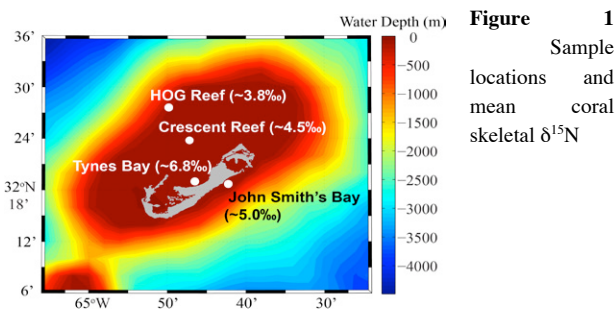


Figure 1
Sample locations and mean coral skeletal $\delta^{15}\text{N}$

Cokriging estimation of soil heavy-metal data obtained from portable X-ray fluorescence spectrometry

XIN-HAI WANG¹, KYOUNG-HO KIM¹, HO-RIM KIM¹,
SANG-IL HWANG², HYEONG-DON KIM³ AND SEONG-TAEK YUN^{1*}

¹Korea University, Department of Earth and Environmental Sciences and KU-KIST Green School, Seoul, South Korea,

styun@korea.ac.kr (* correspondence)

²Korea Environment Institute (KEI), Seoul, South Korea

³Seoul National University, National Instrumentation Center for Environmental Management, Seoul, South Korea

Portable X-ray fluorescence spectrometry (P-XRF) is currently used as a cost-effective and rapid analytical tool for assessing the heavy metal pollution of soil. However, the *in-situ* measured data are frequently unreliable due to soil heterogeneity, which may result in a difficulty to accurately interpret the spatial pattern of pollution status. This study is purposed to evaluate the feasibility of P-XRF to obtain a reliable auxiliary dataset for the cokriging interpolation of soil heavy metal data. For this study, we used analytical results of arsenic concentrations in soil samples ($n=156$) from a metal-polluted site, which were obtained by the conventional chemical leaching method and P-XRF. The both arsenic levels showed a good correlation ($R^2 = 0.72$). The true As pollution map was initially established by an ordinary kriging of 156 data. Then, one third of the total samples (i.e., 52 P-XRF data) were randomly chosen to presume the virtual soil investigation, and two kinds of pollution maps were constructed using the ordinary kriging and cokriging methods. Comparison of the estimated As levels with the true data at total sampling points ($n=156$) showed that the cokriging map is more reliable ($R^2 = 0.89$) than the ordinary kriging map ($R^2 = 0.40$). This study shows the advantage of the cokriging interpretation of P-XRF data to evaluate the spatial distribution of heavy metal pollution of soil.

Study on uranium speciation in the water of a river near phosphate mining area

XIN-YU WANG^{1,2}, ZE-MING SHI^{1,2} AND SHI-JUN NI^{1,2,*}

¹Department of Geochemistry, Chengdu University of Technology, Chengdu, 610059, China;

²Key laboratory of Nuclear Techniques in Geosciences, Chengdu 610059, China (E-mail: wangxinyucdut@gmail.com; shizm@cdut.edu.cn; nsj@cdut.edu.cn.)

Uranium is a toxic and radioactive element for human health. Previous research has revealed that those people who lived in the phosphate mining affected zone, had higher concentration of uranium in blood than those who lived in urban area. Based on the investigation of uranium concentration in a river which flowed through phosphate mining affected zone, the speciation of uranium in the water was discussed in detail.

In this paper, the potential, temperature and pH value were in situ analysed. The concentrations of uranium, other cations and anions were respectively determined by ICP-MS, ICP-OES and IC. According to the above experimental data, the uranium speciation model was constructed. The results show that:

In nearly-neutral pH value range, the uranium speciation distribution in water was mainly controlled by the phosphate concentration of the water. The MUS (major uranium speciation) of the river near the phosphate mining affected zone was $\text{UO}_2(\text{HPO}_4)_2^{2-}$, while the MUS were $\text{UO}_2(\text{CO}_3)_2^{2-}$ and $\text{UO}_2(\text{CO}_3)_3^{4-}$ in water which near the cement factories. When the river flowed through a farmland where the phosphate fertilizer was being used, the MUS in the water was $\text{UO}_2(\text{HPO}_4)_2^{2-}$. But after that site, the MUS of the river changed into $\text{UO}_2(\text{CO}_3)_2^{2-}$ and $\text{UO}_2(\text{CO}_3)_3^{4-}$ because of the increase of pH value and phosphate concentration. In this process, We found the use of phosphate fertilizer would lead to a significant increase of the phosphate concentration in the river. Moreover, the increasing of the phosphate concentration resulted in the hydrolysis of the anion and led to the raise of pH value of the river. Some studies about the relationship between the uranium toxicity and its speciation revealed that, because of the biological preference of element Phosphorus, the speciation of uranyl phosphate had stronger cytotoxicity (bioavailability) than the common speciation of uranyl carbonate.

Holocene changes in fire frequency in the Daihai Lake region (north-central China): Indications and implications for an important role of human activity

XU WANG¹, LINLIN CUI¹, JULE XIAO¹
AND ZHONGLI DING¹

¹Key Laboratory of Cenozoic Geology and Environment, Institute of Geology and Geophysics, Chinese Academy of Sciences, P.O. Box 9825, Beijing, 100029, China; (xuking@mail.iggcas.ac.cn)

Black carbon (BC) content in a sediment core from Daihai Lake, Inner Mongolia, was analyzed to reconstruct a high-resolution history of fires occurring in northern China during the Holocene and to examine the impacts of natural changes and human activities on the fire regime. The black carbon mass sedimentation rate (BCMSR) was disintegrated into two components: the background BCMSR and the BCMSR peak, with the BCMSR peak representing the frequency of fire episodes. Both the background BCMSR and the magnitude of the BCMSR peak display a close relation with the percentage of tree pollen from the same sediment core, suggesting that regional vegetation type would be a factor controlling the intensity of fires. The inferred fire-episode frequency for the Holocene exhibits two phases of obvious increases, i.e., the first increase from <5 to ~10 episodes/1000 yrs occurring at 8200 cal. yrs BP when the vegetation of the lake basin shifted from grasses to forests and the climate changed from warm/dry to warm/humid condition, and the further increase to a maximum frequency of 13 episodes/1000 yrs occurring at 2800 cal. yrs BP when herbs and shrubs replaced the forests in the lake basin and the climate became cool/dry. Both increases in the fire frequency contradict the previous interpretation that fires occurred frequently in the monsoon region of northern China when steppe developed under the cold/dry climate. We thus suggest that human activities would be responsible for the increased frequencies of fires in the Daihai Lake region in terms that the appearance of early agriculture and the expansion of human land use were considered to take place in northern China at ca 8000 and 3000 cal. yrs BP, respectively.

Early Archean ultra-depleted mantle: Evidence from newly discovered ~3.8 Ga trondhjemite in North China

YAFEI WANG^{1*}, XIANHUA LI¹, WEI JIN²
AND JIAHUI ZHANG²

¹Institute of Geology and Geophysics, Chinese Academy of Sciences, Beijing, 100029, China (*correspondence: pengfei4783@163.com; lixh@gig.ac.cn)

²College of Earth Sciences, Jilin University, 130021, China

The scale and degree of early mantle depletion and continental crust growth are poorly constrained because isotopic systems of ancient rocks are susceptible to later disturbances and most reliable Hadean to Archean zircons exhibit enriched isotopic characteristics.

Detailed field and zircon isotopic studies show that our newly discovered ~3.81 Ga trondhjemite was enclosed by ~3.36 Ga migmatite complex, and variable younger ages due to various degree of ancient radiogenic Pb loss, intrusion of leucosome, and a possible new ~3.31 Ga crustal growth event.

The concordant (disc.<5%) ~3.8 Ga zircons with simple oscillatory zonings preserve the primary isotopic signatures, ranging in $\epsilon_{\text{Hf}}(T)$ values from -1.9 ± 0.9 to 6.2 ± 0.7 and $\delta^{18}\text{O}$ from 5.3 ± 0.3 to $7.0 \pm 0.3\text{‰}$. The extremely positive ϵ_{Hf} values exceed values of previously reported contemporaneous zircons and existing depleted mantle Hf isotopic evolutionary models at ~3.8 Ga, providing robust isotopic evidence for the existence of an ultra-depleted mantle source corresponding to significant crustal growth at least 3.8 Gyr ago.

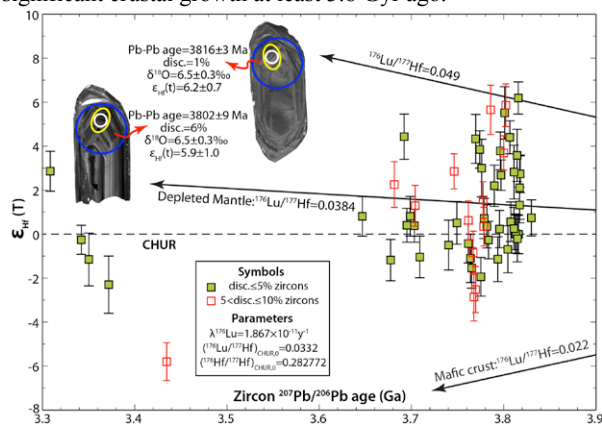


Figure 1: Plot of $\epsilon_{\text{Hf}}(T)$ versus age of disc.<10% zircons in ~3.81 Ga unit with putative reservoirs differentiated at 4.5 Ga and details of two highest ϵ_{Hf} zircons. The highest ϵ_{Hf} value requires a reservoir with $^{176}\text{Lu}/^{177}\text{Hf}$ ratio of 0.049, significantly higher than present-day depleted mantle value of 0.0384, differentiated at 4.5 Ga. The blue circle is ~60 μm in diameter.

Silicate melts under high pressure

YANBIN WANG¹, TATSUYA SAKAMAKI^{1,*},
LAWRIE SKINNER², GUOYIN SHEN³, TONY YU¹, YOSHIO
KONO³, ZHICHENG JING¹ AND CHANGYONG PARK³

¹Cnter for Advanced Radiation Sources, the University of Chicago, Chicago, IL, USA

²Stony Brook University, Stony Brook, NY, USA

³HPCAT, Carnegie Institution of Washington, Argonne, IL, USA

We present our recent data on structural evolution of silicate melts and glasses at high pressures, along with measurements of density, elasticity, and viscosity. High-pressure melt structure studies were conducted using a Paris-Edinburgh Press at the HPCAT beamline 16-BM-B. Acoustic velocities were also measured on silicate glasses. A DIA apparatus was used for melt density measurements based on x-ray absorption at GSECARS beamline 13-BM-D. Structures of polymerized (jadeite – $\text{NaAlSi}_2\text{O}_6$) and depolymerized (diopside, $\text{CaMgSi}_2\text{O}_6$) melts show distinct responses to pressure. In jadeite melt, T-O (T denotes tetrahedrally coordinated Al and Si) bond length, T-T bond length, and T-O-T angle all exhibit rapid and non-linear decrease with increasing pressure to ~3 GPa. In diopside melt, these parameters vary linearly with pressure and change very little. A large viscosity dataset from the literature shows that, with increasing pressure, viscosities of polymerized liquids (including jadeite) first decrease and reach a minimum at around 3 GPa before turning over. On the other hand, viscosities of depolymerized melts (including diopside) increase monotonically with pressure. Molecular dynamics calculations, constrained by the x-ray structural data, were employed to examine details of structural evolution in the two types of liquids. A model will be presented to link structural evolutions to changes in melt properties, such as density and viscosity, with pressure.

Oxygen isotope compositions of Al-rich chondrules from carbonaceous chondrites

Y. WANG^{1*}, W. HSU¹, X. LI², AND Q. LI²

¹Purple Mountain Observatory, Chinese Academy of Sciences, Nanjing 210008, China (*correspondence: y_wang@pmo.ac.cn)

²Institute of Geology and Geophysics, Chinese Academy of Sciences, Beijing 100029, China

Al-rich chondrules (ARCs) are rare objects with >10 wt% bulk Al₂O₃ content. They have petrological, chemical, and oxygen isotopic characteristics intermediate between Ca,Al-rich inclusions (CAIs) and ferromagnesian chondrules (FMCs) [1]. ARCs are an unique window to study the origins of CAIs and chondrules and their genetic relationship.

Eleven ARCs and representative CAIs and FMCs from three CV3 (NWA 2140, NWA 2697, and NWA 989) and Ningqiang chondrites were studied. Olivine, pyroxene, plagioclase, spinel, and Si,Al-rich glasses were analyzed with the Cameca ims-1280 ion microprobe, housed at IGG, Beijing. The oxygen isotope compositions of ARCs form a mixing line with a slope of 0.86±0.04 (Figure 1), close to the CCAM line (slope=0.94) [2]. ARCs have Δ¹⁷O values (0.3~17.9 ‰) intermediate between CAIs (-1.4~-27 ‰) and FMCs (2.4~9.8 ‰), indicating that the precursors of ARCs might be mixtures of CAIs and FMCs. Minerals in individual ARCs are heterogeneous in oxygen isotope compositions, with the biggest Δ¹⁷O variation of 15.4 ‰. This implies that during the formation of ARCs, oxygen isotopic exchange with nebular gases might have occurred.

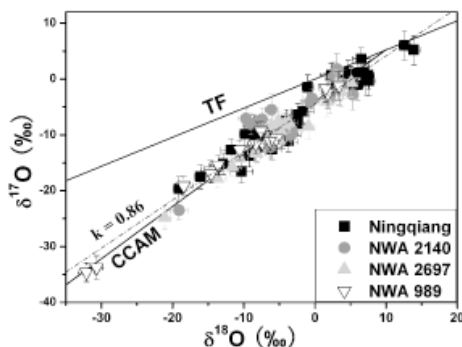


Figure 1: Oxygen isotope compositions of ARCs from Ningqiang and three CV3 chondrites.

[1] Krot & Keil (2002) *MAPS* **37**, 91-111. [2] Yurimoto *et al.* (2008) in *Rev. in Min. & Geochem* **68**, 141-186.

This work was supported by the National Natural Science Foundation (41003026) and the Minor Planet Foundation of China.

Geochemical characteristics of different type reservoirs from the Sinian Dengying Formation in Southeastern Sichuan Basin, China

WANG YONG AND SHI ZEJIN²

¹ Department of Geochemistry, Chengdu University of Technology, Chengdu 610059, China; e-mail: wangyong10@cdut.cn

² State Key Laboratory of Oil and Gas Reservoir Geology and Exploitation, Chengdu University of Technology, Chengdu 610059, China; e-mail: szj@cdut.edu.cn

Reservoirs in Sinian Dengying Formation can be divided into three categories according to genesis, that is, paleo-karst reservoirs related to tectonic uplift, buried dissolution reservoirs due to burial and dissolution and hydrothermal dolomite reservoirs. Compared with surrounding rocks in Dengying Formation, paleo-karst reservoirs had the characteristics of low Na, high Mn, high Fe, low Sr, low carbon isotope and high ⁸⁷Sr/⁸⁶Sr value, generally reflecting the fact that the formation of paleo-karst reservoirs was closely related to fresh water. Buried dissolution reservoirs had the characteristics of high Mn, low Fe and low carbon isotopes. The characteristics of high Mn indicated that buried dissolution reservoirs experienced stronger diagenesis modification in the burial environment, while low Fe and low carbon isotopes were related to dissolution effects of organic acids during burial. Hydrothermal dolomite reservoirs had very low contents of Fe and Sr element, significantly partial negative oxygen isotope, and very high ⁸⁷Sr/⁸⁶Sr value. The formation of these characteristics was related to hydrothermal physical and chemical properties. Three major types of reservoirs in Dengying Formation had significant geochemical response characteristics, which could be taken as geochemical indicators to identify different types of reservoirs.

Lawsonite as a potential repository of Th and REE in subduction zones: Blueschists from Tavşanlı (Turkey)

Y. WANG¹, D. PRELEVIĆ¹, S. FOLEY^{1,2}, S. BUHRE¹,
T. JOHNSON¹ AND T. HÄGER¹

¹Uni Mainz, Mainz, Germany (wangyu@uni-mainz.de)

²CCFS, Dept. Earth and Planetary Sciences, Macquarie University, North Ryde, NSW 2109, Australia

Constraining the processes by which crust is recycled back through the mantle wedge and into volcanic arcs is one of the most challenging issues in modern geochemistry. Discussion is mostly centered around the dichotomy of fluid vs melt transport and subsolidus dehydration vs melting, in which the mobility of Th and REE has particular significance. In this context, production of fluid or melt by breakdown of hydrous minerals such as lawsonite, and the consequences for trace element mobilization remain largely unconstrained.

Here we combine EMP, LAM-ICP-MS and confocal microRaman spectroscopy with THERMOCALC modelling of four samples of lawsonite and garnet bearing blueschist from the Tavşanlı Zone, Turkey, a melange metamorphosed under blueschist to lawsonite-eclogite facies conditions. Our aim was to monitor trace element redistribution during high-pressure–low-temperature metamorphism. Two samples have low concentrations of Th, REE and K, suggesting an essentially oceanic crust protolith, while the other two samples are enriched in K (up to 2.89% K₂O), Th and REE, implying the presence of a continent-derived terrigenous component.

Equilibrium assemblages are lawsonite + glaucophane + chlorite + phengite + titanite + apatite +/- garnet +/- quartz and iron oxides. Garnet is the major host for HREE, phengite contains most LILE and titanite and zircon are the dominant carriers for Nb, Ta and Zr, Hf, respectively. Lawsonite and apatite carry almost all Sr and a significant proportion of the REE. In Th rich samples, lawsonite is extremely enriched (up to 100 ppm) in Th, giving rise to high Th/La ratios up to 1.0, at relatively low Sm/La (down to 0.4).

The high Th/La ratios observed in lawsonite are significantly higher than in average crust and normal arc volcanics, but similar to those in Mediterranean lamproites, rare ultrapotassic orogenic lavas occurring within Alpine-Himalayan belt. This “fingerprint” may result from the incorporation of lawsonite-bearing blueschists into their melting source, and subsequent melting. High Th/La can be liberated only by direct melting, ruling out prograde recrystallization into new mineral phases, which redistribute trace elements differently.

Mercury biogeochemistry and its biomagnification in the fish food web in Three Gorges Reservoir after 175m impoundment

YUCHUN WANG¹ MEI MA^{2A} AND YANG YU¹

¹Department of Water Environment, China Institute of Water Resources and Hydropower Research, Beijing 100038, China. wangyc@iwhr.com; yuyangle@126.com

²State Key Laboratory of Environmental Chemistry and Ecotoxicology, Research Center for Eco-Environmental Sciences, Chinese Academy of Sciences, Beijing 100038, China. mamei@rcees.ac

Three Gorges Reservoir (TGR) is a giant canyon-shaped reservoir located in the lower section of the upper reaches of the Yangtze River. Concern about human consumption of fish contaminated with MeHg had been raised even before the construction of TGR. This study tried to investigate the total mercury concentrations in fish and biomagnification characters of mercury along food chains in TGR after 175m impoundment. We collected eleven fish species from three main stem sections and seven typical tributaries of TGR from 2011 to 2012. Result showed that mercury concentrations in fishes from TGR had not obviously increased after impoundment. But spatial difference was found among different sections of main stem. Due to the enhanced sediment deposition along reservoir, there was a decreasing trend of mercury concentration in fish from upper stream to lower stream within TGR. Mercury concentrations in the fishes from Luoqi in up area of reservoir (88.0µg/kg, average) was significantly higher than those from Wushan in middle area of reservoir (43.1µg/kg, average) and tributaries (57.1µg/kg, average). The mercury concentrations in fish from tributaries were comparable to those from main stem, and there were no significant difference among most tributaries. While Log-transformed mercury contents were consistently correlated with δ¹⁵N values for the fish food web in all sampling sites, the slope of the relationship with δ¹⁵N (biomagnification power value) was significant higher in Shennong River than that in Wanzhou and Wushan section. This indicated that biomagnification power of mercury is greater in tributary than in main stem of TGR. Data of δ¹⁵N and δ¹³C showed that fishes in tributary rely more on pelagic primary production while those in main stem tend to take allochthonous materials carried by runoff. In conclusion, the difference between body type of tributary and main stem after impoundment may be an important reason of different mercury bioaccumulation within TGR.

Uranium(IV) mobility in a mining-impacted wetland

Y. WANG^{1*}, M. FRUTSCHI¹, E. SUVOROVA¹,
V. PHROMMAVANH², M. DESCOSTES², A. OSMAN³,
G. GEIPEL³ AND R. BERNIER-LATMANI¹

¹Ecole Polytechnique Fédérale de Lausanne (EPFL), Environmental Microbiology Laboratory, Lausanne, Switzerland (*presenting author: yuheng.wang@epfl.ch)

²AREVA - Business Group Mines, Direction R&D, BAL 3720C, Tour AREVA, Paris, France

³Helmholtz Center Dresden Rossendorf (HZDR), Institute of Resource Ecology, Dresden, Germany

Uranium is known to accumulate in wetlands through its association with organic-rich soils. The precipitation of relatively insoluble U(IV) minerals under reducing conditions is considered as a means to immobilize U in constructed wetland systems [1]. A wetland in the Limousin region in France, located adjacent to a former U mine was impacted by mining activity for several decades and contains U hotspots (~4,000 ppm) [2]. The concentration of U steadily increases as a function of distance in a stream flowing through the wetland, suggesting U release from the wetland into the stream. We collected soil and porewater samples under anoxic conditions from two selected U hotspots in the wetland as a function of depth and season to assess the geochemical conditions leading to this release. High porewater Fe(II) concentrations suggest that metal-reducing conditions prevail in the wetland soil. Using laser fluorescence spectroscopy (LFS) and X-ray absorption spectroscopy (XAS), we concluded that the predominant U redox state in both porewater and soil was tetravalent. A near constant U(IV) concentration is observed throughout the porewater profile while soil U(IV) is restricted to the top 30 cm. Evidence for U association with colloidal Fe(OH)₂-organic matter assemblages provided a ready explanation for the mobility of porewater U. Furthermore, U in the soil occurs primarily as a non-crystalline U(IV) species corresponding to U(IV) adsorbed onto amorphous Fe-Al-P-Si aggregates. Hence, U(IV) species in the porewater are distinct from those present in the soil. These results show that the form of U(IV) in soil is labile and releases U(IV) to form mobile colloids that ultimately result in the release of U into the stream. The surprising mobility of U(IV) in this system brings into question the often assumed immobilization of U through reduction, particularly in high organic matter environments such as wetlands.

[1] Owen *et al.* (1995) *Ecol. Eng.* **5**, 77-93. [2] Moulin (2008) PhD thesis, Ecole Centrale de Paris.

Nano pore evolutions of shale and coal during petroleum generation process using SANS and pyrolysis

YUNPENG WANG¹ MEI DING^{2A} AND LINGLING LIAO¹

¹ SKLOG, Guangzhou Institute of Geochemistry, Chinese Academy of Sciences, Guangzhou 510640, China

² EES-14, LANL, Los Alamos, NM 87545, USA

This study aims to examine the changes of nano- to microscaled pores of shale (marine and lacustrine) and coal with petroleum generation, retaining and cracking. Pyrolysis was used to define oil and gas window, as well as study the compositions of expelled and retained oil while small-angle neutron scattering (SANS) was used to characterize nano- to microscaled pores of residual source rocks. Oil windows are defined as 0.6-1.3%Ro for shale and 0.5-1.2%Ro for coal; wet gas window are 0.9-3.0% Ro for shale and 0.8-3.0% Ro for coal; dry gas windows are 1.3-3.6%Ro for both shale and coal. In oil window, marine shale oil shows mainly saturated and aromatic fractions, resins and less asphaltene. In gas window, higher saturated fractions is due to its higher stability. Coal oil shows dominant asphaltene fraction with higher aromatic HC, resin, asphaltene and rare saturated HC.

Pore features corresponding to oil and gas windows by SANS show that shale and coal have unique pore features at the scale between 1 to 100 nm. Results also show that pore features change more significantly in coal relative to shale rock during hydrocarbon generation and expulsion from source rocks, presumably due to the much higher organic carbon content of the coal and unique HC fractional compositions (Fig. 1).

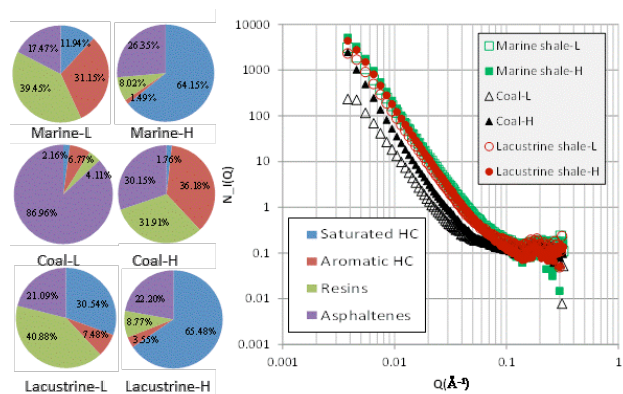


Figure 1 SANS plot of shale and coal in early oil window(L, 0.4%Ro) and post gas window(H,3.8%Ro) as well as the corresponding hydrocarbon(HC) fractional compositions

Accretion of a volatile rich late veneer recorded by CI chondrite-like S/Se and Se/Te in the Earth's mantle

ZAICONG WANG* AND HARRY BECKER

Freie Universität Berlin, Malteserstrasse 74-100, 12249
Berlin, Germany (*contact: zaicongwang@gmail.com)

The history of delivery of volatile elements is of fundamental importance for understanding planetary evolution (Albered, 2009). The detailed origin and history of moderately volatile and atmophile elements in the Earth remains uncertain. The excess of highly siderophile elements (HSE) and chondritic ratios of most HSE in the bulk silicate Earth (BSE) may reflect accretion of a chondritic late veneer of about 0.5 % of Earth's mass after core formation[1,2]. The proportion of volatiles delivered by the late veneer is a key constraint for the budget and the origin of the volatiles in the Earth. At high pressure-temperature conditions, the moderately volatile chalcogen elements S, Se and Te with rather low 50 % condensation temperatures near 700 K are moderately to highly siderophile, thus, if depleted by core formation, their mantle abundances should reflect the composition of the late veneer[3]. Here we determined ratios and abundances of S, Se and Te in the mantle based on new isotope dilution data for post-Archean mantle peridotites with negligible low-temperature alteration. Infiltration and trapping of silicate melt in peridotites have very similar effects on abundances of S, Se and Te as partitioning during open system melting[4,5]. The mean S/Se (2690 ± 700 , 1σ) and Se/Te (7.9 ± 1.6 , 1σ) of mantle lherzolites overlap with CI chondrite values[6]. In contrast, Se/Te of ordinary and enstatite chondrites are significantly different (11-30)[7]. The chalcogen/HSE ratio of the BSE is similar to CM group carbonaceous chondrites, consistent with the view that the HSE signature of the BSE reflects a mixture of slightly volatile depleted carbonaceous chondrite and minor non-chondritic material[8]. Depending on the estimates for the abundances of water and carbon in the BSE (Marty 2012), the late veneer may have supplied a significant proportion of the budget of hydrogen and carbon in the BSE.

[1] Albarède (2009), *Nature*, 461, 1227-1233. [2] Walker (2009) *Chem Erde-Geo* **69**, 101-125. [3] Mann et al. (2012) *GCA* **84**, 593-613. [4] Rose-Weston et al. (2009) *GCA* **73**, 4598-4615. [5] Wang et al. (2013) *GCA* **108**, 21-44. [6] Lorand & Alard (2010) *CG*, **278**, 120-130. [7] Lodders (2003) *J Astrophys* **591**, 1220-1247. [8] Wasson & Kallemeyn (1988) *Phil Trans R Soc A* 325, 535-544. [9] Fischer-Gödde & Becker (2012) *GCA* **77**, 135-156. [10] Marty (2012) *EPLS*, 313-314(0): 56-66.

Origin of deep gas and oil cracking gas potential in Tarim Basin, China

ZHAOYUN WANG¹, YONGXIN LI², AND HONGJU ZHENG³

¹ Research Institute of Petroleum Exploration and Development, Petrochina, Beijing, China, wzy@petrochina.com.cn

² Research Institute of Petroleum Exploration and Development, Petrochina, Beijing, China, lyxin@petrochina.com.cn

³ Research Institute of Petroleum Exploration and Development, Petrochina, Beijing, China, hjzheng@petrochina.com.cn

The marine strata in China is of old age and in high evolution period, and the potential of gas generated from high-overmature source rocks is limited, but the gas exploration of this marine strata in Tarim basin has greatly effective with large gas fields constantly discovered.

This paper brings up the successive gas generation mechanism for the origin of deep marine gas, including three meanings of transformation of gas generation matter, replacement of gas generation time, and change of gas source kitchen. The gas source kitchen of dispersive liquid hydrocarbon inside of source rocks inherits the characteristics of original gas source kitchen, but the gas source kitchen of dispersive & concentrated liquid hydrocarbon outside of source rocks has occurred the spacial change comparing with original gas source kitchen. The above three liquid hydrocarbon can be cracked into gas at high-over mature stage, but the latter is embedded flatter and its time of cracking and gas generation is later than the former, which makes for the late gas accumulations.

This paper creates expulsion oil rate plates of different organic matter abundance through simulation experiments of hydrocarbon generation and expulsion of different organic matter abundance and different lithology source rocks, providing the basis for the reasearch of allocation proportion and quantity of dispersive liquid hydrocarbon inside & outside of source rocks.

This paper demonstrates the quantity, distribution and cracking degree of dispersive soluble organic materials of palaeozoic strata in Tarim basin from the evaluating indicator S_1 of hydrocarbon generating potential, heat-origin asphalt and the fluorescence characteristic of reservoirs, and makes sure of the reality of successive gas generation of organic matter of palaeozoic marine source rocks in Tarim basin, and also calculates the cracking gas quantity of dispersive soluble organic matter in middle and lower Cambrian of Tarim basin. The application of successive gas generation mechanism of organic matter can greatly increase the gas exploration potential and hopeness of palaeozoic strata in Tarim basin, China.

[1] Dai et al (2002) *Xinjiang Petroleum Geology* **23**, 357-365. [2] Zhao et al (2005) *Petroleum Exploration and Development* **32**, 1-7. [3] Liang et al (2000) *Earth Science Frontiers* **7**, 534-547. [4] Zhang et al (2002) *China Petroleum Exploration* **4**, 18-24.

Novel calcite-aragonite sea transition in the terminal Proterozoic

ZHENGRONG WANG¹ JUSTIN AND RIES² CHAO LIU¹

¹Department of Geology and Geophysics, Yale University, New Haven, CT, USA, Zhengrong.wang@yale.edu

²Department of Marine Sciences, University of North Carolina, Chapel Hill, NC, USA, riesjustin@gmail.com

Tectonically driven fluctuations in seawater Mg/Ca are thought to have caused changes in the polymorph mineralogy of platform carbonates throughout Phanerozoic time (Mg/Ca < 2 = calcite seas; Mg/Ca > 2 = aragonite seas) [1]. Previously published elemental analyses of micritic limestones from the terminal Proterozoic Nama Group (552–544 Ma), southern Namibia, show a threshold increase in Sr/Ca (by a factor of 6–7) from 549 to 547 Ma and a decrease in Mg/Ca ratio (by a factor of 5) from 552 to 544, which are both consistent with a transition from primary calcite limestones (Sr-depleted, Mg-enriched) to primary aragonite limestones (Sr-enriched, Mg-depleted) across this interval [2].

To further investigate this potentially novel calcite-aragonite sea transition, we measured the Sr and Mg isotope compositions of the Nama Group carbonates (552–544 Ma) at Yale University. ⁸⁷Sr/⁸⁶Sr ratios are elevated from 0.7090 to 0.7105 between 552 and 549 Ma, and then decline to a relatively stable value of 0.7086 between 549 and 544 Ma. The bulk $\delta^{26}\text{Mg}_{\text{DSM3}}$ values of the carbonates increase steadily from ~ -2.5 to -1.2‰ between 552 and 544 Ma, with a brief excursion down to -3.5‰ at ca. 549 Ma, which coincides with peaks in ⁸⁷Sr/⁸⁶Sr and Mg/Ca ratios.

Theoretical work and empirical observations of modern carbonates show that ²⁶Mg is enriched in the following order: low Mg calcite < high-Mg calcite < dolomite < aragonite [3]. Thus, the increase in $\delta^{26}\text{Mg}$ from 552 to 542 Ma is consistent with an increase in the proportion of primary aragonite with time. Likewise, the decline in ⁸⁷Sr/⁸⁶Sr across the interval is consistent with a transition from a lower-Mg/Ca calcite sea characterized by increased hydrothermal flux of radiogenic Sr (higher ^{87/86}Sr), to a higher-Mg/Ca aragonitic sea characterized by decreased hydrothermal flux of radiogenic Sr (lower ^{87/86}Sr). High-frequency incremental leaching of a set of limestone samples also suggests that the anomalous peaks in ^{87/86}Sr and Mg/Ca around 549 Ma may have resulted from localized diagenetic alteration.

[1] Hardie, LA, 1996, *Geology* 24: 279–283. [2] Ries, J *et al.*, 2009, *Geology* 37: 743–746 [3] Wang *et al.*, 2013, *GCA*, 102: 113–123

Oxygen isotope equilibrium between sulfite and water

SCOTT D. WANKEL^{*1,2}, ALEXANDER S. BRADLEY^{1,3}, DANIEL L ELDRIDGE⁴ AND DAVID T. JOHNSTON^{*1}

¹Dept. of Earth and Planetary Science, Harvard University, Cambridge, MA 02138 (johnston@eps.harvard.edu)

²Dept. of Marine Chemistry and Geochemistry, WHOI, Woods Hole, MA 02540 (sdwankel@whoi.edu)

³Dept. of Earth and Planetary Science, Washington University, St. Louis, MO 63130

⁴Dept of Geology, Univ of Maryland, College Park, MD 20742

Application of the oxygen isotopic composition of sulfate ($\delta^{18}\text{O}_{\text{SO}_4}$) is complicated by rapid equilibration between sulfoxyanions and water. Specifically, the apparent relationship that develops between $\delta^{18}\text{O}_{\text{SO}_4}$ and $\delta^{18}\text{O}_{\text{water}}$ during microbial sulfate reduction is thought to result from rapid equilibrium between water and aqueous intracellular sulfite (SO_3^{2-}) – a reactive intermediate in the sulfate reduction network. Here, we describe the oxygen isotope equilibrium effect between SO_3^{2-} and water, based on experiments conducted over a range of pH (4.5 to 9.8) and temperature (2 to 90°C). Experimental results are consistent with predicted values based on *ab initio* estimates of oxygen isotope equilibrium values among S(IV) species and water and changes in speciation. We find that $\epsilon_{\text{sulfite-water}} = 13.61 - 0.299 \cdot \text{pH} - 0.081 \cdot \text{T}^\circ\text{C}$ such that at a pH (7.0) and temperature (25°C) typifying common experimental conditions of sulfate reducing bacterial cultures, SO_3^{2-} is enriched in ¹⁸O by 9.5‰ ($\pm 0.8\%$) relative to ambient water. By evaluating previously published data within an updated sulfate reduction network, results prove consistent with high enzyme reversibility in the sulfate reduction biochemical network. We show that intracellular SO_3^{2-} exchanges with water up to 3 orders of magnitude faster than internal recycling and that kinetic isotope effects upstream of SO_3^{2-} are required to explain previous laboratory and environmental studies of $\delta^{18}\text{O}_{\text{SO}_4}$ resulting as a consequence of sulfate reduction.

Seawater $\delta^7\text{Li}$: A tracer for global CO_2 consumption by continental silicate weathering?

CHRISTOPH WANNER* AND ERIC L. SONNENTHAL

Lawrence Berkeley National Laboratory, Berkeley, CA, USA,

(*correspondence: cwanner@lbl.gov)

Lithium isotope fractionation has been used as a proxy for silicate weathering and as a tracer in geothermal systems [1,2]. Misra & Froelich [1] recently presented the first record of Cenozoic seawater $\delta^7\text{Li}$ showing an increase of 9‰ over the last 60 Ma. This increase was attributed to increasing riverine $\delta^7\text{Li}$ values caused by a general change in continental silicate weathering behaviour.

Reactive transport modelling was performed using TOUGHREACT [3] to gain insight into the geochemical and isotopic effects of the changing weathering pattern. Simulations considered a granitic aquifer feeding a major river system. Li isotope fractionation was assumed to solely occur during Li incorporation into precipitating secondary minerals, computed using a solid solution approach [4]. Different weathering patterns were simulated by varying the contribution from weathering of unaltered granitic mineral phases (quartz, feldspars, micas), including the precipitation and dissolution of secondary minerals (kaolinite, chlorite) using a dual continuum approach.

Simulated $\delta^7\text{Li}$ values increased with an increasing contribution from weathering of primary granitic mineral phases suggesting that today's heavy riverine and seawater $\delta^7\text{Li}$ values are the result of a "weathering-limited" weathering pattern such as proposed by Misra and Froelich [1]. In contrast, our simulations suggest that low $\delta^7\text{Li}$ values inferred for the Paleocene-Eocene boundary [1] were largely inherited from weathering of previously formed secondary mineral phases associated with little or no Li isotope fractionation. Moreover, total simulated CO_2 consumption by silicate weathering reactions are positively correlated with $\delta^7\text{Li}$ values suggesting that global riverine and seawater $\delta^7\text{Li}$ values are directly linked to the total amount of global CO_2 consumption by continental silicate weathering. For a quantitative correlation, however, more experimental work is needed to better understand Li isotope fractionation processes including identifying key minerals involved and determining corresponding Li isotope fractionation factors.

[1] Misra & Froelich (2012), *Science* 335, 818-823. [2] Millot & Negrel (2007), *Chem. Geol.* 244, 664-678. [3] Xu *et al.* (2011), *Comput. & Geosci.* 37, 763-774. [4] Wanner & Sonnenthal (2013), *Chem. Geol.* 337-338, 88-98.

Noble gas partitioning in CO_2 environments: a supercritical assessment of current assumptions

O. WARR^{1*}, A. MASTERS², C. ROCHELLE³
AND C.J. BALLENTINE¹

¹SEAES, University of Manchester, M13 9PL, UK

(*correspondence: oliver.warr@manchester.ac.uk)

²CEAS, University of Manchester, M13 9PL, UK

³ British Geological Survey, Nottingham, NG12 5GG, UK

Noble gases are powerful inert tracers which can yield key information about physical processes occurring within geological systems. Currently all modelling involving binary phase noble gas partitioning are based on the determinations by Crovetto *et al.* 1982 [1] under conditions that did not require consideration of phase composition, supercriticality nor the effect of non ideality on solute noble gases. Subsequent studies have not investigated these factors; the validity of all current interpretations is based on the assumption that these variables have no effect on noble gas partitioning. However, no published study exists which substantiates this supposition. Assessing the effects these variables have on partitioning will give us a much warranted greater insight and understanding into geological systems that operate under significantly different PVTX conditions.

We present noble gas partitioning results from a supercritical CO_2 - H_2O binary phase system at elevated temperatures and pressures (50-100°C & 90-140 bar). This system was chosen due to a strong current interest in underground storage of anthropogenic CO_2 and their natural analogues for which noble gases have already proven invaluable [2,3]. Partitioning is determined using a combined experimental and numerical simulation-based approach to generate partitioning values which forms the basis of a robust model for predicting partitioning over a wide range of PT conditions. We present our methodology and results which we compare and contrast with values derived from the Crovetto *et al.* dataset. Preliminary findings suggest noble gas partitioning is demonstrably different for a supercritical CO_2 - H_2O system; overall water phase solubility is significantly reduced, especially for the heavier noble gases by up to 60%. This observed disparity appears greatest at higher pressures and lower temperatures although an observable difference is noted across the studied PT range.

[1] Crovetto *et al.* (1982) *J. Chem. Phys.* 76, 1077-1086. [2] Gilfillan *et al.* (2009) *Nature* 458 614-618. [3] Zhou *et al.* (2012) *Geochim. Cosmochim. Acta* 86 257-275.

Global Abyssal Peridotite Constraints on the Upper Mantle

JESSICA M. WARREN¹

¹Stanford University, 450 Serra Mall, Stanford, CA 93405;
warrenj@stanford.edu

Abyssal peridotites are the residues of adiabatic decompression melting beneath ridges. A broad sampling of abyssal peridotites from all major ocean ridges reveals variations in composition that reflect both ridge processes (melting, refertilization) and pre-existing heterogeneity. I present a compilation of geochemical data for abyssal peridotites from 59 localities on 6 major ridge systems (EPR, MAR, SWIR, CIR, AAR, and Gakkel). While the majority of peridotites have been sampled at transform faults, sampling at slow and ultra-slow ridges in the past decade has recovered large suites of on-axis peridotites. Compositional data has now been published for ~1500 peridotites, permitting a detailed look at global variations in the oceanic upper mantle.

I classify peridotites into residual peridotites and four types of veined peridotite: (1) gabbro-veined & plagioclase-bearing peridotite, (2) pyroxenite-veined peridotite, (3) dunite, and (4) cryptically metasomatized peridotite. The veins are generally interpreted to represent incompletely extracted melt or melt-related features retained in peridotite after adiabatic decompression melting. Veined peridotites represent >30% of the dataset. The abundance of veined peridotite indicates that oceanic lithospheric mantle is less depleted than commonly assumed, resulting in recycling of relatively more enriched material at subduction zones.

Residual peridotites provide the best representation of mantle composition following melt depletion and extraction. However, these unveined, residual peridotites define a surprisingly large compositional range, particularly at some individual localities. Modal Cpx varies from 0 to 15%, while spinel Cr/[Cr+Al] varies from 0.1 to 0.6. Individual trace elements vary by one to three orders of magnitude, which corresponds to ~0-12% degree of nonmodal fractional melting. Such variation is at odds with theory, which predicts that the degree of melting beneath ridges should be relatively uniform, except at ultra-slow spreading rates. In addition, some sections of ridge contain highly depleted peridotite associated with thin or absent basaltic crust. Some local-scale variability can be explained by incipient melt-rock reaction to produce dunite, but the pervasive variability at all length-scales indicates that regions of the upper mantle must contain pre-existing heterogeneities. This agrees with isotopic data (available for <100 abyssal peridotites), which require long-term depletions and enrichments in the mantle.

Long-term CO₂ induced reactivity, observations on natural CO₂ analogues and geochemical model predictions

LAURA J. WASCH¹, MARIELLE KOENEN¹
AND SUSANNE NELSKAMP¹

TNO, Princetonlaan 6, P.O. Box 80015, 3508 TA Utrecht, the Netherlands. Laura.wasch@tno.nl

Predicting CO₂ trapping and containment over extended timescales asks for accurate models and well constrained input parameters. CO₂ natural analogues provide good opportunities to study the actual long-term effect of CO₂ on reservoir and caprock. This will provide valuable insight in long-term geochemical processes concerning CO₂ storage. Moreover, natural analogues can help calibrate simulations of the long-term chemical effects of CO₂ storage. Accurate simulations are essential for confirming whether the observed and modelled behaviour of injected CO₂ are in agreement, as required for EU regulations, thereby facilitating successful implementation of CCUS.

We present an integrated approach of petrography, basin modelling and geochemical modelling. Our study is focussed on the Werkendam natural analogue, a Dutch gas field containing > 70% CO₂. The CO₂ was trapped millions of years ago and hence the reservoir has been reacting with CO₂ for prolonged periods of time. In addition to CO₂ induced reactions, reactions related to 'ordinary' diagenesis are expected to have occurred. To distinguish the effect of CO₂ from diagenesis, the Waalwijk methane field was selected as a CO₂ free reference of the same formation. Basin modelling showed that this field has a comparable burial history as Werkendam. Samples from both reservoirs are studied with SEM to assess the differences in the mineral relations. Comparison of the reactions observed in the CO₂ and the CH₄ fields points to differences in mineral dissolution and secondary carbonate formation. The presence of CO₂ appears to enhance feldspar dissolution while facilitating (additional) formation of carbonates such as siderite, dolomite and ankerite. Geochemical modelling with PHREEQC is performed to assess if these reactions associated with CO₂ correspond to the predicted mineral changes. Calibration of the model indicates that the selection of primary mineralogy, especially the minor iron-bearing minerals, has a large effect on predicted CO₂ mineralization.

Detailed mineralogical input and assessment of the burial history is required to calibrate geochemical models which will increase our knowledge on long-term geochemical processes considering CCUS.

Bioweathering of chrysotile asbestos

KIRSTIN E. WASHINGTON*¹, JANE K. WILLENBRING¹
AND BRENDA CASPER²

¹University of Pennsylvania, Department of Earth and
Environmental Sciences, Philadelphia, PA 19104, USA

²University of Pennsylvania, Department of Biology,
Philadelphia, PA 19104, USA

*kirstin.e.washington@gmail.com

The serpentine mineral, chrysotile, is the most common asbestiform mineral at asbestos-contaminated sites. Similar in mechanism to other asbestos minerals, its toxicity is related to the presence of iron, which induces oxidative stress, and the fiber's shape, which can lead to piercing of lung alveoli and induces inflammation.

Previous research has developed the idea that fungi endemic to serpentine substrates (*Fusarium oxysporum* and *Verticillium leptobactrum*) can remove atoms of key elements from asbestos particles, rendering them less toxic [1]. In this study, we investigate natural mechanisms of removal of impurity elements (Fe) and structural cations (Mg, Si) from the chrysotile asbestos fibers. We ran greenhouse experiments using heavy metal accumulating plant species, *Brassica juncea*, *Helianthus annuus*, and *Thlaspi caerulescens*. We also planted the native serpentine grassland species, *Sorghastrum nutans*, whose roots form mutualist relationships with arbuscular mycorrhizal fungi (AMF). We also evaluated the use of fungal exudates to remove iron from asbestiform chrysotile through cultured fungal experiments for different species of *Fusarium*.

We analyzed the iron content of plant tissue, fungal tissue, and iron in solution in fungal growth media and organic acid solutions over time via ICP-OES. We imaged the chrysotile fibers and fungi mycelium using an ESEM to determine the change in mineral structure and aspect ratio over time, and we assessed the change in mineral composition of untreated and treated asbestos samples via XRD. Preliminary data demonstrate that *Brassica juncea* was able to remove an average of 300ppm Fe per gram of plant tissue from the surface of chrysotile asbestos, and there was no difference in plant biomass when compared to plants grown with the addition of fertilizer containing iron. Preliminary results from the fungi treatments show that fungi take up iron but do not liberate the iron into the broth solution.

[1] Daghino, S. *et al.* 2006. ES&T 40: 5793-5798.

Cd isotope fractionation during sorption to Mn oxide at low and high ionic strength

LAURA E. WASYLENKI¹ AND JARED W. SWIHART¹

¹Department of Geological Sciences, Indiana University,
Bloomington, Indiana USA 47405 (lauraw@indiana.edu)

Two potential applications of Cd isotopes motivate this study:

First, some diatoms have evolved to use Cd instead of Zn in their carbonic anhydrase enzyme [1]. Because these diatoms strongly fractionate Cd isotopes [2], marine sediments may preserve isotopic records of Cd utilization and diatom productivity in the past. A recent study [3] indicated that ferromanganese crusts in particular might preserve a straightforward record of global deepwater Cd isotopes.

Second, for freshwater or groundwater contaminated with Cd, sorption to Mn oxyhydroxide particles can be the dominant process retarding mobility of this toxic heavy metal (except in sulfide-rich conditions). If sorption drives a distinctive isotope effect, then determining the extent to which sorption reactions are attenuating flow of Cd may be possible by tracking Cd isotope signatures in soils or water.

To lay groundwork for these potential applications and to investigate fractionation mechanisms for Cd, we conducted sorption experiments using particles of the Mn oxyhydroxide birnessite, both in pure water and in synthetic seawater. Suspensions of synthetic birnessite particles were doped with Cd and allowed to react for 24 hours (pH adjusted to 8-8.5). Dissolved and sorbed Cd pools were separated by filtration, purified by ion exchange chromatography, and analyzed by MC-ICP-MS.

At low ionic strength we observed a constant offset of +0.15‰ ($\Delta^{114/112}\text{Cd}$) between dissolved and sorbed Cd (sorbed is lighter), regardless of proportion sorbed. This is consistent with reversible sorption driving an equilibrium isotope effect. At high ionic strength, the magnitude of fractionation increased with the proportion of Cd adsorbed, suggesting a kinetic or Rayleigh effect. The difference between low and high ionic strength results is likely driven by solution speciation; *chloro-* complexes dominate Cd speciation in synthetic seawater. We hypothesize that the difference in bonding environment between Cd^{2+} and an inner-sphere sorbed complex drives the equilibrium effect at low ionic strength, while fractionation in solution between various *chloro-* complexes becomes important at high ionic strength.

[1] Price & Morel (1990) *Nature* 344, 658. [2] Lacan *et al.* (2006) *Geochim. Cosmochim. Acta.* 70, 5104. [3] Horner *et al.* (2010) *G³*, doi:10.1029/2009GC002987.

Hayabusa-2 – sample return from a near-Earth C-type asteroid (2014-2020): Current status

S. WATANABE*, M. ABE, M. ARAKAWA, M. FUJIMOTO, M. ISHIGURO, K. KITAZATO, N. KOBAYASHI, N. NAMIKI, T. OKADA, S. SUGITA, S. TACHIBANA, S. TANAKA, M. YOSHIKAWA, H. KUNINAKA AND HAYABUSA-2 PROJECT TEAM

*Nagoya U., Nagoya 464-8601. seicoro@eps.nagoya-u.ac.jp

Hayabusa-2 is an asteroid exploration mission to return surface samples of a near-Earth C-type asteroid 1999 JU₃. Because asteroids are the evolved remnants of planetesimals that were the building blocks of planets, detailed observation by a spacecraft and analyses of return samples will provide direct evidence of planet formation and dynamical evolution of the solar system. Moreover, C-type asteroids are expected to preserve the most pristine materials in the solar system, an interacted mixture of minerals, ice, and organic matter. Space missions are the only way to obtain such pristine materials with geologic context and without terrestrial contamination. In order to understand the dynamical and chemical evolution of the solar system by investigating and sampling 1999 JU₃, Hayabusa-2 sets the following scientific objectives: (1) Thermal evolution from planetesimal to near-Earth asteroid, (2) Destruction and accumulation of rubble pile body, (3) Diversification of organics through interactions with minerals and water on planetesimal, and (4) Material circulation in the early solar system. The basic design of the spacecraft is the same as in the original Hayabusa, but many improvements will be made and new technology will be adopted. The on-board instruments necessary for the fulfillment of the scientific objectives are a laser altimeter (LIDAR), a multi-band camera (ONC-T), a near-infrared spectrometer (NIRS3), a thermal infrared imager (TIR) and a wide-angle camera (ONC-W). A small impactor (SCI) will also be aboard for an asteroid-scale impact experiment, which will make a crater of several meters in diameter. The sampler, of which concept and design are also the same as the original Hayabusa, has three projectiles for impact sampling and the sample container has three separate rooms inside for sampling at three different locations, one of which could be ejecta from the artificial impact to sample sub-surface materials.

Hayabusa-2 will be launched in late 2014, arrive on 1999 JU₃ in mid-2018, and fully investigate and sample the asteroid during its 18-month stay. The spacecraft will return to Earth with samples in December 2020. Preliminary integration tests of the spacecraft are now being made, and the current mission status will be presented at the meeting.

Geochemical discrimination of tsunami sediments in Tohoku and Shizuoka area, Japan

T. WATANABE¹*, N. TSUCHIYA¹, C. INOUE¹, A. KITAMURA², T. KOMAI³, S. YAMASAKI¹, R. YAMADA¹, N. HIRANO¹, A. OKAMOTO¹, F.W. NARA¹ AND TOHOKU AND TSUNAMI SEDIMENT RESEARCH GROUP

¹Graduate School of Environmental Studies, Tohoku University, Sendai 980-8579, Japan

²Faculty of Science, Shizuoka University, Shizuoka 422-8059, Japan

³National Institute of Advanced Industrial Science and Technology, Tsukuba 305-8564, Japan

Tsunami sediments from the stricken area

Geochemical studies of modern and past-tsunami sediments were performed to detect a tsunami invasion proxy. In this study, the modern tsunami sediments from the Pacific coast of Tohoku area, Japan (March.11th, 2011), have been analyzed by EDXRF and ICP-MS. In addition, past-tsunami sediments were also taken from the coastal area of Japan (Jogan, ca. 1100 BP; Yayoi, ca. 2000 BP; Sizuoka, ca. 3000 BP) in order to establish a novel method for the geochemical discrimination of invisible tsunami layers, such as mud and thin sand layers.

Na/Ti atomic ratios of tsunami sediment

Na/Ti and Si/Al atomic ratios in the tsunami sediments varied from 2.7 to 22.4 and from 1.7 to 13.6, respectively (Fig. 1). The Na/Ti ratios markedly increased up to ca. 7-22 in the tsunami layers from the northeast (Tohoku area) and middle Japan (Shizuoka prefecture). Our results show that the Na/Ti values are useful indicator of past-tsunami sediment layers.

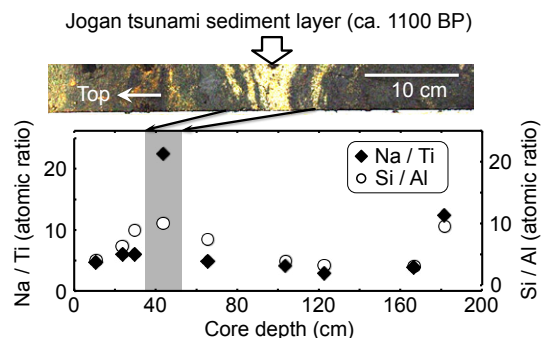


Figure 1: Na/Ti and Si/Al atomic ratios of tsunami sediments (Jogan, ca. 1100 BP) from Sendai plain in Tohoku area, Japan.

Corals at volcanic island of Satsuma Iwo-jima: Implication for a new proxy of hydrothermal events and biological adaptation

T. WATANABE¹, K. KAMIMURA¹, A. YAMAZAKI^{1&2*},
K. OMORI¹, F. LE GUERN³ AND S. KIYOKAWA⁴

¹Grad. Sch. of Science, Hokkaido Univ., Sapporo, 060-0810, JAPAN (*correspondence: nabe@mail.sci.hokudai.ac.jp, k.kanae@frontier.hokudai.ac.jp, zaki@frontier.hokudai.ac.jp, kazuto@mail.sci.hokudai.ac.jp)

²AORI, University of Tokyo, Kashiwa, Chiba, 277-0882, JAPAN(zaki@aori.u-tokyo.ac.jp)

³CNRS, LSCE, Gif sur Yvette, 91190, France (Deceased)

⁴Grad. Sch. of Science, Kyushu Univ. Fukuoka 812-8581 JAPAN (kiyokawa@geo.kyushu-u.ac.jp)

Coral cores from massive corals could record marine environmental and ecological changes in their annual bands with monthly temporal resolution in the present and/or the past. We discovered large massive Porites corals living at active volcanic island of Satsuma Iwo-jima, located 50 km south from Kyushu area, southern part of Japan. Satsuma Iwo-jima provides a unique opportunity to observe marine organism living under extreme environments of volcanic gases emission and different types of hydrothermal activities from sea floor. We collected eleven coral cores from four different conditions around the island to test if corals could record volcanic and hydrothermal activities and how corals could survive in extreme environments such as very low pH condition with CO₂ gasses emission. Coral extension rate for the site near hydrothermal vent was significantly small (1-2mm/year) relative to that for general condition of Porites corals (ca. 10-20 mm/year), suggesting that coral growth was influenced by hydrothermal activity. We will demonstrate our preliminary results of geochemical approaches of $\delta^{18}\text{O}$, $\delta^{13}\text{C}$, Sr/Ca, Mg/Ca, Ba/Ca, and F/Ca in coral skeletons and in surrounding seawater and discuss the possibility for reconstructing the past hydrothermal events and relationship between marine ecosystem and extreme environments at volcanic activity as the analogues for coral adaptation to future ocean acidification.

Applications of neutron beam analysis to study the origins of carbonaceous matter in terrestrial and planetary rocks: A new approach

Y. WATANABE^{1*}, Y. FURUKAWA², T. KAKEGAWA² AND
H. OHMOTO³

¹J-PARC, Ibaraki 319-1195, Japan (*correspondence: yumiko.watanabe@j-parc.jp)

²Tohoku University, Sendai, Miyagi 980-8578, Japan (furukawa@m.tohoku.ac.jp, kakegawa@m.tohoku.ac.jp)

³PSARC and Penn State University, College Park, PA 16802, USA (hqo@psu.edu)

Some of the most fundamental and important questions in the fields of Earth Sciences, Biology and Astrobiology are when, where and how life originated and different species evolved from the common ancestor during the 4.5 billion years history of the Earth. For example, we do not know whether carbonaceous matter in a particular Archean sedimentary rock represents a product of inorganic processes (e.g., Fischer-Tropsch reactions) or a remnant of organisms. Similarly, the origins of carbonaceous matter in meteorites, Mars, and other planetary rocks have been debated.

The origins of carbonaceous matter in terrestrial and planetary materials have been investigated primarily from its chemical, isotopic, and physical characteristics, such as the H/C/N/P ratios, H, C, N, and S isotope ratios, crystal structure, and crystallinity. Here we introduce a new method, an application of neutron beam analysis, to determine the chemical composition and crystal structure of solid carbonaceous matter. Compared to the other techniques using x-ray, such as XRD, an advantage of neutron beam analysis is that it will identify the positions of light elements, particularly hydrogen, in the structure.

We will present the results of our preliminary investigations using neutron scatter analysis, XRD, and Raman spectroscopy on simple organic compounds (e.g., glycine, steroid), micro-organism (e.g., cyanobacteria), and kerogens of various geologic age.

Influence of kinetics on the oxygen isotope composition of calcite

J. WATKINS^{1*}, L.C. NIELSEN², F.J. RYERSON³
AND D.J. DEPAOLO⁴,

¹University of Oregon, Eugene, OR 97403, USA

(*correspondence: watkins4@uoregon.edu)

²Stanford University, Palo Alto, CA 94305, USA

³Lawrence Livermore National Laboratory, Livermore, CA 94550, USA

⁴Lawrence Berkeley National Laboratory, Berkeley, CA 94720, USA

Paleotemperature reconstructions rely on knowledge of the equilibrium fractionation of oxygen isotopes between aqueous solution and calcium carbonate. Although oxygen isotope separation is expected on theoretical grounds, the temperature-dependence remains uncertain because other factors, such as slow exchange of isotopes between dissolved CO₂-species and water, can obscure the temperature signal. This is problematic for crystal growth experiments on laboratory timescales and for interpreting the oxygen isotope composition of crystals formed in natural settings.

We present results from experiments in which inorganic calcite is precipitated in the presence of 0.25 μM dissolved bovine carbonic anhydrase (CA). The presence of dissolved CA accelerates oxygen isotope equilibration between the dissolved carbon species CO₂, H₂CO₃, HCO₃⁻, CO₃²⁻ and water, thereby eliminating this source of isotopic disequilibrium during calcite growth. The experimental results allow us to isolate kinetic oxygen isotope effects occurring at the calcite-water interface during mineral growth.

The oxygen isotope composition of precipitated calcite is lighter than dissolved HCO₃⁻ yet heavier than CO₃²⁻ at pH = 8.3. ¹⁸O uptake into calcite varies with precipitation rate, but the observed rate-dependence is lower than in previous studies where calcite is not precipitated in the presence of dissolved CA. These non-equilibrium effects can be explained in terms of isotopologue-specific reaction rate coefficients. We present a framework of ion-by-ion growth of calcite that reconciles our new measurements with measurements of natural cave calcites that are the best candidate for having precipitated under near-equilibrium conditions. Our findings suggest that isotopic equilibrium between calcite and water is unlikely to have been established in laboratory experiments or in many natural settings. The use of CA in carbonate precipitation experiments offers new opportunities to refine oxygen isotope-based geothermometers and to interrogate environmental variables other than temperature that influence calcite growth rates.

First melt inclusion study of the Sudbury Igneous Complex (Ontario, Canada): Evidence for two-liquid immiscibility and constraints on trace element distribution

KATHLEEN WATTS^{1*}, JACOB J. HANLEY¹, DANIEL KONTAK² AND DOREEN AMES³

¹Saint Mary's University, Halifax, NS, Canada

(*correspondence: kathleen.margot@gmail.com)

²MERC, Laurentian University, Sudbury, ON, Canada

³Geological Survey of Canada, Ottawa, ON, Canada

The 1.85 Ga Sudbury Igneous Complex (SIC), Ontario, Canada, is an intrusive complex representing a crystallized melt sheet formed during a bolide impact. The SIC has been extensively studied due to its rich endowment in magmatic sulfide ores (Ni-Cu-PGEs). In this study, primary melt inclusions hosted in cumulus apatite within three mafic units of the SIC (gabbro, norite and sublayer quartz diorite) are used to decipher the physical and chemical characteristics of the evolving melt sheet as it crystallized.

The compositions of coeval melt inclusions show 2 distinct types: (1) SiO₂-rich, ranging from tonalitic to granodioritic in composition (60-70 wt% SiO₂, up to 11 wt% FeO); and (2) Fe-rich with syenogabbroic to essexitic to alkali gabbroic compositions (27-49 wt% SiO₂, 16-44 wt% FeO). The liquids are interpreted to represent the products of immiscibility (*c.f.* Skaergaard Intrusion [1]).

$D_{\text{Fe-rich melt/Si-rich melt}}$ values range between ~0.7 and ~2 with the exception of V and Co that partition more strongly into the Fe-rich melt ($D > 4$). Microthermometry shows that complete melting of the inclusion contents occurs at ~1100°C, with homogenization (*i.e.*, minimum trapping T; by bubble contraction) between ~1230 and 1300°C, confirming that apatite is an early liquidus phase in melt and trapped melt over a range of temperatures. Preliminary melt inclusion analyses suggest that the earliest melt phase of the SIC, as represented by sublayer quartz diorite, was enriched in Ni and Cu, up to an order of magnitude higher than those liquids trapped in the units stratigraphically higher in the SIC, and may reflect loss of these metals to early sulfide liquids.

The results of this study may lead to the development of parameters that enhance exploration success in mafic-ultramafic systems where post-magmatic processes have severely limited the application of bulk rock chemistry in understanding their petrogenesis.

[1] Jakobsen *et al.* (2005) *Geology* **33**, 885-888.

Effect of magma oxidation state on iron isotope composition of magmatic-hydrothermal minerals

CHRISTINE WAWRYK* AND JOHN D. FODEN

Centre for Tectonics, Research and Exploration, University of Adelaide, South Australia, 5005

(*correspondence: christine.wawryk@adelaide.edu.au)

Do ore minerals precipitated from magmatic-hydrothermal solutions reflect the isotopic composition of the parent magma? We present new stable iron isotope compositions of sulfides from two deposits associated with fractionated, reduced magmas. The Renison tin deposit is associated with magmatic fluids exsolved from an S-type magma [1]. The Hillside deposit is an IOCG skarn associated with an A-type granite of the Hiltaba Suite [2]. Figure 1 compares isotopic composition of host intrusions, pyrite and chalcopyrite from Renison with published data from Grasberg [3] and Xinqiao [4].

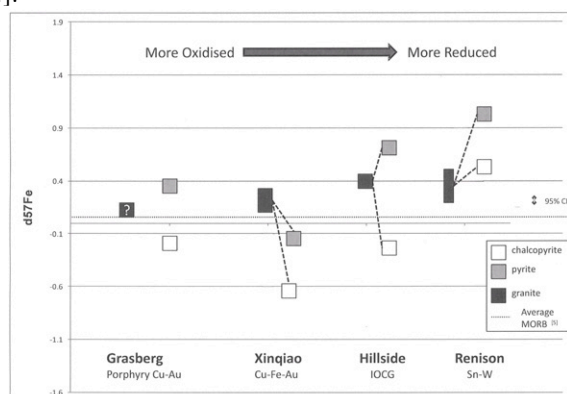


Figure 1. Comparison of $\delta^{57}\text{Fe}$ composition of host intrusions, pyrite and chalcopyrite.

Our results demonstrate that sulfides associated with the reduced Hillside and Renison Granites have, on average, heavier iron isotopic compositions than ore minerals associated with the oxidized GIC, and the Jitou Stock hosting Xinqiao. Our modelling of magma/fluid evolution considers variables such as $f\text{O}_2$, pressure and temperature.

[1] Patterson *et al.* (1981) *Econ Geol* **76** 393-438. [2] Conor *et al.* (2010) *Hydrothermal IOCG and Related Deposits* **3** 147-170 PCG Publ. [3] Graham *et al.* (2004) *Chem Geol* **207** 147-169. [4] Wang *et al.* (2011) *Ore Geol Rev* **43** 194-202. [5] Teng *et al.* (2013) *Geochim Cosmochim Acta* **107** 12-26.

Amino acid binding on oxide surfaces: Results from CTR and surface x-ray anomalous scattering

GLENN WAYCHUNAS¹, JOANNE STUBBS²
AND PETER ENG²

¹Lawrence Berkeley National Laboratory, Earth Sciences
Division, Berkeley, CA, USA

²University of Chicago, Consortium for Advanced Radiation
Sources, Argonne, IL, USA

The interaction and binding of organic species and amino acids with mineral surfaces is a large frontier in geochemistry. As opposed to inorganic sorbates, which interact with a surface by forming covalent and hydrogen bonds, organic structures may have partial or dominant hydrophobic interactions and reduced interaction with waters, multiple charges on a single molecule such as a zwitterion, and very complex multi-site interactions with surface functional groups. These considerations have limited the utility of many studies in the past, with the vast majority involving measurement of uptake concentrations without information on the actual binding geometry or mechanisms. We are developing a program to couple sum-frequency vibrational spectroscopy (SFVS), surface x-ray scattering methods, and computer simulations to characterize organic species topologic interactions with well-known mineral surfaces. Initial investigations examined ethanol as a single monolayer, and as a bulk liquid, on the corundum R-plane (1-102) surface using SFVS. Subsequent studies examining selenomethionine and other heavy atom-substituted amino acids are in progress. This approach enables x-ray surface scattering and anomalous scattering measurements to be correlated with SFVS vibrational information. The complexities and advantages of this approach will be described, as well as most recent results.

Probing quartz for P-T-D paths

LAURA E. WEBB¹, PATRICK G. DYESS¹, KYLE T. ASHLEY², FRANK S. SPEAR³ AND JAY B. THOMAS³

¹University of Vermont, Department of Geology, Burlington, VT, USA, lewebb@uvm.edu, patrick.dyess@gmail.com

²Department of Geosciences, Virginia Tech, Blacksburg, VA, USA, ktashley@vt.edu

³Earth and Environmental Sciences, Rensselaer Polytechnic Institute, Troy, NY, USA, spearf@rpi.edu, thomaj2@rpi.edu

TitaniQ (Ti-in-quartz) thermobarometry of chlorite–staurolite grade metapelites reveals that quartz grains in different fabric domains may record distinct stages of the P-T-D path and, in some cases, preserve detrital [Ti] signatures. Our findings are based on integrated microstructural and petrologic analyses, cathodoluminescence (CL) imaging, and secondary ion mass spectrometry (SIMS) of samples with known tectonic histories collected along an E–W transect across central Vermont, spanning rocks of the Rowe–Hawley Belt (RHB) and the Connecticut Valley–Gaspe Trough (CVG). Rocks of the RHB record crenulation cleavage development during both the Taconic and Acadian orogenies; CVG rocks record similar processes during the Acadian orogeny only. CL and SIMS analyses were conducted on quartz in different microstructural contexts such as in fold hinges, quartz-feldspar cleavage domains, inclusion suites defining internal foliations in garnet, and pressure shadows. Both suites of metapelites lack evidence for significant dynamic recrystallization of quartz; quartz grains predominately display polygonal textures. The dominant CL zoning pattern of quartz is darker rounded–anhedral cores and brighter polygonal rims, indicating an increase in [Ti] from core to rim. In some cases grains record bright cores with dark rims (RHB), or dark cores, bright mantles, and dark rims (CVG). RHB chlorite–garnet grade metapelites yield [Ti] from 0.4–157 ppm; a small fraction of analyses yield [Ti] greater than that predicted for peak metamorphic conditions. Analyses of garnet–staurolite grade CVG metapelites yielded [Ti] of 2.2–9.8 ppm. In both suites, dark cores with low [Ti] are interpreted as quartz growth during burial metamorphism and cleavage development via strain-induced solution transfer. Brighter mantles and rims with increasing [Ti] relative to cores result from quartz-producing metamorphic reactions and continued solution transfer to low strain and quartz-feldspar domains. [Ti]>50 ppm in RHB rocks are interpreted to be inherited detrital signatures and thus likely provide information on sedimentary provenance of the protoliths. These studies highlight the importance that both structural and metamorphic processes play in the cycling of quartz in metapelites and its ability to record P-T-D paths.

Micro-scale complexity in iron-sulfide phases in Precambrian sedimentary rocks determined by coupled spectroscopic, isotopic, and magnetic techniques

SAMUEL M. WEBB^{1*}, JENA E. JOHNSON², SARAH P. SLOTZNICK², JOSEPH L. KIRSCHVINK² AND WOODWARD W. FISCHER²

¹Stanford Synchrotron Radiation Lightsource, Menlo Park, CA 94025, USA (*correspondence: samwebb@slac.stanford.edu)

²California Institute of Technology, Pasadena, CA 91125, USA

The record of sedimentary pyrite forms the foundation for most isotope records working to define the coupled evolution and behavior of the ancient iron and sulfur cycles. In order to assess the strengths and limitations of records derived from pyrite-rich rocks (e.g. iron speciation, sulfur isotope ratios), we need to understand more about the processes that form and alter sedimentary pyrite.

From samples of the Archean/early Proterozoic Transvaal and middle Proterozoic Belt Supergroups, petrography reveals that what might operationally be called sedimentary pyrite has complex textures that hint at a rich process history of sulfur mineralization. A common limitation of virtually all proxy measurements employed to date is that they operate on ‘bulk’ samples, typically gram-sized or larger pieces. As such, they lose the ability to relate geochemistry to petrography at the scale of mineral grains. Many of the sedimentary pyrites in the Transvaal Supergroup exhibit complex redox and electronic structures of S and Fe, with crystals of pyrite, pyrrhotite, and sulfate-bearing minerals throughout.

Parallel application of multiple techniques on the same samples across micron bases spatial scales, provide an opportunity to diagnose issues resulting from post-depositional alteration of sedimentary rocks. We have integrated light and electron microscopy for petrography, electron microprobe and synchrotron XRF for elemental composition, synchrotron X-ray spectroscopy for redox and chemical state, SQUID microscopy for remnant magnetism, and secondary ion mass spectrometry (SIMS) for isotopic composition. The coupling of these tools allows in essence “images” of the proxy data at the micrometer scale, giving a wide array of textural and mineralogical information designed to inform and untangle the complicated histories of these early Precambrian rocks.

Large ^{34}S depletions of reduced sedimentary sulfides at low sulfate concentrations in an iron-rich lake dominated by anaerobic methane oxidation

WEBER H.S.* , THAMDRUP B. AND HABICHT K.S.

Nordic Center for Earth Evolution and Institute of Biology,
University of Southern Denmark, Campusvej 55, 5230,
Odense M, Denmark (*correspondence:
hannah@biology.sdu.dk)

The sediment of Lake Ørn (Denmark) is characterized by a high reactive iron content and a strong methane consumption in the deep sulfate-containing zone reaching ~15 cm depth. Radiotracer studies (^{14}C -methane and ^{35}S -sulfate) confirmed anaerobic oxidation of methane (AOM) and microbial sulfate reduction (SR) and demonstrated the highest AOM rates (up to $40 \text{ nmol cm}^{-3} \text{ day}^{-1}$) at 10-15 cm depth with very low sulfate concentrations ($5\text{--}10 \mu\text{mol L}^{-1}$). We further used stable sulfur isotope analysis and incubation experiments to investigate the interactions of iron, sulfur and methane with particular focus on a hypothetical cryptic sulfur cycle. Isotope analyses revealed substantial ^{34}S depletion in reduced sulfur species with $\delta^{34}\text{S}$ values of down to -15‰ for acid volatile sulfides (H_2S and FeS) and -25‰ for chromium reducible sulfides (S^0 and FeS_2) accumulating in the AOM zone. Anoxic slurry incubations demonstrated $\delta^{34}\text{S}$ values of up to 40‰ in sulfate in the incubations with methane and S^0 respectively, indicating that large sulfur isotope fractionations can be established by a combination of sulfate reduction, sulfide oxidation, AOM and microbial sulfur disproportionation. RNA stable isotope probing was applied to identify key players of the cryptic sulfur cycle.

The cycling and transport of glacially derived iron in Arctic fjord sediments

L.M. WEHRMANN^{1*}, M.J. FORMOLO², J.D. OWENS¹, T. G. FERDELMAN³, R. RAISWELL⁴ AND T.W. LYONS¹

¹University of California, Riverside, Riverside, CA, USA,
laura.wehrmann@ucr.edu, jowens@student.ucr.edu,
timothy1@ucr.edu (* presenting author)

²The University of Tulsa, Tulsa, OK, USA, michael-
formolo@utulsa.edu

³Max Planck Institute for Marine Microbiology, Bremen,
Germany, tferdelm@mpi-bremen.de

⁴University of Leeds, Leeds, UK, r.w.raiswell@leeds.ac.uk

Iron is an essential nutrient for primary production and is strongly connected to glacial-interglacial variations in atmospheric CO_2 concentrations. Glacial runoff rapidly delivers large volumes of potentially bioavailable Fe, produced by mechanical and microbially enhanced chemical weathering in glacial environments, to high latitude oceans. Little is known about the fate of this Fe pool in adjacent coastal marine waters, particularly fjord systems. We investigated the concentration and speciation of Fe in the sediments of three Western Svalbard fjords with the aim of quantifying and understanding the biogeochemical processes of the sedimentary Fe cycle. Results of porewater and solid-phase analyses show that the input of glacially derived Fe plays an important role in the biogeochemical processes in fjord sediments by controlling sulfur and manganese cycling and by providing a large Fe-oxide pool for dissimilatory iron reducers (DIR). Extreme sedimentation rates in the fjords result in elevated Fe accumulation but dilution of the organic carbon pool. From this combination, the sediments show a strong signature of DIR, leading to high dissolved Fe concentrations of up to $800 \mu\text{M}$ in the porewaters of Kongsfjorden and Van Keulenfjorden and correspondingly enhanced benthic Fe flux from the sediment to the water column. Our data point to extensive benthic Fe cycling in Svalbard fjord sediments likely promoted by bioturbation and physical disturbance via iceberg calving. Thus, recycling of iron in fjord sediments may facilitate the transport of this important micronutrient across the fjords while maintaining its bioavailability for fertilization of primary productivity on the adjacent continental shelf. This work complements recent studies on the bioavailability and concentration of Fe in glacial runoff and contributes to the emerging picture that glacially derived Fe may constitute an important component of the global Fe cycle, particularly in high-latitude ocean regions.

Using radium isotopes to determine the residence time of circulated seawater in coastal sediments

WEINSTEIN Y.¹, SHALEM Y.¹, BRINBERG B.¹
AND NOIMEIR Y.¹

¹ Bar-Ilan University, Ramat-Gan 52900, Israel
(*correspondence: weinsty@biu.ac.il)

The circulation of seawater in seafloor sediments and the resultant fluxes of water to the water column are highly important to oceanic mass balances of certain elements and to coastal water quality. The residence time of this water in the sediments is critical to the kinetics, therefore the effectiveness of water-rock interaction, which further affects the delivery of chemicals from the sub-seafloor to the ocean.

We used radium isotopes to decipher about the residence time of circulated seawater in coastal sediments. Seawater is radium-poor, with the activity of ²²⁶Ra (half time of 1605 yrs) on the order 0.1 dpm/L, and those of the short-lived isotopes, ²²⁴Ra and ²²³Ra (half lives of days), being close to zero. On the other hand, activities in pore water of both short and the long-lived isotopes may be 2-3 orders of magnitude higher. Another important consideration is that while the pore water activities of the long-lived ²²⁶Ra are pretty much controlled by desorption, those of the short lived isotopes are mainly controlled by recoil during the disintegration of their thorium radioactive parents. Gonner *et al.* (2008) have shown that pore water attains secular equilibrium for ²²⁶Ra within a few hours, may be less. On the other hand, since ²²⁴Ra in pore water is enriched by recoil due to the disintegration of sediments' ²²⁸Th, the activity of this nuclide may be built-up during a period of up to several weeks, which could be more relevant to the process of seawater circulation (hours to years).

We pumped pore water using mini piezometers from depths of 0.5-2 m in the granular sediments (quartz sands) of Dor Bay (eastern Mediterranean, northern Israel). Water salinities were between 30-39 (eastern Mediterranean water salinity is ~40, psu scale). ²²⁶Ra activities were mostly 2-2.5 dpm/l, though in a few shallow cases (0.5 m), activities dropped to <1 dpm/l. Experiments showed similar ²²⁶Ra activities of 2-3 dpm/l, which suggests that the residence times of pore water are longer than a few hours. Activities of ²²⁴Ra varied between 1.5-6.5 dpm/l, with the deeper water (1.5-2 m) significantly more enriched than the shallow ones (0.5-1 m). In chromatography experiments with the same sediments and coastal seawater, ²²⁴Ra increased from <0.5 to 4 dpm/l at residence times of 1 and 24 hrs, respectively. Assuming uniform sediment characteristics, this suggests that the average age of pore water at 1-2 m depth is about 0.5-2 days.

Low-T hydrothermal fluid evolution

C. G. WEINZIERL^{1*}, W. BACH², F. BÖHM³
M. REGELOUS AND K.M. HAASE¹

¹GeoZentrum Nordbayern, Univ. Erlangen-Nuernberg,
Schlossgarten 5, 91054 Erlangen, Germany
(*correspondence: christoph.weinzierl@fau.de)

²Geoscience Department, Bremen Univ., Klagenfurter Str.,
28359 Bremen, Germany

³GEOMAR Helmholtz Centre for Ocean Research Kiel,
Wischofstr. 1-3, 24148 Kiel, Germany

The chemical and isotopic composition of calcium carbonate veins precipitated within the oceanic crust can be used to infer the composition of their parent fluid [1], and trends of fluid compositions with temperature [2] can be extrapolated to estimate ancient ocean water compositions [3, 4]. Previous studies focused on carbonates from drillcores in ancient oceanic crust, but ophiolites could be used to extend the record of ocean water chemistry further back in time. We evaluated the potential of ophiolites as paleoseawater archives by analysing carbonates from the Cretaceous Troodos Ophiolite of Cyprus.

Variations of fluid Sr/Ca, Mg/Ca, ⁸⁷Sr/⁸⁶Sr and ⁴⁴Ca/⁴⁰Ca with temperature ($\delta^{18}\text{O}$) in the volcanic section of the Troodos Ophiolite display similar trends to data for fluids [2] and carbonates [3, 4] from drilled oceanic crust, indicating that similar processes acted upon the fluids. In accordance with experimental results [5] we found that the formation of saponite and palagonite, and the subsequent precipitation of anhydrite, are responsible for modifying the composition of seawater as it percolates downwards through the oceanic crust. Our data and thermodynamic calculations indicate that anhydrite may form at much lower temperatures ($T < 70^\circ\text{C}$) than previously thought [6], if seawater interacts with basalt.

Our results allow not only to identify fluid evolution pathways affected by mixing of seawater with a more evolved fluid (e.g. Juan de Fuca), but also to show that ophiolites can be used to determine past seawater compositions, and to study the chemical evolution of fluids in greater detail than is possible using samples drilled from oceanic crust, where recovery of interstitial carbonates is less complete.

[1] Coggon *et al.* (2004) *EPSL* **219**, 111 - 128. [2] Elderfield *et al.* (1999) *EPSL* **172**, 151-165. [3] Coggon *et al.* (2010) *Science* **327**, 1114-1117. [4] Rausch *et al.* (2013) *EPSL* **362**, 215-224. [5] Seyfried & Mottl (1982) *Geochim. Cosmochim. Acta* **46**, 985-1002. [6] Bischoff & Seyfried (1975) *Amer. J. Sci.* **278**, 838-860.

“Tuning the Torch” of the Nu Plasma II-ES MC-ICP-MS

D. WEIS^{1*}, K. GORDON¹, L. XING¹, A. BURROWS²,
R. COHEN² AND P. FREEDMAN²

¹Pacific Centre for Isotopic and Geochemical Research,
Department of Earth, Ocean and Atmospheric Sciences,
University of British Columbia, 2207 Main Mall,
Vancouver BC, V6T 1Z4, Canada. *dweis@eos.ubc.ca

²Nu Instruments Ltd, 74 Clywedog Road South, Wrexham
Industrial Estate, Wrexham LL13 9XS, United Kingdom

Since the development in the early 1990s of the first multi-collector inductively coupled plasma mass spectrometer, there has been an unprecedented broadening of isotopic analysis applications in geochemistry, mostly because the ICP source effectively ionizes virtually all elements in the periodic table. The Nu Plasma II-ES is Nu Instruments Ltd.’s latest generation plasma source multi-collector mass spectrometer. The NP II at UBC is equipped with a newly designed ES interface system that increases the overall sensitivity of the instrument. Additionally, the instrument is equipped with an enhanced detector system that includes large dynamic range 55 volt Faraday amplifiers coupled to 16 Faraday detectors plus 5 full-size discrete dynode ion counters. Sensitivity tests across the mass range, from Li to U, reveal a significant increase compared to the previous generation interface. We tested the instrument for stability of mass bias and accuracy of isotopic ratios while measuring oxide production, interface pressure, and other key parameters.

This work demonstrates that the enhanced sensitivity can be achieved with no compromise in either mass bias stability or isotope ratio accuracy. Small sample concentrations of Nd, Hf and Pb are now analyzed to precisions previously attainable only with great analytical effort or by pooling samples. Larger samples show much improved external reproducibility that previously required longer analysis times. The improved ion interface and detector systems on the NP II-ES increase the overall productivity and analytical capability of multi-collector ICP-MS, which is especially advantageous in a multi-disciplinary laboratory.

These improvements open up new avenues in geochemical research with analyses of samples down to sub-ppm levels or with transient signals. They will allow further understanding of the timing and processes, and fingerprinting of sources, in Earth, planetary, biological and medical science.

Matrix-independent calibration of LA-ICP-MS using femtosecond-UV-lasers?

U. WEIS^{1*}, K.P. JOCHUM¹, B. STOLL¹, D. JACOB²,
R. MERTZ-KRAUS² AND M.O. ANDREAE¹

¹Max Planck Institute for Chemistry, Mainz, Germany
(*correspondence: ulrike.weis@mpic.de)

²University of Mainz, Germany

The major limitations regarding accuracy and precision of LA-ICP-MS trace element analysis are elemental fractionation [1] and mass-load-dependent matrix effects [2]. Reducing the pulse width of the laser from the ns to the fs range leads to an improvement of the analytical results, in particular for in-situ isotope ratio measurements [3], where matrix related mass fractionation is considerably reduced. To test matrix-related effects in trace element analysis, we determined the fractionation factors (FF) and element/Ca ratios in reference materials with different matrices (silicate, basalt, phosphate, carbonate) by a Ti-sapphire based fs-UV-LA-ICP-MS. Measurements were performed with different spot sizes (10 – 55 μm), pulse repetition rates (PRR) (10 – 250 Hz) using spot and line scan mode. For comparison, similar experiments were made using 213 nm and 193 nm Nd:YAG lasers and a 193 nm ArF excimer laser.

Our measurements demonstrate that in each case the fs data are more reproducible and less matrix-dependent with respect to FF and mass-load induced matrix effects than the results obtained using the other lasers. The FF are independent of the measuring conditions and of the matrix within about 0.3 - 1 % and 0.5 - 3 % for line scan and spot analysis, respectively. The line scan mode yields unity FF, whereas in the spot analysis mode small, but significantly lower values for the volatile elements Zn (0.88) and Pb (0.93) were observed. The ratios of the lithophile elements Sr, Ba, Rb to Ca are identical for all spot sizes, PRR and materials within about 5%, for both line scan and spot analyses. An extreme dependency of the element ratio with spot size (up to 50%) was found for Pb/Ca and Zn/Ca using spot analysis; however, it is similar for all matrices. This is in contrast to measurements done with the 213 nm Nd:YAG laser, where high spot sizes may lead to different element/Ca ratios compared to low spot sizes. Consequently, the use of fs-UV lasers improves not only high-precision isotope ratio measurements but also trace element analysis. Calibration can be performed reliably for quite different matrices with certified reference materials, e.g. those from NIST [4].

[1] Fryer *et al.* (1995) *Can. Min.* **33**, 303-312. [2] Krosiakova and Günther (2007) *JAAS* **22**, 51-62. [3] Horn *et al.* (2006) *GCA* **70**, 3677-3688. [4] Jochum *et al.* (2011) *GGR* **35**, 397-429.

Bacterial mineral-metalloid redox transformations in aneobic environments

CHRISTOPHER WEISENER^{1*}, RACHEL FRANZBLAU¹ AND NADINE LOICK^{1,2}

¹Great Lakes Environmental Institute for Research, University of Windsor, Windsor, Canada, franzbl@uwindsor.ca*

²Rothamsted Research Institute, NorthWyke, UK

Jarosite minerals are of environmental importance as trace metal scavengers and are involved in metal cycling. A number of metal species can be incorporated into the jarosite structure, including selenium (Se). Se is a trace nutrient, but is toxic in relatively low doses to humans, microbes, and other fauna[1]. Se is present in aqueous systems in its two oxyanion forms; selenate and selenite (SeO_4^{2-} & SeO_3^{2-}). The sulfate group can be completely substituted for selenate in jarosite minerals ($\text{NaFe}_3(\text{SO}_4)_x(\text{SeO}_4)_{2-x}(\text{OH})_6$). Under certain environmental conditions (e.g. pH, ionic strength, anaerobic environment), bacteria use these metals as potential electron acceptors mobilization and reduction from iron hydroxy sulfate minerals. Several species of bacteria have been observed to reduce Se oxyanions to nanoparticulate elemental Se, which is insoluble under most conditions. This pathway potentially poses a vector for mobilization and transport at Se-contaminated sites. The mechanisms pertaining to this research along with toxicity thresholds to model organisms will be discussed.

[1] Winkel (2011) *Environmental Science & Technology* **46**, 571-579.

Diamond-forming fluids: The trace-element perspective

Y. WEISS^{1,3*}, W. L. GRIFFIN² AND O. NAVON¹

¹The Institute of Earth Sciences, The Hebrew University of Jerusalem, Edmund J. Safra Campus, Israel

²CCFS and GEMOC, Dept. of Earth and Planetary Sciences, Macquarie University, NSW, Australia

³Lamont-Doherty Earth Observatory, Columbia University, 61 Rt. 9W, Palisades, NY 10964-1000, USA

(*correspondence: yweiss@ldeo.columbia.edu)

Diamond-forming high-density fluids (HDFs) of different major-element composition share similar incompatible-element characteristics, regardless of their host diamond provenance. All have fractionated REE patterns and variable, mostly negative, anomalies (PM normalized) in K, Rb, Cs, Ti, Zr, Hf, Nb, Ta, Sr and Y relative to Ba, Th, U and REEs of similar compatibility. Two principal patterns, "Planed" and "Ribbed", are characterized by differences in the highly incompatible elements from Ce–Pr. The two patterns are best distinguished using co-variation diagrams of (La, Ce)/(Nb, Rb) vs (U, Th)/(Nb, Rb).

Similarities of canonical ratios, Nb/(Th, U, La) and K/U, between MORB and OIB samples and HDFs with "Planed" patterns suggest that an asthenospheric source for these HDFs is plausible. This idea is strengthened by calculating the composition of sources in equilibrium with "Planed" patterns of silicic HDFs which range between the DMM and more fertile parts of the convecting mantle. The direct production of HDFs with "Planed" patterns by melting the asthenosphere with no need for a pre-metasomatized source, avoids the circular "chicken and egg" reasoning that has plagued diamond and kimberlite genesis. Such asthenosphere-derived enriched fluids can metasomatize the lithosphere to produce the old and new enriched sources that are needed to explain the formation of kimberlites and metasomatized xenoliths.

We suggest that the "Ribbed" incompatible-element pattern in HDFs evolved during percolation of HDFs with "Planed" patterns through a previously metasomatized lithosphere that carries accessory phlogopite, ilmenite and rutile. HDFs that are trapped in growing diamonds very soon after entry retain their "Planed" trace-element characteristics. If they percolate and interact with the accessory minerals, they acquire the "Ribbed" pattern before they are sealed in microinclusions in diamonds. This model explains the decoupling between major- and trace elements in HDFs and the resemblance of incompatible-element patterns of HDFs from different mantle localities; the averaging of large volumes of mantle rocks smooths the effect of small-scale heterogeneities in the subcontinental lithosphere.

Methylated hopanoid biosynthesis and function in modern bacteria

PAULA V. WELANDER^{*1}, JESSICA N. RICCI²,
DIANNE K. NEWMAN² AND ROGER E. SUMMONS³

¹Dept. EESS, Stanford University, Stanford, CA 94305
(*correspondence: welander@stanford.edu)

²Divs. Biology and GPS California Inst. Technology,
Pasadena, CA 91125 USA

³Dept. EAPS, MIT, Cambridge, MA 02139 USA

The majority of life's history has been dominated by microbes whose metabolic inventions have significantly altered the Earth's surface environment and, in turn, impacted the evolution of life on Earth. Because unicellular microorganisms do not readily leave diagnostic morphological fossils, alternative strategies are necessary for studying microbial communities in the context of the Earth's distant past. One predominant strategy is to correlate organic compounds deposited by ancient microbes and preserved in sedimentary rock with lipid molecules produced by extant microorganisms. One such class of biomarkers are the hopanes, pentacyclic triterpenoid lipids that are clearly the diagenetic products of modern day hopanoids. Hopanoids are produced by a diverse set of bacteria and as a result most sedimentary hopanes do not provide any taxonomic specificity below the domain level. However, hopanoids methylated at the C-2 or C-3 position are produced by a limited number of bacterial taxa and thus have the potential to function as robust biomarkers. Traditionally, 2-methyl and 3-methylhopanoids have been utilized as proxies for cyanobacteria and aerobic methanotrophs, respectively. However, our discovery of the two proteins necessary to methylate at the C-2 (HpnP) and C-3 (HpnR) position revealed that the diversity of bacteria capable of producing methylhopanoids was underestimated. Subsequent ecological studies of the C-2 methylase have shown that alphaproteobacterial copies of the *hpnP* gene are found in diverse modern environments while cyanobacterial *hpnP* genes are rarer. Further, physiological studies of a C-3 methylase deletion mutant have demonstrated a potential role for 3-methylhopanoids in survival under nutrient limited conditions. Taken together, these studies illustrate that a proper interpretation of methylhopanes in the rock record requires us to look beyond simple taxonomic classification of methylhopanoid producers. In addition to understanding which organisms produce methylated hopanoids, a deeper knowledge of the physiological function and environmental factors that induce their expression in modern cells is needed.

Changes of the GWP due to shifts from flooded to upland rice cultivation

S. WELLER^{1*}, K. BUTTERBACH-BAHL¹ AND R. KIESE¹

¹Karlsruher Institute of Technology, IKM-IFU, 82467
Garmisch-Partenkirchen, Germany (*correspondence:
sebastian.weller@kit.edu, ralf.kiese@kit.edu,
klaus.butterbach-bahl@kit.edu)

Changes in climate and water distribution resulting in physical or economic water scarcity may have severe effects on rice production systems. Shifting to rotations with non-flooded crops entails pronounced implications in terms of C and N element cycling and associated greenhouse gas (GHG) emissions (CH₄, N₂O, CO₂). Higher soil aeration in upland systems might decrease CH₄ emissions, but increase N₂O emissions ("pollution swapping") and cause losses in soil organic carbon that translate into CO₂ emissions [1, 2].

An automated GHG measuring system was set up at the IRRI farm, Philippines to investigate changes in the total GHGs balance when shifting from flooded to upland rice cultivation in the dry season under consideration of different fertilizer regimes (zero, conventional, improved). The system consists of two analytical sampling units (valve steering and GCs) connected to a total of 18 chambers (2 treatments, 3 fertilizer regimes; 3 replicates).

The highest global-warming potential (GWP) (kg CO₂eq ha⁻¹ season⁻¹) was found for flooded rice without N fertilization. Higher N application in irrigated plots resulted in lower CH₄ emissions. This finding supports theories that ammonium based fertilizers can decrease CH₄ emissions [3, 4]. Total GWPs (CH₄, N₂O) were about 70-80% lower in the upland systems due to lower CH₄ emissions but were offset by lower yields.

Upland rice cultivation using high yield varieties could help to mitigate GHG emissions and reduce water-use in rice production systems while further research of N fertilization-impacts on CH₄ emissions seems necessary.

[1] Reay (2004) *Soil. Biol. Biochem.* **36**, 2059-2065. [2] Stevens & Quinton (2009) *Crit. Rev. Env. Sci. Tec.* **39**, 478-520. [3] Xie *et al.* (2010) *Plant Soil* **326**, 393-401. [4] Cai *et al.* (2007) *Soil Sci. Plant Nutr.* **53**, 353-361.

Integrated analysis of hydrogeologic and biogeochemical processes controlling Technetium mobility at the Hanford site, Washington State, USA

DAWN M. WELLMAN, M. HOPE LEE
AND DANIELLE P. JANSIK¹

¹902 Battelle Blvd, P.O. Box 999, MS K3-62, Richland, WA, USA 99354; dawn.wellman@pnnl.gov; hope.lee@pnnl.gov, danielle.jansik@pnnl.gov

Historic nuclear power and weapons operations resulted in an enduring legacy of approximately six billion cubic meters of radionuclide-contaminated soil and groundwater. Technetium (⁹⁹Tc) is one of the primary risk-driving contaminants and of the most problematic in the environment. At the Hanford Site, over 500 Ci of ⁹⁹Tc was released to the vadose zone as part of past site operations. However, the complex hydrogeology of the subsurface and associated biogeochemical cycles result in a variety of technical, scientific and financial challenges for ⁹⁹Tc remediation efforts.

The mobility of ⁹⁹Tc in the geologic medium is mainly a result of redox chemistry. Long believed to exist as the pertechnetate anion (TcO₄⁻) and predicted to be highly mobile in the predominantly oxidizing groundwaters, with eventual discharge to the Columbia River, ⁹⁹Tc is one of the site's major risk-drivers for remediation. However, recent results have demonstrated the fractionation and persistence of ⁹⁹Tc through the existence of three different species. There are two primary means by which ⁹⁹Tc can be immobilized in subsurface environments: (1) indirect (abiotic) and (2) direct (biotic). Although much has been learned about the physiology and metabolic potential of single microbial species (pure cultures) that immobilize ⁹⁹Tc, major gaps exist in our understanding of the functioning of these and other microorganisms in natural and contaminated ecosystems. To this end, we will present results of an on-going multidisciplinary investigation that provides an integrated, comprehensive understanding of the hydrogeologic, and biogeochemical processes controlling ⁹⁹Tc behavior and fate in complex subsurface system. This information is further being used to develop tools that integrate the chemical and biological reaction network influencing the mobility of ⁹⁹Tc in the subsurface.

Gas geochemistry and soil CO₂ flux in active volcanic areas, China

HSIN-YI WEN¹, TSANYAO FRANK YANG¹, ZHENG FU GUO², CHING-CHOU FU¹, AI-TI CHEN¹
AND MAOLIANG ZHANG²

¹ Department of Geosciences, National Taiwan University
(*correspondence: d99224009@ntu.edu.tw)

² Institute of Geology and Geophysics, Chinese Academy of Sciences

Changbaishan intra-plate volcano and Tengchong hydrothermal area are two of the active volcanic areas in China. In order to better understand current status of magma/hydrothermal activities of the Changbaishan intra-plate volcano and Tengchong hydrothermal area, we have conducted the soil gas survey and bubbling gas sampling from hot springs around the Tianchi crater lake and Rehai geothermal area.

In Changbaishan volcano, the results show that CO₂ is the major component gas for most samples. The maximum value of helium isotopic ratio of 5.8 R_A (where R_A = ³He/⁴He in air) implies more than 60% of helium is contributed by mantle component, while carbon isotope values fall in the range of -5.8 to -2.0‰ (vs. PDB), indicating magmatic source signatures as well. Nitrogen dominated samples, 18Dawgo, have helium isotopic ratio of 0.7 R_A and carbon isotope value of -11.4‰, implying the gas source might be associated with regional crustal components beneath 18Dawgo. The first-time systematic soil CO₂ flux measurements indicate the flux is ca. 22.8 g m⁻² day⁻¹ and 6.8 g m⁻² day⁻¹ at the western and southern flank of Changbaishan, which is at the same level as the background value in the Tatun Volcano Group (24.6 g m⁻² day⁻¹), implying that Changbaishan may not be as active as TVG.

In Tengchong hydrothermal area, the preliminary results show that CO₂ is the major component gas for most samples. The helium and carbon isotopic ratio fall in the range of 0.5 R_A to 3.5 R_A and -4.7 to -1.6‰ (vs. PDB), respectively. We also analyzed the hot springs water. The δD and δ¹⁸O values fall in the range from -59.8 to 84.6‰ and -6.20 to -12.38‰ (vs. SMOW), respectively. Rehai has the highest helium isotopic ratio of 3.5 R_A, which implies ca. 40% of helium is mantle-derived. The δD and δ¹⁸O results implied the water in this area was affected by primary magmatic water. Nevertheless, samples from Banglazhang and Shihchiang hydrothermal areas show much lower helium isotopic ratio of 0.8 R_A and 0.5 R_A, respectively. It suggests that the local tectonic setting plays an important role for the gas degassing in this area.

Geochemical characterization of tire-wear particles

M. WENZEL^{1*}, V. DIETZE², P. STILLE³ AND R. GIERÉ¹

¹Institut für Geo- und Umweltwissenschaften, Albert-Ludwigs-Universität, 79104 Freiburg, Germany, (*correspondence: melanie.wenzel@minpet.uni-freiburg.de)

²Deutscher Wetterdienst, Zentrum für Medizin-Meteorologische Forschung, Referat Lufthygiene, 79104 Freiburg, Germany, (Volker.Dietze@dwd.de)

³Laboratoire d'Hydrologie et de Géochimie de Strasbourg, Université de Strasbourg, UMR 7517 CNRS, 67084 Strasbourg, France, (pstille@unistra.fr)

Tire-wear particles are a basic component of common road dust present in urban environments, and their annual emissions to the environment in Germany are reported to be 60×10^6 kg [1]. The knowledge of their basic characteristics can be useful to trace tire material in environmental dust samples and for the evaluation of possible health effects related to the inhalation of tire-wear particles. For this study, we analyzed particles generated in a closed indoor tire test rig at the Bundesanstalt für Straßentechnik (BAST) from three car tires as well as particles generated by cryogenic milling of shredded waste tires.

Particles ranging in size from $0.2 \mu\text{m}$ to $25 \mu\text{m}$ were characterized with a scanning electron microscope (SEM). All samples contained particles with diameters $<0.6 \mu\text{m}$. According to their morphological and chemical features the particles were divided into characteristic groups. The bulk chemical composition of each sample was distinct, with the total carbon content varying between 28.73 and 83.75 wt%. Inductively coupled plasma mass spectrometry (ICP-MS) data revealed significant variability in the contents of various trace elements (e.g. Pb 3.4 ppm - 437.2 ppm). Characteristic among all samples was a very high Zn content (> 1100 ppm). In addition, the ratios of $^{87}\text{Sr}/^{86}\text{Sr}$, which varied from 0.7089 to 0.7094, and of $^{204}\text{Pb}/^{206}\text{Pb}$, with values between 0.0560 and 0.0570, were found to be characteristic for the tire-wear particles, but differed from the ratios measured for the shredded tires. Comparison of the Pb isotope ratios with literature data [2, 3] from road-related dust samples (e.g. pavement particles or brake-wear) and traffic-related lead sources (e.g. batteries or gasoline) showed that Pb isotope ratios could be used as a tracer for the tire-wear contribution to road dust.

[1] Baumann & Ismaier (1998) *KGK* 51, 182-186. [2] Wijaya *et al.* (2012) *J Geochem Exploration* 118, 68-76. [3] Monna *et al.* (1997) *ES & T* 31, 2277-2286.

Mojave Crater, Mars: One meteorite source crater

S.C. WERNER¹, A. ODY² AND F. POULET²

¹Centre for Earth Evolution and Dynamics, University Of Oslo, Norway (stephanie.werner@fys.uio.no)

²Institut d'Astrophysique Spatiale, Université Paris-Sud, 91405 Orsay cedex, France.

The Mojave Crater on Mars has a diameter of about 55 km; it is situated at 7.5°N and 33.0°W at the joint of Simud and Tiu Valles in Xanthe Terra. It attracted attention for its well preserved landforms resembling the morphology of alluvial fans in arid environments, and suggesting a very young formation age. However, because of its large size, speculations on the age range from late Hesperian to late Amazonian age.

From crater count statistics technique, we here demonstrate that Mojave formed only 2-4 Ma ago. Such a young age makes it a prime candidate for being the ejection source of several groups of martian meteorites. Additional potential links (site mineralogy and presence of an extended ejecta ray pattern) between this crater and the SNCs will be discussed.

Because Mojave formed on old Noachian terrain, it questions the original crystallization age of shergottites. A 4.1 Gyrs old was inferred by debated Pb-Pb isotope ratios (Bouvier *et al.*, 2008, *EPSL* 266, 105-124; Bouvier *et al.*, 2013, *LPSC No. 1719*), whereas some apparently young crystallization ages (173-596 Ma, *Mars Meteorite Compendium, JSC Pub. No. 27672*, the latter is Tissint, which is the oldest, Brennecka *et al.*, 2012, *75th Met Soc abstract No 5157*) are more commonly accepted. We will attempt to reconcile our observations with the debate about the age of shergottites.

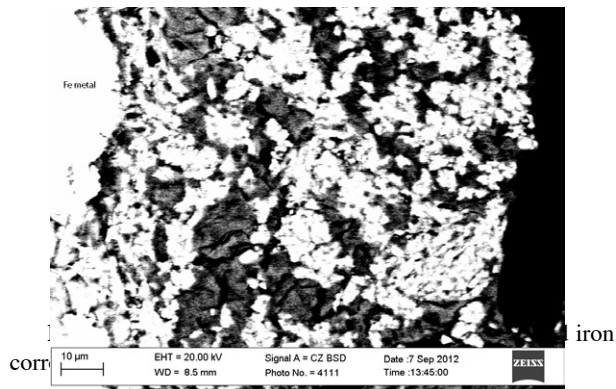
Interaction of corroding iron with bentonite at repository conditions

P. WERSIN^{1*}, A. JENNI¹ AND U.K. MÄDER¹

¹Institute of Geological Sciences, University of Bern, 3012 Bern, Switzerland (*paul.wersin@geo.unibe.ch)

Iron canisters containing high-level nuclear waste surrounded by swelling bentonite backfill are foreseen to be emplaced in geologic formations. Corrosion will release Fe(II) species which will interact with the bentonite. This may induce cementation and clay mineral transformations. The details of this process are still poorly understood. In an in-situ experiment (ABM-1) at the Äspö Hard Rock Laboratory (Sweden), compacted bentonite materials in contact with steel were exposed to temperatures up to 140°C for 2 years. After overcoring, clay samples in contact with the Fe were sampled and analysed with microscopic techniques and μ -Raman spectroscopy. Both sides of an Fe metal structure, the Fe-water and the Fe-clay interfaces were studied.

The Fe-water side reveals a 100-200 μm thick corrosion layer composed of magnetite, siderite, hematite, hydrous ferric oxide. The Fe-clay side exhibits a web-shaped ~ 100 μm thick layer of iron corrosion products (bright) and clay (dark). Siderite and Fe oxyhydroxides could be identified. The clay matrix is somewhat enriched in Fe and partly also in Mg, but no change in A/Si ratio was noted. At a distance of about 1 mm from the metal formation of CaSO_4 is observed. The front enriched in Fe extends 1-2 mm into the clay. Overall, the data suggest an intimate association of iron corrosion product and montmorillonite, but no formation of Fe silicates.



Insights into U-series weathering chronometers from size fraction distribution of U and Th nuclides in Himalayan soils and sediments

A. JOSHUA WEST¹

¹University of Southern California, Department of Earth Sciences, 3651 Trousdale Parkway-ZHS 117, Los Angeles, CA 90089 UNITED STATES; (joshwest@usc.edu)

As a result of varying mobility between different nuclides, disequilibria within the U-series decay chain potentially provides valuable constraints on the timescales of Earth surface processes. Models describing the evolution of both ($^{234}\text{U}/^{238}\text{U}$) and ($^{230}\text{Th}/^{238}\text{U}$) activity ratios during leaching are increasingly used to determine the duration of weathering and sediment transport. However, important assumptions in these models remain untested. While the basic mechanisms driving observed disequilibria during weathering are well-established (e.g. alpha recoil and preferential leaching), the picture remains somewhat fuzzy in terms of how bulk rocks, soils, and sediments, and the complementary dissolved phase, actually acquire their U and Th signature. Important puzzles, such as the reason for ^{234}U enrichment of some bulk solid phases despite the expected more rapid leaching of this nuclide, have yet to be completely resolved.

This study focuses on measurements of the U and Th nuclide abundance in a suite of samples (rocks, soils, sediments, and stream water) from the Middle Hills of Nepal, where solid products of weathering show distinct depletion in soluble elements (e.g. Ca, Na). Bulk soils and sediments have ($^{234}\text{U}/^{238}\text{U}$) above equilibrium ($\delta^{234}\text{U} = +15\text{-}30\%$ relative to equilibrium), increasing with weathering extent in the soil profiles. Variability in $^{234}\text{U}/^{238}\text{U}$ between size fractions of the Nepal soils demonstrates that the ^{234}U enrichment can be quantitatively explained by retention in the very fine ($<0.2\mu\text{m}$) fractions, which have measured $\delta^{234}\text{U} > +100\%$ and REE patterns characteristic of Fe-oxides. These results suggest that bulk solid phase ($^{234}\text{U}/^{238}\text{U}$) > 1 can result from modern weathering processes because of retention in oxide phases.

Observed ($^{230}\text{Th}/^{238}\text{U}$) is highly variable and would imply long (tens to hundreds kyr) weathering duration based on simple models of leaching and decay. These durations require residence times that are inconsistent with the depth of weathering profiles and erosion rates inferred from ^{10}Be inventories in quartz from these locations. One possible explanation is that the measured sediment ($^{230}\text{Th}/^{238}\text{U}$) from these sites may be strongly influenced by grain size sorting.

Mo isotope signature of OAE 2

S. WESTERMANN^{1-2*}, D. VANCE¹, V. CAMERON²,
C. ARCHER¹ AND S.A. ROBINSON³

¹Institute of Geochemistry and Petrology, Dept. of Earth Sciences, ETH Zurich, Switzerland

²Bristol Isotope Group, School of Earth Sciences, University of Bristol, UK.

³Dept. of Earth Sciences, University College London, UK.
(* correspondence: stephane.westermann@bristol.ac.uk)

Understanding variations of redox conditions during oceanic anoxic events (OAEs) is of primary importance, particularly as recent observations and modelling have shown that processes invoked to explain the origin of OAEs are being observed today as a consequence of anthropogenic change.

Here, we compare redox-sensitive trace metal (RSTM) distributions and molybdenum (Mo) isotope variations during a major Cretaceous OAE (OAE 2, Bonarelli event) within the western Tethys and the Northern Atlantic. Whereas RSTM have the potential to provide insights regarding local depositional conditions and processes in paleoceanographic systems, Mo-isotope data can, under certain circumstances, provide quantitative estimates of how the extent of seawater anoxia may have fluctuated in the past.

The RSTM contents indicate more reducing conditions during the OAE 2 interval, reaching from suboxic to euxinic conditions. The RSTM enrichment factors (EFs) also suggest different depositional conditions and paleoceanographic processes between the Tethys and the North Atlantic. Whereas the North Atlantic sites show evidence of weak watermass restriction associated with the action of a particulate shuttle within the water column, the EFs of the Tethyan sections are characteristic of unrestricted marine systems.

Mo isotopes show surprisingly negative values along the Tethyan sections. At the onset of OAE 2, an increasing trend in $\delta^{98/95}\text{Mo}$ is observed with values ranging from -0.6 to 0.6 ‰. During the 2nd half of OAE 2, the $\delta^{98/95}\text{Mo}$ curve shows a progressive shift towards more negative values. In the North Atlantic, Mo isotopes are generally heavier during OAE 2, fluctuating around an average value of 1.1 ‰.

Both the western Tethys and the Northern Atlantic sites show redox variations, reaching anoxic/euxinic conditions. However, light $\delta^{98/95}\text{Mo}$ values in the western Tethys suggest redox conditions may not have been fully euxinic. For the North Atlantic, our results are consistent with fully euxinic conditions and may help to improve our understanding of the global extent of euxinia during OAE 2.

New U-Pb age and $\square\text{Hf}$ signature data of metasedimentary and metabasic rocks of the front of the Southern Brasilia Orogen, south of São Francisco Craton, Brazil

A. WESTIN^{1*} AND M. C. CAMPOS NETO¹

¹Geosciences Institute, University of São Paulo, São Paulo, SP, Brazil (*correspondence: alice.teixeira@usp.br; camposnt@usp.br)

The Brasília Orogen, located on the western and southern margin of the São Francisco Craton, corresponds to a horizontal nappe stack that was regionally transported eastward during the collision between the Paranapanema and Goiás Central Blocks and the Sanfranciscan Plate in the Ediacaran Period [1]. The front of the Southern Brasília Orogen is represented, at the base, by metasediments with lithic nature associated with amphibolite lenses, both objects of this study, followed by metapsamites and metapelites of the Carrancas Group, with a tectonically upper exotic unit of metawackes [2, 3].

The metasediments of the base are paragneiss rich in lithic fragments that vary from plagioclase-quartz-biotite-epidote gneiss with potassic feldspar and hornblende (EG) to epidote-plagioclase-biotite-quartz gneiss with carbonate (QG). Detrital zircons from EG rocks provided U-Pb ages (LA MC ICP MS) that range between 2.04 to 2.18 Ga, with mean peak age of 2.12 ± 13 Ga. The $\square\text{Hf}$ values of this crystals vary from -10.4 to +15.1, with predominance of the positive values. Detrital zircons from the QG rocks indicated a provenance age between 2.00 to 2.19 Ga, with mean peak age of 2.03 ± 11 Ga. The $\square\text{Hf}$ values range from -7.4 to +6.2, with prevalence of the negative values.

The amphibolite lenses are discontinuously interbedded with the paragneiss, predominantly formed by hornblende and plagioclase (andesine), with tholeiitic signature. The mean peak age of this rocks stands in 1.96 ± 22 Ga and the $\square\text{Hf}$ values vary from -16.8 to +23.5.

These data suggest that the deposition of the metasedimentary sequence initiated after 2.0 Ga, with the related basic magmatism starting somewhat around 1.96 Ga. The $\square\text{Hf}$ values also suggest that the source area comprised rocks related to juvenile accretion and rocks having long crustal residence.

[1] Campos Neto, M. C. (2000) *Tect. Evol. S. America*, 335-365. [2] Campos Neto *et al.*, (2011) *JSAES* **32**, 393-406. [3] Westin e Campos Neto (submitted article) *JSAES*.

Impacts of geothermal energy storage on the microbial community composition and activity in shallow systems

ANKE WESTPHAL¹, ANNA JESUBEK², TOBIAS LIENEN¹,
ANDREAS DAHMKE² AND HILKE WÜRDEMANN¹

¹ Helmholtz Centre Potsdam, *German Research Centre for Geosciences GFZ*, wuerdemann@gfz-potsdam.de

² Christian Albrechts Universität zu Kiel, ad@gpi.uni-kiel.de

To investigate the effects of temperature change due to geothermal energy storage on the microbial communities and the fluid geochemistry, soil column experiments using aquifer sediment and acetate added water were performed at 10, 25, 40 and 70°C. Genetic fingerprinting revealed a change in microbial community composition and activities due to elevated temperatures. The highest DNA amount and sulphate reducing bacteria (SRB) specific gene copy number were observed in fluids of the 40°C column. Correspondingly, the highest sulphate reduction rate was detected at 40°C. Thus probably the highest number of SRB was present in this column. Due to the formation of different redox zones in the 10°C column, zones of microbial colonization were observed. In the entrance nitrate and iron reducers were identified, whereas at the outlet fermentative bacteria dominated. At 70°C sulphate reducing conditions predominated and no zoning of microbial colonization was detected. Genetic fingerprinting revealed the dominance of SRB and fermentative bacteria. Methane production was found at 25°C, only. Accordingly, quantification with quantitative polymerase chain reaction (qPCR) proved the highest number of the dominant methanogen *Methanosaeta concilii*.

Reduced C-O-H Volatiles Dissolved in Lunar Picritic Glasses

D.T. WETZEL^{1*}, M.J. RUTHERFORD¹, S.D. JACOBSEN²,
E.H. HAURI³, A.E. SAAL¹, AND S.-M. THOMAS⁴

¹Dept. of Geological Sciences, Brown University, Providence, RI 02912 (*correspondence: Diane_Wetzel@brown.edu)

²Dept. of Earth and Planetary Sciences, Northwestern University, Evanston, IL 60208

³DTM Carnegie Institute of Washington, DC 20015

⁴Dept. of Geoscience, University of Nevada Las Vegas, Las Vegas, NV 89154

The Moon had long been considered dry, until recently, when Saal *et al.* [1,2] used SIMS to measure H₂O dissolved in the lunar picritic glasses. Before this discovery, carbon was considered the primary volatile. The formation of a CO-rich gas phase by graphite oxidation was thought to drive fire fountain eruptions on the Moon producing the glass beads [3]. The natural lunar glasses contain too little dissolved C (below detection limits) to be detected by FTIR spectroscopy. We used the Apollo 15 green glass composition to experimentally determine the solubility and speciation of C in H-bearing graphite-saturated melts. Our experiments show C dissolves in reduced lunar melts ($f_{O_2} < IW-0.55$) as mainly Fe(CO)₅ and to a lesser extent CH₄. Under more oxidizing conditions ($f_{O_2} > IW-0.55$), we find C is dissolved as carbonate in lunar picritic melts. We also determine that twice as much C can be dissolved in oxidized melts compared to the reduced melts.

NanoSIMS measurements [1] of natural glasses suggest that hydrogen is dissolved in large enough quantities (up to ~40 ppm) to be detectable by FTIR spectroscopy. We used Raman and FTIR spectroscopy to study the speciation of H in the natural orange, yellow, and green lunar glasses. We also calculated the absorption coefficients for each glass composition based on our experiments. The synthetic sample spectra were also used as a guide to baseline correct and locate the weak O-H stretching peak in the natural samples. With this work, we are able to determine the abundance and speciation of dissolved volatiles in lunar and other reduced high FeO melts and the effect of planetary degassing on the evolution of an early atmosphere.

[1] Saal A.E. *et al.* (2008) *Nature*, 454, p.192-95. [2] Saal A.E. *et al.* (2009) *Goldschmidt Conf.*, Abst. #A1139. [3] Sato M. (1976) *PLSC 7th*, p.1323-25.

Lithium isotope variation in waters and sediments from lake Donggi Cona and its catchment, China

M. WEYNELL^{1*}, U. WIECHERT¹ AND J.A. SCHÜSSLER²

¹Freie Universität Berlin; Germany (*correspondance: marc.weynell@fu-berlin.de)

²GFZ German Research Centre for Geosciences, Helmholtz Centre Potsdam, Potsdam, Germany

Lithium isotopes are a tracer of weathering at the Earth's surface, as documented from catchments with basaltic [e.g., 1], granitic [e.g., 2] and mixed (carbonate, volcanic and sedimentary) lithologies [e.g., 3]. In this study we examine the behaviour of lithium (Li) and its isotopes in the catchment of lake Donggi Cona, China, which is an open oligotroph freshwater lake in the northeastern part of the Tibetan Plateau. The main inflow drains an area with a high proportion of carbonate rocks and a second inflow is sourced from a catchment with a larger quantity of silicate rocks. In addition, warm springs contribute to the Li budget of the lake. Water chemistry is mainly controlled by carbonate dissolution. With the exception of spring waters, pH values are constant at ~8.8. The dissolved load (DL) of every compartment shows distinct $\delta^7\text{Li}$ values (relative to L-SVEC): main inflow +17.0; minor inflow +20.7; warm springs +11.5 and lake +16.9. Suspended loads and river sediments give $\delta^7\text{Li}$ values from -2.1 to +3.1. However, lake sediments exhibit a narrow range of -1.1 to -0.5 for distal sample locations. Detrital influenced lake sediments show positive $\delta^7\text{Li}$ values of +1.7 and +2.9. Li concentrations (DL) are 37 ng/ml in the lake, 7 to 12 ng/ml in the main inflow, 33 ng/ml in the second inflow and 125 ng/ml in warm spring waters. Li concentrations of suspended loads and sediments are in the range of 20 to 55 $\mu\text{g/g}$. Lithium concentrations and isotope ratios of the lake can be explained by mixing of waters from the 3 sources and by evaporation. High $\delta^7\text{Li}$ values (DL) in the tributaries can be explained by incorporation of light Li into secondary minerals formed in the catchments, which is consistent with low $\delta^7\text{Li}$ values of complementary sediments and suspended loads. However, compared with basaltic catchments, e.g. [1], Li concentrations in the waters are higher and $\delta^7\text{Li}$ values are lower. We suggest that this is due to a distinguished lithology and lower soil formation rates controlled by the climatic regime on the northeastern Tibetan Plateau.

[1] Vigier *et al.* (2009) *EPSL* 287, 434-441; [2] Lemarchand *et al.* (2010) *GCA* 74, 4612-4618; [3] Millot *et al.* (2010) *GCA* 74, 3897-3912.

Regional-scale metasomatism in the Fortescue Group volcanics, Hamersley Basin, Western Australia, constrained through phase equilibria modelling

A.J.R. WHITE*, M. LEGRAS, R.E. SMITH AND P. NADOLL

CSIRO Earth Science and Resource Engineering, Australian Resources Research Centre, 26 Dick Perry Avenue, Kensington, WA 6151, Australia (*correspondance: alistair.white@csiro.au)

Mafic to intermediate volcanic rocks of the Fortescue Group form the lowermost stratigraphic unit of the 100,000 km² Hamersley Basin on the southern margin of the Archaean Pilbara Craton, Western Australia. A regional burial metamorphic gradient extends across the basin from prehnite-pumpellyite facies in the north to greenschist facies in the south [1]. Superimposed on this metamorphic gradient is a heterogeneous distribution of metasomatized rocks characterized by pumpellyite+epidote+quartz assemblages.

Whole-rock geochemical data indicate metasomatism is associated with significant depletions in alkali elements, Mg and first transition series metals, with enrichments in Si and Ca. Such geochemical trends are compatible with sub-sea floor hydrothermal circulation [2].

Phase equilibria modelling with the program THERMOCALC [3], in subsets of the model system Na₂O-CaO-K₂O-FeO-MgO-Al₂O₃-SiO₂-H₂O-Fe₂O₃ (NCKFMASHO), place P-T constraints on the conditions of regional metamorphism and regional-scale metasomatism. 'Least altered', regional metamorphic rocks show a temperature gradient from <200°C in the north, to > 325°C in south, consistent with predicted burial-derived thermal gradients [1]. Highly altered, metasomatized rocks show consistent temperatures of 275 – 300°C, and pressures > 2.5 kbar, across the entire basin.

The calculated temperature for the metasomatized rocks is interpreted to represent the temperature under which hydrothermal alteration occurred. The consistent P-T estimates and geochemical data suggest a common hydrothermal event acting across the entire Hamersley Basin, covering length scales of hundreds of kilometres. This has important implications for the size of metasomatic systems in other metamorphic terranes.

[1] Smith *et al.* (1982) *J. Pet* 23, 75-102. [2] Hannington *et al.* (2003) *Miner Deposita* 38, 393-422. [3] Powell & Holland (1988) *J. Met. Geol.* 6, 173-204.

Towards better Greenland source attribution for IRD via Pb-Pb in feldspar and Ar-Ar in amphibole

WHITE. L.^{1*}, STOREY. C.¹, BAILEY. I.² AND FOSTER. G.²

¹University of Portsmouth, Burnaby Road, Portsmouth.

(*Presenting Author: Lee.white1@myport.ac.uk)

²University of Southampton, European Way, Southampton.

A major uncertainty in future climate predictions involves changes in the mass and areal extent of the Greenland ice sheet (GrIS) and its variability in a warmer climate. Understanding the growth of the GrIS during Pliocene intensification of northern hemisphere glaciation may enable the critical evaluation of existing models and aid in future validation of these models. The provenance of Ice rafted debris (IRD) deposited in marine sediments has great potential to fingerprint regions of present and past iceberg calving in the coastal zones of continental margins. As such, this could potentially be a powerful technique when confining the extent of the GrIS during past climatic intervals. However, the IRD record is only as strong as the onshore land-based record of potential sources.

Two minerals common within IRD that have been used previously and that show great promise in this regard are feldspar and amphibole. Pb isotopes in feldspar record a diagnostic signature of the continental crust within distinct geologic terranes. In particular, Greenland is composed of a number of distinct terranes with proven distinct Pb isotope signatures. Ar-Ar dating of amphiboles records the thermal history of a terrain when it was metamorphosed above or cooled below c. 550°C. Due to distinctive metamorphic histories within different terranes this signature is also potentially diagnostic of a particular source area. The two minerals together could be particularly powerful but only if the potential areas of calving are well-characterised.

Here we present data from fluvio-glacial sediments from sites around the margins of Greenland and discuss their diagnostic characteristics. We then compare these diagnostic geochemical signatures to some circum-Greenland core top IRD samples from numerous offshore sites, acting as a proof of concept. Finally, we present data sets from Mid Pliocene IRD from ODP Site 907, from numerous depths and time intervals, to further develop the proposed method and apply it to a key period in the development of northern hemisphere glaciation.

Indium's aqueous behavior in a stream influenced by acid mine drainage

SARAH JANE O. WHITE^{1,2*}, FATIMA A. HUSSAIN², HAROLD F. HEMOND², ROBERT L. RUNKEL³, KATHERINE WALTON-DAY³ AND BRIANT A. KIMBALL⁴

¹Harvard School of Public Health, 401 Park Dr, Boston, MA 02215 (*correspondence: sjwhite@hsph.harvard.edu)

²MIT, 15 Vassar St, Cambridge, MA 02139

³U.S. Geological Survey, Denver Federal Center, Box 25046, MS 415, Denver, CO 80335

⁴U.S. Geological Survey, 2329 West Orton Circle Salt Lake City, Utah, 84119

Indium is an increasingly important metal in semiconductors and electronics, and its use is growing rapidly as a semiconductive coating (in indium tin oxide) for LCD displays, flat panel displays, and photovoltaic cells. It also has uses in important energy technologies such as LEDs. Despite its rapid increase in use, very little is known about indium's environmental behavior, and concerns are emerging over its health impacts.

One significant flux of indium to the environment is from nonferrous mining and smelting. Mineral Creek is a headwater stream in southwestern Colorado that is severely affected by heavy metal contamination as a result of acid mine drainage. This includes indium concentrations that are 10,000 times those found in natural rivers. There have been a variety of remediation efforts in this watershed, including the installation of bulkheads to reduce water flow from mining tunnels, and removal of tailings piles. These remediation efforts appear to have reduced metal loadings in the system, though they remain above chronic aquatic standards. Indium, however, has not been previously measured, and no standards exist for indium in natural waters. In this work, a pH modification experiment was conducted in August 2005 to investigate the effects of an active remediation proposal to increase the pH of the creek. At the existing pH of ~3, indium concentrations are 6-29 µg/L (10,000x those found in natural rivers), and exist completely in the dissolved phase. Upon raising the pH of the system to > 8, all of the indium became associated with the suspended solid phase, primarily due to sorption to iron-oxides. This work informs how much indium may be mobilized from nonferrous mine wastes globally, and provides much-needed data about the aqueous behavior of indium.

Radioactivity and Neutrino Production in the Oceanic Crust

WILLIAM M. WHITE¹

¹Dept. of Earth & Atmospheric Sciences, Cornell University, Ithaca, NY, 14853 USA, (wmw4@cornell.edu)

Most oceanic crust is created at mid-ocean ridges as magma rises from the mantle to fill the gap between diverging plates. This produces a relatively uniform crustal structure and composition. The upper km of so of the crust consists of basaltic lavas (called mid-ocean ridge basalts or MORB) characterized by low concentrations of incompatible element, including the heat producing elements U, Th, and K. Concentrations show a highly skewed distribution; log-normal means (which provide an estimate of the modal concentrations) are U= 94 ppb, Th = 273 ppb, and K = 1211 ppm, while mean concentrations are U = 119±26 ppb, Th = 404±77 ppb, and K = 1328±71 ppm (quoted uncertainty is 2 standard errors of the mean based on ~2000 analyses; from Gale *et al.*, *G³*, 14, 2013). Back-arc basin basalts have similar Th but higher U and K: 137 ppb U, 399 ppb Th, and 2258 ppm K. The compositions of MORB indicates that they evolve through fractional crystallization within the oceanic crust and hence do not represent the composition of the crust as a whole. Calculations based on the MELTS thermodynamic model suggests MORB have experienced an average of 39% fractional crystallization. Assuming that the composition of the bulk 'fresh' oceanic crust is that of a primitive parent in equilibrium with mantle olivine, bulk 'fresh' oceanic crust is estimated to have 80 ppb U, 260 ppb Th, and 875 ppm K. Simple mass balance then indicates that 'fresh' lower oceanic crust (gabbroic section or layer 3) has 70 ppb U, 220 ppb Th, and 750 ppm K. Assuming the crust is generated by 8% melting, this implies depleted mantle concentrations of 6 ppb U, 21 ppb Th, and 70 ppm K. Hydrothermal processes modify the composition of oceanic crust, increasing K and U by 402 mg/kg and 0.307 mg/kg, respectively (Staudigel, TOC, Chapter 13, 2013). This increases U and K in the bulk oceanic crust to 110 ppb U and 1280 K. A small fraction of the oceanic crust consists of thick ocean plateaus produced by melting over mantle plumes. These plateau basalts have higher U, Th, and K concentrations: ~400 ppb U, ~1300 ppb Th, and ~1369 ppm K. Considering all these factors considered and assuming an average crustal thickness of 7 km for crust created at mid-ocean ridges, total U, Th, and K in the oceanic crust is estimated at 6.62 x 10¹⁴ kg, 1.55 x 10¹⁵ kg, and 762 x 10¹⁸ kg, respectively, producing 0.13 TW of energy (≤1% of the terrestrial total). These masses of U and Th would produce 3.9 x 10⁶ anti-neutrinos per year.

Ion imaging and ion tomography applications in zircon geochronology

M.J. WHITEHOUSE^{1*}

¹Swedish Museum of Natural History, SE-104 05 Stockholm, Sweden (*correspondence: martin.whitehouse@nrm.se)

High spatial resolution secondary ion mass spectrometry (SIMS) has been routinely used in zircon U-Pb geochronology and geochemistry for three decades and has been central to many important geological discoveries. The unique ion microscope capability of the CAMECA IMS 1270/80 instruments, in particular using scanning ion imaging (SII) coupled with high sensitivity, high mass resolution and exceedingly low noise ion-counting multicollection remains however, a relatively underutilised tool in geochronology.

A recent study [1] of Meso- to Paleoproterozoic zircon from gneisses in east Antarctica which have experienced ultra-high temperature (UHT) metamorphism, used scanning ion imaging (SII) both to map the occurrence and measure the isotope ratio of unsupported radiogenic Pb. Numerous micrometre-sized Pb-rich clots were revealed in an 80 x 80 μm imaged area by the SII technique. These clots are independent of the distribution of other elements, notably U and Y, both of which show simple oscillatory zoning, while their elevated ²⁰⁷Pb/²⁰⁶Pb ratios clearly indicate their antiquity. Apart from explaining commonly observed Pb instability and reverse discordance [2] during SIMS analysis of UHT zircon, such ancient Pb redistribution can have implications for the geochronology of zircon from the early Earth [1].

The lateral resolution of an SII analysis is limited to the ca. 2 μm diameter of the primary beam and so the actual size of the Pb-enriched clots remains essentially unconstrained below this level, but is clearly considerably smaller given the relative uniformity in observed clot area. In an extension of the conventional SII study, an investigation of UHT zircon from southern India that exhibit similar Pb-clots, utilised a novel combination of SII and depth profiling, here termed scanning ion tomography (SIT), to add a third dimension to the Pb clots. During a typical SII analysis (comprising 100 scans), the ion beam penetration is < 5 nm and using this method, Pb-rich clots are revealed to have a size typically of only a few nanometers. The ability of SIT to reveal the true length-scale of Pb-isotope redistribution, while still uniquely recording a Pb isotope ratio, considerably aids in constraining models for the processes involved in their generation.

[1] Kusiak *et al.* (2013), *Geology* **41**, 291-294. [2] Williams *et al.* (1984), *Contr. Min. Petrol* **88**, 322-327.

Persistence of early Archean style of crustal growth and near-chondritic mantle into the late Archean

M.J. WHITEHOUSE^{1*} AND A.I.S. KEMP²

¹Swedish Museum of Natural History, SE-104 05 Stockholm, Sweden (*correspondence: martin.whitehouse@nrm.se)

²University of Western Australia, Crawley, WA 6009, Australia (tony.kemp@uwa.edu.au)

The Neoproterozoic Lewisian Complex of north-west Scotland is one of the most extensively studied TTG gneiss terranes on Earth. It has been used to propose and refine models of crustal evolution for over a century, from the early recognition of multiple phases of crustal reworking based on cross-cutting dykes [1] to the more recent “terranes models” proposed for crustal accretion [2]. Interpretation of both geochronology and isotopic data from the Lewisian, however, remains complicated (e.g. [3]) by polyphase metamorphism, which in places attains granulite facies.

In this study, we present cathodoluminescence image-guided ion microprobe U-Th-Pb geochronology and LA-ICP-MS Hf isotopes of zircon separated from representative TTG gneisses across the Scottish mainland and Outer Hebridean Lewisian outcrop. Applying a similar methodology to that outlined in [3], we assign a preferred magmatic protolith age to each zircon population and this age is then used to calculate $\epsilon_{\text{Hf}}(t)$ values.

Over a wide range of protolith ages from > 3.1 Ga to 2.7 Ga, zircon $\epsilon_{\text{Hf}}(t)$ values are, on average, only slightly super-chondritic and show relatively little variation with time. A possible explanation for this trend is that younger TTG magmas are increasingly influenced by recycling of older crust, although few older zircon cores are observed to support such an *ad hoc* interpretation. As an alternative, we propose a tectonic model for the Lewisian in which mafic precursors to the TTG magmas, generated from a mildly depleted to near-chondritic mantle, were rapidly recycled over a period of >400 Ma with little or no direct input of typical contemporaneous depleted-mantle. Similar tectonic scenarios, differing markedly from “modern-style” plate tectonics, have been proposed for the early Archean (e.g. [4]) and our observations from the Lewisian TTG gneisses suggest that, at least locally, similar processes, as well as near-chondritic mantle, may have persisted into the Neoproterozoic.

[1] Peach *et al.* (1907), *Mem. Geol. Surv. GB*. [2] Kinny *et al.* (2005), *J. Geol. Soc. Lond.* 162, 175–186. [3] Whitehouse & Kemp (2010), *Geol. Soc. Lond. Spec. Publ.* 335, 81–101. [4] Naeraa *et al.* (2012), *Nature* 485, 627–630.

Increasing greenhouse gas emissions in circumpolar regions due to climate change-induced permafrost retreat

M. WHITICAR^{*1} J. BHATTI² AND N. STARTSEV²

¹ SEOS, U. Victoria, Victoria, BC, V8W 2Y2, Canada (*correspondence: whiticar@uvic.ca)

² NFC, Canadian Forest Service, Edmonton, AB, Canada

Thawing permafrost peatlands substantially influence northern ecosystems by changing the regional hydrology and mobilizing the vast carbon (C) reserves that results in increased greenhouse gas (GHGs) emissions to the atmosphere. With permafrost distribution controlled largely by topography and climate, our IPY study intensively monitored the local C-cycling processes and GHG fluxes associated with different hydrologic and permafrost environments at 4 sites along a latitudinal climatic gradient of mid-boreal, boreal, low and high subarctic ecoclimatic regions that extend south-north from the Isolated Patches Permafrost Zone (northern Alberta), to the Continuous Permafrost Zone (Inuvik, NWT). Each site encompasses a local hydrologic and vegetation gradient from upland forest and peat plateau to collapse scar.

Our multi-year measurements of peatland profiles and flux chambers for CH₄ and CO₂ concentrations and stable isotope ratios indicate processes, including methanogenesis, methanotrophy, transport and emission that control the distribution of these GHGs. These relationships are modulated by fluctuating local soil water and ecosystem conditions. The gas geochemistry shows that significant surface CH₄ production occurs by both hydrogenotrophic and methyl-fermentative methanogenesis in submerged, anaerobic peats, e.g., collapse scars, whereas methane oxidation is restricted to aerobic, drier environments, e.g., upland sites and peat-atmosphere interface. The most active methanogenesis and emissions are in the actively thawing permafrost sites contrasting with those under continuous permafrost. This degree of methanogenesis is being amplified by the increased rate of warming and the rapid retreat of permafrost in Canada's northern areas (ca. 2.5 km/yr).

For context, the present permafrost and GHG emission situation is compared with the rapid rises in temperature, CH₄ and CO₂ concentrations during the Younger Dryas-Preboreal transition (~11.5yBP). Our pCH₄ and $\delta^{13}\text{C}_{\text{CH}_4}$ work [1] on Pakitsiq, Greenland ice show that the rapid rise in pCH₄ during YD-PB is unlikely to have been due to massive marine gas hydrate release (‘clathrate gun’), but that CH₄ from permafrost retreat after Last Glacial Maximum is a plausible explanation.

[1] Schaefer, *et al.* (2006) *Science* 313, 1109–1112.

Absorbing aerosol radiative effects in the limb-scatter viewing geometry

A. WIACEK¹, R. V. MARTIN^{2,3}, A. E. BOURASSA⁴,
N. D. LLOYD⁴ AND D. A. DEGENSTEIN⁴

¹ Division of Engineering, Saint Mary's University, Halifax, Canada

² Department of Physics and Atmospheric Science, Dalhousie University, Halifax, Canada

³ Harvard-Smithsonian Center for Astrophysics, Cambridge, Massachusetts, USA

⁴ Department of Physics and Engineering Physics, University of Saskatchewan, Saskatoon, Canada

We use the fully 3-D radiative transfer code SASKTRAN to simulate the sensitivity of limb-scatter viewing Odin/OSIRIS satellite measurements to absorbing mineral dust and carbonaceous aerosols, and to sulfate aerosol and ice in the upper troposphere.

At short wavelengths (337 nm, 377 nm, 452 nm), we found that the addition of any aerosol species to an air only atmosphere caused a decrease in single-scattered radiation due to an extinction of Rayleigh scattering in the direction of OSIRIS. The reduction was clearly related to particle size first, with absorption responsible for second-order effects only. Multiple-scattered radiation could either increase or decrease in the presence of an aerosol species, depending both on particle size and absorption. The combined effect led to complex total radiance signatures that generally could not unambiguously distinguish absorbing versus non-absorbing aerosols. However, we found that scene darkening above the aerosol layer is unambiguously due to absorption whereas scene darkening within and below the aerosol layer can simply be the result of a reduction in single-scattered radiance. However, the effect did not exceed 0.2% of the total radiance due to air only for medium-sized carbonaceous aerosols.

A fortuitous, unexpected implication of our analysis is that limb-scatter retrievals of aerosol extinction are insensitive to external information about aerosol absorption.

Stable Sr isotope fractionation in synthetic barite

INOKA H. WIDANAGAMAGE¹, ELIZABETH M. GRIFFITH²,
AND HOWIE D. SCHER³

¹ Department of Geology, Kent State University,
iwidanag@kent.edu

² Department of Earth and Environmental Sciences, University of Texas at Arlington, lgriff@uta.edu

³ Department of Earth and Ocean Sciences, University of South Carolina, hscher@geol.sc.edu

Barite (BaSO₄) is a highly stable and widely distributed mineral that incorporates many elements (e.g., Sr, Ca, Ra) in its crystal lattice making it useful as an archive for geochemical and isotopic signals of environmental change. Abiotic precipitation of barite commonly occurs with mixing of sulfate and barium rich solutions. Barite can also precipitate in association with biological processes, such as bacterial sulfide oxidation. We present stable Sr isotope results ($\delta^{88}\text{Sr}$) from synthetically precipitated barite to elucidate the parameters (e.g., temperature, barite saturation state, solution Sr/Ba) influencing mass dependent Sr isotopic fractionation under abiotic conditions. This work will constrain future studies of stable Sr isotopic fractionation in natural biologically-influenced barite precipitation.

We precipitated barite from solution by adding sulfate to a Sr-Ba solution under various conditions (solution Sr/Ba, temperature, and barite saturation state) that may influence equilibrium and/or kinetic mass dependent stable Sr isotopic fractionation. Isotopic measurements were made on a Thermo Neptune Plus MC-ICPMS at the University of South Carolina using a standard-sample bracketing technique that corrects for instrumental mass bias relative to a Zr reference ratio. All barite samples were less enriched in ⁸⁸Sr relative to the solutions from which they precipitated similar to other isotope systems (e.g., Ca).

In our experiments, Sr isotopic fractionation is influenced by both barite saturation state and temperature. However, neither dominantly controls Sr isotopic fractionation under our experimental conditions. Temperature dependent isotopic fractionation of Sr under our experimental conditions was very weak and negative (-0.0032‰/°C), however the variation of the isotopic data is largely within the analytical uncertainty of the measurement over the temperature range of our experiments, 5 to 40°C. The relationship between $\Delta^{88/86}\text{Sr}_{\text{barite-aq}}$ for all experiments and D_{Sr} was not significant, but was affected by the solution initial barite saturation state, which likely influences precipitation rate. At a constant initial barite saturation state, the relationship is significant and appears to be independent of temperature and (Sr/Ba) ratio.

Lithium isotope variation in rivers and lakes on the Tibetan Plateau

U. WIECHERT^{1*}, M. WEYNELL¹, S. BARVENCIK¹,
AND J. A. SCHUESSLER²

¹Freie Universität Berlin; Germany (*correspondance: wiechert@zedat.fu-berlin.de)

²GFZ German Research Centre for Geosciences, Helmholtz Centre Potsdam, Potsdam, Germany

We report lithium abundances and isotope ratios for lakes, tributaries, and large rivers (Indus, Yarlung Tsangpo and Yellow River) on the Tibetan Plateau. In rivers we found solely calcium-bicarbonate waters, whereas lakes with sodium-chloride and sodium-sulfate waters could be distinguished. The chemical composition of the rivers primarily reflects weathering of rocks in carbonate-rich catchments. In contrast, lake water chemistry is affected by evaporation and crystallization of minerals. This is indicated by a high level of mineralization and an electric conductivity of more than 10 mS/cm, which classifies them as salt lakes. The $\delta^7\text{Li}$ of lake waters varies between +7.0 and +25 relative to L-SVEC. The $\delta^7\text{Li}$ of rivers in the south range from +4.0 to +9.0 and the Yellow River in the NE gives a $\delta^7\text{Li} \sim +18$. The variation of $\delta^7\text{Li}$ in the water samples is, in general, consistent with fractionation of isotopically light lithium in secondary clay minerals during weathering in the catchments [1,2]. However, at the lake Tashi Namtso a systematic isotopic difference between inflow and lake provides evidence for lithium isotope fractionation in the lake. In this example a strong pH change from about 8.2 to 9.8 is observed at the transition from river to lake waters. It is suggested that formation of clay minerals at the transition cause an additional isotopic shift by $\sim 10\%$. In the large rivers of the southern Tibetan plateau low $\delta^7\text{Li}$ are consistent with a transport-limited weathering regime, whereas the rather high $\delta^7\text{Li}$ of the Yellow River favour a weathering-limited transport regime. The results support that riverine lithium isotopes are a powerful proxy for the intensity of silicate weathering in a catchment [3] rather than silicate weathering rates [4]. However, in some areas lithium isotope compositions of the tributaries are affected by sulfate-rich thermal waters. How much this alters the weathering budget of the large rivers is difficult to estimate because evaporates and hot springs, which are important players in the terrestrial lithium cycle, are yet to be constrained.

[1] Huh *et al.* (1998) *GCA* **62**, 2039-2051 [2] Vigier *et al.* (2009) *GCA* **72**, 780-792 [3] Misra & Froehlich (2012) *Sci.* **335**, 818-823 [4] Vigier *et al.* (2009) *EPSL* **287**, 434-441.

Prospective shale gas zones in the Kimmeridgian and Tithonian strata of Polish Lowlands

D. WIĘCŁAW^{1*} AND M.J. KOTARBA¹

¹AGH University of Science and Technology, Mickiewicza 30 St., 30-059 Kraków, Poland (*correspondence: wieclaw@agh.edu.pl)

Kimmeridgian strata in the Norwegian and North Seas are considered to be responsible for hydrocarbon generation of large petroleum conventional accumulations [1]. Although exploration of these strata in Poland did not record commercial accumulation of petroleum, the preliminary studies [2] reveal generation of oil and gas in areas, where the Upper Jurassic strata were covered by thick Cretaceous rocks. In the present study we determinate areas and depth intervals of possible shale gas accumulation in these strata.

Results and discussion

A total of 482 core samples: 242 from the Kimmeridgian and 240 from the Tithonian strata from 40 wells of central part of Polish Lowlands were analysed. Rock-Eval pyrolysis reveals total organic carbon (TOC) contents from 0.14 to 9.6 wt% in the Kimmeridgian samples and from 0.19 to 12.5 wt% in the Tithonian samples. The highest values were recorded in the Upper Kimmeridgian and Lower Tithonian strata (TOC, up to 12.5 wt%, usually above 2 wt%). Rock-Eval, biomarker and kerogen elemental composition data evidence domination of the oil-prone Type-II kerogen in this most prospective sequences. Organic matter mostly is immature or early mature. 1-D modelling of the petroleum generation processes [2] reveal that in selected deeply buried structures in the Łódź Trough, the Upper Jurassic source rocks reached maturities corresponding to peak of oil window (0.7 - 1.0% Ro).

Conclusion

Intense sampling and Rock-Eval analyses enabled authors to designate a ca. 60 m thick marly shale complex at the border of Kimmeridgian and Tithonian strata in Łęczyca-Koło area as the most prospective for shale gas exploration.

The study was financed by the Ministry of Science and Higher Education (Projects Nos. N307 3141 39 and 744/N-IRAN/2010/0).

[1] Espitalie, Lafargue, Eggen (1991) *Spec. Pub. of EAPG*, 1, 49-63. [2] Więclaw, Kosakowski (2011) *Goldschmidt Conference*, 2156.

Tracing local industrial pollution sources with mercury isotopes

JAN G. WIEDERHOLD^{1,2*}, MARTIN JISKRA^{1,2},
ULF SKYLLBERG³, ANDREAS DROTT³, SOFI JONSSON⁴,
ERIK BJÖRN⁴, BERNARD BOURDON^{2,5}
AND RUBEN KRETZSCHMAR¹

¹Soil Chemistry, IBP, ETH Zurich, Switzerland

(*correspondence: wiederhold@env.ethz.ch)

²Isotope Geochemistry, IGP, ETH Zurich, Switzerland

³Forest Ecology and Management, SLU Umeå, Sweden

⁴Chemistry, Umeå University, Sweden

⁵ENS Lyon and CNRS, France

Stable mercury (Hg) isotope analysis offers a promising tool for tracing sources of anthropogenic Hg pollution in the environment. Mass-dependent (MDF) and mass-independent fractionation (MIF) of Hg isotopes results in two-dimensional isotope signatures of different Hg sources and can help understand transformation processes at contaminated sites.

Here, we present Hg isotope data for sediments collected in the vicinity of different industrial pollution sources in Sweden. The sampling sites covered a range of environmental conditions (salinity, organic matter, temperature) and were contaminated with either elemental Hg from the chlor-alkali industry or with phenyl-Hg used as preservative for pulp fibers in the paper industry. In addition to analyzing total sediment digests, a sequential extraction method designed to separate sulfide- and non-sulfide-bound Hg was performed on selected samples. Stable Hg isotope ratios were measured by CV-MC-ICPMS using standard-bracketing (NIST-3133) and Tl addition for mass bias correction.

The sediments exhibited a wide range of total Hg concentrations from 0.8 to 229 $\mu\text{g g}^{-1}$, consisting dominantly of organically-bound Hg(II) and a smaller pool of sulfide-bound Hg. The Hg isotope ratios of the three phenyl-Hg sites displayed nearly identical signatures (MDF $\delta^{202}\text{Hg}$: -0.2 to -0.5‰, MIF $\Delta^{199}\text{Hg}$: -0.05 to -0.10‰). In contrast, the four sites which had been contaminated with elemental Hg showed much greater variations ($\delta^{202}\text{Hg}$: -2.1 to 0.6‰, $\Delta^{199}\text{Hg}$: -0.19 to 0.03‰), but with distinct ranges for the different sites.

The sequential extraction data revealed that the smaller sulfide-bound Hg pool was in some samples up to 1‰ heavier in $\delta^{202}\text{Hg}$ than the dominant organically-bound Hg pool. The selectivity of the sequential extraction procedure was assessed using standard materials prepared with enriched stable Hg isotope tracers, which also allowed to gain insight into the exchange of Hg isotopes between different Hg pools.

Our results suggest that different industrial pollution sources can be distinguished based on their Hg isotope signatures, which can additionally record fractionation processes between different Hg pools in the sediments.

Geochemical and isotopic investigation of fluids from Lahendong geothermal field

B.A. WIEGAND^{1*}, M. BREHME², F. TEUKU¹,
I.A. AMRAN¹, R. PRASETIO¹, Y. KAMAH³
AND M. SAUTER¹

¹Univ. Göttingen, GZG, Goldschmidtstr. 3, 37077 Göttingen, Germany, (bwiegand@gwdg.de)

²Helmholtz Centre Potsdam – GFZ, Telegrafenberg, 14473 Potsdam, Germany, (brehme@gfz-potsdam.de)

³Pertamina Geothermal Energy, Jl.M.H. Thamrin No.9, Jakarta 10340, Indonesia.

Lahendong geothermal field is a high-temperature liquid-dominated system located in North Sulawesi (Indonesia) with a current power production capacity of 80 MW (Operator: Pertamina Geothermal Energy). The geology of the area comprises Late Pliocene to Mid-Pleistocene volcanic rocks of Mount Tondano and younger eruptions, including basaltic and andesitic lavas and pyroclastics [1,2]. Deep reservoir fluids are dominated by Cl-SO₄-HCO₃ and Cl type, while HCO₃-rich and SO₄-HCO₃ type fluids discharge at the surface [2].

We investigated trace elements and naturally occurring isotope systems (D-O, Sr, Ca) in fluids from hot springs, shallow groundwater wells, geothermal production wells, and surface waters from the Lahendong area to elucidate solute sources and geochemical processes in the aquifer. δD and $\delta^{18}\text{O}$ values of the fluid samples suggest a meteoric origin of geothermal groundwaters. Variable trace element concentrations are subject to differences in weathering regime and geochemical equilibrium conditions in the aquifer. Deep fluids are usually characterized by high As (≤ 4 mg/L), Cs (≤ 1.4 mg/L), and Li (≤ 2.3 mg/L) and low Ca and Mg concentrations (≤ 6 mg/L). In turn, surface waters and hot springs have higher Ca and Mg concentrations but are low in As, Cs, and Li content (<0.5 mg/L). $^{87}\text{Sr}/^{86}\text{Sr}$ ratios are lower in surface waters and hot springs (0.7039 – 0.7043), while fluids of the deeper reservoir have higher $^{87}\text{Sr}/^{86}\text{Sr}$ ratios (0.7050 – 0.7057), which suggests differences in the Sr isotope composition of andesitic and basaltic rocks in the reservoir and at the surface. $\delta^{44/40}\text{Ca}$ values vary between -1.50 and 0.09 ‰ and may be employed as an indicator for processes involving dissolved Ca²⁺. These processes include dissolution of minerals, cation exchange, and precipitation of secondary Ca-bearing phases.

[1] Koestono *et al.* (2010) Proceedings World Geothermal Congress 2010; Bali, Indonesia. [2] Utami *et al.* (2007) Proceedings 29th NZ Geothermal Workshop 2007.

Source and speciation of ^{14}C in a cement-based repository for radioactive waste

E. WIELANDT^{1*}, J. SCHENZEL¹ AND G. SCHLOTTERBECK²

¹Paul Scherrer Institute, Laboratory for Waste Management, 5232 Villigen PSI, Switzerland (*correspondence: erich.wielandt@psi.ch)

²University of Applied Sciences Northwestern Switzerland, School of Life Sciences, 4132 Muttenz, Switzerland

Carbon-14 is an important contributor to the annual dose released from a cement-based repository for low- and intermediate-level radioactive waste in Switzerland. To date, performance assessment has to be based on assumptions regarding the speciation and mobility of ^{14}C bearing compounds. It is considered that ^{14}C mainly contributes to dose in its organic form, such as ^{14}C bearing organic compounds, which are only weakly retarded in the cementitious near field.

Compilations of the activity inventories reveal that, in the already existing and future arising of radioactive waste in Switzerland, the ^{14}C inventory is mainly associated with activated steel (~ 85 %). The inventories of activated steel and ^{14}C in the repository are well known. However, the chemical speciation of ^{14}C in the cementitious near field upon release from activated steel is only poorly investigated.

Identification and quantification of the ^{14}C bearing organic compounds formed during the anoxic corrosion of activated steel is a major challenge, firstly due to the low ^{14}C inventory of the material available for the corrosion experiment, and secondly due to the extremely low corrosion rate of steel in alkaline solution (few nm/year). Thus, the development of an analytical method with a very low ^{14}C detection limit is required, such as compound-specific ^{14}C AMS. As a first step towards the development of the technique, batch-type corrosion experiments with non-activated, carbon-containing iron powders were carried out with the aim of identifying potentially ^{14}C bearing organic compounds. The powders were immersed in groundwater- and cement-type solutions and time-dependent changes in the concentrations of dissolved and gaseous carbon species were determined using high-performance ion exclusion chromatography coupled to conductivity detection and mass spectrometry and gas chromatography coupled to mass spectrometry. The conceptual approach for a corrosion study with activated steel along with first results will be discussed.

Irradiation histories of meteoritic inclusions measured by ^{40}K

D. WIELANDT¹ AND M. BIZZARRO¹

¹Centre for Star and Planet Formation, University of Copenhagen, Denmark (wielandt@snm.ku.dk).

The solar and galactic cosmic rays recorded by chondrules and refractory inclusions (CAIs and AOAs) can provide unique information on their formation, transport and storage histories. To explore the irradiation histories of these objects, we have developed novel analytical protocols to accurately measure Ca/K ratios and K-isotopes by thermal ionization mass spectrometry [1]. The low abundance of ^{40}K relative to ^{39}K makes the $^{40}\text{K}/^{39}\text{K}$ ratio a sensitive indicator of spallation, whereby efficient spallogenic production of ^{40}K occurs through proton irradiation of calcium targets by $^{43}\text{Ca}(p,\alpha)^{40}\text{K}$ and $^{44}\text{Ca}(p,n+\alpha)^{40}\text{K}$. Because proton stopping and reaction depths at relevant energies are similar to the sizes of the inclusions, ^{40}K depth profiles can allow us to discriminate between solar and galactic cosmic rays. Further, the common K retains information on precursor irradiation.

We selected well characterized CAIs and AOAs from Efremovka carbonaceous chondrite (CV3red) and chondrules from the NWA 5697 ordinary chondrite (LL3). The three chondrules selected for study have variable U-corrected Pb-Pb dates and ^{54}Cr compositions [2], suggesting lateral transport and storage of these objects in the solar protoplanetary disk for at least ~2 Myr prior to their accretion in the NWA 5697 parent body. All material analyzed show large (i.e. permil to percent) positive ^{40}K anomalies that broadly correlate with Ca/K ratios, consistent with spallation of Ca. The ^{40}K anomalies in the 3 chondrules vary with their absolute Pb-Pb dates, such that the oldest chondrules register the largest doses. At face value, this is consistent with a monotonic irradiation source, suggesting that ^{40}K anomalies were generated during storage in the protoplanetary disk, likely from exposures to galactic cosmic rays. The comparable dosages recorded by CAIs and chondrules suggest a similar transport mechanism, possibly associated with stellar outflows [3]. Similarly to CAIs, we infer that some chondrules formed in the inner regions of the protoplanetary disk were ejected to large orbital distances and drifted back to the accretion regions of chondrites over timescales of a few Myr. We are currently conducting ^{40}K depth profiles of large, well characterised and Pb-Pb dated chondrules to test this conclusion.

[1] Wielandt & Bizzarro (2011) *JAAS* **26**, 366 [2] Connelly *et al.* (2012) *Science* **338**, 651 [3] Shu *et al.* (1996) *Science* **271**, 1545

Sieve textures in impact zircon from Vredefort, South Africa: Implications to impact geochronology

MATTHEW M. WIELICKI* AND T. MARK HARRISON¹

¹Department of Earth and Space Sciences, University of California, Los Angeles, 595 Charles E. Young Drive East, Los Angeles, CA 90095

(*correspondence: mwielicki@gmail.com)

The bombardment history of our planet has major implications for Earth's atmosphere, habitability, near surface conditions, and the delivery of the building blocks of life over its four and a half billion years. Constraining the impact flux to the Earth-Moon system was highlighted by the National Research Council's 2007 report "The Scientific Context for the Exploration of the Moon" as the top priority goal for lunar research. Evidence of the early impact flux has largely been based on interpretations of ⁴⁰Ar-³⁹Ar ages of lunar samples which can be problematic due to the presence of relic clasts, incomplete Ar outgassing, diffusive modification during shock and heating, and exposure to solar wind and cosmic rays [1]. Recent studies [2,3] have utilized zircon from Apollo samples as well as lunar meteorites to better constrain the impact history of the Moon. Sieve textures found in zircon within lunar meteorite SaU 169 have been identified as "poikilitic impact melt zircon formed during equilibrium crystallization of the impact melt" and used to better constrain the age of the Ibridium impact [3]. Such textures had previously not been observed in terrestrial zircon. We report the first terrestrial sieve textures in zircon isolated from Vredefort impactites. Zircons isolated from the granophyre unit show an intimate relationship with pyroxene, similar to that seen in the lunar samples, most likely due to resorption. U-Pb analysis of such grains clearly shows that the zircons have been inherited from the target and are not neo-formed zircon that crystallized from the impact melt and thus should not be used to imply impact events. Pb-loss is highly variable in these samples and the lower intercept age of ~1985±150 Ma agrees well with that of the Vredefort impact [4,5]. Zircon geochronology offers a new tool with which to constrain planetary impact histories however effects on zircon from impact events remain poorly understood and need to be explored terrestrially prior to making interpretations on extraterrestrial samples.

[1] Fernandes *et al.* (2013) *MAPS* **48**, 241-269. [2] Nemchin *et al.* (2008) *GCA* **72**, 668-689. [3] Liu *et al.* (2013) *EPSL* 319-320, 277-286. [4] Kamo *et al.* (1996) *EPSL* **144**, 369-387. [5] Wielicki *et al.* (2012) *EPSL* **321-322**, 20-31

Modeling nanomaterial transport and biouptake in a complex aquatic system: Exploring surface affinity as a predictor of nanoparticle fate

MARK WIESNER^{1,2}, MATHIEU THEREZEIN^{1,2},
FABIENNE SCHWAB^{1,2}, LAUREN BARTON^{1,2},
CHRISTINE HENDREN^{1,2}, GREGORY V. LOWRY^{3,2},
RAJU BADIREDDY^{1,2}, BENJAMIN ESPINASSE^{1,2},
BENJAMIN P. COLMAN^{1,2}, EMILY S. BERNHARDT^{1,2},
JEAN-YVES BOTTERO^{4,2} AND MELANIE AUFFAN^{4,2}

¹Duke University, Durham, NC 27708

²Center for Environmental Implications of Nanotechnology

³Carnegie Mellon University, Pittsburgh, PA 15213

⁴Centre de Recherche et d'Enseignement de Géosciences de l'Environnement, Aix-en-Provence, France

A recent study of silver nanoparticles introduced to a simulated freshwater wetland indicated an initial period of particle removal and associated die-off of some aquatic plants. This talk considers the initial transport and fate of nanoparticles introduced to this system from the standpoint of heteroaggregation, deposition, and dissolution and the implications for short-term impacts on rooted aquatic plants. Simulations show that nanoparticles introduced in a complex, albeit greatly simplified environment exhibit a wide range of behaviors depending on their affinities for each other and their concentrations. The complexity of these interactions appears to be governed by the relative affinity of nanoparticles for each other (autoaggregation) and with background particles (heteroaggregation) and other native surfaces. Surface affinity as a predictor of nanoparticle fate is explored further in the context of interactions with plant surfaces biofilms and the potential for uptake by plants. A functional assay for determining the affinity of nanoparticles for complex mixtures of native particles is evaluated.

The end-Permian mass extinction and its aftermath

PAUL B. WIGNALL

School of Earth and Environment, University of Leeds, UK
(p.wignall@see.leeds.ac.uk)

Our understanding of the timing of the end-Permian mass extinction and subsequent recovery has improved dramatically in the past few years. For long thought to be a protracted affair spread over several million years of the Late Permian, by the 1990s it was re-evaluated as a geologically abrupt crisis. Latest work shows the marine (and probably the terrestrial) extinction to be a two-phased event that straddles the Permian-Triassic boundary whilst the record from higher northern (Boreal) latitudes suggests the extinction phase was somewhat earlier. The ~200 kyr interval between the extinction pulses saw a transient recovery of the benthic fauna. The significance of this improved resolution of extinction timings can be compared with recent advances in both our understanding of ocean redox and sea-surface temperatures at this time. The first pulse of extinction saw the onset of open ocean anoxia but only a transient pulse of low- oxygen conditions whilst the second extinction pulse, in the earliest Triassic, coincides with the long-term establishment of global marine anoxia. The contemporaneous oxygen isotope record of conodont phosphate reveals a rapid temperature rise that persisted long in to the Early Triassic.

The Early Triassic fossil and geochemical record is one of the most extraordinary of the Phanerozoic. Carbon isotope stratigraphy is highly unstable with a series of both positive and negative excursions whilst the oxygen isotope record shows similar instability reflecting major temperature oscillations within an overall exceptionally hot interval. This culminated in the latest Smithian Stage with very light $\delta^{13}\text{C}$ values (~2‰) and $\delta^{18}\text{O}$ values suggestive of equatorial sea-surface temperatures >40°C. The marine invertebrate record is remarkably impoverished for 2 myrs with little in the way of recovery of the benthos whilst nektonic organisms radiated with their usual exuberance. Only after the Late Smithian Thermal Maximum can it be claimed that widespread diversification is underway although not until the Middle Triassic are conditions truly normal in marine and terrestrial habitats.

Experimental study of majorite stability in chromium rich garnets

CH WIJBRANS^{1*}, S KLEMMER¹ AND A ROHRBACH¹

¹Institut für Mineralogie, Universität Münster, Germany,
(*ineke.wijbrans@uni-muenster.de)

Garnet is an important constituent of upper mantle rocks, and is stable over a wide range of pressures. At high pressures (>5GPa), silica is incorporated into the octahedral site in the garnet structure partially replacing aluminium, which results in the so-called majorite component. In mantle rocks, this will cause the pyroxenes to gradually dissolve into garnet with increasing pressure [1]. Majoritic garnets are sometimes found as inclusions in deep diamonds and in mantle peridotites. The silicon content of these garnets is often used to estimate the depth of origin of these samples [2].

In addition to pressure [1], majorite stability is also expected to depend on temperature, composition of the garnet and presence of other Al-bearing phases or melt. For instance, the presence of chromium or ferric iron may decrease majorite stability with increasing pressure. If true, this has implications for the interpretation of the formation depth of diamond inclusions as the Cr/(Cr+Al) ratio is much higher in depleted lithospheric mantle compared to fertile mantle.

To investigate this further, we performed high pressure high temperature experiments in a Walker-type multi anvil press (Bristol design) at pressures between 6 and 14 GPa, and temperatures between 1400 and 1700 °C. Starting materials consist of silicate glasses or oxide mixes in the system $\text{Cr}_2\text{O}_3\text{-CaO-MgO-Al}_2\text{O}_3\text{-SiO}_2$, with varying $\text{Cr}_2\text{O}_3/(\text{Al}_2\text{O}_3+\text{Cr}_2\text{O}_3)$ ratio. Major and minor element concentrations of the phases present were determined by electron microprobe.

All experiments yielded garnet, most contained opx, olivine and (minor) cpx as stable phases. At high temperatures only one pyroxene phase is stable. Preliminary results indicate that for constant pressures and temperatures, the majorite component in garnet decreases with increasing Cr/(Cr+Al) of the bulk composition. However, this effect is most notable at high pressures (>11GPa), at lower pressures this effect is smaller.

[1] Akaogi and Akimoto (1977) *Physics of the Earth and Planetary Interiors* 15, 90-106. [2] Griffin (2008), *Geology* 36, 95-96.

Power stations as a source of atmospheric particulate matter in southern Poland

W. WILCZYŃSKA-MICHALIK^{1*}, R. MORYL¹, B. SUDER¹,
AND M. MICHALIK²

¹Pedagogical University, ul. Podchorążych 2, Kraków, Poland

(*correspondence: wanda.michalik@post.pl),
(renatamoryl@gmail.com; basia_suder@vp.pl)

²Jagiellonian University, ul. Oleandry 2a, Kraków, Poland
(marek.michalik@uj.edu.pl)

High concentration of atmospheric particulate matter in southern Poland is a problem of great meaning. The improvement of this situation needs the recognition of the source of aerosol particles (natural or anthropogenic; local source or long distance transport). Power stations are considered to be an important source of atmospheric pollution in Poland. Changes in fuel used (coal, coal+biomass, biomass) and in combustion technology caused much bigger variability in the composition and morphology of fly ash particles than it was noted in the past when pulverized coal boilers were mainly used. Interpretation of origin of aerosol particles is also more difficult.

Fly ash from coal fired pulverized bed and fluidized bed boilers is similar in chemical composition but mineral composition differs (less mullite and glass in ash from fluidized bed boiler but more coaly irregular particles) as well as morphology of particles. Fly ash from coal and biomass co-combustion in pulverized bed boiler is rich in SiO₂, Al₂O₃, Fe₂O₃, MgO and CaO. Beside quartz, mullite, glass, Fe oxides, Ca, Ca-Mg or Ca-Mg-Fe oxides are present. Aluminosilicate spheres (<1 μm - 50 μm) are accompanied by numerous, usually porous and less regular spheres Ca or Ca-Mg, Ca-Mg-Fe oxides. Fly-ash from fluidized bed boiler fired with biomass is rich in SiO₂ (content of CaO is low; Al₂O₃ very low). Bigger particles are composed of quartz core with reaction rim or of glass, smaller (<1 mm - 10 mm) are represented by glassy spheres or irregular fragments of glassy particles.

Study was supported by NCN grant No. 579/B/P01/2011/40.

Delamination of the North China Craton: A widespread phenomenon or a one-off situation?

S.A. WILDE

Dept. of Applied Geology, Curtin University, Perth, Australia

The North China Craton is widely recognized as the type-example of delamination of an Archean craton and, although it has been extensively investigated over the past decade, many and diverse reasons have been suggested to explain the phenomenon; but with little consensus reached. Although several surface features and the Mesozoic rock record indicate it was operative in the Cretaceous, outstanding issues include: when did delamination/thinning commence; what were the mechanisms involved; was there a link to marginal orogenic belts; was paleo-Pacific plate subduction a controlling factor; and did global tectonic processes play a role? A review of geological data from the Archean to the present-day indicates a number of unique features in the North China Craton that most likely contributed to its 'decratonization' in the Mesozoic [1]. However, were these sufficient to make it a one-off situation or was this process more widespread in the geological past? This has important implications with respect to the preservation of ancient continental crust and thus for models of continental growth. Tomographic studies indicate that other cratonic areas also have thinned lithosphere, but it is uncertain if this, on its own, will ultimately lead to their destruction. Since the thickness of the lithosphere exerts an important control on the deformation of continental blocks when they get dismembered and re-distributed in supercontinent cycles, it is important to identify features that may have resulted from earlier delamination or thinning. Likewise, the fact that certain areas currently involved in collisional events, such as Tibet and Iran, have thickened lithospheres with seismic properties that resemble cratonic areas [2], indicates that 'cratons' may develop by several different mechanisms, perhaps with diagnostic characteristics. Evidence from the North China Craton will be reviewed with respect to the various models proposed to explain delamination/thinning, with the aim of resolving some of the contentious issues and leading toward a consensus.

[1] Yang *et al.* (2008), *Geology* **36**, 467-470; [2] McKenzie & Priestley (2008), *Lithos* **102**, 1-11.

Mobility of inorganic and organic compounds from black shales during unconventional gas production

F.D.H. WILKE^{1,2*}, A. VIETH-HILLEBRAND¹,
R. NAUMANN¹, B. HORSFIELD¹ AND J. ERZINGER^{1,2}

¹GFZ German Research Centre for Geosciences,
Telegrafenberg, 14473 Potsdam, Germany

²University of Potsdam, Department of Earth and
Environmental Sciences, Karl-Liebknecht Str. 24-25,
14467 Potsdam, Germany (*fwilke@gfz-potsdam.de)

Taking into account the envisaged activities of shale gas exploitation and production from black shales in central Europe we see an increasing demand in a quantitative evaluation of possible environmental risks and impacts. For the development of a shale gas play, water is mixed with proppant material (e.g. sand grains) and 0.5 – 1% of additives. Additives, such as acids, biocides, corrosion inhibitors and friction reducers are used to optimize the fracturing job.

Besides of flow-back water a varying amounts of production water will appear at the surface containing various salt compounds, gases, heavy metals, radioactive elements and organics. In order to investigate the mobility of Ca, Fe, S and trace elements such as Co, Cr, Cu, Mn, Mo, Ni, Pb, U, V, Zn and selected organic compounds during hydrofracturing we performed sequential leaching tests with 12 black shales from five locations in Europe and the US. Using five different artificial fracking fluids 24h short-term experiments were carried out at ambient pressure and temperatures of up to 100°C. Two long-term experiments lasting, respectively, 6 and 3 months, respectively, at 100°C / 100bar were performed with selected black shales from Bornholm, Denmark and Lower Saxony, Germany, using a fracking fluid with additives provided by the industry.

We characterized the black shales by XRD, XRF and ICP-MS following HF-HClO₄ dissolution before and after the experiments. Fluids were analysed by ICP-MS, IC, LC-OCD and Gas MS and GC.

The amount of dissolved constituents after the experiment is independent from the pH of the fracking fluid but highly dependent from the element content in the black shale and the buffering capacity of specific components, namely pyrite and carbonates. Shales containing carbonates buffer the solution at pH 7-8. Sulphide minerals (pyrite) become oxidized and generate sulfuric acid (H₂SO₄) leading to a pH of 2-3. Shales containing pyrite but only traces of, or lacking, carbonates give rise to low pH fluids responsible for the much higher concentrations of most dissolved cations (except e.g. Mo, Sr). In each experiment, less than 15% of a certain element contained in the black shale was mobilised into the fluid.

Orogenic Eclogites, Rutile and Trace Element Flux in the Subduction Zone

DARREN J. WILKINSON*, GODFREY FITTON,
AND SIMON L. HARLEY

Grant Institute, The King's Buildings, West Mains Road,
Edinburgh (*correspondance: D.J.Wilkinson@ed.ac.uk)

The geochemical evolution of the continental crust, oceanic crust and mantle is strongly influenced by complex geochemical processes occurring in the subduction zone. However, significant gaps exist in our understanding of these controls on the behaviour of important trace elements. Using orogenic eclogites from the Western Gneiss Region (WGR) of Norway as analogues for subducted oceanic crust, we quantitatively assess the behaviour of many of these elements.

Rare Earth Element (REE) and immobile High Field Strength Element (HFSE) compositions have shown that most Norwegian eclogites have E-MORB to N-MORB protoliths. Using elements thought to be highly immobile (e.g. Nb, Hf), we have estimated the likely total element flux for many more mobile trace elements.

We also assess the role of accessory rutile in controlling HFSE flux from the slab. Nb/Ta as well as Zr/Hf ratios in rutile vary from sub- to superchondritic, yet mean grain compositions appear essentially chondritic (19.9, 34.5 respectively). Whole rock samples reflect this variance on a much larger regional scale, since average ratios for eclogites across the whole WGR are also chondritic. We discuss possible explanations and consequences for heterogeneity in these processes.

The $\epsilon^{182}\text{W}$ isotope composition of the ca. 3920 Ma Acasta Gneiss Complex

M. WILLBOLD^{1,3}, S. J. MOJZSIS² AND T. ELLIOTT³

¹Imperial College London, Earth Science and Engineering, London, SW7 2AZ, United Kingdom; (m.willbold@imperial.ac.uk)

²University of Colorado, Geological Sciences, Boulder, Colorado 80309-0399, USA; mojsis@colorado.edu

³University of Bristol, School of Earth Sciences, Bristol, BS1 8RJ, United Kingdom; (tim.elliott@bristol.ac.uk)

The short-lived ^{182}Hf - ^{182}W decay system ($t_{1/2}$ ca. 9 Myr) is a useful tracer to investigate accretionary and geodynamic processes on the early Earth. Variable enrichments in $^{182}\text{W}/^{184}\text{W}$ – expressed in the conventional $\epsilon^{182}\text{W}$ notation – have been documented in Eoarchean crustal rocks. These data were interpreted by invoking either a ‘Late Veneer’ model [1], or via early Earth differentiation processes ENREF_2 [2]. Here we report the first $\epsilon^{182}\text{W}$ measurements for rocks from the Acasta Gneiss Complex (AGC), a terrane located on the western margin of the Slave craton in the Northwest Territories (Canada). The AGC is the oldest known crustal domain with primary magmatic ages that are about 3,920 Ma [3]. It is also apparent that these rocks inherited a much older (ca. 4,200 Ma) crustal component [4]. Our samples include granitoid gneisses and plagioclase-hornblende schists that define a range in $\epsilon^{182}\text{W}$ values comparable to those found in rocks from the ca. 3,800 Ma Isua Supracrustal Belt in southern West Greenland, which formed the basis of the ‘Late Veneer’ model presented in [1]. Using these new values for the AGC in conjunction with previous data, we test the two models for the W isotopic evolution of bulk silicate Earth in the terminal Hadean. Our results provide new motivation in the search for other daughter products of extinct nuclides (e.g. ^{142}Nd) in the AGC.

[1] Willbold, M. *et al.* *Nature* **477**, 195-198 (2011); [2] Touboul, M. *et al.* *Science* **335**, 1065-1069 (2012); [3] Cates, N.L. *et al.* (in review); [4] Iizuka, T. *et al.* *Geology* **34**, 245-248 (2006).

Archean Mo isotopic evolution: Comparing the Pilbara and the Kapvaal Cratons

M. WILLE¹, F. KURZWEIL¹, S. EROGLU¹
R. SCHOENBERG¹, N. BEUKES
AND M. VAN KRANENDONK³

¹Dept. of Geoscience, University of Tuebingen, Wilhelmstr. 56, 72074 Tuebingen, Germany

²University of Johannesburg, Auckland Park Kingsway Campus, 2006, South Africa

³School of Biological, Earth and Environmental Sciences, University of New South Wales, Kensington, NSW 2052, Australia

The environmental and geochemical circumstances which led to heavy Mo isotopic signatures in Archaean sediments remains elusive. Sufficiently oxidising conditions, which enable mobility of Mo in its highest oxidation state, are generally seen as one precondition for the formation of such an isotopically heavy Mo seawater reservoir. However, interpretation of temporal changes in Mo isotopic compositions stored within ancient sediments is often hampered by the fact that they are strongly influenced by paleo-environmental conditions during sediment formation. As such, sedimentary Mo isotopic signatures different to that of the continental crust are often only qualitative rather than quantitative indicators of changes in environmental redox conditions.

Here we present Mo stable isotope datasets, published and new data, from different 3.46 to 2.5 Ga old sedimentary environments from the Pilbara (Australia) and Kapvaal (South Africa) Cratons, respectively. Mo isotopic results for ≥ 2.76 Ga old sedimentary rocks are within the field of continentally derived detritus, indicating insufficient O_2 levels required to oxidize and mobilize this element. In contrast, Mo isotopic signatures in sediments ≤ 2.7 Ga are isotopically heavier than sedimentary material solely continent derived. Comparing the Pilbara and the Transvaal general trend to heavier Mo isotopic values in Mo isotopic evolution can be seen in both basins approaching 2.5 Ga. These heavier Mo isotopic signatures, in conjunction with the apparent elevated concentrations of other redox sensitive elements, such as U and Re, after 2.7 Ga suggests aquatic mobilization of these elements under sufficient O_2 levels. The comparison of Mo isotopic variations in different contemporary environmental sedimentary setting allows us to ascertain the reasons for the observed Mo isotopic fluctuations.

Temporal evolution of detrital cosmogenic denudation rates in transient landscapes from *in situ*-produced and meteoric ^{10}Be

J.K. WILLENBRING^{1*}; N. M. GASPARINI²,
B.T. CROSBY³, G. BROCARD¹, M.E. OCCHI¹
AND P. BELMONT⁴

¹Department of Earth and Environmental Sciences, University of Pennsylvania, Philadelphia, PA, USA

²Department of Earth and Environmental Sciences, Tulane University, New Orleans, Louisiana, USA

³Department of Geosciences, Idaho State University, Pocatello, Idaho, USA,

⁴Department of Watershed Sciences, Utah State University, Logan, Utah, USA, (*jane.willenbring@sas.upenn.edu)

In equilibrium landscapes, ^{10}Be concentrations within detrital quartz grains are expected to quantitatively reflect basin-wide denudation rates. In transient landscapes, though detrital quartz is derived from both the incising, adjusting lowland and the unadjusted, relict upland, the integrated ^{10}Be concentrations still provide a denudation rate averaged across the two domains. Because field samples using *in situ*-produced ^{10}Be can only provide a snapshot of the current upstream-averaged erosion rate, we employ a numerical landscape evolution model to explore how ^{10}Be derived denudation rates vary over time and space during long-term transient adjustment. Model results suggest that the longitudinal pattern of mean erosion rates is generated by the river's progressive dilution of low-volume, high-concentration detritus from relict uplands by the integration of high-volume, low-concentration detritus from adjusting lowlands. The proportion of these materials in any detrital sample depends on what fraction of the upstream area remains unadjusted.

On shorter timescales, a single storm can induce transience in a landscape. Meteoric ^{10}Be concentrations can be measured in submilligram-sized sediment samples and this attribute enables us to measure suspended sediment through a hydrograph. The meteoric ^{10}Be concentration in river sediment changes with the source areas and fluxes of material supplied to the stream. The average concentration from the couplet of the rising and falling limbs of the hydrograph can differ from the concentration of the sediment that is preserved in depo-centers. Using this short timescale system, we reconsider how to interpret paleoerosion rates from depo-centers derived from meteoric and *in situ*-produced ^{10}Be concentrations.

Temporal Variability of Coastal Rainwater Fe(II) Concentration and Wet Deposition to Surface Seawater

J.D. WILLEY, B.C. RICE, J.J. HUMPHREYS, R.J. KIEBER,
J.R. HELMS, G.B. AVERY AND R.N. MEAD

¹University of North Carolina Wilmington, Department of Chemistry and Biochemistry, Wilmington, NC USA 28403-5932 (*correspondence: willeyj@uncw.edu)

The concentration and stability of dissolved Fe(II) in rainwater collected in Wilmington, North Carolina, USA, have decreased by more than an order of magnitude in the preceding decade. Rainwater Fe(II) during the winter of 2003 was stable for more than 96 hours, whereas in 2011, concentrations decreased by 60% within 4 hours. A decade ago, rainwater Fe(II) was strongly complexed by organic ligands which stabilized it against oxidation. Currently Fe(II) appears to be present in rainwater predominantly as photochemically produced inorganic $\text{Fe}^{2+}(\text{aq})$. Spectral slope data indicates rainwater dissolved organic carbon (DOC) has become less conjugated and smaller in average molecular weight, consistent with less iron complexation. These changes in DOC may result from improved control of automobile emissions. Inorganic $\text{Fe}^{2+}(\text{aq})$ can be rapidly oxidized by H_2O_2 and, in rains with $\text{pH} > 5$ (half of all rains), by O_2 . H_2O_2 has doubled in the last decade due to lower emissions of SO_2 (a sink for H_2O_2), which increases the oxidation rate of $\text{Fe}^{2+}(\text{aq})$ by approximately 30%.

A decade ago, rainwater was a source of soluble Fe(II) to surface seawater, where it is a phytoplankton nutrient. Because of the decreased concentration and stability of Fe(II) in rain, Wilmington NC rainwater is now a much smaller source of soluble Fe(II) to North Atlantic surface seawater, which may reduce primary productivity and hence lower CO_2 uptake in this region.

Iron isotope fingerprinting of mantle mineralogy

HELEN M. WILLIAMS¹ AND MICHAEL BIZIMIS²

¹Dept. Earth Sciences, Durham University, Durham, DH1 3LE, UK; (h.m.williams2@durham.ac.uk)

²Dept. Earth and Ocean Sciences, University of South Carolina, Columbia, SC 29208; (mbizimis@geol.sc.edu)

Mineralogical and lithological variations in the Earth's mantle have important implications for mantle dynamics, magma generation, and the fate of recycled surface material. Directly tracing such variations is challenging. While the elemental and radiogenic isotope compositions of mid oceanic ridge and ocean island basalts (MORB and OIB respectively) are thought to reflect variable amounts of enriched mineralogies within the mantle, in the form of pyroxenite or eclogite derived from oceanic crust or metasomatised lithosphere, directly linking geochemical and mineralogical variation is difficult. Iron (Fe) stable isotopes potentially offer a solution to this problem, as the Fe isotope compositions ($\delta^{57}\text{Fe}$) of mafic rocks primarily reflect mineral-specific partitioning [1, 2]. Here we present Fe isotope data for sub-oceanic lithosphere peridotite and pyroxenite xenoliths from Oahu, Hawaii and demonstrate that Fe isotopes can be used as a new tracer of mantle mineralogical heterogeneity. Pyroxenite $\delta^{57}\text{Fe}$ values are heavy (0.10 to 0.27‰) relative to MORB and OIB ($\delta^{57}\text{Fe} \sim 0.15‰$) [3-6] and reflect isotopic fractionation during magmatic differentiation and pyroxene cumulate formation at the lithosphere-asthenosphere boundary. In contrast, peridotites have light $\delta^{57}\text{Fe}$ values (-0.34 to 0.14‰) that correlate with elemental and radiogenic isotope tracers of melt extraction, providing evidence for Fe isotope fractionation during partial melt extraction and the generation of depleted, low- $\delta^{57}\text{Fe}$ peridotitic residues. The heavy $\delta^{57}\text{Fe}$ values of MORB and OIB relative to mantle peridotites can therefore be explained by partial melting, where isotopically heavy Fe is preferentially concentrated in the melt phase. However, the considerable range in MORB and OIB $\delta^{57}\text{Fe}$ requires a $\delta^{57}\text{Fe}$ -heterogeneous mantle, containing enriched (pyroxenite, heavy $\delta^{57}\text{Fe}$) and depleted peridotite (light $\delta^{57}\text{Fe}$) domains. Iron stable isotopes thus provide a powerful new means of fingerprinting mineralogical variations within the Earth's mantle and identifying depleted and enriched components within the source regions of volcanic rocks.

[1] Weyer & Ionov *EPSL* (2007); [2] Williams *et al.* *EPSL* (2005); [3] Dauphas *et al.* *EPSL* (2009); [4] Teng, *et al.* *Science* (2008) [5] Weyer *et al.* *EPSL* (2005); [6] Teng *et al.* *GCA* (2013).

Analysing conodont $\delta^{18}\text{O}$ by SIMS

I.S. WILLIAMS¹, J.T. TROTTER², M. RIGO³
AND C.R. BARNES⁴

¹Research School of Earth Sciences, Australian National University, Canberra (ian.williams@anu.edu.au)

²School of Earth and Environment, University of Western Australia, Perth ((julie.trotter@uwa.edu.au)

³Department of Geosciences, University of Padova, Padova: (manuel.rigo@unipd.it)

⁴School of Earth and Ocean Sciences, University of Victoria, (Victoria: crbarnes@uvic.ca)

Oxygen isotope compositions of phosphatic conodont microfossils are a more robust indicator of early Paleozoic sea surface temperatures than the O compositions of calcitic brachiopods. SIMS microanalysis allows conodont O compositions to be determined on an $\sim 30 \mu\text{m}$ scale, so the isotopic homogeneity of individual conodont elements and of multiple elements from a single rock sample can be assessed. Analyses can be obtained on very small and/or rare specimens, and targeted on those parts of conodonts that are best preserved. Differences in composition between co-existing species from different biofacies can be measured. SIMS analyses, however, are less precise and more sensitive to differences in the chemical composition of the sample than conventional IRMS analyses. The latter is important because the conodont crown can consist of two tissue types: albid—large ($>100 \mu\text{m}$) crystals containing mostly PO_4 , and hyaline—microcrystals with PO_4 and some CO_3 , and a higher trace element content. Some conodonts also contain poorly mineralised basal tissue that can be isotopically contaminated. In addition, conodont crystal structure can be modified at temperatures above $\sim 100^\circ\text{C}$. No conodont sample is available that is both isotopically uniform and abundant enough to be distributed between SIMS and IRMS labs as an O isotope standard. SIMS measurements are currently referenced to a mineral apatite standard (Durango 3 at ANU), and potential systematic bias is assessed by comparing SIMS and IRMS analyses of large bioapatite samples (e.g. shark enameloid), and of conodonts from the same or closely equivalent rock samples. As part of our study of sea surface temperatures at critical periods of biotic crisis and environmental change in the Paleozoic and Early Mesozoic using conodont O isotopes, we have addressed issues of bias, inter- and intra-conodont heterogeneity, and thermal alteration (as indicated by Colour Alteration Index). In some samples we find O variation within and between elements, but more commonly there is inter- and intra conodont uniformity between genera and species in a single rock sample within the sub-permil precision of the measurements. The rare exceptions have both biological and geological explanations.

Linking fluvial processes and elemental cycling within the Old Rifle, CO aquifer

K.H. WILLIAMS^{1*}, M.J. ROBBINS¹, S.B. YABUSAKI² AND P.E. LONG¹

¹Earth Sciences Division, Lawrence Berkeley National Laboratory, Berkeley, CA 94720, USA, (*correspondence: khwilliams@lbl.gov), (mjrobbins@lbl.gov), (pelong@lbl.gov)

²Pacific Northwest National Laboratory, Richland, WA 99352, USA (yabusaki@pnl.gov)

A successive series of biostimulation experiments within the Old Rifle, CO (USA) aquifer since 2002 have focused on biogeochemical pathways arising from organic carbon injection and its role in mediating the cycling of iron, manganese, sulfur, uranium, vanadium, arsenic, and selenium. While most have concentrated on reductive pathways and their impact on contaminant mobility, recent studies have begun to explore oxidative pathways and their impact on metals dynamics, carbon modification, and the long-term viability of reductive immobilization as a remedial strategy. Insights gained from such experiments have shed light on analogous natural biogeochemical pathways that mediate element cycling in the absence of exogenous carbon amendment. Within the aquifer, such pathways are often seasonal and correlate with excursions in groundwater elevation of 1-2m associated with increased discharge in the Colorado River during spring/summer snowmelt. Imbibition of oxygen bubbles within the capillary fringe associated with such excursions is inferred to be the primary contributor to seasonally oxic groundwater, with its impact on redox-mediated reactions exhibiting close correspondence to intentional introduction of oxidants.

Superimposed upon natural and artificial redox fluctuations are relic signatures of the depositional fabric of alluvial accumulation. Specifically, ferromanganese-encrusted cobbles accumulated as channel fill deposits serve as an effective vector for iron and manganese delivery during incipient accretion of the aquifer materials. Post-depositional redox processes and oxygen incursion associated with groundwater level fluctuations enable redistribution and mineralization of iron and manganese throughout the aquifer, with subsequent implications for carbon and metals transformations. Linking such pathways within the context of a 'porous subsurface bioreactor' constitutes an ambitious yet tractable means for quantifying elemental fluxes at the floodplain and potentially larger scales.

Petrologic implications of magmatic underplating: Observations from the Athabasca granulite terrane

M.L. WILLIAMS^{1*}, S.J. SEAMAN¹ AND G.C. KOTEAS²

¹Dept. of Geosciences, Univ. of Massachusetts, Amherst, MA 01003 (*correspondence: mlw@geo.umass.edu)

²Dept. of Geology, Norwich Univ., Norwich VT

The Chipman mafic dike swarm, Athabasca granulite terrane, Saskatchewan, CA, provides a field example of mafic magmatic intraplating in the deep continental crust. The Chipman dikes were emplaced at 1.0-1.2 GPa (35-40 km) at 1.9 Ga, possibly above a magmatic underplate. The dikes are dominated by Hbl and Pl_a with minor Cpx. Host rocks include the 3Ga Chipman tonalite and 2.6Ga Fehr and Stevenson granites. Several effects of underplating have been documented, including tonalite genesis, granite genesis and contamination, garnet growth, and crustal densification. Only limited melting was induced in the Chipman tonalite during underplating and intraplating. Instead, the mafic dikes themselves were partially melted to Grt + tonalite. Leucosomes occur in strain shadows associated with garnet. Where melting was extensive, individual leucosomes have coalesced and tonalite dikes and veins are common. Within the Fehr granite/gneiss, partial melting was extensive. Leucosome veins, pods, and pools apparently represent the products of several melting reactions, including hydrous modal melting and both biotite and hornblende dehydration melting. Granitic partial melt apparently accumulated in an early (S1) foliation and then was mobilized during formation of a "megacrenulation" into S2. This "pumping" mechanism provides one model for melt segregation in the deep crust. Subsequent Chipman dikes mingled and mixed with the new granitic magma producing a wide range of hybrid compositions. With increasing extent of granite melting, Chipman dikes are more irregular in geometry, apparently trapped by the granite mush. Magmas moving to higher levels probably evolve from mafic to contaminated intermediate and felsic compositions over time. Other granitoids in the region were apparently heated and deformed but not melted during dike emplacement and underplating. One common reaction involves $\text{Opx} + \text{Pl}_a = \text{Grt} + \text{Cpx}$. Extensive Grt production leads to increased density, up to 3.0 g/cm³ even in felsic rocks and may play a role in stabilization and possibly delamination of lower continental crust. Based on the Athabasca example, underplating can initiate a number of positive and negative feedbacks that ultimately result in dramatic and probably irreversible changes in character, rheology, composition of the overlying crust.

Rare Earth Element ore genesis: The Great Unknown

ANTHONY E. WILLIAMS-JONES¹

¹Earth and Planetary Sciences, McGill University, Montreal,
Canada, (anthony.williams-jones@mcgill.ca)

Economic or potentially economic REE deposits are hosted by or genetically associated with alkaline igneous rocks and carbonatites. Primary REE enrichment in silicate magmas depends on the highly incompatible nature of the REE, may be facilitated by fluoride complexation, and occurs at late stages of magma evolution through crystal settling and crystallisation of residual, fluid-saturated liquids including immiscible fluoride melts. Carbonatite magmas likely owe their REE enrichment to the high solubility of the REE, and their preference for the LREE to the similar ionic radii of Ca²⁺ and Ce³⁺; HREE are smaller.

Hydrothermal mobilisation may be essential to the economic viability of many REE deposits. Indeed, the World's largest deposit, Bayan Obo, China, is dominantly hydrothermal. Although aqueous fluoride complexes are widely thought to be the main agent of REE transport, modelling of natural systems suggests that this is not the case. Instead, chloride complexes appear to be responsible for REE transport. Moreover, experiments suggest that REE chloride complexes can cause the observed preferential LREE mobility. Hydrothermal concentration of REE occurs when interaction of acid REE-Cl-bearing fluids with pH-buffering rocks, or mixing with neutral fluids, and/or decreasing temperature, induces REE mineral deposition.

LA-ICPMS²: Laser ablation sampling with combined ICP-Q-MS and MC- ICP-MS detection for simultaneous trace elemental and isotope ratio analyses

JULIAN D. WILLS¹, NICHOLAS LLOYD¹, LOTHAR
ROTTMANN¹, CLAUDIA BOUMAN¹
AND STEVE SHUTTLEWORTH²

¹Thermo Fisher Scientific, Hanna-Kunath-Strasse 11, 28199
Bremen, Germany, (julian.wills@thermofisher.com)

²Photon Machines Inc, USA

In situ analysis by laser ablation offers significant advantages to users in a range of applications including geochronology but interrogating the sample for all of the information required may not be possible in a single measurement. Laser ablation is a destructive sampling technique and while many samples are large enough to allow for multiple analyses on a range of instruments, geochronologically relevant samples are often so small as to preclude multiple analyses. These samples are often unique and once sampled by laser ablation, they are lost and no further information can be extracted.

In this presentation, a system for the simultaneous isotopic and elemental characterization of zircon (ZrSiO₄) is described. A high performance 193nm excimer laser (Photon Machines Analyte G2) is used to sample ~50 μm diameter pits in the zircon, and the He carrier gas containing the entrained sample is split between ICP-Q-MS and MC-ICP-MS systems. A new high performance ICP-Q-MS system (Thermo Scientific iCAP Q) is used for the quantification of trace elements (both transition metals and rare earth elements) and MC-ICP-MS (Thermo Scientific Neptune Plus) is used for high precision Pb and Hf isotope ratio measurements.

The advantages afforded by such combined, simultaneous isotopic and elemental analyses of growth zones of minerals will be highlighted in the presentation

Deep ocean circulation and its link to carbon storage through glacial cycles

D.J. WILSON^{1,2*}, A.M. PIOTROWSKI², A. GALY² AND V.K. BANAKAR³

¹Department of Earth Science and Engineering, Imperial College London, London, SW7 2AZ

(*correspondence: david.wilson1@imperial.ac.uk)

²Department of Earth Sciences, University of Cambridge, Cambridge, CB2 3EQ

³National Institute of Oceanography, Dona Paula, Goa, 403 004, India

Storage of carbon in the deep ocean during glaciation and its release during deglaciation is widely called upon in order to explain glacial-interglacial changes in atmospheric CO₂ [1,2], but the mechanisms involved remain uncertain and the locations of carbon storage are poorly quantified through time. Changes in water mass volumes in the global ocean exert one first order control on carbon storage [3], suggesting a sensitivity of atmospheric CO₂ to reorganisations of ocean circulation. However, modelling studies tend to disagree over the nature and timing of paleoceanographic changes influencing atmospheric CO₂ [4,5].

Better paleoceanographic constraints are therefore required, particularly from the deep Indo-Pacific, which has significant potential for carbon storage during glacial periods. Here we characterise its chemical evolution over the last 250 thousand years using Nd isotopes (ϵ_{Nd}) and benthic carbon isotopes ($\delta^{13}C$) in deep Indian Ocean core SK129-CR2 [6]. The ϵ_{Nd} record indicates a significant glacial reduction in the North Atlantic Deep Water component in Circumpolar Deep Water, consistent with increased oceanic carbon storage [3]. However, the ϵ_{Nd} - $\delta^{13}C$ relationship evolves over the course of each glacial cycle, indicating a changing global distribution of water masses and carbon. During glaciation and early glacial periods, ϵ_{Nd} and $\delta^{13}C$ are decoupled, revealing carbon cycling changes that are independent of Atlantic circulation changes. This decoupling may reflect the processes involved in carbon sequestration in Antarctic Bottom Water at these times. In contrast, coupled ϵ_{Nd} - $\delta^{13}C$ changes during late glacials and deglaciation suggest a close link between deep ocean circulation and carbon release to the atmosphere.

[1] Toggweiler, Russell & Carson (2006), *Paleoceanography* **21**. [2] Sigman, Hain & Haug (2010), *Nature* **466**, 47-55. [3] Skinner (2009), *Clim. Past* **5**, 537-550. [4] Brovkin *et al.* (2007) *Paleoceanography* **22** [5] Hain, Sigman & Haug (2010) *Glob. Biogeochem. Cycle* **24**. [6] Piotrowski *et al.* (2009) *Earth Planet. Sci. Lett.* **285**, 179-189

Co-precipitation of arsenate with calcite – an example from Greece

LENNY H.E. WINKEL^{1,2}, BARBARA CASENTINI³, FABRIZIO BARDELLI⁴, ANDREAS VOEGELIN¹, NIKOLAOS P. NIKOLAIDIS⁵ AND LAURENT CHARLET⁴

¹Eawag: Swiss Federal Institute of Aquatic Science and Technology, Ueberlandstrasse 133, P.O. Box 611, 8600 Duebendorf, Switzerland, lenny.winkel@eawag.ch, andreas.voegelin@eawag.ch

²Swiss Federal Institute of Technology (ETH) Zurich, 8092 Zurich, Switzerland, lwinkel@ethz.ch

³Water Research Institute-National Research Council, Via Salaria, 00015 Monterotondo (RM), Italy, casentini@irsa.cnr.it

⁴Université Joseph Fourier, Grenoble, 1381 rue de la Piscine, 38400 Saint-Martin d'Hères, France, fabrizio.bardelli@gmail.com, charlet38@gmail.com

⁵Technical University of Crete, Polytechniupolis, 73100 Chania, Greece, nikolaos.nikolaidis@enveng.tuc.gr

The uptake of arsenic (As) in calcite may represent an important immobilization process for As in calcareous rocks. Nevertheless, knowledge on this retention mechanism in the natural environment is limited since As incorporation in calcite has mostly been studied on synthetic samples.

We identified very high levels of As (up to 913 mg/kg) in travertine deposits derived from geothermal As-enriched groundwaters on the Greek peninsula Chalkidiki. We analyzed two different types of travertine from this region using both bulk and micro-focused X-ray absorption spectroscopy (XAS and μ -XAS) and micro-focused X-ray fluorescence spectroscopy (μ -XRF) to determine the mechanism of arsenic uptake in the travertines¹. Bulk XAS showed that in all of the studied samples As is present as arsenate (As[V]), and μ -XRF analyses revealed that As is closely associated with the calcite matrix. Iron on the other hand was found to be mainly present as a constituent of clay minerals, of presumably detrital origin, suggesting that Fe-(hydr)oxides were not sufficiently abundant to act as major scavengers for As in the Chalkidiki travertines.

From our results we estimate that the natural travertines could sequester at least 25% of groundwater As(V) via co-precipitation with calcite. The formation of As-enriched calcite is thus an efficient mechanism to immobilize As in the geothermal groundwaters of Chalkidiki and could possibly also occur in other environments characterized by high As and CO₂ contents.

[1] L.H.E. Winkel; B. Casentini; F. Bardelli; A. Voegelin; N.P. Nikolaidis; L. Charlet. *Geochim. Cosmochim. Acta* 2013, 106 99–110.

Role of climatic factors on the terrestrial distribution of selenium

LENNY H.E. WINKEL^{1,2}, BAS VRIENS¹, TIM BLAZINA¹,
RITA SCHUBERT¹, AND C. ANNETTE JOHNSON¹

¹Eawag: Swiss Federal Institute of Aquatic Science and Technology, 8600 Duebendorf, Switzerland, (*correspondence: lenny.winkel@eawag.ch), bas.vriens@eawag.ch, tim.blazina@eawag.ch, rita.schubert@eawag.ch, annette.johnson@eawag.ch

²Swiss Federal Institute of Technology (ETH) Zurich, 8092 Zurich, Switzerland, lwinkel@ethz.ch

Selenium (Se) is of key importance for human health. However, due to the highly uneven global distribution of selenium in agricultural soils, it is estimated that 0.5 to 1 billion people have too low Se intake. As a result Se supplementation and fortification of foods are being increasingly discussed as possible strategies for improving human Se status. Despite observations that the Se distribution in the natural environment is closely related to human health issues and our growing awareness of the importance of this element, the behavior of Se in the natural environment is still poorly understood. It is therefore of major importance to better understand the factors that control this distribution.

The atmosphere is an important transient reservoir for Se, which is largely fed by volatile Se compounds formed via biomethylation in marine and terrestrial environments. In turn, the atmosphere can also function as a source of terrestrial Se when it is returned to the Earth's surface via wet and dry deposition. In this talk we will give new insights into the processes that are relevant to the atmospheric Se reservoir. We will also present new evidence on how climatic conditions play a major role in the large-scale terrestrial Se distribution, both directly as a source of Se (via atmospheric deposition) and indirectly by controlling pedoclimatic regimes and thus Se bioavailability. Therefore, it can be expected that changes in climatic conditions will have a significant impact on the Se distribution in the environment. We will show how climatic factors can be used to predict large-scale terrestrial Se distribution. This will be crucial in helping to understand and prevent future health hazards resulting from the uneven distribution of Se in the environment.

Reconstruction of humid phases in the Caribbean during the Late Pleistocene

SOPHIE WINTERHALDER^{1,2*}, DENIS SCHOLZ¹,
AUGUSTO MANGINI², CHRISTOPH SPÖTL³, THOMAS E.
MILLER⁴, AMOS WINTER⁵, KLAUS PETER JOCHUM⁶
AND JESÚS M. PAJÓN⁷

¹Institute for Geosciences, University of Mainz, J.-J.-Becher-Weg 21, 55128 Mainz, Germany, (*correspondence: sophie.winterhalder@iup.uni-heidelberg.de)

²Institute of Environmental Physics, University of Heidelberg, INF 229, 69120 Heidelberg, Germany,

³Institute of Geology and Palaeontology, University of Innsbruck, Innrain 52, 6020 Innsbruck

⁴Department of Geology, University of Puerto Rico, Mayagüez, PR 00681

⁵Department of Marine Sciences, University of Puerto Rico, Mayagüez, PR 00681

⁶Max Planck Institute for Chemistry, Hahn-Meitner-Weg 1, 55128 Mainz, Germany

⁷National Museum of Natural History, Department of Paleogeography and Paleobiology, La Habana, Cuba

For the Caribbean, high-resolution terrestrial records are mainly available for the Holocene and suggest a linkage to North Atlantic climate variability (e.g. [1]). During the Late Pleistocene climate in the North Atlantic area was also subject to large and rapid changes, which are evident in climate records from Central America as well [2]. We present precise MC-ICP-MS ²³⁰Th/U-dating, together with stable isotope and trace element data from three speleothems from Puerto Rico and Cuba, which grew between 80 and 7 ka BP. Growth phases of Caribbean speleothems are assumed to reflect humid phases in the tropical Atlantic. Stalagmite ENS2 from Puerto Rico grew in several phases (63-61, 40-39, 34-31 and 17-13 ka BP), coinciding with periods of weak East Asian Summer Monsoon recorded in speleothems from China [3]. A large stalagmite from Puerto Rico (Larga1) reveals a variable growth rate between 35 and 17 ka BP. Stalagmite CM from Cuba grew, interrupted by a few short-term hiatuses, between 80 and 7 ka BP. High-resolution multi-proxy (stable isotope and trace element) records from these speleothems are currently in preparation. They will deliver a deeper understanding of climate variability during the Late Pleistocene in the tropical Atlantic region and identify potential teleconnections to the North Atlantic.

[1] Hodell *et al.* (2008). *QSR*. **27**, 1152-1165. [2] Fensterer *et al.* (2012). *The Holocene* **22**, 1405-1412. [3] Wang *et al.* (2001). *Science* **294**, 2345-2348.

H in garnet: Implications for upper mantle H₂O storage capacity

ANTHONY C WITHERS AND MARC M HIRSCHMANN

Dept of Earth Sciences, University of Minnesota, MN, USA

The maximum amount of H₂O that can be stored in mantle minerals without saturation to stabilise a fluid or melt (the H₂O storage capacity) varies as a function of pressure, temperature and peridotite phase assemblage. The systematics of H₂O storage capacity in olivine and pyroxene are relatively well established. The H₂O storage capacity of nominally anhydrous garnet, on the other hand, is poorly understood. Measurements of H in pyropes synthesised in hydrothermal experiments at 1000 °C suggest that the hydrogarnet component becomes destabilised at pressures greater than 7 GPa [1], suggesting that under conditions approaching those of the transition zone, where garnet makes up an appreciable proportion of the mantle, garnet does not contribute significantly to the mantle H₂O storage capacity. Annealing of natural pyrope under similar conditions of P and T, however, suggest that other types of H defect may result in pyrope storage capacities approaching 200 ppm H₂O at 10 GPa [2]. In contrast, H contents in excess of 1000 ppm H₂O were measured in natural, Fe-bearing pyropic garnet that was hydrothermally annealed in the presence of olivine at 1100 °C at pressures up to 9 GPa [3]. If such elevated H₂O storage capacities are applicable to mantle garnet, H₂O fluxed melting of the upper mantle overlying the transition zone would require bulk H₂O concentrations in excess of 600 ppm [4].

We have examined the systematics of H incorporation in pyrope in 24h hydrothermal experiments at 2-8 GPa and 1400 °C. Platinum capsules were loaded with 2 compositional layers such that the upper part of the capsule contained pure pyrope (py) composition and the remainder a mixture of forsterite (fo), enstatite (en) + 5 wt.% Al₂O₃. Buffering of SiO₂ activity by growth of fo and en during experiments was verified by Raman spectroscopy. Grain growth in the py composition layer was facilitated by lack of grain boundary pinning. FTIR spectra of 100-700 μm pyropes from experiments at 4, 6 and 8 GPa all display a characteristic hydrogarnet absorption band. Our preliminary results suggest that H content is close to 235±75 ppm H₂O over this pressure range. At mantle temperatures, it is unlikely that garnet is a major contributor to bulk mantle H₂O storage capacity.

[1] Withers *et al* (1998), *Chem Geol* **147**, 161-171. [2] Lu and Keppler (1997), *Contrib. Mineral. Petrol.* **129**, 35-42. [3] Mookherjee and Karato (2010), *Geophys. Res. Lett.* **37**, L03310. [4] Tenner *et al* (2012), *Contrib Mineral. Petrol.* **163**, 297-316.

Comparison of LDI and ESI to study natural organic matter on the molecular level by FT-ICR mass spectrometry

M. WITT¹

¹Bruker Daltonik GmbH, Bremen, Germany

FT-ICR mass spectrometry of NOM

Fourier Transform ion cyclotron resonance (FT-ICR) mass spectrometry (MS) is a well known method to study natural organic matter (NOM) on the molecular level. Mainly electrospray ionization in negative ion mode is used to detect compounds in this complex mixture. However, also Laser/desorption ionization (LDI) in negative ion mode can be used to study NOM. LDI has been used recently to analyze crude oil by FT-ICR mass spectrometry [1]. LDI has the advantage to be independent of the solvent. Several NOM standards have been analyzed by ESI and LDI for comparison of both ionization techniques. Additionally the effect of collision energy and laser power has been studied.

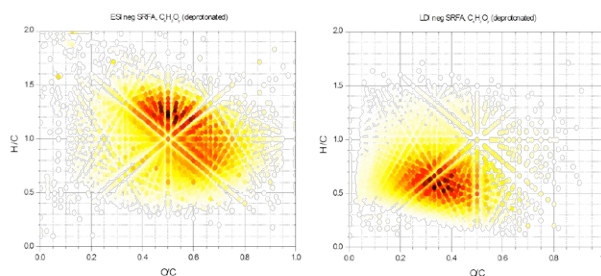


Figure 1: Van Krevelen plots of ESI- and LDI-FT-ICR MS measurement of Suwannee river fulvic acid

Discussion and results

Calculations of the molecular formulas of detected compounds were based on exact mass measurements using ultra-high resolution and high mass accuracy of FT-ICR mass spectrometry. Lower H/C as well as O/C ratios have been observed in LDI than ESI. This effect is shown in the Van Krevelen plots of Suwannee river fulvic acid in Figure 1. Therefore, highly aromatic compounds are ionized using LDI at UV-wavelength of 355 nm.

Collision induced fragmentation results mainly in a loss of CO₂. However, experiments with high laser power results only in a loss of water.

[1] Cho *et al.* (2012) *Anal. Chem.* **84**, 8587-8594.

Determination and comparison of acidic gas ratios at the Stromboli Volcano and Mount Etna obtained by various active alkaline traps

J. WITTMER^{1,*2}, N. BOBROWSKI², M. LIOTTA^{3,4}, G. GIUFFRIDA⁴, S. CALABRESE⁵ AND U. PLATT²

¹University of Bayreuth, Atmospheric Chemistry Research Laboratory, Bayreuth, Germany (*Julian.Wittmer@uni-bayreuth.de)

²University of Heidelberg, Institute of Environmental Physics, Heidelberg, Germany

³Second University of Naples, Dip. DiSTABiF, Caserta, Italy

⁴Istituto Nazionale di Geofisica e Vulcanologia, Palermo, Italy

⁵University of Palermo, Dip. CFTA, Palermo, Italy

Determining volcanic gas composition by direct plume sampling is still challenge in volcanic research. At most volcanoes (e.g. Stromboli volcano, Italy) scientists have to deal with difficult access to the plume, strong atmospheric dilution and varying weather conditions making a high sampling performance necessary.

Besides a more accurate quantification of the main acidic gas compounds (CO₂, SO₂, H₂S, HCl) a reduction of detection limits for less abundant species (HF, HBr, HI) were achieved in this work. For this purpose a Raschig-Tube [1] was modified and utilized for the application on volcanic plumes. The theoretical and experimental absorption properties of the Raschig-Tube (RT) and the Drechsel bottle (DB) [2] set-ups were characterized and afterwards applied simultaneously to the well-established Filter packs technique (FP) in the field (on Stromboli and Mount Etna). The obtained results make a comparison between the set-ups possible and help to point out the potential weakness and strength of each set-up. Additionally, the analytical procedure, including sample preparation, analysis by Titration, Ion Chromatography and Inductively Coupled Plasma Mass Spectrometry, was optimised to accurately quantify molar concentrations of dissolved compounds.

The progress in sampling and analysis led to a significant data set that covers most of the important elements. In particular, less abundant species were quantified more accurately due to the RT technique. Therefore, even iodine could be detected at Stromboli. Besides difficulties to determine fluorine and carbonate, influences of saturation effects on the FP results could be observed and characterized.

[1] Levin *et al.* (1980) *Radiocarbon* **22**, 379-391. [2] Liotta *et al.* (2012) *Geochim. Geophys. Geosyst.*, **13** (5)

Spectroscopic studies of radionuclide adsorption and diffusion

R.A. WOGELIUS^{1*}, A. VAN VEELEN¹, B. ZOU¹, J.R. BARGAR², G.E. BROWN JR.^{2,3}, G. LAW⁴ AND G.W. GRIME⁵

¹Williamson Research Centre, SEAES, Oxford Road, University of Manchester, Manchester M13 9PL, UK (*correspondence:roy.wogelius@manchester.ac.uk)

²Stanford Synchrotron Radiation Lightsource, PO Box 4349, Stanford, California 94309, USA

³School of Earth Sciences, Stanford University, Stanford, California 94305-2115, USA

⁴Centre for Radiochemistry Research, School of Chemistry, University of Manchester, Manchester M13 9PL, UK

⁵Ion Beam Centre, Advanced Technology Institute, University of Surrey, Guildford GU2 7XH, UK

Solute mobility in geochemical fluids depends strongly on both the physical properties of the host lithology as well as mineral surface reactivity. Due to the extremely slow rates of diffusion and the typically dilute concentrations of radionuclides involved in disposal scenarios, constraining physical and chemical processes for use in risk models is challenging. Therefore predictions about the mass transfer of contaminants over time periods pertinent to geological disposal facilities (10⁵ to 10⁶ years) require both reliable measurements of adsorption and robust determinations of diffusive flux. Here we will present results from spectroscopic measurements designed to provide chemical details of the process of surface attachment of key radionuclides (U, Tc, Sr, Cs) to a number of mineral surfaces (magnesite, brucite, portlandite, magnetite, phyllosilicate, K-feldspar, plagioclase feldspar) that will be exposed under a range of repository conditions (pH 6-13, reducing and oxidizing conditions, low and high PCO₂). EXAFS, both standard and polarization dependent, has been used to provide unambiguous information regarding surface adsorbate bonding geometries. Evolution of surface morphology and details of thin films or surface precipitates has been studied using x-ray reflectivity and glancing incidence XRD. Bulk adsorption experiments have also been completed in order to measure mass uptake as a function of concentration. In addition, diffusion through low permeability rock matrices (which include the minerals used in the adsorption studies) has been directly determined via both flow-through (micro-reactor) and *in situ* (Multiple internal reflection-FTIR) experimentation. Direct measurements of contaminant uptake and diffusion length have been completed using proton induced x-ray emission (PIXE) coupled with Rutherford Back-Scattering (RBS).

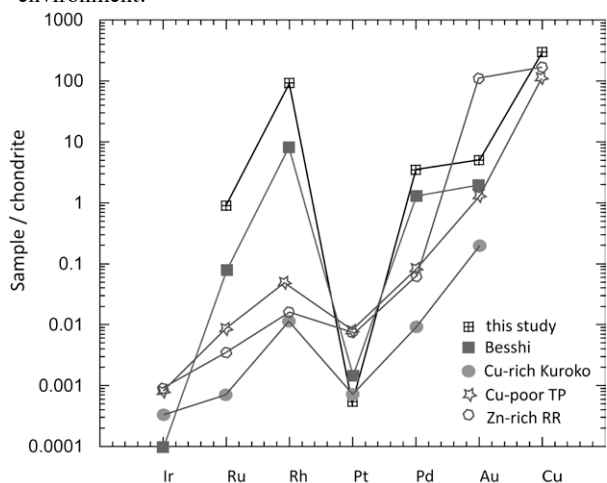
Formation and metamorphism of the Upper Sulfide Zone of the Salt River VMS deposit (South Africa)

CORA C. WOHLGEMUTH-UEBERWASSER^{1,2},
FANUS VILJOEN¹ AND CRAIG R. MCCLUNG¹

¹Paleoproterozoic Mineralization Group (PPM), Department of Mineralogy, University of Johannesburg, South Africa; (cora@geoinventio.de)

²PetroTectonics Centre, Department of Geological Sciences, Stockholm University, Sweden

Sulfides from the upper sulfide zone of the Salt River VMS (South Africa) were analyzed for PGE (platinum group elements), Re, Au, Sb, As, Se, Te, Cr, Co, Ni, Mn, Mo, Ag, Hg and Pb using in-situ LA-ICP-MS (laser ablation-inductively coupled plasma-mass spectrometry) techniques. The analysis of a plethora of trace elements during the ablation of one single spot was possible by using a multi standard approach, involving the analysis of several external standards before, after and between the analysis of unknowns. Chondrite normalized PGE patterns best fit data from Besshi-type deposits, implying the formation within a back-arc basin environment.



This conclusion can be drawn although the Salt River VMS deposit experienced peak amphibolite metamorphism as metamorphism of the deposit was isochemical with respect to the PGE and Au.

Surface topography controls on calcite growth kinetics: From Molecular Dynamics simulations to macroscopic-scale modelling

MARIËTTE WOLTHERS,^{1,2*} DEVIS DI TOMMASO,¹ ZHIMEI DU¹ AND NORA H DE LEEUW^{1,2}

¹Department of Chemistry, University College London, 20 Gordon Street, London WC1 H0AJ, U.K. (* Correspondence: m.wolthers@ucl.ac.uk)

²Department of Earth Sciences-Geochemistry, Utrecht University, P.O. Box 80021, 3508 TA Utrecht, the Netherlands.

Cation dehydration is generally accepted to be the rate-limiting step to ionic crystal growth from aqueous solution. Our classical Molecular Dynamics simulations show a variation in water exchange frequency at structurally distinct calcium sites in the calcite surface of about two orders of magnitude. A process-based calcite growth kinetics model has been re-parameterized, using the water exchange frequencies computed from our molecular dynamics simulations, to represent the attachment frequencies of carbonate and bicarbonate ions. This calcite growth kinetics model illustrates the impact of variations in attachment frequencies on kink-formation frequency (Figure 1), step velocities and bulk growth rate. The calculated frequencies of kink formation show a strong variation with surface structures, which can be amplified further depending on the saturation state and calcium-to-carbonate ratio in the aqueous solution. Modelled and measured step velocities and bulk growth rates are generally in agreement, showing that surface topography might at least partially induce variations in calcite growth rates and step velocities as observed experimentally.

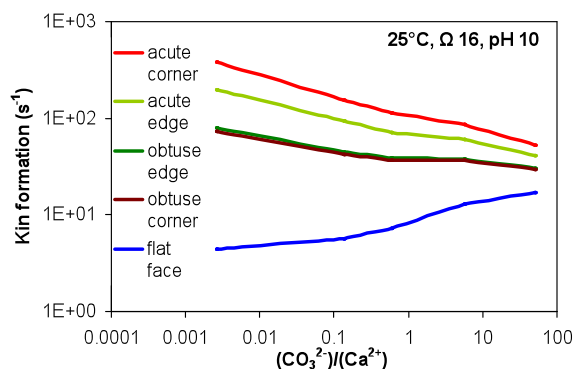


Figure 1: Variation in kink formation frequency with surface topography.

Trace elements in Catanda carbonatitic massif (SW Angola)

WOLKOWICZ STANISŁAW* BOJAKOWSKA IZABELA,
WOLKOWICZ KRYSZYNA, AND SMAKOWSKI TADEUSZ
PGI-NRI, 4 Rakowiecka, 00-975 Warsaw, Poland
(stanislaw.wolkowicz@pgi.gov.pl)

The Catanda carbonatite massif (SW Angola) is built mainly of lapilli and lapilli-ash tuffs, ash tuffs, carbonatites and granulated carbonatites.

The studies covered 43 samples of rocks of the massif. Concentrations of Sc, Y, Li, Ta, Zr, Nb, Th, As, Ba, Co, Cr, Cu, Ga, Hf, Mo, Ni, Pb, Rb, Sr, U, V, Zn and REE were determined by the ICP-MS and ICP-OES methods after dissolving the rocks in aqua regia.

Concentrations of radioactive elements are rather low. U concentrations range from 1 to 20 ppm. Mean levels in tuffs (8.6 ppm) is higher than in lavas (5.9 ppm). Th contents range from 5 to 52 ppm. Mean levels of Th tend to be higher in lavas (30.4 ppm) than in tuffs (28.8 ppm). Nb concentrations range from 14 to 652 ppm, with mean levels equal 383 ppm for tuffs and 285 ppm for lavas. Li contents range from 9 to 55 ppm, attaining 21 ppm at the average. Cr concentrations range from 25 to 161 ppm, being markedly higher in tuffs (49 ppm) than in lavas (33 ppm). Cu contents range from 11 to 356 ppm, being much lower in tuffs than in lavas (29 and 48 ppm at the average, respectively). V concentrations range from 33 to 222 ppm (98 ppm at the average). Zn contents change from 57 to 551 (124 ppm at the average). Ba concentrations change from 250 to 1700 ppm (950 ppm at the average). Sr contents change from 0.08 to 0.54%, with mean levels clearly higher in carbonatite lavas (0.21%) than in tuffs (0.16%). Concentrations of Ga, Hf, Ni, Pb, As and Co are low and poorly differentiated as they appear generally unrelated to petrology. The rocks are also enriched in REE, especially LREE (La, Ce, Pr and Nd). Sum REE contents range from 0.25 to 0.95%. The concentrations were found to be markedly higher in tuffs (avg. 0.33%) than in carbonatite lavas (0.21%).

Carbonatite lavas of the Catanda Massif are characterized by higher mean levels of Cu, Zr, Th and HREE and the tuffs – by higher mean levels of Cr, U, V, Rb, Mo, Zn, Nb, Li and LREE. In turn, concentrations of As, Ba, Ga, Hf, Ni, Pb, Y and Sc appeared not related to the types of rocks of that massif.

Mass-(in)dependent Cd isotope fractionation during evaporation

FRANK WOMBACHER¹ AND MARK REHKÄMPER²

¹ Institut für Geologie und Mineralogie, Universität zu Köln, 50674 Köln, Germany, (fwombach@uni-koeln.de)
² Dept. of Earth Science & Engineering, Imperial College, London SW7 2AZ, UK.

Here, we investigate large mass-dependent (MDF) and very small mass-independent fractionations (MIF) of Cd isotopes that result from the evaporation of liquid Cd into vacuum at 10⁻⁴ mbar and ~180°C [1].

Cadmium stable isotope data were obtained using a Neptune MC-ICP-MS. To resolve small mass-independent anomalies, residual Cd metal samples were analysed at high ion beam intensities typically >20V for ¹¹⁴Cd and long analysis times (30 min.).

MDF in the residual Cd metal samples from vacuum evaporation experiments are well described by Rayleigh distillation with a vapor-residue fractionation factor $\alpha = 0.9900$ for ¹¹⁴Cd/¹¹⁰Cd (i.e. 10.0‰) [1]. The observed fractionation is much less than predicted from kinetic theory ($\alpha_{kin} = (\text{mass } ^{110}\text{Cd} / \text{mass } ^{114}\text{Cd})^{0.5} = 0.9823$; i.e. 17.7‰), a mismatch that is frequently observed, e.g. [2].

The accurate quantification of mass-independent fractionation (MIF) in residual Cd metals required that the large mass-dependent fractionation is accurately corrected. This is facilitated using the generalized power law and normalization to ¹¹⁰Cd/¹¹⁴Cd of the starting material [1]. After correction, deficits ranging from 8 to 28 ppm were well resolved for ¹¹¹Cd/¹¹⁴Cd, ¹¹³Cd/¹¹⁴Cd and ¹¹⁶Cd/¹¹⁴Cd. The observed pattern is in accord with predictions from nuclear charge radii and thus indicate nuclear volume effects [3-6]. The preferential evaporation of ¹¹¹Cd, ¹¹³Cd and ¹¹⁶Cd may result from their more tightly bound 5s electrons and hence weaker metallic bonds in the liquid as previously suggested for Hg [7,8], another group 12 element. The observation of nuclear volume effects thus suggests that (metallic) bonding in the melt results in reduced fractionation factors.

[1] Wombacher *et al.* (2004) *GCA* **68**, 2349–2357. [2] Richter *et al.* (2009) *Chem. Geol.* **258**, 92–103. [3] Bigeleisen (1996) *J. Am. Chem. Soc.* **118**, 3676–3680. [4] Schauble (2007) *GCA* **71**, 2170–2189. [5] Fujii *et al.* (2009) *Chem. Geol.* **267**, 157–163. [6] Rehkämper *et al.* (2011) *Handbook Environ. Isotope Geochem.*, Chap. 8, 125–154. [7] Estrade *et al.* (2009) *GCA* **73**, 2693–2711. [8] Ghosh *et al.* (2013) *Chem. Geol.* **336**, 5–12.

Melts, fluids, crystals, sulphides, metals: Trace element partitioning and geochemical applications

BERNARD J. WOOD

Department of Earth Sciences, University of Oxford, U.K.
(berniew@earth.ox.ac.uk)

First there was Goldschmidt [1], then there was lattice-strain [2], so what else is there to learn about partitioning behaviour? The answer is that we are now getting to the point where the geochemical problems are really interesting. Here are the things I will talk about:

Olivine-liquid partitioning and basalt genesis: Ni partitioning was completely understood long ago [3]. Ni contents of Hawaiian olivines hence seemed to require a pyroxenitic mantle source. New experimental olivine-melt partitioning data indicate however that they can be explained by relatively high temperature of melting of "standard" mantle.

Chalcophile elements in terrestrial and martian basalts: Chalcophile partitioning between sulphide melt and silicate melt is a simple function of the FeO content of the silicate melt. This means we can quantify the influence of residual sulphide on chalcophiles in terrestrial and martian melts. Residual sulphide appears to be critical to basalt generation on Mars.

Crystal-fluid partitioning of trace elements: Although crystal-fluid partitioning is difficult to systematize, applications of the lattice strain approach show that hydrothermal minerals record the compositions of the fluids from which they were generated when corrections for fluid speciation are applied.

The "melt-effect" and trace element partitioning: It is now possible to measure trace element activities in silicate melts using partitioning into metal as a monitor. The data are applicable to determination of melt composition effects on crystal-melt partitioning and other important properties such as volatility.

Metal-silicate partitioning and planetary core formation: We are just getting to grips with the high pressures of core formation on Earth and the effects of the light element in the core on partitioning between core and mantle. For Si, O and S these effects are large for many trace elements.

[1] Goldschmidt, V. M. *Geochemistry*. 730 pp (Clarendon Press, 1954). [2] Blundy, J. D. & Wood, B. J. *Nature* **372**, 452-454 (1994). [3] Hart, S.R. & Davis, K.E. *Earth Planet. Sci. Lett.* **40**, 203-219 (1978)

Temporal evolution of the Raahe-Ladoga Shear Complex, Finland: Constraints from a sheared granitoid in the Pielavesi Shear Zone

J. WOODARD^{1*}, P. TUISKU¹, A. KÄRKI¹ AND H. HUUMA²

¹Department of Geosciences, University of Oulu, FI-90014 Oulu, Finland (*jeremy.woodard@oulu.fi)

²Geological Survey of Finland, P.O. Box 96, FI-02151 Espoo, Finland

The Fennoscandian Shield experienced several stages of brittle - ductile deformation during the Palaeoproterozoic. The Raahe-Ladoga Shear Complex (RLSC) is a ~100 km wide, NW - SE striking set of strongly sheared rocks and intervening crustal blocks in which antecedent structures are preserved. These were formed by long-term and multi-phase Svecofennian convergent tectonic evolution and consist of supracrustal paragneisses and intrusive rocks. The latter are mostly pre- or syn-kinematic granitoids, but distinctly postkinematic granite veins occur in all areas. The Pielavesi Shear Zone (PSZ) in Central Finland is an important shear dominated, N-S striking unit within the RLSC.

At Heinäsuo, in the Pielavesi parish, Central Finland, pre- to syn-kinematic quartz diorite intrudes the PSZ. The quartz diorite has strong N-S foliation, likely developed during or immediately after crystallisation. This intrusion is cut by a late-kinematic, broadly N-S striking blastomylonite. U-(Th)-Pb geochronology of zircon, monazite and titanite are used to place constraints on the timing of deformation and shearing within the PSZ. Samples were collected from both the quartz diorite intrusion and the blastomylonite. Zircons were separated from the quartz diorite using standard gravitational separation methods, while polished chips of the blastomylonite were selected for *in situ* analysis of monazite. These were mounted in epoxy resin and analysed at the NORDSIM laboratory, Swedish Museum of Natural History, Stockholm, Sweden. Titanite was analysed *in situ* from polished thin sections of quartz diorite using LA-ICP-MS at the Geological Survey of Finland, Espoo, Finland.

Zircons have oscillatory zoning patterns in BSE images, characteristic of igneous zircon. Analysis of the zircons resulted in a concordia age of 1884 +/- 6 Ma, providing a magmatic age and constraining an age maximum for deformation in the PSZ. The monazite from the blastomylonite has a concordia age of 1793 +/- 3, placing the brittle - ductile shearing event at ~100 m.y. later. The titanite age, 1780 +/- 23 Ma, also indicates some recrystallisation in the quartz diorite during the late stage shearing event.

The U-Pb in speleothem chronometer: Current progress and future prospects

JON WOODHEAD^{1*} AND ROBYN PICKERING¹

¹School of Earth Sciences, The University of Melbourne, Melbourne, VIC 3010, Australia

The chronology of speleothems by the U-Pb method has reached the point of a robust analytical methodology with enormous, but as yet largely unexploited, potential. A number of applications are beginning to appear relating to climate change, tectonics and human evolution. The next decade will likely see a major expansion of these activities. When coupled with other emerging technologies, the U-Pb chronology of speleothems from selected sites now has the potential to provide novel insights (both palaeotemperature and palaeohumidity) into ancient climate—effectively ‘ancient weather stations’—from around the globe and throughout much of Earth history. Meanwhile studies of included pollens and microscopic animals offer insights into floral/faunal diversity and change through geological time. The ramifications of these many developments will be significant across diverse fields of research, from human evolution, palaeontology and ecosystem development, through studies of weathering and erosion, to the influence of tectonics on landscape evolution.

Some solid solutions involving Fe₄O₅

A.B. WOODLAND¹, K. SCHOLLENBRUCH², M. KOCH³, AND D.J. FROST⁴

¹Inst. Für Geowissenschaften, Universität Frankfurt, 60438 Frankfurt, Germany

²Deutsche Gemmologische Gesellschaft, 55743 Idar-Oberstein, Germany

³Inst. für Geowissenschaften, Universität, Heidelberg, 69120 Heidelberg, Germany

⁴Bayerisches Geoinstitut, Universität Bayreuth, 95440 Bayreuth, Germany

The recently discovered Fe-oxide phase with Fe₄O₅ stoichiometry [1] opens up the potential for this phase being stable in Earth's mantle. This is particularly the case since [2] demonstrated that magnetite breaks down to Fe₄O₅ + Fe₂O₃ at 9-10 GPa over a large range of temperature. Thus it is important to know if this new phase can incorporate other cations and form solid solutions which would expand its stability field in terms of P and T and composition. Experiments have been performed in 3 simple systems: i) Fe₃O₄-Fe₂SiO₄, ii) Fe₃O₄-(Mg,Fe)₂SiO₄, and iii) Fe₃O₄-FeCr₂O₄ over a P-T range of 9-16 GPa and 1100-1300°C.

The Fe₄O₅ phase essentially excludes Si, even when it coexists with stishovite or a Fe³⁺-bearing Fe₂SiO₄-rich spinel. The addition of Mg stabilizes a variety of assemblages in which the Fe₄O₅ phase occurs together with olivine, High-P clinopyroxene, spinelloid V, wadsleyite or ringwoodite. Experiments so far indicate solid solution of up to at least 25 mol % Mg₂Fe₂O₅ component. Molar volumes decrease from 53.76 to 53.55 cm³ mol⁻¹ over this solid solution range. Mg-Fe²⁺ partitioning is such that the Fe₄O₅ phase is the phase richest in Fe in a given assemblage, with $K_d^{\text{phase/Fe4O5}}$ usually <0.14. Cr can also be incorporated in the Fe₄O₅ structure in exchange for Fe³⁺. In the bulk compositions studied, the Fe₄O₅ phase coexists with a spinel and/or a hematite-eskolaite solid solution. Up to 0.92 cats. Cr p.f.u. have been measured so far, implying a Fe₂Cr₂O₅ component of 46 mol %. Molar volumes also decrease with increasing Fe₂Cr₂O₅ content.

[1] Lavina *et al.* (2011) PNAS, **108**, 17281-17285. [2] Woodland *et al.* (2012) Amer Mineral, **97**,1808-1811.

Lead isotope analysis: Removal of ^{204}Hg isobaric interference from ^{204}Pb for U/Pb dating using an (MS/MS capable) ICP-QQQ-MS

GLENN WOODS^{1A} AND JEAN-PIERRE LENER²

¹Agilent Technologies (UK) Ltd. 5500 Lakeside, Cheadle Royal Business Park, Stockport, SK8 3GR United Kingdom

²Agilent Technologies, Avenue des Tropiques, ZA Courtaboeuf 2, BP 12, 91941 Les Ulis, FRANCE

Lead is an element whose isotopic pattern naturally varies more than any other element in the periodic table. The various stable isotopes are derived from uranium and thorium decay ($^{238}\text{U} - ^{206}\text{Pb}$, $^{235}\text{U} - ^{207}\text{Pb}$; $^{232}\text{Th} - ^{208}\text{Pb}$) with the only non-radiogenic isotope being the ^{204}Pb isotope. Lead is an important element for provenance testing (e.g. tracing the origin of an artefact, food product, pollution event etc.) and its isotope analysis has been used in applications as far afield as pollution tracer studies for TEL (tetraethyl lead fuel additive), ore, olive oil & wine origin testing and forensic analysis of bullets.

One of the most important and difficult analyses for lead isotopes is for dating of minerals and Pb containing artefacts. For successful dating, all of the stable isotopes of Pb are required however there is an isobaric overlap from ^{204}Hg on the ^{204}Pb isotope. If any Hg is present in the sample, reagents or as a contaminant in the Ar gas, this would significantly bias the data whether solution or laser analysis is employed.

Removal of the Hg-based isobaric overlap can be achieved by addition of ammonia to a collision-reaction cell (CRC) equipped instrument. Mercury ions undergo rapid charge-transfer reaction in the presence of ammonia (the Hg^+ ion is neutralised to Hg^0 and the charge is passed to the ammonia molecule).

This could lead to the successful removal of Hg isobaric interference from Pb – however the potential issue of new molecular interferences created within the cell remain unless the reaction can be sufficiently controlled by ion pre-selection. This paper demonstrates the benefit of a MS/MS capable ICP-MS for the effective interference-free analysis of lead isotopes.

Increasing spatial resolution of lipid biomarker analysis by LDI FT-ICRMS

L. WÖRMER^{1*}, M. ELVERT¹, J. FUCHSER², J.S. LIPP¹ AND K.-U. HINRICHS¹

¹MARUM and Department of Geosciences, University of Bremen, 28359 Bremen, Germany

²Bruker Daltonik GmbH, 28359 Bremen, Germany

Planktonic archaea and other marine microorganisms are known to adapt their membrane lipids to temperature – a phenomenon exploited in a number of molecular proxies for the reconstruction of past sea surface temperature (SST) from dated sediment cores. One widely applied proxy is the TEX_{86} index [1], which is based on the number of rings in the structure of the archaeal lipid GDGT. Given typical sample sizes and analysis by LC-APCI-MS, such SST records can resolve decadal to millennial variations, dependent on the geological setting examined. Our goal was to combine the temperature proxy potential of lipids in the sedimentological record with the high spatial resolution of laser desorption ionization (LDI) coupled to FT-ICRMS. Micrometer-scale resolution of LDI may produce estimates on sub-decadal to sub-annual scales and potentially provide crucial, previously hidden insights on the heartbeat of past climates.

We demonstrate that LDI FT-ICRMS efficiently ionizes GDGTs and that the high resolving power of FT-ICRMS is crucial for their unequivocal identification. We also observe a strong correlation between TEX_{86} -based SST analysis by LC-APCI-MS and ring distributions obtained by LDI FT-ICRMS, which proves the utility of the proposed method for correctly quantifying the different GDGT species.

We analyzed a several-cm long sediment core segment of Mediterranean Sapropel S1 with a spatial resolution of $200\ \mu\text{m}$, which corresponds to a temporal resolution of about 6 yrs. The observed GDGT distributions are consistent with short-term rhythmic variations of SST with relatively high amplitudes of several °C. Further validation of these trends is ongoing. These first results demonstrate the capacity to obtain a continuous, high resolution profile of GDGTs directly on an intact sediment core, thus setting the stage for lipid-based paleotemperature estimations with unprecedented temporal resolution and suggesting an enormous potential of this approach for future biomarker applications.

[1] Schouten *et al.* (2002), *EPSL* **204**, 265-274.

From zircon date to process rate: Interpreting zircon U-Pb dates in igneous petrology and stratigraphy

JÖRN-FREDERIK WOTZLAW¹ AND URS SCHALTEGGER¹

¹Section of Earth and Environmental Sciences, University of Geneva, CH-1205 Geneva, Switzerland
(joern.wotzlaw@unige.ch; urs.schaltegger@unige.ch)

The precision of single crystal zircon U-Pb dates achievable by isotope dilution thermal ionization mass spectrometry (ID-TIMS) often exceeds our ability to interpret them in the context of magmatic processes. Closing this gap is presently one of the big challenges in high-precision U-Pb geochronology. Recent developments of analytical protocols allowing the analysis of various isotopic ratios and trace element concentrations in tandem with ID-TIMS U-Pb geochronology (e.g., Schoene *et al.*, 2010; Wotzlaw *et al.*, 2013) significantly improved our ability to link the timing of zircon crystallization to specific episodes during the lifetime of a magmatic system. With this contribution, we aim to highlight the potential and limitations of high-precision U-Pb geochronology in petrologic and stratigraphic applications.

We present high-*n* zircon U-Pb datasets of individual eruptive units from large-volume magmatic systems to investigate patterns of zircon crystallization during magma evolution from assembly to eruption. These data-sets display age distributions that point to discrete events of zircon crystallization that can be linked to the thermal evolution of the magmatic systems prior to eruption. When combined with isotopic and chemical information from the same crystals, individual zircons provide snapshots of the chemical and physical state of the magma at the time of zircon crystallization, allowing us to construct time-integrated petrogenetic models. However, in stratigraphic applications, where the desired age information is that of ash bed deposition, the pre-eruptive magmatic history recorded by zircons is a fundamental limiting factor. We use zircon U-Pb dates from ash beds intercalated with astronomically tuned sedimentary sequences in the Mediterranean to test the accuracy of zircon U-Pb derived age models. We evaluate various approaches to estimate ash bed deposition and construct continuous age models employing different fitting algorithms aiming to find a solution to minimize the residual offset between radioisotopic and astronomical time.

[1] Schoene, B., Laskoczy, C., Schaltegger, U., Günther, D., 2010, *Geochimica et Cosmochimica Acta* 74, 7144-7159. [2] Wotzlaw, J.F., Schaltegger, U., Frick, D., Dungan, M., Gerdes, A., Günther, D., 2013, *Geology* (in press).

The research of sulfur early diagenesis cycle driven by AOM and methane-seep environment in the Cold Seep Area, northern South China Sea

DAIDAI WU¹ AND NENGYOU WU²

¹Key Laboratory of Renewable Energy and Gas Hydrate of Guangzhou Institute of Energy Conversion, Chinese Academy of Sciences, Guangzhou 510640, China; (wudd@ms.giec.ac.cn)

²Key Laboratory of Renewable Energy and Gas Hydrate of Guangzhou Institute of Energy Conversion, Chinese Academy of Sciences, Guangzhou 510640, China; (wuny@ms.giec.ac.cn)

Abstract : The South China Sea is located at the junction of three tectonic plates: the Eurasian, the Pacific and the Indian-Australian. The northern continental slope, the South China Sea, is well known for its prospect of oil, gas, gas hydrate resources. Four areas including Taixinan Basin, Northeast Dongsha, Baiyun depression and Qiongdongnan Basin were identified as the most favourable conditions for gas seep or gas hydrate to occur, and were discovered geological, geochemical and biological evidences for cold seeps. In the seabed Cold Seep Area, the sulfate reduction drives by the organic matter oxidation, but mainly drives by anaerobic methane oxidation (AOM). However, the research of AOM-driven sulfate reduction and its important contribution to the sulfur early diagenesis cycle and sulfur buried needs to be studied. In this paper, the sediment cores and cold seep carbonates were collected from the Dongsha and Shenhui Cold Seep Area, northern South China Sea. The main geochemistry characteristics research contains the chemical composition of pore water, the microstructure of sulfates and sulfides authigenic minerals, the distribution and content of intermediate state of sulfur and organic matter sulfide, sulfur and carbon stable isotope fractionation with comprehensive methods such as geochemistry, mineralogy, isotope geochemistry, numerical calculation methods, etc. The target is to identify the sulfate reduction drives by organic matter oxidation or AOM, obtain the proportion of sulfate consumption by AOM in the pore water, the sulfur isotope fractionation characteristics and constraints; establish a sound sulfur cycle path in marine sediment, quantitative assessment the diagenesis burial flux of iron sulfide and sulfate minerals in marine sediments and react the cold seep sedimentary environment characteristics.

Acknowledgments : Funding was provided by the National Natural Science Foundation of China (No. 41003010) and (No. 41273022).

Metasomatic perovskite

FU-YUAN WU*, JING SUN AND CHUAN-ZHOU LIU

Institute of Geology and Geophysics, Chinese Academy of Sciences, Beijing 100029, China,
(wufuyuan@mail.iggcas.ac.cn) (* presenting author),
(sunjing@mail.iggcas.ac.cn),(chzliu@mail.iggcas.ac.cn)

Perovskite is one of the major minerals containing significant amount of U, Th, Sr, Hf and REE, which makes it a suitable mineral for U-Th-Pb dating and Sr-Nd-Hf isotopic analyses by TIMS and in situ techniques[1]. Generally, perovskite is occurred by magmatic crystallization in kimberlitic, kamafugitic, lamproitic, alkaline ultramafic and carbonatitic rocks[2], and rarely in carbonaceous chondrite[3]. Metasomatic perovskite, however, is rarely reported. During this study, metasomatic perovskite from numerous localities were examined for its major, trace elemental compositions, and Sr-Nd isotopic data were used to constrain its petrogenetic history.

The reported metasomatic perovskite includes those from:

1) Mantle peridotite xenolith in kimberlite, South Africa[4]; 2) Rodingite from Changawuzi in Tianshan, China; 3) Skarn formed by contact metamorphism between syenite intrusion and carbonate, Tazheran, Baikal; 4) Chlorite schist formed by dioritic intrusion into limestone in Zlatoust of Urals, Russia, and 5) Chlorite schist probably related to intrusion of the nearby syenite in San Benito of Californian, USA.

Compared with those from kimberlites and alkaline ultramafic intrusions, metasomatic perovskite is relatively stoichiometric with higher amount of Ca and Ti. In terms of trace elements, metasomatic perovskite has variable concentrations of REE, U and Th, but higher concentrations of Zr, Hf and LREE/HREE fractionation, and lower Nb, Ta and Sr.

According to our data, perovskite from Tazheran has the lowest common lead, making it a suitable standard for in situ U-Pb dating. The low Sr concentration makes it impossible to get its Sr isotopic composition using laser ablation. However, most metasomatic perovskites can be determined its Nd isotopic composition by in situ method, except those from San San Benito, which is the most stoichiometric in major elements, and has the lowest REE concentrations.

[1] Yang *et al.* (2009) *Chem. Geol.*, **264**, 24-42. [2] Chakhmouradian and Mitchell (2001) *Can. Mineral.*, **38**, 975-994. [3] Ireland *et al.* (1990) *Earth Planet. Sci. Lett.*, **101**, 379-387. [4] Dawson *et al.* (2001) *Contrib. Mineral. Petrol.*, **140**: 720-733.

Sensitivity of carbonaceous aerosol simulations to aging schemes

SHILIANG WU¹, YAOXIAN HUANG¹,
MANVENDRA DUBEY² AND NANCY FRENCH¹

¹Michigan Technological University, Houghton, MI 49931, USA (slwu@mtu.edu)

²Earth System Observations, Los Alamos National Laboratory, Los Alamos, NM 87545, USA

Carbonaceous aerosols including organic carbon and black carbon have significant implications for both climate and air quality. In the current global climate or chemical transport models, a fixed hydrophobic-to-hydrophilic conversion lifetime for carbonaceous aerosol is generally assumed, which is usually around one day. We have implemented a new detailed aging scheme for carbonaceous aerosols in a chemical transport model (GEOS-Chem) to account for both the chemical oxidation and the physical condensation-coagulation effects, where the aging is affected by local atmospheric environment including atmospheric concentrations of water vapor, ozone, hydroxyl radical and sulfuric acid. The updated conversion lifetime exhibits large spatial and temporal variations with the global average calculated to be 4.3 days. The chemical aging effects are found to be strongest over the tropical regions driven by the low ozone concentrations and high humidity there. The conversion lifetime resulted from chemical aging generally decreases with altitude due to increases in ozone concentration and decreases in humidity. The condensation-coagulation effects are found to be most important for the high-latitude areas, in particular the polar regions, where the τ values are calculated to be up to 15 days. When both the chemical aging and condensation-coagulation effects are considered, the total atmospheric burdens and global average lifetimes of BC (OC) are calculated to increase by 52% (29%) compared to the control simulation. Model evaluation against data from multiple observation networks worldwide shows that the updated aging scheme improves model simulations of carbonaceous aerosols, especially for the remote regions. Further model sensitivity simulations focusing on the continental outflow of carbonaceous aerosols demonstrate that previous studies using the old aging scheme could have significantly underestimated the inter-continental transport of carbonaceous aerosols.

Chemical weathering, atmospheric CO₂ consumption, and the controlling factors of a small silicate watershed in subtropical zone

WEIHUA WU^{1*}, HONGBO ZHENG² AND CHAO LUO¹

¹ Key Laboratory of Surficial Geochemistry, Ministry of Education; School of Earth Sciences and Engineering, Nanjing University, Nanjing 210093, China.

(*correspondence: wuwh@nju.edu.cn)

² School of Geography Science, Nanjing Normal University, Nanjing 210046, China

Hydrochemistry of a small subtropical watershed, the Xishui River draining mainly gneisses and amphibolites is systematically investigated. By collecting samples from source area to river mouth in summer and winter, we discuss temporal and spatial variations of major ion concentrations. An inversion model is used to evaluate different contributions from atmospheric input, anthropogenic activities and rock weathering (silicate, carbonate, and evaporite), and calculate chemical weathering and atmospheric CO₂ consumption rates in the catchment.

The results show: (1) Major ion concentrations in summer are mostly higher than those in winter except for Si, which indicates that influence of intensive weathering, agricultural activities, and acid rain in summer exceeds dilution effect. (2) Contributions from atmospheric input are 13.2 % and 7.8 % in winter and summer, respectively. Anthropogenic activities provide only 2.4 % and 4.2 % major ions to the Xishui River, which has a slight influence on the hydrochemistry. Contributions from silicate weathering are 52.1 % and 48.7 %, and carbonate weathering are 28.4 % and 24.2 %. Therefore, though area of carbonate rocks only accounts for < 5 % of the drainage area, it has an important contribution to major cations in the Xishui River. Contributions from evaporite are 3.8 % and 15.1 % in winter and summer, indicating that influence of temperature on evaporite dissolution is more noticeable. (3) Silicate weathering rates are 0.64–4.44 t/km²y and 4.1–21.2 t/km²y in winter and summer, respectively. The atmospheric CO₂ consumption rates resulted from silicate weathering are 0.31–2.1×10⁵ mol/km²y and 1.94–10.2×10⁵ mol/km²y in winter and summer. The rates in the Xishui River are remarkably lower than those in small watersheds which had higher temperature and rainfall in tropical zone, and are higher than those in small watersheds had similar rainfall but lower temperature in central Europe and eastern France, indicating that temperature may be the most important factor influenced the chemical weathering rates in silicate watersheds.

Physiology, mineralogy and Fe isotope fractionation of Fe(II) oxidation by a marine photoferrotroph - Implications for the deposition of Precambrian BIFs

WENFANG WU^{1,2}, ELIZABETH D. SWANNER², YONGXIN PAN¹, RONNY SCHOENBERG² AND ANDREAS KAPPLER²

¹Institute of Geology and Geophysics, Chinese Academy of Sciences, Beijing, China, wuwenfang@mail.iggcas.ac.cn

²Department of Geoscience, University of Tuebingen, Germany

Anoxygenic photoferrotrophs are capable of photosynthetic Fe(II) oxidation in the absence of oxygen. Because of this ability they were suggested to be involved in the precipitation of oxidized iron minerals in Banded Iron Formations (BIFs) prior to the presence of significant amounts of O₂ on Earth. Although photoferrotrophs are thought to be important for Fe(II) oxidation in ancient oceans, previous studies related to BIFs have focused on freshwater strains [1]. However, marine geochemistry differs from freshwater probably strongly affecting anoxygenic Fe(II) oxidation and consequently the mineralogy and Fe isotope composition of the Fe(III) minerals produced. In this study we therefore quantified cell growth, Fe(II) oxidation rates, Fe isotope fractionation and mineralogy of Fe(III) precipitates during Fe(II) oxidation by the marine photoferrotroph *Rhodovulum iodolum*. We found that the maximum Fe(II) oxidation rate was slower than determined for the freshwater strains. The crystalline Fe(III) oxyhydroxides goethite and lepidocrocite were produced in contrast to the poorly crystalline ferrihydrite that is typically produced by the freshwater strains. During Fe(II) oxidation, the Fe(III) precipitate enriches in the heavier Fe isotopes while the aqueous Fe(II) becomes lighter, consistent with the trend observed for freshwater strains but with a significantly smaller fractionation factor than determined for the freshwater strain *Thiodictyon* F4 [2]. Our experiments demonstrate that anoxygenic phototrophic Fe(II) oxidation shows distinct differences in marine settings compared to experiments done under freshwater conditions and will ultimately allow us to better understand their role in the deposition of oxidized Fe minerals in Precambrian Banded Iron Formations.

[1] Hegler *et al.* (2008) *FEMS Microbiol. Ecol.* **66**: 250-260.

[2] Croal *et al.* (2004) *Geochim. Cosmochim. Acta* **68**: 1227-1242.

Pristane isomerization ratio: Novel maturity index for highly mature and overmature oils

YINGQIN WU^{1,2}, YONGLI WANG^{1*}, TIANZHU LEI¹,
SUPING MA¹, YOUXIAO WANG¹, YUAN GAO¹ AND
YANQING XIA^{1*}

¹Key Laboratory of Petroleum Resources Research, Institute of Geology and Geophysics, Chinese Academy of Science, Lanzhou 730000, China
(wuyingqin001@163.com) (*correspondence: yqxia@lzb.ac.cn, wyl16800@163.com)

²Graduate School of the Chinese Academy of Sciences, Beijing 100049, China

Thermal maturity is an important parameter in assessing petroleum evolution in sedimentary basins. However, the maturity parameters based on biomarkers cannot be applied to highly mature oils ($R_o > 1.5\%$), especially to overmature oils ($R_o > 2.0\%$) (e.g. the sterane and terpane isomerization ratios, methyl phenanthrene index and methyl diamantane index). The reason is that these ratios reach their equilibrium values before or at the onset of the “oil window”. Therefore, the peak hydrocarbon generation stage cannot be assessed using these parameters, particularly for highly mature and overmature crude oils.

In this experiment, pristane isomers were identified in extracts from the coal samples of Junggar Basin, China. From brown coal to subbituminous coal, corresponding to R_o 0.36–2.99 %, the PIR [pristane isomerization ratio = $\{ [6(R)10(R) + 6(S)10(S)] / 6(R)10(S) \}$] ranges from 42 to 97% for the coal extracts. The value of PIR, a molecular maturity parameter, is evaluated by analyzing a series of samples from the Junggar Basin with known values of the molecular maturity parameter based on the sterane and hopane isomerization and methyl phenanthrene index. Changes in the PIR in these highly mature Ai-13 ($R_o > 1.5\%$) and overmature Ha-01 and Ha-02 ($R_o > 2.0\%$) are still obvious and with linear correlation between PIR and R_o . As a result, our results suggest that the PIR is an appropriate indicator of maturity for the highly mature and overmature oils and sediments.

It is clear that the PIR increases with the increasing of R_o , which possibly suggests an isomerization of RS isomer into the RR and/or SS isomer.

In summary, the PIR may be potential interest as it can efficiently be used in measuring the maturity of highly mature oils, sediments and may work throughout the “oil window”. However, the same case may be expected to take place in other molecular parameters, but the current work does not observe the dependence of the PIR on the kerogen type. It is necessary to make further investigation and collect data of the PIR from other samples (elsewhere) in order to attain better results of the present study.

Supported by grants No. XDB03020405, 2012CB214701, NSFC No. 41272147, 41172169, 40672123 and TPR-2012-18.

Elasticity of ferropericlase at lower mantle conditions

ZHONGQING WU^{1,2}, JOÃO F. JUSTO,^{1,3}
AND RENATA M. WENTZCOVITCH¹

¹Department of Chemical Engineering and Materials Science, University of Minnesota, Minneapolis, MN 55455

²Laboratory of Seismology and Physics of Earth's Interior, School of Earth and Space Sciences, University of Science and Technology of China, Hefei, Anhui 230026, China

³Escola Politécnica, Universidade de São Paulo, CP 61548, CEP 05424-970, São Paulo, SP, Brazil

Clarification of the effect of the iron spin state change on properties of Fp is important to address the relative abundance of Fp in the lower mantle. However, recent works addressing this question have reached different conclusions. The calculated density of a pyrolite aggregate with spin crossover-related change in iron partitioning compared well with the density in PREM up to 45 GPa [1]. In contrast, Murakami *et al.*'s analysis of V_s in aggregates with variable amounts of Fp concluded that the lower mantle is more perovskitic than pyrolitic [2].

We investigated the thermoelasticity of Fp by first principles using the DFT+U functional. The calculated thermoelastic coefficients are consistent with available experimental data on samples with various iron concentrations. Results help us to understand some discrepancies among different experimental data sets regarding the shear modulus softening [3,4]. We predict velocities of Fp at lower mantle conditions and suggest that pyrolite is a reasonable compositional model for the lower mantle. Our results show the importance of constraining the elastic properties of minerals without extrapolations for analyses of the thermochemical state of this region.

[1] Irifune *et al. Science* **327**, 193 (2010). [2] Murakami *et al. Nature* **485**, 90 (2012). [3] Crowhurst *et al. Science* **319**, 451 (2008). [4] Marquardt *et al. Science* **324**, 224 (2009).

Anaerobic activity of nitrite-oxidizing microorganisms affects the $\delta^{18}\text{O}$ of dissolved nitrate during microbial denitrification

ANJA WUNDERLICH^{1,2*}, RAINER U. MECKENSTOCK¹ AND FLORIAN EINSIEDL²

¹ Institute of Groundwater Ecology, Helmholtz Center Munich, Ingolstädter Landstraße 1, Neuherberg, Germany (anja.wunderlich@tum.de)

² Technische Universität München, Chair of Hydrogeology, Arcisstrasse 21, Munich, Germany

The stable isotopes of nitrate in water are frequently used to assess denitrification and sources of nitrate in the environment. It was previously assumed for terrestrial environments that a relative increase in $\delta^{18}\text{O}$ of nitrate compared to its $\delta^{15}\text{N}$ of 0.5 is indicative of denitrification.

We anaerobically incubated sediments with natural microbial populations from 3 different anoxic habitats and a pure culture of the nitrite oxidizing bacterium *Nitrobacter vulgaris* in strongly ^{18}O -labeled water with nitrate and adequate electron donors. A significant influence of $\delta^{18}\text{O}$ of water on the $\delta^{18}\text{O}$ of nitrate was found in all experiments. All incubations clearly expressed microbial denitrification. Given oxic conditions, the microbial populations of all incubations were also able to oxidize nitrite. We thus assume the presence of nitrite oxidizing microorganisms in all incubations. As nitrite oxidizers may catalyze the observed isotopic shift in pure cultures, they are likely also the driving parameter of the observed shift in the environmental incubations. This shift questions the stability of predicted $\Delta\delta^{18}\text{O}/\Delta\delta^{15}\text{N}$ ratios in the environment during denitrification. Such a shift in $\delta^{18}\text{O}$ of nitrate under anoxic conditions also questions the validity of nitrate source determination by 2D isotopic fingerprinting, specifically in respect to the $\delta^{18}\text{O}$ axis.

Nitrite oxidizing microorganisms possess a nitrite oxidoreductase enzyme (NXR) which is able to oxidize nitrite as well as reduce nitrate, depending on the redox conditions. Regular denitrifiers possess a nitrate reductase (Nar) which only reduces nitrate irreversibly. We hypothesize that the nitrate reduction reaction at the NXR enzyme by nitrite oxidizing microorganisms is reversible even under anoxic conditions, allowing the incorporation of oxygen-atoms from water into nitrate.



It is likely that a variable activity of nitrite oxidizers in anoxic environments produces a variable shift of $\delta^{18}\text{O}$ of nitrate towards $\delta^{18}\text{O}$ of ambient water and thus varied ratios of $\Delta\delta^{18}\text{O}/\Delta\delta^{15}\text{N}$.

Geochemical impacts of carbon dioxide leakage into carbonate aquifer rocks

ASSAF WUNCH¹, ALEXIS SITCHLER², JOEL MOORE³ AND JOHN E. MCCRAY⁴

¹Hydrologic Science and Engineering Program, Colorado School of Mines, Golden CO 80401, awunsch@mines.edu

² Geology and Geological Engineering Department, Colorado School of Mines, Golden CO 80401, asitchle@mines.edu

³Department of Physics, Astronomy and Geosciences, Towson University, Towson MD 21252, (moore@towson.edu)

⁴ Civil and Environmental Engineering Department, Colorado School of Mines, Golden CO 80401, jmccray@mines.edu

Leakage of CO_2 during geological carbon sequestration can prevent meeting environmental and storage goals. A significant environmental concern is acidification of groundwater with a potential subsequent increase in aqueous metal concentrations due to mineral dissolution and desorption. Even though carbonate aquifers supply about 20% of drinking water worldwide, these aquifers are somewhat neglected in the CO_2 sequestration literature, because carbonate minerals are presumed to buffer pH increases. The common carbonate minerals (calcite, dolomite) are rarely found in pure form in nature, and typically contain metal impurities. Dissolution of these minerals is very sensitive to pH changes, and we hypothesized that metals could be released during carbonate dissolution. Previous studies usually point to sulfide minerals as likely sources of toxic metals. Pressurized experiments containing natural carbonate rocks at elevated CO_2 pressures resulted in elevated aqueous concentrations of Mn, Ni, As, Cr, Sr, Ba, Co, Mo and Tl, with few elements rising above U.S. regulatory limits. Geochemical modeling (constrained by our experimental results) suggest that carbonate minerals may be the dominant contributors to metal release in a carbonate aquifers, not pyrite. Consequently, models that ignore co-release of metals from carbonates may underpredict metal release. However, geochemical modeling also demonstrates that pyrite may be an important source of metals under oxidizing conditions, and that the influence of O_2 partial pressures is equally important that of CO_2 .

Microbial metabolic processes in the deep subsurface - impact on geological energy storage

HILKE WÜRDEMANN^{1*}, DARIA MOROZOVA¹, STEPHANIE LERM¹, ANKE WESTPHAL, MONIKA KASINA¹ LINDA PELLIZZARI¹, HANANAH HALM¹ AND DOMINIK NEUMANN¹

¹Helmholtz Centre Potsdam, GFZ German Research Centre for Geosciences, 14473 Potsdam, Germany

Enhanced process understanding of engineered reservoirs is a prerequisite to optimize the operation of geological storage, to increase the reliability as well as to assess the risks involved. Since microorganisms are very effective geochemical catalysts and their contribution to the mineral alteration and dissolution needs to be investigated.

The microbial diversity of a different reservoirs in the North German Basin, the Upper Rhine Graben, the Molasse Basin and the Styrian Basin was analysed with molecular biological and geochemical methods. Interactions of microbial activity with the geotechnical use of the reservoirs were studied in a pilot plant for CO₂ storage, in bypass systems of a geothermal heat store and in long-term laboratory experiments with rock cores and reservoir fluids. Genetic fingerprinting analyses revealed distinct microbial communities in fluids depending on the temperature, the salinity and the availability of electron donors like organic substances or hydrogen. Cell counting and quantification of 16S rRNA genes and dissimilatory sulfite reductase (*dsrA*) genes by real-time PCR proved different population sizes in fluids, showing higher abundance of Bacteria and sulfate reducing bacteria (SRB) in systems influenced by corrosion. SRB were accounted for corrosion damage and iron sulfide precipitates in the near wellbore area that affected plant reliability adversely.

Geoneutrino detection in the future low-energy neutrino observatory LENA

MICHAEL WURM

Eberhard Karls Universität Tübingen, 72076 Tübingen, Germany

The next-generation liquid-scintillator detector LENA (Low Energy Neutrino Astronomy) will be a versatile tool for the study of low-energy neutrino fluxes. Following up on the first successful measurements of geoneutrinos by the KamLAND and Borexino experiments, LENA is aiming at a high-statistics measurement of the geoneutrino flux above 1.8 MeV. Like its predecessors, LENA will profit from the low energy threshold and the excellent background discrimination capabilities of the liquid scintillator technique, but above all from its in comparison considerably larger target mass of 50 kiloton.

For the preferred experimental site, the Pyhäsalmi mine in central Finland, we expect about 1000 inverse beta decay events per year. Far from the majority of nuclear power plants, the expected geoneutrino signal to reactor neutrino background ratio at this site is of the order of 2:1. Based on the predicted event rate and 10 years of exposure, the geoneutrino flux could be determined at 1% level. This will open the door for a precise determination of the radiogenic contribution to the terrestrial heat flow and the discrimination of geological models. Moreover, the detected geoneutrino spectrum can be evaluated to determine the relative contributions of beta-decays from the uranium and thorium decay chains to the overall neutrino flux. After 10 years, an accuracy of 5% could be reached for the U/Th ratio, thereby reaching a level of precision relevant for the study of terrestrial models.

The volatile content of Mount Etna magma: An FTIR and Raman study of glassy melt inclusions

ROBIN WYLIE

University College London, London WC1E 6BT
(correspondence: r.wylie.11@ucl.ac.uk)

The 1983 eruption of Mount Etna

Mount Etna volcano, Sicily, is amongst the highest emitters of volcanic carbon dioxide worldwide, however the origin of this prolific output is still debated. As such, characterising the occurrence of CO₂ in Mount Etna magmas has important implications for our understanding of deep Earth degassing.

Lavas from the 1983 eruption of Mount Etna have been found to contain native carbon, in the form of graphite and diamond [Adrian Jones, pers. comm.]. This unprecedented observation suggests that this, so far little-studied eruption, may have sampled an unusually deep source of carbon beneath Etna. These lavas therefore represent an ideal target for the further characterisation of the carbon output of this volcano.

By the time they are erupted, lavas are heavily depleted in CO₂, as it begins to degas at large depths within the volcanic system. Melt inclusions are small pockets of magma which become trapped within crystals growing within a magma body, and – as they are isolated from the effects of degassing – can preserve the early volatile composition of magmas. Importantly, the analysis of H₂O together with CO₂ allows the trapping depth of these inclusions to be estimated.

Work plan

Glassy melt inclusions, hosted within olivine phenocrysts from lavas of the 1983 Etna eruption, will be analysed using FTIR (Fourier Transform Infra Red) Spectroscopy, and Raman microscopy, in order to determine the concentrations of dissolved CO₂ and H₂O, respectively, in the glasses. Using the Raman method, the presence of H₂O has already been verified in the inclusions (fig. 1), and FTIR analysis will be performed on the same samples, starting in April 2013.

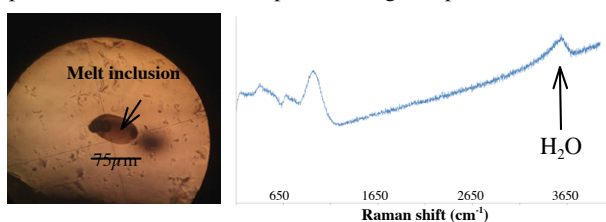


Fig. 1. Left: Sample prepared melt inclusion within its olivine host crystal; Right: Raman microprobe spectrum of the same inclusion, which shows a prominent OH peak indicating the presence of dissolved H₂O.

Seasonal distinction of hydrological variability in speleothem calcite

WYNN, P.M.^{1*} FAIRCHILD, I.J.² SPÖTL, C.³ HARTLAND, A.⁴ MATTEY, D.⁵ COTTE, AND M⁶. FAYARD, B.^{6,7}

¹Lancaster University, Lancaster, UK. (*correspondance p.wynn@lancaster.ac.uk)

²University of Birmingham, Birmingham, UK (fairchij@bham.ac.uk)

³Leopold-Franzens-Universität Innsbruck, Innsbruck, AT. (christoph.spoetl@uibk.ac.at)

⁴University of Waikato, Hamilton, New Zealand. (ahrtland@waikato.ac.nz)

⁵Royal Holloway University of London, UK (mattey@es.rhul.ac.uk)

⁶European Synchrotron Radiation Facility, Grenoble, FR (marine.cotte@esrf.fr)

⁷Université Paris-Sud, F-91405, FR (fayard@lps.u-psud.fr)

Speleothem chemical records have been employed in the reconstruction of environmental change on a broad range of timescales. Whilst sub-annual records are scarce, it is here that one of the research frontiers resides, providing a modern calibration between speleothem proxy and meteorological conditions. Here, we use Synchrotron μ XRF spectrometry at ID21, ESRF, to reveal trace element patterns of Zn, Pb and S within speleothem calcite over three annual cycles. In this way, archived signals are calibrated to modes of trace element incorporation and meteorological conditions. Concentrations of Zn and Pb in speleothem Obi84 show in-phase cyclicity and are attributed to transport in complexes with natural organic matter (NOM) originating from the soil/epikarst above the cave. Peak fluorescent laminae occur on an annual basis, although banding of lower fluorescence intensity reveals multiple events at the sub-annual scale. Meteorological data reveals the delivery of NOM-metal complexes to the speleothem is dependent upon water excess, snowpack condition, and soil microbiological activity. Sulphur demonstrated annual cyclicity, with minimum and maximum concentrations coinciding with winter and summer respectively, dependent upon internal cave atmospheric conditions and the pH value to which cave drip waters degas. At the current resolution of analysis, this represents some of the first evidence linking event-based meteorological records to the trace element content of speleothem calcite and is the initial phase of work which aims at developing records of seasonal infiltration patterns and cave ventilation dynamics, building towards proxy records of winter duration and seasonal infiltration patterns as indices of climatic change.

***In situ* determination of REE in clinopyroxene from syenites**

IRENA WYSOCKA¹ AND EWA KRZEMINSKA¹

¹Polish Geological Institute-National Research Institute, 00-975 Warszawa, 4 Rakowiecka, Poland
(irena.wysocka@pgi.gov.pl);(wa.krzeminska@pgi.gov.pl)

Laser ablation inductively coupled plasma mass spectrometry (LA-ICP-MS) has become widely used method for the geological applications. In this work, the distribution of rare earth elements (REEs) in clinopyroxene (cpx) was studied. Cpx is significant mineral phase in foid syenite to syenite, which are late differentiates of alkaline-ultramafic Carboniferous igneous suite of Tajno and Ełk (Poland). The analyses were restricted to the phenocrysts with about 400 - 500 μm width, chemically classified as a diopside and eagirine augite.

Determination of the trace element concentrations in cpx were performed by laser ablation system LSX-500 (UV Nd:YAG 266 nm, Cetac) connected to the quadruple mass spectrometer (Elan DRC II, Perkin Elmer Sciex). The ablation conditions (spot diameter, energy and pulse rate) were optimised separately for the rocks and the thin sections.

The applied spot size was 50 or 100 μm . Cpxs were analysed for REE and trace element content using frequency of 10 Hz or 5 Hz. The measurements were carried out *in-situ* in the polished rocks and in thin sections (thickness of $\sim 100\text{-}120 \mu\text{m}$). The same thin sections and polished rock samples of each syenite were also imaged by BSE and analyzed by WDS Cameca SX100 electron microprobe at the aim of the determination of the main chemical components. The synthetic silicate certified reference materials NIST 610 and NIST 612 were used for method calibration and BIR-1, BCR-2 and BHVO-2 were used for the verification of the obtained results. Different element oxides were applied as the internal standards and the results were compared.

Based on the performed analyses we have concluded that:

- 1) LA-ICP-MS is appropriate method for *in-situ* measurements in the polished rocks and in thin sections of minerals and results are comparable;
- 2) the pronounced differences in REE content in cpx of different origin were observed;
- 3) the variation of the REE contents in cpx phenocrysts from alkali silicate host rocks may reflect slightly different melt evolution paths of the complexes with (Tajno syenite) and without associated carbonatites (Ełk syenite).

Automated γ -ray spectrometer for monitoring wastes made by non-nuclear industries

XHIXHA G.¹, BEZZON G.P.¹, BROGGINI C.², BUSO G.P.¹, CACIOLLI A.², CALLEGARI I.³, COLONNA T.³, FIORENTINI G.¹, GUASTALDI E.³, KAÇELI XHIXHA M.⁴, MANTOVANI F.⁵, MASSA G.³, MENEGAZZO R.², MOU L.¹
ROSSI ALVAREZ AND C.² AND STRATI V.⁵

¹Legnaro National Laboratory (LNL-INFN), Via dell'Università, 2 - 35020 Legnaro, Padova, Italy – (xhixha@fe.infn.it)

²Padova Section INFN, Via Marzolo 8 - 35131 Padova, Italy – (carlo.broggini@pd.infn.it)

³CGT Center for GeoTechnologies, University of Siena, Via Vetri Vecchi, 34 - 52027 S. Giovanni Valdarno, Italy – (ocallegari@unisi.it)

⁴University of Sassari, Botanical, Ecological and Geological Sciences Department, Piazza Università 21- 07100 Sassari, Italy – (mxhixha@fe.infn.it)

⁵University of Ferrara, Physics Department, Via Saragat, 1 - 44100 Ferrara, Italy – (mantovani@fe.infn.it)

The huge amount of naturally occurring radioactive material (NORM) worldwide generated shows a high level of complexity for disposal purposes because of the high variability of radioactivity enrichment, therefore a case-by-case control is required. We developed a fully automated high-resolution gamma-ray spectrometer, called MCA_Rad system [1], which offers a suitable measurement technique for monitoring huge amounts of NORM. Two coupled HPGe detectors p-type with 60% relative efficiency are accurately shielded allowing to reach an environmental background reduction of two orders of magnitude. Through fully automation of operational processes up to 24 samples can be measured without any human attendance. The absolute efficiency of the MCA_Rad system is estimated by using two point sources, ¹⁵²Eu and a ⁵⁶Co and validated at 5% of relative uncertainty by measuring certified reference materials.

[1] G. Xhixha *et al.*, 2013 J Radioanal Nucl Chem 295:445–457. doi: 10.1007/s10967-012-1791-1

Study on sulfur isotopic composition of acid rain in Nanchang City, China

F. XIA¹, J-Y. PAN¹, S-H CHEN¹, H-M PENG¹ AND P. LIU¹

¹State Key Laboratory Breeding Base of Nuclear Resources and Environmental, East China Institute of Technology, Nanchang 330013, China (xf730@163.com)

The acid rain is sulfuric acid type acid rain in Jiangxi province Nanchang City, its sulfur isotopic composition are different from that of other Cities.

We analyzed the sulfur isotopic composition of rain water from Nanchang City in this paper (Fig 1). The results indicated that the sulfur isotopic composition possesses a seasonal variation trend, isotopically heavier in spring and summer, lighter in autumn and winter. The sources of sulfur in rain water include bio-organic sulfur, anthropogenic sulfur and sulfur from the sea. In spring and summer, the sulfur in rain water comes mainly from anthropogenic sulfur. In autumn and winter, the sulfur in rain water dominantly originates from bio-organic sulfur. The sulfur in rain water from the sea may be very small in percentage.

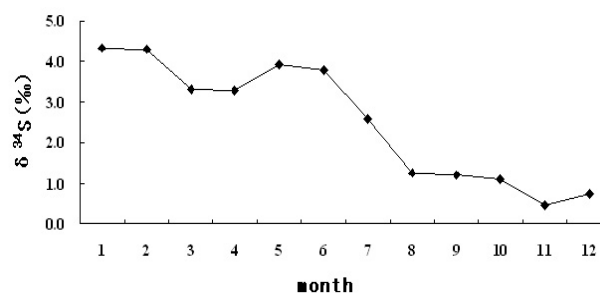


Fig. 1. Seasonal variations in sulfur isotopic composition of the precipitation

This research was jointly supported by the National natural Science Foundation of China (Grant No. 40963004).

[1] Ohizumi T, *et al.* (1997) *Atmos Environ*, **31**(9):1339-1348.
[2] Pichlmayer F, Sehdner W & Seibert P. (1998) *Atmos Environ*, **32**(23): 4075-4085. [3] Xia F, *et al.* (2010) *Geochimica et Cosmochimica Acta*, **74** (11): 1150-1151.

A pathway for aromatic hydrocarbon formation

YANQING XIA^{1*} AND JIANG CHANG¹

¹ Key Laboratory of Petroleum Resources Research, Institute of Geology and Geophysics, Chinese Academy of Science, Lanzhou, China, (yqxia@lzb.ac.cn(*)

Though aromatic hydrocarbons, the important components in petroleum, have been studied extensively, their formation mechanism is poorly understood, except for aromatic steranes, aromatic hopanes, and some sulphur-containing biomarker compounds, which are mainly thiophenes[1]. It is difficult to make clear their formation mechanism by studying the natural aromatic hydrocarbons lonely. During researching on the reaction of sulphur with organic matter by experiment, we found another pathway for aromatic hydrocarbon formation besides the aromatization of cyclanes. Though saturated chain compounds are difficult to become aromatic hydrocarbons, they can react quite easily with elemental sulphur and generate almost all kinds of aromatic hydrocarbons found in petroleum or sediments.

Many researchers have studied the mechanism of natural sulphur incorporation into organic matter by simulation or pyrolysis reactions[2], but the role of sulphur to the formation of common aromatic hydrocarbons in petroleum has not been pay great attention to and the action of sulphur on the organic matter in sediment used to be considered incorporating into carbon skeleton and forming sulphur-containing organic compounds even though Tissot *et* noted that the quantities of aromatic hydrocarbons in petroleum were direct proportion to sulphur[3]. From the present simulation experiment, it is clear that the reaction of sulphur and organic matter not only gives rise to sulphur-containing compounds, but also form non-heterocyclic aromatic hydrocarbons. Natural sediments are rich in saturated compounds and sulphur, so the reaction between them may be one of the most important sources of aromatic hydrocarbons.

[1] Jaap S. Sinninghe Damste and Jan W. de Leeuw. *Org Geochem*, 16(4-6): 1077–1101(1990). [2] Eitan B. Krein and Zeev Aizenshtat. *Org Geochem*, 21(10/11):1015–1025 (1994). [3] B. T. Tissot and D. H. Welte, *Petroleum Formation and Occurrence*, (in Chinese, Petroleum Publishing Company, 1989), 279–281.

The P-T-t path of the UHT granulites from Tongbai orogen, Central China

HUA XIANG¹, ZENG-QIU ZHONG², LI ZHANG², HAN-WEN ZHOU² AND ZE-MING ZHANG¹

¹ State Key Laboratory for Continental Tectonics and Dynamics, Institute of Geology, Chinese Academy of Geological Sciences, Beijing 100037, China

² Faculty of Earth Sciences, China University of Geosciences (Wuhan), Wuhan, China, 430074

Although the U-Pb zircon geochronometer has been widely used for dating metamorphism in moderate- to high-grade rocks, it is generally difficult to link the U-Pb age of zircon to pressure-temperature (P-T) conditions. Fortunately, the textures and chemical compositions (e.g. REEs) of zircon may provide qualitative information for correlating radiometric ages with certain stages in the metamorphic history of a rock. Additionally, zircon Lu-Hf isotopes can be used to constrain the nature of the igneous or metamorphic event in which the zircon grew.

Four stages of metamorphism are recognised in the granulites from Tongbai orogen, including a prograde stage (M1, ca.730–820°C at ca. <6 kbar), peak stage (M2, >920°C and 8.5–9.5 kbar), amphibolite facies retrograde stage (M3, ca. 700°C at ca. 7 kbar) and greenschist facies retrograde stage (M4, ca. 500 °C at ca. 5.8 kbar). Correspondingly, four distinct domains in the metamorphic zircons, which ²⁰⁶Pb/²³⁸U age are ca. 443 Ma, ca. 430 Ma, ca. 419 Ma and ca. 400 Ma respectively, are classified based on CL images, trace elements, U-Pb ages and Hf isotopes. The ca. 443 Ma zircons, which are suggested as the M1 minerals, are characterized by flat HREE pattern, indicating presence of garnet during formation of these zircons. The ca. 430Ma zircons from a semi-pelitic granulite are characterized by strongly depleted HREEs, resulting in low HREE partitioning between zircon and garnet (<1.0), which is consistent with the characteristics of the ultra-high temperature metamorphic zircon. The age of ca. 430 Ma is represented the peak metamorphic age. The ca. 419 Ma zircons occur as rim of the ca. 430 Ma or ca. 443 Ma zircons from a semi-pelitic granulite, and are characterized by relatively rich in HREE. This coincides with the fact of that garnet porphyroblasts were replaced by biotite + plagioclase during the retrograde stage (M3). In a mafic rock, the ca. 400 Ma zircon rims have obviously lower initial ¹⁷⁶Hf/¹⁷⁷Hf ratio than ca. 419 Ma zircons. It is extremely possible that hydrothermal fluids with low ¹⁷⁶Hf/¹⁷⁷Hf ratios were added into the rock during greenschist-facies hydrothermal event at ca. 400 Ma. We argue that the Tongbai UHT granulites is possibly related to the mid oceanic ridge subduction.

Stable Nitrogen Isotope Analysis of Amino Acids by GC/C/IRMS

HUA-YUN XIAO, REN-GUO ZHU AND ZUO-YING YIN

State Key Laboratory of Environmental Geochemistry,
Institute of Geochemistry, Chinese Academy of Sciences,
Guiyang 550002, China

Measurements of the $\delta^{15}\text{N}$ values of individual amino acids have provided very specific information about the biogeochemical, environmental, and ecological processes. The combination of gas chromatography with IRMS has become a hopeful tool for nitrogen isotopic analyses of individual amino acids in mixtures.

Amino acids before isotopic determination need to be derivatized using MTBSTFA and separated by gas chromatography, and gas chromatographic effluents were combusted and sent to the mass spectrometer continuously in a helium carrier stream. The GC column temperature was programmed for the tBDMSi derivatives separation as follows: isothermal 90 °C for 1 min, then heating up to 140 °C at rate of 8 °C/min and keeping it for 5 min, to 220 °C at rate of 3 °C/min and then to 285 °C at rate of 12 °C/min, and hold at final temperature 285 °C for 12.5 min until the elution of the last component. In this study, 0.8 ~ 4.5 nmol of each of the 20 amino acids (Ala, Gly, Val, Leu, Ile, Pro, Asn, Met, Ser, Thr, Phe, Asp, Glu, Lys, Gln, Arg, His, Tyr, Trp and GABA) was injected for isotopic determination.

All the 20 derivatized amino acids could be completely resolved in 60 min by GC program. We found a high isotopic correlation ($R^2=0.9987$, $p<0.0001$) between the determined values and the real values for most of the amino acids except three amino acids (Asn, Gln and Arg) which signals were much depleted. But for the three amino acids, there also existed a high isotopic correlation ($R^2=0.9999$, $p<0.0001$). Reproducible $\delta^{15}\text{N}$ values were obtained within different injected amounts. The reproducibility of all the 20 derivatives was between 0.3‰ and 0.8‰. The mean precision of reproducibility was 0.5‰. After calibration with the 2 correlation equations, the isotopic difference between the calibrated values and the real values was in the range of 0.1‰ to 0.5‰ for the 20 amino acids.

Using the method developed, we successfully analysed the $\delta^{15}\text{N}$ values of 20 free amino acids in tree leaves and barks.

This study work was kindly supported by the National Natural Science Foundation of China through grants 41173027.

Cell Alive System (CAS): A new method of core sample freezing for shore-based biological analyses and sample storage

NAN XIAO¹, YUKI MORONO¹, TAKESHI TERADA², YUHJI YAMAMOTO³, TAKEHIRO HORISE¹ AND FUMIO INAGAKI¹

¹Kochi Institute for Core Sample Research, Japan Agency for Marine-Earth Science and Technology (JAMSTEC),
²Marine Works Japan Ltd., ³Kochi University, Monobe B200, Nankoku, Kochi 783-8502, Japan.

We report a novel freezing technology for the long-term preservation of seafloor core samples. Seafloor core samples recovered by scientific ocean drilling provide unprecedented opportunities to study deep seafloor life and biogeochemical cycles. For the future analyses of cores using newly developed life science technologies, archiving precious core materials under the appropriate condition is fundamental significant. Given such scientific requirements, the Kochi Core Center (KCC), one of the official core repositories of the Integrated Ocean Drilling Program (IODP), has started storing some biological core samples in -80°C deep freezers and/or in liquid N₂ tanks, so called "DeepBIOS" (Deep Biosphere Samples).

To keep quality assurance and control (QA/QC) of the DeepBIOS, the initial freezing process is a key: however, using the conventional way (e.g., quick transfer to deep freezer), it has been confirmed that formation of ice crystals decompose biological signatures. During the JAMSTEC *Chikyu* Expedition 905, we tested a new technology called "Cell Alive System (CAS)", which utilizes magnetic field to vibrate water molecule in the sample, following snap and hence uniform freezing of core samples at the supercooling temperature. The core samples from various depths were sub-sampled, and immediately frozen in the CAS system along with the standard freezing method under the temperature of -20°C, -80°C, and -196°C. Analysis of cell abundance showed that conventional freezing methods decreased the number of microbial cells, whereas the CAS freezing resulted in almost no loss of the cells. We also tested the paleomagnetic characteristics after the CAS freezing, indicating no or very little change in remnant magnetism. No visible changes in volume of sediment was observed after the CAS freezing. Consequently, our results indicate that the CAS freezing technique is highly useful for QA/QC of scientific frozen core samples to preserve intact biological signatures, as well as other non-biological characteristics, for the long-term storage.

The transformation and co-evolution of archaea with its environment assessed by energy quantum

XIANG XIAO*, YU ZHANG, FENGPING WANG^{1,2},
YING HE AND JUNXU

State Key Laboratory of Microbial Metabolism and State Key Laboratory of Ocean Engineering, Shanghai JiaoTong University, Shanghai, 200240, People's Republic of China

*(Correspondence: xoxiang@sjtu.edu.cn)

Archaea are believed as key players in the biogeochemical cycling of basic elements such as carbon, nitrogen, and sulfur in various environments, yet the physiology and functions of many of them remain largely unknown mainly due to difficulties in cultivation and lack of genetic manipulation systems. By the combined utilization of high pressure bioreactors, together with OMICS enabled metabolic potential analysis, synthetic biological technologies, and single cell capturing and sequencing methods, our group aims to reveal the physiology, evolution and functions of some important archaeal groups in the deep-sea environments. As examples, we will highlight our recent progress in the systematic investigation and genetic engineering of piezophilic/thermophilic Thermococcales strains pool from deep-sea hydrothermal vents; and some novel understandings on the physiology, evolution and metabolisms of methane oxidizing archaea-bacteria syntrophic consortia. We propose a "Coevolution and Energy Quantum" (CEQ) theory as a guidance for mathematic model construction to understand the interaction and co-evolution of life and environment.

Skarn Cu-Fe-Au deposits in the East Hubei ore cluster, Middle–Lower Yangtze River metallogenic belt

XIE GUIQING^{1,2}, ZHU QIAOQIAO¹ AND LI WEI¹

¹Institute of Mineral Resources, Chinese Academy of Geological Sciences, Beijing, 100037, China

²MLR Key Laboratory of Metallogeny and Mineral Assessment, Beijing, 100037, China

The East Hubei ore cluster is one of most important skarn Cu-Fe-Au clusters in the Middle–Lower Yangtze River metallogenic belt (MLYR) because it contains >50 skarn Cu-Fe-Au deposits and over 800 km² of igneous rocks, which provides the best sample for studies on the origins of Late Mesozoic igneous and ore-forming event in the MLYR. With respect to mineral systems and metal associations, there are dominantly skarn Cu-Fe, Fe-Cu, Fe and Au deposits, which are all genetically associated with Late Mesozoic granitoids in the East Hubei. Previous studies mainly focused on individual skarn deposits, and comparatively studies among different skarn Cu-Fe-Au deposits have not yet been investigated.

There are similar compositions and mineral assemblages of skarn minerals, such as prograde garnet and pyroxene, among skarn Cu-Fe, Fe-Cu, Fe and Au deposits, and garnets and pyroxenes are dominantly andradite and diopside, respectively. In contrast, obviously differences between sulphur isotope and mineralized-related intrusions in different skarn types have been recognized: (1) The 137–144 Ma skarn Cu-Fe, Fe-Cu and Au deposits are genetically associated with 136–143 Ma diorite and quartz diorite, and the $\delta^{34}\text{S}$ of pyrites and chalcopyrites range from -8 to +12‰; while the 132–133 Ma skarn Fe deposits are genetically associated with 127–133 Ma diorite, quartz diorite and granite, and the $\delta^{34}\text{S}$ of pyrite range from +12 to +20‰. (2) The intrusions related skarn Cu-Fe, Fe-Cu and Au deposits show relatively high Sr/Y (25.1–201), and (La/Yb)_N (8.1–173), and low Yb contents (0.34–1.93 ppm); whereas intrusions-related skarn Fe deposits show relatively low Sr/Y (0.66–75.3), and (La/Yb)_N (2.3–30.0), and high Yb contents (1.07–5.17 ppm). It is proposed that the tationation of Cu, Fe and Au in the East Hubei ore cluster are possible related to different magma sources of intrusion and various evaporitic rocks involved in the formation of these skarn deposits.

Multistage refertilization of an Archean peridotite massif, N. Qaidam orogen (NE Tibet, China)

QING XIONG^{1,2*}, SUZANNE Y. O'REILLY¹, W.L. GRIFFIN¹, N.J. PEARSON¹ AND J.-P. ZHENG²

¹ CCFS and GEMOC, Earth and Planetary Sciences, Macquarie Univ., NSW 2109, Australia (*correspondence: qing.xiong@mq.edu.au)

² State Key Laboratory of GPMR, Faculty of Earth Sciences, China Univ. of Geosciences, Wuhan 430074, China

A garnet (Gt) -facies peridotite massif [1] was involved in the early Paleozoic North Qaidam orogeny that generated ultrahigh-pressure (UHP) rocks during the collision between the Qaidam and Qilian blocks, NE Tibet (China) [2]. Original dunite and harzburgite now enclose fertile lherzolite zones, secondary clinopyroxene (Cpx)-rich lherzolite/wehrlite layers and rare clinopyroxenite dykes. Re-Os isotopic analyses of Fe-Ni-sulfides from the peridotite give Re-depleted model ages up to 3.0 Ga, indicating an Archean origin.

Hf-Nd-Sr-O mineral isotopic data support multiple refertilization episodes for this Archean massif. Lu-Hf isotopic ratios of Gt and Cpx in the dunites distant from the fertile rocks give an isochron age of ~1.5 Ga, similar to their Hf depleted-mantle model ages, suggesting early Mesoproterozoic melt addition from depleted asthenosphere. Parallel layers of Cpx-rich peridotites and pods of Gt+Cpx occur within harzburgite and dunite. Lu-Hf and Sm-Nd isotopic signatures indicate the formation of these secondary peridotite layers and pods was related to a refertilization by basaltic melts from the asthenosphere at ~1.1-0.7 Ga. All peridotitic minerals have moderately evolved initial Sr isotopes (0.70358-0.70873), relative to primitive mantle. Whole-rock and mineral elemental compositions of phlogopite-bearing garnet pyroxenite dykes suggest derivation from arc-related melts. Their mineral Nd-Sr-O isotopic compositions imply an evolved source, probably from subducted continental crust. However, Lu-Hf isotopic data reflect an early Paleozoic depleted-mantle origin. U-Pb ages of zircon and Lu-Hf isochrons and model ages of Gt+Cpx both show that the intrusion of the pyroxenitic melts, derived from asthenosphere contaminated by continental crust, occurred in the early Paleozoic, related to the coeval North Qaidam orogeny.

[1] Xiong *et al.* (2011) *Precambrian Research* **187**, 33-57. [2] Xiong *et al.* (2012) *Lithos* **155**, 125-145.

Gas and Water Distributed Patterns and Influential Factors in the Tight Sandstone Gas Reservoirs of Upper Triassic Xujiache Formation in Hechuan Area of Sichuan Basin, China

ANNA XU¹; ZECHENG WANG² AND CONGSHENG BIAN³

¹ (xan@petrochina.com.cn)

² (wzc@petrochina.com.cn)

³ (bcs_1981@petrochina.com.cn)

The gas and water distribute complicatedly within the Upper Triassic Xujiache-2 tight sandstone in the Hechuan area of Sichuan basin. The origin and formation of water in the gas reservoir is complex. Generally, the wells released gas initially but produced water instead or shut down soon after, and that affected the gas production. Understanding distributed pattern of gas-water and its main influential factors is benefit to the development solutions-making of gas reservoir, enhanced reserves estimation and exploitation profits of such gas reservoir. This paper discusses the correlation of gas-bearing capability with pore-throat size, permeability and porosity, on the basis of reservoir rock research, combined with core mercury injection experiment, gas relative permeability experiment, nuclear magnetic resonance and gas-driving water percolation experiment. We also carried out typical gas reservoir dynamic analysis and synthetic geology research, using single well testing and pilot production data. The conclusions are followings, 1) the pore structures of the Xujiache-2 tight sandstone are dominated by fine or micro-throats, with strong heterogeneity; 2) the gas saturation relates with permeability and pore throat size in the Xujiache-2 gas reservoirs; 3) the Xujiache-2 gas and water have four distribution patterns, i.e. gas reservoir, upper gas with lower water, upper water with lower gas, and gas and water at the same zone; 4) the main controls on the Xujiache-2 gas-water occurrence are gentle-slope setting, pervasively near-source gas charging and heterogeneity of the pore throat.

Geochronology of ore-bearing andesite in the Kuozhenkuola Au deposit, Northern Xinjiang, China

C. XU, T.F. ZHOU*, F. YUAN, Y. FAN, Y.F. DENG
AND D.Y. ZHANG

School of Resources and Environmental Engineering, Hefei University of Technology, Hefei 230009, China
(*correspondence: tfzhou@hfut.edu.cn)

The Sawur gold belt is in the northern Xinjiang, China, which belongs to the central south region of the Central Asian Orogenic Belt. The Kuozhenkuola gold deposit is the largest epithermal gold deposit in this belt, which is spatially associated with andesite.

Zircon La-ICPMS U-Pb age of ore-bearing andesite we picked the ore-bearing andesite in the deposit district by detailed sampling. Furthermore, we tested the zircon U-Pb age of andesite is 339.4±4.8 Ma (MSWD=0.73) by La-ICPMS in Hefei University of Technology. The Kuozhenkuola Au-bearing andesite was intruded in Early Carboniferous Epoch.

The zircon U-Pb age of the mineralized andesite (339.4±4.8 Ma) is similar to the mineralization age (332±2.02 Ma) in Kuozhenkuola Au deposit within error [1], which indicate that Kuozhenkuola Au mineralization was genetically related to the andesitic magma [2]. In Eastern Sawur area, there several Au deposits are found through current exploration, including Berkesidai, Heishantou and Tasite Au deposits [3][4]. This geochronological result affords credit evidence to genetic research of the Early Carboniferous Au mineralization in the regional area.

This research was sponsored by Chinese National Science and Technology Program (2011BAB06B01).

[1] Shen *et al.* (2006) *Sawur Research Report* : 111-117 (in Chinese). [2] Shen *et al.* (2007) *Ore Geology Reviews* **32**: 207-226. [3] Yang *et al.* (2005) *Mineral Deposit*, **24(3)**: 242-263 (in Chinese). [4] Fan *et al.* (2007) *Acta Petrological Sinica* **23(8)**: 1901-1908.

Plutonium Immobilization and Re-mobilization by soil mineral-organic matter matrix compounds in the Far-field of the Savannah River Site (SRS), USA

CHEN XU¹, MATTHEW ATHON¹, YI-FANG HO¹, KATHLEEN A. SCHWEHR¹, DANIEL I. KAPLAN², ROBERTS A. KIMBERLY², NICOLE DIDONATO³, PATRICK G. HATCHER³ AND PETER H. SANTSCHI^{1*}

¹Department of Marine Sciences, Texas A&M University, Building 3029, Galveston, Texas 77553 (*correspondence: santschi@tamu.edu)

²Savannah River National Laboratory, Aiken, SC 29808

³Department of Chemistry & Biochemistry, College of Sciences, Old Dominion University, Norfolk, VA 23529

Pu is believed to be essentially immobile due to its low solubility and high particle reactivity to mineral phase or soil organic matter. For example, in sediments collected from a region of SRS, close to a wetland and a groundwater plume, ^{239,240}Pu concentrations correlated with organic carbon contents. However, previous studies reported Pu can be transported several kilometers in surface water systems through wind/water interactions [2,3]. The role of natural organic matter (NOM) in immobilizing or re-mobilizing Pu thus has been demonstrated. It was found that partitioning coefficients (K_d s) of intact humic acids (HAs) were significantly higher than those were treated with HF, lowering chelating sites for Pu or hydrophobicity differences between the two types HAs. K_d s of Pu (IV) with HAs were higher at low pH (4.4) than those at high pH (7.1), in contrast to the observation of Pu sorption to most mineral phases [4], possibly caused by the increased solubility of HA under more alkaline conditions. Though the colloidal fraction of HAs only accounts for a minor fraction of total OC (<5%) at pH 4.4, Pu binding to HAs accounts for 61-83% of the total added Pu, indicating colloidal organic matter as the mobile Pu carrier in the wetland area. Lastly, ^{239,240}Pu concentrations were found to be positively correlated with particulate hydroxamate and nitrogen contents, indicating binding to siderophores.

[1] Kaplan *et al.* (2007), *ES&T* **41**, 7417-7423. [2] Santschi *et al.* *ES&T* **36**, 3711-3719. (2002). [3] Xu *et al.* (2008) *ES&T* **42**, 8211-8217. [4] Kaplan *et al.* (2006), *ES&T* **40**, 5937-5942.

Petrographical features of the Shilu Fe-polymetallic ore deposit in Hainan Province, South China: implication for ore-deposit type

DERU XU¹, HUAYONG CHEN¹ AND ZHILIN WANG^{1,2}

¹CAS Key Laboratory of mineralogy and metallogeny, Guangzhou Institute of Geochemistry, Chinese Academy of Sciences, Guangzhou 510640, China

²Graduate University of Chinese Academy of Sciences, Beijing 100049, China

The Shilu Fe-polymetallic hematite-rich deposit is situated in the western Hainan Province of South China. This deposit is characterized by upper Fe-rich ores and lower Co-Cu-rich ores, which are mainly hosted within a dominantly metamorphosed submarine siliciclastic and carbonate sedimentary succession of the Proterozoic Shilu Group that has been metamorphosed to greenschist to amphibolite facies. Two types of metamorphosed BIFs, i.e. the quartz itabirites which contain alternating hematite-rich microbands with quartz-rich microbands, and the amphibolitic itabirites which comprise alternating millimeter- to a few tens meter-scale, Fe oxide (magnetite, hematite)-rich bands with calcisilicate (garnet + amphibole + pyroxene + epidote)-rich mesobands to microbands, have been identified within the Shilu Group. A Fe-Co-Cu-rich sulfide facies, represented by the stratabound Co-Cu ores, also characterizes alternating Co-bearing pyrite + Co-bearing pyrrhotite + chalcopyrite macro- to mesobands dominantly with dolomite + calcite ± amphibole and minor with sericite + chlorite + quartz macro- to mesobands. The relic oolitic, pelletoid, colloidal and psammitic textures, and bedding structures which most likely represent primary sedimentary structures often observed in the Shilu itabirites. Hereby, the precursor precipitates to the Shilu deposit are interpreted as Fe-Co-Cu-(Si)-rich chemical sediments intercalated or mixed with variable amounts of detrital components. Input of the Fe, Si, Co and Cu from a mixed source of weathered landmass and sea-floor-derived hydrothermal fluids into a continental margin marine basin separated from an open ocean in fluctuating redox state caused primary sedimentation of the Shilu itabirites and Co-Cu ores via hydrogeneous-sedimentary processes. Further, we consider the Shilu deposit as a BIF (banded iron formation) ore deposit-type (Lake-Superior).

Rapid recovery of seawater ¹⁸⁷Os/¹⁸⁸Os after CAMP magmatism at Triassic-Jurassic boundary

G. XU¹, J.L. HANNAH^{1,2}, H.J. STEIN^{1,2}, R.F. GALIMBERTI³ AND M. NALI³

¹ AIRIE Program, Colorado State University, Fort Collins, CO, USA

Guangping.Xu@colostate.edu (*presenting author)

² CEED Centre of Excellence, University of Oslo, Oslo, Norway

³ Eni E&P, Geology and Geochemistry Labs, Milano, Italy

The Late Triassic–Early Jurassic (T-J) was a time of major global change. The end-Triassic mass extinction is one of the “big five” extinction events of the Phanerozoic. The extinction is proposed to be causally linked with volcanic eruptions from the Central Atlantic Magmatic Province (CAMP)^{[1][2]} which produced low ¹⁸⁷Os/¹⁸⁸Os ratios in seawater at the period boundary. Late Triassic to Early Jurassic organic-rich shales from SE Sicily offer an opportunity to track events across the T-J boundary. Here we present Re-Os geochemistry of Hettangian Streppenosa Formation black shales from Gela #1 drillcore, SE Sicily.

Black shales from the lower Streppenosa Formation, deposited in a deep euxinic intraplatform basin, yield a Model 3 Re-Os age of 200.3 Ma and initial ¹⁸⁷Os/¹⁸⁸Os of 0.87. This Early Jurassic age is nominally younger than the T-J boundary of 201.3 Ma^[3] and the major four pulses of CAMP volcanism, dated between 201.6 and 200.9 Ma^[2].

The seawater ¹⁸⁷Os/¹⁸⁸Os ratio of 0.87 at 200.3 Ma is the highest ratio recorded in Triassic to Early Jurassic seawater^[4]. This ratio stands in contrast to mostly low ratios reported across the T-J boundary, attributed to the sudden initiation of volcanic activity of CAMP^{[1][4]}. Yet the high ¹⁸⁷Os/¹⁸⁸Os coincides with an unusual spike in seawater ¹⁸⁷Os/¹⁸⁸Os at the T-J boundary^[4]. The high ¹⁸⁷Os/¹⁸⁸Os ratio at 200.3 Ma documents minimal contribution of unradiogenic Os from CAMP magmatism, and may also reflect enhanced continental weathering resulting from uplift along newly formed rifted margins. This rapid recovery of seawater ¹⁸⁷Os/¹⁸⁸Os after CAMP volcanic eruption likely reflects the short residence time of Os in seawater (tens of kyr).

Our results confirm that the Os isotope composition of seawater responds rapidly to large volcanic events, further demonstrating the role that seawater Os can play in identifying major environmental changes.

ENI S.p.A. provided samples and financial support.

[1] Cohen & Coe (2002) *Geology*, **30**: 267-270; [2] Blackburn *et al.* (2013) *Science*, DOI: 10.1126/science.1234204; [3] Gradstein *et al.* (2012) *GTS*; [4] Cohen & Coe (2007) *P3*, **244**: 374-390

Selenium geochemical characteristics of Ruorgai plateau wetland, eastern margin of the Qinghai-Tibet Plateau, Southwest China

J.Y. XU^{1*} AND T. WANG²

¹Department of Geochemistry, Chengdu Univ. of Technology, Chengdu 610059, China (*correspondence: xujinyong@cdut.cn; xujinyong@yahoo.cn)

²College of Materials and Chemistry & Chemical Engineering, Chengdu Univ. of Technology, Chengdu 610059, China

Ruorgai wetland is a typical plateau wetland ecosystem in the eastern margin of the Qinghai-Tibet Plateau, southwest China. This area is one of five big pastoral areas in China. On the other hand, the people's health and the development of livestock suffer from selenium deficiency symptom[1].

Here we developed a method for determination of selenium in environment sample by high performance liquid phase inductively coupled plasma-mass spectrometry (HPLC-ICP-MS)[2]. The selenium of rock, soil, water and plant in this area were researched. Conclusions are as follows.

The selenium of rock in this area is generally lower than the crustal abundance. The selenium of the water is much lower than normal drinking water. The selenium of plant is between selenium deficiency areas and normal areas. The selenium of increased with organic matter content in soil.

[1] Kanekura *et al.*(2005) *Clinical and Experimental Dermatology* 30, 346-348. [2] Bird *et al.* (1997) *Journal of Analytical Atomic Spectrometry* 12, 785-788.

Fluid and melt inclusions in the Wulaga gold deposit, Heilongjiang, China

J.H. XU^{1*}, Y.H. WANG¹, H. WEI¹, Q.D. ZENG², J.M. LIU², Y.B. WANG² AND Q. MAO²

¹Department of Resource Engineering, University of Science and Technology Beijing, Beijing 100083 (*correspondence: jiuhuaxu@ces.ustb.edu.cn)

²Institute of Geology and Geophysics, Chinese Academy of Sciences, Beijing 100029

The Wulaga gold deposit, located in northeastern China, is a controversial deposit for its ore genesis[1-3]. The ore bodies are mainly hosted in cryptoexplosive breccia zone within Tuanjiegou plagioclase granite-porphyry of 106~108Ma[4], and in the layer fractures of metamorphic Heilongjiang group. Gold mineralization can be divided into 3 stages: pyrite- early white chalcedony quartz stage (stage I), smoky gray chalcedony quartz - polymetallic sulfide stage (stage II), and carbonate-quartz stage (stage III). Fluid inclusions in stage I are mainly aqueous solutions with homogenization temperatures (Th) of 154°C~355°C, mainly in 230°C~270°C. Salinities of fluid inclusions are 1.3%~8.2%NaCl eqv. Those in stage II are 159°C~196°C, with salinities of 2.2%~3.2%NaCl eqv. Those in stage III are mainly in 170°C~230°C, with salinities of 0.5%~2.9%NaCl eqv. Ore-forming fluids in the main mineralization stages are characterized by mid to low temperatures, low salinities, and lack of CO₂, which is similar with epithermal deposits related with continental volcanic-subvolcanic rocks. There are three types of inclusions in quartz phenocryst of plagioclase granite-porphyry, that is, melt inclusions, primary L-V and L-V-S inclusions, as well as secondary L-V inclusions. Glassy melt inclusions are characterized by acid magma (SiO₂ =69.5~73.8%), with the trapping temperatures higher than 800°C. Secondary L-V inclusions in quartz phenocryst have 210°C~350°C of Th, which are coincided with those of mineralizing stage I (Q1), while salinities (5~7wt%NaCleqv.) are slightly higher than those of Q1. Melt and fluid inclusion study shows that gold mineralization is related with plagioclase granite-porphyry, and it is possible for silicate magma to produce salt-aqueous solution through immiscibility in magmatic differentiation.

[1]Wu (1984) *Geology and Exploration* 20,28-31. [2] Wang *et al.* (2004) *Geotectonica et Metallogenia* 28,171-178. [3] Sun *et al.* (2008) *Geology in China*, 35,1267-1273. [4]Wang *et al.*(2012) *Acta Petrologica Sinica* 28, 557-570.

Relationships between porphyry Cu–Mo mineralization in the Jinshajiang–Red River metallogenic belt and tectonic activity: Constraints from zircon U–Pb and molybdenite Re–Os geochronology

LEILUO XU¹

¹State Key Laboratory of Ore Deposit Geochemistry, Institute of Geochemistry, Chinese Academy of Sciences, Guiyang, 550002, China.

The Jinshajiang–Red River porphyry Cu–Mo metallogenic belt is an important Cenozoic porphyry Cu–Mo mineralization concentrating zone in the eastern Indo–Asian collision zone. New zircon U–Pb and molybdenite Re–Os ages and compilation of previously published ages indicate that porphyry Cu–Mo deposits in the belt did not form at the same time, i.e., the porphyry emplacement and relevant Cu–Mo mineralization ages of the Ailaoshan–Red River ore belt in south range from 36.3 Ma to 34.6 Ma, and from 36.0 Ma to 33.9 Ma, respectively, which are obviously younger than the porphyry emplacement ages of 43.8–36.9 Ma and the relevant Cu–Mo mineralization ages of 41.6–35.8 Ma of the Yulong ore belt in north. Tectonic studies indicated that the Jinshajiang fault system in north and Ailaoshan–Red River fault system in south of the Red river belt had different strike-slip patterns and ages. The right-lateral strike-slip motion of the Jinshajiang fault system initiated at ca. 43 Ma with corresponding formation of the Yulong porphyry Cu–Mo system, whereas the left-lateral strike-slip motion of the Ailaoshan–Red River fault system initiated at ca. 36 Ma with corresponding formation of the Ailaoshan–Red River porphyry Cu–Mo system. Therefore, the different ages of porphyry Cu–Mo systems, between in north and south of the Jinshajiang–Red River belt, indicate that the porphyry Cu–Mo mineralization is closely related to the divergent strike faulting resulted from the Indo Asian collision. The tanslithospheric Jinshajiang–Red River faulting caused partial melting of the enriched mantle sources of alkali-rich porphyries by depressurization or/and asthenospheric heating, and facilitated the migration of alkali-rich magmas and the corresponding formation of alkali-rich porphyries and relevant Cu–Mo deposits in the belt.

The Platinum-Group Element Abundance Patterns of the Meishan Permian-Triassic Boundary, China

L. XU^{1*} AND S. HU²

¹ National Astronomical Observatories, Chinese Academy of Science, Beijing, China (*Email: xul@nao.cas.cn)

² Institute of Geology and Geophysics, Chinese Academy of Science, Beijing, China

It is a long-standing controversy what triggered the extinctions at the Permian-Triassic boundary, the most severe mass extinction in the geologic record (1). We analyzed all PGEs (except for Os) of a set of samples from the GSSP of the P-Tr boundary at Meishan, China. The PGE patterns have important constraints on sources of the P-Tr boundary materials. The data are also compared with previous results of known layers samples (2).

A total of 16 samples from three sections at Meishan were analyzed, which were numbered bed A to H, T, N, and bed O to S, and U. They were treated as blind testing samples, and the location information was released after the experiments. Our data reveal no significant positive PGE anomaly with the Ir contents of 0.003-0.029 ng/g. Compared with previous analyses (2), the abundance of PGEs reached the maximum at layer B-26. The layer B-25 and the pyrite lamina of B-24 (bed C and Q) that is referred to as the P-Tr event boundary, contain the lowest abundance of PGEs.

The P-Tr boundary samples show highly fractionated PGE patterns, distinct from chondrites and iron meteorites. The PGE patterns are parallel to those of Siberian flood basalts and Emeishan flood basalts, especially more similar to the former. The PGE data suggest a possible linkage between the P-Tr boundary event and the eruption of Siberian or Emeishan flood basalts.

[1] Erwin (1994) *Nature* 367, 231-236. [2] Xu *et al.*, (2007) *Chem. Geo.* 246, 55-64.

Synthesis of Symplectite (Fe₃(AsO₄)₂·8H₂O)

LIYING XU^{1,2}, YONGFENG JIA², DETONG JIANG³,
NING CHEN⁴, JOEL REID⁴ AND GEORGE P.
DEMOPOULOS^{1,*}

¹[Department of Mining and Materials Engineering,
University of McGill, Montreal, Canada, H3A 0C5.
(liying.xu@mcgill.ca);(george.demopoulos@mcgill.ca)

²[Institute of Applied Ecology, Chinese Academy of Sci-
ences, Shenyang, China, 110016.]

³[Department of Physics, University of Guelph, Guelph, ON,
Canada, N1G 2W1.]

⁴[Canadian Light Source Inc.University of Saskatchewan,
Saskatoon, Canada. S7N 0X4.]

Symplectite is the crystalline-triclinic ferrous arsenate (Fe₃(AsO₄)₂·8H₂O). It has very low solubility at neutral to slightly alkaline pH (much lower than scorodite). Hence, symplectite could be a dominant compound for arsenic immobilization in suboxic environment, such as in co-precipitated tailings ponds. However, little is known about its synthesis, solubility and structure. The objectives of this work were to study the synthesis methods and to characterize the product using various techniques.

Fe(II) (FeSO₄·7H₂O, 60, 90 mM pH 2, adjusted by HNO₃) and As(V) (Na₂HAsO₄·7H₂O, 40, 70mM, pH 8.6) solutions ere prepared using deoxygenated DI-water in glovebox.

Different synthesis strategies were tested including raising the pH of pre-mixed Fe(II)-As(V) solutions to 4, 5, 6, 8 respectively (denoted as RMP), and mixing Fe(II) and As(V) solutions at fixed pH (4, 5, 6, 8) (denoted as TAP) to precipitate the precursor followed by aging at different temperatures (21, 45, 70 °C). The molar ratio of Fe/As = 1.5 was applied. NaOH (0.25N) and HNO₃ (0.5N) were used to adjust media pH. The solid products were separated by filtration in glovebox and vacuum dried. XRD and SEM were used to characterize the products.

The XRD data indicated the successful synthesis of symplectite. SEM showed that the product was needle-shaped particles. The TAP method is better than RMP for the synthesis of symplectite. The media pH and temperature for precursor precipitation or crystallization during ageing are very important factors. Better crystallinity was obtained at higher temperature. The pH significantly influences the product's purity and re-crystallization. The rate of re-crystallization increased with increasing pH, but the highest pH of 8 was applied to avoid the formation of Fe(OH)₂.

[1] R.B. Johoston. Solubility of symplectite (ferrous arsenate):Implication for reduced groundwaters and other geochemical environments. Soil Sci. Soc. Am. 2007, 71:101-107.

In-situ trace elements and Li, Sr isotopes in peridotite xenoliths from Kuandian, North China Craton: Insights into Pacific slab subduction-related mantle modification

RONG XU¹, YONGSHENG LIU^{1*}, XIRUN TONG¹, ZHAOCHU HU¹, KEQING ZONG¹, HUI LI AND SHAN GAO¹

¹ State Key Laboratory of Geological Processes and Mineral Resources, Faculty of Earth Sciences, China University of Geosciences, Wuhan 430074, China

Trace element, Li and Sr isotopic compositions of major minerals in peridotite xenoliths from Kuandian, North China Craton (NCC) were analyzed *in situ* to investigate Pacific slab subduction-related mantle modification beneath the eastern NCC. The ⁸⁷Sr/⁸⁶Sr ratios are positively correlated with the La/Nb, Ce/Zr and Sr/Y ratios and negatively correlated with the Nb/U ratio for Cpx. Based on the trace element distribution patterns, three types of Cpx were identified. Type 1 Cpx are characterized by significant Nb-Ta-Ti depletions and the highest Sr isotopic ratios; Type 2 Cpx display Nb (or Ta) depletions and highly variable Nb and Ta fractionation; and Type 3 Cpx show no significant Nb or Ta depletion or even weak Ta enrichment and have the lowest Sr isotopic ratios. Some Cpx display a pattern of increasing Ca+Mg±Si from the cores to the rims, indicating addition of Ca+Mg±Si-rich fluids derived from a serpentinized peridotite layer above the subducting slab. These features indicate multiple mantle metasomatism events associated with the ancient subduction of the altered Pacific oceanic crust, which may contribute substantially to the destruction of the eastern NCC.

The Li contents in the Cpx (up to 34.8 ppm) and Opx (up to 28.0 ppm) are typically higher than those in the coexisting Ol (< 9.19 ppm), suggesting silicate melt metasomatism. Furthermore, both pyroxenes and Ol display remarkable zoning patterns in their Li contents and isotopic ratios, indicating a redistribution and disequilibrium fractionation of Li within and/or between minerals. The Li enrichment and low δ⁷Li values in the rims of most Ol, Cpx and Opx may have arisen from diffusive fractionation during Li-rich melt/fluid metasomatic processes. However, the Li depletion and high δ⁷Li in the rims of a few Ol may suggest cooling-induced Li isotope fractionation. Based on the zonation and Li diffusion coefficient at mantle temperatures, a model calculation suggests that the latest Li-rich melt/fluid metasomatic process was a recent event occurring shortly before or during the host magma eruption.

Temporal variations of Fukushima-derived ^{129}I in precipitations

SHENG XU^{1*}, STEWART FREEMAN¹, XIAOLIN HOU²,
AKIRA WATANABE³, KATSUHIKO YAMAGUCHI³
AND LUYUAN ZHANG²

¹Scottish Universities Environmental Research Center, East Kilbride, G75 0QF, UK

(*correspondence: s.xu@suerc.gla.ac.uk)

²Center for Nuclear Technologies, Technical University of Denmark, 4000 Roskilde, Denmark

³Geophysical Institute, Fukushima University, Fukushima 960-1296, Japan

The precipitation samples collected from Fukushima, Japan over 2010-2012 were analyzed for ^{127}I and ^{129}I in order to explore the atmospheric level and behaviour of radioactive iodine released from the Fukushima nuclear accident in 2011. ^{129}I concentration of 1.2×10^8 atom/L in 2010 before the accident dramatically increased about 4 orders of magnitude to 7.6×10^{11} atom/L in March 2011 immediately after the accident with a $^{129}\text{I}/^{127}\text{I}$ ratio up to 6.9×10^{-5} . Afterwards the ^{129}I concentrations in precipitation decreased exponentially to $\sim 3 \times 10^9$ atom/L until October 2011 with a half-life of about 29 days. This decline trend of ^{129}I concentrations in precipitation was interrupted around October 2011 by newly ^{129}I input to the atmosphere, and the elevated ^{129}I concentration in the atmosphere decreased exponentially again. Such a cycle of abrupt increase - exponential decrease occurred three times until present. This temporal variation can be attributed as alternation of ^{129}I dispersion and re-suspension from the contaminated local environment. A $^{129}\text{I}/^{131}\text{I}$ atomic ratio of 16 ± 1 obtained from the rainwater sample is comparable with those estimated by analysis of surface soil samples [1]. Comparison of ^{129}I level in Europe suggests an insignificant effect of ^{129}I released from Fukushima to the ^{129}I level in the Europe.

[1] Miyake *et al.* (2012) *Geochem. J.* **46**, 327-333.

Historical trends of heavy metal pollution recorded in sediments from Lake Qionghai, China

WEI XU, ZE-MING SHI, SHI-JUN NI
AND YING GAO

Department of Geochemistry, Chengdu University of Technology, Key laboratory of Earth Science and Nuclear Techniques in Sichuan Province, Chengdu, 610059, China
(weixuxw@gmail.com; shizm@cdut.edu.cn; nsj@cdut.edu.cn; ying.gao@gmail.com)

Heavy metals are serious pollutants due to their toxicity and long persistence in the environment. Lake sediment cores preserved the geochemical environmental changing record. A sediment core was collected in 2011 from Lake Qionghai, the second largest freshwater lake of Sichuan Province in China, to analyze the heavy metal pollution evolution of the lake.

The sediment core was 46cm in height, and was sectioned at 1cm intervals for the above 30cm while 2cm intervals for the left. The coefficients of variation of As, Cd, Cr, Cu, Hg, Ni, Pb, Zn in the sediment core are 0.32, 0.72, 0.16, 0.08, 0.34, 0.24, 0.19, 0.19, respectively, which indicates Cd varies greatly as a result of human activities, while the other heavy metals have little change mainly due to a natural origin.

The content of Cd increased distinctly and continuously to 0.87g/kg in the surficial six centimetres of the sediment core, indicating the lake had a large quantity of Cd input in the last years. According to the ^{137}Cs dating result, this interval was deposited from 1998 to 2011. Besides, the evaluation by potential ecological risk index method showed Cd in the sediments had pollution risk of medium degree. That means the lake has suffered Cd pollution since 1998.

Spatial-temporal extent of the influence of the Mongol-Okhotsk tectonic regime on China during Mesozoic: Evidence from Mesozoic igneous rocks

WEN-LIANG XU*, FENG WANG, JIE TANG, FU-PING PEI, WEI WANG AND HONG FENG

College of Earth Sciences, Jilin University, Changchun 130061, China (xuw1@jlu.edu.cn)

It has been a controversial issue whether the southward subduction of the Mongol-Okhotsk oceanic plate happen during Mesozoic. The spatial-temporal distributions of the Mesozoic igneous rocks in NE China provide a constraints on this question. Zircon U-Pb dating results indicate that the Mesozoic magmatism in the Argun Massif adjacent to the Mongol-Okhotsk suture can be subdivided into the following stages: ~245 Ma, ~220 Ma, ~200 Ma, ~185 Ma, ~162 Ma, ~142 Ma, and ~125 Ma. The Early Mesozoic igneous rocks (~245 Ma, ~220 Ma, ~200 Ma, and ~185 Ma) consist of a suite of calc-alkaline basalt, basalt-andesite, diorite, and granodiorite. Together with the coeval porphyry Cu-Mo deposits, they reveal the subduction of the Mongol-Okhotsk plate beneath the Argun Massif. The ~162 Ma igneous rocks are composed of trachy-basalt, basaltic trachyandesite, and trachyandesite which display a transitional type between alkaline and subalkaline series, and only occur in the Great Xing'an Range and northern Hebei-western Liaoning provinces. Similarly, ~142 Ma magmatism also only occur in the same area as ~162 Ma igneous rocks and consist of alkaline rhyolite, implying an extensional environment. Taken together, it is suggested that the ~162 Ma and ~142 Ma magmatism could be related to the evolution of the Mongol-Okhotsk tectonic regime and could be generated by the collapse and/or delamination of the thickened lower crust in the Great Xing'an Range and northern Hebei-western Liaoning provinces, which is also supported by two regional unconformability (beneath the Haifanggou Formation and overlying the Tuchengzi Formation, respectively). From north to south, the beginning time of ~162 Ma and ~142 Ma magmatism gradually become younger, further implying that their formations should be attributed to the evolution of the Mongol-Okhotsk tectonic regime. The ~125 Ma igneous rocks are widely distributed in NE China and consist of bimodal igneous rocks in the Great Xing'an Range and Songliao basin as well as a calc-alkaline volcanic rocks in the eastern Heilongjiang-Jinlin provinces, suggesting that the later could be formed under the subduction of the Paleo-pacific plate beneath the Eurasian continent, whereas the former could be generated by the delamination of the thickened lower crust and/or the subduction of the Paleo-pacific plate. This work is supported by 973 program (2013CB429803) and NSFC (41272077).

Tectonic implications for Mid-late-Neoproterozoic rift-related volcanic rocks in China

XUE-YI XU, LIN-QI XIA, ZU-CHUN XIA, XIANG-MIN LI AND ZHONG-PING MA

Xi'an Institute of Geology and Mineral Resources, China Geological Survey, Xi'an, Shaanxi 710054, China

Mid-late-Neoproterozoic rift-related volcanic rocks which had aggregated to form part of the Rodinia Supercontinent by ca. 900 Ma are widespread on several Precambrian in China. These volcanic rocks, which mainly consist of huge volumes of basic rocks and variable amounts of silicic volcanics, with small amounts or absence of intermediate rocks displaying a compositional bimodality, have attracted a number of recent studies. Several lines of evidence show most of these volcanics have a compositional bimodality, and formed in an intra-continental rift setting which may be genetically linked with mantle plumes activities.

On the basis of petrogeochemical data, these basic lavas can be classified into two major types: High Ti/Y and Low Ti/Y types, both of which can be further divided into two subtypes by different Nb/La ratios, respectively. The lavas (Nb/La <0.85) can be accounted for by lithospheric contamination of asthenosphere- (or plume-) derived magmas during their ascent, but parental magmas of others (Nb/La >0.85) may have not undergone such a process.

The rift-related volcanism at end of mid-Neoproterozoic and early-Cambrian coincided temporally with the separating between Australia-East Antarctica, South China and Laurentia and between Australia and Tarim, respectively. The mid-late-Neoproterozoic volcanism in China is the geologic record of broken-up of the supercontinent Rodinia. (This research is supported by Land and Resources Survey Project of China, Grant No. 1212011220649 and the National Natural Science Foundation of China, Grant No. 40872061)

Vanadium dynamics in soils impacted by vanadiferous titanomagnetite ore mining

Y.-H. XU^{1*}, H. BRANDL¹ AND J.-H. HUANG²

¹ Institute of Evolutionary Biology and Environmental Studies, University of Zurich, CH-8057, Zurich, Switzerland (*correspondence: yuhui.xu@ieu.uzh.ch) (helmut.brandl@ieu.uzh.ch)

² Environmental Geosciences, University of Basel, CH-4056, Basel, Switzerland (jen-how.huang@unibas.ch)

Vanadium (V) plays a highly critical role in natural systems due to its potential essence and toxicity to organisms. To date, knowledge about V biogeochemistry is scarce so that assessing the impact of V enriched solids on the terrestrial environment is still difficult. Two soil profiles overlaid with and without ores and mining rests close to the vanadiferous titanomagnetite ore mining site were sampled. We attempted to characterize the mobility of soil V under the influence of mining activities and to estimate the potential risk of V to the adjacent environment by analysing the vertical V distribution, speciation of V oxidation state and its sequential distribution in different organic and mineral fractions. Additionally, HPLC-ICP-MS coupling was taken for speciation of V(V) and V(IV) in water and EDTA extracts of soils to understand V bioavailability and its potential toxicity.

Except the very high V concentrations (784 ppm) in the surface layer composed of mining rests, the soil V concentrations vary little along both soil profiles (343-356 and 143-201 ppm), suggesting the general low V mobility. Speciation of soil V based on sodium carbonate extraction indicates that more than 85% of total V in soil is tetravalent, which is generally rather insoluble and strongly absorbed [1]. Results of sequential extraction show totally different fractionation patterns compared to the other metalloids e.g. arsenic. Vanadium prefers to enrich in crystalline fractions and residues, while arsenic is abundant in poorly crystalline fractions. Interestingly, the proportion of V in the crystalline fraction and residues is independent of the depth (~69%) in the unpolluted soils, but the relevance of these two fractions increases from 52% to 82% with the depth along the polluted soil profile, suggesting the potential influence of mining materials on V binding forms in soils. Pentavalent V predominates in both water and EDTA extracts, reflecting higher mobility of V(V) than V(IV). This further implicates elevated toxicity for the plants and soil organism due to higher toxicity of V(V) compared to V(IV).

[1] Wehrli & Stumm (1989) *GCA* 53, 69-77.

Paleoclimate reconstruct of Late Triassic Xujiahe Formation Sichuan Basin in Southwest China

XU ZHAOHUI¹ WANG ZECHENG² AND HU SUYUN³

¹ Research Institute of Petroleum Exploration and Development, PetroChina, Beijing, China, (tadxu@126.com)

² Research Institute of Petroleum Exploration and Development, PetroChina, Beijing, China, (wangzecheng@petrochina.com.cn)

³ Research Institute of Petroleum Exploration and Development, PetroChina, Beijing, China, (husy@petrochina.com.cn)

Formation of Upper Triassic in Sichuan Basin China is abundant in gas resource, with proved gas resource of more than hundreds of billion cubic meters. As a result, the formation has become an important area for the gas industry of China.

Xujiahe Formation can be divided into six members with a texture of interbedded sandstones and mudstones, like a sandwich. The paleoclimate is an important reason for the texture. Three methods named palynoflora, clay minerals, and eigen elements were used in this paper to reconstruct the paleoclimate when Xujiahe Formation was sediment. Mudstone samples of the six members were taken from six different areas of the entire basin, and then analyzed to reconstruct the paleoclimate, respectively. The palynoflora indicated that the paleoclimate background of Xujiahe Formation was hot and humid, belonging to tropics-subtropics zone. Making use of clay minerals, the ratio of Kaolinite and Illite (K/I) was used to analyze the Paleoclimate, which reduced the ambiguity. Using the ratio of Calcium and Magnesium (Ca/Mg) and Strontium/Barium (Sr/Ba), the details of paleotemperature and paleomoisture (paleosalinity) were analyzed. It can be seen that the paleotemperature and paleomoisture of Xujiahe Formation fluctuated regularly against the setting of tropics-subtropics. Member Xu 1 was formed in transitional facies when the paleoclimate was hot and humid. Member Xu 2 was formed in the climate of hot and arid. When member Xu 3 was formed, the temperature and moisture were all higher than Xu 2. It belonged to palustrine environment. After shortly decrease of temperature and moisture in Member Xu 4, it became hottest and wettest during the period when Member Xu 5 was formed. The temperature and moisture declined slowly in Member Xu 6, and the paleoclimate became relatively warm and aridity. It is the fluctuation of paleoclimate that led to the forming of the sandwich sedimentation structure of Xujiahe Formation in Sichuan Basin Southwest China.

The nature of crustal components in mantle sources for Cenozoic continent basalts in southeastern North China Craton

ZHENG XU, YONG-FEI ZHENG* AND ZI-FU ZHAO

School of Earth and Space Sciences, University of Science and Technology of China, Hefei 230026, China
(*correspondence: yfzheng@ustc.edu.cn)

Cenozoic continental basalts in the southeastern part of the North China Craton exhibit depleted Sr-Nd isotope compositions and OIB-like trace element patterns. It is intriguing what kinds of crustal component were involved in mantle sources for the intraplate basalts. An integrated interpretation of major-trace elements and stable-radiogenic isotope data for these intraplate provides new insights into this issue. Different types of correlations occur between such variables as Ba/Th, Sr/Y, $\epsilon_{Nd}(t)$, (La/Yb)_N and SiO₂, suggesting two types of crustal components in the mantle source: altered oceanic basalt and seafloor sediment. The altered oceanic basalt yields adakitic melt that is characterized by high (La/Yb)_N, Sr/Y and $\epsilon_{Nd}(t)$ but low Ba/Th and SiO₂, whereas the seafloor sediment yields sialic melt that is characterized by low (La/Yb)_N, Sr/Y and $\epsilon_{Nd}(t)$ but high Ba/Th and SiO₂. The OIB-type trace element patterns are interpreted as involvement of the oceanic crust that underwent partial melting outside the rutile stability field. These basalts exhibit low Fe/Zn and high Fe/Mn ratios, suggesting pyroxene-rich source lithology. The depleted Sr-Nd-Hf isotope compositions indicate involvement of juvenile lithospheric mantle.

We propose that westward subduction of the Pacific plate beneath the Eurasian continent serves as the geodynamic mechanism for slab-mantle interaction in oceanic subduction channel for formation of the mantle sources. A MASH mechanism is used to account for petrogenesis of these continental basalts. The subduction-modified oceanic basalt and sediment become melted (M) during subduction to mantle depths of over 100 km. Then the melts assimilated (A) the SCLM wedge peridotite to generate a variety of ultramafic metasomes. These metasomes would be stored (S) at bottom of the SCLM wedge for a long time (maybe 50-100 Myr or longer). Finally, when the continental lithosphere was in extension during the renewed subduction of Pacific plate beneath the Eurasian continent in the Cenozoic, these metasomes were heated (H) by upwelling of the asthenospheric mantle, generating the intraplate basaltic melts.

Evidence for the hydrothermal fluid origin of Sanqisan uranium deposit in China

XU ZHENGQI^{1,2*} AND SONG HAO^{1,2}

¹ Department of Geochemistry and Nuclear Resources Engineering, Chengdu University of Technology, Chengdu 610059, China (*Correspondence: xuzhengqi@cdu.cn)

² Key Laboratory of Nuclear Techniques in Geosciences of Sichuan Province, Chengdu 610059, China

Sanqisan uranium deposit is a typical carbonate-siliceous-pelitic rock-type uranium deposit in Southwestern Guangxi. Through studies of the ore geological features, trace elements, isotope geochemical characteristics and petrology, this paper presents the evidence of hydrothermal activities, and draws the conclusions that magmatism has great significance for the formation of Sanqisan deposit, with the general basic geological features the same as the normal hydrothermal type uranium deposits. 1) Many siliceous bodies, as well as the multiphase quartz vein, have been found in field. The siliceous bodies, with a relatively high uranium content, appear in lenticular shape and a different scope, the big one being 2-3 m thick, 5-6 m long, the small one being only dozens of centimeters. 2) According to microscopic observation, the newly found pyroclastic and phyllite detritus indicate that there are signs of magma activity (or volcanic activity), and show that the main ore-bearing structure is relatively violent with large scale. 3) There are signs of multiphase hydrothermal activity, such as quartzitification, pyritization, carbonatization, etc., which intersperse with each other. 4) From the trace element analysis results, the content of some elements, such as Ni, As, Mo, Zn, Cd, Co, etc. are significantly high, more than 10 to hundreds times higher than the crustal abundance value, and the concentrating coefficient of Sb is 4630. 5) The carbon and oxygen isotopic compositions of hydrothermal calcite of the Sanqisan deposit show obvious genetic characteristics of deep magmatic source. The variation range of $\delta^{13}C$ is -0.709‰~ -3.172‰, and that of $\delta^{18}O$ is -12.451‰~ -14.516‰. 6) According to the U-Pb zircon dating, the ages for the diabase dykes in Sanqisan uranium deposit are 90Ma and 32-47Ma, which are in accordance with the age of the Sanqisan uranium deposit, indicating great significance of magmatism for the mineralization of Sanqisan deposit.

This work is supported financially by the National Natural Scientific Foundation of China (Grants No. 41173059).

Ca²⁺ and Phosphate Ion Transport To and Calcium Phosphate Cluster Nucleation Within Collagen Fibrils In Bone Biomineralization

ZHIJUN XU¹, WEILONG ZHAO¹, YANG YANG²
QIANG CUI³ AND NITA SAHAI¹

¹Department of Polymer Science, University of Akron, Akron, OH 44325-3909, USA. (xu@uakron.edu) (wz24@zips.uakron.edu.) (sahai@uakron.edu.)

²Department of Chemistry and Biochemistry, Rowan University, Glassboro, NJ 08028, USA. (yangy@rowan.edu.)

³Department of Chemistry and Theoretical Chemistry Institute, University of Wisconsin, Madison, WI 53706, USA. (cui@chem.wisc.edu.)

Bone is a composite material consisting of collagen, an insoluble, fibrillar, protein; a non-stoichiometric calcium phosphate (Ca-P) phase idealized to hydroxyapatite (HAP); and soluble proteins. Based on TEM observations for six decades, collagen fibrils are known to be arranged in a hierarchical, “staggered” array, which controls the locations of the earliest nucleation in “hole zones” of the “a and e bands” within the fibril. However, the mechanisms for Ca²⁺ and inorganic phosphate (P_i) ion transport into the fibrils and for Ca-P nucleation in specific locations remain unknown.

We used the structure of collagen mimetic peptides and the 3-D packing structure of collagen molecules within a fibril to construct and optimize the entire collagen fibril structure with regular Molecular Dynamics (MD) simulations. Furthermore, Ca-P cluster formation and water diffusion and density distributions within the fibril were determined using Hamiltonian Replica Exchange Molecular Dynamics (HREMD), which captures even rare nucleation events. Significantly, we found that the lateral space between two adjacent collagen molecules is too small to allow prenucleation clusters larger than ~1nm to enter the fibril and reach the hole zones near the a and e bands where the earliest nucleation is observed by TEM. This result provides constraints on previously proposed mechanisms for calcium phosphate prenucleation cluster transport into the intra-fibrillar space. Further, the charged amino acid side chains (glutamate, aspartate, lysine, arginine) of the e bands are oriented to point into the hole zones, and attract Ca²⁺ and P_i ions electrostatically to form the earliest Ca-P clusters. We have shown for the first time the mechanisms by which the 3D hierarchical structure of collagen controls mineral nucleation from the Å – 10s of nm length-scale.

Carbonate speciation in depolymerized silicate melts (glasses): New evidence from ab initio calculations and ¹³C MAS and static NMR measurements

X. XUE^{1*} AND M. KANZAKI¹

¹Institute for Study of the Earth's Interior, Okayama Univ., Misasa, Tottori 682-0193 Japan (*Correspondence: xianyu@misasa.okayama-u.ac.jp)

Knowledge of the dissolution mechanisms of CO₂ in silicate melts and glasses is indispensable for understanding its effects on physical and thermodynamic properties. For depolymerised silicate compositions, previous IR, Raman and ¹³C MAS NMR studies of quenched glasses all revealed CO₃²⁻ as the dominant species. However, no consensus has been reached as to whether CO₃²⁻ are linked to network-formers (e.g. Si) or bonded to network-modifiers (e.g. Ca) only (referred to as free carbonates hereafter), due to the lack of direct information for spectroscopic features of the former.

Here we report ab initio calculation results (using Gaussian 09) of vibrational frequencies (at B3LYP/6-31+G(d,p), scaled by 0.9685) and ¹³C chemical shift tensors (at HF/6-311+G(2df,p)) for CO₃²⁻ groups bonded to one and two SiO₄/AlO₄ tetrahedra. We also report ¹³C MAS and static NMR results for several ¹³CO₂-bearing depolymerized silicate glasses, e.g. diopside (CaMgSi₂O₆) and Ca-melilite (Ca_{1.5}AlSi₂O₇), prepared by quenching melts at 1.0-1.5 GPa and 1400-1600 °C in a piston cylinder apparatus. The ab initio calculation revealed that the splittings of the ν₃ (asymmetric stretching) doublets for CO₃²⁻ bonded to one or two tetrahedral Si/Al are all large (around 180-480 cm⁻¹). In contrast, experimental data for CO₃²⁻ (bonded only to metal cations) in minerals show ν₃ splitting from zero to moderate, depending on local geometry. Thus, the moderate ν₃ splitting (70-100 cm⁻¹) reported for many depolymerized silicate glasses, which was used as evidence for CO₃²⁻ bonded to one Si (e.g. [1]), should be better viewed as evidence for free carbonates. Our calculations also showed that carbonates bonded to one or two Si/Al all show distinctly different characteristics of ¹³C chemical shift tensors compared to free carbonates, similar to experimental observations for organic carbonates (bonded to one or two C). Our ¹³C MAS and static NMR data for depolymerized silicate glasses are consistent with free carbonates as the dominant species. Its formation would lead to polymerization of the silicate structure.

[1] Blank, JG & Brooker, RA (1994) *Rev. Mineral.* **30**, 157-186.

Organic nitrogen cosmochemistry of ultracarbonaceous micrometeorite

H. YABUTA*, T. NOGUCHI, S. ITOH, S. TSUJIMOTO, N. SAKAMOTO, M. HASHIGUCHI, K. ABE, D. KILCOYNE, A. OKUBO, R. OKAZAKI, S. TACHIBANA, K. TERADA, T. NAKAMURA, M. EBIHARA AND H. NAGAHARA

*Dept. Earth and Space Science, Osaka University, Japan, (hyabuta@ess.sci.osaka-u.ac.jp)

Nitrogen is expected as a critical diagnostic tracer to determine the origin and evolution of organic compounds in the early Solar System. In the meteorite studies, nitrogen molecular and isotopic compositions have been debated separately for some of soluble organic compounds (e.g., amino acids) and insoluble organic solids, respectively. However, more than 10000 kinds of high molecular weight CHONS compounds remained unidentified in the solvent extract of Murchison meteorite (Schmitt-Kopplin *et al.* 2010). For understanding the formation of every discrete N-bearing organic compounds, it is very important to link soluble and insoluble components, by tracing back to more primitive organic chemistry than that of chondritic meteorites.

Amicrometeorite collected from the snow near the Dome Fuji Station, Antarctica, was investigated by SIMS, FIB-SEM, μ -XANES, and TEM in this study. From the micrometeorite, we have found an organic material in size of $\sim 10 \times 20 \mu\text{m}^2$, that is more than twenty times as large as those in chondritic meteorites. The organic material is seeping into epoxy (embedding media), implying partial solubility. Its C- and N-XANES spectra are rich in a variety of nitrogen functional groups, such as imine (C=N), nitrile (C \equiv N), and amide (NHx(C=O)C). The N/C ratio is estimated order of 0.15, which is around five times higher than those of insoluble organic solids from chondritic meteorites (Alexander *et al.* 2007) but similar to some of comet 81P/Wild 2 dust particles (Cody *et al.* 2008). The isotopic imaging reveals that the organic material is likely sulfurized by the surrounding sulfide. The N- and S-rich organic chemistry may be related to a number of soluble CHONS compounds found by Schmitt-Kopplin *et al.* No isotopic anomalies in hydrogen, carbon, and nitrogen are observed ($\delta\text{D} = \sim +100 \pm 300\text{‰}$, $\delta^{13}\text{C} = \sim 0 \pm 70\text{‰}$, $\delta^{15}\text{N} = \sim +100 \pm 110\text{‰}$). The nitrogen isotopic range covers that of α -amino acids in CR chondrite (Pizzarello and Holmes, 2009), but is distinct from that of insoluble organic solids in the same meteorite group (Alexander *et al.* 2007). The TEM mineralogical characterization records a very slight degree of aqueous alteration (Yabuta *et al.* 2013). Thus, the observed N-rich organic chemical characteristics could reflect a original source of amino acids and the other CHONS in meteorites.

REE Geochemistry of ~ 3.2 Ga old BIFs from the Mapepe Formation and Msauli Member, Barberton, South Africa

T.R. YAHAGI^{1*}, K.E. YAMAGUCHI^{1,2}, S. HARAGUCHI³, R. SANO⁴, S. TERAJI⁵, S. KIYOKAWA⁵, M. IKEHARA⁶ AND T. ITO⁷

¹Dept. Chem., Toho Univ. (6112029y@nc.toho-u.ac.jp),

²NASA Astrobiol. Inst., ³Atmosph. & Ocean Res. Inst. (AORI), Univ. of Tokyo,

⁴Japan Chem. Anal. Ctr. (JCAC),

⁵Dept. Earth & Planetary Sci., Kyushu Univ.,

⁶Ctr for Adv. Marine Core Res., Kochi Univ.,

⁷Fac. Edu., Ibaraki Univ.

A popular mechanism for Banded Iron Formation (BIF) deposition is that Fe-oxides were precipitated in deep-water setting by oxidation of dissolved Fe^{2+} supplied from submarine hydrothermal activity, by dissolved oxygen supplied from oxygenic photosynthesis in the surface ocean. When Fe-oxides precipitated, rare earth elements (REEs) were adsorbed on their surface. REE compositions of seawater have been recognized to reflect redox state of seawater and the extent of input from hydrothermal activity. In this study, we aimed to estimate Mesoarchean seawater chemistry based on REE signatures of 3.2 Ga old BIFs.

Samples were collected from outcrops of the Mapepe Fm at the bottom of the Fig Tree Gp and Msauli Member in the Onverwacht Gp, both belonging to the Swaziland Supergroup. Powdered rock samples were analyzed for their major element compositions by XRF at AORI, REE compositions by ICP-MS at JCAC, and oxygen isotope compositions. Samples with $<1.0 \text{ wt.}\% \text{ Al}_2\text{O}_3$ are considered to be "pure chemical precipitates" and thus used for further discussion.

Chondrite-normalized REE patterns of the Mapepe samples show positive Eu anomaly, elevated Y/Ho ratios, and LREE>HREE. Furthermore, there exist positive correlations among the extent of positive Eu anomaly, $\Sigma\text{Fe}_2\text{O}_3$ contents, and Y/Ho ratios. The maximum Y/Ho ratios are surprisingly comparable to the those of the modern ocean. These characteristics suggest a coherent story for BIF deposition; Fe^{2+} emanated from submarine hydrothermal activity was oxidized to Fe^{3+} , which, with enhanced particle reactivity, absorbed dissolved REEs and Y in the 3.2 Ga ocean, producing elevated near-modern Y/Ho ratios. The Msauli samples are mostly enriched in Al_2O_3 and have clastics-dominated REE patterns, suggesting deposition at shallower, more proximal setting.

We also estimate temperature of seawater 3.2 Ga ago from which the BIF precipitated, based on their oxygen isotope compositions of silicate- and Fe-oxide phases.

Intepretation of Cs adsorption behavior based on the EXAFS, TR-DXAFS, and STXM methods

TSUYOSHI YAITA

Japan Atomic Energy Agency, 1-1-1 Koto, Sayo-cho, Sayo-gun, Hyogo 670-5148, Japan

Radioactive cesium in Fukushima has brought serious problem on our daily life since the nuclear reactor accident. Thus, verification test of decontamination of radioactive cesium has been widely carried out in Fukushima. Although this test is usually performed based on the pre-test in laboratory, radioactive cesium, however, was not sometimes able to removed from clay minerals even if used the same method. Based on this backgrounds, we first tried to clarify the adsorption mechanism on clay mineral in detail through the speciation of cesium using the advanced analytical methods such as the synchrotron based EXAFS, TR (time resolved)-DXAFS (SPRING-8), STXM (ALS). Afterwards, we attempted identification of a specific adsorption site in clay minerals.

The adsorbent clay minerals were adopted vermiculite delivered from Fukushima and prepared by adsorption/desorption experiments of stable cesium in laboratory.

Figure 1 shows the time dependent radial structural function of EXAFS by TR-DXAFS. The structural differences dependent on time were able to classified into four processes as follows, 1) diffusion of hydrated cesium in frayed edge site, 2) dehydration, 3) adsorption on clay mineral, 4) closing of frayed edge site and fixing cesium on clay mineral site. In this presentation, we will talk about interpretation regarding the adsorption model based on the these results.

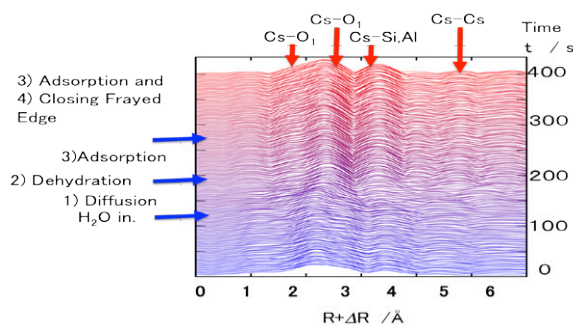


Figure 1: Time resolved radial structural functions of EXAFS for clay mineral-Cs-H₂O system. * Arrows in blue mean changing points of spectral features.

Oxygen isotopes as an indicator of corundums origin

¹V. V. YAKOVENKO ²S. V. VYSOTSKY³
AND A. V. IGNAT'EV

¹Far East Geological Institute, Far East Branch, Russian Academy of Sciences, Vladivostok, Russia(
yakovenko_v.v@mail.ru)

Jewelry corundums have different origins [1]. The purpose of this study was to show dependence of oxygen isotope composition in corundum from genesis. Samples from various fields of the world were studied. The obtained isotope data testify that all studied Corundum-bearing Ural pegmatites showed range from $4.6 < \delta^{18}O < 6.5 \text{ ‰}$. At the same time corundum from pegmatites of the Tazheransky massif showed values within range from $10.6 < \delta^{18}O < 11.9 \text{ ‰}$. Corundum from plagioclases in the ultramafic breccias Tanzania, Polar Ural Mountains and Gvineniya keeps within range from $4.8 \text{ ‰} < \delta^{18}O < 5.5 \text{ ‰}$. Biotite with corundum (Pamir) (7.4 ‰) it was formed of magmatic breccias, most likely under the influence of a mix of fluids: magmatic and metamorphic. Corundum was formed of Alabashka's marble and Pakistan ($19.4 - 19.9 \text{ ‰}$), most likely, as a result of a regional metamorphism of carbonate breccias, at a temperature of 600-6200C under the influence of a metamorphic fluid [2]. Thus, the oxygen isotope composition of corundums in fields metamorphic, pegmatitic and pneumatolitic-hydrothermal is dictated by oxygen isotope composition of the water containing fluid participating in their formation.

[1] E. Ya. Kievlenko, Ornamental Collection Minerals, 1987;
[2] Okrusch M., Bunch T.E., Bank H. // Mineral Deposita (Berlin) 1976. № 11. P.278-297.

(U-Th)/He dating of native gold: Problems and perspectives

YAKUBOVICH O.V.^{1,2}, SHUKOLYUKOV YU.A.^{1,2,*},
SALNIKOVA E.B.², YAKOVLEVA S.Z.²,
GOROKHOVSKY B.M.² AND KOTOV A.B.²

¹ Saint-Petersburg State University, Saint-Petersburg, Russia
[correspondence: olya.v.yakubovich@gmail.com]

² IPGG RAS, Saint-Petersburg, Russia

* deceased

As it has been suggested long time ago helium can easily escapes from crystal structures of minerals. However nowadays earlier preconceived ideas about the quick migration of helium from all materials should be revised.

There is a group of minerals, namely native metals, where the retention of radiogenic helium is rather high. Helium due to its very low solubility in metals tends to form atomic clusters. Migration of such stable clusters needs relatively high temperatures that are close to the metal melting point [1]. Anomalously high retention of radiogenic helium in native metals is experimentally shown on the example of native minerals of platinum. Finding paves the way for creation a novel ¹⁹⁰Pt-⁴He method of isotope geochronology [2].

Aforementioned indicates that theoretically retention of radiogenic helium in native gold also should be high. Taking into account that the concentration of U in native gold varies from first ppb to hundreds of ppm, there are rather high possibility for the direct dating of native gold by the (U-Th)/He method. Importance of this opportunity needs no explanations.

By the way first attempts of the direct (U-Th)/He dating of native gold seems to be inaccurate. Method easily could distinguish events within hundreds of million years. Nevertheless there was large dispersion in obtained ages. And as it become clear nowadays one of the main reasons of this dispersion hides in the problem of the behavior of uranium in native gold. After extended detailed SEM study of native gold it was shown that U and Th mainly occurs in gold as submicron inclusions of phosphates of REE that are very sensitive to secondary processes. In this way reliable age determination of native gold requires careful mineralogical study and appropriate sample preparation as well as special methodological approach for release of radiogenic He from native gold.

[1] Shukolyukov (2012) *Petrology*, **20.1.**, 1-20, [2] Shukolyukov (2012) *Petrology*, **20.6.**, 491-505

Phase equilibria modelling of open system melting: Some implications

CHRIS YAKYMCHUK^{1*} AND MICHAEL BROWN¹

¹University of Maryland, College Park, USA

(*correspondence: cyak@umd.edu)

Decompression melting has been invoked as an important process in tectonics. To evaluate this postulate, the melt production from metapelite and greywacke during high-*T* decompression is evaluated using *P-T* pseudosections calculated in the Na₂O–CaO–K₂O–FeO–MgO–Al₂O₃–SiO₂–H₂O–TiO₂–Fe₂O₃ chemical system. Both closed system (undrained) and open system (drained by episodic melt loss) conditions are investigated. In nature, closed system behaviour is unlikely to be important in crustal differentiation. For drained conditions, at each point along the *P-T* path where the melt fraction reaches 7 mol%, 6/7ths of the melt produced is removed from the bulk chemical composition and a new phase diagram is calculated for the residual composition. First, we consider melt production along schematic *P-T* paths comprising an isobaric heating segment at 1.2 GPa followed by decompression to 0.4 GPa at 750°C, 820°C, and 890°C. The maximum amount of melt produced during decompression occurs at the lowest temperature investigated (750°C). Along this *P-T* path, the melt volume does not reach 7 mol% prior to decompression; during decompression the metapelite generates 15 mol% and the greywacke 12 mol% melt. This amount is significantly less than commonly invoked in some discussions of orogenic collapse. Isobaric heating to 820°C and 890°C produces significantly more melt along the prograde segment, resulting in multiple melt drainage events prior to decompression, which leads to lower melt production during decompression. Second, we consider melt production from the solidus at 1.2 GPa to peak *P-T* of 860°C at 1.8 GPa followed by isothermal decompression to 0.4 GPa. For drained conditions along this schematic *P-T* path, the metapelite generates only 1/4 of the cumulative total of 31 mol% melt during decompression, whereas the greywacke generates 1/3 of the cumulative total of 19 mol% melt during decompression. The effects of melt loss on the dissolution of zircon and monazite are evaluated and the implications for the interpretation of U–Pb ages will be discussed. Some models for the structural and thermal development of migmatite domes and metamorphic core complexes may require reevaluation. In particular, the role of melt transfer through suprasolidus crust and melt accumulation at shallow levels in the anatectic zone should be considered rather than simply invoking the presence of large volumes of melt in decompressing crust.

An application of multivariate statistical analysis using SAS programme to identify heavy metal sources between Cebeci (Kocaeli)-Eregli (Zonguldak), Turkey

F. YALÇIN¹, E. KAYA² AND N. ILBEYLİ^{3*}

¹ Akdeniz University, Department of Mathematics, 07058, Antalya, Turkey, fusunyalcin@akdeniz.edu.tr

² Akdeniz University, Department of Animal Science, 07058, Antalya, Turkey, ebrukaya@akdeniz.edu.tr

³ Akdeniz University, Department of Geological Engineering, 07058, Antalya, Turkey, ilbeyli@akdeniz.edu.tr

The aim of this work is to determine heavy metal contents and their possible causes that represent the variability of The Sakarya Canyon coastal sediments using SAS programme. Results of the previous study were conducted in the same area and obtained by using SPSS programme (Yalcin et al., 2013). The results of analysis show that Zn, Cr, Zr, V, Ni, Pb, Co, Cu, Ga, As, Nb, Al, Sn, Cd, Fe, Mg, Ti and Mn are the highest values of heavy metals. Correlation analysis results display that there are high relationships between concentrations of Zn and Al, Cr and Mg, Ti, Mn, Fe and V. According to PCA, because of the eigen values that are larger than 1, three components are obtained. From the three components which are obtained: first one includes Ti, Mg, V, Mn, Co, Fe, Cr, Nb, second one contains Pb, Zn, Al, Cd and third one consists of Sn, Zr, Cu, Ga. Though, As wasn't included any of these components. The PCA that uses rotated loadings pointed out that first one variance explanation ratio is 42%, second one variance explanation ratio is 19% and finally third one variance explanation ratio is 16%. Considering all three components, total variance explanation ratio is 77%. Furthermore, PCA was performed using varimax transformation in order to obtain more interpretable results. When hierarchical cluster analysis is applied to data, resulting dendrogram showed that highest similarities are between G2, G3 and G4 stations. The similarities between these stations refer to the similarities between the ambient conditions. Regression analysis of the percentage of explanatory (R²) is 0.99 and the results of analysis are shown a high degree of accuracy. According to the data, heavy metals representing different factor groups display genetic similarity.

[1] Yalcin M.G., Simsek G., Ocak S.B., Yalcin F., Kalayci Y., Karaman M.E., "Multivariate Statistics and Heavy Metals Contamination in beach sediments from the Sakarya Canyon, Turkey" Asian Journal of Chemistry, 25 (4), 2059 - 2066 (2013).

Coal petrography and depositional environments relationship of the Tertiary coals from Anatolides (Tokat Region - Turkey)

N. YALÇIN ERIK^{1*} AND F. AY²

¹ Cumhuriyet Univ., Dep. of Geology, Sivas – Turkey (*correspondence: nyalcin@gmail.com)

² Cumhuriyet Univ., Dep. of Anthropology, Sivas – Turkey (farukay@gmail.com)

The study area is situated in the Anatolides, one of the major tectonic units of the Turkey. The aim of the study was to understand depositional environments of the Pliocene and Eocene coal-bearing strata from two different area of the Tokat region, and this is the first detailed investigation on the coal petrographic characterization and the interpretation of coal facies and depositional environment. These Pliocene and Eocene coals are a high ash and sulphur sub-bituminous coal which is petrographically characterised by a high huminite content, mainly gelinite macerals, relatively abundant vitrite, clarite and carbalgilitic microlithotypes. The mineral matter of the studied coal samples are made up mainly of clay minerals and quartz, in which calcite is the dominant mineral phase. Generally, the Pliocene coal has slightly higher ash content than the Eocene coals. Gross calorific values similar between Eocene and Pliocene samples (respectively avr. value 2974.33 and 3051.8 Kcal/kg). These coals have similar huminite reflectance value (average R_{max} values respectively; 0.42% and 0.48%). Based on volatile matter and gross calorific value, Eocene and Pliocene coals can be characterized as "Sub-bituminous B/C" coals. The ultimate analysis shows that these coals are low in carbon content, but have high oxygen and sulphur content. Palynological investigation in this study (especially Ovoidites parvus, the prevalence of the freshwater algae of Ovoidites ligneolus species) supports the development of that kind of vegetation in the Tokat region. Low TPI values indicate predominance of herbaceous and woody derived tissues and increased rate of subsidence that result in the poor preservation of the maceral structures. GI values indicate variable water table and suggest that the mire was not too acidic.

On the basis of the petrological parameters it is concluded that the Artova and Zile coals from Tokat interior are limno-telmatic type, formed in the lagoon in typical this formation conditions.

Chemical speciation of heavy metal elements in indoor dust by XAFS spectroscopy

H. YAMADA^{1*}, H. QIN² AND Y. TAKAHASHI¹.

¹ Hiroshima University, Hiroshima 739-8526, Japan

(*correspondence : m120941@hiroshima-u.ac.jp)

² Institute of Geochemistry, CAS

It is recently concerned that indoor dust can be a source of chemical materials which lead to adverse health effects for children. However, heavy metals in indoor dust have been poorly studied in Japan and China. Our previous study showed that lead (Pb), zinc (Zn), and antimony (Sb) were highly concentrated in indoor dust. Lead has been used for various industrial products, but low-level Pb exposure which leads to adverse health effect for children is concerned. Zinc is an essential element for living organisms, but can be a toxic if ingested excessively. The toxicity of Sb, which is recently recognized as an emerging element found environment, largely depends on the chemical state, especially the oxidation state. Thus, it is important to identify the chemical species of Pb, Zn, and Sb to understand their origins and assess their health effects for children. In this study, X-ray absorption fine structure (XAFS) was performed to identify the chemical species of heavy metal elements included in indoor dust and their origins.

The indoor dust was collected by a vacuum cleaner and, for comparison, soil outside of the same house was collected. The particle size fraction used for the analysis was smaller than 180 μm , the particle range of which can be ingested by children. Lead L_{III}-edge XAFS spectra for indoor dust samples in could be fitted with that of PbCrO₄, which was identified only in the indoor dust. It is suggested that the source of PbCrO₄ which may be derived from pigment possibly used in some materials indoors. Antimony K-edge bulk XANES and μ -XANES spectra of the indoor dust showed that the chemical state of Sb in most of the particles was Sb(V) which has a toxicity lower than Sb(III). Zinc K-edge bulk XANES spectra of the indoor dust collected suggested presence of ZnS originated from indoor materials.

Pu isotope in water column of the Sea of Okhotsk

MASATOSHI YAMADA^{1*}, JIAN ZHENG²
AND TATSUO AONO³

¹ Department of Radiation Chemistry, Institute of Radiation Emergency Medicine, Hirosaki University, Hirosaki, Japan, (*correspondence: myamada@cc.hirosaki-u.ac.jp)

² Research Center for Radiation Protection, National Institute of Radiological Sciences, Chiba, Japan (jzheng@nirs.go.jp)

³ Fukushima Reconstruction Support Headquarters, National Institute of Radiological Sciences, Chiba, Japan (t_aono@nirs.go.jp)

The Sea of Okhotsk is a marginal sea of the western North Pacific Ocean, lying between the Hokkaido Island, the Sakhalin Island, the Kamchatka Peninsula, Kuril Islands and the Siberian coast, and is a highly productive marine ecosystem. Anthropogenic radionuclides such as ²³⁹Pu (half-life: 24,100 yr), ²⁴⁰Pu (half-life: 6,560 yr) and ²⁴¹Pu (half-life: 14,325 yr) mainly have been released into the environment as the result of atmospheric nuclear weapons testing. The objectives of this study are to measure the ²³⁹Pu and ²⁴⁰Pu concentrations and ²⁴⁰Pu/²³⁹Pu atom ratios in seawater from the Sea of Okhotsk and to discuss the transport processes of Pu.

Seawater samples were collected at Stn. CM-06 in the Sea of Okhotsk with acoustically triggered quadruple PVC large-volume sampling bottles during the Canis Minor Expedition of the R/V Hakuho-Maru. The ²³⁹Pu and ²⁴⁰Pu concentrations and ²⁴⁰Pu/²³⁹Pu atom ratios were measured with a double-focusing SF-ICP-MS, which was equipped with a guard electrode to eliminate secondary discharge in the plasma and to enhance overall sensitivity [1].

The ²³⁹Pu and ²⁴⁰Pu concentrations were 1.3 – 1.5 mBq m⁻³ in the surface water and they increased with depth; a broad maximum was identified at 1,000 – 2,000 m depth. The atom ratio of ²⁴⁰Pu/²³⁹Pu showed no notable variation from surface water to deep water of 3,000 m depth. The atom ratios in water column of the Sea of Okhotsk were higher than the mean global fallout ratio of 0.18. However, the atom ratios were slightly lower than those observed in the Japan Sea and the western North Pacific Ocean. The Bikini close-in tropospheric fallout Pu could be transported to the Sea of Okhotsk by ocean currents.

[1] Zheng & Yamada (2007) *Anal. Sci.* **23**, 611-615.

Exposed Pleistocene Kurobegawa Granite (0.8 Ma): LA-ICP-MS and SHRIMP analysis

RYUJI YAMADA¹, HISATOSHI ITO², AKIHIRO TAMURA³, SHOJI ARAI³, KENJI HORIE⁴ AND TOMOKAZU HOKADA⁴

¹National Res. Inst. for Earth Sci. and Disaster Prevention, Ibaraki 305-0006, Japan (ryamada@bosai.go.jp)

²Geosphere Sci. Sector, Central Res. Inst. of Electric Power Industry, Chiba 270-1194, Japan

³Dept. Earth Sci., Kanazawa Univ., Ishikawa 920-1192, Japan

⁴National Inst. of Polar Res., Tokyo 190-8518, Japan

A young exposed pluton represents the recent tectonic uplift and high exhumation because a pluton is a body of intrusive igneous rock that crystallized from slowly cooling magma at depths of several kilometers beneath the surface of the Earth. The youngest exposed pluton reported to date was the Takidani Granodiorite (~ 1.4 Ma) in the Hida Mountain Range of central Japan [1]. Using LA-ICP-MS and SHRIMP U-Pb zircon dating methods, this study demonstrates that the Kurobegawa Granite, situated in the middle of Cretaceous granitic batholith in the Hida Range, is as young as ~ 0.8 Ma [2]. Our data indicate multiple intrusion episodes in this pluton since 10 Ma with a ~ 2-million-year period of quiescence; hence, a future intrusion event is likely within 1 million years.

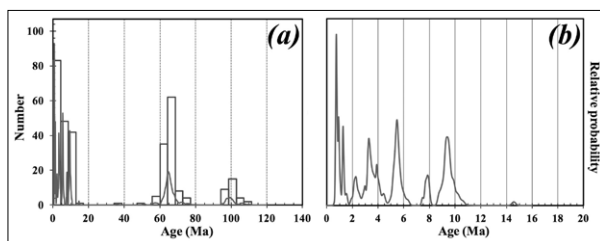


Figure 1: Age distribution of individual zircons. (a) Age distributions (cumulative probability distributions by *Isoplot* 3.75) for 320 grains of granitic origin with ages younger than 140 Ma. The peaks > 20 Ma are at 65 and 100 Ma. (b) Age distributions for 174 grains with ages < 20 Ma. The prominent peaks are 0.8, 1.3, 3.3, 5.5, 7.9, and 9.5 Ma.

[1] Sano, Y., *et al.* Ion microprobe U-Pb dating of Quaternary zircon: implication for magma cooling and residence time. *J. Volcanol. Geotherm. Res.* 117, 285–296 (2002).

[2] Ito, H. *et al.* Earth's youngest exposed granite and its tectonic implications: the 10–0.8 Ma Kurobegawa Granite. *Nature Sci. Rep.* 3, 1306; DOI:10.1038/srep01306 (2013).

Impact history of lunar highlands recorded in MIL 090034, 090036, and 090070 lunar meteorites

A. YAMAGUCHI^{1*}, N. SHIRAI², L.E. NYQUIST³, J. PARK^{4,5}, C-Y, SHIH⁶, M. EBIHARA² AND G.F. HERZOG⁵

¹National Institute of Polar Research, Tachikawa, Tokyo 190-8518, Japan (yamaguch@nipr.ac.jp)

²Tokyo Metropolitan University, Hachioji, Tokyo 192-0397, Japan

³NASA/JSC, Houston, TX77058, USA.

⁴LPI, Houston, TX 77058, USA.

⁵Rutgers University, Piscataway, NJ, USA.

⁶JE-23, ESGC/Jacobs Sverdrup, Houston, TX77258, USA.

Clues from feldspathic lunar meteorites help in understanding lunar crustal evolution. We performed petrological, geochemical, isotopic studies of feldspathic lunar meteorites, MIL 090034 (MIL34), 090036 (MIL36), and 090070 (MIL70) [1,2]. Here, we report petrology and impact history of the three lunar crustal rocks.

MIL34 and MIL70 are crystalline melt breccias. MIL34 contains anorthositic clasts. We found a clast of noritic anorthosite with minor phosphate and zircon that seems to be of Mg-suite rock in MIL34. MIL70 is poorer in clastic components and has coarser-grained melt matrix. Plagioclase compositions of MIL34 and MIL70 peak sharply around An_{96-97} as do those of FAN. Mg numbers of olivine vary from 58–65 with a few higher values. MIL36 is a fragmental or regolith breccia that contains fragments of K, Na-rich feldspar, phosphate, and zircon which are related to KREEP components. Plagioclase compositions vary from $\sim An_{84-98}$ with a broad peak at An_{95-97} .

Bulk chemical compositions are generally consistent with these petrologic data. The REE abundances of MIL34 and MIL70 ($Sm\sim 6\times CI$) are similar, whereas those of MIL36 are much higher ($\sim 30\times CI$) [1]. Also, MIL34 and MIL70 have similar cosmic ray exposure (CRE) ages indicating they are launch paired. MIL36 has a larger CRE age ($\sim >70Ma$) [2].

We suggest that MIL34 and 70 were derived from a large crater: MIL70 was deeply buried in the impact melt sheet, whereas MIL34 was closer to the surface on the basis of CRE and petrologic data. MIL36 was derived from a site near the KREEP-rich terrane. Ar-Ar ages for subsamples of MIL 34 and MIL70 range from 3.50 ± 0.11 to 3.64 ± 0.22 Ga, resp., and are 3.79 ± 0.04 Ga for MIL36.

[1] Shirai *et al.* (2012) *LPSC* 43, #2003. [2] Park *et al.* (2013) *LPSC* 43, #2576.

Natural analogue study on long term alteration of bentonite (2) - Geochemical simulation-

KOHEI YAMAGUCHI¹, HISAO SATOH¹, KUNIAKI AKAHORI¹,
TOMOKO ISHII², JIRO ETO² AND TOSHIAKI OHE³

¹Mitsubishi Materials Corp., Saitama Pref., 330-8508, JAPAN
(kyama@mmc.co.jp)

²Radioactive Waste Management Funding and Research
Center, Tokyo, 104-0052, JAPAN

³Tokai University, Kanagawa Pref., 25-1292, JAPAN

Introduction

In the geological disposal of Japanese TRU waste, it is important to understand the long term alteration of bentonite that is a part of the engineered barrier system. In this study, the geochemical simulations were carried out on natural bentonite suffered from Ca-rich alteration.

Discussion of Results

The alteration of bentonite in a tuffaceous bed at a Japanese island arc basin was focused as natural analogue. Based on the initial minerals estimated by MELTS[1], long term alteration of initial rock was calculated by PHREEQC[2]. In the simulation case, the initial marine sediments deposited in seawater at 5 Ma ago. This sedimentary age was based on experimental analysis of microfossils. In the simulation case, we programed that the sedimentary basin changed to land at 1 Ma ago. At the time, the porewater was set to be a 50:50 mixed rainwater-groundwater because a result of principal component analysis of present groundwater suggests this mixing ratio among rainwater and shallow hot spring water.

As a calculation result, coexistence of Na-, Ca-montmorillonite and zeolite were confirmed (Fig.2) for the past 5Ma. This coexistence is consistent with experimental results.

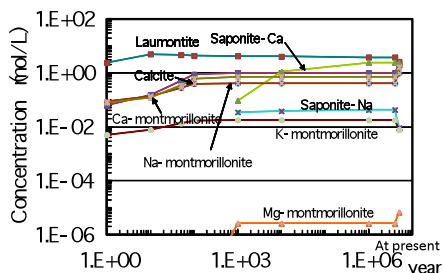


Fig.1 Calculated time-evolution of minerals in bentonite.

This research is a part of "Development of the technique for the evaluation of long-term performance of EBS (FY2007-2012)" under a grant from the Agency of Natural Resources and Energy, the Ministry of Economy Trade and Industry of Japan (METI)

[1] Ghiorsio & Sack (1995) *CMP* **119**, 197-212. [2] Parkhurst & Appelo (1999) *WRIR* 99-4259.

Biogeochemical cycling of nitrogen and carbon in the 3.2 Ga ocean: Results from DXCL-DP, NW Pilbara, Western Australia

K.E. YAMAGUCHI^{1,2}, D. KOBAYASHI¹, K. YAMADA¹,
R. SAKAMOTO³, K. HOSOI⁴, S. KIYOKAWA³,
M. IKEHARA⁴ AND T. ITO⁵

¹Dept. Chemistry, Toho Univ., ²NASA Astrobiol. Inst., ³Dept. Earth & Planetary Sci., Kyushu Univ., ⁴Center for Advanced Marine Core Res., Kochi Univ., ⁵Fac. Edu., Ibaraki Univ.

Records of geochemical cycling of bio-essential, redox-sensitive elements have keys to decipher mysteries of the co-evolution of Earth and life. In order to obtain insight into biogeochemical cycling of those elements and early evolution of microbial biosphere from high-quality samples, we drilled through Mesoarchean strata in coastal Pilbara (Dixon Island-Cleaverville Drilling Project, see [1]), and obtained 3.2 Ga old drillcores (CL1, CL2, and DX) of sulfide-rich black shales in the Cleaverville Group. We conducted a systematic geochemical study involving sequential extractions of Fe, S, C, and N for phase-dependent contents and isotope compositions, in addition to major and trace element analysis, for >80 samples. Here we focus on geochemistry of N and C.

The average C_{org} contents are 0.60, 0.73m and 1.21 wt.% for CL1, CL2, and DX, respectively, with a maximum value of 3.0 wt.%. The $\delta^{13}C_{org}$ values range from -30.7 to -25.7‰ (CL1), -32.6 to -27.8‰ (CL2), and -31.8 to -26.0‰ (DX). The average $\delta^{15}N_{org}$ values are $-3.8 \pm 0.9\text{‰}$ for CL1 and CL2 and $-2.0 \pm 1.0\text{‰}$ for DX, while the $\delta^{15}N_{clay}$ values are $-3.4 \pm 0.6\text{‰}$ for CL1 and CL2, and $-0.1 \pm 2.4\text{‰}$ for DX. These data may be explained by the following processes.

Microbially mediated redox-cycling of nitrogen, possibly involving denitrification and microbial (cyanobacterial?) N_2 -fixation are most likely mechanism to fully explain the obtained data set, while microbially mediated non-redox cycling of NH_3 is also possible. Sources of N are N_2 from the coeval atmosphere and/or NH_3 from submarine hydrothermal activity. Denitrification occurs in anoxic environments where sulfate reducton may also occur, which is supported by sulfur isotope compositions of sulfide in the same sample set. These results are in contrast with a previous study using chert [2], but consistent with more recent study by [3].

This study suggests operation of microbial N in the Mesoarchean. The atmosphere-hydrosphere system would have been sufficiently oxidized to allow redox-cycling of nitrate.

[1] Yamaguchi *et al.* (2009) *Sci. Drill.* **7**, 34-37. [2] Beaumont & Robert (1999) *Precam. Res.* **96**, 63-82. [3] Godfrey & Falkowsky (2009) *Nature Geosc.* **2**, 725-729.

Early sulfide precipitation in basaltic magma intruding into felsic reservoir beneath the summit of Asama volcano: a melt inclusion study for the 2004 eruption

YOSHIKI YAMAGUCHI¹, TOSHISUKE KAWASAKI²,
TAMAMI YAMAGUCHI³ AND YASUSHI OHTA⁴

¹Shinshu university, Japan

(*correspondance: yoshia_ygutti@d4.dion.ne.jp)

²Ehime University, Japan

³Kawasaki Municipal Science Museum, Japan

⁴Pacific Metals Co., Ltd., Japan

During the 2004 eruption of Asama volcano, sulfur-rich basaltic magma repeatedly intruded into a long-lived crystal-rich felsic reservoir beneath the summit. Melt inclusion study of scoria (23 September) revealed that the major phenocrysts (plagioclase, ortho- and clinopyroxene, and Fe-Ti oxides) were principally derived from the felsic magma and the phenocrysts trapped sulfur-poor felsic melt (SiO₂ 67-77 wt%, S mostly <1000 ppm). In contrast, olivine (>Fo₈₀), a rare phenocryst, was derived from basaltic magma, trapping sulfur-rich mafic melt (SiO₂ 48-59 wt%, S <2600 ppm) before the mixing.

Two types of Sulfide precipitates, Cu and Ni-bearing heterogeneous sulfide spherules (Cu <31 wt%, Ni <10 wt%) and homogeneous pyrrhotite, are commonly trapped in olivine phenocryst. And they are also found to be scattered in the glassy groundmass. In contrast, the major phenocrysts includes the only homogeneous pyrrhotite, together with the sulfur-poor felsic melt.

Petrologic observation of the melt and various crystalline inclusions trapped in olivine phenocrysts here provides relevant information about the primary composition of the basaltic magma. The three pieces of information are as follows. 1) Primary large SO₄²⁻ concentration of magma. 2) A high oxygen fugacity condition (> NNO + 1) of magma. 3) Primarily hydrous nature of magma and the consequent boiling of magma during crystallization.

It is likely that, during the ascent of this SO₄²⁻-rich hydrous magma, transformation of sulfur species on cooling from SO₂ to H₂S oxidized iron of magma, and led to the extensive precipitation of sulfide phases in the magma. The sulfur separation from the melt continuously decreased sulfur concentration of magma during the crystallization, hence, the most mafic (SiO₂-poor) and pre-boiling melts have the highest sulfur concentration (2600 ppm).

These petrologic data provide us with valuable information about the sulfur budget and the sulfur supply system. The ascent of the hydrous basalt magma transfers a large amount of sulphur, together with copper and probably other chalcophile metals, from the subduction slabs in the mantle to the felsic reservoir beneath the summit of the frontal volcanoes in central-northeastern Japan.

Apatite inclusions in Hadean zircon from Jack Hills, Australia

S. YAMAMOTO^{1*}, T. KOMIYA¹, M. SHIMOJO¹,
S. SAKATA², K. MAKI² AND T. HIRATA²,

¹Department of Earth Science and Astronomy, The University of Tokyo, Komaba, Meguro, Tokyo, 153-8902, Japan

(*correspondence: syamamot@ea.c.u-tokyo.ac.jp)

²Laboratory for Planetary Sciences, Kyoto University, Japan

Clues about conditions during Hadean era can be deduced from detrital zircons as old as 4.4 Ga preserved in metaconglomerate at Jack Hills in the Narryer Gneiss Complex, Western Australia. Previous investigations of these grains have suggested the existence of a hydrosphere, granitic continental crust and sedimentary cycling [1]. Especially, granitic mineral inclusions, such as quartz, plagioclase and K-feldspar, in Hadean detrital zircons provide strong evidence for the existence of granitic crust on early Earth. However, [2] proposes that inclusions of plagioclase and K-feldspar in zircon do not constrain a source rock. Moreover, *in-situ* U-Pb dating of monazite and xenotime inclusions in 4.25–3.35 Ga detrital zircons from Jack Hills shows ages with 2.68 Ga or 0.8 Ga, suggesting that the most mineral inclusions suffered from metamorphic/metasomatic overprint during late stage metamorphism [3]. These results call for a reassessment of source magma based on mineral inclusions in Hadean zircons.

We investigated apatite inclusions in Hadean zircons using Laser-Raman microscopy, SEM-EDS and electronprobe micro-analyzer (EPMA). Chemistry of apatite inclusions in zircon reflects the chemical compositions of the whole rocks and can characterize the host magma [2, 4]. Although low-abundance of apatite inclusions in detrital zircons from Jack Hills compared to those in granitic rocks suggests a secondary replacement on mineral inclusions [3], we observed 6 primary apatite inclusions with no visible cracks in 106 Hadean zircons. Y₂O₃ and SrO abundances in apatite determined by EPMA negatively correlate, ranging from 0.02 to 0.9 wt% and from 0.08 to below detection limit (0.01 wt%), respectively. High concentrations of Y₂O₃ (>0.4 wt%) and low concentration of SrO (<0.02 wt%) in apatite inclusions in Hadean zircons in Jack Hills are indicative of evolved, felsic host magma >65 wt% SiO₂ [2].

[1] Harrison (2009) *Annu. Rev. Earth Planet. Sci.* **37**, 479-505.

[2] Jennings *et al.*, (2011) *Geology* **39**, 863-866. [3]

Rasmussen *et al.*, (2011) *Geology* **39**, 1143-1146. [4]

Belousova *et al.*, (2002) *J. Geochem. Expl.* **76**, 45-69.

Iron isotopic composition of submarine hydrogenetic, diagenetic, and hydrothermal ferromanganese deposits

K. YAMAOKA^{1*}, D.M. BORROK², A. USUI³
AND H. KAWAHATA⁴

¹Geological Survey of Japan, National Institute of Advanced Industrial Science and Technology, 1-1-1 Higashi, Tsukuba, Ibaraki 305-8567, Japan (*correspondence: k.yamaoka@aist.go.jp)

²School of Geosciences, University of Louisiana at Lafayette, 611 McKinley Street, Lafayette, LA 70504, USA

³Faculty of Science, Kochi University, 2-5-1 Akebono-cho, Kochi 780-8520, Japan

⁴Atmosphere and Ocean Research Institute, The University of Tokyo, 5-1-5 Kashiwanoha, Kashiwa, Chiba 277-8564, Japan

In this study, we measured the iron isotopic compositions ($\delta^{56}\text{Fe}$ relative to IRMM-14) of hydrogenetic, diagenetic, and hydrothermal ferromanganese deposits from the Pacific Ocean (1400–6000 m water depth). The hydrogenetic nodules and crusts had a consistent average Fe isotopic composition of $-0.34 \pm 0.15\text{‰}$ (2σ). Our study contrasts with previous reports that measured larger variations in the $\delta^{56}\text{Fe}$ of these crusts in the Pacific ($-0.59 \pm 0.36\text{‰}$) and the Atlantic ($-0.27 \pm 0.36\text{‰}$) [1]. The consistent $\delta^{56}\text{Fe}$ values imply homogenous Fe isotopic composition of modern deep seawater in the central to northeastern Pacific. Despite differences in mineralogy and chemistry, the average $\delta^{56}\text{Fe}$ of diagenetic nodules ($-0.28 \pm 0.13\text{‰}$) was indistinguishable from the average $\delta^{56}\text{Fe}$ of nodules of hydrogenetic origin. These observations suggest that dissolution and re-precipitation of Fe in sediments resulted in no significant Fe isotope fractionation. In contrast, the recent and fossil hydrothermal manganese deposits from the Izu-Bonin arc showed large variations in $\delta^{56}\text{Fe}$, from -3.43 to $+1.27\text{‰}$. The recent manganese deposits (~30 mm thick) generally consisted of Mn-cemented volcanic sand with high $\delta^{56}\text{Fe}$ values overlying dense gray to black layers of manganese oxides with low $\delta^{56}\text{Fe}$ values. The mixing of different Fe sources is unlikely for such large isotopic variation. Given the proposed formation models [2,3], the most plausible explanation is kinetic Fe isotope fractionation during rapid oxidation of Fe(II) and precipitation of ferric oxides at the seawater-sediment interface.

[1] Levasseur *et al.* (2004) *EPSL*, [2] Usui and Nishimura (1992) *Mar. Geol.*, [3] Hein *et al.* (2008) *JGR*

Intermethod Comparison for K-Ar Dating of Clay Gouge

SEIKO YAMASAKI¹, HORST ZWINGMANN²
AND TAKAHIRO TAGAMI³

¹Geological Survey of Japan, AIST, Tsukuba, Japan, (yamasaki.seiko@aist.go.jp)

²CSIRO ESRE, Perth, Australia, (horst.zwingmann@csiro.au)

³KUEPS Kyoto Univ., Kyoto, Japan, (tagami@kueps.kyoto-u.ac.jp)

K-Ar dating of clay gouge has been reported as a suitable method for direct dating of shallow faults in recent decades. A new “unspiked” K-Ar dating system for clay samples has been set up at the Tono Geoscience Center (TGC), Japan Atomic Energy Agency. The unspiked K-Ar method is applied successfully for age determination of young volcanic rocks, and the method could similar be useful to date young fault gouges. However, there is only one study reported that compares the age data for fault gouges by the conventional “spike” method and unspiked methods [1].

We conducted an intermethod comparison study for K-Ar dating of clay gouge in two laboratories. A unique gouge sample was collected at depth of 252.9 m from a fault on the wall of a shaft at the Mizunami Underground Research Laboratory, central Japan.

Three clay separates (<0.1, <0.4, <2 micron) were measured by the two different K-Ar methods. The conventional K-Ar method was applied at CSIRO and the unspiked method was applied at TGC.

The age data for each fraction with two method agree well in their analytical errors. Because the age calculation parameters are different, the errors of the unspiked method are larger than those of the conventional method. The ages of coarser <2 micron fractions spread slightly, suggesting sample heterogeneity. The obtained illite age range is consistent with the stability field of illite and the main temperature field of brittle deformation within the cooling history of the host granite body of the fault, which was evaluated by apatite and zircon fission-track and K-Ar biotite ages from the host rock.

The consistency of the data between two methods, and the consistency with constraints from other geochronology data, demonstrate the potential of gouge dating with the new analytical system.

[1] Zwingmann *et al.* (2010) *Chem. Geol.* **275**, 176-185

A 150-year variation of Kuroshio transport detected by the nitrate $\delta^{15}\text{N}$ records in coral skeletons

A. YAMAZAKI^{1&2*}, T. WATANABE¹, U. TSUNOGAI³,
F. IWASE⁴ AND H. YAMANO⁵

¹Grad. Sch. of Science, Hokkaido Univ., Sapporo, 060-0810, JAPAN (*correspondence: zaki@frontier.hokudai.ac.jp, nabe@mail.sci.hokudai.ac.jp)

²AORI, University of Tokyo, Kashiwa, Chiba, 277-0882, JAPAN(zaki@aori.u-tokyo.ac.jp)

³Grad. Sch. of Environmental Studies, Nagoya Univ., Nagoya 464-8601, JAPAN (urumu@nagoya-u.jp)

⁴Kuroshio Research Institute, Ohtsuki, Kochi, 788-0333, JAPAN (iwase@kuroshio.or.jp)

⁵NIES, Tsukuba, Ibaraki, 305-8506, JAPAN (hyamano@nies.go.jp)

The Kuroshio Current is the strongest ocean current in the world, driving the physical ocean-atmosphere system with heat transport from tropical to temperate in the North Pacific Ocean. The global environment has dramatically changed over the past 100 years, and the global sea surface temperature has increased by $\sim 1^\circ\text{C}$ since the early 1900s. The response of the Kuroshio to global warming is debatable, however, as the variability of the Kuroshio Current during the past 100 years has not been well understood. In this presentation, we describe the variability of the Kuroshio transport over the past 150 years as reconstructed from the nitrogen isotope composition of coral skeletons ($\delta^{15}\text{N}_{\text{coral}}$). $\delta^{15}\text{N}_{\text{coral}}$ has been used as a proxy to record nitrate $\delta^{15}\text{N}$ values [1-2]. *Porites* coral cores were collected from Tatsukushi Bay, on the Pacific coast of Japan and located on the Kuroshio axis. $\delta^{15}\text{N}_{\text{coral}}$ varied due to a mixture of Kuroshio water and temperate sea surface water. We discuss the relationship between $\delta^{15}\text{N}_{\text{coral}}$ and global warming, PDO, and ENSO.

[1] Yamazaki *et al.* (2011) *Geophys. Res. Lett.* **38**, L19605.

[2] Yamazaki *et al.* (2011) *J. Geophys. Res.* **116**, G04005.

P-V-T equation of state for ϵ -iron up to 80 GPa and 1900 K using the Kawai-type high pressure apparatus

D. YAMAZAKI^{1*}, E. ITO¹, T. YOSHINO¹, A. YONEDA¹,
X. GUO¹, B. ZHANG¹, W. SUN¹, A. SHIMOJUKU¹,
N. TSUJINO¹, T. KUNIMOTO², Y. HIGO²
AND K. FUNAKOSHI²

¹Institute for Study of the Earth's Interior, Okayama Univ., Japan

²Japan Synchrotron Radiation Research Institute, Japan (dy@misasa.okayama-u.ac.jp)

Using the Kawai-type multianvil high pressure apparatus equipped with sintered diamond anvils, we determined the *P-V-T* equation of state of ϵ -iron by means of in situ X-ray observations with synchrotron radiation at pressures up to 80 GPa and temperatures up to 1900 K. The *P-V-T* data set of ϵ -iron was fitted to a single EOS model based on the Mie-Grüneisen equation of state as shown in Fig. 1. The present results indicate the unit cell volume at ambient conditions $V_0=22.15(5) \text{ \AA}^3$, the isothermal bulk modulus $K_{T0}=202(7) \text{ GPa}$ and its pressure derivative $K'_{T0}=4.5(2)$, the Debye temperature $\theta_0=1173(62) \text{ K}$, Grüneisen parameter at ambient pressure $\gamma_0=3.2(2)$, and its logarithmic volume dependence $q=0.8(3)$. Furthermore, thermal expansion coefficient at ambient pressure was determined to be $\alpha_0(\text{K}^{-1})=3.7(2)\times 10^{-5}+7.2(6)\times 10^{-8}(T-300)$ and Anderson-Grüneisen parameter $\delta_T=6.2(3)$. Using these parameters, the density of ϵ -iron at the inner core conditions was estimated to be $\sim 3\%$ denser than the value inferred from seismological observation. This result indicates that certain amount of light elements should be contained in the inner core as well as in the outer core but in definitely smaller amount.

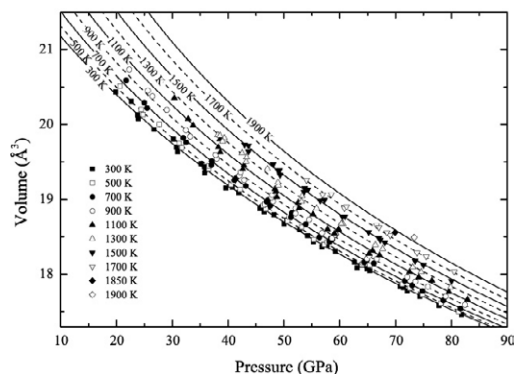


Fig. 1. *P-V* data along isotherms at 300-1900 K.

Zn isotope compositions of the Ediacaran Carbonates, Yangtze Block

B. YAN, X. K. ZHU AND S. H. TANG

Laboratory of Isotope Geology, Institute of geology, Chinese Academy of Geological Sciences, Beijing, 10037, China (yanbin703@163.com)

The sedimentary sequences of the Ediacaran Doushantuo Formation in the Yangtze block are mainly composed of alternating siliciclastic and carbonate rocks and yields abundant preserved animal fossils, thus it is critical for deciphering the evolutionary history of life during the time interval. Zn isotope fractionations are controlled by the biological processes in seawater (Maréchal *et al.*, 2000; Pichat *et al.*, 2003). Thus it can be used to track the evolution of primary productivity in the Ediacaran Period.

The $\delta^{66}\text{Zn}$ values of carbonate rocks in the whole Doushantuo Formation vary from 0.18‰ to 0.81‰ (relative to JMC3-0749L), with an average of 0.48‰, displaying enrichment in Zn heavy isotope. The carbonates $\delta^{66}\text{Zn}$ values of the Doushantuo Formation which comprises the four members have some positive and negative shifts. The $\delta^{66}\text{Zn}$ in the Member 1 increases from 0.41‰ at the base to 0.81‰ at the middle, and declines to 0.34‰ in the upper. The $\delta^{66}\text{Zn}$ of Member 2 increases to 0.65‰ at the base, and decreases to 0.18‰ at the middle. At the upper of the Member 2 and the base of Member 3, the $\delta^{66}\text{Zn}$ values fluctuate around 0.21‰–0.57‰. The $\delta^{66}\text{Zn}$ at the middle of Member 3 begins with an increase from 0.38‰ to 0.80‰, and decrease to 0.32‰ at the uppermost.

Those compositions are significantly higher than average continental crust (~0.2‰–0.3‰; Maréchal *et al.*, 2000; Archer and Vance, 2004). This may suggest that due to biological process control of the Zn isotope composition (Maréchal *et al.*, 2000), Zn light isotope is removed from the surface ocean by primary producers and transported to the deep ocean (Maréchal *et al.*, 2000; Bermin *et al.*, 2006). In that case, the Zn isotope ratios measured in carbonates may record the fluctuations in primary productivity during Ediacaran Period.

Distribution of cadmium and its main influencing factors in the surface sediments from five typical bays in eastern coastal areas of Guangdong Province, South China

WEN YAN, XIAOHUA ZHANG, LIFENG ZHONG AND NAN ZHANG

CAS Key Laboratory of Marginal Sea Geology, South China Sea Institute of Oceanology, Chinese Academy of Sciences, Guangzhou 510301, China (wyan@scsio.ac.cn)

In recent years, with the rapid economic and social development in eastern Guangdong, South China, the environmental state of the coastal waters has aroused great attention by the people. Cadmium (Cd) is a heavy metal with biological non-essential and highly toxic effects, and its special chemical and geochemical properties determines its high degree of risk and difficult to control in the natural environment.

The contents of Cd were determined for 64 surface sediments collected from five typical bays in eastern coastal areas of Guangdong Province, and the distribution characteristics of Cd in surface sediments and their main influencing factors were discussed. Meanwhile, the potential ecological risk indexes were calculated referring to the background value of the continental shelf of South China Sea. The results showed that content ranges of Cd were 0.04~0.58mg/kg, 0.06~6.63 mg/kg, 0.06~0.11mg/kg, 0.04~0.20 mg/kg and 0.08~0.15mg/kg respectively in Zhelin Bay, Shantou Bay, Shanwei Bay, Daya Bay and Dapeng Bay, and different distribution trend appeared in different bay. In Zhelin Bay and Shantou Bay, the Cd content presents a high value in aquaculture areas and in the waters near of Sanbaimen dam and Cape of Good Hope, as well as the end of the Sediment Retention embankment waters, and low Cd content presents in the rest of the waters, close to or below the background values of the continental shelf sediments in the South China Sea. The Cd contents increased from inshore to offshore, west to east in Shanwei Bay, and the high levels of Cd generally appear in the Bay outside in Daya Bay and Dapeng Bay.

Organic carbon and fine-grained component of sediments are not the main factors to control the content and distribution of Cd in the study area. Cd distribution was more influenced by the heavy metal input and hydrodynamic effects, and the aquaculture was also a way to change the depositional environment, so that the spatial distribution of Cd changed.

Acknowledgments: This study was supported by the Key project of NSFC-Guangdong Joint Foundation (U1133002).

Study of lithium isotope in hydrothermal quartz veins from the Qulong porphyry copper deposit in Tibet

YANG DAN^{1,2*}, YANG ZHIMING³ AND HOU ZENGQIAN³

¹Institute of Mineral Resources, CAGS, Beijing 100037, China
(*correspondence: yangd_2004@yahoo.com.cn)

²Key Laboratory of Metallogeny and Mineral Assessment, MLR, Beijing 100037, P.R.China

³Institute of of Geology, CAGS, Beijing 100037, China

Evolution details of ore-forming fluids and the precipitation mechanism of ore mineral have always been the focus of metallogeny research. However, the traditional hydrogen and oxygen isotope tracing method of ore-forming fluid has been strongly questioned in recent years because it is difficult to avoid the impact of secondary inclusions and high-temperature isotope fractionation. In Qulong porphyry copper deposit, a typical representative of Gangdise porphyry copper belt of Tibet, we attempt to use the lithium isotope to trace the origin of ore-forming fluid. We analysed lithium isotopic compositions of different stage quartz veins and altered minerals. Preliminary results show that there is a positive correlation between $\delta^7\text{Li}$ and $\delta^{18}\text{O}_{\text{V-SMOW}}$ of quartz veins. From early quartz vein to late ones, $\delta^7\text{Li}$ and $\delta^{18}\text{O}_{\text{V-SMOW}}$ values decrease synchronously. This trend indicates that the early ore-forming fluid originated from degassed magma water and meteoric water gradually joined in it in late stage. This attempt may provide a reliable and effective tracing method for ore-forming fluid.

Petrogenesis of Early Cretaceous intrusive rocks from southern margin of the North China Craton: Constraints from zircon U-Pb ages and Sr-Nd-Pb-Hf isotopes

D.B. YANG, W.L. XU, F. WANG AND F.P. PEI

College of Earth Sciences, Jilin University, Changchun 130061, China
(yangdb@jlu.edu.cn, xuwl@jlu.edu.cn)

The spatial extent of the influence of the deeply subducted Yangtze slab on the North China Craton (NCC) remains a controversial issue. The zircon U-Pb ages and Sr-Nd-Pb-Hf isotopic data of Early Cretaceous intrusive rocks in Sanmenxia area from the southern margin of the NCC provide a constraint for that. These intrusive rocks, including Gaomiao (GM), Quli (QL), Canfang (CF), and Wangmao (WM) intrusions, consist of quartz diorite porphyry, granodiorite, and granodiorite porphyry.

Zircon U-Pb dating results indicate that the GM, QL, CF, and WM intrusions formed in the Early Cretaceous (129 Ma, 115 Ma, 130 Ma, and 130 Ma, respectively). The occurrence of Neoproterozoic zircons (620 and 542 Ma) and inherited Late Triassic (214 - 225 Ma, n=6) metamorphic zircons within the QL intrusion, suggests that the primary magmas could be derived from partial melting of the Yangtze Craton basement that was superimposed by ultrahigh pressure metamorphism. In contrast, the occurrence of Paleoproterozoic and Archean ages within the GM, CF, and WM intrusions, indicates that their primary magmas were mainly originated from partial melting of the NCC basement.

The GM, QL, CF, and WM intrusions have high SiO_2 (60.65 - 67.62 %) and low MgO (0.35 - 1.15 %). They are enriched in LILEs and LREEs, and depleted in HFSEs and HREEs. The GM, QL, and CF intrusions have strong negative $\epsilon\text{Nd}(t)$ (-22.2 to -16.7) and $\epsilon\text{Hf}(t)$ (-29.6 to -21.4) values as well as low initial $^{206}\text{Pb}/^{204}\text{Pb}$ ratios (17.19 to 17.33), suggesting that they were mainly derived from partial melting of ancient lower crust, whereas the WM granodiorite porphyries have relatively high $\epsilon\text{Nd}(t)$ (-12.5 to -11.9) and $\epsilon\text{Hf}(t)$ (-21.7 to -16.6) values, indicating that they could be derived from partial melting of lower crustal materials with involvement of mantle components.

Taken together, we conclude that the southern margin of the NCC had been influenced by the deeply subducted Yangtze slab during the Triassic.

This research was financially supported by research grants from 973 program (2009CB825005), the NSFC (41002018, 91014004), and NCET.

Structure of Weathered Clastic Crust and Its Significance in Deep Petroleum Exploration

FAN YANG, LIAN-HUA HOU AND CHUN YANG

Research Institute of Petroleum Exploration & Development,
PetroChina, Beijing 100083
China(yf2010@petrochina.com.cn)

Deep, ultra-deep are one of the most important hydrocarbon exploration areas in the future. 96 ultra-deep clastic reservoirs were discovered in the global since 2000, accounting for 91.4% of the total number of ultra-deep reservoirs (IHS, 2011). Most of the ultra-deep reservoirs relate to unconformity, such as Junggar Basin that locates in Western China which develops 13 regional large-middle scale unconformities. Good reservoirs whose porosity above 15% are developed at the burial depth of about 6500m because of the influence of K-J unconformity. Based on clastic outcrops and well cores in Junggar Basin, considering the lithology of weathered layers, different weathering degree of minerals and diversity of element migration capabilities, weathering index of weathered clastic crust was built mainly in view of Fe and Al contents. The weathered clastic crust was divided into 3-layer structure model, which are weathered clay, sandy eluvial zone and muddy eluvial zone. Weathered clay mainly distributed at the slopes and low places, and had an inverse proportional development relationship with the eluvial zone. Analyzing reservoir properties of rock samples from the outcrop and well cores, detailed describing reservoirs beneath the T-P unconformity in western Junggar Basin, the results suggest that the porosity of eluvial zone is greatly improved due to weathering and leaching, but the permeability depends on the clay mineral contents. The higher the clay content, the worse the permeability is. The weathered clay has a high breaking pressure and could be treated as a good cap rock. The lower limits of hydrocarbon exploration depth are greatly downward because of weathering effect. The existence of weathered crust provides effective reservoir-cap rock for hydrocarbon accumulation, enriching an important geological theory and assessment methodology in deep, ultra-deep petroleum exploration.

Re-Os analyses for Ag ores from the Kongsberg mines, southeast Norway

G. YANG^{1*}, H. STEIN^{1,2} AND A. ZIMMERMAN¹,

¹AIRIE Program, Colorado State University, Fort Collins, CO USA (*correspondence: gangyang@colostate.edu)

²CEED Centre of Excellence, University of Oslo, Norway

The Kongsberg silver mines, hosted in Precambrian gneisses, are located along the western margin of the Permian Oslo rift, southeast Norway [1]. Native Ag-bearing late calcite veins are widely distributed in the Kongsberg metallogenic district, along with sphalerite, pyrrhotite, chalcocopyrite, galena, argentite and Co-(Ni) arsenides. The main gangue minerals in the Kongsberg silver mines are calcite, fluorite, quartz, barite and locally coalblende [1].

Re-Os analysis of native Ag provides chemical challenges. Conventional sample digestion using inverse *aqua regia* produces a highly insoluble AgCl precipitate, and thus is not suitable for native Ag or Ag-bearing ores. A modified version of conventional Re-Os chemical procedures [2] was therefore implemented. Hydrochloric acid was removed from the digestion and anion resin exchange column chemistry. To determine Re and Os concentrations and Re-Os isotope systematics, we analyzed pure vein silver, disseminated silver minerals in a fine-grained carbonate-calcite matrix, and nearly-barren calcite. Re and Os concentrations for visibly pure vein silver are 89-108 ppt and 1.1-1.7 ppt, respectively. Re and Os concentrations for disseminated silver minerals are notably enriched at 10.2 ppb and 47 ppt, respectively. And, Re and Os concentrations for calcites are 3.2-6.4 ppb and 16-29 ppt. Petrography suggests that high Re and Os concentrations in the sample with disseminated Ag are derived from small inclusions and intergrowths of other sulfides. A Model 3 isochron age of 436 ± 23 Ma (MSWD = 45, n = 6) was obtained based on pure vein silver, disseminated silver minerals, and calcite with large ranges of $^{187}\text{Re}/^{188}\text{Os}$ and $^{187}\text{Os}/^{188}\text{Os}$ from 311 to 92992 and 0.21 to 671, respectively.

The suggestion of a 436 Ma isochron could allude to an older history than has been assumed for formation of the Kongsberg Ag deposits. Clearly additional work is needed on other Ag-associated sulfides to confirm a pre-Permian, Caledonian age for this historically important ore.

We thank Fred Steinar Nordrum of the Norwegian mining museum for access to Ag-bearing samples from the Kongsberg mines.

[1] Bjørlykke *et al.* (1990) *Tectonophysics* **178**, 109–126. [2] Stein *et al.* (2001) *Terra Nova* **13**, 479–486.

Geochemical characteristics of granites and their relationship to gold mineralization in Yangshan gold deposit, Gansu Province, China

YANG GUICAI^{1,2*}, YUAN SHISONG^{1,2}, QI JINZHONG³
AND GE LIANGSHENG²

¹ School of Earth Science and Resources, China University of Geosciences, Beijing, 10083, China;

² Gold Geological Institute of CAPF, Langfang 065000, Hebei, China;

³ Gold Headquarters of CAPF, Beijing 100055, China

*(Corresponding author: yangguicai_1979@126.com)

Yangshan gold deposit, hosted in the Devonian stratum on the north margin of Bikou Terrane, western Qinling orogenic belt, is a super-large carlin-like gold deposit discovered recently in Gansu Province, China. Many granitic dikes were found in the deposit and had spatial relationship to gold ore bodies. But the genetic relationship between them is still controversial. Studies show that the SiO₂, K₂O and Al₂O₃ of the granites range from 60.64% to 80.77%, 2.27% to 4.32% and 11.83% to 23.71% respectively, and the A/CNK varies from 1.24 to 4.29, which indicate the granites are belong to prealuminous, calc-alkaline. The Granites are also enriched in Cs, U, K, Pb, and depleted in Ba, Nb, La, Ce, Sr, Ti. Rare earth elements (REE) content of the granites is between 14.45×10⁻⁶ and 143.14×10⁻⁶ (average 70.31×10⁻⁶), with La_N/Yb_N ratios of 1.48- 37.26 (average 17.08). Light rare earth elements (LREE) are concentrated evidently and heavy rare earth elements (HREE) are deficient with LREE/HREE ratios of 1.39-19.52 (average 10.12). The REE patterns are characterized by slightly negative Eu anomalies, with δEu=0.50-1.21 (average 0.77). Combining with the analytical data of the major and trace elements, geochronology and Sm/Nd, Rb/Sr and Pb isotope of Yangshan granites, Bikou group volcanic rock and Devonian Sanhekou section stratum from previous work, it is proposed that the granites were derived from partial melting of deep thickening crust (Bikou group volcanic rock) and mixed with Devonian stratum during ascent. That is to say that the ore-forming material of Yangshan gold deposit directly derived from granitic magma, and the Bikou group volcanic rock and Devonian stratum should be the primary source.

Source of fluid during continental subduction and exhumation: *In situ* LA-ICP-MS analysis of Sr-isotope in barite of eclogite from the Sulu UHP terrane, eastern China

H. YANG¹ A. GERDES² L.-F. ZHANG³ AND F.-L. LIU¹

¹ Institute of Geology, Chinese Academy of Geological Sciences, Beijing 100037, China (hyang@cags.ac.cn, lfl0225@sina.com)

² Institut für Geowissenschaften, Mineralogie, Altenhoferallee 1, D-60438 Frankfurt am Main, Germany (gerdes@em.uni-frankfurt.de)

³ School of Earth and Space Sciences, Peking University, Beijing 100871, China (Lfzhang@pku.edu.cn)

Barite occurs as a fluid-bearing mineral in eclogite cores distributed at 0-3000 m depth intervals of the main-hole of the Chinese Continental Scientific Drilling (CCSD) in the Sulu UHP terrane. Based on the petrographic features, barite can be divided into three types, including as inclusions of garnet at the peak ultrahigh-pressure (UHP) metamorphic stage, and as matrix mineral at the early retrogressive eclogite-facies stage and the late retrogressive amphibolites-facies stage. Its formation was genetically associated with fluid activity and metamorphic P-T conditions. This study introduces a new method of *in situ* ⁸⁷Sr/⁸⁶Sr analyses on the barite grains by LA-ICP-MS, and obtains three groups of Sr-isotope ratios related to the different metamorphic stage. The analyzed results show that ⁸⁷Sr/⁸⁶Sr ratios of barite is about ~0.7050, ~0.7067 and 0.7080~0.7125 for the peak UHP metamorphic stage, the early retrogressive eclogite-facies and the late amphibolites-facies stage, respectively, and display an increase trend from UHP metamorphism until late retrogression. This evolutionary characteristics of ⁸⁷Sr/⁸⁶Sr ratios reveal the genetic information of fluid activity during UHP metamorphism and late retrogression. Thereinto, the fluid was mainly a mixed phase from mantle and crust source during the continental subduction, then more external crustal fluid was added during the early exhumation, and finally external crustal fluid became the dominant source when the Sulu UHP terrane was exhumed to the upper crust level.

Molybdenum isotopes during magmatic differentiation

J. YANG¹, C. SIEBERT², J. BARLING¹, P. SAVAGE³,
Y.-H. LIANG¹ AND A. N. HALLIDAY¹

¹ Department of Earth Sciences, University of Oxford, South Parks Road, OX1 3AN, UK (jiej@earth.ox.ac.uk)

² GEOMAR, Helmholtz-Zentrum für Ozeanforschung, Wischhofstrasse 1-3, 24148 Kiel, Germany

³ Department of Earth and Planetary Sciences, Washington University in St. Louis

This study presents the first evidence for the behaviour of molybdenum isotopes during magmatic differentiation. Molybdenum isotopic compositions, as well as rare earth elements (REE), have been determined for a sequence of lavas from Hekla volcano, Iceland, covering a compositional range from basalt to rhyolite (from 46 to 72 wt.% SiO₂), sequentially developed by magmatic differentiation from a cogenetic source. All samples are characterised by identical Mo isotopic composition with $\delta^{98}\text{Mo}$ approximating zero (with an average $\delta^{98/95}\text{Mo}$ of $-0.02\pm 0.1\%$ (2s.d.) relative to an Alfa Aesar standard solution (lot 011895D) [1]). This study therefore reveals that resolvable Mo isotope fractionation is unlikely to occur during such magmatic differentiation. This is consistent with the fact that Mo is consistently incompatible in this suite of lavas; the lack of fractionating phases therefore preserves the original basaltic parent magma composition.

Previous work [2] suggests that Pr and Mo are equally incompatible in basaltic systems. However, in this study it can be seen that Mo becomes more incompatible than Pr in silicic systems. Despite the fact that these are low ¹⁸O magmas, hydrothermal processes and assimilation have had no effect on the Mo isotopic compositions.

Two additional volcanic samples from nearby unrelated volcanos were analysed and are indistinguishable from the Hekla data. This is consistent with a previous study which also indicates a similarity of Mo isotopic signature ($\delta^{98/95}\text{Mo}\sim 0.03\pm 0.12\%$) for riverine bedrocks from the vicinity of Vatnajökull glacier on Iceland [3]. Therefore, the Iceland crust appears to have a very homogeneous Mo isotopic signature ($\delta^{98}\text{Mo}\sim 0\pm 0.1\%$). The insensitivity of the Mo isotope system to igneous differentiation means that it is especially well suited for studies of assimilation and water-rock interaction in magmatic systems.

[1] Greber *et al.* (2012) *Geostand. Geoanalytical Res.* **36**, 291–300. [2] Newsom *et al.* (1986) *Earth Planet. Sci. Lett.* **80**, 299–313. [3] Pearce *et al.* (2010) *Earth Planet. Sci. Lett.* **295**, 104–114.

Thallium isotope geochemistry of early Cambrian black shales and Ni-Mo sulfide ores in South China

YANG JING-HONG¹, JIANG SHAO-YONG^{1,2},
REHKAMPER M³, XUE XC³, PI DH^{1,2} AND ZHU B^{1,4}

¹State Key Laboratory for Mineral Deposits, Department of Earth Sciences, Nanjing University, Nanjing 210093, China

²State Key Laboratory of Geological Processes and Mineral Resources, China University of Geosciences, Wuhan, Hubei, 430074, China

³Department of Earth Sciences & Engineering, Imperial College London, UK

⁴Institute of Isotope Hydrology, School of Earth Sciences and Engineering, Hohai University, Nanjing 210098, China

Thallium has two stable isotopes: ²⁰³Tl (29.5%) and ²⁰⁵Tl (70.5%). The present-day oceanic residence time of Tl is estimated to be ~20 kyr, significantly longer than the mixing time of the oceans (about 1 kyr). Natural Tl isotopic composition shows a variation of about 35 $\epsilon^{205}\text{Tl}$ units in terrestrial samples.

In this study, we analyzed Tl isotopes for the early Cambrian Niutitang Formation black shales and the Ni-Mo sulfide ores from Zunyi, Guizhou province, south China. The Ni-Mo sulfide ore shows the highest Tl concentration (40.5 ppm) and the lowest and negative $\epsilon^{205}\text{Tl}$ (-2.06), similar to seafloor hydrothermal fluid value (-1.9), but different from present-day seawater (-6.0). The black shales show smaller negative $\epsilon^{205}\text{Tl}$ near 0 (0 to -0.17). But the V-rich black shale has slightly higher Tl concentration (7.3 ppm) and lower $\epsilon^{205}\text{Tl}$ value of -0.6. The chert shows similar Tl concentration with the black shale, but significantly higher and positive $\epsilon^{205}\text{Tl}$ (-0.3 to 1.13). Good correlations are observed between $\epsilon^{205}\text{Tl}$ and Mo/TOC, Ni/TOC, and U/TOC.

In summary, the new data of Tl isotopes in black shales are useful tools: 1) To distinguish between oxic and anoxic marine deposits; 2) To identify hydrothermal input of Tl (and other metals) for the early Cambrian black shales and polymetallic Ni-Mo sulfide bed in south China.

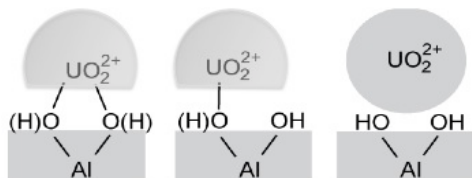
This study is supported by NSFC grant 41273009, 41230102.

Understanding Uranyl adsorption at the water-mineral interface: A theoretical approach

PING YANG*, ERIC J. BYLASKA AND WIBE A DE JONG

W.R. Wiley Environmental Molecular Science Laboratory,
Pacific Northwest National Laboratory, Richland, WA,
99352, USA. (ping.yang@pnl.gov)

In order to understand the physico-chemical properties of actinide complexes in the natural environment, we performed *ab initio* molecular dynamics (AIMD) simulations of the dynamic adsorption processes of uranyl at the water-mineral interfaces. Hydroxylated α -Al₂O₃ surface is an important model system analogues for commonly occurring soil phase such as gibbsite, boehmite, akdalaita, bayerite, etc. Our current focuses are on two targeted questions: 1.) the structure of surface complexation: inner-sphere *versus* outer-sphere; [2] 2.) surface charge effects for adsorption at pH > p*H*_{ZPC}, where partially deprotonated sites present on surface, illustrated in Fig. 1. Both geometric structures and energy profiling of adsorption of uranyl at will be reported.



In acidic environment, we have found that the average distance of uranium to equatorial oxygen atoms is $\sim 2.5 \text{ \AA}$, in good agreement with extended X-ray absorption fine structure (EXAFS) spectroscopy experiment for acidic environment.^[3,4] The coordination number of uranyl to surface oxygens dynamically changes, indicating multidentate bonding interactions occurring at a finite temperature. The surface charges have profound effects on the surface complexation by forming stronger surface adsorption with a shorter bond distance to the deprotonated site, suggesting a lower mobility of uranyl in a basic environment.^[5]

Acknowledgements : This research is supported by the DOE Basic Energy Sciences Heavy Element Program. Part of the computing was performed using the MSC in the EMSL, a national scientific user facility sponsored by the Department of Energy's Office of Biological and Environmental Research located at Pacific Northwest National Laboratory.

[1] P. Nichols, N. Govind, E.J. Bylaska, W.A. deJong, *J. Chem. Theory Comput.* 5, 491 (2009). [2] H. Gecheis, J. Lutzenkirchen, R. Polly, T. Rabung, M. Schmidt, *Chem. Rev.* 113, 1016-1061 (2013) [3] E.R. Sylwester, E.A. Hudson, P.G. Allen, *Geochim. Cosmochim. Acta.* 64, 2431 (2000). [4] MA Denecke, J Rothe, K Dardenne, P Lindqvist-Reis, *Phys Chem Chem Phys*, 5, 939 (2003). [5] P. Yang, E.J. Bylaska, W.A. de Jong, submitted.

Response of epikarst hydrochemical changes to soil CO₂ and weather conditions in Chenqi, SW China

RUI YANG^{1,2}, ZAIHUA LIU^{1,2*}, CHENG ZENG^{1,2}
AND MIN ZHAO^{1,2}

¹State Key Laboratory of Environmental Geochemistry,
Institute of Geochemistry, Chinese Academy of Sciences,
46 Guanshui Road, Guiyang 550002, China
(*correspondence: liuzaihua@vip.gyig.ac.cn)

²Puding Comprehensive Karst Research and Experimental
Station, Inst. Geochem., CAS & Science and Technology
Department of Guizhou Province, Puding 562100, China

Karst-related carbon cycle, as a result of water-carbonate rock-CO₂ gas-aquatic organism interactions, significantly affects global carbon budget. Soil CO₂ is a major chemical driving force for karst process and has significant impact on the water-rock-gas-organism system. However, few studies examined the direct correlations between hydrochemical parameters and soil CO₂ in epikarst systems.

An epikarst spring system in Chenqi, SW China was chosen to monitor soil CO₂ concentration and hydrochemical parameters with high-resolution (interval of 15 min.) and to investigate the responses of hydrochemical changes to soil CO₂ and weather conditions. It was found that both soil CO₂ and rainfall are major driving forces for karst hydrochemical variations. Soil CO₂ effect on hydrochemical variations was reflected in all seasonal, diurnal and storm-scales. There was an increasing CO₂ partial pressure (pCO₂) and electrical conductivity (EC) but a decreasing pH in groundwater caused by the increasing CO₂ in soil during spring-summer growing season, while a decreasing pCO₂ and EC but an increasing pH caused by the decreasing soil CO₂ in autumn-winter dormant season. Similar responses were also found on diurnal scales but with a time lag of a few hours during dry season, showing different groundwater recharge mode as well as the complex supply path (quick flow by conduit or slow flow by fracture). During rainy seasons, hydrochemical variations in epikarst spring were regulated by both dilution and soil CO₂ effects. Under high-intensity rainfall, the dilution effect was dominant, indicated by a quick decrease in EC, pH and calcite saturation (SI_c) but a quick increase in pCO₂. Contrastly, under low-intensity rainfall, soil CO₂ effect was dominant, indicated by an increase in EC and pCO₂ but a decrease in pH and SI_c.

To sum up, this study has shown the high sensitivity and variability of karst process to environmental change, implying that the role of karst process in global carbon cycle needs to be reappraised based on high-resolution monitoring strategy.

Chemical weathering and sediment source-to-sink processes within the Changjiang (Yangtze River) and mountainous river basins (Taiwan)

S. Y. YANG^{1*}, C. LI¹, X. D. WANG¹ AND Y. GUO²

¹State Key Lab. of Marine Geology, Tongji Uni., Shanghai 200092, China (*correspondence: syyang@tongji.edu.cn),

²School of Materials Science and Engineering, Shanghai Uni., Shanghai 200072, China,

The Changjiang is the largest river originating from the Himalayan-Tibetan Plateau and bridges the Eurasian continent and west Pacific Ocean. In comparison, the small-sized mountainous rivers in Taiwan have increasingly attracted research attentions in recent years owing to the unique geologic setting and huge sediment fluxes. Both river systems deliver huge amount of terrigenous matter into East Asian marginal seas, which exerts a great control on marine sedimentation and biogeochemical cycle. Nevertheless, the sediment source-to-sink (S2S) processes are significantly different within these two kinds of river systems.

In this contribution, we attempt to compare the weathering intensity and sediment S2S processes within the Changjiang catchment and Taiwan river basins by using various geochemical proxies. Source rock compositions and chemical weathering intensities in the catchments account for the compositional variations of the fluvial sediments. The CIA, bulk Sr-Nd isotopic compositions and age spectrum of zircon provide good constraints on sediment recycling and evolution of weathered upper continental crust under different tectonic settings. Geochemical composition of the sediment into the sea is complicated by hydrodynamic sorting and changing sediment suppliers in relation to variability of monsoon-induced precipitation in the river basin. Overall, the mountainous Taiwan rivers and the mega-river like Changjiang represent two kinds of typical river systems that shape the earth surface and drive material cycle.

Acknowledgements: This work was supported by NSFC research fund (Grant No: 41076018, 41225020).

Boron isotopic fractionation during magmatic differentiation: A case study of tourmalines from the Nyalam leucogranite-pegmatite system, South Tibetan Himalaya

SHUI-YUAN YANG AND SHAO-YONG JIANG*

State Key Laboratory for Mineral Deposits Research, School of Earth Sciences and Engineering, Nanjing University, Nanjing 210093, PR China

(*correspondence: shyjiang@nju.edu.cn)

The Miocene Nyalam leucogranite-pegmatite system from South Tibetan Himalaya consists of two mica leucogranite (2mg), tourmaline leucogranite (Tg) and pegmatite dykes which were extracted from two mica leucogranite magma. Tourmaline is an important constituent of the Nyalam leucogranite-pegmatite system. Tourmaline in the two mica leucogranite and tourmaline leucogranite occurs mostly as nodular tourmaline-quartz segregations. Tourmaline in the pegmatite consists of isolated, millimeter sized, euhedral crystals. In situ analyses by electron microprobe and LA-MC-ICP-MS reveal a large variation of chemical and boron isotopic compositions of tourmaline from the Nyalam leucogranite-pegmatite system. Most of these tourmalines have high Fe/(Fe+Mg) and Na/(Na+Ca) ratios, and can be considered as a typical magmatic product.

Tourmalines from the Nyalam two mica leucogranite have the $\delta^{11}\text{B}$ values between -15.8 and -12.3% , whereas tourmalines from the tourmaline leucogranite are between -13.1 and -11.4% . The tourmalines from one pegmatite dyke have $\delta^{11}\text{B}$ values of -13.1 to -11.5% . But, tourmalines from another pegmatite dyke have a wide range of $\delta^{11}\text{B}$ values between -13.5 and -7.7% . We consider that the source rock control was important for the boron isotope compositions in the granites. The two mica leucogranite was produced by biotite dehydration melting in biotite-rich metapelites, whereas the tourmaline leucogranite was produced by muscovite dehydration melting in muscovite-rich metapelites. The boron isotope variation from granite to pegmatite indicates that boron isotopic fractionation factually occurred during the magmatic differentiation process in Nyalam leucogranite-pegmatite system. The pegmatitic magma with high primary water concentration is more prone to trigonal $\text{B}(\text{OH})_3$ complexes and therefore ^{11}B is preferentially partitioned into the extracted pegmatitic magma.

Ancient magmatic CO₂ degassing from non-volcanic area in West Taiwan: Helium and carbon isotopic evidences

TSANYAO FRANK YANG¹

¹ Department of Geosciences, National Taiwan University, Taipei 10617, Taiwan (tyyang@ntu.edu.tw)

Representative gas samples of fumaroles, springs, mud volcanoes, natural gases were collected from Taiwan for helium isotopes measurement. Samples from northern and eastern Taiwan exhibit higher ³He/⁴He ratios, which indicates significant mantle-derived signature. The result is not unexpected, since hydrothermal activity is still active at those areas. Nevertheless, some abnormally high ³He/⁴He ratios (up to 6.4 Ra) are obtained from non-volcanic area in western Taiwan. Carbon isotopes of CO₂ and CO₂/³He ratios in those samples are similar with those from mid-ocean ridge basalts, which believed to be derived from upper mantle. Hence, we are able to conclude that they are mantle-derived in origin.

Intrusive magmatism and/or deep normal faults occurred in western Taiwan could be the straight forward way to explain the high helium isotopic ratios observed in non-volcanic area. Considering the possible inversion of tectonic stress from compression to tension, post-collisional magmatism around northern Taiwan may have occurred since late-Pliocene. The model might explain the possible mantle source for northwest Taiwan area, however, it is still unable to demonstrate why there is no any magmatic activity reported since late-Miocene and, presently, the areas are still under severe tectonic compression environment where we found the high helium ratio samples, especially in southwestern Taiwan.

I propose that the high ³He/⁴He ratio gases are not in-situ mantle-derived volatiles. They may be associated with Miocene magmatism and have been trapped by impermeable formation during the stage of basin subsidence before orogenic event occurred. Consequently, the deep normal faults may be reactivated as reverse faults by continuous compressive stress and cut through the capped rock of the gas reservoir. The "old" mantle gases, hence, could be released to surface through the leakage.

Studying crystal growth with NanoSIMS: An example of zircon

WEI YANG^{1*}, YANGTING LIN¹, JIALONG HAO¹, JIANCHAO ZHANG¹, SEN HU¹ AND HUAIWEI NI²

¹ Institute of Geology and Geophysics, Chinese Academy of Sciences, Beijing, China

(*correspondence: yangw@mail.iggcas.ac.cn)

² School of Earth and Space Sciences, University of Science and Technology of China, Hefei, China

Zircon has become one of the most widely used minerals for studying the prehistory and genesis of the host rock, because it is an excellent geochronometer, geochemical tracer and geothermometer. In many applications, the partition of trace elements between zircon and silicate melts is assumed to exhibit Henry's Law behavior and the crystal growth to be an equilibrium process. However, these assumptions may not be fulfilled in natural systems. For example, oscillatory zoning, a predominant texture of igneous zircon, appears to indicate non-equilibrium crystal growth [1].

To better understand origins of oscillatory zoning in zircons, distributions of REE (represented by Ce, Sm, Dy, Lu), Y, Ti, Li and P in zircons have been investigated with Cameca NanoSIMS 50L. The QH igneous zircons with oscillatory zonings display large trace element variations by a factor up to 13.5, with Y ranging from 574 to 7754 µg/g. By contrast, the DMP06-14 metamorphic zircons without oscillatory zonings show much smaller trace element variations by a factor of 1.4, with Y ranging from 477 to 636 µg/g. In the QH zircons, the cathodoluminescence (CL) images and ion images of Y show strong correlations with the CL-dark bands having high Y abundances than those of adjacent CL-bright bands by a factor of 2 to 10. The Y abundances are strongly correlated with the concentrations of P and REE (R² > 0.97). The corrections between P and (Y+REE) can be divided into three groups, with (Y+REE)/P atomic ratios of 3.3, 1.0 and 0.5, respectively, indicating three types of solid solution substitution of phosphates in zircon.

The oscillatory zoning can be well explained by a crystal growth kinetics model associated with substitutions of phosphates. The oscillatory distribution of P in zircon could be controlled by the fluctuation of P/Zr ratio in the melt adjacent to the mineral-melt boundary, because P diffuses slower than Zr in silicate melts. Such a zoned distribution of P in turn controlled the substitution types of phosphates in zircon, and consequently formed the oscillatory distributions of Y and REE in zircon.

[1] Hoskin, P.W.O., Schaltegger, U., 2003. Reviews in mineralogy and geochemistry 53, 27-62.

Strontium, carbon and oxygen isotopic compositions of Silurian on the northern and southern margins of Sichuan Basin, China

YANG WEI¹, ZHANG TINGSHAN² AND XIAOHUI CHEN^{3*}

¹ State Key Lab.of Oil&Gas G&E Engineering, Chengdu, China (rexswp@163.com)

² State Key Lab.of Oil&Gas G&E Engineering, Chengdu, China (zhangtingshan@swpu.edu.cn)

³ State Key Lab.of Oil&Gas G&E Engineering, Chengdu, China (zts_3@sina.com)(* presenting author)

The Sr, C and O isotopic compositions across the stratigraphic section have been obtained in the light of the systematic determinations of $^{87}\text{Sr}/^{86}\text{Sr}$, $\delta^{13}\text{C}$ and $\delta^{18}\text{O}$ values for the Upper Ordovician-Lower Silurian strata in the northern and southern margins of the Sichuan Basin. On the basis of the isotopic Data in combination with the sedimentary facies and tectonic data and the global Silurian regressive-transgressive events, the following conclusions can be drawn:

1. The $^{87}\text{Sr}/^{86}\text{Sr}$ values are commonly higher than the average values of $^{87}\text{Sr}/^{86}\text{Sr}$ for sea water in the geologic records on the southern margin of the basin. This is because the study area was in a ramp setting governed by intraplate palaeocontinent, and the addition of a large amount of terrigenous strontium led to the increase in $^{87}\text{Sr}/^{86}\text{Sr}$ values.

2. The $^{87}\text{Sr}/^{86}\text{Sr}$ values are positively fluctuated at the Upper Ordovician-Lower Silurian Boundary and Rhuddanian-Aeronian boundary, indicating a temporary fall of sea level at that time.

3. The $\delta^{13}\text{C}$ values increased gradually on both the northern and southern margins from the Aeronian to early Sheinwoodian, while the things for $\delta^{18}\text{O}$ values are contrary.

4. The isotopic evolution shows that the Upper Yangtze area was influenced by the Transgressive events from the Rhuddanian to early Sheinwoodian.

Early Paleozoic shale gas reservoir microscopic structure characteristics in southern Sichuan, China

YANG YANG¹ AND ZHANG TS^{2*}

¹ State Key Lab.of Oil&Gas G&E Engineering, Chengdu, China (843850989@qq.com)

² State Key Lab.of Oil&Gas G&E Engineering, Chengdu, China (zts_3@126.com) (* presenting author)

The well-preserved Lower Cambrian (Qiongzhusi Fm) and Lower Silurian (Longmaxi Fm) in the southern Sichuan province, China consists mainly of two lithological associations including shallow marine and lagoonal dark to black shales and shallow marine dark silty shale, with a total thickness of up to 1900 m. Using ESEM, AFM and test data and adsorption/desorption isothermal that produced from Multipoint Brunauer Emmett Teller (MBET) to do multi-researches on the types of reservoir spaces and micro-pore structure characteristics of early Cambrian Qiongzhusi Fm. and early Silurian Longmaxi Fm. shale gas reservoirs in southern Sichuan basin area. The shale gas reservoir spaces of early Cambrian Qiongzhusi Fm. and early Silurian Longmaxi Fm. mainly including residual primary intergranular pores, intercrystal pores, mineral moldic pores, secondary dissolution pores, micropores among clay minerals, organic matter pores. Through the analyses of ESEM and AFM, the micron and nanoscale pore image in the shale can be observed directly, and the pore specific surface area measurement can test samples of nano and micro nano level pores. The authors show that the Qiongzhusi Fm. and Longmaxi Fm. shale gas reservoirs are with great development of micro holes, and provide the large pore volume and surface area for shale gas. But the specific surface area and pore volume of Qiongzhusi Fm. are smaller than that of the Longmaxi Fm. shale. The organic carbon content and kerogen type, clay mineral type and content, and thermal evolution degree is the main factors to control the microscopic pore structure development, among them, the thermal evolution is the most obvious. Along with the thermal evolution degree, the organic carbon content and II kerogen content increase, the numbers of the micro-pore, the specific surface area and pore volume are increased. When the thermal evolution degree developed over a certain value, the specific surface area, pore volume all along with the increase of the degree of thermal evolution decreases sharply.

Research on the Au transport of Lannigou Gold Deposit in Guizhou Province, China

YUPING YANG¹ AND CHENGHUI WANG¹

¹MLR Key Laboratory of Metallogeny and Mineral Assessment, Institute of Mineral Resources, Chinese Academy of Geological Sciences, Beijing 100037, China (*correspondence: ypyang@pku.edu.cn)

Based on the features of ore fluids of Lannigou Gold Deposit in Guizhou Province, China, the experiments of Au-S complex in fluids which were moderate temperature, low salinity and CO₂-rich are carried out in the hydrothermal diamond anvil cell. In-situ measurements of Au species in different systems was obtained with changing temperature, pressure, fluid composition, density and acidity. Finally, fine ore-forming model of Lannigou Gold Deposit will be built and its ore-forming mechanism will be studied according to the geological features of the deposit.

Iron-containing mineral effects on hydrothermal reactions of ketones

ZIMING YANG^{1*}, IAN R. GOULD¹
AND EVERETT L. SHOCK^{1,2}

¹Department of Chemistry & Biochemistry, Arizona State University, Tempe, AZ, 85287 (*correspondence: zyang20@asu.edu)

²School of Earth and Space Exploration, Arizona State University, Tempe, AZ, 85287

Hydrothermal organic transformations occurring in geochemical processes are influenced by the presence of minerals. This work reports the influence of several common iron-containing minerals on the hydrothermal reactions of a model ketone, dibenzylketone (DBK). Ketones are central to many hydrothermal organic functional group interconversions, and DBK was chosen because the mechanisms of its hydrothermal reactions were recently studied in water alone [1]. Under the experimental conditions (300°C, 70 MPa, and up to 168 hours), minerals were found to significantly and specifically influence the hydrothermal reactions of DBK. Quartz (SiO₂) and corundum (Al₂O₃) had no detectable effect compared to water alone, whereas hematite (Fe₂O₃), magnetite (Fe₃O₄), and ferrous sulfide (FeS) all increased DBK reactivity to various extents. Magnetite had the largest effect on the rate of DBK decomposition. Product distributions indicate that magnetite and hematite increase covalent bond fragmentation compared to water alone, whereas reduced products were observed in the presence of ferrous sulfide. The mechanisms of the mineral reactions were investigated using hydrogen balance calculations, dissolved H₂ measurements, and experiments as functions of mineral surface areas. The effects of the iron oxide minerals appear to be mainly attributable to mineral surface-promoted catalytic bond cleavage reactions. In contrast, the reactions with ferrous sulfide are best explained as arising from dissolved inorganic compounds in solution that can deliver hydrogen atoms to the organic reactants, i.e., the ferrous sulfide acted as a reagent.

[1] Yang et al. (2012), *Geochim. Cosmochim. Acta* **98**, 48-65.

100% decomposition of diatomous organic carbon during settlement through ocean columns

SAKI YASUDA^{1*}, YURIKO HARA¹, HIROSI NARAOKA¹
KOZO TAKAHASHI² AND TASUKU AKAGI¹

¹ Kyushu Univ., Fukuoka, 812-8581, Japan
(3sc12028k@s.kyushu-u.ac.jp)

² Hokusei Gakuen Univ., Sapporo, 004-8631, Japan

Introduction

Two major planktonic phases responsible for biological pump are diatoms and coccolithophores. In this study, diatom-frustule dominated settling particles was analyzed for the carbon isotopic ratio to evaluate the decomposition of diatom-derived organic carbon.

The samples of settling particles were collected from two stations in 200 km north and 300 km south of the Aleutian Islands using two sediment traps, which were deployed for one whole year (2008-2009). (1) Wet oxidation was employed to decompose non-refractory organic carbon (NRC) in the trapped samples. The CO₂ from NRC was analyzed for $\delta^{13}\text{C}$. (2) The residue of the wet oxidation was recovered as refractory carbon (RC) and the amount of RC was measured by an elemental analyzer.

Results and Discussion

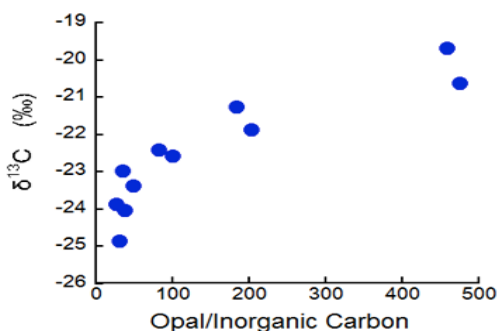


Figure 1: Relationship between $\delta^{13}\text{C}$ of NRC and Opal/Inorganic Carbon

(1) The relationship between carbon isotope ratio of NRC and Opal/Inorganic Carbon ratio is shown in Figure 1. Opal and inorganic carbon represents diatoms and coccolith+foraminifera, respectively. The carbon isotope ratio of the organic carbon in the settling particles was understood as a mixing of two end members with $\delta^{13}\text{C}$ of -19 ‰ and -25 ‰. The results of fitting suggest that the diatom-derived NRC has been almost totally decomposed.

(2) The amount of carbon recovered as RC was near the detection limit and RC was absent in most of the residue samples treated with the wet oxidation.

An insight into negative feedback mechanisms in a recovery phase of the PETM

KAZUTAKA YASUKAWA¹ AND YASUHIRO KATO^{1,2}

¹Department of Systems Innovation, School of Engineering, The University of Tokyo, Tokyo, 113-8656, Japan
(4708722967@mail.ecc.u-tokyo.ac.jp)

²Frontier Research Center for Energy and Resources, School of Engineering, The University of Tokyo, Tokyo, 113-8656, Japan (ykato@sys.t.u-tokyo.ac.jp)

Across the Paleocene-Eocene boundary (PEB), an extreme global warming by 4-8 °C coincided with a rapid and distinct negative carbon isotope excursion (CIE) in both marine and terrestrial environments, which is known as the Paleocene-Eocene Thermal Maximum (PETM). Several lines of evidence from previous studies strongly suggest that a massive and rapid injection of ¹³C-depleted carbon into the ocean-atmosphere system induced the global carbon cycle perturbation and climate change. It is generally considered that, after the culmination of the global warming and CIE, enhanced continental chemical weathering and biological productivity functioned as negative feedbacks by which the excess carbon was removed from the ocean-atmosphere system.

We simulated the global carbon cycle perturbation across the PEB with a simple ocean-atmosphere box model modified from [1]. We calculated mass balances of carbon, calcium, and carbon isotopes regarding ocean and atmosphere boxes, which are connected by terrestrial weathering fluxes depending on atmospheric partial pressure of CO₂ and temperature. Earth system's negative feedbacks which appear to have worked in a recovery phase of the PETM correspond to variations of carbonate and organic carbon burial fluxes in the ocean box.

We compared our simulated results with geologic records from literatures. Our calculated organic carbon burial enhancement causes a transient positive shift in the oceanic carbon isotopes. However, to our knowledge, no such positive shift has been recognized during the PETM. A possible scenario that reconciles the simulated results with geologic records is a globally constant organic carbon burial in the ocean. While intensified continental weathering and nutrient-rich runoff may have resulted in elevated primary production on shelves, the open-ocean productivity decreased with the onset of the PETM [2]. Due to the balance of productivity changes between shelf and open-ocean environments, a global organic carbon burial flux in the ocean may have remained nearly constant across the PEB.

[1] Beerling & Berner (2002) *Global Biogeochem. Cycles*, **16**, 10.1029/2001GB001637. [2] Gibbs *et al.* (2006) *Geology*, **34**, 233-236.

Characteristics of the Eemian from the Greenland Ice Sheet at GISP2

AUDREY M YAU¹

¹ ayau@princeton.edu

The Eemian (115-128ka) is arguably the warmest the Earth's Arctic has been for the past 800ka. Recent data from NEEM (northwestern Greenland) show peak surface temperatures at ~126ka of $8 \pm 4^\circ\text{C}$ above the mean of the past thousand years, and a decrease in elevation of $400 \pm 250\text{m}$ between 128-122ka. Here, we focus on Summit Greenland at GISP2. The depth interval of GISP2 between 2750 and 3040m contains clean, disturbed ice, which is largely warm ice of Eemian age. We have constrained the age of this ice by measuring CH_4 and $\delta^{18}\text{O}_{\text{atm}}$ of O_2 , and analyzing the results in the context of the well-known histories of these gases from the Greenland NGRIP record to 121ka, and the Antarctic EDML and Vostok records beyond 121ka. Dating is not yet definitive but the most parsimonious interpretations align climate at GISP2 with change at NEEM. Dating of 44 sections of the warm, disturbed ice fall predominately into three distinct time periods: 104-107ka, 118-121ka, and 126-128ka. We do not find any evidence for ice between 121.5-125ka. The net change from ~127ka to ~118ka indicates an increase in total air content from 86-98ml/kg (~12%), similar to the change in observed total air content and inferred elevation at NEEM. Over the same interval, we see an increase in $\delta^{18}\text{O}$ of the ice from 128-126ka, and a decrease from 121-118ka, yielding a net increase of ~2‰ (~4°C). CH_4 concentrations in excess of 870ppb were observed at depths greater than 3030m, precluding the ability to date these samples. Our inferred elevation and temperature histories are generally consistent with recent results from NEEM, however we do not observe prevalent melt layers at the summit location.

Xenoliths, XANES and redox-related processes in the cratonic lithosphere

GREGORY M. YAXLEY¹, ANDREW J. BERRY¹,
ALAN B. WOODLAND², BRENDAN J. HANGER¹
AND VADIM S. KAMENETSKY³

¹ Research School of Earth Sciences, The Australian National University, Canberra ACT 0200, Australia

(*correspondence: greg.yaxley@anu.edu.au)

² Institut für Geowissenschaften, Universität Frankfurt, 60438 Frankfurt, Germany

³ ARC Centre of Excellence in Ore Deposits, University of Tasmania, Hobart TAS 7001, Australia

The oxygen fugacity ($f\text{O}_2$) of peridotite upper mantle is predicted to decrease with increasing pressure because of molar volume changes of redox buffering reactions in peridotitic assemblages [1].

Fe K-edge XANES spectroscopy can now be routinely used to measure $\text{Fe}^{3+}/\Sigma\text{Fe}$ (where $\Sigma\text{Fe}=\text{Fe}^{2+}+\text{Fe}^{3+}$) in garnet from peridotite xenoliths [2]. Combined with conventional thermobarometry and experimentally calibrated oxybarometers [1] this enables rapid (30 min. acquisition), precise ($\pm 0.1 \log_{10}$ units) $f\text{O}_2$ determinations at micron-scale spatial resolution, as well as quantitative mapping of the distribution of Fe^{3+} in garnet crystals [3].

We have used the XANES technique [2] at the X-ray Fluorescence Microscopy beamline of the Australian Synchrotron to investigate $f\text{O}_2$ -depth variation in the Siberian Craton (Udachnaya East and Obnazhennaya kimberlites), the Slave Craton (Panda kimberlites) and the Kaapvaal Craton (Kimberley and Wesselton kimberlites).

In the Siberian and Slave cratonic lithosphere the $f\text{O}_2$ of peridotite xenoliths decreases with depth to $\Delta \log_{10} f\text{O}_2^{\text{FMQ}}$ of ≈ -4 to -5 at ≈ 200 - 220 km [1,4]. Such values approach the limiting Fe-Ni precipitation curve. Metasomatic events however, have locally perturbed this trend, and lead to oxidation by 1-2 \log_{10} units [3,4]. In the case of Wesselton, we mapped the Fe^{3+} distribution in compositionally zoned garnets, demonstrating that metasomatic overgrowth rims grew at $f\text{O}_2 > 2 \log_{10}$ units higher than the cores [3] only a very short time before eruption.

Redox conditions in the deep lithosphere are in general too reduced for carbonate melt stability [1,5], unless carbonate activity is substantially reduced by other components (silicates, halides etc).

[1] Stagno *et al.* (2013) Nature doi:10.1038/nature11679; [2] Berry *et al.* (2010) Chem Geol 278, 31-37; [3] Berry *et al.* (2013) Geology, *in press*; [4] Yaxley *et al.* (2013) Lithos 140-141 (142-151); [5] Woodland & Koch (2003) EPSL 214, 295-310.

Petrography and alteration of Cu-mineralization in the Niaz, Meshginshahr, NW Iran

M. YAZDI¹, H. MOHAMMADIAN¹, GH. HOSSENZADEH²
AND F. MASOUDI¹

¹ Faculty of Earth Sciences, Shahid Beheshti University, Iran,
(m-yazdi@sbu.ac.ir)

² Department of Geology, Tabriz University, Iran

The Niaz area is located on the western part of the Cenozoic Alborz–Azerbaijan volcanic belt (Arasbaran sub-zone). The belt is also an important Cu–Mo–Au metallogenic province in northwestern Iran. The exposed rocks in the study area consist of a volcanoclastic sequence, subvolcanic rocks and intermediate to mafic lava flows of Paleogene age. The main host rocks are alkali granite to hornblende-biotite granite, monzonite to monzodiorite which have been intruded by andesitic to andesitic-basalt. Also several andesitic, rhyodacite to microgranite dykes have been intruded to the host rocks. The main host rock is monzonite to monzodiorite porphyry which is the host of main mineralization and alteration.

The geological and geochemical signature shows that the rocks are typical subduction-related magmatic complexes. The field observation, petrography and geochemical study show similarity to typical Cu-porphyry mineralization in the area. The main factors are monzonite stock, typical potassic, phyllic, prophylic and argillic alteration (zonality of the alteration patterns from intense phyllic at the center to outward weak-phyllic, argillic), stock works and disseminated Cu-mineralization, siliceous breccias and various fractures.

Actively forming Kuroko-style massive sulfide mineralisation and hydrothermal alteration at Iheya North, Okinawa Trough

C.J. YEATS^{1*} AND S.P. HOLLIS¹

¹CSIRO Earth Science and Resource Engineering, Kensington, WA 6151, Australia (*correspondence: chris.yeats@csiro.au; steven.hollis@csiro.au)

IODP Expedition 331 drilled five sites at the Iheya North hydrothermal field within the Okinawa Trough backarc basin. At Iheya North, hydrothermal alteration and sulfide mineralisation is hosted in a geologically complex mixed sequence of coarse pumiceous volcanoclastic and fine hemipelagic sediments, overlying dacitic to rhyolitic volcanic substrate.

At Site C0016, coring adjacent to the foot of an actively venting sulfide mound intersected massive sphalerite-(pyrite-chalcopyrite)-rich sulfides that strongly resemble the black ore of the Miocene-age Kuroko deposits of Japan – the first time that such material has been recovered from an active seafloor hydrothermal system. The sulfide mineralisation shows clear microtextural evidence of formation via a combination of surface detrital and subsurface chemical processes, with at least some sphalerite precipitating into void space in the rock. Altered volcanic rocks beneath the massive sulfide exhibit quartz-muscovite/illite and quartz-Mg-chlorite alteration, reminiscent of the proximal footwall alteration typically associated with ancient volcanic-hosted massive sulfide mineralisation.

At the nearby Site C0013, a likely location of recent high-temperature discharge, intense hydrothermal alteration obliterates primary mineralogy and texture. Near surface alteration is dominated by kaolinite and muscovite with locally abundant native sulfur, suggesting acidic fluids; grading to Mg-chlorite dominated assemblages at depths of >5m below sea floor. Late coarse-grained anhydrite veining overprints the earlier alteration and is interpreted to have precipitated from downwelling seawater that penetrated the sediments when hydrothermal activity at the site waned.

Sulfide-bearing samples from Site C0016 and Site C0013 have been sectioned and mapped using scanning electron microscope (SEM) and proton induced X-ray emission (PIXE) techniques for major and trace element composition. Sphalerite from C0016 contains very little iron, which is consistent with the low overall iron budget of the hydrothermal system. PIXE analyses are currently underway and trace elemental distributions revealed by this technique will be presented.

Calcitic corals from the Red Sea as paleohydrological monitors

M. YEHUDAI^{1*}, B. LAZAR¹, N. KOHN¹, Y. SHAKED²,
A. AGNON¹ AND M. STEIN³

¹Institute of Earth Science, The Hebrew University of
Jerusalem, ISRAEL 91904 (maayanchik@gmail.com)

²Interuniversity Institute for Marine Sciences, Eilat ISRAEL
88103

³Geological Survey of Israel, 30 Malkhe Israel St. Jerusalem,
95501 ISRAEL

While pristine aragonite corals provide information on sea level history and coastal tectonics, fossil corals that were altered to calcite (calcified), can be used to establish the chronology of corals diagenesis by freshwater. Such diagenesis is possible provided the corals reside within the saturated zone of freshwater aquifers. Establishing the chronology of freshwater diagenesis in hyperarid areas, such as the Red Sea is extremely useful for reconstruction of past climate fluctuations. Here, we present a new open system U-Th dating method for calculating the time of deposition and the age of diagenesis of calcitic corals from the last interglacial uplifted reef terraces at the northern Red Sea. The calculated age of coral calcification (~120 ka) is similar to closed system U-Th ages determined for aragonite corals from a nearby location[1]. These results suggest that the aragonite corals in this terrace resided in a coastal freshwater aquifer and recrystallized to calcite shortly after their initial formation. Therefore, it appears that wetter (than present) conditions prevailed during MIS5e in the currently hyperarid region of the northern Red Sea. Indication for enhanced runoff activity in this area is provided by ⁸⁷Sr/⁸⁶Sr ratios of foraminifers and fine detritus material from Red Sea cores[2].

[1] Scholz D., Mangini A. and Felis T. (2004), *EPSL* **218**, 163–178. [2] Stein M., Almogi-Labin A., Goldstein S. L., Hemleben C. and Starinsky A. (2007), *EPSL* **261**, 104–119.

Adakite-like volcanism in Boyabat Region, Turkey: Geochemistry and Petrogenesis

N. YESILOREN-GORMUS^{1*} AND A. TEMEL²

¹General Directorate of Mineral Research and Exploration,
06800, Çankaya, Ankara, Turkey (*correspondence:
nihalyg@gmail.com)

²Hacettepe University, Faculty of Engineering, Geological
Engineering Department, 06800, Beytepe, Ankara, Turkey

Cretaceous aged Dodurga volcanics mainly include andesitic (trachyandesite, andesite), dacitic (dacite, trachydacite) volcanic rocks and volcanoclastics. Volcanic rocks have typical hypocrystalline porphyric texture and mineralogically contain amphibole, plagioclase (zoning-polysynthetic twinning), biotite, quartz and opaque minerals, in varying quantity.

Dodurga volcanics have subalkaline and calc-alkaline characteristics. Major, trace and rare earth element data exhibit fractional crystallization which is effective process, in generation of volcanic rocks. Furthermore, effects of crustal contamination and/or subduction zone process were also determined. MORB and Chondrite-normalized spider diagrams indicate LILE, LREE content enrichments, compared with HFS elements. Besides, negative anomalies, observed in Ta, Nb and Ti elements reveal fractional crystallization, subduction and/or crustal contamination effectively, in occurrence of the volcanics. In Dodurga volcanics, SiO₂ content varying between 61%-65.1% (averagely 63.3%), Al₂O₃ between 16.1%-17.8% (averagely 16.9%), Sr between 385.9-611.4 ppm (averagely 505.2 ppm), Y between 5-14.5 ppm (averagely 9.5 ppm), Yb between 0.5-1.3 ppm (averagely 0.9) and Zr/Sm ratio 46.2-89.5 (averagely 65.6) were determined. In (Yb)_N-(La/Yb)_N and Y-Sr/Y diagrams, the majority of Cretaceous Dodurga volcanics scattered in adakite area and partially in the classic arc volcanics were observed. In primitive mantle-normalized spider diagrams, Dodurga volcanics have typically low Nb, Ce and positive Sr contents, compatible with adakite-like volcanics.

According to the partial melting modeling diagrams, the Cretaceous Dodurga volcanics were formed as low degree batch melting of spinel-lherzolite which was a shallow depth lithospheric resource. All geochemical data and especially La/Nb>1 and Ba/Nb>28 ratios show Dodurga volcanics to have typical island arc volcanic characteristics, derived from lithospheric resources.

Atmospheric chemistry and dynamics recorded in the isotopic ordering in O₂ and CO₂

LAURENCE Y. YEUNG,^{1*} EDWARD D. YOUNG,¹ EDWIN A. SCHAUBLE,¹ HAGIT P. AFFEK,² KRISTIE A. BOERING,³ JOHN M. EILER⁴ AND MITCHIO OKUMURA⁵

¹Department of Earth and Space Sciences, University of California, Los Angeles, CA, USA
(*correspondence: lyyeung@ucla.edu)

²Department of Geology & Geophysics, Yale University, New Haven, CT, USA

³Departments of Chemistry and Earth & Planetary Science, University of California, Berkeley, CA, USA

⁴Division of Geological and Planetary Sciences, California Institute of Technology, Pasadena, CA, USA

⁵Division of Chemistry and Chemical Engineering, California Institute of Technology, Pasadena, CA, USA

Molecules in Earth's atmosphere undergo photochemical oxidation while being transported through regions where they are mixed and/or stratified. Chemistry, transport, and mixing all alter the distribution of gases in the atmosphere, and tracing these processes over large spatial and temporal scales is therefore challenging. Concentrations of the short-lived free radical oxidants that drive atmospheric chemistry are especially difficult to quantify due to short chemical lifetimes and spatial and temporal variations in source strengths.

Our studies of O₂ and CO₂ molecules containing more than one rare stable isotope (¹⁸O¹⁸O and ¹⁶O¹³C¹⁸O) suggest that these species preserve signatures of isotope-exchange reactions in the stratosphere and troposphere [1,2]. For instance, ¹⁶O¹³C¹⁸O can be used to constrain the isotopic signature of O(¹D) in the midlatitude stratosphere as well as the chemistry and dynamics of the stratospheric polar vortex. In contrast, atmospheric ¹⁸O¹⁸O traces O(³P) chemistry and stratosphere-troposphere exchange.

Our most recent measurements of ¹⁸O¹⁸O in stratospheric air and in air drawn from the firm layer in Antarctica bolster the case for O(³P) + O₂ isotope exchange reactions governing the distribution of ¹⁸O¹⁸O (i.e., Δ₃₆) throughout the atmosphere. Using these observations together with laboratory experiments and modeling, we show that Δ₃₆ in the atmosphere is sensitive to O(³P) concentrations. Because O(³P) is linked directly to NO₂ and O₃ in the troposphere, Δ₃₆ is a proxy for global NO₂ and O₃ concentrations.

[1] Yeung *et al.* (2012) *J. Geophys. Res.* **117**, D18306. [2] Yeung and Affek *et al.* (2009) *Proc. Natl. Acad. Sci. USA* **106**, 11496-11501.

δ⁶⁶Zn values: An isotopic tool for comprehension of metallurgical slags weathering

N.H. YIN^{1,2,3*}, Y. SIVRY¹, P.N.L. LENS² AND E.D VANHULLEBUSCH³

¹Univ. Paris Diderot, Sorbonne Paris Cité, IPGP, UMR 7154, CNRS, F-75205 Paris, France (*correspondence: yin@ipgp.fr, sivry@ipgp.fr)

²UNESCO-IHE, 2601 DA Delft, The Netherlands (p.lens@unesco-ihe.org)

³Univ. Paris-Est, LGE (EA 4508), 77454 Marne-la-Vallée, France (eric.vanhullebusch@univ-paris-est.fr)

The considered slags are originated from Lead Blast Furnace (LBF) and Imperial Smelting Furnace (ISF) Smelters. LBF and ISF slags contain 9.8 wt% and 8 wt% of Zn respectively, embedded in CaO-SiO-FeO matrix. Complete acid digestions showed that these bulk materials are enriched in heavy isotopes, with δ⁶⁶Zn_{JMC} +0.77 ± 0.06‰ and +0.12 ± 0.06‰ in ISF and LBF in agreement with previous studies [1]. Chemical dissolution kinetics were conducted at fixed pH values (4, 5.5, 7, 8.5 and 10), both in open-air and nitrogen atmospheres.

Zn dissolution was shown to be strongly governed by its mineral bearing phases: Spinel Zn(Al_{0.8}Fe_{0.2})O₄ and Wurtzite (ZnS) in ISF, and Franklinite [(Zn,Mn²⁺,Fe²⁺)(Fe³⁺,Mn³⁺)₂O₄] in LBF. Zn from Spinel phases was more resistant to weathering comparing to Zn from sulfide phases and from glassy silicates matrix. Furthermore, Zn dissolution in both slags was enhanced by the collateral dissolution of matrix elements such as Ca, Fe and Si. At all pHs tested, dissolved Zn of ISF reached higher concentration when there was no secondary precipitates formation like Zincite (ZnO) and Zinc carbonate (ZnCO₃), i.e. under N₂ atmosphere.

Such dissolution was related to extremes zinc isotopic signatures in the leachate solutions collected under open-air atmosphere. Both ISF and LBF displayed the same trend: heavier δ⁶⁶Zn values at low pH than at high pH (i.e. +0.91 ± 0.06‰ and -0.19 ± 0.06‰ at pH 4 and 10, respectively for ISF, and +0.10 ± 0.06‰ and -1.25 ± 0.06‰ at pH 4 and 10 respectively for LBF).

In open-air atm., δ⁶⁶Zn values remained constant with time from 48 to 200hrs (e.g. -0.19 ± 0.08‰ and -0.27 ± 0.06‰, respectively, for ISF), whereas they became enriched in heavier isotopes under N₂ atm. (e.g. +0.07 ± 0.06‰ and +0.71 ± 0.06‰ after 48 hrs and 200 hrs, resp.). This may imply that the absence of secondary precipitates allows more congruent slag dissolution and, thus, weathered Zn reaches isotopic signature closer to the bulk slag.

[1] Sivry, Y., *et al.* (2008) *Chem. Geol.* **255**, 295–304.

Study of Pb isotopic compositions during metallurgical slags leaching experiments

N.H. YIN^{1,2,3}, Y. SIVRY^{1*}, P.N.L. LENS²
AND E.D VANHULLEBUSCH³

¹Univ. Paris Diderot, Sorbonne Paris Cité, IGP, UMR 7154, CNRS, F-75205 Paris, France (*correspondence: sivry@ipgp.fr, yin@ipgp.fr)

²UNESCO-IHE, 2601 DA Delft, The Netherlands (p.lens@unesco-ihe.org)

³Univ. Paris-Est, LGE (EA 4508), 77454 Marne-la-Vallée, France (eric.vanhullebusch@univ-paris-est.fr)

Chemical leaching of both Lead Blast Furnace (LBF) and Imperial Smelting Furnace (ISF) slags were conducted at different pH (4, 5.5, 7, 8.5 and 10) under open air and nitrogen atmospheres. LBF and ISF slags contain 3.62 wt% and 1.26 wt% of Pb, as metallic droplets embedded in CaO-SiO-FeO matrix. According to total acid digestion, ISF slag exhibits a more radiogenic composition ($^{206}\text{Pb}/^{207}\text{Pb}$: 1.1479 ± 0.0018) than LBF ($^{206}\text{Pb}/^{207}\text{Pb}$: 1.0733 ± 0.0018) for which the ratios are comparable to previous studies [1].

Dissolved Pb constantly increases with time in ISF (and to a lesser extent LBF) leaching solutions under open-air atm., which is consistent with SEM imaging of weathered slags, showing the increasing weathering of slag's surface over the long term period, releasing Pb included in metallic droplets. On the contrary, dissolved Pb quickly reaches a plateau under N₂ atm. This difference may be related to Pb precipitates formed in both cases: few Pb(OH)₂ were formed for both LBF and ISF under N₂ atm. at pH 8.5, whereas PbO₂, PbCO₃ and Pb₃(CO₃)₂(OH)₂ are controlling the dissolved Pb under open-air atm. for both slags. Furthermore, the Pb concentration remains higher at pH 10 than at pH 8.5 in both slag leachates, with 4 mg L⁻¹ and 1 mg L⁻¹, resp.

Globally, ISF slag dissolution under open-air atm. is related to a more radiogenic Pb isotopic composition in the leachates, compared to N₂ atm. experiments: $^{206}\text{Pb}/^{207}\text{Pb}$ in leaching solution was typically 1.1569 ± 0.006 and 1.1378 ± 0.002 , resp. at pH 10. Moreover, $^{206}\text{Pb}/^{207}\text{Pb}$ remains close to the bulk slag value at pH 8.5, with values of 1.1495 ± 0.002 and 1.1477 ± 0.002 , under N₂ atm and open-air atm., resp. Under N₂ atmosphere the $^{206}\text{Pb}/^{207}\text{Pb}$ ratio in LBF slag leachate displays extremely radiogenic values compared to initial bulk ratio (i.e. i.e. 1.0806 ± 0.002 and 1.0785 ± 0.001 at pH 8.5 and 10, resp. against 1.0733 ± 0.002). Thus, assuming an homogeneous isotopic composition of lead included in metallic droplets, such results would indicate an isotopic fractionation during dissolution and/or sorption processes.

[1] Komárek *et al.* (2008) *Environ. Int.* **34**(4), 562-577.

Allende Chondrule Chronology Revisited: Eroding Age Gap between CAIs and Chondrules

Q.-Z. YIN¹, A. YAMAKAWA¹, M. SANBORN¹
AND K. YAMASHITA²

¹Department of Geology, University of California at Davis, Davis, CA 95616, USA (qyin@ucdavis.edu)

²Okayama University, Okayama, JAPAN

We have recently suggested [1-3] that carbonaceous chondrites, as undifferentiated primitive objects formed in the protoplanetary disk, were accreted very early, within the first 1 Ma at the beginning of the Solar System. We have further suggested that the current ^{53}Mn - ^{53}Cr data for bulk carbonaceous chondrites [1-3] imply that chondrules in them must also have formed early, given the logical necessity of forming chondrules first before accreting chondrites (we need "sand grains" first to form the cosmic "sandstone"). This argument was supported by examination of Allende chondrules with ultra high precision Mn-Cr isotope systematics [2]. This simple temporal relationship is at odds with the currently accepted paradigm of chondrule chronology of ^{26}Al - ^{26}Mg and some Pb-Pb ages [e.g., 4, 5], which at face value requires a minimum age gap between CAIs and chondrules by 2-3 Ma. However, a younger chondrule age poses a serious dynamic problem for the early solar nebula, known as the "storage problem" [6], namely, how could CAI-sized particle float in the protoplanetary disk for over 2-3 Ma until chondrules form, then accrete together to form chondrite, without facing head wind and spiraling into the Sun rapidly. Gas drag would efficiently remove the CAI-sized dust particles in the solar nebula in a timescale far less than 2-3 Ma. Although some new theoretical models were subsequently developed to solve the long term storage problem of CAIs [e.g. 7], new high precision U-Pb ages once again supported chondrule formation started contemporaneously with CAIs [8]. Since our initial report [2], $^{235}\text{U}/^{238}\text{U}$ isotope composition was shown to be no longer a constant [e.g. 9], thus some of the relative age anchors require readjustment. We will reexamine the emerging stories in the light of new measurements.

[1] Moynier *et al.* (2007) *ApJL*, 671, L181. [2] Yin *et al.* (2009) *LPSC 40th*, A2006. [3] Jenniskens *et al.* [2012] *Science*, 338, 1583. [4] Kurahashi *et al.* (2008) *GCA*, 72, 3865. [5] Connelly *et al.* (2008) *ApJL*, 675, L121. [6] Cameron (1995) *Meteorit.*, 30, 133. [7] Ciesla (2009) *Icarus*, 200, 655. [8] Connelly *et al.* (2012) *Science*, 338, 651. [9] Brennecka *et al.* (2010) *Science*, 327, 449.

Granulite xenolith constraints on the modification of the lower crust beneath the northern margin of the North China craton

Ji-FENG YING*, HONG-FU ZHANG AND YAN-JIE TANG

Institute of Geology and Geophysics, Chinese Academy of Sciences, Beijing 100029, China (*correspondence: jfyfing@mail.iggcas.ac.cn)

It has been well accepted that the lithosphere of the North China craton was severely destroyed in Mesozoic, in that the cratonic thick lithospheric mantle was replaced by mantle with oceanic affinity. A large amount of studies on the peridotite xenoliths entrapped by basalts of varied ages have invariably confirmed such catastrophic transformation. However, it is still unclear whether the crust, especially the lower crust also experiences significant modification or just keep stable and intact since its formation in Archean. A suite of granulite xenoliths captured in Cretaceous alkali basalts in the northern margin of the North China provide valuable constraints on the evolution of the lower crust. These xenoliths are mainly two-pyroxene granulites. We performed in situ U-Pb dating and Hf isotopic analyses on zircons separated from these xenoliths. CL images revealed that the majority of zircons are of igneous origin, though some zircon rims are metamorphically recrystallized. Zircons from one sample are discordant and show an upper intercept age of 2.5 Ga, representing the crystallization age of the protolith, which is consistent with the granulite terrain-based conclusion that the lower crust was mainly formed in 2.5 Ga ago. Apart from the Archean xenoliths, there are samples in which zircons are concordant with ages ranging from 200 to 300 Ma and peaking at 250-280 Ma, their Hf isotopic compositions, with $\epsilon_{\text{Hf}}(t)$ values trending towards positive suggest that mantle materials contributed to the formation of their protoliths. Their relative younger model ages also ruled out their origin of mere remelting of preexisted lower crust, and underplating of mantle-derived magmas plays a considerable role in modifying the lower crust. Furthermore, the timing of magmatic underplating is closely correlated with the closing and subsequent evolution of the Paleo-Asian ocean. We conclude that the modification of the lower crust beneath the northern margin of the North China craton was mainly, if not totally attributed to the southward subduction of Paleo-Asian oceanic slab and subsequent magmatism.

This work is financially supported by the Chinese Academy of Sciences (KZCX2-EW-QN106) and the National Natural Science Foundation of China (91214203).

The comparison experiments of acid leaching and bioleaching of sand-type uranium ore

ZHOU YIPENG^{1,2}, SHEN ZHAOLI¹, SHI WEIJUN²,
LIU JINHUI² AND LIU YAJIE²

¹ China University of Geosciences, Beijing 100083, China

² East China Institute of Technology, Fuzhou, Jiangxi 344000, China

A series of comparison experiments of acid leaching and bioleaching of sand-type uranium ore were conducted in laboratory. The average grade of ore is 0.416%, and the main size of the ore particles was 0.3-0.6mm. *Acidibacillus ferrooxidans* and *Acidibacillus thiooxidans*, by which Fe^{2+} was oxidized to Fe^{3+} to produce ferric acid leaching solution, were employed in the bacterial leaching processes.

For experiments under different conditions, 2.4kg uranium ore were divided into 12 uniform parts and each was put into a 500ml conical flask. Then these 12 flasks were ranged equally into three groups. Sulphuric acid solution was used for ore acidification; concentration of 2.0g/L was for group 1, 3.5g/L for group 2, and 5.0g/L for group 3. When the pH value of leaching system went down below 2.0, bacterial ferric acid solution with different concentration of Fe^{3+} and H_2SO_4 were added into different flask for bioleaching; a uniform acidity was also applied for all individuals in a same group, 2.0g/L was for group 1, 3.5g/L for group 2, and 5.0g/L for group 3; the ferric concentrations of 0g/L, 2.0g/L, 3.5g/L and 5.0g/L were applied respectively for those four flasks of every group.

Results showed that the uranium yield had been influenced by the solution acidity both in acid leaching and bioleaching processes; the yield could be increased by 2-3 percents as the solution acidity rose by 1.5g/L. The yield also determined by leaching technique. Comparing to acid leaching, bioleaching using bacteria solution of 2-5g/L Fe^{3+} could raise the yield by 6-11 percents. However, the leaching efficiency of 5g/L Fe^{3+} did not gain advantage over that of 2g/L; it indicated that concentration of 2g/L of Fe^{3+} in the bacterial leaching process was effective and economical.

This work was financed by the Major State Basic Research Development Program of China (973 Program) (No. 2012CB723101).

Ge/Si atomic ratio of siliceous deposit formed from geothermal water: as an indicator of silica source of BIF

T. YOKOYAMA^{1*} AND H. OHMOTO²

¹Faculty of Science, Kyushu University, Fukuoka 812-8581, Japan (yokoyamatakushi@chem.kyushu-univ.jp)

²Department of Geochemistry, Penn State University, University Park, PA 16802

The source of iron and silica in BIF has been argued for a long period. For the source of iron (Fe²⁺) of BIF, most of the geoscientists agree with the submarine hydrothermal activity. For the source of silica, however, there are different ideas based on the difference in Ge/Si atomic ratio: whether it is hydrothermal or is continental in origin. Hamade *et al.* found that the Ge/Si atomic ratios of iron-poor silica layer in the Brockman BIFs are essentially identical to present-day seawater ($\sim 0.8 \times 10^{-6}$), suggesting that the silica in Fe-poor layers formed from silica derived from the weathering of continental crust (input from river) rather than from hydrothermal fluids [1]. On the other hand, the Ge/Si atomic ratios in the Fe-rich layers are as high as $\sim 20 \times 10^{-6}$, which are similar to those in MOR hydrothermal fluids. In order to well-establish the reliability of Ge/Si atomic ratio as an indicator for the source of silica in Fe-poor layer in BIF, it is essential to show the relationship between Ge/Si atomic ratios in hydrothermal fluid and in siliceous deposit which precipitated directly from the fluid. In this study, we measured the Ge/Si atomic ratios of geothermal waters and siliceous deposits at geothermal power plants.

The distribution ratio of Ge into siliceous deposit from geothermal water was low. The Ge/Si atomic ratio of siliceous deposits formed in geothermal water in the aging tank at the Hatchobaru geothermal power plant was in the range from 3.72 to 5.42×10^{-6} . This values of Ge/Si atomic ratio can be considered to be an indicator showing the hydrothermal origin. The Ge/Si atomic ratio of iron-poor silica layer of Temagami BIF was in the range from 3.3 to 7.9×10^{-6} , suggesting hydrothermal origin.

[1] Hamade *et al.*, *Geology*, 31, 35-38 (2003)

¹⁴²Nd isotope anomaly in chondrite revisited

TETSUYA YOKOYAMA^{1*}, HIROKAZU TAKAHASHI¹
AND HIROSHI YAMAZAKI¹

¹Department of Earth and Planetary Sciences, Tokyo Institute of Technology, Japan. (*: tetsuya.yoko@geo.titech.ac.jp)

Chondrites and differentiated meteorites possess isotope differences from the terrestrial composition for some heavy elements, suggesting heterogeneous isotope distribution in the early Solar System. For Nd, carbonaceous chondrites have ¹⁴²Nd/¹⁴⁴Nd ratios >20 ppm lower than the terrestrial [1]. The finding most likely suggests the occurrence of a large scale silicate differentiation that fractionated Sm-Nd in early history of the Earth when short-lived ¹⁴⁶Sm existed. However, most of the Nd isotope data in chondrites were obtained using incomplete sample digestion that could not dissolve acid resistant, isotopically anomalous presolar grains, resulting in variable ^{145,148,150}Nd/¹⁴⁴Nd ratios [2]. To resolve this issue, we have developed a new method for determining Nd isotope ratios in meteorites with ultra-high precision using a TIMS (TRITON plus at Tokyo Tech), coupled with complete sample decomposition technique using a pressure digestion system (DAB-2, Berghof, Germany). Meteorite samples were put in Teflon inserts together with a mixture of HF, HNO₃ and H₂SO₄. The insert was placed in a stainless jacket and heated at 240 °C for >12 hours under high pressure. The existence of H₂SO₄ facilitated digestion of acid resistant presolar SiC. The resulting solution was dried and dissolved in 1M HCl, and passed through cation exchange resin and Ln spec to isolate Nd. In the TIMS analysis, we monitored ¹⁴⁰Ce interference using a compact discrete dynode, resulting in an excellent analytical precision of ¹⁴²Nd/¹⁴⁴Nd (2 ppm, 2SD) for repeated analysis of 500 ng of JNdi-1 standard. Using the technique, we determined Nd isotope compositions in four chondrites; Murchison (CM2), Saratov (L4), Chergach (H5) and NWA 4814 (R4), as well as terrestrial samples. These chondrites have ¹⁴²Nd/¹⁴⁴Nd ratios of 23 ± 3 ppm lower than the terrestrial samples, although the ^{145,148,150}Nd/¹⁴⁴Nd ratios were not resolvable from the terrestrial. This indicates that Nd isotopes were homogeneously distributed in the early Solar System. Our result supports the existence of an enriched hidden reservoir in the Earth's mantle whose chemical composition is complementary with a depleted mantle that was produced by silicate differentiation in the early history of the Earth while ¹⁴⁶Sm existed.

[1] Boyet and Carlson (2005) *Science* 309, 576. [2] Carlson *et al.* (2007) *Science* 316, 1175.

Speciation and fate of As in calcite formed under anoxic condition

Y. YOKOYAMA^{1*}, T. IWATSUKI² AND Y. TAKAHASHI¹

¹Hiroshima University, Hiroshima 739-8526, Japan

(*correspondence: yoshiyuka@hiroshima-u.ac.jp)

²Tono Geoscience Center, Japan Atomic Energy Agency, Toki, 509-6133, Japan

Speciation analyses for arsenic (As) in natural calcite, precipitated in fracture of deep underground sedimentary strata (Hokkaido, Japan), were performed using micro X-ray fluorescence and XAFS (μ -XRF-XAFS) technique to infer how calcite limit As migration in groundwater system.

Chemical data of pore water and groundwater collected from the sedimentary strata showed that arsenite (As^{III}) is predominant aqueous As species in the water phase. Nevertheless, As in the natural calcite is arsenate (As^{V}) [1]. This inconsistency of As species between calcite and water phases has already been observed in our laboratory experiment [2]. In calcite supersaturated solution, aqueous arsenite could be oxidized to arsenate, which is induced by complexation of arsenate with Ca^{2+} ion [2]. On the other hand, other minerals in the sedimentary strata (Fe oxide, siderite, biotite, and pyrite) contain As as arsenide and arsenite species. These Fe (secondary) minerals are frequent in As-contaminated sediments and considered to be effective sink for As. Among the minerals formed under anoxic condition, only calcite immobilized arsenate even in the arsenite system by selective incorporation of arsenate produced by the complexation-induced arsenite oxidation.

This property differentiates calcite from other minerals as a unique scavenger for As under anoxic condition. Calcite could preserve As as relatively insoluble arsenate from anoxic groundwater, while the arsenide and arsenite in the Fe secondary minerals easily leach from host minerals into aqueous phase depending on the change of the environmental condition such as redox. Mobilization of arsenate from calcite to aqueous phase hardly occur regardless of redox condition. Calcite seemed to be a rare mineral scavenging As as arsenate in groundwater system with low risk of As leaching to natural water. The present study about distribution behavior of As to calcite is also expected to lead a understanding of incorporation mechanism of redox sensitive oxyanions into calcite, which might be a useful tool for reconstruction of paleo-redox environment in which the calcite precipitated.

[1] Yokoyama et al. (accepted) *J. Phys.: Conf. Ser.* [2] Yokoyama et al. (2012) *Geochim. Cosmochim. Acta* **91**, 202–219.

Adsorption experiment of rare earth elements on clay minerals: Implication to the formation of ion-adsorption type REE deposit

KOTARO YONEZU¹, MASAHIRO NISHIDA¹, KOICHIRO WATANABE¹ AND TAKUSHI YOKOYAMA²

¹744 Motooka, Nishi-ku, Fukuoka, 819-0395 Japan, (yone@mine.kyushu-u.ac.jp)

²6-10-1 Hakozaki, Higashi-ku, Fukuoka 812-8581 Japan

Supply of rare earth elements (REE), especially heavy rare earth elements (HREE), highly depends on China. REE are essential for advanced environmental protection technology. HREE ore is mainly produced from ion adsorption type deposit. In order to clarify the role of the surface of clay minerals on the adsorption of REE, the adsorption and desorption (sequential extraction) experiment of REE were demonstrated in this study. Kaolin minerals such as kaolinite and halloysite were focused as adsorbents. In addition to the above experiment, some of hydrothermally altered rocks and clay vein were applied to the desorption experiment.

The adsorption experiments were conducted at room temperature and pH 6 with magnetically stirring in NaNO_3 or NaCl solutions (0.025M and 0.5M). At 0.5M, significant fractionation of REE on clay minerals from LREE to HREE was observed (HREE rich). However, no significant effect of the different electrolyte could be observed on any clay minerals at 0.5M. In order to understand an adsorption mode on clay minerals, the desorption (extraction) experiment were subsequently carried out. Three types of samples are used: REE on montmorillonite, 10Å-halloysite and pyrophyllite. Most of REE, especially LREE were preferentially extracted from montmorillonite and halloysite by neutral salt extraction step, suggesting that those extracted REE are considered to be concentrated by ion exchangeable form. Relatively more strongly adsorbed REE by forming chemical adsorption may be extracted by the following proton exchangeable step.

Feedbacks between biological retention of nutrients, carbon-mineral sorption, and pore space generation along an earthworm invasion chronosequence

KYUNGSOO YOO^{1*}, KIT RESNER¹, AMY LYTTLE¹,
CINDY HALE², ANTHONY AUFDENKAMPE³
AND STEPHEN SEBESTYEN⁴

¹ University of Minnesota, St. Paul, MN 55108, USA
(correspondence*: (kyoo@umn.edu),
(resne005@umn.edu), lytt0004@umn.edu)

² University of Minnesota Duluth, MN 55811, USA
(cmhale@d.umn.edu)

³ Stroud Water Research Center, PA 19311, USA,
(aufdenkampe@stroudcenter.org)

⁴ USDA Forest Service, Northern Research Station, Grand
Rapids, MN 55744, USA (ssebestyen@fs.fed.us)

Partitioning and transport of chemical phases in soils are governed by the complex interactions between competing biotic and abiotic processes that are difficult to quantitatively and mechanically separate. Addressing this challenge, we study an ~200 m long earthworm invasion chronosequence in a hardwood forest in Minnesota. The forests in the Great Lakes region have evolved without native earthworms since the Last Glacial Maximum. Exotic earthworms were recently introduced due to agriculture, recreational fishing, and logging activities. The transect represents an invasion history of ~40 yrs with its invasion front proceeding at a rate of ~5 m/yr. We quantified the degree that biological retention of elements (Si, Ca, P, K), sorption of organic matter on mineral surface, and generation of pore space respond to the arrivals of different earthworm functional groups. Invasive earthworms critically and systematically impact the three key biogeochemical processes. We quantitatively and mechanistically reveal that strong feedbacks among the three processes are present, and that the feedbacks systematically evolve with ongoing earthworm invasion. We determined biomasses and species compositions of earthworms, elemental chemistry (ICP), soil mixing intensity (¹³⁷Cs), and carbon-mineral sorption (BET), and adopted the geochemical mass balance approach with Zr as an immobile element. This study illustrates how and to what degree invasive earthworms – by altering bioturbation and consuming particulate organic matter – cause cascading effects on the dynamics and interactions between nutrients and carbon fluxes.

Light-absorbing aerosol radiative forcing in the Kathmandu Valley during Suskat-ABC Field Campaign

SOON-CHANG YOON¹, SANG-WOO KIM¹,
JIHYOUNG KIM¹, CHAE YOON CHO¹, JIN-YOUNG JUNG²,
AND MAHESWAR RUPARKHETI³

¹ School of Earth and Environmental Sciences, Seoul National
University, Seoul, Korea (yoon@snu.ac.kr)

² Korea Polar Research Institute, Incheon, Korea

³ Institute for Advanced Sustainability, Potsdam, Germany

Light-absorbing aerosols, such as black carbon (BC), are major contributors to the atmospheric heating and the reduction of solar radiation reaching at the earth's surface. In this study, we investigate light-absorption properties of aerosols (i.e., BC mass concentration, aerosol solar-absorption efficiency) in the Kathmandu valley during Sustainable atmosphere for the Kathmandu valley (SusKat)-ABC campaign, from December 2012 to February 2013. Kathmandu City is among the most polluted cities in the world. However, there are only few past studies that provide basic understanding of air pollution in the Kathmandu Valley, which is not sufficient for designing effective mitigation measures (e.g., technological, financial, regulatory, legal and political measures, planning strategies). A distinct diurnal variation of BC mass concentration with two high peaks observed during wintertime dry monsoon period. BC mass concentration was found to be maximum around 09:00 and 20:00 local standard time (LST). Increased cars and cooking activities including substantial burning of wood and other biomass in the morning and in the evening contributed to high BC concentration. Low BC concentrations during the daytime can be explain by reduced vehicular movement and cooking activities. Also, the developmements of the boundary layer height and mountain-valley winds in the Kathmandu Valley paly a crucial role in the temporal variation of BC mass concentrations. Detailed radiative effects of light-absorbing aerosols will be presented.

Origin and distribution of sedimentary organic matter in Yellow Sea and northern East China Sea studied with carbon and nitrogen stable isotopes and radiocarbon

SUK-HEE YOON¹, JONG-GU GAL¹, HI-IL YI²
AND KYUNG-HOON SHIN^{1*}

¹Hanyang University, Department of Marine Sciences and convergent technology, Ansan, Rep of Korea,
(Correspondence: shinkh@hanyang.ac.kr)

²Korean Ocean Research Development Institute, Ansan, Rep. of Korea,

In order to investigate the source and distribution of organic matter in the surface sediment of Yellow Sea and northern East China Sea, we have collected surface sediment samples from more than 300 sampling sites, and have measured their stable carbon and nitrogen isotope ratios. The distributions of organic carbon and nitrogen stable isotopes ratios are described in the entire Yellow Sea and northern East China Sea, indicating apparently lighter carbon isotope ratios at the sites near Sangdong Peninsular. In addition, ¹⁴C values of organic carbon at the surface sediments are also determined at the same sites. ¹⁴C values of organic carbon range from 10930±80 to modern. In the near Sangdong Peninsular, the oldest ¹⁴C age of organic carbon corresponds to the lighter stable carbon isotopes ratios, reflecting large contribution of terrestrial organic carbon. However, ¹⁴C value of organic carbon in the central basin of Yellow Sea is close to modern, which is mainly contributed by marine organic carbon. Other sites in the shelf regions show around 2000 of ¹⁴C age. Some sedimentary organic carbon was younger than 2000 ¹⁴C age in the northern East China Sea where is the area affected by Tsushima Current. In the current study, the ¹⁴C values of organic carbon in the surface sediment of Yellow Sea and northern East China Sea seems to be strongly influenced by the transport of terrestrial organic carbon as well as petroleum derived organic carbon from the coastal regions.

Mineralogical characterization of thermal treated chrysotile and tremolite asbestos in soils

SUNGJUN YOON¹, HYEONYI JEONG², WONJIN MOON³
AND YUL ROH^{4*}

¹Chonnam National University, Gwangju, Korea,
(sungjunyoon8@naver.com)

²Chonnam National University, Gwangju, Korea,
(happy11hyun@nate.com)

³Korea Basic Science Institute, Gwangju, Korea,
(wjmoon@kbsi.re.kr)

⁴Chonnam National University, Gwangju, Korea,
(*correspondence: rohy@jnu.ac.kr)

Asbestos-containing soils occur mainly at ultramafic rocks and hydrothermally altered carbonate rocks in S. Korea. Remediation of asbestos-containing soils is considered a high priority by the Korean Government because these soils, if left untreated, represent a hazard to the environment and human health. Thermal transformation asbestos-containing waste used to detoxify asbestos may potentially be adapted to achieve remediation of the asbestos-containing soils. The objectives of this study were to provide information related to the thermal effects on asbestos and to examine mineralogical characteristics of the thermal treated asbestos-containing soils.

Two soils, a soil weathered from serpentinite rock and a soil weathered from hydrothermally altered carbonate rocks, were selected for thermal treatment and mineralogical characterization. The mineralogical characterization approach was designed to obtain basic information relating to the nature of asbestos in the soils. TG-DTA analysis was used to find the optimum temperature for thermal treatment of the two asbestos-containing soils. PLM, XRD, SEM, TEM and EDS analyses were used to examine the mineralogical properties of asbestos in soils before and after the thermal treatment.

PLM, SEM and TEM analyses showed chrysotile contained in the soil weathered from serpentinite rock and tremolite asbestos contained in a soil weathered from hydrothermally altered carbonate rocks. Chrysotile and tremolite asbestos in soil were transformed to forsterite and diopside at 820°C and 1060°C, respectively. Chrysotile fibers were transformed into rod-shaped forsterite at 820°C. Tremolite asbestos was transformed into non-fibrous diopside 1060°C. The thermal treated asbestos, chrysotile and tremolite asbestos, was non-fibrous. These results indicated that thermal treatment of asbestos-containing soils was effective for detoxification of the asbestos and can be applied to treat the asbestos-containing soils.

Natural radionuclides as tracers in surface water and groundwater interaction

YOON YEOL YOON, SOO YOUNG CHO, KIL YONG LEE,
AND YONG CHUL KIM

Korea Institute of Geoscience and Mineral Resources,
Gwahang-no 124, Yuseong-gu, Daejeon, 305-350,
Korea,(yyyoon@kigam.re.kr, sycho@kigam.re.kr,
kylee@kigam.re.kr, yckim@kigam.re.kr)

Determining the relationship between rivers and adjacent groundwater systems is critical to understanding hydrogeological systems, protecting riverine ecosystems, and managing water resources. Due to its high activities in groundwater, the radionuclide ^{222}Rn is a sensitive natural tracer to detect and quantify groundwater. In this study ^{222}Rn and ^3H were used as a tracer in groundwater and river water interaction.

^{222}Rn and ^3H were used as a natural radiotracer to study groundwater and river water interaction. Study area is used groundwater as a water curtain house in winter, so shortage of groundwater problem is occurred and groundwater-river water interaction was severely varied at this time. This variation was studied with ^{222}Rn and ^3H during water curtain house operation period and the results was showed in figure 1 and the interation difference was compared with upper and below river dam.

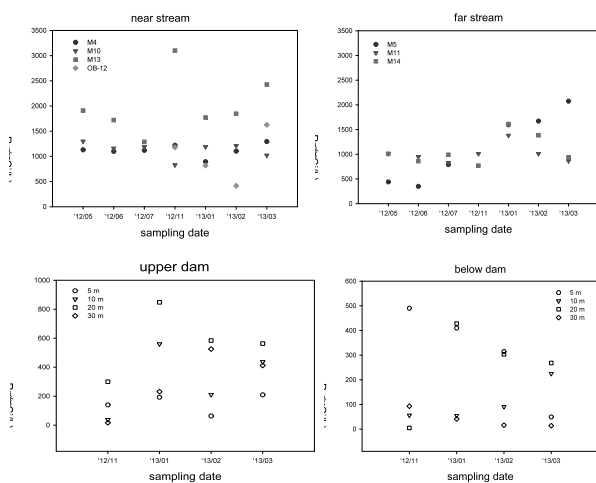


Fig. 1. ^{222}Rn contents variation with water curtain house operation period.

[1] T.Kluge (2007) *Hydrol. Earth Syst. Sci.* **11**, 1621-1631. [2] Ian Cartwright (2011) *J. Hydrol.* **405**, 333-343. [3] N.J. Mullinger (2008) *Geophysical Research Abstracts*, Vol. 10, EGU2008-A-08953 [4] Vasile (2010) *Appl. Radiat. Isotop.* **8**, 1236-1239.

Cathodoluminescence of terrestrial and extraterrestrial halite

E. YOSHIDA¹, H. NISHIDO¹, N. NIMURA²
AND K. NINAGAWA¹

¹Department of Biosphere-Geosphere Science, Okayama
University of Science, 1-1 Ridai-cho, Okayama 700-0005
Japan (correspondence: nishido@rins.ous.ac.jp)

²Okayama Astronomical Museum, 3037-5 Honjou, Asakuchi,
Okayama, 719-0232 Japan

Luminescence of natural alkali halides such as halite and sylvite is characterized by structural defects related to F-center(+p) and V-center(+e). Their CL (cathodoluminescence), however, have not been reported so far. Since asteroidal water was discovered as fluid inclusion in halite from H5 chondrite, Monahans (1998), alkali halides in meteorites have been extensively investigated for understandings of aqueous alteration and thermal metamorphism on the parent body. Therefore, luminescence features of halides can provide valuable information on such issues. In this study we have measured CL spectra of terrestrial halite and ones in meteorites to clarify luminescence centers in various types of halite.

Several halite crystals of terrestrial origin and small halite particles in ureilite meteorites were selected for CL spectral measurements. All samples were prepared using oil while cutting and polishing without water.

All samples exhibit weak blue to greenish blue CL with broad band emissions from 350 to 650 nm. CL spectra corrected for total instrumental response were converted into energy units for spectral deconvolution using a Gaussian curve fitting. The analysis of terrestrial halite results in two emission components at 3.02 eV (410 nm) and at 2.22 eV (557 nm). Former can be assigned to F center and the latter to V center. Halite in ureilite gives two components at 3.10 eV (399 nm) for F center and at 2.61 eV (475 nm), which is different from any luminescence centers previously reported. Therefore, the emission at 2.61 eV might be defect center derived from the damage induced by high-energy radiation in cosmic space.

Mantle wedge metasomatism recorded in LREE-depleted calcic amphibole in the Pinatubo harzburgite xenoliths

M. YOSHIKAWA^{*1}, T. KAWAMOTO¹, Y. KUMAGAI¹,
S. ARAI², A. TAMURA², T. KOBAYASHI³
AND M. OKUNO⁴

¹ Kyoto Univ., Beppu, 874-0903, Japan (*correspondence: masako@bep.vgs.kyoto-u.ac.jp)

² Kanazawa Univ., Kanazawa 920-1192, Japan

³ Kagoshima Univ., Kagoshima 890-0065, Japan

⁴ Fukuoka Univ., Fukuoka 814-0180, Japan

Calcic amphibole-bearing spinel harzburgites from the Pinatubo 1991 dacite are characterized by residual mantle mineral chemistry and abundant fluid inclusions of saline solutions and magnesite in mantle minerals. Some xenoliths have zoned selvages composed of amphibole, phlogopite, plagioclase and orthopyroxene. The peridotite xenoliths show more or less metasomatized textures; fine-grained orthopyroxene-rich parts with amphibole, olivine, spinel, and phlogopite, replacing primary olivines. We determined trace element compositions of amphiboles of the least metasomatized harzburgite using LA-ICP-MS.

Chondrite-normalized trace element patterns of the amphiboles show depletion in LREE with various degrees of negative Ti and positive Sr anomalies, in contrast to LREE enriched amphiboles with negative anomalies of HFSE, Eu and Sr from the selvages. This suggests that the harzburgites were metasomatized before entrainment in the host dacite. Amphiboles inside the harzburgite xenolith show continuous chemistry from magnesiohornblende to tremolite. These amphiboles can be classified into primary and secondary ones in paragenesis and chemical composition. The secondary amphiboles are contained in the fine-grained orthopyroxene rich parts and show relatively low TiO₂ and Al₂O₃, and high SiO₂ and MgO contents. Their trace element patterns are similar to those of primary amphiboles but with lower concentrations. These LREE-depleted amphiboles have been observed in the subcontinental lithospheric mantle peridotites metasomatized by subduction-related hydrous fluids, because hydrous fluids do not carry large amounts of REE [1, 2]. The compositional features of the amphiboles suggest that the primary amphiboles were formed through a reaction between pyroxene and subduction-related SiO₂-rich aqueous fluids and the secondary amphiboles were formed from more diluted fluids at lower temperature conditions.

[1] Vannucci *et al.* (1995) *GCA* **59**, 1763-1771. [2] Downes (2001) *J. Petrol.* **42**, 233-250.

Apparent inverse carbon isotope effects during the anaerobic oxidation of methane

MARCOS YOSHINAGA¹, GUNTER WEGENER^{1,2*},
THOMAS² HOLLER, TOBIAS GOLDHAMMER²,
BENJAMIN BRUNNER², JOHN POHLMAN³,
MARCEL KUYPERS², KAI-UWE HINRICHS¹
AND MARCUS ELVERT¹

¹Marum, Center for Marine Environmental Sciences, University of Bremen, Bremen, Germany (*presenting author)

²Max Planck Institute for Marine Microbiology, Bremen, Germany

³U.S. Geological Survey, Woods Hole Coastal and Marine Science Center, Massachusetts, USA

Large amounts of methane are produced in marine subsurface sediments. Their emission to the hydrosphere is suppressed by microbial consortia, which perform the sulfate-dependent anaerobic oxidation of methane (AOM) in distinct sulfate-methane transition zones (SMTZ). According to conventional isotope systematics, the biological consumption should result in ¹³C-enriched residual methane. Instead, within the SMTZs methane is often depleted in ¹³C, a pattern frequently interpreted as evidence of concomitant methane production.

Here we tested if AOM alone can yield ¹³C-depleted methane. We incubated sediment-free AOM-cultures devoid of background methanogenesis at low sulfate concentrations. As a result of decreasing sulfate availability (<0.5 mM), the system switched from ¹³C-enrichment towards ¹³C-depletion in the methane pool. We explain this apparent inverse carbon isotope effect by AOM-mediated equilibrium isotope exchange, which predominates during sulfate-limited AOM. Our results are representative of SMTZs, where generally low sulfate concentrations prevail. Evidence that ¹³C-depleted methane can form by a non-methanogenic process expands our current understanding of the methane biogeochemistry in marine sediments. Microbially mediated equilibrium isotope exchange might be common in marine subsurface habitats, which are generally characterized by limited substrate availability combined with low energy yields.

Methane production potential of subsurface microbes in Pleistocene sediments from a water-dissolved natural gas field in central Japan

HIDEYOSHI YOSHIOKA*, HANAKO MOCHIMARU
AND SUSUMU SAKATA

Institute for Geo-Resources and Environment, National
Institute of Advanced Industrial Science and Technology
(AIST), 1-1-1 Higashi, Tsukuba 305-8567, Japan
(*correspondence: hi-yoshioka@aist.go.jp)

As much as 20% of the world's natural gas resources is estimated to be of biogenic origin [1]. This implies that subsurface anaerobic microbes are important producers of natural gas. However, it is unclear when and where the microbes produced methane and what kind of substrates they utilize. To address these issues, we investigated microbial methanogenesis in Pleistocene sediments from Minami-Kanto gas field in central Japan. The gas field is widely distributed in the southern area of the Kanto Plain and the gas dissolved in the formation water consists almost solely of biogenic methane [2]. Mochimaru *et al.* found that methanogens are living in the formation water from production wells [3].

Core sediments from the depth of 287-607 m were obtained by drilling, and sludge sediments were collected from the settling ponds which were located downstream of the gas-water separators. Methane production rates from the sediments were measured in the tracer experiments using [¹⁴C]-bicarbonate and [2-¹⁴C]-acetate. Cumulative amounts of methane produced from the sediments were monitored in the long-term (tracer-free) incubation experiments.

The tracer experiments showed that CO₂ reduction was the main pathway of methane production. The highest rate of 1.1 nmol CH₄ cm⁻³ day⁻¹, obtained from the muddy sediment at 607 m, was comparable with those in the sediments from the Blake Ridge gas-hydrate region [4].

In the long-term incubation experiments, intense methanogenesis occurred and continued for a few months. Mass balance evaluation indicated that most of the methane was derived from kerogen. This study has demonstrated that subsurface microbes can utilize a substantial fraction of the recalcitrant sedimentary organic matter as the source of methane production.

[1] Rice (1993) *USGS Professional Paper* **1570**, 583-606. [2] Igari & Sakata (1989) *Geochem. J.* **23**, 139-142. [3] Mochimaru *et al.* (2007) *Geomicrobiol. J.* **24**, 93-100. [4] Wellsbury *et al.* (2002) *FEMS Microbiol. Ecol.* **42**, 59-70.

In-situ iron isotope analysis of pyrite in ca. 3.8 Ga metasediments from Isua supracrustal belt, Greenland

KAZUMI YOSHIYA¹, YUSUKE SAWAKI²,
TSUYOSHI KOMIYA³, SHIGENORI MARUYAMA¹
AND TAKAFUMI HIRATA⁴

¹ Earth Life Science Institute, Tokyo Institute of Technology,
Japan (yoshiya.k.aa@m.titech.ac.jp)

² Dept. of Earth and Planetary Sci., Tokyo Institute of
Technology, Japan

³ Dept. of Earth Sci. and Astro., Komaba, Univ. Tokyo, Japan

⁴ Dept. of Geology and Mineralogy, Kyoto Univ., Japan

The timing of emergence of life still remains one of the unresolved questions in the early Earth. Early life could be identified and characterized by its metabolic processes, which must be deposited and preserved in the old rocks. The oldest (*ca.* 3.8Ga) sedimentary rocks on Earth occur in the Isua supracrustal belt (ISB), southern West Greenland. These rocks have been subjected to until amphibolite facies metamorphism [1,2]. Despite the contribution of the intense thermal metamorphism, carbon isotope compositions from the Isua metasediments suggested the evidence for biological carbon fixation [3,4,5]. Microbial dissimilatory iron reduction (DIR) is also considered to be one of the earliest metabolisms on Earth [6,7]. $\delta^{56}\text{Fe}$ value of Fe²⁺_{aq} generated by DIR is expected to have lower value, whereas negative $\delta^{56}\text{Fe}$ values lower than -1 ‰ are not found in the sedimentary record prior to 2.9Ga. Here, we report the *in-situ* iron isotope analysis of pyrite in sedimentary rocks from the ISB, using femtosecond laser ablation multi-collector ICP-MS technique (fs-LA-MC-ICP-MS)[8]. We obtained a large variation of iron isotope data from -2.41 to +2.35 ‰ in $\delta^{56}\text{Fe}$ values, from 212 points of pyrite grains in 15 rock specimens, including metachert, muddy metachert, BIF, carbonate rock and conglomerate. The distribution of $\delta^{56}\text{Fe}$ values varies depending on the lithology, whereas no correlation could be found between $\delta^{56}\text{Fe}$ values and the metamorphic zone.

Low $\delta^{13}\text{C}$ values of graphite in ISB muddy metachert suggested the existence of biological carbon fixation [5]. $\delta^{56}\text{Fe}$ values of pyrite grains from the same samples show lower $\delta^{56}\text{Fe}$ values, which suggested the occurrence of microbial DIR in the Early Archean.

[1] Nutman (1986), *Precam. Res.* **78**, 1-39. [2] Hayashi *et al.* (2000) *Int. Geol. Rev.* **42**, 1055-1115. [3] Schidlowski *et al.* (1979), *GCA.* **43**, 189-199. [4] Rosing (1999), *Science* **283**, 674-676. [5] Ueno *et al.* (2002), *GCA.* **66**, 257-268. [6] Vargas *et al.* (1998) *Nature* **395**, 65-67. [7] Lovley (2004), *Origins, Evolution, and Biodiversity of Microbial Life.* pp. 301-313. [7] Hirata & Kon (2008), *Anal. Sci.* **24**, 345-353.

A lithospheric mantle source for Etna magmatism

H. PATRICK YOUNG¹, ZHENGRONG WANG¹
AND MARK BRANDON¹

¹Department of Geology and Geophysics, Yale University,
New Haven, CT 06520, USA. (Hobart.young@yale.edu)

Mt. Etna has important geochemical and petrologic similarities with other sodic volcanics in the region. We compared the chemistry of rocks from Mt. Etna with those from other nearby volcanoes (e.g., Pantelleria and Ustica) which have the least contribution from the subducted slabs, in order to better understand the nature of the regional mantle source that is supplying melts for Mt. Etna. We obtained Sr-Nd-Pb-O isotopes, as well as trace and major element data for rocks spanning the ages and compositions of these volcanoes. Among them, lavas from Etna, Pantelleria and Ustica have more radiogenic Pb-isotopes than MORBs. Their mantle-like oxygen isotope composition indicates that the radiogenic component might originate directly from the mantle. Moreover, the isolation of a high- μ (HIMU = old material with initially high U/Pb ratio) source for ~500 Ma is required to generate the Pb isotope compositions in these lavas. Interestingly, these melts are similar to experimental melts of amphibole in peridotite [1]. However, amphibole and most other hydrous silicates are unstable above ~1100 °C, which is significantly below asthenospheric temperatures, requiring that the source veins were frozen into the lithospheric mantle during ingrowth of radiogenic Pb. We suggest that the source of Mt. Etna magmatism might be related to extensional decompression, or alternatively, heating by a hot plume, resulting in melting of a metasomatized sub-continental lithospheric mantle.

[1] Medard *et al.*, 2006, *J. of Petrology*, 47: 481-504

Cerium sequestration in fractures in the upper kilometer of granitoids, SE, Sweden

C. X. YU^{1*}, H. DRAKE¹, M. ÅSTRÖM¹
AND F. MATHURIN¹

¹Linnaeus University, 39182 Kalmar, Sweden

(*correspondence: changxun.yu@lnu.se)

This study seeks to define geochemical processes governing the accumulation and sequestration of Ce in granitoidic fractures down to >700 m depth, revealing past intrusions of oxygenated waters. The fracture coatings (secondary mineral precipitates in open fractures) gathered from the study area (Laxemar, SE Sweden) are characterized by high levels of Ce (Fig. 1b) compared to host rock coccentration (average: 86 ppm, n=65) and show a striking feature of distinct positive Ce anomalies ($Ce_{WN}^* = 1.21-3.95$, n=8) in the uppermost 20 m of the bedrock (Fig. 1a).

Cerium and Mn X-ray absorption spectroscopy (XAS) of selected fracture coatings, together with existing data (e.g. fracture mineralogy and groundwater chemistry), indicate that: (1) Ce(IV) occurs down to c.a. 70 m depth and is exclusively associated with Mn oxides which occur as todorokite and triclinic birnessite as suggested by Mn EXAFS spectra; (2) Since Mn is largely speciated as Mn^{2+} in the present bedrock groundwaters, the Ce(IV)-bearing Mn oxides most probably resulted from oxidative weathering of wall rock and fracture coating minerals when oxygenated waters intruded into the bedrock (down to several hundred meters depth) during deglaciation events (>13000 BP); (3) Unlike other samples, clear XAS features of a poorly-crystalline hexagonal-birnessite-like phase and larger proportion of aqueous Mn^{2+} were observed in the sample with strikingly positive Ce anomaly ($Ce_{WN}^* = 3.95$) (Fig. 1b) at the depth of 0.87 m, suggesting an ongoing dynamic accumulation of Ce(IV), i.e. dissolution and reprecipitation of Mn oxides while Ce(IV)-enriched residue largely remained.

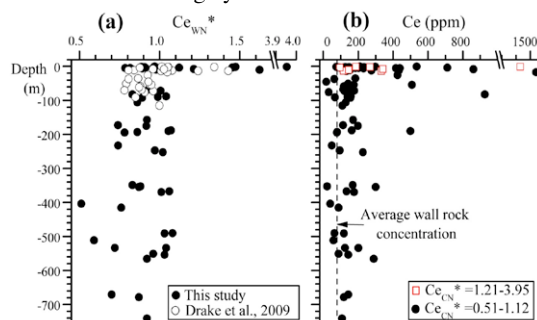


Fig. 1. Distribution of Ce anomalies ($Ce^* = Ce / (La * Pr)^{1/2}$ in WN WN WN WN fracture coatings (a), where WN denotes normalization to average wall rock; and concentrations in the fracture coatings (b).

[1] Drake *et al.* (2009) *Appl Geochem* **24**, 1023–1039.

Oxygen Before Cyanobacteria implied from Magnetotactic Bacteria

HANG YU AND JOSEPH L. KIRSCHVINK

Geological and Planetary Sciences, California Institute of Technology, Pasadena CA 91125, USA
(*correspondence: kirschvink@caltech.edu)

Magnetotactic bacteria (MTB) position themselves magnetically at oxic/anoxic and sulfate/sulfide transitions in redox stratified sediments. As opposed to the earlier polyphyletic idea¹, recent functional gene studies of magnetosome formation support a common origin of MTB²⁻⁴, but their evolutionary relationship with other bacterial groups remains obscure. We analyzed over 700 MTB 16s rRNA sequences to elucidate the origin and evolution of MTB in relation to other Bacterial groups as shown below.

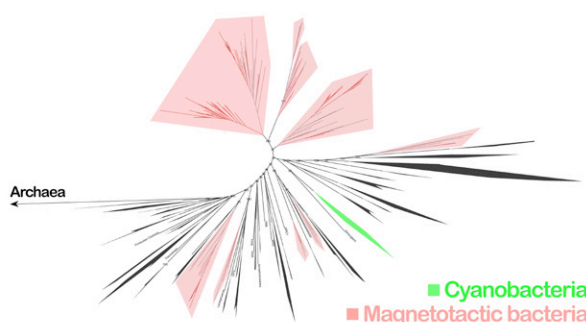


Figure 1. A Bayesian tree showing the molecular phylogeny of Bacteria, with special emphasis on magnetotactic bacteria.

Our phylogenetic analysis suggests a ubiquitous presence of MTB throughout all but the oldest branches of the bacterial tree. Four phyla with MTB appear before the cyanobacterial divergence, indicating a much earlier origin for this group than hypothesized. Horizontal gene transfer is an unlikely explanation based on the genetics and biochemistry of magnetosome formation. This result suggests the presence of pre-Cyano redox stratified environments in the Archaean, such as the peroxide-rich glacial runoff settings where oxygen mediating enzymes may have evolved⁵. Together with peroxidase and reactive oxygen species (ROS) scavenging properties of magnetosomes⁶, MTB might have contributed to the adaptation to oxygen by mediating ROS toxicity in ancient microoxic environments.

[1] Delong *et al.* (1993) *Science* **259**, 803–806. [2] Abreu *et al.* (2011) *ISME J* **5**, 1634–1640. [3] Jogler *et al.* (2011) *PNAS USA* **108**, 1134–1139. [4] Lefèvre *et al.* (2013) *EM* doi:10.1111/1462-2920.12097. [5] Liang *et al.* (2012) *PNAS USA* **103**, 18896. [6] Guo *et al.* (2012) *EM* **14**, 1722–1729.

Eco-geochemistry and Kashin-Beck Disease-A case study in Aba, Sichuan

T. YU¹, Z.F. YANG^{1*}, Q.Y. HOU¹, W.J. MA²
AND L.X. JIN³

¹School of Earth Sciences and Resources, China University of Geosciences, Beijing 100083, China

(*correspondence: zfyang@up-point.com)

²Peking University Health Science Center, Beijing 100191, China

³Sichuan Institute of Geological Survey, Chengdu 610081, China

Kashin-Beck disease (KBD) is a chronic, endemic osteochondropathy (disease of the bone), but it is not clear what is the cause. There are still new cases of KBD in part of the Tibet, Qinghai and Sichuan province in recent years[1], severely damage the wellbeing of the local population.

The distribution characteristics of selenium(Se), calcium(Ca), molybdenum(Mo), iron(Fe), zinc(Zn) and strontium(Sr) in environmental media, plants, animals and human blood, urine and hair in Aba, Sichuan were studied with the theory and method of eco-geochemistry. Elements related to KBD were disclosed. The geochemical processes of migration and transformation of Se and other elements, the healthy risk and the KBD eco-geochemical model of the population in studied area were established. The practical prevention and control measures for KBD in the area were suggested.

It is proved that the Se, Ca, Zn, Fe, Mn, Mo, Sr are all deficient in these environmental media in the area, the Se in soil is 0.12mg/kg on average, far lower than that of in Chengdu Economical Zone 0.28mg/kg and the average of whole country (0.26mg/kg).

New KBD cases are all from inhabitation on the slopes in the valley, where in contrast to the control area, Ca, Se and some other elements in surface soil were severely leached and most soil pH was nearly acidic to neutral.

The results of the present study could be applied to the improvement of the environment in KBD area and reduce the KBD incidence, is an important progress on eco-geochemistry and KBD research.

[1] Tan *et al.* (2002) *The Science of the Total Environment* **28**, 227-235.

Re-evaluation of electron transfer budgets for oxidation and incorporation of bisulfide by dissolved organic matter under anaerobic conditions

ZHIGUO YU^{1,2} AND KLAUS-HOLGER KNORR^{1,2}

¹ Department of Hydrology, University of Bayreuth, Bayreuth, Germany

² present address: Hydrology Group, Institute for Landscape Ecology, WWU Muenster, Germany, (zhiguo.yu@uni-muenster.de)

While it is known that functional groups of organic matter, such as quinones, can reversibly transfer electrons, there is little known about electron transfer (e-transfer) processes in redox reactions of reactive species, such as sulfide, with organic matter.

We investigated the chemical oxidation of H₂S with a reduced (as control) and non-reduced dissolved humic acid (HA), in batch experiments at pH 6 under anoxic conditions. Thereafter, electron transfer budgets were calculated from sulfide consumption and production of oxidized sulfur species formed.

Sulfide reacted rapidly with DOM and thereby regenerated more oxidized forms of sulfur, either inorganic sulfur species (S⁰ and S₂O₃²⁻) or organic products (e.g. as carbon bonded sulfur). Lower concentrations of HA in solution reacted more effectively towards sulfide (25 ppm C: moles S/moles C = 0.024; 75 ppm C: moles S/moles C = 0.015). The main reaction product was S⁰ (making up about 40–50 %), important intermediate was S₂O₃²⁻ (about 13–32 % reaction for 48 hours). Total recovery in the inorganic fraction accounted to 60–78%, while a gap remained in the budget of about 22–40% of sulfur that had presumably added to the HA as organic sulfur. Thus, in all non-reduced HA treatments, 10–30 μmol/L sulfide added to the HA as organic sulfur (22–40%), and X-ray absorption spectroscopy data supported organic sulfur to be approximate zerovalent sulfur. E-transfer capacities of non-reduced HA towards sulfide based on formation of organic sulfur was therefore about 0.8–1.24 μeq/mg C. The amount of electrons transferred to reduced HA was comparable to the difference of e-transferred to oxidized HA minus e-transferred to HA pre-reduced with H₂/Pd.

In conclusion, the results showed that HA chemically reoxidized sulfide under anoxic condition at significant rates, and formed reduced organic sulfur compounds that provided a sink for sulfur and reduces the amount to be recycled.

Uranium reduction on magnetite: An electrochemistry approach

KE YUAN*, RODNEY C. EWING^A AND UDO BECKER

Department of Earth and Environmental Sciences, University of Michigan, Ann Arbor, MI 48109, USA
(*correspondence: keyuan@umich.edu)

Electrochemical methods provide a unique approach that allows one to measure or control the redox environments close to the surface of semiconducting minerals. Cyclic voltammetry and potential step voltammetry have been applied in order to investigate the redox reactions of aqueous uranyl on the electrodes made of bulk and nano-powder of crystalline magnetite. *In-situ* Atomic Force Microscopy and Raman spectroscopy were used to probe the surface morphology and phase change as a function of the redox potential.

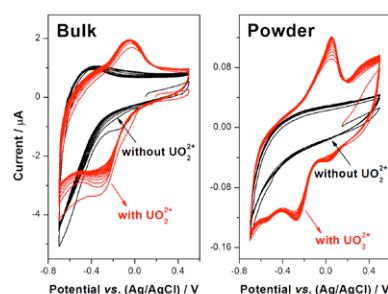


Figure 1: Cyclic voltammetry of the bulk and the powder magnetite electrode in solution with and without uranyl and the AFM height image of the bulk electrode surface after the reaction (220×220nm).

Two sets of redox peaks were found on the cyclic voltammogram of magnetite nano-powder in blank solution, showing its high reactivity, but none was detected on the bulk crystalline electrode. The one-electron reduction from U⁶⁺ to U⁵⁺ was verified by fitting the potential step voltammetry of the crystalline electrode. The U⁶⁺ to U⁵⁺ reduction peak was evident at a more negative potential (-0.33 V vs. Ag/AgCl) on the cyclic voltammetry of the bulk electrode as compared with that of powder electrode (-0.27 V vs. Ag/AgCl). This reflects the slower kinetics of the electron transfer on the bulk magnetite surface. After immersion in a uranyl sulfate solution, the surface roughness of the magnetite increased as the redox potential decreased from -0.22V to -0.30V within one hour. Island-like features of about 20 nm height were found on the magnetite surface, which could be iron hydroxides resulting from the oxidation of magnetite.

Petrogenesis of the Syenite Granites in Kuluketage Block: Constraints from Petro-Geochemistry, Zircon U-Pb Dating and Hf Isotope

Q. YUAN, X.B. LÜ*, X.F. CAO, X.D. WANG
AND E.L. YANG

Faculty of Earth Resources, China University of Geosciences,
Wuhan 430074, China
(*correspondence: lvxb_01@163.com)

Kuluketage block is the best area for Precambrian geology in Xinjiang, NW China. In this paper, we studied the petrology, geochemistry, zircon LA-ICPMS U-Pb chronology and zircon Hf isotope research of Daxigou syenite granite (DSG) which is located in Kuluketage. Zircons from the intrusions display oscillatory zoning and high Th/U ratios (0.16-2.11), implying their magmatic origin. Zircon U-Pb dating results of DSG indicate that they formed in Paleoproterozoic with the weighted $^{207}\text{Pb}/^{206}\text{Pb}$ average age of $1767 \pm 46 \text{ Ma}$, which is coincidentally identical with its associated diorite age within the error range. Studies of petrogeochemistry suggest that DSG belong to medium-sodium and rich-potassium peraluminous calc-alkaline type, rich in Pb, La, Th and LILE, significant poor in HFSE (Gd, Nd, Ta). The chondrite-normalised REE pattern is slightly to the right form. The average $\Sigma \text{ REE}$ is 56.57×10^{-6} ; HREE show moderate fractionation (LREE/HREE averaged 10.28, (La/Yb)_N average of 13.04) N; average (La/Sm)_N of syenite is 4.96, average (Gd/Yb)_N is 1.67 and the δEu , δCe are not obvious. Their initial Hf isotope ratios and Hf two-stage model ages range from -7.74 to -4.02 and 2.74 Ga to 2.67 Ga, respectively. Taken together, it is suggested that DSG is the typical S-type granite and its primary magma could be mainly derived from partial melting of the Neoproterozoic crust and mainly formed in the syn-collision arc environment, which recorded the tectonic-magma activities response of Tarim refers to the amalgamation of the supercontinent Columbia.

Copper-mediated oxidation of hydroquinone under conditions typical of natural saline waters

XIU YUAN¹, A. NINH PHAM², CHRISTOPHER J. MILLER³
AND T. DAVID WAITE⁴

School of Civil and Environmental Engineering, the
University of New South Wales, Sydney, NSW 2052,
Australia

¹ (xiu.yuan@unsw.edu.au,) presenting author;

² (anninh.pham@unsw.edu.au); ³ (c.miller@unsw.edu.au);

⁴ (d.waite@unsw.edu.au.)

Copper (Cu) is an essential transition metal that is involved in a variety of photoreactions and physiological processes. The redox chemistry between cuprous copper (Cu(I)) and cupric copper (Cu(II)) in the upper water column plays a significant role in its speciation, transport and bioavailability [1]. As electron transfer mediators, quinone moieties in natural organic matter (NOM) play important roles in essential biogeochemical processes [2-3]. In this study, detailed kinetic model has been developed to describe the oxidation of 1,4-hydroquinone (H₂Q) by Cu(II) in the presence O₂ in 0.7 M NaCl solution at pH range 6.5 – 8.0. Cu(II) catalyzed the overall oxidation of H₂Q in a strongly pH dependent manner with concomitant formation of benzoquinone and H₂O₂.

The kinetic model indicated the mono-anion HQ⁻ is the active species to reduce Cu(II) with an intrinsic rate constant of $5.0 \times 10^7 \text{ M}^{-1} \cdot \text{s}^{-1}$. While the semiquinone radical (SQ⁻) generated from one-electron oxidation of hydroquinone or one-electron reduction of benzoquinone acts as a chain propagating species, the presence of O₂ in the system is also essential in terms of supplying Cu(II) by continuously oxidizing Cu(I) and rapidly removing SQ⁻ to generate O₂⁻. The development of the kinetic model should assist in understanding and predicting the factors controlling copper transformation, speciation, bioavailability and toxicity in aquatic systems.

[1]. Moffett, J. W.; Zika, R. G. (1988) *Geochim. Cosmochim. Acta* 52, 1849-1857. [2]. Uchimiya, M.; Stone, A. T. (2010). *Aquat Geochem* 16, 173-188. [3]. Uchimiya, M.; Stone, A. T. (2009), *Chemosphere* 77, 451-458.

The genesis of Jadeitite: A viewpoint from Zirconology

T.F. YUI^{1*}

¹Institute of Earth Sciences, Academia Sinica, Taipei, Taiwan
(*correspondence: tfyui@earth.sinica.edu.tw)

Jadeitite is a rare rock type formed in subduction zones. Its genesis has attracted much attention recently. Two formation mechanisms have been proposed: the whole-sale metasomatic replacement and the vein precipitation. These two mechanisms would imply different chemical cycling paths for elements such as Al, Na, Zr and Hf, in subduction zones as a result of different physical-chemical conditions. Correct deciphering of jadeitite genesis around the world could therefore provide important information on subduction environment/processes. Recent advance on in situ micro-analysis of zircons provide a unique opportunity to tackle this issue.

Zircon as an accessory mineral in jadeitite would be either inherited from igneous protolith or recrystallized/newly-formed through metasomatic processes. Theoretically, jadeitite formed from whole-sale metasomatic replacement would contain both types of zircon, while jadeitite formed through vein precipitation may only have metasomatic zircon. Mineral inclusions, trace-element and isotopic compositions, as well as textures of zircon have been employed as criteria to distinguish magmatic from metasomatic zircons in recent studies on jadeitite. Unfortunately, with more case studies, it turns out that none of the criteria mentioned above is conclusive. For example, mineral inclusions of metasomatic origin may actually be pseudo-inclusions in inherited, but not metasomatic, zircons. The resetting rate of trace element compositions and U-Pb isotope system of zircon, as well as zircon texture changes, may not take place “in phase” during zircon recrystallization in association with jadeitite formation. Even with “apparent” metasomatic textures, zircons may not necessarily display metasomatic chemistries or yield metasomatic ages. Only through careful and detailed examination of integrated data can the correct interpretation on the origin of zircons, and hence the genesis of jadeitite, be retrieved. A thorough review shows that most jadeitites that have been studied recently would have formed through whole-sale metasomatic replacement processes. Jadeitite formed through vein precipitation process can only be convincingly identified from north of the Motagua fault, Guatemala.

Inverse Modeling of Asian Dust Emission with MODIS AOT and the SPRINTARS Adjoint Model

KEIYA YUMIMOTO^{1*} AND TOSHIHIKO TAKEMURA²

¹ Meteorological Research Institute, Japan Meteorological Agency, Nagamine 1-1, Tukuba-city, 305-0052, Ibaraki, Japan

(Correspondence; yumimoto@mri-jma.go.jp)

² Research Institute for Applied Mechanism, Kyushu University, Kasuga Park 6-1, Kasuga, 816-8580, Fukuoka, Japan (toshi@riam.kyushu-u.ac.jp)

In this study, we performed inverse modeling of Asian dust using MODIS coarse-mode aerosol optical thickness (AOT) and the adjoint of global aerosol climate model [1] for four years (2005–2008). Gridded (T42 horizontal resolution; approximately $2.8^\circ \times 2.8^\circ$) and daily dust emissions in Asian dust sources were optimized. The adjoint inverse modeling generally increased dust emissions from the Gobi desert, and emphasized the daily and inter-annual variations of dust emission amount, comparing with a priori emission (Figure 1). For a severe dust storm in late March 2007, the peak of dust emission was shifted by one day earlier by the inverse modeling. The inversion results were widely validated independent observations (e.g. lidar observation network).

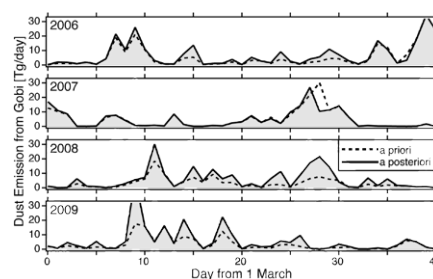


Figure 1. Time series of dust emission in the Gobi desert. Solid and broken lines represent a priori and a posteriori emissions, respectively.

Direct Aerosol Radiative Forcing (DARF) for dust aerosol was estimated with a posteriori dust emissions. The increase of dust emissions led to increases of longwave DARF at both the top of atmosphere and surface. A posteriori DARF exhibits the different trend and the larger inter-annual variations than a priori one.

[1] Yumimoto and Takemura (2013), SPRINTARS/4D-Var Data Assimilation System: Development and Inversion Experiment Based on OSSE Framework, submitted to Geoscientific Model Development.

Geodynamics of the layered mafic – ultramafic intrusions in the East Sayan (Russia)

A. N. YURICHEV* AND A. I. CHERNISHOV

Tomsk State University, Tomsk, Russia
(*juratur@sibmail.com)

Within the Central Asian folded belt, the most of the layered low-titaniferous and high-aluminous peridotite-troctolite-gabbro massifs are comparable with the products of Early Paleozoic island arc magmatism by the time of their formation [1]. In addition, their spatial relation to axial parts of island-arc systems is being discussed. One of the representatives of this formational type is the Talazhin mafic-ultramafic intrusive massif in the northwestern part of the Eastern Sayan studied by us. It is composed of troctolites, which dominate over plagioclones, as well as lenses anorthosite, and gabbro with high anorthite ratio (An_{75-99}). The relatively high Fe content in olivine (Fa_{20}) and similarity in behavior of trace elements to island-arc high-aluminous basalts indicates that the massif rocks are comagmatic with IAB-type volcanites. Mineralogical characteristics of gabbro of the Talazhin massif are similar to the allivalite and eucrite xenoliths in modern island-arc volcanites. The geochemical features of the massif rocks indicate that their generating is a result of crystallization differentiation of high-aluminous olivine-bearing basalt magma. The rocks are characterized by high magnesium at low concentrations of HFSE (Ti, Zr, REE), as well as enrichment in LREE, and the positive Eu-anomaly. Sharp minimums for Ta and Nb, and maximums for Ba and Sr can be seen in the spider diagrams. It is suggested that the formation of the Talazhin massif occurred as a result of magma forming in the suprasubduction setting.

This study was funded by the Russian Ministry of Education and Science (projects 14.B37.21.0686, 14.B37.21.1257).

[1] Izokh A.E. *et al.* (1998) *Russ. Geol. Geophys.* **39**, 1565–1577.

Ordering of isotope composition for H, N and O between planets

H. YURIMOTO^{1*}

¹Hokkaido University, Sapporo 060-0810, Japan
(*correspondence: yuri@ep.sci.hokudai.ac.jp)

Hydrogen, Nitrogen and Oxygen are among the most abundant elements of the universe. Isotopic compositions of these elements between molecules are highly variable in molecular clouds. Due to highly volatile nature of these elements, the chemical forms are easily changed between vapor and solid (ice) by environmental temperature and pressure. Thus, the standard planetary formation model of the solar system suggests that inner planets deplete these elements, but outer planets enrich as major elements. Isotopic compositions for planets of these three elements should be determined spontaneously according to the standard planetary formation processes. Therefore, the isotopic variation between planets would be an important key to clarify how to form planets in the solar system. In this report, we propose new systematic approach to infer isotopic compositions for H, N and O of outer planets.

We have proposed a model for oxygen isotopic evolution in proto-planetary disk [1], and inferred O isotopic compositions of outer planets [2]. The augmented model based on [2] in this study assumes the initial condition of isotopic compositions of molecules observed in molecular clouds and in chondrites, and includes two key points, i.e., 1) temporal preservation of chemical species fractionated in mass and 2) astronomical space separation by dynamic coupling/decoupling due to the chemical form changes for H, N and O in the disk.

The model infer systematic increase of heavier isotope components of H, N and O for outer planets towards increasing radial distance from the sun, whereas relatively uniform isotopic composition for inner planets. Inferred H isotope variations between outer planets are quantitatively consistent with observation data by planet explorations [e.g. 3]. We infer enrichments of ¹⁵N in the order of Jupiter, Saturn, and Uranus/Neptune. The ¹⁵N/¹⁴N ratio of Uranus/Neptune would be larger than the Earth's value. Oxygen isotope systematics between outer planets would be mass independent and ¹⁶O component would be depleted in the order from Jupiter towards Neptune. The isotopic compositions of inner planets suggest significant accretions of ices from outer solar system during planetary growth and as late veneer.

[1] Yurimoto & Kuramoto (2004) *Science* **305**, 1763–1766. [2] Kuramoto & Yurimoto (2005) *In Chondrites and the Protoplanetary Disk* **341**, pp. 181–192. [3] Hartogh *et al.* (2011) *Nature* **478**, 218–220.

Causes of Late Pleistocene Lake Victoria water level change, derived from clumped isotopes in land snails and fresh water mollusks

SHIKMA ZAARUR^{1*}, HAGIT PAFFEK¹ CHRISTIAN TRYON², DANIEL PEPPE³ AND J. TYLER FAITH⁴

¹Yale University, Geology and Geophysics, New Haven, CT, USA (shikma.zaarur@yale.edu)

²New York University, Anthropology, New York, NY, USA

³Baylor University, Geology, Waco, TX, USA

⁴Univ. of Queensland, School of Social Science, Australia

Carbonate clumped isotopes thermometry is based on the dependence of Δ_{47} on carbonate formation temperature. Most marine and fresh water biogenic carbonates agree with the Δ_{47} -T calibration. The clumped isotope thermometry is particularly useful in terrestrial environments where the interpretation of carbonate $\delta^{18}\text{O}$ is limited by difficulty in estimating paleo-water composition.

Clumped isotopes - derived temperatures of land snails are generally higher than the ambient environmental temperatures, but show no evidence for disequilibrium. We attribute these higher body temperatures to eco-physiological snail adaptations. Combined with shell $\delta^{18}\text{O}$, we use these temperatures to calculate snail body water composition, that serves as a paleo-hydrological indicator.

We combine Δ_{47} and $\delta^{18}\text{O}$ in modern and fossil fresh water mollusks and land snails from Rusinga and Mfangano Islands in Lake Victoria to examine lake paleo-hydrology, testing hypotheses about the mechanism of a significant rise in lake level in Lake Victoria ~35-40 ka BP.

Outcrops of paleo-beach deposits ~18 m above the modern day lake levels indicate high water stands at ~35-40 ka BP. Such increase in lake level could be driven by local mean annual precipitation that is significantly greater than modern. However, this is inconsistent with regional climate reconstructions, suggesting that either lake level was controlled by non-climatic factors, or that local climate in the Lake Victoria basin was different than regional patterns of climate across eastern Africa. We analyze modern and fossil shells from this 18 m beach outcrop on Mfangano Island to compare with modern lake water $\delta^{18}\text{O}$ values and to calculate paleo-water compositions. We combine these results with calculated land snail body water $\delta^{18}\text{O}$ from Rusinga and Mfangano Islands, to study hydrological changes of Lake Victoria and to evaluate the relative importance of climate change and tectonics as mechanisms for the Late Pleistocene expansion of Lake Victoria.

A cold slab-mantle interface: Constraints from exceptionally well preserved lawsonite eclogites

THOMAS ZACK¹

¹Department of Earth Sciences, University of Gothenburg, Sweden, (zack@gvc.gu.se)

The area around Halilbagı in the Tavşanlı Zone, Turkey exhibits the largest known continuous unit (>5 km²) at which lawsonite eclogite facies conditions (circa 460- 520°C and 2.2- 2.4 GPa, [1,2]) were attained and peak metamorphic assemblages preserved. Within this area, a wide range of rock types can be found, of which metamafic (lws-gla-omp-grt bearing), Mn-rich metachert (piedmontite-phe-qtz bearing), marble (with aragonite pseudomorphs) and serpentinites (with antigorite) are of particular relevance. Critical is the recent finding of rare lws-epi-chl assemblages at the direct contact between serpentinite lenses and metamafic rocks, interpreted as metasomatic blackwalls formed close to peak metamorphic conditions. This argues for an intimate mixing of mantle-derived and crust-derived components at great depths (in contrast to incorporation of nearby low pressure serpentinites during exhumation).

The exceptional preservation of those mineral assemblages (especially with lawsonite) has been a matter of discussion. Cetinkaplan et al (2008) [1] calls for cooling through continued underplating of crustal material during exhumation. The discovery of a second generation of lawsonite and glaucophane in a chlorite matrix that replaces garnet supports that model, as it confirms the assumption that on the cooling path at temperature below 400°C, lawsonite was still stable. I would like to add that the underplating of very H₂O-poor lithologies (especially cherty limestone of the Afyon Zone) [3] helped to minimize the availability of retrogressing fluids.

These findings imply that the formation of lawsonite eclogite is not only possible in the interior of a downgoing slab, but also in direct contact to the overlying mantle wedge. Therefore it can be concluded that rather low temperatures (460-520°C) are achieved at a depth of ca 70 km at the slab-mantle boundary, and this at moderate to low convergence rates (ca 2 cm/a) after less than 20 Ma of convergence [4]. This places tight constraints on any thermal model of subduction zones, ruling out several recent models predicting much higher slab-mantle temperatures at such depths.

[1] Cetinkaplan *et al.* (2008) *Lithos* **104**: 12-32. [2] Davis & Whitney (2008) *Contr Min Petrol* **156**: 217-241. [3] Candan *et al.* (2005) *Lithos* **84**: 102-124. [4] Okay *et al.* (1998) *Tectonophysics* **285**: 275-299.

Atmospheric trace gases and isotopologues using mid-IR laser direct absorption spectroscopy

MARK ZAHNISER, BARRY MCMANUS, DAVID NELSON, JOANNE SHORER, SCOTT HERNDON, JOSEPH ROSCIOLI, TARA YACOVITCH J AND CODY FLOERCHINGER

Aerodyne Research, Inc., Billerica, Massachusetts, USA

Recent advances in mid-infrared laser technology have greatly facilitated field measurements of atmospheric trace gases to identify and quantify their sources and sinks. Newly available non-cryogenic mid-infrared lasers and detectors, long path length, small volume sampling cells, and advances in direct absorption techniques with have led to smaller, lighter, and more robust instrumentation for measurements from mobile and aircraft platforms, field sites at remote locations, and laboratories for clumped isotopologues. The reliability and reproducibility of the mid-infrared lasers has led to long term monitoring and turn-key operation. Trace gas detection in ambient air at the low part-per-trillion levels are now feasible. Fractional precisions of less than 1 part in 10,000 allow for isotopologue ratio measurements of carbon dioxide, methane, and nitrous oxide at atmospheric mixing ratio levels. Applications to measurements of greenhouse gas emissions of methane and nitrous oxide, high precision measurements of carbonyl sulphide (OCS), measurements of ethane (C₂H₆) to determine sources of methane, and isotopologue measurements of CO₂, CH₄, N₂O and H₂O, will be presented.

TRACE GASES ambient mixing ratios	Frequency cm ⁻¹	1 s std dev [ppt] 210 m 76 m	
CH ₄	1275	100	300
¹³ CH ₄ /CH ₄	1294	1.5‰	
OCS	2050	2	5
CO	2199	40	
N ₂ O	2199	20	
¹⁵ N ¹⁴ NO, ¹⁴ N ¹⁵ NO	2188	3‰	
¹³ CO ₂ , C ¹⁸ O ¹⁶ O	2311	0.1‰	
C ₂ H ₆	2996	20	
¹³ CH ₄ /CH ₄	3057	0.5‰	
CH ₃ D/CH ₄	3060	20‰	

Impacts and LIPs: ¹⁸⁷Os/¹⁸⁸Os signatures across the K-Pg boundary

JESSICA ZAISS¹, GREG RAVIZZA*¹ AND BIGER SCHMITZ²

¹Geology & Geophysics, SOEST, University of Hawaii, Manoa, Honolulu HI 96822 USA. (zaiss@hawaii.edu), c(correspondance: ravizza@hawaii.edu)

²Dept. Geology, Lund University, Solvegatan 12 SE-22362, Lund, Sweden. (Birger.Schmitz@geology.lu.se)

Both impacts and large igneous provinces (LIPs) can introduce unradiogenic Os into the global ocean producing excursions to lower ¹⁸⁷Os/¹⁸⁸Os in pelagic sediments. The ¹⁸⁷Os/¹⁸⁸Os excursion caused by the late Eocene Popigai impact is consistent with abrupt addition of soluble meteoritic Os to the ocean [1]. In contrast, previously reported ¹⁸⁷Os/¹⁸⁸Os excursions related to LIPs show greater variability and longer duration than the Popigai Os excursion. It is well established that the Chicxulub impact event is coincident with the K-Pg mass extinction and that eruption of the Deccan Traps began before, and continued after, the extinction event. Comparison of the Popigai excursion to the Cretaceous-Paleogene (K-Pg) boundary ¹⁸⁷Os/¹⁸⁸Os record provides a means of assessing whether or not eruption of the Deccan liberated significant amounts of mantle-derived Os to the ocean-atmosphere system coincident with the K-Pg mass extinction. In the Equatorial Pacific, South Atlantic and Atlantic-sector of the Southern Ocean the recovery of the marine ¹⁸⁷Os/¹⁸⁸Os record to higher pre-extinction levels [2] closely resembles the shape and duration of the Os recovery from the Popigai impact event. This similarity does not support claims [3] that the main phase of the Deccan volcanism is closely linked to the K-Pg mass extinction. However, an Indian Ocean site (ODP 738C) on the Kerguelen Plateau displays ¹⁸⁷Os/¹⁸⁸Os ratios consistently below those from other ocean basins during the Paleogene. In close proximity to the K-Pg boundary in ODP 738C, the Os-Ir-¹⁸⁷Os/¹⁸⁸Os signature is unequivocally meteoritic. Upsection, low ¹⁸⁷Os/¹⁸⁸Os ratios as far as 4.5m above the boundary (≈ 1.2 M.Y.) are unlikely to be related to the Chicxulub impact event. These low ¹⁸⁷Os/¹⁸⁸Os ratios in the Indian Ocean may be fingerprint of Paleogene LIP activity associated with either the Deccan or Kerguelen, but other interpretations are possible. The marine ¹⁸⁷Os/¹⁸⁸Os record allows large impact events to be differentiated from the emplacement of LIPs, and may preserve regional gradients in seawater ¹⁸⁷Os/¹⁸⁸Os controlled by the proximity to active volcanism.

[1] Paquay *et al.* (2008) *Science* 320, 214-218. [2] Ravizza and Vonderhaar (2012) *Paleoceanography* 27, 10.1029/2012PA002301. [3] Keller *et al.* (2009) *EPSL* 282, 10-23.

Magnetite-hosted melt inclusions from phoscorites and carbonatites (Kovdor, Kola): A hydrous analog of Oldoinyo Lengai natrocarbonatites?

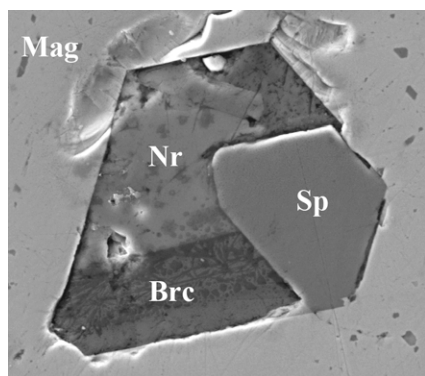
A.N. ZAITSEV^{1,2*} AND V.S. KAMENETSKY³

¹St. Petersburg State University, St. Petersburg 199034, Russia
(*correspondence: burbankite@gmail.com)

²Natural History Museum, London SW7 5BD, UK

³University of Tasmania, Hobart, Tasmania 7001, Australia

Kovdor is a well-studied Devonian complex from the Kola peninsula, Russia consisting of various ultrabasic and alkaline rocks, phoscorites and carbonatites [1]. Silicate minerals composing these diverse rocks often contain primary melt inclusions, particularly in carbonatites, with Na–K–Ca and Na–Mg carbonates as common daughter minerals [2]. Magnetite is a major to minor mineral in Kovdor rocks and SEM study of a mineral from the early-formed calcite-rich phoscorite and calcite carbonatite revealed presences of abundant negative-shaped polymineralic crystallized melt inclusions. SEM/ED analyses and Raman spectroscopy indicate occurrence of various minerals within inclusion including (1) oxides – spinel, baddeleyite, pyrochlore, (2) hydroxides – brucite, (3) silicates – phlogopite, (4) carbonates – nyerereite, eitelite, bradleyite, tychite, calcite, dolomite, (6) phosphates – apatite, (7) halogens – sylvite, and a number of unidentified mineral phases. Coexistence of brucite and unaltered nyerereite in crystallised melt inclusions (Fig.) indicate existence of hydrous and alkali-rich carbonate (\pm phosphate, sulphate) melt from which Kovdor phoscorites and carbonatites were crystallised.



Spinel (Sp), brucite(Brc), nyerereite (Nr) in magnetite (Mag).

[1] Krasnova *et al.* (2004) *Mineral Soc Series* 10, 99-132. [2] Veksler *et al.* (1998) *J Petrol* 39, 2015-2031.

The effect of silicate melt composition on the volatile/melt partitioning of oxidized sulfur

ZOLTAN ZAJACZ¹

¹Inst. of Geochemistry & Petrology, ETH Zürich, Switzerland
(correspondence: zoltan.zajacz@erdw.ethz.ch)

Sulfur is the third most abundant volatile element in magmas and it impacts society via volcanic degassing and by its essential role in the formation of magmatic-hydrothermal ore deposits. Therefore, it is necessary to understand the partitioning of S between silicate melts and exsolving volatile phases. The construction of a thermodynamic model that predicts the volatile/melt partition coefficients of S ($D_S^{\text{volatile/melt}}$) requires the understanding of the dissolution mechanism of S in silicate melts.

I conducted experiments at $P=500$ MPa and $T=1240$ °C in a piston cylinder apparatus to assess the effect of melt composition on $D_S^{\text{melt/volatile}}$, which was used as a measure of the silicate melt's affinity to dissolve oxidized sulfur species. Iron-free, three- and four-component silicate melts were equilibrated with H_2O-S volatiles with $X_S \leq 0.02$ at an fO_2 imposed by the Re-ReO₂ buffer. At these conditions, SO₂ is predicted to be the dominant sulfur species in the volatile phase and S⁶⁺ is the dominant oxidation state of S in the silicate melt. The values of $D_S^{\text{melt/volatile}}$ were calculated by mass balance. The results show that $D_S^{\text{melt/volatile}}$ increases exponentially with the degree of depolymerization of the silicate melt structure expressed with the parameter $NBO/T = [Na+K+2(Ca+Mg)-Al]/(Si+Al)$. At a constant NBO/T of 0.4, $D_S^{\text{melt/volatile}}$ in equilibrium with sodium-aluminosilicate (NAS) melts is more than an order of magnitude higher than in equilibrium with calcium-aluminosilicate (CAS) melts, and more than two orders of magnitude higher than in equilibrium with magnesium-aluminosilicate (MAS) melts. The variation of $D_S^{\text{melt/volatile}}$ in equilibrium with various CNAS and MNAS melts indicates that alkalis are only available for sulfate complexation when they are present in excess compared to the required amount to charge balance for the Si⁴⁺ to Al³⁺ substitution in the melt structure. Calcium has moderate, Mg has very minor affinity to replace alkali elements in this charge balancing role.

At subvolcanic depth, decompression induced degassing of S is more efficient at reducing than at oxidizing conditions, in particular from mafic and peralkaline felsic melts. Effective transfer of S to the ore-forming environment from such magmas requires relatively low fO_2 or advanced degree of crystallization.

Controls on the composition of magmatic volatiles in the crust: Implications for ore genesis and volcanic degassing

ZOLTAN ZAJACZ¹, PHILIP CANDELA², PHILIP PICCOLI²
AND CARMEN SANCHEZ-VALLE¹

¹ IGP, ETH Zürich, Switzerland (correspondence: zoltan.zajacz@erdw.ethz.ch)

² LMDR, University of Maryland, College Park, USA

Volatile elements dissolved in silicate melts not only serve as the driving force for explosive volcanic activity, but also facilitate the formation of magmatic-hydrothermal ore deposits and have a significant impact on the Earth's atmosphere and climate. Though water and CO₂ are the most abundant volatile components in most magmatic systems, the effect of sulfur and halogens on atmospheric chemistry and ore-forming systems is more pronounced.

We will discuss the most important parameters controlling the composition of exsolving magmatic volatiles in the middle to upper crust including numerous new experimental data on the effect of melt composition and P-T on the partition coefficients of S, Cl and some economically important metals such as Au, Cu and Mo.

Experimental data suggests that sulfur is the most easily degassed volatile element after carbon, in particular at relatively low fO_2 (<Ni-NiO) where FeS and H₂S are the dominant sulfur species in the silicate melt and the volatile phase, respectively. Similarly to CO₂, a large fraction of reduced S may be lost from the magma during moderate degree open system degassing induced by decompression. On the other hand, at subvolcanic depth, effective degassing of oxidized sulfur, and in particular Cl will require significant amount of crystallization. Crystallization will promote the transfer of these elements to the volatile phase by decreasing the melt volume, and increasing the volatile/melt partition coefficients by increasing the degree of melt polymerization. The maximum amount of S in the volatile phase is limited to a few mol% by the saturation of sulfide and/or sulfate minerals at P-T- fO_2 conditions typical of subvolcanic reservoirs in arc settings.

Considering metallic elements, Au can be effectively degassed by H₂S-bearing volatiles even from mafic magmas in the early stages of evolution. However, the extraction of Cu will become efficient only from felsic melts exsolving Cl-rich volatiles. The relative timing of saturation in sulfide and volatile phases may have a significant impact on metal extraction efficiencies if the sulfides are fractionated by entrapment in rock forming minerals or gravitational settling.

Biogeochemical poly-barrier qualities in plants

L.V. ZAKHARIKHINA AND YU. S. LITVINENKO

EcoGeoLit Ltd., Moscow, Russia (ecogeolit@mail.ru)

In terms of the ability to accumulate chemical elements in relation to their concentration in the soils, two types of plant species are distinguished, barrier and barrier-free ones.

Our studies of moss and pine purple grass (*Calamagrostis langsdorffii*) show a more complicated correlation of the amounts of elements in the "soil-plant" system. Often the plants show biogeochemical poly-barrier qualities: as the concentration of the element in the soil increases, the barrier mechanism is repeatedly turned on and off.

The graph below shows the poly-barrier display in mosses with respect to Ni, the x axis being the logarithms of the average values for the selected content intervals for the element in soil (lnCs), the y axis being logarithms of average Ni content in mosses (lnCv), growing on these soils (fig. 1).

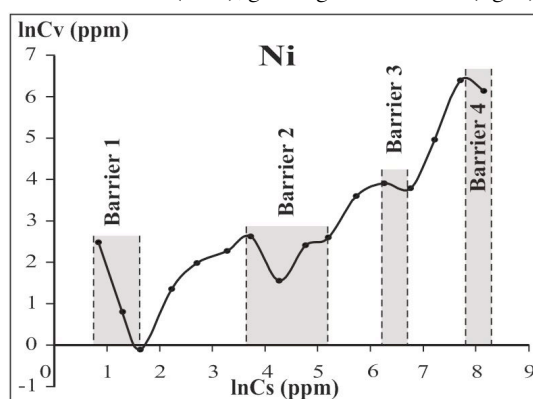


Figure 1: poly-barrier qualities of moss with respect to biological accumulation of Ni.

During the biogeochemical monitoring it is necessary to take into consideration that the cessation of the growth and the decline in the elements in plants are not always connected with the environmental conditions' improvement on the territory. It might as well be conditioned by activation of intermediate biogeochemical barrier. On the other hand, a sharp increase in contents of elements in the vegetation does not definitely mean the deteriorating environmental conditions, it can possibly be the consequence of the barrier being "broken". It is necessary to perform a full ecological-geochemical monitoring of the soils and vegetation to determine biogeochemical poly-barrier qualities in plants.

Heavy metals mobility: Surface water processes (The Copperbelt Case Study)

K. ŽALUDKOVÁ¹ AND J. ZEMAN²

¹Department of Geological Sciences, Masaryk Univ., Brno
611 37, Czech Rep. (voda.dobra@centrum.cz)

²Department of Geological Sciences, Masaryk Univ., Brno
611 37, Czech Rep. (jzeman@sci.muni.cz)

Exemplary well monitored mining areas such as the Copperbelt in Zambia with contaminated reservoirs may provide a better insight into the heavy metals mobility as well as defining principles of the system stability by precipitation or sorption onto either sedimentary clay or organic content at the river bottom sediments.

Processes and heavy metals mobility were evaluated using Surfer[®] Mapping System Ver. 8.00 and Geochemist's Workbench[®] ver. 8.0.11 and 9.0.7 modelling on data acquired in the years 2004 – 2008 during a case study of the semiarid central African Copperbelt in surface waters in the Kafue river and its tributaries, and adjacent soils. Results indicate fluxes and main processes relations affecting the elements mobility.

Mostly all the contamination in tributaries does not exceed limits entering the Kafue river. Important role is attributed to the leaching process, dilution and decomplexation.

The main contaminants Cu and Co mined as a source sulphidic ore are processed in smelters using liming. Fine-grained fraction is washed from the mine waste deposits during rainy seasons and therefore contaminates surface water.

The 4-year monitoring reflected a time evolution and seasonal changes in system parameters. Mostly neutral and slightly alkaline pH decreased down to 2, accompanied by high EC in the vicinity of processing plants and causing metals mobilisation from the bottom sediments.

Griffin and Shimp [1] found the relative mobility of nine metals through montmorillonite and kaolinite: $Cr^{VI} > Se > As^{III} > As^V > Cd > Zn > Pb > Cu > Cr^{III}$. However, the data from the Copperbelt assume the mobility observed in the real environment: $Co = Mn^{II} > Zn > Cu = Mo > Ni > Pb > Zn > Hg$ considering local redox conditions, sediments and subsoil.

Modelling showed the Co concentration was determined by decomplexation of $HCoO_2^-$ and by dissolution of secondary cobalt oxide Co_3O_4 in case of higher Co concentrations. Cu also showed boundary conditions between dissolved $CuOH^+$ Cu^{2+} and precipitates.

[1] Griffin & Shimp (1978) Attenuation of pollutants in municipal landfill leachate by clay minerals. EPA-600/2-78-157, pp. 128 - 135.

Hydrogeochemistry Technogenesis Zone Gold Deposits Baley Ore Field (Eastern Transbaikalia, Russia)

L.V. ZAMANA

INREC of SB RAS, Chita, Russian Federation, 672014
(correspondence: l.v.zamana@mail.ru)

Baley ore field in the middle of the last century was one of the main centers of gold mining in the f. Soviet Union. It is presented adjacent to each other deposits – Baley (BD) and Taseevsk (TD), which were developed respectively in the 1929-1983 and 1948-1995 years. During the period of operation produced more than 450 tons of Au reserves of it in both fields have not been developed.

The ore field is confined to the Mesozoic graben depression, made mainly of sandstones and conglomerates (J_3-K_1). Gold-bearing quartz veins of the BD are located in granodiorite stockwork forming a ledge of the foundation. The total content of sulfides (pyrite, arsenopyrite, chalcopyrite, and others) in the ores is 0.5-5%, and 20% of carbonates and sheet silicates and up to 20%. TD ore in the form of quartz veins and vein mineralization occur in sandstones and contain sulfides and veined minerals in about the same amount [1]. The enclosing sandstones are pyritized.

Different levels of sulfides in the host rocks resulted in the formation of two types of geotechnogenic hydrogeochemical systems with contrasting physical and chemical parameters. In mining objects TD (quarry, waste dumps, tailings) of sulfate acid water with pH less than 3-4 (at least 2.69) and high concentrations of Al, heavy metals, F, Ca, Mg. Identified concentrations reached (mg/l): SO_4^{2-} - 4900, Al - 150.8, Mg - 724.6, Fe - 774.1, Mn - 88.1, Cu - 3.18, Zn - 6.31, Pb - 1.94, Ni - 3.44, Co - 1.08, Cd - 1.1, F - 11.9, As - 1.3. The isotopic composition of sulfate sulfur is lighter than starting sulfides ($\delta^{34}S_{CDT}$ -1.7...-6.5 and -1.18...+1.10‰ respectively), which indicates the involvement of bacterial processes in the oxidation of sulfides and thus enrich acidic waters metals. Water quarry BD is alkaline (pH to 8.40), with relatively low concentrations of ore and petrogenic elements. According to thermodynamic calculations, metals are mainly in ionic form, fluorine, as in the acidic waters of tungsten deposits [2], in the form of complexes with Al. Equilibrium minerals are calculated (quartz, celestine, gypsum, fluoride and etc.).

This work was supported by the RFBR (11-05-98043).

[1] Yurgenson & Grabeklis (1985) In: Mestorojdenia Zabaikalia, 19-32 (in Russian). [2] Zamana & Bukaty (2004) Dokl. Earth Sci. **396** (4), 522-524.

Constraining current oceanic nitrous oxide (N₂O) Emissions and reducing uncertainty for future emissions

L.M. ZAMORA^{1*}, A. KOCK¹, A. OSCHLIES¹
AND H.W. BANGE¹

¹GEOMAR Helmholtz Centre for Ocean Research Kiel, 24105 Kiel, Germany (*correspondence: lzamora@geomar.de)

N₂O is the third most important greenhouse gas, and the 2007 IPCC estimated that oceans provide 10-30% of annual N₂O flux to the atmosphere [1]. The large range in previously estimated oceanic emissions is primarily due to uncertainties in parametrizing microbial N₂O production and consumption within the ocean and to spottiness of data coverage. Here we better constrain ocean N₂O fluxes to the atmosphere by using a complementary dual data-based and modeling approach. First, we estimate current day emissions from the new MEMENTO database, in which gaps in ocean N₂O data coverage have been improved from previous studies [2]. We find oceanic emissions at ~8.6 Tg N₂O yr⁻¹, which falls into the higher end of the 2007 IPCC estimate of 2.8-9.1 Tg N₂O yr⁻¹ emitted from the ocean [1]. Our estimate falls on the high-end of previous estimates primarily due to better data coverage in oceanic N₂O emission hotspots.

The new atmospheric N₂O fluxes from the MEMENTO database gives us valuable insight into the importance of oceanic N₂O emissions. However, improved estimates of the fluxes alone will not allow predictive capacity for future marine N₂O emissions. Therefore, we use the improved present-day emissions estimate calculated here to constrain N₂O parameterizations for a marine biogeochemical model. The marine biogeochemical model incorporates the ranges of literature uncertainties in N₂O biological production and consumption and provides the associated N₂O emissions. Given the known range in current-day fluxes, we are now able to better constrain some of the uncertainties in biogeochemical model parameterizations, thereby enabling a better predictive capacity for future N₂O emissions from the oceans.

[1] Denman *et al.* (2007) in 4th IPCC report, Cambridge Univ. Press. [2] Nevison *et al.* (1995) *J. Geophys. Res.* **100**, 15809-15820.

Tephrostratigraphy and tephrochronology of the Last 130 Ka in the Mediterranean Basin for synchronizing past climatic events

G. ZANCHETTA¹

¹Dipartimento di Scienze della Terra, University of Pisa, Via S.Maria 53, 56126, Pisa, Italy (*correspondance: zanchetta@dst.unipi.it)

With the explosion of palaeoclimatic and palaeoenvironmental research following the concerns related to global warming, few volcanologists could have imagined their role to have changed so dramatically from their traditional focus. In the last two decades, this sector of the scientific community was compelled to move towards a tighter link with Quaternarists, geomorphologists, archaeologists, palaeoceanographers and more in general palaeoclimatologists. Tephrostratigraphy and the identification of tephra layers in different archives will become a mandatory request of many projects for synchronizing archives and improving chronological control of palaeoclimatological records.

The Mediterranean basin is probably one of the most significant areas globally where tephrostratigraphy can reveal its full potential and benefit different disciplines, due to the very large number of explosive volcanoes with very distinctive geochemistries. However, for the correct identification and separation of the different tephra events on distal archives, detailed micro-analytical work is necessary, in some cases including trace elements and observations of peculiar mineralogical associations along with stratigraphic information. Now well dated, chemically well characterized and widely dispersed tephra layers allow us to propose very detailed reconstruction of succession of climatic events for the last 130 ka.

Timing and progression of Mediterranean climate during MIS5 as deduced by Speleothem records from corchia cave (Central Italy)

G. ZANCHETTA^{1*}, R.N. DRYSDALE², J.C. HELLSTROM²,
A.F. FALLICK³, I. COUCHOUD⁴, I. ISOLA⁵,
J. FOHLMESITER⁶, M.F. SANCHEZ GONI⁷
AND E. REGATTIERI¹

¹Dipartimento di Scienze della Terra, University of Pisa, Pisa, Italy (*correspondance: zanchetta@dst.unipi.it)

²University of Melbourne, Victoria, Australia

³SUERC Glasgow, Scotland, UK

⁴Laboratoire EDYTEM, Université de Savoie, France

⁵Istituto Nazionale Geofisica e Vulcanologia, Pisa, Italy

⁶Heidelberg Academy of Science, Heidelberg, Germany

⁸EPHE, UMR-CNR Université Bordeaux, France

Prominent, sub-Milankovitch climatic instability dominates the palaeoclimate record for the last glacial period, particularly in archives sourced from the North Atlantic region. A growing number of studies have suggested this climatic instability affected the Mediterranean basin. We present a continuous, highly resolved (decadal to centennial scale) isotopic record obtained from Corchia Cave. The isotope time series has been assembled by stacking four separate stalagmites records spanning the period between 140 and 90 ka. The lowest $\delta^{18}\text{O}$ values, representing the wettest and probably the warmest interval, started at 130 ka and ending abruptly at 126 ka. A long-term trend of increasing $\delta^{18}\text{O}$ values is present between ca. 126 and 114 ka, which is punctuated by century-scale abrupt events of increasing $\delta^{18}\text{O}$ and $\delta^{13}\text{C}$ values at ca. 126, 123, 121, 119, 116 and 114 ka. Some of these events appear to correlate with cooling events C25-C27 in North Atlantic. Two prominent cooling/drying events are clearly recognizable centred at ca. 109 and 104 ka (corresponding to C24 and C23 cold events in the North Atlantic), which are in excellent agreement with two dry/cold events at Monticchio pollen record in Southern Italy. The record terminated with a cold/dry phase at ca. 88 ka corresponding to C21 cooling in North Atlantic.

Magma storage and ascent conditions beneath Pico And Faial Islands (Azores Islands). A study on fluid inclusions

V. ZANON AND M.L. FREZZOTTI

Vittorio.VZ.Zanon@azores.gov.pt

In the islands of Faial and Pico (the Azores), fluid inclusions are hosted in megacrysts of olivine (Mg#80-88) and clinopyroxene (Mg#79-90) in highly porphyritic lavas and in mineral assemblages of ultramafic xenoliths. Only few inclusions are contained in olivine phenocrysts (Mg#<80) and plagioclases in poorly porphyritic lavas. Trails of late-stage inclusions are predominant over isolated early stage inclusions. The former experienced re-equilibration and consist of pure CO_2 ($T_m = -56.5 \div -57.2$). The latter have the same composition but may contain dypingite or Mg-calcite, which indicates that in earlier times water was present along with CO_2 .

Barometric data indicate that inclusions in xenoliths re-equilibrated at 570-586 MPa (19.7-21.2 km), in poorly porphyritic lavas from fissure zones and at the central volcano of Faial, at 465-508 MPa (16.4-18.1 km), and at Pico Volcano at 342-437 MPa (12.5-16.5 km). Shallow conditions of trapping/re-equilibration were recorded at 156 MPa for the volcano of Faial (5.6 km) and at 194 MPa for the volcano of Pico (7.1 km) in phenocrysts of the mugearites. These pressures correspond to the magma ponding and to its crystallization and can be useful for tracing the progressive thickening of a dense transition zone, below the geophysical Moho. The ability to rapidly withdrawal of the stored magmas from these volcanic systems strictly depends on the different tectonic styles, acting in the transition zone. Tectonics also plays a major role in the evolution of magmas, favouring the formation of small-lived intracrustal reservoirs, not necessarily coaxial with main conduit system.

Evaluation of the pollution in the agricultural grounds irrigated by waters: Case Of The High Valley Of Oued Bounamoussa, Algerian Northeast

¹* L. ZAOUÏ AND ² M. BENSLAMA

¹Département of Pharmacy. Faculty of medical Science. Hadj Iakhder University. Batna. Algeria

^{1,2}Laboratoire grounds and sustainable development, department of Biology. Faculty of Science. Badji Mokhtar University. B.P.12, Annaba, 23000 Algeria Phone : (213)(0)38 87 53 99 (*Lilia_zaoui@yahoo.fr)

The pollution represents a severe problem for the environment because of the discharges cross-posted in rivers and ponds hillsides. Under the influence of the continuous activity of the People), the ground receives and absorbs wastes which form the pollution of subterranean waters. The region of El Tarf is extremely situated northeast Algerian.

With the aim to know the current state of the quality of waters in the region of the Algerian northeast, we led a study which concerns the quality of waters and the grounds of the agro-system of the plain of Bounamoussa situated in the wilaya of El Tarf which is an essentially rural zone where water resources are strongly requested for agricultural activities.

The evaluation of the analyses of grounds and waters in the various points of observation was the object of a treatment of data realized during a cycle allowed to notice that waters of the plain of Bounamoussa are of an even strong average salinity, generally suiting in the irrigation of the tolerant cultures in salts on well drained grounds, very sensitive to the variations of the chemical aspect connected to the irrational use of artificial fertilizers. The evolution of the salinity must be however controlled.

That is why it is imperative, in front of a susceptibility of pollution such as the agricultural irrigation of waters of the plain, to estimate the contents of these chemical elements in the ground, to appreciate really the scale of the risk as well as for knowledge the origins of the contamination of waters of the plain under the influence of the impact of waters of Oued Bounamoussa.

First-principles modeling of hydrolysis reactions for nuclear waste glass forms

P. ZAPOL^{1,2*}

¹Materials Science Division, Argonne National Laboratory, Argonne, IL 60439, USA (*correspondence zapol@anl.gov)²Chemical Science and Engineering Division, Argonne National Laboratory, Argonne, IL 60439, USA

First-principles informed models of dissolution behavior of glass waste forms in aqueous environments can potentially lead to reduced uncertainties in predictions of long-term behavior. As a starting point, we have developed a model using a well characterized crystalline aluminosilicate (orthoclase) that has a known structure, but possess key characteristics of waste form glass, such as compositions with multiple cations, pH dependence and formation of secondary phases in dissolution. A Kinetic Monte Carlo study based on first-principles calculations of barriers for water reactions at neutral, protonated and deprotonated sites provided information on the overall dissolution rate and rate-limiting steps. The dissolution rate far from equilibrium is compared to experiments. We have also extended this approach to multi-component glasses, where we calculated reaction energies and barriers from first-principles. Insights into the molecular-level mechanisms of glass dissolution will be used for a coarser scale modeling. This work is aimed at better understanding of the dissolution behavior and development of predictive models for dissolution rates.

Non-Innocent role of electron-mediating ligands in reductive dissolution of hematite

PIOTR ZARZYCKI¹, DIANA TOCZYDŁOWSKA¹,
SHAWN CHATMAN² AND KEVIN ROSSO²

¹Institute of Physical Chemistry, Polish Academy of Sciences, Warsaw, Poland ²Physical Sciences Division, Pacific Northwest National Laboratory, WA

Reductive iron (III) oxide dissolution is a primary source of soluble ferrous ions in environment [1]. It can be mediated biotically (e.g., by dissimilatory metal reducing bacteria) or abiotically (e.g., by organic reductive pollutants in anthropogenic environment) [1]. The reductive dissolution is promoted by surface protonation, adsorption of chelating electron-donating ligands (e.g., ascorbate, hydroquinone, sulfide) [2,3,4,5] and chelating electron-mediating ligands (e.g., dicarboxylic acids) [1,6]. Despite the decades of research, we still do not fully understand mechanism of iron(III) oxide reductive dissolution on a molecular level. For instance, in some cases addition of the Fe(II) ions facilitates dissolution (e.g., in the presence of oxalate, ascorbate, EDTA) [7,8], whereas in others it inhibits iron reduction (e.g., AH₂DS, microbial systems) [9-11]. The same appears to be true for surface-bound ligands, that is, some are able to promote surface dissolution by assisting Fe(II) detachment (e.g., oxalate, citrate) [9], while others block surface sites (e.g., chromate, arsenate) [1,11]. Surface protonation plays also an important, synergistic role in hematite dissolution [1].

Here we report the molecular modelling and electrochemical studies of the non-innocent role of the electron-mediating ligands bridging the surface ferric ions with the external reductants.

[1] Cornell & Schwertmann (2003) *The Iron Oxides*. Wiley, Weinheim. [2] Afonso *et al.* (1990) *J. Colloid Interface Sci.* **138**, 74-82. [3] Pulton *et al.* (2004) *Geochim. Cosmochim. Acta* **68**, 3703-3715. [4] LaKind & Stone (1989) *Geochim. Cosmochim. Acta* **53**, 961-971. [5] Stack *et al.* (2004) *J. Colloid Interface Sci.* **273**, 442-450. [6] Duchworth & Martin (2001) *Geochim. Cosmochim. Acta* **65**, 4289-4301. [7] Ballesteros *et al.* (1998) *J. Colloid Interface Sci.* **201**, 13-19. [8] Suter *et al.* (1991) *Langmuir* **7**, 809-813. [9] Royer *et al.* (2004) *Environ. Sci. Technol.* **38**, 187-193. [10] Liu *et al.* (2007) *Environ. Sci. Technol.* **41**, 7730-7735. [11] Chang & Matijevic (1983) *J. Colloid Interface Sci.* **92**, 479-488.

LA ICP-MS Trace element and oxygen isotope variation of vanadium-rich Ruby and Sapphire within Mogok Gemfield, Myanmar

KHIN ZAW^{1*}, L. SUTHERLAND², T.F. YUI³, S. MEFFRE¹
AND KYAW THU⁴

¹CODES ARC Centre of Excellence in Ore Deposits, University of Tasmania, Hobart, Tasmania, Australia (*correspondance: Khin.Zaw@utas.edu.au)

²School of Natural Sciences, University of Western Sydney, Penrith, NSW 2751, Australia ²Geoscience, Australian Museum, 6 College Street, Sydney, NSW, Australia

³Institute of Earth Sciences, Academia Sinica, Nankang, Taipei, Taiwan ⁴Geology Department, Yangon University, Yangon, Myanmar

Rubies and sapphires attract scientific and commercial interest, e.g. the renowned Mogok, Myanmar gem field. These gemstones are corundum colored by transition elements within the alumina crystal lattice: sufficient Cr³⁺ gives red in ruby and Fe²⁺, Fe³⁺ and Ti⁴⁺ ionic interactions color sapphires; a minor ion, V³⁺ introduces slate to purple colors and color change effects in some sapphires, but its role in coloring rubies remain enigmatic. Trace element and oxygen isotope values provide genetic signatures for natural corundum and assist geographic typing. Precise LA-ICP-MS analysis of ruby and sapphire from Mogok placer and *in situ* deposits reveal V can exceed 5000 ppm, giving V/Cr, V/Fe and V/Ti ratios up to 26, 78 and 97 respectively. Such values significantly exceed those elsewhere and are focused on a specific area, suggesting a geological control on V-rich ruby distribution. Our results demonstrate that detailed geochemical studies of ruby suites can reveal new gemmological, gem grading and gem exploration insights. They give V a greater role as a ruby tracer, encourage comparisons of V/Cr-variation between ruby suites and widen modelling of ruby genesis.

Parental Growth Media Of Siberian Diamonds – Relation To Kimberlites

D.A. ZEDGENIZOV^{1,2*}, A.L. RAGOZIN^{1,2},
V.S. SHATSKY^{1,3} AND W.L. GRIFFIN⁴

¹Sobolev Institute of Geology and Mineralogy, 3 Koptyuga ave., 630090, Novosibirsk, Russia (*correspondence: zed@igm.nsc.ru)

²Novosibirsk State University, 2 Pirogova str., 630090, Novosibirsk, Russia

³Vinogradov Institute of Geochemistry SB RAS, 1a Favorovskiy str., 664033, Irkutsk, Russia

⁴CCFS/GEMOC, Macquarie University, NSW 2109, Australia

Microinclusions in natural diamonds represent a bulk sample of fluids/melts from which they crystallized [1], and provide a unique opportunity to characterize diamond-forming media and to understand their origin and evolution. In comparison with the worldwide database, the parental fluids/melts in Siberian diamonds (fibrous, cloudy, coated) define a continuous range of carbonatitic to silicic compositions; only a few fall into the first half of the range from carbonatitic to saline. Several individual diamonds show core to rim variations from carbonatitic to silicic or vice versa, or from chloride-carbonate to predominantly carbonatitic.

The trace-element patterns of the microinclusions are generally similar to those of kimberlites and carbonatites, but there are significant differences in major elements. The relative abundance of K in the fluids is significantly higher than observed in the host kimberlite and carbonatites. The pattern of HFSE in the microinclusions shows some depletion in Ti, Zr and Hf. The REE pattern reveals low abundances of the heavy REE and high light REE concentrations. Many samples with carbonatitic composition have a negative anomaly in Y.

These studies have revealed that there are many geochemical features consistent with a genetic link between the diamond-forming media and ephemeral carbonatitic and silicic liquids (HDF's) which may be precursors of the host kimberlite. These HDF's may originate either from the metasomatic influx of volatile agents; some may be liberated by low-degree partial melting of eclogites and peridotites. The absence of any marked correlation of $\delta^{13}\text{C}$ of diamonds with the compositions of their microinclusions suggests that carbon-isotope compositions are generally related to the primary source of diamond-forming HDF's. Some elemental variations may be explained by the fractional crystallization of such fluids/melts, or mixing between liquids with different compositions.

[1] Navon *et al.* (1988) *Nature*. **335**, 784-789.

Bioreduction Of Sb-Substituted Goethite :A Mechanism Of Sb Mobility And Bioavailability?

A. ZEGEYE¹, P. BILLARD¹ AND C. MUSTIN¹

¹ Université de Lorraine, Laboratoire Interdisciplinaire des Environnements Continentaux, UMR 7360, BP 70239 Vandoeuvre-lès-Nancy, F-54506, cedex France (*correspondance: asfaw.zegeye@univ-lorraine.fr)

Antimony (Sb) is the ninth most mined metal for industrial uses worldwide. It is frequently used in a variety of industrial products although Sb and its compounds are considered as pollutants of priority interest. Due to their large surface area and reactive surface properties, iron oxide can be important sorbents of antimony (Sb). The incorporation of Sb into synthetic and natural iron oxides has been demonstrated [1]. However, extensive research is still required to evaluate whether the co-precipitation of antimony with iron oxide can serve as a possible long-term sink.

The aim of this work was therefore to synthesize Sb substituted goethite and to analyze the mobilization of Sb during the bioreduction process by *Shewanella putrefaciens* MR-1, an iron respiring bacteria. Additionally, the bioavailability of Sb was assessed using a whole cell GFP-based bacterial biosensor. Depending on the synthesis pathway, our data show that up to 1% of antimony can be substituted in the goethite structure affecting the coherence domain size of the mineral. The modification of the coherence domain size affects in turn the goethite's bioreduction and the bioavailability of Sb.

[1] Mitsunobu, S., *et al.* (2010): *EST*, 44, 3712-3718.

Nanoscale probing of the reactivity of biologically *versus* chemically formed green rusts

A. ZEGEYE^{1,2*}, M. ETIQUÉ^{1,2}, P. SCHAAF³, C. RUBY^{1,2},
AND G. FRANCIUS^{1,2}.

¹ Université de Lorraine, Laboratoire de Chimie Physique et Microbiologie pour l'Environnement, UMR 7564, Villers-lès-Nancy, F-54601, France (*correspondance: asfaw.zegeye@univ-lorraine.fr)² CNRS, Laboratoire de Chimie Physique et Microbiologie pour l'Environnement, UMR 7564, Villers-lès-Nancy, F-54601, France³ Institut Charles Sadron, CNRS UPR 22, BP 84749, Strasbourg Cedex 2, F-67034, France

Iron containing nanoparticles such as green rusts (GR) display very high reactivity against organic and inorganic contaminants and present a great potential for the remediation of polluted surfaces and subsurfaces. Since GR can either be formed by chemical or biological pathways, an understanding of their reactivity at the nanoscale level is fundamentally necessary for establishing an efficient remediation process. For the first time, we demonstrated that the combination of atomic force microscopy and chemical force microscopy is a powerful platform for probing the reactivity of GR at the nanoscale. In the presence of nitrate, we probed the nano minerals surface of both the chemically and biologically formed GRs, which enabled us to show a significant deprotonation of the H⁺ present on the basal surface of the chemically formed GR, in contrast the biologically formed GR displayed virtually no reaction. Furthermore, by using the free chain model to model the force curves obtained from our spectroscopy data, we showed that the absence of reactivity of the biological GRs was due to the presence of biopolymers on its surface.

Undoubtedly, the experiments and results presented in this study open new avenues for understanding the potential difference in reactivity between biologically and chemically formed GR.

The oldest zircons of Africa - Their implications for Hadean to Archean crust-mantle evolution

A. ZEH^{1*}, A. GERDES¹ AND R. STERN²

¹Goethe University Frankfurt, Altenhöferallee 1, D-60438 Frankfurt am Main, Germany (correspondence: a.zeh@em.uni-frankfurt.de)²Canadian Centre for Isotopic Microanalysis (CCIM), University of Alberta Edmonton, AB T6G 2E3, Canada

More than 450 detrital zircon grains from Limpopo Belt quartzites were carefully investigated by CL/BSE imaging, U-Pb dating, $\delta^{18}\text{O}$, and Lu-Hf isotope analyses in order to get faithful information about the early Earth's crust - mantle evolution. The zircon grains have crystallisation ages between 3.95 Ga and 3.40 Ga, show near chondritic to subchondritic ϵHf_t between +1 to -15 ($\pm 1 \epsilon$ -unit), and $\delta^{18}\text{O}$ mostly between +5.5 and +8.1 ‰ ($\pm 0.2\%$) VSMOW. Trace elements point to zircon formation in (mostly) granitoid rocks.

The new U-Pb-Hf-datasets provide evidence for three distinct crust evolution (ϵHf_t -age) trends. All three trends start from nearly chondritic mantle sources at about 4.5 Ga (trend 1), 4.05 Ga (trend 2), and 3.75 Ga (trend 3), and require $^{176}\text{Lu}/^{177}\text{Hf}$ between 0.018 and 0.020, typical for mafic crust. $\delta^{18}\text{O}$ values mostly above 6.0 ‰ (VSMOW) indicate that the mafic crust has been altered, perhaps by interaction with cold oceanic water.

The new datasets from the Limpopo Belt and compilation of data from worldwide sources indicate a significant ϵHf_t -gap of about 5 epsilon units between trend 1 and 2. Furthermore, they reveal that many zircon analyses plot well below trend 1 (mostly at ages <4.3 Ga), or have (super)chondritic composition between 4.4 and 4.0 Ga. These findings together support an interpretation that the early Earth was covered by a long-lived, but volumetrically insignificant Hadean mafic protocrust, perhaps an unstable "stagnant lid" [1], which was affected by internal reworking [2], and injected and overlain by melts from chondritic and (highly) depleted mantle sources. This mafic protocrust was locally transformed into a TTG crust starting at <4.3 Ga [3], perhaps due to successive resurfacing [4], accompanied by crust cooling and enhanced foundering. Eventually, the complex Hadean protocrust became re-worked completely during new crust formation at <4.05 Ga.

[1] Ernst (2007) *Gondw. Res.* **11**, 38-49. [2] Kemp *et al.* (2010) *EPSL* **296**, 45-56. [3] Harrison *et al.* (2008) *EPSL* **268**, 476-486. [4] Kamber *et al.* (2005) *EPSL* **240**, 276-290.

Ni availability/Ni solid phases in soils and waters from ultramafic complexes in Brazil: A narrow relationship

I. ZELANO^{1,2}, Y. SIVRY^{1*}, C. QUANTIN³, A. GÉLABERT¹, M. THARAUD¹, D. JOUVIN³, E. MONTARGES-PELLETIER⁴, J. GARNIER⁵, R. PICHON³, S. NOWAK⁶, S. MISKAC³, O. ABOLLINO² AND M.F. BENEDETTI¹

¹Université Paris Diderot – Sorbonne Paris Cité – IPGP UMR CNRS 7154 * :sivry@ipgp.fr² Università degli Studi di Torino, Italy

³UMR 8148 IDES, UPS-CNRS

⁴UMR 7569 LEM, CNRS-NancyI

⁵Instituto de Geociências, Universidade de Brasília

⁶Univ. Paris Diderot, Sorbonne Paris Cité ITODYS UMR CNRS 7086

The modification of Ni availability and lability consequently to mining and metallurgical activity was studied in the two ultramafic complexes of Barro Alto and Niquelândia (BA and NIQ, resp., Goiás State, Brazil). Soils, ores, metallurgical wastes as well as surface waters samples were collected.

Stable Isotopic Exchange Kinetic technique (SIEK, [1]) was applied to solid samples to assess both the kinetic of solid-solution transfers and total exchangeable pool of Ni (E_{Ni}). Moreover, for the nearly first time, this technique was performed on natural water samples to quantify the pool of isotopically exchangeable Ni from the suspended particulate matter (SPM) in water, defined here as E_{Ni}^W . Goethite, chlorite, talc and serpentine were identified by XRD, SEM-EDS and TEM as the main Ni bearing phases in SPM located far from metallurgical activity (BA site), while in samples located in the area influenced by metallurgy (NIQ site) Ni was mainly associated to spherical micrometric particles related to fly ash produced by the ore combustion.

This difference in Ni bearing phases between BA and NIQ sites induces a difference of Ni exchangeable pool: up to 565 mg L⁻¹ in NIQ samples (E_{Ni}^W value) while in BA it only reached 62 mg L⁻¹. These E_{Ni}^W values correspond to total exchangeable Ni in SPM (E_{Ni} values) of 49,000 and 2350 mg kg⁻¹ for BA and NIQ sites, resp.

Consequently, sites located in the metallurgy influence area display higher E_{Ni} amount and slower exchanges kinetics, revealing that anthropic activity significantly enhances Ni (bio)availability through the modification of its bearing phases [2].

[1] Sivry *Environ. Sci. Technol* **45** (2011) 6247-6253.[2] Zelano *Coll. Surf.* (2013)

The Isothermal Evaporation Phase Equilibria for Salt – Water System Focused on Zabuye Salt Lake

Y. ZENG^{1,2*}, X. D. YU¹, J. J. LI¹, Y. PENG^{1,2}, S. FENG^{1,2} AND R. L. WANG^{1,2}

¹College of Materials and Chem. & Chem. Eng., Chengdu Univ. of Technology, Chengdu, 610059, P.R. China;

²Mineral Resources Chemistry Key Laboratory of Sichuan Higher Education Institutions, Chengdu, 610059, P. R. China (* correspondence: zengyster@gmail.com)

There are a larger number of salt lakes in the Qinghai – Xizang Plateau, more than 200 salt lakes that spread out over 1 km². Of all salt lakes in Tibet, Zabuye salt lake has distinct characteristics from others, with an area of 247 km², and is famous for its high concentration of potassium, lithium and borate resources. Low concentrations of calcium and magnesium are advantageous for recovering lithium from brine. The potassium reserves of Zabuye Salt Lake is 7.43 million ton, Li₂CO₃ reserves is 1.74 million ton, B₂O₃ reserves is 0.71 million ton.[1] The composition of Zabuye salt lake falls under the complex system which includes lithium, sodium, potassium, carbonate, sulfate, chloride, and borate.

To exploit brine resources, it is essential to make use of local climatic resources such as wind and solar energy for solar pond techniques. The climate in the region of the Zabuye salt lake is windy, arid and the average temperature is about 273 K. Therefore, the isothermal evaporation phase equilibria, which was determined in the laboratory under the similar conditions, can objectively describe the interactions among the brine minerals and reveal the crystallization path of various salts.

By now, a series of researches about the stable and metastable phase equilibria of the salt – water system focused on Zabuye salt lake have been done at 273 K, 288 K, and 298 K.[2-6] Comparisons between the stable and metastable phase diagrams at different temperatures can obtain the information about the crystalloid forms and crystallization zones of salts at multi-temperature. These information, especially the solubilities of salts change with the temperature, co-existing ions, and the total concentration of salts in solution, are useful for the exploiting of brine. However, most of the previous researches focused on temperature above 288 K, and the isothermal evaporation phase equilibria at 273 K are only some subsystems of the complex system, the results are not enough for the comprehensive utilization of the brine, thus, the investigation about the more complex system are necessary.

The authors acknowledge the support of the State 863 Projects (2012AA061704), NNSFC(40673050, 41173071), the Doctoral Foundation of Ministry of Education of China (20115122110001) and the Research Fund from the Sichuan Provincial Education Department (11ZZ009).

[1] Zheng (2010) *Acta Geologica Sinica*. **84**, 1523. [2] Zeng (2004) *J.Chem. Eng. Data*. **49**, 1648. [3] Zeng (2006) *J.Chem. Eng. Data*. **51**, 219. [4] Sang (2006) *J.Chem. Thermodynamics*. **38**, 173. [5] Sang (2010) *CALPHAD*. **34**, 64. [6] Zeng (2010) *J.Chem. Eng. Data*. **55**, 5834.

Aluminum Oxide In Submarine Hydrothermal Sulfide From East Pacific Rise Near 13°N

Z.G. ZENG^{1*} AND H.Y. QI¹

¹ Seafloor Hydrothermal Activity Laboratory of the Key Laboratory of Marine Geology and Environment, Institute of Oceanology, Chinese Academy of Sciences, Qingdao 266071, China (*correspondence: zgzen@ms.qdio.ac.cn)

Seafloor hydrothermal activity is a window into the subseafloor ocean. Studying hydrothermal products aids in understanding the deep processes of hydrothermal circulation. Aluminium (Al) is highly enriched in hydrothermal vent fluids compared to seawater (10–20 $\mu\text{mol/kg}$ versus 10 nmol/kg) [1]. Al in seafloor hydrothermal sulfides is also common both in deposits in mid-ocean ridges and in back-arc basins or volcanic arcs. The Al concentration of seafloor hydrothermal sulfide deposits has received only cursory attention. Previous geochemical studies had shown Al to be present to varying concentration (from 52.8 ppm at North Fiji basin to 4396 ppm at East Pacific Rise (EPR)) in seafloor hydrothermal sulfides, which are believed that Al may be present in clay minerals [2, 3].

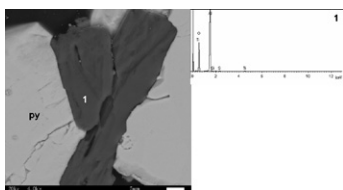


Figure 1: Backscattered electron microprobe images of Al oxide microcrystallite in pyrite from the EPR near 13°N. 1 and Py represent Al-oxide and pyrite, respectively. 1. Energy dispersive X-ray spectrum of Al-oxide microcrystallite.

We report data on the concentration of aluminum in sulfide from EPR near 13°N is from 13.7 ppm to 1071 ppm, which Al is present in Al-oxide. A positive correlation exists between Al and Ti, Zr, Nb, Sr, Ni, Y, and REEs in the sulfides of the EPR near 13°N, which means REEs, Y, Ti, Sr, Ni, Zr, and Nb occur in the minor Al-oxide of the sulfides from the EPR near 13°N.

[1] Von Damm (1995) In: Humphris *et al.* (Eds.), *AGU*, Washington, D.C., pp. 222–247. [2] Fouquet *et al.* (1988) *Marine Geology* **84**, 145–178. [3] Kim *et al.* (2006) *Chemical Geology* **233**, 257–275.

Response Of The Global Nitrogen Cycle To The Great Oxidation Event

A.L. ZERKLE¹, S.W. POULTON², R.J. NEWTON²,
M.W. CLAIRE¹ AND A. BEKKER³

¹Department of Earth and Environmental Sciences, University of St Andrews, St Andrews, Fife, KY16 9AL, Scotland, UK (aubrey.zerkle@ncl.ac.uk; m.claire@uea.ac.uk)

²School of Earth and Environment, University of Leeds, Leeds, LS2 9JT, England, UK (s.poulton@leeds.ac.uk; R.J.Newton@leeds.ac.uk)

³Department of Geological Sciences, University of Manitoba, Winnipeg, Manitoba, R3T 2N2, Canada (Andrey.Bekker@ad.umanitoba.ca)

Nitrogen isotope values in kerogens from the ~2.32 Ga Rooihoogete and Timeball Hill formations (R-TH), South Africa, record a reorganization in global nutrient cycling in response to changes in ocean chemistry during the Great Oxidation Event. These units were deposited immediately after the disappearance of sulfur isotope mass-independent fractionation, indicating that atmospheric O₂ levels rose to greater than 1ppm level. The shales of the R-TH document a dramatic swing in the $\delta^{15}\text{N}$ values of marine organic matter from -14 to +13‰, unprecedented in sedimentary records. The extremely ¹⁵N-depleted values and associated geochemical signatures of iron and carbon preserve evidence for a redox-stratified ocean with primary productivity dominated by anoxygenic photoautotrophs utilizing a large pool of bioavailable ammonium as a nitrogen source. An increase in $\delta^{15}\text{N}$ across the formation boundary represents titration of this ammonium by continued assimilation and nitrification utilizing newly available marine oxidants. In the upper part of this succession, the $\delta^{15}\text{N}$ values settle to around modern values (~+5‰) in both deep- and shallow-water sediments, where they remain for much of the rest of Earth history. We propose that this trend records a change in the dominant form of nitrogen available for global primary productivity, from ammonium to nitrate, as a direct consequence of changes in ocean chemistry. We will present a box model of marine nitrogen concentrations and isotopes to test this hypothesis.

Volumetric properties of multi-electrolyte aqueous solutions at elevated temperatures and pressures

D. ZEZIN¹, T. DRIESNER² AND C. SANCHEZ-VALLE³

¹(denis.zezin@erdw.ethz.ch),

²(thomas.driesner@erdw.ethz.ch.)

³(carmen.sanchez@erdw.ethz.ch)

Aqueous solutions play a vital role for many geological processes in various environments, such as geothermal and magmatic hydrothermal settings or sedimentary basins. In order to perform a detailed geochemical modeling to describe these processes quantitatively, one needs accurate thermodynamic data for all constituents, with aqueous fluid being the essential part of a system. The fluids are typically multi-electrolyte aqueous solutions of a wide range of salinity predominantly comprising chlorides and sulfates of alkali and alkali earth metals. However, the thermodynamic properties of such solutions have remained largely unstudied at elevated temperatures and at pressures above the vapor pressure saturation curve, affecting the accuracy of geochemical modeling at geologically relevant conditions.

We present the results of an experimental study of the volumetric data of multicomponent electrolyte solutions over a wide range of temperatures, pressures, and compositions. This study provides the volumetric properties of aqueous solutions containing binary mixtures of chlorides and sulfates of Na, K, Ca and Mg at temperatures up to 250 °C and pressures up to 70 MPa for ionic strengths up to 12 molal. A vibrating-tube densimeter was used to measure the relative density of aqueous solutions with respect to pure water. The mean apparent molar volume of the electrolyte mixture, calculated from the experimental data, was used for evaluation of the partial molar volume of dissolved components and limiting partial molar volume of these solutes. The obtained data were used for direct evaluation of the pressure dependence on water-rock equilibrium, e.g., anhydrite dissolution and Na-K-(Ca) geothermometry reactions. Such experimental data may also provide important information about the structure of a solution and ionic interactions occurring in aqueous liquids.

The presented experimental data will be employed for the parameterization of thermodynamic models describing the properties of aqueous mixtures of electrolytes. The results of this study will find use in hydrothermal and geothermal fluid-related modeling, petroleum and geothermal reservoir engineering, processing and utilization of industrial brines and CO₂.

Mineralogical evidence of high-fluoride oxidizing fluid in Baiyanghe U-Be-Mo Deposit, Xinjiang, China

CHENGJIANG ZHANG¹, WANG GUO^{1,2}, SONG HAO¹, CHEN FENXIONG² AND WANG BAOQUN²

¹ Chengdu University of Technology, Chengdu 610059, China

(*Correspondence: zcj@cdut.edu.cn)² Geologic Party No. 216, CNNC, Urumqi 830011, China

Baiyanghe uranium-beryllium-molybdenum deposit, located in the western of Xuemisitan volcanic rock belt, is formed in late Palaeozoic mature island-arc environment, the north marginal active belt of Junggar. According to incomplete statistics, the unique similar to this deposit is the Spor uranium-beryllium deposit in Utah, USA, and the elements combination in Spor are U-Be-F, while Baiyanghe deposit are U-Be-Mo-F.

In space, there is both overlap and separation phenomenon exist in uranium-beryllium-molybdenum ore bodies. There are mainly three kinds of spatial relations: Firstly, the uranium-beryllium-molybdenum ore bodies are coincided basically with the space or roughly consistent; Secondly, the single uranium ore body without beryllium and molybdenum; Thirdly, the beryllium and molybdenum ore bodies without uranium.

This type of ore deposits are associated with high silicon-rich fluorine acidic volcanic rocks, and the ore-forming fluid derive from the fluorine-rich gas-liquid containing molybdenum, beryllium and uranium from the immiscibility of the later volcanic magmatism[1,2]. The migration of the three elements in fluid are in various complex forms, such as fluoride, beryllium fluoride complex, carbonate complex, uranyl ions carbonate, the fluoro carbonate of uranium, uranyl ions molybdenum acid radical. Thus, the volatile, such as F and CO₂, play an important role in the migration and precipitation of uranium, beryllium and molybdenum.

The sulfide mineral are rare in Baiyanghe deposit, and the vast oxide minerals, such as hematite, manganite, pyrolusite, indicate that the ore-forming fluid are oxidizing fluid properties. At the late ore-forming stage, there are small amounts of sulfide mineral, such as pyrite, gellenite and molybdenite.

This work is supported financially by the National Natural Scientific Foundation of China (Grants No. 41272100).

[1]Mark D B et al. (2002) Reviews in Mineralogy and Geochemistry 50, 591-691. [2] Greta M E et al.(2002) International Journal of Coal Geology 55, 47-58.

Early diagenesis how to impact C/N and organic isotopic compositions in the Lacustrine Sediments

ZHANG CHENGJUN¹ AND FAN RONG²

¹School of Earth Sciences & Key Laboratory of Mineral Resources in Western China, Lanzhou University, Lanzhou, 730000, China

*(correspondence: cjzhang@lzu.edu.cn)

²College of Resource and Environmental Sciences, Lanzhou University, Lanzhou, 730000, China

C/N, organic carbon isotopic compositions and organic *n*-alkane components have been analyzed in surface sediments from 28 lakes in the Koh Xil area and 26 lakes in the northeastern China. Early diagenesis can impact the ratios of C/N and the values of $\delta^{13}\text{C}_{\text{org}}$ at the beginning of terrestrial and aquatic plants inputting the lake water bodies, and lower the C/N and $\delta^{13}\text{C}_{\text{org}}$ obviously in the process of transferring and accumulation of organic matter. Changed C/N and $\delta^{13}\text{C}_{\text{org}}$ cannot indicate organic sources very accurately. Submerged plants, algae and C4 grasses degrade most intensively in the evolution process of organic matter. Original values of organic isotope may be in the range of -17‰ to -20‰; Organic matter mainly from terrestrial plants changes in minimum and original organic isotope is about -26‰~-30‰; floating aquatic and emergent macrophytes are in the mid, and original isotope is about -20‰~-26‰. In general, organic matter in the lakes is remade with types of organic matter, water characteristics, depth and residue time of lake waterbodies. Organic isotopic compositions of endogenous algae and aquatic merged, submerged and floating plants lower more obviously than that of the terrestrial plants which changed less can indicate primary environments preferably.

Keywords: lake; organic matter; early diagenesis; C/N; organic isotopic composition;

Geochronology of ore-bearing granites in the Baishan Mo Deposit, Eastern Tianshan, Xinjiang

D.Y. ZHANG, T.F. ZHOU*, F. YUAN, Y. FAN, Y.F. DENG AND C. XU

School of Resources and Environmental Engineering, Hefei University of Technology, Hefei 230009, China
(*correspondence: tfzhou@hfut.edu.cn)

The Baishan Mo deposit is located in the eastern section of Jueluotag tectonic belt, Eastern Tianshan, Xinjiang, China. In this study, we sampled the deep (1500m below surface) ore bearing granite from the latest exploration drill core. Furthermore, we tested the zircon U-Pb age of ore-bearing granites is 228.5 ± 8.9 Ma (MSWD=3.1) by La-ICPMS in Hefei University of Technology.

The zircon U-Pb age of the ore-bearing granites (228.5 ± 8.9 Ma) is the same with mineralization age (227.7 ± 4.3 Ma) in Baishan Mo deposit within error [1], which further confirms that Baishan Mo mineralization was genetically related with the granite body[2].

In Eastern Tianshan-Beishan area, there are numerous Mo deposits was found through current exploration, including Donggebi, Huaheitan and Xiaohulishan Mo deposits [3][4]. The Baishan Mo-bearing granite was intruded in Mid Triassic epoch. This geochronological result affords credit evidence to genetic research of the Mid Triassic Mo mineralization in the regional area.

This research was sponsored by Chinese National Science and Technology Program (2011BAB06B01), the National Key Basic Science Research project of China (2007CB411304 and 2001CB409806) and the National Natural Science Foundation of China (40772057).

[1] Zhang *et al.*(2009) *Mineral Deposit* **28(5)** : 663-672 (in Chinese). [2] Zhou *et al.*(2010) *Acta Petrologica Sinica* **26(2)**: 533-546 (in Chinese). [3] Zhu *et al.*(2012) *Chinese Journal of Geochemistry*, **31**: 85-94. [4] Xiao *et al.*(2004) *American Journal of Science* **304**: 370-395.

Metamorphism and *P-T* evolution of high pressure granulite in Chicheng, Northern part of the paleoproterozoic Trans-North China Orogen

DINGDING ZHANG AND JINGHUI GUO

Institute of Geology and Geophysics, Chinese Academy of Sciences, Beijing 100029, China (correspondence: zhangdingx @163.com)

It is widely accepted that the North China Craton formed by collisional amalgamation of the Eastern and the Western Blocks along the central Trans-North China Orogen (TNCO) at ~1.85 Ga. However, the continental subduction process has not been well recorded by previously reported high-pressure (HP) granulites due to lack of prograde metamorphism because of high peak temperature. Recently, we have identified a set of HP mafic granulites with well preserved prograde metamorphism in the Womakeng of ChiCheng, northern part of the TNCO. They developed among a granulite facies mafic to felsic metavolcanic rock association. The prograde metamorphic stage (M1) has been revealed by distinct growth zone of garnet porphyroblasts with inclusion rich core and inclusion free mantle. The peak metamorphic mineral assemblage (M2) consists of Grt and Cpx predominantly with minor Pl, Rut, Amph and Qtz. The Pl+Amph symplectite or corona surrounding garnet and Cpx+Ilm symplectite around titanite documented the post-peak decompression (M3) stage. Phase equilibria modelling by THERMOCALC software yielded a consecutive clockwise *P-T* path with a remarkable prograde metamorphic section, during which the temperatures increase from 630~680 °C to 700~750 °C as coincident increase of pressures from 9~11 kbar to the peak (14~16 kbar). During decompression after peak from 16 kbar to 10 kbar, the temperature keeps increasing from 700~750 °C to 750-800 °C indicating a thermal relaxation, and then decreases as the pressure further descends. The new defined *P-T* path of the HP granulites provide a better metamorphic evidence for the subduction process during the continental collision along the Trans-North China Orogen.

The effect of chemical evolution in ¹³⁷CsCl on radionuclide leaching

F. ZHANG¹, N. A. MARKS¹, J. D. GALE¹, Q. KANG², B. P. UBERUAGA², C. R. STANEK² AND N. HENSON²

¹Nanochemistry Research Institute, Curtin University, PO Box U1987, Perth, Western Australia 6845, Australia
²Los Alamos National Laboratory, Los Alamos, New Mexico 87545, USA

A critical component of nuclear waste disposal strategy is to prevent radionuclides from leaving the waste form and entering the environment. However, radiation damage and leaching studies over the past 30 years have focused on the performance of the candidate waste form at t=0, with far less attention paid to the phase stability, and subsequent durability, during the course of daughter product formation. As a case study in chemical aging, we consider here the system of ¹³⁷CsCl, capsules of which exist in storage pools at Hanford, Washington State. We combine density-functional-theory (DFT) calculations with pore scale modeling to gain a sense of how radionuclide leaching varies as a function of time due to in-growth of the daughter products.

In previous calculations of bulk material we have shown [1,2] that beta-decay of ¹³⁷Cs to stable ¹³⁷Ba generates a rocksalt BaCl daughter phase in which the Ba does not have the expected 2+ oxidation state. This phenomenon is an example of a process we term radioparagenesis [3], in which decay of a major lattice constituent gives rise to a novel solid state daughter phase. Here we study radioparagenesis at surfaces, finding that isolated Ba atoms are most stable in the sub-surface layer, while pairs of Ba atoms have a large binding energy. The Ba atoms also enhance segregation of Cs and Cl vacancies to the surface, suggesting that although Ba will not easily migrate to the surface of the crystal, it significantly modifies the behavior of other defects. In particular, when water interacts with the CsCl surface, the dissolution energy will depend on whether there is Ba nearby or not. Using Schottky defect formation energies derived from DFT, pore-scale modelling simulations were used to predict dissolution of CsCl into water at 20 °C. The models show that the CsCl leaching rate significantly increases when Ba is present, suggesting that chemical aging should be considered as an additional factor in waste form design.

[1] Jiang *et al.* (2009) *Phys. Rev. B* **79**, 132110. [2] Uberuaga *et al.* (2010) *Nucl. Instrum. Meth. B* **268**, 3261-3264. [3] Jiang *et al.* (2010) *Energy & Environ. Science* **3**, 130-135.

Effect of pressure on oxygen fugacities in magma oceans

H. ZHANG AND M. M. HIRSCHMANN*.

310 Pillsbury Drive SE, Minneapolis, MN, 55455 *Presenting
Author: (mmh@umn.edu)

Oxygen fugacities in a magma ocean (MO) may have a crucial influence on removal of siderophile and volatile elements to the core during metal-silicate interaction and may control the composition and redox state of the overlying primitive atmosphere. However, the f_{O_2} prevailing at depth where metal equilibrates with silicate could be quite variable and remains controversial. Importantly, the f_{O_2} at the MO surface may not be similar to that at depth, owing to the effect of pressure on the chemical potentials of redox-sensitive elements, most notably iron.

Iron is the most abundant multi-valent element in silicate melts and so magmatic $Fe^{3+}/\Sigma Fe$ ratios are linked directly to MO f_{O_2} . In a vigorously convecting, well-mixed MO, the variation with depth in the f_{O_2} may be set by a uniform $Fe^{3+}/\Sigma Fe$ ratio of the silicate liquid, which in turn is fixed by magma-metal equilibration at high pressure. To determine this effect, one must know how magmatic $Fe^{3+}/\Sigma Fe$ varies with pressure at known f_{O_2} and temperature. Experiments on an andesitic liquid up to 7 GPa and 1750°C, analyzed by Mossbauer spectroscopy, show that $Fe^{3+}/\Sigma Fe$ ratios decrease with increasing pressure and temperature. If this trend continues at higher pressure, it suggests a MO with fixed $Fe^{3+}/\Sigma Fe$ is more reduced in its shallow portions than it is at depth. However, considering the different compressibilities of Fe^{2+} and Fe^{3+} in silicate liquid, the trend may reverse at higher pressure and experiments above 7 GPa are in progress.

It is clear that the oxidation state of atmospheres overlying MOs may be related to the depth at which equilibrium is established between Fe-rich alloy and silicate, with consequences for evolution of early atmospheres and climate, and the origin of life. If shallow MOs are related to reducing atmospheres and deep high pressure ones related to oxidizing atmospheres, then smaller planets that equilibrate with iron at low pressure may yield early atmospheres rich in CO and H₂. Larger ones equilibrating with Fe at higher pressure, may yield early atmospheres rich in CO₂ and H₂O.

Elasticity and structure of mantle pyroxenes

J S ZHANG¹, L SANG^{1,5}, J D BASS^{2*}, B REYNARD³,
G MONTAGNAC³ AND P DERA⁴

¹Geology Department, University of Illinois, 1301 W Green St., Urbana IL 61801 USA,

²COMPRES, 1301 W Green St., Urbana, IL 61801 USA

³ENS Lyon, FR

⁴GSECARS and University of Chicago IL USA

⁵Texas A&M University

To understand complex upper mantle seismic structure we must know the single-crystal elastic properties of the constituent minerals at high pressures and temperatures. Here we report recent work on the single-crystal elastic properties and phase transitions in Ca-poor orthopyroxene and Ca-rich clinopyroxene at high pressures. The elastic properties of natural orthoenstatite (OEN) and natural diopside have been determined at high pressures to over 14 GPa at room temperature by Brillouin spectroscopy. Single crystals of Fe-bearing orthoenstatite from San Carlos were used in the study. Sound velocity data display a pronounced change upon cold compression to above 12 GPa, and an abrupt change in velocity anisotropy. Single-crystal X-ray structure refinements show that OEN transforms to a new high-pressure phase with space group P21/c, with the transition pressure bracketed between about 10-14 GPa. No evidence of a C2/c structure was observed. Raman spectroscopy on nearly pure Mg OPX, a high-alumina sample, and an Fe-rich sample show that Al and Fe both effect the transition pressure, but that the high-pressure phase is still P21/c in all cases.

The single-crystal elasticity diopside was measured to transition zone pressures using Brillouin spectroscopy. It shows a markedly different behaviour to that of OEN. The C_{ij} 's as a function of pressure were obtained. Aggregate bulk elastic properties are in very good agreement with polycrystalline acoustic measurements. In the case of diopside single-crystal Brillouin and polycrystalline acoustic measurements give highly consistent results.

Data-processing and multi-type anomaly recognition in the geochemical survey in the south slope of the Dongying Depression, East China

LIUPING ZHANG¹, GUOPING BAI² AND YINGQUAN ZHAO³

¹ Key Laboratory of Petroleum Resource, Institute of Geology and Geophysics, Chinese Academy of Sciences, P.O. Box 9825, Beijing 100029, China

² State Key Laboratory of Petroleum Resources and Prospecting, China University of Petroleum, Beijing 102249, PR China

³ Chengdu University of Technology, Sichuan 610059, China

Surface geochemical survey was not widely used in petroleum exploration. To resolve problems in data-processing and anomaly recognition, we have worked up a series of fundamental equations and methods for eliminating surface interference and influences of geological conditions on anomaly intensities and recognizing multi-type anomalies of uni- and multi-variates, by using statistics, fractal geometry, wavelet analysis and artificial neural networks. One of these equations illustrates that the threshold (the boundary between background and micro-seepage anomalies) is determined by means, standard deviations and prior probabilities of background and micro-seepage anomalies when multi-normality is met, and that the traditional equation for the threshold (background mean plus one or two standard deviations) is not correct. In the face of many new equations and methods, it is important how to comprehensively use them to resolve the problems in geochemical surveys. A geochemical survey in the south slope of the Dongying Depression, eastern China provides a good opportunity to address this issue. We iteratively applied the wavelet-analysis-based methods to eliminate the surface interference and geological influence, and statistical methods with new fundamental equations to recognize uni-variate anomalies of seepage and microseepage. And then, multi-variate anomalies of seepage and microseepage were recognized with our fundamental equations and methods. In the results, the seepage anomalies display a string-bead-shaped pattern and are distributed along faults, and the micro-seepage anomalies are ring-shaped and coincide with oil/gas pools, sandbodies or traps. Therefore, processing of geochemical data with our fundamental equations and methods combined in the iterative manner can resolve the complicated problems in data-processing and anomaly recognition and thus greatly improve the predictive capability of surface geochemical survey.

Phenylanthracenes and terphenyls in mesozoic-cenozoic source rocks of the Qaidam Basin, China

MINGFENG ZHANG¹, JINCAI TUO¹, CHENJUN WU^{1,2}
AND RU CHEN^{1,2}

¹Key Laboratory of Petroleum Resources Research, Institute of Geology and Geophysics, Chinese Academy of Sciences, Lanzhou, China
zhangmingfeng_9@hotmail.com)

²Graduate University of the Chinese Academy of Sciences, Beijing, China

Source rocks from an inland lake depositional setting from Mesozoic-Cenozoic formations in the Qaidam Basin (west, China) were analysed for aromatics using capillary gas chromatography-mass spectrometry (GC-MS). The triaromatic members of the new series, Phenylanthracenes (PhNs) and terphenyls (TrPs), are found in different type of source rock (II and III) investigated. The isomeric composition of the phenylanthracenes and terphenyls was found to depend on thermal maturity. In the lower maturity samples abundances of 1-PhN and o-TrP are higher. Increase in sample maturity is indicated by an increase in the relative abundance of 2-PhN as well as m-TrP and p-TrP. Three thermal maturity parameters of the organic matter based on the relative abundances of the PhN and TrP isomers are proposed: $PhNR = 2-PhN/1PhN$, $TrP1 = p-TrP/o-TrP$, and $TrP2 = (m-TrP + p-TrP)/o-TrP[1]$. In general their values are positive correlation versus vitrinite reflectance (Ro) in a range of 0.47-2.75%. While correlation of the conventional biomarker maturity parameters (C_{29} $\alpha\alpha\alpha$ sterane $-20S/(20S+20R)$, C_{31} $\alpha\beta$ hopane $22S/(22S+22R)$, MPI1 ratio) are less apparent with vitrinite reflectance (Ro) in a range of 1.32-2.75%. So the new parameters perhaps are effective reflecting degree of thermal evolution of organic matter in mature-high maturity.

[1] Leszek *et al.* (2001) *Org Geochem*, 32,69-85.

Dissolution kinetics of some femic-silicate minerals in water from 20 to 435°C, 23mpa: Effect of water solvent properties within the critical region

RONGHUA ZHANG*, SHUMIN HU AND XUETONG ZHANG
 Laboratory of Geochemical Kinetics, MLR Key Laboratory of Metallogeny and Mineral Assessment, Institute of Mineral Resources, Chinese Academy of Geological Sciences, Baiwanzhuang Road 26, Beijing 100037, P.R.China
 (*correspondence: zrhsm@pku.edu.cn)

Experiments for measurements steady-state dissolution rates of hedenbergite, diopside, actinolite, garnet, in water were performed using flow through reactor (continuous stirred tank reactor, and packed bed reactor) at temperatures from 25 to 435°C at 23 MPa. Minerals used in experiments are collected from natural, examined through microscope, cleaned and analyzed chemically. Usually, all reactive solutions were undersaturated with respect to the minerals, while run the experiments at high flow rates. A few secondary product phases were found on the reacted surface while using SEM observations. We tested the release ratio of molar concentrations of metal M_i versus molar concentration of Si in outlet solutions $\Delta M_i/\Delta Si$. We found that the dissolutions of those minerals are often incongruent. The dissolution is stoichiometric, when $\Delta M_i/\Delta Si$ is identical to the stoichiometric number N_i in silicate mineral. Dissolution rates (r_{Si}) for hedenbergite, diopside, garnet in water increase with increasing T from 25 to 300°C, and decrease with continued increasing T from 300 to 400°C. The maximum release rates (r_{Si}) for the minerals are always reached at about 300°C. The different metals in the minerals often behave the different release rates at a given temperature. The $r(Ca)$ reach maximum at 200°C; The maximum $r(Na)$, $r(Mg)$, $r(Fe)$ are found at 20 to 100°C. Usually, the rates of Na, Ca, Mg, Fe are often higher than $r(Si)$ at $T < 300^\circ C$, when release rates are controlled by Metal- H^+ exchange reactions. Water properties vary strongly within the region from a sub-critical to a supercritical state: lowering density and dielectric constant in the temperature range 300–400°C, which lead to break the hydrogen bond network of water molecules. Thus water molecules easily break polarized bond, such as Si-O-Si. The hydrolysis of Si-O-Si bond is dominated at $T \geq 300^\circ C$, and thus $r(Si)$ is relatively faster the others. Using SEM and HRTEM, we examined the reacted surface of the minerals at $T \geq 300^\circ C$ and found amorphous leaching layer at the surface, which is a Fe rich, Si-deficient nano layer.

Note: This project is supported by the project of k[2013]01-062-014, SinoProbe-07-02-03, SinoProbe-03-01-2A and 2010G28.

Phosphorus speciation in the sediment profile of Lake Erhai, Southwestern China by fractionation and ^{31}P NMR

R.Y.ZHANG* AND L.Y. WANG

State Key Laboratory of Environmental Geochemistry,
 Institute of Geochemistry, Chinese Academy of Sciences,
 Guiyang 550002, China (*correspondence:
 zhangrunyu@vip.gyig.ac.cn)

Distribution characteristics of phosphorus (P) forms in the sediment profile of Lake Erhai, in Southwestern China has been investigated by sequential extraction and ^{31}P nuclear magnetic resonance spectroscopy (NMR) of NaOH extracts to understand P dynamics and its potential contribution to lake eutrophication. Contents of P fractions varied in the order of NH_4Cl extracted P (NH_4Cl -P) < bicarbonate-dithionite extracted P (BD-P) < HCl-P, Residual-P < NaOH extracted P (NaOH-P). The highly available NH_4Cl -P represented less than 1% of total P (TP). BD-P and NaOH extracted reactive P (NaOH-rP) averaged 39%, while the ratio of Fe/P was higher than 15, indicating low P release from the sediments under permanent oxic condition. The less bio-available HCl-P, NaOH extracted nonreactive P (NaOH-nrP) and Residual-P contributed 61% of TP. Regression analysis revealed that BD-P, NaOH-rP and HCl-P were positively correlated with the contents of Fe and Mn, Al and Fe, and Ca, respectively. The investigation of P compound groups in NaOH extracts by ^{31}P NMR showed that ortho-P and monoester-P were the largest two constituents of the P pool, followed by diester-P, phosphonate and pyro-P. A comparison of vertical variations of P groups in the sediment profile suggested that these compounds were involved in the P recycling to different extents in Lake Erhai. In particular, the lake exhibits high potential for labile P release from the surface sediments, which should be taken into consideration even after the outsourced P runoff ceased.

The early cambrian microbial-like fossils: New insights from their potential for hydrocarbon-generation

TINGSHAN ZHANG^{1*}, ZHAO GUOAN² AND LIU ZCHENG³

¹State Key Lab.of Oil&Gas G&E

Engineering,Chengdu,China

(zts_3@sina.com) (* presenting author)

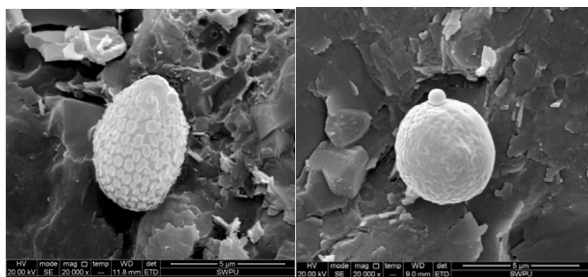
²State Key Lab.of Oil&Gas G&E

Engineering,Chengdu,China (zhaoga@petrochina.com.cn)

³ State Key Lab.of Oil&Gas G&EEngineering,Chengdu,China

(rex_swpu2005@126.com)

The well-preserved Early Cambrian in the southern Sichuan,China consists mainly of two lithological associations including dark to black shales and dark silty shale, with a total thickness of up to 300 m. Some microbial-like fossils(they are similar to the present-day picoplankton and cyanobacteria found in the oceans) have been identified in it. The well-preserved microbial-like structures consist of spheroids about 1.0 μm diameter resembling picoplankton forms (Fig.1).



According to Agawin etc(2000) , more than 90% of all production DOC is the largest reservoir of organic carbon in marine system, even more important is the most of which come from the releasing of picoplankton. The dark to black shales have been recognized under anoxic conditions. Warm climate and anoxic conditions in the Early Cambrian oceans may have facilitated high microbial productivity and organic burial in sediments. Abundant microbially induced organic carbon is from 3 to 7% in E_1 , and their potential for hydrocarbon-generation (shale gas) have been recognized.

[1] Agawin N S R , Duarte C M , Agustí S . Nutrient and temperature control of the contribution of picoplankton to phytoplankton biomass and production[J] . **Limnology and Oceanography**, 2000, 5: 591-600 .

Large perturbations of the carbon cycle during the middle-late Ordovician in Southeastern Poland

TONGGANG ZHANG^{1*}, YANAN SHEN²
AND WIESLAW TRELA³

¹State Key Laboratory of Petroleum Resource and Prospecting, China University of Petroleum at Beijing, Beijing 102249, China (* Correspondence: zhang.tonggang@cup.edu.cn)

²CAS (Chinese Academy of Sciences) Key Laboratory of Crust-Mantle Materials and Environments, School of Earth and Space Sciences, University of Science and Technology of China, Hefei 230026, China

³Polish Geological Institute-National Research Institute, Holy Cross Mts Branch, Zgoda 21, 25-953 Kielce, Poland

It is a puzzle that a major glaciation occurred in the Late Ordovician when greenhouse climatic conditions were prevailing on the Earth. The Late Ordovician glaciation resulted in significant changes in global environment as well as the biosphere. Many reports focused on the environmental changes and the great mass extinction associated with the Late Ordovician glaciation. However, debate still remains in the timing and causes of the transition to the icehouse climate from greenhouse conditions in the Late Ordovician. To investigate the Late Ordovician carbon cycle, we conducted detail analyses of carbon isotopic compositions of organic carbon, TOC, and trace elements in the Ordovician sediments from Poland.

No correlations between TOC and $\delta^{13}C_{org}$ values , low thermal maturity, and global correlations indicate that the primary signal of carbon isotopic compositions were well preserved in the Polish sediments. The Caradocian sediments show low $\delta^{13}C_{org}$ values, rich in TOC, and high V/(V+Ni). In contrast, the Ashgill samples show high $\delta^{13}C_{org}$ values, depleted in TOC, and low V/(V+Ni). Two positive excursions of $\delta^{13}C_{org}$ occurred in the Middle Caradoc and in the Latest Ashgill, respectively. We suggest that anoxic environment developed in the Caradoc Stage have contributed to the burial of organic carbon. Elevated primary productivity indicated by the Ba/Al ratios resulted in positive shift in $\delta^{13}C_{org}$ values of Ashgill sediments those were deposited in an oxic environment. Carbon isotopic records suggest that the transition to an icehouse climate possibly occurred in the Early Ashgill Epoch of Late Ordovician.

NH₄HF₂- assisted digestion of silicate rocks for multi-element analysis by ICP-MS: A new development in open vessel digestion

WEN ZHANG¹, ZHAOCHU HU^{1*}, YONGSHENG LIU¹,
HAIHONG CHEN¹, SHAN GAO¹
AND RICHARD M. GASCHNIG²

¹State Key Laboratory of GPMR, China University of Geosciences, Wuhan 430074, China (*correspondence: zchu@vip.sina.com)

²Department of Geology, University of Maryland, College Park, Maryland 20742, United States

Complete digestion is prerequisite to obtain accurate analytical results for geological samples [1,2]. A new digestion technique using NH₄HF₂ in Savillex screw-top Teflon vials has been developed for multi-element analysis, including felsic rocks that contain refractory minerals such as zircon.

NH₄HF₂ has a higher boiling point (239.5 °C) than conventional acids such as HF, HNO₃ and HCl, which allows for an elevated digestion temperature in open vessels, enabling the decomposition of refractory phases. A digestion time of 2–3 hours for 200 mg NH₄HF₂ in a Savillex Teflon vial at 230 °C is sufficient to digest 50 mg of the felsic rock GSP-2, which is ~6 times faster than using conventional closed-vessel acid digestion at 190 °C (high-pressure PTFE digestion bomb). No insoluble fluorides are present in the final sample solution in this method, even when the sample mass is as large as 200 mg. It appears that the low pressure environment inhibits the formation of insoluble fluorides. The ready production of an ultrapure NH₄HF₂ reagent by sub-boiling distillation makes the proposed NH₄HF₂ digestion method suitable for ultratrace-multielement analyses in various geological samples.

The new method combines the advantages of both the open- and closed-vessel digestion methods, providing us with an effective, simple, economical, and comparatively safe dissolution method.

[1] Lamble & Hill (1998) *Analyst* **123**, 103–133. [2] Tanaka *et al.* (2003) *Anal. At. Spectrom* **18**, 1458–1463.

Nd-Sr isotopic evolution of Asian dust: Tectonic And climatic implications

WENFANG ZHANG^{1*}, GAOJUN LI¹, ZHONG CHEN¹
AND JUN CHEN^{1†}

MOE Key Laboratory of Surficial Geochemistry, Department of Earth Sciences, Nanjing University, Nanjing 210093, China. (*correspondence: nic_langdi@163.com)

The eolian deposits archived in the loess and Pacific pelagic sediments provide important information on the late Cenozoic atmospheric circulation and paleo-environmental condition of the source regions. In recent years, Nd-Sr isotope was widely used to trace the source of eolian dust. Systematic investigation on the Nd and Sr isotopes of potential source materials in recent years provides a solid bases to interpret the Nd-Sr isotopic evolution of Asian dust[1]. Here we present new sedimentary records of Asian dust from Chinese Loess Plateau and Northwest Pacific, which may shed new light on regional tectonic and climatic evolution since the late Oligocene.

The Nd isotope of Chinese loess decreases while the Sr isotope increases progressively during 22-1.2Ma. This record is based a very narrow grain size range (28-45 μm) of silicate fraction so that potential influence of weathering and mineral sorting on Sr isotope is eliminated. Similar Nd-Sr isotopic evolution of Asian dust has also been detected in Northeast Pacific site GPC3[2]. We interpret decreasing Nd isotope and increasing Sr isotopic ratio during 22-1.2Ma may reflect progressive uplift of Northeast Tibetan Plateau. The source region of Asian dust mainly receives debris eroded from North Tibetan Plateau and Gobi Altay Mountains. Compared to Gobi dust, Tibetan materials have much lower Nd isotopic ratio and higher Sr isotopic ratio. Uplift may increase the relative contribution of Tibetan material, and thus shift the Nd and Sr isotope to Tibetan values. Since 1.2 Ma, the loess record indicates that the detritus contribution from Tibet drops rapidly in compare with that from Gobi. As large-scale topographic changes would not be expected in such a short time period, the source shift since 1.2 Ma is interpreted by the differing erosional responses in North Tibetan Plateau and Gobi Altay Mountains to the development of full glacial climate after the middle Pleistocene transition.

However, the patterns of Nd-Sr isotopic evolution observed in Chinese loess and pelagic sediment of Northeast Pacific has not been detected in ODP 1208 core in Northwest Pacific. We find that a separate contribution of pure Gobi dust by winter monsoon may explain the very different pattern recorded in ODP 1208 core. The Nd-Sr isotopic record in ODP 1208 core may reflect competition between Taklimakan dust and Gobi dust, which may have great potential in paleoclimatic and tectonic applications.

[1] Chen *et al.* (2007) *Geochim. Cosmochim. Acta* **71**, 3904-3914. [2] Pettke *et al.* (2002) *Paleoceanography* **17**, 1031.

New dating result of the Caledonian granitoids and related mineralization of Miaoershan-Yuechengling area, South China

WENLAN ZHANG¹, DI ZHANG¹ AND RUCHENG WANG¹

¹ State Key Laboratory for Mineral Deposits Research, School of Earth Sciences and Engineering, Nanjing University, Nanjing 210093, P.R. China

It has been accepted that W-Sn-(Mo) rare metal mineralization in South China are in close association with the Yanshanian granites, whereas the granites of the other ages results in minor metallogenic process. The effect of Caledonian granites on such kind ore deposits is considered to be neglectable. However, more than 100 mineralization pots and deposits are recently found around Miaoershan-Yuechengling area, which are hosted in Indosinian and Caledonian granitoids. This report presents three typical mineralization samples in Luchongping, Shengxianyan and Niutangjie with dating results of host granites and ore minerals.

(1) Luchongping deposit is of greisen-quartz vein type W-Cu mine in the middle south of Miaoershan. The host rock is a middle-fine grained biotite granite with zircon date of 396-402 Ma; (2) Shengxianyan develops a greisen type W-Mo deposit in the south Miaoershan. The host rock is also the middle-fine grained biotite granite with zircon date of 433.5 Ma; (3) Niutangjie is a strata-banded scheelite deposit of skarn type in the southwest margin of Yuechengling. This deposit is a relatively large ore deposit in this area, which has been mined tens of years. Its host rock is fine-grained muscovite granite. The zircon dating results is 411-422 Ma. The mineralization age is 421±24 Ma.

Based on the above dating results, it is suggested that the Caledonian mineralization is of great importance in the studied area. It is revealed that the primary host rocks are those middle-fine grained biotite granites and the major ore mineral is scheelite. This mineralization feature has already been identified from the Yanshanian metallogenic process in the central Nanling area, South China, where the host rock is mainly fine-grained muscovite granite and the major ore mineral is wolframite.

Isotope fractionation by alternative nitrogenases and oceanic anoxic events

X. ZHANG¹, D. M. SIGMAN¹ AND A. M. L. KRAEPIEL¹

¹Princeton University, Princeton, NJ 08544, USA

(*correspondence: xinningz@princeton.edu)

The ¹⁵N/¹⁴N of marine N (quantified by the parameter δ¹⁵N) is used to reconstruct the N cycle in the modern and ancient oceans¹. Anomalously low δ¹⁵N values reaching -5‰ have been measured in sediments from mid-Cretaceous oceanic anoxic events (OAEs)^{2,3}. These low values, which fall below that of newly fixed N from N₂ fixation (currently believed to average -1‰), cannot be explained by current isotopic models.

We show that the δ¹⁵N of newly fixed N can be as low as -7‰, depending chiefly on the type of nitrogenase that catalyzes N₂ fixation. Alternative nitrogenases, which contain catalytic vanadium (V) or iron (Fe) rather than molybdenum (Mo), produce fixed N that is significantly lighter in ¹⁵N than canonical Mo enzymes (-6‰ for V-, -7‰ for Fe-, -2‰ for Mo-nitrogenase), regardless of N₂ fixer phylogeny or metabolism.

Thus, a N cycle in which alternative nitrogenases account for a large fraction of N₂ fixation provides a straightforward explanation for the extremely low δ¹⁵N of OAE sediments. Low Mo bioavailability combined with high Fe inputs under the euxinic conditions proposed for OAEs may have led to greater reliance on alternative nitrogenases. Results indicate that the role of alternative nitrogenases may have been underestimated in low oxygen/sulfidic environments, and understanding their importance in modern environments is imperative.

[1] Sigman *et al.* (2009) *Encyclopedia of Ocean Sciences* 4138-4153. [2] Rau *et al.* (1987) *EPSL* 82, 269-279. [3] Junium & Arthur (2007) *GGG* 8, 1525-2027.

Kinetic study of syenite-water interactions at temperatures from 20°C To 435°C And at pressures up to 36mpa

XUETONG ZHANG*, RONGHUA ZHANG AND SHUMIN HU

Laboratory of Geochemical Kinetics, MLR Key Laboratory of Metallogeny and Mineral Assessment, Institute of Mineral Resources, Chinese Academy of Geological Sciences, Baiwanzhuang Road 26, Beijing 100037, P.R.China
(*correspondence: zhangxuotong@cags.ac.cn)

The kinetics experiments of syenite in water are performed in the temperature range of 20-435°C and at pressures of 23-36MPa using flow through packed bed reactor. The results indicated that the release rates of Si, Al, K and Na of the syenite increase with increasing temperature, and reached maximum values at 400°C. The release rates of Ca, Mg reached maximum values at 200°C. The release rates of Fe reached maximum values at 374°C. Another important impact factor of the reaction between syenite and water is pressure. The release rates of Si did not vary with pressure, as pressure was changed from 23 to 36 MPa. The release rates of K and Al in syenite increase with increasing pressure.

Dissolved metallic elements are abundant in aqueous solutions after water reacted with syenite. The maximum release concentrations and maximum release rates of most metals (Si, Al, K, Na, Fe, Ni, Zn, Cu, Mo, V, Ag, Pb and Ti) are observed at $T \geq 300$ °C, Ca, Mg, Mn, Sr and Ba at 200°C. As a result, fluids that have reacted with syenite are metal-rich fluids. The most metals (Si, Ca and ore-forming elements) easily release in to aqueous solutions at 23 MPa. If increasing pressure from 23 to 36 MPa, most molar concentration ratio of metal Mi vs Si, Mi/M_{Si} in the effluent solutions decreases with pressure.

The in situ measurements of electric conductances of the water-rock interaction system at temperature range from 20-435°C, 23-36MPa were performed using the flow system. The in situ measurements of electric conductances combined the kinetic experiments found that the maximum electric conductances are present at 374-390°C, 23-36MPa, and simultaneously the maximum release rates of Si, Al, K are reached at the same temperature range. This project is supported by the project of k[2013]01-062-014, SinoProbe-07-02-03, SinoProbe-03-01-2A and 2010G28.

Geology and geochemistry of basic intrusive rocks in the eastern fault depression of Liaohe Basin

YAN ZHANG,¹ WEIHUA BIAN¹, YULONG HUANG¹, XIAOJIAN YU¹, YOUFENG GAO² AND HUAFENG TANG¹

¹ College of Earth Sciences, Jilin University, China, yan_zhang@jlu.edu.cn² Research Center of Palaeontology Stratigraphy, Jilin University, China

Basic intrusive rocks are widely developed in the third member of Shahejie formation in the eastern fault depression of Liaohe Basin. Their heat accelerated source rocks maturity, and themselves can be reservoirs. In fact, lots of oil and gas shows have been found in intrusive rocks in eastern fault depression of Liaohe Basin.

According to core of wells, main lithology in the region is diabase. Samples are chosen for geological and geochemistry investigation. Through rock-mineral identification, diabase mainly consist of plagioclase and pyroxene, some pyroxene are altered into chlorite, a small amount of amphibole, quartz, biotite and alkali feldspar.

The composition of diabase shows that diabase in the eastern fault depression of Liaohe Basin is sodic alkaline series rocks. REE appear to negative anomaly of δEu , light REE enrichment, obvious crystallization differentiation, crystallization differentiation degree of light REE is higher than heavy REE. Based on the analysis of geological setting and geochemical characteristic, the intrusive rocks might form in the settings of continental intraplate.

The characteristics of fluid inclusion from Ordovician carbonate reservoirs in Western Ordos Basin

ZHANG YANLING¹, GUO YANRU^A AND LIU JUNBANG³,

¹ Research Institute of Petroleum Exploration & Development, PetroChina, Beijing, 100083, China; zhangyanling07@petrochina.com.cn

² Research Institute of Petroleum Exploration & Development, PetroChina, Beijing, 100083, China; gyr2005@petrochina.com.cn

³ Research Institute of Petroleum Exploration & Development, PetroChina, Beijing, 100083, China; liujunbang@petrochina.com.cn

The study area is located in the western thrust belt region of the Ordos Basin, China. Due to the multi-period tectonic movement and evolution of mechanical mechanism, It resulted in complicated block structure and complicated geological conditions. For western Ordovician reservoir, when were the oil and gas filling accumulation? How many times filling had It experienced? These issues will directly affect effectiveness of the trap and the exploration.

In this study, we respectively carried out samplings of the fluid inclusions in reservoirs of Zhuoxishan group and Kelimoli group Ordovician of QT1, YT1 wells in the Western Basin, made microscopic petrography analysis, homogenization temperature test and microscopic laser Raman microprobe analysis of samples. we analyzed reservoir characteristics of the fluid inclusions of kelimoli and Zhuozishan groups in Ordovician.

There are 4 views: bitumen, hydrocarbon residues, as well as a large number of hydrocarbon fluid inclusions were prevalent in cracks and pores in reservoir of kelimoli group and Zhuozishan group Ordovician which fully shows that oil-gas migration and filling have occurred within the Ordovician reservoirs. Inclusions of microscopic petrography analysis shows 2 issues were prevalent in hydrocarbon filling in Ordovician limestone reservoir. The 1th hydrocarbon inclusions in the Ordovician period were dominated by the dark brown and brown liquid hydrocarbon inclusions, capturing hydrocarbons maturity is relatively low; the 2nd grey-gaseous hydrocarbon inclusions were in the hydrocarbon inclusions, capturing hydrocarbons maturity is relatively high. The first homogenization temperature distribution has a bimodal characteristics of kelimoli group Ordovician; The second homogenization temperature distribution has an asymmetrical single peak, Wide at front and rear is narrow.

Oligocene – Early Miocene North Pacific temperatures based in clumped isotopes in Kamchatka Bivalves

YI GE ZHANG^{1*}, HAGIT AFFEK¹, ANTON OLEINIK², ZHENGRONG WANG¹ AND PING HU¹

¹Department of Geology and Geophysics, Yale University, New Haven, CT 06520-8109

²Department of Geosciences, Florida Atlantic University, Boca Raton, FL 33431

The Oligocene through early Miocene was an important transitional interval in the development of the Neogene "Icehouse World". However, very little is known about the details of ocean temperature evolution at that time, particularly in high-latitude areas. We use clumped-isotope based paleotemperature reconstructions derived from the Oligocene - early Miocene shallow water molluscan faunas coupled with the MBT/CBT-based soil temperature reconstruction and ⁸⁷Sr/⁸⁶Sr dating to examine North Pacific paleoceanography. Fossil mollusks were collected from the Cape Ugol'nyi section in northwestern Kamchatka Peninsula. Sample mineralogy and seasonal signals in $\delta^{18}\text{O}$ along bivalve growth axis suggest that these samples have not experienced significant diagenetic alterations during burial.

Clumped isotope analyses were applied to 2 modern samples and 16 fossil samples, with ⁸⁷Sr/⁸⁶Sr ages range from ~32.6 to 19.9 Ma. In the modern samples, clumped isotopes derived growth temperature is 10-12°C, consistent with satellite-based summer temperatures. Fossil samples have a larger temperature variability, between 21°C and 7°C. Both early Oligocene and early Miocene are warm (~16°C), with the coldest temperature (9°C) found in the late Oligocene, slightly lower than the modern growth season temperature at the same location. This late Oligocene cooling event was obtained from a stratigraphic horizon with ⁸⁷Sr/⁸⁶Sr age of 27.8-29.1 Ma, coinciding with the marine benthic $\delta^{18}\text{O}$ positive excursion Oi2b-Oi2c. Organic biomarkers extracted from a rock sample at the same horizon give a MBT/CBT-based soil temperature estimate of 6°C, in support of a prevailing cold temperature both on land and in the ocean.

The colder-than-today temperatures in the late Oligocene is intriguing because the Oligocene world is thought to be warmer, as suggested by lower global benthic $\delta^{18}\text{O}$ stack and higher atmospheric CO₂. The dramatic cooling during Oi2b may be a consequence of reorganization of surface circulation patterns in the North Pacific, with the cold North Pacific becoming a major source for bottom-water production during this time interval.

Indonesian mineralization event in the Wulashan District, Northwest China: Evidence of isotopic geochronology

Y.M. ZHANG¹, X.X. GU¹, W.L. YANG¹ AND W.P. ZHU²

¹State Key Laboratory of Geological Processes and Mineral Resources, China University of Geosciences, Beijing 100083, P.R. China (bzzym@163.com)

²China Aero Geophysical Survey and Remote Sensing Center for Land and Resources, China

The Wulashan district has a great economic potential for Mo–Au mineralization and attracted wide attentions of geologists. More than thirty ore deposits have been discovered in this region since the late 1980s. Representative deposits mainly include the medium-sized Xishadegai porphyry Mo deposit and the superlarge-sized Hadamengou-Liubagou alkaline-related Mo–Au ore field. Previous opinion of mineralization epoch was Hercynian, however, Indonesian ages have been recognized recently. Re–Os isotopic dating on seven molybdenites from the Xishadegai Mo deposit defines model ages of 223.2–232.6 Ma and an isochron age of 225.4 ± 2.6 Ma, whereas LA-ICP-MS dates on zircon from the Xishadegai host granite yield an age of 245.3 ± 9.6 Ma. Stepwise ⁴⁰Ar–³⁹Ar dates on K-feldspar of auriferous quartz-K feldspar vein (ores) give a plateau age of 217.9 ± 3.1 Ma in the Liubagou deposit, in accordance with the previously reported ⁴⁰Ar–³⁹Ar data (239.8 ± 3.0 Ma) for sericite separated from ores in the Hadamengou deposit. Considering that the dating minerals showed clear co-existing textures with ore-stage mineral assemblages, the mineralization process mainly occurred during early Indonesian. In addition, LA-ICP-MS dates on zircon from associated granitoid (Shadegai granite) give an isochron age of 231.4 ± 3.1 Ma. The geochronological data, together with the regional geological setting, suggest that the early Indosinian (231–245 Ma) magmatic activities induced a coeval magmatic hydrothermal mineralization (218–240 Ma) under a post-collisional extensional setting. This magmatism-mineralization event is significantly recorded and should be highly valued in the north margin of the North China Craton.

The research was funded by the National Natural Science Foundation of China under grants of 40930423 and the Specialized Research Fund for the Doctoral Program of Higher Education (SRFDP, 20130022120016).

Superchondritic Mantle Is Partially Depleted MORB Mantle

YOUXUE ZHANG

Department of Earth & Environmental Sci, Univ of Michigan, Ann Arbor, MI 48109-1005, USA, (youxue@umich.edu)

The composition of the bulk silicate Earth (BSE) is often modeled by the “chondritic” model, in which the refractory and lithophile elements such as REEs in BSE are assumed to have chondritic ratios (Jagoutz *et al.*, 1979; Sun, 1982; Zindler and Hart, 1986; Allegre *et al.*, 1995; McDonough and Sun, 1995; Palme and O’Neill, 2004). Recently, high-precision measurements reveal that ¹⁴²Nd/¹⁴⁴Nd ratios in terrestrial samples are higher than those in chondrites by about 0.2 epsilon units (Boyett and Carlson, 2005, 2006). The results were interpreted to mean that the primordial Sm/Nd ratio in BSE was higher than chondritic ratio, namely superchondritic. Since then, there has been much discussion about the “superchondritic” mantle (Caro *et al.*, 2008, Caro and Bourdon, 2010, Campbell and O’Neill, 2012), although the jury is still out (e.g., Huang *et al.*, 2013; Gale *et al.*, 2013).

If BSE is indeed superchondritic, it is necessary to estimate the SuperChondritic BSE (SC-BSE) composition, to distinguish it from previous BSE composition based on the “chondritic” assumption. The latter is hereafter referred to as chondritic BSE (C-BSE). To estimate SC-BSE composition, isotopic constraints can be converted to the following elemental ratio constraints (Caro and Bourdon, 2010):

$$(\text{Sm/Nd})_{\text{SC-BSE}} \approx 1.06(\text{Sm/Nd})_{\text{C-BSE}};$$

$$(\text{Lu/Hf})_{\text{SC-BSE}} \approx 1.12(\text{Lu/Hf})_{\text{C-BSE}};$$

$$(\text{Rb/Sr})_{\text{SC-BSE}} \approx 0.70(\text{Rb/Sr})_{\text{C-BSE}}.$$

The more incompatible elements are depleted in SC-BSE compared to C-BSE, consistent with depletion of the mantle. To quantitatively examine whether the SC-BSE is partially depleted MORB mantle (DMM), it is necessary to quantify the incompatible element sequence (Sun and McDonough, 1989): **Rb** > **Th** > **U** > **La** > **Ce** > **Sr** > **Nd** > *Pm* > **Sm** ≈ **Hf** > **Eu** > **Gd** > **Tb** > **Dy** > **Ho** > **Er** > **Tm** > **Yb** > **Lu**. The quantification is achieved by comparing DMM composition (Salters and Stracke, 2004; Workman and Hart, 2005) with C-BSE composition (McDonough and Sun, 1995) to define the Compatibility Index (CoI) calculated as $\ln(C_{\text{DMM}}/C_{\text{C-BSE}})$. It was found that the Sm/Nd, Lu/Hf, and Rb/Sr ratios in SC-BSE over those in C-BSE are well related to the difference in CoI between the numerator element and the denominator element, implying that SC-BSE can be regarded as partially depleted DMM. The concentrations of other elements in SC-BSE are then obtained. SC-BSE likely formed by some early depletion event in Earth. The complementary subchondritic material might be in D" layer or in the lower crust.

Geochronological and geochemical constraints on sequences of the Cangshuipu group and their implications for the amalgamation between the Yangtze and Cathaysian blocks

YUZHANG¹, YUEJUN WANG^{1*}, HUICHUAN LIU¹
AND YONGFENG CAI¹

¹ State Key Laboratory of Isotope Geochemistry, Guangzhou Institute of Geochemistry, Chinese Academy of Sciences, Guangzhou 510640, China (*correspondence: yjwang@gig.ac.cn)

This contribution documents a synthesis of geochronological and geochemical analytical data for the Cangshuipu Group, which is composed of the Yinzhuba volcanic agglomerates and Linjiawan conglomerates and represents an angular unconformity between the Lengjiaxi and Banxi Groups in Hunan, South China.

The Yinzhuba volcanic agglomerates are characteristic by high-Mg andesites and dacites, which are enriched in LILEs and depleted in HFSEs and the $\epsilon_{Nd}(t)$ values ranging from -1.7 to -4.7. They are dated at 824 ± 7 Ma and 822 ± 28 Ma by zircon U-Pb analytical technology, representing the formation age of the Yinzhuba volcanic sequences.

The Linjiawan conglomerates are mainly composed of dacite and rhyolite, without high-Mg component. Most of the samples are dominated by quartz and plagioclase phenocryst, minor magnetite, with cryptocrystalline matrix, typical characteristics of felsic volcanic rocks. The youngest zircons from the conglomerates exhibit a weighted mean age of 831 ± 27 Ma, representing the maximum depositional age of the Linjiawan conglomerates.

Integrated with other geological data, the Cangshuipu Group are composed of the the Yinzhuba volcanic agglomerates at the upper part and the Linjiawan conglomerates at the basal part. And the amalgamation of the Yangtze and Cathaysian Blocks along the Jiangnan orogen occurred at ca. 831~822 Ma as a part of an exterior accretionary orogen along the periphery of Rodinia rather than that of the Grenvillian-aged orogenic events.

Building of the Deep Gangdese Arc, South Tibet: Linking granulites, and magmatism and crustal growth in the active continental margin

ZEMING ZHANG, XIN DONG AND HUA XIANG

Institute of Geology, Chinese Academy of Geological Sciences, Beijing 100037, China

The present-day formation of continental crust is generally attributed to magmatic processes in the plate convergence margins and those within intra-plate settings. Therefore, the deep-seated magmatism and metamorphism in active continental margins can provide important clues to understand the formation of the continental crust.

The Gangdese arc along the southern Lhasa terrane is a product of the Mesozoic Andean-type orogeny derived from the northward subduction of the Neo-Tethys. In the Eastern Himalaya, owing to Late Cenozoic rapid uplift and erosion, the high-grade metamorphic Complex is well exposed. Petrological and geochronological studies reveal that the complex experienced intense Paleocene subduction-related magmatism, and almost synchronous granulite-facies metamorphism accompanied by the formation of S-type granites. The subduction-related intrusive rocks show geochemical features typical of continental magmatic arcs. Their zircons yielded the U-Pb ages of 65–56 Ma, and commonly display positive $\epsilon_{Hf}(t)$ values of -3.0 – +11.7, indicating juvenile source. The syn-intrusion high-grade metamorphism indicates that the plutons were emplaced at the middle to lower crustal depth. The S-type granitoids are characterized by peraluminous nature and contain garnet and muscovite. Their zircons yielded the U-Pb ages of 66–55 Ma, and have distinct but negative $\epsilon_{Hf}(t)$ values of -18.4 – -6.8. The inherited detrital zircons from the metasedimentary rocks yielded variable U-Pb ages of 2910–235 Ma. The metamorphic zircons from the metaplutonic and metasedimentary rocks yielded ages of 67 Ma–53 Ma. Phase equilibria modeling shows that the granulite-facies metamorphism and partial melting form under the conditions of 9.7–10.2 kbar and 710–810 °C. We argue that the late Mesozoic compressional orogeny resulted in the deep burial of the Mesozoic sedimentary rocks, and that the accretion and loading of voluminous asthenosphere-derived and deep-stated intrusions resulted in the extensive crustal thickening and heating to generate the granulite-facies metamorphism and S-type magmas.

Iron deposits in China: Distribution, types and tectonic setting

ZHAO-CHONG ZHANG¹ AND TONG HOU¹

¹ State Key Laboratory of Geological Processes and Mineral Resources, China University of Geosciences, Beijing, 100083, China (zczhang@cugb.edu.cn)

All types of iron deposits have been recognized in China, but Banded Iron Formations (BIFs), skarn, Kiruna, submarine volcanic-hosted and Ti–Fe–(V) oxide deposits are the most economically important. However, the high-grade iron ores are predominantly from skarn, Kiruna and submarine volcanic-hosted types although BIFs occupy 48% of total iron reserves in China. The special feature can be ascribed to prolonged interaction of the Central-Asian, the Circum-Pacific and the Tethys–Himalaya systems or absence of strict cratons due to multiple tectonism. BIFs are mainly distributed in the North China Craton (NCC), and Neoproterozoic (ca. 2.5 Ga) metamorphic rocks are the most important hosting rocks, which are primarily meta-volcanic rocks and minor meta-sedimentary rocks. The submarine volcanic-hosted iron deposits are widely distributed in orogenic belts, mostly located in western China, including Tianshan, Beishan, Altay, and western margin of Yangtze Craton (YC). They formed in a considerable age range, from Proterozoic to Mesozoic, but with more than 70% formed in Late Paleozoic, and mostly related to subduction settings. Ti–Fe–(V) oxide deposits are predominantly associated with ca. 260 Ma mafic-ultramafic layered intrusions in the Panxi region, central part of the Emeishan large igneous province and Mesoproterozoic (ca. 1.8 Ga) anorthosite complex in the Chengde region of NCC. The Panxi region is the most important V and Ti ore cluster in the world, and has been genetically attributed to mantle plume event. In contrast, the Mesoproterozoic anorthosite complex have been considered to be related to rift event in NCC. The skarn iron deposits are widespread, concentrically the uplift areas at the margin of down-faulted basins of Eastern China. The hosting rocks are mainly Early Cretaceous intermediate-felsic intrusions, which lithospheric extension following subduction of paleo-Pacific plate. Comparably, the Kiruna iron deposits, commonly associated with dioritic subvolcanic intrusions, are present in the Cretaceous terrigenous volcanic basins in the northern margin of YC, and they were formed in the same tectonic setting with those skarn iron deposits in the eastern China.

Lipid biomarkers in the sediments of Lake El Junco and their possible sources

ZHAOHUI ZHANG¹, PIERRE METZGER²
AND JULIAN P. SACHS³

1. School of Earth Sciences and Engineering, Nanjing University, 22 Hankou Road, Nanjing, 210093, China
2. Université Pierre et Marie Curie, BioEMco, CNRS UMR 7618, 4 Place Jussieu, Paris, France
3. University of Washington, School of Oceanography, Box 355351, Seattle, WA 98195, USA

Lipid biomarkers contained in suspended particles and sediments from Lake El Junco, Galápagos demonstrate for the first time that all three races of the alga *Botryococcus braunii* (A, B & L) have co-existed intermittently during the last 460 years. *Cis* and *trans* C₂₅–C₃₁ *n*-alkadienes and a C₂₉ triene indicated race A, a series of C₃₄H₅₈ botryococenes indicated race B, and a C₄₀H₇₈ hydrocarbon, *trans*, *trans*-lycopadiene indicated race L (Zhang *et al.*, 2007).

Other biomarkers include C₂₅ HBIs from diatoms, long-chain alkenols, diols and a triol, keto-ols, hydroxy acids and keto acids. Saturated and monounsaturated long chain diols from C₃₀ to C₃₆ had terminal hydroxyl groups and hydroxyl groups between the ω16 and ω20 positions. Vicinal diols with hydroxyl groups at ω9 and ω10 were likely from the floating fern *Azolla*. C₃₀ to C₃₆ keto-ols, mid-chain hydroxy and keto acids had mid-chain functional groups at similar positions to the diols, suggesting common origins. The predominance of ω20-hydroxy acids and diols, together with 20,21-dihydroxy-nonacosanoic acid is indicative of an *Azolla* source, while ω16 and ω18 hydroxy acids and diols imply a microalgal source.

Long chain (C₃₀–C₃₆) *n*-chloroalkanes and chloroalkenes have a chlorine atom at the terminal position. The *cis* and *trans* alkenyl chlorides have double bonds near the middle of the hydrocarbon chain. The lipid chain lengths and the positions of functional groups imply a structural relationship between chloroalkenes and some alkenols, diols and (or) hydroxy acids that most likely derive from algae.

A rapid crater detection method for statistics of crater on planetary surface

Z.B. ZHANG*, W. ZUO, G.H. ZHANG AND L. GENG

National Astronomical Observatories, Chinese Academy of Sciences, Beijing, China (*correspondence: zzbin@nao.cas.cn)

Impact craters are key geomorphological structures formed by the collision of a meteoroid, asteroid or comet with a planetary surface. They can accumulate over a long period of subsequent bombardment or slow surface erosion, which provide us with the relative age of the surface unit and more information on the planetary surface geology and its evolution. As statistics of crater form the basis for geologic stratigraphy, planetary surface chronology and so on, automatic crater measurement, detection and derived crater size frequency distribution become a routine activity in planetary science.

There are many publications devoted to various techniques of crater detection, but the efficiency is quite a problem when much of these methods come to high resolution planetary image due to the extremely high computational complexity. In our study, we employ a method derived from face detection technique, which significantly improve the efficiency while remaining a robust performance in two ways: 1) using several Haar-like features to model some basic crater characteristics, such as crater rim, illumination mode, which can be computed very rapidly on a so-called integral image; 2) cascade of classifiers trained by a AdaBoost algorithm [1], where simpler classifiers in previous stages are used to reject the majority of negative targets before more complex classifiers are called upon to make further more complex computation on a promising positive target.

[1] Viola & Jones (2004), International Journal of Computer Vision 57(2), 137–154.

Geochemistry and tectonic significance of Neopaleozoic Granitoid in Alxa Area, Inner Mongolia, China

HONG ZHAO^{1,2*}, BEN DANG^{1,2}, BIN LIANG¹, LU-JUN LIN¹ AND JING REN¹

¹ School of Earth Sciences and Resources, Chang'an University, Xi'an 710054, China;

² Key Laboratory of Western China's Mineral Resources and Geological Engineering, Xi'an 710054, China (*correspondence: xacdzh@126.com)

Alxa area located in the southern edge of Central Asia Orogenic Belt and the western margin of the North China plate. The study area has numerous granite, particularly in the Neopaleozoic (Carboniferous-Permian) granites are most widely distributed, which contain much abundant information of tectonic evolution. Carboniferous-Permian is the key period to the formation and evolution of Central Asian Orogenic Belt. Moreover, Carboniferous-Permian are the most important periods for large-scale mineralization. At the present, the research of granites in geological age, petrogenesis and tectonic setting are very absent. Based on analyzing of geochronology, petrology and geochemical of granitoid in the study area, the Carboniferous-Permian petrogenesis and tectonic setting have been discussed. The results indicate that these granitoid are dominated by monzonitic granite, granodiorite, tonalite, quartz diorite and diorite, which emplaced in Carboniferous, later Early Permian and Late Permian. The samples of Carboniferous are metaluminous, calc-alkalic, I-type granitites, but the samples of Permian are metaluminous to peraluminous, calc-alkalic to alkalic, I-A type granites. These granitoid show not only the characteristics of within plate setting, but also that of subduction zone. And their arc-like geochemical features (such as Nb-Ta depletion) should have been inherited from the protoliths (pre-existing island arc igneous rocks), rather than inflection of their tectonic setting when they formed and contaminated by old crust materials during magma ascending and emplacement. It is concluded by comprehensive analysis that Carboniferous-Permian granitoid of the study area are formed in post-collision tectonic setting, and are the product of the tectonic transition from compression to intraplate extension.

Geochronology and geochemistry of two triassic A-Type granites in South China: Implication for petrogenesis and Indosinian transtensional extension

ZHAO KUI-DONG, JIANG SHAO-YONG AND PU WEI

State Key Laboratory for Mineral Deposits Research, School of Earth Sciences and Engineering, Nanjing University, Jiangsu, 210093, P. R. China

We carried out a detailed study of LA-ICP-MS zircon U-Pb dating, major and trace element compositions, and Sr-Nd-Hf isotope geochemistry of the Caijiang granite in Jiangxi Province and the Gaoxi granite in Fujian Province, South China. Both of the Caijiang and Gaoxi granites were emplaced at Triassic with ages of about 228-230 Ma. Textural examination of the two granites reveals that biotite crystals occur along the boundary of euhedral plagioclase and quartz, which imply the primary magma could be anhydrous. The two granites have high total alkalis contents ($\text{Na}_2\text{O}+\text{K}_2\text{O}=7.81-12.15\%$), high field strength element contents (e.g. $\text{Zr}=240-458\text{ppm}$, $\text{Y}=16.8-38.0\text{ppm}$, $\text{Nb}=13.5-33.8\text{ppm}$ and $\text{Zr}+\text{Nb}+\text{Ce}+\text{Y}=382-604\text{ppm}$), Ga/Al ratios ($10000\times\text{Ga}/\text{Al}=2.41-3.53$). The Caijiang granite has relatively high ($^{87}\text{Sr}/^{86}\text{Sr}$)_i ratios (0.71288-0.72009), low $\epsilon_{\text{Nd}}(t)$ values (-9.9--9.3) and low zircon $\epsilon_{\text{Hf}}(t)$ values (peak value of -7.5). Whole-rock Nd isotopic model ages and zircon Hf isotopic model ages mostly vary from 1.65 to 1.80 Ga. The Gaoxi granite has also high ($^{87}\text{Sr}/^{86}\text{Sr}$)_i ratios (0.71252-0.71356), low $\epsilon_{\text{Nd}}(t)$ values (-13.8) and zircon $\epsilon_{\text{Hf}}(t)$ values (peak value of -12.0). Nd isotopic model ages and zircon Hf isotopic model ages mostly vary from 1.95 to 2.10 Ga. The two granites might be derived from partial melting of pre-Cambrian crustal rocks that had been granulitized during an earlier thermal event. Our study of the Caijiang and Gaoxi granites, together with previous studies on Triassic alkaline syenites (Tieshan and Yangfang) in Fujian Province and A-type granite (Wengshan) in Zhejiang Province in South China, define a wide transtensional tectonic environment in the Cathaysia Block at least lasting from 254 to 225 Ma. When combined with all the available studies for the Indosinian granites and tectonic evolutions in South China, we suggest that the formation of A-type granites was related to the local NE-trending extensional faults which were caused by collision between the South China Block and the Indochina Block or the North China Block.

CO₂ absorption and precipitation in MgCl₂-NH₃·H₂O Solutions: Relevance to CO₂ sequestration

LIANG ZHAO¹, CHEN ZHU¹, SIJIA DONG¹
AND H. HENRY TENG^{1,2}

¹Department of Earth Sciences, Key Laboratory of Surficial Geochemistry, Ministry of Education; Nanjing University, Nanjing, 210093, China; ²Department of Chemistry, The George Washington University, Washington, DC, 20052, USAEmail: (zhaoliang@nju.edu.cn)

Mineral sequestration of CO₂ is one of the safer options in the portfolio of available CCS stratagems. To optimize the absorption of CO₂, numerous approaches, such as MEA/DEA/Ammonia based post combustion scrubbing and O₂/CO₂ recycle combustion, were tested. These methods, however, did not address the costly issue of carbon storage. Following a newly proposed pH-swing CO₂ mineralization process (Kodama, *et al.*, 2008) which showed capability of capturing and storing CO₂ simultaneously, we investigated the rate and kinetic controlling factors for CO₂ absorption and mineralization in MgCl₂-NH₃ solutions. Experiments were carried out at 298 K in solutions of different compositions (0.05-0.2molL⁻¹ MgCl₂) to measure the reaction kinetics using a wetted wall column setup similar to those reported in Pacheco (1998) and Victor (2011). Conditions were maintained where brucite precipitation was not allowed, and magnesium concentration was analyzed by ICP-AES with interval sampling. The absorption solution was then cycled between the column and a jacketed glass reactor with its pH maintained constant and the transmittance at 546 nm monitored in real-time. Preliminary results indicate that initial concentration of Mg in solution has little effect on CO₂ absorption. Although absorption rate increased slightly over time with increasing ammonia addition, pH appeared to be the dominant controlling factor. The higher the solution pH was, the faster the absorption rate increased. Upon reaching saturation, nesquehonite precipitated as indicated by the decreased laser transmittance, leading to rapid addition of aqueous ammonia. However, precipitation of nesquehonite unexpectedly showed little influence on CO₂ absorption, suggesting that the interaction between aqueous CO₂ and OH⁻ or ammonium ions in liquid film may be the rate limit step during the absorption process, further indicating that the gas-liquid interaction barrier should be treated seriously in order to optimize CO₂ capture efficiency. Due to the low gas-liquid reaction area (0.005 m²L⁻¹), extended time period (2-3 hours) was needed to dissolve enough CO₂ for nesquehonite to reach supersaturation. Measured typical absorption rates under these experimental conditions are between 0.000668 mol s⁻¹m⁻² (pH=8.74, pCO₂= 15495Pa, 298K) and 0.001997 mol s⁻¹m⁻² (pH=9.16, pCO₂= 15403Pa, 298K).

Reservoir characteristics of volcanic rocks in the Northeast of Junggar Basin, China

ZHAO XIA^{1*}, ZHANG XIAOFENG², GAO XIAOHUI¹,
HOU LIANHUA¹ AND WEI YANZHAO¹

¹ RIPED, Petrochina, Beijing, China (*correspondence: zhaox601@petrochina.com.cn)² CCAD Petrochina, Beijing, China.

The Junggar basin is a part of central Asia orogenic belt and the Carboniferous is an important transition period of ocean to continent in the basin. Based on the comprehensive analysis of petroleum geology and exploration practice, it is proved that Carboniferous is a primary petroleum exploration domain of this basin, and volcanic rocks are the main reservoir. This paper studied reserved space type and controlling factors of volcanic reservoir, it is basic research for further study of favorable reservoir distribution.

The reservoir characteristics including lithologic characteristics, lithofacies characteristics, pore type, reservoir physical property of the Carboniferous volcanic rocks in the northeast of Junggar basin were analyzed by observing core and thin slice with microscope and scanning electron microscope. The reservoir accumulation type and the main affecting factors of reservoir physical property were also analyzed.

Volcanic cone and weathering crust are two important factors of the distribution of favorable volcanic reservoir. Volcanic reservoirs have three types reservoir space of primary porosity, secondary porosity and fracture in Junggar basin. The reservoir property is controlled by volcanic rock lithology and lithofacies as well as post-reformation function, weathering leaching and structural stress are all beneficial for reservoir property. The cone volcanic mechanism has controlled function to lithology, lithofacies, weathering leaching and corrosion reformation, besides, fracture is well developed in the center of volcanic mechanism.

The cone volcanic mechanism has significant controlling effect for the favorable volcanic reservoir distribution. This conclusion has been confirmed by the gas & oil exploration findings in the Junggar basin. So the cone volcanic mechanism is the important direction for research of the volcanic gas & oil reservoir in this basin.

Tight oil in the continuous sandbody in the A'er Sag of the Erlian Basin, China

XIANZHENG ZHAO¹, LIUPING ZHANG², FENGMING JIN¹,
QUAN WANG¹ AND QIANG LUO¹

¹Huabei Oilfield Company, PetroChina, Renqiu 062552, China²Key Laboratory of Petroleum Resource, Institute of Geology and Geophysics, Chinese Academy of Sciences, P.O. Box 9825, Beijing 100029, China

Since the discovery of the A'er sag with the area of 650 km² in the Erlian Basin of Inner Mongolia in 2006, more than one billion barrels of oil reserves has been found. In the central part of this sag, there is a large syncline without well-developed fault systems except areas along the sag margins. The largest oil pool was discovered in this syncline, within a continuous tight sandbody at the top of the lower part in the first member of the Cretaceous Tengg'e'er Formation (K₁bt^{1L}). In the early stage of exploration, two wells revealed this sandbody with an average porosity of 11.2% and permeability of 40.3 mD in the east slope of this sag. Compaction and carbonate cementation are the main factors reducing porosity and permeability of the sandbody. The sedimentary facies study based on core, logging and seismic data indicated that the sandbody at the top of K₁bt^{1L} is continuous in the main parts of the sag. This continuous sandbody with the buried depths of 1300-2300 m and dip angles of 0-11° is sandwiched by two sets of petroleum source beds. Oil-source correlation of biomarkers illustrates that the oil came mainly from the underlain source bed. We inferred that the porosity, permeability and dip angle of the sandbody decrease from the east slope to the center of the sag and there is a relatively large oil pool without downdip water in the sag-centered area. Twelve wells were then drilled step by step in the sag-centered area. All of them have produced commercial oil after acid-fracturing and revealed a continuous oil pool. This work demonstrated that economically viable oil exists in continuous tight sandbodies with low dip angles even in central areas of small faulted basins if there are source kitchens.

Tectonic control of volcanism in Potassic Volcanic Belt in NE China

ZHAO YONGWEI¹ AND FAN QICHEN²

¹ Key Laboratory of Active Tectonics and Volcano Institute of Geology, CEA, Beijing 100029, China, email: (zilongzhao1981@yahoo.com.cn)² Key Laboratory of Active Tectonics and Volcano Institute of Geology, CEA, Beijing 100029, China, email: (fqc@ies.ac.cn)

Quaternary potassic volcanic rocks are found in several dispersed potassic volcanic fields in Heilongjiang province in NE China, including volcanic fields of Xiaogulihe, Keluo, Wudalianchi, and Erkeshan, composing a North-South trending potassic volcanic belt (PVB) in northeastern China. The volcanic belt extends for about 318 km. All the volcanic fields in the PVB show a 160 degree linear arrangement with a separation distance of about 50 km. Most of volcanoes in PVB are in Wudalianchi and Keluo. Cones in Keluo show 58 degree linear arrangement, and cones in Wudalianchi show 41 degree linear arrangement. Previous volcanism mode proposed that preexisting NE trending rifts controlled the distribution of cones in this belt, while the preexisting NNW-NS trending deep rift may control the upwelling of basaltic magma. Specially, Nen river fault, a pre-existing NNE trending normal fault on the surface and changes into a low angle detachment fault in the deep crust, are thought controlled the volcanism. However, this mode cannot explain the decoupled formation time and emplacement location between the fault or rift and the volcanic activity. The Nen river fault are formed in Mesozoic and Cenozoic, but the belt show apparent volcanism since middle Pleistocene. The volcanic belt are emplaced 100 km far from the detected Nen river fault.

In the context of NE and NNE compression with dextral shearing in NE China in the present day, we propose that the coeval NS trending slip-strike deformation in lithosphere take an important part in controlling the volcanism, resulting in an echelon arrangement of NNE and NNE trending fractures in the deep lithosphere. Although the fractures are short in the lateral, they are vertical deep and can reach to mantle lithosphere, resulting in decompression and melting of magma source rocks. The magma ascends through these fractures, forming violent volcanic activity since middle Pleistocene.

This work was supported by National Natural Science Foundation of China (Grant Nos. 41172305), Fundamental research funds for Central Public Welfare Research Institutes of China Earthquake Administration (Grant No. IGCEA1102)

Non-linear rates of fluid-mineral reaction in metamorphic fluid flow

ZHIHONG ZHAO AND ALASDAIR SKELTON

Department of Geological Sciences, Bolin Centre for Climate Research, Stockholm University, Sweden

It is well known that fluid-mineral reactions record the infiltration histories of fluid tracers (such as H₂O, CO₂ or CH₄) through the Earth's crust [1]. Early studies mainly employed linear reaction rate laws to model metamorphic fluid flow [e.g. 2-4]. Although some studies indicate that a linear reaction rate law is appropriate near equilibrium [e.g. 5, 6], Lasaga [7] concluded that reaction kinetics are likely to be non-linear in most fluid-mineral reactions. Therefore, the main objective of this study is to investigate the effects of non-linear reaction rate laws on metamorphic fluid flow parameterisations obtained using inverting modeling.

The transport model applied to metamorphic fluid flow with non-linear reaction kinetics was numerically solved and incorporated into a general inverse modeling framework based on the differential evolution method. The flux, duration of metamorphic fluid flow and rates of fluid-mineral reactions were constrained for four metamorphic sills with varying Péclet (Pe) and Damköhler (Nd) numbers in the SW Scottish Highlands. It is verified that the linear reaction rate law yields reliable first order estimates of time-averaged and time-integrated fluxes and the duration of metamorphic fluid flow. However, with increasing reaction order, the apparent reaction rate constant changed considerably. The magnitude of this effect is shown to be dependent on the combination of Pe and Nd. Our estimates of apparent reaction rate constants for non-linear reaction kinetics are in agreement with experimentally-based kinetic data based on linear reaction rate laws, but much larger than other measurements based on natural systems [6]. This indicates that accurate quantification of the order of fluid-mineral reactions is important if reaction rates are to be calculated.

- [1] Ague (2003) *Treatise on Geochemistry* **3**, 195-228. [2] Bickle *et al.* (1992) *Am. J. Sci.* **292**, 289-316. [3] Skelton *et al.* (1997) *EPSL* **164**, 527-539. [4] Abart and Sperb (1997) *Am. J. Sci.* **297**, 679-706. [5] Wood and Walther (1983) *Science* **222**, 413-415. [6] Baxter (2003) *Geol. Soc. London* **220**, 183-202. [7] Lasaga (1986) *MinMag* **50**, 359-373.

Permeability of the continental crust – Experimental study and insight from the petrological and seismological data

A.V. ZHARIKOV^{1,3*}, M.V. RODKIN²
AND V.M. VITOVTOVA³

¹Institute of Geology of Ore Deposits, RAS, Moscow, Russia
(*correspondence: vil@igem.ru)

²Institute of Earthquake Prediction Theory and Mathematical
Geophysics, RAS, Moscow, Russia

³Institute of the Experimental Mineralogy, RAS,
Chernogolovka, Russia

Permeability is one of the key properties governing the fluid regime, mass and heat transfer in the continental crust. The results of the laboratory experiments show that the values of rock permeability can change by decimal orders due to the effect of high temperature and pressure. In general it was found that permeability of the continental crust rocks decreases with depth. In contrast, it increases at PT-parameters of progressive metamorphic transformations.

The results of petrologic studies reveal both the marks of long periods of very low permeability and events of high permeability.

The conception when long periods of low permeability are coupled with short periods of high permeability is supported by seismic data. The burst of hypocenters clouds to the Earth surface and/or their systematical movement up to the Earth surface are found using the data of the earthquakes localization. Identification of such events with front of fluid propagation allows to estimate high permeability values as ($>10^{-13} \text{ m}^2$).

However, the mechanism of permeability increase in low and mid-crust is unclear. Moreover, we suggest that some episodes of the crust permeability increase could be related to the positive feedbacks, between microcrack initiation due to rock metamorphic transformations resulting in increase of permeability and active deep fluid infiltration which in its turn accelerates the rate of metamorphic transformations.

Iron and sulfur speciation of sliding mud from Xieliupo Landslide in South Gansu Province, NW China

GUODONG ZHENG¹, SHOUYUN LIANG^{1,2} AND NI ZHANG²

¹ Key Lab Petrol Resources Res, Inst Geol and Geophy, CAS,
Lanzhou 730000, China

² Key Lab Mech Disast Envir W China (Lanzhou Uni), Mini
Edu, Lanzhou 730000, China

Gray and/or black mud materials are often observed within many slipping zones of landslide, especially those landslides in large scale and long history of action, which are always known as sliding mud and considered as a key factor corresponding to landslide development and even the slipping actions. The sliding mud is attractive to many researchers and engineers working on landslide protection. However, there is still a large space to understand the formation mechanism and accumulation process of sliding mud. There are several famous landslides with thick layers of sliding mud in the Longnan district, south part of Gansu province, NW China. In order to check the possible relationship between the sliding mud properties and landslide development, 13 samples were collected from one vertical profile cross the sliding surface of the Xieliupo Landslide and analyzed for their mineral and chemical compositions as well as chemical species of iron and sulfur using XRD, XRF, and Mössbauer spectroscopy and K-edge XANES, respectively. The mineral and chemical composition of the samples showed the sliding mud was different from both the upward debris rock and beneath bedrock, being agreed well with their surface properties such as color and partial sizes. Mössbauer spectroscopy revealed a clear variation of iron species between the sliding mud and the debris and bed rocks. The sliding muds contain much more ferrous iron than the sliding (the debris) rocks and the bedrocks, indicating a relatively stronger reducing condition within the slip zone. In addition, the sliding mud in darker colors near the sliding surface showed much more ferrous iron than the sliding mud in light gray color relatively far from the sliding surface. K-edge XANES also revealed the vertical variation of sulfur species that was similar to iron speciation, the slip zone was enriched with reduced sulfur species and the debris and bed rocks contain relatively much more oxic sulfur species. All data of mineral and chemical composition, and also iron and sulfur species revealed a relatively reducing condition in the slip zone. Such a reducing condition could be favored for the gray and/or black mud materials precipitated and accumulated, and furthermore resulted the weakness of sliding zone along with the process of landslide development.

[1] Zheng *et al.* (2010) *J. Earth Sci.* **21**, 954-960; [2] Zheng *et al.* (2008) *Hyper. Interact.* **186**, 39-52; [3] Zheng *et al.* (2007) *Environ. Geo.* **51**, 1455-1464; [4] Zheng *et al.* (2002) *Hyper. Interact.* **141/142**, 361-367; [5] Zheng *et al.* (2002) *J. Asian Earth Sci.* **20**, 955-963; [6] Zheng *et al.* (2002) *Chin Sci. Bul.* **47**, 2018-2024

Numerical interpretation of laboratory and field data showing CO₂-induced groundwater changes

LIANGE ZHENG¹, RUTH M. TINNACHER¹,
CHARULEKA VARADHARAJAN¹, NICOLAS F. SPYCHER¹,
MARCO BIANCHI¹, PETER S. NICO¹,
JENS T. BIRKHOLZER¹, ROBERT C. TRAUTZ²
AND JOHN D. PUGH³

¹Lawrence Berkeley National Laboratory (LBNL), Berkeley, California 94720

²Electric Power Research Institute (EPRI), Palo Alto, California 94304

³Southern Company Services, Birmingham, Alabama 35291

The potential impact of leaking CO₂ on shallow groundwater quality is one of the issues related to the risk assessment of CO₂ geological sequestration. Here we discuss CO₂-induced geochemical changes in a shallow sandy aquifer at ~ 50 m depth, focusing on the mobilization of trace elements and the underlying chemical mechanisms revealed by a controlled-release field experiment, laboratory tests and numerical modeling. The field test involved a dipole system in which the groundwater was pumped from one well, saturated with CO₂ at the pressure corresponding to the hydraulic pressure of the aquifer, and then re-injected into the same aquifer using a second well. Groundwater samples for chemical analyses were collected in four monitoring wells. A series of lab-scale sequential leaching experiments were also carried out with synthetic groundwater solutions at different pH and CO₂ concentrations. Upon introduction of CO₂, a rapid increase in concentrations of some trace elements (e.g. Ba, Sr) was observed in both the field and lab tests; the lab experiments suggest that metal release was primarily driven by the decrease in groundwater pH from ~8 to ~5. Geochemical modeling was employed to interpret laboratory and field results and gain insights on the mechanisms potentially involved in the CO₂-induced mobilization of trace elements. The increase in concentrations of alkali and alkaline earth metals can be explained by the dissolution of trace amounts of calcite and subsequent calcium-driven cation exchange reactions. Modeling also indicates that the magnitude and extent of metal mobilization depends not only on metal-mineral associations and sediment pH buffering characteristics, but also on the residence time of CO₂-impacted groundwater relative to the rates of metal-release reactions, with the effect of slow reactions only noticeable under conditions of slow groundwater velocity.

Navigating troubled waters

YAN ZHENG^{1,2}

¹Queens College, City University of New York, Flushing, NY 11367, (yan.zheng@qc.cuny.edu)²Lamont-Doherty Earth Observatory of Columbia University, Palisades, NY 10964, (yzheng@ldeo.columbia.edu)

In September 2000, the General Assembly adopted the United Nations Millennium Declaration. Under Article III development and poverty eradication, item 19 states “we resolve further to halve, by the year 2015, ...to halve the proportion of people who are unable to reach or to afford safe drinking water.” In 2012, the Joint Monitoring Program (JMP) of the World Health Organization and UNICEF reported that the drinking water target of the Millennium Development Goal has been achieved. In 2010, the proportion of the global population still using unimproved sources is estimated at only 11 per cent, which is less than half of the 24 per cent estimated for 1990. However, this is based on a proxy indicator for safe drinking water: an improved water source defined as those that, by the nature of their construction, are protected from outside contamination, particularly fecal matter. It is increasingly clear that this proxy indicator is inadequate because naturally occurring chemicals such as arsenic and fluoride that are harmful to humans can render the water unsafe. In addition, poor sanitation frequently leads to fecal contamination of shallow groundwater. Here, occurrences of arsenic in groundwaters in Bangladesh, China and United States are used as examples to illustrate research by hydrogeochemists that have been impactful on safe drinking water supply. A critical contribution made by hydrogeochemists over the last decade was the evaluation of the sustainability of the low arsenic groundwater sources as a safer drinking water source.

Bangladesh is the only country in the world when access to improved water source is reported by the JMP, a correction has been made for arsenic occurrence in groundwater. Based on a national drinking water quality survey conducted in 2009, access to improved water sources containing less than 50 µg/L As was estimated to be 81%. The vast majority of improved water sources in rural Bangladesh is a private, shallow tube well. The rapidly developing China saw the access to improved water increasing from 67% in 1990 to 91% in 2010, with 2/3 of the improved sources being water piped on premises. However, millions of rural Chinese are still exposed to As and F. Likewise, more than 10 million rural Americans relying on private well waters are at risk of exposure to > 10 µg/L As. Much work remain to identify alternative water sources to protect human health.

Zircon U-Pb geochronology of hosting rhyolites and mineralized quartz veins at the Tiemurt Pb-Zn-Cu Deposit: Insights for ore genesis

YI ZHENG^{1,2*}, LI ZHANG² AND YAN-JING CHEN³

¹Dept. of Earth Sciences, Sun Yat-sen University, Guangzhou, China, 510275. (*correspondence: zhengyi@gig.ac.cn)

²Guangzhou Institute of Geochemistry, Chinese Academy of Sciences, Guangzhou, China, 510640³Key Laboratory of Crust and Orogen Evolution, Peking University, Beijing 100871, China

This contribution reports the finding of zircon-bearing rhyolites and mineralized quartz veins at the Tiemurt deposit, which occurs as veins controlled by NW-extending structures in the Devonian volcanic-sedimentary basin of the Altay orogenic belt Xinjiang, China.

The zircons separated from two hosting meta-rhyolites samples yield weighted mean ²⁰⁶Pb/²³⁸U ages of 403.1±5.1 Ma and 393.3±4.9 Ma, respectively. Integrated with their automorphic crystal, the lack of fluid inclusions, high Th/U and high ΣREE values, the ²⁰⁶Pb/²³⁸U ages ranging from 393Ma to 403Ma can be interpreted as the eruption age of the volcanic rocks in the Early Devonian.

The four mineralized quartz samples yield complicated zircon U-Pb ages. At least two age peaks are recognized, ca. 400Ma and ca. 220Ma. The age of ca.400Ma may be the joining age of the hosting volcanics. The zircons with ca. 220Ma age contain abundant hydrothermal fluid inclusions and coincide with the Ar-Ar ages of biotite in the polymetallic quartz veins. Therefore, the age ca. 220 Ma can represent that of the flowing metamorphism fluids migrations.

In term of the geological characteristics, structural, geochemical and geochronological characteristics of the zircon, the Tiemurt Pb-Zn-Cu deposit may be an example of epigenetic orogenic Pb-Zn+Cu systems formed in the settings of intercontinental collision at the Early Trassic of ca.220Ma.

Phosphorus-bearing pyroxenes in flood basalts with native iron, Khungtukun, Polar Siberia, Russia

L.M. ZHITOVA^{1,2*}, V.V. SHARYGIN^{1,2}, V.S. KAMENETSKY³, N.S. KARMANOV¹ AND E.N. NIGMATULINA¹

¹V.S. Sobolev Institute of Geology and Mineralogy SD RAS, Novosibirsk 630090, Russia (*correspondence: zhitova@igm.nsc.ru)²Novosibirsk State University, Novosibirsk 630090, Russia³University of Tasmania, Hobart TAS 7001, Australia

Native iron from the Khungtukun trap intrusion contains melt inclusions, some of which show silicate-silicate liquid immiscibility [1, 2]. We studied in detail composition of the immiscible inclusions (0.2-1 mm). The silicate melts in them represent the aluminosilicate (60-77 wt% SiO₂) and silica-poor, Fe-Ti-Ca-P-rich (in wt%: SiO₂ 15-46; FeO 15-22; TiO₂ 2-7; CaO 11-27; P₂O₅ 5-30) conjugate liquids; one of components mainly occurs as globules in other (Fig. 1).

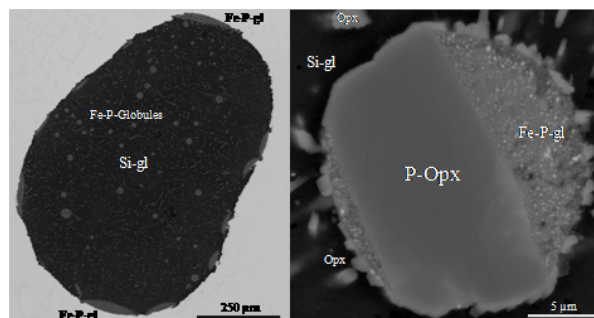


Figure 1: BSE images of an immiscible inclusion in native iron and one of Si-poor, Fe-Ti-Ca-P-rich globules in it.

In contrast with Si-rich part, the Si-poor globules contain ortho- and clinopyroxene with high P₂O₅. Composition of orthopyroxene is (in wt%): SiO₂ 42.2-44.7; P₂O₅ 3.3-4.3 (0.1-0.15 apfu); TiO₂ 2.5-3.2; Al₂O₃ 4.7-6.0; FeO 20.7-22.7; MnO 0.8-0.9; MgO 15.3-18.1; CaO 4.8-6.1; Na₂O 0.05-0.2; Mg# 55-61. Clinopyroxene is richer in P₂O₅ (up to 13 wt%) and has formula Na_{0.05}Ca_{0.55}Fe_{0.7}Mg_{0.6}Ti_{0.1}(Al_{0.4}P_{0.4}Si_{1.2})O₆. In general, Si-poor and P-rich nature of an immiscible liquid and reduced conditions were favourable to incorporation of P in the tetrahedral site in the structures of pyroxenes.

This work is supported by RFB (grant 11-05-00681) and the Government of Russia (grant 14.V37.21.0879).

[1] Ryabov (1989) *Immiscibility in natural glasses*. Nauka, Novosibirsk. [2] Ryabov & Lapkovsky (2010) *Aust J Earth Sci* 57, 707-736.

Carbon-13 and Uranothorianite age dating in the Botogol Alkaline Massif Graphites (Eastern Sayan, Russia)

S.M.ZHMODIK^{1*}, A.G.MIRONOV², N.S.KARMANOV¹,
V.A.PONOMARCHUK¹, D.K.BELIANIN²,
I.S.KIRICHENKO¹ AND A.S. ZHMODIK¹

¹Institute of Geology and Mineralogy SB RAS, Pr. Koptug, 3, Novosibirsk, 630090, Russia (*zhmodik@igm.nsc.ru)

²Geological Institute SB RAS, Av. Sakhyanova, 3, Ulan-Ude, 670000, Russia

Botogol alkali pyroxene and nepheline syenite rock massif located in the Altai-Sayan region in the southwestern part of the Siberian platform's folded framing. Alkaline rocks intruded through carbonate-shale strata of Proterozoic age. Graphite is widespread in alkaline massif rocks and has a form of stockworks, veins and small veinlets as well as disseminated occurrences. There are several types of graphite identified: a massive, tree-like, droplet-like, fishscale-like. Pure graphite containing massive graphite areas with high concentrations of U (up 0.4%) and Th (2%), in the forms of uranothorianite and thorite. There are "crystals" with unusual decay structures founded. Cubic "crystals" (1-3 mm), consisting of graphite filled with concentrically zoned uranothorianite spherulites (30-50 microns). The center of the spherulite consist of a cubic uranothorianite crystal (5-8 microns), surrounded by splitted radially grown crystals of uranothorianite. Mineral occurrences of this type may indicate a joint transport of U, Th and C, in the form of a volatile compounds. The uranothorianites age was determined based on results of chemical analysis using scanning electron microscope MIRA 3 equipped with INCA Wave 500 microanalysis system and defined as 510 ± 13 - 519 ± 10 Ma. This age dating is in the good agreement with the results obtained for the Botogol massif using Rb-Sr isochron (492 ± 11 Ma) and also K-Ar (biotite, 521 and 492 Ma) [1]. These age data indicates that graphite and uranothorianite were formed during the magmatic stage. The isotopic values of carbon in the graphite associated with uranothorianite (in the mikrosamples of ~ 1 mg) were equal to -8.1/-5.7 and pure graphite values are -5.1/-10.7 permille. These data indicate mantle source of carbon. Botogol alkaline massif origination corresponds to the time of Neoproterozoic plume magmatism development (520-460 Ma).

This work was supported by the IP 89 and RFBR 12-05-01164; 12-05-31324.

[1] Nikiforov & Yarmoluk (2007) *Proc. RAS*, 412, 81-86.

Geological characteristics and mineralization stages in the Yaojialing Zinc-Gold ore deposit, Tongling Ore District, Anhui

G.X. ZHONG, T.F. ZHOU* AND Y. FAN

School of Resources and Environmental Engineering, Hefei University of Technology, Hefei 230009, China
(*correspondence: tfzhou@hfut.edu.cn)

The Yaojialing deposit is located in the Tongling ore district, Middle-Lower Yangtze River Belt, East China. The deposit has measured reserves of 1.2 Mt of Zn with an average grade of 3.64%, 32 t of Au (5.02g/t Au), and Pb,Cu and Ag as by-products[1]. The main orebodies, whose shapes mainly include lenticular or bedded, situate along the contact zone with Early Permian limestone of the Qixia Formation and Late Jurassic granodiorite porphyry intrusion or occur inside limestone xenoliths entrapped within the intrusion. The mainly encountered ore minerals include sphalerite, chalcopyrite, galena, pyrite, gold and magnetite, gangue minerals are represented by calcite, quartz, garnet, diopside, vesuvianite, fluorite. Euhedral to anhedral granular texture, metasomatic texture and disseminated-massive structure are considered to be the dominating ore texture and structure. Hydrothermal alteration is well developed and is primarily composed of skarnization, K-feldspar alteration, silicification, carbonatization, sericitization, clayzation. Needs to be emphasized that silicification and carbonatization are closely related to mineralization. The mineralization process of it can be divided into three stages and from early to late they are: (1) skarn stage, which witnesses filling of garnet and diopside in the contact zone or inside the intrusion; (2) oxidization stage, which is the magnetite stage; (3) Quartz-sulfide-carbonate stage, in which most economic Zn and Au mineralization is formed.

Conclusion: From what has been discussed above, it could be inferred that Yaojialing ore deposit is a skarn-type ore deposit.

This research was sponsored by the National Natural Science Foundation of China (40772057).

[1] Wen *et al.* (2011) *Mineral Deposits* 30(3) : 533-546 (in Chinese).

Zircon U–Pb geochronology and Sr–Nd–Hf isotopic geochemistry of the Yuanzhuding Granitoid Porphyry, Shi-Hang Zone, South China: Implications for petrogenesis and Cu–Mo mineralization

LIFENG ZHONG¹, JIE LI², TOUPING PENG² AND BIN XIA³

¹Key Laboratory of Marginal Sea Geology, South China Sea Institute of Oceanology, Chinese Academy of Sciences, Guangzhou 510301, China

²State Key Laboratory of Isotope Geochemistry, Guangzhou Institute of Geochemistry, Chinese Academy of Sciences, Guangzhou 510640, China

³School of Marine Sciences, Sun Yat-sen University, Guangzhou 510006, China

The Shi-Hang zone is an important NE–SW-trending Mesozoic magmatic belt in southern China that is dominated by granites with high $\epsilon\text{Nd}(t)$ values and young TDM model ages. Here, we present zircon U–Pb ages, major and trace element whole-rock compositions, and Sr–Nd–Hf isotope data for the Yuanzhuding porphyritic granitoids, located in the southwest of the Shi-Hang zone, and use these data to determine the origin of this granitoid and its relationship to Cu–Mo mineralization. Zircon U–Pb dating indicates that these granitoids were emplaced in the Later Jurassic (~158 Ma), and they have initial $87\text{Sr}/86\text{Sr}$ ratios of 0.70941–0.71398, $\epsilon\text{Nd}(t)$ values of –3.15 to –2.02, and in situ zircon $\epsilon\text{Hf}(t)$ values of +1.71 to +6.17. Whole-rock geochemical and isotopic data suggest that these granitoids were formed by partial melting of Proterozoic metasedimentary basement within the lower crust, with additional input at relatively high temperatures (~790°C) from basaltic magmas. These magmatic systems are highly oxidized. This process played a crucial role in the development of Cu–Mo mineralization within the Yuanzhuding that is genetically related to these granites. The discovery of the Yuanzhuding deposit indicates that the Shi-Hang zone should be considered prospective for mineral exploration for porphyry Cu–Mo deposits.

Acknowledgments: This study was supported by the Key project of NSFC-Guangdong Joint Foundation (U1133002).

Role of material properties on TiO_2 nanoparticle agglomeration

DONGXU ZHOU^{1,2}, ARTURO A. KELLER^{1,2}ZHAOXIA JI², DARREN R DUNPHY³ AND JEFFREY BRINKER^{3,4}

¹Bren School of Environmental Science and Management, University of California, Santa Barbara

²University of California Center of Environmental Implications of Nanotechnology

³University of New Mexico Center for Micro-Engineered Materials and the Dept. of Chemical Engineering⁴Sandia National Laboratory, New Mexico

Emerging nanomaterials are being manufactured with varying particle sizes, morphologies, and crystal structures in the pursuit of achieving outstanding functional properties. These variations in these key material properties of nanoparticles may affect their environmental fate and transport. To date, few studies have investigated this important aspect of nanoparticles' environmental behavior. In this study, the agglomeration kinetics of ten different TiO_2 nanoparticles (5 anatase and 5 rutile each with varying size) was systematically evaluated. Our results show that, as particle size increases, the surface charge of both anatase and rutile TiO_2 nanoparticles shifts toward a more negative value, and, accordingly, the point of zero charge shifts toward a lower value. The colloidal stability of anatase sphere samples agreed well with DLVO theoretical predictions, where an increase in particle size led to a higher energy barrier and therefore greater critical coagulation concentration. In contrast, the critical coagulation concentration of rutile rod samples correlated positively with the specific surface area, i.e., samples with higher specific surface area exhibited higher stability. Finally, due to the large innate negative surface charge of all the TiO_2 samples at the pH value (pH=8) tested, the addition of natural organic matter was observed to have minimal effect on TiO_2 agglomeration kinetics, except for the smallest rutile rods that showed decreased stability in the presence of natural organic matter.

Mineral characteristics of Tungsten-bearing granite in the Jiangnan orogenic belt: A case study of the Qingyang pluton

JIE ZHOU^{1,2*}, YAO-HUI JIANG¹ AND WEIYA, GE²

¹ State Key Laboratory for Mineral Deposits Research, School of Earth Sciences and Engineering, Nanjing University, Jiangsu, 210093, P.R. China (*correspondence: zhoujie0517@sina.com)

² Nanjing Institute of Geology and Mineral Resources, China, 210016, P.R.China

South China is the most important tungsten-concentrated zone in China and even in the world, famous for the Nanling Tungsten ore belt. A series of Tungsten deposits, related with the late Yangshanian granites, have been recently discovered in the Jiangnan orogen, northeastern Qin Zhou-Hangzhou metallogenic belt. The Qingyang composite granite is one of a tungsten-bearing granites in the east of Jiangnan orogenic belt. It crops out over an area of approximately 750 km². The Baizhangya tungsten-molybdenum deposit was found near this pluton. New LA-ICPMS zircon U-Pb dating suggests that the crystallization age of the Qingyang body is 145.5±0.5Ma. The Qingyang pluton has zircon, apatite, fluorite, titanite, rutile, ilmeite, limonite, anatase and magnetite. The main rock-forming minerals including amphibole, biotite, plagioclase were analysed chemical compositions. The biotite is characterized by high MgO and low FeO contents with high Mg/(Mg+Fe) ratios (0.58-0.61), plotted in the crust-mantle zone. The oxygen fugacity calculated by biotite compositions is above Ni-NiO (NNO). The amphiboles are magnesiohornblende. The pressure of the granite estimated by Al-in-hornblende barometer is 1.79~2.50kbar. An amphibole-plagioclase thermometry and a semiquantitative hornblende thermometer yield a forming temperature of ~714°C. The plagioclase is oligoclase (An~29.5%). The mineral characteristics of Qingyang pluton are different from the Nanling tungsten-bearing S-type granites. The Jiangnan tungsten ore belt is NE-trending and distinct from the Nanling belt in terms of metallogenic age, tungsten-bearing granite type etc. and require further study.

Molecular simulation study of rectorite

ZHOU JINHONG^{1,2*}, LU XIANCAI³, ZHU JIANXI¹, MICHIEL SPRIK⁴, EDO BOEK AND HE HONGPING¹

¹ Key Laboratory of Mineralogy and Metallogeny, Guangzhou Institute of Geochemistry, Chinese Academy of Sciences, Guangzhou 510640, P.R. China

² Graduate University of Chinese Academy of Sciences, Beijing 100049, P.R. China

³ State Key Laboratory for Mineral Deposits Research, School of Earth Sciences and Engineering, Nanjing University, Nanjing 210093, P.R. China

⁴ Department of Chemistry, University of Cambridge, Cambridge CB2 1EW, United Kingdom

⁵ Department of Chemical Engineering, Imperial College London, London SW7 2AZ, United Kingdom

Rectorite is a special kind of clay mineral, consisting of illite layer and smectite layer in a regular order [1]. Rectorite and organo-intercalated rectorite can be applied in many fields. In this study, we use molecular simulations to investigate the interlayer properties of pristine and organo-rectorites. First, we use grand canonical monte carlo and molecular dynamics methods to investigate the hydration properties of rectorite with the comparison with montmorillonite. The results indicate that rectorite shows a similar swelling pattern as montmorillonite but a different interlayer cation distribution [2]. Second, we employ classical molecular dynamic simulations to study the microscopic interlayer properties of HDTMA⁺-intercalated rectorites with and without water at different HDTMA⁺ loading levels [4]. According to our simulations of organo rectorite, we find that as the loading level changes, different configurations of HDTMA⁺ occur. And water addition leads little influence on the mobility of Na⁺, but decreases the mobility of alkyl chains. Also we observe the behaviour of anions in system exceeding 1 CEC.

[1] Weaver (1956) *American Mineralogist* **41**, 202-231. [2] Kawano & Tomita (1992) *Clays and Clay Minerals* **40**, 421-428. [3] Zhou & Lu (2012) *Journal of Physical Chemistry C* **116**, 13071-13078. [4] Cygan & Greathouse & Heinz & Kalinichev (2009) *Journal of Materials Chemistry* **19**, 2470-2481.

Natural gas genetic types in the Northern Margin of the Qaidam Basin, NW China

S. X. ZHOU¹, S. H. GONG^{1,2}, J. LI^{1,2}, D. L. FU^{1,2}
AND H. K. ZHANG^{1,2}

¹ Key Laboratory of Petroleum Resources Research, Institute of Geology and Geophysics, CAS, Lanzhou, 730000 (sxzhou@lzb.ac.cn)

² Graduate University of CAS, Beijing, 1000049

There is abundant natural gas resources present in the northern margin of the Qaidam Basin. Based on chemical composition and carbon isotopic values of natural gases, natural gases can be divided into three different origins. Natural gases in Lenghu and Nabaxian structural belt are typical coal-derived gases with $\delta^{13}\text{C}_1$ ranging from -25.3‰ to -31.0‰ and $\delta^{13}\text{C}_2$ values range from -26.1‰ to -28.2‰. Lower Jurassic mudstone in Yikeyawuru Sag was regarded as main source rocks for these natural gases.

Natural gases in the Mabei and Mahai have different geochemical characteristics, their $\delta^{13}\text{C}_1$ range from -34.3 to -40.9‰, $\delta^{13}\text{C}_2$ values range from -25.0‰ to -27.7‰. It is showed that natural gases in these structural belt are generated probably from Middle Jurassic source rocks.

Special geochemical characteristics for natural gases in the Hulusan, Yahu, Yikeyawuru, Eboliang, Nabei and Jiansan structural belt have been observed. The methane carbon isotope compositions range from -18.1‰ to -22.6‰, and $\delta^{13}\text{C}_2$ values range from -17.6‰ to -23.0‰; some gases show carbon isotopic reversal ($\delta^{13}\text{C}_1 > \delta^{13}\text{C}_2$), this natural gas type maybe related to deep Lower Jurassic or Carboniferous source rocks at high levels of thermal maturity, which is new natural gas exploration field in Qaidam Basin.

This work was supported by partly by the Chinese National Natural Science Foundation (41072105), the Chinese National Major Fundamental Research Developing Project (2011CB201102), the National Special Projects of Science and Technology (2011ZX05008-004-01).

Source And Geochemical Characteristics Of Carbon And Nitrogen In Poyang Lake Sediments

ZHOU WENBIN^{1,2}, HUANG DAN^{1,2}, LOU QIAN^{1,2},
LI LIYANG^{1,2} AND HU CHUNHUA^{1,2*}

¹ School of Environmental and Chemical Engineering, Nanchang University, Nanchang, 330031, China (*correspondence: nchuchunhua@163.com)

² Key Laboratory of Lake Poyang Environment and Resource Utilization, Ministry of Education, Nanchang University, Nanchang, 330029, China

A certain proportion of organic carbon (OC) deposited onto the sediments will be mineralized and the remainder will be buried over geological timescales. The OC that reaches the lake sediment surface will partly be mineralized to CO_2 or CH_4 by heterotrophic microorganisms [1]. Lake is a rather considerable carbon source and sensitively responding to regional and global climate changes [2]. In this paper, we study geochemical proxies of total organic carbon (TOC), N, $\delta^{13}\text{C}$ and $\delta^{15}\text{N}$ in lake sediments of Poyang Lake to estimate its source of organic matter in 2012.

Results show that the organic matters source in sediments were mainly autochthonous in Poyang Lake, of which the terrigenous were less, especially in the south. Before 1970s, sediment organic matters were less affected by human activities, mainly from the deposition of aquatic plants in the northern Poyang Lake. From 1970s in the last century to the present, the main source were constant, however, there were more and more terrigenous. As for in the southern, deposition of aquatic plants were the main source before 1960s. From 1960s to 1980s in the last century, organic matters were mainly derived from soil erosion and death of algae. From 1970s to the present, the source of organic matters were autochthonous and terrigenous. In addition, the terrestrial source of nitrogen were increasing.

[1] Gudasz *et al.* (2010) Nature 466, 478–48. [2] Kling *et al.* (1991) Science 251, 298–301.

LOMU Geochemical Signature Of The Cenozoic Ultrapotassic Volcanic Rocks In NE China: Implications For A Relic Ancient Mantle Segment Beneath The Eastern CAOB

XIN-HUA ZHOU^{1*}, JI-FENG YING¹, YANG SUN¹
AND JI'AN SHAO²

¹ Institute of Geology and Geophysics, Chinese Academy of Sciences, Beijing 100029, China (*correspondence: xhzhou@mail.igcas.ac.cn)

² College of Earth & Space Sciences, Peking University, Beijing 100871, China

In the past several decades, the Sr-Nd-Pb isotopic features of oceanic basalts have been elegantly described as mixtures of depleted mantle (DMM) and a spectrum of enriched endmember components, such as EM I, EM II and HIMU. The applications of these mantle endmembers in the petrogenesis of basalts in continental tectonic setting have revealed that the EM I signature is invariably related with the cratonic subcontinental lithosphere. In this study, we reported a suite of Pleistocene basic, high potassic to ultrapotassic volcanic rocks from NE China. These rocks are characterized with modal leucite and have SiO₂=42-45%, K₂O=9-11% with K₂O/Na₂O as high as 4. Geochemical data show these rocks are highly enriched in REE with extremely fractionated LREE/HREE ratios (55-70), LILE are also enriched without apparent HFSE depletion. Though their ⁸⁷Sr/⁸⁶Sr=0.70558-0.70580 and εNd=-5 - -12 demonstrate a typical EM I affinity, it is more accurate to define it as a LOMU signature in terms of Pb isotopes, as these rocks exhibit very low ²⁰⁶Pb/²⁰⁴Pb (16.34 - 16.45), ²⁰⁷Pb/²⁰⁴Pb (15.27-15.39) which is comparable with other leucite-bearing potassic volcanic rocks found elsewhere in the world, such as Leucite Hill and Smoky Butte in North America. We proposed that these potassic rocks were derived from an ancient (Archean?) phlogopite-rich garnet facies subcontinental lithospheric mantle which is decoupled from the overlying crust that was formed since Neoproterozoic accompanying with the evolution of CAOB. As two Archean cratons, namely the Aldan Shield and North China cratons exist on the northern and southern side of the CAOB, respectively, it is speculate that the mantle source feeding these potassic rocks is likely a relic cratonic segment of either Aldan or North China cratons.

This work is financially supported by the National Natural Science Foundation of China (41173045).

Petrogenesis of the Early Paleoproterozoic Garnet-Bearing Monzonite in the Lushan Area, Southern Margin of the North China Craton

YANYAN ZHOU^{1*}, TAIPING ZHAO² AND MINGGUO ZHAI¹

¹ State Key Laboratory of Lithospheric Evolution, Institute of Geology and Geophysics, Chinese Academy of Sciences, Beijing 100029, China (correspondence: llylz_b3@163.com)

² Key Laboratory of Mineralogy and Metallogeny, Guangzhou Institute of Geochemistry, Chinese Academy of Sciences, Guangzhou 510640, China

LA-ICP-MS zircon U-Pb dating indicate that the garnet-bearing monzonite, exposed in the Lushan area, southern margin of the North China Craton (NCC), formed at 2134±18Ma. Electron microprobe analyses reveal that the magmatic garnets are homogeneous without substantial chemical zoning. They contain 61.94 to 66.39 mol% almandine, 18.60 to 23.40 mol% grossular, 10.06 to 15.11 mol% pyrope and 1.09 to 4.32 mol% spessartine. They have high CaO and low MnO contents with high Fe/Mn ratios, comparable to those crystallized from high pressure basaltic granulite, but different from those in I, S and A type granites. Garnets have strongly LREE-depleted chondrite-normalized REE patterns with limited HREE variation. The MREE show equally partition between garnet and zircon, whereas HREE prefer zircon to garnet, suggesting crystallizing temperatures at 800 to 850°C. Moreover, in terms of the trace element distribution coefficients between zircon and garnet, our data well agree with experimental data at 800°C and granulite-facies samples. Considering strongly various HREE/LREE, and low MgO, we envisage that the host melt of garnet might be ever modified by granitic melts.

The monzonite contains SiO₂ from 57.0 to 58.9 wt% with high K₂O+Na₂O contents (7.46 to 9.14 wt%), consistent with intermediate shoshonite series. The calculated magmatic zircon ε_{Hf}(t) values are mostly positive (+0.02 to +4.10) with T_{DM}^C from 2492 to 2388 Ma, except four analyses give negative ε_{Hf}(t) values (-0.97 to -0.98) with T_{DM}^C from 2508 to 2496 Ma, suggesting that they derived from a depleted mantle-derived basaltic source with contamination of older granitic components. On the basis of their high Zr (598 to 926 ppm) and Zr/Y ratios (17 to 21), and enrichments of Rb, Cs, Ba, Hf, Th, U and REE, similar to OIB, we suggest that they have formed in an intra-plate setting, related to lithospheric thinning and asthenospheric mantle upwelling, further constraining that the NCC probably underwent a rifting event during the Paleoproterozoic (2.2 to 1.95 Ga).

Modelling gas-fluid-mineral interactions in a CO₂ injection analogue site with noble gases

Z. ZHOU^{1*}, M.J. BICKLE², A. GALY², H.J. CHAPMAN²,
N.KAMPMAN², B. DUBACQ², M. WIGLEY², O. WARR¹,
T. SIRIKITPUTTISAK¹ P. HANNAH³
AND C.J. BALLENTINE¹

¹University of Manchester, M13 9PL, UK

(*correspondence: zheng.zhou@manchester.ac.uk)

²Department of Earth Sciences, University of Cambridge,
UK³Full-Spectrum Monitoring, LLC, USA

We carried out an artificial noble gas tracer injection experiment in a CO₂ EOR project in a depleted oil field in the USA. In this experiment, 2 STP litres of ³He and 2 STP litres of ¹²⁹Xe were injected together with the EOR CO₂ stream. Samples were collected both from the CO₂ injector and 4 monitoring wells before, during and after injection.

Natural background of ³He/⁴He and ¹²⁹Xe/¹³²Xe ratios in fluid sampled from this field are 0.07Ra and 0.98 respectively. Measured spiked CO₂ stream has ³He/⁴He and ¹²⁹Xe/¹³²Xe ratios of 49.0Ra and 23.94 respectively. Tracers were detected in monitoring wells both updip and downdip of the injector in a short period after the tracer injection. This is completely different from a simple PHREEQC model prediction that is based on one-dimensional tracer dispersion in a dual porosity column. It reflects the complexity of the reservoir system. Although tracers are present in monitoring wells, the peak tracer ratios are at a level that is orders of magnitude lower than the injected ratios. Simple mass balance calculation assuming phase equilibrium between gas and groundwater shows that water volume involved in this system is 3-4 orders of magnitude higher than the gas volume. This is not reasonable and groundwater alone cannot account for observed tracer concentrations and ratios. Other processes that could affect tracers present in monitoring wells include multi-phase interaction, dissolution into oil, diffusion and adsorption into immobile reservoir porosity, etc. In this presentation, we discuss models that take into account these processes in this complex reservoir system to explain observed data. This work demonstrates huge potential of exploiting artificial noble gases in crustal fluid studies.

Silicon isotopes as a new tool to identify the main cause of the field-lab apparent discrepancy of feldspar dissolution rates

CHEN ZHU¹, CHAO WANG¹ AND GEORG, R.B.²

¹Indiana University, Bloomington, Indiana, USA; ² Water Quality Centre, Trent University, Canada.

(*correspondence: chenzhu@indiana.edu)

In 2004, Zhu, Blum, and Veblen proposed a new hypothesis for explaining the apparent discrepancy between lab-measured and field-estimated feldspar dissolution rates [1]. They identified the coupling of dissolution and precipitation reactions as the main contributor to the apparent discrepancy. In the intervening nine years, we have tested this hypothesis by conducting a series of batch experiments at elevated temperatures [2-5] and numerical simulations of coupled dissolution and precipitation reactions [4, 6]. The results show that taking into account of reaction coupling is able to reduce the gap between the field and lab rates by about two orders of magnitude at elevated temperatures of 200-300 °C [4]. A chapter in volume 70 of *Review in Mineralogy and Geochemistry* [7] has summarized the historical development of the topic and its role in the overall picture of water-rock interaction.

A field study of Si isotopes of groundwater, feldspars, and secondary clays demonstrated the promise of Si isotopes as a new tool to unravel the coupled reactions [8]. We are now employing the new tool for laboratory experiments. A methodology paper on using Si isotopes was just published [9]. This presentation will discuss results of new experimental data, as well as the potentials and pitfalls of this new tool.

[1] Zhu *et al.*, in *Water-Rock Interaction*, R.B. Wanty and R.R.I. Seal (Ed) 2004, A.A. Balkema: Saratoga Springs, New York. 895-899.[2] Fu *et al.*, *Chemical Geology.*, 2009. **91**(3): 955-964. [3] Zhu and Lu, *GCA*, 2009. **73**(11): 3171-3200. [4] Zhu *et al.*, *GCA*, 2010. **74**(14): 3963-3983. [5] Lu *et al.*, *Applied Geochemistry*, 2013. **30**: 75-90 [6] Ganor *et al.*, *Environmental Geology*, 2007. **53**(3): 599-610. [7] Zhu, in *Thermodynamics and kinetics of water-rock interaction*, E.H. Oelkers and J. Schott, Editors. 2009, Mineralogical Society of America. 533-569. [8] Georg *et al*, *GCA*, 2009. **73**(8): 2229-2241.[9] Gruber *et al.*, *GCA*, 2013. **104**: 261-280.

Tracing the sources of sulfur in Beijing rain water with stable isotopes

GUANGXU ZHU¹, QINGJUN GUO^{1*}, HARALD STRAUSS²
AND MARC PETERS¹

¹ Institute of Geographic Sciences and Natural Resources
Research, Chinese Academy of Sciences, Beijing 100101,
China (*correspondence: guojq@igsnr.ac.cn)

² Westfälische Wilhelms-Universität Münster, Corrensstr. 24,
8149 Münster, Germany

Acid rain is one of the prominent atmospheric environmental problems in Beijing, China. The stable isotopes of sulfur were used as environmental tracers of sulfur in rain by tracing its sources and identifying rain sulfur turnover rates. 74 rainwater samples in Beijing were collected between August 2010 and December 2012 and the concentrations of SO_4^{2-} , the sulfur isotopic composition and pH were analyzed. The results showed that mean pH in precipitation was 6.42, the acid rain frequency in 2011 was 26.9% compared to 13.6% in 2012. The concentrations of SO_4^{2-} ranged from 2.23-82.36 mg/L with a weighted average of 22.44 mg/L, whereas the average value of $\delta^{34}\text{S}$ was 4.8 ‰ within range of 2.1‰ and 12.8‰. A pronounced seasonal pattern is discernible for $\delta^{34}\text{S}$ in precipitation with data for the winter (7.0‰) > autumn (5.7‰) > summer (3.9‰) \approx spring (3.8‰), SO_4^{2-} concentration in summer was significantly lower than in the other seasons. $\delta^{34}\text{S}$ indicates that the sources of sulfur in rain water include bioorganic sulfur, anthropogenic sulfur (coal combustion) and sulfur from sea spray. Anthropogenic sulfur contributes the majority to the sulfur in rainwater, especially in winter and autumn. For several rainstorms sulfur dominantly originated from sea spray. Results provided important information about the sulfur sources in rain which will help to decrease acid rain and improve air quality in Beijing.

Financial support by the One Hundred Talents Program of the Chinese Academy of Sciences, the National Natural Science Foundation of China (NSFC No. 41250110528), 863 Program sponsored by Ministry of Science and Technology of China (No. 2013AA06A211) is gratefully acknowledged.

Research On The Super-Long Life Of Deep Carbonate Oil Reservoir

GUANGYOU ZHU¹, SCHUICHANG ZHANG¹ AND JIN SU¹

¹ PetroChina, Research Institute of Petroleum Exploration and Development, Beijing 100083,
(huguangyou@petrochina.com.cn)

Reservoir's destroy is a universal phenomenon and more than one half of the reservoirs are formed later than Oligocene Epoch, which average age is 35 Ma and the average live age is 55 Ma (Macgregor, 1996). As for the ancestral marine basin of China, Palaeozoic marine strata experienced multicycle movements, reservoirs are reformed and destroyed seriously, and there mainly be secondary reservoir. Recently, large ancient deep carbonate reservoirs generated in 290-250 Ma ago have been discovered in the north of Tarim basin. This discovery not only changed the reservoir toplimit age (95Ma) but also brought great belief in exploring ancient reservoir.

The reservoirs distributed in 5500-7200m, and reservoir is Ordovician carbonate, and cap rock is upper Ordovician finely carbonate and mudstone. The oil came from middle-upper Ordovician hydrocarbon source rock in late Permian. Based on hydrocarbon generation history, fluid inclusion, burial history, authigenic Illite K-Ar aging, trap formation and evolution process and so on, the reservoirs formed during 290-250 Ma and were conserved with depth increasing.

For Tarim basin, late Permian is an important generating and expelling hydrocarbon period. Since the Triassic, Ordovician oil reservoirs preserved had been in the process of increasing buried depth with increasing thick cap rock, and the location and form of Ordovician trap are always the same. With depth more than 7000m and reservoir temperature more than 160 °C, the crude oil hasn't been cracked by now, so the zone more deeper is predicted still filled with oil.

Gold tube thermal simulation experiments show that oil cracking depth of Tarim basin is about 7500m and peaked in 9000-9500m combining the compensation effect of the low geothermal gradient and late quickly buried process of Tarim basin. The reservoir temperature of oil cracking is higher than 210°C, and liquid oil can be exist above 9000m. Therefore, the ancient oil reservoirs discovery brings great belief in searching for native marine oil reservoir in complex structure area of Tarim basin, believing the exploring depth can be expanded to 9000m.

[1] Macgregor D.S. Factors controlling the destruction of preservation of giant light oilfields. *Petroleum Geoscience*, 1996, 2: 197-217

The Isotopic Composition Of Selenium In Chinese Coals

JIAN-MING ZHU^{1,2*}, THOMAS M. JOHNSON^{2*},
LIANG LIANG¹ XIANG-LI WANG², HAI-BO QIN¹
AND ZUO-YING YIN¹

¹State Key Lab. of Environmental Geochemistry, Inst. of Geochemistry, CAS, Guiyang, 550002, China.

(zhujianming@vip.gyig.ac.cn) (*present author)

²Department of Geology, University of Illinois at Urbana-Champaign, Urbana, 61801, USA.
(tmjohnsn@illinois.edu)

Selenium generally occurs in relatively high abundance in coals, black shales and other organic-rich rocks. Coal mining, combustion and weathering are the important pollution source in China, which released a large of Se into the environment, increasing its concentration in the air, soils, water and plants, and in some areas of China, Se from coal combustion poses human health concerns. So comprehensive studies on Se isotopes in Chinese coals are very important to understand Se biogeochemical cycling and its geochemical behavior in surface environment^[1].

Here, using HG (hydride generator)-MC-ICP-MS^[2] and a ⁷⁴Se-⁷⁷Se double spike technique to achieve high precision, we determined Se isotopic compositions of Chinese coals from the different coal fields and geological ages. The $\delta^{82/76}\text{Se}$ values ranged from -4.01‰ to 4.75‰ in our samples already analyzed. The overall range of $\delta^{82/76}\text{Se}$ was 8.76‰, indicating Se isotopic variation occurs in a relatively moderate range compared to most shales. Systematic differences in Se isotopic composition between high sulfur and low sulfur (Total S < 1%) Chinese coals were not observed.

However, the Se isotopic composition of coals from different geological ages are different. The average $\delta^{82/76}\text{Se}$ values of Chinese coals formed in Tertiary, Jurassic-Triassic, and Permian-Carboniferous Period are $2.10 \pm 0.74\%$, $-0.07 \pm 0.68\%$, and $1.50 \pm 0.25\%$, respectively. The difference in $\delta^{82/76}\text{Se}$ values may be related to their original precursor plant speices, or further reflect the paleoclimate change, continent weathering situation and depositional plaeoenvironment. Additionally, our results also provide some hope that Se isotopes may be used to trace atmospheric Se sources in the different regions of China.

The work was supported by the National Natural Science Foundation of China (41073017, 41021062) and the Knowledge Innovation Program of the Chinese Academy of Sciences (KZCX2-YW-JC101).

[1] Johnson (2004) *Chem Geol* 201-214. [2]Zhu *et al.* (2008) *Chinese J Anal Chem* 36, 1385-1390.

Geochemistry of Huashan A-Type Granitoid Complex, South China, and its geotectonic significance

ZHU JINCHU

Department of Earth Sciences, Nanjing University, Nanjing 210093, CHINA (jczhu@nju.edu.cn)

The Huashan A-type granitoid complex in NE Guangxi Province, South China, with an exposure of more than 500 km² in area consists of three granitoid bodies: The Huashan main body biotite granite batholith, the Niumiao diorite stock in the SE periphery, and the Tong'an quartz monzonite granite stock in the W periphery. This complex is 160~163 Ma in emplacement age, acidic to intermediate in composition. The mafic enclaves with mingling feature are frequently seen. This complex is characterized by high contents of alkalis (especially K) and enrichment in LILE (Rb, K, Ba, Pb, etc.) and HFSE (Th, U, REE, Y, Nb, Ta, Zr, Hf etc.). The whole rock I_{Sr} values are between 0.70472 ~ 0.70714, $\epsilon_{Nd}(t)$ values between -0.37 ~ -3.21, and $\epsilon_{Hf}(t)$ values of zircons between -2.8 ~ +2.1. These geochemical data indicate an A type feature and significant involvement of mantle materials. Combining the regional geological and geochemical data, we suggest that strong mixing of mantle-derived and crust-derived magmas under an intense crustal extension and thinning environment during the Mid-Late Jurassic period might be the major mechanism for generating the A-type Huashan granitoid complex.

Microbial carbonate precipitation under high alkaline condition and its implications in concrete restoration

TINGTING ZHU¹, CARLOS PAULO¹
AND MARIA DITTRICH^{1*}

¹University of Toronto Scarborough, 1265 Military Trail,
Toronto, ON, M1C 1A4, Canada
(*correspondence: mdittrich@utsc.utoronto.ca)

Microbial carbonate precipitation (MCP) has been demonstrated to have a potential in constructional restoration. The repair of concrete by MCP requires microorganisms that can survive high alkaline conditions in the cracks. Although heterotrophic organisms showed promising results in concrete restoration, they generate contamination (e.g., NH₄⁺) to the environment. This study aims to examine the potential of phototrophic microorganisms for MCP in the cracks of concrete. Among the several autophototrophic strains, PCC8806 showed the highest rate of biomineralization [1]. However, it is unknown whether they can survive under high alkaline conditions and impact MCP.

In this study, carbonate precipitation by PCC8806 under high alkaline conditions has been investigated. Calcium chloride (50 mM) was added to an initial solution, which was prepared from concrete mix by adjusting the pH to 11.7. Ten ml of washed cells, with a concentration of 3.53×10⁹ cells/ml, was inoculated into solution. Another experimental set without bacteria was monitored as control. Samples were taken at the starting point, and after 1h, 2h, 3h, 6h, 18h and 24h to determine the solution composition by atomic adsorption spectroscopy (AAS), and to observe morphology of the precipitates by optical and scanning electron microscopy (SEM), and Atomic Force microscopy. The precipitates were examined by X-ray diffractometry and Raman spectroscopy.

After 24 hours of reaction, the pH dropped 0.5 unit in control and 1 unit with PCC8806. In the presence of PCC8806, the calcium concentration decreased by 5 mM/L by the end of the experiment, while there was no change in control. As it has been confirmed by SEM, a large amount of calcium carbonates with diverse morphologies were formed, some of which were attached to cells. AFM images and Raman spectra indicated that the calcium carbonates were mostly calcites. Our study showed that PCC8806 can survive high alkaline conditions in concrete cracks and strongly impact MCP compared to the abiotic experiments.

[1] Liang *et al.* (2013). *Colloids and Surfaces B: Biointerfaces*, under review.

Mg and Fe isotope constraints on the genesis of Bayan Obo ore deposits, Inner Mongolia, China

X. K. ZHU, J. SUN AND S. Z. LI

Laboratory of Isotope Geology, MLR, Institute of
Geology, CAGS, Beijing, 100037, PR China
(XIANGKUN@CAGS.AC.CN)

The giant polymetallic Bayan Obo REE-Nb-Fe ore deposit is the largest REE deposit in the world. Its origin, however, remains controversial. A number of genetic models have been proposed, including sedimentary origin, magmatic origin, hydrothermal origin or origin with multiple processes. Mg and Fe isotope compositions of H8 Dolomite (the ore-bearing bed), carbonatite dykes nearby, mesoproterozoic sedimentary carbonate and micrite from Sailinhuodong have been systematically investigated to constrain the genesis of Bayan Obo deposit. The results show that δ²⁶Mg_{-DSM3} of the H8 dolomite varies from -1.13‰~0.10‰, with average δ²⁶Mg-DSM3 of -0.53‰, which is closer to those of igneous rocks, but much heavier than micrite carbonate rocks (its δ²⁶Mg ranges from -1.99‰ to -1.93‰). The Fe isotope compositions of the deposit are rather homogeneous with an average in δ⁵⁶Fe values of -0.03‰, which are very different to those of Precambrian sedimentary Fe ores, but similar to those of igneous rocks.

Overall both Mg and Fe compositions are inconsistent with either sedimentary or hydrothermal origin, but consistent with an igneous genesis.

Discussion on the characteristics and influence factors of specific surfaces in argillaceous source rocks

XIAOJUN ZHU¹, JINGONG CAI^{1*}, GUOQI SONG²
AND JUNFENG JI³

¹ State Key Laboratory of Marine Geology, Tongji University, Shanghai 200092, China (*correspondence: jgcai@tongji.edu.cn) ² Shengli Oilfield Company, SINOPEC, Dongying 257015, China

³ State Key Laboratory of Surficial Geochemistry, Nanjing University, Nanjing 210093, China

Samples of argillaceous source rocks were taken at different depth in well S of Dongying Sag (Bohai Basin), and also separated the clay fractions (<2 μ m) to measure the specific surface areas (SSAs) by using nitrogen adsorption method (BET) and ethylene glycol monoethyl ether method (EGME), as well as performing the X-ray diffraction for mineral compositions determination, for discussing the characteristics and influence factors of specific surfaces in argillaceous source rocks. The analysis results show that a) the specific surfaces of argillaceous source rock consist of inner surface and external surface, and clay minerals (smectite in particular) have great contributions to the inner and external surface area in source rocks, however non-clay minerals basically only have external surface, b) the influences of diagenesis to minerals etc. make the evolution of SSAs in burial depth have episodic characteristics, which is much more obviously in the inner surface area in particular, meanwhile there is a strong inhibition for SSAs (especially the inner surface) when the content of carbonate minerals is more than 40%, and it exists a threshold of carbonate minerals content (20~40%) that makes the external surface area stable, c) the inner and external surface in source rocks are more abundant in argillaceous siltstone whose external surface area is large, and the SSAs of mudstone (mainly inner surface) is bigger than the sandstone (chiefly external surface).

According to the difference between inner surface and external surface in argillaceous source rocks, the analyses give the results that the specific surfaces of argillaceous source rocks are influenced by the factors of rock types, mineral compositions and diagenesis, etc., and it is of great significance for the research of organic matter and hydrocarbon occurrence and petroleum exploration and exploitation in argillaceous source rocks, especially should be concerned in the research of unconventional petroleum.

This work was supported by National Natural Science Foundation of China Program (Grant No. 41072089).

Mineralogy and elemental geochemistry of coal in Southeast Chongqing, Southwest China

ZHU ZHENGJIE¹² AND XIANG XIAOJUN¹²³

¹Chongqing Key Laboratory of Exogenic Mineralization and Mine Environment, Chongqing Institute of Geology and Mineral Resources, Chongqing 400042, China;

²Chongqing Research Center of State Key Laboratory of Coal Resources and Safe Mining, Chongqing 400042, China
E-Mail: (zhuzhjie@163.com)

The coal-bearing stratum in the southeast Chongqing coalfield is the Wujiaping Formation (P_{3w}, Late Permian age). Mineralogy and elemental geochemistry of coal in this area were investigated by using inductively coupled plasma mass spectrometry (ICP-MS) and X-ray diffraction (XRD) techniques. The results showed that minerals in the coal are characterized by dominant clay minerals and pyrite, with the minor calcite, quartz and anatase. Compared with the average concentration of the China coal, the element Zr and rare Earth element (REE) in Southeast Chongqing coal is enriched, with the average content of 678.15 μ g/g and 413.95 μ g/g, respectively, approaching the industrial grade of the weathering deposit of Zr and REE. Besides these two elements, concentrations of Li, Sc, Ga are also higher than that in the China and the world coal. However, the element Nb, Ta is depleted, which may be attributed to the lack of tonstein in the coal seam. The model of REE in southeast Chongqing is enriched in LREE, with the LREE/HREE ratio between 1.9 and 7.91. Otherwise, the REE model also showed the negative Eu anomaly, the slightly negative Ce anomaly, similar with that of the Emeishan basalt. Valuable elements Zr, REE are concentrated in southeast Chongqing coal, which would have the potential economic value, and be deserved to research in future.

Garnet and spinel in the Upper Mantle: Results from thermodynamic modeling in fertile and depleted compositions

L. ZIBERNA^{*1,3}, S. KLEMME² AND P. NIMIS³

¹Bayerisches Geoinstitut, Universität Bayreuth, Germany, (correspondence: luca.zibera@uni-bayreuth.de)

²Institut für Mineralogie, Universität Münster, Germany, (stephan.klemme@uni-muenster.de)³Dipartimento di Geoscienze, Università di Padova, Italy, (paolo.nimis@unipd.it)

Spinel–garnet relations in the upper mantle have long been investigated from different perspectives, by means of petrological studies on natural samples (orogenic massifs, xenoliths, diamonds), high-P-T experiments, thermodynamic calculations, and geophysical observations. Here we report a refined thermodynamic model that allows one to predict phase relations and mineral compositions in a wide range of realistic mantle compositions [1]. The generated phase diagrams show that the garnet+spinel stability field is always broad at low temperatures and progressively narrows with increasing T. In lithospheric sections with hot geotherms, garnet coexists with spinel across an interval of 10–15 km, at ca. 50–70 km depths. In colder, cratonic, lithospheric sections, the width of the garnet–spinel transition strongly depends on bulk composition: in fertile mantle, spinel can coexist with garnet to about 120 km depth, while in a strongly depleted harzburgitic mantle spinel is stable to over 180 km depth. These results are in agreement with the observed extension of the Hales gradient zone (a seismic impedance increase in the mantle that is usually attributed to the spinel-to-garnet transition) in various geodynamic settings. The model predicts that formation of chromian spinel inclusions in diamonds is restricted to pressures between 4.0 and 6.0 GPa. The calculated modes of spinel decrease rapidly to less than 1 vol% when garnet enters the equilibrium assemblage, hence spinel grains can be easily overlooked during the petrographical characterization of small mantle xenoliths. The very Cr-rich nature of many spinels from xenoliths and diamonds from cratonic settings may simply be a consequence of their low modes in high-P assemblages and does not require ultra-depleted compositions. The model also shows that large Ca and Cr variations in lherzolitic garnets in equilibrium with spinel can be explained by variations of pressure and temperature along a continental geotherm and do not necessarily imply variations of bulk composition.

[1] Zibera *et al.* (2013), *Contrib. Min. Petrol.*, in press.

Factors controlling the distribution of Neodymium isotopes and REEs in tropical atlantic seawater

M. ZIERINGER¹, M. FRANK^{1*} AND E. HATHORNE¹

¹GEOMAR Helmholtz Centre for Ocean Research Kiel, Wischhofstrasse 1-3, 24148 Kiel, Germany (*mfrank@geomar.de)

Neodymium (Nd) isotopes and rare earth element (REE) patterns are used as tracers of present day ocean circulation and to fingerprint source materials. We present full water column Nd isotopic compositions and dissolved REE distributions in seawater of the tropical Atlantic Ocean. Samples were collected during the GEOTRACES expedition A11 (R/V Meteor) from Las Palmas (Canary Islands) to Port of Spain (Trinidad and Tobago).

Highly variable REE concentrations and associated REE patterns in surface waters reflect different oceanic provinces and prominent local source provenances, such as volcanic islands and dust particles of continental origin. Generally, concentrations in the eastern basin, in particular in the vicinity of the Canary Islands and off the coast of NW Africa, are higher than in the western basin. In the area of the Canary Islands shale-normalized REE patterns are characterized by a strong increase in concentrations of the heavy REEs relative to the light REEs as a consequence of exchange with the volcanic rocks, while further south comparatively flat REE patterns indicate dust dissolution.

Nd concentrations in surface waters range between a minimum of 14 pmol/kg in low salinity waters (< 33.6 psu) originating from the Amazon river and a broad maximum off NW Africa reflecting the dissolution of Saharan dust. This is also reflected in the dissolved Nd isotope compositions, which range from $\epsilon_{Nd} = -12.7$ to -8.4 . The most radiogenic values were measured between Tenerife and Grand Canary and near the Amazon river mouth while the least radiogenic ones are found in the open ocean surface waters off NW Africa, and in the uppermost 100 m of the western basin.

We also present full water column profiles including all major water masses present in the tropical Atlantic Ocean. Southern Ocean sourced intermediate and deep waters are clearly distinct in the eastern and western basins and allow the estimation of mixing proportions between different endmember water masses.

Additional insight into natural $^{185}\text{Re}/^{187}\text{Re}$ of various materials

A. ZIMMERMAN^{1*}, H. STEIN^{1,2} AND J. HANNAH^{1,2}

¹AIRIE Program, Colorado State Univ, Fort Collins, CO
(*correspondance: aaron.zimmerman@colostate.edu)

²CEED Centre of Excellence, University of Oslo, Norway

Following the preliminary work of Zimmerman et al [1] and the impressive results of Miller et al [2], additional investigation into the natural $^{185}\text{Re}/^{187}\text{Re}$ isotopic ratio supports the notion that variability of the ratio may exist in different geological samples and Re-bearing materials.

Four molybdenite samples, including NIST RM 8599 [3], and AIRIE's Re standard solution (RR-4, prepared from potassium perrhenate), were analyzed for their Re isotopic composition (IC) in triplicate. All samples showed elevated Re IC relative to the "true" value of 0.5974 [4]. The analyses followed standard Re-Os procedures except sample Re was liberated with concentrated HNO_3 in open glass beakers rather than Carius tubes. Anion exchange Re separation followed conversion of the solution to HCl form. Single bead Re clean-up resulted in notable NTIMS signal improvement.

NTIMS multi-collector faraday cup measurements are ruled out as causing elevated ICs as RR-4 loaded directly onto outgassed Pt filaments yields the expected ratio (0.59735 ± 0.00044 1 σ stdev, n=6). Excluding two outliers, the mean $^{185}\text{Re}/^{187}\text{Re}$ is 0.5989 ± 0.0014 1 σ stdev (n=16). Interestingly, every sample's IC was above 0.5974 yet there are no systematic correlations between IC and material type or molybdenite geologic setting.

Summarizing the Re IC of the analyzed samples relative to the true value of 0.5974 is difficult because of analytical concerns. The molybdenites selected (save RM 8599) have geologically unusual low Re concentrations between 1ppm and 50ppb. Column chemistry was hampered by extreme Mo:Re and low total Re. RM 8599 and RR-4 amounts were selected to best match the low Re molybdenites. As such, NTIMS signals for all samples were less than ideal. It is therefore difficult to determine whether the elevated Re ICs are analytically robust or biased by anomalous column chemistry and weak signals. Additional analyses using high Re molybdenites along with matching 8599 and RR-4 are in progress to test for biases resulting from low total Re.

[1] Zimmerman *et al.* (2011) *Min. Mag.* **75**, 2287. [2] Miller *et al.* (2009) *J. Anal. Atom. Spect.* **24**, 1069-1078. [3] Markey *et al.* (2007) *Chem. Geol.* **244**, 74-87. [4] Gramlich *et al.* (1973) *J. Res. Nat. Bur. Stand.* **77**, 691-698.

Release of engineered nanomaterials from flexible thin-film photovoltaic cells

YANNICK-SERGE ZIMMERMANN^{1,2},
ANDREAS SCHÄFFER², PHILIPPE F.-X. CORVINI^{1,3}
AND MARKUS LENZ^{1*}

¹ Institute for Ecopreneurship, University of Applied Sciences and Arts Northwestern Switzerland, Gründenstrasse 40, CH-4132 Muttenz, Switzerland

² Institute for Environmental Research (Biology V), RWTH Aachen University, 52074 Aachen, Germany

³ State Key Laboratory of Pollution Control and Resource Reuse, School of the Environment, Nanjing University, Hankou Road 22, 210093, Nanjing, China

* (correspondence: markus.lenz@fhnw.ch)

Organic photovoltaic solar cells (OPVs) are a promising renewable energy technology. In consideration of the anticipated forthcoming large-scale production, the environmental impact of OPVs should be benchmarked to commercially available thin film technologies such as CuInGaSe cells (CIGS). Whereas most research focusses on performance of photovoltaics, little is known on the environmental fate and effect of their constituents such as engineered nanomaterials after their life cycle. CIGS rely on hazardous metal(oids) such as Cu, In, Ga, Se, Mo and Cd. However, also OPV – although based on light-absorbing organic molecules – contain metals such as Al, In, and Ag, some of which applied in nanoparticulate form.

For the first time, this study investigates the leaching behavior of engineered inorganic nanomaterials present in OPV and CIGS. Leaching scenarios investigated under environmentally relevant conditions, like exposition to acidic rain and mechanical stress, were carried out for long term. Metal concentrations were determined by Inductively Coupled Plasma Mass Spectrometry (ICP-MS). This allowed the calculation of the predicted environmental concentrations for different scenarios, which were set in relation to corresponding WHO water limits. Furthermore, models for the observed leaching kinetics of the most relevant metals were determined. Eventually, all released inorganic components were investigated by time-resolved ICP-MS in order to distinguish between dissolved and nanoparticulate states. Our results show that after four months, OPV do not pose any risk to the environment regarding their engineered inorganic nanomaterial content, even under most conservative scenarios. On the other hand, high amounts of Mo, Se and Cd were leaching from CIGS. Under the constraints of this study, these would exceed drinking water limits many times.

Highly equilibrated carbonaceous chondrites

J. ZIPFEL^{1*}, J.-A. BARRAT², CH. GÖPEL³
AND U. LINNEMANN⁴

¹Senckenberg Frankfurt, 60325 Frankfurt, Germany
(*correspondance: jutta.zipfel@senckenberg.de)

²Université de Bretagne Occidentale, 29280 Plouzané Cedex,
France (Jean-Alix.Barrat@univ-brest.fr)

³IPGP, 75238 Paris, France (gopel@ipgp.fr)

⁴Senckenberg Naturhistorische Sammlungen Dresden, 01109
Dresden, Germany (ulf.linnemann@senckenberg.de)

Most carbonaceous chondrites have primitive, unequilibrated textures of petrologic type 3 and lower. Recently a number of extensively metamorphosed carbonaceous chondrites of types 6 were identified. They have O isotopes similar to CR chondrites and were classified as CR metachondrites [1]. The CR relationship is supported by the similarity in bulk compositions of major elements. The FeO-rich mafic mineralogy (Fa~36) distinguishes these meteorites from CR-chondrites. Northwest Africa (NWA) 6901 and those described by [1] are potentially paired meteorites with identical O isotopic composition, mineralogy, and highly equilibrated texture and old single grain phosphate U-Pb age of 4563 ± 13 Ma [2].

We performed analyses of major and trace elements of bulk NWA 6901 by ICP-AES and ICP-MS [3] and of trace elements of merrillites by LA-ICPMS. Bulk NWA 6901 is different from CR chondrites with depletions of refractory elements (Al, Ca and Sc) and moderately volatile elements (K, Na, Ga, and Zn). The phosphates are strongly enriched in LREE with a positive Ce anomaly, a negative Eu anomaly and a subchondritic U/Th ratio. The pattern is the same as the pattern of bulk NWA 6901. Phosphates of basaltic achondrite NWA 011 have a similar pattern suspected to be caused by terrestrial alteration [4]. The absence of common Pb in single phosphate grains suggest, however, that terrestrial alteration in NWA 6901 is at most minor [2].

The fractionated trace elements of phosphate and bulk NWA 6901 are not in accordance with isochemical metamorphism on the CR parent body and can also not be explained by loss and/or gain of trace element rich partial melts. Chemistry and ⁵⁴Cr [5] indicate that NWA 6901 is a new type of carbonaceous chondrite derived from a parent body that formed in a chondritic source region unknown so far.

[1] Bunch T. E. *et al.* 2008. LPSC XXXIX, #1991. [2] Zipfel J. and Linnemann U. (2012) European Mineralogical Conference Vol. 1, EMC2012-503, 2012. [3] Barrat J.-A. GCA 83 (2012) 79–92. [4] Floss Ch. *et al.* (2005) MAPS 40, Nr 3, 343–360. [5] Göpel Ch. *et al.* (2013) this volume.

Silver enrichment in rain under different cloud conditions

ASSAF ZIPORI, DANIEL ROSENFELD AND YIGAL EREL*

The Nadine and Freddy Herman Institute of Earth Sciences,
the Hebrew University of Jerusalem, 91904 Jerusalem,
Israel (*correspondence: yerel@vms.huji.ac.il)

This study follows and records the arrival and activity of AgI in seeded clouds. During four winters while cloud seeding took place, precipitation was collected at three stations in the catchment area of the Sea of Galilee (target stations) and in one station west of the seeding line (control station). Chemical analysis of 23 metals was carried out on more than 4000 rain samples in order to determine the major and trace metal concentrations and enrichment factor with respect to Al (EF), where Al was assumed to represent natural dust. In addition, satellite images were analyzed to characterize the cloud phase (liquid, ice, mixed liquid-ice) and the temperature of the clouds using the EUMETSAT second generation geostationary satellite.

It was found that AgI arrives to the targeted clouds, as indicated by significantly higher EF_{Ag} values there compared with the control station. We found significantly higher EF_{Ag} values in precipitations from mixed-phase clouds compared with precipitation from warm or fully glaciated clouds. This difference was observed only at the target stations and only for Ag (Fig. 1). The observation is consistent with the assertion that AgI contributes actively to the formation processes of precipitation in mixed-phase clouds, where ice nuclei concentrations can be rate determining in precipitation formation. This is also consistent with theoretical predictions about the activity of AgI in clouds.

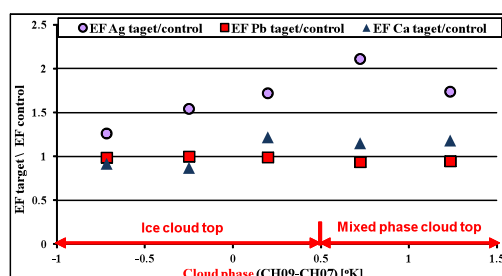


Figure 1: Ratios of EF_{Ag} , EF_{Ca} and EF_{Pb} between the target and the control station at different cloud phase intervals. Liquid clouds > 2 , icy clouds $\approx 0.5-0$, mixed-phase clouds $0.5 - 1.5$. Negative $BTD(CH09-CH07)$ values indicate convective clouds.

Mineralogical and geochemical characteristics of clay deposits from Northwest Gonabad District of clay Deposit (East Iran)

S. ZIRJANIZADEH^{1*}, M. H. KARIMPOUR¹
AND KH. EBRAHIMI¹

¹Department of geology, Faculty of sciences, Mashhad university, Iran.

(*correspondence: Zirjani38@yahoo.com)

Kaolin deposits, situated approximately northwest of Gonabad (east Iran), have been formed by the intrusion of hydrothermal fluids from granite dike and alteration of rhyolite, dacite and rhyodacite related to the Eocene volcanism [1]. Fine clay deposits have been located in this area. The area is covered by the mikaschist, dacite, rhyolite, trachiandesite, lithic tuff and acidic tuff rocks.

The mineralogical compositions are dominated by quartz, kaolinite, dickite, illite, baidelite and minor phases include chlorite, albite, hematite, montmorillonite, pyrite and gypsum. We analyzed for mineralogical and chemical composition, including the rare earth element contents.

Whole rock chemistry shows that samples rich in SiO₂ and Al₂O₃. Enrichment of Sr in altered and partially altered rocks relative to fresh volcanic-rock samples demonstrates retention of Sr and depletion of Rb, Ba, Ca, and K during hydrothermal alteration of sanidine and plagioclase within the volcanic units. The chondrite-normalized Rare earth element patterns of the clay deposits show LREE enrichments ((La/Lu)_{cn} = 6.75 to 57.74) and a negative Eu anomaly. The negative Eu anomaly suggests the alteration of feldspar by hydrothermal fluids [2].

The mineralogical composition, REE contents, main elements discrimination diagram and elemental ratios in these deposits suggest a provenance mainly felsic rocks and also, a high amount of weathering has occurred in Kaolin's source.

[1] Karimpour, MH, Saadat, S., 1384, Report of kaolin deposits in east Iran, 34 pages. [2] Nyakairu G W A, Koeberl C, Kurzweil H (2001) *Geochemical Journal* 35(4): 245.

Anorthosite dikes from Cyprus: Phase relations in the system CaAl₂Si₂O₈ – CaMgSi₂O₆ – Mg₂SiO₄ at 5 Wt.% H₂O

AURELIA ZIRNER¹, CHRIS BALLHAUS¹,
CARSTEN MÜNKER^{1,2} AND CHRISTIAN MARIEN²

¹Universität Bonn, Germany (zirner.aurelia@googlemail.com)

²Universität zu Köln, Germany (c.muenker@uni-koeln.de)

Massive anorthosite dikes are documented for the first time from the Limassol Forest Complex (LFC) of Cyprus, a deformed equivalent of the Troodos ultramafic massif. Both the Troodos and LFC complexes are part of a Cretaceous oceanic crust that formed within a backarc basin 90 Ma ago and was obducted during late Miocene.

From crosscutting relations with the sheeted dike complex, it follows that the anorthosites belong to one of the latest magmatic events on Cyprus. In hand specimen, the rocks appear massive and unaltered, although in thin section magmatic Pl (An₉₃) is partially replaced by Zo. Where magmatic textures are preserved, Pl forms cm-sized, acicular, radially arranged crystal aggregates reminiscent of spinifex textures.

The origin of these anorthosites remains poorly understood. Even though they occur as intrusive dikes, it is evident they cannot represent liquid compositions, at least under dry conditions. Whole-sale melting of a pure An₉₃ would require temperatures in excess of 1450 °C, which is a quite unrealistic temperature of the modern Earth's crust.

We are exploring experimentally if such lithologies can be generated by medium-pressure fractional crystallisation of hydrous basaltic melts followed by decompression-degassing. High p_{H₂O} stabilizes Ol and Spl but tends to suppress Pl, hence may allow the An-component to be accumulated in late-stage melts. Hydrous melts do occur on Cyprus, in form of high-Ca boninites with ~ 5 wt.% H₂O. Experiments are being performed in the Ol-Cpx-Pl-H₂O system, with Ol (Fo₉₅), Pl (An₉₃), and Cpx (Di₉₅) separates as starting materials. The separates are ground, mixed in the desired proportions, then equilibrated with 4 wt.% H₂O at 0.5 GPa total pressure from 1000 to 1300 °C in a piston-cylinder press. Aim is to delineate the An saturation field in the Ol-Cpx-Pl-H₂O system, and assess to what extent Pl can be suppressed as a liquidus phase in a basalt fractionating under hydrous conditions.

Sulphur driven denitrification dominates N-removal in the water column of Lake Lugano

J. ZOPFI¹, C. B. WENK¹, DORA SCHWEIGHOFFER¹, J. BLEES¹, H. NIEMANN¹ AND M. F. LEHMANN¹

¹Department of Environmental Sciences, University of Basel, Basel Switzerland; (jakob.zopfi@unibas.ch)

Besides organotrophic denitrification, alternative pathways, such as anaerobic ammonium oxidation (anammox) or sulphide-dependent denitrification are potentially important for the removal of fixed nitrogen from lakes. We identified the dominant N₂ forming processes in the permanently stratified northern basin of Lake Lugano (Switzerland) using ¹⁵N labelling experiments, molecular and cultivation based microbiological approaches.

Potential rate measurements suggest that anammox can contribute up to 30% to total N₂ formation but denitrification remained the dominant process at all depths. Additional incubation experiments with potential substrates for denitrifying bacteria identified sulphide and thiosulphate as important substrates [1]. Enrichment cultures of sulphide dependent nitrate-reducing bacteria were established to determine the products of sulphur and nitrogen transformations, respectively, and for molecular characterisation.

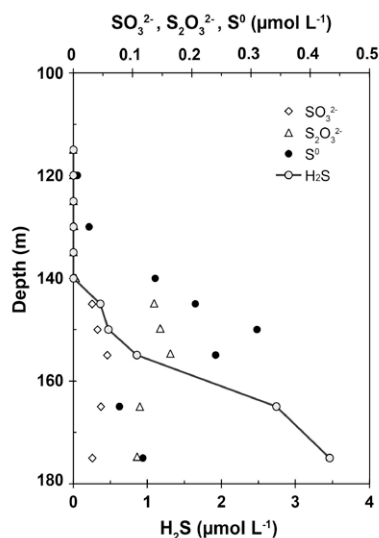


Figure 1: Concentrations of sulphide and sulphur intermediates at the RTZ in the stratified deep northern basin of Lake Lugano

Our study highlights that despite of the mesotrophic nature of the lake and the very low concentrations of sulphur species (Figure 1), water column denitrification is mainly driven by sulphur compounds rather than organic matter.

[1] Wenk *et al.* (2013) *Limnol. Oceanogr.* **58**, 1–12.

Cs and Sr mass transfer constrained via ion beam analysis

B. ZOU¹, T. OHE², G. GRIME³ AND R. WOGELIUS^{1*}

¹Williamson Research Centre, University of Manchester, M13 9PL, UK (*roy.wogelius@manchester.ac.uk)

²Tokai University, 259-1292, Japan ³University of Surrey Ion Beam Centre, GU2 7XH, UK

Micro-Reactor Simulated-Channel (MRSC) methods have been developed to rapidly determine mass transfer coefficients of intact low-permeability rock samples [1,2]. The design uses a thin fluid channel in the centre of the solid system which increases reaction rates due to a high surface area to liquid volume ratio. This enables fast measurements using only small reactor volumes. The MRSC consists of two injection syringe pumps, a reaction unit, an auto sampler, and a drainage tank. Unlike the conventional column method, an intact hard rock sample also produces flat surfaces for direct chemical analysis. ⁹⁰Sr and ¹³⁷Cs isotopes are both of great concern in disposal scenarios, with half-lives of approximately 30 years. In the MRSC experiments presented here, aqueous fluids with dissolved Sr and Cs have been pumped through simulated fractures at constant rates. Breakthrough curves were constructed by time resolved analysis of the effluent solution until steady state was observed. Differences between inlet and outlet concentrations are caused by two dominant processes; 1) diffusion into grain boundaries, micropores, and microfractures, and 2) sorption from the simulated fracture onto mineral surfaces. Mass difference is much higher than would be predicted from surface adsorption, and hence it is concluded that appreciable Sr and Cs has diffused into grain boundaries. In order to further constrain the tracer inventory, an analytical regimen was developed using ion beam techniques. This allowed us to fully characterise the reacted surfaces and to carry out depth-profiling. In particular, we designed these measurements to take advantage of the extremely low background radiation levels at the Sr and Cs K α energies in particle induced X-ray emission (PIXE) analysis in order to accurately quantify Sr and Cs [3]. In addition, the depth profiling capability of Rutherford backscattering spectrometry (RBS) is able to non-destructively constrain diffusion profiles at concentrations down to a few parts per million from areas 1 μ m in diameter. Results of these provide critical constraints on mass transfer parameters produced from MRSC experiments.

[1] Ohe *et al.*, (2012) *Min. Mag.* **76**, 3203–3215. [2] Okuyama *et al.*, (2008). *App. Geochem.* **23**, 2130–2136. [3] Wogelius *et al.* (1992) *Geochim. Cosmochim. Acta*, **56**, 319–334.

Concentration and isotopic analysis of soil gas N₂O in a Japanese tea field

YUN ZOU^{1*}, YUHEI HIRONO², YOSUKE YANAI², SHOHEI HATTORI³, SAKAE TOYODA⁴ AND NAOHIRO YOSHIDA³

¹Department of Environmental Science and Technology, Tokyo Institute of Technology, Japan (*correspondence: zou.y.aa@m.titech.ac.jp)

²NARO Institute of Vegetable and Tea Science, Japan (hirono@affrc.go.jp, yosuke@affrc.go.jp)

³Department of Environmental Chemistry and Engineering, Tokyo Institute of Technology, Japan (hattori.s.ab@m.titech.ac.jp, yoshida.n.aa@m.titech.ac.jp)

⁴Department of Environmental Science and Technology, Tokyo Institute of Technology, Japan (toyoda.s.aa@m.titech.ac.jp)

N₂O is an important trace gas that causes global warming and is indirectly related to destruction of stratospheric ozone layer. Fields planted with tea (*Camellia sinensis*) in Japan have a high potential to emit large amount of N₂O because of the highest level of N fertilizer application. In this study, we focus on the processes leading to high N₂O production in an experimental tea field in Shizuoka, Japan for better arranging N₂O mitigation strategy.

Soil gas samples were collected at four depths in two plots (Plots I and II) at 3 to 7-day interval from May to July, 2012 for concentration and isotopic analysis of N₂O. Surface soils (0-20 cm) were also collected for the analysis of other N-compounds.

Three peaks of N₂O concentration were observed corresponding to fertilization on 8 June and 5 July 2012. Each peak was found after heavy precipitation and a rise in air temperature above 20°C. The site preference of N₂O (SP, the difference in ¹⁵N/¹⁴N ratio between central (α) and terminal (β) N in ^δN-NO) ranged from 0.8‰ to 11.1‰ at the N₂O concentration peaks, suggesting greater (64% to 95%) contribution of bacterial nitrite (NO₂⁻) reduction than hydroxylamine (NH₂OH) oxidation or fungal denitrification. However, on one occasion (21 June at 35 cm depth of Plot I) N₂O had relatively high SP value (18.1‰), indicating an increase in production rate of NH₂OH oxidation or fungal denitrification relative to bacterial NO₂⁻ reduction.

Overall, N₂O in Japanese tea field was mainly produced by bacterial NO₂⁻ reduction under the effects of fertilization and precipitation in warmer (above 20°C) condition.

Clay mineral argon release during frictional shear experiments – Implications for brittle fault dating

H. ZWINGMANN^{1*}, S.A.M. DEN HARTOG² AND A. TODD¹

¹CSIRO ESRE, Bentley, WA 6102, Australia (*correspondance: horst.zwingmann@csiro.au; andrew.todd@csiro.au)

²Department of Earth Sciences, Utrecht University, 3508 TA Utrecht, Netherlands (s.denhartog@uu.nl)

Brittle fault zones comprise synkinematic or authigenic clay minerals such as illite, which can be dated by conventional K-Ar or Ar-Ar dating using micro-encapsulation (Zwingmann *et al.*, 2010). A pre-requirement for dating authigenic fault illite invokes no inheritance of radiogenic Ar.

The retention of Ar in fine grained clay minerals such as illite, occurring in clay rich fault gouge zones, is difficult to measure in nature. Den Hartog *et al.* (2012) describe friction experiments on fine grained mixtures of illite and quartz, performed with the aim of determining the frictional properties and slip stability under (near) in situ subduction megathrust conditions, i.e. at an effective normal stress of 170 MPa, a pore fluid pressure of 100 MPa at 150-500°C and sliding velocities relevant to earthquake nucleation (1-100 μm/s). These experiments allow investigation of Ar isotope retention and diffusion aspects in artificial gouge samples. We present preliminary conventional K-Ar age data on four artificially generated illite gouge samples, obtained from frictional shear experiments ranging from 150 to 450°C under the same pressure regime.

The original Rochester shale yields a Silurian age of 421.4 ± 8.4 Ma as described by Folk (1962). Low temperature (150 °C) frictional shearing experiments reduce the age of the artificial gouge to 218.3 ± 5.0 Ma, still containing more than 70% of radiogenic ⁴⁰Ar. Ar diffusion modeling using a <2 micron clay fraction size indicates negligible diffusion aspects at a temperature of 150 °C. The age data suggests that the frictional shearing of clay gouge affects the clay microstructures and releases radiogenic Ar caused by processes reported in Den Hartog (2012). The 250, 350 and 450°C experiments yield artificial illite gouge ages of 155.0 ± 3.1 Ma, 139.5 ± 2.9 Ma and 74.7 ± 1.5 Ma, respectively. Argon diffusion modeling indicates that diffusion starts to affect the clay mineral gouge ages from 300°C. Further studies are in progress, investigating clay gouge noble gas retention and effects, to constrain timing of fault gouge reactivation in the seismogenic zone.

[1] Den Hartog *et al.* (2012) *EPSL* **353-354**, 240-252 [2] Folk (1962) *J. Sediment Petrol.* **32**, 539-578. [3] Zwingmann *et al.* (2010) *Geology* **38**, 487-490

A	Adaktylou, I.J.	1798	Aguado, R.	1918	Alastuey, A.	2014
Aaberg, I.	Adam, Christian.....	1530	Ague, J.	2012	Albalat, E.	567
Aagaard, P.	Adam, Claudia.....	1256	Àgueda, A.	932	569
Aalto, R.E.	Adam, J.	555	Aguilar-Carrillo, J.	561	Albanese, S.	567
Abad, I.	1636	Aguilera, Á.	999	888
Abadie, C.	2101	1890	920
Abart, R.	2367	Aguñiga, S.	2132	991
.....	Adam, N.	556	562	2111
.....	Adam, V.	556	Aguirre, L.	666	Albani, S.	568
.....	Adams, D.	796	Ahadnejad, V.	562	Albarède, F.	568
.....	1542	Ahm, A.	563	569
.....	Adams, T.J.	1084	Ahmad, F.	1853	749
Abbott, A.	Adamson, D.	608	2444	Albert, P.	569
.....	Adatte, T.	669	Ahmad, M.	2433	1002
Abdel Aal, G.	Adekoya, J.A.	2342	Ahmad, S.	563	2340
Abdelmoula, M.	Adena, K.	557	Ahmadian, J.	961	Albokari, M.	570
Abdelouas, A.	Ader, M.	557	1267	Albrecht, M.	570
Abdesselam, A.	799	1425	977
Abdurrachman, M.	1561	Ahmed, A.H.	606	Albrecht, N.	571
Abe, K.	2130	Ahmed, E.	564	Albuquerque, A.L.	985
Abe, M.	2325	Ahmed, K.M.	1455	1737
Abe, N.	2327	1756	Albuquerque, T.	600
.....	Adkins, J.F.	794	Ahmed, N.	564	Alcorn, C.	2352
.....	817	Ahonen, L.	1457	Aldanmaz, E.	1814
.....	1100	Aichner, B.	1579	Alekhin, Y.	1801
.....	2018	Aiello, I.	1734	Alesci, G.	571
.....	2052	2166	Alessandro, A.	1790
Abelson, M.	Adlakha, E.	558	Airo, A.	1316	Alessi, D.S.	572
Abernethy, F.	Adlassnig, W.	1950	Aiuppa, A.	922	693
Abi-Ghanem, R.	Adler, M.	558	1944	1377
Abollino, O.	600	Aiyesanmi, F.	2342	2278
Abouchami, W.	Adra, A.	1792	Akagi, T.	2554	Alexander, B.	2143
.....	1792	Akahori, K.	2540	Alexander, C.	572
.....	Adriaens, R.	2082	Akçar, N.	2153	Alexander, D.	1496
.....	Aeschbach-Hertig, W.	580	Akçe, M.A.	565	Alexandre, P.	573
Abraham, K.	1111	974	Alexandrov, V.	861
Abramov, O.	1412	Akhtara, S.	2447	Alfayfi, Y.	573
.....	2066	Akinfiyev, N.	1999	Alferyeva, Y.	574
Abreu, J.	2161	2209	Alfredsson, H.	1178
Abu Zeid, N.	Aeschbacher, M.	2126	Akis, I.	614	Algeo, T.	1293
Accaino, F.	Afanasiev, V.	2226	Akizawa, N.	565	Alhashmi, Z.	574
Acero, P.	Affatato, A.	1849	Akmaz, R.M.	2115	Ali, A.	575
Achilles, C.N.	Affek, H.P.	2558	2178	1368
Achouak, W.	2574	Akob, D.	697	Ali Abu El-Rus, M.	575
.....	Afonin, I.	2597	1518	Alías, G.	2351
Achtenhagen, J.	Afonso, J.C.	559	Al, T.	843	Alifirova, T.A.	576
Achterberg, E.P.	1220	2136	Alkan, H.	2219
.....	Agafonov, L.	2106	al Ghabban, A.N.	829	Allan, J.	746
.....	Agangi, A.	560	Al Mukaimi, M.	579	Allan, M.	577
.....	Agee, C.	2391	Al Najem, S.	580	Allard, B.	1210
Aciego, S.	Ageeva, O.	560	1111	Allard, P.	577
.....	Agnon, A.	2557	1360	578
.....	Agostini, F.	561	Al Taky, M.	1269	797
.....	Agostini, S.	819	Al-Balushi, S.	691	Allard, T.	808
.....	873	Al-Kaabi, F.	576	Allègre, C.	900
.....	1035	Al-Saidi, Y.	605	1750
.....	1266	Al-Saleh, A.	581	Allen, Charlotte.	1691
.....	1656	Alabarse, F.	908	2212
Ackerman, L.	1712	Alain, K.	890	Allen, Claire.	1974
.....	Agrawal, A.	2431	Alakangas, Lena	566	Allen, G.	1215
.....	Agrinier, P.	1694	1950	Allen, N.	1930
Acosta-Vigil, A.	2252	Alakangas, Linda	566	Allen-King, R.	578
.....		Alam, M.	1163	Aller, J.	1483
Adabi, M.H.	

Aller, R.....	1083	Amils, R.	999	Andersson, M.p.	883	Anum, S.	2150
Allin, S.	579	1880	938	Aoi, Y.	601
Allison, M.	2084	1890	1270	1121
Alloway, B.	943	2004	1886	Aoki, S.	601
Almeev, R.	1119	2124	1890	2202
.....	2393	Amini, S.	1049	Andersson, Madelen	1537	Aoki, T.....	1825
Almeida, S.....	2384	Ammann, M.	2438	2111	Aono, T.....	2538
Almogi-Labin, A.....	2258	Ammannati, E.	587	2374	Aouizerats, B.	2393
Aloisi, G.....	1290	912	Andersson, Martin	595	Aoyagi, Y.....	1758
.....	1510	Ammawy, M.	1279	2117	Aoyama, M.....	1522
Alonso, R.	1648	Amoako, F.Y.....	588	Andersson, P.....	874	Aoyama, S.....	602
Alonso, U.	580	Amoo, I.	2342	Andrade, C.....	928	Apel, W.....	1564
.....	1716	Amor, M.	588	1788	Apollaro, C.	926
.....	1771	Amorim, N.	1737	Andraut, D.....	595	2409
Alp, E.E.....	948	Amos, R.	1375	751	Appel, P.	901
.....	2085	Amouroux, D.....	1051	1787	Appelo, T.....	602
.....	2199	Amran, I.A.	2491	1953	Applegarth, L.....	2352
Alpermann, T.	581	Amron, T.	1269	André, Laurent.....	1552	Apukhtina, O.B.....	603
Alpers, C.	813	Amrose, S.	2395	André, Luc	553	Aqimidze, K.....	1888
Alpert, P.	1483	Amthauer, G.	1734	969	Aqleh, S.	603
Alphandéry, E.	588	Amyago, D.	2383	Andre-Mayer, A-S.....	1583	Aquilina, A.	604
Alsop, E.....	757	An, Y.M.	1384	Andreae, M.O.	596	Aquilina, L.....	729
.....	2033	Anagnostou, E.	589	1394	Aradhi, K.K.	604
Alt, J.....	1694	2265	1523	Aradi, L.E.	605
Alt-Epping, P.	582	Anand, M.....	589	2268	1618
.....	984	736	2477	1934
Altabet, M.	1209	2314	Andreani, M.....	958	2410
.....	2050	Anand, R.	2328	1961	Aradottir, E.	1178
Altaratz, O.....	1577	Anantha Murthy, K.S.	590	Andresen, A.....	629	2277
Altherr, R.	2318	Anason, Angela Maria	1352	Andresen, G.....	1213	Arae, H.....	1769
.....	2373	Anason, Angela Maria	1684	Andrews, B.....	1219	Arafin, S.....	605
Altmaier, M.....	1017	1834	Andronicos, C.....	1313	Aragón, E.....	2015
.....	2079	Anbar, A.	590	Andujar, J.M.....	1206	Arai, S.	565
Altunsoy, M.	582	853	Anesio, A.M.	1658	606
.....	1906	1198	Anfilogov, V.....	1355	1362
Alvarez, F.....	583	1293	Angel, R.J.....	1840	1484
.....	1950	Anchukaitis, K.....	591	Angeli, F.....	1968	1663
Álvarez-Iglesias, P.....	2095	Ancochea, E.	1194	Angelopoulos, G.....	1136	1772
Alves, A.	583	Anczkiewicz, R.	591	Angyal, J.....	1585	1779
.....	1376	Andeer, P.	1255	Anjos, O.....	596	1811
Amachi, S.....	584	1560	Anma, R.....	1896	2304
.....	1886	Andersen, A.....	592	Annappurna, B.....	597	2305
Amador, E.....	584	Andersen, M.....	592	Annen, C.....	597	2539
Amador-García, A.....	1638	1037	825	2566
.....	2123	1112	2164	Arai, T.....	606
Amalberti, J.....	585	1286	Annesi-Maesano, I.....	598	Arakawa, M.	2470
Amann, M.	1477	1296	Annesley, I.....	1930	Arakawa, T.	2198
Amano, Y.....	1821	Andersen, N.....	1548	Anoshin, G.....	728	Aral, D.	1814
Ambade, B.	585	Andersen, Tom	892	Anoshkina, Y.....	598	Aramendia, M.....	2396
Amelin, Y.....	586	1742	Anquetil, C.	1555	Arana, A.....	620
.....	747	Andersen, Torgeir	1240	Ansdell, K.....	1930	Arancibia, G.....	2122
.....	909	Anderson, D.L.....	593	Ansems, N.	599	Aranovich, L.....	607
.....	957	Anderson, J.....	593	Ansoborlo, E.....	2406	Aransiola, O.....	1392
.....	1349	Anderson, R.....	594	Antelo, J.....	599	Araoka, D.....	607
.....	1721	1369	1086	Araújo, L.....	1587
Amelung, W.....	586	2050	Antler, G.	600	Aravena, R.	608
Amemiya, D.....	2361	Anderson, S.....	1715	633	Arbour, T.	987
Amen, J.	1722	Anderson, T.....	1722	1556	Arce, F.	599
Amend, J.P.....	1547	Anderson-Smith, L.....	673	Antonangeli, D.	1787	1086
.....	1997	Andersson, J.....	1956	2211	Archer, Corey	608
Ames, D.	587	Andersson, K.....	594	Antonelli, M.	805	2389
.....	1665	Antonova, I.....	727	2483
.....	2472	Antunes, I.	600	Archer, Cristina.....	609

Archilla, J.	1013	Arsouze, T.	1537	Auffan, M.	664	Bachet, M.	681
Arcilla, C.	609	Artaxo, P.	620	2320	Bachmann, O.	1016
Arculus, R.J.	610	Artells, E.	2320	Aughterson, R.	1650	1229
.....	684	Artemieva, I.	620	2072	2100
.....	1382	870	Augland, L.E.	629	Baciu, C.	1472
.....	1655	Artioli, G.	621	Augustin, C.	630	Backnäs, S.	638
.....	1835	Arvestål, E.	874	Augustin, N.	2393	Bäckström, M.	2134
.....	2094	Arvidson, R.S.	621	Aulbach, S.	630	Bacon, A.	2058
.....	2338	1087	Aulinas, M.	631	Bacon, C.G.D.	639
Ardau, C.	610	1657	1146	Badanina, I.	639
.....	949	1664	1174	1676
Ardelt, D.	657	Arzilli, F.	622	Ault, R.	1819	Bader, T.	1011
Ardit, M.	611	1673	Aumont, B.	764	Badger, M.	1918
Ardizzone, M.	2416	Asa-Awuku, A.	1175	Auro, M.	2273	Badica, C.	640
Areias, M.	611	Asakawa, S.	1427	Austin, R.	1945	911
Arendt, C.	612	Asano, K.	2302	Austin-Giddings, W.	1927	Badireddy, A.R.	1591
.....	2263	Asano, T.	1821	2027	Badot, P-M.	2260
Arenholz, E.	1941	Aschchepkov, I.	1866	Austrheim, H.	1715	Badro, J.	640
Arey, J.S.	612	Ascher, J.	622	1800	1998
Argles, T.	1796	Ashchepkov, I.	623	2007	2142
Argyaki, A.	613	Ashcroft, H.	623	2377	2211
.....	1459	Ashley, K.	624	Auzende, A-L.	1038	Baer, D.	641
Arias, J.L.	2346	2474	1114	Baeva, A.	790
Arias, R.	932	Ashwal, L.	802	Avanzinelli, R.	587	Baeyens, B.	1687
Arienzo, I.	1692	Asimow, P.D.	624	631	1689
Arienzo, M.	613	673	837	2236
.....	1814	Askhabov, A.	625	912	Baeza, A.	1617
.....	1992	Aslan, Z.	1430	Avery, B.	1456	Baeza-Romero, M.T.	1084
Ariga, D.	614	Asmerom, Y.	625	Avery, G.	2498	Bagard, M-L.	641
Arik, F.	614	Asochakova, E.	626	Aviado, K.B.	632	Bagas, L.	1903
Arima, M.	615	Asogan, D.	626	Avice, G.	632	Bagatin, R.	1699
.....	1436	Assamoi, E.	1617	Ávila, C.Á.	2319	Bağci, U.	816
Arkin, A.P.	826	Assayag, N.	1965	Avino, R.	1958	2178
Arletti, R.	1168	Assbichler, D.	627	Avrahamov, N.	633	Baggenstos, D.	790
.....	1559	Asseva, A.	1866	Avramenko, I.	633	Bai, B.	930
Arlinghaus, H.F.	2065	Asta, M.	1869	717	Bai, G.	2591
Armanious, A.	615	Astilleros, J.M.	627	Axelsson, G.	2277	Baik, M.H.	642
Armbruster, T.	1160	1853	Axelsson, E.	634	Bailey, D.	917
Armienti, P.	616	2081	Ay, F.	2537	Bailey, I.	2486
.....	616	2123	Aydin, F.	634	Bailey, J.	642
Armoza-Zvuloni, R.	2187	Aston, J.	1564	Aydin, N.	635	1405
Armstrong, J.	755	Åström, M.	566	Ayora, C.	554	Bailey, K.	1347
Armstrong, Richard.	1178	691	1143	Bain, P.	1546
Armstrong, Robin.	1001	1008	2346	Bajda, T.	2295
Armstrong McKay, D.I.	617	1709	Ayral, A.	1094	2366
Armytage, R.	617	2568	Ayrault, S.	2091	Bajnoczi, B.	658
Arnarsson, M.	1178	Atekwana, Eliot.	1100	Ayris, P.	1708	Bajo, K-I.	643
Arndt, Nicholas.	1016	Atekwana, Estella.	628	Ayuso, R.	920	Baken, S.	643
.....	1564	1100	Azaroual, M.	1552	Baker, Alex.	1454
.....	2141	Athon, M.	2524	Azer, M.	635	Baker, Alexander.	644
.....	2232	Atkins, A.	628	Azmy, K.	1065	Baker, Andy.	1385
Arndt, Nicholas.	618	Atlas, E.	2139			Baker, B.	1557
.....	2343	Atroschenko, F.	1453	B		Baker, D.R.	809
Arndt, S.	956	Atteia, O.	2173	Baars, O.	636	Baker, E.	1655
Arneth, A.	618	Aubert, M.	1226	Babcsanyi, I.	636	Baker, J.	644
Arnold, G.L.	619	Aubinet, M.	2420	Babchuk, M.	637	916
Arnold, T.	1127	Auclair, D.	682	Babinski, M.	637	925
Arnórsson, S.	1414	Aucour, A-M.	629	Babkin, I.	1557	Baker, L.	645
Arnosti, C.	619	Audétat, A.	1521	Bacak, A.	746	Baker, Michael.	645
.....	1342	2423	Bach, W.	638	Baker, Michael B.	2269
Arranz, E.	2371	Audifred, A.	830	1895	Balakrishnan, S.	1473
Arrio, M-A.	836	Audigane, P.	2353	2476	Balan, E.	715
.....	1038	Aufdenkampe, A.	2563	Bachelet, C.	1157	1972

Balco, G.	2208	Banik, N.L.	1689	Bargar, J.R.	572	Bartley, J.	904
.....	2352	Banner, J.	1761	693	1181
Balcone-Boissard, H.	646	Banothu, D.	649	734	Bartmiński, P.	1660
.....	750	Bantan, R.	2393	1377	Bartoli, O.	657
Baldermann, A.	646	Banuelos, J.L.	1831	1406	663
.....	1845	Banwart, S.	676	1499	Bartolini, G.	2242
Baldini, J.	644	737	1946	Barton, L.	664
Baldoncini, M.	1224	1108	2214	Bartov, G.	978
Baldwin, D.	1449	1258	2275	Barvencik, S.	2490
Balen, D.	647	2038	2278	Basaham, A.	2393
Balitsky, V.	785	2176	2400	Basak, C.	1913
Ball, R.	1215	Bao, D.	650	2505	Basheleishvili, L.	664
Ball, S.M.	1084	1388	Barger, W.	657	Baskaran, M.	655
Balland-Bolou-Bi, C.	647	Bao, H.	650	Barich, A.	657	665
Ballentine, C.J.	648	1274	Baricza, A.	658	1318
.....	703	Bao, P.	2279	Barker, A.K.	960	Bass, J.	2590
.....	776	Bao, Zhengyu	1844	Barker, I.	946	Basso, E.	1174
.....	863	Bao, Zhiwei	651	1795	Bast, R.	665
.....	896	Baptiste, V.	2341	Barker, P.	2225	Bastias, J.	666
.....	1072	Baqués, V.	2351	Barker Jørgensen, B.	1342	Bastrakov, E.	666
.....	1312	Baradello, L.	1849	Barkleit, A.	2109	2209
.....	1385	Barandas, A.	651	Barles, S.	658	Basu, A.	780
.....	1393	Baranova, A.	871	Barley, M.	2435	Basu, S.	667
.....	1484	Baranovskaya, N.	652	Barling, J.	659	1404
.....	2105	652	918	Batanova, V.	667
.....	2195	Baranyi, C.	1342	2548	683
.....	2285	Barao, A.L.	2082	Barnes, C.	2499	2232
.....	2467	Baratoux, D.	653	Barnes, James D.	659	Batelaan, O.	2082
.....	2613	1878	1617	Bateman, K.	1082
Ballèvre, M.	844	Barbagli, A.	653	Barnes, Jessica	589	Bates, S.M.	1252
Ballhaus, C.	1125	Barbante, C.	1126	Barnes, Sarah-Jane	2434	Batet, Ò.	932
.....	1283	Barbecot, F.	1094	Barnes, Stephen J.	618	Batsaikhan, B.	668
.....	1423	Barber, A.	654	660	Battaglia, S.	1947
.....	1447	654	835	Battaglini, R.	1856
.....	1469	Barberi, F.	2067	1732	Baturin, G.	1503
.....	2180	Barbero, L.	655	2434	Bau, M.	928
.....	2621	Barbier, G.	890	Barnetche, D.	1792	1743
Ballouard, C.	1991	Barbieri, E.	655	Baron, S.	660	1987
Balta, B.	2372	Barboni, M.	1445	842	2158
Baltensperger, U.	832	Barbosa, H.	620	Baronas, J.J.	661	2323
Baltog, I.	911	Barbosa, J.A.	2210	Baroni, C.	714	2415
Balzaretti, N.M.	786	Barbosa, N.	2319	Barou, F.	1618	Baublys, K.	1187
.....	908	Barca, D.	2413	Barovich, K.	1939	Bauer, J.D.	668
.....	1828	Barceló, D.	661	Barra, F.	661	Bauer, Katrin.	2154
Balzer, I.	1847	Barclay, J.	1976	2042	Bauer, Kerstin	669
Bambi, A.	814	Bard, E.	833	Barras, C.	1827	Bauguitte, S.	1644
Banakar, V.	2502	2125	Barrat, J-A.	961	Baum, A.	989
Bancon-Montigny, C.	773	Bardelli, F.	1278	1998	Baumann, T.	669
Band, A.	648	2502	2620	1520
Bandfield, J.	584	Barden, H.	656	Barré, P.	1575	Baumberger, T.	670
Banerjee, N.	575	1029	Barrese, E.	840	Baumgartner, L.P.	670
.....	673	Bardi, F.	1859	Barriga, F.J.A.S.	929	724
.....	1368	Bardoux, G.	1575	Barrott, J.	662	753
Banerjee, Y.	649	Barelko, V.	656	Barrow, M.	1216	970
Baneschi, I.	744	Barrows, T.T.	1685	1095
.....	873	Barry, P.	662	2164
.....	911	Barry, T.	648	2175
.....	1010	663	Baumgartner, P.O.	1970
.....	1829	924	Baur, T.	754
Banfield, J.f.	987	2193	Bavec, Š.	671
Banfield, Jill	2440	Barth, M.	1995	Baxter, E.	671
Bange, H.W.	2579	Barthelemy, K.	1227	Bayanova, Tamara	672
Bangs, N.	1480

Bayanova, Tatyana	1159	Beier, C.....	678	Bénard, A.....	684	Berezhnaya, E.....	1013
.....	1757	761	Bender, J.....	1252	2063
Bayarjagal, L.....	668	1154	Bender, K.S.....	2443	Berg, Jasmine.....	688
Baykal, A.....	1908	2038	Bendő, Z.....	1916	Berg, John K.....	689
Bayon, G.....	1110	Beig, G.....	1688	Benedetti, L.....	2106	Berg, Madeleine.....	689
.....	1537	Beinlich, A.....	1715	Benedetti, M.F.....	685	Berg, Michael.....	717
.....	1777	Beirne, E.....	1401	737	2432
Bazhenova, E.....	1060	Bekaroglu, E.....	1048	896	Berg, S.E.....	690
Bazin, L.....	672	Bekker, A.....	679	980	2357
Baziotis, I.....	673	799	1759	Bergantz, G.....	2100
Bazzocchi, F.....	1174	1259	2044	Berger, A.....	1377
Bearcock, J.....	713	1315	2050	Berger, D.....	1743
Beauchamp, B.....	1482	1929	2585	Berger, Jeffrey.....	2158
Beaufort, D.....	1114	2290	Benedetti, R.....	966	Berger, Julia.....	1806
.....	2416	2586	Benedicto, A.....	1143	Berger, Julien.....	690
Beaver, C.....	628	Belando, M.D.....	1697	1771	Berger, T.....	691
Bebout, G.....	673	Belchenko, L.....	2209	Bénézeth, P.....	681	Berggren Kleja, D.....	1235
.....	906	Belien, I.....	837	685	Bergholm, J.....	2216
Beccaluva, L.....	2185	2103	2256	Berglund, S.....	2355
Bechtel, A.....	2026	Belissont, R.....	679	Bengtson, S.....	874	Bergmann, K.....	691
Beck, M.....	674	Belkasem, E.....	680	1366	Bergmann, U.....	656
Becker, Hans-Werner.....	1577	Bell, A.....	680	1843	1029
Becker, Harry.....	674	2215	Benimoff, A.....	686	Bergstrom, R.....	974
.....	1149	Bell, E.....	1342	Benisek, A.....	935	Berhanu, T.A.....	1747
.....	1311	Bellatreccia, F.....	1875	Benko, A.....	2431	Beridze, G.....	715
.....	1416	2018	Benner, S.....	686	Berkelhammer, M.....	1398
.....	1955	Bellefleur, A.....	681	Bennett, P.....	1404	Berkesi, M.....	1972
.....	2465	Bellenger, J-P.....	681	2131	Berman, E.....	641
Becker, K.G.....	840	Beller, H.....	1869	Bennett, V.....	687	Bermell, S.....	1110
Becker, M.....	675	2011	916	Bernabeu, A.....	2095
Becker, S.....	1213	Belliemi, G.....	809	1721	Bernard, D.....	1859
Becker, T.....	1968	1751	Benning, L.G.....	737	Bernard, S.....	692
Becker, U.....	675	2180	765	1597
.....	1078	Bellin, A.....	876	899	2034
.....	2439	Bellot, N.....	682	969	2049
.....	2451	1006	1658	Bernasconi, A.....	692
.....	2570	Bellucci, F.....	682	1732	Bernasconi, S.M.....	895
Becker, V.....	1850	Bellucci, P.....	1701	2076	1443
Beckett, J.....	1713	Belluso, E.....	840	2081	1759
Bedell, J-P.....	629	2416	2254	2408
Bedini, F.....	744	Belmino, I.....	2414	2255	Berndt, C.....	2259
Beerling, D.....	676	Belmont, P.....	2498	Benoit, Magali.....	1020	Berndt, J.....	1476
Begg, G.....	676	Belonoshko, A.....	2146	Benoit, Mathieu.....	972	Berner, U.....	1522
.....	1873	Belousov, I.....	683	1460	2327
Beghein, C.....	677	Belousova, E.....	639	Benslama, M.....	2581	Berner, Z.....	710
Beghin, J.....	577	683	Benson, S.M.....	687	Bernhardt, E.....	1645
.....	1380	727	Bensoussan, N.....	1048	2257
Begue, F.....	677	874	Benuzzi Mounaix, A.....	1237	Bernier, F.....	1377
.....	850	1001	Benvenuti, M.....	1789	Bernier-Latmani, R.....	572
Behn, M.....	678	1194	Benzerara, K.....	688	693
Behrends, T.....	599	1742	921	1377
.....	2398	1836	1135	2046
Behrens, H.....	989	1926	1597	2278
.....	1063	1943	1740	2464
.....	1179	Belova, D.....	684	1780	Berninger, U-N.....	693
.....	1770	Belshaw, N.....	659	Bercovici, D.....	2012	Berro, F.....	694
.....	2249	Beltrando, M.....	659	Berelson, W.M.....	661	Berry, A.J.....	694
.....	2410	2240	1268	1245
Behrens, S.....	1798	Belyanin, D.....	2608	1401	1253
Behzadi, M.....	2111	Belyatsky, B.....	1516	1706	2402
.....		1755	1728	2555
.....		1836	2000	Berryman, E.....	695
.....		Ben Maamar, S.....	890	Bereninger, N.....	1878		

Bertagnini, A.....	891	Bicego, M.....	1587	Biskos, G.....	746	Blazina, T.....	717
.....	935	1842	Bissig, T.....	709	2503
Berthold, C.....	1431	2246	Bisson, M.....	1208	Bleeker, W.....	841
Berthomieu, C.....	1780	Bickle, M.....	703	Bissonette, K.....	2352	1230
Bertics, V.....	2353	856	Biswas, A.....	710	Blees, J.H.....	718
Bertinetti, L.....	2223	942	Biswas, P.....	1389	1849
Bertolino, S.A.R.....	2456	1424	Bitencourt, M.D.F.....	710	2622
Bertran, E.....	695	1703	1095	Blessington, M.....	718
Bertrand, H.....	809	2613	Biwer, C.....	2275	Blichert-Toft, J.....	719
.....	809	Bicocchi, G.....	703	Bizi, M.....	1590	749
.....	1701	Biddanda, B.....	985	Bizimis, M.....	1953	752
.....	2180	Biddle, D.....	952	2499	784
Bessho, H.....	696	Biddle, J.....	1898	Bizzarro, M.....	644	841
Bestel, M.....	696	Bidzhova, L.....	704	711	1035
Betiollo, L.....	1819	Biegel, E.....	2219	732	1230
Beukes, N.J.....	928	Bielser, J.M.....	704	925	1253
.....	1047	Biester, H.....	671	936	1263
.....	2162	Bigalke, N.....	981	1315	2003
.....	2224	Bigorre, S.....	2272	1548	2244
.....	2497	Bijeljic, B.....	574	1633	Bligh, M.....	2437
Beulig, F.....	697	Bijma, J.....	705	1889	Bloch, E.....	1129
Beulke, S.....	1418	1838	1934	Blockley, S.....	2229
Bevilaqua, R.....	697	1987	2152	Blodau, C.....	719
Bey, I.....	2241	Bilal, E.....	1161	2227	1483
.....	2251	1352	2492	Bloethe, M.....	720
Beyer, A.....	698	Bilenker, L.....	680	Bjerg, E.....	1808	Bloise, A.....	840
Beyer, C.....	698	705	Bjerrum, C.J.....	1585	2409
.....	854	2215	2097	Blonder, B.....	720
Beyssac, O.....	699	Billard, P.....	2583	Björck, S.....	898	Blot, R.....	894
.....	1135	Billor, Z.....	1968	Björn, E.....	2491	Blöthe, M.....	1498
.....	1597	Billström, K.....	892	Black, B.....	711	Blowes, D.....	1375
Bezada, M.....	1591	Bindeman, I.....	706	Black, J.....	712	1711
Bezard, R.....	699	706	Black, S.....	1305	Bluhm, H.....	2207
Bezentakos, S.....	746	1008	2408	Blum, A.....	813
Beziat, D.....	1583	1234	Blackburn, T.....	712	1715
Bezzon, G.....	1224	1373	909	Blum, J.....	721
.....	2519	Binder, B.....	1431	Blackie, D.....	1659	Blum, W.E.H.....	2151
Bhandari, N.....	2273	Bindi, L.....	1313	Blackwell, N.....	713	Blumberger, J.....	771
Bhattacharyya, P.....	710	2251	Blaha, V.....	1509	Blundy, J.D.....	825
.....	1455	Bingen, B.....	1476	Blain, S.....	2387	1709
Bhatti, J.....	2488	2183	Blair, N.....	713	1789
Bhowmik, S.K.....	700	Biondi, F.....	707	Blake, D.F.....	1590	1907
Bi, L.....	700	Birck, J.-L.....	707	1794	2147
Bi, X.....	1652	1196	Blake, S.....	924	2220
Bi, Y.....	701	Bird, A.....	708	Blakowski, M.....	714	2315
Biagioni, C.....	1154	Bird, D.....	1142	Blanc, G.....	2276	Blunier, T.....	1062
.....	2412	1399	Blanc, P.....	714	2053
Bialek, J.....	1870	Bird, Laurence.....	1249	1129	Blunt, M.....	574
.....	1902	Bird, Lina.....	708	1552	Bluvshstein, N.....	2095
Bialik, O.M.....	701	Bireta, P.....	2041	Blanca Romero, A.....	715	Blythe, L.S.....	2357
Bian, C.....	2523	Birke, M.....	991	Blanchard, M.....	715	Bo, Y.....	1652
Bian, W.....	2596	2044	1792	Boates, B.....	735
Biancani, P.....	827	2045	1972	Boatta, F.....	721
Bianchi, D.....	702	Birkedal, H.....	709	Blanco, J.D.....	2255	Boaventura, G.....	1983
Bianchi, M.....	2606	1353	Blanpied, C.....	1380	Bobocioiu, E.....	722
Bianchi, T.....	2084	Birkholzer, J.....	2606	Blard, P-H.....	716	Bobrov, A.....	722
Bianchini, G.....	702	Birsa, L.....	911	860	2218
.....	1681	Biscaye, P.E.....	1285	Blaschek, M.....	1067	Bobrov, V.....	728
.....	2185	Bischoff, A.....	2086	Blasioli, S.....	1559	787
Bibikova, E.....	892	Bish, D.L.....	1794	Blättler, C.....	716	1587
Bibring, J-P.....	1878	Bishop, J.J.K.....	1462	Blaud, A.....	2038	1678
.....		Bishop, K.....	1563	Blazhennikova, I.....	633	1735
.....		Bishop, T.....	2365	717	Bobrowski, N.....	2505

Boc, A.	723	Bolarinwa, A.T.	1392	Boris, G.	2213	Botke, W.	748
Bock, M.	2181	Boles, J.R.	731	Borisenko, A.	1830	1319
Bockheim, J.	1799	Bolfan-Casanova, N.	732	Borisover, M.	740	Bouby, M.	1862
Bodinier, J-L.	1076	751	Borovička, J.	1518	Bouchaou, L.	1594
.....	2341	958	Borovinskays, O.	1232	Boucher, B.	748
Bodnar, R.J.	723	2068	Borovkov, N.	741	Bouchet, R.	749
.....	819	2417	Boroznovskaya, N.N.	741	Bouchez, J.	749
.....	999	Bolívar, J.P.	655	1835	967
.....	1050	Bollard, J.	732	Borras, E.	1084	1130
.....	1563	Bollinger, C.	1110	Borrego, C.M.	1634	2168
.....	1934	1408	Borrego, J.	1207	2429
.....	2255	Bolot, M.	733	Borrini, D.	2180	Boudens, R.	750
Bodner, R.	724	Bolotin, J.	1310	Borrok, D.	742	2043
Boehm, F.	724	Bolotov, I.	1677	2542	Boudon, G.	646
.....	1116	Bolou-Bi, E.B.	647	Bortnikov, N.	887	750
Boek, E.	2610	Bolton, E.	2012	Bory, A.	1537	Boudou, J-P.	557
Boekhout, F.	725	Böhlček, C.	635	Bosbach, D.	668	Bougoure, J.	1961
.....	1156	Bomou, B.	733	762	Bouhifd, A.	751
Boerenboom, T.	2134	Bonadiman, C.	1058	963	Bouhifd, M.A.	834
Boering, K.	725	1154	1084	Bouhlila, R.	1829
.....	2558	1164	1296	Bouikine, A.	2235
Boetius, A.	726	1165	1478	Bouillon, S.	1634
Boffa Ballaran, T.	844	Bonal, L.	734	2092	Boullemant, A.	1982
.....	1526	Bonardi, M.L.	2417	Bosc, O.	742	Bouloton, J.	988
.....	1916	Bonasoni, P.	2064	Bosch, D.	743	Boulvais, P.	751
Bogatko, S.	726	Bondarenko, G.	1898	1076	1991
Bogatyrev, L.	727	Bone, S.E.	734	1146	Boulyga, S.	789
Bogdanova, S.	727	2214	Boschero, V.	743	Bouman, C.	1495
Boger, S.	1214	Bonev, N.	906	Boschi, C.	744	1635
Bogina, M.	2188	Bonev, S.	735	1829	2355
Bogush, A.	728	Bonfanti, P.	1165	2424	2501
.....	1028	Bongiolo, E.	2319	Boschi, V.	744	Bouman, H.A.	780
.....	1587	Bonifacie, M.	735	Boschker, H.T.S.	1220	Bour, O.	729
Bogush, G.	1587	810	Bose, S.	1802	Bourassa, A.	2489
Bohaty, S.	1344	Böning, P.	736	Bosle, J.M.	745	Bourdon, B.	752
.....	2389	Bonini, M.	703	Bosse, V.	745	1091
Bohdalkova, L.	1863	Bonnand, P.	736	988	1230
Böhm, F.	1847	2002	2183	1254
.....	2427	Bonnet, J-Y.	2049	Bossioli, E.	746	1300
.....	2476	Bonneville, A.	685	Bostick, B.C.	746	1300
Bohrmann, G.	1613	Bonneville, S.	737	1756	2491
.....	2315	765	2285	Bourg, A.C.M.	752
Bohrson, W.	728	Bonnot, C.A.	737	Bostock, H.	860	Bourg, I.	1484
.....	1975	Bonny, E.	738	2089	Bourgeade, P.	2160
.....	2413	Bonotto, D.M.	738	Boston, K.	747	Bourke, M.	913
Boily, J-F.	729	2066	2093	Bourlès, D.	716
.....	1506	Bontognali, T.	764	Botcharnikov, R.	977	860
.....	2200	Bonville, P.	2332	1063	1374
.....	2238	Bopp, L.	1576	2410	Bourles, O.	860
Boiron, M-C.	679	Borah, K.	2021	Botelho, N.	2013	Bourliva, A.	1176
.....	1582	Borca, C.	925	Bots, P.	2076	Bourotte, C.	753
.....	1930	Borch, T.	2359	Bots, Pieter.	2059	Bourrain, X.	978
Boisson, A.	729	Borchert, M.	739	2081	Bousquet, R.	1873
Boizard, A.	1863	Bordage, A.	1983	Böttcher, M.E.	747	2142
Bojakowska, I.	730	Bordier, L.	2091	985	Bousta, F.	1079
.....	1562	Borensztajn, S.	1511	1173	Boutaleb, S.	1594
.....	2507	Borg, L.	768	1737	Bouven, I.	2089
Bok, F.	730	Borg, S.	739	1775	Bouvier, Anne-Sophie.	670
.....	1783	Borges, A.V.	1634	1890	753
.....	2155	Borghini, G.	740	Botter, C.	1218	970
Bokhari, S.N.H.	731	2025	Bottero, J-Y.	664	Bouvier, Audrey.	754
.....	1734	Borgonie, G.	1553	2320	758
Bol'shakov, A.	1193	2005	Bottini, C.	1044		

Bovet, N.	754	Brandon, A.	617	Brennwald, M.S.	769	Broggini, C.	1224
.....	883	761	769	2519
.....	938	765	1664	Brogna, F.	653
.....	987	1727	2005	Brombacher, A.	705
.....	1781	1838	2288	Bromiley, G.	689
.....	1848	Brandon, M.	2568	2342	777
.....	1886	Brandt, F.	762	2370	1304
Bower, D.	755	963	2424	Bromssen, M.V.	1455
Bowler, C.	755	1084	2426	Bronk Ramsey, C.	2229
Bowles, M.	756	1296	Brenot, A.	770	Brook, E.	790
Bowman, J.	756	1478	1762	1062
Bowman, V.	1869	2092	Brens, R.	770	Brooke, J.	777
Bowring, S.	979	Branson, O.	762	Brest, J.	1014	Brooker, R.	1347
Boyanov, M.	1533	2035	1227	1539
.....	1553	Brantley, S.	834	1891	1728
Boyce, A.	699	976	Bretesché, S.	1205	Brooks, J.R.	1592
.....	1345	1184	Breuer, M.	771	Brooks, P.	881
Boyce, J.	757	2170	Breuer, U.	1478	Brooks, S.	2404
Boyd, E.	757	2266	Breuker, A.	720	Brounce, M.	777
.....	758	2284	890	1446
Boyd, P.	1037	Braschi, E.	763	Brey, G.P.	771	Brousset, L.	2320
Boyet, M.	682	891	1306	Brown, A.	737
.....	754	993	1306	969
.....	758	1102	2206	Brown, C.	778
.....	834	Braschi, I.	1559	2210	Brown, Gordon E., Jr.	778
.....	1006	Brasier, A.T.	763	Brey, T.	1987	1014
.....	1250	927	Breynaert, E.	772	1142
.....	1871	Braucher, Régis	860	Briand, C.	772	1399
.....	2067	Braucher, Régis	716	Briant, N.	773	Brown, Graham	779
Boyle, E.	829	Brauchli, M.	764	Brick, R.	2442	Brown, L.	2172
.....	1092	Brauer, A.	2110	Bridge, J.	2176	Brown, M.	778
Boyle, R.	759	2169	Bridges, J.	2158	779
Bożęcki, P.	759	Bräuer, P.	764	Bridgestock, L.	773	2536
.....	2107	Braun, J.	1203	Briki, M.	774	Brown, R.	2340
Božović, M.	1995	Braun, S.	765	Brinberg, B.	2476	Brown, Shaun T.	780
Bracciali, L.	760	Brauns, M.	1775	Brinker, J.	2609	882
Brack, P.	1095	Bray, A.	737	Brinza, L.	774	Brown, Stephanie	711
Bracke, G.	1256	765	Brioschi, L.	2260	Brown, Jr., G.E.	808
Braconnot, P.	2053	Brazelton, W.	584	Bristow, L.A.	775	1591
Bradbury, M.	1689	766	1451	1645
.....	2236	926	1990	1792
Bradley, A.	1560	2369	Bristow, T.F.	1794	2505
.....	2466	Breeding, C.	766	Britz, S.	775	Browning, T.J.	780
Bradley, C.	1385	Brehme, M.	767	2267	Brownlee, S.	781
Braeckevelt, M.	1764	2491	Broach, C.	2225	Brownlow, R.	1854
Braga, R.	1386	Breillat, N.	767	Broad, K.	630	Bruand, E.	1263
.....	1640	Breitenach, S.	1443	Broadley, M.	648	Brüchert, V.	1007
.....	2354	1759	776	1342
Bragagni, A.	631	Breitkreuz, C.	2221	Brocard, G.	2498	2145
.....	760	Brekhovskikh, V.	894	Brocks, J.	776	Brueseke, M.	1248
.....	1492	Brenan, J.	768	781	1264
Bragin, I.	1453	1809	1110	Brueske, A.	2213
Brahmantyo, B.	1267	Brendler, V.	730	1176	Bruggeman, C.	1020
Brancato, A.	1680	775	1379	Brugger, J.	1598
Brand, A.	1218	2109	Broderick, C.	1095	1627
Brand, U.	1065	2155	2148	1732
Brandl, H.	888	Brenker, F.E.	2267	Brodholt, J.	640	2047
.....	2531	Brennecka, G.	768	2438	Brüggemann, G.	1995
Brandl, P.A.	761	1188	Brodie, E.	1961	Bruisten, B.	776
.....		2345	781
			Broecker, W.S.	1178	Brumsack, H-J.	736
		1285		
		2277		

Brunelli, D.....	655	Bukaemskiy, A.....	1084	Burton, K.....	608	Bylund, D.....	1671
.....	782	1296	796	1672
.....	1739	Bukharova, O.....	790	939	Byrne, J.....	804
.....	1931	2335	1274		
Brunet, F.....	1033	Bulanova, G.....	795	1607	C	
.....	1377	1486	1837	Cabato, J.....	632
.....	1759	2205	1894	Cabestrero, Ó.....	2133
.....	2167	2328	2211	Cabral, R.....	805
Brunner, B.....	619	2442	2263	Cabral Pinto, M.....	805
.....	782	Bull, S.....	1546	2289	Caby, R.....	690
.....	783	Bullen, T.D.....	784	Burton, M.....	797	Cachier, H.....	806
.....	2566	791	797	1617
Brunner, I.....	1656	791	1551	Caciolli, A.....	1224
Bruno, J.....	783	1864	2119	2519
.....	1021	Bullock, L.....	792	Burton-Johnson, A.....	798	Caddick, Mark.....	671
.....	2401	Burant, A.....	792	Busch, A.....	856	Caddick, Mark J.....	624
Bruno, M.....	1840	Burchardt, S.....	690	1424	806
Brunstad, H.....	1588	Burckel, P.....	793	1703	1228
.....	2114	Bureau, H.....	2068	Busch, J.....	798	1717
Bryan, S.E.....	1691	Bureau, S.....	862	Busemann, H.....	896	Cadkova, E.....	1864
.....	2212	Burg, J-P.....	690	Bush, M.....	799	Caetano-Filho, S.....	637
Bryanskaya, A.....	1557	Burgaud, G.....	890	Bush, R.T.....	799	Caggiati, M.....	938
Bryce, J.....	632	Burgess, D.....	1913	1508	Cai, Jia.....	1625
.....	784	Burgess, R.....	648	2398	1739
.....	1263	776	Bushinsky, S.....	1040	2447
.....	2244	793	Bushmin, S.....	1516	Cai, Jingong.....	1233
Bryson, J.....	784	863	Busigny, V.....	588	1603
.....	1262	896	799	2617
Bublikova, T.....	785	1385	835	Cai, M.....	1391
Buccianti, A.....	703	1393	866	1391
.....	785	1484	921	Cai, P.....	807
Büchel, G.....	1210	1700	1561	Cai, Q.....	807
Bucher, H.....	1903	2105	1683	Cai, Yongfeng.....	2599
Buchner, S.....	786	2285	1694	Cai, Yuqi.....	1604
Bucholz, C.....	1127	Burghelea, C.....	1005	Buso, G.P.....	1224	Caillaud, J.....	1191
Buchs, D.....	1970	Burgos, W.....	1549	2519	Caillon, N.....	1543
Buchwald, C.....	786	Burke, A.....	794	Buss, H.L.....	800	Çakıroğlu, R.E.....	808
Buckley, B.....	591	2273	855	Calabrese, S.....	721
Buckley, W.....	2150	Burke, I.....	1635	896	2505
Budakoglu, M.....	1426	Burkhardt, C.....	1091	1005	Calas, G.....	725
.....	1431	1254	Bussian, B.....	1579	778
.....	1524	1475	Bussio, J.....	800	808
.....	2382	1515	Bussmann, I.....	1849	861
Budashkina, V.....	787	Burkhardt, J.....	794	Busso, A.....	1287	964
Budde, G.....	787	Burnard, P.....	585	Bussy, F.....	1273	1133
Budnitskiy, S.....	788	1541	2345	Caldas, R.....	2136
Budyak, A.....	788	1662	Butler, I.....	689	Calibo, M.....	609
Buechel, G.....	698	Burnham, A.D.....	694	Butterbach-Bahl, K.....	1158	Caliebe, W.A.....	2215
Buechele, A.....	2207	795	2479	Calin, N.....	1352
Bueker, P.....	1039	Burnham, M.....	1734	Butterfield, C.....	801	Caliro, S.....	875
Buenning, N.....	1428	Burnley, P.....	795	Butterfield, D.....	1655	1004
Buerger, S.....	789	Burnol, A.....	714	Butterfield, N.....	801	1357
Buffat, A.....	2405	Burow, K.....	698	Butvina, V.....	802	1958
Bugnet, M.....	1795	Burrows, A.....	2477	Buzgar, N.....	2336	Callegari, I.....	1224
Buhl, D.....	747	Burton, A.....	2255	Bybee, G.....	802	2519
.....	1160	Burton, E.D.....	796	Bychkov, A.....	803	Callegaro, S.....	809
Buhre, S.....	2463	1508	1989	809
Bühning, S.I.....	2234	2398	Byerly, B.....	803	Calmano, W.....	1080
Buick, I.....	933			1552	Calmels, D.....	735
Buick, R.....	1110			Bykov, L.....	656	810
Buie, M.....	1512			Bykova, E.....	844	967
Buikin, A.....	789			Bykova, N.....	656	Caltabiano, T.....	1165
Buizert, C.....	790			Bylaska, E.....	2549	Calzolari, G.....	2127

Cam, N.	688	Canovas, P.	758	Carlson, R.W.	758	Casini, L.	838
Cama, J.	822	1887	826	1128
.....	951	2104	827	2002
Camarda, M.	810	Cantarero, I.	2351	1321	Casiot, C.	2052
.....	962	Canti, M.G.	2408	1871	Casman, E.	2257
Came, R.	811	Cantrell, K.	2377	2067	Casper, B.	2469
Cameron, V.	811	Cantucci, B.	820	Carmichael, G.	1688	Cassidy, M.	1400
.....	2389	Canup, R.	1105	Carmichael, R.H.	827	Castagno, K.	2001
.....	2483	Cao, G.	2161	Carn, S.	738	Castanha, C.	2345
Camilli, R.	612	Cao, J.	820	Carneiro, J.	2077	Castilhos, Z.	1080
.....	812	1653	Carniel, L.	908	Castillo, P.	838
Campagnola, S.	812	Cao, M.	821	Carnol, M.	2420	2330
Campbell, A.	823	Cao, T.	821	Caro, G.	828	Castro, A.	2075
.....	1088	Cao, X-F.	2571	841	Castro, Jonathan	2264
Campbell, H.J.	2376	Cao, Y.	1411	1212	Castro, Jose Manuel	839
Campbell, I.	813	Cao, Z-M.	2454	Carozza, D.	702	1918
.....	867	Capaccioni, F.	2180	Carracedo, J.C.	960	Castro, M.C.	839
Campbell, J.L.	2158	Capecchiacci, F.	703	Carraro, A.	828	1973
Campbell, K.	813	Capella, S.	2416	829	Catalano, J.G.	840
Campbell, L.	814	Capezuoli, E.	1443	Carras, M.	1200	1301
Campeny, M.	814	Capilla, R.	985	Carrasco, G.	829	1673
Campos, E.	2122	1737	Carrera, J.	962	Catalano, M.	840
Campos, F.	815	Capizzi, L.	1656	1413	Catalli, K.	2199
Campos, L.	1456	Capo, R.	1965	1655	Cates, N.	841
Campos, M.S.	815	2264	Carriere, M.	1780	1212
Campos, Teresa	894	Caporuscio, F.	822	Carrillo-Chavez, A.	830	1230
Campos, Thomas.	816	Cappelli, C.	822	Carroll, M.R.	622	Cathelineau, M.	679
Campos, W.	2314	Cappuzzo, S.	962	830	841
Campos Neto, M.C.	2118	Capron, E.	1543	1673	1863
.....	2483	Capuano, P.	1958	Carroll, S.	831	1970
Camps-Arbestain, M.	2280	Caracas, R.	722	1704	1991
Camuzcuoglu, M.	816	823	Carruthers, A.	1897	Catillon, G.	1511
Canals, À.	918	844	Carshaw, K.	831	Catling, D.	842
Cancela da Fonseca, L.	928	1916	832	Caumon, M-C.	841
Candela, P.	817	Caracausi, A.	823	Carson, C.	1214	Cauti, F.	1179
.....	2315	824	Carstens, D.	832	Cauuet, B.	660
.....	2577	1617	Cartapanis, O.	833	842
Candelier, Y.	1290	Carapezza, M.L.	2067	Carter, A.	1147	Cavallo, A.	1179
Canepari, S.	2127	Carbone, C.	824	1471	1770
Caner, L.	1114	Carbone, D.	825	Carter, D.	2072	Caves, J.	1894
Canet, C.	2418	Carbone, Samara	1169	Carter, J.	833	Cavicchioli, A.	753
Canfield, D.E.	775	1912	Carter, L.	2220	Cavosie, A.	2386
.....	817	Carbone, Serafina	1680	Carter, M.	834	Cawood, P.A.	984
.....	928	Cardace, D.	766	Cartier, C.	834	2245
.....	936	2369	1250	Cazier, T.	2022
.....	1062	Cardellach, E.	918	Cartigny, P.	835	Ceburnis, D.	843
.....	1249	1831	961	1141
.....	1405	Cardellini, C.	875	1535	1870
.....	1634	1004	1965	1902
.....	1682	1720	Carturan, L.	1126	Ceccato, D.	580
.....	1763	1958	Cartwright, J.	793	Ceccherini, M.	622
.....	1843	Cardenas, M.B.	1451	Caruso, S.	835	Cecile, E.	2014
.....	1990	Cardinal, D.	553	Carvalho, J.	1973	Celejewski, M.	843
.....	2097	969	Carvalho, R.	928	Cembrano, J.	2122
Cang, Y.	1632	Cardman, Z.	619	Carvalho, C.	836	Censi, P.	818
Cangemi, M.	818	Carey, M.	2421	Casacuberta, N.	836	Centler, F.	2329
Canion, A.	818	Caricchi, L.	825	Casagli, N.	1859	Centrella, S.	844
Cannaò, E.	819	Carignan, J.	1051	Casalini, M.	837	Cepedal Hernández, A.	1695
Cannat, M.	1922	2239	Casas-Ruiz, M.	655	Cerkez, E.	2273
Cannata, C.B.	840	Carley, T.	1760	Casciotti, K.	1396	Cernok, A.	844
Cannatelli, C.	819	Carli, C.	2180	Casentini, B.	2502	Cerrato, J.	572
.....	999	Carlone, D.	578	Cashman, K.	837	1377
.....	1050	Carlson, H.K.	826	2103	Cervellino, A.	1223

Cesare, B.	657	Chang, J.	2520	Chauvel, C.	682	Chen, Yang	1278
.....	663	Chang, Q.	1256	862	1599
.....	1934	Chang, T-J.	852	916	1774
.....	2366	Chang, X-Y.	852	965	Chen, Yanjing	2607
Cestelli Guidi, M.	2018	Chang, Y-H.	853	1016	Chen, Yin	1341
Cha, H.J.	845	Channon, M.	853	1143	Chen, Youwei	1652
Chabaux, F.	636	1198	1203	Chen, Yue-Gau	1471
.....	641	Chantel, J.	854	Chavrit, D.	648	Chen, Yuheng	869
.....	845	Chanton, J.	915	863	Chen, Yunke	1629
.....	1192	Chanton, P.	915	2105	Chen, Zhong	2455
.....	1969	Chanyshhev, A.	854	2285	2594
.....	2063	Chao, H-C.	855	Chazot, G.	1033	Chen, Zhongqiang	1542
.....	2160	Chaouachi, M.	2177	Chebbi, I.	588	Cheng, H.	594
Chabot, N.L.	846	Chapela Lara, M.	800	Cheetham, M.D.	1508	1398
Chacko, T.	630	855	Chekhovskaia, T.	2121	Cheng, Jianzhong	1574
.....	1929	Chapligin, B.	1734	Chellman, N.	1270	Cheng, Jun.	1628
.....	2045	Chaplygin, I.	856	Chelnokov, G.	1453	Cheng, Sanyou	869
Chaduteau, C.	1561	2313	Chemnitzer, R.	863	Cheng, Shenggao	937
Chadwick, J.P.	960	Chapman, A.	781	1248	Cheng, Xiaohui	2552
Chae, B-G.	1351	Chapman, E.	2264	Chemtob, S.	864	Cheng, Xinyuan	1284
Chae, S.H.	1566	Chapman, H.	703	Chen, A-T.	864	Cheng, Y.	1688
Chaerun, S.K.	846	856	2480	Chenu, C.	870
Chafe, A.N.	847	942	Chen, B.	865	1409
Chagneau, A.	847	1424	1430	1575
.....	2320	1703	Chen, Cheng-Hong	1118	Cheong, C-S.	1384
Chaka, A.	2275	2613	Chen, Chi-Yen	1118	Cherdynceva, S.	2402
Chakhmouradian, A.	848	Chapman, S.	608	Chen, Chia-Te.	1045	Cherepanova, Y.	620
.....	2039	Chapon, V.	1780	Chen, D.	1653	870
Chakrabarti, K.	1802	Chappaz, A.	857	Chen, Fahu	1387	Cherniak, D.	924
Chakrabarti, R.	649	Chappellaz, J.	857	Chen, Feng	992	Chernikov, R.	2215
Chakraborty, R.	2011	1062	Chen, Fenxiong	2587	Chernow, R.	1035
Chakraborty, Subrata	1243	1200	Chen, Fukun.	1600	Cherns, D.	1215
Chakraborty, Sumit	591	1543	Chen, Haihong	2594	Chernyshev, I.	871
.....	700	Charbonnier, S.	2034	Chen, Heng	2142	887
.....	848	Chareev, Dmitriy	858	Chen, Huayong	1313	Chernyshov, A.	2573
.....	1058	Chareev, Dmitriy	1898	2525	Cheron, S.	1110
.....	1418	Charette, M.	1985	Chen, Jeffrey	685	1408
Chakravadhanula, M.	849	Charles, C.	858	Chen, Jiansheng	1150	Chertkova, N.	871
.....	862	1100	Chen, Jiawei.	865	Cheshire, M.	822
Chalnev, A.	666	2018	Chen, Jie	866	Chesnot, T.	772
Chalot-Prat, F.	849	Charlet, L.	1278	Chen, Jiu-Bin	866	Chetelat, B.	872
Chambefort, I.	677	2432	1643	1643
.....	850	2502	Chen, Jun	1599	Chevillard, M.	2362
Chamberlain, C.P.	1670	Charlier, Bernard	859	1680	Chew, D.	872
.....	1745	Charlier, Bruce	859	2594	Chi Fru, E.	874
Chamberlain, Katy Jane ...	850	Charnock, J.	2183	Chen, K-Y.	864	Chiang, H-W.	873
Chamberlain, Kevin	946	Charpentier, T.	1968	Chen, Liang	2408	Chiarabba, C.	875
Chambers, J.	1024	Charreau, J.	860	Chen, Lingxiao	1393	Chiaradia, M.	809
Champagnac, J-D.	1289	Charrier, P.	1023	Chen, M.	867	1095
Chance, R.	1454	Chartier, F.	1226	Chen, Nan	852	Chiarantini, L.	873
Chand, S.	1588	Chase, Z.	860	Chen, Ning	2528	1829
.....	2139	1728	Chen, R.	1630	Chiari, M.	2127
Chandler, R.	2436	Chassé, M.	861	2591	Chicharro, E.	874
Chandrasekharam, D.	1434	Chatman, S.	861	Chen, S-H	2519	Chien, Y-H.	2452
.....	2217	2582	Chen, Shuwang	867	Chikaraishi, Y.	875
Chanéac, C.	1015	Chatterjee, A.	849	Chen, T-Y.	868	1201
Chaneva, S.	851	862	1387	Childress, L.	713
.....	1851	Chatterjee, C.	2383	Chen, Wei	567	Chillrud, S.	2285
Chaney, R.	2083	Chatterjee, D.	710	Chen, Wei Ting.	868	Chin, E.	659
Chang, C.	851	Chatzitheodoridis, E.	1093	Chen, X.	1615		
Chang, D.	879	Chaussidon, M.	1699				
.....	1924	2141				
Chang, H-H.	1613	2218				

Chiodini, G.....	703	Christiansen, B.c	883	Cipriani, A.	655	Coates, J.D.	826
.....	875	Christiansen, B.c.	1836	740	910
.....	1004	Christianson, K.....	2385	Ćirić, A.	2414	Cobb, K.....	910
.....	1208	Christl, M.	836	Cirino, G.	620	Cobbold, P.	2258
.....	1720	944	Cirpka, O.A.	1027	Cobelo García, A.	1639
.....	1944	1272	1239	Cobenas, G.....	898
.....	1958	1302	Cirrincione, R.	891	Cobert, C.....	751
Chiogna, G.	876	Christmann, G.	1898	Cismasu, C.....	778	Cobert, F.	899
Chipera, S.J.....	1794	Christner, E.	884	Cisternas, M.E.	999	2160
Chirinos, J.	1193	1025	Civetta, L.	2340	Coble, M.	1186
Chirita, P.	640	Christofides, G.	1921	Cividini, D.	1626	Cobourne, G.....	899
.....	876	Christopher, T.	1347	Clæsson, S.	892	Codina-Miquela, R.	1831
.....	911	Christy, A.	1214	Claeys, P.	726	Cody, G.....	1441
Chistyakov, A.	2188	Chrysochoou, M.	884	2399	2255
Chivas, A.	1049	Chu, B.	1652	Clague, D.....	2094	Coe, A.	986
Cho, B.	877	Chu, C-H.	1567	Claiborne, L.....	1760	Coe, H.....	746
Cho, C.Y.	2563	Chu, K.	1931	Claire, M.....	892	Coetsee, E.	1447
Cho, D-L.	877	Chu, M-F.	885	1367	Coffineau, N.	900
.....	1572	Chu, R.	1282	2586	Cogez, A.	900
Cho, Hui Je.....	1384	Chu, X.	885	Claret, F.	847	1750
Cho, Hye-Youn	1351	Chu, Z.....	886	893	Coggon, J.	901
Cho, K.R.	2223	Chubakov, V.	1341	Clark, A.	893	Cohen, Anne	901
Cho, M.	1322	Chudnenko, K.	886	Clark, C.....	894	2459
Cho, S.Y.....	877	1928	1979	Cohen, Anthony	986
.....	2565	Chugaev, Andrey.....	871	2316	Cohen, B.A.	902
Cho, Y.	878	887	Clark, I.D.....	1292	Cohen, Ronald	902
Choi, Heechul	878	Chugaev, Andrey, V.....	2378	Clark, S.M.	1077	Cohen, Roy	2477
Choi, Hyeon-Gyu	878	Chumakov, A.	1985	Clarke, A.....	894	Coke, C.	2318
Choi, Jaeyoung.....	1533	Chung, Chang Soo	1465	Clarke, G.	975	Col, L.	903
Choi, Jong-Woo	879	Chung, Chuan-Hsiung	855	Clarke, L.	895	Colangelo-Lillis, J.....	781
.....	879	1614	Clarkson, M.	895	Colás, V.	903
Choi, Jung Youn	1384	Chung, Sun-Lin	853	Class, C.....	740	Cole, C.	904
Choi, K.Y.	1465	885	Clausen, T.	754	Cole, J.M.....	1285
Choi, Man Sik	845	1567	Clavier, N.	1296	Coleman, D.	904
.....	879	1613	Clay, P.	648	Coleman, Maureen.....	2056
.....	1464	Chung, Sung Lae	1566	896	Coleman, Max.....	905
.....	1924	Church, N.	1262	1393	Coles, B.....	1541
Choi, Min Seok	2203	Chutcharavan, P.	887	2105	Cölfen, H.....	689
Choi, S-H.	1464	Chval, Z.....	1994	Clergue, C.....	896	Colin, A.....	905
Choi, W.Y.	1566	Chvalun, S.	2402	Clerque, C.....	1130	Colin, C.....	1537
Chok, H.	2225	Chwalek, T.	888	Cleveland, C.	1669	Colin, S.	2362
Choo, C-O.	880	Cianflone, G.	2409	Cleverley, J.	739	Colinet, G.....	899
.....	1384	Cibin, G.	694	890	Collerson, K.D.	2202
Chopin, C.	1033	1245	1942	Collin, P-Y.....	2017
Chorney, A.	880	1980	2381	Collings, D.....	906
Chorover, J.	881	Ciborowski, J.....	750	Cliff, J.	835	Collins, A.....	1979
.....	1005	Cicchella, D.....	888	897	2442
.....	1250	Cicconi, M.R.....	622	1054	Collins, B.	1725
Choudhury, I.	1756	2249	1066	Collins, J.	1558
Choung, S.....	881	Ciceri, G.	2242	2435	Collins, N.....	906
Chow, P.....	2199	Ciesielczuk, J.....	889	Clifton, P.	1795	Collins, R.....	907
.....	2310	Ciesla, F.	1515	2386	Collins, W.	593
Chrastny, V.	1756	Ciffroy, P.....	1932	Clog, M.....	897	2230
.....	1864	Cimarelli, C.....	741	Cloquet, C.....	1051	Colman, B.P.....	1645
Christ, A.	1349	Cinque, G.	2018	1052	2257
Christen, R.	1780	Cinti, D.	2171	1268	Colombani, N.....	1059
Christensen, B.	1575	Cioacă, M.E.....	889	Clouser, B.	1540	Colon, D.....	706
Christensen, H.	882	1834	1797	Colonna, T.	1224
Christensen, J.N.	780	Ciobanu, C.....	890	Cluzel, N.....	2151	2519
.....	882	1363	Clyde, W.....	2230	Colpaert, J.....	784
.....	2011	Ciobanu, M-C.....	890	Clymans, W.....	898	Coltelli, M.....	738
Christensen, P.	2104	Cioni, R.	891	Clynne, M.....	2441	Coltice, N.....	1536
Christenson, H.....	883	935				

Coltorti, M.	571	Cooke, David	645	Cottrell, E.	777	Crowe, S.A.	817
.....	1058	914	923	928
.....	1059	1313	1219	1405
.....	1154	Coolen, M.J.L.	2026	1446	1437
.....	1164	Cooper, K.	915	1720	1561
.....	1165	2100	2094	1634
Colussi, A.	1308	2261	Couchoud, I.	1010	1682
Comans, R.	907	Cooper, L.	2094	2037	Crowley, James	2295
.....	1495	Cooper, R.	1370	2580	Crowley, Jim	2240
Comodi, P.	908	Cooper, William	1024	Couder, E.	1712	Crowley, Q.C.	1802
.....	1154	Cooper, William	915	Courtin-Nomade, A.	1163	Cruces, A.	928
Comolli, L.R.	693	Coplen, T.	1761	Cousin, A.	2269	Cruciani, G.	611
Conceicao, H.	2065	Copping, R.	2400	Coutinho, J.	1687	929
Conceicao, R.V.	908	Corbella, M.	918	Couture, R-M.	1312	Cruden, A.	952
Condamine, P.	909	1831	2054	Cruden, S.	618
Condon, D.J.	763	Corcoran, L.	916	Coveney, P.	2293	Cruz, C.	2056
.....	909	Cordier, Carole	916	Cox, A.	1485	Cruz, M.I.F.S.	929
.....	927	2141	Cox, G.C.	923	Cruz, N.	830
.....	1588	Cordier, Catherine	2085	1246	Cruz-Uribe, A.	930
.....	1927	Cordier, P.	917	1343	Cserny, T.	1868
.....	2114	Cordiez, M.	1806	Cox, R.P.	1990	Cubadda, F.	1551
.....	2226	Corella, J.P.	2233	Cox, Simon C.	1847	Cuccuru, S.	838
Condon, E.	827	Corfu, F.	1778	Cox, Stephen	924	2002
Conley, D.J.	898	2054	Coxall, H.	1395	Cui, J.	930
.....	1114	Corkhill, C.	917	Coyte, K.Z.	1021	Cui, L.	931
.....	2274	Cormier, L.	1740	Cozzarelli, I.	2294	2460
Connolly, D.	904	Cornelis, J-T.	918	Craddock, P.	948	Cui, Q.	2533
.....	1273	Cornu, S.	1374	Craddock, R.	1119	Cui, Y.	1739
.....	1608	Coronato, A.	982	Crame, J.A.	1869	Cuirrice, J.	1527
.....	1941	Corral, I.	918	Cramer, E.	924	Cullen, J.	931
Connelly, J.N.	711	Correale, A.	919	Crapster-Pregont, E.	1026	Cuney, M.	1930
.....	732	Corsaro, R.A.	825	Craw, D.	1785	1991
.....	909	919	Crean, D.	925	Curci, G.	932
.....	936	1617	Creaser, R.A.	765	2362
.....	1315	Corselli, C.	964	2386	Curcoll, R.	932
.....	1633	Corsetti, F.	2000	Creech, J.	644	Curik, J.	1509
.....	2152	Cortecchi, G.	1969	916	1863
Connolly, J.A.	1380	Cortes, J.	2031	925	Curran, M.	579
.....	1640	Corvini, P.F.-X.	2619	Creeley, D.	1597	Curtis, B.	2345
Conrad, M.	910	Corvisier, J.	919	Crepisson, C.	2247	Curtius, H.	668
Conroy, J.	910	Corzo, A.	2346	Crespo-Medina, M.	926	Cutts, K.	933
Consoloni, I.	911	Cosca, M.	1101	Criqui, P.	1617	Cvetković, V.	1995
Constantin, C.	876	Cosentino, N.	920	Crisp, J.A.	1794	Cynn, H.	1574
.....	911	Cosenza, A.	920	Crispi, O.	896	2199
Conticelli, S.	587	Cosmidis, J.	921	980	Cypionka, H.	1043
.....	912	Costa, Antonio	1208	Crispini, L.	2025	Czerwiński, J.	2366
.....	1846	Costa, Antonio Carlos	921	Cristofanelli, P.	2064	Czeschel, R.	2272
Conway, T.M.	604	Costa, F.	1293	2127	Czuppon, G.	970
.....	912	1418	Cristofolini, R.	1846		
.....	1092	Costa, Maria Mafalda	1778	Critelli, T.	926	D	
.....	1396	Costa, Michela	922	Crne, A.E.	927	D'Alessandro, W.	721
Cook, C.	2389	Costagliola, P.	1211	Crocitti, M.	1002	1128
Cook, N.	890	1789	Crocket, K.C.	1541	2067
.....	1363	Costea, C.	889	2273	D'Amato, M.	1551
Cook, P.L.M.	913	1017	Crompton, N.	1816	D'Errico, M.	934
.....	1451	Costin, G.	889	Croot, P.	927	D'Hondt, S.	934
Cook, R.L.	913	Cotte, M.	2517	Crosby, B.	2498	2140
.....	1488	Cottle, J.	922	Cross, E.	1514	D'Orazio, M.	911
Cook-Kollars, J.	906	1240	Crosson, E.	2048	2412
Cooke, David	914			2360	D'Oriano, C.	891
.....	1780			Croteau, P.	1514	935
						D'Ovidio, F.	2387
						D'Souza, R.	1067

Da Campo, R.....	1216	Danielczok, A.....	2259	Davies, G.....	905	De Lucia, M.....	968
Dacheux, N.....	1296	Daniele, L.....	1831	1495	1009
Dachs, E.....	935	Daniels, E.....	557	Davies, J Huw.....	663	de Meyer, C.....	970
Dadou, I.....	1576	Daniels, K.....	703	2396	De Min, A.....	809
Daehn, R.....	2236	942	Davies, Joshua.....	950	de Moor, J.M.....	1541
Daeron, M.....	1010	Daniels, M.J.S.....	1084	Davies, M.....	986	de Nooijer, L.....	705
Dahl, T.W.....	857	Danielsson, K.....	943	Dávila, G.....	951	1838
.....	936	Danisik, M.....	943	Dávila-Ramos, S.....	1051	de Oliveira, N.....	1659
Dahl-Jensen, D.....	1720	Dannhaus, N.....	944	Davis, A.....	951	de Pablo, J.....	1410
.....	2385	Dantu, S.....	944	Davis, D.W.....	952	De Paoli, M.....	975
Dahmke, A.....	2484	Danyushevsky, L.....	898	2065	de Parseval, P.....	2183
Dahms, D.....	1715	945	Davis, J.....	1377	De Proft, F.....	726
Dähn, R.....	936	1171	2118	de Rezende, J.R.....	1342
.....	1687	1245	Davis, M.....	1126	de Ronde, C.....	2333
Dahrén, B.....	2357	1546	Davis, R.....	1035	De Rosa, R.....	840
Dai, B.....	1612	1704	Davis, S.....	1480	926
Dai, D.....	937	Darab, J.....	2207	Dawson, G.....	952	977
Dai, J.....	2050	Darchambeau, F.....	1634	1066	1002
Dai, M.....	807	Dardé, B.....	1902	1942	1049
Daines, S.....	937	Dargaud, O.....	1740	Dawson, K.S.....	953	De Saint-Blanquat, M.....	2409
Dainty, J.R.....	1546	Dargent, M.....	945	1181	972
Dairou, J.....	1759	Darling, J.....	946	Day, C.C.....	662	de Silva, S.....	1219
Dal Corso, J.....	938	1795	953	de Soto, F.....	2418
.....	1701	Darmovzalova, M.....	1863	Day, J.....	805	de Souza, G.....	980
Dalai, T.....	1473	Darr, J.....	1195	954	de St Blanquat, M.....	1460
.....	2120	Darrah, T.....	2401	1871	De Toni, G.B.....	710
Dalby, K.N.....	938	Darrouzès, J.....	1584	Dayal, A.M.....	955	De Vivo, B.....	567
.....	1836	Dartois, E.....	946	2121	819
.....	1848	Das, P.....	1285	De Abreu, A.....	729	888
.....	1886	Das, S.....	1833	de Anna, P.....	955	920
Dale, Amy.....	2257	Dasgupta, R.....	947	993	991
Dale, Andrew.....	2270	947	De Astis, G.....	993	999
Dale, Annabel.....	939	1018	de Baar, H.....	956	1050
Dale, C.W.....	939	1677	1541	2111
.....	1362	Dasgupta, S.....	591	2397	De Vleeschouwer, F.....	982
Dalkhaa, C.....	1716	Dash, J.....	2281	De Baere, B.....	957	de Vries, L.M.....	982
.....	1850	Daskalakis, N.....	1817	de Beer, D.....	1241	De Waele, B.....	727
Dalla Fontana, G.....	1126	Dassargues, A.....	2082	1474	De Yoreo, J.....	983
Dalladay-Simpson, P.....	2129	Datta, S.....	1455	De Campos, C.....	1952	2223
Dallai, L.....	744	Daughney, C.....	948	1952	2440
.....	776	Dauphas, N.....	948	de Caritat, P.....	958	De-Pourcq, K.....	1143
.....	911	1107	De Caro, M.....	2184	Deák, J.....	1443
.....	2037	Dautria, J-M.....	1076	De Gaspari, F.....	962	Death, R.....	956
.....	2354	Daval, D.....	926	De Gea, G.A.....	839	Debaille, V.....	957
Dallas, J.....	644	2218	1918	1016
DallOsto, M.....	940	2335	De Giacomo, A.....	828	1343
Dalrymple, D.J.....	827	Davantès, A.....	610	De Gregorio, S.....	810	1872
Dalsgaard, T.....	775	949	962	2357
Daly, J.S.....	1115	Davenport, R.....	1398	De Grouchy, C.....	2247	2399
.....	1871	David, J.....	1360	De Hoog, J.....	963	Debat, P.....	1460
Damgaard, L.R.....	940	David, M.....	2341	de Jong, W.....	2549	DeBièvre, P.....	2417
.....	1964	Davidson, Jon.....	699	de la Rocha, C.....	900	Deblochouse, B.....	772
Daneshvar, E.....	941	972	1114	Debois, T.....	1200
Daneu, N.....	2252	Davies, A.....	600	de la Torre, M.L.....	1206	Deboudt, K.....	1093
Dang, B.....	941	1207	Debret, B.....	958
.....	2601	de Lange, G.J.....	2384	DeCarlo, T.....	901
Danhara, T.....	2116	964	Decesari, S.....	843
Daniel, B.....	1597	2408	959
Daniel, I.....	1059	de Leeuw, N.H.....	965	1169
Danielache, S.....	942	Davidson, Jonathan.....	950	966	1912
.....	2506	2064
.....	1042	de Ligny, D.....	2311	2127
.....	1272	de los Reyes, M.....	1650	Decker, M.....	1688
.....	2373

Declercq, J.	742	Demichelis, R.	971	Dessert, C.	855	Didier, A.	745
.....	959	2022	896	988
Deconinck, J-F.	1777	Demina, L.	971	980	Diella, V.	692
Decrée, S.	751	Demopoulos, G.P.	2528	1130	Diels, J.	2082
.....	960	Demouchy, S.	917	Dettman, D.	2145	Diener, A.	988
Deditius, A.P.	646	2138	Deusner, C.	981	Dieterle, M.	1496
.....	2042	Demouy, S.	972	Deutsch, C.	981	Dieterlen, A.	1168
.....	2064	Dempsey, S.	972	Deutschbauer, A.M.	826	Dietiker, R.	1272
Deegan, F.M.	690	Dempster, T.J.	1354	Devau, N.	1590	Dietrich, M.	989
.....	960	1727	Devey, C.	1035	1770
.....	2357	Den Hartog, S.	2623	2393	Dietrich, W.E.	1462
Deek, A.	832	Den Uyl, P.	2192	Devidal, J-L.	745	Dietze, H.	1083
Deering, C.	677	Denduluri Subba Rao, V. .	973	834	Dietze, V.	989
Deevsalar, R.	961	Denecke, M.A.	1530	988	1168
Defouilloy, C.	961	Deng, F.	973	1078	2481
Degenstein, D.	2489	Deng, H.	1092	1250	Dietzel, M.	646
Degryse, P.	983	Deng, K.	1594	1693	1116
Deino, A.	2051	Deng, T.	1052	Devouard, B.	1693	1775
Deissmann, G.	963	Deng, Yinan.	1234	DeVries, T.	981	1845
Déjeant, A.	964	Deng, Yufeng.	2524	Devulder, V.	983	1847
Del Carlo, P.	1986	Denier van der Gon, H.	974	DeWit, M.	2340	2004
del Moral, C.	1880	Deniz, K.	974	DeYoreo, J.	987	2064
Del Ventisette, C.	1859	1231	Dezileau, L.	2052	2164
Del Villar, L.P.	2401	1498	Dhuime, B.	984	2308
Delavault, H.	965	Dennis, P.	1469	Di Benedetto, F.	1789	Diez Ortiz, M.	1556
.....	1285	Denoyel, R.	1129	Di Chiara-Roupert, R.	845	2040
Delcamp, A.	960	Dentener, F.	1477	Di Giuseppe, D.	1059	Dijkstra, J.	907
Delgado, C.	2384	2394	Di Leo, P.	990	1731
Delgado López, J.M.	1223	Dentz, M.	955	Di Piazza, A.	993	Dildar, N.	990
Delhaye, T.	2314	975	2067	Dilling, J.	2039
Delinardo, M.	966	1561	2427	Dillmann, P.	2379
Delitsky, M.	1259	Deon, F.	767	Di Renzo, V.	919	Dimitriou-Christidis, P.	612
Della Lunga, D.	967	DePaolo, D.	780	Di Roma, A.	1681	Dimova, N.	1940
Della Puppa, L.	1489	2472	Di Salvo, S.	993	Dinale, R.	1126
Della Ventura, G.	1875	Depecker, C.	2417	1102	Dinato, N.	2524
.....	2018	Deque, M.	1184	Di Stefano, G.	1133	Dinelli, E.	888
Dellapenna, T.	579	Dera, P.	1088	Di Tommaso, D.	2506	991
Dellinger, M.	896	2590	Di Traglia, F.	1124	1542
.....	967	Derbeko, I.	976	1859	Ding, F.	1233
.....	1130	Dere, A.	976	Diamond, L.W.	582	Ding, H.	991
Dellwig, O.	747	Derenne, S.	1555	696	1543
.....	2053	Derrey, I.T.	570	984	Ding, L.	2196
.....	2162	977	1172	Ding, M.	2464
Delmas, P.	1023	Derry, L.	978	2136	Ding, T.	992
Delmelle, P.	968	Desaulty, A.M.	978	Dias, A.S.C.A.	929	Ding, X.	992
.....	1708	1762	Dias, I.	1687	1615
Delmonte, B.	714	Desbois, T.	1062	Dias, R.	2318	Ding, Z.	931
DeLong, E.	1405	Deschanel, X.	979	Diaz, J.	1255	2460
.....	1682	Descostes, M.	725	Díaz, R.	985	Dingwell, D.B.	741
Delos, A.	1075	964	1737	1512
Deloule, E.	1103	1863	Dibb, J.	1081	1952
.....	1123	2046	Dick, G.	985	1952
Delpoux, S.	773	2123	1557	1980
DelSontro, T.	2233	2464	2192	Dini, A.	744
Delvaux, B.	918	Descy, J.P.	1634	Dick, H.	986	1829
Delvigne, C.	969	Desmarchelier, J.	1936	Dickson, A.	986	2412
Demaiffe, D.	751	DesOrmeau, J.	979	Dickson, J.	987	2412
Demant, A.	666	1199	Dideriksen, K.	551	Dipple, G.M.	1262
Demarchi, B.	969	Desponds, L.	2405	883	1992
deMenocal, P.	2331	Desrochers, A.	1981	987	Distler, V.	1313
Demény, A.	970	1836	2168	Ditterich, F.	994
Demetriades, A.	2044	2336	2336	Dittmar, T.	1373
.....	2045						

Dittrich, M.....	994	Donnini, M.....	1004	Druhan, J.....	1009	Dunlea, A.....	2140
.....	1938	1004	1719	Dunning, G.R.....	1287
.....	2616	Dontsova, K.....	1005	Druitt, T.H.....	993	Dunphy, D.....	2609
Divan, Y.....	995	Dore, E.....	610	Druteikienė, R.....	1010	Dupraz, C.....	2184
.....	995	Dore, J.....	758	Druzhinin, S.....	1677	Dupraz, S.....	1019
Dixon, D.....	996	Dória, A.....	611	Drysdale, R.N.....	1010	Dupre, B.....	2415
Dixon, E.T.....	1801	Dornhof, R.....	1168	1363	Dupuis, R.....	1020
Dixon, R.....	996	Dorokhov, V.....	656	1936	Duran, C.....	2183
Dixon, S.....	997	dos Santos Pinheiro, G.....	1983	2037	Durand, G.....	672
.....	1926	Dosseto, A.....	1005	2580	Durand-Dubief, M.....	588
Diz, P.....	1641	1049	Du, J.....	1011	Durce, D.....	1020
Djediati, C.....	1496	1693	Du, Z.....	2506	Durham, W.M.....	1021
Djuly, T.....	1474	1741	Du Vivier, A.....	1023	Duro, L.....	1021
Djurhuus, A.....	1273	2293	Duan, W.....	1011	1075
Dmytrieva, S.....	1522	Dosso, L.....	1252	Duan, X.....	1012	Dürr, H.....	1611
Do, H-K.....	997	1256	Duan, Y.....	1012	Dury, M.....	1184
Dobrescu, A.....	998	Doucelance, R.....	682	Duarte, M.A.....	651	Duryea, A.....	812
Dobson, D.....	2438	1006	Dubacq, B.....	703	Dutay, J-C.....	1537
Doering, K.....	1031	Doucet, L-S.....	1359	2613	2397
Doglioni, C.....	998	Dougans, J.....	2363	Dube, B.....	1139	Dutrow, B.....	1120
Dogra, Y.....	2040	Douglas, T.....	1006	Dubesky, C.....	573	Dutta, T.....	1022
Doherty, A.....	999	Doumbia, T.....	1617	Dubessy, J.....	945	Dutton, A.....	1022
Dohmen, R.....	1203	Douvalis, A.....	1185	1582	Duwig, C.....	1023
.....	1577	Dove, M.....	1815	1983	Dvorski, S.....	1024
.....	1686	Dove, P.....	983	Dubey, M.....	2512	Dworkin, J.....	2255
.....	1879	Doveri, M.....	1766	Dubinina, A.....	1013	Dwyer, C.....	1024
Doichinova, V.....	1348	1856	2063	Dyachkov, B.....	1531
Dold, B.....	999	Dowall, D.....	2312	Dubinko, V.....	1013	Dybowska, A.....	1556
.....	1498	Downes, H.....	1007	Dublet, G.....	921	2040
.....	1813	2244	1014	Dye, S.....	1394
.....	2373	2373	1114	Dyer, A.....	814
Dolder, F.....	1000	Downs, K.....	1007	Dubois, M.....	1014	Dyer, J.A.....	1558
Dolejš, D.....	1000	Downs, R.T.....	1629	1148	Dyess, P.....	2474
.....	1290	1794	1616	Dyhr, C.T.....	1314
.....	2247	Doyle, P.....	1515	Dubrovinsky, L.....	844	Dymshits, A.....	722
.....	2283	Døssing, L.N.....	928	1983	1025
Dolgopolova, A.....	1001	Draga, G.....	1126	2235	Dyroff, C.....	884
Domack, E.....	1974	Dragovic, B.....	671	Dubujet, P.....	2055	1025
Domart-Coulon, I.....	1496	Drahota, P.....	1674	Ducea, M.N.....	1015	Dysthe, D.K.....	2086
Dombrowski, N.....	2154	Drake, H.....	691	2267	2093
Domènech, C.....	1021	1008	Duchateau, A.....	1015	Dzierzanowski, P.....	1134
Dominguez-Villar, D.....	1265	1709	Duchemin, C.....	1016	1134
Dominici, R.....	2409	2568	Dufek, J.....	1016	1160
Donahoe, R.....	1001	Dreossi, G.....	1126	Duffy, C.....	2284	Dzombak, D.....	1928
Donahue, N.....	1919	Dresen, G.....	1283	DuFrane, W.....	831	1929
Donard, O.....	1051	Drew, D.....	706	1704		
.....	2239	1008	Dufresne, A.....	890	E	
Donato, P.....	977	Drewitt, J.....	2129	Dugarova, N.....	1159	E. Böttcher, M.....	2053
.....	1002	2247	Duhaut, P-B.....	1297	Ebel, D.....	1026
Dondi, M.....	611	Drewniak, Ł.....	1755	Duke, J.....	996	Eberlei, T.....	1026
Dong, A.....	1002	2023	Dulski, P.....	2049	Ebert, V.....	1520
Dong, D.T.....	584	Drewnick, F.....	1168	Dumas, P.....	1834	1540
Dong, F.....	641	Dreyfus, G.....	1543	Dumas, T.....	1017	1797
Dong, M.....	1193	Driba, D.....	1009	Dumitras, D.G.....	1017	Ebihara, M.....	2534
Dong, Shu.Yi.....	1222	Driesner, T.....	2125	1352	2539
Dong, Sijia.....	2602	2587	1684	Ebrahimi, H.....	982
Dong, X.....	2599	Driouch, Y.....	1460	1834	Ebrahimi Nasrabadi, K.....	2621
Dong, Y.....	1003	Drobniak, A.....	2153	Duncan, Martin.....	1592	Eccles, K.....	906
Donnadieu, F.....	738	Drott, A.....	2491	Duncan, Megan.....	947	Echevarria, G.....	1052
Donnadieu, Y.....	733	Droxler, A.....	1894	1018	Eckert, D.....	1027
.....	1003	Drozd, V.....	1329	Duncan, R.....	1018	Eckert, W.....	558
.....	1343	2146	Dunkel, K.....	1019	Edadasi, L.....	849
.....	1777			Dunkley, D.J.....	1529	862
Donner, E.....	774						

Eddy, M.	1313	Ekblad, A.	1671	Emerson, S.	1040	Espinasse, B.	2320
Edgar, K.M.	589	Eklund, M.	1537	Emmanuel, D.	2014	Esposito, R.	723
Edgcomb, V.	1898	Ekström, S.	1114	Emmanuel, S.	1041	819
Edlmann, K.	1458	El Albani, A.	874	Emmenegger, L.	1041	999
Edmonds, M.	1027	1843	Ende, M.	1042	1050
.....	1326	El Atrassi, F.	1033	Endo, Y.	1042	Essaraj, S.	1582
.....	1347	El Dosuky, B.T.	1162	2373	Esterle, J.	1187
.....	1976	El Galy, M.M.	2194	Eng, P.	2275	Estrada, C.	1050
Edmunds, W.M.	1028	El Goresy, A.	2194	2473	Estradas-Romero, A.	1051
.....	1028	El Korh, A.	1614	Engel, A.	1510	Estrade, N.	1051
Edwards, A.	713	El Korh, A.	1180	Engelbrecht, J.	1786	1052
Edwards, K.	1895	El-Turki, A.	1215	Engelbrekton, A.	910	2239
.....	2037	Elbaz-Poulichet, F.	773	Engelen, B.	1043	Etheridge, D.	579
Edwards, M.	1875	2052	Engelhardt, T.	1043	Etiopie, G.	2153
Edwards, N.	1029	Elderfield, H.	762	Engi, M.	747	Etique, M.	2584
Edwards, R.L.	594	1033	1043	Eto, J.	2540
.....	1398	2029	1180	Etoh, J.	1361
.....	1398	2035	Englert, A.	1044	Etou, M.	1707
Eggenkamp, H.G.M.	1179	Eldridge, D.	2466	Engvik, A.K.	1476	1901
Egger, M.	1029	Eley, Y.	1034	1528	Etoubleau, J.	1110
Egli, M.	622	1943	Enzmann, F.	847	1408
.....	1715	Elfers, B-M.	1034	2177	Etschmann, B.	1598
Eglington, B.	1030	Elhanany, S.	1147	Enzweiler, J.	651	1627
.....	1944	Elio, J.	2401	815	Ettayfi, N.	1594
Eglington, T.I.	2311	Elisha, B.	1035	Eom, H-J.	1461	Ettler, V.	1052
Egorov, K.	1497	Elison Timm, O.	2298	Erambert, M.	2357	1756
Egozcue, J.J.	785	Elkins, L.J.	1035	Erasmus, M.	1553	2370
Eguchi, J.	1679	Elkins-Tanton, L.	711	2005	Ettwig, K.F.	2030
Ehleringer, J.R.	1030	1036	Erba, E.	964	Etzol, C.	1149
Ehlert, C.	1031	1036	1044	Eun, S-H.	1053
Ehlmann, B.	2158	Ellam, R.	1791	Erbanova, L.	1864	Evangelou, M.	704
Ehrig, K.	603	Eller, V.	1951	Erbland, J.	1747	Evans, David	1053
.....	1469	Elliott, B.	2158	2143	Evans, David	1030
Eiche, E.	1031	Elliott, T.	557	Erbs, J.	1170	1944
Eichhubl, P.	2375	631	Erdmann, M.	1111	Evans, J.P.	856
Eichinger, F.	1589	1037	Erdoğan, M.S.	1045	1424
Eigenbrode, J.	1367	1112	Erel, Y.	2106	1703
Eiler, J.	691	1296	2258	Evans, K.	1054
.....	735	1407	2620	Evans, N.J.	821
.....	757	1433	Erez, J.	1053	943
.....	864	1539	1116	1054
.....	897	2018	Ergaliev, G.	1137	1724
.....	1032	2220	Erhardt, A.	1045	Evans, T.W.	1055
.....	1313	2497	Erickson, T.	1046	Evans, W.	1574
.....	1670	Elliott Jr., W.	2225	Eriksson, G.	2146	2199
.....	1967	Ellis, B.	2090	Erkül, F.	1046	Evaristo, J.	1055
.....	1997	Ellis, K.	2050	Erkül, S.T.	1046	Evenstar, L.	1056
.....	2230	Ellwood, M.	1037	Eroglu, S.	1047	Evershed, R.	1610
.....	2269	2089	2497	Evrard, V.	913
.....	2558	Elmaleh, A.	1038	Erpicum, M.	2420	Ewing, R.C.	1056
Einarsson, A.	1837	Elmessbahi, H.	1076	Ersoy, E.Y.	1046	1057
Einsiedl, F.	2515	Elmoulat, M.	1038	Ersoy, H.	1047	2451
Eiriksdottir, E.S.	1032	Elsner, M.	1027	Ertel-Ingrisch, W.	1512	2570
.....	1837	Elvert, M.	697	1952	Ewing, T.	1057
Eisenhauer, A.	724	2166	Erzinger, J.	1847	Expedition 345 Shipboard	
.....	1065	2510	2496	Scientific Party,	1750
.....	1083	Elzinga, E.	2566	Esat, T.	1048		
.....	1116	1039	Escauriaza, C.	1227		
.....	1261	Emberson, L.	1039	Escher, P.	1890	F	
.....	1295	Embile Jr., R.	1040	Escoffier, N.	1048	Faarinen, M.	566
.....	1608	Embley, R.	1655	Escrig, S.	2094	Fabbri, A.	1019
.....	1847	2094	Eskandary, A.	1049	Fabbri, P.	829
.....	2213	Emeis, K-C.	1774	Espanion, V.	1049	Fabian, K.	1067
.....	2427					Fabisch, M.	1396

Facca, G.	1969	Farmer, D.K.	1555	Feng, S.	1946	Ferrigno, F.	1859
Faccenda, M.	1058	Farmer, G.L.	718	2585	Ferry, J.	1080
Facchini, M.C.	843	1065	Feng, X.	1074	Ferullo, G.	567
.....	959	1371	Feng, Y.	1612	Feseker, T.	2259
.....	1169	Farnaaz, S.	2433	Fenn, M.	1999	Fester, T.	1764
.....	1912	Farquhar, J.	805	Fenter, P.	682	Feuillie, C.	1081
.....	2064	817	1663	Feurtet-Mazel, A.	1152
Faccini, B.	1058	1066	2159	Fevrier, L.	1780
.....	1059	1173	Ferard, C.	688	2406
Facq, S.	1059	1367	Ferdelman, T.G.	1074	Fiannacca, P.	891
Fagan, T.J.	1060	1425	1205	Fibiger, D.	1081
.....	1490	Farquhar, S.	1066	1342	1270
Faganeli, J.	1746	1942	Ferlat, G.	2475	Fiebig, J.	1745
Fagel, N.	577	Faucher, G.	1044	Ferlito, C.	1972	2435
.....	1060	Faucon, M-P.	1544	571	Field, E.K.	1535
Fahad, Z.	1061	Faul, K.	2017	977	Field, L.	1082
Fahlbusch, W.	1061	Faure, A.	734	1164	Field, P.	1082
Faïn, X.	1062	Faust, J.	1067	1165	Fietzke, J.	1065
Fairchild, I.J.	1265	Favali, P.	2184	1545	1083
.....	2517	Favara, R.	810	Fernandes, J.	2132	1116
Fairley, J.	950	Favas, P.	1067	Fernandes, T.	1075	1735
Faith, J.T.	2574	Favier, M.	1189	Fernandes, V.	1385	2213
Fall, A.	2375	Fawcett, S.	1200	Fernandez, A.	1075	2393
Fallas Dotti, M.	1062	2050	2308	2427
Fallick, A.E.	763	2222	Fernandez, C.	2097	Fifield, K.	943
.....	927	Fayard, B.	2517	2098	Fike, D.	1083
.....	1433	Fayek, M.	1068	Fernandez, Irene	1076	1565
.....	2363	Fayol, N.	1068	Fernandez, Ivan	1882	1746
.....	2580	Fazzini, M.	1681	Fernandez, J.P.	1207	2001
Fallon, S.	2089	Feakins, S.	1069	Fernandez, L.	1076	2082
.....	2274	Fedele, L.	1934	Fernandez, R.	1383	Filiberto, J.	793
Falloon, T.	849	Federico, C.	721	Fernandez Bastero, S.	1129	Filippi, M.	1674
.....	898	Fedkin, A.	1738	Fernández-Barranco, C.	1077	Filippidis, A.	1176
Falus, G.	1468	Fedortchouk, Y.	1069	Fernandez-Dávila, A.	1173	Filley, T.	1442
.....	1504	2220	Fernández-Díaz, L.	1853	Finck, N.	1862
.....	1618	Fedotov, G.	672	2081	Finessi, E.	1084
Fan, D.	2350	Fegley, B.	1912	2123	Finger, F.	647
Fan, Qiaohui	2302	Fehn, U.	1070	Fernández-Díaz, M.L.	627	Fink, D.	2293
Fan, Qicheng	2604	Fehr, K.T.	741	Fernandez-Gonzalez, M.A.	1195	Finkel, R.	2153
Fan, R.	2588	Fehr, M.	997	1390	Finkeldei, S.	1084
Fan, W.	1615	1070	Fernandez-Martinez, A.	1077	Finlay, A.	1085
Fan, Yang	1388	1926	2440	Finlay, N.	1085
Fan, Yu	2524	2041	Fernández-Remolar, D.	2004	1398
Fanara, S.	2608	Fei, H.C.	2013	Fernández-Roig, M.	1078	2070
.....	2410	Fei, Y.	908	Fernandez-Romar, D.	2124	Finlay, R.	1061
Fancsik, T.	1504	1116	Fernandez.Dávila, A.	1129	1671
Fang, B.	1574	2251	1641	1672
Fang, J.	1063	Feineman, M.	930	Fernando, S.	1078	1700
Fanlo, I.	903	Feingold, G.	894	Fernandoy, F.	666	Finster, K.	1342
Fanning, M.	1196	2239	Férot, A.	732	Fintor, K.	1916
.....	1725	Feldbusch, E.	1071	Ferrand, J.	1079	Fiol, S.	599
.....	2221	Felgate, M.R.	1178	Ferrari, S.	2064	1086
Fantle, M.	1064	Fellhauer, D.	1017	Ferreira, A.	2269	Fiorentini, G.	1086
.....	1261	Fellowes, J.	1072	Ferreira, J.	1079	1224
Faraco, M.T.	1819	Felmy, A.	685	Ferreira, M.	1080	2519
Farges, F.	1079	Fendorf, S.	1406	2133	Fiorentini, M.L.	660
Farina, F.	1064	Feng, C.	1073	2414	835
Farkaš, J.	1065	Feng, H.	1138	Ferreira, P.	1079	1636
.....	1469	2530	Ferreira, T.	928	1732
.....	1864	Feng, L.	1073	Ferreira, V.P.	815	1903
.....	2427	2210	1926
Farley, K.	924	Ferreira da Silva, E.	805	2434
.....	Ferrer, C.	609	Fioretti, A.M.	1934

Fiquet, G.....	2068	Flight, D.....	1649	Fossen, H.	1199	Frank, M.....	868
Firat Ersoy, A.	1087	Flinois, J-S.....	1075	Foster, A.	1499	1031
.....	1231	Flipo, N.....	1048	Foster, C.T.	724	1135
.....	1271	2022	Foster, D.	1120	1209
Firestone, M.	1961	Floerchinger, C.	2575	Foster, G.L.....	589	1271
Fischer, A.	2329	Floess, D.	1095	617	1387
Fischer, Christian	1218	2164	1102	2276
Fischer, Cornelius	621	Flögel, S.....	1991	1236	2618
.....	822	Flood, B.	642	1395	Frank, N.	1537
.....	1087	1405	1475	Frank, S.	1044
.....	1657	Flores, M.	2095	1696	Franke, H.....	1105
.....	1734	Florian, P.	1582	1823	Franke, M.....	1106
Fischer, Horst	1088	Floribal, L.M.....	710	2018	Frankenberg, C.....	1568
Fischer, Hubertus	1904	1095	2265	Frantz, N.	1106
.....	2160	Floury, P.	1096	2486	Franz, G.....	695
.....	2161	Flügge, J.	2267	Foster, L.C.	1083	1234
.....	2181	Fluteau, F.....	1965	Fottova, D.	1863	Franzblau, R.....	948
Fischer, J.	1121	Flynn, G.	1096	Fountoukis, C.....	974	1107
Fischer, R.	823	Flynn, T.	1097	Fouquet, Y.	1225	2478
.....	1088	Foden, J.	1097	1408	Franzen, C.	1107
Fischer, S.....	968	1979	Fowle, D.	1405	2263
.....	1089	2032	Fox, P.	572	Frau, F.	610
Fischer, T.P.	1089	2473	1377	Frazer, R.....	904
.....	1090	Foerstendorf, H.....	1098	Fraga, L.M.....	1819	Frazier, W.	1760
.....	1541	1806	França, Z.....	1547	Freda, C.....	2018
.....	1720	Fohlmeister, J.	2580	Francalanci, L.	631	2357
Fischer, W.W.	1090	Folch, A.	2077	763	Fredin, O.	1108
.....	1286	Foley, N.	920	891	Freedman, P.	2477
.....	1397	Foley, S.....	553	993	Freeman, C.....	969
.....	1565	587	1102	1108
.....	1910	1995	1959	1258
.....	1977	2463	2067	Freeman, K.....	1249
.....	2256	Folliet, N.....	1098	France, J.	1644	Freeman, S.	2529
.....	2474	Fomba, K.W.	1099	1854	Freeze, P.....	1109
Fischer-Gödde, M.	665	1523	France, L.	1103	Frei, D.	933
.....	1091	Fonseca, Rafael	1198	France-Lanord, C.....	749	1064
.....	2059	Fonseca, Raúl O.C.....	760	828	Frei, R.	815
Fisher, C.	1196	1099	1103	873
.....	2409	1283	1143	928
Fisher, R.	1644	1423	Francescon, F.....	692	2075
.....	1854	1809	Franchi, I.	589	2097
Fisk, M.	2269	2390	Francis, A.j	2282	2210
Fitoussi, C.	1091	2437	Francis, Albarède.....	567	2376
.....	1300	Ford, B.....	1100	Francis, J.	1869	2422
Fitton, J.G.....	1607	Ford, D.....	2226	Francisco, P.C.....	1104	Frei, S.	1483
.....	2496	Ford, S.	1455	Francius, G.....	2584	Freissinet, C.	2255
Fitts, J.P.....	857	Forecast, R.....	1395	Francke, H.....	1072	Freitag, S.....	894
.....	1092	1399	François, Camille.....	1104	Freitas, L.	1967
Fitzherbert, J.....	975	Foreman, A.	1100	François, Chabaux	2266	Freitas, M.C.	928
Fitzsimmons, J.....	1092	2018	Francois, L.	1184	1788
Fitzsimons, I.....	2316	Formolo, M.J.	2475	2420	French, D.....	1819
Flachet, M.	2379	Fornaro, A.	753	Francois, R.....	957	French, J.....	1109
Flament, P.	1093	Fornash, K.	1101	François-Regis, O-D.....	2014	French, K.....	1110
Flamigni, L.....	1232	Fornasier, F.....	622	Francomme, J.....	1730	French, N.....	2512
Flanagan, D.	1760	Fornelli, A.	1101	Frandsen, C.....	883	Freslon, N.....	1110
Flehoc, C.	2017	1754	987	Frets, E.	2341
Fleisher, M.	594	Forray, V.	1468	Franěk, J.....	1378	Freund, S.....	1111
Fleitmann, D.....	2424	Förster, B.	630	Frank, A.	1470	Freundt, F.....	580
Flemetakis, S.	1093	Förster, H-J.....	1618	Frank, E.	1105	1111
Flemming, R.....	2342	2221	1778	2066
Fletcher, I.	1800	Forth, M.	1763		Freutel, F.....	1168
Fleurent, L.	1094	Forti, M.C.....	753		Frey, B.....	1656
Fleury, B.....	1094	Fortner, J.....	1389		Frey, H.	1544

Frey, S.....	1112	Fujimura, S.....	1876	Gagnidze, N.....	1888	Galy, A.....	703
Freydier, R.....	773	Fujioka, T.....	1119	Gago-Duport, L.....	1129	1135
.....	2052	Fujishima, K.....	1937	1173	1136
Freyer, G.....	1396	Fujiwara, T.....	553	1641	1196
Freytmuth, H.....	631	Fujiyama, A.....	1439	Gai, H.....	2446	2228
.....	1037	Fukai, I.....	1120	Gailhanou, H.....	1129	2502
.....	1112	Fukuda, M.....	1120	Gaillard, F.....	1706	2613
Frezzotti, M.L.....	1113	Fukui, M.....	1904	Gaillardet, J.....	749	Galy, V.....	699
.....	2226	Fukushi, K.....	601	794	1103
.....	2580	1121	855	2084
.....	2230	2137	866	Galy-Lacaux, C.....	1617
Fricke, H.....	2230	Fukushima, A.....	1438	896	Gamaletsos, P.....	1136
Fridriksson, T.....	1357	Fulignati, P.....	1875	967	1459
Friebel, M.....	1113	Fumagalli, P.....	1121	980	Gamo, T.....	1465
Frierdich, A.J.....	840	2025	1130	1874
Fries, M.....	2255	2334	1643	Gamper, A.....	1137
Frimmel, H.....	1442	Funakoshi, K-I.....	1025	1858	1311
Frings, P.....	1114	2543	Gaines, R.....	1130	1881
Frison, R.....	1223	Funamori, N.....	1122	1249	2260
Fritsch, E.....	1014	Funcke, A.....	705	2000	Gamyamin, G.....	887
.....	1114	Fung, I.....	1462	Gajos, N.....	705	Gamzo, P.....	1829
Fritschle, T.....	1115	Funk, C.....	1568	Gajurel, A.....	1103	Gambavale, G.....	1137
Fritzsche, D.....	1720	Funk, R.....	1122	Gal, J-G.....	2564	Ganeshram, R.....	2363
Frodella, W.....	1859	Furche, M.....	2259	Galán, G.....	1078	Gangloff, S.....	2160
Froehner, S.....	1918	Füri, E.....	2155	Galazka, Z.....	1752	Gannoun, A.....	758
Froelich, P.....	1770	1123	Galbraith, E.....	702	939
Fröllje, H.....	736	1541	Gale, A.....	2059	Ganor, J.....	1186
Froncini, F.....	875	1699	Galé, C.....	1547	1221
.....	1004	Furman, T.....	1525	2371	Gantt, B.....	1744
.....	1004	Furrer, G.....	888	Gale, J.D.....	971	Gao, A-G.....	1138
Frost, D.J.....	698	1715	2022	Gao, F.....	1138
.....	854	Furukawa, T.....	2303	2440	2448
.....	1115	854	2589	Gao, H.....	1628
.....	1116	1123	Galer, S.J.G.....	596	Gao, Jian-Feng.....	1139
.....	1526	1339	956	Gao, Jianfei.....	992
.....	1554	2291	1131	Gao, Jianxin.....	1083
.....	1865	2471	1523	Gao, Jun.....	2280
.....	1916	Furuya, K.....	2310	2368	Gao, L.....	2199
.....	1990	Fusillo, R.....	1124	Galić, A.....	1783	Gao, Q-Q.....	941
.....	2068	Futagami, T.....	1439	Galimberti, R.F.....	2525	Gao, Shan.....	1153
.....	2084	Fuzzi, S.....	1912	Galimov, E.....	1421	1277
.....	2417	2064	Gallagher, M.....	1131	2528
.....	2423	G		Gallagher, T.....	985	2594
.....	2509	G., T.....	2217	Gallego, E.....	1132	Gao, Shuang.....	1139
Fruchter, N.....	1116	Gab, F.....	1125	Gallego-Torres, D.....	1410	Gao, X.....	1140
Früchtl, M.....	1117	Gabay, C.....	1724	1696	2603
Frugier, P.....	1117	Gabellone, T.....	1125	Gallego-Urrea, J.....	943	Gao, Ying.....	2529
Früh-Green, G.L.....	766	Gabitov, R.....	1126	Gallet, S.....	862	Gao, Youfeng.....	2596
.....	2424	Gaboyer, F.....	890	Gallhofer, D.....	1132	Gao, Yu-Ya.....	1140
Frutschi, M.....	2464	Gabrieli, J.....	1126	2431	Gao, Yuan.....	2514
Fu, B.....	1008	Gabrielli, P.....	1126	Galli, G.....	1133	Gaona, X.....	1017
Fu, C-C.....	1118	2374	Galloway, T.....	2040	2079
.....	2480	Gadgil, A.....	2395	Galoisy, L.....	808	Gapais, D.....	1991
Fu, D.....	2611	Gaetani, G.....	901	861	Garasic, V.....	1141
Fu, S-M.....	852	1127	Galuskin, E.....	964	Garbaras, A.....	843
Fu, X.....	1074	1589	1133	1141
Fu, Y.....	1118	Gagan, M.....	1010	Galuskin, E.....	1134	Garbarino, G.....	611
Fuchs, P.....	1119	Gagell, C.....	1127	1134	1787
Fuchs, J.....	2510	Gagen, M.....	591	Galuskina, I.....	1160	Garbe-Schönberg, D.....	1806
Fuchser, J.....	2510	Gaggero, L.....	1128	1134	García, María Gabriela ...	2276
Fuentes, F.....	666	Gagliano, A.L.....	721	1160	Garcia, Michael.....	1692
Fujii, Naoki.....	1793	1128	Galvez, M.....	1135	Garcia, Miguel.....	2079
Fujii, Naoki.....	1837		Garcia, R.....	653
Fujii, T.....	1798						
Fujimoto, M.....	2470						

García	Gauthier, A.	1014	Genske, F.	1154	Ghasemi, H.	1988
de Madinabeitia, S.	1148	Gentili, S.	1154	Gherardi, F.	1969
García del Real, P.	1616	Geoghegan, M.	1258	Gherardi, J.	793
García- Lorenzo, M.	1697	Gauthier-Lafaye, F.	Georg, B.	1221	1537
.....	1697	Gauthiez Putallaz, L.	1738	Ghinet, C.	1161
García-Armisen, T.	1634	2613	1352
García-Gutierrez, M.	580	Gautron, L.	George, A.	605	1684
.....	1143	Gavrieli, I.	George, C.	1155	Ghiorso, M.S.	728
García-Robledo, E.	2346	Georgelin, T.	688	1162
García-Ruiz, J.M.	1899	1155	1223
García-Solsane, E.	2091	Georgiev, Stoyan	1962	Ghoneim, M.	1162
García-Tenorio, R.	2418	Gavrilov, Y.	Georgiev, Svetoslav V.	1156	2194
García-Tortosa, F.J.	2124	Gavrilyuk, A.	1323	Ghorbel, M.	1810
García-Veigas, J.	2244	Gawronski, T.	Geraki, T.	809	Ghorbel, S.	1163
Garçon, M.	862	Gayer, B.	Gaye, B.	1774	Geranmayeh	1802
.....	1143	Gayer, E.	Odomeh, A.	1235	Ghosh, G.	649
Gardel, A.	1191	Gazel, E.	Gerard, E.	1739	1823
Gardien, V.	751	1974	2021
Garg, S.	2437	Ge, Liangsheng	Gérard, M.	725	Ghosh, S.	1802
Garing, C.	1144	Ge, Lu	1156	Ghosh, W.	1163
Garnier, G.	2585	Gebauer, D.	1965	Ghoshal, S.	1164
Garnier, P.	870	1974	Giaccio, L.	888
Garofalini, S.	1144	Geckeis, H.	Gerdes, A.	771	Giacconi, P.P.	571
Garofalo, P.	1145	1064	1164
Garrido, C.J.	657	1306	1165
.....	1194	1672	Giammanco, S.	1133
.....	1266	Geelhoed, J.	2206	1165
.....	1640	Geerlings, P.	2210	1766
.....	1681	Gehin, A.	2316	Giammar, D.	572
.....	2341	Gehlen, M.	2360	1377
.....	1636	Gehrels, G.	2380	1673
Garuti, G.	1636	Geibert, W.	2435	Gianfagna, A.	2261
Garven, G.	731	2547	Giannakourou, A.	1975
Garver, E.	665	2584	Giannossi, M.	828
Garvin, M.C.	2152	Geiger, C.A.	Gerin, C.	1157	Giano, S.I.	990
Garzanti, E.	1143	Germain, D.	2034	Gianola, O.	1166
Gasc, J.	2167	Geiger, F.M.	Germain, Y.	1110	Gianolla, P.	938
Gaschnig, R.M.	1145	German, C.R.	1157	Giarretta, A.	829
.....	1335	Geilert, S.	1158	Gibbs, D.	1724
.....	2096	Geilich, J.	1576	Gibbs, G.V.	1166
.....	2594	Geipel, G.	Gernon, T.	1400	Gibert-Brunet, E.	1094
Gashkina, N.	1777	Geisler, T.	1915	Gibson, B.	1375
Gąsiorrek, M.	1660	Gerringa, L.	1541	Gibson, K.A.	1167
Gasparini, N.	2498	Geisler-Wierwille, T.	Gerschlaue, F.	1158	Giegengack, R.	2244
Gasparini, P.	1146	Geist, D.	Gersonde, R.	868	Giehl, C.	1167
Gasparon, M.	576	Gélabert, A.	792	Gier, J.	2353
.....	1789	Gertisser, R.	1253	Gieré, R.	989
.....	616	1381	1093
.....	631	1381	1168
.....	1146	Gelencsér, A.	Gertner, I.	1159	1218
Gasser, G.	1147	Gélinas, Y.	2433	1650
Gast, P.	2346	Gervilla, F.	661	1688
Gastelum Strozzi, A.	1023	903	1702
Gattacceca, J.	1135	Geller, G.	1159	2481
Gattolin, G.	938	Gellert, R.	1194	2418
Gaucher, C.	815	Gerya, T.	1058	Giering, S.	2418
.....	2075	Geske, A.	1160	Gies, H.	1733
.....	2210	Geslin, E.	1746	Giesler, R.	1448
Gaucher, E.C.	1552	Gemmi, M.	1827	Giestler, G.	1226
Gault, B.	1795	Gen, J.	829	Giffaut, E.	893
Gaup, R.	2003	Genberg, J.	Gfeller, F.	1160	1129
Gautheron, C.	1147	Geng, L.	Gfeller, G.	1904	2109
.....	1157	Geng, X-L.	Ghaleb, B.	1161	Gigli, L.	1168
.....	1157	Gennis, R.	Gharsoo, M.G.	981	Gil Ibaruchi, J.I.	1142

Gil Lozano, C.....	1129	Giraudeau, J.....	1067	Godard, M.....	740	Gómez-Pugnaire, M.T. ...	1640
.....	1173	Girguis, P.....	1373	934	1681
.....	1641	1895	1103	Gonçalves, O.....	596
Gil-Crespo, P-P.....	1171	Gisbert, G.	631	1184	Goncharov, Aleksey	1852
.....	1954	1146	1961	Goncharov, Aleksey	1190
.....	2074	1174	2025	Göncüoğlu, M.C.	808
Gilardoni, S.....	1169	1177	2138	Gondar, D.	599
.....	2064	Gisbert, P.....	1828	2178	1086
Gilbert, B.....	1169	Gislason, S.R.....	1032	Goddéris, Y.....	1003	Gong, H.....	1191
.....	1170	1178	1184	Gong, S.	2611
.....	1576	1225	1343	Gong, X.....	2196
Gilbert, P.	1170	1274	2284	Goni, M.....	1728
Gilbert, S.	945	1406	2420	Gonsior, M.....	1024
.....	1171	1894	Godel, B.....	2434	Gontharet, S.	1191
.....	2406	2277	Godelitsas, A.	1136	1192
Gilcrease, P.	1187	Giubbina, F.....	1456	1185	2063
Gilder, C.....	1728	Giudice, G.	1944	1459	Gonzales, M.....	1261
Giles, D.	890	Giuffrida, G.....	2505	Goderis, S.	2399	Gonzalez, A.G.	1192
.....	1363	Giuffrida, M.	2413	Godfroy, A.....	890	1193
.....	2032	Giuli, G.....	622	Godinho, J.....	1185	1949
Gilfillan, S.....	1172	824	Godon, N.	1094	Gonzalez, Christian.....	1227
.....	1458	2249	1117	González, Cristina.....	1735
Gilgen, S.	1172	Giulianelli, L.	1912	Goekpinar, T.....	1044	Gonzalez, E.....	1697
Gilhooly, W.....	1173	2127	Goemann, K.....	1930	Gonzalez, J.....	1193
.....	2225	Giuliani, A.....	1178	Goettlicher, J.....	1136	Gonzalez Fairen, A.	1129
Gill, B.C.	936	Giuliani, G.....	2242	1185	1173
.....	1173	Giuliani, L.	1179	Gogot, J.....	1982	1641
.....	1252	Giunta, T.	1179	Gogou, A.	1975	González Guadarrama,	
.....	1401	Giuntoli, F.	1180	Goin, J.....	2421	M.D.J.	1194
.....	1725	Gkinis, V.	1180	Gökgöz, A.....	1443	Gonzalez-Davila, M.....	1193
Gill, James.....	1373	2257	Golan, R.....	1186	1949
Gill, Jim.....	2094	Gkritzalis-Papadopoulos,		Golan, T.....	1186	Gonzalez-Jimenez, J.M.....	605
Gill, S.	2333	A.....	1406	Goldberg, T.....	1187	683
Gilles, M.	2014	Gladish, E.....	2024	2041	903
Gillet, P.	1614	Glamoclija, M.	2255	Golden, J.....	1629	1159
Gillis, K.....	1184	Glancy, S.	2094	Goldenberg, E.....	1218	1194
.....	1750	Glass, J.	1181	Goldhammer, T.....	2166	1802
Giménez, J.....	1410	Glaus, M.A.	696	2566	Gonzalez-Lopez, J.	1195
Gimeno, D.....	631	Glaus, R.....	1122	Golding, S.....	952	Gonzalez-Toril, E.	999
.....	1146	Glavin, D.	2255	1066	Goodall, I.C.A.....	1084
.....	1174	Glazman, H.	1147	1187	Goodall, J.....	1195
.....	1177	Glazner, A.	904	1470	Goodge, J.....	1196
.....	1910	1181	1754	Goodrich, C.....	1758
Gimmi, T.....	696	Gledhill, M.	1182	1942	Göpel, C.....	707
.....	1174	Glennon, M.	1182	Goldmann, A.	1188	1196
Gin, S.	1094	Gloaguen, E.....	2362	1188	2620
.....	1927	Glud, R.N.	913	Goldstein, R.....	1160	Göransson, H.	1656
Ginnane, C.	713	1183	Goldstein, S.L.....	740	Gorbachev, N.....	1197
Ginoux, P.	1175	1451	1189	1502
Gioda, A.....	1705	Gminski, R.	1168	2258	Gorczyk, W.....	1197
Gioia, D.....	990	Gnecco, E.....	1971	Golovin, A.	1359	Gordanić, V.....	1198
Gioncada, A.	1124	1971	2189	2243
Giordano, G.....	812	Gniese, C.	2024	Goltsin, N.	1516	2414
Giordano, M.....	1175	Gnos, E.....	1377	Golubev, V.	871	Gordon, G.	853
Giordano, P.	2242	Gobbi, G.P.....	959	Gomes, E.	1189	1198
Giorgioni, M.	1176	Gobechiya, E.....	772	Gomes, Maria	2318	1293
.....	1379	Gocmez, G.....	1183	Gomes, Maya.....	1190	Gordon, K.	1712
Giouri, K.	1176		Gomes, P.....	1207	2477
Giovanardi, T.	1177	2384	Gordon, S.M.	979
.....	1545		Gómez-Gras, D.....	918	1199
Girard, J-P.....	1662	1831	Goren, O.	1260
Girardclos, S.	2233		Gómez-Morales, J.....	1223	Gorge, C.....	967
Girardin, C.	1575	1130

Gorji, L.	1665	Grasemann, B.	1026	Griffin, W.L.	605	Grundy, J.	2041
Gorman, J.	1199	Grasineau, N.	1342	676	Grybos, M.	2089
Gorokhovskiy, B.	2536	Grassa, F.	810	683	Gu, C.	2199
Gorrotkategi, P.	1200	823	1140	Gu, X.X.	1222
Gorski, C.	1200	1944	1159	2598
Gosar, M.	671	Grasse, P.	1031	1194	Gu, Y.	1647
.....	991	1209	1215	Gu, Z.	1222
Gosnold, W.	1201	Grassineau, N.	1209	1328	Guagliardi, A.	1223
Goswami, J.N.	1672	Grataloup, S.	1019	1337	Gualda, G.A.R.	1223
Goto, A.	1201	Grathoff, G.	1845	1802	1760
Goto, D.	1202	Grathwohl, P.	1210	1813	Gualtieri, A.	840
Göttlicher, J.	627	Gratton, Y.	1576	1872	1224
.....	1459	Gratwohl, P.	1239	1873	Guan, J.	1332
Gottschalk, M.	1202	Grau Crespo, R.	966	1943	Guan, Y.	757
Gottsmann, J.	1789	Grauel, A-L.	2408	2019	1313
Götze, J.	1618	Graves, C.	2259	2140	Guastaldi, E.	653
.....	2221	Gravley, D.	677	2452	1224
Götze, L.C.	1203	950	2478	2519
Goudeau, M-L.	2408	Grawunder, A.	1210	2523	Gube, M.	2425
Goudemand, N.	1903	Gray, D.	2043	2583	Gudbrandsson, S.	1225
Gouin, J.	2362	Gray, J.E.	1211	Griffith, E.	2150	Gueguen, B.	1225
Gould, I.	2553	Gray, W.	1114	2489	Guéguen, F.	1226
Gourcy, L.	770	1211	Griffith, G.	713	Gueibe, J.	1060
Gourlan, A.T.	1203	Grčman, H.	671	Griffiths, G.	1215	Guenther, W.	1226
.....	1537	Greau, Y.	1337	Griffiths, M.	1216	Guerbois, D.	1227
.....	2029	Greber, N.D.	1212	Griffiths, T.A.	1216	1891
Gousgouni, M.	1459	Green, Damon	626	Grilli, R.	1217	Guerra, P.	1227
Gouze, P.	1144	Green, David	849	Grime, G.	2505	Guerrot, C.	767
.....	1961	Green, H.	1936	2622	978
Govaerts, J.	1204	Greenwood, J.	757	Grishina, S.	1217	2017
Govers, G.	2082	Greenwood, P.	2364	Grivé, M.	1021	Guevara, A.	1708
Govil, P.	1204	Greer, J.	1212	Groat, L.	948	Guevara, V.	1228
Govindaraju, -.	590	Grefe, I.	1213	1218	Guglielmino, F.	825
Grabs, T.	1563	Gregg, D.	1650	Grobe, R.	1111	Guibaud, G.	2089
Grady, M.	2255	Gregoire, M.	1058	Grobety, B.	1218	Guidi, M.	873
Graf, J.	1205	1078	Grocholski, B.	2199	911
Graham, C.	777	1460	Grocke, S.	1219	1010
Graham, D.	648	1713	Grodzicki, M.	935	Guidry, M.	1664
.....	1655	2007	Gröger-Trampe, J.	1219	Guignot, N.	1787
.....	1752	Gregory, D.	1245	Grohmann, C.	1698	Guilbaud, R.	1228
Graham, G.	1292	1546	Groleau, A.	1048	1348
Graham, I.	683	Greig, A.	1010	2252	Guillaume, D.	1488
Grambow, B.	1205	1178	Grolimund, D.	925	1983
.....	1206	2369	Gronewold, J.	1445	2183
Gramenitskiy, E.	574	Greiner, M.	1213	Gros, J.	612	Guillaumet, M.	1133
Grandal, E.M.	1108	Gresta, S.	1680	Gros, O.	723	Guillet, M.	916
Grandbois, R.	1597	Grew, E.	1214	2173	Guillong, M.	1229
Grande Gil, J.A.	1206	1629	Grosbois, C.	1163	Guillot, B.	1098
.....	1207	Grey, N.	1398	Gröschel, A.	1806	2434
.....	2384	Greyer, M.	2425	Grose, C.	1220	Guillot, T.	1229
Grandia, F.	2401	Griban, J.	1214	Gross, J.	757	Guillou, V.	1374
Granet, M.	636	2122	Grosse, J.	1220	Guimaraes, F.	1610
Graney, J.	2264	Grice, K.	776	Grossi, C.	932	Guimaraes, L.F.	1230
Grange, M.	1207	2364	Grosso, N.R.	1558	Guinoiseau, D.	1643
.....	1414	Griera, A.	918	Grotek, I.	1221	Guitreau, M.	752
Grangeon, S.	893	1831	Grotzinger, J.	691	841
Granieri, D.	797	Griesshaber, E.	1853	1565	1230
.....	1208	1590	Gulaya, E.	2144
Grant, K.	1943	Grousset, F.	1537	Güleç, N.	1814
Grant, T.	1208	Grove, T.L.	859	1907
Grantham, G.	1298	Grozdev, V.	1962	Gullu, B.	974
Grasby, S.	1482	Gruber, C.	1221	1231
.....	2321	Gründger, F.	2272	1498

Gültekin, F.	1087	Guzman, M.	1237	Haley, B.	552	Hammouda, T.	834
.....	1231	Guzmics, T.	1238	2276	1006
.....	1271	Guzzetti, F.	1004	Halfar, J.	1083	1250
Gumus, L.	1431	1004	Halicz, L.	2188	Hamzehie, Z.	1425
Gunnarsson, I.	1178	Guzzo, J.	897	2324	Han, D.	1251
.....	1414	Gvozdaite, R.	1010	Halim, S.	2297	Han, J-S.	879
.....	2277	Gwak, H-Y.	1466	Hall, A.	1243	1350
Gunnarsson Robin, J.	1445	Gwosdz, S.	1238	Hall, C.M.	839	Han, K.M.	1251
Gunnlaugsson, E.	1178	Gyollai, I.	1916	1544	Han, R.	2011
.....	2277			Hall, J.	2277	Hanan, B.	1252
Günther, A.	741	H		Hall, R.	798	1256
Günther, D.	1122	Ha, K.	1351	972	1428
.....	1232	Haase, C.	767	Hallberg, K.	713	1525
.....	1272	Haase, K.	678	Halldorsson, S.	1243	Hanchar, J.M.	847
.....	2297	761	1244	2310
Guo, C.L.	1232	1111	Halliday, A.	2548	Hancock, L.G.	1252
Guo, H.	2118	1154	Halliday, Alex.	659	Hand, M.	593
Guo, Jinghui.	886	1443	1244	1939
.....	2589	2038	1607	2230
Guo, Junfeng.	1233	2476	1894	2442
Guo, M.	1233	Haba, M.	1239	2289	Handler, M.	916
Guo, Q.	1234	Haberer, C.M.	1239	Hallis, L.J.	1244	925
.....	1311	Habicht, K.S.	1990	Hallmann, C.	1110	Handley, H.	1253
.....	1954	2475	1581	Handley, K.	572
.....	2614	Habig, J.	1520	Halm, H.	2516	1377
Guo, W.	1560	1540	Halpin, J.	1245	Hanger, B.	1253
Guo, X.	2543	1797	1546	2555
Guo, Yanru.	2597	Habler, G.	1026	Halse, H.R.	694	Hanley, J.	587
Guo, Yun.	2550	1216	1245	748
Guo, Z.	2480	2148	Halton, A.	924	1254
Guoan, Z.	2593	Habraken, W.	2223	Halverson, G.P.	923	1449
Gupta, M.	641	Hachicho, N.	1240	1097	1665
Gupta, S.	2021	Häckel, F.	1443	1246	2472
Gurenko, A.	706	Hacker, B.	781	1343	Hannah, J.L.	1156
.....	1123	1240	Ham, B.	1533	1323
.....	1234	1494	Hama, T.	1246	2258
Gurnis, M.	1282	1533	Hamahiga, K.	1440	2356
Gurrieri, S.	810	2224	Hamamoto, M.	696	2525
.....	962	Haderlein, S.	1392	1247	2619
Gürtler, S.	2155	Haeckel, M.	981	Hamaoka, H.	1793	Hannah, P.	2613
Guseva, N.	2383	1241	Hamed, A.	959	Hannon, A.C.	899
Gussone, N.	747	1608	Hamelin, C.	1247	Hans, U.	1254
.....	2455	Haese, R.	712	1922	Hansel, C.	786
Gust, D.A.	2212	Haffert, L.	1241	Hames, W.	1248	1255
Gustafsson, J.P.	643	1608	1968	1560
.....	710	Hafizoglu, E.	1183	Hamester, M.	863	2404
.....	1235	Hagadorn, J.	1246	1248	2423
.....	1551	Häger, T.	2463	Hamilton, J.F.	1084	Hansen, V.	1255
Gustaytis, M.	1235	Haider, N.	1452	Hamilton, L.	2173	Hansmeier, C.	1256
.....	1815	Haider, S.	965	Hamilton, S.	1187	Hanson, C.A.	1342
Gustin, M.	882	Haigis, V.	674	Hamilton, T.	758	Hansson, M.	1904
Gutjahr, M.	1236	Hain, M.	1241	1249	Hansteen, T.H.	1083
.....	2059	1242	Hamm, L.	983	Hanyu, T.	1256
Gutzmer, J.	1752	1369	874	2178
.....	2224	Hakala, A.	1929	1249	2319
Guyodo, Y.	836	Hakdaoui, M.	1038	1843	Hanzel, J.	1257
.....	2332	Hakim, S.S.	2168	Hammond, C.	1250	Hao, J.	1614
Guyot, F.	588	Halas, S.	747	Hammond, D.E.	661	Hao, Jialong.	2551
.....	1236	Halder, D.	710	1268	Hao, Jiaqing.	1388
.....	1237	Hale, C.	2563	Hammond, S.	1070	Hao, L.	1646
.....	1759	Halevy, I.	701	1344	Hao, W.	2448
.....	1767	1242			Hao, X.	1647
.....	2325					Hara, Y.	2554

Harada, N.	1120	Haskell, W.Z.....	1268	Hawkesworth, C.	984	Heinrich, C.A.	1132
.....	1257	Hasliger, E.	991	2245	1280
Haraguchi, D.	2291	Hassaan, M.	1269	Hawley, S.	1274	2431
.....	2337	Hassan, A.	1269	Hay, M.	813	2436
Haraguchi, S.	2534	Hassan, T.	1269	Hayashi, D.	1837	2441
Hardiagon, M.	1258	Hassani, Y.	598	Hayes, C.	594	Heinrich, W.	1283
Hardiman, M.	569	Hassannezhad, A.A.	995	1369	2048
Harding, J.	969	Hassellöv, M.	943	Hayes, K.	701	2049
.....	1108	Hassenkam, T.	1270	Hayles, J.	1274	Heinz, D.	1088
.....	1258	Hassnezhad, A.	995	Hayoz, P.	991	Heistek, R.	1280
Hardisty, D.	1259	Hastings, M.	1081	Hazarika, P.	1275	Heister, K.	994
Harir, M.	1024	1270	Hazemann, J-L.	1627	1281
.....	1294	Haszeldine, S.	1172	1643	2001
Harju, E.	1259	Hatcher, P.G.	1882	1983	Heizler, M.	1281
Harlavan, Y.	1260	2524	Hazen, R.M.	1050	Hékinian, R.	2199
.....	2324	Hathorne, E.	904	1081	Held, A.	2139
Harley, S.	2496	1271	1275	Held, P.	2368
Harlov, D.	1260	2618	1276	Helena, S.	2056
.....	2358	Hatipoglu, E.	1231	1571	Hélie, J-F.	1792
Harmer, S.	948	1271	1629	Hellebrand, E.	2094
.....	1261	Hatta, M.	2198	Hazotte, A.	1276	Heller, H-P.	1752
Harmon, M.	1442	Hattendorf, B.	1232	He, D.	1277	Heller, M.	927
Harouaka, K.	1261	1272	He, Hongping.	2610	Hellmann, R.	949
Harpold, A.	881	Hattori, K.	558	He, Huaiyu.	1277	Hellstrom, J.	1010
Harpp, K.	1956	605	He, J.	1278	1282
Harrington, G.A.	2228	963	He, T.	1278	1363
Harris, C.	690	1911	He, Y.	2522	1936
.....	960	Hattori, S.	1042	He, Z.	2448	2037
.....	2357	1042	Head, I.M.	1342	2580
Harris, E.	1892	1272	Heald, C.	1514	Helmberger, D.	1282
Harris, J.W.	1840	2623	Healy, R.M.	1084	Helms, J.	2498
Harris, L.B.	1068	Hatzikonstantinou, N.	1185	Heaman, L.	950	Helmy, H.	1283
Harris, N.	1796	Hauff, F.	1111	1095	Helpa, V.	1283
Harris, P.	1182	1956	1929	Helz, G.	1284
Harris-Hellal, J.	714	Haug, G.	1241	2045	Hemati, M.	2299
Harrison, A.L.	1262	1242	Hearty, P.	2033	Hembury, D.J.	1284
.....	1992	1369	Heavens, N.	568	1316
Harrison, G.	596	Haug, T.J.	1455	Heberling, F.	1279	Hemming, S.R.	1285
Harrison, M.	2493	Haule, K.	902	2326	2389
Harrison, R.	784	Hauri, E.H.	555	Hébrard, E.	1700	Hemminsson, C.	1358
.....	1262	711	Heck, S.	1862	Hemond, C.	1285
Harrison-Buck, E.	1263	805	Heckman, K.	1659	Hemond, H.	2486
Harsh, J.	987	1382	Hedges, L.	2440	Hemp, J.	1090
.....	1109	1692	Heeschen, K.	1105	1286
Hart, C.	709	1865	Hegedűs, E.	1504	1910
Hart, E.	1263	1956	Hegner, E.	1600	Hendel, R.	2444
Hart, W.	1264	1978	2244	Henderson, G.M.	662
Harte, B.	1264	2108	Heikal, M.T.S.	1162	780
.....	1265	2199	1279	953
Hartland, A.	1265	2205	2194	973
.....	2517	2255	Heiko, P.	1236	1151
Hartley, A.	1056	2450	Heikoop, J.	780	1284
Hartmann, Jan Frederik ...	1266	2484	Heiland, K.	2174	1316
Hartmann, Jens	1786	Hauser, A-C.	1273	Heim, C.	1008	1323
Hartnett, H.	1885	Hauser, P.	888	Heim, K.	1098	1329
Harvey, J.	1266	Häusler, K.	2162	Heim, N.A.	1939	1331
Harvilla, P.	1669	Hauzenberger, C.	1808	Hein, J.	608	1937
Haschke, M.	1267	1866	1499	1977
Hasegawa, W.	1267	Havig, J.	758	Hein, S.	1579	2436
Hashiguchi, M.	2534	Haviv, I.	2106	Heimesch, B.	2420	Henderson, M.	2183
Hashimoto, K.	1826	Havranek, R.	1130	Heinold, B.	2317	Henderson, P.	858
Hashizume, K.	1268	Hawes, I.	883	Heinonen, J.	1657	Hendrickson, S.	1553
.....	1699	Hawkes, J.	1273		Hendry, K.	1286

Henehan, M.J.	1475	Hertkorn, N.	1024	Hilton, D.R.	648	Hirschmann, M.	1304
.....	1696	1294	662	2504
Henjes-Kunst, F.	2354	Herut, B.	600	863	2590
Henkel, Steven	2003	1975	1090	Hiscock, M.	1304
Henkel, Susann	1287	Hervé, F.	666	1243	Hissler, C.	2266
.....	1991	Herwartz, D.	1294	1244	Hitchcock, A.P.	1798
.....	2253	Herzberg, C.	1295	1814	Hnatyshin, D.	2386
Henkel, T.	1393	Herzlieb, S.	1311	2105	Ho, Y-F.	2524
Henley, R.	1708	Herzog, G.	2539	2357	Hoàng, T.B.H.	1688
.....	2333	Hess, K-U.	741	Hilton, R.	1136	Hoareau, G.	733
.....	1041	1980	1299	Hobbie, E.	784
Henne, S.	1041	1980	Hily-Blant, P.	734	Hobbs, B.	1197
Hennig, C.	668	2428	Hin, R.C.	1300	Hochella, Jr, M.	1396
Henriques, S.B.A.	1287	Hesse, F.	2329	Hindshaw, R.	1300	2405
Henry, D.	1120	Hesselbo, S.P.	2376	Hinkel, K.	1799	Hochstetler, D.L.	876
Henry, L.	1288	Hetland, E.	612	Hinkle, M.A.G.	840	Hockaday, W.	1338
Hensen, C.	1608	Hettipathirana, T.	1584	1301	Hockmann, K.	1305
Henson, N.	2589	Heubeck, Christoph	1818	Hinman, N.	1024	Hodierne, C.	2083
Henton - De Angelis, S. ...	2428	Heubeck, Christoph	1316	Hinrichs, K-U.	697	Hodson, M.E.	774
Hepburn, L.E.	604	Heuer, V.	697	756	969
Herbst, F-A.	1764	1553	1055	1305
Herbst, M.	586	2166	1087	2408
Herceg, M.	620	Heuser, A.	1099	1301	Hoefler, C.E.	1306
Herd, R.	1976	1295	1356	1306
Herde, H.	1659	1423	1405	Hoefler, H.E.	771
Herdsmann, R.	592	Heuser, J.	1296	1553	1306
Hergt, J.M.	852	Heusser, L.	1069	1557	1306
.....	1288	Hewitt, D.	942	1730	2206
.....	1683	Hewton, M.	1691	2157	2210
.....	1936	Hezel, D.	675	2166	Hoeger Luque, T.	1307
.....	2369	Hibberson, W.	849	2201	Hoehler, T.	926
Hering, D.	1107	Hibbert, K.	1296	2234	2369
Hering, J.	2179	Hicks, K.	1039	2510	Hoelzemann, J.	816
Herman, D.	2345	Hicks, S.	1558	2566	Hoernle, K.	1373
Herman, F.	1289	Hidaka, H.	1239	Hinton, R.	1407	Hoeschen, C.	1307
Hermann, J.	747	1297	Hippe, K.	1302	Hoeschen, T.	1307
.....	1148	Hidalgo Moreno, C.	1023	Hippler, D.	1234	Hoff, C.	784
.....	1289	Hidas, K.	1618	Hirakawa, S.	2116	Hoffmann, D.	2163
.....	1402	Hiemstra, T.	1297	Hirano, H.	2301	Hoffmann, J.E.	933
.....	1640	1309	Hirano, Naoto	1302	1308
.....	1911	Hierro, A.	655	1663	2296
.....	2262	Higashino, F.	1298	Hirano, Nobuo	2470	Hoffmann, K-H.	1433
.....	2338	Higgie, K.	2341	Hirano, N.	1540	Hoffmann, M.	1308
.....	2402	Higgins, J.A.	701	1797	Hoffmann, N.	2259
Hermanska, M.	1290	716	Hirao, N.	1772	Hoffmann, T.	745
Hermoso, M.	1290	1241	1884	Hoffmann-Jäniche, C.	1764
Hernandez, C.	1697	Hignette, M.	1496	Hirata, T.	601	Hoffnagle, J.	2257
Hernández, L.	2015	Hignette, T.	1496	1303	Hofmann, Albrecht	740
Hernandez Sanchez, M.T.	1291	Higo, T.	2283	1885	1309
Hernandez-Cordoba, M. ...	1697	Higo, Y.	2543	2116	Hofmann, Annette.	1309
Hernandez-Puentes, P.	1291	Hihose, T.	2521	2202	Hofmann, Axel	553
Herndon, S.	2575	Hilaret, N.	2167	2303	560
Hernlund, J.	1536	Hilamo, R.	1169	2541	969
Herod, M.N.	1292	Hildebrand-Habel, T.	2456	2567	Hofmann, S.	1310
Herold, A.	2219	Hilkert, A.	1410	Hiroi, Y.	1436	Hofmann, T.	1418
Herrero Albillos, J.	784	Hillaire-Marcel, C.	1161	Hirono, Y.	2623	1554
.....	1262	1537	Hirose, Katsumi	1457	1714
.....	1292	Hillamo, R.	1867	1303	1840
Herrin, J.	1007	Hillenbrand, C-D.	1912	1436	2156
.....	1293	1974	1860	2430
Herrmann, A.	1293	Hills, L.V.	1585	Hirsch, A.	1296	Hofstetter, T.B.	1200
Herrmann, H.	764	1585	1310
.....	1099
Herrmann, M.	1518

Hogarth, G.....	1195	Hong, G.H.	1318	Hough, R.....	1942	Hu, X.....	1334
Hogg, A.....	943	1465	2381	Hu, Yang.....	1496
Hoglund, L.....	2394	Hong, K.S.....	2203	Houghton, B.....	1027	Hu, Yongxia.....	2128
Hohl, S.....	1311	Hong, M.....	2322	1326	Hu, Z.....	1277
Höhler, K.....	2259	Hong, T.....	2191	Houot, S.....	1575	1335
Hokada, T.....	1769	Hong, Y.....	1317	Houseman, G.....	1327	2528
.....	2304	Hongju, Z.....	2454	Hout, C.....	2271	2594
.....	2539	Hood, D.....	1318	Houzay, J-P.....	1380	Hua, J.....	2454
Hökerek, S.....	582	Hooijschuur, J-H.....	905	Hövelmann, J-E.....	2007	Hua, R.....	1335
.....	1906	Hoose, C.....	1936	Hovis, G.....	1327	Huang, B-S.....	1525
Holbourn, A.....	1637	2259	Hovius, N.....	1136	Huang, Daikuan.....	1574
Holcomb, M.....	901	Hopcroft, P.....	2163	2228	Huang, Dan.....	1331
.....	1722	Hope, J.....	1110	Howard, D.....	1253	2611
Holden, N.E.....	1311	Hopkins, J.....	1319	Howell, D.....	Huang, F.....	1073
.....	2417	Hopkins, M.....	841	1215	1336
Holdgate, G.....	852	1319	1328	Huang, Jen-How.....	2531
Holdship, P.....	1284	Hopp, J.....	1243	Howes, E.....	705	Huang, Jin-Xiang.....	1337
Hole, M.....	1762	Hoppe, P.....	2268	Hoyer, M.....	1328	Huang, Jing.....	1336
Holland, G.....	1312	Hoppie, B.....	1320	Højlund, F.....	1675	Huang, Junhua.....	1337
.....	2195	Hopwood, J.....	914	Hronsky, J.M.A.....	676	Huang, Junhuang.....	1651
Holland, H.....	2244	Hora, J.....	1320	1873	Huang, Ko-Chun.....	1338
Hollanda, M.H.....	2319	Horan, M.....	1321	Hrubiak, R.....	1329	Huang, Kuo-Fang.....	594
Holler, T.....	2566	Horbe, A.M.C.....	596	2146	Huang, L.....	1627
Hollingham, M.....	1312	Hori, M.....	1321	Hruska, J.....	1509	Huang, Q.....	2196
Hollings, Pete.....	645	Horie, K.....	1322	Hsieh, I-J.....	1613	Huang, Rixiang.....	1338
.....	1378	2304	Hsieh, Y-T.....	1151	Huang, Rui.....	1339
Hollings, Pete.....	1313	2539	1316	Huang, Shan.....	1339
Hollingsworth, N.....	1195	Horiguchi, K.....	1322	1329	Huang, ShiChun.....	1073
Hollis, S.....	2556	Horita, J.....	1323	Hssaisoune, M.....	1594	1336
Hollister, L.....	1313	Horiuchi, M.....	1123	Hsu, C-W.....	1613	1340
Holloway, J.....	1538	Horn, I.....	570	Hsu, H.....	1330	Huang, Shichun.....	1371
Holm, N.G.....	647	977	Hsu, L.....	1579	1922
.....	1314	1559	Hsu, W.....	2462	Huang, Xiaoxian.....	1340
.....	1358	1879	Hu, B.....	1330	Huang, Xingxing.....	774
Holm, P.M.....	1314	Horner, T.J.....	1323	Hu, Chaoyong.....	1331	Huang, Yaoxian.....	2512
Holmden, Chris.....	1315	Hornibrook, E.....	1610	Hu, Chunhua.....	1331	Huang, Yi.....	1341
Holmden, Chris.....	1785	Horsfield, B.....	692	2611	Huang, Yu.....	1341
Holme, C.....	2385	2496	Hu, D.....	1335	Huang, Yulong.....	2596
Holmes, J.....	1211	Horstwood, M.....	760	Hu, H.....	1932	Hubbard, C.....	910
Holmes, M.....	794	1324	Hu, J.....	1332	Huber, C.....	2185
Holmes, V.....	869	1927	Hu, L.....	1574	Huber, J.....	1373
Holmström, S.J.M.....	564	2226	Hu, M.....	948	Hubert, A.....	1342
.....	647	Horváth, P.....	647	2085	Hubert, C.R.....	1342
Holst, J.....	1315	Hoshino, T.....	1324	Hu, N.....	2458	Hubert-Théou, L.....	1246
.....	2227	1793	Hu, Peiqing.....	1332	1343
Holt, K.....	1195	2323	Hu, Ping.....	2597	Hublet, G.....	1343
Holtz, F.....	977	Hosoi, K.....	2540	Hu, R.....	1118	Huck, C.....	1344
.....	1770	Hossain, M.....	1455	1652	Huckriede, H.....	747
.....	2410	Hosseinzadeh, G.....	2556	Hu, Sen.....	1614	Hudgins, T.....	1344
Homann, M.....	1316	Hou, K.....	1325	2527	Hudson-Edwards, K.....	1398
.....	1818	2330	2551	Huenges, E.....	1589
Hombourger, C.....	2119	Hou, Lianhua.....	1333	Hu, Shumin.....	1333	Huertas, F.J.....	822
Homoky, W.B.....	604	Hou, Lianhua.....	2546	2592	Huettel, M.....	1501
.....	973	2603	2596	Huey, L.G.....	1081
.....	1316	Hou, Q.....	2569	Hu, Suyun.....	1333	Hug, S.....	2179
.....	1323	Hou, S.....	1325	1388	2422
.....	1764	Hou, T.....	1326	2454	Hughes, H.....	1345
Homolova, V.....	1317	2600	2455	Hughes, N.....	1725
Honda, T.....	1457	Hou, X.....	2529	2531	Huguenot, D.....	1948
Hondoh, T.....	1904	Hou, Z.....	1631	Hu, Wenjie.....	2330	Huh, Y.....	1376
Honey, D.J.....	1182	2330	Hu, Wenxuan.....	851	Huhma, H.....	2508
Hong, B.....	1317	2545	1334	Humayun, M.....	1149
Hong, F.....	1388	Houben, S.....	2389	2457	Hummel, M.....	2259

Hummel, W.	1345	Ibsen, C.	709	Ionov, D.A.	684	Ivarsson, M.	1366
.....	2327	1353	827	1841
Hummer, D.	755	Icenhower, J.	1968	1359	Iversen, B.B.	1166
.....	1346	2207	1852	Ivleva, N.P.	669
.....	1517	Ichikawa, H.	1438	Ireland, Thomas	2335	1520
Humphreys, E.	1346	Ida, S.	1229	Ireland, Trevor R.	867	Ivy-Ochs, S.	1302
.....	1591	Iddon, F.	1354	2367	2153
Humphreys, J.	2498	Iden, S.	2061	Isaac, C.	660	Iwamori, H.	1500
Humphreys, M.	1347	Ideta, K.	2136	835	1816
.....	1976	Iezzi, G.	1179	Isenbeck-Schröter, M.	580	1888
Humphreys-Williams, E.	1347	1545	1111	Iwamoto, Y.	1366
.....	1728	1770	1266	Iwano, H.	2116
Huneau, F.	2276	Iglakova, A.	1354	1360	Iwase, F.	2543
Hunsche, M.	794	2066	2066	Iwata, T.	2310
Hunt, L.	Ignatiev, A.	788	Isensee, K.	1735	Iwatani, H.	2306
Hunter, J.	1514	2535	Ishida, A.	1360	Iwatsuki, T.	1821
Hunter, R.	1496	Igumentseva, M.	1355	Ishidoshiro, K.	1361	2562
Huo, X.	2453	Iizuka, Y.	1904	Ishiguro, M.	2470	Iyer, S.	1285
Huot, S.	1161	Ijiri, A.	1355	Ishihara, M.	643	Izawa, M.	673
Hurley, D.	1744	Ikawa, R.	1707	Ishii, T.	1361	Izawa, S.	1367
Hurowitz, J.	864	Ikehara, M.	1765	1837	2291
.....	2158	2534	2138	2337
Hursthouse, A.	1348	2540	2540	Izmer, A.	2395
Hurtgen, M.	923	Ilbeyli, N.	2537	Ishikawa, A.	601	2396
.....	1190	Ildefonse, B.	1103	1362	Izon, G.	1367
.....	2001	2025	1500		
Husband, K.	1348	Ilenia, A.	1790	2178		
Husen, A.	1063	Illera, V.	1870	2202	J	
Huss, G.R.	1244	Illies, A.	1968	2319	Jabeen, I.	575
Hussain, F.	2486	Imai, A.	1714	Ishikawa, M.	1298	1368
Husson, J.	1445	Imai, N.	1883	Ishikawa, T.	1438	Jaber, M.	688
Huston, D.	1944	Imfeld, G.	636	2115	1155
Hutcheon, I.	1515	Immenhauser, A.	747	2438	Jabłońska, M.	1368
.....	1716	1160	Ishimaru, S.	1362	1369
Hutchins, D.	1037	1847	1484	Jaccard, S.	1369
Hutchinson, R.	1349	Imre, K.	1510	2305	Jack, D.	1338
.....	1935	Inagaki, F.	1324	Ishimura, T.	2301	Jack, T.	2431
Huxman, T.	1005	1355	Ishiyama, D.	1879	Jacks, G.	1455
Huyskens, M.	586	1356	Ishizuka, O.	1256	Jackson, Chris	1370
.....	1349	1439	2305	Jackson, Colin	1370
Hwang, Jin Ju	1384	1517	Ismail, R.	1363	Jackson, M.	805
Hwang, Jong-Yeon	1350	1793	Isnard, H.	1226	Jackson, S.	587
Hwang, S-I.	2459	2323	Isola, I.	1010	1139
Hwang, Y.	1533	Inagawa, N.	2521	1363	1324
Hyatt, N.	917	1356	2037	1501
.....	925	1811	2580	Jackson, V.	996
Hybler, J.	1970	Ineson, J.	1869	Ispas, S.	1364	Jacob, D.	587
Hyde, B.	575	Inglis, E.	1400	Issartel, J.	2320	2477
Hynek, B.	1350	Inglis, J.	1913	Itai, T.	1364	Jacob, K.H.	1371
Hyobu, Y.	1364	2033	Italiano, F.	1472	Jacobs, J.	1476
Hystad, G.	1629	Ingrin, J.	1357	Ito, A.	1365	Jacobsen, Stein B.	1340
Hyun, J-H.	1351	2183	Ito, E.	2543	1371
Hyun, S.P.	1351	2417	Ito, H.	2539	1922
Iacono Marziano, G.	922	Inguaggiato, S.	1357	Ito, M.	1793	Jacobsen, Steven D.	2484
		Iñiguez Pacheco, J.E.	1358	Ito, Takashi	2534	Jacobson, A.D.	1023
		Inisheva, L.	1358	2540	1045
I		Innocent, C.	978	Ito, Takeshi	1821	1785
Iacovino, K.	1352	Inomata, S.	2310	Itoh, S.	1901	Jacobson, G.	2048
Iacumin, P.	2271	Inoue, C.	2470	2534	Jacobson, M.	1372
Iancu, A.M.	1161	Intrieri, E.	1859	Itoh, T.	1439	Jacobson, S.	2094
.....	1352	Ion, A.	1017	Itose, S.	643	Jacq, V.	1372
.....	1684	1359	Ivanova, A.	1365	Jacquemet, N.	1983
Iancu, G.O.	2336			Ivanova, E.	1452	Jacques, C.	1708
Ianni, A.	1353						

Jacques, D.	1204	Jean, D.	2014	Jia, G.	1387	Joachim, B.	648
Jacques, G.	1373	Jean-Noel, R.	2014	Jia, Y.	2528	896
Jaekel, U.	1373	Jeandel, C.	1381	Jiang, D.	2528	1393
Jaffe, D.	882	1537	Jiang, F.	1387	2105
Jaffe, P.R.	1339	2091	Jiang, H.	1388	Joachimski, M.M.	2435
Jagercikova, M.	1374	Jebbar, M.	890	1598	Jocher, G.	1394
Jagoutz, O.	678	Jébrak, M.	1068	Jiang, L.	650	Jochum, K.P.	596
.....	1166	1818	1388	1394
.....	1374	Jeffery, A.	1381	Jiang, M.	2204	1504
Jahn, B-M.	862	Jeffries, T.	722	Jiang, Q.	821	1768
Jahn, S.	674	1347	Jiang, Shao Yong	1150	2268
.....	739	1728	1498	2477
.....	1375	1934	2548	2503
.....	1505	Jeffroy, M.	2311	2550	Joelsson, L.	1395
Jakobsen, R.	2375	Jégo, S.	947	2602	Joelsson, M.L.T.	2216
James, Rachael H.	904	Jehlicka, J.	1889	Jiang, Shu-Dong	1389	Jogo, K.	1515
.....	997	Jenkins, D.	1525	Jiang, Simin	1774	Johannessen, B.	948
.....	1473	Jenkins, W.J.	858	Jiang, T.	2280	Johannessen, K.	1455
.....	1608	1382	Jiang, Wei	790	John, C.M.	939
.....	1926	Jenkyns, H.C.	938	2005	1142
.....	1941	1701	Jiang, Wei-Teh	1338	1160
James, Richard	748	2059	Jiang, Xiaoyan	1652	1443
Jameson, J.	764	Jenner, F.	1382	Jiang, Xu	952	1480
Jamieson-Hanes, J.	1375	2094	Jiang, Yi	1389	1662
Jamtveit, B.	2093	Jenni, A.	936	Jiang, Yongbin	1386	2390
Janasi, V.A.	583	1000	Jiang, Youlu	650	John, E.H.	589
.....	1095	1383	1624	1395
.....	1230	Jennings, G.	1870	Jianu, D.	1957	John, S.G.	604
.....	1376	2267	2267	912
Janeczek, J.	1368	Jensen, T.	1213	Jiao, Z.	1654	1092
.....	1369	Jeon, C.M.	1569	Jigau, G.	2336	1396
Jang, K.	1376	Jeon, H.	1383	Jilbert, T.	1029	2083
Janin, M.	1285	Jeong, B-G.	1464	1390	John, T.	1403
Janot, N.	572	Jeong, Gi-Young	1463	Jimenez, A.	1195	1528
.....	1377	Jeong, Gyo-Cheol	880	1390	1674
.....	1406	1384	Jimenez, J.L.	1555	1979
.....	2044	Jeong, H.	2564	Jiménez Garcia, N.	1391	2086
Janots, E.	1377	Jeong, J.T.	642	1391	Johnsen, R.	2031
.....	1538	Jeong, Y-J.	1384	2272	Johnson, A.	2503
Janoušek, V.	1378	Jepson, L.	648	Jimenez-Espejo, F.J.	1526	Johnson, B.	713
.....	1493	1385	1696	Johnson, C.	1396
.....	2360	Jercinovic, M.	2172	Jimenez-Espinosa, R.	1291	Johnson, G.	1716
Jansen, N.	1378	2231	2124	Johnson, H.	1808
Jansik, D.	2480	Jespersen, H.T.	551	Jiménez-Millán, J.	1077	Johnson, James W.	1397
Janssen, C.	1117	Jesušek, A.	2484	1291	Johnson, Jason.	2264
.....	2186	Jetten, M.S.M.	2030	Jimoh, M.T.	1392	Johnson, Jena E.	1090
.....	2216	Jew, A.	1591	1392	1286
Janssens-Maenhout, G.	2394	Jex, C.	1385	Jin, B.	1392	1397
Jansson, J.	2345	Jézéquel, D.	921	Jin, F.	2603	2474
Jara, C.	2015	1561	Jin, Lixin	2569	Johnson, Karen.	1085
Jaron, I.	2113	2252	Jin, Luying	821	1398
Jarrett, A.	781	Ji, H.	774	Jin, Q.	1669	2070
.....	1176	1386	Jin, W.	2461	Johnson, Kathleen	644
.....	1379	Ji, Jian-Qing	1601	Jin, Y.	1492	1331
Jasim, A.	1379	Ji, Junfeng	1278	1821	1398
Jaupart, C.	1682	1599	Jin, Z.	1393	Johnson, M.S.	1042
Javakhishvili, Z.	853	1603	1596	1272
Javaux, E.J.	1380	1680	Jing, Z.	854	1395
Javoy, M.	1380	2617	2461	1399
.....	1423	Ji, W-Q.	1386	Jinhui, L.	2560	1744
Jayananda, M.	1268	2383	Jiricka, D.	1930	1747
Jayaram, G.N.	590	Ji, Z.	2609	Jiskra, M.	2491	2216
Jayne, J.	1514		Jitaru, P.	1544	2373

Johnson, N.....	1142	Jordan, N.	1098	Kaden, P.	1530	Kamber, B.S.....	637
.....	1399	1107	Kadi, K.	1383	872
Johnson, Peter	1400	2109	Kadioglu, S.....	1415	927
Johnson, Peter	1246	Jordan, T.....	920	Kadinkiz, G.....	1045	1131
Johnson, Thomas M.....	1977	Jorge, S.	702	Kadioglu, Y.K.	565	1422
.....	2197	Jorissen, F.....	1746	974	1422
.....	2430	1827	1231	1448
.....	2615	Joseph, C.	2155	1415	1959
Johnson, Tim	779	Josso, P.....	1408	1416	Kamei, A.....	601
.....	2463	Joubert, L.....	2005	1498	Kamenetsky, V.S.....	560
Johnson, Tom M.	978	Jourdan, F.....	1408	Kadlag, Y.....	1416	603
Johnson, W.....	1521	Jouvin, D.	2585	Kaegi, R.....	1417	814
Johnston, C.....	884	Jouzel, J.	1543	2179	1178
Johnston, D.T.....	695	Jovanović, D.....	1198	2422	1253
.....	786	2243	Kageyama, M.	2053	1423
.....	1173	Jowitt, S.....	2182	Kagi, H.	1239	1469
.....	1400	Joy, B.....	573	Kagoshima, T.	1417	1930
.....	1401	Joye, S.	633	Kah, M.....	1418	2180
.....	1560	Jørgensen, B.B.	1055	Kahl, M.....	1418	2199
.....	1706	1409	Kahl, W-A.	638	2555
.....	2246	Jørgensen, J.	1315	Kahmen, A.....	2110	2576
.....	2466	Ju, P.	774	Kahya, A.....	1419	2607
Johnston, S.	796	Juarez, S.	870	Kaiden, H.....	2304	Kameyama, S.....	2310
.....	1401	1409	Kaigorodova, E.....	1419	Kamilli, K.	2139
Jolayemi, O.	1402	Juárez-López, K.	1051	Kaiser, J.	1213	Kamimura, K.	2471
Jolis, E.M.	2357	Jubany, I.	1410	1933	Kaminski, E.	1423
Jolivet, J-P.....	1015	Juchelka, D.	1410	2392	Kaminski, U.....	989
Jollands, M.....	1402	Jugo, P.	1411	Kajdas, B.	1420	1168
Jolley, D.	924	Juhin, A.	1038	Kajino, M.....	2176	Kaminsky, F.....	1424
.....	1762	Juhl, K.	938	Kakegawa, T.....	1123	Kampman, N.....	703
Jollivet, P.....	1117	Juillot, F.....	808	1339	856
.....	1927	1014	1826	942
Jomori, Y.....	1403	1114	1901	1424
.....	1766	1858	2291	1703
Jonas, L.	1403	Julie, C.....	958	2471	2613
Jonckheere, R.....	2105	Jun, Y.	1391	Kakonyi, G.	1108	Kamyshny, A.	720
Jones, Aaron.....	1404	Jung, Hae-Jin	1461	Kaksonen, A.	2328	1173
Jones, Adrian.....	667	Jung, Haemyeong	1411	Kaleowda, Y.	1261	1425
.....	1328	Jung, Hee-Won.....	1412	Kalinichev, A.....	1420	Kan Bostanci, A.....	1426
.....	1404	Jung, J-Y.	2563	1636	1468
.....	2404	Jung, M.....	1412	1843	Kanakidou, M.	1817
Jones, B.	1529	Jung, Sejin	1411	Kalinina, V.	2190	2419
Jones, C.	817	Jung, Stefan	1963	Kalinovich, I.....	578	Kanakin, S.....	2253
.....	1405	Junginger, A.	2430	Kalinowski, B.	1709	Kananian, A.	1425
.....	1682	Junkermann, W.	2139	Kaliwoda, M.....	2115	Kandeler, E.	994
.....	1763	Jurado, A.	1413	2123	1984
Jones, D.....	1405	Juranyi, F.....	696	2178	Kaneko, Makoto	1426
Jones, J.	1611	Justo, J.	2514	Kalkan, B.....	1077	Kaneko, Masanori.....	1427
Jones, L.	2005	K		Kallay, N.....	1995	Kanematsu, M.....	1869
Jones, Morgan	1406	Kaal, J.	2280	Kallmeyer, J.....	1043	Kaneoka, I.....	2349
Jones, Morris	1406	Kaasalainen, H.	1414	1421	Kang, K-G.....	1412
Jones, R.	1407	Kabengi, N.	884	Källström, K.	1021	1460
Jones, T.	1180	1516	Kalmychkov, G.....	1982	Kang, Q.....	2589
Jöns, N.....	638	Kabius, B.....	1941	Kalogiros, J.....	746	Kang, S.	1427
Jonson, E.	2436	Kaceli Xhixha, M.	1224	Kaltenbach, A.	1812	2078
Jonsson, C.M.....	943	2002	Kalvig, P.	1451	Kani, T.	1428
Jonsson, H.	2239	2519	2150	Kanner, L.	1428
Jonsson, S.....	2491	Kaczmar, F.	1372	Kamah, Y.....	767	Kanzaki, M.	1429
Joordens, J.....	2430	Kaczmarek, K.....	705	2491	2533
Joosu, L.	1407	Kaczmarek, M-A.....	1414	Kamaleeva, A.	1421	Kanzaki, Y.	1429
Jordan, Guntram.....	693	Kadar, E.....	1415		Kanzari, A.....	1156
Jordan, Gyozo	2426					Kao, C-C.....	1574
						Kao, S-J.....	1299

Kao-Kniffin, J.	1799	Kasten, S.	756	Kelemen, P.B.	678	Kersten, M.	1450
Kaown, D.	1430	1266	1444	1450
.....	1461	1287	1444	1511
.....	1572	1991	1935	2177
Kaplan, Daniel I.	1597	2253	2321	Kertész, Z.	1510
.....	2524	Kasting, J.	1435	2399	Kervévan, C.	1552
Kaplan, Dilber	1430	Kästner, M.	1240	Keller, A.	2609	Keskin, M.	1905
Kappler, A.	804	1764	Keller, B.	1445	2378
.....	1431	Kaszuba, J.	1831	Keller, C.	1747	Kessler, A.J.	1451
.....	1479	Katerrer, T.	1575	Keller, J.	569	Kessler, J.	1940
.....	1798	Kato, C.	1436	2340	Kestenare, E.	2387
.....	1967	Kato, M.	1436	2452	Ketcham, R.	1147
.....	2126	Kato, Y.	1663	Keller, L.	1693	1226
.....	2294	2554	Keller, N.	1445	Ketterer, M.	655
.....	2513	Katsev, S.	1437	1655	Kettler, R.	718
Kara-Gülbay, R.	1045	Katsura, M.	1247	2094	Keul, N.	705
Karabel, S.B.	1431	Katz, A.	810	Kellermeier, M.	689	1838
.....	1468	883	Kelley, D.	584	Keulen, N.	1451
.....	2382	Katzir, Y.	1035	Kelley, K.	777	Kevorkian, R.	1634
Karamalidis, A.	792	1186	923	Khaled, B.	1788
.....	1928	Kaufman, J.	2000	1219	Khan, C.	952
.....	1929	Kausch, M.	1914	1446	Khan, S.	1452
Karaman, M.	1426	Kavner, A.	1346	2055	Kharanzhevskaya, J.	1452
.....	2382	Kawabata, H.	2178	2094	Kharitonova, N.	1453
Karasava, O.N.	684	Kawagucci, S.	1437	Kelley, M.	893	2384
Karato, S-I.	1432	1826	Kelley, S.	924	Kharkhordin, I.	1453
.....	1912	Kawahata, H.	607	1370	Khatiwala, S.	1977
.....	2012	1438	Kellom, M.	2033	Khin Zaw,	1539
Kargin, A.	1432	2301	Kelly, L.	1446	Khodja, H.	2068
Karimpour, M.H.	2621	2542	Kelly, S.	1646	Khondoker, R.	1454
Karion, A.	2048	Kawai, K.	1438	Kelly, T.	2386	Khoury, H.	1454
Kärki, A.	2508	Kawai, M.	1439	Kelsey, D.	593	Khromykh, S.	1503
Karki, B.	2250	Kawai, T.	1826	Kemner, K.	1097	Kibria, G.	1455
Karlin, T.	1904	Kawakami, H.	1120	1533	Kichanov, V.	1455
Karlsson, N.	2385	Kawakami, T.	1298	1553	Kichanova, V.	1455
Karlsson, S.	1210	1439	Kemp, A.I.S.	1513	Kiddle, E.	597
Karlsson, Teemu	638	Kawamoto, K.	2115	1926	Kieber, R.	1456
Karlsson, Torbjörn	594	Kawamoto, T.	1440	2409	2498
.....	2289	1484	Kemp, D.	1869	Kieffer, I.	2320
Kármán, K.	1472	1751	Kemp, T.	2488	Kieft, T.L.	1535
Karmanov, N.	1558	1855	Kendall, B.	1447	1553
.....	2189	2566	Kendrick, M.A.	1178	Kienel, U.	2081
.....	2607	Kawamura, Katsuyuki	1861	Kennedy, Ben M.	677	Kierczak, J.	1456
.....	2608	Kawamura, Kunio	1440	2428	2370
Karmasz, D.	1562	Kawano, T.	1522	Kennedy, Bianca	1447	Kiese, R.	1158
Karpoff, A-M.	2416	Kawasaki, T.	2541	Kennedy, M.	1176	2479
Kasama, T.	1262	Kawata, Y.	1441	Kenney, J.	594	Kieser, W.E.	1292
Kasemann, S.A.	1407	Kaya, E.	2537	1448	Kietäväinen, R.	1457
.....	1433	Kayser, S.	817	Kenny, G.	1448	Kikawada, Y.	1457
.....	1648	Kazahaya, K.	1322	Kent, A.	915	Kikuchi, R.K.P.	1948
.....	1881	Kazantseva, L.	2028	Kent, P.	1517	Kilburn, M.	1458
Kashima, D.	1060	Kazil, J.	894	Kerber, L.	2087	2435
Kashiwabara, T.	614	Keays, R.	2182	Kerestedjian, T.	903	Kilcoyne, D.	2255
.....	1433	2343	Kerisit, S.	861	2534
Kashyap, C.S.A.	1434	Kebukawa, Y.	1441	1968	Kilgallon, R.	1458
Kasina, M.	1434	Kehrwald, N.	1126	Kerr, A.	1345	Kilias, S.	1459
.....	1435	Keiding, J.	1442	Kerr, J.	1449	Kilic, C.O.	974
.....	2516	Keiluweit, M.	1442	Kerr, M.	1449	1231
Kasparbauer, K.	1483	1845	Kerstel, E.	1200	Kilic, S.	1459
Kassahun, A.	1435	1961	1520	Kilthau, W.	1483
.....		Keith, M.	1443	1540	Kilzi, M.	1460
.....		Kele, S.	1443	1797	Kim, Bo-Kyong.	1350
.....		2277	Kim, Byung-Gon.	1053

Kim, Byung-Hyo.....	1464	Kinsman-Costello, L.	985	Klaus, A.....	1184	Knope, M.L.....	1939
Kim, C.J.	1318	Kipfer, R.....	769	Klaver, M.....	1474	Knopf, D.	1483
Kim, D.....	1571	769	Kleber, M.....	1442	Knorr, K-H.....	1483
Kim, Heejung	1430	1664	1845	1840
Kim, Ho-Rim	1460	2005	1961	2570
.....	2459	2342	Kleespies, P.	1218	Knorr, W.	618
Kim, Hun-Mi.....	1461	2370	Klein Gebbinck, C.....	1475	Ko, B.....	1411
.....	1572	2424	Kleine, T.....	1091	Kob, W.....	1364
Kim, HyeKyeong	1461	Kipfstuhl, S.	2385	1254	Koba, K.....	1855
Kim, Hyeong-Don.....	2459	Király, C.....	1468	1475	Kobayashi, D.	2540
Kim, Hyojin	1462	Kiran Yildirim, D.	1426	1515	Kobayashi, K.	1484
Kim, Hyun S.	1462	1431	2249	Kobayashi, M.....	1484
Kim, J.	1925	1468	Kleinhanns, I.C.....	1476	2285
Kim, Jae Gon	1569	2382	2162	Kobayashi, N.	2470
Kim, Jhoon	1573	Kirat, G.....	635	Kleinpeter, J.....	1168	Kobayashi, Takamichi ...	2291
Kim, Jihyoung.....	2563	Kirby, M.....	1069	Kleinschrodt, R.....	2390	Kobayashi, Tetsuo	1484
Kim, Juhyun	1463	Kirchen, S.....	2259	Klemd, R.....	1443	2566
Kim, Kangjoo.....	1463	Kirchenbauer, M.	1469	Klemme, S.	1476	Kobayashi, Tomoyuki....	1876
.....	1464	2390	2215	Köbberich, M.....	1485
Kim, Kyoung-Ho	668	Kirdyanov, A.....	2415	2494	Kober, B.....	1111
.....	997	Kirichenko, I.	2608	2618	Kober, F.....	1302
.....	1412	Kirillov, M.....	1531	Klepeis, K.	2271	Koch, B.....	2157
.....	1460	Kirino, Y.	696	Kleybocker, A.....	1434	Koch, J.....	1122
.....	1569	Kirk, M.....	1455	Klima, R.L.....	846	1232
.....	2459	Kirk, R.....	1469	Klimkin, A.	1354	1272
Kim, Mi Seon.....	1464	Kirkby, J.	832	1477	Koch, M.	2509
Kim, Min-Gyu.....	881	Kirsch, K.	1470	Klimont, Z.	1477	Koch-Müller, M.....	1042
Kim, Min-Seob	1350	Kirschbaum, A.	1813	2394	Kochergina, Y.....	555
Kim, Minkyung.....	881	Kirschhock, C.E.A.	772	Klimuszko, E.	1221	1485
Kim, Sang-Eun.....	2389	Kirschvink, J.	1397	1478	Kock, A.....	2579
Kim, Sang-Tae	668	2474	Klinkenberg, M.....	762	Kocot, Y.....	2163
.....	817	2569	1478	Kodirov, O.....	1486
.....	1475	Kirsimäe, K.	1407	Klinkhammer, G.....	1479	Koehler, I.	1431
Kim, Sang-Woo	2563	Kirste, D.	1470	Klötzli, U.	1046	Koenen, M.	2468
Kim, Seok-Hwi	1464	Kirstein, L.	1407	Klueglein, N.	1479	Koepke, J.	816
Kim, So Jin.....	1384	1471	Kluesner, J.	1480	1103
Kim, Suk Hyun	1318	Kirtland Turner, S.	1471	Kluge, T.	1142	1111
.....	1465	Kis, B-M.....	1472	1160	Koga, K.....	805
Kim, Sung-Han	1351	Kisakürek, B.....	1847	1443	1127
Kim, Taehoon	1570	Kiseeva, K.	1472	1480	Kogarko, L.....	789
Kim, Taejin	1465	1768	Klügel, A.	1119	2235
Kim, Yeongkyoo.....	1466	Kiselev, A.....	2259	1481	Kögel-Knabner, I.	994
Kim, Yong Chul.....	877	Kisku, P.C.	1473	1963	1307
.....	2565	Kiss, J.	1504	Klüglein, N.	804	2001
Kim, Yong H.....	1462	Kistner, M.	1437	Klunder, M.	956	Kogiso, T.	1440
Kim, Yoonsup.....	1924	Kita, K.....	1899	Klүpfel, L.	1200	1773
Kim, Young Ho.....	1465	Kitagawa, H.....	1189	2126	2202
Kim, Young Il	1318	Kitajima, K.....	1080	Klymenko, N.	2121	Koh, D-C.....	1430
.....	1465	Kitamura, Akihisa	2470	Knauss, K.G.....	926	Koh, H.....	1572
Kim, YoungJae	1466	Kitamura, Akira.....	2292	949	Köhler, M.....	1743
Kim, Yumi	1427	Kitanidis, P.K.	876	2118	Köhler, P.	2160
Kimball, B.	2486	Kitazato, K.	2470	Knesel, K.....	1691	2161
Kimoto, K.	615	Kiyokawa, S.	2304	Knicker, H.	1481	Köhler, S.J.	1563
Kimura, J-I.....	2285	2471	2280	1840
King, H.E.	1403	2534	Knies, J.	1067	1847
.....	1674	2540	1108	Kohn, N.....	2557
King, P.	2158	Kjarsgaard, B.A.....	760	1482	Kohn, S.C.....	795
.....	2269	2312	2139	1486
King, R.	645	Kjær, H.....	2385	Knights, K.....	1482	2205
King, S.	1467	Kjærgaard, H.....	1042	Knipping, J.	2249	2328
Kingsley, R.	1428	Kjeldsen, K.U.....	1342	Knoll, A.....	2246	2442
Kinoshita, N.	1467	Klar, J.K.	1473	Knöller, K.....	702	Kohn, T.....	615
Kinouchi, K.....	1366	Klatt, J.	1474	Knope, K.....	2159	Kohut, M.....	1487

Koike, Makoto.....	1899	Konyshev, A.....	1735	Kothe, E.	588	Krausova, K.	1511
Koike, Mizuho.....	1487	Konzett, J.....	1487	698	Krauße, T.	2425
Kojima, H.....	1906	Koo, M.....	877	2425	Kreidenweis, S.	1960
Kok, J.	568	Kooijman, E.....	1494	Kotler, P.	1503	Kreissig, K.	1511
Kokh, M.	1488	2224	Kotov, A.	2207	1541
.....	1983	Kool, D.M.....	2030	2536	Kremer, I.....	2335
Kolb, J.	1903	Koopmans, G.F.....	1495	Kotova, O.....	1986	Kremser, V.....	1512
Kolic, P.E.	1488	Koornneef, J.	1495	2358	Krengel, T.	1266
Kolodny, Y.....	2188	Kopf, S.....	1496	Kotzer, T.	1930	Kretke, K.....	1512
Kolonis, S.....	603	1670	Kouchi, A.....	1246	1592
Kolpakov, V.	1531	Kopitz, J.....	2167	1711	Kretzschmar, R.	1513
Kolpakova, M.....	1489	Kopp, C.	1496	1874	1758
Komai, T.	2470	Kopylova, M.....	Koukina, S.	1503	2491
Komarek, M.	1489	1497	Koutsovitits, P.....	1866	Kreutzmann, A-C.....	688
.....	2394	2226	Kouvarakis, G.....	746	Krevor, S.	1923
Komatsu, D.	1490	Koralay, D.B.....	1497	Kouzmanov, K.....	1983	Kribek, B.....	1052
Komatsu, M.....	1490	Koralay, T.....	974	Kovac, R.	2054	1756
Komelkov, A.	1136	1231	Kovacs, C.....	827	Krieger, U.	1137
Komissarov, A.....	1722	1498	Kovács, I.....	1504	Kriete, C.....	1734
Komiya, T.	601	Korehi, H.....	1498	1585	Kripounoff, A.....	1110
.....	606	Koren, I.....	1071	1618	Kristensen, M.....	2385
.....	1303	1577	1839	Kristinsdóttir, B.....	1513
.....	1500	Korkmaz, S.....	1045	1972	Krivonogov, S.	728
.....	2129	Kornes, R.I.	2456	Kovács, Z.....	1934	1587
.....	2202	Korolev, N.....	1190	Kovalchuk, E.	1432	1678
.....	2541	Koron, N.....	1746	2031	Krmíček, L.	1514
.....	2567	Koroneos, A.....	673	Kovalev, K.....	1830	2376
Komorowski, J-C.....	2413	1921	Kowal-Linka, M.	1504	Kroger, R.....	2391
Konagaya, N.....	1440	Korsakov, A.....	1757	Kowalski, Piotr.....	1505	Kroll, J.....	1514
Konagaya, W.....	1491	Korte, C.	2075	Kowalski, Piotr M.....	715	Krom, M.D.....	1917
Konc, Zoltán.....	1972	2097	1505	1975
Konc, Zoltan.....	1194	2376	Kozai, N.....	1882	Kronast, F.....	784
Könczöl, M.....	1168	2422	Kozin, P.	1506	Kronz, A.....	1320
Kondo, Y.....	1899	Korte, L.	1648	Kozlov, A.....	1477	Krot, A.	1315
.....	2113	Korup, O.....	2293	Kozlu, H.....	1506	1515
Kondratyeva, L.....	728	Korzh, V.	1499	Kozmenko, O.....	1507	1822
Kone, M.....	1491	Koschinsky, A.	1499	Kozyreva, I.	1507	Kroutil, O.	1994
Konečný, P.....	647	1987	Kraal, P.	1508	Krüger, M.....	1238
Koneev, R.....	1001	2158	Krabbenhöft, A.....	2427	1391
Kong, C.	2435	Koshida, K.....	1500	Krabbenhof, K.....	807	1391
Kong, Xiang.....	2191	2202	Kraemer, S.....	2149	2024
Kong, Xiang-Zhao.....	2108	Kosjanenko, A.	1500	Kraepiel, A.M.L.....	636	2219
.....	2368	Kosjanenko, D.....	1500	681	2272
Konhauser, K.O.....	1431	Kosler, J.....	1324	2595	Kruger, S.J.	928
König, S.....	1492	1493	Kraft, S.....	2276	Kruijer, T.S.	1515
.....	1619	1501	Kragie, S.X.....	1508	Krumwiede, D.....	1032
.....	1782	Kossel, E.....	981	Krahner, K.....	675	Kruspan, P.....	1168
Könneke, M.....	1087	Kostin, A.	1313	Krall, L.....	1509	Kryachko, V.....	1313
.....	1730	Kostinski, A.....	1577	2364	Krylov, D.	1294
Konno, U.....	1437	Kostka, J.	818	Kram, P.....	944	Krymskiy, G.....	1477
Konno, Y.....	1492	915	1509	Krymsky, R.....	1516
.....	1821	1501	Krämer, U.	1798	Kryza, R.	1502
Kono, Y.....	2247	Kostopoulos, D.....	1093	Kraml, M.	1111	Krzemińska, E.....	2518
.....	2461	Kostrovitsky, S.....	1497	Krapez, B.	799	Kubicki, J.....	884
Konopásek, J.	1493	Kostylew, J.....	1502	2030	1516
Konopelko, D.....	1001	Kostyuk, A.....	1197	Krasnobaev, A.	2385	1517
Konôpková, Z.....	595	1502	Krasnova, T.	1159	1663
.....	2129	Kotarba, M.J.....	2490	Krassován, K.	1510	2061
Konovalenko, S.....	1493	Koteas, C.	2172	Krasuska, J.....	730	Kubo, M.....	926
.....	1494	2500	Krause, S.....	1510	Kubo, Y.....	1355
Konrad, G.....	1031	Kotelnikov, A.....	2433	1849	1356
Konstantinidis, K.....	1501	Krause, T.	2139	1517
Kontak, D.	2472	Krause-Nehring, J.....	2430	Kubrová, J.....	1518

Kuchenbecker, M.	637	Kurnosov, A.	1526	Labidi, J.	1179	Lanci, L.	2037
Kuder, T.	2329	1916	1535	Lancianese, V.	991
Kudo, M.	643	Kuroda, J.	1526	Labolle, F.	641	1542
Kuentz, D.	2031	1893	2160	Landais, A.	672
Kuesel, K.	1518	Kuroiwa, K-I.	1440	Labonté, J.M.	1535	1543
Kuga, M.	1519	Kuryak, A.	1477	Labrosse, S.	1536	2053
Kuhn, G.	1519	Kurz, M.D.	1149	1536	Landenberger, B.	1725
.....	2059	1527	1682	Landing, W.	1951
Kuhn, K.	1714	1956	Labs, S.	668	Landis, R.C.	1558
Kühn, Melanie	1520	Kurzweil, F.	1527	Lacan, F.	551	1931
Kühn, Michael	968	2497	1537	2041
Kühnreich, B.	1520	Kusano, N.	1528	Lacerda, L.D.	2210	Landsberg, J.	1520
.....	1540	1675	2414	1540
.....	1797	1854	Lachhman, D.	1819	1797
Kuhnt, W.	1637	Kuscu, M.	1419	Lachner, J.	836	2277
.....	2276	Kusebauch, C.	1528	Lachniet, M.	625	Lane, S.	2322
Kührt, E.	2346	1674	Lacrampe-Couloume, G.	1312	Lang, S.	766
Kuhs, W.F.	2177	Küsel, K.	697	1553	Lang, Y-C.	991
Kuippers, G.	1730	1396	1931	1543
Kujawinski, E.	1521	2451	2195	Lange, B.	1544
Kukkonen, I.	1457	Kusiak, M.A.	1529	Ladenberger, A.	1537	Lange, C.B.	1120
Kularatne, K.	1521	Kustka, A.	1529	2111	Lange, H.	2312
Kulik, D.	1522	Kutzer, A.	1530	2374	Lange, R.	1544
.....	2092	Kuwae, M.	1793	Laeufer, A.	1476	Lange, S.	1481
.....	2326	Kuypers, M.M.M.	688	Laevsky, Y.	2407	Langenhorst, F.	1676
Kuloyo, K.	1553	1205	Lafay, R.	1538	Langer, G.	705
Kuloyo, O.	2005	1530	Lafortune, S.	2055	1838
Kumagai, M.	1364	1900	Lafreniere, M.	1538	Langlet, D.	1746
Kumagai, Y.	1484	2566	Lagaria, A.	1975	Langmuir, C.	2094
.....	2566	Kuzmin, A.	1136	Lago, M.	1547	Langone, A.	1101
Kumamoto, Y.	1522	Kuzmin, Dmitrii	1755	2371	1177
Kumar, A.	596	Kuzmin, Dmitry	2232	Lagos, M.	1136	1386
.....	1523	Kuzmin, M.I.	2452	Lagostina, L.	1055	1545
Kumar, B.	597	Kuzmina, O.	1531	Lagroix, F.	836	2147
.....	2028	Kuzyura, A.	722	2332	Laniyan, T.	1877
.....	2029	1531	Lahajnar, N.	1774	Lanoisellé, M.	1644
Kumar, M.S.	1769	Kvashnina, Kristina	739	Lahera, E.	1643	Lansard, B.	2387
Kummer, N-A.	1328	1245	Lai, C-K.	1539	Lanson, M.	1377
Kummer, S.	2174	1530	Lai, Peixin.	820	Lanza, R.	2037
Kump, L.	906	Kvashnina, Kristina O.	2215	Lai, Peter.	1923	Lanzafame, G.	1164
.....	1064	Kwaśniak-Kominek, M.	1532	Lai, T-H.	1118	1545
.....	1523	Kwiecien, O.	2026	Lai, Y-J.	1539	Lanzirotti, A.	2027
.....	1524	Kwon, C.W.	1532	Lair, G.J.	2038	2083
Kumral, M.	1431	Kwon, M.J.	1533	2151	2290
.....	1468	Kylander-Clark, A.	1240	Lajeunesse, E.	980	Lapen, T.	617
.....	1524	1494	Lakshthanov, L.Z.	684	Laperche, V.	714
.....	2382	1533	1540	Lapham, L.	747
Kumud, S.P.	2021	Kyle, R.	2027	Lalonde, K.	654	Laporte, D.	585
Kundu, A.K.	710	Kyono, A.	755	654	909
Kunihiro, T.	1793	Kyriakopoulos, K.	2090	Lamb, K.	1540	1258
Kunii, M.	2176	Kyser, K.	573	1797	Larcher, D.	1767
Kunimoto, T.	2543	1534	Lambelet, M.	1541	Large, R.	1245
Kuninaka, H.	2470	L		2273	1546
Kunzmann, M.	1246	L'Ecuyer, T.	2239	Lambert, J-F.	688	1704
Kuo, E.	1650	L'Helguen, S.	1372	1155	Larionov, A.	672
.....	2072	L'Heureux, Z.	1514	Lamborg, C.	2404	2122
Kuo-Chen, H.	1525	La Rubia-García, M.D.	1077	Lamoureux, S.	1538	2262
Kupcik, T.	1689	La Spina, A.	1165	Lamy, I.	1832	Larionova, Y.	2122
Kupper, S.	2346	1551	Lan, D-Z.	2454	2262
Kurakalva, R.M.	604	Laaksonen, A.	959	Lan, T.F.	1541	Lariviere, A.	1496
Kurganskaya, I.	1657	Labasque, T.	729	1662	
Kurita, K.	653		Lan, Z.	1542	
Kurkcuoglu, B.	1525		Lana, C.	2121	

Larner, F.	1546	Lawrence, D.	2386	Lech, D.	1562	Lee, X.	1574
.....	1556	Laycock, A.	1556	2219	Lee, Yeonjin.....	1567
.....	2040	2040	Lecher, A.	1940	Lee, Yongjae	1574
.....	2041	2041	Leconte, M.	1562	Lee, Yongmoon.....	1574
Larocque, M.	1792	Layne, G.D.	2086	Lecumberri-Sanchez, P.	1563	Lee, Young Jae.....	1466
LaRowe, D.E.	1547	Layton-Matthews, D.	573	2255	Leemreize, H.	709
Larrea, P.	1547	2333	Ledesma, J.	1563	Lefebvre, V.	1003
.....	2371	Lazar, B.	1186	Ledevin, M.	1564	Lefèvre, G.	949
Larsen, K.	1315	1556	Lee, B.	1564	1575
.....	1548	1593	Lee, Carina.....	1565	Lefevre, R.	1575
.....	2126	2188	Lee, Chaehyang	1565	Lefort, S.	1576
Larsen, S.	1964	2557	Lee, Chang-Min	1466	Lefticariu, L.	2443
Larsen, T.	1548	Lazar, C.	1557	Lee, Cin-Ty A.	567	Legendre, L.	1158
Larson, D.	1795	1730	659	1576
.....	2386	Lazareva, E.	1235	1838	Legrand, M.	1062
Larson, L.	1549	1557	2193	1217
Larson, P.	592	1558	Lee, Dal-Heui	1566	LeGrande, A.	591
.....	1549	1815	Lee, Der-Chuen.....	1566	Legras, B.	733
Larson, S.Å.....	1550	Lazareva, O.	1558	Lee, G.	1567	leGras, M.	2485
Larson, T.	1550	Lazaro, P.	2191	Lee, Hao-Yang.....	885	Lehahn, Y.	1577
Larsson, M.A.	1551	Lazarov, M.	1559	1567	Lehmann, B.	1578
Lasaga, A.	1880	2015	Lee, Hsiao-Fen.....	1568	Lehmann, J.	1605
Lassin, A.	1129	Lazzeri, K.	673	Lee, Hyun Mi.....	1318	Lehmann, K.	869
.....	1552	Lazzeri, M.	715	Lee, J.	1925	Lehmann, M.F.	718
Lassiter, J.	803	Le Borgne, M.	1798	Lee, Jae-Chul	1463	832
.....	1552	Le Borgne, T.	729	Lee, Jaehwa.....	1573	1849
Lathem, T.	2135	955	Lee, Jaeseok	1411	2259
Latta, D.	1553	1561	Lee, Jaiyoung	1571	2622
Lattanzi, P.	610	le Bris, N.	1158	Lee, Jin-Yong	1430	Lehn, G.	1023
.....	1211	Le Champion, P.	1739	Lee, Jong Ik	1570	Lehne, E.	1578
.....	1789	Le Coustumer, P.	2276	Lee, Joohan	1570	Lehnert, K.	1579
Lau, B.	1338	Le Godec, Y.	689	Lee, Jun-Jeong	1384	Lehnik-Habrink, P.	1579
Lau, G.	2321	Le Guillou, C.	1577	Lee, Jung Hwa	1569	Lehtinen, T.	2038
Lau, M.	1535	Le Hir, G.	733	Lee, Jung-Eun	1568	Lei, Liangqi.....	1580
.....	1553	1003	Lee, Kang-Kun	1430	Lei, Lidan	1337
Laubach, P.	2197	1343	1461	Lei, R.	1580
Laube, J.	579	1965	1572	Lei, T.	1233
Laudon, H.	1840	Le Losq, C.	1096	Lee, Khanghyun.....	879	2514
Laumann, S.	1554	Le Mignot, E.	1583	Lee, Kil Yong	877	Lei, W.	1581
.....	2156	Le Moigne, F.	2418	2565	1629
Launeau, P.	2164	Le Pennec, J-L.	1730	Lee, Kyung-Jin	1569	Leidel, L.	976
Laurenz, V.	1554	Le Roex, A.	1619	Lee, L.	831	Leider, A.	1581
Lauretta, D.	1760	le roux, G.	577	832	2408
Lavallée, Y.	2428	982	Lee, Mi Jung	1570	Leira, M.	928
Lavé, J.	716	le Roux, P.	1619	Lee, Michelle Hope	1564	Leis, A.	646
.....	860	Le Roux, V.	1527	1570	2164
.....	1103	1589	1963	Leisen, M.	1582
Laverman, A.M.	723	2341	2480	Leisner, T.	2259
.....	1048	Lead, J.	2040	Lee, N.	1571	Leithold, L.	713
.....	1227	Leake, J.	676	Lee, S. J.	1925	Leitner, J.	2268
.....	1555	Leanni, L.	860	Lee, Sang Heon.....	1464	Lelli, M.	1856
.....	1795	Lear, C.H.	589	Lee, Sang Soo	682	Lelong, G.	861
.....	2022	Leardini, L.	1559	2159	1133
Laverne, C.	1694	Learman, D.	1560	Lee, Sanghoon	1571	Lemarchand, D.	1192
.....	1739	Learned, J.	1394	Lee, Seong-Sun	1461	1582
Lavi, A.	1555	Leavitt, W.	695	1572	2063
Lavigne, F.	2413	1560	Lee, Seung Ryeol.....	1572	Lemieux-Dudon, B.	672
Lavkulich, L.	918	Lebeau, O.	799	Lee, So J.	1251	Lemini, J.	1967
Law, G.T.W.	2400	921	1573	Lemke, K.	1583
.....	2505	1561	1925	2256
Law, R.D.	624	Lebeau, T.	1276	Lee, Sung Keun	1573	Lener, J-P.	1584
.....	1717	Lebedev, V.A.	2378	Lee, W-S.	879	1584
Lawler, M.	2227	1350	2510

Leng, M.....	2225	Lever, M-A.....	1055	Li, Long	1090	Liang, Yanci	1605
Leng, W.....	1282	Levi, E.....	1556	1553	1606
Lenhardt, N.....	1402	Levin, N.E.....	1592	2195	Liang, Yu-Hsuan.....	1607
Lenkey, L.....	1585	1932	Li, Maowen.....	821	Liang, Yunfeng	1484
Lenniger, M.....	1585	Levison, H.....	1512	Li, Meihan	1595	Liao, J.....	1331
Lens, P.....	2558	1592	Li, Qiong.....	1599	Liao, Libing	2453
.....	2559	Levitan, M.....	1593	Li, Qiu-Li.....	1623	Liao, Lingling	2464
Lenton, T.....	937	Levresse, G.....	830	2462	Liao, Yipeng	820
.....	1586	1751	Li, Shanshan	2445	Liao, Yuantao	1607
.....	1763	Levy, E.J.....	1593	Li, Shilei	1599	Libowitzky, E.....	1042
Lenz, C.....	1586	Lewin, E.....	900	Li, Shizhen.....	1002	Lichtner, P.....	982
Lenz, M.....	704	Lewis, K.....	2158	2616	Lichtschlag, A.....	1608
.....	1305	Leybourne, M.....	2333	Li, Shuang-Qing	1600	Lie, J-E.....	1108
.....	2023	Leys, C.....	1819	Li, Shuguang.....	2447	Liebetrau, V.....	1241
.....	2432	Lezama-Pacheco, J.....	572	Li, Shuning	1592	1510
.....	2619	1377	1932	1608
Leombruni, A.....	1021	2278	Li, Siliang	1332	2427
Leonard, G.....	1319	Lgourma, Z.....	1594	Li, Tao	1600	Liebrich, M.....	1434
Leone, L.....	2026	Li, A.....	1387	Li, Tiegang	1387	Liebscher, A.....	968
Leonel, J.....	1587	Li, Bao.Hua.....	1222	Li, Ting	2128	1089
.....	2246	Li, Baogang	2446	Li, Tingyong	1011	2049
Leonova, G.....	728	Li, Ben.....	1542	Li, Wei.....	2522	Liebske, C.....	1115
.....	1587	Li, Cai.....	774	Li, Wei-Ran	1601	Lienen, T.....	2484
.....	1678	Li, Chao.....	1612	Li, Xian-Hua.....	885	Liermann, H-P.....	595
.....	1735	Li, Chao.....	700	1140	844
Lepchina, C.....	1214	1594	1542	Lifton, N.....	1609
Lepekhina, E.....	2122	2550	2461	Likhanov, I.....	1609
Lepland, A.....	927	Li, Chao.....	1651	2462	Lilley, M.D.....	670
.....	1407	Li, Chengzhan	1331	Li, Xiang-Min.....	2530	766
.....	1588	Li, Chongying	1595	Li, Xiao-Dong.....	1601	1655
.....	2114	Li, Chuangju.....	651	Li, Xuan Qi.....	1602	Lim, D-I.....	1924
.....	2139	2525	Li, Xue.....	1461	Lim, H.....	1463
.....	2400	Li, Da.....	1595	Li, Xue-Fang.....	1602	1565
Lepot, K.....	1588	1615	Li, Yan.....	1603	Lim, K.....	1610
Lerch, T.....	1409	Li, Dong-Mei.....	852	1645	Lima, Alexandre	1610
Leresche, S.....	2175	Li, Dongsheng	983	Li, Yin.....	1615	Lima, Ana Teresa.....	1281
Lerm, S.....	1589	2223	Li, Yingjie.....	869	1611
.....	2516	Li, F.....	1393	Li, Yingli	1603	1611
Lerouge, C.....	893	1596	Li, Yong.....	1233	Lima, Annamaria	567
Leroy, P.....	1590	Li, Gaojun	1596	1625	819
Leshner, M.....	618	1600	Li, Yongxin.....	1604	888
.....	2343	2347	2465	920
Leshin, L.....	1590	2594	Li, You-Lian	2011	1050
.....	2158	Li, Guanglai.....	2012	Li, Yuan.....	1679	2111
Lesniewski, R.....	1997	Li, Guangming	821	Li, Yuefen.....	1191	Lima, G.....	608
Lesniok, M.....	1368	Li, Hsiu-Ping	1597	2446	Lima, J.C.D.....	786
.....	1369	Li, Hui.....	2528	Li, Zheng-Hua	902	Limonta, M.....	1143
Lesourd, S.....	1191	Li, Jia Jia	1946	Li, Zhenzhen	1604	Lin, C-H.....	1568
Leue, M.....	2259	2585	Li, Zhihong	1002	Lin, D.....	1612
Leuenerge, D.....	1904	Li, Jiahua	2287	Li, Zhiming.....	821	Lin, Jun	1647
Leuenerger, M.....	1543	Li, Jie.....	2609	Li, Zhiyang	1387	Lin, Jung-Fu.....	1365
.....	2027	Li, Jilei.....	2280	Liall, G.....	653	1612
Leupin, O.X.....	1174	Li, Jin.....	2611	Lian, E.....	1594	Lin, L-J.....	941
Lev, O.....	1147	Li, Jin Wen	2013	Liang, Bin.....	2601	2601
Levander, A.....	749	Li, Jinhua	688	Liang, Biqing	1605	Lin, S.....	1613
.....	1346	1597	Liang, Handong	1605	Lin, T-H.....	1613
.....	1591	1740	1606	Lin, Xiaomao	1722
Levard, C.....	778	Li, Jiying	1437	Liang, Huaying	2286	Lin, Xueju	915
.....	1591	Li, Juan	1624	Liang, J.....	1606	1501
.....	1645	Li, K.....	1598	Liang, L.....	2615	Lin, Y.....	1614
.....	2257	Li, Ling.....	1598	Liang, S.....	2605	Lin, Yangting	2551
Levenson, Y.....	1041	Li, Liyang	1331	Liang, Y.-H.....	2548	Lin, Yen-Po.....	1614
Lévêque, J.....	1191	2611		Lin Thu Aung,	873

Linage, B.	1553	Liu, FuLai	1623	Liu, Yue	2446	Lopez, R.	599
.....	2005	1625	Liu, Yun	1602	1086
Lindsay, J.	699	1739	1626	López Sánchez, D.E.	1639
.....	943	2447	1632	López Sánchez-Vizcaíno,	
Lindsay, M.	1553	2547	2309	V	1266
Ling, H-F.	1615	Liu, Hai	1293	Liu, Zaihua.....	2549	1640
Ling, M.	1615	Liu, Hongyan	1646	Liu, Zhicheng.....	1632	1681
.....	2286	Liu, Hou-Chun.....	855	Livens, F.	925	Lopez-Capel, E.	2070
Lingadevaru, M.	590	Liu, Hsin-Ting	1566	Livermore, B.D.....	1633	López-Fernández, M.	1638
Linnemann, U.	2620	Liu, Huan	1624	Livi, K.	1633	2123
Lintern, M.	1616	Liu, Hui	852	Llirós, M.	1634	López-García, J.Á.	874
Lintner, B.	1568	Liu, Huichuan	2599	Lloret, E.	980	Lopez-Garcia, P.	688
Liotta, A.	1616	Liu, James T.	700	Lloyd, A.	1978	Lopez-Gomez, J-L.	1716
Liotta, M.	721	Liu, Jiangsi	1651	Lloyd, K.	1634	López-Gutiérrez, J.M.	1639
.....	1617	Liu, Jianhui	1625	Lloyd, Nicholas S.	1635	López-Pamo, E.	999
.....	2505	Liu, Jianming	2526	1791	1890
Liousse, C.	806	Liu, Jiguo	1621	2501	2132
.....	1617	Liu, Jingao	2439	Lloyd, Nick	2489	López-Serna, R.	1413
Lipp, J.S.	890	Liu, Jingdong	1624	Lo, C-H.	1567	Löppmann, S.	1799
.....	1301	Liu, Juan	1941	Lo Bue, N.	2184	Lorand, J-P.	1492
.....	2510	Liu, Junbang	2597	Lo Giudice Cappelli, E. ..	1637	1641
Liptai, N.	1618	Liu, Junfeng	1625	Lo Pò, D.	1640	Lorenz, B.	754
.....	1934	Liu, Liang	2011	Lobato, L.	2314	Lorinczi, P.	1327
Lisiecki, L.	1955	Liu, Lianwen	2194	Lobus, N.	1503	Loring, J.	685
Lisowiec, K.	1618	Liu, Lin	1003	Loch, J.P.G.	1611	Losa-Adams, E.	1129
.....	2221	Liu, M.	941	Lockwood, C.	1635	1173
Lissner, M.	1619	Liu, N.	951	Lockwood, G.	1144	1641
Litasov, K.	854	Liu, Ping	2519	Locmelis, M.	1636	Loseth, H.	2258
.....	1025	Liu, Ping-Ping	1626	Loewy, S.	659	Lothenbach, B.	1642
.....	1619	Liu, Pinghua	1623	Lofts, S.	2334	Lottermoser, B.	1857
.....	2189	1625	Loganathan, N.	1420	Lou, Q.	2611
.....	781	2447	1636	Loucks, R.	1642
Littke, R.	781	Liu, Q.	1626	1843	Loudin, L.C.	1801
Little, S.	592	Liu, R.	1458	Lohan, M.	773	Loughrey, L.	1691
.....	1620	Liu, Shengao.....	2447	1037	Lounejeva, E.	1245
.....	2389	Liu, Suet	1442	1291	1546
Little, T.	979	Liu, Taoze	991	1637	Lourantou, A.	1543
Litvak, M.	881	1627	1937	Louvat, P.	737
Litvak, V.	1407	Liu, Tsung-Kwei	864	Lohmann, K.	839	749
Litvin, Y.	722	1118	Lohmann, U.	2181	772
.....	1531	Liu, Weihua	739	2241	866
.....	1620	1627	Lohmar, S.	2122	967
.....	2235	Liu, Wenjing	1627	Loick, N.	2109	1130
Litvinenko, Y.	1621	Liu, Xiandong.....	1628	2478	1149
.....	2577	Liu, Xiao-Ming.....	1629	Lokhov, K.	1106	1643
Liu, Bang	1621	Liu, Xiaohuan	1628	Lomakina, A.	1638	1858
Liu, Bao-Jian	1601	Liu, Xiaoming.....	770	Lombi, E.	774	Louvel, M.	1643
Liu, Baojian	1332	Liu, Xijun	1920	Lomenech, C.	2109	Love, G.	1565
Liu, Chao	1622	Liu, Xin.	2280	2406	2079
.....	2466	Liu, Ya Ming	1630	Long, P.	572	Lövgren, L.	1644
Liu, Chaohui.....	1622	Liu, Yajian	1581	1377	1645
.....	1623	1629	2197	Lowe, D.R.	2256
Liu, Chuan-Zhou	1623	Liu, Yan	1630	2500	Lowenstein, T.	2244
.....	2512	Liu, Yanan	1973	Longerich, H.	1193	Lowry, D.	1644
Liu, Cong-Qiang	872	Liu, Yi-Wei	1631	1521	1854
.....	991	Liu, Yifei	1604	Longnecker, K.	1781	Lowry, G.V.	778
.....	1543	Liu, Ying	1652	Longo, A.	1133	792
.....	1627	Liu, YingChao	1631	Longo, V.	1165	1591
.....	2308	Liu, Yong-Sheng	1153	Longpré, M-A.	1481	1645
Liu, D.	1647	1277	990	Lowson, C.	1918
Liu, Fu	1330	1335	Lopano, C.	1929	Loy, A.	1342
.....		2528	Lopes, J.	1967	Loyaux Lawniczak, S.	556
.....		2594		Loyd, S.	2000

Lu, A.	1603	Luo, M.	1653	Ma, W.	2569	Maffioli, P.	1891
.....	1645	Luo, Q.	2603	Ma, X.	865	Magalhães, V.H.	2455
Lu, Jianjun	1624	Luo, S.	820	Ma, Z-P.	2530	Magdans, U.	1733
Lu, Jiemin	1550	1653	Maas, R.	1178	Maggi, V.	568
Lu, Jilong	1646	Luo, Weijun	1011	1214	Magiera, T.	1668
Lu, Jinmei	566	Luo, Wenyun	1647	1423	Magna, T.	555
Lu, P.	1646	1469	1661	1668
Lu, S.	1647	Luo, Xianrong	1654	2369	2214
Lu, Xiancai	1624	Luo, Xurong	992	Mabry, J.C.	1541	Magnin, V.	979
.....	1628	Luo, Y.	766	1662	Magnuson, T.	1570
.....	2610	840	Macalady, J.	1249	Magny, M.	2037
Lu, Xiaowei	1338	Lupker, M.	749	Macchi Ceccarani, G.	1063	Magot, M.	2379
Lü, Xin-Biao	2571	1103	Macdonald, F.	765	Maguffin, S.C.	1669
Lu, Xinze	1447	1289	1622	Magyar, J.	1669
Lu, Y.	594	1302	MacDonald, J.	1662	Magyar, P.	1670
Lu, Zheng-Tian	790	Lupton, J.	1655	Macedonio, G.	1208	Mahaffy, P.	869
.....	2005	2094	Macera, P.	1146	1590
Lu, Zunli	1259	Luquot, L.	951	Machado, W.	985	Maher, K.	1009
.....	1647	1144	1737	1142
Luais, B.	679	1655	Machesky, M.	884	1399
.....	1626	Luster, J.	1656	1517	1670
.....	2141	Lustrino, M.	1656	1663	1719
Luca, B.	2218	2331	2061	1867
Lucas, A.	2043	Luther, G.	1667	1663	2213
Lucassen, F.	1648	Luttge, A.	621	Machida, S.	1663	Maheshwari, P.	1671
Lucazeau, F.	1682	1087	Mächler, L.	1664	Mahmood, S.	1061
Lucchetti, G.	824	1657	Macías-Vázquez, F.	2280	1671
Lucchi, F.	1102	Luttinen, A.	1657	Mack, E.E.	1931	1671
Lüchinger, N.	2297	Lüttner, E.J.	1931	Mackensen, A.	1974	1672
Luchs, T.	1306	Lutz, S.	1658	MacKenzie, A.B.	2364	1700
Lucot, E.	2260	Lützenkirchen, J.	1309	Mackenzie, F.	1664	Mahowald, N.	568
Ludden, J.	1648	1658	Mackizadeh, M.A.	1665	Mahy, G.	1544
.....	1649	Lybrand, R.	1659	MacIannan, J.	1027	Maibam, B.	1672
Lüders, T.	2272	Lydie, B.	2014	MacLeod, C.J.	1103	Maier, M.	1360
Lüders, V.	1563	Lyon, I.	1393	Macmillan, E.	1598	Maier, R.	1005
Luetzenkirchen, J.	1995	Lyons, J.	1399	MacMillan, M.	1665	1250
Luffi, P.	567	1659	Macpherson, C.	699	Maier, W.	1105
Luginbuehl, S.	1649	Lyons, T.W.	590	798	Maillot, F.	1673
Lugmeier, J.	1307	592	972	1792
Lugovic, B.	1141	604	1253	Mailloux, B.	1553
Luguet, A.	760	1173	1666	2285
.....	901	1245	MacPherson, G.	1313	Maimaiti, M.	1673
.....	1492	1252	1666	Mair, V.	1126
.....	1619	1259	MacRae, C.	739	Maison, A.	664
.....	1782	1546	Madai, F.	1040	Maisons, G.	1200
.....	2437	1620	Madden, A.	2294	Majidi, P.	2191
Luhmann, A.J.	2108	1904	Madé, B.	847	Major, J.	2131
.....	2368	1977	1129	Majumdar, A.S.	1674
Lukens, W.	2207	2062	Maden, C.	769	Majzlan, J.	588
Lukšienė, B.	1010	2475	2342	1674
Lumpkin, G.	1650	Lythgoe, P.	814	2424	Makabe, A.	1855
.....	1650	Lyttle, A.	2563	Mäder, U.	936	Makarova, I.	2432
.....	2072	Lyubutin, I.	1365	1000	Maki, K.	2202
Lundby, C.	769	1383	1383	2541
Lundeen, R.A.	1651	M	1667	Madison, A.	1667	Makio, M.	1528
Lundstrom, C.	705	Ma, C.	757	Madland, M.	2456	1675
.....	2197	1661	Madonna, F.	1667	Maklhoufi, Y.	2017
Lunt, D.	1869	Ma, M.	2463	Madureira, P.	1686	Makovicky, E.	1675
Luo, C.	2513	Ma, N.	2088	Maeder, U.	2482	2126
Luo, G.	1337	Ma, R.	778	Maenhaut, W.	1141	Malaspina, N.	1676
.....	1651	1645	Maes, A.	772	Maldonado, M.	931
Luo, J.	1652	Ma, S.	2514	Maes, N.	1020	Malik, D.	1993
Luo, L.	1652	Ma, T.	1003	Maffert, A.	2263		

Malitch, K.	639	Marchesini, I.	1004	Marris, H.	1093	Martins, H.C.B.	1079
.....	1676	1004	Marrocchi, Y.	1519	1698
Malkin, S.Y.	2174	Marchev, P.	1962	Marroni, M.	808	2130
Mallik, A.	1677	Marchi, S.	748	Marsac, R.	1689	Martins, J.M.F.	1788
Mallmann, G.	1099	Marchina, C.	702	1862	1832
Malone, E.	2173	1681	Marsal, F.	2379	Martins, L.	2318
Malov, A.	1677	Marcinko, C.	1639	Marsala, A.	1689	Martins, V.	1698
Malthe-Sørenssen, A.	2093	Marcolli, C.	1137	Marschall, H.R.	1199	Martma, T.	1588
.....	2377	Marconi, D.	1396	1690	Martucci, A.	1559
Maltsev, A.	728	Marcoux, E.	767	2169	1699
.....	1587	Marcoux, M.	743	Marschall, P.	2096	Martucci, G.	1902
.....	1678	Marcucci, E.	1350	Marshall, C.	1690	Marty, B.	632
.....	1735	Marcus, D.	985	1889	1123
Malyshev, S.	1175	Maresca, J.A.	1405	Marshall, Dan.	1691	1417
Malyshkin, S.	1477	1682	Marshall, David.	1808	1519
Malz, N.	1678	Mareschal, J-C.	1682	Marshall, V.	1691	1541
Manatschal, G.	1957	Marhan, S.	1984	Marsico, R.	2423	1662
Mancini, L.	622	Marien, C.	2621	Marske, J.	1692	1699
Mandaliev, P.	1758	Marillo Sialer, E.	1054	Martelli, M.	824	1700
Mandon, C.	738	1683	919	1908
Maneck, J.	1532	Marin-Carbonne, J.	1683	1617	Marty, N.	1552
Mangas, J.	814	Marincea, S.	1017	1692	Marui, A.	1707
Mangiacapra, A.	1958	1161	Märten, A.	1743	Maruoka, Y.	1440
Mangini, A.	2503	1352	Martens, J.A.	772	Marupakula, S.	1700
Mann, G.	831	1684	Martí, V.	1410	Maruyama, S.	606
.....	832	Marini, L.	694	Martin, Adam.	763	1303
Manninen, H.	959	926	Martin, Ashley.	1693	1438
Manning, Christina.	1679	1684	Martin, Audrey.	1693	2282
Manning, Craig.	1346	1685	Martin, F.	1486	2567
.....	1679	2409	Martin, H.	1694	Marxer, H.	1701
.....	2358	Marino, G.	1696	Martin, I.	2386	Maryunani, K.A.	1267
Manning, D.	2070	Marinoni, A.	959	Martin, J.	1085	Marz, C.	603
Manning, P.	656	2127	Martin, L.	1289	1991
.....	1029	Marinoni, N.	692	Martin, P.	1562	Marzoli, A.	809
Mansaray, Z.	1425	Mariotti, A.	1795	Martin, R.	2489	809
Mansoor, B.	2444	Mariotti, V.	2053	Martin-Benito, D.	591	1701
Mantegazzi, D.	2125	Mark, D.	2229	Martín-Romero, F.	2418	1751
Manthilake, G.	854	Markl, G.	2318	Martindale, M.	2220	2180
.....	1953	2452	Martinelli, G.	1947	Masaki, S.	1702
Mantilla, L.C.	709	Markle, B.	1180	Martinierie, P.	1933	Masalaite, A.	1141
Mantovani, F.	1224	Marks, K.	1501	Martínez, A.	932	Masanori, M.	601
.....	1341	Marks, M.A.W.	1167	Martinez, Carmen Enid.	2083	Masatsugu, Y.	552
.....	2002	2318	Martínez, Cristina.	2351	Maschowski, C.	1168
.....	2519	2452	Martínez, Fernando.	2055	1702
Manuel, J.	814	Marks, N.	1650	Martínez, Francisco.	2034	Masciocchi, N.	1223
Manuella, F.	1680	2072	Martínez, I.	1135	Masetti, G.	1856
Mao, C.	1680	2589	1694	Mashhour, I.	570
Mao, F.	1621	Marmier, N.	2109	Martínez, L.	1697	Mashukov, A.	1703
Mao, Q.	2526	Marquard, J.	1685	Martínez, R.	1688	Mashukova, A.	1703
Mao, X.	1193	Marquardt, C.	1689	1695	Maskell, A.	942
Mapani, B.	2405	Marquardt, K.	1529	Martínez, S.	1697	1424
Mapes, R.	1760	1686	Martínez Abad, I.	1695	1703
Maphanga, S.	1553	Marquer, D.	733	Martínez-Boti, M.A.	1102	Maslennikov, V.	1245
.....	2005	Marques, A.F.A.	929	1696	1546
Marakovic, G.	1858	1686	Martínez-García, A.	1369	1704
Marang, L.	1932	Marques, R.	1687	Martínez-Legorreta, F.	1378	Maslennikova, S.	1704
Marca, A.	1469	Marques Fernandes, M.	1687	Martínez-Ruiz, F.	1696	Mason, A.J.	2436
Marchand, C.	1858	1689	Martínez-Sánchez, M.J.	1697	Mason, B.	1897
Marchandise, S.	2091	2236	1697	Mason, H.	831
Marchant, I.	1400	Marquez, J.E.	1688	Martinotti, V.	2242	1704
Marchesi, C.	1266	Marquez, M.	2180	Martins, C.	1672	Mason, P.	851
.....	1640	Marquillas, R.A.	2210	1783
.....	1681	Marrapu, P.	1688	1850

Masoudi, F.	2556	Matthies, R.	1711	McAlister, J.	1718	McLennan, S.M.	2158
Masqué, P.	836	Matthiesen, J.	1890	McAlpine, S.R.B.	684	2269
.....	1075	Matthieu, M.	1537	McAnena, A.	1718	McLeod, C.	1727
Massa, G.	1224	Mattiel, N.	577	McCabe-Glynn, S.	1398	McLeod, G.W.	1354
.....	2519	Mattielli, N.	982	McCaffrey, K.	1666	1727
Massion, A.	2320	1016	McCammon, C.	1116	McLoughlin, N.	2435
Massoli, P.	1169	1060	2247	McMahon, S.	1728
Masson-Delmotte, V.	1543	1712	McCann, C.	1398	McManus, J Barry	1892
Massone, C.	1705	Mattioli, M.	1712	McClain, Craig R.	1939	2575
Massonne, H-J.	1705	Matushkin, N.	2407	McClain, Cynthia	1009	McManus, James	552
.....	1799	Matusiak-Matek, M.	1713	1719	661
.....	1799	2007	McClelland, H.	1290	1620
Massuyeau, M.	1706	Matusik, J.	2366	McClelland, J.	794	1728
Masters, A.	2467	Matveeva, S.	1989	McClung, C.R.	2506	McManus, Jerry	1288
Masterson, A.	1401	Matys Grygar, T.	1864	McCollom, T.	1350	McMillan, P.	1729
.....	1706	Matzen, A.	1713	McConachy, T.	1719	McMurry, P.	2227
Mastrocicco, M.	1059	Maugeri, R.	1165	McConnell, B.	1115	McMurtry, G.M.	1541
Masuda, H.	1707	Maulana, A.	1714	McConnell, J.	1062	McNeill, K.	1651
Masunaga, S.	1707	Mauri, F.	715	1270	McNeill, V.F.	1729
Masy, J.	1591	1972	1720	2135
Mata, J.	2132	Maurice, L.	749	McCormick, B.	1720	McSween, H.	2372
Matchan, E.	1966	967	McCoy-West, A.	1721	Mead, R.	1456
Mateeva, T.	1957	Maurice, P.	1714	McCray, J.	1470	2498
Matei, E.	911	Maurice, S.	1590	1831	Meador, T.B.	1301
Maters, E.	1708	2269	2515	1730
Mateus, A.	2314	Mavris, C.	622	McCuaig, T.C.	1926	Meakin, P.	2093
Mather, T.	1708	1715	McCubbin, F.	1721	Meana-Prado, M.F.	784
Mathes, M.	2325	Mavrogenes, J.	1382	2255	Measures, C.	2198
Mathiessen, J.	1270	Mavromatis, V.	693	2391	Mechie, J.	1525
Mathieu, L.	1918	742	McCulloch, M.	1722	Meckenstock, R.	2515
Mathieu, O.	1191	1715	2359	Meckler, N.	1443
Mathurin, F.	566	1858	McCurry, M.	1008	1759
.....	691	1878	McCutcheon, J.	1992	2424
.....	1709	2000	McDade, C.	882	Médard, E.	909
.....	2568	2165	McDermitt, D.	1722	1693
Matjuschkin, V.	1306	Maxfield, P.	1610	McDermott, C.	1458	1730
.....	1709	May, J-H.	2293	McDonald, B.	1054	2085
Matlakowska, R.	1710	May, M.	1634	1724	Medici, L.	828
Matmon, A.	2106	Mayali, X.	1961	McDonald, I.	1345	Medjoubi, K.	2184
Matott, L.S.	578	Mayer, B.	668	McDonald, K.J.	2035	Medvedeva, E.	2385
Matson, C.	645	997	McDonough, W.	1145	Meeussen, J.	1731
Matsui, H.	1899	1370	1341	Meffre, S.	945
Matsui, A.	1366	1716	1723	1171
Matsumoto, I.	1710	1726	2096	1539
.....	2378	1850	McDowell, S.	1723	2032
Matsumoto, Takeshi.	1120	1999	1760	2582
Matsumoto, Toru.	1711	Mayer, K.U.	957	McGee, D.	1992	Méheut, M.	715
.....	2361	1262	McGinnity, P.	1639	1020
Matsunaga, A.	1960	Mayes, W.	1635	McGlynn, S.	1181	1731
Matsuno, J.	2361	Mayhew, L.	2321	McInerney, M.	1724	Mehta, V.	1673
Matsuo, M.	1321	Maynard, J.	2290	McInnes, B.	1054	Mei, Y.	1627
Matsuoka, H.	1267	Mayor, M.	1374	1724	1732
Matsuoka, T.	1484	Mayordomo, N.	1716	McIntosh, J.	881	Meibom, A.	1496
Matsushima, T.	2361	1771	McIntosh, K.	1480	1838
Matsuya, M.	643	Mayorova, N.	1531	McIntyre, C.	2311	Meidla, T.	1981
Matsuzaki, H.	1356	Mayr, C.	2123	McKenzie, J.	764	Meier, D.B.	1732
.....	1811	Mazevet, S.	1237	McKenzie, R.	1725	2030
.....	1881	Mazumdar, A.	1163	McKeown, D.	2207	Meier, M.	1218
Matter, J.	1178	1717	McKibbin, S.	1725	Meima, J.	1733
.....	1935	1945	McKiernan, B.	1726	Meis, S.	1733
.....	2277	Mazza, S.E.	1717	McLachlin, K.	1935	Meisel, T.	731
Mattey, D.	2517	Mazzucchelli, M.	1177	McLean, N.	1726	1734
Matthews, A.	592	1545		Meisenhelder, K.	1035
Matthews, J.	1740						

Meißner, S.	1210	Mertzimekis, T.	1136	Michalik, M.	1420	Miller, Calvin	1723
Meister, P.	1734	1185	1434	1760
Meixner, A.	1648	1459	1505	Miller, Christopher	572
.....	1881	Mesbah, A.	979	1753	Miller, Christopher	2571
Méjean, G.	1217	Mesfin, K.	1178	2495	Miller, D.	1867
Mejía, L.M.	1735	2277	Michalkova, Z.	1489	Miller, H.	2321
Melcher, F.	570	Meskhidze, N.	1744	Michalopoulos, P.	1753	Miller, J. Scott	902
Melenevsky, V.	1735	1744	Michel, F.M.	778	Miller, Jodie	2405
Melezhik, V.A.	763	Messina, A.	920	1758	Miller, John	1926
.....	927	999	Micheletti, F.	1101	Miller, Jonathan	1760
.....	2162	Messini, P.	613	1754	Miller, Kelly	1760
Melgarejo, J.C.	814	Metcalfe, I.	1349	Michibayashi, K.	2138	Miller, Kerri	1761
Meliksetian, K.	1850	Metcalfe, K.	1130	Michon, L.	1149	Miller, Kevin	1589
Melnik, A.	1736	Methner, K.	1745	Micic, V.	1554	Miller, N.	1761
Melo, G.	966	Metreveli, G.	1745	2156	Miller, R.	1949
Memeti, V.	1736	Métrich, N.	935	Middag, R.	956	Miller, T.E.	2503
Menard, G.	1737	1790	2397	Millet, M-A.	1319
Méndez-Vicente, A.	1735	2413	Middleburgh, S.	1650	Millett, J.	1762
Mendoza, U.	985	Metz, C.	669	2072	Millot, R.	978
.....	1737	Metzger, E.	1746	Middleton, A.	1754	1762
Mendoza-Flores, A.	1738	1827	2381	Milloux, M-J.	1191
Mendybaev, R.	1738	Metzger, J.G.	1746	Midende, G.	751	Mills, B.	1763
.....	2218	Metzger, P.	2600	Miecznik, J.	1221	775
Menegazzo, R.	1224	Meunier, J-D.	1747	1478	1763
.....	2519	Meusinger, C.	1399	Mielcarek, J.	2039	Mills, H.	2037
Ménez, B.	1739	1747	Mielnicki, S.	1755	Mills, Rachel A.	604
.....	1931	Mewafy, F.	628	Mietelski, J.W.	1769	973
.....	1974	Meydan, A.F.	2342	1933	1316
.....	2325	Meyer, C.	674	Mifsud, C.	1119	1323
Meng, E.	1739	Meyer, Hanno	1734	Migdisov, A.	2397	1764
Meng, H.	1628	Meyer, Hans Peter	1141	Migdisova, N.	1755	Mills, Ryan	904
Menguy, N.	1740	Meyer, J.	1373	Migorsky, V.	1777	Milne, A.	1037
.....	1792	Meyer, Katja M.	1748	Mihajlov, I.	1756	1291
.....	2332	1939	Mihaljevič, M.	1052	1637
Menicucci, A.	1740	Meyer, Kyle	1748	1756	Milodowski, A.	1082
Menneken, M.	1476	Meyer, Melanie	1749	1864	2073
Mennon, M.	2038	Meyer, Michael R.	1749	2370	Milosan, I.	1017
Menot, G.	2125	Meyer, N.	586	2394	Milot, J.	842
Menozi, D.	1741	Meyer, R.	1184	Mihalopoulos, N.	746	Miltner, A.	1240
Menzies, C.D.	1847	1750	1975	1764
Menzies, M.	569	Meyer, Stefan	2062	2419	Milu, C.	1957
.....	1002	Meyer, Steffi	1474	Mihira, T.	1758	Milucka, J.	688
.....	2340	Meynadier, L.	900	Mikhail, S.	1328	1205
Merchel, S.	1752	1537	2255	1765
Mercier, F.	2379	1750	2442	1900
Mercolli, I.	1172	Meysman, F.J.R.	2174	Mikhalevko, V.	1126	Milzer, G.	1067
Mercury, L.	1741	2284	Mikheev, E.	1757	Mimura, K.	1588
Merfort, I.	1168	Meyzen, C.	809	Mikheev, V.	1703	Minaev, V.	1494
Merino, E.	1742	1751	Mikhno, A.	1757	Minami, H.	1765
Merkel, B.	2154	Mezger, K.	634	Mikouchi, T.	1490	Minami, M.	1403
.....	2159	665	1758	1766
.....	2212	1830	2152	Minami, T.	1491
.....	2224	Mia, S.	1297	Mikutta, C.	1758	Minardi, I.	694
Merle, R.	1742	Mibe, K.	1440	Milani, S.	1840	Miner, K.	2431
Merlini, M.	1121	1751	Milazzo, M.	721	Ming, D.W.	1794
Mernagh, T.	666	Michael, P.	1752	Milesi, V.	1759	2158
.....	2209	2094	Milewski, A.	1038	Minissale, A.	1766
Merroun, M.L.	1638	Michalak, P.P.	1618	Milke, R.	1203	Minitti, M.E.	846
.....	2123	1752	1208	2269
Mersch-Sundermann, V. .	1168	2221	Millán, I.	895	Minofar, B.	1767
Merschel, G.	1743	1443	Minoletti, F.	1290
Merten, D.	1210	1759	Minoura, K.	1826
.....	1743	Millar, I.	663	Minshull, T.	597
Mertz-Kraus, R.	2477

Miot, J.	1767	Mohammadzadeh, H.	1776	Montgomery, D.	1558	Morgan, Jason P.	1790
Miraj, H.	1049	Möhler, O.	1540	Montinaro, A.	1783	1791
Miranda, C.R.	697	2259	Montlucon, D.	2311	Morgan, Jennifer.	853
Miranda, R.	753	Mohn, G.	1957	Montouillout, V.	1858	Morgan, L.	1791
Mirolo, F.	1768	Mohwinkel, D.	1499	Montross, S.	1538	Morgan, W.J.	1791
Mironov, A.	2608	Moine, B.	1250	Moog, H.	1783	Morgenroth, W.	595
Mironovich, A.	1365	Moirogiorgou, K.	1851	Mook, J-S.	1351	668
Mischel, S.	1768	Moiroud, M.	1777	Moola, P.	1784	2129
Mishima, K.	1769	Moise, T.	1555	Moon, E.	1940	Morguñ, J-A.	932
Mishra, Biswajit.	1275	Moiseenko, T.	1777	Moon, H.S.	1351	Moricz, F.	1040
Mishra, Brundaban.	1802	Moita, P.	1778	Moon, J.	996	Moriguti, T.	1071
Mishra, H.	1308	Mojzsis, S.J.	752	Moon, S-H.	1460	Morikawa, N.	1322
Mishra, Snigdha.	955	841	Moon, W.	2564	Morin, G.	737
Mishra, Suchismita.	1769	1105	Moorbath, S.	939	778
Misiti, V.	1179	1212	Moore, C.M.	780	808
.....	1770	1230	Moore, G.	1784	836
Miska, S.	2585	1319	Moore, J.	1785	921
Misra, S.	1770	1778	2515	1014
Missana, T.	580	2497	Moore, L.	723	1103
.....	1143	Mokhtari, M.A.A.	2111	Moore, O.W.	800	1227
.....	1716	Molinero, J.	982	Moore, W.	807	1792
.....	1771	2355	858	1858
.....	2079	Molleman, B.	1297	1785	1891
Mitchell, A.H.G.	1567	Möller, A.	1873	Moorsom, B.	648	2332
.....	1613	2142	Moosdorf, N.	1786	Morin, S.	2143
Mito, S.	1441	Möller, C.	1956	Moosmüller, H.	1786	Morishita, T.	601
.....	2353	Möller, I.	1238	Moradpour, M.	1833	2305
Mitra, S.	1591	Möller, K.	747	Moraes, E.	897	Moritz, A.	1792
Mitrofanov, F.	672	Mollo, S.	1179	Moraes, R.	1938	Moriwaki, E.	1827
Mitrovica, J.	2033	1545	Moragas, M.	2351	Moriya, K.	1438
Mitsunobu, S.	1771	1770	Morales, L.	1208	1793
Miura, K.	1201	1779	1283	2301
Miura, M.	1772	2147	2048	Moriyama, S.	2136
Miura, Y.N.	878	Moncoffre, N.	2109	Morales, V.	1227	Morizet, Y.	1258
Miyahara, M.	1614	Mondal, S.K.	1779	Moran, S.B.	594	1706
.....	1772	1802	Morana, C.	1634	Mormul, R.	1114
.....	1884	Mondani, L.	1780	Morand, G.	1787	Moroni, M.	835
Miyaji, A.	1773	Monga, O.	870	Morbideilli, A.	1512	Morono, Y.	1324
Miyaji, T.	2204	1778	2094	1793
Miyajima, N.	844	Monks, P.S.	1084	948	2323
Miyake, A.	1711	Monnereau, M.	653	Moreau-Fournier, M.	948	2521
Miyawaki, J.	2136	Monnier, L.	1902	Moreira, D.	688	Morookian, J.M.	1794
Miyazaki, J.	1855	Monnington, A.	1780	Moreira, Manuel.	1535	Moroz, T.	1987
Miyoshi, A.	1773	Monoz, C.	830	1787	Morozov, I.	1638
Mizernaya, M.	1531	Monsef, I.	2020	1922	Morozova, D.	1435
Mizuguchi, Y.	1517	Montagna, C.P.	1781	2087	1794
Mo, S.	1774	Montagna, P.	1537	Moreira, Manuel.	985	1841
Mo, X.	2330	1722	1737	2516
Moallemi, A.	1833	Montagnac, G.	2590	Moreira, S.	928	Morozova, L.	672
Möbius, J.	1774	Montagnat, M.	672	1788	Morozova, V.	1557
Mobley, M.	2058	Montagnat, M.	1766	Morel, C.	2405	Morrill, P.	766
Mochalov, A.	1775	Montanari, D.	1781	Morel, F.M.M.	636	Morris, B.	1391
.....	2207	Montanari, G.	1932	Morel, J.L.	1052	Morris, G.A.	1537
Mochimaru, H.	2567	Montanari, S.	1782	Morel, M-C.	1788	1857
Modolo, G.	963	Montanini, A.	2585	Morelli, G.	1789	2111
.....	1084	Montarges-Pelletier, E.	1206	Moreno, T.	2014	Morris, P.	858
Moeck, I.	767	Montavon, G.	956	Moreto, C.	966	Morris, R.V.	1794
Moehler, O.	1797	Monteiro, F.	966	Moretti, H.	1789	Morrison, S.M.	1794
Moeller, I.	2155	Monteiro, L.	1127	Moretti, R.	1096	Mörth, M.	874
Moeller, K.	1775	Monteleone, B.	1735	1790	Mortimer, R.	1635
Mogollón, J.	756	Monteleone, S.	1766	Morey, P.	869	1917
Mohammad, F.	1776	Montes-Hernandez, G.	1538	Morgan, D.J.	737	Morton, D.	2129
Mohammadian, H.	2556	1782	850	Mortyn, P.G.	1696

Moryl, R.	2495	Mugnaioli, E.	1970	Münker, C.	675	Müter, D.	2168
Moser, D.	946	Muhling, J.	1800	933	Mutlu, H.	1814
.....	950	2030	1469	Mutter, A.	1815
.....	1795	Mukai, H.	1800	1512	Mutum, R.S.	849
.....	2386	Mukasa, S.B.	632	1678	862
Mosselmans, J.F.W.	694	1165	1809	Myagkaya, I.	1235
.....	774	1344	1955	1815
.....	1245	1801	1964	Myers, J.	2240
Mosser-Ruck, R.	841	Mukhamadiyarova, R.	1801	2390	Myhill, R.	1115
.....	1970	Mukherjee, R.	1802	2415	Mykyczuk, N.	1945
Mostefaoui, S.	745	Mukhopadhyay, D.	591	2621	Myneni, S.	1816
.....	988	Mukhopadhyay, J.	1802	Munnecke, A.	2435	2429
Moteki, N.	1899	Mukhopadhyay, S.	1340	Munnik, F.	1752	Myojo, K.	1816
.....	2113	1803	2221	Myriokefalitakis, S.	1817
Mothet, A.	1795	1803	Munoz, A.	1084	Myrow, P.	1725
.....	2173	Mukotaka, A.	1804	Munoz, Manuel	958	Myska, O.	1509
Motoyama, I.	1120	Mulch, A.	1745	1377		
Motschmann, U.	2346	Mulholland, D.	1983	Munoz, Marguerite	1810	N	
Mottram, C.	1796	Mulkidjanian, A.	1804	Münsterer, C.	1272	Naafs, B.D.A.	839
Mou, L.	1224	Mullan, M.R.	826	Muntean, M.	2394	1918
.....	2519	Mullen, E.	1805	Munteanu, M.	889	Nabelek, P.	948
Mouchel, J-M.	1227	Müller, Albert	1342	Müntener, O.	1057	Nabhan, S.	1316
Mouchel-Vallon, C.	764	Müller, Axel	1108	1095	1818
Moucka, F.	2229	Müller, B.	888	Murakami, C.	1698	Nabi, D.	612
Moulas, E.	1093	1876	Murakami, M.	1810	Nadeau, O.	1818
Mountjoy, G.	899	2347	Murakami, T.	1429	Nadeau, S.	1819
Moura, C.A.V.	2065	Müller, E.	1683	Murali, R.	1910	Nadoll, P.	1819
Mousavi, S.Z.	1796	1805	Muramatsu, Y.	583	2485
Mouvet, C.	752	1965	1356	Naegler, T.	1422
Mouzakis, K.	1831	Müller, H.	1627	1811	Nagahara, H.	1820
Mowlem, M.	1406	Müller, I.	2207	1876	2534
Moy, C.	1045	Müller, Katharina	1806	1881	Nagai, Y.	1820
Moyano, F.	870	2155	1886	Nagano, T.	2361
.....	1575	Müller, Konrad	1099	2349	Nagao, J.	1492
Moyard, S.	1552	Müller, P.	2005	Murashko, M.	1134	1821
Moyce, E.	1082	Müller, S.	1806	1134	Nagao, K.	1239
Moyen, J.F.	1104	Müller, T.	1577	1160	1484
.....	1797	Müller, U.	569	Murata, A.	1522	Nagaoka, M.	1467
.....	1846	Müller, Werner	1394	Muratli, J.	1728	Nagaoka, T.	1821
.....	2419	Müller, Wolfgang	967	Murayama, Masafumi	1765	Nagashima, K.	1244
Moyer, E.	733	1053	Murayama, Mitsuhiro	1396	1315
.....	1520	1265	Murè, F.	1165	1515
.....	1540	1599	Muroi, R.	1811	1822
.....	1797	Mullins, O.	1807	648	2416
.....	2277	Mulvaney, R.	579	Murphy, B.	2251	Nagel, T.	1283
.....	948	1904	Murphy, C.	1385	Nagender, N.	1822
.....	961	Mumin, H.	1807	Murphy, D.	2080	Nägler, T.F.	747
.....	1798	Munda, P.	1833	1514	1212
.....	1998	Munday, D.	1808	Murphy, J.	1812	1775
.....	2142	Mundl, A.	1808	1812	1830
.....	2214	Mungall, J.	1809	Murphy, Melissa	1812	Nagy, S.	1916
Mozley, P.	939	Munger, Z.	578	Murphy, Michael	637	Naidu, D.	1823
Mucci, A.	654	Munhá, J.	1788	Murphy, R.	1813	1823
.....	1576	2314	1943	Naidu, P.K.	1823
.....	1667		Murray, J.	1813	Naik, Smita	1823
Muehe, E.M.	1798			Murray, R.	2140	Naik, Sushant	1823
Mueller, C.W.	1307			Murray, S.	613	Najman, Y.	760
.....	1799			1814	Najorka, J.	1454
Mueller, Paul	1120			Murton, B.	2387	Nakada, R.	1824
Mueller, Peter	790			Muschitiello, A.	1101	Nakagawa, F.	1490
Mueller, T.	1799			1754	Nakagawa, T.	2229
Muenker, C.	1034			Musiani, M.	573	Nakagawa, Y.	1824
Muggeridge, A.H.	939			Mussi, A.	917	Nakai, S.	1256
				Mustin, C.	2583	Nakajima, J.	2302

Nakama, A.	1322	Naude, K.	2405	Németh, B.	1839	Nickel, C.	1845
Nakamachi, K.	1457	Naumann, R.	2039	Nenes, A.	1839	Nickel, M.	1342
Nakamatsu, Y.	1426	2496	2135	Nicklin, I.	575
.....	1825	Naumenko, M.	1830	Nescher, P.	2175	Nico, P.	1442
.....	2204	Naumov, E.	1830	Nestola, F.	1845
Nakamura, E.	1071	Nauret, F.	909	611	1961
.....	2307	1730	809	2345
Nakamura, H.	1899	Navarre-Sitchler, A.	1470	1840	2606
Nakamura, M.	1711	1831	Neubauer, E.	1714	Nicol, A.	950
.....	1825	Navarrete, J.	1937	1840	Nicoli, G.	1846
.....	1902	Navarro-Ciurana, D.	918	2430	Nicoll, R.S.	1349
Nakamura, R.	1826	1831	Neubeck, A.	1841	Nicollet, C.	958
Nakamura, Takamichi	1821	Navasardyan, G.	1850	Neubert, N.	2213	Nicotra, E.	977
Nakamura, Tomoki	2534	Navel, A.	1832	Neufeld, J.	703	1846
Nakamura, Toshio	1826	Navon, O.	2478	942	2413
Nakanishi, T.	1467	Navozov, O.	1503	Neugebauer, I.	2169	2427
Nakano, T.	2361	Navrotsky, A.	1832	Neuland, M.	2062	Nie, S.	1429
Nakashima, K.	2283	Nayak, B.	1833	Neumann, A.	1296	Niedermann, S.	1457
Nakashima, S.	696	Nazarenko, I.	1168	Neumann, D.	1794	1485
.....	1247	Nazarian Samani, P.	1833	1841	1847
.....	1891	Nazima, V.	1453	2516	Niedermayr, A.	1116
Nakata, Y.	1711	Nazzareni, S.	1834	Neumann, U.	1431	1847
Nakaya, S.	1707	Ndayisaba, C.	2370	Neumeier, S.	963	2004
Nale, S.	1480	Neacsu, A.	1834	1084	Nielsdottir, M.N.	1182
Nali, M.	2525	Neal, A.	1455	1296	Nielsen, A.R.	1848
Nalini Jr, H.	2121	Nebel, O.	684	Neupane, G.	1001	Nielsen, Lars Peter	940
Nam, I.H.	1569	1835	Neuville, D.R.	948	1964
Nam, K-H.	880	2380	1096	Nielsen, Laura	2472
.....	1384	Nebera, T.	741	1562	Nielsen, M.r.	1848
Namgung, S.	1567	1835	1582	Nielsen, Mike	983
Namiki, N.	2470	Nedel, S.	883	1842	2223
Namjesnik, D.	1995	1836	1858	Nielsen, S.	608
Namur, O.	859	Nedialkov, R.	704	2085	1527
Namba, K.	1426	Nedosekova, I.	1836	2311	2041
.....	1882	Neely, R.	1837	Neven, I.	956	Niemann, H.	718
Nanbu, S.	942	Neff, D.	2379	Neves, P.	1842	1849
Nance, J.	817	Negishi, H.	1811	Nevolko, P.	1830	2134
Nancharaiah, Y.V.	2282	Negishi, K.	1837	New, A.	1529	2259
Nancy Ion Microprobe	Negrel, P.	767	Newcombe, M.	2269	2622
Team,	2080	770	Newman, D.K.	708	Nies, D.H.	2047
Nanson, G.	1119	1762	1496	Niessner, R.	669
Nara, F.	1826	Negulescu, E.	2110	2056	1520
.....	2470	Nehrke, G.	705	2479	Nieto, F.	2124
Naraoka, H.	1765	1838	Newton, R.J.	938	Nieto, J.M.	554
.....	1827	Neidhardt, H.	710	2213	Nieto Yabar, D.	1849
.....	2554	Neil, H.	860	2586	Nieto-Moreno, V.	1696
Nardelli, M.P.	1827	2089	Newville, M.	2290	Niggemann, J.	2166
Nardi, L.V.S.	710	Neiva, A.M.R.	1287	Nezbeda, I.	2229	Nightingale, M.	1716
.....	1828	Nekrasov, A.	1197	Ngo, H.	1592	1726
Nardin, E.	1003	Nekrasov, S.	803	Ngombi-Pemba, L.	1843	1850
Nardoux, P.	1780	Nelskamp, S.	2468	Ngouana W., B.F.	1420	Nigmatulina, E.	2607
Narog, M.	1866	Nelson, D.	1892	1636	Nikiforov, A.	1893
Nascimento, R.S.C.	815	2575	1843	Nikogosian, I.	851
Nasdala, L.	1226	Nelson, H.	1644	Ni, H.	1844	1850
.....	1586	Nelson, L.	1343	2551	1851
Nash, W.	1828	Nelson, R.K.	612	Ni, Q.	1335	Nikolaeva, I.	803
Nasri, N.	1829	Nelson, W.	1838	1844	Nikolaidis, N.	1851
Nastos, P.	1185	Nemchin, A.A.	897	Ni, S-J.	1341	2502
Natali, C.	744	1046	2460	Nimis, P.	1840
.....	873	1207	2529	1852
.....	1829	1414	Nicholls, I.	1661	2618
Natarajan, S.	2281	1529	2032	Nimmo, F.	1024
Näthe, K.	596	1742	Nichols, A.	905	1852

Nimura, N.....	2565	Noone, D.	910	O	Obst, M.	1479
Ninagawa, K.....	1528	1428	O'Brien, C.	1798
.....	1675	1860	O'Brien, David.....	1967
.....	2565	Noordmann, J.	1188	O'Brien, Diane.....	Occhi, M.	2498
Nindiyasary, F.....	1853	Noorian Ramsheh, Z.....	1861	O'Connell, D.	Occhipinti, P.	932
Ning, Q.....	1853	Nordlund, Å.....	1315	Och, L.	1615
Nisbet, E.	1209	Nordstrom, K.....	813	O'Connor, C.	1876
.....	1644	Noritake, F.....	1861	O'Connor, Patrick.....	2347
.....	1854	Noronha, F.....	2130	O'Connor, Peter.....	Oda, K.	1876
Nishida, M.....	2562	Norrfors, K.	1862	O'Day, P.....	Odom-Parker, K.....	2271
Nishido, H.	1528	Norris, A.	1724	Odukoya, A.	1877
.....	1675	1862	O'Dowd, C.	Oduro, H.	1425
.....	1854	Norris, R.D.	1236	1877
.....	2565	2416	Ody, A.	1878
Nishijima, M.	1884	Nos, J.	1863	2481
Nishimura, K.....	607	2123	O'Driscoll, B.	Oeggl, K.....	1126
Nishino, S.F.....	1310	Noseck, U.	775	Oehlerich, M.	2123
Nishio, Y.	607	2267	Oelkers, E.H.....	693
Nishioka, J.....	1874	Nosova, A.	1432	O'Leary, M.....	742
Nishiyama, N.....	696	2122	O'Loughlin, E.....	765
Nishizaki, R.	1855	Not, C.	1060	926
Nishizawa, M.	602	Nothstein, A.....	1031	959
.....	1855	Novak, M.....	1863	1032
Nishizawa, S.....	1854	1864	O'Neal, K.	1032
Nishri, A.	2188	Novakova, T.	1864	O'Neil, J.	1178
Nisi, B.	1856	Novella, D.	1115	O'Neill, C.	1225
.....	2401	1865	O'Neill, H.S.C.....	1381
Nitani, H.	1837	Novembre, D.	1910	1715
Nitkina, E.	672	Nowak, I.	1865	1878
Nitschke, W.....	708	Nowak, M.....	1167	2165
Nitta, S.....	1123	1431	Oelze, M.....	2058
Nittler, L.	572	1701	Oeser, M.....	1879
.....	1856	1996	O'Reilly, S.Y.....	Ofner, J.....	2139
Niu, Y.	2279	Nowak, S.	2585	Ogawa, N.	875
Nizamoff, J.....	2074	Nowak, T.....	1219	1427
Noble, S.....	1588	Nowell, G.	798	Ogawa, Y.	1879
.....	2114	901	Oggerin, M.....	1880
.....	2225	2312	Oggiano, G.....	838
Noble, T.....	1857	Nozaka, T.	1750	1128
.....	1930	Nozaki, T.	1526	2002
Nobre Silva, I.	1857	1893	Oguri, K.	1826
Nodder, S.....	1037	2137	Oh, H.	1924
Noel, V.	921	Nøhr-Hansen, H.....	1585	Oh, M.	1571
.....	1858	Ntaflos, T.....	623	Oh, S-S.....	1412
.....	1891	1269	Ohara, Y.....	1838
Noetzel, U.	1584	1713	2055
Nofuentes, M.....	932	1808	Ohe, T.	1361
Nogthai, Y.....	1598	1866	2540
Noguchi, T.....	2534	2007	O'Riordan, S.....	2622
Nogueira, A.	2130	Ntounoglou, K.	1176	O'Neill, H.	Ohira, I.....	1884
Noimeir, Y.....	2476	Nuccio, E.	1961	O'Reilly, S.Y.....	Ohishi, Y.....	1860
Noireaux, J.	1858	Nudelman, F.	2223	1884
Noiriel, C.....	743	Nunan, N.	870	Oalmann, J.....	Ohkouchi, N.....	875
.....	1859	1409	1427
Nolan, M.	1720	Nunes, L.	596	Oba, Y.....	Öhlander, B.....	1950
Nolesini, T.....	1859	1866	Obata, H.....	Ohmoto, H.....	880
Nomikou, P.	1459	Nurhati, I.	829	1880
Nomosatryo, S.....	817	Nuriel, P.....	1867	2471
Nutman, A.	1405	Nutman, A.	687	Obenholzner, J.H.....	2561
Nomura, R.	1436	Nuttin, L.	1867	Oberhänsli, R.	Ohnemüller, F.	1881
.....	1860	Nyirő-Kósa, I.....	1868	Oberti, R.	Ohnenstetter, M.....	2047
Nonell, A.	1226	2343	Öborn, Ingrid.....	
		Nyquist, L.....	2539	Öborn, Ingrid.....	

Ohno, Takeshi	1303	Oliveras, V.	1078	Orians, K.	1718	Owano, T.	641
.....	1356	Olivi, L.	664	Orihashi, Y.	1896	Owen, J.	1903
.....	1811	Oliviero, E.	1157	2203	Owens, J.D.	1904
.....	1876	Olofsson, M.	1672	Oristaglio, M.	2012	2475
.....	1881	Olsen, J.	1353	Orlandi, P.	2412	Owens, R.	1894
Ohno, Tsutomu	1882	Olsen, M.B.	1315	Orlando, A.	2180	Oyabu, I.	1904
Ohnuki, T.	1426	1889	Oron, S.	1053	Oyan, V.	1905
.....	1702	Olsson, B.	2216	Oropeza, D.	1193	Oyungerel, S.	1166
.....	1882	Olsson, J.	551	Orosz, L.	1585	Ozaki, K.	1905
.....	2204	Olsson, M.H.M.	754	Orphan, V.J.	953	Ozawa, H.	1303
Ohsawa, S.	1267	1886	1181	Ozawa, K.	565
Ohsumi, T.	1883	1890	1496	1820
Ohta, A.	1403	Omelson, S.	731	1670	Ozawa, S.	1614
.....	1766	Omeregic, E.	1890	1896	1772
.....	1883	Omori, K.	1793	Orr-Ewing, A.	1897	1906
Ohta, J.	1884	Omori, S.	606	Orsega, E.F.	2395	Özçelik, O.	582
Ohta, Y.	2541	Omori, Y.	2310	Orsi, A.	1897	1906
Ohtake, M.	1711	Ona-Nguema, G.	588	Orsi, G.	2340	Özdemir, Y.	1905
.....	2361	808	Orsi, W.	1898	1907
Ohtani, E.	854	836	Orsini, P.	820	Ozerskiy, A.	1907
.....	1025	1227	Ortega-Huertas, M.	1696	Ozerskiy, D.	1907
.....	1614	1792	Osadchii, E.	858	Ozima, M.	1908
.....	1619	1858	1898	Ozkanlar, A.	893
.....	1772	1891	1985	Özkul, M.	1443
.....	1884	2332	Osadchii, V.	1898	Ozturk, A.	1908
.....	2189	Onda, Y.	2306	Osborne, A.	868	Özvan, A.	1909
Ohwada, M.	1322	Ong, R.	609	Oschkinat, H.	1481		
Oi, T.	1457	Onga, C.	1891	Oschlies, A.	2272	P	
Oiler, J.	1885	Oni, O.	2053	2579	Pace, C.	1910
OIsson, C.	2145	Onishi, Hidejiro	1793	Oshima, N.	1899	Pace, L.A.	1090
OIyan, V.	1909	Onishi, Hiroji.	1257	Osman, A.	2464	1286
Ojwang', L.	913	Ono, Shigeaki	1751	Ossorio, M.	1899	1910
Okabayashi, S.	1303	1892	Ostertag-Henning, C.	581	Pacevski, A.	1559
.....	1885	Ono, Shuhei	1395	1219	Pacey, A.	1666
Okabe, N.	1886	1397	1900	Pacheco, F.	2351
Okada, T.	2470	1445	2065	Pacheco, J.	1381
Okamoto, A.	2470	1651	Oswald, K.	1900	Pacheco, N.	1973
Okaue, Y.	1707	1877	Oswald, S.	798	Pack, A.	1294
.....	1901	1892	Oswald, V.	1669	Padilla, A.	1760
Okawa, A.	1457	Onodera, J.	1257	Ota, Y.	1487	Padrón-Navarta, J.A.	1266
Okazaki, R.	2534	Onoue, T.	1893	Otake, T.	1901	1640
Okhrimenko, D.V.	1886	2137	Otemuyiwa, B.	840	1681
Okie, J.	1887	Onstott, T.C.	869	Othmane, G.	921	1911
Okland, I.	1887	1535	Otsu, E.	1901	2380
Okrostsvaridze, Avtandil	1888	1553	Ottavi-Pupier, E.	1902	Paganelli, E.	655
Okrostsvaridze, Avto	853	2005	Otten, W.	870	782
Okubara, P.	1109	2195	Ottesen, R.T.	1182	Page, Laurence.	2150
Okubo, A.	2534	Onufrienok, V.	1893	Otto-Bliesner, B.	568	Page, Lilianne	1911
Okui, W.	1820	Oo Than,	873	Outrequin, M.	2119	Pagel, M.	1147
.....	1888	Opdyke, B.	1894	Ouyang, B.	1624	Pagès, A.	776
Okumura, M.	2558	Opfergelt, S.	1708	Ouyang, F.	1654	Paglione, M.	1169
Okumura, S.	1302	1894	Ouyang, Z.	1614	1912
.....	1825	Opitz, S.	1518	Ovadnevaite, J.	843	Pahlevan, K.	1778
.....	1902	Oppelt, A.	1895	1141	1912
Okuno, M.	2566	Oppenheimer, C.	1352	1870	Pahnke, K.	1913
Olcott Marshall, A.	1690	Oppenheimer, J.	837	1902	Pai, S.	1514
.....	1889	2103	Overholt, W.	1501	Paige, D.	1259
Olde Venterink, H.	1656	Orberger, B.	1268	Ovtcharova, M.	704	Pailles, C.	2320
Oleinik, A.	2597	Orcutt, B.	1895	1903	Pajón, J.M.	2503
Olenick, L.L.	2356	Orejana, D.	1742	Owada, H.	1837	Pál-Molnár, E.	1916
Oliva, P.	2415	Orekhov, Andrey	2402	2138	Pal'yanova, G.	886
Oliveira, A.	1610	Orekhov, Anton	2402	Owada, S.	2291	Palacz, Z.	1913
Oliveira, S.	600	Orgogozo, L.	743	2337	Palazzo, L.	828

Palchan, D.	2258	Parbhoo, A.	1923	Parro Garcia, V.	2124	Pavlovskaya, A.	741
Paliewicz, C.	2024	Parello, F.	721	Parruzot, B.	1927	Pawley, A.	1393
Palladino, D.M.	1063	1128	Parshin, A.	788	Pawlowsky-Glahn, V.	785
Pallot-Frossard, I.	1079	Parez, S.	1994	1928	Payne, Jonathan L.	1748
Pallud, C.	1914	Parinos, C.	1975	Parsons, C.	2054	1939
Palme, H.	1914	Parinos, K.	1753	Parthasarathy, H.	1928	2213
.....	1915	Paris, E.	2249	1929	Payne, Justin	1939
.....	2423	Paris, G.	817	Parthiban, G.	1822	1943
Palmer, Martin.	1400	1643	Partin, C.	1929	Payot, B.D.	1779
.....	1406	2052	Pašalić, S.	1210	Paytan, A.	1045
.....	1915	Parisatto, M.	1675	Pasanen, A.	638	1940
Palmer, Matthew R.	1329	2366	Pasava, J.	1864	Pe-Piper, G.	1921
Palomino, J.	2132	Parisot, J.C.	1156	Pascal, M.	1930	Peach, D.	1649
Palumbo-Roe, B.	713	Pariyar, S.	794	Pascual, R.	1930	Peacock, C.L.	628
Palya, A.	673	Park, Chan-Soo.	1924	Pasini, V.	1739	1732
Pamato, M.G.	1916	Park, Changkun.	1822	1931	1926
Pamukcu, A.	1760	Park, Changyong.	1923	Passchier, S.	2389	1940
Pan, G.	1917	2247	Passeport, E.	1931	Pearce, Carolyn.	685
Pan, J-Y.	2519	2461	Passey, B.	1932	861
Pan, Yaodong.	1917	Park, Hosik.	878	Passey, S.	1762	1553
Pan, Yongxin.	2513	Park, Hyung Soo.	2431	Pasten, P.	1227	1941
Panagiotopoulos, C.	1918	Park, Jaebong.	1463	Pasti, L.	1699	Pearce, Christopher.	1941
.....	1975	Park, Jong-Kyu.	879	Pastor, L.	1932	Pearce, Jonathan.	2102
Pancost, R.D.	589	Park, Jisun.	2539	Paszowski, M.	1933	Pearce, Julie.	1066
.....	839	Park, Jong-Kyu.	879	Patchineelam, S.R.	1080	1470
.....	1291	1924	1737	1942
.....	1610	Park, Joonbeom.	1572	2133	Pearce, M.	739
.....	1918	Park, M.E.	1411	2414	1942
Pandey, O.P.	1919	1573	Patel, K.S.	2113	Pearson, A.	1299
Pandis, S.	974	1925	Patelli, A.	580	Pearson, D.G.	760
.....	1919	Park, R.S.	1573	Paterson, D.	1253	1492
Pandolfi, L.	808	1925	Patey, M.D.	2143	2312
Panetta, T.	1546	1925	Pathirana, S.	1933	2437
Pang, B.	1920	Park, S.	879	Patko, L.	1618	Pearson, N.J.	903
Panighello, S.	2395	1924	1934	1140
Pankhurst, M.	1920	Parker, B.	608	1972	1159
Pankhurst, R.	1001	Parkhurst, D.	602	Paton, C.	1315	1194
Pankratov, I.	1147	Parkinson, Ian J.	736	1548	1215
Pantoja, S.	1120	939	1934	1324
Paolieri, M.	1789	Parkinson, Ian P.	796	2227	1328
Paonita, A.	824	859	Patrick, A.	1790	1337
.....	919	997	Pattanaik, J.K.	1473	1802
.....	922	1070	2120	1813
.....	1617	1473	Pattelli, G.	1211	1836
Papadopoulos, A.	1176	1926	Patterson, D.	1724	1873
.....	1921	1941	Patterson, W.	1935	1939
Papadopoulou, L.	1176	2002	Pattison, P.	936	1943
Papale, P.	1781	2263	Paukert, A.	1935	2140
Papanikolaou, D.	1459	2289	Paukert, M.	1936	2452
Papaspyrou, S.	2346	Parks, J.	1875	Paul, B.	1010	2523
Papendick, S.	1187	Parman, S.	1370	1936	Pearson, P.N.	589
Papineau, D.	1431	Parmenter, A.	952	Paul, Manoj.	1067	1236
.....	2327	2136	Paul, Maxence.	773	1395
Pappalardo, G.	1667	Parmentier, M.	1552	1937	Pease, V.	1857
Paquay, F.	1921	Parmigiani, A.	2185	2041	Pedentchouk, N.	1034
Paquet, M.	1922	Parra, L.A.	1926	Paula-Santos, G.	637	1943
Paquette, J-L.	745	Parrenin, F.	1543	Paulatto, M.	597	2144
.....	972	Parrish, R.	760	Paulino Lima, I.G.	1937	Pedersen, J.H.	1588
.....	988	1796	Paulo, C.	1938	Pedersen, R.B.	670
.....	2183	1927	2616	929
Paradis, S.	2386	2027	Pavan, M.	1938	1247
Parai, R.	1803	2226	Pavese, A.	692	1887
.....	1922	Parro, V.	2004	Pavlova, O.	1982	2162

Pedesseau, L.....	1364	Perez, Andréa.....	2379	Petersen, S.....	1443	Philippot, P.....	1104
Pedone, M.....	1944	Perez, Anne.....	1948	Peterson, B.....	1119	1683
Pedrosa-Soares, A.....	637	Pérez, C.....	1949	Peterson, C.....	1955	1700
Peđziwiatr, A.....	1456	Perez, Pamela.....	2122	Peterson, E.....	2380	1805
Pegg, I.....	2207	Pérez, Pedro.....	1899	Peterson, L.....	1167	1965
Pehrsson, S.....	1030	Perez, V.....	1697	Peterson, M.....	1801	2184
.....	1944	Perez Fodich, A.....	1950	1956	2400
Pei, F.....	2530	Pérez Rodríguez, N.....	1950	Peterson, R.....	573	Phillips, D.....	852
.....	2545	Perez-Almeida, N.....	1193	Peterson, A.....	1513	1178
Pei, R.F.....	2013	1949	1956	1966
Peiffer, S.....	1840	Pérez-López, R.....	554	2150	Philp, P.....	2329
Peiffert, C.....	1863	Perez-Sirvent, C.....	1697	Petit, J.....	1712	Phipps, S.....	1385
Peketi, A.....	1945	1697	Petit, S.....	2416	Phrommavanh, V.....	725
Pelivan, I.....	2346	Pérez-Soba, C.....	1742	Petitjean, C.....	1562	964
Pellerin, A.....	695	Perinelli, C.....	616	Petkov, V.....	1170	1863
.....	1945	Perkins, W.....	713	Peto, M.....	1803	2123
Pelleter, E.....	1408	Perko, J.....	1204	Petrenko, V.....	790	2464
Pelletier, J.....	881	Perlman, D.H.....	636	Petrescu, L.....	1957	Phyo Maung Maung,.....	873
Pellin, M.....	951	Perlwitz, J.P.....	1949	Petret, C.....	747	Pi, D-H.....	2548
Pellizzari, L.....	1435	Perminova, T.....	652	Petri, B.....	1957	Piani, L.....	1966
.....	2516	Pernice, M.....	1496	Petrillo, Z.....	1958	2049
Pelorosso, B.....	1165	Peron, O.....	1276	Petrishcheva, E.....	1958	Piantone, P.....	1552
Pelt, E.....	845	Perrett, G.....	2158	2148	Piasecki, A.....	1967
.....	1192	Perrette, Y.....	2037	Petron, G.....	2048	Piazolo, S.....	1185
Pemba, L.....	874	Perrino, C.....	2127	Petrone, C.M.....	763	Picard, A.....	1734
Pena, J.....	1946	Perrot, V.....	1951	1102	1967
.....	2214	Perry, A.....	568	1959	Piccarreta, G.....	1101
.....	2395	Persson, I.....	1235	Petrosino, P.....	2111	1754
Peng, H-M.....	2519	Persson, P.....	594	Petrov, A.....	1477	Piccoli, P.....	778
Peng, J.....	1118	1448	Petrovic, M.....	1413	817
Peng, P.....	1330	1951	Petrus, J.....	872	2315
Peng, S.....	807	2026	1959	2577
Peng, T.....	2609	2289	Pett-Ridge, J.....	1442	Pichat, S.....	793
Peng, Y.....	1946	Pertsev, A.....	560	1845	Pichavant, M.....	2419
.....	2585	Perucchi, A.....	1834	1961	Pichler, T.....	2234
Penizek, V.....	1756	1972	Petta, R.....	816	Pichon, R.....	2585
Penkin, M.....	789	Peruchena, J.I.....	1639	Petters, M.....	1744	Pickard, M.....	1525
Penkman, K.....	969	Perugini, D.....	1952	1960	Pickering, R.....	2509
Penn, R.L.....	836	1952	Pettke, T.....	1145	Pickford, M.....	2145
.....	1170	Peruzzo, L.....	829	1212	Pickles, J.....	2220
Penna, P.....	2242	2366	1649	Pidgeon, B.....	897
Penner, J.....	1365	Pesce, G.....	1953	1960	Piechotta, C.....	1579
.....	1617	Peslier, A.....	617	2334	Piepenbrock, A.....	2126
Pennino, V.....	823	1953	Peuble, S.....	1961	Pierce, Elizabeth.....	2389
Pennisi, M.....	702	Pesquera, A.....	1142	Peucker-Ehrenbrink, B.....	794	Pierce, Eric.....	987
.....	1947	1171	1962	1968
Penniston-Dorland, S.....	1199	1954	Peuget, S.....	979	Pieronek, J.....	1968
Pepi, S.....	1849	2074	Peytcheva, I.....	1132	Pierotti, L.....	1969
Peppe, D.....	2574	Petaev, M.....	1371	1962	Pierre, B.....	2014
Peppe, S.....	1084	Petelet-Giraud, E.....	770	2431	Pierret, M-C.....	1969
Perales, J.F.....	1410	Peter, T.....	1137	Peyton, B.....	1963	2260
Perdrial, J.....	881	Peterman, E.....	2231	Pfänder, J.....	1678	Pierson-Wickmann, A-C.....	1843
Pereira, A.S.....	786	Peters, C.A.....	1092	1963	Pietramellara, G.....	622
Pereira, G.S.....	583	Peters, J.....	758	2105	Pietranik, A.....	2221
.....	1376	Peters, K.....	1578	Pfeffer, C.....	1964	2370
Pereira, Inês.....	1560	Peters, L.....	2385	Pfeifer, M.....	1964	Pietro, M.....	824
Pereira, Inês A. C.....	1947	Peters, M.....	1954	Pham, A.N.....	2571	Pietruszka, A.....	1692
Periera, Natan Silva.....	815	2614	Phan, T.....	1965	Pignatelli, I.....	841
.....	1948	Peters, N.....	1352	Philippe, S.....	1191	1970
.....	2210	Peters, Shanan.....	1130	Philippini, V.....	2406	Pik, R.....	860
Peresypkin, V.....	1503	Peters, Stefan T.M.....	1034	Pilet, S.....	1970
.....	2208	1955	Pimentel, A.....	1381
Perez, Alida.....	583	1964

Pimentel, C.	1971	Playà, E.	2351	Polyakov, V.	1985	Pouteau, V.	1409
.....	1971	Plümpfer, O.	638	Polyanskiy, O.P.	1985	Powell, J.	1415
Pimentel, Marcio	1983	1979	2407	Powell, W.	1943
Pimentel, Marcio Martins ..	815	Poaty, B.	1163	Pompilio, M.	935	Power, I.M.	1262
Pin, C.	682	Pockalny, R.	2140	1418	1992
.....	1078	Podgornykh, N.	1988	1834	Power, M.	1993
.....	1737	2189	1986	Pradler, I.	2158
Pina, C.M.	1971	Podladchikov, Y.Y.	1979	Ponaryadov, A.	1986	Prado, B.	1023
.....	1971	Podlaha, O.	603	Ponepal, M.	2154	Prakapenka, V.	844
Pinay, G.	2173	Podlesskii, K.K.	1980	Pongetti, F.	1133	908
Pinheiro, L.M.	2455	Podosek, F.	1699	Ponnuram, A.	1987	1088
Pinilla, C.	715	Poe, B.	1179	Ponomarchuk, A.	1987	Pramana, S.	1293
.....	1972	1980	1988	Prasannakumar, V.	1994
Pinna, R.	1147	Poertner, H-O.	1981	Ponomarchuk, V.	1987	Prasetio, R.	1993
Pintér, Z.	1504	Pogge von Strandmann,		1988	2491
.....	1972	P.A.E.	855	2008	Prata, F.	738
Pinti, D.L.	1268	1274	2608	Pratas, J.	1067
.....	1360	1433	Ponomarev, Y.	1477	Pratesi, G.	2180
.....	1792	1539	Pontikes, Y.	1136	Pratheesh, P.	1994
.....	1973	1878	Ponzevera, E.	1110	Pratomo, I.	2413
.....	1993	1894	Pooralizadeh, M.	1988	Prave, A.R.	763
Pinto, A.	1973	1981	Pop Ristova, P.	2234	927
Pinzer, B.	2177	2376	Popov, D.	936	1433
Piotrowska, N.	577	Pogodaeva, T.	1638	Popova, J.	1989	Prechova, E.	1864
.....	982	1982	Popp, T.	2385	Predota, M.	1663
Piotrowski, Alexander	1135	Pogozheva, E.	727	Porcelli, D.	2289	1994
.....	1974	727	Porter, D.	2091	Preis, Y.	728
.....	2069	Pogrzeba, M.	1753	Pöschl, U.	1989	2144
.....	2502	Pohlman, J.	2566	Pósfai, M.	1868	Prelević, D.	1656
Piotrowski, Alexander	1291	Pointing, M.	1284	2343	1995
Piovano, E.	2276	Poirier, A.	923	Posner, E.S.	1990	2222
Pipon, Y.	2109	1319	Posth, N.R.	1431	2463
Piquer, J.	914	1343	1990	Preocanin, T.	1995
Piro, J-L.	1737	Poitrasson, F.	551	Postnikov, A.	727	Presnyakov, M.	1365
Pisapia, C.	1739	715	Potel, S.	2362	Pretet, C.	1422
.....	1974	1983	Potizil, C.	795	Preto, N.	938
Pisonero, J.	1735	Pokhilenko, L.N.	576	558	Preud'homme, H.	1996
Pistolesi, M.	891	2189	Potter, E.	1993	Preunkert, S.	1217
.....	935	Pokhilenko, N.	2189	1980	Preuss, O.	1996
.....	1124	Pokrovski, G.	1488	Potuzak, M.	1980	Price, David.	1119
Pitcher, B.	1975	1983	Poujol, M.	1991	Price, David.	1349
.....	2413	Pokrovsky, Oleg	1677	Poulain, L.	1169	Price, J.B.	1997
Pitra, P.	844	2415	Poulet, F.	833	826
Pitta, P.	1975	1152	1878	Price, M.N.	826
Pizarro, G.	1227	Pokrovsky, Oleg S.	1152	2481	Price, Richard.	2265
Pizzino, L.	1976	1192	Poulson, S.	1827	Price, Roy E.	1547
Plá Cid, C.	1828	2000	Poulton, S.	603	1997
Plá Cid, J.	1828	Polerecky, L.	1474	895	Prié, F.	1543
Plagnes, V.	772	Poli, G.	673	1187	Pries, C.	2345
Plaïl, M.	1976	Poli, S.	663	1228	Prieto, M.	1390
Planavsky, N.	1090	1121	1348	2077
.....	1259	1676	1367	2081
.....	1977	1984	1379	Prikhodko, V.	1866
.....	1977	2334	1718	Přikryl, J.	1998
Plancherel, Y.	1977	Poll, C.	994	1991	Primeau, F.	981
Planer-Friedrich, B.	1978	1984	2253	Primm, O.	657
Plank, T.	1978	Pollard, D.	1184	2586	Pring, A.	1598
.....	2094	Pollastri, S.	1224	Pourmand, A.	1992	Pringle, E.	961
.....	2100	Polly, R.	1279	Pourret, O.	899	1998
Planquette, H.	1941	Polo, L.A.	1230	960	Pringle, K.	831
Plante, A.F.	2270	Poluzzi, V.	959	1408	832
Plata, A.	2351	1169	1544	Prinzhofer, A.	1759
Platt, U.	2505	2064	1695	Probst, A.	1004
Plavsa, D.	1979	Polyak, V.	625	2362	Probst, J-L.	1004

Procesi, M.	2171	Pushkarev, E.	2006	Querol, X.	940	Raitzsch, M.	705
Proemse, B.	1999	Puskar, L.	1449	2014	Rajamanickam, M.	2023
.....	2322	Putlitz, B.	1095	Queyron, M.	629	Rajasekar, C.R.S.	1164
Proenza, J.A.	1159	2175	Quijano, M.L.	839	Rajpert, L.	2023
Prokofiev, V.	1999	Putnis, A.	1019	1918	Rakoczy, J.	2024
Prokopenko, M.G.	1268	1403	Quirico, E.	734	Rakotonandrasana, T.	615
.....	2000	1674	2014	Rakotondrazafy, R.	615
Prokopiev, V.	1354	1800	2049	Ramalho, R.	557
Prokrovsky, O.S.	641	2006	Quirk, J.	676	Ramos, A.R.	1947
Prokushin, A.	641	2098	Quispe, D.L.	554	Ramos, F.	2024
.....	2000	2099			Rampe, E.B.	1794
.....	2415	Putnis, C.V.	1185			Rampone, E.	740
Prol-Ledesma, R.M.	1051	2006	R		2025
.....	1194	2007	Rabbia, O.	2015	Ramsey, M.	2025
Prommer, H.	2173	2098	Rabe, K.	2015	Ramstedt, M.	2026
Pronk, G.J.	994	2099	Rabideau, A.	578	Ranaivoson, M.	615
.....	2001	Puziewicz, J.	1713	Rabiet, M.	2089	Randlett, M-È.	2026
Provencal, R.	641	2007	Rabindra, R.N.T.	2016	2233
Provost, A.	1258	Pyryaev, A.	1987	Rabung, T.	1689	Ranjan, S.	2027
.....	2151	1988	2079	Ranville, J.	2430
Proyer, A.	627	2008	Rabus, R.	2016	Rao, A.	689
Prudencio, I.	1687	Pystin, A.	2008	Rach, O.	2110	Rao, P.H.	597
Prunier, J.	1969	Pystina, J.	2009	2169	2028
.....	2260	Python, M.	1772	Rachwał, M.	1668	Rao, S.	1477
Pruseth, K.L.	1275			Raco, B.	1856	Rao, Wanxiang	1332
Prusik, K.	1134	Q		Rad, S.	2017	Rao, Wenbo	1917
.....	1134	Qafoku, O.	685	Raddatz, J.	2427	Rao, Y.	937
Pruss, S.	2001	Qi, C.	1249	Raddatz, T.	2251	Rao, Z.	1387
Prüßmann, T.	1530	Qi, H.Y.	2586	Rademacher, L.	2017	Rap, A.	2248
Prytulak, J.	2002	Qi, Jinzhong	2547	Radic, A.	551	Rapprich, V.	1485
Psarakis, M.	1656	Qi, Jun	2010	Radica, F.	1875	Rasbury, T.	1927
Ptacek, C.	1375	Qi, L.	889	2018	2027
.....	1558	Qi, M.	2010	Radke, J.	1410	Rashchenko, S.	2028
Pu, W.	2602	Qi, S.	567	Radtke, G.	1740	Rasheed, M.A.	597
Puccini, A.	838	Qin, H-B.	2538	Radtke, M.	1752	2028
.....	2002	2615	Radway, J.	1483	2029
Puceat, E.	1537	2196	Rae, J.	1100	Rashid, H.	2029
.....	1777	Qin, J.	2196	2018	Rasigraf, O.	2030
Puchol, N.	860	Qin, K.	821	Raepsaet, C.	2068	Rasmussen, B.	1800
Puchtel, I.S.	2003	Qin, L.	2011	Raetz, M.	2032	2030
.....	2067	Qin, M.	1650	Rafter, P.	981	Rasmussen, C.	881
.....	2348	2072	1396	1659
.....	2439	Qin, T.	1073	2019	Rasmussen, D.	2441
Pudlo, D.	2003	Qin, Z.	2445	2050	Rasmussen, S.O.	967
Puente-Sánchez, F.	2004	Qiu, H.	2010	Ragazzola, F.	1083	Rasoazanamparany, C.	2031
.....	2124	Qiu, J-S.	2011	Raggi, A.	1551	Rass, I.	2031
Puffer, J.	686	Qiu, Lin	2012	Ragon, M.	688	Rastogi, N.	2032
Pugh, C.W.	2443	Qiu, Liwen.	2012	Ragozin, A.	2019	Ratschbacher, L.	1494
Pugh, J.	2606	Qiu, S.	1027	2190	1678
Puglisi, G.	797	Qiu, X.	2136	2583	2224
.....	825	Qu, H.Y.	2013	Rahav, E.	1975	Rau, C.	2035
Puigdomenech, I.	2364	Qu, W.	1118	Rahgoshay, M.	2020	Raub, T.	1622
Pujades, E.	1413	Quantin, Cathy	1878	Rahman, Z.	1693	Raveggi, M.	2032
Pujol, M.	1700	Quantin, Cécile.	2585	Rahn, M.	2020	Ravelo, C.	2050
Pulice, I.	990	Quaranta, G.	556	Rahul, P.	2021	Ravizza, G.	1064
Pullin, M.	1553	Quaranta, V.	828	Rai, N.	905	1921
Purdy, D.J.	2212	Quartieri, S.	1168	2129	2416
Purgstaller, B.	2004	1559	Rai, S.	2021	2575
Purser, G.	2005	Quatrini, P.	1128	Raimonet, M.	1048	Raymo, M.	2033
.....	2073	Quattrocchi, F.	820	2022	Raymond, J.	757
.....	2102	1133	Raiswell, R.	2475	2033
Purtschert, R.	790	2171	Raiteri, P.	971	Raynaud, D.	672
.....	2005	Queiroz, H.	2013	2022	1543
					2440		

Reaman, D.....	1088	Reich, M.....	583	Ren, Z.L.....	2050	Ricci, J.N.....	2056
Reason, C.....	2222	661	Renard, F.....	2086	2479
Recanati, A.....	2034	1950	Renema, W.....	1053	Riccobono, F.....	832
Recchia, S.....	2334	2042	Renna, M.R.....	1545	Rice, B.....	2498
Recham, N.....	1767	2122	2354	Richard, L.....	1759
Reche, J.....	2034	Reichart, G-J.....	705	Renne, P.....	1533	2057
Rečnik, A.....	2252	Reichert, B.....	1256	1968	Richards, D.....	2226
Reddington, C.....	831	Reichert, M.....	1840	2051	Richards, J.....	1807
.....	832	Reick, C.....	2251	2051	2057
Reddy, C.M.....	612	Reid, Joel.....	2528	2248	Richnow, H-H.....	1238
Reddy, K.J.....	2035	Reid, Jonathan.....	1897	2417	1391
Reddy, S.....	1046	Reid, M.....	749	Rennert, T.....	1307	1391
.....	1414	2042	Renneson, M.....	899	2272
.....	2434	Reid, N.....	2043	Rennie, V.....	600	2329
Redfern, S.....	689	Reid, T.....	750	2052	Richoz, S.....	895
.....	762	2043	Renno, A.....	1752	Richter, A.....	730
.....	784	Reijnen, M.....	657	Renock, D.....	675	Richter, Daniel.....	2058
.....	2035	Reiller, P.....	2044	1692	Richter, Detlev.....	1160
Redler, C.....	2036	2406	Renzulli, A.....	1712	1738
Redolfi, M.....	2036	Reimann, C.....	1537	1918	2058
Redou, V.....	890	2044	Repeta, D.....	2396	2218
Reece, J.....	1819	2045	Resano, M.....	1147	Richter, G.....	561
Reed, R.....	2430	Reimers, C.....	552	Resing, J.....	1655	Rickaby, R.....	1290
Reeder, R.....	2273	1728	Resner, K.....	2563	1647
Rees, G.....	1449	Reimink, J.....	2045	Resongles, E.....	2052	2059
Reese, B.....	2037	Reimus, P.....	780	Resplandy, L.....	1576	Rickard, A.R.....	1084
Regattieri, E.....	1010	Reiners, P.....	1226	Rethemeyer, J.....	1799	Rickli, J.....	1271
.....	1363	Reinhard, C.T.....	1181	Rettenwander, D.....	1734	1300
.....	2037	1904	Reuning, L.....	781	2059
.....	2580	1977	Reutenauer, C.....	2053	Ridame, C.....	1372
Regelink, Inge.....	2038	2079	Reutsky, V.....	1507	Ridgwell, A.....	956
Regelink, Inge C.....	1495	Reinhard, D.....	1795	Reverdatto, V.....	1609	1395
Regelous, M.....	678	2231	Revil, A.....	1590	1748
.....	761	2386	Revill, A.....	2274	1918
.....	1012	Reinhardt, P.....	2068	Revsbech, N-P.....	775	2018
.....	2038	Reinholz, U.....	1752	Rewerski, B.....	1755	2060
.....	2476	Reinsch, B.....	2046	Rey, D.....	2095	2060
Regenberg, M.....	1637	Reis, A.....	2046	Rey, P.....	1104	Ridley, M.....	1517
Regenspurg, S.....	767	Reis, N.J.....	1819	Reyes, A.....	2333	1663
.....	1072	Reisberg, L.....	809	Reyes, C.....	2053	2061
.....	2039	1583	Reymond, C.....	2405	Ridolfi, F.....	1692
.....	2411	2047	Reynard, B.....	2590	Riedel, B.....	1746
Regis, D.....	1043	Reissner, C.....	1586	Rezaei, M.....	2191	Riedel, T.....	2061
Regnarsson, E.....	551	Reith, F.....	2047	Rezaei-Kahkhaei, M.....	2054	Riedinger, N.....	2062
Reguir, E.....	848	Reitner, H.....	991	Rezaie, M.....	2344	Riedo, A.....	2062
.....	2039	Reitz, A.....	964	Rezanezhad, F.....	1312	Ries, J.....	2466
Reguzzoni, M.....	2040	Rella, C.....	2048	2054	Rigato, V.....	580
Rehder, G.....	1409	2360	Rezza, C.....	567	Righi, S.....	1063
Rehkämper, M.....	773	Rella, S.....	2372	653	Righter, K.....	1693
.....	956	Relvas, J.....	929	Rhede, D.....	1216	Rigo, M.....	938
.....	1187	1973	1260	2499
.....	1323	Remeikis, V.....	843	2148	Rigo, V.....	697
.....	1454	1010	2221	Rihs, S.....	845
.....	1511	1141	Rhenals Garrido, D.R.....	2055	1192
.....	1541	Remmert, P.....	2048	Rhodes, R.....	1062	2063
.....	1546	Rempel, K.....	1627	Ribeiro, J.....	2055	Riishuus, M.S.....	690
.....	1556	2049	Ribeiro, M. Anjos.....	611	Rijkenberg, M.....	1182
.....	1937	Remusat, L.....	663	1079	1541
.....	2040	1966	2056	Rikhvanov, L.....	652
.....	2041	2049	Ribeiro, Maria Luisa.....	1287	Rilling, S.....	632
.....	2507	Ren, H.....	2050	Ribeiro, S.....	2132	Rimondi, V.....	1211
.....	2548	Ren, J.....	2601	Riccardi, M.P.....	1174	1789
Reible, D.....	2041	Ren, Y.....	1327		Rimskaya-Korsakova, M.....	2063

Rinaldi, M.	843	Robinson, S.	1869	Rogers, K.	1350	Rosario, B.	2014
.....	1169	2483	2255	Rosciglione, A.	1692
.....	2064	Roca, F.J.	1410	Rogers, N.	2275	Roscioli, J.	2575
Rinder, T.	2064	Rocchi, S.	2412	Roghi, G.	938	Rose, A.L.	1508
Ring, U.	2381	Rocha, A.	2133	Roh, Y.	1427	2437
Rinnen, S.	2065	Rocha, C.	1895	1463	Rose, C.	2082
Rios, D.C.	2065	Rocha, F.	1687	1565	Rose, J.	2320
Riser, S.	1040	Rochat, L.	1970	2078	Rose-Koga, E.	805
Risgaard-Petersen, N.	940	2073	2564	1127
.....	1964	Roche, D.	1543	Rohrbach, A.	2078	1737
Risi, C.	1568	664	2494	Rosenberg, A.	2083
.....	2053	Roche, N.	664	Rohrmüller, J.	1963	Rosenfeld, C.	2083
Riße, A.	2065	Rochelle, C.	1082	Rohrsen, M.	2079	Rosenfeld, D.	2620
Risse-Buhl, U.	1518	2005	Roho, H.	2079	Rosenheim, B.	1075
Ritschel, T.	2066	2073	1476	2084
Ritter, S.	2066	2102	Roldan, N.W.	1476	2308
.....	2066	2467	Roldan, A.	965	Rosenthal, A.	2084
Ritz, C.	672	Rocher, V.	2022	Rolfe, S.	1258	Roshchina, I.	1593
Rivas-Sánchez, M.D.L.L.	2117	Rochez, G.	2271	Rolle, M.	876	Rosi, M.	1124
Rivera, M.J.	2384	Rocholl, A.	2074	1239	Roskosz, M.	948
Rivers, E.R.	1035	Röckmann, T.	1117	1392	2085
Rivers, M.	2290	1933	Rollion-Bard, C.	1126	2218
Rizo, H.	2067	2134	1342	Rosling, A.	1061
Rizzo, A.L.	823	2186	1626	Rosner, M.	2085
.....	824	Roda-Robles, E.	1142	1683	Rosoldi, M.	1667
.....	919	1171	1805	Ross, A.	1007
.....	1472	1954	2080	Ross, C.	1999
.....	1617	2074	2141	Ross, N.L.	1166
.....	1692	Rode, M.	1210	Roman-Ross, G.	1021	Rossano, S.	1079
.....	2067	Rodionov, N.	1106	2355	1948
Rizzo, L.	620	Rodkin, M.	2605	Romaniello, S.	592	628
Ro, C-U.	1461	Rodler, A.	2075	1293	Rosbach, S.	628
Robbins, M.	2500	Rodó, X.	932	Romanini, D.	1062	Rosset, R.	1617
Robbins, S.	1187	Rodrigo-Gamiz, M.	1696	1200	Rossi, M.	968
Roberge, M.	2068	Rodrigues, B.	1610	1217	Rossi, P.	2046
Robert, F.	1966	Rodríguez, A.	1067	Romano, C.	812	Rossi Alvarez, C.	1224
.....	2034	Rodríguez, C.	2075	993	2002
.....	2068	Rodríguez, G.M.	562	1980	2519
Roberts, B.	2084	Rodríguez, N.	1880	2427	Rossier, M.	2297
Roberts, E.	1724	2004	2428	Rossman, G.	864
Roberts, J.	800	2124	Romanov, A.	1676	1661
.....	1402	Rodríguez, R.	1213	Romanova, I.	2080	Rosso, K.	771
.....	2069	Rodríguez, Sedelia	2076	2407	861
Roberts, K.A.	2524	Rodríguez, Sergio	1949	Romanova, T.	2209	907
Roberts, Natalie.	2069	Rodríguez Galán, R.M.	2077	Romer, R.	1514	1553
Roberts, Nick M.W.	1927	Rodríguez-Aranda, J.P.	2133	1563	1941
.....	2245	Rodríguez-Blanco, J.d.	899	2222	2582
Roberts-Semple, D.	2071	Rodríguez-Blanco, Juan		Romero, F.M.	561	Rost, D.	951
Robertson, A.H.F.	2380	Diego	551	Romero, O.E.	833	Rostási, Á.	1868
Robertson, E.	2070	2076	Romero-Gonzalez, M.	680	Rostom, F.	2086
Robertson, J.	618	2081	1108	Roszjar, J.	2086
Robertson, S.	1085	2336	1638	Rotenberg, E.	1555
.....	1398	Rodríguez-Escalas, P.	2077	2176	Roth, A.	752
.....	2070	Rodríguez-Germade, I.	2095	Romero-Viana, L.	2081	1230
Robinson, A.	1919	Rodríguez-Navarro, A.B.	1077	Romo, J.A.	562	Roth, G.	1530
Robinson, L.F.	594	Rodríguez-R, L.M.	1501	Roncal-Herrero, T.	2081	Rothe, J.	1530
.....	794	Rodushkin, I.	1950	Ronchi, B.	2082	Rother, G.	1831
.....	2071	Roecker, S.	1525	Roncucci, N.	561	Rothery, D.	2087
.....	2273	Roehl, U.	2389	Ronen, Z.	558	Rothschild, L.	1937
Robinson, M.	1650	Roelofse, F.	2351	Rontani, J-F.	1918	Rotolo, S.	919
.....	2072	Roeske, T.	1271	Rooney, A.	1348	Rötting, T.	1655
Robinson, P.T.	1215	Roffey, A.	1195	Root, R.	1250	Rottmann, L.	2501
.....	2072	Rogalev, A.	1038	Rosa, J.	596	Roubinet, C.	1787
Robinson, R.	1299	Rogalla, D.	1577	Rosa, M.L.S.	2065	2087

Rouchon, V.	2088	Ruiz Hernandez, S.	966	Saaltink, M.	962	Sakamoto, H.	1837
Rouff, A.	2088	Ruiz-Agudo, E.	2006	1829	Sakamoto, N.	2534
Rouget, M.L.	1110	2007	Saar, M.O.	2108	Sakamoto, R.	2540
Roulleau, E.	1973	2099	2368	Sakamoto, Y.	1901
Rousseau, J.	2089	Rumble, D.	2290	Saarikoski, S.	1912	Sakata, Shuhei	601
Rousseva, S.	2038	Runkel, R.	2486	Saathoff, H.	1520	1885
Rousteau, A.	896	Ruparkheti, M.	2563	1540	2116
Rouwane, A.	2089	Ruppert, H.	1061	1797	2202
Rouxel, Olivier	1225	2099	2259	2541
.....	2090	Ruprecht, P.	1978	Sabari Prakasan, M.R.	2109	Sakata, Susumu	2567
Rouxel, Olivier	1843	2094	Sabau, A.	2109	Sakellariadou, F.	2116
Rouzaud, J-N.	1889	2100	Săbău, G.	2110	Sakuma, H.	2117
Rovere, A.	2033	2100	Sachs, J.	2600	Sala, H.	1287
Rowe, E.	1851	Rusakov, V.	2101	Sachse, D.	2081	Šala, M.	2395
Rowe, Mark	2436	Rusanov, I.	2208	2110	Salas, E.	830
Rowe, Michael	592	Rushmer, T.	770	2169	Salazar Mora, C.A.	2118
.....	2090	1636	Sadati, N.	2111	Salazar-Camacho, C.	2117
Roy, J.	626	2101	Sadeghi, M.	1537	Saldi, G.D.	926
Roy, M.	1728	Rushton, J.	2102	2111	949
Roy-Barman, M.	2091	Rusin, A.	2385	2374	2118
Roychoudhury, A.	2091	Russell, L.	1169	Sadekov, A.	1126	Saleeby, J.	781
.....	2429	2102	Sadooni, F.	764	Salerno, G.	1165
Rozanov, A.	2092	Russell, S.	1539	Saeed, S.	1776	1551
Rozov, K.	762	Russo, C.	1479	Saenger, E.H.	2177	2119
.....	2092	Russo, G.	1958	Safar, Z.	1611	Salikhov, R.	623
Røyne, A.	2086	Russo, R.	1193	Saffarzadeh, A.	2112	Saliot, A.	1372
.....	2093	Russo, S.	1849	Safonov, O.	656	Saliot, P.	2119
Ruan, J.	1011	Rust, A.	837	802	Salm, N.	1360
.....	1331	1379	2112	Salnikiva, C.	1214
Rubatto, D.	747	2103	Sagar, N.	2433	Salnikova, E.	2262
.....	970	Rustad, James	2104	Sagawa, T.	1793	2536
.....	1043	Rustad, James	2103	Sageman, B.	1023	Salova, T.	2213
.....	1104	Ruszkowski, D.	2219	Saha, A.	1184	Salpeteur, I.	991
.....	1148	Rusznayak, A.	1518	Sahai, N.	2533	Salters, V.	1951
.....	2093	Rutgers van de Loeff, M.	1271	Sahajpal, R.	1285	Salvado, J.A.	578
.....	2380	Rutherford, M.J.	2108	Sahoo, S.K.	1769	Salvi, S.	1488
Rubie, D.C.	1554	2484	Sahu, B.L.	2113	1583
.....	1990	Rutledge, A.	2104	Sahu, L.	2113	Samadi, R.	2120
.....	2094	Rutte, D.	2105	Sahu, S.	1688	2205
.....	2423	Ruzie, L.	648	Sahy, D.	1588	Samankassou, E.	747
Rubin, K.	1655	863	2114	Samanta, S.	2120
.....	2094	896	Said, N.	1926	Sampaio, G.	2121
Rubino, M.	579	1393	Saiki, H.	2292	Samperio, G.	1193
Rubio, B.	2095	2105	Sainctavit, P.	836	Samperio-Jiménez, F.	2418
Rubol, S.	1022	Ryabenko, E.	1209	1038	Samperton, K.	1445
Ruby, C.	2584	Ryabkov, Y.	1986	Saint Blanquat, M.D.	2164	Sampietro, D.	2040
Rudashevsky, V.	1506	Ryabov, V.	2106	Saito, Mak	2114	Sampson, B.	1546
Rudich, Y.	1555	Ryb, U.	2106	Saito, Masafumi	2373	Samsoni-Todorova, O.	2121
.....	2095	Rybacki, E.	1283	Saito, Mitsuyo	1793	Samsonov, A.	1214
Rudnick, R.	770	Ryerson, F.	640	Saito, N.	2283	2122
.....	835	2211	Saito, T.	1276	2262
.....	1145	2472	Saitoh, Y.	2115	Samuel, H.	653
.....	1341	Ryu, J-S.	2203	Saka, S.	2115	Sanati, S.	1025
.....	2096	Rzepa, G.	759	2178	Sanborn, M.	2559
Rudolph, V.	952	2107	Sakaguchi, A.	2302	Sánchez, A.	562
.....	1187	Rzepka, P.	1040	2306	Sánchez, M.E.	1142
Rueedi, J.	2096	2107	Sakaguchi, I.	643	Sanchez, P.	2122
Ruggieri, G.	703	S		Sakai, H.	1121	Sanchez Goni, M.F.	2580
Rügnér, H.	1210	Saal, A.E.	1956	Sakai, T.	1772	Sánchez-Castro, I.	1638
Ruhl, M.	2097	2108	1884	2123
Ruiz, C.	2097	2199	Sakamaki, T.	2461	Sanchez-Espana, J.	1549
.....	2098	2484	Sakamoto, F.	1702	Sánchez-Navas, A.	2075
Ruiz Agudo, C.	2098			1882		

Sánchez-Pastor, N.	627	Santos Neto, E.	2269	Sauter, M.	767	Schaper, J.	1483
.....	1853	Santos-Neves, J.	2133	1993	Schaub, P.	936
.....	2123	Santosh, D.	2028	2491	Schauble, E.A.	1731
Sanchez-Roa, C.	2124	Santosh, M.	1979	Sautter, V.	2269	2558
Sánchez-Román, M.	1880	Santschi, P.H.	1597	Sauvage, J.	2140	Schauer, A.	2257
.....	2004	2524	Sauvage, L.	2141	Schauer, R.	2174
.....	2124	Sanz-Montero, M.E.	2133	Sauzeat, L.	2141	Schaumann, G.E.	1745
Sanchez-Valle, C.	2125	Sapart, C.J.	2134	Savage, J.	2142	2149
.....	2361	Saphton, M.	2406	Savage, P.	1998	Schaumburg, K.	551
.....	2577	Šapolaitė, J.	1010	2142	Scheepmaker, R.	1568
.....	2587	Sapunar, M.	1995	2548	Scheiber, J.	1841
Sanchi, L.	2125	Saqib, N.	2134	Savarino, J.	1747	Scheinost, Andreas	1017
Sand, K.K.	1848	Sârbu, C.	2135	2143	Scheinost, Andreas C.	2263
.....	2126	Sareen, N.	2135	Savelieva, G.	683	Schenato, F.	908
.....	2336	Sarjoughian, F.	1267	Savenko, A.	2143	Schenk, O.	1578
.....	2391	1425	Savina, M.	951	Schenkeveld, W.	2149
Sander, M.	615	Sarkozy, L.	1540	Savinykh, Y.	2144	Schenzel, J.	2492
.....	1200	1797	Savov, I.	906	Scher, H.	2150
.....	2126	2277	1266	2489
Sander, S.G.	1158	Sarma, D.S.	1805	2144	Scherer, E.E.	665
.....	1576	Sarmiento, J.	980	Sawada, Y.	2145	787
Sanders, R.	2418	Sarrasin, L.	1948	Sawaki, Y.	2567	2224
Sandhage-Hofmann, A.	586	Sarrazin, P.C.	1794	Sawicka, J.E.	2145	2249
Sandrini, S.	2127	Sarret, G.	629	Sawyer, G.	797	Scherstén, A.	1513
Sandström, B.	1509	Sarti, E.	1699	2119	1956
.....	2364	Sasaki, K.	1367	Saxena, S.	1329	2150
Sanematsu, K.	2127	2136	2146	Schiano, P.	2151
Sanfilippo, A.	2128	Sasaki, O.	1825	Sayadyan, G.	1159	Schiattarella, M.	990
Sang, L.	2590	Sasaki, Y.	1821	Sayama, M.	2146	Schiavi, F.	2151
Sang, S.	2128	Sasamoto, H.	696	Sayit, K.	1252	Schiefer, J.	2038
Sanial, V.	2387	Saso, J.	2136	1525	2151
Sankar, M.S.	1455	Sasselov, D.	1371	Sazonov, A.	1893	Schierz, A.	2041
Sanloup, C.	2129	Satish-Kumar, M.	1298	Scambelluri, M.	819	Schijf, J.	2152
.....	2247	Sato, H.	1893	1979	Schiller, M.	644
Sano, R.	2534	2137	2201	925
Sano, Y.	864	Sato, M.	1120	Scanlon, R.	1182	1315
.....	1360	1257	1482	1548
.....	1417	Sato, S.	1490	Scanza, R.	568	1889
.....	1487	Sato, Tomohiko	2129	Scarlato, P.	2147	1934
.....	1816	Sato, Tsutomu	893	Scarsi, P.	1243	2152
.....	1973	1104	Schaaf, P.	2584	Schilling, F.	674
.....	2129	Satoh, H.	1361	Schadt, C.	915	Schilling, J-G.	1428
Sansjofre, Pierre	2130	2138	Schaefer, T.	685	Schimmelmann, A.	2153
Sansjofre, Pierre	1246	2540	Schaefer, B.F.	1812	Schimmelpfennig, I.	2153
Sant'Ovaia, H.	2130	Sator, N.	1098	1920	Schinke, R.	1399
Santaella, C.	664	2434	Schaef, J.M.	2153	Schinteie, R.	781
.....	2320	Satou, M.	1356	Schaeffer, A-K.	1958	Schipek, M.	2154
Santana-Casiano, J.M.	1193	Satsukawa, T.	2138	2148	Schippers, A.	720
.....	1949	Sattler, T.	2139	Schaelchli, J.	1651	890
Santelli, C.	2404	Satyanarayanan, M.	973	Schäfer, J.	2276	1498
Santi, I.	2234	Satyro-Ferreira, S.	2414	Schäfer, T.	847	2015
Santiago Ramos, D.	2201	Sauer, B.	1061	893	2024
Santillan, E.	2131	Sauer, S.	1588	1075	Schkade, U-K.	2039
Santini, T.	2131	2139	1689	Schlaeppli, K.	2154
Santisteban, M.	1206	Saunders, A.	648	1862	Schlegel, M.	876
.....	1207	2193	2320	911
.....	2384	Saunders, J.	1248	Schäffer, A.	2619	Schlenz, H.	1296
Santofimia, E.	1890	2140	Schaller, M.	1703	Schloemer, S.	2155
.....	2132	Saunders, M.	2391	Schaltegger, U.	1095	Schlömann, M.	2024
Santos, G.	943	2435	1903	Schlömer, S.	2250
Santos, J.F.	1778	2148	Schlosser, C.	780
.....	2132	2511	900
Santos Carballal, D.	965	1473

Schlotterbeck, G.	2492	Schoenemann, S.	1180	Schulz, T.	675	Segre, E.	1555
Schluechter, C.	2153	2257	1734	Seibert, S.	2173
Schmahl, W.W.	1853	Schofield, P.F.	774	1809	Seidel, T.	2099
.....	2123	1245	1955	Seifert, J.	1764
Schmalenberger, A.	737	Schöler, H.F.	2139	Schulze-Lefert, P.	2154	Seitaj, D.	2174
Schmandt, B.	1346	Schollenbruch, K.	2509	Schumacher, J.C.	1690	2284
.....	1591	Scholz, D.	745	2169	Seither, A.	2174
Schmeide, K.	2155	1768	Schüngel, M.	2390	Seitsonen, A.	2434
Schmid, D.	2156	2163	Schüpbach, S.	1904	Seitz, H-M.	2210
Schmid, T.	994	2503	Schüssler, J.A.	2485	Seitz, J.	1243
Schmidt, A.	2156	Scholz-Ahrens, K.	1295	Schuster, R.	1141	Seitz, S.	2175
Schmidt, C.	739	Schön, W.	2164	Schuth, S.	570	Seke, A.	1198
.....	989	Schönbächler, M.	2041	1879	2414
.....	2157	Schöne, B.R.	2204	2015	Sekine, T.	2291
Schmidt, D.	2018	2435	Schütrumpf, K.	2169	Sekisova, V.	2175
Schmidt, F.	2157	Schöpa, A.	2164	Schwab, F.	2257	Sekiyama, T.T.	2176
Schmidt, J.A.	1272	Schorr, S.	1203	Schwanenthal, J.	2407	Sekusak, M.	1141
.....	1399	Schott, J.	681	Schwark, L.	2364	Selby, D.	1023
Schmidt, K.	2158	693	Schwartz, J.	2271	1348
Schmidt, Mariek E.	2158	926	Schwartz, S.	958	Selector, S.	1999
.....	2269	1152	Schwartz, T.	2259	Self, S.	1381
Schmidt, Max W.	1166	1184	Schwartzman, D.	2170	Šelih, V.S.	2395
.....	1300	1858	Schwarz-Sampera, U.	1105	Seliman, A.	2176
Schmidt, Moritz	2159	2165	1443	Sell, K.	2177
Schmidt, N.	2159	2256	Schwarzenbach, Esther ...	2170	Sellers, W.	1029
.....	2212	2284	Schwarzenbach,		Selroos, J-O.	2355
Schmidt, Sabine	2276	Schotterer, U.	1126	Esther M.	2424	Seltmann, R.	1001
Schmidt, Sonja	870	Schrag, D.	1298	Schwarzkopf, L.M.	2357	Semeniuk, D.	931
Schmidt-Mumm, A.	890	Schreiber, A.	692	Schwedt, A.	688	Semenova, D.	1987
.....	1363	Schreiner, K.	2084	Schwehr, K.A.	1597	2008
Schmidtko, S.	2272	Schrenk, M.	766	2524	Semiz, B.	2177
Schmitt, Anne-Désirée	641	926	Schweigert, M.	1764	Sempéré, R.	1918
.....	2160	2165	Schweighoffer, D.	2622	Sen, A.D.	2178
.....	943	2369	Schwientek, M.	1210	Sen, E.	1525
Schmitt, Axel K.	946	Schrezenmeir, J.	1295	Schwier, A.	2135	Sen, G.	2076
.....	1008	Schrifer, D.	1259	Schwieters, J.B.	1495	Sen, P.	1525
.....	1320	Schröder, C.	1798	2355	Sena, E.	620
Schmitt, J.	2160	Schröder, J.	2166	Sciarra, A.	1976	Senda, R.	1256
.....	2161	Schroder, T.	1731	2171	1362
.....	2181	Schroeder, C.	1431	Scoates, James	2171	2178
Schmitt-Kopplin, P.	1024	Schubert, C.J.	718	Scoates, Jon	2171	2319
.....	1294	832	Scofield, A.	1705	Sendula, E.	1468
Schmitz, B.	2575	1482	Scopelliti, G.	1018	Senger, R.	2096
Schmitz, M.	1246	1900	Scott, C.	832	Şengüler, İ.	582
.....	2295	2026	2248	Senn, A-C.	2179
Schnabel, C.	1639	2139	Scott, J.M.	2392	2422
Schnaiter, M.	2259	2166	Scott, P.	1284	Senn, D.	2233
Schneider, R.	2423	2233	1977	Seoung, D.	1574
Schneider, T.	2161	Schubert, M.	2167	Scott, S.	1686	Sepahi, Ali A.	2179
Schnetger, B.	747	Schubert, R.	2503	Scott, T.	1379	Sepahi, Ali Asghar	1776
.....	2162	Schubnel, A.	2167	Scribano, V.	2172	Seppi, R.	1126
Schnurr, A.	1689	Schuessler, J.A.	1394	Scrivener, K.	2231	Sequeira Braga, M.A.	1207
Schoenbaechler, M.	1321	2168	Seaman, S.	2172	Sergeev, I.	1985
Schoenberg, R.	1047	2315	2500	Sergeev, S.	1516
.....	1476	2490	Searle, R.	2387	Sergeeva, M.	1358
.....	1527	Schüler, D.	2343	Sebestyen, S.	2563	Serov, P.	672
.....	1950	Schulin, R.	1305	Sebilo, M.	723	Serrano, A.M.	620
.....	2162	Schulmann, K.	1957	772	Serrano, L.	2180
.....	2294	Schultz, L.N.	2168	1795	Serrano, S.	1870
.....	2497	Schultz, M.	1688	2173	Sert, A.S.	1426
.....	2513	Schulz, H-M.	692	Secchi, F.	838	Servais, P.	1634
Schoene, B.	1445	Schulz, M.	800	Seetharam, S.	1204	Serventi, G.	2180
.....	2163		Seghedi, I.	1132	Sesartic, A.	2181

Sessions, A.L.	817	Shatskiy, A.	854	Shi, W.	2196	Shock, E.	757
.....	953	1025	Shi, Xiangming	807	758
.....	1496	1619	Shi, Xiaoping	1774	1885
.....	1565	2189	Shi, Xuefa	1118	1887
.....	1967	Shatsky, V.	2019	Shi, Y.	2284	2104
.....	2056	2190	Shi, Ze-Ming	2460	2553
.....	2269	2583	2529	Shofner, G.	2142
Seth, B.	2160	Shaw, Alison	2055	Shi, Zhenqing	1109	Shollenberger, Q.	853
.....	2161	Shaw, Andrey	1798	Shi, Zongbo	1415	Shorter, J.	2575
.....	2181	Shaw, S.	2076	1975	Shozugawa, K.	1321
.....	Shaw, Samuel	628	2197	Shu, Q.	771
.....	1082	Shibata, H.	2283	2206
.....	2059	Shibata, Y.	1317	2206
.....	Shaybekov, R.	2190	Shiel, A.	1712	Shuang, Y.	2206
.....	Shchekina, T.	574	2197	Shubenkova, O.	1982
.....	Shcherbinina, E.	986	Shields, G.	1615	Shuh, D.	2207
.....	Shchukarev, A.	1506	Shih, C-Y.	2539	2400
.....	2026	Shikazono, N.	1879	Shukolyukov, A.	2351
.....	2191	2198	Shukolyukov*, Y.	1775
.....	Shea, D.	2198	2207
.....	Sheibi, M.	1988	Shiller, A.	2198	2536
.....	2191	Shillington, D.	678	Shukurov, N.	1486
.....	Sheik, C.	2192	Shilobreeva, S.	1694	Shulga, N.	2208
.....	Sheikh Zakariaee, S.J.	2120	Shim, S-H.	2199	Shuller-Nickles, L.	1318
.....	Sheldon, N.	985	Shima, S.	1427	Shulmeister, J.	2379
.....	1132	Shimada, A.	2361	Shumlyanskyy, L.	892
.....	2192	Shimaoka, T.	2112	Shurkhuua, T.	1574
.....	Sheldrick, T.	2193	Shimizu, A.	2285	Shusta, S.	2269
.....	Shelley, M.	1054	Shimizu, Kei	2199	Shuster, D.	2208
.....	1724	Shimizu, Kenichi	2200	2352
.....	Shen, B.	2193	Shimizu, Kenji	2200	Shuttleworth, S.	626
.....	Shen, C-C.	873	Shimizu, M.	2201	2501
.....	Shen, G.	2310	Shimizu, N.	1127	Shuvaeva, O.	1235
.....	2461	1735	1557
.....	Shen, J.	1332	2200	2209
.....	Shen, X.	1011	2201	Shvarov, Y.	2209
.....	Shen, Y.	2593	Shimoda, G.	2202	Shvetsova, I.	1507
.....	Sheng, D.	807	Shimojo, M.	2202	Shyu, J.B.H.	873
.....	Sheng, G.D.	1596	2541	Siade, A.	2173
.....	Sheng, X.	2194	Shimajuku, A.	2543	Sial, A.N.	815
.....	Sherbov, B.	1558	Shin, D.B.	1384	1948
.....	Sherif, M.I.	1162	Shin, H.S.	1924	2210
.....	2194	2203	Sickinger, M.	2451
.....	Sherlock, S.	924	Shin, K-H.	2564	Sides, I.	1027
.....	Sherman, Dave	956	Shin, S-K.	1925	Siebel, W.	2318
.....	Sherman, David M.	639	Shinjoe, H.	1896	Siebenaller, L.	1583
.....	2195	2203	Sieber, M.	2210
.....	Sherwood Lollar, B.	1312	Shiotsu, H.	1702	Siebert, C.	2548
.....	1553	2204	Siebert, Christopher	1607
.....	1892	Shipboard Scientific Party, I.E.3.	1184	1837
.....	1931	Shirai, K.	2129	Siebert, J.	2211
.....	2195	2204	640
.....	Shestakov, S.	1928	Shirai, N.	2539	810
.....	Shevalier, M.	1716	Shiraishi, F.	1771	1787
.....	1850	Shirdashtzadeh, N.	2120	2211
.....	Shevliakova, E.	1175	2205	Siégel, C.	2212
.....	Shi, G.	992	Shirey, S.B.	802	Siegel, K.	2436
.....	Shi, H.	1646	1252	Siegler, M.	1259
.....	Shi, J.	1625	2205	Sieland, R.	2154
.....	2447	2330	2159
.....	Shi, P.	2146	2450	2212
.....	Shi, Ren-Deng	1215	2220	Siemens, J.	1125
.....	Shi, Rendeng	2196	Shiryaev, A.	1741	Siena, F.	1058
.....	Shi, S.	1961	Shmulovich, K.	1741	2185

Sierau, B.	2259	Sinton, J.M.	863	Smart, S.	2222	Soendergaard, A.	1213
Sigfusson, B.	1178	2105	Smeets, P.	2223	Sohrin, Y.	1491
.....	1784	Sinyutkina, A.	1452	2223	1824
.....	1998	Sio, C.K.I.	948	Smekhova, A.	1038	2303
.....	2277	2085	Smellie, J.	2364	Sokol, E.	1507
Sigl, M.	1720	Sirikitputtisak, T.	2218	Smerdon, B.D.	2228	Sokolova, E.	2232
Sigman, D.	1241	Sirio, C.	2613	Smirnov, S.	2232	Soktoev, B.	652
.....	1242	Sirotkina, E.	824	Smit, M.	2224	Soldati, A.	837
.....	1369	Sitchler, A.	2218	Smith, Albertus	2224	Soldatova, A.	801
.....	1396	Sitnikova, M.A.	2515	Smith, Allison	702	Soler, A.	2077
.....	2019	Sitte, J.	1498	Smith, Andrew	579	Soler, J.M.	951
.....	2050	Sivan, O.	2219	Smith, Andrew Christopher	2225	1174
.....	2222	558	2225	2233
.....	2459	600	Smith, Andrew J.	2400	Solismaa, L.	638
.....	2595	633	Smith, Caroline	1007	Sollberger, S.	2233
Sigstam, T.	615	1556	2255	Sollich, M.	2234
Sigurdardottir, H.	1178	1593	Smith, Chris	795	Solodukhina, M.	2234
.....	2277	Sivry, Y.	2050	1486	Solomon, D.K.	2228
Sigurdsson, I.	1234	2558	2205	Solomon, S.	1856
Siljestroem, S.	2255	2559	2328	Solopova, N.	2235
Silva, C.	928	2585	2442	Solovova, I.	789
Silva, E.	1687	Sjöberg, S.	1644	Smith, Christopher	2225	856
Silva, Joao	2132	Sjöstedt, C.	1235	Smith, Christopher	2226	2235
Silva, Juan Carlos	2213	Skelton, A.	2604	Smith, Colin	2274	Soltermann, D.	2236
Silver, E.	1480	Skidmore, M.	758	Smith, D.	771	Somarin, A.	2236
Silvester, E.	1449	Skinner, L.	2461	Smith, Eugene	2031	Sommer, J.	1099
Simakin, A.	706	Skłodowska, A.	1710	Smith, Evan	2226	Sommer, S.	2353
.....	2213	1755	Smith, F.	2227	Sommerdijk, N.	1602
Simanova, A.A.	1946	2023	Smith, I.	2265	2223
.....	2214	2219	Smith, James	2227	2223
Šimčková, M.	2214	Sklyarov, E.	2253	Smith, Joanne	1136	Somogyi, A.	2184
Simionovici, A.	1342	Skogby, H.	1834	2228	Son, M.	878
.....	1564	Skora, S.	2220	Smith, M.	2029	Sondag, F.	1983
Simkus, D.	1553	Skouri-Panet, F.	688	Smith, R.	2485	Song, Chul H.	1251
Simmons, A.	780	Skovbjerg, L.L.	1886	Smith, Scott	853	1462
Simmons, W.	2074	Skrzypek, E.	1957	Smith, Stanley D.	2228	1573
Simon, A.	680	Skulan, J.	1198	Smith, V.	569	1925
.....	705	Skvortsova, V.	2220	2229	1925
.....	1344	Skyllberg, U.	2491	2340	Song, Cian	1580
.....	2215	Slaby, E.	1618	Smith, W.	2229	Song, G.	2617
.....	2310	Sláma, J.	1493	Smits, R.	2230	Song, H.	2237
Simon, J.	1791	Slater, G.F.	1312	Smolders, E.	643	2532
Simon, P.	1741	1553	Sneha, S.	2021	2587
Simon, R.	1185	2195	Snell, K.	2230	Song, K-Y.	2237
Simon, S.	2215	Slater, L.	628	Snellings, R.	2231	Song, Seckwhan	1463
Simone, D.	2216	Slater, N.	2024	Snider, J.	894	1565
Simonetti, A.	868	Slater, R.	980	Snider, M.	985	Song, Shuguang	1411
Simons, S.	1742	Slaugenwhite, J.	1589	Snoeyenbos, D.	2231	2279
Simonsson, M.	2216	Sleighter, R.	1882	Snow, J.	1184	2445
Simpson, D.	974	Sloan, L.	1428	1750	Song, X.	2238
Sims, K.W.W.	612	Sloan, S.	807	1838	Song, Yen-Fang	1605
.....	1035	Slomp, C.P.	964	Snow, L.	1018	Song, Yinxian	1680
Singh, Anshuman	578	1029	Snyder, Glen T.	583	Sonke, J.	2238
Singh, Atinderpal	2032	1390	Snyder, Glen T.	1950	2239
Singh, B.	2217	2284	Soares, T.	2414	Sonnenthal, E.	1935
Singh, D.	2032	Slotznick, S.	2474	Soballa, E.	1530	2467
Singh, H.K.	2217	Slowey, N.	1100	Sobolev, A.	667	Sonzogni, C.	2298
Singh, R.	605	Słaby, E.	2221	683	Sorooshian, A.	2239
Singh, Satinder Pal	2217	Słodczyk, E.	2221	706	Sortino, F.	2067
Singh, Sunil Kumar	2217	Smakowski, T.	2507	2232	Sossi, P.	1097
Sinha, A.	1398	Smalley, C.P.	939	Sodemann, H.	644	2240
Sinninghe Damsté, J.	1991	Smart, K.	2222	Soderholm, L.	2159	Soto, J.G.	993
.....			Soe Thura Tun,	873	Soubrand, M.	1163

Souders, K.	1193	Spivak, A.	2235	Steele, A.	755	Sterckeman, T.	1052
.....	2240	Spivak, D.A.	1488	2255	Sterl, A.	2397
Souhaut, M.	2387	Spolaor, A.	1126	Steele, J.	1181	Stern, Richard	950
Soule, A.	2094	Sposito, G.	734	Steele-MacInnis, M.	723	1328
Souli, H.	2055	1946	1050	1929
Sousa, D.	966	2214	2255	2045
Sousa Brito, J.	805	Spotl, C.	1768	Steen, A.	619	2584
Sousa Santos, G.	2241	2163	1634	Stern, Robert	2055
Soustelle, V.	2341	2503	Stefani, V.	908	2305
Southam, G.	1992	2517	Stefansson, A.	1414	Stetzer, O.	2259
.....	2047	Spots, T.	758	1445	Steutner, R.	2155
Southworth, R.	1328	Spracklen, D.	832	1784	2263
Souza, I.	897	2248	1998	Stevens, G.	933
Sovacool, B.	2241	Sprain, C.	2248	2256	1064
Soyama, H.	1268	Spruk, M.	1628	Stefurak, E.J.T.	2256	1846
Søager, N.	1314	2610	Stegemeier, J.	2257	Stevenson, E.	612
Sørensen, H.O.	883	Sprung, P.	665	Stehmeier, L.	1370	2192
.....	2336	1099	Steig, E.	1180	2263
Sørli, R.	1108	1475	2257	Stevenson, R.	1818
Špaček, P.	555	2249	Stein, H.J.	1156	Stewart, A.-M.	2264
.....	1668	Spycher, N.	2606	1323	Stewart, B.	1965
Spadini, L.	1788	Squyres, S.	2158	2258	2264
.....	1832	Srinivasa Sarma, D.	973	2356	Stewart, D.	1635
Spagnoli, D.	1170	2023	2525	Stewart, J.	2265
Spagnoli, F.	2242	Srinivasan, B.	2281	2546	Stewart, R.	2265
.....	2242	1919	2619	Steyl, G.	1447
Spahiu, K.	783	Srivastava, R.P.	1919	Stein, M.	1189	Stickler, C.P.	646
Spain, J.C.	1310	St. C. O'Neill, H.	2240	1556	Stille, P.	641
Spak, S.	1688	Stabile, P.	2249	1593	845
Spampinato, L.	1165	Stachel, T.	1328	1593	989
Spandler, C.	1402	Stachowitch, M.	1746	2258	1969
Spangenberg, J.	1496	Stackhouse, S.	2250	2557	2160
.....	1496	2438	Stein, R.	1593	2260
Sparkes, R.	1136	Stadelmann, G.	1226	Steinbrückner, D.	2154	2266
Sparks, David	1108	Stadler, S.	2250	Steinhardt, P.	1313	2481
Sparks, Donald L.	1558	Staff, R.	2229	2251	Stinchcomb, G.	2266
Sparks, S.	597	Stagno, V.	908	Steinhardt, W.	1313	Stipp, S.L.S.	551
Sparrow, K.	1940	1116	Steininger, R.	627	595
Spasić-Jokić, V.	1198	2251	1136	684
.....	2243	Stahl, H.	1608	1185	754
.....	2414	Stahr, D.	624	1459	883
Spaulding, D.	2243	Stalder, R.	1487	Steinke, I.	2259	938
Spear, F.	624	Stamati, F.	1851	Steinle, L.I.	1849	987
.....	2474	Stanek, C.	2589	2259	1270
Spear, J.	2056	Stanelle, T.	2241	Steinmann, M.	2260	1540
.....	2321	2251	Steinmann, Y.	2260	1781
Spear, N.	2244	Staniszewski, Y.	2252	Steinweg, J.	915	1836
Speelmanns, I.	1099	Stankevičius, Ž.	2313	Stelluti, I.	2261	1848
Spence, A.	2244	Stankiewicz, A.	1578	Stelten, M.	2261	1848
Spencer, C.J.	2245	Stanković, N.	2252	Steltenpohl, M.	629	1886
Spengler, D.	2245	Stanley, R.H.R.	1268	Stemmerik, L.	2097	1890
Spera, A.	2246	Starikova, A.	2253	Steneck, R.S.	1083	2117
Spera, F.	728	Stark, G.	1659	Stennett, M.	917	2126
Sperling, E.	2246	Starkey, N.	589	925	2168
Spero, H.	1740	Startsev, N.	2488	Stenni, B.	1126	2336
Spetsius, Z.	623	Staubwasser, M.	1287	Stensgaard, B.	1903	Stirling, C.	1812
Spice, H.	2247	2253	Stensland, A.	670	Stix, J.	1481
Spicuzza, M.J.	1035	Staudigel, H.	2254	Stepanaukas, R.	1535	Stixrude, L.	2250
.....	1588	Stawski, T.M.	2254	Stepanov, A.	2262	Stock, C.	702
.....	2386	Stearns, M.	1533	Stepanov, V.	2262	Stockdale, A.	2334
.....	2399	Stedra, V.	1509	Stepanova, A.	2262	Stocker, R.	1021
Špillar, V.	2247	Steeffel, C.	1859	Stepanova, M.	1863	Stockhecke, M.	2026
Spiro, T.	801	1869	1863	
Spivack, A.	2140		Stephan, T.	951	

Stockmann, M.	775	Stuart, Finley M.	2357	Sumino, H.	648	Suzuki, S.	1367
.....	2267	Stuart, G.	1327	863	2291
Stoica, A.	2267	Stubbs, J.	2275	1484	Suzuki, T.	942
Stojic, A.N.	2268	2473	2285	Suzuki, Yoshinori	2292
Stoll, B.	1394	Stumpf, R.	2276	2349	Suzuki, Yoshio	2361
.....	2268	Stumpf, T.	1310	Summa, V.	828	Suzuki-Muresan, T.	1206
.....	2477	Stupar, Y.	2276	Summons, R.E.	1110	Suzzane, O.	2196
Stoll, Heather	1735	Sturges, W.	579	1565	Svensden, C.	1556
Stoll, Heather M.	1291	Sturm, M.	1876	2056	2040
Stolpe, B.	2040	2166	2364	Svensson, A.	967
Stolper, D.	2269	2347	2479	2385
Stolper, E.M.	757	Sturm, P.	1041	Sun, Jian	2616	Svensson, U.	982
.....	2158	Stute, M.	1178	Sun, Jianlin	1652	Sverjensky, D.	1050
.....	2269	1756	Sun, Jing	2512	1059
Stolpovsky, K.	2270	2277	Sun, Jing	746	1081
Stone, J.	2359	Stutz, E.	1540	2285	1571
Stone, M.M.	2270	1797	Sun, Wei	2543	1629
Stoops, G.	1156	2277	Sun, Weidong	651	1633
Storelvmo, T.	2181	Stylo, M.	693	1606	2292
Storey, C.	1263	2278	1615	Swadling, J.	2293
.....	2486	Su, Chih-Chieh	699	2286	Swander, Z.	2293
Storm, S.	943	Su, Chunming	2278	Sun, X.	2286	Swanner, E.	1431
Storme, J-Y.	2271	Su, F.	1277	Sun, Yang	2612	2294
Stotskaia, A.	1503	Su, J.	2279	Sun, Yongge	2287	2513
Stott, L.	1428	2614	Sun, Youbin	717	Swanson, D.	1027
Stowasser, C.	1062	Su, L.	2279	Sun, Yuanyuan	2287	Swanson, L.	680
Stowell, H.	2271	Su, W.	2280	Sun, Z.	2288	Swart, P.	613
Straaten, N.	1391	Suarez De Tangil, M.	1949	Sundal, A.	2288	630
.....	2272	Suarez-Abelenda, M.	2280	Sundby, B.	1667	1814
Strachan, R.	708	Suárez-Suárez, A.	1342	Sundman, A.	2289	Swartz, J.M.	2071
Stracke, A.	1154	Subashri, R.	2281	Sung-Yup, K.	1517	Swedlund, P.	948
.....	2222	Subramanian, B.	1488	Sunnetci, M.O.	1047	Sweeney, C.	2048
Strakhovenko, V.	2432	Suchy, M.	1292	Surble, S.	2068	Sweeten, B.	1763
Stramma, L.	2272	Suckow, A.	2281	2109	Swietlicki, E.	1912
Strasser, M.	2062	Suda, K.	2282	Suresh, P.O.	1005	Swihart, J.	2469
Strati, V.	1224	Suda, S.	1960	Surkus, B.	989	Swindle, A.	2294
.....	2519	Suder, B.	2495	Surmik, D.	1504	Syed, H.F.	1434
Strauss, H.	1234	Suginohara, A.	1060	Surono,	2413	Sylvester, P.	1193
.....	1783	Sugita, S.	878	Sushchevskaya, N.	1755	1324
.....	1954	2470	Sushchevskaya, T.	1989	1929
.....	2614	Sugitani, K.	1588	Sutcliffe, C.	2289	2240
Streit, L.	2321	Sugiura, N.	1487	Suter, J.	2293	2295
Strekopytov, S.	1454	1816	Sutherland, L.	2582	Synal, A.	1272
Strnad, L.	1864	Sugiyama, K.	1758	Sutton, Sally	2290	Synal, H.A.	836
Strohenger, C.	764	Sugiyama, N.	1584	Sutton, Stephen	1096	Syromyatnikov, K.	1593
Strollo, C.	1960	Suja, E.	2282	2290	Szabó, C.	605
Strong, C.	1398	Sukenaga, S.	2283	Suvorov, Y.	1353	658
Strongin, D.	2273	Sukhorukov, V.P.	1985	Suvorova, E.	572	1468
Stroud, R.	572	Suksi, J.	2364	1377	1504
Strous, M.	1150	Sulak, M.	2283	2464	1618
Struck, U.	747	Suleimenov, O.	2183	Suzuki, Akio	1025	1839
.....	1137	Sulli, A.	823	Suzuki, Atsushi	1438	1934
.....	1890	Sullivan, L.A.	799	2301	1972
.....	2260	1508	Suzuki, C.	2291	2410
Struve, T.	2273	Sullivan, P.	2284	Suzuki, Katsuhiko	1362	2426
Struyf, E.	1114	Sulpizio, R.	1789	1526	Szala, B.	2295
.....	2082	Sultanov, D.	1197	1826	2366
.....	2274	Sulu-Gambari, F.	2284	1893	Szamosfalvy, Á.	1468
Strzepek, K.	2274	Sumi, T.	1467	2137	Szidat, S.	843
Stuart, Fin M.	1056	Sumii, T.	2203	2178	Szilas, K.	2296
.....	1814	2319	Szurmanova, Z.	1864
.....	2275	Suzuki, Kentaroh	1202	Szymkiewicz, M.	1755
Stuart, Finlay	1172

T

Tabersky, D.....	1122	Takami, H.....	1439	Tanis, E.....	680	Teixeira, R.	2318
.....	2297	Takamori, H.	2136	2310	Teixeira, W.	2319
Tacconi Stefanelli, C.....	1859	Takano, S.....	1824	Tanner, M.	1232	Tejada, M.L.	2319
Tachibana, S.....	2297	2303	Tannou, I.....	2311	Telfeyan, K.	1455
.....	2470	Takano, Y.	1427	Tanteri, L.....	1859	Tella, M.....	2320
.....	2534	Takegawa, N.	1899	Tao, Shizhen	1140	Tellini, F.	829
Tachikawa, K.	833	Takehara, M.	1322	Tao, Shuqin.....	2311	Telouk, P.....	569
.....	1537	2304	Tao, T.	1011	784
.....	2298	Takemura, T.	2572	Tappa, M.....	1791	Telus, M.....	948
Tack, L.	751	Takeoka, H.	1793	Tappe, S.....	2222	Temel, A.	1730
Tacker, C.....	2298	Takeuchi, A.	2361	2312	2557
Taddeucci, J.	1326	Takeuchi, M.	2304	Tappero, R.	1092	Temgoua, L.G.....	2320
Tagami, T.	1267	Takigawa, A.	1711	Taran, Olga	2312	Templeton, A.	2321
.....	2299	2297	Taran, Oxana	1557	2321
.....	2542	Takimoto, K.	1467	Taran, Y.	1357	Ten, G.	2196
Taghipour, B.	1665	Talla, D.....	1586	2313	Teng, F.....	948
.....	2299	Talling, P.	1400	Tarantino, S.C.....	1038	1615
Tagliabue, A.....	2397	Tamas, C.G.....	660	Tarascon, J-M.....	1767	1738
Tagliavini, E.....	1912	842	Taraškevičius, R.	2313	2218
Tagma, T.	1594	Tamura, A.	565	Tarran, G.A.....	780	Teng, H.H.	2322
Taisne, B.	2300	1362	Tartakovsky, A.	955	2602
Tait, A.	2363	1663	Tartese, R.....	589	Tennant, A.	2322
Tait, Kim.....	946	1772	2314	Tennent, N.H.	2395
Tait, Kimberly.....	575	1779	Tarvainen, T.	1537	Tepe, N.	2323
.....	1795	1811	Tassan-Got, L.	1147	Terada, K.	2534
Tajcmanova, L.	1287	2305	1157	Terada, T.....	1793
.....	2300	2539	Tassi, F.	703	2323
Tajika, E.....	1905	2566	1856	2521
Takada, A.....	2301	Tamura, Y.	2305	Tassinari, C.....	1788	Teraji, S.....	2534
Takagi, H.....	2301	Tan, M.	1011	2314	Terranova, U.....	965
Takagi, T.	607	2306	Tateno, S.....	1303	Teske, A.	619
Takahashi, E.....	1825	Tan, S.	2257	828	1557
.....	1888	Tanabe, K.....	2204	Tateo, F.....	829	1730
.....	2302	Tanabe, S.....	1364	1701	Tessalina, S.	1830
Takahashi, H.	2561	Tanaka, A.	1490	Tatsumi, Y.	1256	Tessier, E.	1051
Takahashi, K.	1257	Tanaka, K.	2302	Tattitch, B.	1709	Teste, G.....	1543
.....	2554	2306	2315	Testemale, D.	1562
Takahashi, S.	1874	Tanaka, M.	614	Tatyana, C.....	2213	1627
Takahashi, T.....	2178	2307	Tatyanin, G.....	559	1643
Takahashi, Y.	614	Tanaka, R.	2307	Tatzel, M.....	2315	Tetsuo, I.	2218
.....	1433	Tanaka, S.....	2470	Tavares de Morais, E.	2088	Teuku, F.....	2491
.....	1695	Tanaka, T.....	2438	Taviani, M.	2359	Teutsch, N.....	2324
.....	1773	Tandy, S.	1305	Tay, Y.Y.	1293	Tevlin, A.....	1812
.....	1824	Tang, C-G.....	2308	Taylor, G.J.....	1244	Teyssier, C.	1199
.....	2302	Tang, H.....	2596	Taylor, J.....	1846	Tfaily, M.....	915
.....	2303	Tang, Jianwu	1075	2316	Thaler, C.	2325
.....	2306	2308	Taylor, Lawrence.....	662	Thalmann, B.	1417
.....	2307	Tang, Jie	2309	Taylor, Lyla	676	Thambidurai, P.	1434
.....	2338	2448	Taylor, P.....	1608	Thamdrup, B.	775
.....	2538	Tang, M.....	2530	Taylor, Rebecca.....	931	1351
.....	2562	Tang, R-T.....	1613	Taylor, Rich.....	2316	1451
Takahata, N.....	864	Tang, S.	2544	Tazoe, H.	2317	2070
.....	1360	Tani, K.....	1256	Teagle, D.A.	1847	2375
.....	1417	Taniguchi, S.	1842	Tebo, B.	801	2475
.....	1487	2246	1667	Thanthiriwatte, K.S.....	996
.....	1816	Tanimizu, M.	1824	Tecce, F.	1113	Thapalia, A.	742
.....	2129	2115	Tegen, I.....	2251	Tharaud, M.	588
Takai, K.....	602	2303	2317	1746
.....	1826	2438	Tegetmeyer, H.	1150	2585
.....	1855	Tanimoto, H.	2310	Teiber, H.....	2318	Thebaud, N.	1903
Takaki, Y.....	1439	1965	Teitler, Y.....	1965	Theou-Hubert, L.	923
Takamasa, A.	1769	1841	Teitz, S.....	1841	Theye, T.....	2110

Thibault, N.	2422	Tiepolo, M.	911	Tomilenko, A.	2189	Tournassat, C.	893
Thieme, J.	2325	1128	2332	1552
Thiemens, M.	2326	1177	Tomiyasu, F.	2340	Tourney, J.	1398
Thien, B.	2326	1386	Tomkins, A.	1054	Town, R.	2349
Thiery, A.	2320	1545	2182	Townsend, A.	860
Thil, F.	2091	2128	Tomlinson, E.	569	Toyama, C.	1356
Thirlwall, M.	708	2331	2340	1811
.....	1599	2354	Tommaseo, C.	2341	2349
.....	1679	Tierney, J.	2331	Tommasi, A.	917	Toyoda, A.	1439
Thoenen, T.	1522	Tikunova, N.	1557	1618	Toyoda, Sakae	1804
.....	2327	Tilgner, A.	764	2341	2623
Thomalla, S.	2222	Till, J.	2332	Tommasini, S.	763	Toyoda, Shoichi	1881
Thomas, A.L.	973	Timina, T.	2189	837	Toyoshima, K.	2129
.....	2436	2332	Tomonaga, Y.	769	Trail, D.	841
Thomas, C.W.	624	Timm, C.	1319	769	Trakal, L.	1489
Thomas, E.	1647	2333	2026	Trambouze, O.	890
Thomas, J.	624	Timmerman, A.	1428	2342	Tranter, M.	2350
.....	2474	Timmermann, A.	2298	Tomori, W.	2370	Tranzer, O.	1021
Thomas, K.	1397	Timms, N.	1046	2342	Trappitsch, R.	951
Thomas, P.	2014	1942	Tompa, É.	1868	Tratnyek, P.	2350
Thomas, R.	2087	Timofeev, A.	2333	2343	Trautz, R.	2606
Thomas, S-M.	2484	Tinnacher, R.	2606	Tonarini, S.	819	Travé, A.	2351
Thomazo, C.	2327	Tipping, E.	2334	873	Travin, A.	1503
Thompson, C.	685	Tiraboschi, C.	2334	2201	1757
Thompson, Lonnie	1126	Tirado, J.	1022	Tong, X.	1277	Trcera, N.	1079
.....	2374	Tishin, P.	559	2528	1377
Thompson, Lucy	2158	2335	Tonidandel, D.	1126	1948
Thompson, M.	1760	Tison, J-L.	2134	Tonnelier, N.	2343	Tredoux, M.	1283
Thompson, W.G.	2071	Tissandier, L.	2085	Tonoue, R.	696	1447
Thomson, A.R.	795	Tissot, F.L.H.	948	Tooth, S.	1119	2351
.....	2205	1992	Toplis, Michael	1878	Treiman, A.H.	757
.....	2328	2085	Toplis, Mickael J.	653	1794
Thomson, J.	964	2335	Toprak, E.	2259	2158
Thornber, S.	917	Tobin, M.	1449	Torabi, G.	2205	2269
Thorne, R.	2328	Tobler, D.J.	1732	Torapava, N.	2344	Trela, W.	2593
Thorogood, G.	1650	2126	Torfstein, A.	1189	Tremaine, P.	2352
.....	2072	2336	Torkian, A.	2344	Tremblay, M.	2208
Thorseth, I.H.	670	Toczydlowska, D.	2582	Torn, M.	2345	2352
.....	1887	Todd, A.	2623	Tornare, E.	2345	Tremosa, J.	2353
Thorsnes, T.	1588	Todd, E.	2094	Tornos, F.	1880	Tretyachenko, V.	2122
Thouement, H.A.A.	2329	Tofan, E.	2336	Tornow, C.	2346	Treude, T.	1510
Thresher, R.	2274	Togo, Y.	2302	Toro, J.	1965	1849
.....	2359	Tokarev, I.	633	Török, K.	1839	2259
Thu, K.	2582	717	Torrelles, X.	1733	2353
Thullner, M.	2329	2337	Torres, E.	2346	Treusch, A.	1763
Thura, O.	1613	Tokoro, C.	1367	Torres, M.	2347	Triadó-Margarit, X.	1634
Thybo, H.	620	2291	Torres, N.	888	Tribet, M.	979
Tian, C.	1003	2337	2347	Tribuzio, R.	1782
Tian, Lijun	1011	Tokunaga, K.	2338	Torres-Ruiz, J.	1171	2128
Tian, Liyan	2330	Tokunaga, T.	1884	1954	2331
Tian, S.	1631	Tokuyama, H.	1765	2074	2354
.....	2330	Toli, K.	1185	Toth, M.	658	2354
Tian, W.	867	Tollan, P.M.E.	684	Totsche, K.U.	1257	Trincherro, P.	2355
Tiano, L.	775	2338	1518	Trindade, R.	637
Tibuleac, C.	2385	Tolstikhin, I.	2339	2066	2130
Tice, M.	1316	Tolstov, A.	1558	Touboul, M.	2003	Trinquier, A.	2355
Tiede, K.	1418	Tolstykh, N.	2339	2067	Tripathy, G.	2356
.....		Tomascak, P.	2027	2348	Troch, P.	881
.....		Tomaschek, F.	1742	2439	Troiano, J.M.	2356
.....		Tomašových, A.	1065	Toucanne, S.	1110	Troll, V.R.	690
.....		2427	Toulhoat, N.	2109	960
.....		Tombrou, M.	746	Toure, P.R.	2348	2357
.....			Trombino, L.	1156

Trompetter, W.....	850	Tumiati, S.....	2334	Uchida, M.....	1317	Ustaömer, T.	2380
Tronnes, R.G.....	1115	2365	2372	Usui, A.....	2542
.....	2357	Tuner, S.....	770	Uchino, K.....	643	Utsunomiya, S.....	1426
Tropnikov, E.....	2358	Tuo, J.....	1630	Uchiyama, I.....	1439	1702
Tropper, P.....	2358	2591	Udina, N.....	1358	1825
Trots, D.M.....	1526	Turchyn, A.V.....	600	Udry, A.....	2372	2204
.....	1916	2052	Uebe, R.....	2343	Uvarova, Y.....	2381
Trotta, M.....	653	2286	Uecker, R.....	1752	Uysal, Ibrahim.....	2115
Trotter, J.....	1722	2365	Uematsu, M.....	2310	2178
.....	2359	Turek, P.....	2295	Ueno, Y.....	602	Uysal, Ibrahim.....	1046
.....	2499	2366	1042	Uysal, T.....	1691
Trouvé, G.....	1168	Turina, A.....	2366	1272	1754
.....	1702	Türke, A.....	638	1769	2379
Troyer, L.....	2359	Turner, B.....	807	2282	2381
Trønnes, R.....	595	Turner, E.....	1422	2340	Uzasci Sultanyan, S.....	1431
Trubač, J.....	2360	Turner, M.....	555	2373	1468
Truche, L.....	841	1636	Uenver-Thiele, L.....	2373	2382
.....	945	2367	Uesugi, K.....	1860		
Trudinger, C.....	579	2367	1902	V	
Trumbull, R.....	1442	Turner, S.....	555	2361	Vaca-Escobar, K.....	1633
.....	2436	699	Uesugi, M.....	1902	Vaccaro, C.....	1681
Tryon, C.....	2574	1154	Uglietti, C.....	2374	1849
Tsagaraki, T.M.....	1975	1253	Uhlbäck, J.....	1537	Vadeboncoeur, M.....	784
Tsai, F.T-C.....	1038	1636	2111	Vadlamani, R.....	2383
Tsai, T.....	2360	1812	2374	Vaishlya, O.....	2383
Tsapakis, M.....	1975	1920	Ukar, E.....	2375	Vaishya, A.....	1870
Tsay, A.....	2361	2367	Uldahl, A.....	2375	Vaitl, T.....	1044
Tschauner, O.....	2310	2367	Ullmann, C.V.....	2075	Vakh, A.....	2384
Tsiola, A.....	1975	Turpault, M-P.....	1192	2376	Vakh, E.....	2384
Tsuchiya, M.....	875	1446	2422	Val, S.....	1617
Tsuchiya, N.....	1298	1582	Ulloa, O.....	775	Valente, T.....	1206
.....	1826	2063	Ulmer, P.....	1649	1207
.....	1879	Turunen, K.....	638	2334	2384
.....	2470	Tütken, T.....	2368	Ulmer, S.....	1701	Valentine, D.L.....	612
Tsuchiya, T.....	1237	Tutolo, B.M.....	2108	Ulrich, Andrea.....	1876	2269
.....	1438	2368	Ulrich, Andreas.....	2259	Valentine, G.....	2031
Tsuchiyama, A.....	1711	Tuysuz, N.....	903	Ulrich, Ania.....	1491	Valera, P.....	888
.....	1860	Tuzson, B.....	1041	Ulrich, M.....	1491	Valeria, D.R.....	1790
.....	1902	2186	Ulrych, J.....	2376	Valizer, P.....	2385
.....	2361	Twing, K.....	766	Ulven, O.I.....	2377	Vall, S.A.....	1022
Tsuda, A.....	2310	926	Um, W.....	881	Vallelonga, P.....	2385
Tsujimoto, S.....	2534	2369	2377	Valley, J.W.....	1035
Tsujino, N.....	2543	Tye, A.....	2228	Umeda, T.....	2378	1080
Tsukamoto, K.....	2138	Tyler, J.....	1864	Umemura, T.....	2198	1588
Tsuno, K.....	947	Tyler, C.....	2040	Umezawa, Y.....	2115	2386
Tsunogai, U.....	1490	Tyliszczak, T.....	762	Ummenhofer, C.....	591	2399
.....	2543	1798	Ünal, E.....	2378	Valsami-Jones, E.....	1556
Tsutsumi, M.....	1324	2035	Ünal, N.....	582	2040
Tsutsumi, Y.....	1322	2207	1906	Valstar, J.....	1851
Tuba, G.....	587	Tympel, J.F.....	2369	Ünal-İmer, E.....	2379	Valverde-Vaquero, P.....	874
Tuccella, P.....	932	Tyroller, L.....	2370	Uno, Masaoi.....	1888	van Acken, D.....	765
.....	2362	Tyrrell, T.....	617	Uno, Masaoki.....	1816	2386
Tucker, J.....	1803	Tyson, G.....	1187	Unrine, J.....	645	van Aken, H.....	1541
Tuduri, J.....	2362	Tyszka, R.....	1456	Unterricker, S.....	2105	van Beek, P.....	2387
Tuerena, R.....	2363	2370	Urios, L.....	2379	Van Bergen, M.....	851
Tuff, J.....	2363	Tzamos, E.....	1176	Urosevic, M.....	2380	1152
Tuisku, P.....	2508			Uroz, S.....	1446	1850
Tulej, M.....	2062	U		Urquhart, H.....	1991	1851
Tulipani, S.....	2364	Uberuaga, B.P.....	2371	Urrutia, P.....	1114	van Breukelen, B.M.....	2077
Tullborg, E-L.....	1509	2589	Ushikubo, T.....	1588	2329
.....	1550	Ubide, T.....	1547	2386	van Calsteren, P.....	2387
.....	2364	2371	Usman, S.....	1394		
Tulloch, A.....	2271			Ustaömer, P.A.....	2380		

Van Cappellen, P.	599	van Oort, F.	1575	Vaughn, B.	1180	Vezzoni, S.	2412
.....	1312	Van Orman, J.	2108	Vaury, V.	1795	2412
.....	1611	van Riel, K.P.G.L.	2398	2173	Viana, M.	2014
.....	2054	Van Roosbroek, N.	2399	Vautour, G.	1973	Viani, A.	1224
.....	2182	van Rossum, B.	1481	Vaz Dos Santos Neto, E.	2088	Vicars, W.	2143
.....	2388	Van Tendeloo, L.	772	Vazquez, J.	2042	Viccaro, M.	1846
.....	2388	van Veelen, A.	2400	2261	1975
van de Flierdt, T.	773	2505	Vazquez-Rodriguez, A.	2404	2172
.....	1344	van Westrenen, W.	905	Vázquez-Suñé, E.	1413	2413
.....	1454	2129	Vecht, A.	2404	2427
.....	1541	van Zomeren, A.	907	Vedanti, N.	1919	Vickers, M.	2059
.....	1937	Van Zuilen, M.	2162	Veeramani, H.	2405	Vidal, C.M.	2413
.....	2041	2184	Veizer, J.	2427	Vidal, L.	2298
.....	2273	2400	Veksler, I.	1442	Vidal, M.	2133
.....	2389	Vance, D.	592	Velasquez, M.	2314	2414
van de Löcht, J.	2390	811	Velasquez, G.	1583	Vidal-Gavilan, G.	2077
van de Loch, R.	2391	956	Velivetskaya, T.	788	Videau, G.	1075
Van De Moortele, B.	1961	1485	Venceslau, S.S.	1947	Vidović, M.	1198
van den Boorn, S.	603	1615	Vennemann, T.	669	2243
van den Kerkhof, A.M.	571	1620	2405	2414
van der Laan, G.	784	1696	Ventura, G.	1179	Viehmann, S.	2415
van der Loeff, M.	836	2059	1545	Viehweger, B.	697
van der Lubbe, J.	2430	2389	1770	1405
van der Meer, A.	2392	2483	Ventura, M.	1548	Vieillard, P.	1129
van der Meer, Q.H.A.	2392	Vandeginste, V.	2390	Venugopalan, V.P.	2282	Vieira, L.	1983
Van der Putten, N.	898	Vandenkoornhuysse, P.	890	Ver, N.	1687	Viers, J.	641
van der Veen, C.	1933	Vander Kaaden, K.	2391	Ver Loren		2000
.....	2134	Vanderford, M.	2329	Van Themaat, E.	2154	2052
van der Werf, G.	2393	Vanderstraten, A.	982	Verch, A.	2391	2415
van der Zaan, B.	2038	Vandevenne, F.	2082	Verchovsky, A.	667	Vieth-Hillebrand, A.	2496
van der Zwan, F.	2393	Vandieken, V.	1342	789	Vigier, N.	2416
Van Dingenen, R.	2394	1351	2235	Vigliaturo, R.	2416
van Dongen, B.	656	Vanek, A.	1756	2406	Vigouroux, E.	2417
Van Dover, C.	2201	2394	Verchovsky, S.	1328	Vikor, Z.	1585
Van Driessche, A.E.S.	1899	Vanhaecke, F.	983	Vercouter, T.	2406	Viljoen, F.	2343
van Duin, A.	1517	2395	Verdoux, P.	1076	2506
van Elteren, J.T.	2395	2396	Vereecken, H.	586	Villa, I.M.	634
Van Gaelen, N.	2082	Vaniman, D.T.	1794	Verheyden, S.	577	847
van Geen, A.	1508	Vanneste, H.	982	Verheyen, D.	2082	1830
.....	1756	Vanniere, B.	2037	Vermeesch, P.	1054	2417
van Geldern, R.	2250	Vannucchi, P.	2398	2407	Villa-Alfageme, M.	1639
van Genuchten, C.	2395	Vannucci, R.	1177	Verney-Caron, A.	1948	2418
van Heck, H.	2396	Van Tongeren, J.A.	779	Vernikovskaya, A.	2407	Villacis-Garcia, M.	1633
van Heerden, E.	1535	2399	Vernikovskiy, V.	2407	Villalobos, M.	561
.....	1553	Vapnik, Y.	1134	Veronesi, M.	718	1633
.....	2005	1134	Verplanck, P.	718	1738
Van Heghe, L.	2396	1160	Versteegh, E.A.A.	1305	2117
van Hengstum, P.J.	2436	Varadharajan, C.	2606	2408	Villanueva-Estrada, R.E.	1194
van Heuven, S.	956	Varela, M.	1633	Versteegh, G.	2408	2418
van Hinsberg, V.	2397	Vargas, G.	583	Verstraete, M.	823	Villanueva-González, P.	2418
van Hullebusch, E.	1079	Vasconcelos, C.	764	Vervoort, J.	1196	2419
.....	1948	Vasconcelos, P.M.	2401	2409	Villaros, A.	874
.....	2558	Vaselli, O.	703	Veselovsky, F.	1509	1194
.....	2559	1211	1863	1742
van Hulten, M.	2397	1618	Vespasiano, G.	2409	Villermaux, E.	1561
van Hunen, J.	644	1856	Vetere, F.P.	1179	Vilmin, L.	1048
Van Keken, P.	648	1934	1770	2022
Van Kranendonk, M.	1527	2401	2410	Vince, E.	1832
.....	2497	Vasiliev, A.	2402	Vetlényi, E.J.	2410	Vindel, E.	1831
van Leeuwen, J.	2038	Vasilyev, P.	2402	Vetrov, V.	2411	Vineesh, T.C.	1822
Van Loon, L.R.	696	Vasyukova, E.	2403	Vetter, A.	2411	Vinha Silva, M.M.	805
.....	1174	Vasyukova, O.	2403	Veyalko, I.	2407	
van Ooijen, J.	956	Vauchez, A.	2341	Vezzalini, G.	1168	

Vinograd, V.....	762	Vollmer, C.....	1476	Wada, I.....	2441	Wälle, M.....	1689
.....	1279	1577	Wade, Benjamin.....	890	2441
.....	2092	Vollmer, M.K.....	2426	Wade, Bridget.....	1395	Wallin, B.....	566
Vinther, B.....	2385	Vollstaedt, Hauke.....	1608	Wade, J.....	623	Wallmann, K.....	1031
Violaki, K.....	1975	Vollstaedt, Hauke.....	2427	1768	2270
.....	2419	Vologina, E.....	1876	2363	2427
Violette, A.....	2420	2347	Wade, M.....	1398	Walowski, K.....	2441
Viollier, E.....	1746	Voltolini, M.....	622	Wadham, J.....	1300	Walsh, A.....	2442
Virgili, G.....	694	von Aulock, F.W.....	2428	Wadhwa, M.....	768	Walsh, S.....	831
Visconti, G.....	2362	von Blanckenburg, F.....	944	1188	1704
Vishnevskaya, I.....	2420	2058	Waelbroeck, C.....	793	Walshe, J.....	1819
Visschedijk, A.....	974	2168	1537	Walter, M.J.....	795
Visscher, P.T.....	2184	2315	Waelle, M.....	2431	1486
Visser, B.....	2005	2429	Waerenborgh, J.....	1687	1728
Viti, C.....	809	von der Handt, A.....	2020	Wagener, A.....	1705	2205
.....	2261	2452	Wagner, D.....	2102	2328
Vitkova, M.....	1052	von der Heyden, B.....	2429	Wagner, N.....	800	2442
Vitova, T.....	1530	von der Kammer, F.....	1714	Wagner, S.....	1520	Walter, S.R.....	2356
Vitovtova, V.....	2605	1840	1540	Walters, C.....	2443
Vizio, C.....	2416	2430	1797	Walters, E.R.....	2443
Vlach, S.R.F.....	1307	von Quadt, A.....	704	Wagner, Thomas.....	603	Walther, C.....	2344
Vladimirov, A.....	1503	1132	1187	Walton, E.....	950
.....	1531	1229	1991	Walton, R.....	1258
.....	1757	1962	Wagner, Thomas.....	1522	Walton, W.....	827
.....	2421	2431	1689	Walton-Day, K.....	2486
Vlasova, N.....	1450	von Strandmann, P.....	2211	2436	Walzer, U.....	2444
Vlassopoulos, D.....	1870	Vona, A.....	812	Waight, Tod.....	2357	Wan, A-M.....	1853
.....	2421	993	Waight, Tod E.....	2392	2444
Vlastélic, I.....	1737	1779	Waillace, L.....	1514	Wan, L.....	1621
Voegelin, Andrea R.....	1212	2427	Wainer, K.A.I.....	2436	Wan, Q.....	2445
.....	2075	2428	Wainwright, A.N.....	2437	Wan, S.....	1191
.....	2422	Vonhof, H.....	613	Waite, D.....	1671	Wanamaker, A.....	1631
Voegelin, Andreas.....	1200	2430	2437	Wang, Bao-Li.....	1601
.....	1417	Voordouw, G.....	2431	2571	Wang, Baohua.....	1920
.....	1876	Voorhies, A.....	985	Wakabayashi, D.....	1122	Wang, Baoli.....	2449
.....	2179	Voronin, K.....	2407	Wakabayashi, Y.....	1060	Wang, Baoqun.....	2587
.....	2422	Vorontsov, A.....	2452	Wakaki, S.....	2438	Wang, Bing.....	1574
.....	2502	Vosel, Y.....	2432	Wakita, S.....	1515	Wang, Chao.....	2445
Voelker, B.....	2294	Voss, B.....	794	Walder, I.....	1040	Wang, Chao.....	2613
.....	2423	Vougiokakakis, G.E.....	1959	2107	Wang, Chengyu.....	992
Voelker, T.....	1255	Vrána, S.....	1378	Walder, P.....	1040	Wang, Chien-Ying.....	1525
Vogel, Andreas.....	1218	Vriens, B.....	2432	Waldmann, S.....	1219	Wang, Chun-Chieh.....	1605
Vogel, Antje Kathrin.....	2423	2503	Waldron, S.....	1172	Wang, Chung-Che.....	873
Vogel, Manja.....	2263	Vrkljan, M.....	1141	Walia, V.....	1118	Wang, Chung-Ho.....	1605
Vogel, Monica.....	2424	Vroon, P.....	1152	Walker, A.....	2438	Wang, Chunjiang.....	2446
Vogel, N.....	769	1474	Walker, J.....	1897	Wang, Chunyan.....	1844
.....	2424	1835	Walker, R.....	886	Wang, D.....	1191
Vogl, J.....	2085	Vrublevskii, V.....	1159	1199	2446
.....	2425	2433	1871	Wang, Fang.....	1623
Vogt, C.....	1108	Vuba, S.....	2433	2003	1625
.....	1734	Vuilleumier, R.....	1972	2067	2447
Vogt, K.....	1197	2434	2348	Wang, Fangyue.....	2447
Vogt, T.....	1574	Vukmanovic, Z.....	2434	2439	Wang, Feiyu.....	2448
Voinot, A.....	1582	Vysotskiy, S.....	2535	Walker, S.....	2439	Wang, Feng.....	1138
.....	2063	W		Wall, C.....	2171	2309
Voisin, C.....	1203	W. Friedrich, M.....	2053	Wall, F.....	2440	2448
Voistinova, E.....	1452	Wacey, D.....	2435	Wall, J.....	695	2530
Voit, A.....	2425	Wachniew, P.....	1660	1945	2545
Völgyesi, P.....	2426	Wacker, L.....	1272	Wallace, A.f.....	987	Wang, FengPing.....	2449
Völker, C.....	1139	1302	Wallace, Adam.....	2440	2522
Volkman, J.....	2196	Wacker, U.....	1745	Wallace, P.....	723	Wang, Fushun.....	1654
Volkova, N.....	1757	2435	1124	2449
.....	2421	2441	Wang, Guizhi.....	807

Wang, Guo	2587	Wang, Yong Lei	2013	Watanabe, N.	1246	Weiping, F.....	2448
Wang, Hao Lin	2013	Wang, Yongbin	2526	1711	Weis, D.	918
Wang, Hongjun	1604	Wang, Yongli	2514	1874	1712
Wang, Hua.....	1607	Wang, Youxiao	2514	Watanabe, S-I.	2470	1805
Wang, Huajian.....	2450	Wang, Yu.....	2279	Watanabe, Takahiro	1826	2477
.....	2457	Wang, Yu.....	2463	2470	Weis, U.	1394
Wang, Jianhua	2255	Wang, Yu.....	873	Watanabe, Takeshi.....	1427	2268
.....	2450	Wang, Yuan	1671	Watanabe, Tsuyoshi.....	2471	2477
Wang, Jianwei	2451	Wang, Yuchun	2463	2543	Weisberg, M.....	1026
Wang, Juanjuan	2451	Wang, Yue	1002	Watanabe, Yasushi	607	Weisenburger, S.....	1530
Wang, K-L.....	2452	Wang, Yuejun	2599	2127	Weisener, C.....	750
Wang, Lianxun	2452	Wang, Yuheng	778	Watanabe, Yoshio.....	1769	948
Wang, Lichao	1334	1792	Watanabe, Yumiko	880	1107
Wang, Lijuan	2453	2464	Watanabe, Yumiko	2471	2043
Wang, Liying	2592	Wang, Yunpeng	2464	Watanabe, Yumiko	1267	2109
Wang, M.....	2453	Wang, Yunshuen	864	Waterton, P.....	942	2478
Wang, Qi Lian	872	Wang, Zaicong	2465	Watkins, J.	2472	Weisner, M.....	2257
Wang, Quan.....	2603	Wang, Zecheng.....	1222	Watson, A.	1763	Weiss, D.....	1454
Wang, Quan.....	700	1388	Watson, E.B.....	1126	1546
Wang, Rucheng	1628	1598	1317	1937
.....	2595	2454	Watson, P.....	1082	Weiss, H.....	1156
Wang, Ruiju	1388	2523	Watt, S.	1400	Weiss, S.....	668
.....	2454	2531	Watts, Kathleen.....	2472	Weiss, Y.....	2478
Wang, Ruilin	2585	Wang, Zhaoyun	1604	Watts, Kathryn	1008	Weiss-Penzias, P.....	882
Wang, Shan-Shan	2454	2465	Wawer, M.	1668	Weijden, B.	2288
Wang, Shuhong	2455	Wang, Zheming	1673	Wawryk, C.....	2473	Welander, P.V.	2056
Wang, Tao	2458	Wang, Zhen	2239	Waychunas, G.A.....	1077	2479
Wang, Tijian.....	1340	Wang, Zhengrong	1622	1170	Welding, K.....	1722
Wang, Tong	2526	2012	2275	Welker, J.M.....	1592
Wang, Tongshan	1598	2330	2440	Weller, R.A.....	2272
.....	2455	2466	2473	Weller, S.	2479
Wang, Wei.....	2309	2568	Weaver, K.....	1009	Wellman, D.....	2480
.....	2530	2597	1719	Wellmann, E.	1431
Wang, Wei-Ning	1389	Wang, Zhengyang	820	Webb, E.	1368	Wellpott, A.....	1644
Wang, Wengxia.....	2456	Wang, Zhilin.....	2525	Webb, G.	1422	Wen, H-Y.....	1568
Wang, Xiang	866	Wang, Zhiqiang	865	Webb, L.	624	2480
Wang, Xiang-Dong	2571	Wangermez, W.....	772	2474	Wen, M.	1654
Wang, Xiang-Li.....	1977	Wankel, S.	786	Webb, S.M.....	1090	Wen, Y.	1318
.....	2615	2466	1397	Weng, Y.....	2385
Wang, Xiao	2456	Wanner, C.....	2467	2474	Wenk, C.B.....	718
Wang, Xiao Yuan	2458	Wanyan, Q.....	1632	Weber, H.S.	2475	2622
Wang, Xiaodan	2550	Ward, L.....	1763	Weber, K.....	1218	Wenke, A.	1111
Wang, Xiaofang	1652	Ward, N.	799	Weber, P.	1845	Wensaas, L.....	2258
Wang, Xiaohong	1394	Wardlaw, G.D.....	612	Webster-Brown, J.	1961	Wentzovitch, R.....	2514
Wang, Xiaolin	851	Waroszewski, J.....	1456	Wegener, G.....	883	Wenzel, M.....	989
.....	1334	Warr, L.N.....	1845	1301	2481
.....	2457	Warr, O.....	703	1890	Wenzel, T.....	2318
Wang, Xiaomei	2450	2467	2566	2452
.....	2457	2613	Wehrli, B.	1900	Wenzhöfer, F.....	726
Wang, Xiaoxia.....	2458	Warren, C.	1796	2026	Werner, R.....	1956
Wang, Xin-Hai.....	2459	Warren, J.	934	2233	Werner, S.C.....	2481
Wang, Xingchen.....	2459	1527	Wehrmann, H.....	1373	Wersin, P.....	2482
Wang, Xinyu	2460	2468	Wehrmann, L.M.....	2475	Wesolowski, D.....	682
Wang, Xiuyu	1831	Warren, L.....	2131	Wei, C.	1819	1663
Wang, Xu	931	Warrier, R.B.....	839	Wei, Hailun	1594	West, A.J.....	1786
.....	2460	Wasch, L.....	2468	Wei, Hao	2526	2347
Wang, Yafei	2461	Washington, K.....	2469	Wei, Y.....	2603	2482
Wang, Yanbin	854	Wåstegard, S.....	898	Weider, S.	1856	West, K.	1931
.....	2167	Wasylenki, L.	2469	Weigand, A.	2222	Westall, F.....	1342
.....	2461	Watanabe, A.	2529	Weigand, M.	2050	Westermann, S.....	2483
Wang, Yanhai	2526	Watanabe, K.....	1714	WeiJun, S.	2560	Westin, A.	2483
Wang, Ying	2462	2562	Weinstein, Y.	2476	Westphal, A.....	1589
Wang, Yong	2462	2562	Weinzierl, C.....	2476	2484

Wetzel, D.T.	2484	Wiegand, B.A.	767	William, G.	2196	Wirth, R.	692
Weyer, S.	570	1993	Williams, B.	2436	949
.....	977	2491	Williams, C.	814	1203
.....	1188	Wiegand, M.	1442	Williams, Earle	596	1208
.....	1188	Wieland, E.	936	Williams, Elizabeth	2084	1283
.....	1559	2492	Williams, Emma	1454	1424
.....	1879	Wielandt, D.	1315	Williams, H.	939	1529
.....	2015	2492	1274	Withers, A.	2504
.....	2213	Wieler, R.	1302	2499	Withers, P.	656
Weynell, M.	2485	1515	Williams, I.S.	891	Witrant, E.	1933
.....	2490	1699	2499	Witt, A.	1320
Whaler, C.	777	2424	Williams, K.	572	Witt, M.	2157
Whan, T.	1382	Wielicki, M.	2493	1377	2504
Wheat, G.	1895	Wiens, Roger	1590	2197	Wittebroodt, C.	2379
Whitaker, F.	1125	Wiens, Roger C.	2269	2500	Wittmann, H.	944
.....	1379	Wiersberg, T.	1072	Williams, M.	2172	Wittmer, J.	2505
White, Alistair	2485	1457	2231	Wlodyka, R.	1160
White, Art F.	800	Wieser, M.	573	2500	Wodicka, N.	1929
White, J.	1180	1726	Williams, Terry	1650	Wogelius, R.	656
White, L.	2486	1761	Williams, Trevor	2389	1029
White, S.J.	2486	2322	Williams-Jones, A.E.	2333	2400
White, T.	976	Wiesner, M.R.	664	2397	2505
White, W.	2487	1645	2403	2622
Whitehouse, M.J.	805	2493	2501	Wohlgenuth-Ueberwasser,	
.....	892	Wigley, M.	703	Williamson, C.	2321	C.C.	2506
.....	1008	2613	Williford, K.H.	1588	Woillez, M-N.	2053
.....	1115	Wignall, P.	2213	Willner, A.	1799	Wold, S.	1862
.....	1383	2494	Wills, J.	2501	Wolf, A.S.	624
.....	1528	Wijbrans, I.	1476	Wilson, A.H.	1308	Wolf, M.	847
.....	1529	2494	Wilson, C.J.N.	850	Wolf-Gladrow, D.	900
.....	1865	Wijbrans, J.R.	2371	859	1139
.....	2086	Wijker, R.S.	1310	1319	Wolff, P.E.	816
.....	2400	Wiklund, J.	599	Wilson, D.	2502	Wolff-Boenisch, D.	1178
.....	2487	Wilczynska-Michalik, W.	1753	Wilson, G.	2248	1225
.....	2488	2495	Wilson, J.	1395	Wolke, R.	764
Whitelam, S.	2440	Wilde, S.A.	1529	Wilson, P.A.	617	Wollack, E.A.	846
Whitesides, G.	2312	2386	1894	Wolock, C.	2246
Whithouse, M.	851	2495	Wilson, R.	2159	Wolthers, M.	1211
Whiticar, M.	2488	Wilhelm, C.	988	Wilson, S.A.	1262	2506
Whitney, D.L.	1101	Wilhelm, S.	1037	Wimpenny, J.	1343	Wołkiewicz, K.	2507
.....	1199	Wilke, F.D.H.	2496	2193	Wołkiewicz, S.	730
Whittle, R.	1869	Wilke, M.	739	2261	1221
Whyte, L.	1945	989	Wing, B.	695	1478
Wiacek, A.	2489	2215	835	2507
Wibberley, E.	1486	Wilkes, H.	2110	923	Wombacher, F.	1034
Wichser, A.	1876	Wilkinson, D.	2496	1945	1122
Wick, L.	1240	Will, T.	1442	Winguth, A.	1647	1512
.....	2329	Willbold, M.	1296	Winkel, L.	704	2041
Widanagamage, I.	2489	2497	717	2507
Widdowson, M.	637	Wille, M.	1047	2432	Wood, B.	623
Widom, E.	1547	1527	2502	1472
.....	2031	1835	2503	1713
Widory, D.	978	2162	Winkler, B.	668	1768
Wiechert, U.	1113	2497	2092	1828
.....	2485	Willenbring, J.	744	Winkler, P.	2227	1862
.....	2490	1055	Winkler, R.	2048	2363
Wieclaw, D.	2490	2160	Winter, A.	2503	2397
Wieczorek, M.	653	2161	Winterhalder, S.	2503	2508
Wieczorek, R.	1064	2469	Wintsch, R.P.	1750	Wood, R.	895
Wiedenbeck, M.	2025	2498	Wirick, S.	1096	Woodard, J.	2508
.....	2074	Willett, S.	1289	2290	Wooden, J.	1723
Wiederhold, J.G.	2491	Willey, J.	1456	1760
Wiederin, D.	1082	2498				

Woodhead, J.D.	1683	Wulf, S.	2340	Xiong, F.	2072	Yakovleva, S.	2536
.....	1936	Wunder, B.	695	Xiong, Q.	2523	Yakubovich, O.	1775
.....	2226	1042	Xiong, X.	2446	2207
.....	2369	1208	Xu, A.	2523	2536
.....	2509	2048	Xu, Chao	2524	Yakymchuk, C.	2536
Woodland, A.	1713	Wunderlich, A.	2515	Xu, Chen	1597	Yalcin, F.	1459
.....	2373	Wunsch, A.	1470	2524	2537
.....	2509	2515	Xu, D.	2525	Yalcin, M.G.	1459
.....	2555	Würdemann, H.	1434	Xu, G.	1156	Yalcin Erik, N.	1906
Woods, G.	2510	1435	2525	2537
Woodward, E.M.S.	780	1589	Xu, H.	2287	Yamada, A.	1272
.....	1316	1794	Xu, Jinyong	2526	Yamada, H.	2538
.....	1329	1841	Xu, Jiuhua	2526	Yamada, K.	2540
.....	1637	2484	Xu, Jun	2522	Yamada, M.	2317
.....	2363	2516	Xu, L.	1614	2538
Wookey, J.	2438	Wurm, M.	2516	Xu, Leiluo	2527	Yamada, Ryoichi	2470
Worden, J.	1568	Wurz, P.	2062	Xu, Li	1617	Yamada, Ryuji	2539
Worden, R.	941	Wuttig, K.	927	Xu, Li	1365	Yamagata, T.	2317
Wörmer, L.	1055	Wyatt, N.	1637	Xu, Lin	2527	Yamaguchi, A.	1239
.....	2510	Wyborn, L.	666	Xu, Liukang	1722	1772
Wörner, G.	571	Wylie, R.	2517	Xu, Liying	2528	1906
.....	1280	Wynn, P.M.	2225	Xu, M.	2309	2539
.....	1320	2517	Xu, R.	2528	Yamaguchi, Katsuhiko	2529
Wotzlaw, J-F.	2148	Wysocka, I.	2113	Xu, S.	2529	Yamaguchi, Kohei	1361
.....	2511	2518	Xu, T.	1652	2540
Wright, D.	2293	X		Xu, T.	1652	Yamaguchi, Kosei E.	1765
Wright, K.	2321	Xanthos, S.	1136	Xu, Wei	2529	2534
Wrighton, K.	572	Xavier, A.M.	908	Xu, Wenli	1607	2540
Wtight, I.	2406	Xavier, R.	966	Xu, Wenliang	2530	Yamaguchi, N.	584
Wu, Changzhi	1580	2224	2545	Yamaguchi, T.	2541
Wu, Cheng Yun	1222	Xhixha, G.	1224	Xu, Wenliang	2309	Yamaguchi, Y.	2541
Wu, Chenjun	1630	2002	2448	Yamakawa, A.	2559
.....	2591	2519	Xu, X-Y.	2530	Yamamoto, J.	1302
Wu, Dai-She	2187	Xi, B.	2196	Xu, Y.	1614	2349
Wu, Daidai	2511	Xia, B.	2609	Xu, Yan	681	Yamamoto, Masahiro	1826
Wu, Francis	1525	Xia, F.	2519	Xu, Yi Ming	1232	Yamamoto, Masanobu	1793
Wu, Fu-Yuan	1177	Xia, L-Q.	2530	Xu, Yigang	1615	Yamamoto, S.	601
.....	1386	Xia, X-R.	2191	Xu, Yu-Hui	2531	1438
.....	1613	Xia, Y.	2514	Xu, Zhaohui	2531	2202
.....	1623	2520	Xu, Zheng	2532	2541
.....	2331	Xia, Z-C.	2530	Xu, Zhengjiu	1844	Yamamoto, Y.	2521
.....	2383	Xiang, H.	2010	Xu, Zhengqi	2237	Yamano, H.	2543
.....	2512	2520	2532	Yamaoka, K.	2542
.....	1600	2599	Xu, Zhifang	1627	Yamasaki, Seiko	2542
Wu, Jia-De	1600	Xiang, X.	2206	Xu, Zhijun	2533	Yamasaki, Shinichi	1826
Wu, Jichun	2287	Xiao, H-Y.	2187	Xue, B.	2446	2470
Wu, L-J.	1601	2521	Xue, C.J.	1222	Yamasaki, Shinya	1882
Wu, Minchao	618	Xiao, J.	931	Xue, G.	1691	Yamashina, Y.	1121
Wu, Mong Sin	1069	2460	Xue, X.	1429	Yamashita, K.	2559
Wu, N.	2511	2521	2533	Yamato, P.	844
Wu, Shiliang	2512	Xiao, N.	1132	Xue, Y.	867	Yamazaki, A.	2471
Wu, Songtao	930	Xiao, S.	2193	Xue, Z-C.	2548	2543
Wu, Weihua	1917	2522	Xue, Zichen	956	Yamazaki, D.	2543
.....	2513	Xiao, X.	2445	Xue, Ziqiu	1441	Yamazaki, H.	2561
Wu, Wenfang	2294	Xiao, Yi	571	2353	Yamazaki, R.	1769
.....	2513	Xiao, Yilin	2199	Y		Yan, B.	2544
Wu, X-L.	846	Xiao, Yuming	2310	Yabusaki, S.	2500	Yan, H.	1923
Wu, Ye	1429	2522	Yabuta, H.	2534	Yan, W.	2455
Wu, Yingqin	2514	Xie, G.	2287	Yacovitch, T.	2575	2544
Wu, Yuanqiao	719	Xie, L.	1331	Yahagi, T.R.	2534	Yan, Y.	886
Wu, Zhengquan	1653	Xie, Shucheng	1651	Yaita, T.	2535	Yanai, Y.	2623
Wu, Zhongqing	1073	1301	Yajie, L.	2560	Yanful, E.	2342
.....	1336	Xing, L.	2477	Yakovenko, V.	2535	Yang, Chengfan	1594
.....	2514						

Yang, Chun	2546	Yao, M.	1682	Yonezu, K.	1714	Yudovskaya, Marina	856
Yang, Dan	2545	Yao, Q-Z.	1389		2562	Yui, T-F.	2572
Yang, Debin	2545	Yao, X.	1628	Yoo, E-J.	879		2582
Yang, Dongsheng	1920	Yao, Y.	1391	Yoo, J.	1193	Yumimoto, K.	2572
Yang, E-L.	2571	Yasuda, K.	1711	Yoo, K.	2563	Yun, S-T.	668
Yang, Fan	2546	Yasuda, S.	2554	Yoon, P.	1351		997
Yang, Fang	1574	Yasuhara, A.	1758	Yoon, Soon-Chang	2563		1412
Yang, Gang	2258	Yasukawa, K.	2554	Yoon, Suk-Hee	2564		1460
	2356	Yates, M.	1214	Yoon, Sungjun	2564		1569
	2546	Yau, A.	2555	Yoon, Yook	877		2459
Yang, Guicai	2547	Yaxley, G.M.	1253	Yoon, Yoon Yeol	877	Yurgenson, G.	2234
Yang, Hong	1625		1306		1430	Yurichev, A.	2573
	2547		2402		2565	Yurimoto, H.	643
Yang, Hsian-Ming	1567		2555	Yoshida, E.	2565		1901
Yang, J.	1614	Yazdi, M.	1861	Yoshida, N.	1272		2573
	2548		2111		1804	Yürür, T.	1525
Yang, Jiehua	1118		2556		2623		
Yang, Jing-Hong	2548	Yeager, C.	1597	Yoshida, S.	1769	Z	
Yang, Jingsui	1215	Yeats, C.	2556	Yoshida, T.	1825	Zaarur, S.	2574
	2072	Yebra-Rodríguez, Á.	1077	Yoshida, Z.	1882	Zabel, M.	756
Yang, Jung-Seok	1533	Yechieli, Y.	633	Yoshie, N.	1793		2166
Yang, K.	2410		1556	Yoshikawa, H.	1821	Zaccarini, F.	1636
Yang, Li	572		1593		2292	Zacháry, D.	2426
	1377	Yeh, G.	1960	Yoshikawa, Makoto	2470	Zack, T.	2574
	1859	Yehudai, M.	2557	Yoshikawa, Masako	1484	Zafra, C.	2351
Yang, Liyan	1580	Yen, A.S.	1794		2566	Zagorsky, V.	2421
Yang, M.	1654	Yesiloren-Gormus, N.	2557	Yoshinaga, M.	2201	Zaharescu, D.	1005
Yang, P.	2549	Yeung, L.	2558		2566	Zaheer Hasan, S.	597
Yang, R.	2549	Yi, F.	1647	Yoshino, T.	2543		2028
Yang, Shou Ye	700	Yi, H-I.	2564	Yoshioka, H.	2567		2029
	1594	Yi, J.	820	Yoshiya, K.	1303	Zahiri, R.	995
	2550	Yi, K.	1924		2567		995
Yang, Shui-Yuan	2550	Yin, B.	1232	Yoshiyuki, I.	1605	Zahn, A.	884
Yang, Shun-Chun	1566	Yin, N.H.	2558	You, C-F.	855	Zahniser, M.	1892
Yang, Tao	1150		2559		1614		2575
Yang, Tiffany	1591	Yin, Q-Z.	957	Youbi, N.	1701	Zaiss, J.	2575
Yang, Tsanyao Frank	864		1343	Young, E.	864	Zaitsev, A.	848
	1118		2193		2094		2175
	1568		2261		2558		2576
	2480		2559	Young, H.P.	2568	Zajac, K.	719
	2551	Yin, Zuo-Ying	2615	Young, K.	692	Zajacz, Z.	705
Yang, W.	1614	Yin, Zuo-Ying	2521	Yttri, K.E.	843		1238
Yang, Wei	2551	Ying, J-F.	2560	Yu, Changxun	2568		1254
Yang, Wei	2552		2612	Yu, Chaoqi	1595		1686
Yang, Wei-Long	2598	Yipeng, Z.	2560	Yu, Hang	2569		2361
Yang, Xiaolin	2446	Yokochi, R.	2335	Yu, Hongyu	1885		2410
Yang, Xiaoyong	1615	Yokoyama, A.	1467	Yu, Tao	2569		2576
	2286	Yokoyama, Tadashi	696	Yu, Tony	2461		2577
Yang, Yang	1138	Yokoyama, Takushi	1707	Yu, Xiaojian	2596	Žák, J.	2360
Yang, Yang	2533		1901	Yu, Xu Dong	1946	Zakharikhina, L.	2577
Yang, Yang	2552		2561	Yu, Xudong	2585	Zalaszewicz, J.	1502
Yang, Yu Ping	2553		2562	Yu, Y.	2463	Žaludková, K.	2578
Yang, Yuanyuan	2446	Yokoyama, Tetsuya	1071	Yu, Z.	2570	Zamana, L.V.	2578
Yang, Yueheng	886		1816	Yuan, F.	2524	Zammit, C.	2047
Yang, Zhaoping	1501		1820	Yuan, Kaiqing	677	Zamora, L.M.	2579
Yang, Zhiming	2545		1888	Yuan, Ke	675	Zamponi, M.	696
Yang, Zhongfang	2569		2307		2570	Zanchetta, G.	911
Yang, Zhou	1601		2561	Yuan, Q.	2571		1010
Yang, ZhuSen	1631	Yokoyama, Y.	2338	Yuan, S.	2547		1363
	2330		2562	Yuan, Xiu	2571		2037
Yang, Ziming	2553	Yoneda, A.	2543	Yuan, Xuyin	1680		2579
Yans, J.	2271	Yoneda, S.	1297	Yubuta, K.	1758		2580
Yao, C.	2449	Yonemochi, S.	1647	Yudovskaya, Marina	1313	Zanda, B.	1196

Zane, G.	695	Zhang, Gui Hua	2601	Zhang, Xuetong	1333	Zhao, Yuyan.....	1646
.....	1945	Zhang, Guo Ping.....	872	2592	Zhao, Zhi-Qi	1543
Zanella, E.	2037	Zhang, Haikun	2611	2596	Zhao, Zhihong	2604
Zanetti, A.	740	Zhang, Hong	2286	Zhang, Yan	2596	Zhao, Zhiqi.....	1627
.....	1177	Zhang, Hongluo.....	2590	Zhang, Yanbin	886	Zhao, Zi-Fu	2532
.....	1545	Zhang, Hui	1074	Zhang, Yanglin	1332	Zhaoli, S.	2560
.....	2354	Zhang, J.	1614	Zhang, Yanling	2597	Zharikov, A.	2605
Zanon, V.	2580	Zhang, Jiahui	2461	Zhang, Yi Ge	2597	Zheng, C.....	2161
Zaoui, L.	2581	Zhang, Jianchao.....	2551	Zhang, Yihan	2309	Zheng, F.	1774
Zapol, P.	2581	Zhang, Jie	1387	Zhang, Yingjie	1650	Zheng, G.	2605
Zarkadas, C.	1136	Zhang, Jin S	2590	Zhang, Yong Mei.....	1222	Zheng, Hang	1187
Zarzycki, P.	861	Zhang, Jing	1654	2598	Zheng, Hongbo	2513
.....	2582	Zhang, Junwen.....	1003	Zhang, Youxue	1844	Zheng, Hongju	2465
Zaw, K.	2582	Zhang, Li	1063	1978	Zheng, Jian	2538
Zazzeri, G.	1644	2520	2598	Zheng, Jianping.....	2523
Zcheng, L.	2593	2607	Zhang, Yu	2522	Zheng, Liange	2606
Zedgenizov, D.	2019	Zhang, Lifei	1011	Zhang, Yuan	1612	Zheng, Linjie.....	1491
.....	2190	2547	Zhang, Yuzhi	2599	Zheng, Xiangmin	1336
.....	2583	Zhang, Like	1574	Zhang, Zeming.....	2010	Zheng, Xinyuan.....	1977
Zega, T.	1760	Zhang, Liuping	2591	2520	Zheng, Yan	2606
Zegeye, A.	2583	2603	2599	Zheng, Yi	2607
.....	2584	Zhang, Luyuan.....	2529	Zhang, Zhan	682	Zheng, Yong-Fei	2532
Zeh, A.	2316	Zhang, Maoliang	2480	1663	Zhilicheva, O.....	560
.....	2584	Zhang, Meiyi	1917	Zhang, Zhaochong	1326	Zhitova, L.....	2607
Zeitvogel, F.	1479	Zhang, Min	1920	2453	Zhiyanski, M.	1348
Zelano, I.	2585	Zhang, Mingfeng	2591	2600	Zhmodik, A.	2608
Zelenski, M.	2313	Zhang, Nan	2544	Zhang, Zhaohui.....	2600	Zhmodik, S.....	1557
Zema, M.	1038	Zhang, Ni	2605	Zhang, Zhaoming.....	1650	1558
Zeman, J.	2578	Zhang, P.	1011	Zhang, Zhaoqing	2330	1815
Zemskaya, T.	1638	Zhang, Rongchi	1647	Zhang, Zhirong	2196	2608
.....	1982	Zhang, Ronghua	1333	Zhang, Zhou Bin	2601	Zhong, G.	2608
Zender, C.....	568	2592	Zhao, D-M.	1138	Zhong, Lichun	1341
Zeng, C.	2549	2596	Zhao, G.	1622	Zhong, Lifeng	2544
Zeng, G.	1011	Zhang, Runyu	2592	Zhao, H.	941	2609
Zeng, Q.	2526	Zhang, Saijing	1597	2601	Zhong, Z.	2010
Zeng, Y.	1946	Zhang, Shoupeng	1603	Zhao, Jian-Xin	2379	2520
.....	2585	Zhang, Shuang	2012	Zhao, Jing	1598	Zhornyak, L.....	1363
Zeng, Z.G.	2458	Zhang, Shuichang	2279	Zhao, Jiyong	948	Zhou, C.	2193
.....	2586	2450	2085	Zhou, D.	2609
.....	1597	2457	Zhao, Jun	2227	Zhou, G-T.	1389
Zeren, N.....	1597	2614	Zhao, K-D.	2602	Zhou, Han-Wen.....	2520
Zerkle, A.	817	Zhang, Si-Ting.....	2309	Zhao, Laishi	1335	Zhou, Huaiyang.....	986
.....	1066	Zhang, Tingshan	1632	Zhao, Liang.....	1774	Zhou, Jie.....	2610
.....	1367	2552	2602	Zhou, Jie.....	931
.....	2586	2552	Zhao, Meixun.....	2311	Zhou, Jing	1601
Zernack, A.	2265	2593	Zhao, Min	2549	Zhou, Jinhong	2610
Zetsch, C.	2139	Zhang, Tong	1255	Zhao, N.	829	Zhou, Lian.....	1335
Zettlitzer, M.....	1794	1560	Zhao, Q.	1334	Zhou, Limin	1336
Zeyer, T.	1213	2404	Zhao, Taiping.....	2612	Zhou, Mei-Fu	1626
Zezin, D.	2587	2423	Zhao, Tong.....	1627	2072
Zhai, Mingguo.....	1330	Zhang, Tonggang.....	2593	Zhao, W.	2533	Zhou, Meng.....	2387
Zhai, Minhhuo.....	2612	Zhang, Wei	1341	Zhao, X.	1614	Zhou, P.	1331
Zhai, X.	1222	Zhang, Wen	1335	Zhao, Xia	1140	Zhou, Q.	1337
Zhang, B.	2543	2594	2603	Zhou, R.	1237
Zhang, Chengjiang	2587	Zhang, Wenfang	2594	Zhao, Xianzheng.....	2603	Zhou, S.....	2611
Zhang, Chengjun	2588	Zhang, Wenlan	2595	Zhao, Xiao-Feng	852	Zhou, T.	2524
Zhang, Chunming.....	2454	Zhang, Xianwei	1917	Zhao, Y	2113	2608
Zhang, Chunming.....	2454	Zhang, XiaoFeng	2603	Zhao, Yin	1583	Zhou, W.	1331
Zhang, Dayu	2524	Zhang, Xiaohua	2544	Zhao, Yingquan	2591	2611
.....	2588	Zhang, Xiaoran	2196	Zhao, Yiying	1191	Zhou, Xiaoli	1259
Zhang, Dezhong	1011	Zhang, Xinning.....	681	Zhao, Yongwei	2604	1647
Zhang, Di.....	2595	2595	Zhao, Yue	2330	Zhou, Xinhua	2612
Zhang, Dingding	2589	Zhang, XinXu	2449	Zhao, Yusheng.....	2310	Zhou, Xuan	2446
Zhang, Feiwu.....	2589						
Zhang, Fucun.....	1003						

Zhou, Yanyan.....	2612	Zipori, A.....	2620
Zhou, Yu.....	1387	Zirjani Zadeh, S.....	2621
Zhou, YueHeng.....	2449	Zirner, A.....	2621
Zhou, Z.....	703	Ziveri, P.....	1696
.....	2613	Zolensky, M.....	1758
Zhu, Baoli.....	2030	Zong, K.....	1277
Zhu, Bi.....	2548	2528
Zhu, Biao.....	2345	Zonneveld, K.....	2408
Zhu, C.....	1221	Zopfi, J.....	718
.....	1646	2622
.....	2602	Zoroglu, O.....	1231
.....	2613	Zotiadis, V.....	613
Zhu, D.....	2330	Zotzmann, J.....	2039
Zhu, Guangxu.....	1234	Zou, B.....	2505
.....	1954	2622
.....	2614	Zou, C.....	1333
Zhu, Guangyou.....	2279	Zou, Y.....	2623
.....	2614	Zouiten, C.....	2415
Zhu, Jialei.....	1340	Zucchini, A.....	908
Zhu, Jian-Ming.....	2615	1154
Zhu, Jianxi.....	2610	Zuend, A.....	1137
Zhu, Jinchu.....	2615	Zulauf, G.....	2380
Zhu, L.....	2194	Zuo, W.....	2601
Zhu, Q.....	2522	Zuschin, M.....	1746
Zhu, Ren-Guo.....	2521	Zwick, A.....	1983
Zhu, Rixiang.....	1277	Zwingmann, H.....	1108
Zhu, Rong.....	1055	2542
Zhu, Rukai.....	930	2623
.....	1333	Zykov, S.....	1677
Zhu, T.....	2616	Zyryanova, L.....	741
Zhu, W.P.....	2598		
Zhu, Xiangkun.....	1002		
.....	2544		
.....	2616		
Zhu, Xiangyu.....	1624		
Zhu, Xiaojun.....	2617		
Zhu, Ying.....	1039		
Zhu, Yong.....	994		
Zhu, Yongxuan.....	1317		
Zhu, Yujiao.....	1628		
Zhu, Z.....	2617		
Zibera, L.....	2618		
Ziegler, K.....	864		
Ziegler, M.....	1443		
.....	1759		
Ziemann, P.....	1960		
Zieringer, M.....	2618		
Ziervogel, K.....	619		
Zimmer, M.....	1072		
.....	1847		
Zimmerman, A.....	2546		
.....	2619		
Zimmerman, S.....	2153		
Zimmermann, C.....	2047		
Zimmermann, G.....	767		
Zimmermann, L.....	1699		
.....	1700		
Zimmermann, U.....	2456		
Zimmermann, Y-S.....	2619		
Zinke, L.....	2037		
Zinkutè, R.....	2313		
Zipfel, J.....	1196		
Zipfel, Jutta.....	2620		